NCHRP

REPORT 725

NATIONAL COOPERATIVE HIGHWAY RESEARCH PROGRAM

Guidelines for Analysis Methods and Construction Engineering of Curved and Skewed Steel Girder Bridges

TRANSPORTATION RESEARCH BOARD
OF THE NATIONAL ACADEMIES

TRANSPORTATION RESEARCH BOARD 2012 EXECUTIVE COMMITTEE*

OFFICERS

CHAIR: **Sandra Rosenbloom,** *Professor of Planning, University of Arizona, Tucson*
VICE CHAIR: **Deborah H. Butler,** *Executive Vice President, Planning, and CIO, Norfolk Southern Corporation, Norfolk, VA*
EXECUTIVE DIRECTOR: **Robert E. Skinner, Jr.,** *Transportation Research Board*

MEMBERS

J. Barry Barker, *Executive Director, Transit Authority of River City, Louisville, KY*
William A.V. Clark, *Professor of Geography and Professor of Statistics, Department of Geography, University of California, Los Angeles*
Eugene A. Conti, Jr., *Secretary of Transportation, North Carolina DOT, Raleigh*
James M. Crites, *Executive Vice President of Operations, Dallas-Fort Worth International Airport, TX*
Paula J. C. Hammond, *Secretary, Washington State DOT, Olympia*
Michael W. Hancock, *Secretary, Kentucky Transportation Cabinet, Frankfort*
Chris T. Hendrickson, *Duquesne Light Professor of Engineering, Carnegie-Mellon University, Pittsburgh, PA*
Adib K. Kanafani, *Professor of the Graduate School, University of California, Berkeley*
Gary P. LaGrange, *President and CEO, Port of New Orleans, LA*
Michael P. Lewis, *Director, Rhode Island DOT, Providence*
Susan Martinovich, *Director, Nevada DOT, Carson City*
Joan McDonald, *Commissioner, New York State DOT, Albany*
Michael R. Morris, *Director of Transportation, North Central Texas Council of Governments, Arlington*
Tracy L. Rosser, *Vice President, Regional General Manager, Wal-Mart Stores, Inc., Mandeville, LA*
Henry G. (Gerry) Schwartz, Jr., *Chairman (retired), Jacobs/Sverdrup Civil, Inc., St. Louis, MO*
Beverly A. Scott, *General Manager and CEO, Metropolitan Atlanta Rapid Transit Authority, Atlanta, GA*
David Seltzer, *Principal, Mercator Advisors LLC, Philadelphia, PA*
Kumares C. Sinha, *Olson Distinguished Professor of Civil Engineering, Purdue University, West Lafayette, IN*
Thomas K. Sorel, *Commissioner, Minnesota DOT, St. Paul*
Daniel Sperling, *Professor of Civil Engineering and Environmental Science and Policy; Director, Institute of Transportation Studies; and Acting Director, Energy Efficiency Center, University of California, Davis*
Kirk T. Steudle, *Director, Michigan DOT, Lansing*
Douglas W. Stotlar, *President and CEO, Con-Way, Inc., Ann Arbor, MI*
C. Michael Walton, *Ernest H. Cockrell Centennial Chair in Engineering, University of Texas, Austin*

EX OFFICIO MEMBERS

Rebecca M. Brewster, *President and COO, American Transportation Research Institute, Smyrna, GA*
Anne S. Ferro, *Administrator, Federal Motor Carrier Safety Administration, U.S.DOT*
LeRoy Gishi, *Chief, Division of Transportation, Bureau of Indian Affairs, U.S. Department of the Interior, Washington, DC*
John T. Gray II, *Senior Vice President, Policy and Economics, Association of American Railroads, Washington, DC*
John C. Horsley, *Executive Director, American Association of State Highway and Transportation Officials, Washington, DC*
Michael P. Huerta, *Acting Administrator, Federal Aviation Administration, U.S.DOT*
David T. Matsuda, *Administrator, Maritime Administration, U.S.DOT*
Michael P. Melaniphy, *President and CEO, American Public Transportation Association, Washington, DC*
Victor M. Mendez, *Administrator, Federal Highway Administration, U.S.DOT*
Tara O'Toole, *Under Secretary for Science and Technology, U.S. Department of Homeland Security, Washington, DC*
Robert J. Papp (Adm., U.S. Coast Guard), *Commandant, U.S. Coast Guard, U.S. Department of Homeland Security, Washington, DC*
Cynthia L. Quarterman, *Administrator, Pipeline and Hazardous Materials Safety Administration, U.S.DOT*
Peter M. Rogoff, *Administrator, Federal Transit Administration, U.S.DOT*
David L. Strickland, *Administrator, National Highway Traffic Safety Administration, U.S.DOT*
Joseph C. Szabo, *Administrator, Federal Railroad Administration, U.S.DOT*
Polly Trottenberg, *Assistant Secretary for Transportation Policy, U.S.DOT*
Robert L. Van Antwerp (Lt. Gen., U.S. Army), *Chief of Engineers and Commanding General, U.S. Army Corps of Engineers, Washington, DC*
Barry R. Wallerstein, *Executive Officer, South Coast Air Quality Management District, Diamond Bar, CA*
Gregory D. Winfree, *Acting Administrator, Research and Innovative Technology Administration, U.S.DOT*

*Membership as of March 2012.

NATIONAL COOPERATIVE HIGHWAY RESEARCH PROGRAM

NCHRP REPORT 725

Guidelines for Analysis Methods and Construction Engineering of Curved and Skewed Steel Girder Bridges

Donald W. White
GEORGIA INSTITUTE OF TECHNOLOGY
Atlanta, GA

Domenic Coletti
HDR ENGINEERING, INC.
Raleigh, NC

Brandon W. Chavel
HDR ENGINEERING, INC.
Chicago, IL

Andres Sanchez
HDR ENGINEERING, INC.
Pittsburgh, PA

Cagri Ozgur and Juan Manuel Jimenez Chong
PAUL C. RIZZO ASSOCIATES, INC.
Pittsburgh, PA

Roberto T. Leon
VIRGINIA POLYTECHNIC INSTITUTE AND STATE UNIVERSITY
Blacksburg, VA

Ronald D. Medlock and Robert A. Cisneros
HIGH STEEL STRUCTURES, INC.
Lancaster, PA

Theodore V. Galambos
UNIVERSITY OF MINNESOTA
Minneapolis, MN

John M. Yadlosky
HDR ENGINEERING, INC.
Pittsburgh, PA

Walter J. Gatti
TENSOR ENGINEERING
Indian Harbor Beach, FL

Gary T. Kowatch
THE MARKOSKY ENGINEERING GROUP
Youngwood, PA

Subscriber Categories
Bridges and Other Structures • Highways

Research sponsored by the American Association of State Highway and Transportation Officials
in cooperation with the Federal Highway Administration

TRANSPORTATION RESEARCH BOARD

WASHINGTON, D.C.
2012
www.TRB.org

NATIONAL COOPERATIVE HIGHWAY RESEARCH PROGRAM

Systematic, well-designed research provides the most effective approach to the solution of many problems facing highway administrators and engineers. Often, highway problems are of local interest and can best be studied by highway departments individually or in cooperation with their state universities and others. However, the accelerating growth of highway transportation develops increasingly complex problems of wide interest to highway authorities. These problems are best studied through a coordinated program of cooperative research.

In recognition of these needs, the highway administrators of the American Association of State Highway and Transportation Officials initiated in 1962 an objective national highway research program employing modern scientific techniques. This program is supported on a continuing basis by funds from participating member states of the Association and it receives the full cooperation and support of the Federal Highway Administration, United States Department of Transportation.

The Transportation Research Board of the National Academies was requested by the Association to administer the research program because of the Board's recognized objectivity and understanding of modern research practices. The Board is uniquely suited for this purpose as it maintains an extensive committee structure from which authorities on any highway transportation subject may be drawn; it possesses avenues of communications and cooperation with federal, state and local governmental agencies, universities, and industry; its relationship to the National Research Council is an insurance of objectivity; it maintains a full-time research correlation staff of specialists in highway transportation matters to bring the findings of research directly to those who are in a position to use them.

The program is developed on the basis of research needs identified by chief administrators of the highway and transportation departments and by committees of AASHTO. Each year, specific areas of research needs to be included in the program are proposed to the National Research Council and the Board by the American Association of State Highway and Transportation Officials. Research projects to fulfill these needs are defined by the Board, and qualified research agencies are selected from those that have submitted proposals. Administration and surveillance of research contracts are the responsibilities of the National Research Council and the Transportation Research Board.

The needs for highway research are many, and the National Cooperative Highway Research Program can make significant contributions to the solution of highway transportation problems of mutual concern to many responsible groups. The program, however, is intended to complement rather than to substitute for or duplicate other highway research programs.

NCHRP REPORT 725

Project 12-79
ISSN 0077-5614
ISBN 978-0-309-25839-5
Library of Congress Control Number 2012942265

COPYRIGHT INFORMATION

NOTICE

The project that is the subject of this report was a part of the National Cooperative Highway Research Program, conducted by the Transportation Research Board with the approval of the Governing Board of the National Research Council.

The members of the technical panel selected to monitor this project and to review this report were chosen for their special competencies and with regard for appropriate balance. The report was reviewed by the technical panel and accepted for publication according to procedures established and overseen by the Transportation Research Board and approved by the Governing Board of the National Research Council.

The opinions and conclusions expressed or implied in this report are those of the researchers who performed the research and are not necessarily those of the Transportation Research Board, the National Research Council, or the program sponsors.

The Transportation Research Board of the National Academies, the National Research Council, and the sponsors of the National Cooperative Highway Research Program do not endorse products or manufacturers. Trade or manufacturers' names appear herein solely because they are considered essential to the object of the report.

Published reports of the

NATIONAL COOPERATIVE HIGHWAY RESEARCH PROGRAM

are available from:

Transportation Research Board
Business Office
500 Fifth Street, NW
Washington, DC 20001

and can be ordered through the Internet at:

http://www.national-academies.org/trb/bookstore

Printed in the United States of America

THE NATIONAL ACADEMIES

Advisers to the Nation on Science, Engineering, and Medicine

The **National Academy of Sciences** is a private, nonprofit, self-perpetuating society of distinguished scholars engaged in scientific and engineering research, dedicated to the furtherance of science and technology and to their use for the general welfare. On the authority of the charter granted to it by the Congress in 1863, the Academy has a mandate that requires it to advise the federal government on scientific and technical matters. Dr. Ralph J. Cicerone is president of the National Academy of Sciences.

The **National Academy of Engineering** was established in 1964, under the charter of the National Academy of Sciences, as a parallel organization of outstanding engineers. It is autonomous in its administration and in the selection of its members, sharing with the National Academy of Sciences the responsibility for advising the federal government. The National Academy of Engineering also sponsors engineering programs aimed at meeting national needs, encourages education and research, and recognizes the superior achievements of engineers. Dr. Charles M. Vest is president of the National Academy of Engineering.

The **Institute of Medicine** was established in 1970 by the National Academy of Sciences to secure the services of eminent members of appropriate professions in the examination of policy matters pertaining to the health of the public. The Institute acts under the responsibility given to the National Academy of Sciences by its congressional charter to be an adviser to the federal government and, on its own initiative, to identify issues of medical care, research, and education. Dr. Harvey V. Fineberg is president of the Institute of Medicine.

The **National Research Council** was organized by the National Academy of Sciences in 1916 to associate the broad community of science and technology with the Academy's purposes of furthering knowledge and advising the federal government. Functioning in accordance with general policies determined by the Academy, the Council has become the principal operating agency of both the National Academy of Sciences and the National Academy of Engineering in providing services to the government, the public, and the scientific and engineering communities. The Council is administered jointly by both Academies and the Institute of Medicine. Dr. Ralph J. Cicerone and Dr. Charles M. Vest are chair and vice chair, respectively, of the National Research Council.

The **Transportation Research Board** is one of six major divisions of the National Research Council. The mission of the Transportation Research Board is to provide leadership in transportation innovation and progress through research and information exchange, conducted within a setting that is objective, interdisciplinary, and multimodal. The Board's varied activities annually engage about 7,000 engineers, scientists, and other transportation researchers and practitioners from the public and private sectors and academia, all of whom contribute their expertise in the public interest. The program is supported by state transportation departments, federal agencies including the component administrations of the U.S. Department of Transportation, and other organizations and individuals interested in the development of transportation. **www.TRB.org**

www.national-academies.org

COOPERATIVE RESEARCH PROGRAMS

CRP STAFF FOR NCHRP REPORT 725

Christopher W. Jenks, *Director, Cooperative Research Programs*
Crawford F. Jencks, *Deputy Director, Cooperative Research Programs*
Waseem Dekelbab, *Senior Program Officer*
Danna Powell, *Senior Program Assistant*
Eileen P. Delaney, *Director of Publications*
Hilary Freer, *Senior Editor*

NCHRP PROJECT 12-79 PANEL
Field of Design—Area of Bridges

Edward P. Wasserman, *Modjeski and Masters, Nashville, TN* (Chair)
David J. Kiekbusch, *Wisconsin DOT, Madison, WI*
Paul V. Liles, Jr., *Georgia DOT, Atlanta, GA*
Thomas P. Macioce, *Pennsylvania DOT, Harrisburg, PA*
Gichuru Muchane, *North Carolina DOT, Raleigh, NC*
Hormoz Seradj, *Oregon DOT, Salem, OR*
Yuan Zhao, *Texas DOT, Austin, TX*
Fassil Beshah, *FHWA Liaison*
Frederick Hejl, *TRB Liaison*

FOREWORD

By Waseem Dekelbab
Staff Officer
Transportation Research Board

This report contains guidelines on the appropriate level of analysis needed to determine the constructability and constructed geometry of curved and skewed steel girder bridges. Required plan details and submittals are included in the guidelines. When appropriate in lieu of a 3D analysis, the guidelines also introduce improvements to 1D and 2D analyses that require little additional computational costs. The report will be of immediate interest to bridge and construction engineers.

Curved and skewed steel girder bridges can experience significant three-dimensional deflections and rotations. These deformations should be considered in design and in the detailing of cross-frames and the fit-up of cross-frames during erection. The consequences of ignoring these deformations include potential fit-up problems during girder erection, over-run or under-run of deck thicknesses, misalignment of deck joints, mismatched stages in staged construction projects, deviations from intended deck cross-slopes and profiles, and unintended dead load stresses in the structural components. Depending on the severity of the bridge geometric conditions, a simple analysis solution may be adequate, or a more refined analysis may be required.

In addition, curved and skewed steel deck-girder bridges may be unstable during erection. The behavior of these structures at various stages of construction can be quite complex. Depending on the specific configuration of the structure, different levels of analysis techniques may be required to adequately assess the stability of the structure and the possible need for temporary shoring, bracing, or other means to ensure stability during erection. Longer spans, more severe curvature, and more severe skew exacerbate the magnitude of the above effects and may lead to construction problems, claims, and accidents. Therefore, greater attention to erection engineering analysis, preparation of erection plans, and review of erection plans is needed as a function of the span length, horizontal curvature, and magnitude of the skew.

Research was performed under NCHRP Project 12-79 by Dr. Donald W. White, School of Civil and Environmental Engineering at the Georgia Institute of Technology, Atlanta, GA. The objectives of NCHRP Project 12-79 were to develop (1) guidance on selecting analytical methods for design and (2) recommendations on the level of erection analysis, erection plan detail, and submittals for skewed and/or horizontally curved steel deck-girder bridges.

A number of deliverables are provided as appendices. Only Appendix A—Glossary of Key Terms Pertaining to Cross-Frame Detailing and Appendix B—Recommendations for Construction Plan Details and Level of Construction Analysis are published herein. Other

appendices are not published but are available on the TRB website by searching on *NCHRP Report 725*. These appendices are titled as follows:

- APPENDIX C—Evaluation of Analytical Methods for Construction Engineering of Curved and Skewed Steel Girder Bridges
- APPENDIX D—Benchmark Problems
- APPENDIX E—Executive Summaries of Study Bridges
- APPENDIX F—Early Correspondence with Owners and Agencies
- APPENDIX G—Owner/Agency Policies and Procedures
- APPENDIX H—Design Criteria for New Bridge Designs
- APPENDIX I—Extended Summaries of Study Bridges
- APPENDIX J—Bridge Drawings
- APPENDIX K—Organization of Electronic Data

CONTENTS

Note: Many of the photographs, figures, and tables in this report have been converted from color to grayscale for printing. The electronic version of the report (posted on the Web at www.trb.org) retains the color versions.

AUTHOR ACKNOWLEDGMENTS

The research reported herein was performed under NCHRP Project 12-79 by the School of Civil and Environmental Engineering at the Georgia Institute of Technology, Atlanta, Georgia. The Georgia Institute of Technology was the contractor for this study, with the Georgia Tech Research Foundation serving as the Fiscal Administrator.

Dr. Donald W. White, professor, Georgia Institute of Technology, was the project director and principal investigator. Mr. Domenic Coletti, PE, senior professional associate, HDR Engineering, Inc., was the co-principal investigator. The research involved a substantial collaborative effort among Georgia Tech; HDR Engineering; Markosky Engineering Group, Inc.; High Steel Structures, Inc.; Tensor Engineering; and Dr. Theodore V. Galambos. The authors of this report were Dr. White, Mr. Coletti, Dr. Brandon W. Chavel, PE, professional associate, HDR Engineering; Dr. Andres Sanchez, bridge designer, HDR Engineering (formerly graduate research assistant, Georgia Tech); Dr. Cagri Ozgur, engineering associate II, Paul C. Rizzo Associates, Inc. (formerly graduate research assistant, Georgia Tech); Dr. Juan Manuel Jimenez Chong, project engineering associate, Paul C. Rizzo Associates (formerly graduate research assistant, Georgia Tech); Dr. Roberto T. Leon, PE, professor, Virginia Polytechnic Institute and State University (formerly professor, Georgia Tech); Mr. Ronald D. Medlock, PE, director-technical services, High Steel Structures; Mr. Robert A. Cisneros, PE, chief engineer, High Steel Structures; Dr. Galambos, professor emeritus, University of Minnesota; Mr. John M. Yadlosky, PE, senior professional associate and vice president, HDR Engineering; Mr. Walter J. Gatti, president, Tensor Engineering; and Mr. Gary T. Kowatch, PE, project manager, Markosky Engineering Group.

The Tennessee Department of Transportation (TDOT) provided substantial supplementary funding for field instrumentation of Bridge EICCR22a by the Georgia Institute of Technology research team for the purpose of verifying the veracity of the 3D FEA models as a standard for comparison of 1D and 2D methods. TDOT, Bell and Associates Construction L.P., and Powell Construction Co., Inc., provided substantial assistance to the field study. The supplementary funding from TDOT and the cheerful assistance from all of the above parties are gratefully acknowledged.

SUMMARY

Guidelines for Analysis Methods and Construction Engineering of Curved and Skewed Steel Girder Bridges

Horizontally curved and/or skewed bridges generally exhibit significant torsional displacements. Twisting of the girders, and of the overall bridge as a structural system, is unavoidable in these structures. Steel I-girder and tub-girder bridges have performed well in a vast majority of the cases involving horizontal curvature and skew in highway bridge engineering. Indeed, they are arguably the premier design option for handling of curved and skewed roadway alignments. However, in situations where problems have occurred, they often have been during, or related to, the construction. Furthermore, these problems often have involved issues in addressing the torsional response.

Within the structural design profession, little has been published in the way of guidelines or recommendations on the level of structural analysis sufficient for the construction engineering of curved and skewed steel I- and tub-girder bridges. The key construction engineering considerations for these types of structures include the following:

1. The prediction of the deflected geometry at the intermediate and final stages of the construction,
2. Determination and assessment of cases where the stability of a structure or unit needs to be addressed,
3. Identification and alleviation of situations where fit-up may be difficult during the erection of the structural steel, and
4. Estimation of component internal stresses during the construction and in the final constructed configuration.

Bridges with significant span lengths, curvature, and/or skew generally require detailed planning of the erection procedures and sequences such that lifting and assembly of their spatially deformed components is achievable. Conversely, shorter bridges with minor curvature and skew can be built with less attention to the construction engineering. With respect to all of the above considerations, it is important that an appropriate level of analysis is applied for the task at hand.

This research has systematically evaluated the accuracy of various 1D (line-girder analysis based) as well as 2D-grid structural analysis procedures to assess when the simplified 1D and 2D methods are sufficient and when 3D methods may be more appropriate for prediction of the constructability and of the constructed geometry of curved and/or skewed steel girder bridges. Both steel I-girder and tub-girder bridges are addressed. A method of estimating the accuracy of conventional 1D line-girder and 2D-grid procedures as a function of the bridge geometry is provided. In addition, a number of improvements to conventional line-girder and 2D-grid methods of analysis are developed, which provide substantial benefits at little

additional computational cost. Furthermore, cases where locked-in forces from steel dead load fit (SDLF) or total dead load fit (TDLF) detailing of cross-frames should be considered using an accurate 2D-grid or 3D finite element analysis are explained, and procedures for incorporating the corresponding initial lack-of-fit displacements in these analysis methods are provided. Finally, the project has developed guidelines on the level of construction analysis, plan detail, and submittals for curved and skewed steel girder bridges. These guidelines are suitable for direct incorporation into specifications or other guideline documents.

CHAPTER 1

Background

1.1 Problem Statement

At larger span lengths, tighter curvatures and/or sharper skews, assurance of fit-up, control of the component stresses, and control of the constructed geometry are critical attributes in the construction engineering of steel girder bridges. Significantly curved and/or skewed bridges generally exhibit significant torsional deformations, along with associated significant cross-frame forces, potential for uplift at bearings, and other effects. These attributes must be considered in the design, detailing, and construction of these structures. Conversely, straight bridges with negligible skew respond predominantly in a manner involving vertical girder displacements with little or no torsional response.

Bridge engineers have a wide array of approximate and refined analysis and design tools at their disposal for the assessment of constructability. It is important that the right tool is selected for the job at hand. Furthermore, it is essential that construction plans and submittals adequately convey the information necessary to build a given structure safely without unnecessary delays or rework. With regard to these attributes, the key construction engineering considerations for steel I- and tub-girder bridges are as follows:

- **Prediction of the deflected geometry at the intermediate and final stages of the construction.** During steel erection stages, it can be necessary in some cases to limit the structural displacements to avoid fit-up difficulties. In addition, it is particularly important for the engineer to be able to predict the deflected geometry under the steel dead load, prior to the placement of the deck concrete, as well as under the total dead load, after placement of the deck and various appurtenances. It should be noted that, in general, there is no such thing as a "conservative" prediction of the structural displacements. Over-prediction of the displacements can be just as bad as under-prediction when considering the control of the constructed geometry. The deflections during the concrete deck placement generally need to be evaluated to assess that the deck thickness, cross-slopes, superelevations, and grade are within tolerances, the dead load rotations are limited at the bearings, the separate units are sufficiently aligned at deck joints, and the separate phases are matched in phased construction projects.

Detailers and fabricators use long-established practices for various types of steel structures in which they detail and fabricate the steel components such that the parts do not fit together when they are in their unloaded (unstressed and undeformed) geometry. This initial lack of fit of the undeformed components is used to compensate for some of the displacements that occur under load, and it can facilitate or hinder the assembly of the unshored, partially shored, or shored structure depending on the procedures and the erection conditions. In curved and/or skewed I-girder bridges, the corresponding practices are commonly termed *steel dead load fit* (*SDLF*)

or *total dead load fit* (*TDLF*) detailing of the cross-frames. These detailing methods entail the fabrication of the cross-frames in a geometry that does not fit-up with the connection work points on the initially fabricated (cambered and plumb) girders. The corresponding internal locked-in forces twist the girders in a direction opposite to that corresponding to the torsional displacements under the bridge steel or total dead load. Due to the combined dead load and locked-in force effects, the girders deflect into a position where their webs are approximately plumb under the steel dead load, for SDLF, or under the total dead load, for TDLF. In certain cases, the dead load and locked-in force effects approximately cancel each other, such that the net final stresses due to the torsional deformations are approximately zero; however, in other cases these internal effects are additive (i.e., the locked-in forces increase the internal stresses).

Numerous bridges also are built in which all the components are detailed ideally to fit-up in their undeformed geometry. This method of detailing is commonly referred to as *no-load fit (NLF)*. When NLF detailing is used, the girders are plumb in the theoretical zero load condition when connected to the cross-frames, but due to the torsional deformations, they deflect into a position in which their webs are out of plumb, or laid over, under the action of the steel and total dead loads.

There are various advantages and disadvantages to all of the above methods of detailing, and generally, different methods work well for different bridge types and geometries. Furthermore, it is important to note that the above descriptions are from the perspective of the structural analysis and behavior of steel I-girder bridges. However, the detailer and the fabricator do not conduct any structural analysis. When SDLF or TDLF detailing is used, the detailer and fabricator work solely with the specified steel dead load and total dead load cambers of the girders. The specified steel or total dead load cambers are subtracted from the initially fabricated (cambered and plumb) girder geometries and the cross-frames are detailed to fit between the girders in the anticipated plumb steel or total dead load final geometry. The torsional interactions between the individual girders and the overall structural system, via the attached cross-frames as the structure deforms under the loads, is only indirectly and approximately considered.

SDLF and TDLF detailing are very effective at achieving *approximately* plumb steel girder webs at the targeted dead load condition. However, the resulting effects on the structural responses are quite complex and are generally not well understood. This has led to the current state of practice where the AASHTO LRFD Specifications (AASHTO, 2010) Article C6.7.2 state that for curved I-girder bridges, " . . . the Engineer may need to consider the potential for any problematic locked-in stresses in the girder flanges or the cross-frames or diaphragms. . . ." However, due to the lack of detailed knowledge of the locked-in stresses that can be generated, no guidance is provided regarding when the influence of these stresses needs to be considered in the design. The de facto standard practice is that these effects are rarely, if ever, included in design calculations. That is, the implicit assumption in the structural design of steel I-girder bridges is no-load fit (NLF). The components are implicitly assumed to fit-up perfectly in their undeformed condition under zero load. As a result, regardless of the level of sophistication of the structural analysis, the structural displacements, internal forces, and internal stresses used in current practice are in error to the extent that the locked-in responses due to SDLF or TDLF detailing are important.

The lack of understanding of SDLF and TDLF detailing effects has led, in some instances, to conflicting job requirements, such as stating that TDLF detailing should be used and that the I-girder webs should be plumb under the steel dead load condition, or stating that no significant locked-in forces shall be generated and that the I-girder webs should be plumb in the final dead load condition. The I-girder webs can be plumb only under one loading due to the fact that curved and skewed bridges displace torsionally under load. SDLF detailing targets approximately plumb webs in the steel dead load condition, while TDLF detailing targets approximately plumb webs under the final dead load. However, these detailing practices produce locked-in forces due to the corresponding fabricated initial lack of fit between the undeformed (cambered and plumb)

no-load geometry of the girders and the fabricated geometry of the cross-frames. These forces can be both additive and subtractive with the dead load forces in the structure.

Appendix A provides summary definitions of key terms pertaining to cross-frame detailing. It is essential that the reader understand these definitions to facilitate study and interpretation of the corresponding results and discussions throughout this report.

- **Determination and assessment of cases where stability effects may be important.** In curved and/or skewed structures, stability effects show up as significant second-order amplification of the displacements and the corresponding internal forces and stresses. In cases where they experience significant stability-related limit states, curved and skewed structures do not exhibit a "bifurcation" from a primary load-displacement response. Rather, the structural displacements increase at an increasing rate as the stability limit of the structure is approached. In cases where the structure is stability critical, second-order amplification can significantly impact the prediction and control of the constructed geometry. In girder bridge structures, large second-order amplification generally should be avoided in the structure's final constructed condition as well as during the concrete deck placement. However, the engineer needs to be able to anticipate and/or predict a problem in order to prevent it. Lastly, it is important to note that large second-order amplification may not present any significant problem during intermediate stages of steel erection, unless the amplified displacements lead to difficulty with fit-up of the structural components.
- **Identification and alleviation of situations where fit-up may be difficult during the erection of the structural steel.** Due to a combination of (1) structural component or unit weights, (2) the deflections of the steel components under their self-weight during a specific erection stage, as well as (3) the stiffnesses of the components (i.e., the component resistances to being deformed by come-alongs, jacks, cranes, etc. such that their connections can be made), some situations involving tight curves, sharp skews, and/or long spans may be particularly problematic for the erector to fit the structural components together. These situations generally must be identified and addressed by the development of suitable erection plans. It is well known that TDLF detailing of the cross-frames in I-girder bridges tends to increase the forces required for fit-up. This is because the cross-frames do not fit together with the girders (without some force fitting) until the girder total dead load vertical deflections have occurred in the final constructed configuration (including the influence of the concrete slab weight). The girders are not yet subjected to the total dead load, nor are they connected together in the final constructed geometry, during a given intermediate steel erection stage.

In cases where cross-frames or other secondary framing must be included in shop assembly, the fabricator is not likely to choose TDLF. Inclusion of such framing in a shop assembly is rare and only necessary in complex framing situations, such as a single-point urban interchange (SPUI), where girders of varying lengths and curvature are joined by multiple short, stiff diaphragms. For such situations, the fabricator will likely choose SDLF or NLF so that the steel can be assembled in the yard without the weight of the deck present. In such cases, it is good for the erector to be aware of the assembly requirements so that the field assembly procedure can closely mimic the shop support conditions inasmuch as the jobsite conditions will allow.

- **Estimation of component internal stresses during construction and in the final constructed condition.** AASHTO LRFD Article 6.10.3 requires various checks of factored forces and stresses in steel girder bridges during construction. These include the following:
  1. Prevention of any nominal yielding under factored loads (neglecting initial steel residual stress effects) during the construction.
  2. Checking of strength limit states, which in some cases, can occur prior to nominal yielding of the structural components.

3. Prevention of girder web bend buckling or shear buckling during the construction, such that the out-of-plane deflections of the (initially out-of-flat) girder webs are limited.
4. Limiting of girder flange lateral bending stresses (to $0.6F_y$) to ensure the applicability of the AASHTO resistance equations for the girder strength limit states, and practically, to limit the magnitude of the flange lateral bending deformations.
5. Control of tensile stresses in the concrete deck, to limit the potential for significant deck cracking.

Generally speaking, the structural analysis used for assessing the construction conditions must be sufficiently accurate such that, at the least, all major contributors to the structural responses are accounted for (including all major contributions to the structural displacements, e.g., any significant deformations in attachment details). It is important for engineers to understand if, and when, the responses of curved and/or skewed steel girder bridges are impacted significantly by (1) SDLF or TDLF detailing effects and/or (2) structural stability (i.e., second-order amplification) effects, in addition to the primary effects associated with the bending and twisting of these structures under load.

- **Development of sufficient construction plans and submittals.** Given the application of a sufficient level of structural analysis for a given job, it is also important that the construction plans and procedures contain adequate detail to properly convey the job requirements as a function of the bridge and construction complexity. Bridges with significant span lengths, curvature, and/or skew generally require detailed planning of the erection procedures and sequences such that lifting and assembly of their spatially deformed components is achievable. Longer bridges typically require placement of the deck concrete in multiple stages. Setup of the concrete from prior stages and, in some cases, during the current stage, can have a significant influence on the final geometry and the ultimate performance of the structure. Conversely, shorter bridges with minor curvature and skew can be built with less attention to the construction engineering. With respect to all of the above considerations, it is important that an appropriate level of effort is applied for the task at hand. More complete guidelines are needed in current practice (2012) regarding the level of construction analysis, plan detail, and submittals for curved and/or skewed steel girder bridge structures.

1.2 Current Knowledge

Substantial progress has been achieved in recent years with the streamlining and unification of the AASHTO LRFD (2010a and b) provisions for general steel girder bridges. These Specifications provide more organized and explicit guidance on design for constructability than ever before. Also, recent AASHTO/NSBA Guidelines and Guide Specifications (AASHTO/NSBA, 2003, 2006, 2007, and 2011) provide numerous useful and important recommendations. In addition, many state DOTs have developed substantial constructability guidelines, such as PennDOT (2004), TxDOT (2005), and NCDOT (2006). However, while these documents provide important recommendations applicable to curved and/or skewed steel girder bridges, they target a broad range of steel bridge construction. The construction engineering of highly curved and/or skewed bridges is a highly specialized topic. NCHRP Project 12-79 seeks to develop recommendations that can be fully integrated with the present Specifications and Guidelines to better address the unique attributes of curved and/or skewed steel girder bridges.

In recent years, the capabilities for simulation of physical tests using advanced 3D finite element analysis (FEA) has progressed to the point that, in numerous areas, the results from physical experiments can be reproduced readily and quite reliably. There is great potential for advanced 3D FEA simulation methods to be used as a tool for more comprehensive assessment of various levels of analysis and calculation suitable for design. Nevertheless, similar to the

results from experimental testing, the results from an FEA test simulation are only as good as the accuracy of

- The detailed geometry (e.g., plate thicknesses, deck-slab thicknesses, haunch depths, girder web depths, bearing heights, bearing plan locations, etc.),
- The load and displacement boundary conditions, including any thermal loading conditions where important, and bearing restraints with finite stiffness or flexibility where important,
- The assumed initial conditions (e.g., initial residual stresses, geometric imperfections, any lack of fit between components in their unloaded condition, etc.),
- The constitutive relationships for the various constituent materials, including attributes such as early stiffness and strength gain of the deck concrete at a given casting stage, or between stages when the deck is placed sequentially in multiple stages, creep and shrinkage deformations of the concrete, concrete micro-cracking in tension, and concrete tension stiffening due to interaction with the deck reinforcing steel, and
- The kinematic assumptions and/or constraints imposed by structural theories and/or associated with the assumed interconnection between various components (e.g., the modeling of stay-in-place metal deck forms tied to the girders by flexible strap details; also, the composite interconnection between the steel girders and the concrete slab, including local short-term and creep deformation of the concrete in the vicinity of shear studs etc., particularly if accounting for early concrete stiffness gains).

The consideration of above attributes should not detract from the use of advanced 3D FEA test simulations. In many respects, the above attributes are more easily specified, controlled, and quantified in sophisticated 3D FEA models than in physical tests. Also, in certain situations, many of the above attributes have an inconsequential effect on the structural response. However, similar to successful experimental testing procedures, the execution of refined test simulations requires great care in the creation and setup of the models. This is particularly the case where advanced simulation capabilities are not facilitated well by simplified computer user interfaces. As stated well by Hall et al. (1999), "3D FEA models are not all the same."

The current knowledge about the true accuracy of different methods of analysis for curved and/or skewed steel girder bridges is limited. NCHRP Project 12-79 provided an opportunity to gain substantial insights into the behavior of curved and skewed steel bridge structures, as well as the accuracy of various methods of analysis for these structures, by comparing the results from practical design-analysis methods to the results from refined 3D FEA test simulations. The NCHRP Project 12-79 research is the first time that the overall analysis and construction engineering of curved and/or skewed steel girder bridges has been studied in a systematic manner, considering a large sample of bridges representative of the range of structures encountered in practice, to develop improved guidelines for practice.

1.3 Objectives and Scope of This Research

The objectives of NCHRP Project 12-79 are to provide the following:

1. An extensive evaluation of when simplified 1D or 2D analysis methods are sufficient and when 3D methods may be more appropriate for prediction of the constructability and of the constructed geometry of curved and/or skewed steel girder bridges, and
2. A guidelines document providing recommendations on the level of construction analysis, plan detail, and submittals for curved and skewed steel girder bridges suitable for direct incorporation into specifications or guidelines.

Both I- and tub-girder bridges are addressed.

The first major objective starts with the assessment of the accuracy of "base" or "conventional" 1D (line-girder) and 2D-grid methods of analysis, representing current standards of care in the profession. These assessments lead to the identification of a number of important improvements that can be made to the current simplified methods of analysis. Various improvements are addressed that

1. Are easy to implement in structural engineering practice, and
2. Result in substantial improvements in the ability of the methods to capture the physical responses with minimal additional calculation effort.

In recognition of the importance of integration with structural analysis and design software in structural engineering practice, specific considerations with respect to software implementation also are addressed. The identification of when stability effects (i.e., second-order amplification effects) are significant, as well as the calculation of these effects when they are important, is considered. In addition, a thorough evaluation of the influence of steel dead load fit (SDLF) and total dead load fit (TDLF) detailing of the cross-frames in steel I-girder bridges is conducted. The research focused on the first objective is summarized in the NCHRP Project 12-79 Task 8 report, "Evaluation of Analytical Methods for Construction Engineering of Curved and Skewed Steel Girder Bridges," Appendix C of the contractors' final report.

The second major objective is addressed by the NCHRP Project 12-79 Task 9 report "Recommendations for Construction Plan Details and Level of Construction Analysis," which is included as Appendix B of this document. The Task 9 report provides a detailed description of considerations necessary for the development of construction plans. This information is provided in a specification format, complete with a commentary. In addition, the Task 9 report synthesizes key recommendations from the Task 8 research into a specification form.

1.4 Organization of This Report

Chapter 2 of this report provides a brief overview of the research approach used in NCHRP Project 12-79. Chapter 3 highlights the major findings from this research and their applications.

Section 3.1 summarizes the results from the core NCHRP Project 12-79 research involving the assessment of the "base" or "conventional" 1D line-girder and 2D-grid methods of analysis, representing the current standards of care in the profession. A matrix of scores is provided, indicating the general accuracy of each of the methods for determining different types of responses. This section also gives several examples of how the matrix of scores should be applied.

Section 3.2 discusses detailed results behind the assessment of the conventional analysis methods in Section 3.1 and focuses on key improvements that can be made to the current simplified methods of analysis identified in Task 8 of the NCHRP Project 12-79 research. Section 3.3 then summarizes essential results from the portion of the NCHRP Project 12-79 research focused on evaluating the influence of steel dead load fit (SDLF) and total dead load fit (TDLF) methods of detailing the cross-frames in steel I-girder bridges. This is followed by Section 3.4, which gives a synthesis of the overall pros and cons of no-load fit (NLF), steel dead load fit (SDLF), and total load fit (TDF) detailing of cross-frames, and Section 3.5, which provides a few basic recommendations for selection of cross-frame detailing methods in I-girder bridges. Chapter 3 concludes with Section 3.6, which highlights key construction engineering recommendations captured in NCHRP Project 12-79 Task 9.

Chapter 4 emphasizes the most important findings of the NCHRP Project 12-79 research, provides specific recommendations for application and implementation of the findings, and describes areas where further research would be valuable.

Appendix A provides summary definitions of key terms pertaining to cross-frame detailing. It is essential that the reader understand these definitions to facilitate study and interpretation of the corresponding results and discussions throughout this report. Appendixes B and C contain the reports for Tasks 8 and 9, addressing the two major objectives of the NCHRP Project 12-79 research. In addition, Appendix D contains a Task 7 report that provides specific written documentation on three of the 76 bridges considered in the NCHRP Project 12-79 studies. Appendix E provides a short summary of each of the bridges studied by the NCHRP Project 12-79 researchers, emphasizing the primary considerations addressed by each bridge. Appendixes F and G, respectively, show an early survey sent to owners/agencies in July 2008 and provide a brief summary of policies and practices pertaining to the analysis and design of curved and/or skewed steel girder bridges at the beginning of the NCHRP Project 12-79 research. Appendix H summarizes the criteria used for the parametric study bridges designed and evaluated during the core NCHRP Project 12-79 research. The parametric study designs were developed to reflect a comprehensive range of potential curved and/or skewed steel girder bridge attributes and geometries based on current practices. Appendix I provides a more detailed summary of results for each of the existing, example, and parametric bridges studied by the project, while Appendix J provides the engineering drawings for all of the bridges. Detailed electronic data from the complete set of analysis studies is available as one of the project's Task 8 products. Finally, Appendix K explains the organization of the project electronic data. Please note that Appendixes C through K are not published herein but are available at the TRB website by searching on *NCHRP Report 725*.

CHAPTER 2

Research Approach

This chapter provides a brief summary of the approach used in addressing the objectives of the NCHRP Project 12-79 research. The primary project tasks were:

- Task 1. Review and evaluation of pertinent research,
- Task 2. Synthesis of owner/agency policies,
- Task 3. Identification of existing bridges,
- Task 4. Identification of geometric factors,
- Task 5. Selection of range and levels of geometric factors,
- Task 6. Selection of existing and parametric design bridges,
- Task 7. Analytical studies,
- Task 8A. Data reduction and assessment of analysis procedures,
- Task 8B. Development of improvements to simplified methods, and
- Task 9. Development of guidelines.

The following descriptions are organized and arranged in the order of these tasks.

2.1 Review and Evaluation of Pertinent Research

The first task of the research was to review and evaluate pertinent domestic and international research on the basis of applicability, conclusiveness of findings, and usefulness for the development of guidance for selecting analytical methods for the construction engineering of curved and/or skewed steel girder bridges. An extensive bibliography of the pertinent research was developed, including abstract summaries of research in progress, conference and workshop presentation slides, research reports, and archival journal papers. The references were scanned, indexed, and loaded into an internal database for ease of document access. The bibliography was focused primarily on references since 1993. Since Zureick et al. (1994) developed a comprehensive bibliography of the published literature on curved I- and box-girder bridges before 1994, the bibliography focused only on references not identified by the earlier bibliography for any citations prior to 1994.

2.2 Synthesis of Owner/Agency Policies and Practices

The second project task was to synthesize current owner/agency policies and practices related to the construction engineering, construction plan preparation, and construction plan review for the above structure types. During this task, the project team coordinated its work with the

AASHTO/NSBA Steel Bridge Collaboration Task Group 13, which conducted a "Survey of Current Practice in Steel Girder Design" during the early stages of the NCHRP Project 12-79 research. The project team also conducted its own survey, which was sent to the 50 state bridge engineers and bridge engineering contacts as well as the Commonwealth of Puerto Rico, the District of Columbia, and the bridge engineering contacts of various other owner agencies. The mailing, (see Appendix F of the contractors' final report), included a short slide presentation summarizing the focus of Project 12-79, requested pertinent bridge cases (descriptions and plans) encountered in the recipient's practice that fit the criteria highlighted in the slides (summarized in the third project task below), and asked for input on state policies and practices regarding analysis methods and construction engineering of curved and/or skewed steel girder bridges.

Thirty-one responses were received. Of these, 20 provided one or more bridges that fit the criteria provided with the mailing, 12 states provided specific input regarding their policies and practices, and 9 states responded but indicated that they did not have any relevant information to provide. In addition to the specific request regarding state policies and practices, the project team researched various state policies and practices available via the Web. Appendix G of the contractors' final report contains a summary of the policies and practices from several representative states. The results of the AASHTO/NSBA Steel Bridge Collaboration Group Task Group 13 (TG13) Survey of Current Practice also are discussed in this appendix. The TG13 and Project 12-79 efforts were complementary to one another, with the TG13 efforts focusing on synthesis of current practices and practical recommendations concerning analysis methods, while the Project 12-79 focus was directed at identifying specific representative bridges and specific state policies and practices.

2.3 Identification of Existing Bridges

During Task 3, the project collected more than 130 representative curved and/or skewed steel girder bridges based on a specific set of selection criteria. These included the bridges provided by the states as well as bridges from the professional practice of the project team members and various consultants contacted by the project team.

The primary criteria posed for the collection of existing bridges were:

- Availability of quality field instrumentation data, or at least field observations, particularly during intermediate stages of construction,
- Availability of detailed construction and erection plans, and
- Successful construction but with significant challenges or concerns about the state of stress, etc.

Cases involving generally acknowledged poor practices, such as the inappropriate use of oversize holes or inadequate attachment of cross-frames leading to loss of control of the structural geometry, were specifically ruled out from consideration.

One of the key existing bridges identified for the NCHRP Project 12-79 studies was an eight-span curved I-girder fly-over ramp in Nashville, Tennessee, in which the Tennessee Department of Transportation gave the Georgia Institute of Technology researchers the opportunity to instrument and monitor the girders throughout the erection of the steel and the placement of the concrete deck. The results of this research are documented in Dykas (2012).

The collected bridges, which are documented in the project's Task 8 report (Appendix C of the contractors' final report), showed a wide diversity in span arrangements, span lengths, span-to-width ratios, horizontal curvature, skew angles, and skew patterns (i.e., radial, non-radial, parallel, and non-parallel supports). In the Task 8 report, the collected bridges are summarized

succinctly in the form of sketches of their overall plan geometry, along with a title block listing specific bridge geometric parameters.

2.4 Identification of Geometric Factors

In its fourth task, the project team developed a list of various geometric factors that potentially could have a significant impact on the accuracy of simplified methods of analysis. It was clear that if NCHRP Project 12-79 was to consider analysis accuracy for curved and/or skewed steel I- and tub-girder bridges, then the project would need to consider the following factors in the design of its parametric studies:

- Some measure of the horizontal curvature and
- Some quantification of the skew magnitude and pattern.

Furthermore, it was apparent that the bridge responses, and hence the analysis accuracy, can be affected significantly by the magnitude of the span lengths as well as the span length-to-width ratios. Longer span bridges tend to be affected more substantially by dead load effects, potentially resulting in more significant stability considerations during construction. In addition, beyond a certain span length, I-girder bridges are more likely to need partial or full-span horizontal flange-level bracing systems to ensure adequate stability and sufficient resistance to lateral loads during construction. Flange lateral bracing systems cause corresponding portions of the structure to act as "pseudo-box girders," fundamentally changing the behavior of the structural system. Furthermore, longer span bridges generally exhibit larger overall deflections. These larger overall deflections can lead to larger relative deflections at certain locations in the structural system, which can sometimes be problematic during construction. Longer span bridges often have a smaller ratio of the girder spacing relative to the girder depths, and typically have larger girder depth-to-flange-width ratios. These attributes can fundamentally affect various relative deflections in the structure as well as the local and overall behavior and analysis accuracy at the different stages of construction.

In addition, the bridge span length-to-width ratios can significantly impact the influence of skew. Skewed bridges with smaller span length-to-width ratios tend to have more significant load transfer to the bearing lines across the width of the structure and hence more significant "nuisance stiffness" effects that need to be addressed in the design. Furthermore, relatively narrow horizontally curved bridges experience a greater torsional "overturning component" of the reactions, which tends to increase the vertical reactions on the girders farther from the center of curvature and decrease the vertical reactions on the girders closer to the center of curvature. Of equal or greater importance, these types of bridges potentially can experience significant global second-order amplification of their displacements. In addition, relatively wide horizontally curved bridges can have more substantial concerns related to overturning at intermediate stages of the steel erection, prior to assembly of the girders across the full width of the bridge cross-section. These spans become more stable as additional girders are erected and connected by cross-frames across the width of the bridge. Wide horizontally curved bridges also can cause greater concerns associated with overturning forces during deck placement.

Lastly, it was apparent that the bridge responses (and the analysis accuracy) can be significantly affected by whether the spans are simply supported or continuous. Simple-span bridges tend to have larger deflections for a given geometry and potentially can be more difficult to handle during construction. Although simple-span girders can see negative bending during erection (due to lifting or temporary support from holding cranes, etc.), continuous spans have more significant negative bending considerations. Furthermore, particularly in I-girder bridges,

continuous-span bridges can have significant interactions between adjacent spans with respect to both major-axis bending as well as the overall torsional response.

All of the above factors can have a substantial influence on the many detailed structural attributes of steel I-girder and tub-girder bridges. Also, there can be significant interactions between these factors in terms of their influence on the bridge responses, as well as the accuracy of different bridge analysis methods.

If one considers the many detailed attributes of steel I- and tub-girder bridge structural systems and their members and components addressed subsequently, the combinations and permutations of potential bridge designs become endless. Hence, it was decided that the most practical way of covering the design space of curved and/or skewed I-girder and tub-girder bridges was to consider a range of practical combinations and permutations of the following primary factors:

- Span length of the bridge centerline, L_s,
- Deck width normal to the girders, w, (in phased construction projects, w is determined separately for each bridge unit),
- Horizontal curvature, of which the most appropriate characterization is discussed below,
- Skew angle of the bearing lines relative to the bridge centerline, θ (equal to zero for bridges in which the bearing lines are not skewed),
- Skew pattern of the bearing lines, of which the most appropriate characterization is discussed below, and
- Span type, simple and various types of continuous spans.

2.5 Selection of Range and Levels of Geometric Factors

As part of its fifth task, the project team compiled a summary of the range of values encountered for the above primary factors, as well as for various other geometric factors, considering the existing bridges collected in Task 3. This summary is documented in the project's Task 8 research report (see Appendix C of the contractors' final report). Given, this summary and the project team's knowledge of maximum practical limits on the values, the primary factor ranges and levels shown in Table 2-1 were selected.

Several nomenclature terms for categorizing the collected existing bridges as well as the bridges studied analytically in the project research appear in Table 2-1. These are the terms ICCR, TCCR, ICSS, TCSS, ICCS, and TCCS. The complete categories and their designations, which are used extensively throughout the remainder of this report, are as follows for the I-girder bridges:

- Simple-span, straight, with skewed supports (ISSS),
- Continuous-span, straight, with skewed supports (ICSS),
- Simple-span, curved, with radial supports (ISCR),
- Continuous-span, curved, with radial supports (ICCR),
- Simple-span, curved, with skewed supports (ISCS), and
- Continuous-span, curved, with skewed supports (ICCS).

The same designations are used for the tub-girder bridges, except the first letter in the designation starts with a "T" rather than an "I."

A specific geometric factor used to characterize the bridge horizontal curvature is introduced in Table 2-1. This is the bridge torsion index:

$$I_T = \frac{s_{ci}}{s_{ci} + s_{co}} \qquad \text{Eq. 1}$$

Table 2-1. Primary factor ranges and levels for the NCHRP Project 12-79 main analytical study.

Factor	I-girder bridges	Tub-girder bridges
Type of span	Simple, 2-span continuous, and 3-span continuous with one balanced end span and one end span equal in length to the main center span. Use the above 3-span continuous bridges as base ICCR and TCCR cases. Consider both 2- and 3-span continuous bridges for the ICSS and TCSS cases. Consider only 2-span continuous cases for the ICCS and TCCS designs. Consider at least one 2-span continuous bridge with a significant unbalance between the span lengths.	
Maximum span length of bridge centerline, L_s	150, 225, and 300 ft. for simple spans 150, 250, and 350 ft. for continuous spans (measured along the curve)	
Deck width, w	30 ft. (1 to 2 traffic lanes + shoulders and barriers) 80 ft. (4 to 5 traffic lanes + shoulders and barriers	30 ft. (1 to 2 traffic lanes + shoulders and barriers)
Torsion Index, I_T	0.58 to 0.71 for ISCR bridges 0.66 to 0.88 for ICCR bridges	0.72 to 0.87 for TSCR bridges 0.69 to 1.14 for TCCR bridges
Skew angle relative to the bridge centerline, θ	20^o, 35^o, 50^o, and 70^0 but with θ at the inside edge of the deck $\leq 70^o$ in curved spans	15^o and 30^o, plus additional sensitivity studies with variations up to ±15° from zero skew
Skew pattern	Consider the $\pm$ combinations of skew angles shown in Figure 2-1 (for straight bridges) and Figure 2-2 (for curved bridges), but using $\theta = 35$ and 70^o for I-girder bridges and $\theta = 15$ and 30^o for tub-girder bridges. Limit the ratio of the span lengths along the edges of the deck, L_2/L_1, to a maximum value of 2.0 in all cases. Limit the difference in orientation of adjacent bearing lines to a maximum of 90^o in all cases. Give preference to typical (i.e., non-exceptional) bridge geometries.	

The terms in this equation, illustrated in Figure 2-3, are:

- s_{ci}, the distance between the centroid of the deck and the chord between the inside fascia girder bearings, measured at the bridge mid-span perpendicular to a chord between the intersections of the deck centerline with the bearing lines, and
- s_{co}, the distance between the centroid of the deck and the chord between the outside fascia girder bearings, measured at the bridge mid-span perpendicular to a chord between the intersections of the deck centerline with the bearing lines.

The torsion index I_T is an indicator of the overall magnitude of the torsion within a span. It is a strong indicator of the tendency for uplift at the bearings under the nominal (unfactored) dead loads. This parameter was selected over various other factors that could be used to characterize the horizontal curvature effects on the bridge behavior and analysis accuracy, because it can be used to set minimum practical values for the radius of curvature of a span for a given deck width.

A value of $I_T = 0.5$ means that the centroid of the deck area is mid-way between the chords intersecting the outside and inside bearings. This is the ideal case where the radius of curvature

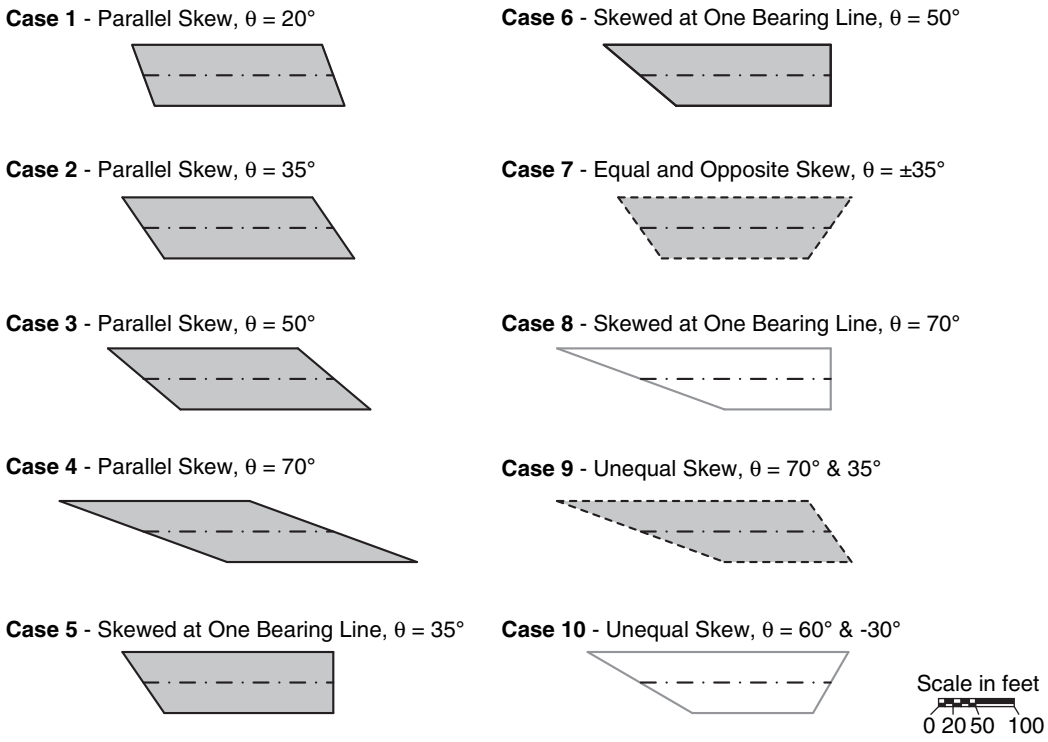

Figure 2-1. Potential skew combinations for straight I-girder bridge spans with w = 80 ft. and L_s = 250 ft. (sketches with a dashed border are considered unusual; unshaded sketches with a grey border are considered exceptional).

is equal to infinity and the skew is zero, (i.e., a straight tangent bridge). A value of $I_T = 1.0$ means that the centroid of the deck area is located at the chord line between the outside bearings. This implies that the bridge is at incipient overturning instability, by rocking about its outside bearings under uniform self-weight. For a curved radially supported span, the denominator in Equation 1, $s_{ci} + s_{co}$, is equal to $w_g \cos(L_s/2R)$, where w_g is the perpendicular width between the fascia girders.

The NCHRP Project 12-79 research identified that simple-span I-girder bridges with $I_T \geq 0.65$ are often susceptible to uplift at the bearings under nominal (unfactored) dead plus live load. Similarly, for simple-span tub-girder bridges with single bearings on each tub, $I_T = 0.87$ was identified as a limit beyond which bearing uplift problems are likely. The maximum values of 0.71 and 0.87 for the ISCR and TSCR bridges shown in Table 2-1 are similar to, and the same as, these values respectively. Continuous-span bridges can tolerate larger I_T values due to the continuity with the adjacent spans. Therefore, the maximum I_T values shown in Table 2-1 are larger for the ICCR and TCCR bridges.

Figures 2-1 and 2-2 are referenced in Table 2-1 for the consideration of the skew pattern in straight and curved bridges, respectively.

2.6 Selection of Existing and Parametric Design Bridges

Task 6 of the NCHRP Project 12-79 research involved the selection of various existing and parametric design bridges for detailed analytical study. The project's Task 8 research report provides a detailed discussion of the considerations in the selection of the study bridges. An initial preliminary selection of these bridges was conducted at the start of Task 7 of the

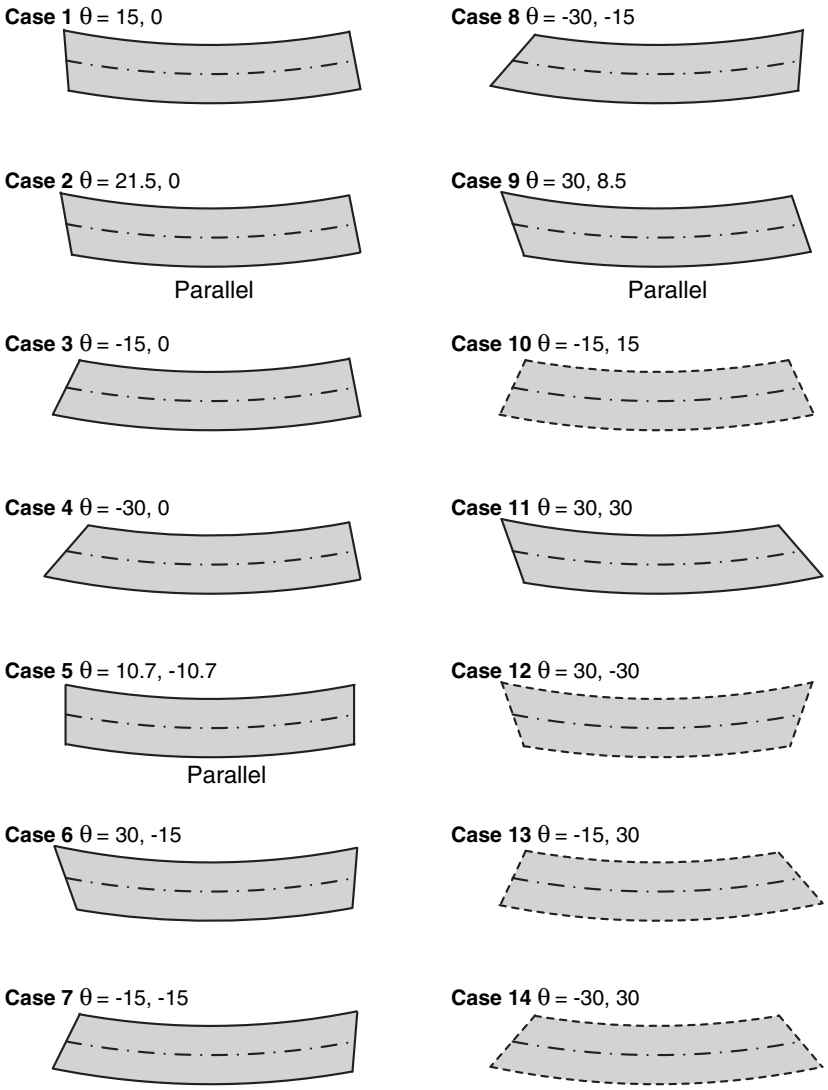

Figure 2-2. Example potential skew and horizontal curvature combinations for curved tub-girder bridge spans with w = 30 ft., L_s = 150 ft., and R = 400 ft. (sketches with a dashed border are considered unusual).

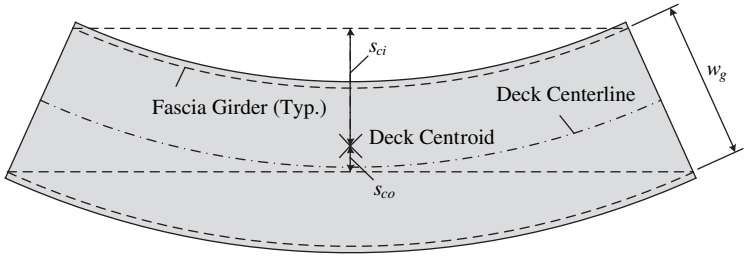

Figure 2-3. Illustration of parameters used in calculating I_T.

research (i.e., the specific analytical studies discussed in the next section). These selections were revisited and revised at various subsequent stages, based on information learned during the analytical studies. A total of 58 I-girder and 18 tub-girder bridges were considered by the project at the completion of its analytical studies. In addition, another 10 tub-girder bridges were studied that involved taking several of the above tub-girder bridges and varying the skew angle at one of the bearing lines to study the sensitivity of the bridge response and the analysis accuracy to skew effects. Of the 86 total bridges studied, 16 were existing I-girder bridges and 5 were existing tub-girder bridges. In addition, three of the I-girder bridges and two of the tub-girder bridges studied were detailed example designs taken from prior AISI, NSBA, NCHRP, and NHI developments.

Throughout the project documentation, the various bridges are referred to by their category (e.g., ISCR, ICCS, TCCS, etc.), preceded by the letters:

- E if the structure is an "existing" bridge,
- X if the structure is an AISI, NSBA, NCHRP, or NHI "example" bridge, and
- N if the structure is a "new" parametric bridge design.

A unique number is appended to the end of the designation to arrive at the specific bridge name. Therefore, for example, the 8-span continuous I-girder ramp flyover in Nashville, Tennessee, studied by the NCHRP project team, has the designation EICCR22a (the number "22a" was selected in this case to group this bridge with other Tennessee EICCR bridges considered within the project research without modifying the numbers that had already been assigned to the other EICCR bridges).

For all of the above bridges, the erection sequences used in the bridge construction were considered, or hypothetical erection sequences were developed where the specific erection sequences were not known. Various critical stages of the construction were then selected for study. In general, from 4 to 10 construction stages were selected for analysis with each bridge. As a result, more than 500 construction stages were considered in total, including the execution of multiple analysis methods for each stage.

For the $58 - 16 - 3 = 39$ additional "new" I-girder bridges and the $28 - 10 - 5 - 2 = 11$ "new" tub-girder bridges, hypothetical parametric designs were developed by the practicing design members of the project team. These $39 + 11 = 50$ bridges were complete designs satisfying the current AASHTO LRFD Specifications requirements. Specific supplementary criteria used for the design of these parametric bridges are explained in Appendix H of the contractors' final report. It is important to note that the results of simply varying design parameters without checking Specification requirements can be misleading. The AASHTO requirements were satisfied for the parametric study bridges such that the research could establish appropriate relationships between bridge design variables and recommended levels of analysis and construction engineering effort.

It should be noted that the study of 86 different bridges, as well as more than 500 construction stages, is not enough to develop a relevant data set for valid statistical assessment of analysis accuracy, given the vast range of potential situations that can be encountered during construction. However, the evaluations of the accuracy are certainly a large representative sample of the results that can be encountered in professional practice. Furthermore, a major focus of the project research, in Task 8 below, was the identification of mechanistic causes of the errors observed in the simplified analysis calculations, as well as the development of specific improvements to the simplified methods. By adopting this approach in the project research, various improvements were identified that are relatively easy to implement and lead to substantial gains in the general accuracy of the simplified methods.

2.7 Analytical Studies

Task 7 of the NCHRP Project 12-79 research involved the development and execution of a large number of analysis studies aimed at identifying when simplified 1D and 2D analysis methods are sufficient for the evaluation of the constructability and the prediction of the constructed geometry of curved and/or skewed steel girder bridges. Results from the Task 7 research are provided in written report form for three benchmark cases extracted from the larger studies. This report is included as Appendix D of the contractors' final report.

Three main levels of design analysis were considered in the NCHRP Project 12-79 research: 1D or line-girder analysis, 2D-grid (or grillage) analysis, and general 3D finite element analysis (FEA). The specifics of the methods evaluated in each of these categories are summarized in the sections below. Chapter 2 of the Task 8 project report, Appendix C to the contractors' final report, provides a more detailed description of each of the methods.

2.7.1 1D Line-Girder Analysis

The first level of analysis targeted in the NCHRP Project 12-79 research was a conventional line-girder analysis including approximations such as the V-load (Richardson, Gordon & Associates, 1976; USS, 1980; Grubb, 1984; Poellot, 1987) and M/R (Tung and Fountain, 1970) methods to account for horizontal curvature effects. For these 1D solutions, a commonly available commercial line-girder analysis program, STLBRIDGE (Bridgesoft, 2010) was used to analyze the behavior for straight skewed I- and tub-girder bridges. The 1D analysis of curved, and curved and skewed, I-girder bridges was based on the V-load method using the software VANCK (NSBA, 1996).

The 1D analysis of curved and skewed tub-girder bridges was based on a line-girder analysis coupled with supplementary calculations implemented by the project team based on the M/R Method. In addition, a useful method developed in the NCHRP Project 12-79 research for estimating the internal torque due to skew was implemented within the calculations for skewed tub-girder bridges. The recommended procedure is summarized subsequently in Section 3.2.6 of this report.

Furthermore, for the estimation of the flange lateral bending stresses and the bracing forces in tub-girder bridges, the component force equations developed originally by Fan and Helwig (1999 and 2002), supplemented by additional equations presented in Helwig et al.(2007) for the calculation of external intermediate cross-frame forces and the top flange lateral bracing (TFLB) system strut forces in Pratt systems, are used. Section 2.7 of the Task 8 report provides a detailed summary of these equations.

Lastly, one additional improvement developed in the NCHRP Project 12-79 research is included in the calculation of the top flange average longitudinal normal stresses in tub-girder bridges. An additional local "saw-tooth" contribution to these stresses that comes from the longitudinal component of the TFLB diagonal forces is included in the project calculations. These additional "saw-tooth" stresses are discussed in Section 3.2.6 of this report.

2.7.2 2D-Grid Analysis

To evaluate conventional 2D-grid methods of analysis, two commercially available software packages, employed by many bridge designers, were used to analyze the behavior of the same bridges considered with the above 1D methods: the software MDX (MDX, 2011) for analysis using a conventional 2D-grid approach, and a subset of the capabilities of the general-purpose LARSA-4D (LARSA, 2010) software for analysis using a conventional 2D-frame approach. In

the subsequent presentations in this report, the LARSA-4D software is referred to as Program P1 and the MDX software is referred to as Program P2.

The 2D-frame model is referred to as such, even though the nodes in this model have 6 degrees of freedom (dofs) (3 translations and 3 rotations), because the entire structural model is created in a single horizontal plane. As discussed in Section 2.3 of the NCHRP Project 12-79 Task 8 report (see Appendix C to the contractors' final report), if the structural model is constructed all in one plane with no depth information being represented, and if the element formulation does not include any coupling between the traditional 2D-grid dofs and the other dofs (which is practically always the case), 2D-frame models do not provide any additional forces or displacements beyond those provided by ordinary 2D-grid solutions. Assuming gravity loading normal to the plane of the structure, all the displacements at the three additional nodal dofs in the 2D-frame solution are zero. All of these conditions are satisfied by the LARSA-4D models developed in the NCHRP Project 12-79 research. Therefore, the 2D-frame and 2D-grid procedures are conceptually and theoretically synonymous. Unfortunately, the programs typically do not provide identical results for various reasons, some of which are addressed in the subsequent discussions.

For the estimation of the flange lateral bending stresses and the bracing component forces in tub-girder bridges, NCHRP Project 12-79 used the same component force equations described above for the 1D-methods in its 2D-grid solutions.

In a limited number of cases, 2D-grid calculations for the staged placement of the concrete deck were evaluated in the NCHRP Project 12-79 research. These calculations were conducted using a refinement on the basic 2D-grid modeling approach implemented in the MDX software system. For these calculations, once the deck was made composite with the girders in a staged construction analysis, the composite deck was modeled using a flat shell finite element model and the girders were represented by 6 dof per node frame elements with an offset relative to the slab. This modeling procedure is commonly referred to as a plate and eccentric beam (PEB) approach. In the PEB analyses of staged deck placement conducted by the project team, the concrete was assumed to be fully effective at the beginning of the stage just after the one in which it is placed.

In addition, a limited number of additional "specialized" 2D-grid solutions were performed in the NCHRP Project 12-79 research using the first-order analysis capabilities of a thin-walled open-section (TWOS) frame element implemented in the educational program MASTAN2 (MASTAN2, 2011; McGuire et al., 2000). The TWOS frame element in MASTAN2 contains a seventh nodal warping degree of freedom, or a total of 14 nodal dofs per element. The specific element implemented in the MASTAN2 software, discussed in detail in McGuire et al. (2000), assumes a doubly symmetric cross-section such that the girder cross-section shear center is at the same position as the cross-section centroid. Therefore, the element is strictly not capable of representing the detailed response of singly symmetric bridge I-girders. However, in the 2D-grid models created with the MASTAN2 element, all the girder and cross-frame reference axes were modeled at the same planar elevation, and no depth information (e.g., bearing position relative to the reference axis of the girders, load height above the girder reference axis, etc.) was included in the model. As such, only the three conventional 2D-grid dofs plus the additional warping dof have non-zero displacement values and the influence of the shear center height relative to the height of the cross-section centroid does not enter into the first-order TWOS 2D-grid solutions.

2.7.3 3D Finite Element Analysis

The ABAQUS software system was used to conduct linear elastic (first-order) design-analysis solutions as well as detailed geometric nonlinear (second-order) elastic "simulation" studies in the NCHRP Project 12-79 research. Furthermore, for selected cases from the full suite of 86

bridges considered in the NCHRP Project 12-79 analytical studies, ABAQUS was used to conduct full nonlinear (material and geometric nonlinear) test simulations. Where possible, extant bridges were evaluated, and if those bridges had been instrumented, the test simulation results were validated against measured responses. The ABAQUS geometric nonlinear solutions were taken as the benchmarks to which all the simplified elastic analysis solutions were compared. Furthermore, the ABAQUS full nonlinear test simulation models were utilized as "virtual experiments" to evaluate questions such as the influence of different practices on the structural capacity of the physical bridges.

Generally speaking, any matrix analysis software where the structure is modeled in three-dimensions may be referred to as a three-dimensional finite element analysis (3D FEA). The NCHRP Project 12-79 research adopts the more restrictive definition of 3D FEA stated by AASHTO/NSBA G13.1 (2011). According to G13.1, an analysis method is classified as 3D FEA if:

1. The superstructure is modeled fully in three dimensions,
2. The individual girder flanges are modeled using beam, shell, or solid type elements,
3. The girder webs are modeled using shell or solid type elements,
4. The cross-frames or diaphragms are modeled using truss, beam, shell, or solid type elements as appropriate, and
5. The concrete deck is modeled using shell or solid elements (when considering the response of the composite structure).

Section 2.8 of the Project Task 8 report (Appendix C to the contractors' final report) provides a detailed description of the specific finite element modeling procedures employed for the elastic first- and second-order 3D FEA solutions as well as the full nonlinear test simulations conducted in the NCHRP Project 12-79 research.

One additional 3D FEA solution (using a less restrictive definition of the term) is employed for limited additional checking and verification of the above linear elastic and geometric nonlinear 3D FEA solutions in the NCHRP Project 12-79 research. This approach involves a second TWOS frame element implemented in the GT-Sabre software (Chang, 2006; Chang and White, 2008). The GT-Sabre TWOS frame element formulation accommodates the geometrically nonlinear modeling of singly symmetric I-girders, where the cross-section shear center and centroid are located at different elevations. In addition, in the GT-Sabre software, all of the girder reference axes (taken as the shear-center axis) are modeled at their correct physical elevations, and all of the individual cross-frame members are modeled explicitly at their precise elevation in the physical bridge. The connection of these components to the girder reference axes is accomplished by the use of rigid offsets. Furthermore, the height of the girder reference axes above the bearings is modeled by rigid offsets, and the load height of the slab dead weight effects is included in the element formulation. Therefore, the GT-Sabre model captures all the essential three-dimensional attributes of the structure geometry. This approach is referred to as a TWOS 3D-frame method in the project's Task 8 report. Specific comparisons of the geometric nonlinear results from GT-Sabre and ABAQUS are discussed subsequently in Section 3.2.4 of this report.

2.8 Data Reduction and Assessment of Analysis Procedures

Task 8A of the NCHRP Project 12-79 research involved extensive data reduction and interpretation of the results from the various studies of Task 7. The detailed results of this research are documented in the Task 8 report, "Evaluation of Analytical Methods for Construction Engineering of Curved and Skewed Steel Girder Bridges," Appendix C to the contractors' final report. Key results from this task are summarized in Chapter 3 of this report.

2.9 Development of Improvements to Simplified Methods

Task 8B of the NCHRP Project 12-79 research involved the identification of various shortcomings of the conventional simplified analysis methods studied in Tasks 7 and 8A and the development of specific improvements to these methods that lead to significantly better accuracy at little additional effort or cost. Specific calculations, as well as important considerations in the software implementation of these methods, were addressed.

Several of the key improvements for the analysis of tub-girder bridges have already been outlined in Sections 2.7.1 and 2.7.2, and, with the exception of the saw-tooth top-flange major-axis bending stress effects, were included as part of the "conventional" analysis calculations evaluated in Tasks 7 and 8 of the research. This is because these improvements are all implemented as part of 1D line-girder calculations as well as "post-processing" calculations to determine top flange lateral bending stresses and bracing component forces given the internal major-axis bending moments and torques determined either from the 1D or 2D analysis procedures. These improvements are discussed in more detail in Section 3.2.6 of this report.

The key improvements for the analysis of I-girder bridges require implementation within software if they are to be used efficiently in design practice. Furthermore, it is valuable to illustrate the critical inadequacies of the conventional methods to emphasize the importance of making the recommended improvements. Therefore, for I-girder bridges, the above Tasks 7 and 8 focus on evaluation of the accuracy of the simplified methods without the benefit of these improvements. The critical shortcomings of the conventional models and the essential improvements developed in the NCHRP Project 12-79 research are as follows:

- **The conventional 2D-grid models used in current practice substantially underestimate the girder torsional stiffnesses in I-girder bridges.** This is because the software considers only the St. Venant torsional stiffness of the girders. The contribution of warping torsion to the girder responses is generally neglected. It is interesting to note that competent structural engineers would never discount the girder warping rigidity EC_w, and thus use only the girder St. Venant torsional stiffness GJ, when evaluating the lateral-torsional buckling (LTB) resistance of I-girders. Doing so would underestimate the girder LTB resistances in practical constructed geometries so drastically that the I-girders would become useless. Yet, it is common practice to completely discount the girder warping rigidity when conducting a structural analysis. This practice generally results in dramatic over-estimation of the structural displacements when curved I-girders are modeled with nodes along the arc between the cross-frame locations. Furthermore, it tends to discount the significant transverse load paths in highly skewed bridges, since the girders are so torsionally soft (in the structural model) that they are unable to accept any significant load from the cross-frames causing torsion in the girders. As such, the cross-frame forces can be under-estimated to a dramatic extent.

In the Project 12-79 Task 8B research, this limitation is addressed by the development of an *equivalent St. Venant torsion constant* that accounts approximately for the girder stiffness from warping torsion. Section 3.2.2 of this report makes the case for this essential improvement.

- **The conventional 2D-grid models commonly use an equivalent beam stiffness model for the cross-frames that substantially misrepresents the cross-frame responses.** Fortunately, in many I-girder bridges, cross-frame deformations are small enough compared to the girder displacements such that the cross-frames perform essentially as rigid components in their own plane. However, in cases of significantly skewed I-girder bridges having "nuisance stiffness" transverse load paths (Krupicka and Poellot, 1993) and/or in general wide I-girder bridges, the deformations of the cross-frames can be a significant factor in the overall bridge response.

The Project 12-79 Task 8B research addressed this issue by the development of equivalent beam elements that capture the "exact" in-plane response for various cross-frame configurations. Section 3.2.3 of this report makes the case for this essential improvement.

- **The conventional 2D-grid models do not address the calculation of girder flange lateral bending in skewed I-girder bridges.** The current AASHTO LRFD Specifications Article C6.10.1 states:

  > In the absence of calculated values of f_ℓ from a refined analysis, a suggested estimate for the total f_ℓ in a flange at a cross-frame or diaphragm due to the use of discontinuous cross-frame or diaphragm lines is 10.0 ksi for interior girders and 7.5 ksi for exterior girders. These estimates are based on a limited examination of refined analysis results for bridges with skews approaching 60 degrees from normal and an average D/b_f ratio of approximately 4.0. In regions of the girders with contiguous cross-frames or diaphragms, these values need not be considered. Lateral flange bending in the exterior girders is substantially reduced when cross-frames or diaphragms are placed in discontinuous lines over the entire bridge due to the reduced cross-frame or diaphragm forces. A value of 2.0 ksi is suggested for f_ℓ, for the exterior girders in such cases, with the suggested value of 10 ksi retained for the interior girders. In all cases, it is suggested that the recommended values of f_ℓ be proportioned [apportioned] to dead and live load in the same proportion as the unfactored major-axis dead and live-load stresses at the section under consideration. An examination of cross-frame or diaphragm forces is also considered prudent in all bridges with skew angles exceeding 20 degrees.

The above recommendations are intended as coarse estimates of the total unfactored stresses associated with the controlling strength load condition. Hence, for an example location in a straight skewed bridge governed by the STRENGTH I load combination, with discontinuous cross-frames over only a portion of the bridge and with a ratio of dead load stress to total stress (dead plus live load) of ⅓, the nominal total *dead load* flange lateral bending stress in the exterior girders may be taken as 7.5 ksi × ⅓ = 2.5 ksi. If discontinuous cross-frame lines are used throughout the entire bridge, then using this same example dead-to-live-load ratio, f_ℓ may be taken equal to 2.0 ksi × ⅓ = 0.7 ksi. In both of these cases, the dead load f_ℓ values may be taken as 10.0 × ⅓ = 3.3 ksi on the interior girders.

In lieu of using a more rational method of determining the flange lateral bending effects, the NCHRP Project 12-79 research recommends that the value of f_ℓ from the above AASHTO (2010) provisions should be combined additively with the results from other estimates for the effects of overhang bracket loads and horizontal curvature when using 1D (line-girder) and 2D-grid analysis methods. However, the variety of geometries and framing conditions in highway bridges is extensive, involving a large range of skew, length, width, number of spans, and curvature combinations. Therefore, the above recommendations are very coarse estimates. Section 3.2.4 describes a method to more closely predict the f_ℓ stresses caused by skew effects within a 2D-grid analysis.

- **None of the analysis calculations commonly employed in current bridge design practice address the calculation of internal locked-in forces due to cross-frame detailing.** Yet, AASHTO (2010) Article C6.7.2 states that for curved I-girder bridges, " . . . the Engineer may need to consider the potential for any problematic locked-in stresses in the girder flanges or the cross-frames or diaphragms . . . " This article goes on to state, "The decision as to when these stresses should be evaluated is currently a matter of engineering judgment. It is anticipated that these stresses will be of little consequence in the vast majority of cases and that the resulting twist of the girders will be small enough that the cross-frames or diaphragms will easily pull the girders into their intended position and reverse any locked-in stresses as the dead load is applied." This statement reflects a limited understanding of the detailed behavior associated with the locked-in forces due to steel dead load fit (SDLF) or total dead load fit (TDLF) detailing of the cross-frames. One major misconception in this statement is that these forces are canceled by the dead load effects calculated by the 2D-grid analysis or 3D FEA. This implicit assumption

is false. The 2D-grid and 3D FEA calculations, conducted without the modeling of initial lack-of-fit effects, only give the internal forces in the bridge associated with no-load fit (NLF) detailing. Any locked-in forces, due to the lack of fit of the cross-frames with the girders in the undeformed geometry, add to (or subtract from) the forces determined from the 2D-grid or 3D FEA design analysis. Fortunately, at many locations in a given bridge, the SDLF or TDLF detailing effects tend to be opposite in sign to the internal forces due to the dead loads. Therefore, the 2D-grid or 3D FEA solutions for the stresses at these locations are conservative (potentially, undesirably so). However, there are important locations where the SDLF or TDLF detailing effects and the dead load effects can be additive. These locations depend on the characteristics of the bridge geometry.

Substantial effort was invested in the NCHRP Project 12-79 research to thoroughly evaluate the detailed behavior associated with the conceptually simple SDLF and TDLF detailing of the cross-frames in steel I-girder bridges. Sections 3.3 through 3.5 highlight the major findings and applications of this work. However, possibly the most important point related to the locked-in forces caused by SDLF and TDLF detailing is that they can be included in 2D-grid or 3D FEA calculations with relative ease and with little computational expense. Section 3.2.5 discusses how these locked-in force effects can be included in both of these types of analysis.

- **Little guidance is available in the current literature on methods that can be used to estimate fit-up forces.** In order to evaluate the potential for fit-up difficulties in the field for a given steel erection stage, generally, the engineer must conduct some evaluation of the corresponding fit-up forces. Better and more complete guidelines for conducting these types of analysis would be very useful. Section 3.3.5 of this report highlights major NCHRP Project 12-79 Task 8B findings that address this need.

2.10 Development of Guidelines for the Level of Construction Analysis, Plan Detail, and Submittals

The tenth task of the NCHRP Project 12-79 studies involved the development of guidelines for the level of construction analysis, plan detail, and submittals for curved and skewed steel girder bridges. As noted previously, this major objective of the project is addressed by the Task 9 report "Recommendations for Construction Plan Details and Level of Construction Analysis," which is included as Appendix B of this document. Section 3.6 of this report outlines the major recommendations from these guidelines.

CHAPTER 3

Findings and Applications

3.1 Evaluation of Conventional Simplified Analysis Methods

A substantial number of studies were conducted as part of NCHRP Project 12-79 to determine the ability of approximate 1D and 2D methods of analysis to capture the behavior predicted by refined 3D finite element models.

This chapter summarizes the findings and applications from the above research. Section 3.1.1 first addresses procedures for checking of (and in many cases, preventing) large second-order amplifications. Once these considerations are addressed, attention can be focused on selecting a suitable method of analysis for estimating the primary (i.e., first-order) forces, stresses, and displacements. Section 3.1.2 presents an overall scoring matrix for use in selecting the appropriate analysis type for I-girder bridges. Sections 3.1.3 and 3.1.4 provide examples illustrating how the scoring matrix should be used. Sections 3.1.5 and 3.1.6 parallel the above sections and focus on tub-girder bridges.

Sections 3.1.2 through 3.1.6 focus on the evaluation of conventional methods of 1D line-girder and 2D-grid analysis (i.e., methods of 1D line-girder and 2D-grid analysis representative of the current standards of care in the bridge design profession). However, as noted in the statement of the objectives and scope of this research (Section 1.3) and in the summary of Task 8B of the project, development of improvements to simplified methods (see Section 2.9), substantial research effort was devoted to identifying the major causes of shortcomings in the conventional methods and to the development of easily implemented, low-cost solutions that provide substantial improvements to these methods. Sections 3.2 through 3.4 describe these improvements.

The ultimate goal of the NCHRP Project 12-79 research is to provide substantive recommendations on the level of construction analysis, plan detail, and submittals for curved and skewed steel girder bridges. The project's Task 9 report, "Recommendations for Construction Plan Details and Level of Construction Analysis," included as Appendix B of this document, addresses this goal. Section 3.6 of this chapter provides an overview of this guidelines document.

3.1.1 Checking for (and Preventing) Large Second-Order Amplification

3.1.1.1 Global Second-Order Amplification

In certain situations, steel I-girder bridges can be vulnerable to overall (i.e., global) stability-related failures during their construction. The noncomposite dead loads must be resisted predominantly by the steel structure prior to hardening of the concrete deck. Relatively narrow

I-girder bridge units (i.e., units with large span-to-width ratios) may be susceptible to global stability problems rather than cross-section or individual unbraced length strength limit states (Yura et al., 2008).

Furthermore, due to second-order lateral-torsional amplification of the displacements and stresses, the limit of the structural resistance may be reached well before the theoretical elastic buckling load. Therefore, in curved and/or skewed bridge structures sensitive to second-order effects, simply ensuring that the loads for a given configuration are below an estimated global elastic buckling load is not sufficient. Large displacement amplifications can make it difficult to predict and control the structure's geometry during construction well before the theoretical elastic buckling load is reached.

Possible situations with the above characteristics include widening projects on existing bridges, pedestrian bridges with twin girders, phased construction involving narrow units, and erection stages where only a few girders of a bridge unit are in place. In all of these cases, the problem unit is relatively long and narrow.

The NCHRP Project 12-79 research recommends a simple method that can be used to alert the engineer to undesired response amplifications due to global second-order effects. The linear response prediction obtained from any of the first-order analyses can be multiplied by the following amplification factor:

$$AF_G = \frac{1}{1 - \frac{M_{\max G}}{M_{crG}}} \qquad \text{Eq. 2}$$

where M_{maxG} is the maximum total moment supported by the bridge unit for the loading under consideration, equal to the sum of all the girder moments, and

$$M_{crG} = C_b \frac{\pi^2 sE}{L_s^2} \sqrt{I_{ye} I_x} \qquad \text{Eq. 3}$$

is the elastic global buckling moment of the bridge unit (Yura et al., 2008). In Equation (2.25), C_b is the moment gradient modification factor applied to the full bridge cross-section moment diagram, s is the spacing between the two outside girders of the unit, E is the modulus of elasticity of steel,

$$I_{ye} = I_{yc} + \frac{b}{c} I_{yt} \qquad \text{Eq. 4}$$

is the effective moment of inertia of the individual I-girders about their weak axis, where I_{yc} and I_{yt} are the moments of inertia of the compression and tension flanges about the weak-axis of the girder cross-section respectively, b and c are the distances from the mid-thickness of the tension and compression flanges to the centroidal axis of the cross-section, and I_x is the moment of inertia of the individual girders about their major-axis of bending (i.e., the moment of inertia of a single girder).

Yura et al. (2008) developed Equation 3 considering multiple girder systems with up to four girders in the cross-section of the bridge unit. The individual girders were assumed to be prismatic and all the girders were assumed to have the same cross-section. The engineer must exercise judgment in applying this equation to general I-girder bridge units with stepped or other non-prismatic cross-sections, as well as cases where the different I-girders have different cross-sections.

In addition to providing an estimate of the second-order effects on the overall girder displacements, Equation 2 also can be used to predict potential increases in the girder stresses. Hence, to address potential second-order amplification concerns with narrow structural units, the results of an approximate 1D or 2D analysis should be amplified, using Equation 2, prior to conducting the constructability checks required by AASHTO LRFD Article 6.10.3. The limit states in Article 6.10.3 are:

- Nominal initial yielding due to combined major-axis bending and flange lateral bending,
- Strength under combined major-axis and flange lateral bending,
- Bend buckling or shear buckling of the girder webs,
- Reaching a flange lateral bending stress of $0.6F_y$, and
- Reaching the factored tensile modulus of rupture of the concrete deck in regions not adequately reinforced to control the concrete crack size.

Section 2.9 of the NCHRP Project 12-79 Task 8 report provides a detailed example showing the results of these calculations for an example narrow bridge unit that experienced construction difficulties (over-rotation of the bridge cross-section) during the deck placement.

The NCHRP Project 12-79 research suggests that Equation 2 should be used to detect possible large response amplifications during preliminary construction engineering. If the amplifier shows that a structure will exhibit significant nonlinear behavior during the deck placement, then in many cases, the scheme adopted for the construction should be revisited. In these cases, by conducting a detailed 3D FEA of the suspect stages, one often may find that the physical second-order amplification is somewhat smaller than predicted by the above simple estimate. If the second-order amplification is still relatively large in the more refined model, one should consider reducing the system response amplification by providing shoring or by bracing off of adjacent units. If AF_G from Equation 2 is less than approximately 1.1, it is recommended that the influence of global second-order effects may be neglected.

If it is found necessary to construct a structure that has potentially large response amplification during the deck placement, the engineer should perform a final detailed check of the suspect stages using a second-order (geometric nonlinear) 3D FEA. (It is recommended that this scenario with an AF_G larger than approximately 1.25 should be considered as requiring an accurate second-order 3D FEA.) In addition, it will be necessary to ensure that the deck placement does not deviate from the assumptions of the analysis in any way that would increase the second-order effects. Obviously, in most cases, it is best to stay away from these issues.

Substantial second-order effects during the steel erection may be a concern in some situations; however, particularly during the earliest stages of the steel erection, if the steel stresses are small and if the influence of the displacements on fit-up is not a factor, large second-order amplification of the deformations typically does not present a problem.

Steel tub girders generally have as much as 100 to more than 1,000 times the torsional stiffness of a comparable I-girder section. Therefore, when steel tub girders are fabricated with proper internal cross-frames to restrain their cross-section distortions as well as a proper top flange lateral bracing (TFLB) system, which acts as an effective top flange plate creating a pseudo-closed cross-section with the commensurate large torsional stiffness, lateral-torsional buckling is rarely a concern. Furthermore, second-order amplification in bridge tub girders is rarely of any significance even during lifting operations and early stages of the steel erection. However, overturning stability of curved tub girders, or tub-girder bridge units, can be a significant issue if it is not properly identified and addressed. Overturning stability considerations are addressed in Section 3.1.1.3.

3.1.1.2 Second-Order Amplification of Flange Lateral Bending between Cross-Frame Locations

Design-analysis compression flange lateral bending estimates usually are based on a first-order analysis. They do not consider any potential amplification of the bending between cross-frame locations due to second-order effects. That is, they do not consider equilibrium on the deflected geometry of the structure in the evaluation of the stresses. The corresponding "local" second-order flange lateral bending stresses (local to a given unbraced length between cross-frames) can be estimated by multiplying the first order f_ℓ values by the following amplification factor discussed in Article 6.10.1.6 of the AASHTO LRFD Specifications:

$$AF = \frac{0.85}{1 - f_b / F_{cr}} \geq 1.0 \qquad \text{Eq. 5}$$

where F_{cr} is the *elastic* lateral-torsional buckling stress for the compression flange, based on the unbraced length L_b between the cross-frames, and f_b is the maximum major-axis bending stress in the compression flange within the targeted unbraced length. It should be noted that when Equation 5 gives a value less than 1.0, AF must be taken equal to 1.0; in this case, the second-order amplification of the flange lateral bending is considered negligible.

When determining the amplification of f_ℓ in horizontally curved I-girders, White et al. (2001) indicate that for girders with $L_b/R \geq 0.05$, F_{cr} in Equation 5 may be determined using $KL_b = 0.5L_b$. For girders with $L_b/R < 0.05$, they recommend using the actual unsupported length L_b in Equation 5. The use of $KL_b = 0.5L_b$ for $L_b/R \geq 0.05$ gives a better estimate of the amplification of the bending deformations associated with the approximate symmetry boundary conditions for the flange lateral bending at the intermediate cross-frame locations and assumes that an unwinding stability failure of the compression flange is unlikely for this magnitude of the girder horizontal curvature. Figure 3-1 illustrates the flange lateral deflections associated with the horizontal curvature effects, as well as the unwinding stability failure mode for a straight elastic member.

3.1.1.3 Overturning Stability

Two straight dashed lines are drawn along the length direction of the plan sketches in Figure 3-2. One of the dashed lines is the chord between the fascia girder bearings on the outside of the curve. The other is the chord between the fascia girder bearings on the inside of the curve. Also shown on the plan sketches is the symbol "x," which indicates the centroid of the deck area (and hence the approximate centroid of dead weight of the structure). For bridges that are more highly curved (smaller R), the centroid (x) is closer to the outside chord line. If the curvature is

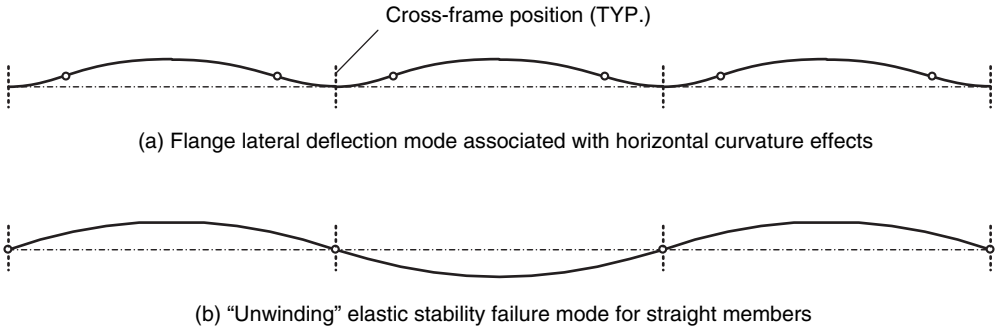

Figure 3-1. Second-order elastic deflection of a horizontally curved flange versus the unwinding stability failure mode of the compression flange in a straight member.

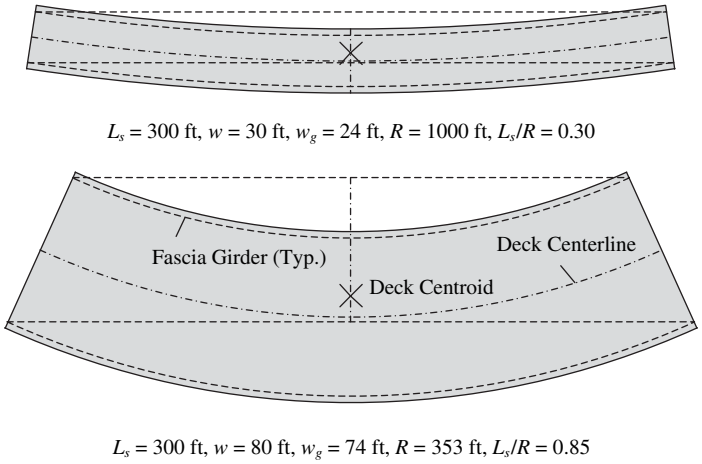

Figure 3-2. Plan geometries of two representative simple-span horizontally curved bridges with L_s = 300 ft.

such that the centroid is positioned directly over the outside chord line, then all the bridge reactions have to be zero except for the reactions at the outside bearings. That is, the bridge unit is at the verge of tipping about its outside bearings (assuming a single span, simply supported ends, and no hold-downs at the other bearings). This is obviously an extreme condition. Even a bridge with a much smaller curvature (larger radius of curvature) would require hold-downs at bearings closer to the center of curvature to handle uplift and equilibrate (or balance) the structure weight. The more common practice is to avoid uplift at any of the bearings.

As noted previously in Section 2.5, the bridge torsion index I_T provides a rough indication of the tendency for uplift at the bridge bearings. I_T is equal to 1.0 for the extreme hypothetical case where the deck centroid is located on the chord between the bearings on the outside of the curve, as discussed previously. It is equal to 0.5 for a straight bridge with zero skew. The NCHRP Project 12-79 research studies identified that simply supported I-girder bridges with $I_T \geq 0.65$ are often susceptible to uplift at some of the bearings under the nominal (unfactored) dead plus live loads. Similarly, for simple-span tub-girder bridges with single bearings on each tub, $I_T = 0.87$ was identified as a limit beyond which bearing uplift problems are likely. Continuous-span bridges can tolerate larger I_T values due to the continuity with adjacent spans.

It should be emphasized that I_T is only a rough indicator of uplift or overturning problems. It is relatively easy to calculate, but it is based on the idealization that the structure weight is uniformly distributed over the slab area. Also, when considering intermediate stages of the steel erection, it should be noted that until all the girders are erected and connected together sufficiently with cross-frames, the width of the bridge cross-section is only equal to the perpendicular distance between the connected girders on the inside and the outside of the curve. (I_T can be determined using this approximation for intermediate stages of the steel erection.) In addition, it should be noted that individual spans of continuous-span bridges may be supported essentially in a simple-span condition during some of the intermediate steel erection stages. Lastly, it should be noted that on highly curved bridge units, it may be useful to start the placement of the deck concrete on the inside of the curve to avoid a potential bearing uplift or overturning stability issue.

3.1.2 Selection of Analysis Methods for I-Girder Bridges

A quantitative assessment of the accuracy of conventional 1D line-girder and 2D-grid analysis methods was obtained in the NCHRP Project 12-79 research by identifying several error measures

that compared the conventional approximate (1D and 2D method) solutions to 3D FEA benchmark solutions. Using these quantitative assessments, the simplified methods of analysis were graded based on a scoring system developed to provide a comparative evaluation of the accuracy of each analysis method with regard to its ability to predict various structural responses.

Table 3-1 summarizes the results for the various methods and responses monitored for I-girder bridges. The grading rubric was as follows:

- A grade of A is assigned when the *normalized mean error* is less than or equal to 6 percent, reflecting excellent accuracy of the analysis predictions.

Table 3-1. Matrix for recommended level of analysis—I-girder bridges.

Response	Geometry	Worst-Case Scores		Mode of Scores	
		Traditional 2D-Grid	1D-Line Girder	Traditional 2D-Grid	1D-Line Girder
Major-Axis Bending Stresses	C ($I_C \leq 1$)	B	B	A	B
	C ($I_C > 1$)	D	C	B	C
	S ($I_S < 0.30$)	B	B	A	A
	S ($0.30 \leq I_S < 0.65$)	B	C	B	B
	S ($I_S \geq 0.65$)	D	D	C	C
	C&S ($I_C > 0.5$ & $I_S > 0.1$)	D	F	B	C
Vertical Displacements	C ($I_C \leq 1$)	B	C	A	B
	C ($I_C > 1$)	F	D	F	C
	S ($I_S < 0.30$)	B	A	A	A
	S ($0.30 \leq I_S < 0.65$)	B	B	A	B
	S ($I_S \geq 0.65$)	D	D	C	C
	C&S ($I_C > 0.5$ & $I_S > 0.1$)	F	F	F	C
Cross-Frame Forces	C ($I_C \leq 1$)	C	C	B	B
	C ($I_C > 1$)	F	D	C	C
	S ($I_S < 0.30$)	NA[a]	NA[a]	NA[a]	NA[a]
	S ($0.30 \leq I_S < 0.65$)	F[b]	F[c]	F[b]	F[c]
	S ($I_S \geq 0.65$)	F[b]	F[c]	F[b]	F[c]
	C&S ($I_C > 0.5$ & $I_S > 0.1$)	F[b]	F[c]	F[b]	F[c]
Flange Lateral Bending Stresses	C ($I_C \leq 1$)	C	C	B	B
	C ($I_C > 1$)	F	D	C	C
	S ($I_S < 0.30$)	NA[d]	NA[d]	NA[d]	NA[d]
	S ($0.30 \leq I_S < 0.65$)	F[b]	F[e]	F[b]	F[e]
	S ($I_S \geq 0.65$)	F[b]	F[e]	F[b]	F[e]
	C&S ($I_C > 0.5$ & $I_S > 0.1$)	F[b]	F[e]	F[b]	F[e]
Girder Layover at Bearings	C ($I_C \leq 1$)	NA[f]	NA[f]	NA[f]	NA[f]
	C ($I_C > 1$)	NA[f]	NA[f]	NA[f]	NA[f]
	S ($I_S < 0.30$)	B	A	A	A
	S ($0.30 \leq I_S < 0.65$)	B	B	A	B
	S ($I_S \geq 0.65$)	D	D	C	C
	C&S ($I_C > 0.5$ & $I_S > 0.1$)	F	F	F	C

[a] Magnitudes should be negligible for bridges that are properly designed & detailed. The cross-frame design is likely to be controlled by considerations other than gravity-load forces.

[b] Results are highly inaccurate due to modeling deficiencies addressed in Ch. 6 of the NCHRP 12-79 Task 8 report. The improved 2D-grid method discussed in this Ch. 6 provides an accurate estimate of these forces.

[c] Line-girder analysis provides no estimate of cross-frame forces associated with skew.

[d] The flange lateral bending stresses tend to be small. AASHTO Article C6.10.1 may be used as a conservative estimate of the flange lateral bending stresses due to skew.

[e] Line-girder analysis provides no estimate of girder flange lateral bending stresses associated with skew.

[f] Magnitudes should be negligible for bridges that are properly designed & detailed.

- A grade of B is assigned when the normalized mean error is between 7 percent and 12 percent, reflecting a case where the analysis predictions are in "reasonable agreement" with the benchmark analysis results.
- A grade of C is assigned when the normalized mean error is between 13 percent and 20 percent, reflecting a case where the analysis predictions start to deviate "significantly" from the benchmark analysis results.
- A grade of D is assigned when the normalized mean error is between 21 percent and 30 percent, indicating a case where the analysis predictions are poor, but may be considered acceptable in some cases.
- A score of F is assigned if the normalized mean errors are above the 30 percent limit. At this level of deviation from the benchmark analysis results, the subject approximate analysis method is considered unreliable and inadequate for design.

The normalized mean error used in the assessment of the above grades is calculated as

$$\mu_e = \frac{1}{N \bullet R_{FEAmax}} \sum_{i=1}^{N} e_i \qquad \text{Eq. 6}$$

where N is the total number of sampling points along the bridge length in the approximate model, R_{FEAmax} is the absolute value of the maximum response obtained from the FEA, and e_i is the absolute value of the error relative to the 3D FEA benchmark solution at point *i:*

$$e_i = \left| R_{approx} - R_{FEA} \right| \qquad \text{Eq. 7}$$

The summation in Equation 6 is computed for each girder line along the full length of the bridge. The largest resulting value is reported as the normalized mean error for the bridge. The error measure μ_e is useful for the overall assessment of the analysis accuracy since this measure is insensitive to local discrepancies, which can be due to minor shifting of the response predictions, etc. The normalized local maximum errors, e_i/R_{FEAmax}, generally are somewhat larger than the normalized mean error. Also, in many situations, unconservative error at one location in the bridge leads to comparable conservative error at another location. Hence, it is simpler to not consider the sign of the error as part of the overall assessment of the analysis accuracy.

In Table 3-1, the scoring for the various measured responses is subdivided into six categories based on the bridge geometry. These categories are defined as follows:

- Curved bridges with no skew are identified in the geometry column by the letter "C."
- The curved bridges are further divided into two subcategories, based on the connectivity index, defined as:

$$I_C = \frac{15000}{R(n_{cf}+1)m} \qquad \text{Eq. 8}$$

where R is the minimum radius of curvature at the centerline of the bridge cross-section in feet throughout the length of the bridge, n_{cf} is the number of intermediate cross-frames in the span, and m is a constant taken equal to 1 for simple-span bridges and 2 for continuous-span bridges. In bridges with multiple spans, I_C is taken as the largest value obtained from any of the spans.

- Straight skewed bridges are identified in the geometry column by the letter "S."
- The straight skewed bridges are further divided into three subcategories, based on the *skew index*:

$$I_S = \frac{w_g \tan\theta}{L_s} \qquad \text{Eq. 9}$$

where w_g is the width of the bridge measured between fascia girders, θ is the skew angle measured from a line perpendicular to the tangent of the bridge centerline, and L_s is the span

length at the bridge centerline. In bridges with unequal skew of their bearing lines, θ is taken as the angle of the bearing line with the largest skew.
- Bridges that are both curved and skewed are identified in the geometry column by the letters "C&S."

Two letter grades are indicated for each of the cells in Table 3-1. The first grade corresponds to the worst-case results encountered for the bridges studied by NCHRP Project 12-79 within the specified category. The second grade indicates the mode of the letter grades for that category (i.e., the letter grade encountered most often for that category).

It is useful to understand the qualifier indicated on the "C&S" bridges, i.e., "($I_C > 0.5$ & $I_S > 0.1$)" in Table 3-1. If a bridge has an $I_C < 0.5$ and an $I_S > 0.1$, it can be considered as a straight-skewed bridge for the purposes of assessing the expected analysis accuracy. Furthermore, if a bridge has an $I_C > 0.5$ and an $I_S \leq 0.1$, it can be considered as a curved radially supported bridge for these purposes.

Table 3-1 can be used to assess when a certain analysis method can be expected to give acceptable results. The following examples illustrate how this table should be used.

3.1.3 I-Girder Bridge Level of Analysis Example 1

Consider a horizontally curved steel I-girder bridge with radial supports, "very regular" geometry (constant girder spacing, constant deck width, relatively uniform cross-frame spacing, etc.), and $I_C < 1$, for which the engineer wants to perform a traditional 2D-grid analysis to determine the forces and displacements during critical stages of the erection sequence. (It should be noted that if I_C is calculated for an intermediate stage of the steel erection in which some of the cross-frames have not yet been placed, the number of intermediate cross-frames n_{cf} in Equation 8 should be taken as the number installed in the erection stage that is being checked. In addition, the radius of curvature R and the constant m should correspond to the specific intermediate stage of construction being evaluated, not the bridge in its final erected configuration.)

For the girder major-axis bending stresses and vertical displacements (f_b and Δ), the results are expected to deviate somewhat from those of a 3D analysis in general, since a worst-case score of B is assigned in Table 3-1 for these response quantities. The worst-case normalized mean error in these results from the 2D-grid analysis will typically range from 7 percent to 12 percent, compared to the results from a refined geometric nonlinear benchmark 3D FEA. However, one can expect that for most bridges, the errors will be less than or equal to 6 percent, based on the mode score of A for both of these responses.

Therefore, in this example, if the major-axis bending stresses and vertical displacements are of prime interest, a 2D-grid model should be sufficient if worst-case errors of approximately 12 percent are acceptable. Given that the bridge has "very regular" geometry, it is likely that the f_b and Δ errors are less than or equal to 6 percent. (The worst-case score is considered as the appropriate one to consider when designing a bridge with complicating features such as a poor span balance, or other "less regular" geometry characteristics.)

It is important to note that the engineer can compensate for potential unconservative major-axis bending stress errors in the design by adjusting the performance ratios targeted for the construction engineering design checks. For example, for the above bridge, the engineer may require that the performance ratios be less than or equal to 1/1.12 = 0.89 or 1/1.06 = 0.94 for the girder flexural resistance checks to gain further confidence in the adequacy of the resulting design. Conversely, over-prediction or under-prediction of the vertical displacements can be equally bad. Nevertheless, 12 percent or 6 percent displacement error may be of little consequence if the magnitude of the displacements is relatively small, or if the deflections are being calculated at an early stage of

the steel erection and it is expected that any resulting displacement incompatibilities or loss of geometry control can be subsequently resolved. However, if the magnitude of the displacements is large, or if it is expected that the resulting errors or displacement incompatibilities may be difficult to resolve, the engineer should consider conducting a 3D FEA of the subject construction stage to gain further confidence in the calculated displacements. This step in the application of Table 3-1 is where the bridge span length enters as an important factor, since longer-span bridges tend to have larger displacements.

It should be noted that compared to the creation of 3D FEA models for overall bridge design, including the calculation of live-load effects, the development of a 3D FEA model for several specific construction stages of potential concern involves a relatively small amount of effort. This is particularly the case with many of the modern software interfaces that facilitate the definition of the overall bridge geometry.

For calculation of the girder flange lateral bending stresses and the cross-frame forces in the above example bridge, the worst-case errors are expected to be larger, on the order of 13 percent to 20 percent (corresponding to a grade of C for both of these responses). However, the mode score is B, and since the bridge has a very regular geometry, it is likely that the normalized mean error in the flange lateral bending stresses and cross-frame forces is less than 12 percent. If these errors are acceptable in the engineer's judgment, then the 2D-grid analysis should be acceptable for the construction engineering calculations. As noted above, the engineer can compensate for these potential errors by reducing the target performance indices. In addition, with respect to the flange lateral bending stress, it should be noted that the f_ℓ values are multiplied by ⅓ in the AASHTO ⅓ rule equations. Therefore, the errors in f_ℓ have less of an influence on the performance ratio than errors in f_b when considering the strength limit state. When checking the AASHTO flange yielding limit for constructability, both f_ℓ and f_b have equal weights though. Based on these considerations, the simplest way to compensate for different potential unconservative errors in the f_ℓ and f_b values is to multiply the calculated stresses from the 2D-grid analysis by 1.20 and 1.12 (or 1.12 and 1.06) respectively prior to checking the performance ratios.

3.1.4 I-Girder Bridge Level of Analysis Example 2

Consider a straight steel I-girder bridge, with skewed supports and a skew index $I_s = 0.35$ (corresponding to the intermediate erection stage being evaluated), for which the engineer wants to perform a traditional 2D-grid analysis to determine the forces and displacements.

After reviewing Table 3-1, it is observed that for the major axis bending stresses and vertical deflections, a worst-case score of B is shown for straight skewed I-girder bridges with $0.30 < I_S \leq 0.65$. Furthermore, it can be observed that the mode of the scores for these bridge types is a B for the major-axis bending stresses and an A for the vertical displacements. Therefore, a properly prepared conventional 2D-grid analysis would be expected to produce major-axis bending stress and vertical deflection results that compare reasonably well with the results of a second-order elastic 3D FEA, such that the normalized mean error would be expected to be less than or equal to 12 percent.

If the layout of the cross-frames in the skewed bridge is such that overly stiff (nuisance) transverse load paths are alleviated, the engineer may expect that the error in the displacement calculations may be close to 6 percent or less. In this case, the engineer should be reasonably confident in the 2D-grid results for the calculation of the displacements. As noted in the previous example, the potential unconservative errors in the stresses can be compensated for in the construction engineering design checks; however, positive or negative displacement errors are equally bad.

The girder layover (i.e., the relative lateral deflection of the flanges) at the skewed bearing lines is often of key interest in skewed I-girder bridges. Table 3-1 shows that the girder layover calculations essentially have the same magnitude of error (i.e., the same resulting grades, as the girder vertical displacements). This is because properly designed and detailed skewed bearing line cross-frames are relatively rigid in their own planes compared to the lateral stiffness of the girders. Hence, the girder layovers are essentially proportional to the girder major-axis bending rotations at the skewed bearing lines.

For the calculation of the cross-frame forces and/or the girder flange lateral bending stresses in the above example, one should observe that the conventional 2D-grid procedures are entirely unreliable. That is, the scores in Table 3-1 are uniformly an F. The reason for this poor performance of the traditional 2D-grid methods is the ordinary modeling of the girder torsional properties using only the St. Venant torsional stiffness *GJ*/*L*. The physical girder torsional stiffnesses are generally much larger due to restraint of warping (i.e., flange lateral bending) effects. In addition, for wide skewed bridges and/or for skewed bridges containing specific overly stiff (nuisance) transverse load paths, the limited accuracy of the cross-frame equivalent beam stiffness models used in conventional 2D-grid methods may lead to a dramatic loss of accuracy in the cross-frame forces.

Lastly, conventional 2D-grid methods generally do not include any calculations of the girder flange lateral bending stresses due to skew. Hence, the score for the calculation of the flange lateral bending stresses is also an F in Table 3-1.

3.1.5 Selection of Analysis Methods for Tub-Girder Bridges

Similar to the I-girder bridges, a quantitative assessment of the analysis accuracy of tub-girder bridges was obtained in the NCHRP Project 12-79 research by focusing first on the normalized mean errors in the approximate (1D and 2D method) solutions for the girder major-axis bending stresses, internal torques and vertical displacements, compared to benchmark 3D FEA results. Using the quantitative assessments, the various methods of analysis were assigned scores in the same manner as the scoring for the I-girder bridge responses. Table 3-2 summarizes the scores for the above responses in tub-girder bridges.

Table 3-2. Matrix 1 for recommended level of analysis—tub-girder bridges.

Response	Geometry	Worst-Case Scores		Mode of Scores	
		2D-P1	1D-Line Girder	2D-P1	1D-Line Girder
Major-Axis Bending Stresses	S	B	B	A	B
	C	B	C	A	B
	C&S	B	C	B	B
Girder Torques	S	F	F	D	F
	C	D	D	A	B
	C&S	F	F	A	B
Vertical Displacements	S	B	B	A	A
	C	A	B	A	A
	C&S	B	B	A	A
Girder Layover at Bearing Lines	S	B	B	A	A
	C	NA[a]	NA[a]	NA[a]	NA[a]
	C&S	B	B	A	A

[a] Magnitudes should be negligible where properly designed and detailed diaphragms or cross-frames are present.

It is interesting that the Table 3-2 scores for the major-axis bending stresses and vertical displacements are relatively good. However, the worst-case scores for the internal torques are generally quite low. These low scores are largely due to the fact that the internal torques in tub-girder bridges can be sensitive to various details of the framing, such as the use and location of external intermediate cross-frames or diaphragms, the relative flexibility of these diaphragms as well as the adjacent internal cross-frames within the tub girders, skewed interior piers without external cross-frames between the piers at the corresponding bearing line, incidental torques introduced into the girders due to the specific orientation of the top flange lateral bracing system members (particularly for Pratt-type TFLB systems), etc. Jimenez Chong (2012) provides a detailed evaluation and assessment of the causes for the errors in the girder internal torques for the tub-girder bridges considered in the NCHRP Project 12-79 research.

Similar to the considerations for I-girder bridges, the external diaphragms and/or cross-frames typically respond relatively rigidly in their own plane compared to the torsional stiffness of the girders (even though the tub-girder torsional stiffnesses are significantly larger than those of comparable I-girders). Therefore, the girder layovers at skewed bearing lines tend to be proportional to the major-axis bending rotation of the girders at these locations. As a result, the errors in the girder layover calculations obtained from the approximate methods tend to be similar to the errors in the major-axis bending displacements.

The connectivity index, I_C, does not apply to tub-girder bridges. This index is primarily a measure of the loss of accuracy in I-girder bridges due to the poor modeling of the I-girder torsion properties. For tub-girder bridges, the conventional St. Venant torsion model generally works well as a characterization of the response of the pseudo-closed section tub girders. Hence, I_C is not used for characterization of tub-girder bridges in Table 3-2. Furthermore, there is only a weak correlation between the accuracy of the simplified analysis calculations and the skew index I_S for tub-girder bridges. Therefore, the skew index is not used to characterize tub-girder bridges in Table 3-2 either. Important differences in the simplified analysis predictions do exist, however, as a function of whether the bridge is curved, "C," straight and skewed, "S," or curved and skewed, "C&S." Therefore, these characterizations are shown in the table.

It should be noted that there was a measureable decrease in the accuracy of the 2D-grid solutions for the tub-girder bridges obtained with Program P2 compared to Program P1. Since the research team had greater control over the calculations, as well as more detailed information regarding the specifics of the procedures in Program P1, the P1 results are presented in Table 3-2 as being the most representative of the results achievable with a 2D-grid procedure.

In addition to the above assessments, the accuracy of the bracing component force calculations in tub-girder bridges is assessed separately in Table 3-3. It is useful to address the accuracy of these response calculations separately from the ones shown in Table 3-2 since the simplified bracing component force calculations take the girder major-axis bending moments, torques, and applied transverse loads as inputs and then apply various useful mechanics of materials approximations to obtain the force estimates. That is, there are two distinct sources of error in the bracing component forces relative to the 3D FEA benchmark solutions:

1. The error in the calculation of the input quantities obtained from the 1D line-girder or 2D-grid analysis, and
2. The error introduced by approximations in the bracing component force equations.

Chapter 2 of the NCHRP Project 12-79 Task 8 report provides an overview of the bracing component force equations evaluated here, which are used frequently in current professional practice. It should be noted that the calculation of the top flange lateral bending stresses in tub girders is included with the bracing component force calculations. This is because these stresses

Table 3-3. Matrix 2 for recommended level of analysis—tub-girder bridges.

Response	Sign of Error	Geometry	Worst-Case Scores		Mode of Scores	
			2D-P1	1D-Line Girder	2D-P1	1D-Line Girder
TFLB Diagonal Force	Positive (Conservative)	S	D	D	D	C
		C	D	F	B	F
		C&S	D[a]	F	B	F
		Pratt TFLB System	C	F	A	F
	Negative (Unconservative)	S	F[b]	C		
		C	--[c]	--		
		C&S	--	--		
		Pratt TFLB System	--	--		
TFLB & Top Internal CF Strut Force	Positive (Conservative)	S	C	C		
		C	F	F		
		C&S	F	F[d]		
		Pratt TFLB System	F	F		
	Negative (Unconservative)	S	C	C		
		C	--	A		
		C&S	--	C		
		Pratt TFLB System	D	D		
Internal CF Diagonal Force	Positive (Conservative)	S	NA[e]	NA[e]		
		C	F	F		
		C&S	F	F		
		Pratt TFLB System	--	F[f]		
	Negative (Unconservative)	S	NA[e]	NA[e]		
		C	--	--		
		C&S	--	D		
		Pratt TFLB System	B	--		
Top Flange Lateral Bending Stress (Warren TFLB Systems)	Positive (Conservative)	S	C	C		
		C	F	F		
		C&S	F	F[d]		
	Negative (Unconservative)	S	C	C		
		C	--	A		
		C&S	--	C		

[a] Modified from a C to a D considering the grade for the C and the S bridges.

[b] Large unconservative error obtained for bridge ETSSS2 due to complex framing. If this bridge is considered as an exceptional case, the next worst-case unconservative error is -15 % for NTSSS2 (grade = C).

[c] The symbol "--" indicates that no cases were encountered with this score.

[d] Modified from a B to an F considering the grade for the C bridges.

[e] For straight-skewed bridges, the internal intermediate cross-frame diagonal forces tend to be negligible.

[f] Modified from an A to an F considering the grade for the C and C&S bridges.

are influenced significantly by the interaction of the top flanges with the tub-girder bracing systems.

The NCHRP Project 12-79 research observed that in many situations, the bracing component force estimates are conservative relative to the 3D FEA benchmark solutions. Therefore, it is useful to consider a signed error measure for the bracing component force calculations. In addition, the bracing component dimensions and section sizes often are repeated to a substantial degree throughout a tub-girder bridge for the different types of components. Therefore, it is useful to

quantify the analysis error as the difference between the maximum of the component forces determined by the approximate analysis minus the corresponding estimate from the 3D FEA benchmark, that is:

$$e_{\max} = \left(R_{approx.max} - R_{FEA.max}\right) / R_{FEA.max} \quad \text{Eq. 10}$$

for a given type of component. The grades for these responses were assigned based on the same scoring system used for the assessments based on the normalized mean error with one exception: Separate grades were assigned for the positive (conservative) errors and for the negative (unconservative) errors in Table 3-3. In situations where no negative (unconservative) errors were observed in all of the bridges considered in a given category, the symbol "—" is shown in the cells of the matrix, and the cells are unshaded.

The mode of the grades is shown only for the top flange diagonal bracing forces in Table 3-3. The mode of the grades for the other component force types is not shown because of substantial positive and negative errors in the calculations that were encountered in general for the tub-girder bridges and because, in cases where a clear mode for the grades existed, the mode of the grades was the same as the worst-case grade.

In addition to the above considerations, it should be noted that current simplified estimates of the tub-girder bridge bracing component forces are generally less accurate for bridges with Pratt-type top flange lateral bracing (TFLB) systems compared to Warren and X-type systems. A small number of tub-girder bridges with Pratt-type TFLB systems were considered in the NCHRP Project 12-79 research. Therefore, the composite scores for these bridges are reported separately in Table 3-3.

3.1.6 Tub-Girder Bridge Level of Analysis Example

Consider a horizontally curved steel tub-girder bridge with a Warren top flange lateral bracing system and skewed supports for which the engineer wants to perform a traditional 2D-grid analysis to determine the forces and displacements during critical stages of the erection sequence. The bridge has a "very regular" geometry (constant girder spacing, constant deck width, a relatively uniform top flange lateral bracing [TFLB] system and internal cross-frame spacing, solid plate end diaphragms, single bearings for each girder, etc.).

A properly prepared 2D-grid analysis would be expected to produce major axis bending stresses and vertical deflections with mean errors less than 12 percent relative to a rigorous 3D FEA solution, since the worst-case score assigned for both of these quantities is a B in Table 3-2 for the subject "C&S" category. Furthermore, it can be observed that the mode of the scores for the vertical displacements is an A; hence, given the "very regular" geometry of the above bridge, it is expected that the vertical displacements most likely would be accurate to within 6 percent.

Unfortunately, the worst-case score is an F for the 2D-grid estimates of the internal torques in the C&S bridges. As noted previously, this low score is due to the fact that the internal torques in tub-girder bridges can be very sensitive to various details of the framing, such as the use and location of external intermediate cross-frames or diaphragms, the relative flexibility of these diaphragms as well as the adjacent internal cross-frames within the tub girders, skewed interior piers without external cross-frames between the piers at the corresponding bearing line, incidental torques induced in the girders due to the specific orientation of the top flange lateral bracing system members (particularly for Pratt-type TFLB systems), etc. Fortunately though, the web and bottom flange shear forces due to the internal torques are often relatively small compared to the normal stresses associated with the major-axis bending response of the

girders. Furthermore, the mode of the scores for the internal torques is an A from Table 3-2. Therefore, the engineer must exercise substantial judgment in estimating what the expected error may be for the internal torque from a 2D-grid analysis and in assessing the impact of this error on the bridge design. As noted for I-girder bridges, one can compensate for any anticipated potential unconservative error in the internal force or stress response quantities by scaling up the corresponding responses by the anticipated error, or by adjusting the target values of the performance ratios.

Based on Table 3-3, the worst-case score for the positive (conservative) error in the calculation of the TFLB diagonal forces in the above example is a D, whereas the mode of the scores is a B. The table shows that no unconservative errors were encountered in this calculation for the tub-girder bridges studied in NCHRP Project 12-79. Since the example bridge is "very regular," the engineer may assume that the TFLB diagonal force calculations are conservative, but reasonably accurate, relative to the refined 3D FEA benchmark values.

For both the TFLB and top internal cross-frame strut forces and the internal cross-frame diagonal forces in C&S bridges, Table 3-3 shows a grade of F for the conservative error. Also, the table shows that no unconservative errors were encountered in the NCHRP Project 12-79 calculations for these responses. Therefore, the engineer can assume that the forces for these components, as determined from a 2D-grid analysis plus the bracing component force equations, are highly conservative. It should be noted that the forces in the top struts of the internal cross-frames near exterior diaphragm or exterior cross-frame locations can be very sensitive to the interaction of the external diaphragm or cross-frame with the girders. These forces should be determined based on consideration of statics at these locations, given the forces transmitted to the girders from the external diaphragm or cross-frame components. NCHRP Project 12-79 did not consider these component forces in its error assessments.

Lastly, Table 3-3 shows that the tub-girder top flange lateral bending stresses tend to be estimated with a high degree of conservatism by 2D-grid methods combined with the bracing component force equations. In addition, no unconservative errors were encountered in the tub-girder bridges studied by NCHRP Project 12-79 for the top flange lateral bending stresses. Therefore, the engineer can also assume that these stress estimates are highly conservative.

3.2 Improvements to Conventional Analysis Methods

Various essential improvements to conventional methods of analysis were developed during the course of the NCHRP Project 12-79 research. In all cases, the project team strived to identify specific sources of errors relative to 3D FEA benchmark solutions and then to develop solutions to these errors by addressing the inadequacies in the conventional models at a fundamental structural mechanics level. In addition, solutions were sought that provided substantial benefits, yet involved little computational expense and were relatively easy to implement in software. The following sections highlight these major improvements.

First, Section 3.2.1 introduces a basic simply supported I-girder bridge used for illustration purposes in a number of the subsequent sections. This bridge was designed and tested at the FHWA Turner-Fairbank Highway Research Center in prior FHWA research (Jung, 2006; Jung and White, 2008). The bridge has substantial horizontal curvature and zero skew. Furthermore, the bridge was designed at, or slightly above, a number of limits in the AASHTO LRFD Design Specifications. Therefore, this structure is particularly sensitive to a number of parameters that influence the accuracy of simplified analysis methods. Because of the fact that the bridge is relatively basic and easily modeled in a short amount of time, due to the sensitivity of the structure to attributes influencing the analysis accuracy, and since the calculations are backed up by a large

number of experimental measurements, this bridge is an excellent case for discussion of analysis error sources as well as analysis improvements.

Section 3.2.1 is followed by four sections that describe four key improvements to conventional 2D-grid analysis methods recommended by the NCHRP Project 12-79 research for I-girder bridges:

1. Use of an equivalent St. Venant torsion constant for the I-girders that accounts approximately for the contribution of warping (i.e., flange lateral bending) to the girder torsional stiffnesses,
2. Use of equivalent beam models for the cross-frames that better capture the true bending and shear racking stiffnesses of various types of cross-frames used in I-girder bridges,
3. Direct calculation of flange lateral bending stresses in skewed or curved and skewed I-girder bridges based on the cross-frame forces calculated from the above improved 2D-grid procedures, and
4. 2D-grid (or 3D FEA) calculation of locked-in forces due to steel dead load fit (SDLF) or total dead load fit (TDLF) detailing of the cross-frames in curved and/or skewed I-girder bridges.

The first three of the above sections focus on the recommended calculations and their implementation, as well as the resulting improvement of the analysis results. However, the fourth of these sections focuses just on the recommended calculations and their implementation. A longer discussion is necessary to convey the detailed characteristics of the locked-in force effects from SDLF or TDLF detailing. These considerations are addressed in depth in Section 3.3.

3.2.1 The FHWA Test Bridge

Figure 3-3 shows key particulars of the geometry for a 90 ft. span curved I-girder bridge tested in 2005 at the FHWA Turner-Fairbank Highway Research Center (Jung, 2006; Jung and White, 2008). This bridge is introduced here because it is used for illustration purposes in a number of the subsequent sections. The reader is referred to the Task 8 report (Appendix C of the contractors' final report), and to Sanchez (2011), Ozgur (2011) and Jimenez Chong (2012) for similar results to those discussed in Sections 3.2.2 through 3.2.6 for a wide range of bridges.

The radius of curvature of the centerline of the FHWA Test Bridge was 200 ft. and the bridge cross-section contained three I-girders spaced at 8.75 ft. Figure 3-4 shows a photo of the bridge after the girders G3 and G2 were placed on the supports and the cross-frames were installed. The fascia girder on the outside of the curve (G1) is blocked on the laboratory floor toward the right-hand side of the photo. It should be noted that the naming of the outside girder as G1 and the inside girder as G3 follows the naming convention adopted within the NCHRP Project 12-79 project research. The above referenced research reports refer to the outside girder as G3 and the inside girder as G1.

The total width of the 8-in. concrete deck was 23.5 ft., with 3.0-ft. overhangs outside the fascia girders. The bridge was constructed using V-type cross-frames composed of circular tube section members. These HSS 5 × ¼-in. members had areas comparable to the member areas that would have been required for this bridge with other more common cross-frame section types. However, the tube-member cross-frames facilitated the measurement of the cross-frame forces, since the tubes were essentially instrumented as load cells.

The FHWA Test Bridge was designed with a number of characteristics that pushed or slightly exceeded the limits of prior AASHTO curved I-girder bridge specifications, as well as some of the limits in the current AASHTO (2010) LRFD Specifications, as follows:

- Intermediate cross-frames were employed at only three cross-sections within the bridge span, resulting in a subtended angle between the cross-frames of $L_b/R = 0.1125$. This is slightly larger than the maximum limit of $L_b/R = 0.10$ specified in AASHTO (2010) Article 6.7.4.2.

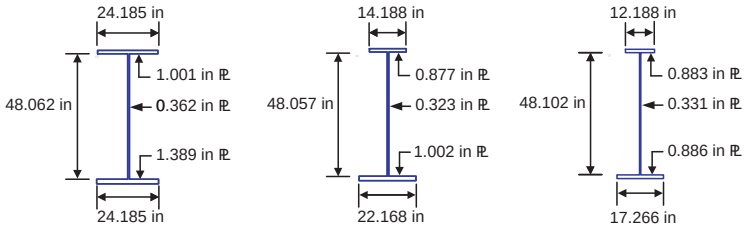

(a) G1 cross-section (b) G2 cross-section (b) G3 cross-section

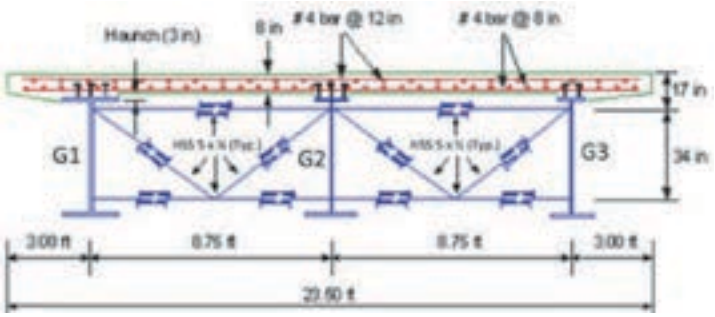

(d) Bridge cross-section

L_s = 90 ft., R = 2000 ft., w = 23.5 ft.

(e) Bridge plan view

Figure 3-3. FHWA Test Bridge (EISCR1) geometry.

Figure 3-4. FHWA Test Bridge (EISCR1) during the steel erection, with cross-frames attached between girders G2 and G3 (Jung, 2006; Jung and White, 2008).

- The fascia girder on the outside of the curve (G1) utilized a hybrid HPS 70W bottom flange. Hybrid curved girders were not permitted in the AASHTO Specifications at the time of the FHWA research. The use of grade 70 steel allowed the bottom flange thickness for Girder G1 to be reduced from approximately 2 in. if grade 50 steel had been used.
- Due to the grade 70 bottom flange on G1, the 48-in. web depth for this girder slightly violates the arc-span length-to-depth requirements in AASHTO (2010) Article 2.5.2.6.3. However, this bridge satisfies the *Span*/800 deflection limit of AASHTO Article 2.5.2.6.2.
- The web slenderness D/t_w of all the girders was close to the AASHTO (2010) limit of 150 for straight and curved transversely stiffened web panels.
- Transverse stiffening of the girder webs varied from a maximum of close to $d_o/D = 3$ in all the girders near the mid-span of the bridge to $d_o/D < 1$ near the supports for Girder G1. Prior AASHTO Specifications have required a much tighter spacing of web transverse stiffeners in curved I-girder webs.
- The top compression flange slenderness $b_{fc}/2t_{fc}$ was slightly larger than 12, which is the maximum limit on the flange slenderness specified in AASHTO LRFD Article 6.10.2.2.
- Both girders G1 and G2 were sized close to the AASHTO (2010) strength limits.

The tight radius of curvature ($R = 200$ ft.) combined with the use of only three intermediate cross-frames ($n_{cf} = 3$) results in a value of I_C of 18.75 from Equation 8 for this bridge in its final constructed condition. Therefore, this bridge significantly exceeds the $I_C \leq 1$ limit utilized for scoring the accuracy of the simplified analysis methods in Table 3-1. As noted previously, the NCHRP Project 12-79 research found that the connectivity index, I_C, tended to correlate well with the magnitude of the errors exhibited by conventional 2D-grid methods.

Figures 3-5 and 3-6 show several photos of the test bridge during its construction.

3.2.2 Improved I-Girder Torsion Model for 2D-Grid Analysis

As noted previously, the conventional use of just the St. Venant term (GJ/L) in characterizing the torsional stiffness of I-girders results in a dramatic underestimation of the true girder

Figure 3-5. FHWA Test Bridge, overhang brackets attached to the fascia girder on the outside of the curve (Girder G1 per the NCHRP Project 12-79 naming convention, Girder G3 in reports and papers on the FHWA research) (Jung, 2006; Jung and White, 2008).

Figure 3-6. FHWA Test Bridge placement of the slab concrete (Jung, 2006; Jung and White, 2008).

torsional stiffness. This is due to the neglect of the contributions from flange lateral bending, that is, warping of the flanges, to the torsional properties. Even for intermediate steel erection stages where some of the cross-frames are not yet installed, the typical torsional contribution from the girder warping rigidity (EC_w) is substantial compared to the contribution from the St. Venant torsional rigidity (GJ). It is somewhat odd that structural engineers commonly would never check the lateral-torsional buckling capacity of a bridge I-girder by neglecting the term EC_w and using only the term GJ. Yet, it is common practice in conventional 2D-grid methods to neglect the warping torsion contribution coming from the lateral bending of the flanges.

The NCHRP Project 12-79 Task 8B research observed that an *equivalent torsion constant*, J_{eq}, based on equating the stiffness GJ_{eq}/L_b with the analytical torsional stiffness associated with assuming warping fixity at the intermediate cross-frame locations and warping free conditions at the simply supported ends of a bridge girder, potentially could result in significant improvements to the accuracy of 2D-grid models for I-girder bridges. This observation was based in part on the prior research developments by Ahmed and Weisgerber (1996), as well as the commercial implementation of this type of capability within the software RISA-3D (RISA, 2011). The term L_b in the stiffness GJ_{eq}/L_b is the unbraced length between the cross-frames.

When implementing this approach, a different value of the equivalent torsional constant J_{eq} must be calculated for each unbraced length having a different L_b or any difference in the girder cross-sectional properties. Furthermore, it is important to recognize that the use of a length less than L_b typically will result in a substantial over-estimation of the torsional stiffness. Therefore, when a given unbraced length is modeled using multiple elements, it is essential that the unbraced length L_b be used in the equations for J_{eq}, not the individual element lengths.

By equating GJ_{eq}/L_b to the torsional stiffness (T/ϕ) for the open-section thin-walled beam associated with warping fixity at each end of a given unbraced length L_b, where T is the applied end torque and ϕ is corresponding relative end rotation, the equivalent torsion constant is obtained as:

$$J_{eq(fx-fx)} = J\left[1-\frac{\sinh(pL_b)}{pL_b}+\frac{[\cosh(pL_b)-1]^2}{pL_b\sinh(pL_b)}\right]^{-1} \qquad \text{Eq. 11}$$

Similarly, by equating GJ_{eq}/L_b to the torsional stiffness (T/ϕ) for the open-section thin-walled beam associated with warping fixity at one end and warping free boundary conditions at the opposite end of a given unbraced length, one obtains:

$$J_{eq(s-fx)} = J\left[1-\frac{\sinh(pL_b)}{pL_b\cosh(pL_b)}\right]^{-1} \qquad \text{Eq. 12}$$

Section 6.1.2 of the Task 8 report shows a complete derivation of these equivalent torsion constants.

The assumption of warping fixity at all of the intermediate cross-frame locations is certainly a gross approximation. TWOS 3D-frame analysis (see Section 2.7.3 for a description of this terminology) generally shows that some flange warping (i.e., cross-bending) rotations occur at the cross-frame locations. However, the assumption of warping fixity at the intermediate cross-frame locations leads to a reasonably accurate characterization of the girder torsional stiffnesses pertaining to the overall deformations of a bridge unit as long as:

- There are at least two I-girders connected together, and
- They are connected by enough cross-frames such that the connectivity index I_C is less than 20 ($I_C \leq 20$).

Therefore, the FHWA Test Bridge in its final constructed condition represents essentially the maximum limit at which the above approach provides a sufficient solution.

3.2.2.1 Comparison of the Vertical Displacement Results from Various Approaches for the FHWA Test Bridge

Figure 3-7 shows representative results for the vertical displacement of Girder G1 of the FHWA Test Bridge under the nominal (unfactored) total dead load, i.e., the self-weight of the structural steel plus the weight of the concrete deck, with all the loads being resisted by the noncomposite structure. The benchmark 3D FEA prediction, 4.49 in. downward deflection of the centerline of G1 at its mid-span, matches closely with the results from the physical test (Jung, 2006; Jung and White, 2008). Figure 3-8 shows a rendering of the magnified bridge vertical deflections from the 3D FEA solution.

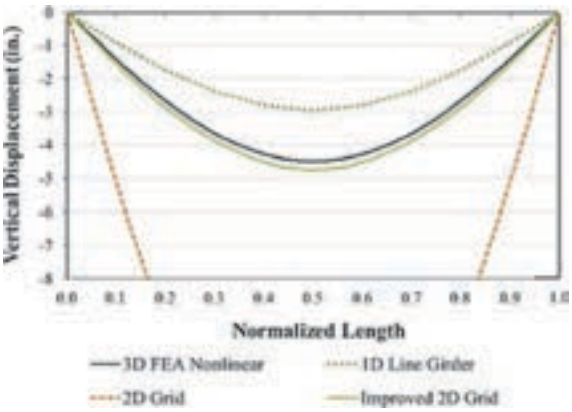

Figure 3-7. FHWA Test Bridge (EISCR1) vertical displacements in fascia girder on the outside of the curve under total dead load (unfactored).

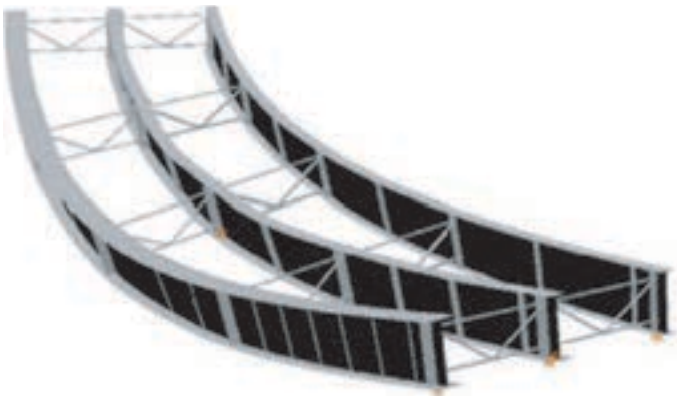

Figure 3-8. Magnified deflected geometry of EISCR1 under total dead load, from 3D FEA (displacements scaled 20x, initial vertical camber not scaled).

The 1D-line girder solution in Figure 3-7 is obtained using the V-load method, applying the primary loads as well as the V-loads to Girder G1 on the outside of the horizontal curve, and analyzing the uniaxial bending deformations of the member subjected to these loads. Unfortunately, this solution under-predicts the vertical displacement of Girder G1 by 33.4 percent. The actual displacements are larger due to the coupling between the girder mid-span vertical displacements and the twisting deformations, particularly the twisting deformations of the girder near the supports. That is, the twisting of the girder near the supports produces corresponding additional vertical displacements at the mid-span.

In the 2D-grid analyses, the girders are modeled by four elements within each of their unbraced lengths, with the nodes being positioned along the circular arc between the cross-frames. Only one conventional 2D-grid solution is shown in the plot. However, essentially the same results are obtained by models built in MDX and LARSA-4D, as well as one other 2D-grid model created using a third independent code for this problem. The improved method of modeling the cross-frames discussed in Section 3.2.3 is employed for all the 2D-grid solutions discussed in this section.

One can observe that the improved 2D-grid solution, based on the use of J_{eq}, predicts a slightly larger mid-span displacement of Girder G1 than obtained in the 3D FEA solution (4.73 in. versus 4.49 in.). Furthermore, it should be noted that the benchmark 3D FEA solution shown here includes geometric nonlinearity. However, if the 3D FEA simulation model is run as a geometrically linear (first-order analysis) solution, the mid-span displacements reduce to only 4.40 in. Therefore, the second-order effects on the vertical displacements are only about 2 percent for this structure and loading. The improved 2D-grid solution over-estimates the 3D FEA linear elastic solution by 7.5 percent and over-predicts the 3D FEA geometric nonlinear benchmark solution by 5.3 percent.

Conversely, the conventional 2D-grid solutions predict a displacement of 15.37 in. at the mid-span of G1, 342 percent larger than the benchmark result. Obviously, this discrepancy between the 2D-grid prediction and the physical result is some cause for concern.

Table 3-4 summarizes the above numerical results and presents a number of additional solutions for the vertical displacement of Girder G1. The only solution that is dramatically in error is the conventional 2D-grid solution discussed above. Interestingly, if the girders are modeled using only one straight conventional element between each of the cross-frames, the predicted displacement is 4.35 in. (3.1 percent smaller than the benchmark solution). Furthermore, the same

Table 3-4. FHWA Test Bridge (EISCR1) mid-span vertical displacement of Girder G1 (ΔG1) under total dead load (unfactored) for different 2D-grid girder discretizations and idealizations, cross-frames modeled using shear deformable beam element (ΔG1 = 4.49 in., second-order 3D FEA; ΔG1 = 4.40 in., first-order 3D FEA).

2D-grid discretization and idealization	Δ_{G1} (in.)
Four conventional elements within each L_b, nodes located on the circular arc	15.37
One conventional element within each L_b, straight between each CF	4.35
Four conventional elements within each L_b, straight between each CF	4.35
Four elements within each L_b, nodes located on the circular arc, using J_{eq}	4.73
Four elements within each L_b, straight between each CF, using J_{eq}	4.28
One element within each L_b, straight between each CF, using J_{eq}	4.28
Four TWOS beam elements within each L_b, nodes located on the circular arc	4.42
Four TWOS beam elements within each L_b, straight between each CF	4.34
Four TWOS beam elements within each L_b, nodes located on the circular arc, warping fixed at the intermediate CF locations	4.32
Four TWOS beam elements within each L_b, straight between each CF, warping fixed at the intermediate CF locations	4.28
Four TWOS beam elements within each L_b, nodes located on the circular arc, all girder J values taken equal to zero	4.43
One TWOS beam element within each L_b, straight between each CF	4.38
One TWOS beam element within each L_b, straight between each CF, warping fixed at the intermediate CF locations	4.32

displacement solution is obtained if the girders are modeled with four elements positioned along the straight chord between each of the cross-frames. If the improved 2D-grid model is used with only one straight element between each of the cross-frames, or with four elements positioned along the straight chord between each of the cross-frames, the predicted displacement is 4.28 in. (4.7 percent smaller than the benchmark solution).

One solution to the above problem that some engineers might consider is to simply never represent any unbraced length with the nodes positioned along the curved arc of an I-girder member when using conventional methods. However, this can lead to an awkward handling of situations where the same model is used to analyze girders with different numbers of cross-frames inserted in the structure at an early intermediate stage of construction. In addition, a common practice for modeling of staged deck placement in 2D-grid programs such as MDX is to use conventional frame elements to model portions of the bridge that are not yet composite, but then to connect these elements to a plate representation of the slab once the slab has been activated for a given stage. Usually, it is desirable to use more than one plate element within each unbraced length for modeling of the structure in its composite condition. Furthermore, it is desirable to model the slab with nodes along arcs about the center of curvature (assuming a circular arc). Therefore, it is desirable to also position the I-girder element nodes along the circular arcs between the cross-frames.

Several additional 2D-grid solutions are provided at the bottom of Table 3-4 using the TWOS frame element in MASTAN2 (MASTAN2, 2011; McGuire et al., 2000). The reader is referred to Section 2.7.2 for a discussion of the meaning of a TWOS 2D-grid analysis. One can observe that this element predicts a displacement of 4.42 in. (1.6 percent smaller than the benchmark solution) when four elements are used between each of the cross-frames and the nodes are positioned along the circular arc, whereas a displacement of 4.34 in. (3.3 percent smaller than the benchmark solution) is obtained when four elements are used with the nodes positioned along a straight chord between the cross-frames.

Another interesting solution is one obtained using the TWOS frame element if the warping is artificially fully fixed at the intermediate cross-frame locations rather than being modeled as a

continuous function along the girder lengths. In this case, the displacement prediction is reduced to 4.28 in. (4.5 percent smaller than the benchmark displacement). This demonstrates the accuracy of assuming full fixity at these locations, subject to the limitations discussed in the development of the improved 2D-grid procedure (i.e., at least two I-girders connected together, and $I_C \leq 20$). The accuracy of these solutions is not influenced significantly if the girders are modeled using only one element between the cross-frames for the evaluation of the non-composite behavior of this bridge.

Lastly, it is interesting to investigate the influence of completely neglecting the St. Venant torsional contribution to the stiffness within the Mastan TWOS 2D-grid analysis. In this case, the solution with four elements modeled along the circular arcs between the cross-frames increases from 4.42 in. to 4.43 in. The torsional stiffness of the I-girders is dominated by the restraint of flange warping, once the girders are sufficiently connected together such that I_C is less than approximately 20. It should be noted that if the improved 2D-grid model is used to predict the vertical displacements for the girder pair G2-G3, connected together by the bearing-line cross-frames and only a single intermediate cross-frame, the results are very poor. In this case, the connectivity index I_C is equal to 38. However, if G2 and G3 are connected together by three intermediate cross-frames, as shown in Figure 3-4, the accuracy of the improved 2D-grid prediction is comparable to that demonstrated above.

One question that could be asked relative to the implementation of the improved 2D-grid model is the following: Will the improved 2D-grid model work properly when used to model composite conditions with a plate-eccentric beam approach? Separate studies conducted in the NCHRP Project 12-79 research indicate that the improved 2D-grid model works sufficiently with a plate representation of the slab as long as one handles the calculation of the girder bottom flange lateral bending stresses properly. Chang and White (2008) have shown in previous research that, if TWOS 3D-frame elements are used to model the steel I-girders, and if these elements are constrained by rigid offsets to a shell representation of the slab, the bottom flange lateral bending stresses predicted by the TWOS element are drastically underestimated. This is because the slab bending stiffness, along with the rigid link of the TWOS element to the slab, essentially prevents any lateral bending of the bottom flange in the TWOS model (unless special procedures are invoked to release the torsional constraint of the TWOS element by the slab model). As noted above, these issues are not encountered for the improved 2D-grid element with the use of J_{eq}, as long as the flange lateral bending stresses (f_ℓ) are calculated properly. The calculation of f_ℓ is addressed subsequently in Section 3.2.4.

3.2.2.2 Mechanical Explanation of the Large Error in the Conventional 2D-Grid Procedure with the Nodes Positioned along a Circular Arc

Consider the idealized 2D-frame representation of an I-girder unbraced length between two cross-frames shown in Figure 3-9. All the degrees of freedom at the end nodes are constrained with

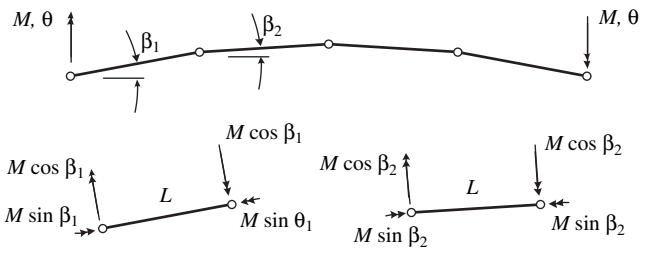

Figure 3-9. Behavior for a chorded representation of a curved girder using four straight elements.

the exception of the rotational dof corresponding to the applied end moments. In addition, all of the dofs are free at the interior nodes in this model. The reason for the dramatic over-prediction of the vertical displacements by the conventional 2D-grid procedure shown in the previous section is due to the fact that statics requires that a portion of the bending moment transmitted to the elements must be taken by element torsion (when the elements are modeled along a circular arc). However, the torsional stiffness of the elements is drastically underestimated by the St. Venant torsional stiffness GJ/L, where L is the length of each of the individual elements.

The bending end rotations in the idealized problem shown in Figure 3-9 can be calculated with relative ease, using the principle of virtual work, as:

$$1 \cdot \theta = (1 \cdot \sin\beta_1)\frac{(M\sin\beta_1)L}{GJ} + (1 \cdot \cos\beta_1)\frac{(M\cos\beta_1)L}{EI} + (1 \cdot \sin\beta_2)\frac{(M\sin\beta_2)L}{GJ} + (1 \cdot \cos\beta_2)\frac{(M\cos\beta_2)L}{EI} \quad \text{Eq. 13}$$

After some algebra, Equation 13 may be expressed as:

$$\theta = \frac{ML}{EI}\sum_i \left[\frac{EI}{GJ}\sin^2\beta_i + \cos^2\beta_i\right] \quad \text{Eq. 14}$$

Clearly, one can obtain a significant contribution from the torsional term in this equation, i.e., the first term inside the brackets.

If one substitutes the relevant parameters for Girder G1 of the previous problem into Equation 14, i.e., I = 37,600 in^4, J = 29.4 in^4, L = 70.45 in., β_1 = 0.04218 radians and β_2 = 0.01462 radians, along with the yield moment of the G1 cross-section, $M = M_{yG1}$ = 5,564 ft-kips = 66,768 in-kips, one obtains θ = 0.0369 radians. This prediction matches precisely with the first-order elastic MASTAN2 solution for this problem. If the improved 2D-grid procedure with $J_{eq(fx\text{-}fx)}$ = 688.3 in.^{4} is employed, the predicted value for θ is 0.00983 radians. Finally, if the more rigorous TWOS frame element solution is employed, where C_w = 1,662,000 in.^{6} for Girder G1, equal end rotations of θ = 0.00889 radians are obtained. The rotations predicted by the recommended improved 2D-grid model are 10.6 percent larger than the more rigorous predictions from the TWOS frame element. Correspondingly, the conventional 2D-grid solution over-predicts the end rotations by 315 percent.

3.2.2.3 Comparison of the Major-Axis Bending Stresses from Various Approaches for the FHWA Test Bridge

Figures 3-10 and 3-11 show the results from the different methods of analysis for the major-axis bending stresses in the FHWA Test Bridge Girder G1 (on the outside of the horizontal curve) and Girder G3 (on the inside of the horizontal curve) respectively. It should be noted that these results are shown at the factored load level, i.e., 1.5 of the total dead load, associated with the Strength IV loading condition.

One can observe that the major-axis bending stress at the mid-span of Girder G1 is under-predicted by 12.3 percent in the 1D line-girder solution conducted using the V-load method. All of the other solutions are very comparable. Therefore, it can be concluded that the poor vertical displacement estimate for Girder G1 does not impact the accuracy of the conventional 2D-grid estimate of the major-axis bending stress in this problem.

The percentage accuracy of the results is not as good for Girder G3. However one should notice that the scale on the vertical axis of the plot in Figure 3-11 is highly magnified compared to the

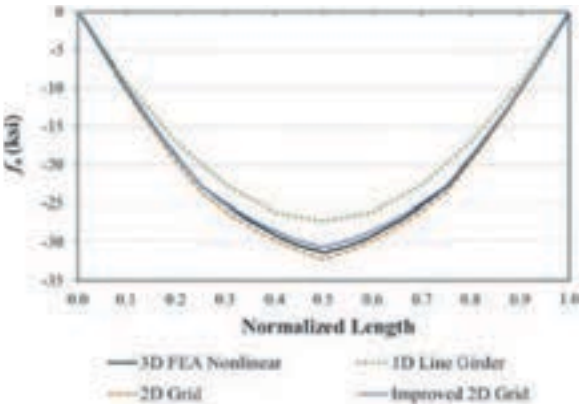

Figure 3-10. FHWA Test Bridge (EISCR1) top flange major-axis bending stresses in the fascia Girder G1 on the outside of the curve under the Strength IV load combination (1.5 × total dead load).

scale in Figure 3-10. It may be more useful to consider the differences between the maximum predicted stresses when considering the errors for Girder G3 in this bridge. The maximum major-axis bending stress in the 3D FEA simulation model is 8.1 ksi. The corresponding maximum predicted by the improved 2D-grid method is 9.9 ksi versus 10.8 ksi by the conventional 2D-grid solution. The 1D line-girder (V-load) solution exhibits the largest error in this problem, predicting a maximum major-axis bending stress of only 4.1 ksi. Furthermore, the 1D solution does not capture any semblance of the shape of the stress diagram from the benchmark.

3.2.3 Improved Equivalent Beam Cross-Frame Models

Figure 3-12 shows the geometry of the V-type cross-frames used in the FHWA Test Bridge. The cross-frames are 34 in. deep and $L = 8.75$ ft. = 105 in. wide between the work points at the girder centerlines. The areas of all the tube members are $A = 3.73$ in.^{2} In this section, various

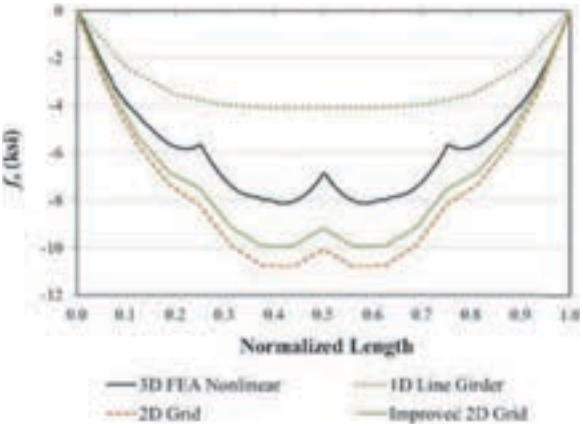

Figure 3-11. FHWA Test Bridge (EISCR1) top flange major-axis bending stresses in the fascia Girder G3 on the inside of the curve under the Strength IV load combination (1.5 × total dead load).

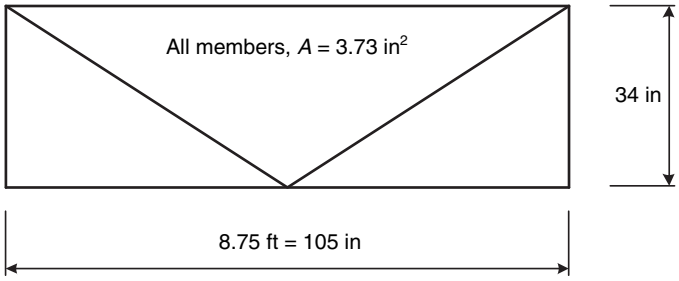

Figure 3-12. Cross-frame configuration, FHWA Test Bridge.

idealized beam solutions are compared to the "exact" equivalent beam stiffnesses of this cross-frame, where the "exact" solutions are taken as the stiffnesses from an explicit truss representation of the cross-frames in their own plane. The most appropriate simplified equivalent beam modeling of the cross-frames becomes apparent by evaluating these results.

3.2.3.1 Equivalent Beam Stiffness Based on the Flexural Analogy Approach

Figure 3-13 illustrates the calculation of the equivalent moment of inertia for the cross-frames in the FHWA Test Bridge using the "flexural analogy" approach discussed as one of two commonly used options in the AASHTO/NSBA (2011) G13.1 document "Guidelines for Steel Girder Bridge Analysis." This is the default option for calculation of the cross-frame equivalent beam stiffness in the MDX software. The lighter arrows in the figure represent displacement constraints at the corner nodes of the cross-frame. The truss support reactions corresponding to the loading applied in the figure are shown with these arrows. The cross-frame is effectively supported as a propped cantilever and is loaded by an end moment at its simply supported end in the flexural analogy approach. It is fixed against rotation and vertical displacement at its left-hand side and restrained against vertical movement at its right-hand side in the figure. A couple composed of equal and opposite unit loads is applied to the top and bottom joints on the right-hand side. The associated horizontal displacements of the truss are determined via a

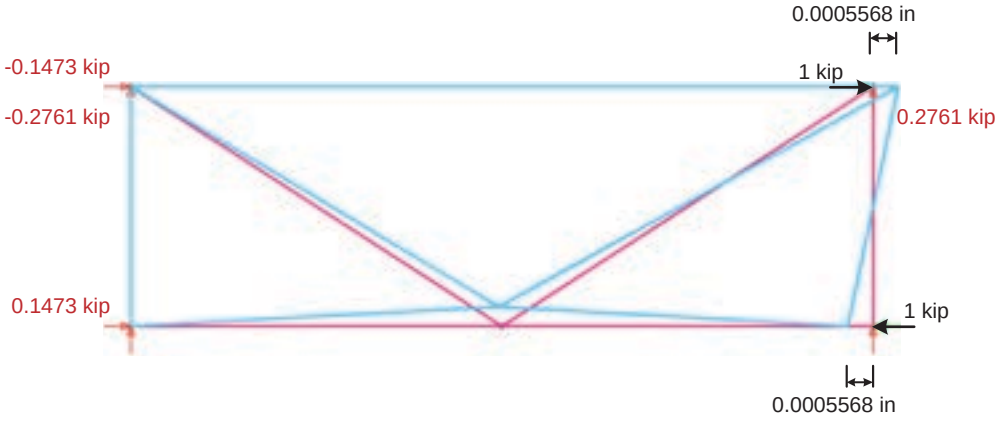

$\theta = 2(0.0005568)/34 = 0.00003275$ radians $= ML/4EI_{eq} = (34)(105)/4(29000)I_{eq}$

$I_{eq} = 940$ in^4

Figure 3-13. Calculation of equivalent moment of inertia based on the flexural analogy method.

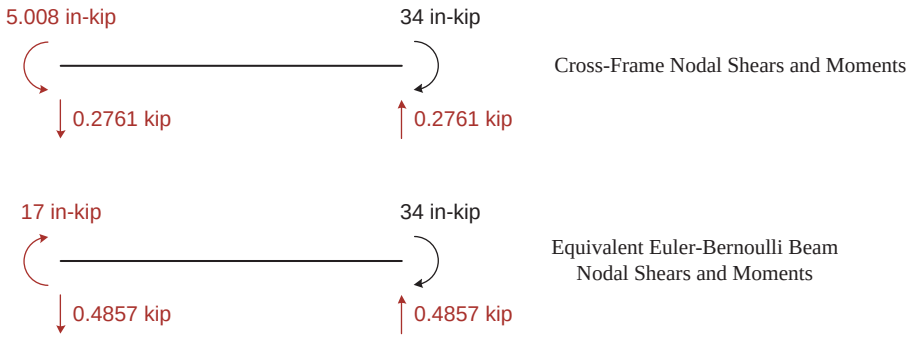

Figure 3-14. Cross-frame nodal shears and moments and equivalent Euler-Bernoulli beam shears and moments based on flexural analogy method.

structural analysis. The equivalent beam moment of inertia, I_{eq}, is then calculated by equating the corresponding rotation at the right-hand side to the Euler-Bernoulli beam rotation $M/(4EI_{eq}/L)$, as shown in the figure.

Figure 3-14 compares the physical cross-frame end shears and moments to the nodal shears and moments in the equivalent Euler-Bernoulli beam. One can observe that the moment induced at the left-hand side of the physical cross-frame is much smaller than the "carry-over moment" of one-half of the applied end moment in the equivalent Euler-Bernoulli beam element. In fact, it is even of the opposite sign. Correspondingly, the vertical shear forces induced in the physical cross-frame are much smaller than the ones associated with the equivalent beam based on the flexural analogy. These smaller internal forces are due to the shear raking deformations in the physical truss system. The equivalent Euler-Bernoulli beam does not consider any beam shear deformations.

3.2.3.2 Equivalent Beam Stiffness Based on the Shear Analogy Approach

Figure 3-15 illustrates the second common method of determining an equivalent beam stiffness discussed by the AASHTO/NSBA (2011) G13.1 document. This approach is termed the shear analogy method. In this approach, the cross-frame is supported as a fixed-fixed beam subjected to a transverse shear force. In the figure, all of the truss dofs are fixed on the left-hand side,

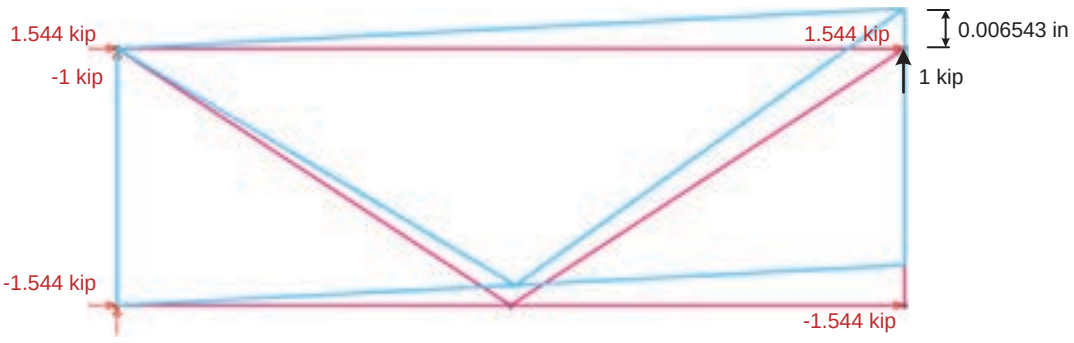

$$\Delta = 0.0006543 \text{ in} = PL^3/12EI_{eq} = (1)(105)^3/12(29000)I_{eq}$$

$$I_{eq} = 508 \text{ in}^3$$

Figure 3-15. Calculation of equivalent moment of inertia based on the shear analogy method.

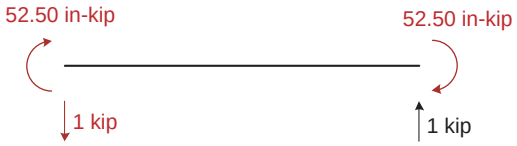

Figure 3-16. Cross-frame nodal shears and moments and equivalent Euler-Bernoulli beam shears and moments based on shear analogy.

the horizontal dofs are constrained on the right-hand side, and the truss is subjected to a unit vertical load on the right-hand side. It should be noted that the vertical members at the sides of the cross-frames represent the stiffness of the girder webs and connection plates, which typically involves a larger effective area than the cross-frame members themselves. The unit load is applied on the right-hand side and the truss is supported on the left-hand side in Figure 3-15 such that no deformations of the end vertical elements come into play. The equivalent beam cross-frame stiffness is obtained by equating the relative end deflection to the Euler-Bernoulli beam solution $P/(12EI_{eq}/L^3)$.

Figure 3-16 shows the nodal shears and moments for both the physical cross-frame and the equivalent Euler-Bernoulli beam in this problem. That is, the nodal shears and moments are identical for the equivalent beam idealization and the physical truss in this case. However, it should be noted that a large portion of the vertical displacement in the physical truss is due to shearing type deformations whereas the Euler-Bernoulli beam does not include any consideration of shear deformations. Therefore, the equivalent moment of inertia is in essence "artificially reduced" to account for these large shearing deformations in the shear analogy approach.

3.2.3.3 Equivalent Beam Stiffness for a Timoshenko Beam Element

Figure 3-17 illustrates the first step of a more accurate approach for the calculation of the cross-frame equivalent beam stiffnesses. This approach simply involves the calculation of an equivalent moment of inertia, I_{eq}, as well as an equivalent shear area A_{seq} for a shear-deformable (Timoshenko) beam element representation of the cross-frame. In this approach, the equivalent

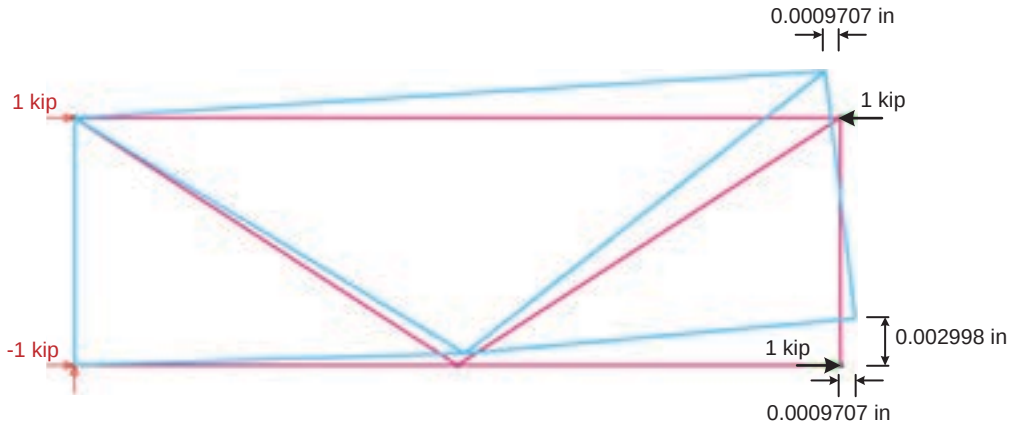

$$\theta = 2(0.0009707)/34 = 0.0000571 = ML/EI_{eq} = 34(105)/29000I_{eq}$$

$$I_{eq} = 2156 \text{ in}^4$$

Figure 3-17. Calculation of equivalent moment of inertia based on pure bending.

moment of inertia is determined first based on pure flexural deformation of the cross-frame (zero shear). The cross-frame is supported as a cantilever at one end and is subjected to a force couple applied at the corner joints at the other end, producing constant bending moment. The associated horizontal displacements are determined at the free end of the cantilever, and the corresponding end rotation is equated to the value from the beam pure flexure solution $M/(EI_{eq}/L)$. One can observe that this results in a substantially larger I_{eq} and that this EI_{eq} represents the "true" flexural rigidity of the cross-frame.

In the second step of the improved calculation, using an equivalent Timoshenko beam element rather than a Euler-Bernoulli element, the cross-frame is still supported as a cantilever but is subjected to a unit transverse shear at its tip. Figure 3-18 shows the corresponding displacements and reactions for this model, as well as the Timoshenko beam equation for the transverse displacement and the solution for the A_{seq} of the FHWA Test Bridge cross-frame.

It should be noted that the end rotation of the equivalent beam in Figure 3-18 is

$$\theta = VL^2/2EI_{eq} - V/GA_{seq}$$

$$= 1(105)^2/2(29000)(2156) - (1)(2.6)/(29000)(2.008) = 0.00004352 \text{ radians}$$

However, from the deflected shape in Figure 3-18, $\theta = 2(0.001499)/34 = 0.00008818$ radians. Therefore, it can be observed that the shear-deformable Timoshenko beam element is not able to match the "exact" kinematics of the cross-frame.

Figure 3-19 compares the physical cross-frame end shears and moments to the nodal shears and moments for the equivalent Timoshenko beam for the case of a propped cantilever subjected to end moment. One can observe that the Timoshenko beam comes much closer to fitting the force response of the cross-frame, compared to the earlier result with the Euler-Bernoulli beam element in Figure 3-14. However, it can be seen that the Timoshenko beam shear forces are still 2.9 percent smaller than those of the physical truss, and the left-hand end moment is 16.5 percent larger than the "actual" left end moment. The left-hand moment is in the correct direction though in Figure 3-19, whereas in the previous Figure 3-14, the left-hand end moment is not even in the correct direction.

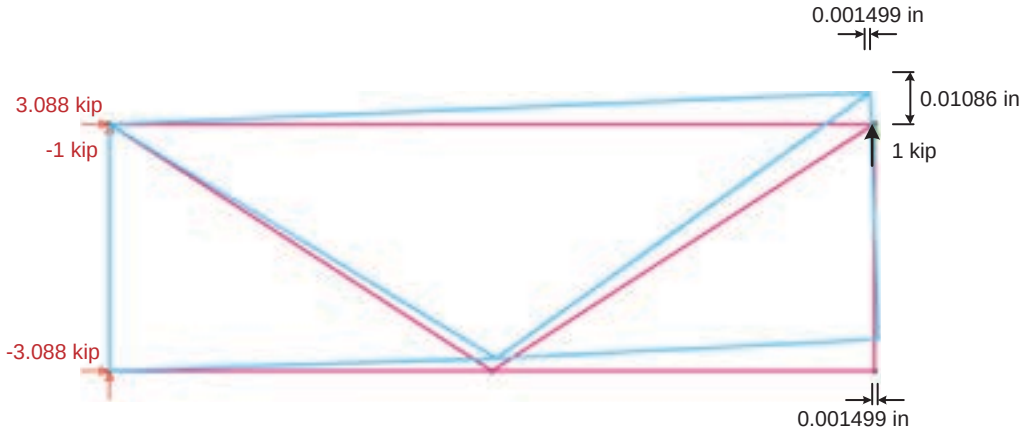

$$\Delta = 0.01086 \text{ in} = VL^3/3EI_{eq} + VL/GA_{eq}$$
$$= 1(105)^3/3(29000)(2156) + (1)(105)(2.6)/29000A_{seq}$$
$$A_{seq} = 2.008 \text{ in}^2$$

Figure 3-18. Calculation of equivalent shear area based on tip loading of the cross-frame supported as a cantilever.

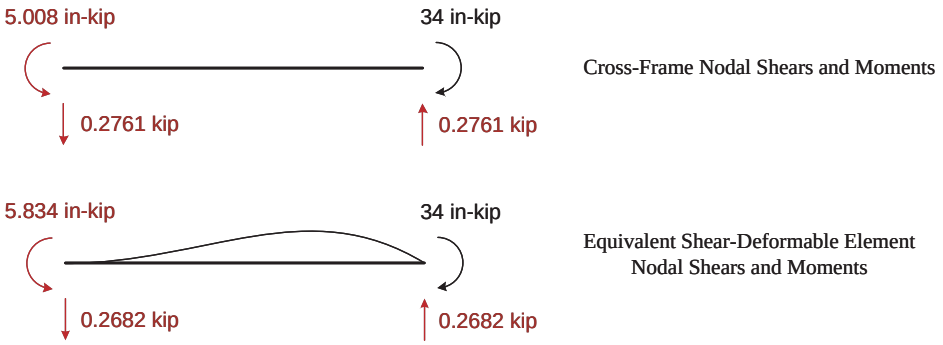

Figure 3-19. Cross-frame nodal shears and moments and equivalent shear-deformable beam shears and moments.

3.2.3.4 Overall Comparison of Cross-Frame Models

Table 3-5 provides a detailed comparison of the force and displacement results for the three different equivalent beam elements described in the above compared to the "exact" results for the physical truss model of the cross-frame from Figure 3-12. All the "exact" solutions are shown in bold. It can be observed that the equivalent Euler-Bernoulli beams are able to fit the exact solution for only one response, whereas the Timoshenko beam is able to fit the exact solution for two responses. Furthermore, the Timoshenko beam provides a closer approximation to the physical truss results in the cases where the fit is not exact. This is due to the fact that the Timoshenko element is able to represent both flexure and shear deformations. The approximations are due in part to the fact that the Timoshenko beam formulation considered here is a close representation of prismatic solid web members. The truss-type cross-frame deformations generally lead to different stiffness results than provided by a prismatic solid web member though.

It can be shown that the Timoshenko beam element provides a closer approximation of the physical cross-frame behavior compared to the Euler-Bernoulli beam for all other types of cross-frames typically used in I-girder bridges as well, including X and inverted V cross-frames with top and bottom chords, as well as X and V cross-frames without top chords. However, similar to the above demonstrations, the Timoshenko beam model is only able to provide an exact fit for two of the five responses listed across the rows of Table 3-5.

Given the "exact" equivalent beam stiffness values developed in the above solutions, the next logical refinement is to develop generic X, V, inverted-V, X without top chord, and V without top chord models with variable width and height and variable cross-section area for the cross-frame members (including different cross-section areas for the different members). Section 6.2.2 of the Task 8 report describes the development of one "exact" equivalent beam element of this form as well as a rather easy implementation of this element as a user-defined element within the LARSA 4D software system. Sanchez (2011) provides detailed developments of this form for all of the above cross-frame types.

3.2.3.5 Influence of the Cross-Frame Equivalent Beam Stiffness Model on the Vertical Displacement Results in the FHWA Test Bridge

Table 3-6 shows the influence of the different equivalent beam stiffness models considered in the above developments on the vertical displacement at the mid-span of the fascia girder (G1) on the outside of the horizontal curve in the FHWA Test Bridge. It can be observed that the 2D-grid model using the Timoshenko equivalent beam element generally provides the best estimate of the models developed in the above section. The results provided by the "exact" equivalent beam model of the test bridge cross-frame are essentially the same as those obtained using the

Table 3-5. Comparison of equivalent beam responses to the physical truss cross-frame model responses for the V-type cross-frame of Figure 3-12.

CF Model	I_{eq} (in^4)	A_{seq} (in^2)	M_{far}/M_{near} propped cantilever subjected to end moment	Transverse deflection of cantilever in pure bending (M = 34 in-k)	Transverse deflection of tip-loaded fixed-fixed member (V = 1 k)	End rotation of propped cantilever (M = 34 in-k)	Cantilever in pure bending, end rotation (M = 34 in-k)
Euler-Bernoulli element with I_{eq} based on flexural analogy	940	NA[a]	+0.5	6.88E-3 inches	3.54E-3 inches	**3.27E-5 radians**[b]	13.1E-5
Euler-Bernoulli element with I_{eq} based on shear analogy	508	NA[a]	+0.5	12.7E-3 inches	**6.55E-3 inches**	6.06E-5 radians	24.9E-5
Timoshenko beam element	2156	2.01	-0.172	**3.00E-3 inches**	6.23E-3 inches	3.28E-5 radians	**5.71E-5 radians**
Physical truss model	--	--	-0.147	**3.00E-3 inches**	**6.55E-3 inches**	**3.27E-5 radians**	**5.71-5 radians**

[a] The shear area is effectively ∞ for the Euler-Bernoulli beam element.

[b] Exact values are shown in bold font.

Timoshenko beam formulation. The predicted mid-span displacement is 8.7 percent larger using the model with the Euler-Bernoulli element based on the shear analogy. This demonstrates that the cross-frame model can have a measurable influence on the prediction of the constructed geometry. The absolute difference in the displacements is relatively small for the test bridge; however, for a longer span, the difference could be more consequential.

The last row of Table 3-6 gives the solution obtained if the cross-frame torsional stiffness is neglected (i.e., $J = 0$) for the cross-frame equivalent beam element. One can observe that this results in little change in the bridge vertical displacement.

3.2.3.6 FHWA Test Bridge Cross-Frame Forces Predicted by Different Methods

Figure 3-20 shows the forces calculated in the two cross-frames at the mid-span of the FHWA Test Bridge from the various methods of analysis. One can observe that, of the various solutions,

Table 3-6. FHWA Test Bridge (EISCR1) mid-span vertical displacement of Girder G1 (Δ_{G1}) under total dead load (unfactored) for different 2D-grid cross-frame idealizations, girders modeled using J_{eq} and four elements in each L_b, nodes located on the circular arc (Δ_{G1} = 4.49 in., second-order 3D FEA; Δ_{G1} = 4.40 in., first-order 3D FEA).

Cross-frame idealization	Δ_{G1} (in.)
Shear-deformable (Timoshenko) beam element – I = 2156 in^4, A_s = 2.01 in^2, J = 39.8 in^4	4.73
Equivalent Euler-Bernoulli beam element based on flexural analogy – I = 940 in^4, A_s = ∞, J = 39.8 in^4	4.87
Equivalent Euler-Bernoulli beam element based on shear analogy – I = 508 in^4, A_s = ∞, J = 39.8 in^4	5.14
Shear deformable (Timoshenko) beam element – I = 2156 in^4, A_s = 2.01 in^2, J = 0 in^4	4.74

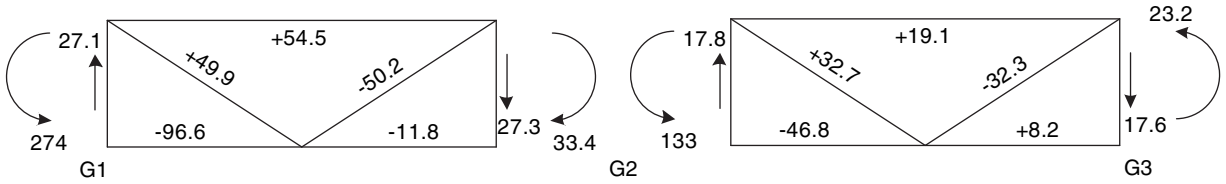

(a) 3D FEA benchmark

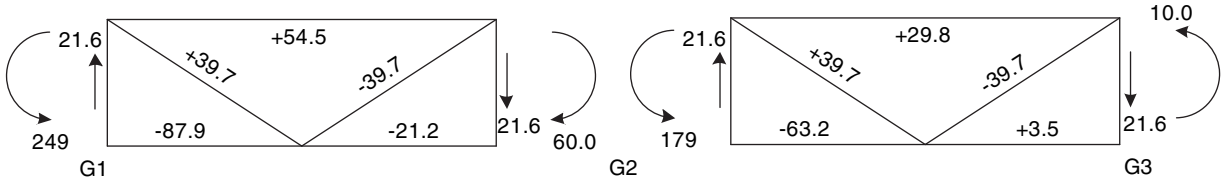

(b) V-Load

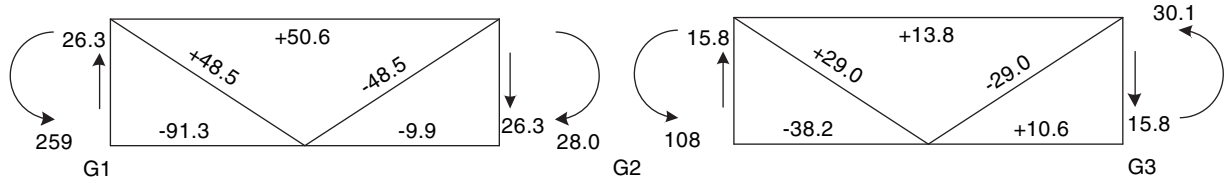

(c) Conventional 2D-grid, cross-frame equivalent beam stiffness based on flexural analogy

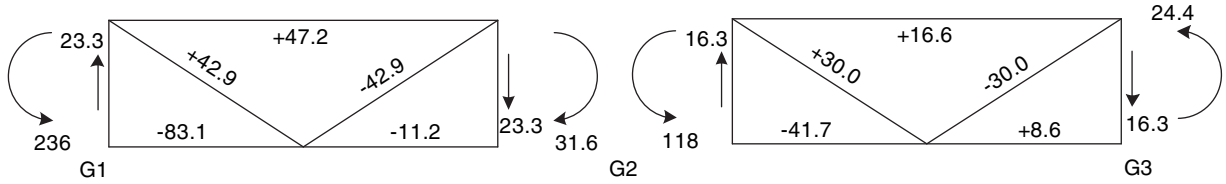

(d) Improved 2D-grid, cross-frame equivalent beam stiffness based on Timoshenko beam model

(e) TWOS 2D-grid, cross-frame equivalent beam stiffness based on Timoshenko beam model

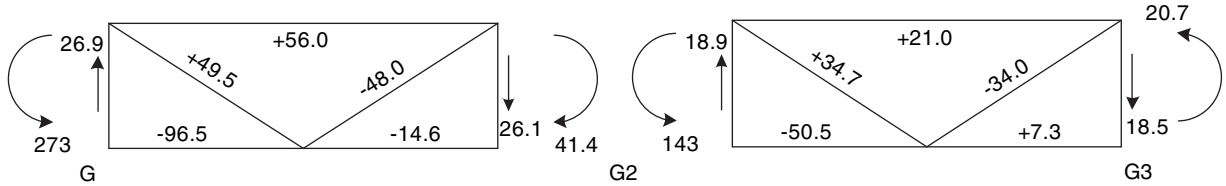

(f) TWOS 3D-frame, explicit modeling of cross-frames by beam and truss elements

Figure 3-20. FHWA Test Bridge (EISCR1) unfactored (nominal) cross-frame dead load forces calculated at mid-span by different methods (units: ft-kip moments, kip forces).

only the TWOS results shown in Figure 3-20e and f give results that never deviate more than 3 kips from the 3D FEA benchmark solution. (The percentage errors can be large even for these solutions in cases where the cross-frame forces are small. However, these percentage errors are not of any consequence when the cross-frame member sizes are repeated throughout the structure and sized for the most critical demand.) The TWOS 3D-frame solution shown in Figure 3-20f gives the best correlation with the 3D FEA benchmark. This is because this is the only "simplified" solution that accounts for:

1. The second-order effects in the calculation of the cross-frame forces (although the second-order effects are only a few percent for this structure and loading, as discussed previously in Section 3.2.2.1), and
2. The location of the various components and entities through the depth of the structure (i.e., the girder centroids and shear centers, the cross-frame depths and locations through the depth of the girders, the load height of the concrete slab, and the location of the bearings relative to the girder centroidal and shear center axes).

Nevertheless, all of the 2D-grid solutions as well as the V-load solution give reasonable results for this bridge. The maximum error in the prediction of the maximum cross-frame bottom chord force is -14.0 percent, corresponding to the improved 2D-grid solution shown in Figure 3-20d, while the maximum error in the maximum cross-frame diagonal force is -20.4 percent, corresponding to the V-load method solution shown in Figure 3-20b. It is clear that the V-load method gives the greatest misrepresentation of the true cross-frame vertical shear forces. This is due to the fact that the V-load method is based on an assumption of "equal vertical stiffness" across all the girders at each of the intermediate cross-frame locations.

The concept of equal vertical stiffness in the above means that, if each girder were considered in isolation, and if a unit load were applied at each girder in succession, the same vertical displacement would be obtained. However, the girders can never be physically isolated from each other in any meaningful way for calculation of these so-called vertical stiffnesses. Isolating the girders requires the application of artificial boundary conditions to them, which changes the way they respond to the load. An implicit assumption of an equal vertical stiffness from each girder is invoked in the derivation of the coefficient *C* used in calculating the V-load as a function of the number of girders in the bridge system (NHI, 2011). Since the "equal vertical stiffnesses" can never be calculated in any meaningful way, they can never be checked. Conceptually, the girder vertical stiffnesses can be thought of typically as being very different though, even in radially supported bridges with a "very regular" geometry such as the FHWA Test Bridge, at least when the structure is highly curved. This is because the outside girder generally must resist substantially more load.

It should be noted that in the calculation of the results shown for the simplified methods in Figure 3-20b through e, part of the solution involves the calculation of the contribution from the overhang eccentric bracket loads. These load effects are approximated based on the AASHTO LRFD Equation (C-6.10.3.4-2) and are shown in Figure 3-21.

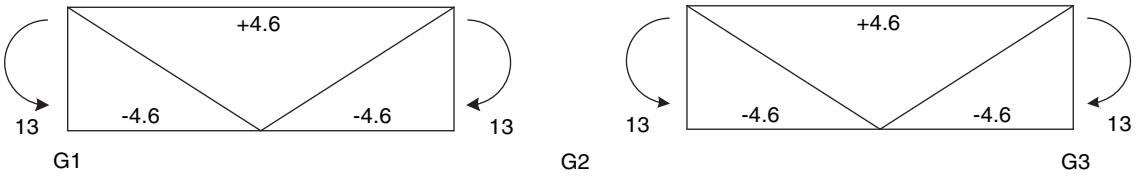

Figure 3-21. FHWA Test Bridge (EISCR1) unfactored (nominal) cross-frame dead load forces due to eccentric bracket loads (units: ft-kip moments, kip forces).

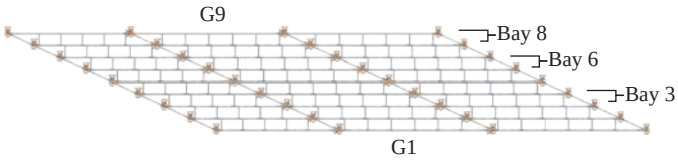

Figure 3-22. Framing plan of Bridge NICSS16.

3.2.3.7 Improved Prediction of Cross-Frame Forces in Skewed I-Girder Bridges

Figure 3-22 shows a sketch of the framing plan for Bridge NICSS16 from the NCHRP Project 12-79 Task 7 analytical studies. This is a continuous-span structure with an extreme parallel skew of its bearing lines of 70°, combined with an 80-ft.-wide deck ($w = 80$ ft.), a perpendicular distance between its fascia girders of $w_g = 74$ ft., and 120-, 150- and 150-ft. span lengths. As a result, its skew index I_S is 1.69 from Equation 9. The skew index captures the tendency for the development of substantial transverse load paths in I-girder bridge structures and is used as a key term in scoring the accuracy of the simplified methods of analysis in Table 3-1. This bridge is framed with staggered cross-frame lines, which reduces the large forces developed particularly in the transverse direction between the obtuse corners of each span. However, these forces still are significant.

Figures 3-23 through 3-25 show the cross-frame forces calculated in Bay 3 (between Girders G2 and G3), Bay 6 (between Girders G3 and G4, and Bay 8 (between Girders G6 and G7)

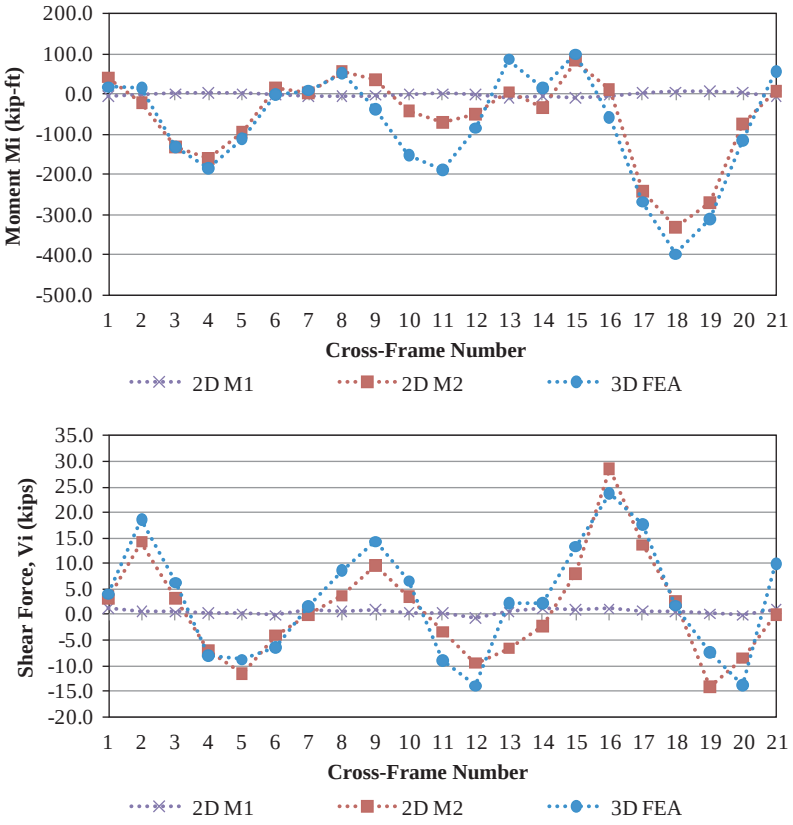

Figure 3-23. Bridge NICSS16 cross-frame forces in Bay 3 (between Girders G3 and G4) under total dead load (unfactored) from conventional 2D-grid analysis (M1), improved 2D-grid analysis (M2), and 3D FEA.

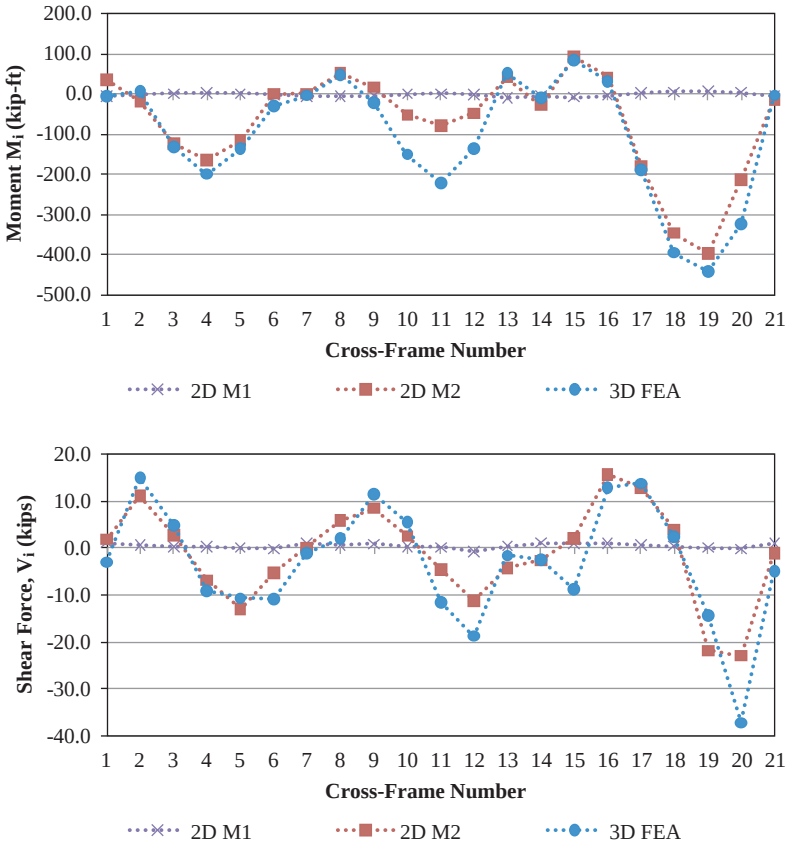

Figure 3-24. Bridge NICSS16 cross-frame forces in Bay 6 (between Girders G6 and G7) under total dead load (unfactored) from conventional 2D-grid analysis (M1), improved 2D-grid analysis (M2), and 3D FEA.

in the Bridge NICSS16 using the conventional 2D-grid approach, the improved 2D-grid method, and the 3D FEA benchmark simulation. The improved 2D-grid solution implemented here uses the J_{eq} girder torsion model discussed in Section 3.2.2 as well as the "exact" equivalent beam element discussed Section 3.2.3 and described in detail in the Task 8 report (Appendix C of the contractors' final report).

The first plot in each of the figures cited above shows the nodal moment at the ends of the cross-frames toward the bottom of the plan view shown in Figure 3-22. The second plot shows the vertical shear transferred by each cross-frame. The horizontal axis shows the cross-frame number within each of the bays, starting from the left-hand end of the bridge in Figure 3-22 and progressing to the right-hand end. The forces are calculated assuming no-load fit detailing of the cross-frames for simplicity of the discussion. Steel dead load fit (SDLF) and total dead load fit (TDLF) detailing effects are addressed subsequently in Sections 3.2.5 and 3.3.

From the above plots, it is apparent that the conventional 2D-grid solution predicts essentially zero cross-frame forces throughout the NICSS16 bridge structure. The primary reason for this behavior is the dramatic under-estimation of the girder torsional stiffnesses due to using only the St. Venant torsional stiffness term (GJ/L) in the 2D-grid idealization. Conversely, the improved 2D-grid method provides a reasonably good estimate of the cross-frame forces in this extreme structure, compared to the benchmark 3D FEA solutions.

The results in Figures 3-23 through 3-25 for the above skewed I-girder bridge, combined with the results in Figure 3-7 for the FHWA Test Bridge highlight the importance of using a

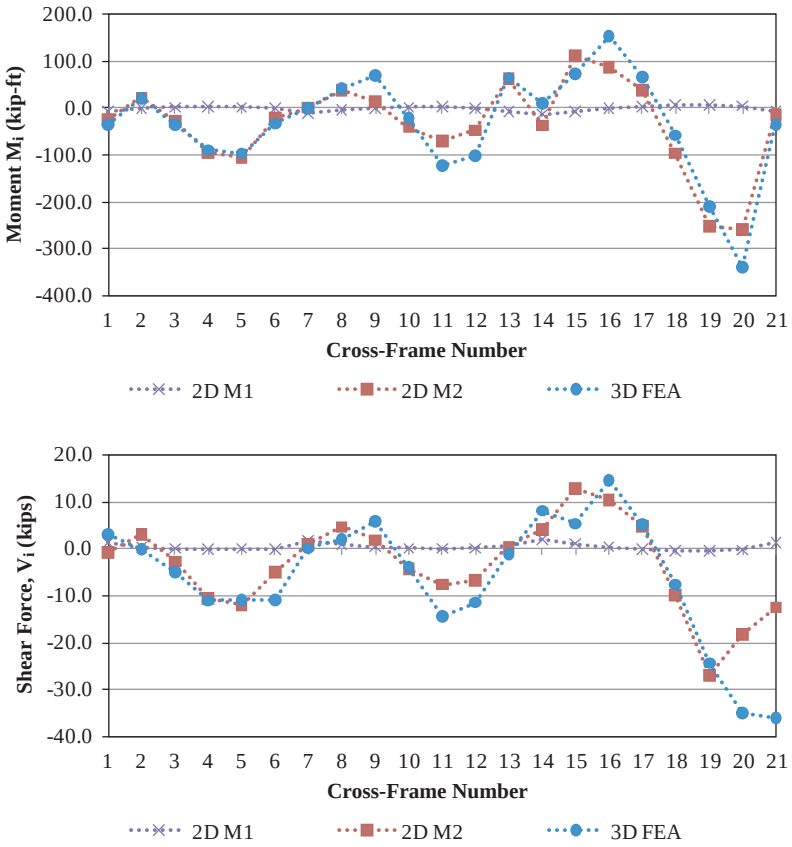

Figure 3-25. Bridge NICSS16 cross-frame forces in Bay 8 (between Girders G8 and G9) under total dead load (unfactored) from conventional 2D-grid analysis (M1), improved 2D-grid analysis (M2), and 3D FEA.

better I-girder torsion model than the simplistic one commonly used in conventional 2D-grid methods. Furthermore, the results in Table 3-6 clearly show the importance of also using a better representation of the cross-frame stiffnesses in bridges where the cross-frame deformations start to have some influence on the overall structure response. Of major importance is the fact that these improvements require little additional computational expense, and their software implementation is relatively straightforward. However, professional software implementation of these methods is essential for them to be used efficiently in practice. Manual calculation and input of the corresponding improvements into the software is too laborious to be workable given common professional time constraints.

3.2.4 Improved Calculation of I-Girder Flange Lateral Bending Stresses from 2D-Grid Analysis

Given the above improvements in the I-girder and cross-frame stiffness representations, it is still essential to address the calculation of the flange lateral bending stresses in curved and/or skewed I-girder bridges. This section recommends specific improvements in these calculations.

Figure 3-26a shows the plan view of Bridge NISSS16 considered in the NCHRP Project 12-79 Task 7 analytical studies. This is a 150-ft. simple-span straight bridge with an 80-ft.-wide deck ($w = 80$ ft.), a perpendicular distance between its fascia girders of 74 ft., and a skew of 50 degrees at its left-hand abutment. These geometry factors produce a skew index of $I_s = 0.59$, placing this

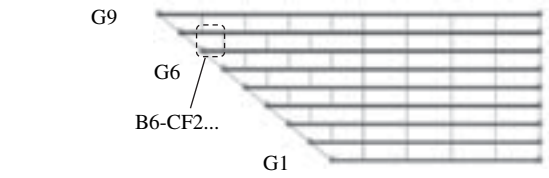

(a) Plan view of Bridge NISSS16

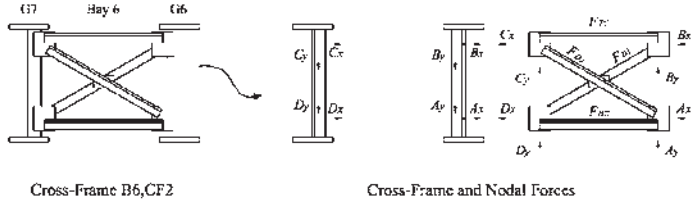

(b) Forces transferred from cross-frame B6-CF2 to Girders G6 and G7

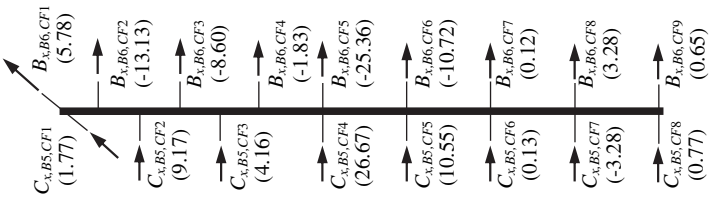

(c) Top flange of Girder G6 subject to the horizontal components of the nodal forces

Figure 3-26. Calculation of lateral bending stresses in the top flange of Girder G6, in Bridge NISSS16 under total dead load (unfactored).

bridge just inside the second category of straight-skewed bridge structures in the scoring system of Table 3-1.

Figure 3-26b illustrates the forces in cross-frame 2 (CF2) of Bay 6 in this structure and the corresponding statically equivalent nodal horizontal and vertical forces transferred to the I-girders at the cross-frame chord levels. These horizontal forces can be transformed to statically equivalent lateral forces applied at the flange levels of the I-girders by determining the couple associated with these horizontal forces and then multiplying the chord-level couple forces by the ratio of the cross-frame depth to the girder depth between the flange centroids, d_{CF}/h. In typical 2D-grid solutions, $C_x = -D_x$ and $B_x = -A_x$, and thus the forces shown in Figure 3-26b are the couple forces.

Figure 3-26c shows the top flange forces applied to Girder G6 in this bridge, determined from the improved 2D-grid method discussed in the previous sections. The forces are still labeled "C_x" and "B_x," for simplicity of the presentation. It should be noted that the chord-level couple forces shown in Figure 3-26b are multiplied by (d_{CF}/h) to determine the flange-level forces.

Given a general statical free-body diagram of a girder flange, such as the one shown for Girder G6 in the figure, one would expect that the subsequent determination of the flange lateral bending stresses is an easy strength of materials calculation. If the girder is also horizontally curved, the equivalent radial lateral loads corresponding to the horizontal curvature can be included in the free-body diagram. Furthermore, eccentric bracket loads from the overhangs can be included on fascia girders.

Unfortunately, the solution for the flange lateral bending stresses is not this simple. The problem is that the girder torsional stiffnesses, upon which the above calculation of the cross-frame

forces is based, include a contribution both from the girder warping torsion as well as the girder St. Venant torsion. As such, a portion of the above forces is transferred (by the interaction of the flange with the girder web) into the internal St. Venant torsion in the girders. More specifically, corresponding small but undetermined distributed lateral forces are transferred to the flange from the web in Figure 3-26c. Because of this effect, if the statical free-body diagram shown in Figure 3-26c is used to calculate the girder flange lateral bending stresses, slight errors accumulate as one moves along the girder length.

Solutions to this problem include:

1. Use the girder torsional rotations and displacements along with the detailed open-section thin-walled beam stiffness model associated with J_{eq} to directly determine the flange lateral bending stresses. This results in an imbalance in the flange lateral bending moments on each side of the intermediate cross-frames (since J_{eq} is based on the assumption of warping fixity at the cross-frame locations). This moment imbalance could be re-distributed along the girder flange to determine accurate flange lateral bending moments. A procedure analogous to elastic moment distribution could be utilized for this calculation. Although this approach is a viable one, it is relatively complex. Therefore, it was not pursued in the NCHRP Project 12-79 research.
2. Focus on an approximate local calculation in the vicinity of each cross-frame, utilizing the forces delivered to the flanges from the cross-frames as shown in Figure 3-26c. Because of its relative simplicity, this approach was selected in the NCHRP Project 12-79 research.

It should be noted that the girder flange lateral bending stresses are calculated directly and explicitly from the element displacements and stiffnesses in the TWOS 2D-grid and TWOS 3D-frame solutions. Therefore, these methods provide the best combination of accuracy and simplicity for the grid or frame element calculation of the flange lateral bending stresses. However, the disadvantage of this approach is the additional complexity of the element formulation and the requirement that an additional warping degree of freedom has to be included in the global structural analysis.

Figure 3-27 illustrates the simplified approach adopted in the NCHRP Project 12-79 research for calculating the I-girder flange lateral bending moments given the statically equivalent lateral loads transferred at the flange level from the cross-frames. The calculation focuses on a given cross-frame location and the unbraced lengths, *a* and *b,* on each side of this location. For simplicity of the discussion, only the force delivered from the cross-frame under consideration

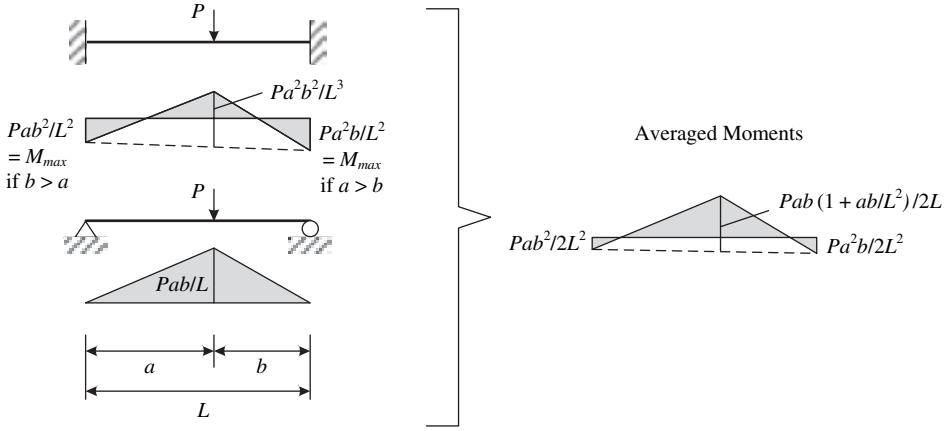

Figure 3-27. Lateral bending moment, M_ℓ in a flange segment under simply supported and fixed-end conditions.

is shown in the figure, and the cross-frame is assumed to be non-adjacent to a simply supported end of the girder. In general, the lateral forces from horizontal curvature effects and/or from eccentric bracket loads on fascia girders also would be included. Two flange lateral bending moment diagrams are calculated as shown in the figure, one based on simply supported end conditions and one based on fixed-end conditions at the opposite ends of the unbraced lengths. For unbraced lengths adjacent to simply supported girder ends, similar moment diagrams are calculated, but the boundary conditions are always pinned at the simply supported end. The cross-frame under consideration is located at the position of the load P in the sketches. In many situations, the moments at the position of the load are the controlling ones in the procedure specified below.

Given the moment diagrams for the above cases, the project Task 8B research determined that an accurate-to-conservative solution for the flange lateral bending moments and stresses is obtained generally by:

1. Averaging the above moment diagrams, and
2. Taking the largest averaged internal moment in each of the unbraced lengths as the flange lateral bending moment for that length.

This solution is repeated cross-frame location by cross-frame location along the length of the girders and the largest moment from the two solutions obtained for each unbraced length is taken as the estimate of the flange lateral bending moment in that unbraced length. (For the unbraced lengths at girder simply supported ends, only one solution is performed.)

The above procedure recognizes that the true flange lateral bending moment is bounded by the "pinned" and "fixed" moment diagrams (neglecting the small St. Venant torsional contributions from the interaction with the web) and ensures that the flange lateral bending moments required for static equilibrium are never underestimated. Also, the average of the pinned and fixed moment diagrams is analogous to the use of the approximation $qL_b^2/10$ rather than $qL_b^2/12$ when estimating the flange lateral bending moments due to horizontal curvature, where q is the equivalent flange radial load. In addition, the above solution is insensitive to any inaccuracies in the calculation of the cross-frame forces as described in Sections 3.2.3.6 and 3.2.3.7.

Figure 3-28 illustrates the accuracy associated with using the procedure from Figure 3-27 for the NISSS16 Bridge. One can observe that the flange lateral bending stresses from the 3D FEA simulation model are predicted quite well. The recommended procedure of using the maximum of the internal moments from the calculations for the two adjacent cross-frames for each unbraced

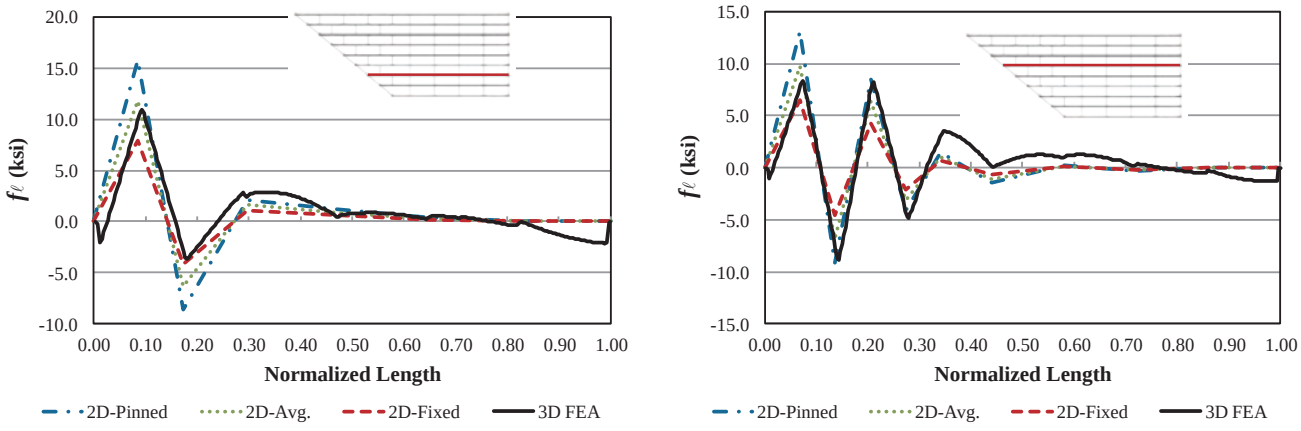

(a) Girder G3 (b) Girder G6

Figure 3-28. Bridge NISSS16 flange lateral bending stresses under total dead load (unfactored).

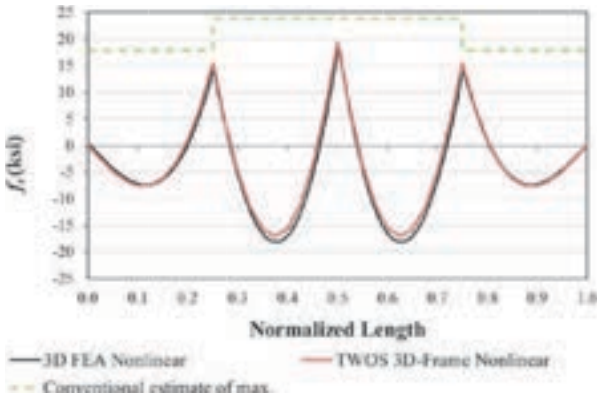

Figure 3-29. FHWA Test Bridge (EISCR1) flange lateral bending stresses in Girder G1 under Service IV load combination (1.5 × total dead load).

length as the flange lateral bending moment value tends to be somewhat conservative in extreme cases where the dimensions *a* and *b* are substantially different.

Figure 3-29 compares the results of simplified calculations of the maximum flange lateral bending stresses for the different unbraced lengths to the 3D FEA benchmark solution for the fascia girder (G1) on the outside of the curve in the FHWA Test Bridge. For curved radially supported I-girder bridges with relatively regular geometry, the basic "conventional" estimate from the AASHTO LRFD equation (C4.6.1.2.4b-1), using a coefficient of $N = 12$ rather than 10, works quite well. In the FHWA Test Bridge calculations, the results from the above improved calculations give essentially the same results as those obtained from the AASHTO equation. However, the AASHTO equation is obviously much simpler. Nevertheless, for bridges having non-zero skew, the improved method is able to account in a rational manner for the skew effects. The net result is a significantly improved estimate of the girder flange lateral bending stresses compared to the coarse values recommended in AASHTO (2010) Article C6.10.1.

It should be emphasized that the AASHTO LRFD equation (C4.6.1.2.4b-1) gives an estimate of the maximum flange lateral bending moment in a given unbraced length. Therefore, in Figure 3-29, the simplified solution is shown just as a constant value within each unbraced length.

Lastly, in Figure 3-29, the TWOS 3D-frame geometric nonlinear solution is provided along with the 3D FEA benchmark result to illustrate the high accuracy achievable with this TWOS solution. However, as stated in the Task 8 report (Appendix C of the contractors' final report), the TWOS approach was not pursued as an improved simplified solution in the NCHRP Project 12-79 research due to the additional complexities associated with its implementation.

3.2.5 Calculation of Locked-In Forces Due to Cross-Frame Detailing

This section addresses the fourth major improvement recommended by the NCHRP Project 12-79 research for the simplified 2D-grid analysis of curved and/or skewed I-girder bridges. However, it is important to note that this improvement also applies to 3D FE design analysis. This section addresses the calculation of locked-in forces due to steel dead load fit (SDLF) or total dead load fit (TDLF) cross-frame detailing. The emphasis here is predominantly on the calculation aspects. Section 3.3 addresses the broader attributes of the behavior and the question of when the locked-in forces due to the detailing of the cross-frames should be considered in the design. Appendix A provides summary definitions of key terms pertaining to cross-frame

detailing. It is essential that the reader understand these definitions to facilitate study and interpretation of the corresponding results and discussions throughout the report.

As noted previously, regardless of whether the analysis is a 2D-grid or a 3D FEA method, it can only give the bridge internal forces associated with no-load fit (NLF) detailing if it is conducted without the modeling of initial lack-of-fit effects. Any locked-in forces, due to the lack of fit of the cross-frames with the girders in the undeformed geometry, add to (or subtract from) the forces determined from the 2D-grid or 3D FEA design-analysis solutions. Fortunately, with some qualifications (discussed subsequently in Section 3.3), the SDLF or TDLF detailing effects tend to be opposite in sign to the internal forces due to the dead loads in straight-skewed bridges. Therefore, the 2D-grid or 3D FEA solutions for the cross-frame forces and the flange lateral bending stresses are conservative when they neglect the SDLF or TDLF initial lack-of-fit effects. Unfortunately, in some cases, these solutions can be prohibitively conservative. In addition, unfortunately, for curved radially supported structures, the cross-frame forces and girder maximum flange lateral bending stresses tend to be increased by the SDLF or TDLF detailing effects (see the subsequent discussions in Section 3.3). For generally curved and skewed bridges, the effects can go both ways.

Technically, it is relatively easy to include the influence of locked-in forces in either 2D-grid or 3D FEA calculations. Basically, the calculation amounts simply to the inclusion of an initial stress or initial strain effect. This is similar to the handling of thermal strains and deflections. Therefore, for cases where the initial lack-of-fit effects are important, including them in the analysis should not provide any significant hardship in terms of modeling effort or computational expense. Of course, as emphasized with the other key improvements recommended in the previous sections, the implementation of the calculations into professional software is essential for the methods to be used efficiently by the design engineer. In addition, it is essential for engineers to understand the methods, calculations, and potential issues; therefore, the software methods need to be well documented.

3.2.5.1 Key Conceptual Configurations Associated with SDLF and TDLF Detailing

To understand the calculation of the locked-in forces due to SDLF or TDLF detailing of the cross-frames, it is essential to first understand the basic geometry calculations associated with these methods. These calculations do not require any structural analysis, but rather, they utilize the specified girder camber profiles to determine the fabricated geometry of the cross-frames.

Figure 3-30 illustrates four different configurations associated with SDLF or TDLF detailing. Geometric factors such as cross-slope, super-elevation, and profile grade line are not shown in the figure for clarity. The cross-frame shown in the figure is assumed to be an arbitrary one within the bridge span (considerations at bearing line cross-frames are addressed subsequently). The two configurations used by structural detailers are Configurations 1 and 4. In Configuration 1, the girders are assumed to be blocked and under zero load with their webs vertical in their initially fabricated (cambered and plumb) geometry. If either TDLF or SDLF detailing is employed, the cross-frame, if connected to the girder on one side, will not fit up with the connection on the other side. This is because the cross-frame geometry is detailed to fit between the girder connection work points, assuming that the girder webs remain vertical while the corresponding camber values are taken out of the girders at the cross-frame location. If TDLF detailing is employed, Configuration 4 is the idealized girder geometry, with plumb webs and with the *total* dead load camber taken out of both of the girders. Correspondingly, if SDLF detailing is used, Configuration 4 is the idealized plumb girder geometry with the *steel* dead load camber taken out of both of the girders. Therefore, given the total dead load or steel dead load camber profiles, the TDLF or SDLF calculation is simply a geometrical one for the detailer and fabricator.

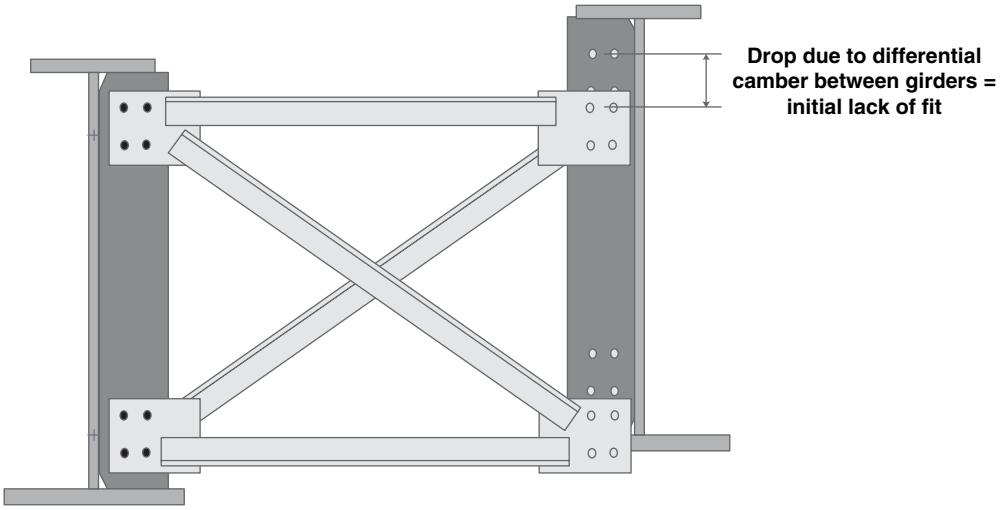

(a) Configuration 1 – No-load geometry before connecting the cross-frames

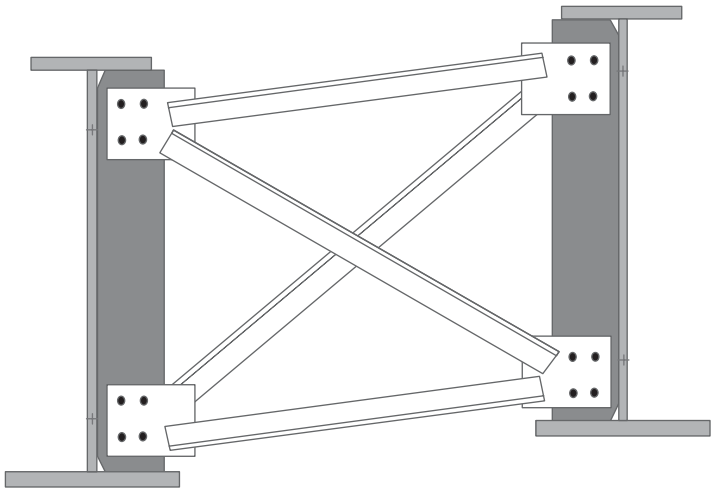

(b) Configuration 2 – Girders "locked" in the initial no-load, plumb and cambered geometry, cross-frames subjected to initial strains and initial stresses to connect them to the girders

Figure 3-30. Important conceptual configurations associated with total (or steel) dead load fit detailing (geometric factors such as cross-slope, super-elevation, and profile grade line are not shown for clarity).

(continued)

In order to include the initial lack-of-fit effects due to the above procedures in the structural analysis, Configuration 2 needs to be considered. It should be emphasized that Configuration 2 is never experienced in the physical bridge. However, this configuration is very convenient for setting up the analysis of the SDLF or TDLF effects. In this configuration, the girders are conceptually "locked" into position in their no-load ideally plumb geometry, and the cross-frames are conceptually deformed (i.e., forced) into the position where they fit up with the corresponding points on the girder connection plates. In many cases, the drops due to the differential camber, labeled in Configuration 1, are sufficiently large such that substantial initial strains need to be induced into the cross-frames in order for the connection points to fit up. This is not a problem, since the girders have been artificially locked in their no-load plumb position in this configuration. This is similar to the conceptual model used in the calculation of thermal loading effects, where the structure "nodes" are initially locked into position, the temperature changes are applied

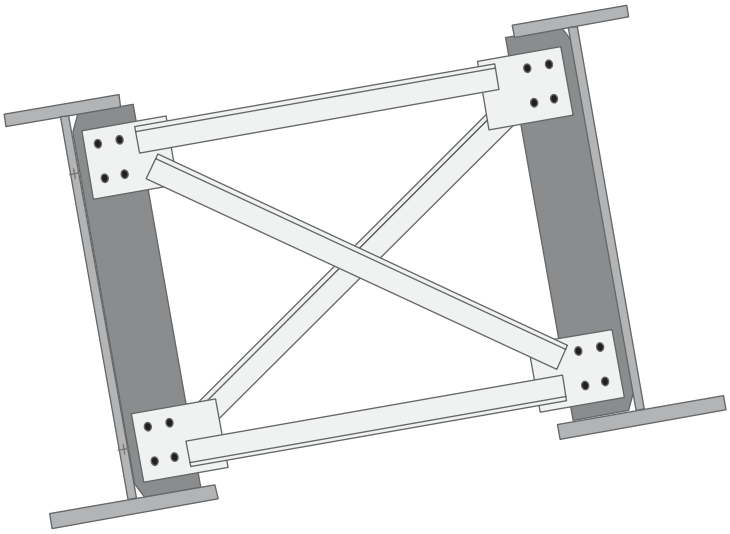

(c) Configuration 3 – Theoretical geometry under no-load (dead load not yet applied), after resolving the initial lack of fit by connecting the cross-frames to the girders, then "releasing" the girders to deflect under the lack-of-fit effects from the cross-frames

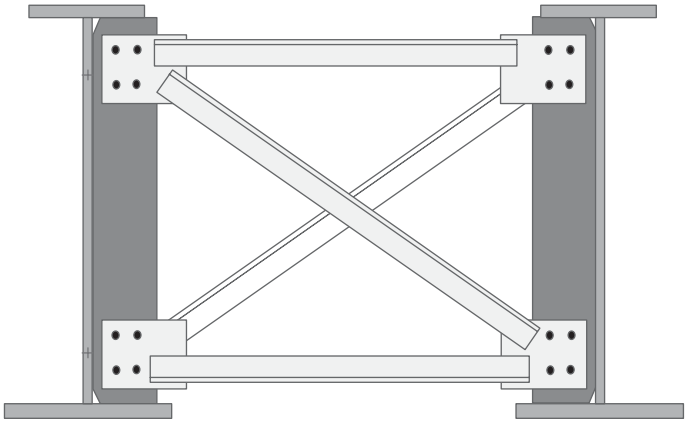

(d) Configuration 4 – Geometry under the combined effects of the total (or steel) dead load plus the locked-in internal forces due to the dead load fit detailing

Figure 3-30. (Continued).

to the model, producing initial stresses, and then the nodes are "released" and the structure is allowed to deform due to the "fixed-end" forces induced at the nodes when everything was initially "locked up."

Configuration 3 represents the geometry achieved by the structure once the girders are "unlocked" and allowed to deform under the fixed-end forces induced from the cross-frames at the connection points in Configuration 2. It should be emphasized that, conceptually, the dead loads (i.e., the self-weight of the steel and the dead weight of the concrete deck) have not been applied to the structure yet in Configuration 3. Therefore, similar to Configuration 2, this configuration also is never directly experienced by the bridge. However, the internal forces and stresses induced in Configuration 3 are the locked-in values due to the SDLF or TDLF detailing effects. When the corresponding steel or total dead load is added to this configuration, Configuration 4 (the state of the bridge under the combined dead load and locked-in force effects) is achieved.

The goal of TDLF or SDLF detailing is to achieve approximately plumb girder webs under the total dead load or the steel dead load respectively. Once the girders are released from their locked

positions in Configuration 2, the cross-frames tend to "spring back" or "elastically rebound." Since the cross-frames tend to be relatively stiff in their own planes compared to the resistance of the individual girders to lateral bending and twisting, the cross-frames tend to snap-back close to their original undeformed geometry. However, this cannot occur without the twisting of the girders, since compatibility must be maintained between the cross-frame connection points and the corresponding points on the girder connection plates. As a result, the girders are twisted into the position shown in Configuration 3.

When the dead load (i.e., the total dead load or the steel dead load) is applied conceptually to the bridge, starting in Configuration 3, the structure tends to bend and twist under the load such that the geometry shown in Configuration 4 is achieved. The sketch of Configuration 4 shown in Figure 3-30d implies TDLF detailing, since the bridge cross-slopes, etc., are not shown in the figure and the drawing indicates that both of the girders have deflected to the same final elevation. For TDLF detailing, the girder webs are approximately plumb in this condition under the total dead load.

If SDLF detailing is employed, the additional camber associated with the concrete dead load (plus any additional camber for dead load from appurtenances, etc.) still remains in the girders in Configuration 4. However, in this case, the girder webs are approximately plumb under the *steel* dead load.

It should be noted that the twisting induced into the girders in Configuration 3 is largely due to the differential camber between the girders in Configuration 1. Furthermore, the differential camber in Configuration 1 is due to the different vertical displacements that occur in the girders due to the bending and twisting of the structure under the applied loads. Therefore, the displacements that the cross-frames tend to "pull" into the girders in Configuration 3 are approximately equal and opposite to the displacements at these locations under the corresponding total or steel dead load.

3.2.5.2 Calculation of the Initial Strains, Initial Stresses or Initial Forces Associated with SDLF or TDLF Detailing of the Cross-Frames

The calculation of the initial strains generated in the cross-frames in Configuration 2 of Figure 3-30b simply involves the identification of the nodal positions of the girder connection work points in the desired "final" Configuration 4, as well as the corresponding nodal positions of the girder connection work points in Configuration 2. (Note that the Configuration 2 girder nodal positions are the same as the nodal positions in Configuration 1 since the girders are in their undisplaced no-load plumb-web geometry in both of these configurations.) The difference between the nodal positions in Configurations 2 and 4 gives the displacements that the cross-frame is subjected to in order to connect it with the girders in Configuration 2.

- **Calculation of the initial strains, initial stresses, or initial forces in 3D FEA software.** Figure 3-31 shows a spatial representation of Configurations 2 and 4 for a hypothetical location within a bridge span. It should be noted that, if the individual cross-frame members are represented explicitly by truss and/or beam elements, the calculated initial strain is simply the axial extension of the individual members associated with the above displacements. If beam elements are employed for the individual cross-frame members, it is generally sufficient to assume that these elements are "pinned" to the girder connection work points at their ends, such that only axial deformation is produced by the displacements from Configuration 4 to Configuration 2. The engineer may wish to insert rotational releases explicitly in the model at the end of the cross-frame members in many situations where they are modeled by beam elements. However, the bending rigidity of the individual cross-frame members is typically sufficiently small such that including or not including the rotational releases is not of any significance.

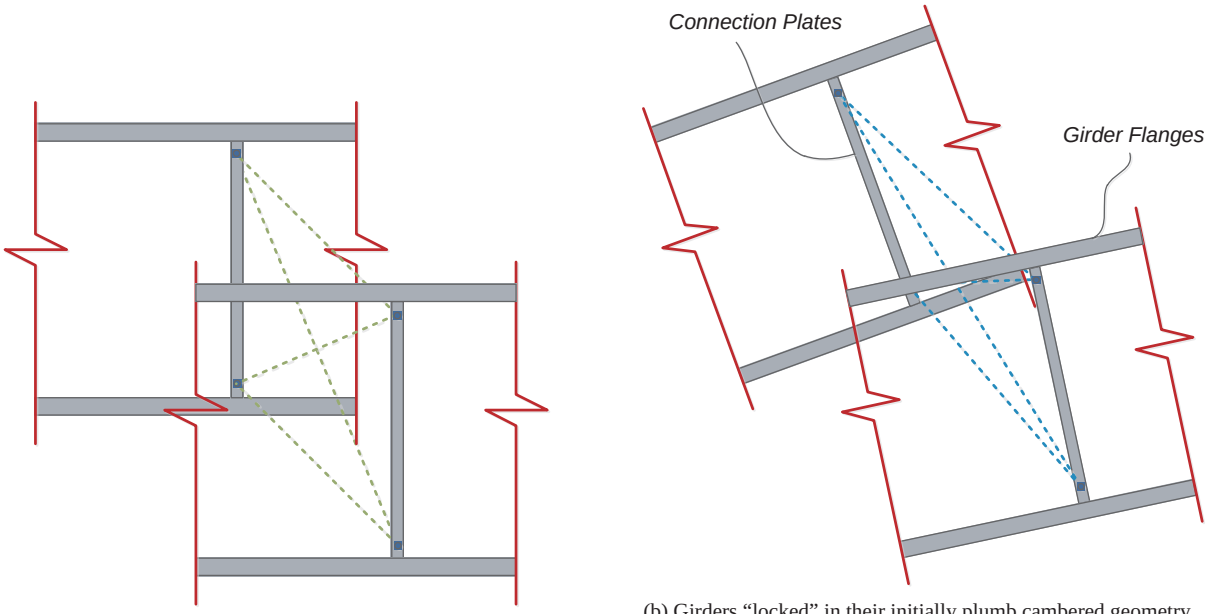

(a) Girders in the final geometry (Configuration 4)

(b) Girders "locked" in their initially plumb cambered geometry, cross-frames subjected to initial strains to connect to the girders (Configuration 2)

Figure 3-31. Configurations used for calculation of initial strains in cross-frame members due to initial lack of fit.

Once the cross-frame element initial (axial) strains are calculated, the corresponding initial stresses are determined simply by multiplying the strains by the elastic modulus of the material. The initial strains and initial stresses are simply a computational device to determine the locked-in force effects. Therefore, even if the initial stress is larger than the material yield strength, the material behavior should be assumed to be linear elastic. The initial cross-frame member forces are determined simply by multiplying the initial stress by the cross-frame area.

It should be noted that the implementation of the above calculations requires that the software, and the structural elements used in the software, must have either initial stress or initial strain capabilities. Any software that already is capable of modeling thermal loading has these capabilities.

Calculation of the initial strains and initial forces in cross-frame equivalent beam elements. If the cross-frames are represented by equivalent beam elements, the calculations are exactly the same as in the above discussion. However, the displacements at the two cross-frame end connection work points are resolved into element end displacements and end rotations. These element end displacements and rotations are then applied to the equivalent beam element. Assuming the use of a structural element for the equivalent beam, the best approach is to calculate the initial forces induced by the above displacements from Configuration 4 to Configuration 2. These forces are then handled as initial fixed-end forces in the equivalent beam element. This procedure requires that the beam element implementation must be able to handle initial fixed-end forces (e.g., fixed-end forces due to thermal loading, fixed-end forces due to internal element loads, etc.). If this is the case, the implementation of the "initial force" effects is relatively straightforward.

As noted above, elements that are able to handle thermal loading already include these effects. In addition, elements that incorporate the calculation of fixed-end forces from internal loading between the nodes already include this type of effect.

3.2.5.3 Handling of Cross-Frame Initial Strains and Initial Stresses (or Initial Forces) at Skewed Bearing Line Cross-Frames

The computational handling of the initial lack-of-fit or locked-in force effects at bearing line cross-frames is essentially no different than described in the above section. However, the behavior is somewhat different since the girders cannot displace vertically at the bearings and because the skewed cross-frames impose a twist into the girders associated with the girder major-axis bending rotation at the bearings. Figure 3-32 illustrates the rotations, due to applied loads within the bridge span, at the end of a girder connected to a skewed bearing line cross-frame. A fixed bearing is assumed at this position to simplify the discussion.

The girder web and the bearing line cross-frame are assumed to be plumb in the current configuration shown in the figure. The double arrow perpendicular to the girder web represents the major-axis bending rotation of the girder, ϕ_x, about the fixed point. This rotation induces the longitudinal displacement Δ_z at the top flange of the girder. However, since the girder is attached to the skewed bearing line cross-frame, the top flange can only displace significantly in the direction normal to the plane of the cross-frame. This is indicated by the arrow labeled Δ. The cross-frame deflects essentially only by rotating about its longitudinal axis through the fixed point. This is shown by the double-arrow vector ϕ. In order to maintain compatibility between the girder and the cross-frame, the top flange of the girder must deflect by the vector component labeled Δ_x in the figure. Therefore, the girder web lays over by the deflection Δ_x relative to the fixed point. This deflection, divided by the height *h*, gives the girder twist rotation ϕ_z.

Figure 3-33 shows an alternate plan view of the behavior illustrated in Figure 3-32, except that the rotations are in the opposite direction to the rotations associated with the structure's dead loads. If one considers the "deflections" of the girders due to the camber, the typical upward displacement in the spans induces a major-axis bending rotation at the bearing line shown by the double arrows normal to the girders in Figure 3-33 (using the right-hand rule). That is, if the bearing stiffener/connection plate at the bearing is placed normal to the flanges, this stiffener is rotated to a non-vertical position in the initial cambered, no-load, plumb geometry of the girder. This is comparable to Configuration 1 in Figure 3-30a. In order to fit-up with the girders in Configuration 2, the bearing line cross-frames have to be rotated about their

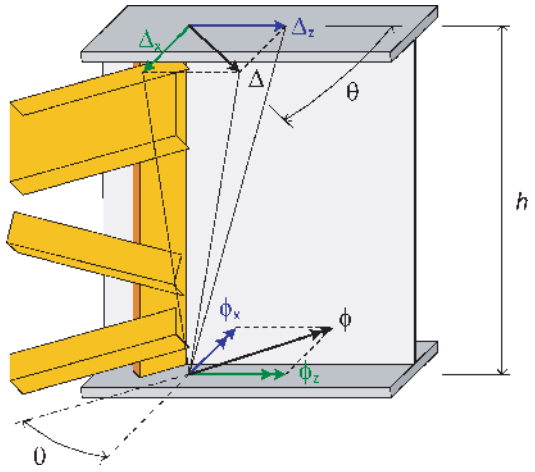

Figure 3-32. Illustration of the girder major-axis bending and twist rotations required for compatibility at a skewed bearing line cross-frame.

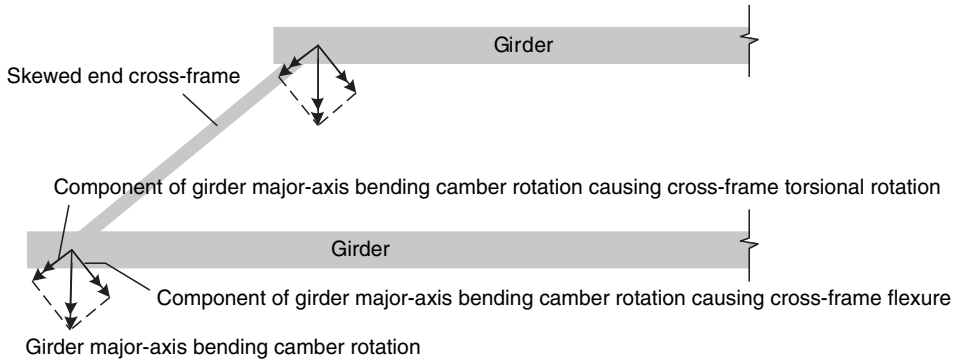

Figure 3-33. Flexural and torsional rotation components at the ends of a skewed end cross-frame due to the girder major-axis bending camber rotations.

longitudinal axis, and then (because of the skewed geometry), strained into position to connect them with the rotated connection plates in the initial cambered no-load, plumb geometry of the girders (i.e., assuming no drops between the girders at the bearing line, the bearing line cross-frames have to be deformed from their rectangular geometry in Configuration 1 into a parallelogram geometry in Configuration 2, assuming equal ϕ at both ends of the cross-frame). When the girders are then "unlocked" and "released," the cross-frames elastically rebound approximately to their initial rectangular geometry and force a twist into the girders opposite to the direction that they twist under the dead loads. This corresponds to Configuration 3 in Figure 3-30c. However, the girders only lay over at the bearing lines. They cannot displace vertically.

It should be noted that skewed intermediate cross-frames involve a combination of the two effects shown in the above for the intermediate cross-frames in Figure 3-30 and for the skewed bearing line cross-frames in Figures 3-32 and 3-33. That is, at skewed intermediate cross-frames, the girders are subjected to twisting due to the differential vertical displacements between the cross-frame connection points on the girders as well as the compatibility of the rotations between the girders and the skewed cross-frames at the connection points.

3.2.6 Simplified Analysis Improvements for Tub-Girder Bridges

Significant improvements also were developed for the simplified analysis of curved and skewed tub-girder bridges in the NCHRP Project 12-79 Task 8B research. These improvements are of a somewhat different nature though, since tub-girder bridges are fundamentally different from I-girder bridges. The key improvements for tub girders were:

1. The development of an improved method for estimating the influence of skew on tub-girder internal torques using basic 1D analysis procedures,
2. The investigation of the influence of skew (and torsion due to skew) on the cross-section distortion of box-girders, and
3. The calculation of local effects from the longitudinal components of the axial forces in the diagonals of the top flange lateral bracing (TFLB) system, which result in "saw-tooth" type local spikes in the longitudinal normal stresses in tub-girder top flanges.

These improvements are described briefly in the following subsections. The NCHRP Project 12-79 Task 8 report (Appendix C of the contractors' final report) and Jimenez Chong (2012) provide more detailed discussions of these improvements.

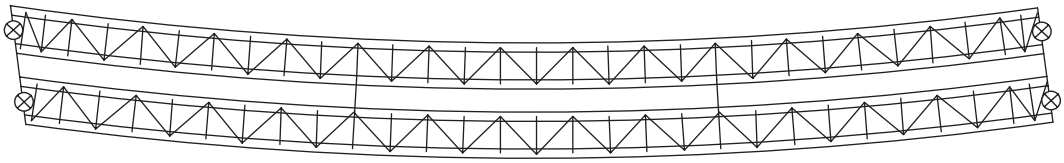

Figure 3-34. Plan view of Bridge NTSCS29.

3.2.6.1 Improved Estimation of Tub-Girder Internal Torques in 1D Line-Girder Analysis Methods

Figure 3-34 shows a plan view of Bridge NTSCS29 analyzed in the NCHRP Project 12-79 Task 7 studies. This is a 225-ft. span simply supported curved and skewed tub-girder bridge with a horizontal radius of curvature of 820 ft., a deck width of 30 ft., and a skew angle of 15.7° at the left-hand abutment. The bearing line at the right-hand abutment is radial. The girders are each supported on single bearings at their ends, and the structure is built with two intermediate external cross-frames. The top flange lateral bracing (TFLB) system in this bridge is a Warren-type truss system.

Figure 3-35 compares the internal torques calculated with two different line-girder analyses of this bridge (including the use of the M/R method for estimating the effects of the horizontal curvature), to two different 3D FEA benchmark simulations. The lighter dotted curve in the figure shows the results for the internal torque calculated solely by using the conventional M/R method without any accounting for the skew effects at the left-hand end. The bold dotted curve shows the combination of this conventional calculation with a separate additional estimate of the internal torque due to the left-hand end skew. The two 3D FEA solutions for the internal torque shown in the plot are:

1. A 3D FEA solution of the bridge as shown in Figure 3-34, indicated by the dark solid line, and
2. A 3D FEA solution of the bridge constructed without any intermediate external cross-frames, indicated by the light dashed line.

One can observe that the M/R solution, combined with the improved method of estimating the internal torque, gives a close representation of the response of the bridge if it did not have any intermediate external cross-frames tying the girders together along the span length. Furthermore, the left-most intermediate external cross-frame appears to cause a shift in the internal torque on

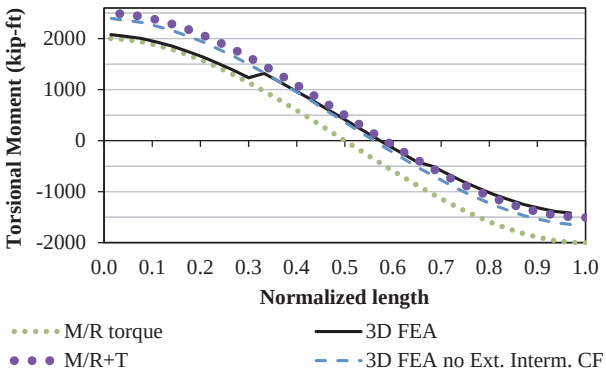

Figure 3-35. Comparison of total dead load torsional moments (unfactored) in the girder on the outside of the horizontal curve of Bridge NTSCS29 predicted by 1D analysis assuming rigid end diaphragms versus 3D FEA.

one side, given by just the M/R method solution, and on the other side, given by the combination of the M/R method with the improved method of estimating the internal torque due to skew. The right-most external cross-frame does not appear to have any significant influence on the internal torque.

The improved method of estimating the internal torque due to skew involves the relatively simple idealization that the bearing line diaphragms (or cross-frames) are rigid in their own plane with respect to torsional stiffness of the tub girders. Although tub girders generally have substantially larger torsional stiffness than I-girders, the bearing line diaphragms or cross-frames are relatively short in length. Therefore, particularly in relatively narrow tub-girder bridges, these components may be approximated reasonably well as acting rigidly in their own plane. As a result, once the major-axis bending rotations are estimated for the tub girders at a bearing line, the same type of rotational compatibility rules as discussed in Section 3.2.5.3 apply.

The NCHRP Project 12-79 research has not addressed analysis of the effect of external intermediate cross-frames or diaphragms via a 1D analysis in the context of the above procedures. A number of the conceptual idealizations used in the development of the V-load method for I-girder bridges may be helpful for the development of such procedures. However, the tedious nature of the adjustments to the 1D solutions may outweigh the benefits of these procedures, given that the use of 2D-grid methods should be quite feasible in current practice (2012).

3.2.6.2 Investigation of the Influence of Skew (and Torsion Due to Skew) on the Cross-Section Distortion of Box-Girders

AASHTO LRFD Article 6.7.4.3 generally requires the use of intermediate internal diaphragms or cross-frames in steel box girders to control cross-section distortion due to torsional loads. Cross-section distortion of box girders is caused by external torsional loads that are not distributed in proportion to the St. Venant shear flow. It is well known that the distortional behavior of a box girder is dependent on the manner in which the external torque is applied to the member. Fan and Helwig (2002) have developed equations for estimating the distortional bracing forces developed in internal diaphragm and cross-frame components by horizontal curvature effects and by eccentric vertical applied loads. However, to the knowledge of the NCHRP Project 12-79 research team, no prior studies have been conducted to understand and to estimate the influence of distortion due to skew.

Evaluations of the tub-girder bridges studied in NCHRP Project 12-79 Tasks 7, 8, and 9 research have indicated that the tub-girder internal cross-frame forces tend to be negligible in straight-skewed tub-girder bridges and that these forces tend to be predicted conservatively by the Fan and Helwig (2002) equations in curved tub-girder bridges. It appears that the development of internal torsional moments in tub girders, due to support skew, is similar to the shear flow associated with St. Venant uniform torsion. This is largely because the support diaphragms restrain the distortion of the girder cross-sections at the skewed supports. As such, the discrete torque induced in the girders at the skewed supports is predominantly a St. Venant torque.

Figure 3-36 shows two basic geometries that can be used to gain some further understanding of this problem: (1) a straight simply supported box girder with a square cross-section and 30° skew at its right-hand end, and (2) a horizontally curved, simply supported box girder having the same cross-section. The span length of these girders is L_s = 150 ft., and the girders are subjected to vertical loads representative of the weight from the placement of a concrete deck. The square box depth is set to $D = L_s/25 = 72$ in. and the web thickness is set to $t_w = 0.5$ in. The top and bottom flange thickness is also set to $t_f = 0.5$ in. for simplicity. The radius of curvature of the second girder is taken as $R = 400$ ft. Solid plate diaphragms with $t = 1$ in. are used at the ends of the boxes, but no intermediate internal diaphragms or cross-frames are employed along the spans. Both box girders are supported continuously across their bottom flange at the supports.

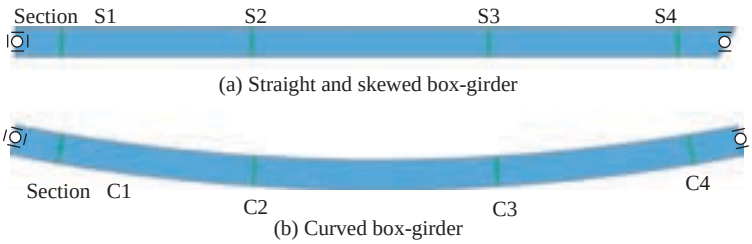

Figure 3-36. Straight skewed and curved box girders used for study of distortion effects.

In Figures 3-37 and 3-38, the cross-section warping deformation is illustrated via a side view and the cross-section distortion is illustrated via a cross-section view from the 3D FEA at the four cross-sections labeled in Figure 3-36. Although the torsion is also smaller in the first case, the warping deformations, as well as the cross-sectional distortion deformations, are also small relative to the torsional deformations. Conversely, in the second case, the distortion of the box is quite evident. This is predominantly due to effective radial forces due to the horizontal curvature coming from the flanges.

3.2.6.3 Calculation of "Saw-Tooth" Longitudinal Normal Stresses in the Top Flanges of Tub Girders

Figure 3-39 shows a simplified free-body diagram illustrating the forces *Q* and *P* delivered to one of the top flanges of a tub girder at the connection of the top flange lateral bracing (TFLB)

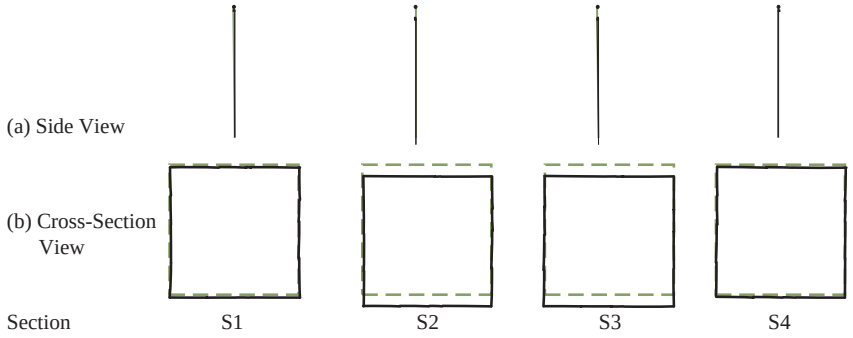

Figure 3-37. Deformed cross-sections in the straight skewed box girder.

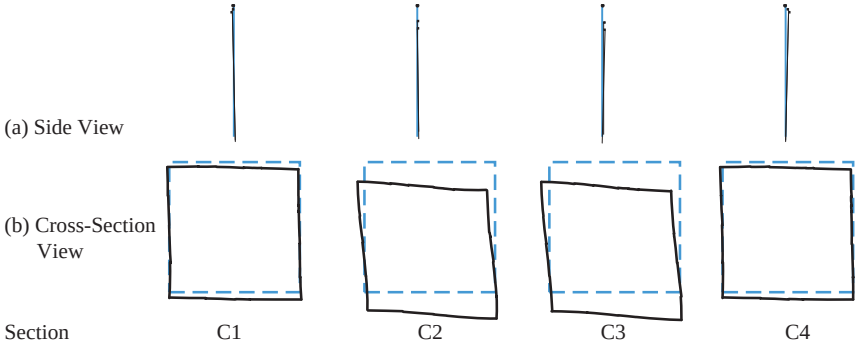

Figure 3-38. Deformed cross-sections in the curved box girder.

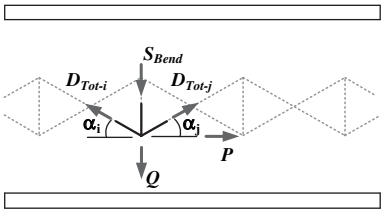

$$P = D_{Tot-i}\cos\alpha_i - D_{Tot-j}\cos\alpha_j$$

$$Q = D_{Tot-i}\sin\alpha_i + D_{Tot-j}\sin\alpha_j - S_{Bend}$$

Figure 3-39. Interaction of forces between top flange lateral bracing and girder top flange for Warren and X-type layouts.

system to the girder. For cases where the tub girder is resisting significant torsion, the diagonal forces often are dominated by the torsion and the forces in the diagonals alternate from tension to compression in the consecutive panels. In these cases, the effects of the tension and compression forces due to the torsion are additive in their contribution to *P*. Therefore, the tub-girder flanges are acted upon by a longitudinal concentrated load at the intersection of the diagonals with the flanges.

Although the predominant flange stress is the major-axis bending stress, which is commonly estimated as $f_b = M/S_{x.top}$, where M is the major-axis bending moment at the cross-section under consideration and $S_{x.top}$ is the elastic section modulus to the top flange, neglecting the contribution of the TFLB system, the above axial load P has an important local effect on the flange stresses. Interestingly, the resulting top flange average normal stress tends to follow a saw-tooth pattern in which the saw-tooth "jump" in stress is essentially $P/b_f t_f$. The saw-tooth effect appears as a $+ P/2b_f t_f$ fluctuation about the "mean" value $f_b = M/S_{x.top}$ (see Figure 3-40). The researchers obtained the best accuracy of the simplified calculations relative to 3D FEA benchmark results when this saw-tooth effect is added to the stress f_b with $S_{x.top}$ determined as explained above.

Figures 3-42 and 3-44 show example results comparing the top flange longitudinal normal stresses (labeled generally as f_b) from 3D FEA simulation models to the "conventional" calculation of the top flange major-axis bending stress as $f_b = M/S_{x.top}$ from a 2D-grid model (neglecting the contribution of the TFLB system in determining $S_{x.top}$). These results correspond to the two simple-span tub-girder bridges shown in Figures 3-41 and 3-43. The first bridge (NTSSS2) is a straight-skewed 150-ft. span tub-girder bridge with 30° parallel skew, a 30-ft. wide deck, and

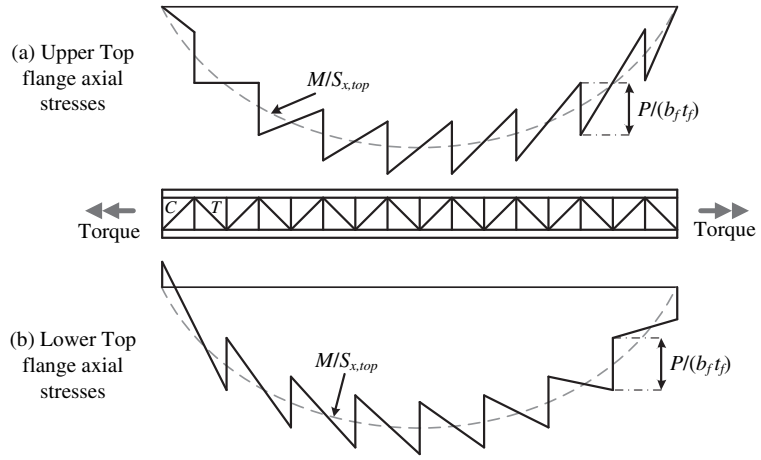

Figure 3-40. Top flange saw-tooth major-axis bending stresses due to interaction with the flange level lateral bracing system.

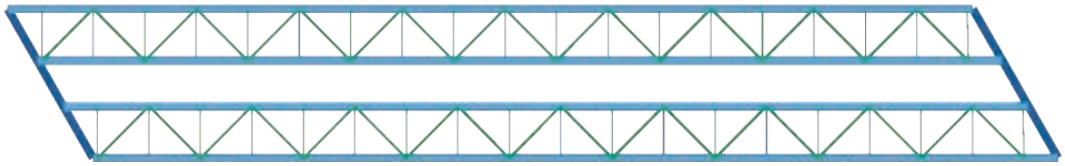

Figure 3-41. Plan view of Bridge NTSSS2.

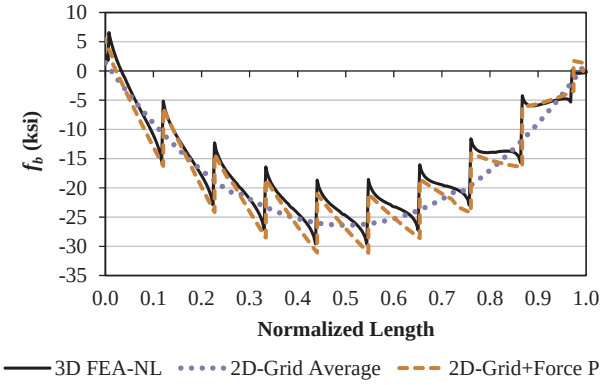

Figure 3-42. Bridge NTSSS2 exterior top flange normal stresses on Girder G1.

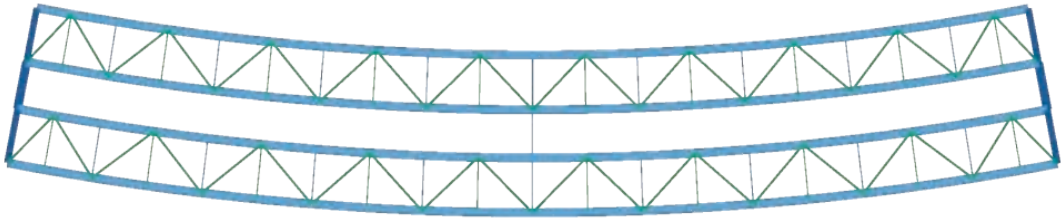

Figure 3-43. Plan view of Bridge NTSCR1.

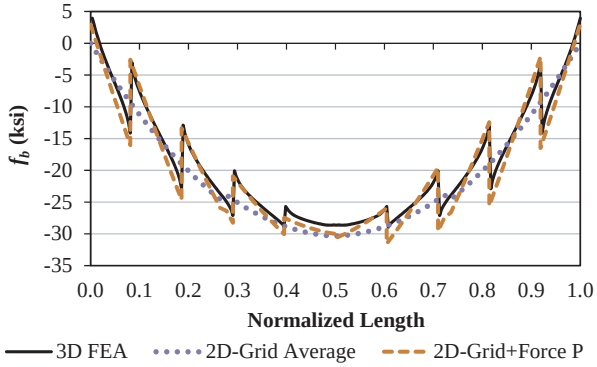

Figure 3-44. Bridge NTSCR1 exterior top flange normal stresses on Girder G1.

no intermediate external diaphragms within its span. The second case (NTSCR1) is a curved 150-ft. span, radially supported structure with a 30-ft. wide deck, and a horizontal radius of curvature $R = 400$ ft.

The 2D-grid estimates of the top flange major-axis bending stresses are excellent in both of these examples. Correspondingly, this result is reflected in the mode grade of A for the calculation of the major-axis bending stresses in straight-skewed and curved radially supported tub-girder bridges in Table 3-2 of Section 3.1.5.

Interestingly, the internal torque is constant (and solely due to the skew) in the straight-skewed bridge. Conversely, the internal torque is maximum at the supports and zero at the mid-span in the horizontally curved structure. These variations in the internal torque are reflected clearly in the saw-tooth patterns shown in Figures 3-42 and 3-44. The "jump" associated with the saw-tooth is constant throughout the length of the bridge in Figure 3-42, while this jump is maximum toward the ends of the bridge and relatively small near the mid-span in Figure 3-44. In cases such as the one in Figure 3-44, the saw-tooth stresses result in a significant local increase in stress above the conventionally calculated f_b in the region of maximum moment. This effect can also occur in the negative moment region of continuous-span bridges.

3.3 Influence of Locked-In Forces Due to SDLF or TDLF Detailing of Cross-Frames

This section provides a summary of the findings of the NCHRP Project 12-79 Task 8B research pertaining to the influence of steel dead load fit (SDLF) and total dead load fit (TDLF) detailing of the cross-frames in curved and/or skewed I-girder bridges. Two examples are extracted from the large suite of structures considered in the Task 7 studies for this purpose. The first example is a simple-span straight bridge with a substantial parallel skew; the second example is a horizontally curved, radially supported structure. The results presented show the impact of the above detailing methods on a relatively complete set of important responses including:

- Bridge displacements (i.e., the constructed geometry),
- Cross-frame forces, and
- Girder flange lateral bending stresses.

This is followed by a broader discussion of key considerations, including the questions:

- When is it important or essential to consider locked-in force effects due to SDLF or TDLF detailing in the design?
- When can SDLF or TDLF initial lack-of-fit effects be considered as incidental?
- To what extent can standard connection tolerances relieve the locked-in internal forces induced by SDLF or TDLF detailing?

Appendix C of the contractors' final report provides a more detailed summary of results for the wide range of bridges studied in the NCHRP Project 12-79 research. Appendix A provides summary definitions of key terms. It is essential that the reader understand these definitions to facilitate study and interpretation of corresponding results and discussions throughout this report.

3.3.1 Straight-Skewed Bridge Example

Figure 3-45 shows the framing plan for a 300-ft. straight simple-span I-girder bridge with a 70° parallel skew of its bearing lines. The bridge has an 80-ft.-wide deck (i.e., $w = 80$ ft.) and 74-ft. spacing between its fascia girders. This geometry produces a skew index of $I_S = 0.68$, which places

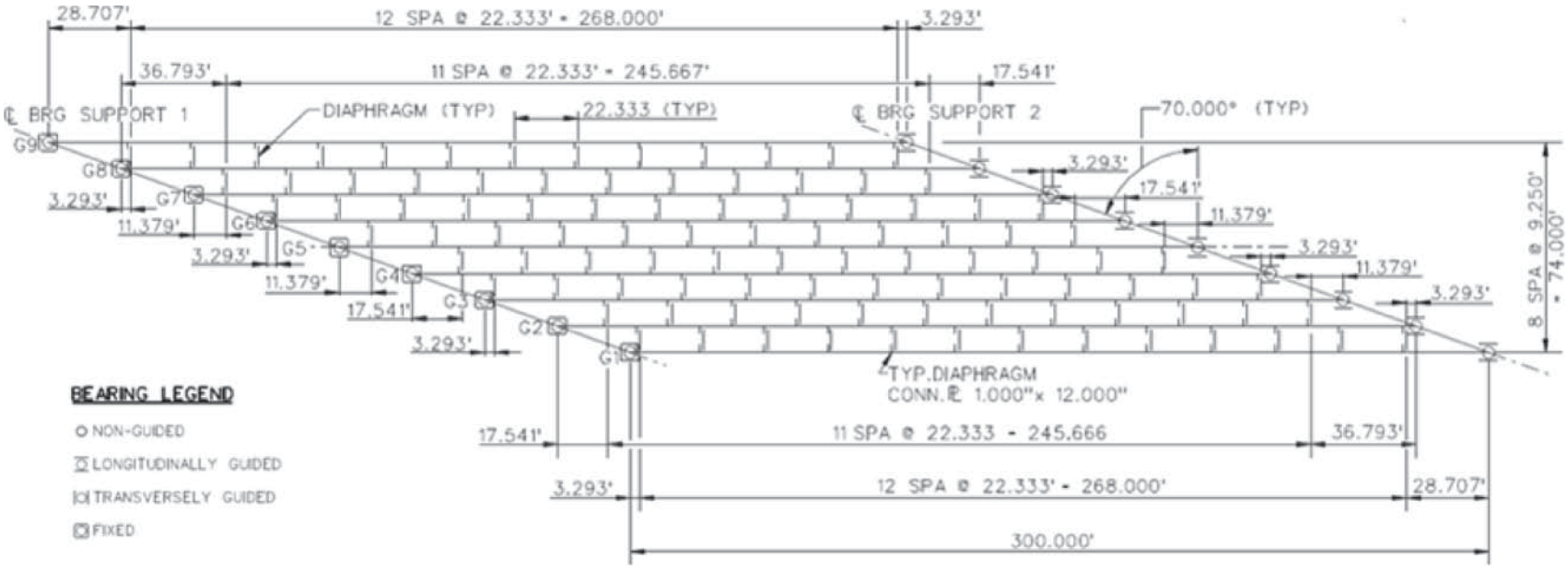

Figure 3-45. NISSS54 framing plan.

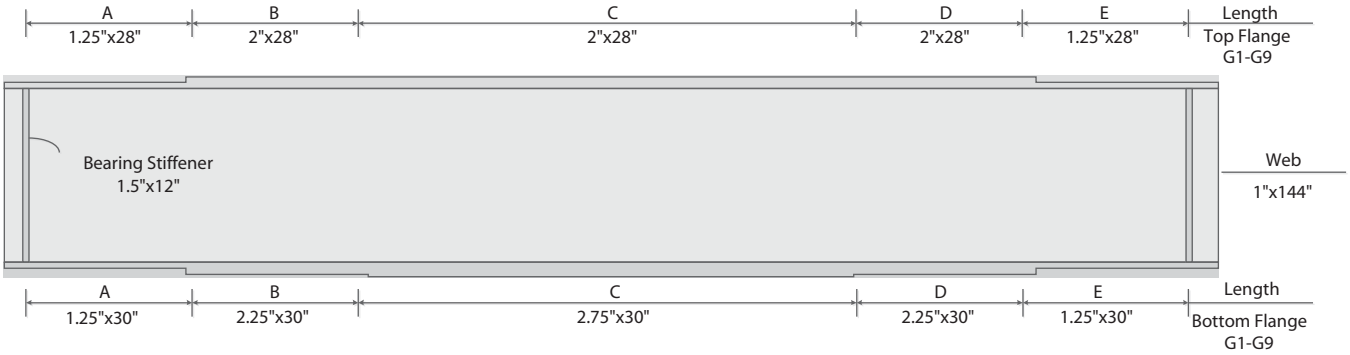

Figure 3-46. NISSS54 girder plate dimensions.

this structure in the third and most difficult "S" category of Table 3-1. Figure 3-46 and Table 3-7 give the girder dimensions, and Table 3-8 gives the cross-frame member sizes. The bridge uses staggered cross-frames to alleviate "nuisance" transverse stiffness effects due to the large skew.

3.3.1.1 Bridge Deflections

It is useful to first consider how this example bridge deflects under its total construction dead load. This can be accomplished by conducting a 3D FEA of the structure assuming no-load fit (NLF) of the cross-frames. Figure 3-47 shows a plan view of the magnified deflected geometry. One can observe that the girders are subjected to substantial layover (i.e., twist rotations) at the bearing lines. This is due to the compatibility between the girders and the heavily skewed bearing line cross-frames, as discussed previously in Section 3.2.5.3. The bearing line cross-frame deflections involve predominantly a rotation about the skewed bearing line, highlighted by the double arrows in the figure (right-hand rule). The large 70° skew induces girder end twists (denoted by ϕ_z in the previous Figure 3-32) approximately equal to $\phi_x \tan(70°) = 2.75\ \phi_x$, where ϕ_x is the girder end major-axis bending rotation. Twists of a similar but different magnitude are induced by the intermediate cross-frames due to the fact that they frame into the girders at different positions along the girder spans. The overall twisting of the girders is a rather complicated pattern, involving twist rotations in opposite directions at the girder ends.

3.3.1.2 Girder Cambers and Camber Differences

Based on the prior discussions in Section 3.2.5.1, it should be clear that the SDLF and TDLF detailing effects are driven largely by the girder camber profiles, or more specifically, by the differences between the camber profiles at each of the cross-frame positions. Figures 3-48 and 3-49 show two different camber profiles for this bridge, the first one based on a 1D line-girder analysis and the second based on a 3D FEA assuming NLF. Figure 3-50 shows the differential values for the 3D FEA girder cambers.

Table 3-7. NISSS54 girder plate lengths (ft.).

Girder	A	B	C	D	E
G1-G9	45	45	45	45	45

Table 3-8. NISSS54, cross-frame member sizes.

Cross-Frame Type	Top Chord	Diagonals	Bottom Chord
Interior (X type)	L6x6x1	L6x6x1	L6x6x1
End (Inverted V)	WT6x53	WT6x60	WT9x38

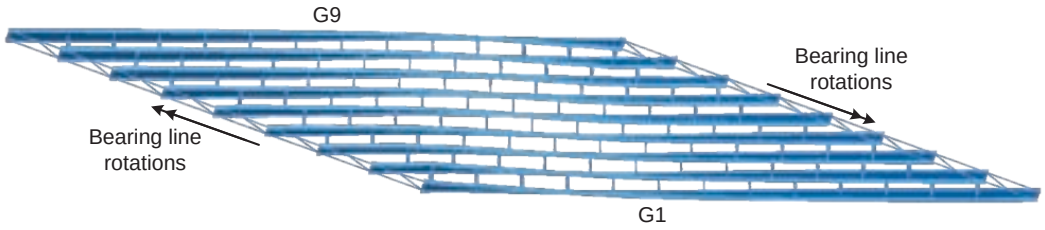

Figure 3-47. Bridge NISSS54 total dead load deflected geometry for the case of NLF detailing of the cross-frames (scale factor = 10x).

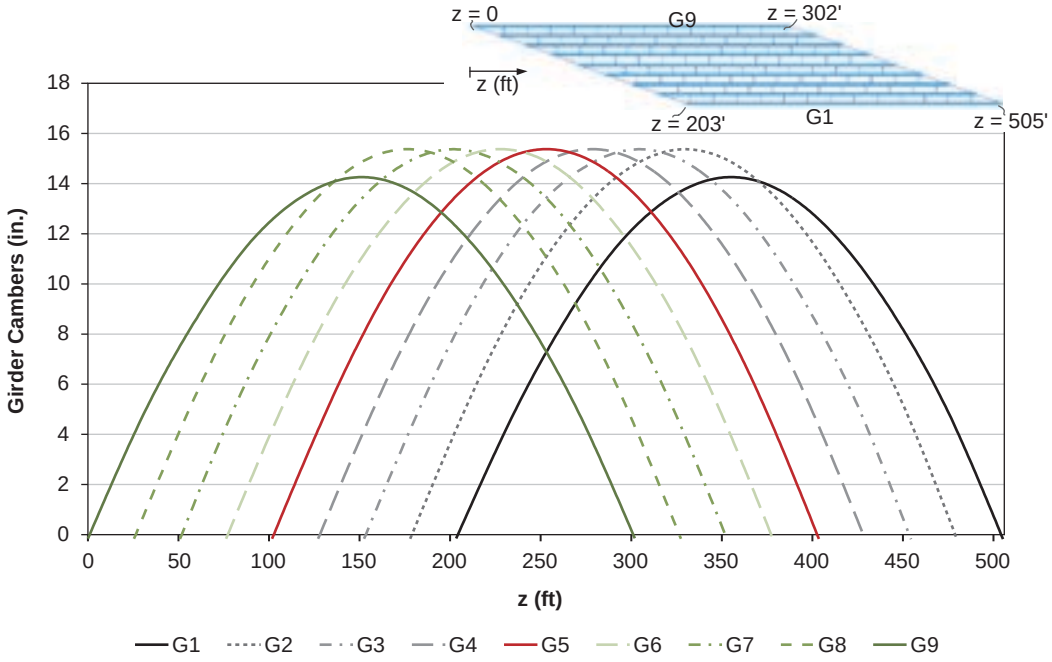

Figure 3-48. Bridge NISSS54 total dead load camber profiles from line-girder analysis.

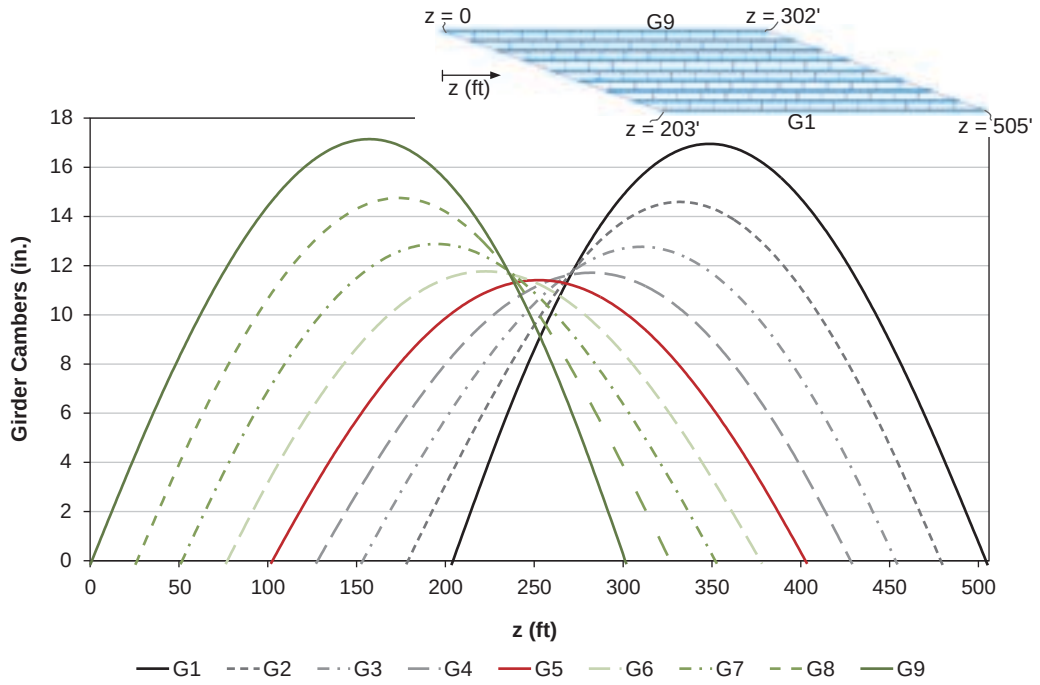

Figure 3-49. Bridge NISSS54 total dead load camber profiles from 3D FEA.

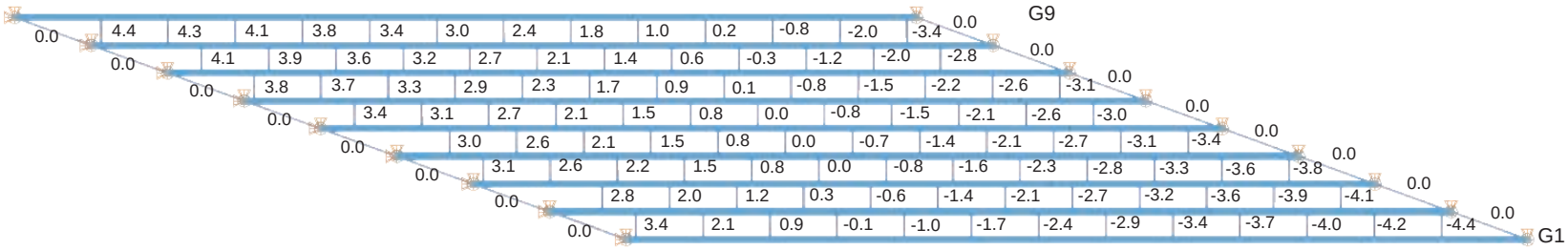

Figure 3-50. Bridge NISSS54 total dead load camber differences (differential camber values) between girders, taken from the camber profiles based on the 3D FEA vertical deflections.

Each of the curves in Figures 3-48 and 3-49 is the total dead load camber profile for a single girder. Only the total dead load cambers are shown to keep the discussion focused and brief. The focus of the subsequent discussions is on the TDLF detailing of the cross-frames and its effects. For TDLF detailing, the cross-frames are fabricated to fit to the girder connection work points in the conceptual geometry where the girder webs are still plumb but the total dead load cambers have been removed from the girders. The TDLF detailing induces twists in the girders in the opposite directions from those shown in Figure 3-47.

The horizontal axis in Figures 3-48 and 3-49 is the longitudinal coordinate "z" along the length of the bridge. The origin for the z coordinate is located at the bearing on Girder G9 at the left-hand acute corner of the structure. Therefore, the left-most curve in the plots is the camber profile for Girder G9. Correspondingly, the right-most curve, ending at $z = 505$ ft., is the camber profile for Girder G1.

One can observe that the 3D FEA camber profiles are substantially smaller for the girders near the center of the bridge width. This is due to the substantial transverse load path between the obtuse corners of the bridge, developed via the cross-frames (even though the cross-frames are staggered throughout the length of the bridge to reduce these effects). The differential cambers shown in Figure 3-50 are based on the girder cambers determined from the 3D FEA vertical deflections. The implications of using the line-girder analysis total dead load vertical displacements versus the 3D FEA vertical displacements for setting the total dead load cambers are discussed subsequently.

3.3.1.3 System Deflections Due to Initial Lack-of-Fit Effects

Figure 3-51 shows the deflections of the NISSS54 Bridge after, first, the cross-frames conceptually are connected to the girders (Configuration 2 of the previous Figure 3-30b), then the girders are "unlocked" and "released" from their initial no-load plumb geometry such that they are deformed by the cross-frames into the Configuration 3 shown in Figure 3-30c. That is, Figure 3-51 shows the "final" deformed geometry due to the cross-frame locked-in force effects (from the TDLF detailing of the cross-frames) if, by some means, the bridge dead load were not yet applied to the structure. One can observe that the bridge deformations in Figure 3-51 are approximately the opposite of the deflections shown previously in Figure 3-47.

Figure 3-52 shows the layover of the girders corresponding to the deflections in Figure 3-51, where the term "layover" is defined as the lateral deflection of the girder's top flange relative to its bottom flange. The plot in Figure 3-52 is similar to the previous plots of the girder cambers in that (1) the horizontal axis is the horizontal z coordinate in the bridge plan view, measured from the bearing at the left-hand acute corner; and (2) each curve gives the layover of a different girder at the various positions along the length.

Upon studying Figure 3-52 carefully, one can observe that the "curvature" of the fascia girder layover curves (i.e., the darkest solid curves in Figure 3-52) is largest near the acute corners

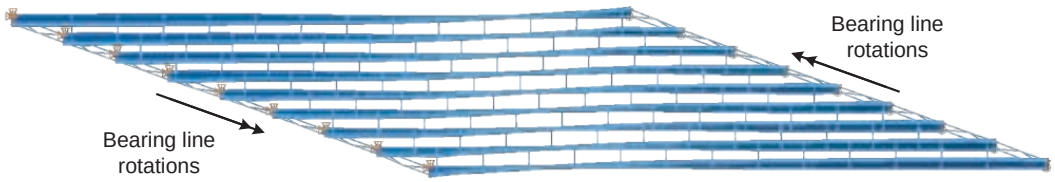

Figure 3-51. Bridge NISSS54 "Configuration 3" deflected geometry under no-load due solely to the initial lack of fit associated with the TDLF detailing of the cross-frames (camber profiles based on 3D FEA vertical deflections).

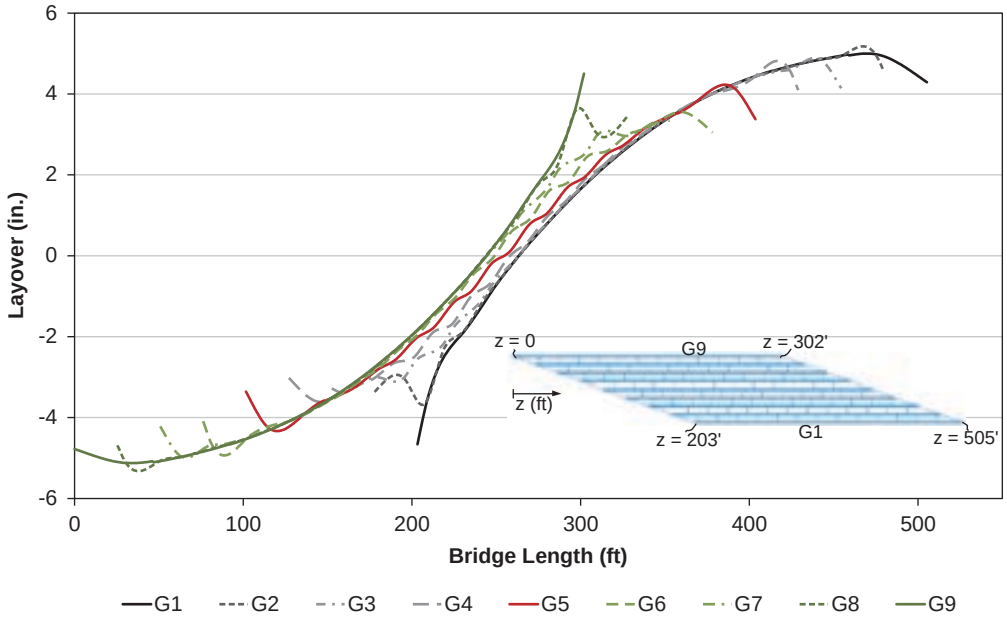

Figure 3-52. Bridge NISSS54 girder "Configuration 3" layovers due to the initial lack of fit associated with the TDLF detailing of the cross-frames.

of the span. This indicates that the TDLF detailing results in substantial "locked-in" flange lateral bending of the fascia girders at the acute corners. In addition, one can observe that the curvature of the layover curves for the interior girders is even more dramatic in the vicinity of the skewed bearing lines at each end of the bridge. Furthermore, if one looks carefully at the curves in the middle of the plot, it can be seen that the inner-most girders are subject to noticeable "back-and-forth" twisting actions. This is due to the use of the staggered cross-frames throughout the bridge, causing the load transfer between the obtuse corners to pass from cross-frame to cross-frame by twisting and flange lateral bending of the girders.

3.3.1.4 Approximate Canceling of Dead Load Layovers by Dead-Load Fit Effects

Figure 3-53 shows the girder layovers in Bridge NISSS54 due solely to the total dead load. That is, these are the layovers associated with the deflected geometry illustrated previously in Figure 3-47. One should note that the girder values in Figure 3-53 are approximately equal and opposite the corresponding girder values in Figure 3-52. However, it should be emphasized that the values in these two plots are not *exactly* equal and opposite to one another.

If one considers the application of the *steel* dead load to the bridge, resulting in the deflections of the girders from Configuration 3 to an intermediate configuration between 3 and 4 shown in the previous Figure 3-30c and d, the resulting girder layovers are the ones plotted in Figure 3-54. As one would expect (once the typical effect of TDLF on the girder layovers is understood), the girder webs are not plumb under the steel dead load. This is because TDLF detailing gives approximately plumb webs under the total dead load, but the total dead load has not been applied at the time of this graph.

Next, if the concrete dead weight is added to the structure (assumed to be applied non-compositely to the bridge for simplicity of the example), the girders finally reach the conceptual Configuration 4 shown previously in Figure 3-30d. The resulting girder layovers corresponding to this configuration are obtained by summing the results from Figures 3-52 and 3-53 and are

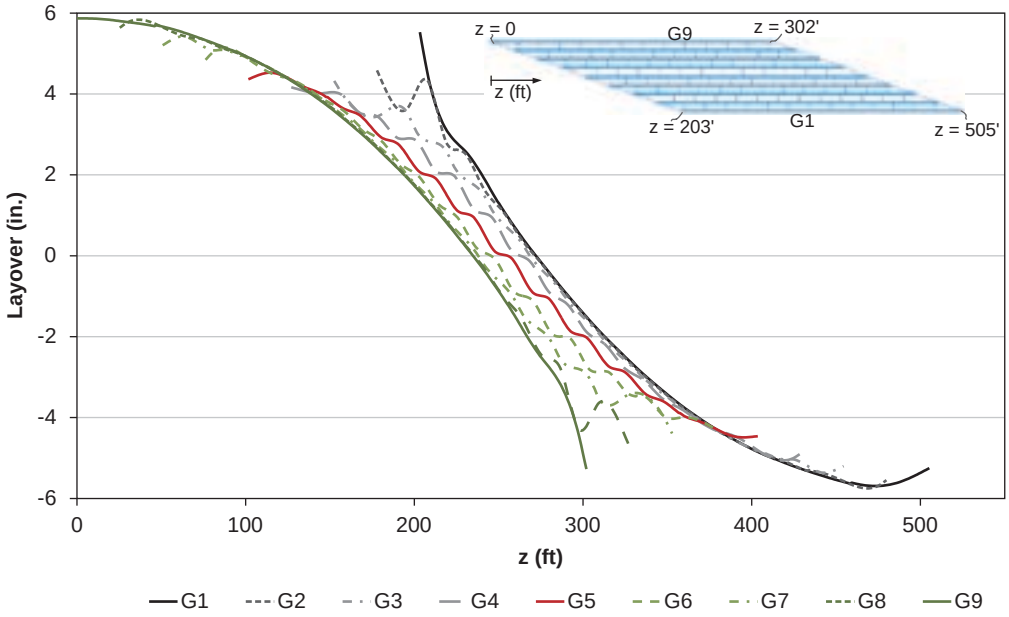

Figure 3-53. Bridge NISSS54 girder layovers solely due to the total dead load.

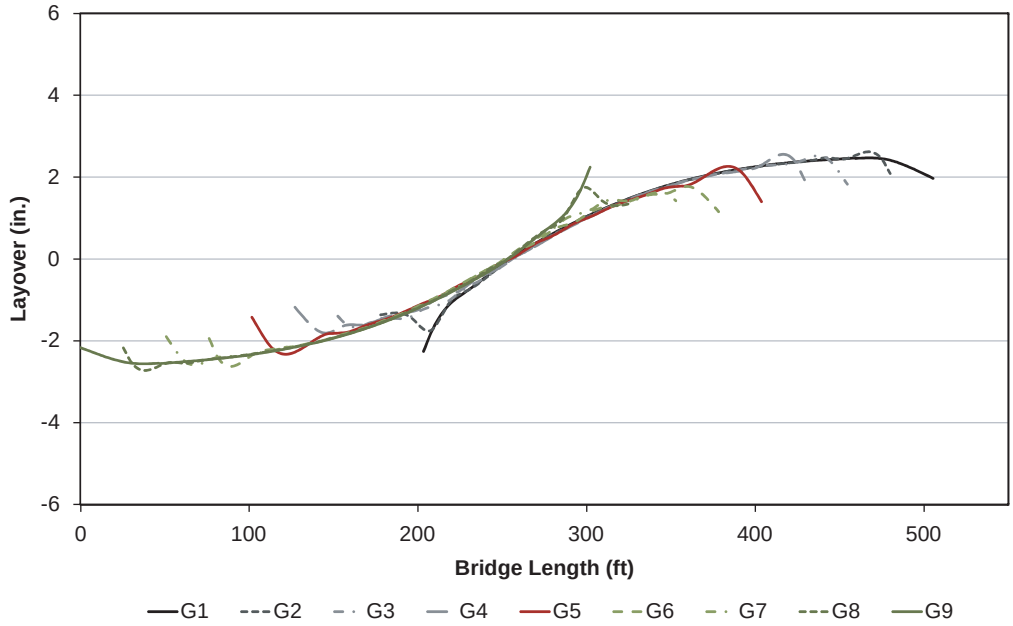

Figure 3-54. Bridge NISSS54 girder layovers under steel dead load (due to the effects of TDLF detailing of the cross-frames plus the steel dead load effects) for the case where the cross-frames are detailed for TDLF.

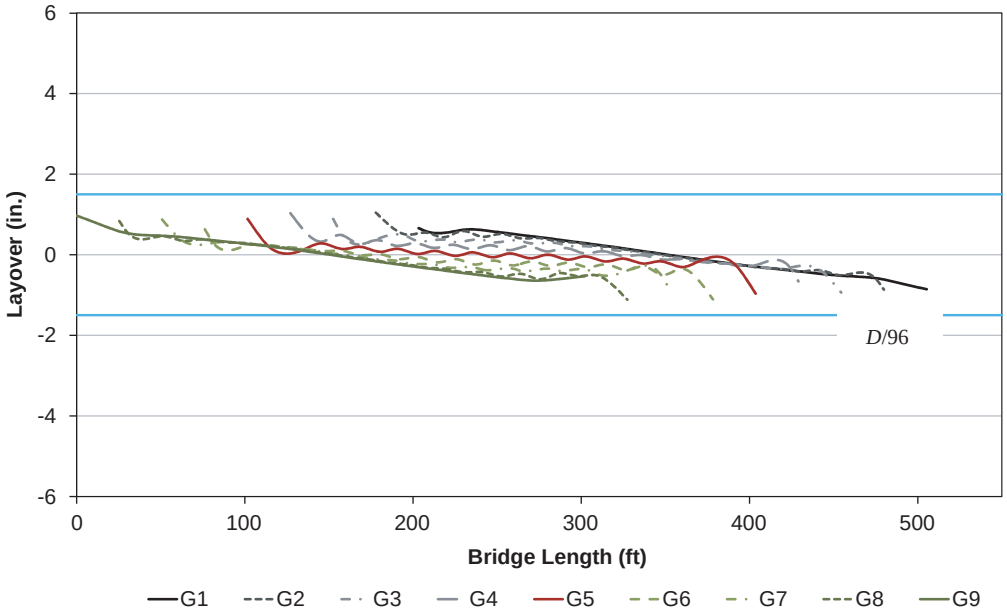

Figure 3-55. Bridge NISSS54 girder "Configuration 4" layovers under total dead load (due to the combined effects of TDLF detailing of the cross-frames and the total dead load effects) for the case where the cross-frames are detailed for TDLF.

shown in Figure 3-55. Many engineers would expect that the girder webs would be perfectly plumb in "Configuration 4" under the total dead load, since TDLF detailing was employed and the same analysis solutions were used consistently throughout the above developments. They would also expect that the girder flange lateral bending stresses would be perfectly zero in this "Configuration 4." However, neither of these assumptions is correct. One can observe from Figure 3-55 that there is still a measurable amount of girder twisting (and corresponding flange lateral bending), particularly in the inner-most girders. Nevertheless, the layover of the webs is within the tolerance of $D/96 = 144$ in./96 = 1.5 in. Therefore, the webs may be considered as "approximately plumb."

The reason why the layovers are not zero in Figure 3-55, as well as why the corresponding girder flange lateral bending stresses discussed subsequently are not zero, is because of the following facts:

- The girders are twisted in the direction opposite to the total dead load displacements (in Figure 3-52) by concentrated lateral loads applied from the cross-frames.
- However, the torsional displacements of the girders under the total dead load, shown in Figure 3-53, are due to the distributed self-weight of the steel as well as the distributed concrete dead load.
- The concentrated lateral loads from the cross-frames, which induce the girder deflections due to the TDLF detailing, cannot possibly produce girder layovers exactly equal and opposite to the effects of the distributed dead loads acting on the girders.

3.3.1.5 Final Girder Vertical Deflections and Vertical Elevations

Figure 3-56 shows the vertical deflections versus the normalized length along the fascia Girder G1 as well as the inner-most Girder G5 for the extreme example skewed I-girder bridge (NISSS54). (The girder normalized length coordinates vary from zero at the bearing at the left end of the bridge to 1.0 at the bearing on right end of the bridge.)

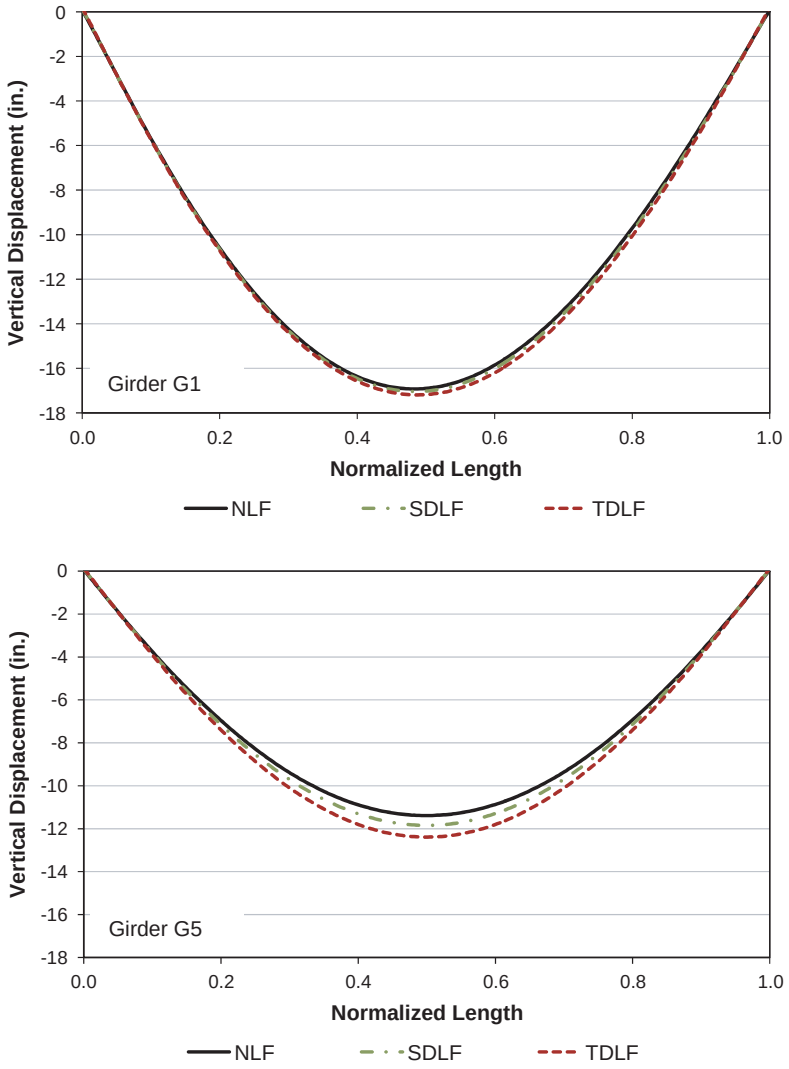

Figure 3-56. Bridge NISSS54 "Configuration 4" vertical deflections under total dead load for different cross-frame detailing methods.

The results for the final (or total) dead load vertical displacements in these plots are shown considering each of the three main cross-frame detailing methods: NLF, SDLF, and TDLF. It can be observed that the mid-span displacements in Girder G5 are slightly smaller at the mid-span when NLF detailing is used. However, the vertical displacements are relatively insensitive to the type of cross-frame detailing. This is generally the case for all straight bridges. The vertical displacements of the fascia girders are essentially the same for all of the detailing methods.

The above displacements can be added to the 3D FEA camber profiles of Figure 3-49 to obtain the final total dead load elevations of the girders. One can observe that the fascia girders are essentially at a "zero" elevation along their full length, whereas the interior Girder G5 has a final "flat" geometry for NLF detailing and is slightly less than 1 in. below the "zero" elevation for TDLF detailing.

3.3.1.6 Cross-Frame Forces

The choice of NLF, SDLF, or TDLF detailing affects more than the girder displacements and stresses. It also can have a significant effect on the cross-frame forces. Figure 3-57 shows the

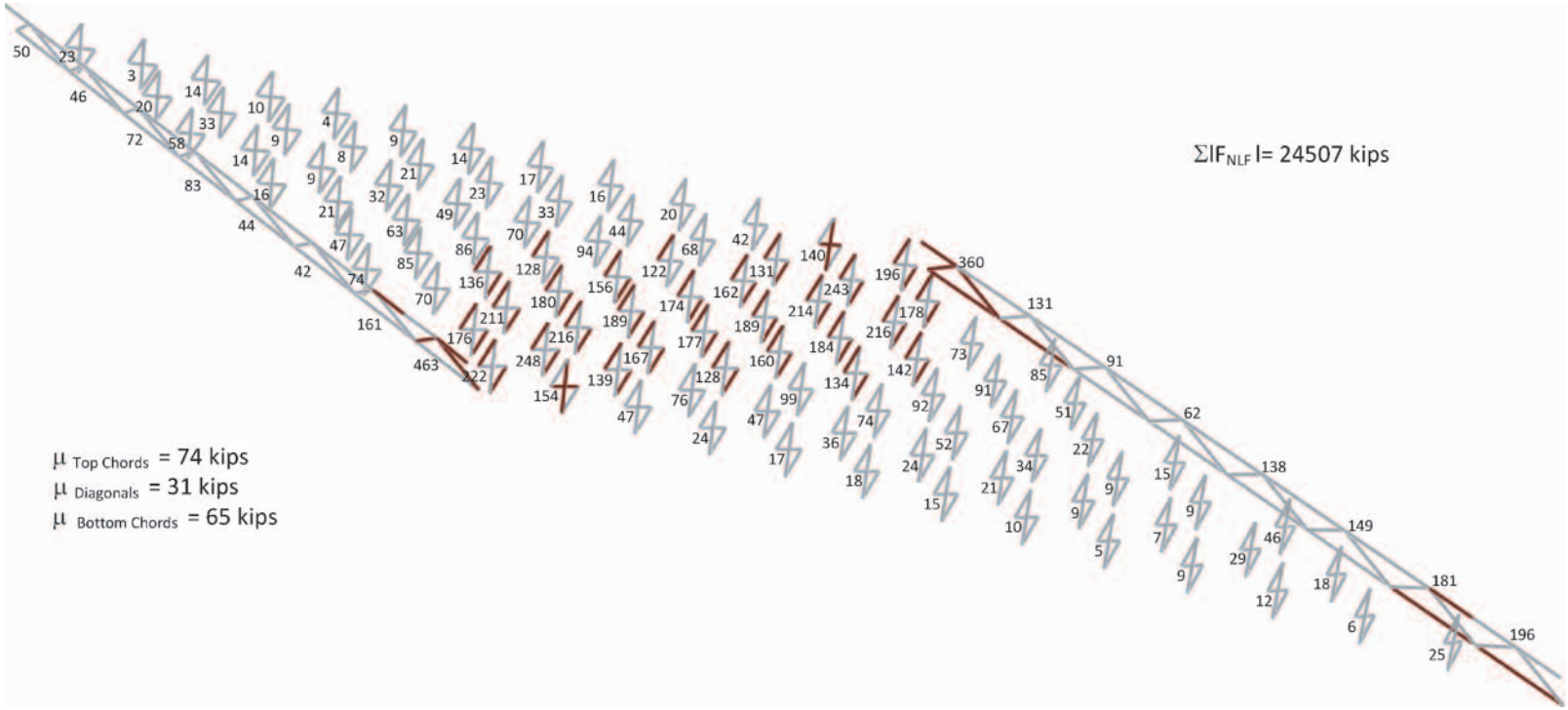

Figure 3-57. Bridge NISSS54 maximum amplitude of the component axial forces in each of the cross-frames under total dead load, NLF detailing of the cross-frames.

maximum magnitude of the total dead load member axial forces in each cross-frame throughout the NISSS54 Bridge for the ideal case where the cross-frames are fabricated NLF. Figure 3-58 parallels Figure 3-57, but shows the total dead load member axial forces in each of the cross-frames for the situation where the cross-frames are fabricated TDLF. One can observe that, in the NLF case, the cross-frame forces are relatively large in the vicinity of the short transverse load path between the obtuse corners of the bridge. The members having the largest axial force appear in bold in Figure 3-57. It should be noted that the figure also shows the mean of the cross-frame member force magnitudes for the cross-frame top chord, the cross-frame diagonals, and the cross-frame bottom chords. In addition, the sum of absolute value of all the cross-frame member forces, $\Sigma|F_{NLF}|$, is shown in the upper right-hand corner of the figure.

Conversely, in Figure 3-58, the cross-frame member axial forces along the short diagonal direction between the obtuse corners are relatively small (but not equal to zero). In this case, the maximum forces are in the diagonals of several "nuisance stiffness" cross-frames that frame into the girders very close to the skewed bearing lines. If these nuisance stiffness cross-frames are offset a sufficient distance from the bearing lines, as discussed subsequently, all of the final total dead load cross-frame forces are relatively small compared to the forces in the NLF case. However, the cross-frame forces generally are increased due to the TDLF detailing effects in the regions near the acute corners of the deck. One can observe that the chord forces are significantly smaller on average in Figure 3-58, but the average diagonal forces are larger compared to Figure 3-57. This is mainly due to the extremely large forces in the cross-frame diagonals at the acute corners, caused by the small offset distance of these cross-frames from the bearing line. These large forces are due to interactions between the first intermediate cross-frame near the acute corners with the bearing line cross-frames and the corresponding need to introduce a large force into the intermediate cross-frame to "pull" the fascia girders back to an approximately plumb position under the total dead load.

Section 8.2.1 of the Task 8 report (Appendix C of the contractors' final report) recommends that the first intermediate cross-frames should be placed a minimum distance of

$$a = \max(1.5D, 0.4b) \qquad \text{Eq. 15}$$

from the bearing line to alleviate the "nuisance stiffness" effects associated with the above spike in the cross-frame forces, where D is the girder depth and b is the second unbraced length within the span from the bearing line.

Figures 3-59 and 3-60 show solutions comparable to the ones in Figures 3-57 and 3-58, but corresponding to the steel dead load condition. The values for the maximum cross-frame forces in these figures are somewhat representative of the difficulty the erector may encounter in fitting up the cross-frames with the girders in an unshored erection scenario. It is apparent from Figure 3-59 that, for the case with NLF detailing, the greatest difficulty may be encountered with the cross-frames located near the bearing lines and along the short diagonal direction. However, for the case of TDLF detailing, the largest cross-frame forces occur near the acute corners. In particular, it is apparent that some of the cross-frame diagonals near the acute corners may be particularly difficult to install. Again, these "nuisance stiffness" effects can be relieved by using a more appropriate offset distance from the bearing line for these cross-frames. This result demonstrates an important fact that fit-up problems tend to be exacerbated by TDLF detailing of the cross-frames.

From Figures 3-57 through 3-60 as a whole, it is apparent that the locked-in force effects in the cross-frames tend to substantially relieve the cross-frame dead load forces in the short, stiff diagonal direction. However, the "locked-in" cross-frame forces in the vicinity of the acute corners tend to be additive with the dead load effects. Also, it is apparent that the TDLF

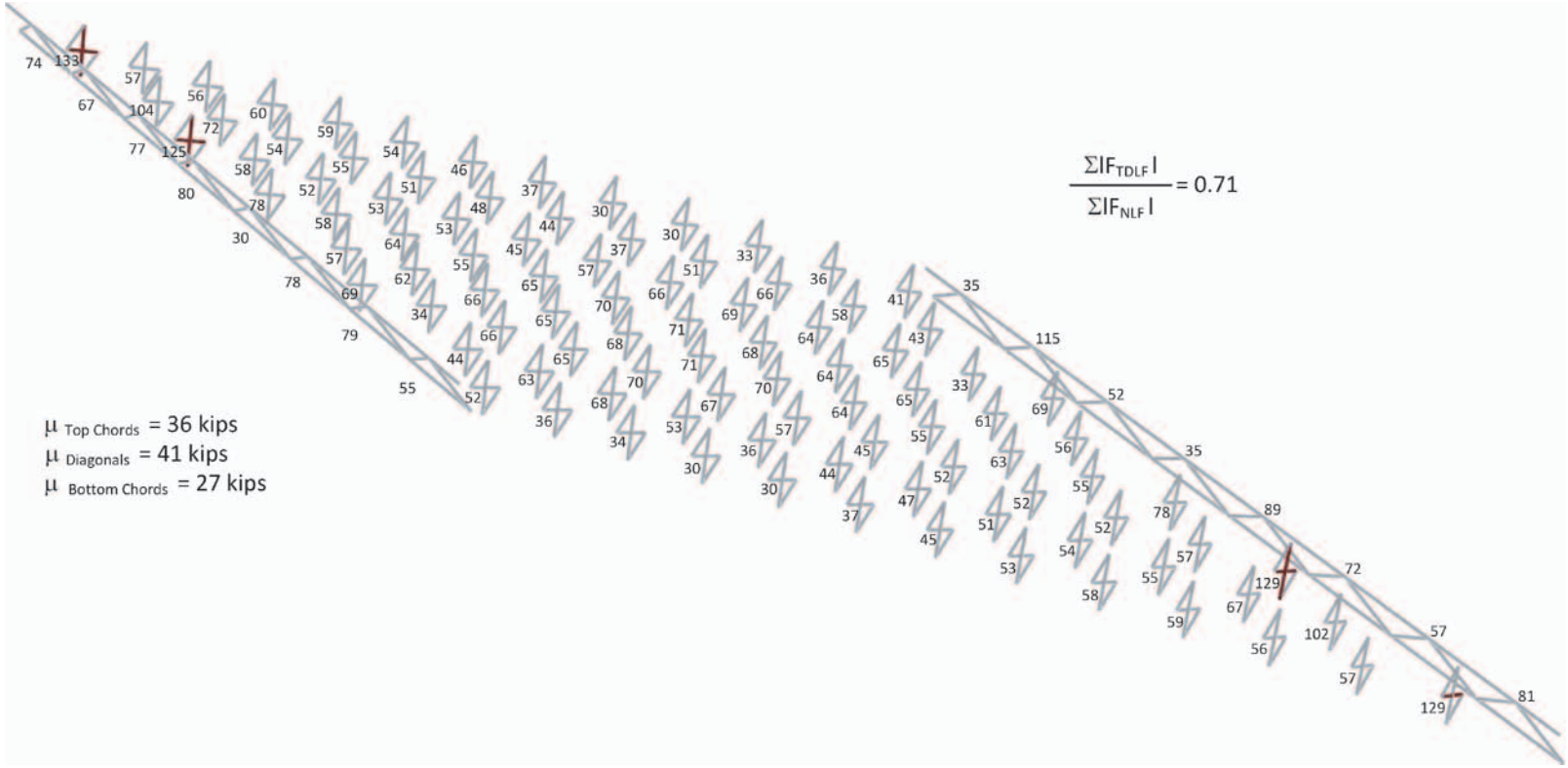

Figure 3-58. Bridge NISSS54 maximum amplitude of the "Configuration 4" component axial forces in each of the cross-frames under total dead load, TDLF detailing of the cross-frames.

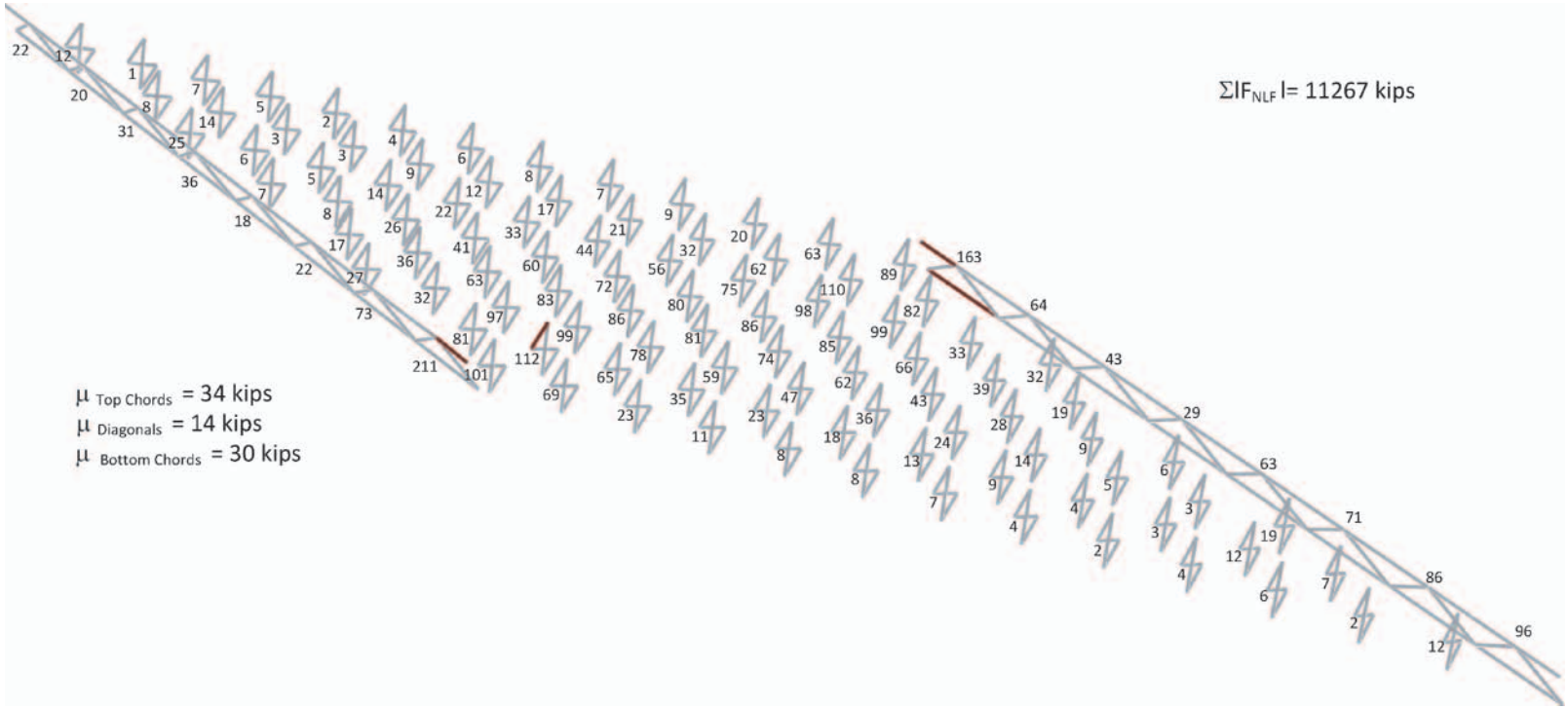

Figure 3-59. Bridge NISSS54 maximum amplitude of the component axial forces in each of the cross-frames under steel dead load, NLF detailing of the cross-frames.

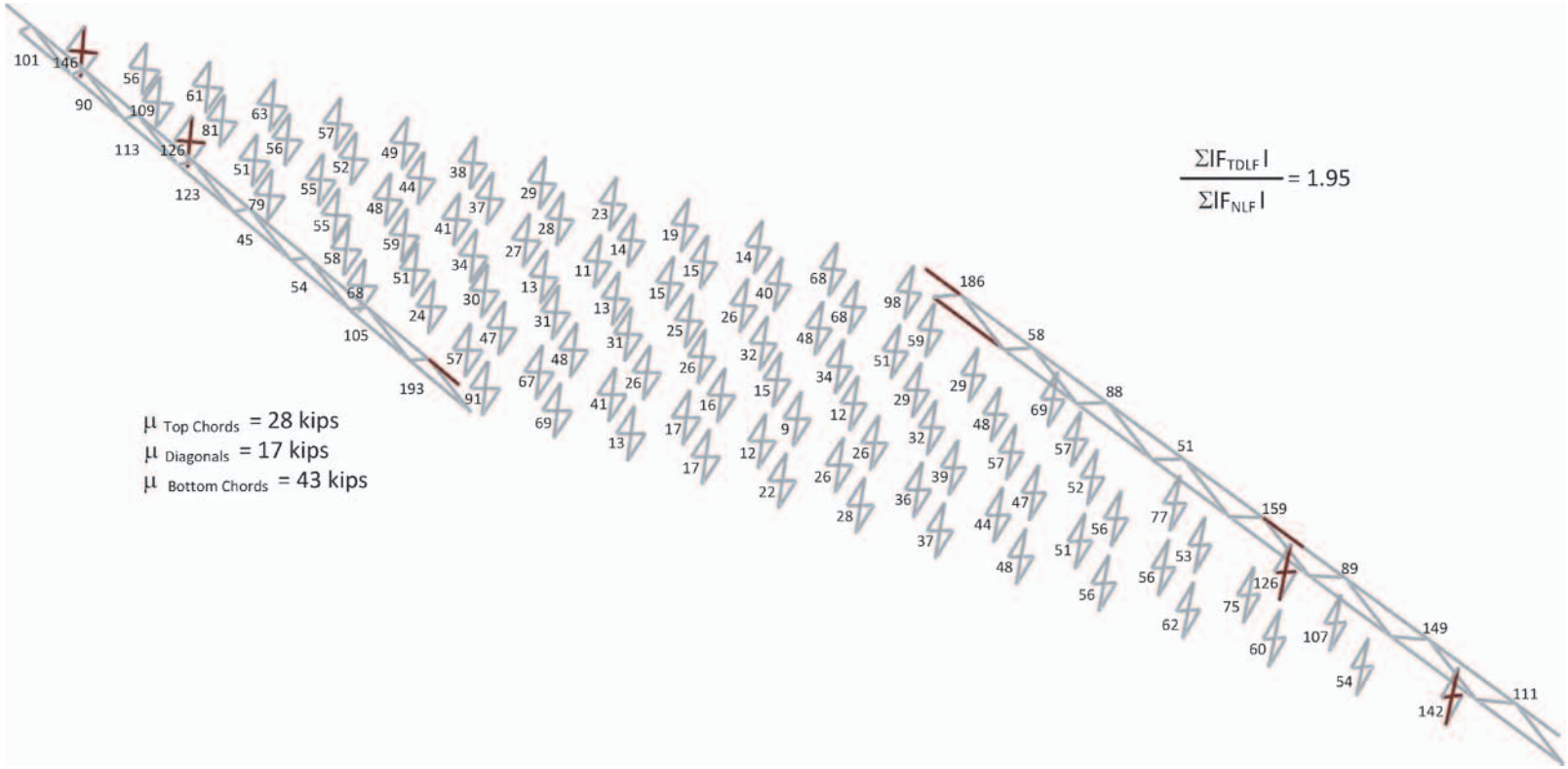

Figure 3-60. Bridge NISSS54 maximum amplitude of the component axial forces in each of the cross-frames under steel dead load, TDLF detailing of the cross-frames.

detailing of the cross-frames tends to exacerbate fit-up problems during the steel erection (due to the fact that the total dead load deflections have not yet been fully taken out of the girders by the application of the total dead loads). Lastly, it should be noted that for NLF detailing of the cross-frames, the forces needed to connect the structure together are theoretically zero if the girders are supported in their no-load position. Therefore, shoring of the girders is a good way to facilitate the erection when NLF detailing is used.

3.3.1.7 Girder Flange Major-Axis and Lateral Bending Stresses

Figure 3-61 shows the top flange major-axis and lateral bending stresses for the fascia Girder G1 and for the inner-most Girder G5 of Bridge NISSS54. The plots in this figure again show the results for all the methods of detailing the cross-frames: NLF, SDLF, and TDLF. Similar to the results for the vertical deflections in G1 and G5, the major-axis bending stresses in these straight girders are relatively insensitive to the type of cross-frame detailing. However, the girder flange lateral bending stresses are substantially affected by whether the detailing of the cross-frames is NLF, SDLF, or TDLF. This should not be surprising given the above results for the girder layovers and cross-frame forces.

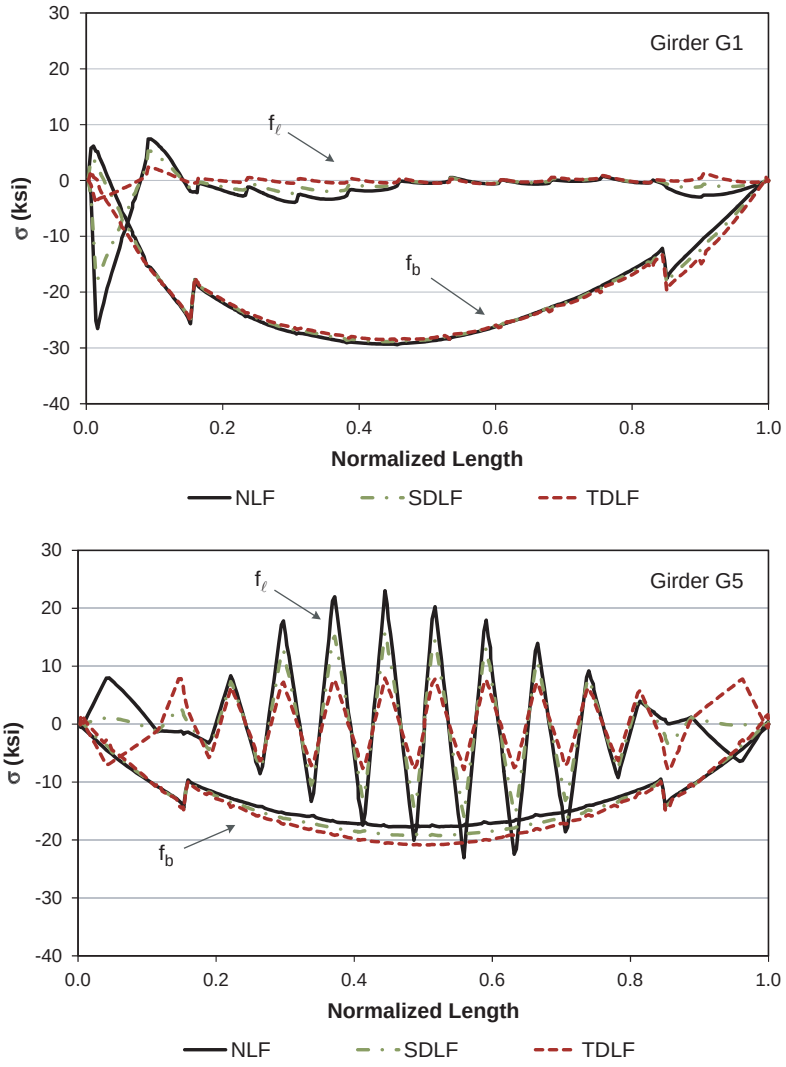

Figure 3-61. Bridge NISSS54 "Configuration 4" top flange stresses under total dead load for different detailing methods.

The girder flange lateral bending stresses are the smallest when TDLF detailing is used. Many engineers expect that if TDLF detailing is used, the flange lateral bending stresses will be essentially zero (under the total dead load condition). This is not generally the case for the same reasons as explained in Section 3.3.1.4. In the fascia girder, the flange lateral bending stress is still approximately 3 ksi near the left-hand end (see the top plot in Figure 3-61). This is related to the same nuisance stiffness effects of framing a number of the cross-frames in too close to the supports observed in Section 3.3.1.6. If the problem cross-frames are offset further from the bearing line, the flange lateral bending stresses in the fascia girder are essentially negligible. It should be noted that some small lateral bending stresses are induced in the top flange of the fascia girder due to the overhang loads.

For the interior Girder G5, significant flange lateral bending stresses are still encountered even for the case of TDLF detailing. These stresses are due to the fact that the locked-in concentrated lateral forces acting on Girder G5 from the cross-frames are not able to cancel the torsional actions of this girder under the distributed total vertical dead load. The maximum flange lateral bending stresses, however, are actually reduced by more than a factor of two by the TDLF detailing effects in Girder G5.

3.3.2 Curved Radially Supported Bridge Example

Figure 3-62 provides the framing plan for a 150-ft. simple-span curved radially supported I-girder bridge with a radius of curvature at its centerline of $R = 438$ ft., a deck width of $w = 30$ ft., and four I-girders spaced at 8 ft. apart. This bridge, named NISCR2, has a connectivity index of $I_C = 4.89$, which places it in the second category of the "C" bridges of Table 3-1. It is expected that a conventional 2D grid analysis may have some difficulty in capturing all the responses of this structure. Figure 3-63 and Table 3-9 give this bridge's plate girder dimensions, and Table 3-10 gives the sizes of its cross-frame members. A number of the attributes of this bridge are simpler than those of the previous example. However, this bridge is important to illustrate several key considerations with respect to SDLF and TDLF detailing effects on horizontally curved geometries.

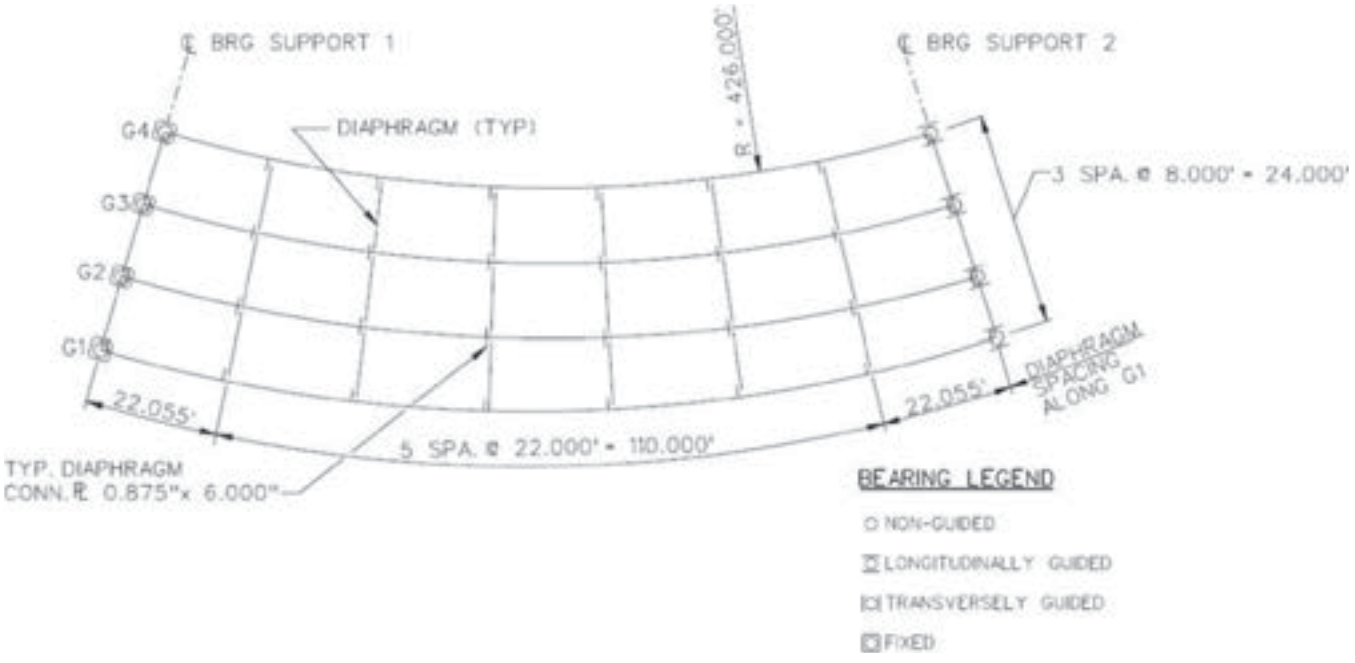

Figure 3-62. Bridge NISCR2 framing plan.

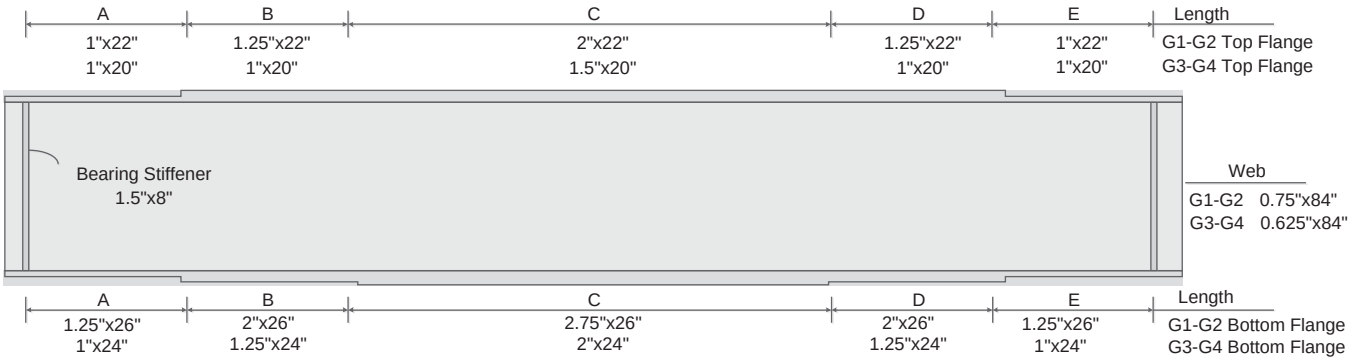

Figure 3-63. NISCR2 girder plate dimensions.

3.3.2.1 Bridge Deflections

Figure 3-64 shows a plan view of the Bridge NISCR2 magnified deformed geometry due to its total dead load. One can observe that there is an overall twisting of the bridge cross-section and all of the girders are laying over in the same direction. However, the layover at the radial supports is zero.

3.3.2.2 Girder Cambers and Camber Differences

As noted in the previous example in Section 3.3.1, SDLF and TDLF detailing are driven by the girder camber profiles or, more specifically, by the differential camber at the cross-frame locations. Figure 3-65 shows the total dead load differential cambers for Bridge NISCR2. One can observe that all the cambers are negative values, indicating that in all cases, the girders with a smaller horizontal radius of curvature have smaller dead load deflections in this bridge. Similar to the previous example, the discussions are focused on the behavior for TDLF detailing of the cross-frames unless noted otherwise.

3.3.2.3 System Deflections Due to Initial Lack-of-Fit Effects

Figure 3-66 shows the deflections of NISCR2 after the cross-frames are first connected to the girders in "Configuration 2" (see Figure 3-30b), second, the girders are "unlocked" and "released" from their initial no-load plumb geometry, and third, the girders are deformed by the cross-frames into Configuration 3 (described in Figure 3-30c). In other words, Figure 3-66 shows the "final" deformed geometry due to the locked-in forces caused by the TDLF detailing of the cross-frames.

Table 3-9. NISCR2 girder plate lengths (ft.).

Girder	A	B	C	D	E
G1	20.0	20.0	74.1	20.0	20.0
G2	19.6	19.6	72.8	19.6	19.6
G3	19.3	19.3	71.5	19.3	19.3
G4	18.9	18.9	70.2	18.9	18.9

Table 3-10. NISCR2 cross-frame member sizes.

Cross-Frame Type	Top Chord	Diagonals	Bottom Chord
Interior (X type)	L6x6x0.75	L6x6x0.75	L6x6x0.75
End (Inverted V)	L6x6x0.75	L6x6x0.75	L6x6x0.75

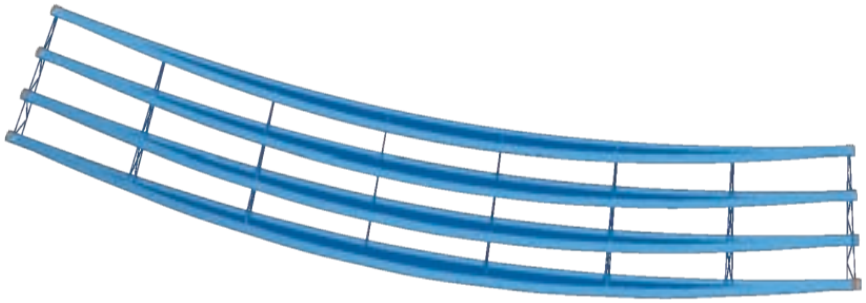

Figure 3-64. Bridge NISCR2 total dead load deflected geometry for the case of NLF detailing of the cross-frames (scale factor = 20x).

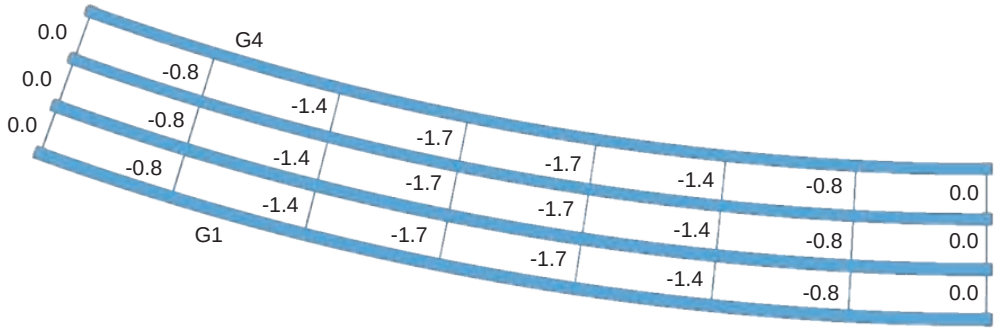

Figure 3-65. Bridge NISCR2 total dead load camber differences (differential camber values) between girders.

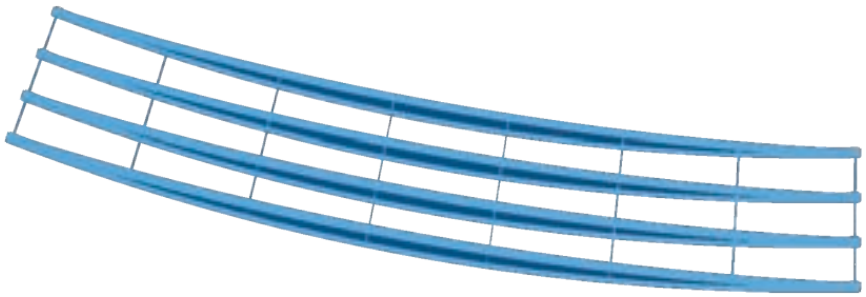

Figure 3-66. Bridge NISCR2 "Configuration 3" deflected shape due to the initial lack-of-fit effects from TDLF detailing of the cross-frames (scale factor = 20x).

One can observe that the bridge deformations in Figure 3-66 are approximately the opposite of the deflections shown in Figure 3-64. Similar to the previous example, they are not exactly equal and opposite.

3.3.2.4 Approximate Canceling of Dead Load Layovers by Dead-Load Fit Effects

Figure 3-67 shows the girder layovers in this bridge once the steel and concrete dead load effects have been added to deflect the structure conceptually from the previously discussed "Configuration 3" to "Configuration 4" (see Figure 3-30c and d). Results similar to those obtained in the previous skewed bridge example are observed in that each of the girder

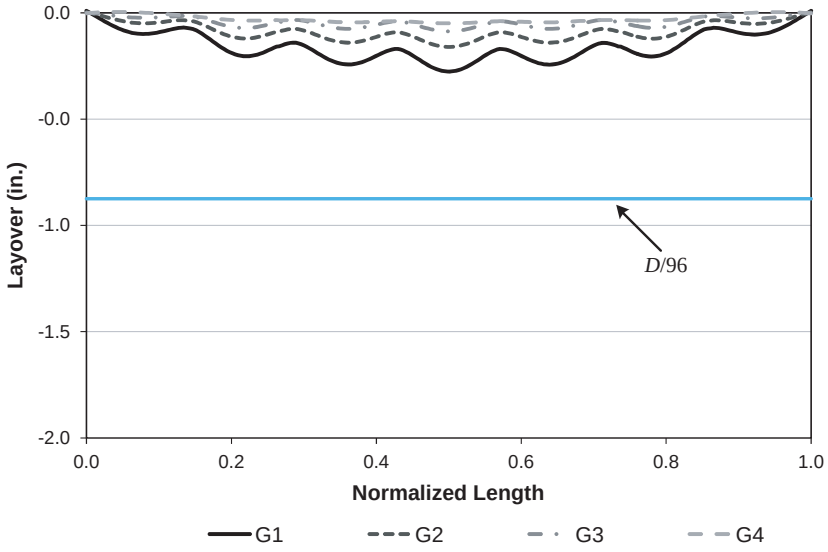

Figure 3-67. Bridge NISCR2 "Configuration 4" girder layovers under total dead load for the case where the cross-frames are detailed for TDLF.

layovers is strictly non-zero; however, the final layovers are well within the typical tolerance of $D/96 = 84$ in./96 = 0.875 in. Also, as stated previously, the layovers cannot possibly be expected to be exactly equal to zero because the TDLF detailing effects are applied to the girders as concentrated lateral loads from the cross-frames, whereas the total dead load layovers are caused by distributed vertical loads.

Figure 3-68 illustrates the girder layovers in Bridge NISCR2 under the steel dead load when TDLF detailing of the cross-frames is used. Clearly, the girders are not plumb under the steel dead load. They are still rotated in the direction opposite to the direction that they twist under the action of the vertical loads. However, these layovers also satisfy the $D/96$ tolerance. Lastly,

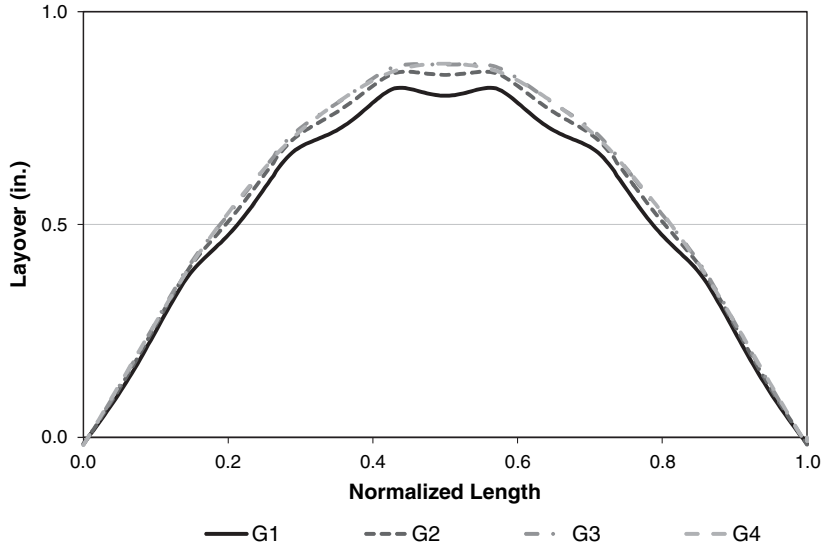

Figure 3-68. Bridge NISCR2 girder layovers under steel dead load for the case where the cross-frames are detailed for TDLF.

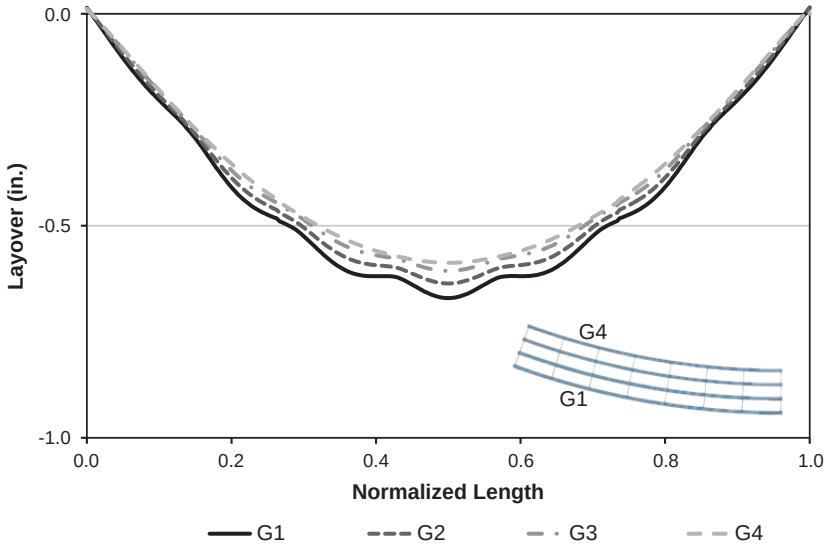

Figure 3-69. Bridge NISCR2 girder layovers under steel dead load for the case where the cross-frames are detailed for NLF.

Figure 3-69 shows the girder layovers under the steel dead load for the case of NLF detailing of the cross-frames, while Figure 3-70 indicates the corresponding layovers under the total dead load. It can be observed that the layovers under the total dead load violate the above *D*/96 tolerance. Nevertheless, rigorous test simulation studies show that this layover does not have any measurable effect on the system capacity.

3.3.2.5 Final Girder Vertical Deflections

Figure 3-71 shows the vertical deflections along the length of the fascia Girder G1 on the outside of the horizontal curve as well as the fascia Girder G4 on the inside of the curve of Bridge NISCR2. The results in these plots are shown for each of the three main cross-frame detailing

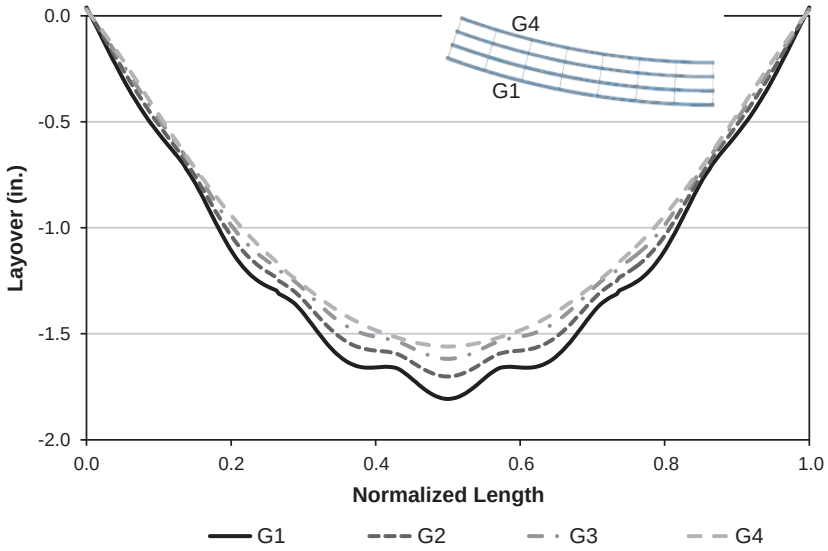

Figure 3-70. Bridge NISCR2 girder layovers under total dead load for the case where the cross-frames are detailed for NLF.

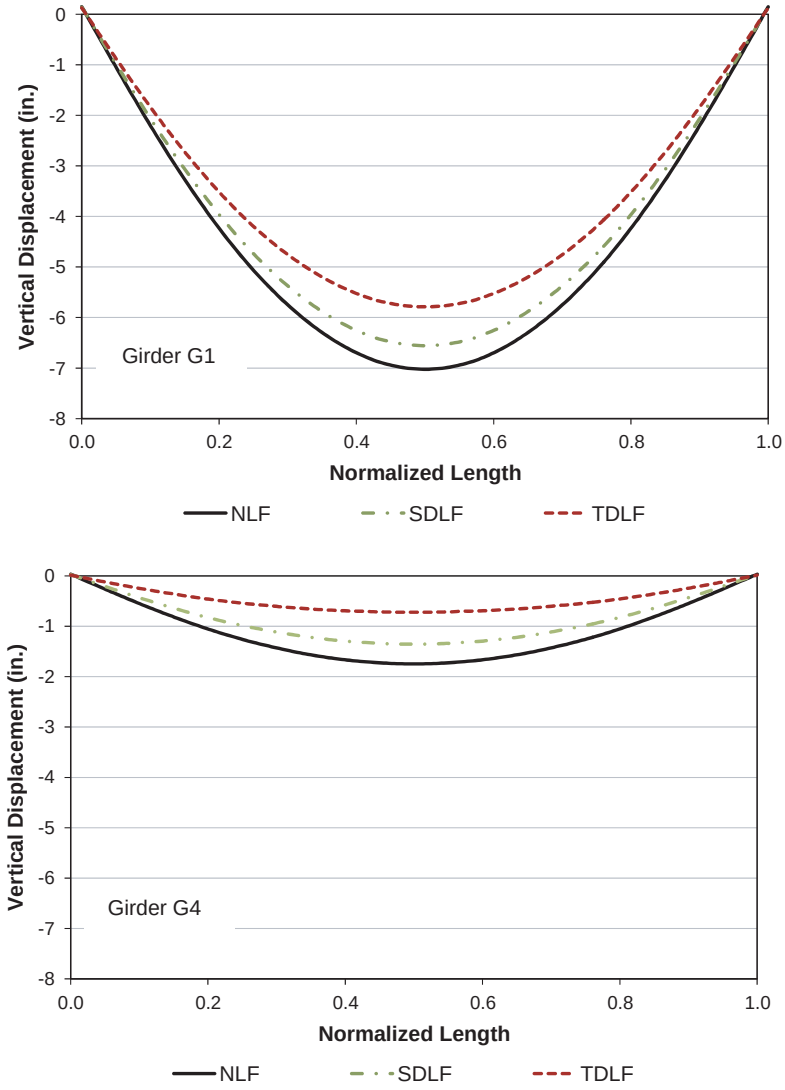

Figure 3-71. Bridge NISCR2 vertical deflections under total dead load for different cross-frame detailing methods.

methods: NLF, SDLF, and TDLF. One can observe that the percentage differences between these vertical displacement solutions are significantly larger than observed in the previous straight bridge example. Generally, the vertical displacements in horizontally curved bridges tend to be affected to a larger degree by the SDLF and TDLF detailing effects than in straight bridges. The mid-span vertical displacement of G1 in this specific example is 7 percent smaller than the solution for NLF when SDLF detailing is used. It is 17 percent smaller when TDLF detailing is employed.

One other important observation that should be made from Figure 3-71 is that the influence on the vertical displacements from the SDLF detailing (i.e., the differences between the SDLF and NLF curves) are similar for all of the girders in the NISCR2 Bridge. The SDLF detailing reduces the displacements of all the girders equally by approximately 0.4 in. This statement also can be made regarding the influence of the TDLF detailing on the girder vertical displacements. The TDLF detailing reduces all the girder displacements by approximately 1.2 in. This is a general finding for all curved radially supported bridges and is demonstrated subsequently for several other bridges of this type.

3.3.2.6 Cross-Frame Forces

Figures 3-72 through 3-74 show the individual cross-frame member axial forces under the total dead load in the NISCR2 Bridge for the cases of NLF, SDLF, and TDLF detailing of the cross-frames, respectively. These figures indicate that the cross-frame chord forces are not significantly affected in this bridge by the type of cross-frame detailing. However, all the diagonal forces are significantly increased. The increase in the mean of the axial force in the diagonals is 35 percent for SDLF detailing versus NLF. The increase is 100 percent for TDLF detailing of the cross-frames.

Correspondingly, Figures 3-75 through 3-77 show the individual cross-frame member axial forces under the steel dead load in the NISCR2 Bridge for NLF, SDLF, and TDLF. As discussed previously, the internal cross-frame forces in these solutions provide an indication of any potential difficulty regarding the fit-up of the cross-frames with the girders during the steel erection. One can observe again that the chord forces are not affected significantly

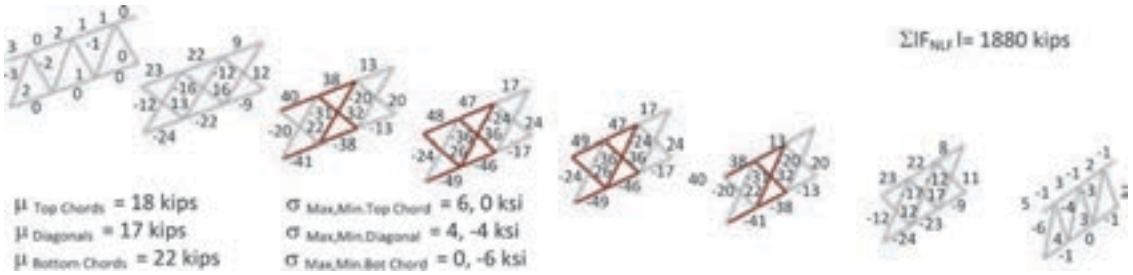

Figure 3-72. Bridge NISCR2 maximum amplitude of the component axial forces in each of the cross-frames under total dead load, NLF detailing of the cross-frames.

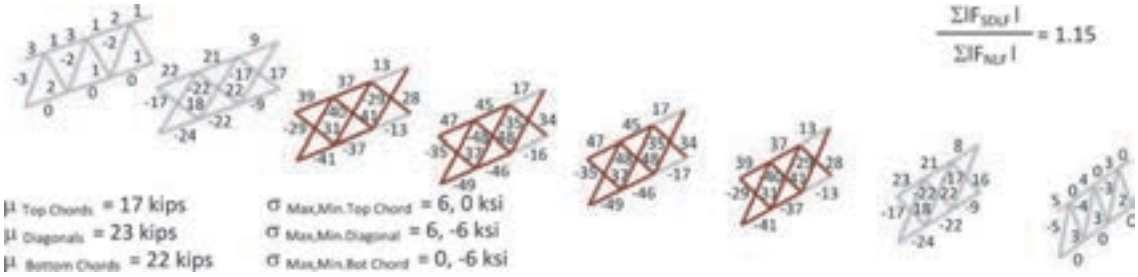

Figure 3-73. Bridge NISCR2 maximum amplitude of the component axial forces in each of the cross-frames under total dead load, SDLF detailing of the cross-frames.

Figure 3-74. Bridge NISCR2 maximum amplitude of the component axial forces in each of the cross-frames under total dead load, TDLF detailing of the cross-frames.

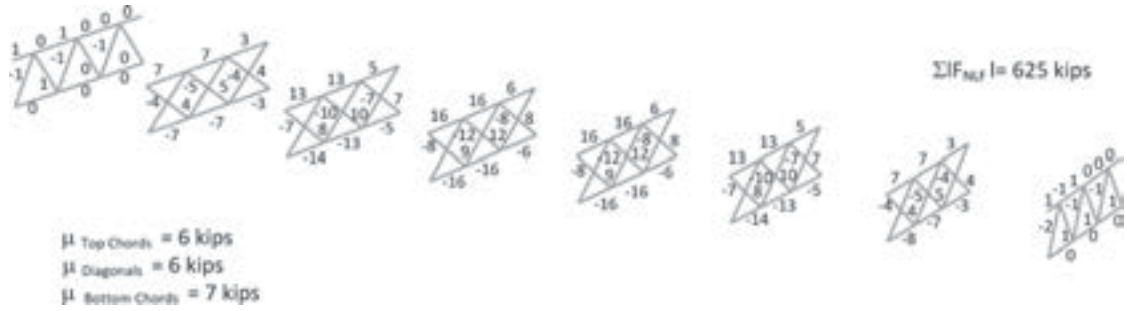

Figure 3-75. Bridge NISCR2 maximum amplitude of the component axial forces in each of the cross-frames under steel dead load, NLF detailing of the cross-frames.

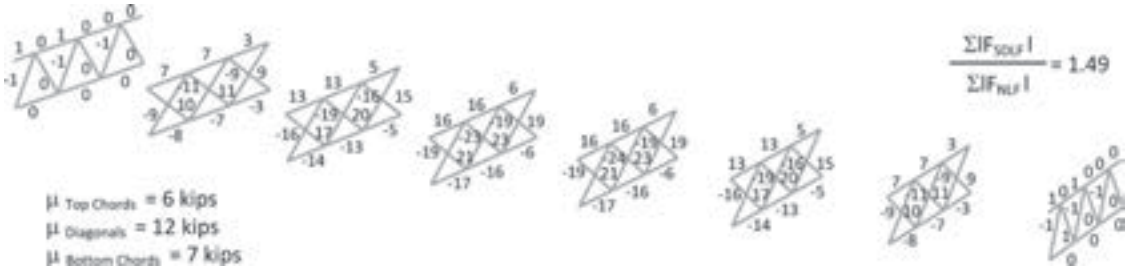

Figure 3-76. Bridge NISCR2 maximum amplitude of the component axial forces in each of the cross-frames under steel dead load, SDLF detailing of the cross-frames.

Figure 3-77. Bridge NISCR2 maximum amplitude of the component axial forces in each of the cross-frames under steel dead load, TDLF detailing of the cross-frames.

by the cross-frame detailing type. However, the mean of the diagonal forces is increased by 100 percent from the NLF detailing to the SDLF case, and 283 percent from NLF to TDLF. Based on the results in Figure 3-77, one can conclude that the span length and radius of curvature for NISCR2 is such that the cross-frame fit-up forces are expected to be manageable for any of the methods. However, for a comparable bridge with a tighter radius curvature and/or a longer span length, the above percentage differences may be of greater significance.

Based on the full set of bridge studies performed within NCHRP Project 12-79, the locked-in forces in the cross-frame diagonals always tend to be additive with the dead load effects when SDLF or TDLF detailing is used on curved radially supported bridge structures. Also, the chord forces tend to be increased, but not as much so. These are important findings. One can conclude that locked-in force effects generally should be considered when sizing the cross-frames in horizontally curved I-girder bridges. (These conclusions are independent of the specific sequence of girder erection, since assuming the structure remains elastic, and neglecting aspects such as

friction at the supports and non-zero connection tolerances, the bridge is a conservative elastic system for which the responses are path independent.)

3.3.2.7 Girder Flange Major-Axis and Lateral Bending Stresses

Figure 3-78 gives the top flange major-axis and flange lateral bending stresses for Girders G1, G2, and G4 in the NISCR2 Bridge. The plots in this figure again show the results for all the methods of detailing the cross-frames: NLF, SDLF, and TDLF. One can observe that the major-axis bending stress in the girders is insensitive to the type of cross-frame detailing. This is a common result for horizontally curved structures, even though the girder vertical displacements exhibit some sensitivity to these attributes. This sensitivity is related to the coupling between the girder vertical displacements and the twist deformations in curved members.

Conversely, the curved I-girder flange lateral bending stresses show some sensitivity to the cross-frame detailing type. This is due to the fact that, in a curved radially supported bridge, the locked-in cross-frame forces due to SDLF or TDLF detailing tend to displace the flanges laterally, and in a direction opposite to the direction the girders are tending to bend and twist under the vertical loads. These actions occur over the full span length of the girders. In the specific case of the NISCR2 Bridge, as well as other generally curved and radially supported structures, the flanges act effectively as continuous-span beams loaded effectively by uniformly distributed lateral loads coming from the horizontal curvature. The cross-frames are the supports for these effective continuous-span beams.

The influence of SDLF or TDLF detailing on the effective continuous span beams is to essentially "pre-stress" the flanges by displacing their supports in the direction opposite to the equivalent horizontal curvature loading. On the inside Girder G4 of NISCR2, this "pre-stressing" is the dominant effect, essentially shifting the entire flange lateral bending moment diagram throughout the span. However in Girders G1 and G2, this pre-stressing effect is manifested predominantly in an increase in the flange "negative bending" moments and flexural stresses (using the above continuous-span beam analogy). These "negative bending stresses" are relatively small in this bridge, but they are increased by a maximum of approximately 20 percent due to SDLF detailing and 66 percent due to TDLF detailing.

3.3.3 General Considerations

3.3.3.1 Key Results from Studies of the Ford City Bridge (EICCR11)

Because of its relative simplicity, Bridge NISCR2 considered in the previous section is useful to illustrate the influence of SDLF and TDLF cross-frame detailing effects on general horizontally curved bridges. Furthermore, this structure is illustrative of the behavior for reasonably "regular" curved I-girder bridges with relatively short-to-moderate span lengths.

The Ford City Bridge (EICCR11) shown in Figures 3-79 through 3-81 represents the most extreme case encountered in the NCHRP Project 12-79 research regarding the influence of the cross-frame detailing method on the girder layovers, vertical displacements, and flange lateral bending stresses. This three-span continuous I-girder bridge has one straight end span of length 321 ft., a straight center span of 445 ft., and a highly curved end span of 292 ft. The minimum radius of curvature in the curved span is 511 ft. Furthermore, the bridge has a relatively narrow deck with $w = 48.2$ ft. given its span lengths. The torsion index on its curved span (Equation 1) is $I_T = 0.87$. In addition, its four girders are 14 ft. deep and are spaced at 13.5 ft. apart. The circles in Figure 3-81 are highlighting a come-along beam that is being used to stabilize the curved girder during lifting. A cable goes up to a lifting beam from each end of the come-along beam.

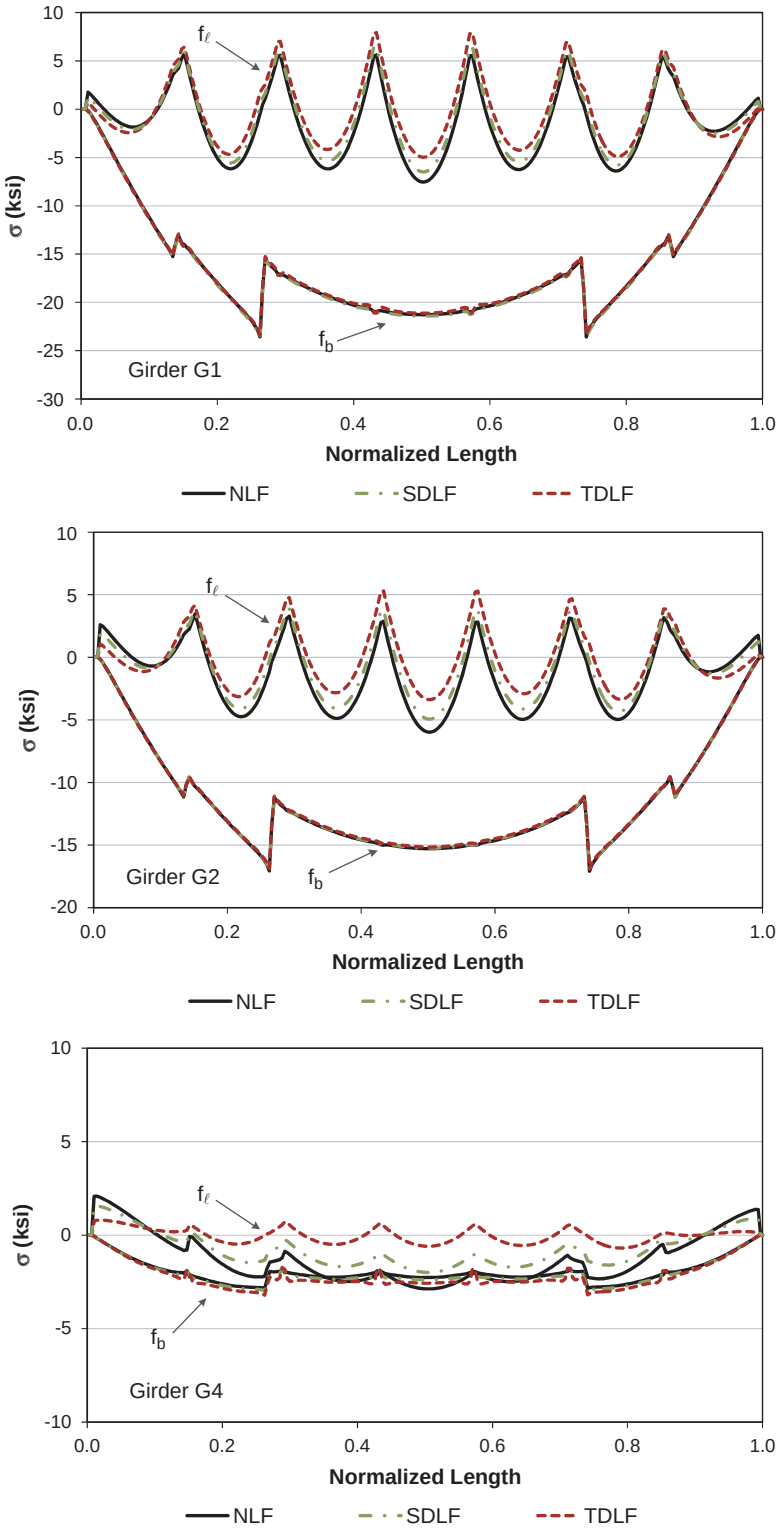

Figure 3-78. Bridge NISCR2 top flange stresses under total dead load for different detailing methods.

Figure 3-79. Ford City Bridge (EICCR11) (Chavel, 2008).

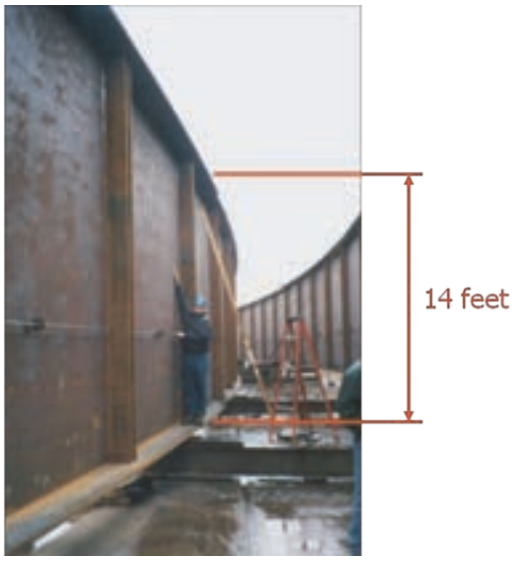

Figure 3-80. Ford City Bridge (EICCR11) girder depth and spacing (Chavel, 2008).

Figure 3-81. Ford City Bridge (EICCR11) installation of drop-in segment (Chavel, 2008).

The combination of the above attributes, along with various other factors, make the Ford City Bridge possibly one of the most challenging curved I-girder bridges that has ever been erected. This bridge was not originally designed with a top flange lateral bracing (TFLB) system, but one was provided as shown in Figure 3-79 to facilitate the steel erection and concrete deck placement. This bridge was studied without a TFLB system in the NCHRP Project 12-79 research so that legitimate comparisons could be made between the 3D FEA simulations and simplified 1D line-girder and 2D-grid methods (since the 1D line-girder and 2D-grid solutions are generally not sufficient for I-girder bridges with TFLB systems).

Figure 3-82 provides a plan view of three magnified displaced shapes from the 3D FEA simulation model of the Ford City Bridge. These images illustrate the influence of the different methods of cross-frame detailing on the torsional and lateral bending response of the bridge. It is apparent that there are substantial layovers, lateral movements, and span interactions in the bridge if it is constructed with NLF detailing. SDLF detailing reduces these deformations substantially, whereas TDLF detailing gives effectively plumb webs under the total dead load. Unfortunately, because of the size and close spacing of the girders on this bridge, TDLF detailing results in prohibitive fit-up forces. Therefore, SDLF detailing, or possibly detailing for an intermediate condition between NLF and SDLF, is the best option for this bridge. Based on the analytical studies from the NCHRP Project 12-79, NLF detailing tends to minimize the cross-frame internal forces under the intermediate and final steel dead load conditions in curved radially supported bridges and also tends to minimize the forces required to fit-up the steel in these structure types.

Figure 3-83 plots the girder layovers associated with the deflected geometries from Figure 3-82 and shows that the maximum layovers under the total dead load are 3.6 in. when SDLF detailing is used. The NCHRP Project 12-79 research studies show that these displacements do not have any significant impact on the strengths. Generally, if the stability (second-order amplification) checks of Sections 3.1.1.1 and 3.1.1.2 are satisfied and the cross-frames satisfy stability bracing requirements (Helwig, 2012), the influence of girder layover on the structural resistance is sufficiently addressed and does not need to be considered any further.

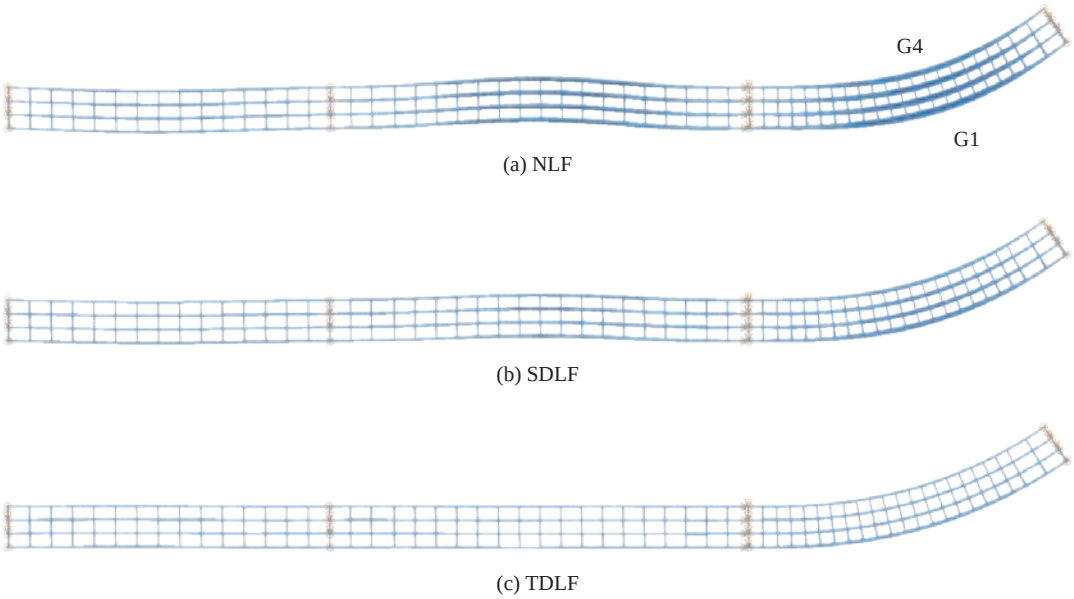

Figure 3-82. Ford City Bridge (EICCR11) deflected shape under total dead load for different detailing methods (scale factor = 10x).

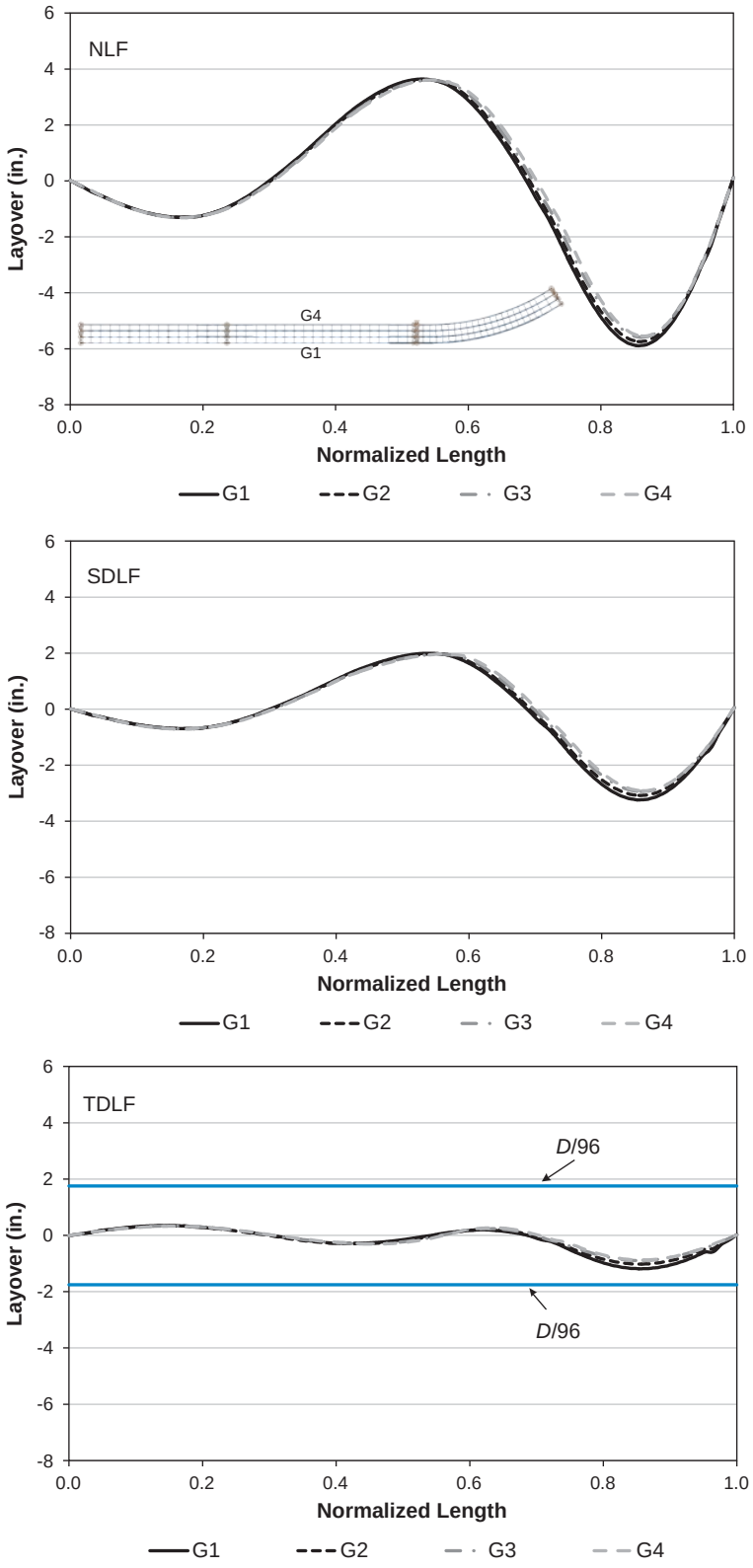

Figure 3-83. Ford City Bridge (EICCR11) girder layovers under total dead load for different detailing methods.

Figure 3-84 shows the vertical deflections from the above 3D FEA simulations of the Ford City Bridge. One can observe that the maximum vertical displacement on Girder G1 under the total dead load is 19.1 in. if NLF detailing were used, 16.9 in. if SDLF detailing were used, and 14.9 in. for TDLF detailing. Girder G4 experiences a more dramatic effect on its vertical deflections due to the span torsional interactions. The curved span on G4 sees a maximum downward displacement of 3.2 in. with NLF detailing of the cross-frames, a maximum upward displacement of 1.7 in. with SDLF detailing, and a maximum upward displacement of 3.4 in. with TDLF detailing. These differences are large enough such that it is clear that the influence of the type of cross-frame detailing would need to be considered in setting the girder cambers in this bridge.

As noted previously for the NISCR2 Bridge (see Section 3.3.2.5 and Figure 3-71), SDLF or TDLF detailing tends to have a similar effect on all of the girder vertical displacements within a given bridge. In Figure 3-84, one can observe that the vertical displacements of all the girders are reduced by the SDLF and TDLF detailing effects in the right-hand curved end-span of the Ford City Bridge. Correspondingly, all the vertical displacements are increased by these effects in the

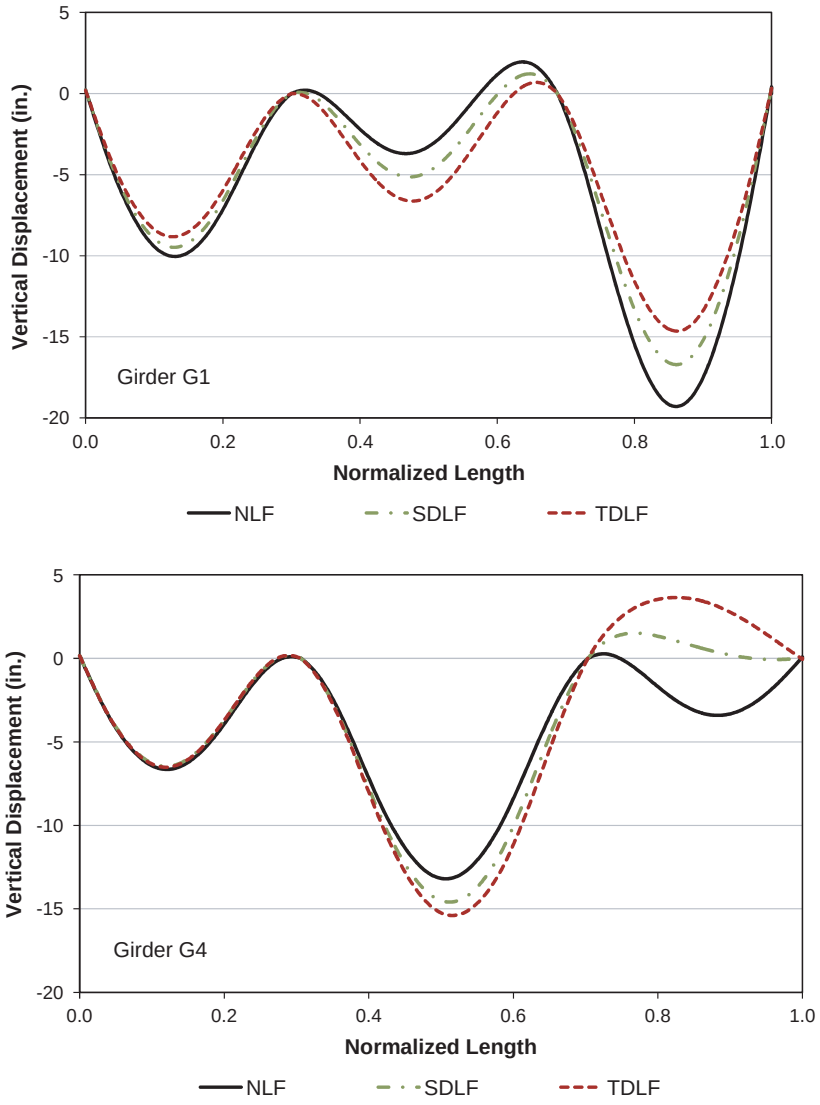

Figure 3-84. Ford City Bridge (EICCR11) vertical deflections under total dead load for different detailing methods.

middle span. The SDLF and TDLF influences on the Girder G1 and G4 displacements, given by the differences between the SDLF and NLF and the TDLF and NLF curves, are somewhat different in the Ford City Bridge however. This is due to the interaction between the continuous spans.

3.3.3.2 Consideration of the Influence of Cross-Frame Connection Tolerances on the Development of Locked-in Forces Due to SDLF or TDLF Detailing

One question that may be asked regarding the influence of SDLF or TDLF detailing is whether small connection tolerances can add up to relieve the locked-in forces to a substantial degree. This question can be evaluated in an informative but simplified fashion using the FHWA Test Bridge (EISCR1) considered in prior Section 3.2. Figure 3-85 shows an isometric view of the 3D FEA simulation model for this structure, illustrating the undeformed geometry as well as the "Configuration 3" geometry explained previously in Figure 3-30c. This is the conceptual configuration in which the girders are "unlocked" and "released" such that the cross-frames impose deformations on them due to the initial lack of fit. However, the vertical loads conceptually have not been applied to the structure at this stage.

Figures 3-86 and 3-87 show the vertical displacements and the flange major-axis and lateral bending stresses under the total dead load (unfactored) for the cases where the cross-frames are detailed for NLF and for TDLF. These results closely parallel the results presented previously in Figures 3-71 and 3-78 for Bridge NISCR2. Basically, the method of detailing can have a significant influence on both of these quantities in horizontally curved I-girder bridge structures.

Figure 3-88 shows the corresponding cross-frame forces in the test bridge associated with NLF and TDLF detailing of the cross-frames. These results show the same trends as illustrated earlier for the NISCR2 Bridge in Figures 3-72 and 3-74 (i.e., the cross-frame diagonal forces can be increased substantially by the use of TDLF detailing in horizontally curved bridges). Similar results are obtained for SDLF detailing, but the increase in the cross-frame forces is smaller.

It is useful to plot the responses induced solely due to the TDLF detailing, to understand their magnitudes before addressing the connection tolerance question. Figure 3-89 shows the vertical displacements induced in Girder G1 on the outside of the horizontal curve and in Girder G3 on the inside of the horizontal curve corresponding to the deformed "Configuration 3" geometry from Figure 3-85. One can observe that comparable vertical displacements are induced in both girders due to the effects of the TDLF detailing (consistent with the previous results shown in Figures 3-71 and 3-84). Figure 3-90 shows the corresponding major-axis and flange lateral bending stresses in the girders due to the initial lack-of-fit effects from the TDLF detailing method, and

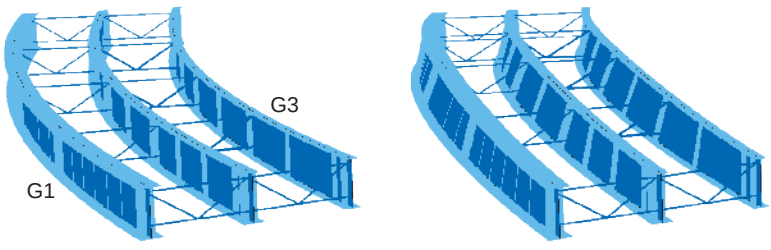

Figure 3-85. FHWA Test Bridge (EISCR1) undeflected geometry and "Configuration 3" deflected geometry due solely to the initial lack of fit from TDLF detailing of the cross-frames.

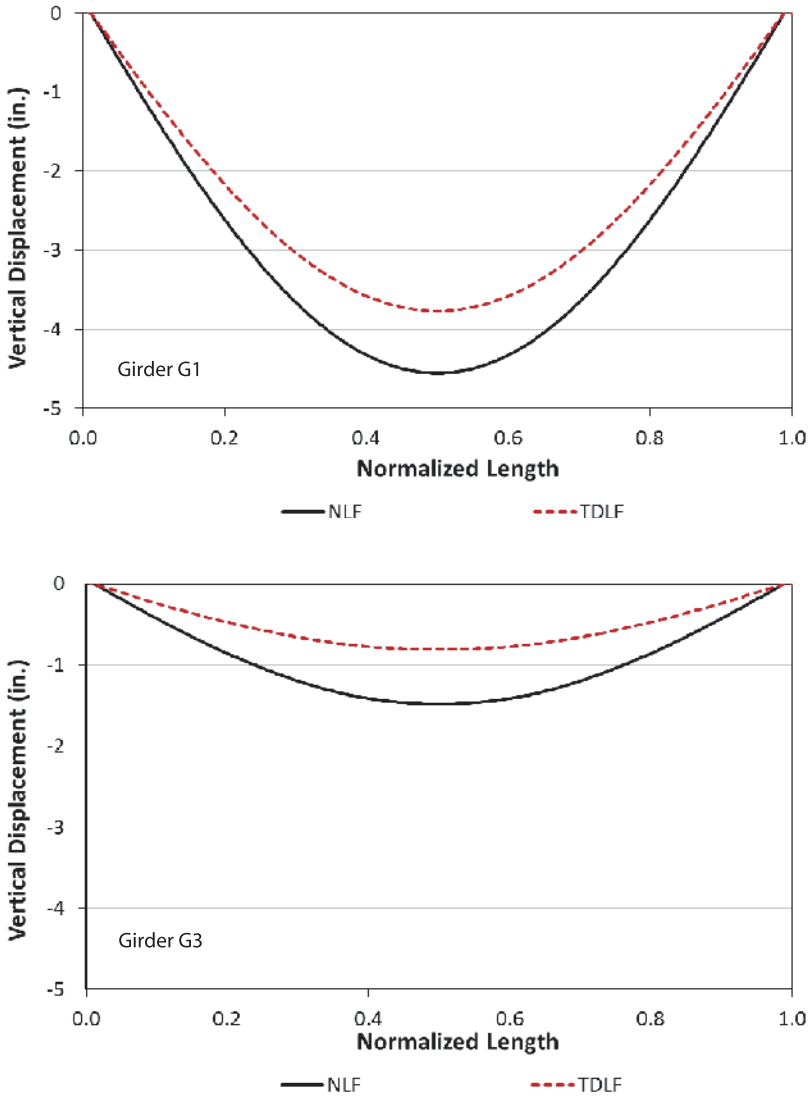

Figure 3-86. FHWA Test Bridge (EISCR1) vertical displacements under total dead load (unfactored) for NLF versus TDLF detailing of the cross-frames.

Figure 3-91 shows the "Configuration 3" cross-frame forces (note that the cross-frame forces in Figure 3-91 are not exactly equal to the difference between the cross-frame forces in Figures 3-88a and 3-88b due to small second-order effects).

Figure 3-92 illustrates the loading mechanism causing a reduction in the downward vertical displacements in all of the girders due to TDLF detailing in the FHWA Test Bridge. Basically, the locked-in forces in the intermediate cross-frames generate an internal couple that is applied to each of the girders at the intermediate cross-frame locations. These couples are balanced by couples in the opposite direction at the bridge bearing lines. The applied internal couples at the intermediate cross-frames twist the girders in the opposite direction from the direction they displace under the total dead load. However, because of the horizontal curvature, the girders cannot twist in this fashion without the girder vertical displacements also being reduced.

In order to obtain a "representative upper-bound" estimate of "slip" at the connections due to small connection tolerances, two scenarios were considered as shown in Figure 3-93. In the first

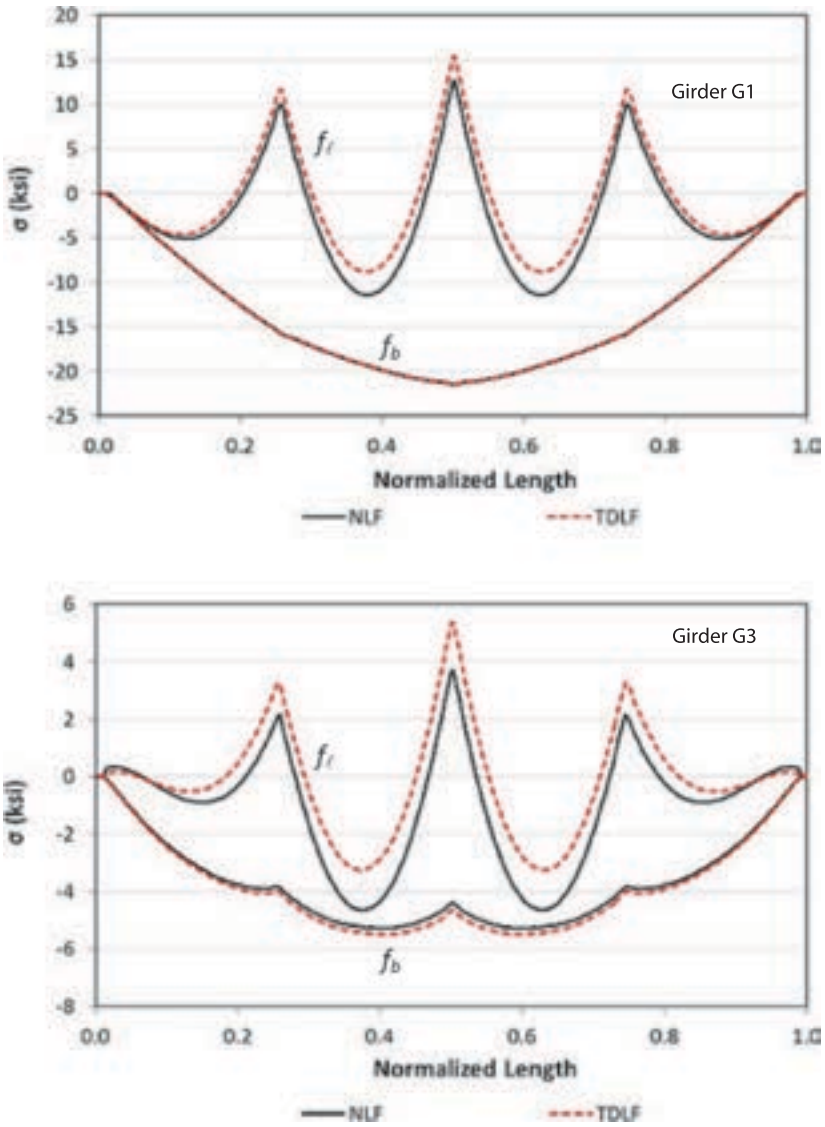

Figure 3-87. FHWA Test Bridge (EISCR1) major-axis bending and flange lateral bending stresses under total dead load (unfactored) for NLF versus TDLF detailing of the cross-frames.

scenario, a ⅛-in. axial movement, or "slip," was assumed in *all* the intermediate cross-frame diagonals of the test bridge. The bridge deformations due to these connection movements are shown in the top image of Figure 3-93. In the second scenario, a ⅛-in. "slip" was assumed in both chords of the three intermediate cross-frames in the direction of their dead load and TDLF axial forces. The deformations corresponding to these movements are shown in the bottom image of Figure 3-93. Figures 3-93 through 3-95 show plots of the corresponding induced girder vertical displacements, flange major-axis and lateral bending stresses, and cross-frame forces due to the first scenario above, and Figures 3-96 through 3-98 show plots of these responses due to the second scenario.

The above ⅛-in. magnitude is obtained by assuming standard size bolt holes 1/16-in. larger than the fasteners and assuming that nominally (or on average) the bolts are in the center of the holes. Then, assuming two plies in every connection, the ideal "slip" that can occur at a given connection is 1/16-in. This value is then multiplied by two to account for the ideal influence of the connection slip at each end on the elongation or shortening of each member.

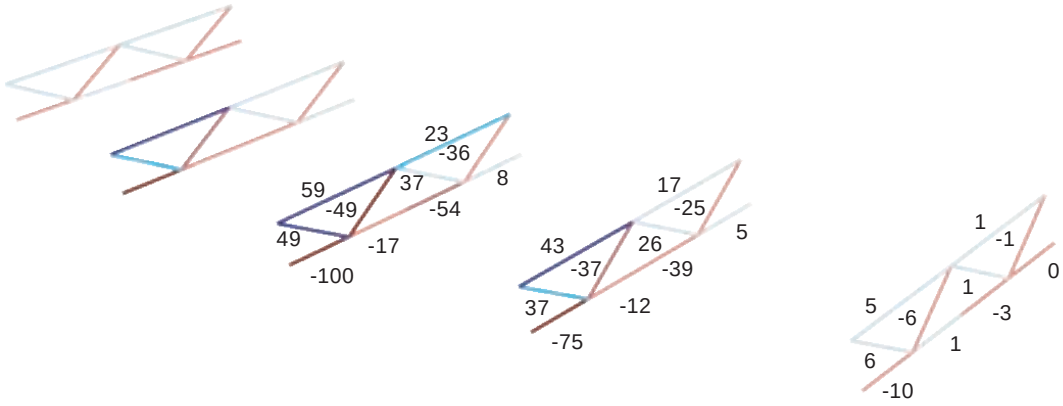

(a) NLF detailing

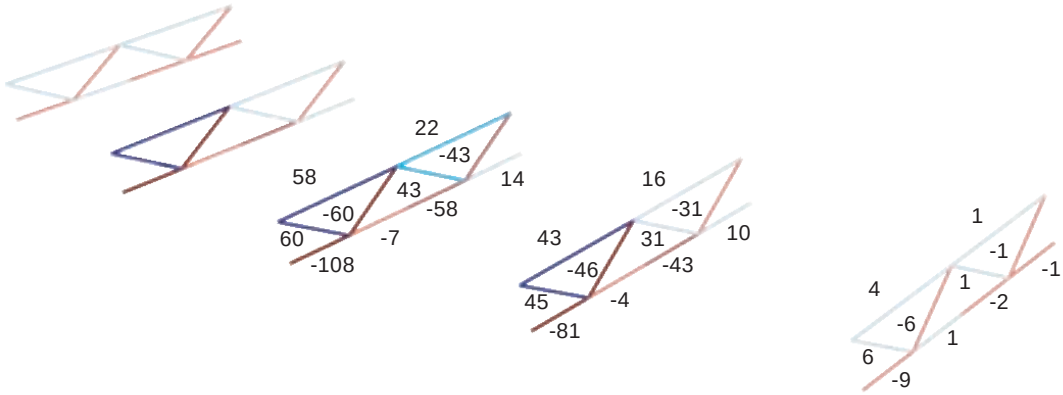

(b) TDLF detailing

Figure 3-88. Cross-frame forces under total dead load (unfactored) for NLF versus TDLF detailing of the cross-frames.

By comparing the values in the above plots, one can observe that the locked-in forces from the TDLF detailing can indeed be reduced to some extent by "joint slip" within standard connection tolerances. However, in this bridge, the TDLF effects are significantly larger than the effects of these "slip" displacements. The other key point that can be noted by considering the above influence of the "slip" displacements is that the use of oversize holes to allow adjustment in the structure basically amounts to giving up control of the geometry by the amount that the connections can move. In addition, the connections have to be engaged before the cross-frames can brace the girders.

This example again shows that the locked-in forces in the cross-frames generally are additive with the dead load effects when SDLF or TDLF detailing is used on curved radially supported bridge structures. Therefore, one can conclude that locked-in forces generally should be considered when sizing the cross-frames in horizontally curved I-girder bridges.

Figures 3-99 and 3-100 provide a combined summary of the above results in terms of the influences of TDLF detailing, as well as the upper-bound connection tolerance movements on the vertical displacements and the girder layovers. The dark solid curve in these figures shows the results for NLF detailing of the cross-frames, and the dashed curve shows the results with TDLF. The light solid curve illustrates the combined results of TDLF detailing along with the ⅛-in. slip in each of the cross-frame diagonals. Finally, the dot-dash curve shows the result of a ⅛-in. slip in all of the internal cross-frame members (diagonals and chords), in the direction of their axial forces, combined with the influence of the TDLF detailing.

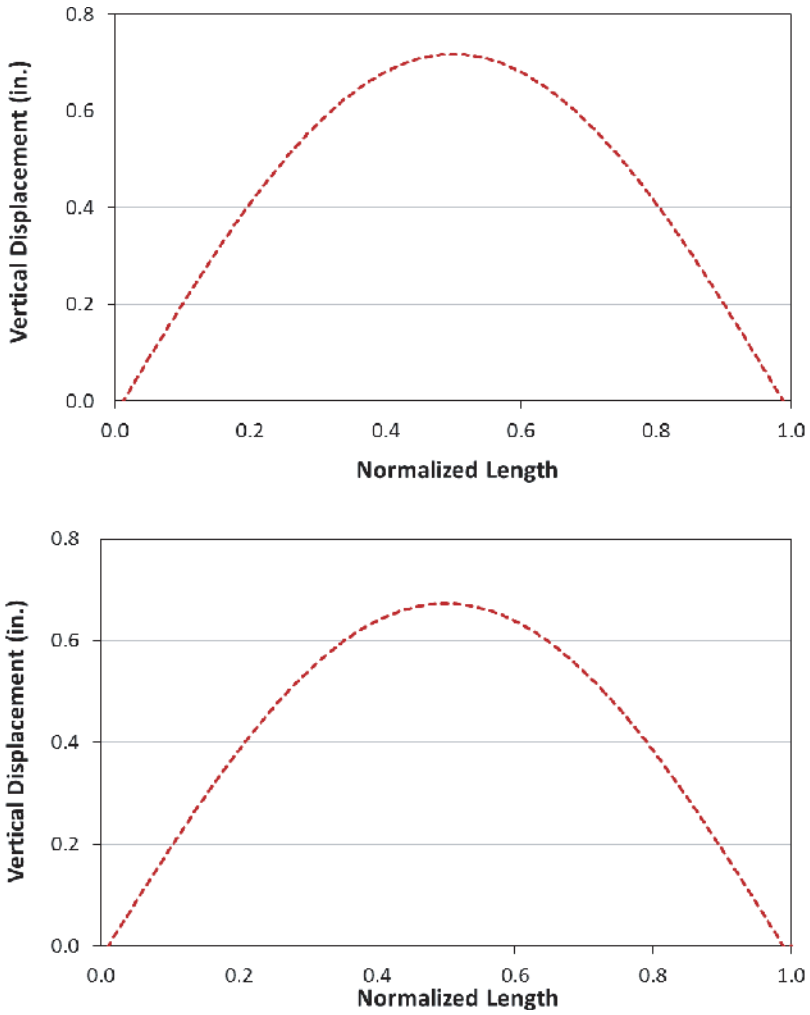

Figure 3-89. FHWA Test Bridge (EISCR1) "Configuration 3" vertical displacements solely due to the initial lack-of-fit effects from TDLF detailing of the cross-frames.

One can conclude that "slip" due to standard connection tolerances within the cross-frames can indeed reduce the influence of TDLF detailing by a significant fraction. However, this is based on a representative upper-bound effect of standard connection tolerances. Indeed, if the TDLF detailing is successful at achieving its objective of approximately plumb webs under the total dead load, then the corresponding girder locked-in vertical deflections, internal stresses, and cross-frame forces would be induced. Similar results are obtained for SDLF detailing, but again, the SDLF effects are smaller (and hence the potential influence of connection tolerances tends to be larger with respect to these effects). In horizontally curved bridges, it can be concluded that TDLF and SDLF detailing effects generally should be included in the structural analysis, since they tend to produce an additive effect on the girder "negative" flange lateral bending stresses and on the cross-frame forces.

3.3.3.3 Potential Influence of Other Connection Tolerances

The previous section considered several scenarios giving an indication of the influence of representative cross-frame connection tolerances on the final constructed geometry, the cross-frame forces, and the girder major-axis and flange lateral bending stresses in the FHWA Test Bridge (EISCR1). It was shown that these connection tolerances can indeed have a measurable effect.

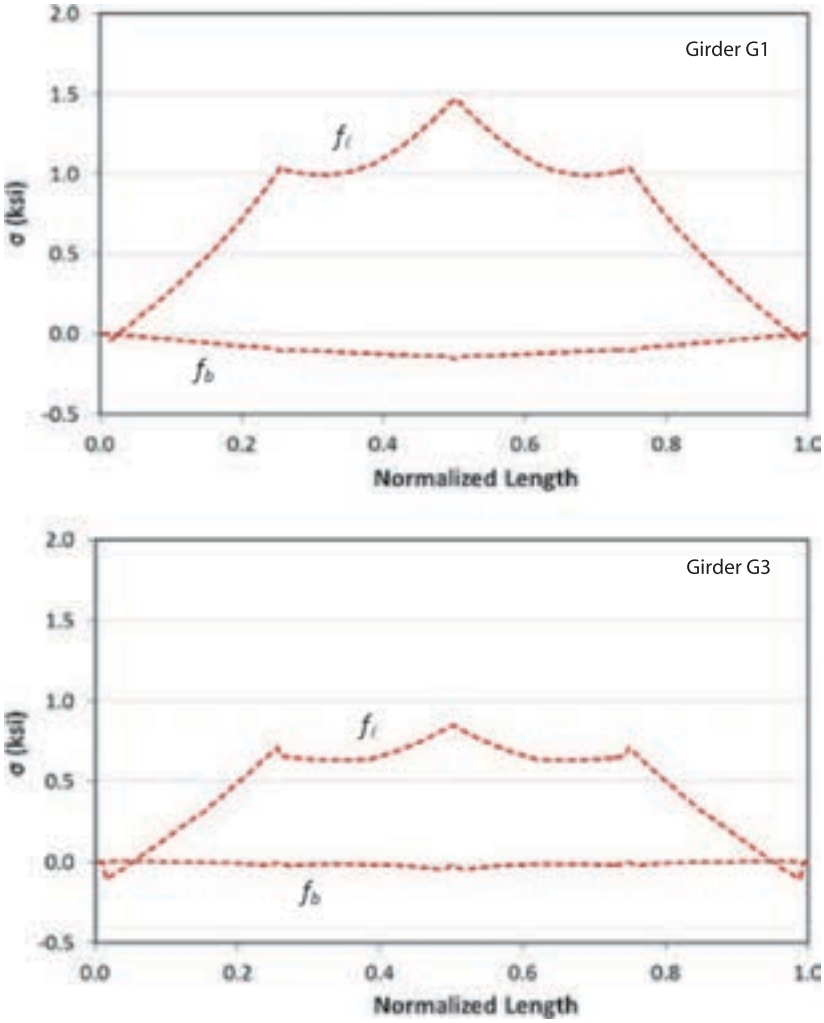

Figure 3-90. FHWA Test Bridge (EISCR1) "Configuration 3" top flange major-axis and lateral bending stresses solely due to the initial lack-of-fit effects from TDLF detailing of the cross-frames.

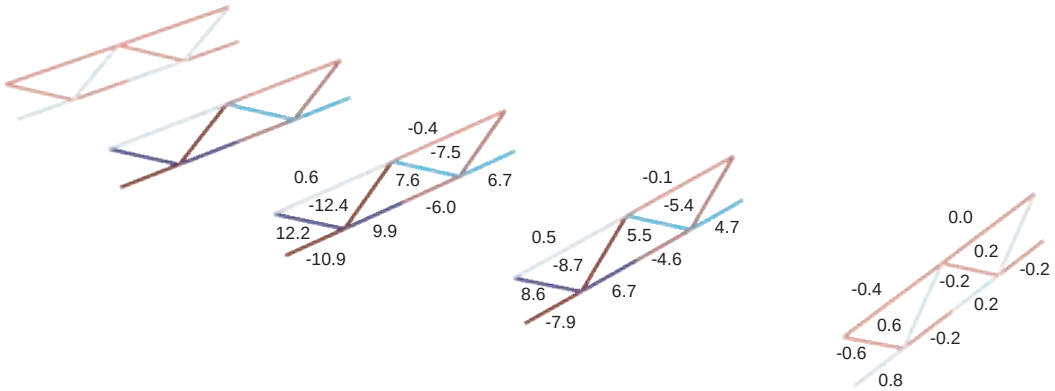

Figure 3-91. FHWA Test Bridge (EISCR1) "Configuration 3" cross-frame forces solely due to the initial lack-of-fit effects from TDLF detailing of the cross-frames.

However, the influence on the overall displacements is not as large as erectors would commonly expect for more general structures based on experience. The discussion below addresses one example scenario where the connection tolerance effects can be significantly larger.

Figure 3-102 illustrates the potential impact of a relative "slip" between the top and bottom of a girder splice. In this case, the impact of the displacement Δ_{slip} between the top and the bottom of the splice is multiplied by the length-to-depth ratio (L/D) of the girder field section. Basically, whenever there is a significant ratio of this sort, there is a lever effect that can have a substantial influence on the constructed geometry. This "lever effect" can also occur across the width of the bridge due to the types of cross-frame connection "slip" displacements discussed in the previous section. However, the FHWA Test Bridge is not wide enough relative to its length to exhibit a significant "lever effect" of the cross-frame connection slip displacements.

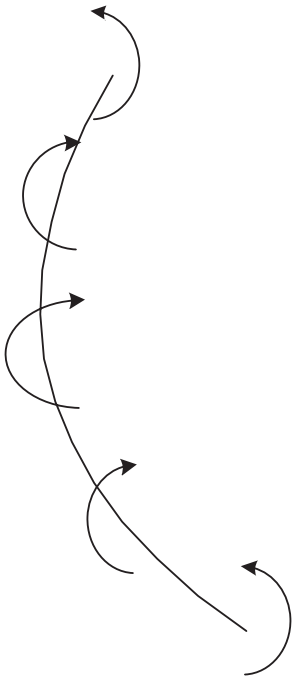

Figure 3-92. Loading mechanism associated with an increase in all the girder vertical displacements due to TDLF detailing in the FHWA Test Bridge (EISCR1).

3.3.4 When Should Locked-in Forces from SDLF or TDLF Detailing be Considered in a Structural Design Analysis?

Table 3-11 summarizes the recommendations and their corresponding rationale from Ozgur (2011) pertaining to the question: When must locked-in forces from SDLF or TDLF detailing be considered in the structural design analysis? Alternately, this question can be phrased as: When can a curved and/or skewed I-girder bridge be designed based on an analysis that assumes NLF detailing, but then the cross-frames are detailed subsequently for either SDLF or TDLF without any significant consequences? The answers are listed in terms of the key bridge responses and are all based on the assumption that the girder cambers are based on

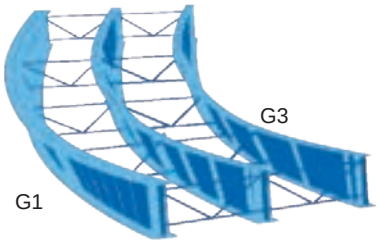

Deformations due to +1/8 inch "slip" in all intermediate cross-frame diagonals (scale factor = 100x)

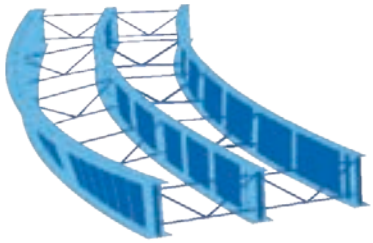

Deformations due to +1/8 inch "slip" in all intermediate cross-frame top and bottom chords (scale factor = 100x)

Figure 3-93. FHWA Test Bridge (EISCR1) deformed geometry solely due to ⅛-in. "slip" in the direction of the internal load in all the intermediate cross-frame diagonals and due to ⅛-in. slip in the direction of the internal load in all the intermediate cross-frame chords.

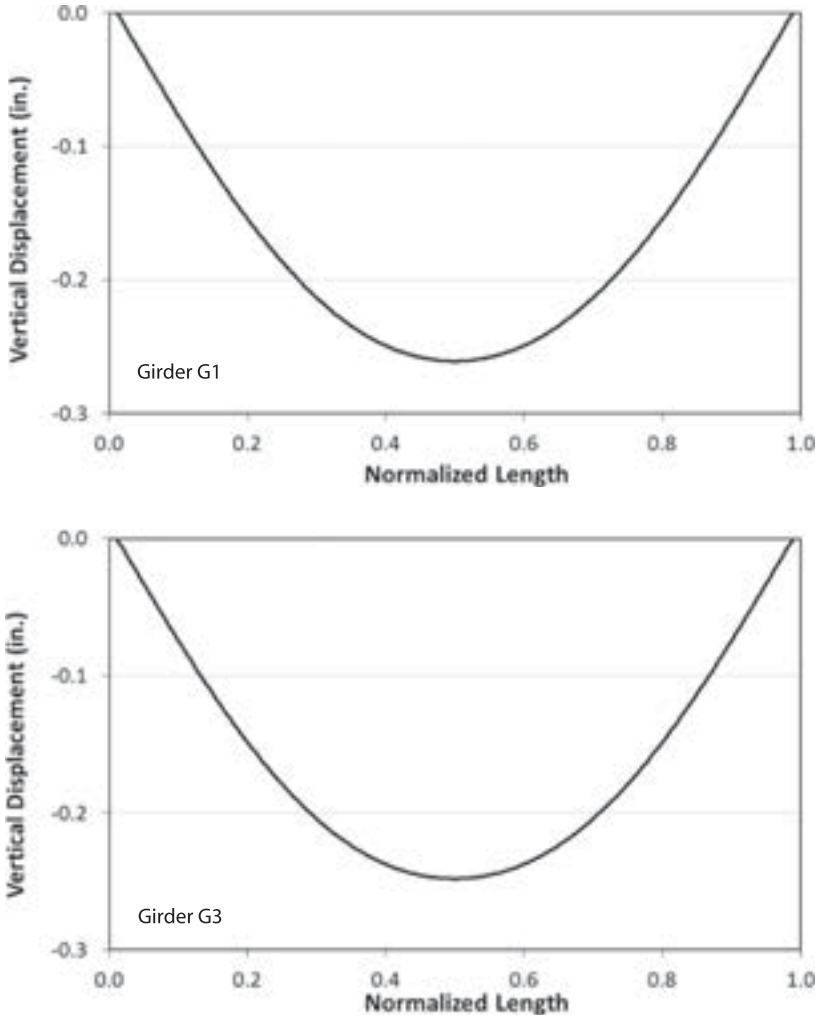

Figure 3-94. FHWA Test Bridge (EISCR1) vertical displacements solely due to ⅛-in. slip in the direction of the internal load in all of the intermediate cross-frame diagonals.

an accurate 2D-grid or 3D FE analysis (see Appendix A for a definition of these terms). These findings are derived from the detailed study of the various bridges analyzed in the NCHRP Project 12-79 Task 8A research.

Based on the basic illustrative examples in Sections 3.3.1 to 3.3.3, one can observe clearly that the answer to the above questions is different for straight-skewed and horizontally curved, radially supported bridges. Furthermore, in short, it can be stated that the influence of SDLF and TDLF detailing on bridges that have both horizontal curvature and skew can involve any combination of the attributes shown for the above distinct bridge types. However, the requirements for when lack-of-fit effects need to be included in the analysis are the same for horizontally curved, radially supported bridges and horizontally curved bridges with skewed supports. Therefore, the rules in Table 3-11 are listed for straight-skewed and skewed and/or curved bridges.

Influence of cross-frame connection tolerances. From the presentations in Sections 3.3.3.2 and 3.3.3.3, clearly connection "slip" displacements can have a substantial influence on the constructed geometry as well as the internal force state in the erected structure. However, this fact

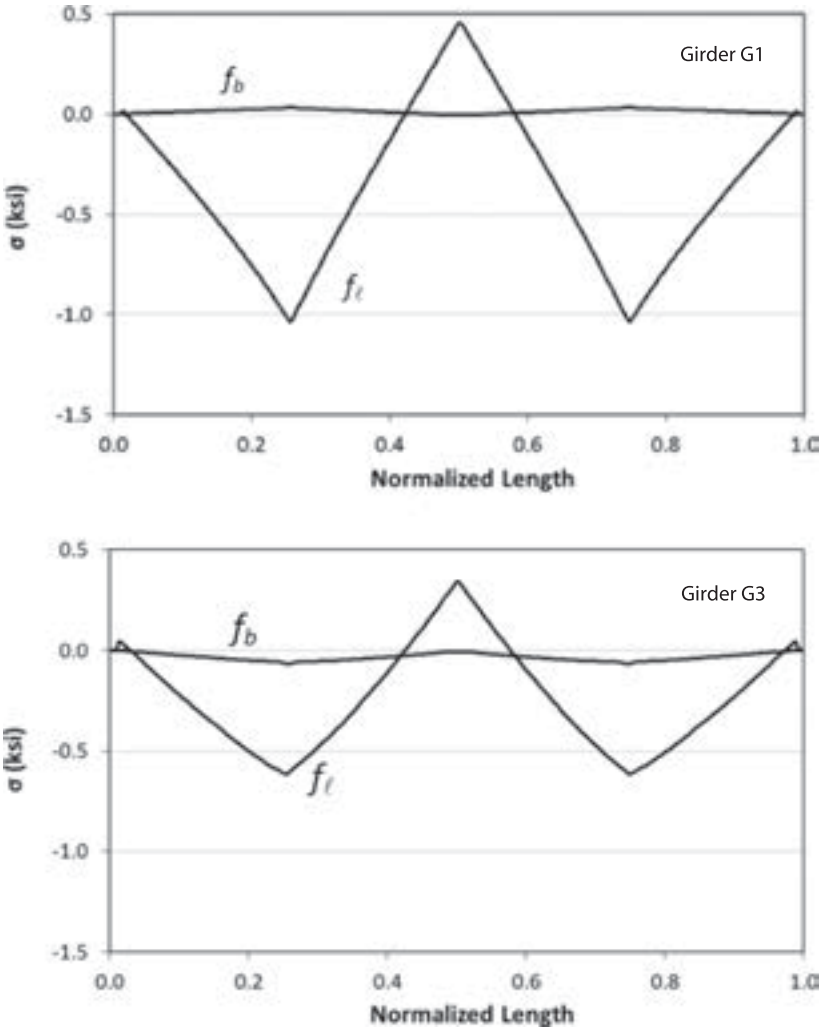

Figure 3-95. FHWA Test Bridge (EISCR1) major-axis bending and flange lateral bending stresses solely due to ⅛-in. slip in the direction of the internal load in all of the intermediate cross-frame diagonals.

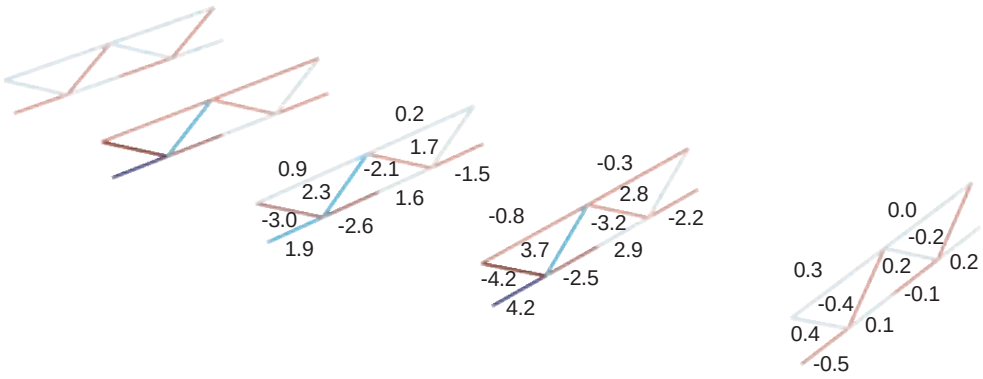

Figure 3-96. FHWA Test Bridge (EISCR1) cross-frame forces solely due to ⅛-in. slip in the direction of the internal load in all of the intermediate cross-frame diagonals.

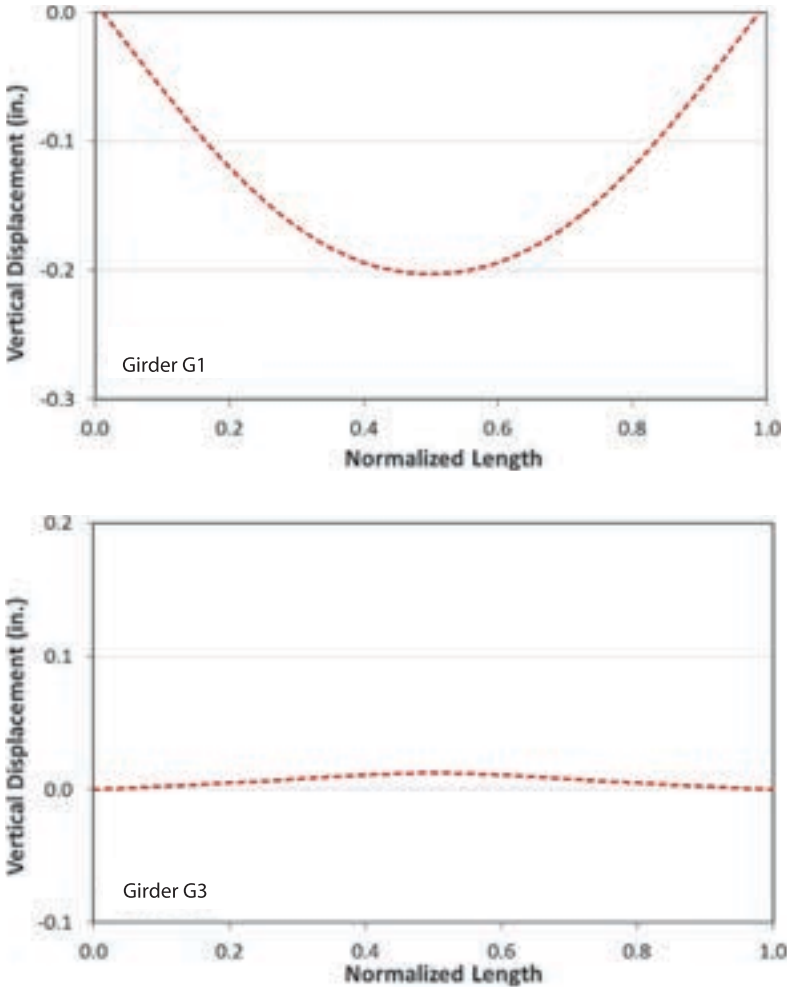

Figure 3-97. FHWA Test Bridge (EISCR1) vertical displacements solely due to ⅛-in. slip in the direction of the internal load in all of the intermediate cross-frame chords.

should not be used as a justification for neglecting initial lack-of-fit effects and the calculation of locked-in forces due to SDLF or TDLF detailing in the structural analysis. Given the above examples and discussions, it is clear that the effects of SDLF and TDLF detailing on the cross-frame forces and girder flange lateral bending stresses are typically additive in curved radially supported I-girder bridges. When these types of structures have longer spans and/or tighter curvatures, the influence of SDLF and TDLF detailing on the girder vertical displacements can be significant. If the cross-frame detailing is indeed successful in controlling the girder layovers, as it is intended to do, these locked-in forces have to exist. However, it is evident that "standard" connection tolerances can nullify much of the SDLF or TDLF detailing effects for bridges with shorter spans or smaller horizontal curvature. Interestingly, when this is the case, the small initial lack of fit is an indication that the cross-frame detailing effects are sufficiently small such that NLF detailing may be a good option.

Impact of using girder cambers from a line-girder analysis in cambering the girders and in SDLF or TDLF detailing of the cross-frames. Table 3-11 is based on the assumption that the girder cambers are determined from an accurate 2D-grid or 3D FE analysis. Some very interesting behavior occurs if the displacements from a line-girder analysis are used in setting the girder

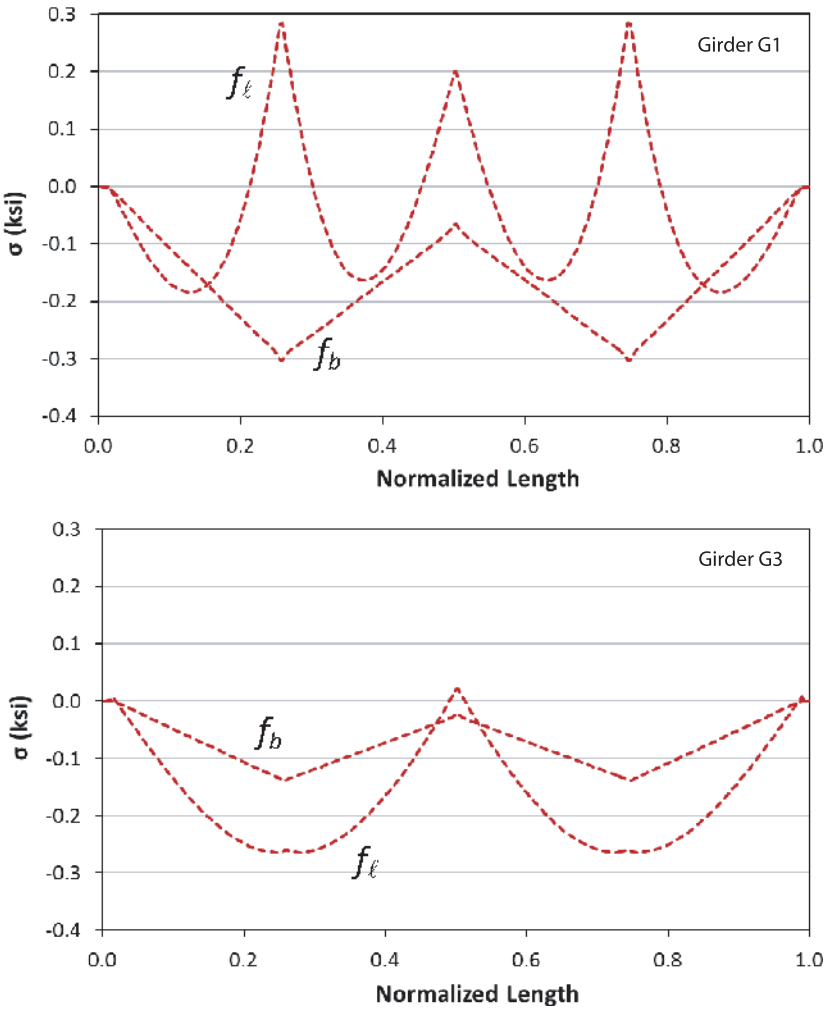

Figure 3-98. FHWA Test Bridge (EISCR1) major-axis bending and flange lateral bending stresses solely due to ⅛-in. slip in the direction of the internal load in all of the intermediate cross-frame chords.

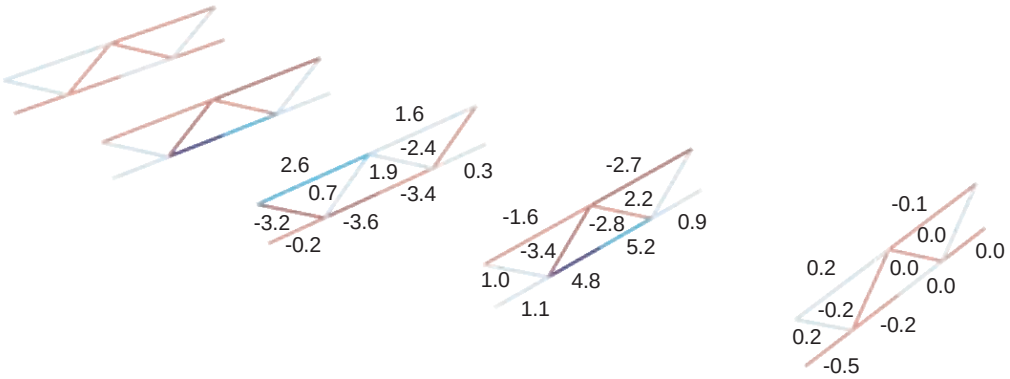

Figure 3-99. FHWA Test Bridge (EISCR1) cross-frame forces solely due to ⅛-in. slip in the direction of the internal load in all of the intermediate cross-frame chords.

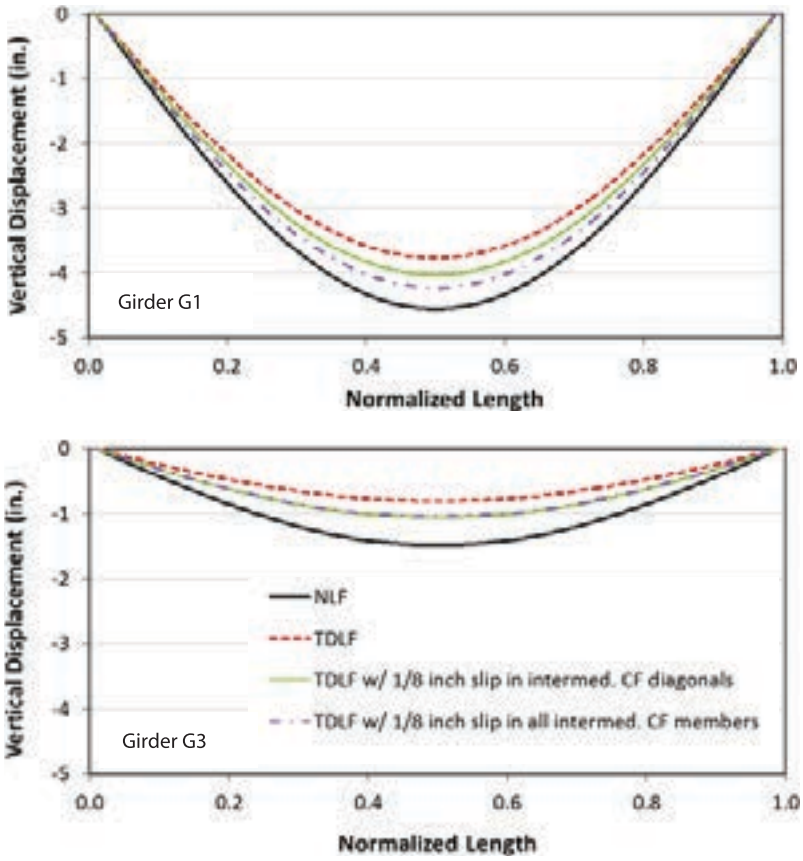

Figure 3-100. FHWA Test Bridge (EISCR1) vertical displacements under the total dead load, based on NLF detailing of the cross-frames, TDLF detailing of the cross-frames with zero tolerance in the fit-up of the connections, and TDLF detailing of the cross-frames with ⅛-in. slip in the direction of the internal load in the intermediate cross-frame diagonals or in all the intermediate cross-frame members.

cambers and detailing the cross-frames for SDLF or TDLF. This behavior, and its implications on the analysis requirements, is detailed below.

- **Steel dead load (SDL) response of straight-skewed bridges with the cross-frames fabricated for SDLF based on line-girder analysis cambers.** For any straight-skewed bridge, if the steel dead load (SDL) cambers are obtained from a line-girder analysis, and if the cross-frames are detailed for SDLF based on these cambers, then theoretically there is zero lack of fit between the girders and the cross-frames *in an idealized unshored SDL configuration* where, prior to engaging the cross-frames, all the girders are placed on the supports and allowed to deflect under the self-weight of the steel. The girder webs are plumb in this configuration, since there is no interaction with the cross-frames. When the cross-frames are detailed for SDLF based on this configuration, they fit-up perfectly with the girders in this configuration without any forcing. Therefore, interestingly, the use of line-girder analysis for SDL gives the "optimum" SDL cambers in that the total cross-frame forces and total flange lateral bending stresses in the SDL condition will be zero. These statements are all predicated on including the correct tributary weights from the cross-frames in the above line-girder analysis.

  Very interestingly, but as should be expected based on a fundamental understanding of the analysis of initial lack-of-fit effects from Section 3.2.5, an accurate 2D-grid or 3D FE analysis

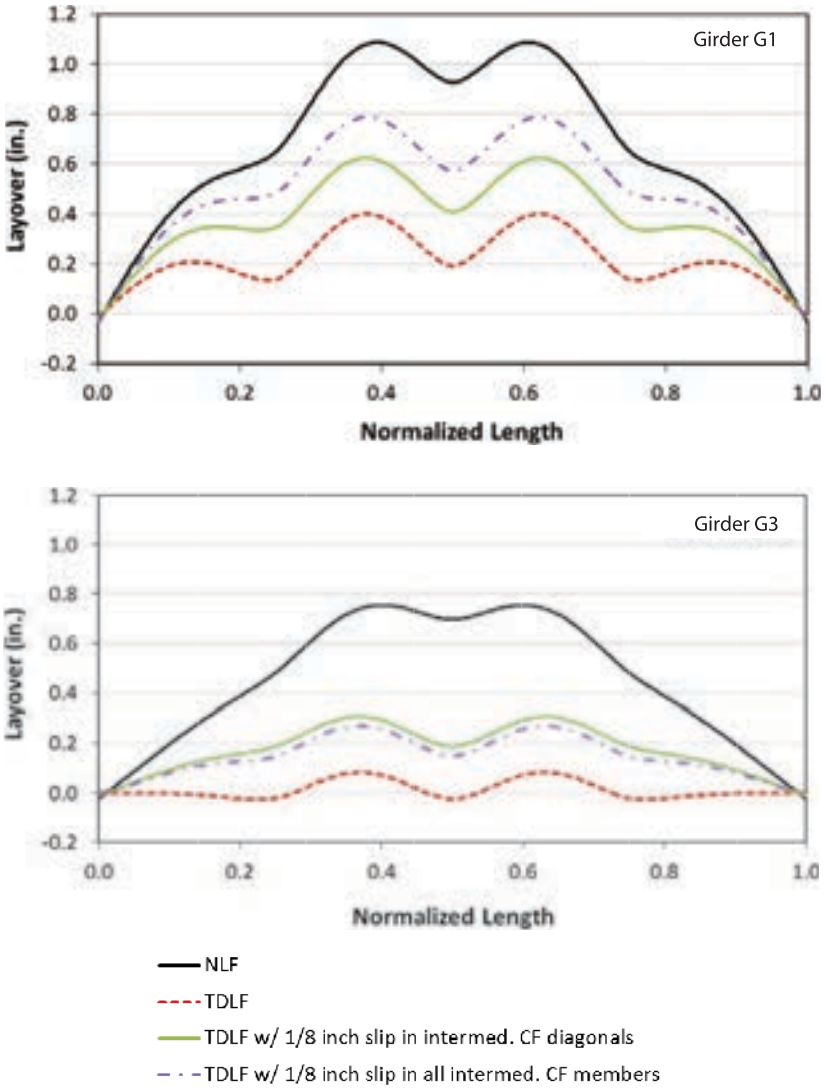

Figure 3-101. FHWA Test Bridge (EISCR1) girder layovers under total dead load, based on NLF detailing of the cross-frames, TDLF detailing of the cross-frames with zero tolerance in the fit-up of the connections, and TDLF detailing of the cross-frames with ⅛-in. slip in the direction of the internal load in the intermediate cross-frame diagonals or in all the intermediate cross-frame members.

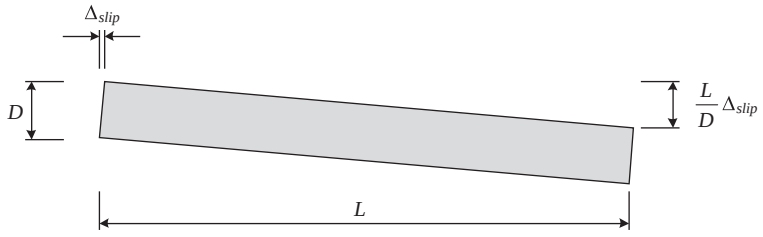

Figure 3-102. Influence of a relative slip between the top and bottom of a girder splice.

Table 3-11. Summary recommendations and rationale for when the initial lack of fit from SDLF or TDLF detailing should be considered in an accurate 2D-grid or 3D FE analysis (based on the assumption that the cambers are determined from an accurate 2D-grid or 3D FE analysis).

Response	Bridge Type	Lack of Fit Required?	Rationale
Major-axis bending stress f_b	Straight-Skewed Skewed &/or Curved	No	Locked-in f_b is negligible.
General girder vertical displacements, layovers, and final elevations	Straight-Skewed	No	The vertical displacements are insensitive to initial lack-of-fit effects.
	Skewed &/or Curved	Yes	Girder vertical displacements can be affected significantly by cross-frame detailing effects.
Girder layovers in the DL condition corresponding to the type of cross-frame detailing	Straight-Skewed Skewed &/or Curved	No	Approximately plumb webs are obtained.
Cross-frame forces and girder flange lateral bending stresses	Straight-Skewed	Conditionally No	As long as: (1) The first intermediate cross-frames are offset based on Equation 15, and (2) The cross-frames are symmetrical about their mid-length (e.g., no Z-type cross-frames), separate single-size intermediate and bearing-line cross-frames can be designed conservatively and used throughout the bridge based on the maximum member forces obtained from an accurate 2D-grid or 3D FE analysis neglecting lack-of-fit effects (top chord members designed for the maximum tension and the maximum compression determined in the top chord at the cross-frames throughout the bridge, bottom chord members designed similarly, and diagonal members designed similarly). One cross-frame type can be designed for all the intermediate cross-frames, and another for the bearing line cross-frames. In addition, the girder flange lateral bending stresses tend to be predicted conservatively from an accurate 2D-grid or 3D FE analysis neglecting lack-of-fit effects given above caveat Number 1 (e.g., see Figure 3-61). Unfortunately, for bridges with larger skew indices, the conservatism of designing single-size cross-frames in the above fashion can be prohibitive. Since the distribution of the internal cross-frame forces based on NLF detailing (see Figure 3-57) can be very different from that obtained based on SDLF or TDLF detailing (see Figure 3-58), the only alternative if the cross-frames are detailed for SDLF or TDLF is to account for the corresponding locked-in force effects in the analysis. In addition, note that generally, the total forces in the SDL condition (SDL + locked-in, e.g., see Figure 3-60) need to be considered.
	Skewed &/or Curved	Yes	The cross-frame forces and girder flange lateral bending stresses generated by the cross-frame detailing effects tend to be additive with the dead load effects.

of the same straight-skewed bridge matches exactly with the above line-girder analysis results, *but only if initial lack-of-fit effects are considered in the analysis (and only if the lack-of-fit effects are calculated based on the cambers from the line-girder analysis).* Although there is no lack of fit between the cross-frames and the girders in the above SDL condition, there is a lack of fit between the cross-frames and the girders *in the initially fabricated (cambered and plumb) girder geometry.* Therefore, locked-in forces are generated by the SDLF detailing. These locked-in cross-frame forces are exactly equal and opposite to the cross-frame forces from the SDL, and the corresponding locked-in girder flange lateral bending stresses are exactly equal and opposite to the SDL girder flange lateral bending stresses. Assuming that the structural system remains elastic, and neglecting aspects such as friction at the supports and non-zero connection tolerances, the bridge response is unique. That is, regardless of the sequence in which the structure is erected, if the cross-frames are detailed for SDLF based on the cambers from the above line-girder analysis, the total internal cross-frame forces and the girder flange lateral bending stresses are theoretically zero in the final SDL configuration. In summary, *an accurate 2D-grid or 3D FE analysis has to include the initial lack-of-fit effects* (i.e., the corresponding locked-in forces need to be calculated in the analysis) *to properly capture the bridge behavior corresponding to this "optimum" SDL camber-SDLF detailing combination.* The key attributes of this "optimum" combination are summarized again in Table 3-14.

It is important to note that the total dead load (TDL) line-girder analysis responses for a bridge fabricated with the above "optimum" SDL camber-SDLF detailing combination *typically will not be accurate.* The only way to obtain accurate TDL results in general for the above type of bridge is to conduct an accurate 2D-grid or 3D FE analysis *including the initial lack-of-fit effects.*

- **Total dead load (TDL) response of straight-skewed bridges with the cross-frames fabricated for TDLF based on line-girder analysis cambers.** It is very interesting to note that, in many situations, if the TDL cambers are obtained from a line-girder analysis, the total TDL cross-frame forces and girder flange lateral bending stresses tend to be minimized (relative to the results with other cross-frame detailing options). However, these forces and stresses generally are not zero. This is because of (1) the interaction between the girders and cross-frames in the 3D structural system once the cross-frames are engaged, (2) the influence of non-equal loading effects on the fascia girders and the interior girders, (3) the influence of eccentric loads applied to the fascia girders from overhang brackets, and (4) the interaction between the girders and a composite concrete deck, for any construction stages where the deck has gained significant early stiffness and strength. However, in cases with relatively equal load effects on the fascia and interior girders, and if the torsion from eccentric overhang loads on the fascia girders is estimated from a separate analysis, the TDL line-girder analysis results are reasonably accurate for the above case. This fact can be understood by considering the behavior for the "optimum" SDL camber-SDLF detailing combination, and then realizing that the comparable TDL camber-TDLF detailing combination works approximately the same. Similar to the previous summary, *an accurate 2D-grid or 3D FE analysis has to include the initial lack-of-fit effects to properly capture the bridge behavior for this TDLF camber-TDLF detailing combination.* The reader is referred to the Task 8 report (Appendix C of the contractors' final report), Section 7.5.1, for an example illustrating these results. Ozgur (2011) provides additional detailed examples and results.

  Lastly, it is important to note that the steel dead load (SDL) line-girder analysis responses for a bridge fabricated with the above TDL camber-TDLF detailing combination *typically will not be accurate.* The only way to obtain accurate SDL results in general for the above type of bridge is to conduct an accurate 2D-grid or 3D FE analysis *including the initial lack-of-fit effects.*
- **Use of cambers obtained from a V-load analysis on curved or curved and skewed I-girder bridges.** As shown previously in Table 3-1 of Section 3.1.2, the vertical displacements obtained from a 1D line-girder (V-load) analysis can be in error by as much as 20 percent for curved radially supported bridges with $I_C \leq 1$ (C grade in Table 3-1), and by as much as 30 percent for

curved radially supported bridges with $I_C > 1$ (D grade in Table 3-1). For curved and skewed I-girder bridges, Table 3-1 shows an F grade for the vertical displacements. Therefore, generally the use of a V-load analysis to set the camber profiles in curved or curved and skewed bridges should be discouraged. For curved, or curved and skewed I-girder bridges, the displacements used to set the girder cambers and to establish the cross-frame drops for SDLF or TDLF detailing of the cross-frames generally should be based on an accurate 2D-grid or 3D FE analysis. Regarding whether the initial lack-of-fit effects should be included in the structural design analysis, Table 3-11 then applies.

Section 7.5.2 of the Task 8 report (Appendix C of the contractors' final report) discusses an interesting fact that the V-load analysis results for simple-span radially supported I-girder bridges approximate the physical responses obtained using TDLF detailing better than the responses for SDLF or NLF detailing. This appears to be due to the fact that the girder webs are held in an approximately plumb position at the cross-frame locations when TDLF detailing is used. Ozgur (2011) provides some additional discussion of this behavior.

3.3.5 Estimation of Steel Erection Fit-Up Forces Including SDLF or TDLF Effects

The identification of potential fit-up difficulty during steel erection and the development of erection plans that avoid or alleviate this difficulty is a key task for the erection engineer. This task is often handled based on experience and using relatively simple analysis tools. However, in some situations with longer spans, tighter curves, and sharper skews, a relatively rigorous estimate of the forces required to fit-up the steel may be desirable at certain intermediate stages. This section outlines one recommended process for determining these estimates.

The basic concepts are relatively simple and can be listed as follows:

1. Select a given erection stage where fit-up of the steel is a concern. Numerous factors enter into the decision about which erection stages may need to be evaluated. In very broad terms, fit-up difficulty is typically due to some combination of structural component or unit weights, deflections of the steel components under their self-weight, component resistances to being deformed by come-alongs, jacks, cranes, etc., such that their connections can be made, and site conditions or restrictions that limit the erector's ability to provide temporary supports and/or to apply forces to make a given connection. In many situations, the greatest fit-up difficulty occurs when the connections are made for one of the last girders to be erected in a given span. This is because the incompatibility in the displacements may be significant between the portion of the structure that is already erected, particularly if the structure has significant deflections under its self-weight, and a relatively lightly loaded girder that is being assembled. In addition, the locked-in forces due to SDLF or TDLF detailing of the cross-frames tend to build up as more and more components are connected. It is important to note that there are as many steel dead load configurations as there are erection stages. SDLF detailing commonly is based on the final erected configuration. Therefore, if SDLF detailing is used, the girder webs generally are not close to plumb under steel dead load until all the steel is erected. Particularly when TDLF detailing is used, the locked-in forces can be a significant fraction of the internal forces in the steel during the steel erection.
2. Analyze the structure in the specific configuration attained immediately after the targeted connection is made. The calculated force in the targeted connection at this stage is a direct indicator of the forces that need to be applied to make the connection. This is because, just prior to making the connection, the connection force is, of course, zero. As noted previously, the locked-in forces from any initial SDLF or TDLF lack of fit between the cross-frames and the girders in their initial fabricated (cambered and plumb) geometry can be significant in some cases. These lack-of-fit effects can be included in the analysis with relative ease using

the procedures discussed previously in Section 3.2.5. The actual forces that the erector must apply are, of course, generally different from the above connection force. However, given the connection force that needs to be developed, along with the selection of rigging and other equipment, reasonable estimates can be made of the actual forces the erector will need to apply.

If the estimated fit-up forces are too large, manipulate the temporary supports, holding cranes, and other devices to limit the displacement incompatibility (the lack of fit in the deformed geometry) that needs to be resolved at the stage just prior to making the connection.

3.4 Pros and Cons of Different Cross-Frame Detailing Methods

There is much variety in the industry across the United States regarding practices and preferences pertaining to the detailing of the cross-frames to affect the constructed geometry of curved and/or skewed bridges and to achieve successful erection of the structural steel. In many cases, this variety of practices does not mean that one method is "wrong" or another answer is "better." Rather, there is often more than one right answer, and successful practices vary widely based on local preferences, local strengths, and specific characteristics of a given bridge.

In recognition of the above, this section aims to synthesize the wide range of information about each of the main cross-frame detailing methods (NLF, SDLF, and TDLF) learned from the NCHRP Project 12-79 studies in the form of "pro facts," "con facts," and commentary about these facts and their implications and applications to the two basic types of I-girder bridges addressed in the previous sections: straight-skewed and horizontally curved radially supported. The intent is to provide a reasonably comprehensive accounting of the various factors that can influence the choice of a method, so that designers, detailers, fabricators, erectors, and owners have information readily at hand.

Tables 3-12 through 3-17 provide a synthesis of the pro facts, con facts, and commentary for straight-skewed bridges while Tables 3-18 through 3-23 provide this information for horizontally curved radially supported bridges. These tables are followed by a short discussion of horizontally curved bridges with significant skew of their bearing lines and detailing for special cases such as widening projects, phased construction, and specific tub-girder bridge considerations.

As would be expected, horizontally curved bridges with significant skew generally exhibit a combination of the characteristics detailed in the above tables for straight-skewed and curved radially supported bridges. If the skews increase the girder length on the outside of the curve,

Table 3-12. Pro facts and commentary, straight-skewed I-girder bridges with NLF detailing—no lack of fit between the cross-frames and the girders in the fabricated (cambered and plumb) no-load geometry of the girders (Configuration 1 of Figure 3-30); plumb girder webs in the no-load state after connecting the cross-frames (Configurations 2 and 3 of Figure 3-30).

Pro Facts:	Commentary:
• The steel fits together with zero applied force in the no-load condition.	• This facilitates erection in a shored configuration approximating the theoretical no-load condition. However, erection under other shored or unshored conditions is practically always achievable for straight-skewed bridges, particularly if SDLF detailing is used. Furthermore, NLF detailing leads to other undesirable consequences on straight-skewed bridges as discussed in Table 3-13.
• The locked-in forces are zero.	• As a result, the structural analysis is simpler. When the cross-frames are detailed for NLF, the cross-frame forces are theoretically as analyzed by the designer for SDL, TDL, and LL+I. No additional locked-in forces are present.

Table 3-13. Con facts and commentary, straight-skewed I-girder bridges with NLF detailing.

Con Facts:	Commentary:
• Due to differential displacements and rotations between the girders, the steel does not fit together in an unshored SDL condition without applying forces.	• This is not a problem for smaller spans and/or smaller skew indices. However, for longer span lengths and larger skew indices, temporary shoring or hold cranes will likely be required. The erector may encounter fit-up difficulty if the girders are not supported by holding cranes or temporary supports such that their dead load deflections are limited. • In some cases, the erector may have to affect the relative vertical elevation of the girders, in addition to twisting a girder, to install a cross-frame. Affecting the relative girder vertical elevations typically is much more difficult to accomplish. In straight-skewed bridges, this problem can be alleviated by (1) temporary shoring or hold cranes, if NLF detailing is used, (2) the use of SDLF detailing and allowing the steel to deflect to its unshored SDL profile (this may require temporary shoring or holding to that profile; also, see the subsequent discussion of the "optimum" girder SDL cambers for SDLF detailing in straight-skewed bridges), and (3) generally, offsetting the first intermediate cross-frames relative to the bearing lines based on Equation 15 of Section 3.3.1.6, $a \geq \max(1.5D, 0.4b)$.
• The girders twist (i.e., lay over) under any dead load conditions. At highly skewed end bearing lines, the TDL layover of the girders tends to be large.	• More expensive bearings may be required in some instances at heavily skewed bearing lines, unless the dead load rotations are accommodated by modifying the bevels of the sole plates (note that beveled sole plates are already common in many bridges to accommodate grade changes along the length of the bridge). • The deck dead load lateral deflections due to girder layover must be addressed in the alignment of any deck joints. • Substantial layover of the girders under the TDL (in the final constructed condition) may be visually objectionable. • The NCHRP Project 12-79 research, as well as other prior research studies, has shown that the influence of girder layovers on the system ***strength*** is negligible as long as the checks for global stability, stability between the cross-frame locations, and bracing of the girders are satisfied. • If desired, the layover of the girders at the completion of the erection can be estimated accurately, based on the Table 3-1 guidance. These layovers may be specified on the engineering drawings to indicate the expected geometry.
• The locked-in forces are zero, since the girders are not "reverse twisted" during the installation of the cross-frames.	• At the end of the construction (i.e., under TDL conditions), the internal cross-frame forces and girder flange lateral bending stresses tend to be larger (compared to the results with other cross-frame detailing methods) due to the effects of torsion, since these forces and stresses are not offset by any locked-in force effects that would have been introduced by initial lack of fit in the no-load condition if the SDLF or TDLF cross-frame detailing methods were used.

the skew effects tend to amplify the horizontal curvature effects (i.e., the bridge tends to exhibit a significant overall twist rotation of its cross-section within the span). If there is a sharp skew that increases the length of the girder on the inside of the curve, the bridge tends to behave more like a straight-skewed structure.

In cases involving widening projects and/or phased construction where new cambered girders are placed next to an existing decked girder line under total dead load, detailing the cross-frames to fit between the steel dead load profile of the new girders and the total dead load profile of the decked girders at the time of the erection is one option. Another option is to not provide any cross-frame diagonals to transfer shear between the new and existing girders until after the deck is placed on the new girders.

Because of the inherent torsional stiffness of the tub girders, and to maintain equal heights of the webs on both sides of the tubs, these girder types are commonly detailed with their cross-section rotated parallel to the bridge cross-slope in the initial no-load configuration. The bearing-line diaphragms are commonly detailed so that they can be subassembled, then fitted

Table 3-14. Pro facts and commentary, straight-skewed I-girder bridges with SDLF detailing—cross-frames fabricated such that they do not fit-up with the girders in their fabricated (cambered and plumb) no-load geometry (Configuration 1 of Figure 3-30); the erector must generally "reverse twist" the girders during the installation of the cross-frames to achieve fit-up (Configuration 3 of Figure 3-30).

Pro Facts:	Commentary:
• Locked-in forces are generated by the initial lack of fit between the cross-frames and the girders in their fabricated (cambered and plumb) no-load geometry.	• The girder webs will be approximately plumb at the end of the steel erection. This results in a web plumb condition, which is easy to measure and inspect at a time when the erector is still on site and the deck has not yet been cast (thus allowing better opportunity to correct any misalignments). • The girder vertical displacements are relatively insensitive to the lack-of-fit effects from SDLF detailing in straight-skewed I-girder bridges. • The internal cross-frame forces and girder flange lateral bending stresses tend to be minimized under the SDL conditions (compared to the results from other methods of cross-frame detailing). The corresponding TDL forces and stresses (at the end of the construction) generally still are significant, but are reduced relative to the results for NLF detailing. • The tendency for uplift at bearings (e.g., uplift at bearings located at the acute corners of a simply supported bridge plan) is minimized under the SDL conditions (compared to the other methods of cross-frame detailing). This is a direct result of the internal cross-frame forces being minimized.
• At highly skewed end bearing lines, the TDL layover of the girders is smaller than that for NLF detailing.	• Depending on the skew angle of the bearing line and the rotation capacity of the bearings, the layover of the girders at the bearing line may be acceptable.
• The lack of fit between the cross-frames and the girders, *under any unshored SDL erection conditions*, tends to be small compared to the results from other methods of cross-frame detailing (this applies only to straight-skewed bridges).	• For straight-skewed bridges, the girder unshored SDL deflections during the steel erection tend to largely offset the SDL cambers, even though the SDL cambers are based on the state at the completion of the steel erection. • The discussion below of the "optimum" SDL cambers requires a thorough understanding of the behavior, but aids in understanding these general statements.

(continued on next page)

to the girder bottom flange and web assemblies in the shop (i.e., they are detailed for no-load fit [NLF]). The stiffeners are kept normal to the bottom flange (AASHTO/NSBA, 2006). At a skewed bearing line, if the diaphragm plate also is kept normal to the flanges, this means the major-axis bending camber rotation of the girders (at the bearing) must be accounted for in determining the fabricated profile of the diaphragm plate. Otherwise, the profile geometry of the diaphragm plate will not fit-up with the profile geometry of the tub girders without some forcing.

Intermediate external cross-frames (or diaphragms) in tub-girder bridges can be installed no-load fit (NLF) or a special steel dead load fit (SDLF) to the tub girders in their unshored deflected position under the steel self-weight (special because both the vertical deflections and the torsional rotations of the tub girders are considered). This latter detailing of the intermediate external cross-frames allows them to be installed theoretically without having to apply any force to the girders, assuming that the girders are in an unshored deflected position at the time of the installation. These cross-frames are subsequently effective to help restrain relative torsional movement between the tub girders during the placement of the deck (although, they are not effective in restraining the relative movements between the tub girders under the steel self-weight). If the cross-frames are detailed for this special SDLF, they will then

(text continues on page 133)

Table 3-14. (Continued).

Pro Facts:	Commentary:
• Line-girder analysis provides the "optimum" SDL cambers for SDLF detailing of the cross-frames *in straight-skewed bridges*.	• This statement applies only to straight-skewed bridges and only to SDLF detailing. • "Optimum" means that the total cross-frame forces and girder flange lateral bending stresses in the SDL condition, produced by the sum of the SDL forces and the locked-in forces (from the lack of fit in the NL geometry due to SDLF detailing), are minimized. • If the girder SDL camber is obtained from a line-girder analysis, then theoretically, there is zero lack of fit between the girders and the cross-frames *in an idealized unshored SDL configuration* where, prior to engaging the cross-frames, all the girders are placed on the supports and allowed to deflect under the self-weight of the steel. • The girder webs are plumb in this condition, since there is no interaction with the cross-frames. • If the girders are detailed for SDLF based on the above cambers, zero force is required to fit-up the cross-frames with the girders in the above *idealized unshored SDL configuration*. • Correspondingly, once all the cross-frames are fully connected in this configuration to complete the steel erection, the internal cross-frame forces and the girder flange lateral bending stresses will be zero. • Assuming that the structural system remains elastic, and neglecting aspects such as friction at the supports and non-zero connection tolerances, the bridge response is unique. That is, regardless of the sequence in which the structure is erected, if the cross-frames are detailed for SDLF based on the cambers from a line-girder analysis, the internal cross-frame forces and the girder flange lateral bending stresses are theoretically zero in the final SDL configuration. • Although there is no lack of fit in the above idealized SDL condition, there is a lack of fit between the cross-frames and the girders *in the initially fabricated (cambered and plumb) girder geometry*. Therefore, locked-in forces are generated by the SDLF detailing. • If the SDL cambers are obtained based on an accurate 2D-grid or 3D FE analysis, rather than a line-girder analysis, the sum of the SDL and lack-of-fit forces will be non-zero even though the cross-frames are detailed for SDLF. This is because the interaction between the girders and cross-frames in the 3D structural system modifies the girder SDL displacements from the values discussed above. The torsional effects of the distributed vertical loads (the self-weight of the steel) cannot be perfectly offset by the locked-in concentrated forces at the cross-frame locations. Generally, the above sum of the SDL forces and the locked-in forces is not negligible, but tends to be relatively small as long as the first intermediate cross-frames are sufficiently offset from the bearing lines based on Equation 15 of Section 3.3.1.6, $a \geq \max(1.5D, 0.4b)$.

Table 3-15. Con facts and commentary, straight-skewed I-girder bridges with SDLF detailing.

Con Facts:	Commentary:
• Locked-in forces are generated.	• In general, an accurate 2D-grid or 3D FE analysis is required to accurately assess the bridge responses at the end of the construction (i.e., under TDL conditions), as well as for any conditions other than SDL. Generally, for $I_S > 0.30$, accurate calculation of the responses by line-girder analysis is possible only for the SDL condition, and only if the SDL cambers are set based on the line-girder analysis.
• The locked-in forces are not sufficient to offset the TDL forces in the final constructed condition.	• At the TDL level, the cross-frame forces and girder flange lateral bending stresses can be significant, and need to be considered in the design, although they are smaller than when NLF detailing is used. • At the end of the construction (i.e., under TDL conditions), the cross-frame forces and girder flange lateral bending stresses tend to be larger than for the case of TDLF detailing, although these forces and stresses are smaller than for NLF detailing. • Line-girder analysis provides an accurate characterization of SDL vertical deflections and major-axis bending stresses in straight-skewed bridges, if the cross-frames are detailed for SDLF using the line-girder analysis cambers. For any other conditions and/or combinations with SDLF detailing, line-girder analysis can provide erroneous predictions of the girder vertical deflections and major-axis bending stresses. The magnitude of the errors is strongly correlated with the skew index I_S. • When the concrete deck is placed and other appurtenances are added to the bridge, the resulting cross-frame forces can be substantial in bridges with a large skew index, due to the torsional interactions within the system. In general, if SDLF detailing is used, accurate calculation of the cross-frame forces and flange lateral bending stresses in the TDL condition (from the sum of the TDL effects plus the locked-in force effects) requires the use of an accurate 2D-grid or 3D FE analysis including the modeling of the initial lack of fit.
• At highly skewed end bearing lines, the TDL layover of the girders still may be large.	• More expensive bearings may be required in some instances at heavily skewed bearing lines, unless the dead load rotations are accommodated by modifying the bevels of the sole plates (note that beveled sole plates are already common in many bridges to accommodate grade changes along the length of the bridge). • The deck dead load lateral deflections due to girder layover must be addressed in the alignment of any deck joints. • Substantial layover of the girders under the TDL (in the final constructed condition) may be visually objectionable. • The NCHRP Project 12-79 research, as well as other prior research studies, has shown that the influence of girder layovers on the system ***strength*** is negligible as long as the checks for global stability, stability between the cross-frame locations, and bracing of the girders are satisfied.
• For longer spans, the difference between the girder SDL displacements obtained from a line-girder analysis versus an accurate 2D-grid or 3D FE analysis can be significant.	• This is due to the interaction between the girders and the cross-frames in the 3D system. However, as noted in the pros for SDLF detailing, setting the cambers and the SDLF detailing based on a line-girder analysis tends to minimize the lack of fit between the girders and the cross-frames in any unshored SDL erection conditions. • If the SDL camber is based on line-girder analysis, an accurate 2D-grid or 3D FE analysis can reproduce the line-girder analysis (and the physical/actual) vertical deflections, but only if lack-of-fit effects are included in the analysis. An accurate 2D-grid or 3D FE analysis does not give the correct girder vertical displacements for a bridge where the SDL cambers are based on line girder analysis, unless the lack-of-fit effects are included in the analysis.

Table 3-16. Pro facts and commentary, straight-skewed I-girder bridges with TDLF detailing—cross-frames fabricated such that they do not fit-up with the girders in their fabricated (cambered and plumb) no-load geometry (Configuration 1 of Figure 3-30); the erector must essentially "reverse-twist" the girders during the installation of the cross-frames to achieve fit-up (Configuration 3 of Figure 3-30).

Pro Facts:	Commentary:
• Locked-in forces are generated by the initial lack of fit between the cross-frames and the fabricated (cambered and plumb) no-load geometry of the girders.	• The girder webs will be approximately plumb at the end of the construction (i.e., at the TDL level). • The girder vertical displacements are relatively insensitive to the lack-of-fit effects from TDLF detailing in straight-skewed I-girder bridges. • The internal cross-frame forces and girder flange lateral bending stresses (due to the sum of the dead load effects plus the locked-in force effects) tend to be minimized under the TDL conditions (compared to the results from other methods of cross-frame detailing). • The tendency for uplift at bearings (e.g., uplift at bearings located at the acute corners of a simply supported bridge plan) is minimized under the TDL conditions, compared to the other methods of cross-frame detailing. • The final internal force and stress state and the girder deflections in the TDL condition can be approximated from a line-girder analysis, if the TDL cambers are set based on a line-girder analysis and the cross-frames are detailed for TDLF. However, the accuracy of the line-girder analysis degrades as a function of the bridge skew index. A line-girder analysis predicts zero cross-frame forces and zero flange lateral bending stresses. The sum of the TDL effects plus the locked-in force effects generally is not zero, although this sum tends to be minimized as noted above. • Line-girder analysis provides an accurate characterization of the TDL vertical deflections and major-axis bending stresses in straight-skewed bridges, as long as the cross-frames are detailed for TLDF using the TDL line-girder analysis cambers. For any other loading conditions combined with TDLF detailing (e.g., the SDL vertical deflections of a bridge using TDLF detailing), line-girder analysis can provide erroneous predictions of the girder vertical deflections and major-axis bending stresses. The magnitude of these errors is strongly correlated with the skew index I_S.
• The TDL layover of the girders is approximately zero, even at highly skewed end bearing lines.	• This minimizes the total, long-term (permanent) rotation demand on the bearings. Also, this allows the use of a target TDL geometry in which the girders are assumed to be plumb for the layout of deck joints, etc.
• On bridges with constant cross-slope, detailing for TDLF allows the cross-frames to be built identically, with one fabrication set-up and one piece-mark for multiple frames.	• This makes the fabrication of the cross-frames more efficient and economical and facilitates the handling of the cross-frames during the erection.

Table 3-17. Con facts and commentary, straight-skewed I-girder bridges with TDLF detailing.

Con Facts:	Commentary:
• Significant locked-in forces are generated.	• In general, a more complex analysis is required for any conditions other than TDL. Even for evaluating the TDL condition, an accurate 2D-grid or 3D FE analysis, including the influence of the initial lack of fit between the cross-frames with the girders in their fabricated (cambered and plumb) no-load geometry, is necessary to obtain accurate cross-frame forces and girder flange lateral bending stresses for bridges with larger skew indices. • In some cases, the cross-frame forces and girder flange lateral bending stresses under the SDL (due to the sum of the steel dead weight plus the locked-in force effects) at a given stage of steel erection can be larger than the corresponding TDL values at the end of the construction. If the bridge girders are connected to the cross-frames and supported in a configuration between the SDL and NL conditions, these forces and stresses can be even larger. *Therefore, during interim stages of the steel erection, the locked-in force effects can be significant and should be considered in the design.* It should be noted that the locked-in forces tend to be smaller at the earlier stages of the steel erection. These forces build up as more and more components are assembled into the structural system. • The corresponding forces and stresses under the TDL (at the end of the construction), due to the sum of the dead load effects plus the locked-in force effects, are relatively small compared to the results from the other methods of cross-frame detailing. However, generally, they are not negligible unless the skew index is smaller than $I_S = 0.30$. These non-zero cross-frame forces and girder flange lateral bending stresses are due to the interaction between the girders and the cross-frames (as well as the girders and the slab for construction stages after portions of the concrete deck start to act compositely). The torsional effects of the distributed dead loads cannot be perfectly offset by the locked-in concentrated forces at the cross-frame locations.
• The girder webs will not be plumb under the NL or SDL conditions, once the girders are connected to the cross-frames. The girders will be laid over in the opposite direction from the direction in which they twist under the application of the dead loads.	• The bearings at support lines with significant skew can be subjected to relatively large rotation demands under various NL and SDL conditions during erection and prior to placement of the concrete deck. However, these rotations are temporary and are not additive with the rotation demands due to live loads. If necessary, blocking may be used to protect the bearings at these locations. • If desired, the layover of the girders at the completion of the steel erection can be estimated from an accurate 2D-grid or 3D FE analysis. These layovers can be specified on the engineering drawings to indicate the expected geometry.
• Caution: The girders can be plumb only under one TDL condition.	• If there are significant DC2 loads (such as a substantial utility load, barrier rail load, or wall load), the designer must decide under which TDL the girders should be plumb.
• Caution: Various incidental effects may have an influence on the bridge TDL responses.	• If early stiffness gain on the concrete deck from prior deck casting stages, or from set-up of the concrete during a given stage, is expected to be a factor, these effects would need to be considered in the calculation of the TDL displacements, internal forces, and internal stresses. In addition, other incidental effects such as tipping restraint at the bearings, participation of the metal deck forms, temporary timber struts between girders, welding of rebar between shear studs on adjacent girders, etc., can influence the response and may need to evaluated when ***estimating*** the TDL displacements, internal forces, and internal stresses.
• The lack of fit between the cross-frames and the girders is *maximized under any shored or unshored SDL erection conditions*, compared to the results from other methods of cross-frame detailing.	• For longer spans and larger skew indices, the forces required to fit-up the cross-frames with the girders during the steel erection can be substantial. This is because the TDL major-axis bending deflections have not yet occurred (since only the steel self-weight load is on the structure). Furthermore, for longer spans, the girders tend to be deeper, the girders tend to be more closely spaced relative to their depth, the flanges tend to be larger, and overall, the girders tend to be harder to deform to resolve the incompatibility in displacements between the cross-frames and the girders under the SDL. • The girder SDL deflections typically can be used to reduce the lack of fit between the girders and the cross-frames in an unshored SDL erection condition. In many situations, this may be sufficient to limit the magnitude of the forces the erector will need to apply to get the steel to fit up.

Table 3-18. Pro facts and commentary, curved radially supported I-girder bridges with NLF detailing—no lack of fit between the cross-frames and the girders in the fabricated (cambered and plumb) no-load geometry of the girders (Configuration 1 of Figure 3-30); girder webs plumb in the no-load state after connecting the cross-frames (Configurations 2 and 3 of Figure 3-30).

Pro Facts:	Commentary:
• The steel fits together with zero applied force in the no-load condition.	• This facilitates erection in a shored configuration approximating the theoretical no-load condition. However, erection under other shored or unshored conditions should be feasible for smaller spans and/or smaller curvature.
• The locked-in forces are zero.	• As a result, the structural analysis is simpler. When the cross-frames are detailed for NLF, the cross-frame forces are theoretically as analyzed by the designer for SDL, TDL, and LL+I. No additional locked-in forces are present.
• NLF detailing tends to minimize the total cross-frame forces, as well as the girder flange "negative" lateral bending moments over the cross-frame locations.	• This is because the locked-in cross-frame forces due to SDLF or TDLF detailing of the cross-frames tend to be additive with the SDL and TDL cross-frame forces in curved radially supported bridges (see the subsequent "con" discussions for SDLF and TDLF cross-frame detailing). • This statement is true both for situations where temporary shoring or hold cranes are used to support the girders in a near NL condition, as well as for unshored SDL or TDL conditions. • The girder flange lateral bending moments tend to be the largest at the cross-frame locations. The girder flanges act in lateral bending effectively like continuous-span beams. The cross-frames act as the supports for these analogous continuous-span beams (see the subsequent "con" discussions for SDLF and TDLF cross-frame detailing). • This statement applies only to curved radially supported bridges.
• NLF detailing tends to minimize the fit-up forces required during the steel erection, since the girders are not "reverse twisted" during the installation of the cross-frames.	• In curved radially supported bridges, since the cross-frame connection forces at any intermediate stage of the steel erection tend to be smallest when NLF detailing is used, the force required to install a given cross-frame at a given intermediate stage also tends to be minimized by NLF detailing. This is because the cross-frame connection force at the intermediate stage is equal to the force that has to be developed into the cross-frame if it were installed just prior to this stage. Before the cross-frame is installed, the connection force is zero, since the cross-frame is unconnected. • This statement is true both for situations where temporary shoring or hold cranes are used to support the girders in a near NL condition, as well as for unshored SDL conditions • This statement applies only to curved radially supported bridges.
• The differential vertical displacements between the girders are comparable for both NLF and SDLF in curved radially supported bridges.	• In some cases, the erector may have to affect the relative vertical elevation of the girders, in addition to twisting a girder, in order to install a given cross-frame. • Curved girders tend to twist as well as deflect vertically under their self-weight. The girder twisting tends to increase the girder vertical deflections. This is beneficial in facilitating the fit-up to steel that has already been erected (if working from the inside of the curve to the outside of the curve in erecting the girders). The steel that has already been erected will be over-rotated relative to its final SDL configuration. If working from the outside to the inside of the curve, the girders can be interconnected first near the mid-span, and the self-weight of the added girder can be used to reduce the over-rotation of the partially erected bridge cross-section. • These attributes work essentially the same in bridges with either NLF or SDLF detailing. • See the subsequent discussion under the pros for SDLF detailing. • This statement applies only to curved radially supported bridges.

Table 3-19. Con facts and commentary, curved radially supported I-girder bridges with NLF detailing.

Con Facts:	Commentary:
• The girders will be twisted (laid over) under any dead load conditions.	• Layover of the girders is restrained essentially to zero by the bearing-line cross-frames at radial bearing lines. • Layover of the girders within the span is more difficult to detect and therefore tends not to be visually objectionable. • The NCHRP Project 12-79 research, as well as other prior research studies, has shown that the influence of girder layovers on the system ***strength*** is negligible as long as the checks for global stability, stability between the cross-frame locations, and bracing of the girders are satisfied.
• Because there are no locked-in forces, the girders see larger "positive" flange lateral bending moments between the cross-frames.	• The "negative" flange lateral bending moments at the cross-frame locations are typically the largest moments. Therefore, NLF detailing of the cross-frames tends to give smaller maximum flange lateral bending moments.

Table 3-20. Pro facts and commentary, curved radially supported I-girder bridges with SDLF detailing—cross-frames fabricated such that they do not fit-up with the girders in their fabricated (cambered and plumb) no-load geometry (Configuration 1 of Figure 3-30); the erector must essentially "reverse twist" the girders during the installation of the cross-frames to achieve fit-up (Configuration 3 of Figure 3-30).

Pro Facts:	Commentary:
• Locked-in forces are generated by the initial lack of fit between the cross-frames and the girders in their fabricated (cambered and plumb) no-load geometry.	• The girder webs will be approximately plumb at the end of the steel erection. This results in a web plumb condition that is easy to measure and inspect at a time when the erector is still on site and the deck has not yet been cast (thus allowing better opportunity to correct any misalignments).
• The layover of the girders within the span will be smaller than that for NLF detailing.	• In curved radially supported bridges, the "reverse twisting" of the girders required to install the cross-frames induces internal forces that twist the girders in the opposite direction from that which they tend to roll under the dead load. This occurs at all of the cross-frames along a given span. As a result, the overall "global" twisting of the girders, and the corresponding lateral bending of the girder flanges, is reduced along the full span lengths.
• The differential vertical displacements between the girders are comparable for both NLF and SDLF in curved radially supported bridges.	• In some cases, the erector also may have to affect the relative vertical elevation of the girders in order to install a given cross-frame. • Curved girders tend to twist as well as deflect vertically under their self-weight. The girder twisting tends to increase the girder vertical deflections. This is beneficial in facilitating the fit-up to steel that has already been erected (if working from the inside of the curve to the outside of the curve in erecting the girders). The steel that has already been erected will be over-rotated relative to its final SDL configuration. If working from the outside to the inside of the curve, the girders can be interconnected first near the mid-span, and the self-weight of the added girder can be used to reduce the over-rotation of the partially erected bridge cross-section. • These attributes work essentially the same in bridges with either SDLF or NLF detailing.
• Some fabricators and erectors believe that bridges with cross-frames detailed for SDLF generally are easier to fit-up under unshored SDL erection conditions.	• The analytical evidence suggests that this is the case for straight-skewed bridges. However, the analytical evidence suggests that the forces required to fit up the steel under unshored SDL erection conditions are somewhat larger when SDLF detailing is used in curved radially supported bridges. • The fit-up forces often are very comparable for curved radially supported bridges with either SDLF or NLF detailing of the cross-frames.

Table 3-21. Con facts and commentary, curved radially supported I-girder bridges with SDLF detailing.

Con Facts:	Commentary:
• Locked-in forces are developed within the structural system.	• An accurate 2D-grid or 3D FE analysis, including the influence of the initial lack of fit between the cross-frames with the girders in their fabricated (cambered and plumb) no-load geometry, is necessary to account accurately for these effects.
• On average, the locked-in cross-frame forces due to SDLF or TDLF detailing are additive with the SDL and TDL cross-frame forces in curved radially supported bridges.	• For SDLF or TDLF detailing, the girder flanges in curved radially supported bridges work effectively like continuous-span beams over the cross-frames in the lateral direction. The SDLF or TDLF detailing effects are akin to pre-stressing these effective continuous-span beams by displacing their supports (the cross-frames) in the direction opposite to that which these supports displace under the SDL or TDL. This "pre-stressing" increases the continuous-span beam reactions (i.e., the cross-frame forces) and increases the beam negative moments over the supports (i.e., the flange lateral bending moments over the cross-frame locations).
• The girder flange maximum lateral bending stresses tend to be increased by the effects of SDLF or TDLF detailing.	• The predominant SDLF or TDLF detailing effect is in the cross-frame diagonals, and is associated with a racking of the cross-frames that accomplishes the compensating deflections necessary for the girder webs to be plumb in the targeted dead load condition. • Assuming that the bridge remains elastic, and neglecting aspects such as friction at the supports and non-zero connection tolerances, these responses are independent of the sequence of erection. • Generally, the locked-in forces need to be calculated in the analysis to obtain accurate cross-frame forces.
• The girders still will be laid over within the spans under the TDL, although the layover will be smaller than for NLF detailing of the cross-frames.	• Layover of the girders is restrained essentially to zero by the bearing-line cross-frames at radial bearing lines. • Layover of the girders within the span is difficult to detect and therefore tends not to be visually objectionable. • The NCHRP Project 12-79 research, as well as other prior research studies, has shown that the influence of girder layovers on the system ***strength*** is negligible as long as the checks for global stability, stability between the cross-frame locations, and bracing of the girders are satisfied.
• In curved bridges, SDLF detailing tends to reduce the vertical deflections. The required cambers will tend to be over-predicted by an analysis that neglects lack-of-fit force effects.	• The change in the vertical deflections due to SDLF detailing is usually relatively small. However, in extreme cases such as the Ford City Bridge example (see Figure 3-84), this change can be several inches. • This can reduce the concrete deck haunch to a thickness that is not desirable or can lead to problems in achieving the desired deck elevations along the spans. • Generally, the locked-in forces need to be calculated in the analysis to obtain accurate girder cambers.
• The differential vertical displacements between the girders are comparable for both SDLF and NLF in curved radially supported bridges.	• SDLF detailing has approximately the same effect on the vertical displacements for all the girders at any given cross-section of the bridge. The overall rotation of the bridge cross-section tends to not be significantly affected. Therefore, the influence of SDLF detailing on the differential vertical displacements between the girders is small (i.e., there is no significant benefit of SDLF versus NLF, or vice versa, in resolving vertical displacement incompatibilities during erection).
• In curved, radially supported bridges, SDLF detailing tends to increase the fit-up forces required during the steel erection somewhat relative to NLF detailing.	• In curved radially supported bridges, since the cross-frame connection forces at any intermediate stage of the steel erection tend to be increased due to the locked-in forces from SDLF detailing, the force required to install a given cross-frame into the system at a given intermediate stage tends to be increased. This is because the cross-frame connection force at a given intermediate stage is equal to the force that has to be developed into the cross-frame if it were installed just prior to this stage. Before the cross-frame is installed, the connection force is zero, since the cross-frame is unconnected.

Table 3-22. Pro facts and commentary, curved radially supported I-girder bridges with TDLF detailing—cross-frames fabricated such that they do not fit-up with the girders in their fabricated (cambered and plumb) no-load geometry (Configuration 1 of Figure 3-30); the erector must essentially "reverse twist" the girders during the installation of the cross-frames to achieve fit-up (Configuration 3 of Figure 3-30).

Pro Facts:	Commentary:
• Locked-in forces are generated by the initial lack of fit between the cross-frames and the girders in their fabricated (cambered and plumb) no-load geometry.	• The girder webs will be approximately plumb at the end of the construction (i.e., at the TDL level). However, it is most important that the girder webs be plumb at the bearing lines. The cross-frames at radial bearing lines enforce this, regardless of the type of cross-frame detailing. • In curved radially supported bridges, the "reverse twisting" of the girders required to install the cross-frames induces internal forces that twist the girders in the opposite direction from that which they tend to roll under the dead load. This occurs at all the cross-frames along a given span. As a result, the overall "global" twisting of the girders, and the corresponding lateral bending of the girder flanges, is reduced along the full span lengths. For TDLF detailing of the cross-frames, the twisting of the girders is approximately zero at the cross-frame locations at the end of the construction (i.e., at the TDL level). • For curved radially supported bridges, the final internal cross-frame forces and the girder flange lateral bending stresses from a V-load analysis tend to correlate well with the corresponding physical responses associated with TDLF detailing of the cross-frames. However, the accuracy of V-load analysis for predicting the girder vertical deflections degrades as a function of the horizontal curvature.

Table 3-23. Con facts and commentary, curved radially supported I-girder bridges with TDLF detailing.

Con Facts:	Commentary:
• Locked-in forces are developed within the structural system.	• An accurate 2D-grid or 3D FE analysis, including the influence of the initial lack of fit between the cross-frames with the girders in their fabricated (cambered and plumb) no-load geometry, is necessary to account accurately for all of the effects of the locked-in forces. • For curved radially supported bridges, the final internal cross-frame forces and the girder flange lateral bending stresses from a V-load analysis tend to correlate well with the corresponding physical responses associated with TDLF detailing of the cross-frames. However, the accuracy of V-load analysis for predicting the girder vertical deflections degrades as a function of the horizontal curvature.
• On average, the locked-in cross-frame forces due to TDLF or SDLF are additive with the TDL and SDL cross-frame forces in curved radially supported bridges.	• For TDLF or SDLF detailing, the girder flanges in curved radially supported bridges work effectively like continuous-span beams over the cross-frames in the lateral direction. The TDLF or SDLF detailing effects are akin to pre-stressing these effective continuous-span beams by displacing their supports (the cross-frames) in the direction opposite to that which these supports displace under the TDL or SDL. This "pre-stressing" increases the continuous-span beam reactions (i.e., the cross-frame forces) and increases the beam negative moments over the supports (i.e., the flange lateral bending moments over the cross-frame locations).
• The girder flange maximum lateral bending stresses tend to be increased by the effects of TDLF or SDLF detailing.	• The predominant TDLF or SDLF detailing effect is in the cross-frame diagonals and is associated with a racking of the cross-frames that accomplishes the compensating deflections necessary for the girder webs to be plumb in the targeted dead load condition. • Assuming that the bridge remains elastic, and neglecting aspects such as friction at the supports and non-zero connection tolerances, these responses are independent of the sequence of erection. • Generally, the locked-in forces need to be calculated in the analysis to obtain accurate cross-frame forces.

(continued on next page)

Table 3-23. Continued.

Con Facts:	Commentary:
• Under SDL, the girders will be laid over in the opposite direction from the direction in which they twist under the application of the dead loads.	• These rotations are temporary and are not additive with the rotations due to live load.
• In curved radially supported bridges, TDLF detailing tends to reduce the vertical deflections. The required cambers will tend to be over-predicted by an analysis that neglects lack-of-fit force effects.	• The change in the vertical deflections due to TDLF detailing can potentially be of significance. In the extreme Ford City Bridge example (see Figure 3-84), this change was as much as approximately 5 in. • This can reduce the concrete deck haunch to a thickness that is not desirable or can lead to problems in matching the desired deck elevations at a given location along the spans. • The calculation of locked-in forces generally should be included in the analysis to predict accurate girder cambers.
• The differential vertical displacements between the girders are not significantly affected by TDLF detailing.	• In curved radially supported bridges, TDLF detailing influences the girder twists and the girder vertical deflections. However, the overall rotation of the bridge cross-section tends not to be significantly affected. Therefore, the influence of TDLF detailing on the differential vertical displacements between the girders is small in these types of structures (i.e., there is no significant benefit of TDLF versus NLF or SDLF detailing in resolving vertical displacement incompatibilities during erection).
• In curved radially supported bridges, TDLF detailing tends to increase the fit-up forces required during the steel erection relative to the results for both SDLF and NLF detailing.	• In curved radially supported bridges, since the cross-frame connection forces at any intermediate stage of the steel erection tend to be increased due to the locked-in forces from TDLF detailing, the force required to install a given cross-frame into the system at a given intermediate stage tends to be increased. This is because the cross-frame connection force at a given intermediate stage is equal to the force that has to be developed into the cross-frame if it were installed just prior to this stage. Before the cross-frame is installed, the connection force is zero, since the cross-frame is unconnected.
• The lack of fit between the cross-frames and the girders is *maximized under any shored or unshored SDL erection conditions*, compared to the results from other cross-frame detailing methods.	• For longer spans and larger skew indices, the forces required to fit-up the cross-frames with the girders during the steel erection can be substantial. This is because the TDL major-axis bending deflections have not yet occurred (since only the steel self-weight load is on the structure).
• Caution: The girders can be plumb only under one TDL condition.	• If there are significant DC2 loads (such as a substantial utility load, barrier rail load or wall load), the designer must decide under which TDL the girders should be plumb.
• Caution: Various incidental effects may have an influence on the bridge TDL responses.	• If early stiffness gain on the concrete deck from prior deck casting stages, or from set-up of the concrete during a given stage, is expected to be a factor, these effects would need to be considered in the calculation of the TDL displacements, internal forces, and internal stresses. In addition, other incidental effects such as tipping restraint at the bearings, participation of the metal deck forms, temporary timber struts between girders, welding of rebar between shear studs on adjacent girders, etc. can influence the response and may need to evaluated when ***estimating*** the TDL displacements, internal forces, and internal stresses.

need to be installed with the girders in their deflected steel dead load positions. If the cross-frames are installed before temporary supports or holding cranes are removed, NLF detailing is necessary. Due to the torsional stiffness of tub girders, force-fitting of the cross-frames generally is not an option. In most cases with longer-span tub-girder bridges, there are multiple field sections along the spans and shoring to the approximate no-load condition is preferred.

3.5 Selection of Cross-Frame Detailing Methods for I-Girder Bridges

Based on the summaries in Section 3.4, it is apparent that different methods of cross detailing work well for different I-girder bridge geometries. Furthermore, in many cases, steel I-girder bridges can be built successfully using a wide range of methods. Generally, the appropriate selection of a cross-frame detailing method depends in large part on the priority that one assigns to the various objectives and tradeoffs. Therefore, in the view of the NCHRP Project 12-79 research team, it is important to allow flexibility in any recommendations for selecting cross-frame detailing methods. However, given the detailed pros and cons discussed in Section 3.4, a few basic trends become apparent. These trends are explained in this section.

For straight-skewed bridges with $I_S \leq 0.30$, TDLF detailing is typically a good option:

- The girder webs will be approximately plumb under the targeted TDL.
- The TDL cross-frame forces and girder flange lateral bending stresses will be canceled out in large part by the TDLF locked-in forces. As such, the cross-frame forces and girder flange lateral bending stresses tend to be minimized under the targeted TDL. In addition, these forces and stresses tend to be negligible, given $I_S \leq 0.30$.
- Fit-up concerns during the steel erection should be minimal, given $I_S \leq 0.30$.
- Line girder analysis provides a reasonable estimate of the responses under TDL, given that the cross-frame forces and the girder flange lateral bending stresses are negligible.
- The twist rotation of the girders in the SDL condition can be estimated as $\phi_z = \phi_x \tan \theta$ at skewed bearing lines, where ϕ_x is the sum of the initial camber and the SDL girder major-axis bending rotations and θ is the skew angle, equal to zero for zero skew. The girder SDL twist rotation at cross-frames normal to the girders within the spans may be estimated as $\phi_z = \Delta_y / s$, where Δ_y is the differential vertical displacement between the cross-frame ends due to sum of the initial TDL camber and the SDL displacements. These layovers can be specified on the engineering drawings to indicate the expected geometry at the completion of the steel erection (the direction of the layovers under SDL will be opposite to those due to the TDL).
- Potential "incidental" effects such as non-calculated early stiffness gains of the concrete, tipping restraint at the bearings, participation of metal deck forms, temporary timber struts between girders, welding of rebar between studs on adjacent girders, etc., potentially should be considered when setting the TDL cambers. The accounting for these effects requires engineering judgment regarding specific construction practices and characteristics and cannot be well quantified as of this writing. The engineer may consider reducing the TDL cambers (based on ideal conditions) to ensure that the girders are not "over-cambered" or specifying a cross-frame detailing method somewhere between TDLF and SDLF, but not both of these ad hoc compensating measures. In ordinary practice, these types of effects are often neglected without any apparent detrimental influence.
- The first intermediate cross-frames generally should be positioned at an offset distance $a \geq \max(1.5D, 0.4b)$, where D is the girder depth and b is the second unbraced length within the span adjacent to the offset from the bearing line. This is intended to alleviate local spikes in the cross-frame forces and corresponding potential fit-up difficulty due to nuisance stiffness effects. (In basic terms, the first intermediate cross-frame needs to be far enough away from

the bearing line so that one end of the girder offset length can be pulled over relative to the other without requiring excessive force.)

For straight-skewed bridges with small-to-moderate span lengths and $I_S > 0.30$, TDLF detailing is typically a good option:

- The girder webs will be approximately plumb under the targeted TDL.
- The TDL internal forces and stresses due to the system torsional effects will be offset in large part by the TDLF locked-in forces. As such, the cross-frame forces and girder flange lateral bending stresses will tend to be minimized under the targeted TDL.
- Fit-up during the steel erection should be feasible, given the small-to-moderate span length.
- Generally, significant cross-frame forces and girder flange lateral bending stresses will exist in the TDL condition and in other loading conditions. Accurate calculation of these values requires an accurate 2D-grid or 3D FE analysis, including the calculation of locked-in forces due to the initial lack-of-fit effects. Since the locked-in forces are comparable in magnitude to the internal forces due to the TDL effects, the internal forces from an accurate 2D-grid or 3D FE analysis neglecting the initial lack-of-fit effects will be substantially in error (e.g., compare the forces in Figure 3-57 versus those in Figure 3-58).
- The twist rotation of the girders in the SDL condition can be estimated as $\phi_z = \phi_x \tan \theta$ at skewed bearing lines, where ϕ_x is the sum of the initial camber and the SDL girder major-axis bending rotations and θ is the skew angle, equal to zero for zero skew. The girder SDL twist rotation at cross-frames normal to the girders within the spans may be estimated as $\phi_z = \Delta_y/s$, where Δ_y is the differential vertical displacement between the cross-frame ends due to the sum of the initial TDL camber and the SDL displacements. These layovers can be specified on the engineering drawings to indicate the expected geometry at the completion of the steel erection.
- Potential "incidental" effects such as non-calculated early stiffness gains of the concrete, tipping restraint at the bearings, participation of metal deck forms, temporary timber struts between girders, welding of rebar between studs on adjacent girders, etc., potentially should be considered when setting the TDL cambers. The accounting for these effects requires engineering judgment regarding specific construction practices and characteristics and cannot be well quantified as of this writing. The engineer may consider reducing the TDL cambers (based on ideal conditions) to ensure that the girders are not "over-cambered" or specifying a cross-frame detailing method somewhere between TDLF and SDLF, but not both of these ad hoc compensating measures. In ordinary practice, these types of effects are often neglected without any apparent detrimental influence.
- The first intermediate cross-frames generally should be positioned at an offset distance $a \geq \max(1.5D, 0.4b)$, where D is the girder depth and b is the second unbraced length within the span adjacent to the offset from the bearing line. This is intended to alleviate local spikes in the cross-frame forces and corresponding potential fit-up difficulty due to nuisance stiffness effects. (In basic terms, the first intermediate cross-frame needs to be far enough away from the bearing line so that one end of the girder offset length can be pulled over relative to the other without requiring excessive force.)

For straight-skewed bridges with large span lengths and $I_S > 0.30$, SDLF detailing, or detailing between SDLF and TDLF, typically are good options:

- In these cases, a potential consideration is the alleviation of fit-up difficulty during the steel erection. SDLF detailing tends to minimize the fit-up difficulty for straight-skewed bridges, but may result in significant layover of the girders at highly skewed bearing lines under the TDL. In the experience of some erectors, long-span straight-skewed bridges with TDLF detailing do not present any major problems with respect to fit-up. Ozgur (2011) discusses a 267-ft. span skewed bridge erection procedure in which TDLF detailing was used and the bridge was erected quite successfully by using the steel dead load deflections to alleviate fit-up problems.

- The tendency for excessive layover at highly skewed bearing lines can be addressed by a combination of the cross-frame detailing, the use of beveled sole plates, and/or by using bearings with a larger rotation capacity. If TDLF detailing is used, the layover is addressed entirely by the cross-frame detailing.
- For SDLF detailing, the girder webs will be approximately plumb under the SDL at the completion of the steel erection.
- For other than SDLF detailing of the cross-frames, the twist rotation of the girders in the SDL condition can be estimated as $\phi_z = \phi_x \tan \theta$ at skewed bearing lines, where ϕ_x is the sum of the initial camber and the SDL girder major-axis bending rotations and θ is the skew angle, equal to zero for zero skew. The girder twist rotation at cross-frames normal to the girders within the spans may be estimated as $\phi_z = \Delta_y/s$, where Δ_y is the differential vertical displacement between the ends of the cross-frame due to the sum of the initial TDL camber and the SDL displacements. These layovers can be specified on the engineering drawings to indicate the expected geometry at the completion of the steel erection.
- Generally, significant cross-frame forces and girder flange lateral bending stresses will exist in the TDL condition and in other loading conditions. Accurate calculation of these values requires an accurate 2D-grid or 3D FE analysis, including the calculation of locked-in forces due to the initial lack-of-fit effects. Since the locked-in forces are comparable in magnitude to the internal forces due to the corresponding dead load effects (e.g., SDL for SDLF and TDL for TDLF), the internal forces from an accurate 2D-grid or 3D FE analysis neglecting the initial lack-of-fit effects will be substantially in error (e.g., compare the forces in Figure 3-57 versus those in Figure 3-58).
- The first intermediate cross-frames generally should be positioned at an offset distance $a \geq \max(1.5D, 0.4b)$, where D is the girder depth and b is the second unbraced length within the span adjacent to the offset from the bearing line. This is intended to alleviate local spikes in the cross-frame forces and corresponding potential fit-up difficulty due to nuisance stiffness effects. (In basic terms, the first intermediate cross-frame needs to be far enough away from the bearing line so that one end of the girder offset length can be pulled over relative to the other without requiring excessive force.)

For curved bridges with radial supports, NLF detailing, or detailing between NLF and SDLF, typically are good options:

- NLF detailing tends to minimize the cross-frame forces as well as the "negative" girder flange lateral bending moments over the cross-frame locations, since there are no additive locked-in force effects due to initial lack of fit.
- Because the cross-frame forces tend to be minimized, the analytical evidence shows that the fit-up forces required to erect the steel tend to be minimized. However, the experience of some fabricators and erectors is that curved radially supported bridges are easier to fit-up under unshored SDL erection conditions if SDLF detailing is used. The use of SDLF detailing on curved radially supported I-girder bridges is a common practice in the industry, although bridges of this type have been detailed and constructed without difficulty using NLF detailing. It is recommended that the expanded use of NLF detailing should be explored and monitored on selected projects to further validate the NCHRP Project 12-79 findings.
- Layover of the girder webs occurs within the spans, but this layover is more difficult to detect visually and is not of any significance with respect to the bridge structural resistance as long as the checks for global stability, stability between the cross-frame locations, and bracing of the girders are satisfied. If the girder layovers within the span are judged to be excessive, the engineer may wish to employ a flange level lateral bracing system to stiffen the structure, particularly for longer span bridges.
- For NLF detailing, the structural analysis is simplified, since there are no initial lack-of-fit effects.

- For other than NLF detailing, the locked-in force effects in the cross-frames and in the "negative" girder flange lateral bending moments at the cross-frame positions tend to be additive with the dead load effects (compare Figure 3-73 to Figure 3-72, 3-74 to 3-72, 3-76 to 3-75, and 3-77 to 3-75, see Figures 3-78 and 3-87, compare Figure 3-88b to 3-88a, and see Figures 3-90 and 3-91). Accurate calculation of these values requires an accurate 2D-grid or 3D FE analysis, including the calculation of locked-in forces due to the initial lack-of-fit effects. Since the locked-in forces tend to be additive with the internal forces due to the dead load effects, the internal forces from an accurate 2D-grid or 3D FE analysis neglecting the initial lack-of-fit effects tend to underestimate the true forces.

For curved bridges with *sharply skewed* supports, *minor horizontal curvature* and small span lengths, TDLF detailing is typically a good option:

- In these cases, limiting the girder layover at the skewed bearing lines is the overriding consideration.
- The tendency for the cross-frame forces and the girder "negative" flange lateral bending moments (due to horizontal curvature effects) to be increased by the TDLF detailing can be accounted for by conducting an accurate 2D-grid or 3D FE analysis, including the calculation of locked-in forces due to the initial lack-of-fit effects. Since the locked-in forces are comparable in magnitude to the internal forces due to the dead load effects, the internal forces from an accurate 2D-grid or 3D FE analysis neglecting the initial lack-of-fit effects will be substantially in error.
- The first intermediate cross-frames generally should be positioned at an offset distance $a \geq \max(1.5D, 0.4b)$, where D is the girder depth and b is the second unbraced length within the span adjacent to the offset from the bearing line. This is intended to alleviate local spikes in the cross-frame forces and corresponding potential fit-up difficulty due to nuisance stiffness effects. (In basic terms, the first intermediate cross-frame needs to be far enough away from the bearing line so that one end of the girder offset length can be pulled over relative to the other without requiring excessive force.)

For curved bridges with moderately skewed supports, and small to moderate span lengths, detailing of the cross-frames anywhere between NLF and TDLF can be a good option:

- In this case, the engineer should select the cross-frame detailing method to balance between (1) limiting the dead load twist rotations at the skewed bearing lines, (2) alleviating the larger additive locked-in forces associated with TDLF detailing on a curved bridge, and (3) facilitating fit-up during the steel erection.
- Often SDLF detailing is a good "middle of the road" option for these bridge types.
- For other than NLF detailing, the locked-in force effects due to the horizontal curvature in the cross-frames and in the "negative" girder flange lateral bending moments at the cross-frame positions tend to be additive with the dead load effects. Accurate calculation of these values requires an accurate 2D-grid or 3D FE analysis, including the calculation of locked-in forces due to the initial lack-of-fit effects. Since the locked-in forces tend to be additive with the internal forces due to the dead load effects, the internal forces from an accurate 2D-grid or 3D FE analysis neglecting the initial lack-of-fit effects tend to underestimate the true forces.

For curved bridges with skewed supports and large span length, SDLF detailing, or detailing between SDLF and NLF, is typically a good option.

- In these cases, the overriding consideration is the alleviation of fit-up difficulty during the steel erection. SDLF detailing tends to minimize the fit-up difficulty in the vicinity of highly skewed bearing lines and is often preferred by fabricators and erectors for these types of bridges. However, SDLF detailing may result in significant layover of the girders at highly skewed bearing lines under the TDL. NLF detailing tends to minimize the fit-up difficulty

with respect to horizontal curvature effects (based on analytical evidence), but provides no compensation for the layover of the girders at highly skewed bearing lines.
- The tendency for excessive layover at highly skewed bearing lines can be addressed by a combination of the cross-frame detailing, the use of beveled sole plates, and/or by using bearings with a larger rotation capacity.
- For SDLF detailing, the girder webs will be approximately plumb under the SDL at the completion of the steel erection.
- For other than NLF detailing, the locked-in force effects in the cross-frames and in the "negative" girder flange lateral bending moments at the cross-frame positions tend to be additive with the dead load effects due to the horizontal curvature. Accurate calculation of these values requires an accurate 2D-grid or 3D FE analysis, including the calculation of locked-in forces due to initial lack-of-fit effects. Since the locked-in forces associated with the combined skew and horizontal curvature can be comparable in magnitude to the internal forces due to the dead load effects, the internal forces from an accurate 2D-grid or 3D FE analysis neglecting the initial lack-of-fit effects can be substantially in error.
- The first intermediate cross-frames generally should be positioned at an offset distance $a \geq \max(1.5D, 0.4b)$, where D is the girder depth and b is the second unbraced length within the span adjacent to the offset from the bearing line. This is intended to alleviate local spikes in the cross-frame forces and corresponding potential fit-up difficulty due to nuisance stiffness effects. (In basic terms, the first intermediate cross-frame needs to be far enough away from the bearing line so that one end of the girder offset length can be pulled over relative to the other without requiring excessive force.)

3.6 Construction Engineering Recommendations

The main focus of this research was the improvement of analysis methods for erection analysis and prediction of constructed geometry of steel girder bridges. However, the construction engineering recommendations represent perhaps the most important results of this work, and they are likely to be the most easily implemented to provide direct benefit to the industry.

The recommendations in regard to construction engineering are organized into four categories, represented by the subsections of this report presented below. The specific recommendations, however, are best presented in their full and complete form, which appears in the NCHRP Project 12-79 Task 9 report, "Recommendations for Construction Plan Details and Level of Construction Analysis." This document is included as Appendix B of this report. This appendix provides specific guidelines and commentary on recommendations for construction plan details and recommendations for methods of structural analysis and calculations. These guidelines are comprehensive and address all aspects of erection engineering plans and calculations. An owner-agency could adopt the guidelines as a complete specification, could reference the guidelines in their erection specifications, or could adopt all or portions of the guidelines in their specifications.

To further facilitate immediate implementation of these recommendations, this appendix has been deliberately written in a format and with language that can be directly adopted by AASHTO via a revision to the AASHTO/NSBA Steel Bridge Collaboration Guide Specification S10.1 – 2007, *Steel Bridge Erection Guide Specification.*

3.6.1 Recommendations for Construction Plan Details

The reader is referred to Section 2 of Appendix B, which provides detailed and comprehensive recommendations with commentary, organized in a format that would easily lend itself to the

- Plan of work area
  - Permanent and temporary structures shown
  - All roads, railroad tracks, waterways, clearances, utilities, potential conflicts shown
  - Material (steel) storage areas shown
- Erection sequence
  - Step-by-step procedure—figures and narrative dictating work
  - Delivery location of components shown
  - Crane locations shown
  - Temporary support, hold cranes, blocking, tie-downs shown
  - Load restrictions for certain stages (i.e., wind)
- Crane information
  - Crane type, pick radii, boom length shown
  - Approximate crane pick points shown
  - Crane pick weights shown
  - Hold crane loads
- Details of lifting devices and special procedures
- Bolting requirements
- Bearing blocking and tie-down details
- Temporary supports
  - Details of structure shown
  - Load capacities
- Jacking devices and procedures

Figure 3-103. Erection plan and procedures checklist.

development of approval checklists. Figure 3-103 provides the summary checklist developed in this portion of NCHRP Project 12-79's Task 9.

3.6.2 Recommendations for Methods of Structural Analysis and Other Calculations

The reader is referred to Sections 3.1 through 3.6 of Appendix B for summary recommendations on methods of structural analysis and other calculations. Section 3.1 provides an introduction to this topic. Section 3.2 specifically provides quantitative guidance on the accuracy of various analysis methods, organized according to key parameters related to bridge geometry and framing. These analysis accuracy tables are supplemented with examples illustrating their use. Section 3.3 specifically provides guidelines on calculations for structural adequacy and especially stability of the steel framing during construction, as well as guidance on myriad associated issues such as cantilever girders, uplift, temporary hold cranes and support loads, bearing, cross-frames, and bracing. Section 3.5 specifically addresses miscellaneous calculations and recommendations for crane pick locations, alignment of field splice and cross frame connections, and support conditions. Section 3.6 provides a useful calculation checklist. This checklist is shown as Figure 3-104 for ease of reference.

3.6.3 Design and Construction Considerations for Ease of Analysis via Improved Behavior

There are a number of ways to improve analysis accuracy while simultaneously improving the behavior and constructability of steel girder bridges by means of wisely establishing

- Complete analysis of erection sequence
    1. Proper level of analysis used
    2. Support conditions modeled appropriately at all stages
- Correct design criteria employed
- Correct loads investigated
- Complete checks of structural adequacy of bridge components
- Complete checks of stability of girder and bridge system
- Second-order amplification effects addressed as needed
- Girder reactions checked for uplift
- Temporary hold crane loads computed
- Temporary support loads computed
- Bearing capacity and rotation checks
- Cross frame and bracing placement
- Checks of structural adequacy of temporary supports and devices
    1. Falsework towers
    2. Girder tie-downs
    3. Lifting beams
    4. Jacking devices
- Crane pick location calculations
- Checks of displacements at field splices
- Checks of displacements for cross frame placement

Figure 3-104. Calculation checklist.

the framing plan for the structure and by avoiding problematic details. Problematic details are in fact a significant enough topic to warrant separate discussion in Section 3.6.4 of this report.

A wisely established framing plan is one that provides clean, direct load paths and specifically avoids use of secondary bracing members (such as cross-frames) in locations where they would be anticipated to carry significantly high loads as a function of displacement compatibility. Examples include the use of lean-on bracing or omitting selected cross-frames near supports in severely skewed bridges, as cited in Krupicka and Poellot (1993).

3.6.4 Problematic Physical Characteristics and Details to Avoid

The reader is referred to Section 3.7 of Appendix B for a discussion of problematic characteristics and details such as oversize or slotted holes, narrow bridges or bridge units, V-type cross-frames without top chords, bent-plate connections in I-girder bridges, long span I-girder bridges without top flange lateral bracing systems, partial-depth end diaphragms in tub-girder bridges, non-collinear external intermediate diaphragms in tub-girder bridges, and two-girder bearing systems at tub-girder supports.

CHAPTER 4

Conclusions and Recommendations

4.1 Summary

Based on the results of the research conducted on this project, the following conclusions may be drawn:

- Conventional 1D line-girder and 2D-grid methods of analysis are capable of predicting accurate construction responses in many situations; however, there are definite bridge geometries where significant reductions in accuracy can be expected. This research has provided a scoring method engineers can utilize as an aid to gage the accuracy of these simplified tools. Several examples are provided illustrating how the scoring system can be applied most effectively.
- The research identified a number of critical shortcomings in commonly used conventional methods and, in each case, provided mechanistic evaluations of the reasons for the shortcomings and recommended improved procedures that remove or alleviate these flaws. For I-girder bridges, the key critical flaws identified were:
  1. The common dramatic underestimation of I-girder torsional stiffnesses by using solely the St. Venant torsional stiffness GJ/L in 2D-grid analysis methods. This flaw was addressed by the development and use of an equivalent St. Venant torsion constant that approximates the increase in the girder torsional stiffnesses due to the restraint of warping.
  2. The common usage of equivalent beam elements for cross-frames that are unable to capture the physical load-deformation characteristics of these components. This problem was addressed by developing a procedure to obtain relatively accurate equivalent beam properties using a Timoshenko beam approximation rather than a Euler-Bernoulli equivalent beam element. In addition, "exact" equivalent beam elements were developed for a complete range of practical I-girder bridge cross-frame types.
  3. The lack of any direct method of evaluating flange lateral bending stresses due to skew in I-girder bridges. The NCHRP Project 12-79 research developed an approximate procedure that works directly with the more accurate values of the cross-frame forces obtained using the above two improvements.
  4. The lack of consideration of locked-in force effects associated with SDLF and TDLF detailing of the cross-frames. These locked-in forces are due to the lack of fit between the cross-frames and the girders in the initially fabricated (cambered and plumb) girder geometry. This issue was addressed by recommending a streamlined procedure for calculating these effects using cross-frame element initial strains, initial stresses, or initial (fixed-end) forces. Thorough case study examples were presented to provide practical guidance for when the influence of the above locked-in effects should be considered in design.

Several areas of important improvements were also identified for tub-girder bridge analysis:

1. A method was developed for simplified estimation of the internal torques due to skew in tub girders,

2. The impact of skew on box-girder cross-section distortion was directly evaluated and it was shown that the distortion associated with skew effects is typically minor, and
3. A method of accounting for a localized spike or "saw-tooth" in the longitudinal average normal stress distribution in the top flanges of tub girders, caused by the interaction with diagonals in the top flange lateral bracing (TFLB) system, was developed.

- Lastly, this research developed a guidelines document providing recommendations on the level of construction analysis, plan detail, and submittals for curved and skewed steel I- and tub-girder bridges. These guidelines were developed in a specification and commentary format suitable for direct incorporation into other specifications or guideline documents.

4.2 Recommendations for Implementation

The recommendations for implementation of the results of this research are aimed at evolutionary improvements to the current state of practice for steel girder bridge engineering. These recommendations are primarily focused on the following items, which relate directly to the original scope of the research:

1. **Improvements to Conventional Analysis Methods:** Specifically, improvements to the modeling of I-girder torsional stiffness, the modeling of cross-frames' overall stiffness in 2D-grid analyses, the calculation of flange lateral bending stresses from 2D-grid analyses, calculation of fit-up forces due to cross-frame detailing, and simplified analysis improvements for tub-girder bridges.
2. **Definition of Erection Engineering Tasks:** Specifically, a detailed list of recommended items to investigate as part of the erection engineering effort, with commentary, building on existing engineering guidelines as currently published by AASHTO.
3. **Recommendations for Appropriate Level of Analysis Refinement:** Specifically, a set of simple tables providing "letter grade" assessments of the anticipated accuracy of various analysis methods (1D and conventional 2D-grid vs. 3D benchmark solutions) corresponding to the framing and geometry of a given bridge.

The first of these recommendations takes the form of explicit definition of the suggested improvements. The implementation of most of these recommendations would have to be undertaken voluntarily by the structural engineering software industry, but it is hoped that market pressures would encourage implementation. The implementation of the remainder of these improvements would be through education of the design community.

It is recommended that the second and third recommendations would take the form of a guidelines document, published by AASHTO in the form of a guide specification that could be adopted, referenced, or excerpted by the various state DOTs. Various modifications to the AASHTO (2010 and 2010b) Specifications could be provided to make the Specifications consistent with the detailed guidelines.

4.2.1 Improvements to Conventional Analysis Methods

This research produced a number of recommendations for improvements to conventional analysis methods. These recommendations are detailed in Section 3.2 of this report. A summary of these recommendations with implementation strategies is provided in Table 4-1.

4.2.2 Definition of Erection Engineering Tasks

Currently, there is no nationally recognized guideline addressing erection engineering and erection plans for curved and/or skewed steel girder bridges. The closest nationally recognized

Table 4-1. Analysis improvements and recommendations for implementation.

Improvement	Report Section	Description	Implementation Strategy
Improved I-Girder Torsion Model for 2D-Grid Analysis	3.2.2	Current 2D-grid methods typically neglect warping stiffness, which is a key parameter in the torsional stiffness of an I-girder. Methods for improving the torsional model of an I-girder are provided.	Provide specific methodologies (presented in this report) to the bridge software industry and encourage their implementation in commercial bridge design software. Provide education (through this report and through associated presentations/publications) on this topic to the bridge engineering community. Encourage implementation in commercial bridge design software.
Improved Equivalent Beam Cross-Frame Models	3.2.3	Current 2D-grid methods use simplified models of cross-frame stiffness that mispredict cross-frame load-deformation characteristics. A method for improving the modeling of cross-frame stiffness is provided.	
Improved Calculation of I-Girder Flange Lateral Bending Stresses	3.2.4	Current 2D-grid methods use a simplified approach for calculation of I-girder flange lateral bending stresses and do not provide any direct calculation of flange lateral bending stresses due to skew effects. An improved method is provided.	
Calculation of Locked-in Forces due to Cross-Frame Detailing	3.2.5	Currently, bridge engineers do not typically include locked-in forces in bridge design. Guidance on proper evaluation of lack-of-fit forces is provided.	Provide specific methodologies (presented in this report) to the bridge software industry and encourage their implementation in commercial bridge design software. Provide education (through this report and through associated presentations/publications) on this topic to the bridge engineering community. Encourage implementation in commercial bridge design software.
Simplified Analysis Improvements for Tub-Girder Bridges	3.2.6	2D-grid analysis is not capable of directly predicting all responses in tub girders, particularly with regard to internal framing responses. Improvements for simplified analysis methods are provided.	
Estimation of Fit-up Forces	3.3.5	Currently, bridge engineers do not typically evaluate fit-up forces in a consistently correct manner. Guidance on proper evaluation of fit-up forces is provided.	Provide education (through this report and through associated presentations/publications) on this topic to the bridge engineering community. Software implementation of the recommended improvements from Sections 3.2.2 through 3.2.5 will permit the estimation of fit-up forces using simplified 2D-grid methods in I-girder bridges. Implementation of Section 3.2.5 to 3D FEA methods is essential for comprehensive evaluation of fit-up forces using these methods. The improvements recommended in Section 3.2.6 are not directly related to the evaluation of fit-up forces in tub-girder bridges.

guideline is the AASHTO/NSBA Steel Bridge Collaboration Guide Specification S10.1 – 2007, *Steel Bridge Erection Guide Specification.*

This report addresses this lack of guidance in Appendix B, Recommendations for Construction Plan Details and Level of Construction Analysis. This appendix provides specific guidelines and commentary on recommendations for construction plan details and recommendations for methods of structural analysis and calculations. These guidelines are comprehensive and address all aspects of erection engineering plans and calculations. An owner-agency could adopt the guidelines as a complete specification, could reference the guidelines in their erection specifications, or could adopt all or portions of the guidelines in their specifications.

4.2.3 Recommendations for Appropriate Level of Analysis Refinement

Section 3.1 of this report outlines simplified equations to check for (and prevent) large second-order amplification in I-girder bridges. When tub girders are fabricated with proper internal cross-frames to restrain their cross-section distortion as well as a proper top flange lateral bracing (TFLB) system, second-order amplification of the overall deformations is practically nonexistent. Simplified rules are provided for identifying cases where overall overturning stability and potential uplift at bearing locations is more likely in both I-girder and tub-girder bridges.

A basic scoring table is provided for assessing the anticipated accuracy of 1D line-girder and conventional 2D-grid methods as a function of the framing and geometry of a given bridge. With the implementation of the recommended improvements to the conventional 2D-grid methods, the accuracy of a 2D-grid analysis is improved to the extent that comparable solutions to 3D FEA are obtained for the assessment of gravity-load responses during construction as long as:

- There are at least two I-girders connected together, and
- They are connected by enough cross-frames such that the connectivity index

$$I_C = \frac{15000}{R\left(n_{cf}+1\right)m}$$

is less than 20 ($I_C \leq 20$).

4.2.4 Recommendations for Specific Revisions to AASHTO Documents

The research accomplished by NCHRP Project 12-79 covers both design engineering and erection engineering, as well as detailing, fabrication, and erection of steel girder bridges. As a result, there are some areas where more than one option exists for specific implementation of the recommendations of this project in the form of revisions to AASHTO documents. In some cases, a single recommendation for revisions to AASHTO documents is provided below; in other cases, when appropriate, a second recommendation is listed as an option.

Also, as previously mentioned in Section 4.2.1, the success of the recommendations resulting from this research related to improvements to conventional analysis methods are critically dependent upon implementation in commercial software. Specific updates to provisions in the AASHTO LRFD Bridge Design Specifications are important to provide the endorsement and authority of AASHTO behind these recommendations, while these provisions must be written in a way to maintain freedom for software providers and engineers to use any legitimate method of analysis that provides sufficient accuracy for a given design. Detailed presentation of the procedures in AASHTO guidelines documents is critical for end users to understand the methods and how to use them.

Thus, the four primary options for implementation of specific revisions to AASHTO documents are:

1. Revisions to the AASHTO LRFD Bridge Design Specifications.
2. Revisions to the AASHTO LRFD Bridge Construction Specifications.
3. Revisions to appropriate AASHTO/NSBA Steel Bridge Collaboration Guideline or Guide Specification documents.
4. Separate publication and dissemination to the bridge industry.

A key advantage to implementation in an AASHTO/NSBA standard is that doing so will offer thorough vetting of practice recommendations with broad representation, including owners, design engineers, engineers who perform erection calculations and analysis, fabricators, and contractors.

The specific recommendations are listed in Table 4-2, with primary (and if appropriate, secondary) implementation suggestions.

4.3 Further Research Needs

The NCHRP Project 12-79 research has provided a relatively comprehensive assessment and synthesis of the adequacy of simplified 1D and 2D analysis methods for prediction of the constructability and of the constructed geometry of curved and/or skewed steel girder bridges. A guidelines document has been developed based on this research, providing recommendations on the level of construction analysis, plan detail, and submittals for curved and skewed steel girder bridges. Nevertheless, there are a number of related areas that merit further study:

- **Fit-up Practices—**A focused, comprehensive investigation of the impact of various decisions and procedures on the fit-up of steel girder bridges during erection would be very fruitful. A fit-up decision is made on every steel bridge project and usually, due to lack of other direction, the decision is made by the fabricator. The decision impacts constructability of the bridge members during erection, loads in the steel bridge system, and the final bridge geometry. This practice has been customary from the earliest days of steel bridge construction, but there has been little study of actual implications of the decision. This investigation should address the various impacts on fit-up forces, locked-in stresses, and final constructed geometry. The collective knowledge of fit-up issues in the steel bridge industry today (2012) is based almost entirely on qualitative experience. Partial knowledge of each aspect of the issues is typically highly compartmentalized: steel detailers, fabricators, and erectors have knowledge and preferences on detailing practices, designers have knowledge and preferences on how to perform structural analysis for final conditions, and owners have knowledge and preferences regarding the final geometry of bridges.

  A comprehensive knowledge of all aspects of these issues by all parties is lacking. Furthermore, all parties only have limited understanding regarding the possible implications of detailing methods on the structural behavior. This research should involve more than just the application and exercise of sophisticated analytical tools; the analytical assessments will be most useful if they are coupled with high-resolution, high-quality field measurements. The emphasis should be placed on I-girder bridges with NLF, SDLF, and TDLF detailing, but some assessment of the specific causes of fit-up issues in tub-girder bridges also would be a valuable contribution.
- **Early Concrete Deck Stiffness and Strength—**More extensive coupled field and analytical evaluation of the effects of early concrete deck stiffness and strength gains, including the influence of staged concrete deck placement would be very valuable. Prior research addressing this consideration shows generally that significant early stiffness and strength gains can exist. However, the studies have been limited to only a few bridges and a few parameters of the

(continued on page 154)

Table 4-2. Recommendations for specific revisions to AASHTO documents.

Recommendation	Report Section	Implementation Suggestion	Comments
Checking for (and Preventing) Large Global Second-Order Amplification	NCHRP Report 725 § 3.1.1.1	PRIMARY: Provide §3 .2.2 to the AASHTO/NSBA Steel Bridge Collaboration for vetting by the industry and for organization and publication in one or more AASHTO/NSBA Steel Bridge Collaboration documents. The initial recommendation of the research team would be for the Collaboration to consider publication of the content of § 3.2.2 in the AASHTO/NSBA Steel Bridge Collaboration Document G13.1, Guidelines for Steel Girder Bridge Analysis. G13.1 does not presently address simplified estimation of global second-order amplification of girder stresses and displacements. Provide a requirement in Article 6.10.1.6 of the AASHTO LRFD Bridge Design Specifications that potential global second-order amplification shall be considered. Provide Eqs. 2 through 4 as one approach for estimating global second-order amplification in Article C6.10.1.6, and provide guidance for when global second-order amplification is apt to be of concern (e.g., long narrow bridge units with a limited number of girders).	There is no significant precedent for prescribing modeling specifics to this high a level of detail in the AASHTO LRFD Bridge Design Specifications. Generally, designers are allowed leeway in choosing specific modeling strategies, provided they understand the implications of their decisions.
		SECONDARY:P rovide education (through this report and through associated presentations/publications) on this topic to the bridge engineering community.	

(continued on next page)

Table 4-2. (Continued).

Recommendation	Report Section	Implementation Suggestion	Comments
Second-Order Amplification of Flange Lateral Bending Stresses between Cross-Frame Locations	NCHRP Report 725 § 3.1.1.2	PRIMARY: Provide § 3.2.2 to the AASHTO/NSBA Steel Bridge Collaboration for vetting by the industry and for organization and publication in one or more AASHTO/NSBA Steel Bridge Collaboration documents. The initial recommendation of the research team would be for the Collaboration to consider publication of the content of § 3.2.2 in the AASHTO/NSBA Steel Bridge Collaboration Document G13.1, Guidelines for Steel Girder Bridge Analysis. G13.1 presently does not address the characteristic of the flange lateral bending amplification illustrated by Figure 3-1. Provide Figure 3-1 and a brief discussion of the behavior for Article C6.10.1.6 of the AASHTO LRFD Bridge Design Specifications.	There is no significant precedent for prescribing analysis specifics to this high a level of detail in the AASHTO LRFD Bridge Design Specifications. Generally, designers are allowed some leeway between choosing to use simpler, more conservative methods vs. more complicated, more refined methods when evaluating second-order effects and when choosing design strategies to minimize or mitigate such effects, provided they understand the implications of their decisions.
		SECONDARY: Provide education (through this report and through associated presentations/publications) on this topic to the bridge engineering community.	
Overturning Stability	NCHRP Report 725 § 3.1.1.3	PRIMARY: Provide a paragraph for Article C6.10.3.1 that introduces the torsion index I_T (Eq. 1) and Figure 2-3 and discusses the use of I_T as a rough indicator of situations when uplift at bearings should be considered.	This is a simple revision to the AASHTO specifications that would be of value to designers.

Improved I-Girder Torsion Model for 2D-Grid Analysis	NCHRP Report 725 § 3.2.2	PRIMARY: Provide § 3.2.2 to the AASHTO/NSBA Steel Bridge Collaboration for vetting by the industry and for organization and publication in one or more AASHTO/NSBA Steel Bridge Collaboration documents. The initial recommendation of the research team would be for the Collaboration to consider publication of the content of § 3.2.2 in the AASHTO/NSBA Steel Bridge Collaboration Document G13.1, Guidelines for Steel Girder Bridge Analysis. G13.1 does not presently address the flaws associated with under-representation of I-girder torsional stiffness by using the conventional *J* and neglecting the flange warping stiffness. Provide a specific paragraph for Article 4.6.2.2.1 of the AASHTO LRFD Bridge Design Specifications indicating that the warping stiffness of steel I-girder flanges shall be considered in the structural analysis when the I-girders are subjected to torsion. Provide a specific paragraph to introduce Eqs. 11 and 12, for J_{eq}, and Eq. 8, for I_C (used to define the limits of applicability of $J_{eq)}$ immediately after the presentation of Eqs. (C4.6.2.2.1-1) through (C4.6.2.2.1-3) in Article C4.6.2.2.1 of the AASHTO LRFD Bridge Design Specifications. Explain that the direct use of open-section thin-walled beam theory, or a general 3D FEA, are other ways of considering steel I-girder flange warping stiffness. Provide a brief explanation of the potential pitfalls of not considering the girder flange warping stiffness in the structural analysis. Provide a reference to the updated AASHTO/NSBA Collaboration Document G13.1 for more detailed information. Provide a discussion of the modeling problem illustrated by Figure 3-9, complete with this figure, in Article C4.6.1.2.4b of the AASHTO LRFD Bridge Design Specifications. Provide a requirement that the flange warping stiffness shall be accounted for in the modeling of curved steel I-section members in Article 4.6.1.2.4b.	There is no significant precedent for prescribing modeling specifics to this high a level of detail in the AASHTO LRFD Bridge Design Specifications. Generally, designers are allowed leeway in choosing specific modeling strategies provided they understand the implications of their decisions.
		SECONDARY: Publish specific methodologies (presented in this report), present them to the bridge software industry, and encourage their implementation in commercial bridge design software.	

(continued on next page)

Table 4-2. (Continued).

Recommendation	Report Section	Implementation Suggestion	Comments
Improved Equivalent Beam Cross-Frame Models	NCHRP Report 725 § 3.2.3	PRIMARY: Provide § 3.2.3 to the AASHTO/NSBA Steel Bridge Collaboration for vetting by the industry and for organization and publication in one or more AASHTO/NSBA Steel Bridge Collaboration documents. The initial recommendation of the research team would be for the Collaboration to consider publication of the content of § 3.2.3 in the AASHTO/NSBA Steel Bridge Collaboration Document G13.1, Guidelines for Steel Girder Bridge Analysis. G13.1 currently presents the "flexural analogy" and "shear analogy" methods of modeling cross-frames without discussion of their flaws. Provide a requirement in Article 6.7.4.1 of the AASHTO LRFD Bridge Design Specifications that flexural and shear deformation should be considered in the modeling of cross-frames as equivalent beam elements, and provide a reference to G13.1 for detailed discussion from Article C6.7.4.1.	There is no significant precedent for prescribing modeling specifics to this high a level of detail in the AASHTO LRFD Bridge Design Specifications. Generally, designers are allowed leeway in choosing specific modeling strategies provided they understand the implications of their decisions. Presently, there is no discussion regarding equivalent beam modeling of cross-frames in the AASHTO LRFD Bridge Design Specifications.
		SECONDARY: Publish specific methodologies (presented in this report), present them to the bridge software industry, and encourage their implementation in commercial bridge design software.	
Improved Calculation of I-Girder Flange Lateral Bending Stresses	NCHRP Report 725 § 3.2.4	PRIMARY: Provide § 3.2.4 to the AASHTO/NSBA Steel Bridge Collaboration for vetting by the industry and for organization and publication in one or more AASHTO/NSBA Steel Bridge Collaboration documents. The initial recommendation of the research team would be for the Collaboration to consider publication of the content of § 3.2.4 in the AASHTO/NSBA Steel Bridge Collaboration Document G13.1, Guidelines for Steel Girder Bridge Analysis. G13.1 presently does not explain how I-girder flange lateral bending stresses can be calculated given the equivalent flange level lateral forces transmitted by the cross-frames. Provide a brief discussion of the recommended calculation of I-girder flange lateral bending stresses in Article C6.10.1 of the AASHTO LRFD Bridge Design Specifications, with reference to G13.1 for detailed discussion.	There is no significant precedent for prescribing modeling specifics to this high a level of detail in the AASHTO LRFD Bridge Design Specifications. Generally, designers are allowed leeway in choosing specific modeling strategies provided they understand the implications of their decisions.
		SECONDARY: Publish specific methodologies (presented in this report), present them to the bridge software industry, and encourage their implementation in commercial bridge design software.	

Calculation of Locked-in Forces Due to Cross-Frame Detailing	NCHRP Report 725 § 3.2.5	PRIMARY: Provide § 3.2.5 to the AASHTO/NSBA Steel Bridge Collaboration for vetting by the industry and for organization and publication in one or more AASHTO/NSBA Steel Bridge Collaboration documents. The initial recommendation of the research team would be for the Collaboration to consider publication of the content of § 3.2.5 in the AASHTO/NSBA Steel Bridge Collaboration Document G13.1, Guidelines for Steel Girder Bridge Analysis. Provide minor updates to Article C6.7.2 of the AASHTO LRFD Bridge Design Specifications to clarify the multiple uses of the term "erected position" and to clarify that locked-in cross-frame forces and negative flange lateral bending stresses are generally additive with the dead load effects in curved radially supported bridges, with references to G13.1 for detailed discussion.	The need for detailed analytical evaluation of locked-in forces due to cross-frame detailing varies from bridge to bridge (as explained in § 3.3.4 of this report), and this type of analysis is currently not commonly performed in practice. At this time, the best strategy is to publicize the issues, provide education on how to address these issues, and seek industry input in formulating policy regarding the need, and best practices, for detailed analytical evaluations.
		SECONDARY: Provide education (through this report and through associated presentations/publications) on this topic to the bridge engineering community. Encourage implementation in bridge design software.	
Simplified Analysis Improvements for Tub-Girder Bridges	NCHRP Report 725 § 3.2.6	PRIMARY: Provide § 3.2.6 to the AASHTO/NSBA Steel Bridge Collaboration for vetting by the industry and for organization and publication in one or more AASHTO/NSBA Steel Bridge Collaboration documents. The initial recommendation of the research team would be for the Collaboration to consider publication of the content of § 3.2.6 in the AASHTO/NSBA Steel Bridge Collaboration Document G13.1, Guidelines for Steel Girder Bridge Analysis.	There is no significant precedent for prescribing modeling specifics to this high a level of detail in the AASHTO LRFD Bridge Design Specifications. Generally, designers are allowed leeway in choosing specific modeling strategies provided they understand the implications of their decisions. Presently, there is no discussion of the detailed component force equations from Fan and Helwig (1999 and 2002) in the AASHTO LRFD Bridge Design Specifications. These equations are discussed in the AASHTO/NSBA Steel Bridge Collaboration Document G13.1. The research team recommends that G13.1 is the preferred location for discussion of these details.
		SECONDARY: Provide education (through this report and through associated presentations/publications) on this topic to the bridge engineering community.	

(continued on next page)

Table 4-2. (Continued).

Recommendation	Report Section	Implementation Suggestion	Comments
Estimation of Fit-up Forces	NCHRP Report 725 § 3.3.5	PRIMARY: Provide § 3.3.5 to the AASHTO/NSBA Steel Bridge Collaboration for vetting by the industry and for organization and publication in one or more AASHTO/NSBA Steel Bridge Collaboration documents. The initial recommendation of the research team would be for the Collaboration to consider publication of the content of § 3.2.2 in the AASHTO/NSBA Steel Bridge Collaboration Document G13.1, Guidelines for Steel Girder Bridge Analysis.	The need for detailed analytical evaluation of locked-in forces due to cross-frame detailing varies from bridge to bridge (as explained in § 3.3.4 of this report), and this type of analysis is currently not commonly performed in practice. At this time, the best strategy is to publicize the issues, provide education on how to address these issues, and seek industry input in formulating policy regarding the need, and best practices, for detailed analytical evaluations. If appropriate discussions are developed by the AASHTO/NSBA Collaboration, references to this material should be provided in commentary to Articles 11.6.4.2 and 11.6.5 of the AASHTO LRFD Bridge Construction Specifications.
		SECONDARY: Provide education (through this report and through associated presentations/publications) on this topic to the bridge engineering community.	
Definition of Erection Engineering Tasks	Task 9 Report § 2	PRIMARY: Provide the Task 9 report to the AASHTO/NSBA Steel Bridge Collaboration for vetting by the industry and for organization and publication in one or more AASHTO/NSBA Steel Bridge Collaboration documents. The initial recommendation of the research team would be for the Collaboration to consider publication of the content of the Task 9 report in the AASHTO/NSBA Steel Bridge Collaboration Guide Specification S10.1, Steel Bridge Erection Guide Specifications.	§ 2 of the Task 9 report is titled Recommendations for Construction Plan Details and addresses all aspects of the documentation of the erection plan for a steel girder bridge, including both drawings and calculations. This section of the Task 9 report is already written in the format of "requirement" and associated "commentary." As such, it can be adopted easily and directly into either the S10.1 Guide Specification or the AASHTO LRFD Bridge Construction Specifications. Adoption in either document would allow national dissemination of the guidelines and provide bridge owners the opportunity to adopt the guidelines directly, by reference as a whole or in parts, or by means of transferring some or all of the provisions into their own specifications and policy documents. The primary recommendation of publication via an AASHTO/NSBA Steel Bridge Collaboration Guideline or Guide Specification reflects the recommendation of the research team to publish a single, cohesive, comprehensive guideline document that addresses the entire set of steel bridge erection documentation requirements, including both erection engineering calculations and plans.
		SECONDARY: Package § 2 of the Task 9 report in its entirety as a ballot item for incorporation into the AASHTO LRFD Bridge Construction Specifications in a revision of § 11.2.2 – Erection Drawings.	

Recommendations for Appropriate Level of Analysis Refinement	NCHRP Report 725 § 3.1 Task 9 Report § 3.2	PRIMARY: Provide the Task 9 report to the AASHTO/NSBA Steel Bridge Collaboration for vetting by the industry and for organization and publication in one or more AASHTO/NSBA Steel Bridge Collaboration documents. The initial recommendation of the research team would be for the Collaboration to consider publication of the content of the Task 9 report in the AASHTO/NSBA Steel Bridge Collaboration Guide Specification S10.1, Steel Bridge Erection Guide Specifications. SECONDARY: Rewrite § 3.2 of the Task 9 report into the format of a ballot item for incorporation into the AASHTO LRFD Bridge Construction Specifications in a revised and re-titled version of § 11.6.4.2. The proposed new title of this section would be Evaluation of Stability, Stresses, and Constructed Geometry During Erection.	The recommendations regarding the appropriate level of analysis refinement are the heart of the research results of NCHRP Project 12-79, and these recommendations should receive as wide and intense a distribution as possible. However, a brief presentation of these recommendations is not feasible. As can be seen in § 3.1 of NCHRP Report 725 or § 3.2 of the Task 9 report, the matrices for recommended level of analysis are large and warrant substantial commentary and examples. For this reason, the primary recommendation of the research team is to publish these recommendations in a document where a more lengthy presentation of the guidelines is more appropriate. The more flexible intent and format of the AASHTO/NSBA Steel Bridge Collaboration documents provides such a mechanism. Publication of these recommendations in the AASHTO LRFD Bridge Design Specifications or LRFD Bridge Construction Specifications is possible, but less desirable due to concerns that the length of the presentation would undesirably encumber the presentation and understanding of the recommendations. The primary recommendation of publication via an AASHTO/NSBA Steel Bridge Collaboration Guideline or Guide Specification reflects the recommendation of the research team to publish a single, cohesive, comprehensive guideline document that addresses the entire set of steel bridge erection documentation requirements, including both erection engineering calculations and plans. These particular analysis recommendations blur the line between design and construction. Therefore the secondary recommendation to publish these recommendations in the AASHTO LRFD Bridge Construction Specifications (rather than the AASHTO LRFD Bridge Design Specifications) reflects the opinion of the research team that this type of analysis is heavily dependent on the individual contractor's chosen erection sequence and erection methods. This type of engineering analysis is not typically the responsibility of the engineer who develops the design documents for bidding, but rather is the responsibility of the contractor's engineer who develops/analyzes the contractor's specific erection plan.

(continued on next page)

Table 4-2. (Continued).

Recommendation	Report Section	Implementation Suggestion	Comments
Guidelines on Calculations for Structural Adequacy and Stability	Task 9 Report § 3.3	PRIMARY: Provide the Task 9 report to the AASHTO/NSBA Steel Bridge Collaboration for vetting by the industry and for organization and publication in one or more AASHTO/NSBA Steel Bridge Collaboration documents. The initial recommendation of the research team would be for the Collaboration to consider publication of the content of the Task 9 report in the AASHTO/NSBA Steel Bridge Collaboration Guide Specification S10.1, Steel Bridge Erection Guide Specifications.	The primary recommendation of publication via an AASHTO/NSBA Steel Bridge Collaboration Guideline or Guide Specification reflects the recommendation of the research team to publish a single, cohesive, comprehensive guideline document that addresses the entire set of steel bridge erection documentation requirements, including both erection engineering calculations and plans. These particular analysis recommendations blur the line between design and construction. Therefore the secondary recommendation to publish these recommendations in the AASHTO LRFD Bridge Construction Specifications (rather than the AASHTO LRFD Bridge Design Specifications) reflects the opinion of the research team that this type of analysis is heavily dependent on the individual contractor's chosen erection sequence and erection methods. This type of engineering analysis is not typically the responsibility of the engineer who develops the design documents for bidding, but rather is the responsibility of the contractor's engineer who develops/analyzes the contractor's specific erection plan.
		SECONDARY: Rewrite § 3.3 through 3.6 of the Task 9 report into the format of a ballot item for incorporation into the AASHTO LRFD Bridge Construction Specifications in a revised and re-titled version of § 11.6.4.2. The proposed new title of this section would be Evaluation of Stability, Stresses, and Constructed Geometry during Erection.	
Guidelines for Structural Adequacy of Temporary Components	Task 9 Report § 3.4	Same as for Task 9 report, § 3.3	Same as for Task 9 report, § 3.3
Miscellaneous Calculations and Recommendations	Task 9 Report § 3.5	Same as for Task 9 report, § 3.3	Same as for Task 9 report, § 3.3
Calculation Checklist	Task 9 Report § 3.6	Same as for Task 9 report, § 3.3	Same as for Task 9 report, § 3.3

Problematic Characteristics and Details to Avoid	Task 9 Report § 3.4	PRIMARY: Provide the Task 9 report to the AASHTO/NSBA Steel Bridge Collaboration for vetting by the industry and for organization and publication in one or more AASHTO/NSBA Steel Bridge Collaboration documents. The initial recommendation of the research team would be for the Collaboration to consider publication of the content of the Task 9 report in the AASHTO/NSBA Steel Bridge Collaboration Guide Specification S10.1, Steel Bridge Erection Guide Specifications. SECONDARY: Rewrite § 3.3 through 3.7 of the Task 9 report into the format of a ballot item for incorporation into the AASHTO LRFD Bridge Design Specifications in a new section, § 6.7.8. The proposed new title of this section would be Problematic Details to Avoid.	The recommendations related to problematic details to avoid are focused on the effect of these details on erection of steel girder bridges. Although this is more clearly a design issue since these decisions are typically made by the design engineer long before the contract is let to a contractor, these specific recommendations do not necessarily rise to the level of prescriptive specification requirements. Thus, the primary recommendation of publication via an AASHTO/NSBA Steel Bridge Collaboration Guideline or Guide Specification reflects the recommendation of the research team to publish a single, cohesive, comprehensive guideline document that addresses the entire set of steel bridge erection documentation requirements, including both erection engineering calculations and plans, and the associated hope that design engineers also will read this document and implement design strategies that will facilitate easy erection of steel girder bridges. The secondary recommendation of publication in the AASHTO LRFD Bridge Design Specifications in a new § 6.7.8 reflects the difficulty in placing these general recommendations in a specific section of the design code. As a compromise, a new section of the code is proposed. A third option could be considered, where the individual recommendations are scattered through the code in sections more directly related to each individual recommendation’s specific subject.

concrete mix design and methods of construction. A more comprehensive understanding of the actual early-age behavior during and after placement of concrete decks is needed if engineers are to take optimum advantage of the early strength gains. Furthermore, as noted in the NCHRP Project 12-79 research, there is no such thing as a conservative displacement prediction. Sufficient measurements and corresponding analytical predictions are needed to allow the calculation of confidence limits for the predicted displacements during and after the concrete deck placement.

- **Innovative Framing Arrangements—**Further studies of innovative framing arrangements to mitigate nuisance stiffness effects in skewed girder bridge construction would be useful. For example, as detailed in the Task 8 report of the NCHRP Project 12-79 research, further research should be conducted to investigate the use of skewed intermediate cross-frames at angles larger than 20°, combined with a split-pipe connection detail to mitigate the problems of connecting to the girders at a sharp skew angle. As demonstrated in the NCHRP Project 12-79 research, nuisance stiffness effects are mitigated best by making the intermediate cross-frames parallel to the bearing lines in parallel-skew bridges and by "fanning" the intermediate cross-frames between the skewed bearing lines in bridges with non-parallel skew. The behavior of straight and curved bridges with these arrangements should be investigated in more detail, including the consideration of other impacts that these cross-frame arrangements may have on the design behavior and construction.
- **Tub Girders with Pratt TFLB Systems—**The impact of Pratt top flange lateral bracing (TFLB) system layouts on the internal forces in tub-girder bridges needs to be better understood. The NCHRP Project 12-79 research showed that a conventional 2D-grid analysis, coupled with commonly used tub-girder bridge component force equations, has particular difficulty in predicting the response of these types of bridges. Further improvements to 2D-grid analysis methods may be possible to make these methods viable for the design of tub-girder bridges with Pratt TFLB systems.
- **Live-Load Effects—**Lastly, the emphasis of the NCHRP Project 12-79 research was on analysis for construction engineering of steel girder bridges. Parallel studies should be conducted to evaluate the accuracy of simplified methods of analysis for the prediction of the live-load response of bridges. Of concern is the tedious nature and limited accuracy of traditional load distribution factor calculations for horizontally curved and/or skewed girder bridges as a function of the complexity of the bridge geometry. Engineers need to better understand the limits of their analysis calculations regarding the live-load response of steel girder bridge systems.

References and Bibliography

AASHTO (2010). AASHTO LRFD *Bridge Design Specifications,* 5th Edition with 2010 Interim Revisions, American Association of State Highway and Transportation Officials, Washington, D.C.

AASHTO (2010b). *AASHTO LRFD Bridge Construction Specifications,* 3rd Edition with 2010 and 2011 Interim Revisions, American Association of State Highway and Transportation Officials, Washington, D.C.

AASHTO/NSBA (2011). *Guidelines for the Analysis of Steel Girder Bridges,* G13.1, AASHTO/NSBA Steel Bridge Collaboration, American Association of State Highway and Transportation Officials, Washington, D.C. and National Steel Bridge Alliance, Chicago, IL.

AASHTO/NSBA (2007). *Steel Bridge Erection Guide Specification,* S10.1, AASHTO/NSBA Steel Bridge Collaboration, American Association of State Highway and Transportation Officials, Washington, D.C. and National Steel Bridge Alliance, Chicago, IL.

AASHTO/NSBA (2006). *Guidelines for Design Details,* G1.4, AASHTO/NSBA Steel Bridge Collaboration, American Association of State Highway and Transportation Officials, Washington, D.C. and National Steel Bridge Alliance, Chicago, IL.

AASHTO/NSBA (2003). *Guidelines for Design for Constructibility*, G12.1, AASHTO/NSBA Steel Bridge Collaboration, American Association of State Highway and Transportation Officials, Washington, D.C. and National Steel Bridge Alliance, Chicago, IL.

Ahmed, M.Z. and Weisberger, F.E. (1996). "Torsion Constant for Matrix Analysis of Structures Including Warping Effect," *International Journal of Solids and Structures,* Elsevier, 33(3), 361–374.

Bridgesoft, Inc. (2010). "STLBRIDGE, Continuous Steel Bridge Design," http://bridgesoftinc.com/

Chang, C.-J. (2006). "Construction Simulation of Curved Steel I-Girder Bridges," doctoral dissertation, School of Civil and Environmental Engineering, Georgia Institute of Technology, Atlanta, GA, 340 pp.

Chang, C.-J. and White, D.W. (2008). "Construction Simulation of Curved Steel I-Girder Bridge Systems," report to Federal Highway Administration, School of Civil and Environmental Engineering, Georgia Institute of Technology, Atlanta, GA, 285 pp.

Chavel, B.W. (2008). "Construction and Detailing Methods of Horizontally Curved Steel I-Girder Bridges," Ph.D. dissertation, Swanson School of Engineering, University of Pittsburgh, Pittsburgh, PA, 357 pp.

Dykas, J. (2012). "Field Measurements during Erection of Ramp B Bridge Over I-40," master's thesis, School of Civil and Environmental Engineering, Georgia Institute of Technology, Atlanta, GA, May.

Fan, Z.F. and Helwig, T. (2002) "Distortional Loads and Brace Forces in Steel Box Girders," *ASCE Journal of Structural Engineering,* V. 128, No. 6, June 2002, pp. 710–718.

Fan, Z.F. and Helwig, T. (1999). "Behavior of Steel Box Girders with Top Flange Bracing," *Journal of Structural Engineering,* August 1999, ASCE, pp. 829–837.

Grubb, M. (1984). "Horizontally Curved I-Girder Bridge Analysis: V-Load Method," *Transportation Research Record 289,* 1984, pp. 26–36.

Hall, D.H., Grubb, M.A., and Yoo, C.H. (1999). *NCHRP Report 424: Improved Design Specifications for Horizontally Curved Steel Girder Highway Bridges*, Transportation Research Board, NRC, Washington, D.C.

Helwig, T. (2012). "Bracing System Design," *Steel Bridge Design Handbook,* Office of Bridge Technology, Federal Highway Administration.

Helwig, T., Yura, J., Herman, R., Williamson, E., and Li, D. (2007). "Design Guidelines for Steel Trapezoidal Box Girder Systems," Technical Report No. FHWA/TX-07/0-4307-1. Center for Transportation Research, University of Texas at Austin, TX, 84 pp.

Jimenez Chong, J.M. (2012). "Construction Engineering of Steel Tub-Girder Bridge Systems for Skew Effects," Ph.D. dissertation, School of Civil and Environmental Engineering, Georgia Institute of Technology, Atlanta, GA, 276 pp.

Jung, S.K. (2006) "Inelastic Strength Behavior of Horizontally Curved Composite I-Girder Bridge Structural Systems," doctoral dissertation, School of Civil and Environmental Engineering, Georgia Institute of Technology, Atlanta, GA, 811 pp.

Jung, S.K. and White, D.W. (2008) "Inelastic Strength Behavior of Horizontally Curved Composite I-Girder Bridge Structural Systems," report to Federal Highway Administration, School of Civil and Environmental Engineering, Georgia Institute of Technology, Atlanta, GA, 731 pp.

Krupicka, G. and Poellot, B. (1993). "Nuisance Stiffness," *Bridgeline,* 4(1), HDR Engineering, Inc., 3 pp.

LARSA (2010). "LARSA 4D, The Complete Software for Bridge Engineering," http://www.larsa4d.com/products/larsa4d.aspx

MASTAN2 (2011)." MASTAN2, Interactive Structural Analysis Program that Provides Preprocessing, Analysis, and Postprocessing Capabilities," http://www.mastan2.com/

McGuire, W., Gallagher, R.H,, and Ziemian, R.D. (2000). *Matrix Structural Analysis,* 2nd Edition, Wiley, NY.

MDX (2011). "MDX Software, The Proven Steels Bridge Design Solution," http://www.mdxsoftware.com/

NCDOT (2006). *Computing Non-Composite Dead Load Deflections on Steel Bridges,* Memorandum to Project Engineers and Project Design Engineers, G.R. Perfetti, State Bridge Design Engineer, North Carolina Department of Transportation, October 19, 2006, http://www.ncdot.org/doh/preconstruct/highway/structur/polmemo/m101906.pdf

NHI (2011). "Analysis and Design of Skewed and Curved Steel Bridges with LRFD, Reference Manual," NHI Course No. 130095, Publication No. FHWA-NHI-10-087, National Highway Institute, Federal Highway Administration, 1,476 pp.

NSBA (1996). "V-Load Analysis and Check (VANCK), User Manual, Version 1.0," National Steel Bridge Alliance and American Institute of Steel Construction.

Ozgur, C. (2011). "Influence of Cross-Frame Detailing on Curved and Skewed Steel I-Girder Bridges," Ph.D. dissertation, School of Civil and Environmental Engineering, Georgia Institute of Technology, Atlanta, GA, 398 pp.

PennDOT (2004). *Steel Girder Bridges Lateral Bracing Criteria and Details,* BD-620M, Pennsylvania Department of Transportation, http://www.dot.state.pa.us/Internet/BQADStandards.nsf/bd2005?openfrm

Poellot, W. (1987). "Computer-Aided Design of Horizontally Curved Girders by the V-Load Method." *Engineering Journal,* AISC, Vol. 24, No. 1, First Quarter 1987, pp. 42–50.

Richardson, G. and Associates (1963). "Analysis and Design of Horizontally Curved Steel Bridge Girders," United States Steel Structural Report, ADUSS 88-6003-01.

RISA (2011). "Superior Structural Engineering Software for Analysis and Design," RISA Technologies LLC," http://www.risatech.com/

Sanchez, T.A. (2011). "Influence of Bracing Systems on the Behavior of Steel Curved and/or Skewed I-Girder Bridges during Construction," Ph.D. dissertation, School of Civil and Environmental Engineering, Georgia Institute of Technology, Atlanta, GA, 335 pp.

Tung, D. and Fountain, R. (1970). "Approximate Torsional Analysis of Curved Box Girders by the M/R-Method," *AISC Engineering Journal,* July 1970, AISC, pp. 65–74.

TxDOT (2005). *Preferred Practices for Steel Bridge Design, Fabrication and Erection,* Texas Steel Quality Council and Texas Department of Transportation, Austin, TX, 37 pp.

United States Steel Corporation (1965), "Highway Structures Design Book," ADUSS 88-1895-01, Vol. 1.

White, D.W., Zureick, A.H., Phoawanich, N.P., and Jung, S.K. (2001). "Development of Unified Equations for Design of Curved and Straight Steel Bridge I Girders," Final Report to AISI, PSI Inc. and FHWA, October, 547 pp.

Yura, J., Helwig, T., Herman, R., and Zhou, C. (2008). "Global Lateral Buckling of I-Shaped Girder Systems," *Journal of Structural Engineering,* 134(9), 1,487-1,494.

Zureick, A., Naqib, R., and Yadlosky, J.M. (1994). "Curved Steel Bridge Research Project," Interim Report I, Synthesis, FHWA Contract No. DT FG61-93-C-00136, FHWA, McLean, VA, December.

APPENDIX A

Glossary of Key Terms Pertaining to Cross-Frame Detailing

It is essential that the reader thoroughly understand the fundamental meaning of a number of the terms used in this report pertaining to cross-frame detailing, in order to facilitate study and interpretation of the corresponding results and discussions throughout the report. These terms and their definitions are as follows, listed in alphabetical order.

- **Accurate 2D-Grid Analysis.** A 2D-grid analysis that incorporates the improved I-girder torsion model of Section 3.2.2, the improved equivalent beam cross-frame model of Section 3.2.3, the improved method of calculating girder flange lateral bending stresses of Section 3.2.4, and when SDLF or TDLF detailing are employed, the procedure for calculating locked-in forces of Section 3.2.5.
- **Accurate 3D FE Analysis.** A 3D-FEA model that is capable of matching the benchmark 3D FEA responses of the Task 7 report (Appendix D of the contractors' final report) as well as the FHWA Test Bridge benchmarks of Sections 3.2.2.1, 3.2.2.3, 3.2.3.6, 3.2.4, and 3.3.3.2 (Figures 3-85 through 3-91) with a normalized mean error (Equation 6) less than or equal to 6 percent. This corresponds to an A grade in Table 3-1 of Section 3.1.2. When SDLF or TDLF detailing are employed, an accurate 3D FEA must account for the corresponding locked-in forces using a procedure such as the one presented in Section 3.2.5. As shown in Section 3.3, the locked-in forces from the (beneficial) initial lack of fit of the cross-frames and girders generally has a substantial effect on the distribution of internal forces and stresses.
- **Conservative Elastic System.** A structural system in which the response to any loading is unique (i.e., path independent), and in which, if the loading were removed, the system would return to its original undeformed geometry. Steel girder bridges are commonly idealized as conservative elastic systems for their erection analysis. Based on the assumptions that (1) yielding does not occur at any location within the structure, (2) any slip associated with frictional forces developed at the supports is negligible such that the supports may be idealized as non-frictional, and (3) slip within the structural connections (cross-frame connections to the girders, girder splices, etc.) is negligible, a structural analysis model can be developed of all the connected components/members/units for any steel erection stage and the gravity loads can simply be "turned on" to determine the unique response of the structure for that stage. Structural analysis of staged concrete deck placement is not unique because the "strain-free" position of the concrete deck, when its early stiffness first becomes significant for a given stage, depends on the sequence in which the concrete deck is placed. Staged concrete deck placement analysis is commonly handled by considering the bridge as an "incrementally conservative elastic system" in which the structure is analyzed elastically for the concrete loading increment associated with each stage, using a selected constant concrete elastic stiffness for the portions of the deck that have significant early stiffness.
- **Cross-Frame Drop.** The change in elevation between the ends of a fabricated cross-frame. For NLF detailing, the cross-frame drops are taken equal to the drops between the girders in

the initial fabricated (plumb and cambered) geometry. For SDLF or TDLF detailing of the cross-frames, the intermediate cross-frame drops are different from the corresponding girder drops. For SDLF detailing, the steel dead load cambers are subtracted from the above total drops between the girders to obtain the cross-frame drops. For TDLF detailing, the total dead load cambers are subtracted from the above total drops between the girders to obtain the cross-frame drops.

- **Fit-Up Forces.** The forces required to physically bring the components together and complete a connection during the erection of the steel. These forces can be influenced by initial lack-of-fit effects from SDLF or TDLF detailing of the cross-frames, but generally, they are distinctly different from the forces associated with the initial lack of fit between the girders and the cross-frames in their initially fabricated no-load geometry.
- **Initial Lack of Fit.** For analysis of SDLF or TDLF effects, the displacement incompatibility between the connection work points on the cross-frames and the corresponding points on the girders, with the cross-frames and girders in their initially fabricated no-load geometry, and in the context of this report, with plumb cambered initial girder geometry. For SDLF or TDLF detailing of cross-frames in I-girder bridges, the cross-frame may be considered to be connected to the initially plumb and cambered girder on one side, and the initial lack of fit is the displacement incompatibility with the work points on the girder on the other side. It should be noted that for cross-frames that are not normal (perpendicular) to the girders, there are generally two contributions to the initial lack of fit: (1) the difference in the vertical camber between the work points on the connected girders and (2) the major-axis bending rotations of the girders at the girder work points (see Figures 3-31 through 3-33). The initial no-load geometry defines the reference state of the corresponding conservative elastic system at which the strain energy is equal to zero. Hence, the no-load configuration is the only appropriate configuration to use as a basis for determining the corresponding lack-of-fit forces in the structure.
- **Lack-of-Fit Analysis.** A structural analysis in which locked-in forces are determined based on the initial lack of fit between the connection points within the structure. The designer can conduct a lack-of-fit analysis without any applied dead load on the structure to calculate the specific locked-in forces in the structure, or the steel dead load or total dead load may be included in the analysis to determine the total force effects in the structure for the selected steel dead or total dead load loading condition.
- **Lack-of-Fit Analysis Configuration 1.** The physical initial no-load (undeformed, unstrained) geometry of the cross-frames and of the fabricated (cambered and plumb) girders under theoretical zero load (see Figure 3-30a). One should note that defining the initial no-load (undeformed, unstrained) geometry of the structure is key to any structural analysis. The stresses and forces in the system are based on the deformations from this configuration, including any lack-of-fit effects.
- **Lack-of-Fit Analysis Configuration 2.** An idealized (fictitious) configuration, used for the structural analysis, in which the girders are assumed to be "locked" in their initial no-load, plumb and cambered geometry, and the cross-frames are deformed to connect them to the girder connection work points (see Figure 3-30b). For a 3D FEA, the structural analysis calculates cross-frame member initial axial strains or initial axial stresses based on a position vector analysis involving the initial lack of fit of the cross-frames to the girder connection work points. For an accurate 2D-grid analysis, the structural analysis calculates corresponding initial equivalent beam element "fixed-end forces" corresponding to the deformations required to achieve compatibility with the girder connection work points.
- **Lack-of-Fit Analysis Configuration 3.** The idealized deformed configuration reached by the structural system under no-load (dead load not yet applied), after resolving the initial lack of fit by connecting the cross-frames to the girders in Configuration 2, then "releasing" the locked girders to deflect under the lack-of-fit effects from the cross-frames.

- **Lack-of-Fit Analysis Configuration 4.** The final geometry reached under the targeted steel dead load or total dead load condition once the steel dead load or total dead load has been added to the structure, i.e., the geometry under the combined effects of the steel (or total) dead load plus the locked-in forces due to the SDLF or TDLF detailing of the cross-frames.
- **Layover.** The lateral deflection of the girder top flange relative to its bottom flange associated with twisting.
- **Locked-In Forces.** The internal forces induced into the structural system by force-fitting the cross-frames and girders together. These internal forces would remain if the structure's dead load were theoretically removed. In straight-skewed bridges, the locked-in forces due to SDLF or TLDF detailing are largely opposite in sign to corresponding dead load effects, but they can be additive with the dead load effects in some locations. In curved radially supported bridges, the locked-in forces due to SDLF or TDLF detailing largely are additive with the corresponding dead load effects. The locked-in forces are never "removed" by corresponding dead load forces, but when they are opposite in sign to these forces, they can be "balanced" by the corresponding dead load forces.
- **No-Load Fit (NLF) Detailing.** A method of detailing of the cross-frames in which the cross-frame connection work points fit-up perfectly with the corresponding work points on the girders, without any force fitting, in the initial undeformed cross-frame geometry, and with the girders in their initially undeformed fabricated (cambered and plumb) geometry.
- **Steel Dead Load Fit (SDLF) Detailing.** A method of detailing of the cross-frames in which the cross-frame connection work points are detailed to fit-up perfectly with the corresponding points on the girders with the steel dead load camber vertical displacements and rotations subtracted out of the initial total camber of the girders. Also referred to commonly as "erection fit." Detailers and fabricators work solely with the girder cambers specified on the engineering drawings to set the cross-frame drops associated with the SDLF detailing. The girders are assumed to be displaced from their initially fabricated (cambered and plumb) position to the targeted *plumb* steel dead load condition. Any twisting of the girders associated with the three-dimensional interactions with the cross-frames and overall structural system are not directly considered in these calculations.
- **Total Dead Load Fit (TDLF) Detailing.** A method of detailing of the cross-frames in which the cross-frame connection work points are detailed to fit-up perfectly with the corresponding points on the girders with the total dead load camber vertical displacements and rotations subtracted out of the initial total camber of the girders. Detailers and fabricators work solely with the girder cambers specified on the engineering drawings to set the cross-frame drops associated with the TDLF detailing. The girders are assumed to be displaced from their initially fabricated (cambered and plumb) position to the targeted *plumb* total dead load condition. Any twisting of the girders associated with the three-dimensional interactions with the cross-frames, slab, and overall structural system are not directly considered in these calculations. Also referred to commonly as "final fit."
- **Total Forces.** The forces due to the combination of the dead load effects in the targeted condition plus the locked-in force effects from SDLF or TDLF detailing of the cross-frames.
- **Uniqueness.** The attribute of a conservative elastic structural system in which the state of stress and strain in the structure is path independent, i.e., in the context of steel bridge erection, independent of the sequence of erection. This assumption is a common staple of structural analysis for design. The unique solution depends not only on the targeted loading state (e.g., steel dead load or total dead load). It also depends on any specific initial lack of fit between the structural components. The influence of connection slip within tolerances also can be included to obtain a unique solution for a given slip, as demonstrated in Section 3.3.3.2. However, the influence of connection "slip" within standard connection tolerances generally is considered to be negligible for structural design purposes.

APPENDIX B

Task 9 Report—Recommendations for Construction Plan Details and Level of Construction Analysis

NATIONAL COOPERATIVE HIGHWAY RESEARCH PROGRAM

PROJECT NO. NCHRP 12-79

Recommendations for Construction Plan Details and Level of Construction Analysis

TASK 9 REPORT

Prepared for
NCHRP
Transportation Research Board
Of
The National Academies

Brandon W. Chavel
HDR Engineering, Inc.
Chicago, IL

Domenic Coletti
HDR Engineering, Inc.
Raleigh, NC

Donald W. White
Georgia Institute of Technology
Atlanta, GA

February 29, 2012

TRANSPORTATION RESEARCH BOARD

WASHINGTON, D.C.
2006
www.TRB.org

CONTENTS

SUMMARY

Recommendations for Construction Plan Details and Level of Construction Analysis

Difficulties can arise during the construction of curved and skewed steel girder bridges when an erection plan does not contain sufficient details or when the construction analysis does not properly account for the three-dimensional behavior of the structure. The erection plan, construction analysis, and other computations for curved and skewed steel girder bridges must be sufficient to account for the complex behavior of these bridge types.

This document provides recommendations regarding the content of construction plans for curved and skewed steel I-girder bridges. Guidelines for selecting the appropriate methods of analysis for the construction analysis of I-girder and tub-girder bridges are also provided. The guidelines for selecting the appropriate methods of analysis focus on commonly used 1D, 2D, and 3D analytical approaches in current structural engineering practice (2011). Guidelines pertaining to the calculations developed to support the erection plan and procedures also are provided within this document. This document focuses on the plans, analysis methods, and other calculations conducted for the construction engineering of curved and/or skewed steel girder bridges. It does not address the wide range of additional overall considerations in the complete design and analysis of these types of bridges, such as the design of the structure in its final constructed condition for vehicular live load effects.

The major objectives of these recommendations are to help engineers:

1. Ensure that construction plans, methods of analysis, and other calculations for curved and/or skewed steel girder bridges, as affected by the structure's geometry and other construction conditions, are generally sufficient for predicting the constructed geometry (to facilitate fit-up),
2. Ensure stability during all stages of erection, and
3. Achieve better consistency in construction plans, methods of analysis, and other calculations for a given degree of the bridge's geometric, structural, and construction complexity.

Contractors and Contractors' Engineers can use this document as a guide in developing construction plans, performing calculations, and selecting the appropriate analysis methods. Bridge Owners can use this document as a checklist to verify that the Contractor and the Contractor's Engineer have developed an appropriate construction plan and calculation submittal.

CHAPTER 1

Introduction

1.1 Problem Statement

In current practice (2011), the construction of curved and/or skewed steel girder bridges is sometimes hampered by insufficient erection plans and procedures or computations. Within the industry, little has been published in the way of guidelines or recommendations on the level of detail for construction plans for curved and/or skewed steel girder bridges, or on the level of detail regarding engineering calculations for the construction engineering. Furthermore, the industry is lacking guidelines on choosing the proper analytical methods for investigating the steel erection sequence of curved and/or skewed steel girder bridges.

1.2 Objectives

This document outlines key recommendations regarding the level of effort for development of construction plans and calculations for curved and/or skewed steel girder bridges at the construction engineering stage. This document also provides recommendations regarding the appropriate methods of structural analysis for evaluating the structural behavior and predicted geometry of the bridge during the various stages of construction.

This document is written in an effort to make the development of construction plans, calculations, and methods of analysis more consistent for curved and/or skewed steel girder bridges. Contractors and Contractors' Engineers can use this document to guide them in developing construction plans, performing calculations, and selecting the appropriate analysis methods. Bridge Owners can use this document as a checklist to verify that the Contractor and the Contractor's Engineer have developed an appropriate construction plan and calculation submittal.

1.3 Organization

This report is divided into two main sections. Section 2 provides recommendations regarding the level of detail that should be used in the development of erection plans and procedures for curved and/or skewed steel girder bridges. This section is written in a style and format similar to design code provisions, including the development of Commentary sections for many of the erection plan recommendations.

Section 3 defines the levels of construction analysis that should be considered for curved and skewed steel girder bridges based upon the complexity of the structure. These guidelines are summarized from the studies conducted as part of NCHRP Project 12-79, "Guidelines for Analytical Methods and Erection Engineering of Curved and Skewed Steel Deck-Girder Bridges." This section also provides details regarding particular calculations for consideration by engineers developing construction plans and procedures.

CHAPTER 2

Recommendations for Construction Plan Details

2.1 Introduction

The AASHTO/NSBA Steel Bridge Collaboration document S10.1, "Steel Bridge Erection Guide Specification," (AASHTO/NSBA, 2007) highlights the minimum requirements for the development of steel girder erection procedures, including steel erection drawings and calculations. The recommendations provided herein use and build upon this AASHTO/NSBA document based on studies conducted as part of NCHRP Project 12-79. Contractors and Engineers developing erection plans for steel erectors are encouraged to use these recommendations so that erection plans are uniform and complete. Bridge Owners are encouraged to adopt these recommendations as a guide to verify that erection plans submitted by the Contractor contain the necessary details and procedures.

2.2 Erection Procedure Drawings Recommendations

2.2.1 General

The Contractor shall submit a detailed erection plan and procedures to the Owner for each structural unit, prepared by or under the supervision of a licensed Professional Engineer (or a qualified Structural Engineer where applicable). The detailed erection plan and procedures shall contain drawings and calculations (see Section 3) that support the erection plan and procedures. The plan and procedures shall address all requirements for erection of the structural steel into the final designed configuration and satisfy all written Owner comments prior to the start of erection. As a minimum, the erection plan and procedures shall include the items cited in the sections that follow.

2.2.1.1 General—Commentary

The qualifications of the Engineer preparing the erection plan and procedures should reflect knowledge, training, and experience in steel erection, and demonstrated abilities to resolve problems related to steel bridge erection. Complex or monumental structures should have specific requirements noted in the Contract. The erection procedure should be submitted as soon as possible after the Contract award. The submission dates and review period should be agreed upon by the Owner and the Contractor as soon as possible after the Contract award, so that sufficient time is allotted for review by the Owner. Erectors are encouraged to attend prebid and preconstruction meetings to help understand the complexities associated with the steel erection well in advance. Projects that involve complex erection or multi-agency reviews can be expected to require additional time for review of the submitted erection plan and procedure. In these cases, submission dates and review periods should be agreed upon by the Contractor and all agencies conducting reviews. Furthermore, in some cases, coordination with the Fabricator and Detailer may be necessary, as the preparation of shop detailing drawings and geometric calculations will be delayed until the erection plan and procedure is approved.

2.2.2 Plan of Work Area

The erection plan shall contain a plan of the work area showing the bridge, the permanent support structures (piers and abutments), roads, railroad tracks, waterways (including dimensions for navigational channel, and navigational clearance required during construction), overhead and underground utilities, structures and conditions that may limit access, right-of-way and property lines, material (steel) storage areas, and other information that may be pertinent to the steel erection.

2.2.2.1 Plan of Work Area—Commentary

The plan of work area drawing should provide a general overview of the area where the bridge is to be erected. It allows all involved to see site conditions, access routes and staging areas, as well as utilities, roadways, existing structures, or other possible site constraints and better understand why a certain procedure or detail is specified within the erection plans and procedures.

2.2.3 Erection Sequence

The erection plan shall contain the erection sequence for all members noting the use of temporary support conditions, such as holding crane positions, temporary supports, falsework, etc. The erection sequence shall be shown in an illustrative plan view of the bridge for each erection stage, highlighting the structural components to be erected, lifting crane locations for primary member picks, and any temporary support conditions that are necessary during the particular stage. The illustrative plan view shall be accompanied with a written narrative of the procedure to be followed by the steel erector, which shall clearly state items such as structural components to be erected, use of temporary supports, use of temporary bracing, hold cranes, etc. Member reference marks, when reflected on the erection plan, should be the same as used on the shop detail drawings.

2.2.3.1 Erection Sequence—Commentary

The erection sequence should clearly indicate specific structural components to be erected at a given stage, such as the girders, cross frames, lateral bracing, etc. The erection sequence should also clearly indicate lifting crane positions, as well as any temporary support conditions necessary to facilitate a certain erection stage, such as temporary supports, holding crane positions, tie-down stability provisions, blocking of the bearings, etc. The erection sequence drawings should be treated as the detailed instructions for construction of the bridge and should be written as, and followed as, mandatory directives. If an item is not clearly shown or described, problems could arise during steel erection.

2.2.4 Delivery Location

The erection plan shall indicate the primary member delivery location and orientation.

2.2.4.1 Delivery Location—Commentary

The maximum crane lift radius is often controlled by the material delivery location, hence it is necessary to indicate the delivery location on the erection plan.

2.2.5 Crane Information

The erection plan shall show the location of each crane to be used for each primary member pick (see Section 2.2.3), the crane type, the crane pick radius, the crane support methods (mats, barges, etc.), and the means of attachment to the girders being lifted or supported.

The erection drawings also shall show a capacity chart or table for each crane configuration, boom length, counterweight requirements, and pick weights required to do the proposed work. The erection drawings also shall indicate any potential obstructions to crane operations such as existing structures, utilities, etc. Any calculations related to evaluation of crane capacity and crane stability also shall be included. The crane types shall be agreed upon by the Contractor and Contractor's Engineer, to ensure that the crane types are available to the Contractor and can access the work site.

2.2.5.1 Crane Information—Commentary

When the steel erection takes place on a navigable waterway, the configuration of the barge(s), loading sequence, and stability provisions (tie-downs, piles, etc.) shall be provided in the erection plan. Communication between the Contractor and the Contractor's Engineer is vital to ensure the cranes assumed by the Engineer are available to the Contractor. Providing the crane types, pick radii, pick weight, boom lengths, possible obstructions, etc., in the erection plans will help to prevent crane interferences, overloads, or failures during the steel erection.

2.2.6 Primary Member Crane Pick Information

The erection plan shall include the lifting weight of the primary member picks, including all rigging and pre-attached elements (such as cross-frames or splice plates). The erection plan shall also include the approximate center of gravity locations for the primary member picks of curved girders and assemblies.

2.2.6.1 Primary Member Crane Pick Information—Commentary

The lifting weights and the approximate centers of gravity for each pick will provide the steel erector with necessary information to safely lift various components. The centers of gravity provided on the plans should be taken as approximate locations, as these are typically calculated assuming nominal material sizes and approximations of minor items such as bolted connections, etc. The actual center of gravity locations should reasonably match these approximate locations and will aid the steel erector in determining the proper lifting location in the field.

2.2.7 Lifting Devices and Special Procedures

The erection plan shall include the details, weight, capacity, and arrangement of all rigging (beam clamps, lifting lugs, etc.) and all lifting devices (such as spreader and lifting beams) required for lifting primary members. The erection plan also shall specify whether rigging or lifting devices are to be bolted or welded to permanent members, including the method and time (shop or field) of attachment and capacity, as well as methods, time, and responsibility for removal.

As necessary, the erection plan shall provide special lifting/handling procedures for any primary member with potential stability or slenderness issues.

2.2.7.1 Lifting Devices and Special Procedures—Commentary

Assumptions regarding the weight of rigging, spreader beams, etc., should be included in the erection plan. Explicitly indicating all details related to rigging and spreader or lifting beams will help to ensure that the appropriate devices are being properly used in the field.

Straight slender beams, traditionally defined as those having a length of the shipping piece to flange width ratio (L/b) greater than 85, are prone to lateral torsional buckling and require particular attention during lifting/handling operations. This limiting length to flange width ratio for curved beams is smaller than 85, and in some cases has been taken as low as a value of 10. The flange width

(b) should be taken as the smallest width flange within the field section being lifted. Other types of structural members also may have slenderness and/or stability issues that should be addressed in the erection plans as appropriate.

2.2.8 Bolting Requirements

The erection plan shall indicate the bolting requirements for field splices and cross-frame (or diaphragm) connections.

For bolted splice connections of primary members, and bolted connections of diaphragms or cross frames that brace I-girders, fill at least 50 percent of holes in the connection prior to crane release with either erection bolts in a snug tight condition, or full-size erection pins (a.k.a., "drift pins"), using bolts for at least half of the filled holes (i.e., at least 25 percent of all holes). Sufficient erection pins shall be used near the outside corners of splice plate and at member ends near splice plate edges to ensure alignment. The filled holes shall be uniformly distributed across the connection.

2.2.8.1 Bolting Requirements—Commentary

Steel I-girders depend on their connections to adjacent girders through bracing members for their stability and stiffness during steel erection. This is especially true for curved steel girders, as the cross frames serve as primary load carrying members. Therefore, loosely connected cross frames should not be used during steel girder bridge erection, as this may compromise the girder alignment (geometry control) and stability.

The bolting requirements for girder field splices during steel erection need to be considered as well. In accordance with the AASHTO LRFD Bridge Construction Specifications, Article 11.6.5, "splices and field connections shall have one-half of the holes filled with bolts and cylindrical erection pins (half bolts and half pins) before installing and tightening the balance of the high strength bolts." In addition, the Contractor's Engineer developing the erection plan must ensure that the number of bolts or erection pins to be used provides enough capacity for transfer of loads for the given stage of steel erection.

2.2.9 Bearing Blocking and Tie-Down Details

The erection plan shall indicate the blocking and/or tie-down details for the bridge bearings, as necessary.

2.2.9.1 Bearing Blocking Details—Commentary

Depending on their details, bridge bearings may allow movement (translation) in any direction and/or rotation about any axis. During steel erection, in addition to other stability provisions, the bearings may require blocking to prevent or limit the translational movements and rotations. In addition, bearings may need temporary tie-downs to prevent uplift at various stages during construction. The Contractor's Engineer (CE) should determine the blocking and/or tie down requirements such that the structure remains stable during all stages of erection and such that the behavior of the physical structure is consistent with the behavior assumed in the analysis and the erection plans. The CE should ensure that the bearings are not overloaded or over-rotated at any stage during the construction.

2.2.10 Load Restrictions

Restrictions regarding wind and construction dead and live loadings shall be included on the erection plan, as necessary.

2.2.10.1 Load Restrictions—Commentary

Limits may be placed on wind velocities during lifting of girder field pieces or during various stages of erection when the structure is only partially complete. The limitations on wind velocities are intended to prevent girder overstress and/or instabilities that could be caused by certain wind speeds and the associated wind pressure loading. Calculations may show that a girder or girder system may not be stable at a certain wind velocity, and this needs to be communicated to the Contractor and Steel Erector via the erection plan. If appropriate, the erection plans should include instructions and details for temporary support or tie-down of partially completed structures during high wind conditions.

The erection plans should also explicitly state restrictions on construction live loads (vehicles, equipment, personnel, etc.) and construction dead loads (formwork/falsework, stored materials, etc.). Inadvertent overloading by construction loads can affect the geometry control and also can lead to structural collapse.

2.2.11 Temporary Supports

The erection plan shall include the location of any temporary support structures (see Section 2.2.3), as well as details of the temporary support structure itself. If the temporary support is to be prefabricated (selected from a supplier's catalogue), the type and capacity shall be clearly defined in the erection plan; lateral capacity as well as vertical capacity requirements shall be considered as appropriate. If the temporary support is to be constructed by the Contractor on site, a complete design with full details, including member sizes, connections, and bracing elements, shall be provided in the erection plans. In either case, details regarding the upper grillage and temporary bearing assembly (i.e., details of how the steel girders will bear on the temporary support) also shall be included in the erection plan. In addition, all foundation requirements for temporary support structures shall be provided in the erection plan.

The erection plan shall indicate the location of hold cranes used to provide temporary support to the steel assembly (see Sections 2.2.3 and 2.2.5). The hold crane type, capacity, boom lengths, pick radius, and means of attachment to the girders also shall be indicated in the erection plan.

The erection plan shall include the location and details for temporary tie-downs that are required to facilitate the steel erection. At a minimum, the details shall include the tie-down, girder attachment devices, and anchoring devices.

2.2.11.1 Temporary Supports—Commentary

In many cases, temporary supports are essential for the construction of a steel girder bridge. As such, they should be clearly detailed in the erection plan, whether the support is a falsework tower, hold crane, tie-down, bearing blocking, or other support.

2.2.12 Jacking Devices

The erection plan shall indicate jacking devices required to complete the steel erection. Their location, type, size, and capacity shall be clearly indicated on the erection plan, as well as their intended use, sequence of engagement, load level, and any other key parameters of their operation.

2.2.12.1 Jacking Devices—Commentary

In some cases, jacking devices may be required at temporary support structures, or at the permanent supports, for alignment of the structure during the erection process. If the erection plan does indeed require jacking devices, they should be clearly indicated in the erection plan to alert the Contractor to their need, and their intended use should be explicitly presented.

2.3 Erection Plan and Procedures Checklist

- Plan of Work Area
  - Permanent and temporary structures shown
  - All roads, railroad tracks, waterways, clearances, utilities, potential conflicts shown
  - Material (steel) storage areas shown
- Erection Sequence
  - Step-by-step procedure–figures and narrative dictating work
  - Delivery location of components shown
  - Crane locations shown
  - Temporary support, hold cranes, blocking, tie-downs shown
  - Load restrictions for certain stages (i.e., wind)
- Crane Information
  - Crane type, pick radii, boom length shown
  - Approximate crane pick points shown
  - Crane pick weights shown
  - Hold crane loads
- Details of Lifting Devices and Special Procedures
- Bolting Requirements
- Bearing Blocking and Tie-Down Details
- Temporary Supports
  - Details of structure shown
  - Load capacities
- Jacking Devices and Procedures

CHAPTER 3

Recommendations for Methods of Structural Analysis and Calculations

3.1 Introduction

Calculations by the Contractor's Engineer investigating the steel erection sequence are required to substantiate the erection plan and procedures submitted for a given project. This section presents guidelines regarding these calculations. It also provides recommendations on the appropriate methods of analysis to employ when investigating the adequacy of the erection sequence of a curved or skewed steel girder bridge. These guidelines and recommendations are a synthesis of studies conducted as part of NCHRP Project 12-79, "Guidelines for Analytical Methods and Erection Engineering of Curved and Skewed Steel Deck-Girder Bridges." Detailed background to these guidelines can be found in the Task 8 report of Project 12-79, "Guidelines for Selecting Analytical Methods for Construction Engineering of Curved and Skewed Steel Girder Bridges."

3.2 Recommendations on Methods of Analysis

A substantial number of studies were conducted as part of NCHRP Project 12-79 to determine the ability of approximate 1D and 2D methods of analysis to capture the behavior predicted by refined 3D finite element models. To evaluate 1D methods, a commonly available commercial line-girder analysis program, STLBRIDGE (Bridgesoft, 2010), was used to analyze the behavior of straight skewed I- and tub-girder bridges. The 1D analysis of curved, and curved and skewed, I-girder bridges was based on the V-load method (Richardson, Gordon & Associates, 1976; United States Steel, 1980) using the software VANCK (NSBA, 1996). The 1D analysis of curved, and curved and skewed, tub-girder bridges was based on a line-girder analysis coupled with additional calculations based on the M/R method (Tung and Fountain, 1970). To evaluate 2D methods, two commercially available software programs, typically employed by bridge designers, were used to investigate the behavior of these same bridges: the software MDX (MDX, 2011) for analysis using a conventional 2D-grid approach and the capabilities of LARSA-4D (LARSA, 2010) for analysis using a conventional 2D-frame approach. To evaluate linear elastic 3D finite element analysis methods, the software program ABAQUS was used to investigate the behavior of these same bridges. The 1D, 2D, and linear elastic 3D analysis results were compared to benchmark nonlinear "simulation" 3D finite element analysis solutions, also prepared using the software program ABAQUS, including the modeling of 2nd-order effects (geometric nonlinearity). Where possible, extant bridges were evaluated and if those bridges had been instrumented, the nonlinear simulation benchmark analysis results were validated against measured responses.

3.2.1 I-Girder Bridges

A quantitative assessment of the analysis accuracy was obtained by identifying error measures that compared the approximate (1D and 2D methods) solutions to the 3D FEA benchmark

solutions. Using the quantitative assessments, the various methods of analysis were ranked based on a scoring system developed to provide a comparative evaluation of each analysis method with regard to the accuracy of its analysis predictions for various structural responses.

Table 3.1 summarizes the scoring system for the various methods and behaviors monitored. The scoring criteria are as follows:

- A grade of A is assigned when the normalized mean error is less than or equal to 6 percent, reflecting excellent accuracy of the analysis predictions.
- A grade of B is assigned when the normalized mean error is between 7 percent and 12 percent, reflecting a case where the analysis predictions are in "reasonable agreement" with the benchmark analysis results.

Table 3.1 Matrix for Recommended Level of Analysis – I-Girder Bridges.

Response	Geometry	Worst-Case Scores		Mode of Scores	
		Traditional 2D-Grid	1D-Line Girder	Traditional 2D-Grid	1D-Line Girder
Major-Axis Bending Stresses	C ($I_C \leq 1$)	B	B	A	B
	C ($I_C > 1$)	D	C	B	C
	S ($I_S < 0.30$)	B	B	A	A
	S ($0.30 \leq I_S < 0.65$)	B	C	B	B
	S ($I_S \geq 0.65$)	D	D	C	C
	C&S ($I_C > 0.5$ & $I_S > 0.1$)	D	F	B	C
Vertical Displacements	C ($I_C \leq 1$)	B	C	A	B
	C ($I_C > 1$)	F	D	F	C
	S ($I_S < 0.30$)	B	A	A	A
	S ($0.30 \leq I_S < 0.65$)	B	B	A	B
	S ($I_S \geq 0.65$)	D	D	C	C
	C&S ($I_C > 0.5$ & $I_S > 0.1$)	F	F	F	C
Cross-Frame Forces	C ($I_C \leq 1$)	C	C	B	B
	C ($I_C > 1$)	F	D	C	C
	S ($I_S < 0.30$)	NA[a]	NA[a]	NA[a]	NA[a]
	S ($0.30 \leq I_S < 0.65$)	F[b]	F[c]	F[b]	F[c]
	S ($I_S \geq 0.65$)	F[b]	F[c]	F[b]	F[c]
	C&S ($I_C > 0.5$ & $I_S > 0.1$)	F[b]	F[c]	F[b]	F[c]
Flange Lateral Bending Stresses	C ($I_C \leq 1$)	C	C	B	B
	C ($I_C > 1$)	F	D	C	C
	S ($I_S < 0.30$)	NA[d]	NA[d]	NA[d]	NA[d]
	S ($0.30 \leq I_S < 0.65$)	F[b]	F[e]	F[b]	F[e]
	S ($I_S \geq 0.65$)	F[b]	F[e]	F[b]	F[e]
	C&S ($I_C > 0.5$ & $I_S > 0.1$)	F[b]	F[e]	F[b]	F[e]
Girder Layover at Bearings	C ($I_C \leq 1$)	NA[f]	NA[f]	NA[f]	NA[f]
	C ($I_C > 1$)	NA[f]	NA[f]	NA[f]	NA[f]
	S ($I_S < 0.30$)	B	A	A	A
	S ($0.30 \leq I_S < 0.65$)	B	B	A	B
	S ($I_S \geq 0.65$)	D	D	C	C
	C&S ($I_C > 0.5$ & $I_S > 0.1$)	F	F	F	C

[a] Magnitudes should be negligible for bridges that are properly designed & detailed. The cross-frame design is likely to be controlled by considerations other than gravity-load forces.

[b] Results are highly inaccurate due to modeling deficiencies addressed in Ch. 6 of the NCHRP 12-79 Task 8 report. The improved 2D-grid method discussed in this Ch. 6 provides an accurate estimate of these forces.

[c] Line-girder analysis provides no estimate of cross-frame forces associated with skew.

[d] The flange lateral bending stresses tend to be small. AASHTO Article C6.10.1 may be used as a conservative estimate of the flange lateral bending stresses due to skew.

[e] Line-girder analysis provides no estimate of girder flange lateral bending stresses associated with skew.

[f] Magnitudes should be negligible for bridges that are properly designed & detailed.

- A grade of C is assigned when the normalized mean error is between 13 percent and 20 percent, reflecting a case where the analysis predictions start to deviate "significantly" from the benchmark analysis results.
- A grade of D is assigned when the normalized mean error is between 21 percent and 30 percent, indicating a case where the analysis predictions are poor, but may be considered acceptable in some situations.
- A grade of F is assigned if the normalized mean errors are above the 30 percent limit. At this level of deviation from the benchmark analysis results, the subject approximate analysis method is considered unreliable and inadequate for design.

The normalized mean error is calculated as

$$\mu_e = \frac{1}{N \cdot R_{FEA\max}} \sum_{i=1}^{N} e_i$$

where N is the total number of sampling points along the length in the approximate model, R_{FEAmax} is the absolute value of the maximum response obtained from the FEA, and e_i is the absolute value of the error relative to the 3D FEA benchmark solution evaluated at point *i:*

$$e_i = \left| R_{approx} - R_{FEA} \right|$$

The summation in the above is computed for each girder line along the full length of the bridge, and the largest resulting value is reported as the normalized mean error for the bridge. The error measure μe is useful for the overall assessment of the analysis accuracy since this measure is insensitive to isolated discrepancies, which can be due to minor shifting of the response predictions, etc. The normalized local maximum errors, e_i / R_{FEAmax} are generally somewhat larger than the normalized mean error. Also, in many situations, unconservative error at one location in the bridge leads to comparable conservative error at another location. Hence, it is simpler to not consider the sign of the error as part of the overall assessment of the analysis accuracy.

In Table 3.1, the scoring for the various measured responses is subdivided into six categories based on the bridge geometry. These bridge categories are defined as follows:

- Curved bridges with no skew are identified in the Geometry column by the letter "C."
- The curved bridges are further divided into two subcategories, based on the connectivity index, I_C defined as:

$$I_C = \frac{15000}{R\left(n_{cf} + 1\right)m}$$

where R is the minimum radius of curvature, n_{cf} is the number of intermediate cross-frames in the span, and m is a constant taken equal to 1 for simple-span bridges and 2 for continuous-span bridges. In bridges with multiple spans, I_C is taken as the largest value obtained from any of the spans.

- Straight-skewed bridges with no curvature are identified in the geometry column by the letter "S."
- The straight-skewed bridges are further divided into three subcategories, based on the skew index, I_S. where I_S is taken as:

$$I_S = \frac{w \tan\theta}{L_s}$$

where w is the width of the bridge measured between fascia girders, θ is the skew angle measured from a line perpendicular to the tangent of the bridge centerline, and L_s is the span

length at the bridge centerline. In bridges with unequal skew at the bearing lines, θ is taken as the angle of the bearing line with the largest skew.
- Bridges that are both curved and skewed are identified in the geometry column by the letters "C&S."

Two letter grades are indicated for each of the cells in Table 3. The first letter grade corresponds to the worst-case results encountered from either of the two 2D-grid solutions considered in the NCHRP Project 12-79 studies, or from the 1D-line girder calculations, within each of the specified categories. The second letter grade indicates the mode of the letter grades for that category, i.e., the letter grade encountered most often for that category.

Table 3.1 can be used to determine when a certain analysis method can be reasonably expected to produce acceptable results. The following two examples illustrate how Table 3.1 is to be used.

3.2.1.1 I-Girder Bridge Level of Analysis Example 1

Consider a horizontally curved steel I-girder bridge with radial supports, "regular" geometry (constant girder spacing, constant deck width, relatively uniform cross-frame spacing, etc.), and $I_C \leq 1$, for which the engineer wants to perform a traditional 2D-grid analysis to determine the forces and displacements during critical stages of the erection sequence. (It should be noted that if I_C is calculated for an intermediate stage of the steel erection in which some of the cross-frames have not yet been placed, the number of intermediate cross-frames n_{cf} in Eq. 8 should be taken as the number installed in the erection stage that is being checked. In addition, the radius of curvature R and the constant m should correspond to the specific intermediate stage of construction being evaluated, not the bridge in its final erected configuration.)

For the girder major-axis bending stresses and vertical displacements (f_b and Δ), the results are expected to deviate somewhat from those of a 3D analysis in general, because a worst-case score of B is assigned in Table 3.1 for all of these response quantities. The worst-case normalized mean error in these results from the 2D-grid analysis will typically range from 7 to 12 percent, as compared to the results from a refined geometric nonlinear 3D FEA. However, one can expect that for most bridges, the errors will be less than or equal to 6 percent, based on the mode score of A for both of these responses.

Therefore, in this example, if the major-axis bending stress results and vertical displacement results are of prime interest, a 2D-grid model should be sufficient if worst-case errors of approximately 12 percent are acceptable. Given that the bridge has very "regular" geometry, it is likely that the f_b and Δ errors are less than or equal to 6 percent. (The worst-case score is considered as the appropriate one to consider when designing a bridge with complicating features such as a poor span balance, or other "less regular" geometry characteristics.)

It is important to note that the engineer can "compensate" for potential unconservative major-axis bending stress errors in the design by adjusting the target performance ratios desired for the construction engineering analysis. For example, with the above bridge, the engineer may require that the performance ratio be less than or equal to 1/1.12 = 0.89 or 1/1.06 = 0.94 for the girder flexural resistance checks to gain some further confidence in the adequacy of the analysis. Conversely, over-prediction and under-prediction of the vertical displacements can be equally bad. Nevertheless, 12 percent or 6 percent displacement error may be of little consequence if the magnitude of the displacements is relatively small, or if the deflections are being calculated at an early stage of the steel erection and it is expected that any resulting displacement incompatibilities or loss of geometry control can be subsequently resolved. However, if the magnitude of the displacements is large, or if it is expected that the resulting errors or displacement incompatibilities may be difficult to resolve, the engineer should consider conducting a 3D FEA of the subject construction stage to gain further confidence in the calculated displacements. This step

in the application of Table 3.1 is where the bridge span length enters as an important factor, since longer-span bridges tend to have larger displacements.

It should be noted that compared to the creation of 3D FEA models for overall bridge design, including calculation of live load effects, the development of a 3D FEA model for several specific construction stages that may be of concern involves a relatively small amount of effort. This is particularly the case with many of the modern software interfaces that facilitate the definition of the overall bridge geometry.

For calculation of the girder flange lateral bending stresses and the cross-frame forces in the above example bridge, the worst-case errors are expected to be larger, on the order of 13 percent to 20 percent (corresponding to a grade of C for both of these responses). However, the mode score is B, and since the bridge has very regular geometry, it is likely that the normalized mean error in the flange lateral bending stresses and cross-frame forces is less than 12 percent. If these errors are acceptable in the engineer's judgment, then the 2D-grid analysis should be acceptable for the construction engineering calculations. As noted above, the engineer can compensate for these potential errors by reducing the target performance indices. With respect to the flange lateral bending stress, it should be noted that the f_λ values are multiplied by ⅓ in the AASHTO ⅓ rule equations. Therefore, the errors in f_λ have less of an influence on the performance ratio errors than errors in f_b. When checking the AASHTO flange yielding limit for constructability, both f_λ and f_b have equal weights though. Based on these considerations, the best way to compensate for different potential unconservative errors in the f_λ and f_b values is to multiply the calculated stresses from the 2D-grid analysis by 1.20 and 1.12 (or 1.12 and 1.06) respectively prior to checking the performance ratios.

3.2.1.2 I-Girder Bridge Level of Analysis Example 2

Consider a straight steel I-girder bridge with skewed supports and a skew index, $I_s = 0.35$ (corresponding to the intermediate erection stage being evaluated), for which the engineer wants to perform a traditional 2D-grid analysis to determine the forces and displacements during critical stages of the erection sequence.

After reviewing Table 3.1, it is observed that for major-axis bending stresses and vertical deflections, a worst-case score of B is shown for straight skewed I-girder bridges with $0.30 < I_S \leq 0.65$. Furthermore, it can be observed that the mode of the scores for these bridge types is a B for the major-axis bending stresses and an A for the vertical displacements. Therefore, a properly prepared conventional 2D-grid analysis would be expected to produce major-axis bending stress and vertical deflection results that compare reasonably well with the results of a second-order elastic 3D FEA, such that the normalized mean error would be expected to be less than or equal to 12 percent.

If the layout of the cross-frames in the skewed bridge is such that overly stiff (nuisance) transverse load paths are alleviated, the engineer may expect that the error in the displacement calculations may be close to 6 percent or less. In this case, the engineer should be reasonably confident in the 2D-grid results for the calculation of these responses. As noted in the previous example, the potential unconservative errors in the stresses can be compensated for in the construction engineering design checks; however, positive or negative displacement errors are equally bad.

The girder layover at the skewed bearing lines is often of key interest in skewed I-girder bridges. Table 3.1 shows that the girder layover calculations have essentially the same magnitude of errors and resulting grades as the girder vertical displacements. This is because the skewed bearing line cross-frames are generally relatively rigid in their own planes compared to the stiffness of the girders. Hence, the girder layovers are essentially proportional to the girder major-axis bending rotations at the skewed bearing lines.

For the calculation of the cross-frame forces and/or the girder flange lateral bending stresses in the above example, one can observe that the conventional 2D-grid procedures are entirely unreliable. That is, the scores in Table 3.1 are uniformly an F. The reason for this poor performance of the traditional 2D-grid methods is the ordinary modeling of the girder torsional properties using only the St. Venant torsional stiffness GJ/L. The physical girder torsional stiffnesses are generally much larger due to restraint of warping, i.e., flange lateral bending, effects. In addition, for wide skewed bridges and/or for skewed bridges containing specific overly stiff (nuisance) transverse load paths, the limited accuracy of the cross-frame equivalent beam stiffness models used in conventional 2D-grid methods may lead to a dramatic loss of accuracy in the cross-frame forces.

Lastly, conventional 2D-grid methods generally do not include any calculations of the girder flange lateral bending stresses due to skew. Hence, the score for the calculation of the flange lateral bending stresses is also an F in Table 3.1.

Chapter 6 of the NCHRP 12-79 Task 8 report, "Guidelines for Selecting Analytical Methods for Construction Engineering of Curved and Skewed Steel Girder Bridges," recommends several important modifications to conventional 2D-grid procedures that are relatively simple for software providers to implement yet provide substantial improvements in the analysis accuracy. To realize the benefits of these improvements in typical bridge design practice it will be necessary for commercial 2D-grid software providers to implement these types of improvements, since manual implementation of the improvements tends to be cumbersome and time consuming for the engineer. Therefore, this document focuses solely on the accuracy of conventional 2D-grid and 1D line-girder procedures.

3.2.2 Tub-Girder Bridges

Similar to the I-girder bridges, a quantitative assessment of the analysis accuracy of tub-girder bridges was obtained by focusing first on the normalized mean errors in the approximate (1D and 2D method) solutions for the girder major-axis bending stresses, internal torques, and vertical displacements, compared to benchmark 3D FEA results. Using the quantitative assessments, the various methods of analysis were assigned scores in the same manner as the scoring discussed in Section 3.1.1 for the I-girder bridge responses. Table 3.2 summarizes the scores for the above responses in tub-girder bridges.

It is interesting that the Table 3.2 scores for the major-axis bending stresses and vertical displacements are relatively good. However, the worst-case scores for the internal torques are generally quite low. These low scores are largely due to the fact that the internal torques in tub-girder bridges can be sensitive to various details of the framing, such as the use and location of external intermediate cross-frames or diaphragms, the relative flexibility of these diaphragms as well as the adjacent internal cross-frames within the tub-girders, skewed interior piers without external cross-frames between the piers at the corresponding bearing line, incidental torques introduced into the girders due to the specific orientation of the top flange lateral bracing system members (particularly for Pratt-type TFLB systems), etc. Jimenez Chong (2012) provides a detailed evaluation and assessment of the causes for the errors in the girder internal torques for the tub-girder bridges considered in the NCHRP Project 12-79 research.

Similar to the considerations for I-girder bridges, the external diaphragms and/or cross-frames typically respond relatively rigidly in their own plane compared to the torsional stiffness of the girders. Therefore, the girder layovers at skewed bearing lines tend to be proportional to the major-axis bending rotation of the girders at these locations. As a result, the errors in the girder layover calculations obtained from the approximate methods tend to be similar to the errors in the major-axis bending displacements.

Table 3.2 Matrix 1 for Recommended Level of Analysis – Tub-Girder Bridges.

Response	Geometry	Worst-Case Scores		Mode of Scores	
		Traditional 2D-Grid	1D-Line Girder	Traditional 2D-Grid	1D-Line Girder
Major-Axis Bending Stresses	S	B	B	A	B
	C	B	C	A	B
	C&S	B	C	B	B
Girder Torques	S	**F**	**F**	D	**F**
	C	D	D	A	B
	C&S	**F**	**F**	A	B
Vertical Displacements	S	B	B	A	A
	C	A	B	A	A
	C&S	B	B	A	A
Girder Layover at Bearing Lines	S	B	B	A	A
	C	NA[a]	NA[a]	NA[a]	NA[a]
	C&S	B	B	A	A

[a] Magnitudes should be negligible where properly designed and detailed diaphragms or cross-frames are present.

The connectivity index, I_C does not apply to tub-girder bridges, since this index is primarily a measure of the loss of accuracy in I-girder bridges due to the poor modeling of the girder torsion properties. For tub-girder bridges, the conventional St. Venant torsion model generally works well as a characterization of the torsional response of the pseudo-closed section tub-girders. Hence, I_C is not used for characterization of tub-girder bridges in the table. Furthermore, there is only a weak correlation between the accuracy of the simplified analysis calculations and the skew index I_S for tub-girder bridges. Therefore, the skew index is not used to characterize tub-girder bridges in Table 3.2 either. Important differences in the simplified analysis predictions do exist, however, as a function of whether the bridge is curved, "C," straight and skewed, "S," or curved and skewed "C&S." Therefore, these characterizations are shown in the table.

In addition, to the above quantitative assessments, the calculation of bracing component forces in tub-girder bridges is assessed separately in Table 3.3. It is useful to address the accuracy of these response calculations separately from those shown in Table 3.2 since the simplified bracing component force calculations take the girder major-axis bending moments, torques, and applied transverse loads as inputs and then apply various useful mechanics of materials approximations to obtain the force estimates. That is, there are two distinct sources of error in the bracing component forces relative to the 3D FEA benchmark solutions:

1. The error in the calculation of the input quantities obtained from the 1D line-girder or the 2D-grid analysis, and
2. The error introduced by approximations in the component force equations.

Chapter 2 of the NCHRP Project 12-79 Task 8 report provides an overview of the most commonly employed bracing component force equations evaluated here. It should be noted that the calculation of the top flange lateral bending stresses in tub girders is included as one of the bracing component force calculations. This is because these stresses are influenced significantly by the interaction of the top flanges with the tub-girder bracing systems.

The NCHRP Project 12-79 research observed that in many situations the bracing component force estimates are conservative relative to the 3D FEA benchmark solutions. Therefore, it is useful to consider a signed error measure for the bracing component force calculations. In addition, the bracing component dimensions and section sizes often are repeated to a substantial degree throughout a tub-girder bridge for the different types of components. Therefore, it is useful to

quantify the analysis error as the difference between the maximum of the component forces determined by the approximate analysis minus the corresponding estimate from the 3D FEA benchmark, i.e.:

$$e_{\max} = \left(R_{approx.max} - R_{FEA.max} \right) / R_{FEA.max}$$

for a given type of component. The grades for these responses were then assigned based on the same scoring system as that used for the assessments based on normalized mean error with one exception: Separate grades were assigned for the positive (conservative) errors and for the negative (unconservative) errors in Table 3.3. In situations where no negative (unconservative) errors were observed in all of the bridges considered in a given category, the symbol "—" is shown in the cells of the matrix and the cells are unshaded.

The mode of the grades is shown only for the top flange diagonal bracing forces in Table 3.3. The mode of the grades for the other component force types are not shown because of substantial positive and negative errors in the calculations that were encountered in general for the tub-girder bridges, and because, in cases where a clear mode for the grades existed, the mode of the grades was the same as the worst-case grade.

In addition to the above considerations, it should be noted that current simplified estimates of the tub-girder bridge bracing component forces are generally less accurate for bridges with Pratt-type top flange lateral bracing (TFLB) systems compared to Warren and X-type systems. A small number of tub-girder bridges with Pratt-type TFLB systems were considered in the NCHRP Project 12-79 research. Therefore, the composite scores for these bridges are reported separately in Table 3.3.

3.2.2.1 Tub-Girder Bridge Level of Analysis Example

Consider a horizontally curved steel tub-girder bridge with a Warren top flange lateral bracing system and skewed supports for which the engineer wants to perform a traditional 2D-grid analysis to determine the forces and displacements during critical stages of the erection sequence. The bridge has "regular" geometry (constant girder spacing, constant deck width, a relatively uniform top flange lateral bracing [TFLB] system and internal cross-frame spacing, solid plate end diaphragms, single bearings for each girder, etc.).

A properly prepared 2D-grid analysis would be expected to produce major-axis bending stresses and vertical deflections with mean errors less than 12 percent relative to a rigorous 3D FEA solution, since the worst-case score assigned for both of these quantities is a B in Table 3.2 for the subject "C&S" category. Furthermore, it can be observed that the mode of the scores for the vertical displacements is an A, and hence, given the "regular" geometry of the above bridge, it is expected that the vertical displacements most likely would be accurate to within 6 percent.

Unfortunately, the worst-case score is an F for the 2D-grid estimates of the internal torques in the "C&S" bridges. As noted previously, this low score is due to the fact that the internal torques in tub-girder bridges can be very sensitive to various details of the framing, such as the use and location of external intermediate cross-frames or diaphragms, the relative flexibility of these diaphragms as well as the adjacent internal cross-frames within the tub-girders, skewed interior piers without external cross-frames between the piers at the corresponding bearing line, incidental torques induced in the girders due to the specific orientation of the top flange lateral bracing system members (particularly for Pratt-type TFLB systems), etc. Fortunately though, the web and bottom flange shear forces due to the internal torques are often relatively small compared to the normal stresses due to the major-axis bending response of the girders. Furthermore, the mode of the scores for the internal torques is an A from Table 3.2. Therefore, the engineer must exercise substantial judgment in estimating what the expected error may be for the internal

Table 3.3 Matrix 2 for Recommended Level of Analysis – Tub-Girder Bridges.

Response	Sign of Error	Geometry	Worst-Case Scores		Mode of Scores	
			Traditional 2D-Grid	1D-Line Girder	Traditional 2D-Grid	1D-Line Girder
TFLB Diagonal Force	Positive (Conservative)	S	D	D	D	C
		C	D	**F**	B	**F**
		C&S	D[a]	**F**	B	**F**
		Pratt TFLB System	C	**F**	A	**F**
	Negative (Unconservative)	S	**F**[b]	C		
		C	--[c]	--		
		C&S	--	--		
		Pratt TFLB System	--	--		
TFLB & Top Internal CF Strut Force	Positive (Conservative)	S	C	C		
		C	**F**	**F**		
		C&S	**F**	**F**[d]		
		Pratt TFLB System	**F**	**F**		
	Negative (Unconservative)	S	C	C		
		C	--	A		
		C&S	--	C		
		Pratt TFLB System	D	D		
Internal CF Diagonal Force	Positive (Conservative)	S	NA[e]	NA[e]		
		C	**F**	**F**		
		C&S	**F**	**F**		
		Pratt TFLB System	--	**F**[f]		
	Negative (Unconservative)	S	NA[e]	NA[e]		
		C	--	--		
		C&S	--	D		
		Pratt TFLB System	B	--		
Top Flange Lateral Bending Stress (Warren TFLB Systems)	Positive (Conservative)	S	C	C		
		C	**F**	**F**		
		C&S	**F**	**F**[d]		
	Negative (Unconservative)	S	C	C		
		C	--	A		
		C&S	--	C		

[a] Modified from a C to a D considerting the grade for the C and the S bridges.

[b] Large unconservative error obtained for bridge ETSSS2 due to complex framing. If this bridge is considered as an exceptional case, the next worst-case unconservative error is -15 % for NTSSS2 (grade = C).

[c] The symbol "--" indicates that no cases were encountered with this score.

[d] Modified from a B to an F considering the grade for the C bridges.

[e] For straight-skewed bridges, the internal intermediate cross-frame diagonal forces tend to be negligible.

[f] Modified from an A to an F considering the grade for the C and C&S bridges.

torque from a 2D-grid analysis, and in assessing the impact of this error on the bridge design. As noted previously in Section 3.2.1.1 and 3.2.1.2 for I-girder bridges, one can compensate for any anticipated potential unconservative error in the internal force or stress response quantities by scaling up the corresponding responses by the anticipated error, or by adjusting the target values of the performance ratios.

Based on Table 3.3, the worst-case score for the positive (conservative) error in the calculation of the TFLB diagonal forces in the above example bridge is a D whereas the mode of the scores is

a B. The table shows that no unconservative errors were encountered in this calculation for the tub-girder bridges studied in NCHRP Project 12-79. Since the example bridge is "very regular," the engineer may assume that the TFLB diagonal force calculations are conservative, but reasonably accurate, relative to the refined 3D FEA benchmark values.

For both the TFLB and top internal cross-frame strut forces and the internal cross-frame diagonal forces in "C&S" bridges, Table 3.3 shows a grade of F for the conservative error. Also, the table shows that no unconservative errors were encountered in the NCHRP Project 12-79 calculations for these responses. Therefore, the engineer can assume that the forces for these components, as determined from a 2D-grid analysis plus the bracing component force equations, are highly conservative. It should be noted that the forces in the top struts of the internal cross-frames at exterior diaphragm or exterior cross-frame locations can be very sensitive to the interaction of the external diaphragm or cross-frame with the girders. These forces should be determined based on consideration of statics at these locations given the forces transmitted to the girders from the external diaphragm or cross-frame components. NCHRP Project 12-79 did not consider these component forces in its error assessments.

Lastly, Table 3.3 shows that the tub-girder top flange lateral bending stresses tend to be estimated with a high degree of conservatism by 2D-grid methods combined with the bracing component force equations. In addition, no unconservative errors were encountered in the tub-girder bridges studied by NCHRP Project 12-79 for the top flange lateral bending stresses. Therefore, the engineer also can assume that these stress estimates are highly conservative.

3.3 Guidelines on Calculations for Structural Adequacy and Stability

Calculations to substantiate the structural adequacy and stability of the bridge system for each step of the steel erection should be submitted with the erection plan. The calculations should be done in accordance with design criteria established by the Owner, or as stated in the contract plans. This section provides guidelines regarding these calculations. These guidelines should by no means be construed as providing a comprehensive "checklist" of items needing evaluation for erection of any steel girder bridge; each project is unique and may have particular issues requiring the attention of the Contractor's Engineer. Only basic guidelines and suggested evaluation items are presented herein.

3.3.1 Design Criteria

The calculations supporting the erection plan and procedures should be completed in accordance with the AASHTO LRFD Bridge Design Specifications, the AASHTO LRFD Bridge Construction Specifications, and the AASHTO Guide Design Specifications for Bridge Temporary Works, unless otherwise directed by the Owner or the contract documents.

3.3.2 Loads and Load Combinations

The calculations supporting the erection plan and procedures shall consider all applicable loads. Typical load considerations include permanent dead load, construction dead load, construction live load, and wind loads.

Permanent dead loads typically include the self-weight of the structural members and detail attachments. Construction dead and live loads may consist of deck placement machinery, Contractor's equipment, deck overhand brackets, concrete formwork, or other similar attachments applied in the appropriate sequence.

Wind loads shall be considered in each step of the steel erection analysis and are to be computed in accordance with the established design criteria. Provisions should be made by the Contractor's Engineer to ensure that girders are stable in wind events. It is permissible to set limits on maximum wind velocities during steel erection, but these limits must be clearly stated in the erection plan. In some cases, it may be advisable and/or necessary to include provisions in the erection plan for temporary supports and/or tie-downs to address high wind conditions.

Load combinations should be in accordance with the project design criteria, and typically in accordance with the AASHTO LRFD Bridge Design Specifications, unless otherwise agreed to by the Owner.

3.3.3 Girder and System Stability

The calculations supporting the erection plan and procedures shall verify the stability both of individual girders and of the entire erected steel framing for each step of the bridge erection. These calculations are highly dependent upon the particular features of the bridge being erected and also of the particular sequence of erection of each part of the bridge. The assumptions used in the analysis should directly and fully conform to all steps and all details in the erection plan.

The constructability provisions of Article 6.10.3 of the AASHTO LRFD Bridge Design Specifications should be referenced by the Contractor's Engineer when investigating structural adequacy and stability during steel erection. A partial list of suggested evaluation items and guidelines regarding appropriate investigations are as follows.

3.3.3.1 Single Girder Stability

Particular attention should be given to the lateral torsional buckling capacity of a singly erected I-girder. One of the most critical stages during I-girder erection is when the first girder has been erected but not yet connected to adjacent girders in the cross section. Assuming the girder is adequately braced at the supports, and there is no additional bracing within the span, the unbraced length for the girder will be the distance between supports. Long unbraced lengths typically correspond to very low lateral torsional buckling capacity of the girder. Tub-girders typically have much higher lateral torsional buckling capacity, but only if provided with a properly designed top flange lateral bracing system that provides for quasi-closed section behavior of the girder.

Global overturning stability is also a concern for single curved girders, whether I- or tub-girders. The offset of the center of gravity of the girder from a chord line drawn between the support points results in an overturning moment. Single girders are typically afforded little or no torsional restraint at their supports unless tie downs or bracing, or temporary shoring or hold cranes, are provided.

3.3.3.2 Multi-Girder (Global) Stability

A girder system may be vulnerable to global buckling during the steel erection sequence and/or during deck placement. Narrow, long span segments during steel erection are the most susceptible to this global buckling phenomenon. Methods to investigate the global stability of girder systems are available (Yura et al., 2008).

3.3.3.3 Second-Order Amplification Estimates

Second-order amplification of the girder lateral-torsional stresses may cause a loading condition that exceeds the design capacity of the girders or other components. In this situation, the lateral-torsional displacement of the girder results in additional torsional loading in a nonlinear manner. In addition, the displacement amplifications may complicate the prediction and control the structure's geometry during erection. Although second-order amplification should be considered in the

erection analysis of any steel girder bridge, structures that are more susceptible to second-order amplification include widening of an existing bridge with one, two, or a few girders, pedestrian bridges with two-girder systems, phased construction where the various phases may have only one, two, or a few girders erected, and the interim stages of erection of larger bridges where only a few girders are in place in a given erection stage.

A relatively simple method for identifying potentially adverse response amplifications due to second-order effects was developed as part of NCHRP Project 12-79. In this method, the linear response prediction obtained from any first-order analysis is multiplied by the following amplification factor (AF_G):

$$AF_G = \frac{1}{1 - \frac{M_{\max G}}{M_{crG}}}$$

where M_{maxG} is the maximum total moment supported by the bridge unit for the loading under consideration, equal to the sum of all the girder moments, and M_{crG} is the elastic global buckling moment of the bridge unit, which may be estimated using the equation

$$M_{crG} = C_b \frac{\pi^2 sE}{L_s^2} \sqrt{I_{ye} I_x}$$

(Yura et al., 2008). In this equation, C_b is the moment gradient modification factor applied to the full bridge cross-section moment diagram, s is the spacing between the two outside girders of the unit, E is the modulus of elasticity of steel,

$$I_{ye} = I_{yc} + \frac{b}{c} I_{yt}$$

is the effective moment of inertia of the individual I-girders about their weak axis, where I_{yc} and I_{yt} are the moments of inertia of the compression and tension flanges about the weak axis of the girder cross-section respectively, b and c are the distances from the mid-thickness of the tension and compression flanges to the centroidal axis of the cross-section, and I_x is the moment of inertia of the individual girders about their major-axis of bending (i.e., the moment of inertia of a single girder). Yura et al. (2008) provide a number of examples illustrating the calculation of M_{crG}.

3.3.3.4 Cantilever Girders

During the various stages of erection of most steel girder bridges there are often cases where field sections of girders are supported in a cantilevered position. Typically, these intermediate cantilever conditions were not addressed by the Design Engineer during the original bridge design, so it is incumbent on the Contractor's Engineer to investigate these conditions. For long cantilevers, lateral torsional buckling will typically govern over yielding of the section. To examine cantilevers, the lateral torsional buckling capacity can be estimated using the procedures provided in Galambos (1998), Ziemian (2010), or a similar appropriate method. For curved girders, additional consideration needs to be given to the torsional forces that develop due to the offset centroid of the cantilever.

3.3.4 Uplift

Uplift at temporary and permanent supports during steel erection should be accounted for in the development of the erection plan and procedures. Typically, uplift is undesirable and should be prevented, either by changing the erection plan or by providing tie-down restraints. If uplift

is indicated in the analysis but no tie-down restraint is provided, then the analysis should recognize the absence of vertical restraint at that particular support by modeling the boundary condition appropriately. Curved or skewed I-girder bridge systems are particularly susceptible to uplift during various stages of steel erection due to the torsional twisting of the system caused by curvature and/or skew. Incorrect consideration of uplift invalidates the analysis; if not considered correctly, uplift can result in girder alignment and/or other problems as steel erection progresses.

3.3.5 Temporary Hold Cranes

The computations for hold crane loads (if hold cranes are used) should be included in the erection plan calculations. Hold cranes are used to apply an upward load at some location with the span of a girder, thereby reducing the load carried by the girder. Oftentimes, the hold crane load is used to reduce the girder flexural moment due to self-weight (and any other applied loads) to a level at which the moment is less than the lateral-torsional bucking capacity. Typically, a hold crane should not be considered as a brace point in the evaluation of the lateral torsional buckling capacity of a girder; in most cases, the crane cable and crane system are flexible and not capable of providing the lateral resistance necessary to be considered as a brace point.

3.3.6 Temporary Support Loads

The erection plan calculations should include computations for the loads on temporary supports provided at critical stages of the erection sequence. These loads may include vertical and lateral reactions from the superstructure, self-weight of the temporary support, wind loads on the temporary support, etc.

3.3.7 Bearings

Computed bearing rotations during construction should not exceed the rotational capacity of the bearing. The erection plan calculations should include these bearing rotations. Skewed bridges are particularly vulnerable to twisting about the longitudinal axis of the girder. During steel erection, the girder could be rotated beyond the rotational capacity of the bearing, regardless of the vertical load on the bearing.

3.3.8 Cross Frames and Bracing

The placement of the cross frames and other bracing members should be substantiated through calculations that support the erection plan and procedures. The required number of cross frames to be installed before the girders are released from the lifting crane should be verified with calculations and clearly indicated in the erection plan. The cross frames and bracing members and their associated connections must be structurally adequate, and they must also provide sufficient stiffness to the bridge system.

The presence, and correct installation of, cross frames in curved or skewed steel I-girder bridge erection is an important issue. During steel erection, the erector may choose to install the minimum required number of cross frames when initially erecting the girders, so as to decrease erection time, allowing a follow-up crew to install the remaining cross frames later. Therefore, correct determination of the minimum number of required cross frames to prevent lateral torsional buckling of the girders is critical to ensuring the stability of the girders during erection. Yura (1998) provides a general method to check whether cross frames in a girder system provide sufficient bracing for the girders. Additional calculations may be required to check that individual cross frame members and connections have adequate capacity.

3.4 Structural Adequacy of Temporary Components

Calculations to substantiate the structural adequacy and stability of any and all temporary support components for each step of the steel erection should be submitted with the erection plan. Additionally, calculations supporting the use of lifting beams, lifting devices (rigging), and jacking devices should be included in the calculation submittal. The calculations should be done in accordance with design criteria established by the Owner, or as stated in the contract plans.

3.4.1 Temporary Supports

Calculations indicating the load capacity and verifying the stability of any temporary supports should be included in the computations supporting the erection plan and procedures. Temporary support structures should be designed to carry vertical and lateral loads resulting from the proposed erection sequence. As necessary, calculations for the design of an upper grillage, temporary bearings, and foundations should also be included. The elevation of the bearing support (bearing seat elevation) at the top of the temporary support structure should be computed and provided in the erection plan. The bearing seat elevations at the temporary supports can aid the steel erector in controlling the geometry of the structure during steel erection.

3.4.2 Girder Tie-Downs

Calculations indicating the load capacity of girder tie-downs at any location should be included in the computations supporting the erection plan and procedures. The tie-downs may be used to resist wind loads, uplift, lateral dead load forces resulting from horizontal curvature, or other loads.

3.4.3 Lifting Beams and Devices

Calculations verifying the load capacity of Contractor-fabricated lifting devices such as lifting beams, spreader beams, welded lugs, beam clamps, etc., should be provided in the computations supporting the erection plan and procedures. When applicable, manufacturers' certification or catalog cuts for pre-engineered devices should be included with the calculations.

3.4.4 Jacking Devices

Calculations for jacking devices, including jacking loads, jack type, etc., should be included with the erection plan calculations. Also, a detailed jacking procedure should be developed and included in the erection plan.

3.5 Miscellaneous Calculations and Recommendations

3.5.1 Crane Pick Locations

The Contractor's Engineer often provides calculations for the approximate pick locations for girder erection. These approximate crane pick locations should be determined with consideration of the centroid of the entire assembly being lifted into place, including the girder as well as any attached cross frames, splice plates, stiffening trusses, or other attached items.

Figure 3.1 provides equations helpful in the computation of the centroids of various curved shapes.

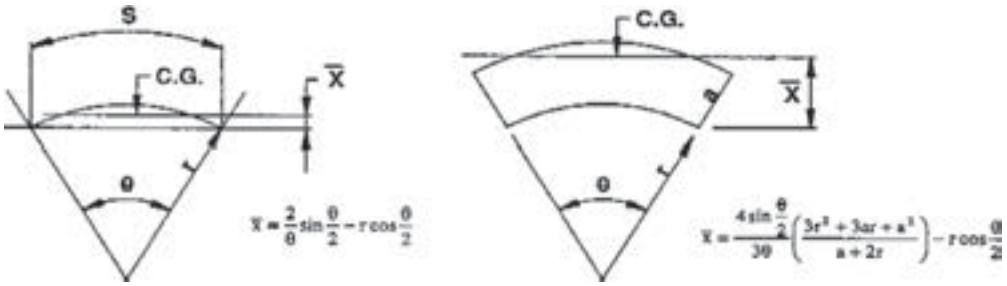

(a) (b)

Figure 3.1 Center of gravity for approximate pick points during lifting: (a) circular arc, (b) sector of annulus.

3.5.2 Alignment of Field Splice Connections

Using the erection analysis results, the Contractor's Engineer should evaluate the lateral and vertical displacements and rotations at field splice locations of previously erected girders in relation to the next girder segment being erected. Oftentimes, the field splice location will be at the end of the girder that is cantilevered over an interior support, and displacements and rotations may be significant enough to hinder the Contractor's attempts to align bolt holes in bolted field splice connections. Vertical displacements and end rotations at the end of the previously placed, cantilevered section may result in the end of the girder being out of position and out of alignment relative to the next field section being erected, which is often in a level, neutral position when being lifted. Lateral displacements are caused by the natural behavior of a curved steel girder to rotate outward from the radius of curvature. Since the next girder piece being lifted into place will typically be in a vertically plumb position, laterally displaced cantilever tips of the previously erected girder could cause alignment issues.

3.5.3 Alignment of Cross Frame Connections

Using the erection analysis results, the Contractor's Engineer should verify that the lateral displacements and girder rotations do not cause problems in erecting cross frames, whether cross frames are installed before or after girders are released from the lifting crane. Long unbraced girder lengths may result in significant out-of-plane rotations and displacements of the top and bottom flanges. Curvature and skew also produce potentially significant girder displacements and rotations. If the rotations and displacements are too large, the Contractor may have difficulty aligning connections.

Contractors typically use various methods to correct these types of misalignments, including the use of temporary hold cranes, jacks, come-alongs, or other means. In certain situations, these means may prove insufficient. In extreme cases, the inherent stiffness of the girders is such that enough force cannot be practically applied to pull the connections into alignment, or alternately the amount of force required to pull the connections into alignment would damage the structure.

3.5.4 Support Conditions

The boundary (support) conditions assumed in the erection analysis should accurately reflect the actual support conditions in the structure at all stages of erection (including accurate consideration of any and all temporary supports). If the character of the support at a location changes during the steel erection, this should be accurately addressed in the analysis model. Improper modeling of boundary conditions leads to erroneous results and invalidates the analysis.

3.6 Calculation Checklist

- Complete analysis of erection sequence
  - Proper level of analysis used
  - Support conditions modeled appropriately at all stages
- Correct design criteria employed
- Correct loads investigated
- Complete checks of structural adequacy of bridge components
- Complete checks of stability of girder and bridge system
- Second-order amplification effects addressed as needed
- Girder reactions checked for uplift
- Temporary hold crane loads computed
- Temporary support loads computed
- Bearing capacity and rotation checks
- Cross frame and bracing placement
- Checks of structural adequacy of temporary supports and devices
  - Falsework towers
  - Girder tie-downs
  - Lifting beams
  - Jacking devices
- Crane pick location calculations
- Checks of displacements at field splices
- Checks of displacements for cross frame placement

3.7 Problematic Characteristics and Details to Avoid

3.7.1 Oversized or Slotted Holes

The use of oversized or slotted holes in gusset and connection plates can decrease significantly the stability bracing efficiency of cross-frames. In addition, the control of the deformed bridge geometry can also be affected since cross-frames are necessary to integrate the girders and make them deform as a unit rather than as independent components. Therefore, it is not recommended to use this scheme as a solution to erecting cross-frames at stiff locations such as the regions near skewed supports.

3.7.2 Narrow Bridges or Bridge Units

In some cases, I-girder bridges can be susceptible to large response amplifications due to global second-order effects. Widening projects of existing bridges, pedestrian bridges with twin girders, phased construction, and erection stages where only a few girders of the bridge are in place, are some examples of structures that can be susceptible to considerable global second-order amplifications. When potential amplifications of the system stress and displacement responses are a concern, it is recommended to study the structure with refined 3D FEA or an approximate method based on amplified responses of a linear analysis solution.

3.7.3 V-Type Cross-Frames without Top Chords

Cross-frames are needed to stabilize I-girders prior to hardening of the concrete deck. In some cases, V-type cross-frames without top chords may not be able to perform this function. The flexural stiffness of this type of cross-frame is substantially smaller than other configurations (i.e. X-type or V-type with top chord). Therefore, its ability to provide stability bracing needs to be con-

sidered carefully during design. Studies conducted on an existing structure that uses V-type cross-frames without top chords illustrates the importance of including the top chord (Sanchez, 2011).

3.7.4 Bent-Plate Connections in I-Girder Bridges

Bent-plate details can introduce excessive flexibility in the system, affecting the stability bracing capacity of skewed cross-frames. Due to this limitation, designers should consider the use of other connection details that do not represent a detriment to the system performance. Details such as the half-pipe stiffener and the reinforced bent-plate are options that can be used to connect skewed cross-frames at angles larger than 20°.

3.7.5 Long-Span I-Girder Bridges without Top Flange Lateral Bracing Systems

Flange level lateral bracing systems are recommended for long-span bridges since second-order amplification and global flange lateral bending effects can be more critical for longer spans as the stresses are more dominated by dead load effects. Flange level lateral bracing systems help to control the bridge geometry and eliminate the second-order effects as these systems cause portions of the structure to act as pseudo-box girders.

3.7.6 Partial-Depth End Diaphragms in Tub-Girder Bridges

Partial-depth end diaphragms often are used when they are the only solution due to the project geometric constraints. When possible, such a detail should be avoided in the practice because it changes the local and global behavior of the system. At the local level, the top flange lateral bracing system will lose continuity close to the end diaphragm. This results in a redistribution of forces through a different load path to reach the end of the girder. Also, the end panel will experience comparatively more deformation with respect to the adjacent panels, thus having a direct impact in the adjacent elements that control the cross section distortion, such as the internal cross-frames. The global consequences include a significant increase of the girder deflections and rotations due to the increased flexibility caused by partial-depth end diaphragms. If partial-depth end diaphragms are used, the resulting behavior of the system needs to be carefully investigated and, in many cases, will require a more refined analysis.

3.7.7 Non-Collinear External Intermediate Diaphragms in Tub-Girder Bridges

When tub-girder bridges require external intermediate cross-frames or support diaphragms to control differential displacements between girders, or reaction force distribution, the internal and external components should be collinear to avoid undesired behavior at the connecting locations.

3.7.8 Two-Bearing System at Tub-Girder Support

The use of twin bearing support under a single tub-girder typically requires a more refined analysis and, in general, should be avoided for curved and/or skewed bridges. In the curved and/or skewed bridges, an ideal twin bearing system could be used to transfer part or all of the associated torque to the support rather than follow the end diaphragm mechanism. In most cases, common bridge bearings are not able to resist upward forces and, consequently, the bridge could experience uplift at one of the twin bearings while the other bearing could be subjected to the entire vertical load, possibly exceeding the bearing design force.

References

AASHTO/NSBA Steel Bridge Collaboration (2007). *Steel Bridge Erection Guide Specification,* American Association of State Highway and Transportation Officials/National Steel Bridge Alliance, Washington, D.C.

AASHTO (2008). Guide Design Specifications for Bridge Temporary Works, 1st edition with Interim Revisions through 2008, American Association of State Highway and Transportation Officials, Washington, D.C.

AASHTO, LRFD Bridge Design Specifications (2010). 5th edition, American Association of State Highway and Transportation Officials, Washington, D.C.

AASHTO, LRFD Bridge Construction Specifications (2010). 3rd edition, American Association of State Highway and Transportation Officials, Washington, D.C.

Bridgesoft, Inc. (2010). "STLBRIDGE, Continuous Steel Bridge Design," http://bridgesoftinc.com/

Galambos, T.V. (1998). *Guide to Stability Design Criteria for Metal Structures*, 5th edition, Wiley, New Jersey.

Jimenez Chong, J.M. (2012). "Construction Engineering of Steel Tub-Girder Bridge Systems for Skew Effects," Ph.D. dissertation, School of Civil and Environmental Engineering, Georgia Institute of Technology, Atlanta, GA, 276 pp.

LARSA (2010). "LARSA 4D, The Complete Software for Bridge Engineering," http://www.larsa4d.com/products/larsa4d.aspx

MDX (2011). "MDX Software, The Proven Steels Bridge Design Solution," http://www.mdxsoftware.com/

NSBA (1996). "V-Load Analysis and Check (VANCK), User Manual, Version 1.0," National Steel Bridge Alliance and American Institute of Steel Construction.

Quadrato, C., Battistini, A., Frank, K., Helwig, T., and Engelhardt, M. (2010). "Improved Cross-Frame Connection Details for Steel Bridges with Skewed Supports," *Transportation Research Record 2200,* 29-35, Transportation Research Board, Washington, D.C.

Richardson, Gordon, & Associates (1976) (now Pittsburgh office of HDR, Inc.), *FHWA Curved Girder Workshop Manual.*

Sanchez, T.A. (2011). "Influence of Bracing Systems on the Behavior of Steel Curved and/or Skewed I-Girder Bridges during Construction," Ph.D. dissertation, School of Civil and Environmental Engineering, Georgia Institute of Technology, Atlanta, GA, 2011.

Tung, D.H.H. and Fountain, R.S. (1970). "Approximate Torsional Analysis of Curved Box Girders by the M/R Method," *AISC Engineering Journal,* Vol. 7, No. 3, 1970.

United States Steel Corporation (1984). *V-Load Analysis (ADUSS 88-8535-01).*

Yura, J., (1993). "Fundamentals of Beam Bracing," *Is Your Structure Suitably Braced? – Structural Stability Research Council Annual Stability Conference Proceedings,* Milwaukee, WI, April 6-7: 1-1.20.

Yura, J., Helwig, T., Herman, R., and Zhou, C., (2008). "Global Buckling of I-Shaped Girder Systems," *Journal of Structural Engineering,* ASCE, 134(9), 1487-1494.

Ziemian, R. (2010). *Guide to Stability Design Criteria for Metal Structures,* 6th edition, Wiley, New Jersey.

Abbreviations and acronyms used without definitions in TRB publications:

AAAE	American Association of Airport Executives
AASHO	American Association of State Highway Officials
AASHTO	American Association of State Highway and Transportation Officials
ACI–NA	Airports Council International–North America
ACRP	Airport Cooperative Research Program
ADA	Americans with Disabilities Act
APTA	American Public Transportation Association
ASCE	American Society of Civil Engineers
ASME	American Society of Mechanical Engineers
ASTM	American Society for Testing and Materials
ATA	American Trucking Associations
CTAA	Community Transportation Association of America
CTBSSP	Commercial Truck and Bus Safety Synthesis Program
DHS	Department of Homeland Security
DOE	Department of Energy
EPA	Environmental Protection Agency
FAA	Federal Aviation Administration
FHWA	Federal Highway Administration
FMCSA	Federal Motor Carrier Safety Administration
FRA	Federal Railroad Administration
FTA	Federal Transit Administration
HMCRP	Hazardous Materials Cooperative Research Program
IEEE	Institute of Electrical and Electronics Engineers
ISTEA	Intermodal Surface Transportation Efficiency Act of 1991
ITE	Institute of Transportation Engineers
NASA	National Aeronautics and Space Administration
NASAO	National Association of State Aviation Officials
NCFRP	National Cooperative Freight Research Program
NCHRP	National Cooperative Highway Research Program
NHTSA	National Highway Traffic Safety Administration
NTSB	National Transportation Safety Board
PHMSA	Pipeline and Hazardous Materials Safety Administration
RITA	Research and Innovative Technology Administration
SAE	Society of Automotive Engineers
SAFETEA-LU	Safe, Accountable, Flexible, Efficient Transportation Equity Act: A Legacy for Users (2005)
TCRP	Transit Cooperative Research Program
TEA-21	Transportation Equity Act for the 21st Century (1998)
TRB	Transportation Research Board
TSA	Transportation Security Administration
U.S.DOT	United States Department of Transportation

Project No. NCHRP 12-79 **COPY NO. 1 of 20**

EVALUATION OF ANALYTICAL METHODS FOR CONSTRUCTION ENGINEERING OF CURVED AND SKEWED STEEL GIRDER BRIDGES

TASK 8 REPORT

Prepared for
NCHRP
Transportation Research Board
of
The National Academies

Donald W. White, Georgia Institute of Technology, Atlanta, GA
Andres Sanchez, HDR Engineering, Inc., Pittsburgh, PA
Cagri Ozgur, Paul C. Rizzo Associates, Inc., Pittsburgh, PA
Juan Manuel Jimenez Chong, Paul C. Rizzo Associates, Inc., Pittsburgh, PA
February 29, 2012

ACKNOWLEDGMENT OF SPONSORSHIP

This work was sponsored by one or more of the following as noted:

☑ American Association of State Highway and Transportation Officials, in cooperation with the Federal Highway Administration, and was conducted in the **National Cooperative Highway Research Program,**

☐ Federal Transit Administration and was conducted in the **Transit Cooperative Research Program**,

☐ American Association of State Highway and Transportation Officials, in cooperation with the Federal Motor Carriers Safety Administration, and was conducted in the **Commercial Truck and Bus Safety Synthesis Program,**

☐ Federal Aviation Administration and was conducted in the **Airports Cooperative Research Program,**

which is administered by the Transportation Research Board of the National Academies.

DISCLAIMER

Project No. NCHRP 12-79

EVALUATION OF ANALYTICAL METHODS FOR CONSTRUCTION ENGINEERING OF CURVED AND SKEWED STEEL GIRDER BRIDGES

TASK 8 REPORT

Prepared for
NCHRP
Transportation Research Board
of
The National Academies

Donald W. White, Georgia Institute of Technology, Atlanta, GA
Andres Sanchez, HDR Engineering, Inc., Pittsburgh, PA
Cagri Ozgur, Paul C. Rizzo Associates, Inc., Pittsburgh, PA
Juan Manuel Jimenez Chong, Paul C. Rizzo Associates, Inc., Pittsburgh, PA

February 29, 2012

Table of Contents

List of Figures

List of Tables

Executive Summary

In current practice (2012), the construction of curved and/or skewed steel girder bridges is sometimes hampered by misconceptions regarding the three-dimensional behavior of these structures. The deflections of curved and skewed girder bridges intrinsically involve torsion of the bridge cross-section and of the individual girders. The resulting 3D movements can affect the fit-up of cross-frames or diaphragms during the steel erection. Furthermore, they can influence the control of the deck thickness, the final deck slopes and superelevations, the dead load rotations at bearings, the alignment of units at deck joints, and the matching of stages in phased construction projects. Depending on the severity of the bridge geometric conditions and the specific needs regarding the geometry control, a simple analysis solution may be sufficient to assess these considerations or a more refined analysis may be necessary.

This document provides guidelines for the selection of analytical methods for the design of skewed and/or horizontally curved steel girder bridges for construction. Both steel I- and tub-girder bridges are addressed. Emphasis is placed on the assessment of when simplified 1D or 2D analysis methods are sufficient, and when 3D methods may be more appropriate for assessment of constructability demands and prediction of the constructed geometry of curved and/or skewed structures.

The report first scrutinizes a number of commonly used 1D, 2D and 3D analysis idealizations to provide a detailed understanding of the underlying assumptions and basic limits of applicability of the methods. A number of established extensions of typical 1D and 2D analyses are discussed that allow the engineer to obtain the broadest potential range of information with these methods when they are applicable. Secondly, several key geometry related bridge indices are identified that can be utilized as aids to identify when different simplified approximations may be suspect. These indices are then used as a part of guidelines for the selection of analytical methods.

Interestingly, although vertical deflections and girder major-axis bending stresses may be estimated with reasonable accuracy in a large number of situations, the cross-

frame forces and girder flange lateral bending stresses in skewed I-girder bridges are essentially impossible to determine with any confidence using 1D line-girder and conventional 2D-grid analysis methods. The problems lie in general with the lack of any ability to capture transverse load paths using the 1D methods, and the gross errors associated with neglecting the true girder warping torsion stiffness and the cross-frame stiffness characteristics in conventional 2D-grid methods. Modifications to conventional 2D-grid analysis methods are provided, however, which result in reliable predictions over a wide range of I-girder bridges.

This study also addresses the difficult questions of what types of cross-frame detailing are most effective for different bridge geometries, and when should locked-in force effects due to the detailing of cross-frames be considered in the calculation of I-girder bridge responses. Recommended procedures are provided for determining locked-in force effects for cases in which these effects need to be included. In addition, guidelines are provided for the selection of cross-frame detailing methods as a function of the bridge geometry.

Lastly, the report discusses a number of design and construction considerations that can be implemented to alleviate the demands on the methods of structural analysis by improving the bridge behavior, various problematic physical characteristics, details and practices are outlined, and important potential pitfalls associated with 1D, 2D and 3D analysis techniques are highlighted.

1. Introduction

1.1 Problem Statement

Curved and/or skewed steel I- and tub-girder bridges can experience significant 3D deflections and rotations. In general, 3D deflections and rotations must be considered in the design, detailing and construction engineering of these bridge types. The 3D movements can affect the fit up of cross-frames or diaphragms during the steel erection. Furthermore, they can influence the control of the bridge geometry, including the deck thickness, the final deck slopes and superelevations, the dead load rotations at the bearings, the alignment of units at deck joints, and the matching of stages in phased construction projects. Depending on the severity of the bridge geometric conditions and the specific needs regarding the geometry control, a simple analysis solution may be sufficient or a more refined analysis may be necessary.

Longer span bridges tend to be affected more substantially by dead load effects, potentially resulting in more significant stability considerations during construction. In curved and/or skewed structures, these effects are manifested predominantly in the second-order amplification of the deflections and internal stresses. During intermediate erection stages, it is important that the physical component stresses are limited, including any significant second-order effects, such that there is no significant onset of inelastic deformations and no component strength limits are exceeded. Conversely, shorter span bridges tend to be dominated more by live load effects; thus, these bridges tend to be less affected by construction loading conditions.

Longer span bridges generally exhibit larger deflections; hence, the accuracy of the deflection predictions can be more critical. Shorter span bridges have smaller deflections and are thus less apt to experience problems due to the movements of the structure during construction. One of the key instances where the deflections during construction can be a factor is during the placement of the deck. Inaccurate prediction of the system deflections can result in over-run or under-run of the deck thickness, deviations from intended deck slopes and superelevations, local dips in deck elevation that are susceptible to ponding, unintended bearing rotations, misalignment of units at

deck joints, and/or mismatched stages in phased construction projects. Since the overall deflections are larger in longer span bridges, the relative deflections that drive the above concerns are also larger. Control of the geometry during the placement of the deck is an essential consideration in the construction of curved and skewed girder bridges, particularly for bridges with longer spans.

Structural engineers currently have a wide array of approximate and refined analysis and design tools at their disposal. It is important that the right tool is selected for a given bridge. In addition, there are a number of specific cross-frame detailing practices typically used to economically control, i.e., to compensate for, the 3D deflections and rotations in curved and skewed I-girder bridges. The application of and the implications of these practices need to be better understood so that they can be applied in the most effective ways.

Bridges with significant span lengths, curvature and skew generally require careful planning of the erection procedures and sequences such that lifting and fit-up of their spatially deformed components and subassemblies is achievable. Longer and/or wider bridges also may require placement of the deck in multiple stages. Setup of the concrete from prior stages, and in some cases during the current stage, can have a significant influence on the final geometry and on the ultimate performance of the deck. Some wide bridges may require construction in multiple longitudinal phases, with the corresponding problems of connecting new steel to a completed structure, and the matching of deck elevations between adjacent phases. On the other hand, shorter bridges with minor curvature and skew often can be built with less attention to the construction engineering. With respect to all the above considerations, it is important that the appropriate level of effort is applied for the task at hand.

1.2 Objectives

This document outlines the key characteristics of various simplified 1D and 2D analysis methods. It provides guidelines for when these methods are sufficient as well as recommendations for when more sophisticated 3D analysis capabilities may be warranted for assessment of the constructability and prediction of the final constructed geometry of

curved and/or skewed steel girder bridges. Both I-girder and tub-girder bridges are addressed. These guidelines are based on extensive information collected from prior and current research, input from bridge owner and consultant policies and practices, and fundamental studies of the accuracy of the simplified methods of analysis conducted by NCHRP Project 12-79, "Guidelines for Analytical Methods and Erection Engineering of Curved and Skewed Steel Deck-Girder Bridges." This report focuses on the accuracy of analysis methods commonly used to determine the strength, stability, and constructability of curved and/or skewed steel girder bridges under the action of their self-weight and various loads imposed during construction operations. In addition, a number of improvements are recommended to conventional analysis techniques that are necessary to eliminate several critical flaws identified by the NCHRP Project 12-79 research.

1.3 Organization

This report is subdivided into eleven main chapters. Chapter 2 aims to establish the framework for the discussions in the other chapters by providing an overview of the common structural analysis tools available in current (2012) practice for analysis of curved and/or skewed steel girder bridges. Namely, these are:

1) Line-girder (1D) methods,
2) 2D-grid methods,
3) 2D-frame methods,
4) Plate and eccentric beam methods,
5) Conventional 3D-frame methods,
6) Thin-walled open-section (TWOS) 3D-frame methods, and
7) 3D Finite Element Analysis (FEA) methods.

The essential idealizations and approximations are summarized for each of these methods. In addition, Chapter 2 discusses specific hand calculation equations commonly used with the 1D and 2D methods, second-order amplification estimates for displacements and stresses in cases where stability effects may be important, and analysis of composite action between the bridge deck and the steel structure, including staged deck placement and consideration of early stiffness and strength gains of the concrete. Chapter

2 closes with a discussion of response attributes that generally cannot be captured by 1D and 2D methods. Of course, in cases where these attributes are not an important factor in the response of the structure, these limitations do not significantly impact the accuracy of the analysis. However, clearly if any of these attributes is expected to be an important contributor to particular structural actions, the engineer must utilize an analysis method capable of capturing the contribution when evaluating these actions.

Chapter 3 defines several key indices identified by NCHRP 12-79 as the most useful for characterizing the importance of curvature and skew on the accuracy of analysis methods for steel girder bridges. Subsequently, these indices are employed as aids to identify when simpler methods of analysis are sufficient as well as when more sophisticated methods should be applied. In addition, this chapter comments on the broad range of factors that generally can influence the detailed behavior of these types of structures.

Chapter 4 provides an overview of the NCHRP 12-79 studies leading to the recommendations of this report. The emphasis of this chapter is on the design and development of a large parametric study of curved and skewed I- and tub-girder bridge systems conducted in the NCHRP research.

Chapter 5 summarizes the core results of the parametric studies conducted by NCHRP 12-79. A scoring method is introduced and utilized to quantify the ability of the different methods of analysis for predicting essential responses. Unfortunately, for a number of responses pertaining to I-girder bridges, the accuracy of commonly used (conventional) simplified methods is essentially binary. That is, either a given method works well or its usage is very suspect. The reasons for this behavior are explained in Chapter 6. Chapter 6 also recommends specific improvements to conventional 2D-grid methods for the analysis of I-girder bridges developed in the NCHRP 12-79 research.

Chapter 7 addresses the consideration of locked-in force effects associated with cross-frame detailing methods commonly used to achieve approximately plumb girder webs at targeted stages of I-girder bridge construction. The highly complex bridge behavior associated with these relatively simple cross-frame detailing practices is

explained through a series of examples. Specific conditions are shown where the locked-in forces from cross-frame detailing should be considered in the design. In addition, specific analysis procedures for determining the locked-in force effects are presented. It is emphasized that these locked-in forces are beneficial in that they provide a simple and cost-effective means of achieving plumb webs under a given dead load condition. However, in certain cases, these effects need to be considered in determining vertical deflections and setting cambers, and in evaluating the structural resistances. Lastly, Chapter 7 discusses several special cases where a 1D (line-girder) analysis (with proper extensions where needed) tends to produce sufficiently accurate results for all the essential response quantities (including locked-in forces), as well as when an accurate structural analysis without including the locked-in forces potentially can be used to estimate the maximum cross-frame forces and girder flange lateral bending stresses in I-girder bridges.

In many situations, the need for a more sophisticated type of analysis can be reduced or eliminated by intelligent and prudent decisions made during the design and construction engineering. Chapter 8 discusses a number of considerations that can ease the demands on the structural analysis via improved structural behavior.

Chapter 9 discusses specific characteristics, practices and details that can lead to major difficulties in the ability to predict the response of the structure during construction, and therefore should be used very carefully or sparingly if they are used at all. Lastly, Chapter 10 summarizes key pitfalls in 1D, 2D and 3D methods of analysis for construction engineering of curved and/or skewed girder bridges. Chapter 11 summarizes the recommendations of this report in a concise form.

1.4 Scope and Intended Audience of this Report

This report presents the results of the NCHRP 12-79 research on methods of analysis in a summary form for engineers interested in accessing the details of the research behind the subject recommendations. Readers interested in a concise implementation of the NCHRP 12-79 recommendations in a code-type format oriented toward current practice should first view the companion Task 9 report "Recommendations for Construction Plan Details and Level of Construction Analysis." Readers interested in a concise summary of the improvements to simplified methods of analysis and their application, should first consult the NCHRP 12-79 Final Report.

2. Overview of Methods (Types) of Analysis

2.1 Line-Girder (1D) Analysis

Line-girder analysis is the most basic method used in the engineering of girder bridges. In this method, the bridge girders are analyzed individually, and their interaction with the bracing system is ignored or accounted for only in a coarse fashion. The loads during steel erection are commonly taken as those acting directly on each girder, but various approaches are used for distributing the subsequent dead loads. NHI (2007) suggests that when the width of the deck is constant, the girders are parallel and have approximately the same stiffness, and the number of girders is not less than four, the permanent load of the wet concrete deck may be distributed equally to each of the girders in the cross-section. Article 4.6.2.2.4 of (AASHTO, 2010) indicates that wearing surface and other distributed loads may be assumed uniformly distributed to each girder in the cross-section of curved steel bridges. However, (NHI, 2011) emphasizes that heavier DC_2 line loads such as parapets, barriers, sidewalks or sound walls should not be distributed equally to all the girders. If the overhang widths and/or the concrete barrier loads are large, engineers commonly use the lever rule (AASHTO, 2010) to distribute the overhang and barrier loads to the girders. Alternatively, some state DOTs assign 60 % of the barrier weight to the exterior girders and 40 % to the adjacent interior girders (NHI, 2007). If the lever rule is used, the portion of the dead load assigned to the fascia girders is increased, while the loads on the interior girders are reduced. NHI (2010) points out that estimating the distribution of DC_2 line loads to the individual girders for line girder analysis is particularly difficult in skewed bridges since the loads may only be on one side of the bridge over significant portions of the span. In addition, NHI (2007) indicates equal distribution of distributed loads can be suspect for skews larger than 10 degrees. Considering all these factors, the distributed dead loads were assigned to the girders based on tributary area in the 1D analyses conducted by the NCHRP 12-79 project team. Parapet loads were considered in the design of parametric study bridges in the NCHRP 12-79 research, but these bridge designs were conducted using 2D-grid and Plate-eccentric beam analysis procedures discussed subsequently.

Typically, various other supplementary calculations are added to the basic line-girder estimates to account for important effects not inherently included in the 1D idealization. The next two sections summarize calculations commonly utilized to extend the line-girder method to the analysis and design of horizontally curved I- and tub-girder bridges. Section 2.1.3 then summarizes equations for estimating flange lateral bending stresses in I-girders and in the top flange of tub girders due to eccentric overhang bracket loads on fascia girders, and due to horizontal curvature effects. Section 2.1.4 addresses the estimation of girder layovers, and Section 2.1.5 recommends a procedure for estimating the torques due to skew effects in tub girders when a line-girder analysis is used.

2.1.1 V-Load Method

The V-load method extends the capabilities of a 1D line-girder analysis to address horizontal curvature effects in I-girder bridges. The method was originally developed by Richardson, Gordon, and Associates (presently the Pittsburgh office of HDR Engineering, Inc.) and was published in the *"USS Structural Report, Analysis and Design of Horizontally Curved Steel Bridge Girders"* (USS, 1965). The V-load method has been used for more than four decades in the preliminary and final design of curved I-girder bridges. This section discusses the background of the method to highlight its attributes and applicability for the analysis of I-girder bridges. The derivations are based on the work presented in Grubb (1984) and Poellot (1987).

Consider the simply-supported curved I-girder shown in Figure 2.1a, which is subjected to a major-axis uniform bending moment, M, via forces applied at its ends. The corresponding flange axial forces, T, are approximately equal to M/h, where h is the distance between the flange centroids. A differential element of the top flange with an arc length $ds = R\ d\theta$ is extracted from the girder, where R is the horizontal radius of curvature of the girder. Figure 2.1b shows a free body diagram (FBD) of this flange segment. The longitudinal components of the forces, T_x, cancel each other. However, the radial components

$$T_y = \frac{M}{h}\frac{d\theta}{2} \tag{2.1}$$

are additive. Therefore, a uniformly distributed internal force

$$q = \frac{2T_y}{ds} = \frac{M}{Rh} \tag{2.2}$$

transferred via the web, is necessary to balance these components. Upon multiplying both sides of this equation by the radius R, one can observe that the flange axial force, T, is equal to qR.

(a) Axial forces in the top flange due to uniform moment

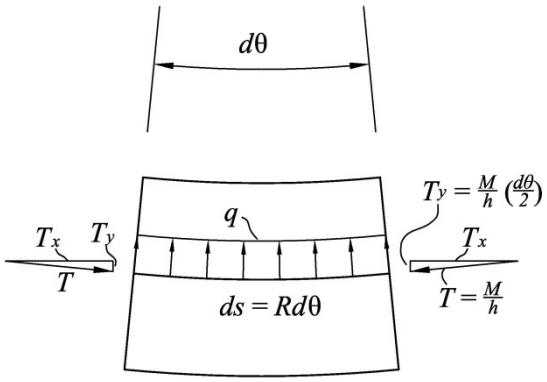

(b) Free body diagram of the flange segment

Figure 2.1. Curved girder subjected to a uniform major-axis bending moment.

The above uniformly distributed force, q, subjects the flanges to lateral bending. Hence, in a two-girder system such as the one depicted in Figure 2.2a, the flanges behave like continuous-span beams in the lateral direction, while the cross-frames act like the continuous-span beam supports. The girders G1 and G2 in this figure are subjected to major-axis bending moments $M_1(x)$ and $M_2(x)$, respectively, where x is the coordinate measured along the arc length of the girders. For equilibrium of the exterior girder at the first intermediate cross-frame in Figure 2.2b the reaction at the level of the cross-frame chords, H_1, must be approximately equal to $q_1 L_{b1} h/h_{CF}$, where h_{CF} is the depth between

the centerline of the cross-frame chords and L_{b1} is the distance between cross-frames measured along the centerline of G1 (assumed constant). By substituting $q_1 = M_1/R_1h$, one obtains

$$H_1 = \frac{M_1 L_{b1}}{R_1 h_{CF}} \tag{2.3}$$

where R_1 is taken as the radius of curvature of the girder at location 1. The moment in this equation, M_1, is taken as the value at the cross-frame position, i.e., $M_1 = M_1(L_{b1})$.

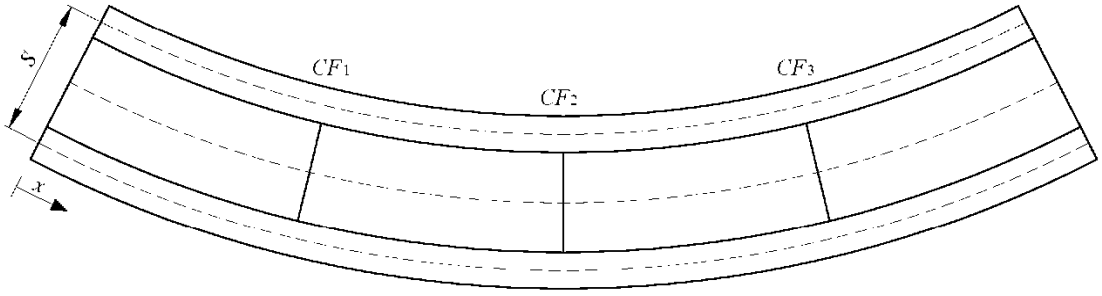

(a) Plan view of the two-girder system

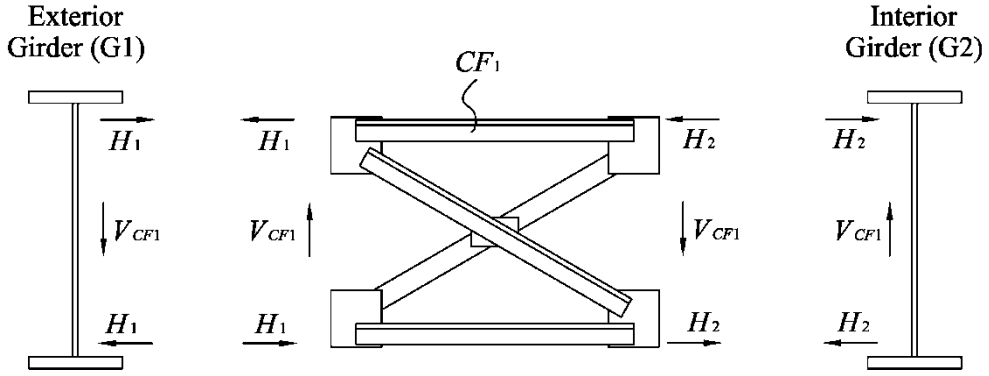

(b) Free body diagram of the first intermediate cross-frame

Figure 2.2. Interaction of forces in a curved girder system.

The reaction at the bottom chord level is the same as H_1, but is in the opposite direction, since the moment causes compression in the top flange and is assumed to cause an equal tension in the bottom flange. Similarly, for the interior girder, G2, the reaction, H_2, may be written as

$$H_2 = q_2 L_{b2} = \frac{M_2 L_{b2}}{R_2 h_{CF}} \tag{2.4}$$

where $M_2 = M_2(L_{b2})$. Note that $L_{b1}/R_1 = L_{b2}/R_2$ may be written as a common value L_b/R, such that $H_1 = M_1 L_b/Rh_{CF}$ and $H_2 = M_2 L_b/Rh_{CF}$.

In the cross-frame shown in Figure 2.2b, moment equilibrium requires that

$$V_{CF1} = \frac{(H_1 + H_2)h_{CF}}{S} = \frac{M_1 + M_2}{RS/L_b} \tag{2.5}$$

These vertical forces are a direct effect of the horizontal curvature, and are known as the V-loads. In Eq. 2.5, the subscript *CF*1 is used to emphasize that this is a load at the first intermediate cross-frame position. Similarly, the loads at the other cross-frame positions can be found by substituting the corresponding moments M_1 and M_2, accordingly. In the exterior girder, G1, the additional moments caused by the downward action of the V-loads, M_{1s}, add to the moments produced directly by the gravity loads, M_{1p}. In the interior girder, G2, these loads are in opposite directions, so the resulting moments are subtracted from the gravity load moments. Therefore, the total moment in a particular cross-section of girder G1, M_1, is equal to $M_{1p} + M_{1s}$. Likewise, for the interior girder, $M_2 = M_{2p} + M_{2s}$. Moreover, at any cross-frame position, $M_{1s} \cong -M_{2s}$ (L_1/L_2), where L_1 and L_2 are the arc-span lengths of G1 and G2, respectively. For practical cases, the term (L_1/L_2) is close to one, so $M_{1s} \approx -M_{2s}$. Given this approximation, the sum of the total moments in G1 and G2, $M_1 + M_2$, may be taken as $M_{1p} + M_{2p}$. Substituting this result into Eq. 2.5, one has

$$V_{CF1} = \frac{M_{1p} + M_{2p}}{RS/L_b} \tag{2.6}$$

Given the above approximations, the girders can be analyzed independently using a line-girder analysis. The curved girders are represented with equivalent straight girders of length L_1 and L_2, and they are subjected to the gravity loads plus the V-loads.

The above development can be extended to consider cases with more than two girders. As explained by Poellot (1987), the V-loads in a multi-girder system are the total

vertical loads delivered to the girders from the cross-frames (equal to the difference in the cross-frame shear forces on the interior girders). The V-load delivered to the girder farthest from the bridge centerline is calculated as

$$V = \frac{\sum M_p}{CRS/L_b} \tag{2.7}$$

The V-loads delivered to the other girders are assumed to vary linearly between a value of zero for any girder at the bridge centerline to the maximum value predicted by Eq. 2.7 for the girder(s) farthest from the centerline. The constant *C* in this equation depends on the number of girders in the structure. Table 2.1 shows the values of *C* for systems with up to ten girders. These constants are derived based on the above assumption.

Table 2.1. Values of the *C* coefficient.

Girders	Coefficient
2	1
3	1
4	10/9
5	5/4
6	7/5
7	14/9
8	12/7
9	15/8
10	165/81

The V-load idealization basically assumes: (1) approximately equal vertical stiffness of all the girders (defined by a unit load applied at a given cross-frame location, divided by the vertical deflection at that location due to the unit load), and (2) a linear variation in vertical displacements across the bridge cross-section due to overall torsion. In general, the V-load method is reasonably accurate for cases that closely satisfy the above assumptions used in its derivation. However, for bridges with skewed supports, staggered cross-frame patterns, etc., a line-girder analysis based on the V-load method may not be sufficient. For those cases, a 3D FEA model, or 2D-grid model with the recommended improvements discussed in Chapter 6 (which captures the interaction

between the structural components more accurately than conventional 2D-grid methods), may be required. These aspects are discussed in the subsequent sections of this report.

2.1.2 M/R Method

The M/R method is a simplified tool for estimating the torsional effects due to curvature in general box girders. This method, which was first introduced by Tung and Fountain (1970), applies an equivalent distributed torsional moment M/R to an individual girder, where M is the major-axis bending moment and R is the radius of curvature. This method assumes that each of the box-girders in the bridge cross-section deforms independently from the other girders for a given span. That is, any interaction between the girders due to their interconnection via the bridge deck and/or intermediate external diaphragms is neglected. The assumptions behind the method are explained by Figure 2.3, which shows a free-body diagram for a box girder differential segment *ds*. The equivalent force at the flange levels, *M/h*, is the same as the force *T* in Figure 2.1.

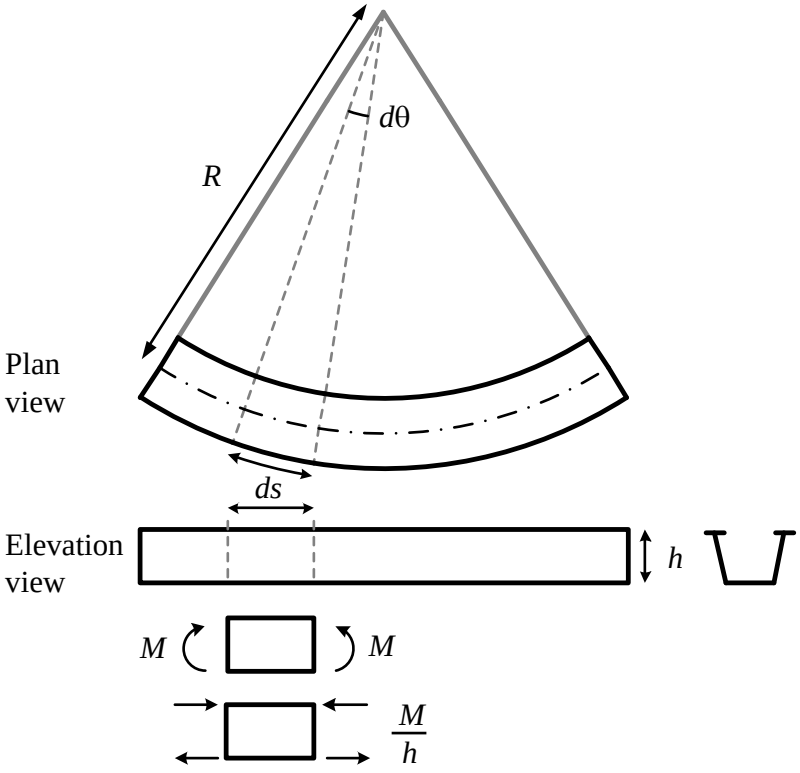

Figure 2.3. Force equilibrium in a segment of a box girder.

As in the V-load method developments explained in Section 2.1.1, the unbalanced flange-level lateral force due to the curvature at the given segment $ds = R\,d\theta$ is obtained as

$$T_y = 2\left(\frac{M}{h}\frac{d\theta}{2}\right) = \frac{M}{h}\frac{ds}{R} \tag{2.8}$$

By dividing both sides of this equation by *ds*, one obtains the equivalent distributed lateral loads at the top and bottom of the section

$$q = \frac{H}{ds} = \frac{M}{h}\frac{ds}{R}\frac{1}{ds} = \frac{M}{Rh} \tag{2.9}$$

These loads produce an equivalent distributed torsional moment *M/R* shown in Figure 2.4, which is identical to the effect of the flange-level distributed lateral load shown in the previous section.

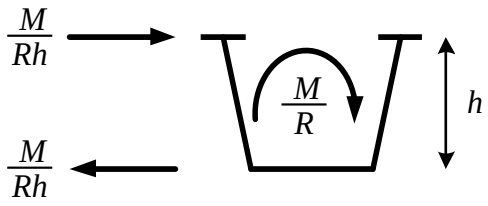

Figure 2.4. M/R torsional moment.

Next, given the specific *M/R* method assumption of no interactions between the girders along the span length, the internal torsional moment at a given position *s* can be found, considering a free body diagram of the girder segment from zero to *s*, and assuming cos(*L*/*R*) = 1.0 (i.e., assuming a small subtended angle over the length *s*), as

$$T(s) = T_{\text{support}} - \int_0^s \frac{M(s)}{R}\,ds \tag{2.10}$$

where *M(s)* is the distribution of the major-axis bending moment along the length. In addition, the contribution from the span to the end torsional reaction at $s = 0$ may be determined as

$$T_{\text{support}} = \frac{1}{L}\int_0^L \frac{M(s)}{R}(L-s)ds \tag{2.11}$$

by solving the statically indeterminate problem of a span subjected to a distributed torque with twisting fully restrained at each end. The contribution to the torsional reaction at the other end of the span is determined by placing the origin for *s* at that end.

For a simple span bridge subjected to uniformly distributed vertical load *w*, the corresponding internal torsional moment from Eq. (2.11) is

$$T(s) = \frac{wL^3}{24R} - \frac{ws^2(3L-2s)}{12R} \tag{2.12}$$

For continuous span bridges, the M/R procedure requires the assumption that the torsion in each span is independent of the other adjacent spans. The above equations are then applied to each span of the bridge. The integration in Eqs. (2.10) and (2.11) is commonly carried out numerically.

2.1.3 Calculation of Flange Lateral Bending Stresses, f_ℓ

Torsion induces girder flange lateral bending stresses, f_ℓ, in the top flanges of tub-girders and in both flanges of I-girders. Several primary sources of girder torsion in I-girder bridges are:

- Eccentric overhang bracket loads
- Horizontal curvature effects
- Support skew effects

In tub-girders, two additional sources of top flange lateral bending are:

- The continuity effects between single-diagonal top flange lateral bracing and the girder top flanges, and
- The lateral component of transverse compression stresses in inclined girder webs.

The AASHTO Specifications require the consideration of these stresses in construction checks. Methods commonly used to estimate the first set of these stresses in design are discussed next. The additional tub-girder stress estimates are addressed subsequently in Section 2.7.

2.1.3.1 Flange Lateral Bending due to Overhang Bracket Loads

The maximum flange lateral bending stress due to overhang bracket loads can be estimated in a given unbraced length of fascia girders as

$$f_\ell = \frac{w_\ell L_b{}^2 / 12}{S_{yf}} \tag{2.13}$$

where w_ℓ is a lateral uniformly distributed load imposed on the flange by the overhangs, calculated by dividing the moment from the distributed loads on the overhang by the depth of the overhang brackets (see Figure 2.5), L_b is the distance between cross-frames, and S_{yf} is the elastic section modulus of the flange. The above equation is based on the assumption of approximate symmetry boundary conditions for the flange lateral bending at the cross-frame locations. Correspondingly, the term in the numerator is basically the end moment for a fixed-fixed beam. In Eq. (2.13), the value 12 is sometimes changed to 10, to recognize the fact that the flange may not be fully fixed (per symmetry boundary conditions) at the cross-frame locations (the value 12 is used in all the NCHRP 12-79 calculations). In many situations, the highest levels of flange lateral bending stress occur at the cross-frame positions; therefore, the stresses calculated with Eq. 2.13 represent reasonable estimates for design.

When considering concentrated loads on the overhangs (P_ℓ), for example from the wheel loads of a screed rail, one may wish to use the equation

$$f_\ell = \frac{P_\ell L_b / 8}{S_{yf}} \tag{2.14}$$

where $P_\ell = P(e/h)$, and e is the eccentricity of the concentrated load.

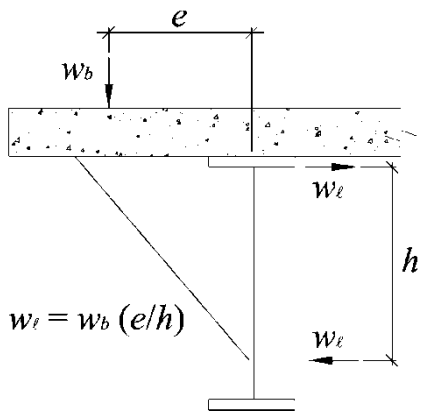

Figure 2.5. Determination of the uniformly distributed load w_ℓ.

It is important generally to ensure that the bracket loads applied to the I-girder web are sufficiently close to the bottom flange such that there is negligible distortion of the web from the reaction at the bottom of the overhang bracket (Ohio DOT, 2008; Roddis et al., 2005). Note that if the bracket cannot be located close to the bottom flange (approximately 6 inches), then it may be necessary to verify that the bracket load will not distort the web, or some type of additional bracing support may be required.

2.1.3.2 Flange Lateral Bending due to Horizontal Curvature

The flange lateral bending stresses due to horizontal curvature can be estimated at the cross-frame locations using the formula

$$f_\ell = \frac{ML_b^{\,2}/12\,Rh}{S_{yf}} \tag{2.15}$$

This equation is essentially the same form as Eq. 2.13, but with an assumed uniformly distributed lateral load, $q = M/Rh$, derived from the V-load method, and substituted for w_ℓ (see Section 2.1.1). In Eq. 2.15, the moment M typically is taken as the total major-axis bending moment at a particular cross-frame location resulting from the action of the gravity loads and the V-loads, i.e., $M = M_p + M_s$. In the fascia girder on the outside of the curve, the combined effects of the horizontal curvature and the overhang bracket loads are considered simultaneously by adding the results of Eqs. (2.13) and (2.15). Similar to the application of Eq. (2.13), engineers sometimes use a coefficient of 10 rather than 12

in Eq. (2.15), as an attempt to ensure a conservative estimate of the flange lateral bending stress. The coefficient 12 is used in all the NCHRP 12-79 studies,

In Eq. 2.15, the elastic section modulus for a typical rectangular flange, S_{yf}, is equal to $(t_f b_f^3/12)/(b_f/2)$, where b_f and t_f are the flange width and thickness, respectively. Since the flange area, A_f, is equal to $b_f t_f$, the section modulus can be expressed as $S_y = A_f \cdot b_f/6$. In addition, the moment, M, is equal to $f_b S_x$, where f_b is the major-axis bending stress and S_x is the strong-axis elastic section modulus to the flange under consideration. Substituting these parameters into Eq. 2.15, the flange lateral bending stress can be expressed as

$$f_\ell = \frac{f_b}{2} \frac{S_x}{A_f h_o} \frac{L_b}{R} \frac{L_b}{b_f} \tag{2.16}$$

This form of the equation for f_ℓ highlights the fundamental factors influencing the flange lateral bending stresses induced by the horizontal curvature (in the context of the above idealizations). Note that if the girder is doubly-symmetric and the contribution of the web to the girder moment of inertia is relatively small, $S_x/(A_f h_o) \approx 1$. In this case, the f_ℓ stress is simply equal to one-half of the product of the major-axis bending stress f_b, the sub-tended angle between the cross-frames L_b/R, and the flange length-to-width ratio L_b/b_f.

2.1.3.3 Flange Lateral Bending due to Skew Effects

There is limited guidance in current practice on how to calculate the f_ℓ stresses resulting from skew effects when an I-girder bridge is evaluated using a line-girder or a conventional 2D-grid analysis. In lieu of providing a predictor method, AASHTO LRFD Article C6.10.1 states:

"In the absence of calculated values of f_ℓ from a refined analysis, a suggested estimate for the total f_ℓ in a flange at a cross-frame or diaphragm due to the use of discontinuous cross-frame or diaphragm lines is 10.0 ksi for interior girders and 7.5 ksi for exterior girders. These estimates are based on a limited examination of refined analysis results for bridges with skews approaching 60 degrees from normal and an average D/b_f ratio of approximately 4.0. In regions of the girders with contiguous cross-frames or diaphragms,

these values need not be considered. Lateral flange bending in the exterior girders is substantially reduced when cross-frames or diaphragms are placed in discontinuous lines over the entire bridge due to the reduced cross-frame or diaphragm forces. A value of 2.0 ksi is suggested for f_ℓ, for the exterior girders in such cases, with the suggested value of 10 ksi retained for the interior girders. In all cases, it is suggested that the recommended values of f_ℓ be proportioned [apportioned] to dead and live load in the same proportion as the unfactored major-axis dead and live load stresses at the section under consideration. An examination of cross-frame or diaphragm forces is also considered prudent in all bridges with skew angles exceeding 20 degrees."

The above recommendations are intended as coarse estimates of the total *unfactored* stresses associated with the controlling Strength load condition. Hence, for an example location in a straight skewed bridge governed by the STRENGTH I load combination, with discontinuous cross-frames over only a portion of the bridge and with a ratio of dead load stress to total stress (dead plus live load) of 1/3, the nominal total *dead load* flange lateral bending stress in the exterior girders may be taken as 7.5 ksi x 1/3 = 2.5 ksi. If discontinuous cross-frame lines are used throughout the entire bridge, then using this same example dead-to-live load ratio, f_ℓ may be taken equal to 2.0 ksi x 1/3 = 0.7 ksi. In both of these cases, the dead load f_ℓ values may be taken as 10.0/3 = 3.3 ksi on the interior girders.

In the case that a more rational method of determining the flange lateral bending effects is not used (the subsequent Section 6.4 of this report provides a more rational method that can be used as part of an improved 2D-grid analysis), the NCHRP 12-79 research recommends that the value of f_ℓ from the above AASHTO (2010) provisions should be combined additively with the results from Eqs. (2.13) and/or (2.15) to account for the effects of overhang bracket loads and horizontal curvature. However, the variety of geometries and framing conditions in highway bridges is extensive, involving a large range of skew, length, width, number of span, and curvature combinations. Therefore, the above recommendations are very coarse estimates. The subsequent Section 6.4 introduces a 2D-grid approach to more closely predict the f_ℓ stresses caused by skew effects.

2.1.3.4 Local Amplification of Flange Lateral Bending between Cross-Frames

The f_ℓ stress estimates discussed in the above sections are based on a first-order analysis. They do not consider any potential amplification that may occur between cross-frames due to second-order effects. That is, they do not consider equilibrium on the deflected geometry of the structure in the evaluation of the stresses. The corresponding second-order response amplification can be estimated by multiplying the first-order f_ℓ stresses by the amplification factor discussed in Article 6.10.1.6 of the AAHSTO LRFD Specifications,

$$AF = \frac{0.85}{1 - f_b / F_{cr}} \geq 1.0 \tag{2.17}$$

where F_{cr} is the elastic buckling stress for the compression flange, based on lateral-torsional buckling of the unbraced length L_b between the cross-frames, and f_b is the maximum major-axis bending stress in the compression flange within the targeted unbraced length. It should be noted that when Eq. (2.17) gives a value less than 1.0, *AF* must be taken equal to 1.0; in this case, the second-order amplification of the flange lateral bending is considered negligible.

When determining the amplification of f_ℓ in horizontally curved I-girders, White et al. (2001) indicate that for girders with $L_b/R \geq 0.05$, F_{cr} in Eq. (2.17) may be determined using $KL_b = 0.5L_b$. For girders with $L_b/R < 0.05$, they recommend using the actual unsupported length L_b in Eq. (2.17). The use of $KL_b = 0.5L_b$ for $L_b/R \geq 0.05$ better approximates the amplification of the bending deformations associated with the approximate symmetry boundary conditions for the flange lateral bending at the cross-frame locations, and assumes that an unwinding stability failure of the compression flange is unlikely for this magnitude of the girder horizontal curvature. Figure 2.6 illustrates the flange lateral deflection mode associated with the horizontal curvature effects as well as the unwinding stability failure mode for a straight elastic member.

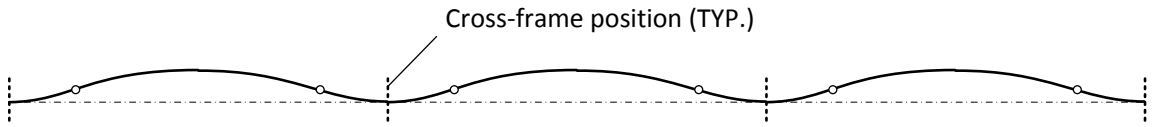

(a) Flange lateral deflection mode associated with horizontal curvature effects

(b) "Unwinding" elastic stability failure mode for straight members

Figure 2.6. Elastic deflection mode of a horizontally curved flange and unwinding stability failure mode of the compression flange in a straight member.

The use of $KL_b = L_b$ for $L_b/R < 0.05$ guards against the amplification of flange deformation modes that are affine to the simply-supported flange buckling condition (shown in Figure 2.6b) in less highly curved flanges, and guards against a potential unwinding stability failure of the compression flange in these cases.

2.1.4 Estimation of Girder Layovers

The cross-frames at skewed bearing lines tend to rotate about their own skewed axis and warp (twist) out of their plane due to the girder rotations. However, typically the cross-frames are relatively rigid compared to the girders in their own plane. Figure 2.7 shows representative I-girder top flange deflections and rotations at a hypothetical fixed bearing location along a skewed bearing line, where θ is the skew angle (taken as the angle between the normal to the girders at their ends and the tangent to the skewed bearing line, thus $\theta = 0$ for zero skew), ϕ_z is the girder torsional rotation at the skewed bearing line, ϕ_x is the major-axis bending rotation at the skewed bearing line, Δ_z is the longitudinal deflection of the top flange due to the major-axis bending rotation, Δ_x is the girder layover due to the torsional rotation, and h may be approximated as the distance between the centroids of the flanges.

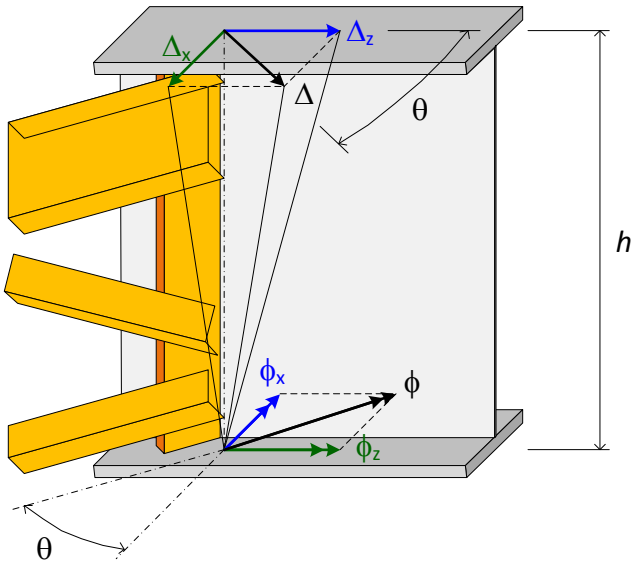

Figure 2.7. Girder top flange deflections and rotations at a fixed bearing location along a skewed bearing line.

The skewed orientation of the cross-frame forces the major-axis bending rotation and the torsional rotation of the girder to be coupled at the bearing, based on the assumption that the in-plane cross-frame deformations are small compared to the displacements. As shown in Ozgur and White (2007), by assuming small rotations such that $\tan(\phi) \cong \sin(\phi) \cong \phi$, the longitudinal deflection of the top flange due to the major-axis bending rotation can be derived from the geometry as

$$\Delta_z = h\phi_x \tag{2.18}$$

where ϕ_x is measured in radians. Also, the layover of the girders at the skewed bearing due to the torsional rotations can be expressed as

$$\Delta_x = h\phi_z \tag{2.19}$$

where ϕ_z is measured in radians. Furthermore, because of the kinematic constraint induced by the in-plane rigidity of the cross-frames, the coupling relationship between the twist and the major-axis bending rotations is

$$\phi_z = \phi_x \tan(\theta) \tag{2.20}$$

Therefore, the layover of the girder at the skewed bearing line (i.e., the lateral displacement of the top flange relative to the bottom flange) is forced to be

$$\Delta_x = h\phi_x \tan(\theta) = \Delta_z \tan(\theta) \tag{2.21}$$

to maintain compatibility between the girders and cross-frames.

In the case of a non-fixed bearing, Eq. (2.21) still gives the girder layover at the bearing, i.e., the relative lateral displacement of the top and bottom flanges. However, the bottom flange is able to translate based on the degrees of freedom of the bearing.

It is emphasized that properly designed cross-frames often are relatively rigid compared to the girders in I-girder bridges. Taking advantage of this assumption, also the layovers of the girders along the spans may be estimated. Figure 2.8 shows representative girder deflections and rotations for an intermediate cross-frame location where Δ_y is the differential vertical displacement between the girders due to dead loads and *s* is the girder spacing.

The layovers within the span can be estimated from the line-girder analysis vertical displacements, assuming negligible cross-frame in-plane deformations and cross-frames framed normal to the girders, as (Sanchez, 2011)

$$\Delta_x = h\ \Delta_y / s \tag{2.22}$$

Figure 2.8 illustrates the definitions of the variables in Eq. (2.22).

Although the above kinematics is illustrated in the context of an I-girder bridge in this figure, the above equations also can be applied similarly to tub-girders to estimate the relative lateral displacements between their top and bottom flanges at skewed bearing lines (Eq. 2.21) and at external intermediate diaphragm locations (Eq. 2.22). In addition, these results may be divided by the depth *h* to estimate the girder twist rotations (Eq. 2.20).

The next section takes advantage of these developments to estimate tub-girder torques.

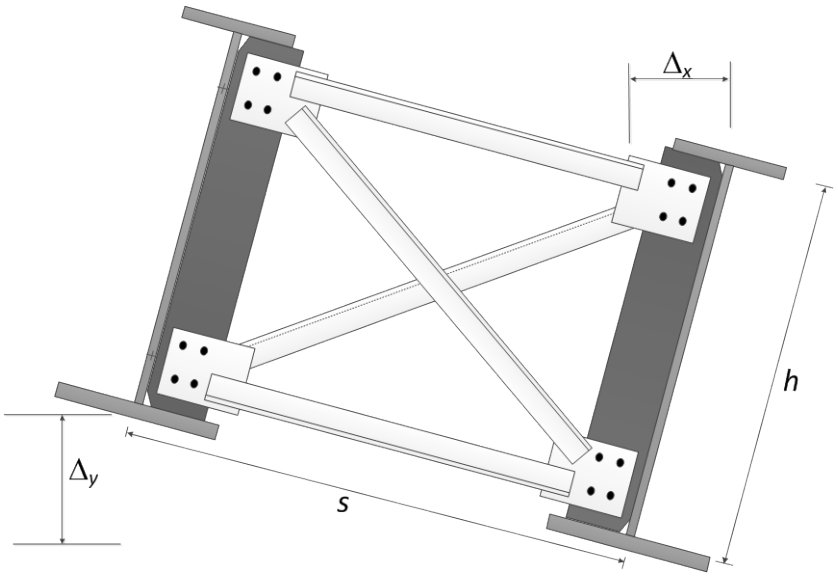

Figure 2.8. Magnified girder deflections and rotations at an intermediate cross-frame location.

2.1.5 Estimation of Tub-Girder Torques due to Skew Effects

The effect of skewed supports on the girder torques in tub-girder bridges can be explained by a few simple mechanistic models. The basic kinematic assumption is the one discussed in the previous section, i.e., the external diaphragms at the supports are effectively rigid in their own plane, while they provide relatively little restraint to the tub girders in their out-of-plane direction. Such assumptions are reasonable approximations since the external diaphragms are usually solid stiffened plates of relatively small length compared to the length of the girders, leading to relatively large in-plane stiffness. Furthermore, the diaphragms are typically I-sections and therefore their torsional stiffness is relatively small compared to that of the tub girders.

As the girders deflect vertically, they rotate about the line between the bearings at the supports. Similarly, the diaphragms, acting approximately as rigid plates in their own plane, rotate about the lines connecting the bearings. When the support line is skewed, the diaphragm thus forces the girders to twist to maintain compatibility (see Figure 2.9).

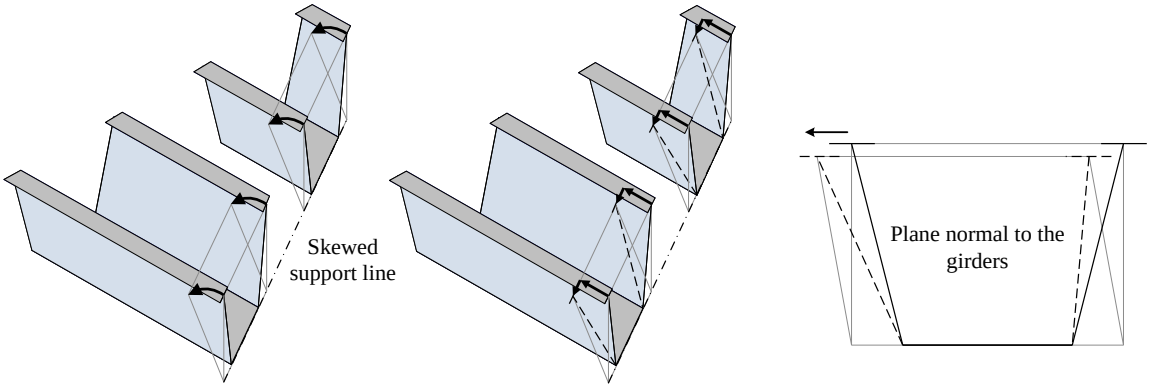

End rotation about the support line

Girder top-flange displacements due to the rotation about the support line

Lateral displacements due to compatibility with the end diaphragms

Figure 2.9. Lateral displacements due to rotation about the line of the support in a tub-girder bridge.

The above behavior is essentially the same as that described in Figure 2.7, and its basic overall impact on the tub girders can be understood by modeling a straight bridge composed of two tub girders with end diaphragms and no intermediate internal diaphragms in a 2D-grid analysis. The support diaphragms are modeled effectively as rigid components in their own plane and as highly flexible components out of their plane. Given the rigid in-plane assumption, the diaphragms have two rotation components relative to the axis of the girders, one corresponding to the major-axis bending rotation of the girders and one corresponding to twist rotation of the girders (see Figure 2.10).

When the corresponding model at the opposite end of the girders is considered, it can be observed that the girder ends can twist by equal or different amounts and in the same or opposite direction depending on the relative skew angle of the bearing lines at the girder ends. Figure 2.11 shows two configurations, one with parallel skew and one with an equal but opposite skew angle. Figure 2.11a illustrates the behavior for the parallel skew case. In this situation the girders experience equal twist but in opposite directions at their ends. This produces a constant torque in the girders. Figure 2.11b illustrates the case when the skew angles are equal but opposite in sign. In this special case, the girder ends twist the same amount and in the same direction. This results in a rigid body girder rotation and zero internal torque in the girders. Other skew

configurations would result in unequal twist of the ends resulting in a constant torque proportional to the relative angle of twist between the girder ends.

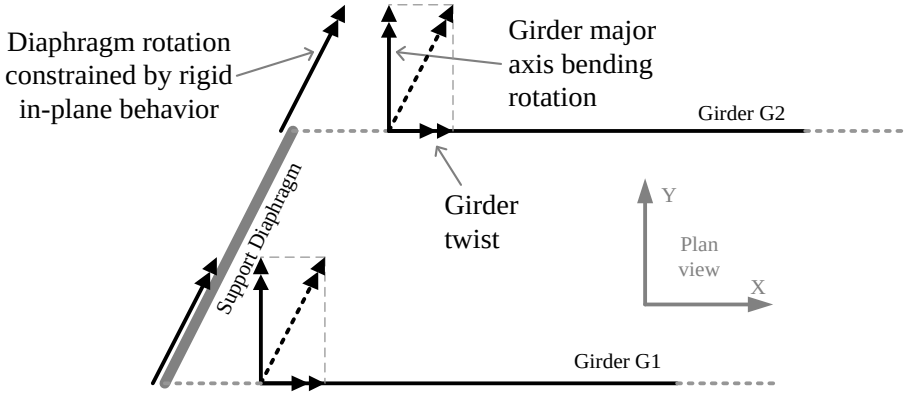

Figure 2.10. Rigid diaphragm rotation mechanism at a skewed support of a tub-girder bridge.

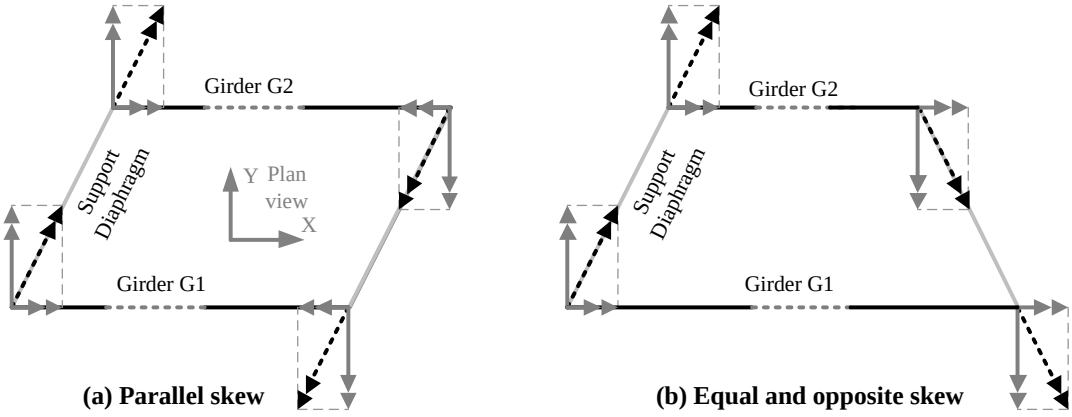

Figure 2.11. Girder end rotations in a tub-girder bridge with parallel skew of the bearing lines and with equal and opposite skew of the bearing lines.

The assumption that the end diaphragms are rigid in their own plane, produces an upper-bound estimate of the relative angle of twist between the girder ends. This can be used with a torsional model of the individual girders, in a line-girder analysis, to obtain an upper-bound estimate of the tub-girder torques due to the skew (Jimenez Chong, 2012).

As an example application, the above procedure is used to estimate the torsional moments in the simple-span curved and skewed tub-girder bridge NTSCS29 studied in NCHRP 12-79 (the bridge name designations are explained in Chapter 4). The bridge is a twin tub-girder system with a span of L = 225 ft. and a skewed support at its left-hand end with $\theta = 15.7°$. The bridge framing plan is shown in Figure 2.12.

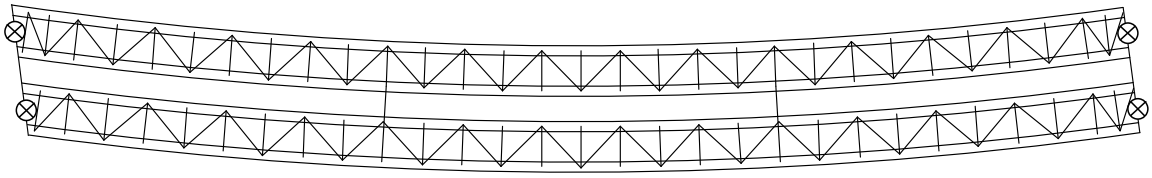

Figure 2.12. Plan view of NTSCS29.

The girder torsional moments are estimated by multiplying the girder torsional stiffness GJ/L by the girder twist rotation at the left-hand bearing line ϕ_z (since the right-hand abutment does not have any skew). The girder end twist rotation can be estimated from the end major-axis bending rotation ϕ_x and the support skew angle θ, using Eq. (2.20). By substituting the simply-supported end major-axis bending rotation, $\phi_x = wL^3/(24EI)$ into Eq. (2.20) and then substituting Eq. (2.20) into the stiffness equation $T = GJ\phi_z/L$, the upper-bound estimate of the torsional moment due to skew is obtained as $T = wL^2GJ \tan\theta /(24EI)$, where w is the vertical distributed load, I and J are the bending and torsional properties of the tub girder and E and G are the material elastic properties. By using the ratio E/G=2.6, the torsional moment in the simple-span single tub-girder is then estimated as

$$T = \frac{wL^2 J}{64.2I}\tan\theta \tag{2.23}$$

Figure 2.13 illustrates the torsional moments in the exterior girder of bridge NTSCS29, obtained from the integration of the 3D FEA stresses on the girder cross-section, as well as the M/R Method estimates with and without the torsional moment T due to the skew. The results from a 3D FEA model without the two intermediate external diaphragms shown in Figure 2.12 are also included in the plot. Jimenez Chong (2012)

studies the evaluation of the internal torques in curved and/or skewed tub-girder bridges by the different methods in detail for a relatively wide range of tub-girder bridges.

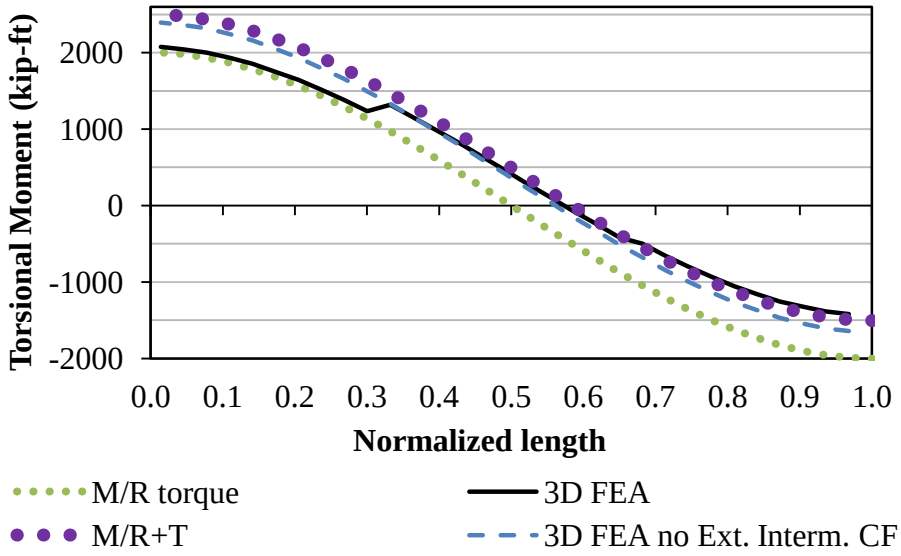

Figure 2.13. Comparison of torsional moments in the exterior girder of Bridge NTSCS29 predicted using refined and approximate analysis methods.

The above bridge has two intermediate external diaphragms as illustrated in Figure 2.12. These diaphragms influence the torsional response due to the shear and moment that they transmit between the girders. The plot in Figure 2.13 shows that the estimated girder torque is very close to the torque from the 3D FEA if the bridge is modeled without any intermediate external diaphragms. In the case with the external intermediate diaphragms, the approximate equations still give a conservative estimate of the maximum girder torque. Furthermore, the maximum errors in the predictions by the simplified calculations are very similar to the estimated additional torque generated by the skew effects. It can be observed that the intermediate external cross-frames assist in activating another source of torque in the overall bridge cross-section, i.e., a torsional couple developed by equal and opposite shear forces in the adjacent girders.

Given the above estimate of the tub girder torques, one must generally consider the moment equilibrium between the tub girder and the support diaphragm as shown in Figure 2.14. If the diaphragm is assumed to have negligible torsional stiffness, the tub

girder torque must be balanced by an internal major-axis bending moment in the tub-girder, in addition to the moment restraint provided by the in-plane stiffness of the diaphragm. This in turn influences the overall vertical bending deflections of the tub girder. This additional effect on the vertical bending deflections typically is neglected in the above type of hand estimate and the results at this stage are taken as a coarse line-girder estimate of the tub-girder bridge response.

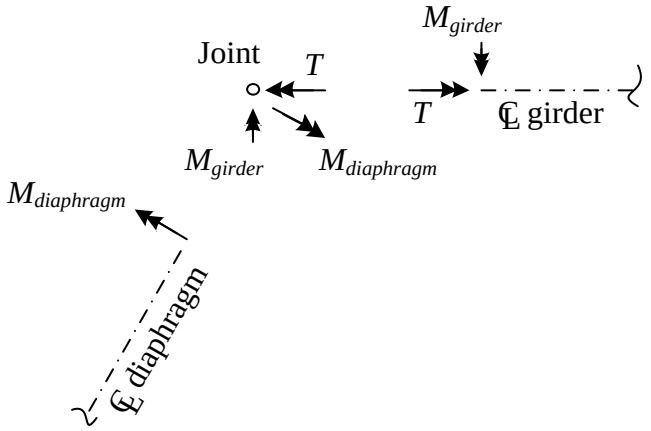

Figure 2.14. Idealization of moment equilibrium at the joint between a tub girder and its support diaphragm.

In bridges that contain intermediate external diaphragms, the behavior is more complex. External intermediate diaphragms typically are provided to control the specific differential displacements between the girders that can affect the transverse bending of the deck and the deck thickness profile (see Figure 2.15). Tub-girder bridges with external intermediate diaphragms generally require a more refined model than a line-girder analysis to properly account for the coupling of the tub-girders by the intermediate diaphragms. However, Helwig et al. suggest an approach that accommodates the use of a line girder analysis. For simplicity, Helwig et al. (2007) recommend the design of tub-girder bridges for their final constructed condition assuming no intermediate external diaphragms or cross-frames. This is followed by the provision of external cross-frames solely to control the profile of the slab thickness during the placement of the concrete deck. They give expressions for sizing the external intermediate cross-frames based on

the criterion of controlling the girder differential deflections that influence the deck thickness profile.

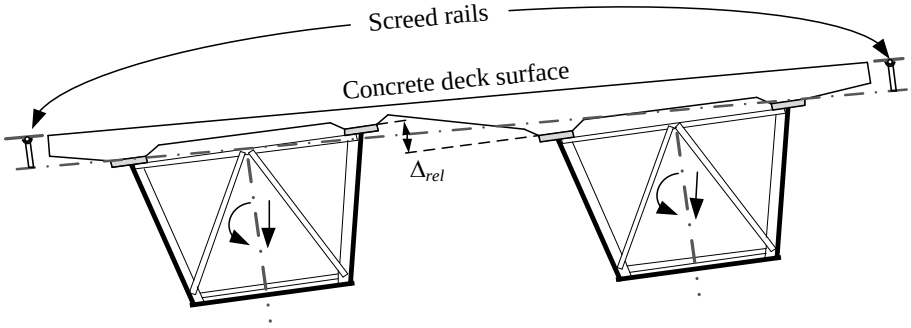

Figure 2.15. Exaggerated deck profile in a tub-girder bridge due to independent deflections of two tub-girders.

2.2 2D-Grid Analysis

The 2D-grid method is an approximate analysis technique commonly used in the design of steel I- and tub-girder bridges. In the most basic and common 2D-grid approach, the girders and cross-frames are modeled as line elements that have three degrees-of-freedom (dofs) per node, two rotational and one translational (see Figure 2.16). The rotational dofs capture the girder major-axis bending and torsional response, and the translational dof corresponds to the vertical displacements. Figure 2.17 shows a perspective view of bridge XICCS7 to illustrate the characteristics of the 2D-grid models (see Chapter 4 for a discussion of the various bridges studied in the NCHRP 12-79 research).

The vertical depth of the superstructure is not considered at all in the 2D-grid models. The girders and their cross-frames or diaphragms are theoretically connected together at a single common elevation, implicitly taken as the centroidal axis of girders (i.e., the axes of all the girders are assumed to bend without any longitudinal or lateral displacement at the connections with the axes of the diaphragms or cross-frames, even if the centroids of the different girders, cross-frames and diaphragms are at different depths). All the bearings and all of the diaphragms and cross-frames theoretically are located at this same elevation in the model. The software calculates only the vertical displacements and the rotations within the plan of the bridge. The popular software

packages DESCUS I and II (Best Center, 2011) and MDX (MDX Software, 2011) both utilize these idealizations. In the NCHRP 12-79 research, the MDX as well as the LARSA 4D software (LARSA, 2010) are used for the analysis studies conducted using 2D-grid models. In the remainder of this report, the LARSA and MDX programs are referred to as program P1 and program P2, respectively.

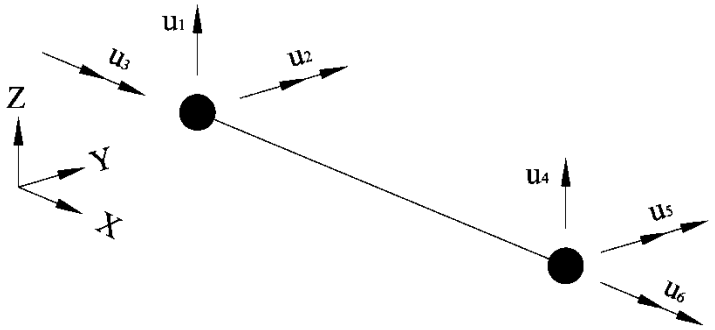

Figure 2.16. Schematic representation of the general two-node element implemented in computer programs for 2D-grid analysis of I-girder bridges.

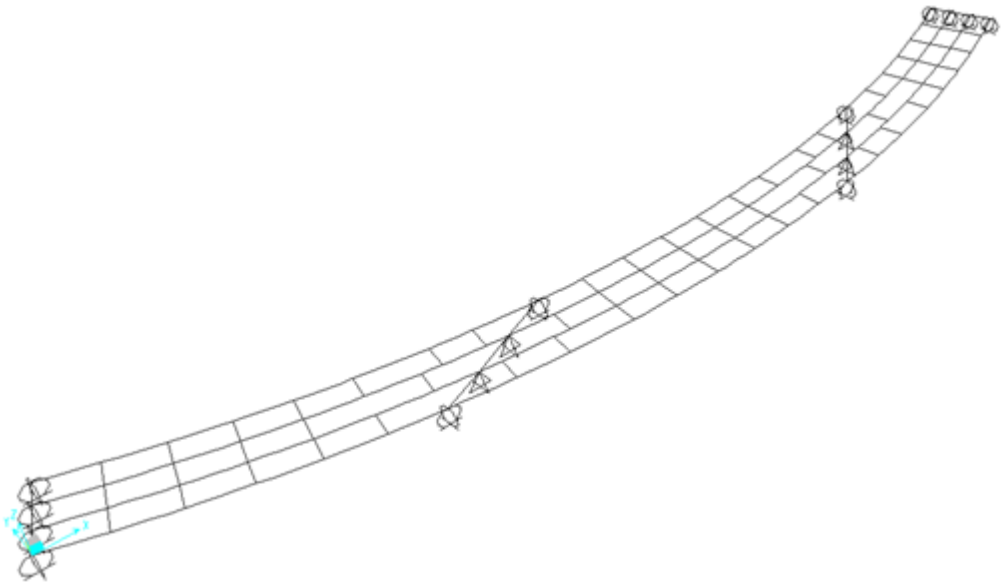

Figure 2.17. 2D-grid model of Bridge XICCS7.

It should be noted that all conventional 2D-grid analyses evaluated in the NCHRP 12-79 research involved the use of the physical girder St. Venant torsion constant, *J*, in setting the torsional properties of the girders, as well as the shear analogy method discussed subsequently in Section 6.2.1 for determining the cross-frame stiffnesses unless noted otherwise.

2.3 2D-Frame Analysis

When using general-purpose software packages, 2D-grid models typically are constructed using beam or frame elements that have six dofs per node. As shown in Figure 2.18, these elements have three translational and three rotational dofs at each node. In this figure, the dofs that are essential to construct a 2D-grid model are u_3, u_4, u_5, u_9, u_{10}, and u_{11}. These implementations are distinguished from the analysis types discussed in Section 2.2 by referring to them as 2D-frame methods.

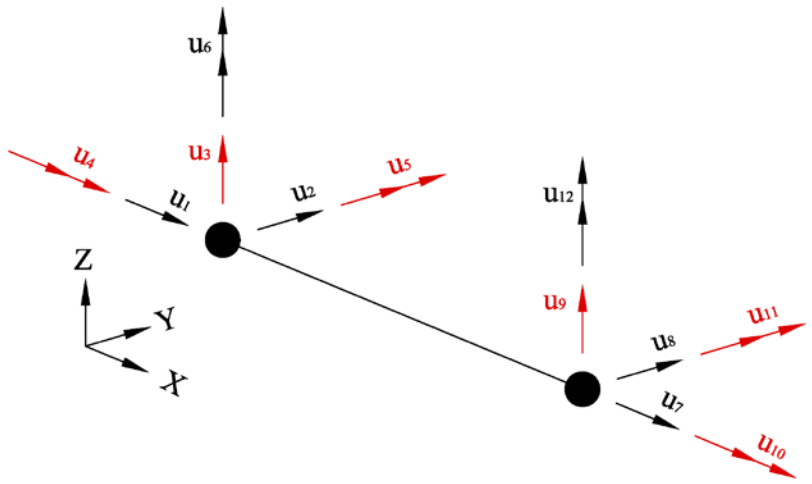

Figure 2.18. Schematic representation of the general two-node element implemented in computer programs for 2D-frame analysis of I-girder bridges.

If the structural model is constructed all in one plane, with no depth information being represented, and if the element formulations do not include any coupling between the conventional 2D-grid dofs and the additional dofs (which is practically always the case), 2D-frame models actually do not provide any additional information beyond the ordinary 2D-grid solutions. Assuming gravity loading normal to the plane of the structure, all the displacements at the three additional nodal dofs will be zero. Therefore, *for purposes of discussion in this report, 2D-frame models are also referred to as 2D-grid*. Nevertheless, the 2D-grid implementation in LARSA 4D discussed in this report is specifically a 2D-frame model.

2.4 Plate and Eccentric Beam Analysis

The MDX Software system implements a second type of model for the analysis of I- and tub-girder bridges that is commonly referred to as a plate and eccentric beam model. In this idealization, the composite bridge deck is modeled using flat shell (or plate) finite elements and the girders are modeled using 6 dof per node frame elements (total of 12 dofs per element, see Figure 2.18) with an offset relative to the slab (see Figure 2.19).

The plate and eccentric beam model is used typically for analysis of composite bridge structures in their final constructed configuration. In the NCHRP 12-79 research, this type of modeling approach was used in the design of various parametric study bridges. Specifically, it was used for the design analysis of the bridges in their final constructed condition. The reader is referred to Chapter 4 for an overview of the various bridges considered in the NCHRP research.

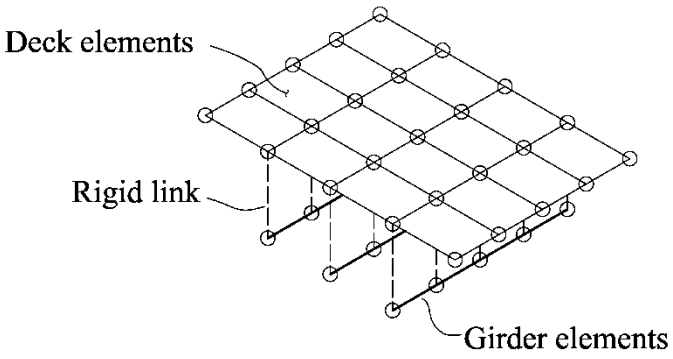

Figure 2.19. Schematic representation of the plate-and-eccentric-beam model.

2.5 Conventional 3D-Frame Analysis

An analysis model may be referred to as a conventional 3D-frame if:

- The structure is modeled using the above 3D frame elements and the centroid and shear center of the girders are modeled at their actual spatial locations,
- The actual location of the cross-frames or diaphragms through the depth is modeled (typically using a single frame element to represent each entire cross-frame or diaphragm between the points of connection to the other components)

- Rigid offsets are used to represent the differences in the depths between the girders, the cross-frames, and the bridge bearings.

It is important to note that this type of model generally provides little to no additional accuracy in representing the bridge responses for I-girder bridges, unless accurate girder torsional stiffnesses and accurate cross-frame generalized stiffnesses are employed. This is because the typical torsional stiffness used by the elements shown in Figure 2.18 is simply *GJ /L*. However, it is well known that the physical I-girder stiffnesses are dominated by the nonuniform torsion associated with warping of the cross-section (i.e., lateral bending of the flanges). In most situations with I-girder bridges, the St. Venant torsional stiffness *GJ/L* is so small, compared to the physical torsional stiffness, any results influenced by torsion have essentially no resemblance to the true physical responses if only the St. Venant torsional response is included. Adjustments to rectify this problem are addressed subsequently in Section 6.1 of this report.

For tub-girder bridges, the torsional response of the semi-closed section tends to be captured relatively well by conventional 3D-frame elements. Therefore, the 3D-frame method is reasonably accurate provided that the tub-girder bracing systems are properly designed. However, there are a number of common approximations in 3D-frame models that can potentially lead to some loss of accuracy. These include:

- Conventional 3D-frame elements typically do not account for differences between the shear center axis and the centroidal axis in their formulation, and
- The width and depth of the tub-girder cross-sections are typically very similar to the length and depth of the external cross-frames. However, the 3D-frame model represents all of these elements as lines.

With respect to the second point, the transfer of shear and moment from the external cross-frames or diaphragms to the tub-girders involves internal diaphragms or cross-frames in the cross-section, as shown in Figure 2.20. The detailed force transfer between the external and internal cross-frames, the webs, the top flanges and the bottom flanges involves more degrees of freedom than included in the 3D-frame models. Therefore, some type of simplified idealization is necessary for 3D-frame models to

represent the detailed responses in these regions. Furthermore, it should be noted that, if the internal cross-frames or diaphragms at these locations have any significant flexibility within their plane, the resulting deformations cause distortion of the tub-girder cross-section.

In many situations where the width of the structure is relatively small compared to the span lengths, the internal and external cross-frames or diaphragms are likely to be sufficiently stiff relative to the girders such that they perform essentially as rigid components in their plane with respect to the overall response of the bridge.

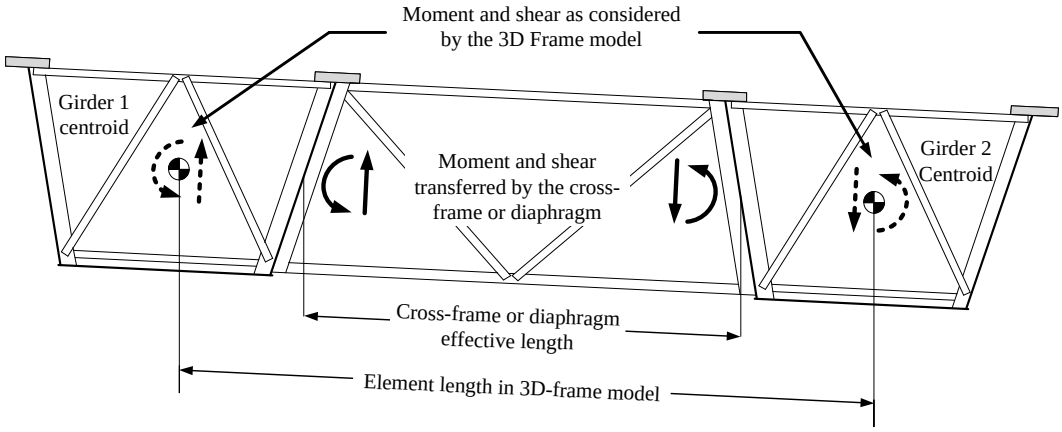

Figure 2.20. Moment and shear force transfer from the external cross-frames or diaphragm to the tub-girders.

2.6 Thin-Walled Open-Section (TWOS) 3D-Frame Analysis

The most accurate frame (i.e., line) element model for I-girder bridges is designated here as a Thin-Walled Open-Section (TWOS) 3D-frame model. This name is used to refer to bridge models constructed with a frame element having seven dofs per node, three translations, three rotations and one warping dof. A schematic representation of a line element having these characteristics is shown in Figure 2.21. The warping degrees of freedom are numbered 7 and 14 in the sketch. This type of element can be utilized to provide a highly accurate characterization of bridge I-girder torsional responses. Typically, this type of element has been used along with comprehensive modeling of the depth information throughout the structure, i.e., representation of the girder shear center and centroidal axes, modeling of the cross-frames, and representation

of bearings all at their corresponding depths (Chang, 2006; Huang, 1996). Selected studies have been conducted in the NCHRP 12-79 research using this type of element as implemented by Chang (2006) in the program GT-Sabre. GT-Sabre not only includes a refined open-section thin-walled beam theory representation of the I-girders, but it also includes the modeling of all the individual cross-frame components (i.e., the separate modeling of the cross-frame chords and diagonals using individual frame elements). In GT-Sabre, the individual elements representing the cross-frame members are tied to the girder nodes by rigid offsets.

The TWOS 3D-frame modeling approach is capable of matching the results of 3D FEA quite closely, with the exception that it is not able to capture the influence of I-girder web distortion on the physical responses. Web distortion can be an important factor when modeling composite I-girder torsional responses (Chang, 2006; Chang and White, 2008), but otherwise, its effect is typically inconsequential. In basic terms, if a TWOS element is tied to a slab via a rigid link, similar to the plate and eccentric beam modeling approach, the slab will incorrectly restrain the lateral bending of the bottom flange unless special modeling procedures, such as those discussed by Chang (2006), are invoked.

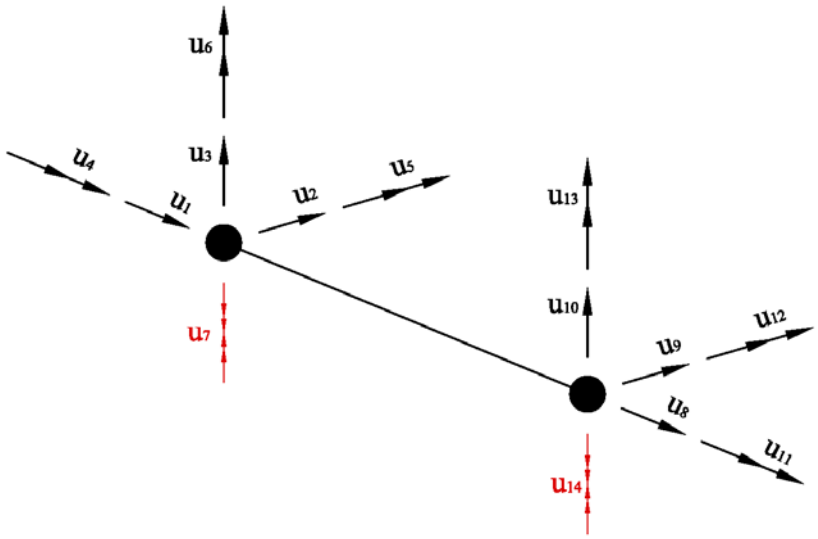

Figure 2.21. Schematic representation of a general two-node 3D TWOS frame element implemented in computer programs of I-girder bridges.

As discussed by Chang (2006), there are a number of other complexities that are difficult to handle in the implementation of 3D TWOS frame elements. These include the modeling of continuity conditions at cross-section transitions (e.g., changes in flange thickness and/or width), and the modeling of the continuity conditions for bifurcated girders (three girder elements framing into a common node). In addition, GT-Sabre (Chang, 2006) is the only known software that correctly displays the detailed three-dimensional deformed geometry from a TWOS 3D-frame analysis. Most TWOS 3D-frame elements have been implemented only in a structural engineering research setting, and either do not include any capability for graphical display of the deflected geometry at all, or display the deformed geometry only as the deformed centroidal axis of the member. Although advanced simulation software systems such as ABAQUS (Simulia, 2010), typically can graphically render the 3D I-section geometry, they do not graphically display the detailed warping deformations of 3D TWOS frame elements when they render the displaced geometry of the structure. As a result of the above complexities, as well as the fact that with increasing computer speeds, large degree of freedom 3D FEA computations can be conducted in a small amount of time, 3D FEA generally is preferred over TWOS 3D-frame analysis for design of steel girder bridges when line-girder or 2D-grid methods do not suffice.

2.7 Calculation of Component Forces Given the Line-Girder or 2D-Grid Analysis Results for Tub-Girder Bridges

Due to the idealization of the tub-girders, cross-frames and diaphragms as “line” elements in the above line-girder, 2D-grid, or 3D-frame approaches, the analysis of tub-girder bridges by any of these methods requires additional calculations to estimate the forces in the bracing components, as well as the stresses in the tub-girders. The bracing components include the top horizontal truss, also known as the top flange lateral bracing (TFLB) system, and the different components of the internal and external cross-frames and diaphragms at intermediate locations and at the supports.

To ensure good accuracy in the evaluation of the component forces in curved and skewed tub-girder bridges, the overall analysis must accurately capture the effects of curvature and skew. In general, conventional line-girder analysis calculations do not

include skewed support effects. However, they include a separate torsional analysis of the individual girders, via the M/R method discussed previously in Section 2.1.2, to account for the influence of horizontal curvature on the girder torques. As shown in Section 2.1.5, reasonable 1D analysis approximations can be obtained for the influence of the skew on the girder torques, particularly when there are no intermediate external diaphragms and the tub girders deflect independently of one another within each span length. 2D-grid methods directly include the effect of the curvature and skew, as well as the influence of intermediate external cross-frames or diaphragms, provided that the external intermediate and support diaphragms and cross-frames are accurately represented in the model.

Estimates of the vertical displacements can be obtained directly from 1D line-girder, 2D-grid and 3D-frame analyses. However, to obtain the girder stresses and the forces in the bracing components, additional calculations are needed.

The TFLB system in tub-girders creates a quasi-closed box section which significantly increases the girder torsional stiffness and strength. To estimate this behavior in a simplified way, Kollbrunner (1966) developed the Equivalent Plate Method (EPM) in which the top truss is replaced by an equivalent plate of a given thickness depending on the top truss characteristics. EPM expressions exist for Warren, Pratt and X-type top truss configurations (Helwig et al., 2007).

In the NCHRP 12-79 studies, the tub-girder top flange lateral bending response as well as all the bracing element forces are calculated using component force equations summarized in (Helwig et al., 2007), supplemented by a small number of additional calculations recommended by (Jimenez Chong, 2012). In broad conceptual terms, these equations address the following:

- The girder top flange major-axis bending stresses are calculated from two contributions: (1) the "average" major-axis bending stress, $f_b = M/S_{x,top,}$ where $S_{x,top}$ is the elastic section modules of the girder calculated neglecting any contribution from the TFLB system, plus (2) a "saw-tooth" stress effect due to the local effects of the longitudinal forces transferred to the top flanges from the TFLB system (Jimenez Chong, 2012).

- The TFLB diagonal forces, D_{tot}, are determined from the girder torques and the girder major-axis bending moments as the sum of two contributions, D_{EPM} and D_{Bend}. The contribution D_{EPM} is obtained from a girder pseudo closed-section torsional analysis, and the contribution D_{Bend} is obtained by considering the axial deformations of the girder top flanges due to flexure and the continuity of the TFLB struts and diagonals with the top flanges.
- The TFLB transverse strut force S_{tot} is obtained from two contributions: (1) the force S_{Bend} required to equilibrate the lateral component of the diagonal forces at the joints of the TFLB system, and (2) the force S_{Lat} caused by the lateral component of the transverse normal forces in the sloping webs required to resist the distributed vertical loads applied to the top flanges of the tub girder.
- The lateral bending stresses in the tub-girder top flanges, $f_{\ell\ Tot}$, are calculated generally from three effects: (1) the effect of the lateral forces S_{Bend} coming from the TFLB struts, $f_{\ell\ Bend}$ (this effect is zero for X-type TFLB systems, but is non-zero due to the "back-and-forth" loading effects on the flanges from the deformations of the top flange truss in Warren-type TFLB systems), (2) the effect of the lateral component of the transverse normal forces in the tub-girder sloping webs required to resist the distributed vertical loads applied to the girder top flanges, $f_{\ell p}$, and (3) the influence of the horizontal curvature of the top flanges $f_{\ell\ M/Rh}$ from Eq. (2.15). In addition, the influence of overhang bracket loads per Eqs. (2.13) and (2.14) is included on the outside flanges of fascia girders.
- The forces in the internal cross-frame diagonals D and the forces in the internal cross-frame top chords S are obtained from tub-girder cross-section distortional force equations developed by (Fan and Helwig, 2002). These forces depend upon the spacing between the internal cross-frames measured along the girder length, s_K, and they are driven by the effects from the equivalent distributed torque M/R associated with the horizontal curvature as well as an eccentricity effect of the vertical loads w, which are assumed to be applied to the top flanges.
- The forces in the intermediate external cross-frame diagonals F_D, the top chord, F_T, and the bottom chord, F_B, are determined based on the spacing between the

external cross-frames along the length of the bridge, as well as the exterior and interior girder rotations and vertical displacements at the external cross-frame locations, obtained from an analysis neglecting the intermediate external cross-frames. These equations were developed by Li (2004) specifically to control the relative deformations shown in Figure 2.15 for two-girder systems.

Jimenez Chong (2012) provides a detailed overview of the background and development of the various component force equations. The following sections document all the specific component force calculations utilized in the NCHRP 12-79 studies. Section 2.7.8 provides a definition of all the variables used in the equations.

2.7.1 Input

2.7.1.1 Major-Axis Bending Moment, M

The girder major-axis bending moment distribution is directly obtained from a 1D or 2D analysis.

2.7.1.2 Torque, T

The girder torsional moment is directly obtained from a 2D-grid analysis. With a 1D line-girder analysis, the torsional moment distribution is calculated independently for each girder and each span as follows. At a location *s*, the torsional moment due to curvature is given by:

$$T_{C0} = \frac{1}{L}\int_0^L \frac{M(s)}{R}(L-s)\,ds \tag{2.24}$$

$$T_C(s) = T_{C0} - \int_0^s \frac{M(s)}{R}\,ds \tag{2.25}$$

Concentrated torques are applied to the girders from the skewed supports. The girder internal torque from the skew in each span is obtained by determining a twist rotation at each end of the span (ends 1 and 2) and then multiplying the total relative twist between the two ends by the St. Venant torsional stiffness *GJ*/*L*. The resulting constant torque in a given span due to skewed supports is given by:

$$T_S = -\frac{GJ}{L}(\phi_{y1}\tan\theta_1 + \phi_{y2}\tan\theta_2) \tag{2.26}$$

The total torque is equal to the sum of the torque due to curvature and due to skew:

$$T(s) = T_C(s) + T_S \tag{2.27}$$

2.7.1.3 Average Major-Axis Bending Stress

The top flange "average" major-axis bending stress is calculated as

$$f_b = \frac{M}{S_{x,top}} \tag{2.28}$$

where $S_{x,top}$ does not include any contribution from the TFLB system.

2.7.1.4 Vertical Displacements, Δ

The vertical displacements are directly obtained from the 1D or 2D analysis.

2.7.1.5 Girder Twist Rotations, ϕ

The girder twist rotations for 2D analysis are directly obtained from the analysis. For 1D analysis the twist rotations are estimated as follows. At a location *s*, the twist rotation due to curvature is given by:

$$\phi_{x,C}(s) = \frac{1}{R}\left(1 + \frac{EI}{GJ}\right)\Delta(s) \tag{2.29}$$

The twist rotation due to skew is calculated at each support by the equation

$$\phi_{xi} = -\phi_{yi}\tan(\theta_i) \tag{2.30}$$

and the distribution along the span length is assumed to vary linearly as

$$\phi_{x,S}(s) = \phi_{x1} - (\phi_{x1} - \phi_{x2})\frac{s}{L} \tag{2.31}$$

The total girder twist rotations are equal to the sum of those due to curvature and those due to skew:

$$\phi_x(s) = \phi_{x,C}(s) + \phi_{x,S}(s) \tag{2.32}$$

2.7.2 Equivalent Plate Method

The Equivalent Plate Method allows the estimation of the girder torsional constant as

$$J = \frac{4A_0^2}{\sum_i b_i / t_i} \tag{2.33}$$

The top truss contribution to the system torsional behavior is estimated by replacing the truss by a fictitious equivalent plate. The equivalent plate thickness t^* can be determined for different truss layouts and cross-sectional areas of the diagonals and struts.

2.7.3 Warren TFLB Systems

The following sketch illustrates the general layout of a Warren TFLB System.

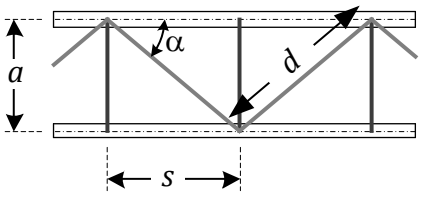

Figure 2.22. Warren TFLB system.

2.7.3.1 Equivalent Plate Thickness

The equivalent plate thickness for a Warren TFLB system is calculated using

$$t^* = \frac{E}{G}\frac{sa}{\left[\frac{d^3}{A_d} + \frac{2s^3}{3A_f}\right]} \tag{2.34}$$

2.7.3.2 TFLB Diagonal Forces

The separate contributions to the TFLB diagonal forces in a Warren TFLB system are determined as follows.

Torsion contribution

$$q = \frac{T}{2A_0} \tag{2.35}$$

$$D_{Torsion} = \frac{qa}{\sin\alpha} \tag{2.36}$$

Bending contribution

$$K_1 = \frac{d}{A_d} + \frac{a}{A_s}\sin^2\alpha + \frac{s^2}{2b_f^2 t_f}\sin^2\alpha \tag{2.37}$$

$$D_{Bend} = \frac{f_b s\cos\alpha}{K_1} \tag{2.38}$$

Other contributions

The lateral components of the transverse forces in the inclined girder webs are assumed to be developed entirely by the TFLB struts.

The influence of distortion on the TFLB diagonal forces is assumed to be negligible.

Total TFLB diagonal forces

$$D_{Tot} = D_{Torsion} + D_{Bend} \tag{2.39}$$

2.7.3.3 TFLB Strut Forces

The transverse strut forces in a Warren TFLB system are determined using the following equations.

Torsion contribution

$$S_{Torsion} = D_{Tot,i}\sin\alpha_i + D_{Tot,j}\sin\alpha_j \tag{2.40}$$

This is typically neglected, and is not considered in the base calculations employed in the NCHRP 12-79 research.

Bending contribution

$$S_{Bend} = -D_{Bend}\sin\alpha \tag{2.41}$$

Transverse load contribution

$$p = \frac{w}{2}\tan\phi \tag{2.42}$$

$$S_{Lat} = ps \tag{2.43}$$

Girder distortional contribution

$$S_{Dist} = \pm\frac{s_K b}{4A_0}\left(\frac{b}{a}ew - \frac{M}{R}\right) \tag{2.44}$$

S_{Dist} affects only the struts that also serve as internal cross-frame top chords.

The only significant girder distortions are assumed to be due to eccentricity of the vertical load *w*, and due to the horizontal curvature effects.

Other contributions

At external cross-frame locations, significant TFLB strut forces may be developed. These forces should be estimated by basic principles considering the overall force paths and joint equilibrium for the bracing components.

Total TFLB strut forces

$$S_{Tot} = S_{Bend} + S_{Lat} + S_{Torsion} + S_{Dist} \tag{2.45}$$

2.7.3.4 Intermediate Internal Cross-Frame Diagonals

Distortion effects due to eccentric vertical load and due to horizontal curvature are assumed to be the only contributor to the internal cross-frame diagonal forces,

$$D = \pm\frac{s_K L_{DK}}{2A_0}\left(\frac{M}{R} - \frac{b}{a}ew\right) \tag{2.46}$$

2.7.3.5 Top Flange Lateral Bending

The tub-girder top flange lateral bending stresses are determined using the following equations.

Major-axis bending contribution (from interaction with TFLB system)

$$f_{\ell,Bend} = \frac{1.5s}{b_f^2 t_f} S_{Bend} \tag{2.47}$$

Horizontal curvature contribution

$$f_{\ell,M/Rh} = \frac{0.6Ms^2}{Rhb_f^2 t_f} \tag{2.48}$$

Transverse load contribution

$$f_{\ell,p} = \frac{0.6ps^2}{b_f^2 t_f} \tag{2.49}$$

Total top flange lateral bending stresses

$$f_{\ell,Tot} = f_{\ell,p} + f_{\ell,M/Rh} + f_{\ell,Bend} \tag{2.50}$$

2.7.3.6 Top Flange Major-Axis Bending Stresses

The top flange major-axis bending stresses are determined generally as follows. The longitudinal force transferred to the top flange at the panel points of the Warren TFLB system may be calculated as

$$P = D_{Tot,i} \cos\alpha_i - D_{Tot,j} \cos\alpha_j \tag{2.51}$$

The corresponding "jump" in the flange major-axis bending stress at these locations is taken as

$$f_{b,TFLB} = f_b \pm \frac{P}{2b_f t_f} \tag{2.52}$$

The $P/2b_f t_f$ stress causes a reduction of the axial stress on one side of the top truss panel point and an increase at the other side. Between the panel points the stress is assumed to vary linearly, causing a saw-tooth distribution of the flange major-axis bending stresses along the length of a tub-girder.

It should be noted that the saw-tooth portion of the flange major-axis bending stresses is not included in the error assessment for f_b conducted in the NCHRP 12-79

research. This is because conventional software, such as MDX, does not include this contribution to the major-axis bending stress in its calculations.

2.7.4 X-Type TFLB Systems

The following sketch shows the general configuration of an X-type TFLB system

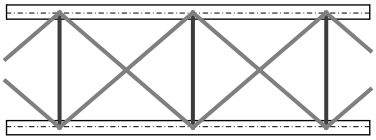

Figure 2.23. X-type TFLB system.

2.7.4.1 Equivalent Plate Thickness

The equivalent plate thickness for an X-type TFLB system is calculated using

$$t^* = \frac{E}{G}\frac{sa}{\left[\frac{d^3}{2A_d} + \frac{s^3}{6A_f}\right]} \tag{2.53}$$

2.7.4.2 TFLB Diagonal Forces

The separate contributions to the TFLB diagonal forces in an X-type TFLB system are determined as follows.

Torsion contribution

$$q = \frac{T}{2A_0} \tag{2.54}$$

$$D_{Torsion} = \frac{qa}{2\sin\alpha} \tag{2.55}$$

Bending contribution

$$K_2 = \frac{d}{A_d} + \frac{2a}{A_s}\sin^2\alpha \tag{2.56}$$

$$D_{Bend} = \frac{f_b s\cos\alpha}{K_2} \tag{2.57}$$

Other contributions

The lateral components of the transverse forces in the inclined girder webs are assumed to be developed entirely by the TFLB struts.

The influence of distortion on the TFLB diagonal forces is assumed to be negligible.

Total TFLB Diagonal Forces

$$D_{Tot} = D_{Torsion} + D_{Bend} \tag{2.58}$$

2.7.4.3 TFLB Strut Forces

The transverse strut forces in a Warren TFLB system are determined using the following equations.

Torsion contribution

$$S_{Torsion} = D_{Tot,i} \sin \alpha_i + D_{Tot,j} \sin \alpha_j \tag{2.59}$$

This is typically neglected, and is not considered in the base calculations.

Bending contribution

$$S_{Bend} = -2D_{Bend} \sin \alpha \tag{2.60}$$

Transverse load contribution

$$p = \frac{w}{2} \tan \phi \tag{2.61}$$

$$S_{Lat} = ps \tag{2.62}$$

Girder distortional contribution

$$S_{Dist} = \pm \frac{s_K b}{4A_0} \left(\frac{b}{a} ew - \frac{M}{R} \right) \tag{2.63}$$

S_{Dist} is assumed to affect the struts that also serve as internal cross-frame top chords.

The only significant girder distortions are assumed to be due to eccentricity of the vertical load *w*, and due to the horizontal curvature effects.

Other contributions

At external cross-frame locations, significant TFLB strut forces may be developed. These forces should be estimated by basic principles considering the overall force paths and joint equilibrium for the bracing components.

Total

$$S_{Tot} = S_{Bend} + S_{Lat} + S_{Torsion} + S_{Dist} \tag{2.64}$$

2.7.4.4 Intermediate Internal Cross-Frame Diagonal Forces

Distortion effects due to eccentric vertical load and due to horizontal curvature are assumed to be the only contributor to the internal cross-frame diagonal forces.

$$D = \pm \frac{s_K L_{DK}}{2A_0}\left(\frac{M}{R} - \frac{b}{a} ew\right) \tag{2.65}$$

2.7.4.5 Top Flange Lateral Bending

The tub-girder top flange lateral bending stresses in X-type TFLB systems are determined using the following equations.

Major-axis bending contribution (from interaction with TFLB system)

$$f_{\ell,Bend} = 0 \tag{2.66}$$

Horizontal curvature contribution

$$f_{\ell,M/Rh} = \frac{0.6Ms^2}{Rhb_f^2 t_f} \tag{2.67}$$

Transverse load contribution:

$$f_{\ell,p} = \frac{0.6ps^2}{b_f^2 t_f} \tag{2.68}$$

Total

$$f_{\ell,Tot} = f_{\ell,p} + f_{\ell,M/Rh} + f_{\ell,Bend} \tag{2.69}$$

2.7.4.6 Top Flange Major-Axis Bending Stresses

The top flange major-axis bending stresses are determined generally as follows. The longitudinal force transferred to the top flange at the panel points of the X-type TFLB system may be calculated as

$$P = D_{Tot,i} \cos \alpha_i - D_{Tot,j} \cos \alpha_j \tag{2.70}$$

The corresponding "jump" in the flange major-axis bending stress at these locations is taken as

$$f_{b,TFLB} = f_b \pm \frac{P}{2 b_f t_f} \tag{2.71}$$

The $P/2b_f t_f$ stress causes a reduction of the axial stress at one side of the top truss work point and an increase at the other side. Between the work points, the stress is assumed to vary linearly causing a saw-tooth distribution of the flange major-axis bending stresses along the length of a tub-girder.

It should be noted that the saw-tooth portion of the flange major-axis bending stresses is not included in the error assessment for f_b conducted in the NCHRP 12-79 research. This is because conventional software, such as MDX, does not include this contribution to the major-axis bending stress in its calculations.

2.7.5 Pratt TFLB Systems

The following sketch illustrates the general layout of a Pratt TFLB System.

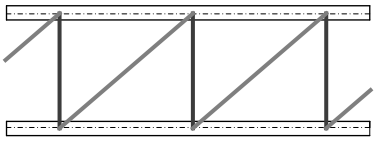

Figure 2.24. Pratt TFLB system.

2.7.5.1 Equivalent Plate Thickness

The equivalent plate thickness for a Pratt TFLB system is calculated using

$$t^* = \frac{E}{G}\frac{sa}{\left[\frac{d^3}{2A_d} + \frac{s^3}{6A_f}\right]} \tag{2.72}$$

2.7.5.2 TFLB Diagonal Forces

The separate contributions to the TFLB diagonal forces in a Pratt TFLB system are determined as follows.

Torsion contribution

$$q = \frac{T}{2A_0} \tag{2.73}$$

$$D_{Torsion} = \frac{qa}{\sin\alpha} \tag{2.74}$$

Bending contribution

$$K_1 = \frac{d}{A_d} + \frac{a}{A_s}\sin^2\alpha + \frac{s^2}{2b_f^2 t_f}\sin^2\alpha \tag{2.75}$$

$$D_{Bend} = \frac{f_b s\cos\alpha}{K_1} \tag{2.76}$$

Other contributions

The lateral components of the transverse forces in the inclined girder webs are assumed to be developed entirely by the TFLB struts.

The influence of distortion on the TFLB diagonal forces is assumed to be negligible.

Total

$$D_{Tot} = D_{Torsion} + D_{Bend} \tag{2.77}$$

2.7.5.3 TFLB Strut Forces

The transverse strut forces in a Pratt TFLB system are determined using the following equations.

Torsion contribution

$$S_{Torsion} = qa \tag{2.78}$$

Bending contribution

$$S_{Bend} = -D_{Bend} \sin \alpha \tag{2.79}$$

Transverse load contribution

$$p = \frac{w}{2} \tan \phi \tag{2.80}$$

$$S_{Lat} = ps \tag{2.81}$$

Girder distortional contribution

$$S_{Dist} = \pm \frac{s_K b}{4A_0} \left(\frac{b}{a} ew - \frac{M}{R} \right) \tag{2.82}$$

S_{Dist} is assumed to affect the struts that also serve as internal cross-frame top chords.

The only significant girder distortions are assumed to be due to eccentricity of the vertical load *w*, and due to the horizontal curvature effects.

Other contributions

At external cross-frame locations, significant TFLB strut forces may be developed. These forces are not considered in the base calculations.

Total

$$S_{Tot} = S_{Bend} + S_{Lat} + S_{Torsion} + S_{Dist} \tag{2.83}$$

2.7.5.4 Intermediate Internal Cross-Frame Diagonals

Distortion effects due to eccentric vertical load and due to horizontal curvature are assumed to be the only contributor to the internal cross-frame diagonal forces.

$$D = \pm \frac{s_K L_{DK}}{2A_0} \left(\frac{M}{R} - \frac{b}{a} ew \right) \tag{2.84}$$

2.7.5.5 Top Flange Lateral Bending

The tub-girder top flange lateral bending stresses in Pratt TFLB systems are determined using the following equations.

Major-axis bending contribution (from interaction with TFLB system):

$$f_{\ell,Bend} = \frac{1.5s}{b_f^2 t_f} S_{Bend} \tag{2.85}$$

Horizontal curvature contribution

$$f_{\ell,M/Rh} = \frac{0.6Ms^2}{Rhb_f^2 t_f} \tag{2.86}$$

Transverse load contribution

$$f_{\ell,p} = \frac{0.6ps^2}{b_f^2 t_f} \tag{2.87}$$

Total

$$f_{\ell,Tot} = f_{\ell,p} + f_{\ell,M/Rh} + f_{\ell,Bend} \tag{2.88}$$

2.7.5.6 Top Flange Major-Axis Bending Stresses

The top flange major-axis bending stresses are determined generally as follows. The longitudinal force transferred to the top flange at the panel points of the X-type TFLB system may be calculated as

$$P_{Pratt} = D_{Tot} \cos\alpha \tag{2.89}$$

$$f_{b,TFLB} = f_b \pm \frac{P_{Pratt}}{2b_f t_f} \tag{2.90}$$

The $P_{Pratt}/2b_f t_f$ stress causes a reduction of the axial stress at one side of the top truss work point and an increase at the other side. Between the work points, the stress is assumed to vary linearly causing a saw-tooth stress distribution of the flange major-axis bending stresses along the length of a tub-girder.

2.7.6 External Intermediate Cross-Frame Forces

The forces in the diagonals of external intermediate cross-frames are calculated using the equation

$$F_D = 4GJ\frac{\left(L_i\phi_{w,ext} + L_e\phi_{w,\text{int}} - K_{e1}\Delta_{w,rel}\right)}{K_{e2}} \tag{2.91}$$

whereas the forces in the top and bottom chords are obtained using

$$F_T = \frac{4GJ\left(\phi_{w,ext} - \phi_{w,\text{int}}\right) - F_D L_K\left(L_e - L_i\right)}{h_k\left(L_i + L_e\right)} \tag{2.92}$$

$$F_B = \pm F_D\cos\psi - F_T \tag{2.93}$$

where the variables in these equations are

$$L_K = h_K\cos\psi + L_T\sin\psi \tag{2.94}$$

$$K_{e0} = 1 + \left(1 + \frac{EI}{GJ}\right)\left(1 - \cos\frac{\beta_0}{2}\right) \tag{2.95}$$

$$K_{e1} = \frac{L_i + L_e}{a + c} \tag{2.96}$$

$$K_{e2} = K_{e0}K_{e1}\frac{L_i^3 + L_e^3}{12\left(EI/GJ\right)}\sin\psi + 2L_iL_eL_K \tag{2.97}$$

2.7.7 Support Diaphragms

The following equations from Helwig et al. (2007) are used for as a basic strength and stiffness criterion for the support diaphragms in the NCHRP 12-79 project research.

Strength requirement

$$A_{d,strength} = \frac{T_1 + T_2}{L_d\left(0.58F_y\right)} \tag{2.98}$$

Stiffness requirement

$$x_r = \left(a + b_f\right)/2 \tag{2.99}$$

$$A_{d,stiffness} = \frac{(T_1 + T_2)\, x_r}{0.0125 G L_d} \tag{2.100}$$

2.7.8 Variables Used in the Equations

The definitions of the variables used in the tub-girder bridge component force equations are as follows. Figure 2.25 illustrates several of the key variables.

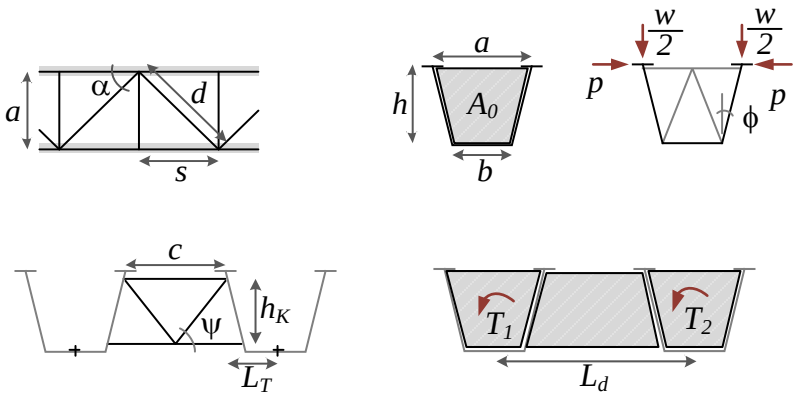

Figure 2.25. Illustration of the displacement, force and stress variables for tub-girder components (two girder systems).

A_0 = area enclosed by box.

$A_{D,stiffness}$ = external end diaphragm cross section area stiffness requirement.

$A_{D,strength}$ = external end diaphragm cross section area strength requirement.

A_d, A_s = cross section area of TFLB diagonal and strut.

D = internal CF diagonal axial force.

$D_{Torsion}, D_{Bend}$ = TFLB diagonals torsional and bending force components.

D_{Tot} = TFLB diagonal axial forces.

$D_{Tot,i}, D_{Tot,j}$ = TFLB diagonal axial forces in two consecutive panels.

E = steel elasticity modulus.

F_D, F_T, F_B = external CF diagonal, top and bottom chord axial forces.

F_y = steel yield strength.

G = steel shear modulus.

I = tub-girder cross-section moment of inertia.

J = St Venant tub-girder torsional constant.

K_1, K_2 = EPM constants for TFLB force calculation.

K_{e0}, K_{e1}, K_{e2} = constants for external intermediate CF force calculation.

L_d = diaphragm length between supports.

L_{DK} = length of internal CF diagonal.

L_i, L_e = internal and external girder CL lengths.

L_K = constant for external intermediate CF force calculation.

L_T = external CF top chord distance to tub centerline.

M = girder bending moment.

R = radius of horizontal curvature of girder.

$S_{Lat}, S_{Bend}, S_{Dist}, S_{Torsion}$ = TFLB struts lateral, bending, distortional and torsion force components.

S_{Tot} = TFLB strut axial forces.

$S_{x,top}$ = top flange section modulus.

T = total girder torsional moment

T_C, T_S = girder torsional moments due to curvature and skew.

T_1, T_2 = girder end torques.

a = box girder top width.

b = bottom flange width.

b_f = top flange width.

c = external CF top chord length.

d = TFLB diagonal length.

e = effective eccentricity of resultant distributed load.

f_b = average top flange major-axis bending stress.

$f_{b,TFLB}$ = top flange major-axis bending stress including the TFLB interaction.

$f_{\ell,Bend}, f_{\ell,p}$ = lateral force and major-axis bending components of lateral bending.

$f_{\ell,M/Rh}$ = influence of the horizontal curvature of the top flanges lateral force to lateral bending.

$f_{\ell,Tot}$ = total top flange lateral bending stress.

h = box girder depth.

h_d = end diaphragm depth.

h_K = external CF chords distance.

p = lateral component of the normal force *w* due the sloping webs.

q = torsion shear flow.

s = TFLB panel length.

s_K = spacing between internal CF measured along the girder length.

t_d = end diaphragm thickness.

t_f = top flange thickness.

x_r = constant for diaphragm force calculation.

w = distributed vertical load per unit length assumed to be applied at the top flange.

α = TFLB diagonal angle.

α_i, α_j = TFLB diagonal angles in two consecutive panels.

β_0 = subtended angle.

$\Delta_{w,rel}$ = relative vertical displacement between girders at external CF location.

$\phi_{w,ext}, \phi_{w,\text{int}}$ = interior and exterior girder twist rotations at CF location.

ϕ = web slope.

ψ = external CF diagonal angle.

2.8 3D Finite Element Analysis (FEA)

2.8.1 3D FEA Procedures for Design Analysis

Generally speaking, any matrix analysis software where the structure is modeled in three dimensions may be referred to as a three-dimensional finite element analysis (3D FEA). This report adopts the more restrictive definition of 3D FEA stated by

AASHTO/NSBA G13.1 (2011). According to G13.1, an analysis method is classified as a 3D FEA if:

1) The superstructure is modeled fully in three dimensions,
2) The individual girder flanges are modeled using beam, shell or solid type elements,
3) The girder webs are modeled using shell or solid type elements,
4) The cross-frames or diaphragms are modeled using truss, beam, shell or solid type elements as appropriate, and
5) The concrete deck is modeled using shell or solid elements (when considering the response of the composite structure).

It is important to recognize that the finite element method generally entails the use of a large number "elements" that are small in dimension compared to the structural dimensions that influence the responses to be evaluated. Furthermore, there are many detailed decisions that either explicitly or implicitly can impact the results, and therefore it is important to recognize that not all 3D FEA models are the same. When creating a 3D FEA model, the engineer (explicitly, or implicitly) selects a theoretical representation for the various parts of the structure (e.g., 3D solid, thick shell, thin shell, Timoshenko beam, Euler-Bernoulli beam, etc.), a mesh density sufficient to ensure convergence of the FEA numerical approximations within an acceptable tolerance, an element formulation type such as a displacement-based, flexibility-based or mixed formulation, an interpolation order for the different element response quantities (e.g., linear or quadratic order interpolation of the element internal displacements), a numerical integration scheme for evaluation of the element nodal forces and stiffnesses (e.g., standard Gauss quadrature, Gauss-Lobatto integration, etc.), and procedures for calculating, extrapolating, and smoothing or averaging of element internal stresses and strains.

The handling of the above attributes, as well as various other important analytical and numerical considerations, is beyond the scope of this document. However, with the exception of the first two of the above considerations, these decisions are more within the realm of finite element software development rather than the domain of engineering

design and analysis. The engineer generally should understand the broad aspects of the assumptions and limitations of the 3D FEA procedures, to ensure their proper application. Furthermore, generally he or she should conduct testing and validation studies with the software to ensure that the methods work as intended and that they provide correct answers for relevant benchmark problems.

Different analysis objectives, although they may be applied to the same structure, generally require different finite element models. For example, 3D FEA can be very useful for performing refined local stress analysis of complex structural details. This is not the objective within the context of this report. The recommendations in this report address the calculation of accurate:

- Elastic girder vertical deflections, lateral deflections, and rotations,
- Elastic girder major-axis bending stresses, or the corresponding bending moments, flange lateral bending stresses, web shear forces, and for tub girders, bottom flange shear stresses,
- Elastic cross-frame component axial forces,
- Elastic diaphragm major-axis bending stresses and web shear stresses, or the corresponding bending moments, and web shear forces, and
- Where composite action is considered, elastic slab normal and shear stresses and strains.

Basically, the objective of the 3D FEA models targeted in this report is the accurate calculation of all the bridge responses utilized by the AASHTO LRFD Specifications for the *overall* design of curved and/or skewed steel I- and tub-girder bridge structures.

There are various 3D FEA modeling strategies that can accomplish this objective. The approach recommended by the NCHRP 12-79 research, and utilized by the project team for their three-dimensional elastic finite element design analyses (i.e., 3D FEA analyses conducted for the purpose of design or design checking) entails the use of:

- A general-purpose 4-node quadrilateral Reissner-Mindin (shear-deformable) shell element for modeling I- and tub-girder webs, tub-girder bottom flanges, and the concrete deck slab, as well as a compatible 3-node triangular shell element, used sparingly for modeling of the concrete deck at skewed bearing lines (tub-girder webs and bottom flanges are modeled at skewed bearing lines by "fanning" the geometry of the quadrilateral elements).
- A compatible 2-node shear-deformable beam element for modeling I-girder flanges, tub-girder top flanges, bearing stiffeners, connection plates, intermediate transverse stiffeners, longitudinal stiffeners, and the "lips" of tub-girder bottom flanges extending outside of the webs.
- A 2-node shear-deformable beam element for modeling of cross-frame chords. The cross-frame chords are modeled at their physical location through the depth of the structure. Their connections into the girders are modeled generally using multi-point constraints so that the FEA discretization through the depth of the webs does not have to be adjusted to place nodes at the specific cross-frame chord depths. In effect, this rigidly connects the cross-frame chords at the location where they intersect the mid-thickness of the girder webs without the need for a web node at that location.
- A 2-node truss element for modeling of cross-frame diagonals, and for modeling of flange-level lateral bracing.
- Connector elements, if desired, to model the interconnection between the slab and the steel girders, but otherwise, rigid multi-point constraints (effectively acting as rigid beam elements) between the top flanges of the girders and the mid-thickness of the slab.

Figure 2.26 shows a segment of a three I-girder bridge unit illustrating the finite element representations of the various structural steel components.

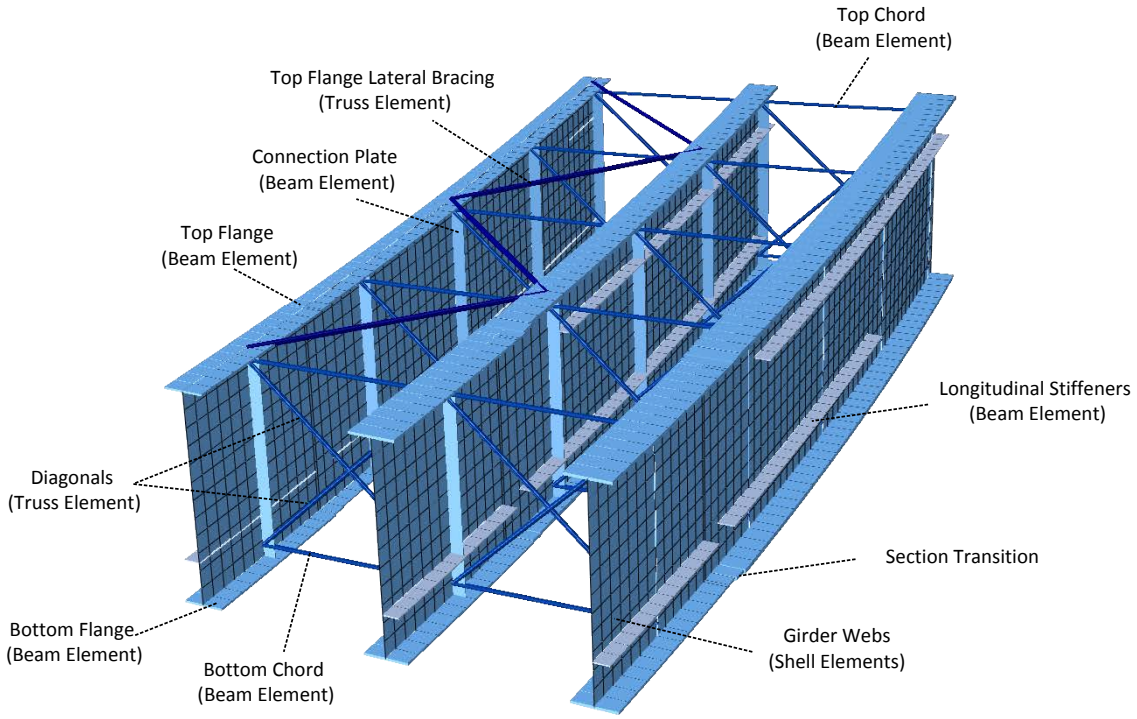

Figure 2.26. Example of recommended 3D FEA modeling approach on a segment of a three-I-girder bridge unit.

All of the bridge components are modeled at their physical geometric locations using the nominal dimensions, with the exception that the girder webs are modeled between the centerlines of the girder flanges. Therefore, the flanges are at the correct physical depth in all cases, and the model of the web has an overlap of t_f /2 with the flange areas. This is comparable to the manner in which joint size often is neglected in the modeling of frame structures; the resulting additional web area is on the order of the steel area from web-flange fillet welds, while the web-flange fillet welds are not explicitly included in the model.

At transitions in girder flange thickness, the centerline of the flange elements shifts with the change in thickness as shown in Figure 2.27. Therefore, the depth of the girder web also shifts with changes in the flange thickness in the FEA model. The average of the two flange areas is used within a one-element transition length along the flange at these locations. The transition element is located on the side of the transition with the larger flange area.

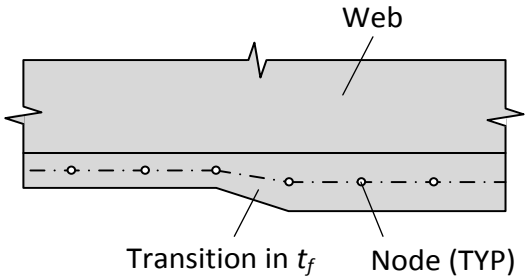

Figure 2.27. FEA Model at a flange thickness transition.

In addition to the above, the recommended 3D FEA modeling approach invokes the following idealizations:

- Similar to the above modeling idealizations, all beam and truss elements representing bracing members are connected directly into the work point locations at the mid-thickness of the girder webs, or in the case of flange-level lateral bracing, at the web-flange juncture.
- In I-girders, the support bearings are modeled as a point vertical support at the web-flange juncture, whereas in tub-girders, they are modeled as a point vertical support at the intersection of the bottom flange and an end diaphragm. At the bearing location, the beam element representations of the flange and of the bearing stiffeners enforce plane sections to remain plane across the width of the flange and distribute the point reaction into the web. In addition, for the tub-girders, a rigid rectangular patch with dimensions equal to those of the sole plate is modeled on the bottom flange. The girder model is generally free to rotate about the point support location, and horizontal displacement constraints representing guided bearings are placed at the point support where applicable.
- The substructure is modeled as a rigid support, including any temporary towers for construction. (This is an idealization in the NCHRP 12-79 research targeted at simplifying the scope of the studies, and is not believed to be a factor affecting the assessment of the accuracy of simplified models of the superstructure.)
- Uplift at bearings is modeled, where desired (or necessary), by using a "one-directional" support.

- The girder cambers are included explicitly for I-girder bridges. Practically speaking, this can be important in some cases where the second-order amplification becomes significant. In addition, it can aid the understanding of the calculations in cases where lack-of-fit effects are included to model the influence of the detailing of the cross-frames in I-girder bridges. Otherwise, the explicit modeling of the girder cambers is not believed to be an important consideration.
- Both geometrically linear (linear elastic) and geometrically nonlinear (second-order elastic) behavior of the elements are considered.
- Any superelevation, grade and vertical curve are not included in the models. It is believed that in most situations in practice, the bridge response to vertical (gravity) loads during construction is not significantly influenced by these attributes.
- The weights of the structural steel components are modeled as distributed body loads of 490 pcf in all of the finite elements. If necessary, additional concentrated loads are applied at cross-frame end nodes to represent the additional weight of connection elements and miscellaneous steel.
- The weights of formwork (10 psf) and the concrete slab including the reinforcing steel (150 pcf) are modeled using equivalent vertical line loads at the middle of the top flanges of the girders. The influence of eccentric loads on the slab overhangs, supported by overhang brackets, is modeled as a force couple composed of equal and opposite horizontal distributed loads, one at the level of the top flange and one at the level of the bottom of the overhang brackets. (Unless noted otherwise, the bottom of the overhang brackets is assumed to frame in at the bottom flange in the NCHRP 12-79 studies).
- The weight of construction equipment is neglected in most cases in the NCHRP 12-79 studies since the accuracy of the simplified methods can be assessed without including these loads.
- When and where the girders are composite, the concrete slab is modeled at its nominal physical location, including the depth of the haunch (i.e., the depth of the bolsters) over the girder flanges. If the slab overhang is tapered, the overhang is

modeled using the average slab thickness within the overhang region. The nominal thickness of the slab at the haunch is included in the FEA models.

- Steel erection stages are modeled by activating the portion of the steel structure for that stage and "turning on" the corresponding gravity loads.
- Holding cranes are modeled as a rigid vertical point support with no horizontal restraint at the hold location.
- Tie downs are modeled as rigid point supports.
- Staged deck placement and/or early stiffness gain of the concrete are modeled, where desired, by incrementally "turning on" and subsequently increasing the stiffness of the concrete as appropriate from stage to stage.

One of the important considerations in conducting a 3D FEA is the discretization of the various structural components into a sufficiently dense mesh to ensure acceptable convergence of the FEA approximations. The required mesh density generally varies with the FEA element theory, formulation and implementation. However, the best performing elements in various software packages usually tend to have roughly similar mesh density requirements (in terms of number of nodes) for a given theory and formulation type.

ABAQUS 6.10 (Simulia, 2010) is the specific software utilized for all the NCHRP 12-79 3D FEA studies. This software was selected because of its acclaim as one of the premier platforms for sophisticated physical test simulation. Model generators were developed by the NCHRP 12-79 researchers that permitted a streamlined comprehensive description of complete I- and tub-girder bridge structures for the above purpose. That is, for the purposes of the NCHRP 12-79 research, it was desired to be able to conduct comprehensive strength test simulations, where needed, including stability effects, the onset of distributed yielding in the steel components due to the combination of the applied stresses and initial residual stresses, and the strength of the concrete slab in tension and compression. Given the development of these capabilities, obviously the same general tools can be used to create elastic FEA design-analysis models. The specific ABAQUS elements utilized and the corresponding FEA discretization selected for the design analyses were as follows:

- For the I- and tub-girders, generally 12 S4R shell elements were utilized through the web depth. The S4R element is a linear-order (i.e., linear displacement field) 4-node quadrilateral Reissner-Mindlin displacement-based shell element with reduced integration. For geometric nonlinear analysis, the element is formulated for large strain. The number of shell elements along the girder lengths was selected such that all the shell elements in the web have an aspect ratio close to 1.0.
- The flanges of the I-girders, the top flanges of the tub girders, the various stiffeners, and the cross-frame connection plates were modeled using the B31 element, which is a two-node beam element compatible with the S4R shell element.
- The bottom flanges of the tub-girders were modeled generally using 20 S4R elements through their width. One B31 element was used on each side of the bottom flange to model the "lips" of the bottom flange that project beyond the intersection of the flange with the webs.
- The solid plate diaphragms in tub-girder bridges were modeled using S4R elements for their web and B31 elements for their flanges. The trapezoidal geometry of the diaphragm webs was represented by "fanning out" the S4R element geometries.
- The cross-frame chords also were modeled using B31 elements.
- The cross-frame diagonals as well as any flange-level lateral bracing were modeled using the T31 truss element.
- Where composite action was considered, the deck was modeled using S4R shell elements, and where needed at skewed bearing lines, the compatible 3-node triangular S3R shell element. The FEA mesh discretization utilized for the slab was generally coarser than the FEA mesh discretization utilized for the steel girders. The slab was modeled by one shell element along the bridge length for every two shell elements in the top flanges in the NCHRP 12-79 studies. Correspondingly, the slab discretization was set in the transverse direction of the bridge so that the slab elements have an aspect ratio approximately equal to 1.0.

The above FEA discretization is relatively dense compared to the coarser mesh requirements (i.e., minimum number of elements) expected to be sufficient for convergence of the elastic stresses in the majority of problems. Based on benchmark testing with the ABAQUS software, the use of 8 S4R elements through the web depth is expected to be sufficient in most problems for elastic analysis.

It should be noted generally that geometric nonlinear elastic FEA solutions, using the above models, were utilized as the primary standard for assessment of the different simplified 1D and 2D models in the NCHRP 12-79 research.

2.8.2 3D FEA for Physical Test Simulation

In recent years, the capabilities for simulation of physical tests using advanced 3D finite element analysis (FEA) has progressed to the point that, in numerous areas, the results from physical experiments can be reproduced readily and quite reliably. However, similar to successful experimental testing, the execution of test simulations requires great care. This is particularly the case where advanced simulation capabilities are not facilitated well by the software user interfaces. It should be noted that the results from an FEA test simulation are only as good as the accuracy of:

- The detailed geometry (e.g., plate thicknesses, deck-slab thicknesses, haunch depths, girder web depths, bearing heights, bearing plan locations, etc.),
- The load and displacement boundary conditions,
- The assumed (or nominal) initial conditions (e.g., initial internal residual stresses, geometric imperfections, any lack-of-fit between components in their unloaded condition, etc.),
- The constitutive relationships for the various constituent materials,
- The kinematic assumptions and/or constraints imposed by the structural theories.

The consideration of the above attributes should not detract from the use of advanced 3D FEA test simulations. In many respects, the above attributes are more easily specified, controlled and quantified in sophisticated 3D FEA models than in physical experiments.

In the NCHRP 12-79 research, 3D nonlinear FEA test simulations were conducted, where needed, using ABAQUS (Simulia, 2010). These simulations generally include realistic modeling of the steel three-dimensional stress-strain response and the modeling of initial residual stresses due to the manufacturing and fabrication of the steel. In these FEA solutions, 20 S4R shell elements were employed through the depth of the webs, primarily to capture the spread of yielding through the web depth, and the other finite element discretizations were refined accordingly. In addition, the I-girder flanges and the top flanges of the tub girders were modeled using 12 S4R shell finite elements in these studies. The modeling of the flanges with shell finite elements for the test simulation studies is primarily for two purposes:

1) The refined shell element discretization across the flange width facilitates the modeling of flange longitudinal residual stresses, and
2) The shell elements allow the consideration of multi-dimensional plasticity effects, although it is expected that the inelastic response of the flanges is associated predominantly with the longitudinal normal stress and strain.

The reader is referred to (Jimenez Chong, 2012; Ozgur, 2011; and Sanchez, 2011) for detailed discussions of inelastic test simulation analyses.

2.9 Global Second-Order Amplification Estimates

In certain situations, steel I-girder bridges can be vulnerable to stability related failures during their construction. The noncomposite dead loads must be resisted by the steel structure prior to hardening of the concrete deck. I-girder bridge units with large span-to-width ratios may be susceptible to global stability problems rather than cross-section or individual unbraced length strength limit states (Yura et al., 2008). In fact, due to second-order lateral-torsional amplification of the displacements and stresses, the limit of the structural resistance may be reached well before the theoretical elastic buckling load. Therefore, in structures sensitive to second-order effects, simply ensuring that the loads for a given configuration are below estimated global elastic buckling level is not sufficient. Furthermore, large displacement amplifications can make it difficult to predict and control the structure's geometry during construction. Possible situations with these

characteristics include widening projects of existing bridges, pedestrian bridges with twin girders, phased construction, and erection stages where only a few girders of a bridge unit are in place, and thus the unit is relatively long and narrow.

Bridge EISCS4 (see Figure 2.28) is an existing structure with these characteristics studied in NCHRP 12-79 (see Chapter 4 for a discussion of the bridges considered in this project and their naming). This structure had a three-girder unit with a span of 256 ft. that experienced large second-order amplifications during its construction. This unit, composed of girders G15 to G17, was the third phase of a construction project erected next to Phases I and II consisting of 14 girders that had been previously constructed.

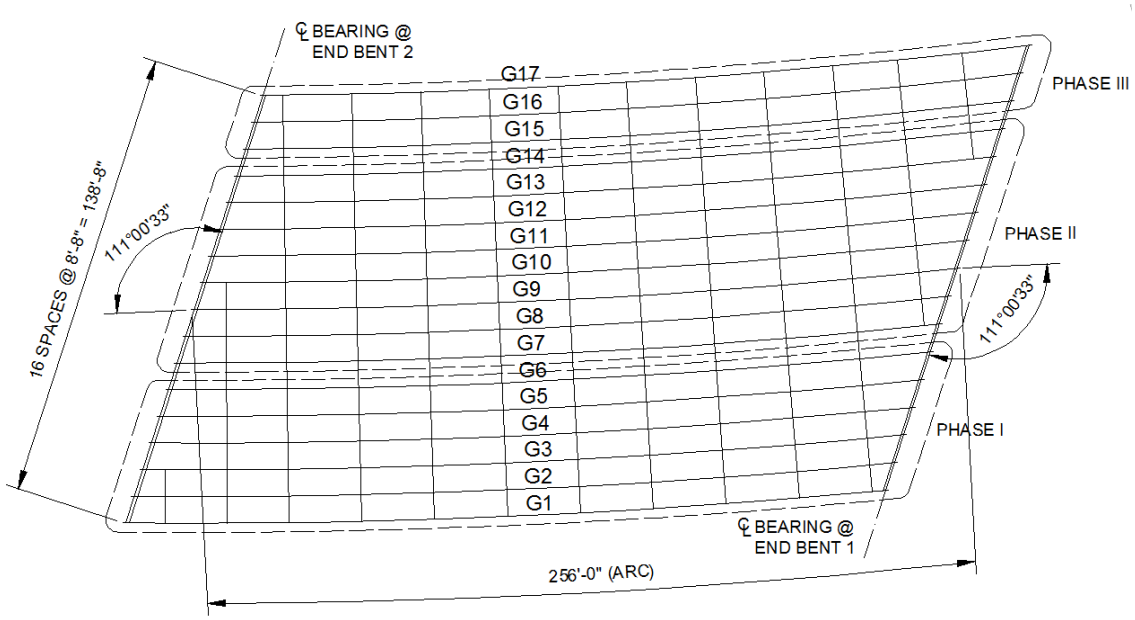

Figure 2.28. Plan view of EISCS4.

The concrete deck in the three-girder unit was placed starting at Bent 1 and moving toward Bent 2. By the time approximately two-thirds of the deck had been placed, the vertical deflections in girder G15 were considerably larger than in girder G14. As a result, there was a significant difference between the slab elevations for Phases II and III. At this point, it was decided to halt the concrete placement. The three-girder unit had deflected more than anticipated, and the structure was potentially at the point of incipient collapse. More detailed descriptions of the bridge and the studies conducted to

assess its performance are presented in (Sanchez, 2011) and in Appendices E and I of the NCHRP 12-79 Final Report.

To accurately capture the behavior of a long-and-narrow bridge unit with these characteristics, a geometric nonlinear (i.e., second-order) 3D FEA is generally required. Figures 2.29 and 2.30 show the major-axis bending stress response, f_b, and the vertical displacements for girder G15 (the girder farthest from the center of curvature) obtained from a second-order (nonlinear) and first-order (linear) elastic 3D FEA of the above Phase III unit. In addition, these figures show the predictions obtained from a line-girder analysis (1D model) conducted using the V-load method, as well as the results from a 2D-grid analysis. These figures show that the simplified solutions provide a close estimate of the first-order 3D FEA predictions. However, the second-order amplification of the responses is not captured by any of these analyses, since all of these analyses are first-order. The first-order analyses are conducted at the Total Dead Load (TDL) level, which is equal to the sum of the structure's self-weight (SDL), the additional dead load due to the weight of the metal deck forms (ADL), and the concrete load (CDL). The responses obtained from the second-order analysis are shown at a lower load level (75 % of the CDL). This is because the geometrically nonlinear 3D FEA predicts that the structure becomes unstable at 75 % of the CDL.

A simple method that can be used to alert the engineer to these potential undesired response amplifications due to second-order effects is recommended in the NCHRP 12-79 research. The linear response prediction obtained from any of the first-order analyses can be multiplied by the following amplification factor:

$$AF_G = \frac{1}{1 - \frac{M_{maxG}}{M_{crG}}} \tag{2.101}$$

where M_{maxG} is the maximum total moment supported by the bridge unit for the loading under consideration, equal to the sum of all the girder moments, and

$$M_{crG} = C_b \frac{\pi^2 sE}{L_s^2} \sqrt{I_{ye} I_x} \tag{2.102}$$

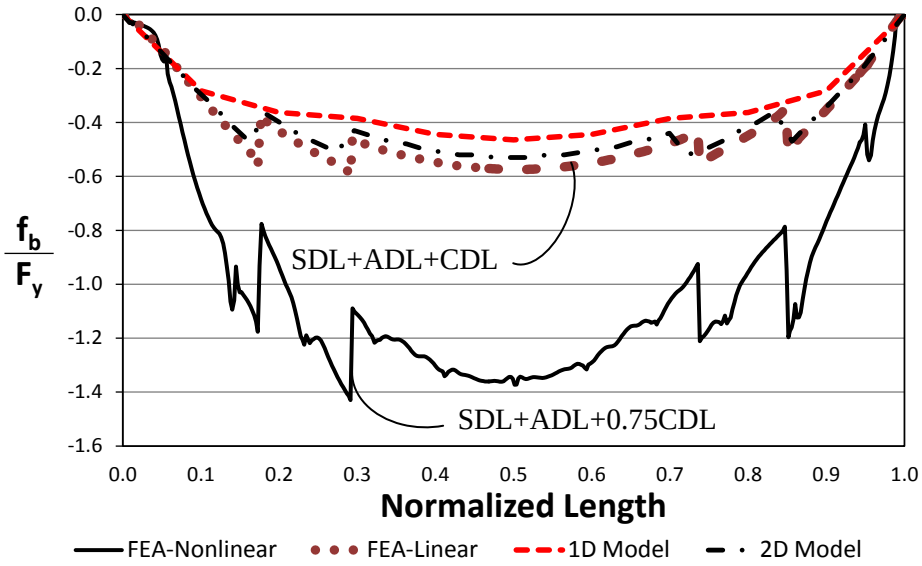

Figure 2.29. Comparison of major-axis bending stresses in girder G15 predicted using refined and approximate analysis methods (SDL = Steel Dead Load; ADL = Additional Dead Load due to metal deck forms; CDL = Concrete Dead Load).

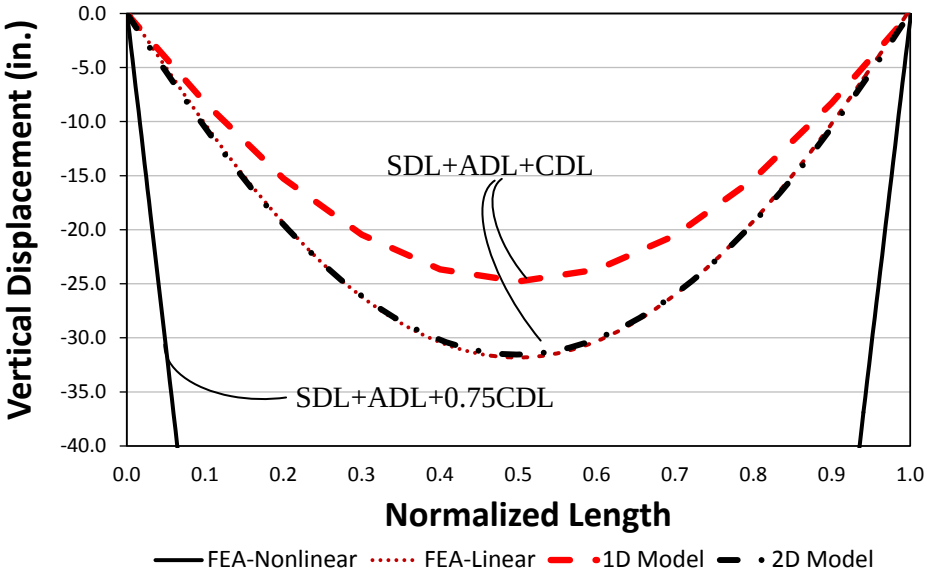

Figure 2.30. Comparison of vertical displacements in girder G15 predicted using refined and approximate analysis methods.

is the elastic global buckling moment of the bridge unit (Yura et al., 2008). In Eq. (2.102), C_b is the moment gradient modification factor applied to the full bridge cross-section moment diagram, s is the spacing between the two outside girders of the unit, E is the modulus of elasticity of steel,

$$I_{ye} = I_{yc} + (b/c)I_{yt} \quad (2.103)$$

is the effective moment of inertia of the individual I-girders about their weak axis, where I_{yc} and I_{yt} are the moments of inertia of the compression and tension flanges about the weak-axis of the girder cross-section respectively, b and c are the distances from the mid-thickness of the tension and compression flanges to the centroidal axis of the cross-section, and I_x is the moment of inertia of the individual girders about their major-axis of bending.

Yura et al. (2008) developed Eq. (2.102) considering multiple girder systems with up to four girders in the cross-section of the bridge unit. The individual girders are assumed to be prismatic and all the girders are assumed to have the same cross-section. For Phase III of EISCR4, $\gamma_{crG} = M_{crG} / M_{maxG} = 0.60$ corresponding to the nominal (unfactored) total dead load, using the sum of the maximum mid-span moments for the three girders for the calculation of M_{maxG}, and using the largest girder cross-section for the calculation of M_{crG}. Even when the largest mid-span cross-section (girder G15) is used for the calculation, Eq. (2.102) still provides a conservative prediction of the rigorous global buckling load level of $\gamma_{crG} = 0.85$ obtained from a 3D FEA eigenvalue buckling analysis. The use of the largest cross-section in Eq. (2.102) can be justified in this problem based on the logic that:

- G15 is the girder farthest from the center of curvature, and therefore, this girder has a greater influence on the global buckling resistance, and
- The mid-span cross-section of the girders provides the dominant contribution to the global elastic LTB resistance.

A global buckling load level of $\gamma_{crG} = M_{crG} / M_{maxG} = 0.24$ is obtained relative to the nominal (unfactored) total dead load if the smallest cross-section at the mid-span of the girders is used, and $\gamma_{crG} = 0.40$ is obtained if the average girder cross-section dimensions are used to determine I_x and I_{ye} in Eq. (2.103).

Figure 2.31 shows the vertical displacements at the mid-span of girder G15 vs. the fraction of the TDL obtained from the linear and nonlinear FEA models. In addition, a

response curve obtained by multiplying the first-order response by the amplification factor of Eq. (2.101), using γ_{crG} = 0.85, is shown in the figure. This calculation generally provides a conservative estimate of the amplified responses. Clearly, the vertical deflection of girder G15 is excessive well before the elastic buckling load level of γ_{crG} = 0.85 is reached.

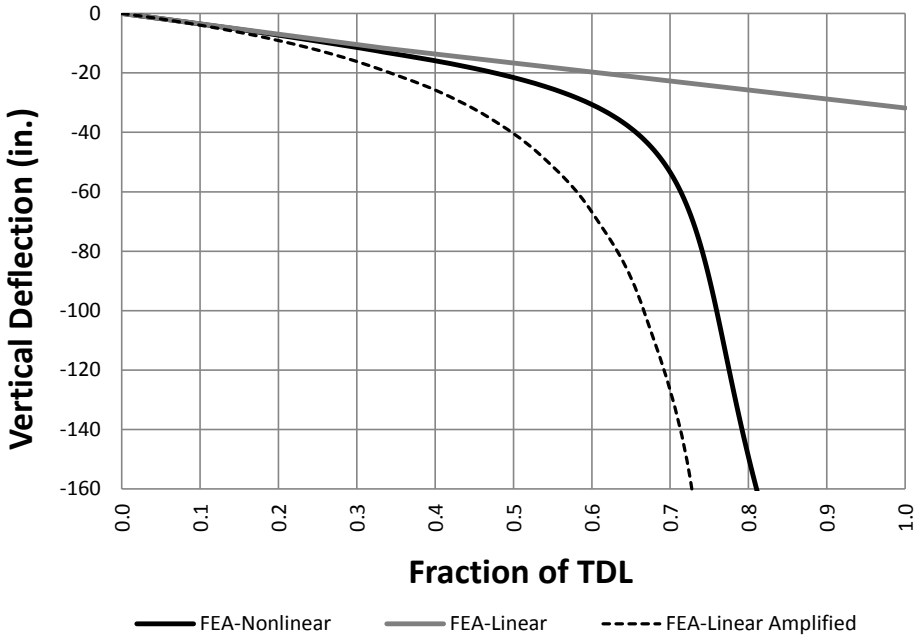

Figure 2.31. Vertical deflection at mid-span of girder G15 vs. the fraction of the TDL.

In addition to providing an estimate of the second-order effects on the girder displacements, the above amplification factor equation also can be used to predict the corresponding amplification of the girder stresses. Hence, the results of an approximate 1D or 2D analysis can be amplified, using Eq. (2.101), to conduct the constructability checks required by AASHTO LRFD Article 6.10.3. These checks are:

- Nominal initial yielding due to combined major-axis bending and flange lateral bending,
- Strength under combined major-axis and flange lateral bending (referred to as the 1/3 rule),
- Web bend buckling, and

- A maximum limit on the flange lateral bending stress of $0.6F_y$.

To illustrate the method, the load level at which the above three-girder unit violates the AASHTO constructability checks is determined using two different approaches:

- A "rigorous" solution in which 3D FEA is used to determine the global eigenvalue buckling resistance (γ_{crG} = 0.85) as well as to solve directly for the second-order load-deflection response in the critical girder G15, and
- The combined use of the global elastic buckling resistance computed using Eq. (2.102) (γ_{crG} = 0.60), the use of the 1D V-load method to estimate the girder G15 linear elastic responses, and the use of Eq. (2.101) to amplify these responses.

The results from these two sets of calculations are then substituted into the AASHTO constructability checks to determine the fraction of the TDL at which the different checks are violated. Table 2.2 summarizes the results. The check associated with web bend buckling is not included here since it does not govern for this bridge. The terms f_{bu} and f_ℓ in the table are the major-axis bending and flange lateral bending stresses predicted by the *second-order (geometric nonlinear)* 3D FEA in the first set of analysis and by the *first-order (linear) elastic* line-girder analysis with the V-load extensions in the second set of analyses. As shown in the table, the checks conducted using the simplified manual equations provide a conservative estimate of the nonlinear FEA predictions. For the case study bridge unit, both procedures predict that the 1/3 rule strength check using the girder G15 elastic global buckling stress for ϕF_{nc}, is the controlling limit state check.

Table 2.2 shows that the simplified analysis can be used to obtain a conservative estimate that this bridge unit is approaching a dangerous condition. That is, the simplified analysis predicts a lower fraction of the TDL at which the checks are breached, compared to the 3D FEA solution. Although the results may be judged to be too conservative for final design, the approximate calculations provide a warning of the magnitude of the amplifications expected in the system due to the nonlinear response.

Table 2.2. AASHTO constructability checks using simplified line-girder (V-load) analysis with global amplification factor and refined 3D FE analysis results.

Limit State	Analysis Type	AF_G	TDL fraction	f_{bu} (ksi)	f_ℓ (ksi)
Nominal yielding AASHTO Eq. 6.10.3.2.1-1	Nonlinear FEA	NA	0.560	39.90	30.10
	Simplified	3.736	0.440	17.52	1.16
1/3 rule strength based on elastic global buckling, AASHTO Eq. 6.10.3.2.1-2	Nonlinear FEA	NA	0.540	33.00	21.00
	Simplified	2.132	0.319	12.70	0.84
$f_\ell \leq 0.6F_y$ AASHTO Eq. 6.10.1.6-1	Nonlinear FEA	NA	0.615	NA	42.00
	Simplified	27.54	0.579	NA	1.52

Regarding the specific case study bridge unit, one can observe from the nonlinear 3D FEA that the structure experiences substantial second-order amplification of the girder G15 major-axis bending stress in addition to the flange lateral bending stress. In fact, because of the relatively large radius of curvature and the relatively minor effects of skew on this narrow and long bridge unit, the first-order flange lateral bending stresses are particularly small. This causes the one-third rule strength interaction check to be more critical than the flange nominal yielding check.

Lastly, it should be noted that although a second-order analysis could be conducted using the 2D-frame model described in Section 2.3, this does not provide any useful results since the corresponding girder torsional stiffness representation (i.e., GJ/L) is poor. Only the 3D FEA provides an accurate analysis of the girder 3D lateral-torsional responses. (This limitation of the conventional 2D-grid procedures is addressed further in Section 6.1, although second-order analysis with the improved 2D-grid method is not recommended either. As the global buckling load level is approached, the approximations associated with the improved 2D-grid calculations are amplified; hence, although the improved 2D-grid methods work well for linear elastic analysis, they do not have sufficient resolution for reliable second-order analysis.)

The NCHRP 12-79 research suggests that Eq. (2.101) can be used to detect possible large response amplifications during preliminary construction engineering. If the

amplifier shows that a structure will exhibit significant nonlinear behavior during the deck placement, the scheme adopted for the construction should be revisited. By providing additional shoring or by bracing off of adjacent units, the system response amplifications can be reduced. If it is found necessary to construct a structure that has potentially large response amplification during the deck placement, the engineer should perform a final check of the suspect conditions using a second-order (geometric nonlinear) 3D FEA. In addition, the construction processes must be monitored carefully, since the structure will be sensitive to any changes in the structural conditions, to ensure that the construction proceeds as assumed.

Substantial nonlinearity during the steel erection may be a concern in some situations; however, if the steel stresses are small and if the influence of the displacements on fit-up is not a factor, large second-order amplification of the deformations may not present any issue during the steel erection. These considerations are discussed further in Section 3.1.1.

2.10 Analysis Including the Effects of Early Concrete Stiffness and Staged Deck Placement

The application of a concrete slab to a steel girder bridge is a complex analysis problem, particularly on longer and/or wider bridges. When initially placed on the steel girders, the wet concrete offers no structural capacity or stiffness to the system and represents nothing more than a gravity load. However, as the concrete begins to cure it develops stiffness and affects the overall stiffness of the structure. Topkaya et al. (2003; 2004a & b) have evaluated the effects of early stiffness gain of the deck concrete for steel girder bridges. These investigators have shown that the interface between shear studs and the deck concrete can transfer considerable force only a few hours after the start of the concrete placement. In addition, they have shown that significant local crushing may occur if the studs are highly loaded at early ages, resulting in a loss of stiffness in the final constructed condition.

In most cases involving reasonable size deck casting stages, the job parameters are set such that early stiffness gain can be neglected within a given stage. In addition, for

most simple-span bridges, the job parameters are commonly set such that the concrete can be placed in a single stage, without any significant stiffness gain of the concrete prior to the completion of the stage. In some cases, the construction specifications may require the use of set-retarding concrete additives to keep the concrete fluid longer and avoid the need to consider early concrete stiffness. Nevertheless, in situations such as continuous placement of a large bridge deck, it may be prudent to investigate the effects of the onset of early composite action.

In continuous-span steel bridges, it is common that the deck will be placed in multiple stages. The main goal of this technique of using separate stages is to minimize deck cracking over the piers. As such, a typical sequence requires that the positive moment regions be placed first, followed by the negative moment zones (days later, after the positive moment regions have sufficiently cured). The variation in the concrete stiffness properties from stage-to-stage needs to be accounted for when computing stresses or resistances, and it can be of substantial importance to the control of the bridge geometry, when determining deflections and girder cambers. The eventual accumulated moments, shears and deflections at a given location generally are different from a staged analysis than from an analysis assuming simultaneous placement. In addition, the maximum flexural demands may be reached at some sections at an intermediate stage of the construction rather than in the final constructed condition when staged deck placement is considered. Uplift can be a concern and should be checked when evaluating deck placement sequences, particularly for relatively light continuous-span framing with heavy concrete loads in adjacent spans.

The above considerations also apply to steel girder bridges built using phased construction. In addition, for phased construction, some girders in a given construction stage may have a reduced composite section due to the proximity of a longitudinal construction joint in the deck. The different section properties that these girders have, as the construction progresses, must be accounted for when evaluating strength and serviceability, and also, when estimating girder deflections and cambers.

The modeling of staged deck placement and incremental (stage-to-stage) increases in the concrete stiffness is possible in numerous 3D FEA software systems used in current practice (2012), and is also available in some 2D-grid software packages. For example, the MDX platform (MDX, 2011) has the ability to incrementally include slab segments in the analysis model, within a 2D-grid idealization. In addition, the program settings allow the user to set full, partial or non-composite action to simulate the effects of early concrete stiffness. Recent work by Stith (2010) includes the consideration of staged concrete deck placement via 3D FEA in the program UT-Bridge.

In the NCHRP 12-79 research, a limited number of studies of staged concrete deck placement focused on comparisons of solutions obtained using MDX to 3D-FEA results using the ABAQUS software system. The primary focus of the Project 12-79 studies was on the prediction of the bridge responses prior to the participation of the concrete deck.

2.11 Analysis of I-Girders During Lifting

Straight I-girders may be susceptible to buckling and curved I-girders may be susceptible to excessive deflection during lifting operations. Essa and Kennedy (1993) provide recommendations to maximize the buckling capacity of doubly-symmetric prismatic I-section members based on the position of the lift clamps along the length of the field section. Their recommendations are developed for cases involving a single spreader beam. Essa and Kennedy observe that the buckling capacity is largest when the lift clamps are placed near the quarter points. However, the buckling capacity is most sensitive to the position of the lift clamps when they are placed in these positions. If the lift clamps are moved either toward the middle or the ends of the member, the buckling capacity sharply decreases.

For the lifting of more general singly-symmetric horizontally-curved non-prismatic I-girders, the software UT Lift (Farris, 2008) is available to evaluate the girder pick locations. UT Lift calculates both the girder rigid body rotation as well as the deformations under self-weight for the lifted girder. The program also reports major-axis bending, flange lateral bending and warping normal stresses, as well as the critical

buckling load of the lifted girder. The program's analysis calculations are based on a Thin-Walled Open-Section (TWOS) 3D-Frame model.

The analysis of I-girders during lifting is not addressed in this report. The focus of this report is on analysis of bridge systems in their partially or fully erected construction conditions.

2.12 Responses that a Line-Girder Analysis Cannot Model

In line-girder models, the girders in the system are analyzed independently. For the noncomposite structure, the loadings acting on each individual girder are determined based on tributary area or by other simplified lateral distribution assumptions. The V-load method extends the capabilities of a line-girder analysis to include horizontal curvature effects in I-girder bridges. However, this method does not include any information about skew, and therefore, it is not able to accurately capture the effects of skewed supports. The software VANCK (used for the V-load calculations in the NCHRP 12-79 research), may be applied to a skewed bridge, but inherently, this program does not address skew effects. This highlights the following important question that the engineer should always raise before utilizing a particular software system or set of calculation equations: Does the software or do the equations account for the important characteristics of the problem at hand? Just because a software package accepts the input parameters for a given structure does not make it applicable for the problem at hand.

For tub-girder bridges, the M/R method provides a way to include the torsional moments due to curvature in a 1D line-girder analysis; however, this method cannot model the effect of external intermediate diaphragms, which potentially can introduce large forces and cause significant differences in the physical response (see Figure 2.13) when the external diaphragms are used to control the girder relative displacements as shown in Figure 2.15.

Support skews generally introduce a transverse load path in the structure. In I-girder bridges, loads are transferred laterally from girder to girder through the cross-frames, subjecting the system to torsion. Since the line-girder analysis does not contain any information regarding the cross-frame contributions to the system response, it cannot

predict the collateral effects of skew. In particular, the cross-frame forces and flange lateral bending stresses associated with the skew are responses that cannot be captured with this method. In addition, Sanchez (2011) shows that in some cases, the major-axis bending stresses and the vertical displacements also can be influenced significantly by the skew effects. Furthermore, it is important to note that if the accuracy of the simplified vertical deflection estimates is degraded, the estimates of the girder layovers also is affected. For tub-girder bridges a traditional line-girder analysis does not include the skew effects; however, these effects can be included with reasonable accuracy when there are no external intermediate diaphragm, as explained in Sections 2.1.4 and 2.1.5.

Fortunately, in many structures the effects of skew are minor. Limits for when it is necessary to capture the skew effects in the analysis of I-girder bridges are proposed in Chapters 3 and 5 of this report. In Section 3.1.2, a "skew index" that relates the skew angle with the width and the span length of the bridge is introduced. For I-girder bridges, the collateral skew effects are observed to be relatively small when the skew index is less than 0.30. This is shown in the quantitative assessment of the approximate analysis methods discussed in Section 5.1. Hence, even though a line-girder analysis is not able to capture the responses mentioned previously, this inaccuracy does not have an important effect on the structural behavior in bridges having indices below this limit. For structures with indices above this limit, the skew effects generally have a significant influence on the system responses. For these structures, a more refined method of analysis should be considered.

2.13 Responses that a 2D-Grid Analysis Cannot Model

In 2D-grid analyses, most of the overall structural components of the bridge are included in the model. Specifically, 2D-grid models are capable of representing the girders and the cross-frames and/or diaphragms. In many cases, all the cross-frames, diaphragms and girders are modeled with elements that are based on Euler-Bernoulli beam theory. In some situations, models are created based on Timoshenko beam theory to consider shear deformations. The capabilities of an element formulated with these theories generally are not sufficient to represent the physical behavior of the structural components. In particular, the poor representation of the torsional stiffnesses of the I-

girders, as well as the poor representation of the cross-frame generalized flexural-shear stiffnesses results in an inaccurate prediction of the bridge responses in certain cases.

Tub-girder bridges are in some respects more easily modeled by 2D-grid methods than I-girder bridges. This is because the tubs act as pseudo-closed sections. As such, warping torsion typically does not need to be considered (assuming an adequate top-flange lateral bracing system and adequate restraint of cross-section distortion by the internal cross-frames). Tub-girder bridges, however, experience modeling difficulties due to the finite size of the cross section relative to the external diaphragms and cross-frames. In 2D-grid analyses, the tub-girders are represented as line elements at their centroid but the offset from the support to the girder centroid is ignored. Similarly, the girder rotations are estimated about the girder centroid but the actual center of rotation can be offset from this location. For multiple girder systems, the external intermediate diaphragm lengths are modeled from the girder centerlines. In cases where the flexibility of the external and/or internal diaphragms or cross-frames has a significant effect on the system response, the force transfer and the deformations within the vicinity of these components are more complex than can be represented accurately by traditional 2D-grid or 3D-frame elements.

Section 5.1 shows quantitatively the results obtained for 58 I-girder bridges studied in NCHRP 12-79 and the influence of the simplifications used in the 2D- grid models on the prediction of the structural behavior. The studies conducted in this research show that, for I-girder bridges, the basic beam or frame elements commonly available in analysis and design software packages can give poor predictions of the displacements in cases involving the following attributes, or certain combinations of these attributes:

- The bridge is highly curved,
- The girders are connected by only a few cross-frames,
- There is a small number of girders in the bridge cross-section (final or during an intermediate stage of construction).

The poor predictions are tied largely to a poor characterization of the true girder torsional stiffnesses by the common St. Venant torsional stiffness idealization, GJ/L. The

analysis models in common software packages do not include the torsional stiffness associated with the warping (or lateral bending) of the I-girder flanges. However, the girder warping response dominates the girder torsional stiffness for essentially all practical geometries. This can be understood by considering a basic I-section member subjected to an end torque, as shown in Figure 2.32. The majority of the torsional stiffness comes from the cross-bending of the flanges for essentially all practical lengths when one considers bridge girder type I-sections. The girder torsional stiffness is even larger if the warping of the flanges is restrained at both ends of the member.

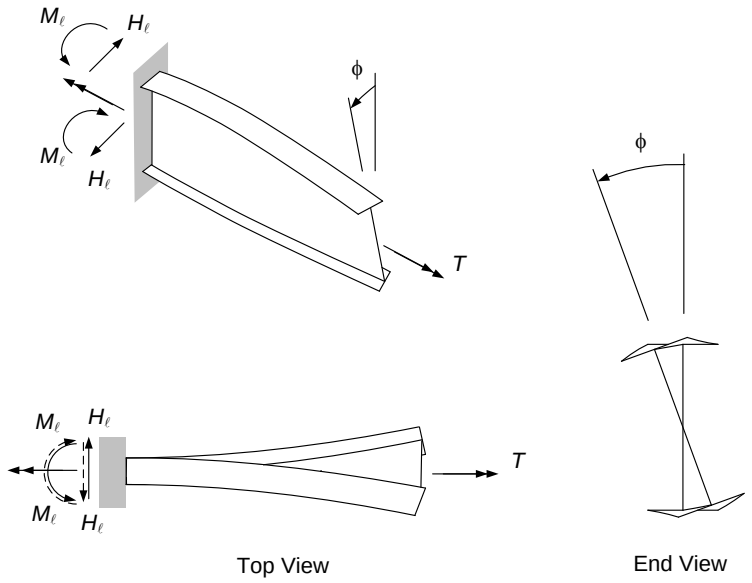

Figure 2.32. Example I-section member subjected to torsion.

It is important to note that horizontal curvature significantly influences the impact of the poor representation of the girder torsional response, and that horizontal curvature can have a dominant effect on the overall analysis accuracy. However, horizontal curvature is not the only factor that can influence the accuracy of 2D-grid methods. Straight skewed bridges having multiple lines of discontinuous (staggered) cross-frames also can be sensitive to the girder torsional stiffnesses used in the analysis models versus the physical torsional stiffness of the girders. Since the skew induces torsion in the I-girders, the predictions obtained from the 2D-grid model of a straight-skewed I-girder system can be inaccurate for bridges having a skew index equal or larger than 0.30.

Specifically, the cross-frame forces and the resulting f_ℓ stresses can be severely underpredicted. For bridges below this limit, the skew effects are relatively minor. Hence, although a conventional 2D-grid analysis may not be able to capture the distribution of transverse forces that result from skew, these effects may be neglected in the design.

The investigations conducted for the bridges studied in NCHRP 12-79 (see Chapter 4) show that the inaccurate representation of the torsional properties of the I-girders can have a minor effect on the major-axis bending stress responses. As shown in the quantitative assessment of the 58 I-girder and 18 tub-girder bridges considered in these studies, the major-axis bending stresses are less sensitive to poor torsion models than the vertical displacements. On the other hand, the torsion model has a significant influence on the vertical displacement predictions in curved I-girder bridges. Due to the lack of consideration of warping torsion in the conventional 2D-grid element formulations, the vertical displacements are commonly over-predicted in curved structures.

Another response of interest for the design of steel girder bridges is the cross-frame forces resulting from horizontal curvature and support skew. When conducting a 2D-grid analysis of a bridge structure, there are two particular practices that can affect the accuracy of the internal force predictions. The first practice is the modeling of the cross-frames. In grid analyses, the cross-frames are typically represented by an equivalent prismatic beam element. In conventional practice, the cross-section properties of the beam element are determined typically by equating either the flexural or the shear stiffness of an explicit model of the cross-frame to the corresponding beam element stiffness (Coletti and Yadlosky, 2007; AASHTO-NSBA, 2011). Some of the subtle attributes of the equivalent beam cross-frame modeling can be understood by considering the three in-plane co-rotational (i.e., deformational) degrees of freedom (dofs) at the ends of a cross-frame. As shown in Figure 2.33, one possible set of these co-rotational dofs involves the rotations at the connection plates on each side of the cross-frame as well as the relative axial extension of the cross-frame between the connection plates at say the mid-depth of the girders. The element equations for the full set of six dofs in the plane of the cross-frame are obtained from the co-rotational set by fundamental rigid-body kinematics and beam element equilibrium (Sanchez, 2011). If one uses an equivalent

prismatic Euler-Bernoulli beam element to represent the cross-frame, the corresponding co-rotational stiffness terms are

$$\begin{bmatrix} EA/L & 0 & 0 \\ 0 & 4EI/L & 2EI/L \\ 0 & 2EI/L & 4EI/L \end{bmatrix} \tag{2.104}$$

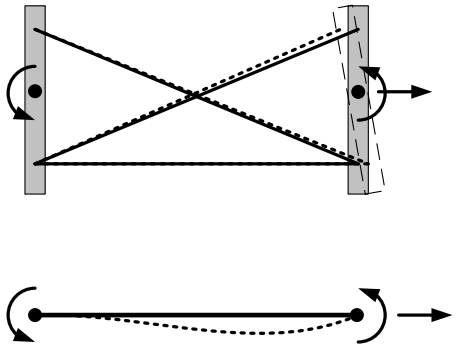

Figure 2.33. Typical cross-frame and equivalent beam element shown with their co-rotational (i.e., deformational) dofs.

If a Timoshenko beam or Reissner-Mindlin beam formulation is used, additional terms will appear in the bending stiffness coefficients that account for the beam shear deformations. In either case, each of the columns in the stiffness matrix gives the forces due to unit displacement at one of the dofs with the other dofs held fixed at zero displacement. If one imposes a unit relative displacement at the axial dof on the X-type frame in Figure 2.33, one will obtain bending moments at the two rotational dofs. This is because the center of axial stiffness of the cross-frames and the mid-height of the girders are not at the same elevation. Consequently, axial lengthening or shortening of the cross-frame between the girders is coupled with the cross-frame bending rotations at the centerline of the connection to the girders. Physically, the ends of the cross-frame cannot rotate relative to one another without some spreading apart or pulling together of the girders. In addition, if one considers the rotational degrees of freedom, it should be recognized that even if the primary rotational stiffness ($4EI/L$ in the Euler-Bernoulli beam element) is matched to the corresponding “true” cross-frame stiffness, the ratio of the off-diagonal rotational stiffness term to the primary rotational stiffness in the true cross-

frame generally will not be the same as the ratio of these terms in the equivalent beam element (e.g., $(4EI/L)/(2EI/L) = 2$ to 1 in the Euler-Bernoulli beam formulation).

The second practice that has an important role in the prediction of the cross-frame forces, as well as potentially the prediction of the behavior of the entire bridge structure, is the representation of the torsional rigidity of the I-girders. As previously stated, the formulation of the element used to represent the I-girders in 2D-grid models typically considers only the St. Venant or pure torsion contribution to the stiffness (GJ/L) and neglects the contribution from flange warping stiffness. In general, this limitation not only has a considerable influence in the prediction of the girder responses; also, it can have a substantial impact on the prediction of the cross-frame forces.

Figure 2.34 shows that the bending dofs for the cross-frames correspond to the torsional dofs of the girders. Only these dofs are shown in the figure to simplify the sketch. In the figure, Nodes 2 and 3 are connected; therefore, the bending moments in the cross-frames, $M_{1\text{-}CF}$, and the torsional moments in the girders, $T_{2\text{-}G}$, generally must balance with one another at this common joint (note that this figure could represent the behavior at the end bearing-line cross-frames of a bridge, but in general, other girder and/or cross-frame elements may frame into this common joint).

Generally, due to the limited capabilities of 2D-grid models to represent the actual torsional stiffness of the girders, the results obtained for $T_{2\text{-}G}$ and $M_{1\text{-}CF}$, will be severely underestimated. The neglect of the flange warping contributions to the stiffness results in a girder torsion model that is considerably more flexible than the physical girders. This means that even though the cross-frames are included in a 2D-grid analysis model, the girders respond as if they were disconnected since they do not have any torsional stiffness to react the cross-frame forces. This is observed particularly in straight and skewed I-girder bridges where the cross-frames are perpendicular to the girders. Since the *torsional* dofs of the girders are connected to *bending* dofs of the cross-frames, the cross-frame forces predicted from a 2D model also will be underpredicted. In fact, the cross-frame forces obtained from refined 3D FEA in straight-skewed with skew indices larger than

0.3 are often considerable, whereas conventional 2D-grid analyses indicate that these forces are essentially zero.

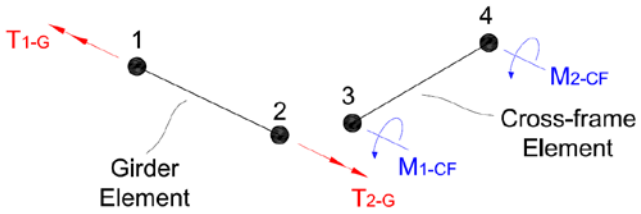

Figure 2.34. Interaction of girder and cross-frame stiffnesses.

Given that the cross-frame forces cause lateral bending in the girder flanges, it is necessary to have an accurate prediction of the cross-frame forces to compute the expected levels of the girder flange f_ℓ stress. Hence, conventional 2D-grid models are not able to predict the flange lateral bending responses with reasonable accuracy. However, as in the case of the cross-frame forces, the flange lateral bending stresses in skewed bridges with a skew index less than 0.30 may be neglected for design purposes.

Sections 6.1 and 6.2 explain the development of modeling techniques that improve the accuracy of the conventional 2D-grid models and extend their applicability to structures with complex geometries. As shown in these sections, a better representation of the cross-frames and of the torsional properties of the I-girders can significantly increase the accuracy of a 2D-grid analysis.

3. Bridge Characterization with Respect to Curvature and Skew

This chapter discusses five key indices identified by NCHRP 12-79 as being the most useful for characterizing the importance of skew and curvature on the response of steel girder bridges and the ability of simplified methods to capture this response. The first index is an estimate of the global second-order amplification of the bridge displacements and stresses, AF_G. This index should be checked to determine whether the stability effects are significant in cases such as relatively narrow and/or long units with a small number of girders. The second two indices are termed the skew index, I_S, and the connectivity index, I_C, and are used in Chapter 5 as an aid to identify when the simpler methods of analysis are sufficient and when more sophisticated methods should be applied for the construction engineering of curved and/or skewed I-girder bridges. The last two indices are termed the torsion index, I_T, and the girder length index, I_L. These indices are used in Chapter 4 as part of the characterization of curved and/or skewed bridges for the design of the project analytical studies. Section 3.2 provides an overview of broad factors that generally can influence the detailed behavior of curved and/or skewed steel girder bridges. These factors were considered in the development of a wide range of bridge geometries and configurations studied within the NCHRP 12-79 research. Chapter 4 discusses these factors and provides an overview of the NCHRP 12-79 studies that serve as input for the guidelines provided in this report.

3.1 Key Bridge Response Indices

3.1.1 Global Second-Order Amplification Factor, AF_G

The potential importance of the global second-order amplification of the vertical and lateral displacements, and of the corresponding girder major-axis and flange lateral bending stresses, is emphasized in Section 2.9. In that section, an equation for AF_G is recommended for making a basic conservative estimate of the second-order amplification. If the corresponding amplified major-axis bending and flange lateral bending stresses do not violate the required AASHTO Article 6.10.3 constructability checks, then strictly speaking, the AASHTO constructability requirements are satisfied. However, one should note that as the physical second-order amplification becomes large, the structural

response becomes sensitive to minor variations in the load and support conditions, as well as any other characteristics that influence the stiffness. Therefore, for construction stages such as the placement of the concrete deck, it is advisable to restrict the estimated AF_G (Eq. 2.101) to a maximum value of approximately 1.25, or perform a 3D FEA of the structure to assess the second-order amplification more carefully. It is recommended that if AF_G from Eq. (2.101) is smaller than 1.10, the global second-order amplification of the structural responses may be neglected. If the designer is concerned about the potential underestimation of design stresses or forces, the design can be conducted using a capacity ratio of 0.9. However, it should be noted that there is no such thing as a conservative prediction of deflections in the context of the control of the constructed geometry of a bridge.

For intermediate steel erection stages, larger values of AF_G should be acceptable as long as the amplified stresses are sufficiently low. The AASHTO Article 6.10.3 yielding and one-third rule strength checks are expected to provide sufficient constructability limits in these cases, without the need to directly assess the structure's amplified deflections. It is important to note that in typical intermediate erection stages, the girder stresses are well below the AASHTO constructability limits.

There are various precedents for the above limits of $AF_G = 1.10$ and $AF_G = 1.25$ in the literature, but the rationale for these types of limits hinges largely on ones confidence in not overpredicting the ratio of the theoretical elastic buckling load of the structure to the design load under consideration, $\gamma_{crG} = M_{crG} / M_{maxG}$. At $AF_G = 1.10$, an underprediction of 10 % for γ_{crG} results in an underestimate in AF_G of approximately 2 %. At $AF_G = 1.25$, an underprediction of 10 % for γ_{crG} results in an underestimate in AF_G of approximately 3 %. At $AF_G = 2.0$, an underproduction of 10 % for γ_{crG} results in an underestimate in AF_G of approximately 12 %.

3.1.2 Skew Index, I_S

The skew index, I_S differentiates bridges where the skew effects are expected to be more significant from those where the collateral effects of skew are relatively small. This index is defined as

$$I_S = \frac{w_g \tan\theta}{L_s} \tag{3.1}$$

where w_g is the width of the bridge measured between the centerline of the fascia girders, θ is the skew angle, and L_s is the span length. In bridge spans with unequal skew of the bearing lines, θ is taken as the largest skew angle of the supports. In continuous-span bridges, one index is determined for each span. Figure 3.1 illustrates the variables required to calculate the skew index.

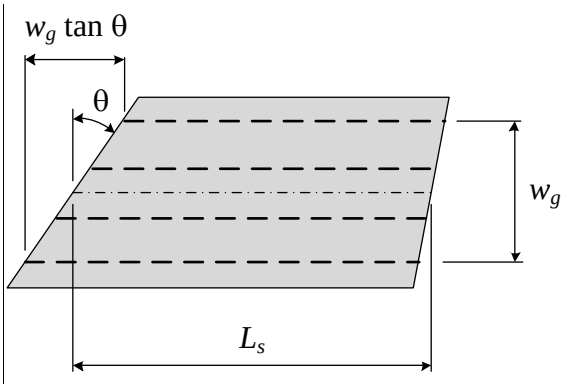

Figure 3.1. Parameters for the definition of the skew index.

The studies conducted in the NCHRP 12-79 research show that the effects of skew, which are largely related to the bridge transverse stiffness and transverse load paths, tend to increase with a larger skew index. Specifically, the levels of flange lateral bending stresses, cross-frame forces, and girder layovers tend to increase with increases in the skew index. The results obtained from 24 straight and skewed I-girder bridges studied in the project show that a value of the skew index of 0.30 differentiates bridges that are more sensitive to the skew from the ones that are less influenced by skew. For most of the structures above this limit, the stress ratio f_ℓ / f_b, which is one of the most suitable parameters to characterize the skew effects, is more than 0.3 in regions of the bridge where the cross-frames are staggered. That is, in these bridges, the levels of flange lateral bending stress are more than 30 % of the major-axis bending stresses, f_b, which may be considered as a large flange lateral bending effect. This limit parallels the limit suggested in the Commentary to Article 6.7.4.2 of AASHTO (2010), which states that for curved bridges, "A maximum value of 0.3 may be used for the bending stress ratio (i.e., f_ℓ / f_b)."

A second limit on the skew index, where the skew effects not only cause large values in the responses associated with the lateral bending of the girder flanges, but also can significantly influence the major-axis bending responses is 0.65. In bridges where I_S is above this limit, the influence of the skew on the girder major-axis bending stresses, f_b, as well as the girder vertical displacements can be significant. Below this limit, the influence of skew on these quantities tends to be small.

To illustrate the use of the skew index, the construction sequence of bridge NISSS14 is discussed (see Chapter 4 for a description of the NCHRP 12-79 studies and bridge naming conventions). Figure 3.2 shows three of the four stages of this bridge's construction considered below. Stage 3, not shown, corresponds to the condition where three girders have been erected and the cross-frames have been installed between the girders.

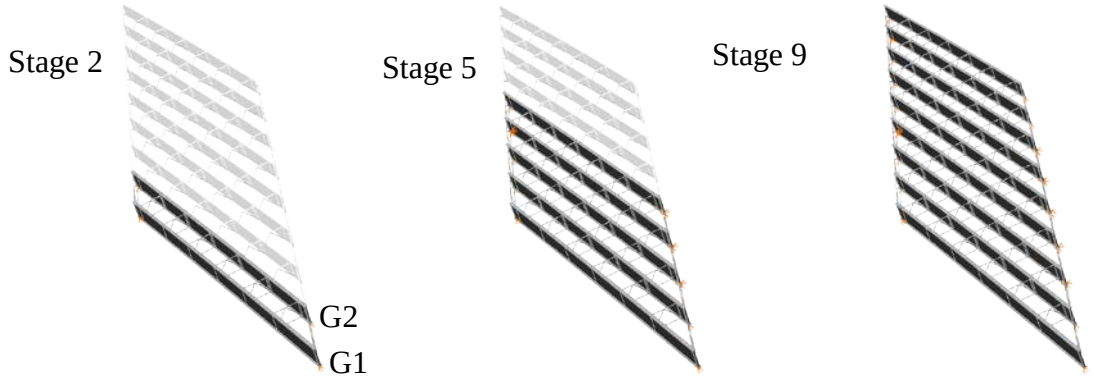

Figure 3.2. Erection stages investigated in bridge NISSS14.

In this bridge, the spacing between the girders is 9.25 ft., the span length is 150 ft., and the skew angle is 70 degrees. Hence, the skew index for Stage 2 is

$$I_S = \frac{9.25\,\text{ft} \times \tan 70^{\circ}}{150\,\text{ft}} = 0.17$$

Similarly, for Stages 3, 5, and 9 the skew index is 0.34, 0.68, and 1.36, respectively.

Figure 3.3 shows the f_b and f_ℓ plots of girders G1 and G2 for each of the stages. The plots contain three responses: the f_b and f_ℓ stresses obtained from the 3D FEA and the f_b stress obtained from a 1D line girder analysis. The bending stresses from the 1D

analyses are based only on the individual weights of the girders. These analyses do not consider the influence of the internal forces in the cross-frames resulting from the skew effects. Since the cross-section dimensions of G1 and G2 are the same and the only loading considered is the structure's self-weight, the line girder analysis predictions for G1 and G2 are also the same and do not change during the construction simulation.

From these plots, it is evident that as the construction progresses and the geometry of the bridge changes, the skew effects become more important. It is observed that in Stage 2, the influence of the skew is negligible, since the horizontal components of the cross-frame forces do not cause considerable levels of f_ℓ. Also, the f_b stresses associated with major-axis bending are dominated by the gravity load effects on each girder. The vertical components of the forces from the cross-frames are too small to influence the response. Hence, the 1D line-girder analysis is a good match to the benchmark. As more girders are erected, the influence of the skew is more noticeable. In Stage 5 for example, when five girders have been erected, the level of the f_ℓ stresses is significant compared to the f_b stresses. Furthermore, the effect of the cross-frame shear forces is particularly noticeable since the line girder analysis prediction of f_b deviates considerably from the benchmark response. In the 1D analysis, the participation of the cross-frames is not included, so the forces transferred by the bracing system do not contribute to the predictions. A similar trend is observed for Stage 9, when the structure's erection is completed. The plots show that the forces transferred through the cross-frames have a considerable impact in the performance of the structure at this stage.

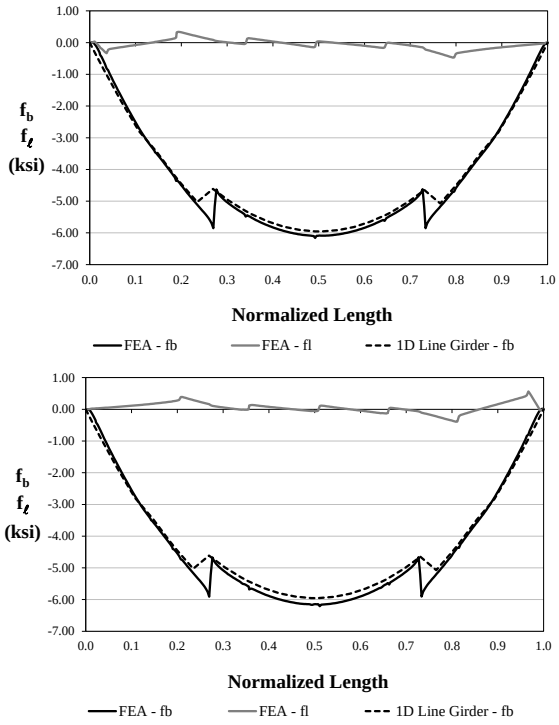

Girder G1 Girder G2

(a) Stage 2 (I_{SE} = 0.17)

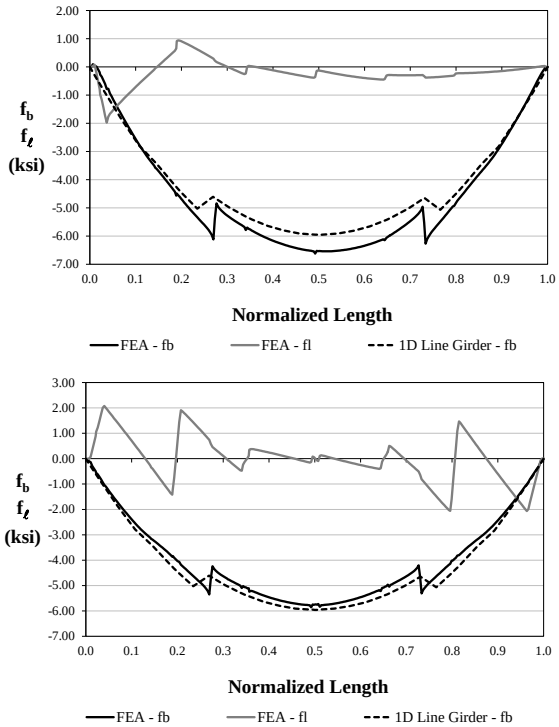

Girder G1 Girder G2

(b) Stage 3 (I_{SE} = 0.34)

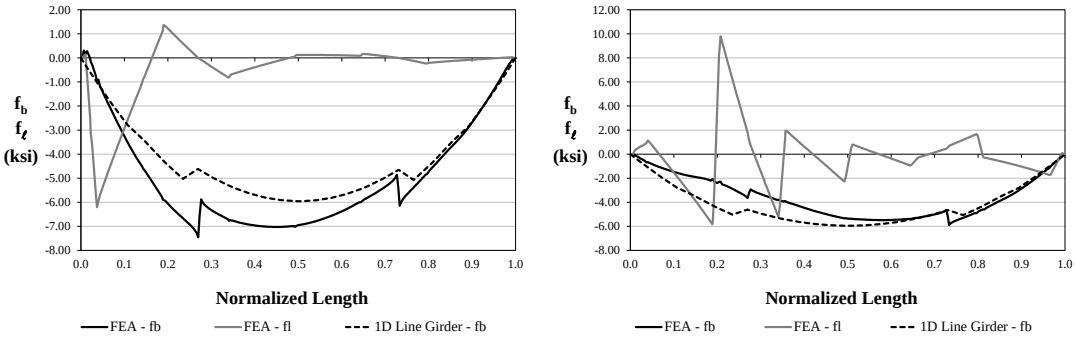

Girder G1 Girder G2

(a) Stage 5 (I_{SE} = 0.68)

Figure 3.3. Stress responses in the top flanges of girders G1 and G2 of bridge NISSS14 during four construction stages.

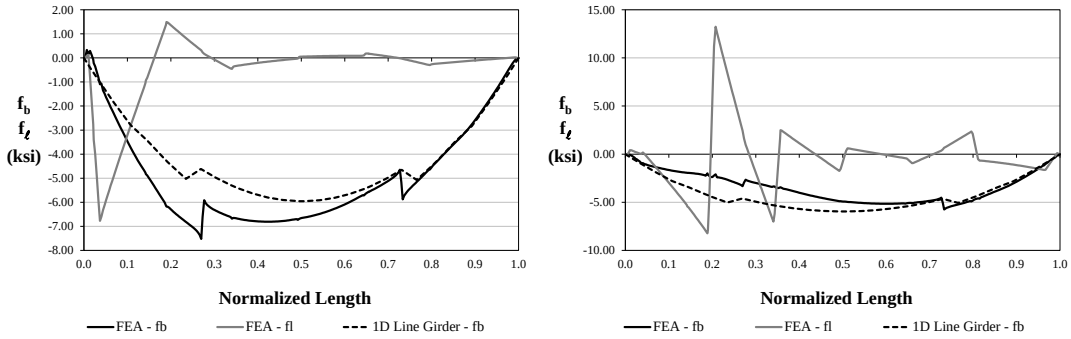

Girder G1 Girder G2

(b) Stage 9 (I_{SE} = 1.36)

Figure 3.3 (continued). Stress responses in the top flanges of girders G1 and G2 of bridge NISSS14 during four construction stages.

The above analyses also demonstrate that the behavior of a skewed bridge depends on more than just the severity of the skew. The skew angle by itself does not determine the magnitude of the collateral skew effects. Instead, it is the combination of the span length, the bridge width (between the fascia girders), the skew angle, and the distribution of the cross-frames in the bridge layout that determines the structural behavior. The proposed skew index relates the first three of these parameters, which define the geometry of the bridge. As discussed, as the index increases, so does the influence of the skew on the system response. Also, it should be noted that in the construction stages investigated for this bridge, the responses in Stages 5 and 9, which have indexes of 0.68 and 1.36, are more significantly affected by the skew compared to Stages 2 and 3, where the index is close to and less than 0.30.

The above construction simulation also highlights an important aspect regarding the accuracy of the 1D model predictions. By comparing the predictions obtained from the 1D and 3D analyses, it is observed that even when the line girder solution deviates from the physical response, in general, the difference in the major-axis bending stress magnitudes tends to be minor. For example, at the mid-span of girder G1, Stage 9, the f_b stress obtained from the 3D model is -6.65 ksi. At the same position, the 1D model predicts a stress of -5.96 ksi, resulting in a difference of 0.69 ksi. For design purposes, this difference is negligible. Therefore, many engineers would conclude that the 1D

model is sufficient to represent the expected structural behavior of this bridge. However, it is important to notice that the 1D model does not provide any information regarding the cross-frame forces and girder flange lateral bending stresses, which according to the AASHTO Specifications must be included in the construction checks when the lateral bending is significant. Hence, although the 1D analysis may capture approximately the major-axis bending response of the girders, it does not provide the information needed to design all the structural components. Additional studies that show the validity of the skew index as a method used to characterize the influence of skew on the structural behavior are provided in Sanchez (2011).

3.1.3 Connectivity Index, I_C

The studies conducted in the NCHRP 12-79 research show that in curved radially supported I-girder bridges, the cross-frame spacing (or the number of intermediate cross-frames within the span) is a key indicator of the accuracy of the results obtained from 2D-grid analyses. In conventional 2D-grid models, the representation of the torsional stiffness of the I-girders is dramatically underestimated since the contributions of warping to the girder stiffness are neglected. If the bridge is significantly curved and/or the girders are not closely connected by cross-frames, the results obtained from these 2D-grid models do not properly represent the structural behavior of the curved bridge during construction. Chapter 6 provides an extensive discussion regarding this topic. The errors are tied largely to the coupling between major-axis bending and torsion in curved girders.

A trend that is noticeable in curved radially supported bridges is that the accuracy of the analysis is roughly proportional to the radius of curvature, R, and to the span length to unbraced length ratio, L_s / L_b. In a straight bridge connected with a typical number of cross-frames needed to make the structure behave as a unit, $R = \infty$ and the L_s / L_b ratio is large. Also, the accuracy of the results obtained from 2D-grid models should be within acceptable limits. On the other hand, if the structure has a tight radius of curvature and/or is connected with a small number of cross-frames, giving a smaller L_s / L_b ratio, the results of the conventional 2D-grid models may be suspect. In addition, continuous-span I-girder bridges tend to be able to tolerate smaller values of R and L_s / L_b for a given error tolerance.

Based on the above observations, the following ad hoc connectivity index is proposed to characterize when the results from a 2D-grid analysis may not be sufficiently accurate:

$$I_C = 15{,}000 \frac{1}{R} \frac{1}{m} \frac{L_{b.avg}}{L_s} = \frac{15{,}000}{R(n_{cf}+1)m} \tag{3.2}$$

where R is the radius of curvature of the bridge centerline in units of ft., m is a constant equal to 1 for simple-span bridges and 2 for continuous-span bridges, $L_{b.avg}$ is the average unbraced length between the cross-frames within the span, L_s is the span length at the bridge centerline, and n_{cf} is the number of intermediate cross-frames within the span. In continuous-span bridges, R and n_{cf} can vary from span to span. Therefore, I_C is calculated for each span, and the largest value is taken as the index for the full bridge.

In the NCHRP 12-79 studies, 14 curved radially-supported I-girder bridges were studied to determine the ability of the simplified methods to capture the responses predicted by refined 3D models (see Chapter 4 of this report, and Appendices E and I of the NCHRP 12-79 Final Report). From the results of this study it was determined that bridges with $I_C > 1$ tend to exhibit large errors from conventional 2D-grid analyses, while for $I_C \leq 1$, the 2D-grid analysis predictions are significantly better. Chapter 5 discusses the categorization of the curved and radial bridges as function of I_C in further detail.

To illustrate the use of this index, consider Bridge EISCR1 depicted in Figure 3.4a. This is a simple-span bridge with a radius of curvature equal to 200 ft. The girders are connected with five cross-frames. For this structure, I_C = 15,000/200/(3+1) = 18.75; therefore a conventional 2D-grid analysis may not be sufficient to capture the expected behavior. Conversely, Figure 3.4b shows the plan view of Bridge EICCR15, a two-span structure with 10 intermediate cross-frames in the first span and 13 intermediate cross-frames in the second. For this bridge, I_{C1} = 15,000/1,921/2/(10+1) = 0.35 and I_{C2} = 15,000/1,921/2/(13+1) = 0.28. Therefore, I_C = 0.35 < 1.0. Hence, the results obtained from the 2D-grid analyses should closely represent the benchmark responses.

The connectivity index is determined empirically based on the NCHRP 12-79 studies. In essence, this index evaluates “how curved is the bridge?” and “how well

connected are the girders?" for conventional 2D-grid analysis purposes. It should not be used for any other purpose than identifying I-girder bridges where the results of a conventional 2D-grid analysis may or may not be reliable. It is not intended to be used in design to determine the number of cross-frames or the cross-frame spacing, for example, since it applies only to assessment of the inadequacies of the traditional 2D-grid calculations. It is emphasized that if a 3D analysis (or a 2D-grid analysis including the recommendations of Chapter 6) is conducted, the engineer will have the required information to dimension the structural members and check the different strength and serviceability limit states according to the requirements of the AASHTO LRFD Specifications, regardless of whether I_C is above or below 1.0.

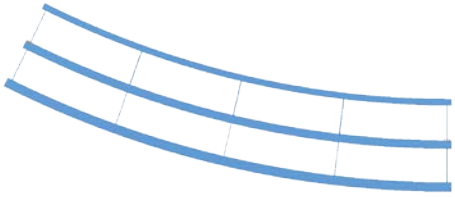

L_1 = 90 ft. / R = 200 ft. / w = 23.5 ft.

(a) Bridge EISCR1

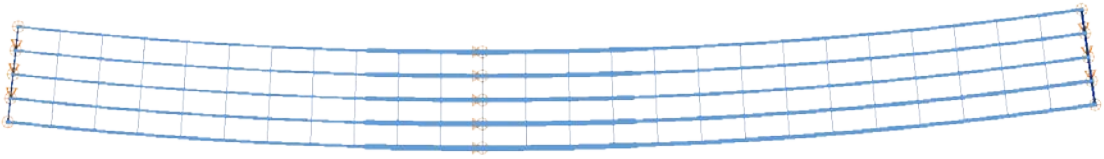

L1 = 210 ft., L2 = 271 ft. / R = 1921 ft. / w = 48.9 ft.

(b) Bridge EICCR15

Figure 3.4. Examples for the calculation of I_C in curved and radial bridges.

3.1.4 Torsion Index, I_T

Regarding the characterization of horizontal curvature effects on the bridge behavior and the corresponding analysis accuracy, the non-dimensional factor L_s/R, which is the subtended angle of a span's centerline expressed in radians, is important (see Figure 3.5). However, the maximum practical values of L_s/R can vary substantially as a function of the width of the structural system. The maximum L_s/R is more limited in relatively narrow bridges because of the greater tendency for overall overturning of the

structure (or structural unit). This characteristic is illustrated by the plan sketches of the two hypothetical simple-span bridges shown in Figure 3.6. Both bridges have span lengths of L_s = 300 ft. and a constant horizontal radius of curvature *R*. However, one bridge has a 30 ft. wide deck while the other has an 80 ft. wide deck. The deck overhang width is 3 ft. on each side for both bridges. If one considers a representative uniformly distributed deck weight loading on these two structures, the subtended angle between the supports L_s/R needs to be much smaller for the narrower structure to avoid uplift at the inside fascia girder supports, i.e., the supports closer to the center of curvature.

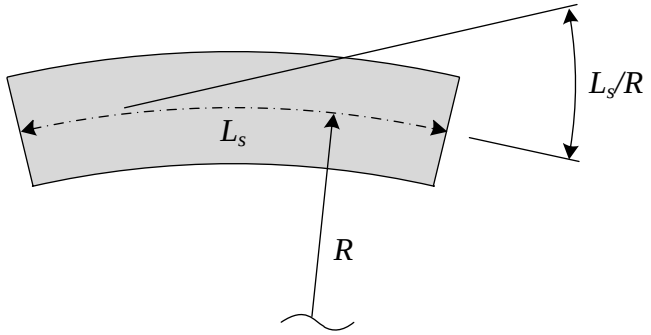

Figure 3.5. Subtended angle of a span's centerline, L_s/R.

Two straight dashed lines are drawn along the length direction of the plan sketches in Figure 3.6. One of the dashed lines is the chord between the fascia girder bearings on the outside of the curve. The other is the chord between the fascia girder bearings on the inside of the curve. Also shown on the plan sketches is the symbol "x", which indicates the centroid of the deck area (and hence the approximate centroid of dead weight of the structure). For bridges that are more highly curved (smaller *R*), the centroid (x) is closer to the outside chord line. If the curvature is such that the centroid (x) is positioned directly over the outside chord line, then all the bridge reactions have to be zero except for the reactions at the outside bearings. That is, the bridge unit is at the verge of tipping about its outside bearings (assuming a single span, simply-supported ends, and no hold-downs at the other bearings). This is obviously an extreme condition. Even a bridge with a much smaller curvature (larger radius of curvature) would require hold downs at bearings closer to the center of curvature to equilibrate (or balance) the structure weight assuming a uniform distribution over the deck area.

The following "torsion index" is an indicator of the overall magnitude of the torsion within a bridge (or bridge unit) span, and is a strong indicator of the tendency for uplift at the bearings:

$$I_T = \frac{s_{ci}}{s_{ci} + s_{co}} \tag{3.3}$$

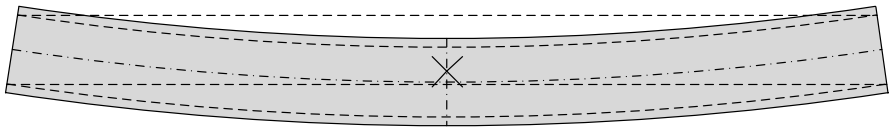

L_s = 300 ft, w = 30 ft, w_g = 24 ft, R = 1000 ft, L_s/R = 0.30

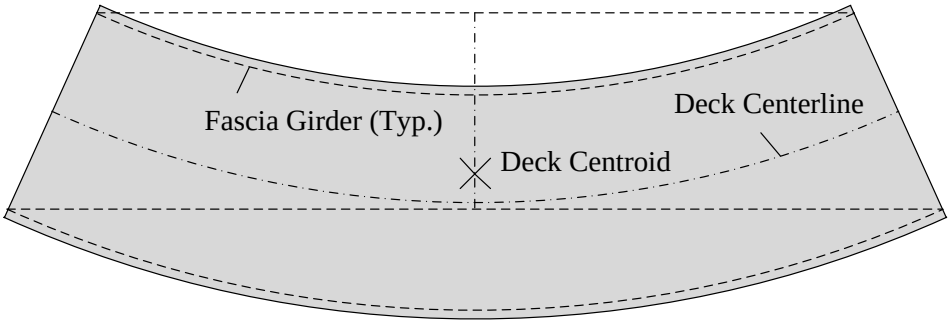

L_s = 300 ft, w = 80 ft, w_g = 74 ft, R = 353 ft, L_s/R = 0.85

Figure 3.6. Plan geometries of two representative simple-span horizontally-curved bridges with L_s = 300 ft.

The terms in this equation, illustrated in Figure 3.7, are:

- s_{ci}, the distance between the centroid of the deck and the chord between the inside fascia girder bearing locations, measured at the bridge mid-span perpendicular to a chord between the intersections of the deck centerline with the bearing lines, and
- s_{co}, the distance between the centroid of the deck and the chord between the outside fascia girder bearing locations, measured at the bridge mid-span perpendicular to a chord between the intersections of the deck centerline with the bearing lines.

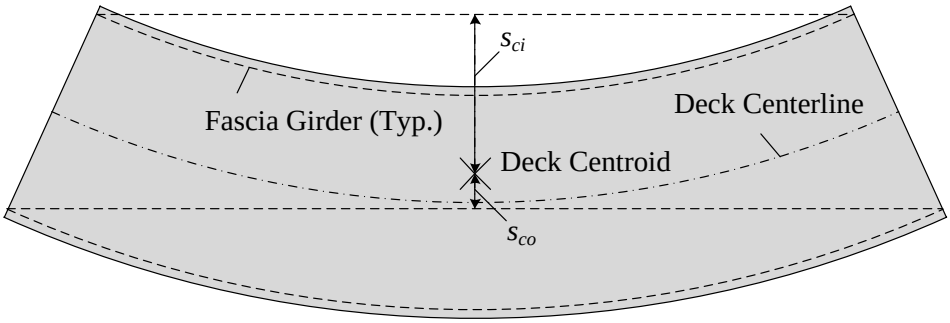

Figure 3.7. Illustration of terms in the equation for I_T.

A value of I_T = 0.5 means that the centroid of the deck area is mid-way between the chords intersecting the outside and inside end bearings. This is the ideal case where the radius of curvature is equal to infinity and the skew is zero, i.e., a straight tangent bridge. A value of I_T = 1.0 means that the centroid of the deck area is located at the chord line between the outside bearings. This implies that the bridge is at incipient overturning instability, by rocking about its outside bearings under uniform self-weight. For a curved radially-supported span, the denominator in Eq. (3.3), $s_{ci} + s_{co}$, is equal to $w_g \cos(L_s/2R)$.

As noted above, the torsion index is related to the magnitude of the overall torsion that exists in the bridge (or bridge unit) span, due to the eccentricity of its self-weight. Furthermore, it is a strong indicator of the potential for uplift at the inside bearings. In the NCHRP 12-79 research, it has been observed that simple-span I-girder bridges with a torsion index of 0.65 and higher are susceptible to uplift at the bearings (Ozgur, 2011). Continuous-span bridges can tolerate higher indices due to the stabilizing effect of the continuity with the adjacent spans. However, the continuity with the adjacent spans generally varies during the steel erection. The torsion index can be calculated for an intermediate steel erection stage using the width between the outside and inside girders during that stage. $I_T > 0.65$ can serve as a rough indicator of when the engineer should check carefully for uplift during the stage.

Tub-girder bridge bearings are typically closer to the bridge centerline and also tub girders are more efficient at resisting overall torsion; therefore, the torsion index in tub-girder bridges tends to be larger than that for an I-girder bridge with the same deck geometry.

3.1.5 Girder Length Index, I_L

The last key index recommended in the NCHRP 12-79 research for characterizing the demands on the methods of analysis with respect to the handling of curvature and skew effects is the girder length index, I_L. This index is usually expressed as

$$I_L = \frac{L_L}{L_S} \tag{3.4}$$

where L_L is the span length of the longest fascia girder and L_S is the span length of the shortest fascia girder within each span. For the curved and skewed bridges considered in the NCHRP 12-79 project research, this definition is modified to

$$I_L = \frac{L_1}{L_{ng}} \tag{3.5}$$

where L_1 is the span length of fascia girder number 1, and L_{ng} is the span length of the highest numbered fascia girder. In the NCHRP 12-79 research, all the curved bridges are displayed in a "concave up" orientation with girder G1 located on the outside of the curve at the bottom of the sketch. Therefore, for the curved radially-supported bridges, I_L is generally somewhat larger than 1.0. If a bridge is curved and skewed, I_L is increased from this value if the skew increases the length of the outside fascia girder. Correspondingly, I_L is decreased and may be less than 1.0 if the fascia girder on the outside of the curve is decreased in length by the skew.

In continuous-span bridges, one index is determined for each span, and the value most different from 1.0 is used to represent the bridge.

The NCHRP 12-79 studies actually indicate that the previous four indices are sufficient to form decisions about the selection of the different methods of analysis. However, the girder length index I_L is an additional parameter indicative of the tendency for differential vertical deflections across the bridge width. The value of I_L is 1.0 for straight bridges with parallel bearing lines, whereas it can be a relatively large number if the bridge is wide and has a significant difference between the skew of adjacent bearing lines. Therefore, one might expect that of two bridges with a large skew index, I_S, the

demands on the analysis may be greater if the index I_L is larger. This trend is not borne out in the NCHRP project studies however. It is believed that the satisfaction of the AASHTO Specification requirements in the bridge designs diminishes the importance of I_L.

3.2 Other Factors

The second and third indices discussed in Section 3.1 (I_S and I_C) are the basis of the scoring system presented in Chapter 5 to assess the ability of the approximate methods to capture the structural responses during the construction of steel I-girder bridges. The first index, AF_G, is used as an indicator of when second-order amplification of the responses may be significant, and the fourth index, (I_T) is used as an indicator of when bearing uplift considerations may be particularly significant. In addition to these indices, NCHRP 12-79 investigated the influence of various other factors that may affect the structural behavior and the analysis accuracy during construction. Span length, radius of curvature, support skew, number of spans and other parameters were variables considered to assess the geometry of the bridges included in the research studies. Chapter 4 discusses these parameters in detail along with criteria for the selection of the bridge geometries that were studied.

4. Design of NCHRP 12-79 Analytical Studies

4.1 Introduction

Curved and/or skewed bridge structures with different geometries can respond in dramatically different ways during their various stages of construction; therefore, extensive studies of a wide range of bridge structures are necessary to gain a true understanding of the accuracy of different analysis methods and the effect of this accuracy on the structural performance.

It should be emphasized that both over-prediction and underprediction of displacements can be equally bad in cases where certain relative deflections are critical. Furthermore, one should not specify a simple blanket accuracy requirement on all the analysis deflections. Specific deflections should be considered, and in cases where the deflections are sufficiently small, larger inaccuracies can be tolerated.

It is important that the accuracy of simplified analysis methods be evaluated using actual bridge designs that satisfy either prior and/or current AASHTO design criteria. The results of simply varying bridge parameters without checking Specification requirements can be misleading. AASHTO requirements must be satisfied for the study bridges to allow the research to establish appropriate relationships between bridge design variables and recommended levels of analysis and construction engineering effort.

One of the early tasks of NCHRP 12-79 was to identify existing bridges representing a spectrum of various combinations of span arrangement, span length, curvature, bridge widths and skew. It was desired to consider both simple and continuous-spans, and that preference would be given to bridges that had:

- Good instrumented field data or at least good field observations, particularly data and observations during intermediate stages of construction and
- Detailed construction plans,

and in which

- The design and construction satisfied prior and/or current AASHTO Specifications and established recommendations, yet construction challenges were encountered or certain attributes resulted in concerns about the final state of stress in the girders, etc.

Bridges where technical challenges were addressed very successfully as well as cases where there were some significant problems were sought. However bridges involving generally acknowledged poor practices, e.g., inappropriate use of oversize or slotted holes, inadequate attachment of cross-frames during construction, etc., were not considered. The focus of Project 12-79 was on analysis and design using appropriate practices. Analysis requirements for forensic investigation of bridges with faulty details were not addressed. However, it was desired for the studies to shed light on the ability of analysis methods to highlight faulty erection schemes, etc., given appropriate design details.

Once the above existing bridge collection effort was completed, then the geometric factors influencing the analysis, design and construction of the bridges were identified. Finally, the ranges and number of levels of these factors were selected for subsequent analytical study.

The following sections provide a detailed description of each of the above steps.

4.2 Identification and Collection of Existing Bridges

Figures 4.1 through 4.6 summarize the overall characteristics of the existing I-girder bridges contributed to NCHRP 12-79 from various owners and consultants. These figures show sketches of the overall plan geometry of the deck and of the bearing lines. Although the number of pages used to illustrate the various geometries is relatively large, these sketches convey a great deal of useful information in a succinct fashion. All the linear dimensions indicated in the sketches are provided in units of feet and all the angular dimensions are provided in degrees. These figures subdivide the collected existing I-girder bridges into the following categories:

- Simple-span, Straight, with Skewed supports (ISSS),
- Continuous-span, Straight, with Skewed supports (ICSS),
- Simple-span, Curved, with Radial supports (ISCR),
- Continuous-span, Curved, with Radial supports (ICCR),
- Simple-span, Curved, with Skewed supports (ISCS), and
- Continuous-span, Curved, with Skewed supports (ICCS).

Each of the bridge sketches in Figures 4.1 through 4.6 has a title block containing the following information:

1. An identification label, composed of the letter "E" for "Existing" followed by the above symbols indicating the bridge category, and ending with the bridge number for that category, e.g., bridge "EISCR1" in Figure 4.3.
2. A description of the structure, composed of the bridge name and/or location.
3. A summary of the basic geometry information about the bridge, enclosed in parentheses. For instance, in Figure 4.3, the basic geometry information for the single EISCR bridge includes:
    - The span length of the bridge centerline (measured along the horizontal curve),
    - The horizontal radius of curvature of the bridge centerline, and
    - The out-to-out width of the bridge deck perpendicular to the bridge centerline.

    This information is conveyed symbolically in the figure caption as "(LENGTH/RADIUS/WIDTH)." The other categories have similar but different basic geometry information. This information is summarized symbolically in each of their figure captions. The skew angle of the bearing lines is represented by the symbol θ. This angle is taken as zero when a bearing line is perpendicular to the centerline of the structure, that is, when the bearing line does not have any skew.
4. The symbol "*", at the end of the parentheses delimiting the basic geometry information, if the bridge has erection plans. No symbol is shown if the bridge does not have erection plans.

5. The organization that provided the drawings for each bridge. This information is delimited by square brackets, i.e., "[FHWA]" in Figure 4.3.

Other pertinent information is provided underneath the plan sketch of each of the bridges. This information includes data such as the number of girders in the bridge cross-section, whether test or field data is available for the structure, references to papers or reports containing test data or documentation of previous research on the bridge, and brief notes regarding successes or difficulties for certain bridges. Note that one scale is utilized for all the simple-span bridges, whereas a slightly smaller scale is used for all the continuous-span bridges.

Figures 4.7 through 4.12 summarize the overall characteristics of the existing tub-girder bridges. These figures are organized in a similar fashion to Figures 4.1 through 4.6.

The various existing bridges shown in Figures 4.1 through 4.12 served two purposes:

1. The composite of all the existing bridges was an aid to the project team in gauging the range and level of geometries that should be considered within the main parametric studies of the Project.

2. A number of the existing bridges that best fit the Project's criteria for the analytical studies, discussed in Section 4.1, were selected for detailed study and inserted into the complete parametric study matrix, discussed subsequently in this chapter.

One can observe that there is a significant diversity of geometries among the existing bridges. This is particularly true for the skewed bridges. It was clear from these sketches that both the skew angle and the skew pattern (i.e., radial, non-radial, parallel and non-parallel bearing arrangements) must be studied. It was not sufficient to focus solely on bridges with parallel bearing lines if the complete implications of skew were to be addressed.

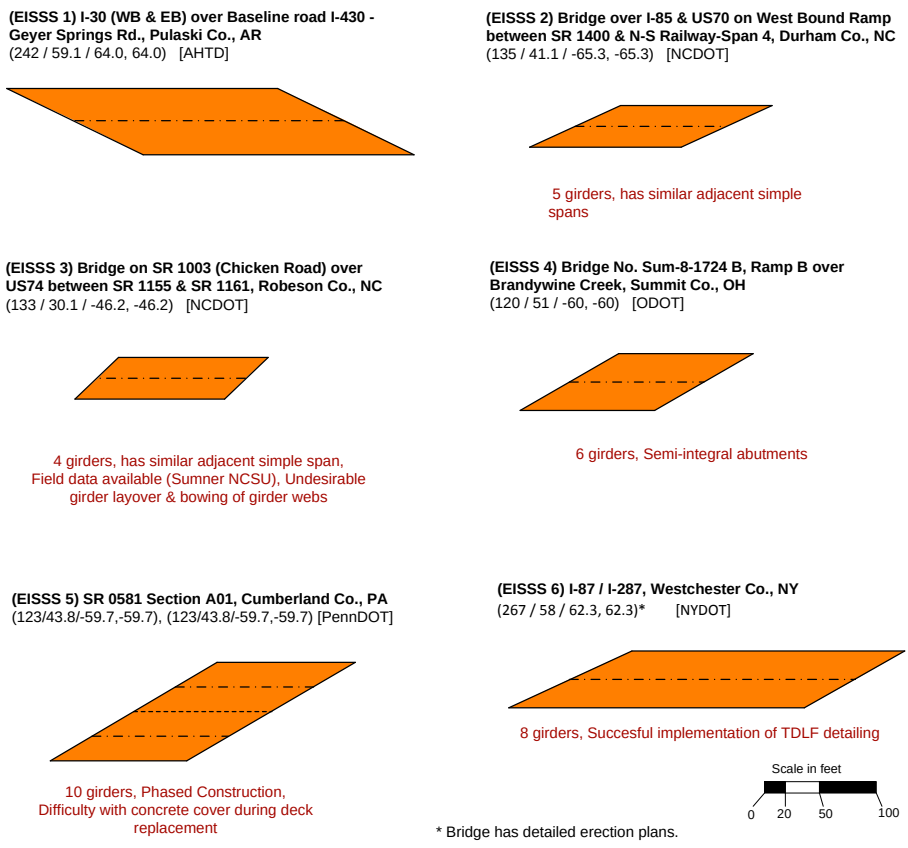

Figure 4.1. Existing I-girder bridges, Simple-span, Straight with Skewed supports, (EISSS #) Description (LENGTH / WIDTH / θ_{Left}, θ_{Right}) [Source].

(EICSS 1) Steel Overpass Sunnyside Road I.C. (I-15B) Over I-15 , Bonneville Co., ID
(160, 160 / 95.2 / -35.2, -35.2, -35.2) [ITD]

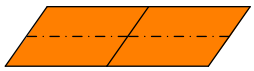

Two-span continuous, 9 girders,
Field data available,
Successful implementation of total dead load fit detailing

(EICSS 2) I-235 EB over E.University Ave., Polk Co., IA
(239, 257, 220 / 74.3 / 58, 61.8, 38, 38) [Iowa DOT]

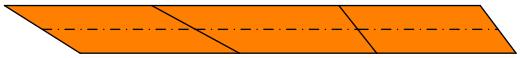

Three-span continuous, 8 girders,
Difficulty installing cross-frames during erection

(EICSS 3) Ramp C over EB I-80, IA
(80, 144, 80 / 26 / -15, -15, -15, -15) [Iowa DOT]

Three-span continuous, 5 girders,
Integral abutments

(EICSS 4) L40 over IA 60, Osceola Co., IA
(145, 148 / 33.2 / 41.0, 41.0, 41.0) [HDR]

Two-span continuous, 4 girders

(EICSS 5) W.BD. RTE. 350 Over I-435 state road from RTE. 40 to RTE. 350 about 2 miles NW of Raytown, Jackson Co., MO
(120, 170, 170, 120 / 40.7 / 56.0, 56.0, 56.0, 56.0, 56.0) [HDR]

Four-span continuous, 5 girders

(EICSS 6) E.BD. RTE. 350 over S.BD I-435 state road from RTE. 40 to RTE. 350 about 2 miles NW of Raytown, Jackson Co., MO
(190, 250, 190, 120 / 40.7 / 56.0, 56.0, 56.0, 56.0) [HDR]

Three-span continuous, 5 girders

(EICSS 7) Bridge over the Castor River, State Road from U.S. 67 to Route 51 about 8 miles S.E. of Frederick Town, Madison Co., MO
(143, 185, 143, 143 / 38.7 / -55.0, -55.0, -55.0, -55.0, -55.0) [HDR]

Four-span continuous, 5 girders

(EICSS 8) Milepost 63.83 Route 300 Bridge over NYS Thruway, NY
(120, 120 / 40.8 / 58.5, 58.5) [NYSDOT]

Two-span continuous, 8 girders,
Field data available (NYSDOT),
Very shallow plate girders (27 in deep).

(EICSS 9) Bridge No. Sum-27 I-1186 R, I-27 I NB & Ramp A Over SR 8, Summit Co., OH
(73, 120, 84, 52 / 91.8 to 95.1 / -48.5, -48.5, -48.5, -48.5, -48.5) [ODOT]

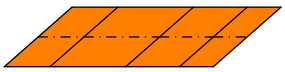

Four-span continuous, 11 girders, Semi-integral abutments

(EICSS 10) SR 0031 over Penn Turnpike, Somerset Co., PA
(161, 161 / 42.3 / -69.5, -69.5, -69.5) [HDR]

Two-span continuous, 5 girders

(EICSS 11) US 82 Mainlane Underpass at 9th Street, Lubbock Co., TX
(182, 172 / 70 / -53.7, -53.7, -53.7) [TxDOT]

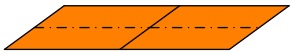

Two-span continuous, 9 girders,
Lean on cross-frame system,
Studied by Zhou (2006),
Field data is not published yet

(EICSS 12) US 82 Mainlane Underpass at 19th Street WB, Lubbock Co., TX
(150, 139 / 47 / -59.6, -59.6, -59.6) [TxDOT]

Two-span continuous, 6 girders,
Lean on cross-frame system

(EICSS 13) SR 90 Broadway Avenue Interchange, WA
(155, 177 / 87.7 / -56.8, -56.8, -56.8) [WSDOT]

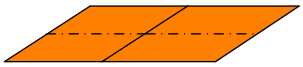

Two-span continuous, 9 girders,
Made use of partial slip of cross-frame bolts during erection

(EICSS 14) Bridge over BNSF Railroad Gillette-Moorcroft East BNSF RR Separation, Campbell Co., WY
(111, 163, 111 / 40.3 / 45, 45, 45, 45) [WYDOT]

Three-span continuous, 5 girders

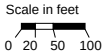

Figure 4.2. Existing I-girder bridges, Continuous-span, Straight with Skewed supports, (EICSS #) Description (LENGTH1, LENGTH2, ... / WIDTH / θ_{Left}, ..., θ_{Right}) [Source].

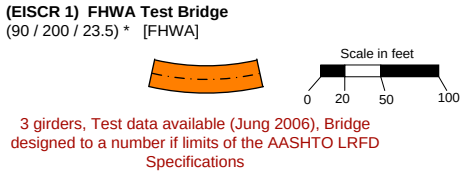

Figure 4.3. Existing I-girder bridges, Simple-span, Curved with Radial supports, (EISCR #) Description (LENGTH / RADIUS / WIDTH) [Source].

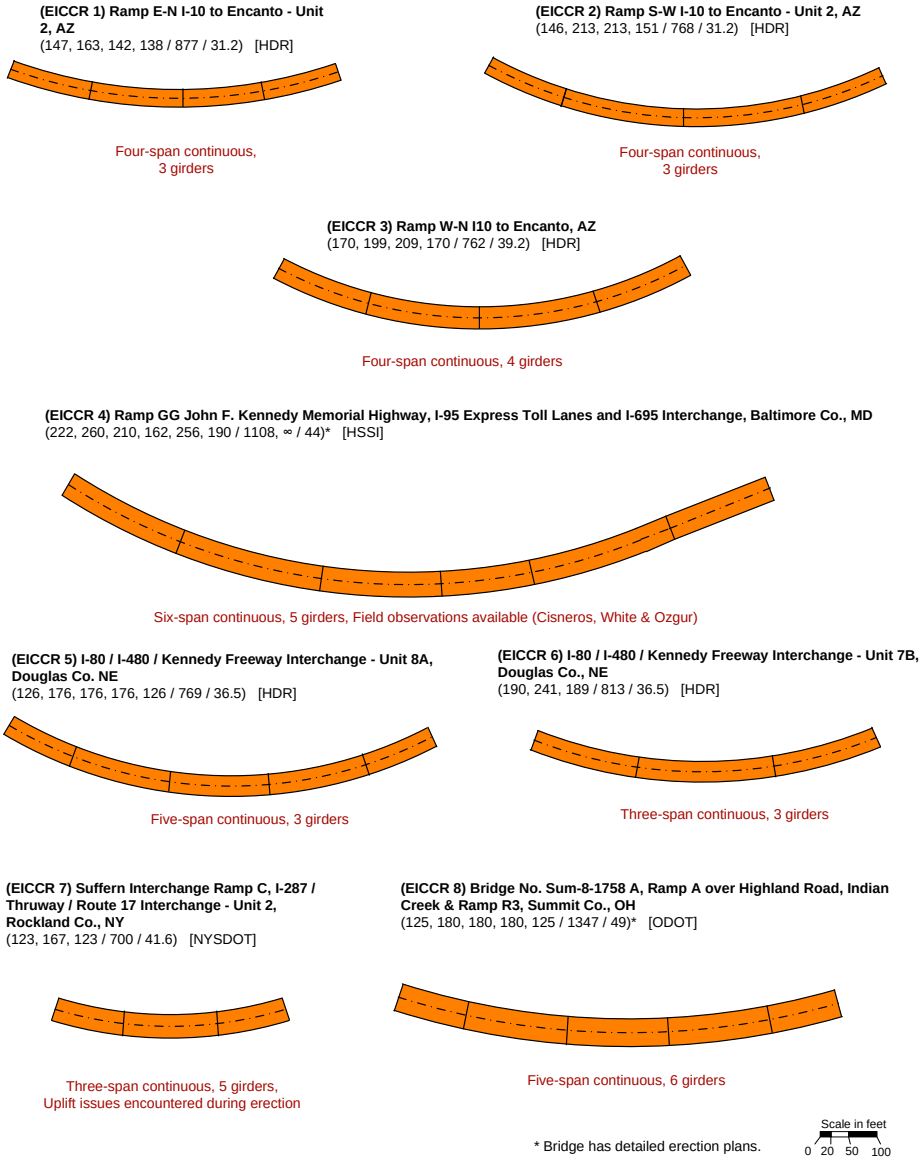

Figure 4.4. Existing I-girder bridges, Continuous-span, Curved with Radial supports, (EICCR #) Description (LENGTH1, LENGTH2, ... / RADIUS1, RADIUS2, .../ WIDTH) [Source].

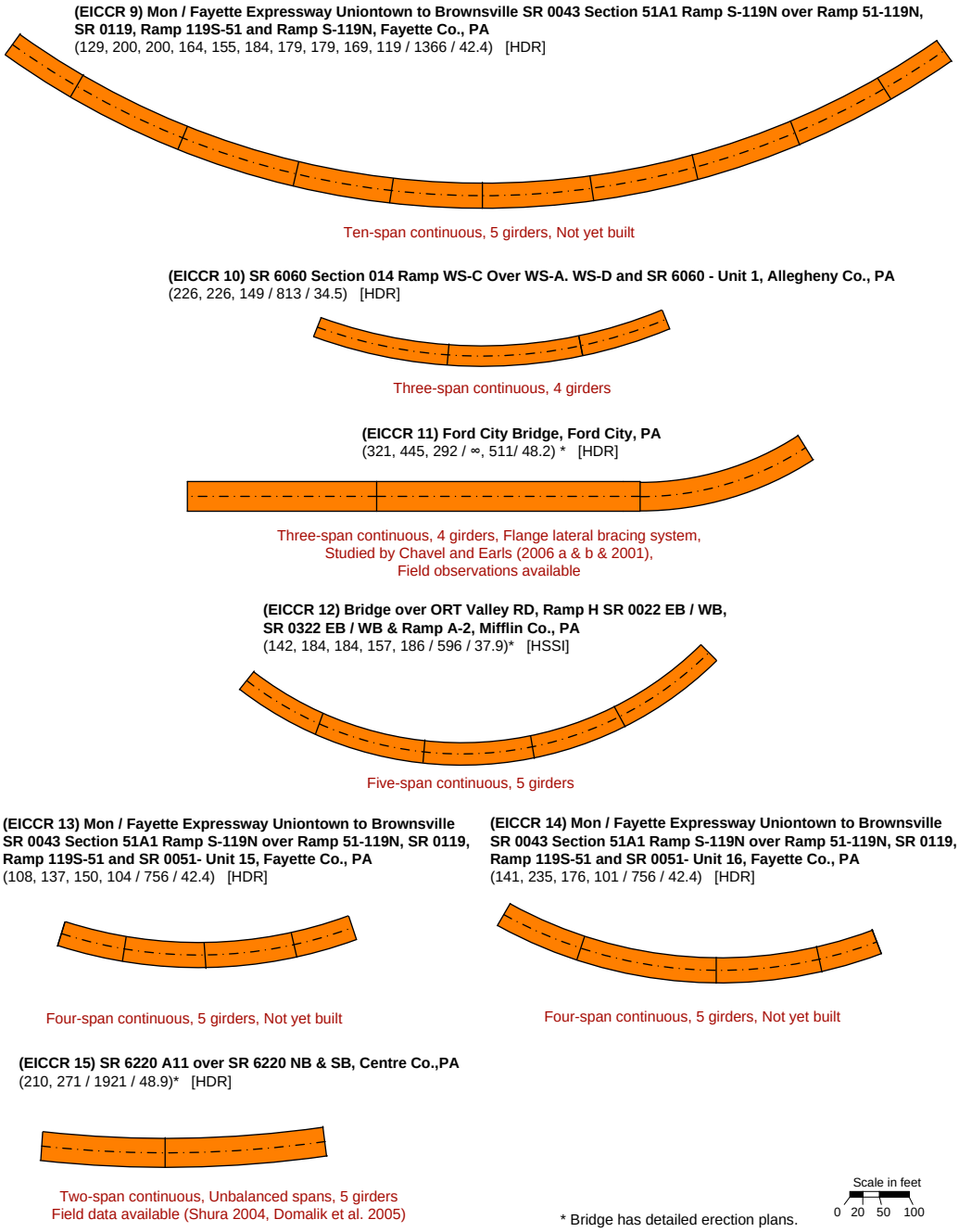

Figure 4.4. (continued). Existing I-girder bridges, Continuous-span, Curved with Radial supports, (EICCR #) Description (LENGTH1, LENGTH2, ... / RADIUS1, RADIUS2, .../ WIDTH) [Source].

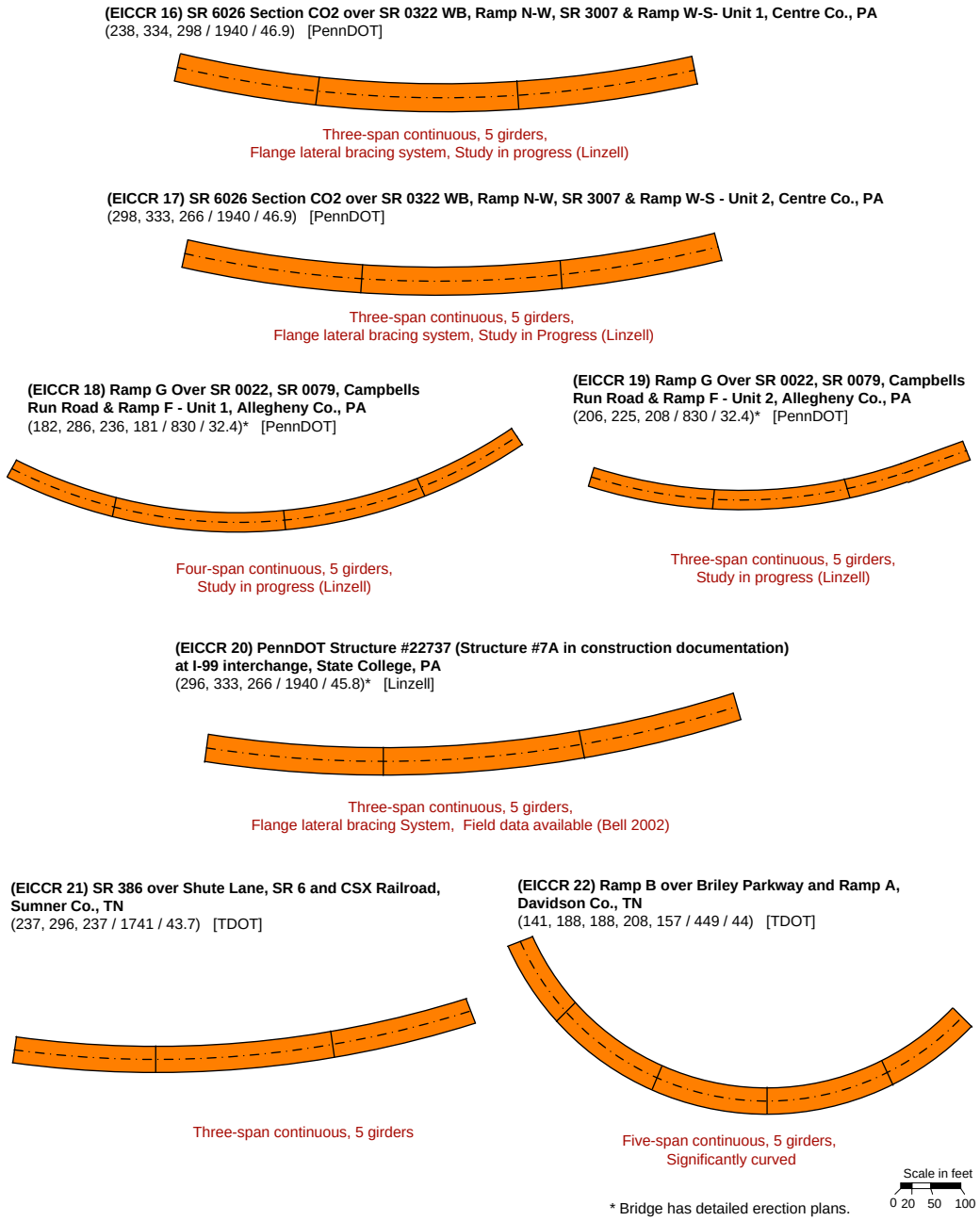

Figure 4.4. (continued). Existing I-girder bridges, Continuous-span, Curved with Radial supports, (EICCR #) Description (LENGTH1, LENGTH2, ... / RADIUS1, RADIUS2, .../ WIDTH) [Source].

Figure 4.4. (continued). Existing I-girder bridges, Continuous-span, Curved with Radial supports, (EICCR #) Description (LENGTH1, LENGTH2, ... / RADIUS1, RADIUS2, .../ WIDTH) [Source].

(EISCS 1) Relocated Route 44 Connector "B" over existing Cherry Street, Kingston & Plymouth, Plymouth Co., MA
(106 / 441 / 29.2 / 51.5, 37.7)* [HSSI]

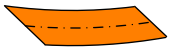

4 girders

(EISCS 2) Bridge over US 401 SBL on US 1 NBL Between Raleigh & Wake Forest, Wake Co., NC
(201 / 2888 / 58.2 / 64.3, 58.9) [NCDOT]

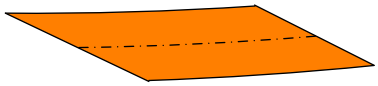

8 girders

(EISCS 3) SR 8002 Ramp A-1, King of Prussia, PA
(151 / 279 / 35.6 / 50.8, 0) * [HDR]

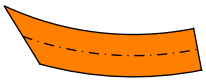

6 girders, Studied by Chavel and Earls (2003) & Chavel (2008), Field observations available

(EISCS 4) Long Shoals Road Overpass, Buncombe Co., NC
(252/2269/27.3/-18.4,-24.7), (251/2306/45.3/-18.1,-24.3), (250/2340/24/-17.8,-23.9) * [NCDOT]

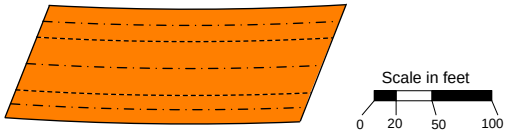

17 girders, Field observations available, Construction in 3 Phases

* Bridge has detailed erection plans.

Figure 4.5. Existing I-girder bridges, Simple-span, Curved with Skewed supports, (EISCS #) Description (LENGTH / RADIUS / WIDTH / θ_{Left}, θ_{Right}) [Source].

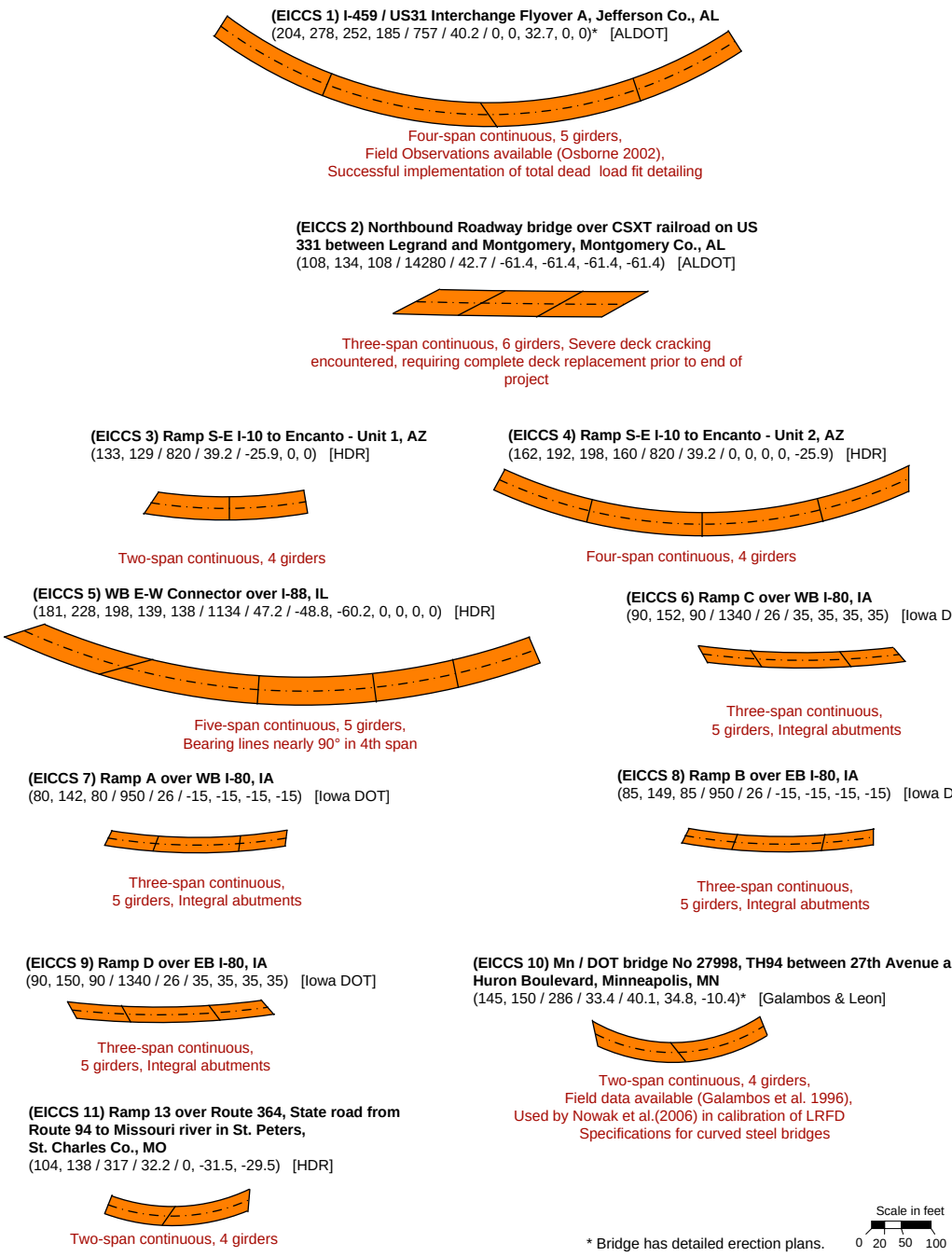

Figure 4.6. Existing I-girder bridges, Continuous-span, Curved with Skewed supports, (EICCS #) Description (LENGTH1, LENGTH2, ... / RADIUS / WIDTH / θ_{Left}, ..., θ_{Right}) [Source].

(EICCS 12) SNI-A-BAR Rd. Over I-435 state road from RTE. 40 to RTE. 350 about 3.6 miles NW of Raytown, Jackson Co., MO
(60, 102, 92, 50 / 881 / 50.2 / -2.4, -6.4, -13.0, -18.9, -22.3) [HDR]

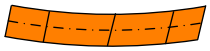

Four-span continuous, 5 girders

(EICCS 13) Bridge 5, West Dodge. 129th St. to I-680, Douglas Co., NE
(118, 128, 145 / 712, ∞, 699 / 32.7 / 0, 18.4, 18.8, 0) [HDR]

Three-span continuous, 4 girders

(EICCS 14) Abbott Drive Bridge, Abbott Drive over UPRR, Douglas Co., NE
(179, 168 / 1125, ∞ / 85.2 / -38, -42, -42) [HDR]

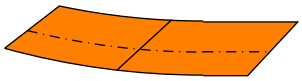

Two-span continuous, 8 girders,
Two different depths of cross-frames and girders

(EICCS 15) Suffern Interchange Ramp C, I-287 / Thruway / Route 17 Interchange - Unit 1, Rockland Co., NY
(148, 158 / 700 / 41.6 / 0, -49.5, -31.8) [NYSDOT]

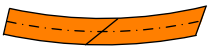

Two-span continuous, 5 girders,
Uplift issues encountered during erection

(EICCS 16) Bridge on Ramp BD over Greensboro Western Urban Loop, -RPCA-, and -CD- Between Bryan Blvd & US 220, Guilford Co., NC
(173, 171, 170 / 754 / 48.4 / 5.6, -2.6, 0, 0) [HDR]

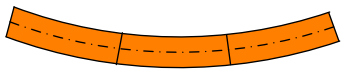

Three-span continuous, 5 girders

(EICCS 17) Bridge on Ramp BD over Bryan Blvd. and -RPD- between US 220 and Bryan Blvd, Guilford Co., NC
(117, 159 / 1574 / 48.4 / 0, 1.1, 0) [HDR]

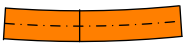

Two-span continuous, 5 girders

(EICCS 18) Bridge on Ramp CA over Bryan Blvd, and Ramp D between I-40 and Bryan Blvd, Guilford Co., NC
(107, 100, 110 / 754 / 48.4 / 0, -0.5, 0, 0) [HDR]

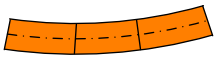

Three-span continuous, 5 girders

(EICCS 19) Bridge on Ramp CA over, Greensboro Western Urban loop, -RPD-, and -CD- BTN I-40 and Bryan Blvd, Guilford Co., NC
(100, 94, 82, 86 / 754 / 48.4 / 0, 0, 8.8, 2.6, 0) [HDR]

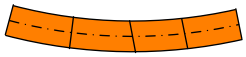

Four-span continuous, 5 girders

(EICCS 20) Bridge No. Sum-8-1757 B, Ramp B over Highland Road, Indian Creek & Ramp R3 & I-271, Summit Co., OH
(115, 170, 151, 182, 146 / 1347 / 49 / 0, 0, -20.7, 0, 0, 0)* [ODOT]

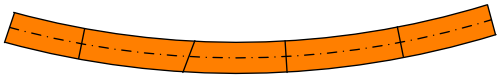

Five-span continuous, 6 girders

(EICCS 21) Grande Ronde River Bridge, Westbound Grande Ronde River Bridge Sec. Old Oregon Trail Hwy., Union Co., OR
(253, 177 / 951 / 50.9 / -31.1, -19.4, -27) [ODOT]

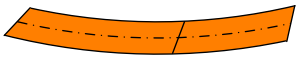

Two-span continuous,5 girders,
Stage 1, independent bridge structure in a phased construction

(EICCS 22) Grande Ronde River Bridge, Eastbound Grande Ronde River (Upper Perry) Bridge Sec. Old Oregon Trail Hwy., Union Co., OR
(240, 177 / 951 / 42.9 / -6.7, -20.4, -28.7) [ODOT]

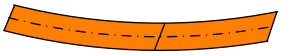

Two-span continuous, 4 girders

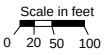

* Bridge has detailed erection plans.

Figure 4.6. (continued). Existing I-girder bridges, Continuous-span, Curved with Skewed supports, (EICCS #) Description (LENGTH1, LENGTH2, ... / RADIUS / WIDTH / θ_{Left}, ..., θ_{Right}) [Source].

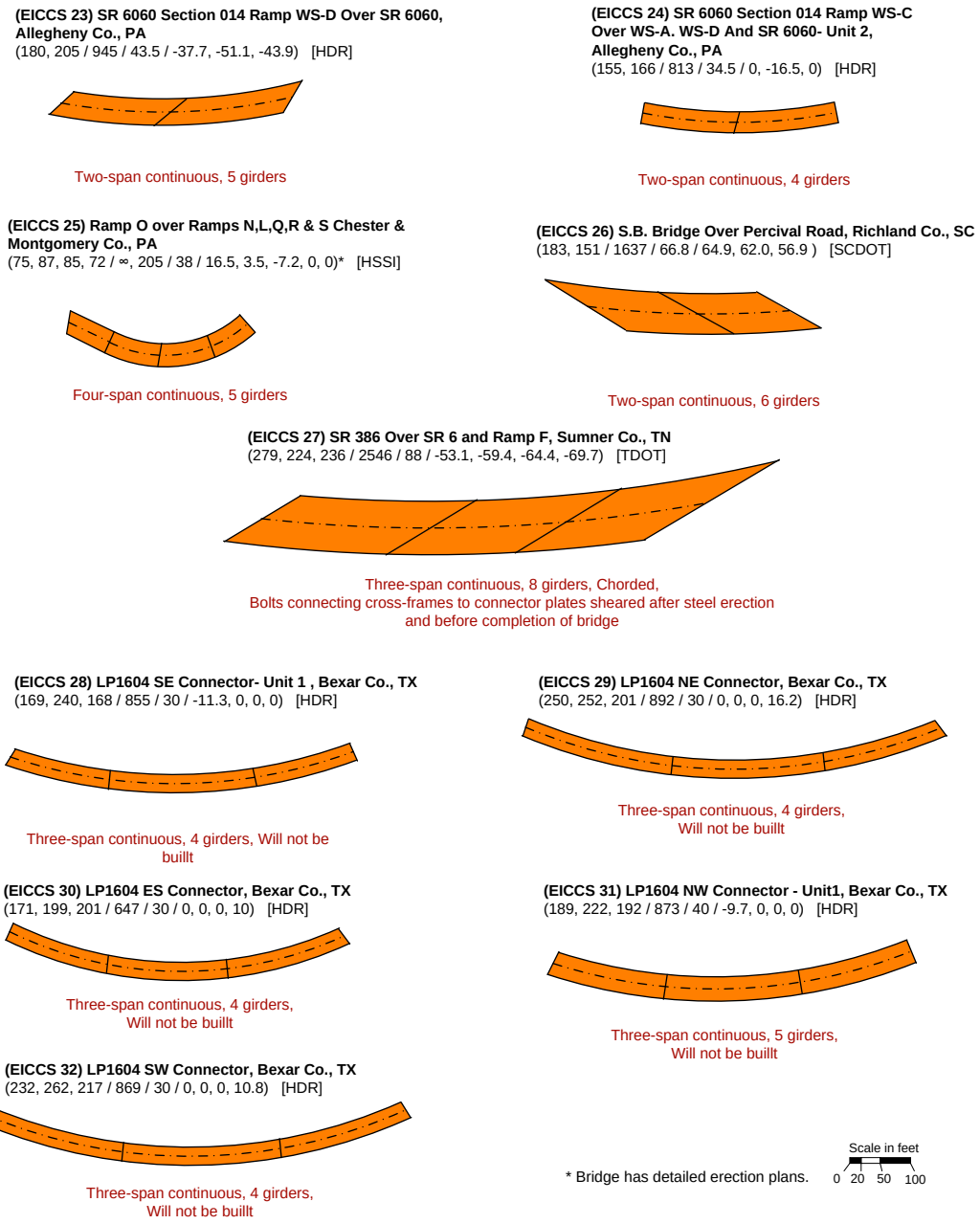

Figure 4.6. (continued). Existing I-girder bridges, Continuous-span, Curved with Skewed supports, (EICCS #) Description (LENGTH1, LENGTH2, ... / RADIUS / WIDTH / θ_{Left}, ..., θ_{Right}) [Source].

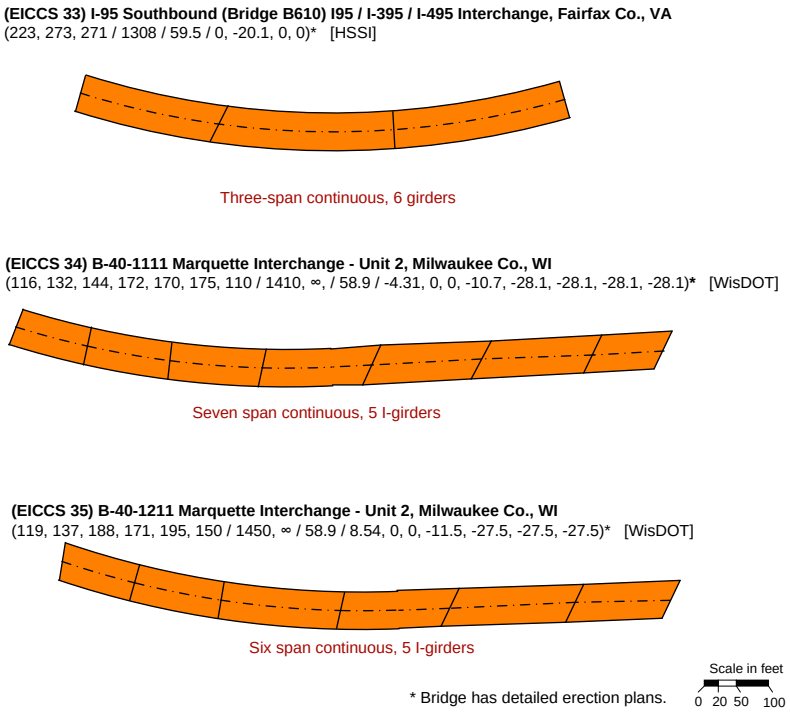

Figure 4.6. (continued). Existing I-girder bridges, Continuous-span, Curved with Skewed supports, (EICCS #) Description (LENGTH1, LENGTH2, ... / RADIUS / WIDTH / θ_{Left}, ..., θ_{Right}) [Source].

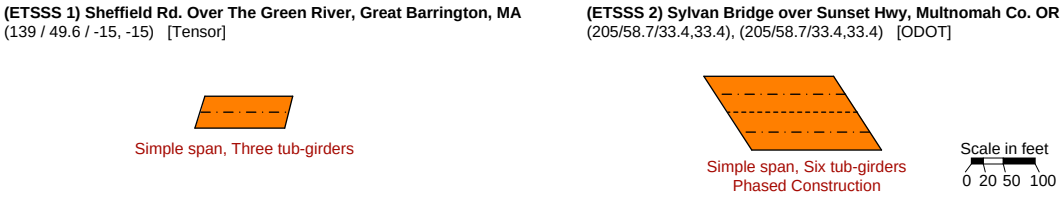

Figure 4.7. Existing Tub-girder bridges, Simple-span, Straight with Skewed supports, (ETSSS #) Description (LENGTH / WIDTH / θ_{Left}, θ_{Right}) [Source].

(ETCSS 1) Rte. 853 / Division St. Over Naugatuck River, Ansonia, CT
(260, 190 / 67.8 / -22.9, -22.9, -22.9) [Tensor]

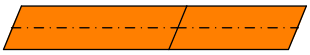

Two span continuous, Four tub-girders
Dramatically different span lengths

(ETCSS 2) US-75 Underpass at Churchill Way, Dallas TX
(139, 133, 100 / 83.0 / -34.1, -34.1, -34.1, -34.1) [HDR]

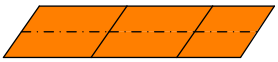

Three span continuous, Five tub-girders

(ETCSS 3) Bridge #564, Woodway Dr Overpass, Harris Co, TX
(140, 169, 121 / 69.2 / 30.2, 30.2, 30.2, 30.2) [Tensor]

Three span continuous, Four tub-girders

(ETCSS 4) Bridge #574, North Post Oak Rd Underpass, Harris Co, TX
(60.4, 124, 144, 138, 83.6 / 73.0 / -38, -38, -38, -38, -38, -38) [Tensor]

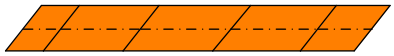

Five span continuous, Six tub-girders

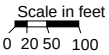

Figure 4.8. Existing Tub-girder bridges, Continuous-span, Straight with Skewed supports, (ETCSS #) Description (LENGTH1, LENGTH2, … / WIDTH / θ_{Left}, …, θ_{Right}) [Source].

(ETSCR 1) NB Cross Island Pkwy to EB I495, Queens Co, NY
(101 / 484 / 25)* [HSSI]

Simple span, Two tub-girders

(ETSCR 2) Ramp M over I-71 NB, Hamilton Co, OH
(207 / 458, ∞ / 40) [ODOT]

Simple span, Two tub-girders

Figure 4.9. Existing Tub-girder bridges, Simple-span, Curved with Radial supports, (ETSCR #) Description (LENGTH / RADIUS / WIDTH) [Source].

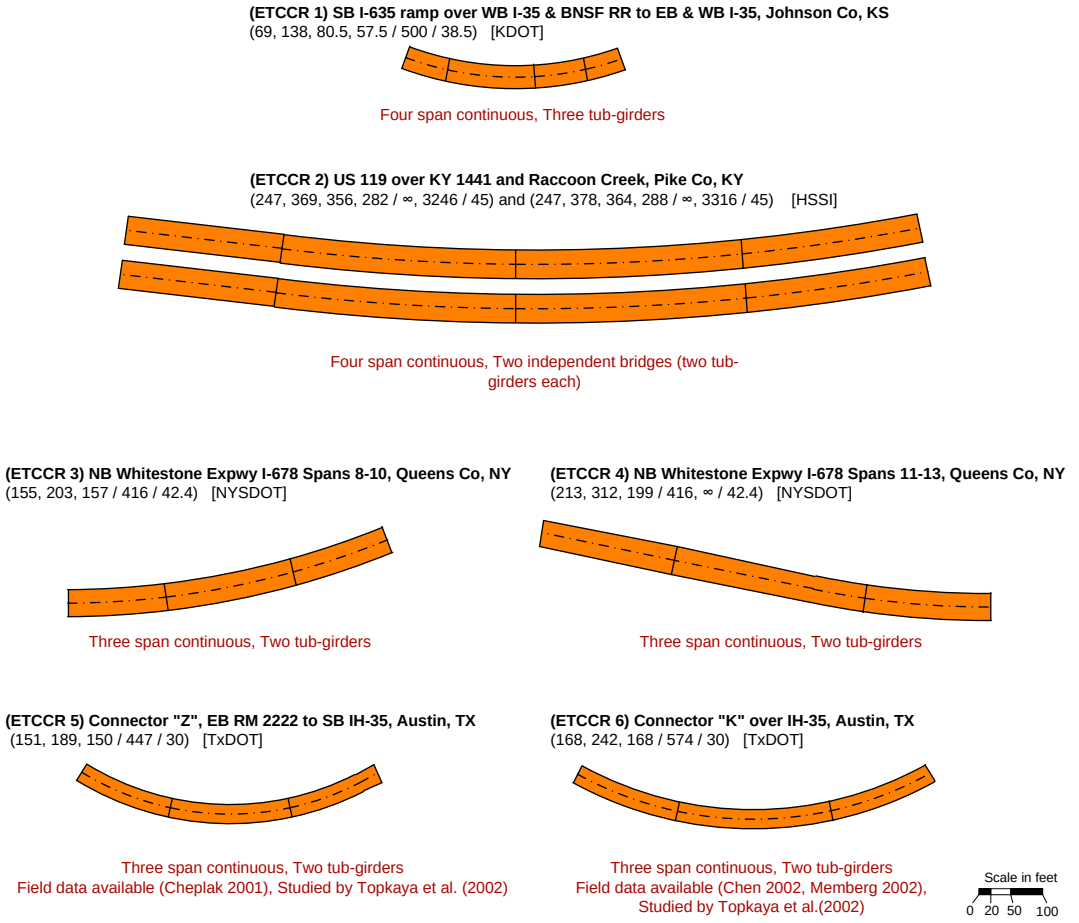

Figure 4.10. Existing Tub-girder bridges, Continuous-span, Curved with Radial supports, (ETCCR #) Description (LENGTH1, LENGTH2, … / RADIUS1, RADIUS2, … / WIDTH) [Source].

(ETCCR 7) DC02 Spans 1&2 IH-30 PGBT Interchange, Dallas, TX
(164, 164 / 895 / 29) [HDR]

Two span continuous, Two tub-girders

(ETCCR 8) DC03 Spans 13&14 IH-30 PGBT Interchange, Dallas, TX
(155, 155 / 1010 / 29) [HDR]

Two span continuous, Two tub-girders

(ETCCR 9) DC03 Spans 15&16 IH-30 PGBT Interchange, Dallas, TX
(170, 170 / 1010 / 29) [HDR]

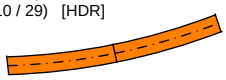

Two span continuous, Two tub-girders

(ETCCR 10) DC03 Spans 1, 2&3 IH-30 PGBT Interchange, Dallas, TX
(149, 189, 149 / 1010 / 29) [HDR]

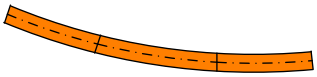

Three span continuous, Two tub-girders

(ETCCR 11) DC03 Spans 4&5 IH-30 PGBT Interchange, Dallas, TX
(167, 191 / 1010 / 29) [HDR]

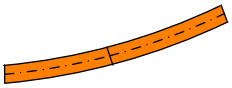

Two span continuous, Two tub-girders

(ETCCR 12) DC04 Spans 22&23 IH-30 PGBT Interchange, Dallas, TX
(165, 165 / 2060 / 29) [HDR]

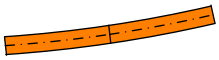

Two span continuous, Two tub-girders

(ETCCR 13) DC04 Spans 24, 25&26 IH-30 PGBT Interchange, Dallas, TX
(204, 254, 204 / 2060 / 29) [HDR]

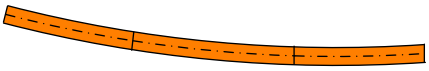

Three span continuous, Two tub-girders

(ETCCR 14) Connector EB North Beltway 8 to NB I-45, Houston, TX
(186, 286, 180 / 895 / 40.8) [TxDOT]

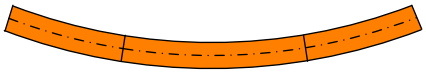

Three span continuous, Two tub-girders
Field data available (Fan 1999)

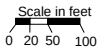

Figure 4.10. (continued). Existing Tub-girder bridges, Continuous-span, Curved with Radial supports, (ETCCR #) Description (LENGTH1, LENGTH2, … / RADIUS1, RADIUS2, … / WIDTH) [Source].

Figure 4.10. (continued). Existing Tub-girder bridges, Continuous-span, Curved with Radial supports, (ETCCR #) Description (LENGTH1, LENGTH2, … / RADIUS1, RADIUS2, … / WIDTH) [Source].

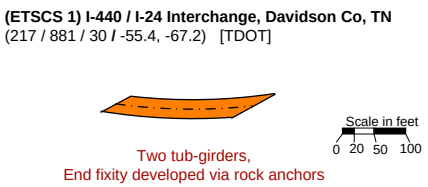

Figure 4.11. Existing Tub-girder bridges, Single-span, Curved with Skewed supports, (ETSCS #) Description (LENGTH / RADIUS / WIDTH / θ_{Left}, θ_{Right}) [Source].

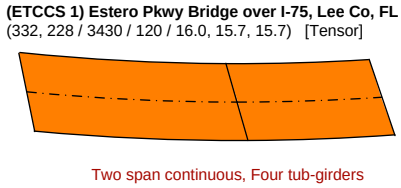

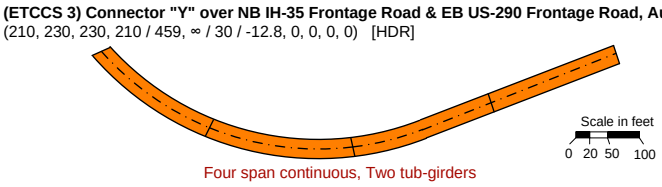

Figure 4.12. Existing Tub-girder bridges, Continuous-span, Curved with Skewed supports, (ETCCS #) Description (LENGTH1, LENGTH2, … / RADIUS1, RADIUS2, … / WIDTH / θ_{Left}, …, θ_{Right}) [Source].

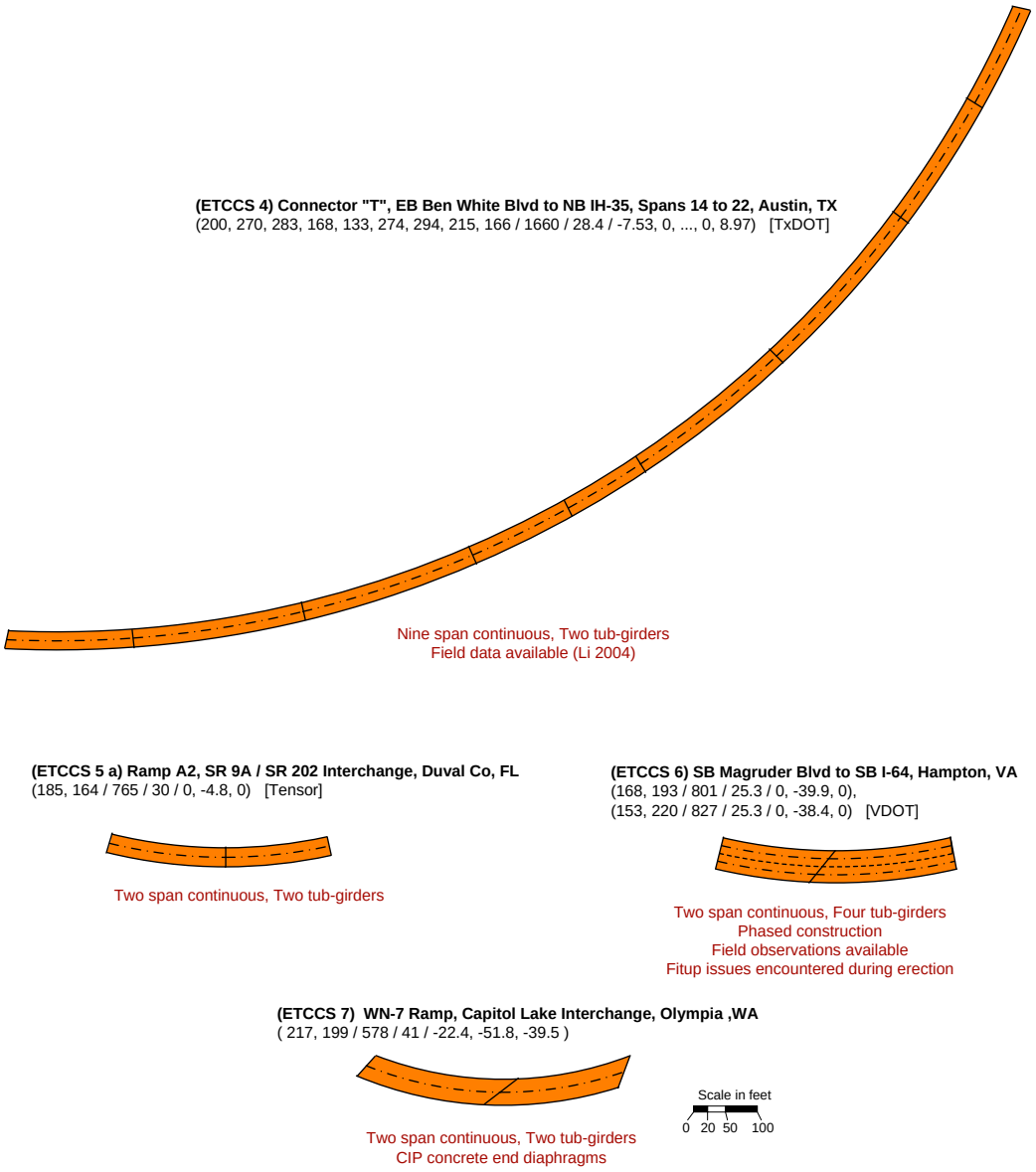

Figure 4.12. (continued). Existing Tub-girder bridges, Continuous-span, Curved with Skewed supports, (ETCCS #) Description (LENGTH1, LENGTH2, … / RADIUS1, RADIUS2, … / WIDTH / θ_{Left}, …, θ_{Right}) [Source].

Only twelve of the I-girder bridges in the above figures had both (1) measurements or field observations of some type during construction as well as (2) detailed construction plans. Four tub-girder bridges had measurements or field observations of some type during construction and six tub-girder bridges had detailed construction plans. Furthermore, the extent of the field measurements was generally limited. Detailed field measurements and observations were taken for the bridge EICCR22a by the NCHRP 12-79 project team during the course of the NCHRP 12-79 research (Leon, 2011). A number of the bridges were indicated as being very successful projects, with the bridge responding as predicted with respect to aspects such as initial layover of the webs but with the girders approaching a plumb condition under total dead load. A number of cases were cited as having a range of field problems including difficulty of fit-up, or unexpected final geometries.

In addition to the above existing bridges, a number of useful detailed LRFD example bridge designs have been published in the recent literature. Figure 4.13 summarizes the plan geometries of several of these hypothetical bridges. The straight, non-skewed bridges in these examples were selected as base-line problems for the project calculations. That is, they were selected to gage the accuracy of the analysis methods for bridges without any curvature or skew. The results for these cases serve as useful base-line benchmarks for decisions about the levels of accuracy sufficient for bridges with more complex geometries.

The selection of the existing and example bridges for inclusion in the Project overall parametric study is addressed subsequently in the discussion of the main analytical studies.

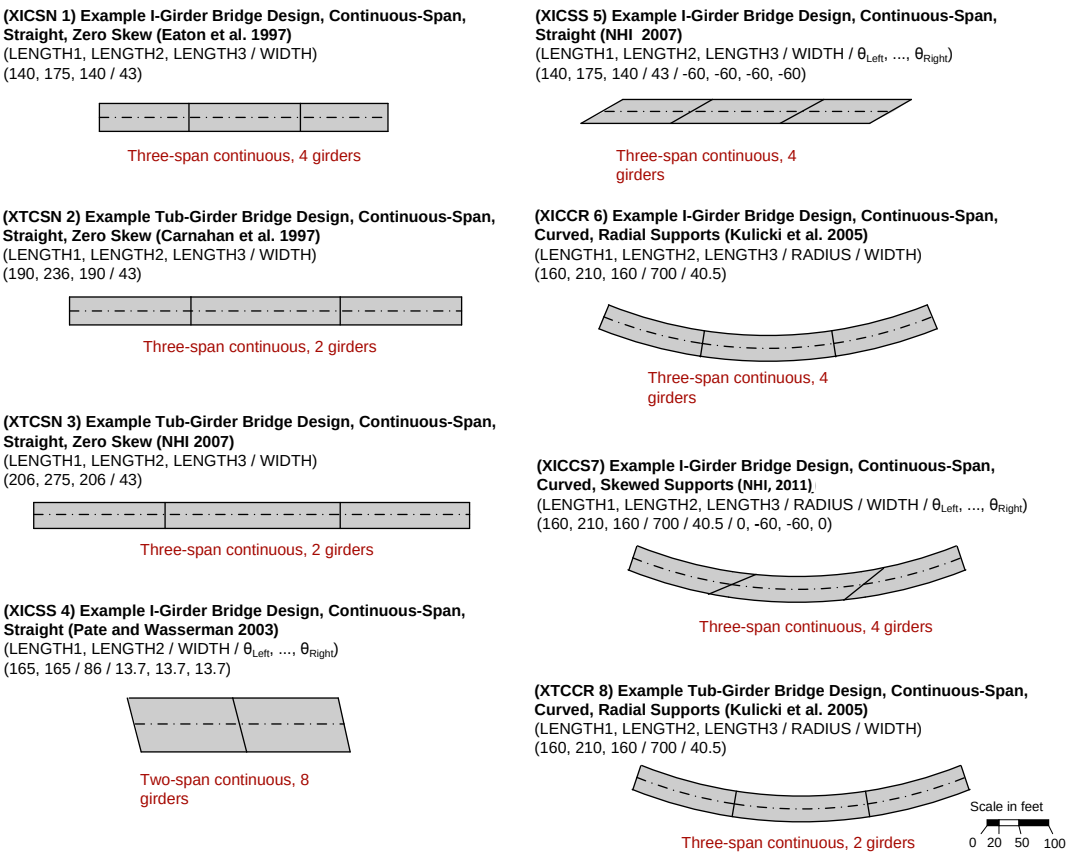

Figure 4.13. AASHTO LRFD example bridge designs.

4.3 Selection of Geometric Factors

4.3.1 Identification of Primary Geometric Factors

It was clear that if NCHRP 12-79 was to consider analysis accuracy for curved and/or skewed steel I- and tub-girder bridges, then the project would need to consider the following factors in the design of its parametric studies:

- Some measure of the horizontal curvature and
- Some quantification of the skew magnitude and pattern.

Furthermore, it was apparent that the bridge responses, and hence the analysis accuracy, can be affected significantly by the magnitude of the span lengths as well as the span length-to-width ratios. Longer span bridges tend to be affected more substantially by dead load effects, potentially resulting in more significant stability considerations during

construction. In addition, beyond a certain span length, I-girder bridges are more likely to need partial or full-span horizontal flange-level bracing systems to ensure adequate stability and sufficient resistance to lateral loads during construction. Flange lateral bracing systems cause portions of the structure to act as "pseudo-box girders," fundamentally changing the behavior of the structural system. Furthermore, longer bridges generally exhibit larger overall deflections. These larger overall deflections can lead to larger relative deflections at certain locations in the structural system, which can sometimes be problematic during construction. Longer span bridges often have a smaller ratio of the girder spacing relative to the girder depths, and typically have larger girder depth-to-flange-width ratios. These attributes can fundamentally affect various relative deflections in the structure as well as local and overall behavior and analysis accuracy at the different stages of construction.

In addition, the bridge span length-to-width ratios can significantly impact the influence of skew. Skewed bridges with smaller span length-to-width ratios tend to have more significant load transfer to the bearing lines across the width of the structure, and hence more significant "nuisance stiffness" effects that need to be addressed in the design. Furthermore, relatively narrow horizontally curved bridges experience a greater torsional "overturning component" of the reactions, which tends to increase the vertical reactions on the girders further from the center of curvature and decrease the vertical reactions on the girders closer to the center of curvature. In addition, relatively wide horizontally-curved bridges can have more substantial concerns related to overturning at intermediate stages of the steel erection, prior to assembly of the girders across the full width of the bridge cross-section. These spans become more stable as additional girders are erected and connected by cross-frames across the width of the bridge. Wide horizontally-curved bridges also can have greater concerns associated with overturning forces during deck placement.

Lastly, it was apparent that the bridge responses (and the analysis accuracy) can be significantly affected by whether the spans are simply-supported or continuous. Simple-span bridges tend to have larger deflections for a given geometry, and potentially can be more difficult to handle during construction. Although simple-span girders can see

negative bending during erection (due to lifting or temporary support from holding cranes, etc.), continuous-spans have more significant negative bending considerations. Furthermore, particularly in I-girder bridges, continuous-span bridges can have significant interactions between adjacent spans with respect to both major-axis bending as well as the overall torsional response.

All of the above factors can have a substantial influence on the many detailed structural attributes of steel I-girder and tub-girder bridges. Also, there can be significant interactions between these factors in terms of their influence on the bridge responses, as well as the accuracy of different bridge analysis methods.

If one considers the many detailed attributes of steel I- and tub-girder bridge structural systems and their members and components addressed subsequently, the combinations and permutations of potential bridge designs become endless. Hence, it was decided that the most practical way of covering the design space of curved and/or skewed I-girder and tub-girder bridges was to consider a range of practical combinations and permutations of the following primary factors:

- Span length of the bridge centerline, L_s,
- Deck width normal to the girders, w, (in phased construction projects, w is determined separately for each bridge unit)
- Horizontal curvature, of which the most appropriate characterization is discussed below,
- Skew angle of the bearing lines relative to the bridge centerline, θ,
- Skew pattern of the bearing lines, of which the most appropriate characterization is discussed below, and
- Span type, simple and various types of continuous-spans.

4.3.1.1 Characterization of Horizontal Curvature

The NCHRP 12-79 project team identified the torsion index, I_T, discussed in Section 3.1.4 as a useful measure of the degree of curvature of the bridge spans at an early stage of the project. This parameter is closely related to the magnitude of the overall torsion that exists in the bridge (or bridge unit).

For curved simple-span radially supported I-girder bridges, the NCHRP 12-79 project team selected horizontal curvature values by first conducting basic estimates to determine the largest curvature (smallest *R*) that could be tolerated without having uplift at the most critical bearing location(s) under nominal dead plus live loads. This value of *R* was used as the most extreme value for the horizontal curvature. This radius of curvature then was increased 1.5 times to obtain cases with smaller curvature (larger *R*). This approach produced lower- and upper-bound values of I_T equal to 0.58 and 0.71 respectively. Continuous-span bridges can tolerate higher torsion indices due to continuity with the adjacent spans. Therefore, for curved continuous-span radially supported I-girder bridges, lower and upper bound values of I_T were obtained as 0.66 and 0.88 respectively.

Similarly, for curved simple-span radially supported tub-girder bridges, the smallest radius of curvature was estimated to avoid uplift at the supports under nominal dead load plus live loads. Tub-girder bridges tend to have relatively high torsion indices compared to I-girder bridges with similar deck geometry due to the shorter length between the fascia girder bearings. The estimated minimum radius of curvature was then increased 1.5 times. This resulted in lower and upper bound values of I_T equal to 0.72 and 0.87 respectively. For continuous-span radially supported tub-girder bridges, the lower and upper bound values of I_T were obtained as 0.69 and 1.14 respectively.

4.3.1.2 Characterization of Skew Pattern

There are a number of factors related to the representation of the skew pattern for practical designs. Figure 4.14 shows a number of possible combinations of θ values and skew patterns on individual straight I-girder bridge spans with w = 80 ft. and L = 250 ft. In general, various combinations of these arrangements are practical for continuous-span bridges. The first four cases in the figure have parallel bearing lines, that is, equal skew of the end supports. The four values of skew shown are 20, 35, 50 and 70^o. The 20^o skew case is significant since the AASHTO LRFD Specifications permit the cross-frames to be oriented parallel to the bearing lines up to this limit. The 70^o skew case is the maximum skew angle considered in prior NCHRP studies on deck effective widths (Chen, 2005). In addition, as summarized subsequently, this is the maximum value of the skew

encountered in the existing I-girder bridges shown in the previous section. The 35° skew is considered as a practical median skew value between zero and 70°, and 50° was selected as an appropriate large skew angle between 35° and the relatively extreme value of 70°.

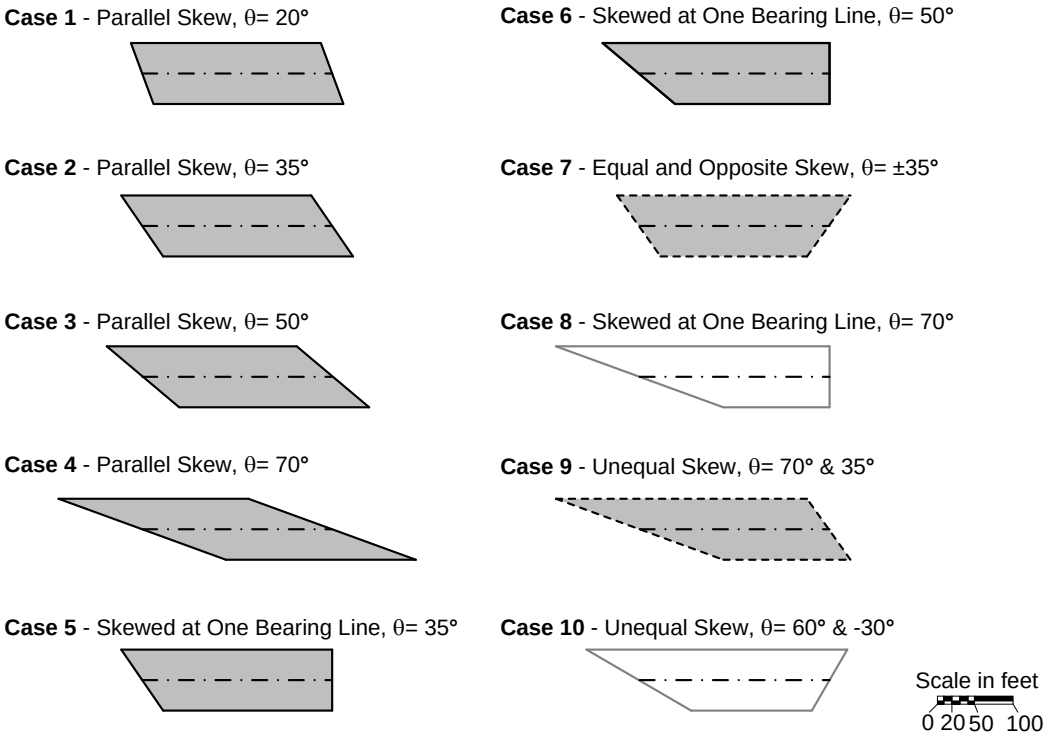

Figure 4.14. Potential skew combinations for straight I-girder bridge spans with w=80 ft. and L_s=250 ft.

The other sketches in Figure 4.14 show a number of representative unequal skew arrangements on individual straight spans in I-girder bridges. Cases 5 and 6 in the figure entail a situation where, due to a site geometry constraint existing at only one position, only one of the bearing lines is skewed. Case 7 shows a possible case where the bearing lines are skewed equally but in opposite directions. This case is considered to be more unusual, or exceptional. However, interestingly, the bearing line orientations for this case are exactly what one would encounter with a curved radially-supported span and L_s/R = 0.70. The outline of the deck is dashed in this case to highlight the fact that this geometry is considered exceptional. Case 8 is similar to Cases 5 and 6, but with a 70° skew. This case illustrates a situation where, due to the extreme skew of the left-hand bearing line, the span length on one side of the deck is more than two times that on the other side of

the deck, i.e., $L_2/L_1 > 2$. A value of $L_2/L_1 = 2$ was considered to be a practical maximum limit by the NCHRP 12-79 project team. It should be noted that if the span length of the centerline were larger, or if the deck width w were smaller for this case, this L_2/L_1 limit would not be exceeded. The outline of the deck geometry for Case 8 is shown as a grey line and the deck plan is shaded white to emphasize that this deck geometry is considered impractical. The above L_2/L_1 limit can be satisfied with $\theta = 70^o$ if the bearing lines are parallel as in Case 4, or if the bearing lines are unequally skewed such as in Case 9. Lastly, Case 10 shows an extreme situation of unequal skew in opposite directions for the two bearing lines. In this case, the bearing lines are oriented at 90^o relative to one another. The project team decided that one would practically never encounter a relative angle between adjacent bearing lines of more than 90^o. This type of bearing arrangement could occur for example if the span were crossing the corner of a rectangular lot and the bearing lines had to be placed parallel to the sides of the lot. Note that $L_2/L_1 > 2$ for Case 10; however, if the span is larger or the deck width is smaller, the $L_2/L_1 \leq 2$ limit could be satisfied.

The skew arrangements on straight tub-girder bridges can be similar to those considered in Figure 4.14. However, tub-girder bridges generally tend to have smaller skew values, due to the expected sensitivity of these types of bridges to skew effects as well as the fabrication difficulties and increased cost associated with complex skewed diaphragm connection details.

Figure 4.15 shows the various possible combinations of horizontal curvature and approximately $\pm$ 15 and 30^o skew on individual tub-girder bridge spans with $L_s = 150$ ft., $w = 30$ ft. and $R = 400$ ft. Again, various combinations of these arrangements are possible for continuous-span bridges. The skew and horizontal curvature combinations in Figure 4.15 are similar to those shown for the straight bridge spans in Figure 4.14. However, whereas a number of patterns with positive and negative skew produce the same net geometry in straight bridges, these positive and negative skew values give different geometries in similar curved bridges, due to the horizontal curvature. Fourteen total combinations are shown in Figure 4.15 that need to be considered in general. A large number of these combinations may be considered as exceptional cases and are drawn

with dashed lines. Note that for Cases 2, 5 and 9 in Figure 4.15, the magnitudes of the skew angles are modified slightly to make the bearing lines parallel.

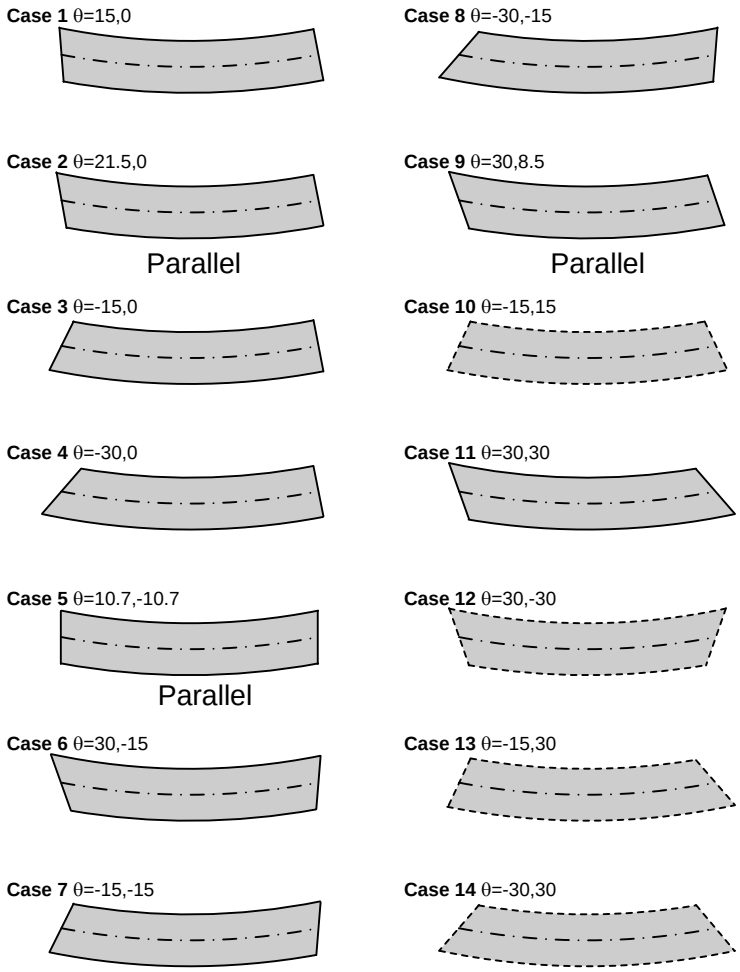

Figure 4.15. Example potential skew and horizontal curvature combinations for curved tub-girder bridge spans with w = 30 ft., L_s = 150 ft. and R = 400 ft.

The possible combinations of skew and horizontal curvature for I-girder bridges are similar to those shown in Figure 4.15, except that as noted previously, somewhat larger skew values can be accommodated generally in I-girder bridges. However, the extent of these patterns is limited by:

- A maximum limit on the ratio of the span lengths of the outside and inside edges of the deck, L_{so}/L_{si}, of 2, and
- A maximum limit on the orientation of adjacent bearing lines of 90^o

similar to the limits discussed previously for the straight skewed bridges. Lastly, for highly-curved spans, the Project team recognized that the skew angle at the inside edge of the deck can be substantially larger than that at the deck centerline. This is illustrated by Figure 4.16. It was decided that it is not practical for the skew angle at the inside edge of the deck to be greater than 70^o in these cases.

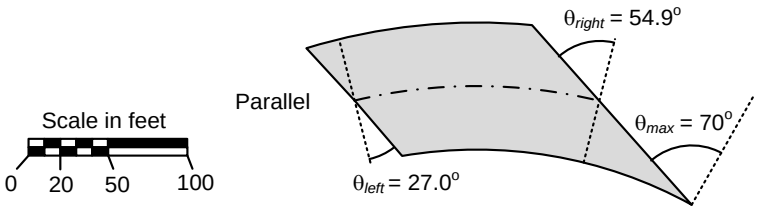

Figure 4.16. Highly-curved span with a skew angle of 70° at the inside edge of the deck and 54.9^o at the centerline of the deck, w = 80 ft., L_s = 150 ft., R = 308 ft.

All of the above factors can have a substantial influence on the many detailed structural attributes of steel I-girder and tub-girder bridges. Also, there can be significant interactions between these factors in terms of their influence on the bridge responses, as well as the accuracy of different bridge analysis methods.

4.3.2 Synthesis of Primary Factor Ranges from the Collected Bridges

Upon synthesis of the primary factors from the existing bridges collected by NCHRP 12-79, the following ranges of these factors were observed:

- Span length, L_s
  - I-Girder
    - 120 to 254 ft. (straight simple-spans with skewed supports)
    - 90 ft. (curved simple-spans with radial supports)
    - Only one bridge was identified as curved simple-span with radial supports; this was the FHWA Test bridge, EISCR1.
    - 106 to 252 ft. (curved simple-spans with skewed supports)
    - 119 to 445 ft. (straight continuous-spans with zero skew)
    - 73 to 257 ft. (straight continuous-spans with skewed supports)
    - 101 to 334 ft. (curved continuous-spans with radial supports)
    - 50 to 279 ft. (curved continuous-spans with skewed supports)

- Tub-Girder
  - 139 to 205 ft. (straight simple-spans with skewed supports)
  - 101 to 207 ft. (curved simple-spans with radial supports)
  - 217 ft. (curved simple-spans with skewed supports)
  - Only one bridge was identified as curved simple-span with skewed supports; this was the bridge ETSCS1.
  - 57.5 to 373 ft. (curved continuous-spans with radial supports)
  - 153 to 332 ft. (curved continuous-spans with skewed supports)

- Deck width (per unit in cases involving phased construction), *w*
  - I-Girder
    - 24 to 87.5 ft. (spans with skew)
    - 30 to 71 ft. (spans with radial supports, with the exception of the EISCR1 FHWA test bridge, which was 23.5 ft.)
  - Tub-Girder
    - 25 to 45 ft. (spans with two tub-girders)
    - 36 ft. to 120 ft. (spans with more than two tub-girders)

- Torsion Index, I_T
  - I-Girder
    - 0.48 to 0.87
  - Tub-Girder
    - 0.50 to 1.14 (spans with two tub-girders; an I_T larger than 1.0 is possible due to continuity with adjacent spans)
    - 0.50 to 0.84 (spans with more than two tub-girders)

- Skew angle of the bearing lines relative to a tangent to the bridge centerline, θ
  - I-Girder
    - 0 to 69.5^o (straight bridges)
    - 0 to 64.3^o (curved bridges)
  - Tub-Girder
    - 0 to 12.8^o (spans with two tub-girders, excluding the ETCCS7 bridge, which had CIP concrete end diaphragms and non-typical bearing details)
    - 0 to 38.9^o (spans with more than two tub-girders)

- Skew pattern
  - I-Girder
    - The bearing lines were parallel in most of the collected I-girder bridges.
    - One straight bridge (EICSS2) has $\theta = 61.8^o$ & 38^o in one span.
    - One curved bridge (EICCS15) has $\theta = 0^o$ & 49.5^o resulting in a 19.8^o differ-ence in orientation between the bearing lines in one span.
    - One curved bridge (EICCS5) has $\theta = 0^o$ & 60.2^o resulting in a 72^o difference in orientation between the bearing lines in one span.

- Tub-Girder

  All the skewed spans have non-parallel bearing lines for the collected bridges that are composed of two tub-girders.

  One curved bridge with two tub-girders (ETCCS3) has $\theta = 0^o$ & 12.8^o and a 39.0^o difference in orientation between the bearing lines.

  One curved bridge with two tub-girders (ETCCS7) has $\theta = 51.8^o$ & 39.5^o and a 32.0^o difference in orientation between the bearing lines; however, this bridge has cast-in-place (CIP) concrete end diaphragms and non-typical bearing details.

  Most of the skewed spans with more than two tub-girders have parallel bearing lines.

  One two-span continuous curved bridge with four tub-girders (ETCCS6), constructed in two phases with two girders in each phase, has $\theta = 0^o$ & 38.9^o and a difference in orientation of 53.8^o between the bearing lines in one span. However, no cross-frames or diaphragms are placed between the girders at the interior bearing line on this bridge, and this bridge does not contain any internal intermediate cross-frames or diaphragms.

- Type-of-span
  - I-Girder

    Most of the collected I-girder bridges are continuous-span.

    Ratio of exterior-to-interior span lengths: 0.56 to 1.25

    Ratio of adjacent interior span lengths: 0.63 to 1.0

    Ratio of span lengths, 2-span continuous: 0.77 to 1.0
  - Tub-Girder

    Most of the collected tub-girder bridges are continuous-span.

    Ratio of exterior-to-interior span lengths: 0.49 to 1.0

    Ratio of adjacent interior span lengths: 0.49 to 1.0

    Ratio of span lengths, 2-span continuous: 0.69 to 1.0

    A fraction of the bridges with more than two tub-girders are simple-span.

The values for several additional "secondary" parameters discussed in the above, but not selected as primary factors were:

- Span length to deck width ratio, L_s/w (per unit in phased construction jobs)
  - I-Girder

    0.55 to 14.77 (spans with skew)

    1.67 to 8.83 (curved spans with radial supports)
  - Tub-Girder

    2.80 to 8.76 (radially-supported spans with two tub-girders)

    4.66 to 10.35 (skewed spans with two tub-girders)

    0.83 to 3.83 (skewed spans with more than two tub-girders)

- Subtended angle of the span's centerline, L_s/R
  - I-Girder

    0.0 to 0.57 radians (32.6^o)
  - Tub-Girder

0.0 to 0.68 radians (39.0^o) (spans with two tub-girders)
0.07 to 0.28 radians (16.0^o) (spans with more than two tub-girders)

In addition to the above parameters, several additional key indices that correlate with the accuracy of different simplified analysis methods were identified during the course of the NCHRP 12-79 research. These indices are discussed in Chapter 3. The ranges of values among the collected bridges for these indices are as follows.

- Skew index, I_S
  - I-Girder
    0.05 to 1.93
  - Tub-Girder
    0.08 to 0.77 (spans with two tub-girders)
    0.01 to 0.18 (spans with more than two tub-girders)
- Connectivity index, I_C
  - I-Girder
    0.35 to 18.75
  - Tub-Girder
    The connectivity index is not applicable to tub-girder bridges
- Girder length index, I_L
  - I-Girder
    1.0 to 1.51
  - Tub-Girder
    1.0 to 1.09

4.3.3 Selection of Primary Factor Ranges and Levels

Table 4.1 shows the ranges and levels of the primary factors that were selected for the main analytical study of NCHRP 12-79. These primary factors are discussed in detail in the preceding sections.

The first row of Table 4.1 addresses the type of span. This factor is addressed in a similar fashion for both the I- and tub-girder bridges. Three-span continuous designs with one balanced end span and one end span of equal length to the main span capture both the behavior associated with drop-in spans as well as the interactions between balanced and unbalanced continuous-spans. However, two-span continuous bridges are apt to be more sensitive to skew effects. Also, the potential combinations of skew arrangements become large as the number of spans is increased. Many of these combinations would have a minor effect on the final analysis accuracy assessments though, due to the fact that the

influence of the skew at a particular bearing line tends to die out as one moves several spans away from this bearing line. Furthermore, long multi-span curved bridges often may have only a few skewed bearing lines because of geometry constraints at a particular location, whereas it may be possible to orient other bearing lines radially. This can be understood by considering cases such as EICCS1 and EICCS5 in Figure 4.6. In these structures, one would quickly reach the maximum practical θ value of approximately 70^o if, for instance, all the bearing lines were parallel.

It was desired to study several continuous-span bridges that had significant unbalanced span lengths. This consideration was addressed by inserting selected existing bridges into the matrix of parametric study bridges. Also, bridges with more than three spans were considered by insertion of a number of existing bridges into the overall parametric study matrix.

The second row of Table 4.1 shows the values selected for the span length. For both I- and tub-girder bridges, the selected lengths for simple-spans were 150, 225 and 300 ft. and the selected lengths for continuous-spans were 150, 250 and 350 ft. The maximum span length of L_s = 350 ft. was selected to match the maximum value targeted by the AASHTO (2010) Specifications. All but one span of one of the existing I-girder bridges had span lengths smaller than 350 ft., although three of the existing I-girder bridge units had spans larger than 300 ft. The span larger than 350 ft. is one of the straight spans of the Ford City bridge (EICCR 11). In current (2012) practice, horizontal flange lateral bracing systems often are considered for span lengths of 250 ft. or more, but spans of 250 ft. may be acceptable without flange level lateral bracing systems in certain cases. A span length of L_s = 150 ft. is a rough lower-bound value at which welded girders are generally required.

Table 4.1. Primary factor ranges and levels for the NCHRP 12-79 main analytical study.

Factor	I-girder bridges	Tub-girder bridges
Type of span	Simple, 2-span continuous, and 3-span continuous with one balanced end span and one end span equal in length to the main center span. Use the above 3-span continuous bridges as base ICCR & TCCR cases. Consider both 2- and 3-span continuous bridges for the ICSS and TCSS. Consider only 2-span continuous cases for the ICCS and TCCS designs. Consider at least one 2-span continuous bridge with a significant unbalance between the span lengths.	
Maximum span length of bridge centerline, L_s	150, 225 & 300 ft. for simple-spans 150, 250 & 350 ft. for continuous-spans (measured along the curve)	
Deck width, *w*	30 ft. (1 to 2 traffic lanes + shoulders & barriers) 80 ft. (4 to 5 traffic lanes + shoulders & barriers	30 ft. (1 to 2 traffic lanes + shoulders & barriers)
Torsion Index, I_T	0.58 to 0.71 for ISCR bridges 0.66 to 0.88 for ICCR bridges	0.72 to 0.87 for TSCR bridges 0.69 to 1.14 for TCCR bridges
Skew angle relative to the bridge centerline, θ	20^o, 35^o, 50^o & 70^0 but with θ at the inside edge of the deck $\leq 70^o$ in curved spans	15^o & 30^o, plus additional sensitivity studies with variations up to ±15° from zero skew
Skew pattern	Consider the $\pm$ combinations of skew angles shown in Figure 4.14 (for straight bridges) and Figure 4.15 (for curved bridges), but using θ = 35 & 70^o for I-girder bridges and θ = 15 & 30^o for tub-girder bridges. Limit the ratio of the span lengths along the edges of the deck, L_2/L_1, to a maximum value of 2.0 in all cases. Limit the difference in orientation of adjacent bearing lines to a maximum of 90^o in all cases. Give preference to typical (i.e., non-exceptional) bridge geometries.	

Of the existing tub-girder bridges, only the two interior spans of the parallel US 119 bridges over KY 1441 and Raccoon Creek in Pike Co., KY (bridge ETCCR 2) have span lengths greater than 350 ft., although there are two other tub-girder bridges with spans larger than 300 ft.

The third row of Table 4.1 shows the selected deck widths for the parametric study bridges. For the I-girder bridge parametric designs, deck widths of 30 ft. and 80 ft. were selected by the project team. Only 30 ft. deck widths were considered in the new parametric designs for the tub-girder bridges. This smaller 30 ft. width is representative of one- to two-lane bridges, whereas the larger 80 ft. width is representative of structures with four to five lanes. A large number of the existing tub-girder bridges are one to two lane ramp type structures. Therefore, it was recommended that the Project should focus predominantly on these types of structures in its studies of tub-girder bridge system behavior and analysis accuracy. The less common tub-girder bridges having more than two girders were addressed by including one of these existing bridge cases in the overall parametric study matrix. However, this bridge involved phased construction, with each of the phases having two tub girders.

The combinations of L_s from 150 to 350 ft. with w from 30 to 80 ft. give span length to the bridge width, L_s/w, ranging from 150/80 = 1.88 to 350/30 = 11.7. The maximum value for this range is slightly larger than the maximum L_s/w of 7.90 and 8.29 for the existing I- and tub-girder bridges. It was believed that these larger values should be studied to fully address the bridge responses and analysis accuracies for these practical but more extreme geometry conditions.

The fourth row of Table 4.1 gives the selected ranges and levels for the torsion index I_T. The implications of I_T ranging from 0.5 to 1.0 have been discussed in Section 3.1.4. This parameter was used in establishing the horizontal radius of curvature R for the ISCR/TSCR and ICCR/TCCR designs, given the span length L_s and the deck width w. The horizontal radius of curvature obtained for the ISCR/TSCR designs was then employed for other new curved ISCS/TSCS parametric bridge designs. Similarly, the horizontal radius of curvature obtained for the ICCR/TCCR designs was employed for the other new curved ICCS/TCCS parametric bridge designs. A maximum limit on L_s/R

of 1.0 was imposed on the parametric designs. This limit can govern for shorter spans with wide decks and is somewhat larger than the maximum L_s/R of 0.57 and 0.68 radians for the collected existing I- and twin tub-girder bridges. Nevertheless, it was believed that $L_s/R = 1.0$ is a practical extreme that should be addressed in the parametric study design. Wide bridges with these larger L_s/R values may require special handling during the steel erection and/or deck placement.

The fifth row of Table 4.1 shows the selected ranges and levels of the skew angle θ. As noted previously, AASHTO (2010) allows the cross-frames to be framed parallel to the bearing lines in I-girder bridges with $\theta \leq 20^o$. Furthermore, it was expected that the effects of skew may be sufficiently small such that a line girder analysis may work quite adequately for certain cases at this skew level. A value of 70^o is a reasonable maximum limit for θ in I-girder bridges. This value was the maximum considered in studies of deck effective widths by Chen (2005), and represents roughly the largest skew angle encountered in the existing bridges. Smaller skew angles of 15 and 30^o were targeted for the tub-girder parametric study designs. In addition, a range of skew angles of $\pm 15^o$ from zero skew were considered in separate 3D FEA studies (with no separate consideration of the simplified analysis methods) to understand the influence of skew on the tub-girder bridge responses in greater detail.

Lastly, the sixth row of Table 4.1 explains the recommended variations of the skew pattern considered. These variations are understood most easily by viewing the actual deck plan geometries for various hypothetical new bridge designs. The reader is referred to Section 4.3.4 for these illustrations.

4.3.4 Selection of the Analytical Study Bridges

The following sub-sections summarize the key characteristics of the I- and tub-girder bridges selected for the NCHRP 12-79 analytical studies, given the ranges and levels of the primary factors identified in Section 4.3.3. To arrive at the analytical study design, the research team first developed a full factorial design matrix involving all the above factors and levels. This led to more than 500 I-girder bridges and more than 250 tub-girder bridges that would need to be studied. Fortunately, a number of these

combinations and permutations could be considered impractical or unbuildable. However, even after the impractical and unbuildable cases were eliminated, the total number of bridges arrived at in the study design was relatively large. Therefore, some prioritization of the bridges was necessary within the full range of practical designs. As noted by Montgomery (2004), "If the experimenter can reasonably assume that certain high-order interactions are negligible, information on the main effects and low-order interactions may be obtained by running only a fraction of the complete factorial experiment. These fractional factorial designs are among the most widely used types of designs for product and process design and for process improvement." In the context of the Project 12-79 analytical study design, this involved the elimination of individual bridges or groups of bridges where the interaction between the primary factor effects was expected to be relatively small. Furthermore, a number of bridges in which the combination of factors led to:

- Exceptional (i.e., particularly unusual) structures, or
- Designs that were very similar in one or more characteristics to other designs

were eliminated.

Once these selections were completed, the library of existing bridges summarized in Figures 4.1 through 4.12 was searched for bridges that:

- Matched closely with the analytical study design selections, and
- Satisfied the criteria described in Section 4.1.

In a few cases, modifications were made to the analytical study design to include existing bridges that were particularly good candidates based on the criteria specified in Section 4.1. In addition, several of the Example bridges from Figure 4.13 that matched closely with the analytical study design selections were selected for inclusion in the analytical study. The remaining bridges in the study design were targeted as "New" bridges, indicating that they were to be fully designed by the project team using the AASHTO LRFD Specifications and current common standards of care.

The initial design of the suite of bridges arrived at, based on the above process, involved approximately 100 bridges. The bridges were then subdivided into smaller suites for execution of the analytical studies. Various milestones were identified at which the study bridge selections were reevaluated based on what was learned from the completed studies. The resulting final study targeted 58 I-girder bridges and 18 tub-girder bridges in total.

The following sections first discuss several base straight, non-skewed study bridges considered at the beginning of the Project, followed by straight skewed simple and continuous-span cases, then simple and continuous-span curved bridges with radial supports, and finally curved and skewed simple- and continuous-span bridges. Each of these sections includes summary sketches of the bridge deck plans and bearing-line geometries corresponding to the designs along with a title block for each of the bridges containing:

1) An identification label, composed of the letter "X" for the "eXample" bridge designs, followed by the symbols explained at the beginning of Section 4.2, indicating the bridge category (e.g., ISSS, ICSS, etc.), and ending with the bridge number for that category. Two additional categories, ICSN and TCSN, are introduced in Figure 4.17. The "CSN" designation stands for Continuous-span, Straight, with Non-skewed supports. For example, the first eXample bridge in Figure 4.17 is labeled "XICSN 1."
2) An identification label, composed of the letter "E" for the "Existing" bridges, followed by the above symbols indicating the bridge category, and ending with the bridge number for that category, e.g., bridge "EISSS 3" in Figure 4.18.
3) An identification label, composed of the letter "N" for the "New" bridge designs, followed by the above symbols indicating the bridge category, and ending with the bridge number for that category, e.g., bridge "NISSS 1" in Figure 4.18.
4) A summary of the basic geometry information about the bridge, enclosed in parentheses. For instance, in Figure 4.18, the basic geometry information includes:

- The span length of the bridge centerline,
- The out-to-out width of the bridge deck perpendicular to the bridge centerline (provided for each unit in phased construction jobs), and
- The skew angle with respect to centerline of the bridge for both bearing lines.

This information is conveyed symbolically in the figure caption as "(LENGTH/WIDTH/θ_1, θ_2)." The other categories have similar but different basic geometry information. This information is summarized symbolically in each of the figure captions. The skew angle of the bearing lines is represented by the symbol θ. This angle is taken as zero when a bearing line is perpendicular to the centerline of the structure, that is, when the bearing line does not have any skew.

All of the figures referenced in the following sub-sections adopt the following conventions:

- Typical or common geometries are sketched using a solid black outline,
- Geometries considered unusual or exceptional are sketched using a black dashed outline,
- A few bridge geometries that are considered impractical or unbuildable are sketched using a solid light-grey outline. (The only cases shown that are impractical or unbuildable are a few bridges with high skew and relatively small length-to-width ratios, where if the bridge span was longer or the deck was narrower, the geometry would indeed be possible.)
- The deck plans for the selected eXample bridges are shaded and cross-hatched,
- The deck plans for the selected Existing bridges are shaded with a textured background,
- The deck plans for the selected New bridges are shaded with a solid background,
- The deck plans of bridges that were not selected for study are white or unshaded,
- The bridge unit centerlines are indicated by a "dot-dash" line, and
- The different phases in phased construction bridges (i.e., bridges constructed as a number of separate longitudinal units) are delineated by dashed lines.

4.3.4.1 Straight Non-skewed Base-Line Comparison Cases (XITSN 1 and XTCSN 3)

The straight non-skewed "base-line" bridges are illustrated in Figure 4.17. The analysis accuracy results for these cases serve as useful indicators or benchmarks for decisions about the levels of accuracy sufficient for bridges with more complex geometries. Both of these bridges are carefully documented example designs.

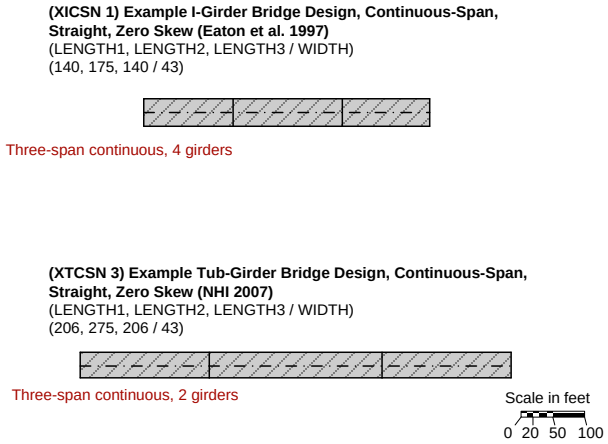

Figure 4.17. eXample Straight Non-skewed bridges used as base comparison cases, (LENGTH1, LENGTH2, LENGTH3 / WIDTH).

4.3.4.2 Simple-Span Bridges, Straight, with Skewed Supports (ISSS and TSSS)

Figure 4.18 shows the 60 total combinations and permutations for the ISSS bridges obtained considering:

- The ten combinations of skew magnitude and pattern for the straight bridges illustrated previously in Figure 4.14, {(θ_{Left}, θ_{Right}) = (20^o,20^o), (35^o,35^o), (50^o,50^o), (70^o,70^o), (35^o,0^o), (50^o,0^o), (35^o,-35^o), (70^o,0^o), (70^o,35^o), (60^o,-30^o)},
- The three values for the length L_s (L_s = 150, 225 and 300 ft.), and
- The two values for the deck width w (w = 30 and 80 ft.)

Figure 4.18. Existing and New I-Girder bridges, Simple-span, Straight with Skewed Supports, EISSS or NISSS (LENGTH / WIDTH / θ_{Left}, θ_{Right}).

In Figure 4.18, one can observe that the selected ISSS bridges emphasize smaller L_s/w and larger θ. The influence of the skew is expected to be significant for the bridges in the 3rd and 4th rows. The selected unequal skew cases in the 6th row parallels the selections in the 3rd row, except for NISSS33 and NISSS36. Bridge NISSS37, in the 7th row, is an interesting case in that the orientation of its bearing lines is the same as in the curved design NISCR10 (shown subsequently). The inclusion of this bridge allows for a comparison of the effects of bearing orientation alone in NISSS37 versus the effects of horizontal curvature in NISCR10. In addition, several parallel skew cases are considered in Figure 4.18, with an emphasis on the bridges with larger L_s/w and moderate skew angle (e.g. NISSS2), as well as a wider bridge with a 20 degrees of skew (NISSS11).

EISSS3 is one of two adjacent simple-span highly-skewed grade separation structures on SR 10003 (Chicken Road) over US 74 in Robeson County, NC. This bridge was closely monitored during construction, and field data relating to undesirable girder layover and bowing of the girder webs has been collected by Morera (2010). The availability of the field data and the successful construction, but with some concerns about the state of the girders, made this bridge a worthwhile candidate for study. Figure 4.19 shows several photos of this bridge.

Figure 4.19. EISSS3, Bridge on SR 1003 (Chicken Road) over US74 between SR 1155 and SR 1161, Robeson Co., NC (Morera, 2010).

EISSS5 is selected due to its large skew angle and short span length. Moreover, EISSS6 is selected since this bridge is constructed with TDLF detailing and provides extensive information about the erection practices to eliminate the fit-up problems. This bridge was provided by High Steel Structures, Inc. Figure 4.20 shows a photo of EISSS6 during steel erection.

Figure 4.20. EISSS6, Bridge on Westchester Co., NY (courtesy of R. Cisneros, High Steel Structures, Inc.).

Figure 4.21 shows the 24 total combinations and permutations for the TSSS (tub-girder) bridges obtained considering:

- Eight combinations of skew magnitude and pattern for the straight bridges are: $\{(\theta_{Left}, \theta_{Right}) = (15°,15°), (30°,30°), (15,0°), (15°,15°), (30°,0°), (30°,15°), (30°,-15°), (30°,-30°)\}$,
- Three values for the length L_s (L_s = 150, 225 and 300 ft.), and
- One value for the deck width w (w = 30 ft.)

Three of the four tub-girder bridges selected in this category have the shortest span length of 150 ft. The selection of short-span cases is based on the fact that the torsional effects due to skew are likely to be larger for the shorter spans. The short-span bridges selected are NTSSS1 and NTSSS2 with parallel skewed supports of 15° and 30°,

and NTSSS4 with equal but opposite skew of 16°. NTSSS4 was modified to a skew angle of 16° in order to make the orientation of the supports similar to the curved and radially supported bridge NTSCR1 shown subsequently. NTSSS4 also highlights the equal and opposite skew case discussed in Section 4.3.1.2 and shown in Figure 4.15.

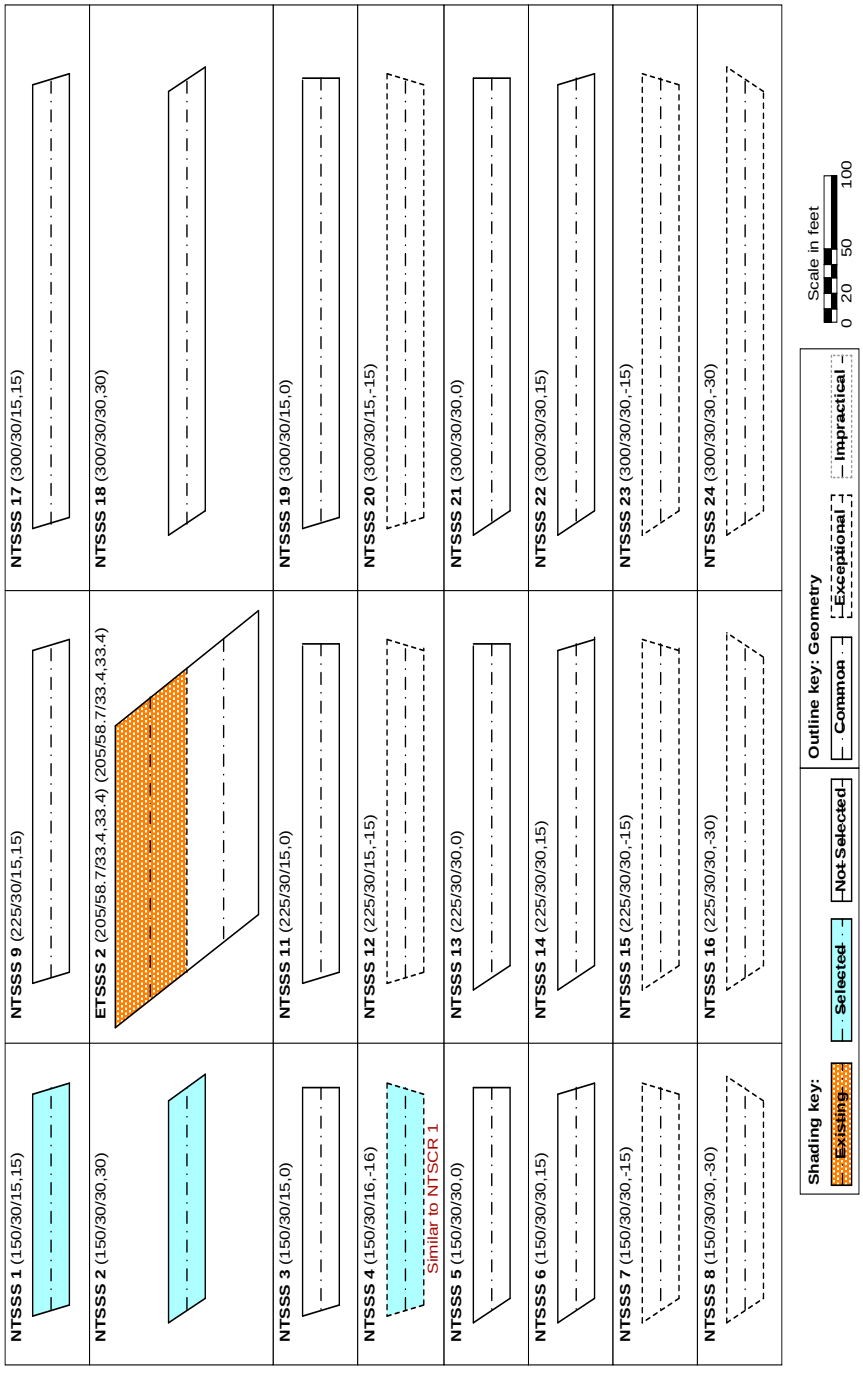

Figure 4.21. Existing and New Tub-girder bridges, Simple-span, Straight with Skewed supports, ETSSS or NTSSS (LENGTH / WIDTH / θ_{Left}, θ_{Right}).

In addition to the above bridges, the NTSSS10 bridge was selected to study the influence of an increase in the span length when the skew support angle is kept constant. The NTSSS10 bridge was replaced by the existing ETSSS2 (Sylvan Bridge). The Sylvan bridge (Figure 4.22) has a span length of 205 ft. and was constructed in two individual longitudinal phases with deck widths of 58.7 ft. and parallel skewed supports of 33.4°.

Figure 4.22. ETSSS 2, Sylvan Bridge over Sunset Highway, Multomah Co., OR (courtesy of Homoz Seradj, Oregon DOT).

4.3.4.3 Continuous-Span Bridges, Straight, with Skewed Supports (ICSS and TCSS)

Figure 4.23 shows four of the six groups of ICSS bridges. The six groups correspond to the combinations of three span lengths and the two deck widths. Two different widths 30 and 80 ft. were considered for L =150 ft. in Figure 4.23, but only 80 ft. wide bridges were considered for L = 250 and 350 ft. This is because the effect of skew was expected to be smaller for the narrower longer-span bridges. Furthermore, for the bridges with L = 250 and 350 ft. and w = 30 ft. are not shown since these combinations and permutations were found to be exceptional due to their large length-to-width ratios.

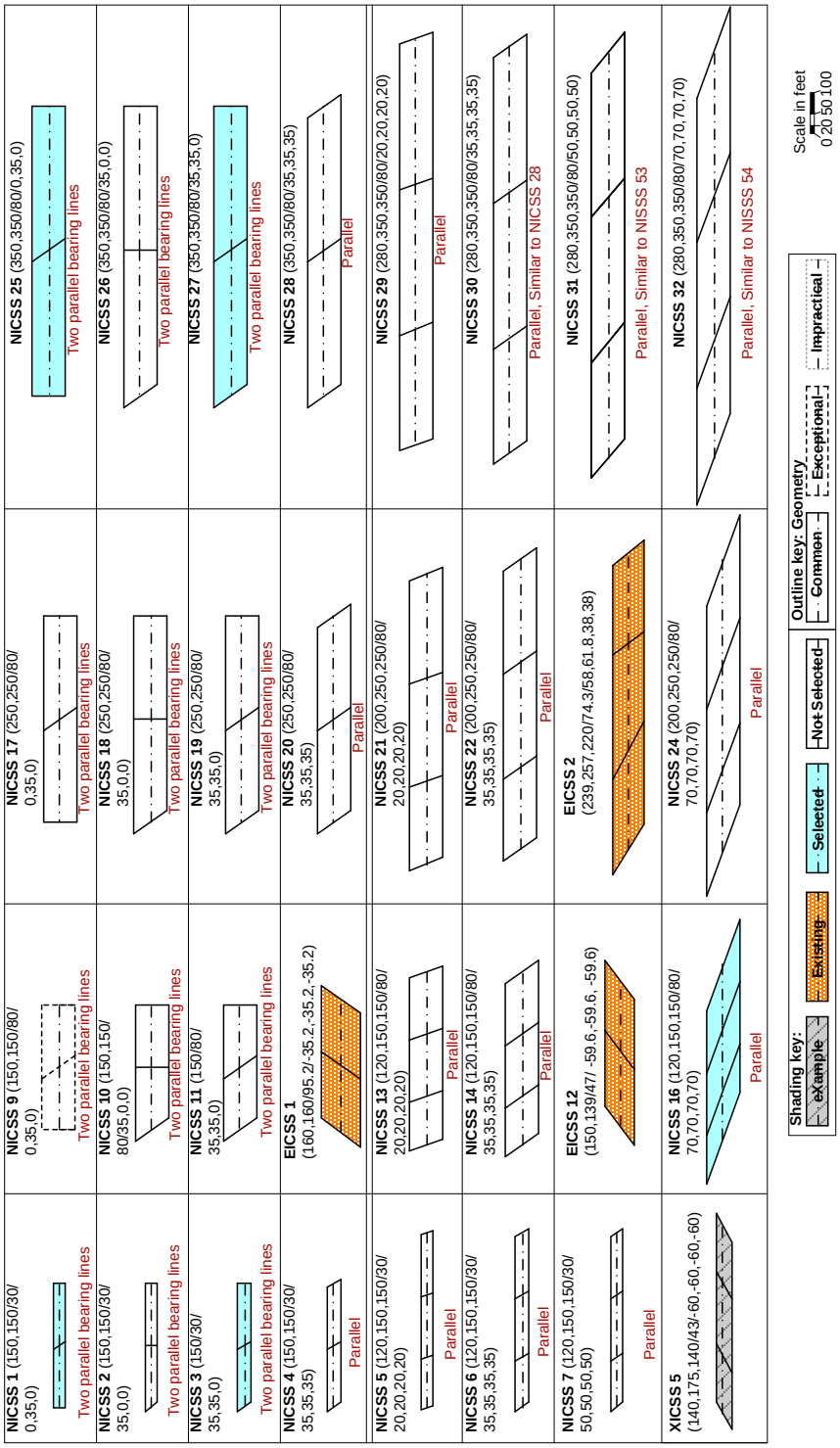

Figure 4.23. Existing, eXample and New I-girder bridges, Continuous-span, Straight with Skewed supports, EICSS, XICSS or NICSS (LENGTH1, LENGTH2, ... / WIDTH / θ_{Left}, …, θ_{Right}). The columns in the matrix for (L = 250 ft., w = 30 ft.) and (L = 350 ft., w = 30 ft.) are not shown.

In Figure 4.23, the top four rows of the matrix include four two-span continuous bridges with unequal skew and one case with parallel skew. Only values of $\theta = 35^o$ were considered for these selected cases.

The case with the parallel skew (EICSS1) is a steel overpass on Sunnyside Road Interchange, (I-15B) over I-15, in Bonneville County, ID. This bridge represents a successful implementation of total dead load fit detailing, which aims to ensure that the webs are plumb under the total steel plus concrete dead load. Both field observations and field data are available for this bridge. Figure 4.24 shows the gap at the sole plate at one of the bearings of this bridge under the steel dead load. Although daylight is apparent between the sole plate and the elastomeric bearing pad on one side under the steel dead load condition, the girders rotated as expected during the deck placement such that full contact was established with the elastomeric pads. Figure 4.25 shows the lack of fit between one of the girder connection plates and the bolt holes in a cross-frame during the steel erection on this bridge. This was expected and intentional due in part to the total dead load fit of the cross-frames. That is, the holes in the girder connection plates and in the cross-frame plates had to be aligned. This hole alignment was achieved on the Sunnyside Road job using drift pins without any other mechanical aid.

Trends in the behavior for other skews were targeted by the ISSS cases in Figure 4.18 and the ICCS cases discussed subsequently (see Figure 4.41). The last four rows of Figure 4.23 are three-span continuous designs with parallel skew. Two cases with unequal skew and a narrower deck, NICSS1 and 3, were selected for L = 150 ft. and two comparable cases but with the wider deck, NICSS25 and 27, were selected for L = 350 ft. Parallel skews with the extreme skew angles were considered by selecting bridges XICSS5 and NICSS16, with L = 150 ft. and w = 30 ft. and 80 ft. for the 3-span continuous designs.

The bridge XICSS5 is taken from the NHI Course No.130081A-D (NHI, 2007), which is an LRFD eXample design developed by Grubb et al. (2007) for the National Highway Institute. Since detailed design calculations are shown for this structure, it was selected to serve as an excellent example for the benchmarking.

Figure 4.24. EICSS1, Steel Overpass Sunnyside Road I.C. (I-15B) over I-15, Bonneville Co. ID, gap at sole plate under steel dead load; the girders rotated during the deck placement such that full contact was established with the elastomeric pads (courtesy of Matt Farrar, ITD).

Figure 4.25. EICSS1, Steel Overpass Sunnyside Road I.C. (I-15B) over I-15, Bonneville Co. ID, bolt hole alignment during erection; for this job, drift pins were used to align the holes without mechanical aid (courtesy of Matt Farrar, ITD).

In addition, several cases involving 3-span continuous designs with parallel skews were selected due availability of similar Existing bridges in the literature:

- EICSS2 is located at I-235 EB over E. University Ave., Polk County, IA. This bridge, recommended by Iowa DOT, had difficulty with the installation of cross-frames during the steel erection. According to Iowa DOT, the fabricator detailed and fabricated the cross-frames for the final dead load condition, i.e., total dead load fit. The problem was resolved by requiring the fabricator to supply new cross-frames that were detailed for steel dead load fit. The bridge has an interesting combination of a relatively wide deck, and substantial unequal skew of the bearing lines. Therefore, it represents a potentially useful case where total dead load fit detailing may be problematic.
- EICSS12 is located at US 82 main lane underpass at 19th stress west bound, Lubbock County, TX. This bridge is one of several suggested by TxDOT. This bridge involves a field implementation and evaluation of the use of lean-on cross-frames to alleviate issues of nuisance stiffness in significantly skewed bridges and to eliminate cross-frame diagonals within a large portion of the bridge framing. The design and construction of this bridge are discussed by Helwig et al. (2003). Field data are reported by Romage (2008). This bridge provided an outstanding potential opportunity for validation or verification of the refined analysis methods utilized in the NCHRP research versus available experimental and analytical results.

Figure 4.26 shows the combinations and permutations for the two and three continuous-span TCSS (tub-girder) bridges considering:

- Eight combinations of skew magnitude and pattern for the two-span straight bridges: {(θ_{Left}, θ_{Right}) = (0°, 15°,0°), (0°, 0°, 15°), (0°, 15°, 15°), (15°, 15°, 15°), (0°, 30°, 0°), (0°, 0°, 30°), (0°, 30°, 30°), (30°, 30°, 30°)},
- Two combinations of skew magnitude and pattern for the three-span straight bridges: {(θ_{Left}, θ_{Right}) = (15°, 15°, 15°), (30°, 30°, 30°)},
- Two values for the length L_s (L_s = 150, 250 ft.), L_s = 350 ft. are not shown, and

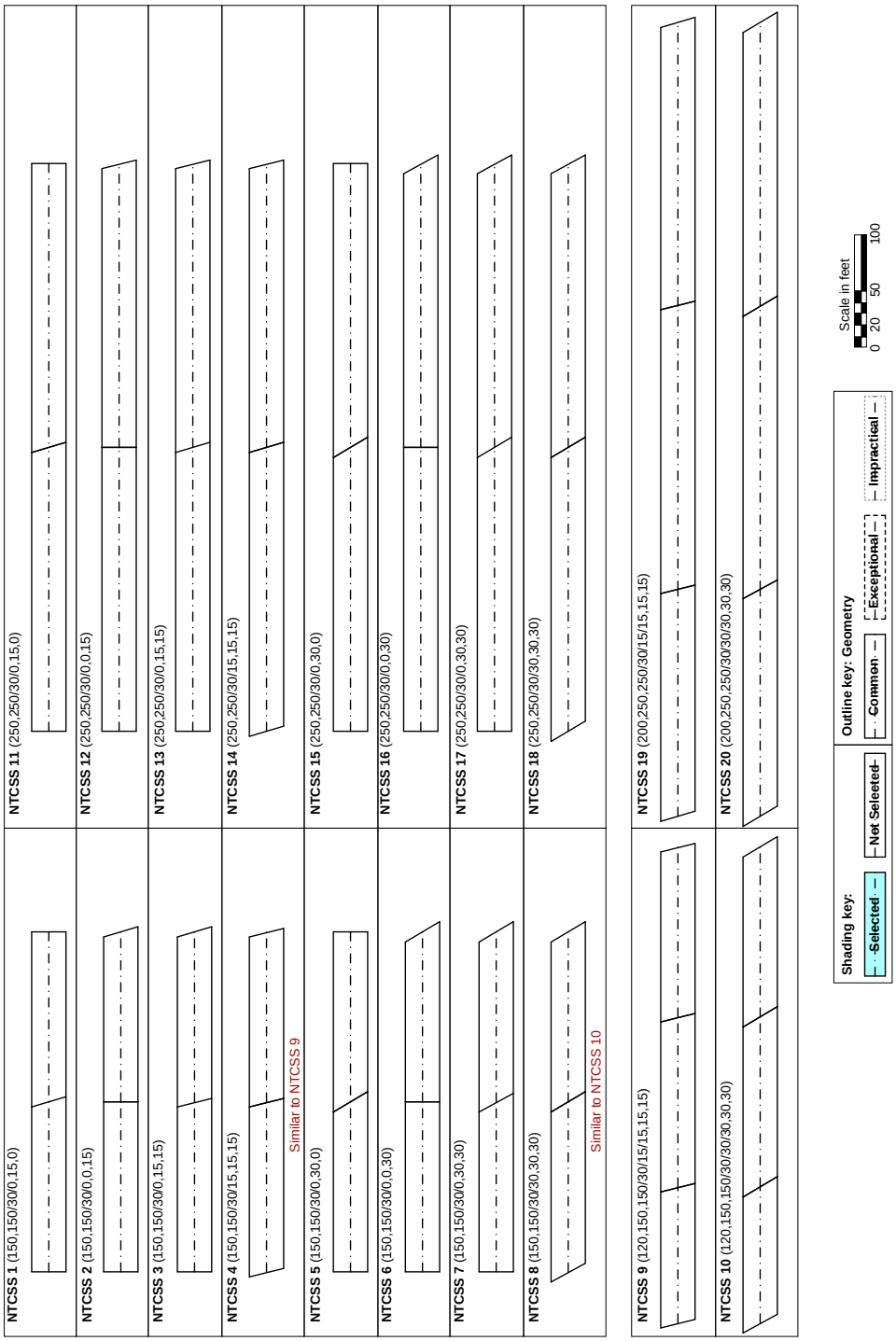

Figure 4.26. New Tub-girder bridges, Continuous-span, Straight with Skewed supports, NTCSS (LENGTH1, LENGTH2, … / WIDTH / θ_{Left}, …, θ_{Right}). The columns in the matrix for (L = 350 ft., w = 30 ft.) are not shown.

- One value for the deck width w (w = 30 ft.)

None of the continuous-span tub-girder bridges shown in Figure 4.26 were selected. It was decided to focus on the other categories for these bridge types, since the interactions between the spans tend to be less significant in tub-girder bridges, the basic influence of skew could be studied more clearly on simple-span bridges, and curved tub-girder bridges are more common than straight ones for narrow two-tub girder systems. It was anticipated that the torsional behavior of curved and straight bridges would be very similar, due to the relatively small torsional interaction of the spans in continuous-span tub-girder bridges.

4.3.4.4 Simple-Span Bridges, Curved, with Radial Supports (ISCR and TSCR)

Figure 4.27 shows the 12 total combinations including three values for the span length (L_s =150, 225 and 300 ft.), the two values for the deck width (w = 30 and 80 ft.), and the two values for the radius of curvature; one corresponding to the largest curvature (smallest R) without having uplift at the most critical bearing location(s) under nominal dead plus live loads and other one corresponding to the smaller curvature (larger R) for the ISCR bridge designs. Seven of the 12 ISCR bridges in Figure 4.27 are selected. These designs are intended to establish the main trends regarding the structural behavior as a function of horizontal curvature and deck width for the different span lengths.

EISCR1 was inserted into the parametric study, which was a very useful case for initial benchmarking and verification of various analysis methods, including simplified 1D I-girder bridge analysis methods coupled with V-load calculations, as well as virtual test simulations procedures. This is due to the following characteristics of this test bridge:

- There were a large number of channels of instrumentation collected and reduced at various stages of the steel erection, deck placement, and loading of this bridge in its final composite condition. This is one of the largest bridge structures ever tested indoors under carefully controlled conditions.
- The geometry of this structure is relatively basic, and should be one of the cases most amenable to simplified analysis.

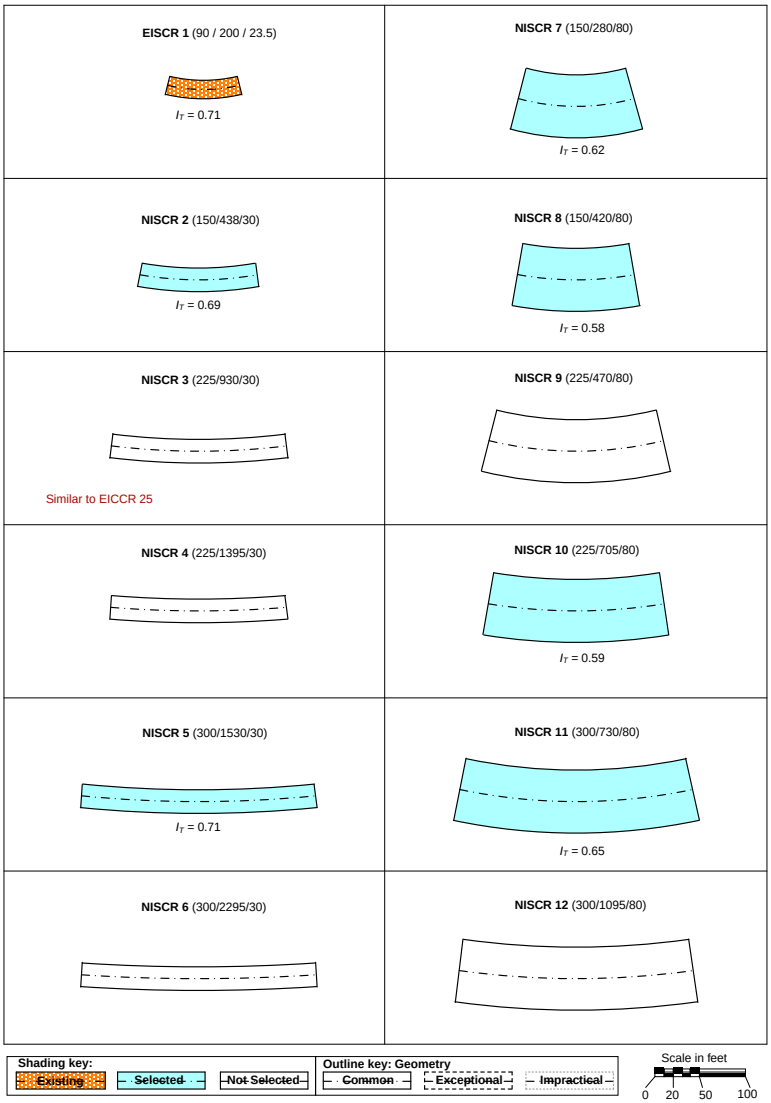

Figure 4.27. Existing and New I-girder bridges, Simple-span, Curved with Radial supports, EISCR or NISCR (LENGTH / RADIUS / WIDTH).

- This test bridge was designed at or slightly above a number of maximum limits in the AASHTO LRFD Specifications. Hence a number of its characteristics are likely to accentuate the effect of certain analysis and/or design approximations.

Jung (2006) and Jung and White (2008) provide a detailed discussion of the characteristics and the behavior of this test bridge. These references also provide substantial prior results from FEA simulation models similar to the types of simulation models that are employed in the NCHRP research. Figure 4.28 shows a view of the FHWA test bridge at an intermediate stage of the steel erection, when the first two of the

three girders in this bridge had been placed on their support bearings and connected together by cross-frames.

Figure 4.28. EISCR1, FHWA Test Bridge (Jung, 2006, Jung and White, 2008).

Figure 4.29 shows the 6 combinations for the TSCR (tub-girder) bridges obtained considering:

- Three values for the span length L_s (L_s = 150, 225 and 300 ft.),
- One value for the deck width w (w = 30 ft.), and
- Two values of the curvature radii R for each span length.

NTSCR1 and NTSCR2 (I_T = 0.83 and 0.72) were selected to study for the effects for different curvature at the shorter span length. One bridge, NTSCR5 (I_T = 0.87), was selected to study the effect of larger span length for similar I_T.

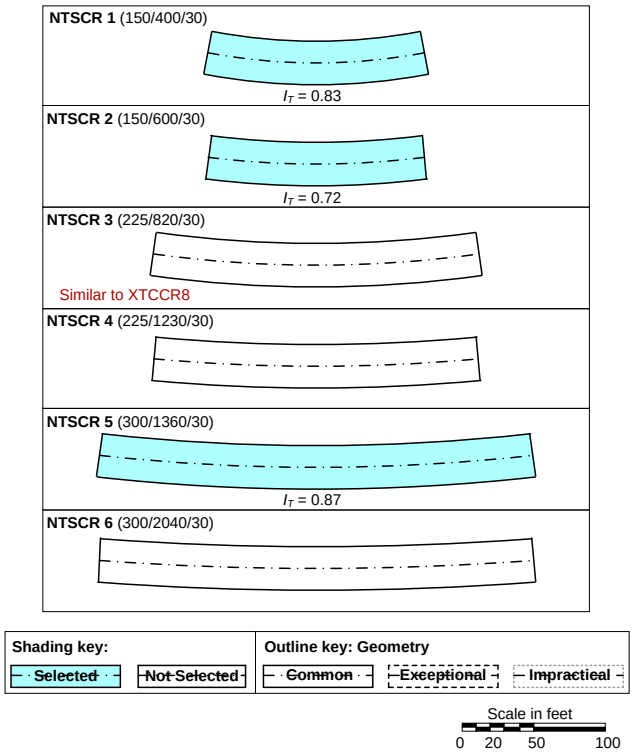

Figure 4.29. New Tub-girder bridges, Simple-span, Curved with Radial supports, NTSCR (LENGTH / RADIUS / WIDTH).

4.3.4.5 Continuous-Span Bridges, Curved, with Radial Supports (ICCR and TCCR)

Figure 4.30 shows 12 total combinations of L_s (= 150, 250 and 350 ft.), w (= 30 and 80 ft.) and the two conceptual values for the radius of curvature discussed previously in Section 4.3.1.1, for the ICCR bridges. The first radius of curvature corresponds to the largest curvature (smallest R) without having uplift at the most critical bearing location(s) under nominal dead plus live loads and the second corresponds to 1.5 times this R value.

In Figure 4.30, all of the cases with the narrower deck are selected, as shown in the first column of this parametric study design matrix, except NICCR5. The selection is mainly driven by the Existing bridge designs. EICCR22a was selected since it has extensive field observations and measurements, reported by Leon et al. (2011). Figure 4.31 shows a photo of EICCR22a during its steel erection.

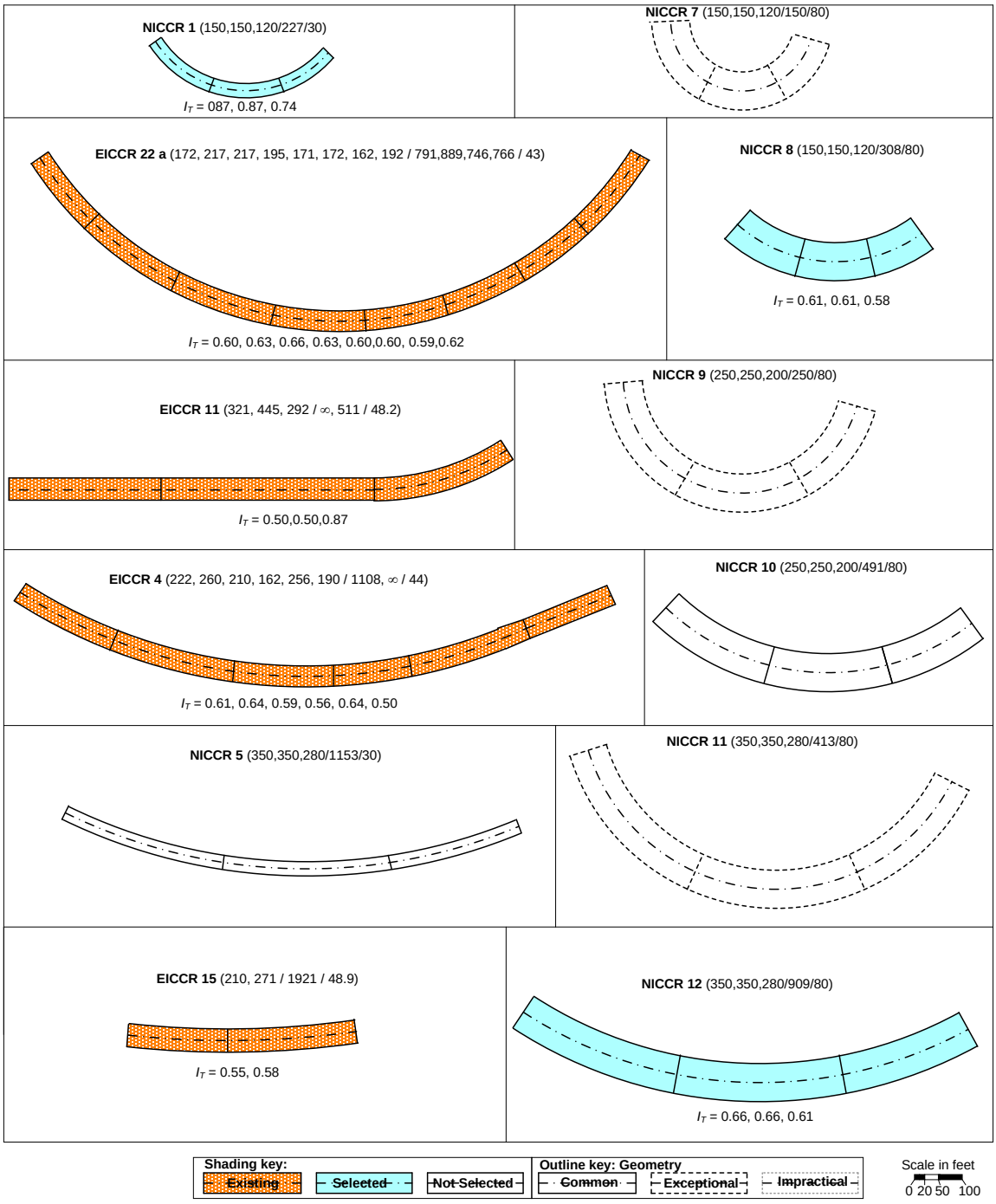

Figure 4.30. Existing, eXample and New I-girder bridges, Continuous-span, Curved with Radial supports, EICCR, XICCR or NICCR (LENGTH1, LENGTH2, ... / RADIUS / WIDTH).

Figure 4.31. EICCR22a, Bridge No. 12 Ramp B over I-40, Robertson Avenue Project, Davidson Co., TN.

EICCR11, which is the Ford City Bridge, in Ford City, PA, was inserted into the analytical study since it represents an important model case where due to combinations of long spans, deep girders with relatively close spacing compared to the girder depths, and relatively tight curvature, substantial erection challenges had to be addressed in the erection engineering of the structure. This bridge has been studied thoroughly in prior work by Chavel and Earls (2006a & b; 2001) as well as by Chang (2006). Hence, it represented another valuable case that can be used to validate the analysis and design methods. Figure 4.32 shows an overall photo of the Ford City bridge during its steel erection. Figure 4.33 emphasizes the overall depth of the girders relative to their horizontal spacing. Figure 4.34 provides several snapshots during the installation of a key drop-in segment on this bridge. The circles in these photos are highlighting a come-along beam that is being used to stabilize the curved girder during lifting. A cable goes to the lifting beam from each end of the come-along beam.

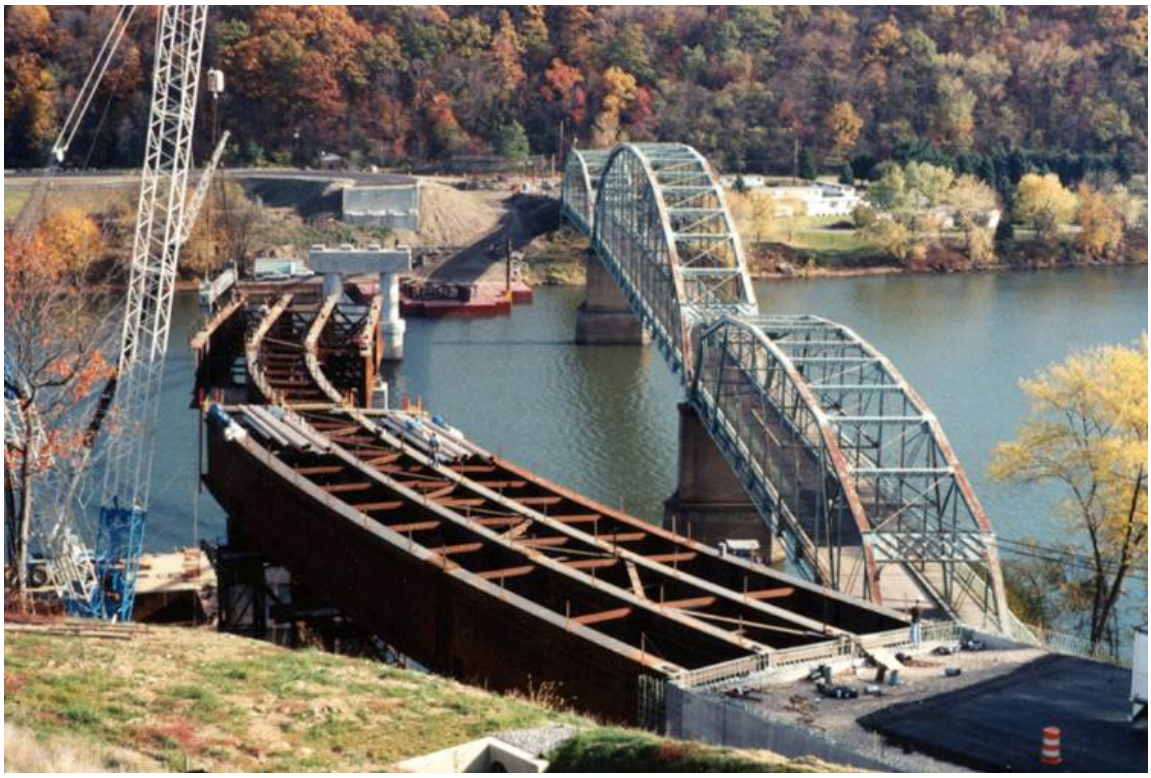

Figure 4.32. EICCR11, Ford City Bridge, Ford City, PA (Chavel, 2008).

Figure 4.33. EICCR11, Ford City Bridge, Ford City, PA, girder depth and spacing (Chavel, 2008).

Figure 4.34. EICCR11, Ford City Bridge, Ford City, PA, installation of drop-in segment (Chavel, 2008).

EICCR4 is one of the units of Ramp GG, John F. Kennedy Memorial Highway, I-95 Express Toll Lanes and I-695 Interchange, Baltimore County, MD. High Steel Structures, Inc. did the fabrication and the steel erection for this bridge. Several members of the NCHRP 12-79 team visited the job site with the High Steel engineers to observe the erection of a drop-in segment on the second span from the right hand end of this bridge in the sketch during August 2007. Figure 4.35 is a photo of the bridge just prior to installation of this drop-in segment.

EICCR15 is located at SR 6220 A11 over SR 6220 NB and SB, Centre County, PA. This bridge was studied experimentally and analytically by Shura (2004) and is discussed by Domalik et al. (2005). Due to its unequal span lengths (ratio of the span lengths of 0.77), this bridge exhibits important torsional interactions between its two spans. The shorter span actually twists in the direction opposite from the torsional deformation of the longer span. That is, the downward deflection of girders toward the outside of the curve

in the longer span corresponds to an upward deflection of the girders toward the inside of the curve on the shorter span. As a result, this bridge was selected to serve as an important case for assessment of the sufficiency or limitations of various simplified analysis methods.

Figure 4.35. EICCR4, Ramp GG John F. Kennedy Memorial Highway, I-95 Express Toll Lanes and I-695 Interchange, Baltimore Co., MD (courtesy of R. Cisneros, High Steel Structures, Inc.).

In addition, two of the three cases with wider decks and smaller curvature (larger *R*) were considered in the second column of the matrix. The wider-deck cases with tighter curvature in Figure 4.30 were considered to be exceptional designs. The influence of wide decks with tight curvatures was expected to be captured sufficiently via the combination of the ISCR and ISCS bridges.

Figure 4.36 is based on the combinations for the TCCR (tub-girder) bridges with three continuous-spans considering:

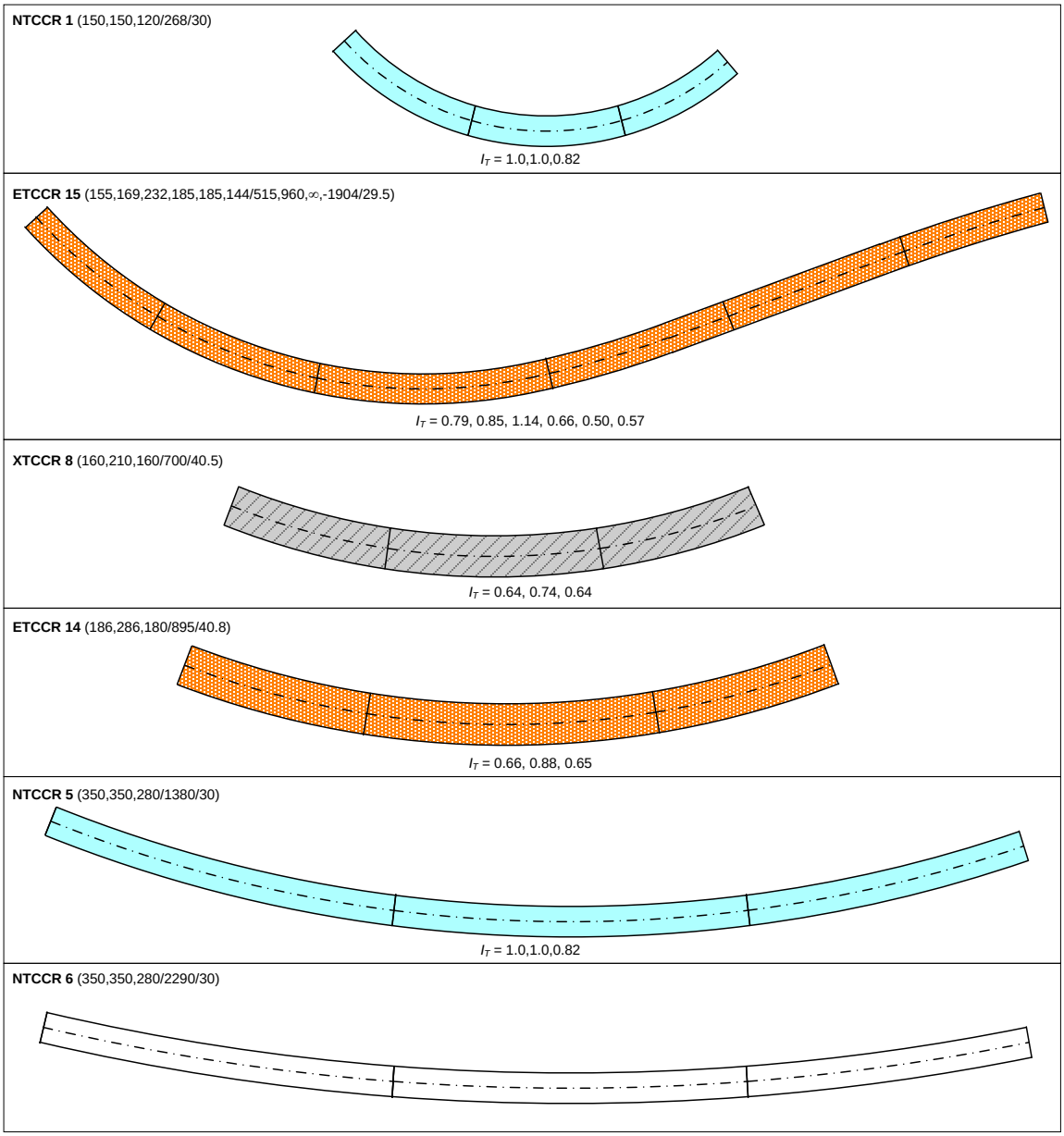

Figure 4.36. Existing, eXample and New Tub-girder bridges, Continuous-span, Curved with Radial supports, ETCCR, XTCCR or NTCCR (LENGTH1, LENGTH2, … / RADIUS / WIDTH).

- Three values for maximum the span length L_s (L_s = 150, 250 and 350 ft.),
- One value for the deck width w (w = 30 ft.), and
- Two conceptual values of the radius of curvature R as discussed in Section 4.3.1.1, the first corresponding to the largest curvature (smallest R) possible

without having uplift at the most critical bearing location(s) under nominal dead plus live loads, and the second corresponding to a radius of curvature of 1.5 times this value.

Five continuous-span tub-girder bridges were selected as this is the most common configuration for tub-girder bridges used as access ramps for highway interchanges. The extreme cases NTCCR1 and NTCCR5 were selected to provide information for sharp curve and large span lengths while the intermediate cases were replaced by existing and example bridges (ETCCR15, XTCCR8 and ETCCR14). ETCCR15 is a six span bridge located in Milwaukee, WI and is part of the Marquette Interchange (see Figure 4.37), XTCCR8 is a design example developed by Kulicki et al. (2005), and ETCCR14 is a three-span bridge instrumented and studied by Fan (1999), located in Houston, TX.

Figure 4.37. ETTCR 15, Unit B-40-1122 of the Marquette Interchange, Milwaukee, WI (courtesy of Tony Shkurti, HNTB Corporation).

4.3.4.6 Simple-Span Bridges, Curved, with Skewed Supports (ISCS and TSCS)

Figure 4.38 displays four of the 12 groups of I-girder bridges considering:

- The twelve combinations of skew magnitude.
- The two values for length, L_s = 150 and 300 ft.
- The two values for the deck width w = 30 and 80 ft.
- The four values of radius of curvature R = 438, 280, 420 and 730 ft. which were selected from ISCR bridges.

Since the effects of skew are generally larger in wider bridges for a given span length, emphasis was placed on bridges with the wider decks in the design of the ISCS studies.

In addition, none of the bridges with 225 ft. span length are considered in Figure 4.38. This is because it was expected that the interactions between the effects of the curvature and skew on I-girder bridges can be captured sufficiently by studying the ISSS, ICSS, ISCR, ICCR, ISCS and ICCS bridges with L_s = 150 ft.

One case with L_s = 300 ft., the case with the wider deck and tighter curvature, was included to investigate the interaction effect on a longer-span design where some type of flange-level lateral bracing system is likely.

In Figure 4.38 one can observe that the bridges in the 2nd and 3rd rows of 1st, 2nd and 3rd columns were selected except NSCS1 and NSCS3 for analytical studies. These bridges were selected to capture the behavior with respect to the variation in the L_s /w and L_s /R ratios. NISCS9 was selected to capture the effect of parallel skewed bearings along with curvature effects.

EISCS3 was inserted into the design matrix. This bridge is SR 8002 Ramp A-1, in King of Prussia, PA, studied extensively by Chavel and Earls (2003) and Chavel (2008) in their prior research (see Figure 4.39). Moreover, the third phase of the EISCS4 was inserted into the study matrix since this phase experienced large differential displacements with respect to the adjacent units due to its large length-to-width ratio.

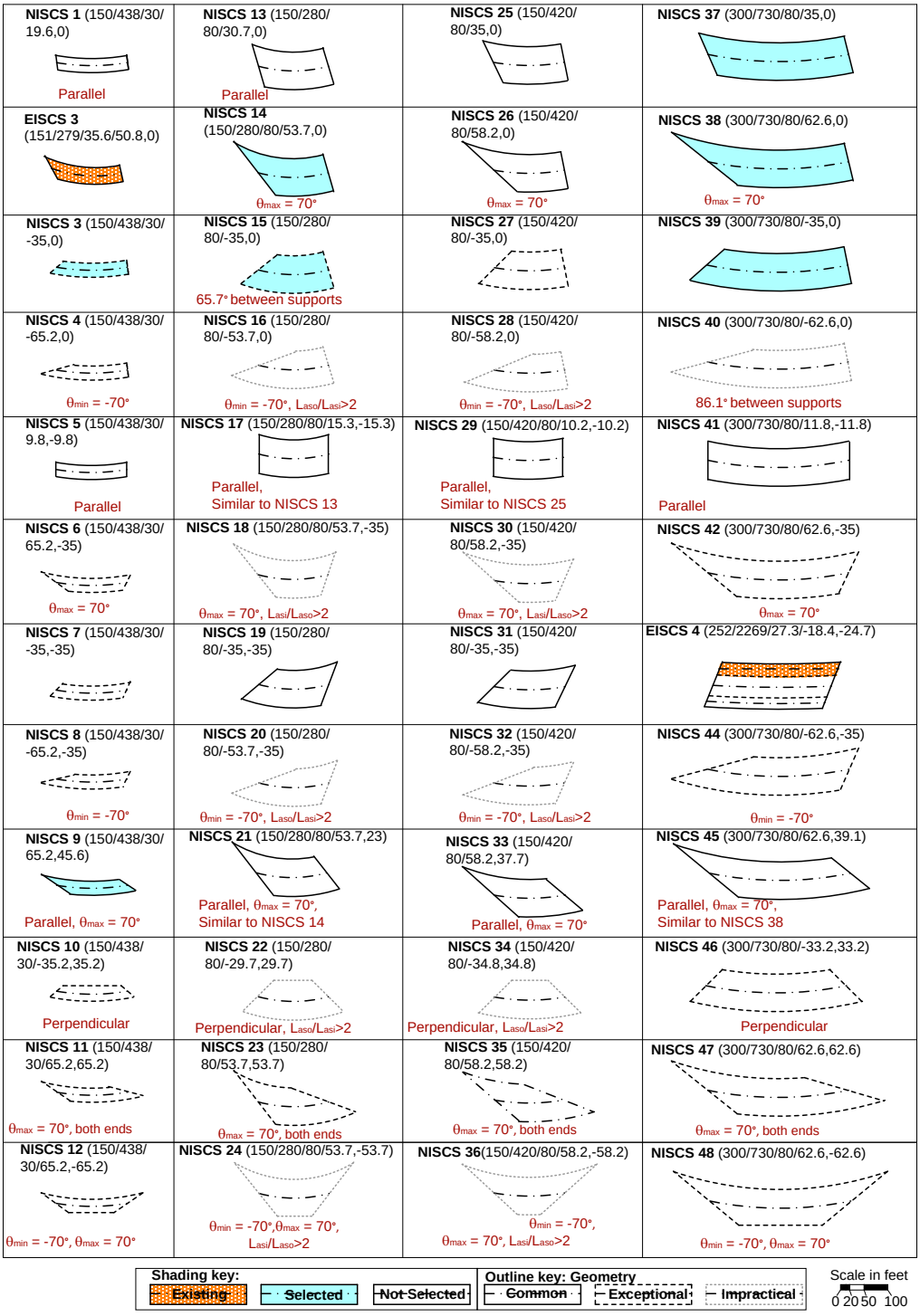

Figure 4.38. Existing and New I-girder bridges, Simple-span, Curved with Skewed supports, EISCS or NISCS (LENGTH / RADIUS / WIDTH / θ_{Left}, θ_{Right}). The columns in the matrix for (L = 150 ft., w =30 ft., R = 292 ft.), (L = 225 ft., w =30 ft., R = 930 and 1395 ft.), (L = 225 ft., w =80 ft., R = 470 and 705 ft.), (L = 300 ft., w =30 ft., R = 1530 and 2295 ft.) and (L = 300 ft., w =80 ft., R = 1095 ft.) are not shown.

Figure 4.39. EISCS3, SR 8002 Ramp A-1, King of Prussia, PA (Chavel and Earls, 2003).

Figure 4.40 displays the possible combinations for the TSCS (tub-girder) bridges considering:

- Twelve combinations of skew magnitude within the ranges of ±30° and two additional configurations for parallel skew previously shown in Figure 4.15,
- Two values for length, L_s =150 and 225 ft., L_s = 300 ft.and their associated radius values are not shown,
- One value for the deck width w =30 ft., and
- Four values of radius of curvature R = 400, 600, 820 and 1230 ft.which are selected from TSCR bridges

The selected cases (NTSCS5 and NTSCS29) have parallel supports since these configurations represent the most likely scenarios for skewed supports combining 150 and 225 ft.spans and skewed supports up to 15.7°. The NTSCS5 bridge is similar to

NTSSS4 shown in Figure 4.21, which has an equal and opposite skew angle at its abutments. The NTSCS29 bridge has skew at only one of its supports.

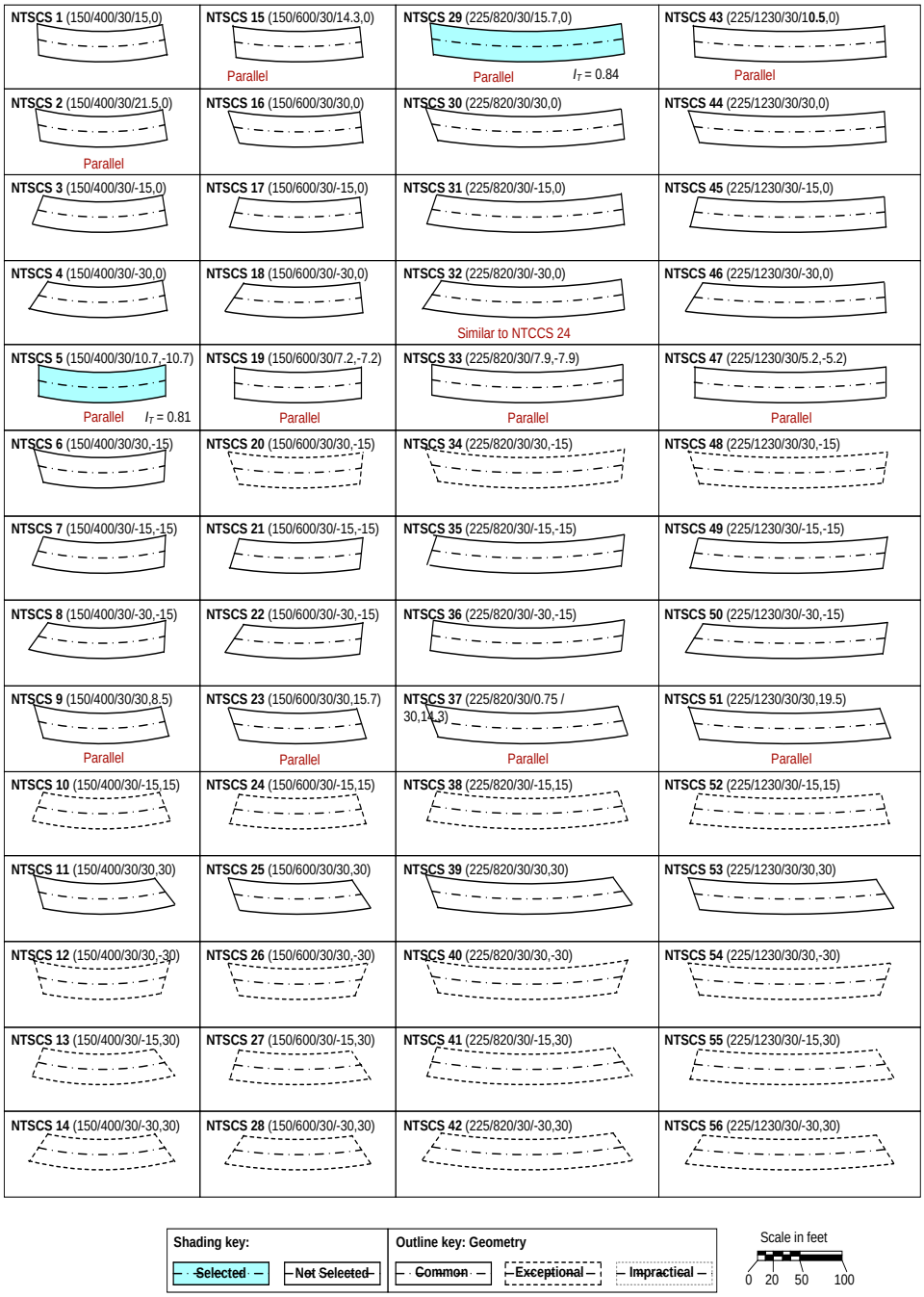

Figure 4.40. New Tub-girder bridges, Simple-span, Curved with Skewed supports, NTSCS (LENGTH / RADIUS / WIDTH / θ_{Left}, θ_{Right}). The columns in the matrix for (L = 350 ft., w = 30 ft., R = 1390 and 2085 ft.) are not shown.

4.3.4.7 Continuous-Span Bridges, Curved, with Skewed Supports (ICCS and TCCS)

Figure 4.41 shows six of the 12 possible groups of ICCS bridges. Note that the *R* values selected for the ICCR bridges (Figure 4.30) were used also for the subsequent ICCS designs in Figure 4.41. Rows 1 through 3 of the parametric study design matrix shown in this figure correspond to different orientations of the bearing lines relative to the curved geometry, but with the bearing lines parallel (or near parallel in cases where the skew angle is limited by $\theta = +70^{o}$ at the inside edge of the deck). The bridges in the fourth row are similar to those in row 1, but with zero skew at the bearing line at the right hand end of the bridge. Three of the four combinations of deck width and horizontal curvature for L = 150 ft.are considered in columns 1 through 3 of this matrix. Narrow 250 ft.continuous-spans with the tighter curvature are considered in the fourth column. This case was included because ramp type structures with roughly 250 ft.span lengths are very common. The last two columns of Figure 4.41 show 350 ft.two-span continuous bridges with 80 ft.wide decks and each of the values of horizontal curvature determined previously. The narrower bridges were not considered for these span lengths, since it was expected that the influence of skew will be more minor for these bridges. Lastly, all the 150 ft.span bridges in column 1 of the Figure 4.41 test matrix were selected. In addition, all the 250 and 350 ft.span bridges in columns 4 and 6 were selected except the ones with perfect symmetry about the center pier (NICCS15 and 23) and NICCS22 since this bridge is similar to NICCR12. The case with perfect symmetry about the center pier was believed to be less common for these types of bridge geometry. The two non-exceptional cases with the wider decks were considered in the third column of this parametric study design matrix. NICCS11 was not selected since this bridge is similar to NICCR8 in Figure 4.30.

EICCS 10 was inserted into the design matrix. This is the MN DOT Bridge No. 27998, TH94 between 27th Avenue and Huron Boulevard in Minneapolis, MN. This bridge has been studied extensively, both experimentally and analytically, by Galambos et al. (1996). Also, it has been used by Nowak et al. (2006) as part of the calibration of the AASHTO LRFD Specifications for curved steel bridges. Therefore, this bridge was

selected to be of particular value in relating the implications of analysis accuracy in the context of structural reliability calibration and assessment of strengths.

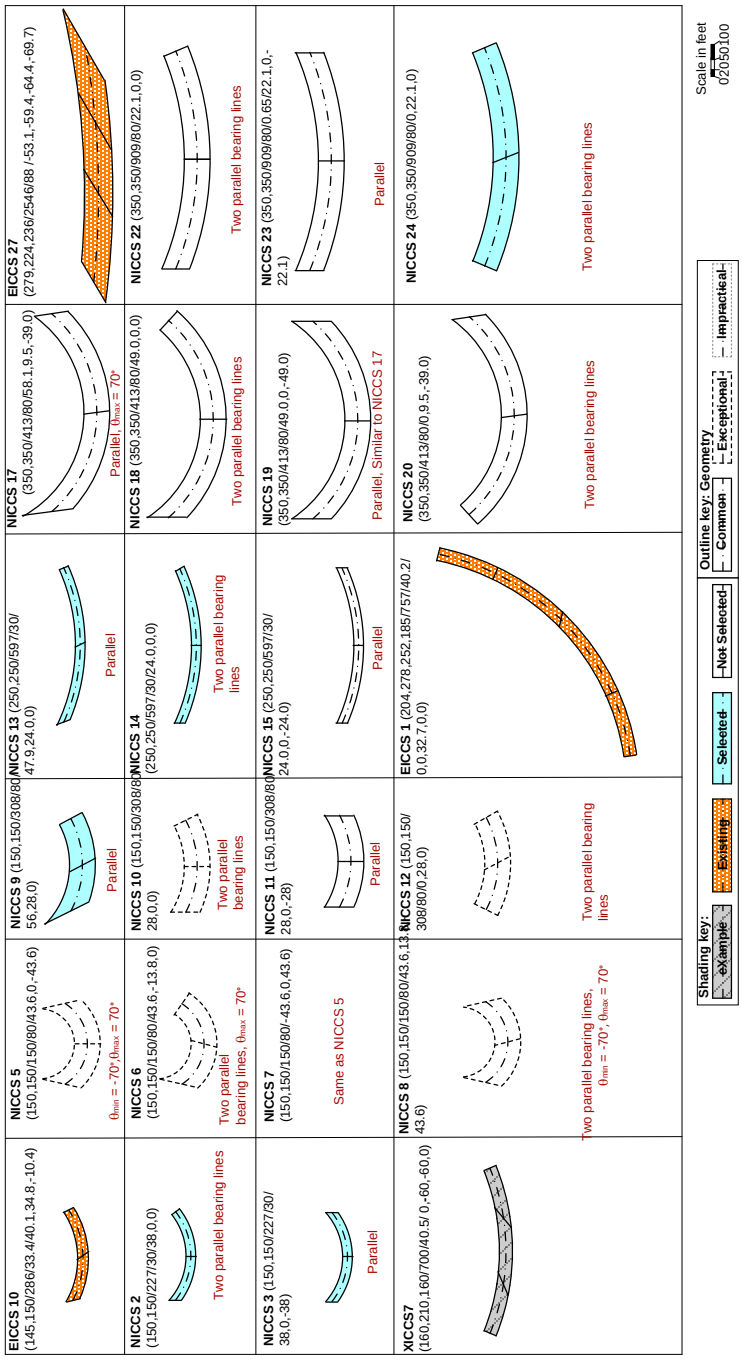

Figure 4.41. Existing and New I-girder bridges, Continuous-span, Curved with Skewed supports, EICCS or NICCS (LENGTH1, LENGTH2, ... / RADIUS / WIDTH / θ_{Left}, …, θ_{Right}). The columns in the matrix for (L = 150 ft., w =30 ft., R = 438 ft.), (L = 250 ft., w =30 ft., R = 1179 ft.), (L = 250 ft., w =80 ft., R = 250 and 491 ft.), (L = 350 ft., w =30 ft., R = 1153 and 2291 ft.) are not shown.

EICCS1 was also inserted into the parametric study matrix. This bridge is the I-459 / US31 Interchange Flyover A in Jefferson County, AL. The construction of this bridge was observed and thoroughly documented by Osborne (2002). This bridge represents a successful implementation of total dead load fit detailing on a significantly curved span with one pier location that is substantially skewed relative to a radial line. Figure 4.42 shows a photo looking along the length of the bridge at the skewed bearing line during construction. Figure 4.43 shows another snapshot of the steel erection.

Figure 4.42. EICCS1, I-459 / US31 Interchange Flyover A, Jefferson Co. AL (Osborne, 2002).

Figure 4.44 shows the two-span continuous TCCS (tub-girder) bridges considering:

- Eight combinations of skew magnitude and pattern when only one support is skewed in the rage of ±30° and two additional configurations when two supports are skewed to accommodate three parallel support lines,
- Two values for the length L_s (L_s = 150 and 250 ft.), L_s = 350 ft.and their associated radius values are not shown,
- Two values of the curvature radii R for each span length, and
- One value for the deck width w (w = 30 ft.)

Figure 4.43. EICCS1, I-459 / US31 Interchange Flyover A, Jefferson Co. AL (Osborne, 2002).

In this category several cases fall into the exceptional cases since a 30° skew for curved bridges distorts the geometry at the support lines causing undesired layouts for a narrow configuration. Two existing bridges with an intermediate skewed support were included in this category (ETCCS5a and ETCCS6) and a third case was selected NTCCS22.

NTCCS22, which has a moderate skew of 20° at one abutment, was selected because this configuration results in two parallel support lines. ETCCS5a, which is located at the SR 9A and SR202 interchange in Duval Co. FL, has an intermediate support that is skewed at 4.8°. These two bridges were targeted to gain insight about the effect of skew at an intermediate support and at the abutment.

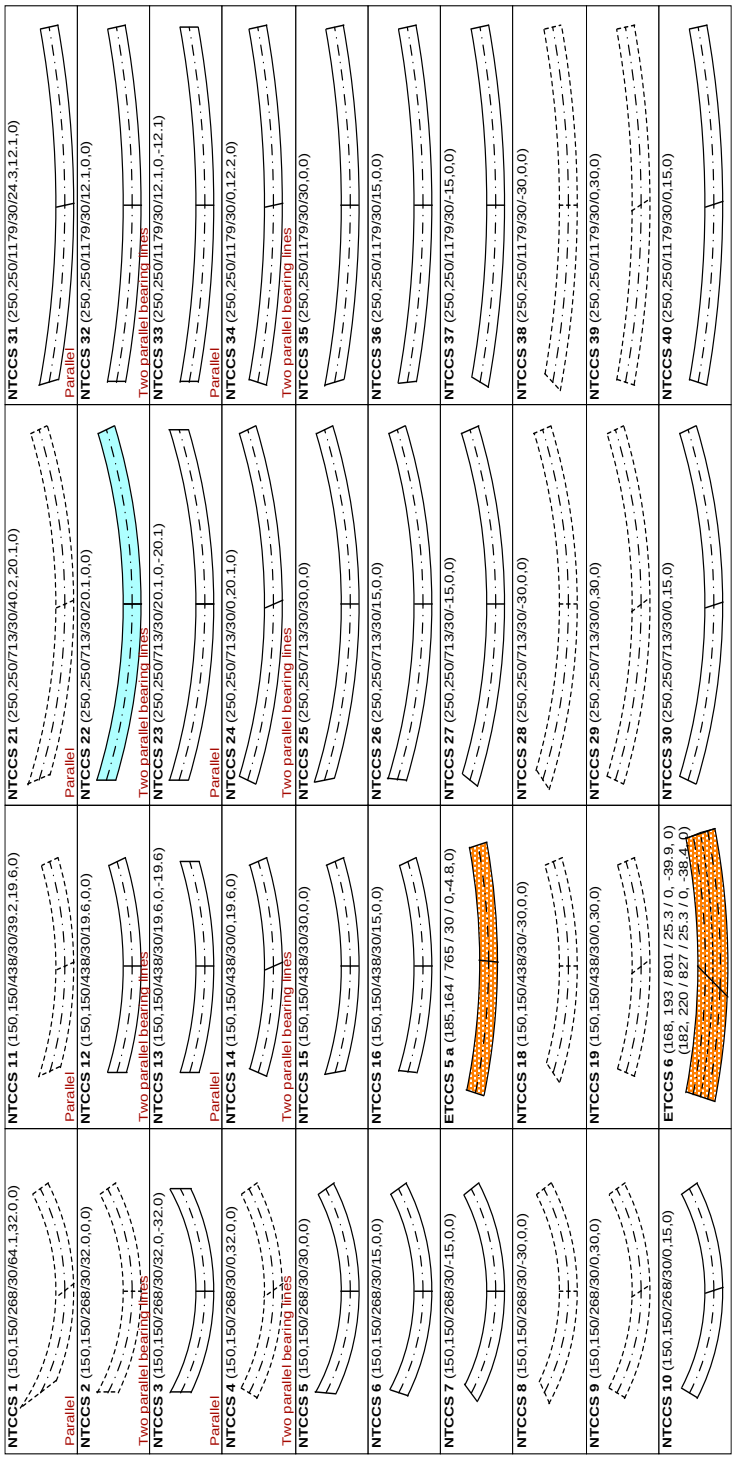

Figure 4.44. Existing and New Tub-girder bridges, Continuous-span, Curved with Skewed supports, ETCCS or NTCCS (LENGTH1, LENGTH2, … / RADIUS / WIDTH / θ_{Left}, …, θ_{Right}). The columns in the matrix for (L = 350 ft., w = 30 ft., R = 1380 and 2291 ft.) are not shown.

ETCCS6 is the Magruder Blvd. bridge over I-64 in Hampton, VA. This bridge was constructed in two phases, with 2 tub-girders each phase, and has a maximum skew angle of 40° at the interior phase. This bridge does not include any external cross-frames or diaphragms between the girders at its skewed interior support, and it does not contain any intermediate external diaphragms between the girders within its spans. Figure 4.45 shows the underside of the completed Magruder Blvd. bridge.

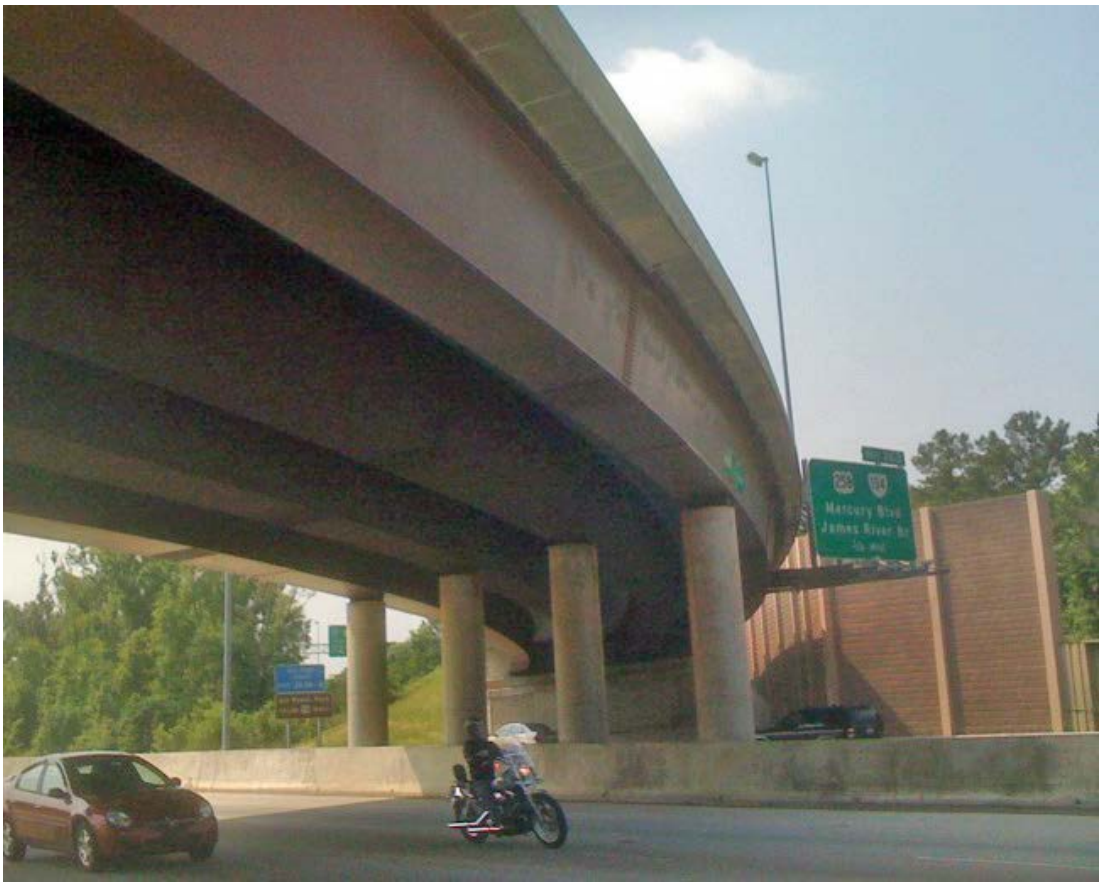

Figure 4.45. ETCCS6, McGruder Blvd. bridge over I-64 in Hampton, VA.

4.3.4.8 Tub-Girder Skew Sensitivity Studies

Skew sensitivity studies were performed for six of the above tub-girder bridges to assess the impact of skew on the simplified torsional moment estimates. No changes to the tub-girder bridge original designs were made but minor modifications were made to accommodate the changes on the framing plan. The bridges and their variations are NTSSS2 (30°, 15° and 0°), NTSSS4 (16°, 10° and 0°), NTSCS5 (10.7° and 0°),

NTSCS29 (15.7° and 0°), ETCCS5a (-4.8°, 0°, -10° and 10°) and NTCCS22 (20.1° and 0°). The first angle in the above parentheses corresponds to the original design. The bridge layouts of the sensitivity studies are shown in Figure 4.46.

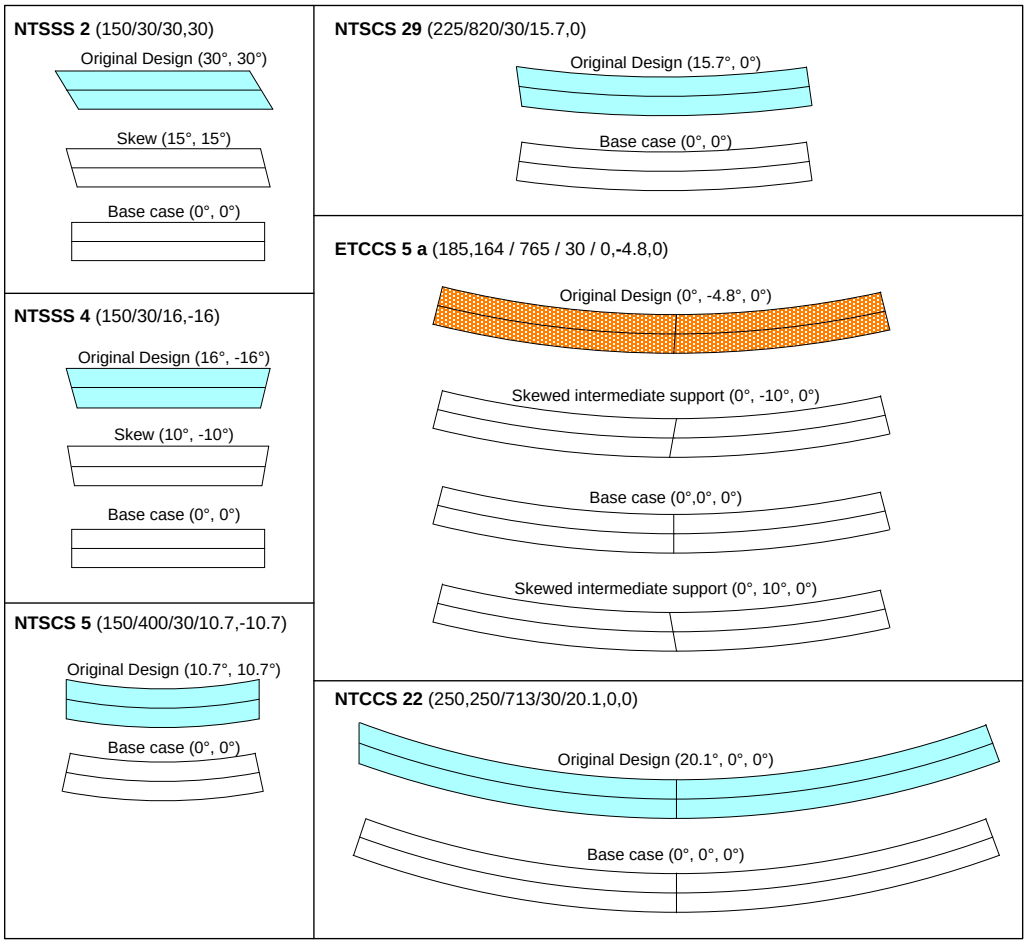

Figure 4.46. Cases considered in the tub-girder bridge sensitivity studies.

4.3.5 Final Summary of the Parametric Study Bridges

Tables 4.2 and 4.3 provide an overall summary of the number of New, Existing and eXample bridges developed in the above parametric study design for each of the major groups of bridges. Eighty-six bridges were selected in total, including 58 I-girder bridges and 28 tub-girder bridges, or 26 existing bridges and 60 parametric study designs.

Table 4.2. Overall summary of New, Existing and eXample I-girder bridges.

Description		Cases
eXample I-girder, Continuous-span, Straight, No skew (Base comparison case)		**1**
ISSS	(EISSS) Existing, I-girder, Simple-span, Straight, Skewed supports	3
	(XISSS) eXample, I-girder, Simple-span, Straight, Skewed supports	0
	(NISSS) New, I-girder, Simple-span, Straight, Skewed supports	12
	Total: ISSS	**15**
ICSS	(EICSS) Existing, I-girder, Continuous-span, Straight, Skewed supports	3
	(XICSS) eXample, I-girder, Continuous-span, Straight, Skewed supports	1
	(NICSS) New, I-girder, Continuous-span, Straight, Skewed supports	5
	Total: ICSS	**9**
ISCR	(EISCR) Existing, I-girder, Simple-span, Curved, Radial supports	1
	(XISCR) eXample, I-girder Simple-span, Curved, Radial supports	0
	(NISCR) New, I-girder Simple-span, Curved, Radial supports	6
	Total: ISCR	**7**
ICCR	(EICCR) Existing, I-girder, Continuous-span, Curved, Radial supports	4
	(XICCR) eXample, I-girder, Continuous-span, Curved Radial supports	0
	(NICCR) New, I-girder, Continuous-span, Curved Radial supports	3
	Total: ICCR	**7**
ISCS	(EISCS) Existing, I-girder, Simple-span, Curved, Skewed supports	2
	(XISCS) eXample, I-girder, Simple-span, Curved, Skewed supports	0
	(NISCS) New, I-girder, Simple-span, Curved, Skewed supports	7
	Total: ISCS	**9**
ICCS	(EICCS) Existing, I-girder, Continuous-span, Curved, Skewed supports	3
	(XICCS) eXample, I-girder, Continuous-span, Curved, Skewed supports	1
	(NICCS) New, I-girder, Continuous-span, Curved, Skewed supports	6
	Total: ICCS	**10**
Total: Existing I-girder bridges		16
Total: eXample I-girder bridges		3
Total: New I-girder bridges		39
Total: I-girder bridges		58

Appendix E of the NCHRP 12-79 final report provides a concise summary of the most important considerations for each of the bridges (one-third to one-half page per bridge), while Appendix K explains the organization of the detailed electronic data for each of the bridges. Appendix I of the final report provides a more detailed summary of the results for each of the bridges.

Table 4.3. Overall summary of New, Existing and eXample tub-girder bridges.

Description		**Cases**
eXample Tub-girder, Continuous-span, Straight, No skew (Base comparison case)		**1**
TSSS	(ETSSS) Existing, Tub-girder, Simple-span, Straight, Skewed supports	1
	(XTSSS) eXample, Tub-girder, Simple-span, Straight, Skewed supports	0
	(NTSSS) New, Tub-girder, Simple-span, Straight, Skewed supports	3
	Total: TSSS	**4**
TCSS	(ETCSS) Existing, Tub-girder, Continuous-span, Straight, Skewed supports	0
	(XTCSS) eXample, Tub-girder, Continuous-span, Straight, Skewed supports	0
	(NTCSS) New, Tub-girder, Continuous-span, Straight, Skewed supports	0
	Total: TCSS	**0**
TSCR	(ETSCR) Existing, Tub-girder Simple-span, Curved, Radial supports	0
	(XTSCR) eXample, Tub-girder Simple-span, Curved, Radial supports	0
	(NTSCR) New, Tub-girder Simple-span, Curved, Radial supports	3
	Total: TSCR	**3**
TCCR	(ETCCR) Existing, Tub-girder, Continuous-span, Curved, Radial supports	2
	(XTCCR) eXample, Tub-girder, Continuous-span, Curved, Radial supports	1
	(NTCCR) New, Tub-girder, Continuous-span, Curved Radial supports	2
	Total: TCCR	**5**
TSCS	(ETSCS) Existing, Tub-girder, Simple-span, Curved, Skewed supports	0
	(XTSCS) eXample, Tub-girder, Simple-span, Curved, Skewed supports	0
	(NTSCS) New, Tub-girder, Simple-span, Curved, Skewed supports	2
	Total: TSCS	**2**
TCCS	(ETCCS) Existing, Tub-girder, Continuous-span, Curved, Skewed supports	2
	(XTCCS) eXample, Tub-girder, Continuous-span, Curved, Skewed supports	0
	(NTCCS) New, Tub-girder, Continuous-span, Curved, Skewed supports	1
	Total: TCCS	**3**
Total: Existing Tub-girder bridges		5
Total: eXample Tub-girder bridges		2
Total: New Tub-girder bridges		11
Total: Additional skew sensitivity studies		10
Total: Tub-girder bridges		28

5. Assessment of Conventional Simplified Methods of Analysis

NCHRP 12-79 has conducted a wide range of studies on the bridges introduced in Chapter 4 to determine the ability of the approximate 1D and 2D methods of analysis to capture the behavior predicted by refined 3D FEA models. The line-girder (1D) analyses of straight I- and tub-girder bridges, as well as curved tub-girder bridges, were performed using the STLBRIDGE package (Bridgesoft, Inc., 2010). The line-girder analyses of curved I-girder bridges were based in the V-load method using the program VANCK (NSBA, 1996). The line-girder analyses of curved tub-girder bridges were modified using a spreadsheet implementation of the M/R Method (Tung and Fountain, 1970). In addition, the line-girder analysis results for skewed tub-girder bridges were modified using the developments described in Sections 2.1.5 and 2.7.1.2. The simplified 2D-grid analyses were conducted using the LARSA 4D (LARSA, 2010) and MDX (MDX Software, 2011) software systems.

A quantitative assessment of the analysis accuracy was obtained by identifying error measures that compare the simplified approximate solutions to the 3D second-order elastic FEA benchmarks. The approach to quantify the error is as follows. First, an error function is defined as the absolute value of the difference between the FEA representation and the approximate analysis response, as shown in Figure 5.1. The errors are calculated at the locations along the length of the girders where the responses are sampled in the approximate method. Next, the error function is used to calculate the normalized mean error, μ_e. This index provides an *overall* measure of the performance of the approximate models and is calculated as:

$$\mu_e = \frac{1}{N \cdot R_{FEA,max}} \sum_{i=1}^{N} e_i \tag{5.1}$$

where N is the total number of sampling points along the girder length used in the simplified analysis, $R_{FEA,max}$ is the absolute value of the maximum response obtained from the FEA benchmark, and e_i is the absolute value of the error relative to the 3D FEA benchmark solution at point i. In this equation, the mean error is normalized with respect to the maximum value of the response obtained from the FEA to avoid a comparison of "small numbers to small numbers." For example, the vertical displacements near the supports in a simple-span bridge are relatively small. The percent error in the response prediction relative to the physical displacement may be

large at these locations, but the deflections are small compared to the deflections expected near mid-span. Hence, in Eq. (5.1), the errors are weighted with respect to the maximum value of the response. In addition, by dividing the error by $R_{FEA,max}$, the influence of the load magnitude is removed from the analyses. Given this practice, the mean errors can be compared for different bridges.

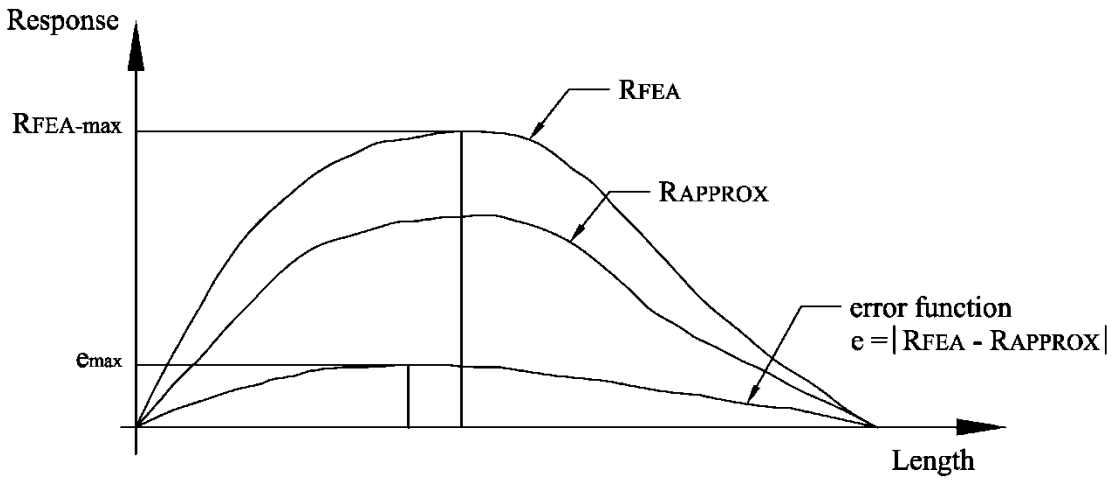

Figure 5.1. Schematic representation of the error function.

5.1 Assessment of I-Girder Bridges

Table 5.1 shows the percent normalized mean errors in the major-axis bending stresses and vertical displacements obtained for the 58 I-girder bridges studied in the NCHRP 12-79 research. These bridges are divided into six different groups based on their geometry. The first group corresponds to the curved radially-supported bridges (labeled as "C") with connectivity indices $I_C > 1$. As discussed in Section 3.1.3, the connectivity index provides an indication of when the inaccurate representation of the girder torsional stiffness in conventional 2D-grid models tends to have a significant impact on the overall error. The second group includes curved and radial bridges with $I_C \leq 1$. The straight and skewed structures (labeled as "S") are subdivided based on the skew index I_S, which differentiates the bridges where skew has a minor influence on the structural behavior from those where the collateral effects from the skew are more important (see Section 3.1.2). The groups correspond to $I_S < 0.30$, $0.30 \leq I_S < 0.65$, and $I_S \geq 0.65$. The sixth group contains the curved and skewed bridges studied in the project (labeled as "C&S"). It is important to note that the skew and curvature indices, I_S and I_C should not be used in combination to estimate the accuracy of the approximate models in a curved and skewed bridge.

No clear trends in the normalized mean errors were identified as a combined function of I_S and I_C with the exception that, as the skew or the horizontal curvature approaches zero, then the error characteristics should approach the values shown for the "C" and the "S" categories respectively.

Table 5.1 compares the results of the first-order (*geometrically linear*) 3D FEA, 2D-grid, and 1D analysis results to the predictions obtained from elastic *second-order* 3D FEA. In the table, f_b is the major-axis bending stress and Δ_z is the vertical displacement. A mean error value is calculated for each response on each girder of the bridges. The values reported in Table 5.1 are the largest mean errors determined by inspecting the values obtained for each girder in a given bridge.

Upon inspection of the results in Table 5.1, the following important trends can be observed:

Second-Order Amplification

The results obtained from the first-order 3D FEA show that the response amplifications due to second-order effects are negligible in most of the bridges. With the exception of bridges NISCR5 and EISCS4, the differences between the linear and nonlinear FEA results are less than 10 %. For bridges NISCR5 and EISCS4, the analyses show that these long-and-narrow structures experience significant global second order amplification. Section 2.9 discusses this behavior in the context of bridge EISCS4. It should be noted that unless noted otherwise, the benchmark second-order stresses in Table 5.1 are evaluated at 1.5 times the nominal dead load, corresponding to the AASHTO LRFD Strength IV load combination. However, the benchmark second-order displacements are evaluated at the nominal (unfactored) dead load level.

It is recommended that the loss of accuracy due to large global second-order amplification should be addressed separately from the other factors affecting accuracy. The estimated global second-order amplification, AF_G (Eq. 2.101), is relatively large for the above two bridges. As noted in Section 2.9, if the AASHTO constructability checks do not pass due to a large AF_G, this should be taken as an indication that a second-order 3D FEA may need to be conducted, or the design should be changed to avoid the large second-order effects. Therefore, these bridges are excluded from the subsequent error syntheses.

Table 5.1. I-girder bridge percent normalized mean errors compared to 3D second-order elastic FEA for major-axis bending stresses (f_b) and vertical displacements (Δ_z).

Group	Bridge Name	I_S	I_C	I_T	I_L	3D-FEA Linear		2D-Grid - P1		2D-Grid - P2		1D	
						f_b μ_e	Δz μ_e	f_b μ_e	Δz μ_e	f_b μ_e	Δz μ_e	f_b μ_e	Δz μ_e
C ($I_C \leq 1$)	EICCR22a	0	0.98	0.66	1.11	0	0	6	3	4	2	10	6
	NICCR12	0	0.69	0.66	1.18	1	1	8	7	8	4	9	8
	EICCR11	0	0.67	0.87	1.17	9	4	11	7	9	3	12	16
	EICCR4	0	0.68	0.64	1.09	1	1	4	3	6	3	7	5
	NISCR5[a]	0	0.58	0.71	1.02	20	9	18	1	15	4	14	19
	EICCR15	0	0.35	0.58	1.05	3	1	5	3	6	2	12	11
C ($I_C > 1$)	EISCR1	0	18.8	0.71	1.09	1	1	8	157	10	147	11	20
	NISCR7	0	6.70	0.62	1.30	1	1	22	90	17	117	15	13
	NISCR2	0	4.89	0.69	1.06	3	2	6	38	5	32	6	15
	NISCR8	0	4.46	0.58	1.19	1	0	11	91	12	97	13	29
	NICCR1	0	4.13	0.87	1.11	0	0	11	96	7	5	8	10
	NICCR8	0	3.04	0.61	1.63	0	0	9	57	9	53	7	5
	NISCR10	0	1.93	0.59	1.11	1	1	12	40	10	37	17	17
	NISCR11	0	1.08	0.65	1.11	5	2	13	44	6	14	13	16

[a] NISCR5 is excluded from the error synthesis since this bridge has large second-order amplification. The stresses and displacements for this bridge are reported at 1.5 and 1.0 of the TDL respectively.

Table 5.1 (continued). I-girder bridge percent normalized mean errors compared to 3D second-order elastic FEA for major-axis bending stresses (f_b) and vertical displacements (Δ_z).

Group	Bridge Name	I_S	I_C	Max. I_T	Max. I_L	3D-FEA Linear		2D-Grid - P1		2D-Grid - P2		1D	
						f_b μ_e	Δz μ_e	f_b μ_e	Δz μ_e	f_b μ_e	Δz μ_e	f_b μ_e	Δz μ_e
S ($I_S \leq 0.30$)	XICSN1	0	0	0.50	1.00	0	0	4	3	3	3	5	6
	NISSS2	0.11	0	0.50	1.00	1	0	5	4	5	2	8	5
	EISSS3[b]	0.24	0	0.50	1.00	4	6	9	9	9	9	10	12
	NISSS6	0.19	0	0.53	1.21	4	2	5	2	7	3	5	2
	NISSS11	0.18	0	0.50	1.00	0	0	4	4	2	1	4	4
	NISSS37	0.18	0	0.54	1.44	2	1	3	2	2	1	10	6
	NISSS53	0.29	0	0.50	1.00	1	1	5	5	5	5	5	6
	NISSS56	0.30	0	0.53	1.34	4	2	5	1	4	1	8	6
	NICSS1	0.11	0	0.52	1.25	1	1	2	3	2	11	4	3
	NICSS3	0.11	0	0.52	1.25	1	0	3	2	3	8	4	3
	NICSS25	0.15	0	0.52	1.16	0	1	2	3	2	4	3	3
	NICSS27	0.15	0	0.52	1.16	1	1	3	3	3	3	4	3

[b] EISSS3 is excluded from the error synthesis since this bridge has large second-order amplification and is unable to support the total dead load (TDL). The stresses and displacements reported in the table for this bridge are at 1.3 and 1.0 of the TDL respectively.

Table 5.1 (continued). I-girder bridge percent normalized mean errors compared to 3D second-order elastic FEA for major-axis bending stresses (f_b) and vertical displacements (Δ_z).

Group	Bridge Name	I_S	I_C	Max. I_T	Max. I_L	3D-FEA Linear		2D-Grid - P1		2D-Grid - P2		1D	
						f_b μ_e	Δz μ_e	f_b μ_e	Δz μ_e	f_b μ_e	Δz μ_e	f_b μ_e	Δz μ_e
S ($0.30 < I_S \leq 0.65$)	NISSS4	0.44	0	0.50	1.00	3	3	9	6	7	6	10	7
	EISSS5	0.54	0	0.50	1.00	2	2	7	6	4	6	9	8
	EISSS6	0.43	0	0.50	1.00	3	0	9	5	7	2	6	6
	NISSS36	0.40	0	0.55	1.49	3	1	9	2	7	2	8	3
	XICSS5[c]	0.53	0	0.50	1.00	1	1	NA	NA	16	12	NA	NA
	EICSS1[c]	0.42	0	0.50	1.00	0	0	NA	NA	11	12	NA	NA
	XICSS5	0.53	0	0.50	1.00	1	1	12	8	6	7	16	12
	EICSS1	0.42	0	0.50	1.00	0	0	4	4	4	6	8	3
	EICSS2	0.50	0	0.55	1.35	1	0	6	6	6	6	9	8
	NISSS13	0.60	0	0.50	1.00	1	1	6	5	5	6	5	5
	NISSS16	0.59	0	0.58	1.83	2	2	9	6	8	6	9	7
	EICSS12	0.58	0	0.50	1.00	1	0	7	5	4	3	7	7
S ($I_S > 0.65$)	NISSS14	1.36	0	0.50	1.00	4	0	27	26	26	27	28	27
	NICSS16	1.69	0	0.50	1.00	1	0	15	12	15	16	15	13
	NISSS54	0.68	0	0.50	1.00	4	2	17	16	16	13	16	13

[c] Considering staged deck placement in the 3D FEA and in Program 2

Table 5.1 (continued). I-girder bridge percent normalized mean errors compared to 3D second-order elastic FEA for major-axis bending stresses (f_b) and vertical displacements (Δ_z)

Group	Bridge Name	I_S	I_C	I_T	I_L	3D-FEA Linear		2D-Grid - P1		2D-Grid - P2		1D	
						f_b μ_e	Δz μ_e	f_b μ_e	Δz μ_e	f_b μ_e	Δz μ_e	f_b μ_e	Δz μ_e
C&S	EISCS3	0.25	2.99	0.68	0.86	1	1	7	25	5	5	19	38
	NISCS3	0.11	3.44	0.71	1.18	4	2	10	2	5	1	29	23
	NISCS9	0.35	3.11	0.63	0.88	2	1	10	36	10	5	24	23
	NISCS14	0.67	4.46	0.55	0.65	0	0	9	76	7	3	10	15
	NISCS15	0.36	4.46	0.67	1.88	1	1	19	74	14	12	11	16
	NISCS37	0.35	1.03	0.35	0.62	1	1	9	42	23	36	37	40
	NISCS38	0.48	0.94	0.59	0.68	1	0	4	39	4	5	15	18
	NISCS39	0.17	1.21	0.68	1.32	7	3	13	53	10	2	10	17
	EISCS4[d]	0.04	0.55	0.64	1.00	53	52	41	48	43	48	43	50
	EICCS10	0.16	2.19	0.73	1.07	0	0	10	25	10	19	14	12
	NICCS2	0.13	3.67	0.87	1.24	0	0	7	36	4	3	9	10
	NICCS3	0.13	3.30	0.81	0.98	1	0	17	62	5	4	11	13
	XICCS7	0.36	1.33	0.65	1.51	0	0	12	21	9	9	15	6
	NICCS9	0.73	3.04	0.58	0.77	0	0	13	73	5	7	8	21
	NICCS13	0.11	1.05	0.85	0.98	2	1	7	21	3	2	10	13
	NICCS14	0.04	1.12	0.88	1.04	2	1	6	21	4	3	11	11
	EICCS1	0.08	0.99	0.80	1.25	1	1	10	20	29	5	30	14
	EICCS27	0.92	0.17	0.47	0.90	1	0	15	10	17	7	18	11
	NICCS24	0.09	0.46	0.68	1.18	1	1	6	19	3	1	7	6

[d] EISCR4 is excluded from the error synthesis since this bridge has large second-order amplification and is unable to support the total dead load (TDL). The stresses and displacements reported in the table for this bridge are at 82 % of the TDL.

It is recommended that the factor AF_G (Eq. 2.101) should be calculated and used in performing the AASHTO constructability checks for two and three-girder units (or intermediate stages of the steel erection), as well as for relatively narrow units or intermediate stages with L_s/w_g ratios greater than about five. In addition, in I-girder bridges involving lean-on bracing systems, the lean-on effects from all the girders being stabilized must be considered. The reader is referred to Helwig et al. (2005) and Hermann et al. (2005) for presentation of simplified procedures for checking girder system stability including lean-on effects.

Although the analysis results considered are based on the final constructed geometry of the bridge for NISCR5, and the final constructed geometry of the bridge unit that experienced excessive displacements for EISCS4, these results are representative of results that can be expected for other intermediate stages of the steel erection where the partially completed structure is composed of only a few girders and/or is relatively narrow compared to the span length.

In addition to global second-order amplification due to stability effects, the potential local second-order amplification of the flange lateral bending should be checked between the cross-frame locations in bridge I-girders. Equation 6.10.1.6-4, from AASHTO LRFD Article 6.10.1.6, serves generally as an accurate to conservative estimate of this local second-order amplification. In particular, large values of the *AF* estimated by this equation on fascia girders may indicate a condition where the flange lateral bending due to overhang eccentric bracket loads and/or horizontal curvature may lead to excessive torsional rotations that can cause local dips in the deck elevations between cross-frames. These rotations can be exacerbated by web distortional deformations in cases where the height of the overhang brackets is significantly less than the girder web depths. Therefore, local web distortional deformations on fascia girders always should be checked.

Lastly, the benchmark 3D-FEA model of the "S ($I_S \leq 0.30$)" bridge EISSS3 is unable to support the factored total dead load (1.5 x TDL) due to large second-order amplification associated with the flexibility of the V-type cross-frames without top chords utilized in this structure. Therefore, EISSS3 is excluded from further consideration in the synthesis of the errors below. V-type cross-frames without top chords often do not have sufficient stiffness to brace the I-girders prior to the deck becoming composite. Their effectiveness may often depend on incidental stiffnesses developed by the formwork or other construction devices serving as top

chord elements. These incidental stiffnesses can be highly variable and difficult to gage or to control, and thus the use of V-type cross-frames can result in significant difficulties in the ability to predict the physical constructed geometry in the field. Therefore, as discussed subsequently in Chapter 9, V-type cross-frames without top chords should be used with extreme caution.

2D-Grid Solutions

Several observations can be made regarding the 2D-grid solutions from Table 5.1:

- The 2D-grid solutions from Programs P1 and P2 are very similar for the major-axis bending stresses in all the cases of Table 5.1, with the exception of only three of the "C&S" bridges, NISCS37, NICCS3, and EICCS1. Program P1 gives significantly better f_b results for NISCS37 and EICCS1, whereas P2 gives much better f_b results for NICCS3. There is no clear reason why the solutions differed significantly for just these three bridges.
- For all the "C" bridges and for all the "S" bridges, the vertical displacement solutions are very similar from both 2D-grid programs with the exception of bridges NICCR1 and NISCR11, where program P2 gives much better results. Similar to the above cases, there is no clear reason for the larger error exhibited by P1 for just these two bridges.
- For the "S" bridges with $I_S \leq 0.30$ and $0.30 < I_S < 0.65$, all of the conventional 2D-grid solutions for the major-axis bending stresses and vertical displacements are reasonably good (a more quantitative assessment of the errors as a function of the bridge type is presented in the next section). However, for the "S" bridges with $I_S > 0.65$, the conventional 2D-grid solutions give relatively poor predictions for both the major-axis bending stresses and the displacements. The reason for this behavior is discussed in detail subsequently in Chapter 6. Basically, due to the poor (highly flexible) girder torsion model, the conventional 2D-grid solutions are unable to capture the transverse load paths that develop in skewed bridges with large I_S values.
- For the "C" bridges with $I_C > 1$, both the 2D-grid programs P1 and P2 give poor displacement solutions in the majority of the cases. The only cases of this group where the results are reasonably accurate are the P2 solutions for bridges NICCR1 and NISCR11. A key reason for this behavior is explained below.

- For the “C&S” bridges, the displacement results are reasonably accurate for the 2D-grid program P2, with the exception of bridges NISCS37 and NICCS10 (after excluding EISCS4 due to large AF_G). However, the 2D-grid program P1 exhibits very large displacement errors for the majority of the “C&S” bridges. NISCS3 and EICCS27 are the only bridges that have reasonably accurate displacement predictions from P1. A key reason for this behavior, as well as for the above poor displacement results for the “C” bridges with $I_C > 1$, is explained below.

The key reason for the poor displacement results in the last two of the above observations is the use of multiple elements between the cross-frame locations in modeling the curved girders in these structures. As noted at the beginning of this chapter, the models in program P1 were created using four elements between each of the cross-frames for all of the bridges, and the program P2 models were created with a “high-resolution mesh” for all of the bridges, which typically means that P2 also uses four elements between each cross-frame member. However, P2 was also set up to include the effect of the composite slab via the Plate-Eccentric Beam approach in subsequent solutions. The P2 Plate-Eccentric Beam solution is effectively just a 2D-grid solution prior to the slab being made composite. Unfortunately, program P2 is unable to create a high-resolution mesh in its Plate-Eccentric Beam solution when a bridge has skew, and hence P2 defaults back to a “low-resolution mesh” in these situations. With a low-resolution mesh in P2, only one element is utilized between each of the cross-frame members.

Interestingly, contrary to what one might expect, the use of a single element between the cross-frame locations results in more accurate solutions with the conventional 2D-grid procedures. The reason for this behavior can be explained in basic terms by considering an isolated conventional 2D-grid model of an I-section member, subjected to uniform moment along a circular arc between two cross-frame locations, i.e., equal and opposite end moments (see Figure 5.2). The vector direction of the moments, by the right-hand rule, is indicated by the double arrows in the figure. In the common “high-resolution” representation of this curved member, the arc is modeled with four straight elements, with each of the nodes located along the arc. Major-axis bending moments perpendicular to the chord between the member ends resolve into both a major-axis bending and a torsional component within the individual elements. If one considers the equilibrium at one of the intermediate nodes, major-axis bending in one element is

generally resolved into both major-axis bending and torsion in the next element. However, unfortunately, in the conventional methods, the torsional model substantially underestimates the true stiffness of the I-girder, since only the St. Venant term (GJ/L) is considered. The torsional stiffness coming from the restraint of warping, related to the cross-section rigidity term EC_w, is neglected. As such, the twisting deformations are grossly over-estimated.

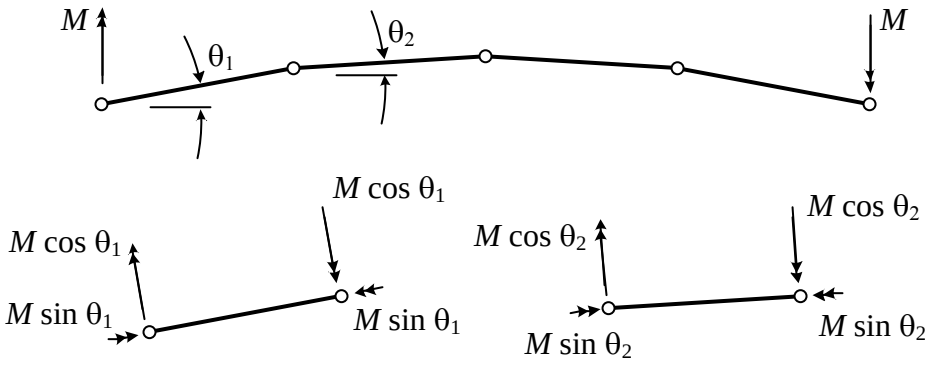

Figure 5.2. Behavior for a chorded representation of a curved I-girder using four straight elements.

Furthermore, because of the curved geometry (represented in a chorded fashion by the four elements in Figure 5.2), the small torsional stiffness reduces the overall stiffness of the approximate model in resisting vertical deflection. The twisting of one element causes not only a torsional rotation in the next element, but because of the change in orientation of the elements in the chorded representation of the arc, it causes major-axis bending rotation and corresponding vertical deflections in the next element. Furthermore, the overall major-axis bending rotational stiffness that this member provides to the rest of the bridge, about an axis perpendicular to its chord and at its ends, is reduced by the above effects. This results in an increase in the vertical deflections at other locations in the bridge.

Interestingly, if a curved I-girder is represented by only one straight element between its cross-frame locations, the cross-frames are able to resist the components of the moments that cause twisting of the girder. As a result, the overall model of the bridge structure responds in a much stiffer fashion. This same behavior is obtained if multiple elements are used between the cross-frames with the overall geometry represented as a straight chord between the cross-frames.

(This helps explain why the vertical deflections in straight skewed I-girders are still represented reasonably well with a high resolution mesh).

Modeling of the girders as straight segments between the cross-frames tends to improve the results in the conventional 2D-grid analysis of curved bridges, since in effect, this approach completely neglects the influence of the horizontal curvature between the cross-frames (with the exception of separate calculations to estimate girder flange lateral bending stresses). Studies conducted with "C&S" bridges to address this peculiarity demonstrate that the responses obtained from the P1 models, when the discretization is reduced to one element between every set of cross-frames, are essentially the same as with the P2 models.

Completely neglecting the horizontal curvature effects between the cross-frames of course cannot generally produce an accurate model either. Therefore, using a coarse grid of elements with only one straight element between each cross-frame is not generally recommended as a proper way to obtain accurate predictions. It should be noted that the "C&S" bridges NISCS37 and EICCS10 have relatively poor displacement predictions in spite of the fact that the P2 solutions were based on a single element between each of the cross-frames. Nevertheless, in many bridges, the girder arcs between the cross-frames are small enough such that a single element between the cross-frames should be sufficient to accurately represent the overall curved geometry of the structure (assuming that a more accurate girder torsional stiffness than the conventional GJ/L is employed, as discussed in Chapter 6). The flange lateral bending stresses between the cross-frames can still be estimated using "component stress" equations such as Eqs. (2.13) through (2.17), or by more accurate means as discussed subsequently in Chapter 6.

Chapter 6 discusses modeling practices that can be implemented to improve the predictions obtained from 2D-grid analyses. The practices discussed in Chapter 6 are based on the principles of structural mechanics, and do not rely on the discretization level used in the model. The large errors associated with the more refined discretization are due to the dramatic under-representation of the girder torsional stiffness in the conventional 2D-grid models, along with the coupling between twist rotations and vertical displacements in curved members.

1D Line-Girder Solutions

The 1D line-girder results in Table 5.1 exhibit the following characteristics:

- The solutions are reasonably good for all the "C" bridges with $I_C < 1$. However, for the "C" bridges with $I_C > 1$, the errors are somewhat larger for several of the bridges, particularly for the displacements. It should be emphasized that the connectivity index, I_C, relates primarily to the influence of the poor girder torsion model on the overall results in conventional 2D-grid solutions. However, some correlation of the errors with I_C is evident also for the line-girder analysis solutions.
- For the "S" bridges, the 1D line-girder solutions are comparable in accuracy to the conventional 2D-grid solutions in all cases. The accuracy is reasonably good using both the 1D and the conventional 2D grid procedures for the $I_S \leq 0.30$ and the $0.30 < I_S \leq 0.65$ bridges. However, both of these types of solutions show relatively large errors for the major-axis bending stresses and the vertical displacements for the bridges with $I_S > 0.65$. Similar to the conventional 2D-grid solutions, 1D line-girder analysis is unable to capture any information about the transverse load paths in the structure. These load paths tend to be a significant characteristic of the overall bridge response in bridges with large I_S values. Of course, engineers would not generally expect to capture the transverse load paths from a 1D line-girder analysis. However, they may expect that these load paths are captured by a 2D-grid solution.
- For the "C&S" bridges, the errors relative to the 3D FEA benchmarks from the 1D-line girder analyses are highly variable. There are no clear trends in the data, other than the fact that the large errors are obviously due to the combination of skew with horizontal curvature. The V-load method does not have any mechanisms for including the influence of skew within its estimates, and therefore, one must expect significant errors with increasing values of skew with this approach. One can observe that the 1D analysis accuracy tends to be better for some of the bridges that have small I_S values. However, this is not generally the case since, in a curved bridge, the orientation of the skew (positive or negative) can have a substantial effect on the resulting bridge geometry.

Staged Deck Placement

For the continuous-span bridges XICSS5 and EICSS1, Table 5.1 shows data both for analyses where staged deck placement was not considered (generated by building the analysis models and simply "turning the gravity loads on") and for analyses where staged deck placement was considered in the 3D FEA and the conventional 2D-grid solutions. The solutions where the staged deck placement was considered are highlighted by the shaded rows for XICSS5 and EICSS1 in Table 5.1. Program P2 was utilized to conduct the 2D-grid solutions for these bridges. In fact, the Plate Eccentric Beam modeling capabilities of this program were employed to represent the participation of the composite concrete deck. The deck concrete from previous stages was assumed to become fully effective in both the 3D FEA and the Plate Eccentric Beam solutions. Other assumptions are possible regarding the early-age stiffness of the concrete deck; however, the above assumptions are sufficient to evaluate the accuracy of the Plate Eccentric Beam solutions versus the 3D FEA benchmarks. In regions of the bridges where the concrete deck is not fully effective, the Plate Eccentric Beam solution effectively defaults to a conventional 2D-grid solution.

The major-axis bending stress and vertical displacement errors for the above two bridges are reasonable, but are slightly larger for the analyses considering the staged deck placement. The scope and number of these studies is not sufficient to draw broad conclusions regarding the accuracy of the Plate-Eccentric Beam models for general staged deck placement analysis. As noted at the end of Section 2.10, the primary focus of the NCHRP 12-79 research was on the overall accuracy of the 1D line-girder and 2D-grid results independent of the participation of the concrete deck.

5.1.1 Synthesis of Errors in Major-Axis Bending Stresses and Vertical Displacements for I-Girder Bridges

Table 5.2 shows the number of I-girder bridges within specific ranges of the normalized mean errors for the major-axis bending stresses and the vertical displacements from Table 5.1. Both of the 2D-grid programs P1 and P2 are considered, as well as the 1D analysis results. The selected error ranges are assigned letter grades based on the following criteria:

A: $\mu_e \leq 6$ %

B: $6\ \% < \mu_e \leq 12$ %

C: $12\ \% < \mu_e \leq 20$ %

D: $20\ \% < \mu_e \leq 30$ %

F: $\mu_e > 30$ %

This grading scheme is somewhat arbitrary and was set based on the experience of the NCHRP 12-79 project team. The recommended use of this grading scheme is addressed subsequently. Depending on the type of response and the consequences of the error, different ranges of error can be acceptable for different calculations on different jobs. In any case, it is believed that most engineers would agree that analysis results that do not deviate more than 6 % from a highly refined benchmark solution are indeed highly accurate. In addition, analysis results where the errors are larger than 30 % relative to a rigorous benchmark solution might be considered as highly unreliable.

All of the linear 3D FEA results in the non-shaded rows of Table 5.1 fall within the A range for the bridges considered with a two minor exceptions, f_b for EICCR11 and f_b for NISCS39 which have errors or 9 and 7 % respectively. The differences between the 3D FEA linear and second-order analysis results in Table 5.1 are due solely to second-order effects. Bridges EICCR11 and NISCS39 are two of the most extreme geometries considered in the NCHRP 12-79 project. EICCR11 is the Ford City Bridge, which is a continuous-span four girder bridge with a 329 ft.curved span, an adjacent 417 ft.straight span, and a 48.3 ft.total deck width. Therefore, it is not surprising that this bridge would have significant second-order effects. These effects are detectable using Eq. (2.101) (see Section 2.9). NISCS39 is a wide 300 ft.simple-span curved bridge with a skew that increases the length of the girder on the outside of the curve.

Although the potential existence of significant second-order effects in the final erected configuration of this bridge would not be detected by the criteria discussed previously, this bridge nearly nearly achieves an A grade. Given these assessments, the 3D linear FEA results are not considered in Table 5.2. Table 5.2 focuses solely on the accuracy of the 2D-grid and 1D line-girder analysis solutions.

Two rows are highlighted for each of the bridge groups and analysis methods in Table 5.2. The row corresponding to the error range with the largest errors exhibited for a given bridge group and analysis solution is highlighted by a dark shade. In addition, the row corresponding to the most frequently occurring error range (i.e., the mode) is highlighted by a light shade, unless this range is the same as the error range with the largest errors.

The highlighted rows in Table 5.2 are used to generate final simplified scores for each of the bridge groups and analysis methods in Tables 5.3 and 5.4. The letter grades provided in Table 5.3 correspond to the worst-case score in Table 5.2, whereas the grades in Table 5.4 correspond to the most frequently occurring score, i.e., the mode score. Various footnotes are provided in Table 5.3 to identify the reasons for the worst-case scores.

Overall, one can observe the following from Tables 5.3 and 5.4:

- Both of the 2D-grid programs have worst-case grades of B and A as long as $I_C \leq 1$ for the "C" bridges, and as long as $I_S < 0.65$ for the "S" bridges. The mode of the grades in these categories is predominantly an A.
- For the "C" bridges with $I_C > 1$, the worst-case grades for f_b are a D and a C, while the mode of the grades is a B. However, the vertical displacements receive an F even for the mode of the grades, indicating that there are a large number of bridges where the displacement results might be considered unacceptable.
- For the "C" bridges with $I_C \leq 1$, the 1D methods (i.e., line-girder analysis with the V-load method) receive a worst-case score of B for both the major-axis bending stresses and C for the displacements.
- For the "C" bridges with $I_C > 1$, the 1D displacement calculations get a minimum grade of D and a mode of the grades of C. Both the worst-case and mode of the grades for the major-axis bending stresses is a C for this group.

Table 5.2. Number of I-girder bridges within specified error ranges for major-axis bending stress and vertical displacement for each of the types of bridges considered.

Type of Bridge	Number of Bridges	Error Range	Number of Bridges within Error Range					
			Major-Axis Bending Stress			Vertical Displacement		
			2D-P1	2D-P2	1D	2D-P1	2D-P2	1D
C ($I_C \leq 1$)	5	A: ≤ 6%	3	3	0	3	**5**	2
		B: 7-12%	**2**	**2**	5	**2**	0	2
		C: 13-20%	0	0	0	0	0	**1**
		D: 21-30%	0	0	0	0	0	0
		F: >30%	0	0	0	0	0	0
C ($I_C > 1$)	8	A: ≤ 6%	1	2	1	0	1	1
		B: 7-12%	5	5	3	0	0	1
		C: 13-20%	1	**1**	**4**	0	1	5
		D: 21-30%	**1**	0	0	0	0	**1**
		F: >30%	0	0	0	**8**	**6**	0
S ($I_S < 0.30$)	11	A: ≤ 6%	**11**	9	8	**11**	10	**11**
		B: 7-12%	0	**2**	**3**	0	**1**	0
		C: 13-20%	0	0	0	0	0	0
		D: 21-30%	0	0	0	0	0	0
		F: >30%	0	0	0	0	0	0
S ($0.30 \leq I_S < 0.65$)	10	A: ≤ 6%	3	6	2	9	9	4
		B: 7-12%	**7**	**4**	7	**1**	**1**	**6**
		C: 13-20%	0	0	**1**	0	0	0
		D: 21-30%	0	0	0	0	0	0
		F: >30%	0	0	0	0	0	0
S ($I_S \geq 0.65$)	3	A: ≤ 6%	0	0	0	0	0	0
		B: 7-12%	0	0	0	1	0	0
		C: 13-20%	2	2	2	1	2	2
		D: 21-30%	**1**	**1**	**1**	**1**	**1**	**1**
		F: >30%	0	0	0	0	0	0
C&S ($I_C > 0.5$ & $I_S > 0.1$)	18	A: ≤ 6%	3	9	0	1	12	2
		B: 7-12%	11	5	9	1	4	4
		C: 13-20%	**4**	2	5	2	1	7
		D: 21-30%	0	**2**	3	5	0	3
		F: >30%	0	0	**1**	**9**	**1**	**2**

Table 5.3. Worst-case I-girder bridge scores for major-axis bending stress and vertical displacement.

Type of Bridge	Worst Case Scores					
	Major-Axis Bending Stress			Vertical Displacement		
	2D-P1	2D-P2	1D	2D-P1	2D-P2	1D
C ($I_C \leq 1$)	B	B	B	B	A	C[e]
C ($I_C > 1$)	D[a]	C[a]	C	F	F	D[f]
S ($I_S < 0.30$)	A	B[b]	B	A	B[g]	A
S ($0.30 \leq I_S < 0.65$)	B	B	C[c]	B[h]	B[i]	B
S ($I_S \geq 0.65$)	D	D	D	D	D	D
C&S ($I_C > 0.5$ & $I_S > 0.1$)	C	D	F[d]	F	F[j]	F

[a] One bridge, NISCR7, has a mean error of 22 % and 17 % for Programs P1 and P2 repectively. This is believed to be due to the combined poor girder torsion model and inaccurate cross-frame stiffness model along with the large width of this bridge. Program P1 has somewhat larger errors than Program P2 because the curved girders were subdivided into multiple elements along each unbraced length in the Program P1 solution.

[b] One bridge with unequal skew, NISSS6, has a mean error of 7 %.

[c] One bridge with parallel 60° skew, XICSS5, has a mean error of 16 % due to transverse load path (nuisance stiffness) effects.

[d] One bridge, NISCS37, has a mean error of 37 %. The V-load method removes load from the girder on the inside of the curve in this bridge, but the inside girder is the longest because of the skew. The V-load method is not able to capture the corresponding larger bending within the inside girder.

[e] One bridge, EICCR11, has a mean error of 16 %. This larger error is due to torsional interactions between the spans in this continuous-span bridge, which are not captured accurately by the V-Load Method.

[f] One bridge, NISCR8, has a mean error of 29 %. The V-Load Method does not accurately capture the major-axis bending stresses in the interior girders (e.g., Girders 4 and 5) of this wide 9-girder bridge

[g] One bridge, NICSS3, has a mean error of 8 %, due to over-prediction of the displacements in the first span (having parallel skew) and under-prediction of the displacements in the second span (having unequal skew).

[h] One bridge with parallel 60° skew, XICSS5, has a mean error of 8 % due to transverse load path (nuisance stiffness) effects.

[i] One bridge with unequal skew, NICSS1, has a mean error of 11 %.

[j] One bridge, NISCS37, has a mean error of 36 %. This is believed to be due to lack of ability of the poor torsional stiffness model in conventional 2D-grid solutions to capture substantial torsional interactions between the girders.

Table 5.4. Mode of I-girder bridge scores for major-axis bending stress and vertical displacement.

Type of Bridge	Mode of Scores					
	Major-Axis Bending Stress			Vertical Displacement		
	2D-P1	2D-P2	1D	2D-P1	2D-P2	1D
C ($I_C \leq 1$)	A	A	B	A	A	B
C ($I_C > 1$)	B	B	C	**F**	**F**	C
S ($I_S < 0.30$)	A	A	A	A	A	A
S ($0.30 \leq I_S < 0.65$)	B	A	B	A	A	B
S ($I_S \geq 0.65$)	C	C	C	C	C	C
C&S ($I_C > 0.5$ & $I_S > 0.1$)	B	A	C[a]	**F**	A	C

[a] Modified from B to C considering the grade for the C ($I_C > 1$) and S ($I_S > 0.65$) bridges

- For the "S" bridges with $I_S \geq 0.65$, both the major-axis bending stresses and the vertical displacements have a worst-case score of D and a mode of the grades of C in all the methods.
- For the "C&S" bridges, the major-axis bending stresses received worst-case grades of C and D with programs P1 and P2 respectively. Furthermore, the 1D analysis major-axis bending stresses scored a worst-case grade of F due to one bridge exhibiting very poor results, while most of the bridges scored in the B range. The displacements generally were very poor for program P1 (due to the discretization of the girder unbraced lengths into multiple elements), whereas they were usually quite good for program P2, due to the defaulting of the element discretization to a low-resolution mesh, although one bridge still fell within the F range with program P2).

It is useful to understand the qualifier indicated on the "C&S" bridges, i.e., "($I_C > 0.5$ & $I_S > 0.1$)" in Tables 5.3 and 5.4. If a bridge has an $I_C < 0.5$ and an $I_S > 0.1$, it can be considered as a straight-skewed bridge for the purposes of assessing the expected analysis accuracy. Furthermore, if a bridge has an $I_C > 0.5$ with an $I_S \leq 0.1$, it can be considered as a curved radially-supported bridge for these purposes.

5.1.2 Generalized I-Girder Bridge Analysis Scores

Table 5.5 provides a synthesis of the analysis scores for the various I-girder bridge responses from traditional 2D-grid and 1D-line girder methods at large. This table addresses the accuracy of the calculations for major-axis bending stresses, vertical displacements, cross-frame forces, flange lateral bending stresses, and girder layovers at the bearings.

Key observations that can be drawn from Table 5.5 are discussed below:

Major-Axis Bending Stresses and Vertical Displacements

For the first two responses in Table 5.5, the major-axis bending stresses and the vertical displacements, the worst-case and mode letter grades are taken as the lower of the scores for programs P1 and P2 in Tables 5.3 and 5.4.

Cross-Frame Forces

The accuracy for the third through fifth responses in Table 5.5 can be estimated based on the grades from the first two responses when considering the "C" bridges. The results for the third response in these bridge types, the cross-frame forces, are roughly one letter grade less in accuracy compared to the major-axis bending stresses when evaluated by the traditional 2D-grid methods. This reduced accuracy is due to the substantial under-representation of the girder torsional stiffnesses and the crude representation of the cross-frame stiffnesses by prismatic beam elements in these methods. However, for curved girder bridges the cross-frame forces are comparable in accuracy to the major-axis bending stresses for the 1D-line girder method (i.e., line girder analysis with the V-load method adjustments).

For the straight-skewed bridges with minor skew, i.e., the "S (I_S < 0.30)" bridges, the gravity load cross-frame forces tend to be relatively small; therefore, the corresponding analysis errors are not of any consequence. However, for straight bridges with larger skew indices, the major flaws of the 2D-grid methods associated with the poor girder torsion model and the poor cross-frame models essentially render the cross-frame force estimates as useless. In addition, the 1D-line girder analysis models do not provide any information about the cross-frame forces due to the skew effects. Therefore, both the traditional 2D-grid and the 1D-line girder analysis methods get an F for these cases.

Table 5.5. Generalized I-girder bridge scores.

Response	Geometry	Worst-Case Scores		Mode of Scores	
		Traditional 2D-Grid	1D-Line Girder	Traditional 2D-Grid	1D-Line Girder
Major-Axis Bending Stresses	C ($I_C \leq 1$)[g]	B	B	A	B
	C ($I_C > 1$)	D	C	B	C
	S ($I_S < 0.30$)[h]	B	B	A	A
	S ($0.30 \leq I_S < 0.65$)	B	C	B	B
	S ($I_S \geq 0.65$)	D	D	C	C
	C&S ($I_C > 0.5$ & $I_S > 0.1$)	D	F	B	C
Vertical Displacements	C ($I_C \leq 1$)	B	C	A	B
	C ($I_C > 1$)	F	D	F	C
	S ($I_S < 0.30$)	B	A	A	A
	S ($0.30 \leq I_S < 0.65$)	B	B	A	B
	S ($I_S \geq 0.65$)	D	D	C	C
	C&S ($I_C > 0.5$ & $I_S > 0.1$)	F	F	F	C
Cross-Frame Forces	C ($I_C \leq 1$)	C	C	B	B
	C ($I_C > 1$)	F	D	C	C
	S ($I_S < 0.30$)	NA[a]	NA[a]	NA[a]	NA[a]
	S ($0.30 \leq I_S < 0.65$)	F[b]	F[c]	F[b]	F[c]
	S ($I_S \geq 0.65$)	F[b]	F[c]	F[b]	F[c]
	C&S ($I_C > 0.5$ & $I_S > 0.1$)	F[b]	F[c]	F[b]	F[c]
Flange Lateral Bending Stresses	C ($I_C \leq 1$)	C	C	B	B
	C ($I_C > 1$)	F	D	C	C
	S ($I_S < 0.30$)	NA[d]	NA[d]	NA[d]	NA[d]
	S ($0.30 \leq I_S < 0.65$)	F[b]	F[e]	F[b]	F[e]
	S ($I_S \geq 0.65$)	F[b]	F[e]	F[b]	F[e]
	C&S ($I_C > 0.5$ & $I_S > 0.1$)	F[b]	F[e]	F[b]	F[e]
Girder Layover at Bearings	C ($I_C \leq 1$)	NA[f]	NA[f]	NA[f]	NA[f]
	C ($I_C > 1$)	NA[f]	NA[f]	NA[f]	NA[f]
	S ($I_S < 0.30$)	B	A	A	A
	S ($0.30 \leq I_S < 0.65$)	B	B	A	B
	S ($I_S \geq 0.65$)	D	D	C	C
	C&S ($I_C > 0.5$ & $I_S > 0.1$)	F	F	F	C

[a] Magnitudes should be negligible for bridges that are properly designed & detailed. The cross-frame design is likely to be controlled by considerations other than gravity-load forces.

[b] Results are highly inaccurate due to modeling deficiencies addressed in Ch. 6 of the NCHRP 12-79 Task 8 report. The improved 2D-grid method discussed in this Ch. 6 provides an accurate estimate of these forces.

[c] Line-girder analysis provides no estimate of cross-frame forces associated with skew.

[d] The flange lateral bending stresses tend to be small. AASHTO Article C6.10.1 may be used as a conservative estimate of the flange lateral bending stresses due to skew.

[e] Line-girder analysis provides no estimate of girder flange lateral bending stresses associated with skew.

[f] Magnitudes should be negligible for bridges that are properly designed & detailed.

Table 5.5 (continued). Generalized I-girder bridge scores.

---

[g] $I_C = \dfrac{15,000}{R(n_{cf}+1)m}$ is the "connectivity index" (see Section 3.1.3 and Eq. (3.2)), where R is the radius of curvature of the bridge centerline in units of ft., n_{cf} is the number of intermediate cross-frames within the span, and m is a constant equal to 1 for simple-span bridges and 2 for continuous-span bridges.

[h] $I_S = \dfrac{w_g \tan\theta}{L_s}$ is the "skew index" (see Section 3.1.2 and Eq. (3.1)), where w_q is the width of the bridge measured between the centerline of the fascia girders, θ is the skew angle (equal to zero for zero skew), and L_s is the span length.

Flange Lateral Bending Stresses

For the fourth response in Table 5.5, the flange lateral bending stresses, the accuracies from the conventional 2D-grid and the 1D-line girder analysis methods for the "C" bridges, are roughly the same grade as the major-axis bending stresses. This can be understood by recognizing that the flange lateral bending stresses are generally calculated from Eqs. (2.13) through (2.16) in these methods (see Sections 2.1.3.1 and 2.1.3.2). Therefore, the estimate of the maximum flange lateral bending stress from horizontal curvature within the different unbraced lengths, from Eq. (2.15) or (2.16), is proportional to the estimate of the major-axis bending stress. Given that the "proportionality factors" multiplying f_b in Eq. (2.16) provide a reasonable (albeit coarse) estimate of the horizontal curvature effects within each of the unbraced lengths, the accuracy of the flange lateral bending stresses is roughly as good as the accuracy of the major-axis bending stresses in the "C" bridges.

Unfortunately, for the same reasons as described above for the cross-frame forces, the estimates of the flange lateral bending stresses in the "S" and "C&S" bridges are unusable when $I_S \geq 0.30$. The flange lateral bending stress accuracy for the "C&S" bridges with $I_S \leq 0.10$ may be taken roughly as the grade corresponding to its I_C value from the "C" bridges.

Girder Layover at Bearings

As discussed in Section 2.1.4, the girder layovers at skewed bearing lines are closely related to the girder major-axis bending rotations at the bearings, which are in turn closely tied to the vertical displacements within the spans. Therefore, the grades for the 2D-grid and the 1D-line girder estimates of these layovers, the fifth set of responses in Table 5.5, may be taken directly from the scores for the vertical displacements. Of course, the layover at non-skewed bearing lines is essentially zero. Therefore, these estimates are Not Applicable (NA) for the "C" bridges.

5.1.3 Assessment Examples for I-girder bridges

Curved I-Girder Bridge: Figure 5.3 shows the plan view of EICCS1, a basic simple-span bridge with radial supports. It is desired to determine the ability of the approximate analysis methods to capture the behavior of this structure prior to the slab becoming composite, according to the scores shown in Table 5.5.

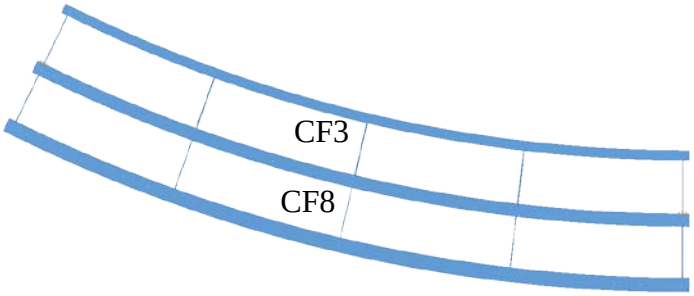

L_{as} = 90 ft./ R = 200 ft./ w = 23.5 ft

Figure 5.3. EICCS1 - Curved and radial simple span I-girder bridge.

This bridge is a relatively simple structure that satisfies the assumptions of the V-load method derivation. For this bridge, the connectivity index is

I_C = 15,000/[(3+1)·200·1] = 18.8 > 1.0

According to Table 5.5, the mode grades for the 1D line-girder and 2D-grid models are:

Response	Analysis Method	
	2D-Grid	1D Line-Girder
f_b	B	C
Vertical deflections	F	C
Cross-frame forces	C	C
f_ℓ	C	C
Girder layovers at bearings	NA	NA

The mode grades may be considered as the more appropriate characterization of the accuracy of this bridge because this bridge is “very regular” in its geometry. The worst-case score is likely the more appropriate one to use when designing a bridge with complicating features such as a poor span balance, or “less regular” geometry characteristics.

Figures 5.4 through 5.6 show the major-axis bending responses on the outside and inside fascia girders of the structure. The vertical displacements in Figure 5.4 are shown at the total noncomposite dead load level (TDL), while f_b in Figures 5.5 and 5.6 is shown at 1.5 times TDL (corresponding to the AASHTO Strengh IV load combination). As shown in Figure 5.4, the vertical displacements are severely over-predicted by the 2D-grid model. The solution obtained from a 1D line-girder model is a better representation of the benchmark. By comparing Figures 5.5 and 5.6, it is observed that the approximate methods properly capture f_b in the outside girder; while in the inside girder, the differences are more noticeable. Since the scores are determined with respect to the girder with the largest errors, which in this case is the inside fascia girder, the score for f_b is B and C for the 2D and 1D methods, respectively.

Figure 5.7 shows the results obtained for the flange lateral bending stresses. In addition, Table 5.6 shows the cross-frame forces calculated from the 2D-grid and the 3D FEA solutions. As in the case of the major-axis bending responses, the scores are a good representation of the predictions obtained with the approximate models. This example shows that the scores are in agreement with the predictions obtained from the approximate analyses.

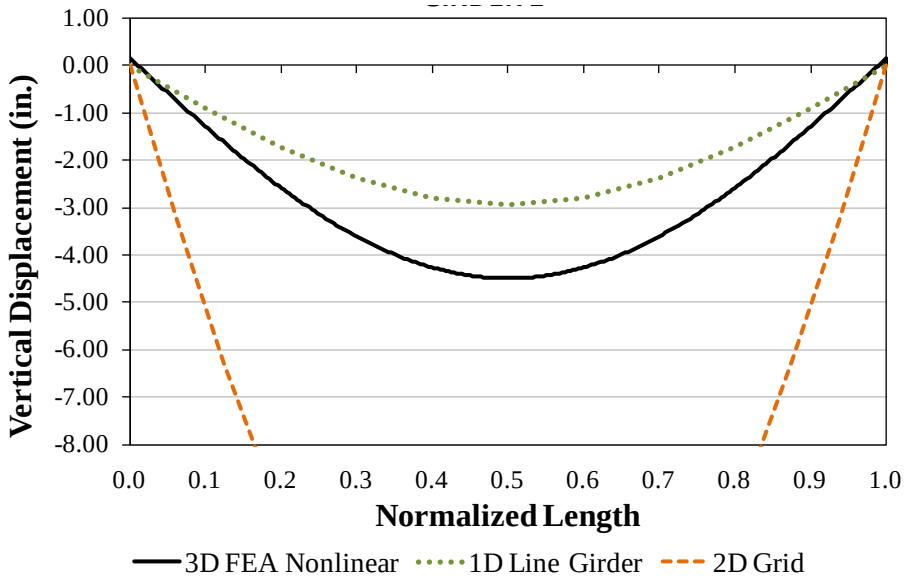

Figure 5.4. Vertical displacements for the fascia girder on the outside of the curve in bridge EISCR1.

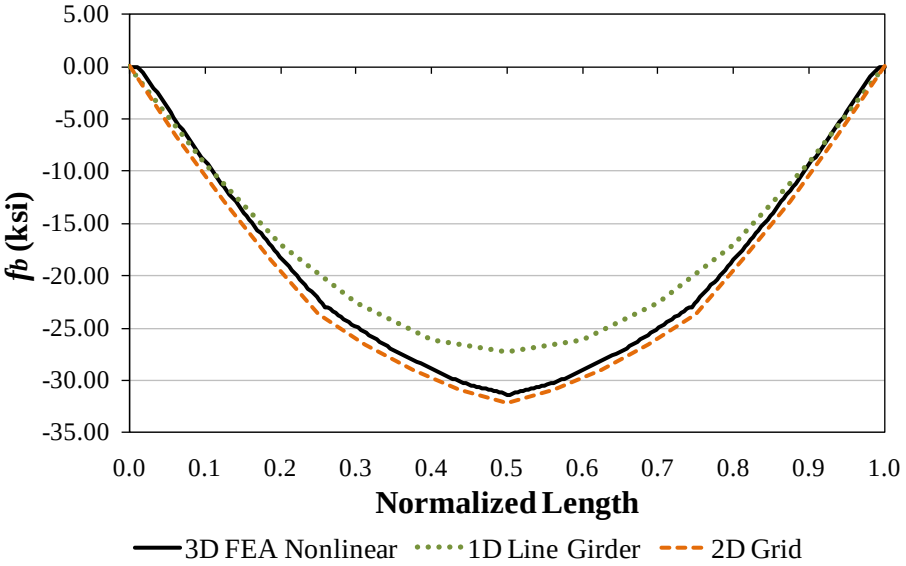

Figure 5.5. Top flange major-axis bending stresses in the fascia girder on the outside of the curve in bridge EISCR1.

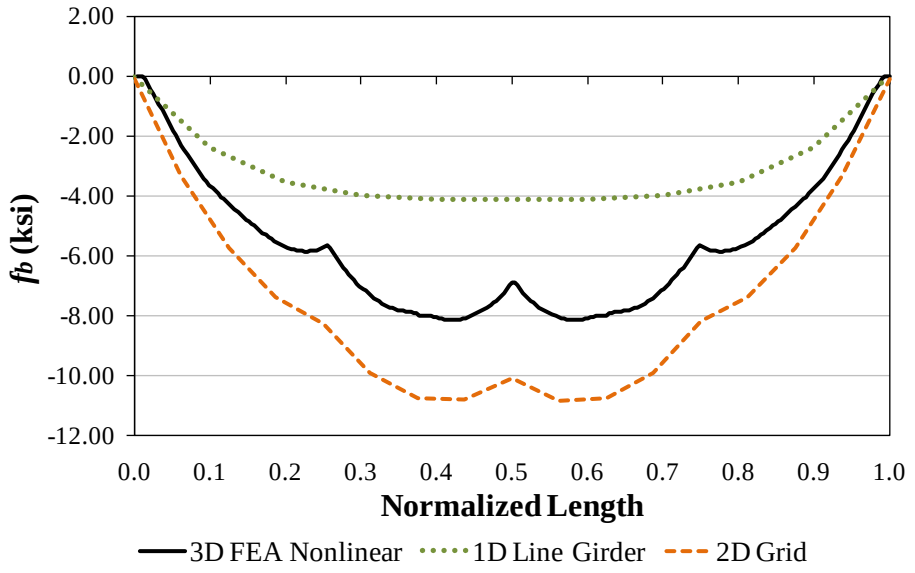

Figure 5.6. Top flange major-axis bending stresses in the fascia girder on the inside of the curve in bridge EISCR1.

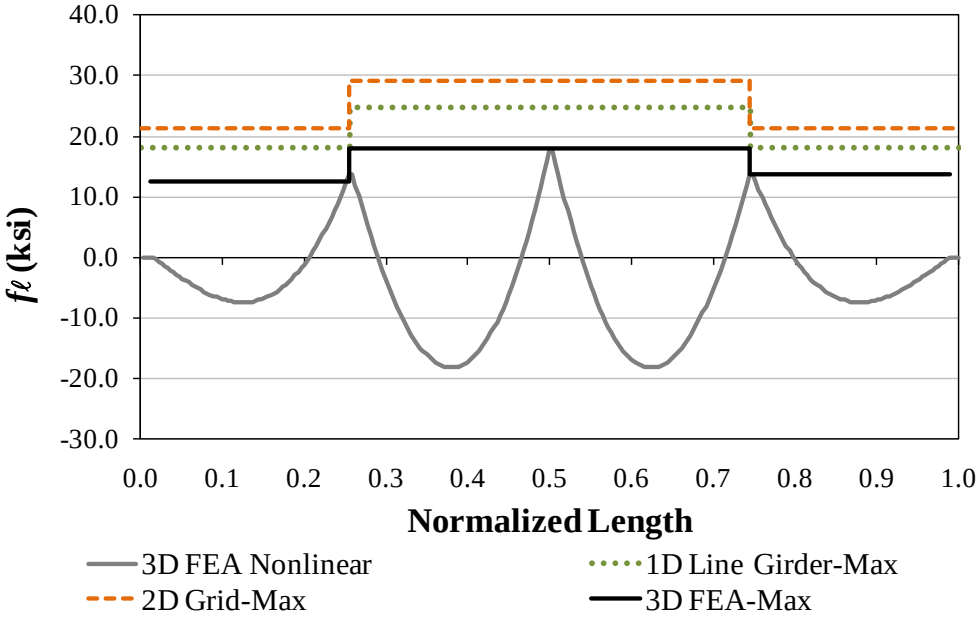

Figure 5.7. Flange lateral bending stresses in the outside fascia girder of bridge EISCR1.

Table 5.6. Cross-frame forces predicted with the 2D-grid and the 3D FEA

Member	CF 3		CF8	
	2D-Grid	3D FEA	2D-Grid	3D FEA
TC	26.6	19.1	24.6	54.5
BC1	-43.1	-46.8	-52.3	-96.6
BC2	-10.1	8.25	3.2	-11.81
D1	23.3	32.7	39.2	49.9
D2	-23.3	-32.3	-39.2	50.2

Skewed I-Girder Bridge: The straight I-girder bridge shown in Figure 5.8, NICSS16, is a severely skewed structure. It is desired to estimate the accuracy of the predictions obtained from a line-girder and a 2D-grid analysis for this bridge, according to the scores shown in Table 5.5.

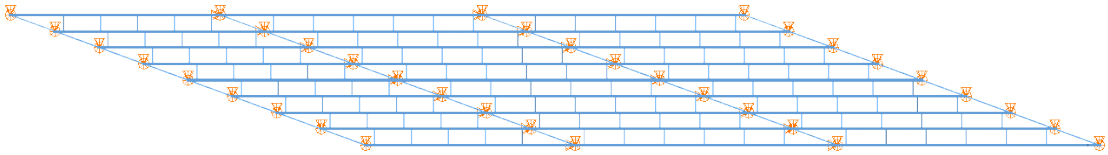

L_1 = 120 ft., L_2 = 150 ft., L_3 = 150 ft./ w = 74 ft./ $\theta_1 = 70^o$, $\theta_2 = 70^o$, $\theta_3 = 70^o$, $\theta_4 = 70^o$

Figure 5.8. NICSS 16 - Straight and skewed continuous I-girder bridge.

The skew indices for each span in this structure are 1.69, 1.36, and 1.36, respectively. These indices are above the 0.65 limit. Hence, it is expected that the skew effects have a significant contribution to the system response. The following are the mode scores for a bridge with these characteristics:

Response	Analysis Method	
	2D-Grid	1D Line-Girder
f_b	C	C
Vertical deflections	C	C
Cross-frame forces	F	F
f_ℓ	F	F
Girder layovers at bearings	C	C

As discussed in the previous example, the mode scores may be considered to be the more appropriate ones here, since the bridge is reasonably "regular," i.e., no severe span imbalance, no significant differences in skew angle of the bearing lines, and no significant variations in the framing of the cross-frames.

Figures 5.9 and 5.10 show the predictions obtained for the girder vertical displacements and stresses in the structure. For simplicity of the discussions, these responses correspond to no-load fit detailing of the cross-frames. As shown in Figure 5.9, both analysis methods overpredict the displacements and stresses in Spans 1 and 3, and slightly underpredict the displacements in Span 2. Similarly, the major-axis bending stresses shown in Figure 5.10, f_b, follow the same trend. In general, it may be considered that the accuracy of the predictions is reasonable.

Conversely, the responses associated with the flow of transverse forces in the system are not captured by the approximate methods. As shown in the stress plot, the local f_ℓ levels are as high as 43 ksi in Span 3. The cross-frame forces associated with the high f_ℓ levels are shown in Figure 5.11. To simplify the observations, they are shown in terms of the cross-frame shear and bending moments rather than in individual chord and diagonal forces. The figure includes the responses obtained from the 3D FEA, a traditional grid analysis, and a grid analysis conducted with the practices recommended in Chapter 6. As shown in the figure, the forces obtained from the traditional grid model are essentially zero. This is due to the limited representation of the cross-frames and the girder torsional stiffness in the traditional method. The plots illustrate that, in this bridge, the physical cross-frame forces are large However, the traditional grid analysis is not able to capture these forces; hence, it is assigned a grade of F.

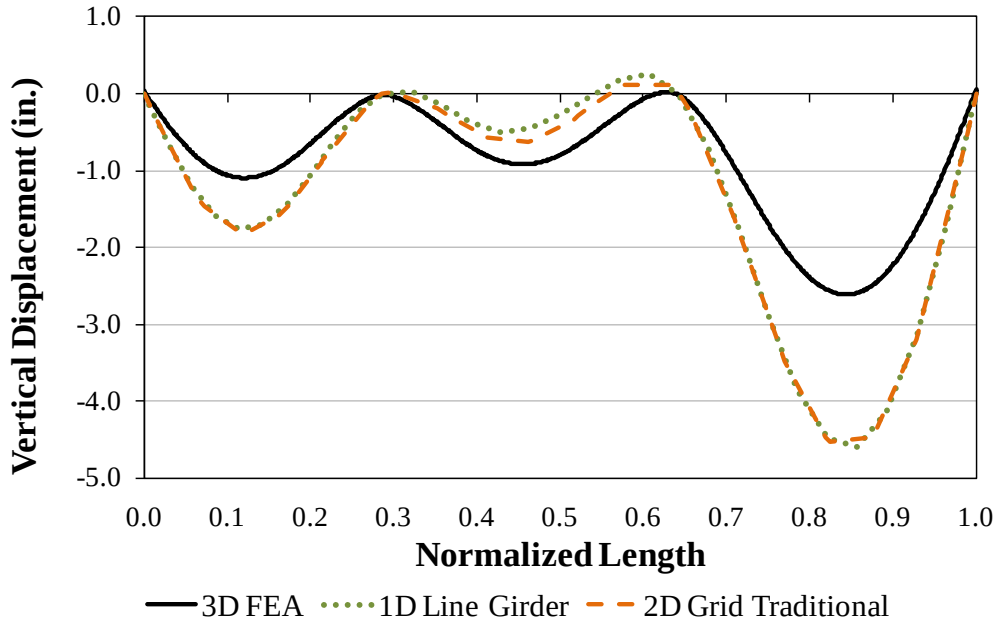

Figure 5.9. Vertical displacement of girder G5 in bridge NICSS16.

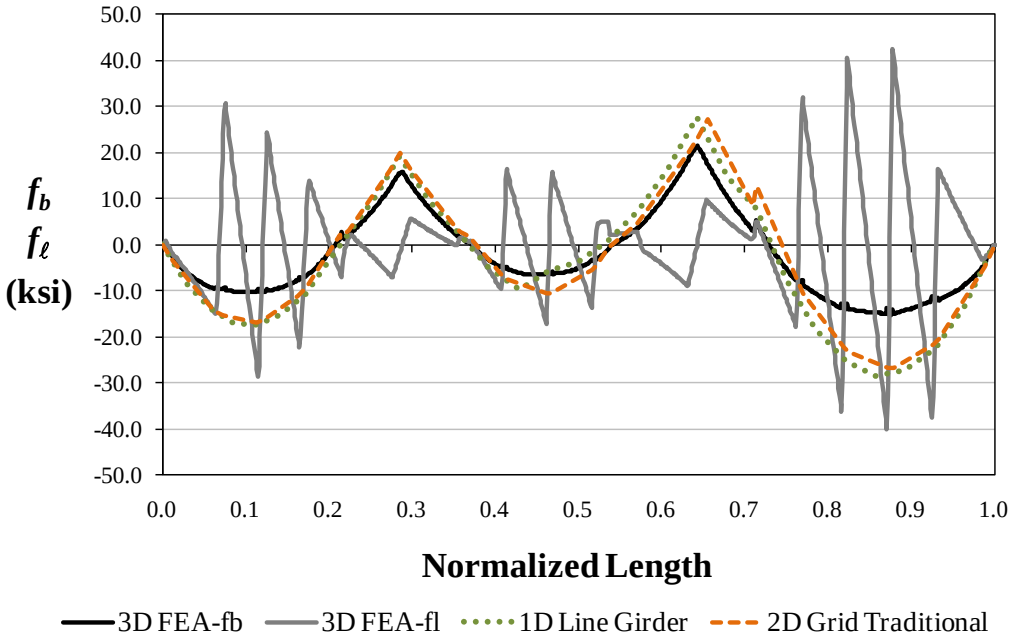

Figure 5.10. Top flange stresses in girder G5 of bridge NICSS16.

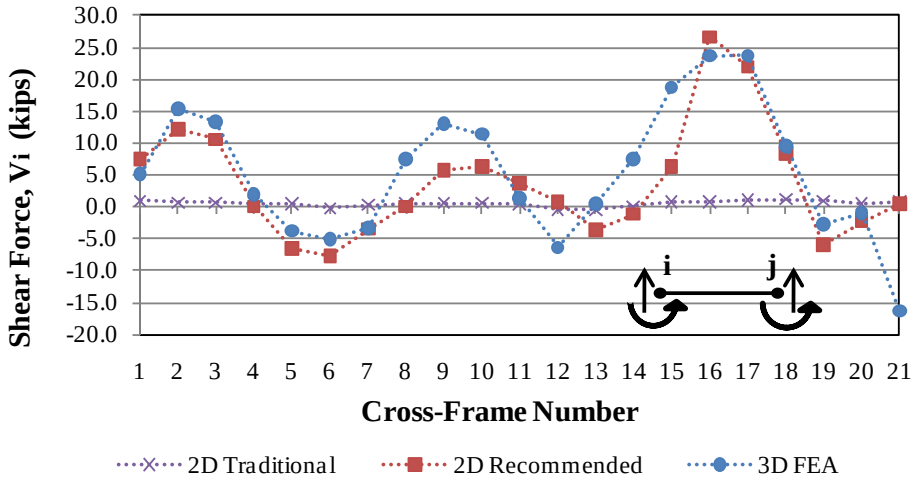

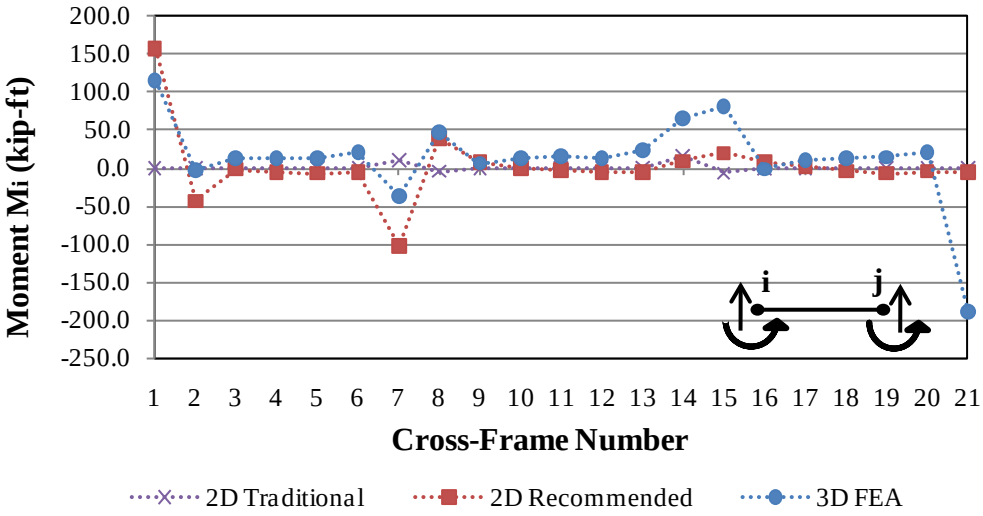

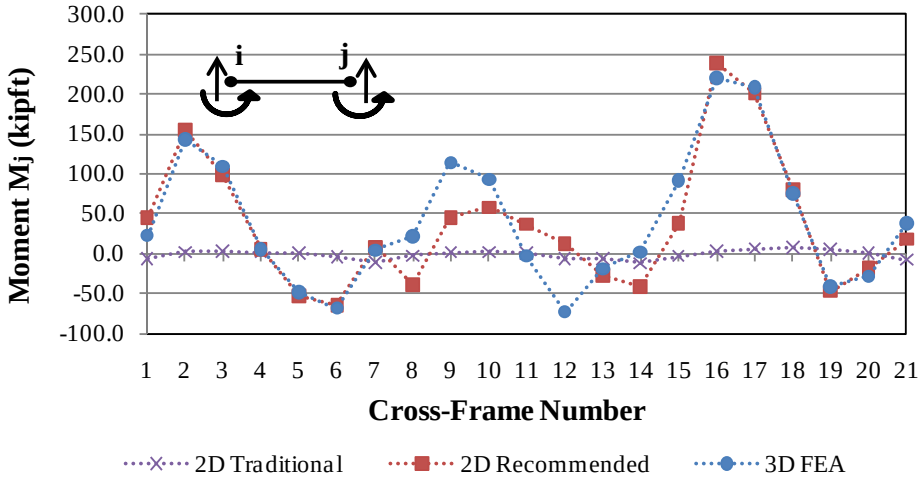

Figure 5.11. Cross-frame forces in Bay 1 (G1-G2) of NICSS16.

5.2 Assessment of Tub-Girder Bridges

Analytical studies also were conducted for the tub-girder bridges introduced in Chapter 4 to determine the ability of the approximate 1D line-girder and 2D-grid methods to capture the behavior predicted by refined 3D FEA models for these bridge types. The software setups used for these studies have already been described at the beginning of Chapter 5. For the simplified 2D-grid solutions the external cross-frames and diaphragms were modeled using the "shear analogy" approach (see Section 6.2.1) with the distance from web-to-web of the tub-girders at the mid-depth of the tubs for the length of the external elements, to determine the moment of inertia of an equivalent Euler-Bernoulli beam element, then using this moment of inertia with the length between the centerline of the tub-girders in the 2D-grid solution. This approach tends to under-estimate the true external diaphragm or cross-frame stiffness, but is a common design practice. A limited number of studies were conducted in which rigid offsets were assumed from the centerline of the tub-girders to the web at the external cross-frame or diaphragm connection. These models indicated that the differences in the girder displacements and internal torsional moments were negligible using either of these modeling approaches.

The tub-girder torsional properties were determined using the Equivalent Plate Method (Kollbrunner and Basler, 1969). The bracing forces were calculated using the component force equations outlined in Section 2.7 in LARSA, in which the results from LARSA were input to a spreadsheet for further calculation. Comparable calculations are handled internally in MDX. The MDX software used one element between each of the panel points of the top flange lateral bracing system for modeling of skewed bridges. Otherwise, a "high-resolution mesh" was used in MDX, i.e., nodes in addition to those at brace locations were placed at twentieth points of the spans, but not closer than span/40 from a brace or support location. The line-girder analyses in STLBRIDGE were conducted with ten elements per span.

The saw-tooth top-flange force effect discussed in Section 2.7 was not included in the calculation of the major-axis bending stresses, in order to focus on the accuracy corresponding to conventional practice (and thus obtain theoretically comparable results between the LARSA-based and MDX-based solutions). The use of the "average" major-axis bending stress, $f_b = M / S_{x.top}$, and the modeling of the external cross-frames and diaphragms neglecting rigid offsets

from the centerline of the tub-girders reflect conventional analysis modeling standards of care in professional bridge design practice.

In the following, the normalized mean errors from Eq. (5.1) are presented for the major-axis bending stresses, vertical displacements and girder torsional moments obtained for the 18 tub-girder bridges studied in the NCHRP 12-79 research. However, for the assessment the analysis accuracy for the top flange lateral bracing (TFLB) and internal cross-frame (CF) axial forces, the signed errors for the maximum response are reported. In many designs, it is common to use the same size bracing members along the length of the bridge since this minimizes the detailing efforts and reduces the possibility of construction errors. As such, the top flange lateral bracing and cross-frame components are designed for the maximum axial forces found throughout the length of the bridge. Due to this practice, it is useful to assess the accuracy of the bracing forces by reporting the signed error for the maximum response for each of the different types of components. Furthermore, due to some of the subsequent simplified calculations being substantially conservative, it is useful to reference the signed error to convey that information. The sign on the error is positive for conservative estimates and unconservative for negative estimates. The reporting of these errors is grouped by: (1) the top flange lateral bracing diagonals, (2) the internal cross-frame diagonals, and (3) the combined top flange lateral bracing struts and internal cross-frame top chords.

Table 5.7 compares the program P1 and P2 2D-grid estimates as well as the1D analysis estimates for the major-axis bending stresses and vertical displacements to the predictions obtained from the geometric nonlinear elastic 3D FEA benchmarks. In the table, f_b is the major-axis bending stress, Δ_z is the vertical displacement and T is the torsional moment. A mean error is calculated for each response on each girder of the bridges. The values reported by Table 5.7 are the largest mean errors determined by inspecting the values obtained for each girder in a given bridge. The differences between the linear and geometric nonlinear 3D FEA were negligible and therefore are not shown. The torsional moments results were not obtained from program P2 and therefore the accuracy of the results are not evaluated for this case.

Table 5.7. Tub-girder bridge percent normalized mean errors compared to geometric nonlinear elastic 3D FEA for major-axis bending stresses (f_b), vertical displacements (Δ_z) and torsional moment (T).

Group	Bridge Name	2D-Grid – P1			2D-Grid – P2		1D		
		f_b μ_e	Δ_z μ_e	T μ_e	f_b μ_e	Δ_z μ_e	f_b μ_e	Δ_z μ_e	T μ_e
C	NTSCR1	7	5	5	12	13	10	6	7
	NTSCR2	5	3	6	8	9	8	4	11
	NTSCR5	8	6	8	19	10	12	8	11
	NTCCR1	5	2	6	8	6	7	4	14
	ETCCR15	5	2	20	6	3	7	3	26
	XTCCR8	5	3	23	7	3	8	12	27
	ETCCR14	6	2	12	36	11	17	8	13
	NTCCR5	6	3	3	8	4	6	2	5
S	XTCSN3	3	2	19	5	5	6	6	23
	NTSSS1	4	5	31	11	7	5	1	18
	NTSSS4	4	1	30	6	5	7	3	53
	NTSSS2	8	7	27	19	13	11	5	10
	ETSSS2	5	2	28	10	2	9	7	30
C&S	NTSCS5	7	6	3	21	13	12	7	14
	NTSCS29	7	7	3	15	11	9	4	9
	ETCCS5a	10	6	22	5	5	6	5	29
	ETCCS6	6	2	43	22	3	7	2	33
	NTCCS22	5	4	3	8	8	6	3	11

In Table 5.7 and in the following discussions, the tub-girder bridges are divided into three groups based on their geometry: curved radially-supported bridges (labeled as “C”), straight and skewed structures (labeled as “S”) and curved and skewed bridges (labeled as “C&S”). The connectivity index, I_C, does not apply to tub-girder bridges. This index is primarily a measure of the loss of accuracy in I-girder bridges due to the poor modeling of the I-girder torsion properties. For tub-girder bridges, the conventional St. Venant torsion model generally works well as a characterization of the response of the pseudo-closed section tub-girders. Hence, I_C is not used for characterization of tub-girder bridges in Table 5.7. Furthermore, there is only a weak correlation between the accuracy of the simplified analysis calculations and the skew index I_S for tub-girder bridges. Therefore, the skew index is not used to characterize tub-girder bridges in Table 5.7 either. Important differences in the simplified analysis predictions do exist, however,

as a function of whether the bridge is curved, "C," straight and skewed, "S," or curved and skewed "C&S."

Similarly, Table 5.8 compares the maximum bracing axial force results from the 2D-grid and 1D analyses to the predictions obtained from the geometric nonlinear elastic 3D FEA benchmarks. In this table, the signed errors for the maximum response are reported for the top flange lateral bracing diagonals (TFLB Diag.), internal cross-frame diagonals (CF Diag.), and the combined top flange lateral bracing struts and internal cross-frame top chords (TFLB & Top CF Strut) for the reasons discussed above.

Table 5.8. Tub-girder bridge percent errors for maximum values of responses compared to geometric nonlinear elastic 3D FEA for the bracing system forces.

Group	Bridge Name	2D-P1			2D-P2			1D		
		TFLB Diag.	CF Diag.	TFLB & Top CF Strut	TFLB Diag.	CF Diag.	TFLB & Top CF Strut	TFLB Diag.	CF Diag.	TFLB & Top CF Strut
C	NTSCR1	8	30	24	55	80	-26	33	19	-1
	NTSCR2	7	27	25	58	74	-7	33	16	5
	NTSCR5	18	36	37	61	91	75	57	17	1
	NTCCR1	12	73	21	54	87	-42	34	90	-2
	XTCCR8	1	200	171	97	265	-18	27	264	54
	ETCCR14	0	241	93	148	51	-80	140	23	48
	NTCCR5	21	71	66	49	99	10	49	60	21
S	NTSSS1	-4	NA[a]	12	165	NA[a]	17	15	NA[a]	6
	NTSSS4	23	NA[a]	13	67	NA[a]	33	-16	NA[a]	6
	NTSSS2	-15	NA[a]	18	119	NA[a]	4	22	NA[a]	15
	ETSSS2	-55	NA[a]	-18	9	NA[a]	-37	15	NA[a]	-16
C&S	NTSCS5	17	24	17	65	75	-30	40	7	-15
	NTSCS29	5	29	35	84	83	-11	14	16	-4
	ETCCS6	12	52	4	46	110	20	51	-24	9
	NTCCS22	8	73	49	97	141	3	25	107	3
Pratt TFLB	ETCCR15	0	NA[b]	-3	-41	NA[b]	-75	56	NA[b]	-19
	XTCSN3	40	NA[a]	49	-74	NA[a]	-84	48	NA[a]	58
	ETCCS5a	0	-12	-3	26	123	-40	1	4	22

[a] The component force equations summarized in Section 2.7 predict negligible forces on the internal CF forces in straight tub-girders.

[b] ETCCR15 uses internal solid plate diaphragms rather than internal CF.

An additional group is shown in Table 5.8 corresponding to the bridges that had a Pratt TFLB system. The simplified analysis methods generally have more difficulty in accurately predicting the bracing forces for these bridges.

5.2.1 Accuracy of the Vertical Displacements, Major-Axis Bending Stresses and Torsional Moments

Upon inspection of the results corresponding to Table 5.7, the following important trends can be observed:

Second-Order Amplification

The results obtained from the first-order 3D FEA show that the response amplifications due to second order effects are negligible for all the tub-girder bridges. Steel tub-girders generally have as much as 100 to more than 1000 times the torsional stiffness of a comparable I-girder section. Therefore, when steel tub girders are fabricated with proper internal cross-frames to restrain their cross-section distortions as well as a proper top flange lateral bracing (TFLB) system, which acts as an effective top flange plate creating a pseudo-closed cross-section with the commensurate large torsional stiffness, second-order amplification is rarely of any significance even during lifting operations and early stages of the steel erection.

2D-Grid Solutions

Based on Table 5.7, several observations can be made regarding the 2D-grid solutions for the major-axis bending stresses, vertical displacements and torsional moments:

- The 2D-grid solutions from program P1 give better estimates than program P2 for the major-axis bending stresses and vertical displacements in all the cases in Table 5.7 with the exception of ETCCS5a. The ETCCS5a bridge uses a Pratt TFLB. The larger errors in the estimates for this bridge are due to the internal behavior associated with the bracing system (e.g., the Pratt TFLB system is not symmetric about the centerline of the tub-girders). Without knowing the details of the internal implementation in program P2, no conclusions can be drawn to confirm that program P2 has better accuracy for bridges using Pratt TFLB systems.
- There is no clear distinction in the results for the major-axis bending stresses and vertical displacements for the different groups “C”, “S” or “C&S”. This means that there is no

clear effect of curvature or skew on the accuracy of the major-axis bending stresses or vertical displacements in the simplified tub-girder bridge analysis solutions.

- Only the torsional moments from program P1 were collected. The errors are the largest for the "S" bridges. However, the groups "C" and "C&S" also have errors that are comparable to those of the "S" group.
- The torsional moment estimates for bridges ETCCR15 and XTCCR8 exhibit the largest errors in the "C" group. ETCCR15 has an irregular TFLB layout using Pratt trusses. The orientation of the TFLB diagonals varies throughout the bridge length. These characteristics (i.e., the non-symmetry relative to the centerline of the tub-girders and the variation in the orientations along the length) are believed to induce a behavior difficult to estimate by simplified 2D and 1D analysis methods. There is no clear reason why the solutions differed for bridge XTCCR8.
- The torsional results are reasonably accurate for three of the "C&S" bridges. The bridge ETCCS5a has large errors. This appears to be due again to the use of a Pratt TFLB system. The bridge ETCCS6 exhibits very large errors in the simplified analysis methods. The reason for this behavior appears to be the lack of external diaphragms at its intermediate pier.
- The torsional moment estimates for the "S" group exhibit errors larger than group "C&S". The "C&S" group bridges have smaller errors even when the independent effects of skew are expected to be comparable to those on the "S" group. However, the effects of curvature are large enough to reduce the relative differences. The reason for the reduced accuracy in the "S" bridges is explained below.

The diaphragm modeling is believed to be an important reason for the lack of accuracy in the internal torsional moments from the 2D-grid analyses. As noted previously, the 2D-grid approach used in the NCHRP 12-79 analytical studies tends to under-estimate the cross-frame or diaphragm stiffnesses. However, it appears that these components behave almost rigidly in many cases due to the small aspect ratio and the stiffening of the diaphragms. Nevertheless, as noted previously, a limited number of studies were conducted in which rigid offsets were assumed from the centerline of the tub-girders to the web at the external cross-frame or diaphragm connection. These models indicated that the differences in the girder displacements and internal

torsional moments were negligible using either of these modeling approaches. Therefore, the results collected in the NCHRP 12-79 research are still inconclusive with respect to this consideration.

In addition, the internal bracing response appears to influence the accuracy of the simplified methods in predicting the internal torsional moments. The bridges that are expected to be subjected to constant internal torsional moments exhibited a slightly nonlinear distribution of the internal torques. It appears that the variation of the internal torques from a constant value is related to the TFLB strut lateral forces which follow a similar distribution. The shape also suggests possible correlation with the girder major-axis bending moment or the strut forces induced by major-axis bending. It should be noted that constant total internal torques taken by the full bridge cross-section can be obtained by simple statics in some of these bridges, given the bridge support reactions. The requirement of constant total internal torque on the full bridge cross-section is satisfied. However, the individual girders themselves do not exhibit constant internal torques along their lengths. The reader is referred to Jimenez Chong (2012) for a detailed assessment of the internal torsion estimates from the simplified methods.

Other errors are attributed to the discretization level of the bridge model; however, these errors are considered minor compared to the effects discussed above.

1D Line-Girder Solutions

The 1D line-girder results in Table 5.7 exhibit the following characteristics:

- The vertical displacements and major-axis bending stress solutions are reasonably good for all the bridges and are comparable to the corresponding 2D-grid results.
- For the “S” and “C&S” bridges, the 1D line-girder solutions for the vertical displacements and major-axis bending stresses exhibit better accuracy than the conventional 2D-grid program P1 solutions in the majority of the cases; however, there is no clear reason why the line-girder analysis solutions are better for these cases.
- The torsional moment errors from the line-girder analyses are less than or equal to 14 %. The torsional moment estimates for the ETCCR15, XTCCR8, ETCCS5a and ETCCS6 bridges appear to exhibit larger errors for the same reasons discussed previously regarding the 2D-grid solution accuracy.

- Similar to the 2D-gird solutions above, the torsional moment estimates for the “S” group exhibited errors larger than those from the “C&S” group. The internal bracing behavior is expected to cause these errors as explained previously; however, an additional reason for the reduced accuracy in the “S” bridges is explained below.

Additional errors in the line-girder analyses are attributed to the effects of the external intermediate cross-frames, since the 1D method is unable to capture any information about the transverse load paths in the bridge system through these components. The external intermediate cross-frames transfer forces between girders that modify the major-axis bending moments, torsional moments, and shears in the girders. When skewed external intermediate cross-frames are used, the cross-frames connect at different relative girder lengths resulting in additional transferred force between the girders, since the relative vertical displacements that these cross-frames control are expected to be larger. The effects of external intermediate cross-frames are again more noticeable in straight bridges since the effect in curved bridges is relatively small when compared to the overall combined torques from the curvature and skew.

5.2.2 Accuracy of Bracing Forces

2D Grid Solutions

As with the vertical displacements and major-axis bending stresses, the 2D-grid solutions from program P1 give better estimates than program P2 for the top flange lateral bracing diagonals forces (TFLB Diag.), internal cross-frame diagonal forces (CF Diag.) and the combined top flange lateral bracing strut and internal cross-frame top strut (TFLB & Top CF Strut) for the majority of the cases in Table 5.8. The larger errors in program P2 are attributed to the coarser discretization used for skewed bridges and the internal process for the evaluation of the bracing forces. Since the internal process for program P2 is proprietary, there is no information to confirm the specific differences in the component force calculations between programs P1 and P2. Therefore, only the results from program P1, which explicitly use the component force equations, are discussed below.

The following observations can be drawn from the program P1 results in Table 5.8:

- The TFLB diagonal forces directly depend on the major-axis bending and torsional moments and, consequently, the errors are larger for the “S” group where the torsional

responses are estimated less accurately. For the “C” and “C&S” bridges, the accuracy is improved and the estimates are all conservative. The accuracy is affected largely by the accuracy of the torsional moment estimates. The large negative error for bridge ETSSS2 of -55 % is related to the complex internal forces generated by the interior pier supports oriented at a significant skew angle in this bridge without any cross-frames or diaphragms along this bearing line.

- The interior intermediate cross-frame diagonal force estimates show large conservative errors for the “C” and “C&S” groups. These forces are negligible for the “S” group, and therefore, these errors are not addressed. The interior intermediate cross-frame diagonal forces are assumed to depend only on the distortional components of the applied loads (Fan and Helwig, 2002). The largest distortional contribution is the *M*/*Rh* distributed lateral load which is characterized by the major-axis bending moments. Since the major-axis bending stresses are captured accurately by the program P2, it is concluded that the conservative estimates in the above forces are caused by the assumption that the internal cross-frames provide the only resistance to cross-section distortion (i.e., zero resistance to cross-section distortion from the girder cross-section itself).
- The combined TFLB & top cross-frame strut force estimates exhibit large conservative errors for the majority of the bridges, with the exception of the bridges that use a Pratt TFLB system. These bracing forces depend on a combination of the major-axis bending moment and torsional moments. The “S” group exhibits smaller errors for these forces. This result is believed to be related to the reduced accuracy of the torsional moment estimates for these bridges.
- Additional localized errors are attributed to the interaction of the external intermediate cross-frames and the internal cross-frames. At the locations that align to the external intermediate cross-frames there is a transverse load path that the component force equations do not consider. This effect causes force increases in the adjacent bracing components.

The bracing force estimates exhibit larger errors than the flange major-axis bending and vertical displacement estimates for the majority of the cases. However, many of these errors are conservative. For bridges using Pratt TFLB layouts, the component force equations exhibit a

poorer performance caused by the interaction between these bracing components and the rest of the structural system.

1D Line-Girder Solutions

The 1D line-girder solutions for the bracing component forces in Table 5.8 exhibit larger errors than the corresponding responses provided by the program P1 2D-grid solution. These errors are a consequence of the effects discussed previously in Section 5.2.1. Additional errors are caused by the discretization level used in the 1D line-girder implementation, which results in some of the bracing component forces not being calculated based on their actual positions, but rather based on the closest tenth point.

The following sections synthesize the analysis errors using a grading scheme similar to the one presented in Section 5.1 for I-girder bridges.

5.2.3 Synthesis of Errors in Major-Axis Bending Stresses and Vertical Displacements for Tub-Girder Bridges

Table 5.9 shows the number of tub-girder bridges within specific ranges of the normalized mean errors for the major-axis bending stresses and the vertical displacements based on Table 5.7. Both of the 2D-grid programs P1 and P2 are considered, as well as the 1D analysis results. The specific selected error ranges are assigned letter grades based on the criteria described previously for I-girder bridges.

The highlighted rows in Table 5.9 are used to generate simplified scores for each of the bridge groups and analysis methods in Tables 5.10 and 5.11. The letter grades provided in Table 5.10 correspond to the worst-case scores in Table 5.9, whereas the grades in Table 5.11 correspond to the most frequently occurring score, i.e., the mode score.

Overall, one can observe the following from Tables 5.10 and 5.11:

- For the major-axis bending stresses and vertical displacements, the 2D-grid program P1 and the 1D line-girder analysis get worst-case grades of B and A. The mode of the grades for these analysis solutions is predominantly an A.

- For the major-axis bending stresses and vertical displacements, the 2D-grid program P2 gets worst-case grades of F and C. The mode of the grades in these categories is predominantly a B.
- For the torsional moments, the 2D-grid program P1 and 1D line-girder analysis have worst-case grades of F. However, the mode of the grades in these categories is a B for the 1D analysis of the "C&S" and "C" bridges and an A for the 2D-grid results. The "S" bridges have the lowest mode grades in general, D for the 2D-grid P1 solution and F for the 1D line-girder analysis solution.

Table 5.9. Number of tub-girder bridges within specified error ranges for major-axis bending stress and vertical displacement for each of the types of bridges considered.

Type of Bridge	Number of bridges	Error range	Number of Bridges within Error Range							
			Major-Axis Bending Stress			Vertical Displacement			Girder Torques	
			2D-P1	2D-P2	1D	2D-P1	2D-P2	1D	2D-P1	1D
C	8	A: ≤ 6%	6	1	1	**8**	4	5	5	1
		B: 7-12%	**2**	5	6	0	3	**3**	1	3
		C: 13-20%	0	1	**1**	0	**1**	0	1	2
		D: 21-30%	0	0	0	0	0	0	**1**	**2**
		F: >30%	0	**1**	0	0	0	0	0	0
S	5	A: ≤ 6%	4	2	2	4	3	4	0	0
		B: 7-12%	**1**	2	**3**	**1**	1	**1**	0	1
		C: 13-20%	0	**1**	0	0	**1**	0	0	1
		D: 21-30%	0	0	0	0	0	0	3	1
		F: >30%	0	0	0	0	0	0	**2**	**2**
C & S	5	A: ≤ 6%	2	1	2	4	2	4	3	0
		B: 7-12%	**3**	1	**3**	**1**	2	**1**	0	2
		C: 13-20%	0	1	0	0	**1**	0	0	1
		D: 21-30%	0	**2**	0	0	0	0	1	1
		F: >30%	0	0	0	0	0	0	**1**	**1**

Table 5.10. Tub-girder bridge worst-case scores for major-axis bending stress, vertical displacements, and torques.

Type of Bridge	Worst-Case Scores							
	Major-Axis Bending Stress			Vertical Displacement			Torque	
	2D-P1	2D-P2	1D	2D-P1	2D-P2	1D	2D-P1	1D
S	B	C	B	B	C	B	**F**	**F**
C	B	**F**	C	A	C	B	D	D
C&S	B	**F**[a]	C[b]	B	C	B	**F**	**F**

[a] Modified from D to F based on the score for the C bridges

[b] Modified from B to C based on the score for the C bridges

Table 5.11. Mode of tub-girder bridge scores for major-axis bending stress, vertical displacements, and torques.

Type of Bridge	Mode of Scores							
	Major-Axis Bending Stress			Vertical Displacement			Torque	
	2D-P1	2D-P2	1D	2D-P1	2D-P2	1D	2D-P1	1D
S	A	B	B	A	A	A	D	F
C	A	B	B	A	A	A	A	B
C&S	B	D	B	A	B	A	A	B

5.2.4 Synthesis of Errors in Bracing Forces for Tub-Girder Bridges

Table 5.12 categorizes the bracing force errors in a manner similar to Table 5.9. However, in this table, the numbers are collected for both positive (conservative) and for negative (unconservative) errors. Several of the estimated bracing forces fall into F grades. The errors are affected significantly by the low accuracy of the torque estimates. However, the majority of the estimates fall into the conservative categories meaning that the simplified methods still provide usable estimates for these cases.

5.2.5 Generalized Tub-Girder Bridge Analysis Scores

Tables 5.13 and 5.14 give the generalized analysis scores for the various tub-girder bridge responses corresponding to the traditional 2D-grid and 1D-line girder methods at large. Table 5.13 addresses the accuracy of the calculations for major-axis bending stresses, girder torques, vertical displacements, and girder layovers at the bearings, whereas Table 5.14 addresses the accuracy of the calculations for the top flange lateral bracing, internal cross-frames and flange lateral bending stresses.

Tables 5.13 and 5.14 are derived by using just the grades from program P1 as being representative of the true accuracy of 2D-grid methods. Clearly, there was a measurable decrease in the overall accuracy of the 2D-grid solutions for the tub-girder bridges obtained with program P2 compared to program P1. Furthermore, the research team had greater control over the procedures, as well as more detailed information regarding the specifics of the calculations, with program P1.

Table 5.12. Number of tub-girder bridges within specified error ranges for the maximum values of the bracing system forces for each of the types of bridges considered.

Type of Bridge	Number of Bridges	Error Range	Number of Bridges within Error Range								
			TFLB Diag.			TFLB & Top CF Strut			CF Diag.		
			2D-P1	2D-P2	1D	2D-P1	2D-P2	1D	2D-P1	2D-P2	1D
C	7	+F: >30%	0	**7**	**6**	**4**	**1**	**2**	**5**	**7**	**3**
		+D: 21-30%	**1**	0	1	3	0	1	2	0	1
		+C: 13-20%	1	0	0	0	0	0	0	0	3
		+B: 7-12%	**3**	0	0	0	1	0	0	0	0
		+A: ≤ 6%	2	0	0	0	0	2	0	0	0
		-A: ≤ 6%	0	0	0	0	0	**2**	0	0	0
		-B: 7-12%	0	0	0	0	1	0	0	0	0
		-C: 13-20%	0	0	0	0	1	0	0	0	0
		-D: 21-30%	0	0	0	0	1	0	0	0	0
		-F: >30%	0	0	0	0	**2**	0	0	0	0
S	4	+F: >30%	0	**3**	0	0	**1**	0			
		+D: 21-30%	**1**	0	**1**	0	0	0			
		+C: 13-20%	0	0	**2**	**2**	1	**1**			
		+B: 7-12%	0	1	0	1	0	0			
		+A: ≤ 6%	0	0	0	0	1	**2**			
		-A: ≤ 6%	1	0	0	0	0	0			
		-B: 7-12%	0	0	0	0	0	0			
		-C: 13-20%	1	0	**1**	**1**	0	**1**			
		-D: 21-30%	0	0	0	0	0	0			
		-F: >30%	**1**	0	0	0	**1**	0			
C&S	4	+F: >30%	0	**4**	**2**	**2**	0	0	**2**	**4**	**1**
		+D: 21-30%	0	0	1	0	0	0	2	0	0
		+C: 13-20%	**1**	0	1	1	**1**	0	0	0	1
		+B: 7-12%	**2**	0	0	0	0	**1**	0	0	1
		+A: ≤ 6%	1	0	0	1	1	1	0	0	0
		-A: ≤ 6%	0	0	0	0	0	1	0	0	0
		-B: 7-12%	0	0	0	0	1	0	0	0	0
		-C: 13-20%	0	0	0	0	0	1	0	0	0
		-D: 21-30%	0	0	0	0	**1**	0	0	0	**1**
		-F: >30%	0	0	0	0	0	0	0	0	0
Pratt TFLB	3	+F: >30%	**1**	0	**2**	**1**	0	**1**			
		+D: 21-30%	0	**1**	0	0	0	1			
		+C: 13-20%	0	0	0	0	0	0			
		+B: 7-12%	0	0	0	0	0	0			
		+A: ≤ 6%	**2**	0	1	0	0	0			
		-A: ≤ 6%	0	0	0	**2**	0	0			
		-B: 7-12%	0	0	0	0	0	0			
		-C: 13-20%	0	0	0	0	0	**1**			
		-D: 21-30%	0	0	0	0	0	0			
		-F: >30%	0	**2**	0	0	**3**	0			

Table 5.13. Generalized tub-girder bridge scores for girder major-axis bending stresses, torques, and displacements.

Response	Geometry	Worst-Case Scores		Mode of Scores	
		2D-P1	1D-Line Girder	2D-P1	1D-Line Girder
Major-Axis Bending Stresses	S	B	B	A	B
	C	B	C	A	B
	C&S	B	C[b]	B	B
Girder Torques	S	F	F	D	F
	C	D	D	A	B
	C&S	F	F	A	B
Vertical Displacements	S	B	B	A	A
	C	A	B	A	A
	C&S	B	B	A	A
Girder Layover at Bearing Lines	S	B	B	A	A
	C	NA[a]	NA[a]	NA[a]	NA[a]
	C&S	B	B	A	A

[a] Magnitudes should be negligible where properly designed and detailed diapharagms or cross-frames are present.

[b] Modified from B to C based on the score for the C bridges.

In Tables 5.13 and 5.14, there are several cases where the letter grade for the "C&S" bridges was lowered from the result derived from Table 5.12 because a grade for a "C" or an "S" bridge was lower. The table footnotes indicate when these modifications were made. It should be noted that in Table 5.13, the "C&S" mode scores of A and B for the prediction of the internal torques by the 2D-grid and the 1D line-girder solutions are not modified. This is because the torque due curvature is typically much larger than the torque due to skew, and the contribution of the torque due to curvature tends to be estimated more accurately in general.

Key observations that can be drawn from Tables 5.13 and 5.14 are as follows:

Table 5.14. Generalized tub-girder bridge scores for bracing system forces and flange lateral bending stresses.

Response	Sign of Error	Geometry	Worst-Case Scores		Mode of Scores	
			2D-P1	1D-Line Girder	2D-P1	1D-Line Girder
TFLB Diagonal Force	Positive (Conservative)	S	D	D	D	C
		C	D	F	B	F
		C&S	D[a]	F	B	F
		Pratt TFLB System	C	F	A	F
	Negative (Unconservative)	S	F[b]	C		
		C	--	--		
		C&S	--	--		
		Pratt TFLB System	--	--		
TFLB & Top Internal CF Strut Force	Positive (Conservative)	S	C	C		
		C	F	F		
		C&S	F	F[c]		
		Pratt TFLB System	F	F		
	Negative (Unconservative)	S	C	C		
		C	--	A		
		C&S	--	C		
		Pratt TFLB System	D	D		
Internal CF Diagonal Force	Positive (Conservative)	S	NA[d]	NA[d]		
		C	F	F		
		C&S	F	F		
		Pratt TFLB System	--	F[e]		
	Negative (Unconservative)	S	NA[d]	NA[d]		
		C	--	--		
		C&S	--	D		
		Pratt TFLB System	B	--		
Top Flange Lateral Bending Stress (Warren TFLB Systems)	Positive (Conservative)	S	C	C		
		C	F	F		
		C&S	F	F[c]		
	Negative (Unconservative)	S	C	C		
		C	--	A		
		C&S	--	C		

[a] Modified from a C to a D considerting the grade for the C and the S bridges.

[b] Large unconsevative error obtained for bridge ETSSS2 due to complex framing. If this bridge is considered as an exceptional case, the worst case unconservative error is -15 % for NTSSS2 (grade = C).

[c] Modified from a B to an F considering the grade for the C bridges.

[d] For straight-skewed bridges, the internal intermediate cross-frame diagonal forces tend to be negligible.

[e] Modified from an A to an F considering the grade for the C and C&S bridges.

Major-Axis Bending Stresses, Vertical Displacements and Girder Layovers

In these categories the worst-case letter grades are dominated by B grades (see Table 5.13). The 1D line-girder falls into the C grade for the major-axis bending stresses in C and "C&S" bridges; however, this should be expected as the complexity of three-dimensional response is not completely represented in the line-girder analysis model. The mode grades are dominated by A's, particularly for the vertical displacements. In summary the simplified analysis methods show good agreement in the prediction of major-axis bending stresses, vertical displacement and girder layovers. For tub-girder bridges the lesser accuracy should be expected from the line-girder analysis since the interaction between the girders cannot be modeled.

Girder Internal Torques

The 2D-grid and 1D-line girder models represent the bridge in terms of idealized longitudinal and transverse equivalent beams. However, the torsional behavior is complex since it involves the interaction of numerous components including the support diaphragms, external intermediate cross-frames, top flange lateral bracing systems, etc. Consequently, the lack of modeling accuracy of each of these components adds up and the worst-case estimates fall to an F grade in curved and/or skewed bridges.

The torque behavior is more difficult to predict accurately as the complexity of the bridge increases. Uniform spacing of internal bracing and of TFLB system panel points, reduced interaction between adjacent girders by elimination of intermediate external bracing, and accurate modeling of support diaphragms generally leads to better torque estimates. Bridges with complex deck geometry, non-uniform brace spacing, multiple external intermediate cross-frames between girders, skewed supports, large eccentric vertical loading, etc., should consider the use of 3D FEA to achieve an accurate representation of the torsional response.

Bracing Forces

Several of the estimated bracing forces in Table 5.14 fall to F grades. The errors are largely caused by the low accuracy on the torque estimates. However, the majority of the estimates fall into the conservative categories meaning that the simplified methods still provide usable estimates.

5.2.6 Assessment Example for Tub-girder Bridges

Curved and Skewed Tub Girder: Figure 5.12 illustrates the TFLB layout of the simple-span tub-girder bridge NTSCS5 having parallel skewed supports. It is desired to determine the ability of the approximate methods of analysis to estimate its responses.

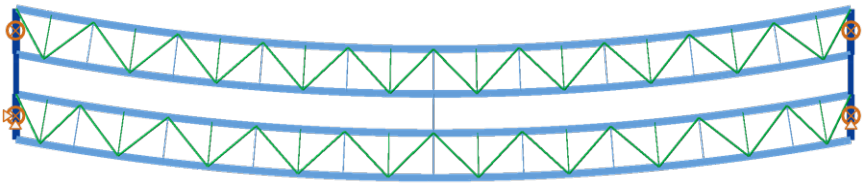

L_{as} = 150 ft./ R = 400 ft./ w = 30 ft./ θ_1 = 10.7°, θ_2 = -10.7°

Figure 5.12. Curved and skewed simple span tub-girder bridge NTSCS5.

The levels of accuracy of the 1D line-girder and 2D-grid models, based on the mode scores in Tables 5.13 and 5.14, are:

Response	Analysis Method	
	2D-grid	1D Line-Girder
f_b	B	B
Girder Torques	A	B
Vertical Deflections	B	B
Girder Layovers	B	B
f_ℓ	F (conservative)	F (conservative)
TFLB & CF forces	F (conservative)	F (conservative)

This structure is reasonably “regular” in its geometry, with uniform spacing of the internal intermediate cross-frames and of the TFLB system panel points along its length

with the exception of the panels near the skewed ends, only one external intermediate diaphragm located at the middle of the span, and approximate symmetry about its mid-span. Therefore, the mode scores are considered as more appropriate for estimating the accuracy of the simplified analysis methods rather than the worst-case scores.

Figure 5.13 shows the vertical displacements and Figure 5.14 shows the girder stresses at the total noncomposite dead load level (unfactored). As noted previously, when steel tub girders are fabricated with proper internal cross-frames to restrain their cross-section distortions as well as a proper top flange lateral bracing (TFLB) system, which acts as an effective top flange plate creating a pseudo-closed cross-section with the commensurate large torsional stiffness, second-order amplification is rarely of any significance even during lifting operations and early stages of the steel erection. Therefore, the nominal stresses unfactored dead load stresses may be scaled by the appropriate load factors to conduct any strength checks.

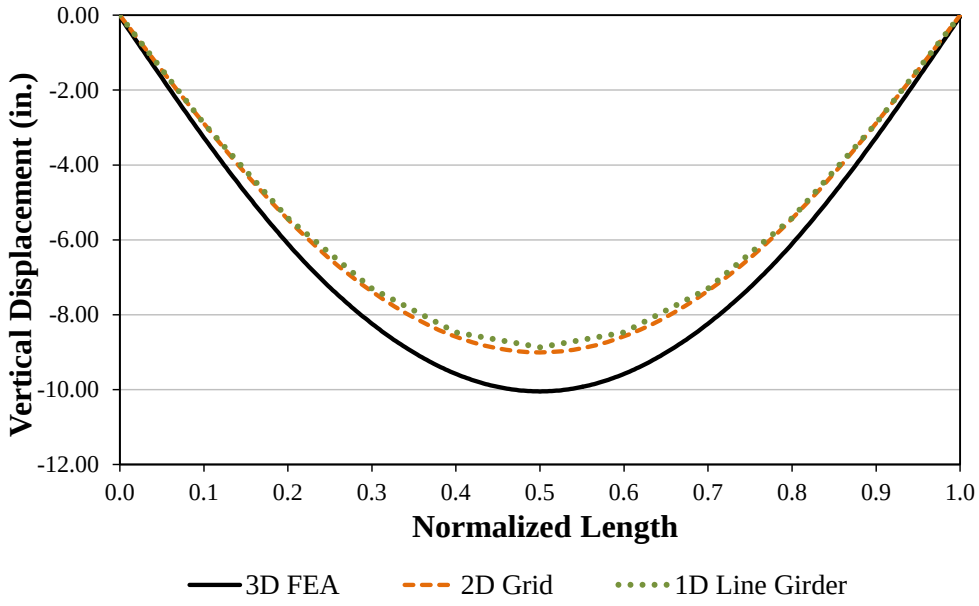

Figure 5.13. Vertical displacements at the centerline of the girder on the outside of the curve in bridge NTSCS5.

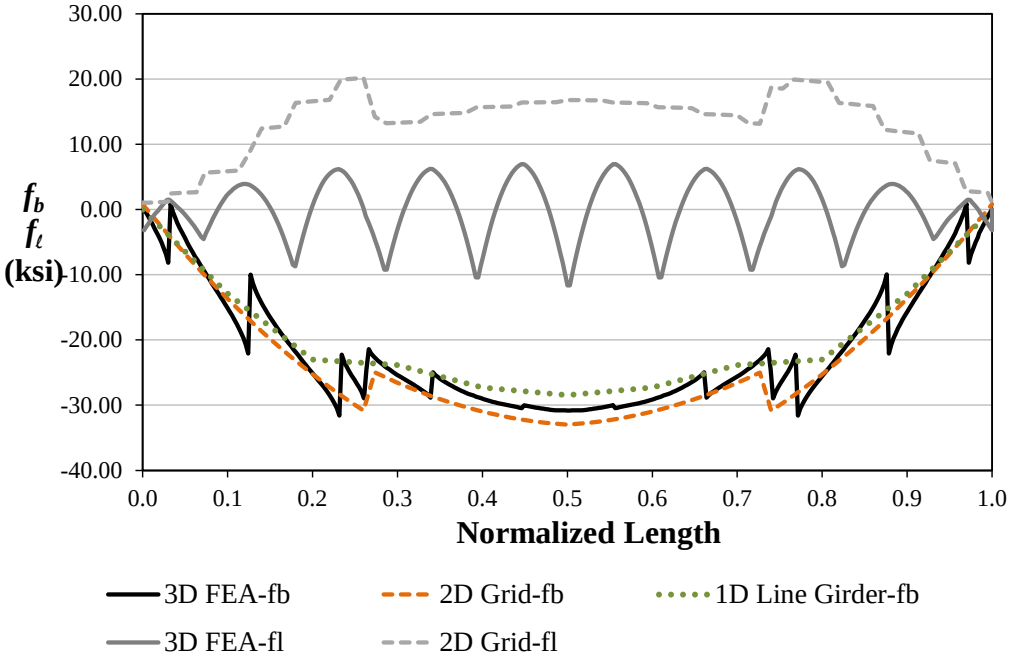

Figure 5.14. Flange major-axis and lateral bending stresses on the outside top flange of the girder on the outside of the curve in bridge NTSCS5.

The top flange lateral bending stresses are estimated conservatively by the 2D-grid calculations. It should be noted that the 2D-grid curve for these stresses is essentially just an estimated envelope curve for the maximum flange lateral bending stresses. The estimated peak flange lateral bending stresses are nearly two times the physical maximum values, and are not located at the same position as the true peak values. Similar predictions (not shown) are obtained using the line-girder analysis calculations. Hence, the grade of F for the top flange lateral bending stresses in Table 5.14 is representative. The vertical deflections are predicted within a normalized mean error of 6 % by both the 2D-grid and the line-girder analysis in this problem.

Figure 5.15 shows the internal torques predicted in the girder on the outside of the curve in NTSCS5. It can be observed that the internal torques are predicted very accurately in this problem, both from the 2D-grid and the 1D line-girder solutions. Because of the equal and opposite skews at the end bearing lines and the symmetry about

the mid-span, the internal torque due to skew is small in this problem. The curvature effects dominate the total torque. This performance justifies the mode scores of A and B for prediction of the torques by the simplified analysis solutions. The internal torques are calculated directly from the structural analysis in the 2D-grid solution. The M/R method does not provide any estimate of the girder internal torques due to skew. However, as discussed in Section 2.1.5, the tub-girder internal torques can be estimated reasonably well for simple, "regular" geometries by considering the major-axis bending responses from the M/R method along with the assumption that the bearing line diaphragms are effectively rigid, to calculate the girder relative end twists in each span. The relative end twists can then be multiplied by the St. Venant torsional stiffness (GJ/L) to obtain an estimate of the internal torques.

Figure 5.16 shows the axial forces for the TFLB system along the length of the exterior girder in NTSCS5. To facilitate the visualization of the results the forces are grouped as positive and negative values, and consecutive results (in every other panel of the TFLB system) are joined by a line.

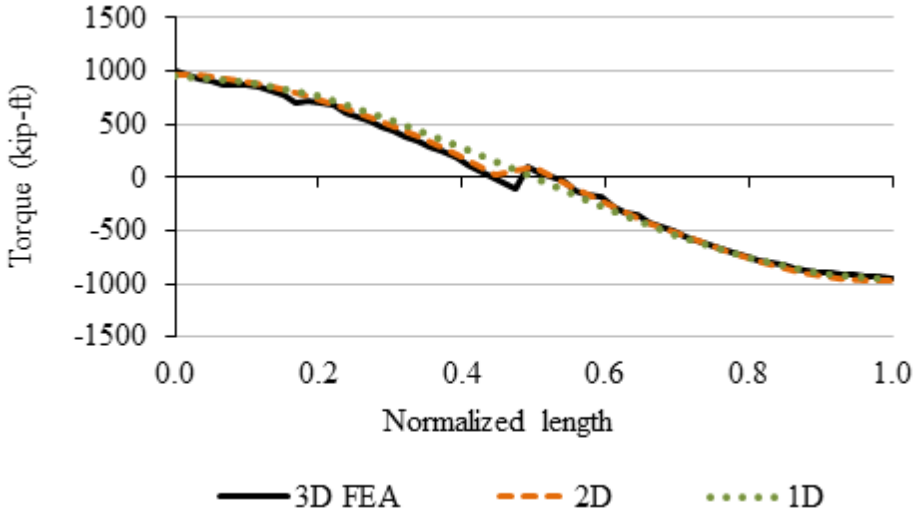

Figure 5.15. Internal torques for the girder on the outside of the horizontal curve in bridge NTSCS5.

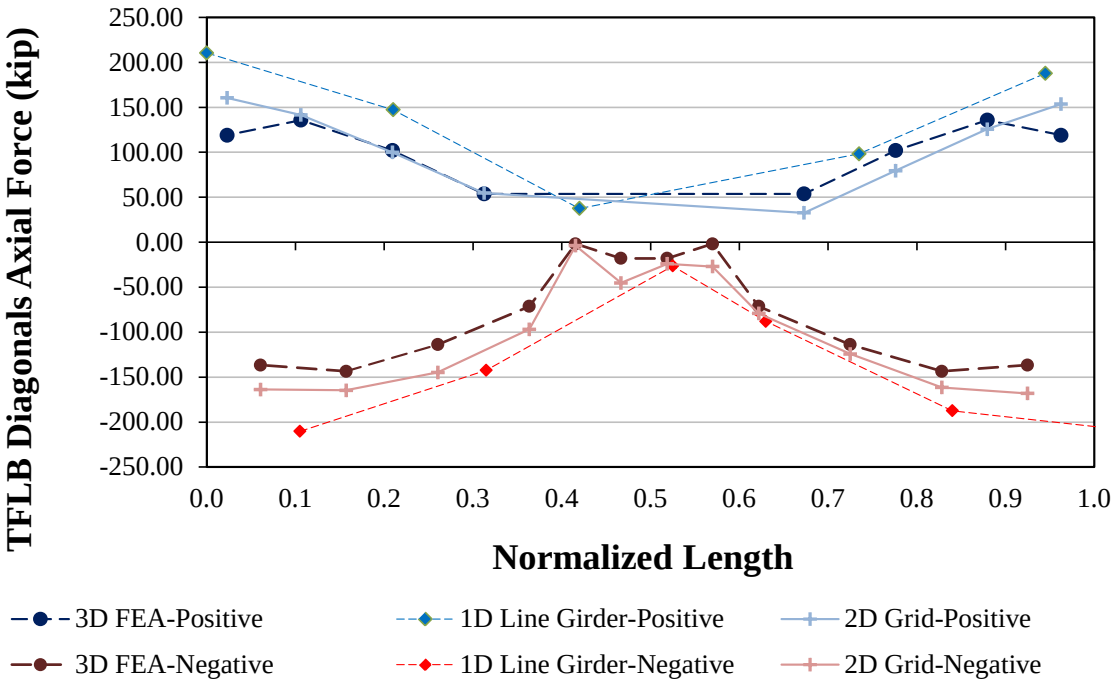

Figure 5.16. Axial forces in the TFLB system diagonals of the girder on the outside of the curve in the NTSCS5 bridge.

One can observe that the overall trends in the predictions from both types of simplified analysis methods are reasonably good, but that the line-girder analysis results generally are significantly conservative relative to the 3D FEA benchmarks. This plot shows that the mode scores of B for the 2D-grid methods are justified, and indicates that scores better than the mode score (F in this case) are certainly attainable with the line-girder analysis solutions.

Figure 5.17 shows the predictions from the 2D-grid and 1D line-girder analyses for the NTSCS5 bridge. Both the 2D-grid and the line-girder analysis predictions appear to be reasonably good in predicting the overall trends in this case, which may seem to be at odds with the grade of F for these responses in Table 5.14. However, upon a closer inspection from Table 5.8, one can observe that the errors in the prediction of the

maximum forces are + 24 % and +7 % here, whereas these errors are significantly larger for the other “C&S” bridges.

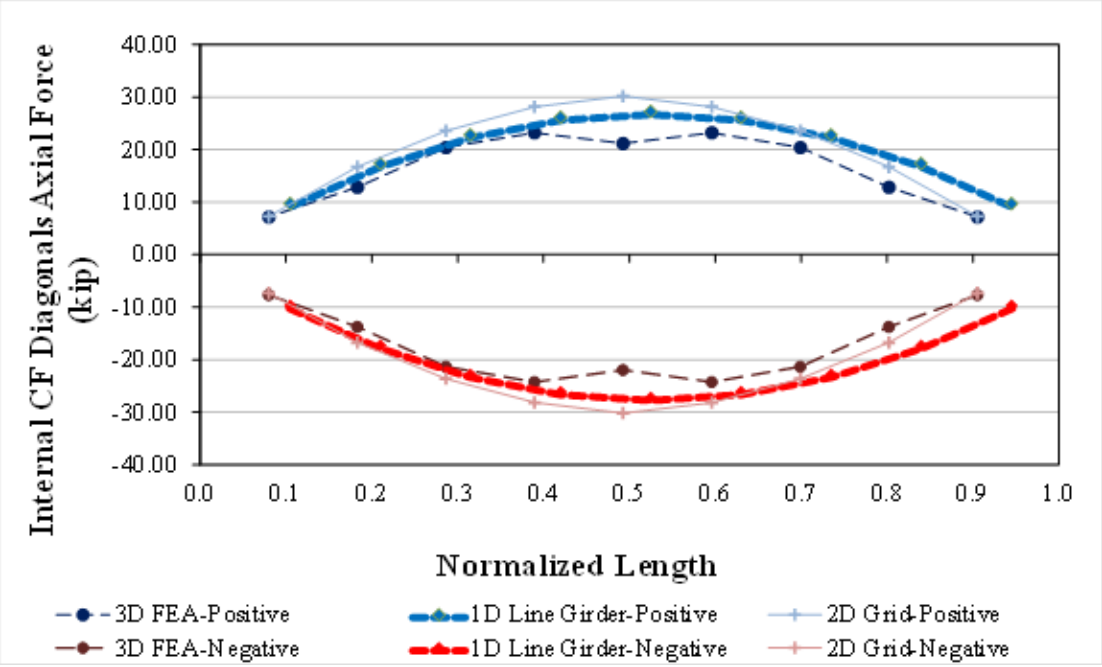

Figure 5.17. Axial forces in the intermediate internal cross-frame diagonals of the girder on the outside of the horizontal curve in the NTSCS5 bridge.

Figure 5.18 compares the line-girder and 2D-grid analysis results for the axial forces in the top chord of the intermediate internal cross-frames in the exterior girder of the NTSCS5 bridge. There are two forces, one on each side of the diagonals, at each position along the bridge length. The force values at these positions are joined together by a vertical line, and the values at the adjacent intermediate internal cross-frames are also connected together by a line to highlight the differences between the two forces. One can observe that the trends in the maximum force in these components are estimated reasonable well for this bridge. The maximum force is over-predicted by 17 % in the 2D-grid solution, whereas this force is predicted quite accurately by the 1D line-girder analysis solution.

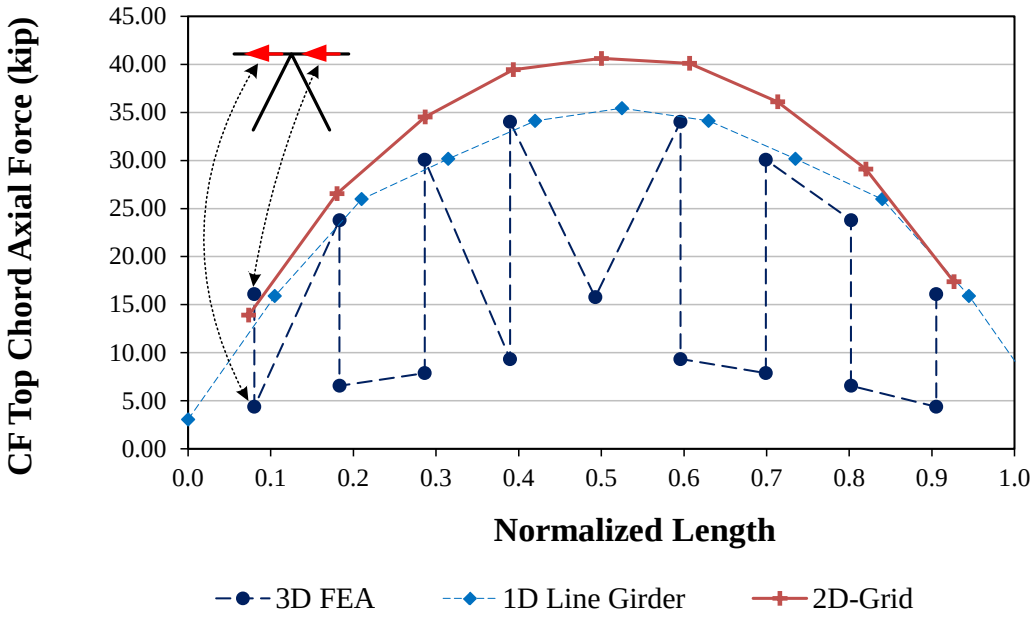

Figure 5.18. Axial forces in the top chord of the intermediate internal cross-frames in the exterior girder of the NTSCS5 bridge.

Lastly, Figure 5.19 shows the results for the 2D-grid analysis predictions of the axial forces in the TFLB struts of the exterior girder for the example bridge. These are the transverse components in the TFLB system at the locations where there is no intermediate internal cross-frame. It can be observed that these forces are predicted quite conservatively by the corresponding component force equations in this case. This is consistent with the conservative F grade shown for this response for the "C&S" bridges in Table 5.14.

The reader is referred to Jimenez Chong (2012) for a more comprehensive summary of example results, similar to the above, from the other tub-girder bridges studied in the NCHRP 12-79 research.

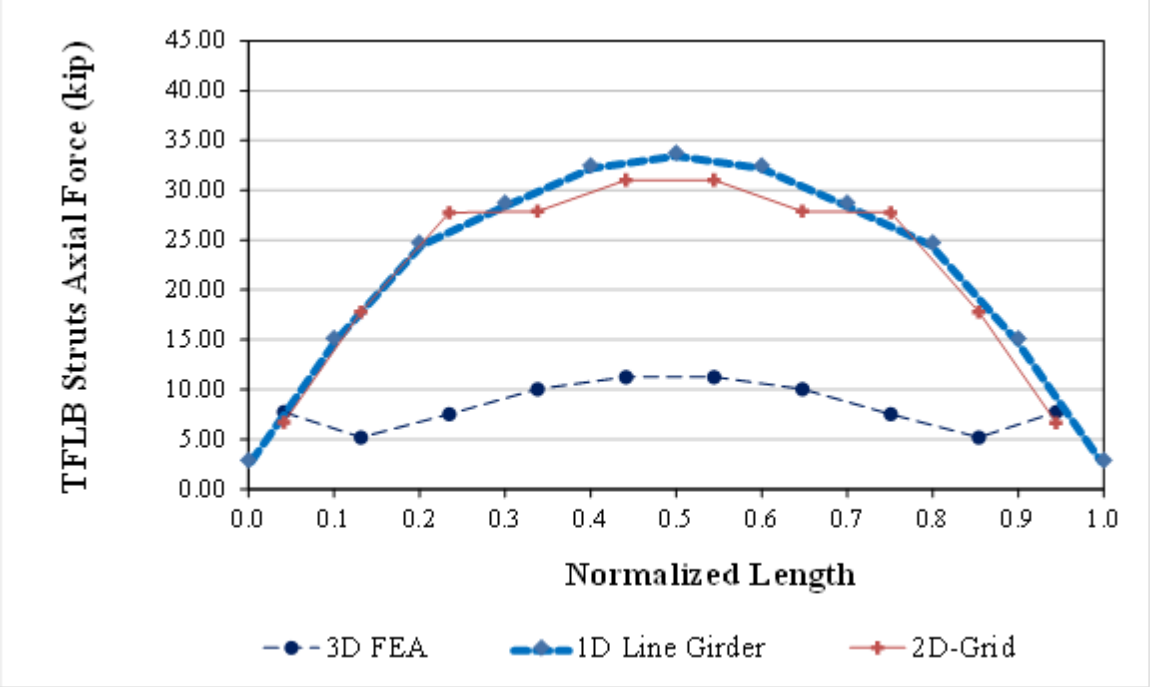

Figure 5.19. TFLB strut axial forces in the exterior girder of the NTSCS5 bridge.

6. Recommended I-Girder Bridge 2D-Grid Analysis Improvements

Chapter 2 provides a broad description of 2D-grid analysis procedures. In the present chapter, the 2D-grid analysis techniques are studied in more detail. Conventional methods used in practice to construct a grid model for the analysis and design of steel I-girder bridges are discussed first to highlight the severe limitations of these approaches. Next, improved modeling techniques are introduced that can be implemented with relative ease in 2D-grid analysis software for a better representation of the structural behavior of I-girder bridges.

6.1 I-Girder Torsional Stiffness for 2D-Grid Analysis

In a thin-walled open-section member, there are two components of torsion resistance, namely the St. Venant or pure torsion resistance and the flange warping or non-uniform torsion resistance. Horizontal curvature, support skew, and overhang eccentric loads subject steel I-girders to torsion. Hence, properly capturing the torsional properties in a curved and/or skewed steel I-girder bridge is essential to obtain an accurate prediction of the structure's performance during construction. Unfortunately, the conventional approaches commonly used to construct 2D-grid models do not have the ability to properly represent the torsion properties of I-section girders. Generally, they only implement the St. Venant torsion component, which results in a substantial misrepresentation of some of the structural responses of interest during the structure's construction.

Consider a beam in cantilever subjected to the external torque, M_z, shown in Figure 6.1a. Due to the applied torque, the free end of the beam rotates an angle ϕ, and the flanges displace laterally, where $u_f = \phi \cdot h/2$, assuming small rotations, and where h is the distance between flange centroids. In this member, the total internal torque is equal to

$$M_z(z) = M_s(z) + M_w(z) \tag{6.1}$$

where the first component, M_s, corresponds to the Saint Venant torsion and the second component, M_w, is the warping torsion. The first component is defined as

$$M_s(z) = GJ\frac{d\phi}{dz} \tag{6.2}$$

where G is the steel shear modulus of elasticity and J is the torsion constant of the girder cross-section. To obtain the warping contribution to the internal torque, one can consider analyzing the flanges as if they are subjected to lateral bending. The warping torque along the longitudinal axis of the beam, z, can be decomposed and represented by a force couple such that $M_w(z) = V_\ell(z) \cdot h$. The forces $V_\ell(z)$, which have an opposite sign in each flange, cause lateral bending of the flanges.

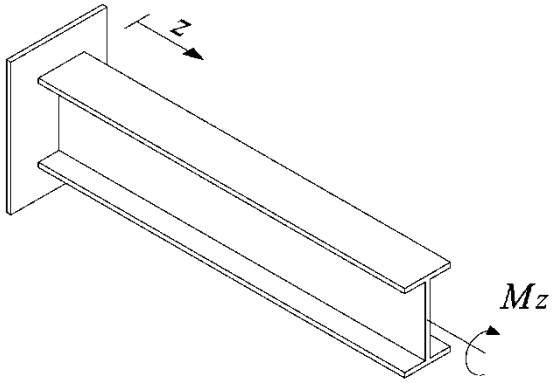

(a) Cantilever beam subject to torque M_z

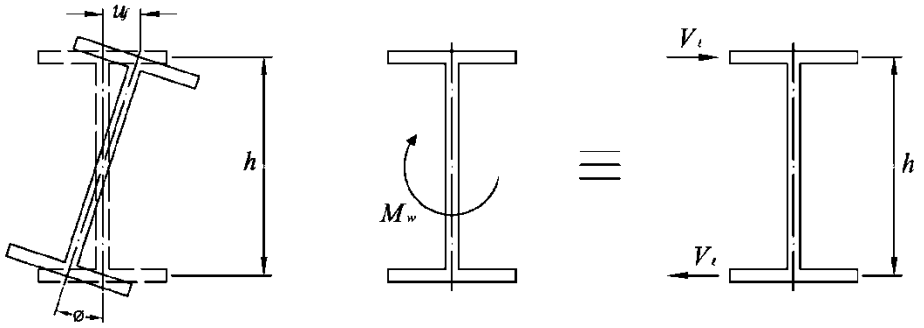

(b) Decomposition of the warping moment, M_w, in an equivalent force couple

Figure 6.1. Warping torsion in a cantilever beam.

The governing differential equation for bending in one of the flanges may be used to determine the flange lateral bending moment, $M_\ell(z)$, and the shear force $V_\ell(z)$,

$$EI_f \frac{d^2 u_f(z)}{dz^2} = EI_f \frac{h}{2} \frac{d^2 \phi(z)}{dz^2} = -M_\ell(z) \tag{6.3}$$

$$V_\ell = \frac{dM_\ell(z)}{dz} = -EI_f \frac{h}{2} \frac{d^3 \phi(z)}{dz^3} \tag{6.4}$$

where E is the modulus of elasticity of the steel, and I_f is the flange moment of inertia about the strong axis. Hence, the warping torsion component is

$$M_w = V_\ell h = -EC_w \frac{d^3 \phi(z)}{dz^3} \tag{6.5}$$

In the above equation, C_w is the warping constant, which is defined as

$$C_w = I_f \frac{h^2}{2} \tag{6.6}$$

The warping constant defined in Eq. (6.6) is valid for doubly-symmetric sections. The formulae to compute C_w in singly symmetric sections are available in the literature (Ziemian, 2010). The governing differential equation for a straight I-section girder subject to torsion is found by substituting Eqs. (6.2) and (6.5) into Eq. (6.1), giving

$$M_z(z) = GJ \frac{d\phi}{dz} - EC_w \frac{d^3 \phi(z)}{dz^3} \tag{6.7}$$

As shown in Eq. (6.7), the twist angle and the applied torsion moment in an I-section beam are related through a third order linear differential equation. This equation is not suitable for implementation using an element with six dofs per node. Hence, an alternate solution is to ignore the term related to flange warping, and assume that the response is dominated by St. Venant torsion. With this simplification, the governing differential equation is reduced to

$$M_z(z) = GJ \frac{d\phi}{dz} \tag{6.8}$$

If the applied torque is constant, Eq. (6.8) can be integrated over the beam length (or bracing points) to obtain a linear relationship between M_z, and ϕ, so that

$$M_z = \frac{GJ}{L}\phi \tag{6.9}$$

The term GJ/L is the torsional stiffness of the beam ignoring the warping contribution. It is important to note that the elements used in software packages for modeling of the girders commonly assume only this contribution to the torsional stiffness.

In box or closed-section members, pure torsion dominates the response, and thus the warping effects are minor. However, in an I-girder the torsional resistance is dominated by flange warping. In general, in members with thin-walled open sections, the effects of warping must be included to properly capture the torsional response. Curved and skewed steel I-girder bridges are inherently subjected to torsion. Therefore, the accuracy of the results obtained from the 2D-grid analysis of a curved and/or skewed bridge can be influenced by the assumptions considered when representing the girder torsional stiffness.

6.1.1 Modeling of Warping Contributions via Thin-Walled Open-Section (TWOS) 3D-Frame Analysis

A better representation of the I-girder torsion properties is implemented in some computer programs via an additional warping dof that is provided at each node of the beam or frame element, as shown in Figure 2.21 (dofs u_7 and u_{14}). Various researchers have developed elements formulated with 14 dofs that include warping deformations. As discussed in Section 2.6, these types of elements may be referred to as Thin-Walled Open-Section (TWOS) 3D-Frame elements. These elements generally provide an accurate representation of the physical behavior of non-composite I-girders subjected to torsion (Yang and McGuire, 1984; Chang, 2006). However, these types of elements must be applied cautiously for I-girders in their composite condition (Chang, 2006). This is because these elements do not account for distortional deformation of an I-girder web into an S shape. When the deck hardens, it provides substantial restraint to both the lateral displacement and the twist of the top flange. However, the bottom flange is still able to move due to the web out-of-plane flexibility. Hence, the bottom flange lateral displace-

ments and the bottom flange lateral bending stresses, f_ℓ, may not be properly captured by a TWOS 3D-frame analysis. A 3D FEA as defined in Section 2.8.1 is able to capture these web distortion effects, by virtue of the modeling of the webs by shell finite elements.

6.1.2 Modeling of Warping Contributions in 2D-Grid Analysis via an Equivalent Torsion Constant

Another technique that can be implemented to better capture the torsional properties of an I-girder in a 2D-grid model is the use of an equivalent torsion constant, J_{eq}, as proposed by Ahmed and Weisgerber (1996). The determination of the equivalent torsion constant is further explained in the following.

The general solution of the governing differential equation for a constant torque between the beam supports (or bracing points) is

$$\phi(z) = \frac{M_z z}{GJ} + A_1 \sinh(pz) + A_2 \cosh(pz) + A_3 \tag{6.10}$$

in which

$$p^2 = \frac{GJ}{EC_w} \tag{6.11}$$

In Eq. (6.10), the constants A_1, A_2, and A_3, depend upon the end boundary conditions. For a beam with the flanges fixed against warping at its ends, these boundary conditions are $\phi(0) = \phi(L) = 0$ and $\phi'(0) = \phi'(L) = 0$. Applying these boundary conditions to Eq. (6.10) gives the following results:

$\phi(0) = 0$: $\quad A_2 + A_3 = 0$

$\phi'(0) = 0$: $\quad A_1 p + \frac{M_z}{GJ} = 0$

$\phi'(L) = 0$: $\quad A_1 p \cosh(pL) + A_2 p \sinh(pL) + \frac{M_z}{GJ} = 0$

and

$$A_1 = -\frac{M_z}{GJp}$$

$$A_2 = \frac{M_z}{GJ}\frac{\cosh(pL)-1}{p\sinh(pL)}$$

$$A_3 = -\frac{M_z}{GJ}\frac{\cosh(pL)-1}{p\sinh(pL)}$$

Substituting the constants A_1, A_2, and A_3 in Eq. (6.10), the twist angle in a beam with warping fixed flanges and subjected to a constant torque is equal to

$$\phi(z) = \frac{M_z z}{GJ} - \frac{M_z}{GJ}\sinh(pz) + \frac{M_z}{GJ}\frac{\cosh(pL)-1}{p\sinh(pL)}\cosh(pz) - \frac{M_z}{GJ}\frac{\cosh(pL)-1}{p\sinh(pL)} \tag{6.12}$$

From the above equation, the relative twist between the beam ends is

$$\phi = \frac{M_z}{GJ}\left[L - \frac{\sinh(pL)}{p} + \frac{\cosh(pL)-1}{p\sinh(pL)}\cdot\cosh(pL) - \frac{\cosh(pL)-1}{p\sinh(pL)}\right] \tag{6.13}$$

or

$$\phi = M_z\frac{L}{GJ_{eq}} \tag{6.14}$$

where J_{eq} is the equivalent torsion constant for the case where flange warping is fully fixed at the beam ends, defined as

$$\begin{aligned} J_{eq(fx-fx)} &= J\left[1 - \frac{\sinh(pL)}{pL} + \frac{\cosh(pL)-1}{pL\sinh(pL)}\cdot\cosh(pL) - \frac{\cosh(pL)-1}{pL\sinh(pL)}\right]^{-1} \\ &= J\left[1 - \frac{\sinh(pL)}{pL} + \frac{\left[\cosh(pL)-1\right]^2}{pL\sinh(pL)}\right]^{-1} \end{aligned} \tag{6.15}$$

With the equivalent torsion constant, $J_{eq(fx\text{-}fx)}$, it is possible to simulate the torsional stiffness of an I-girder with warping-fixed ends. This equivalent torsion constant may be substituted into the grid model to capture more properly the girder properties.

The above derivation can be used to model the torsional rigidity of the interior girder segments, which are the segments defined between two intermediate cross-frames. At the girder ends, the flanges typically are free to warp. For the end segments, defined between the end and the first intermediate cross-frame, the equivalent torsion stiffness may be determined assuming that the warping boundary conditions are fixed-free at the segment ends. In this case, the boundary conditions necessary to determine the constants A_1, A_2, and A_3 are $\phi(0) = \phi(L) = 0$ and $\phi''(0) = \phi'(L) = 0$. Applying these boundary conditions to Eq. (6.10) gives the following results:

$\phi(0) = 0$: $\quad A_2 + A_3 = 0$

$\phi''(0) = 0$: $\quad A_2 p^2 = 0$

$\phi'(L) = 0$: $\quad A_1 p \cosh(pL) + \frac{M_z}{GJ} = 0$

and

$$A_1 = -\frac{M_z}{GJ}\frac{1}{p\cosh(pL)}$$

$$A_2 = A_3 = 0$$

Substituting these constants in Eq. (6.10), the rotation angle in a beam with free-fixed warping conditions subject to a constant torque is equal to

$$\phi(z) = \frac{M_z z}{GJ} - \frac{M_z}{GJ}\frac{\sinh(pz)}{p\cosh(pz)} \tag{6.16}$$

and

$$\phi = \frac{M_z L}{GJ}\left(1 - \frac{\sinh(pL)}{pL\cosh(pL)}\right) \tag{6.17}$$

Therefore, for an exterior girder segment, the equivalent torsion constant is equal to

$$J_{eq(fr-fx)} = J\left(1-\frac{\sinh(pL)}{pL\cosh(pL)}\right)^{-1} \tag{6.18}$$

This implementation of the equivalent torsion constant provides a simple method to approximate the overall torsional stiffness of I-girders. For the analysis of an I-girder bridge, J_{eq} is calculated taking L as the distance between cross-frames. Then the torsion constant J is defined in the program using the calculated value of J_{eq}. With this technique, the typical 12-dof frame element available in commercial programs can be used to construct traditional 2D-grid models that are a closer representation of the physical structure than models constructed using conventional practices, where the flange warping contributions are neglected.

Even though the use of the equivalent torsion constant represents a potential improvement for 2D-grid modeling techniques, there is a limitation that has to be considered. In reality, warping is not fully fixed at the girder bracing points (i.e., the relative flange lateral bending rotations are not zero at the cross-frame positions). In a particular flange segment, which is defined by the distance between bracing points, warping restraint is provided by the adjacent segments. In reality, at the segment ends, the flange warping resembles a partially restrained condition. Unfortunately, it is not practical to provide further guidelines on how to determine the equivalent torsion coefficient other than assuming fixed-fixed warping for interior girder segments and free-fixed for the end segments. In general, it is not feasible to capture the girder torsional stiffness exactly unless the actual flange warping displacements at the nodes of the analysis model are known. However, the response predictions obtained from analyses of bridges with challenging geometries and complex bracing systems with equivalent torsion constants calculated based on fixed-fixed and pinned-fixed warping conditions are significantly more accurate than the responses obtained from analyses that ignore the warping contributions (Sanchez, 2011).

Another factor to consider is the calculation of the equivalent torsion constant for different girder segments in the structure. The distance between cross-frames varies depending on how the engineer configures the bracing system in the bridge. As shown in Figure 6.2, cross-frames may be provided at one or both sides of the girder, and the distance between them is not necessarily the same. In the figure, Segments 2 and 3 have different unbraced lengths. Therefore a different equivalent torsion constant must be determined for each segment. In a skewed bridge, different unbraced lengths are common near the skewed supports. Therefore, it is necessary to compute a J_{eq} for each of the different unbraced lengths.

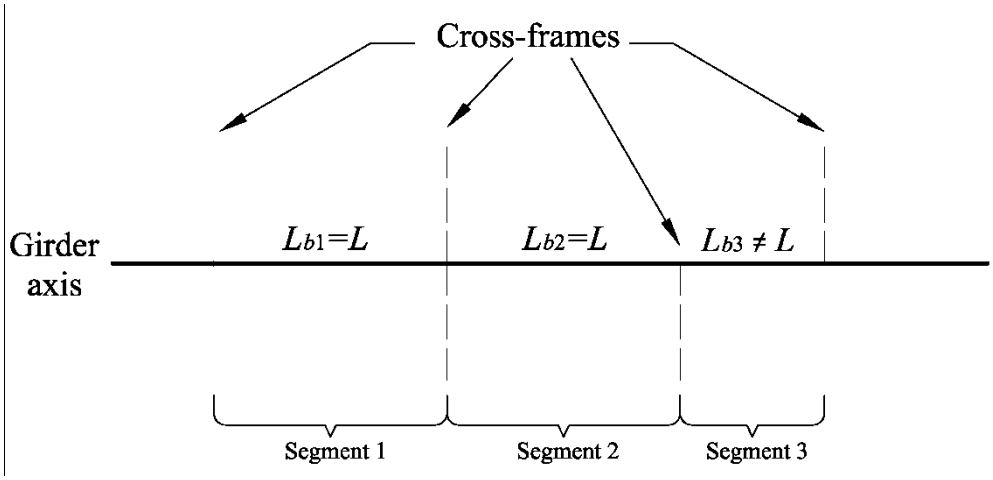

Figure 6.2. Definition of unbraced length for computation of the effective torsion constant, J_{eq}.

6.2 Cross-Frame Element Stiffnesses

In this section, the modeling techniques used to represent the cross-frames in 2D-grid analyses are studied. First, the conventional practices are presented and analyzed, emphasizing their accuracy and their limitations to represent the physical behavior of the cross-frames in the bridge. Next, two-node elements that capture the physical behavior of the X-type, V-type and inverted V-type cross-frames are developed and implemented in LARSA 4D (LARSA, 2010), a software system commonly used for design of steel bridges.

6.2.1 Conventional Cross-Frame Modeling Techniques used in 2D Grid Models

In conventional 2D-grid analysis, the cross-frames are modeled using the same type of element used to model the girders. The frame element based on the Euler-Bernoulli beam theory is used commonly to represent what in reality is a group of elements with the configuration of a truss. Figure 6.3 shows the 2D-grid model and 3D FEA representation of Bridge XICSS7. As shown in the figure, the chords and diagonals that constitute the cross-frame are modeled as a single line element. The section properties of the line element used to represent the cross-frames are determined using ad hoc procedures, such as discussed in Coletti and Yadlosky (2007) and NHI-AASHTO (2010).

One procedure that is used to determine the moment of inertia, I_{eq}, of the equivalent beam element focuses on a particular flexural stiffness of the cross-frame, and is hence referred to as the "flexural analogy" method. As depicted in Figure 6.4, a model of the cross-frame is constructed with boundary conditions that resemble a propped cantilever beam. A force couple is applied at the left-hand end of the cross-frame, resulting in the horizontal displacements Δ_t and Δ_b. Then the rotation angle, θ, is calculated as $\theta = (\Delta_t + \Delta_b)/d$. In the equivalent beam element, the moment $M = P \cdot d$ is applied the left-hand end. It is required that the rotation in this node be equal to the rotation θ obtained from the analysis of the cross-frame. If shear deformations are ignored, the rotation angle in the equivalent beam is defined as $\theta = (M \cdot L)/(4EI_{eq})$. Hence, the moment of inertia of the equivalent beam is:

$$I_{eq} = \frac{ML}{4E\theta} \tag{6.19}$$

The equivalent moment of inertia found from this expression is used in the definition of the elements that represent the cross-frames in the 2D model of the bridge.

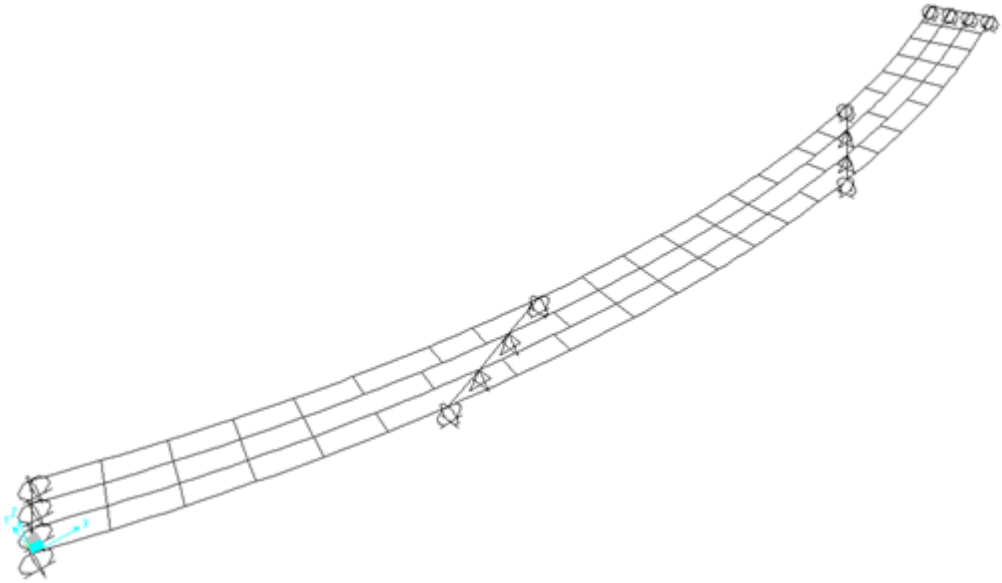

a) 2D Grid model

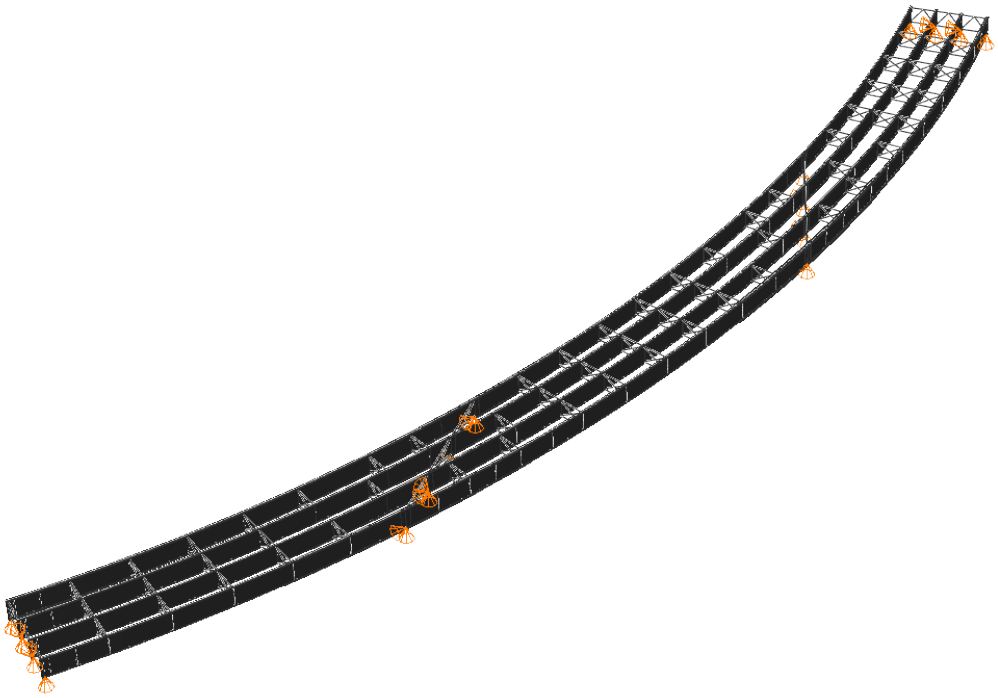

b) 3D FEA model

Figure 6.3. 2D grid and 3D FEA models of XICSS7.

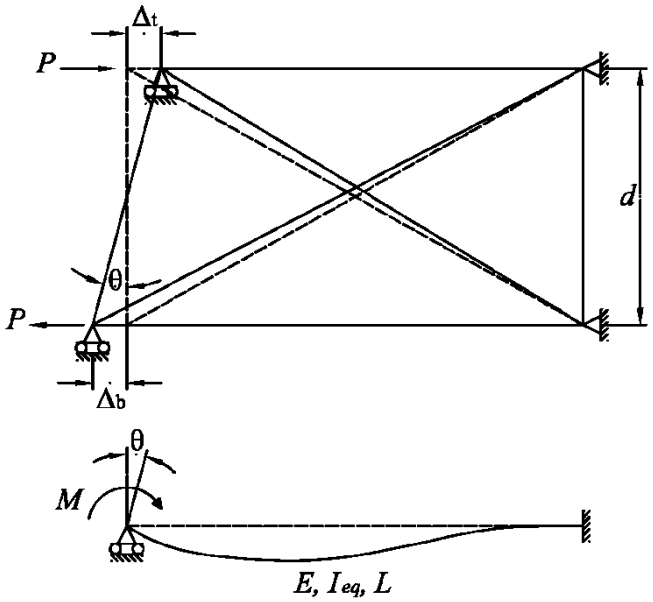

Figure 6.4. Flexural analogy model used in conventional practice to find the moment of inertia of the equivalent beam (adapted from Coletti and Yadlosky (2007)).

Another approximate procedure used to determine the moment of inertia of the equivalent beam elements is the "shear analogy" method. As depicted in Figure 6.5, in this method, the cross-frame is modeled with boundary conditions that allow only the vertical displacement of one of the ends. The force *P* is applied at the end that is free to move and the vertical deflection is captured. In the equivalent beam, the deflection due to this load is equal to $\Delta = (PL^3)/(12EI_{eq})$. Therefore, the moment of inertia used in the 2D-grid models to represent the cross-frames based on this method is:

$$I_{eq} = \frac{PL^3}{12E\Delta} \tag{6.20}$$

These procedures are highly approximate. It is clear that for a cross-frame, two substantially different equivalent moments of inertia can be obtained, depending on which model is used. Both the flexural analogy and shear analogy methods only capture a part of the structural behavior of the cross-frames and are not necessary a realistic representation of these bridge components.

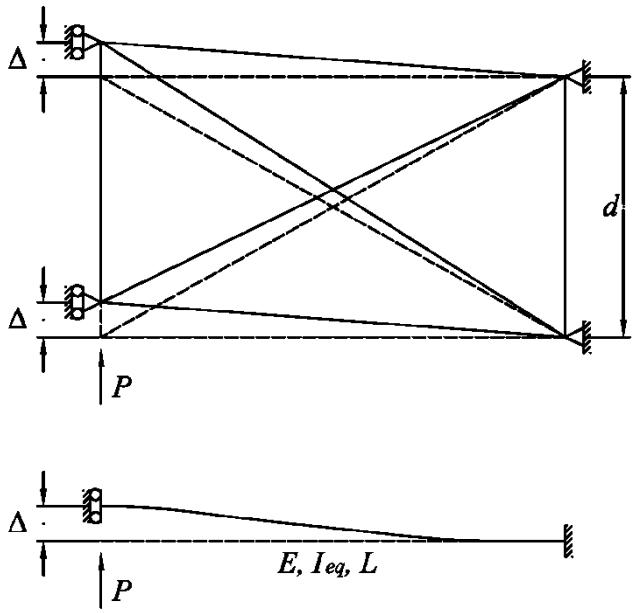

Figure 6.5. Shear analogy model used in conventional practice to find the moment of inertia of the equivalent beam (adapted from Coletti and Yadlosky (2007)).

In many cases, the responses predicted by 2D models constructed using the above procedures are close to the benchmark solutions obtained from 3D FEA analyses. As shown in (Sanchez, 2011), even for bridges with complex geometries, the approximate representation of the cross-frames often does not result in significant differences with respect to the 3D FEA predictions. In particular, the major-axis bending responses of the girders obtained from 2D-grid models constructed with these standard practices are often a close representation of the benchmark solutions. The reason for this incongruence is that in many cases, the cross-frame in-plane rigidity is much larger than the girder torsional rigidity of the I-girders.

The response affected the most by modeling the cross-frames with these ad hoc procedures is the internal forces in the cross-frame elements. In addition, the cross-frame forces generally have a significant influence on the flange lateral bending responses in I-girder bridges. To properly capture the flow of the transverse forces that results from horizontal curvature and support skew and the associated lateral bending response of the girders, it is necessary to perform the analysis with a more realistic model of the cross-frames. If the cross-frame forces are not computed accurately, it is not possible to obtain an accurate prediction of the f_ℓ stresses, either.

The practices used to model the cross-frames along with the poor representation of the torsion stiffness of the I-girders are the most significant limitations of the traditional methods used to conduct 2D-grid analysis. In the next section, simple two-node elements that are a more realistic representation of the cross-frame contributions to the system behavior are developed.

6.2.2 Improved Representation of the Cross-Frames in 2D-Grid Models

In the conventional methods commonly used to model the cross-frames, the structural properties of these components are not properly captured. It is evident that to overcome the limitations of the equivalent beam elements used to model the cross-frames, it is required to capture more efficiently their contributions to the system response. This can be done by applying the direct stiffness method to a model of the physical cross-frame and recovering the coefficients that constitute its stiffness matrix. For this purpose, consider the X-type cross-frame depicted in Figure 6.6a and its line element representation. For simplicity only the in-plane representation (3-dof per node) in shown in the figure. If the connection plates are assumed to be rigid, and the rotational continuity is neglected at the element connections in the plane of the cross-frame, it is possible to apply unit displacements to each of these dofs to recover the stiffness coefficients as shown in Figure 6.6b. Since in the cross-frame plane the chords and the diagonals are simply connected, the coefficients depend exclusively on the axial stiffness of the cross-frame elements. Note that for the formulation of the stiffness matrix, it is necessary to consider that the top chord, bottom chord, and the diagonals can have different cross-sections, i.e., different areas, A_t, A_b, A_{d1}, and A_{d2}, respectively. It is important to formulate the two-node element considering these characteristics, so it can handle cases such as cross-frames without top-chords (i.e., $A_t = 0$), or with only one diagonal (i.e., A_{d1} or $A_{d2} = 0$). The generality of an element formulated considering different element cross-sections is also beneficial when modeling bearing line cross-frames. The top-chord of these cross-frames generally has a larger section than the rest of the elements since it supports the deck joint.

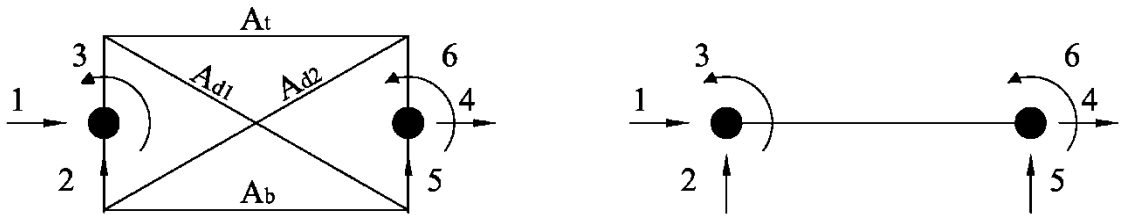

Physical Cross-Frame **Two-Node Element Representation**

a) Reduction of the physical cross-frame to a two-node element

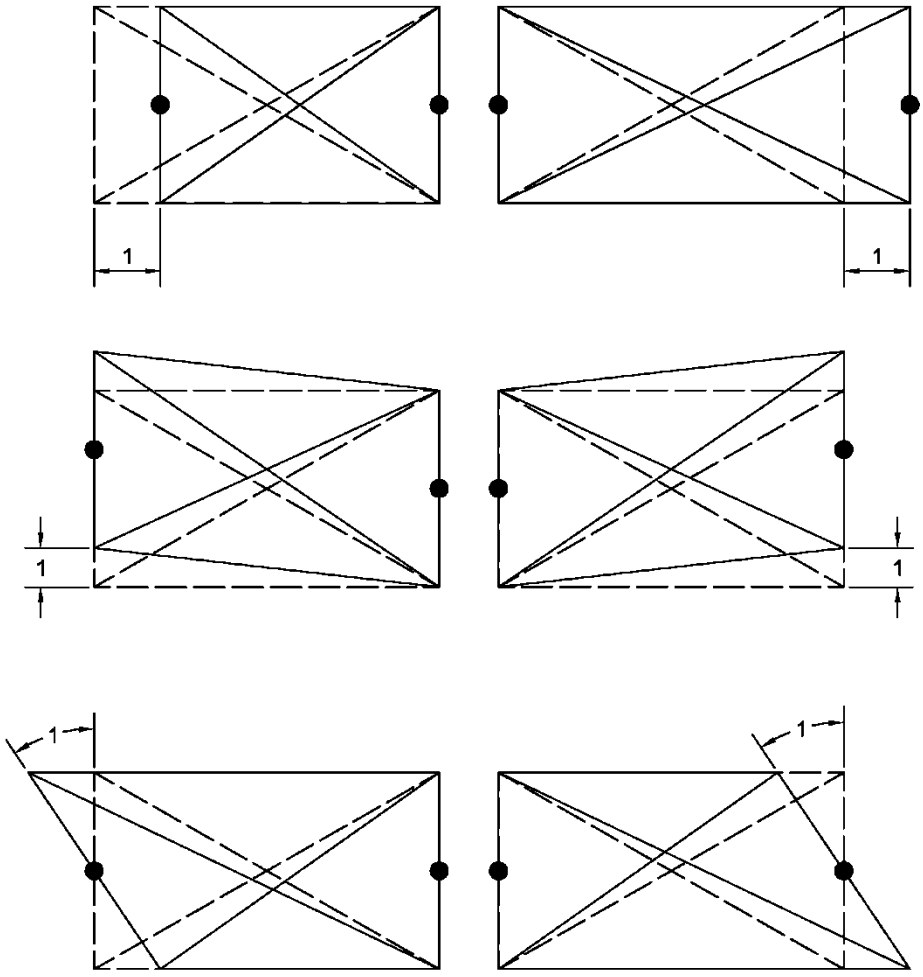

b) Unit displacements for the determination of the stiffness matrix coefficients

Figure 6.6. Determination of the stiffness matrix to represent the X-type cross-frame with a two-node beam element.

The coefficients of the first column of the stiffness matrix are determined by applying a unit displacement at dof 1. The forces in the cross-frame elements due to the applied displacement are shown in Figure 6.7. The coefficients are recovered from this free-body diagram, as shown in the same figure. Applying the same methodology to the other eleven dofs, it is possible to form the 12-by-12 stiffness matrix to represent the three-dimensional two-node element. The details of this formulation are provided in (Sanchez, 2011). Figure 6.8 shows the six-by-six stiffness matrix of the X-type cross-frame, which captures its in-plane behavior.

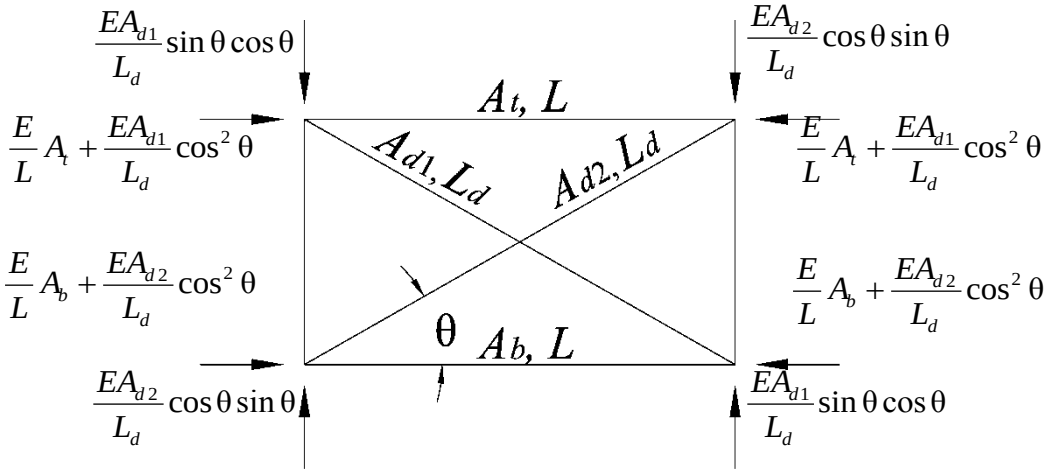

$$k_{11}: \quad \frac{E}{L}\left(A_b + A_t\right) + \frac{EL^2}{L_d^{\,3}}\left(A_{d1} + A_{d2}\right)$$

$$k_{12}: \quad \frac{ELh}{L_d^{\,3}}\left(A_{d2} - A_{d1}\right)$$

$$k_{13}: \quad \frac{Eh}{2L}\left(A_b - A_t\right) + \frac{EhL^2}{2L_d^{\,3}}\left(A_{d2} - A_{d1}\right)$$

$$k_{14}: \quad -\frac{1}{L}\left(A_b + A_t\right) - \frac{L^2}{L_d^{\,3}}\left(A_{d1} + A_{d2}\right)$$

$$k_{15}: \quad \frac{Lh}{L_d^{\,3}}\left(A_{d1} - A_{d2}\right)$$

$$k_{16}: \quad \frac{h}{2L}\left(A_t - A_b\right) + \frac{hL^2}{2L_d^{\,3}}\left(A_{d2} - A_{d1}\right)$$

Figure 6.7. Stiffness coefficients associated with dof 1 – X-type cross-frame.

This two-node element is an accurate representation of the contributions of an X-type cross-frame to the system behavior. In comparison to the equivalent beam elements introduced previously, this element captures all the sources of deformation in the cross-frames; in addition, it considers the coupling between the different dofs. Given that its formulation handles cross-frames with different sections for the chords or the diagonals, it can handle cross-frames without top-chords or with a single diagonal. Due to its simplicity, it has the ability to capture the physical cross-frame behavior via a line element.

This element can be implemented in any computer software to conduct 2D-grid analyses of I-girder bridges and overcome the limitations of the conventional models. This cross-frame model has been implemented and tested in the LARSA 4D software package (LARSA, 2010). This software package is selected for the study because of its versatility to handle custom element definitions. The program architecture facilitates the implementation the elements, so they can be used readily in the analyses of steel girder bridges. The tests conducted to determine the ability of the developed cross-frame models and their results are reported in (Sanchez, 2011).

Figure 6.9 shows the stiffness matrix of the two-node element based on Euler-Bernoulli beam theory. By comparing the matrix of this Euler-Bernoulli beam element and the matrix of the X-type cross-frame, it is evident that the equivalent beam cannot capture the physical behavior of these structural components. The chord and diagonal areas and the height and width of the cross-frame are the six variables needed to compute the cross-frame stiffness matrix. The matrix of the Euler-Bernoulli beam, however, only has two properties, A_{eq} and I_{eq}, that can be manipulated to represent the cross-frame. In conventional practice, when the cross-frames are modeled with beam elements based on the shear analogy method, the equivalent moment of inertia is, in effect, calculated from the equation for the term $k_{22.}$ Similarly, when the flexural analogy method is used to determine the beam properties, I_{eq} is calculated from the equation for k_{33}. Hence, instead of constructing a model of the cross-frame to determine the equivalent moment of inertia from Eqs. (6.19) or (6.20), the same approximate I_{eq} can be directly computed from the equations obtained from the terms k_{22} or k_{33}, respectively

$$k = E\begin{bmatrix}
\frac{1}{L}(A_b+A_t)+\frac{L^2}{{L_d}^3}(A_{d1}+A_{d2}) & \frac{Lh}{{L_d}^3}(A_{d2}-A_{d1}) & \frac{h}{2L}(A_b-A_t)+\frac{hL^2}{2{L_d}^3}(A_{d2}-A_{d1}) & -\frac{1}{L}(A_b+A_t)-\frac{L^2}{{L_d}^3}(A_{d1}+A_{d2}) & \frac{Lh}{{L_d}^3}(A_{d1}-A_{d2}) & \frac{h}{2L}(A_t-A_b)+\frac{hL^2}{2{L_d}^3}(A_{d2}-A_{d1}) \\
\frac{Lh}{{L_d}^3}(A_{d2}-A_{d1}) & \frac{h^2}{{L_d}^3}(A_{d1}+A_{d2}) & \frac{h^2L}{2{L_d}^3}(A_{d1}+A_{d2}) & \frac{Lh}{{L_d}^3}(A_{d1}-A_{d2}) & -\frac{h^2}{{L_d}^3}(A_{d1}+A_{d2}) & \frac{h^2L}{2{L_d}^3}(A_{d1}+A_{d2}) \\
\frac{h}{2L}(A_b-A_t)+\frac{hL^2}{2{L_d}^3}(A_{d2}-A_{d1}) & \frac{h^2L}{2{L_d}^3}(A_{d1}+A_{d2}) & \frac{h^2}{4L}(A_b+A_t)+\frac{h^2L^2}{4{L_d}^3}(A_{d1}+A_{d2}) & \frac{h}{2L}(A_t-A_b)+\frac{hL^2}{2{L_d}^3}(A_{d1}-A_{d2}) & -\frac{h^2L}{2{L_d}^3}(A_{d1}+A_{d2}) & -\frac{h^2}{4L}(A_b+A_t)+\frac{h^2L^2}{4{L_d}^3}(A_{d1}+A_{d2}) \\
-\frac{1}{L}(A_b+A_t)-\frac{L^2}{{L_d}^3}(A_{d1}+A_{d2}) & \frac{Lh}{{L_d}^3}(A_{d1}-A_{d2}) & \frac{h}{2L}(A_t-A_b)+\frac{hL^2}{2{L_d}^3}(A_{d1}-A_{d2}) & \frac{1}{L}(A_b+A_t)+\frac{L^2}{{L_d}^3}(A_{d1}+A_{d2}) & \frac{Lh}{{L_d}^3}(A_{d2}-A_{d1}) & \frac{h}{2L}(A_b-A_t)+\frac{hL^2}{2{L_d}^3}(A_{d1}-A_{d2}) \\
\frac{Lh}{{L_d}^3}(A_{d1}-A_{d2}) & -\frac{h^2}{{L_d}^3}(A_{d1}+A_{d2}) & -\frac{h^2L}{2{L_d}^3}(A_{d1}+A_{d2}) & \frac{Lh}{{L_d}^3}(A_{d2}-A_{d1}) & \frac{h^2}{{L_d}^3}(A_{d1}+A_{d2}) & -\frac{h^2L}{2{L_d}^3}(A_{d1}+A_{d2}) \\
\frac{h}{2L}(A_t-A_b)+\frac{hL^2}{2{L_d}^3}(A_{d2}-A_{d1}) & \frac{h^2L}{2{L_d}^3}(A_{d1}+A_{d2}) & -\frac{h^2}{4L}(A_b+A_t)+\frac{h^2L^2}{4{L_d}^3}(A_{d1}+A_{d2}) & \frac{h}{2L}(A_b-A_t)+\frac{hL^2}{2{L_d}^3}(A_{d1}-A_{d2}) & -\frac{h^2L}{2{L_d}^3}(A_{d1}+A_{d2}) & \frac{h^2}{4L}(A_b+A_t)+\frac{h^2L^2}{4{L_d}^3}(A_{d1}+A_{d2})
\end{bmatrix}$$

Figure 6.8. Two-node element stiffness matrix, two-dimensional representation of the X-type cross-frame.

$$k = E\begin{bmatrix}
\frac{A_{eq}}{L} & 0 & 0 & -\frac{A_{eq}}{L} & 0 & 0 \\
0 & \frac{12I_{eq}}{L^3} & \frac{6I_{eq}}{L^2} & 0 & -\frac{12I_{eq}}{L^3} & \frac{6I_{eq}}{L^2} \\
0 & \frac{6I_{eq}}{L^2} & \frac{4I_{eq}}{L} & 0 & -\frac{6I_{eq}}{L^2} & \frac{2I_{eq}}{L} \\
-\frac{A_{eq}}{L} & 0 & 0 & \frac{A_{eq}}{L} & 0 & 0 \\
0 & -\frac{12I_{eq}}{L^3} & -\frac{6I_{eq}}{L^2} & 0 & \frac{12I_{eq}}{L^3} & -\frac{6I_{eq}}{L^2} \\
0 & \frac{6I_{eq}}{L^2} & \frac{2I_{eq}}{L} & 0 & -\frac{6I_{eq}}{L^2} & \frac{4I_{eq}}{L}
\end{bmatrix}$$

k_{11}: $A_{eq}=(A_b+A_t)+\left(L^3/{L_d}^3\right)(A_{d1}+A_{d2})$

k_{12}: $0=\left(Lh/{L_d}^3\right)(A_{d2}-A_{d1})$

k_{13}: $0=(h/2L)(A_b-A_t)+\left(hL^2/2{L_d}^3\right)(A_{d2}-A_{d1})$

k_{16}: $0=(h/2L)(A_t-A_b)+\left(hL^2/2{L_d}^3\right)(A_{d2}-A_{d1})$

k_{22}: $I_{eq}=\left(h^2L^3/12{L_d}^3\right)(A_{d1}+A_{d2})$

k_{23}: $I_{eq}=\left(h^2L^3/12{L_d}^3\right)(A_{d1}+A_{d2})$

k_{33}: $I_{eq}=\left(h^2/16\right)(A_b+A_t)+\left(h^2L^3/16{L_d}^3\right)(A_{d1}+A_{d2})$

k_{36}: $I_{eq}=\left(-h^2/8\right)(A_b+A_t)+\left(h^2L^3/8{L_d}^3\right)(A_{d1}+A_{d2})$

Figure 6.9. Comparison of the stiffness matrices of the X-type cross-frame and the Euler-Bernoulli beam.

Another type of element that is sometimes used to represent the cross-frames is based on Timoshenko beam theory. This element incorporates the contributions of the shear deformations to the beam response. Figure 6.10 shows the stiffness matrix of the line element formulated with this theory. In this element an additional variable, the shear area, A_v, can be manipulated in combination with the full cross-section area A_{eq} and the moment of inertia I_{eq} to represent the cross-frames with equivalent beams. Section 3.2.3 of the NCHRP 12-79 Final Report shows that the use of the Timoshenko beam element can provide substantial improvement in the modeling accuracy for a V-type cross-frame, and points out that other cases such as X-frames with or without a top chord can be modeled with good accuracy. However, this model is not sufficient to fully capture the cross-frame behavior. As mentioned before, it is necessary to define six variables to fully represent the cross-frame stiffness. Since there are only three section properties that can be modified in the equivalent Timoshenko beam (A_{eq}, A_v, and I_{eq}), this type of element is insufficient to fully model a general X-type cross-frame. However, for an X-type cross-frame that has the same top and bottom chord areas, as well as equal diagonal areas (not necessarily the same as those for the top and bottom chord), the Timoshenko beam element is capable of exactly matching the stiffness of the cross-frame.

$$k = E\begin{bmatrix}
\frac{A_{eq}}{L} & 0 & 0 & -\frac{A_{eq}}{L} & 0 & 0 \\
0 & \frac{12A_vGI_{eq}}{L\left(A_vGL^2+12EI_{eq}\right)} & \frac{6A_vGI_{eq}}{A_vGL^2+12EI_{eq}} & 0 & -\frac{12A_vGI_{eq}}{L\left(A_vGL^2+12EI_{eq}\right)} & \frac{6A_vGI_{eq}}{A_vGL^2+12EI_{eq}} \\
0 & \frac{6A_vGI_{eq}}{A_vGL^2+12EI_{eq}} & \frac{4I_{eq}\left(A_vGL^2+3EI_{eq}\right)}{L\left(A_vGL^2+12EI_{eq}\right)} & 0 & -\frac{6A_vGI_{eq}}{A_vGL^2+12EI_{eq}} & \frac{2I_{eq}\left(A_vGL^2-6EI_{eq}\right)}{L\left(A_vGL^2+12EI_{eq}\right)} \\
-\frac{A_{eq}}{L} & 0 & 0 & \frac{A_{eq}}{L} & 0 & 0 \\
0 & -\frac{12A_vGI_{eq}}{L\left(A_vGL^2+12EI_{eq}\right)} & -\frac{6A_vGI_{eq}}{A_vGL^2+12EI_{eq}} & 0 & \frac{12A_vGI_{eq}}{L\left(A_vGL^2+12EI_{eq}\right)} & -\frac{6A_vGI_{eq}}{A_vGL^2+12EI_{eq}} \\
0 & \frac{6A_vGI_{eq}}{A_vGL^2+12EI_{eq}} & \frac{2I_{eq}\left(A_vGL^2-6EI_{eq}\right)}{L\left(A_vGL^2+12EI_{eq}\right)} & 0 & -\frac{6A_vGI_{eq}}{A_vGL^2+12EI_{eq}} & \frac{4I_{eq}\left(A_vGL^2+3EI_{eq}\right)}{L\left(A_vGL^2+12EI_{eq}\right)}
\end{bmatrix}$$

Figure 6.10. Stiffness matrix of a beam element including shear deformations (Timoshenko beam).

The above discussion shows that neither the Euler-Bernoulli beam nor the Timoshenko beam have the characteristics required for an exact representation of general X-type cross-frames. The two approximate methods used in conventional practice (i.e., the flexural analogy method and the shear analogy method) yield different cross-frame properties that capture only one part of the cross-frame behavior. Therefore, the equivalent beam concept generally is not an accurate representation of the structural behavior of these components. This section illustrates the development of the two-node element for the X-type cross-frame. Sanchez (2011) also discusses the development of the V-type and inverted V-type cross-frames, which are other configurations commonly used for girder bridges. For these types of cross-frames, the Timoshenko beam element is not able to capture the exact physical stiffness properties. The most significant errors in the approximation are for V-type cross-frames without a top chord, where the cross-frame flexural stiffness is critically dependent upon the characteristics of the bottom chord and the connection plates in the vicinity of the joint at the cross-frame mid-length.

The two-node equivalent beam elements developed by (Sanchez, 2011) can be implemented in any computer program used to conduct 2D-grid analyses. In the NCHRP 12-79 research, these elements were implemented in the LARSA 4D program since this software facilitates the inclusion of user-defined elements. However, the cross-frame two-node elements can be implemented in other programs that have user-defined elements, or by software developers, with minor effort.

6.3 Cross-Frame Forces

In 2D-grid models, the primary analysis output is the joint displacements. These displacements are multiplied by the corresponding element stiffness coefficients to calculate the joint forces. To obtain the forces in the chords and diagonals of the cross-frames, the joint forces commonly are decomposed as shown in Figure 6.11. The V_i and V_j shears are essentially the same; the difference between them is equal to the weight of the cross-frame. This effect is negligible, so the largest of these forces is typically selected and equally divided between the top and bottom nodes of the cross-frame (assuming an X-type cross-frame). In most of the other cross-frame types, a single diagonal frames into the girders at each end of the cross-frame, and therefore, the shear

force is applied to the cross-frame node corresponding to this diagonal. In the case of a V-type cross-frame with no top chord, the flexural stiffness of the cross-frame is highly dependent upon the flexural properties provided by the combination of the bottom chord and any connection plates across the joint at the cross-frame mid-length. In this case, the distribution of the shear between the diagonal and the bottom chord is statically indeterminate, but it is reasonable to assume that any shear is taken predominantly by the diagonal.

In most situations in girder bridges, the axial forces, P_i and P_j, are negligible. In the case that they are not, they are also equally divided between the top and bottom nodes. This is necessary to satisfy equilibrium, assuming that the reference axis of the equivalent beam element is located at the mid-depth of the cross-frame.

The left and right moments, M_i and M_j, are decomposed into force couples with magnitude equal to M/h and applied to the cross-frame nodes. Once this is accomplished, the forces in the chords and the diagonals can be obtained by statics.

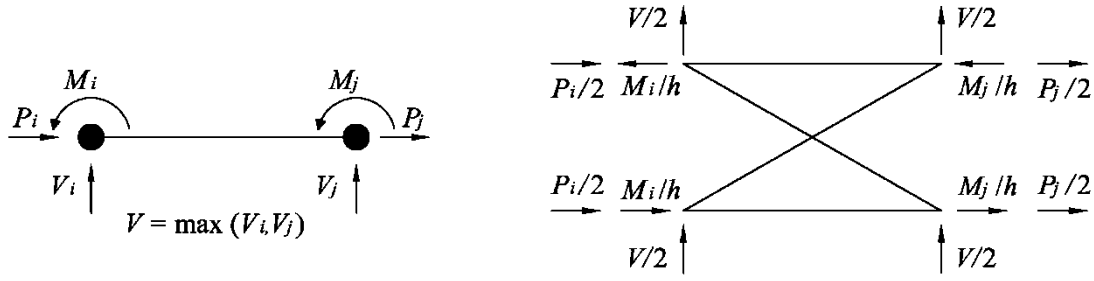

Joint Forces - 2D Analysis

Nodal Forces in the Cross-Frame

Figure 6.11. Conventional practices for determination of cross-frame member forces from 2D-grid analysis results.

It is important to note that, in general, when the cross-frame geometry is symmetric about the equivalent beam reference axis, as in the case of an X-type cross-frame with equal diagonals and equal top and bottom chords, the axial and bending responses of the cross-frame are fully uncoupled. For the Timoshenko beam element (Figure 6.10), this behavior is captured by the zero terms in the stiffness matrix, and for this specific cross-frame case, the corresponding terms in Figure 6.8 are also zero. However, if the cross-frame is not symmetric about the equivalent beam reference axis,

its exact stiffness properties involve coupling between the cross-frame bending and axial degrees of freedom. For instance, for a V-type cross-frame without a top chord, the flexural deformations tend to occur approximately about the bottom chord around the mid-length of the cross-frame. This deformation causes and axial displacement at the nodal positions of the equivalent beam element (assuming that the equivalent beam element is located at the mid-depth of the cross-frame). These axial displacements in turn correspond to weak-axis flexure of the I-girders.

The above coupling is fully captured in any explicit modeling of the cross-frames in a 3D FEA, and it is fully captured in the equivalent beam element stiffness matrices developed by Sanchez (2011). Furthermore, this coupling can be included in any 2D-Frame model of a girder bridge. However, it is common to neglect all the specific depth information such as the actual position of the cross-frames relative to the mid-depth of the girders, the location of the girder shear centers and cross-section centroids relative to the girder mid-depths, and the elevation of the bearings in 2D-Frame models. Therefore, there are other potential sources of significant approximations associated with the cross-frame axial stiffnesses in 2D-Frame models.

If the “exact” cross-frame equivalent beam models are used, they should be used in a 2D-Frame approach. Furthermore, it is acceptable to model all of the components in a common plane, to formulate the singly-symmetric girder stiffnesses using the equations detailed in Section 6.1.2 along with the appropriate girder cross-section warping constant (neglecting the effect of the shift in the shear center relative to the cross-section centroid), and neglecting other height effects such as the depth of the bearings. All of the improved 2D-grid solutions presented from the NCHRP 12-79 research are conducted in this way. Alternately, the Timoshenko beam element (Figure 6.10) provides a significantly improved approximation for all types of cross-frames. This element neglects the coupling between the axial and flexural degrees of freedom, consistent with the assumptions commonly employed for 2D-grid analysis.

In the recommended exact two-node equivalent beam elements, the forces in the chords and diagonals of the cross-frames are calculated considering the fundamental force-displacement relationships from the element stiffness matrices. The forces are

computed by recovering the joint displacements to determine the element deformations. The deformations are then multiplied by the corresponding stiffness coefficients to obtain the element forces. Applying this criterion, the forces in the chords and the diagonals of an X-type cross-frame are:

$$F_{TC} = \frac{E \cdot A_t}{L}\left[\left(u_4 - u_1\right) + \frac{h}{2}\left(u_3 - u_6\right)\right] \tag{6.21}$$

$$F_{BC} = \frac{E \cdot A_b}{L}\left[\left(u_4 - u_1\right) + \frac{h}{2}\left(u_6 - u_3\right)\right] \tag{6.22}$$

$$F_{D1} = \frac{E \cdot A_{d1}}{2L_d^{\,2}}\left[2L\left(u_4 - u_1\right) + 2h\left(u_2 - u_5\right) + Lh\left(u_3 + u_6\right)\right] \tag{6.23}$$

$$F_{D2} = -\frac{E \cdot A_{d2}}{2L_d^{\,2}}\left[2L\left(u_1 - u_4\right) + 2h\left(u_2 - u_5\right) + Lh\left(u_3 + u_6\right)\right] \tag{6.24}$$

where u_i is the displacement at dof i. Figure 6.6 shows the dof numbering associated with the displacements and the orientation of Diagonals 1 and 2. Similar equations for the computation of the forces in V-type and inverted V-type cross-frames are provided in (Sanchez, 2011).

6.4 Calculation of I-Girder Flange Lateral Bending Stresses Given Cross-Frame Forces

In a steel I-girder bridge, the flange lateral bending stresses, f_ℓ, that result from the horizontal curvature and the skew effects must be considered in the design of the structure. As required by the AASHTO Bridge Specifications (AASHTO, 2010), these stresses are combined with the major-axis bending stresses to conduct the strength checks in the noncomposite and composite structure. However, at present, there is limited guidance on how to determine the f_ℓ stresses associated with skew.

In a skewed bridge, the cross-frames induce forces in the I-girders, subjecting their flanges to lateral bending stresses, f_ℓ. Currently, the only methods to compute these cross-frame forces are via refined 3D frame models that explicitly include the warping stiffness contributions, or via a rigorous 3D FEA. However, with some exceptions, these

analysis methods are used predominantly for research purposes or for bridges with particularly complex geometry, since significant effort may be required to construct the model and post-process the results (many of the emerging software systems provide substantial reductions in these efforts).

To obtain the flange lateral bending stresses, f_ℓ, it is necessary to have an accurate prediction of the cross-frame forces. In the approximate 1D line-girder analysis methods, the forces in the cross-frames due to the skew are not captured; therefore, it is not feasible to determine these f_ℓ stresses with a 1D analysis. Similarly, as shown in the second case study of Section 5.1.3, due to the poor representation of the cross-frame in-plane properties and the poor representation of the torsional characteristics of the I-girders, the 2D-grid models developed with conventional techniques often substantially underpredict the physical cross-frame forces. For these reasons, and in the absence of an alternative predictor, the AASHTO Bridge Specifications (AASHTO, 2010), Article C6.10.1 provides the coarse estimates for the flange lateral bending stresses discussed previously in Chapter 2. Unfortunately, no estimates are provided within the AASHTO Specifications for the corresponding cross-frame forces.

In this section, a method to estimate the f_ℓ stresses in straight and skewed bridges is introduced. Bridge NISSS16 is used to illustrate the calculations. Figure 6.12a shows the plan view of the bridge. It is intended to capture the flange lateral bending stresses in the top flange of girder G6. Figure 6.12b shows the free-body diagram of the second cross-frame in Bay 6, B6-CF2. The cross-frame forces (i.e., F_{TC}, F_{D1}, F_{D2}, and F_{BC}) are transferred to the girders in the form of nodal forces (*A*, *B*, *C*, and *D*). The horizontal and vertical components of the vertical loads are determined by applying the equilibrium equations at nodes A to D, such that:

$$
\begin{aligned}
A_x &= -F_{BC} - F_{D2}\cos(\theta) \\
A_y &= -F_{D2}\sin(\theta) \\
B_x &= -F_{TC} - F_{D1}\cos(\theta) \\
B_y &= F_{D1}\sin(\theta) \\
C_x &= F_{TC} + F_{D2}\cos(\theta) \\
C_y &= F_{D2}\sin(\theta) \\
D_x &= F_{BC} + F_{D1}\cos(\theta) \\
D_y &= -F_{D1}\sin(\theta)
\end{aligned}
\tag{6.25}
$$

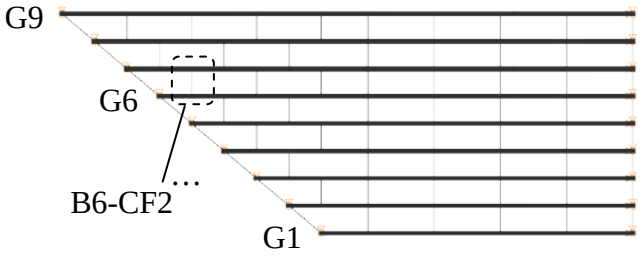

(a) Plan view of Bridge NISSS16

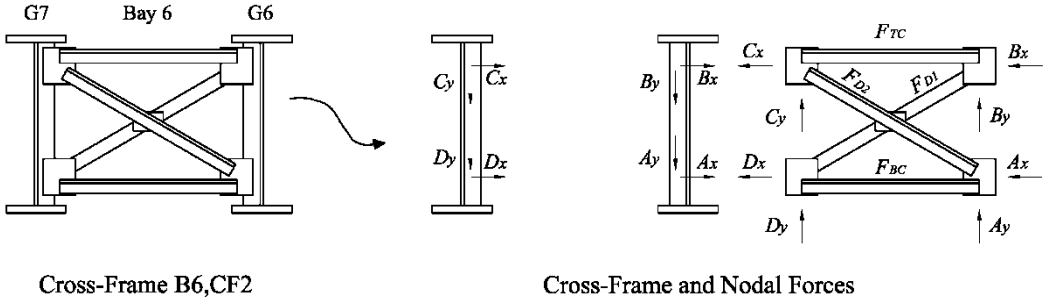

(b) Forces transferred from cross-frame B6-CF2 to girders G6 and G7

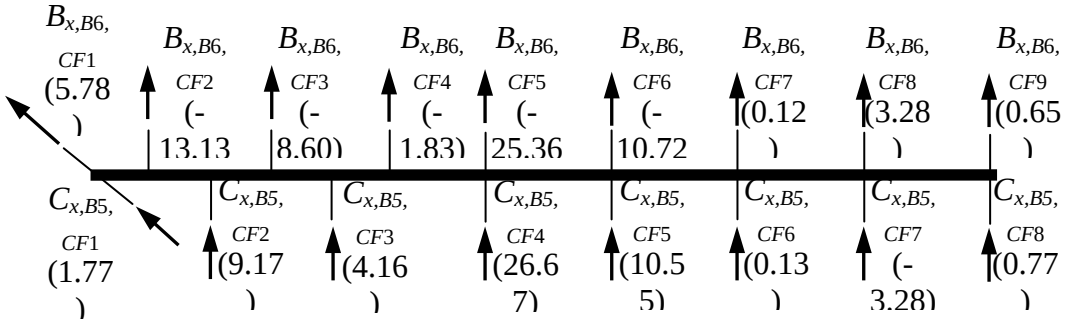

(c) Top flange of girder G6 subject to the horizontal components of the nodal forces

Figure 6.12. Determination of cross-frame forces as the first step in the calculation of flange lateral bending, top flange of girder G6, NISSS16, at TDL level.

where θ is the angle between the chords and the diagonals. Next, the lateral forces A_x and B_x are converted to statically-equivalent lateral forces at the level of the girder flanges, based on a girder cross-section free-body diagram. For simplicity of notation, these converted flange-level forces are referenced using the same symbols in the following.

Given the various flange level forces applied from the cross-frames, the girder flanges are isolated from the rest of the structure and subjected to the horizontal components of the nodal forces, as illustrated in Figure 6.12c. Notice that the C_x force components of the cross-frames in Bay 5 are applied on one side of the flange, while the B_x components of the Bay 6 cross-frames are applied on the other side. The magnitudes of the forces acting on the flange under consideration are included in the figure. They are computed with Eqs. (6.21) to (6.24), by using the cross-frame force estimates obtained from the improved 2D-grid analysis of this bridge. The 2D-grid model is constructed following the recommendations discussed in Sections 6.1 and 6.2.

The above nodal lateral forces are the source of the lateral bending in the flange of girder G6; however, only the forces acting in the region where the cross-frames are staggered cause large flange lateral bending stresses in bridge NISSS16. As shown in Figure 6.12c, the forces in the region where the cross-frames are contiguous can be larger than those where they are staggered, but these lateral forces tend to cancel each other out. For example, in the intermediate contiguous cross-frame line that is closest to the skewed support, the forces are 26.67 kips and -25.36 kips, and the resultant is 1.31 kips. Hence, although the nodal forces are larger than at other locations, the force resultant causes a minor effect on the flange lateral bending. The cross-frames, and the connections between the cross-frames and the girders, however, must be designed considering these forces.

Another important aspect to consider regarding this approximate procedure is that the nodal lateral forces are not completely balanced in Figure 6.12c. This is because the girder torsional stiffnesses, upon which the calculation of the cross-frame forces is based, include a contribution both from the girder warping torsion as well as the girder St. Venant torsion. As such, a portion of the above forces is transferred (by the interaction of the flange with the girder web) into the internal St. Venant torsion in the girders. More

specifically, corresponding small but undetermined distributed lateral forces are transferred to the flange from the web in Figure 6.12c.

In the case of the flange under consideration, the unbalance calculated by adding all the lateral forces acting on the flange (including the lateral components of the forces from the skewed bearing line cross-frames) is -2.58 kips. If the distributed lateral load transferred from the web is added to the above nodal lateral forces, the flange would be in equilibrium.

Solutions to this problem include:

(1) Use the girder torsional rotations and displacements along with the detailed open-section thin-walled beam stiffness model associated with J_{eq} to directly determine the flange lateral bending stresses. This results in an imbalance in the flange lateral bending moments on each side of the intermediate cross-frames (since J_{eq} is based the assumption of warping fixity at the cross-frame locations). This moment imbalance could be re-distributed along the girder flange to determine accurate flange lateral bending moments. A procedure analogous to elastic moment distribution could be utilized for this calculation. Although this approach is a viable one, it is relatively complex. Therefore, it was not pursued in the NCHRP 12-79 research.

(2) Focus on an approximate local calculation in the vicinity of each cross-frame, utilizing the forces delivered to the flanges from the cross-frames as shown in Figure 6.12c. Because of its relative simplicity this approach was selected in the NCHRP 12-79 research.

It should be noted that the girder flange lateral bending stresses are calculated directly and explicitly from the element displacements and stiffnesses in the TWOS 2D-grid and TWOS 3D-frame solutions. Therefore, these methods provide the best combination of accuracy and simplicity for the grid or frame element calculation of the flange lateral bending stresses. However, the disadvantage of this approach is the additional complexity of the element formulation, and the requirement that an additional warping degree of freedom has to be included in the global structural analysis.

Figure 6.13 illustrates the simplified approach adopted in the NCHRP 12-79 research for calculating the I-girder flange lateral bending moments given the statically-equivalent lateral loads transferred at the flange level from the cross-frames. The calculation focuses on a given cross-frame location and the unbraced lengths, *a* and *b*, on each side of this location. For simplicity of the discussion, only the force delivered from the cross-frame under consideration is shown in the figure, and the cross-frame is assumed to be non-adjacent to a simply-supported end of the girder. In general, the lateral forces from horizontal curvature effects and/or from eccentric bracket loads on fascia girders also would be included. Two flange lateral bending moment diagrams are calculated as shown in the figure, one based on simply-supported end conditions and one based on fixed end conditions at the opposite ends of the unbraced lengths. For unbraced lengths adjacent to simply-supported girder ends, similar moment diagrams are calculated, but the boundary conditions are always pinned at the simply-supported end. The cross-frame under consideration is located at the position of the load *P* in the sketches. In many situations, the moments at the position of the load are the controlling ones in the procedure specified below.

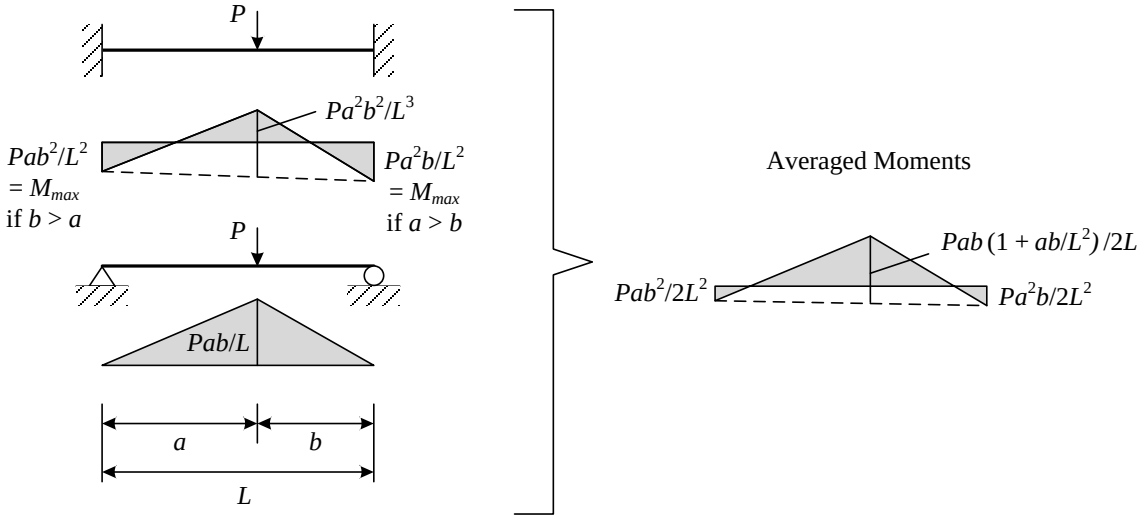

Figure 6.13. Lateral bending moment, M_ℓ, in a flange segment under simply-supported and fixed-end conditions.

Given the moment diagrams for the above cases, the NCHRP 12-79 research determined that an accurate to conservative solution for the flange lateral bending moments and stresses is obtained generally by:

(1) Averaging the above moment diagrams, and

(2) Taking the largest averaged internal moment in each of the unbraced lengths as the flange lateral bending moment for that length.

This solution is repeated cross-frame location by cross-frame location along the length of the girders and the largest moment from the two solutions obtained for each unbraced length is taken as the estimate of the flange lateral bending moment in that unbraced length. (For the unbraced lengths at girder simply-supported ends, only one solution is performed.)

The above procedure recognizes that the true flange lateral bending moment is bounded by the “pinned” and “fixed” moment diagrams (neglecting the small St. Venant torsional contributions from the interaction with the web) and ensures that the flange lateral bending moments required for static equilibrium are never underestimated. Also, the average of the pinned and fixed moment diagrams is analogous to the use of the approximation $qL_b^2/10$ rather than $qL_b^2/12$ when estimating the flange lateral bending moments due to horizontal curvature, where q is the equivalent flange radial load. In

Figure 6.14 shows the plots of the response predictions obtained using the above approach and the results obtained from the 3D FEA for the top flange of Girders G3 and G6. The plots include the responses for fully fixed and simply supported end conditions. Additionally, a trace that represents the average between these two responses is also included. As shown in these plots, the estimates obtained with the proposed approach and using the results derived from the improved 2D-grid model are a reasonable representation of the benchmark. As expected, the responses predicted by the FEA lay between the predictions determined assuming fully fixed and pinned ends, and are accurately estimated by taking the average of the last two predictions.

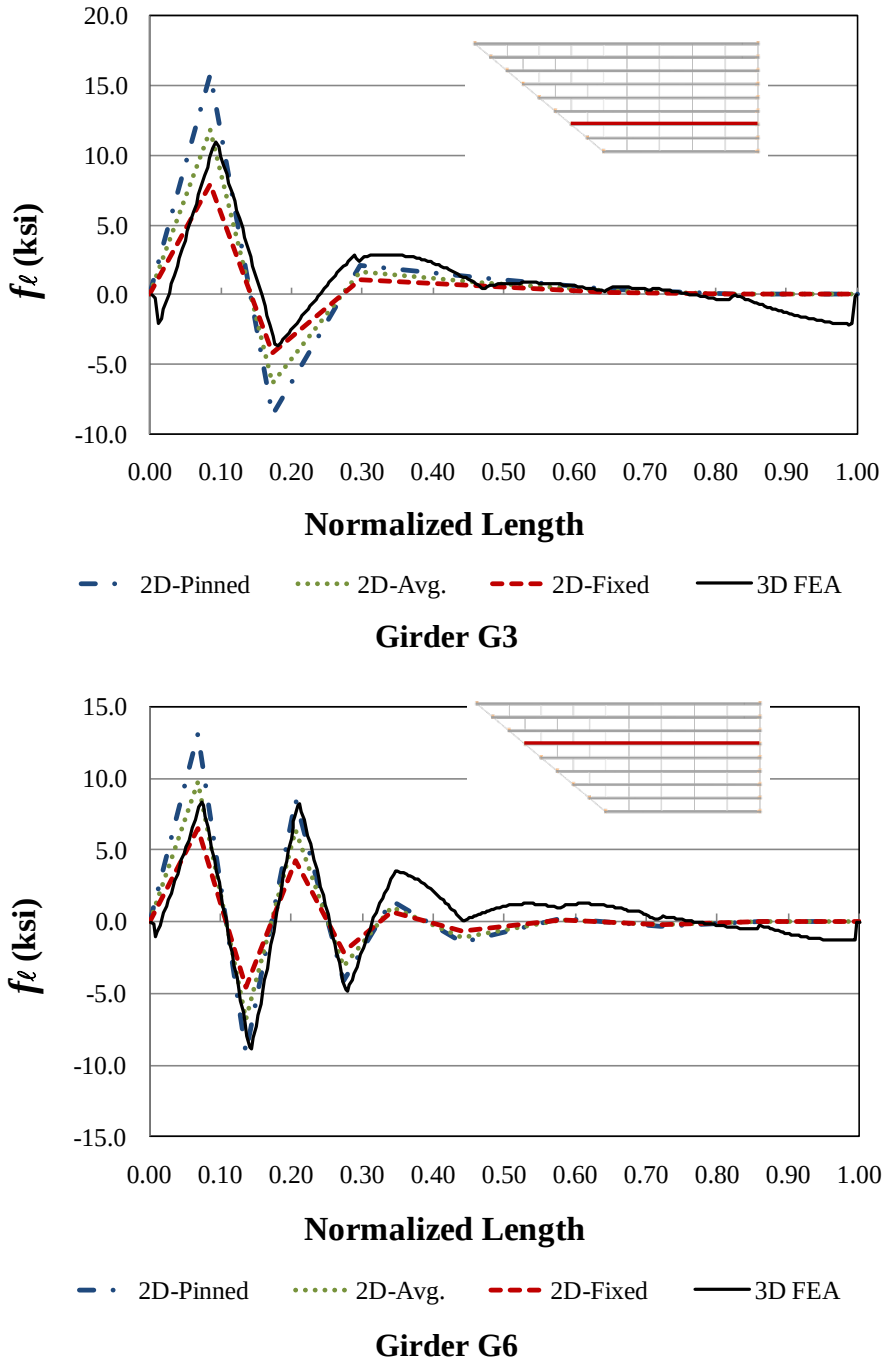

Figure 6.14. Flange lateral bending stresses in Bridge NISSS16 at TDL level.

It should be emphasized that to predict the flange lateral bending stresses using the proposed method, it is necessary to first have an accurate prediction of the cross-frame forces. Hence, the results of a 2D-grid analysis conducted with conventional practices cannot be used for this purpose. The cross-frame forces should be obtained from an analysis where the recommendations of Sections 6.1 and 6.2 are implemented in the model.

6.5 . Summary of Proposed Improvements for the Analysis of I-Girder Bridges using 2D-Grid Analysis

The previous sections highlight the characteristics of the 2D-grid models and the limitations of the conventional techniques to properly represent the behavior of an I-girder bridge during construction. Essentially, there are two modeling practices that can considerably affect the accuracy of the analyses. The first practice is related to the representation of the torsional properties of the I-girders. In computer programs commonly used for 2D-grid modeling, the torsional resistance of the I-girders is formulated considering only the pure or St. Venant torsion contributions. The other factor that can affect the response predictions of a 2D-grid analysis is the model used to represent the cross-frames. In most of cases, the cross-frames are modeled using an equivalent beam element, which is based on the Euler-Bernoulli beam theory.

The improved modeling techniques discussed in this chapter can be implemented with minor effort in design offices. The equivalent torsion constant as a means to simulate the warping contributions to the girder torsional stiffness is a concept that requires a simple manipulation of the cross-section properties in the model definition. This modification, however, can improve the predictions obtained from a grid model of bridges where the torsional responses have a major role in the structural response, as is the case of curved and/or skewed bridges.

Similar to the girder torsional properties, a better representation of the cross-frames can be accomplished by formulating two-node elements that consider all the stiffness contributions to the system response. The elements developed in the NCHRP 12-79 research were included and tested in the LARSA 4D program since the architecture of this software allows the inclusion of user defined finite elements. However, the

element potentially could be implemented in the library of any commercial software used for bridge engineering.

Finally, it is worth emphasizing on the relevance of an accurate model of cross-frames and girder torsional stiffness. In many structures, wide fluctuations in cross-frame stiffness do not have a significant effect in the structural responses. Similarly, in some cases, the poor torsion model of the girders does not represent a considerable source of error. The studies conducted in this research show that in straight and skewed bridges with skew indices below 0.30, torsion induced by skew is minor and the participation of the cross-frames may be negligible. Hence, bridges of these characteristics are insensitive to the cross-frame and girder torsional stiffness model. In fact, a line girder analysis may be sufficient in these cases. However, when the index goes above this limit, due to the torsion that the girders experience as a result of the transverse load path, the system becomes more sensitive to the torsion model and changes in the cross-frame stiffness. In bridges with $I_S \geq 0.30$, it is important how the torsional girder stiffnesses and the cross-frame in-plane stiffnesses are represented in the program since they can have a substantial influence on the system responses.

In curved and skewed bridges it is not clear how the horizontal curvature and the support skew interact to determine when the structure is sensitive to the cross-frame and girder torsional stiffness models. For these bridges, the NCHRP 12-79 research shows that it is difficult to determine limits on when a traditional 2D-grid analysis provides acceptable results. For these structures it is suggested to implement the approaches discussed in this chapter to obtain accurate predictions.

7. Consideration of Locked-In Forces in I-Girder Bridges due to Cross-Frame Detailing

7.1 Cross-Frame Detailing Methods

Curved and skewed I-girder bridges exhibit significant torsional displacements of the individual girders and of the overall bridge cross-section. As a result, the girder webs can be plumb only in one configuration. If the structure is built such that the webs are plumb in the ideal no-load position, they generally cannot be plumb under the action of the structure's steel or total dead load. The deflected geometry resulting from these torsional displacements can impact the fit up of the members (i.e. come-along and jacking forces), the erection requirements (crane position and capacities, number of temporary supports and tie downs), and the bearing cost and type. Furthermore, significant layover (i.e., relative lateral deflection of the flanges associated with twisting) can be visually objectionable. This is particularly the case at piers and abutments.

If the torsional deflections are large enough, then the cross-frames often are detailed with a lack-of-fit that induces opposing torsional displacements to offset the dead load torsional rotations. As explained in the AASHTO LRFD Specifications Article C6.7.2 (2010), different types of cross-frame detailing are used to achieve approximately plumb webs in the theoretically no-load, steel dead load, or total dead load conditions. These methods are summarized below.

No-Load Fit (NLF): For NLF detailing, the cross-frames are fabricated to fit the girders in their cambered, plumb, no-load geometry without inducing any locked-in forces (i.e., there is no lack-of-fit). Figure 7.1 illustrates the behavior associated with NLF detailing at a representative intermediate cross-frame in the no-load geometry and under the action of the dead loads. (Geometric factors such as cross-slope, super-elevation and profile grade line are not shown in this figure and in the subsequent figures for clarity.) The cross-frame is assumed to be normal to the girders for purposes of the following discussion. The girders deflect from their plumb no-load geometry into an out-of-plumb

position under the action of the dead loads. In Figure 7.1, this twisting of the girders is driven primarily by the larger vertical deflection of the girder on the right compared to the one on the left. Since the cross-frame deformation is relatively small within its plane, the cross-frame induces a twist into the girders due to the differential vertical displacements.

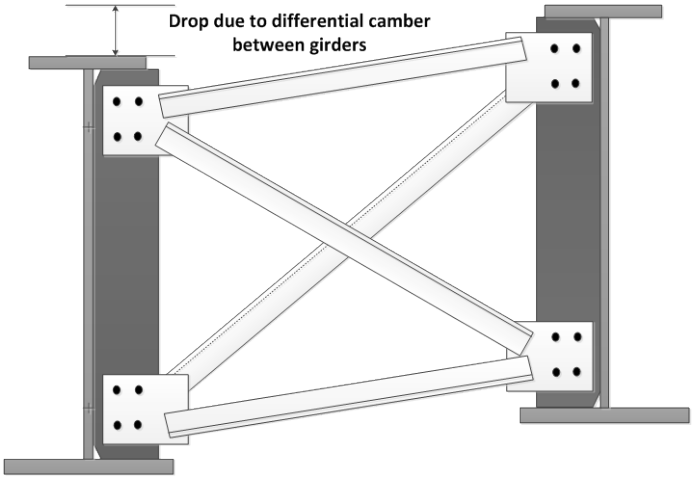

(a) No-load geometry

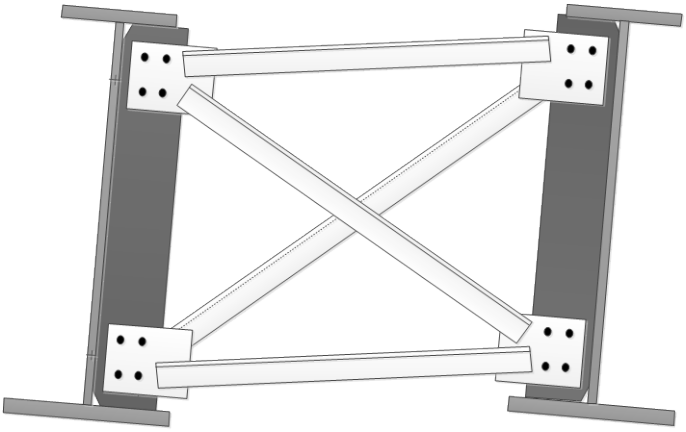

(b) Under the action of dead loads

Figure 7.1. Illustration of the behavior associated with No-Load Fit (NLF) detailing at intermediate cross-frames (geometric factors such as cross-slope, super-elevation and profile grade line are not shown for clarity).

In addition, as explained in Section 2.1.4, the cross-frames at skewed bearing lines tend to rotate about their own skewed axis and warp (twist) out of their plane. However, the cross-frame in-plane stiffnesses are again relatively large compared to the

girder lateral and torsional stiffnesses. Therefore, the girders must lay over at any skewed bearing line to maintain compatibility with the cross-frames under the dead load rotations at the bearing line. This is illustrated by Figure 7.2, which is repeated from Figure 2.7 for ease of reference.

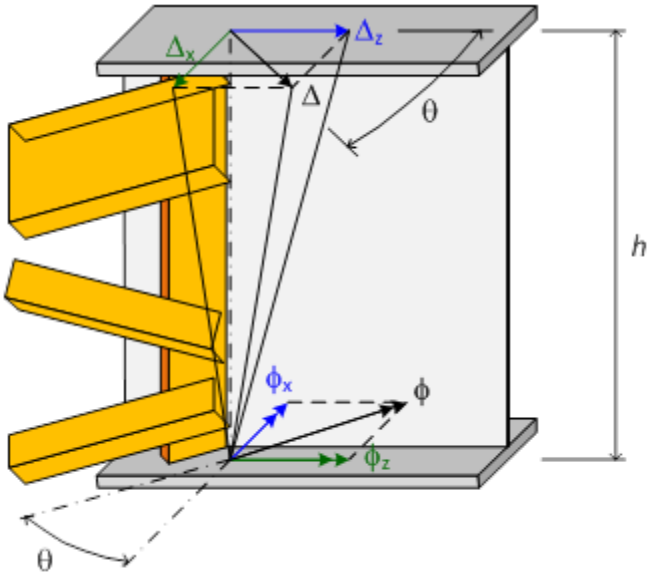

Figure 7.2. Girder top flange deflections and girder rotations at a fixed bearing location on a skewed bearing line.

The above two sources of girder layover work both jointly and independently. That is, if the bearing line cross-frames were theoretically taken out, the layovers at the bearing lines caused by the intermediate cross-frames would be somewhat different (but generally in the same direction). Similarly, if the bearing line cross-frames were left in and the intermediate cross-frames taken out, the girder layovers would be different at the intermediate cross-frame locations, although the direction of the layover tends to be the same.

Total Dead Load Fit (TDLF): For TDLF detailing, the cross-frames are fabricated to fit to the girders in their ideal final plumb position under total dead load (that is plumb webs but with the total dead load vertical deflections subtracted from the initial girder camber). Figure 7.3 illustrates the behavior associated with TDLF detailing at an intermediate cross-frame (assumed normal to the girders) before it is connected to girders in the no-

load geometry, after it is connected to girders in the theoretical no-load position (if the cross-frames could be connected to the girders without any dead load on the structure), and under the total dead load. The intermediate cross-frame does not fit-up with the girder connection points in the no-load geometry since it is fabricated for the final plumb geometry. Also, as noted above, the cross-frame is relatively stiff in its own plane. Therefore, the girders, which are relatively flexible, must be twisted in a direction opposite to their dead load torsional rotations to make the connections to the cross-frame. However, under the action of the total dead loads, the girder webs rotate back to an approximately plumb position. The lack-of-fit between the girders and the cross-frame, due to the differential vertical camber, induces additional locked-in internal stresses and corresponding deformations in the structure when the girders and cross-frames are forced together to make their connections.

All of the illustrations of the deflections, rotations and deformations in Figure 7.3 correspond to a generic location within the span. To achieve a web plumb condition under the total dead load at a skewed bearing line, the opposite of the layover under the total dead load is applied at this location initially (i.e., due to the initial lack-of-fit). Based on the assumption that the in-plane cross-frame deformations are relatively small, this is achieved by fabricating the end cross-frames to fit the final geometry of the girders, but attaching the cross-frames to the girders in their initial cambered geometry. It is commonly assumed that the girder end connection plates, which are also the bearing stiffeners, are vertical in the reference geometry shown in Figure 7.2. Due to the total dead load camber, the girder end connection plates are rotated by the negative of the total dead load major-axis bending rotations shown in Figure 7.2 ($-\phi_x$) to achieve the initial cambered geometry. Correspondingly, if the cross-frames at the bearing line are to be connected to the girders in the theoretical no-load geometry, the girder top flange must be laid over by the negative of the dead load layover shown in Figure 7.2 ($-\Delta_x$). In this work, the girders are assumed to be fabricated with plumb webs in their initial no-load geometry. Therefore, the girder top flange in Figure 7.2 must be forced over by $-\Delta_x$ to make the connection to the bearing line cross-frame in the ideal no-load condition.

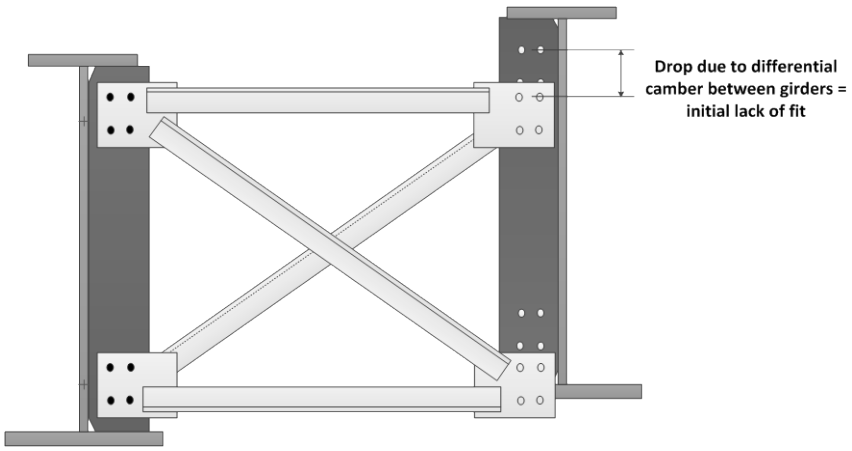

(a) No-load geometry before connecting the cross-frames

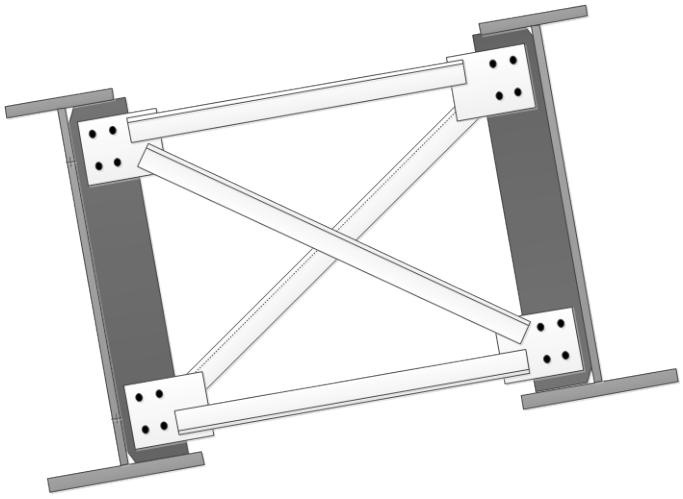

(b) No-load geometry after connecting the cross-frames

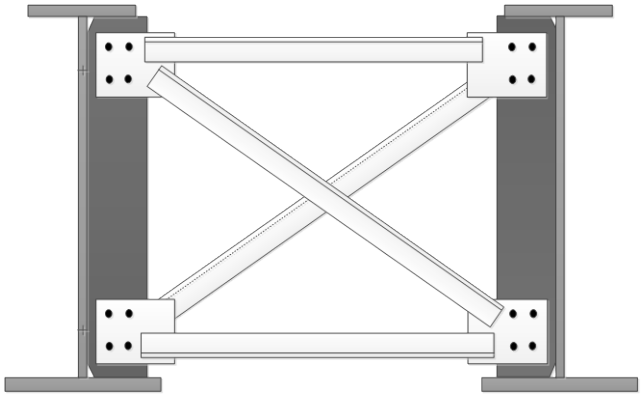

(c) Under the total dead load

Figure 7.3. Illustration of the behavior associated with Total Dead Load Fit (TDLF) detailing at intermediate cross-frames (geometric factors such as cross-slope, super-elevation and profile grade line are not shown for clarity).

When the total dead load has been applied to the structure, the girders "unwind" under the application of the load such that they come back to an approximately plumb position in the final constructed configuration. The girders deflect into the approximately plumb position shown in Figure 7.3(c) at the intermediate cross-frame locations, the girders rotate approximately back to the plumb reference geometry at the skewed bearing lines, and the end connection plates (i.e., the bearing stiffeners) rotate approximately back to the vertical position at the bearings.

Steel Dead Load Fit (SDLF): For SDLF detailing, the cross-frames are fabricated to fit the girders in their idealized final plumb position under the steel dead load (that is plumb webs but with the steel dead load vertical deflections subtracted from the initial girder camber). SDLF detailing is similar to TDLF detailing in that locked-in stresses and deformations are developed due to a lack-of-fit. However, the lack-of-fit between the cross-frames and girders in the no-load geometry for SDLF is often smaller than that due to TDLF. When SDLF is used, the webs rotate back to an approximately plumb position under the action of the *steel* dead loads.

7.2 Procedures for Determining Locked-In Forces

As demonstrated in the subsequent sections of this chapter, the locked-in forces in the bridge system associated with SDLF and TDLF detailing are generally of comparable magnitude to the corresponding steel or total dead load forces. For example, in a straight-skewed I-girder bridge constructed with TDLF detailing of the cross-frames, the locked-in cross-frame forces and girder flange lateral bending stresses are nearly equal and opposite to the corresponding total dead load values. As such, the final cross-frame forces and girder flange lateral bending stresses (equal to the sum of the locked-in and total dead load values) tend to be relatively small. Engineers typically expect this once it is understood that the girders are essentially "reverse twisted" by the initial lack-of-fit associated with the TDLF detailing, but then they "unwind" back to their plumb geometry under the total dead loads. Since the girders unwind back to an approximately plumb position under the total dead load, it is anticipated that the corresponding flange lateral bending stresses and the cross-frame forces are small.

When an engineer conducts an accurate 2D-grid analysis using the improvements discussed in Chapter 6, or an accurate 3D FEA using methods such as those outlined in Section 2.8.1, one might expect that the corresponding internal cross-frame forces and girder flange lateral bending stresses are calculated accurately. Unfortunately, if the cross-frames are detailed for anything other than NLF, the calculated internal distribution and magnitude of the cross-frame forces and girder flange lateral bending stresses will be substantially different from the values in the physical bridge. Without the calculation of the locked-in forces due to the initial lack-of-fit between the cross-frames and the girders, an accurate 2D-grid or 3D FE analysis captures only the *applied* dead load effects.

Technically, the inclusion of the lack-of-fit effects from SDLF or TDLF detailing in analysis is relatively straightforward. Analysis solutions for the locked-in forces associated with DLF detailing are fundamentally no different than typical lack-of-fit problems students first solve in undergraduate Strength of Materials; however, the lack-of-fit due to DLF detailing is generally a 3D geometry problem. One way of capturing the influence of cross-frame detailing is to construct a full model of any intermediate erection stage of the bridge with the girders in their initial no-load cambered and plumb positions, with the cross-frames connected to the girders, and with initial strains introduced into the cross-frames corresponding to the initial lack-of-fit caused by the cross-frame detailing. An analysis of this specific stage is then performed by simply including the cross-frame member initial strains in the analysis and “turning gravity on.”

The initial strains corresponding to the lack-of-fit are introduced to each cross-frame member. These strains are calculated by using the cross-frame member length in the final dead load position, which is the fabrication length of the cross-frame members, (Configuration A) and length between the work points of the girders in the initially-plumb cambered geometry (Configuration B). Figure 7.4 shows an example intermediate cross-frame. The differential cambers between the girders often generate large initial axial strains in the cross-frame members. However, this is not a problem physically, since the initial strains are just an analytical device to determine the locked-in forces. The actual strains in the structure are generally much smaller.

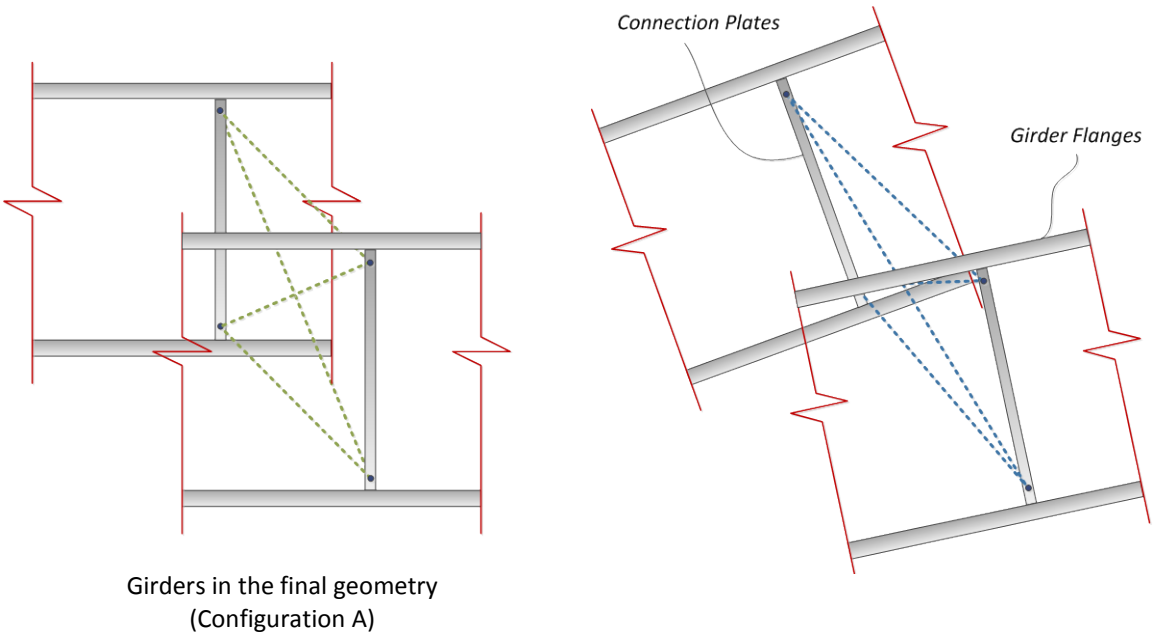

Figure 7.4. Configurations used for calculation of initial lack-of-fit strains in cross-frame members.

The initial strains should be calculated based on the element formulation. If the element formulation is based on engineering strain, then the initial strains may be expressed as

$$\varepsilon_{\text{initial strain}} = \frac{L_{\text{Configuration.B}} - L_{\text{Configuration.A}}}{L_{\text{Configuration.A}}} \tag{7.1}$$

On the other hand, if the element formulation is based on the log strain for example, then the initial strains should be calculated as the log strains (Ozgur, 2011). It should be noted that the length changes of the intermediate cross-frame members are mainly due to the differential vertical cambers between the girders (the steel dead load cambers for SDLF or the total dead load cambers for TDLF), assuming that the cross-frames are normal to the girders, whereas at skewed bearing-line cross-frames, they are mainly due to the component of the girder major-axis bending rotations, due to the girder cambers, causing in-plane distortion of the cross-frames. At skewed intermediate cross-frames, there is a contribution both from the differential vertical cambers and the component of the girder

major-axis bending rotations (due to the camber) causing in-plane distorton of the cross-frames.

In 2D-grid analysis models, the cross-frames typically are modeled with single equivalent beam elements. It is possible to include the initial lack-of-fit effects in the analysis using the equivalent beam elements presented in Chapter 6 and in Sanchez (2011), as well as using conventional beam elements. For this purpose, the initial nodal forces associated with the lack-of-fit between the girders and cross-frames are calculated by taking the product of the cross-frame equivalent beam element stiffness matrices with the following equivalent beam element lack-of-fit displacements:

- For intermediate cross-frames that are normal to the girders, the differential total dead load camber (for TDLF) or the differential steel dead load camber (for SDLF) (see Figure 7.5).
- For cross-frames on skewed bearing lines, the cross-frame end rotations caused by the girder total dead load camber rotations (for TDLF) or the steel dead load camber rotations (for SDLF) (see Figures 7.6 and 7.7).
- For skewed intermediate cross-frames, a combination of the above two effects.

It should be noted that the twisting of the cross-frames has a negligible effect on initial lack-of-fit forces; therefore, the twisting of the cross-frames can be neglected when calculating the initial lack-of-fit forces.

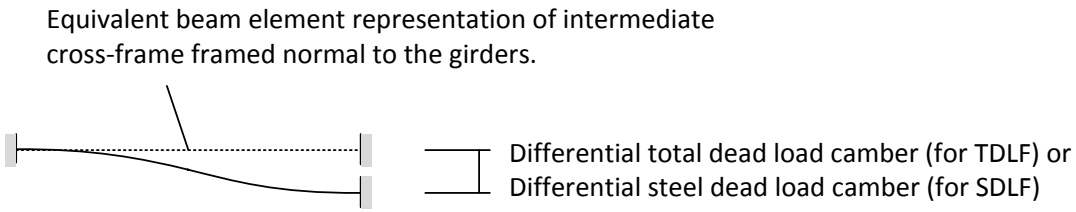

Figure 7.5. Imposed differential vertical camber to calculate initial lack-of-fit forces in the plane of an intermediate cross-frame framed normal to the girders.

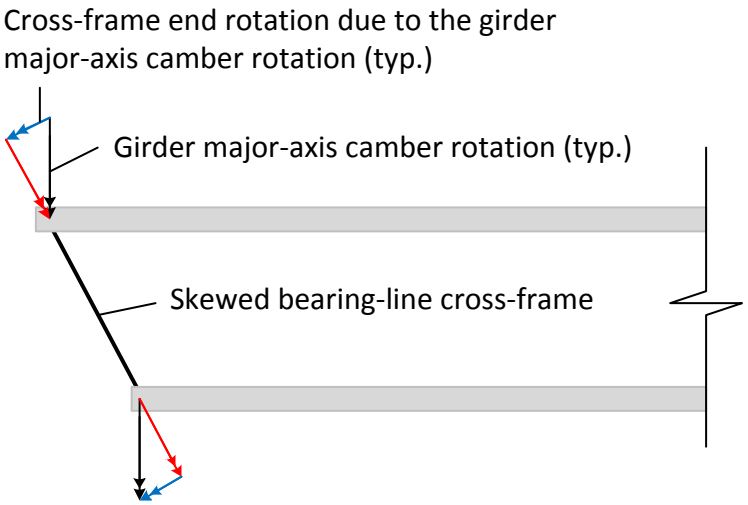

Figure 7.6. Illustration of the cross-frame initial lack-of-fit bending rotations caused by the girder camber rotations for a skewed bearing-line cross-frame.

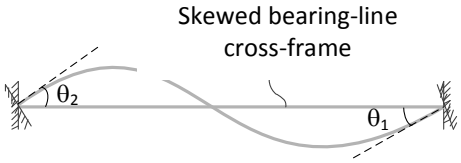

Figure 7.7. View of imposed initial lack-of-fit rotations on bearing-line cross-frame, used to calculate the initial lack-of-fit forces in the plane of a bearing-line cross-frame.

7.3 Impact of Locked-in Forces

Although AASHTO Article C6.7.2 (2010) states that engineers may need to consider the potential for any problematic locked-in stresses for horizontally curved I-girder bridges, engineers practically never include the inherent lack of fit in their structural analysis in current practice. However, the locked-in forces can significantly influence the girder layovers, the cross-frame forces, and the girder major-axis bending and/or flange lateral bending stresses in certain cases. It is important to understand when these forces due to lack-of-fit can be neglected and when they need to be considered in design, and how they can be calculated when they need to be accounted for.

7.3.1 Girder Layovers

As noted previously, bridge I-girders in curved and/or skewed bridges generally can be plumb only in one load condition. The cross-frames are relatively stiff within their planes compared to the torsional stiffness of the I-girders. Therefore, a common assumption is that the girders can be twisted and forced to fit the cross-frames under any lack-of-fit. However, twisting of the girders can be difficult in cases where the twist is coupled significantly with major-axis bending rotations and vertical deflections. This is often the case for curved girders for example. The ultimate goal with any DLF (Dead Load Fit, i.e., TDLF or SDLF) detailing is to obtain plumb webs at the targeted load level by using the rigidity of the cross-frames to impose girder torsional rotations opposite to the dead load torsional rotations. Within the span, the direction of the torsional rotations is mainly driven by the differential vertical camber (assuming that the cross-frames are normal to the girders). At the bearing lines, it is driven mainly by the rotational compatibility with the bearing line cross-frames and the direction of the girder end rotations due to the camber. The differential vertical camber between the girders and the rotational compatibility at the bearing lines associated with the girder camber rotations are the primary sources of the lack-of-fit for SDLF and TDLF detailing.

Figures 7.8 and 7.9 show a representative set of total dead load girder camber profiles and the corresponding differential camber between the girders for a straight I-girder bridge with parallel skew and curved I-girder bridge with radial supports respectively. In these figures, the sign of the differential camber is positive when the girder with the larger number has the larger camber. For instance, the differential camber between girders G2 and G1 at the bottom left corner of the bridge in Figure 7.8(b) is +3.4, meaning that the camber is 3.4 inches higher in girder G2 at the first intermediate cross-frame from the bearing line. Conversely, the differential camber between girders G8 and G9 at the upper right corner of the bridge is -3.4 inches, indicating that the camber in G8 is 3.4 inches higher than in G9 at the first intermediate cross-frame. The differential camber between the girders can be either positive or negative depending on the difference between the girder camber profiles at the cross-frame locations, as illustrated in Figure 7.10.

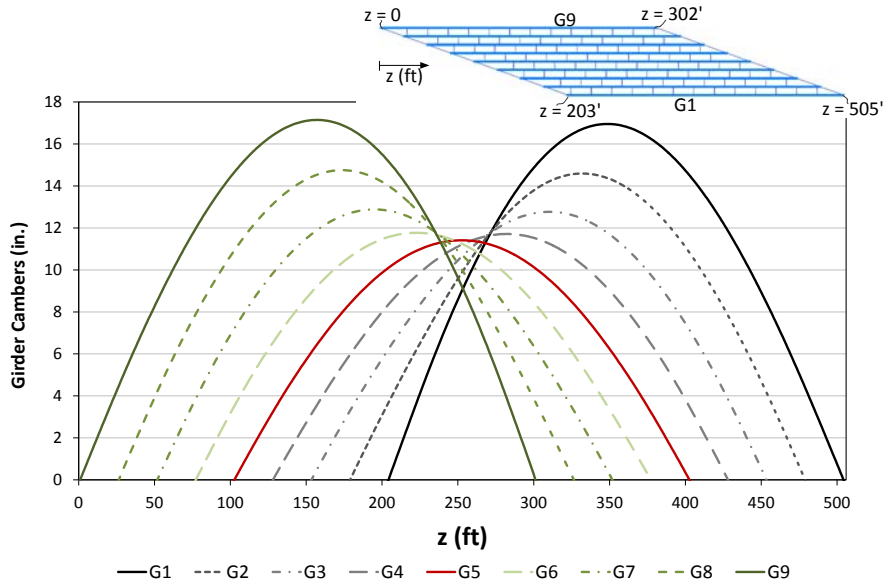

(a) Girder cambers under total dead load

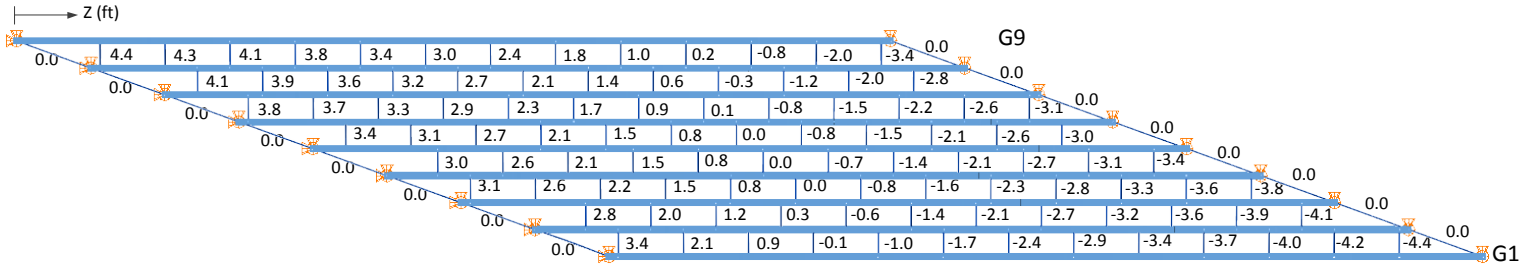

(b) Differential camber between the girders

Figure 7.8. NISSS54, Girder cambers and the differential camber between the girders obtained from FEA vertical deflections.

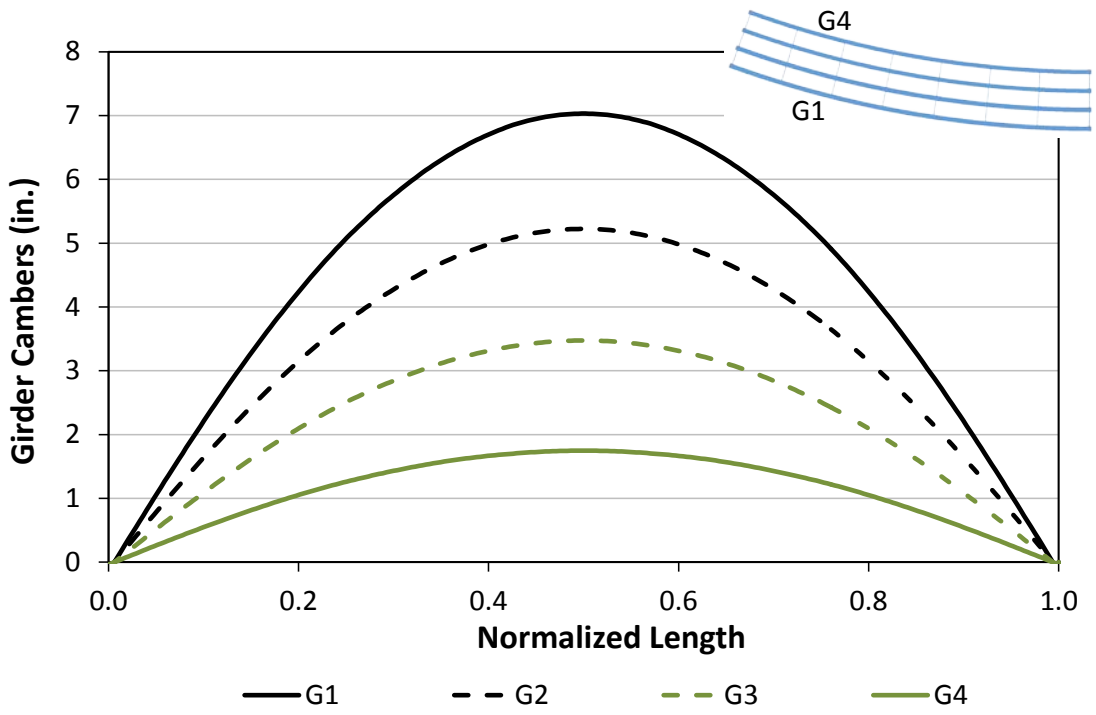

(a) Girder cambers under total dead load

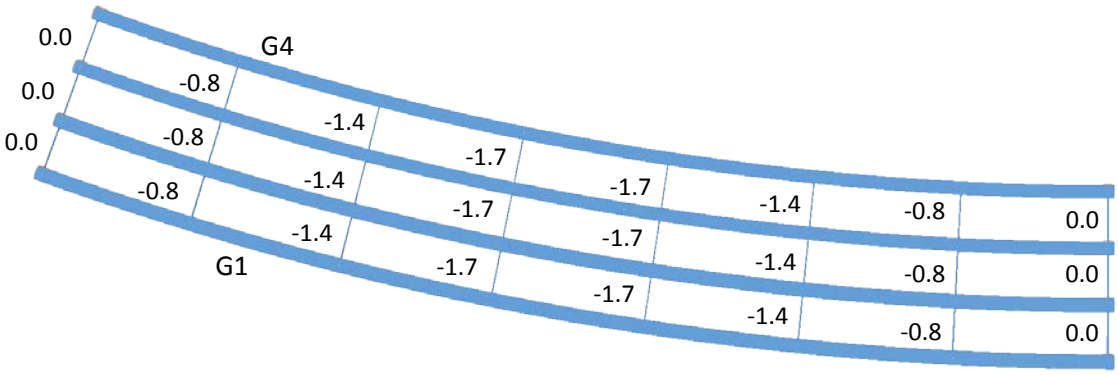

(b) Differential camber between the girders

Figure 7.9. NISCR2, Girder cambers and the differential camber between the girders obtained from FEA vertical deflections.

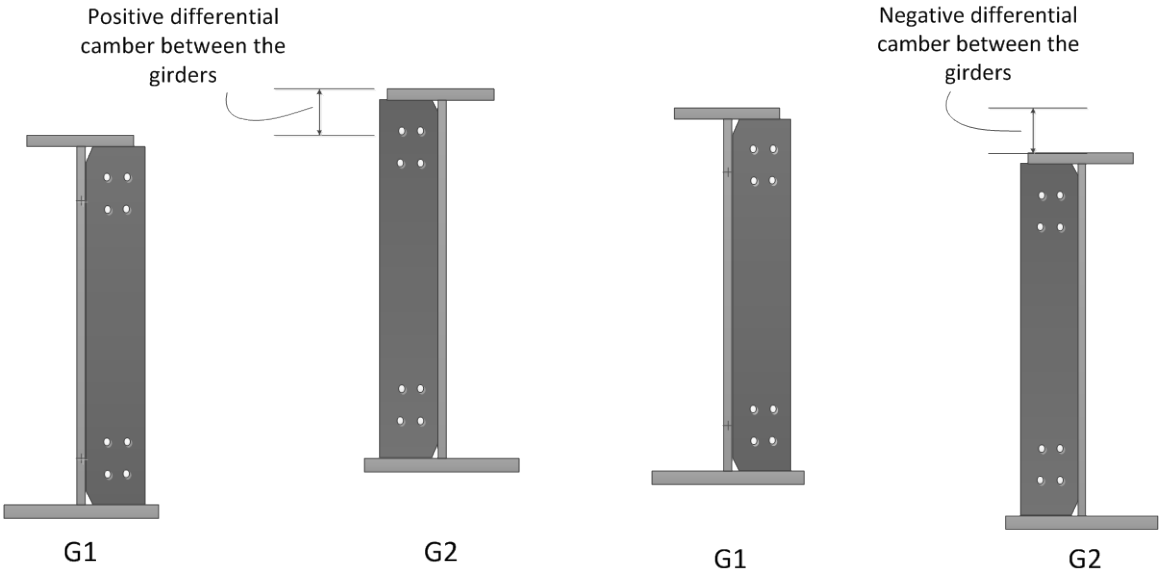

(a) Positive differential camber between the girders

(b) Negative differential camber between the girders

Figure 7.10. Representative sketch of positive and negative differential camber between the girders (geometric factors such as cross-slope, super-elevation and profile grade line are not shown for clarity).

For DLF (Dead Load Fit, i.e., TDLF or SDLF) detailing of the intermediate cross-frames, the girders need to be twisted to connect the cross-frames between them. The movements at the intermediate cross-frames are illustrated in Figure 7.11 for locations with positive and negative differential camber between the girders in the no-load geometry. In the case of straight bridges with parallel skew orientations, both positive and negative differential camber are obtained between the girders since the parallel skew orientation of the bearing lines offsets the camber profiles of the girders as shown in Figure 7.8(a). For instance, the camber profiles for the fascia girders G1 and G9 are the same; however, the left-hand bearing location for G1 is located at a z coordinate of 203 ft., i.e., G1 starts at 203 ft. into the span of G9. The opposite sign of the differential cambers at each end of the bridge results in a twisting of the girders, due to the lack of fit of the cross-frames, that is in opposite directions at the two ends. These lack-of-fit twist rotations are in turn opposite in sign relative to the twist rotations of the girders under dead load.

For curved-radially supported bridges, the differential camber between the girders is always negative, moving from the girders that are farther from the center of curvature toward the center of curvature, due to larger deflection of the "outside" girders compared to the "inside" girders. This enforces a twist opposite to the layovers caused by the dead loads

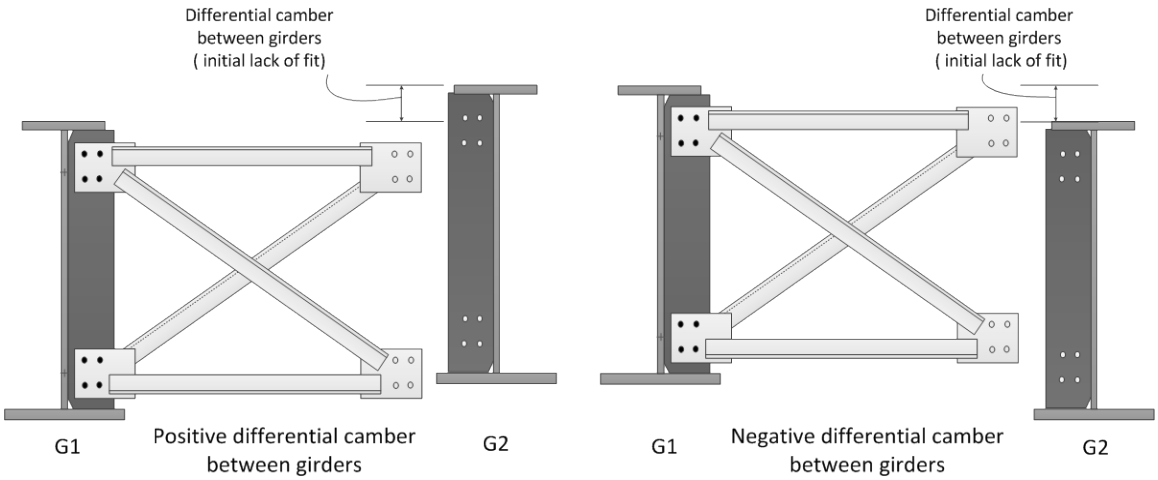

(a) Initially plumb no-load geometry of girders

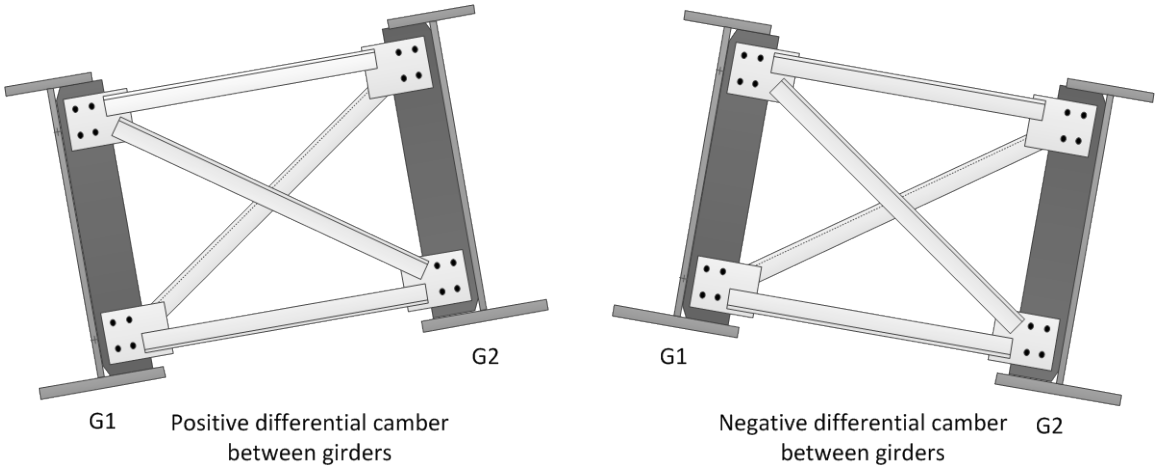

(b) Cross-frames connected in ideal initial no-load geometry

Figure 7.11. Induced girder twist at intermediate cross-frame locations for positive and negative differential camber between girders in ideal no-load geometry (geometric factors such as cross-slope, super-elevation and profile grade line are not shown for clarity).

The compensating girder layovers generated by DLF detailing are never exactly equal and opposite to the dead load layovers. (The term “DLF detailing” is used here and in the following discussions to indicated either SDLF or TDLF detailing.) This is mainly because:

- The stress state due to the torsional effects of the dead load cannot possibly be matched exactly by the cross-frame forces induced by the DLF detailing. The difference between the girder stress state induced by the locked-in forces and the girder stress state associated with the dead load torsion causes additional deformations within the structure.
- The girder camber profiles may have been obtained from an analysis that does not fully capture the true interactions between the girders associated with the three-dimensional response of the bridge. Furthermore, the SDLF and TDLF detailing practice of working just with the differential vertical cambers generally neglects other torsional interactions between the girders and the rest of the structure that occur via the cross-frames.

As a result, slight deviations from the plumb configuration are observed generally at the targeted load conditions. However, (Ozgur, 2011) shows that the layover of the girders at the targeted load conditions tends to be less than a tolerance of $\pm D/96$, where D is the web depth, regardless of the bridge type and geometry.

Figures 7.12 and 7.13 illustrate the deflected shape of the representative straight-skewed bridge from Figure 7.8 (NISSS54) under the steel and total dead loads respectively. Each of these figures shows the magnified deflections associated with each of the three main types of cross-frame detailing. Similarly, Figures 7.14 and 7.15 illustrate the magnitudes of the girder layovers of this straight-skewed bridge under the steel and total dead load respectively for each of the types of cross-frame detailing. The girder layovers are plotted along the length of bridge starting from the left acute corner. The NISSS54 bridge has a large skew index (I_S = 0.68), indicating that the influence of skew is large on the response of the structure and on the accuracy of the simplified methods of analysis. The torsional rotations at the bearings due to the total dead load are more than 0.04 radians in this structure.

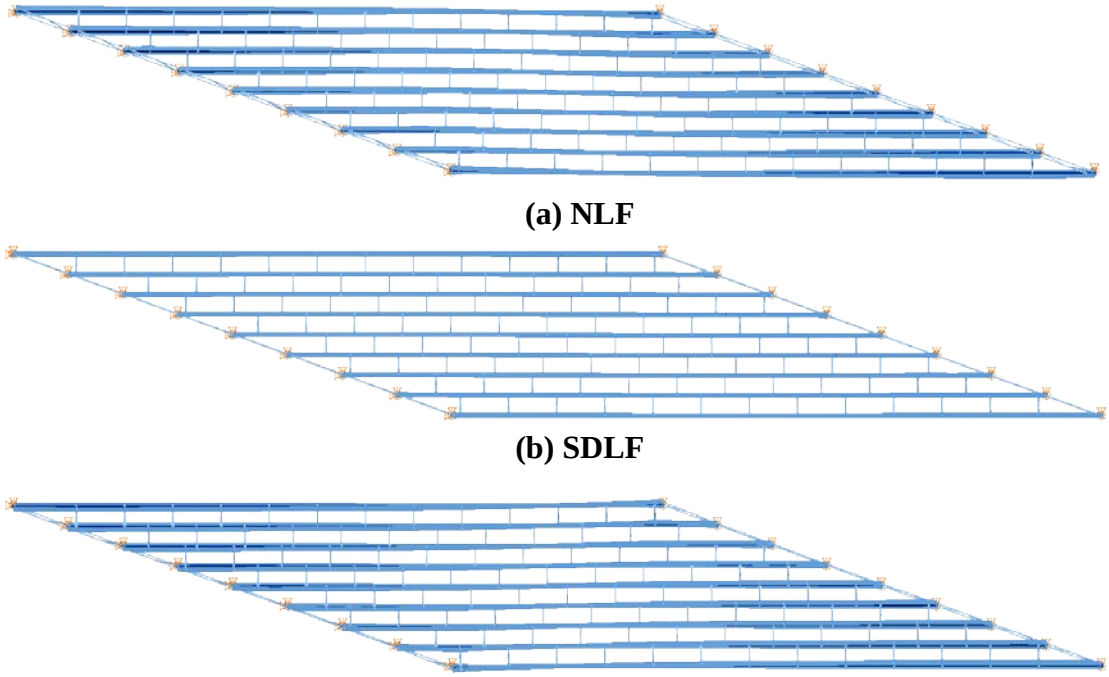

(a) NLF

(b) SDLF

(c) TDLF

Figure 7.12. NISSS54, Deflected shape under steel dead load for different types of detailing methods (magnified by 10x).

Approximately plumb girders are obtained under the steel dead load if the bridge is constructed with SDLF detailing as shown in Figures 7.12(b) and 7.14(b). For TDLF detailing, the cross-frames are detailed such that they approximately compensate for the total dead load deflections. Therefore, layovers in the opposite direction from those due to the total dead load are obtained under the *steel dead load* when TDLF detailing is used, as shown in Figures 7.12(c) and 7.14(c). However, approximately plumb girders are obtained for the bridge where the cross-frames are detailed for TDLF, once the total dead load is placed on the bridge, as illustrated in Figures 7.13(c) and 7.15(c).

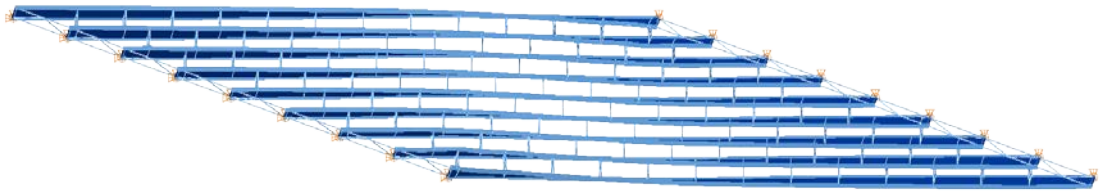

(a) NLF

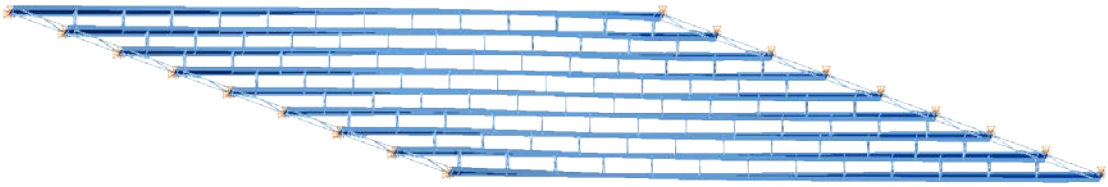

(b) SDLF

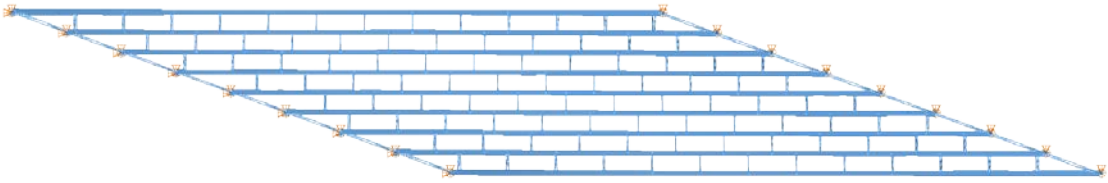

(c) TDLF

Figure 7.13. NISSS54, Deflected shape under total dead load for different types of detailing methods (magnified by 10x).

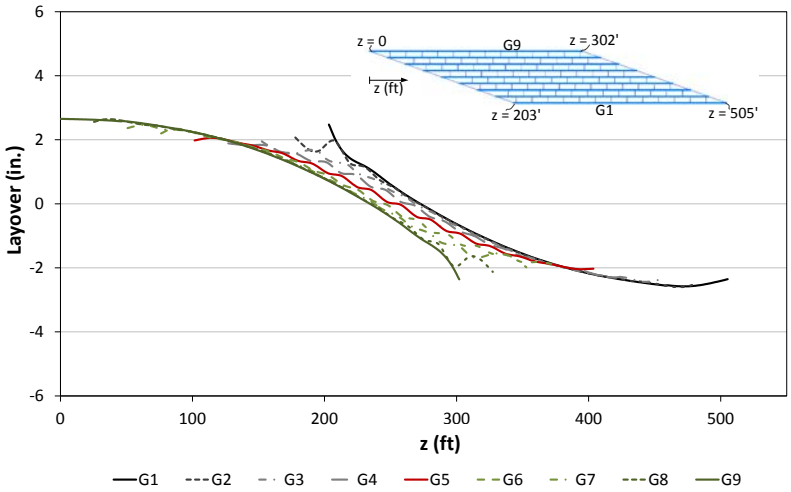

(a) NLF

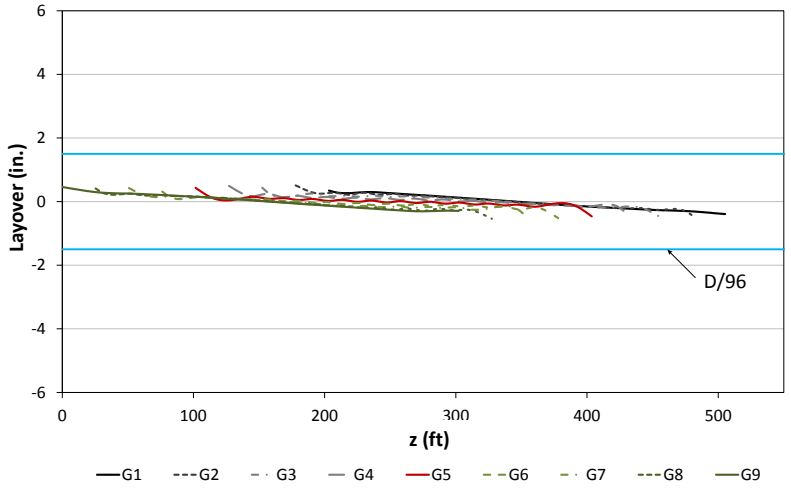

(b) SDLF

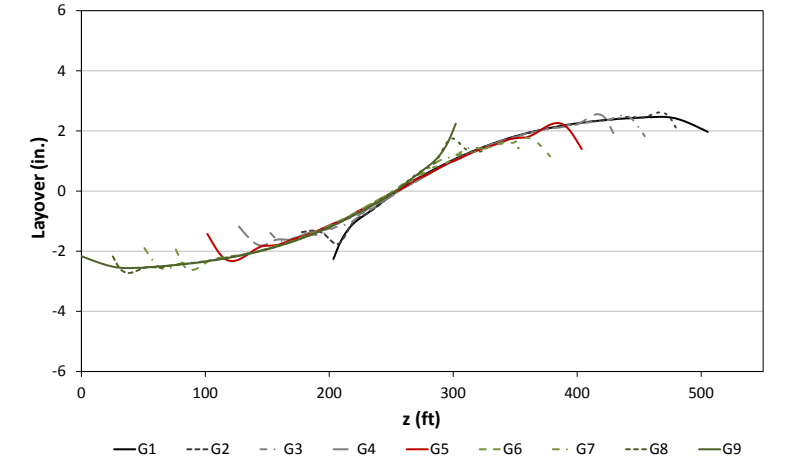

(c) TDLF

Figure 7.14. NISSS54, steel dead load girder layovers associated with different types of detailing methods.

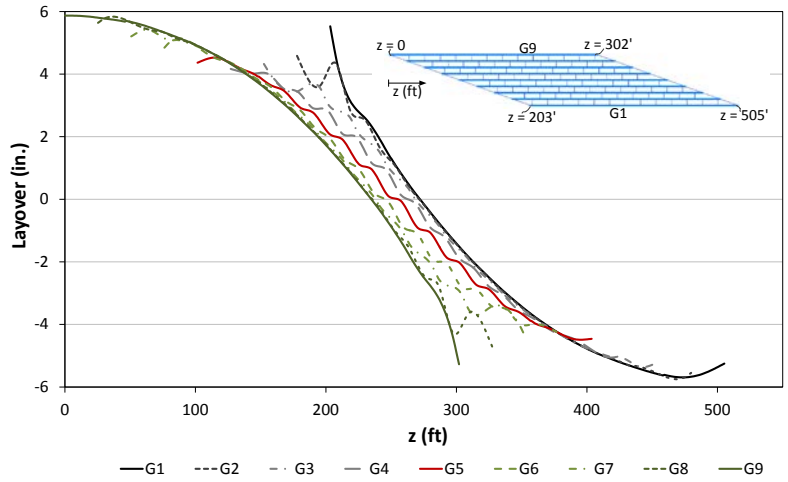

(a) NLF

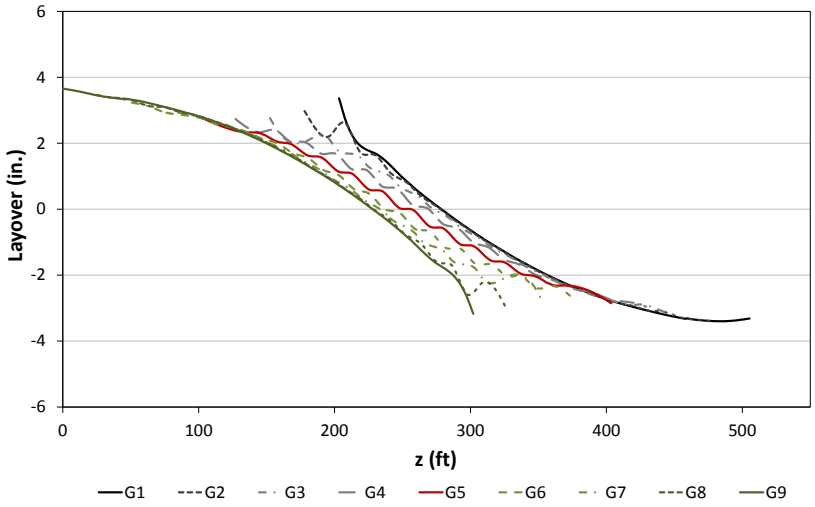

(b) SDLF

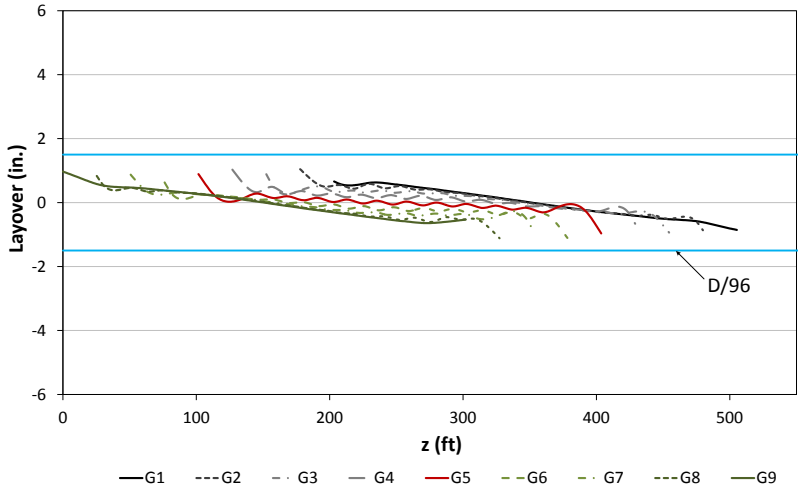

(c) TDLF

Figure 7.15. NISSS54, total dead load girder layovers associated with different types of detailing methods.

7.3.2 Cross-Frame Forces

Straight-Skewed I-girder Bridges

In straight-parallel skewed bridges constructed with NLF detailing, relatively large forces tend to be developed in the cross-frames along the shorter (and stiffer) diagonal direction between the corners of the structure. Figure 7.16 illustrates this transverse load path in the NISSS54 bridge by indicating the magnitude of the largest component force in each of the intermediate cross-frames, normalized by the largest cross-frame component force. The cross-frames with ratios larger than 0.5, located between the obtuse corners of the bridge, are highlighted by a different shade.

For straight bridges constructed with TDLF detailing, the locked-in cross-frame forces are approximately equal and opposite to the total dead load forces in the regions having the largest transverse stiffness, i.e., in the highlighted region of Figure 7.16. However, the locked-in forces in the cross-frames tend to be substantially different than the dead load forces outside of this region.

Large locked-in forces can be developed outside the stiff transverse load paths depending on the relative lateral stiffness of the adjacent girders and the differential camber. These “problem” cross-frame locations are typically at intermediate cross-frames that are at framed too close to the skewed bearing lines.

It should be emphasized that the dead load cross-frame forces from a NLF analysis are not the opposite of the locked-in forces from a lack-of-fit analysis or vice-versa. These two sets of forces can be close to being equal and opposite in the regions of the bridge having the largest transverse stiffness (highlighted in Figure 7.16), but in other regions, they can be substantially different. This is because stresses and deformations induced by DLF detailing are not exactly the same as the stresses and deformations induced by the dead loads.

In the bridge shown in Figure 7.16, the cross-frames in the vicinity of the short direction between the obtuse corners of the plan tend to have their total dead load forces mostly relieved by the effects of the TDLF detailing, while the cross-frames in the

vicinity of the acute corners tend to have their total dead load forces increased relative to the NLF case. Figures 7.17 and 7.18 show the distribution of the largest total dead load cross-frame component axial forces in each of the cross-frames throughout the NISSS54 bridge associated with NLF and TDLF detailing cases respectively. The most highly loaded cross-frame members are highlighted in the darker color, while the more lightly loaded cross-frame members are shaded light grey. One can observe that the cross-frame forces along the stiff diagonal direction are significantly reduced by the TDLF detailing, but they are not zero. In addition, the forces in several of the cross-frame diagonals near the acute corners are significantly increased.

In straight-skewed bridges constructed with TDLF detailing, cross-frames located along the stiff transverse load paths may see their largest forces during the steel erection since the locked-in cross-frame forces are not yet relieved by the dead load forces from the deck weight. Conversely, straight bridges constructed with SDLF detailing tend to see the lowest cross-frame forces under the steel dead load.

Curved-Radially Supported I-girder Bridges

The behavior of curved bridges with respect to cross-frame detailing is significantly different than straight bridges. In curved-radially supported bridges, locked-in cross-frame forces due to SDLF or TDLF detailing tend to add with the dead load forces in the cross-frame members, although it should be noted that SDLF detailing generally results in smaller locked-in forces compared to TDLF detailing. Figures 7.19 and 7.20 illustrate the maximum amplitude of the total dead load component axial forces in each of the cross-frames for the curved-radially supported bridge considered in Section 7.3.1 (NISCR2). Figure 7.19 shows the results for NLF detailing, whereas Figure 7.20 shows the results for TDLF detailing. The maximum locked-in cross-frame forces occur in the cross-frames close to the mid-span. This is because the lack-of-fit between the girders and cross-frames is largest at these locations.

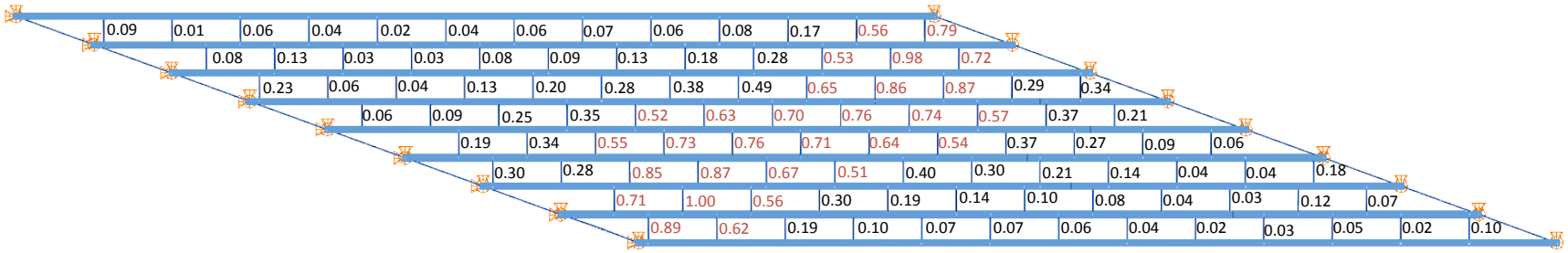

Figure 7.16. NISSS54, Normalized maximum amplitude of the component axial forces in each of the cross-frames under total dead load (NLF detailing).

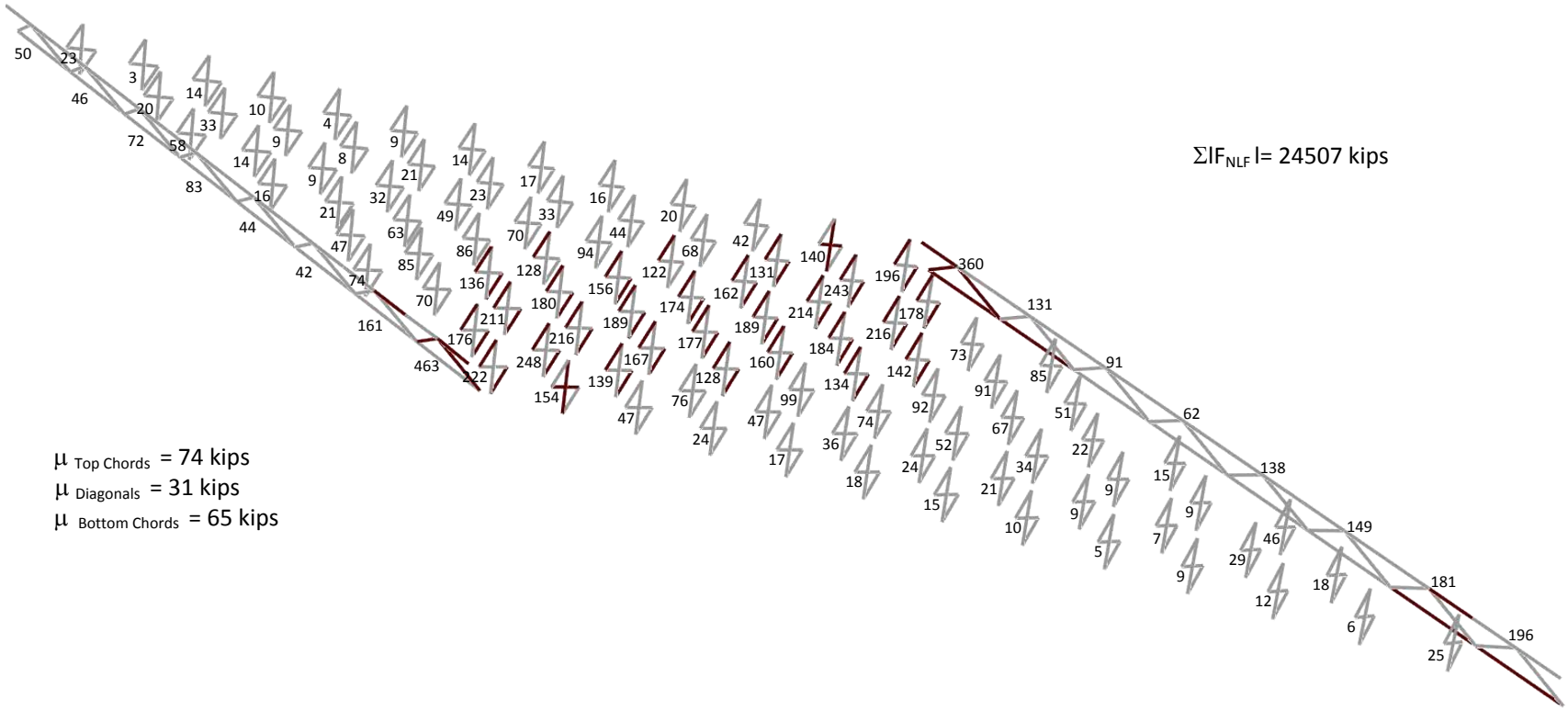

Figure 7.17. NISSS54, maximum amplitude of the component axial forces in each of the cross-frames under total dead load (NLF detailing).

.

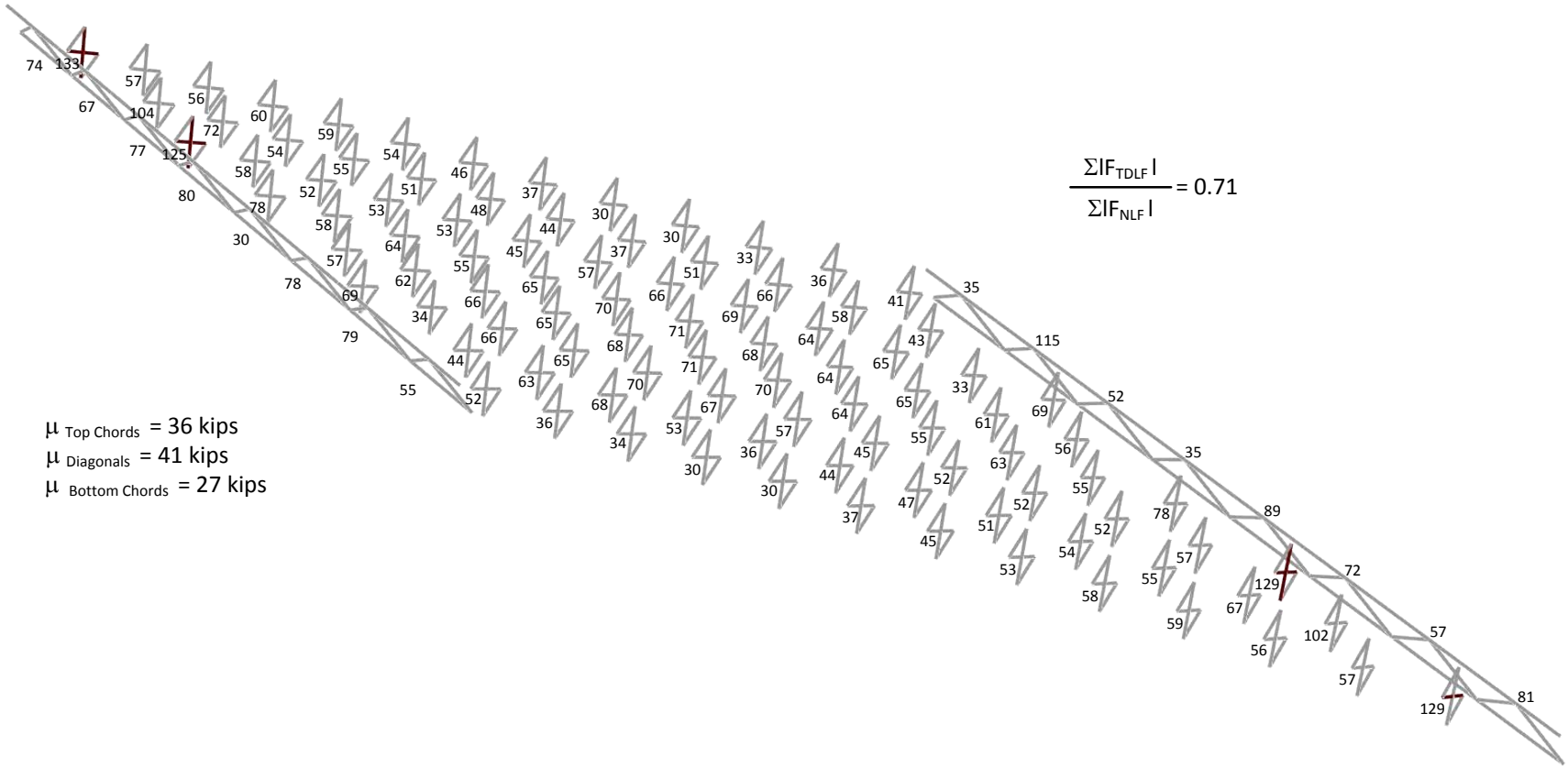

Figure 7.18. NISSS54, maximum amplitude of the component axial forces in each of the cross-frames under total dead load plus the TDLF detailing effects.

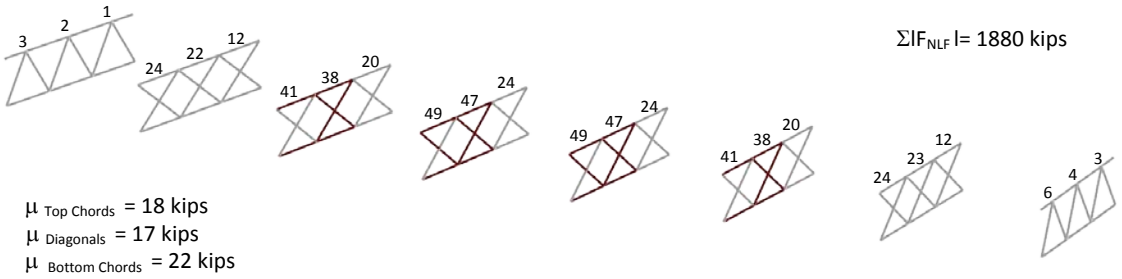

Figure 7.19. NISCR2, maximum amplitude of the component axial forces in each of the cross-frames under total dead load (NLF detailing).

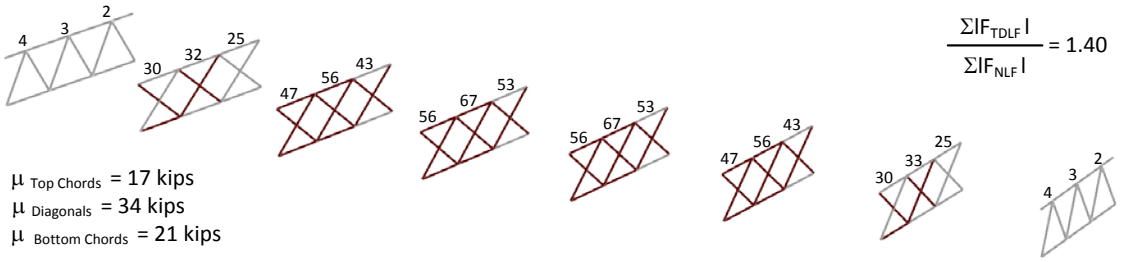

Figure 7.20. NISCR2, maximum amplitude of the component axial forces in each of the cross-frames under total dead load plus the TDLF detailing effects.

7.3.3 Vertical Displacements

In current practice, the girder camber diagrams are practically always determined without considering locked-in force effects. However, locked-in forces due to SDLF or TDLF detailing potentially can have a significant influence on the vertical deflections. Hence, the physical bridge may exhibit different vertical deflections than assumed in setting the cambers. This can lead to deviations from the predicted final deck profile and final girder elevations.

Straight-Skewed I-girder Bridges

For straight and skewed bridges, the locked-in forces from SDLF or TLDF detailing tend to have a small effect on the vertical displacements. This is because there is little to no coupling between the individual girder vertical displacements and the individual girder twisting for straight I-girders. Figure 7.21 shows total dead load vertical deflections for the straight-skewed NISSS54 bridge considering each of the types of cross-frame detailing. It can be observed that there is essentially no difference in the vertical deflections of the two fascia girders due to the type of cross-frame detailing in

this bridge. Both of these girders exhibit approximately 17 inches of vertical deflection at their mid-span under the total dead load regardless of the method of cross-frame detailing. The middle girder (Girder 5) has slightly more than 12 inches of vertical deflection under the total dead load if TDLF detailing is used, whereas it has slightly more than 11 inches of vertical deflection if NLF detailing is used. These small differences in the vertical deflections are due to the restraint from the stiff transverse load path discussed in Section 7.3.2. That is, part of the total dead load tributary to girder G5 is distributed transversely to the bearing lines by the staggered cross-frames framing between the obtuse corners of the bridge. The development of the forces along this path causes significant flange lateral bending in girder G5.

The total dead load vertical deflections generally are compensated for by the total vertical camber in the girders. In current practice, the above differences in the NLF and TDLF vertical deflections due to the initial lack-of-fit between the girders and cross-frames are practically never accounted for. One can conclude that the 1 inch difference in the vertical deflection of Girder 5 is relatively minor. It can be accommodated in the girder haunch depths when setting the forms for the concrete deck (if the contractor anticipates the above behavior).

Curved-Radially Supported I-girder Bridges

Conversely, for curved-radially supported bridges, the locked-in forces due to SDLF or TDLF detailing generally have a significant effect on the vertical displacements of the girders. This is due to the significant coupling between the major-axis bending and torsion in curved I-girders. Figure 7.22 shows a representative example from the bridge NISCR5. The outside girder displacement is reduced by approximately 6 inches due to the TDLF detailing effects, while the inside girder vertical deflection is reduced by approximately 4 inches. It should be noted that this bridge is a relatively extreme case also involving significant global second-order amplification due to the long span and narrow width of the structure.

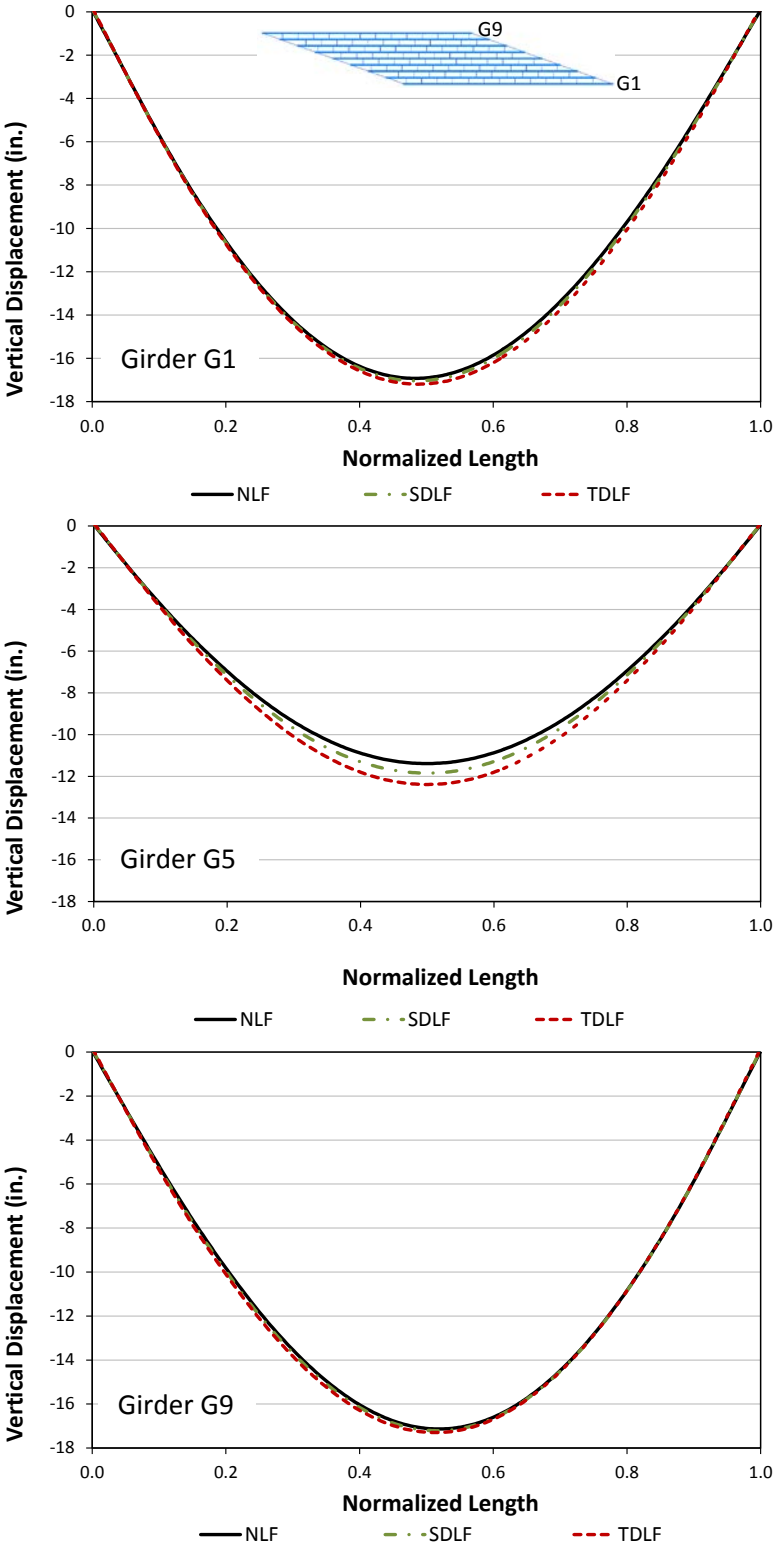

Figure 7.21. NISSS54, Vertical deflections under total dead load associated with different detailing methods.

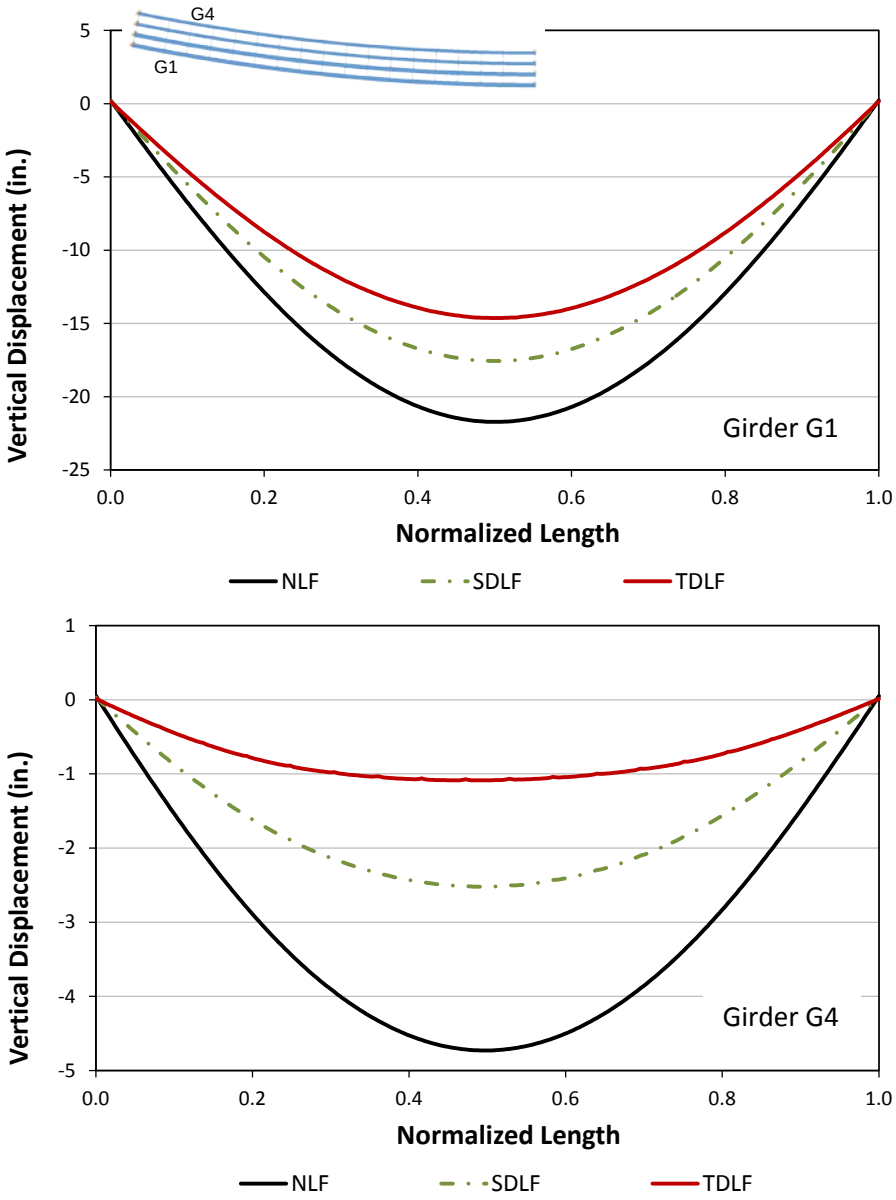

Figure 7.22. NISCR5, Vertical deflections under total dead load associated with different detailing methods.

7.3.4 Major-Axis Bending Stresses, f_b

The NCHRP 12-79 research studies show that the changes in the girder major-axis bending stress predictions are minor due to either SDLF or TDLF detailing for both straight-skewed and curved-radially supported bridges. For straight I-girder bridges, this can be understood by observing the general lack of coupling between torsion and major-axis bending in straight I-girders. For curved I-girder bridges, this can be understood by

considering a basic simply-supported curved I-girder with torsionally simply-supported end conditions subjected to transverse loads as shown in Figure 7.23. The girder torsional deformations near the end supports have a substantial impact on the mid-span vertical displacements. However, the girder internal major-axis bending moments and the corresponding major-axis bending stresses at the mid-span are not affected significantly by the horizontal curvature.

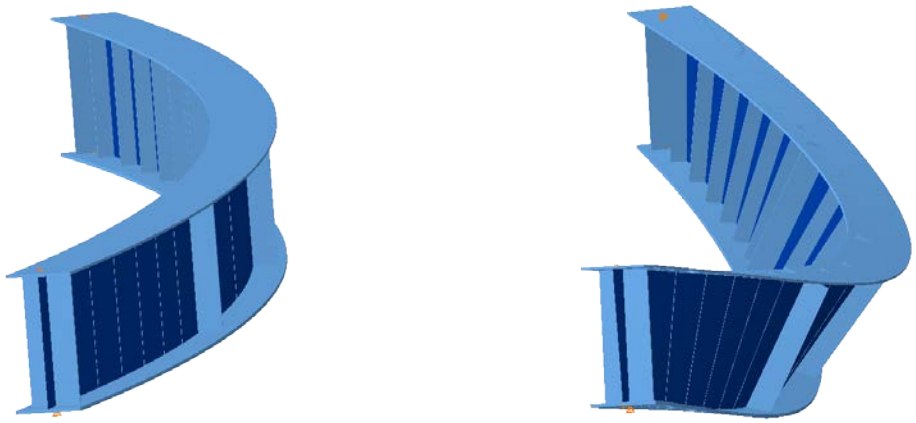

(a) Undeformed shape **(b) Magnified Deflected shape**

Figure 7.23. Illustrative curved girder deformations under dead loads.

7.3.5 Girder Flange Lateral Bending Stresses, f_ℓ

Straight-Skewed I-girder Bridges

The girder flange lateral bending stresses under the total dead load are reduced significantly in straight-skewed bridges due to DLF detailing. If SDLF detailing is used, the smallest flange lateral bending stresses tend to occur under the steel dead load. Conversely, if TDLF detailing is used, the smallest flange lateral bending stresses tend to occur under the total dead load. In these cases the girders largely unwind into their approximately plumb positions under the corresponding dead load effects.

Engineers sometimes conclude that since the girders were plumb in their no-load condition, and since they are also plumb in the targeted dead load condition, the girder flange lateral bending stresses are zero, the cross-frame forces are zero, and the girders

respond essentially in the manner assumed in a line girder analysis when the bridge is in the targeted dead load condition. However, it is important to note that the girder flange lateral bending stresses generally do not completely vanish due to the differences between the locked-in stresses from the DLF detailing and the stresses related to the torsion of the girders under the targeted dead load. There are several reasons for this behavior:

- In particular, local peaks in girder flange lateral bending stresses, as well as cross-frame forces, can be observed due to "nuisance stiffness effects" at locations such as intermediate cross-frames that are located too close to skewed bearing lines. The stresses in the girders due to locked-in force effects do not tend to match the torsional stresses due to the three-dimensional loading effects in these regions.
- Furthermore, when staggered cross-frames are utilized such as in the NISSS54 bridge, there is substantial flange lateral bending in the interior girders due to the transverse load transfer effects. The interior girder flanges are loaded "back-and-forth" in opposing directions by the cross-frames. The corresponding flange lateral bending in these girders is generally reduced, but it is not completely nullified by the locked-in force effects.
- Lastly, in the fascia girders, significant flange lateral bending can occur in some cases due to eccentric overhang bracket loads. These bending effects are of course not nullified by the locked-in forces from DLF detailing. The NCHRP 12-79 research shows that flange lateral bending stresses in the fascia girders often are predominantly due to eccentric overhang bracket loads and are not significantly affected by any of the detailing methods.

In cases with contiguous intermediate cross-frame lines, the total flange lateral bending stresses associated with DLF detailing are found to be close to zero except in the fascia girders and at cross-frame locations with nuisance stiffness effects (Ozgur, 2011).

Figure 7.24 shows selected girder major- and minor-axis flange bending stresses under total dead load for the different types of detailing methods in the NISSS54 bridge. In this structure, the major-axis bending stresses in the fascia girders are essentially unaffected by the type of cross-frame detailing. The maximum total dead load flexural

stress in the top flange of these girders is 30 ksi. The total dead load major-axis bending stresses in the middle girder (Girder 5) are slightly increased for the TDLF detailing case, consistent with the larger vertical displacements in Girder 5 for TDLF detailing. However, the differences in the stresses for the major-axis bending of Girder 5 are relatively minor. The maximum f_b in Girder 5 is approximately 20 ksi under the total dead load for the TDLF detailing case.

The flange lateral bending stresses are relatively small in the fascia girders for all the methods of detailing in the NISSS54 bridge, and are predominantly due to eccentric overhang bracket loads with the exception of the locations near the obtuse corners of the bridge. At the obtuse corners, relatively large lateral forces are introduced into the fascia girders from the chords of the first two intermediate cross-frames near the bearing lines. This causes a "spike" in the flange lateral bending stresses near the ends of the fascia girders. This spike in f_ℓ is largest for the NLF detailing case. It is reduced by the locked-in stresses introduced into the girders in the cases of SDLF and TDLF detailing.

The total dead load lateral bending stresses are significant in Girder 5 regardless of the method of cross-frame detailing. They are largest for the NLF detailing case, reaching peak values of nearly 22 ksi near the mid-span. These flange lateral bending stresses are reduced by the lack-of-fit effects introduced into the girders by SDLF or TDLF detailing. The resulting maximum total dead load f_ℓ values are approximately 15 ksi for SDLF detailing and 8 ksi for TDLF detailing. These significant flange lateral bending stresses in Girder 5 are due to the use of the staggered cross-frames in this bridge and the "back-and-forth" load transfer effects mentioned previously. Staggered cross-frames generally are expected to reduce the magnitude of the cross-frame forces that need to be resisted due to the skew effects, but they introduce "back-and-forth" lateral loads on the girder flanges in the middle regions of the bridge. These forces are highest near the mid-span of the middle girders because these locations are in the middle of the stiff transverse load path first discussed in Section 7.3.2.

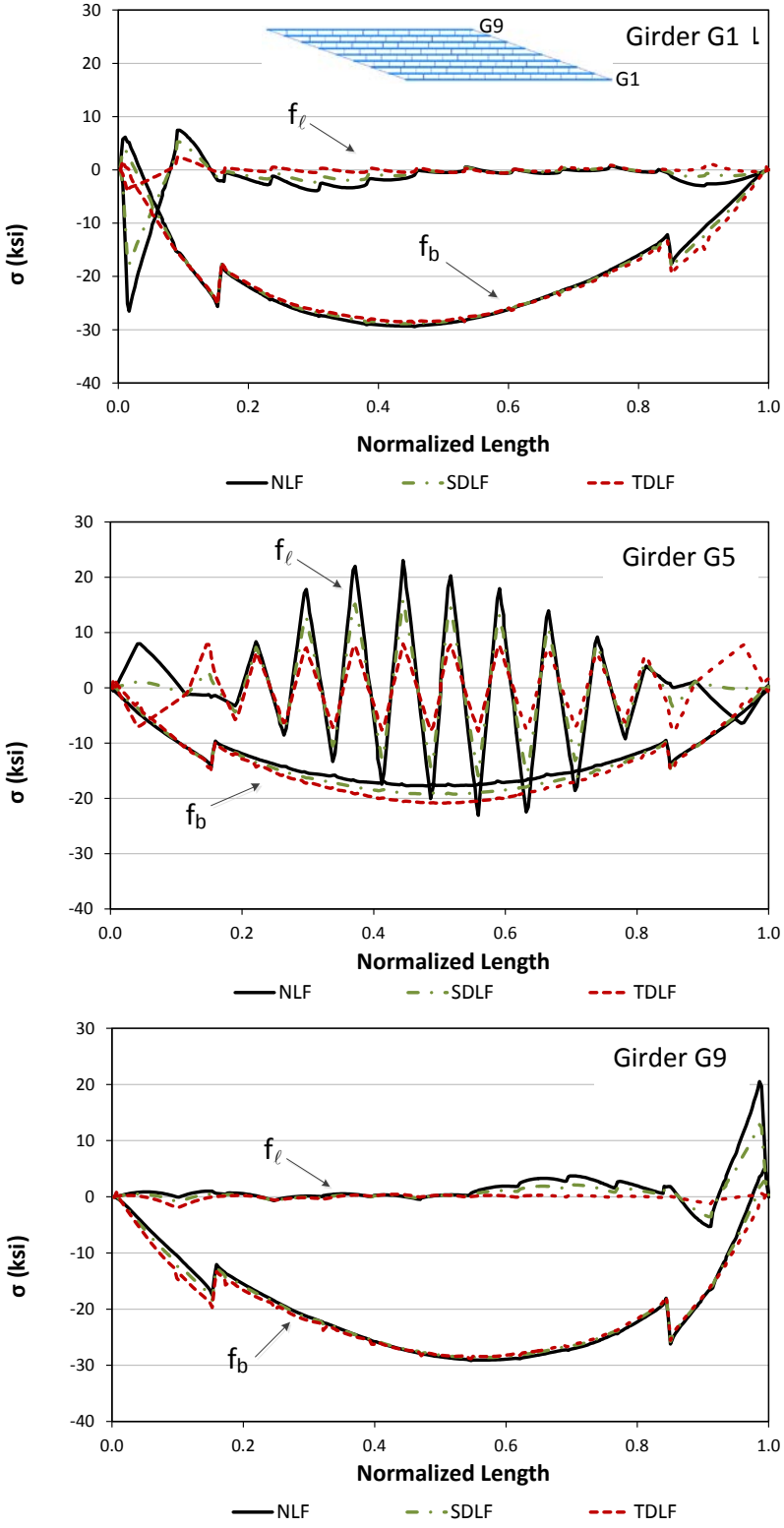

Figure 7.24. NISSS54, top flange stresses under total dead load for different detailing methods.

There is no “spike” in the flange lateral bending stresses in Girder 5 near its ends. This is because the forces coming into the girder from the intermediate cross-frames near the support are not as large in Girder 5 as in the exterior fascia girders. The predominant lateral bending action on Girder 5 is near the middle of the span. Unfortunately, this is also where the major-axis bending stresses are the highest.

Curved-Radially Supported I-Girder Bridges

For curved-radially supported bridges, the “local” flange lateral bending effects between the cross-frames due to the horizontal curvature, i.e., the effects associated with Eq. (2.16), are not influenced by the DLF detailing. However, DLF detailing of curved bridges induces an overall global lateral bending in the girder flanges in the direction:

- opposite to the overall lateral bending of the girders due to the torsional rotation of the bridge cross-section,
- opposite to the bending within the girder unbraced lengths between the cross-frames, and
- in the same direction as the “negative” flange lateral bending stresses due to the continuity of the curved flanges across the cross-frame locations.

That is, the locked-in forces due to DLF detailing tend to reduce the overall “global” girder flange lateral bending stresses in curved bridges. Figure 7.25 illustrates this effect in the NISCR2 bridge. In many curved bridge structures, this overall flange lateral bending effect is relatively minor. However, in some cases, such as narrow curved bridge units, this effect can be substantial. These effects are relatively minor in the NISCR2 bridge, although the percentage change in the flange lateral bending stresses on the inside girder is somewhat large.

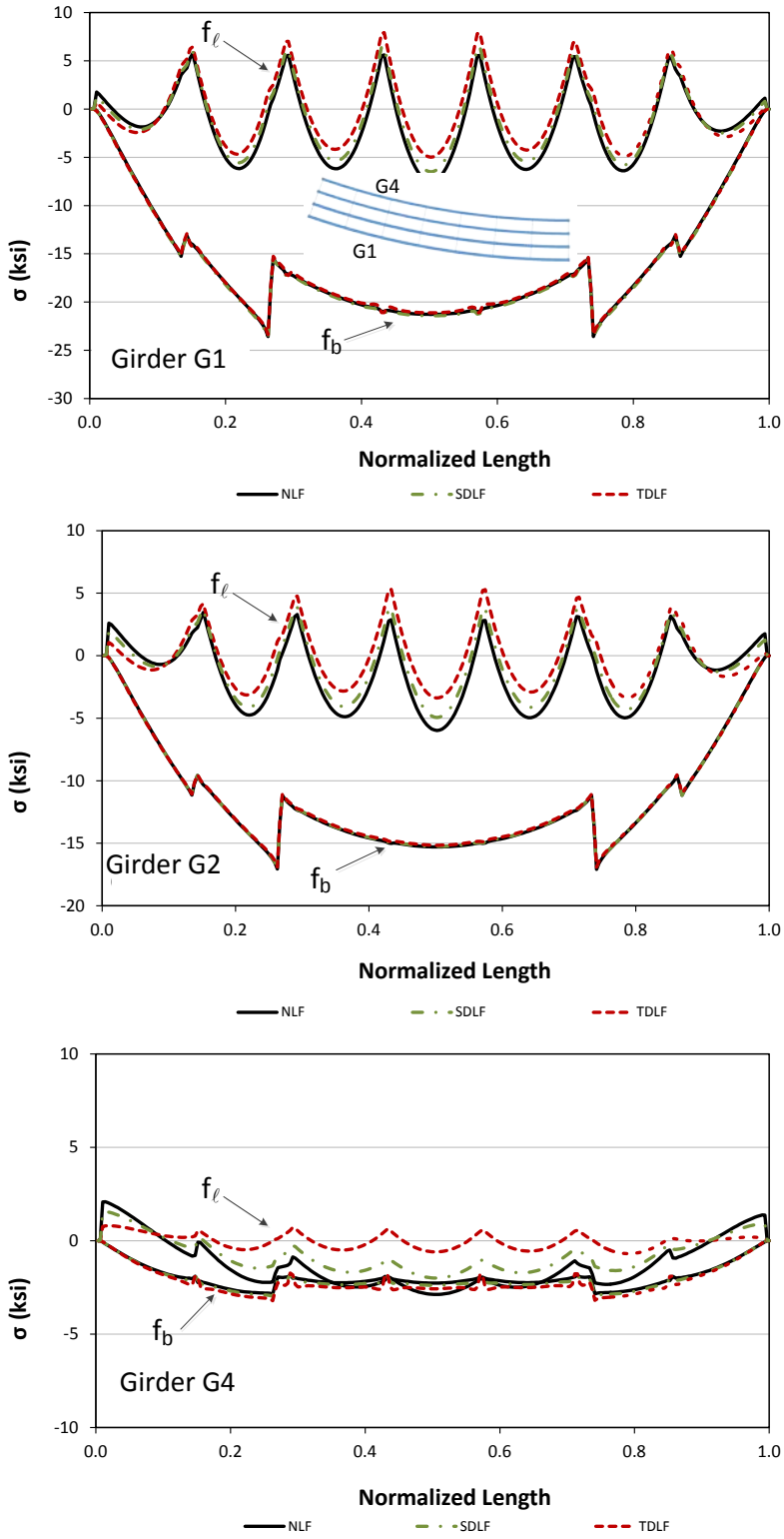

Figure 7.25. NISCR2, Top flange stresses under total dead load for different detailing methods.

7.4 Impact of Locked-in Force Effects on Strength

Locked-in force effects tend to be additive with the dead load responses for the cross-frame forces and the maximum ("negative") girder flange lateral bending stresses in curved and radially-supported bridges. The AASHTO LRFD Specifications provide explicit provisions for checking of strength during construction. Ozgur (2011) observes that additional locked-in force effects due to DLF detailing do not affect the bridge system strength significantly assuming that the cross-frames are sized adequately and that the critical components are the girders. In fact, Ozgur (2011) demonstrates that locked-in force effects can increase the strength of the curved bridges that are susceptible to overall second-order effects or significant overall (global) flange lateral bending. One example of this bridge type is provided in Section 2.9. Unfortunately, DLF detailing of horizontally curved bridges tends to increase the cross-frame member forces.

Example load-deflection curves from two bridges studied by the NCHRP 12-79 project, NISCR2 and NISCR5, are shown in Figures 7.26 and 7.27 respectively. The applied load fraction (ALF) is the multiple of the nominal total dead load applied to the bridge.

NISCR2 is a shorter bridge (150 ft.span) with a 30 ft.deck width that shows relatively little influence of the type of detailing on the overall bridge capacity. However, NISCR5 is a more extreme 300 ft.simple-span bridge with a 30 ft.deck width and no flange-level lateral bracing system. This bridge experiences significant second-order effects under the total dead load. It is only able to develop 1.34 times the total dead load before reaching its capacity for the case with NLF detailing. However, with TDLF detailing, the overall torsional rotations are reduced, thus reducing the second-order amplification and resulting in a load capacity of 1.54 times the nominal total dead load.

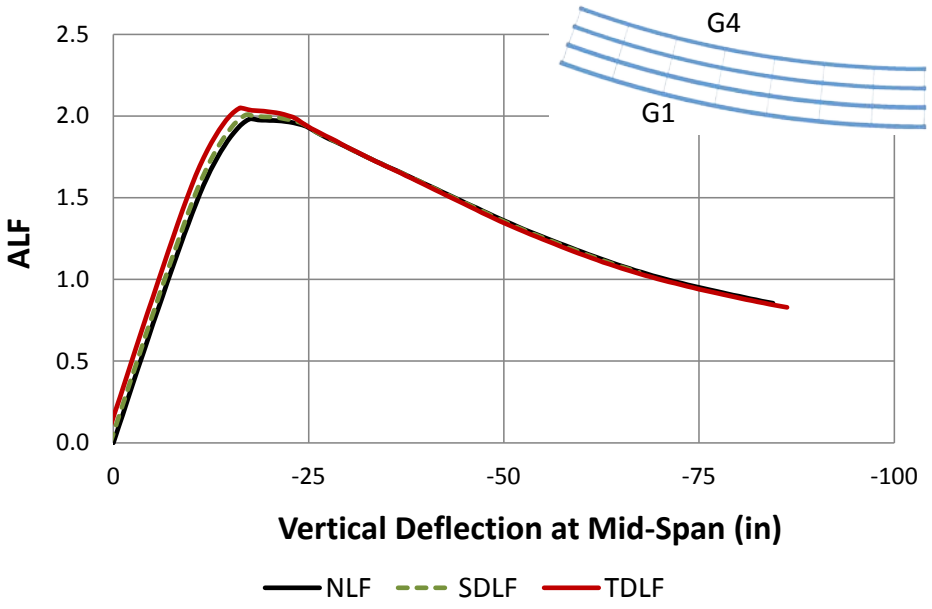

Figure 7.26. NISCR2, vertical displacements at the mid-span of Girder G1 versus the fraction of the total dead load for different detailing methods.

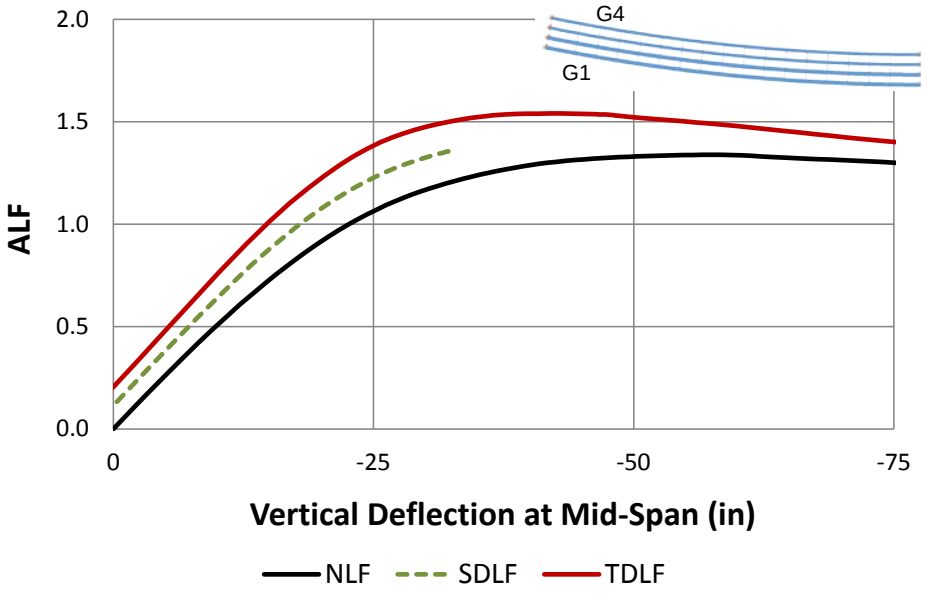

Figure 7.27. NISCR5, vertical displacements at the mid-span of Girder G1 versus the fraction of the total dead load for different detailing methods.

7.5 Special Cases

7.5.1 Special Cases where a Line Girder Analysis Predicts Accurate Results for Straight-Skewed Bridges

Engineers widely use line-girder analysis solutions to design straight skewed I-girder bridges. The corresponding analysis predictions impact the responses associated with the detailing of the cross-frames since the camber profiles are set based on these predictions. Figure 7.28 shows two sets of total dead load girder camber profiles for the bridge NISSS54, one based on line-girder analysis and one based on 3D-FEA. The 3D-FEA solution is conducted assuming NLF detailing, which neglects the small influence of the SDLF or TDLF cross-frame detailing on the corresponding vertical displacements. It is obvious that the line-girder analysis solutions are not capable of capturing any interactions of the individual girders with the NISSS54 bridge system.

In the line-girder analyses, the girders are modeled individually disregarding any interactions with the other framing. The dead loads applied to the individual girders are based on their tributary areas, and the interactions between the cross-frames and girders are neglected. Therefore, the line-girder analyses do not predict any torsion of the girders. Of course, if the cross-frames are detailed for SDLF or TDLF, and if this detailing works as intended, then the girders ideally will not be subjected to any torsion under the steel dead load or the total dead load respectively. Hence, it may be possible that a line-girder analysis will be sufficient to capture the physical vertical displacements and major-axis bending stresses with good accuracy for straight skewed bridges, constructed with DLF detailing, under the load level at which the girder webs are theoretically plumb.

Ozgur (2011) shows that if Total Dead Load Fit (TDLF) detailing is used on straight skewed I-girder bridges (i.e., the cross-frames are detailed for plumb webs in the final dead load condition), and if the girder cambers are set based on the results from 1D line-girder analyses, the locked-in stresses due to the cross-frame detailing come very close to canceling the stresses due to the torsion of the girders under the total dead load condition. As such, the physical girder layovers are approximately zero under the total dead load, and the basic 1D line girder analysis flexural model is sufficient to capture the physical vertical displacement and major-axis bending stresses with good accuracy. This result is

essentially independent of the magnitude and pattern of the support skews. Furthermore, Ozgur (2011) illustrates that the cross-frame forces along the stiff diagonal direction, as well as the corresponding flange lateral bending stresses, are significantly reduced if the bridge is constructed with TDLF detailing based on the cambers from line girder analysis. However, they are not zero. Unfortunately, the line girder analysis does not provide any predictions for these non-zero flange lateral bending stresses and the cross-frame forces.

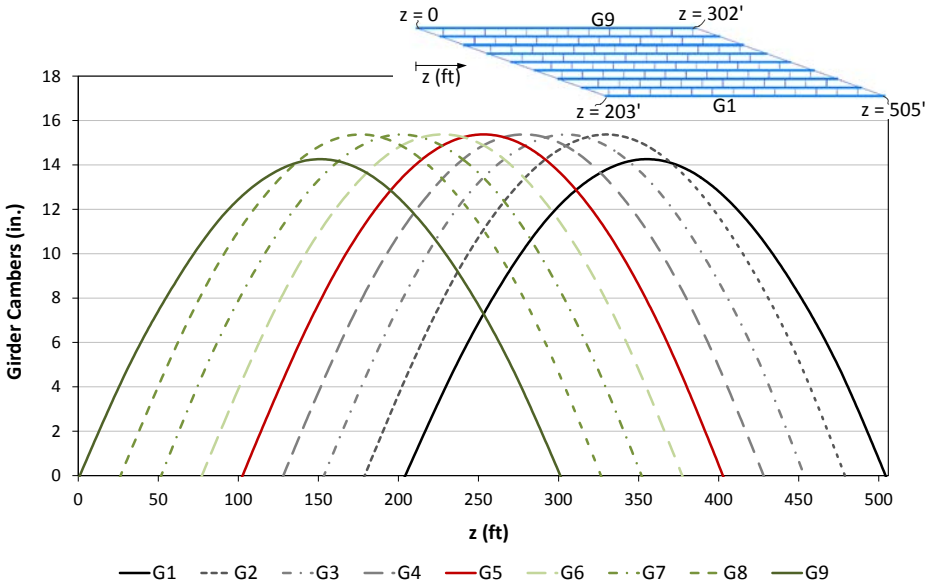

(a) Line girder analysis

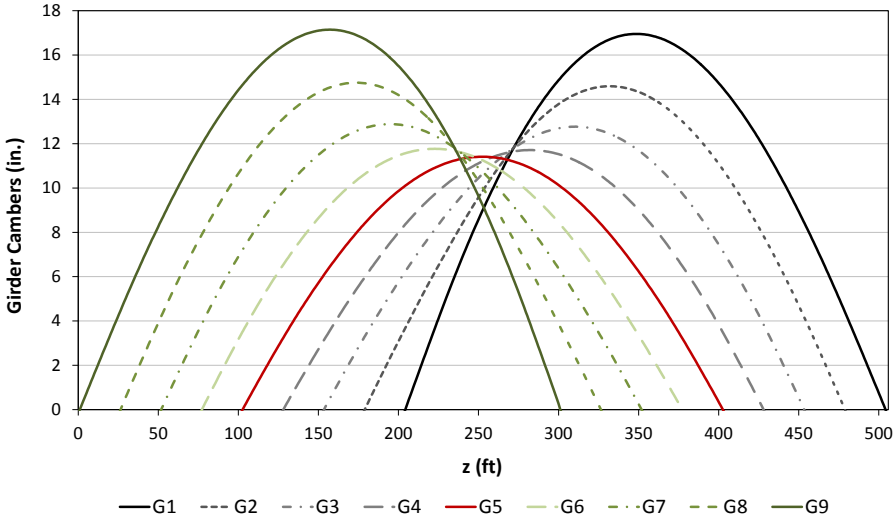

(b) 3D FEA

Figure 7.28. NISSS54, Girder camber profiles, obtained from different analysis solutions.

Figure 7.29 shows the final total dead load vertical displacements and girder major-axis bending and flange lateral bending stresses for NLF and TDLF detailing based on the line-girder analysis cambers in the NISSS54 bridge. Also, this figure illustrates the stress predictions from the line-girder analysis solutions. Interestingly, the 3D-FEA solutions demonstrate the fact that the physical vertical displacements and major-axis bending stresses in straight-skewed I-girder bridges tend to match well with the line girder analysis solutions when TDLF detailing is used along with the line-girder analysis cambers. Also, the flange lateral bending stresses are significantly reduced relative to the responses for NLF detailing.

Unfortunately, the line-girder analysis predictions generally do not produce accurate results for cases other than the dead load condition that the cross-frames are detailed for. For instance, for the above case with TDLF detailing, line-girder analysis generally does not give an accurate prediction of the steel dead load responses.

Similarly, Ozgur (2011) shows that if Steel Dead Load Fit (SDLF) detailing is used on straight-skewed I-girder bridges (i.e., if the cross-frames are detailed to fit to plumb webs in the completed steel dead load condition), and if the girder cambers are set based on the results from 1D line girder analyses, a basic 1D line girder analysis is sufficient to obtain accurate predictions of the girder major-axis bending stresses and displacements under steel dead load. The girder flange lateral bending stresses and the cross-frame forces are essentially zero in the steel dead load condition in this case.

The correctness of this solution can be understood by considering a hypothetical case of a straight-skewed I-girder bridge erection in which all the girders are set on the bearings and the top chord of the cross-frames is connected between all the girders, but otherwise the cross-frames are not engaged. In this situation, the girders remain plumb and deflect vertically under the steel dead load exactly as predicted by the line girder analysis. If the cross-frames are detailed such that they fit-up perfectly with the connection workpoints on the girders in this geometry, then obviously the bottom chord connections can be made between the cross-frames and the girders without applying any force, the cross-frames will have zero force under the steel dead load, and the girder flange lateral bending stresses will be zero.

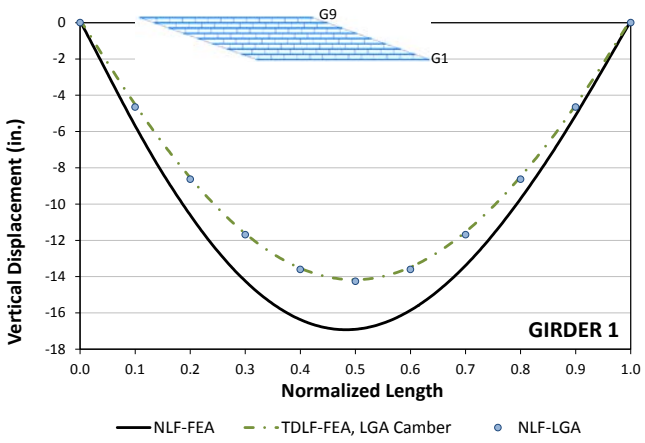

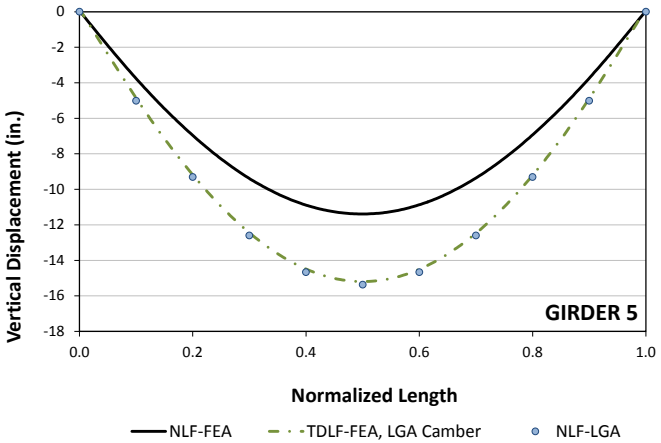

(a) Vertical Displacements

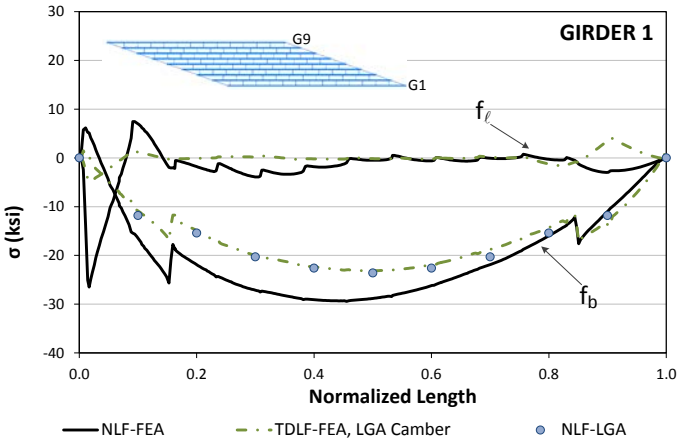

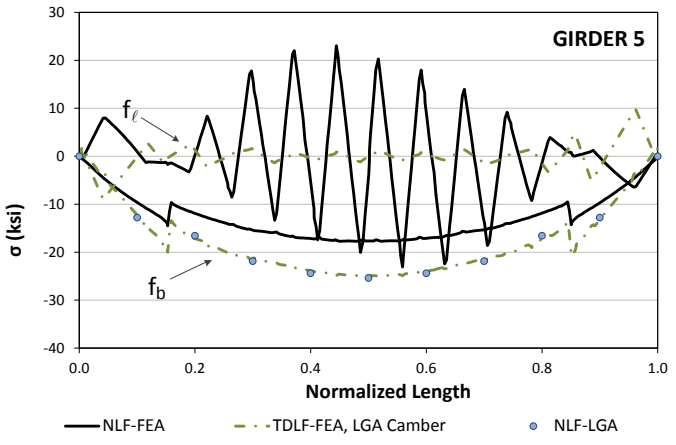

(b) Top Flange Stresses

Figure 7.29. NISSS54, total dead load vertical deflections and top flange stresses associated with NLF and TDLF detailing where the cambers are set based on line girder analysis results.

This solution is achieved via an accurate 2D-grid analysis (satisfying the recommendations of Chapter 6), or via the above 3D FEA, by including the effect of the corresponding lack-of-fit between the girders and the cross-frames in the initial no-load geometry. This lack-of-fit induces cross-frame forces and girder flange lateral bending stresses that in this ideal case are equal and opposite to the cross-frame forces and girder flange lateral bending stresses in the three-dimensional structural system under the steel dead load. Interestingly, if the cambers are obtained as the negative of the vertical displacements associated with this three-dimensional response (Figure 7.28b), the locked-in forces will tend to offset the dead-load forces in the cross-frames under the steel dead load such that the sum of these two effects will be relatively small. However, the resulting cross-frame forces are not zero, and the corresponding flange lateral bending stresses are not zero. The cambers determined from the line girder analysis (Figure 7.28a) are the ones that produce locked-in forces, due to the corresponding initial lack-of-fit, that perfectly offset the steel dead load cross-frame forces.

7.5.2 Special Cases where Line Girder Analysis with the V-load Approximation Predicts Accurate Results for Curved Radially-Supported Bridges

Line-girder analysis, using the V-load approximation to account for horizontal curvature effects, is used widely for the analysis and design of curved bridges with radial supports. In the V-Load analysis, curved girders are modeled as straight girders by using the girder length along the arc. In addition to dead loads, which are based on the tributary area of the girders, vertical loads are applied along each span at the connection points of the cross-frames with girders. The V-load approximations tend to provide good estimates of the girder stresses and cross-frame forces for simple-span curved radially-supported bridges. However, variations in flange lateral bending stress predictions can be observed due to the overall lateral bending of the flanges. Moreover, the vertical displacement predictions can be off due to the coupling between vertical displacements and torsional rotations of the girders.

Figure 7.30 shows total dead load girder camber profiles of the NISCR2 bridge, constructed with NLF detailing based on V-load approximations and 3D-FEA. It can be

observed from this figure that that the V-load approximations underpredict the vertical displacements of this bridge.

Ozgur (2011) shows that if Total Dead Load Fit (TDLF) detailing is used on simply-supported curved I-girder bridges with radial supports (i.e., the bridges are detailed to have plumb webs in their final dead load condition), and if the girder cambers are set based on the results from the 1D line-girder analyses with the V-load approximation, the locked-in stresses due to the cross-frame detailing reduce the overall (global) flange lateral bending effects. As such, the physical girders are approximately plumb under total dead load and the flange lateral bending stresses are solely due to overhang bracket loadings and horizontal curvature effects. That is, the "global" lateral bending of the flanges due to the overall torsional rotation of the bridge cross-section (which results in out-of-plumbness of the girder webs along the span) is taken out by the corresponding locked-in forces. As a result, the basic 1D line-girder analysis flexural model provides a good representation of the physical vertical displacement and major and minor axis bending stresses. However, the V-load solutions still do not produce accurate results for the cross-frame forces, which tend to be increased significantly due to TDLF detailing. It should be noted that torsional rotation of the bridge cross-section under general dead load is unavoidable though. Therefore, the V-load analysis does not necessarily produce accurate results for other dead load conditions in which the webs are not essentially plumb at the cross-frame locations. In addition, for continuous-span bridges, other factors enter which can lead to errors in the simplified method. For instance, the V-load method does not capture the tendency for the vertical reactions at intermediate supports on the inside of the horizontal curve in a continuous-span bridge to be somewhat larger due to the transverse load paths provided by the cross-frames.

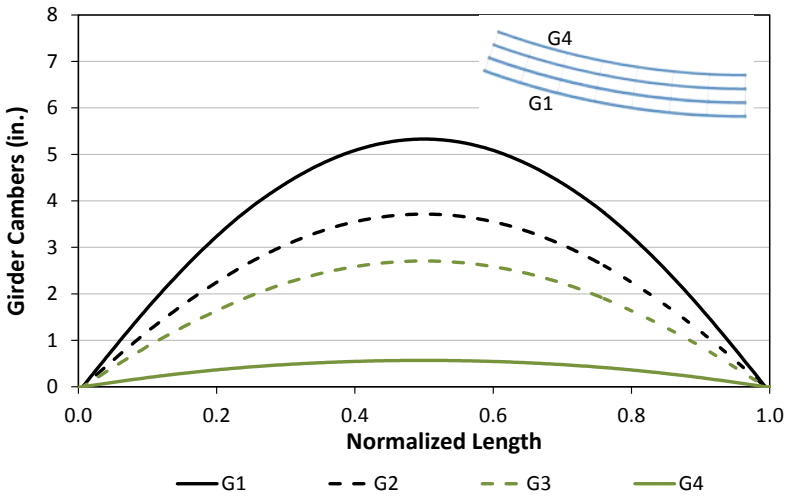

(a) Camber based on line girder analysis

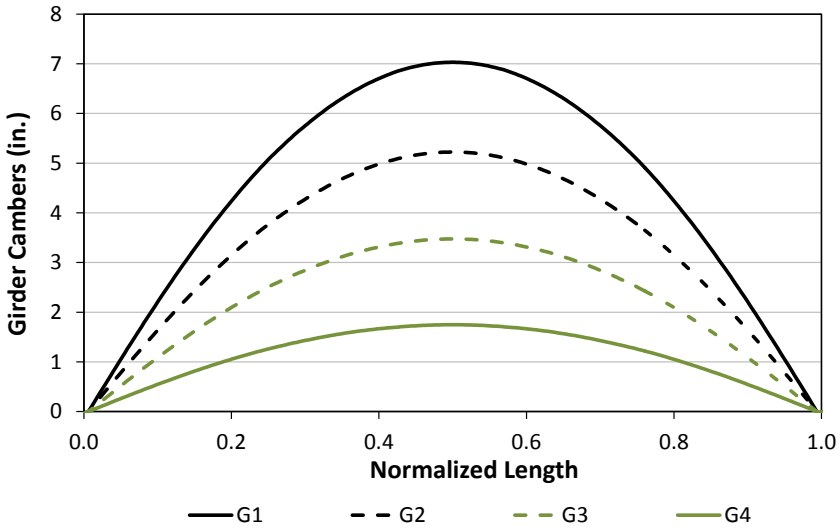

(b) Camber based on FEA deflections

Figure 7.30. NISCR2, Total dead load cambers obtained from line girder and finite element analysis solutions.

Figure 7.31 illustrates the total dead load vertical displacements and girder major-axis bending and flange lateral bending stresses for NLF and TDLF detailing based on the cambers from line girder analysis (with V-load adjustments included) in the NISCR2 bridge. Also, Figure 7.31 shows the V-load analysis predictions. The physical vertical displacements, girder major-axis and flange lateral bending stresses associated with TDLF detailing are captured accurately by the V-load analysis predictions if the girder cambers are set based on the V-load analysis solutions.

Similarly, if Steel Dead Load Fit (SDLF) detailing is used on curved I-girder bridges with radial supports (i.e., the bridges are detailed to have plumb webs in the completed steel dead load condition) and, if the girder cambers are set based on the results from 1D line-girder analyses, a basic 1D line-girder analysis (with the V-load method adjustments) is sufficient to obtain accurate predictions of the girder stresses and displacements in the steel dead load condition. Unfortunately, in this case, the V-load analysis generally does not produce accurate results with respect to the physical girder vertical displacements, major and minor axis bending stresses for other than the steel dead load condition.

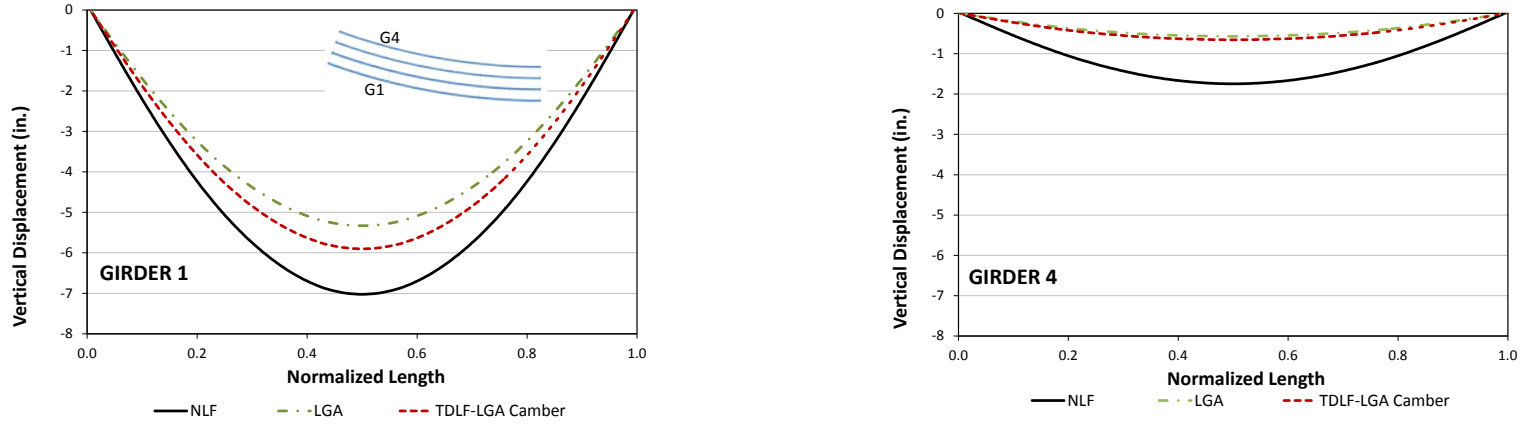

(a) Vertical Displacements

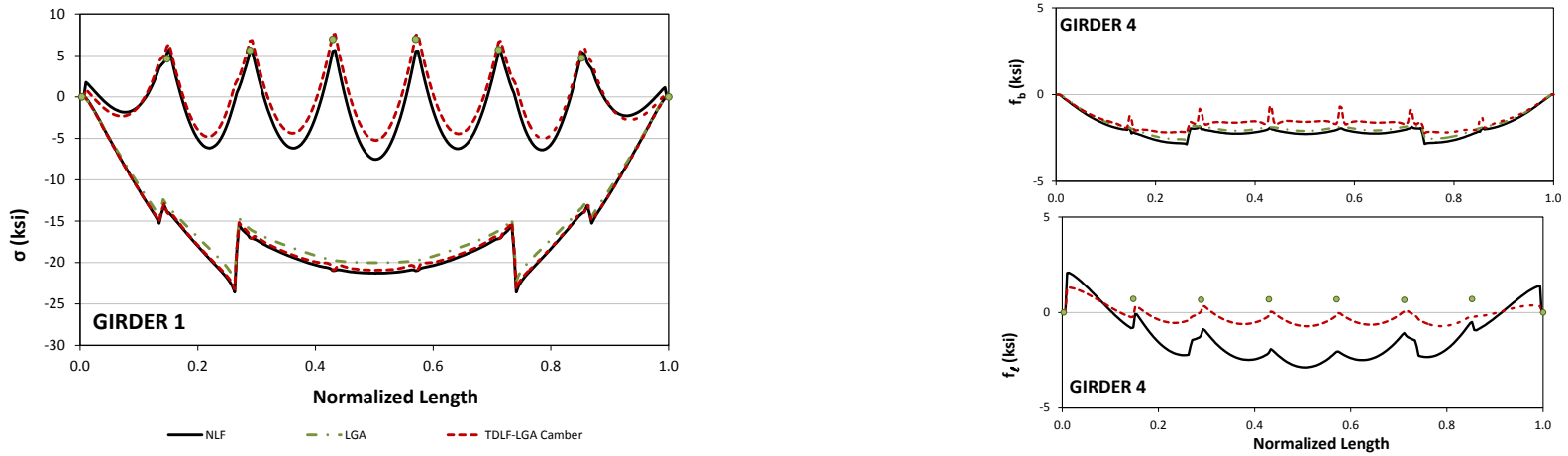

(b) Top Flange Stresses

Figure 7.31. NISSS54, total dead load vertical deflections and top flange stresses associated with NLF and TDLF detailing where the cambers are set based on line girder analysis results.

7.5.3 Estimating Maximum Dead-Load Fit Cross-Frame Forces and Girder Flange Lateral Bending Stresses Using an Analysis Based on NLF Detailing

In current practice (2012), cross-frame members of straight-skewed bridges are commonly sized without considering the locked-in forces from SLDF or TDLF detailing of the cross-frames. However, the physical member-by-member cross-frame forces corresponding to the sum of the dead load effects plus the locked-in forces from the DLF detailing can differ substantially from those obtained from an accurate 2D-grid or 3D FE analysis assuming NLF detailing.

In the previous sections, it is shown that SDLF or TDLF detailing of straight-skewed bridges tends to develop locked-in cross-frame forces due to the initial lack-of-fit that are approximately equal and opposite to the dead load stresses in the region having the largest transverse stiffness, i.e., the shortest diagonal direction across the bridge plan. However, the locked-in forces in the cross-frames can be substantially different from the dead load stresses outside this region. Ozgur (2011) shows that the locked-in cross-frame forces can be relatively large for cross-frames at the vicinity of the skewed bearing lines outside the short diagonal direction across the bridge plan.

For skewed I-girder bridges, (Ozgur. 2011) provides a minimum ratio of adjacent unbraced lengths at the first intermediate cross-frame offset from a bearing line such that large relative lateral stiffness from the adjacent bearing line and large magnitudes of the differential camber between the girders (and corresponding substantial initial lack-of-fit vertical displacements) can be alleviated. This ratio is discussed in detail in Chapter 8. If the minimum ratio of the adjacent unbraced lengths at the first intermediate cross-frame offset from a bearing line is larger than approximately 0.4, large spikes in the locked-in cross-frame forces in this cross-frame tend to be eliminated. Furthermore, it is noted that the maximum cross-frame forces obtained from a 3D FEA assuming NLF detailing are an accurate to conservative estimate of the maximum cross-frame forces for the physical bridge using either SDLF or TDLF detailing. Therefore, separate single-size intermediate and bearing-line cross-frames can be designed conservatively and used throughout the bridge based on the maximum member forces obtained from an accurate 2D-grid or 3D

FE analysis neglecting lack-of-fit effects (top chord members designed for the maximum tension and the maximum compression determined in the top chord at the cross-frames throughout the bridge, bottom chord members designed similarly, and diagonal members designed similarly). One cross-frame type can be designed for all the intermediate cross-frames, and another for the bearing-line cross-frames. In addition, the girder flange lateral bending stresses tend to be predicted conservatively from an accurate 2D-grid or 3D FE analysis neglecting lack-of-fit effects given the above caveat.

For curved I-girder bridges, the DLF detailing effects tend to add with the dead load forces in the cross-frames; therefore, the influence of DLF detailing on the cross-frame forces, as well as on the girder flange lateral bending stresses at the cross-frames, generally needs to be included in curved bridges. Fortunately, NLF is often a good option for curved radially-supported bridges.

For curved and skewed bridges constructed with SDLF or TDLF detailing, the above effects can go both ways depending on the location within the structure and the relative magnitudes and directions of the curvature and skew.

Unfortunately, for bridges with larger skew indices, the conservatism of designing single-size cross-frames in the above fashion can be prohibitive. Since the distribution of the internal cross-frame forces based on NLF detailing (see Figure 7.17) can be very different from that obtained based on SDLF or TDLF detailing (see Figure 7.18), the only alternative if the cross-frames are detailed for SDLF or TDLF is to account for the corresponding locked-in force effects in the analysis. In addition, note that generally, the total forces in the steel dead load condition (i.e., the steel dead load forces plus the locked-in forces) need to be considered. For cases with TDLF detailing, the locked-in force effects may be significantly larger than the steel dead load effects.

8. Design and Construction Considerations for Ease of Analysis Via Improved Behavior

8.1 Limiting the Values of the Bridge Response Indices

The skew effect, torsion, and girder length indices discussed in Chapter 3 can be used to predict potential difficulties in the early stages of the design of steel girder bridges. Whenever it is practical, the bridge geometry should be laid out so the indices are as close to the values of a straight bridge with normal supports, i.e., $I_S = 0$, $I_T = 0.5$, and $I_L = 1.0$.

Coletti et al. (2010) discuss procedures to reduce the severity of the skew effects in straight bridges. In all cases, the efforts are aimed at simplifying the structure's geometry, which in terms of the proposed indices, is equivalent to reducing the value of the skew index. As discussed in Section 3.1.2, the possible complications associated to the skew in both the analysis and the construction of the structure are lessened when I_S is less than 0.30.

Similarly, the torsion index, I_T, is a tool that can be used to detect undesired girder uplift as early as in the preliminary design of a curved and/or skewed bridge (see Section 3.1.4). As discussed in Ozgur (2011), a suggested limit of the torsion index to avoid uplift under nominal (unfactored) dead plus live load in simple-span I-girder bridges is 0.65. If I_T is above this limit in a given structure, the engineer should anticipate that significant uplift issues may need to be addressed. Similarly, for simple-span tub-girder bridges with single bearings on each tub, $I_T = 0.87$ was identified as a limit beyond which bearing uplift problems are likely. Continuous-span bridges can tolerate larger I_T values due to the continuity with the adjacent spans.

8.2 I-Girder Bridge Design Considerations

8.2.1 Minimum Ratio of Adjacent Unbraced Lengths at First Cross-Frame Offset from a Bearing Line

Ozgur (2011) provides recommendations on how far from the bearing line the first intermediate cross-frame should be connected, so that the forces in the cross-frame components are at acceptable levels. Figure 8.1 shows the variation in the relative lateral stiffness of the offset length and the adjacent unbraced length, χ_{Offset}, versus the ratio of these two lengths,

$$\alpha = \frac{\text{Offset length}}{\text{Adjacent unbraced length}}$$

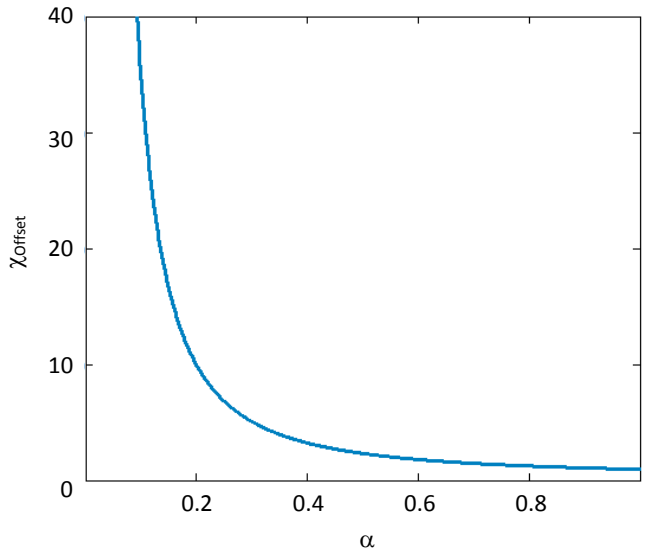

Figure 8.1. Relative lateral stiffness of offset length and the adjacent unbraced length versus the ratio of the two lengths.

at the first intermediate cross-frame from a bearing line. Figure 8.2 shows an example of these two lengths. Ozgur (2011) suggests that the minimum value of α, should be at least 0.4 since the relative lateral stiffness increases significantly for smaller ratios. Conventionally, engineers use at least 1.5 times the depth of the web as the offset for the first intermediate cross-frame. This limit should also be observed. However, for the

bridges with severe skew and long spans, the first intermediate cross-frame should be offset by a greater length than this conventional distance (i.e., $a \geq 0.4b$).

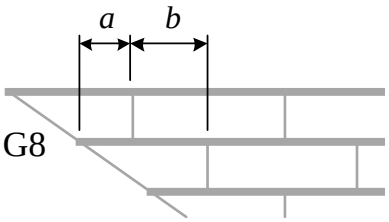

a = offset distance for G8
b = adjacent unbraced length for G8

Figure 8.2. Illustration of offset distance and adjacent unbraced length.

8.2.2 Framing of Cross-Frames to Mitigate Skew Effects

The magnitude of the collateral skew effects depends highly on the configuration of the bracing system. If the cross-frames are laid out so they do not "interfere" with the rotations that the girders experience at the bearing lines, the flange lateral bending stresses, and the cross-frame forces are relatively small. Based on this concept, Sanchez (2011) recommends a scheme that can be implemented in the design of straight I-girder bridges to mitigate the undesirable effects of skew. The approach is to place the cross-frames following an orientation similar to the skew. This practice relaxes the large forces in the cross-frames and the associated girder flange lateral bending stresses that may result due to skew effects. The basic principle is to connect the girders at the points where the layovers are similar, so the twists induced by the cross-frames are reduced (Sanchez (2011) shows that most of the contributions to cross-frame forces and flange lateral bending come from enforcing layover compatibility). In cases where the skew of the bearing lines is unequal, the cross-frames can be placed in a "fanned" configuration. With this layout of the bracing system, the effects of the skew decrease as compared to a configuration where the cross-frames are connected perpendicular to the girder longitudinal axis. Figure 8.3 shows an example of this mitigation scheme. The structure depicted in the figure is Bridge NISSS16. The cross-frame layout shown in Figure 8.3a is the layout that was considered for the studies of Task 6.

Table 8.1 shows the results of the analyses conducted using both configurations. If the cross-frames are fanned out from the point where the projection of the bearing line intersect (Figure 8.3b), the cross-frame forces decrease significantly as compared to the responses obtained with the original configuration. In addition, this reduction of the cross-frame forces also results in a decrease in the flange lateral bending stresses. The only potential negative of this approach is that the cross-frames have different lengths for each cross-frame line. Section 9.4 discusses several options for the connection of these cross-frames to the girders. Further illustrations of the potential improvements of the structural behavior of skewed I-girder bridges are presented in Sanchez (2011).

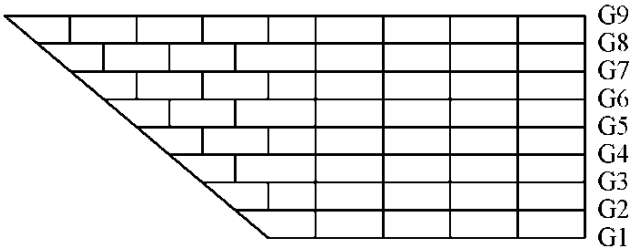

(a) Framing plan of NISSS16 with the cross-frames oriented perpendicular to the longitudinal axis of the girders (Layout 1)

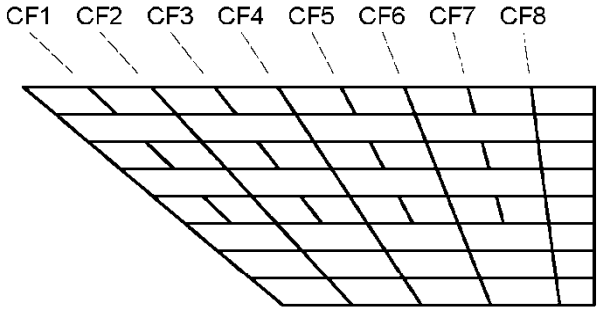

(b) Fanned cross-frame configuration with girders grouped in pairs to diminish the skew effects (Layout 2)

Figure 8.3. Different cross-frame configurations implemented in bridge NISSS16.

Table 8.1. Maximum forces in the cross-frames, predicted for two different cross-frame layouts, bridge NISSS16, TDL level.

Element	Cross-Frame Layout	Number of Interior Cross-Frames	Maximum Compression Force (kips)	Maximum Tension Force (kips)
Top Chord	(1)	48	9.3	62.6
	(2)	44	1.4	46.4
Diagonals	(1)	48	33.9	34.2
	(2)	44	15.4	15.2
Bottom Chord	(1)	48	58.0	8.6
	(2)	44	42.4	0.9

8.2.3 Selection of Cross-Frame Detailing Methods

Given the results discussed in Chapter 7, it should be apparent that different methods of cross-frame detailing work well for different I-girder bridge geometries. Furthermore, in many cases, steel I-girder bridges can be built successfully using a wide range of methods. Generally, the appropriate selection of a cross-frame detailing method depends in large part on the priority that one assigns to various objectives and tradeoffs. The NCHRP 12-79 project main report discusses these objectives and tradeoffs in detail, and provides a number of general recommendations. A few of these considerations are discussed in brief below.

Alleviating layover of the girders at bearing lines

As mentioned in Chapter 2, girder layovers under dead load are unavoidable at skewed bearing lines when NLF detailing is used. The torsional rotation capacity of the bearings can be insufficient if the layovers are excessive. Therefore, for bridges that have a sharp skew of their bearing lines, particularly the bearings at a simply-supported end of a bridge, alleviating the excessive layover of the girders at these positions is a primary objective of SDLF or TLDF detailing of the cross-frames.

The most commonly used bearing types are plain elastomeric bearings and steel reinforced elastomeric bearings. Typical maximum rotational capacities of the above

bearing types are 0.01 radians for elastomeric bearings and 0.04 radians for steel reinforced elastomeric bearings (NHI, 2011). Figures 8.4 and 8.5, from (Ozgur, 2011), show the admissible bearing rotation limits as a function of the skew angle and major-axis bending rotation at the bearing. Figure 8.4 is developed for plain elastomeric bearings while Figure 8.5 is developed for steel reinforced elastomeric bearings. Percentages of the maximum rotational capacity of the bearing are provided to accommodate the fact that part of the rotation is taken up by live loads.

In these figures, if the intersection point of the skew angle and ϕ_x for a bridge falls below the targeted bearing rotation curve, the bridge can be detailed for NLF detailing without exceeding the targeted maximum dead load rotation. Otherwise, SDLF or TDLF detailing should be considered to reduce the layovers, or other solutions such as the use of beveled sole plates or more expensive bearings that can accommodate the larger rotations should be evaluated. It should be noted that beveled sole plates are already common in many bridges to accommodate grade changes along the length of the bridge.

Facilitating Fit-Up During the Steel Erection

In addition to the above, the engineer must be aware of the fact that the type of the detailing also can impact the erection requirements. There are various attributes that result in coupling between the twist rotations and other rotations and between the twist rotations and other displacements in curved and skewed I-girder bridges. These include:

- Skewed end cross-frames create a coupling between the girder torsional and major-axis bending rotations (see Figure 2.7 or Figure 7.2)
- Intermediate cross-frames perpendicular to the members enforce the same layovers between the adjacent girders at the cross-frame locations.
- Major-axis bending rotations and vertical displacements are coupled with torsional rotations in curved girders.

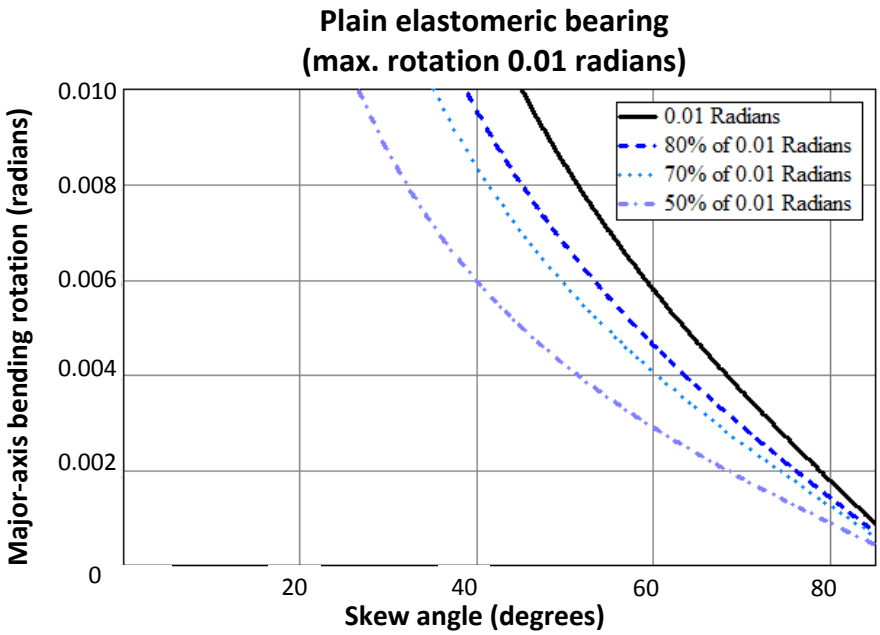

Figure 8.4. Torsional rotation levels for plain elastomeric bearings for given major-axis bending rotation and skew angle of the bearing.

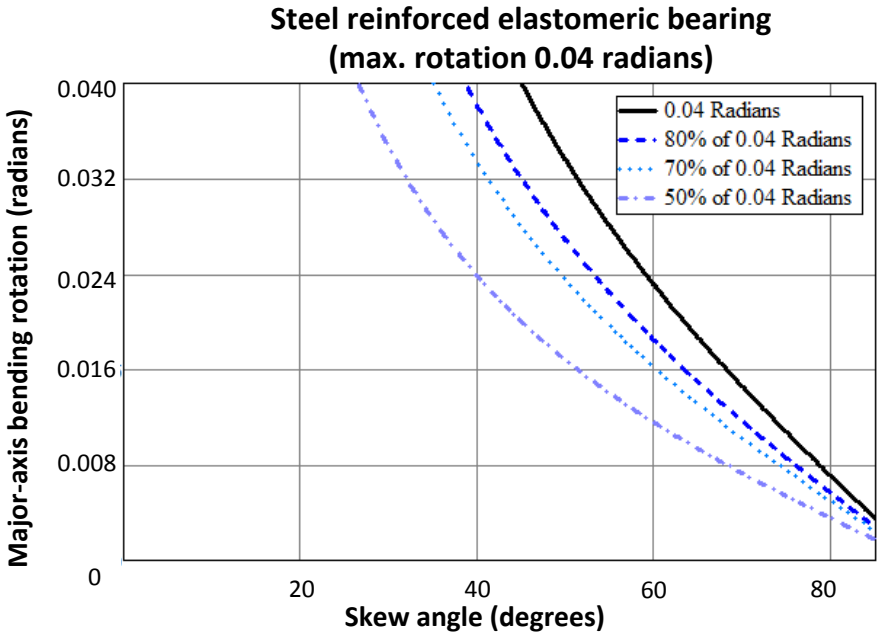

Figure 8.5. Torsional rotation levels for steel reinforced elastomeric bearings for given major-axis bending rotation and skew angle of the bearing.

For bridges constructed with NLF detailing, any variation from the no-load geometry due to dead load deflections requires fit-up forces to assemble the cross-frames in bridges constructed with NLF. In addition, for bridges constructed with TDLF detailing, fit-up forces are required at any stage due to lack-of-fit between the cross-frames and girders (since the total dead load is not yet in place on the girders at the time of the steel erection). In either case, large fit-up forces can be required if the girders need to be displaced vertically since the girders generally have large stiffness against major-axis bending deformations. These cases are more likely to occur at the locations with large differential vertical displacements between the girders, close spacing between cross-frames, and deformations for each of the above "coupled interactions" that unfortunately can be somewhat different from one another. One key location where these factors are combined is at intermediate cross-frames that are framed close to skewed bearing lines). SDLF detailing often reduces the incompatibilities between the cross-frames and the girders close to sharply-skewed bearing lines.

It should be noted that the forces required to assemble the structure during the erection can depend significantly on the erection procedures. The selected erection procedure can have a considerable effect on the dead load deflections during erection. For instance using temporary supports for bridges constructed with NLF detailing or using the dead load deflections during the erection for bridges constructed with DLF detailing can reduce any potential large differential vertical displacements. Therefore, fit-up forces can be reduced based on the selected erection scheme. All these attributes need to be considered when selecting a particular detailing method.

General Considerations

For straight-skewed bridges, SDLF or TDLF detailing are effective ways to control the plumbness of the girders, but the minimum ratio of the offset length to the adjacent unbraced length at the first cross-frame from a bearing line should be taken to be at least 0.4 to avoid large locked-in cross-frame forces. TDLF detailing is typically a good option (or the cross-frames can be detailed for an intermediate condition between TDLF and SDLF) for cases where SDLF detailing does not limit the bearing rotations to

less than the admissible bearing rotation capacity. It should be noted that in straight-skewed bridges the fit-up forces tend to be minimal for SDLF detailing and reduced significantly for TDLF detailing if the steel dead load deflections are used during the erection of the steel.

For curved-radially supported bridges, NLF detailing is generally an effective approach since the locked in stresses due to SDLF and TDLF detailing are additive with the dead load stresses. The fact that the cross-frame forces tend to be smallest with NLF detailing of these types of bridges (in any dead load condition) is also an indicator that the fit-up of the steel during the steel erection is easier with NLF detailing. The effect of the resulting girder layovers on the strength tends to be small (less than approximately 3 %). For cases with three or more girders, the true system capacities tend to be larger than those implied by the AASHTO LRFD strength calculations regardless of the method of cross-frame detailing (assuming that the system capacity is governed by the strength of the girders, i.e., the cross-frames have adequate strength). This is because the girders generally are able to provide some redistribution of forces to other locations in the bridge after the first girder limit state is reached.

For I-girder bridges with combined curvature and skew, NLF detailing is effective for the cases where the bearing rotation limits are not exceeded (see Figures 8.4 and 8.5) as long as fit-up problems near highly-skewed bearing lines are not exacerbated. Otherwise, SDLF detailing is often a better option for curved and skewed I-girder bridges. In the case of SDLF detailing of curved and skewed bridges, the engineer should consider the locked-in vertical displacements and locked-in force effects in the design. This is because the locked-in force effects are largely additive with the dead load effects with respect to the cross-frame forces and the girder maximum (“negative”) flange lateral bending stresses.

8.3 Tub-Girder Bridge Design Considerations

8.3.1 Avoid Flange Connections of Diaphragms where Practicable

As discussed previously in Section 2.1.5, the external support diaphragms play an essential role in the torsional behavior of the system in tub-girder bridges. Also it has been discussed that the behavior of the diaphragms is based mainly on their in-plane stiffness while their out-of-plane response is relatively small compared to the system stiffness.

Previous studies (Helwig et al., 2007) have shown that the flanges of the diaphragms often do not need to be connected to the tub-girders. The recommended practice is that the top flange of the diaphragms should not be connected to the top of the girder as long as the behavior of the diaphragm is dominated by shear. This occurs when the diaphragm length to depth is less than about 5, a limit that is frequently met by tub-girder bridge diaphragms. The 3D FEA studies performed for this research agree with the findings by (Helwig et al., 2007). These recommendations are applicable to full depth diaphragms only.

8.3.2 Avoid Skewed Intermediate Support Diaphragms

Intermediate support diaphragms connect the tub-girders to distribute the reaction forces between consecutive girders and restrain the girder cross-section rotations. However, for continuous span bridges with skewed pier supports, avoiding the external support diaphragms can be a good design decision. The ETCCS6 (Magruder Blvd Bridge) shown in Figures 4.44 and 4.45 uses this approach. The plan layout for this bridge is illustrated in Figure 8.6 where the bearing supports are denoted as crossed circles. In this figure, it can be observed that the girders are not connected at the skewed intermediate pier. The omission of the external support diaphragms avoids complex details at the skewed bearing line, and avoids additional torsional-flexural interactions from the skew that would have introduced large forces into the bridge. The girders have sufficient torsional stiffness such that the external support diaphragms may not be necessary in situations like this. In cases such as this bridge, where there are significant

span differences between the girders due to the skew, external intermediate cross-frames or diaphragms perpendicular to the girders within the spans may be useful to control relative displacements between the girders leading to uneven deck thickness.

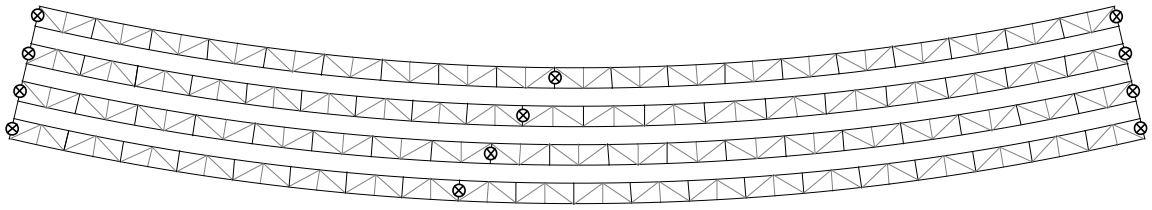

Figure 8.6. Plan view of the ETCCS6 bridge (McGruder Boulevard Bridge) showing intermediate bearing line without external diaphragms.

8.4 Construction Considerations

Forces required to assemble the structure during erection can depend significantly on the erection procedures (e.g., selection of temporary shoring towers, selection of holding cranes, etc.) and the sequence of erection, as well as the type of cross-frame detailing, although the final steel dead load geometry is unique. However, in many cases, the erection procedures may be driven by the site constraints.

Generally, it is more efficient to erect the girders from the outside of the curve to the inside of the curve for curved systems. Erecting girders from outside to inside is preferred since the top flanges of curved girders tend to lay-over in the direction away from the center of curvature under their dead load. Erecting subsequent girders from the outside (girders further away from the center of curvature) to the inside (girders closer to the center of curvature), the self-weight of the components being assembled into the partially erected structure helps to rotate the previously erected girders back into the desired geometry. If the girders are erected from inside to outside, large forces may be required in certain cases to lift the outside girder of the partially erected structure to achieve fit-up with a new outside girder.

I-girder bridges generally experience 3D deflections during erection, due to torsion, which can reduce or increase the displacement incompatibilities between connection points of the structural components. Also, for the given erection stage, displacement

incompatibilities between connections can be different for different types of cross-frame detailing.

For NLF detailing, the cross-frames are detailed such that they connect to the girders in no-load geometry. However, differential displacements between girders can develop due to dead loads during erection. For I-girder bridges constructed with NLF detailing, temporary supports (falsework) can be used to control the differential vertical deflections between adjacent girders by limiting the dead load deflections and stabilizing the bridge during erection. This is particularly important for I-girder bridges with large span lengths. Relatively large differential vertical deflections due to dead loads can cause fit-up problems.

For I-girder bridges with large span-to-width ratios, the girder deflections and stresses tend to be amplified due to global second-order (stability) effects, as discussed in Section 2.9. Excessive girder layovers and large differential vertical displacements due to second-order amplification can lead to fit-up problems or can cause a failure during erection. However, these problems can be eliminated by the use of temporary supports. Moreover, significant reduction in the girder stresses and cross-frame forces are observed for long and narrow I-girder bridge units.

Large differential vertical displacements can be observed between different parallel bridge units. Figure 8.7 shows a representative bridge NISCS37 where large differential vertical displacements are observed for a particular erection stage, as shown in Figure 8.8. Large fit-up forces can be required to connect the different bridge units. However, temporary supports can reduce the differential vertical displacements between adjacent girders by limiting the dead load deflections. As a result, fit-up forces required to connect the cross-frames can be significantly reduced, particularly for bridges constructed with NLF detailing. Ozgur (2011) shows that that providing temporary supports across the width of the bridge between the units significantly reduces the large differential vertical deflections, as illustrated in Figure 8.9 for the bridge NISCS37.

Steel Dead Load Fit (SDLF) detailing of I-girder bridges tends to minimize the fit-up forces (and stresses) during the steel erection in straight bridges, unless the bridge is essentially supported in its no-load condition during the erection. This is because the steel dead load deflections (and deformations) in the various partially erected units often are close to the final steel dead load deflections (and deformations). However, in curved radially-supported bridges, the fit-up forces generally tend to be increased by using SDLF or TDLF detailing (since the cross-frame forces generally tend to be increased by the corresponding locked-in forces in these types of bridges).

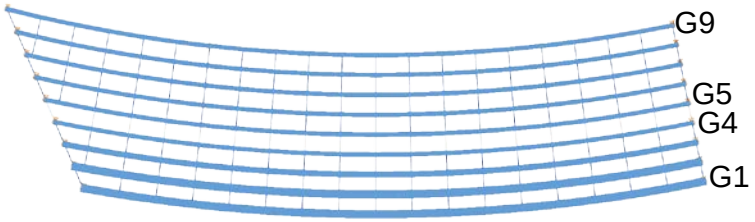

(i) NISCS37, Possible example of an erection stage.

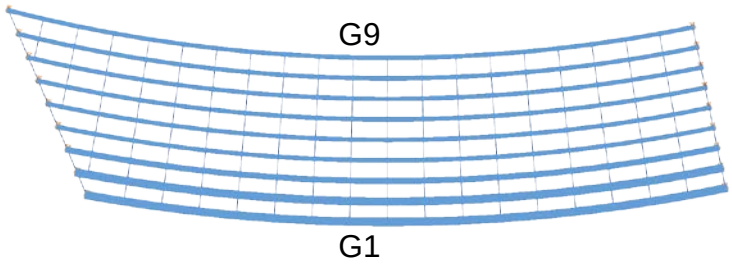

(ii) NISCS37, Completed steel structure.

Figure 8.7. NISCS37, illustration of long narrow units during construction.

If one provides sufficient temporary supports, holding cranes, etc. such that the partially erected structure is essentially in a no-load condition, then No-Load Fit (NLF) detailing minimizes the fit-up forces.

Total Dead Load Fit (TDLF) detailing generally leads to larger fit-up forces since the steel structure has not yet experienced the concrete dead load, but the cross-frames are detailed to fit up with the girders once the total dead load cambers are taken out of the girders.

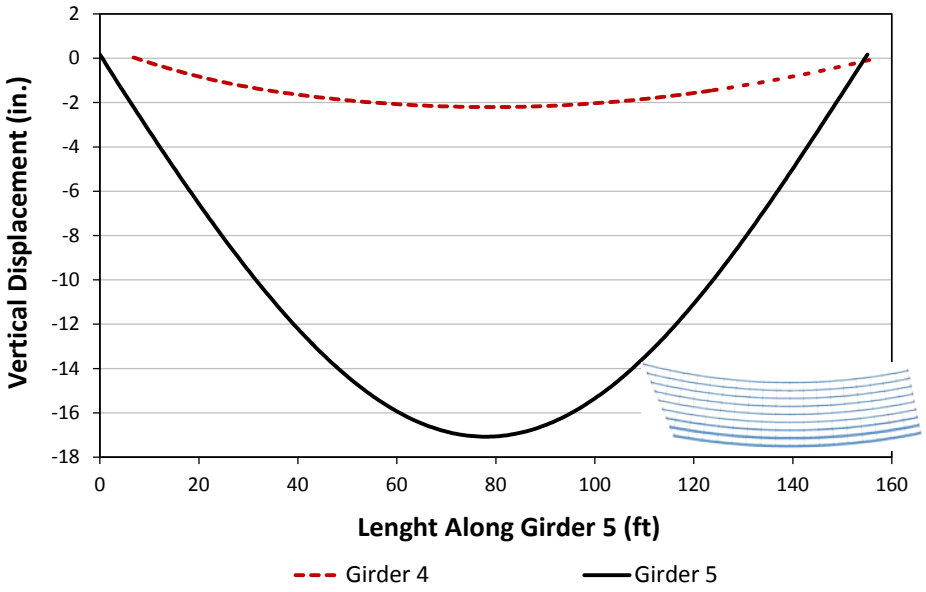

Figure 8.8. NISCS37, Vertical displacements for G4 and G5.

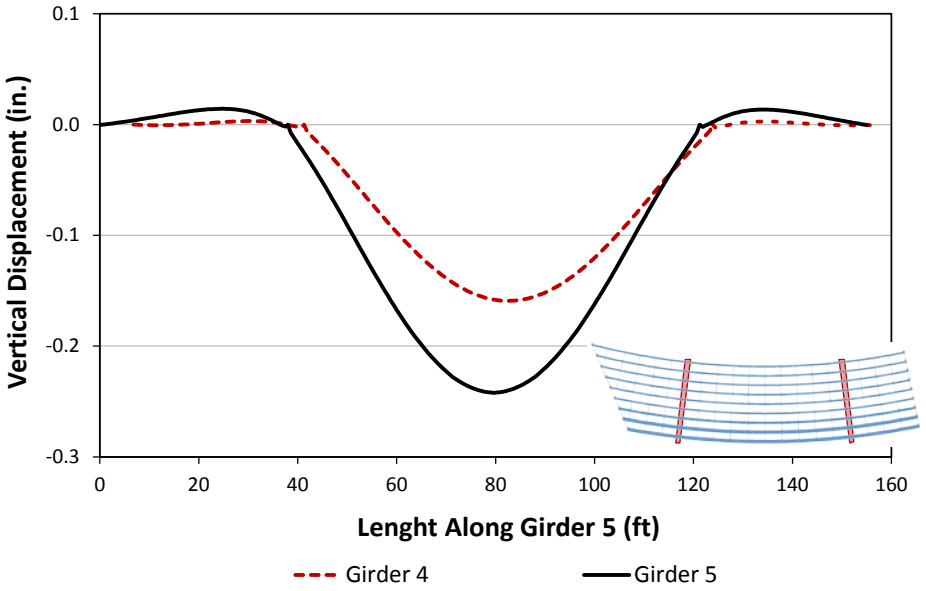

Figure 8.9. NISCS37, illustration of temporary supports between bridge units to minimize differential vertical displacements.

9. Problematic Physical Characteristics and Details

9.1 Oversize or Slotted Holes, Partially-Connected Cross-Frames

In curved and/or skewed bridges, the intermediate cross-frames stabilize the girders at all construction stages. In addition, the cross-frames participate in the control of the deformed geometry of the bridge, facilitating the deck placement. In some cases, erectors prefer not to install a selected number of cross-frames for deck placement operations, especially cross-frames that are close to the supports in skewed bridges. Instead, these cross-frames are erected in an element-by-element basis once the concrete has hardened. This practice, however, may be a detriment to the system performance. Potential amplifications due to second-order effects and other stability related problems are some of the consequences of not erecting all the cross-frames in the bridge. Therefore, prior to the deck placement, it is recommended to erect all the components of the steel structure. Moreover, the fasteners that connect cross-frames and girders must be tightened according to the design requirements.

Another technique that is sometimes used to overcome the difficulties of erecting cross-frames near skewed supports is the use of oversized or slotted holes. With larger holes in the gusset and connection plates, it is possible to maneuver and install the cross-frames with relative ease. However, there are cases where the fasteners do not bear on the surfaces of the gusset and connection plates, reducing the efficiency of the connection. In these cases, the stability bracing efficiency of the cross-frames and their ability to participate in the control of the bridge deformed geometry can be influenced significantly. Hence, it is not recommended to use this technique as a solution to the problem of installing cross-frames located near skew ends. Instead, the cross-frames can be detailed according to the guidelines discussed in Chapter 7. An appropriate detailing method can be used to facilitate the steel erection and in general, to enhance the structural performance of the bridge.

In summary, it is important to note that the cross-frames are the primary means of establishing the vertical alignment and bracing of the girders during the construction of I-

girder bridges. Leaving out a cross-frame, or providing oversize or slotted holes and leaving the connections loose amounts to removal of a brace and release of some control of the geometry.

9.2 Narrow Bridge Units

Under certain circumstances, I-girder bridges can be susceptible to large response amplifications due to global second-order effects. Contrary to local stability related problems that involve individual unbraced lengths (see Section 9.3), structures with relatively large spans-to-width ratios are sensitive to global nonlinear behavior. As discussed in Section 2.9, these structures may experience excessive displacements that can compromise the bridge constructability and in some cases, its structural integrity. Some examples of structures with these characteristics are: widening projects of existing bridges, pedestrian bridges with twin girders, phased construction, and erection stages where only a few girders of the bridge are in place.

When the bridge strength is a concern, the equations proposed by Yura et al. (2008) can be applied to estimate the system buckling load of I-girder bridges. These equations give a simple approximation of the theoretical load level at which a perfectly straight system will bifurcate into its buckled configuration. However, the physical bridge may experience excessive amplification of its lateral-torsional displacements associated with horizontal curvature, skew, unbalanced construction loads, and dissimilar girders long before reaching the theoretical buckling load level.

The amplification factor, AF_G, can be used to anticipate possible large second-order amplifications of girder stresses and displacements on a long-and-narrow bridge unit. To improve the structural performance, it is desirable to limit the value of AF_G to less than approximately 1.25 under the total dead load. If this index is above this limit, there is a potential for the structure to experience undesired deflections that may affect the construction process; specifically, the concrete deck placement. It is important to point out that bridges with $AF_G \geq 1.25$ do not necessarily need to be redesigned to avoid global second-order amplification. The construction process can be modified to reduce this index. For example, the use of temporary shoring towers at mid-span represents a

significant reduction of AF_G. However, it is best for this level of second-order amplification to be avoided by appropriate consideration at the design stage whenever possible.

If a bridge has a sufficient number of girders, so that its width is comparable to its span length, global second order amplifications may be negligible. A decision based on engineering judgment is required to assess when a bridge structure is vulnerable to global second-order amplification. The factor AF_G is the means to quantify this behavior.

9.3 V-Type Cross-Frames without Top Chords

Cross-frames stabilize the I-girders prior deck hardening. In some cases, V-type cross-frames without top chords may not be able to perform this function. The flexural stiffness of this type of cross-frame is substantially smaller than in any other configuration; therefore, its ability to provide stability bracing needs to be scrutinized during design. Studies conducted in an existing structure that used this cross-frame configuration, illustrate the importance of including the top chord. Figure 9.1 shows the plan view of a bridge located in SR1003 (Chicken Road) bridge over US 74, Robeson Co., NC. This bridge was instrumented to monitor its behavior during construction. The field measurements and corresponding original analytical studies are documented in Morera and Sumner (2009).

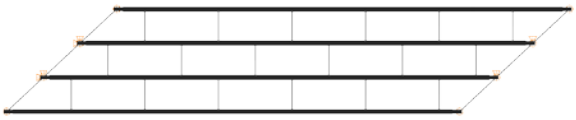

L = 133 ft./ w= 30.1 ft./ $\theta_1 = 46.2^0$, $\theta_2 = 46.2^0$

Figure 9.1. EISCS3 bridge layout.

To investigate the influence of the missing top chord on the structural behavior of this bridge, two cross-frame models are considered in the NCHRP 12-79 research. In the first analysis, the bridge is modeled to represent the as-built condition, without

intermediate cross-frame top chords. In the second analysis, the top chords are included. Figure 9.2 shows a 3D view of both models.

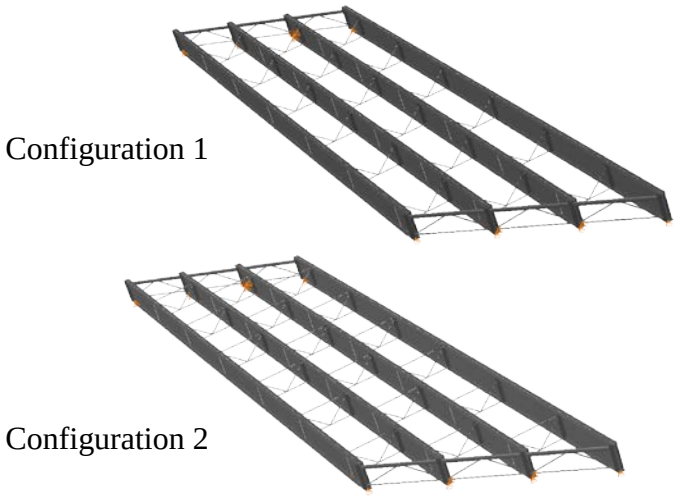

Figure 9.2. Intermediate cross-frame configurations implemented in the analyses.

As observed in the stress and layover plots for the fascia girder, G1, in Figure 9.3, the flange lateral bending response is affected substantially by the presence of the top chord. The results from the analysis conducted with the first configuration show that large lateral displacements may occur in this girder due to the lack of bracing of the top flange. Similarly, the levels of flange lateral bending stress are very high in the segment between 0.4 and 0.7 of the girder length. These two responses indicate that if the incidental contributions from components such as stay-in-place forms, ties between the girders provided by the contractor, and other devices provided to facilitate the concrete placement are not considered, the bridge exhibits substantial second order amplifications, at the TDL level. Sanchez (2011) shows that when the steel structure is properly braced, the influence of the SIP forms on the system responses during the concrete placement is negligible.

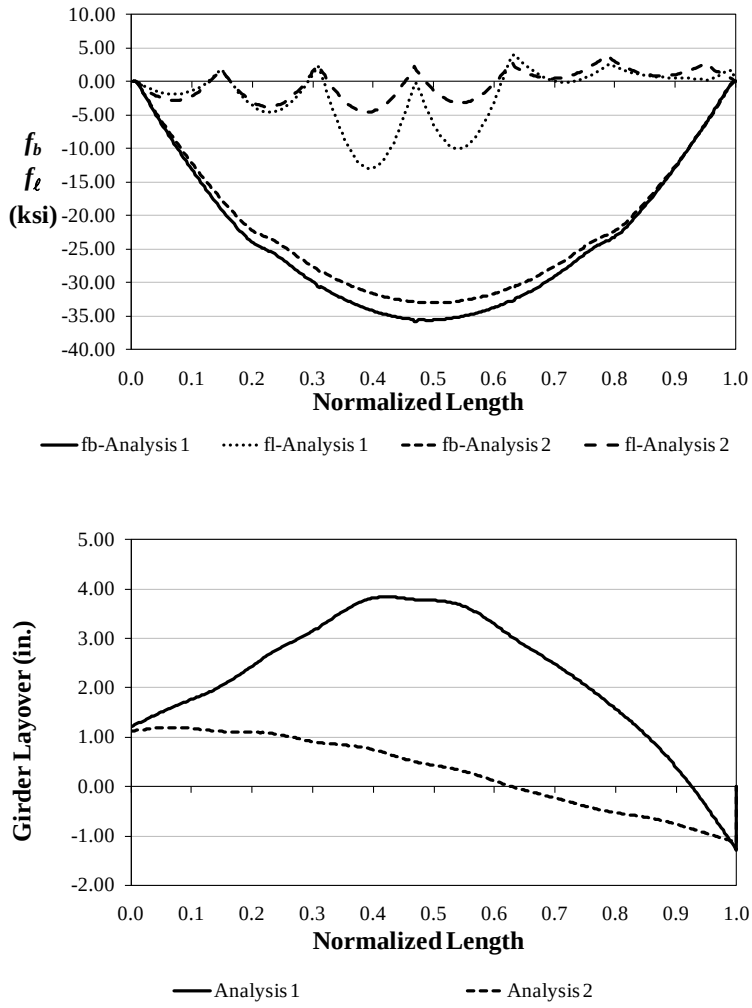

Figure 9.3. Comparison of stresses and relative lateral displacements for EISCS3 with and without a top chord in the cross-frames (Analysis 1 does not have a top chord whereas Analysis 2 has a top chord).

9.4 Connections at Skewed Cross-Frame Locations

Bracing systems have a fundamental role on the behavior of curved and skewed I-girder bridges during construction. In steel bridges, cross-frames are provided to integrate the structure, transforming the individual girders into a structural system that can support larger loads than when the girders work separately. For this purpose, cross-frames must have enough strength and stiffness so they can properly brace the I-girders when the structure is subjected to the noncomposite loads (Ziemian, 2010).

In skewed bridges, the bearing line cross-frames are commonly oriented parallel to the skew. When the cross-frames are skewed at angles less than or equal to 20^o, the connection plates are welded to the girder web, as shown in Figure 9.4(a). At larger angles it is difficult to perform the weld between the connection plate and the web. When the skew is larger than 20^o, a bent-plate detail is used commonly to connect the cross-frames to the girders, as depicted in Figure 9.4(b). The bent-plate detail facilitates the fabrication and erection of skewed cross-frames; however, it also can introduce excessive flexibility in the cross-frames and affect its stability bracing capacity.

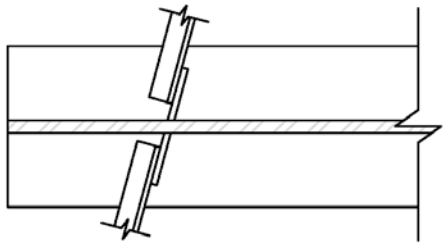

(a) Connection at skew angles equal to or less than 20^o

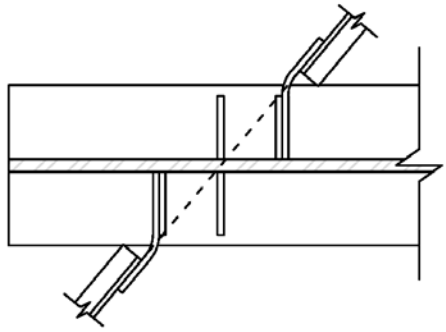

(b) Bent-plate connection detail for skew angles larger than 20^o

Figure 9.4. Typical connection details used for skewed cross-frames.

To overcome this limitation, Quadrato et al. (2010) propose the use of a half-pipe stiffener (see Figure 9.5(a)). This detail substantially improves the I-girder bridge structural performance. The advantage of this detail is that due to its circular contour, it is possible to connect the cross-frames at angles larger than 20^o, without affecting their bracing capacity. In addition to the half-pipe stiffener, Sanchez (2011) proposes a detail

that can be implemented to stiffen the bent-plates. As shown in Figure 9.5(b), the bent-plate can be reinforced to reduce its flexibility by providing stiffeners near the top and bottom flange. Also, a stiffener at the web mid-depth could be provided to increase the rigidity of the bent plate.

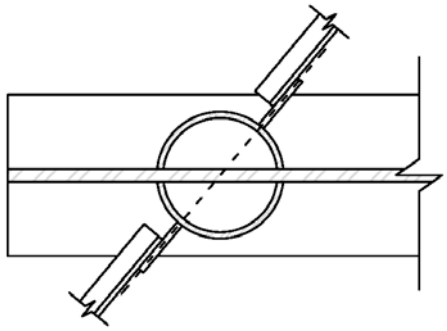

(a) Half-pipe stiffener (adapted from Quadrato et al. (2010))

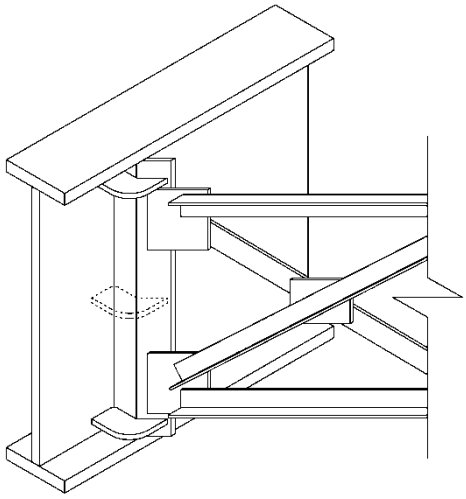

(b) Stiffened bent-plate

Figure 9.5. Improved connection details used for skewed cross-frames.

The improved details shown in Figure 9.5 may be used in combination with the recommendations provided in Section 8.2.2 to mitigate the undesired effects of skew. As discussed in that section, “fanned” configurations can be used in the design of straight I-girder bridges, to layout the intermediate cross-frames and reduce the cross-frame forces and the flange lateral bending stresses.

9.5 Long-Span I-Girder Bridges without Top Flange Lateral Bracing Systems

In many bridges, the second-order effects are expected to be quite small. However, second-order amplification due to global flange lateral bending can be large for individual curved I-girders or for a small number of girders with close spacing relative to the span length. Additionally, second-order amplification and global flange lateral bending effects can be more critical for longer spans without flange level lateral bracing since the stresses are more dominated by dead loads in longer spans. For long-span I-girder bridges without flange level lateral bracing, the overall bridge system can exhibit second-order global lateral deflections without significant twisting of the girders.

Figure 9.6 shows the undeflected and deflected geometry (magnified by 20x) of the bridge NISCR11 under total dead load from the NCHRP project studies. The bridge is 80ft wide and has a 300 ft.span length. However, it does not have a flange-level lateral bracing system. Figure 9.7 shows the magnitudes of the total dead load deflections of girder G1 from first- and second-order analyses. Also, Figure 9.8 shows the girder layovers under total dead load. Although the bridge NISCR11 has nine girders, overall flange lateral bending of the flanges is observed due to lack of flange-level lateral bracing system (see Figures 9.9 and 9.10). Figure 9.11 demonstrates the top flange stresses for the outside girder under total dead load. It should be noted from Figure 9.11 that the girder flange lateral bending stresses are amplified due to the global flange lateral bending effects. This example illustrates that as the span length become relatively large, I-girder bridges without a flange-level lateral bracing system can exhibit significant overall (global) second-order effects during the deck placement, even when the bridge cross-section has a relatively large number of girders.

It is suggested from the NCHRP 12-79 studies that I-girder bridges with spans longer than 200 ft.should be checked for global stability under potential critical stages of construction unless a flange level lateral bracing system is employed. Flange level lateral bracing systems are useful to control the geometry since they cause portions of the structure to act as pseudo-box girders such that large response amplifications due to global second-order effects can be eliminated.

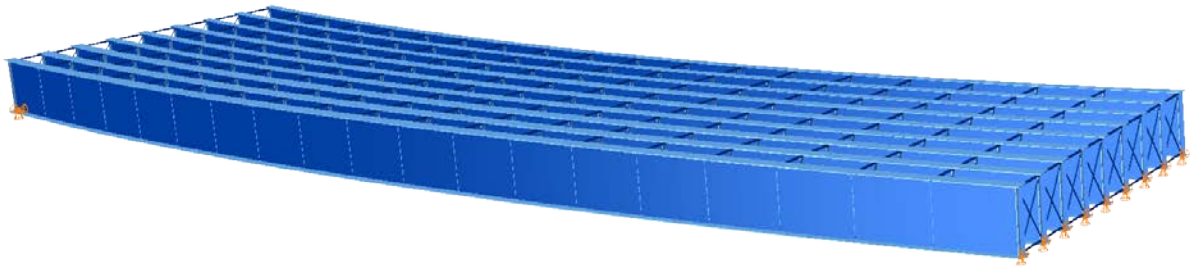

(a) Undeflected Geometry

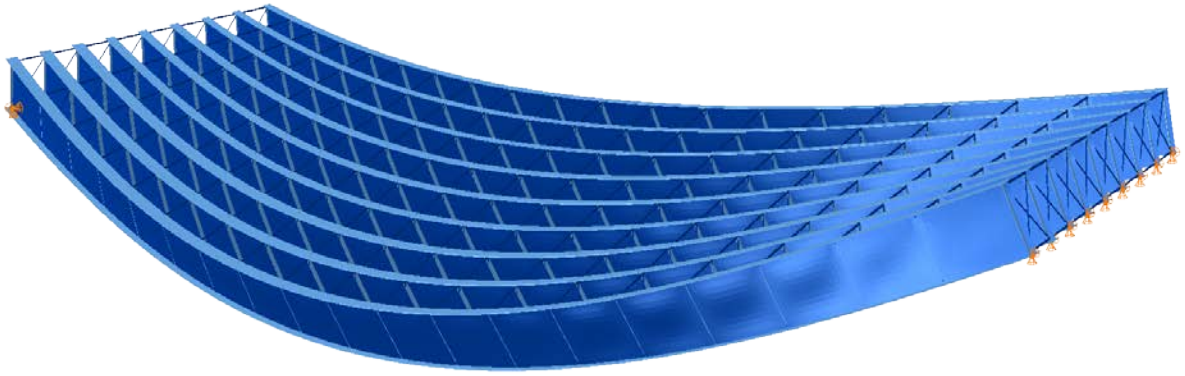

(b) Deflected Geometry

Figure 9.6. NISCR11, undeflected and deflected geometry under total dead load (Magnified by 20x).

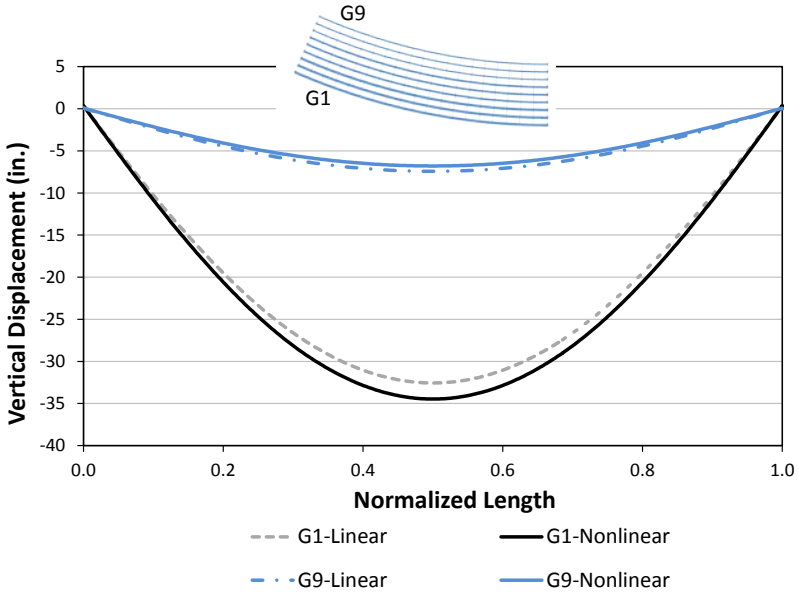

Figure 9.7. NISCR11, total dead load vertical displacements from first- and second-order analyses.

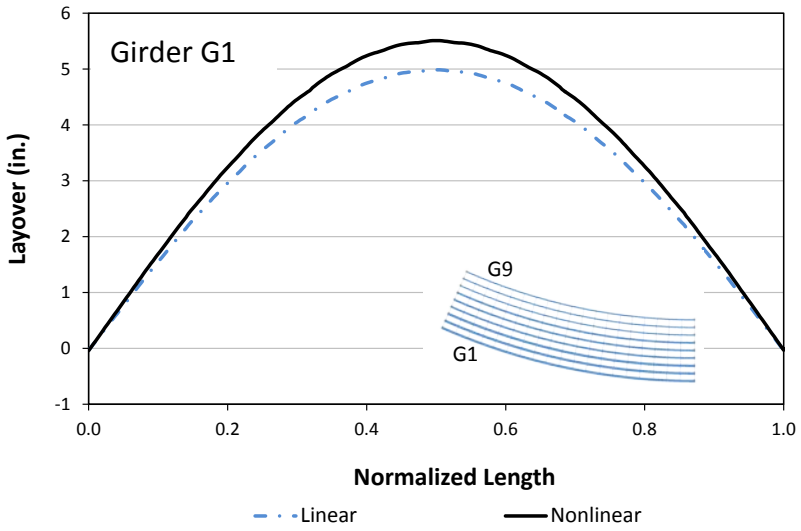

Figure 9.8. NISCR11, Total dead load layovers in Girder G1 from first- and second-order analyses.

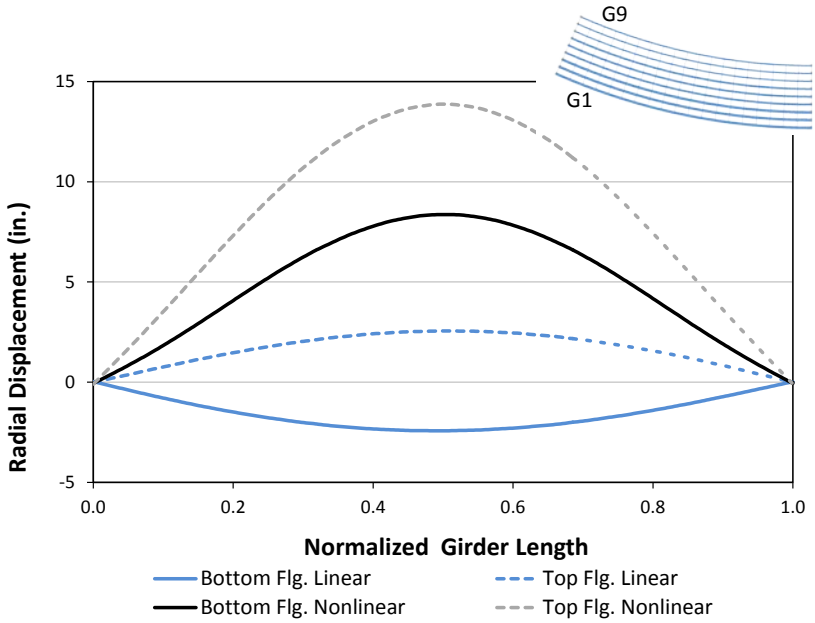

Figure 9.9. NISCR11, Girder G1 total dead load radial displacements from first- and second-order analyses.

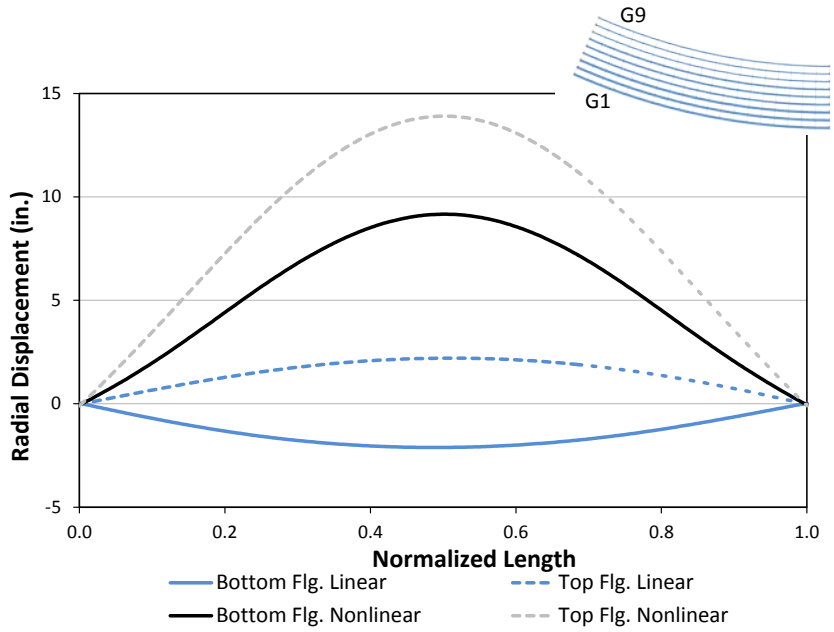

Figure 9.10. NISCR11, Girder G9 total dead load radial displacements from first- and second-order analyses.

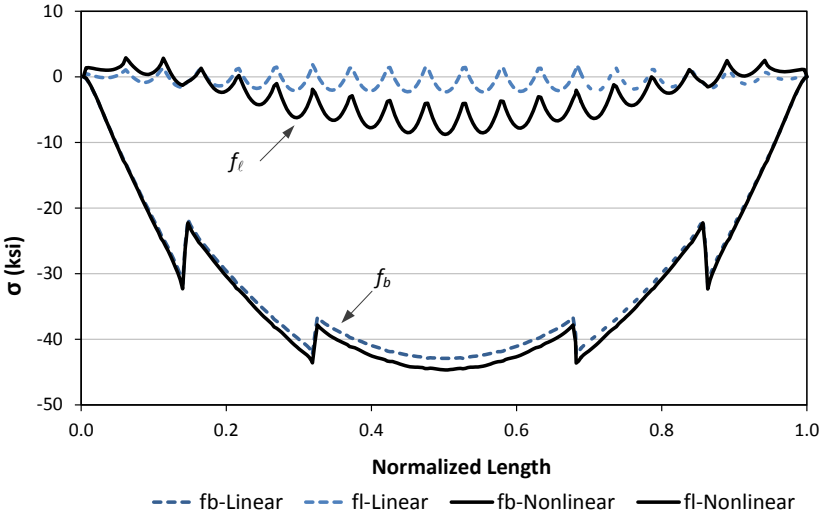

Figure 9.11. NISCR11, Girder G1 top flange stresses under total dead load.

9.6 Partial Depth End Diaphragms (Tub-Girder Bridges)

Partial depth end diaphragms have been used in some of the existing bridges collected but not selected for the analytical studies in NCHRP 12-79. This type of detail should be avoided because it changes the local and global behavior (Helwig et al., 2007). At the local level, the top flange lateral bracing system will lose continuity close to the end diaphragm meaning that the force is redistributed through a different load path to reach the end of the girder. Also, the end panel will experience more deformation with respect to the adjacent panels, having a direct impact in the adjacent elements that control the cross section distortion, such as the internal cross-frames.

The global consequences include a significant increase of the girder deflections and rotations. If both ends of a span experience twist rotations due to diaphragm deformations, the entire span experiences these rotations (essentially as an overall rigid-body rotation of the entire span). Furthermore, significant diaphragm flexibility conflicts with the rigid diaphragm simplification discussed in Section 2.1.5.

9.7 Non-Collinear External Intermediate Cross-frames or Diaphragms in Tub-Girder Bridges

When tub-girder bridges require external intermediate cross-frames or support diaphragms for relative displacement control between the girders or the distribution of reactions to the supports, the internal and external components should be collinear to avoid undesired behavior at the connection locations. Figure 9.12a shows a sketch where the external cross-frame is skewed but the corresponding internal cross-frames are not collinear. In this case, the upper corners of the external cross-frame are aligned with the corresponding elements of the internal components at the connecting points *A* and *B* in the figure. However, the bottom corner of the cross-frame at *C* has an offset along the girder axis. The sloped webs cause the points *C* and *D* to be offset from the bottom corners of the internal cross-frames. This detail could lead to undesired local stresses as the load path between the cross-frames at the lower part of the girder would be interrupted.

One way to avoid this detail is to make the internal and external cross-frames or diaphragms collinear as shown in Figure 9.12b. This detail keeps the main cross-frame forces all in one plane.

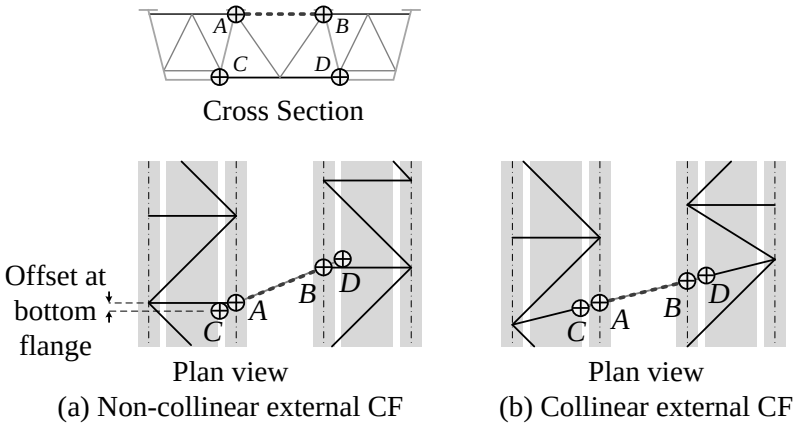

Figure 9.12. Detail of non-collinear and collinear external diaphragms in tub-girder bridges.

9.8 Use of Twin Bearings on Tub-Girders

One possible solution for the tub-girder bearing design is to provide more contact points so that the load taken by each bearing is reduced, thus potentially reducing the associated costs of the bearings. In the case of tub-girder bridges, it is possible to use more than one support bearing at each girder due to the width available at the bottom flange. In straight non-skewed bridges twin bearings are able to share the load equally. However, the reactions on these types of bearings can be very different from one another in curved and/or skewed configurations.

In curved and/or skewed cases, an ideal twin bearing system would transfer a major portion of the girder end torque to the support directly rather than through shear force transfer in the external diaphragms. However, it is common to see uplift at one of the twin supports while the other takes the entire vertical load, potentially exceeding the bearing design force.

In summary, the use of twin bearing on tub-girders creates a situation where the bearing reactions can be sensitive to minor effects potentially causing uplift, and in general, should be avoided for other than straight bridges.

10. Analysis Pitfalls

Chapter 2 provides a detailed description of the analysis methods used in the design of steel girder bridges. Sections 2.1 to 2.8 discuss the characteristics of the 1D, 2D, and 3D models, highlighting their virtues and limitations. In addition, the discussions in Sections 2.12 and 2.13 focus on the structural responses that 1D and 2D models are not able to capture due to the assumptions and simplifications used in the analyses. In this chapter, the analysis methods are revisited to discuss additional aspects that need to be considered when predicting the behavior of steel girder bridges during construction. The following sections discuss practices to avoid when modeling a bridge structure with a given analysis method. In particular, the pitfalls associated with the different analysis methods, which can result in misleading predictions of the structural responses, are presented.

10.1 Line Girder Analysis

- Global second-order amplifications cannot be captured. In general, this analysis method should not be used in cases where the global amplification factor, AF_G, is greater than 1.25 (see Sections 2.9 and 3.1.1).
- With this analysis method, accurate dead load stresses and vertical deflections are obtained in straight-skewed I-girder bridges only when analyzing the dead load condition corresponding to the type of cross-frame detailing. The dead load cross-frame forces and girder flange lateral bending stresses tend to be small in these conditions. However, significantly larger cross-frame forces and flange lateral bending stresses can be encountered at other erection stages.
- Girder cambers predicted by line-girder models may be inaccurate in straight and skewed bridges with large cross-frame forces. Specifically, if the skew index, I_S, is greater than 0.65 (see Sections 3.1.2 and 5.1), the displacements predicted by a line-girder analysis may not be reliable since they do not capture the significant transverse load paths and the correspondingly large forces transferred through the cross-frames.

- In straight and skewed bridges, interactions between the girders via cross-frames and/or diaphragms and/or via the slab generally cannot be captured. If the skew index, I_S, is greater than 0.30, the cross-frame forces and the flange lateral bending stress levels may be significant. In these cases, the results obtained from a line-girder model may be insufficient to predict all the structural responses required to make a complete assessment of the structural behavior.
- Line girder analysis cannot generally account for the influence of a flange level bracing system, and the interaction of the I-girders with this system.
- With this analysis method, the additional vertical deflections in curved I-girders due to substantial coupling between bending and torsion cannot be captured.
- In line-girder analysis, the effects of two bearings under a single tub-girder cannot be directly analyzed. There are cases where the rotations in a tub-girder are sufficiently large to cause uplift at one of the bearings.
- Line-girder analysis is unable to capture the continuity effects associated to the torsional response in continuous-span I-girder bridges.
- Line-girder analysis cannot capture any lateral or radial movement of the structure.
- A 1D analysis is unable to capture dead-load-fit detailing effects since this analysis type does not consider the contributions of cross-frames.

10.2 2D-Grid Analysis

- Global second-order amplifications cannot be captured. In general, it is suggested that this analysis method should not be used in cases where the global amplification factor, AF_G, is greater than 1.25 (see Sections 2.9 and 3.1.1).
- 2D-grid models do not include any depth information in the analysis. Hence, structural responses where the depth information is necessary to obtain accurate predictions cannot be properly captured by this analysis method. Some of the bridge depth attributes generally include:
    - Cross-frame chord depths and positions with respect to the centroid of the girders,
    - Differences between centroidal and shear center axes,

    - Eccentricity between the location of bearings and the girder centroids, and
    - Coupling between axial and bending deformations in cross-frames.
    - Flange-level lateral bracing systems in I-girder bridges and the interaction of these systems with the girders.
- Conventional 2D-grid girder torsion models significantly underestimate the girder torsional stiffnesses, often resulting in an underestimation of cross-frame forces in I-girder bridges. This limitation also can result in a significant over-prediction of the vertical displacements and girder layovers in curved I-girder bridges.
- Conventional 2D-grid cross-frame models cannot represent the physical responses of the cross-frames. This effect can be important in situations such as wide bridges, or bridges containing substantial nuisance stiffness effects causing large cross-frame forces. In straight and skewed I-girder bridges where the skew index, I_S, is greater than 0.30, the cross-frames should be modeled following the recommendations of Chapter 6 to obtain an accurate prediction of the cross-frame forces and of the overall system behavior.
- The response predictions in curved I-girder bridges are sensitive to the level of discretization used in the model. In general, the solutions obtained from a conventional 2D-grid analysis conducted with a refined mesh are less accurate than those obtained from a model with a relatively coarse mesh. This, however, does not necessarily mean that a model with a coarse mesh is the best option to analyze a curved I-girder bridge. The recommendations provided in Chapter 6, which are based on principles of structural mechanics, can be implemented in a 2D-grid analysis to obtain accurate responses, and do not depend on secondary factors such as the level of mesh refinement.
- Conventional 2D-grid models cannot represent the torsional response of I-girders; therefore, they cannot properly predict the responses when the structure has a minimum number of restraints, for example, during lifting.
- Conventional 2D-grid models are not able to capture dead-load-fit cross-frame forces. A more accurate representation of the torsional stiffness and the cross-frame model,

as the discussed in Chapter 6, is required to properly capture the effects of DLF detailing.

10.3 3D-Frame Analysis

- For I-girder bridges, any 3D-frame models that are not a Thin-Walled Open-Section (TWOS) model tend to significantly underpredict the actual girder torsional stiffnesses. Hence, the 3D-Frame models conducted with a poor representation of girder torsional stiffness have essentially the same limitations as the 2D-grid models discussed in the previous section.
- If TWOS 3D-frame elements are tied to a deck model via rigid links, the bottom flange lateral bending displacements can be substantially over-constrained and under-estimated.

10.4 3D Finite Element Analysis

- 3D FEA solutions are generally more sensitive to specific physical details of the structure and to assumptions about the detailed responses. The modeling techniques and methods used to represent the physical characteristics of the structure should be carefully studied before applying them for design purposes. For example, there are several options to model the offset existing between the top flange of the steel girders and the concrete deck centroids. One option is to provide rigid beam elements to simulate this offset. Another option is to include multi-point constraints. The second is not only the most efficient technique in terms of computational resources, but also eliminates any numerical problems that may result from including overly stiff elements in the model.
- Various contributions to flexibility, which may be included implicitly in simpler models, have to be modeled explicitly, with sufficient mesh refinement, to properly capture the effects.
- Large horizontal reactions due to the transverse restraint from guided or fixed bearings may not be present in the physical structure, due to local damage.

- Eigenvalue buckling analysis using 3D FEA generally produces a large number of web buckling modes. Therefore, other types of models are necessary to assess the girder or system overall stability.
- Various contributions to stiffness must be modeled in greater detail in 3D FEA models. For example, connection plates must be modeled properly to avoid false web distortional bending at the cross-frame connections.
- Insufficient refinement of the FEA mesh or discretization of the FEA. For instance, if solid elements are used to model plates, typically more than one element is needed through the thickness. In general the engineer should check convergence of the FEA solution for the key structural responses
- Detailed “incidental” contributions to stiffness, such as the contributions of stay-in-place metal deck forms (which are sensitive to construction practices), are difficult to include in the analysis.
- The orientation of guided or fixed bearings must represent the physical restraints given by the bearings. However, this is a consideration only after the connections to the bearings have been completed and the bearings have been unblocked, etc. In many situations, this is at the end of the steel erection but prior to the placement of the deck concrete.
- Efficient or time productive 3D FEA depends critically on the availability of sophisticated analysis processing capabilities for creation of the models and for synthesis of results; commercial capabilities provided by professional software are becoming increasingly more powerful.
- Locked-in-forces generally need to be included in the 3D FEA of curved I-girder bridges constructed with SDLF or TLDF detailing. They also need to be included in straight-skewed I-girder bridges with large skew indices, to obtain an accurate calculation distribution and magnitude of the cross-frame forces that is not overly conservative.

10.5 All Analysis Methods

- Sources of potential flexibility must be recognized, for example:
    - Flexibility of bent-plates at the connections of skewed cross-frames,
    - Bending of webs due to partial height overhang brackets, and
    - Flexibility of straddle bents, and
    - Sources of flexibility associated within the substructure.

  If it is deemed that these flexibility contributions may have a significant influence on the structural performance, one can generally obtain the best resolution in accounting for their effects by conducting a 3D FEA.
- The engineer must be wary of significant second-order effects in cases such as narrow bridge units, long-span bridges without top-flange lateral bracing systems, and bridges with V-type cross-frames without top chords. Only a nonlinear 3D FEA can capture properly the behavior of structures with these characteristics.
- A good practice always is to check that the sum of reactions is equal to the total applied loads. This includes checking of negative vertical reactions in 2D and 3D models since they are an indication of girder uplift. In 1D analyses, the torsion index, I_T, discussed in Chapter 3 can be used as an indicator of potential girder uplift that may occur due to curvature and/or skew effects.
- Another possible pitfall that is not completely related to the analysis methods, but must be considered when assessing the constructability of a steel girder bridge is the consideration of all critical stages in the partially erected structure. The engineer generally must recognize and analyze specific stages where the structural stability or the control of the deformations in the structure is a concern. The global stability amplifier AF_G discussed in Sections 2.9 and 3.1.1 provides some insight with respect to these considerations.

11. Summary

This chapter provides a summary of the salient guidelines for analysis of curved and/or skewed steel I- and tub-girder bridges, and factors that influence the analysis needs. The chapter is organized into several sections addressing common questions often faced by steel bridge designers and construction engineers.

11.1 When is a Line-Girder Analysis Not Sufficient?

The following are a synthesis of cases when a line-girder analysis is not sufficient:

- Bridges or bridge units where the global amplification of the responses, AF_G, is larger than 1.25 under the nominal (unfactored) total dead load. The global amplification factor AF_G may be estimated as

$$AF_G = \frac{1}{1 - \frac{M_{\max G}}{M_{crG}}} \tag{2.101}$$

where M_{maxG} is the maximum total moment supported by the bridge unit for the loading under consideration, equal to the sum of all the girder moments, and

$$M_{crG} = C_b \frac{\pi^2 sE}{L_s^2} \sqrt{I_{ye} I_x} \tag{2.102}$$

is the elastic global buckling moment of the bridge unit (Yura et al., 2008). In Eq. (2.102), C_b is the moment gradient modification factor applied to the full bridge cross-section moment diagram, s is the spacing between the two outside girders of the unit, E is the modulus of elasticity of steel,

$$I_{ye} = I_{yc} + (b/c) I_{yt} \tag{2.103}$$

is the effective moment of inertia of the individual I-girders about their weak axis, where I_{yc} and I_{yt} are the moments of inertia of the compression and tension flanges about the weak-axis of the girder cross-section respectively, b and c are the distances from the mid-thickness of the tension and compression flanges to the

centroidal axis of the cross-section, and I_x is the moment of inertia of the individual girders about their major-axis of bending.

Long and/or narrow I-girder bridge units with two or three I-girders can easily violate this limit. Tub-girder bridge units fabricated with proper internal cross-frames to restrain their cross-section distortions as well as a proper top flange lateral bracing (TFLB) system, which acts as an effective top flange plate creating a pseudo-closed cross-section with the commensurate large torsional stiffness, would rarely violate this limit.

- I-girder bridges or bridge units employing a flange level lateral bracing system. Line-girder analysis generally is not capable of accurately modeling the overall interaction of the girders as a pseudo-box structural system.
- Curved and/or skewed I-girder bridges detailed for NLF, where the tolerable error in any of the response quantities is smaller than that associated with the applicable score provided in Table 5.5. The tolerable error is largely a matter of the engineer's judgment and is generally a function of the magnitude of the construction stresses and displacements as well as various job conditions. The construction stresses and displacements are in turn largely influenced by the bridge span lengths.
- Curved and/or skewed tub-girder bridges, where the tolerable conservative or unconservative error in any of the response quantities is smaller than that associated with the scores provided in Tables 5.13 an 5.14. The tolerable error is largely a matter of the engineer's judgment and is generally a function of the magnitude of the construction stresses and displacements as well as various job conditions. The construction stresses and displacements are in turn largely influenced by the bridge span lengths.
- Straight I-girder bridges with a skew index $I_S > 0.30$, detailed for SDLF or TDLF. The skew index is defined as

$$I_S = \frac{w_g \tan\theta}{L_s} \tag{3.1}$$

where w_g is the width of the bridge measured between the centerline of the fascia girders, θ is the skew angle (equal to zero for zero skew), and L_s is the span length.

The I-girder major-axis bending stresses and vertical deflections can be estimated with good accuracy for the total dead load condition if TDLF detailing is used, or for the steel dead load condition, if SDLF detailing is used. However, the cross-frame forces and the girder flange lateral bending stresses may be relatively large in the targeted DLF condition, and generally may not be neglected.

- Curved radially-supported I-girder bridges constructed with SDLF or TDLF detailing. For these types of I-girder bridges, the I-girder major-axis bending, flange lateral bending stresses and vertical deflections can be estimated with good accuracy for the total dead load condition if TDLF detailing is used, or for the steel dead load condition, if SDLF detailing is used (assuming adjustment based on the V-Load method). However, a line-girder analysis conducted with the V-load method does not address the locked-in forces generated in the cross-frames under the targeted dead load condition. Therefore, a line-girder (V-Load) analysis is not sufficient to estimate the cross-frame forces in this case. Note that NLF detailing is often a good choice for curved radially-supported bridges.
- Curved and skewed I-girder bridges, detailed for SDLF or TDLF. For these types of bridges, the applicability of the V-Load method tends to break down.

11.2 When is a Traditional 2D-Grid Analysis Not Sufficient?

- Bridges or bridge units where the global amplification of the responses, AF_G, is larger than 1.25 under the nominal (unfactored) total dead load. Long and/or narrow I-girder bridge units with two or three I-girders can easily violate this limit. Practical tub-girder bridge units would rarely violate this limit.
- I-girder bridges or bridge units employing a flange level lateral bracing system. 2D-grid analysis generally is not capable of accurately modeling the overall interaction of the girders as a pseudo-box structural system.

- Curved and/or skewed I-girder and tub-girder bridges, where the tolerable error in any of the response quantities is smaller than that associated with the score provided in Tables 5.5 or Tables 5.13 and 5.14 respectively. The tolerable error is largely a matter of the engineer's judgment and is generally a function of the magnitude of the construction stresses and displacements as well as various job conditions. The construction stresses and displacements are in turn largely influenced by the bridge span lengths.

11.3 When is the Improved 2D-Grid Analysis Method Not Sufficient?

- Bridges or bridge units where the global amplification of the responses, AF_G, is larger than 1.25 under the nominal (unfactored) total dead load. Long and/or narrow I-girder bridge units with two or three I-girders can easily violate this limit. Practical tub-girder bridge units would rarely violate this limit.
- I-girder bridges or bridge units employing a flange level lateral bracing system. Line-girder analysis generally is not capable of accurately modeling the overall interaction of the girders as a pseudo-box structural system.
- Situations where a single I-girder is being analyzed.
- Cases with two or more I-girders connected together but where the connectivity index I_C is greater than or equal to 20. The connectivity index is defined as

$$I_C = \frac{15,000}{R(n_{cf}+1)m} \tag{3.2}$$

where R is the radius of curvature of the bridge centerline in units of ft., n_{cf} is the number of intermediate cross-frames within the span, and m is a constant equal to 1 for simple-span bridges and 2 for continuous-span bridges.

11.4 When does 3D FEA provide the most benefits?

- If the estimated global second-order (stability) effects are significant under any construction configuration, based on AF_G, it is advisable to revise the configuration, or if that is not feasible, perform a second-order 3D FEA of the

configuration to better ascertain the physical response. The existence of significant second-order effects indicates that the structure is sensitive to minor variations in its stiffness as well as its loadings. In these circumstances, the higher resolution possible with a well-conceived 3D FEA model can be beneficial and the construction operations should be monitored closely to ensure that the assumed conditions are in place. Although a quality second-order Thin-Walled Open Section (TWOS) 3D Frame model can provide comparable solutions, the 3D FEA modeling approaches discussed in this report are more general and more commonly available. Either of these approaches can be useful for analysis of I-girder stability and second-order deflections and stresses under lifting and early stages of erection.

- In cases where the effects of holding cranes, tie-downs and other rigging need to be assessed, 3D FEA provides the most direct ability to explicitly model the specific boundary conditions. This type of solution may be important in some situations for estimating stresses and deflections regardless of whether second-order effects are significant or not.
- 3D FEA provides the highest resolution for modeling of interactions between a composite slab and the steel I- or tub-girders, including the ability to account for web distortional flexibility, which is an important attribute of the torsional response of composite I-girders. 3D FEA also provides the highest resolution for representation of staged concrete deck placement effects.
- 3D FEA provides the most reliable characterization of the complex interactions between bridge tub-girders and their bracing systems. The various interactions of the diaphragms, cross-frames, and top-flange lateral bracing with the separate tub-girder flanges and webs are difficult to capture using line element (3D frame or 2D grid) models.
- Similarly, I-girder bridge systems with flange-level lateral bracing systems tend to act as pseudo-box structures. In situations where the participation of flange-level lateral bracing is expected to be an important part of the dead load response, direct modeling of the structure by 3D FEA is essential.

- In cases of larger horizontal curvatures and/or skews, where the tolerable error in any of the response quantities is smaller than that associated with the score provided for the simpler methods in Tables 5.5, 5.13 and 5.14 as applicable, 3D FEA provides the best accuracy for a given set of anticipated or idealized construction conditions.
- 3D FEA provides the highest resolution for analysis of SDLF and TDLF detailing effects.

11.5 When Should the Engineer Analyze for Lack-of-Fit Effects due to SLDF or TDLF Detailing?

Curved I-girder bridges constructed using SDLF or TDLF detailing (referred to generally as DLF detailing) always should be analyzed for locked-in force effects. This is because:

- DLF detailing can have a significant impact on the vertical displacements in curved I-girder bridges.
- DLF detailing tends to increase the cross-frame forces in curved I-girder bridges.
- DLF detailing tends to increase the "negative" lateral bending stresses in curved I-girder flanges, i.e., the stresses at the cross-frames, which act like continuous-span beam supports resisting the flange lateral bending.

However, it should be noted that the results of the NCHRP 12-79 studies indicate that NLF detailing is often a good choice for curved radially-supported I-girder bridges.

In addition, in general, lack-of-fit effects need to be included in an accurate 2D-grid or 3D FE analysis to obtain an accurate representation of the physical distribution and magnitude of the cross-frame forces within a straight-skewed I-girder bridge constructed with SDLF or TDLF detailing. As discussed in Section 7.5.3, the cross-frame forces and girder flange lateral bending stresses can be estimated accurately to conservatively, to design a single-size intermediate cross-frame and a separate single size bearing line cross-frame for use throughout a bridge, using an analysis that neglects the lack-of-fit effects. However, for bridges with larger skew indices, the conservatism may

be prohibitive. If the single-size cross-frames are judged to be excessively large, an analysis that includes the influence of the lack-of-fit effects generally will produce much more economical results.

11.6 When Should Global Stability Effects Be Considered?

Global stability effects should be considered via a 3D FEA for any construction configuration involving concrete deck placement where AF_G from Eq. (2.101) is greater than 1.25. In addition, I-girder bridges with spans longer than 200 ft.should be checked for global stability under potential critical stages of construction unless a flange level lateral bracing system is employed. In some longer span I-girder bridges without flange level lateral bracing, the overall bridge system can exhibit overall second-order global lateral deflections even with a large number of girders in the bridge cross-section (see the discussion of bridge NISCR11 in Section 9.5). If AF_G from Eq. (2.101) is less than 1.10, it is recommended that the influence of global second-order effects may be neglected.

For intermediate steel erection stages, larger values of AF_G should be acceptable as long as the amplified stresses are sufficiently low. The AASHTO Article 6.10.3 yielding and one-third rule strength checks are expected to provide sufficient constructability limits in these cases, without the need to directly assess the structure's amplified deflections. It is important to note that in typical intermediate erection stages, the girder stresses are well below the AASHTO constructability limits.

11.7 When Should No-Load Fit Cross-Frame Detailing Be Avoided?

- No-Load Fit (NLF) cross-frame detailing should generally be avoided when the bridge experiences layovers at skewed bearings that are larger than the remaining tolerance once the live load rotations are deducted from the bearing torsional rotation capacity.
- At highly-skewed bearing lines in straight or horizontally-curved bridges, NLF detailing can lead to increased fit-up difficulty in the vicinity of the supports. Therefore, for longer-span bridges with highly-skewed bearing lines, NLF should generally be avoided.

11.8 When Should SDLF or TDLF Cross-Frame Detailing Be Avoided?

- The results of the NCHRP 12-79 research suggest that SDLF and TDLF detailing should be avoided in sharply-curved radially-supported bridges unless the girder layovers within the spans are larger than a tolerable value based on the visual appearance of the deflected structure. (Even in this case, the addition of a flange-level lateral bracing system should be considered to stiffen the structure rather than using SDLF or TDLF detailing to control the layover within the spans.) This is because these methods of detailing increase the cross-frame forces and the "negative" flange lateral bending stresses as discussed in Section 11.5. In addition, due to the significant torsional-flexural coupling in horizontally-curved I-girders, and due to the fact that in many bridges, the concrete dead load is substantially larger than the steel dead load, Total Dead Load Fit (TDLF) detailing can potentially lead to large fit-up forces (since the girders may need to be displaced vertically as well as twisted to achieve fit-up). This problem tends to be exacerbated for longer span lengths.
- For curved and skewed bridges, the analytical results of the NCHRP 12-79 research suggest that SDLF and TDLF detailing should be avoided whenever they are not needed to satisfy bearing twist rotation tolerances, and as long as fit-up of the girders at highly skewed bearing lines. If DLF detailing is needed to control the girder layovers and/or reduce fit-up concerns at the bearing lines, SDLF detailing should be considered first. If this is not sufficient to satisfy the bearing twist rotation tolerances, the minimum level of DLF detailing between SDLF and TDLF should be used. This approach balances the use of DLF detailing to control the bearing rotations with the importance of limiting the fit-up forces in the structure. As with the above case, longer spans tend to exacerbate fit-up problems. One can observe from these considerations that SDLF detailing may often be a good "middle of the road" option on these types of bridges.

11.9 When Should No-Load Fit Cross-Frame Detailing be Used?

- The NCHRP 12-79 analytical results indicate the NLF detailing of the cross-frames is commonly a good option for horizontally-curved radially-supported bridges, since this type of detailing tends to minimize the cross-frame forces and corresponding maximum ("negative") girder flange lateral bending stresses due to horizontal curvature effects. However, the experience of some fabricators and erectors is that curved radially-supported bridges are easier to fit-up under unshored SDL erection conditions if SDLF detailing is used. The use of SDLF detailing on curved radially-supported I-girder bridges is a common practice in the industry, although bridges of this type have been detailed and constructed without difficulty using NLF detailing. It is recommended that the expanded use of NLF detailing should be explored and monitored on selected projects to further validate the NCHRP 12-79 findings.
- NLF detailing tends to minimize fit-up forces in the rare situation where the girders and cross-frames may need to be assembled in a shored configuration approximating the theoretical no-load condition. However, erection under other shored or unshored conditions is practically always achievable for straight-skewed bridges.

11.10 When Should Steel Dead Load Fit Cross-Frame Detailing be Used?

- The NCHRP 12-79 analytical results indicate that SDLF cross-frame detailing is a good option for minimizing fit-up forces in the vicinity of sharply-skewed bearing lines during steel erection under unshored or partially-shored conditions. Therefore, particularly for longer spans with a combination of sharp skew of the bearing lines along with horizontal curvature, SDLF detailing is typically a good choice.

11.11 When Should Total Dead Load Fit Cross-Frame Detailing be Used?

- For straight-skewed I-girder bridges, the coupling between the girder torsional response and the girder major-axis bending response is smaller than in curved I-girder bridges. In this case, the use of TDLF detailing gives a bridge in which the webs are approximately plumb under total dead load. Of course, since skewed bridges twist under the application of any vertical loads, the webs will not be plumb under any other loading condition (e.g., they will rotate out-of-plumb under any live load).
- For longer span bridges with large skew, one can have significant differential vertical cambers between adjacent girders. TDLF detailing may still be a viable option for many of these cases, but fit-up of the structural steel during the erection may need to be evaluated. In these situations, the girders may need to be displaced vertically as well as twisted to achieve fit-up. The fit-up can be facilitated by using the girder steel dead load deflections, i.e., allowing the girders to deflect under their self-weight, and detailing the cross-frames for SDLF.

12. References

AASHTO (2010). AASHTO LRFD *Bridge Design Specifications*, 5th Edition, American Association of State Highway and Transportation Officials, Washington, DC.

AASHTO – NSBA (2011). "G13.1-2010, Guidelines for the Analysis of Steel Girder Bridges," AASHTO – NSBA Steel Bridge Collaboration.

Best Center (2011). "Descus I, Design and Analysis of Curved I-Girder Bridge System" http://best.umd.edu/software/descus-i/

Best Center (2011). "Descus II, Design and Analysis of Curved I-Girder Bridge System" http://best.umd.edu/software/descus-ii/

Bridgesoft, Inc. (2010). "STLBRIDGE, Continuous Steel Bridge Design" http://bridgesoftinc.com/

Chang C.-J. (2006). "Construction Simulation of Curved Steel I-Girder Bridges," Doctoral Dissertation, School of Civil and Environmental Engineering, Georgia Institute of Technology, Atlanta, GA, 340 pp.

Chang, C.-J., and White, D.W. (2006). "Construction Simulation of Curved I-Girder Bridge Systems," *Annual Proceedings*, Structural Stability Research Council, San Antonio, TX, 93-114.

Chen, B. (2005). "Top-Flange Lateral Bracing Systems for Trapezoidal Steel Box-Girder Bridges," Doctoral Dissertation, Department of Civil, Architectural, and Environmental Engineering, University of Texas at Austin, Austin, TX, pp. 134.

Choo, T-W., Linzell, D.G., Lee J.I., Swanson, J.A. (2005). "Response of a Continuous, Skewed, Steel Bridge, during Deck Placement, *Journal of Constructional Steel Research*, Elsevier Ltd., pp. 567-586.

Coletti, D., and Yadlosky, J. (2007). “Analysis of Steel Girder Bridges – New Challenges,” *Proceedings*, World Steel Bridge Symposium, National Steel Bridge Alliance, New Orleans, LA, 21 pp.

Coletti, D.A., Chavel, B.W., and Gatti, W.J. (2009), “The Problems of Skew,” *Proceedings*, World Steel Bridge Symposium, National Steel Bridge Alliance, San Antonio, TX.

Essa, H.S. and Kennedy, D.J.L. (1993). “Distortional Buckling of Steel Beams,” Structural Engineering Report No. 185, Department of Civil Engineering, University of Alberta, Edmonton, Alberta, Canada, pp.356.

Fan, Z.F. and Helwig, T. (1999). “Behavior of Steel Box Girders with Top Flange Bracing”, *Journal of Structural Engineering*, August 1999, ASCE, pp. 829-837.

Fan, Z.F. and Helwig, T. () “Brace Forces Due to Box Girder Distortion,” *ASCE Journal of Structural Engineering*, V. 128, No. 6, June 2002, pp. 710-718.

Fan, Z.F. (1999). “Field and Computational Studies of Steel Trapezoidal Box Girder Bridges,” Doctoral dissertation, Civil and Environmental Engineering Department, University of Houston, 300 pp.

Farris, J.F. (2008). “Behavior of Horizontally Curved I-Girder Bridges during Construction,” M.S. Thesis, Department of Civil, Architectural, and Environmental Engineering, University of Texas at Austin, Austin, TX, pp. 152.

Fisher, S. (2006). “Development of a Simplified Procedure to Predict Dead Load Deflections of Skewed and Non-Skewed Steel Plate Girder Bridges,” M.S. Thesis, School of Civil Engineering, North Carolina State University, Raleigh, NC, 360 pp.

Grubb, M. (1984). “Horizontally Curved I-Girder Bridge Analysis: V-Load Method” Transportation Research Record, No. 289, 1984, pp. 26-36.

Helwig, T., Yura, J., Herman, R., Williamson, E. and Li, D. (2007). “Design Guidelines for Steel Trapezoidal Box Girder Systems,” Technical Report No.

FHWA/TX-07/0-4307-1. Center for Transportation Research, University of Texas at Austin, TX, 84 pp.

Helwig, T., Herman, R. and Zhou, C. (2005). “Lean-On Bracing for Steel Bridge Girders with Skewed Supports,” *Proceedings of the Annual Technical Session and Meeting*, Montreal, Quebec, Structural Stability Research Council, Univ. of Missouri - Rolla, Rolla, MO, 295-306.

Herman, R., Helwig, T., Holt, J., Medlock, R., Romage, M. and Zhou, C. (2005). “Lean-On Cross-Frame Bracing for Steel Girders with Skewed Supports,” *Time for Steel, Steel for Time*, Proceedings, 2005 World Steel Bridge Symposium, National Steel Bridge Alliance, 10 pp.

Huang, W.-H. (1996). “Curved I-Girder Systems,” Ph.D. dissertation, Department of Civil and Environmental Engineering, University of Minnesota, Minneapolis, MN.

Jimenez Chong, J.M. (2012). “Construction Engineering of Steel Tub-Girder Bridge Systems for Skew Effects,” Ph.D. Dissertation, School of Civil and Environmental Engineering, Georgia Institute of Technology, Atlanta, GA, 276 pp.

Kim Roddis, W.M., Kulseth, P., and Liu, Z. (2005). “TAEG 2.0: Torsional Analysis for Exterior Girders,” Kansas Department of Transportation, KS, 81 pp.

Kollbrunner, C. and Basler, K. (1966), “Torsion in Structures”, Springer-Verlag, New York.

Kulicki, J. M., Wassef, W. G., Smith, C., Johns, K. (2005) “AASHTO-LRFD Design Example Horizontally Curved Steel Box Girder Bridge,” NCHRP Project No. NCHRP 12-52, National Cooperative Highway Research Program, Transportation Research Board, National Research Council, 148 pp.

Leon, R., White, D., Dykas, J., Bhuiyan, M., Ozgur, C., Jimenez, J., Sanchez, A., (2011) “Field Monitoring and Computational Studies of a Horizontally Curved Steel Girder Bridge During Construction,” Report to Tennessee Department of

Transportation, School of Civil and Environmental Engineering, Georgia Institute of Technology, Atlanta, GA, September (to appear).

Norton, E.K., Linzell, D.G., Laman, J.A. (2003). "Examination of Response of a Skewed Steel Bridge Superstructure during Deck Placement," *Journal of the Transportation Research Board*, 1845, pp. 66-75.

LARSA (2010). "LARSA 4D, The Complete Software for Bridge Engineering," http://www.larsa4d.com/products/larsa4d.aspx

Li, D. (2004). "Behavior of Trapezoidal Box Girders with Skewed Supports", Doctoral dissertation, Department of Civil and Environmental Engineering, University of Houston, Houston, TX, 251 pp.

MDX (2011). "MDX Software, The Proven Steels Bridge Design Solution" http://www.mdxsoftware.com/

NHI (2007). "Load and Resistance Factor Design (LRFD) for Highway Bridge Superstructures," Design Manual, NHI Course No. 130081, 130081A-130081D, Publication No. FHWA-NHI-07-035, National Highway Institute, Federal Highway Administration, 1982 pp.

NHI (2011). "Analysis and Design of Skewed and Curved Steel Bridges with LRFD, Reference Manual", NHI Course No. 130095, Publication No. FHWA-NHI-10-087, National Highway Institute, Federal Highway Administration, 1476pp.

NSBA (1996). "V-Load Analysis and check (VANCK), User Manual, Version 1.0," National Steel Bridge Alliance and American Institute of Steel Construction.

Ohio DOT Seminar (2008). "Ohio DOT Seminar, Overview of New Practices and Policies," Ohio Department of Transportation, OH. http://www.dot.state.oh.us/

Ozgur, C. (2011), "Influence of Cross-Frame Detailing on Curved and/or Skewed Steel I-Girder Bridges," Ph.D. Dissertation, School of Civil and Environmental Engineering, Georgia Institute of Technology, Atlanta, GA

Ozgur, C. and White, D.W. (2007). “Behavior and Analysis of a Curved and Skewed I-Girder Bridge,” *Proceedings*, World Steel Bridge Symposium, National Steel Bridge Alliance, Chicago, IL, 18 pp

Poellot, W. (1987). “Computer-Aided Design of Horizontally Curved Girders by the V-Load Method.” *Engineering Journal*, AISC, Vol. 24, No. 1, First Quarter 1987, pp. 42-50.

Quadrato, C., Battistini, A., Frank, K, Helwig, T., and Engelhardt, M. (2010). “Improved Cross-Frame Connection Details for Steel Bridges with Skewed Supports,” Transportation Research Record, No. 2200, 2010, pp. 29-35.

Richardson, G. and Associates (1963). “Analysis and Design of Horizontally Curved Steel Bridge Girders,” United States Steel Structural Report, ADUSS 88-6003-01

Sanchez, T.A. (2011), “Influence of Bracing Systems on the Behavior of Steel Curved and/or Skewed I-Girder Bridges during Construction,” Ph.D. Dissertation, School of Civil and Environmental Engineering, Georgia Institute of Technology, Atlanta, GA

Shah, D.M. (2007), “Effective Flange Width Evaluation for Prestressed Concrete Bulb-Tee Girder Bridges,” M.S. Thesis, Department of Civil Engineering, The State University of Buffalo, NY, 131 pp.

Simulia (2010). “Abaqus, Realistic Simulations” http://www.simulia.com

Stith, J.C. (2010). “Predicting the Behavior of Horizontally Curved I-Girders during Construction.” Doctoral Dissertation, Department of Civil, Architectural, and Environmental Engineering, University of Texas at Austin, Austin, TX, pp. 330.

Topkaya, C., and Williamson, E. (2003). “Development of Computational Software for Analysis of Curved Girders under Construction Loads,” *Computers and Structures*, May 2003, Elsevier Ltd., pp. 2087-2098.

Topkaya, C., Williamson, E., and Frank, K. (2004a). “Behavior of Curved Steel Trapezoidal Box-Girders during Construction.” *Engineering Structures*, Elsevier, 26(6), 721-733.

Topkaya, C., Yura, J., and Williamson, E. (2004b). “Composite Shear Stud Strength at Early Concrete Ages,” *Journal of Structural Engineering*, ASCE, pp. 952-959.

Tung, D. and Fountain, R. (1970). “Approximate Torsional Analysis of Curved Box Girders by the M/R-Method,” *AISC Engineering Journal*, July 1970, AISC, pp. 65-74.

United States Steel Corporation (1965), “Highway Structures Design Book,” ADUSS 88-1895-01, Vol. 1.White, D.W., Zureick, A.H., Phoawanich, N.P. and Jung, S.K. (2001). “Development of Unified Equations for Design of Curved and Straight Steel Bridge I Girders,” Final Report to AISI, PSI Inc. and FHWA, October, 547 pp.

Yang, Y.B. and McGuire, W. (1984). “A procedure for analyzing space frames with partial warping restraint”, *International Journal for Numerical Methods in Engineering*. 20 (1984) 1377–1389.

Yura, J., Helwig, T., Herman, R. and Zhou, C. (2008). “Global Lateral Buckling of I-Shaped Girder Systems,” *Journal of Structural Engineering*, 134(9), 1487-1494.

Ziemian, R. (2010). Guide to Stability Design Criteria for Metal Structures, 6th Edition, Wiley, New Jersey.

Project No. NCHRP 12-79 **COPY NO. 1 of 20**

BENCHMARK PROBLEMS

TASK 7 REPORT

Prepared for
NCHRP
Transportation Research Board
of
The National Academies

Donald W. White, Georgia Institute of Technology, Atlanta, GA
Andres Sanchez, HDR Engineering, Inc., Pittsburgh, PA
Cagri Ozgur, Paul C. Rizzo Associates, Inc., Pittsburgh, PA
Juan Manuel Jimenez Chong, Paul C. Rizzo Associates, Inc. Pittsburgh, PA

February 29, 2012

ACKNOWLEDGMENT OF SPONSORSHIP

This work was sponsored by one or more of the following as noted:

☑ ☐ American Association of State Highway and Transportation Officials, in cooperation with the Federal Highway Administration, and was conducted in the **National Cooperative Highway Research Program,**

☐ ☐ Federal Transit Administration and was conducted in the **Transit Cooperative Research Program**,

☐ ☐ American Association of State Highway and Transportation Officials, in cooperation with the Federal Motor Carriers Safety Administration, and was conducted in the **Commercial Truck and Bus Safety Synthesis Program,**

☐ ☐ Federal Aviation Administration and was conducted in the **Airports Cooperative Research Program,**

which is administered by the Transportation Research Board of the National Academies.

DISCLAIMER

Project No. NCHRP 12-79

BENCHMARK PROBLEMS

TASK 7 REPORT

Prepared for
NCHRP
Transportation Research Board
of
The National Academies

Donald W. White, Georgia Institute of Technology, Atlanta, GA
Andres Sanchez, HDR Engineering, Inc., Pittsburgh, PA
Cagri Ozgur, Paul C. Rizzo Associates, Inc., Pittsburgh, PA
Juan Manuel Jimenez Chong, Paul C. Rizzo Associates, Inc. Pittsburgh, PA

February 29, 2012

Table of Contents

List of Figures

List of Tables

Executive Summary

The engineer generally should understand the broad aspects of the assumptions and limitations of the modeling strategies, to ensure their proper application, and generally, he or she should conduct testing and validation studies with the software to ensure that the methods work as intended and that they provide correct answers for relevant benchmark problems.

This document provides a series of formal benchmark cases that can be used to evaluate several analytical methods. The benchmark cases are presented in a combined drawing/report/data file format. The drawings indicate the characteristics of the structure, with all key structural element sizes and dimensions, material properties, bearing conditions, design loads, etc.

This task indicate modeling assumptions (load and displacement boundary conditions, stiffness modeling assumptions, etc.) and bridge descriptions and benchmark results in a data format easily accessed for comparison to the results of alternate proposed analysis methods.

1. Introduction

In this report, two I-girder bridges and one tub girder bridge studied in Task 7 of the NCHRP 12-79 research are presented as a set of benchmark cases that can be used to evaluate other analytical methods. These models are presented in a combined drawing/report/data file format. The drawings indicate the characteristics of the structure, with all key structural element sizes and dimensions, material properties, bearing conditions, design loads, etc. Also, the modeling assumptions, which include boundary conditions, loading assumptions, stiffness modeling assumptions, etc., are included. The data shown in this report in graphical format is provided also in electronic form as spreadsheets and other data files. In this way, designers and software developers should be able to identify all key parameters of the benchmark solutions, run their analysis using consistent parameters, and compare the results.

2. I-Girder Bridges

2.1 Bridge XICSS5

XICSS5 is a three span continuous straight I-girder bridge with the span lengths of 140ft, 175ft and 140ft with parallel abutments skewed at 60°. This structure is an example bridge studied in "Load and Resistance Factored Design for Highway Bridge Superstructures" (FHWA-NHI, 2007a & 2007b). Figure 2.1 shows the perspective and plan views of XICSS5 with key dimensions. The girders are labeled from bottom to top as Girder 1 to Girder 4 (G1-G4).

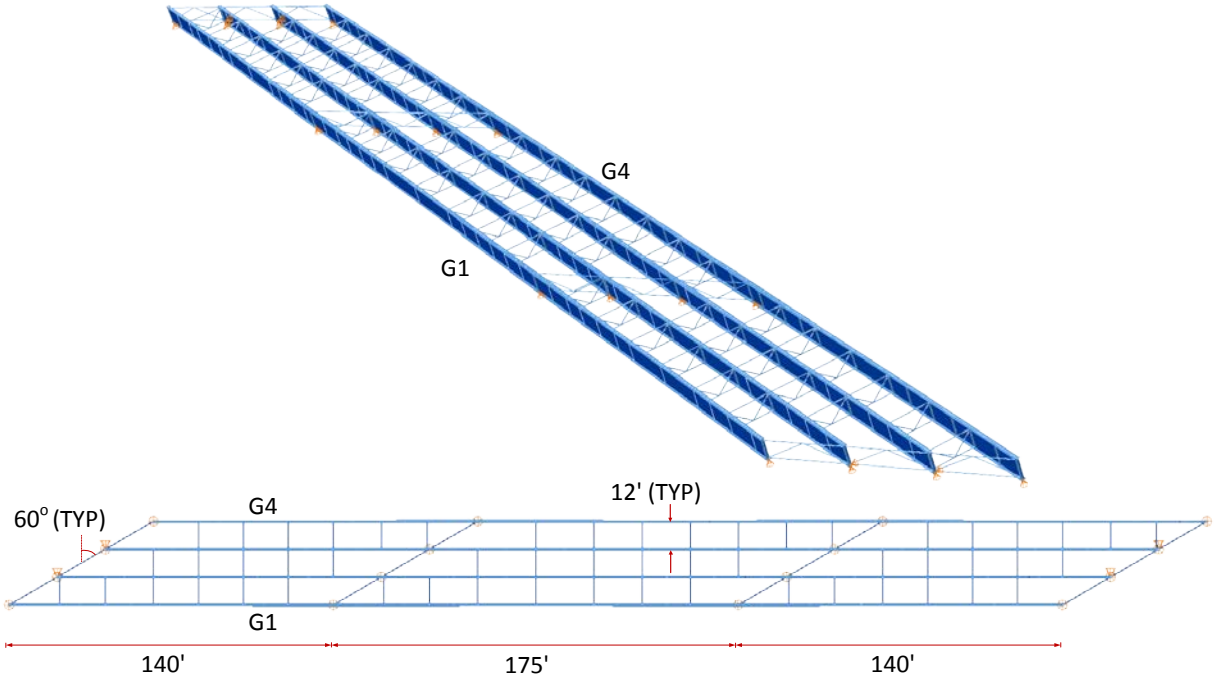

Figure 2.1. XICSS5, perspective and plan views.

The assumed bearing restraints for 3DFEA models are tabulated in Table 2.1. Moreover, Figure 2.2 shows the framing plan of XICSS5. Girder plate dimensions are illustrated in Figure 2.3. The intermediate cross-frames are V-type, and inverted V-type cross-frames are used at abutments and at the interior bents. The cross-frame member sizes are summarized in Table 2.2. Also, typical bridge cross-section is shown in Figure 2.4. The weight of the formwork (10 psf), and the slab reinforcing steel plus the wet concrete (150 psf) is applied to the top flanges as uniformly distributed line loads based

on the tributary width of each girder across the cross-section of the bridge. In addition, the overhang brackets used for resisting the weight of wet concrete and formwork at the fascia girders are considered. In the model, the steel properties are E_s = 29000 ksi and F_y = 50 ksi. Similarly, the concrete properties are E_c = 3600 ksi and f''_c = 4 ksi. Additionally, Figure 2.5 provides the deck placement sequence of the bridge.

Table 2.1. XICSS5, assumed bearing restraints in 3D FEA models.

Girder #	Abutment 1	Pier 1	Pier 2	Abutment 2
1	Free	Free	12000 kip/ft Longitudinally	Free
2	Guided Longitudinally	24000 kip/ft Transversely	12000 kip/ft Longitudinally and 24000 kip/ft Transversely	Guided Longitudinally
3	Guided Longitudinally	24000 kip/ft Transversely	12000 kip/ft Longitudinally and 24000 kip/ft Transversely	Guided Longitudinally
4	Free	Free	12000 kip/ft Longitudinally	Free

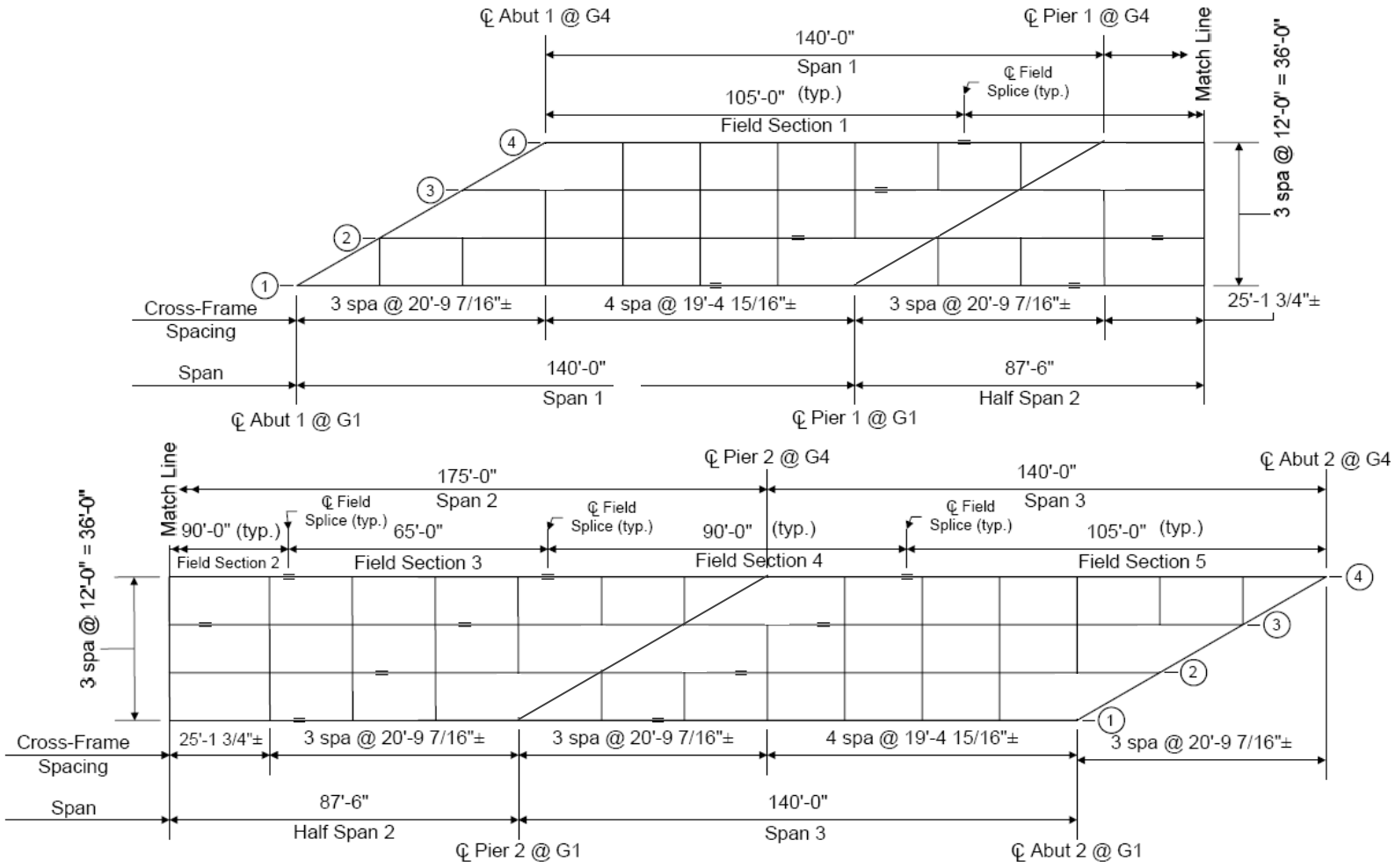

Figure 2.2. XICSS5, framing plan.

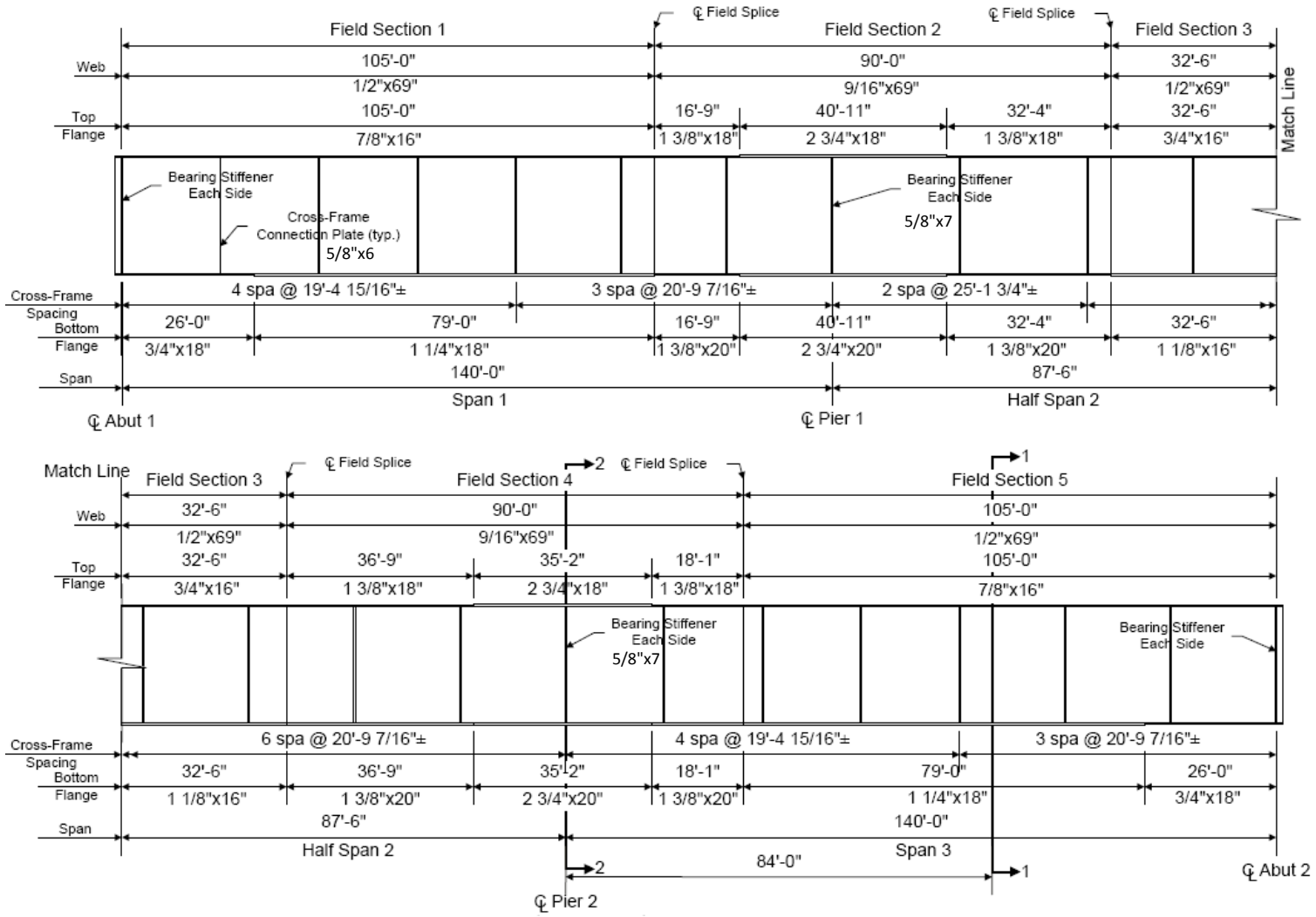

Figure 2.3. XICSS5, girder plate dimensions.

Table 2.2. XICSS5, cross-frame member sizes.

Cross-Frame Type	Top Chord	Diagonals	Bottom Chord
Interior (V)	L6x6x1/2	L6x6x5/8	L6x6x5/8
End (Inverted V)	L6x6x1/2	L6x6x5/8	L6x6x5/8

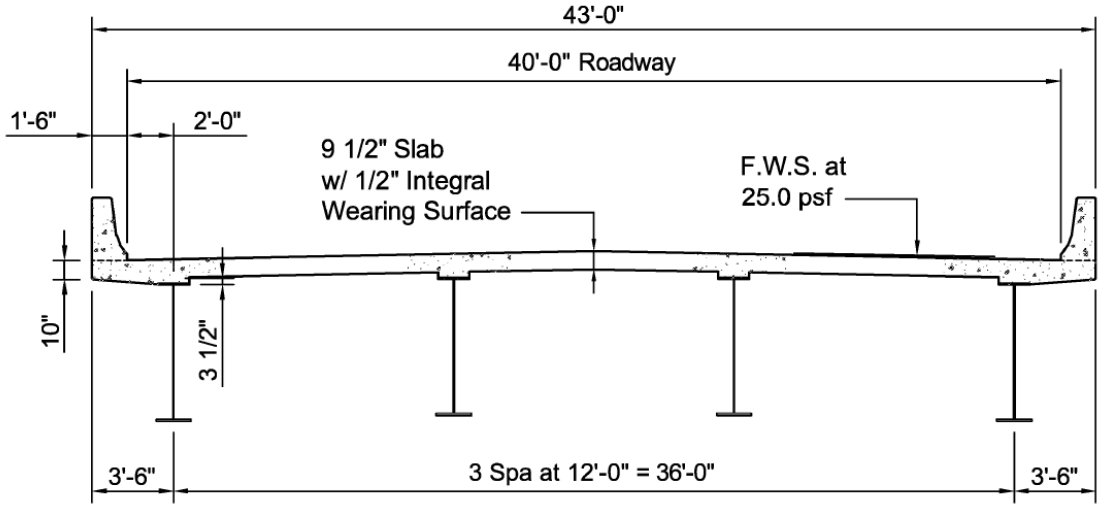

Figure 2.4. XICSS5, typical bridge cross-section.

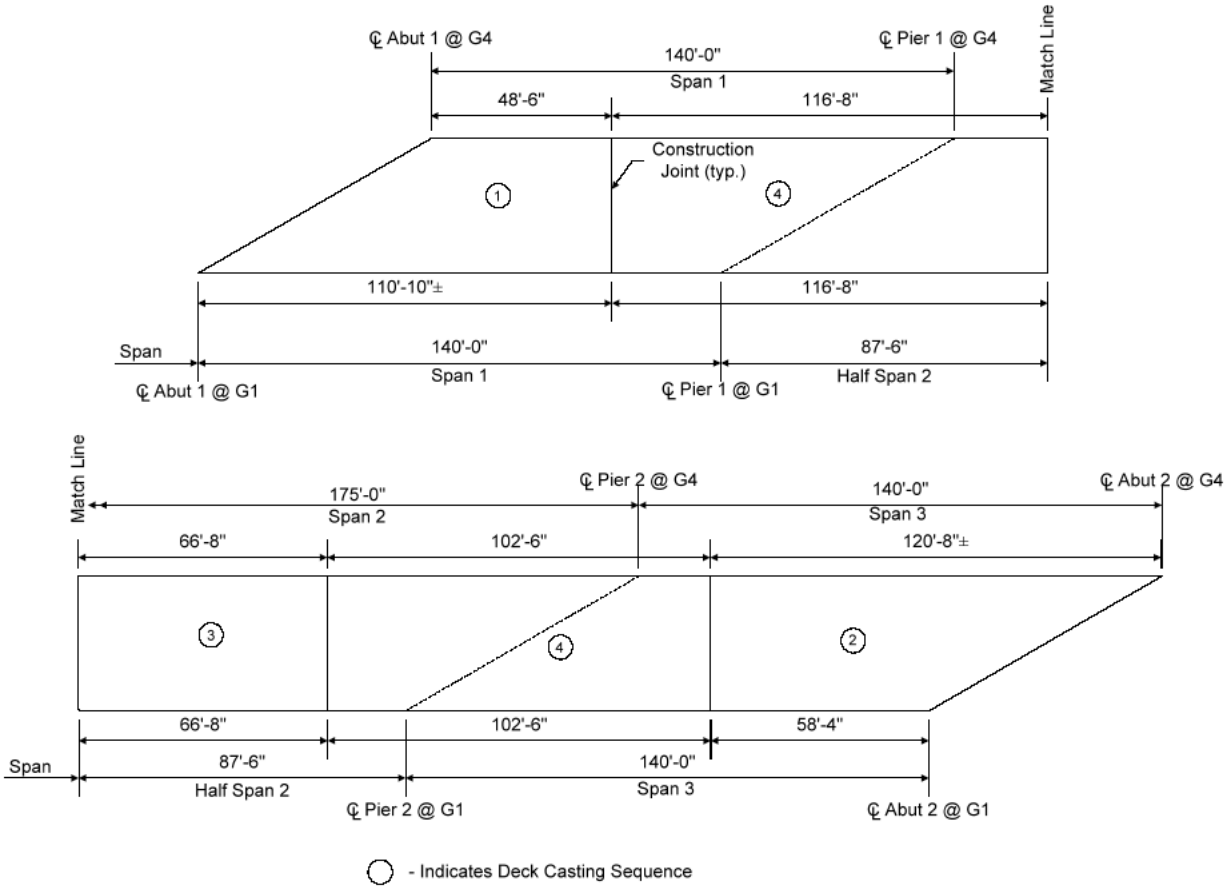

Figure 2.5. XICSS5, deck placement sequence.

2.1.1 Summary of Results

The following plots show the results obtained from the geometrically nonlinear 3D FEA, which represents the benchmark model, and from the approximate methods. The other curves illustrate the nature of the approximations by the simplified models. One can observe that the discrepancy between the simplified model predictions and the benchmark 3D FEA solutions is large at certain locations. Figures 2.6 and 2.7 illustrate the vertical displacements and girder layovers respectively. Figures 2.8 and 2.9 show total dead load girder major-axis bending and flange lateral bending stresses respectively. All the responses are shown at the total noncomposite dead load (TDL). The data used to generate the plots is available in electronic format.

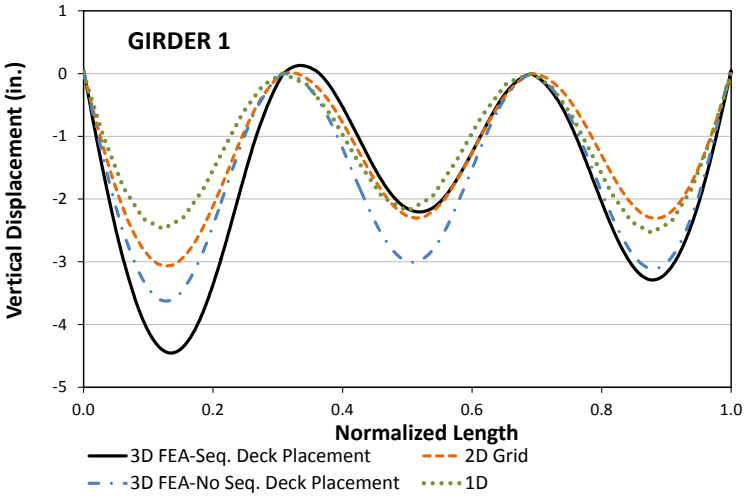

(i) Girder 1

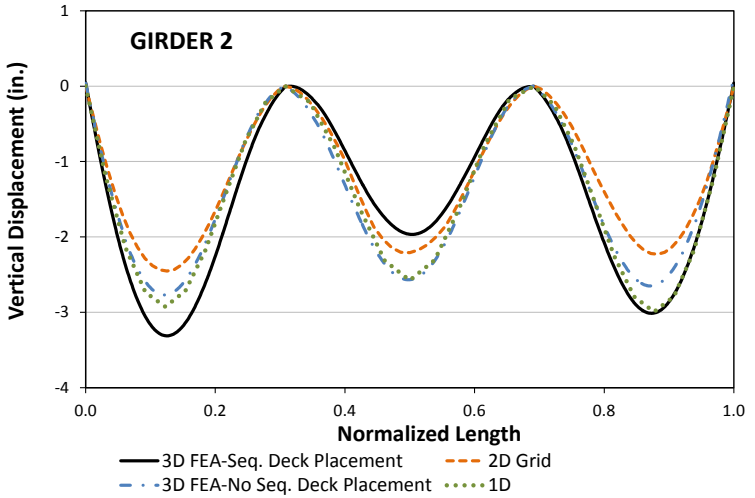

(ii) Girder 2

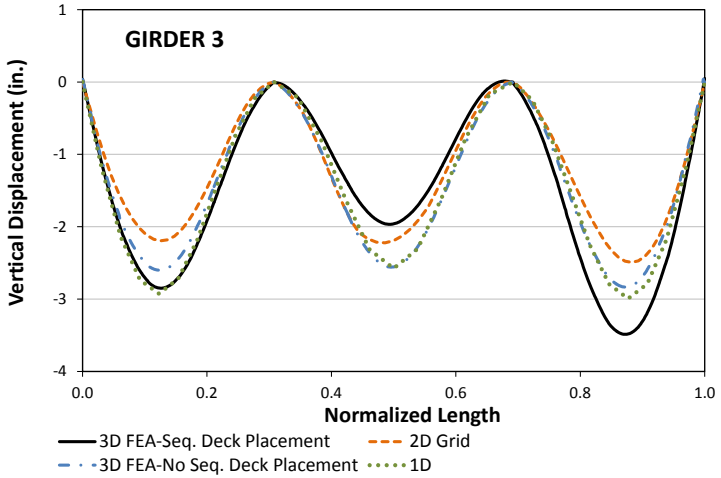

(iii) Girder 3

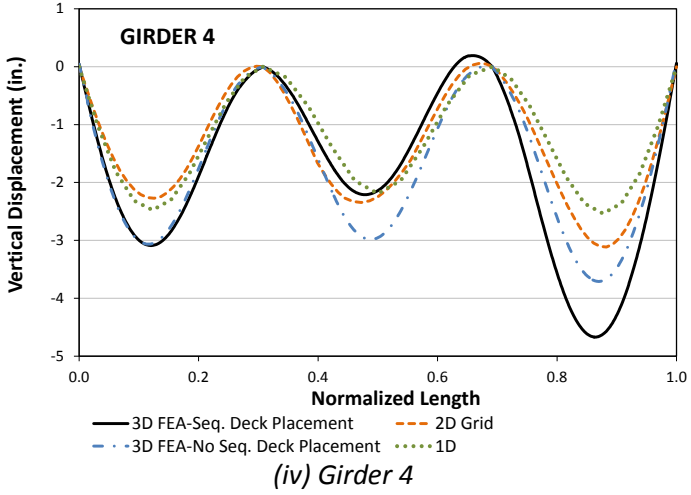

(iv) Girder 4

Figure 2.6. XICSS5, vertical displacements under nominal total dead load.

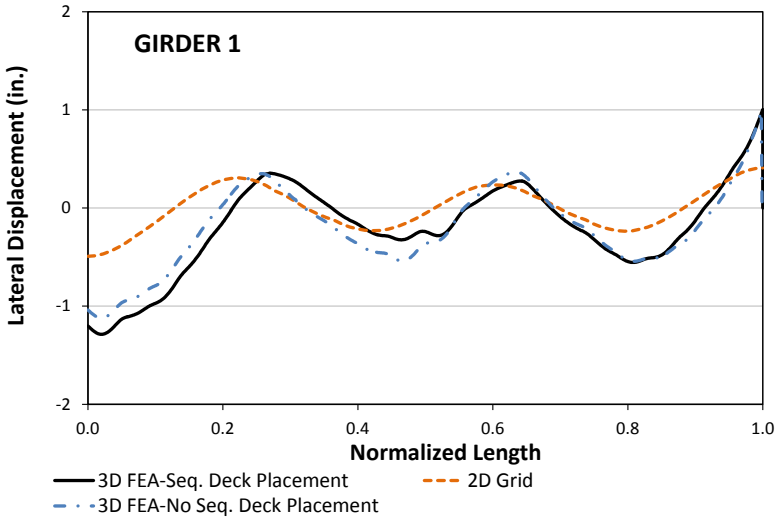

(i) Girder 1

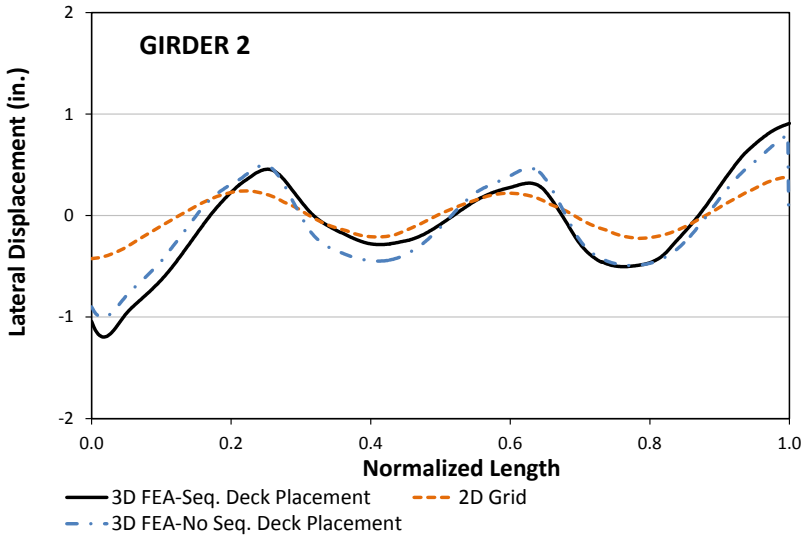

(ii) Girder 2

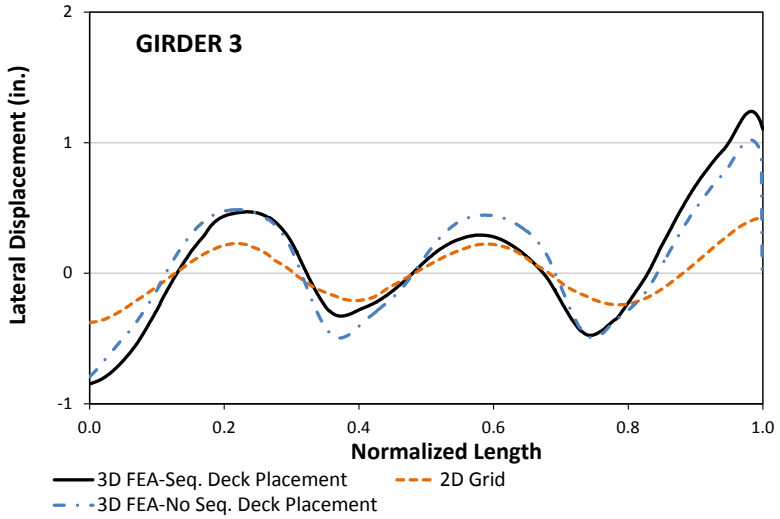

(iii) Girder 3

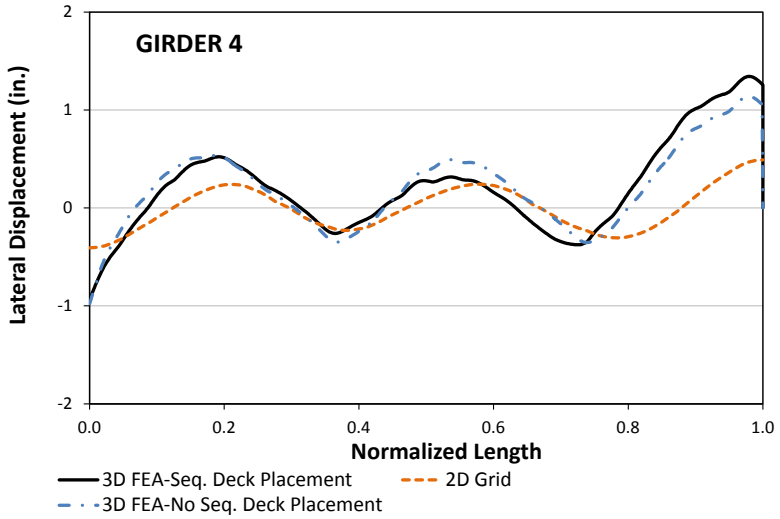

(iv) Girder 4

Figure 2.7. XICSS5, lateral displacements under nominal total dead load.

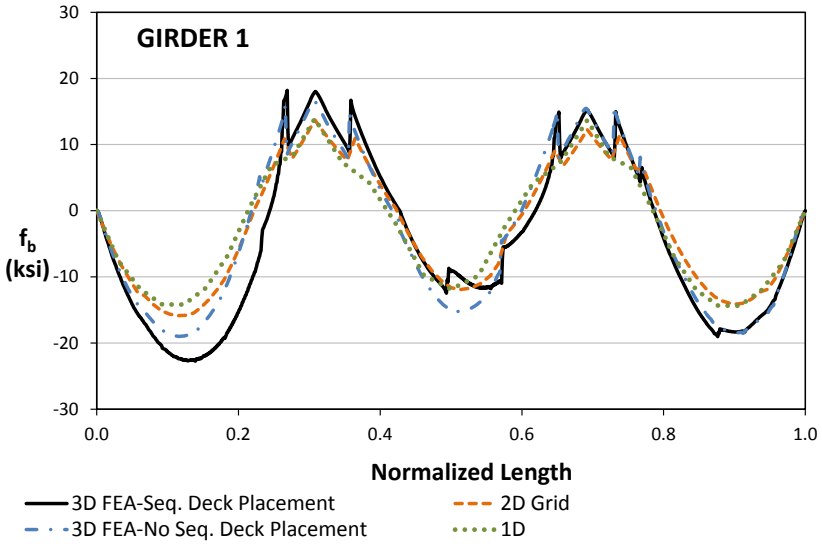

(i) Girder 1

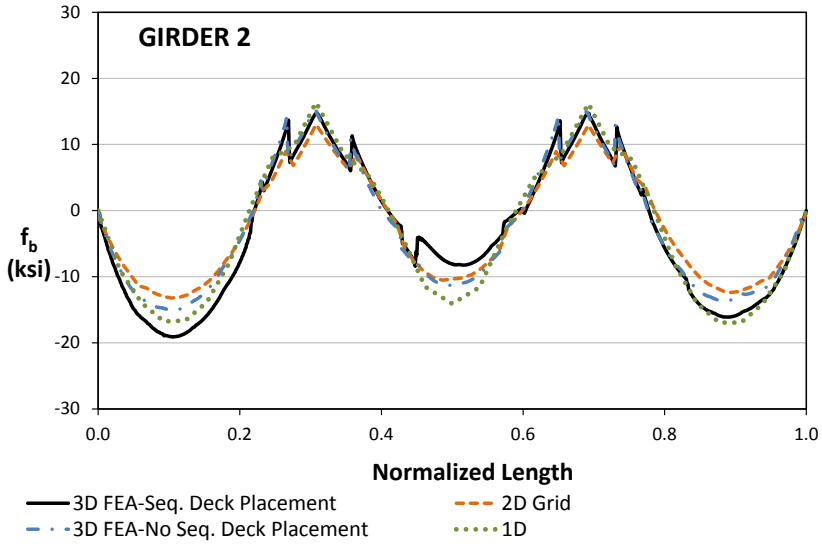

(ii) Girder 2

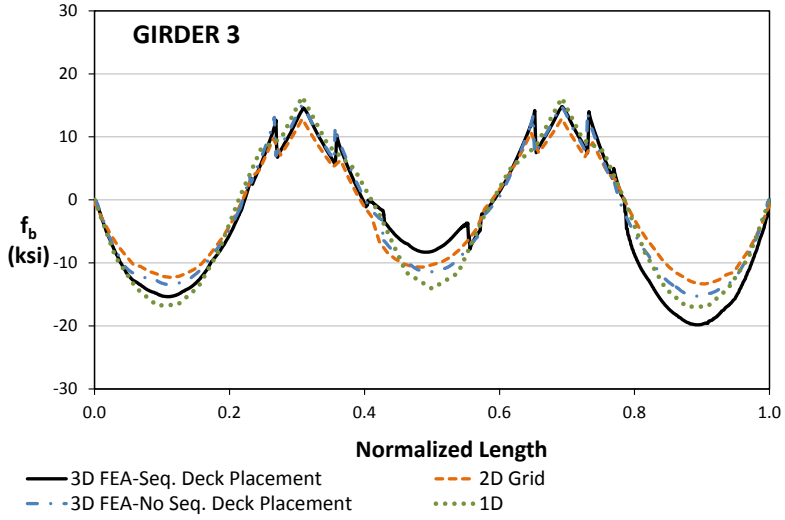

(iii) Girder 3

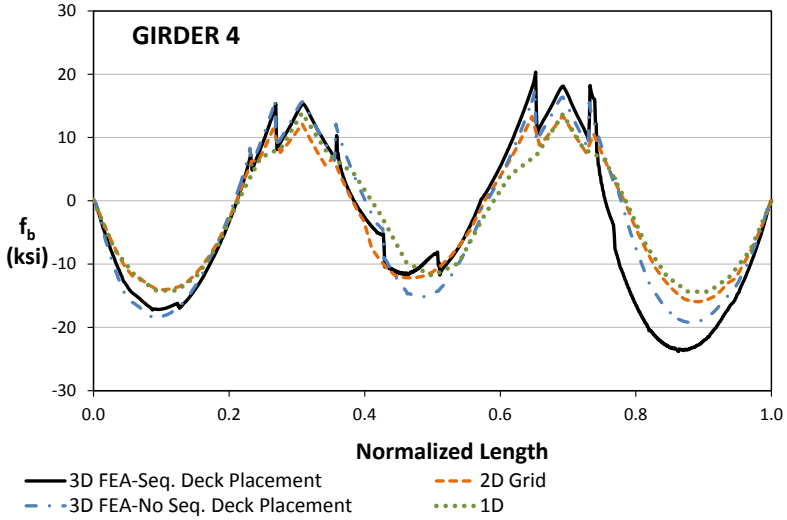

(iv) Girder 4

Figure 2.8. XICSS5, top flange major-axis bending stresses under nominal total dead load.

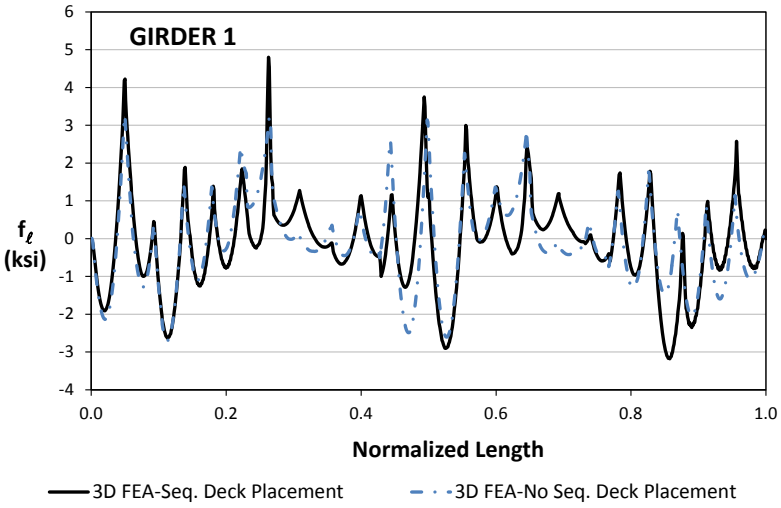

(i) Girder 1

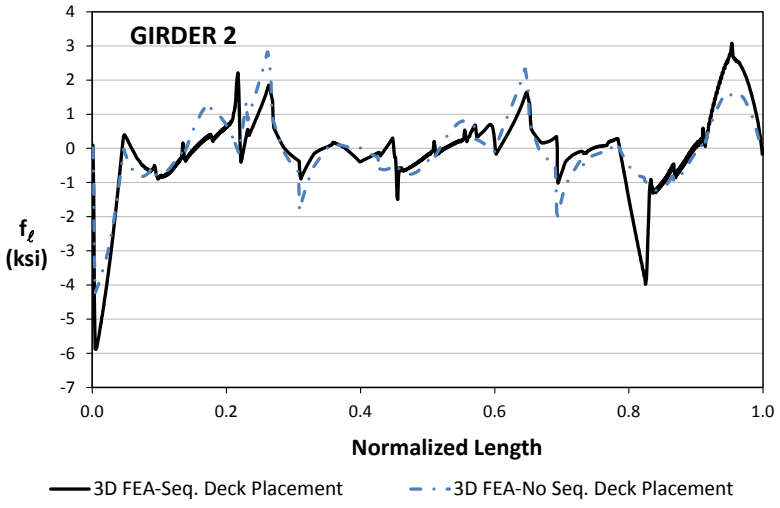

(ii) Girder 2

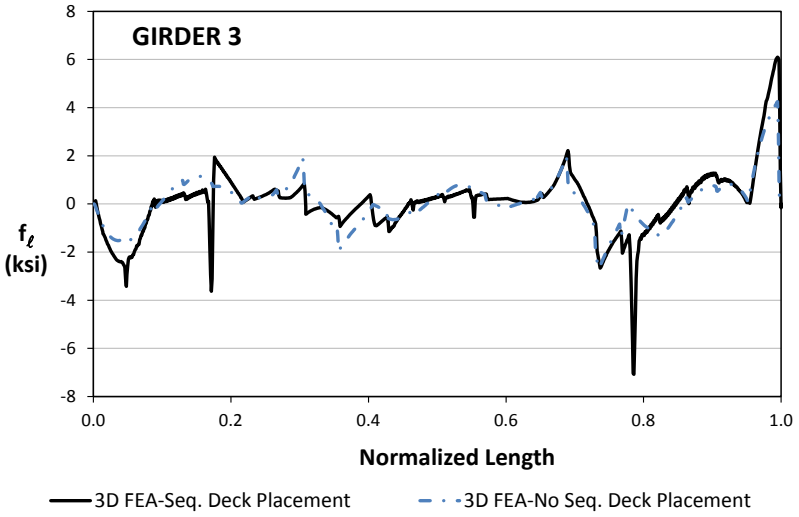

(iii) Girder 3

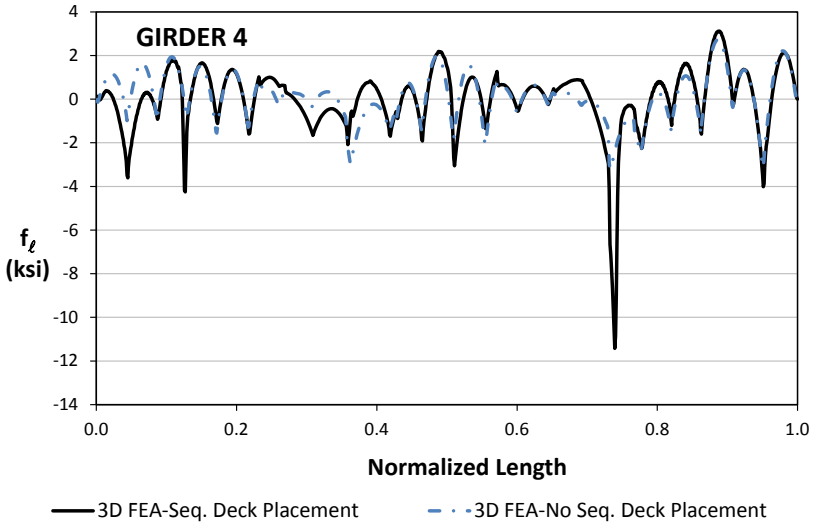

(iv) Girder 4

Figure 2.9. XICSS5, top flange minor-axis bending stresses under nominal total dead load.

2.2 Bridge XICCS7

This structure is an example bridge studied in “Load and Resistance Factored Design and Analysis of Skewed and Curved Steel Bridges” (FHWA-NHI, 2010a & 2010b). It is a three-span four-girder bridge with the interior supports skewed 60 degrees. The span lengths are 160 ft, 210 ft, and 160 ft. The radius of curvature is 700 ft, and the girders are spaced 11 ft apart. This structure is selected as a benchmark problem since it has a complex geometry that includes horizontal curvature and support skew. Figure 2.10 shows the plan view of the bridge. Figure 2.11 depicts the bridge cross-section with the slab information and the dimensions of the cross-frame elements. Figure 2.12 illustrates the girder elevations. The material properties and loading conditions are the same as in Bridge XISSS5.

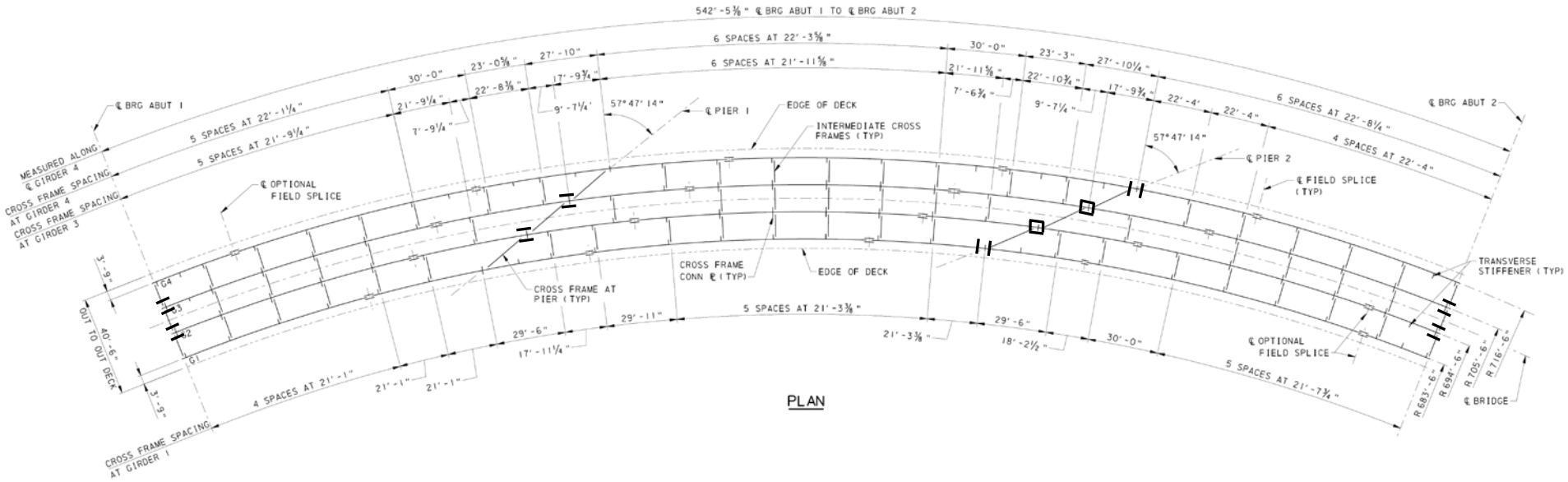

Figure 2.10. XICCS7, framing plan.

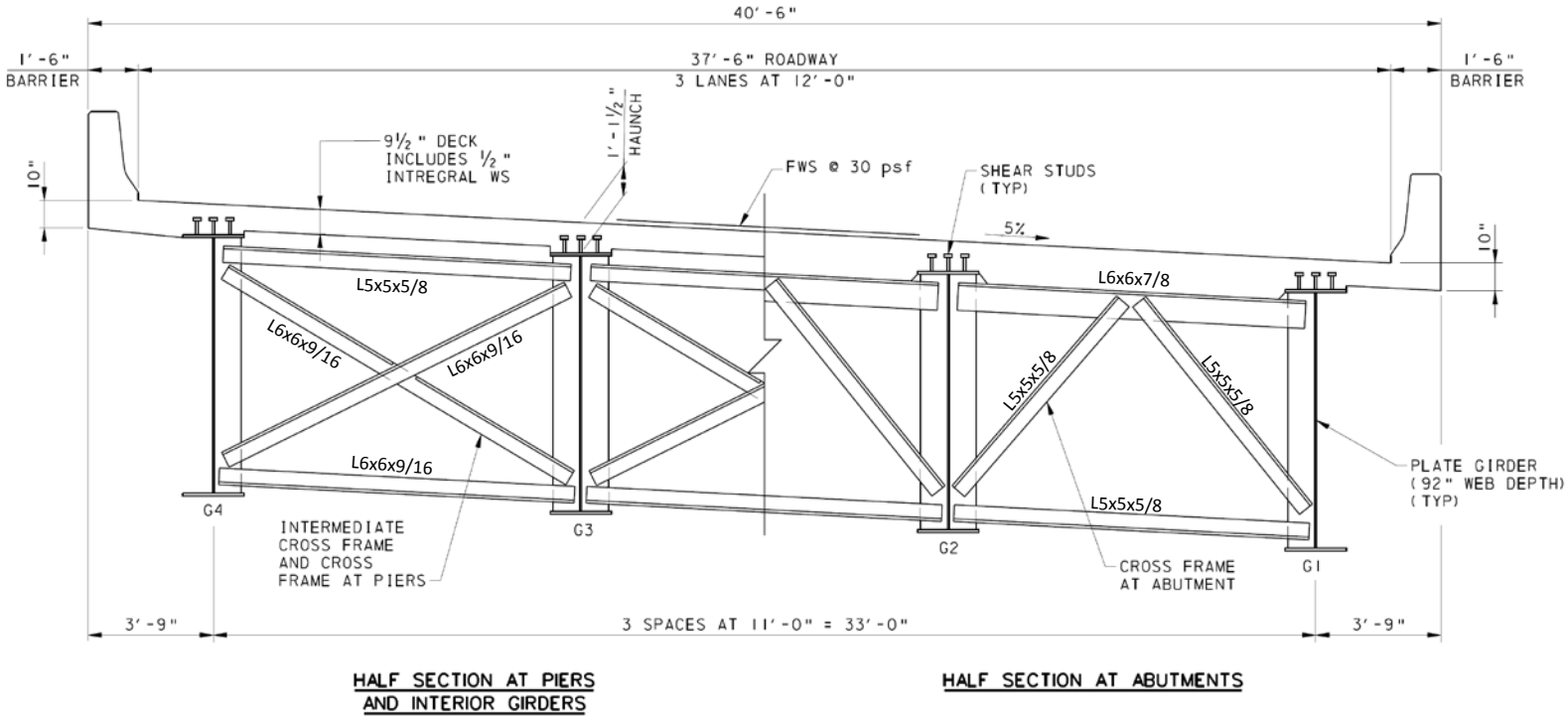

Figure 2.11. XICCS7, bridge cross-section.

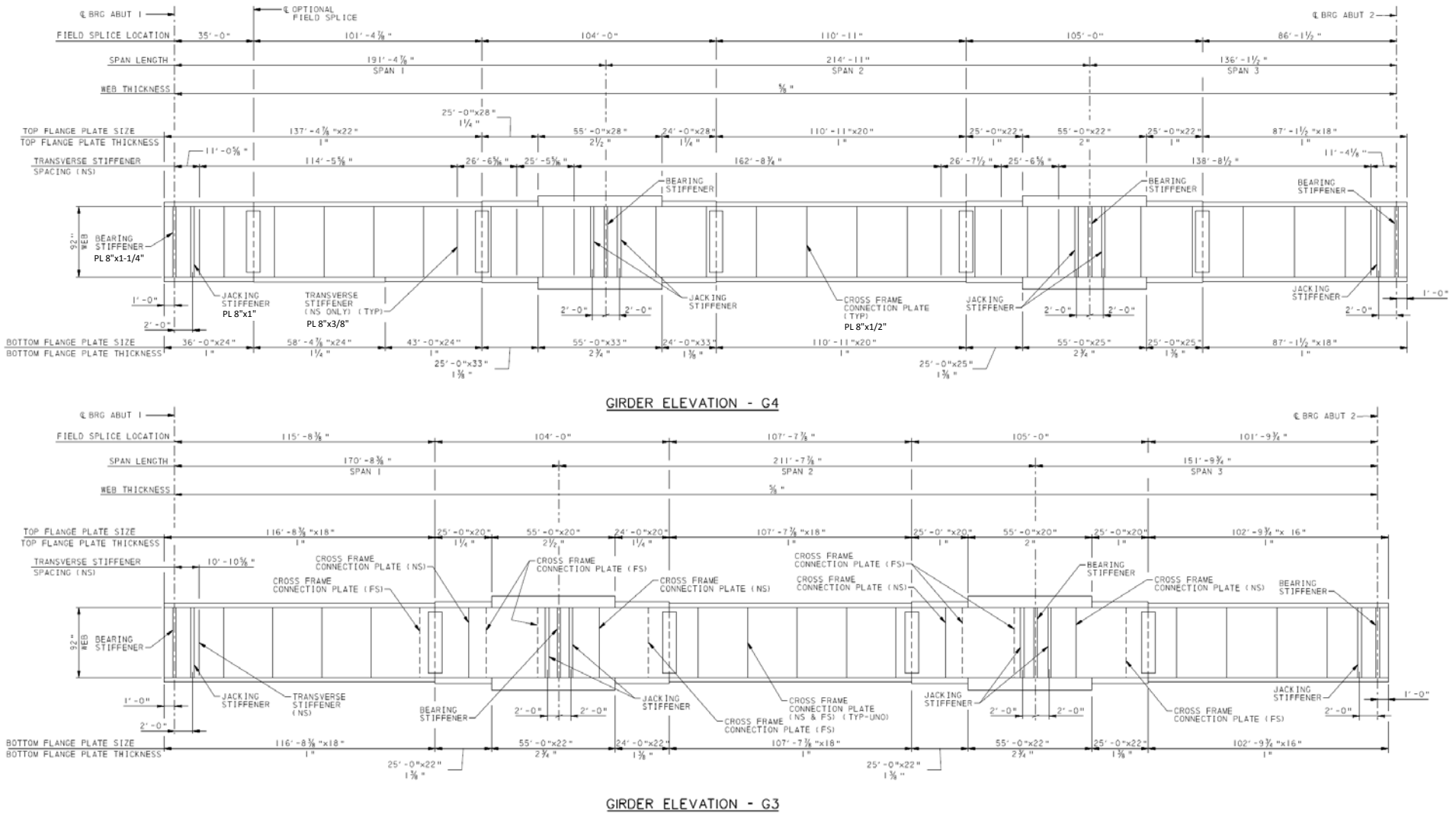

GIRDER ELEVATION - G4

GIRDER ELEVATION - G3

Figure 2.12. XICCS7, girder elevations.

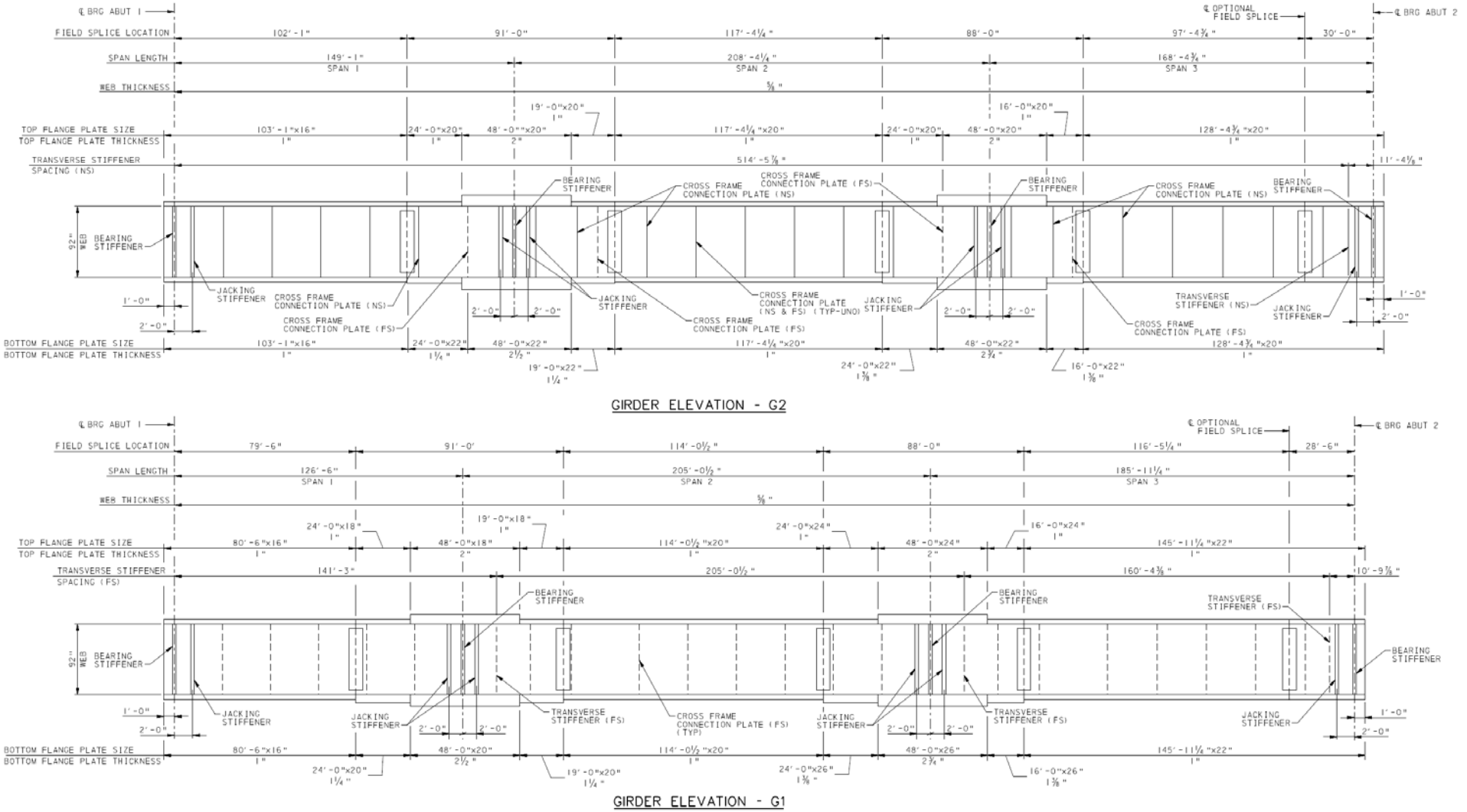

Figure 2.12. XICCS7, girder elevations (continued).

2.2.1 Summary of Results

The following plots show the results obtained from the nonlinear 3D FEA, which represents the benchmark model, as well as the characteristics of the approximations from the simplified methods. One can observe that the discrepancy between the simplified model predictions and the benchmark 3D FEA solutions is large at certain locations. Figures 2.13 and 2.14 illustrate the vertical displacements and girder layovers respectively. Figure 2.15 shows total dead load girder major-axis bending stresses. Similarly, Figure 2.16 shows the flange lateral bending stresses in the girders, predicted by the refined geometric nonlinear FEA. All the responses are shown at the total noncomposite dead load (TDL). The data used to generate the plots is available in electronic format.

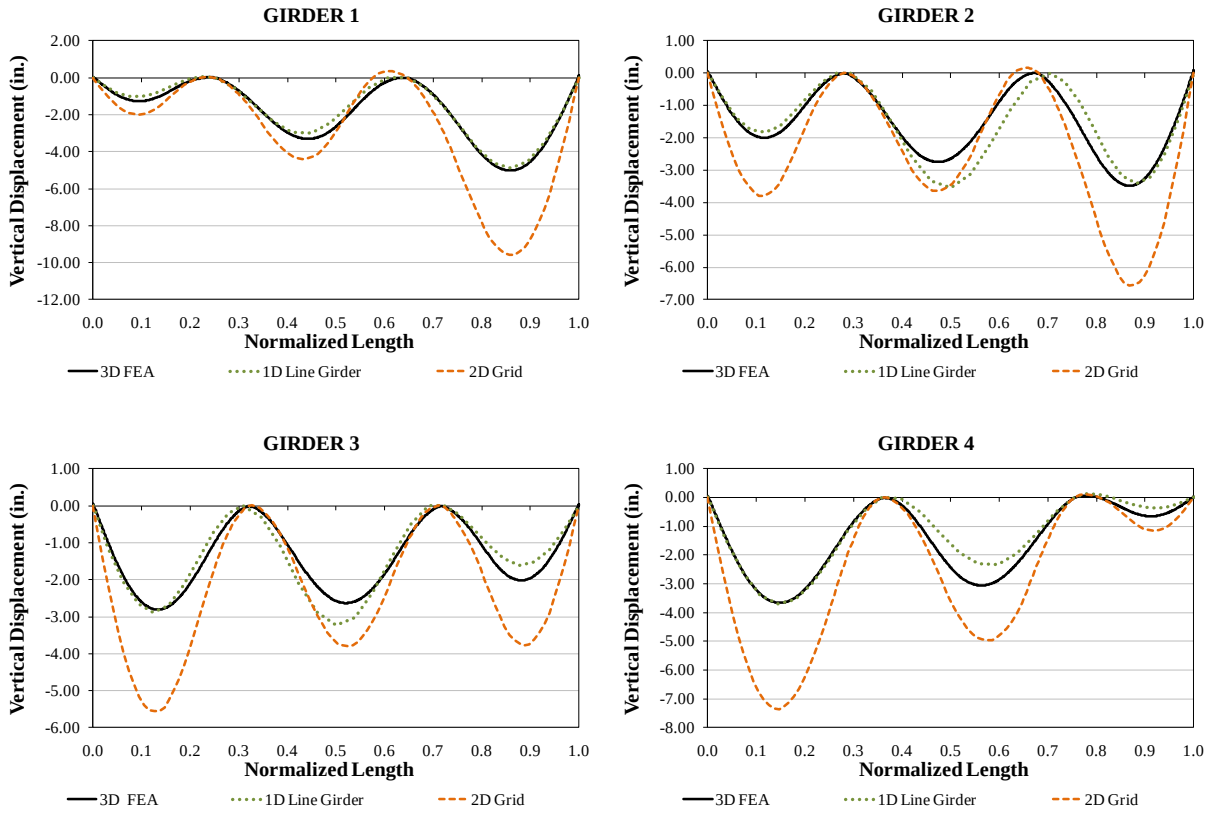

Figure 2.13. XICCS7, girder vertical displacements under total dead load.

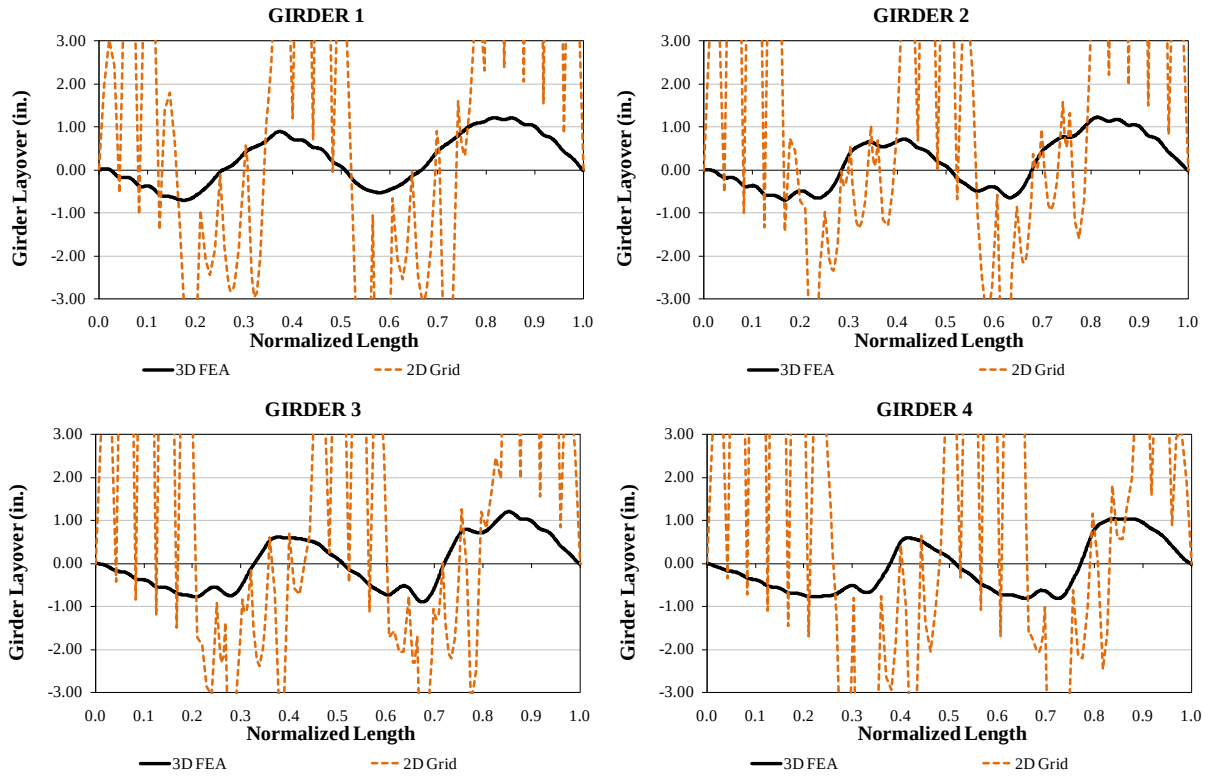

Figure 2.14. XICCS7, girder layovers under total dead load.

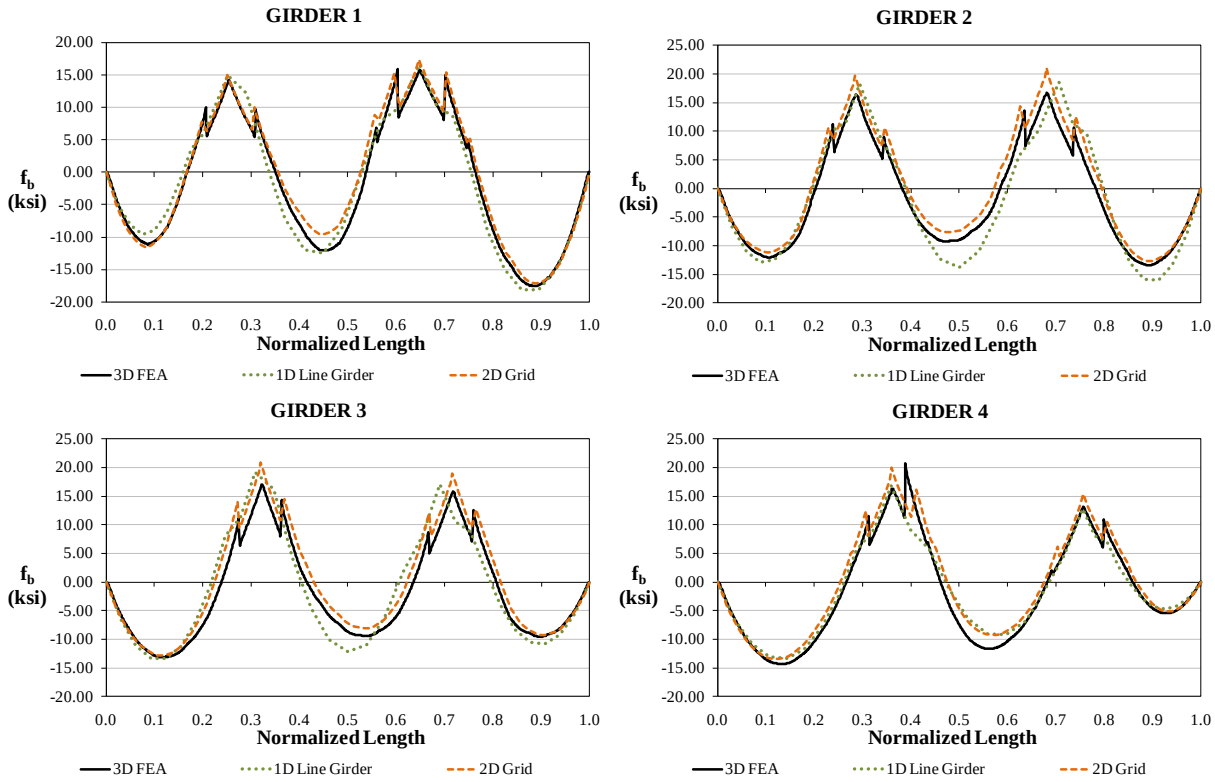

Figure 2.15. XICCS7, girder major-axis bending stresses under total dead load.

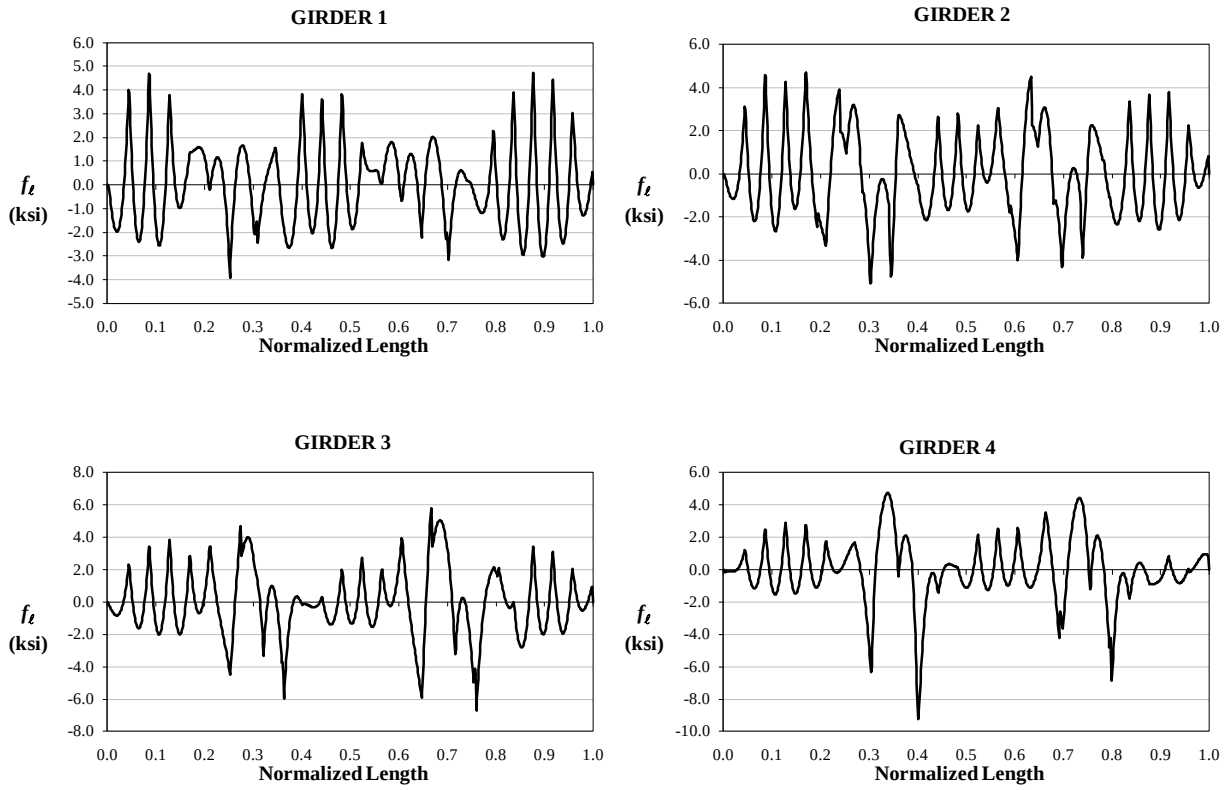

Figure 2.16. XICCS7, lateral bending stresses in the top flanges under total dead load.

3. Tub-Girder Bridges

3.1 Bridge XTCCR8

XTCCR8 is a three span continuous curved twin tub-girder bridge. It has spans of 160 ft, 210 ft and 160 ft measured along the centerline of the bridge and radius of 700 ft. Supports are radial with respect to the bridge centerline, the bridge deck is 40.5ft wide and 9.5 in thick. This structure is a design example studied in "AASHTO-LRFD Design Example Horizontally Curved Steel Box Girder Bridge" from the NCHRP Project 12-52 (Kulicki et al, 2005).

To illustrate the bridge geometry, Figure 3.1 shows the framing plan with span dimensions with respect to the centerline. In the plan view shown the girders are labeled from bottom to top as girder G1 to girder G2. Figure 3.2 illustrates the typical bridge cross-section. The assumed bearing restraints for 3D-FEA models are tabulated in Table 3.1, the original design uses twin-bearing configuration but it was modified to use single bearings since the double bearing configuration reported a torsional constraint that is not possible to accomplish in a real bridge.

The internal cross-frames are spaced at 16 ft for Spans 1 and 3 and 15 ft for Span 2, the cross-fames use an inverted-V configuration with cross-section area of 5 in^2 for chords and diagonals. The top flange lateral bracing system uses a Warren-type truss with constant panel size defined by the internal cross-frame spacing, the diagonals are WT9x48.5 and the struts are defined by the internal cross-frame top chords. Internal and external support diaphragms are solid plate diaphragms 1/2 in thick, the internal diaphragm has four vertical stiffeners of 5.5 in by 1/2 in and the external diaphragm has top and bottom flanges of 8 in by 1 in.

The tub-girder plate dimensions are illustrated in Figure 3.3 and plate lengths are tabulated in Table 3.2. The bottom flange is longitudinally stiffened by a WT8x28.5 at the negative moment regions (64 ft to the left and 45 ft to the right of Support 2 and similarly for Support 3), at these locations the bottom chord of the cross-frame was raised to prevent interference with the longitudinal stiffener. The webs are stiffened transversally by 5.5 in by 1/2 in plates that serve as the internal cross-frame connection plates.

The weight of the formwork (10 psf), and the slab reinforcing steel plus the wet concrete (150 psf) is applied to the top flanges as uniformly distributed line loads based on the tributary width of each girder across the cross-section of the bridge. In addition, the overhang brackets used for resisting the weight of wet concrete and formwork at the fascia webs are considered. In the model, the steel properties are E_s = 29000 ksi and F_y = 50 ksi. Similarly, the concrete properties are E_c = 3600 ksi and f''_c = 4 ksi.

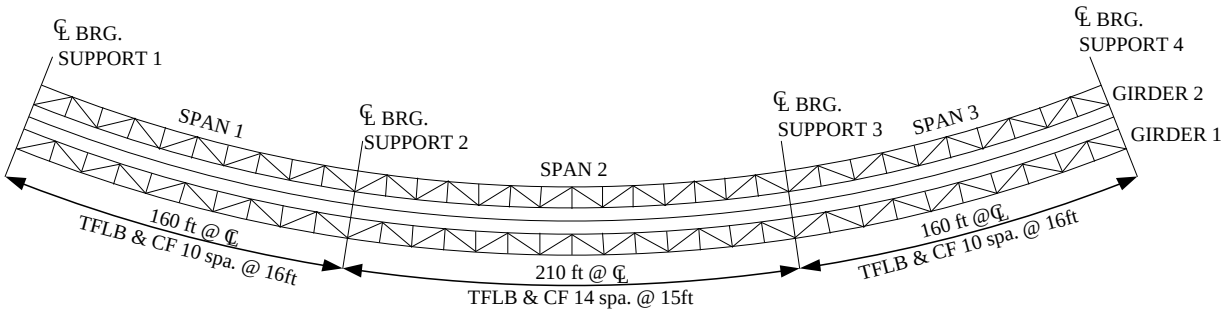

Figure 3.1. XTCCR8, framing plan and general dimensions.

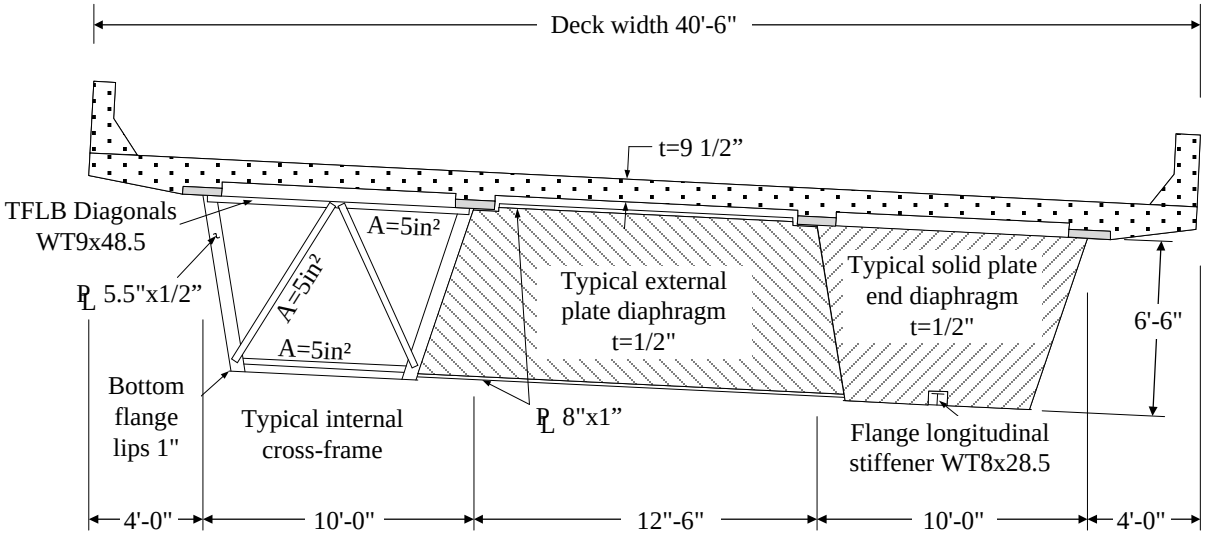

Figure 3.2. XTCCR8 cross-section.

Table 3.1. XTCCR8, assumed bearing restraints in 3D FEA models.

Girder #	Support 1	Support 2	Support 3	Support 4
1	Fixed single support at center of bottom flange	Free single support at center of bottom flange	Free single support at center of bottom flange	Single support at center of bottom flange Guided Longitudinally
2	Free single support at center of bottom flange	Free single support at center of bottom flange	Free single support at center of bottom flange	Free single support at center of bottom flange

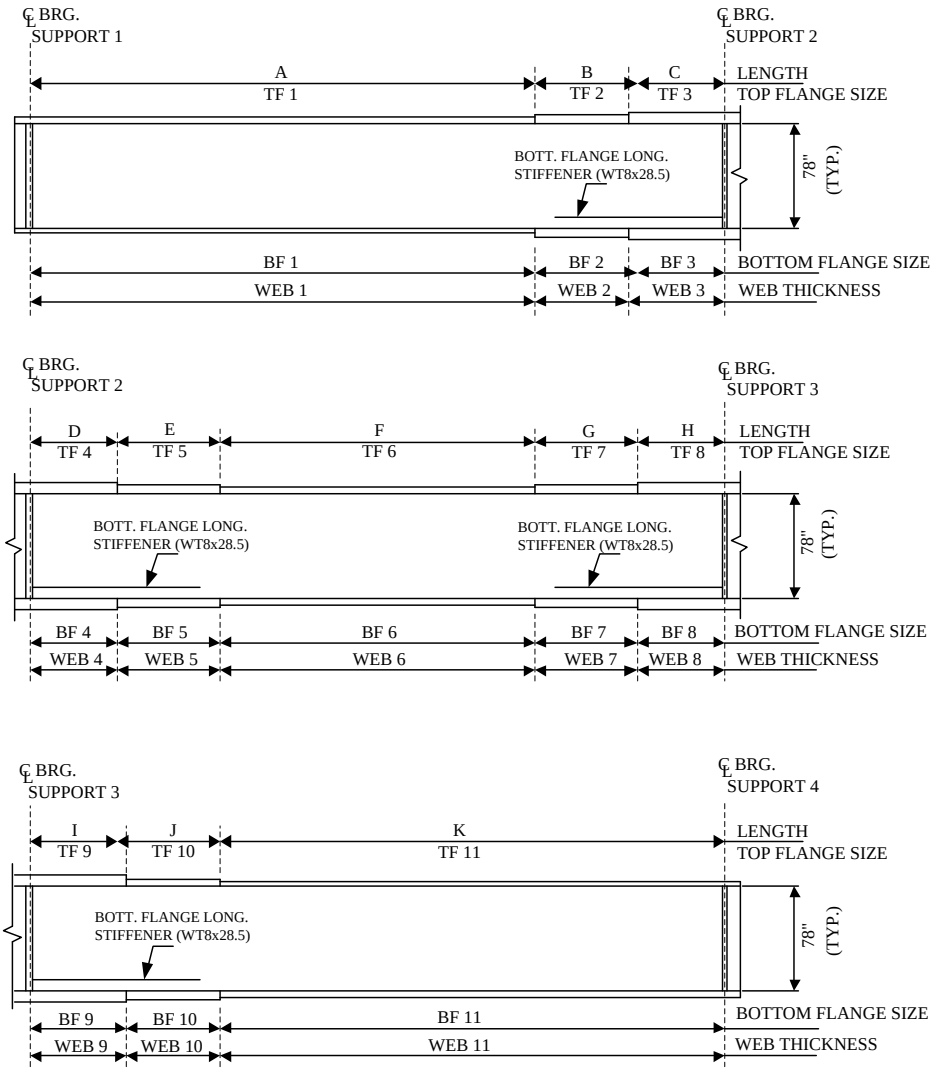

Figure 3.3. XTCCR8 plate dimensions.

Table 3.2. XTCCR8 plate dimensions.

Length @ Bridge CL		Top Flange	Girder 1		Girder 2		Bottom Flange	Girder 1		Girder 2	
Section	Dim (ft)		b_f (in)	t_f (in)	b_f (in)	t_f (in)		b_f (in)	t_f (in)	b_f (in)	t_f (in)
A	120	TF1	16	1	16	1	BF1	83	0.625	83	0.625
B	24	TF2	18	1.5	18	1.5	BF2	83	1	83	1
C	16	TF3	18	3	18	3	BF3	83	1.5	83	1.5
D	15	TF4	18	3	18	3	BF4	83	1.5	83	1.5
E	30	TF5	18	1.5	18	1.5	BF5	83	1	83	1
F	120	TF6	16	1	16	1	BF6	83	0.75	83	0.75
G	30	TF7	18	1.5	18	1.5	BF7	83	1	83	1
H	15	TF8	18	3	18	3	BF8	83	1.5	83	1.5
I	16	TF9	18	3	18	3	BF9	83	1.5	83	1.5
J	24	TF10	18	1.5	18	1.5	BF10	83	1	83	1
K	120	TF11	16	1	16	1	BF11	83	0.625	83	0.625

3.1.1 Summary of Results

The following plots show the results obtained from the geometric nonlinear 3D FEA, which represents the benchmark model, and from the simplified methods. One can observe that the discrepancy between the simplified model predictions and the benchmark 3D FEA solutions is large at certain locations. All the responses are shown at the total noncomposite dead load (TDL). The data used to generate the plots is available in electronic format.

The following figures show the results for the vertical displacements (Figure 3.4), the top flange and bottom flange relative lateral displacements (Figure 3.5), top flange major axis bending stresses (Figure 3.6), top flange lateral bending stresses (Figure 3.7), top flange lateral bracing diagonals axial forces (Figure 3.8), internal cross-frame top chord axial forces (Figure 3.9) and internal cross-frame diagonal axial forces (Figure 3.10).

Results for vertical displacements and major axis stresses are reported for the 3D FEA, 2D Grid and 1D Line Girder methods. The other results are reported only for the 3D FEA and 2D Grid methods.

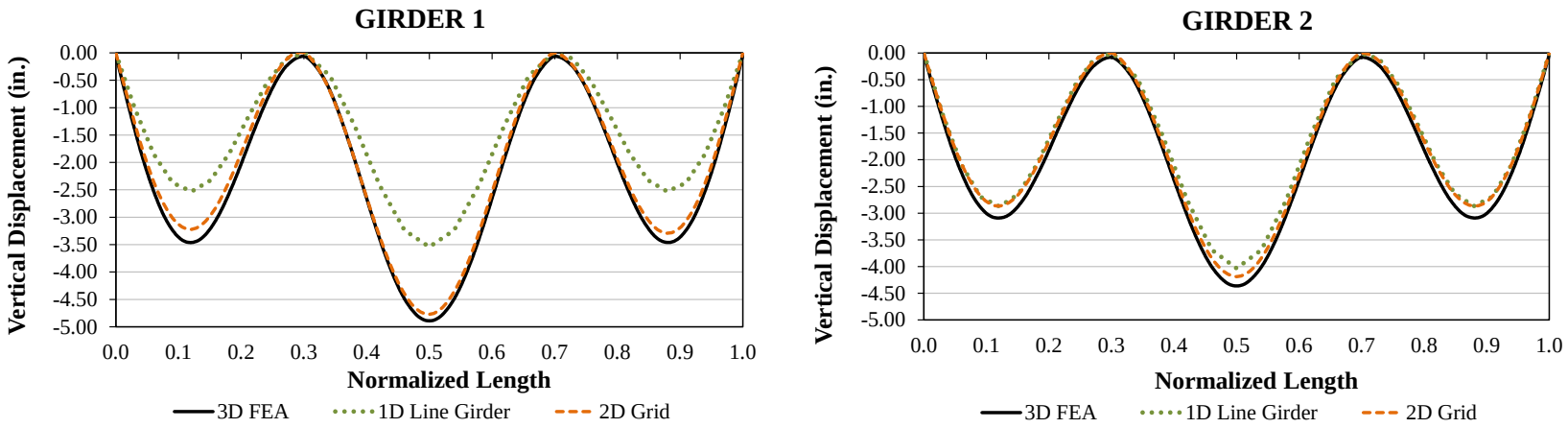

Figure 3.4. XTCCR8, vertical displacements under nominal total dead load.

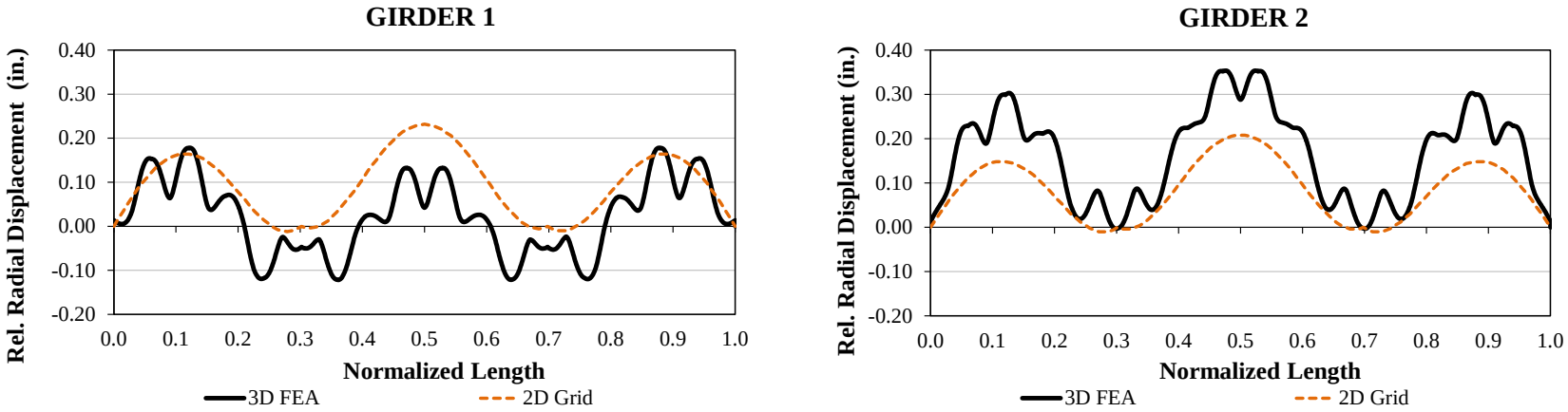

Figure 3.5. XTCCR8, lateral displacements under nominal total dead load.

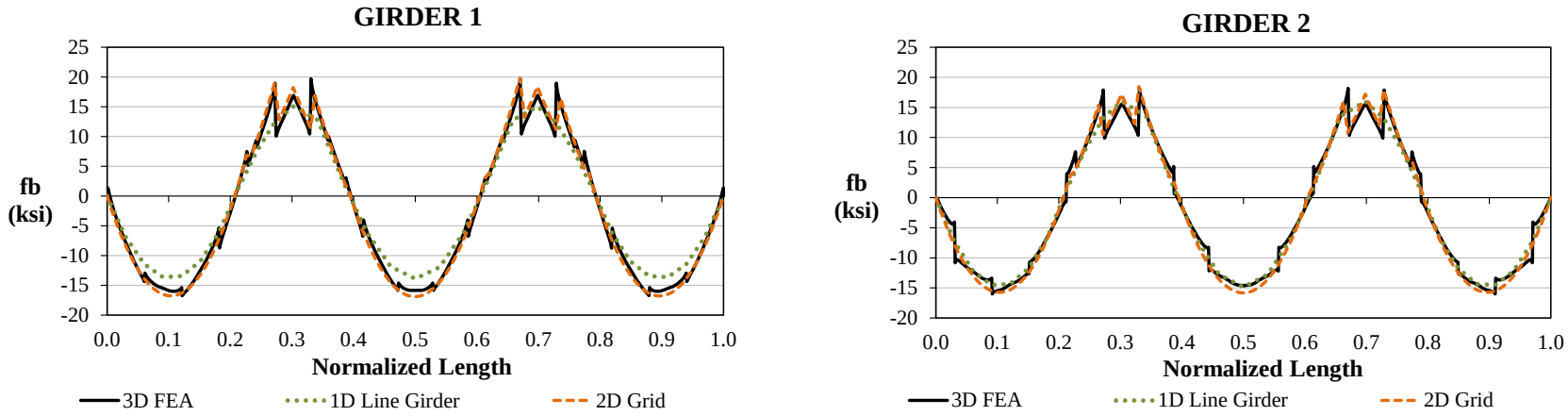

Figure 3.6. XTCCR8, top flange major-axis bending stresses under nominal total dead load.

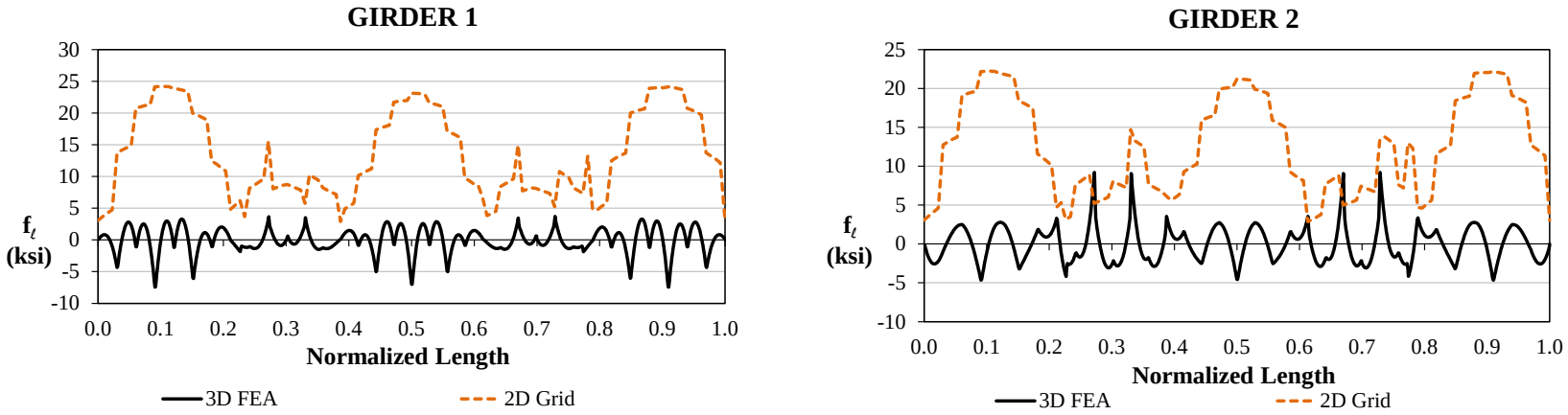

Figure 3.7. XTCCR8, top flange minor-axis bending stresses under nominal total dead load.

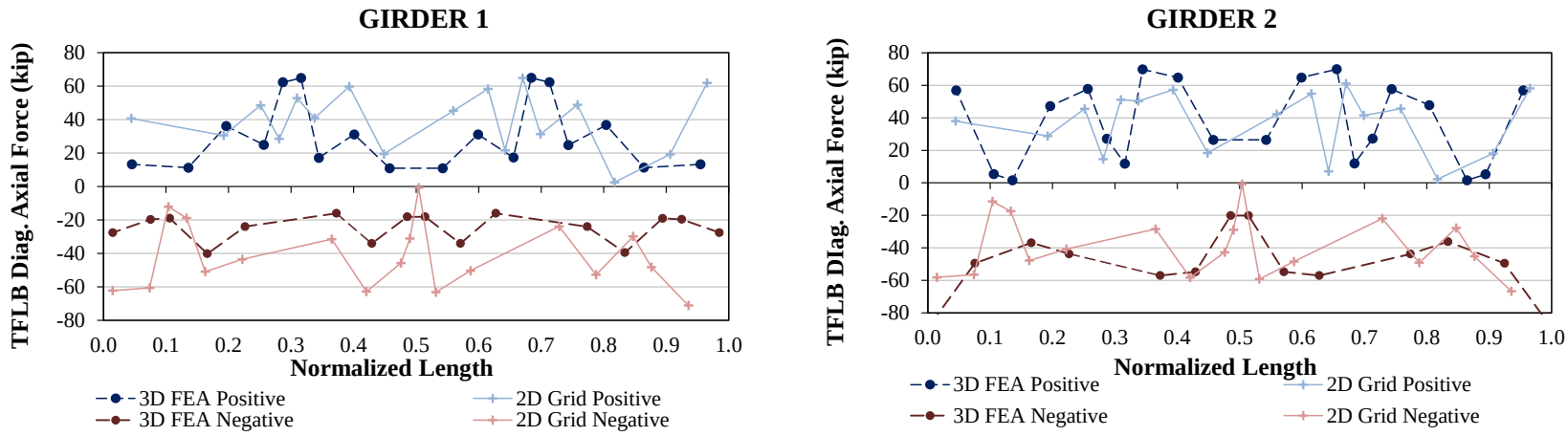

Figure 3.8. XTCCR8, top flange lateral bracing diagonals axial forces under nominal total dead load.

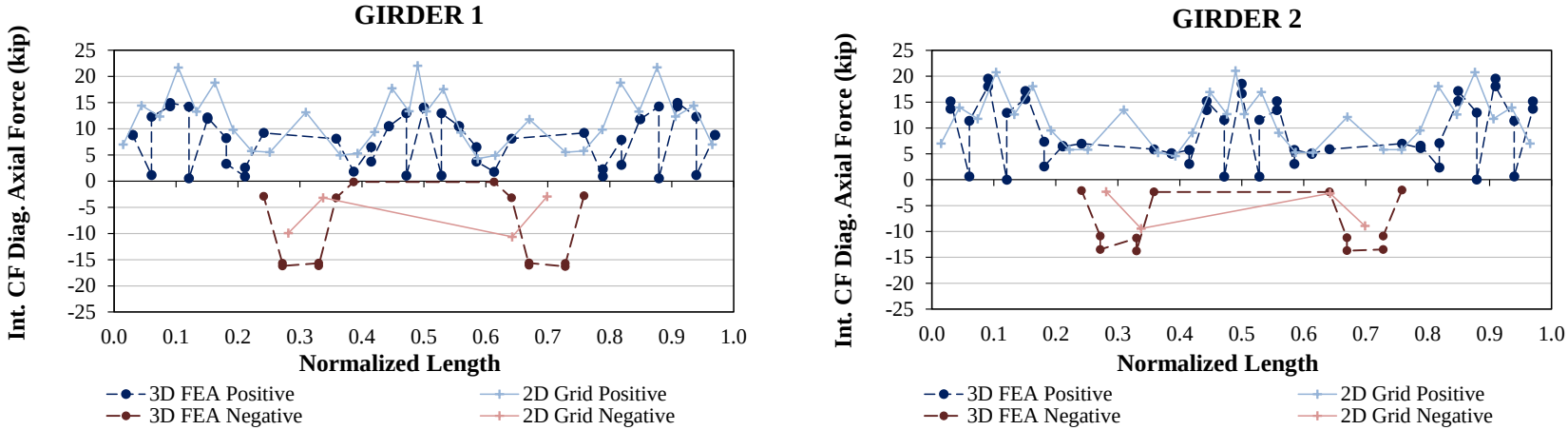

Figure 3.9. XTCCR8, internal cross-frame top chords axial forces under nominal total dead load.

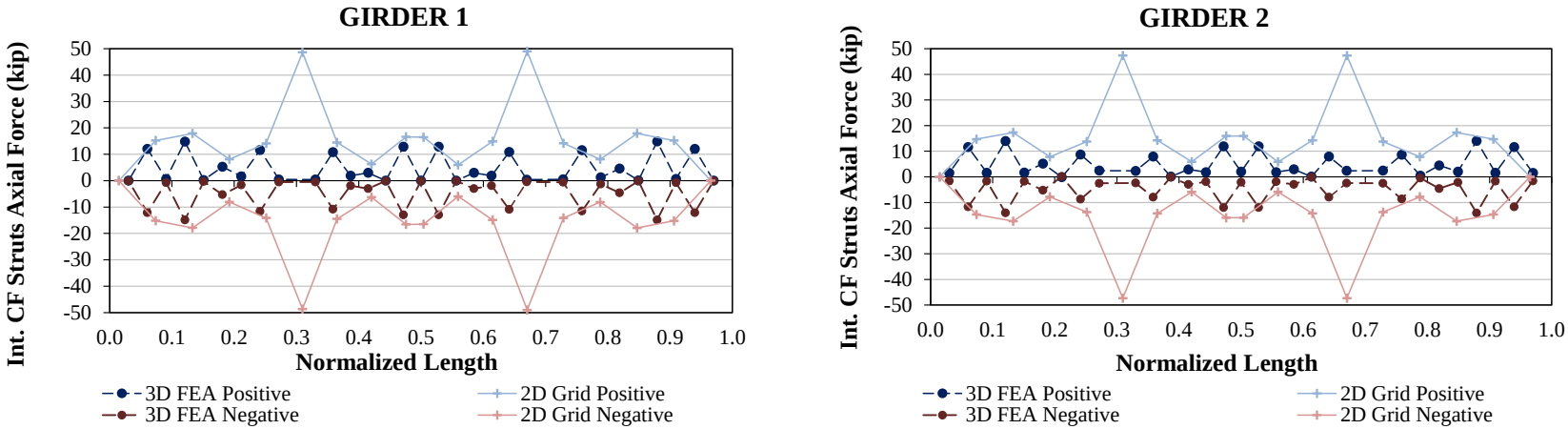

Figure 3.10. XTCCR8, internal cross-frame diagonals axial forces under nominal total dead load.

4. References

Kulicki, J. M., Wassef, W. G., Smith, C., Johns, K. (2005) "AASHTO-LRFD Design Example Horizontally Curved Steel Box Girder Bridge," NCHRP Project No. NCHRP 12-52, National Cooperative Highway Research Program, Transportation Research Board, National Research Council, 148 pp.

NHI/FHWA (2007). "Load and Resistance Factor Design (LRFD) for Highway Bridge Superstructures", Design Manual, NHI Course No. 130081, 130081A-130081D, Publication No. FHWA-NHI-07-035, National Highway Institute, Federal Highway Administration, 1982 pp.

NHI/FHWA (2011a). "Load and Resistance Factored Design and Analysis of Skewed and Curved Steel Bridges," Design Manual, NHI Course No. 130095, Publication No. FHWA-NHI-10-087, National Highway Institute, Federal Highway Administration, 1476 pp.

NHI/FHWA (2011b). "Load and Resistance Factored Design and Analysis of Skewed and Curved Steel Bridges," Participant Workbook, NHI Course No. 130095, Publication No. FHWA-NHI-10-086, National Highway Institute, Federal Highway

Appendix E. Executive Summary of Study Bridges

This appendix provides an executive summary of the bridges that are studied in the NCHRP 12-79 research. The bridges are presented in alphabetical and numerical order within the following bridge categories:

(1) ICSN: I-girder, Continuous-span, Straight, No-skew,
(2) ISSS: I-girder, Simple-span, Straight, Skewed supports,
(3) ICSS: I-girder, Continuous-span, Straight, Skewed supports,
(4) ISCR: I-girder, Simple-span, Curved, Radial supports,
(5) ICCR: I-girder, Continuous-span, Curved, Radial supports,
(6) ISCS: I-girder, Simple-span, Curved, Skewed supports,
(7) ICCS: I-girder, Continuous-span, Curved, Skewed supports,
(8) TCSN: Tub-girder, Continuous-span, Straight, No-skew,
(9) TSSS: Tub-girder, Simple-span, Straight, Skewed supports,
(10) TSCR: Tub-girder, Simple-span, Curved, Radial supports,
(11) TCCR: Tub-girder, Continuous-span, Curved, Radial supports,
(12) TSCS: Tub-girder, Simple-span, Curved, Skewed supports,
(13) TCCS: Tub-girder, Continuous-span, Curved, Skewed supports.

The basic geometry information, key indices, and a summary of important observations are provided for each bridge. For the Existing bridges (indicated by an “E” in front of the above designations), the location information and key information about the physical structure are listed. For the eXample bridges, designated by an “X” in front of the above designations, the reference citation for the example calculations is provided.

(E1) ICSN (I-girder, Continuous-span, Straight, No skew)

E1.1 XICSN1 (L_1 = 140 ft, L_2 = 175 ft, L_3 = 140 ft / w = 43 ft, 4 girders)

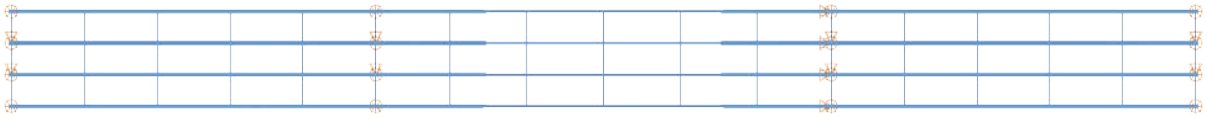

- Reference: (Eaton, et al. 1997).
- I_{S1} = 0, I_{S2} = 0, I_{S3} = 0 / I_{L1} = 1.0, I_{L2} = 1.0, I_{L3} = 1.0 / I_{T1} = 0.5, I_{T2} = 0.5, I_{T3} = 0.5
- Differences in the fascia and interior girder responses due to different applied loadings.

(E2) ISSS (I-girder, Simple-span, Straight, Skewed supports)

E2.1 EISSS3 (L_1 = 133 ft / w = 30.1 ft / θ_1 = -46.2°, θ_2 = -46.2° / 4 girders)

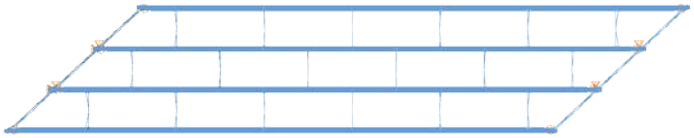

- Bridge on SR 1003 (Chicken Road) over US 74 between SR 1155 & SR 1161, Robeson Co., NC
- Undesirable girder layover and bowing of the girder webs occurred during construction.
- I_{S1} = 0.24, I_{L1} = 1.0, I_{T1} = 0.50
- Significant second-order amplification due to the absence of the top chord in the interior V-type cross-frames.
- Neither the 1D line girder nor the 2D-grid analysis captures the second-order amplification.
- Failure due to lateral torsional buckling of the interior girder occurs at 1.2 times the total dead load (TDL).

E2.2 EISSS5 (L_1 = 123 ft / w = 43.8 ft /θ_1 = -59.7°, θ_2 = -59.7° / 5 girders)

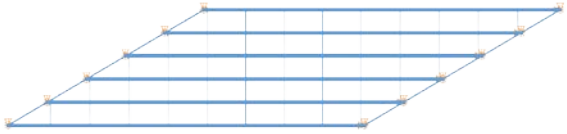

- SR 0581 Section A01, Cumberland Co., PA
- One unit of a phased construction project. Difficulty was encountered with the concrete cover during the deck replacement.
- I_{S1} = 0.54, I_{L1} = 1.0, I_{T1} = 0.50
- The approximate analysis methods accurately capture the responses of the bridge during the steel erection.
- At the total dead load (TDL) level, the bridge experiences second-order amplification that is not captured by the 1D and 2D models. This nonlinear behavior is associated with the limited bracing provided by the V-type cross-frame without top chords.

E2.3 EISSS6 (L_1 = 267 ft / w = 58 ft /θ_1 = -62.3°, θ_2 = -62.3°, 8 girders)

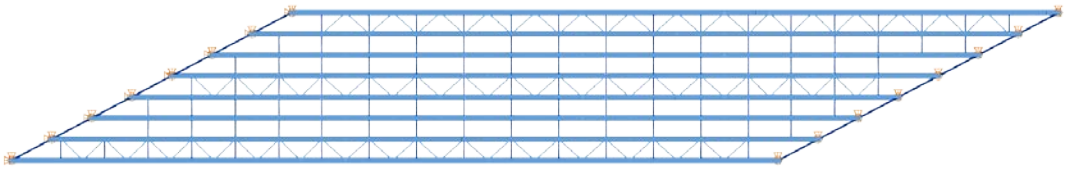

- I-87 / I-287, Westchester Co., NY
- Successful implementation of TDLF detailing. The steel dead load deflections were used to alleviate fit-up problems during the steel erection.
- I_{S1} = 0.43, I_{L1} = 1.0, I_{T1} = 0.50
- Importance of erection sequence for the methods of detailing.
- Estimation of the required layovers during construction.
- Influence of methods of detailing on girder responses and cross-frame forces.

E2.4 NISSS2 (L_1 = 150 ft / w = 30 ft /θ_1 = 35°, θ_2 = 35°, 4 girders)

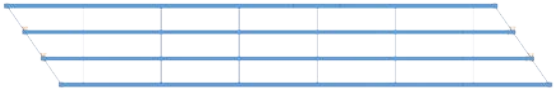

- I_{S1} = 0.11, I_{L1} = 1.0, I_{T1} = 0.50
- The influence of the skew is minor on the behavior of this structure (I_S < 0.30). The girder responses are accurately predicted by1D line girder and the 2D-grid analyses for the different erection stages.
- Minor variation in the flange lateral bending stresses between cross-frames due to second-order effects.

E2.5 NISSS4 (L_1 = 150 ft / w = 30 ft /θ_1 = 70°, θ_2 = 70°, 4 girders)

- I_{S1} = 0.44, I_{L1} = 1.0, I_{T1} = 0.50
- Slight variation in the vertical displacement and girder major-axis bending stress predictions of by1D line girder and the 2D-grid analyses, since I_S is approaching 0.65.
- Significant flange lateral bending due to small offset distance of the first intermediate cross-frame from the skewed bearing

E2.6 NISSS6 (L_1 = 150 ft / w = 30 ft /θ_1 = 50°, θ_2 = 0° / 4 girders)

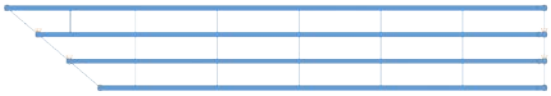

- I_{S1} = 0.19, I_{L1} = 1.21, I_{T1} = 0.53
- The influence of the skew is minor on the behavior of this structure. The girder responses are accurately predicted by the approximate methods for the different erection stages.

E2.7 NISSS11 (L_1 = 150 ft / w = 80 ft /θ_1 = 20°, θ_2 = 20° / 9 girders)

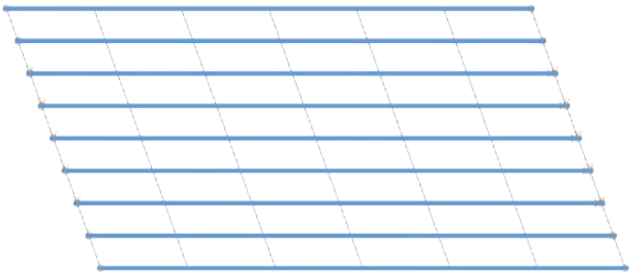

- I_{S1} = 0.18, I_{L1} = 1.0, I_{T1} = 0.50
- Due to the relatively simple geometry of this bridge, its behavior is accurately captured by the approximate methods of analysis.
- The use of inclined cross-frames helps reduce the flange lateral bending stresses to a negligible level.

E2.8 NISSS13 (L_1 = 150 ft / w = 80 ft /θ_1 = 50°, θ_2 = 50°, 9 girders)

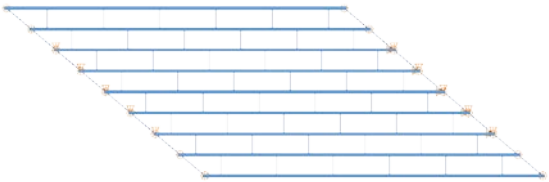

- I_{S1} = 0.60, I_{L1} = 1.0, I_{T1} = 0.50
- Girder responses are accurately predicted by the approximate methods.

E2.9 NISSS14 (L_1 = 150 ft / w = 80 ft /θ_1 = 70°, θ_2 = 70° / 9 girders)

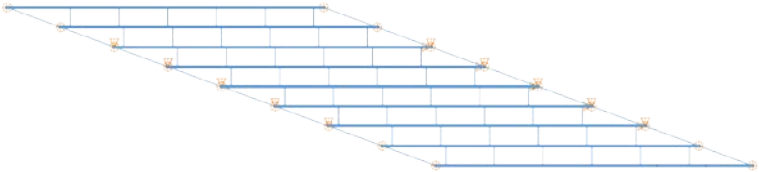

- I_{S1} = 1.36, I_{L1} = 1.0, I_{T1} = 0.50
- The skew effects are particularly important in this bridge. Very large cross-frame forces and levels of flange lateral bending stress are observed at the TDL level.
- Similarly, the skew effects have a considerable participation on the system response during the steel erection.
- The 1D and 2D analyses do not adequately predict the behavior of the bridge both during the steel erection and during the placement of the deck.

E2.10 NISSS16 (L_1 = 150 ft / w = 80 ft /θ_1 = 50°, θ_2 = 0° / 9 girders)

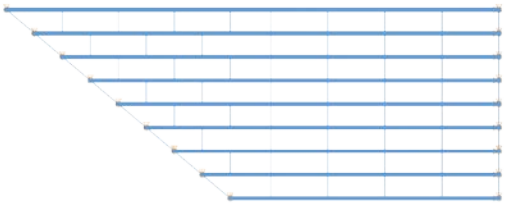

- I_{S1} = 0.59, I_{L1} = 1.83, I_{T1} = 0.58
- The use of staggered cross-frames relaxes the “nuisance stiffness” problem, but results in considerable levels of flange lateral bending stresses.
- At the TDL level, the cross-frame element forces are between 64 kips in compression and 153 kips in tension. Due to these large forces, the dimensions of the cross-frames and their connections can become impractical.

E2.11 NISSS36 (L_1 = 225 ft / w = 80 ft /θ_1 = 50°, θ_2 = 0°, 9 girders)

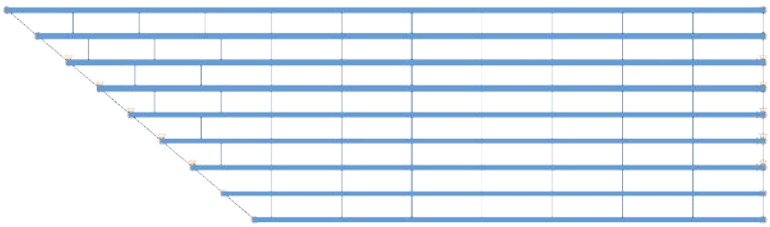

- I_{S1} = 0.40, I_{L1} = 1.49, I_{T1} = 0.55
- Significant flange lateral bending stresses at the girder ends since intermediate cross-frames enforce the same layovers between adjadjacent girders at the cross-frame locations.
- Illustration of the coupling between major-axis bending rotations and torsional rotations at the skewed bearings.

E2.12 NISSS37 (L_1 = 225 ft / w = 80 ft /θ_1 = 28.6°, θ_2 = -28.6°, 9 girders)

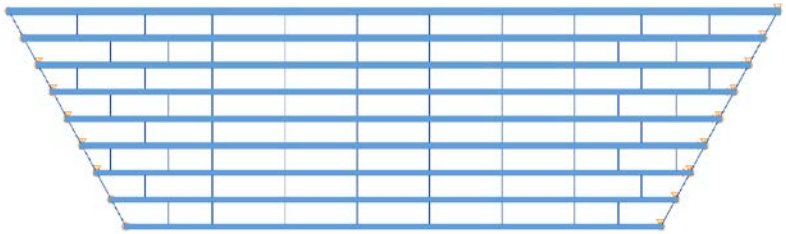

- I_{S1} = 0.18, I_{L1} = 1.44, I_{T1} = 0.54
- The influence of the skew is minor on the behavior of this structure (I_S < 0.30). The girder responses are accurately predicted by1D line girder and the 2D-grid analyses for the different erection stages.
- Illustration of the coupling between major-axis bending rotations and torsional rotations at the skewed bearings.

E2.13 NISSS53 (L_1 = 300 ft / w = 80 ft /θ_1 = 50°, θ_2 = 50°, 9 girders)

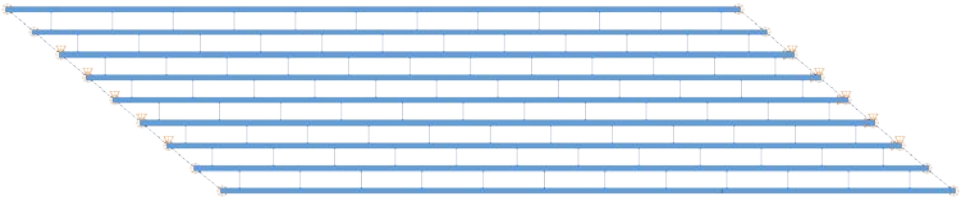

- I_{S1} = 0.29, I_{L1} = 1.0, I_{T1} = 0.50
- The influence of the skew is minor on the behavior of this structure (I_S < 0.30). The girder responses are accurately predicted by1D line girder and the 2D-grid analyses for the different erection stages.
- Illustration of the coupling between major-axis bending rotations and torsional rotations at the skewed bearings.
- Significant second-order amplification in the global flange lateral bending stresses since flange-level lateral bracing is not provided.

E2.14 NISSS54 (L_1 = 300 ft / w = 80 ft /θ_1 = 70°, θ_2 = 70° / 9 girders)

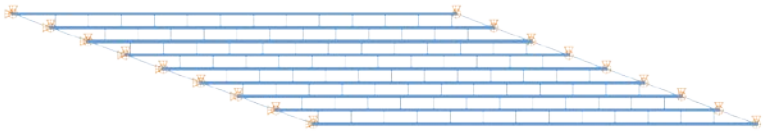

- I_{S1} = 0.68, I_{L1} = 1.0, I_{T1} = 0.50
- In this bridge, the flange lateral bending stress levels reach very high values (e.g., 65 ksi) at the TDL loading level.
- Similarly, the forces in the cross-frames are in the order of 324 kips in compression and 467 kips in tension.
- The approximate analysis methods are not able to properly predict the behavior of the structure either during the steel erection or in the completed configuration.

E2.15 NISSS56 (L_1 = 300 ft / w = 80 ft /θ_1 = 50°, θ_2 = 0° / 9 girders)

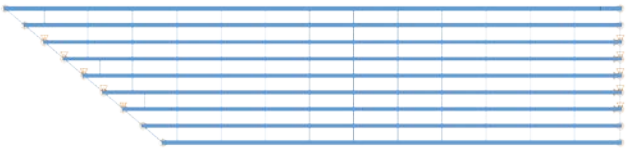

- I_{S1} = 0.30, I_{L1} = 1.34, I_{T1} = 0.53
- The girder responses throughout the construction process are properly captured for this bridge by the 1D and 2D methods of analysis. However, the forces in some of the cross-frames are considerable large (above 100 kips) at the TDL level. These forces cannot be predicted by the approximate methods.

(E3) ICSS (I-girder, Continuous-span, Straight, Skewed supports)

E3.1 EICSS1 (L_1 = 160 ft, L_2 = 160 ft / w = 95.2 ft / θ = -35.2° (all bearing lines), 9 girders)

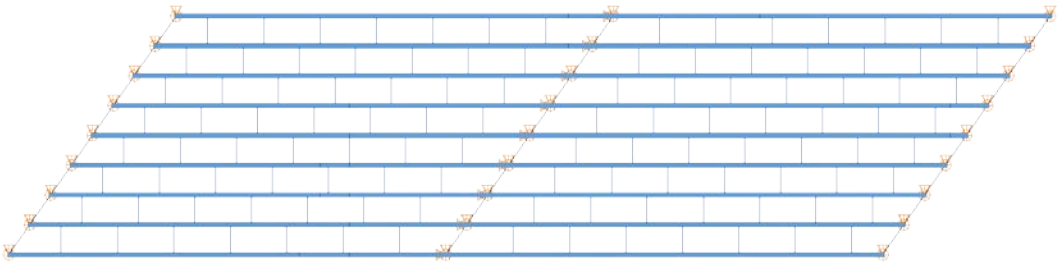

- Steel Overpass, Sunnyside Road I.C. (I-15B) over I-15, Bonneville Co., ID
- Successful implementation of total dead load fit detailing.
- I_{S1} = 0.42, I_{S2} = 0.42 / I_{L1} = 1.0, I_{L2} = 1.0 / I_{T1} = 0.50, I_{T2} = 0.50
- Comparison of the results associated with the staged deck placement.
- Differences in the girder stresses and vertical displacements of 3D-FEA solutions due to staged deck placement.
- Influence of cross-frame detailing methods on the girder responses

E3.2 EICSS2 (L_1 = 239 ft, L_2 = 257 ft, L_3 = 220 ft / w = 74.3 ft / θ_1 = 58°, θ_2 = 61.8°, θ_3 = 38°, θ_4 = 38°, 8 girders)

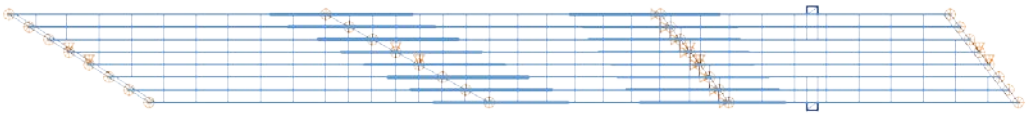

- I-235 EB over E. University Ave., Polk Co., IA
- Difficulty installing cross-frames during erection.
- I_{S1} = 0.50, I_{S2} = 0.46, I_{S3} = 0.26 / I_{L1} = 1.0, I_{L2} = 1.35, I_{L3} = 1.0 / I_{T1} = 0.48, I_{T2} = 0.55, I_{T3} = 0.50.
- Tracking nuisance stiffness issues.
- Large cross-frame forces along stiff transverse load paths.
- Overall deflection behavior due to the different cross-frame detailing methods.
- Influence of method of detailing on girder responses and cross-frame forces

E3.3 EICSS12 (L_1 =150 ft, L_2 = 139 ft, w = 47 ft, θ = 59.6°, 6 girders lean-on cross-frame system)

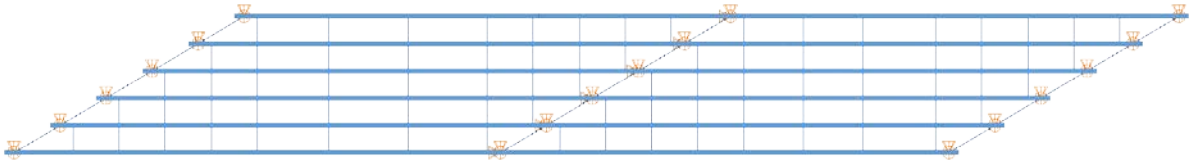

- US 82 Mainlane Underpass at 19th Street WB, Lubbock Co., TX
- Lean-on cross-frame system.
- I_{S1} = 0.53, I_{S2} = 0.58 / I_{L1} = 1.0, I_{L2} = 1.0 / I_{T1} = 0.50, I_{T2} = 0.50
- Girder responses are accurately predicted by1D line girder and the 2D-grid analyses.

E3.4 NICSS1 (L_1 = 150 ft, L_2 = 150 ft / w = 30 ft / θ_1 = 0°, θ_2 = 35°, θ_3 = 0° / 9 girders)

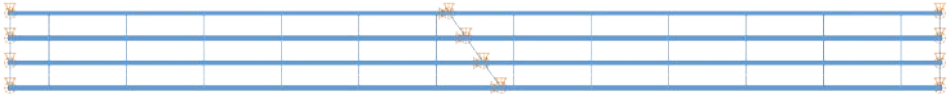

- I_{S1} = 0.11, I_{S2} = 0.11 / I_{L1} = 1.25, I_{L2} = 1.25 / I_{T1} = 0.48, I_{T2} = 0.52
- The 1D and 2D models accurately represent the behavior of this structure. The girder responses are captured properly for all the erection stages and in the final configuration.

E3.5 NICSS3 (L_1 = 150 ft, L_2 = 150 ft / w = 30 ft /θ_1 = 35°, θ_2 = 35°, θ_3 = 0°, 4 girders)

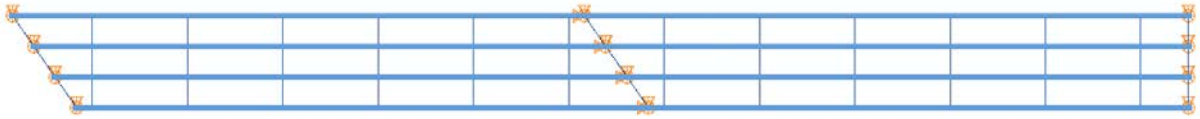

- I_{S1} = 0.11, I_{S2} = 0.11 / I_{L1} = 1.0, I_{L2} = 1.25 / I_{T1} = 0.50, I_{T2} = 0.52
- Uplift during erection Stages 1 and 3 at the piers.
- The influence of the skew is minor on the behavior of this structure (I_S < 0.30). The girder responses are accurately predicted by1D line girder and the 2D-grid analyses for the different erection stages.

E3.6 NICSS16 (L_1 = 350 ft, L_2 = 350 ft / w = 80 ft / θ_1 = 0°, θ_2 = 35°, θ_3 = 0°/ 4 girders)

- I_{S1} = 1.69, I_{S2} = 1.36, I_{S3} = 1.36 / I_{L1} = 1.0, I_{L2} = 1.0, I_{L3} = 1.0 / I_{T1} = 0.50, I_{T2} = 0.50, I_{T3} = 0.50
- The cross-frame forces in this structure reach values that are between 62 kips in compression and 74 kips in tension at the TDL level.
- The flange lateral bending stresses reach values of 25 kips at the same load level.
- The approximate analysis methods are not able to properly predict the behavior of the structure neither during the steel erection nor in the completed configuration.

E3.7 NICSS25 (L_1 = 350 ft, L_2 = 350 ft / w = 80 ft / θ_1 = 0°, θ_2 = 35°, θ_3 = 0°/ 4 girders)

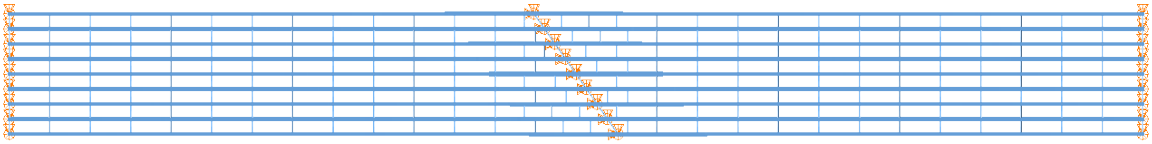

- I_{S1} = 0.15, I_{S2} = 0.15 / I_{L1} = 1.16, I_{L2} = 1.16 / I_{T1} = 0.48, I_{T2} = 0.52
- The major-axis bending responses in the girders are accurately captured by the approximate models. However, near the middle support, there are large forces in the cross-frames, in the order of 120 kips, that cannot be captured by the 1D and 2D models.

E3.8 NICSS27 (L_1 = 350 ft, L_2 = 350 ft / w = 80 ft /θ_1 = 35°, θ_2 = 35°, θ_3 = 0°, 9 girders)

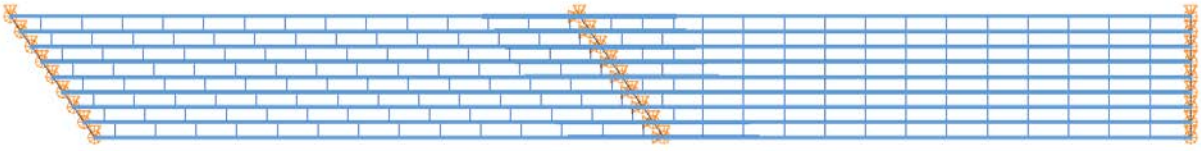

- I_{S1} = 0.15, I_{S2} = 0.15 / I_{L1} = 1.0, I_{L2} = 1.16 / I_{T1} = 0.50, I_{T2} = 0.52
- Influence of large span lengths on girder responses.
- Significant second-order amplification of the global flange lateral bending stresses since flange-level lateral bracing is not provided.

E3.9 XICSS5 (L_1 = 140 ft, L_2 = 175 ft, L_3 = 145 ft / w = 43 ft / θ_1 = -60°, θ_2 = -60°, θ_3 = -60° / 4 girders)

- I_{S1} = 0.53, I_{S2} = 0.43, I_{S3} = 0.53 / I_{L1} = 1.0, I_{L2} = 1.0, I_{L3} = 1.0 / I_{T1} = 0.50, I_{T2} = 0.50, I_{T3} = 0.50
- The effects of the skew in this bridge are moderate. The cross-frame forces are around 45 kips, and the flange lateral bending stresses are in the order of 4 ksi.
- The approximate analysis methods capture the response of the structure as predicted by the 3D FEA.

(E4) ISCR (I-girder, Simple-span, Curved, Radial supports)

E4.1 EISCR1 (L_1 = 90 ft / R = 200 ft / w = 23.5 ft / 3 girders)

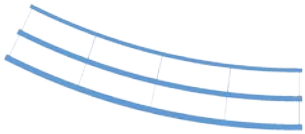

- FHWA Test Bridge.
- Bridge designed to a number of limits of the AASHTO LRFD Specifications. Extensive test date available (Jung, 2006; Jung and White, 2008).
- I_{S1} = 0, I_{L1} = 1.09, I_{T1} = 0.71, I_{C1} = 18.8
- The influence of the poor torsion model implemented in the 2D-grid analysis is notorious in this bridge when more than one element is used to model the girders between the cross-frames. The grid model over estimates the vertical deflections during the steel erection and when the structure is completed.
- The 1D line girder analysis based on the V-load method provides a good estimate of the girder responses.

E4.2 NISCR2 (L_1 = 150 ft/ R_1 = 438 ft / w = 30 ft, 4 girders)

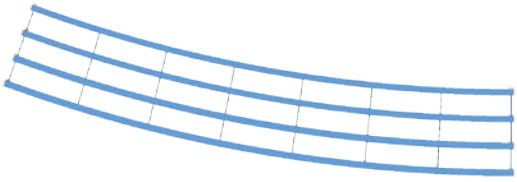

- I_{S1} = 0, I_{L1} = 1.06, I_{T1} = 0.69, I_{C1} = 4.89
- Illustration of the coupling between major-axis bending and torsional rotations due to curvature effects.
- Poor prediction of the vertical displacements and layovers due to poor torsional modeling of girders when more than one element is used to model the girders between the cross-frames.
- Nonlinearity in the flange lateral bending stresses due global flange lateral bending effects.

E4.3 NISCR5 (L_1 = 300 ft/ R_1 = 1530 ft / w = 30 ft, 4 girders)

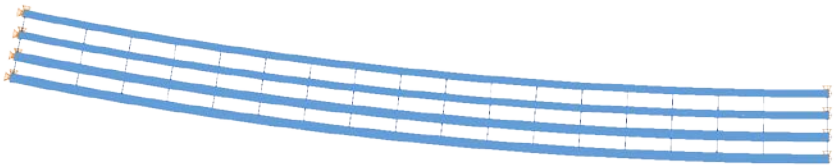

- I_{S1} = 0, I_{L1} = 1.02, I_{T1} = 0.71, I_{C1} = 0.58
- Importance of using temporary supports during construction.
- Poor prediction of the layovers due to poor torsional modeling of girders when more than one element is used to model the girders between the cross-frames..
- Second-order amplification of the flange lateral bending stresses due global flange lateral bending effects since the bridge has large length-to-width ratio.

E4.4 NISCR7 (L_1 = 150 ft / R = 280 ft / w = 80 ft / 9 girders)

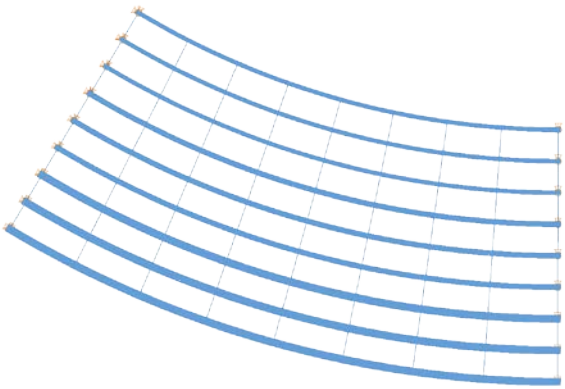

- I_{S1} = 0, I_{L1} = 1.30, I_{T1} = 0.62, I_{C1} = 6.70
- The torsion model that neglects the warping contributions used in the 2D analysis results in a significant mis-prediction of the girder responses. Due to this limitation, the vertical displacements and girder layovers are not accurately captured by the 2D model.
- Since this structure satisfies the assumptions used in the formulation of the V-load method, the simplified line girder analysis is able to predict the bridge behavior as described by the 3D model.

E4.5 NISCR8 (L_1 = 150 ft / R = 420 ft / w = 80 ft / 9 girders)

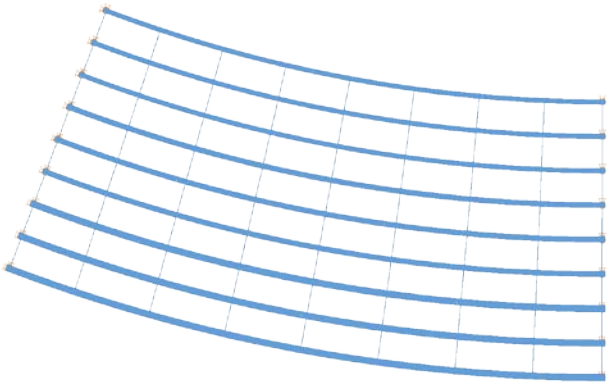

- I_{S1} = 0, I_{L1} = 1.19, I_{T1} = 0.58, I_{C1} = 4.46
- The bridge behavior is misrepresented by the 2D model. The line girder analysis yields better result predictions than the grid model.
- The lack of a term that represents the flange warping contributions to the girder torsion stiffness has a very important influence in the response prediction of this structure.

E4.6 NISCR10 (L_1 = 225 ft / R = 705 ft / w = 80 ft / 9 girders)

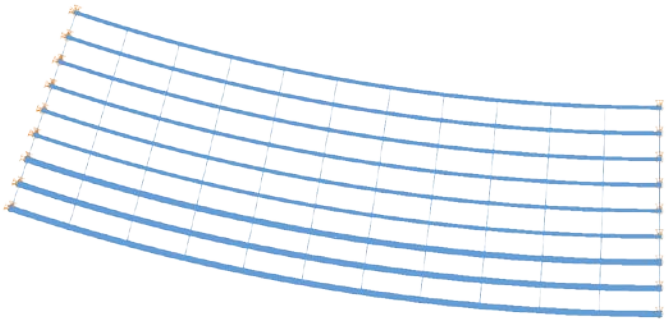

- I_{S1} = 0, I_{L1} = 1.11, I_{T1} = 0.59, I_{C1} = 1.93
- The effects of the curvature are not accurately captured by the 2D model. There is a significant over prediction of the vertical displacements and the girder layovers.
- The 1D model is a closer representation of the structure's behavior. The major-axis bending responses are properly predicted by the model based on the V-load method. Similarly, the flange lateral bending stress responses are well predicted by this analysis method.

E4.7 NISCR11 (L_1 = 300 ft/ R_1 = 730 ft / w = 80 ft, 9 girders)

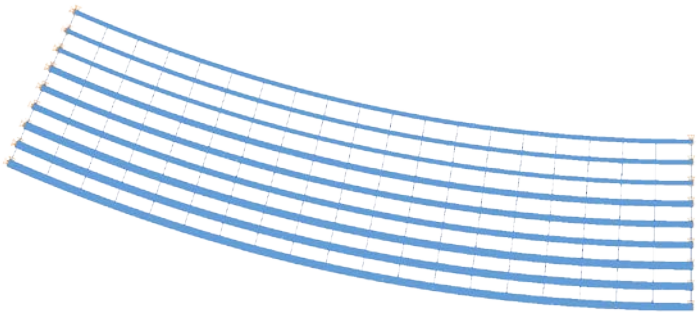

- I_{S1} = 0, I_{L1} = 1.11, I_{T1} = 0.65, I_{C1} = 1.08
- Illustration of the coupling between major-axis bending and torsional rotations due to curvature effects.
- Poor prediction of the vertical displacements and layovers due to poor torsional modeling of girders when more than one element is used to model the girders between the cross-frames..
- Poor prediction accuracy in the flange lateral bending stresses due global nonlinear effects since flange-level lateral bracing is not provided.

(E5) ICCR (I-girder, Continuous-span, Curved, Radial supports)

E5.1 EICCR4 (L_1 = 219 ft, L_2 = 260 ft, L_3 = 211 ft, L_4 = 162 ft, L_5 = 256 ft, L_6 = 190 ft / R_1 = 968 ft, $R_{2,3,4}$ =1108 ft, R_5 =968 ft, ∞ , R_6 = ∞ / w = 44 ft, 5 girders)

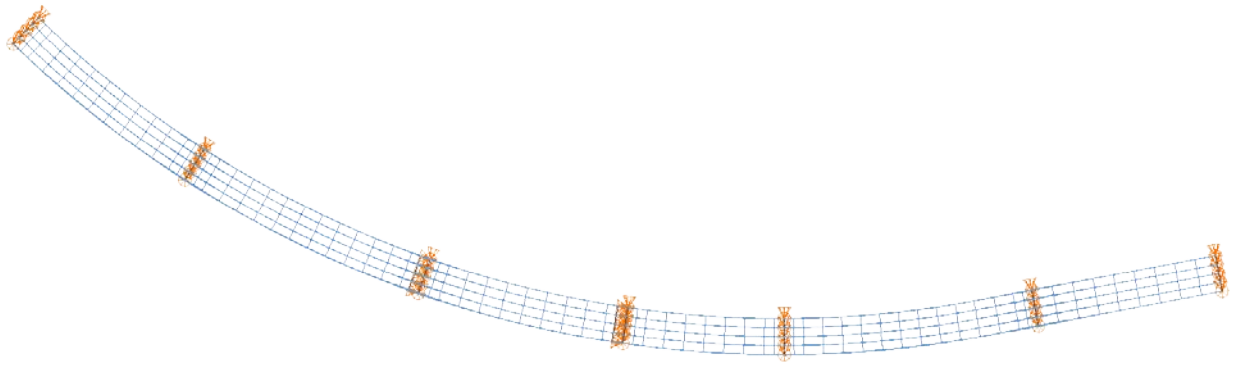

- Ramp GG John F. Kennedy Memorial Highway, I-95 Express Toll Lanes and I-695 Interchange, Baltimore Co., MD
- Relatively long spans and narrow deck. Successful implementation of SDLF detailing.
- I_{S1} = 0, I_{S2} = 0, I_{S3} = 0, I_{S4} = 0, I_{S5} = 0, I_{S6} = 0 / I_{L1} = 1.09, I_{L2} = 1.07, I_{L3} = 1.07, I_{L4} = 1.07, I_{L5} = 1.09, I_{L6} = 1.0 / I_{T1} = 0.61, I_{T2} = 0.64, I_{T3} = 0.59, I_{T4} = 0.56, I_{T5} = 0.64, I_{T6} = 0.50 / I_{C1} = 0.60, I_{C2} = 0.45, I_{C3} = 0.56, I_{C4} = 0.68, I_{C5} = 0.52, I_{C6} = 0
- Poor prediction of the vertical displacements and layovers due to poor torsional modeling of girders when more than one element is used to model the girders between the cross-frames..
- Overestimation of the flange lateral bending stresses during erection.

E5.2 EICCR11 (L_1 = 322 ft, L_2 = 417 ft, L_3 = 329 ft / $R_{1,2}$ = ∞, R_3 = 511 ft / w = 48.3 ft, 4 girders)

- Ford City Bridge, Ford City, PA
- Extreme geometry exacerbating fit-up during the steel erection. Studied extensively by Chavel and Earls (2006a & b; 2001).
- I_{S1} = 0, I_{S2} = 0, I_{S3} = 0 / I_{L1} = 1.0, I_{L2} = 1.0, I_{L3} = 1.17 / I_{T1} = 0.50, I_{T2} = 0.50, I_{T3} = 0.87 / I_{C3} = 0.67
- Influence of flange lateral bracing system on girder responses
- Poor prediction of the vertical displacements and layovers due to poor torsional modeling of girders when more than one element is used to model the girders between the cross-frames.
- Illustration of the overall deflected geometries associated with different types of cross-frame detailing.
- Influence of method of cross-frame detailing on girder responses.
- Influence of method of cross-frame detailing on cross-frame forces.
- Demonstration of the significant locked-in force effects due to DLF detailing.

E5.3 EICCR15 (L_1 = 210 ft, L_2 = 271 ft / R = 1921 ft / w = 48.9 ft, 5 girders)

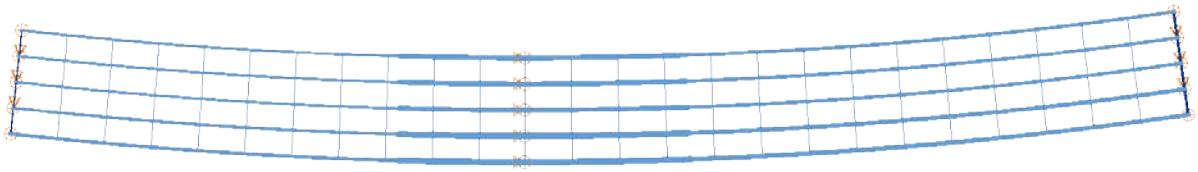

- SR 6220 A11 over SR 6220 NB & SB, Centre Co., PA
- Unbalanced spans. Documentation and field data provided in (Shura, 2004; Domalik, et al., 2005)
- I_{S1} = 0, I_{S2} = 0, / I_{L1} = 1.05, I_{L2} = 1.05 / I_{T1} = 0.55, I_{T2} = 0.58 / I_{C1} = 0.35, I_{C2} = 0.28
- Poor prediction of the vertical displacements and layovers due to poor torsional modeling of girders when more than one element is used to model the girders between the cross-frames..
- Illustration of displacement interactions due to continuity effects in adjacent spans..

E5.4 EICCR22a (L_1 =172 ft, L_2 = 217 ft, L_3 = 217 ft, L_4 =195 ft, L_5 = 171 ft, L_6 = 172 ft, L_7 = 162 ft, L_8 = 192 ft / R_1 =791 ft, R_2 = 889 ft, $R_{3,4,5,6,7}$ = 746 ft, R_8 =766 ft (best fit to spiral curve) / w = 43 ft, 5 girders)

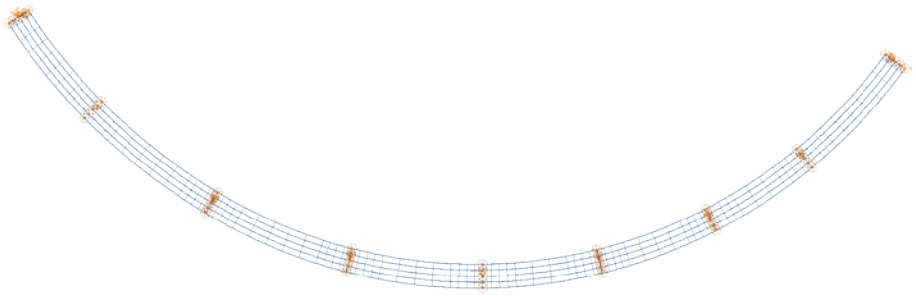

- Bridge No. 12, Ramp B over I-40, Robertson Avenue Project, Davidson Co., TN
- Successful implementation of NLF detailing. Extensive instrumentation placed on the girders prior to their erection. The bridge response was monitored throughout the steel erection, and he concrete deck placement. In addition, live load tests were conducted upon the completion of the bridge prior to opening to traffic. The field studies are documented in (Dykas, 2012).
- I_{S1} = 0, I_{S2} = 0, I_{S3} = 0, I_{S4} = 0, I_{S5} = 0, I_{S6} = 0, I_{S7} = 0, I_{S8} = 0 / I_{L1} = 1.11, I_{L2} = 1.09, I_{L3} = 1.11, I_{L4} = 1.11, I_{L5} = 1.11, I_{L6} = 1.11, I_{L7} = 1.11, I_{L8} = 1.11 / I_{T1} = 0.60, I_{T2} = 0.63, I_{T3} = 0.66, I_{T4} = 0.63, I_{T5} = 0.60, I_{T6} = 0.60, I_{T7} = 0.59, I_{T8} = 0.62 / I_{C1} = 0.95, I_{C2} = 0.65, I_{C3} = 0.77, I_{C4} = 0.84, I_{C5} = 0.91, I_{C6} = 0.84, I_{C7} =0.92, I_{C8} = 0.98
- Poor prediction of the vertical displacements and layovers by 2D-Grid analysis, when multiple elements are used between the cross-frame locations, due to poor torsional modeling of girders.

E5.5 NICCR1 (L_1=150 ft, L_2=150 ft, L_3=120 ft/ R=227 ft / w=30 ft / $\theta_1 = 0^o$, $\theta_2 = 0^o$, $\theta_3 = 0^o$, $\theta_4 = 0^o$/ 4 girders)

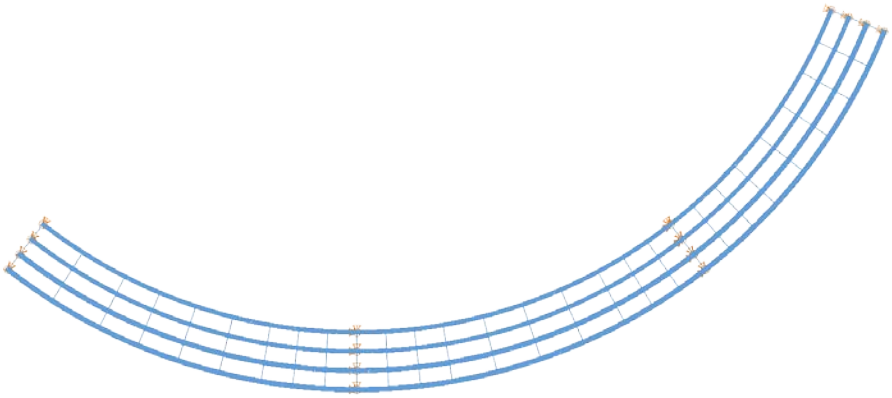

- I_{S1} = 0, I_{S2} = 0, I_{S3} = 0 / I_{L1} = 1.11, I_{L2} = 1.11, I_{L3} = 1.11 / I_{T1} = 0.87, I_{T2} = 0.87, I_{T3} = 0.74 / I_{C1} = 3.67, I_{C2} = 3.30, I_{C3} = 4.13
- Except for the major-axis bending stresses, the girder responses are mis-predicted by the 2D-grid model. The poor representation of the torsion model has a large influence on the response prediction when more than one element is used to model the girders between the cross-frames..
- The 1D girder line model based on the V-load method yields accurate predictions of the system response.

E5.6 NICCR8 (L_1 = 150 ft, L_2 = 150 ft, L_3 = 120 ft / $R_{1,2,3}$ = 308 ft/ w = 80 ft, 9 girders)

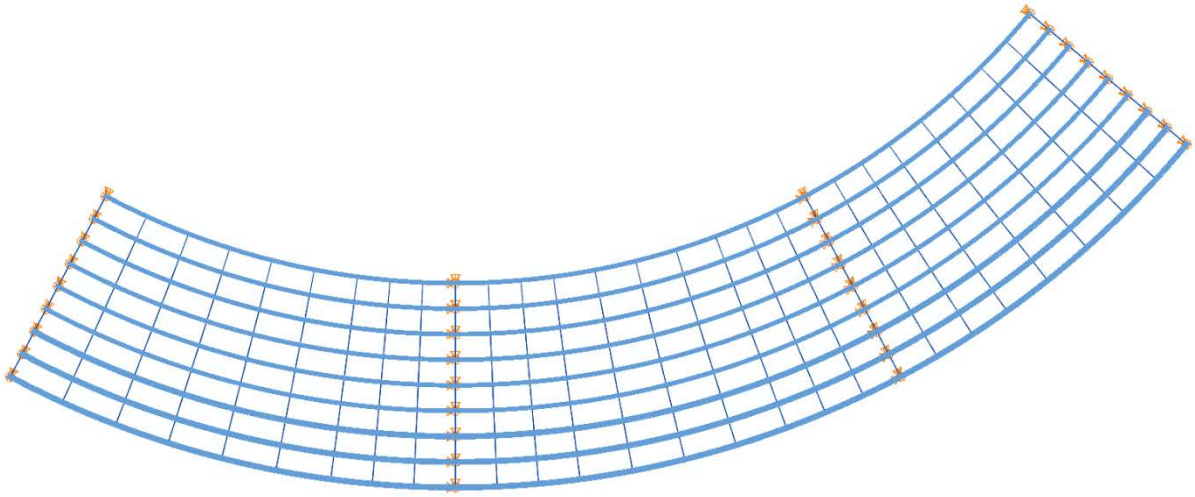

- I_{S1} = 0, I_{S2} = 0, I_{S3} = 0 / I_{L1} = 1.63, I_{L2} = 1.63, I_{L3} = 1.63 / I_{T1} = 0.61, I_{T2} = 0.61, I_{T3} = 0.58 / I_{C1} = 2.71, I_{C2} = 2.43, I_{C3} = 3.04
- Poor prediction of the vertical displacements and layovers due to poor torsional modeling of girders when more than one element is used to model the girders between the cross-frames..
- Tendency for uplift problems during erection due to severe horizontal curvature

E5.7 NICCR12 (L_1=350 ft, L_2=350 ft, L_3=280 ft/ R=909 ft / w=80 ft / θ_1=0 °, θ_2=0 °, θ_3=0 °, θ_4=0 °/ 9 girders)

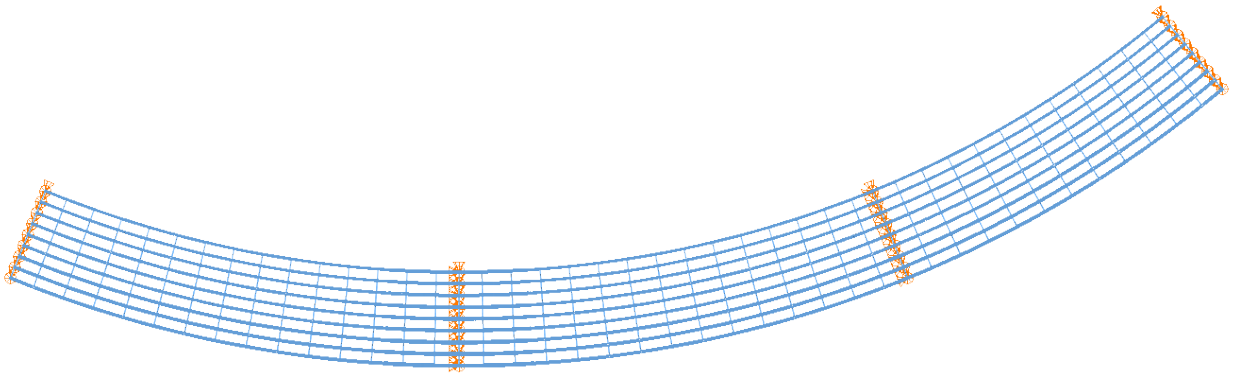

- I_{S1} = 0, I_{S2} = 0, I_{S3} = 0 / I_{L1} = 1.18, I_{L2} = 1.18, I_{L3} = 1.18 / I_{T1} = 0.66, I_{T2} = 0.66, I_{T3} = 0.61 / I_{C1} = 0.55, I_{C2} = 0.55, I_{C3} = 0.69
- The 1D and 2D approximate analysis methods yield results that are an accurate representation of the benchmark responses for the final configuration at the TDL level.
- The flange lateral bending stress responses predicted with the V-load formula are close to those predicted with the 3D FEA.

(E6) ISCS (I-girder, Simple-span, Curved, Skewed supports)

E6.1 EISCS3 (L_1 = 153 ft / R = 279 ft / w = 35.6 ft / θ = 52.4° and 0, 6 girders)

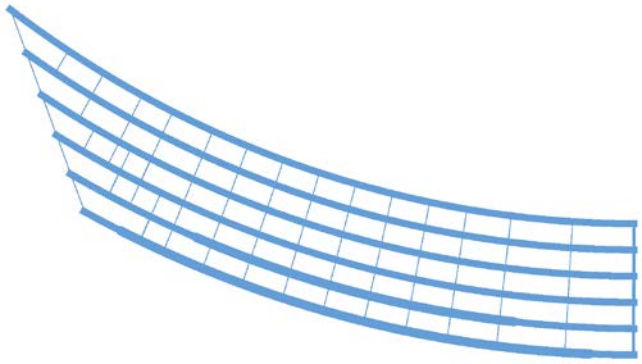

- SR 8002 Ramp A-1, King of Prussia, PA
- Holding crane had to be left on the bridge until four girders were erected. Studied extensively by Chavel and Earls (2003) and Chavel (2008).
- I_{S1} = 0.25, I_{L1} = 0.86, I_{T1} = 0.68, I_{C1} = 2.99
- Illustration of the overall deflections due to curvature and skewed bearings.
- Poor prediction of the vertical displacements and layovers due to poor torsional modeling of girders when more than one element is used to model the girders between the cross-frames..
- Influence of locked-in stresses due to steel dead load fit detailing on girder responses.
- Tendency for uplift during the construction if the bridge is constructed with NLF detailing.

E6.2 EISCS4 (L_1 = 252 ft / R = 2269 ft / w = 26.6 ft / θ_1 = -24.71°, θ_2 = -18.36°/ 3 girders)

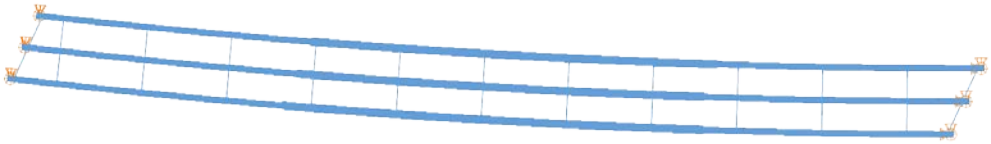

- Long Shoals Road Overpass, Buncombe Co., NC
- Third phase in a three-phase construction project. This three-girder unit over-rotated during the placement of its deck. The deck was removed, then shoring and bracing was provided to the span, and the deck was successfully placed.
- I_{S1} = 0.04, I_{L1} = 1.0, I_{T1} = 0.64, I_{C1} = 0.55
- The structure experiences large amplifications in the girder responses due to second order effects.
- This bridge highlights the importance of conducting a nonlinear analysis via a 3D FEA to properly predict the behavior of a long-and-narrow system.
- The 1D and 2D models are based on linear analysis; hence, they do not capture the expected response of the bridge.

E6.3 NISCS3 (L_1 = 150 ft / R = 436 ft / w = 30 ft / θ_1 = -35°, θ_2 = 0° / 4 girders)

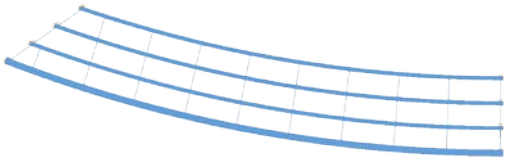

- I_{S1} = 0.11, I_{L1} = 1.18, I_{T1} = 0.71, I_{C1} = 3.44
- In this structure the orientation of the skew makes the girders twist in the same direction as the rotations in the girders due to the curvature. Hence, the effects of the skew and the curvature are additive.
- The combination of the curvature and the skew induces flange lateral bending stresses that are in the order of 25 ksi. None of the approximate analysis methods are able to capture this response.
- Similarly, the deflection predictions obtained from the 1D and 2D analyses do not captured the expected response, as predicted by the 3D FEA.

E6.4 NISCS9 (L_1 = 150 ft / R = 438 ft / w = 30 ft / θ_1 = 65.2°, θ_2 = 45.6° / 4 girders)

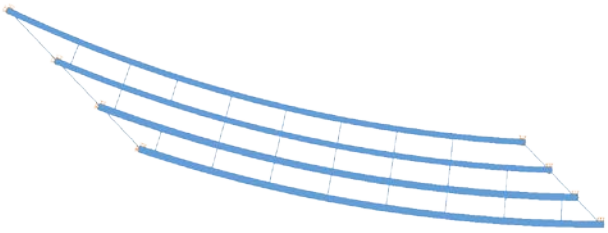

- I_{S1} = 0.35, I_{L1} = 0.88, I_{T1} = 0.63, I_{C1} = 3.11
- In this structure the effects of the skew in the left support counteracts the effects of the horizontal curvature. In the right support, these effects are additive since they both make the girders rotate in the same direction.
- Due to its complex geometry, the approximate 1D and 2D methods do not capture the behavior of the bridge properly. The vertical displacements and girder rotations are severely misrepresented by the approximate models.

E6.5 NISCS14 (L_1 = 150 ft / R_1 = 280 ft/ w = 80 ft /θ_1 = 53.7°, θ_2 = 0°, 9 girders)

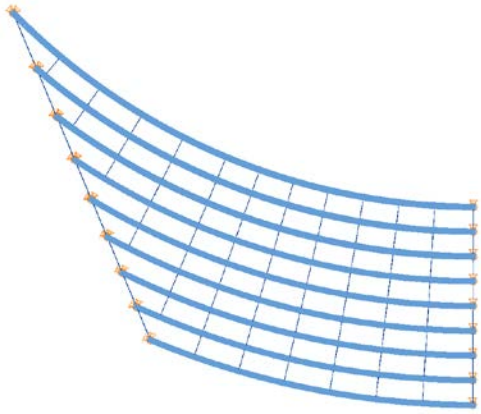

- I_{S1} = 0.67, I_{L1} = 0.65, I_{T1} = 0.55, I_{C1} = 4.46
- Poor prediction of the vertical displacements and layovers due to poor torsional modeling of girders when more than one element is used to model the girders between the cross-frames..

E6.6 NISCS15 (L_1 = 150 ft / R_1 = 280 ft/ w = 80 ft /θ_1 = -35°, θ_2 = 0°, 9 girders)

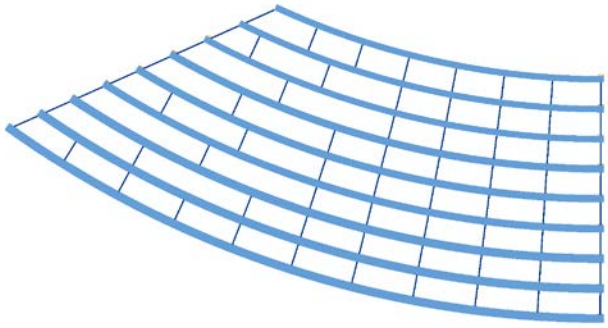

- I_{S1} = 0.36, I_{L1} = 1.88, I_{T1} = 0.67, I_{C1} = 4.46
- Demonstration of the overall bridge deflections due to curvature and skewed bearing lines
- Poor prediction of the vertical displacements and layovers due to poor torsional modeling of girders when more than one element is used to model the girders between the cross-frames..
- Poor prediction of the results due to uplift

E6.7 NISCS37 (L_1 = 300 ft / R_1 = 730 ft/ w = 80 ft /θ_1 = 35°, θ_2 = 0°, 9 girders)

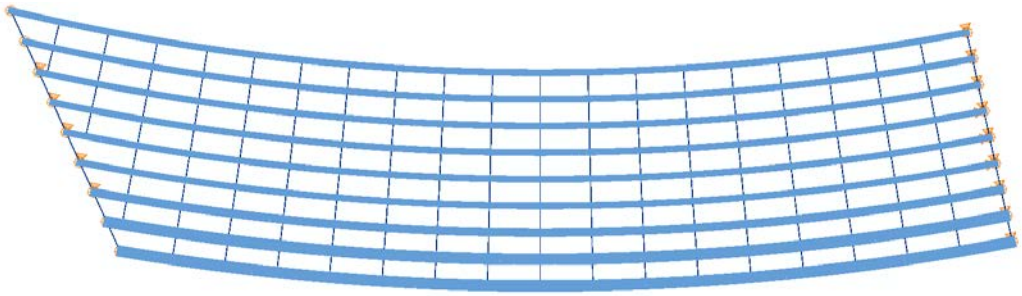

- I_{S1} = 0.35, I_{L1} = 0.93, I_{T1} = 0.62, I_{C1} = 1.03
- Demonstration of the importance of erection sequence on fit-up of the components.
- Poor prediction of the vertical displacements and layovers due to poor torsional modeling of the girders.

E6.8 NISCS38 (L_1 = 300 ft / R = 730 ft / w = 80 ft / θ_1 = 62.6°, θ_2 = 0° / 9 girders)

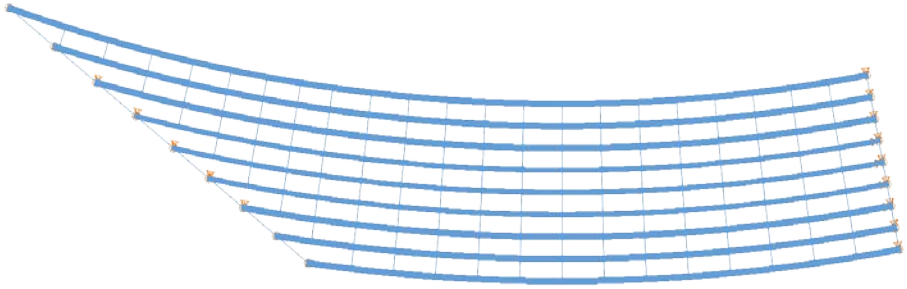

- I_{S1} = 0.48, I_{L1} = 0.68, I_{T1} = 0.59, I_{C1} = 0.94
- The interaction between the skew and the curvature is not captured by the approximate models. Except for the major-axis bending stresses, the rest of responses are inaccurately predicted by the 1D and 2D analyses.
- The inaccuracy of the results obtained from the 2D model is mostly due to the inability of this analysis method to represent the torsion properties of the I-girders.
- Due to the skew, significant levels of flange lateral bending stress are observed near the skewed end.

E6.9 NISCS39 (L_1 = 300 ft / R = 730 ft / w = 80 ft / θ_1 = -35°, θ_2 = 0° / 9 girders)

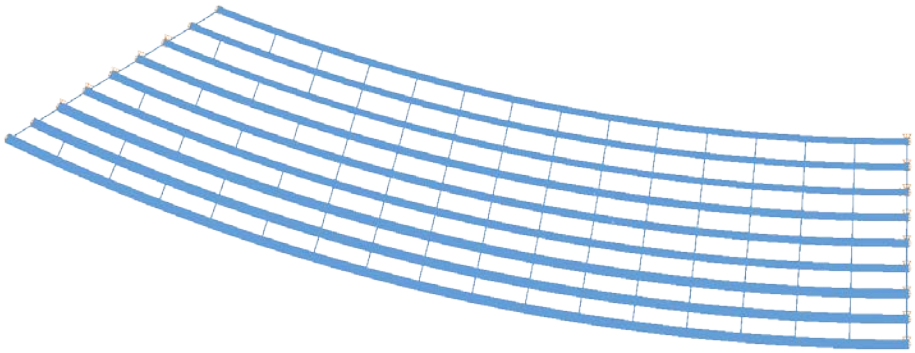

- I_{S1} = 0.17, I_{L1} = 1.32, I_{T1} = 0.68, I_{C1} = 1.21
- In this bridge, the effects of the skew are added to the effects of the horizontal curvature. The girders twist in the same direction, inducing larger levels of flange lateral bending stresses and layovers.
- The approximate analyses yield results that are different to those predicted by the 3D FEA. The main reason is the inability of the girder line and grid models to properly capture the effects of the skew.

(E7) ICCS (I-girder, Continuous-span, Curved, Skewed supports)

E7.1 EICCS1 (L_1 = 204 ft, L_2 = 278 ft, L_3 = 252 ft, L_4 = 185 ft / R = 757 ft / w = 40.2 ft / $\theta_1 = 0^o$, $\theta_2 = 0^o$, $\theta_3 = 32.7^o$, $\theta_4 = 0^o$, $\theta_5 = 0^o$, 5 girders)

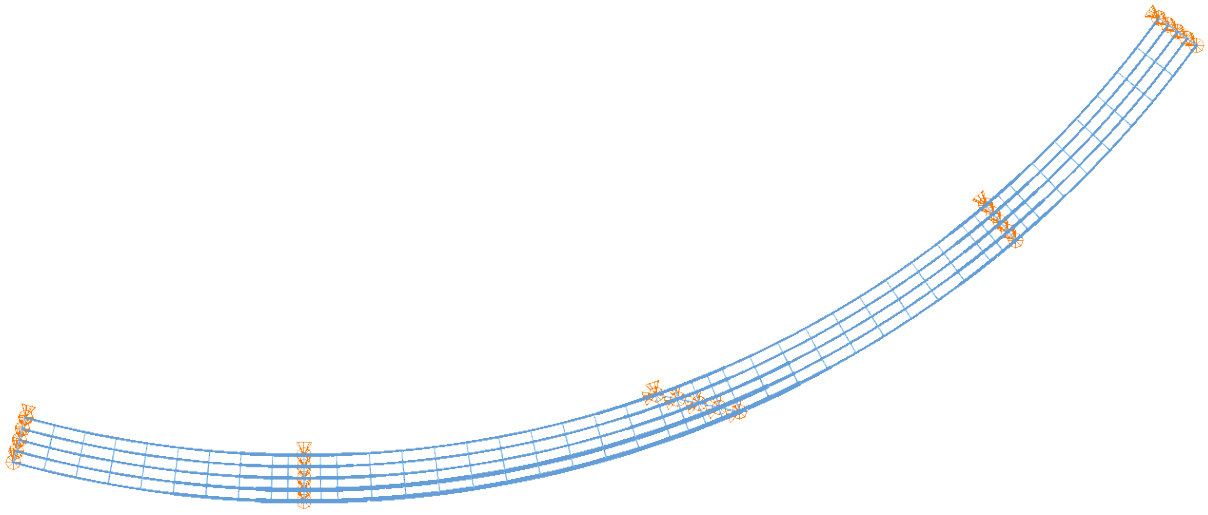

- US 31 Interchange Flyover A, Jefferson Co., AL
- Successful implementation of total dead load fit detailing. Extensive documentation of fabrication and erection provided by Osborne (2002).
- I_{S1} = 0, I_{S2} = 0.08, I_{S3} = 0.08, I_{S4} = 0 / I_{L1} = 1.05, I_{L2} = 1.25, I_{L3} = 0.85, I_{L4} = 1.05 / I_{T1} = 0.65, I_{T2} = 0.80, I_{T3} = 0.70, I_{T4} = 0.62 / I_{C1} = 0.99, I_{C2} = 0.66, I_{C3} = 0.66, I_{C4} = 0.99
- None of the approximate methods capture the expected responses of this structure, as predicted by the 3D model.
- In the case of the 1D model, it cannot capture the influence that the intermediate skewed support has on the behavior of the bridge.
- In the case of the 2D analysis, the torsion stiffness model that neglects the contribution of flange warping has a severe effect in the response predictions.

E7.2 EICCS10 (L_1=145 ft, L_2=150 ft / R=286 ft / w=33.4 ft / θ_{left} = 40.1°, θ_{mid} = 34.8°, θ_{right} = -10.4°, 4 girders)

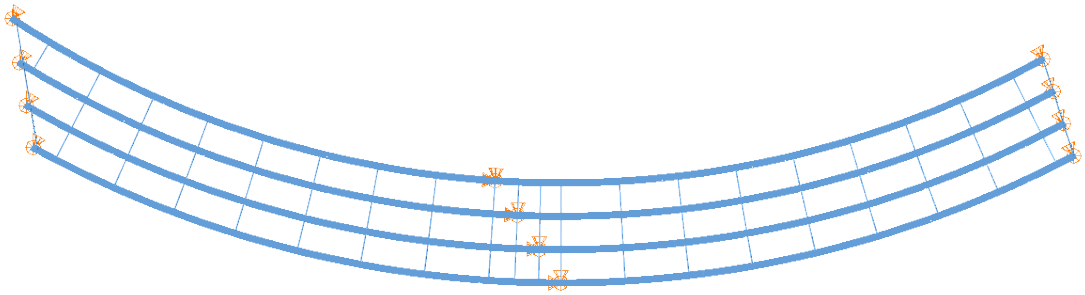

- MN/DOT bridge No. 27998, TH94 between 27th Avenue and Huron Boulevard, Minneapolis, MN
- Instrumented extensively and studied by Galambos et al. (1996). Used by Nowak, et al. (2006) in calibration of LRFD Specifications for curved steel bridges.
- I_{S1} = 0.16, I_{S2} = 0.13, / I_{L1} = 1.07, I_{L2} = 1.07 / I_{T1} = 0.73, I_{T2} = 0.72 / I_{C1} = 2.19, I_{C2} = 2.19
- The 2D model does not capture accurately the displacement responses of the bridge due to the poor torsion model used in the analysis when more than one element is used to model the girders between the cross-frames.
- The 1D girder line analysis yields better results than those obtained from the grid analysis.

E7.3 EICCS27 (L_1 = 279 ft, L_2 = 224 ft, L_3 = 236 ft / R = 2546 ft / w = 88 ft / θ_1 = -53.1°, θ_2 = -59.4°, θ_3 = -64.4°, θ_4 = -69.7°, 8 girders)

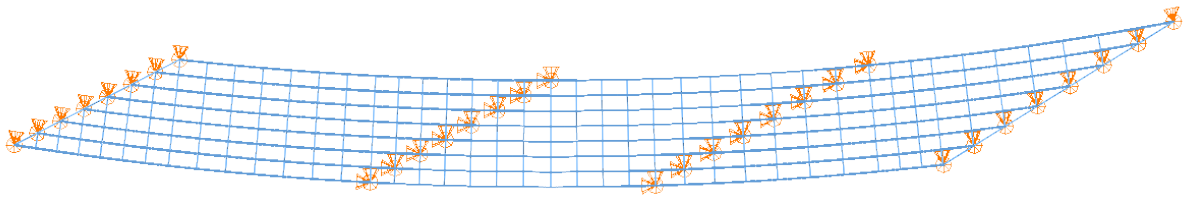

- SR 386 over SR 6 and Ramp F, Sumner Co., TN
- Bolts connecting cross-frames to connection plates sheared after the steel erection and before completion of the bridge.
- I_{S1} = 0.48, I_{S2} = 0.75, I_{S3} = 0.92 / I_{L1} = 0.96, I_{L2} = 0.90, I_{L3} = 0.94 / I_{T1} = 0.51, I_{T2} = 0.49, I_{T3} = 0.47 / I_{C1} = 0.14, I_{C2} = 0.16, I_{C3} = 0.17
- The bridge responses are properly captured by the approximate models.
- The poor representation of the torsion stiffness on the 2D analysis does not have a significant impact in this bridge.

E7.4 NICCS2 (L_1 = 150 ft, L_2 = 150 ft/ R = 227 ft / w =30 ft / θ_1 = 38°, θ_2 = 0°, θ_3 = 0°, 5 girders)

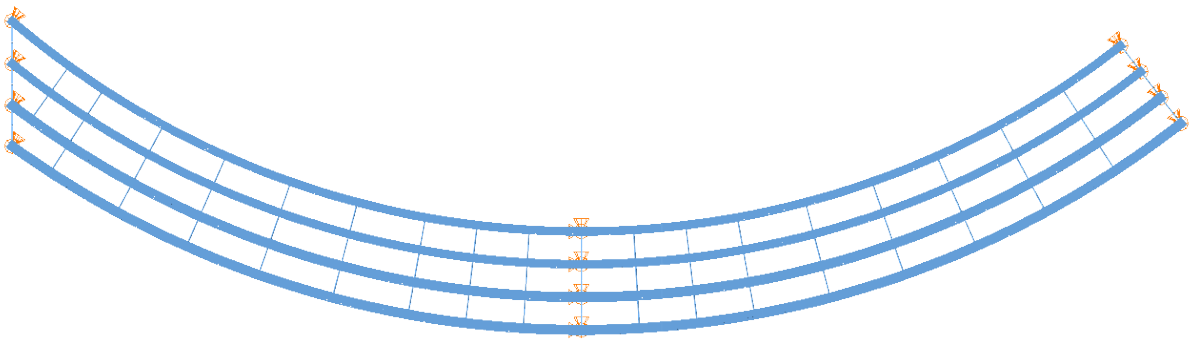

- I_{S1} = 0.13, I_{S2} = 0, / I_{L1} = 0.98, I_{L2} = 1.24 / I_{T1} = 0.81, I_{T2} = 0.87 / I_{C1} = 3.30, I_{C2} = 3.67
- The 2D model does not capture accurately the displacement responses of the bridge due to the poor torsion model used in the analysis when more than one element is used to model the girders between the cross-frames.
- The 1D girder line analysis yields better results than those obtained from the grid analysis.

E7.5 NICCS3 (L_1 = 150 ft, L_2 = 150 ft / $R_{1,2}$ = 227 ft/ w = 30 ft /θ_1 = 38°, θ_2 = 0°, θ_3 = -38°, 4 girders)

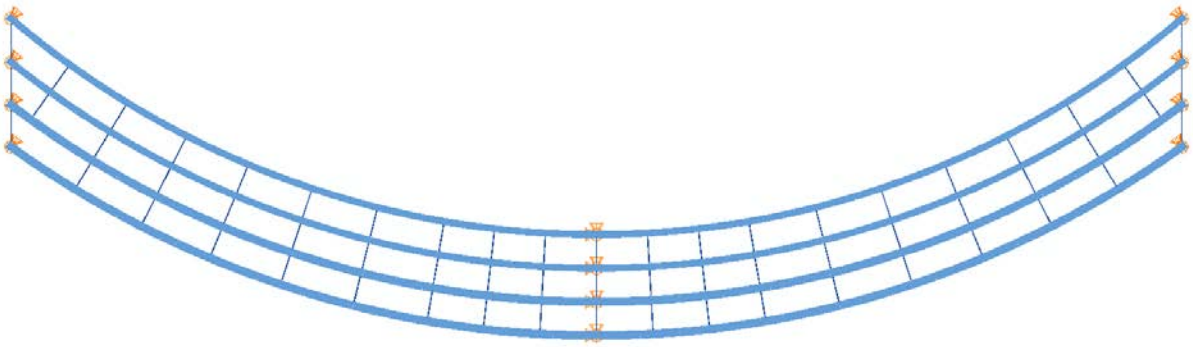

- I_{S1} = 0.13, I_{S2} = 0.13, / I_{L1} = 0.98, I_{L2} = 0.98 / I_{T1} = 0.81, I_{T2} = 0.81 / I_{C1} = 3.30, I_{C2} = 3.30
- Poor prediction of the vertical displacements and layovers due to poor torsional modeling of girders when more than one element is used to model the girders between the cross-frames..
- Tendency for uplift problems during erection
- Overestimation of the flange lateral bending stresses at negative moment regions.

E7.6 NICCS9 (L_1 = 150 ft, L_2 = 150 ft / $R_{1,2}$ = 308 ft/ w = 80 ft /θ_1 = 56°, θ_2 = 28°, θ_3 = 0°, 9 girders)

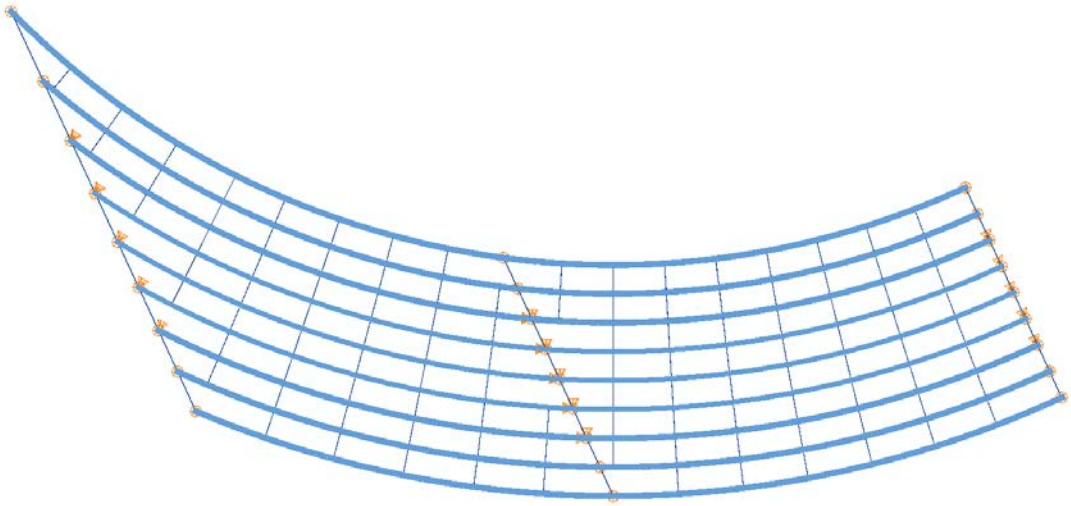

- I_{S1} = 0.73, I_{S2} = 0.26, / I_{L1} = 0.77, I_{L2} = 0.98 / I_{T1} = 0.53, I_{T2} = 0.58 / I_{C1} = 2.21, I_{C2} = 2.71
- Poor prediction of the vertical displacements and layovers due to poor torsional modeling of girders when more than one element is used to model the girders between the cross-frames..
- Tendency for uplift problems during erection stages due to severe horizontal curvature.
- Comparison of the improved grid solutions against benchmark solutions.
- Other assumptions with grid solutions that can cause differences in the responses against benchmark solutions.

E7.7 NICCS13 (L_1 = 250 ft, L_2 = 250 ft / $R_{1,2}$ = 597 ft/ w = 30 ft /θ_1 = 47.9°, θ_2 = 24°, θ_3 = 0°, 4 girders)

- I_{S1} = 0.11, I_{S2} = 0.04, / I_{L1} = 0.98, I_{L2} = 0.99 / I_{T1} = 0.84, I_{T2} = 0.85 / I_{C1} = 1.05, I_{C2} = 1.05
- Poor prediction of the vertical displacements and layovers due to poor torsional modeling of girders when more than one element is used to model the girders between the cross-frames.
- Poor prediction of the flange lateral bending stresses by grid analysis solutions.
- Global second-order effects during construction since there is no temporary supports.

E7.8 NICCS14 (L_1 = 250 ft, L_2 = 250 ft / $R_{1,2}$ = 597 ft/ w = 30 ft /θ_1 = 24°, θ_2 = 0°, θ_3 = 0°, 4 girders)

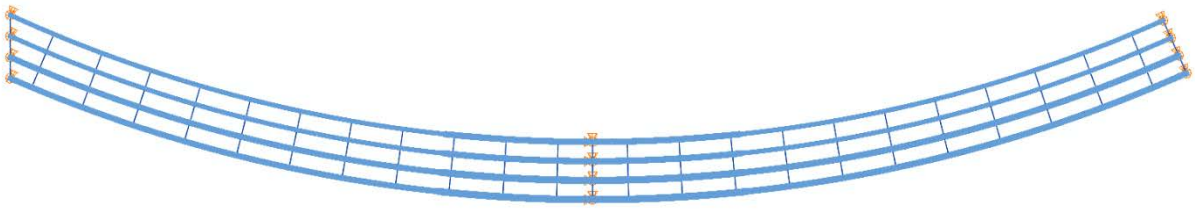

- I_{S1} = 0.04, I_{S2} = 0, / I_{L1} = 0.99, I_{L2} = 1.04 / I_{T1} = 0.85, I_{T2} = 0.88 / I_{C1} = 1.12, I_{C2} = 1.12
- Poor prediction of the vertical displacements and layovers due to poor torsional modeling of girders when more than one element is used to model the girders between the cross-frames.

E7.9 NICCS24 (L_1 = 350 ft, L_2 = 350 ft / R =909 ft / w = 80 ft /θ_1 = 0°, θ_2 = 22.1°, θ_3 = 0°, 9 girders)

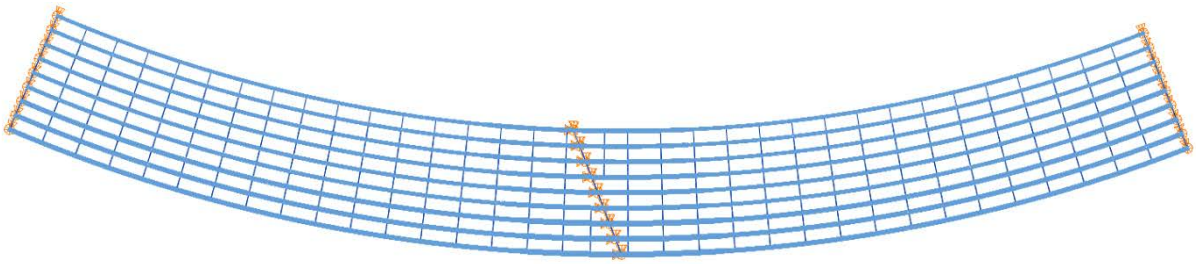

- I_{S1} = 0.09, I_{S2} = 0.09, / I_{L1} = 1.18, I_{L2} = 1.00 / I_{T1} = 0.68, I_{T2} = 0.65 / I_{C1} = 0.46, I_{C2} = 0.46
- Importance of using temporary supports for large span lengths
- Poor prediction of the vertical displacements and layovers due to poor torsional modeling of girders when more than one element is used to model the girders between the cross-frames.

E7.10 XICCS7 (L_1=160 ft, L_2=210 ft, L_3=160 ft/ R=700 ft / w=40.5 ft / θ_1=0 °, θ_2=-60 °, θ_3=-60 °, θ_4=0 °/ 4 girders)

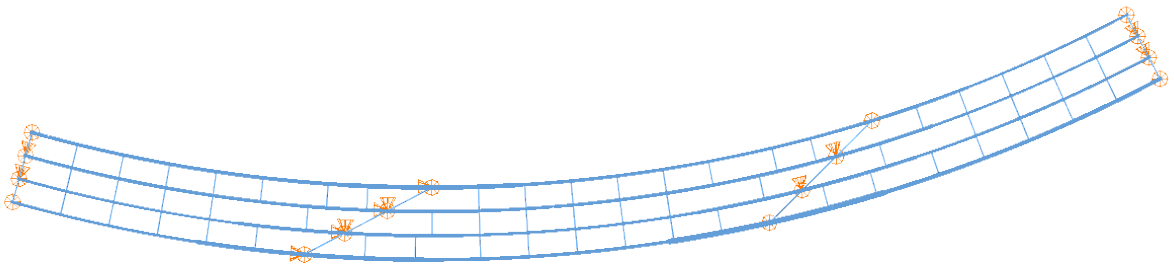

- Reference: (NHI, 2011)
- I_{S1} = 0.36, I_{S2} = 0.27, I_{S3} = 0.36 / I_{L1} = 0.73, I_{L2} = 1.05, I_{L3} = 1.51 / I_{T1} = 0.55, I_{T2} = 0.64, I_{T3} = 0.65 / I_{C1} = 1.33, I_{C2} = 0.97, I_{C3} = 1.33
- The vertical displacement and layover responses are not properly captured in the 2D-grid model due to the limitations of the girder torsion model used in the analysis.
- The 1D girder line model yields results that are comparatively better than those obtained from the grid analysis. For this bridge, the skew effects are moderate, so the 1D analysis predictions are close to the obtained from the 3D FEA.

(8) TCSN (Tub-girder, Continuous, Straight, No Skewed Supports)

8.1 XTCSN3 (L_1 = 206 ft, L_2 = 275, L_3 = 206 ft / w = 43 ft, 2 tub-girders)

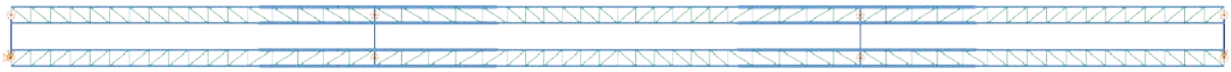

- Reference: (Carnahan, et al., 1997)
- I_{S1} = 0, I_{S2} = 0, I_{S3} = 0 / I_{L1} = 1.0, I_{L2} = 1.0, I_{L3} = 1.0 / I_{T1} = 0.5, I_{T2} = 0.5, I_{T3} = 0.5
- Internal torsional force caused by the Pratt TFLB system.
- 1D and 2D methods do not capture internal torsional moments and in consequence the forces in the bracing elements are not correctly predicted by Helwig et al. expressions.
- Predicted TFLB force distribution follows the bending moment diagram while they should follow the shape of the torsional moment diagram which is similar to the shear force distribution.

(9) TSSS (Tub-girder, Simple-span, Straight, Skewed supports)

9.1 ETSSS2 (L_1 = 205 ft / w = 113 ft / θ=33.4°, θ=33.4°, 6 tub-girders, phased construction, two units of 3 girders each)

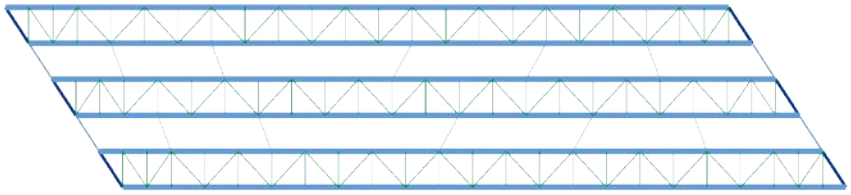

- Sylvan Bridge over Sunset Hwy., Multomah Co., OR
- One unit in a six tub-girder phased construction project.
- I_{S1} = 0.13 / I_{L1} = 1.0 / I_{T1} = 0.5
- Cross-flames are used between girders during stages studied are flexible providing reduced torsional interaction as compared to rigid plate diaphragms.
- Double bearing configuration used at each girder end. Negative reactions found at one of each bearings.
- In 2D analyses the double bearing can be modeled by using an additional rigid member between the bearings.
- Skewed external intermediate cross frames used only during construction. Offset at cross-frames bottom chords due to web slope.
- TFLB and top flange interaction is noticeable as saw-tooth shaped top flange major-axis bending stresses.

9.2 NTSSS1 (L_1 = 150 ft / w = 30 ft / θ=15°, θ=15°, 2 tub-girders)

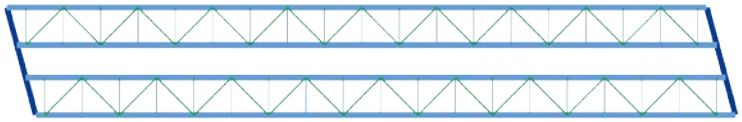

- I_{S1} = 0.03 / I_{L1} = 1.0 / I_{T1} = 0.5
- Torsion due to skew not captured by ordinary 1D analysis. Mechanics approach can provide an approximate torsional moment to apply to 1D model.
- 2D-Grid analysis prediction of the torsional moment depends on the model of the external end diaphragm. The torsional response is mostly insensitive to diaphragm plate thicknesses within a range of commonly used values.
- 3D FEA reports TFLB and girder top flange interaction not captured by 1D or 2D methods. The top flange major axis bending stress distribution has a saw-tooth pattern matching the position of the TFLB locations.
- Plan layout does not permit the use of intermediate cross-frames
- Constant torsional moment on the girders causing a constant force on the TFLB

9.3 NTSSS2 (L_1 = 150 ft / w = 30 ft / θ=30°, θ=30°, 2 tub-girders)

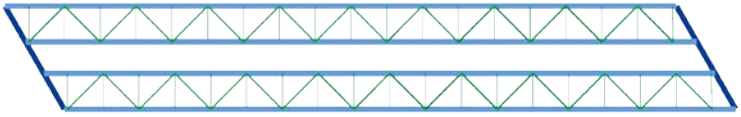

- I_{S1} = 0.06 / I_{L1} = 1.0 / I_{T1} = 0.5
- Increased skew angle with respect to NTSSS1, torsional effects increased.
- Same TFLB interaction as reported on NTSSS1.

9.4 NTSSS4 (L_1 = 150 ft / w = 30 ft / θ=30°, θ=-30°, 2 tub-girders)

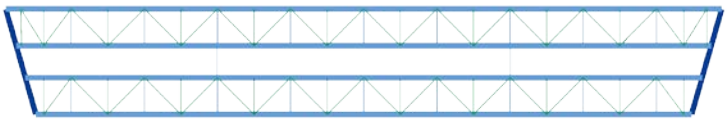

- I_{S1} = 0.03 / I_{L1} = 1.06 / I_{T1} = 0.48
- Due to the equal and opposite skew of the bearing lines, the girder torsional moment is zero, however, the girders exhibit a rigid body twist about their longitudinal axis.
- Girder twist rotation can cause fit-up and slab thickness issues if not accounted for.
- TFLB forces remain low due to rigid body rotation and zero torsional moment.
- No evidence of TFLB and top flange interaction.

(10) TSCR (Tub-girder, Simple-span, Curved, Radial supports)

10.1 NTSCR1 (L_1 = 150ft / R = 400 ft / w = 30 ft, 2 tub-girders)

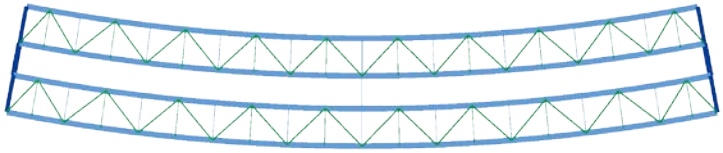

- I_{S1} = 0 / I_{L1} = 1.04 / I_{T1} = 0.83
- Effects of torsional forces are correctly predicted by all the types of analysis.
- Intermediate cross-frame at span center does not affect the vertical displacements or major axis bending stresses predictions for 1D Line-Girder and 2D-Grid analyses.
- TFLB and top flange interaction is noticeable as saw-tooth shaped major axis bending stresses.

10.2 NTSCR2 (L_1 = 150ft / R = 600 ft / w = 30 ft, 2 tub-girders)

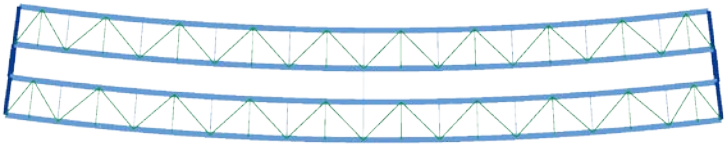

- I_{S1} = 0 / I_{L1} = 1.03 / I_{T1} = 0.72
- Reduced curvature with respect to NTSCR1 (higher curvature radius) proves reduced effects due to skew.
  TFLB and top flange interaction is noticeable as saw-tooth shaped major axis bending stresses. When compared to NTSCR1 the saw-tooth height is reduced.

10.3 NTSCR5 (L_1 = 300 ft / R = 1360 ft / w = 30 ft, 2 tub-girders)

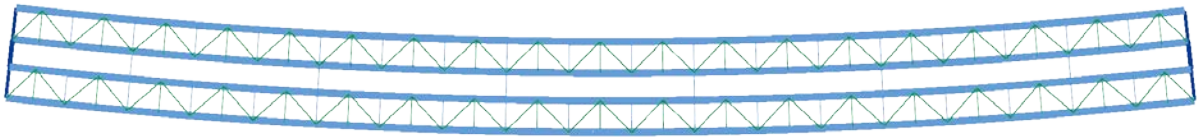

- I_{S1} = 0 / I_{L1} = 1.01 / I_{T1} = 0.87
- Longer span layout uses deeper tubs reducing the bottom flange width.
- Linear and Non-Linear 3D FEA analyses results report negligible differences.
- TFLB and top flange interaction is noticeable as saw-tooth shaped major axis bending stresses.

(11) TCCR (Tub-girder, Continuous-span, Curved, Radial supports)

11.1 ETCCR14 (L_1 = 189 ft, L_2 = 291 ft, L_3 = 183 ft / R = 896 ft / w = 40.8 ft, 4 tub-girders)

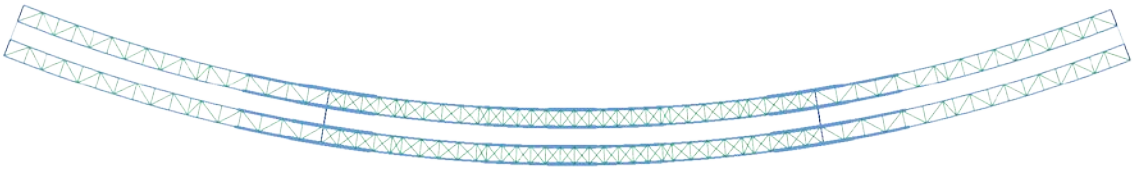

- Connector EB North Beltway 8 to NB I-45, Houston, TX
- Studied extensively by Fan (1999).
- I_{S1} = 0, I_{S2} = 0, I_{S3} = 0 / I_{L1} = 1.02, I_{L2} = 1.02, I_{L3} = 1.02 / I_{T1} = 0.66, I_{T2} = 0.88, I_{T3} = 0.65
- TFLB and top flange interaction is noticeable as saw-tooth shaped major axis bending stresses at spans 1 and 3 with Warren-type top truss, no noticeable interaction at center span with X-type top truss system.

11.2 ETCCR15 (L_1 = 155ft, L_2 = 169 ft, L_3 = 232ft, L_4 = 185ft, L_5 = 185ft, L_6 = 144ft / R = 515ft, 960ft, ∞, -1904ft / w = 29.5ft, 2 tub-girders)

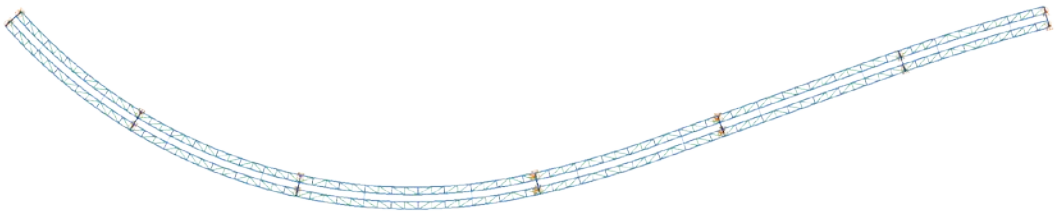

- B-40-1122 Marquette Interchange, Milwaukee, WI
- Change in sign of horizontal curvature along the length.
- I_{S1} = 0, I_{S2} = 0, I_{S3} = 0, I_{S4} = 0, I_{S5} = 0, I_{S6} = 0 / I_{L1} = 1.03, I_{L2} = 1.03, I_{L3} = 1.03, I_{L4} = 1.01, I_{L5} = 1.00, I_{L6} = 1.01 / I_{T1} = 0.79, I_{T2} = 0.85, I_{T3} = 1, I_{T4} = 0.66, I_{T5} = 0.50, I_{T6} = 0.57
- Bridge has alternating Pratt layout for TFLB and internal solid plate diaphragms.
- TFLB and top flange interaction is noticeable as saw-tooth shaped major axis bending stresses. TFLB layout reduced the number of saw-tooth locations.

11.3 NTCCR1 (L_1 = 150 ft, L_2 = 150 ft, L_3 = 120 ft / R = 268 ft / w = 30 ft, 2 tub-girders)

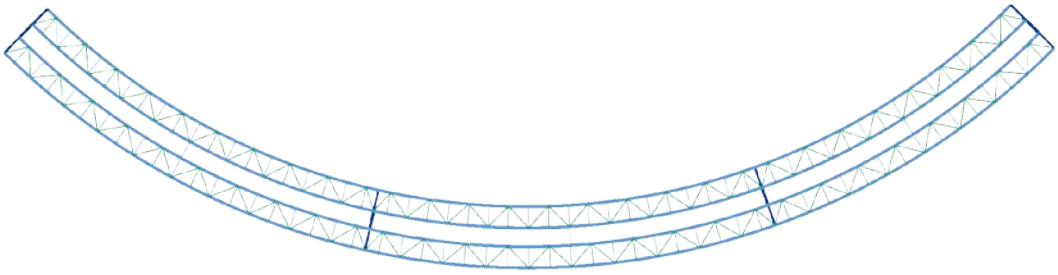

- I_{S1} = 0, I_{S2} = 0, I_{S3} = 0 / I_{L1} = 1.06, I_{L2} = 1.06, I_{L3} = 1.06 / I_{T1} = 1, I_{T2} = 1, I_{T3} = 0.82
- TFLB and top flange interaction is noticeable as saw-tooth shaped major axis bending stresses. Interaction increased due to curvature.

11.4 NTCCR5 (L_1 = 350ft, L_2 = 350 ft, L_3 = 280 ft / R = 1380 ft / w = 30 ft, 2 tub-girders)

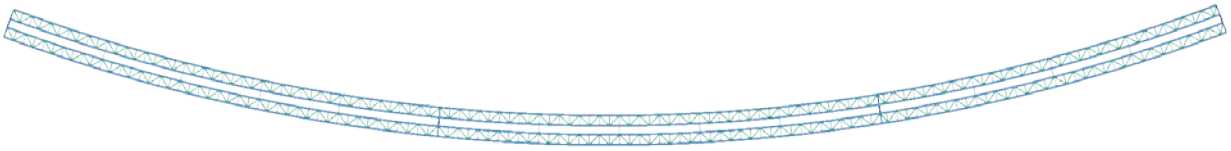

- I_{S1} = 0, I_{S2} = 0, I_{S3} = 0 / I_{L1} = 1.01, I_{L2} = 1.01, I_{L3} = 1.01 / I_{T1} = 1, I_{T2} = 1, I_{T3} = 0.82
- Linear and Non-Linear 3D FEA analyses results report negligible differences.
- TFLB and top flange interaction is noticeable as saw-tooth shaped major axis bending stresses.

11.5 XTCCR8 (L_1 = 160 ft, L_2 = 210 ft, L_3 = 160 ft / R = 700 ft / w = 40.5 ft, 2 tub-girders)

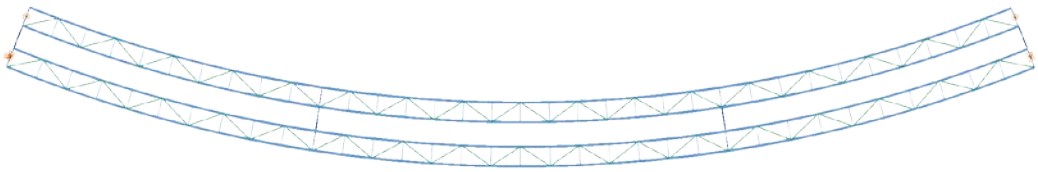

- Reference: (Kulicki et al., 2005)
- I_{S1} = 0, I_{S2} = 0, I_{S3} = 0 / I_{L1} = 1.03, I_{L2} = 1.03, I_{L3} = 1.03 / I_{T1} = 0.64, I_{T2} = 0.74, I_{T3} = 0.64
- Double bearing per girder modeled as single bearing.
- TFLB and top flange interaction is noticeable as saw-tooth shaped major axis bending stresses.

(12) TSCS (Tub-girder, Simple-span, Curved, Skewed supports)

12.1 NTSCS5 (L_1 = 150ft / R = 400 ft / w = 30 ft / θ_1 =10.7°, θ_2 =-10.7°, 2 tub-girders)

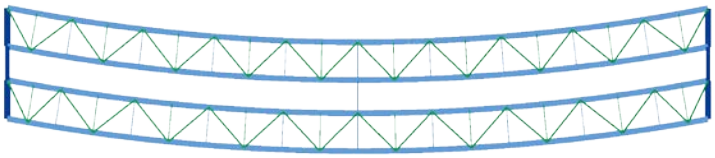

- I_{S1} = 0.02 / I_{L1} = 1.00 / I_{T1} = 0.81
- Lateral displacements start at non-zero value at skewed support locations. 2D-Grid matches the results.
- TFLB and top flange interaction is noticeable as saw-tooth shaped major axis bending stresses.

12.2 NTSCS29 (L_1 = 225ft / R = 820 ft / w = 30 ft / θ_1 =15.7°, θ_2 =0°, 2 tub-girders)

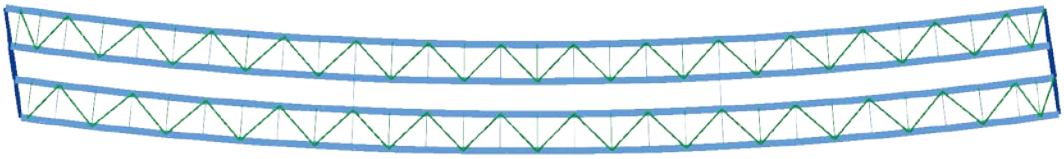

- I_{S1} = 0.02 / I_{L1} = 1.00 / I_{T1} = 0.84
- Lateral displacements start at non-zero value at skewed support location. 2D-Grid matches the results.
- Skew adds to torsion due to curvature increasing the torque at left support and reducing at right support.
- TFLB and top flange interaction is noticeable as saw-tooth shaped major axis bending stresses.

(13) TCCS (Tub-girder, Continuous-span, Curved, Skewed supports)

13.1 ETCCS5a (L_1 = 183 ft, L_2 = 161 ft / R = 765 ft / w = 36.2 ft / θ_1 = 0°, θ_2 = 4.8°, θ_3 = 0°, 2 tub-girders)

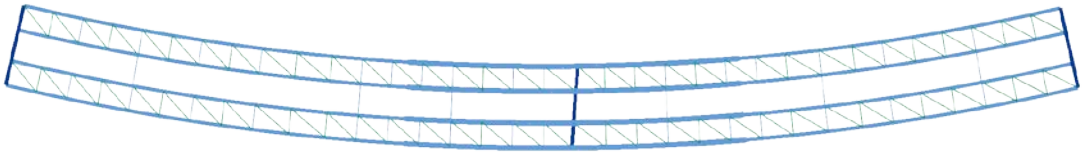

- Ramp A2, SR 9A / SR 202 Interchange, Duval Co., FL
- Small skew at intermediate bearing line.
- I_{S1} = 0.01, I_{S2} = 0.01 / I_{L1} = 1.02, I_{L2} = 1.03 / I_{T1} = 0.70, I_{T2} = 0.67
- Intermediate skew increases the curvature effects on the left span while the skew counteracts the curvature on the left span. This effect is more noticeable when the angle of the skewed support is larger.
- TFLB and top flange interaction is noticeable as saw-tooth shaped major axis bending stresses.

13.2 ETCCS6 (L_1 = 160 ft, L_2 = 207 ft / R = 814 ft / w = 50.5 ft / θ_1 = 0°, θ_2 = 39.2°, θ_3 = 0°, 4 tub-girders)

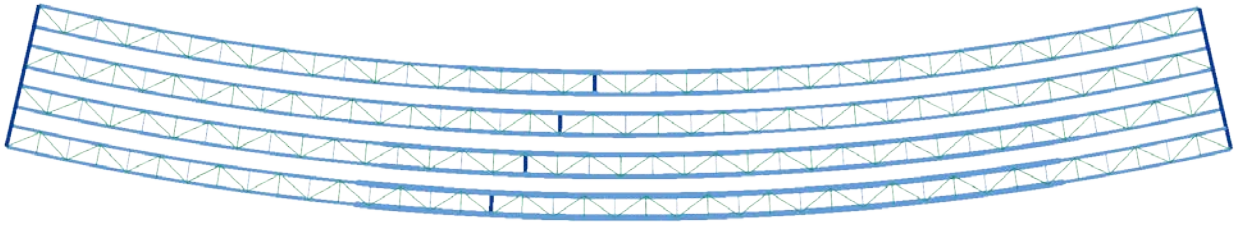

- McGruder Blvd. to SB I-64, Hampton, VA
- Constructed in two phases of two tub-girders each. Fit-up issues encountered during erection.
- I_{S1} = 0.06, I_{S2} = 0.05 / I_{L1} = 0.95, I_{L2} = 1.07 / I_{T1} = 0.70, I_{T2} = 0.84 (Stage 1 - Interior)
- I_{S1} = 0.06, I_{S2} = 0.04 / I_{L1} = 0.95, I_{L2} = 1.06 / I_{T1} = 0.68, I_{T2} = 0.95 (Stage 2 - Exterior)
- Staged construction of 2 tub-girders each.
- The lack of external diaphragms at the interios pier helps avoiding the torsional effects due to skew but girder rotations are increased.
- Heavily skewed intermediate supports must have collinear diaphragms and cross frames to avoid geometric problems with sloped webs.
- Relative vertical displacements of the most extreme flanges have differences of 8in on the completed 4 tub-girder bridge mainly due to the increased relative length of the internal to external girders. These vertical displacements are usually accommodated in the camber but must be predicted accurately.
- TFLB and top flange interaction is noticeable as saw-tooth shaped major axis bending stresses.

13.3 NTCCS22 (L_1 = 250 ft, L_2 = 250 ft / R = 713 ft / w = 30 ft / θ_1 =20.1°, θ_2 =0°, θ_3 =0°, 2 tub-girders)

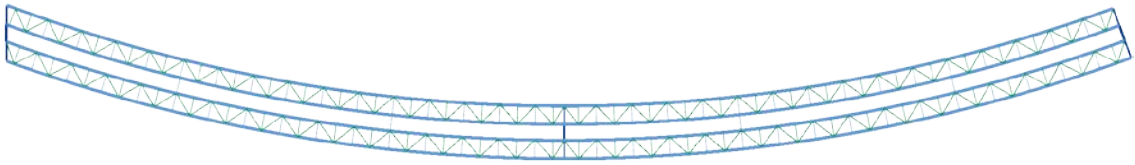

- I_{S1} = 0.02, I_{S2} = 0 / I_{L1} = 1.00, I_{L2} = 1.02 / I_{T1} = 0.98, I_{T2} = 1
- Lateral displacements start at non-zero value at skewed support location. 2D grid matches the results.
- Skew and curvature torsional forces counteract.
- TFLB and top flange interaction is noticeable as saw-tooth shaped major axis bending stresses.
- Linear and Non-Linear 3D FEA analyses results report negligible differences.

APPENDIX F

EARLY CORRESPONDENCE WITH OWNER AND AGENCIES

This appendix shows the materials mailed to 50 state bridge engineers or bridge engineering contacts as well as the bridge engineer for Puerto Rico.

Georgia Institute of Technology

School of Civil and Environmental Engineering

July 2, 2008

_____

_____

_____

___

RE: NCHRP 12-79, Request for curved and/or skewed steel deck-girder bridge descriptions and plans, & information pertaining to policies and procedures pertaining to curved and/or skewed steel deck-girder bridge construction

Dear _____:

Georgia Tech, under the AASHTO-sponsored National Cooperative Highway Research Program (NCHRP), is conducting Project 12-79, "Guidelines for Analytical Methods and Erection Engineering of Curved and Skewed Steel Deck-Girder Bridges." The objectives of this research are:

(1) Develop Guidelines for when simplified 1D or 2D analysis methods are sufficient and when 3D methods may be more appropriate for predicting the constructability and the final constructed geometry of curved and/or skewed steel deck-girder bridges

(2) Develop Recommendations on the level of construction analysis, construction plan detail and submittals for curved and skewed steel deck-girder bridges for direct incorporation into specifications or guidelines.

Both I- and tub-girder bridges will be addressed. Attached, please find a copy of slides that provide some further details about the project.

In Tasks 1 and 2 of the project, we are synthesizing various policies and practices pertaining to the construction engineering of the above bridge types. Also, we are identifying a small suite of existing bridges that we will target in our initial analysis studies. Our criteria for selection of existing bridges are described on slides 12-15.

We would be grateful if you can recommend any particular bridge cases (descriptions and plans) you have encountered in your practice that fit these criteria, and also for any input on your policies and practices regarding analysis methods and construction engineering of steel deck girder bridges. It would be most helpful if we can receive your input by July 25, 2008. My contact information is shown in the footer below.

Thank you in advance for your time and assistance. Best regards.

Sincerely,

Donald W White

Donald W. White
Professor, Structural Engineering, Mechanics and Materials
NCHRP 12-79 Project Principal Investigator

School of Civil and Environmental Engineering
790 Atlantic Drive, Atlanta, Georgia 30332-0355
PHONE 404·894·5839 CELL 678-895-5451 FAX 404·894·2278
E-MAIL: dwhite@ce.gatech.edu

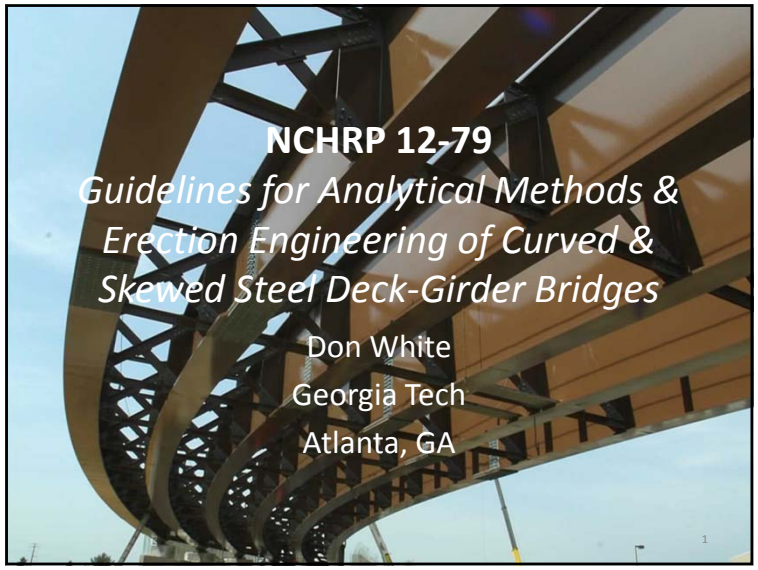

Objectives

1. **Guidelines**
   - When are certain simplified 1D or 2D analysis methods sufficient?
   - When are 3D methods more appropriate?
     for assessing constructability
     and for predicting the constructed geometry
2. **Recommendations**
   - Level of analysis
   - Plan detail
   - Submittals

2

Project Team

Georgia Institute of Technology — Don White (PI), Roberto Leon

HDR — Domenic Coletti (co-PI), John Yadlosky, Brandon Chavel, Tom Howell

The Markosky Engineering Group Inc. — Gary Kowatch, Matthew Walerysiak, Samuel Beachy

High Steel Structures — Ronnie Medlock, Bob Cisneros

tensor engineering — Walter Gatti

T.V. Galambos

3

Panel

- **Mr. Ed Wasserman**, Tennessee DOT (chair)
- **Mr. David Kiekbusch**, Wisconsin DOT
- **Mr. Paul Liles, Jr.**, Georgia DOT
- **Mr. Tom Macioce**, Pennsylvania DOT
- **Mr. Vasant Mistry**, FHWA
- **Dr. Gichuru Muchane**, NC DOT
- **Mr. Hormoz Seradj**, Oregon DOT
- **Dr. Yuan Zhao**, Texas DOT
- **Dr. Joseph Yura,** University of Texas, Austin
- **Dr. Fassil Beshah**, FHWA Liason
- **Mr. Frederick Hejl**, TRB Liason
- **Mr. David Beal**, NCHRP Senior Program Officer
- **Ms. Danna Powell**, Senior Program Assistant

4

Goals

- CLARITY WRT TECHNICAL CONSIDERATIONS
- INFORMATION!....

5

Scope

Analytical study
30 months
~12 Existing Bridges
~60 parametric bridge designs
~60 I-Girder bridges
~12 Tub-girder bridges
w/ radial supports

6

Research Approach

Task 1 – Review lit. & synthesize policies & practices

Task 2 – Identify existing bridges

Task 3 – Select geometric factors & ranges of study

Tasks 4 to 6 – Develop, propose & execute an expanded work plan

Task 7 – Prepare benchmark analysis cases

Task 8 – Prepare Guidelines for selecting analytical methods

Tasks 9 & 10 – Develop & finalize Recommendations for construction analysis, plan detail & submittals

Task 11 – Submit Final Report

7

Work Schedule

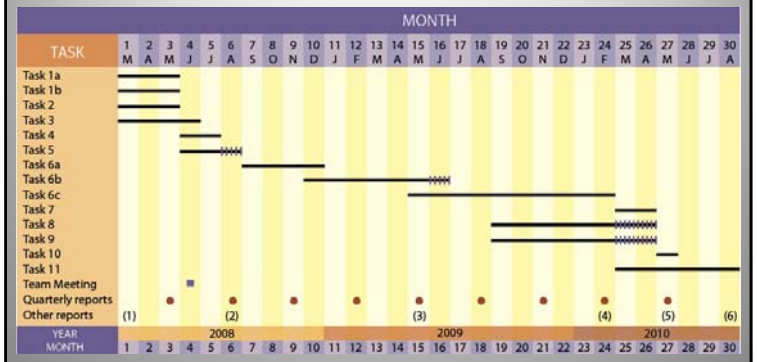

(1) Amplified Research Plan
(2) Interim report on findings from Tasks 1-4 & data archiving & sharing plan

8

T1 – Synthesis of Policies & Practices

- AASHTO LRFD Design & Construction Specs.
- AASHTO/NSBA Guidelines & Guide Specs.
- State Policies & Practices
- Other Research
- NSBA TG13 – Methods of Analysis
  - ***Theme: "How to make your complex bridges simple without making your simple bridges complex"***

9

T2 – Identification of Existing Bridges

- Spectrum of :
  - ***Span arrangements***
  - ***Span lengths***
  - ***Horizontal curvature***
  - ***Bridge widths***
  - ***Skew angles***


I-95 SB over I-395 NB , Fairfax Co., VA

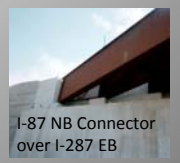
I-87 NB Connector over I-287 EB

10

T2 – Identification of Existing Bridges

- Emphasis on cases where:
  - **Design and construction satisfied prior &/or current AASHTO Specs. & established recommendations, ***BUT***
  - **Construction challenges were encountered or**
  - **Certain attributes resulted in concerns about the final state of stress in the girders, etc.**

11

T2 – Identification of Existing Bridges

- Cases involving generally acknowledged poor practices, e.g.,
  - **Inappropriate use of oversize holes**
  - **Inadequate attachment of cross-frames during construction**

  will not be considered

12

T2 – Identification of Existing Bridges

- Other criteria…
  - **Significant technical challenges addressed very successfully**
  - **Availability of response measurements & observations, particularly during intermediate stages of construction**
  - **Short of having this kind of detailed information…**
    - ***Preference given to bridges having detailed erection plans***

13

Anticipated Research Results

- Better prediction of constructed geometry
  - **Reductions in fit-up problems during girder erection**
  - **Reductions in over-run or under-run of deck thicknesses**
  - **Reductions in misalignment of deck joints**
  - **Reductions in mismatched stages in staged construction projects**
  - **Reductions in deviations from intended deck cross-slopes & profiles**

14

Anticipated Research Results

- Better understanding of the effects of girder web out-of-plumbness
  - **Better decisions regarding target condition for plumbness (TDLF, NLF, etc.)**
  - **Reductions in stability problems**
  - **Appropriate handling of locked-in stresses due to TDLF or SDLF detailing, when these effects are important; clear guidelines on when these effects can be neglected**

15

Anticipated Research Results

- Better preduction of erection stresses & girder stability conditions
  - **Reductions in stability problems during girder erection**
  - **Reductions in situations having unintended/uncalculated significant contributions to displacements**

16

Anticipated Research Results

- *OVERALL*
  - ***Better understanding of critical issues associated with complex steel deck-girder bridges***
  - ***Flexible, clear and consistent standards of care***
  - ***Efficient, safe & economical design & construction of curved & skewed steel deck-girder bridges over a broad range of complexities encountered in practice***

17

THANKS FOR YOUR ATTENTION
Please provide Questions/Comments/Input!

APPENDIX G

OWNER/AGENCY POLICIES AND PROCEDURES

Task 2 of NCHRP Project 12-79 involved the synthesis of pertinent owner/agency policies and practices. To this end:

1. The Project Team coordinated with AASHTO/NSBA Steel Bridge Collaboration Task Group 13 (TG13), which completed a Survey of Current Practice in Steel Girder Design in Summer 2008.

2. The Project Team conducted its own survey of current policies and procedures in Summer 2008.

3. The Project Team reviewed a number of guideline documents, including (but not limited to):

   - The AASHTO/NSBA document G12.1 – 2003, *Guidelines for Constructability*,
   - The AASHTO/NSBA document S10.1 – 2007, *Steel Bridge Erection Guide Specification*,
   - NCHRP Synthesis 345 – *Steel Bridge Erection Practices*, and
   - Vol. 1, Ch. 14 of the *Highway Structures Design Handbook, Steel Erection for Highway, Railroad and other Bridge Structures*.

G.1 AASHTO/NSBA STEEL BRIDGE COLLABORATION TASK GROUP 13 SURVEY

The AASHTO/NSBA Steel Bridge Collaboration formed Task Group 13 in May 2007, with the mission of developing guidelines for the analysis of steel bridges. One of the Task Group's first objectives was to survey the current practices of steel girder design throughout the US. The Task Group wanted to see how the various owner-agencies and other organizations are designing various types of steel girder bridges with the following goals in mind:

- Assessing the current state of practice in steel girder design,
- Noting trends in steel girder design,
- Collecting guidelines, methods, and tools,
- Collating a set of "best practices" guidelines and suggestions for publication in an AASHTO/NSBA Steel Bridge Collaboration steel girder design document.

The survey addressed a wide variety of steel girder bridge types. If there was a particular type of steel girder bridge that a given organization did not typically design, they were encouraged to feel free to skip that section of the survey, or to offer opinions as to how they would approach that type of design if they were to perform it.

In order to establish a consistent context for communication of policies and practices, the survey included definitions of various analysis methods, which are listed below:

- *Hand Analysis Methods:* Any analysis/design method that can be performed completely by hand (even if it is sometimes or often programmed into a spreadsheet or computer program). Examples include the Moment Distribution Method, the V-Load Method, the M/R Method, etc.
- *Line Girder Analysis Methods:* Any analysis/design method that isolates a single tangent girder from the rest of the superstructure system and evaluates that girder individually, with the rest of the superstructure system considered only by means of boundary conditions, live load distribution factors, etc.
- *Grid Analysis Methods:* The characterization as a Grid analysis in this survey was indicated to mostly address 2D Grid or Grillage analysis methods. This includes any analysis/design method that includes a computerized structural analysis model where the superstructure is typically modeled as a two-dimensional array of nodes and line elements, and where the girders and cross frames or diaphragms are typically modeled using line elements, where the analysis displacements are solely vertical displacements and rotations about axes in a horizontal plane, and where the loads considered are primarily out of plane vertical (gravity) loads. Two variants are listed below ("Plate and Eccentric Beam Grid" and "3D Grid"). The survey participants were asked that if they use one of these variants (or another variant) to please indicate so in their survey responses.
- *"Plate and Eccentric Beam Grid" Analysis Methods:* A variant on 2D Grid/Grillage analysis model, where the deck is modeled using plate or shell elements, while the girders and cross frames are still modeled using line elements, offset from the deck elements. The survey participants were asked that if they perform Grid analyses using methods that address some of these refinements, to please indicate so in their survey responses.
- *"3D Grid" Analysis Methods:* This is a modification of a 2D Grid analysis, where more degrees of freedom are modeled. Some typical additions that separate 3D Grid methods from 2D Grid methods include modeling of warping stiffness and warping response of I-shaped girders, modeling of the shear stiffness of cross frames or diaphragms, and modeling of girder supports, lateral bracing, and/or cross-frames or diaphragms at their physical elevation within the structure. The survey participants were asked that if they perform Grid analyses using methods that address some of these refinements, to please indicate so in your survey responses.
- *3D Analysis Methods:* Any analysis/design method that includes a computerized structural analysis model where the superstructure is modeled fully in three dimensions, including: modeling of girder flanges using line/beam elements or plate/shell/solid type elements; modeling of girder webs using plate/shell/solid type elements; modeling of cross frames or diaphragms using line/beam, truss, or plate/shell/solid type elements (as appropriate) and modeling of the deck using plate/shell/solid elements.

A total of 37 state DOTs responded to the survey. These surveys were grouped and collectively titled the "AASHTO responses." Most AASHTO surveys were filled out in a relatively complete manner in terms of answering the "check box" questions, but expanded commentary by the survey respondents was sporadic.

A total of six responses were received from railroad bridge engineers, representing either railroad owner-agencies or consulting engineers who specialize in railroad bridge engineering. These surveys were grouped and collectively titled "AREMA responses." In general, the AREMA surveys were not

completely filled out – the respondents typically limited their comments to the tangent (straight) plate girder / rolled beam questions.

A total of seven responses were received from others during the initial phase of the survey (Task Group 13 is currently soliciting more responses to the survey from designers outside of DOT organizations). Four of these were from consulting engineers, two from owner-agencies other than US state DOTs, and one from a fabricator/erector. These surveys were grouped and collectively titled "At Large responses." Most At Large surveys were filled out in a relatively complete manner in terms of answering the "check box" questions, but expanded commentary by the survey respondents was sporadic.

G.2 NCHRP 12-79 PROJECT TEAM SURVEY

The NCHRP 12-79 Project Team also conducted a focused survey of owner/agency practices and procedures. The Project Team recognized the work already accomplished by TG13 and chose to conduct a focused survey directed primarily at the state DOTs (see Appendix F). All 50 states as well as the commonwealth of Puerto Rico were contacted. The Project Team sent a brief introductory letter, accompanied by a brief description of the NCHRP 12-79 Project and the Project Team, along with a request for existing bridge plans and for any policies, procedures, or comments associated with analysis methods and construction engineering for steel deck girder bridges.

Thirty-one of the 51 contacted owner/agencies responded in some way to this request for information and input. The responses included a large number of existing bridge as well as a number of policy, procedure, and/or guideline documents.

G.3 DISCUSSION OF POLICIES, PROCEDURES AND PRACTICES OF VARIOUS OWNER/ AGENCIES

G.3.1 Overall Trends and Comments

As might be expected, there were wide variations in the responses to various survey questions from the state DOTs. Each state is somewhat unique in terms of how much of their bridge design and construction volume consists of steel girder bridges, as well as being unique in the specific nature of their steel girder bridges. Some states do no steel girder design or construction at all, while other states use steel girders extensively in a wide range of simple and complex bridge applications. Some states use steel girders primarily in simple applications (e.g., tangent, non-skewed rolled beams and plate girders), while other states use steel girders primarily in complex applications (e.g., longer spans, curved girder bridges, etc.) where prestressed concrete girders or other types of bridges are not feasible. As a result, there is understandably some fairly wide scatter in the responses to many of the questions in the survey.

However, many general trends were also apparent. There appears to be a growing interest in some of the more subtle nuances of steel girder behavior and analysis as designers face more challenging steel bridge projects featuring longer spans and more severe curvature and skew. But at the same time, there is still a great reliance in, and confidence in, simple, tried and true analysis methods.

The following general points can be drawn from the surveys:

- Some states are realizing a need for more careful analysis for some of the more complex steel girder bridges they are increasing faced with.

- Some states feel content with their current tools and methods. This is often linked to trends in those states which are not leading them to face more complex steel bridge design and construction projects.

- Among all states, even among the subset of states that are facing more complex steel girder bridges and are considering the need for more rigorous analysis methods, there is a wide variety of practices being used for steel girder bridge design.

More detailed summaries of the answers to the various survey questions are presented below, grouped to match the titled sections of the survey.

G.3.2 Responses to General Questions

In terms of identified needs for better guidance in the area of analysis of steel girder bridges:

- There were numerous references to a desire for a better understanding of the behavior and analysis of skewed bridges.

- There were several references to a desire for a better understanding of the behavior and analysis of curved girder bridges.

- There were several references to a desire for a better understanding of constructability of steel girders, stability of steel girders during construction, and behavior of steel girders through all stages/phases of construction.

In terms of types or classes of steel girder bridges where there have been more than occasional problems during construction, where the problems can be traced back to issues with the original analysis and design:

- There were several references to issues with staged (or phased) construction.

- There were several references to issues with dead load deflections.

- There were several references to issues with skewed bridges.

One state responded with a very interesting story of a curved bridge which exhibited a deflected shape upon erection that was significantly different from the deflected shape predicted by the originally used grid analysis. The structure subsequently needed to be reanalyzed during construction using a non-linear 3D analysis to address second order effects. The state believes this to be an example of where a grid analysis approach “was not sufficient to capture the behavior of the structure and are looking to establish some possible guidelines for curved structures regarding the level of analysis that needs to be performed depending upon geometry and complexity.”

*G.3.2.1 Responses to Questions About Tangent (Straight) Steel Plate Girders or Rolled Beams with No Skew or Limited Skew (**S**kewed less than 20° from Nonskewed)*

Tangent (straight) steel plate girders or rolled beams with no skew or limited skew were listed as being commonly used by approximately 60% of the responding states. They are used in both integral end bent and conventional end bent applications. They are typically used in both simple span and continuous applications, on both narrow and wide bridges. They are used in a wide range of span lengths, with medium span lengths (100' to 250') being most prevalent.

Some form of line girder analysis, often by hand calculations, but more often by in house or commercial software, is by far the most prevalent design method being used. A wide range of software packages (ten or more different commercial packages, and probably an equal or greater number of in-house software packages) are being used.

A similarly wide range of reference documents are used as guidelines for these designs.

A wide variety of comments were received regarding widening and/or staged construction, including a few problems, but there did not appear to be a significant link from any problems directly to the analysis methods used.

G.3.2.2 Responses to Questions About Tangent (Straight) Steel Plate Girders or Rolled Beams, Significantly Skewed (Skewed More than 20° from Nonskewed)

As might be expected, tangent (straight) steel plate girders or rolled beams, significantly skewed, were listed less often as being routinely used, but still nearly half of the responding states listed them as being routinely used.

The use of integral end bents with skewed tangent girder bridges with is less frequent than with non-skewed tangent girder bridges, and even the states that routinely use integral end bents with skewed tangent girder bridges typically limit the permissible skew.

These types of bridges are typically used in both simple span and continuous applications, on both narrow and wide bridges. They are used in a wide range of span lengths, with medium span lengths (100' to 250') being most prevalent.

Again, as for non-skewed tangent girder bridges, some form of line girder analysis, often by hand calculations, but more often by in house or commercial software, is by far the most prevalent design method being used. Again, as for non-skewed bridges, a wide range of software packages is being used.

However, for these skewed tangent girder bridges, the use of either a grid analysis or a 3D analysis is more prevalent, being mentioned 8 times for non-skewed bridges, but 16 times for skewed bridges.

Special considerations and limitations mentioned for skewed bridges were more specific than for non-skewed bridges, with several responses mentioning special consideration being given to cross frame analysis, design, and detailing.

Most of the issues associated with widening and/or staged construction for skewed tangent girder bridges seem to be similar to those listed for non-skewed tangent girder bridges.

G.3.2.3 Responses to Questions About Curved Steel Plate Girders or Rolled Beams with No Skew or Limited Skew (Skewed less than 20^o from Nonskewed)

Curved steel plate girder or rolled beam bridges with no skew or limited skew were reported as being less frequently used than tangent (straight) girder bridges, but still more than half of the responding states reported using them either routinely or occasionally, with some mention that steel girders are often selected for curved bridges, if there is no way to avoid curvature on the bridge.

The use of integral end bents with curved steel girder bridges appears to be much less common than for tangent (straight) girder bridges.

Curved steel girder bridges appeared to be more commonly used in continuous rather than simple span applications, although simple span applications were certainly not rare. Curved steel girder bridges also appeared to be more commonly used in narrow bridge applications rather than wider bridge applications. They are used in a wide range of span lengths, once again with medium span lengths (100' to 250') being most prevalent.

In terms of analysis methods used, the VLOAD method, either by hand or via a computer program, was listed as being used or recommended by 18 of the responding states, although two of those respondents mentioned DESCUS or MDX as their VLOAD software package, which seemed odd since DESCUS and MDX are better known as grid analysis programs. Meanwhile 23 of the responding states said that they used or recommended grid analysis for curved, non-skewed bridges, and 7 of the responding states said that they used or recommended 3D analysis. (Recall that for this question, the respondents were directed to indicate all methods that apply, hence the number of responses sums to more than the 37 responding states). So, in summary, the VLOAD method appeared to still be popular and commonly used, although grid analysis methods appeared to be most prevalent for these types of structures, with 3D analysis methods being the least prevalent.

In terms of limitations, none of the responding states specifically indicated limits on span length or degree of curvature for any given analysis approach (VLOAD, grid, or 3D), although one state hinted that limits on when to move from grid to 3D were being evaluated.

There was much less comment on widening and/or staged construction of curved, non-skewed bridges than was provided for tangent (straight) girder bridges. Of perhaps the most significance were a few comments indicating that curved steel bridges were seldom, if ever, widened, at least in some states.

G.3.2.4 Responses to Questions About Curved Steel Plate Girders or Rolled Beams, Significantly Skewed (Skewed more than 20^o from Nonskewed)

The trend for less application with more complexity continued as curved steel girder bridges with significant skew were listed as less frequently used than curved non-skewed steel girder bridges.

The use of integral end bents for curved steel girder bridges with significant skew was even less than for curved, nonskewed steel girder bridges.

Curved steel girder bridges with significant skew appeared to be more commonly used in continuous rather than simple span applications, although simple span applications were certainly not rare. Curved

steel girder bridges with significant skew also appeared to be more commonly used in narrow bridge applications rather than wider bridge applications. They are used in a wide range of span lengths, once again with medium span lengths (100' to 250') being most prevalent.

Versus curved, non-skewed steel girder bridges, curved steel girder bridges with significant skew were less likely to be analyzed by the VLOAD method, although the VLOAD method was still listed as used or recommended by 13 of the responding states. Meanwhile, the use of grid or 3D analysis methods was more likely for curved steel girder bridges with significant skew, with grid analysis methods being used or recommended by 20 of the responding states, and 3D analysis methods being used or recommended by 10 of the responding states. (Recall that for this question, the respondents were directed to indicate all methods that apply, hence the number of responses sums to more than the 37 responding states). So, in summary, the VLOAD method appeared to still be popular and commonly used, but less so than for curved, non-skewed bridges, with grid analysis methods appearing to still be most prevalent for these types of structures, but with 3D analysis methods being more popular for curved, significantly skewed bridges than for curved, non-skewed bridges.

Few comments were received regarding limitations or special considerations, or for wider bridges and/or staged construction.

G.3.2.5 Responses to Questions About Tub Girders or Box Girders

Much less response was received regarding tub or box girders than was received regarding rolled beams and plate girders. In general, it appeared that tub or box girders are much less common among the states.

In terms of analysis methods, the trends for steel tub or box girders seemed to match the trends for rolled beams and plate girders, with line girder analysis methods being more prevalent than grid or 3D analysis methods for tangent (straight) girder bridges, and grid analysis methods, and to a lesser extent 3D analysis methods, being more prevalent for curved girder bridges. There was however, a noticeable shift toward more refined methods being preferred for tub or box girders vs. rolled beams or plate girders, i.e., for tangent tub or box girders there was a greater percentage of votes for grid analysis than was seen for tangent rolled beams or plate girders, and likewise for curved tub or box girders there was a greater percentage of votes for 3D analysis than was seen for curved rolled beams or plate girders.

G.3.2.6 Responses to Questions About Bridges with Significantly Complex Framing Plans (Variable Girder Spacing, Bifurcation of Girders, Elevated Tee-Intersections, Single Point Urban Interchanges, etc.)

There was little response to these questions and few if any trends were observed. Single Point Urban Interchanges (SPUIs) were mentioned as becoming more prevalent. Line girder, grid, and 3D analysis methods were all listed as being recommended by nearly equal numbers, but not much could be drawn from that voting given the wide range of structures covered by this question and the lack of much in the way of expanded responses from the survey respondents.

G.3.3 Specific Examples of Individual State DOT Policies and Practices

The examples listed below represent only a sampling of individual state DOT policies and practices and are not meant to be an exhaustive listing either with regard to the number of states mentioned nor with regard to the breadth of each state's guidelines. Any notable omissions of specific states or their

specific guidelines is unintentional. At this stage in the project, the various policies and procedures are being synthesized by the Project Team without making any value judgments.

A number of state DOTs have developed stand-alone documents related to steel bridge design, detailing, fabrication, and/or erection, including:

- Caltrans has the *Preferred Practices for Steel Plate Girder Bridge Design, Fabrication, and Erection*, 2002
- TxDOT has the *Texas Steel Quality Council Preferred Practices for Steel Bridge Design, Fabrication, and Erection*, 2005
- There are also the *Mid-Atlantic States Structural Committee for Economical Fabrication (SCEF) Standards*

The Caltrans document was developed by Caltrans, whereas the Texas and Mid-Atlantic States documents were developed by volunteer committees comprised of various owner and industry representatives. These documents are generally very thorough and comprehensive, but are focused on design, detailing, and fabrication issues and offer only limited guidance on analysis issues.

Florida DOT (FDOT) has some explicit guidelines on analysis methods summarized in Table G.1

Table G.1 Explicit Florida DOT guidelines.

Analysis Type	Bridge Type
1D	Straight bridges w/ skews < 10 degrees
2D (grid)	Straight bridges w/ skews > 10 degrees Curved bridges w/ radius >700’
3D	Curved bridges w/ radius <700’

FDOT also has some explicit requirements related to scope and responsible party for constructability checks and erection plans.

Pennsylvania DOT (PennDOT) provides analogous guidelines for curved bridges in their design manual (DM4), where they require that curved girder bridges be analyzed using a “refined method of analysis” which they later define as either a 3D finite element method or a 2D grillage analogy.

Idaho DOT (ITD) has a specific policy and guidelines on prediction of twist in tangent girder bridges with skewed supports, based on simple geometric relationships. ITD also recommends assuming

uniform dead load deflection among all girders (interior and exterior) during slab placement. ITD also recommends consideration of fascia girder twist deformations due to overhang loads, referencing AASHTO LRFD and KDOT guidelines.

Illinois DOT (IDOT) has a standard special provision requiring submittal of a detailed Erection Plan prepared by an Illinois PG. They also require submittal of erection engineering calculations. In addition, the original designer is required to fully investigate at least one erection sequence. IDOT's bridge design manual offers some guidance on how to deal with skewed and curved structures: for severely skewed bridges (>45º), they allow use of an assumed 10 ksi lateral flange bending stress. They also provide guidance on how to consider composite action (typically not considered in negative moment regions on straight or mildly curved girders, considered in more severely curved bridges, with the definition of "curved" being consistent with AASHTO GHC-4). IDOT requires the use of standard holes in the plans for curved girder bridges, but also requires that the connection be designed as if oversize holes were being use (to allow for "a measure of redundancy"). They require detailing for the webs to be plumb at the steel dead load condition.

North Carolina DOT (NCDOT) has a comprehensive Structure Design Manual that addresses steel girder bridge design with some specific design guidelines and some specific detailing suggestions. But more significant are their recent guidelines related to adjustments to dead load deflections in tangent steel girder bridges. NCDOT sponsored extensive research at North Carolina State University to perform field measurements and analytical studies to develop a method for adjusting line girder analysis results to account for girder spacing, skew, interior vs. exterior girder effects, etc. The resulting guidelines are presented in the form of simple equations, but an accompanying spreadsheet which automates the calculations is also offered. The goal of this research and NCDOT's position in general is to try to find ways to use simpler analysis methods whenever possible, while recognizing some of the limitations of these simpler methods and providing procedures for adjusting the results of simpler analyses to better approximate actual behavior in more complex structures.

Ohio DOT (ODOT) recently adopted new policies related specifically to skewed bridges. These include:

- For bridges with skew angles less than 30 degrees, the effects of skew do not have to be considered.

- For bridges with skew angles between 30 and 45 degrees, the differential deflection between beams must be less than the beam spacing divided by 100. If not, a refined analysis must be performed and the beams may have to be redesigned or other measures may have to be taken.

- For bridges with skew angles greater than 45 degrees, a refined analysis must be performed. If the girder twist is greater than 1/8 inch per foot, the beams either have to be redesigned or other measures may have to be taken.

- The effects of twisting of the overhang bracket are to be investigated.

APPENDIX H

DESIGN CRITERIA FOR NCHRP 12-79 PROJECT NEW BRIDGE DESIGNS

This appendix summarizes the criteria applied for the design of new hypothetical bridges considered in NCHRP 12-79's Task 7 parametric studies. The various considerations are presented in an overall outline form.

H.1 GENERAL

In general all requirements of the AASHTO *LRFD Bridge Design Specifications*, 4th edition, with 2008 interim revisions were followed. Where specific AASHTO guidelines were not available, or where the AASHTO specifications allowed for designer discretion, then the guidelines listed below governed.

In addition to the specific guidelines enumerated below, the parametric study bridge designs also followed generally accepted design and detailing practices. Typical reference documents used (and cited below) included, but were not limited to:

- Texas Steel Quality Council, Preferred Practices for Steel Bridge Design, Fabrication, and Erection, (TxDOT 2005),
- AASHTO/NSBA G12.1-2003, Design for Constructability,
- HDR, *Bridgeline* (Various editions)
- AASHTO, GHC-4 (2003), Guide Specifications for Horizontally Curved Steel Girder Highway Bridges with Design Examples for I-Girder and Box-Girder Bridges,
- NHI Course 130081 Design Manual (NHI 2007), and
- NSBA, Steel Bridge Design Handbook, Chapter 8 – Stringer Bridges, 2006.

H.2 MATERIALS

All structural steel was assumed to be ASTM A 709, Gr. 50 W except as follows:

- Any "existing bridges" included in the study were modeled using their specified materials.
- HPS 70W was not considered in the "non-existing" parametric study bridges for the following reasons:

    1. Hybrid girders are not widely used

    2. Hybrid girders introduce another level of complexity to the overall problem statement. It was decided that analysis trends would be easier to see without adding the question of "how does the use of hybrid girders affect the results?"

H.3 FATIGUE

The designers assumed good detailing practices were followed and designed girders assuming Category C' for transverse stiffener-to-flange and transverse stiffener-to-web weld conditions controlled (ref.: AASHTO LRFD Table 6.6.1.2.3-1)

H.4 LIVE LOAD DEFLECTIONS

In order to follow design practices which are still prevalent throughout the US, the parametric study bridges generally were designed to comply with the optional live load deflection control criteria of AASHTO LRFD § 2.5.2.6.2. The more stringent criteria for bridges subjected to pedestrian loads were not considered. These criteria were used as "guidelines" not as absolute limits; deflections as much as 10% beyond the AASHTO criteria were considered acceptable.

H.5 DECK DESIGN

Assumed a 9 1/2" thick concrete deck (including a ½" sacrificial wearing surface), f'_c = 4.0 ksi, nominal unit weight 0.150 kcf.

H.6 DECK LONGITUDINAL REINFORCING

The guidance provided by AASHTO LRFD § 6.10.1.7 was followed.

In the design of the girders in the negative moment regions (i.e., in the girder resistance checks, but not in the structural analysis as outlined below), the deck was considered ineffective. However, the longitudinal deck reinforcing was considered effective.

For all analyses, as suggested in AASHTO LRFD C4.5.2.2, uncracked section properties were assumed for the entire deck (in both positive and negative moment regions).

H.7 SHEAR CONNECTORS

The basic assumption was that shear connectors were provided throughout the length of all bridges, based on the recommendations in AASHTO LRFD § 6.10.10.1.

H.8 INTERMEDIATE DIAPHRAGMS / CROSS FRAMES FOR I-GIRDER BRIDGES

General Configurations:

- Girders with Web Depth $\leq$ 48": Solid diaphragms are common (ref.: Texas Steel Quality Council, *Preferred Practices for Steel Bridge Design, Fabrication, and Erection*, 2005, pg 2-25, AASHTO/NSBA G12.1-2003, pp 20-21, NCDOT *Structure Design Manual*, 2007, pg 6-36 and Fig. 6-98). For consistency in this study, assumed bent plate diaphragms, depth approximately 80-90% of web depth.
- Girders with Web Depth > 48" and spacing/web depth (s/d) ratio $\leq$ 1.5, assumed X-frame cross frames with top and bottom chords (ref.: HDR *Bridgeline*, Vol. 13, No. 1, pg. 3 and AASHTO/

NSBA G12.1-2003, pg. 20). Used single angle sections for chord and diagonals if possible; used WT sections for chords and diagonals if absolutely necessary by design.

- Girders with Web Depth > 48" and s/d ratio > 1.5, assumed inverted K-frame cross frames with top chords (ref.: HDR *Bridgeline*, Vol. 13, No. 1, pg 3 and AASHTO/NSBA G12.1-2003, pg 20). Used single angle sections for chord and diagonals if possible; used WT sections for chords and diagonals if absolutely necessary by design.

Addressing "Nuisance Stiffness" Issues in Skewed Bridges:

- Selectively omitted diaphragms / cross-frames near supports in order to reduce the effects of undesirable transverse stiffness ("nuisance stiffness"). Followed suggestions in the article "Nuisance Stiffness" (HDR *Bridgeline*, Vol. 4, No. 1, 1993, pp 1-3). For consistency among designs in the research project, use of "lean-on" bracing concepts was considered only on a limited basis (this approach is not yet fully implemented nationally).

Spacing:

- Cross frame / diaphragm spacing in horizontally curved bridges was selected so as to limit lateral flange bending stresses. The spacing was initially determined using Eq. C9-1 in AASHTO GHC-4 (2003), with the target bending stress ratio $r_\sigma = | f_\ell / f_b |$ set at 0.30. The spacing was generally limited to a maximum value of 25' in order to result in a reasonably "typical" framing plan.
- Cross frame / diaphragm spacing in tangent, skewed bridges was selected to maximize the spacing. The general target was approximately 25' spacing.

Design:

- Generally followed design procedures as presented in HDR cross frame design spreadsheets developed for recent design projects, but consideration of connection details and their design were omitted. The focus was only on chord and diagonal member design in order to establish reasonable member sizes for use in the analysis models.

Connections:

- It was assumed that all connections were fully effective for analysis modeling purposes.

Cross Frame / Diaphragm Modeling in 2D and 3D Analysis Models:

- In 2D Grid analysis models, truss-type cross frames must be modeled using an equivalent single line element. The cross sectional properties for the equivalent line element were determined using one of the two methods outlined in *Analysis of Steel Girder Bridges – New Challenges* (Coletti and Yadlosky 2007). The specific choice of the "shear stiffness" approach was made early on in Task 7 following a brief study.
- In 2D Grid analysis models, plate-type diaphragms were modeled using an equivalent single line element. The determination of the cross sectional properties for that single line element was a

relatively straight-forward direct application of the cross sectional properties of the actual diaphragm.

- In 3D FEM models, the cross frame or diaphragms were modeled in detail, with each of the chords and diagonals of truss-type cross frames modeled directly, and with the full web depth of plate-type diaphragms modeled directly, with flanges modeled using line elements on the top and bottom of the web plate element.

H.9 END DIAPHRAGMS / CROSS-FRAMES FOR I-GIRDER BRIDGES

As a general rule, the same guidelines were followed as for intermediate diaphragms / cross-frames for I-girder bridges, except that the top chord was assumed to be a channel section extending up to support the edge of the deck (ref.: AASHTO/NSBA G12.1-2003, pg 22).

H.10 PIER DIAPHRAGMS / CROSS-FRAMES FOR I-GIRDER BRIDGES

As a general rule, followed the same guidelines as for intermediate diaphragms / cross-frames for I-girder bridges.

H.11 HORIZONTAL LATERAL BRACING FOR I-GIRDER BRIDGES

Horizontal lateral bracing was provided when necessary; the initial guideline assumption was that it would be considered primarily for the 350' span range I-girder bridges. As a design goal, lateral bracing requirements were met whenever possible by providing only top flange lateral bracing; this is consistent with current common design practice and is done to avoid the situation of bottom flange lateral bracing which is subject to significant live load effects after deck placement. The extent of lateral bracing was limited to a minimum number of bays and panels required to achieve stability and control stresses induced by wind loading. In general, the guidance in the NSBA Steel Bridge Design Handbook Example 1, pp. 50-52 was followed. As a design target, lateral bracing was designed to limit lateral deflections caused by wind loading to a value of approximately L/300 (ref.: 2006 draft of NHI Course 130081 Design Manual, Vol. 1, pg. 2.69).

H.12 INTERNAL INTERMEDIATE DIAPHRAGMS FOR TUB-GIRDER BRIDGES

In general, the suggestions and references presented by Coletti, et al. (2006), Practical Steel Tub Girder Design, regarding spacing and sizing of internal intermediate diaphragms were followed. In particular, a likely spacing configuration was to set the top flange lateral bracing bay spacing approximately equal to the tub girder internal top flange center to center web spacing, and to provide internal intermediate diaphragms at a spacing double that of the top flange lateral bracing bay spacing. The internal intermediate diaphragms consisted of inverted K-frames, with the top chord forming part of the top flange lateral bracing system. Typically the top chord was a WT section, while the diagonals were angle sections.

Member loads in internal intermediate diaphragms were calculated as follows:

- For Approximate Method (M/R) and 2D Grid Analysis models: Followed the guidance offered by Fan and Helwig (2002), "Distortional Loads and Brace Forces in Steel Box Girders."

- For 3D FEM analysis models: Direct force results were obtained from the model.

Chord and diagonal members were designed, but consideration of connection details and their design were omitted.

H.13 EXTERNAL INTERMEDIATE DIAPHRAGMS FOR TUB-GIRDER BIRDGES

In general, the suggestions and references presented by Coletti, et al. (2006), Practical Steel Tub Girder Design, regarding spacing and sizing of external intermediate diaphragms were followed. In addition, recent work by Helwig, et al . (2007), in *Design Guidelines for Steel Trapezoidal Box Girder Systems*, was followed to perform preliminary calculations related to the need and suggested spacing of external intermediate diaphragms. In general, full depth truss-type diaphragms (inverted K-frame with top chords) were used and were assumed to remain in place after deck placement. Partial depth plate-type diaphragms are becoming more popular recently, but to date full depth truss-type diaphragms have been more widely used. WT and angle sections were considered for the chords and diagonals based on loading and detailing requirements.

Member loads in internal intermediate diaphragms were calculated as follows:

- For Approximate Method (M/R) models: N/A. The M/R Method was typically limited to use on single tub-girders.
- 2D Grid Analysis models: Used the procedures recommended by and associated with the MDX program for converting internal forces in the equivalent line elements used for diaphragm modeling to member forces in the actual truss-type external diaphragms.
- For 3D FEM analysis models: Direct force results were obtained from the model.

Chord and diagonal members were designed, but consideration of connection details and their design were omitted.

H.14 INTERNAL AND EXTERNAL DIAPHRAGMS AT SUPPORTS

In general, the suggestions and references presented by Coletti, et al. (2006), Practical Steel Tub Girder Design, regarding sizing of internal and external diaphragms at supports were followed. Full depth plate diaphragms were used for both internal and external diaphragms at supports. Top and bottom flanges for these diaphragms were discontinuous across the entire width of the girder system, following recent research and recommendations by Helwig, et al. (2007), *Design Guidelines for Steel Trapezoidal Box Girder Systems*.

Member loads in internal and external diaphragms at supports were calculated as follows:

- For Approximate Method (M/R) models and 2D Grid Analysis models: Followed the guidance presented by Coletti, et al. (2006), Practical Steel Tub Girder Design, for evaluation of simple free body diagrams.
- For 3D FEM analysis models: Direct force results were obtained from the model.

Overall flange sizes and web thicknesses were designed, but consideration of connection details and their design as well as consideration of access openings (manholes) was omitted.

H.15 TOP FLANGE LATERAL BRACING

In general, the suggestions and references presented by Coletti, et al. (2006), Practical Steel Tub Girder Design, regarding spacing and sizing of top flange lateral bracing were followed. In particular, a likely spacing configuration was set the top flange lateral bracing bay spacing approximately equal to the tub girder internal top flange center to center web spacing, and to provide internal intermediate diaphragms at a spacing double that of the top flange lateral bracing bay spacing. In general, WT and angle sections were used to form the top flange lateral bracing system. The top flange lateral bracing system conformed to a Warren Truss arrangement. Pratt Truss configurations were not used unless modeling an "existing bridge" which used such a configuration.

Member loads in the top flange lateral bracing system were calculated as follows:

- For Approximate Method (M/R) models and 2D Grid Analysis models: Followed the guidance presented by Fan and Helwig (1999), "Behavior of Steel Box Girders with Top Flange Bracing."
- For 3D FEM analysis models: Direct force results were obtained from the model.

Top flange lateral bracing members were designed, but consideration of connection details and their design as well as consideration of access openings (manholes) was omitted.

H.16 GIRDER DESIGN PERFORMANCE RATIOS

In general, all performance ratios (demand/capacity) were kept at or below a maximum value of 1.0.

H.17 INELASTIC DESIGN / MOMENT REDISTRIBUTION

Inelastic design and moment redistribution (as provided for in Appendix B6 of AASHTO LRFD) was generally not considered. All of the parametric study bridges were designed to meet all requirements while remaining fully elastic. If an existing bridge was designed using inelastic design or moment redistribution provisions, that design however, was not changed (none of the bridges considered were designed in this way).

H.18 GIRDER SPACING FOR I-GIRDER BRIDGES

Two main deck widths were proposed for the study bridges: 30' and 80'.

- 30' Deck Width Bridge: Used 3'-6" overhangs with 3 girders spaced at 11'-6".
- 80' Deck Width Bridge: Used 3'-6" overhangs with 7 girders spaced at 12'-2".

(ref.: AASHTO/NSBA G12.1-2003, pg 1)

H.19 GIRDER DEPTH FOR I-GIRDER BRIDGES

- Variable web depth girders were not considered.
- Target span/depth ratio: AASHTO LRFD Table 2.5.2.6.3-1 suggests minimum ratios for simple spans and continuous spans for both the noncomposite steel section depth and the overall composite section depth. However, a more practical target is to use the recommendation for minimum total composite section depth as the recommended web depth (ref NSBA SBDH Example 1, pg 8). Therefore, for simple spans targeted a web depth of 0.040L and for continuous spans target a web depth of 0.032L, where L is the total span length.

H.20 WEB SIZING FOR I-GIRDER BRIDGES

In general, web thickness was selected to result in an unstiffened or "partially stiffened" web design (ref.: Texas Steel Quality Council, *Preferred Practices for Steel Bridge Design, Fabrication, and Erection*, 2005, pg 2-10; *NSBA Steel Bridge Design Handbook, Chapter 8 – Stringer Bridges*, pg. 8-11, NHI Course 130081 Design Manual, Volume 2, pg 2.124).

H.21 FLANGE SIZING FOR I-GIRDER BRIDGES

Flange widths were generally set to be roughly 20% to 30% of the web depth (the Texas Steel Quality Council, *Preferred Practices for Steel Bridge Design, Fabrication, and Erection*, 2005, pg 2-7 recommends 30% or greater, but many designers contacted feel this is too wide). Curved girders may tend to the wider end of the above range, while straight girders may tend toward the narrower end of this range. This is wider than the AASHTO LRFD 6.10.2.2 specified minimum flange width, $b_f \geq D/6$. These were not considered as absolute limits, and engineering judgment was exercised to develop designs which satisfied current norms for constructible, economical designs. Top flanges were generally different widths than bottom flanges. In general, bottom flange widths were held constant over the entire length of a bridge, while top flange widths were allowed to change at field splices if warranted. In addition, the ratio of field section length, L, to flange width, b, was not allowed to exceed 85, i.e., $L/b \leq 85$ (ref.: AASHTO LRFD Eqn. C6.10.3.4-1; Texas Steel Quality Council, *Preferred Practices for Steel Bridge Design, Fabrication, and Erection*, 2005, pg 2-7; other references).

The absolute minimum flange width was 12" (ref.: NHI Course 130081 Design Manual, Volume 2, pg 2.113). The typical minimum flange width was 14".

Typically, as is relatively commonly accepted for composite construction, the bottom flange was typically wider than the top flange (ref.: NHI Course 130081 Design Manual, Volume 2, pg 2.118).

Minimum flange thickness was ¾" (ref.: NHI Course 130081 Design Manual, Volume 2, pg 2.116; AASHTO/NSBA G12.1-2003, pg 2).

Flange transitions were addressed on a case by case basis typically following engineering and fabrication suggested guidelines such as those found in AASHTO/NSBA G12.1-2003, pp 5-6 and *NSBA Steel Bridge Design Handbook, Chapter 8 – Stringer Bridges*, pg. 8-8.

H.22 GIRDER SPACING FOR TUB-GIRDER BRIDGES

Two main deck widths were proposed for the study bridges: 30' and 80'.

- 30' Deck Width Bridge: Used 3'-6" overhangs with 2 girders. The girders had a C-C web spacing of 7'-6" to 8'-6", depending on the web depth which affects bottom flange width. An absolute minimum bottom flange C-C web spacing of 4'-0" was observed (ref.: Coletti, et al. (2006), Practical Steel Tub Girder Design) with a minimum bottom flange C-C web spacing of 4'-6" desired.
- 80' Deck Width Bridge: Used 3'-6" overhangs with 4 or 5 girders. Girders typically had a C-C web spacing of 8'-0" to 10'-6", depending on the web depth which affects bottom flange width. Shorter span bridges were assumed to likely have 5 narrower girders, while longer span bridges would likely have 4 wider girders.

H.23 GIRDER DEPTH FOR TUB-GIRDER BRIDGES

- Variable web depth girders were not considered.
- The guidance provided in Coletti, et al. (2006), Practical Steel Tub Girder Design, was followed; minimum web depth was 5'-0". Target steel girder section depth ranged between roughly L/25 and L/35, where L is the span length for simple spans, and 0.80 times the span length for continuous spans. The shallower end of this range was the preferred design target in general.

H.24 WEB SIZING FOR TUB-GIRDER BRIDGES

In general, web thickness was selected to result in an unstiffened or "partially stiffened" web design (ref.: Texas Steel Quality Council, *Preferred Practices for Steel Bridge Design, Fabrication, and Erection*, 2005, pp 2-10 & 2-17; *NSBA Steel Bridge Design Handbook, Chapter 8 – Stringer Bridges*, pg. 8-11, NHI Course 130081 Design Manual, Volume 2, pg 2.124).

H.25 FLANGE SIZING FOR TUB-GIRDER BRIDGES

Top flange widths were set following guidance similar to that followed for I-girder flanges.

The minimum flange width for 150' span bridges was 14". For the 250' and 350' span bridges, the minimum top flange width was 20". At 14", gusset plates would be required for connection of the top flange lateral bracing. At 20", the top flange lateral bracing members can be bolted directly to the girder top flange, which is preferred.

Bottom flange widths were set 4" wider than the C-C web spacing at the bottom flange.

Minimum flange thickness was ¾" (ref.: NHI Course 130081 Design Manual, Volume 2, pg 2.116; AASHTO/NSBA G12.1-2003, pg 2; Texas Steel Quality Council, *Preferred Practices for Steel Bridge Design, Fabrication, and Erection*, 2005, pg 2-16).

The bottom flange b/t ratio was limited to 80 in positive moment regions, a limit which has been cited by fabricators as helpful in avoiding problems with distortion of the bottom flange during welding (Texas Steel Quality Council, *Preferred Practices for Steel Bridge Design, Fabrication, and Erection*, 2005, pp 2-16). Older AASHTO proposed guide specifications have suggested a maximum b/t limit of 120, but 80 is considered more representative of current practice.

Flange transitions were addressed on a case by case basis typically following engineering and fabrication suggested guidelines such as those found in AASHTO/NSBA G12.1-2003, pp 5-6 and *NSBA Steel Bridge Design Handbook, Chapter 8 – Stringer Bridges*, pg. 8-8.

H.26 STIFFENERS

Stiffeners and related details (transverse intermediate stiffeners, bearing stiffeners, cross frame connection plates, etc.) were designed using the current AASHTO LRFD criteria. Stiffener spacing, as it affects the shear capacity of the girder web, were determined as part of the design.

The use of longitudinal web stiffeners was avoided for the 150’ and 250’ span length parametric bridges. Longitudinal stiffeners were considered as appropriate for the 350’ span I-girder bridges.

The use of longitudinal bottom flange stiffeners was avoided for the tub girder bridges, since the bottom flange b/t ratios were anticipated to be well below the range where longitudinal flange stiffeners offer benefits. Most of the tub girders studied had relatively narrow bottom flanges.

H.27 BEARINGS

It was assumed that all bridges were supported on steel-laminated elastomeric (neoprene) bearings, with one bearing per girder for both I-girders and tub-girders.

Bearing restraints were determined on a case by case basis, but generally followed common design practices such as:

- Longitudinal direction: One set of “fixed” bearings was provided at one support; bearings at all other supports were “free” or “guided.”
- Transverse direction: Generally accepted good practices were followed in deciding bearing fixity details. In most cases, one bearing per support was “fixed”; all other bearings were “free” or “guided.”
- Curvature: The direction of longitudinal movement for “guided” bearings was oriented along the direction of anticipated thermal movement (ref.: Coletti and Yadlosky (2007), “Analysis of Steel Girder Bridges – New Challenges.” Consideration was given to the use of circular bearings in cases of severe curvature or skew.

H.28 DESIGN FOR STEEL ERECTION

In general, the girders were sized and the erection schemes were determined such that the erection conditions would not control the girder sizing. However, as erection stresses were determined through the study, if it became necessary to resize girders in order to satisfactorily address an erection situation, the typical decision was to resize the girder rather than to reconfigure the erection scheme. All models of a given bridge were adjusted as necessary in that scenario. This is consistent with current AASHTO design guidance placing responsibility on the Engineer of Record to determine at least one constructible erection scheme as part of the design process (reference AASHTO LRFD §2.5.3). In some extreme cases where constructability was clearly anticipated to be a controlling factor in the design, the erection analysis was conducted before, or in parallel with, the design modeling.

Appendix I. Detailed Summary of Study Bridges

This appendix provides a detailed summary of the bridges studied in the NCHRP 12-79 research. Important observations are discussed for each bridge. The bridges are presented in alphabetical and numerical order within the following bridge categories:

(1) ICSN: I-girder, Continuous-span, Straight, No-skew,
(2) ISSS: I-girder, Simple-span, Straight, Skewed supports,
(3) ICSS: I-girder, Continuous-span, Straight, Skewed supports,
(4) ISCR: I-girder, Simple-span, Curved, Radial supports,
(5) ICCR: I-girder, Continuous-span, Curved, Radial supports,
(6) ISCS: I-girder, Simple-span, Curved, Skewed supports,
(7) ICCS: I-girder, Continuous-span, Curved, Skewed supports,
(8) TCSN: Tub-girder, Continuous-span, Straight, No-skew,
(9) TSSS: Tub-girder, Simple-span, Straight, Skewed supports,
(10) TSCR: Tub-girder, Simple-span, Curved, Radial supports,
(11) TCCR: Tub-girder, Continuous-span, Curved, Radial supports,
(12) TSCS: Tub-girder, Simple-span, Curved, Skewed supports,
(13) TCCS: Tub-girder, Continuous-span, Curved, Skewed supports.

I1.1 XICSN1 (eXample, I-girder, Continuous-span, Straight, No skew)

Bridge Description :

AISI LRFD Example developed originally by Eaton et al. 1996

Category Data:

L_1 = 140 ft, L_2 = 175 ft, L_3 = 140 ft / w = 43 ft, 4 girders.

References:

AISI LRFD Example Developed by Eaton et al. (1996)

Cross-Frame Detailing Method: NLF

Erection Stages Analyzed: 7 (Analyses are performed assuming NLF)

Deck Placement Sequence: 4 Stages (Analyses are performed assuming no staged deck placement)

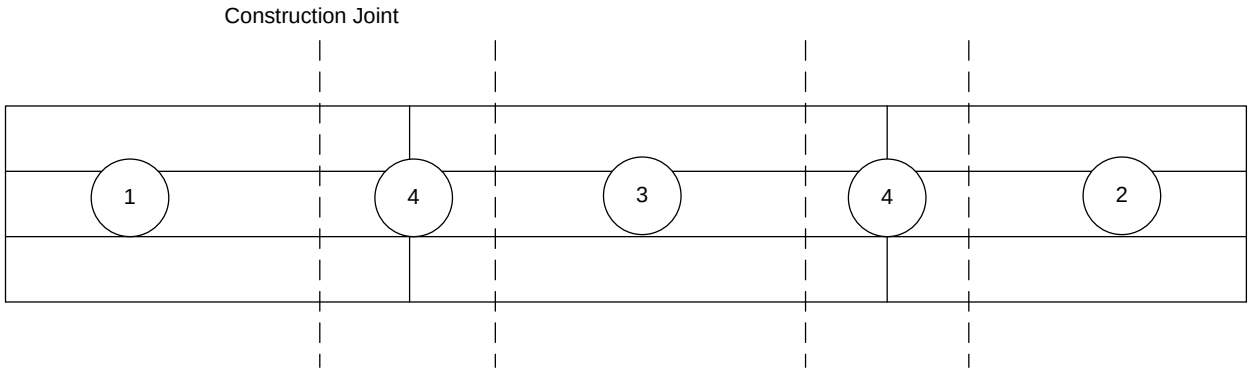

Staged deck placement. End span positive moment regions placed 1st, followed by middle span positive moment region, and finally by placement of the concrete over the piers.

Bridge Perspective & Plan Views:

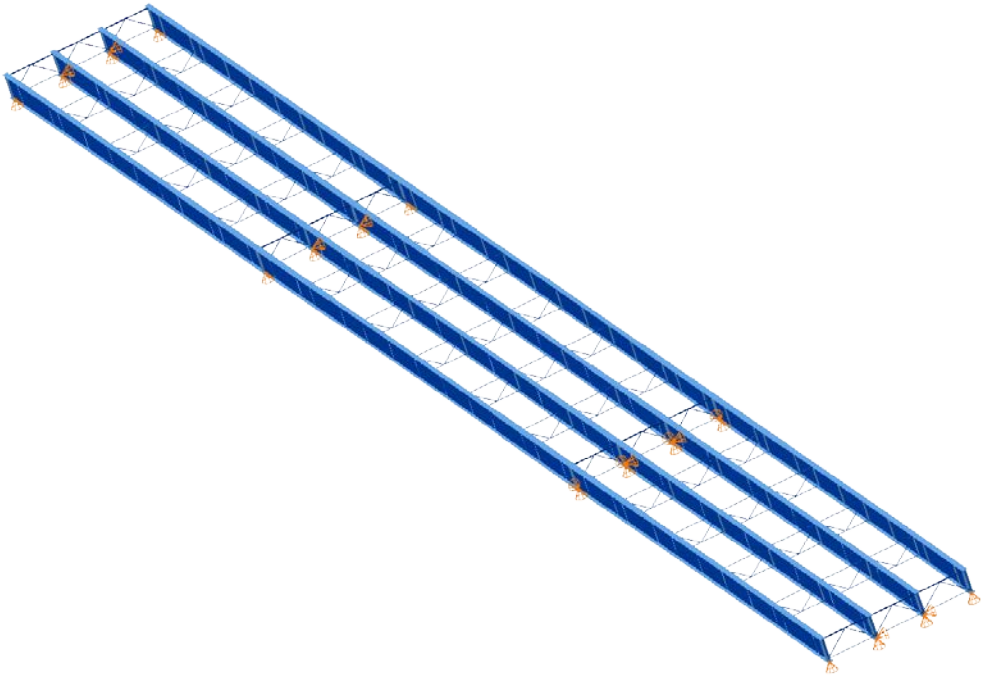

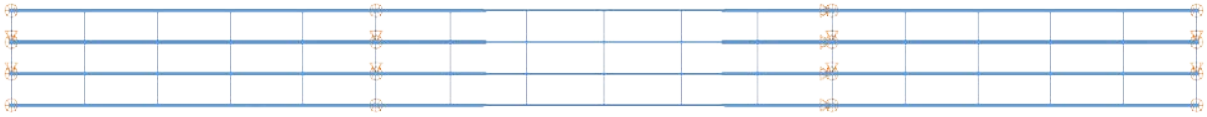

Abbreviated Analysis Results:

This straight, non-skewed bridge is targeted to allow us to assess the baseline accuracy of the various analysis methods for zero skew and zero curvature. Figure 1 shows the vertical displacements under steel dead load. It also provides the top flange major-axis bending stresses under steel dead load. Figs. 8 and 9 clearly illustrate that all approximate analysis methods predict responses successfully. Figures 3 and 4 show girder 1 vertical displacements and major-axis bending stresses. Additionally, Fig. 5 shows the major-axis bending stresses for girder 2. It is clear from Figs. 3 and 4 that the predictions are off for 1D and MDX results. However, the predictions are very close for Fig. 5. The difference in the predictions is due to the assumptions of the tributary area of the deck and the distribution of the loads. These differences are small and can be handled in haunches during pouring the deck.

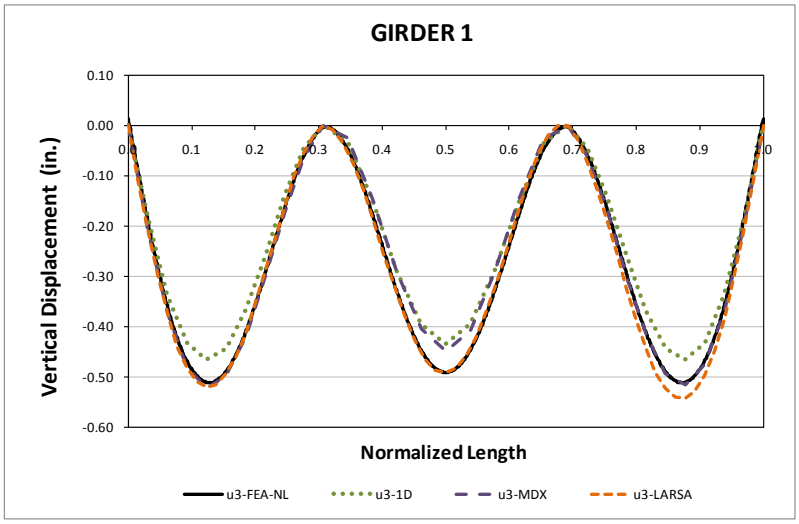

Fig. E.2.5-1.XICSN1, Top Vertical displacements under steel dead load.

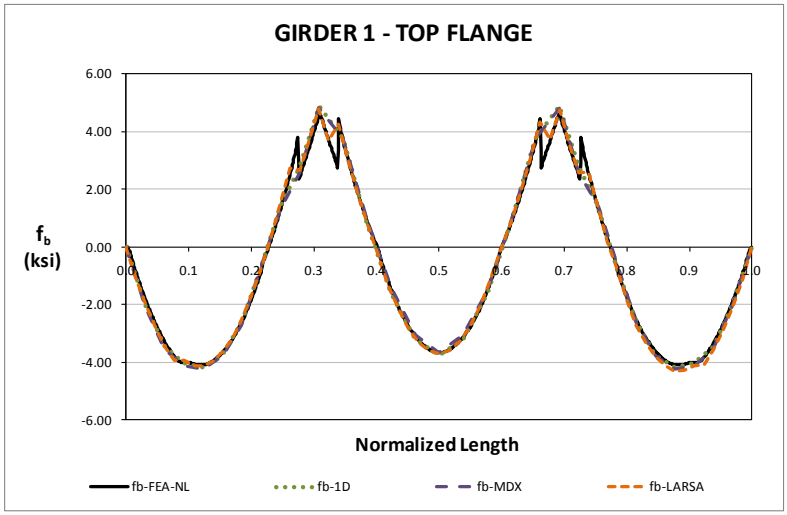

Fig. E.2.5-2.XICSN1, Major-axis bending stresses under steel dead load.

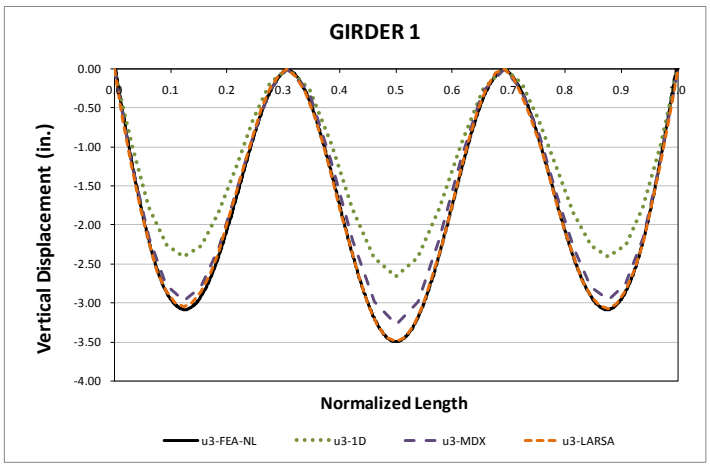

Fig. E.2.5-3.XICSN1, Vertical displacements under total dead load.

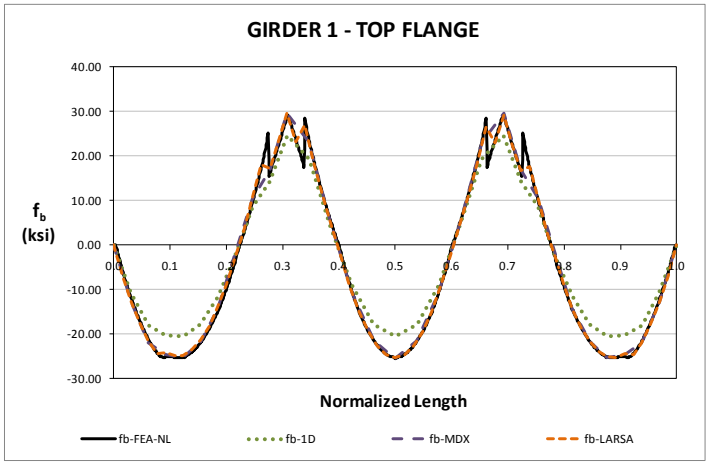

Fig. E.2.5-4.XICSN1, Major-axis bending stresses under total dead load.

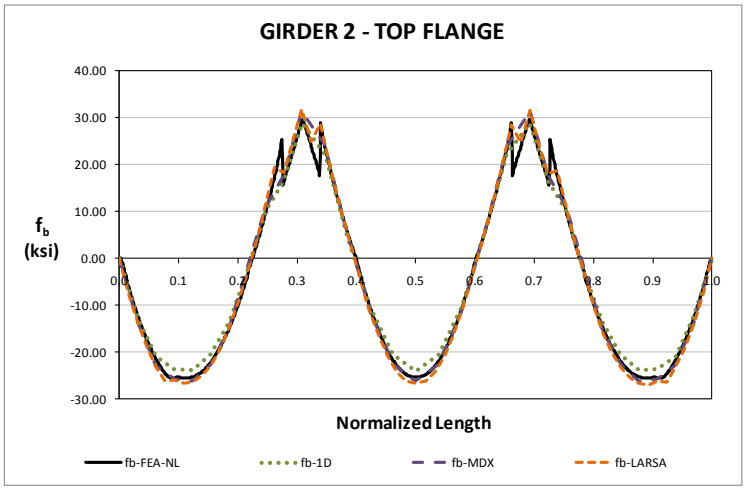

Fig. E.2.5-5.XICSN1, Major-axis bending stresses under total dead load.

I2.1 EISSS3 (Existing, I-girder, Simple-span, Straight, Skewed supports)

Bridge Description:

Bridge on SR 1003 (Chicken Road) over US 74 between SR 1155 & SR 1161, Robeson Co., NC

Category Data:

L = 133 ft / w = 30.1 ft / $\theta_{left} = \theta_{right}$ = 46.2°, 4 girders

References:

Morera and Sumner (2009)

Cross-Frame Detailing Method: NLF

Steel Erection Stages Analyzed: Four

Deck Placement Sequence: One stage

Bridge Perspective & Plan Views:

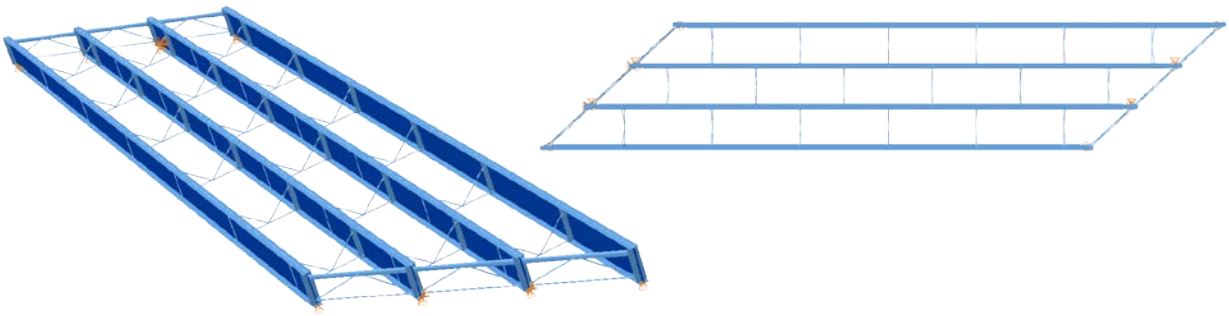

Abbreviated Analysis Results:

In this bridge the absence of the top chord elements in the cross-frames and their influence on the structural behavior is studied. The sensitivity of this parameter and the capabilities of the approximate methods to capture the behavior of the bridge are discussed. In addition, a comparison between the results obtained from a first-order and a second-order analysis is presented.

The construction of the bridge starts with the erection of the two interior girders, G3 and G4. The analysis comparison for both vertical and radial displacements indicates that the 2D grid model captures accurately the behavior of the bridge as represented by the 3D model. Figure 1 shows these responses in girder G4 for this erection stage. The same trend is observed in the major-axis bending stress response, as shown in Figure 2.

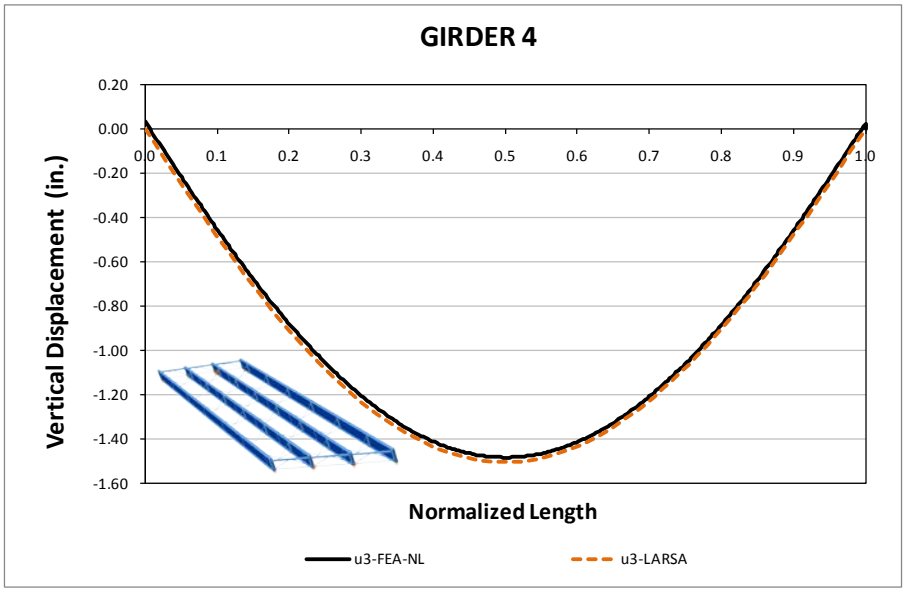

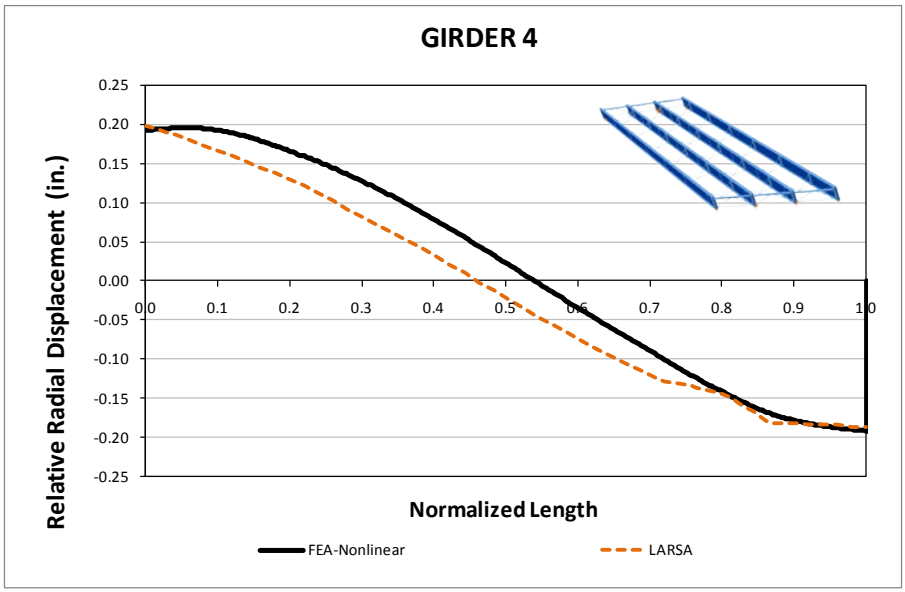

Fig. 1. EISSS 3, Vertical and Relative Radial Displacements for Girder G4 – Stage 1

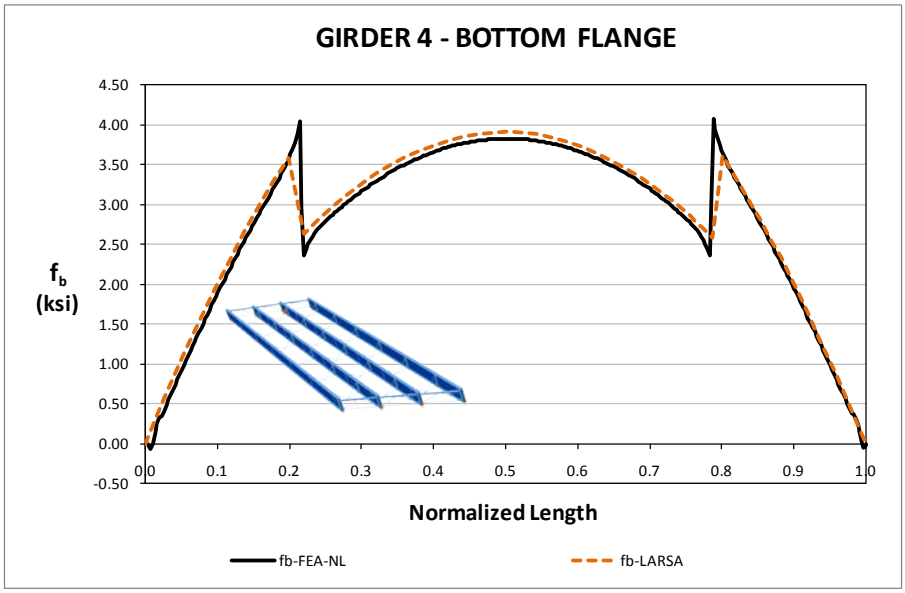

Fig. 2. EISSS 3, Major-Axis Bending Stress Comparison for Girder G4 – Stage 1

The response of the bridge at the end of the deck placement is studied in Stage 4. A comparison of the bridge behavior as predicted by the 1D and 2D approximate methods versus the 3D FE model is presented next. Figure 3.a shows the vertical displacement comparison for the fascia girder, G4. From the figure it is inferred that the vertical displacement predictions are close between the different methods. It is observed that the approximate analyses are very consistent with the 3D FEA linear representation. In fact, this is expected, given the disability of these methods to capture the second-order effects. The 2D model radial displacement prediction, however, is not a reliable approximation of the FEA response, as seen in Figure 3.b. In other bridges considered in this study, the lateral deflections have been predicted accurately at the cross-frame locations because the 2D analyses are able to correctly capture the overall layover of the structure. This behavior is attributed to the fact that at the bracing points, the response of the bridge is dominated by the rotation of the group of girders. In the current case, the group interaction does not exist since the cross-frame top chords that brace the girders are not present. Thus, the lateral displacements are controlled by the rotation of each individual girder, attribute that a 2D grid analysis cannot capture.

In the case of the major-axis bending stresses, the predictions are similar for the different analyses, as shown in Figure 4. In general, the main difference between the 1D and 2D model predictions and the nonlinear FE model is due to the presence of second-order effects.

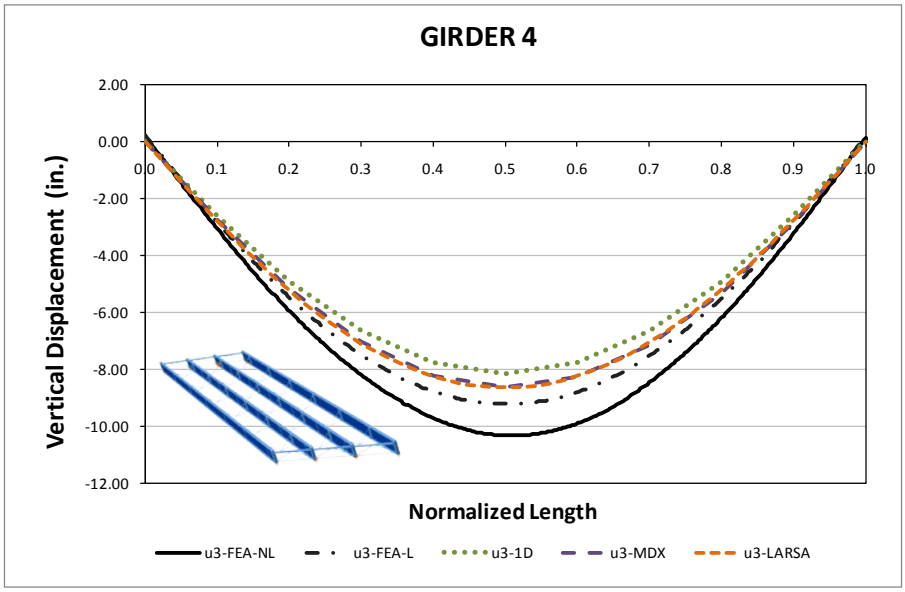

a) Vertical Displacements

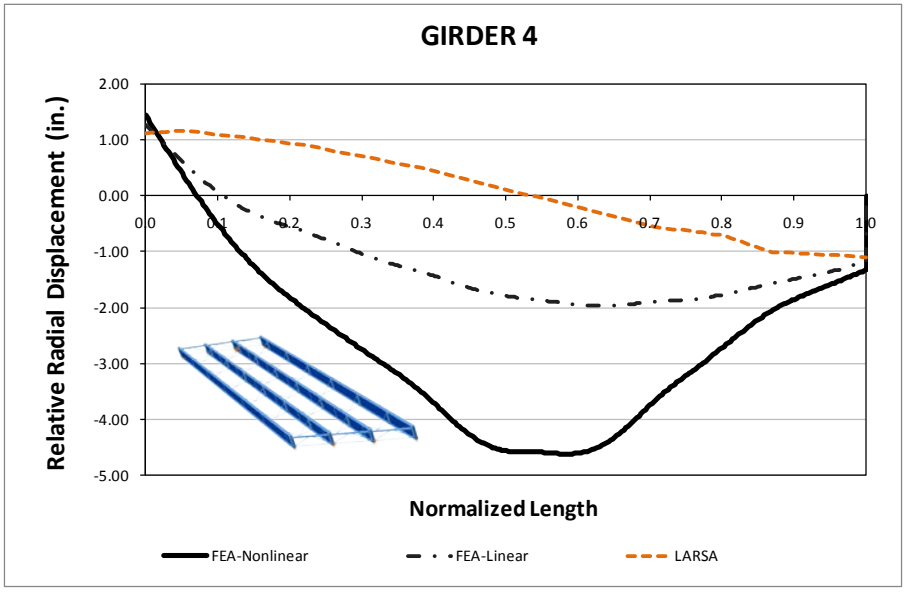

b) Radial Displacements

Fig. 3. EISSS 3, Comparison of Displacement Responses – Stage 4

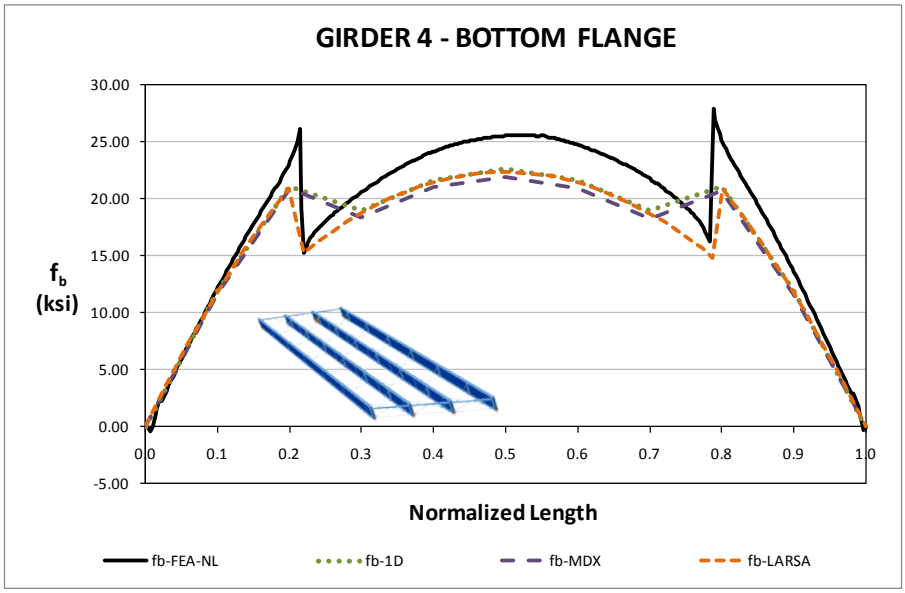

Fig. 4. EISSS 3, Comparison of Major-axis Bending Responses – Stage 4

The dissimilarities observed between the first-order and second-order analyses are associated with the absence of the cross-frame top chord. During the concrete placement these elements provide lateral bracing to the girders, making them act as a group and increasing the structural stability of the system. An evidence of the second-order effects and their influence in the structural integrity can be derived from an inspection of the relative radial displacements. As shown, they are much larger for the nonlinear FEM than for the linear model. This is an indication that the fascia girder is close to a collapse due to lateral-torsional buckling. The nonlinear FE analysis shows that the system collapses at 1.2 times the nominal total construction dead load (steel plus concrete loads).

Conclusions:

The absence of top chord elements in the cross-frames seems to change significantly the structural behavior in a bridge. The lack of these bracing elements in the top flange of the I-girders increases their susceptibility to stability problems. This is of particular importance during the deck placement, when the construction dead loads are supported only by the steel structure. As a result, the typical problems related to a poorly braced system such as excessive lateral deflections, susceptibility to lateral-torsional buckling, magnification of the second order effects, etc., show up in the structural behavior. At this point, the performance and influence of nonstructural elements or that are not considered in the design need to be examined. Namely, the stay-in-place metal deck forms, the formwork, and other attachments done to facilitate the construction might be contributing to prevent the system from failure. However, careful consideration should be given when relying on these elements for structural purposes. In our research, their stiffness contributions to the system need to be included by correctly modeling the nonlinear interaction between them and the steel structure.

I2.2 EISSS5 (Existing, I-girder, Simple-span, Straight, Skewed supports)

Bridge Description:

SR 0581 Section A01, Cumberland Co., PA

Category Data:

L = 123 ft / w = 87.5 ft / $\theta_{left} = \theta_{right}$ = 59.7°, 6 girders

References:

Bridge recommended for study by Mr. Macioce, PennDOT Chief Bridge Engineer

Cross-Frame Detailing Method: NLF

Steel Erection Stages Analyzed: Four

Deck Placement Sequence: One stage

Bridge Perspective & Plan Views:

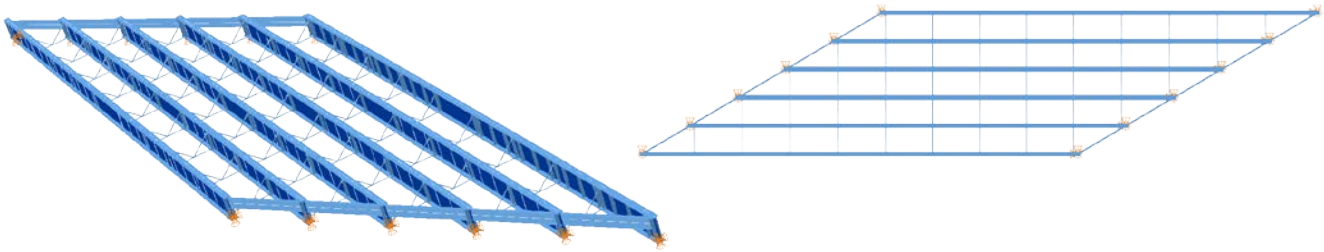

Abbreviated Analysis Results:

Three particular aspects of this bridge are studied to determine their influence in the prediction of its behavior, using the 1D and 2D analysis methods. Namely, the influence of the parallel skewed supports, the absence of the top chords in the cross-frames, and the influence of the number of girders are assessed.

The initial construction stage is studied first. In this stage, the two interior girders, G5 and G6, are placed on the bearings. This stage is considered vulnerable to stability problems given that at this point, the structure is not compact. For this stage, the responses predicted by the 2D grid model match accurately the benchmark prediction. The vertical and lateral displacements obtained from the 2D and 3D models, as shown in Figures 1.a and 1.b for the interior girder, G6, are practically the same. The 2D model is able to capture the opposite rotations that occur at each support as a result of the skew. Likewise, the major-axis bending response of the 2D model resembles the FE model representation, as shown in Figure 2.

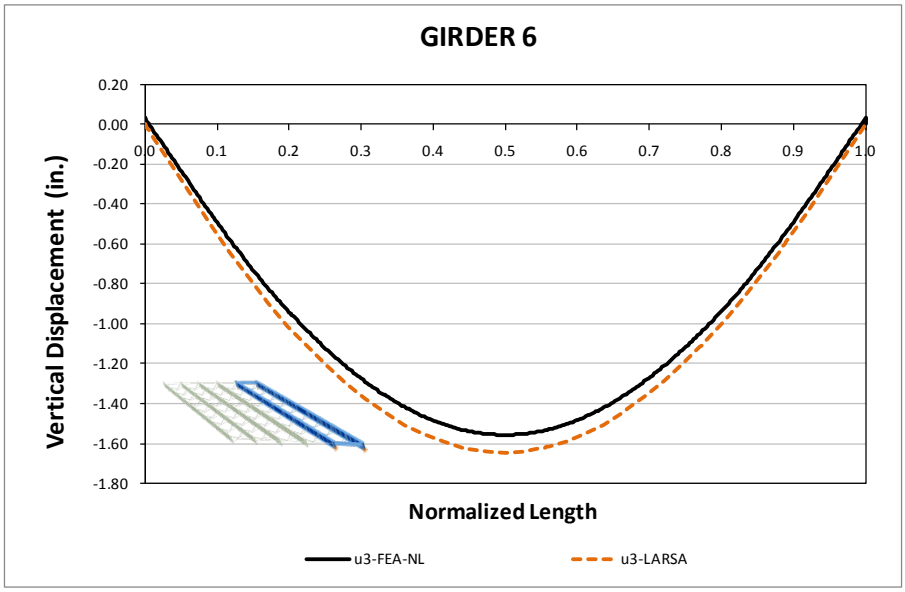

a) Vertical Displacements

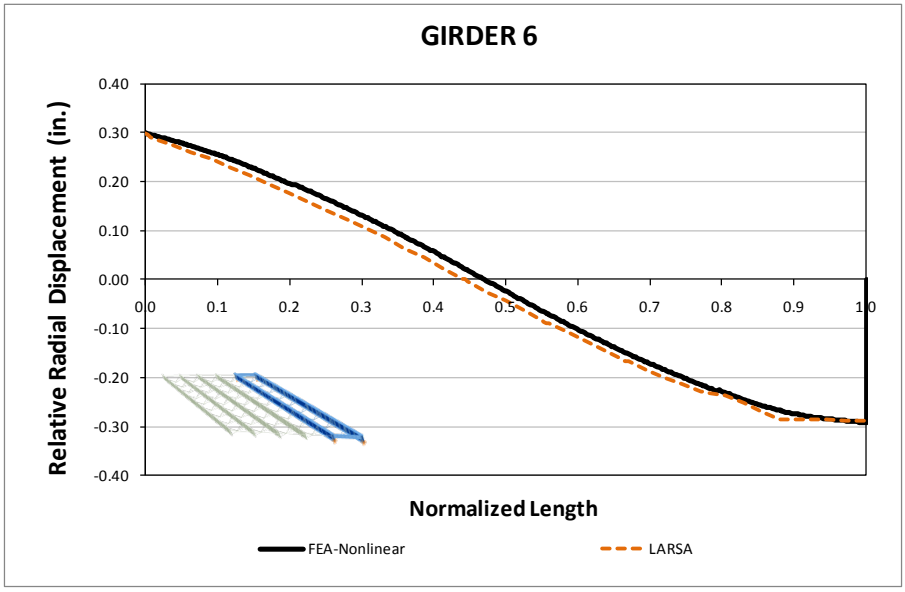

b) Radial Displacements

Fig. 1. EISSS 5, Comparison of Displacement Responses – Stage 1

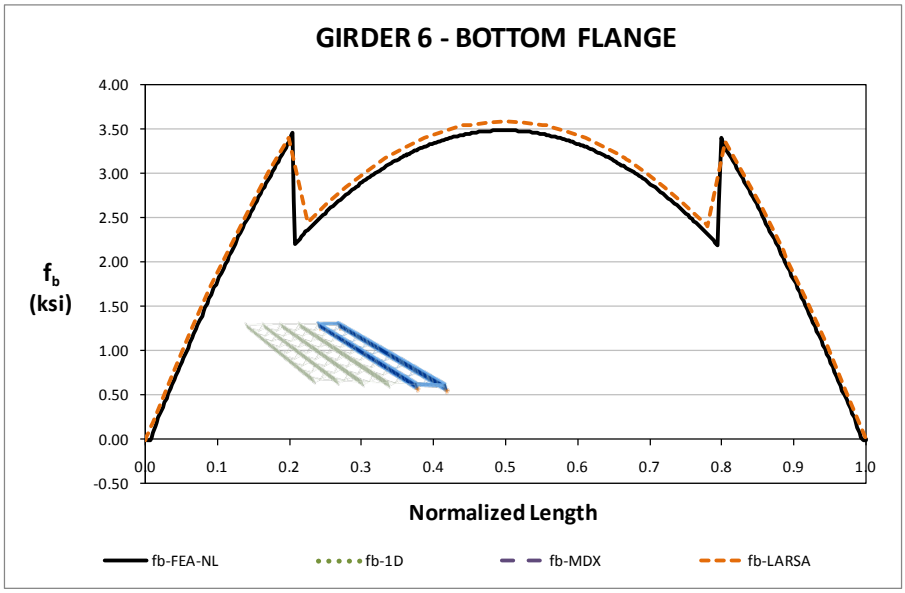

Fig. 2. EISSS 5, Comparison of Major-axis Bending Responses – Stage 1

The behavior of the bridge at the end of the construction is studied next. Figures 3.a and 3.b show the responses for the vertical and radial displacements, respectively. As shown, the 1D and 2D estimations of the vertical displacements at the total dead load condition are coherent with the 3D model values. In the case of the radial displacements, the 2D grid model captures accurately the layover of the girders at the supports. Within the supports, however, the predictions do not match each other with the same precision. The reason for this difference is the level of bracing that the girder has along its length. At the supports, the girders are connected with heavy W-sections that enforce the same radial deformations of all the girders of the system. In the interior, the cross-frames do not provide the same level of bracing as in the supports. As a consequence of not having a top chord in the cross-frames, the girders are less restrained to rotate independently about their longitudinal axes. The global rotation of the system, as mentioned for previous bridges, is efficiently captured by the 2D grid model at the bracing points. The response within the braced points, where the girders behave independently, is not well represented by the 2D analysis.

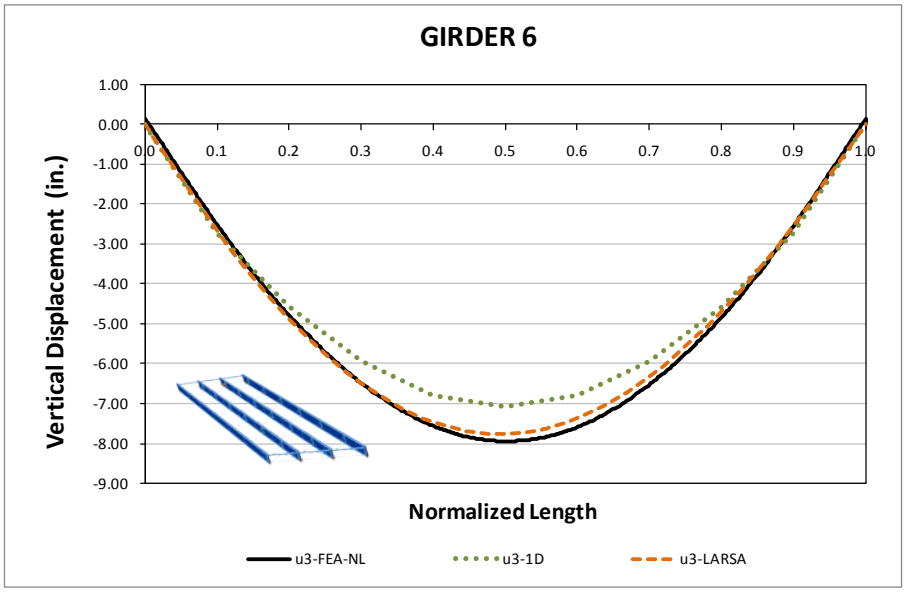

a) Vertical Displacements

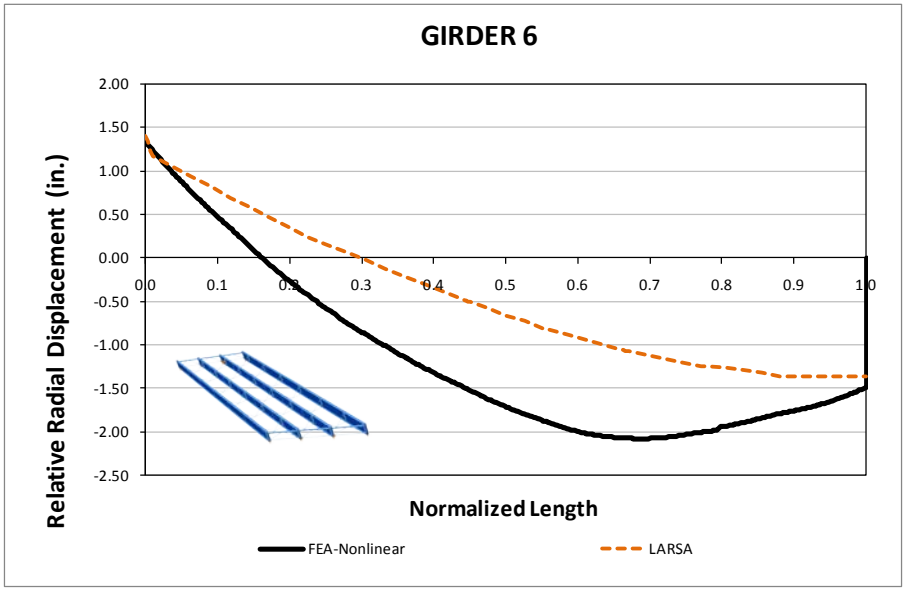

b) Radial Displacements

Fig. 3. EISSS 5, Comparison of Displacement Responses at the TDL Condition

Conclusions:

The effect of not having a top chord in the cross-frames on the behavior of the bridge is not captured correctly by the 2D grid model. In general, the 2D representations are able to model the response of the structural system, but not of independent girders. Thus, if the bridge is not well connected by providing lateral bracing, the elements in the structure deform independently and not as a sole group. Consequently, the actual response is misrepresented by the 2D analysis.

I2.3 EISSS6 (Existing, I-girder, Simple-span, Straight, Skewed supports)

Bridge Description:

I-87 NB Connector over I-287, Westchester Co., NY

Category Data:

L_1 = 267 ft / w = 58 ft /θ_1 = -62.3^o, θ_2 = -62.3^o, 8 girders

Cross-Frame Detailing Method: TDLF

Erection Stages Analyzed: 4 (Analyses are performed assuming NLF, SDLF and TDLF)

Deck Placement Sequence: 1 Stage

Bridge Perspective & Plan Views:

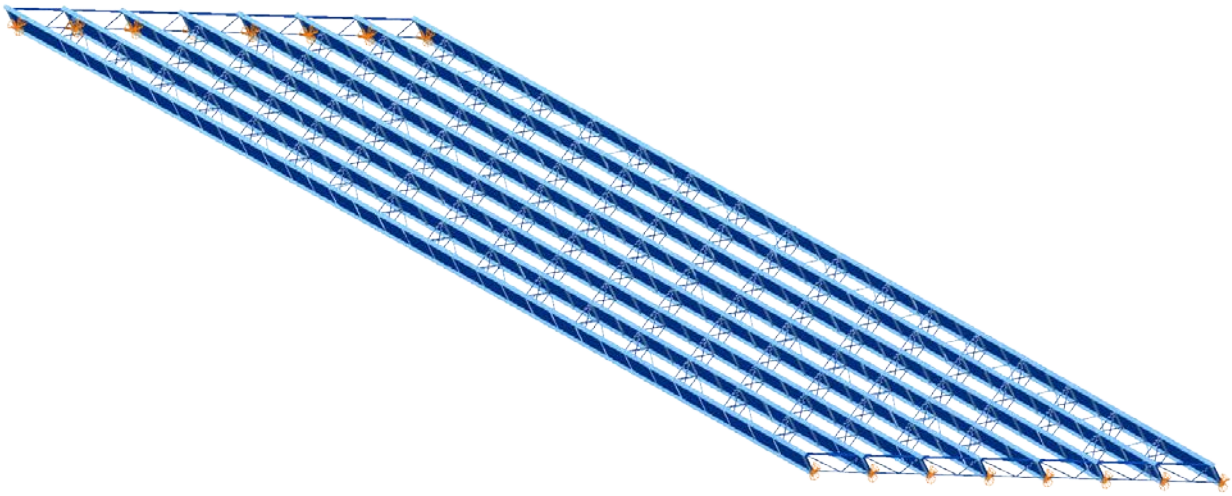

G8

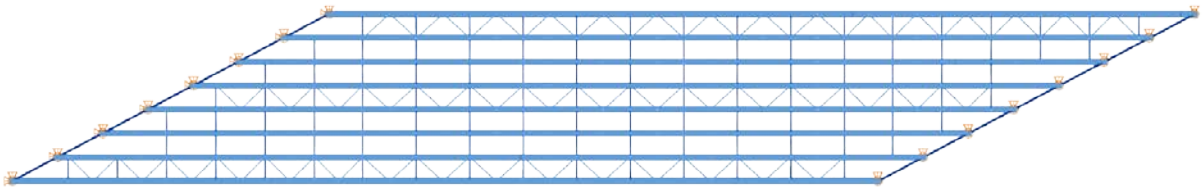

G1

Abbreviated Analysis Results

Figure 1 shows the different analysis stages which are considered to evaluate the different analysis methods.

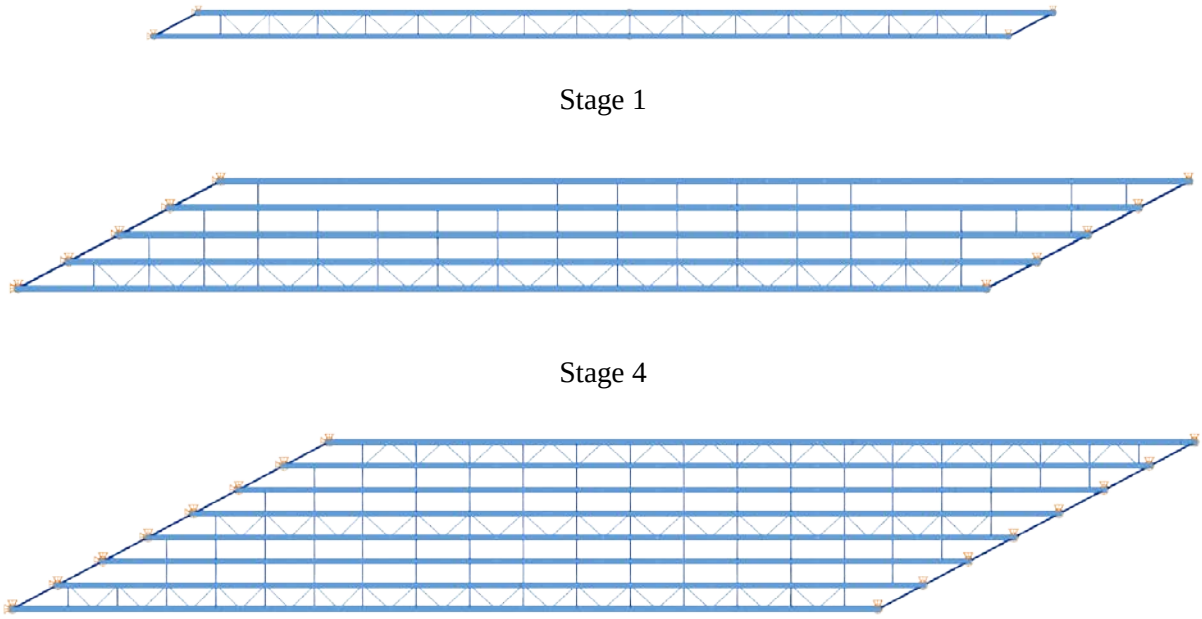

Stage 1

Stage 4

Stage 9 & 10

Fig. 1. EISSS6, Considered different analysis stages.

Importance of erection sequence for the methods of detailing

Plumb girders are targeted for final dead load level by choosing TDLF detailing. EISSS6 is detailed for TDLF which means that cross-frames are fabricated such that they fit the girders in their final dead load condition. Therefore, cross-frames do not fit to the girders in the no-load geometry due to lack-of-fit. Girders have to be twisted and forced to make the connection with the cross-frames. TDLF detailing reduces the girder layovers at the skewed bearing lines. Depending on the lack-of-fit between the girders and cross-frames, installation of the cross-frames can be challenging. The erection sequence of this bridge is prepared such that the additional forces required to assemble the cross-frames are minimum.

The erection of this bridge start with the girder lines 4 and 5. Figure 2 provides the undeflected and deflected geometry of stage 1 due to lack-of-fit forces for TDLF detailing in the no load geometry. TDLF detailing creates a compensating twist opposite to the dead load rotations due to lack-of-fit between girders and cross-frames. Girder lines 4 and 5 are pre-assembled as a pair first by first installing the cross-frames in the middle of the span. The other cross-frames are installed working from middle of the span out toward ends by jacking up or down at ends. The connections are made easily since the structure is in pair and it is easy to twist the girder flanges since they are relatively flexible compared to cross-frames. This pair is assembled in the field and placed into position by using cranes. This stage is followed by assembling of the girder line 6 to the girder lines 4 and 5. Then girder lines 7 and 8 are erected similarly. Similar erection sequence is followed for girder lines 3, 2 and 1.

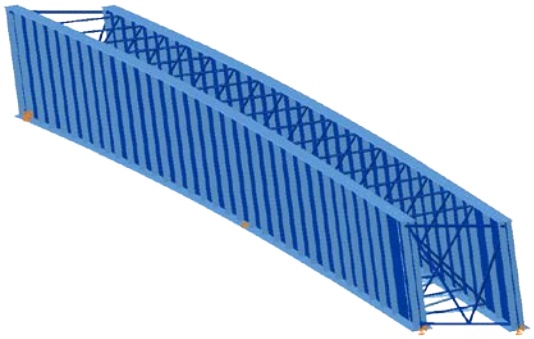

Undeflected Geometry

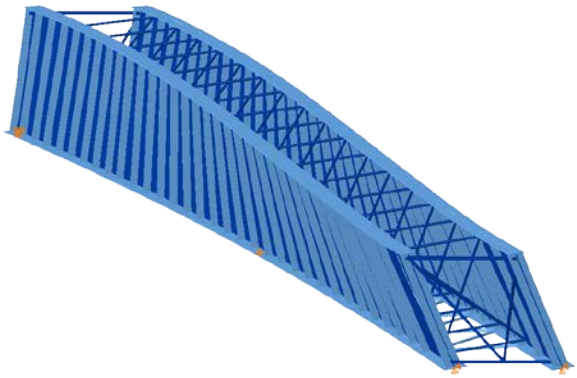

Deflected Geometry

Fig. 2. EISSS6, Stage 1, undeflected and Deflected geometry (magnified by 10x) at no load geometry due to lack-of-fit for TDLF detailing.

Stage 4 is also selected to provide information about fit-up of cross-frames. In this stage girder line 8 is assembled to girder line 7. The erection for this stage is as follows:

1. Girder line 8 is brought to the steel dead load profile by jacking down the false work towers (cranes are also used to hold the girder in a stable configuration).
2. Cross frames that are in the middle of the span is installed (1/4 of the total cross-frames). These are the easiest cross-frames to install since they are at the most flexible point of the bridge.
3. Temporary X-braces at each ends and also temporary struts at extreme ends of the girder are installed to keep the girder spacing constant and stabilize the structure. Figure 3 provides the temporary X-bracing locations and temporary struts. Furthermore, Figs. 4 and 5 illustrate the temporary X-bracing and temporary struts.

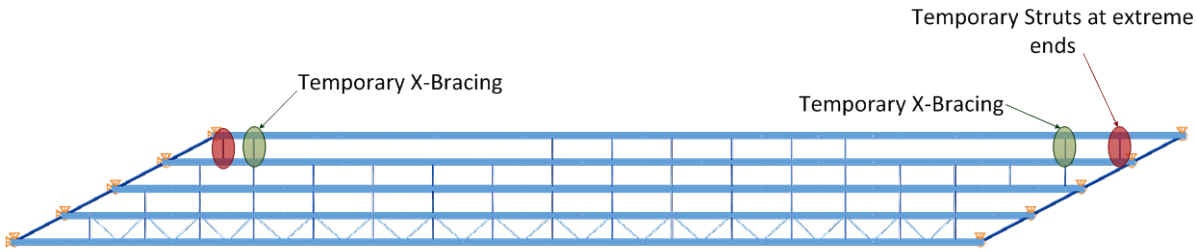

Fig. 3. EISSS6, Stage 4 location of the temporary X-braces and temporary struts.

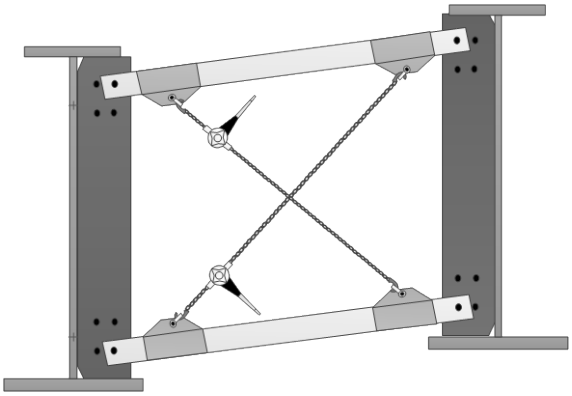

Fig. 4. EISSS6, Representation of the temporary X-braces.

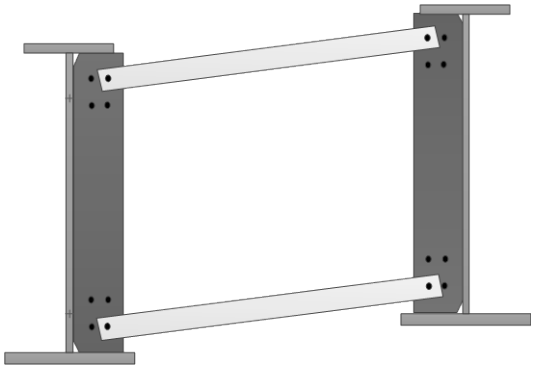

Fig. 5. EISSS6, Representation of the temporary struts.

Stage 4 is followed by installing the cross-frames starting from the mid-span towards the abutments. However, Stage 4 is selected to investigate the fit-up of the cross-frame for TDLF detailing. Figure 6

provides the undeflected and deflected geometry of stage 4 under steel dead load for TDLF detailing. As discussed before, TDLF detailing creates opposite rotational displacements compared to the dead load rotations. Three cross-frame locations are selected for further investigation and illustrated in Fig. 7. Differential deflections between the adjacent girders are maximized at these cross-frame locations that are close to the bearing lines. For TDLF, cross-frames are fabricated to fit the girders under total dead load condition. Therefore, lack of fit between the girders and the cross-frames will influence the come along and jacking forces during construction. The drop at the selected cross frame locations are 2.98",2.96" and -2.32" for CF-1 through 3 respectively. If the erector selects to install these cross-frames in the no-load geometry, the girder flanges at these locations have to be laterally twisted by 3.78", 3.75" and -2.94" to make connection for the cross-frame members at locations of 1 through 3 respectively. This can require very large forces come along and jacking forces. However, in the erection scheme discussed above girders are brought to their steel dead load profiles. Girders layover due to the once the steel dead load profile is achieved. In this stage the girders layover by 1.44", 1.88" and 1.29" and drop reduced to 1.90", 2.06" and 1.36" for cross-frame locations 1 through 3 respectively. Girders have to be twisted at these locations to install the cross-frames. Cross-frames are rigid compared to the girders so the required layover of the girder that are described above can be calculated at each cross-frame location by using the formula,

$$\Delta_{x\ Required} = \mathrm{D}\left(\frac{\Delta_{yTDL} - \Delta_{yConst}}{\mathrm{s}}\right) - \Delta_{xConst} \quad (1)$$

where Δ_{yTDL} is the total dead load drop, Δ_{yConst} is the vertical deflection and Δ_{xConst} is the layover at the particular stage considered. For the cases where the layover of girder flanges is not known the required layover of the girder can be conservatively estimated from,

$$\Delta_{x\ Required} = \mathrm{D}\left[\left(\frac{\Delta_{yTDL} - \Delta_{yConst}}{\mathrm{s}}\right) - \left(\frac{\Delta_{yConst}}{\mathrm{s}}\right)\right] \quad (2)$$

Table 7.2.1 compares the required layovers for Stage 4 for the installation of the diagonal chords of the selected cross-frames.

Table 7.3.1. EISSS6, Required layovers to make install diagonals of the selected cross-frames in Stage 4.

Cross-Frame Number	Required Layovers (in)		
	FEA	Eq. 1	Eq. 2
1	0.99	0.97	1.05
2	0.76	0.73	1.48
3	0.45	0.44	0.52

As a result, the come-along and jacking forces are reduced significantly by using the advantage of dead load deflections during the construction. Temporary X-bracings and temporary struts can be very useful to minimize the fit-up forces while maintaining the stability of bridge geometry by allowing flexibility to the girders to deform.

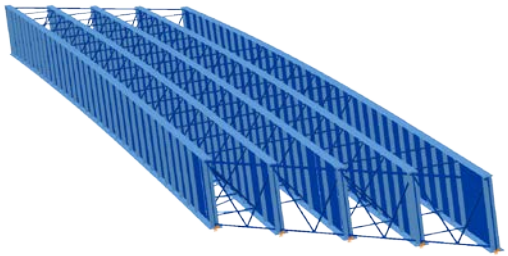

Perspective View

Plan View

Undeflected Geometry

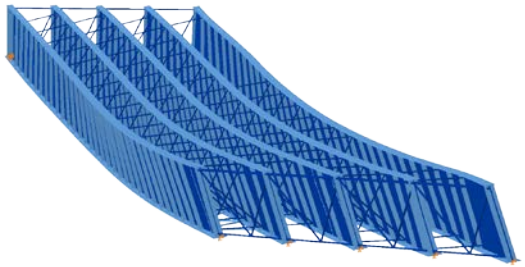

Perspective View

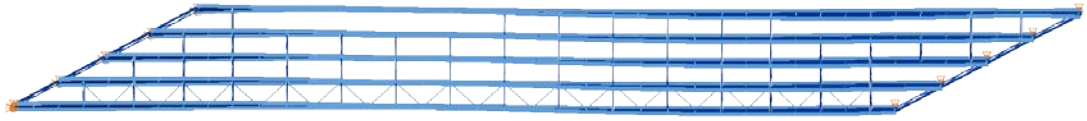

Plan View

Deflected Geometry

Fig. 6. EISSS6, Stage 4 undeflected and Deflected geometry (magnified by 10x) under steel dead load for TDLF detailing.

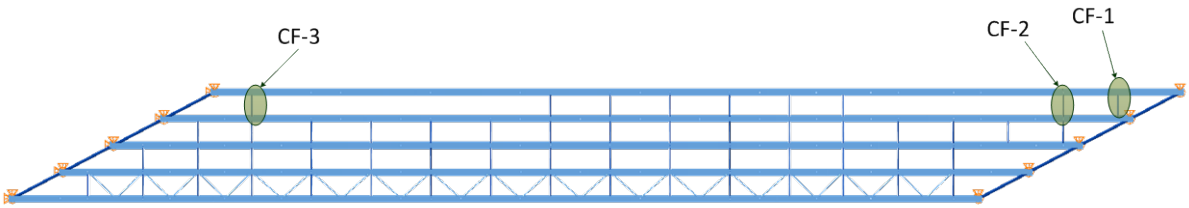

Fig. 7. EISSS6, Selected cross-frame locations.

Influence of cross-frame detailing on girder responses and cross-frame forces

NLF, SDLF and TDLF detailing responses are compared under total dead load. Girders can be plumb only in one configuration during the construction due to the 3D deflections of the bridge. Figure 3 shows the girder 1 layovers along the length of the girder for different detailing methods. It should be noted that the girders are approximately plumb conditions only for TDLF detailing.

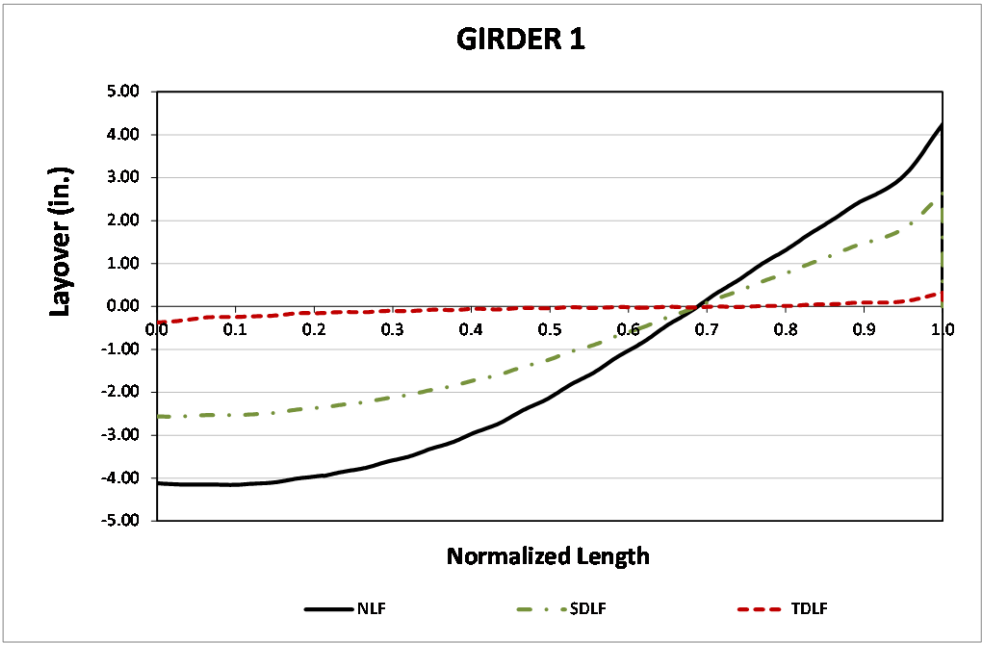

Fig. 8. EISSS6, Girder 1 girder layovers under total dead load due to detailing methods.

Figure 4 provides the girder 1 vertical deflections under total dead load due to different detailing methods. It is clear from Fig.4 that detailing has negligible effect on the vertical deflections. Figure 5 show the girder top flange stresses under total dead load for different detailing methods. Major-axis bending stresses are not influenced by the detailing methods. Flange lateral bending stresses are smaller due to the continuous pattern of the cross-frames. However, TDLF detailing further reduce the flange

lateral bending stresses. Larger reductions are observed for the intermediate girders. The reduction is smaller on the top and bottom girders since most of these stresses are generated by the overhang bracket loads.

For cross-frame forces, it is found that the most loaded diagonals are at the obtuse corner for NLF detailing. This is because the transverse stiffness of the structure is largest at these locations. Detailing the bridge with TDLF reduces these cross-frame forces along these transverse load paths under total dead load. However, at the acute corners TDLF detailing induces forces due to higher drops at these locations. These cross-frame forces are not offset by the dead load effects. Typical results are observed for the other straight and skewed bridges. Some of the other findings for straight and skewed bridges can be listed as follows

- For TDLF detailing, cross-frame forces are highest under steel dead load
- For NLF detailing, cross-frame forces are highest under total dead load.
- For SDLF detailing, cross-frame forces are lowest under steel dead load.

For this bridge, the largest cross-frame force for TDLF under steel dead load is found as 86 kips at the acute corner (15ksi) whereas the largest cross-frame force is found as 99 kips at the obtuse corner (17 ksi) under total dead load. The maximums are close to each other so in terms of sizing the cross-frame members the cross-frame detailing does not require additional concern. It should be noted that these forces can be significantly different for other bridges which might need special attention on sizing the cross-frame members depending on the drop, girder length, girder spacing.

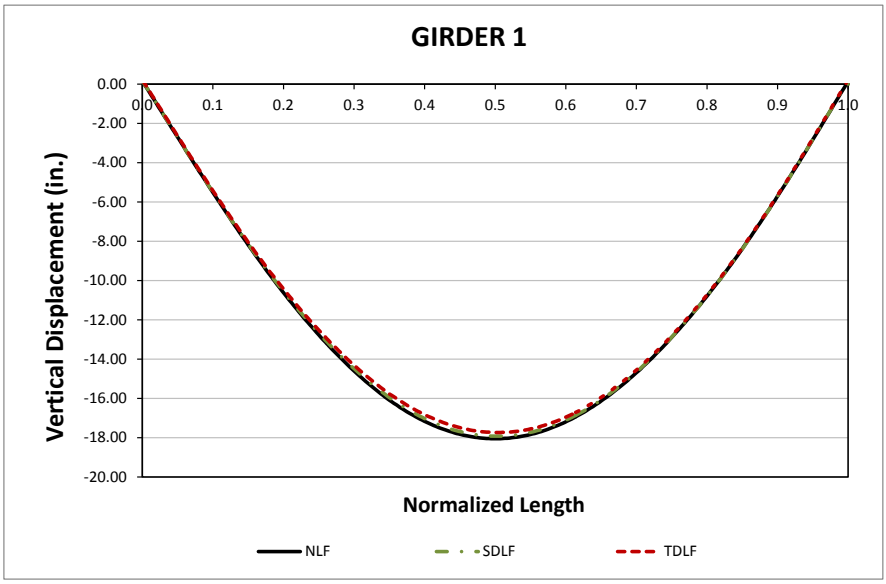

Fig. 9. EISSS6, Girder 1 vertical displacements under total dead load due to detailing methods.

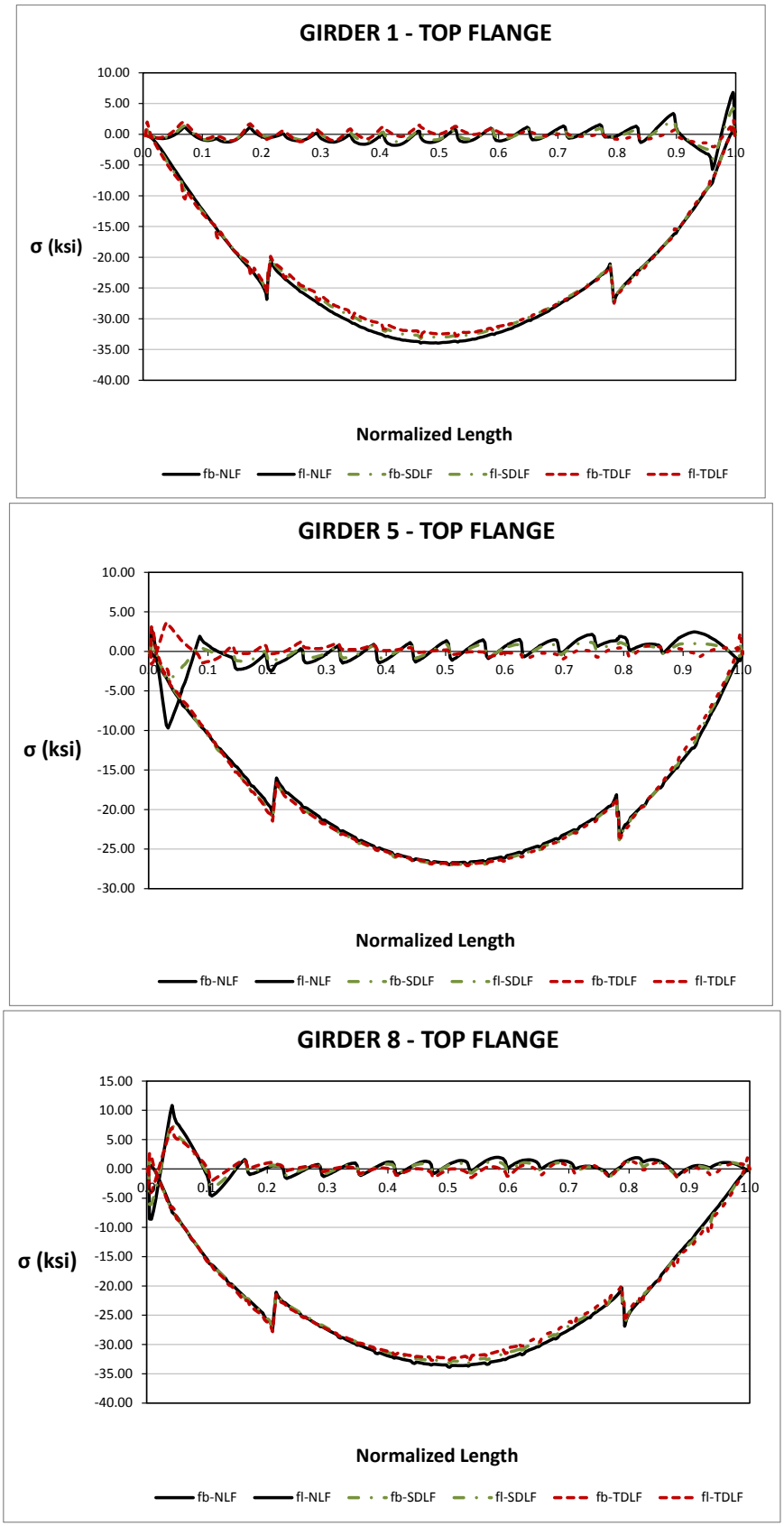

Fig. 10. EISSS6, Girder top flange stresses under total dead load due to detailing methods.

I2.4 NISSS2 (New, I-girder, Simple-span, Straight, Skewed supports)

Category Data:

L_1 = 150 ft / w = 30 ft /θ_1 = 35°, θ_2 = 35°, 4 girders

Cross-Frame Detailing Method: NLF

Erection Stages Analyzed: 5 (Analyses are performed assuming NLF)

Deck Placement Sequence: 1 Stage

Bridge Perspective & Plan Views:

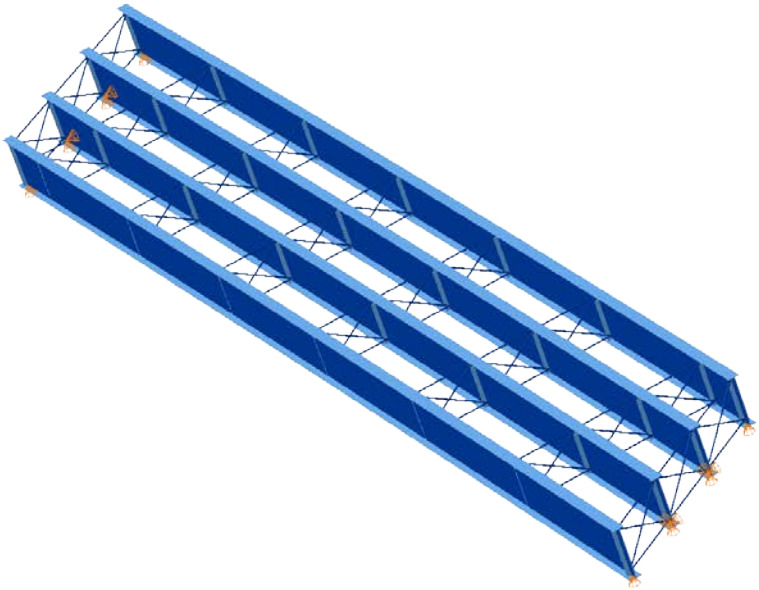

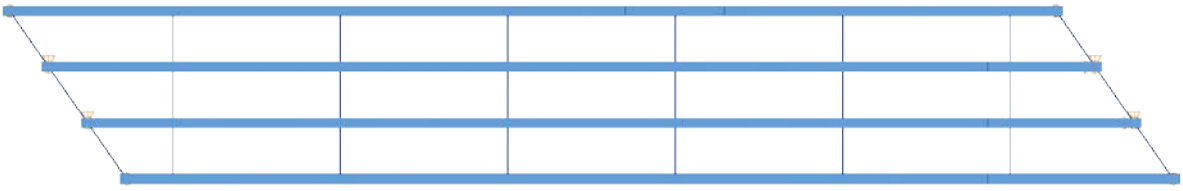

Abbreviated Analysis Results

Figure 1 provides the vertical displacements of the bottom girder (Girder 1) under total dead load. It can be seen from Fig.1 that approximate analysis methods predict the vertical displacements accurately for this bridge.

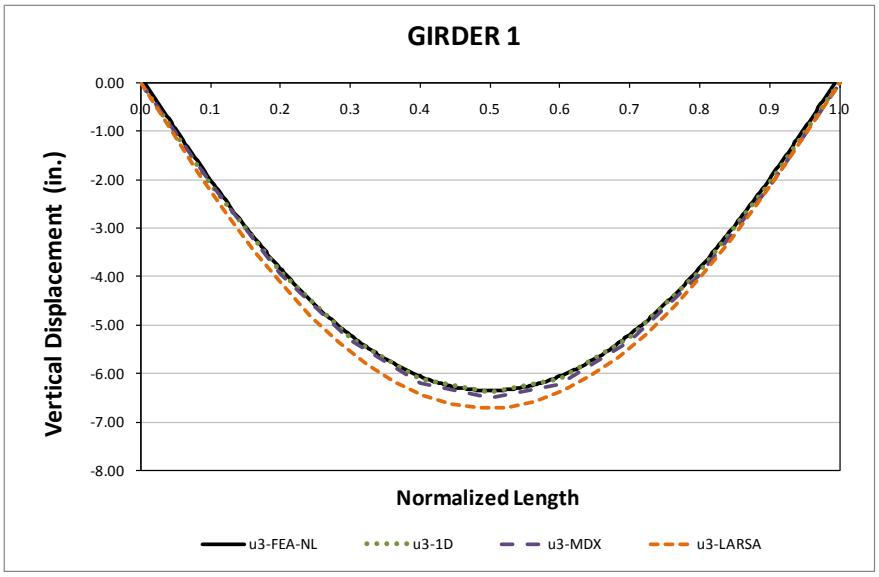

Fig. 1. NISSS2, Vertical displacements under total dead load for NLF detailing.

Figure 2 shows the relative lateral displacement predictions for girder 1 under total dead load. It is clear from Fig. 2 that the end layovers are predicted accurately. Furthermore, the relative lateral displacements are accurately predicted within the span by grid solutions.

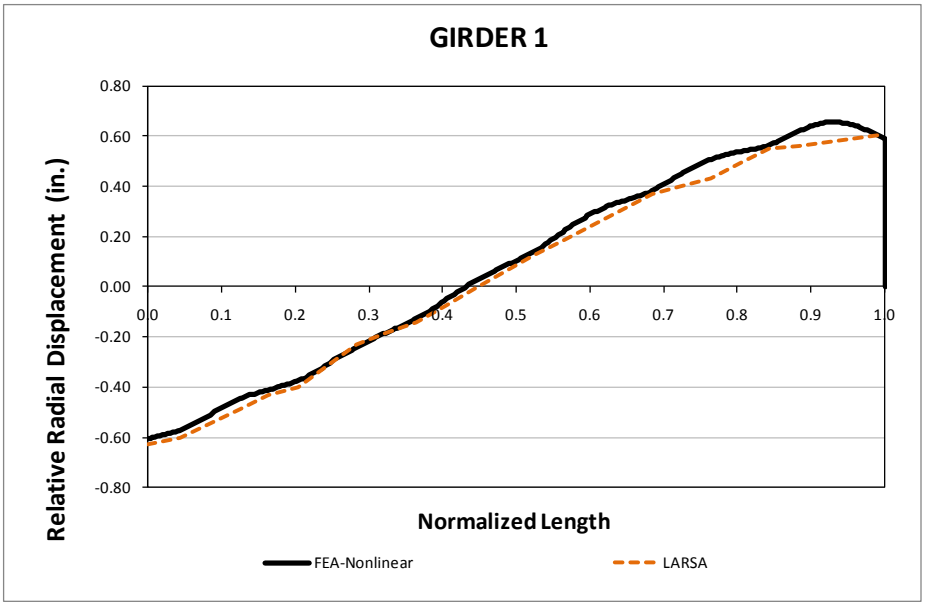

Fig. 2. NISSS2, Relative lateral displacements under total dead load for NLF detailing.

Figure 3 provides top flange major-axis bending stress predictions of bottom girder under total dead load. The major-axis bending stresses are accurately predicted by approximate methods for girder 1. This case is observed for all girders.

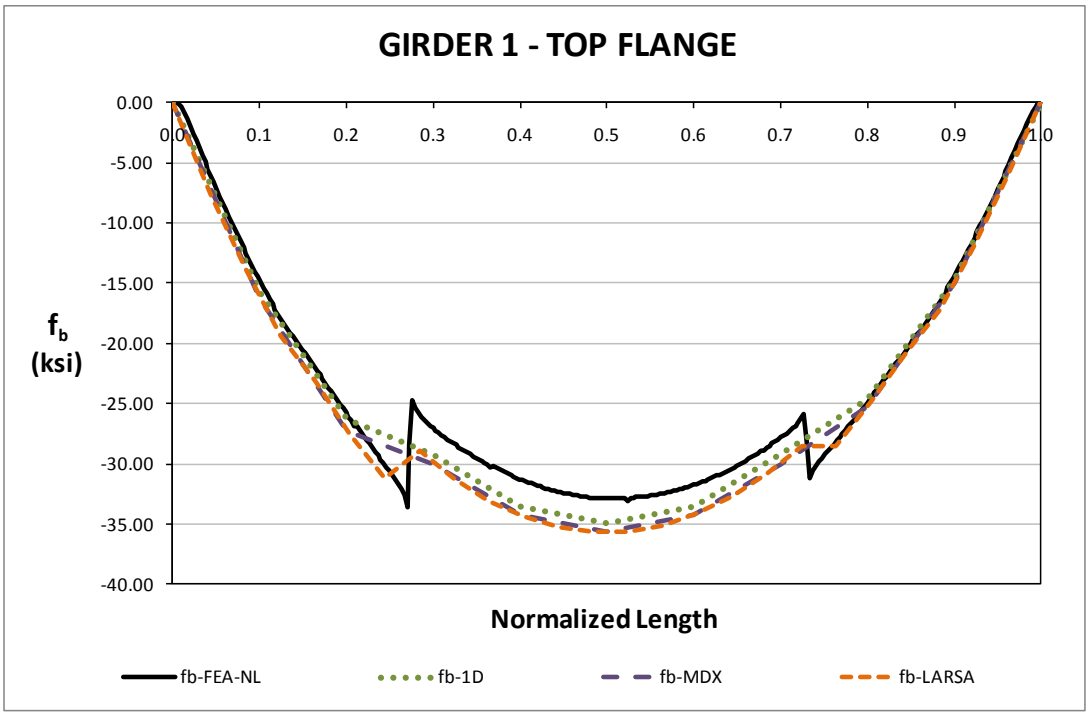

Fig. 3. NISSS2, Major-axis bending stresses under total dead load for NLF detailing.

Generally, in the case of straight bridges the flange lateral bending stresses are not obtained from software. Figure 7 provides the top flange lateral bending stresses of girder 1 predicted by linear and geometric nonlinear 3D FEA analysis results under total dead load. Although the skew angle is small for this bridge, high nonlinearity is observed for the flange lateral bending stresses. This is believed to be due to the large unbraced length of girders. An unbraced length of 24 ft is used for this bridge.

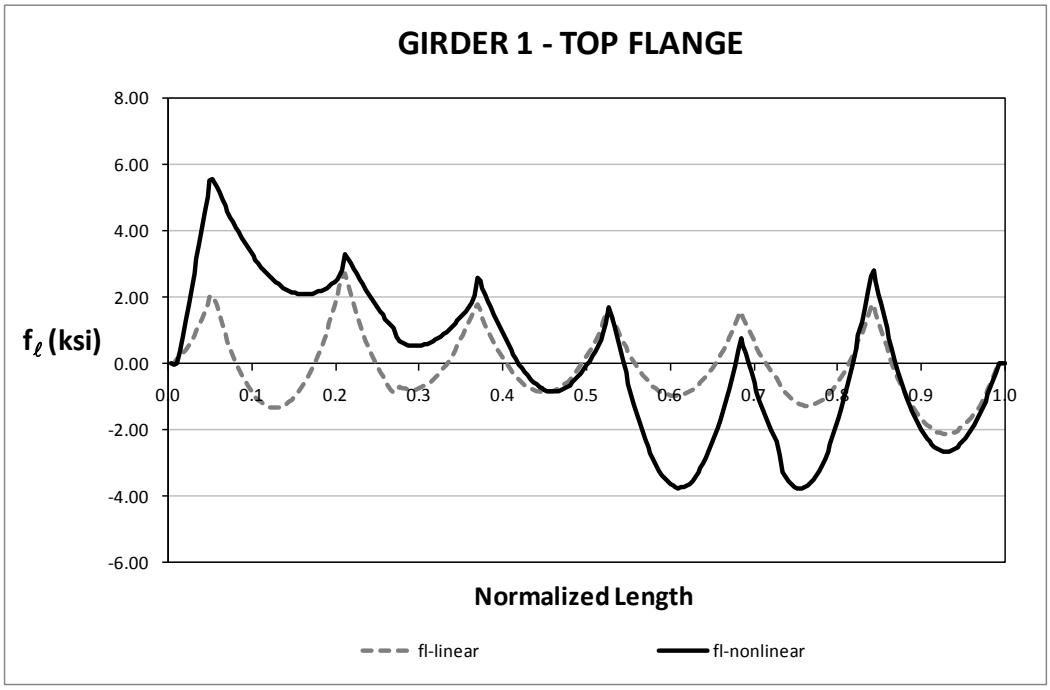

Fig. 4. NISSS2, Flange lateral bending stresses under total dead load for NLF detailing.

Conclusions:

Displacement and major-axis responses are predicted well by approximate analysis methods.

Although there are small differences in the vertical displacements, they can be handled in the haunches while pouring the deck. The end layovers are accurately predicted by approximate analysis methods. Major-axis bendig stresses are predicted well by approximate analysis methods.

Generally, in the case of straight bridges the flange lateral bending stresses are not obtained from software. High nonlinearity in the flange lateral bending stresses is observed for this bridge due to the large unbraced lengths.

I2.5 NISSS4 (New, I-girder, Simple-span, Straight, Skewed supports)

Category Data:

L_1 = 150 ft / w = 30 ft /θ_1 = 70°, θ_2 = 70°, 4 girders

Cross-Frame Detailing Method: NLF

Erection Stages Analyzed: 5 (Analyses are performed assuming NLF)

Deck Placement Sequence: 1 Stage

Bridge Perspective & Plan Views:

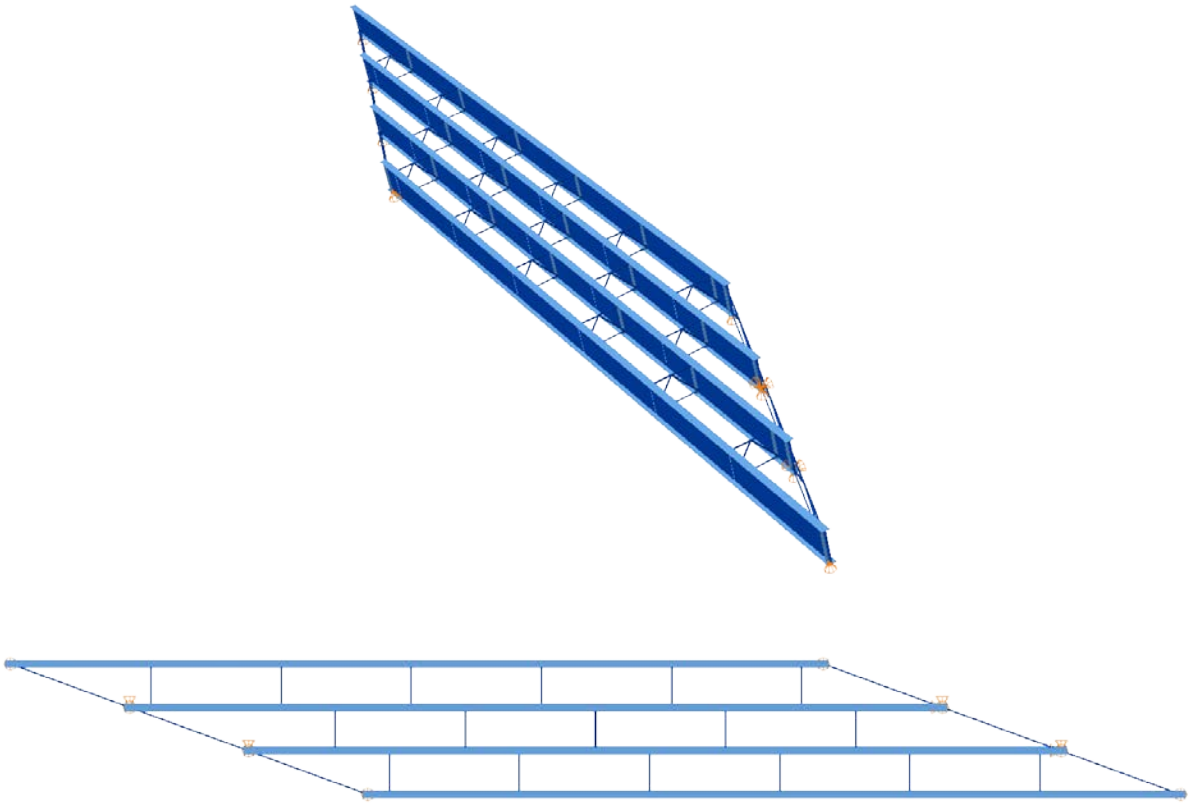

Abbreviated Analysis Results

Figure 1 shows the overall deflected shape of the bridge under total dead load. The deflections are magnified by 15 times. It should be noticed that the layover of the top flange of the bottom girder is upwards on the left skewed bearing due to compatibility between girders and cross-frames. On the other hand the layover is downwards on the right skewed bearing. The direction is opposite due to the skew direction.

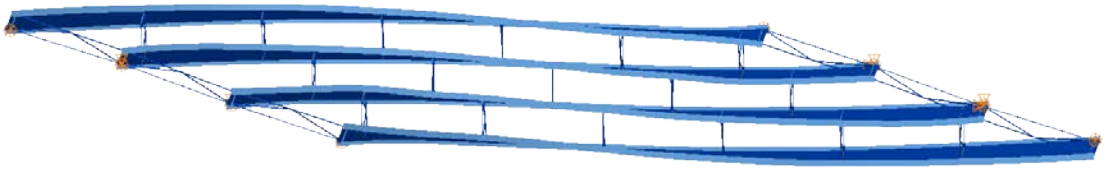

Fig. 1. NISSS4, Overall deflected shapes under total dead load for NLF detailing (Magnified by 15x).

Figure 2 provides the vertical displacements of the bottom girder (Girder 1) under total dead load. Although there are small variations in the vertical displacement predictions, Fig. 2 shows that the approximate methods predict the vertical displacements accurately. Moreover, the small difference in the predictions of the vertical displacements can be handled in the haunches. Figures 3 and 4 show the relative lateral displacement predictions for girders 1 and 2 respectively under total dead load. The layovers are around 3 inches on the skewed bearing. It should be noticed from Figs. 3 and 4 that end layovers are predicted accurately. However, there are small variations in the predictions compared to benchmark solutions within the span.

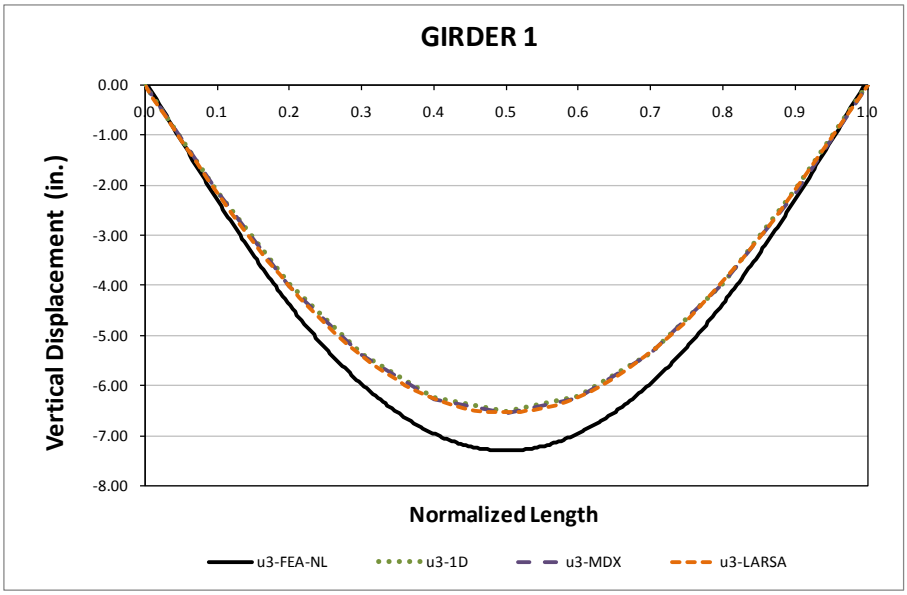

Fig. 2. NISSS4, Vertical displacements under total dead load for NLF detailing.

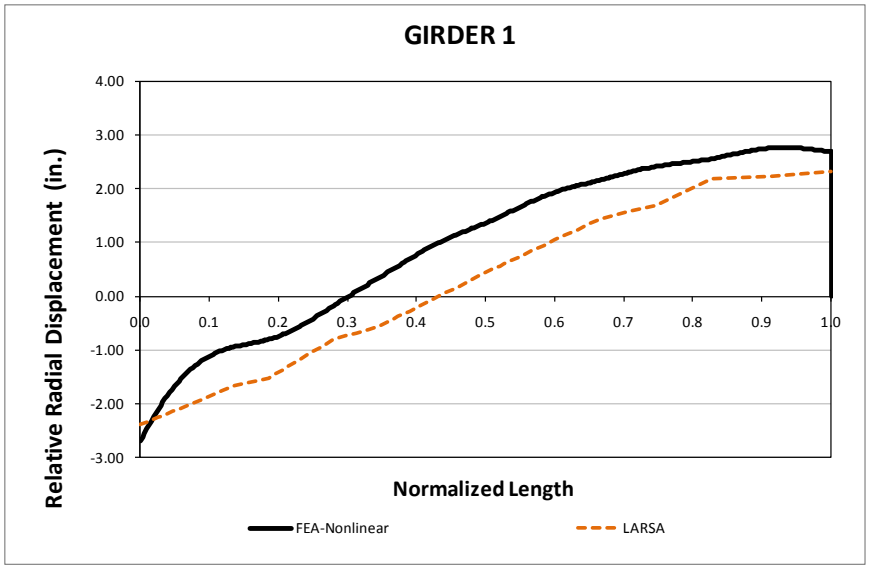

Fig. 3. NISSS4, Relative lateral displacements under total dead load for NLF detailing.

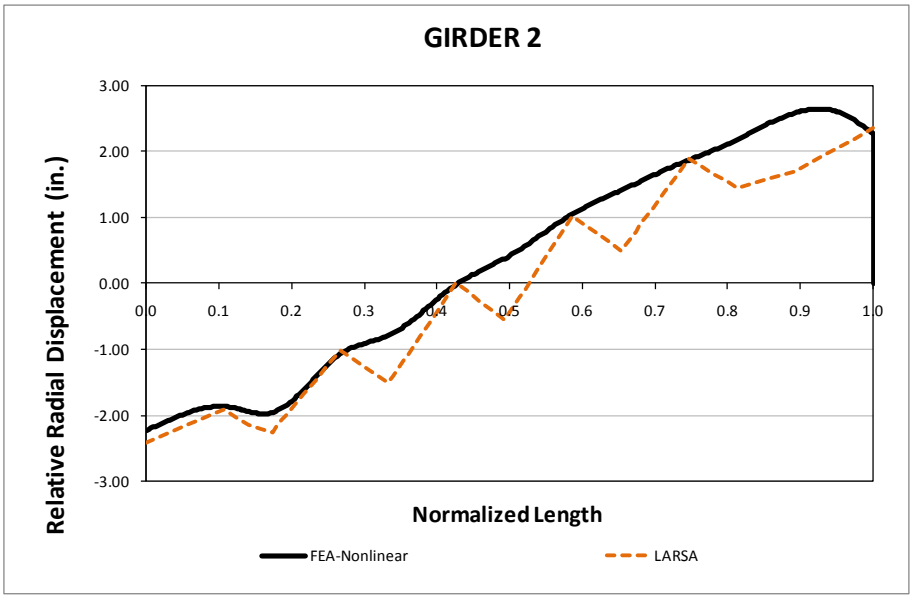

Fig. 4. NISSS4, Relative lateral displacements under total dead load for NLF detailing.

Figure 5 provides top flange major-axis bending stress predictions for bottom girder under total dead load (Girder 1). Although all the approximate analysis methods perform in a similar fashion, there are small variations in the stress predictions compared to the benchmark solutions. Figs. 6, 7 and 8 show top flange major-axis bending stresses of girders 2, 3 and 4. If one looks at Figs. 5 to 8 in order, the variations in the stresses due to the effect of skew on the major-axis bending predictions can be seen clearly. For instance, the prediction error for girder 2 major-axis bending stresses gets higher close to the left side of the mid-span, whereas the error is maximum on girder 3 close to the right side of the mid-span.

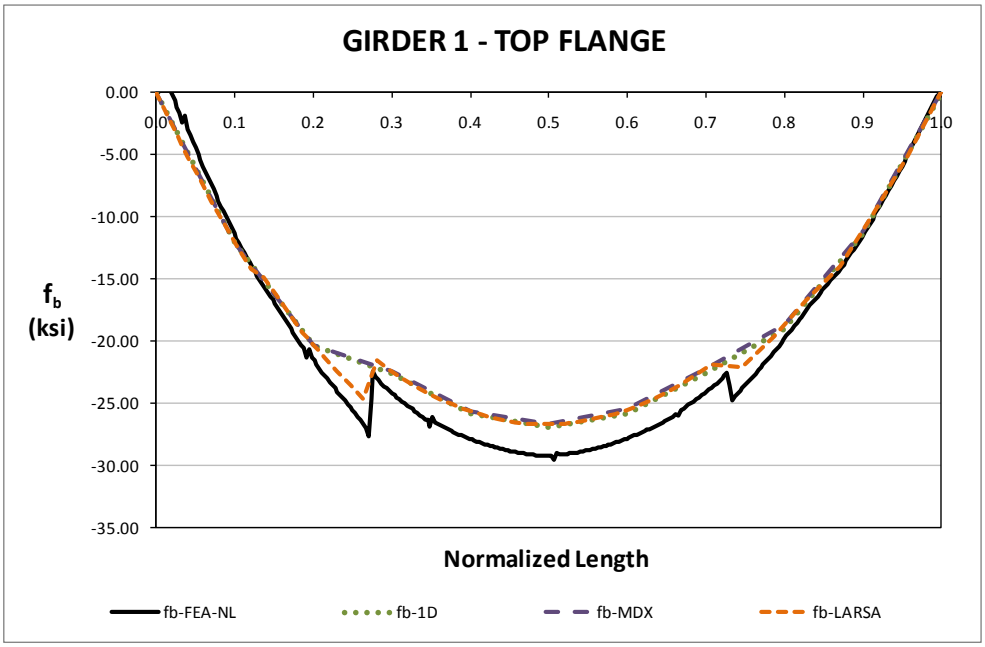

Fig. 5. NISSS4, Major-axis bending stresses under total dead load for NLF detailing.

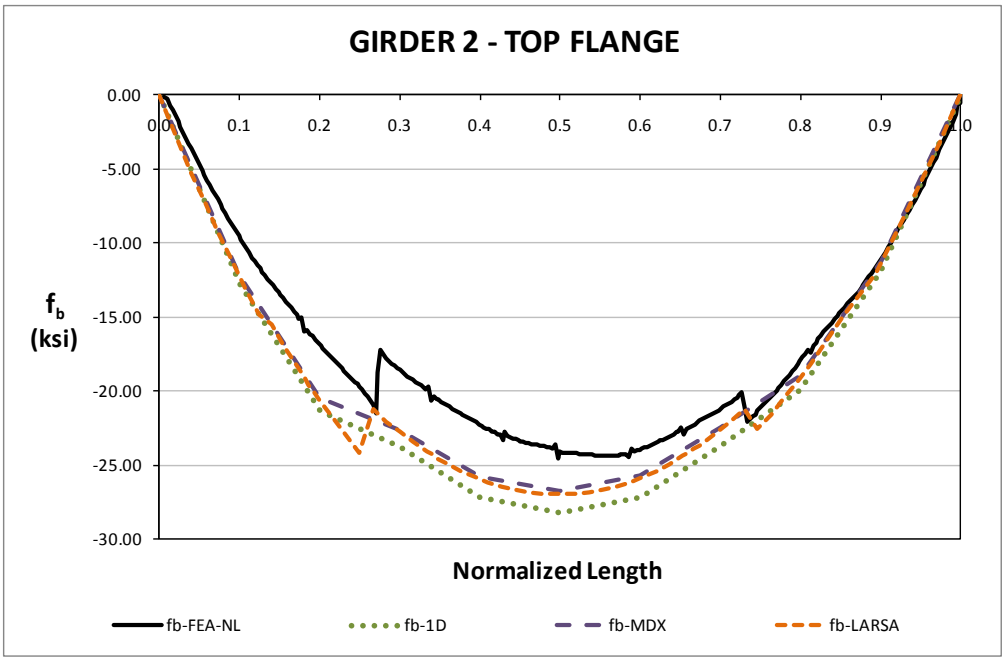

Fig. 6. NISSS4, Major-axis bending stresses under total dead load for NLF detailing.

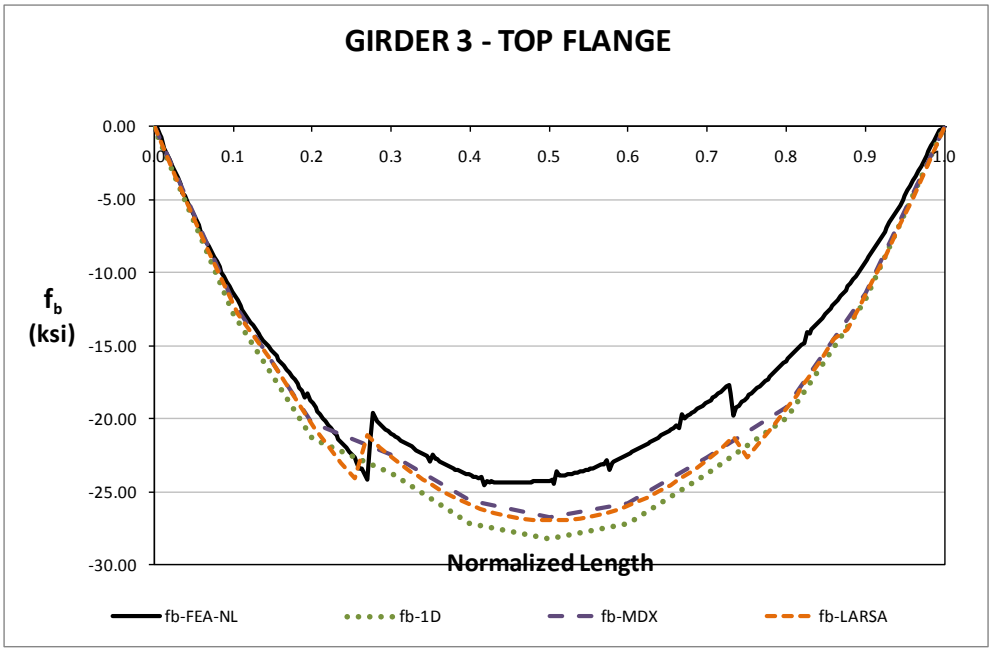

Fig. 7. NISSS4, Major-axis bending stresses under total dead load for NLF detailing.

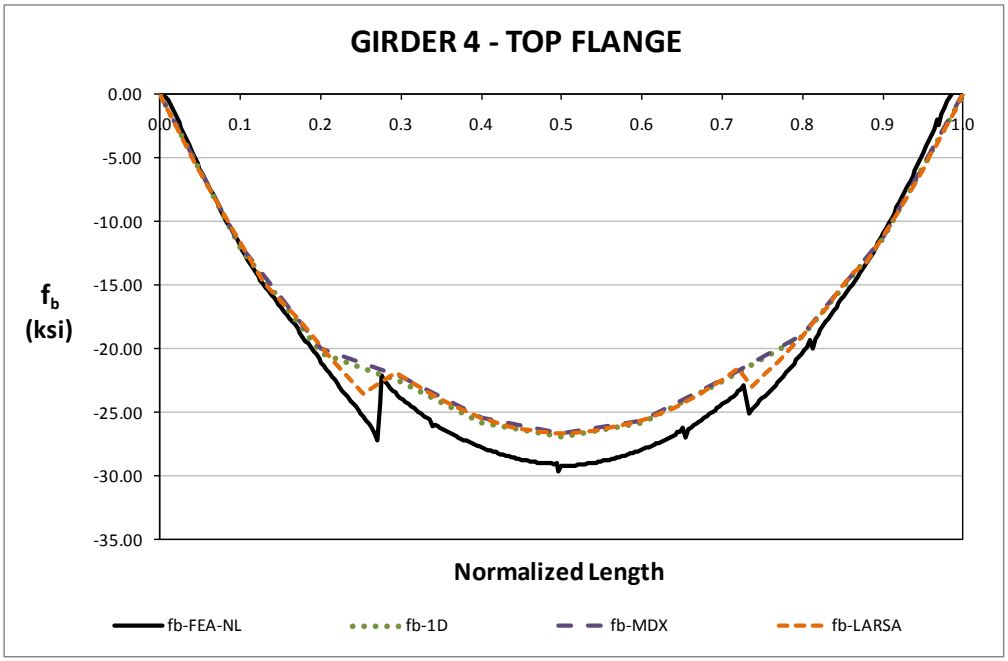

Fig. 8. NISSS4, Major-axis bending stresses under total dead load for NLF detailing.

Staggered cross-frame pattern is used for this bridge. This layout of cross-frames reduces the magnitude of the cross-frame forces at the expense of increasing lateral bending stresses in the girder flanges. Figure 9 shows the flange lateral bending stresses of girders 1 and 2 whereas Fig. 10 shows the flange lateral bending stresses of girders 3 and 4. These figures clearly illustrate that the maximum flange lateral bending stresses occur at the interior girders due to the staggered pattern. The greatest stress usually occurs on those girders from the cross-frames close to the skewed bearings. Figure 11 provides the cross-frames that cause high flange lateral bending stresses on girders. Also, high flange lateral bending stresses away from the skew bearing are observed on the fascia girders. These stresses are caused primarily by overhang bracket loadings.

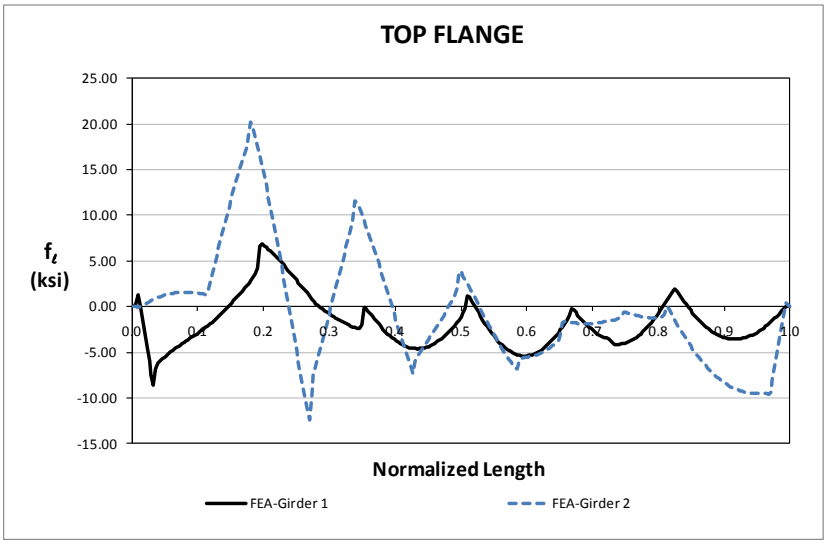

Fig. 9. NISSS4, Flange lateral bending stresses under total dead load for NLF detailing.

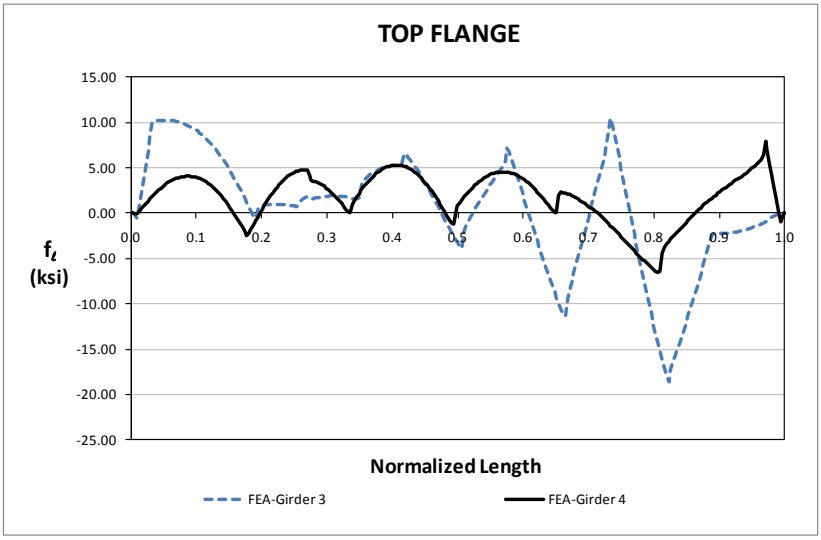

Fig. 10. NISSS4, Flange lateral bending stresses under total dead load for NLF detailing.

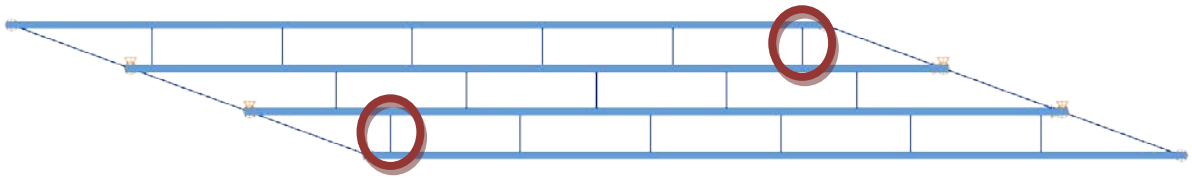

Fig. 11. NISSS4, Cross-frames that causes the highest flange lateral bending stresses in girders.

Conclusions:

Although there are small differences in the vertical displacements, they can be handled in the haunches while pouring the deck. The end layovers are accurately predicted by approximate analysis methods. Major-axis bending stresses are predicted well by approximate analysis methods.

Although the flange lateral bending stresses are not reported for straight bridges from the approximate analysis methods, depending on the skew angle large flange lateral bending stresses can be observed. The magnitude of the flange lateral bending stresses depends on the magnitude of the skew and staggered pattern of the cross-frames. The greatest flange lateral bending stress usually occurs on girders due to perpendicular cross-frames close to the skewed bearings or within the span where high transverse stiffness is observed.

I2.6 NISSS6 (New, I-girder, Simple-span, Straight, Skewed supports)

Category Data:

L_{as} = 150 ft / w = 30 ft / θ_1 = 50 °, θ_2 = 0 °/ 4 girders

Cross-Frame Detailing Method: NLF

Erection Stages Analyzed: Four

Deck Placement Sequence: One stage, deck thickness = 9.5 in.

Bridge Perspective & Plan Views:

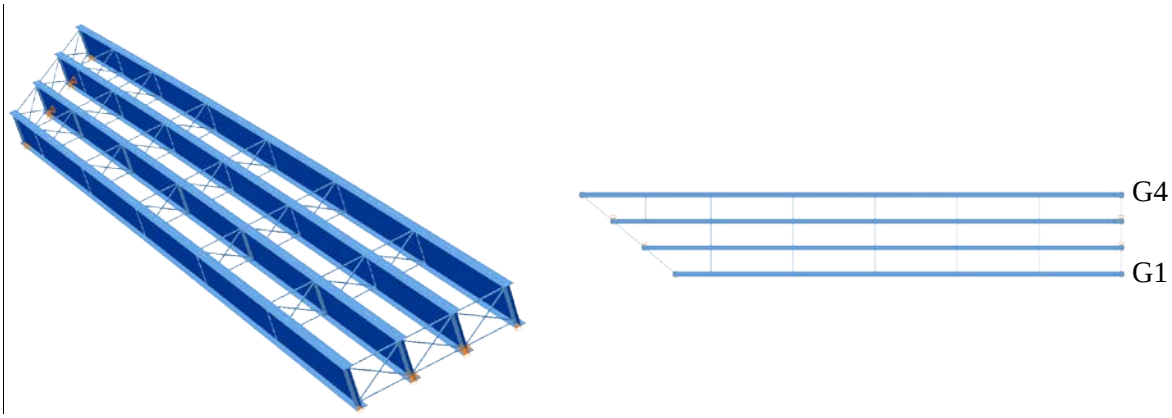

Abbreviated Analysis Results:

This bridge is a relatively short span structure with a high skew in one support. The effects of the skew and unequal girder lengths are studied in this structure. Three stages are considered for the study. The first stage is the case where there is a single girder in place (G1). For this stage, a holding crane is provided at mid-span to prevent a stability failure. In Stage 2, girders G1 and G2 are erected, and the holding crane released. The final state, Stage 5, considers the total dead load condition with wet concrete. Figure 1 shows the 3D FEA representations of the three stages considered in this report.

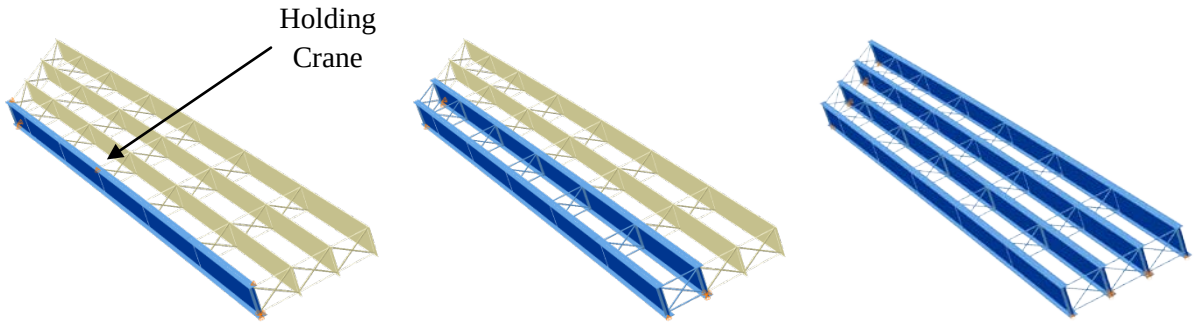

Fig. 1. Analyzed Construction Stages

The major-axis bending stresses for girder G1 in Stage 1 are plotted in Figure 1. As shown, the 2D grid response fits accurately the benchmark 3D prediction. This is an expected result given that this case simply represents a girder with supports at the ends and at mid-span under its own weight. Similar results are observed for Stage 2. The 2D grid representation captures the 3D model prediction accurately for stresses and displacements. Figure 3 shows the stress response for girder G1 at Stage 2.

For the first two construction stages, the lateral bending response is negligible. Flange lateral bending stresses and girder layovers are very small and do not require a consideration in the analysis of these stages.

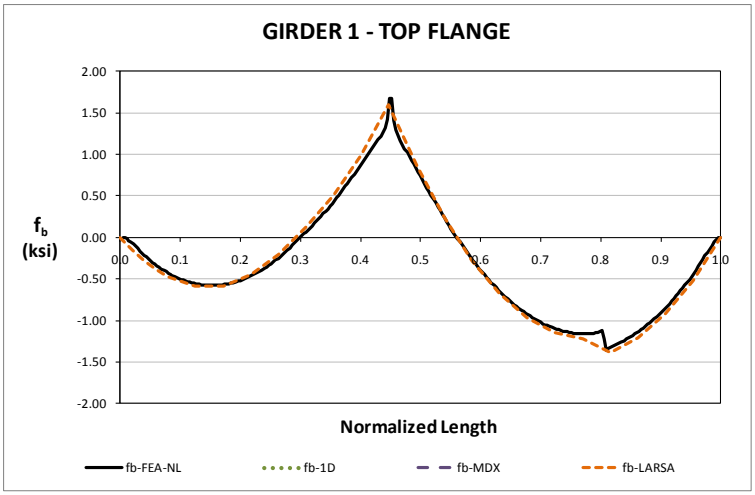

Fig. 2. Major-axis Bending Stresses, Stage 1

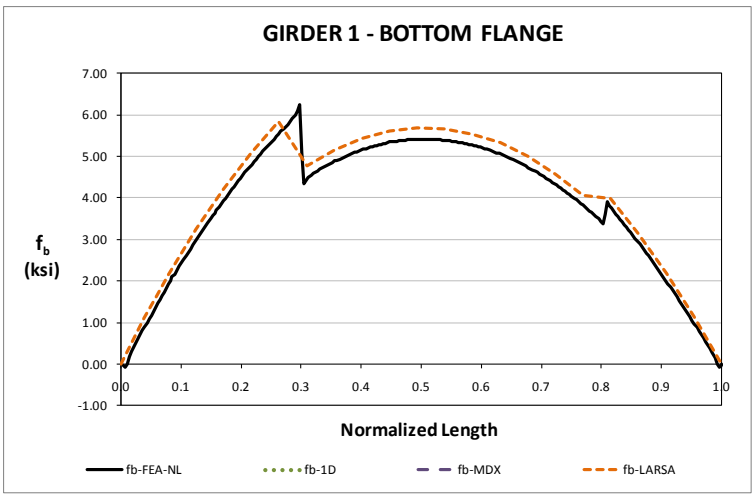

Fig. 3. Major-axis Bending Stresses, Stage 2

The stress and displacement predictions of girder G1 during the concrete placement (Stage 10) are shown in Figures 4 and 5, respectively. These two plots are representative of the results obtained in the rest of girders. As shown in the figures, the approximate 1D and 2D analysis methods reflect with accuracy the expected responses, as predicted by the 3D model.

For this final stage, there are flange lateral bending stresses in girder G1 that should be considered in the design of the bridge. Figure 6 shows that approximately 0.09 the length of the girder, the flange lateral bending stress is 15 ksi. This is a result of the use of staggered cross-frames at the vicinities of the left support. It is also observed that a considerable magnification of the stress as a result of the second order effects.

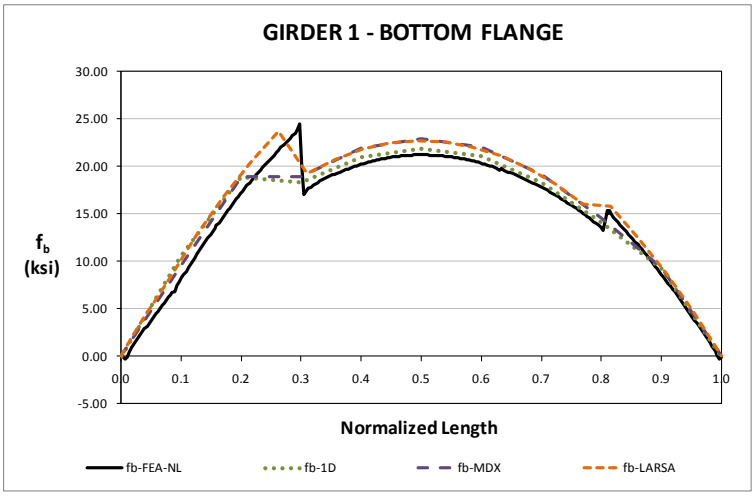

Fig. 4. Major-axis Bending Stresses, Stage 10

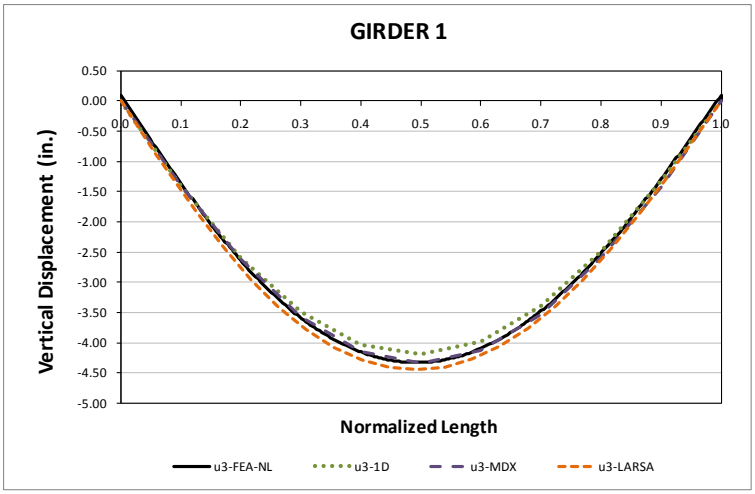

Fig. 5. Vertical Displacements, Stage 10

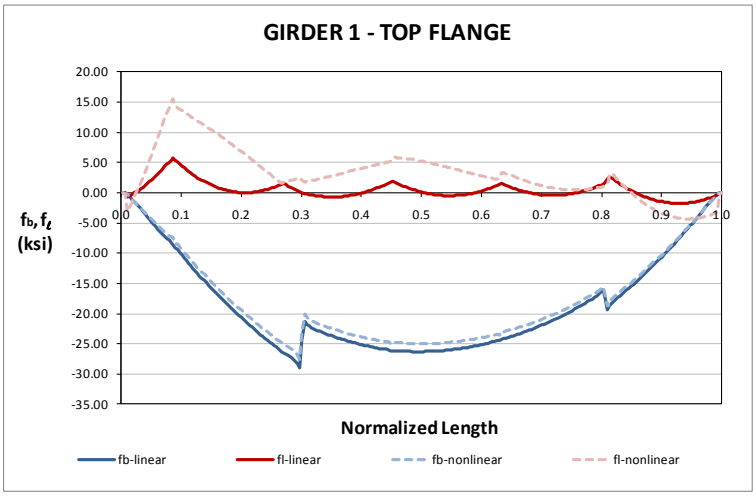

Fig. 6. FEA Stress Predictions, Stage 10

I2.7 NISSS11 (New, I-girder, Simple-span, Straight, Straight supports)

Category Data:

L_{as} = 150 ft / w = 80 ft / θ_1 = 20 °, θ_2 = 20 °/ 9 girders

Cross-Frame Detailing Method: NLF

Erection Stages Analyzed: Three

Deck Placement Sequence: One stage, deck thickness = 9.5 in.

Bridge Perspective & Plan Views:

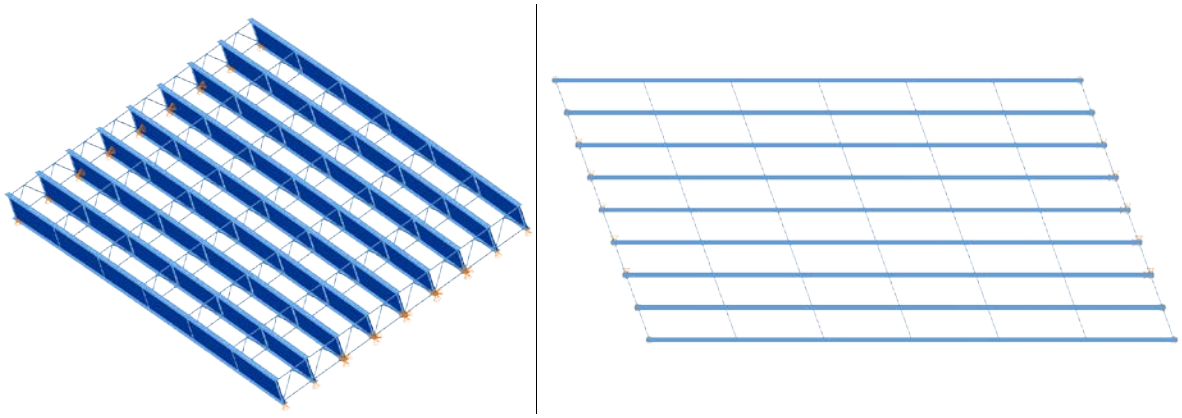

Abbreviated Analysis Results:

This bridge is a relatively simple structure. The skew angle is only 20^0, and the cross-frames are oriented parallel to the skew. The steel erection starts with the placement of girder G1. At the supports, the girder displacements are restrained with tie-downs, and a holding crane is provided at mid-span to prevent stability failure problems. The next girder, G2, is placed and connected to girder G1 with the cross-frames, and then, the holding crane is released. The rest of girders are added sequentially, following the same scheme. The structure is considered to be stable for the

Three stages have been selected to study the construction of this bridge. Stage 1 corresponds to the erection of the first girder, G1. Stage 2 corresponds to the state where two girders are in place without the holding crane. In Stage 10, the steel structure has been completed and the concrete poured. In this stage composite action has not been reached, and only the steel structure is resisting the loadings. Figure 1 shows the plan view of the three stages studied.

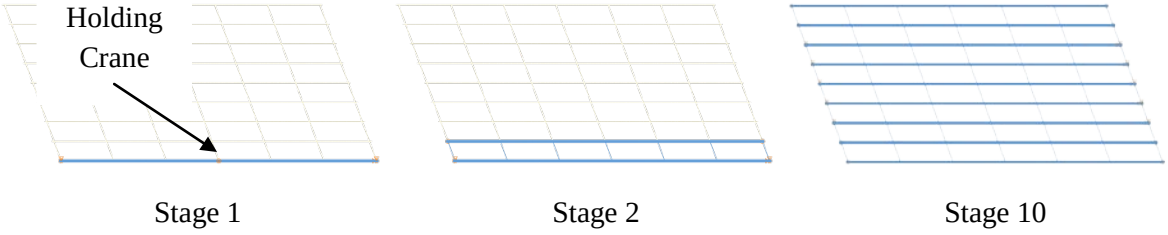

Fig. 1. Analyzed Construction Stages

The results obtained for this bridge from the approximate 1D and 2D analyses are accurate for all the responses, during all the studied construction stages. Figure 2 shows the major-axis bending stresses in girder G1, for Stage 2. As show, the 2D grid response fits accurately the response predicted by the 3D FEA model. The same characteristics are observed for the vertical displacements, as shown in Figure 3.

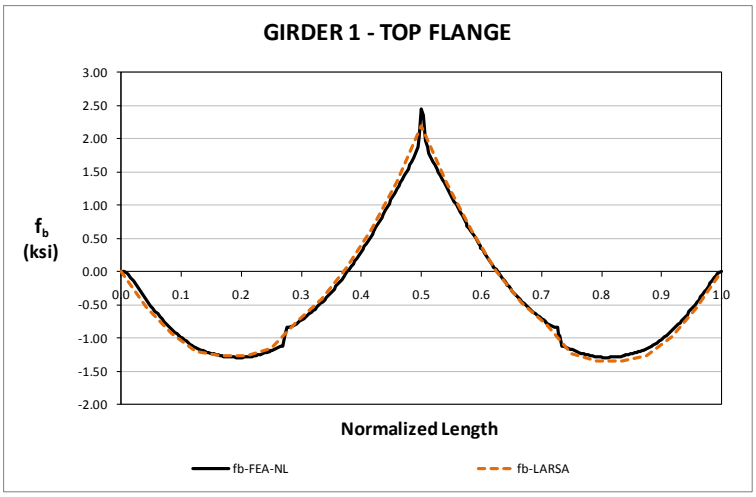

Fig. 2. Major-axis Bending Stresses, Stage 1

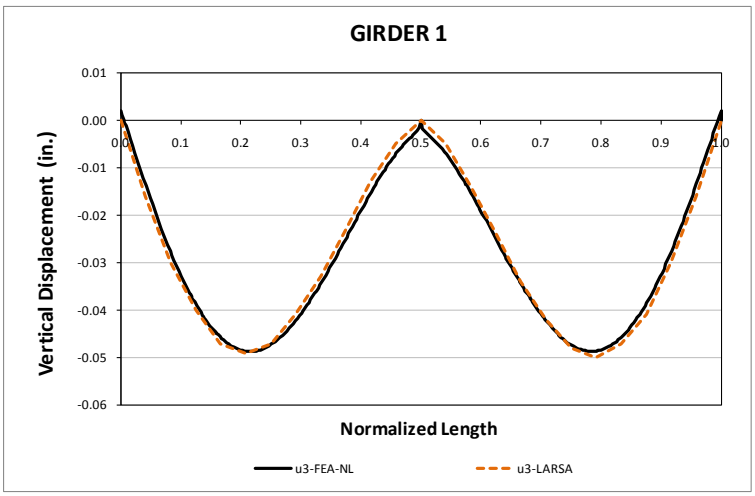

Fig. 3. Vertical Displacements, Stage 1

For Stage 10, the major-axis bending stress response is shown in Figure 4. The responses predicted by the line girder and the two 2D grid analysis methods are an accurate representation of the 3D model response. Figure 5 shows that the vertical displacements are also accurate for this stage, and Figure 6 shows the correspondence between the 2D grid and 3D FEA models for relative lateral displacements. A comparison of flange lateral bending stresses is not shown in this report. Due to the small skew angle and the orientation of the cross-frames, these stresses are negligible.

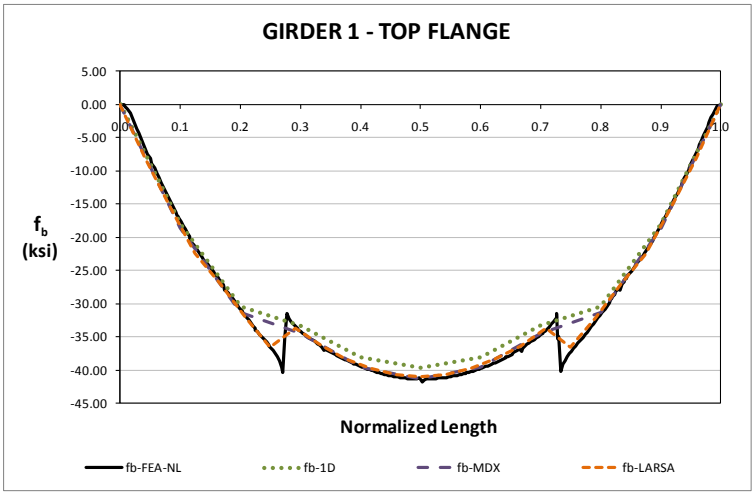

Fig. 4. Major-axis Bending Stresses, Stage 10

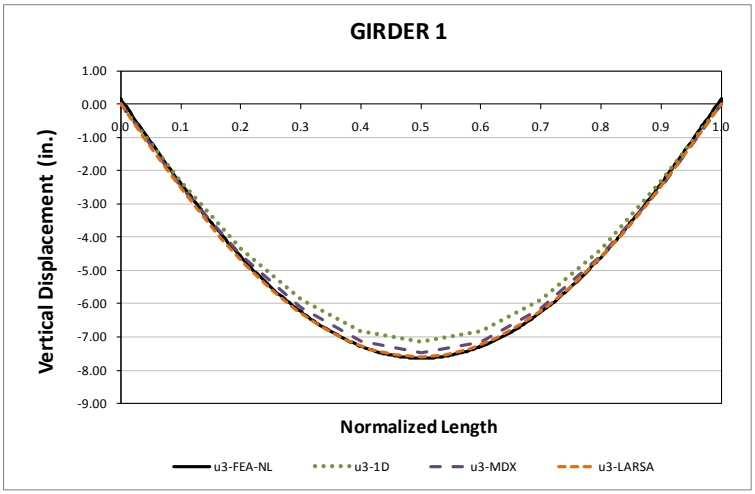

Fig. 5. Vertical Displacements, Stage 10

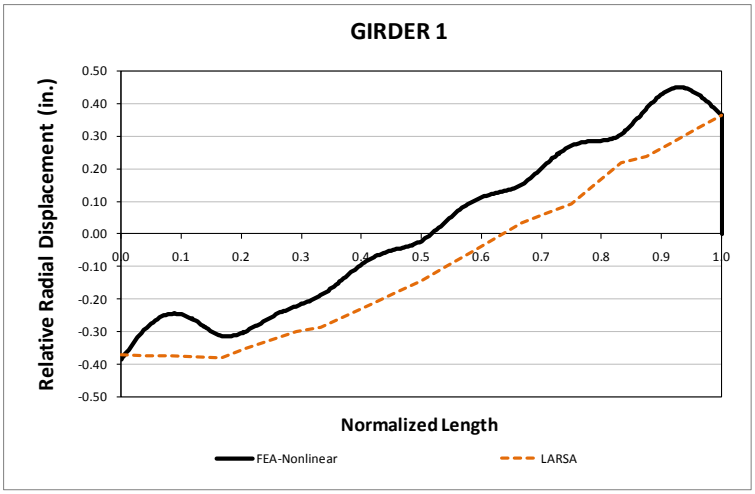

Fig. 6. Relative Radial Displacements, Stage 10

Conclusions:

The geometry of this bridge is relatively simple. As expected, the approximate methods provide reliable results for the major-axis bending responses and the relative lateral displacements. In fact, a simple line girder analysis would be enough to predict the geometry and the stresses of this bridge during construction.

It is also concluded that it might not be required to predict the flange lateral bending response of this bridge. The small skew and the parallel orientation of the cross-frames result in small differential deflections that do not induce considerable levels of flange lateral bending stress.

I2.8 NISSS13 (New, I-girder, Simple-span, Straight, Skewed supports)

Category Data:

L_1 = 150 ft / w = 80 ft /θ_1 = 50°, θ_2 = 50°, 9 girders

Cross-Frame Detailing Method: NLF

Erection Stages Analyzed: 6 (Analyses are performed assuming NLF)

Deck Placement Sequence: 1 Stage

Bridge Perspective & Plan Views:

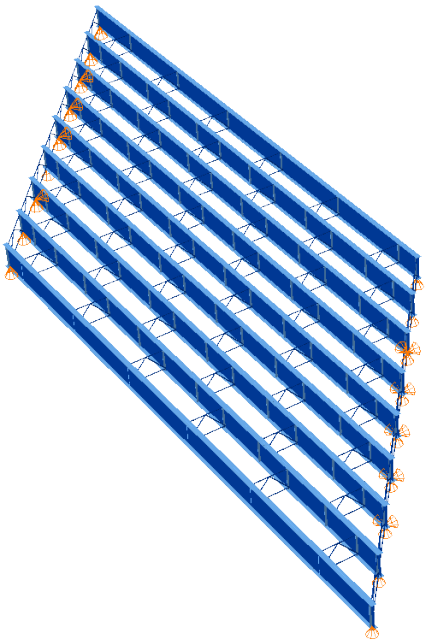

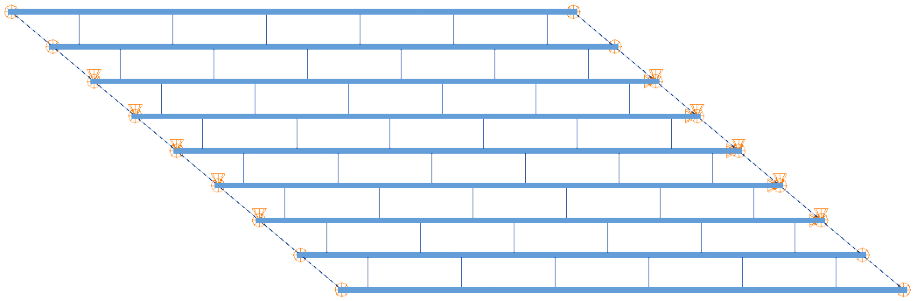

Abbreviated Analysis Results

Although various stages are investigated for this bridge, the total dead load condition is chosen to illustrate the most important observations. Figures 1 and 2 show the vertical displacements of the bottom girder (Girder 1) and girder 2 respectively. Approximate analysis methods predict the vertical displacements accurately compared to the benchmark solution. The predictions are better for the interior girders. This is mainly because the loading is more uniform. The assumptions for handling overhang bracket loads decrease the accuracy of the deflection predictions for the approximate analysis methods. Very good accuracy in the prediction of the vertical displacements is observed for the steel dead load case.

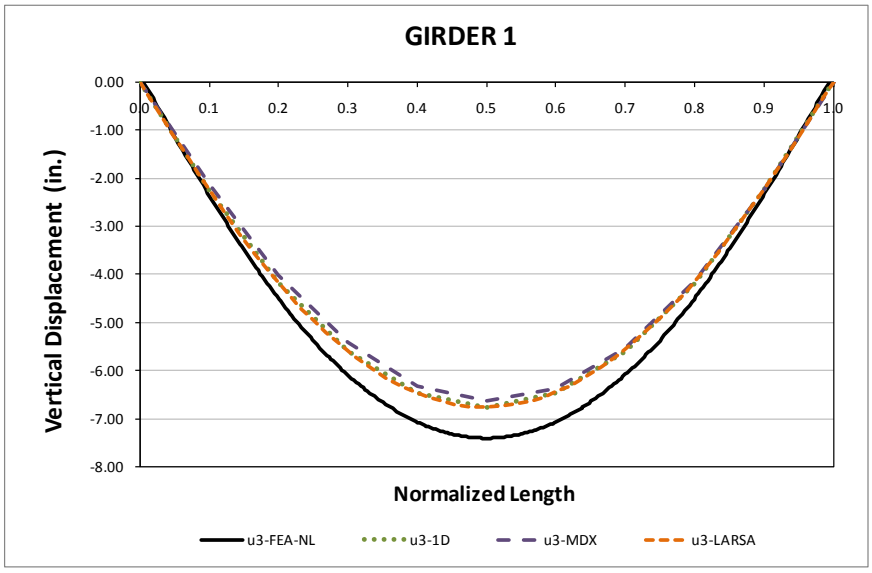

Fig. 1. NISSS13, Vertical displacements under total dead load for NLF detailing.

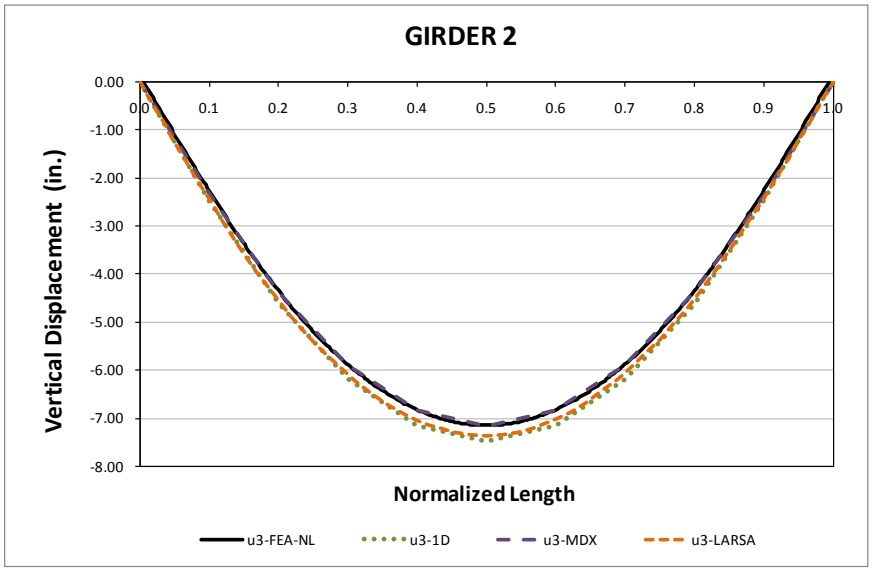

Fig. 2. NISSS13, Vertical displacements under total dead load for NLF detailing.

Figures 3, 4 and 5 provide the relative lateral displacements for girders 1, 2 and 3 respectively. The zigzag pattern is observed for the interior girders due to the staggered pattern of the cross-frames. The predictions are less accurate for the bottom girder (Girder 1). However, the difference between the results gets increasingly smaller from girder 1 to girder 3. This is also the case for the stage under steel dead load. Moreover, the end layovers are predicted accurately by 2D grid solutions.

Figure 6 provides the major-axis bending stress predictions for the bottom girder under steel dead load. Although all the approximate analysis methods perform in a similar fashion, there are small variations in the stress predictions compared to the benchmark solutions.

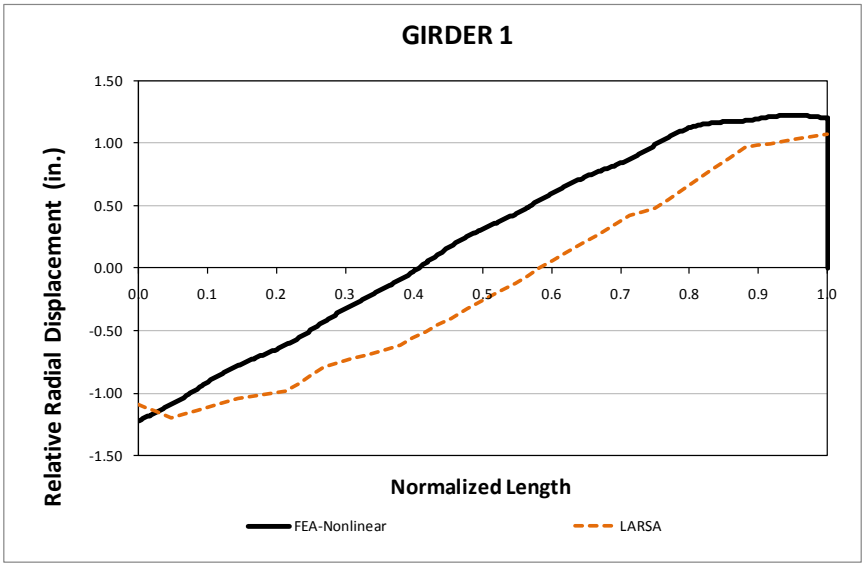

Fig. 3. NISSS13, Relative lateral displacements under total dead load for NLF detailing.

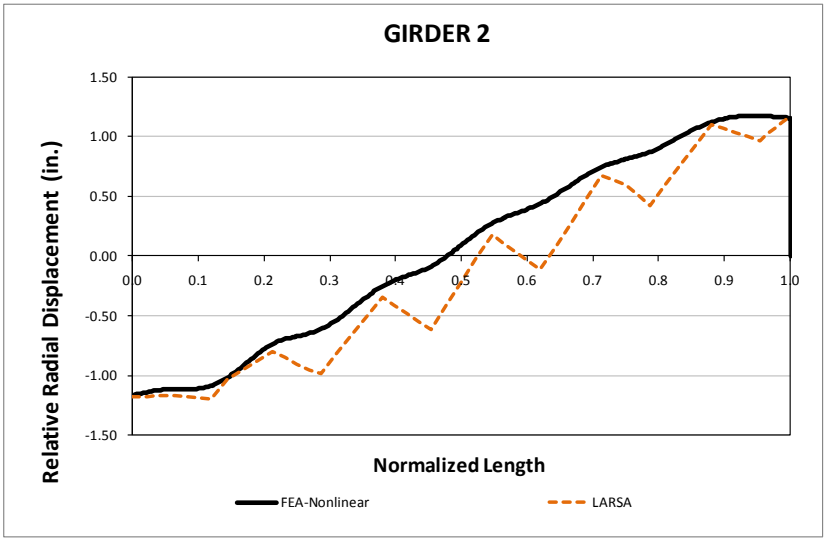

Fig. 4. NISSS13, Relative lateral displacements under total dead load for NLF detailing.

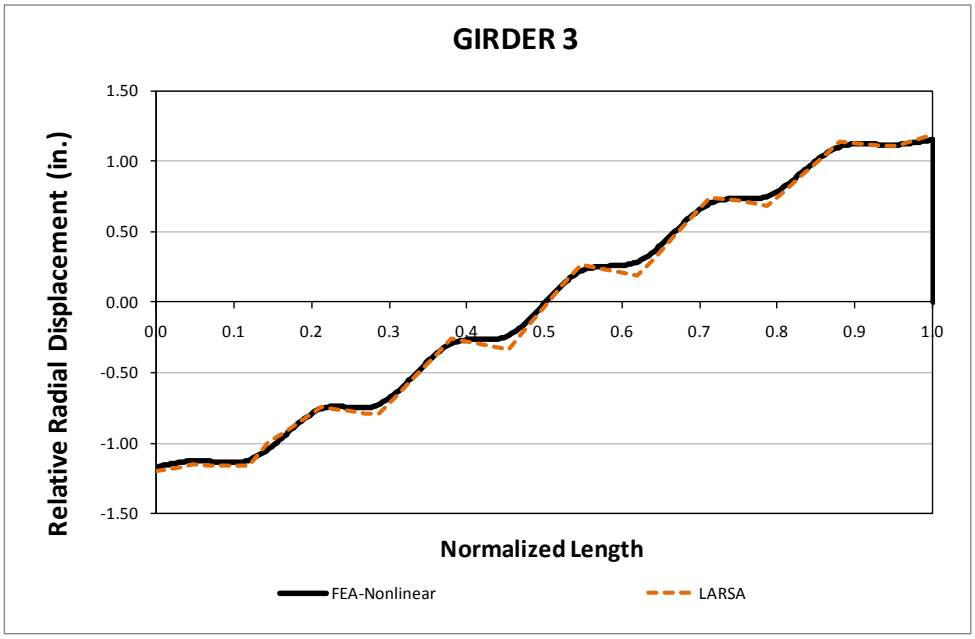

Fig. 5. NISSS13, Relative lateral displacements under total dead load for NLF detailing.

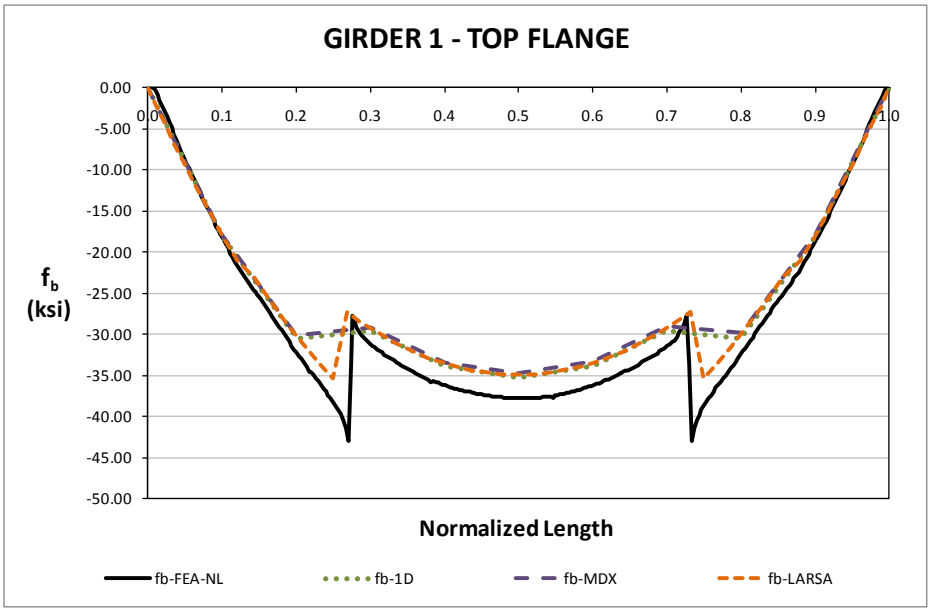

Fig. 6. NISSS13, Major-axis bending stresses under total dead load for NLF detailing.

Conclusions:

Approximate analysis methods performed well for predicting deflections and stresses. The error of predictions gets smaller for the interior girders. The assumptions for handling overhang bracket loads lead to differences in vertical and lateral displacements. However, the differences in the vertical displacements can be handled in the haunches. Zigzag pattern is observed for the lateral displacements due to the staggered pattern of the cross-frames.

I2.9 NISSS14 (New, I-girder, Simple-span, Straight, Straight supports)

Category Data:

L_{as} = 150 ft / w = 80 ft / θ_1 = 70 °, θ_2 = 70 °/ 9 girders

Cross-Frame Detailing Method: NLF

Erection Stages Analyzed: Three

Deck Placement Sequence: One stage, deck thickness = 9.5 in.

Bridge Perspective & Plan Views:

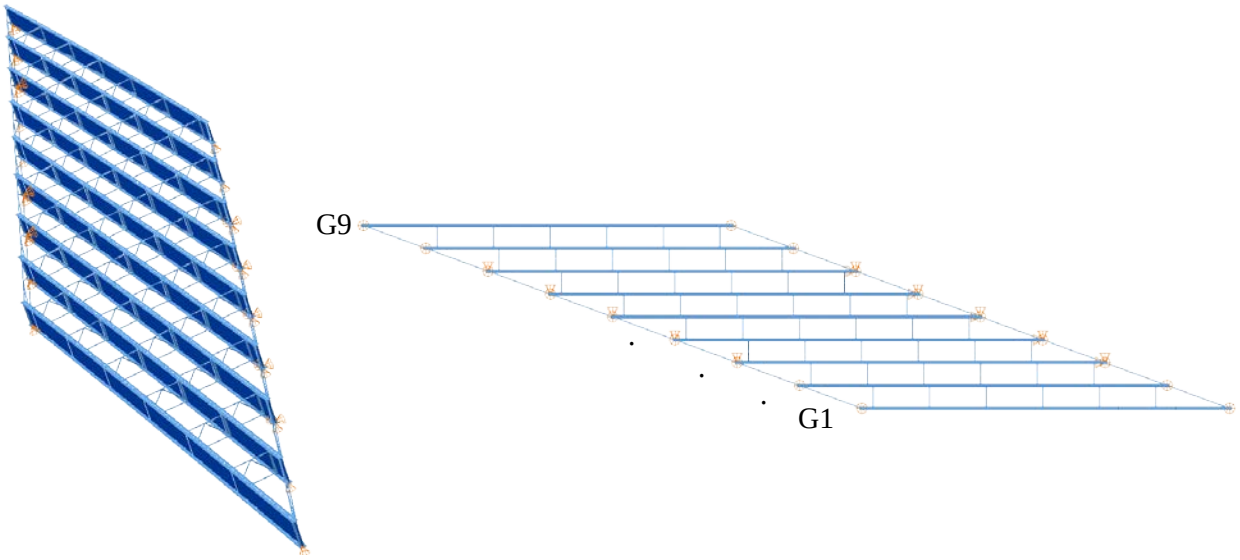

Abbreviated Analysis Results:

This parametric bridge represents an extreme case of a high skew combined with a large width. The steel erection starts with the placement of girder G1. At the supports, the girder displacements are restrained with tie-downs, and a holding crane is provided at mid-span to prevent stability failure problems. The next girder, G2, is placed and connected to girder G1 with the cross-frames, and then, the holding crane is released. The rest of girders are added sequentially following the same scheme.

Three stages have been selected to study the construction of this bridge. Namely, Stages 2, 5, and 10 are considered in the study. Stage 2 corresponds to the state where two girders are in place without the holding crane. In Stage 5, the first five girders are positioned on the bearings. In Stage 10, the steel structure has been completed and the concrete poured. In this stage, also known as the total dead load condition (TDL), composite action has not been reached, and only the steel structure is resisting the loadings. Figure 1 shows the plan view of the three stages studied.

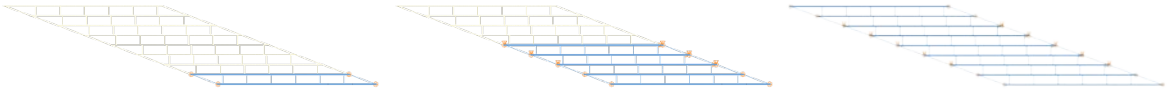

Stage 2 Stage 5 Stage 10

Fig. 1. Analyzed Construction Stages

The results obtained for this bridge from the approximate 1D and 2D analyses are accurate for all the responses, for the first erection stages. Examples of the stress and vertical displacement responses at Stage 2 are shown in Figure 2 and 3, respectively. As the erection progresses, however, the approximate analysis predictions differ from the 3D model results. As shown in Figure 4, at the steel dead load condition (SDL), i.e., when the steel structure has been completed, the 1D and 2D analysis predictions are not an accurate representation of the benchmark. The same characteristics are observed for the vertical displacements, as shown in Figure 5.

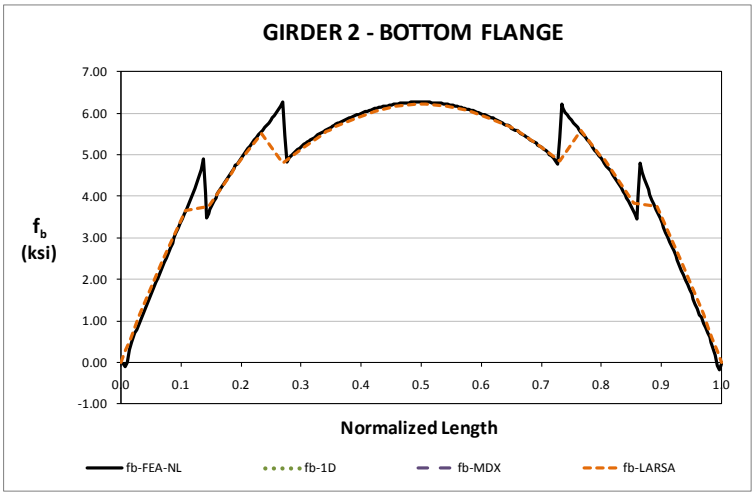

Fig. 2. Major-axis Bending Stresses, Stage 2

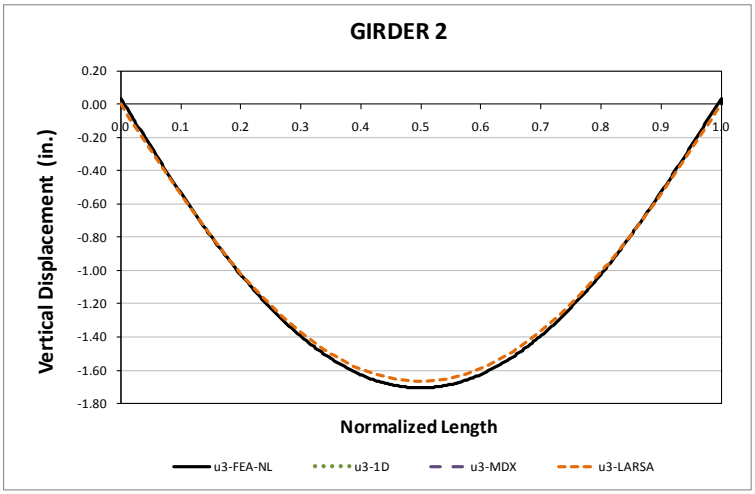

Fig. 3. Vertical Displacements, Stage 2

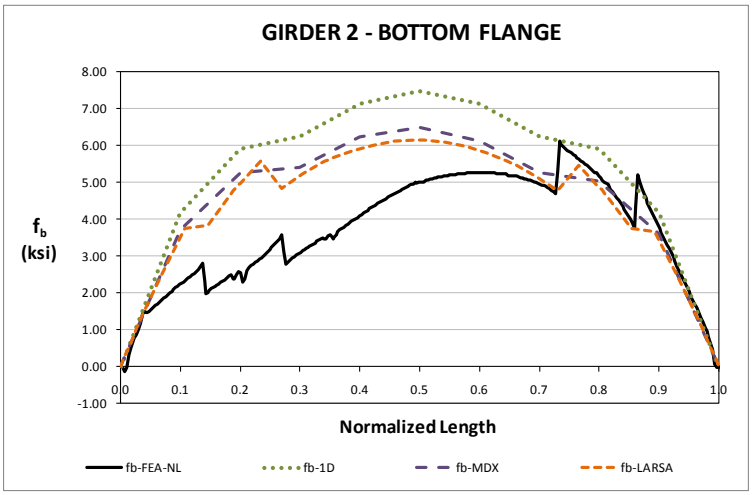

Fig. 4. Major-axis Bending Stresses, SDL Condition

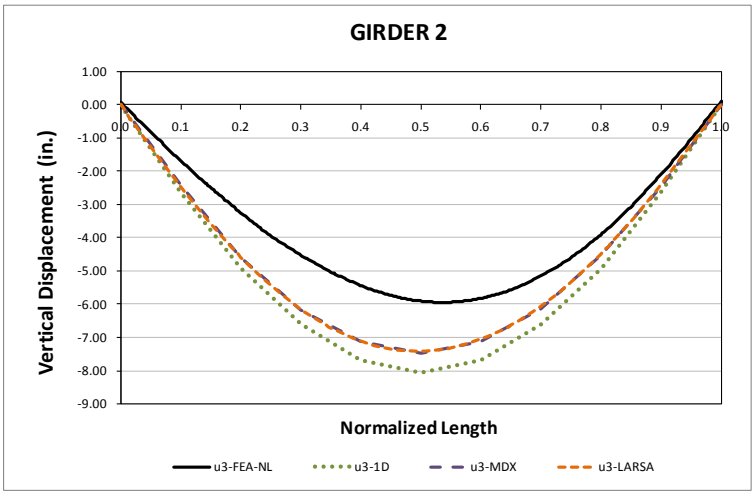

Fig. 5. Vertical Displacements, Stage 10 (TDL)

It is important to notice that due to the contour of the bridge, it is not possible to use contiguous cross-frames across the width. Thus, the use of staggered cross-frames is the only option to avoid problems associated to "nuisance stiffness." This practice, however, results in an increase of the flange lateral bending response and its associated stresses, f_ℓ. Figure 6 shows the results from the 3D FE model for girder G5 at the SDL condition. Both linear and nonlinear responses are included in this plot. As shown in the figure, the levels of flange lateral bending stress are substantial, and even larger than the stresses produced due to major-axis bending, f_b. The same trend is observed for the TDL condition, as shown in Figure 7. In this case, the f_ℓ stress levels are over the yield limit of 50 ksi, while the major-axis bending stresses are in the order of 25 ksi. These plots highlight the importance of considering the flange lateral bending effects in the design of the bridge.

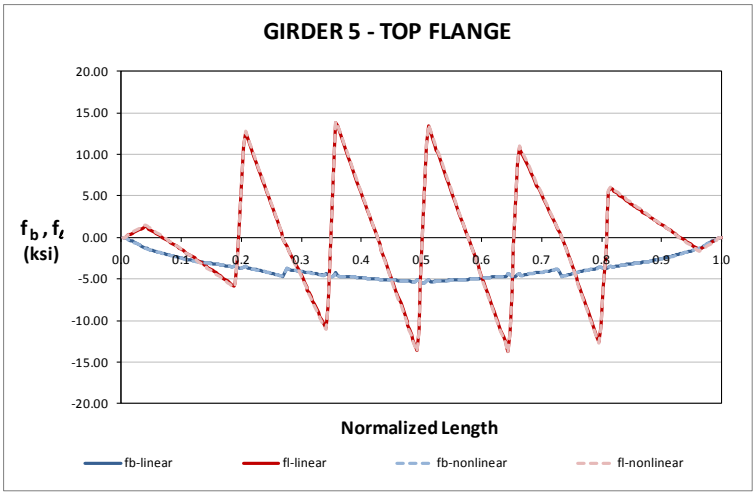

Fig. 6. f_b and f_l predictions, 3D FEA, SDL Condition

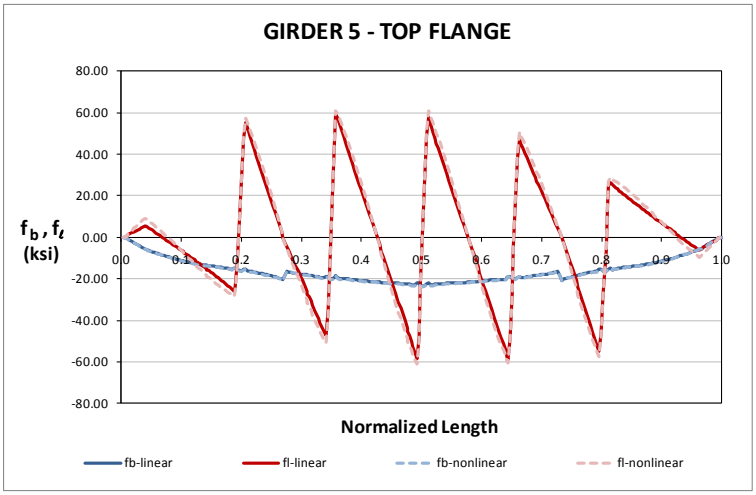

Fig. 7. f_b and f_l predictions, 3D FEA, Stage 10 (TDL)

Conclusions:

Currently, there is no guidance on how to evaluate the effects of the skew at the supports and its correspondent flange lateral bending stresses other than the recommendation of the AASHTO 2010 Bridge Design Specifications, Section C6.10.1. This guideline, however, only applies to bridges that have skews of up to 60 degrees, and does not cover the present case. Therefore, the only method to predict the expected flange lateral bending response in this bridge is by mean of a 3D FE model.

I2.10 NISSS16 (New, I-girder, Simple-span, Straight, Skewed supports)

Category Data:

L_{as} = 150 ft / w = 80 ft / θ_1 = 50 °, θ_2 = 0 °/ 9 girders

Cross-Frame Detailing Method: NLF

Erection Stages Analyzed: Four

Deck Placement Sequence: One stage, deck thickness = 9.5 in.

Bridge Perspective & Plan Views:

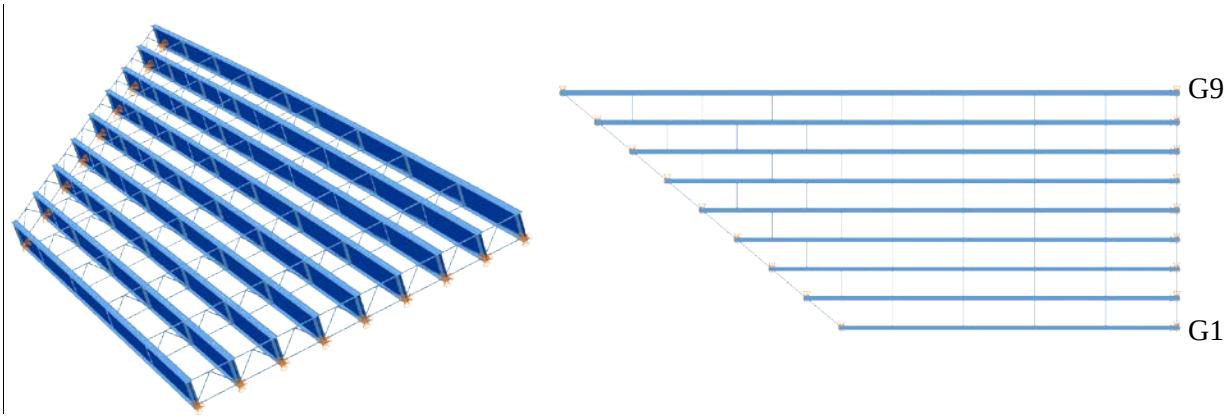

Abbreviated Analysis Results:

This bridge is an excellent case to study the skew effects. The difference in skew angles between the left and right supports results in girders of unequal lengths. This accentuates the differential deflection effects.

The three construction stages shown in Figure 1 are studied in this report. Stage 1, where one girder is in place with a holding crane provided at mid-length is studied first. In the second stage, two girders, G8 and G9 are in place, without any aid of cranes. It is considered that at this stage the two girder group is stable, so there is no need to provide extra supporting points. Finally, in Stage 10, the nine girders are in place and the weight of the wet concrete is applied to the structure.

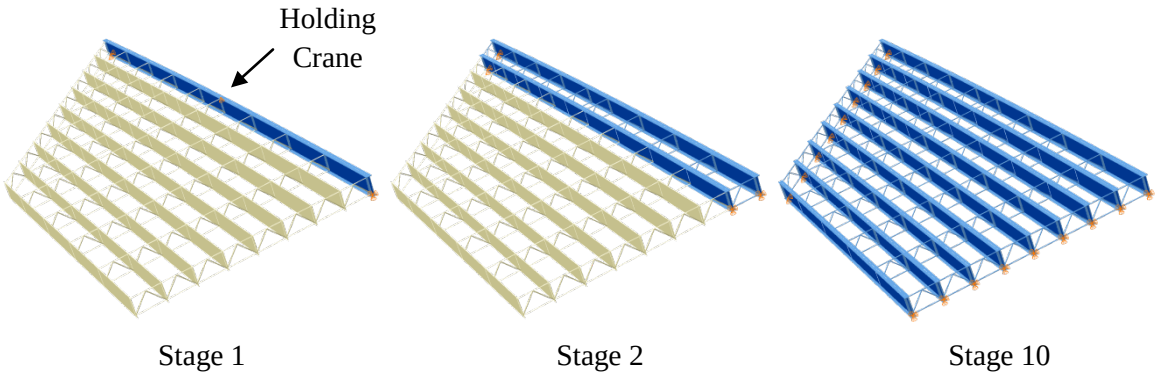

Fig. 1. Analyzed Construction Stages

The plot of major-axis bending stresses of the girder erected in Stage 1 is shown in Figure 2. As shown, the 2D grid model representation captures the response accurately for this stage. This is an expected result, given that in this stage represents the case of a simple straight girder that has an intermediate support.

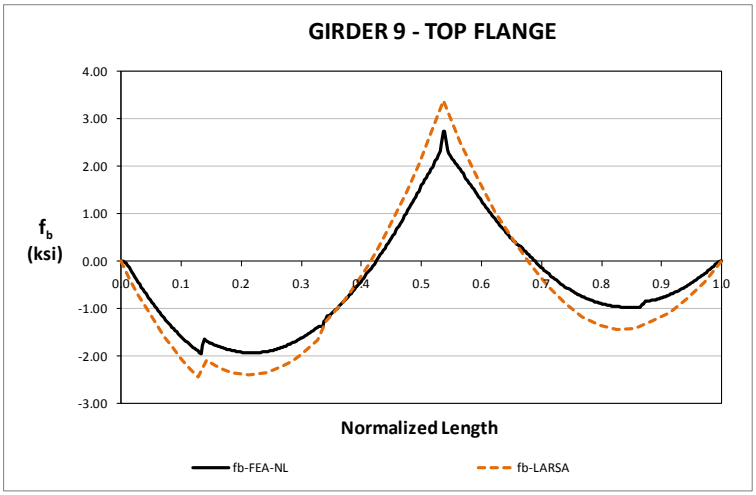

Fig. 2. Major-axis Bending Stresses, Stage 1

A comparison of the vertical and lateral displacements in girder G8 for Stage 2 is shown in Figures 3 and 4, respectively. As shown, the predictions obtained from the approximate method are consistent with the responses obtained from the FEA model. The relative lateral displacements are best predicted at the support locations. Notice that girder rotations are expected only at the skewed support. At the right support, where the bearing line is perpendicular to the girders, the lateral displacement is zero.

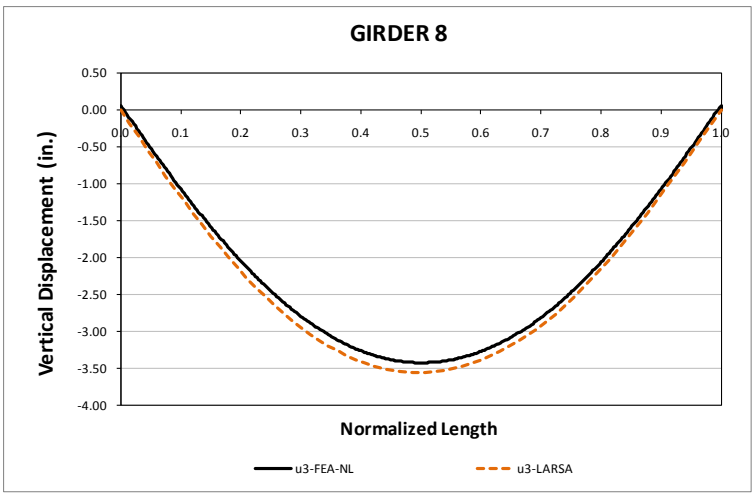

Fig. 3. Vertical Displacements, Stage 2

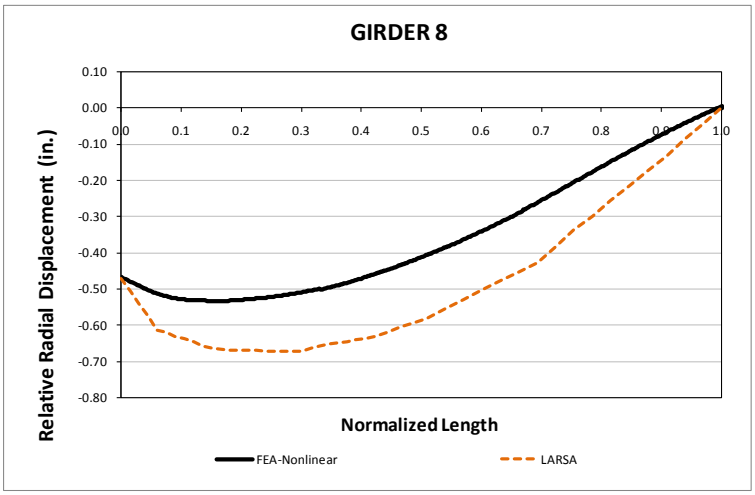

Fig. 4. Relative Lateral Displacements, Stage 2

For the final configuration, Stage 10, the predictions of the major-axis bending stresses are accurately predicted by the 1D and 2D methods of analysis. As shown in Figure 5, a line girder analysis or a grid analysis proves to be sufficient to capture the response.

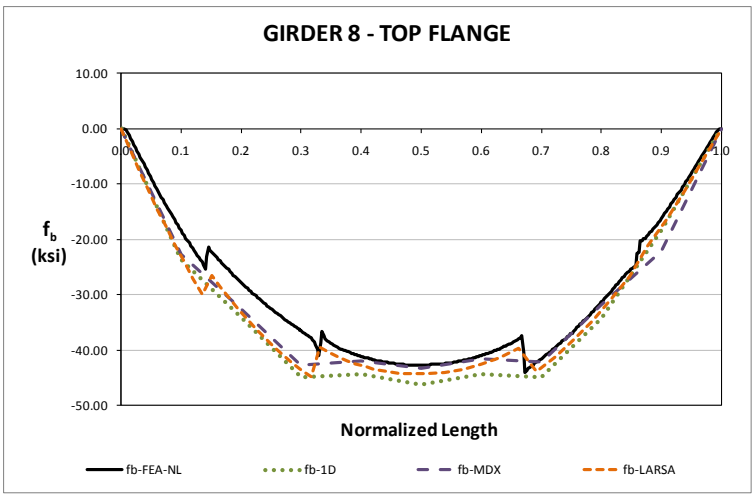

Fig. 5. Major-axis Bending Stresses, Stage 10

Due to the skew at the left support and the use of staggered cross-frames to overcome the nuisance stiffness problem, significant levels of flange lateral bending stresses are observed in the girders. Figure 6 shows a plot that includes both major-axis bending stresses and flange lateral bending stresses for the top flange of girder G6. This girder has the highest levels of flange lateral bending stress in the total dead load condition. The figure includes the FEA results of linear and geometric nonlinear analyses. As shown, the flange develops lateral bending stress levels in the order of 14 ksi at 0.14 the girder length. For this case, the recommendation given in the AASHTO Bridge Design Specification (2010), Section C6.10.1 to estimate these stresses is unconservative. The possible reason is that this bridge is a severe case of support skew combined with unequal girder lengths.

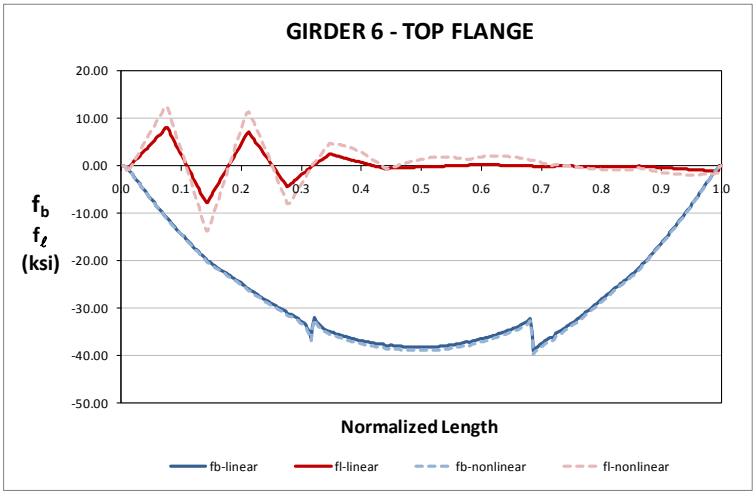

Fig. 6. FEA Stress Predictions, Stage 10

I2.11 NISSS36 (New, I-girder, Simple-span, Straight, Skewed supports)

Category Data:

L_1 = 225 ft / w = 80 ft /θ_1 = 50°, θ_2 = 0°, 9 girders

Cross-Frame Detailing Method: NLF

Erection Stages Analyzed: 5 (Analyses are performed assuming NLF)

Deck Placement Sequence: 1 Stage

Bridge Perspective & Plan Views:

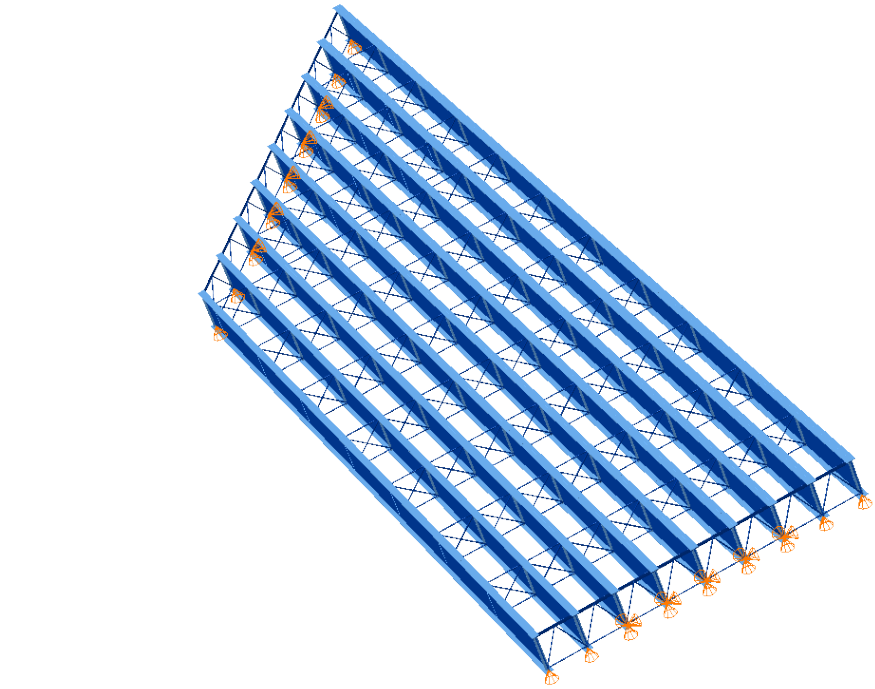

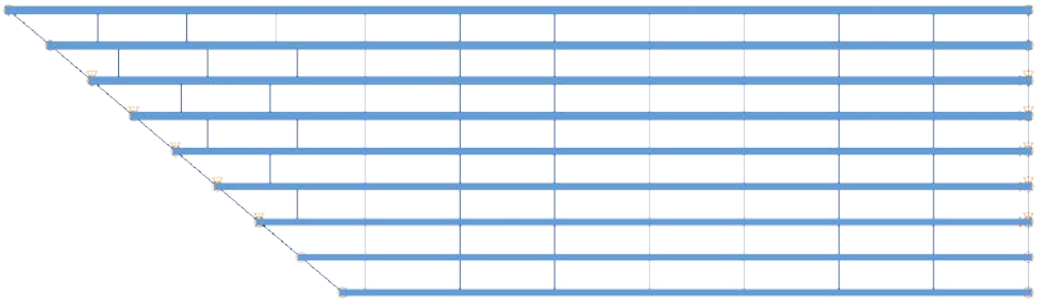

Abbreviated Analysis Results

Figure 1 shows the overall deflected shape of the bridge under total dead load. The deflections are magnified by 15 times. It should be noticed that the layover of the top flange of the bottom girder is upwards on the left skewed bearing due to compatibility between girders and cross-frames. On the other hand there is no layover is on the right bearing.

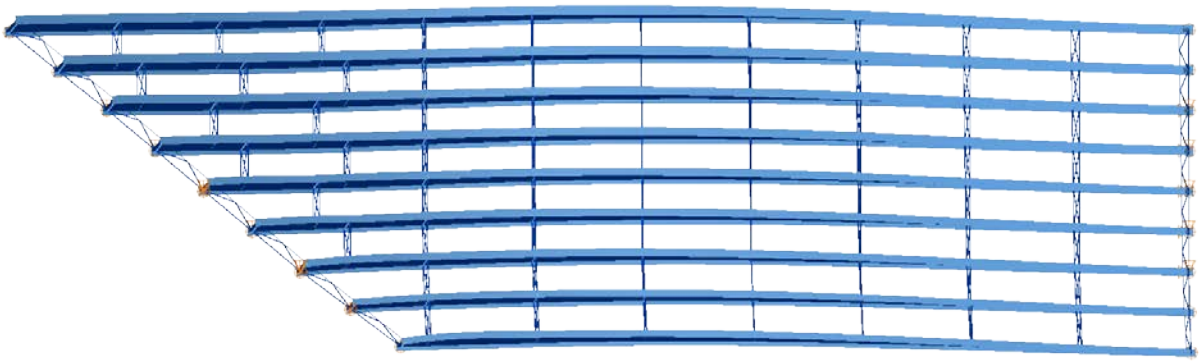

Fig. 1. NISSS36, Overall deflected shapes under total dead load for NLF detailing (Magnified by 15x).

Figure 2 provides the vertical displacements of the bottom girder (Girder 1) under total dead load. The predictions are off about 1 in from the benchmark solutions for girder 1. However, this difference is not critical and can be handled in haunches. Figure 3 shows the vertical displacements of the top girder (Girder 9). This girder is the critical girder for this bridge since it has the longest length among the other girders. Figure 3 shows that the vertical displacements are accurately predicted by the approximate methods. Figures 4 and 5 show fascia girder relative lateral displacement predictions under total dead load. It is clear from Figs. 4 and 5 that the end layovers are predicted accurately at the skewed ends. Furthermore, the layovers are accurately predicted within the span by grid solutions.

Figures 6 and 7 provide fascia girder top flange major-axis bending stress predictions under total dead load. The major-axis bending stresses are accurately predicted by approximate methods for girders 1 and 9. This is the case for all girders.

Figure 8 provides the top flange lateral bending stresses of girders 1, 5 and 9. Only the benchmark solutions are provided since there is no flange lateral bending stress predictions for the approximate analysis solutions. Staggered cross-frame pattern is used towards the skewed bearing to soften the structure. Therefore, higher flange lateral bending stresses are expected on girders towards the skewed end. Girder 5 is chosen since the interior girders tend to get higher flange lateral bending stresses due to the staggered pattern. Staggered cross-frame pattern reduces the magnitude of the cross-frame forces at the expense of increasing lateral bending stresses in the girder flanges. It should be noted from Fig. 8 that flange lateral bending stresses are very small towards the straight end. Furthermore, the top girder has the smallest flange lateral bending stresses compared to other girders. This is mainly because there are no perpendicular cross-frames on this girder that are close to the skewed bearings.

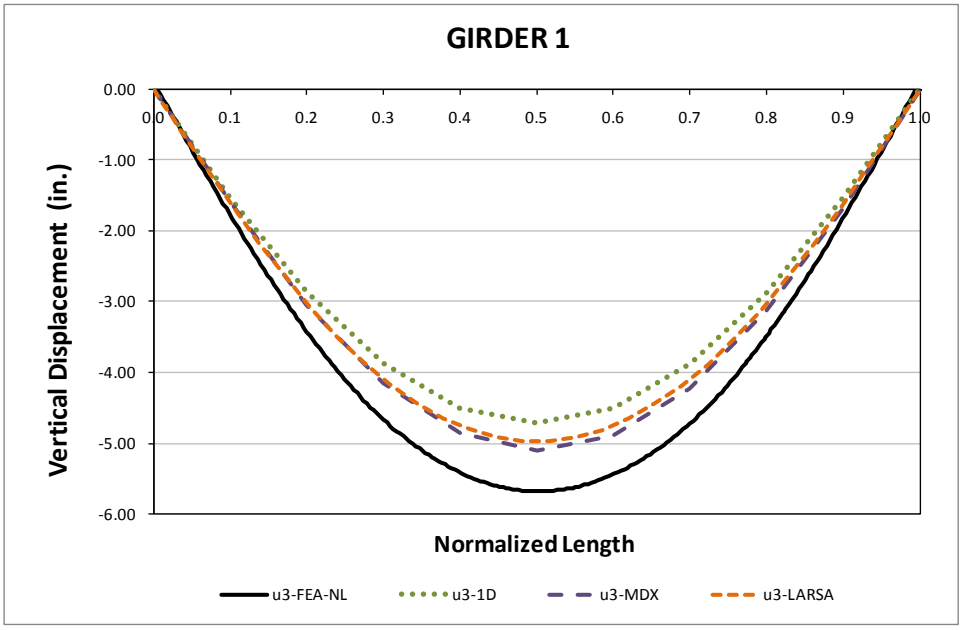

Fig. 2. NISSS36, Vertical displacements under total dead load for NLF detailing.

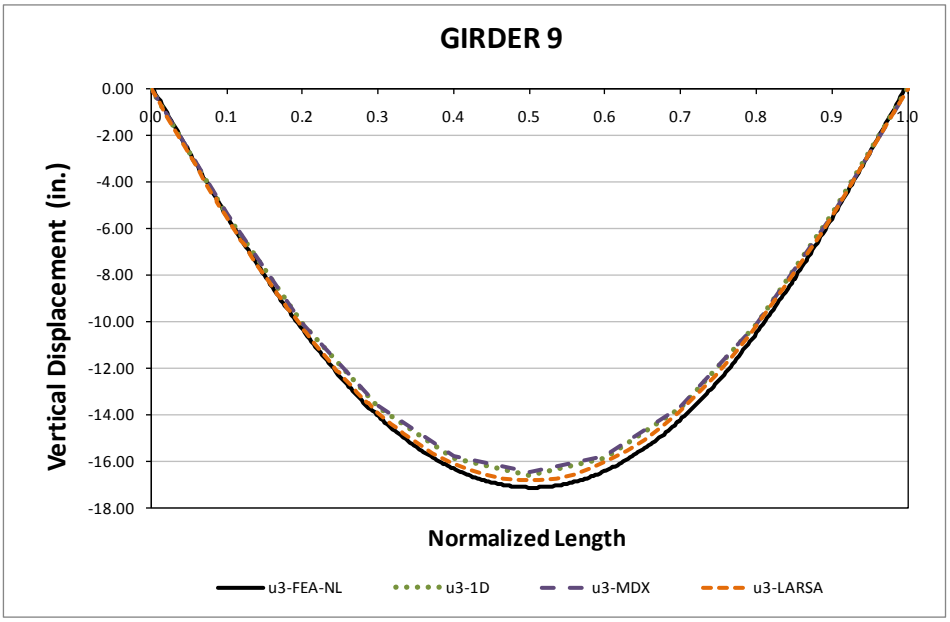

Fig. 3. NISSS36, Vertical displacements under total dead load for NLF detailing.

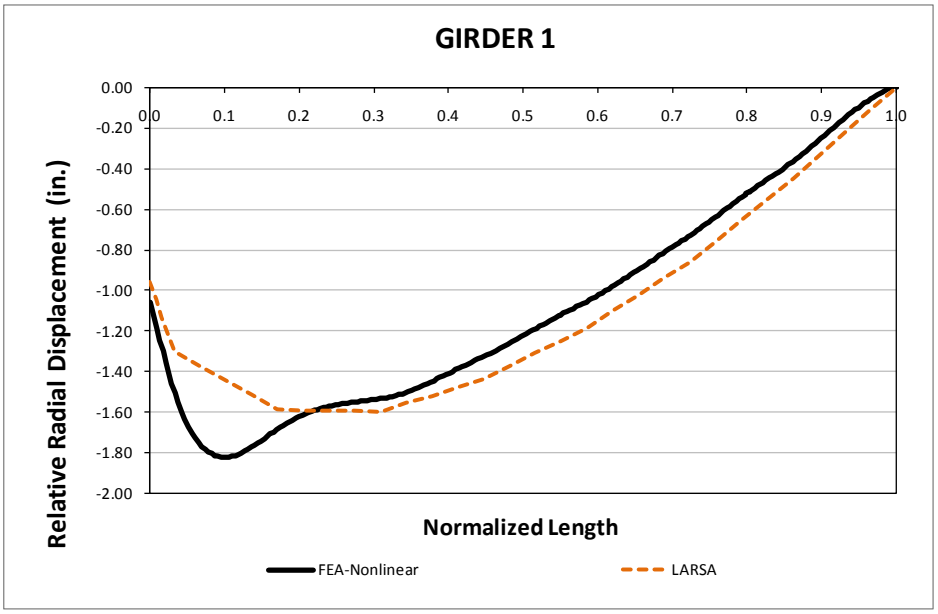

Fig. 4. NISSS36, Relative lateral displacements under total dead load for NLF detailing.

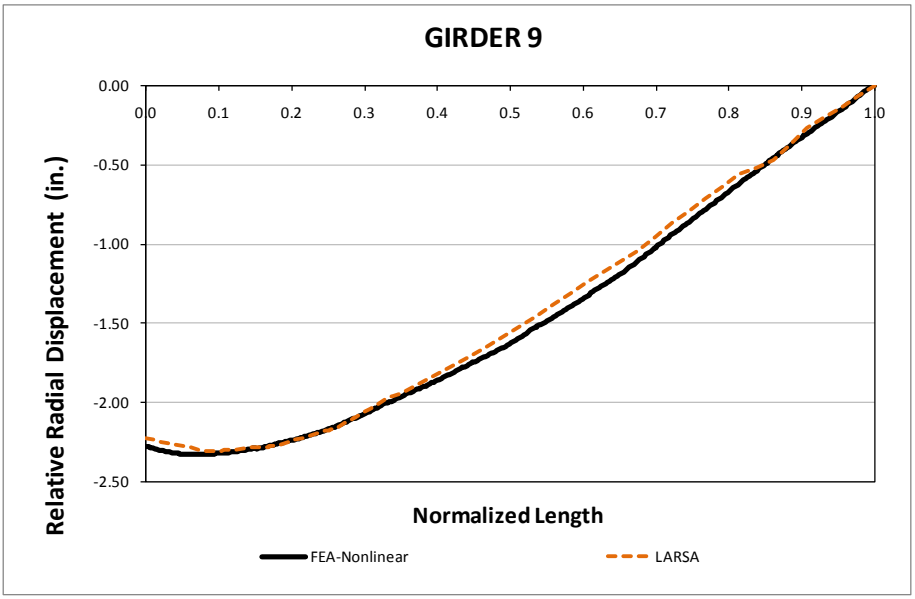

Fig. 5. NISSS36, Relative lateral displacements under total dead load for NLF detailing.

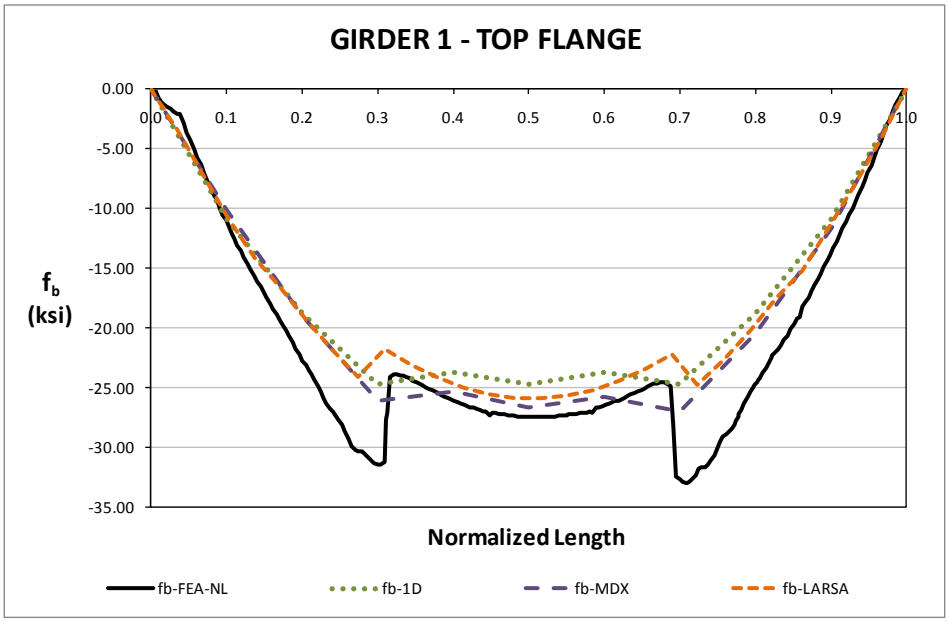

Fig. 6. NISSS36, Major-axis bending stresses under total dead load for NLF detailing.

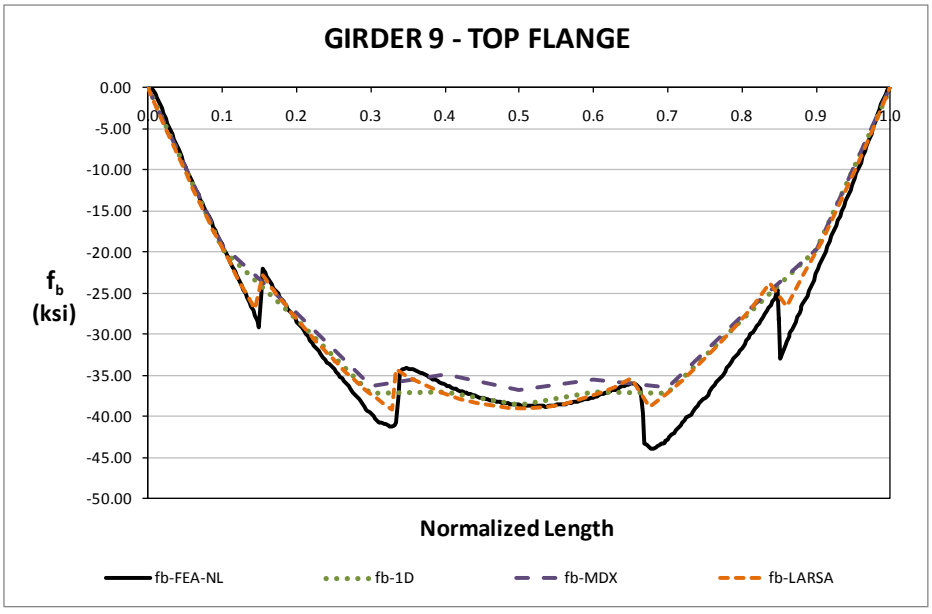

Fig. 7. NISSS36, Major-axis bending stresses under total dead load for NLF detailing.

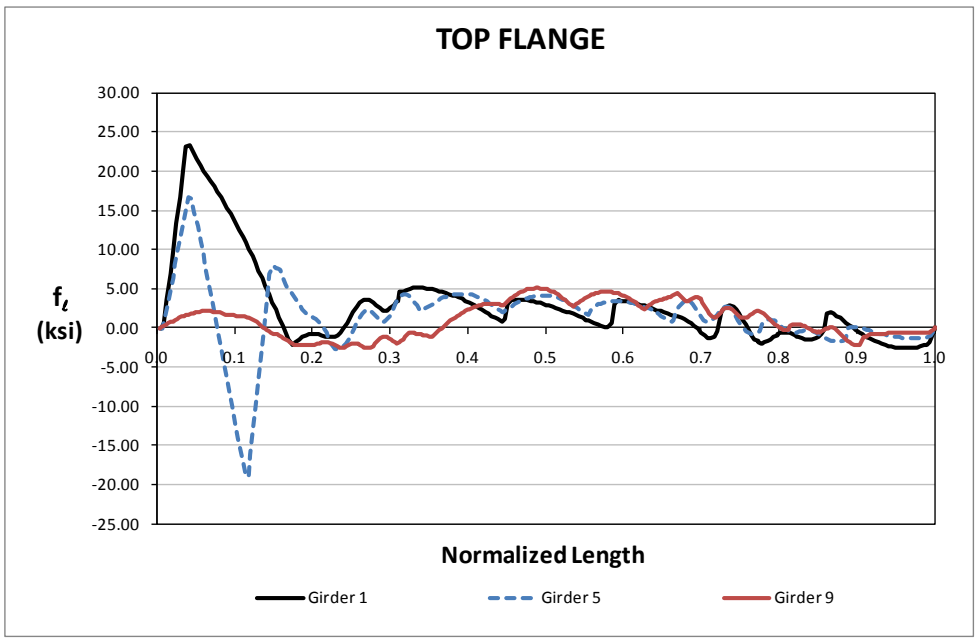

Fig. 8. NISSS36, Flange lateral bending stresses under total dead load for NLF detailing.

Conclusions:

Although there are small differences in the vertical displacements, they can be handled in the haunches while pouring the deck. The end layovers are accurately predicted by approximate analysis methods. Major-axis bendig stresses are predicted well by approximate analysis methods.

High flange lateral bending stresses are observed for the skewed straight bridges especially when the staggered cross-frame pattern is used. These high flange lateral bending stresses should be considered in design. Staggered cross-frame pattern reduces the magnitude of the cross-frame forces at the expense of increasing lateral bending stresses in the girder flanges. The greatest flange lateral bending stress usually occurs on girders due to perpendicular cross-frames close to the skewed bearings. Generally interior girders experience higher flange lateral bending stresses due to the staggered pattern of the cross-frames.

I2.12 NISSS37 (New, I-girder, Simple-span, Straight, Skewed supports)

Category Data:

L_1 = 225 ft / w = 80 ft /θ_1 = 28.6°, θ_2 = -28.6°, 9 girders

Cross-Frame Detailing Method: NLF

Erection Stages Analyzed: 5 (Analyses are performed assuming NLF)

Deck Placement Sequence: 1 Stage

Bridge Perspective & Plan Views:

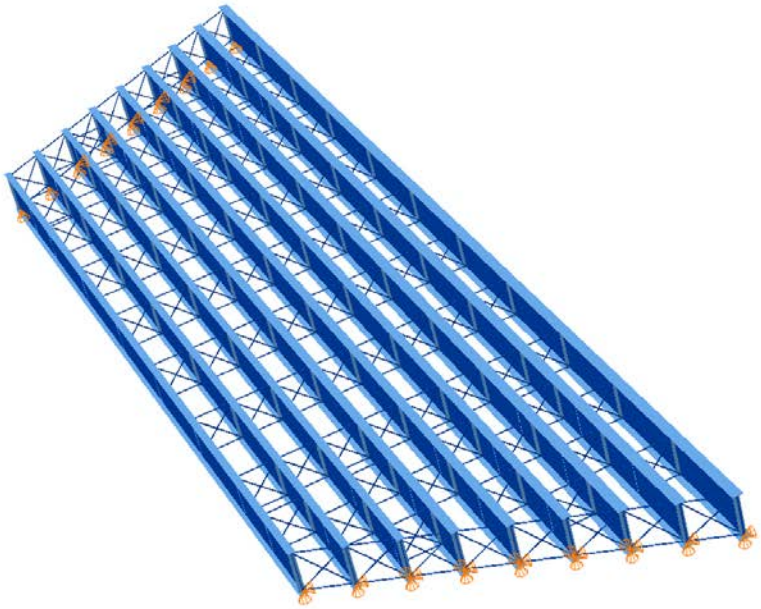

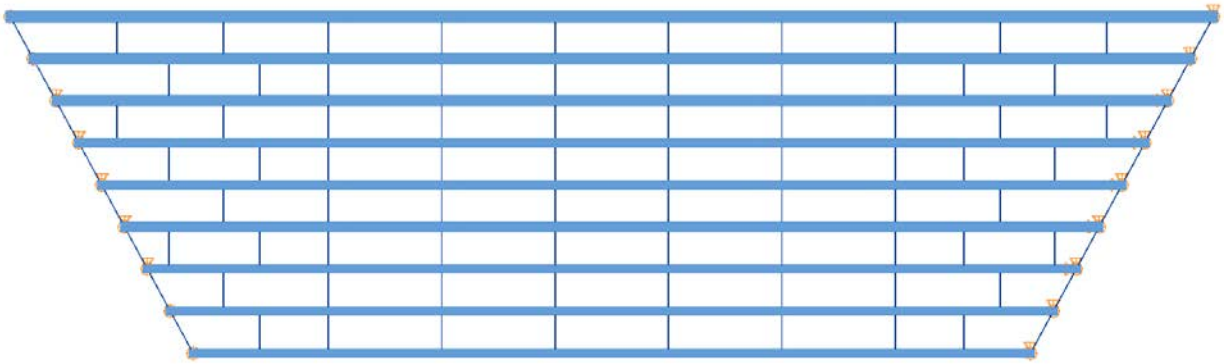

Abbreviated Analysis Results

Figure 1 shows the different analysis stages which are considered to evaluate the different analysis methods. Total dead load results are shown in this document since there are good correlation between the analysis results predicted by different analysis methods.

Stage 2

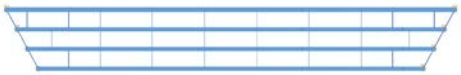

Stage 4

Stage 8

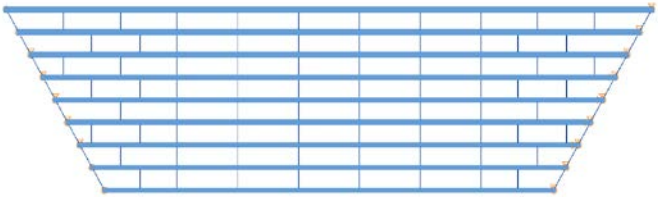

Stage 9 & 10

Fig. 1. NISSS37, Considered different analysis stages.

Figure 2 provides the vertical displacements of the bottom girder (Girder 1) under total dead load. Figure 3 shows the vertical displacements of the top girder (Girder 9). This girder is the critical girder for this bridge since it has the longest length among the other girders. Figures 2 and 3 show that the vertical displacements are accurately predicted by the approximate methods. Figures 4 and 5 show fascia girder relative lateral displacement predictions under total dead load. It should be noted that the ends of the girders are deflecting in the same direction due to the skew pattern. It is clear from Figs. 4 and 5 that the end layovers are predicted accurately at the skewed ends. Furthermore, the layovers are accurately predicted within the span by grid solutions.

Figure 6 provides fascia girder top flange major-axis bending stress predictions under total dead load. The major-axis bending stresses are accurately predicted by approximate methods for girder 9. This is the case for all girders for all different stages as well.

Usually there are no flange lateral bending stress predictions for approximate methods for straight bridges. Flange lateral bending stresses are small for this bridges mainly because of continuous cross-frame pattern. It should be noted that local maximums are observed closed to the skewed bearings due to the skew angle.

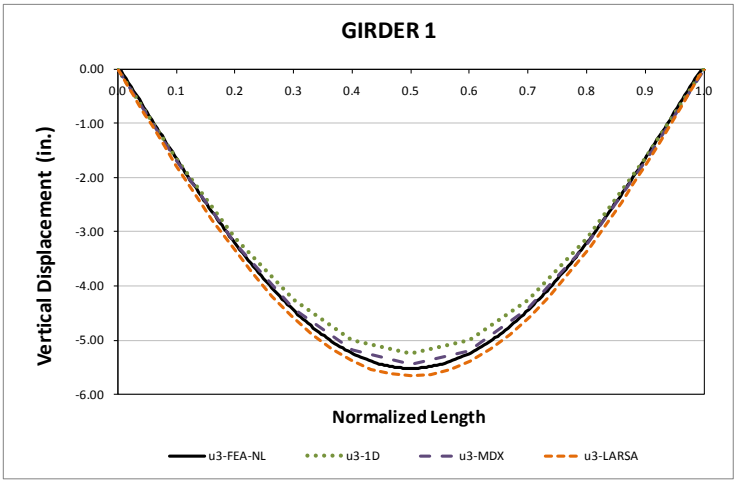

Fig. 2. NISSS37, Vertical displacements under total dead load for NLF detailing.

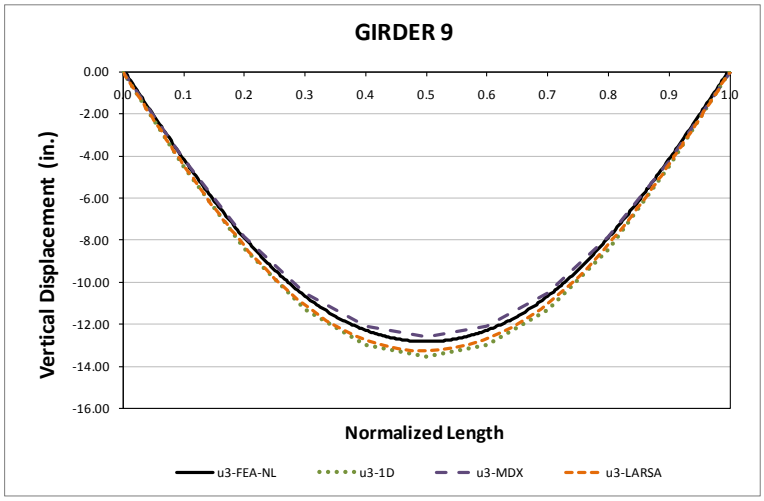

Fig. 3. NISSS37, Vertical displacements under total dead load for NLF detailing.

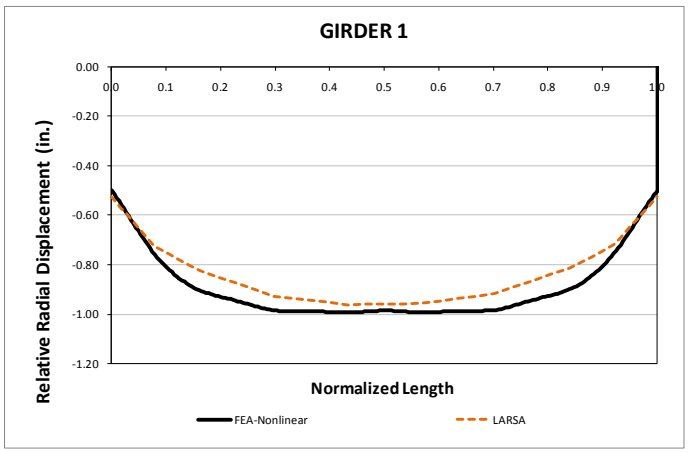

Fig. 4. NISSS37, Relative lateral displacements under total dead load for NLF detailing.

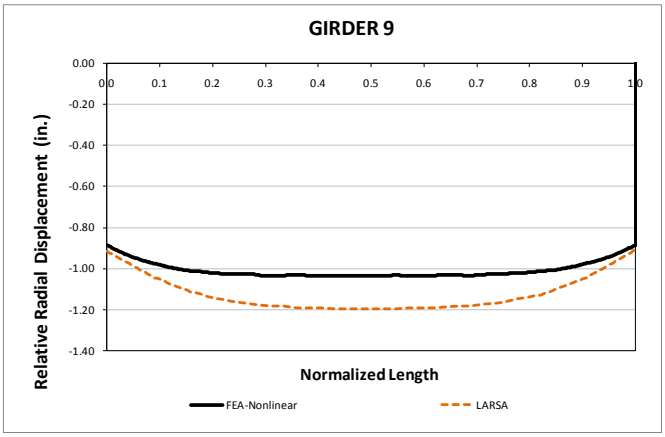

Fig. 5. NISSS37, Relative lateral displacements under total dead load for NLF detailing.

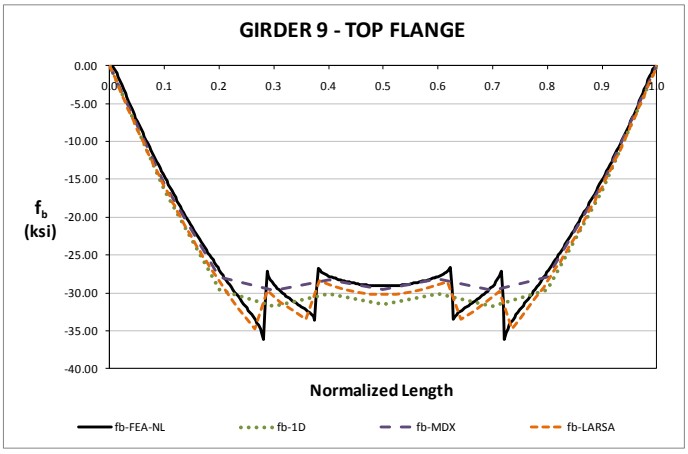

Fig. 6. NISSS37, Major-axis bending stresses under total dead load for NLF detailing.

Conclusions:

Vertical displacements, end layovers and stresses are accurately predicted by approximate analysis methods for all different analysis methods.

Continuous cross-frame pattern provide small flange lateral bending stresses. However, flange lateral bending stresses are small for this bridge. Local maximums are observed at the skewed bearing lines

I2.13 NISSS53 (New, I-girder, Simple-span, Straight, Skewed supports)

Category Data:

L_1 = 300 ft / w = 80 ft /θ_1 = 50^o, θ_2 = 50^o, 9 girders

Cross-Frame Detailing Method: NLF

Erection Stages Analyzed: 5 (Analyses are performed assuming NLF)

Deck Placement Sequence: 1 Stage

Bridge Perspective & Plan Views:

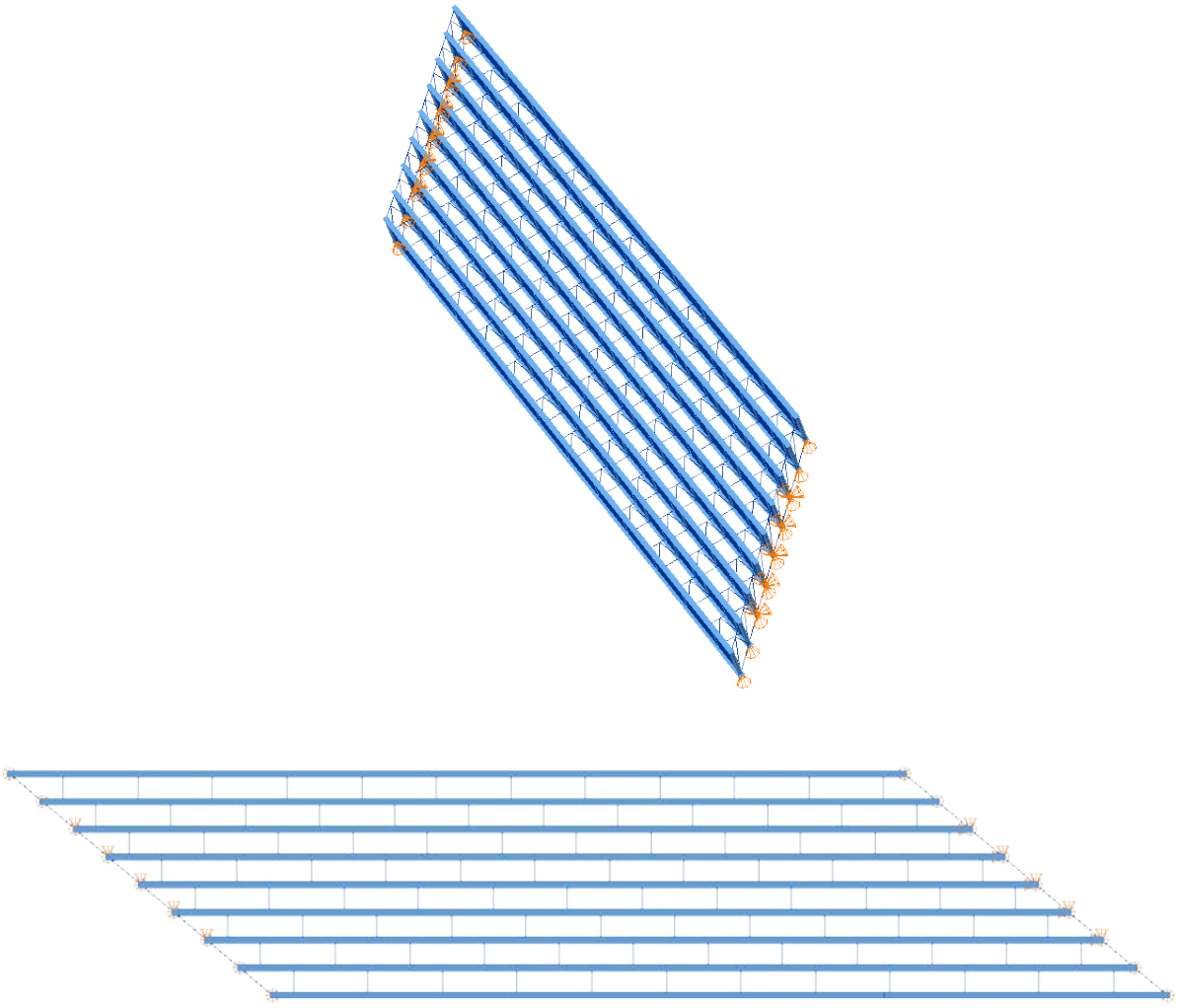

Abbreviated Analysis Results

Responses for total dead load are the focus of the following discussions. This stage is selected since the approximate methods perform well under steel dead load and other stages. Figure 1 shows the overall deflected shape of the bridge under total dead load. The deflections are magnified by 20 times. It should be noticed from Fig.1 that the layover of the top flange of the bottom girder is upwards on the left skewed bearing due to compatibility between girders and cross-frames. On the other hand the layover is downwards on the right skewed bearing. The direction is opposite due to the skew direction.

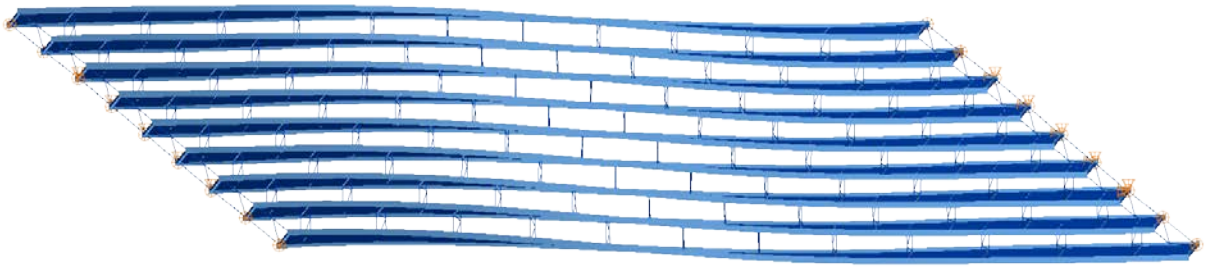

Fig. 1. NISSS53, Overall deflected shapes under total dead load for NLF detailing (Magnified by 20x).

Figure 2 provides the vertical displacements of the bottom girder (Girder 1) under total dead load. The predictions are off from the benchmark solutions about 1.5 inches for girder 1. However, this difference is not critical and can be handled in haunches. Figure 3 shows the vertical displacements of the middle girder (Girder 5). It can be seen from Fig.3 that the displacement predictions by approximate methods are closer to the benchmark solutions.

Figures 4 and 5 show the relative lateral displacement predictions for girders 1 and 5 respectively under total dead load. It is clear from Figs. 4 and 5 that the end layovers are predicted accurately. Furthermore, the layovers are accurately predicted within the span by grid solutions except in the case of the fascia girders.

Figure 6 provides top flange major-axis bending stress predictions of bottom girder under total dead load. The major-axis bending stresses are accurately predicted by approximate methods for girder 1. This is case for all girders.

Generally, in the case of straight bridges the flange lateral bending stresses are not obtained from software. However, second-order effects can be more critical for longer spans since the stresses are more dominated by dead load in longer spans. Therefore, it is important to check the nonlinearity in the system. Figures 7 and 8 provide the top flange lateral bending stresses of girders 1 and 5 predicted by linear and geometric nonlinear analysis results. It is clear from Fig. 7 that the nonlinearity in the flange lateral bending stresses of the bottom girder is high. Also, the flange lateral bending stresses tend to be larger because of the staggered cross-frame pattern. Local maximums are observed at the places close to the skewed ends where girders are tied together with perpendicular cross-frames.

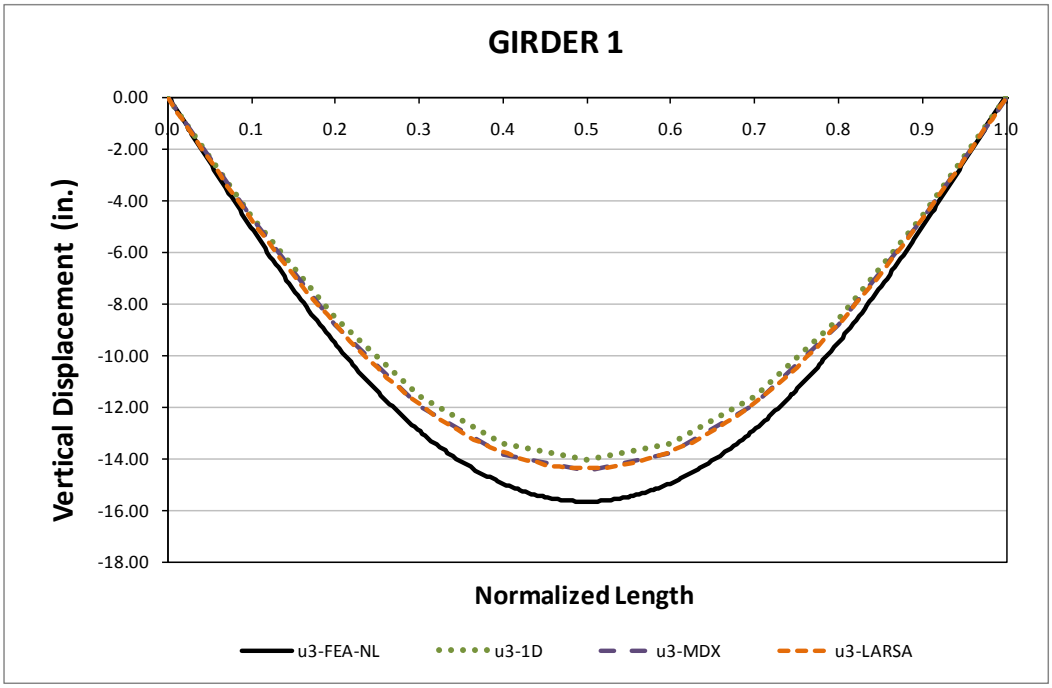

Fig. 2. NISSS53, Vertical displacements under total dead load for NLF detailing.

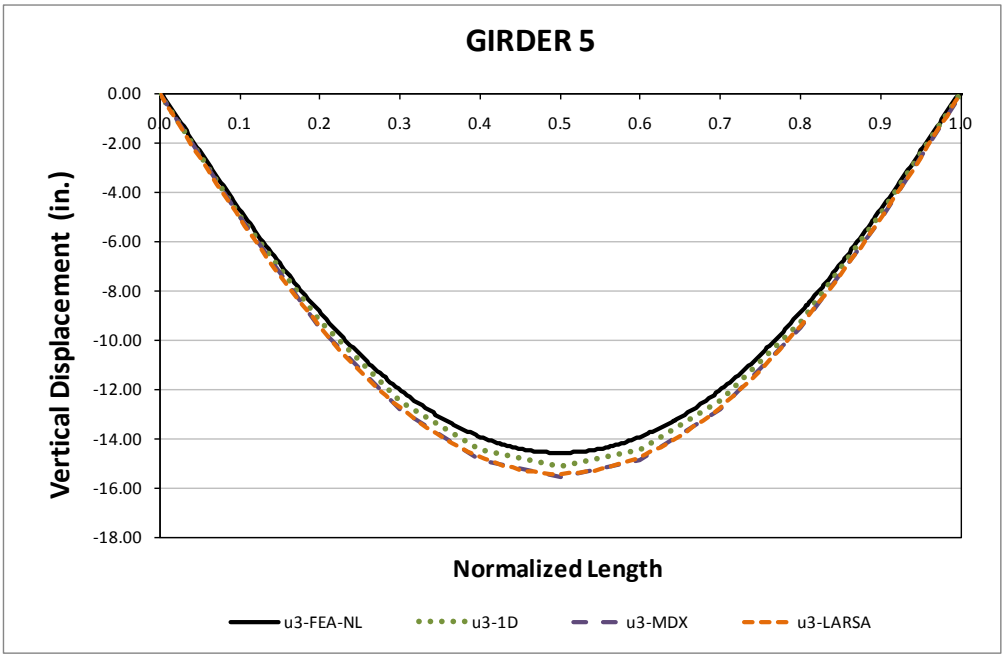

Fig. 3. NISSS53, Vertical displacements under total dead load for NLF detailing.

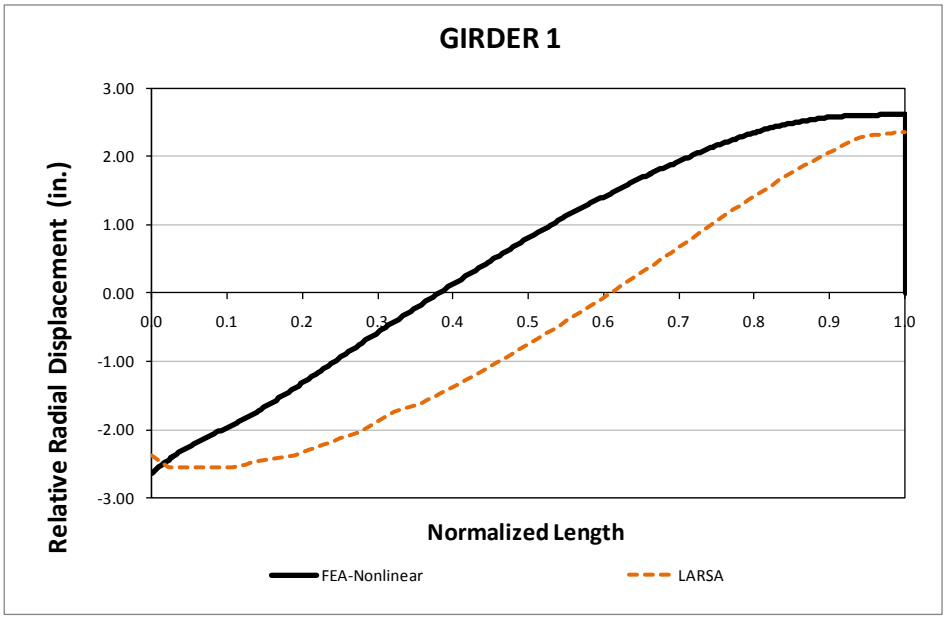

Fig. 4. NISSS53, Relative lateral displacements under total dead load for NLF detailing.

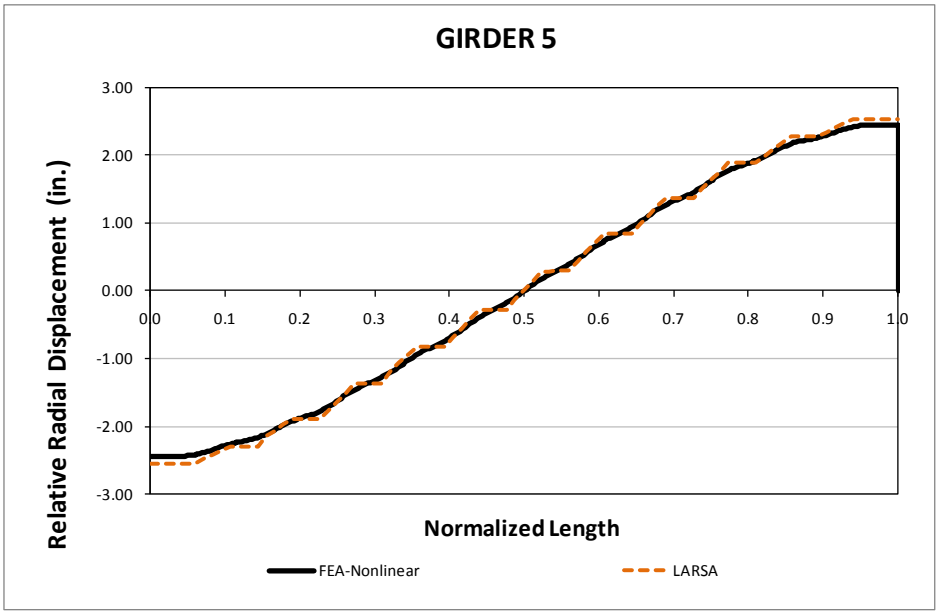

Fig. 5. NISSS53, Relative lateral displacements under total dead load for NLF detailing.

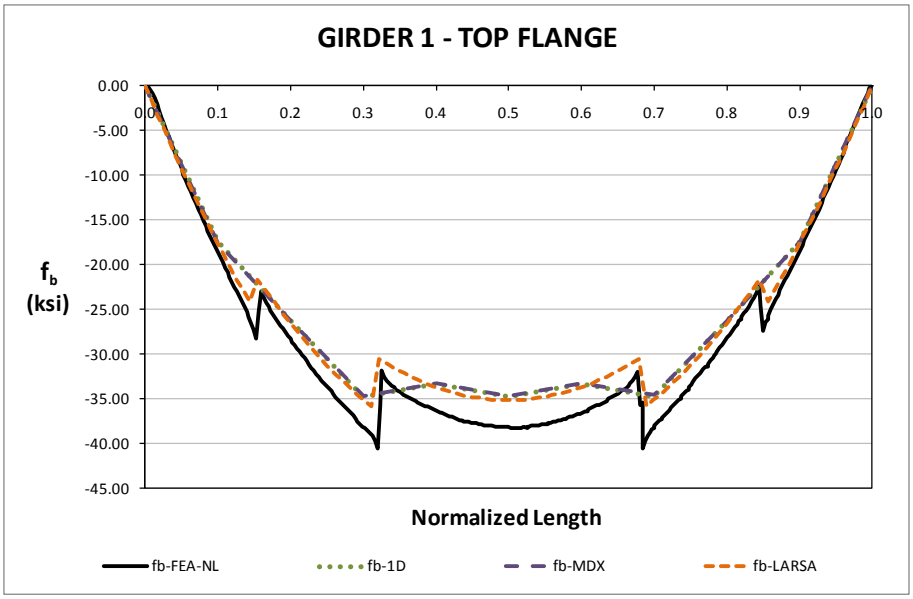

Fig. 6. NISSS53, Major-axis bending stresses under total dead load for NLF detailing.

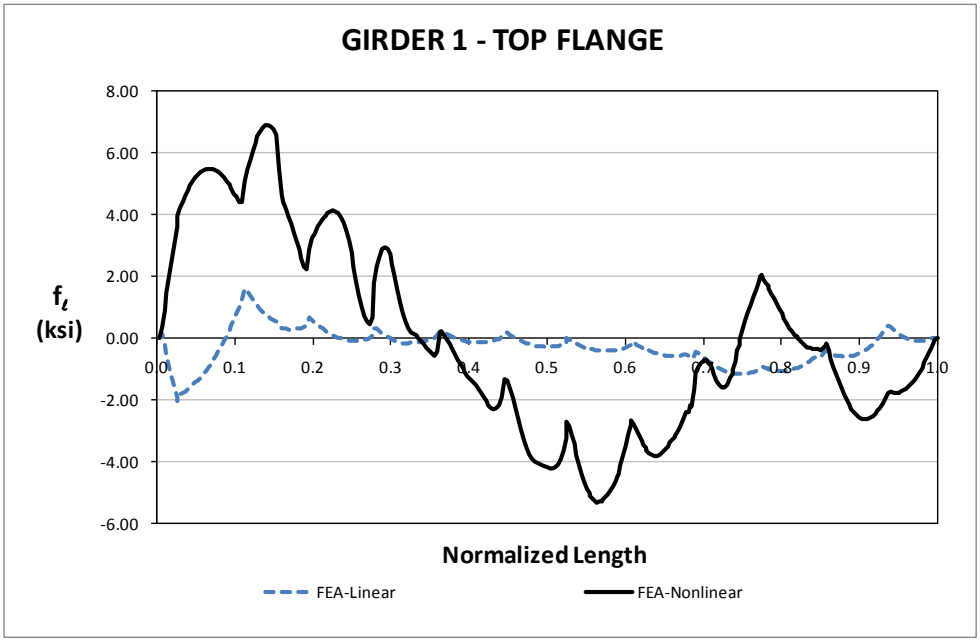

Fig. 7. NISSS53, Flange lateral bending stresses under total dead load for NLF detailing.

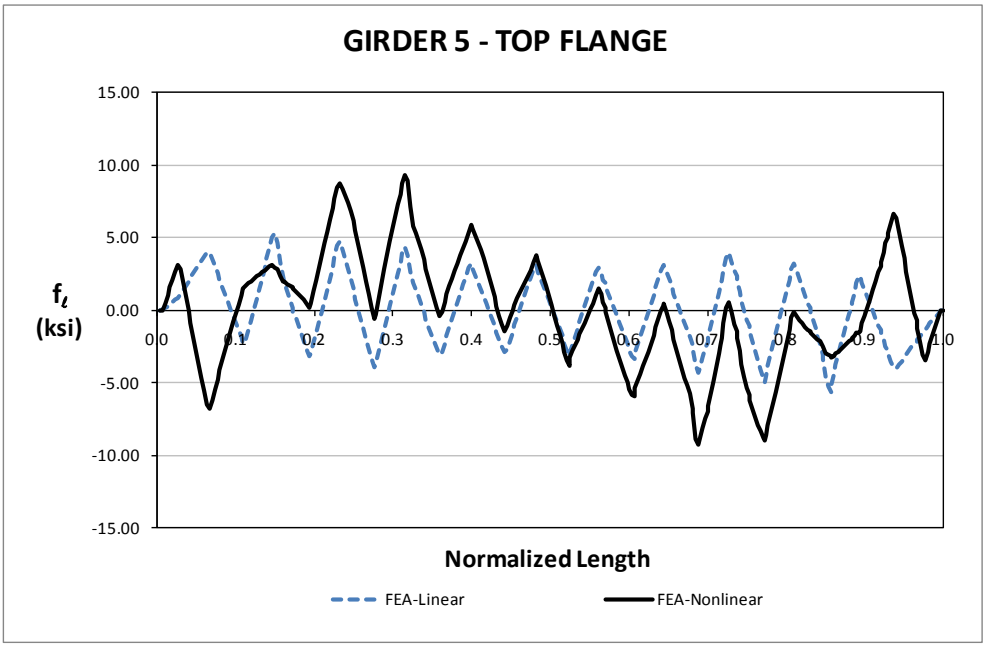

Fig. 8. NISSS53, Flange lateral bending stresses under total dead load for NLF detailing.

Conclusions:

Although there are small differences in the vertical displacements, they can be handled in the haunches while pouring the deck. The end layovers are accurately predicted by approximate analysis methods. Major-axis bending stresses are predicted well by approximate analysis methods.

Generally, in the case of straight bridges the flange lateral bending stresses are not obtained from software. However, this might lead to error due to ignorance of second order effects. High flange lateral bending stresses are observed for the skewed straight bridges especially when the staggered cross-frame pattern is used. These high flange lateral bending stresses should be considered in design. Staggered cross-frame pattern reduces the magnitude of the cross-frame forces at the expense of increasing lateral bending stresses in the girder flanges. The greatest flange lateral bending stress usually occurs on girders due to perpendicular cross-frames close to the skewed bearings. Additionally, bridge I-girder systems are more prone to stability effects when longer spans are used. This is because higher dead load major-axis bending stresses tend to occur for longer spans. Further studies are needed to assess when the second-order amplification effects may become significant, and how to best estimate them using simple checks, in these types of structures.

I2.14 NISSS54 (New, I-girder, Simple-span, Straight, Skewed supports)

Category Data:

L_{as} = 300 ft / w = 80 ft / θ_1 = 70 °, θ_2 = 70 °/ 9 girders

Cross-Frame Detailing Method: NLF

Erection Stages Analyzed: Four

Deck Placement Sequence: One stage, deck thickness = 9.5 in.

Bridge Perspective & Plan Views:

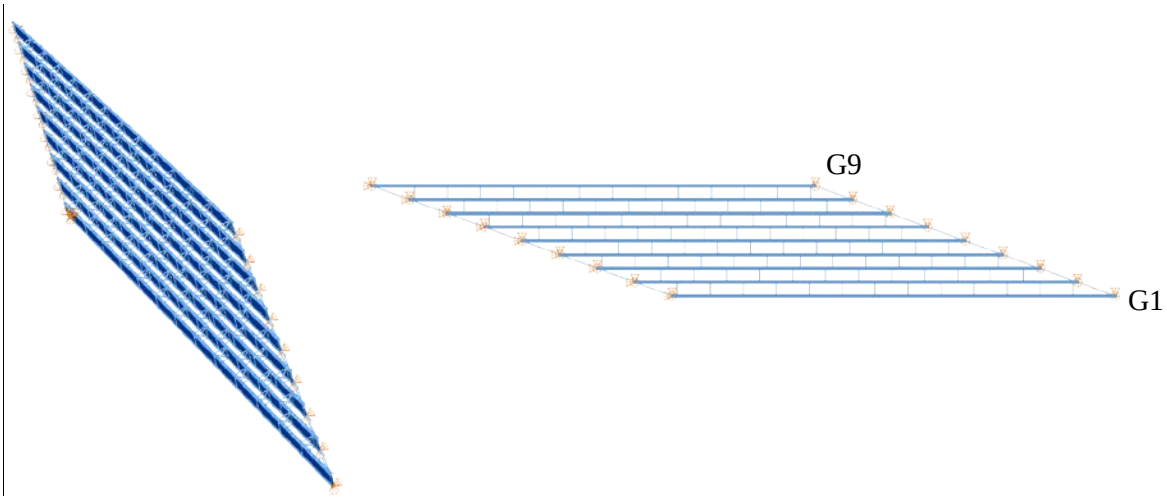

Abbreviated Analysis Results:

There are two important aspects in the geometry of this bridge that are studied: it is highly skewed and has a relatively long span. This bridge has the highest skew angle that is studied in the set of parametric simple span bridges. Thus, it is an extreme case to study the skew effects and the accuracy of the simplified analysis methods to capture the structural behavior.

Three stages are selected to observe the behavior of the bridge during the construction simulation. The plan view of these stages is shown in Figure 1. The first is Stage 2, where the first segments of girders G1 and G2 are in place. Two shoring towers, one on each girder segment, are provided to support them before their completion. The next construction stage studied is Stage 7, where three girders have been erected and a segment of girder G4 is in place. For this stage the shoring towers have been removed since the structure is considered to be stable. The final stage is Stage 19. The concrete deck has been poured at this stage and noncomposite action is assumed.

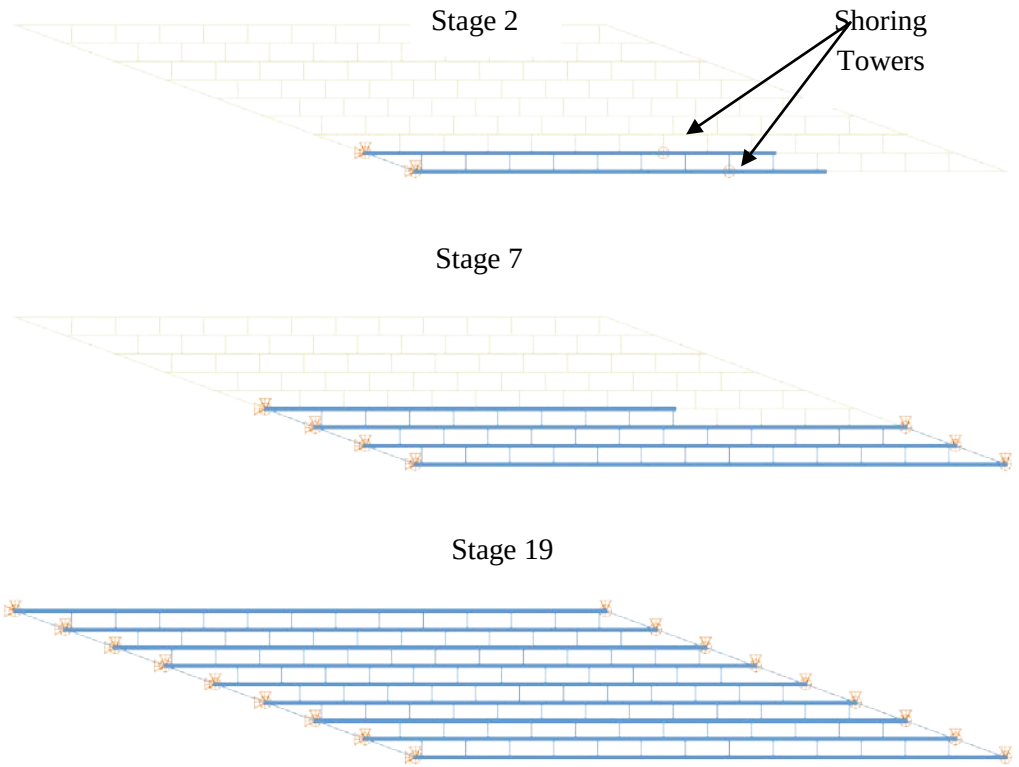

Fig. 1. Analyzed Construction Stages

Figure 2 shows the major-axis bending stress predictions obtained with the 2D and 3D models for the exterior girder G1. As shown, the prediction is accurate for this stage. For Stage 7, the bending stresses as predicted by each method are different. As shown in Figure 3, the section of girder G4 that is connected to the other three girders causes a stress response that is not captured accurately by the 2D grid model. These differences might not be considerable for design purposes since the stresses are relatively low. However, this construction stage represents a challenging scenario were the approximate analysis does not provide the expected results.

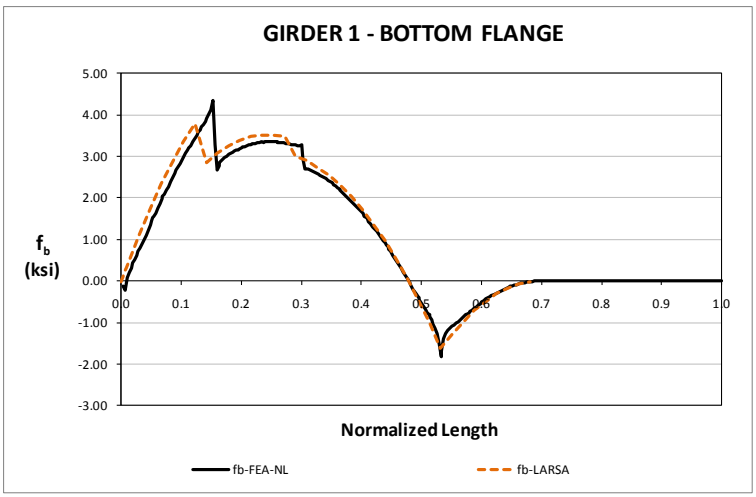

Fig. 2. Major-axis Bending Stresses, Stage 2

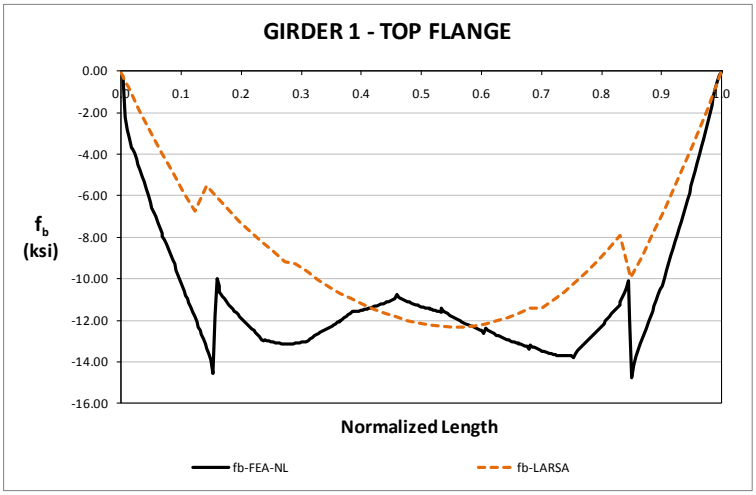

Fig. 3. Major-axis Bending Stresses, Stage 7

For the final configuration, the 1D and 2D analyses provide results that are not in agreement with the benchmark responses. Figure 4 shows the major axis bending stresses in the bottom flange of girder G4. Results for this girder are shown since it is the one with the largest differences between analysis predictions. As shown in the plot, differences of approximately 15 ksi are observed between predictions. Therefore, in this case, the approximate methods might be judged to be not suitable for design.

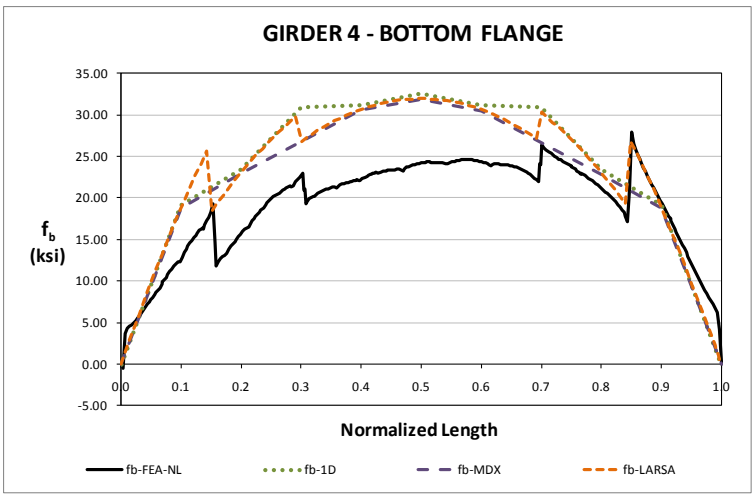

Fig. 4. Major-axis Bending Stresses, Stage 10

As a result of the staggered cross-frames, very large levels of flange lateral bending stresses are observed in this bridge. Figure 5 shows the results obtained from the linear and nonlinear 3D FEA models. It is observed that lateral bending stress levels that might be judged as not permissible are present in the girder flanges.

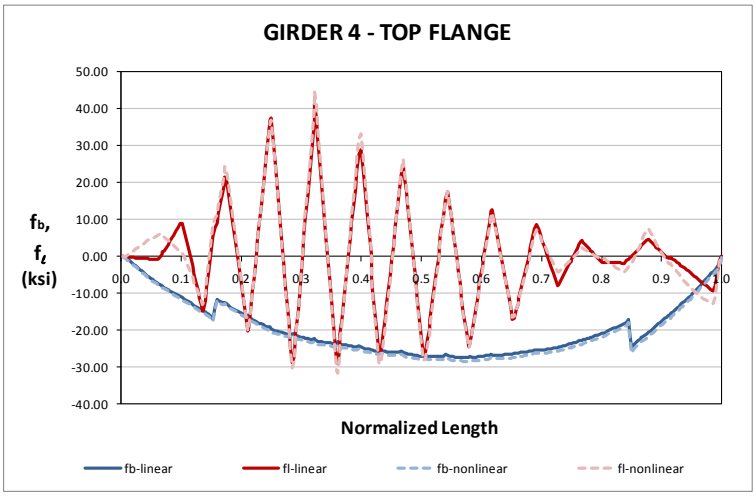

Fig. 5. FEA Stress Predictions, Stage 10

I2.15 NISSS56 (New, I-girder, Simple-span, Straight, Skewed supports)

Category Data:

L_{as} = 300 ft / w = 80 ft / θ_1 = 50 °, θ_2 = 0 °/ 9 girders

Cross-Frame Detailing Method: NLF

Erection Stages Analyzed: Four

Deck Placement Sequence: One stage, deck thickness = 9.5 in.

Bridge Perspective & Plan Views:

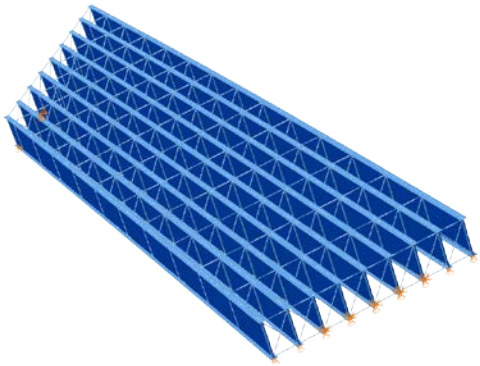

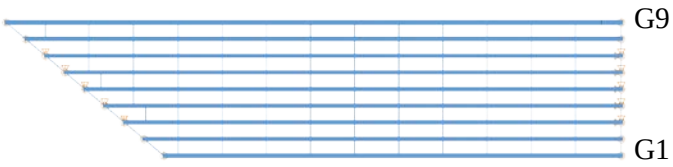

Abbreviated Analysis Results:

There are two important aspects in the geometry of this bridge that are studied: it is highly skewed and has a relatively long span. This bridge has a large skew angle at the left end and a normal support at the right end. Due to this support configuration, the girder lengths vary across the bridge. In this long span structure, the skew effects and the difference in girder lengths are studied to determine the convenience of the use of the simplified analysis methods for its analysis.

Four stages are selected to observe the behavior of the bridge during the construction simulation. The plan view of these stages is shown in Figure 1. The first is Stage 10, where the totality of girder G9 is in place and the first segments of girders G1 to G8 are also erected. A holding crane at approximately mid-span of girder G9 is provided to prevent stability problems, given that at this stage, the left portion of this girder does not have any lateral support. Next, the left portion of girder G8 is erected and the holding crane of girder G9 is removed, as shown in the figure corresponding to Stage 11. It is considered that at this stage, the group formed by girders G8 and G9 is stable, so the crane can be removed. Subsequently, the erection of the left portions of the girders continues in a similar fashion. In Stage 17, the behavior of the bridge is studied before the completion of the steel structure. At this stage, only the left portion of girder G1 remains to be erected. Finally, in Stage 19, the bridge is studied at the total dead load condition (TDL). The concrete deck has been poured at this stage and noncomposite action is assumed. The deck is not shown for visualization purposes.

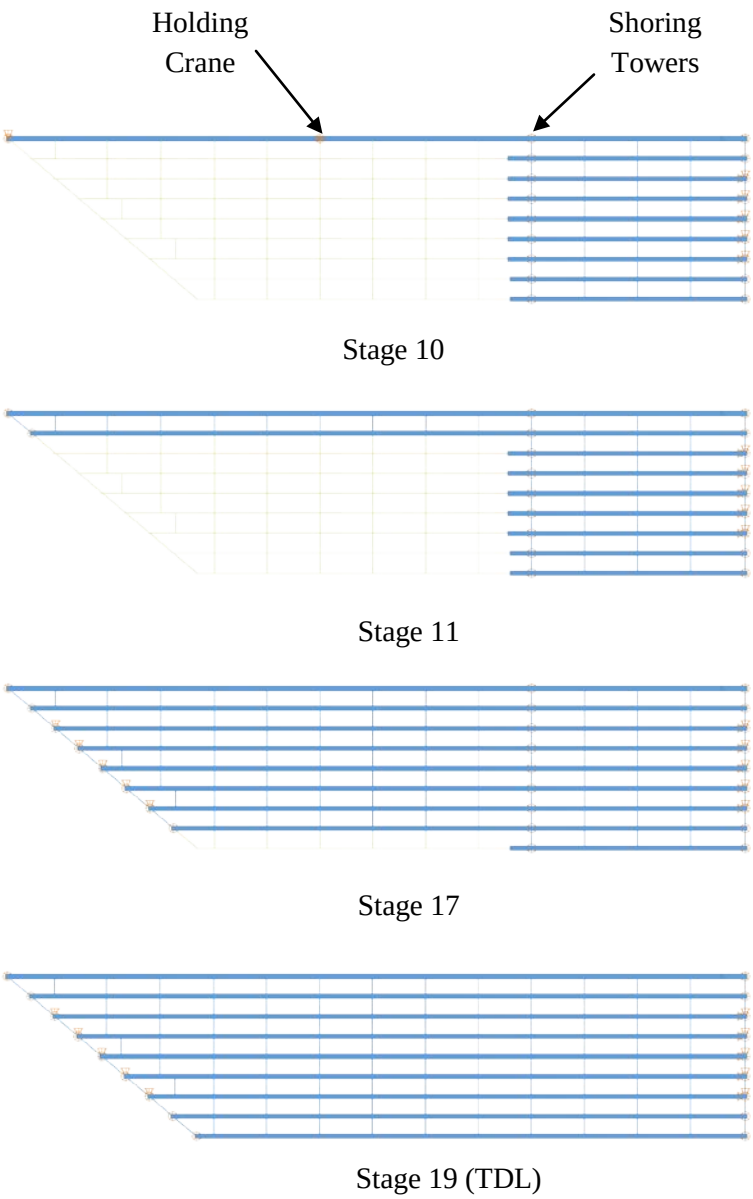

Fig. 1. Analyzed Construction Stages

Figure 2 shows the major-axis bending stress predictions obtained with the 2D and 3D models for the exterior girder G1 at Stage 10. As shown, the grid model represents accurately the benchmark response. Similarly, the vertical displacement predictions are the same for the two models, as shown in Figure 3.

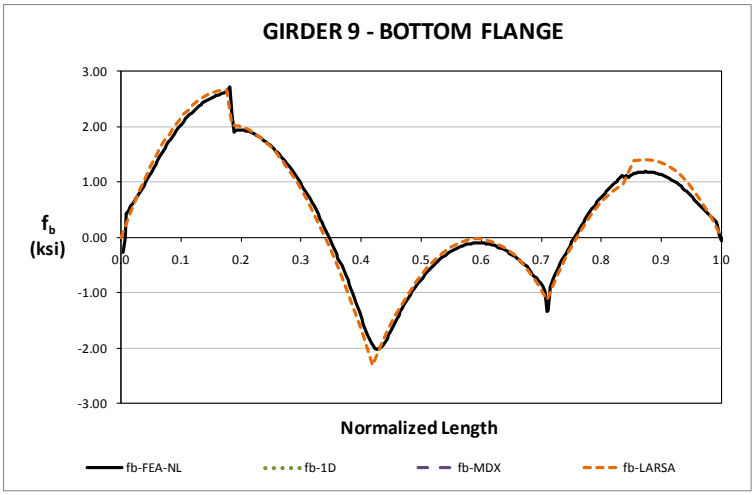

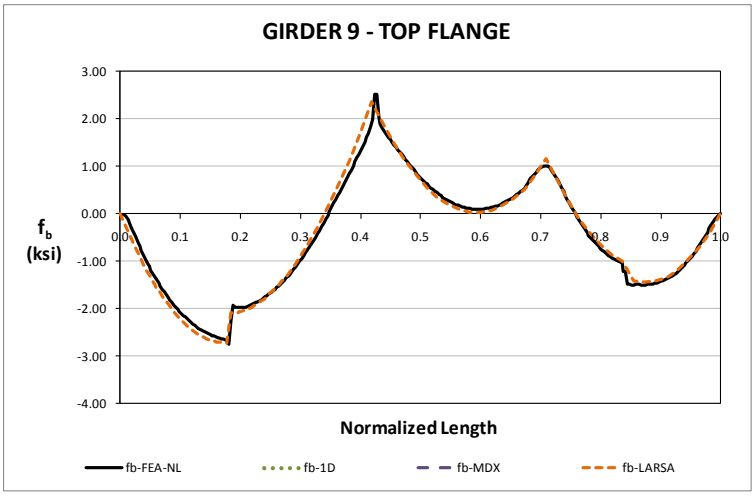

Fig. 2. Major-axis Bending Stresses, Stage 2

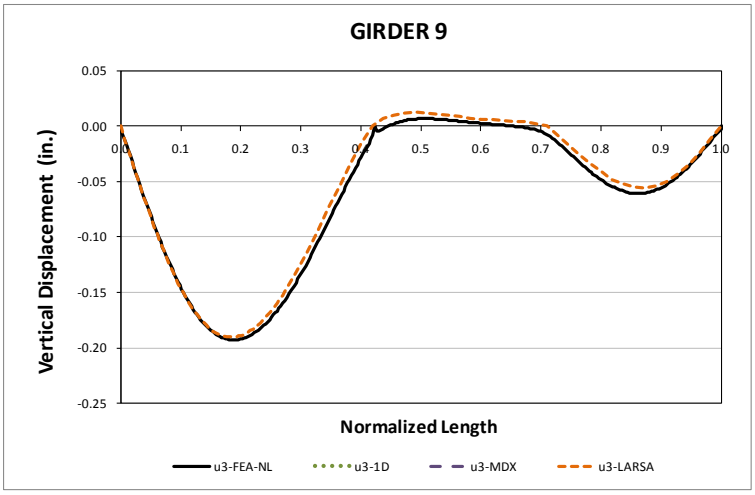

Fig. 3. Vertical Displacements, Stage 10

The accuracy of the 2D grid model predictions as compared to the expected 3D FE model responses is consistent for the rest of intermediate stages. Figure 4, for example, shows the major-axis bending stress prediction for the top flange of girder G1, at Stage 11. As seen in the plot, the approximate response fits accurately the refined solution.

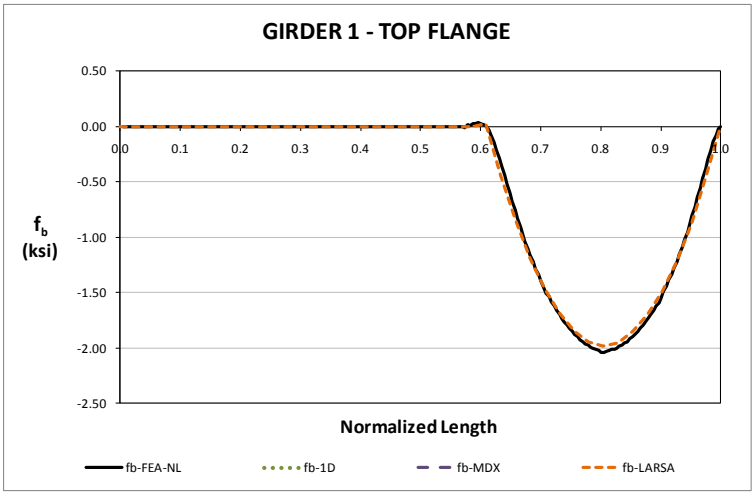

Fig. 4. Major-axis Bending Stresses, Stage 11

Comparisons of the 1D and 2D analysis predictions versus the 3D model responses are conducted at the total death load condition, Stage 19. Figure 5 shows the plot of the major-axis bending stress response for the bottom flange of girder G9. As shown, the 1D and 2D models are an accurate representation of the expected response. The same pattern is observed in the displacement predictions. Figures 6 and 7 show the vertical and lateral displacement predictions, respectively. The displacement result comparisons obtained for this bridge are similar to the observed in other straight and skewed bridges. The limited capability of the 2D grid models to simulate torsion of the I-girders seems to have a minor effect in the prediction of both the girder vertical and lateral displacements. Thus, the support skew does not influence significantly the layover response prediction in these simplified analyses.

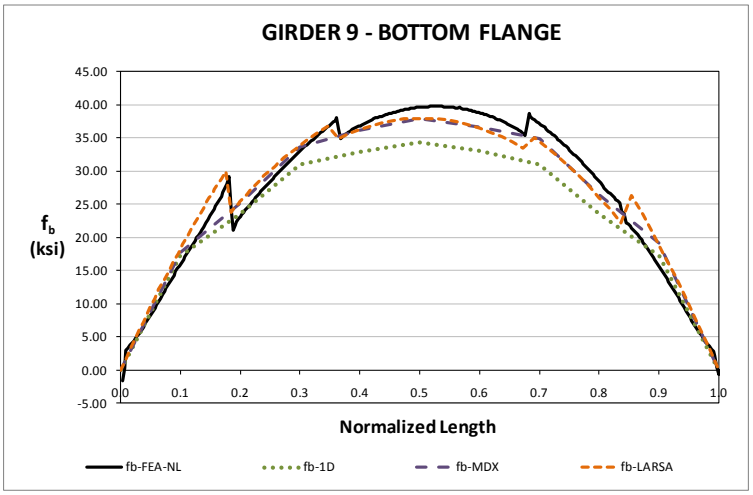

Fig. 5. Major-axis Bending Stresses, Stage 19

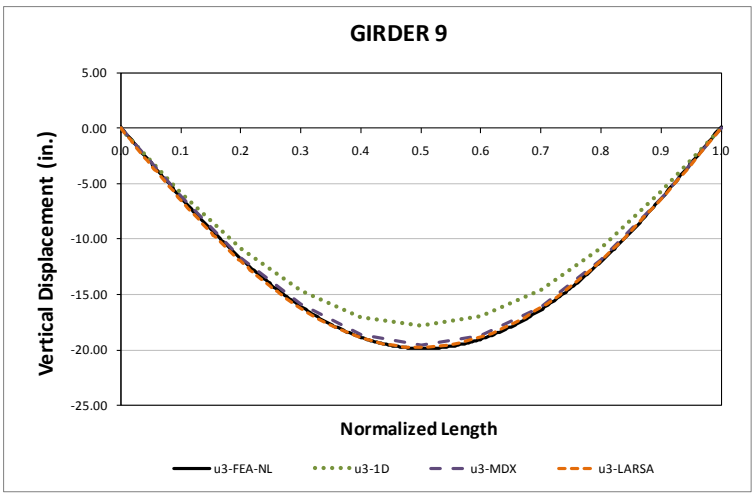

Fig. 6. Vertical Displacements, Stage 19

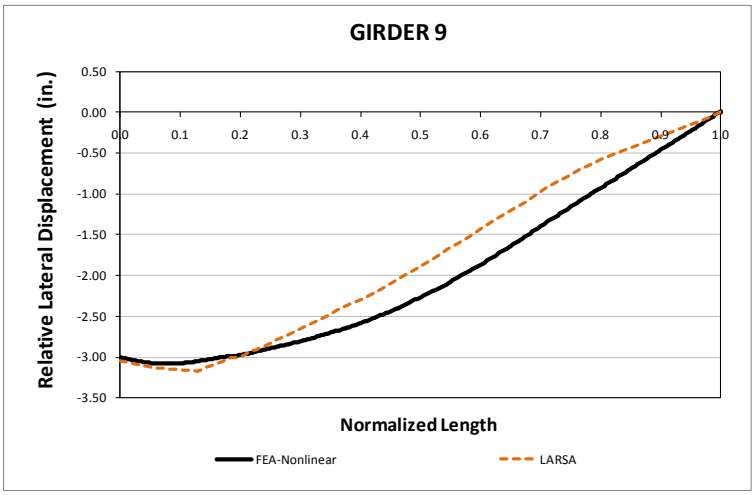

Fig. 7. Lateral Displacements (Layover), Stage 19

I3.1 EICSS1 (Existing, I-girder, Continuous-span, Straight, Skewed supports)

Bridge Description :

Steel Overpass Sunnyside Road I.C. (I-15B) Over I-15, Bonneville Co., ID

Category Data:

L_1 = 160 ft, L_2 = 160 ft / w = 95.2 ft / θ = -35.2^o (all bearing lines), 9 girders

Cross-Frame Detailing Method: TDLF

Erection Stages Analyzed: 7 (Analyses are performed assuming NLF & TDLF)

Deck Placement Sequence: 2 Stages

This bridge was forwarded by ITD as an example of successful implementation of total dead load fit detailing.

Bridge Perspective & Plan Views:

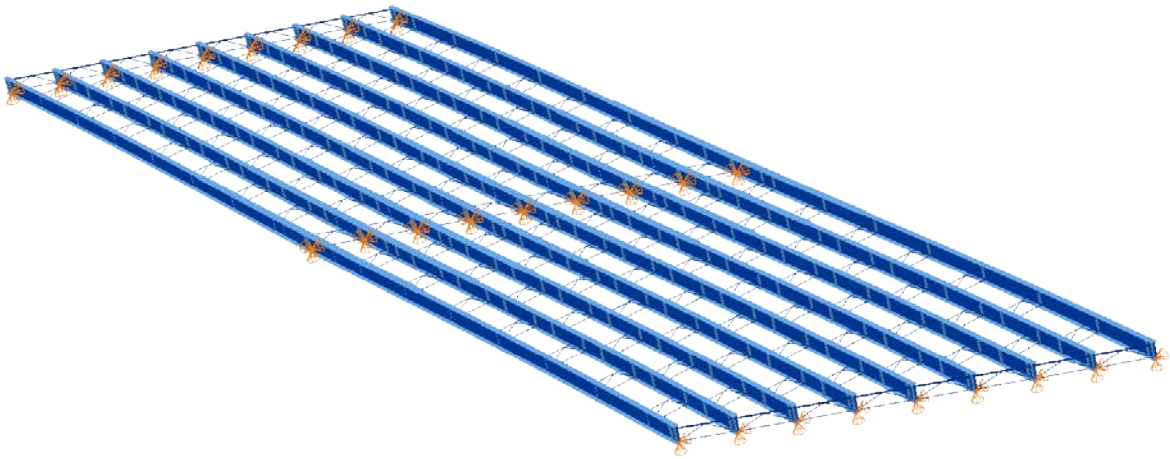

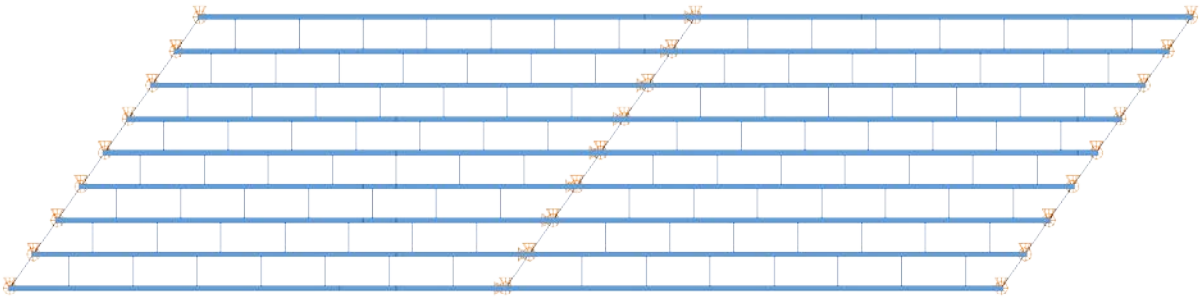

Abbreviated Analysis Results:

The final total dead load stage is selected for discussion of this bridge due to successful implementation of total dead load fit detailing (TDLF). Staged deck placement is considered for analyzing the total dead load configuration. This stage is illustrated in Fig. 1. Two different deck pouring sequences are suggested in the engineering drawings for this bridge: parallel pouring with respect to skew angle or perpendicular pouring with respect to girders. For the ease of analysis the perpendicular deck pouring sequence is selected. Both NLF and TDLF analyses are performed to understand the behavior. Figures 2 and 3 compare the relative radial displacements of girder 1 under total dead load by staged deck analysis. Figure 2 is obtained for NLF whereas Fig. 3 is obtained for TDLF. Figure 4 and 5 shows the deflections of the girders at the different deck stages for NLF and TDLF respectively. It is observed from these figures that girder flanges are approximately plumb positions under total dead load for TDLF whereas they are out of plumb for NLF. It is clear from the deflected shapes under the steel dead load that at this stage girders are twisting in opposite directions due to the lack of fit forces in the TDLF detailing method. It should be noted that in both of the Figs. 2 and 3 2D LARSA predictions are obtained for NLF. The 2D LARSA predictions are good if the NLF results are considered. Moreover, it is observed that the radial deflections are close to 3D FEA predictions along the length at all points. This is the general observation for straight bridges. However, 2D LARSA solutions cannot predicted the relative radial displacements accurately for TDLF. This is mainly because the lack of fit stresses are neglected in 2D LARSA solutions.

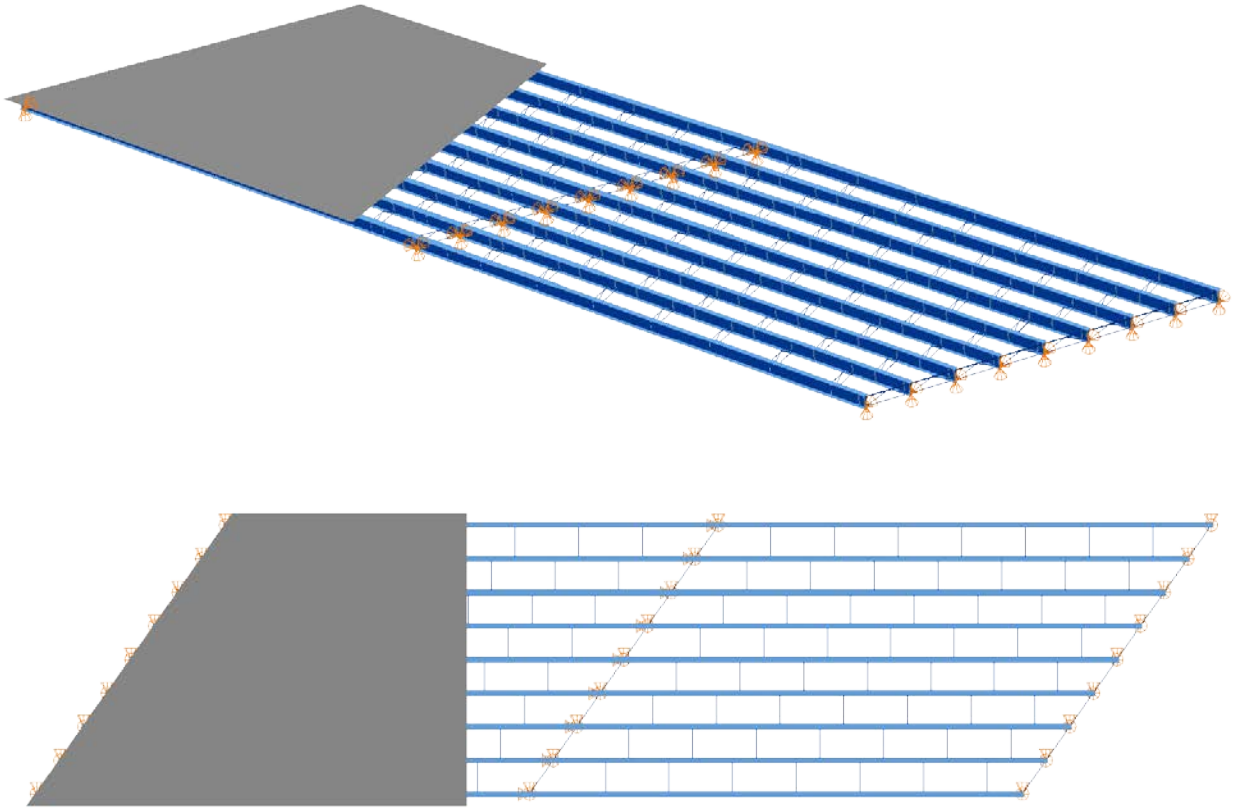

Fig. E.2.4-1. EICSS1, Considered deck placement stage.

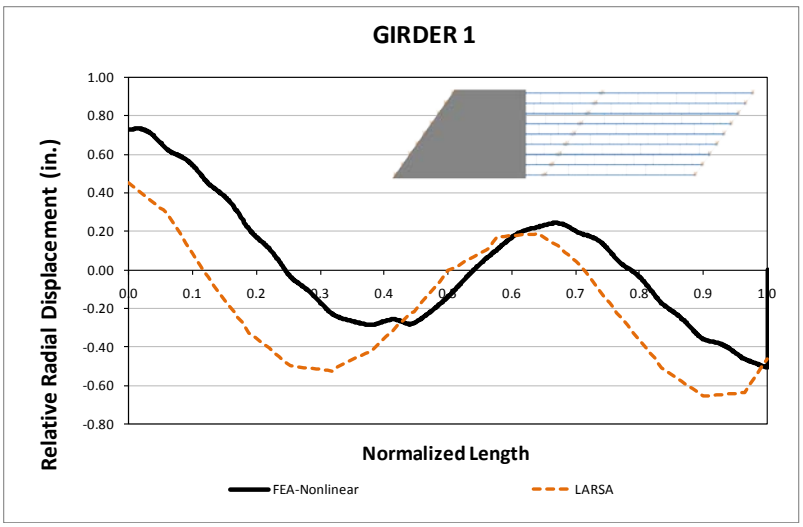

Fig. E.2.4-2. EICSS1, Relative radial displacements under total dead load for NLF detailing.

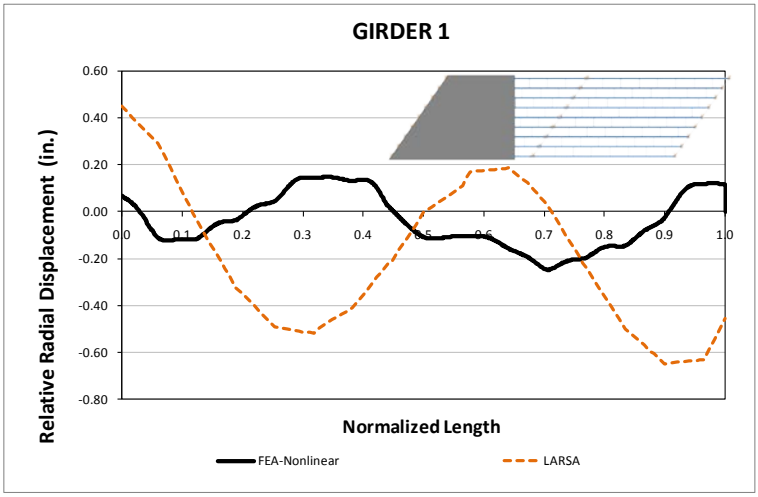

Fig. E.2.4-3. EICSS1, Relative radial displacements under total dead load for TDLF detailing.

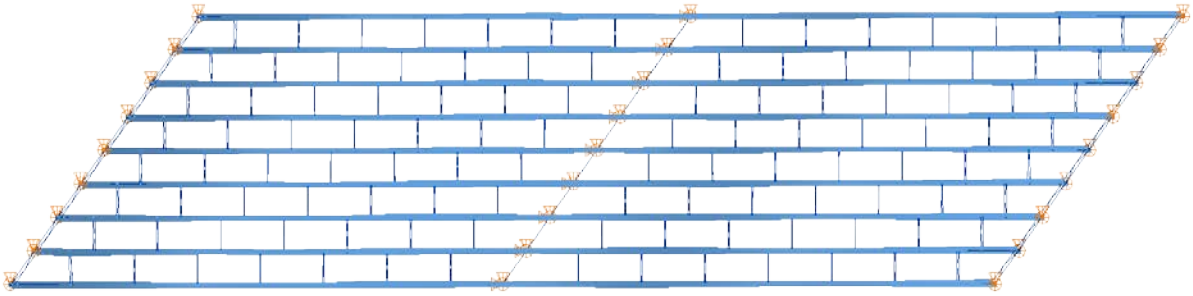

Deflected Shape under steel dead load for NLF detailing

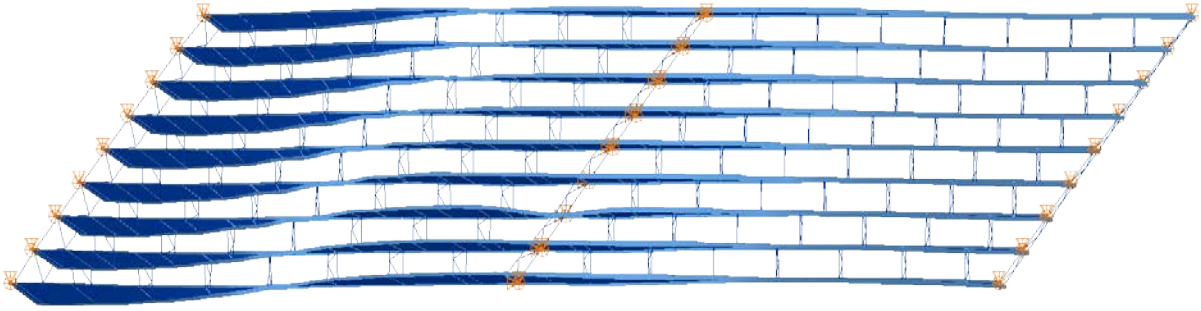

Deflected shape for deck stage 1 for NLF detailing

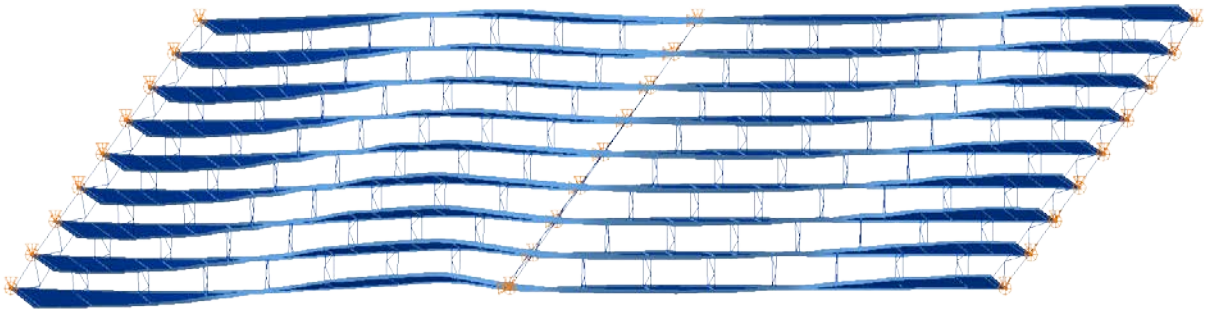

Deflected shape for total dead load at deck stage 2 for NLF detailing

Fig. E.2.4-4. EICSS1, Overall deflected shapes at different deck placement stages for NLF detailing (Magnified by 100x).

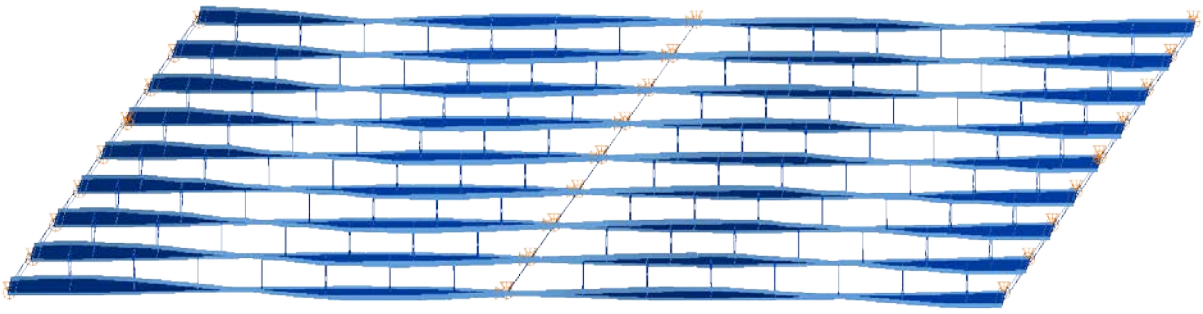

Deflected Shape under steel dead load for TDLF detailing.

Deflected shape for deck stage 1 for TDLF detailing.

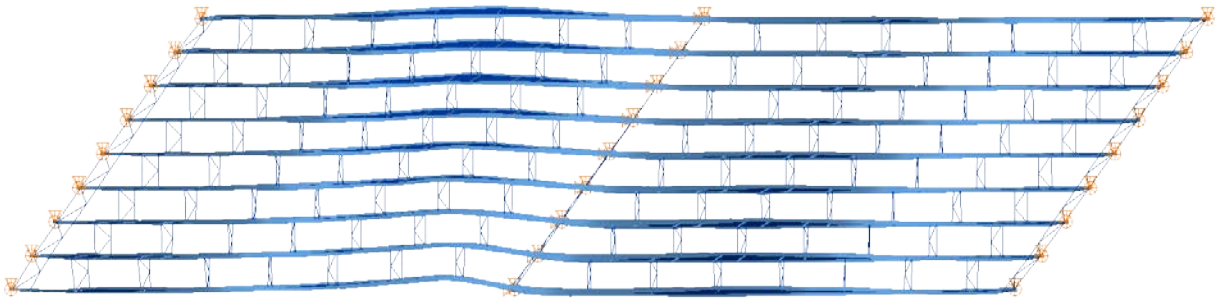

Deflected shape for total dead load at deck stage 2 for TDLF detailing

Fig. E.2.4-5. EICSS1,.Overall deflected shapes at different deck placement stages for TDLF detailing (Magnified by 100x).

The Girder 1 vertical displacements under total dead load are compared in Fig. 6. The displacements are larger in the 3D FEA model in the region where the deck is placed first. This may affect the camber

values of the girders. Figure 7 shows the major-axis bending responses under total dead load. The accuracy of the approximate methods is low for this case. However, this is mainly because approximate methods usually does not consider staged deck placement analysis. The responses usually are obtained by placing the deck in one stage. Therefore, it is important to understand the difference by running the 3D FEA solutions. Figures 8 and 9 show the major-axis bending stresses for girder 1 and girder 9 respectively for comparing staged deck analysis versus pouring the deck in one staged. Figure 8 clearly illustrates the increase due to staged analysis. However once we looked the girder 9 we observed that there is no difference in the response. The effect of staged deck analysis is fully observed at girder 1 whereas these effects are negligible at girder 9. This local effect on girder 1 can be seen clearly at the last stage of Fig. 4 where the first stage of the deck is finished. Figures 10 and 11 illustrate the flange lateral bending stresses for girder 1 and girder 9 respectively for comparing staged analysis versus the pouring the all deck in one stage. Similar to major-axis bending stress responses there are additional stresses on girder 1. It is expected that if the parallel deck pouring option is considered for this bridge the deck is placed such that the vertical deflections of the girders are expected to be similar. In this case, the difference in the stress is more likely to be distributed to all girders and less stress concentrations are expected.

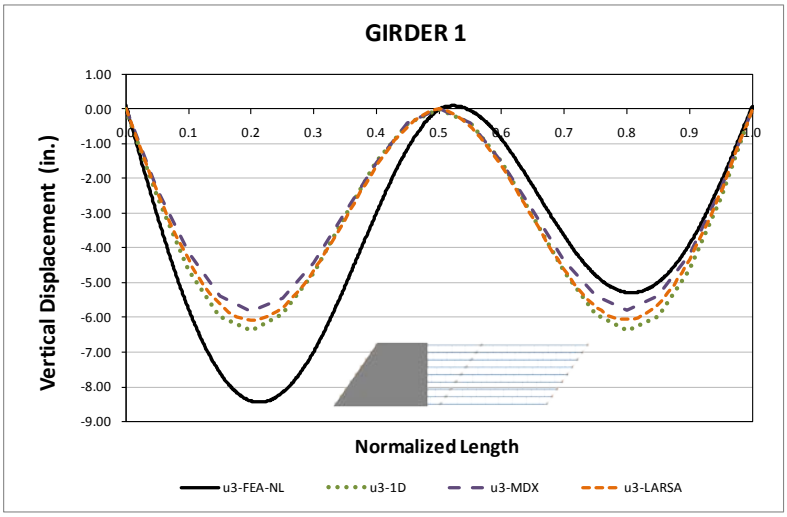

Fig. E.2.4-6. EICSS1, vertical displacements under total dead load for TDLF detailing.

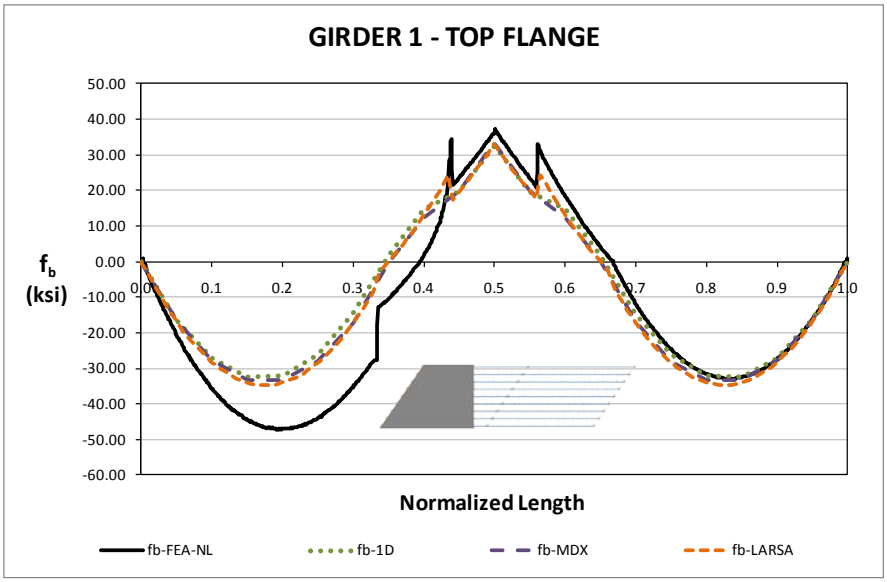

Fig. E.2.4-7. EICSS1, major-axis bending stresses under total dead load for TDLF detailing.

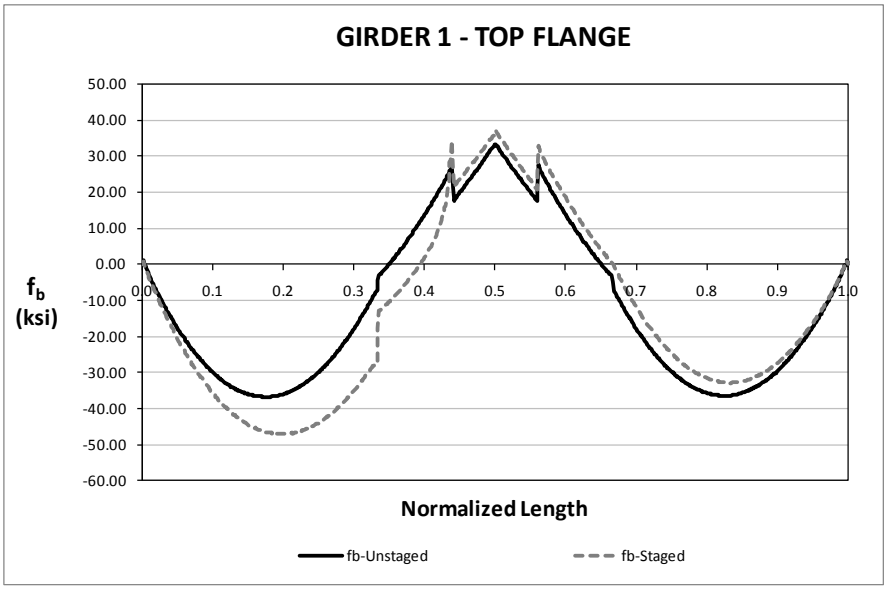

Fig. E.2.4-8. EICSS1, major-axis bending stresses under total dead load for TDLF detailing assuming staged deck analysis vs. no staged deck analysis

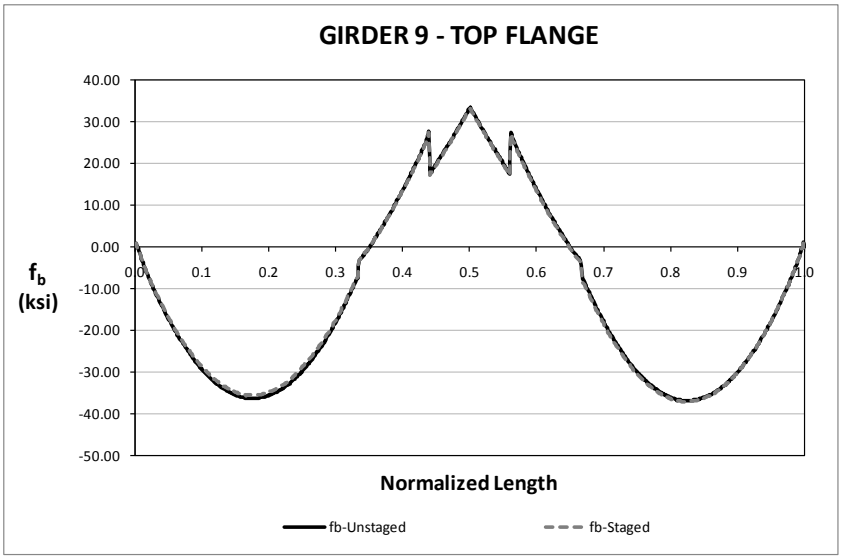

Fig. E.2.4-9. EICSS1,.Major-axis bending stresses under total dead load for TDLF detailing assuming staged deck analysis vs. no staged deck analysis.

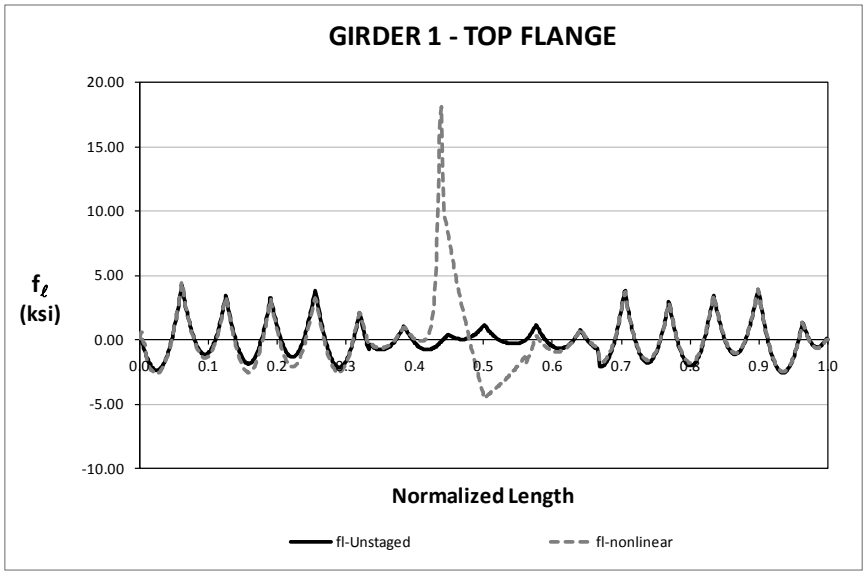

Fig. E.2.4-10. EICSS1, flange lateral bending stresses under total dead load for TDLF detailing assuming staged deck analysis vs. no staged deck analysis.

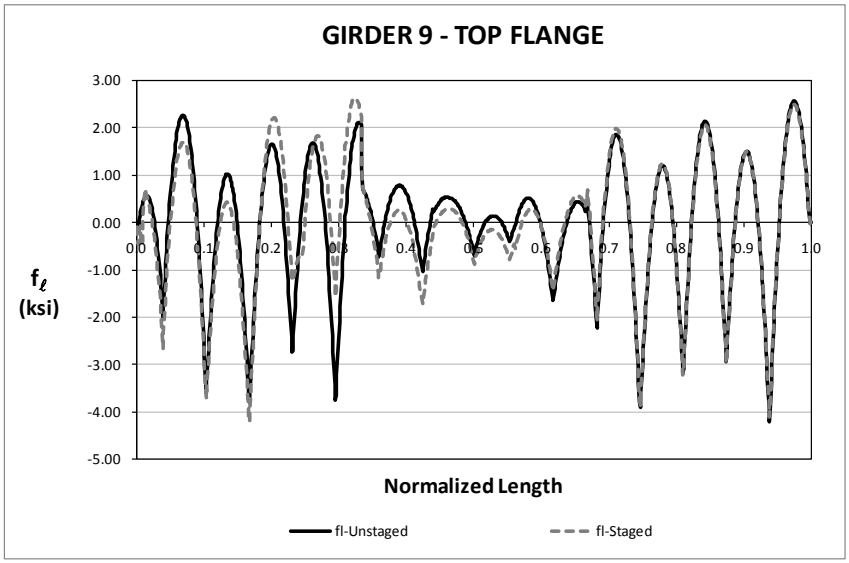

Fig. E.2.4-11. EICSS1, flange lateral bending stresses under total dead load for TDLF detailing assuming staged deck analysis vs. no staged deck analysis.

Conclusions:

In general, different detailing methods may introduce additional stresses in the components due to lack of fit between cross-frames and girders that might affect the system behavior. These additional stresses are usually neglected by designers which lead to poor prediction of radial displacements and behavior.

Approximate methods usually do not consider staged deck placement analysis. The responses usually are obtained by placing the deck in one stage. Detailed staged deck analysis results show that the displacements are larger in 3D FEA model in the region where the deck is placed first. This may affect the camber values of the girders. Moreover, the perpendicular deck pouring in skewed bridges may induce additional local stress concentrations on girders. In the case of parallel pouring with respect to skewed bearings less stress concentrations are expected.

I3.2 EICSS2 (Existing, I-girder, Continuous-span, Straight, Skewed supports)

Bridge Description :

I-235 EB over E. University Ave., Polk Co., IA

Category Data:

L_1 = 239 ft, L_2 = 257 ft, L_3 = 220 ft / w = 74.3 ft / θ_1 = 58°, θ_2 = 61.8°, θ_3 = 38°, θ_4 = 38°, 8 girders

Cross-Frame Detailing Method: SDLF

Erection Stages Analyzed: 9 (Analyses are performed assuming NLF, SDLF & TDLF)

Deck Placement Sequence: 11 Stages (Analyses are performed assuming no staged deck placement).

This bridge was one of several recommended to us by Mr. Norm McDonald and his staff at the Office of Bridges and Structures, Iowa DOT. difficulty installing the cross-frames during erection is observed. The fit-up issues that were encountered can be summarized as follow:

- Cross frames were designed to be erected under steel DL only condition. The connections were designed to handle any additional stresses from final DL condition.
- Assumptions were not stated on the plans (per policy at the time)
- Fabricator detailed and fabricated the cross frames for final DL condition
- Contractor was not able to install the cross frames as fabricated
- Fabricator's proposal to slot existing holes to facilitate the installation was rejected by the State in accordance with current policies
- The problem was resolved by requiring the fabricator to supply new cross frames

Bridge Perspective & Plan Views:

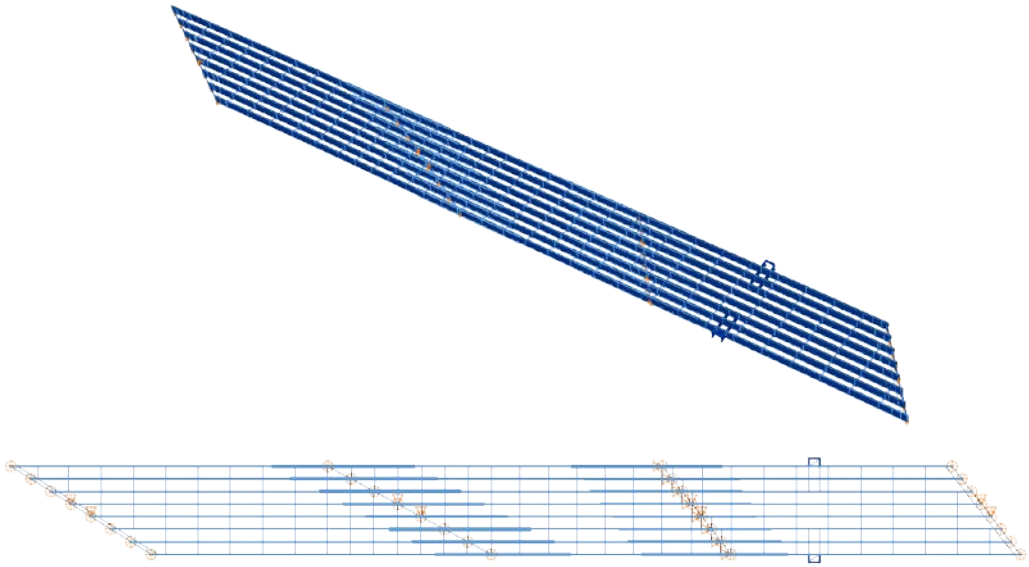

Abbreviated Analysis Results:

Figures 1 and 2 shows vertical and relative lateral displacement results of girder 1 under steel dead load. Although the bridge is very wide and have high and different skew angles on different skews, all analysis methods predict the response accurately. It should be noted from Fig. 2 that the lateral displacements are well predicted by 2D LARSA model. In general for the straight bridges we observe good lateral deflection predictions from 2D LARSA models. It appears that the effect of the lack of warping rigidity in the girder models is not as big of a factor affecting the analysis accuracy for straight skewed bridges, compared to horizontally curved bridges. Figure 3 shows the major-axis bending stresses, which is again well predicted by the different analysis methods.

Also the erection stages of this bridge are investigated since difficulty installing the cross-frames during erection is observed by Norm McDonald and his staff at the Office of Bridges and Structures, Iowa DOT. Although the displacement and stress results are well predicted by all analysis methods as shown for the steel dead load case, high cross frame forces are observed at the vicinity of the skewed bearing lines. This is due to the "Nuisance stiffness". "Nuisance stiffness" is characterized as unwanted stiffness in secondary members, other primary members, or connections, producing undesirable load paths in a structural system (Krupicka and Poellot 1993). Skewed supports are one of the type bridge details where unwanted stiffness can occur. Krupicka and Poellot (1993) provide a fairly extensive discussion of various design and detailing options to reduce the effects of nuisance stiffness in highly skewed bridge structures. They point out that these problems are particularly severe on wide bridges with heavy skew. One of their suggestions to avoid this problem is by interrupting the load path by eliminating selected cross-frames from a given line or shifting the cross-frames slightly to eliminate framing directly into a bearing location. Figure 4 shows the cross-frame lines that may cause nuisance stiffness.

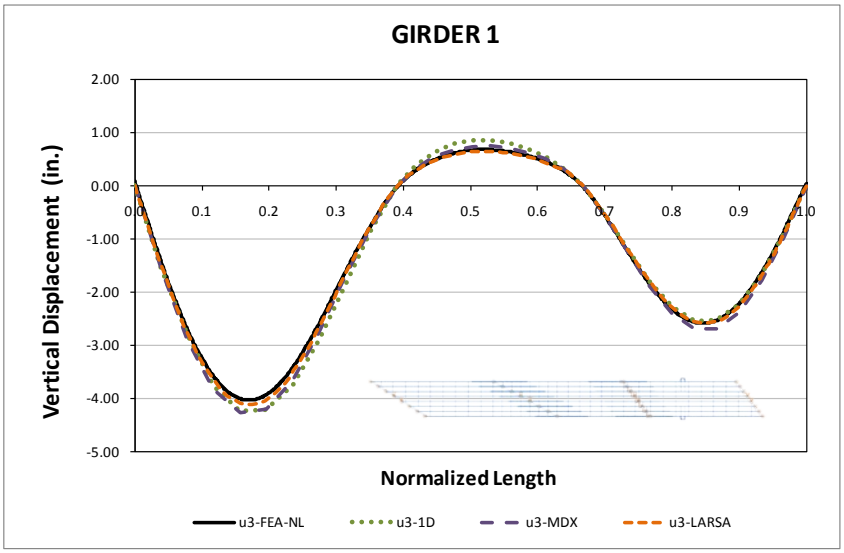

Fig. E.3.4-1. EICSS2, Vertical displacements under steel dead load for NLF detailing.

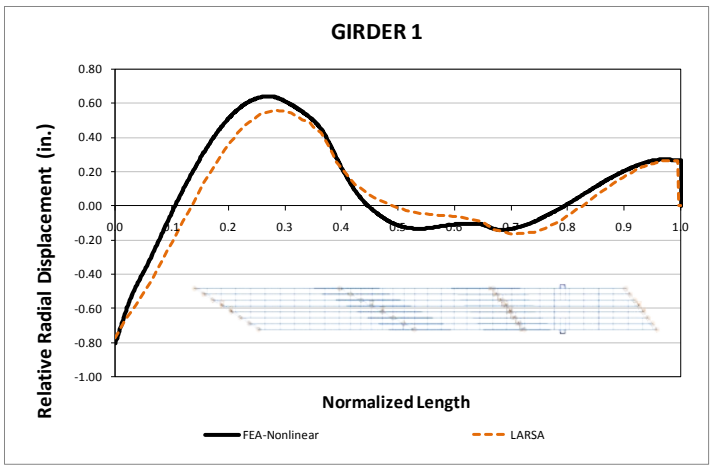

Fig. E.3.4-2. EICSS2, Relative lateral displacements under steel dead load for NLF detailing.

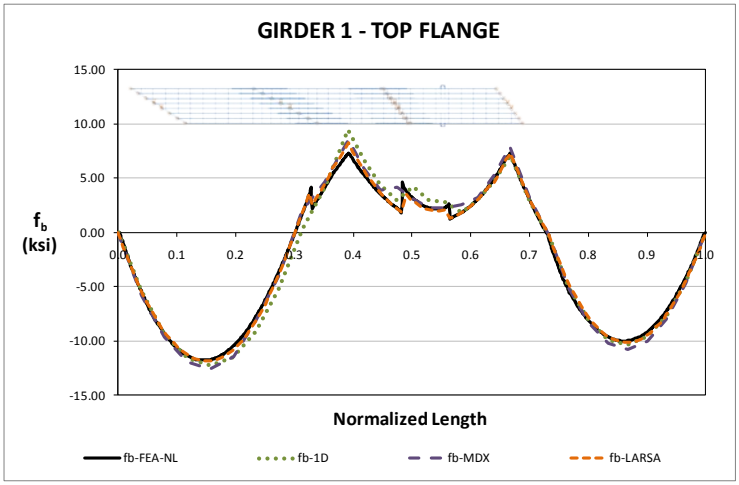

Fig. E.3.4-3. EICSS2, Major-axis bending stresses under steel dead load for NLF detailing.

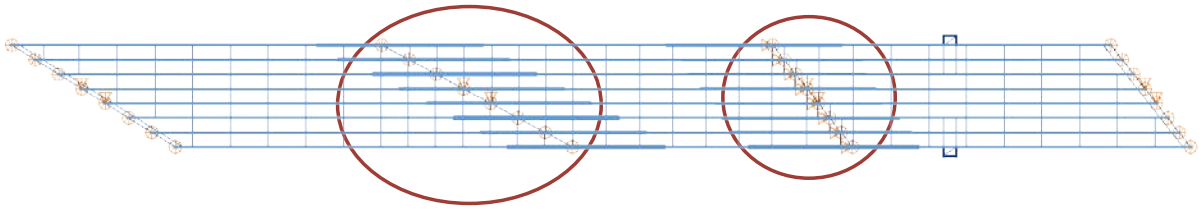

Fig. E.3.4-4. EICSS2, Configuration of the cross-frame lines where relatively large forces are attracted.

This bridge is also analyzed with SDLF and TDLF cross-frame detailing methods by using 3D-FEA. The results are compared with NLF results to illustrate the differences. Usually these different detailing methods may introduce additional stresses in the components due to lack of fit between cross-frames and girders that might affect the system behavior. These additional stresses are usually neglected by designers. This is believed to not present any significant problem for many bridges, but the project team expects that there is some limit at which the effect of the locked in stresses should be considered (as indicated by the

AASHTO LRFD Specifications). Some stages of this bridge are selected to illustrate the effect of these additional responses.

Figures 5 and 6 show relative lateral displacement of the bottom girder (Girder 1) under steel dead load and total dead load for different detailing methods. It is observed from Fig. 5 that the girders are approximately plumb position under steel dead load for SDLF whereas they are out-of-plumb for other methods. Moreover, it should be noted from Fig. 5 that the girders are deflecting in opposite direction when TDLF and NLF relative lateral displacements are considered. Opposite lateral deformations for TDLF detailing is caused by the lack of fit between cross-frames and girders. It is should be observed from Fig. 6 that the girders are plumb only when TDLF detailing method is considered. Figure 7 provides girder 1 vertical displacements under total dead load for different detailing methods. It is observed from Fig.7 that the difference in the deflections are small and can be avoided in the design. Figure 8 shows girder 1 stress responses under total dead load for different detailing methods. It is clear from Fig. 8 that there are no major differences in the major-axis bending stress responses due to lack of fit forces. Again, these small differences can be tolerated in the original design. Additionally, Fig. 8 illustrates that flange lateral bending stresses are reduced when TDLF is used. The difference for the flange lateral bending stresses is bigger on interior girders.

Although there are no major differences for vertical displacements and stress responses, fit up problems are observed in the field. Although SDLF detailing method is targeted, the cross-frames are detailed and fabricated for final DL condition. This lead to fit up problems in the field. Therefore, it is worthwhile to check the cross-frame stresses under steel and total dead load to understand the consequences of these detailing methods. Tables 1 and 2 show cross-frame stresses under steel and total dead load for different detailing methods respectively. The cross-frame stresses are important under steel dead load since this is the end of the steel erection. Table 1 illustrates that high cross-frame stresses for bottom chords are obtained for NLF and TDLF detailing under steel dead load. The high cross-frame stresses are discussed previously for NLF detailing. The main reason of having high stresses are due to the “Nuisance stiffness” at the vicinity of the skewed bearing lines. Likewise high stresses are observed at the similar locations for TDLF detailing. These high stresses are indication of the fit up problems during the erection. On the other hand, it is observed from Table 2 that high cross-frame forces under total dead load can be reduced by applying different detailing methods. It should be noted that TDLF detailing method can provide lowest cross-frame stresses for the final design values under total dead load. However, this may lead to fit up difficulties during the erection. Therefore, SDLF is the most appropriate cross-frame detailing method for this bridge.

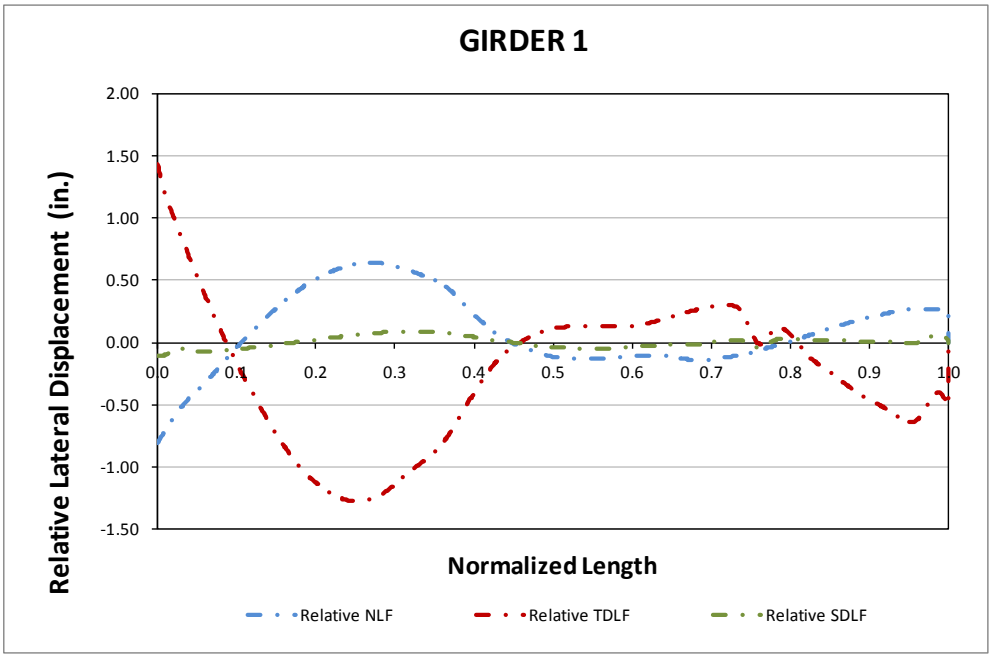

Fig. E.3.4-5. EICSS2, Relative lateral displacements under steel dead load for different detailing methods.

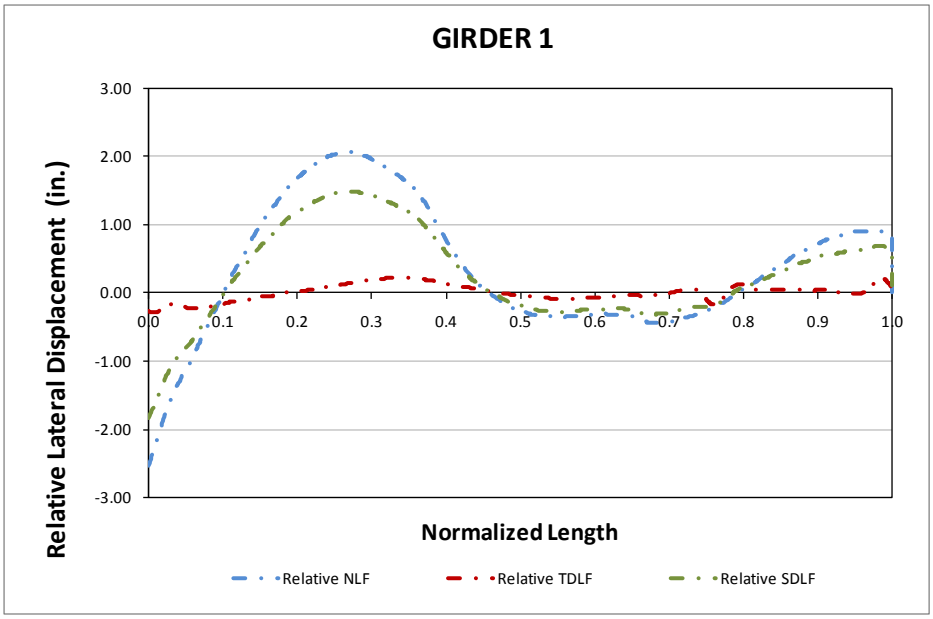

Fig. E.3.4-6. EICSS2, Relative lateral displacements under total dead load for different detailing methods.

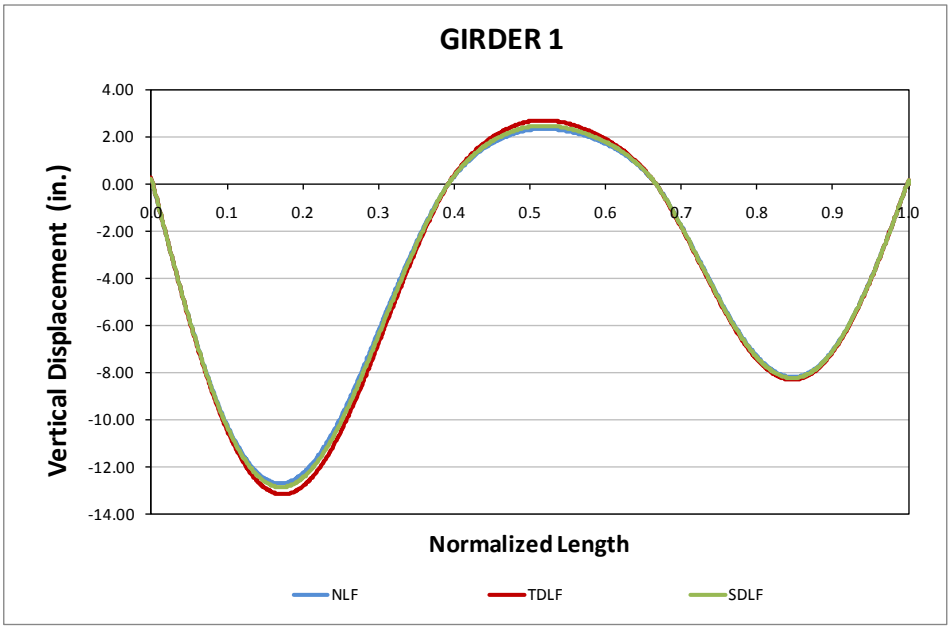

Fig. E.3.4-7. EICSS2, Vertical displacements under total dead load for different detailing methods.

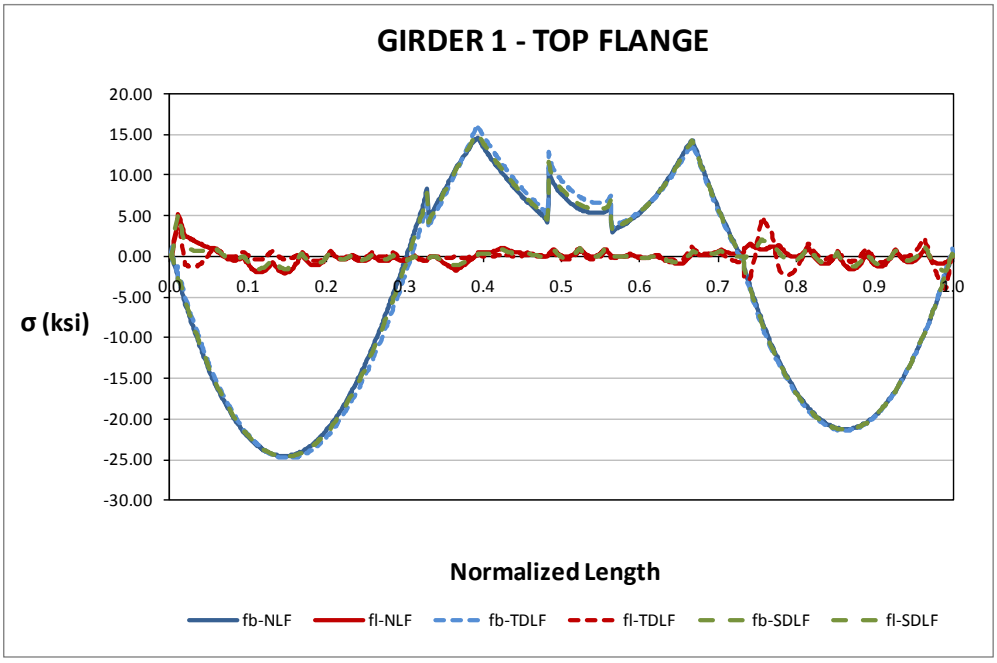

Fig. E.3.4-8. EICSS2, Stress responses under total dead load for different detailing methods.

Table. E.3.4-1. Maximum and minimum cross-frame stresses under steel dead load for both detailing methods.

Steel Dead Load (ksi)						
Detailing	Top Chord		Bottom Chord		Diagonal	
Method	Max.	Min	Max.	Min	Max.	Min
NLF	0.3	-0.6	8.7	-14.8	4.1	-1.8
SDLF	0.3	-0.2	4.3	-4.4	1.5	-1.5
TDLF	1.3	-1.0	22.3	-12.7	4.2	-7.3

Table. E.3.4-2. Maximum and minimum cross-frame stresses under total dead load for both detailing methods.

Total Dead Load (ksi)						
Detailing	Top Chord		Bottom Chord		Diagonal	
Method	Max.	Min	Max.	Min	Max.	Min
NLF	1.1	-1.5	27.8	-44.9	11.8	-5.5
SDLF	1.1	-0.9	20.7	-33.9	8.5	-4.3
TDLF	1.0	-0.8	13.0	-13.2	4.5	-4.6

Conclusions:

The behavior is well predicted by all analysis methods for this bridge. It is observed that the lateral deflections are close to 3D FEA predictions along the length at all points. This is the general observation for straight bridges.

High cross-frame forces are observed at the vicinity of the skewed bearing lines. This is due to the "Nuisance stiffness" which is characterized as unwanted stiffness in secondary members, other primary members, or connections, producing undesirable load paths in a structural system (Krupicka and Poellot 1993).

This bridge is also analyzed by using SDLF and TDLF cross-frame detailing methods. The results are compared with NLF results to illustrate the differences. Usually these different detailing methods may introduce additional stresses in the components due to lack of fit between cross-frames and girders that might affect the system behavior. These additional stresses on vertical displacements and major-axis bending stresses are found to be negligible for this bridge. However, big differences in the cross-frame stresses are observed. it is predicted that these high cross-frame stresses under steel dead load may be an indication of fit up problems in the field. It is concluded from the results that SDLF is the most appropriate cross-frame detailing method for this bridge.

I3.3 EICSS12 (Existing, I-girder, Continuous-span, Straight, Skewed supports)

Bridge Description :

US 82 Mainline Underpass at 19th Street WB, Lubbock, TX

Category Data:

L_1 =150 ft, L_2 = 139 ft, w = 47 ft, θ = 59.6°, 6 girders lean-on cross-frame system

References:

The bridge has been studied analytically in a number of papers and reports developed by colleagues at UT Austin, as previously documented, and measurements on this bridge are documented in the M.S. thesis by Romage (2008). Although Project 12-79 does not aim to undertake specific research on lean-on cross-frame bracing systems, this bridge provides an outstanding opportunity for validation or verification of the refined analysis methods utilized in Project 12-79 versus experimental and other analytical results.

Cross-Frame Detailing Method: NLF

Erection Stages Analyze: 5 (Analyses are performed assuming NLF)

Deck Placement Sequence: 1 Stage

This bridge is one of several suggested by TxDOT. This bridge involves a field implementation and evaluation of the use of lean-on cross-frames to alleviate issues of nuisance stiffness in significantly skewed bridges and to eliminate cross-frame diagonals within a large portion of the bridge framing.

Bridge Perspective & Plan Views:

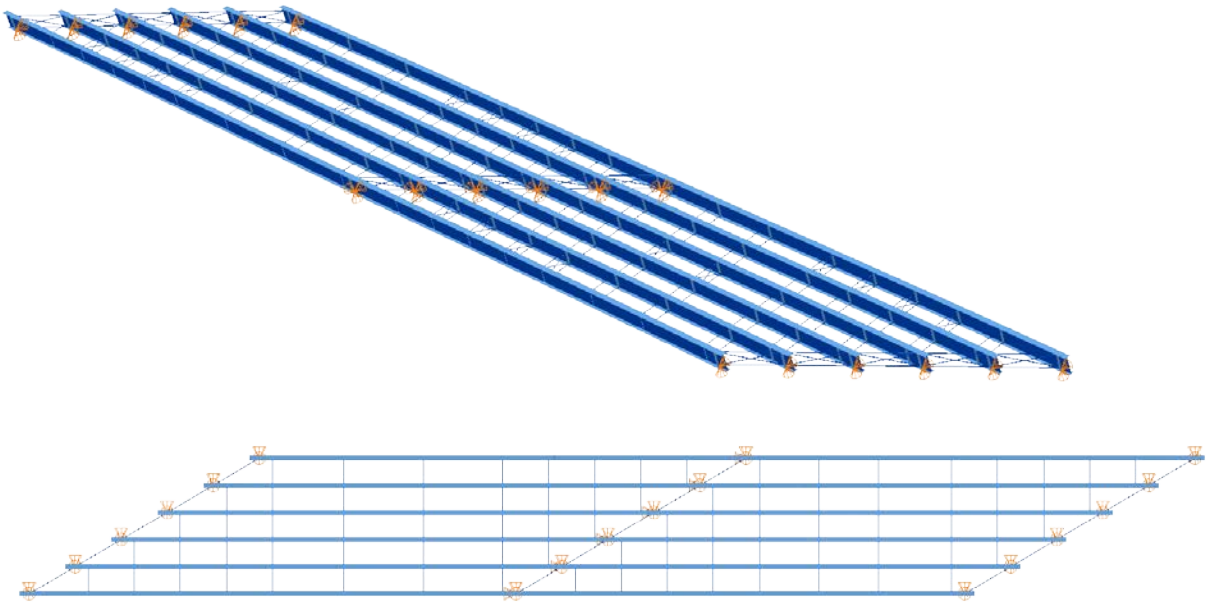

Abbreviated Analysis Results:

Figures 1 and 2 show the vertical and relative radial displacements of the outside girder (Girder 1) under total dead load predicted by different analysis methods. Moreover, Fig. 3 provides the top flange major-axis bending stresses under total dead load. Displacements are well predicted by different analysis methods. In general, the major-axis bending stresses are accurately predicted.

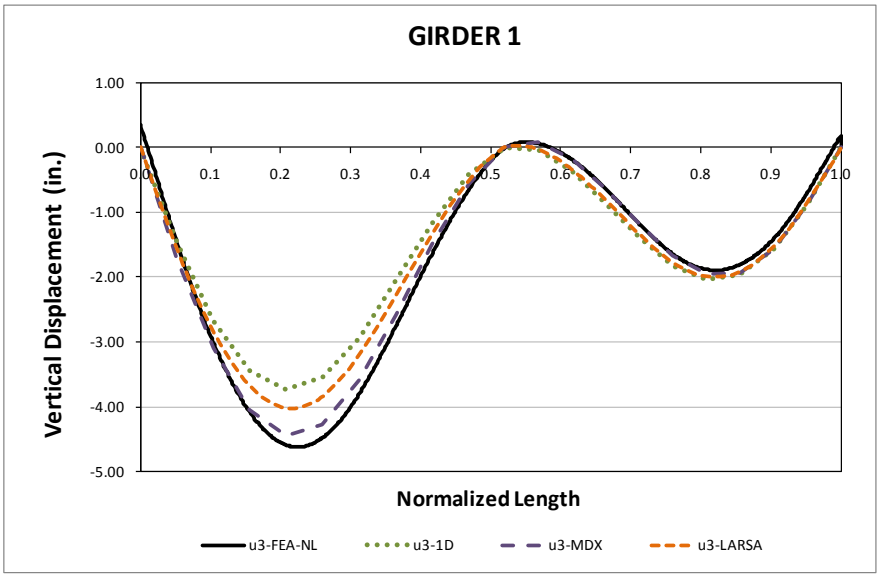

Fig. E.4.4-1. EICCR4, Vertical displacements under total dead load.

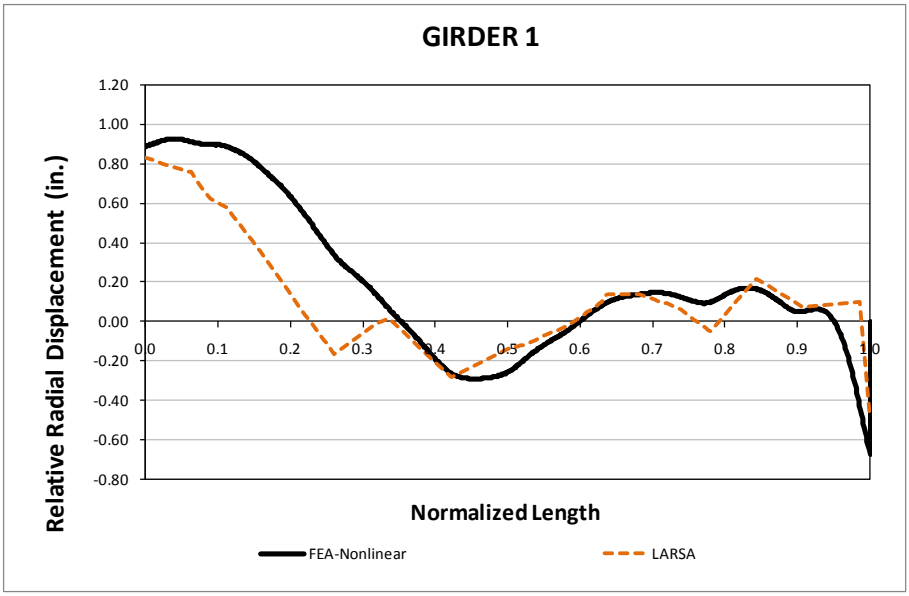

Fig. E.4.4-2. EICCR4, Relative radial displacements under total dead load.

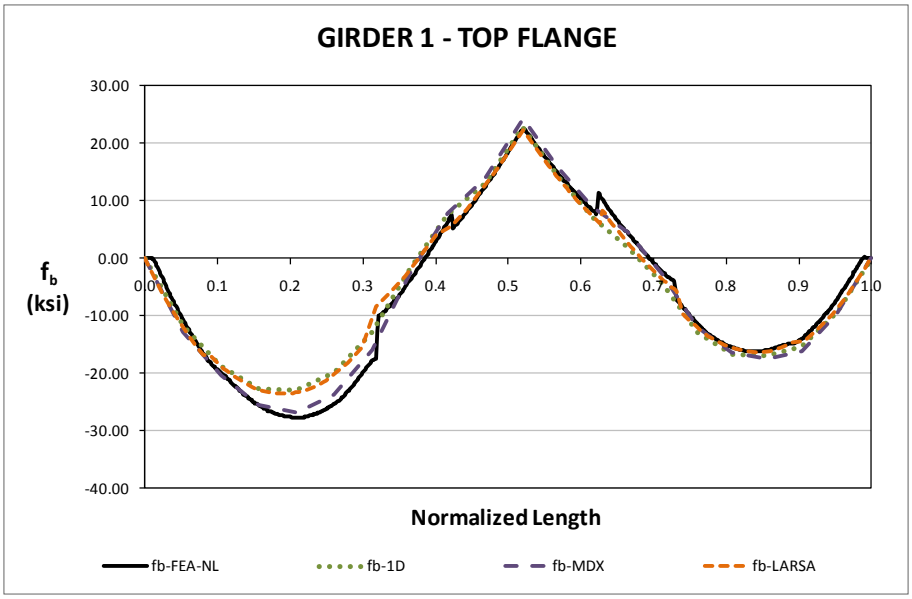

Fig. E.4.4-3. EICCR4, Major-axis bending stresses under total dead load.

I3.4 NICSS1 (New, I-girder, Continuous-span, Straight, Skewed supports)

Category Data:

L_1 = 150 ft, L_2 = 150 ft / w = 30 ft / $\theta_1 = 0^o$, $\theta_2 = 35^o$, $\theta_3 = 0^o$, 4 girders

Cross-Frame Detailing Method: NLF

Erection Stages Analyzed: Five

Deck Placement Sequence: One stage, deck thickness = 9.5 in.

Bridge Perspective & Plan Views:

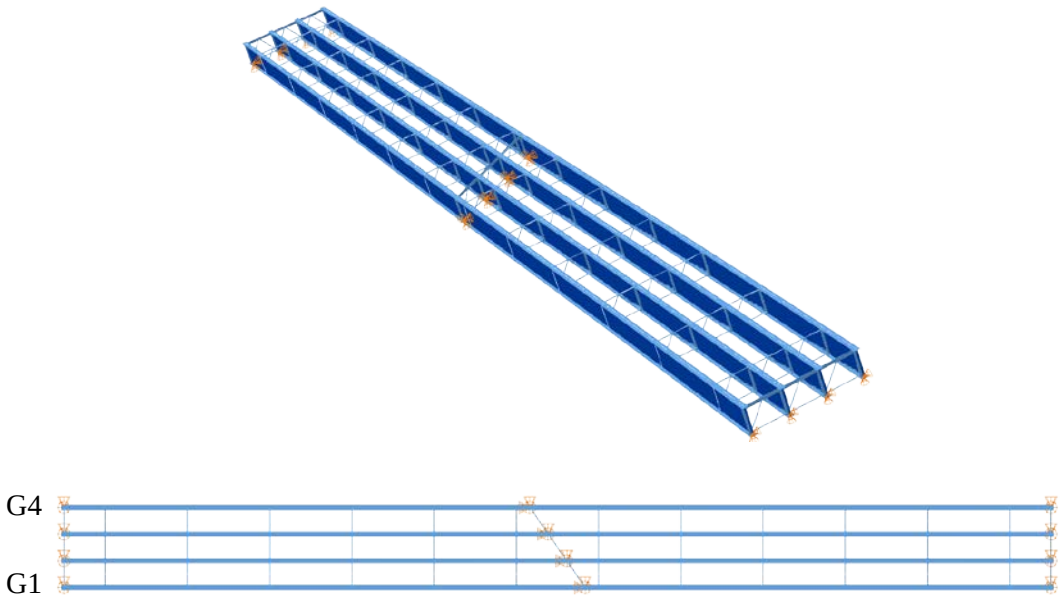

Abbreviated Analysis Results:

In this bridge, the effects of the intermediate support skew and the span continuity are studied. The studied erections stages are shown in Figure 1. The steel erection starts with the placement of girder G1 over the left span. At the supports, the girder displacements are restrained with tie-downs, and a holding crane is provided at approximately mid-span to prevent stability failure problems. The next girder, G2, is placed and connected to girder G1 with the cross-frames, and then, the holding crane is released. Girders G3 and G4 are erected sequentially, following the same scheme to complete the erection of the structure in Span 1. The remaining segments of the four girders over Span 2 are erected next, starting from girder G1 to girder G4.

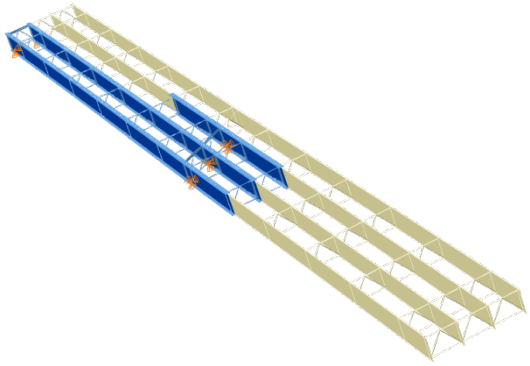

Stage 3

Stage 5

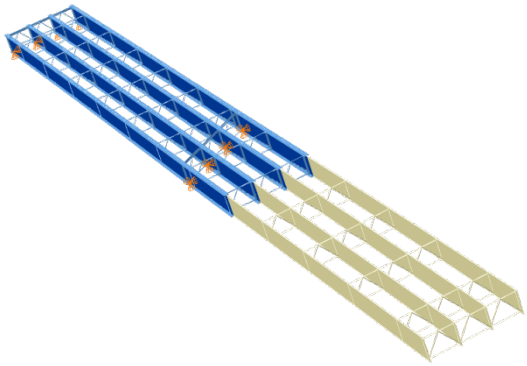

Stage 6

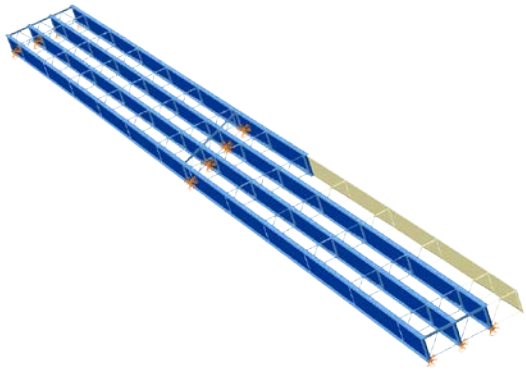

Stage 9

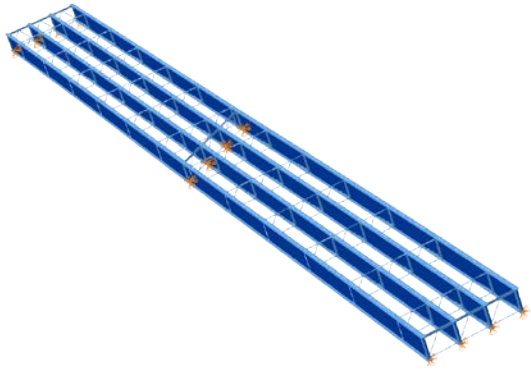

Stage 11 (TDL)

Fig. 1. Analyzed Construction Stages

The results obtained for this bridge from the approximate 1D and 2D analyses are accurate for all the responses, in all the studied construction stages. Figure 2 shows the major-axis bending stresses in the bottom flange of girder G3, for Stage 5. As show, the 2D grid response fits accurately the response predicted by the 3D FEA model. The same characteristics are observed for the vertical displacements, as shown in Figure 3.

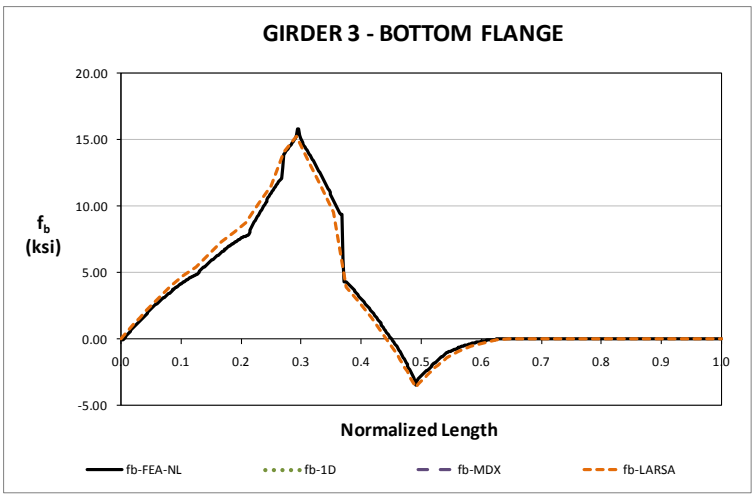

Fig. 2. Major-axis Bending Stresses, Stage 5

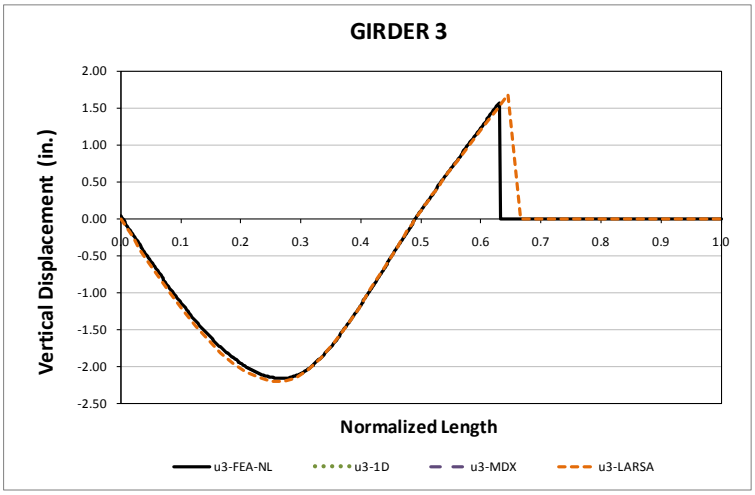

Fig. 3. Vertical Displacements, Stage 5

For Stage 11, the major-axis bending stress response is shown in Figure 4. The responses predicted by the girder line and the two 2D grid analysis methods are an accurate representation of the 3D model response. Figure 5 shows that the vertical displacements are also accurate for this stage, and Figure 6 shows the correspondence between the 2D grid and 3D FEA models for relative lateral displacements. A comparison of flange lateral bending stresses is not shown in this report. Due to the relatively small skew angle and the orientation of the cross-frames, these stresses are negligible.

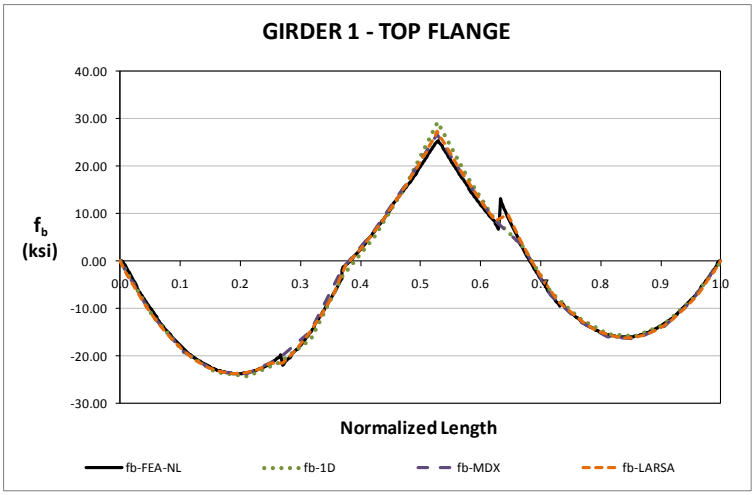

Fig. 4. Major-axis Bending Stresses, Stage 11

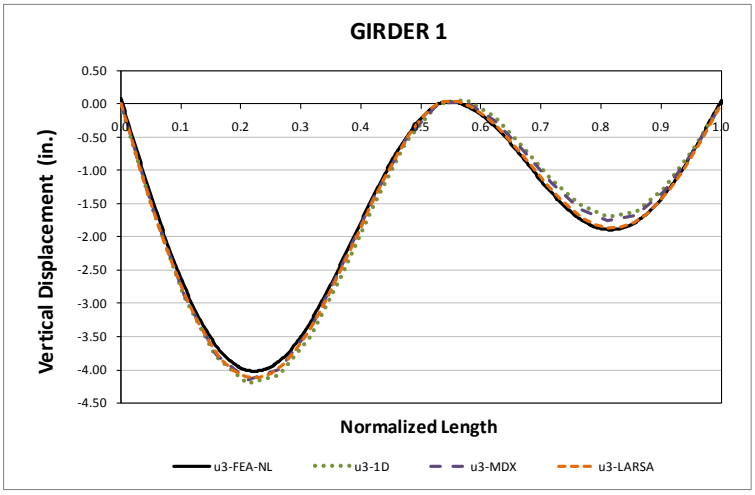

Fig. 5. Vertical Displacements, Stage 11

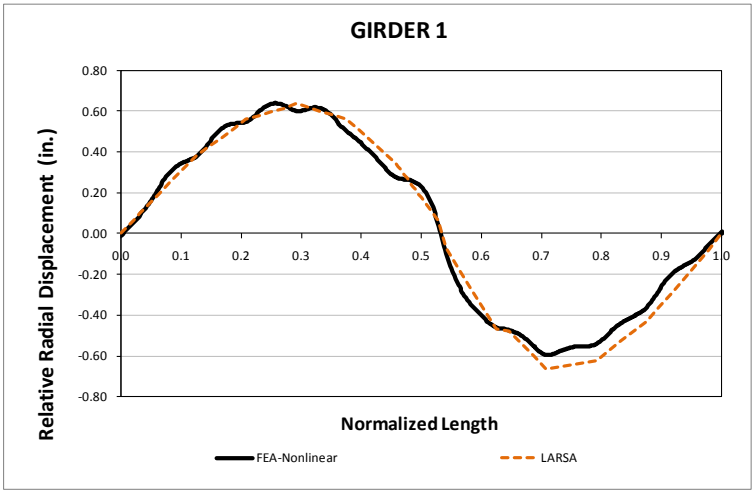

Fig. 6. Relative Radial Displacements, Stage 11

Conclusions:

The geometry of this bridge is relatively simple. As expected, the approximate methods provide reliable results for the major-axis bending responses and the relative lateral displacements. In fact, a simple girder line analysis would be enough to predict the geometry and the stresses of this bridge during construction.

It is also concluded that it might not be required to predict the flange lateral bending response of this bridge. The small skew and the parallel orientation of the cross-frames result in small differential deflections that do not induce considerable levels of flange lateral bending stress.

I3.5 NICSS3 (New, I-girder, Continuous-span, Straight, Skewed supports)

Category Data:

L_1 = 150 ft, L_2 = 150 ft / w = 30 ft /θ_1 = 35^o, θ_2 = 0^o, θ_3 = 0^o, 4 girders

Cross-Frame Detailing Method: NLF

Erection Stages Analyzed: 6 (Analyses are performed assuming NLF)

Deck Placement Sequence: 1 Stage

Bridge Perspective & Plan Views:

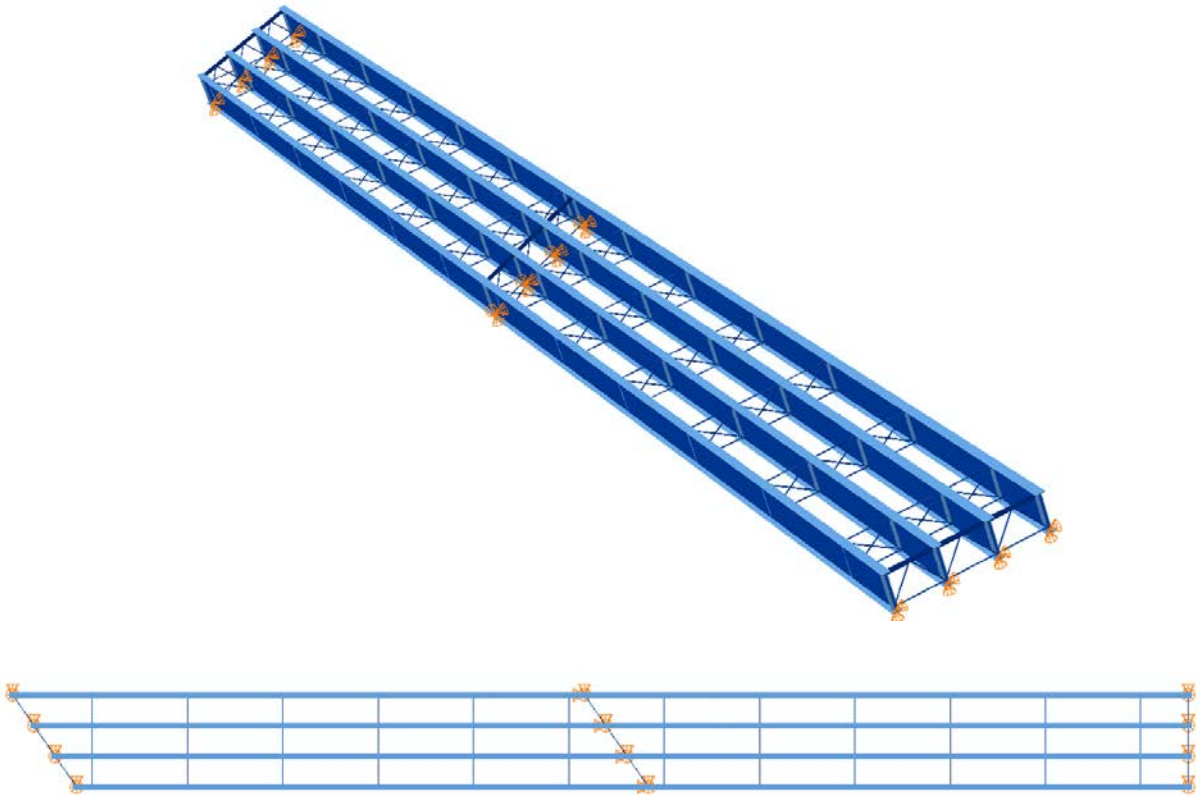

Abbreviated Analysis Results

Figure 1 shows the different analysis stages which are considered to evaluate the different analysis methods. Uplift is observed at Stages 1 and 3 for girders 2 and 3. However the uplift in stages 2 and 3 is captured by Larsa results. The results are not shown here since there is good correlation and the values are small. Total dead load results are provided here in detail since this is the highest load level.

Stage 1

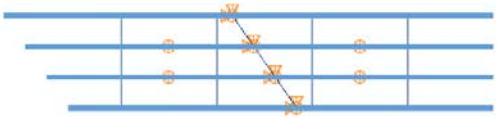

Stage 3

Stage 6

Stage 8

Stage 12 & 13

Fig. 1. NICSS3, Considered different analysis stages.

Figure 2 provides the vertical displacements of the bottom girder (Girder 1) under total dead load. Figure 3 shows the vertical displacements of the top girder (Girder 9) under total dead load. Vertical displacements are accurately predicted by the approximate methods.. There are minor differences between the results which can handled in haunches. Figures 4 and 5 show fascia girder relative lateral displacement predictions under total dead load. It is clear from Figs. 4 and 5 that the end layovers are predicted accurately at the skewed ends. Furthermore, the layovers are accurately predicted within the span by grid solutions.

Figures 6 and 7 provide fascia girder top flange major-axis bending stress predictions under total dead load. The major-axis bending stresses are accurately predicted by approximate methods for girders 1 and 9. This is the case for all girders.

Figure 8 provides the top flange lateral bending stresses of all girders which is predicted by nonlinear geometric analysis. Continuous cross-frame pattern provides smaller flange lateral bending stresses compared to the staggered pattern. However on the fascia girders one should expect higher flange lateral bending stresses due to overhang bracket loading on the fascia girders.

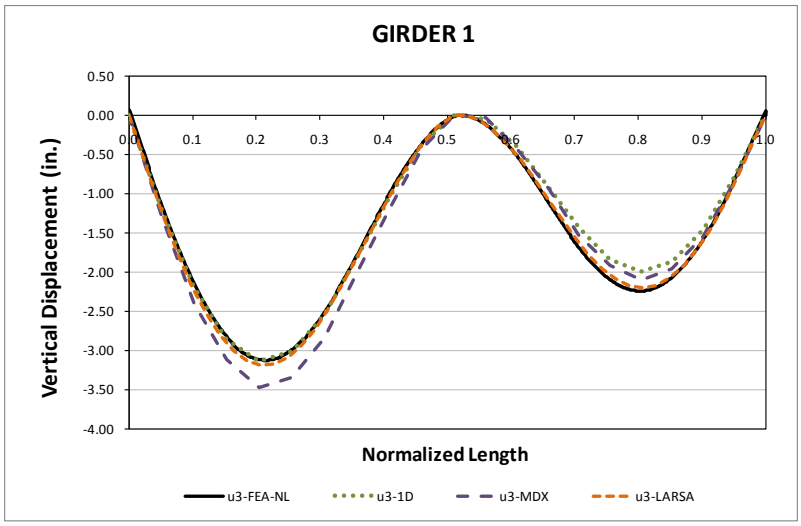

Fig. 2. NICSS3, Vertical displacements under total dead load for NLF detailing.

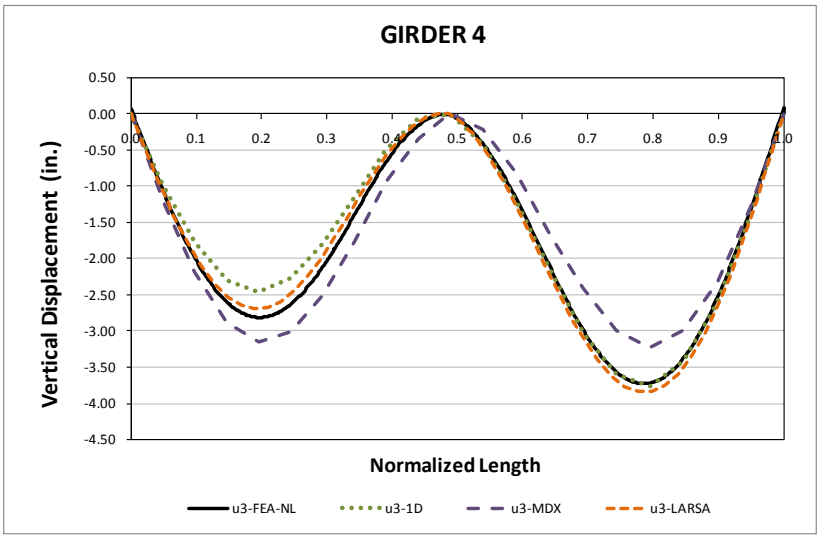

Fig. 3. NICSS3, Vertical displacements under total dead load for NLF detailing.

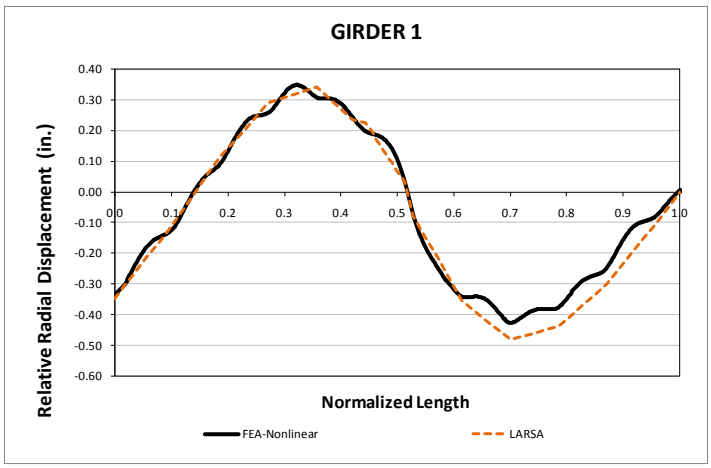

Fig. 4. NICSS3, Relative lateral displacements under total dead load for NLF detailing.

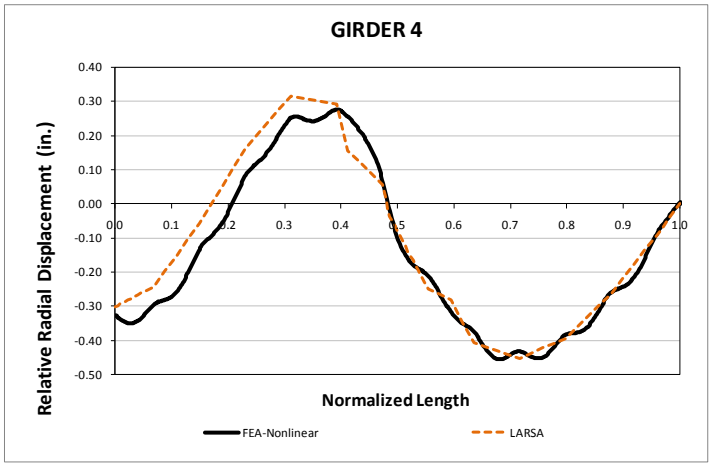

Fig. 5. NICSS3, Relative lateral displacements under total dead load for NLF detailing.

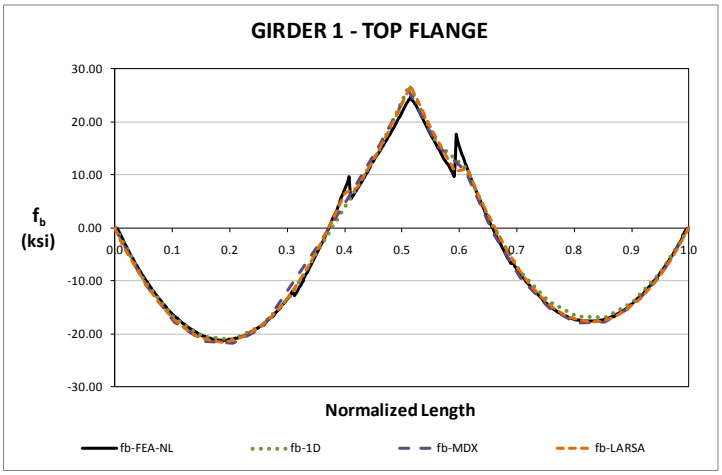

Fig. 6. NICSS3, Major-axis bending stresses under total dead load for NLF detailing.

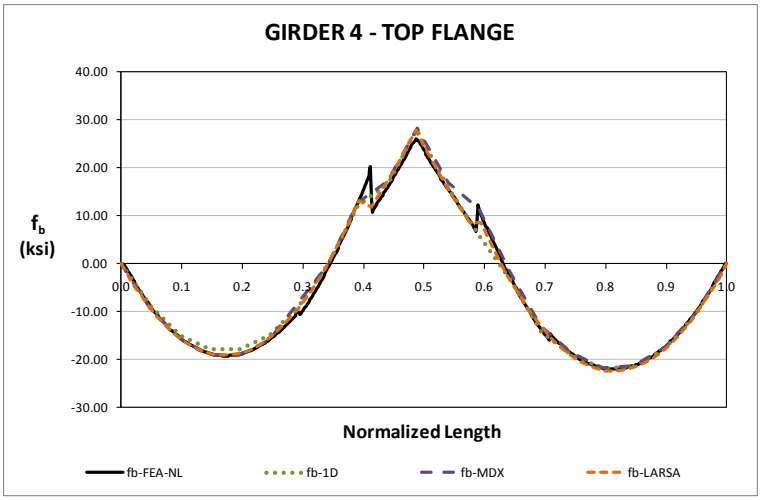

Fig. 7. NICSS3, Major-axis bending stresses under total dead load for NLF detailing.

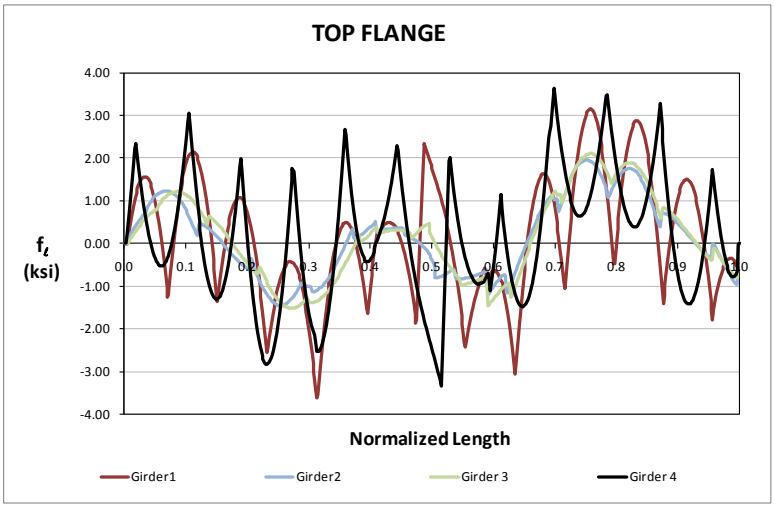

Fig. 8. NICSS3, Flange lateral bending stresses under total dead load for NLF detailing.

I3.6 NICSS 16 (New, I-girder, Continuous-span, Straight, Skewed supports)

Category Data:

L_1 = 120 ft, L_2 = 150 ft, L_3 = 150 ft / w = 80 ft / θ_1 = 70 °, θ_2 = 70 °, θ_3 = 70 °, θ_4 = 70 °, 9 girders

Cross-Frame Detailing Method: NLF

Erection Stages Analyzed: Six

Deck Placement Sequence: One stage, deck thickness = 9.5 in.

Bridge Perspective & Plan Views:

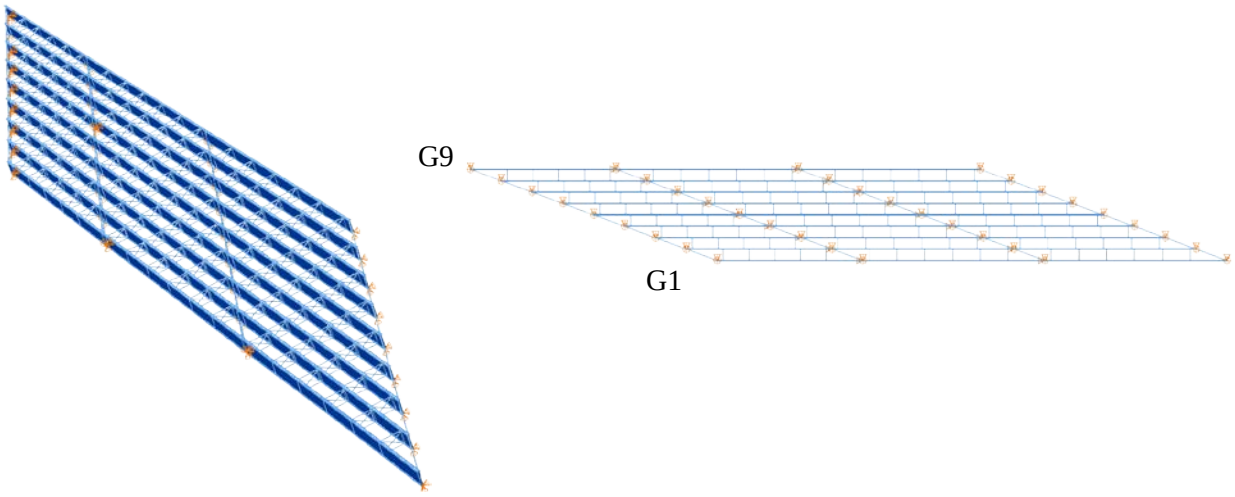

Abbreviated Analysis Results:

This parametric continuous bridge represents an extreme case of a high skew combined with a large width. The steel erection starts with the placement of girders G1 to G9 in Span 1. Stage 2 corresponds to the state where G1 and G2 are in place. The construction of the bridge follows the same scheme with the erection of the girder segments in Span 3. In Stage 11, the first pair of girders in this span has been erected. In Stage 18, the construction of the structure over Spans 1 and 2 is completed. The last phase starts with erection of the G1 drop-in segment in Span 2, Stage 19. In the last stage, the bridge behavior is studied under the total dead load condition.

Stage 2

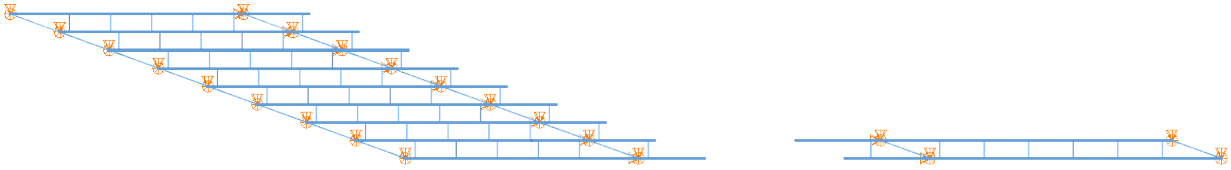

Stage 11

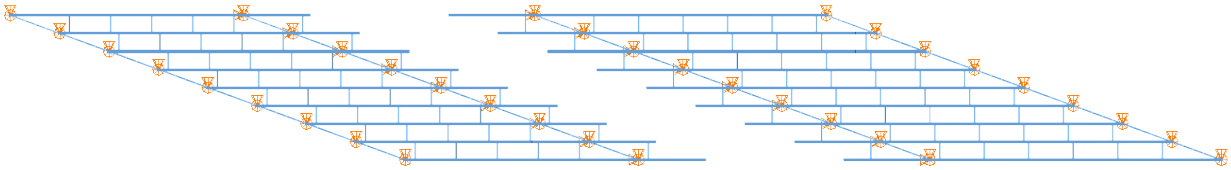

Stage 18

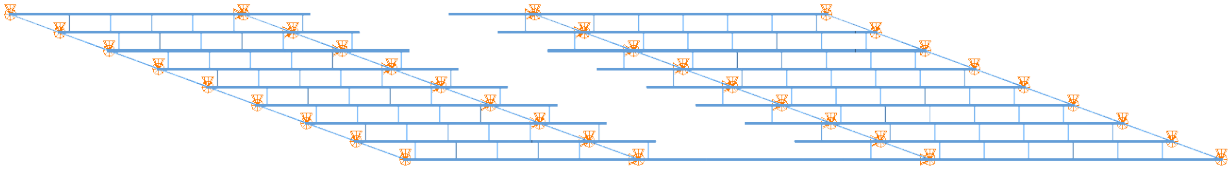

Stage 19

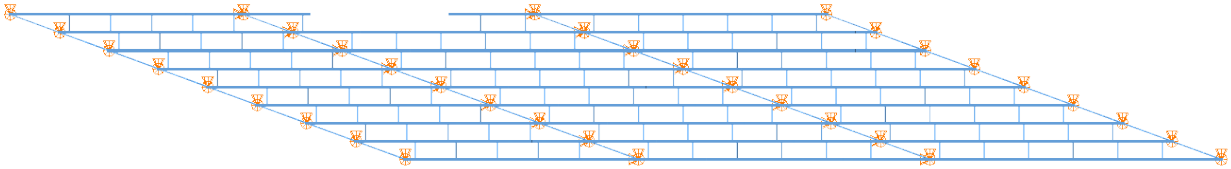

Stage 26

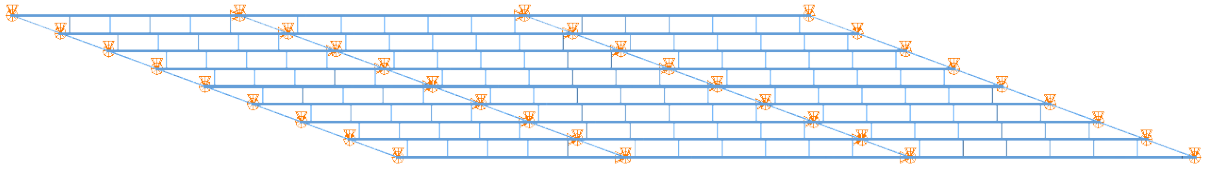

Stage 28 (TDL)

Fig. 1. Analyzed Construction Stages

The results obtained for this bridge from the approximate 1D and 2D analyses are accurate for all the responses, for the first erection stages. Examples of the stress and vertical displacement responses for girder G9 at Stage 1 are shown in Figures 2 and 3, respectively.

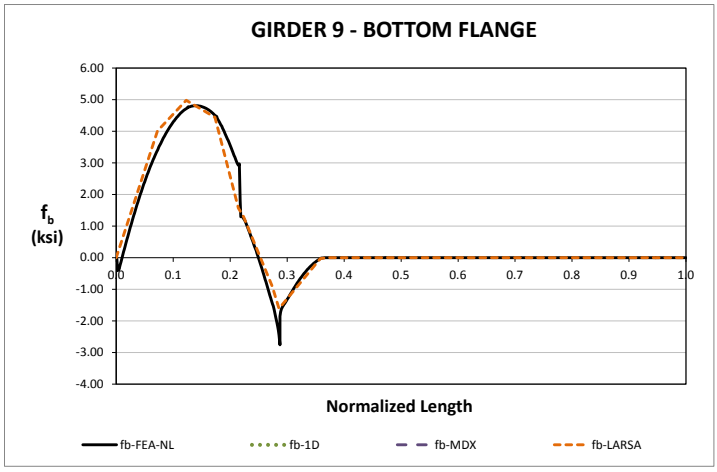

Fig. 2. Major-axis Bending Stresses, Stage 11

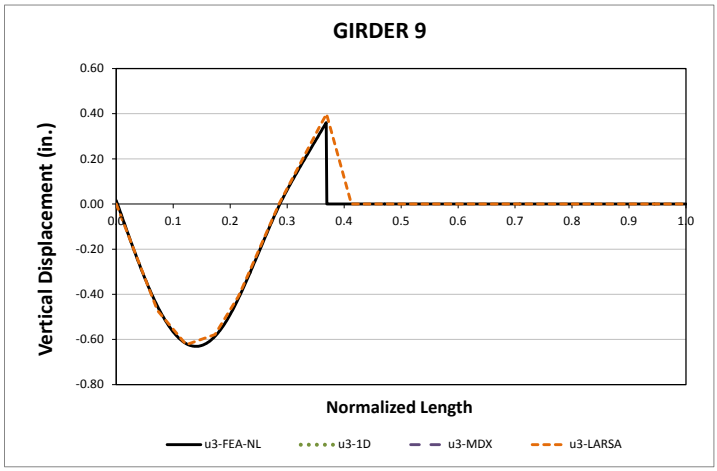

Fig. 3. Vertical Displacements, Stage 11

It is important to notice that due to the geometry of the bridge, it is not possible to use contiguous cross-frames across the width. Thus, the use of staggered cross-frames is the only option to avoid problems associated to "nuisance stiffness." This practice, however, results in an increase of the flange lateral bending response and its associated stresses, f_ℓ. Figure 4 shows the results from the 3D FE model for girder G4 at the SDL condition. Both linear and nonlinear responses are included in this plot. As shown in the figure, the levels of flange lateral bending stress are substantial, and even larger than the stresses produced due to major-axis bending, f_b. The same trend is observed for the TDL condition, as shown in Figure 5. In this case, the f_ℓ stress levels are near the yield limit of 50 ksi, while the major-axis bending stresses are in the order of 15 ksi. These plots highlight the importance of considering the flange lateral bending effects in the design of the bridge.

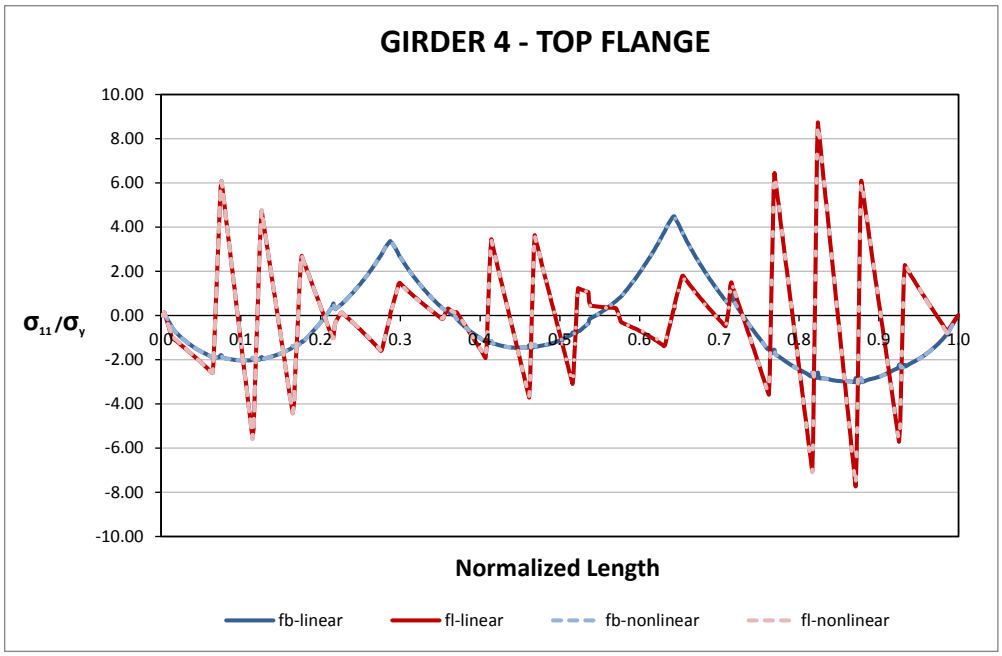

Fig. 4. f_b and f_l predictions, 3D FEA, SDL Condition

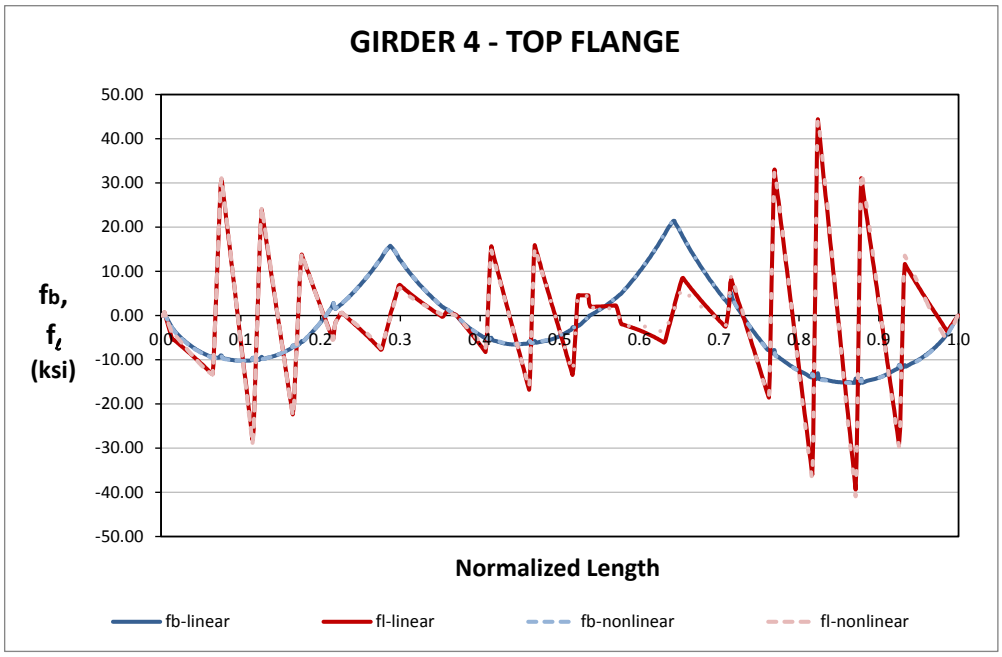

Fig. 5. f_b and f_l predictions, 3D FEA, Stage 10 (TDL)

Conclusions:

Currently, there is no guidance on how to evaluate the effects of the skew at the supports and its correspondent flange lateral bending stresses other than the recommendation of the AASHTO 2010 Bridge Design Specifications, Section C6.10.1. This guideline, however, only applies to bridges that have skews of up to 60 degrees, and does not cover the present case. Therefore, the only method to predict the expected flange lateral bending response in this bridge is by mean of a 3D FE model.

I3.7 NICSS25 (New, I-girder, Continuous-span, Straight, Skewed supports)

Category Data:

L_1 = 350 ft, L_2 = 350 ft / w = 80 ft / $\theta_1 = 0^o$, $\theta_2 = 35^o$, $\theta_3 = 0^o$, 4 girders

Cross-Frame Detailing Method: NLF

Erection Stages Analyzed: Five

Deck Placement Sequence: Three Stages, deck thickness = 9.5 in.

Bridge Perspective & Plan Views:

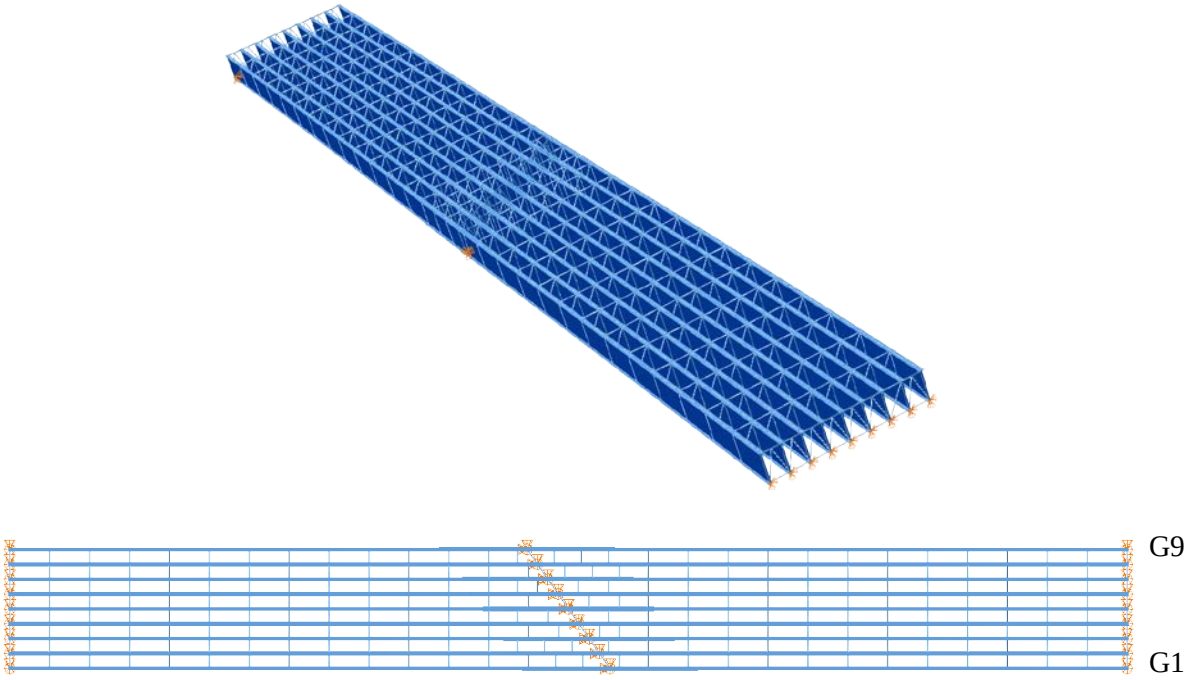

Abbreviated Analysis Results:

In this bridge, the effects of the intermediate support skew and the span continuity are studied. The studied erection stages are shown in Figure 1. The steel erection starts with the placement of girders G1 to G9 over the left span (Stage 9). The girders are divided in five segments due to their length (700 ft in total). Towers are placed across the bridge to support the girders. Subsequent girder segments are erected following the same procedure upon completion of the structure in Stage 47 (SDL condition). In Stage 48, the structure is studied under the total deck load condition corresponding to the deck placement.

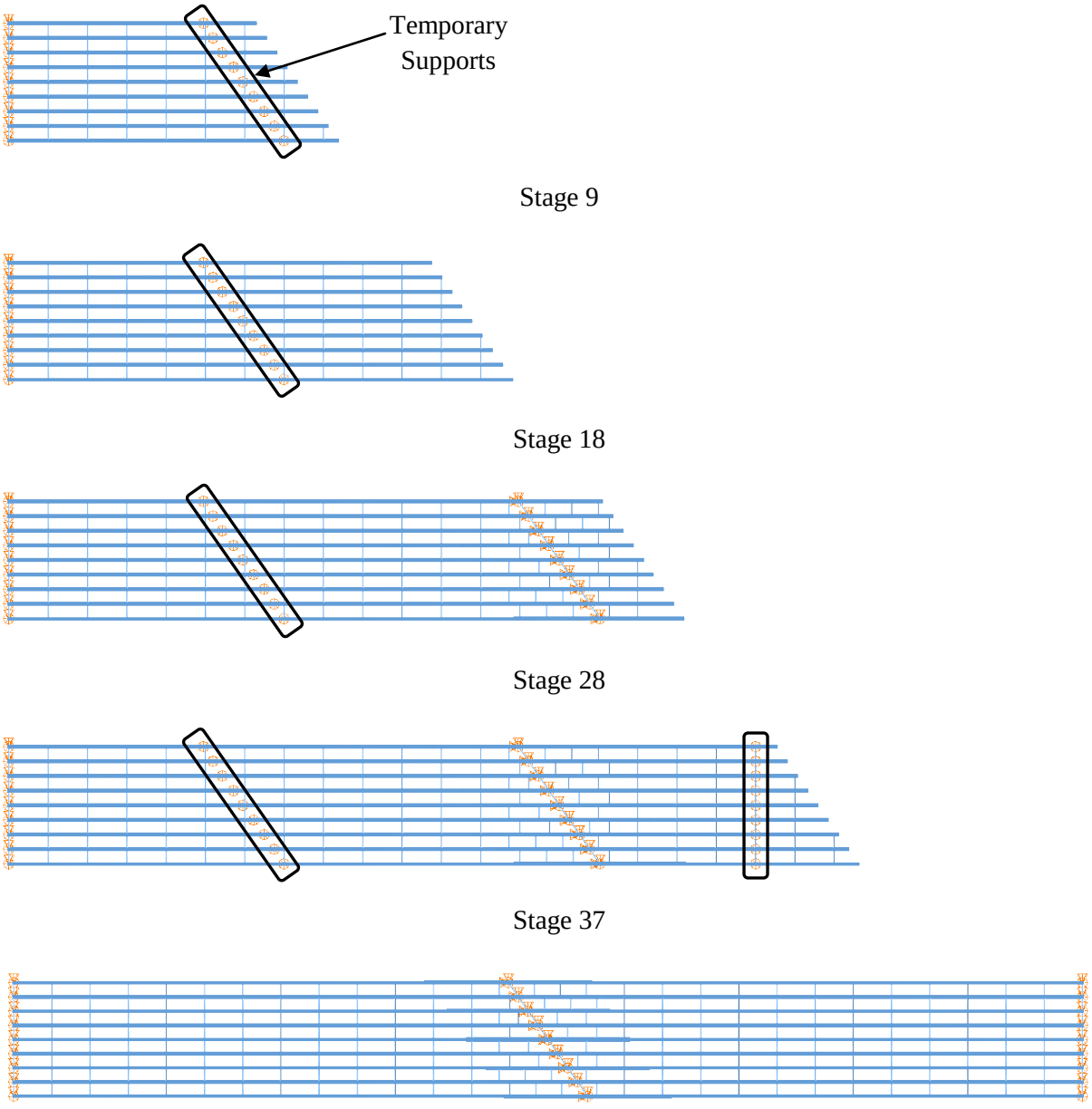

Fig. 1. Analyzed Construction Stages

The predictions obtained from the 1D and 2D analyses for this bridge are accurate in all the studied stages. For example, Figure 2 shows the major-axis bending stresses in the bottom flange of girder G3, for Stage 9. The figure shows that the 2D grid response fits accurately the response predicted by the 3D FEA model. Similarly, the vertical displacements are properly predicted by the 2D grid model, as shown in Figure 3.

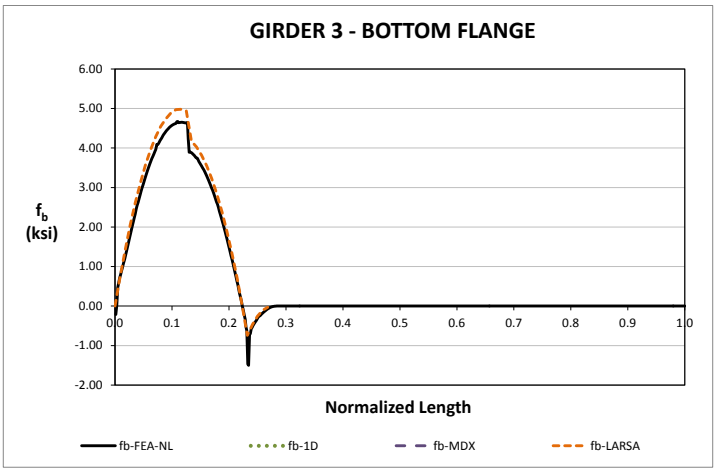

Fig. 2. Major-axis Bending Stresses, Stage 9

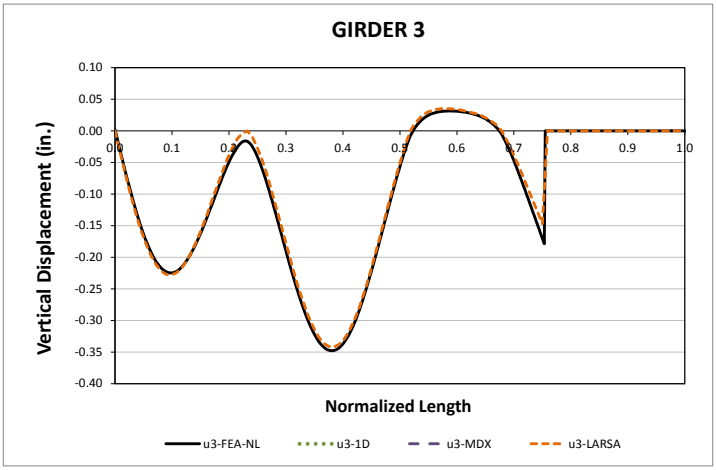

Fig. 3. Vertical Displacements, Stage 9

For Stage 48, the major-axis bending stress response is shown in Figure 4. The responses predicted by the girder line and the two 2D grid analysis methods are an accurate representation of the 3D model response. Figure 5 shows that the vertical displacements are also accurate for this stage, and Figure 6 shows the accuracy of the 2D grid model to predict the relative lateral displacements obtained from the 3D FEA. The flange lateral bending stresses are small for this bridge. Due to the relatively small skew angle and the orientation of the cross-frames, these stresses are negligible.

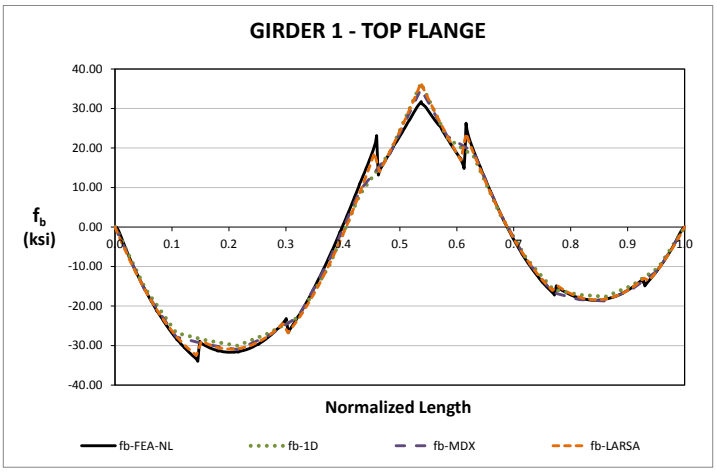

Fig. 4. Major-axis Bending Stresses, Stage 48

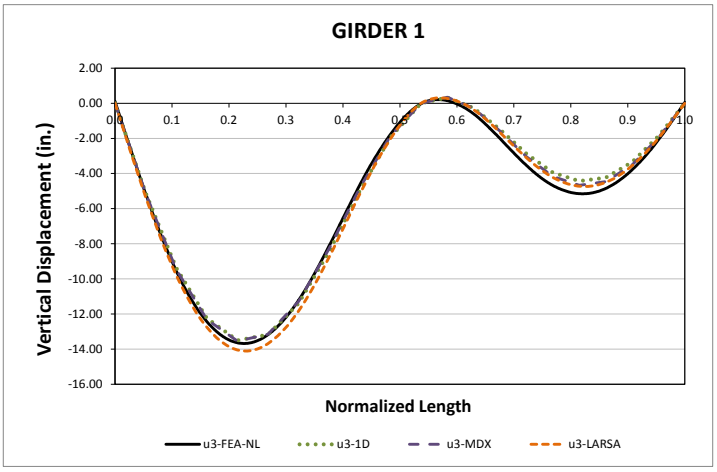

Fig. 5. Vertical Displacements, Stage 48

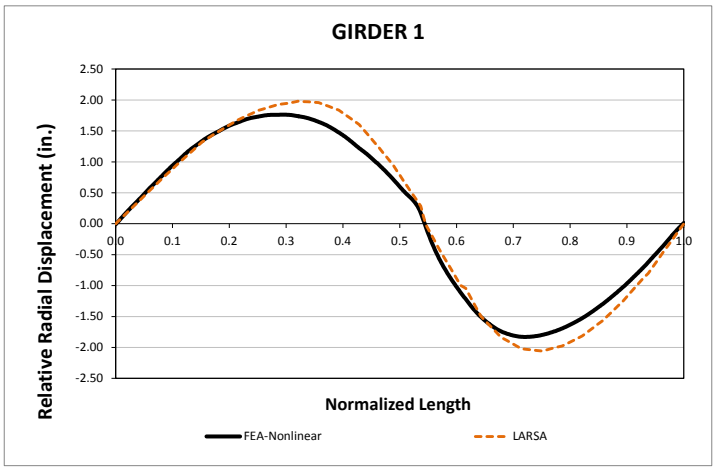

Fig. 6. Relative Radial Displacements, Stage 48

Conclusions:

This bridge has relatively large dimensions as compared to other structures that are part of the parametric study. Regardless its magnitude, the bridge does not have significant irregularities in its geometry that could accentuate the three dimensional response observed in other of the studied bridges. The effects of the skew are negligible, as shown in Figure 6, where the girder layovers are less than 2.0 in. over the 700 ft of the bridge length. Therefore, a simple girder line analysis would be enough to predict the geometry and the stresses of this bridge during construction.

I3.8 NICSS27 (New, I-girder, Continuous-span, Straight, Skewed supports)

Category Data:

L_1 = 350 ft, L_2 = 350 ft / w = 80 ft /θ_1 = 0°, θ_2 = 35°, θ_3 = 0°, 9 girders

Cross-Frame Detailing Method: NLF

Erection Stages Analyzed: 7 (Analyses are performed assuming NLF)

Deck Placement Sequence: 1 Stage

Bridge Perspective & Plan Views:

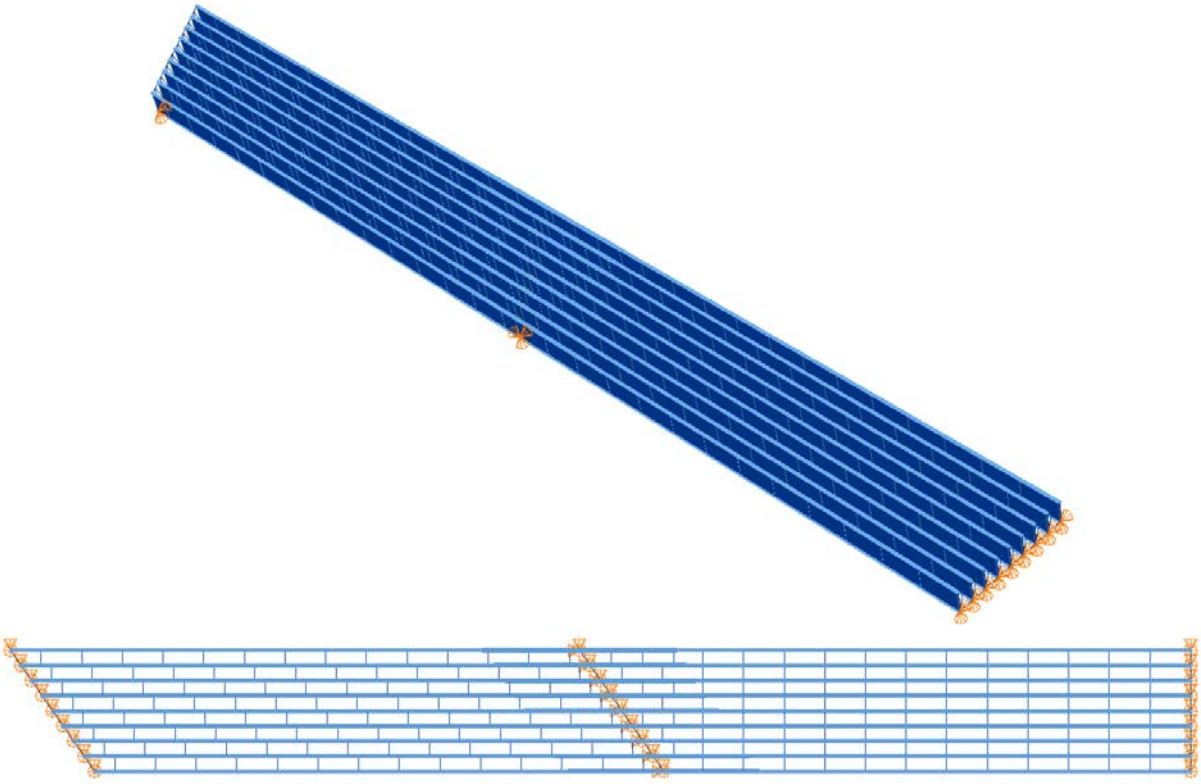

Abbreviated Analysis Results

Figure 1 shows different analysis stages which are considered to evaluate the different analysis methods.

Figure 2 provides the vertical displacements of the bottom girder (Girder 1) under total dead load. Figure 3 shows the vertical displacements of the top girder (Girder 9) under total dead load. Vertical displacements are accurately predicted by the approximate methods. There are minor differences between the results which can be handled in haunches. Figures 4 and 5 show fascia girder relative lateral displacement predictions under total dead load. It is clear from Figs. 4 and 5 that the end layovers are predicted accurately at the skewed ends. However, the layovers cannot captured accurately within the span by grid solutions. This reasons for this behavior is explained in the previous reports. Figure 6 shows the lateral deflections of the top and bottom flanges from linear and nonlinear 3D FEA for Girder 9. It is observed form Fig. 6 that the deflection patterns of the top and bottom flanges are significantly different for linear and nonlinear solutions. Although the layover of the girders is similar for linear and nonlinear analyses the top and bottom flanges shift laterally due to the overall geometric nonlinearity. Longer span lengths in bridges exacerbate the nonlinear effects since the major-axis bending stresses gets larger. Figures 7 and 8 provide fascia girder top flange major-axis bending stress predictions under total dead load. The major-axis bending stresses are accurately predicted by approximate methods for girders 1 and 9. This is the case for all girders.

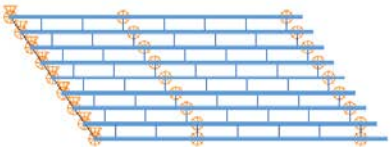

Stage 18

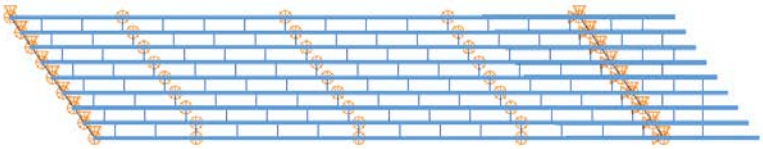

Stage 36

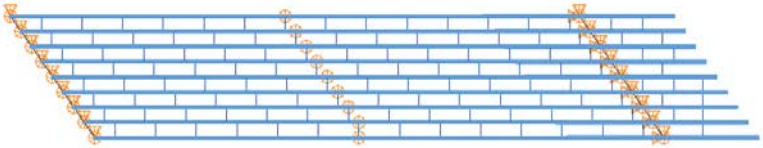

Stage 37

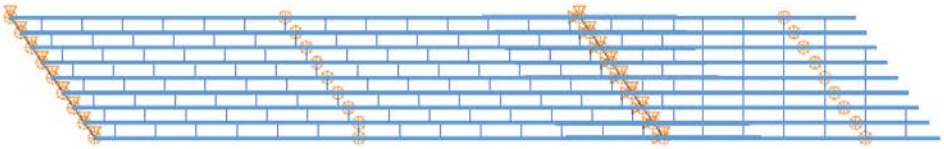

Stage 46

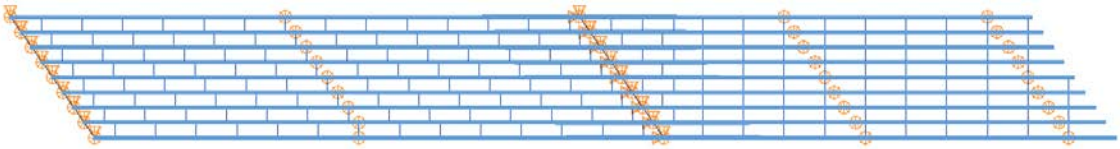

Stage 55

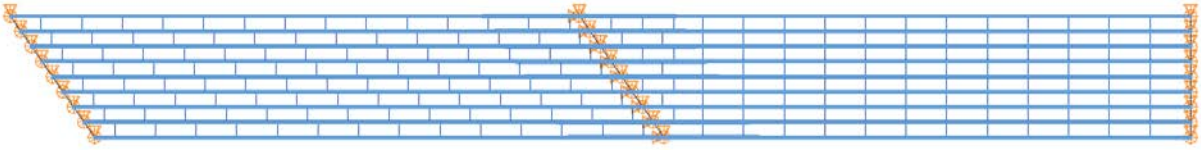

Stage 66 & 67

Fig. 1. NICSS27, Considered different analysis stages.

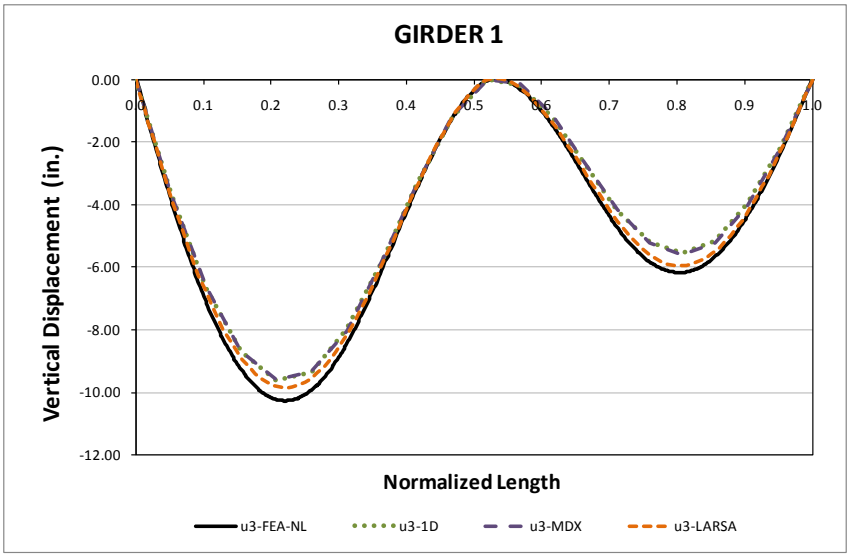

Fig. 2. NICSS27, Vertical displacements under total dead load for NLF detailing.

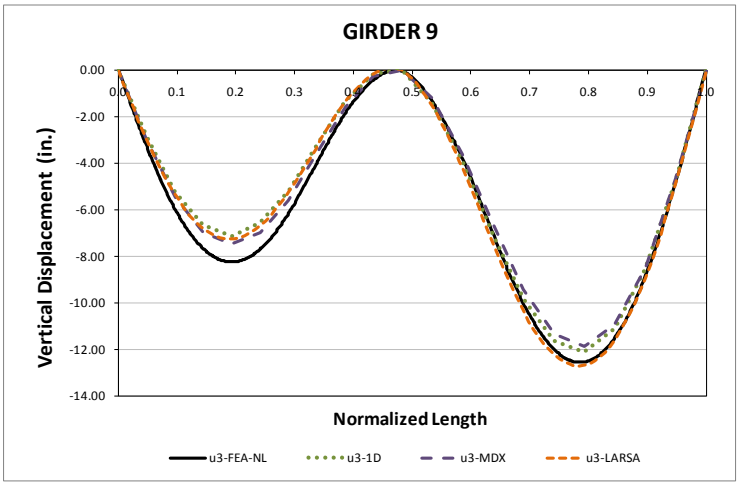

Fig. 3. NICSS27, Vertical displacements under total dead load for NLF detailing.

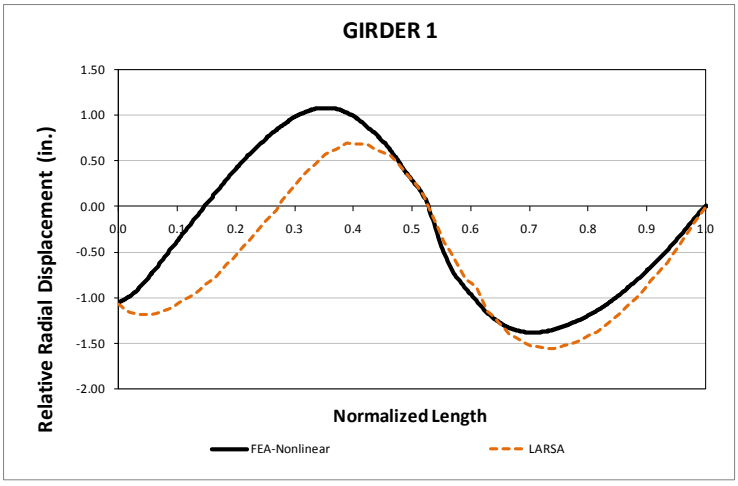

Fig. 4. NICSS27, Relative lateral displacements under total dead load for NLF detailing.

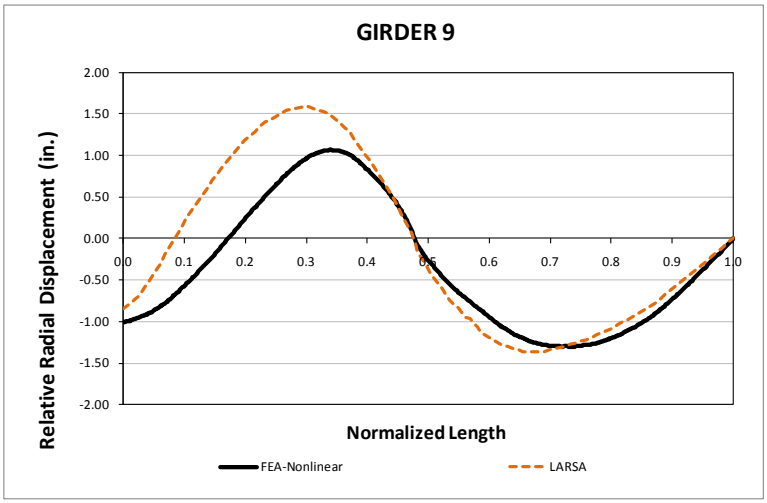

Fig. 5. NICSS27, Relative lateral displacements under total dead load for NLF detailing.

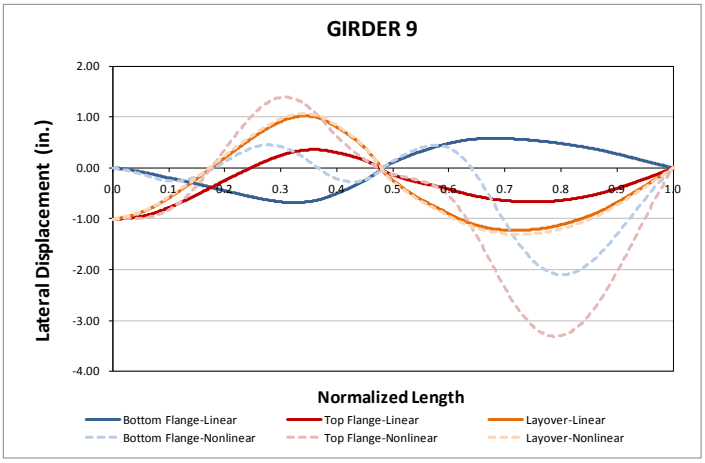

Fig. 6. NICSS27,lateral displacements under total dead load for NLF detailing.

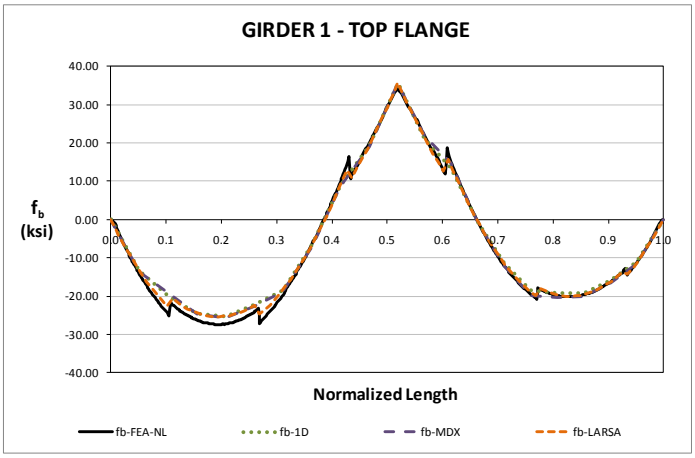

Fig. 7. NICSS27, Major-axis bending stresses under total dead load for NLF detailing.

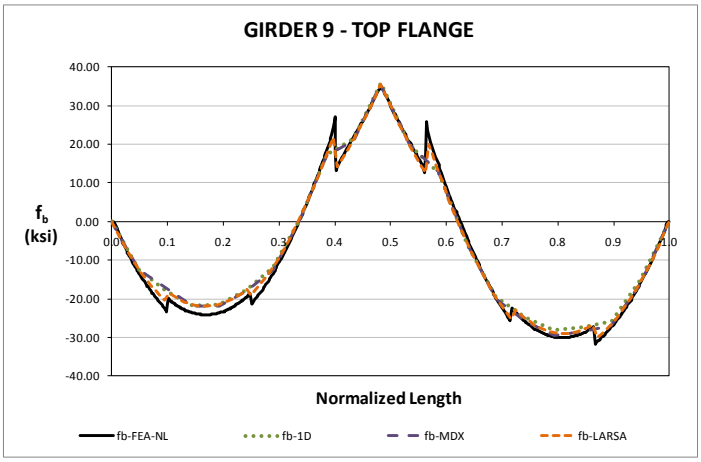

Fig. 8. NICSS27, Major-axis bending stresses under total dead load for NLF detailing.

I3.9 XICSS5 (eXample, I-girder, Continuous-span, Straight, Skewed supports)

Bridge Description:

NHI continuous straight skewed I-girder bridge example, documented in NHI Course No. 130081A-D (Design Manual, Design Examples), 2007

Category Data:

L_1 = 140 ft, L_2 = 175 ft, L_3 = 140 ft / w = 43 ft / θ = -60^o (all bearing lines), 4 girders.

References:

NHI Course No. 130081A-D (Design Manual, Design Examples), 2007

Cross-Frame Detailing Method: NLF

Steel Erection Stages Analyzed: Eight

Deck Placement Sequence: Four stages

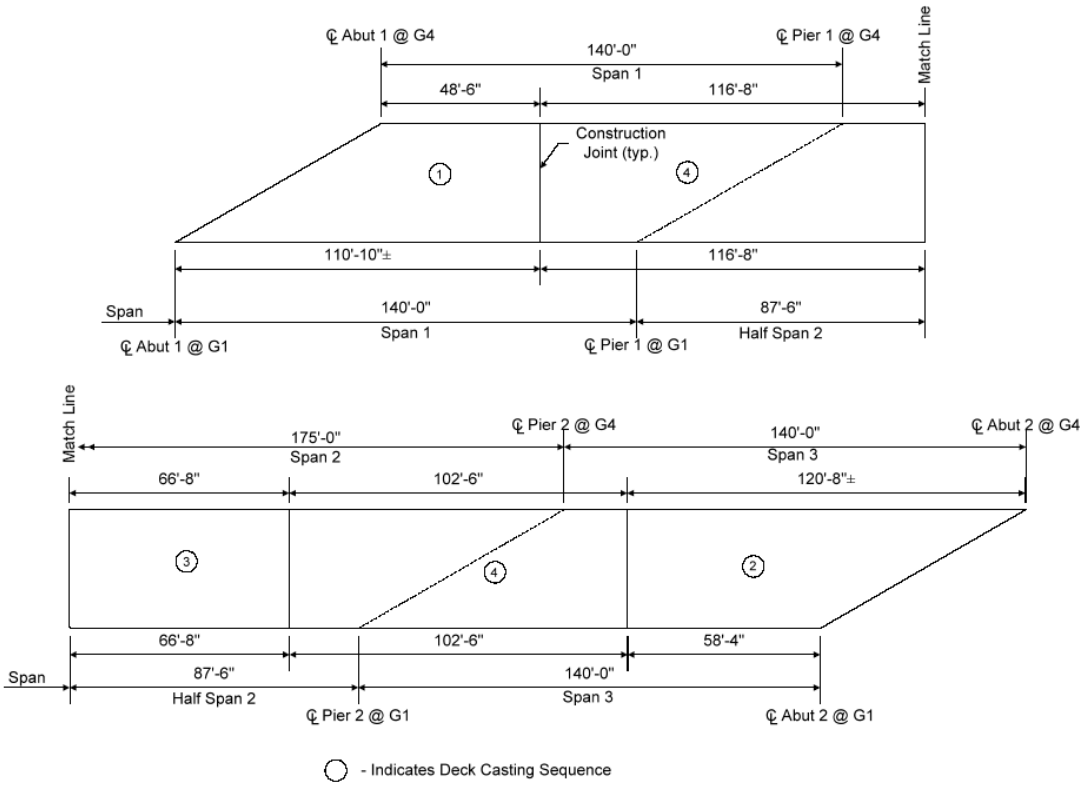

Bridge Perspective & Plan Views:

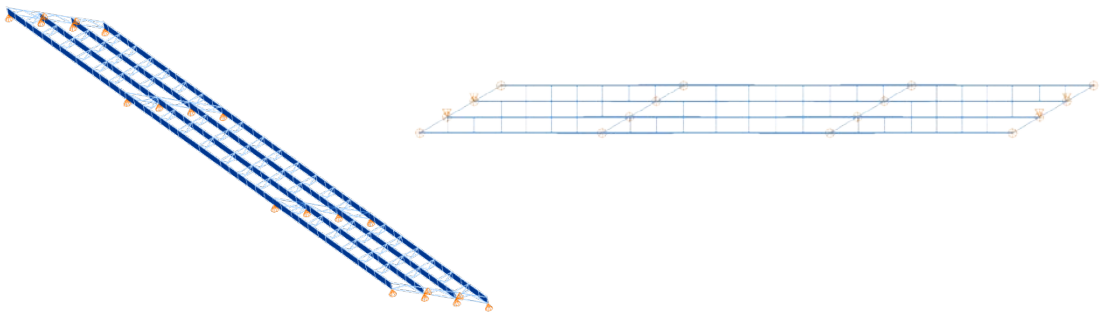

Abbreviated Analysis Results:

In this bridge the effects of the skewed parallel supports as well as continuity over the intermediate supports are investigated. In addition, the influence of sequential deck placement on the behavior of the bridge is studied.

Figure 1.a shows the vertical displacement response of Girder G2 for the steel dead load condition for the completed structure (Stage 12). As shown in the figure, this response is accurately predicted by all the methods. The differential deflections introduced by the parallel skewed supports have minimal influence in the behavior of the bridge for this particular response. With respect to the relative radial displacements of the top and bottom flanges (i.e., the layover of the girders), the limitations of the 2D grid model to represent the torsional behavior of the structure are more evident. Figure 1.b shows this response for the same girder. As shown, the magnitude of the displacements is under predicted; however, both responses have a similar trend. A similar behavior is observed in the other three girders of the bridge.

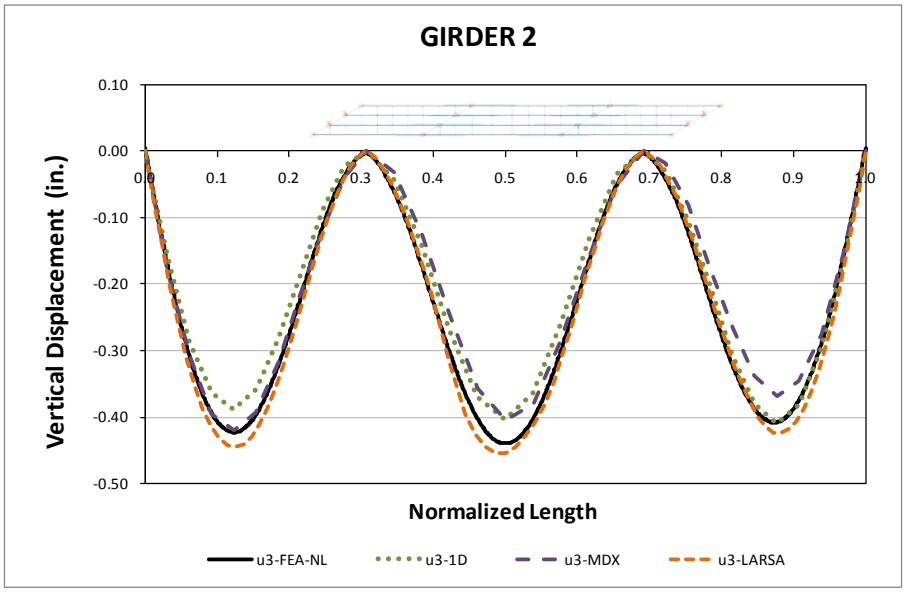

a) Vertical Displacements

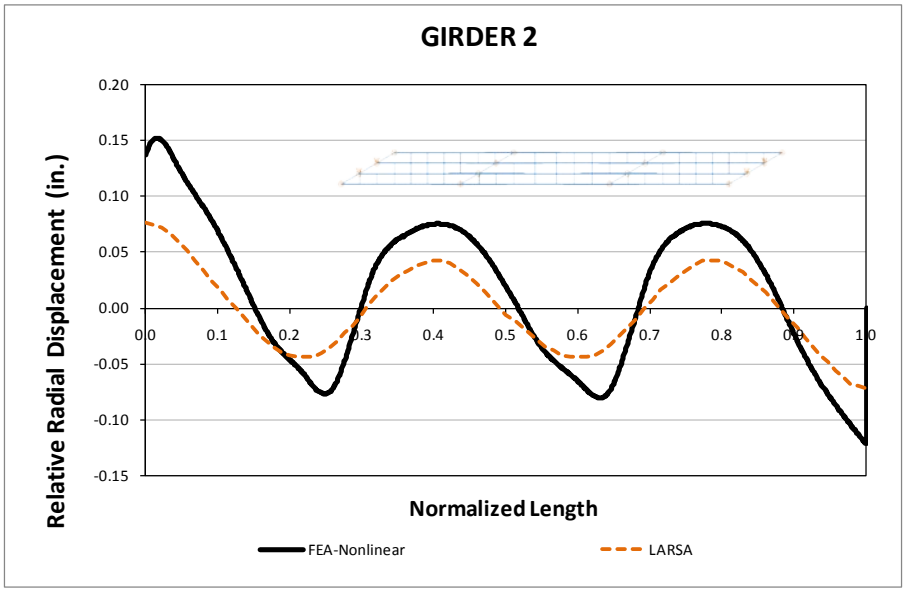

b) Relative Radial Displacements

Fig. 1. XICSS5, Comparison of Displacement Response – Stage 12

The major-axis bending stress response is also accurately represented by the approximate methods. Figure 2 shows the comparison for the top flange of girder G2. As shown, a line girder analysis is sufficient to capture the response as predicted by the 3D reference model. Similarly, the Larsa 2D grid model captures the stress response accurately. The MDX solution predicts somewhat larger major-axis bending stresses compared to the other solutions; the reason for this result has not been determined at the present time. As with the displacements, the skew effect is negligible for this response, having accurate representations for both the positive and negative moment regions. The same trend is observed in the rest of the girders of the bridge.

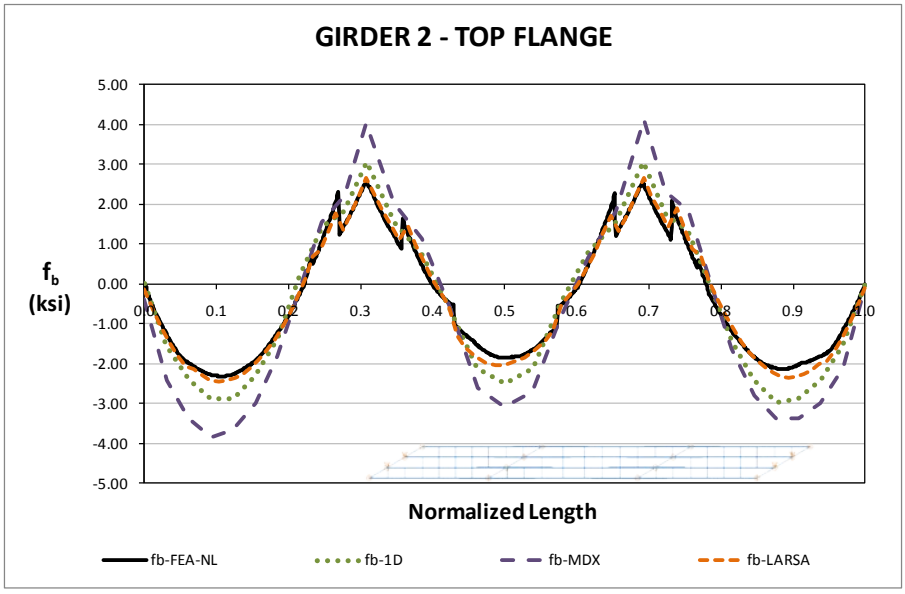

Fig. 2. XICSS5, Comparison of Major-Axis Bending Stress Response – Stage 12

Other aspects studied in this bridge are the effects of the deck placement sequence on the behavior. For this purpose two FE models were analyzed; one that followed the proposed sequence and another that considered the application of the concrete load in a single step. The second model is equivalent to the case where the concrete for the entire deck is placed at once. For identification purposes, the first model is referred to as "SDP," for "Sequential Deck Placement," and the second model as "NSDP."

Figure 3 shows the comparison between vertical deflections for the SDP and NSDP models in girder G2. It is observed from the plot that the deck placement sequence has a moderate influence on this response. In the proposed deck placement sequence the positive moment regions of the exterior spans are placed first. As expected, the deflections are larger in these spans. When the concrete in the positive moment region in the interior span is placed, the deflections in the center span are smaller than those predicted by the NSDP model, since the end spans work compositely. In addition, the upward displacements in the end spans due to the center span concrete load are not as large due to the composite action of the end spans. The overall result is that the sequential deck placement tends to increase the deflections in the regions where the concrete is placed first and decrease them in other regions.

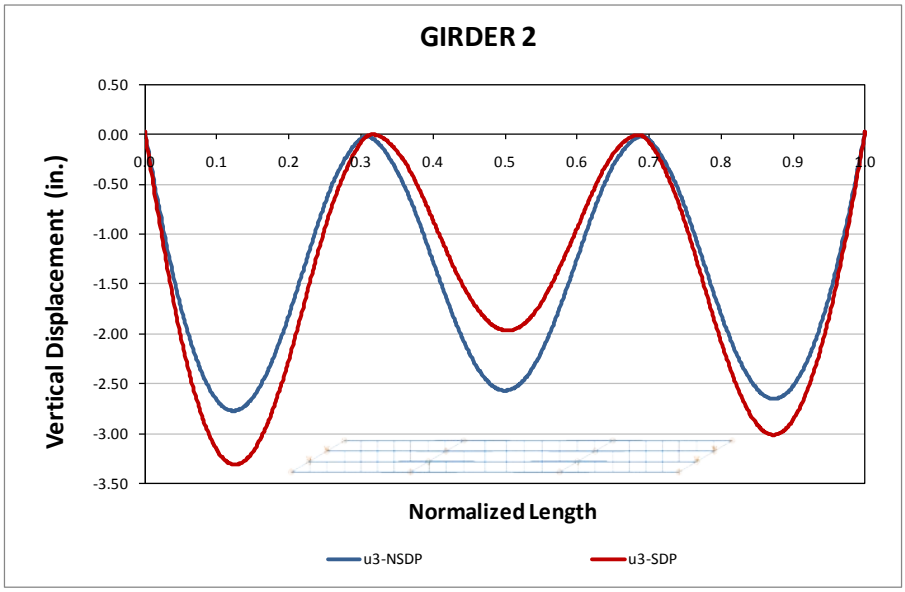

Fig. 3. XICSS5, *Comparison of Vertical Displacement Responses between a Sequential Deck Placement Analysis and a Single Step Analysis – Girder G2*

With respect to the lateral displacements, the influence of the sequential deck placement is small for this bridge. Figure 4 shows the relative radial displacement responses for the two analyzed cases in girder G2. It is observed that the deck placement sequence tends to increase the magnitude of the displacements in the spans where the concrete is placed first, and decrease them in the last regions. However, these effects are rather small.

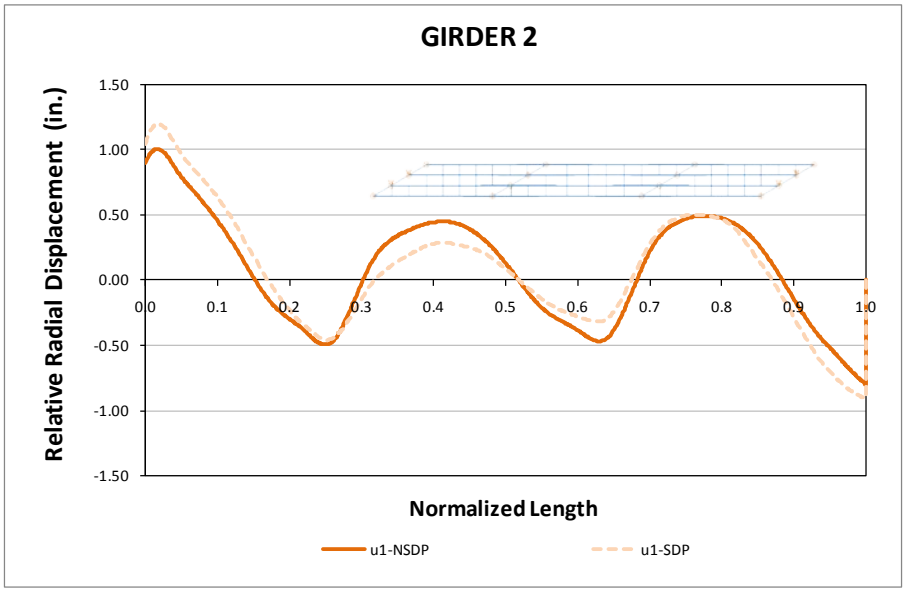

Fig. 4. XICSS5, Comparison of Relative Radial Displacement Responses between a Sequential Deck Placement Analysis and a Single Step Analysis – Girder G2

Figure 5 shows a comparison of the major-axis bending stresses in the top flange. The responses are similar from all of the models. As in the previous cases, the response is larger in the first pouring regions and smaller in the last region. In the negative moment regions, where the concrete is placed last, the responses are essentially the same. Notice also that in this bridge, the flange lateral bending stresses are very small and are not significantly affected by the casting sequence.

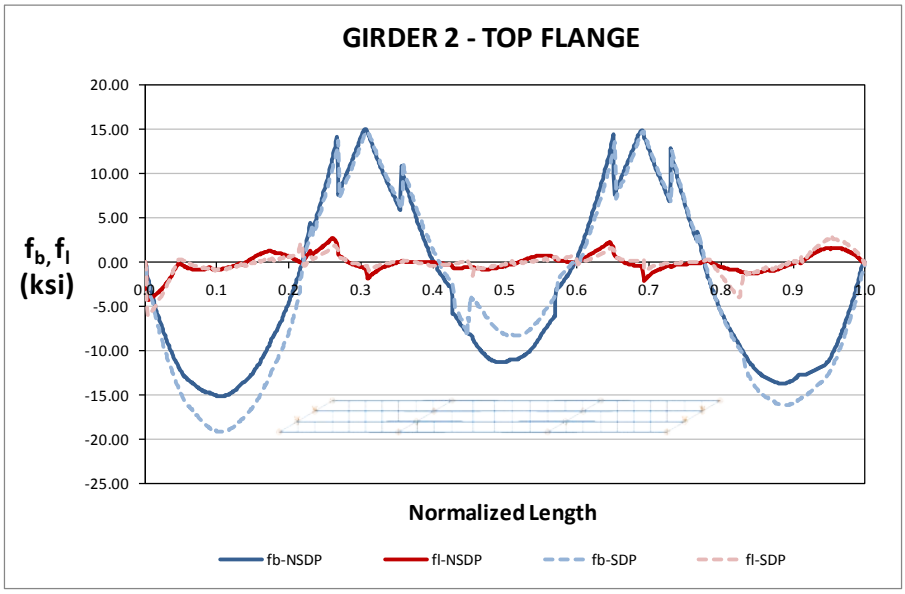

Fig. 5. XICSS5, Comparison of Bending Stresses between a Sequential Deck Placement Analysis and a Single Step Analysis – Girder G2

Conclusions:

In this bridge, the effects of parallel skewed supports and the continuity of spans are analyzed. It is apparent from this study that the skew has little effect in the system response. The geometry in terms of vertical and radial displacements is not substantially affected by these factors. All the methods are accurate enough to capture the expected behavior of the bridge. The same conclusion is drawn for the major-axis bending stresses. A 1D analysis seems to be sufficient for computing these stresses.

The analysis of the bridge response considering the hardening of the concrete due to the sequential deck placement appears to have a minor effect as compared to a one-step deck placement analysis. In general, the response magnitudes for displacements and stresses are increased in the regions where the concrete is placed first and reduced in the last regions. The largest effects are observed in the vertical displacement response. This is a factor that generally should be considered when determining the camber of the bridge girders. For the rest of responses, an analysis using the 1D or 2D methods considering the deck placement in a single step is sufficient for design purposes.

I4.1 EISCR1 (Existing, I-girder, Simple-span, Curved, Radial supports)

Bridge Description:

FHWA Curved Composite I-Girder Test Bridge

Category Data:

L_{as} = 90 ft / R = 200 ft / w = 23.5 ft, 3 girders

References:

Jung and White (2008), Chang and White (2008)

Cross-Frame Detailing Method: NLF

Steel Erection Stages Analyzed: Three

Deck Placement Sequence: One stage

Bridge Perspective & Plan Views:

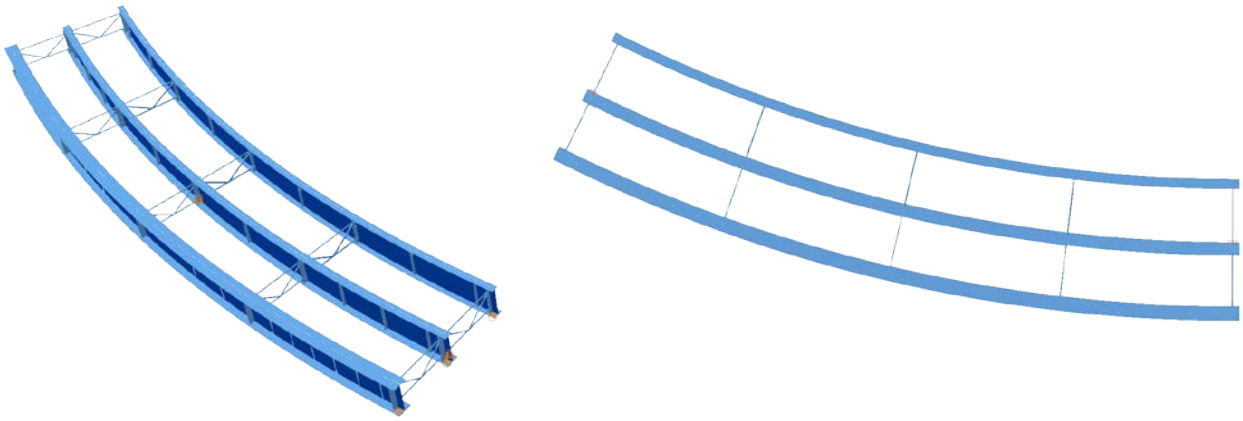

Abbreviated Analysis Results:

The FHWA Test Bridge is one of the simplest structures studied in the NCHRP 12-79 Project. It is comprised of just three I-girders, two end cross-frames and three interior cross-frames. However, this is one of the most challenging bridges for simplified analysis models to capture the structural behavior. For many of the responses analyzed, the results obtained from the approximate methods differ substantially from the 3D FE model. For Stage 1, with just the interior and middle girders erected (Girders G2 and G3), the vertical displacements as well as the major axis bending stresses, f_b, are significantly different in the simplified analysis models compared to the rigorous 3D FEA solution. Figure 1.a shows that the 2D grid model vertical displacements are almost an order of magnitude larger than the benchmark in girder G2. Similarly, the relative radial displacements are misrepresented. Figure 1.b shows that the 2D model predicts the radial displacements much better at the position of the cross-frames than within the unbraced lengths. However, even at the cross-frame locations, the 2D model predicts radial displacements that are more than two times the displacements predicted in the 3D analysis.

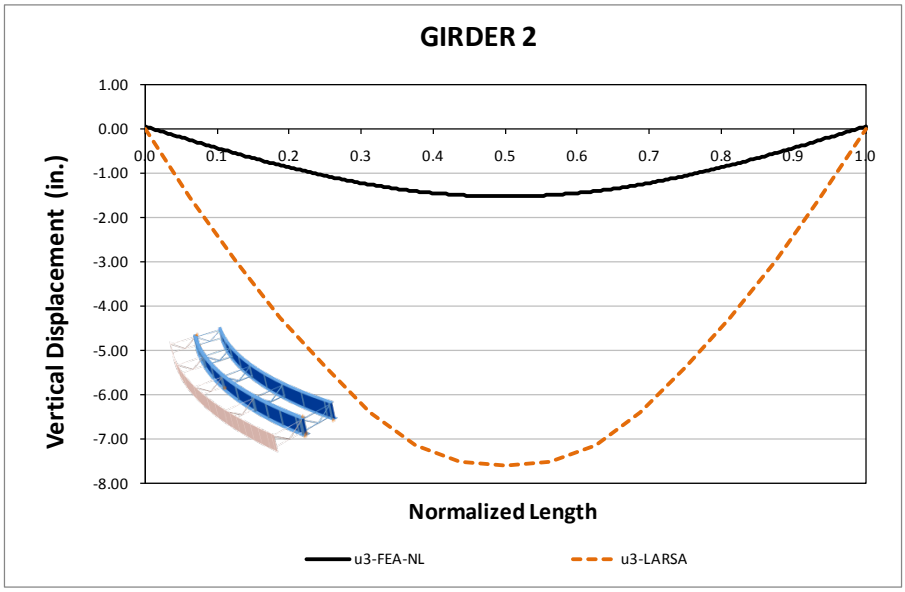

a) Vertical Displacements

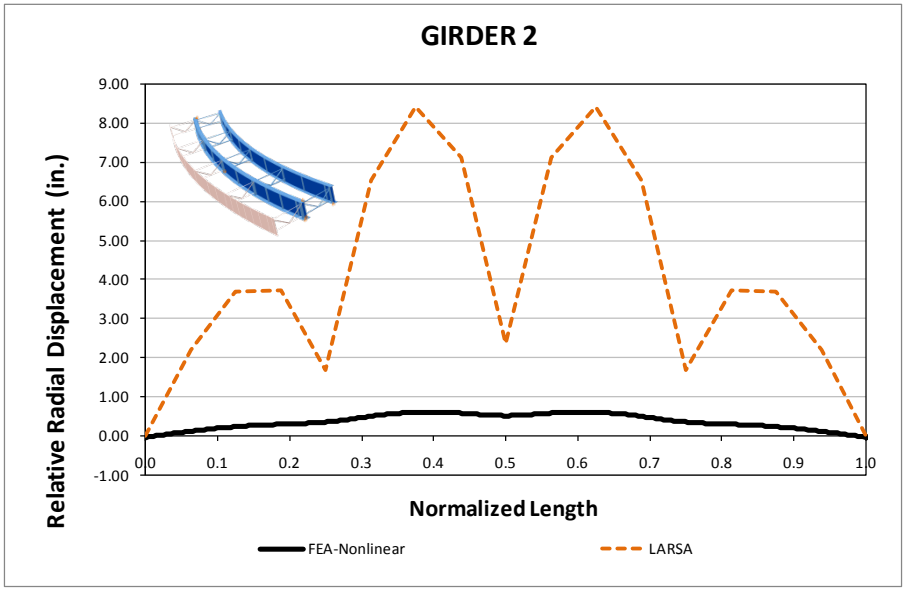

b) Relative Radial Displacements

Fig. 1. EICSR1, comparison of displacements – Stage 1.

A similar trend is observed in the major-axis bending stress response f_b. Figure 2 shows a comparison between the f_b predicted by 2D and 3D models for the bottom flange of girder G3. The response predicted by the approximate method is shifted substantially with respect to the 3D model response. However, the 2D solution closely predicts the variation in f_b relative to the cross-frame positions in each of the unbraced lengths. Thus, for this particular stage, it can be said that the major-axis bending behavior of the individual member is captured by the grid model, but the group response and the transfer of the loading from one girder to the adjacent one through the cross-frames are not captured correctly.

The flange lateral bending stress, f_ℓ, prediction is not considered for this case. The 2D model does not directly provide results for this response. These stresses are predicted using the formula in the AASHTO LRFD commentary, originally developed with the V-Load method, which uses an equivalent flange radial distributed load proportional to the major-axis moment. Since the major-axis bending response is substantially misrepresented, the flange lateral bending response cannot be expected to be accurate.

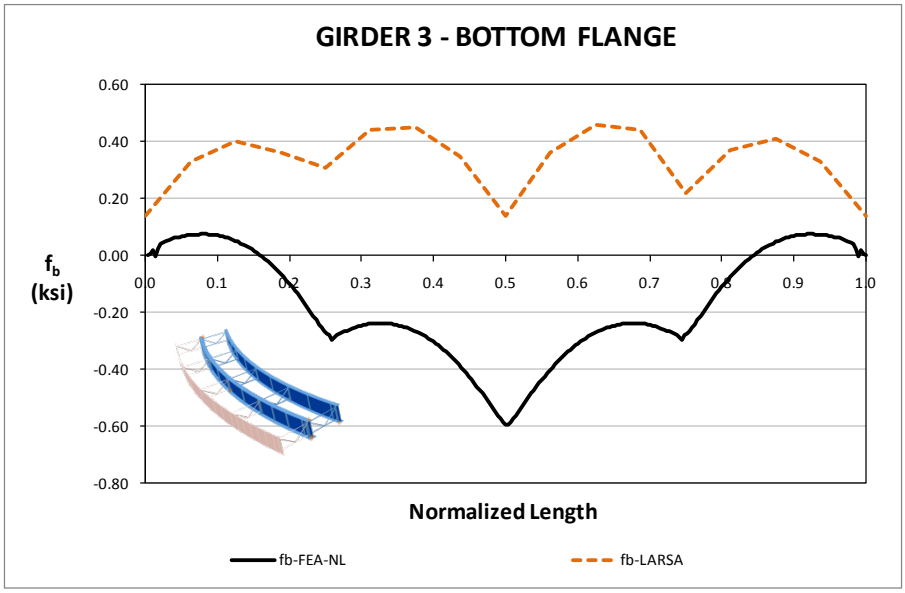

Fig. 2. EISCR1, comparison of major-axis bending stresses – Stage 1

The response of the bridge at the end of the deck placement (Stage 4) is summarized next. For this stage, the results available from the 1D analysis (using the implementation of the V-Load method in VANCK) and two 2D grid models are considered for comparison against the 3D model. Figure 3.a shows the vertical displacement response for the exterior girder, G1. The trend observed for the 2D grid models in Stage 1 is again observed here. That is, the 2D grid predictions are poor. The 1D analysis provides the best fit to the 3D model prediction. In the case of the radial displacements, presented in Figure 3.b, the 2D model representation is close to the benchmark solution at the cross-frame locations. Within the unbraced lengths, the 2D model overestimates the displacements giving invalid results.

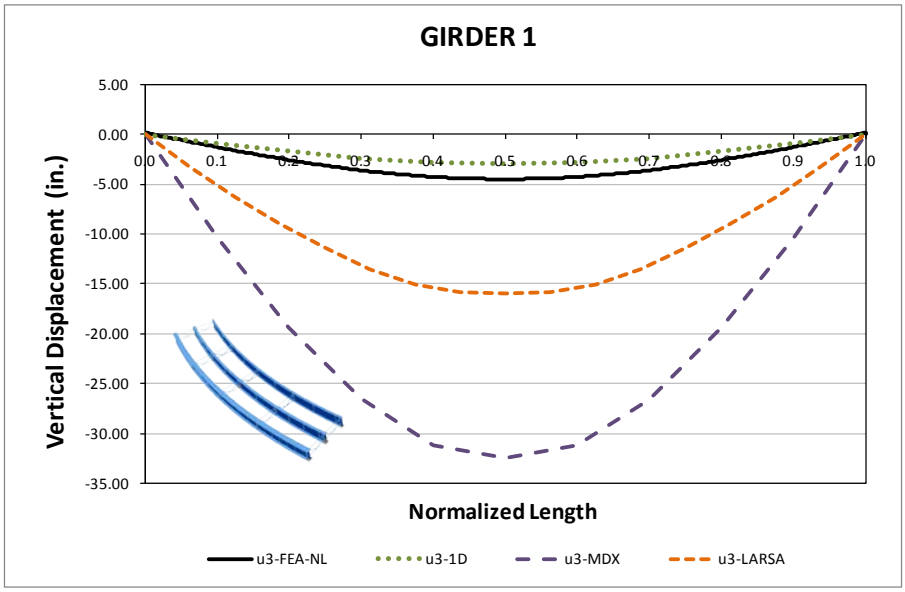

a) Vertical Displacements

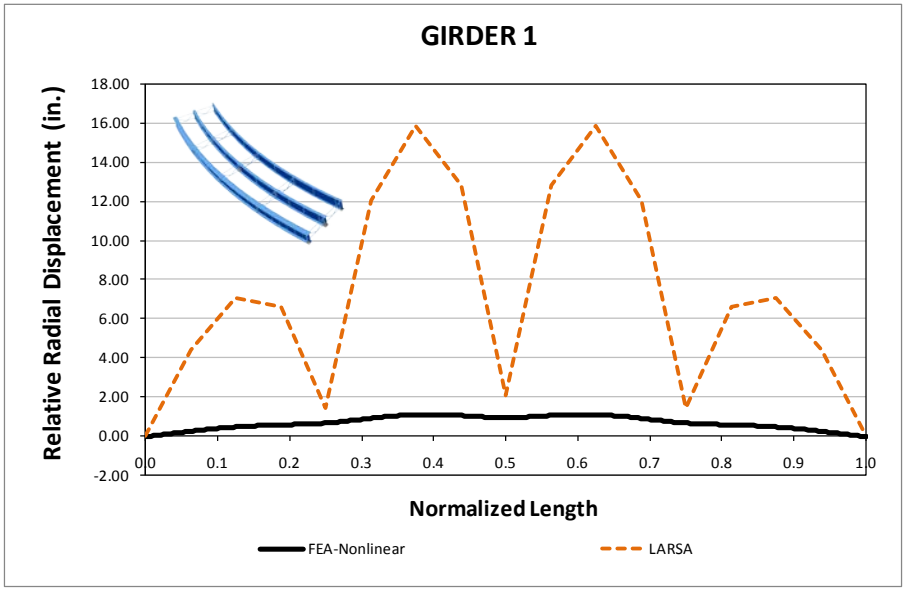

b) Relative Radial Displacements

Fig. 3. EISCR1, comparison of displacements – Stage 4.

For the major-axis bending stresses, the approximate method predictions and the benchmark responses are compared for the exterior and the interior girders. Figures 4.a and 4.b show the responses for the bottom flanges of girders G1 and G3, respectively. As shown in the figures, the exterior girder response is predicted accurately by all the methods, while the interior girder response is overestimated by the 2D grid analyses and underestimated by the line girder analysis. The reasons for this difference are apparently associated with the transfer of the loads through the cross-frames and the consideration of the warping contributions to the overall stiffness of the system. The incapability of the 2D grid models to capture warping deformations appears to be the primary cause for the disparities observed for G3. The cross-

frames are essentially rigid compared to the flexibility of the girders in this problem; hence, errors in the representation of the cross-frame stiffnesses do not have any important effect for this bridge.

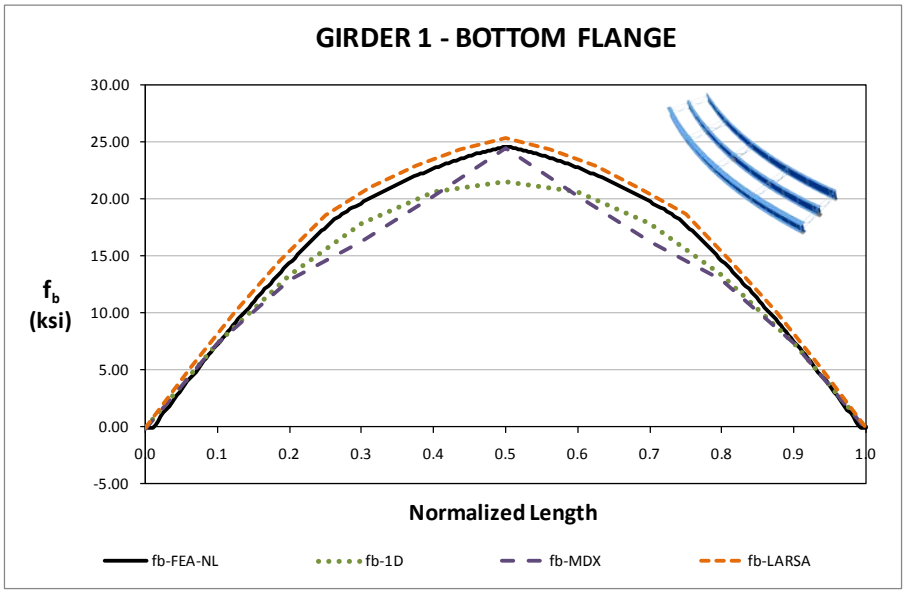

a) Exterior Girder, G1

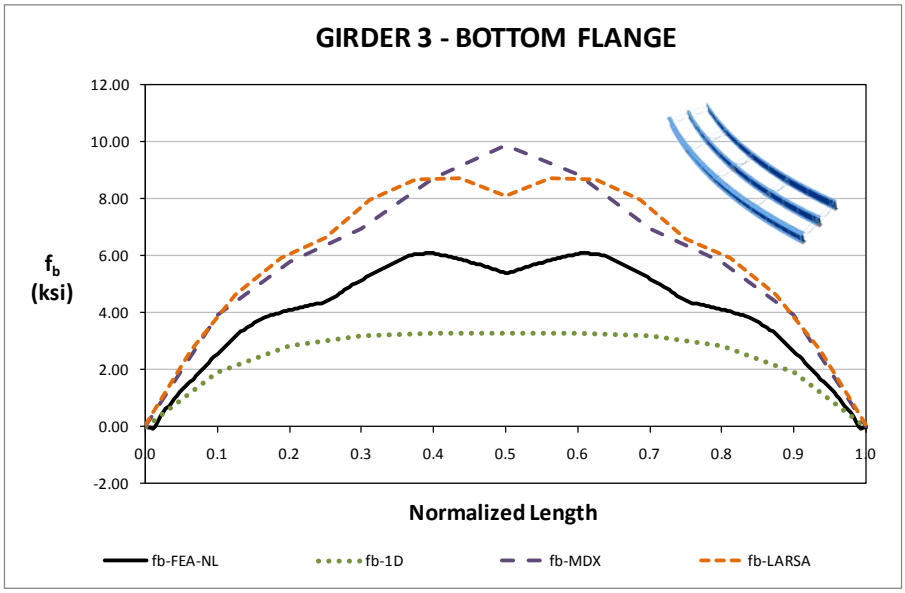

b) Interior Girder, G3

Fig. 4. EISCR1, comparison of major-axis bending stresses – Stage 4.

A comparison of the flange lateral bending stresses is shown in Figure 5 for the bottom flange of girder G1. The results obtained from the formula in the AASHTO commentary, often referred to as the V-Load formula, provide a good estimate of the results obtained from the rigorous FEA solution at the braced points. Note that the V-load formula takes the maximum moment within each unbraced length as one of its inputs and gives an estimate of the maximum flange lateral bending stress in each of the unbraced lengths. Therefore, Fig. 5 shows a single constant value for the f_ℓ from the V-load equation in each

unbraced length. The 3D FEA solution gives the only calculation of the actual distribution of the f_ℓ values along the girder length. To facilitate the comparison with the simplified analysis results, the dark black line, labeled FEA-max, plots the maximum f_ℓ (determined from the rigorous 3D FEA solution for each unbraced length) as a constant value for each unbraced length.

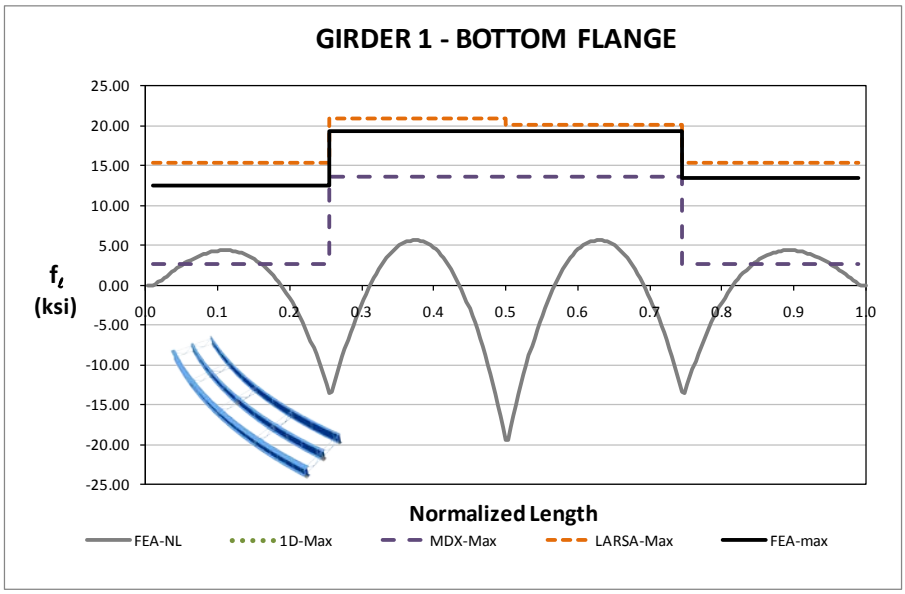

Fig. 5. EISCR1, comparison of flange lateral bending stresses – Stage 4.

Conclusions:

Although this bridge is relatively basic, it is an excellent case to test the capabilities of the approximate methods for predicting the different responses. The larger unbraced lengths in this bridge exacerbate the effect of neglecting the warping stiffness contributions to the error in the prediction of vertical displacements for the 2D grid models. A 1D girder line analysis proves to be a better representation for evaluating this response. With respect to the radial displacements, it is observed that the 2D models are able to capture the overall layover of the bridge at the cross-frame locations. However, they are not able to capture the twisting of the individual girders between these brace points. This is a consequence of the lack of any consideration of warping torsion by the 2D-grid I-girder elements.

The major-axis bending stress response is less affected by the lack of consideration of warping torsion in the simplified analysis models. The approximation of the cross-frame responses by a single beam element may be a key factor that can affect the predictions in some bridges. However, for this bridge, the cross-frames respond nearly as rigid components. The influence of the cross-frame models on the bridge responses will be studied in more detail in the future, considering other bridges where the cross-frame deformations are more significant.

In the case of the flange lateral bending stress responses, the V-Load formula seems to be a good predictor of this response for this bridge. Its accuracy, however, depends on the accuracy in the prediction of the major-axis bending response.

I4.2 NISCR2 (New, I-girder, Simple-span, Curved, Radial supports)

Category Data:

L_1 = 150 ft/ R_1 = 438 ft / w = 30 ft, 4 girders

Cross-Frame Detailing Method: NLF

Erection Stages Analyzed: 5 (Analyses are performed assuming NLF)

Deck Placement Sequence: 1 Stage

Bridge Perspective & Plan Views:

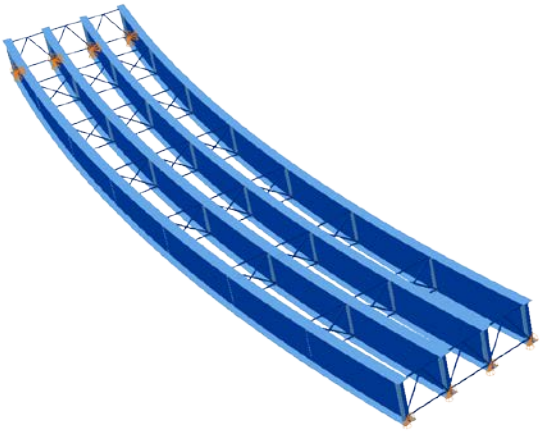

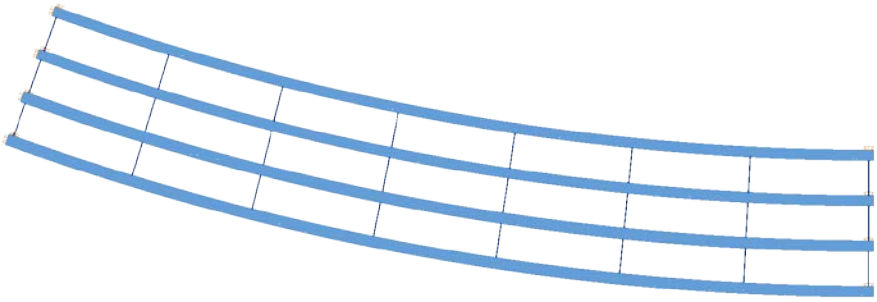

Abbreviated Analysis Results

Figure 1 shows the deflected shape of the bridge under the total dead load. Deflections are magnified by 25 times. It is observed from Fig. 1 that the top flanges are deflecting downward due to horizontal curvature. Figure 2 provides the vertical deflections for the outside girder (Girder 1) under the total dead load. Figure 2 shows that vertical deflections cannot be predicted accurately by any simplified analysis method. This is due to the inability of 1D and 2D solutions to account for the warping rigidity of the I-girders. Previous studies show that L_b/R ratio can affect the accuracy of predictions of the approximate methods. As L_b/R ratio gets smaller, better vertical displacement predictions are obtained from 2D grid analysis solutions. The effect of neglecting warping stiffness for 2D grid analysis methods becomes negligible for small L_b/R ratios. However, L_b/R ratio of 0.049 is obtained for this bridge, which results in error in the prediction of vertical displacements. Moreover, approximate methods cannot capture the nonlinearity of the system. Figure 3 shows relative radial displacement predictions under total dead load. Although previous studies show that 2D methods predict the relative radial displacements better at the cross-frame locations than within the unbraced lengths, small errors are observed at the cross-frame locations. This is believed to be from the global nonlinearity of the system.

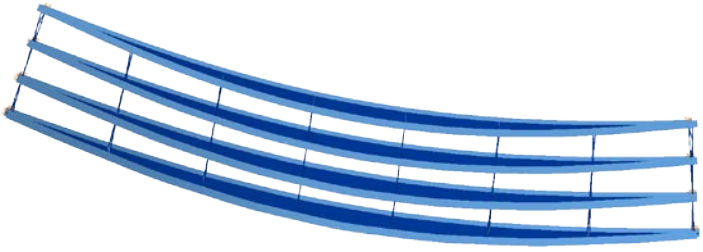

Fig. 1. NISCR2, Deflected shape under total dead load (Magnified 25x).

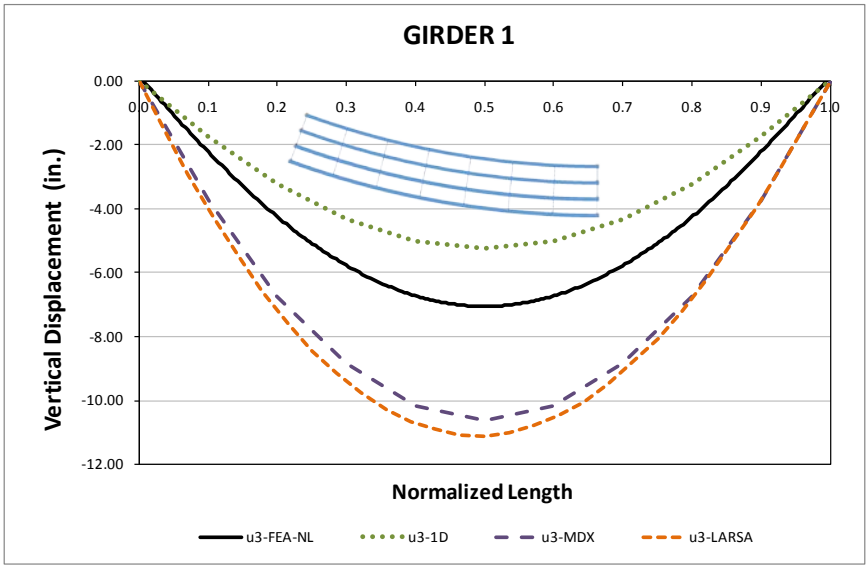

Fig. 2. NISCR2, Vertical displacements under total dead load for NLF detailing.

Figures 4 and 5 show fascia girder major-axis bending predictions predicted by 3D FEA linear, 3D FEA nonlinear and approximate methods under total dead load. The stress predictions are close to each other

for the outside girder. However, one can observe that there is a big difference in the predictions for the inside girder. This difference is primarily due to the nonlinearity of the system. Approximate methods cannot capture these nonlinear effects. Figure 6 shows the flange lateral bending stress predictions of the outside girder under total dead load. The main source of nonlinearity is due to global effects. 2D predictions are derived from the major-axis bending stresses. Flange lateral bending calculations for approximate methods are good as long as the major-axis bending stress predictions are close to the benchmark solutions. Although the stress predictions are close to each other on the outside girder, the calculated flange lateral bending stresses are off from the benchmark solutions. Similar to NISCR11, the global nonlinearity is dominant for this bridge. The actual second order amplifier is calculated as 1.369 for this bridge by comparing the 3D linear and nonlinear solutions. This kind of nonlinearity cannot be predicted by the amplifier equations described in AASHTO Article 6.10.1.6. This is because the amplifier equations are derived for individual unbraced lengths

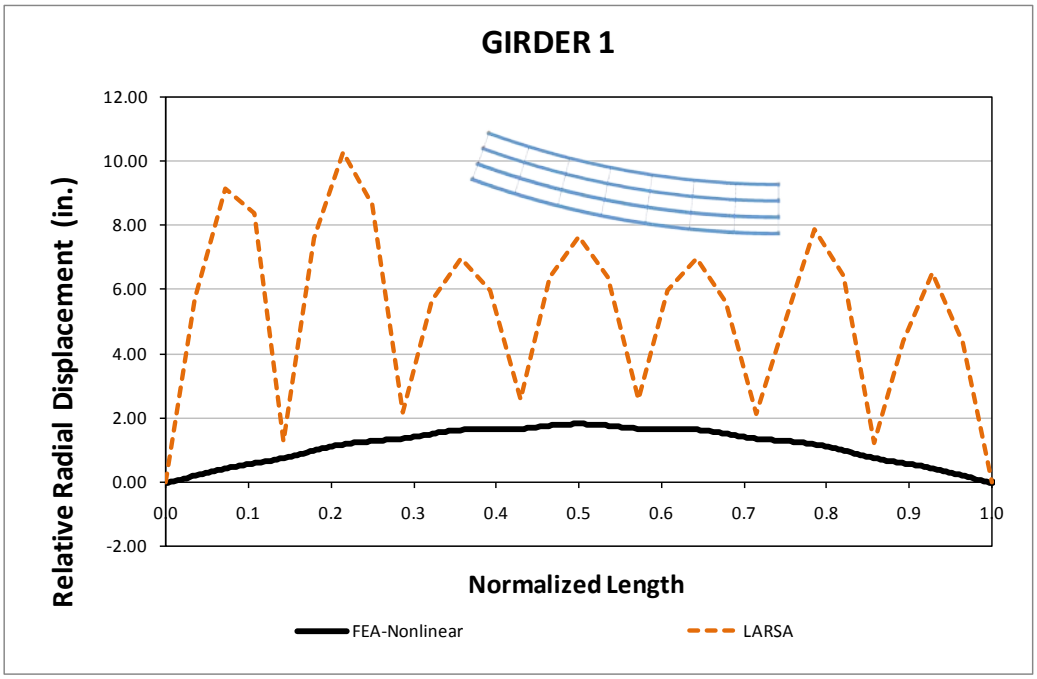

Fig. 3. NISCR2, Relative radial displacements under total dead load for NLF detailing.

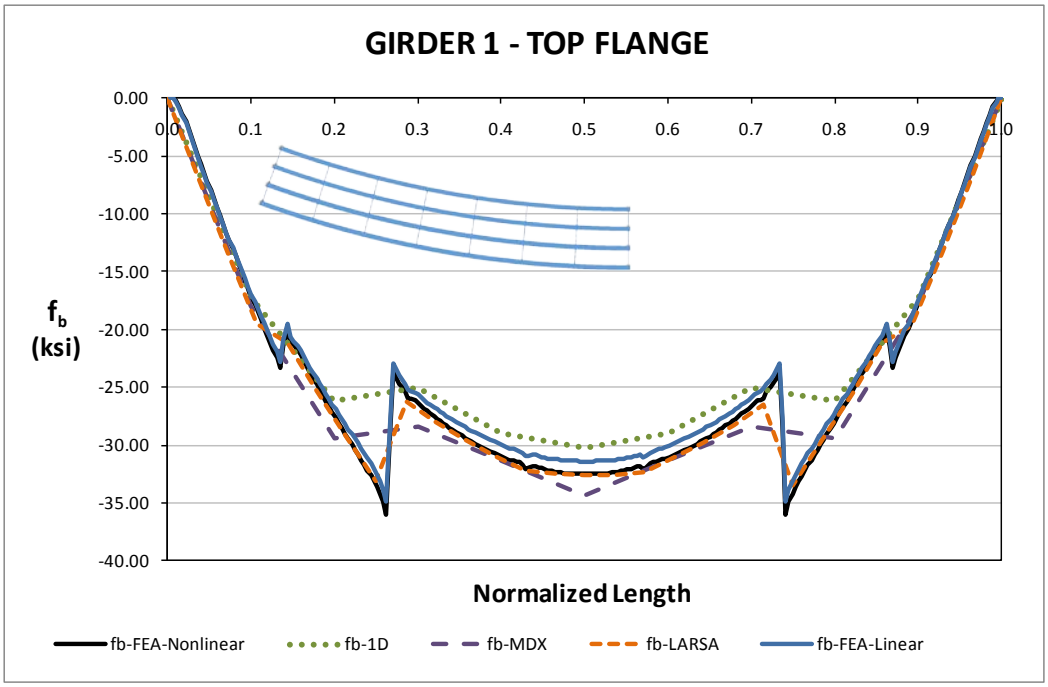

Fig. 4. NISCR2, Major-axis bending stresses under total dead load for NLF detailing.

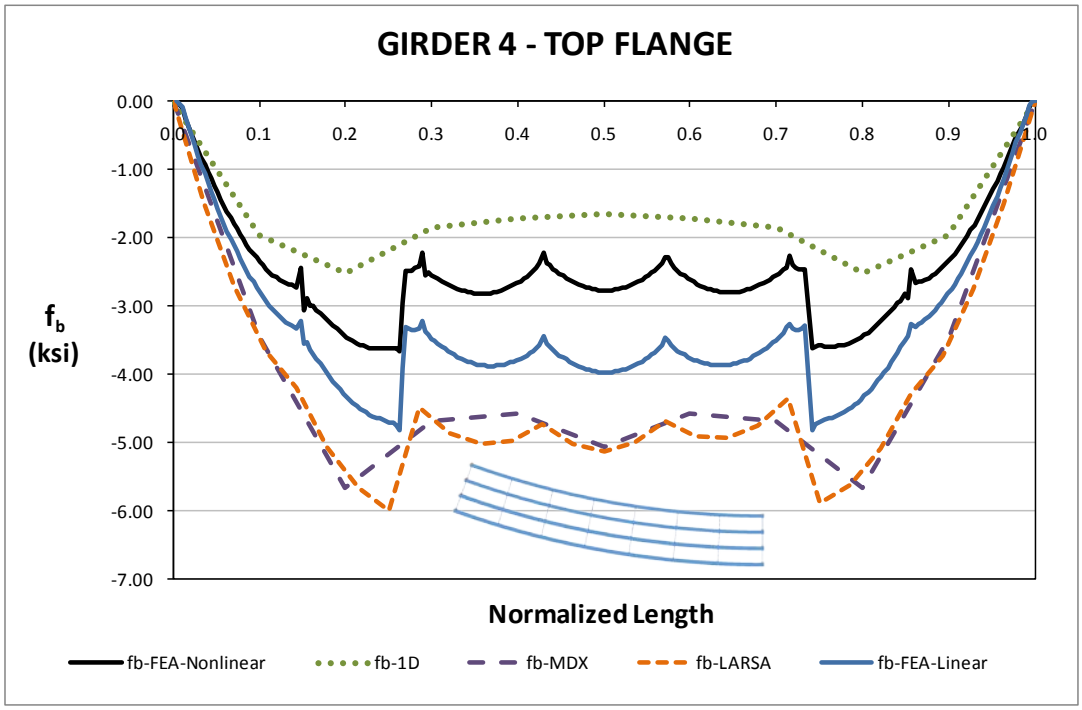

Fig. 5. NISCR2, Major-axis bending stresses under total dead load for NLF detailing.

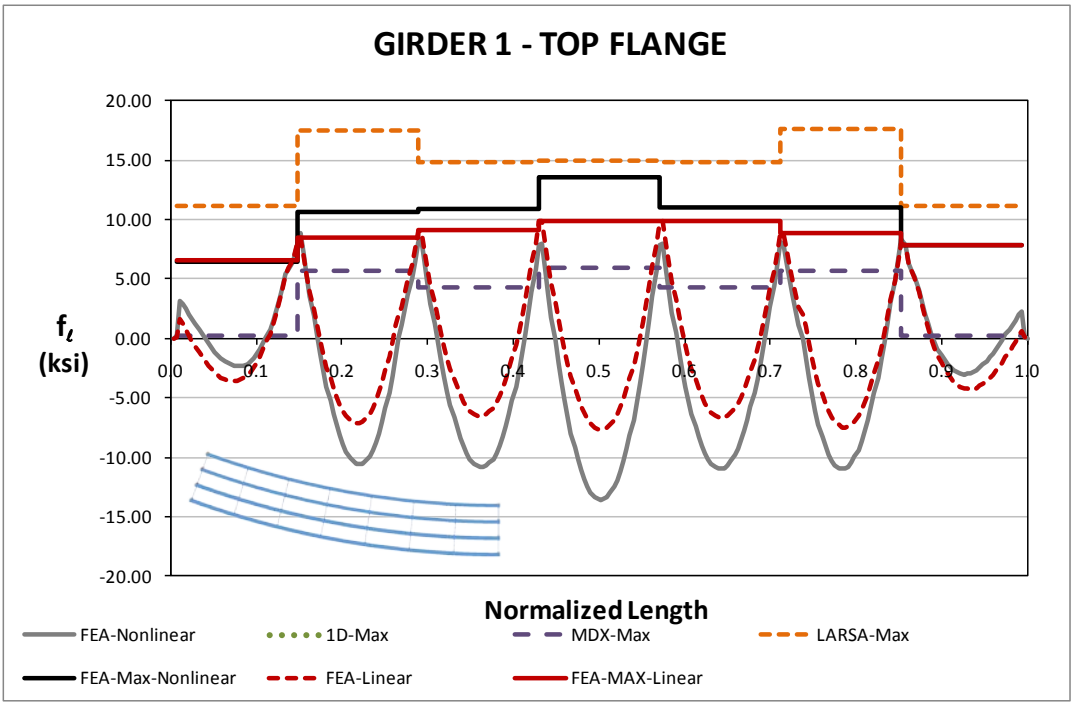

Fig. 6. NISCR2, Minor-axis bending stresses under total dead load for NLF detailing.

Conclusions:

It is observed from this bridge that the effect of neglecting the warping stiffness contributions lead to error in the prediction of vertical displacements for 2D grid models. Previous studies show that small L_b/R ratio increases the prediction accuracy of 2D grid solutions, as the effect of neglecting warping stiffness becomes negligible. However, L_b/R ratio of 0.049 results in error in the prediction of vertical displacements for this bridge.

In the case of radial displacements, it is observed that the 2D grid models better predict the relative radial displacements at the cross-frame locations. However, they are off within the unbraced lengths. Additionally, the displacements at the cross-frame locations are not very accurate due to high nonlinearity of the system.

Major axis bending stresses seem to be less affected by the warping contributions. However, nonlinearity in the system leads to prediction error mainly in the inside girder. Flange lateral bending stress response predictions are good as long as the major-axis bending responses are predicted accurately. This is mainly because they are derived from the major-axis bending stresses by using the V-Load formula. Although the stress predictions are close to each other on outside girder, the calculated flange lateral bending stresses are off from the benchmark solutions. This is due to the inability of the approximate methods to account for nonlinear effects.

It is important to identify the sources of nonlinearity. For this bridge, the source of nonlinearity is due to global nonlinear effects which cannot be predicted by the AASTHO amplifier equation. This is because this equation is derived for individual unbraced lengths.

I4.3 NISCR5 (New, I-girder, Simple-span, Curved, Radial supports)

Category Data:

L_1 = 300 ft/ R_1 = 1530 ft / w = 30 ft, 4 girders

Cross-Frame Detailing Method: NLF

Erection Stages Analyzed: 5 (Analyses are performed assuming NLF)

Deck Placement Sequence: 1 Stage

Bridge Perspective & Plan Views:

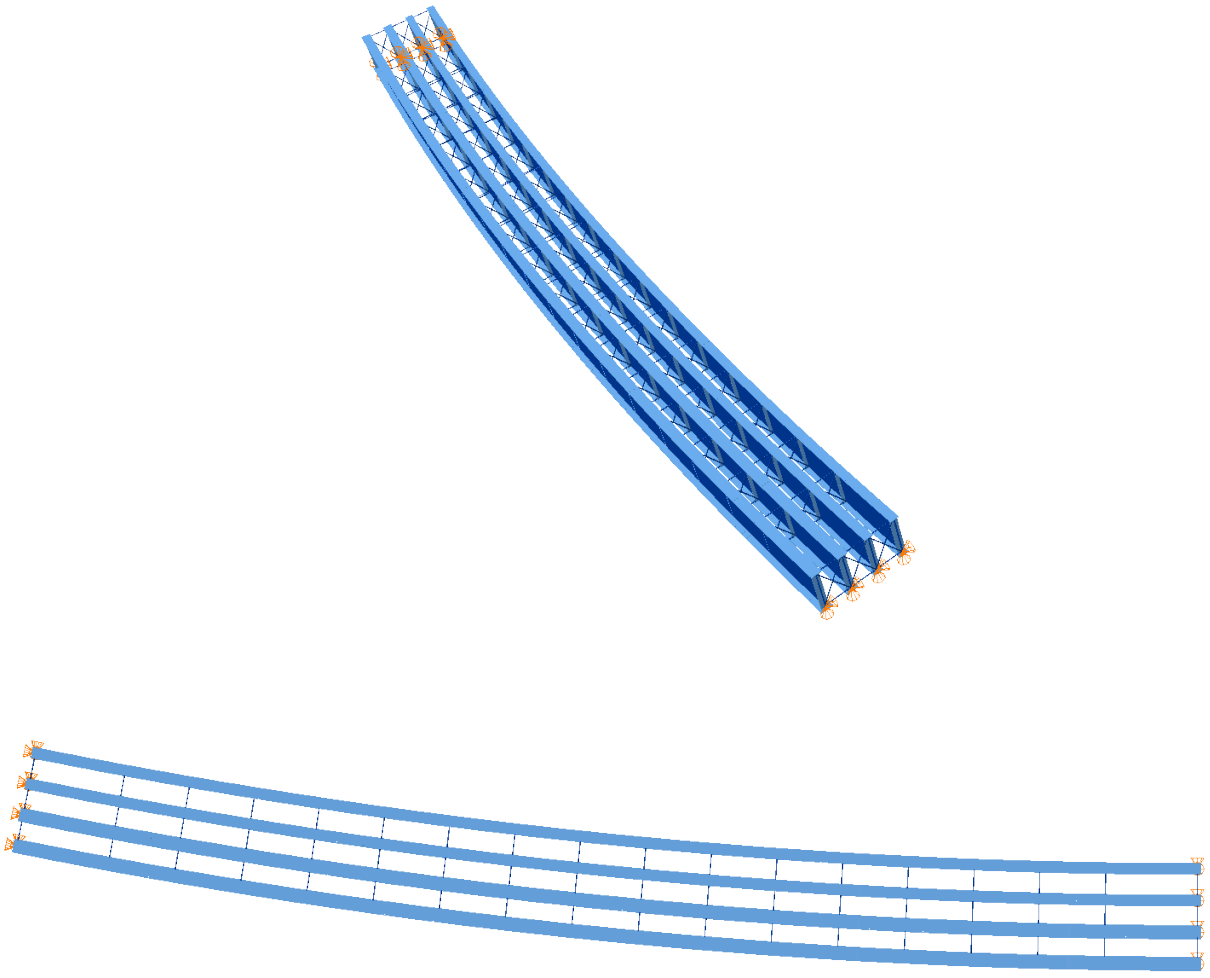

Abbreviated Analysis Results

This bridge is placed on the study matrix with its large span length, tight curvature and narrow width. Temporary supports are used during the erection of the girders due to their long length. This stage is selected to illustrate the change in the deflections and the stresses due to the removal of temporary support at completion of the steel structure. Figure 1 shows the stage where the erection of the steel structure is finished but still has temporary support. Figure 2 shows the vertical deflections of the outside girder under its own weight with temporary support. It is clear from Fig. 2 that vertical displacements are small and predicted accurately with the grid analysis methods. Figure 3 provides the relative radial displacements of the outside girder for the stage with temporary supports. It is observed from Fig 3. that 2D methods predict the relative radial displacements accurately at the cross-frame locations, whereas within the unbraced lengths the predictions are not comparable. This is mainly because the 1D and 2D solutions do not account for the warping rigidity of the I-girders. Figure 4 shows major-axis bending predictions of the outside girder with temporary support. The stress predictions are close to each other, and small values are obtained for the outside girder. Figure 5 provides flange lateral bending stress predictions of the outside girder with temporary support. Flange lateral bending calculations for approximate methods are good as long as the major-axis bending stress predictions are close to the benchmark solutions. Figure 5 shows that flange lateral bending stresses can be calculated accurately by using the grid analysis solutions. Using of temporary support may lead to decreased system response during the construction, which is believed to achieve an easier erection.

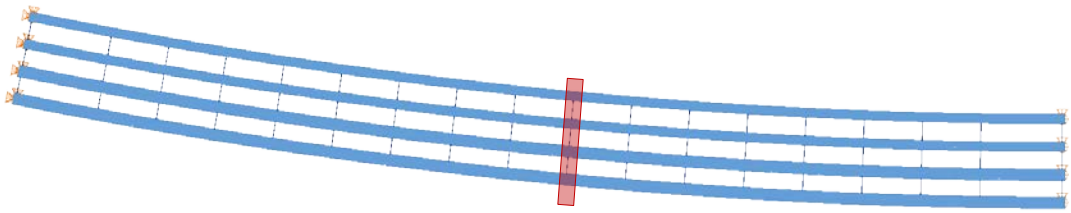

Fig. 1. NISCR5, Completed steel structure with temporary support.

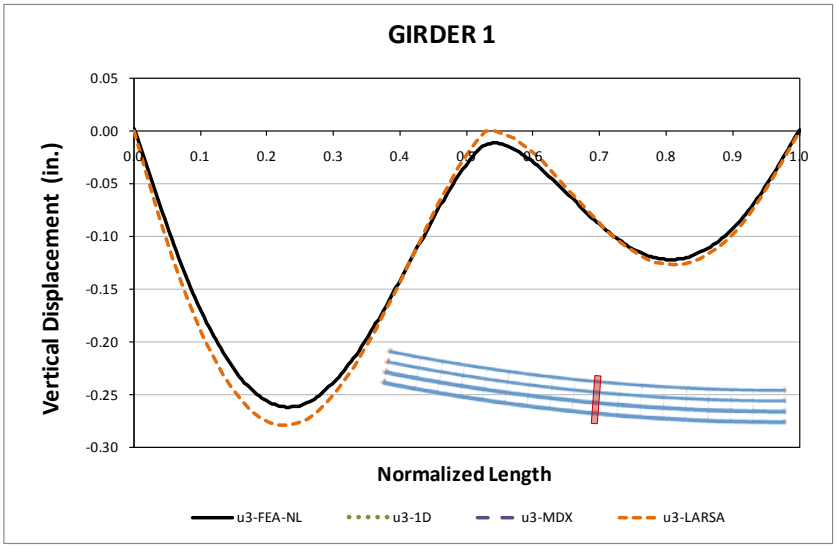

Fig. 2. NISCR5, Vertical displacements with temporary supports.

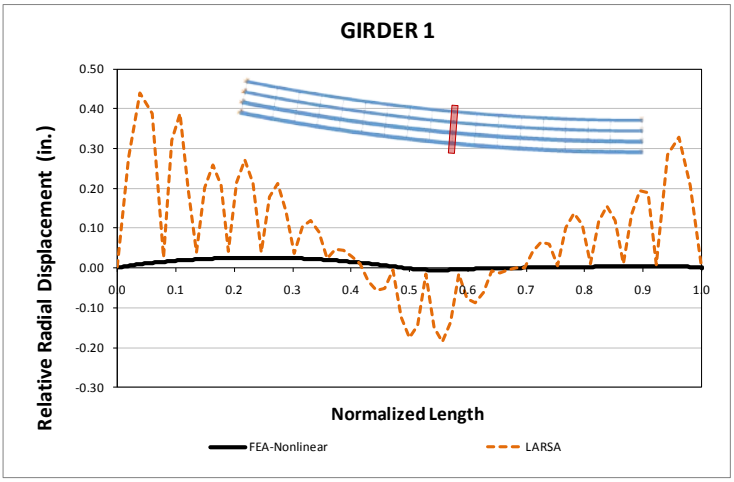

Fig. 3. NISCR5, Relative radial displacements with temporary supports.

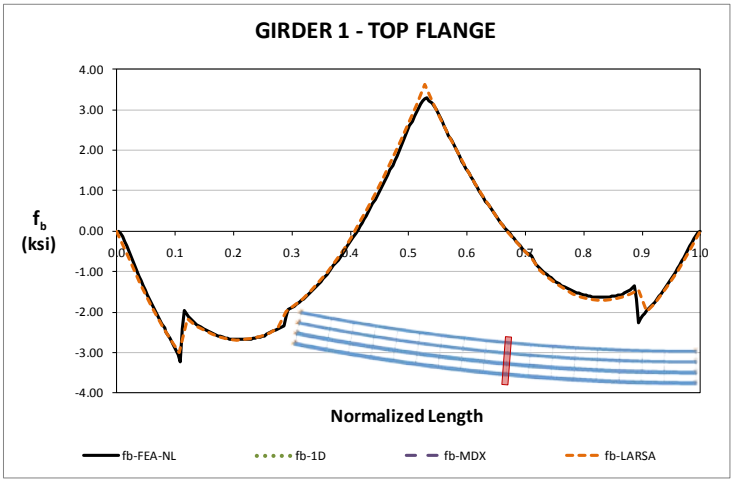

Fig. 4. NISCR5, Major-axis bending stresses with temporary supports.

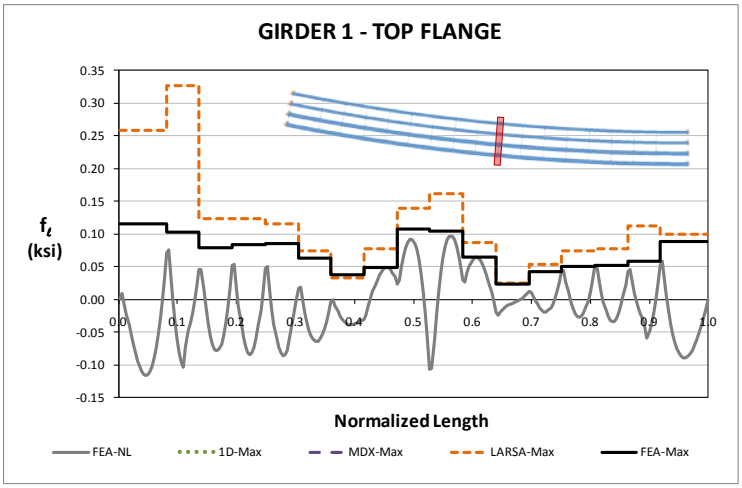

Fig. 5. NISCR5, Flange lateral bending stresses with temporary supports.

Figure 6 shows the vertical deflections of the outside girder under its own weight without temporary support. This stage is the steel dead load case. Vertical displacements are predicted accurately with 2D analysis methods. However, performance of 1D analysis methods is not good. Figure 7 provides the relative radial displacements of the outside girder under steel dead load. It is observed from Fig 7.that 2D methods predict the relative radial displacements accurately at the cross-frame locations whereas within the unbraced lengths the predictions are not comparable. This is a similar observation to that made for the stage with temporary supports. Figure 8 show major-axis bending predictions of the outside girder with temporary support. The stress predictions are close to each other. Figure 9 provides flange lateral bending stress predictions of the outside girder under steel dead load. Although the 2D grid predictions for the major-axis bending stresses are good, the nonlinearity in the system increases the flange lateral bending stresses. Therefore, the nonlinearity of the flange lateral bending stresses leads to underestimation of flange lateral bending stresses, which is calculated by grid analysis solutions. As a result, flange lateral bending stresses cannot be estimated by using the equations for this bridge.

Responses under total dead load are also considered since displacements and stresses are higher for that stage which may cause high nonlinearity and stability problems. This is mainly because second-order effects can be more critical for longer spans since the stresses are more dominated by dead load in longer spans. Figure 10 provides the outside girder vertical deflections under total dead load. It is clear from Fig. 10 that 2D grid methods perform well whereas 1D methods do not. The good prediction of 2D grid analysis methods is mainly because of the small L_b/R ratio (=0.011). Previous studies show that as L_b/R ratio gets smaller, better vertical displacement predictions are obtained from 2D grid analysis solutions. This is because the effect of neglecting the warping stiffness becomes negligible for 2D grid solutions. Figure 11 shows the relative radial displacements of the outside girder. Similar to previous observations, 2D grid methods predict the relative radial displacements better at the cross-frame locations than within the unbraced lengths.

Figure 12 shows factored major-axis bending predictions of the outside girder under total dead load. AASHTO requires engineers to obtain the stress responses from factored loading if nonlinearity is significant. The stress predictions including linear 3D FEA solutions are off from the benchmark solution. High nonlinearity and significant uplift are observed under the factored 3D nonlinear analysis, which causes big differences in the predictions. This behavior can only be captured by performing a second order analysis.

Figure 13 shows the flange lateral bending stress predictions of the outside girder under total dead load. The nonlinearity in the results is significant. Therefore, the responses deviate from the benchmark solutions significantly. None of the second order amplifications are believed to capture this behavior. The nonlinearity in the system is due to the long span length and uplift. It is obvious from these figures that second order analysis is needed for this bridge.

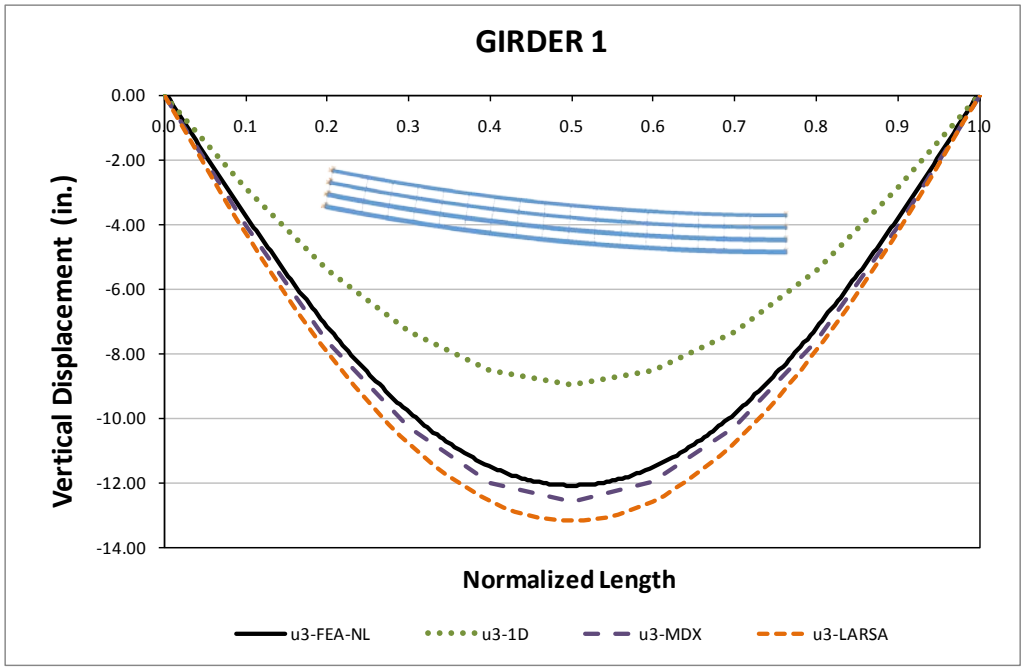

Fig. 6. NISCR5, Vertical displacements under steel dead load for NLF detailing.

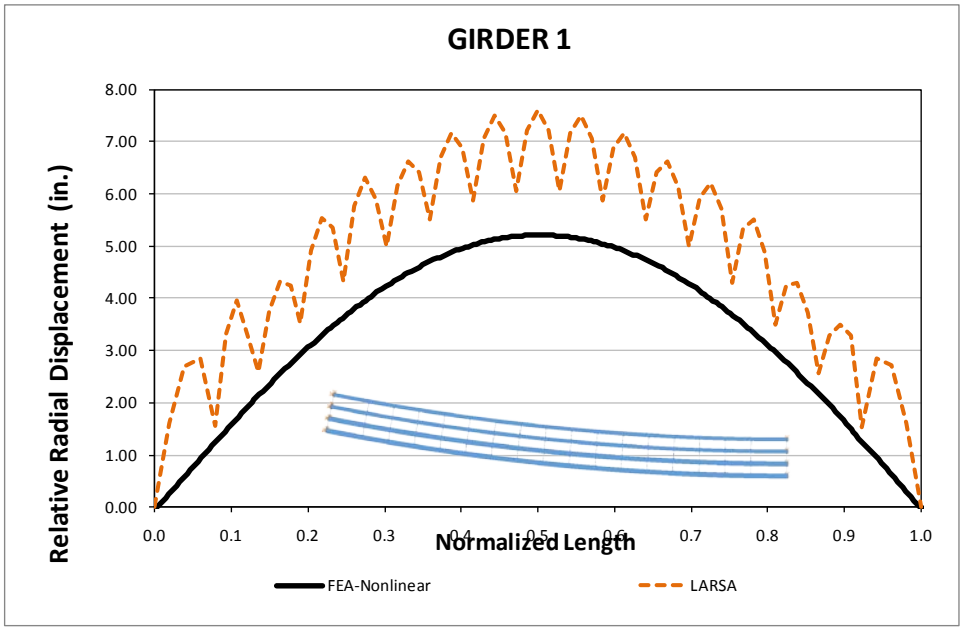

Fig. 7. NISCR5, Relative radial displacements under steel dead load for NLF detailing.

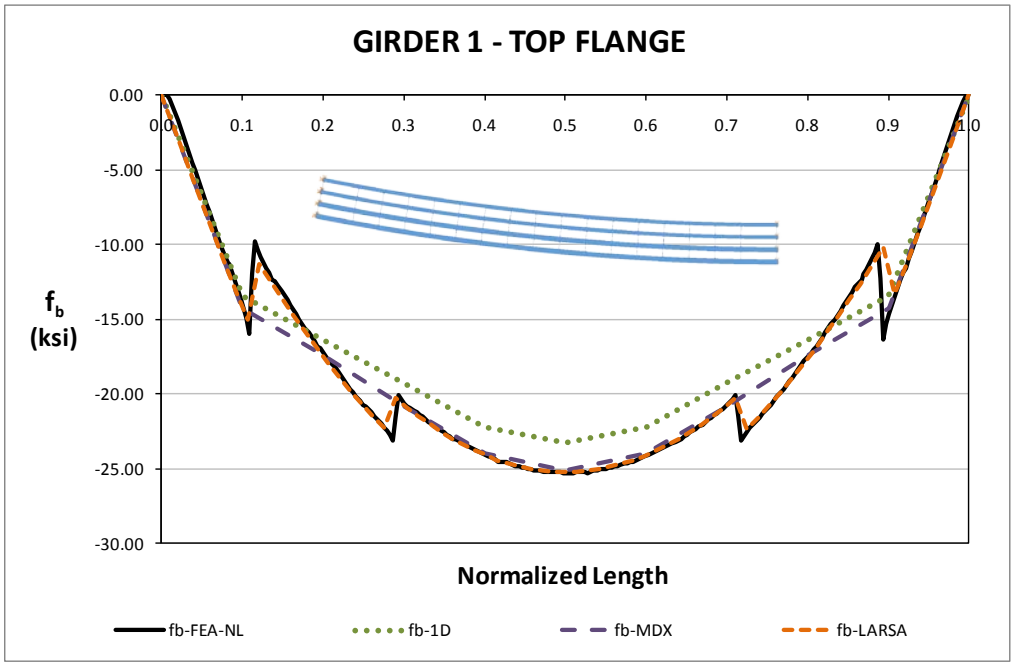

Fig. 8. NISCR5, Major-axis bending stresses under steel dead load for NLF detailing.

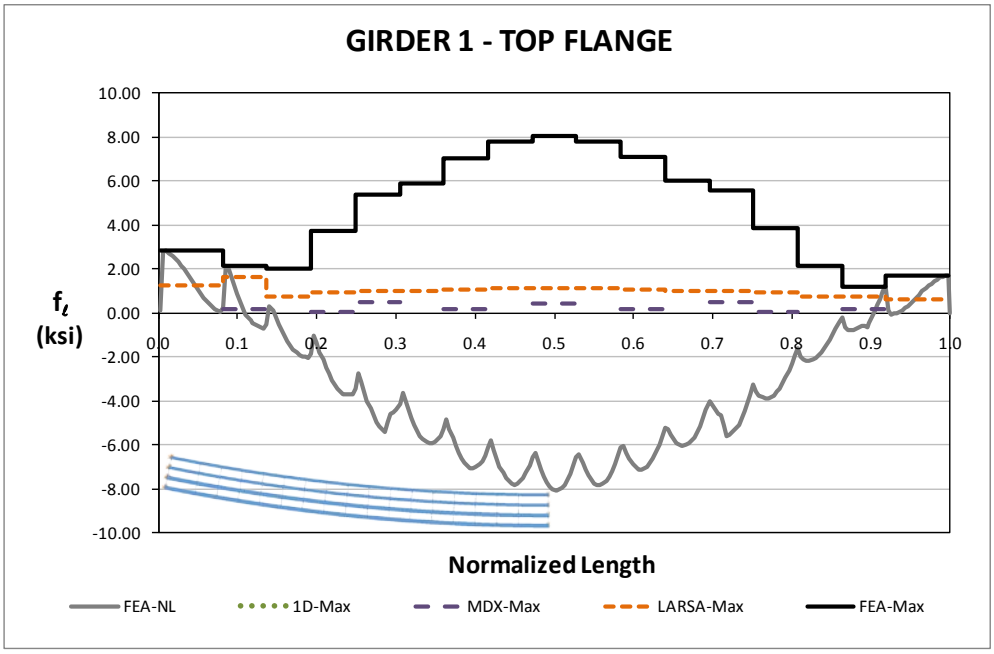

Fig. 9. NISCR5, Flange lateral bending stresses under steel dead load for NLF detailing.

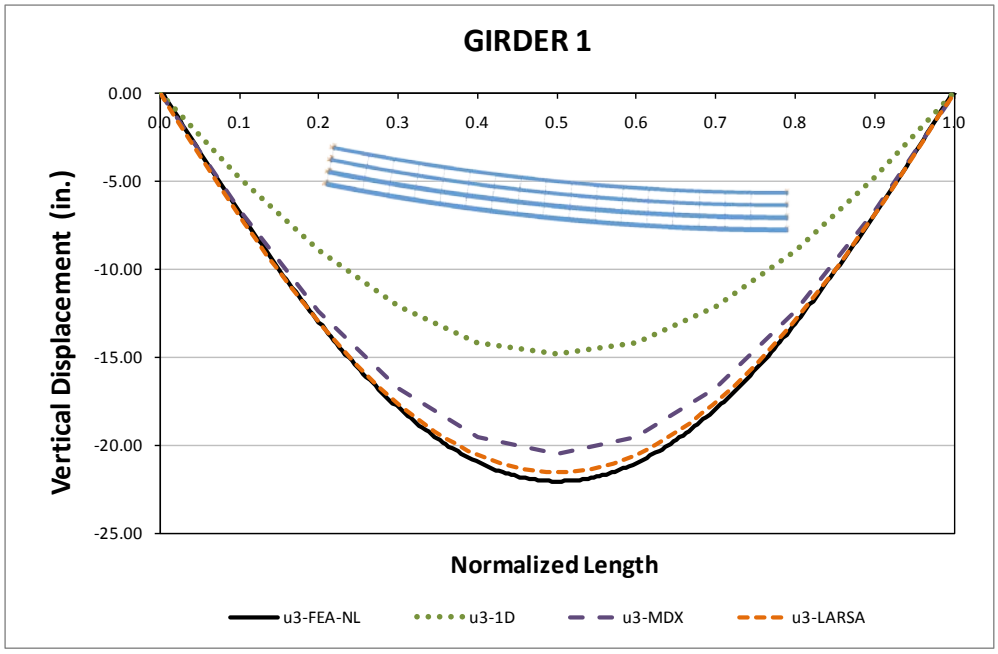

Fig. 10. NISCR5, Vertical displacements under total dead load for NLF detailing.

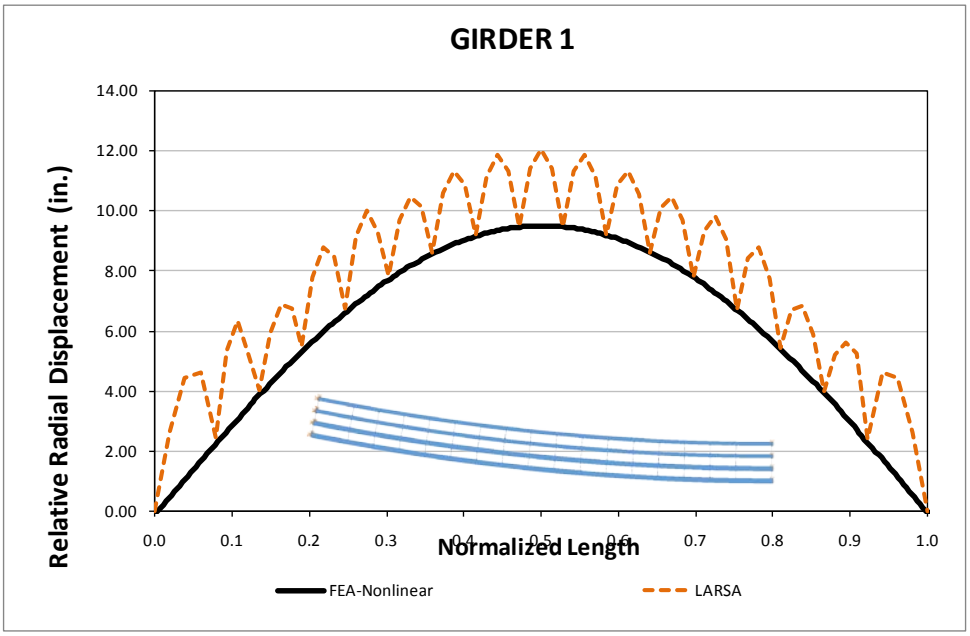

Fig. 11. NISCR5, Relative radial displacements under total dead load for NLF detailing.

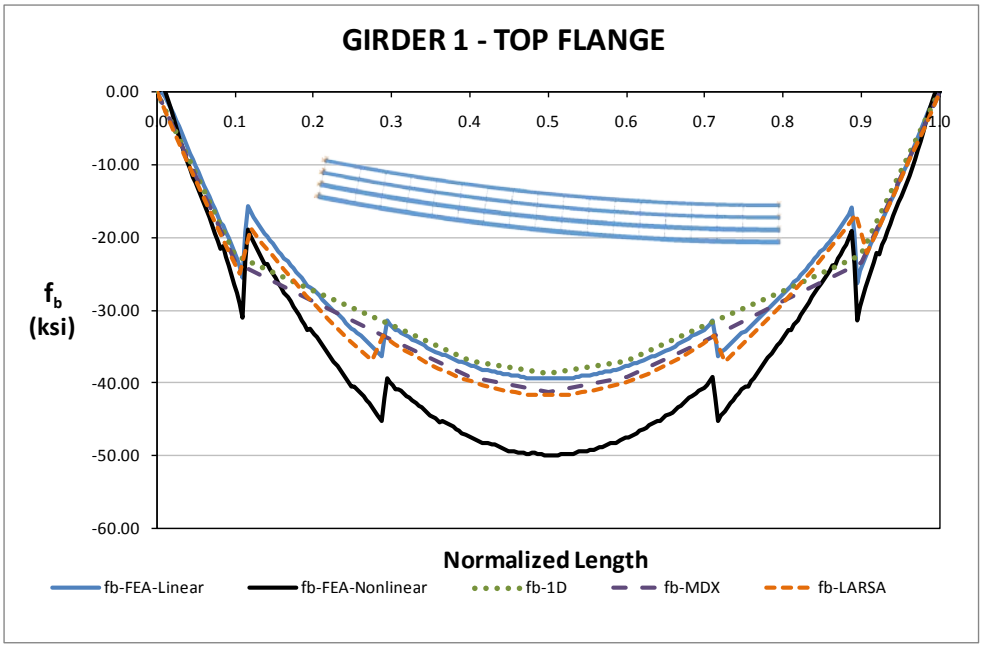

Fig. 12. NISCR5, Major-axis bending stresses under total dead load for NLF detailing.

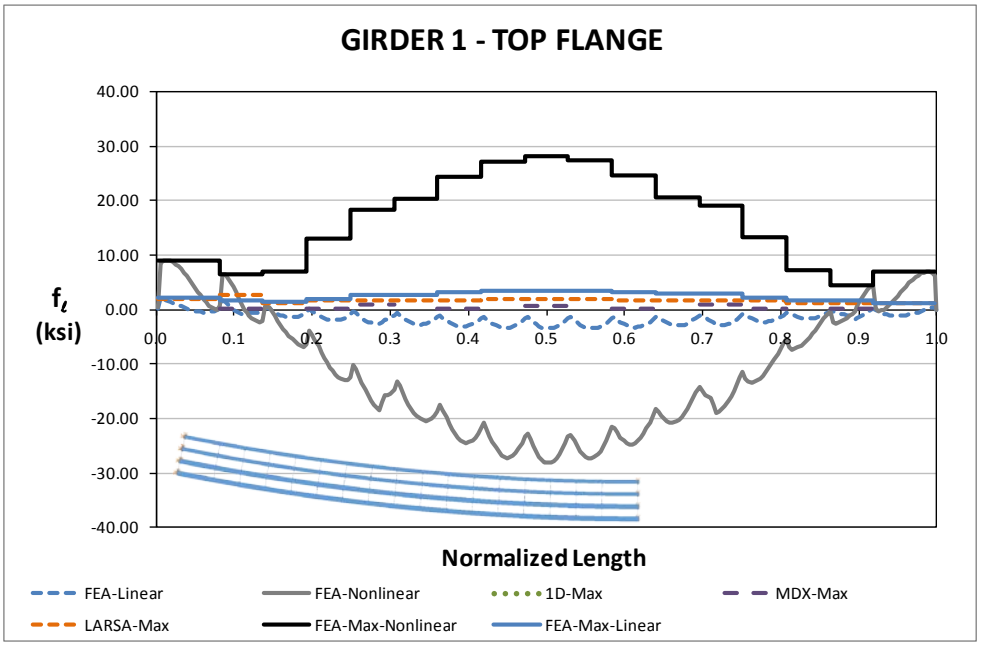

Fig. 13. NISCR5, Flange lateral bending stresses under total dead load for NLF detailing.

Conclusions:

It is expected that temporary supports can help to reduce the magnitude of stresses and displacements for long span bridges. Temporary supports may lead to fewer fit up problems in the field for longer spans.

Vertical displacements and the major-axis bending stresses are predicted accurately by all analysis methods for this bridge under steel dead load and during construction. The relative radial displacements are predicted well at the cross frame locations. On the other hand, flange lateral bending stresses are underestimated by all methods due to nonlinearity of the system.

Vertical displacements and the major-axis bending stresses are predicted accurately by 2D and linear 3D FEA analysis methods for this bridge under total dead load. The accurate predictions of the vertical displacements are due to the small L_b/R ratio (=0.011). The effect of neglecting warping stiffness for 2D grid analysis methods becomes negligible for small L_b/R ratios. Also, relative radial displacements are predicted well at the cross frame locations. Significant uplift is observed by nonlinear FEA (benchmark solution) under factored total dead load. This behavior leads to significant errors in the prediction of major-axis bending and flange lateral bending stresses by linear 3D FEA and approximate methods. Second order analysis is needed to evaluate the accurate behavior of this bridge.

I4.4 NISCR7 (New, I-girder, Simple-span, Curved, Radial supports)

Bridge Description:

Category Data:

L_{as} = 150 ft / R = 280 ft / w = 80 ft / $\theta_1 = 0^o$, $\theta_2 = 0^o$/ 9 girders

References:

Cross-Frame Detailing Method: NLF

Erection Stages Analyzed: Five

Deck Placement Sequence: One stage, deck thickness = 9 in.

Bridge Perspective & Plan Views:

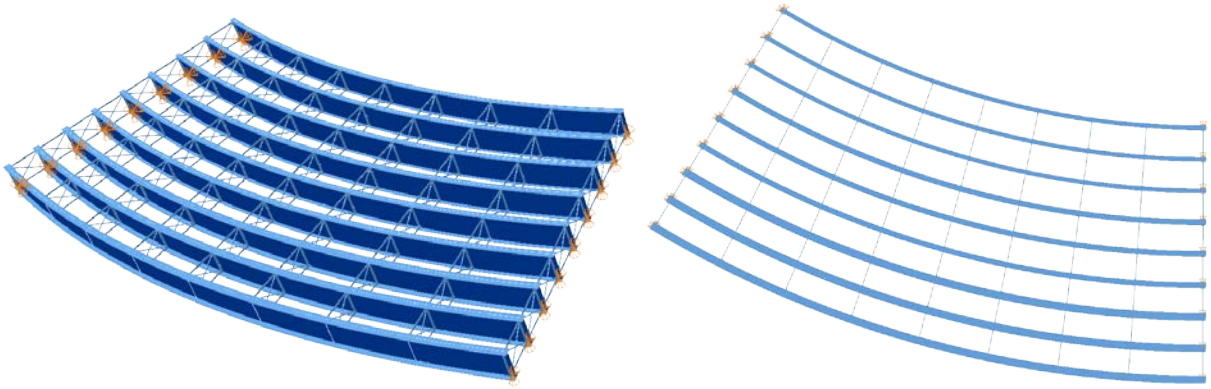

Abbreviated Analysis Results:

This bridge has a relatively short span and a large width. It has the tightest curvature among all the cases studied in the set of simple span parametric bridges. Thus, this bridge is an exceptional case to study the effects of an extreme horizontal curvature and a large width.

Three construction stages are presented in this report. The stages where two, five, and nine girders are in place are studied to observe the changes in the behavior of the bridge, as the construction progresses. The last stage corresponds to the finalized structure, when all the girders and cross-frames have been erected, and the concrete deck has been poured. For this stage, the concrete is assumed to be wet; therefore, no composite action is considered. Figure 1 shows a sequence of the construction and the studied erection stages. For visualization purposes, the deck is not shown in Stage 10.

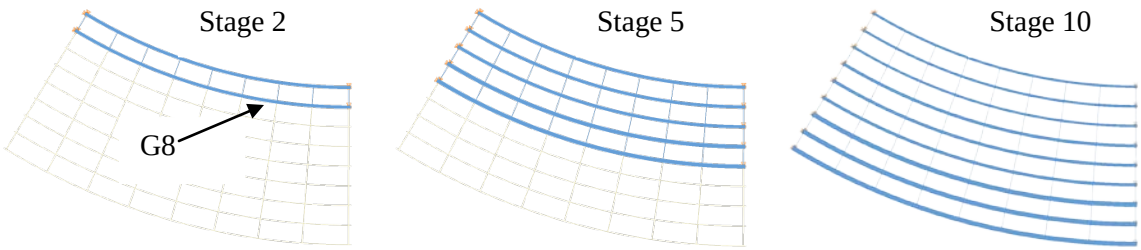

Fig. 1. Analyzed Construction Stages

For the above construction stages, the responses of the approximate 1D and 2D analyses are compared to the results obtained from the more rigorous 3D FEA model. In this report, the comparisons are shown for the second interior girder, G8, since it is present in the three studied erection stages.

The lateral displacement predictions are compared first. Figure 2 shows the plots corresponding to this response. As observed in the plots, the accuracy of the 2D Larsa model prediction increases as the simulation of the bridge construction progresses. The mean error between the approximate predictions and the 3D models decreases from 199% for Stage 2 to 1.6% for Stage 10. It is important to mention that these percentage errors are computed considering the response values only at the cross-frame locations. The lateral displacements obtained from the 2D model within the unbraced length of the girders are a misrepresentation of the actual behavior, due to the limited capabilities of the grid model to represent the torsional rigidity of the girders.

From these plots it is observed that the accuracy of the grid analysis largely depends on the degree of connectivity of the girders. As the erection of more structural components take place, the system consolidation increases, and the structure responds as a sole unit rather than as a set of individual girders.

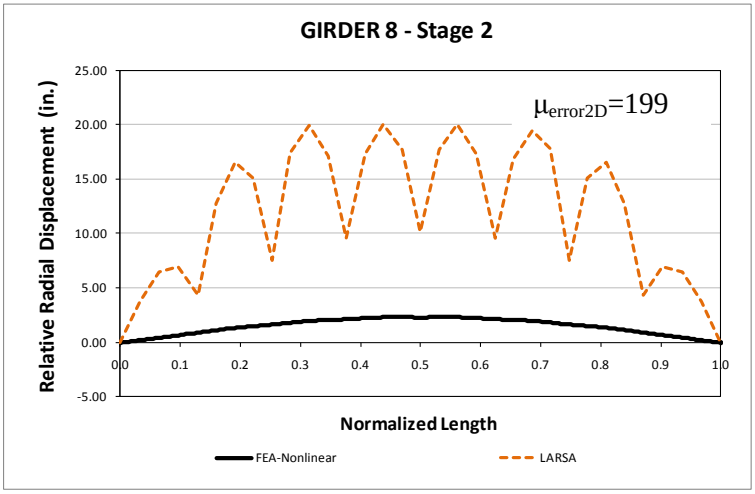

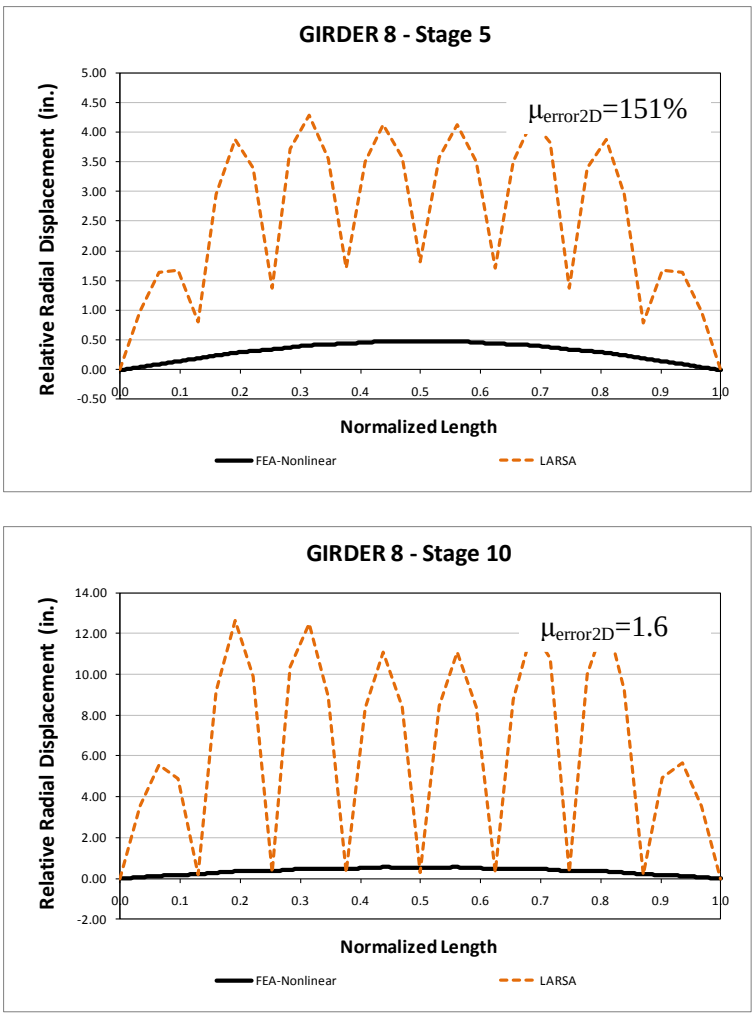

Fig. 2. Comparison of Relative Radial Displacements

In the case of the vertical displacement predictions, the observations are different. As shown in Figure 3, the discrepancies between the 2D predictions and the expected deflections are significant for all stages. The mean error for Stage 2 is 360%, 350% for Stage 5, and 500% for Stage. This shows that vertical deflections in a curved bridge cannot be obtained from a 2D grid analysis.

A comparison of vertical displacement predictions using the approximate 1D and 2D analysis methods for Stage 10 is also shown in Figure 3. As shown, the 1D prediction is the closest to the benchmark response. The limitations in the formulation of the girder torsional rigidity in the 2D grid models affect severely the accuracy of the results. For this particular case, the use of a line girder analysis to calculate vertical deflections might be considered sufficient for design.

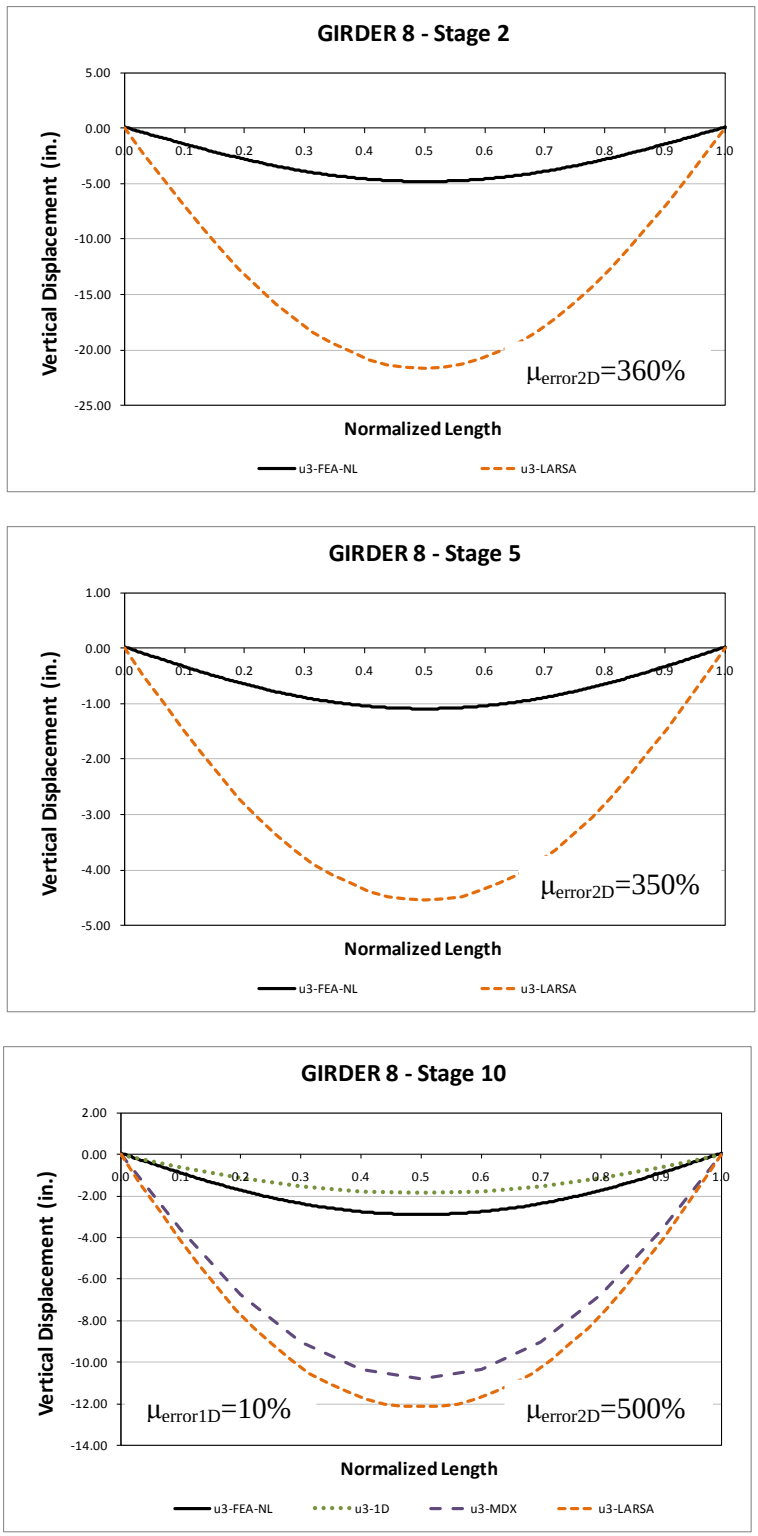

Fig. 3. Comparison of Vertical Displacements

In the case of major-axis bending stresses, the predictions obtained from the approximate methods are consistent with the 3D model responses for all the stages. As shown in Figure 4, the 2D grid model was able to capture the responses for Stages 2 and 5 with small errors. For Stage 10, the accuracy of the 2D grid model decreased, but these results could still be considered valid for design. In the case of the 1D analysis prediction, it is also a reasonable representation of the benchmark. The 10.2% mean error in the predictions might be considered to be acceptable.

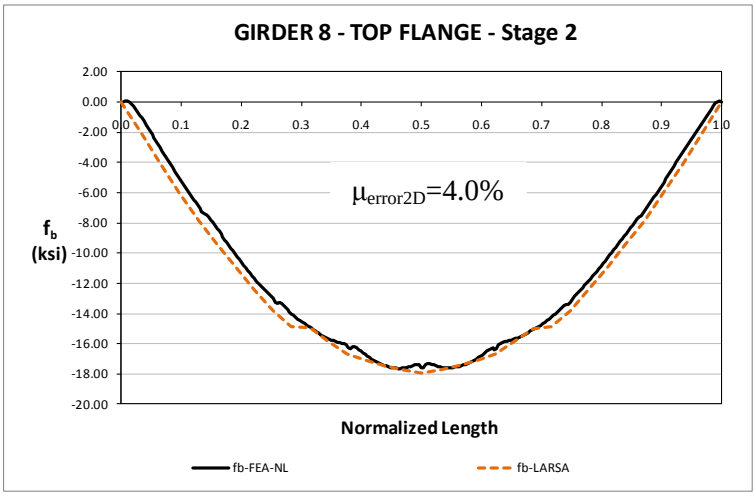

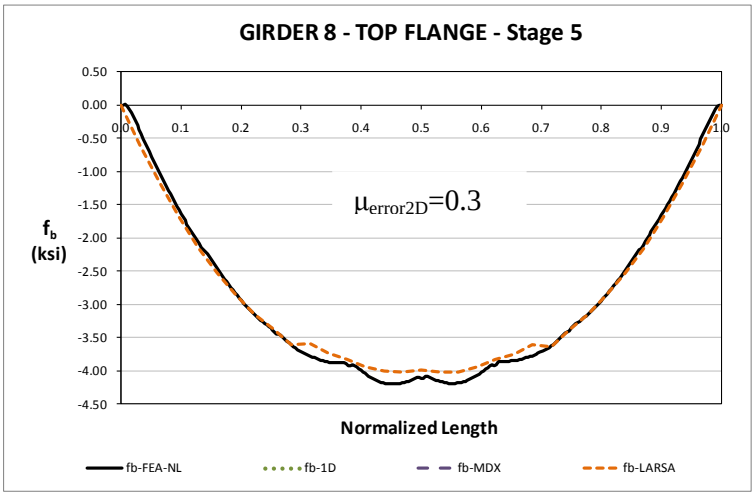

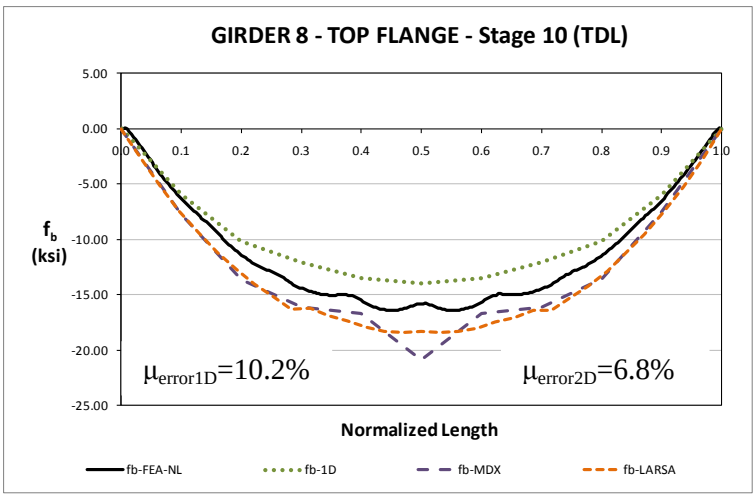

Fig. 4. Comparison of Major-axis Bending Stresses

The comparison of the flange lateral bending stresses for Stage 10 in shown in Figure 5. The 2D model prediction is based on the V-Load formulation that considers the major-axis bending stress response to predict the flange lateral bending stress levels. As shown in the figure, the trends between the 2D and 3D models are similar. In general, the 2D model responses over predict the stress levels by a approximately a factor of two.

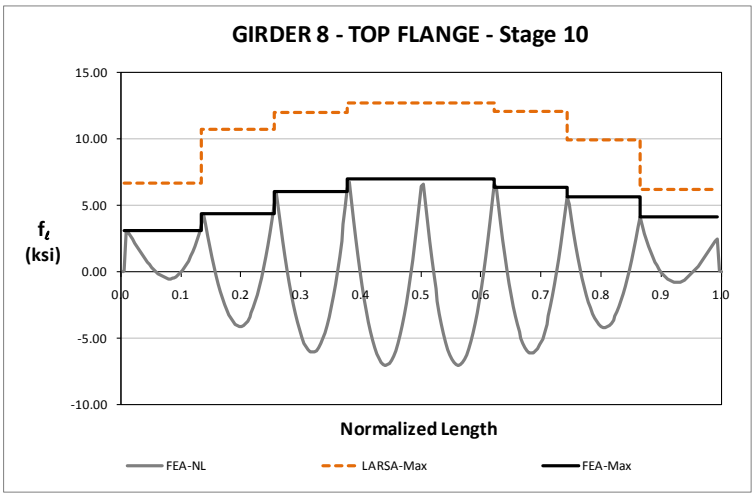

Fig. 5. Comparison of Flange Lateral Bending Stresses

Conclusions:

This bridge shows the influence of a tight radius of curvature in the response prediction obtained from approximate 1D and 2D analysis methods. From the analyses above, it is observed that the predictions improve as the connectivity of the bridge increases. The largest differences between the 2D grid analyses and the 3D FEA models are observed for Stage 2, when only two girders are in place. The vertical displacements, however, are not captured by the 2D grid models for any of the stages. The lack of a warping term in the formulation of the torsional stiffness introduces errors in the displacement estimations that are not tolerable for design.

I4.5 NISCR8 (New, I-girder, Simple-span, Curved, Radial supports)

Bridge Description:

Category Data:

L_{as} = 150 ft / R = 420 ft / w = 80 ft / $\theta_1 = 0^o$, $\theta_2 = 0^o$/ 9 girders

References:

Cross-Frame Detailing Method: NLF

Erection Stages Analyzed: Three

Deck Placement Sequence: One stage, deck thickness = 9 in.

Bridge Perspective & Plan Views:

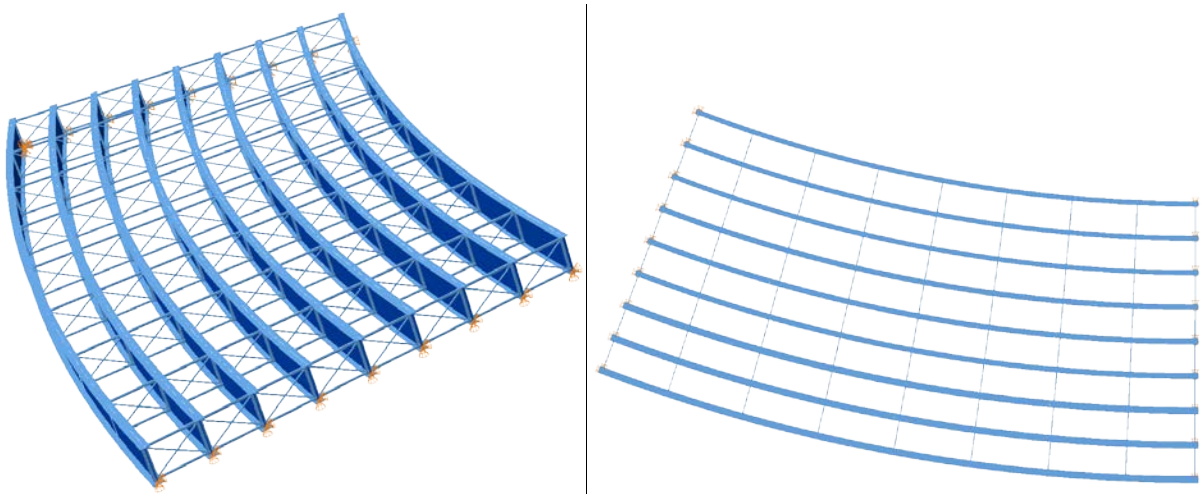

Abbreviated Analysis Results:

In this bridge the effects of a wide width versus a relatively short span are studied. The span to width ratio is 1.88, and has an intermediate radius of curvature. Three stages of construction have been selected to investigate the behavior of the bridge. Stage 1 corresponds to the erection of the exterior girder. A holding crane is provided at midspan to provide additional stability to the girder until girder G2 is erected. In Stage 2, G1 and G2 are connected with the cross-frames and no other means of support is provided besides the supports at the abutments. The last stage studied is Stage 10. This stage corresponds to the total dead load condition, when the concrete has been placed, but there is not composite action. Figure 1 shows the 3D views of the three stages studied.

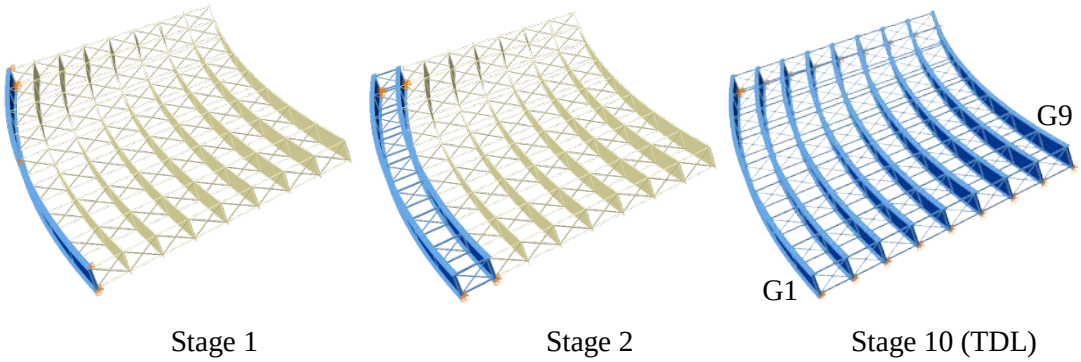

Fig. 1. Analyzed Construction Stages

For the above construction stages, the responses of the approximate 1D and 2D analyses are compared to the results obtained from the more rigorous 3D FEA model. In this report, the comparisons are shown for the second interior girder, G1, since it is present in the three studied erection stages.

During the erection of the erection of the exterior girder, Stage 1, the girder behaves is continuously supported due to the presence of the holding crane at midspan. Figure 2 show the vertical displacements predictions for this stage. As shown in the plot, the Larsa 2D grid model over predicts the displacement by approximately a factor of two. This behavior is consistent with the observations done in other bridges, where due to the inability of the grid model to represent the warping stiffness of the I-girders, the expected vertical displacements are misrepresented. The prediction of the major-axis bending stresses, however, is accurate for the same stage. Figure 2 shows the stress responses predicted by the 3D FEA benchmark and the 2D grid model. It is observed that the limitations of the model to represent the torsional properties of the I-girder do not affect this response.

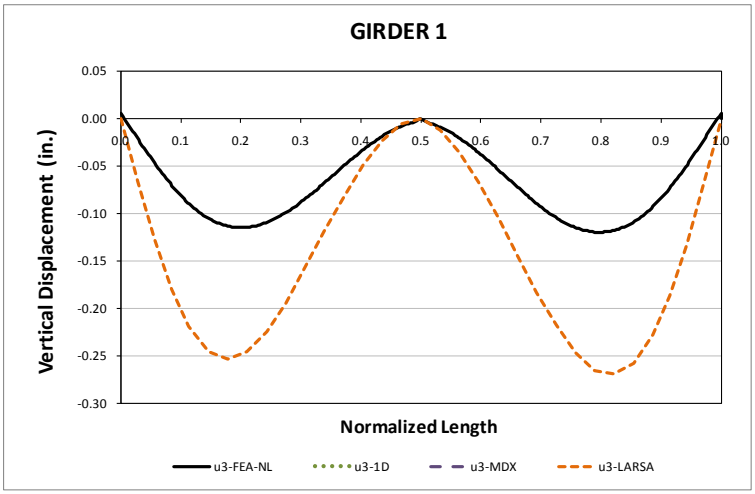

Fig. 2. Comparison of Vertical Displacements, Stage 1

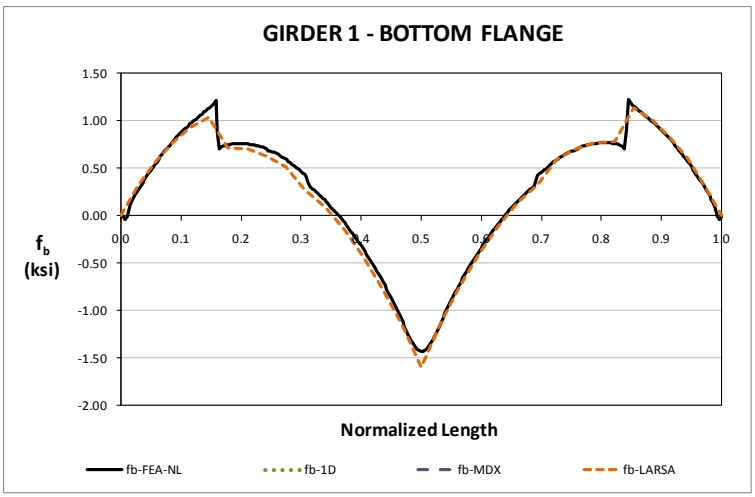

Fig. 3. Comparison of Major-axis Bending Stresses, Stage 1

The prediction of vertical displacements for the steel dead load condition, SDL, is studied next. Figure 4 shows a comparison between the approximate 1D and 2D analysis results and the 3D FEA benchmark. The limitations of the 2D grid model discussed previously affect the response, which results in an over prediction of the displacements. The 1D method, based on the V-Load formulation captures in a more accurate way the expected response. In the case of the lateral displacements, these are best captured at the cross-frame positions, as shown in Figure 5. Within the unbraced length, the 2D grid model is not capable of representing the expected response due to the lack of a warping term in the torsional stiffness formulation of the model.

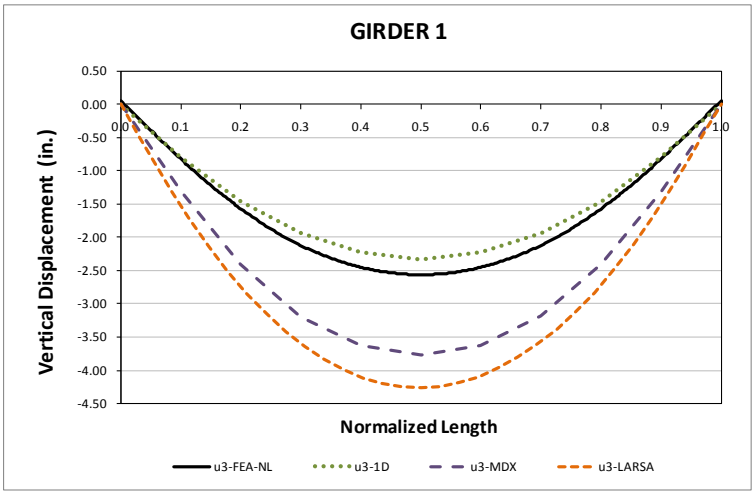

Fig. 4. Comparison of Vertical Displacements, SDL

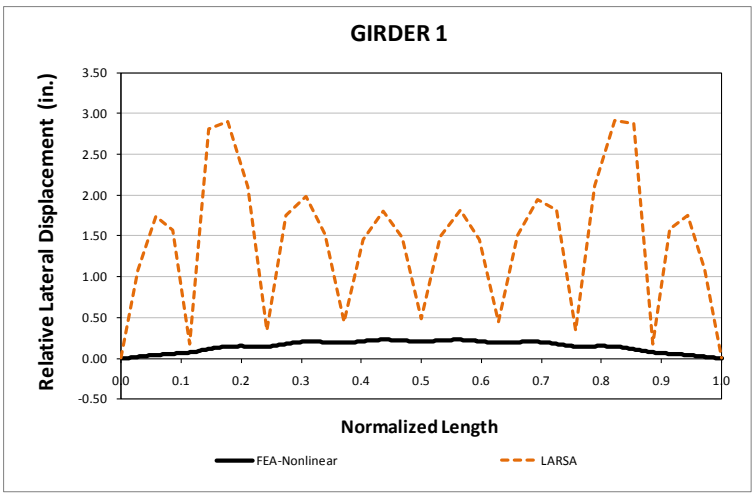

Fig. 5. Comparison of Lateral Displacements, SDL

The stress levels at the total dead load condition are discussed next. Figure 6 shows the major-axis bending response as predicted by the different methods. It is observed that both the 1D and 2D models accurately captured the response predicted by the 3D model. Similarly, the flange lateral bending stress predictions obtained from the Larsa model results are a fair representation of the expected results. As shown in Figure 7, the Larsa prediction is an upper bound of the 3D model response. This is consistent with the results of other curved bridges, where the prediction of the flange lateral bending stress levels using the results of a 2D grid analysis are a conservative estimate of the 3D model predictions.

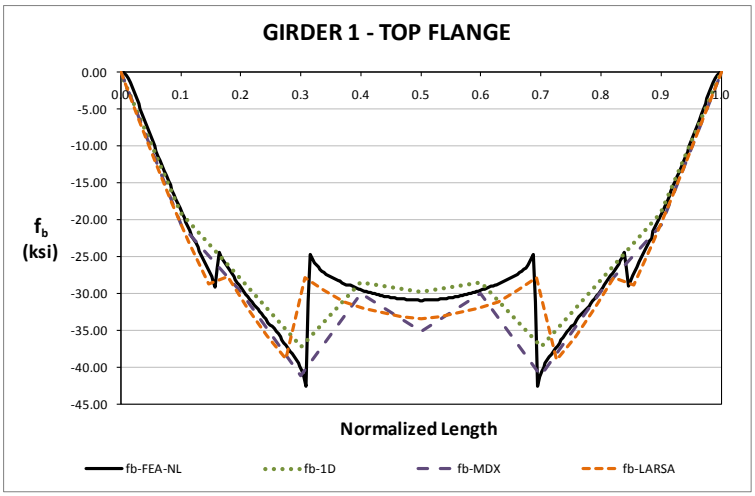

Fig. 6. Comparison of Major-Axis Bending Stresses, TDL

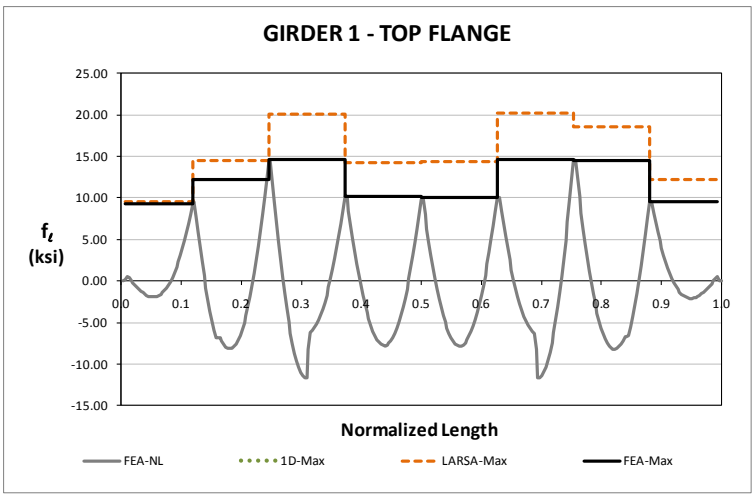

Fig. 7. Comparison of Flange Lateral Bending Stresses, TDL

I4.6 NISCR10 (New, I-girder, Simple-span, Curved, Radial supports)

Category Data:

L_{as} = 225 ft / R = 705 ft / w = 80 ft / $\theta_1 = 0^o$, $\theta_2 = 0^o$/ 9 girders

Cross-Frame Detailing Method: NLF

Erection Stages Analyzed: Five

Deck Placement Sequence: One stage, deck thickness = 9 in.

Bridge Perspective & Plan Views:

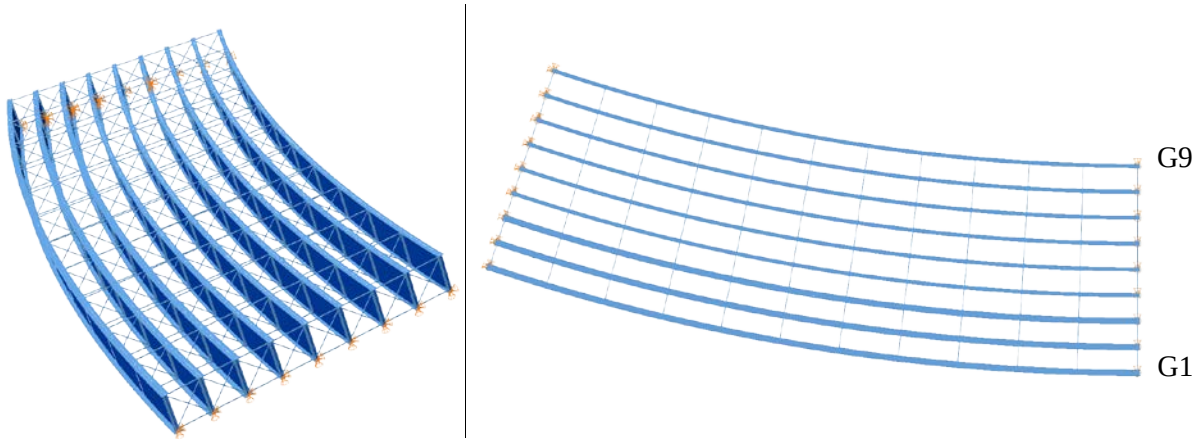

Abbreviated Analysis Results:

This is a relatively wide bridge with a moderate curvature. Due to its long span, shoring towers are provided for erection of girders G1 to G5 at approximately mid-span. The girders are divided in two sections of two thirds and one third of the total length, respectively (i.e., 150 ft and 75 ft approximately). The steel erection starts with the placement of the first section of the exterior girder, G1, over the abutment and the shoring tower, and continues with the erection of girders G2 to G5 following the same scheme. Next, the second sections of these girders are spliced in the air, completing the erection of the first five girders of the structure. The subsequent girders are erected without the aid of more shoring towers. The first and second sections of girder G6 to G9 are erected by connecting them to the girders placed previously (i.e., G1 to G5) without any intermediate support. The same procedure is followed to complete the structure with girders G7 to G9. The shoring towers in girders G1 to G5 are removed once the steel structure has been completed and before the concrete deck is poured.

In this report, three erection stages have been selected to study the behavior of the bridge and compare the predictions between the different analysis methods. Figure 1 shows the plan view of Stages 2, 13, and 16. The last stage represents the condition where the full construction dead load is applied and supported by the steel structure. At this stage, the concrete is not hardened to consider composite action.

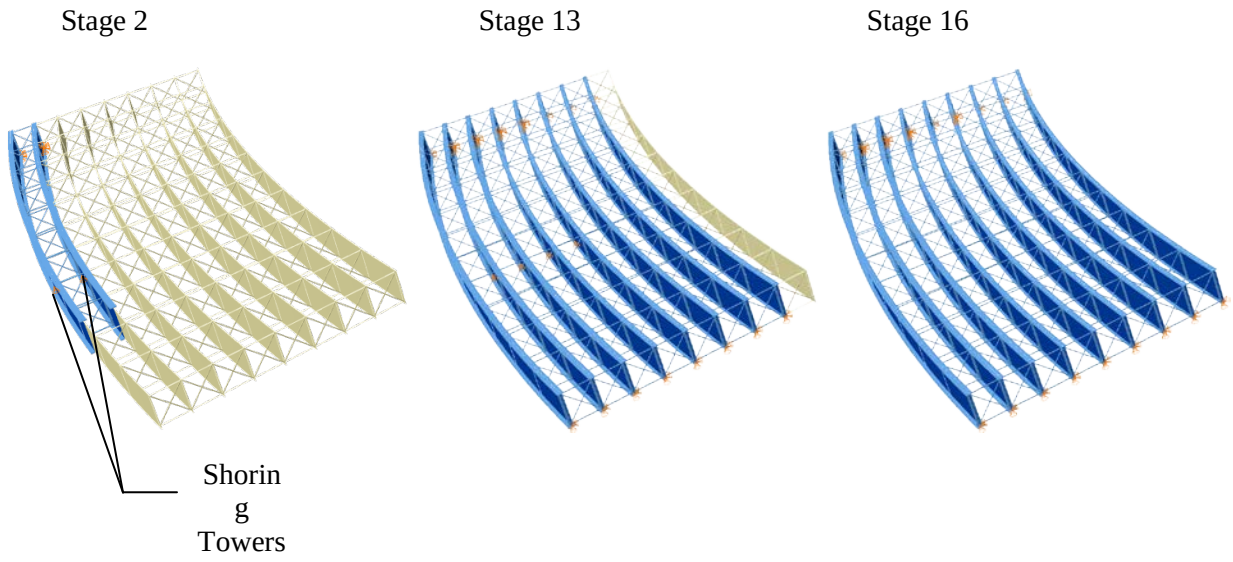

Fig. 1. Analyzed Construction Stages

The major-axis bending response is studied first. The stress response for the top flange of the exterior girder, G1, in Stage 2 is shown in Figure 2. As shown in the figure, the 2D grid model representation captures accurately the 3D FEA prediction. In the case of the vertical displacements, the approximate representation does not present the same level of accuracy. As shown in Figure 3, the 2D grid prediction overestimates the expected displacements. This is observation is consistent with the results obtained in from the analysis of other curved bridges. The lack of a term that considers the contribution of flange warping in the torsional stiffness of the I-girders results in misrepresentations of the actual vertical displacements.

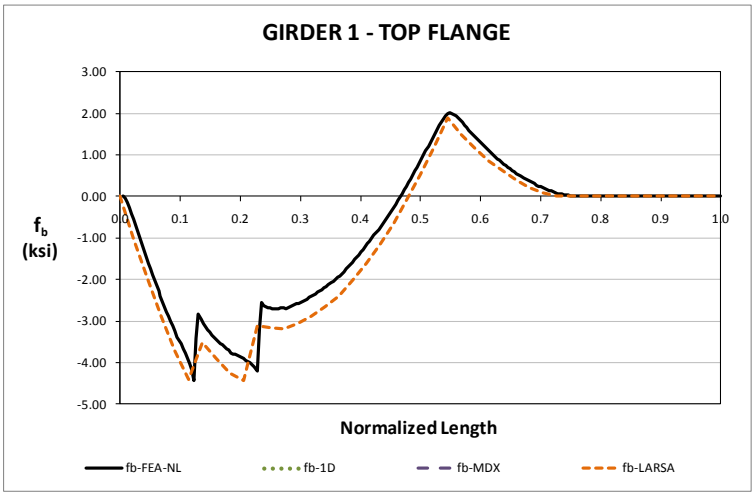

Fig. 2. Comparison of Major-Axis Bending Stresses, Stage 2

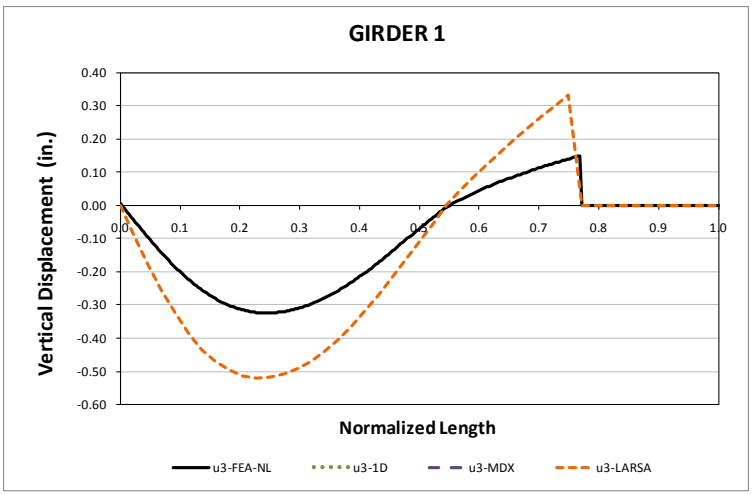

Fig. 3. Comparison of Vertical Displacements, Stage 2

For Stage 13, where eight girders are erected, the major-axis bending stress predictions do not have the same level of accuracy observed for Stage 2. Figure 4 shows the response for the bottom flange of girder G8. In this stage, the largest discrepancies between the 2D and 3D models are observed for this girder. Even the responses are significantly different, the largest difference occurs that mid-span is 1.5 ksi.

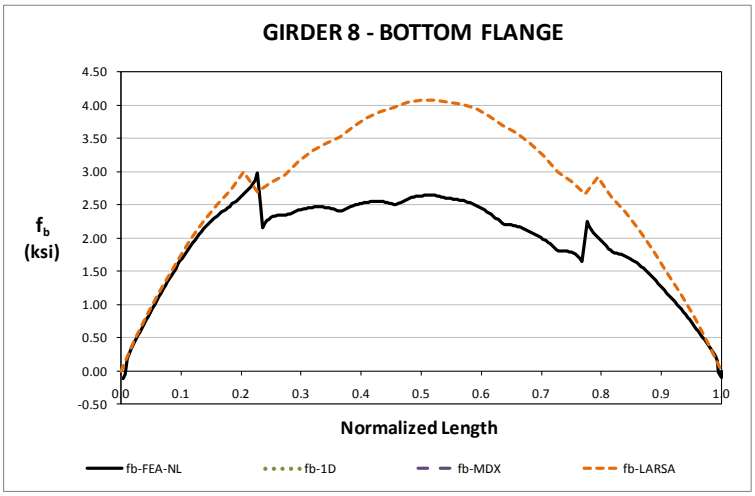

Fig. 4. Comparison of Major-axis Bending Stress, Stage 13

For the final configuration, when the total construction dead load is applied to the structure, the approximate predictions are more accurate. As shown in Figure 5, the 1D and 2D predictions are a close representation of the benchmark. For design purposes, the responses obtained from the approximate models could be considered to be sufficient. In the case of the vertical displacements, the 2D grid analysis limitations result in a poor prediction of this response, as shown in Figure 6. The approximate 1D analysis is a much closer representation of the 3D FEA solution.

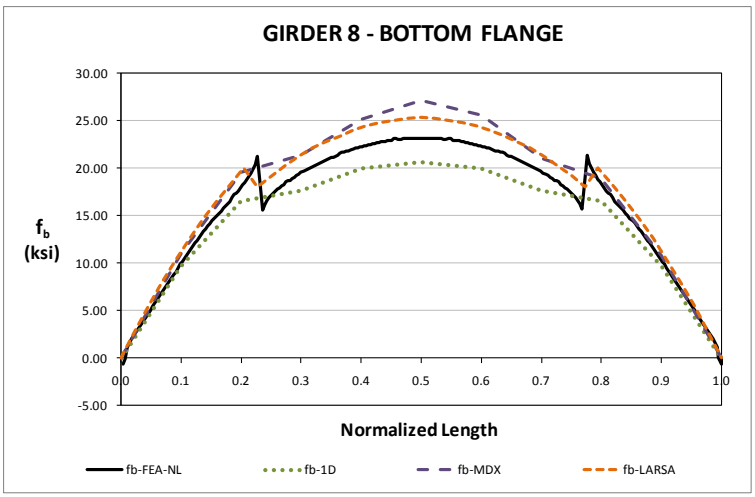

Fig. 5. Comparison of Major-axis Bending Stress, Stage 16

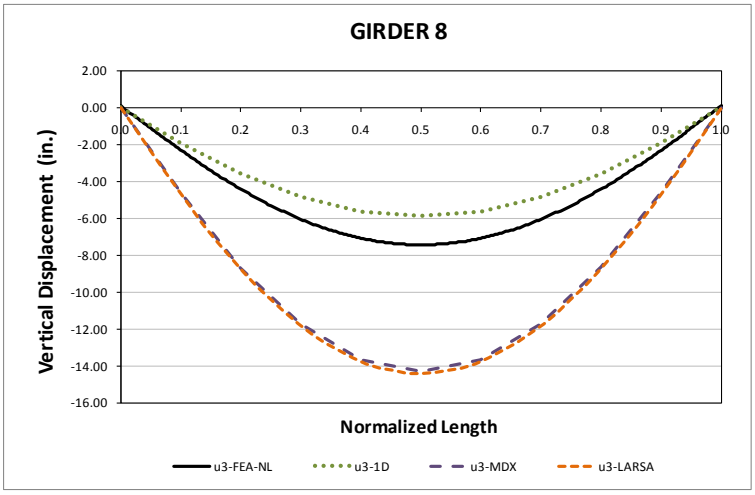

Fig. 6. Comparison of Vertical Displacement Predictions, Stage 16

The flange lateral bending response for Stage 16 is shown in Figures 7 and 8. The relative lateral displacements are accurately predicted by the 2D grid analysis at the cross-frame locations, as depicted in Figure 7. This is a typical result that is also observed in many of the curved bridges studied previously. For the prediction of the layover of the girders during construction, the response obtained from the 2D model could be considered only at the bracing points. A straight line that joins the predictions between two cross-frame positions might be sufficient to describe the response within the unbraced length.

The computation of flange lateral bending stresses based on the V-Load formulation proves to be accurate for this bridge. Figure 8 shows that the approximate predictions are consistent with the 3D FEA model predictions. This is an expected result given that this bridge does not have skewed supports or any other factor that can affect the response.

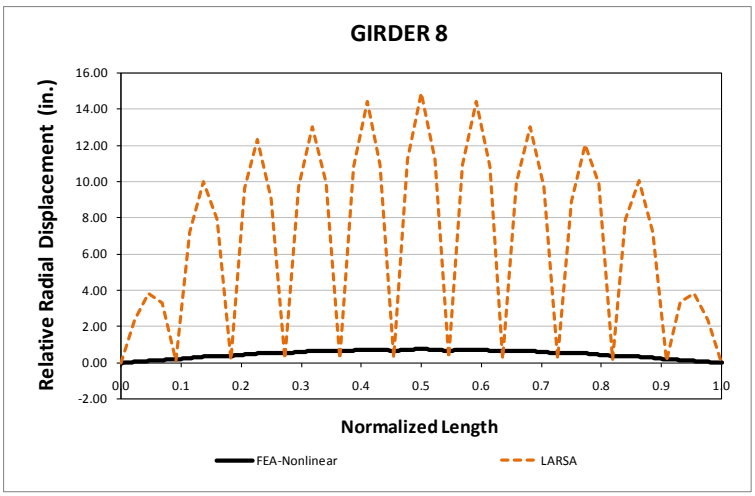

Fig. 7. Comparison of Relative Radial Displacement Predictions, Stage 16

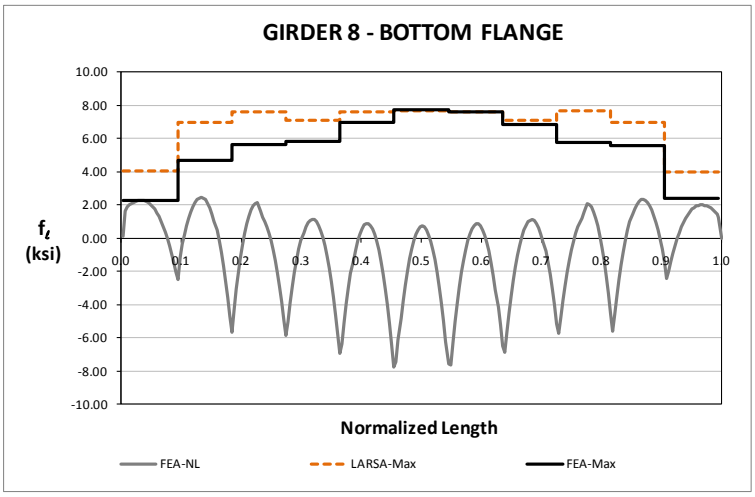

Fig. 8. Comparison of Flange Lateral Bending Stress Predictions, Stage 16

I4.7 NISCR11 (New, I-girder, Simple-span, Curved, Radial supports)

Category Data:

L_1 = 300 ft/ R_1 = 730 ft / w = 80 ft, 9 girders

Cross-Frame Detailing Method: NLF

Erection Stages Analyzed: 5 (Analyses are performed assuming NLF)

Deck Placement Sequence: 1 Stage

Bridge Perspective & Plan Views:

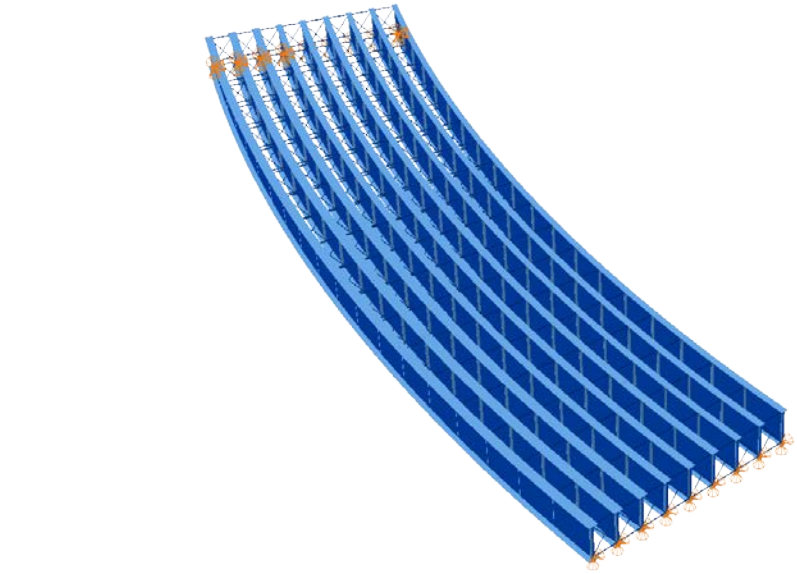

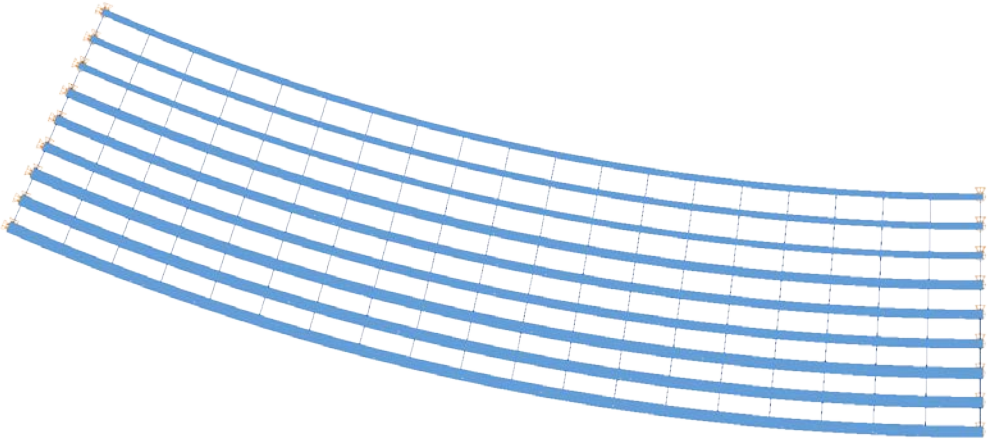

Abbreviated Analysis Results

Figure 1 shows the deflected shape of the bridge under the total dead load. Deflections are magnified by 15 times. Due to curvature, top flanges of the girders layover towards outside within the span wher as due to radial supports no girder layover is observed at the supports. Figures 2 and 3 provide facial girder vertical deflections under the total dead load. Girder 1 is the outside and girder 9 is the inside girder. Figures 2 and 3 show that the deflections cannot be predicted accurately by any simplified analysis method. Moreover, 1D analysis predicts the vertical deflections in the opposite direction for girder 9. The error in the 1D method predictions is believed to be due to the method's inability to predict overall load pattern of the bridge. The error in the 2D grid solutions is primarily because 2D grid solutions do not account for the warping rigidity of the I-girders. Previous studies show that L_b/R ratio can affect the accuracy of predictions of the approximate methods. As L_b/R ratio gets smaller, better vertical displacement predictions are obtained from 2D grid analysis solutions. The effect of neglecting warping stiffness for 2D grid analysis methods becomes negligible for small L_b/R ratios. However, L_b/R ratio of 0.022 is obtained for this bridge, which results in error in the prediction of vertical displacements.

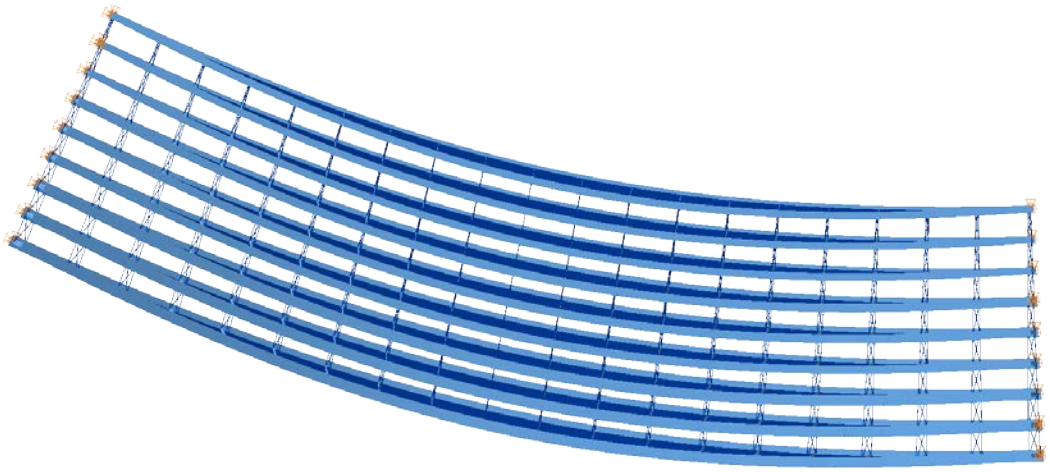

Fig. 1. NISCR11, Deflected shape under total dead load (Magnified by 15x).

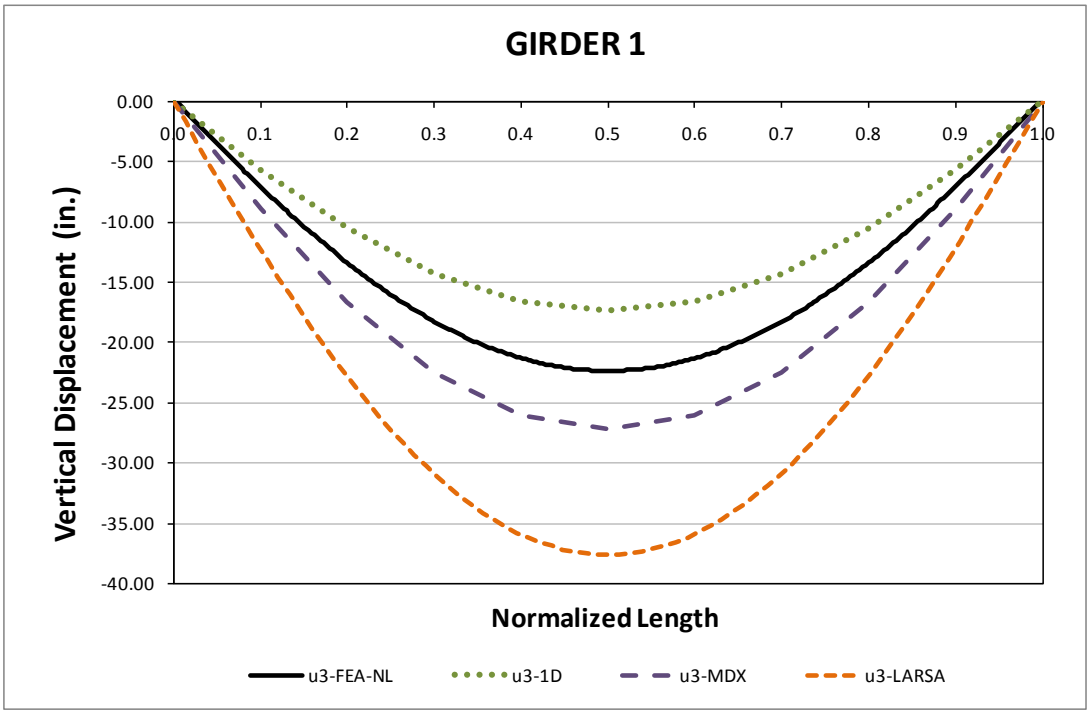

Fig. 2. NISCR11, Vertical displacements under total dead load for NLF detailing.

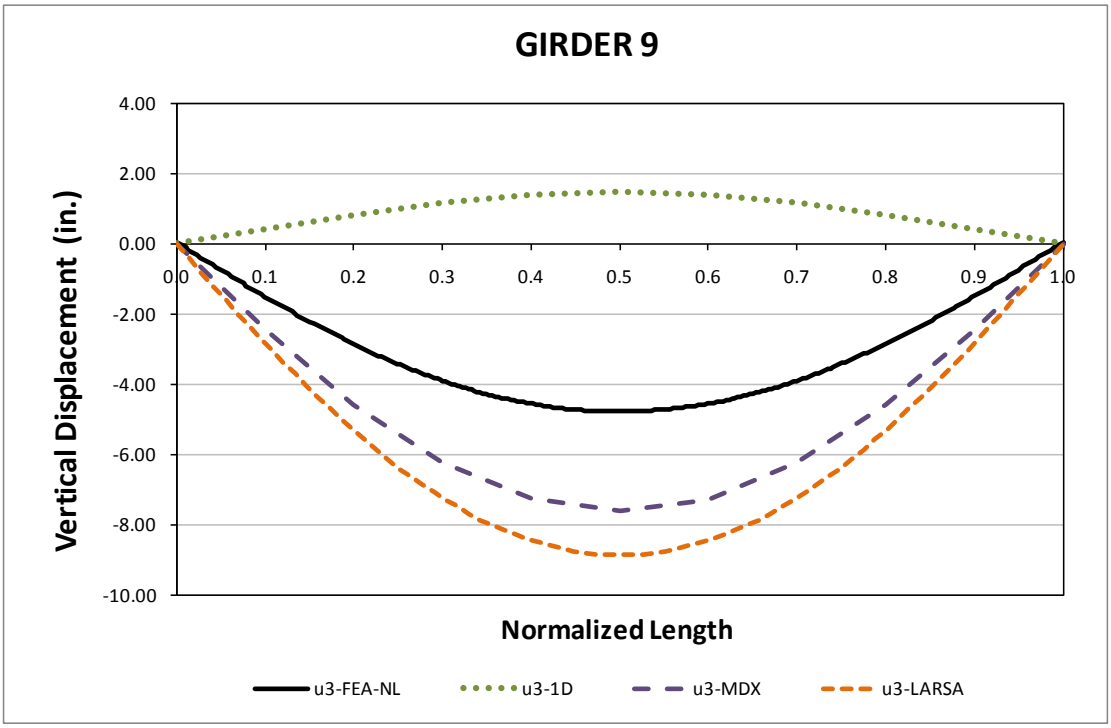

Fig. 3. NISCR11, Vertical displacements under total dead load for NLF detailing.

Figures 4 and 5 show fascia girder relative radial displacement predictions under total dead load. Usually 2D methods predict the relative radial displacements better at the cross-frame locations than within the unbraced lengths, but it is observed in this case that they cannot predict the radial displacements accurately for this bridge. This is believed to be because of the global nonlinearity of the system.

Figures 6 and 7 show the major-axis bending predictions of the outside and inside girders under total dead load. The stress predictions are close to each other for the outside girder. However, one can observe that there is a big difference in the predictions for the inside girder. This difference results primarily from the nonlinearity of the system. Approximate methods cannot capture these nonlinear effects.

Figure 8 shows the flange lateral bending stress predictions of the outside girder under total dead load. The nonlinearity in the results is significant due to global effects. Large span length and small girder spacing exacerbates the global effects in curved bridges.2D predictions are derived from the major-axis bending stresses. Flange lateral bending calculations for approximate methods are good as long as the major-axis bending stress predictions are close to the benchmark solutions. Although the stress predictions are close to each other on outside girder, the calculated flange lateral bending stresses are off from the benchmark solutions. This is mainly because approximate methods cannot account for nonlinear effects. This is mainly because approximate methods cannot account for nonlinear effects. The amplifier equation which is described in AASHTO Article 6.10.1.6, is used to account for the second order effects. The equation can be written as

$$f_l = \left[\frac{0.85}{1 - \frac{f_{bu}}{F_{cr}}}\right] f_{l1} \geq f_{l1}$$

where $f_{\ell 1}$ is the first order flange lateral bending stress, f_{bu} is the largest compressive major-axis bending stress throughout the unbraced length in the flange under consideration and F_{cr} is the elastic lateral torsional buckling stress. However, this equation is established by considering braced beam-column members whose ends are restrained by the other framing. Therefore, the equation does not handle the nonlinearity due to global effects. The actual second order amplifier is calculated as 3.68 for this bridge by comparing the 3D linear and nonlinear solutions. It is important to identify the sources of nonlinearity. The behavior can be only captured by conducting second-order analysis.

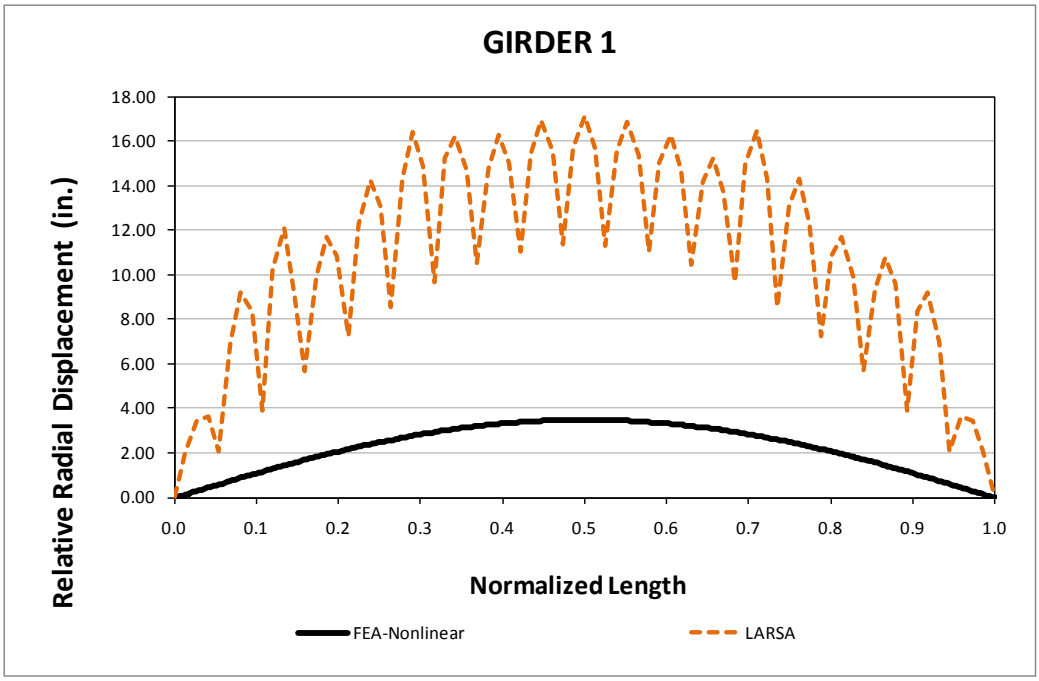

Fig. 4. NISCR11, Relative radial displacements under total dead load for NLF detailing.

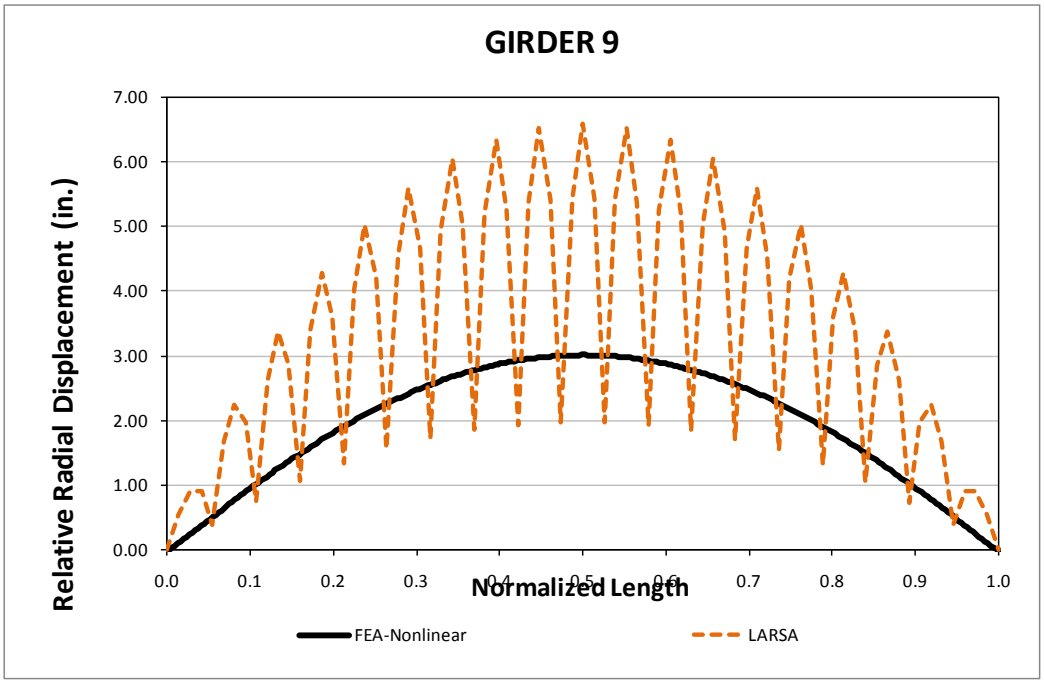

Fig. 5. NISCR11, Relative radial displacements under total dead load for NLF detailing.

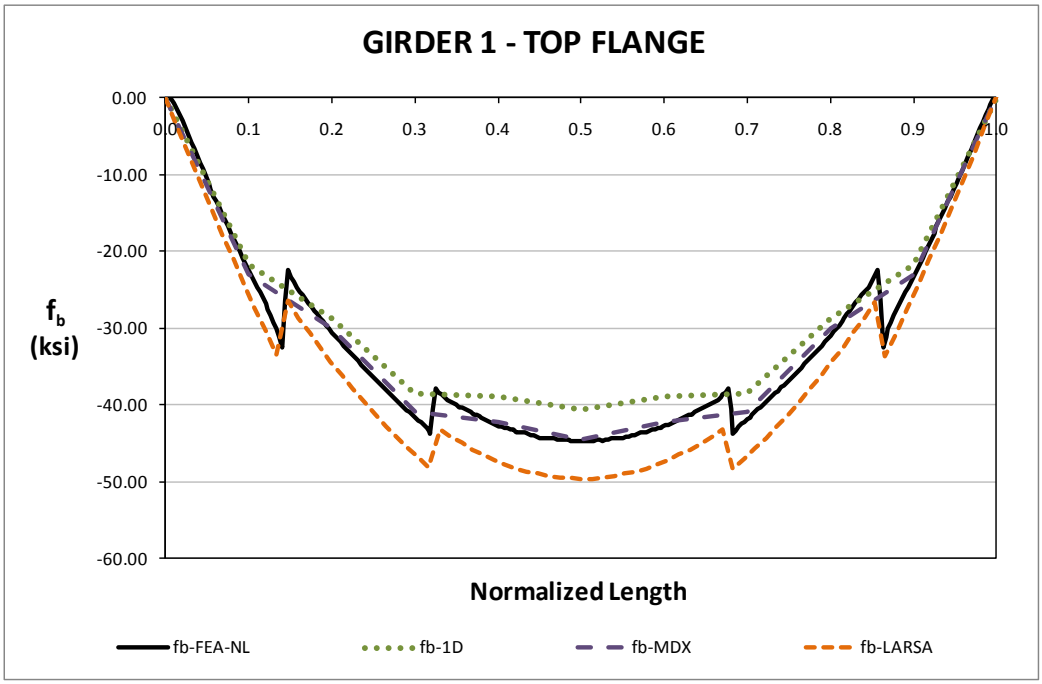

Fig. 6. NISCR11, Major-axis bending stresses under total dead load for NLF detailing.

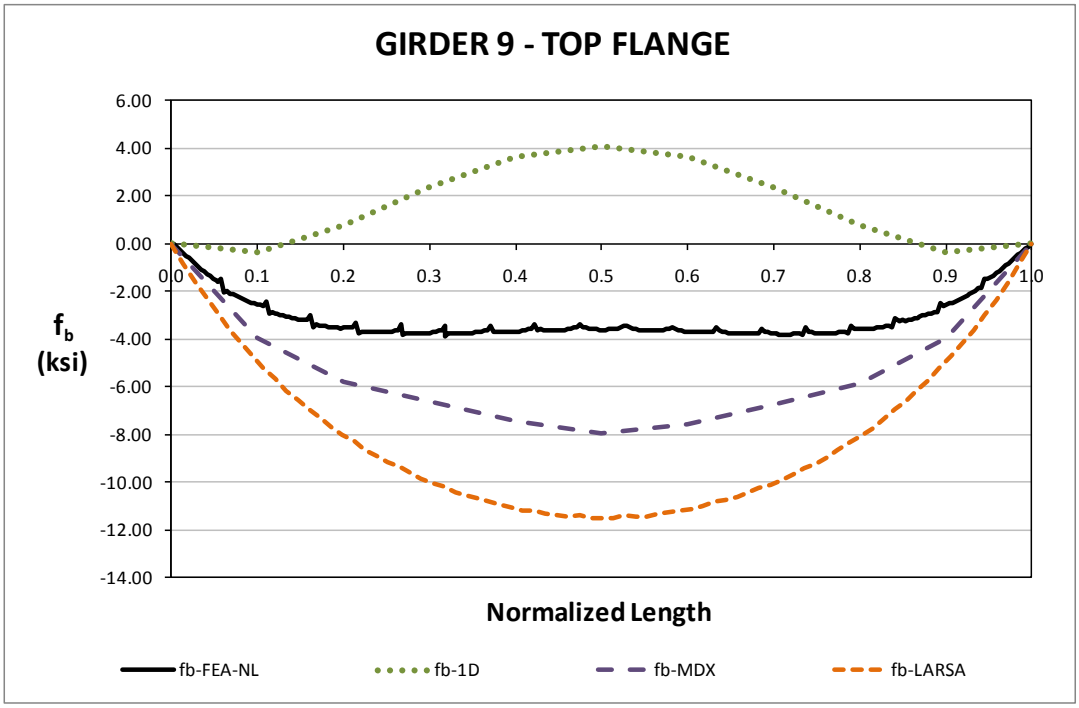

Fig. 7. NISCR11, Major-axis bending stresses under total dead load for NLF detailing.

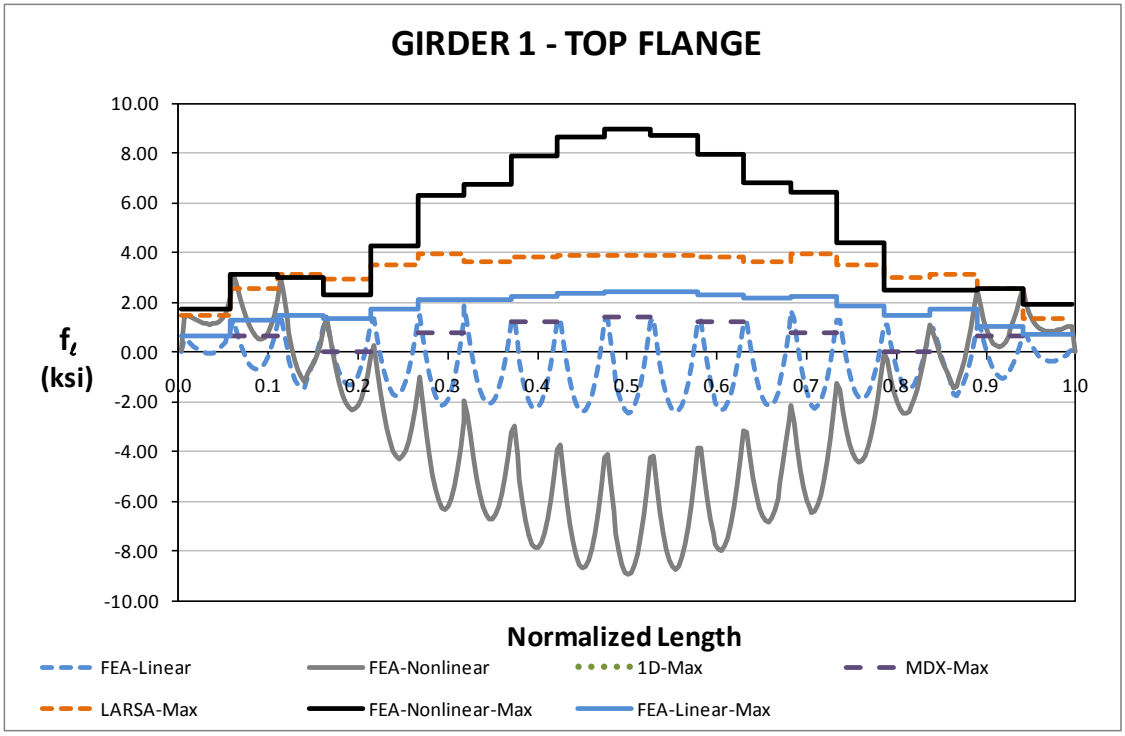

Fig. 8. NISCR11, Minor-axis bending stresses under total dead load for NLF detailing.

Conclusions:

It is observed from this bridge that neglecting the warping stiffness contributions can lead to error in the prediction of vertical displacements for 2D grid models. Small L_b/R ratio increases the prediction accuracy of 2D grid solutions as the effect of neglecting warping stiffness becomes negligible.

In the case of radial displacements, it is observed that the 2D grid models cannot predict the relative radial displacements accurately along the length. It is also observed that the error of predicting relative radial displacements is smaller at the cross-frame locations than the error obtained within the unbraced lengths. However, relative radial displacements are not very accurate at the cross-frame locations due to high nonlinearity of the system.

The major axis bending stresses seem to be less affected by the warping contributions. However, the nonlinearity in the system leads to prediction errors mainly in the inside girder. Flange lateral bending stress response predictions are good as long as the major-axis bending responses are predicted accurately. This is mainly because they are derived from the major-axis bending stresses by using the V-Load formula. Although the stress predictions are close to each other on the outside girder, the calculated flange lateral bending stresses are off from the benchmark solutions. This is primarily because approximate methods cannot account for nonlinear effects. It is also bserved that the nonlinearity in this bridge is due to the global nonlinear effects which cannot be captured by the AASHTO amplifier equations. This is because this equation is derived for individual unbraced lengths. It is concluded for that bridge that second order analysis is needed to capture the better accuracy for the flange lateral bending stresses. It is important to identify when the second order analysis is needed.

I5.1 EICCR4 (Existing, I-girder, Continuous-span, Curved, Radial supports)

Bridge Description :

Ramp GG John F. Kennedy Memorial Highway, I-95 Express Toll Lanes and I-695 Interchange, Baltimore Co, MD

Category Data:

L_1 = 219 ft, L_2 = 260 ft, L_3 = 211 ft, L_4 = 162 ft, L_5 = 256 ft, L_6 = 190 ft / R_1 = 968 ft ,1108 ft, $R_{2,3,4}$ =1108 ft, R_5 =968 ft, ∞ , R_6 = ∞ / w = 44 ft, 5 girders

Cross-Frame Detailing Method: NLF

Erection Stages Analyzed: 16 (Analyses are performed assuming NLF)

Deck Placement Sequence: 10 Stages (Analyses are performed assuming no staged deck placement).

Erection of portions of the structure observed in the field by White and Ozgur (GT), Erection engineering for this job performed by Cisneros (HSSI), detailed erection plans available.

Bridge Perspective & Plan Views:

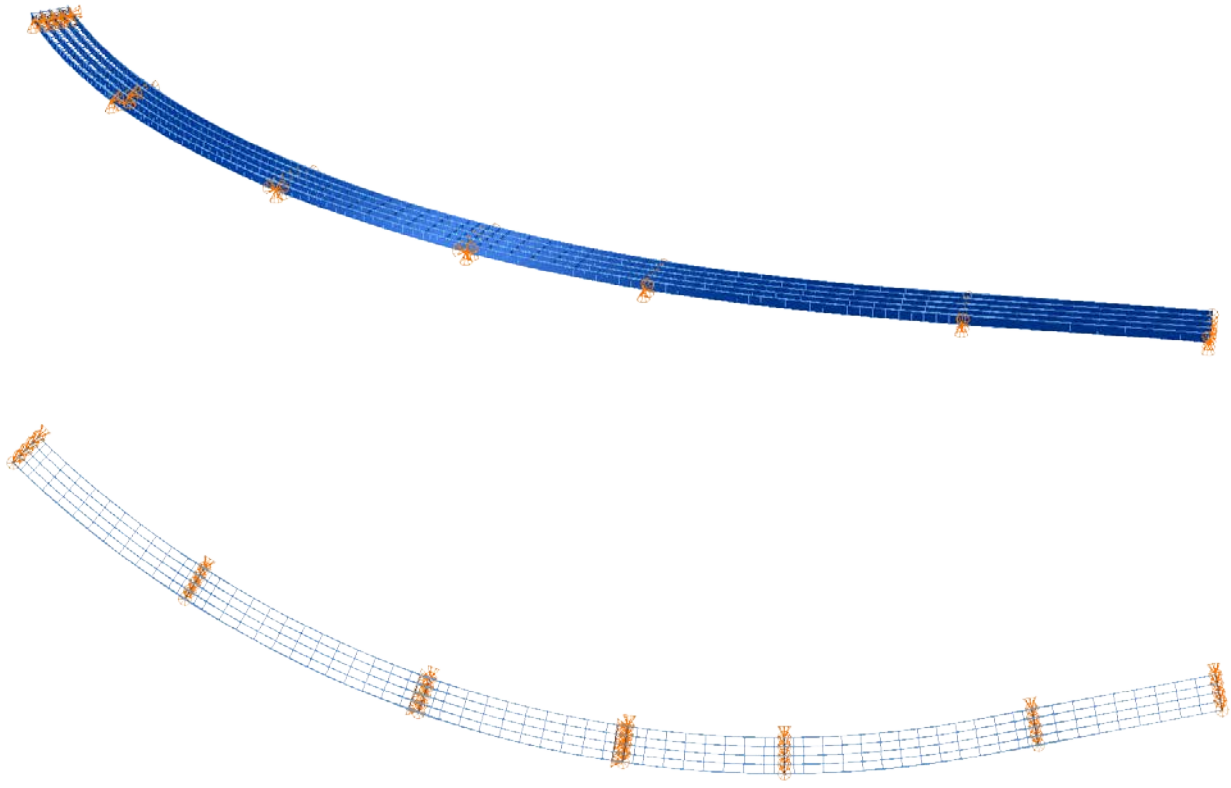

Abbreviated Analysis Results:

Figures 1 and 2 show the vertical and relative radial displacements of the outside girder (Girder 1) under steel dead load predicted by different analysis methods. Figures 3 and 4 provide the top flange major-axis and flange lateral bending stresses under steel dead load respectively. Vertical displacements are well predicted by different analysis methods excluding 1D results. The relative radial deflections predictions from 2D LARSA solutions are good at the cross-frame locations. In general, the major-axis bending stresses are accurately predicted. Therefore, the flange lateral bending predictions are reasonable for the simplified analysis solutions. However, this might not be the case for other cases. A particular erection stage is selected to illustrate this. Figure 5 shows the perspective and plan view of the selected stage. This stage is selected due to the erection of a long girder with large, unbraced lengths. There are two tie downs close to the end of the girder, and the girder is stabilized more with the holding crane as can be seen from Fig. 5. Figure 6 shows the vertical displacements of the outside girder (Girder 1) predicted by different analysis methods. The results are in good correlation for this particular erection stage. Figure 7 shows the major-axis bending stresses of this stage and again the results are in agreement. Figure 8 provides the flange lateral bending stresses for Girder 1. Although the major-axis bending stresses are in agreement, it is clear from Fig. 8 that flange lateral bending stresses are overestimated at the place where we have the longer unbraced length. Usually these stresses are calculated from major-axis bending stresses by using the formula:

$$f_\ell = 0.6\, f_b \frac{L_b}{R} \frac{L_b}{b_f}$$

where L_b is the unbraced length, R is the radius of curvature, f_b is the major-axis bending stress and b_f is the flange width. For the cases similar to Fig. 5 this formula overestimates the flange lateral bending stresses due to the large unbraced lengths. Therefore, this equation is not applicable for the erection stages where the unbraced lengths are large. Figure 9 shows the flange lateral bending stresses for G2 predicted by using the formula shown above. It is obvious from Fig. 9 that this equation gives reasonable estimates for the sections where all the cross-frames are connected.

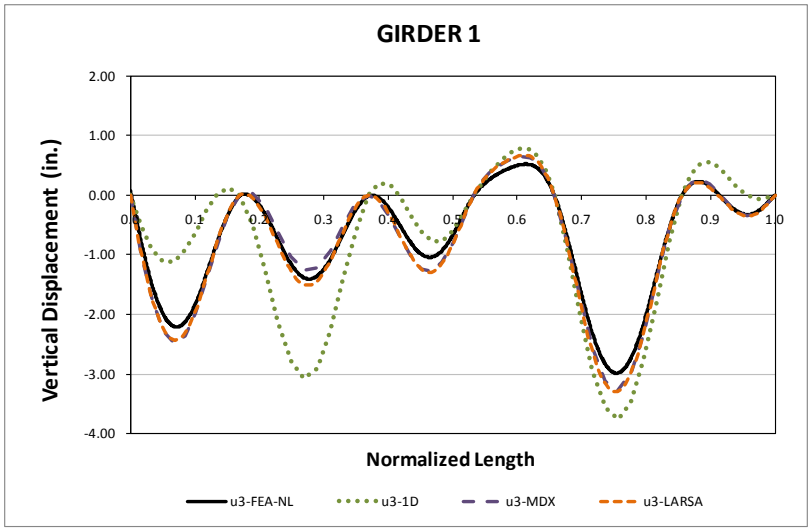

Fig. E.4.3-1. EICCR4, Vertical displacements under steel dead load.

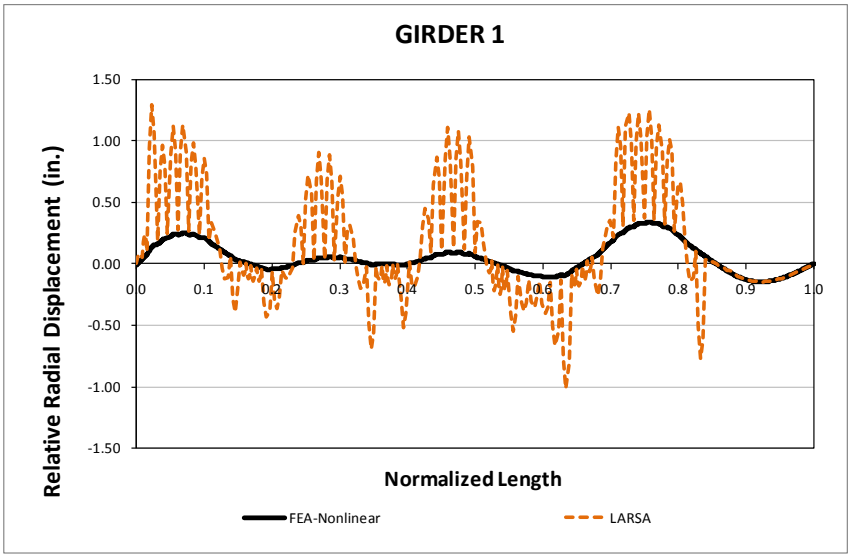

Fig. E.4.3-2. EICCR4, Relative radial displacements under steel dead load.

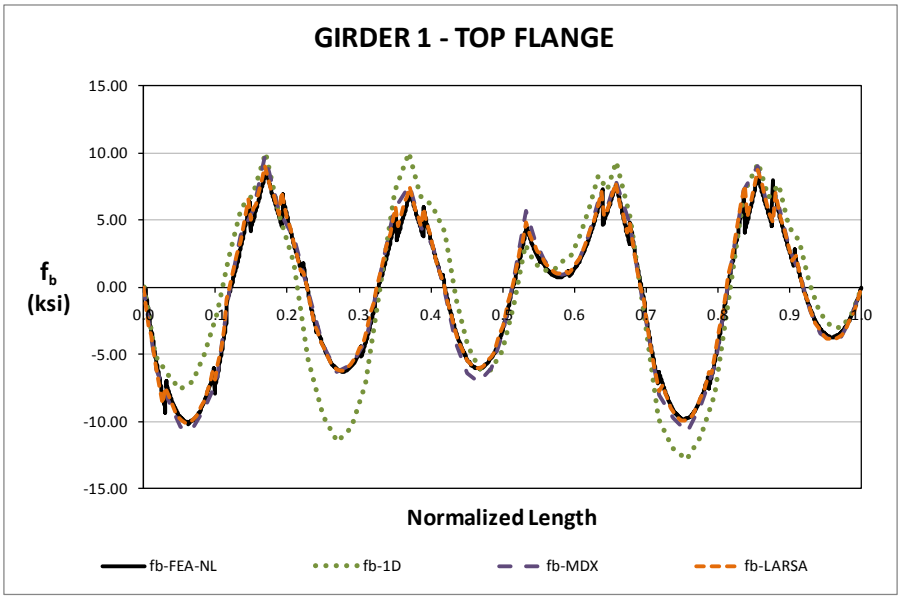

Fig. E.4.3-3. EICCR4, Major-axis bending stresses under steel dead load.

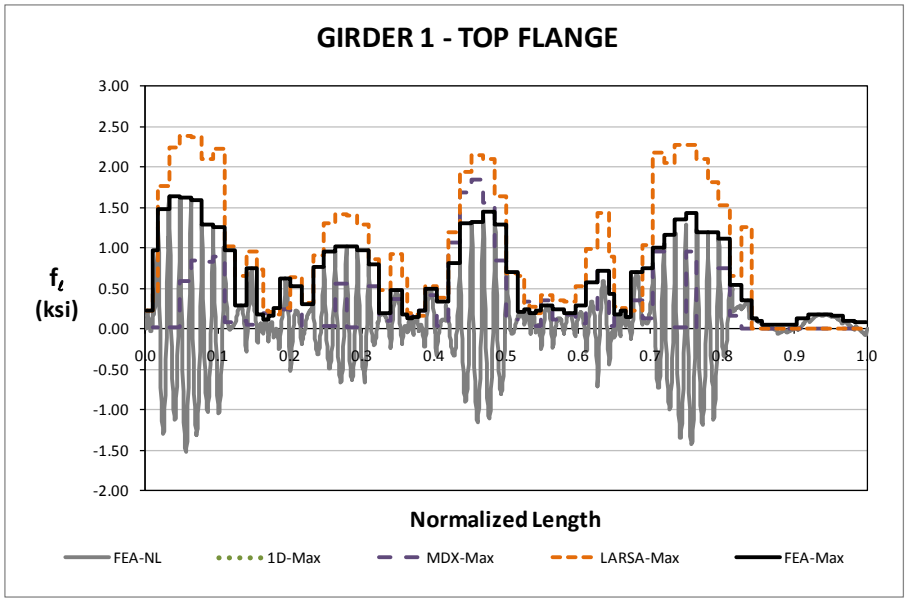

Fig. E.4.3-4. EICCR4, Flange lateral bending stresses under steel dead load.

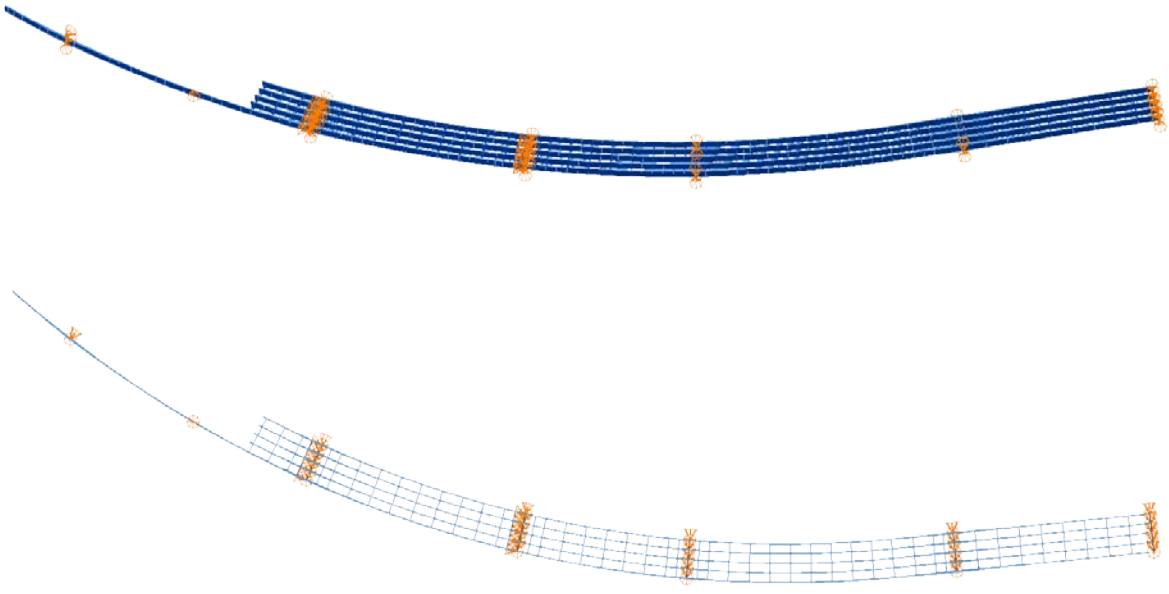

Fig. E.4.3-5. EICCR4, Perspective and plan view of a particular stage.

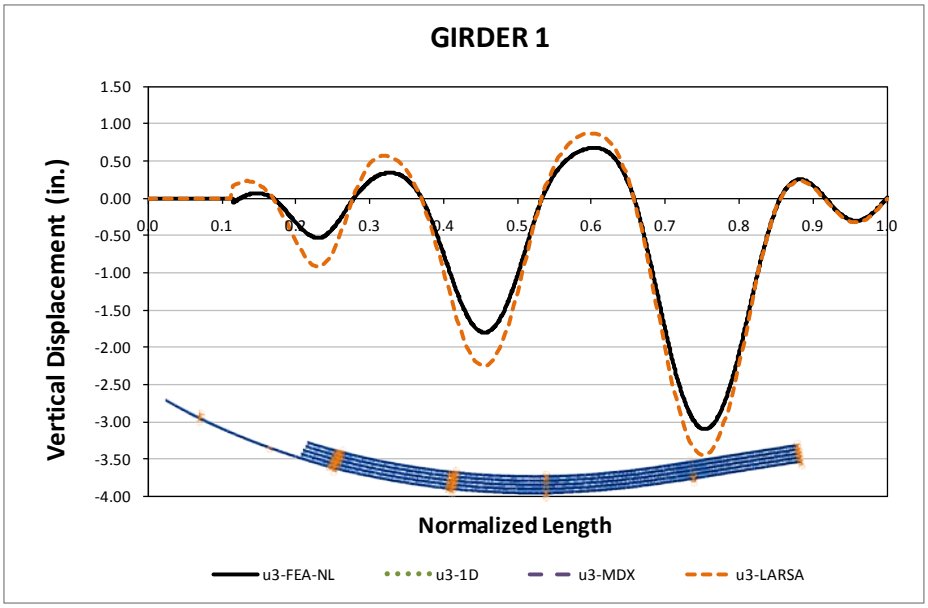

Fig. E.4.3-6. EICCR4, Vertical displacements under steel dead load.

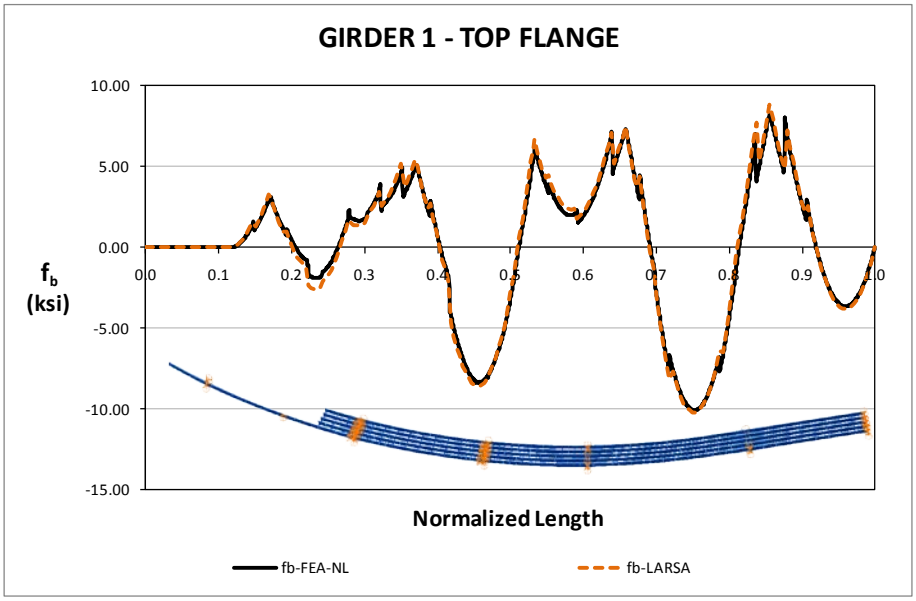

Fig. E.4.3-7. EICCR4, Major-axis bending stresses under steel dead load.

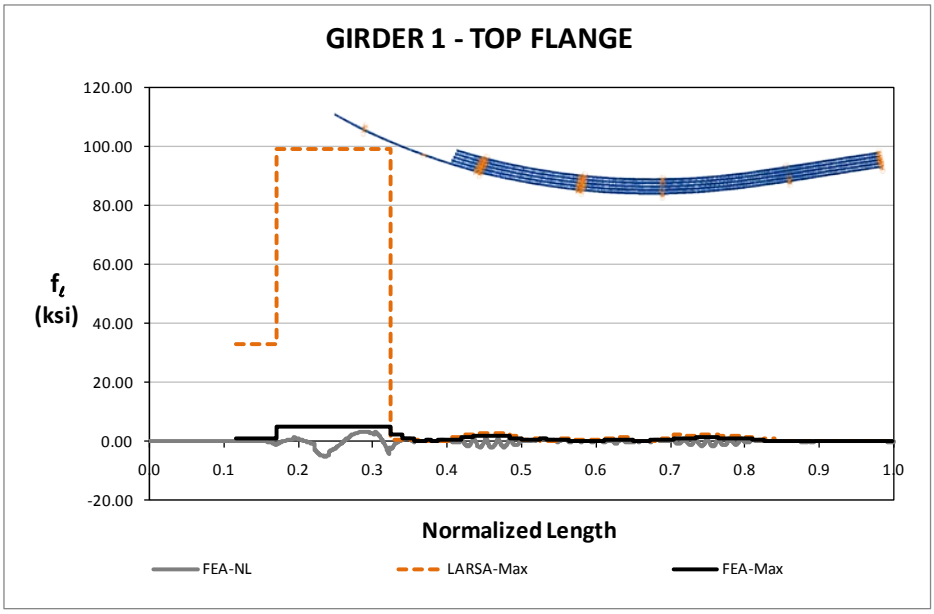

Fig. E.4.3-8. EICCR4, Flange lateral bending stresses under steel dead load.

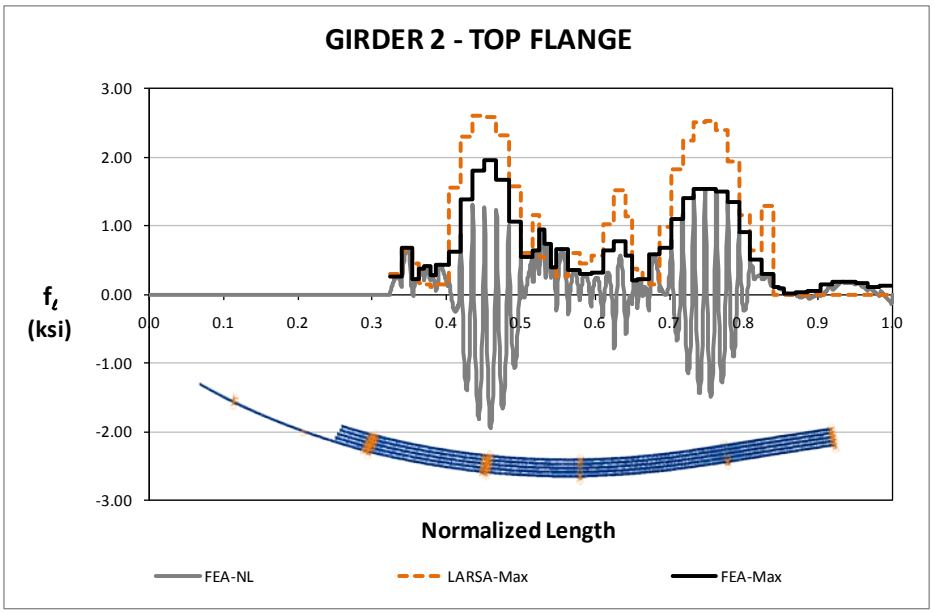

Fig. E.4.3-9. EICCR4, Flange lateral bending stresses under steel dead load.

I5.2 EICCR11 (Existing, I-girder, Continuous-span, Curved, Radial supports)

Bridge Description :

Ford City Bridge, Ford City, PA

Category Data:

L_1 = 322 ft, L_2 = 417 ft, L_3 = 329 ft / $R_{1,2} = \infty$, R_3 = 511 ft / w = 48.3 ft, 4 girders

References:

Studied originally by Chavel and Earls 2006a & b & 2001–flange lateral bracing system, field observations available.

Cross-Frame Detailing Method: NLF

Erection Stages Analyzed: 14 (Analyses are performed assuming NLF, SDLF, TDLF)

Deck Placement Sequence: 7 Stages (Analyses are performed assuming no staged deck placement)

Due to its substantial span length, combined with the depth and spacing of the I-girders, this bridge presented significant challenges during its erection. Dr. Chavel has studied this bridge extensively in his prior research. There are numerous complexities tied to the fabrication and erection of this bridge. However, as a result of Dr. Chavel's prior work and the significant information available regarding erection plans and observations of the bridge during erection, this bridge is a valuable one for the project team to include in its studies.

Bridge Perspective & Plan Views:

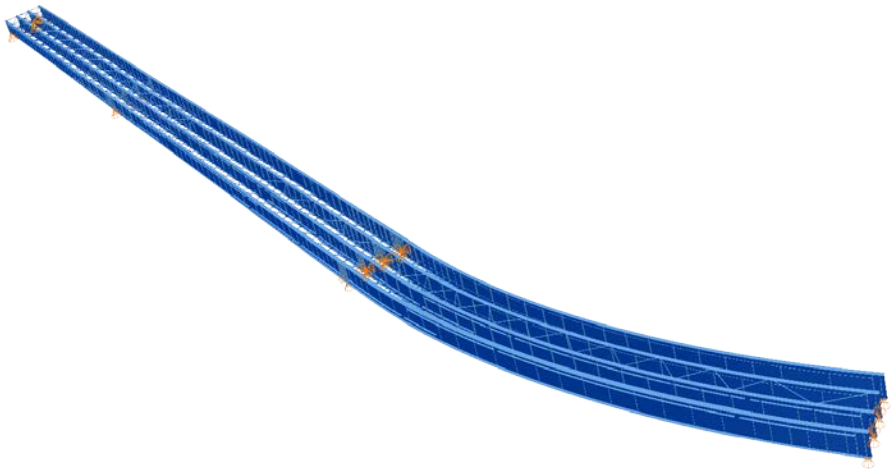

Abbreviated Analysis Results:

Although there is no top flange lateral bracing in the original design, flange lateral bracing systems are placed after the design is completed by the contractor for two reasons: 1) to control lateral deflections due to wind loading during construction, and 2) to try to help "zip up" the bridge to control the geometry associated with detailing errors. Certain members were loosened and others tightened as they fit up and finished off cross frame connections to solve the problems due to detailing. The 3D FEA models are run with and without the flange lateral bracing to illustrate the difference in the behavior under total dead load for NLF detailing. Figures 1, 2 and 3 show outside girder (Girder 1) vertical, radial displacements and stresses under total dead load respectively. Girder 2 stresses are shown in Fig. 4. It is observed from Fig. 1 that the vertical displacements change slightly due to usage of flange lateral bracing. Also, it is clear from Fig.2 that radial displacements are reduced when the flange lateral bracings are used. It should be noted from Fig.3 that the major-axis bending stresses are not affected significantly by the flange lateral bracing system. However, the flange lateral bending stresses are reduced drastically for the curved portion of the bridge for all girders. In contrast, flange lateral bending stresses for the straight portion are increased due to the additional forces that are coming from the flange lateral bracing. This behavior is more obvious in Fig. 4.

In all other analysis comparisons the flange lateral bracing system is removed to be consistent with the approximate analysis methods. Figures 5 and 6 show vertical and relative radial displacements of the outside girder (Girder 1) under steel dead load predicted by different analysis methods. Figure 7 provides the top flange major-axis bending stresses under steel dead load. Although the major-axis bending stress predictions are predicted well for this bridge, the accuracy of the displacement predictions is rather poor. Similar results are obtained under the total dead load. These results are illustrated in Figs. 8, 9 and 10.

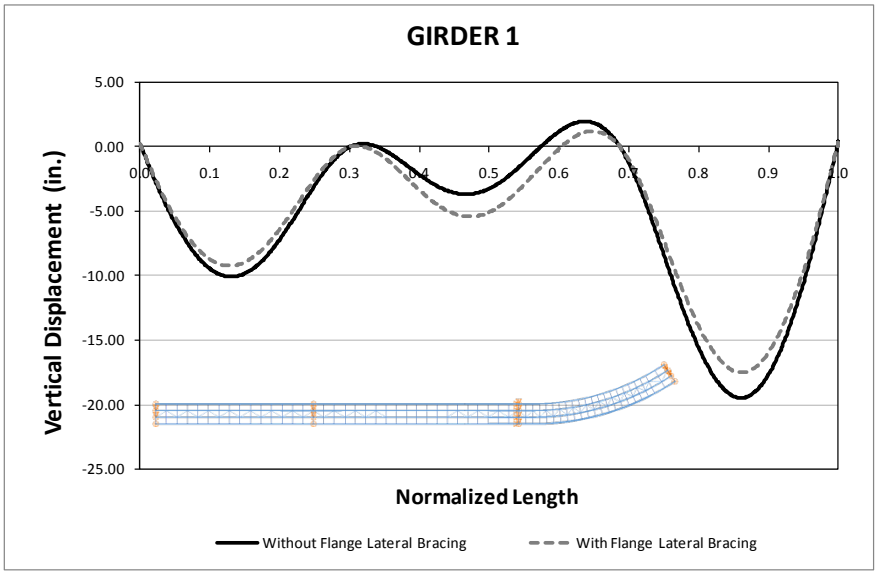

Fig. E.3.3-1. EICCR11, Vertical displacements under total dead load (NLF).

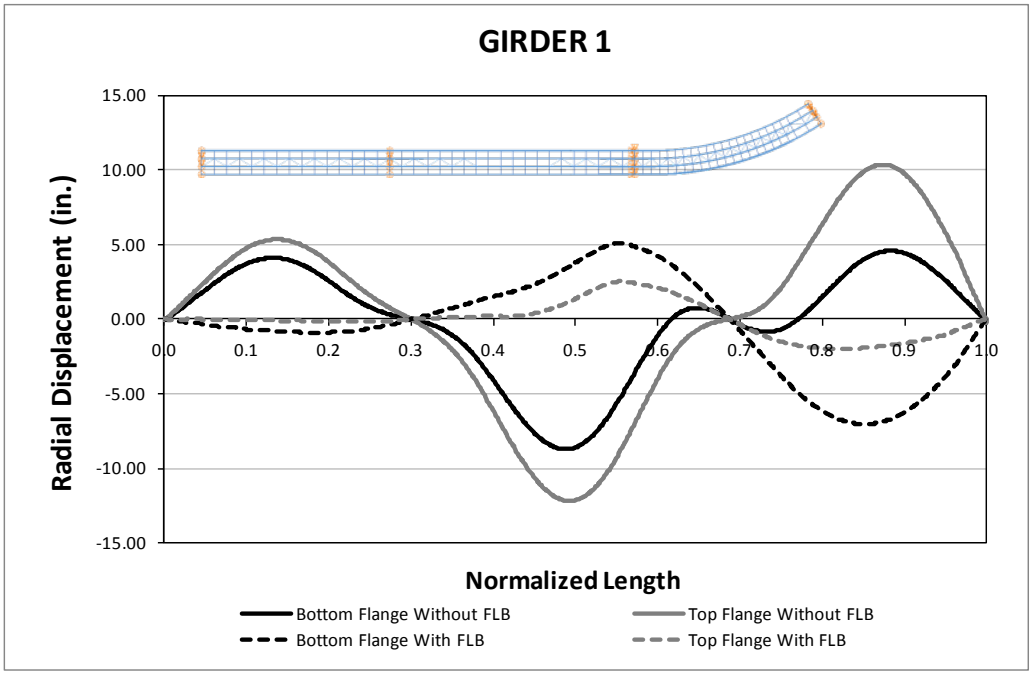

Fig. E.3.3-2. EICCR11, Radial displacements under total dead load (NLF).

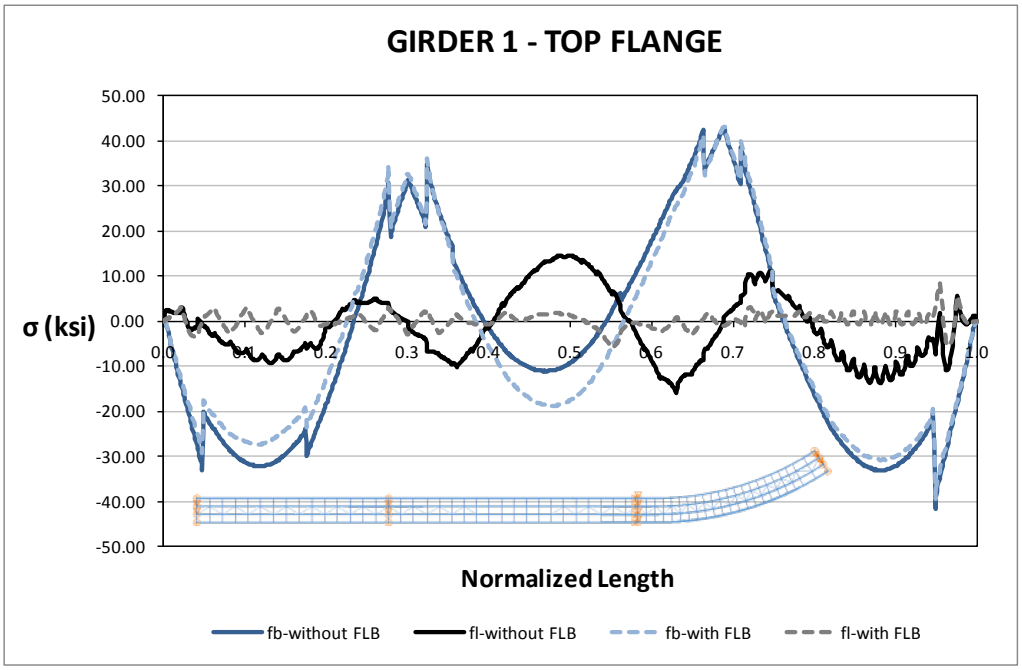

Fig. E.3.3-3. EICCR11, Major-axis and flange lateral bending stresses under total dead load (NLF).

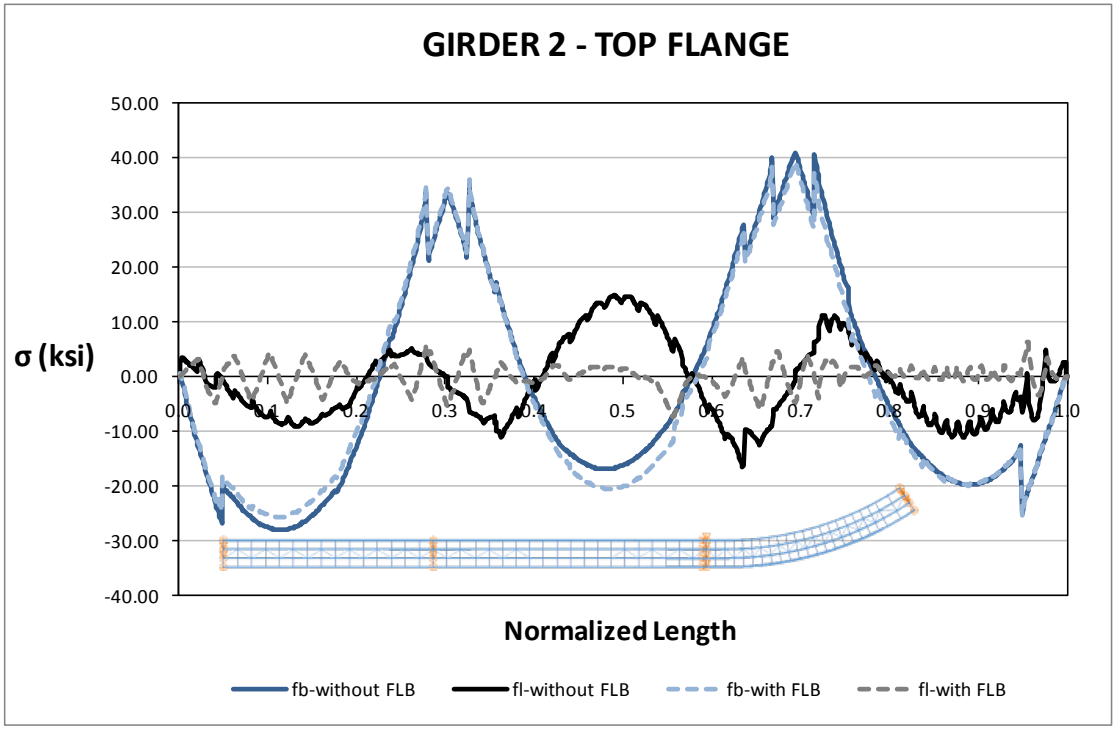

Fig. E.3.3-4. EICCR11 Major-axis and flange lateral bending stresses under total dead load (NLF).

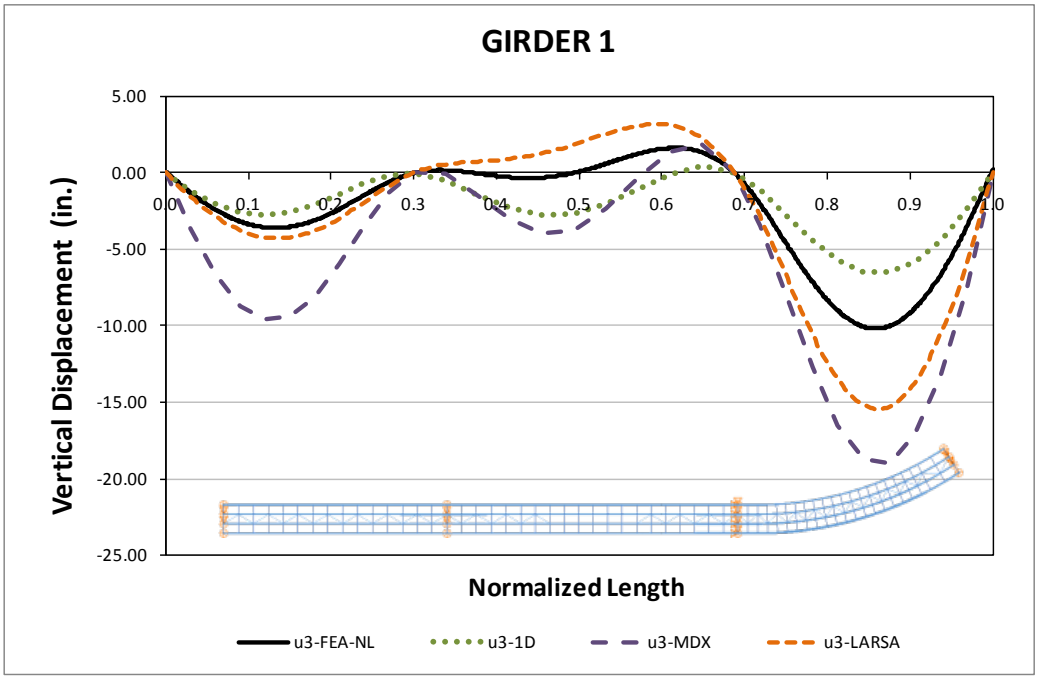

Fig. E.3.3-5. EICCR11, Vertical displacements under steel dead load.

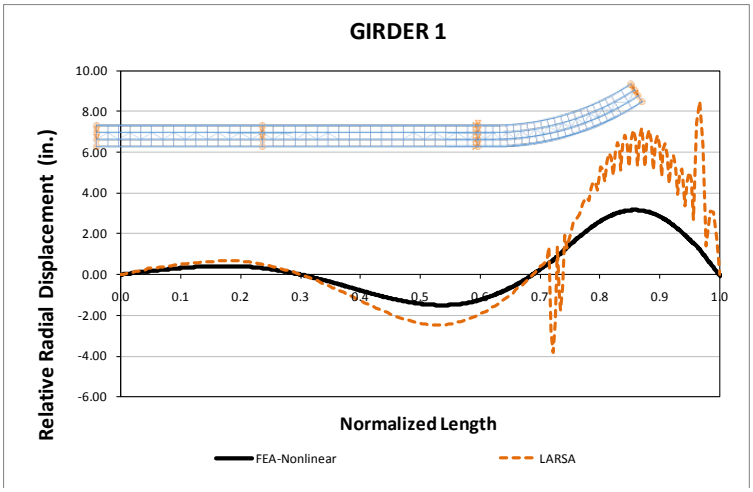

Fig. E.3.3-6. EICCR11, Relative radial displacements under steel dead load.

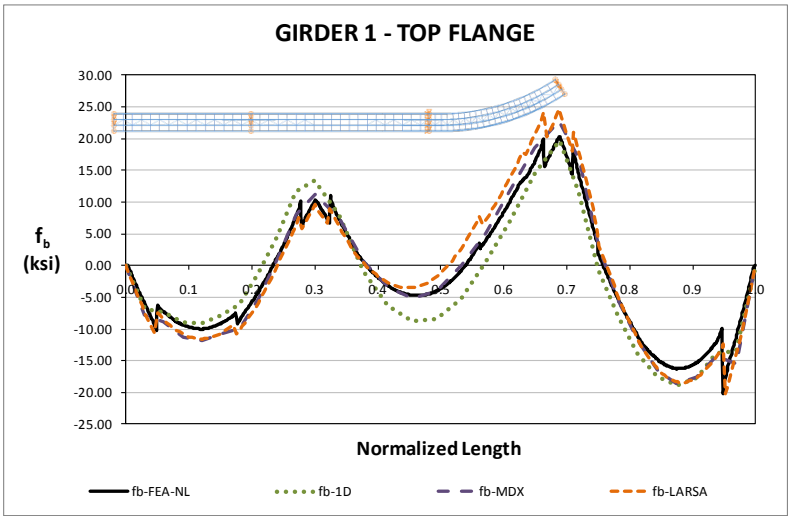

Fig. E.3.3-7. EICCR11, Major-axis bending stresses under steel dead load.

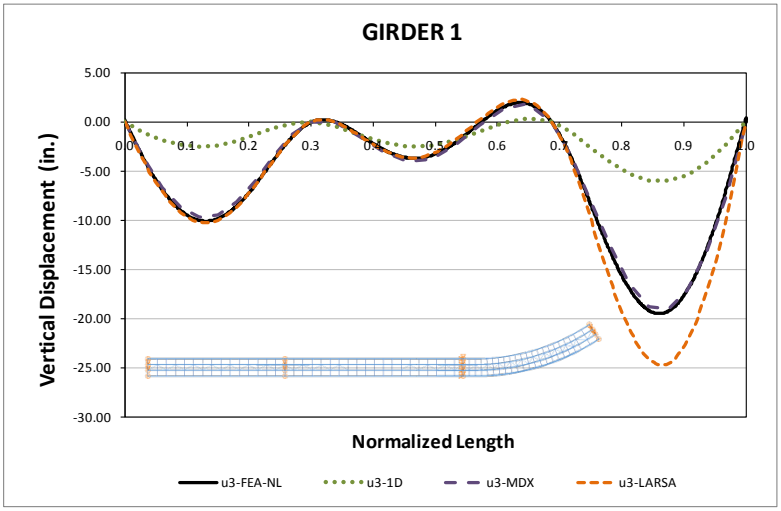

Fig. E.3.3-8. EICCR11, Vertical displacements under total dead load.

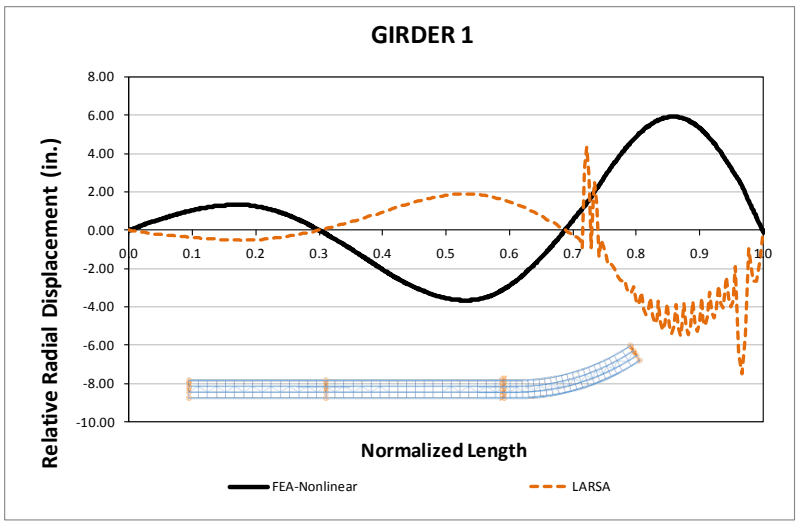

Fig. E.3.3-9. EICCR11, Relative radial displacements under total dead load.

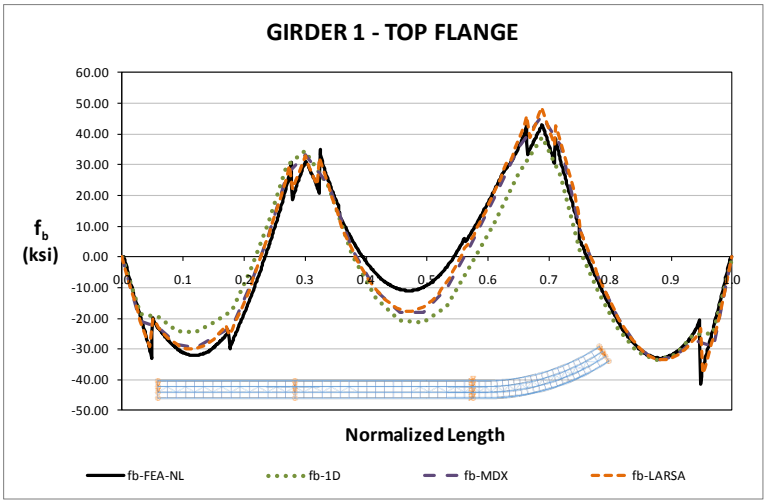

Fig. E.3.3-10. EICCR11, Major-axis bending stresses under total dead load.

Additional study is conducted to investigate the consequences of applying different detailing methods. Both SDLF and TDLF detailing methods are applied to this bridge on the 3D FEA platform. In all analyses the flange lateral bracing system is removed to be consistent with the original design. Figure 11 shows the stress responses of the outside girder (Girder1) under total dead load for different detailing methods. The results from Fig. 11 illustrate that flange lateral bending stresses are reduced significantly by applying TDLF detailing. However, it is also observed from this figure that major-axis bending stresses increase by 4 ksi due to TDLF detailing. Usually different detailing methods may introduce additional stresses and deflections in the components due to lack of fit between cross-frames and girders that might affect the system behavior. These additional responses are usually neglected by designers, which may cause problems during construction. The problems rise because these additional deflections cannot be tolerated during the deck pouring. Furthermore, additional deflections may affect the deflected shape drastically, which needs to considered in the camber diagram to avoid fit up problems.

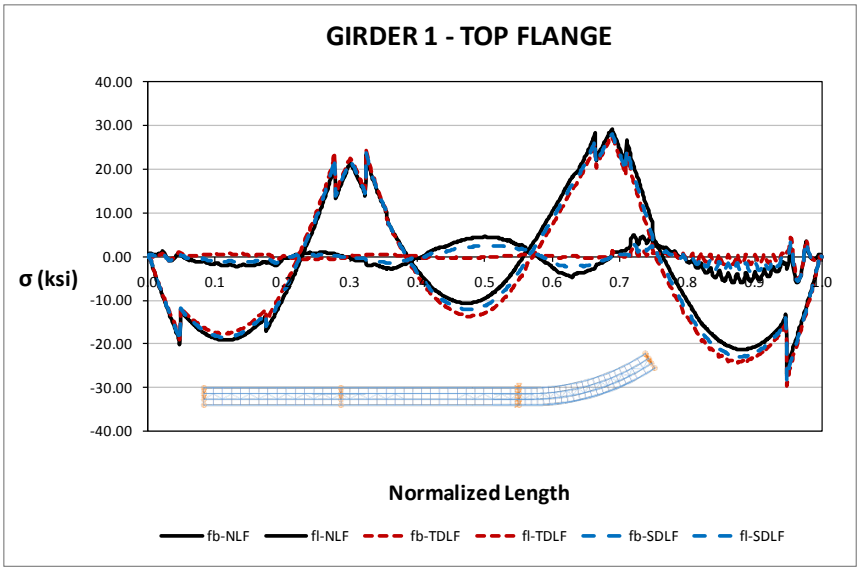

Fig. E.3.3-11. EICCR11, Major-axis and flange lateral bending stresses under total dead load for different detailing methods.

Figure 12, 13 and 14 show the deflections of the girders at the different stages for NLF, SDLF and TDLF respectively. It is observed from these figures that girder flanges are approximately plumb positions under steel dead load for SDLF whereas they are out of plumb for NLF and TDLF. Likewise, it is observed from these figures that girder flanges are approximately plumb positions under total dead load for TDLF whereas they are out of plumb for NLF and SDLF. Figure 15 illustrates the relative radial displacement of the outside girder (Girder 1). It is clear from the deflected shapes under the steel dead load that at this stage girders are twisting in opposite directions due to the lack of fit forces in the TDLF detailing method. Figures 16 and 17 show vertical displacements for outside (Girder 1) and inside girder (Girder 4) under total dead load for different detailing methods. It is clear from Figs. 16 and 17 that the difference in the deflections due to different detailing methods are high and cannot be tolerated anywhere. This is due to the additional deflections induced by the lack of fit forces. Additionally, it is clear that the camber of girders which is obtained based on the NLF deflections doesn't take into account these additional deflections if the TDLF or SDLF detailing method is used. This difference is more likely to cause fit up problems in the field. To avoid this problem, the cambered geometry of the girders needs to be updated if one wants to apply SDLF or TDLF detailing methods. Figure 18 shows the overall deflected shape of the bridge under total dead load for TDLF detailing with the updated camber. If the deflected shapes under total dead load of Figs. 14 and 18 are compared, it is observed that the girders are closer to plumb positions. Figure 19 shows the relative radial displacements of the outside girder obtained from TDLF detailing with initial (NLF camber) and updated camber. It is also clear from Fig. 19 that the girders are closer to the plumb positions. Figure 20 provides the vertical displacements of the outside girder obtained from TDLF detailing with initial and updated camber. It should be noted that the difference in the results is small and can be tolerated in the haunch.

It is also important to check the cross-frame forces for different detailing methods. Table 1 shows the maximum and minimum cross-frame forces obtained for different detailing methods. It is clear that the cross-frame forces increased for SDLF and TDLF detailing methods.

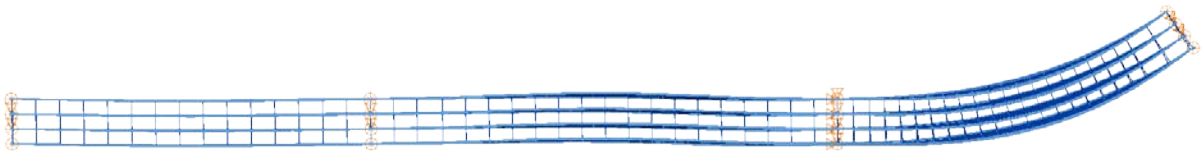

Deflected Shape under steel dead load for NLF detailing

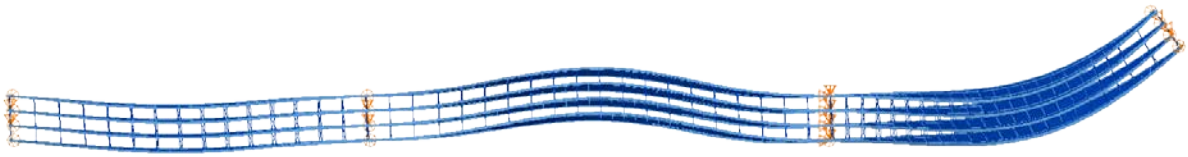

Deflected Shape under total dead load for NLF detailing

Fig. E.3.3-12. EICCR11, Overall deflected shapes at different stages for NLF detailing (Magnified by 25x).

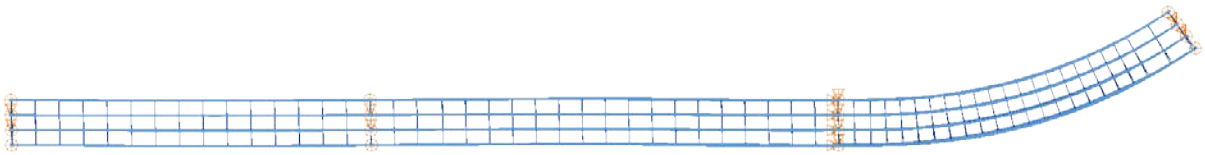

Deflected Shape under steel dead load for SDLF detailing

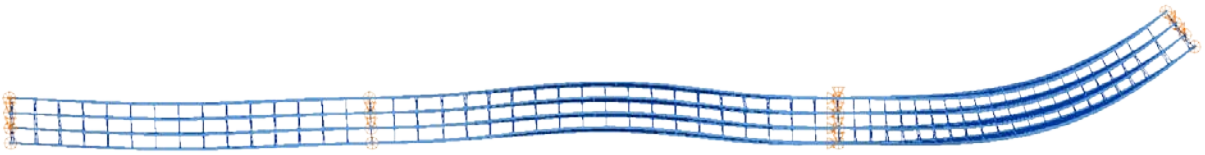

Deflected Shape under total dead load for SDLF detailing

Fig. E.3.3-13. EICCR11, Overall deflected shapes at different stages for SDLF detailing (Magnified by 25x).

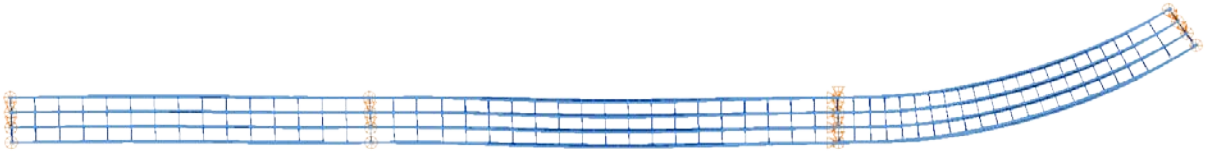

Deflected Shape under steel dead load for TDLF detailing

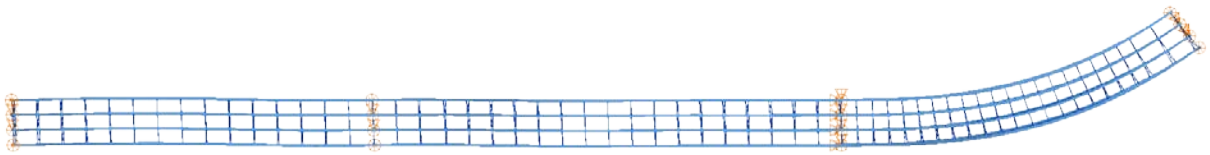

Deflected Shape under total dead load for TDLF detailing

Fig. E.3.3-14. EICCR11, Overall deflected shapes at different stages for TDLF detailing (Magnified by 25x).

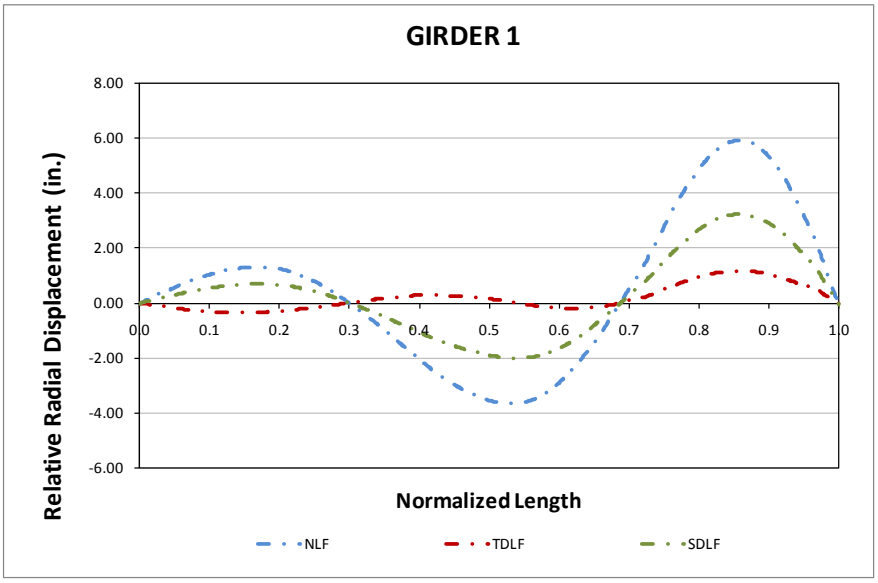

Fig. E.3.3-15. EICCR11, Relative radial displacements under total dead load for different detailing methods.

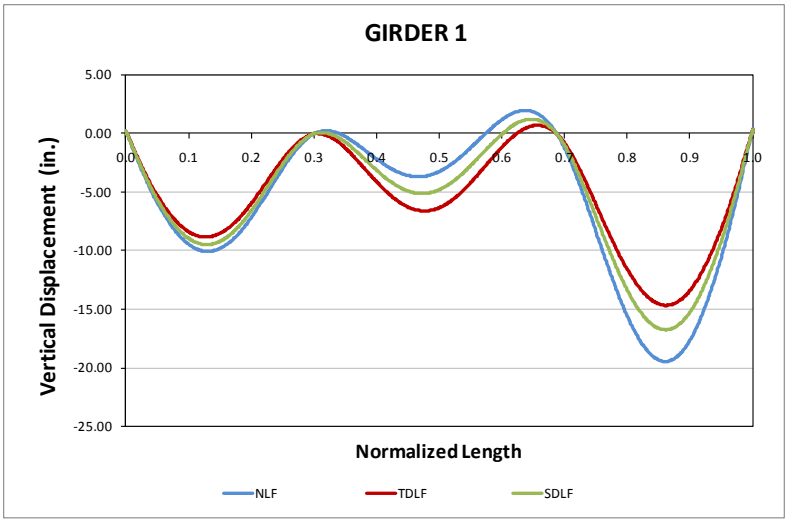

Fig. E.3.3-16. EICCR11, Vertical displacements under total dead load for different detailing methods.

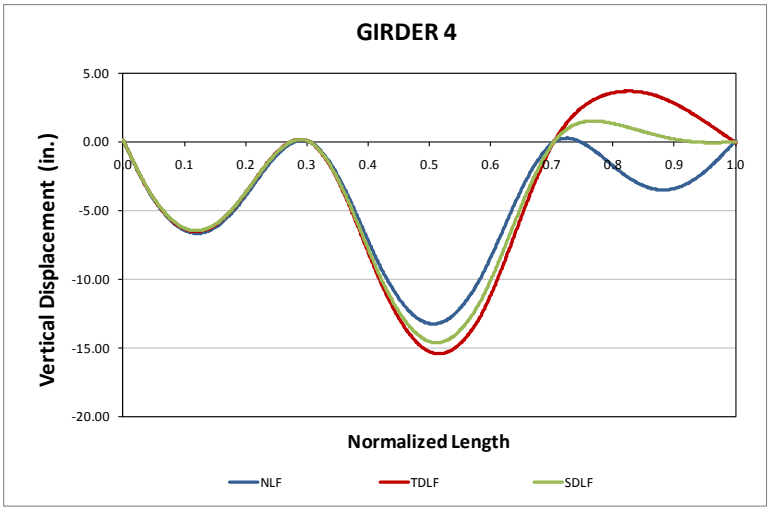

Fig. E.3.3-17. EICCR11, Vertical displacements under total dead load for different detailing methods.

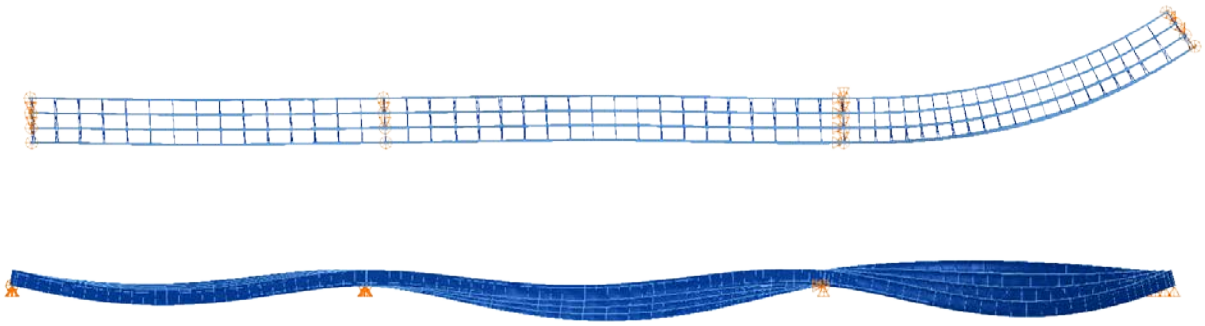

Fig. E.3.3-18. EICCR11, Overall deflected shapes under total dead load for TDLF detailing with the updated camber (Magnified by 25x).

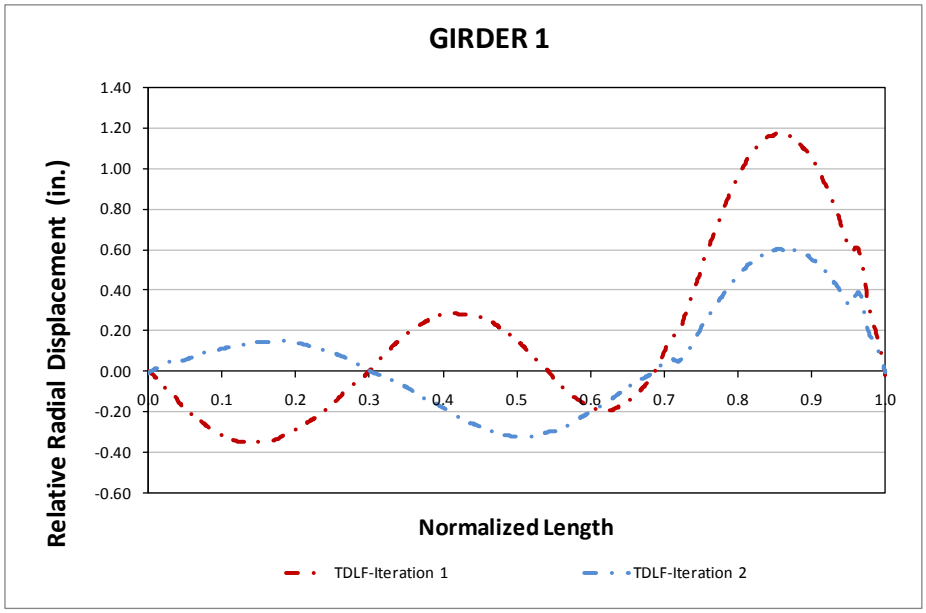

Fig. E.3.3-19. EICCR11, Relative radial displacements under total dead load for TDLF detailing with initial and updated camber.

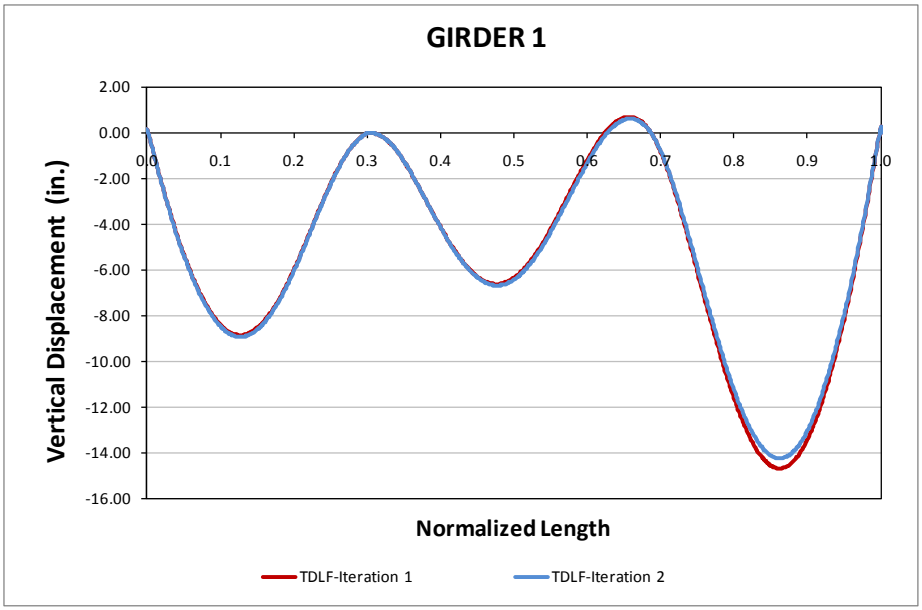

Fig. E.3.3-20. EICCR11, Vertical displacements under total dead load for TDLF detailing with initial and updated camber.

Steel Dead Load (ksi)						
Detailing	Top Chord		Bottom Chord		Diagonal	
Method	Max.	Min	Max.	Min	Max.	Min
NLF	3.9	-0.8	0.8	-3.9	2.0	-1.9
SDLF	4.4	-0.8	0.6	-4.8	4.0	-4.0
TDLF	4.8	-1.0	0.7	-5.4	5.6	-5.7

Total Dead Load (ksi)						
Detailing	Top Chord		Bottom Chord		Diagonal	
Method	Max.	Min	Max.	Min	Max.	Min
NLF	7.8	-2.0	1.6	-7.7	4.6	-4.6
SDLF	8.0	-2.2	1.8	-8.4	6.2	-6.3
TDLF	8.2	-2.4	1.9	-8.9	7.7	-7.9

Conclusions:

Flange lateral bracing can be used to control radial displacements for long span bridges. The flange lateral bending stresses at the curved part of the bridge reduced significantly by using flange lateral bracing systems. However, flange lateral bending stresses are increased for the straight portion due to the additional forces resulting from the flange lateral bracing.

In general, different detailing methods may introduce additional stresses in the components due to lack of fit between cross-frames and girders. These additional stresses might affect the system behavior. However, they are usually neglected by designers, leading to poor prediction of radial displacements and behavior. In this bridge, these additional responses are too large to avoid and affect the camber of the girders, which may cause fit up problems. Cross frame forces are also a good indication for selecting the right detailing method.

I5.3 EICCR15 (Existing, I-girder, Continuous-span, Curved, Radial supports)

Bridge Description :

SR 6220 A11 over SR 6220 NB & SB, Centre Co., PA

Category Data:

L_1 = 210 ft, L_2 = 271 ft / R = 1921 ft / w = 48.9 ft, 5 girders

References:

Studied originally by Shura (2004) & Domalik et al. (2005), More recently studied by Linzell, Neulong & Seo (2008)

Cross-Frame Detailing Method: NLF

Erection Stages Analyzed: 7 (Analyses are performed assuming NLF)

Deck Placement Sequence: 4 Stages (Analyses are performed assuming no staged deck placement)

Bridge Perspective & Plan Views:

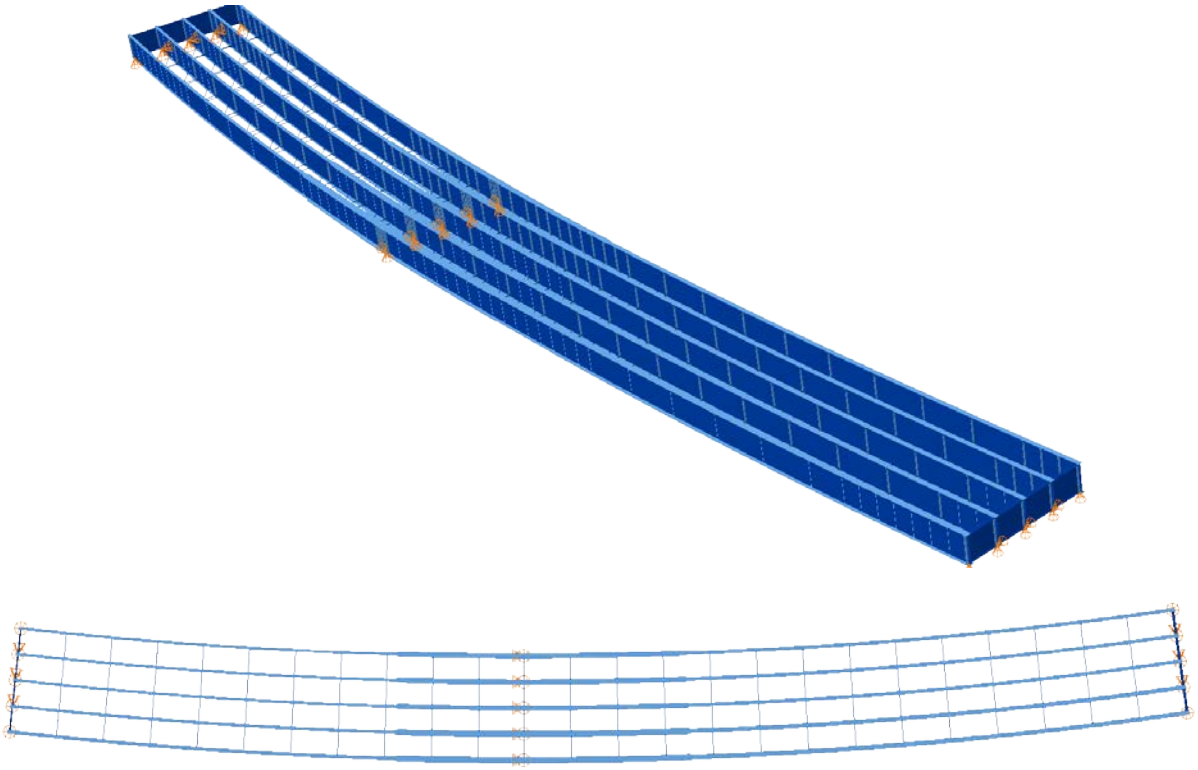

Abbreviated Analysis Results:

Due to the difference in the span lengths, this bridge exhibits a twist of its cross-section in the shorter span that is opposite in direction to the twist of the bridge cross-section in the longer span. This bridge has been referred to by some as exhibiting a response analogous to the "wringing of a towel." This behavior is illustrated by 3D FEA models in Fig. 1 under steel dead load. The deflections are magnified by 50 times. As mentioned before in the longer span the top flanges twist left due to differential deflections between girders whereas in the short span these deflections are in opposite directions. The opposite twist in shorter span is due to the behavior of the long span.

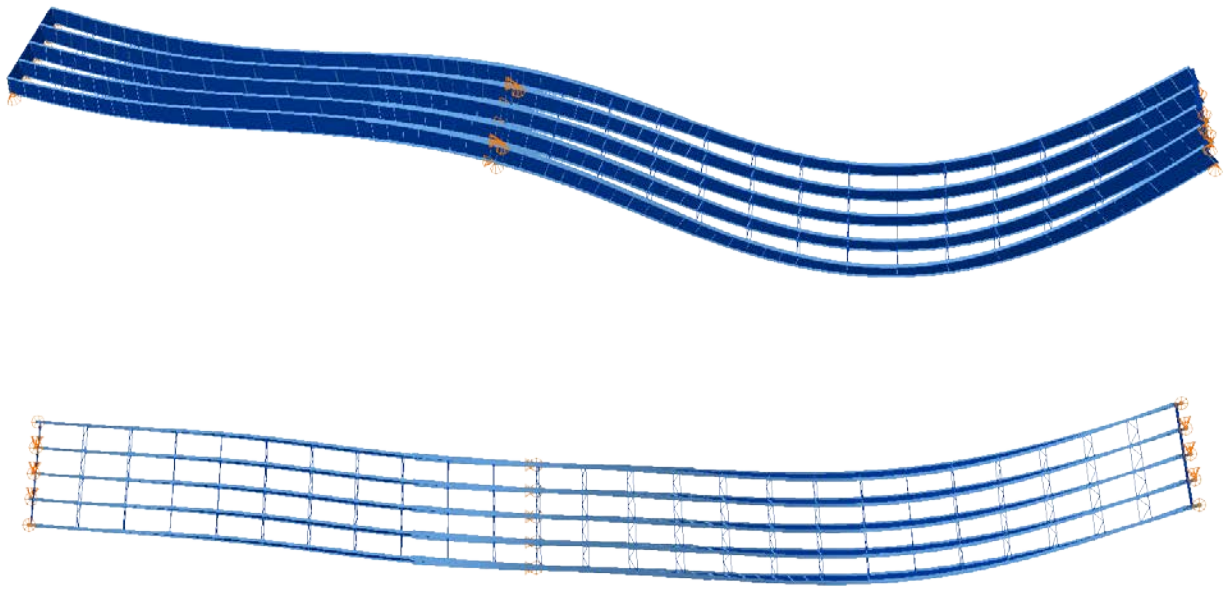

Fig. E.2.3-1. EICCR15, Deflected shape under steel dead load (Magnified by 50x).

Vertical deflections are presented in Fig. 2. The direction of the vertical deflections are opposite for each span. The longer span deflects downward where the shorter span deflects upward. The behavior on the shorter span is dominated by the behavior of the longer span. All the approximate methods predict this behavior well except the 1D method. It should be noted that L_b/R values are small for this bridge (0.001) which decreases the warping of flanges which leads to better prediction of displacements from 2D models. Figure 3 shows the relative radial displacements under steel dead load. 2D LARSA predictions are close enough at the places where we have cross-frames and between the unbraced lengths the behavior cannot predicted due to lack of warping stiffness in 2D LARSA models. This is the general case observed for curved bridges. Figure 4 shows the top flange major-axis bending stresses for the outside girder. Stresses are well predicted except 1D method for this bridge.

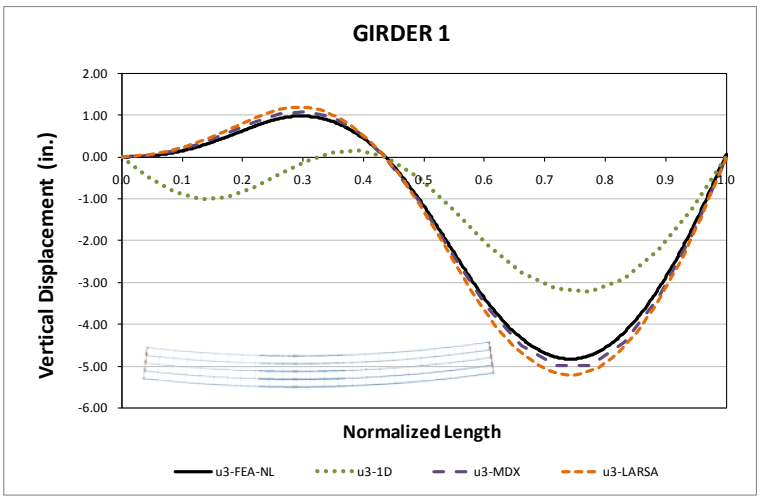

Fig. E.2.3-2. EICCR15, Vertical displacements under steel dead load.

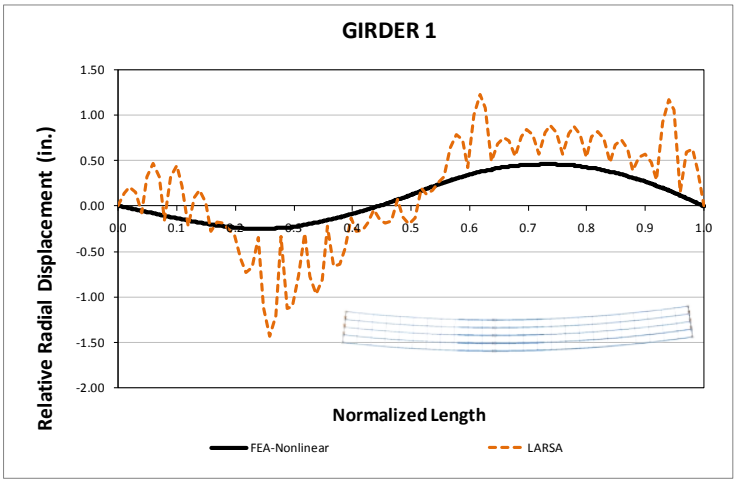

Fig. E.2.3-3. EICCR15, Relative radial displacements under steel dead load.

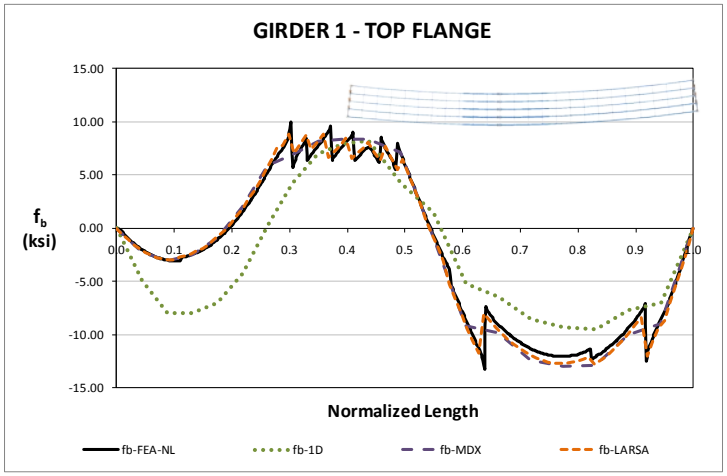

Fig. E.2.3-4. EICCR15, Major-axis bending stresses under steel dead load.

Conclusions:

Although the simplified methods neglect the warping stiffness of the girders, the prediction accuracy of vertical displacements are very good. This is mainly due to the small unbraced lengths of this bridge. Radial displacements are well predicted at the cross-frame locations by 2D LARSA models but between the unbraced lengths the behavior cannot predicted due to lack of warping stiffness in 2D LARSA models. This is the general case observed for curved bridges.

I5.4 EICCR22a (Existing, I-girder, Continuous-span, Curved, Radial supports)

Bridge Description:

Bridge No. 12: Ramp B over Ramp G, Robertson Ave.-Briley Parkway, I-40, Ramp E, Ramp A and Urbandale Road, Davidson County, TN

Category Data:

L_1 =172 ft, L_2 = 217 ft, L_3 = 217 ft, L_4 =195 ft, L_5 = 171 ft, L_6 = 172 ft, L_7 = 162 ft, L_8 = 192 ft / R_1 =791 ft, R_2 = 889 ft, $R_{3,4,5,6,7}$ = 746 ft, R_8 =766 ft (best fit to spiral curve) / w = 43 ft, 5 girders

Cross-Frame Detailing Method: NLF

Erection Stages Analyzed: 9

Deck Placement Sequence: 6 stages

(1) Positive moment regions of spans 8, 7 & 6

(2) Positive moment regions of spans 1, 2 & 3

(3) Negative moment regions over bents 1, 1-A, and 2

(4) Negative moment regions over bents 4, 5 and 6

(5) Positive moment region over bents 4 and 5, and negative moment region over bent 3

(6) Short lengths at the two ends of the bridge.

Bridge Perspective & Plan Views:

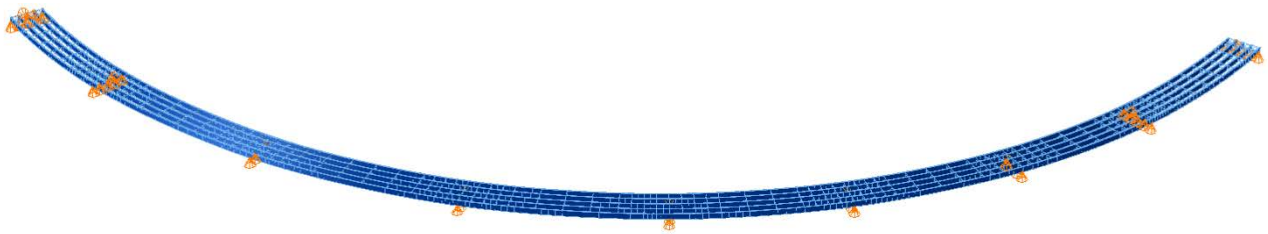

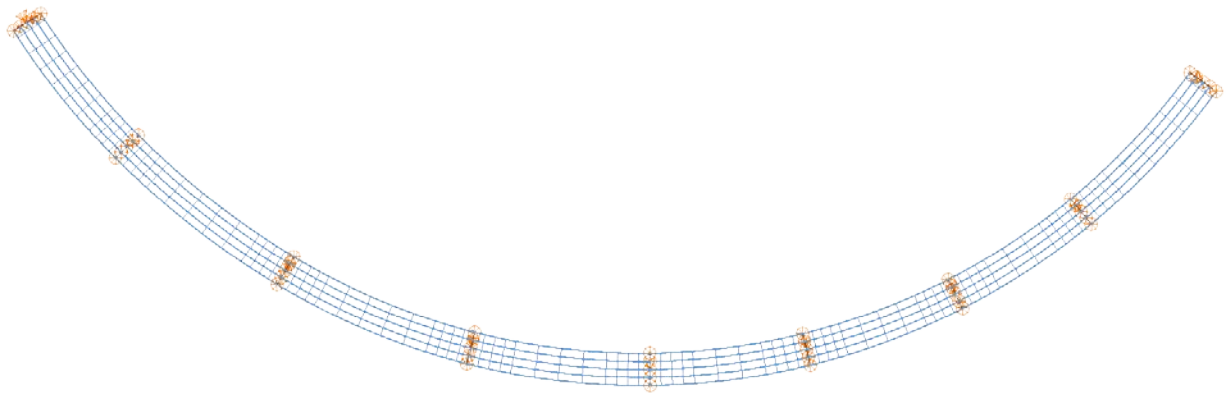

Abbreviated Analysis Results

A large number of results have been reported previously in the 1st Quarterly report of 2009 for the Ramp B bridge. These results were based on a hypothetical erection plan developed by the NCHRP 12-79 project team. Updated analyses of the nine stages of the actual bridge erection have been completed by the NCHRP 12-79 team. The final concrete deck placement sequence is eminent, but has not yet been established, at the end of this reporting period. An overview of the steel erection was provided in Appendix 3 of the previous quarterly report. The powerpoint slides in Appendix 3 of this report explain the instrumentation placed on Ramp B, show comparisons of predictions from 3D FEA and measurements from the field work, and summarize various analysis results.

I5.5 NICCR1 (New, I-girder, Continuous-span, Curved, Radial supports)

Category Data:

L_1 = 150 ft, L_2 = 150 ft, L_3 = 120 ft/ R = 227 ft / w = 30 ft / $\theta_1 = 0^o$, $\theta_2 = 0^o$, / $\theta_3 = 0^o$, $\theta_4 = 0^o$/ 4 girders

Cross-Frame Detailing Method: NLF

Erection Stages Analyzed: Seven

Deck Placement Sequence: Five stages, deck thickness = 9.5 in.

Bridge Perspective & Plan Views:

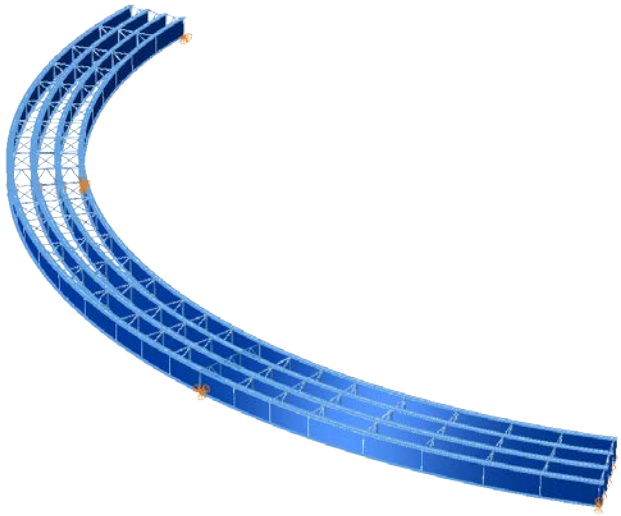

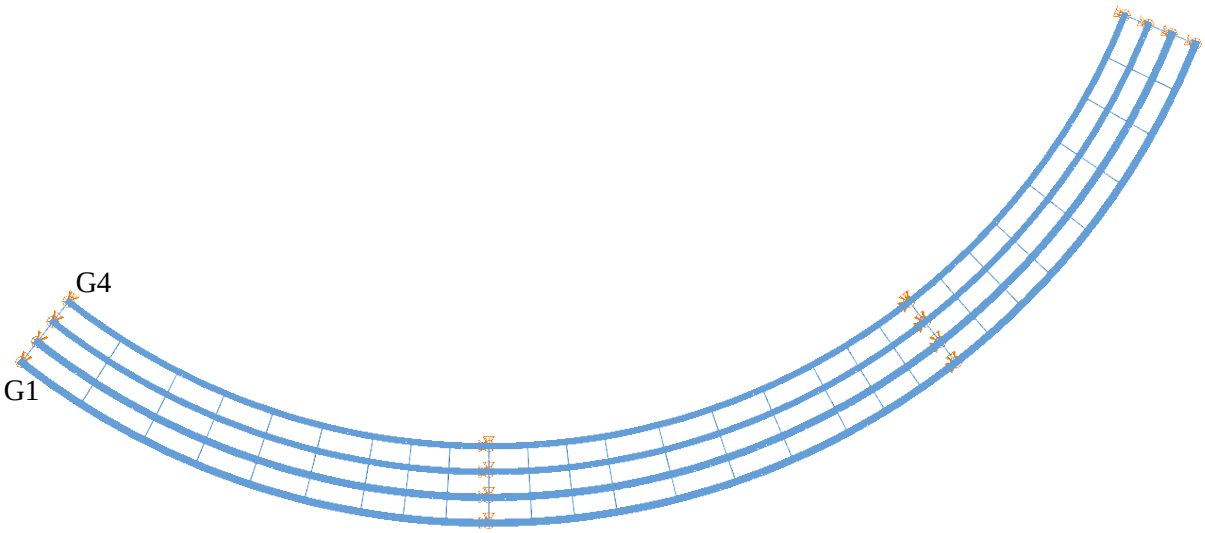

Abbreviated Analysis Results:

The erection of this bridge starts at the left end, with the placement of the first segment of girder G1. A temporary support is provided near the right end of the segment. Following the same procedure, girders G2 to G4 are placed. Next, the second segment of girder G1 is lifted and connected to the segment erected previously (Stage 8). In this operation, the girder is supported on the first interior bent, and cantilevers out from this support approximately 50 ft. The steel erection continues with the placement of girder G1 over Span 3, as shown in Figure 1, Stage 10. A holding crane at midspan prevents the girder buckling, at this stage. In subsequent steps, girders G2, G3, and G4 are erected with the same procedure, as shown for Stages 11 and 13 in Figure 1. Next, in Stages 14 to 17, the drop-in segments in Span 2 are erected to finish the structure. Stage 18 represents the total dead load condition of the structure.

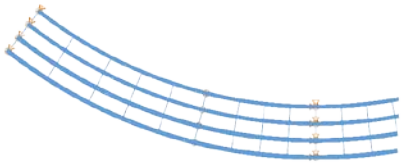

Stage 8

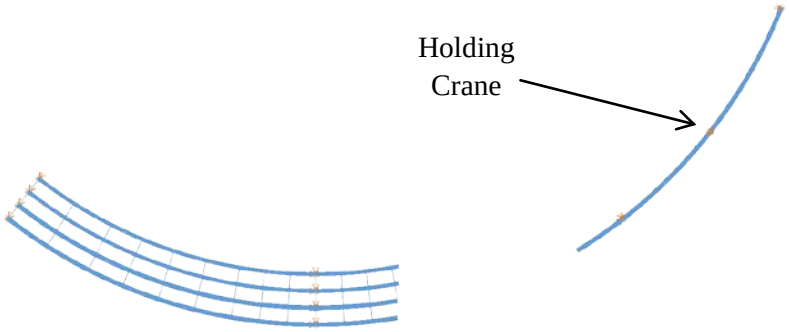

Stage 10

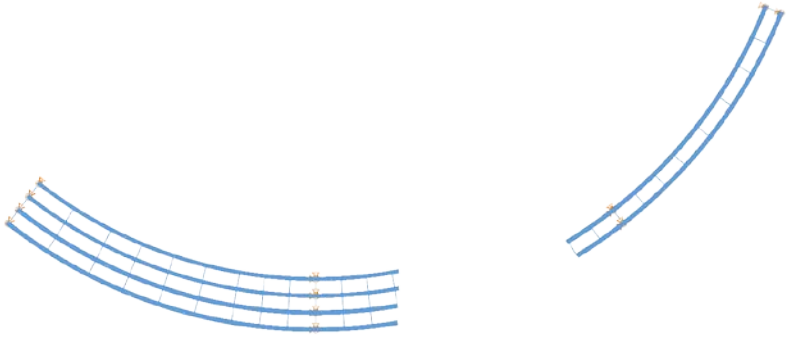

Stage 11

Fig. 1. Analyzed Construction Stages

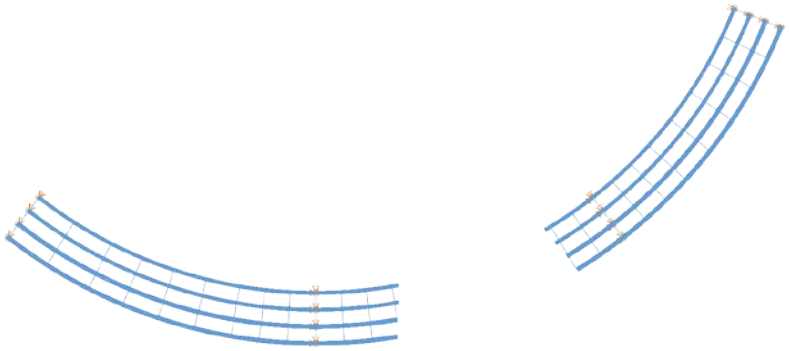

Stage 13

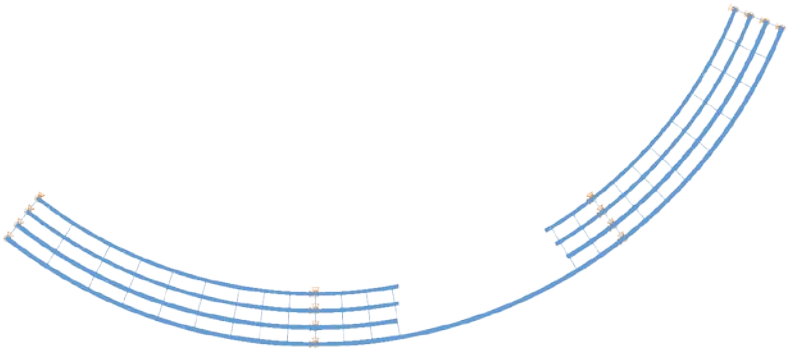

Stage 14

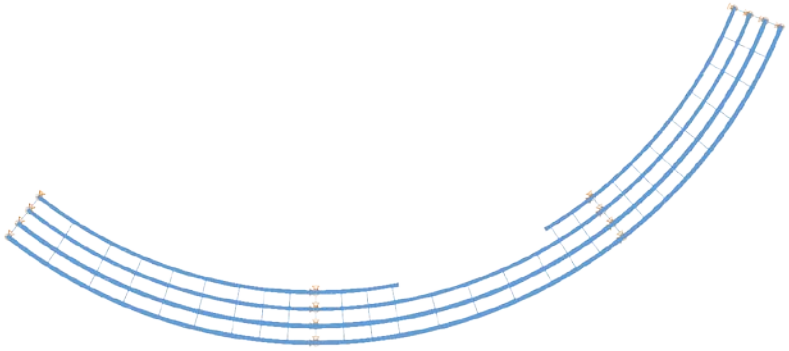

Stage 16

Fig. 1. Analyzed Construction Stages (Continued)

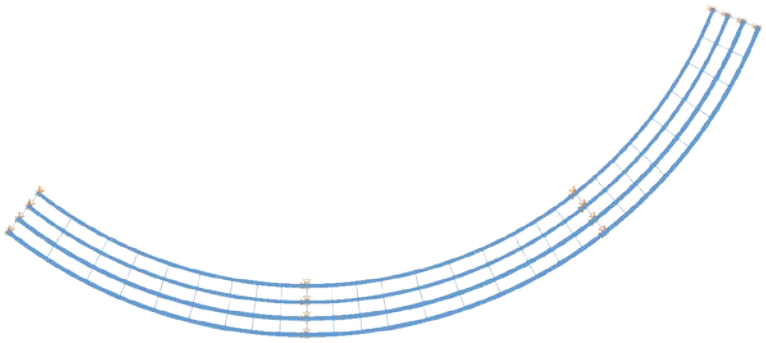

Stage 18 (TDL)

Fig. 1. Analyzed Construction Stages (Continued)

The major-axis bending response is studied first. The stress response for the top flange of the exterior girder, G1, in Stage 11 is shown in Figure 2. As shown in the figure, the 2D grid model representation captures accurately the 3D FEA prediction. In the case of the vertical displacements, the approximate representation does not present the same level of accuracy. As shown in Figure 3, the 2D grid prediction overestimates the expected displacements. This is observation is consistent with the results obtained in from the analysis of other curved bridges. The lack of a term that considers the contribution of flange warping in the torsional stiffness of the I-girders results in misrepresentations of the actual vertical displacements.

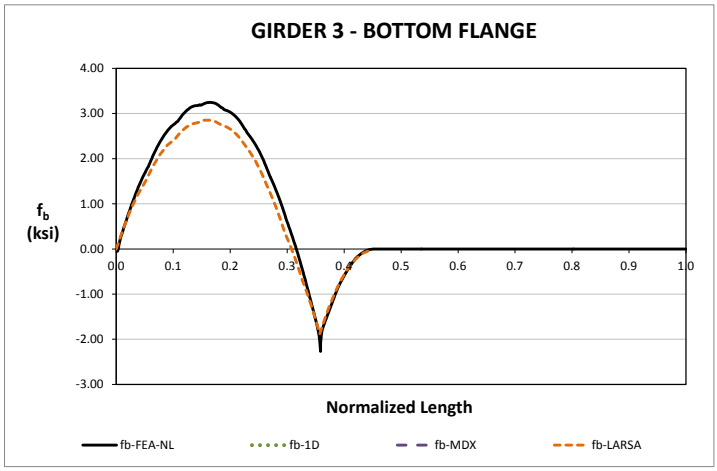

Fig. 2. Comparison of Major-Axis Bending Stresses, Stage 11

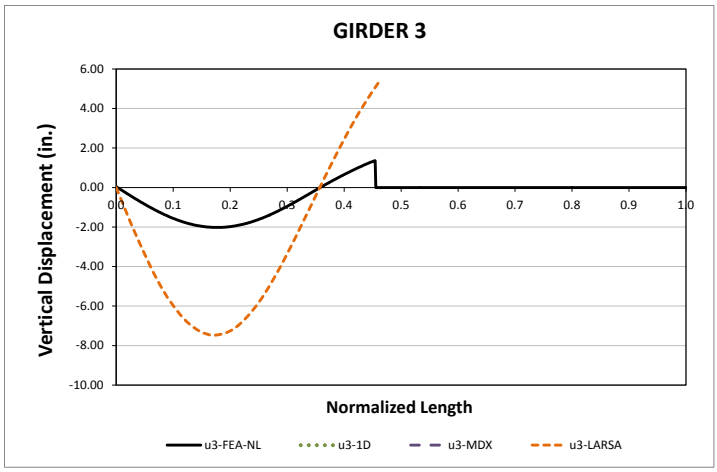

Fig. 3. Comparison of Vertical Displacements, Stage 11

For the final configuration, when the total construction dead load is applied to the structure, the approximate predictions are more accurate. As shown in Figure 4, the 1D and 2D predictions are a close representation of the benchmark. In the case of the vertical displacements shown in Figure 5, the 2D grid analysis accuracy is about the same as in the plot shown in Figure 3. In the case of the 1D analysis, both stresses and deflections are captured accurately for this bridge.

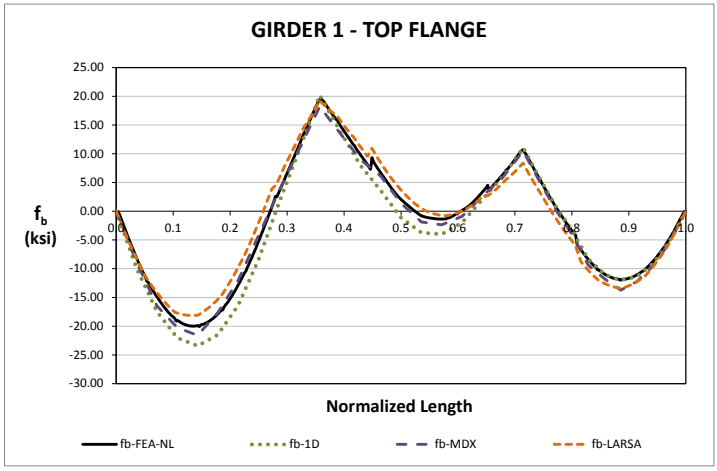

Fig. 4. Comparison of Major-axis Bending Stress, Stage 18

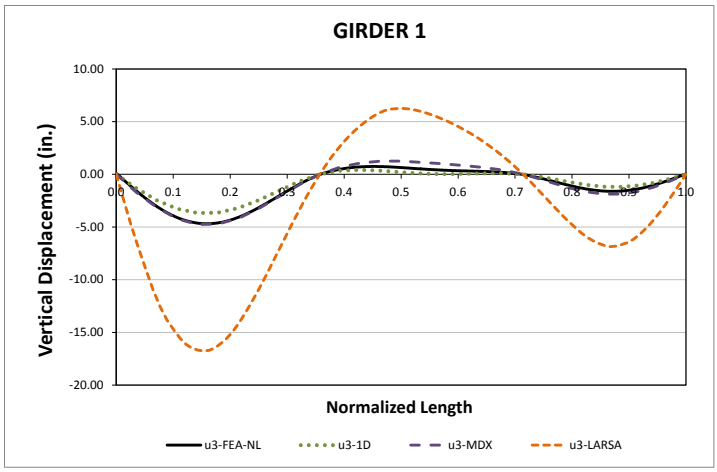

Fig. 5. Comparison of Vertical Displacement Predictions, Stage 18

The flange lateral bending response for Stage 18 is shown in Figures 6 and 7. The relative lateral displacements are accurately predicted by the 2D grid analysis at the cross-frame locations, as depicted in Figure 6. This is a typical result that is also observed in many of the curved bridges studied previously. For the prediction of the girder layover during construction, the response obtained from the 2D model could be considered valid only at the bracing points. A straight line that joins the predictions between two cross-frame positions might be sufficient to describe the response within the unbraced length.

The computation of flange lateral bending stresses based on the V-Load formulation proves to be accurate for this bridge. Figure 7 shows that the approximate predictions are consistent with the 3D FEA model predictions.

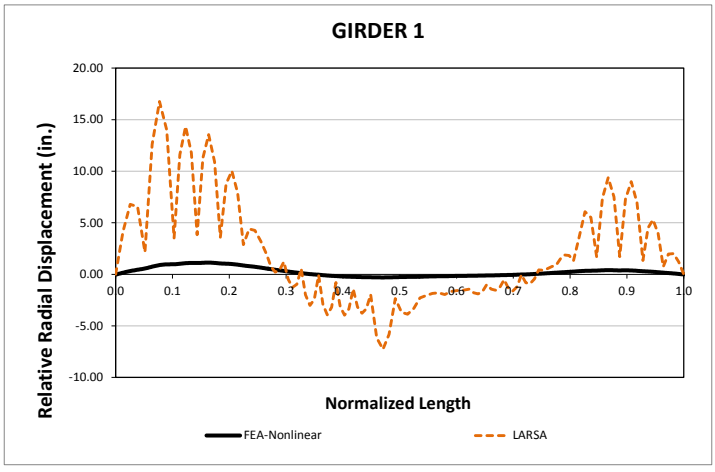

Fig. 6. Comparison of Relative Radial Displacement Predictions, Stage 18

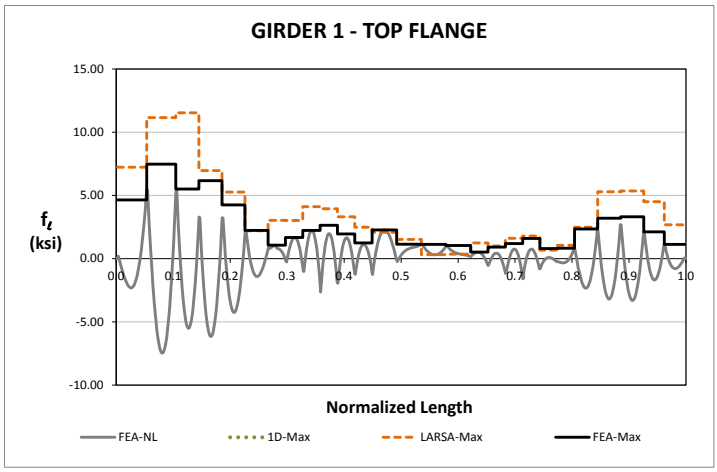

Fig. 7. Comparison of Flange Lateral Bending Stress Predictions, Stage 18

I5.6 NICCR8 (New, I-girder, Continuous-span, Curved, Skewed supports)

Category Data:

L_1 = 150 ft, L_2 = 150 ft, L_3 = 120 ft / $R_{1,2,3}$ = 308 ft/ w = 80 ft, 9 girders

Cross-Frame Detailing Method: NLF

Erection Stages Analyzed: 7 (Analyses are performed assuming NLF)

Deck Placement Sequence: 1 Stage

Bridge Perspective & Plan Views:

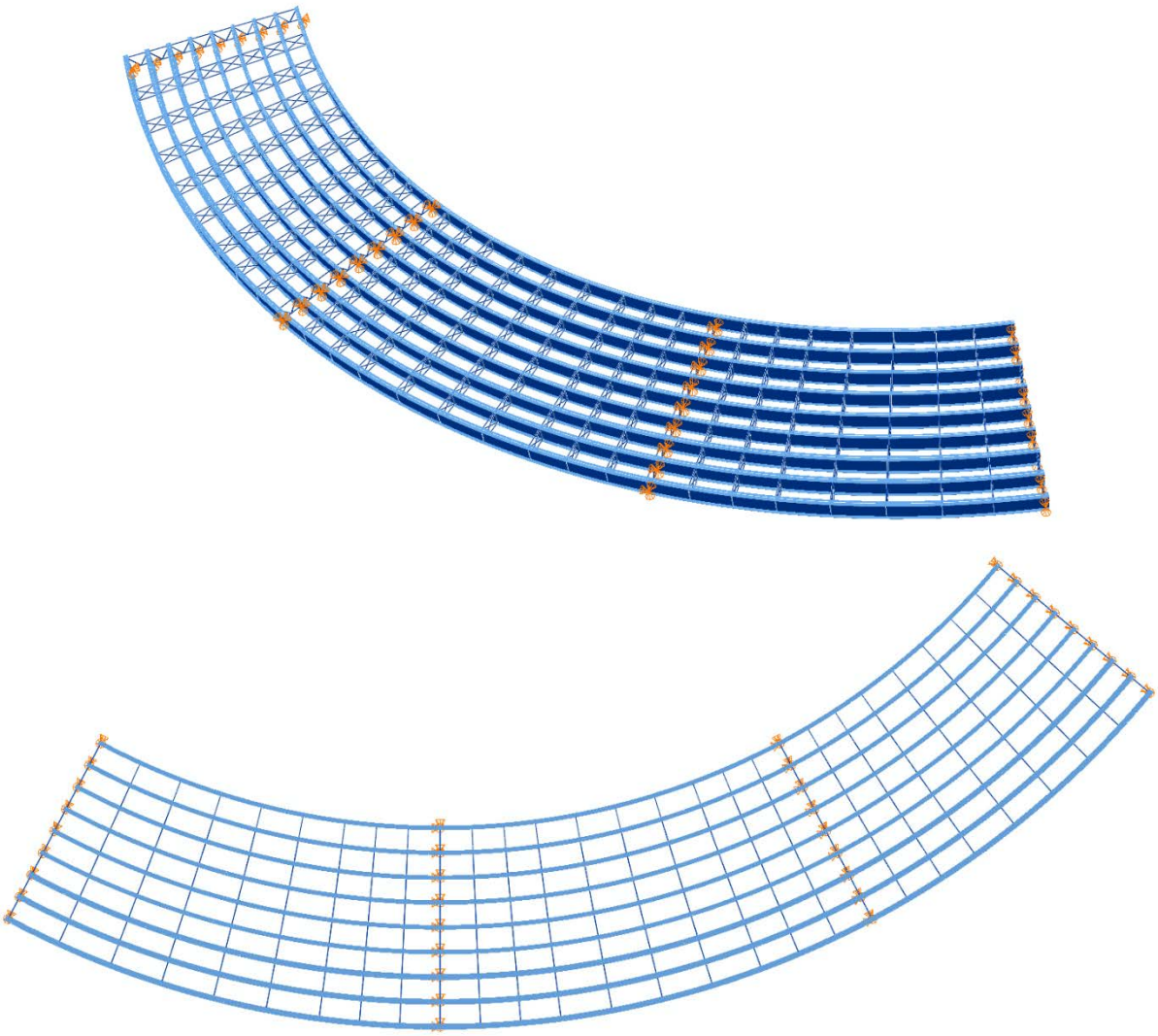

Abbreviated Analysis Results

Figure 1 shows the different analysis stages which are considered to evaluate the different analysis methods. Stage 2 results are provided here since significant observations are made from this stage. Figure 2 shows the deflected shape of Stage 2. Displacement results are magnified by 10x. Uplift of 13 kips is observed on the second girder which is also captured by LARSA solutions.

Figures 3 and 4 show girder 1 and 2 relative radial displacement predictions for stage 2. It should be noted for Figs. 3 and 4 that layovers are way over predicted by the refined LARSA grid solutions . Figures 5 and 6 show girder 1 and 2 vertical displacement predictions for stage 2. Refined LARSA grid solutions cannot predict the vertical displacements accurately. This is mainly due to incapability of the 2D grid models to capture warping deformations between the cross-frame locations. As mentioned in the previous reports, coarser LARSA grid models provide better results since only one elements are use between the brace points.

Figure 7 shows girder 1 major-axis bending stress predictions for stage 2. It is clear that the major-axis bending stresses are predicted well by grid analysis methods. Figure 8 shows girder 1 flange lateral bending stresses.

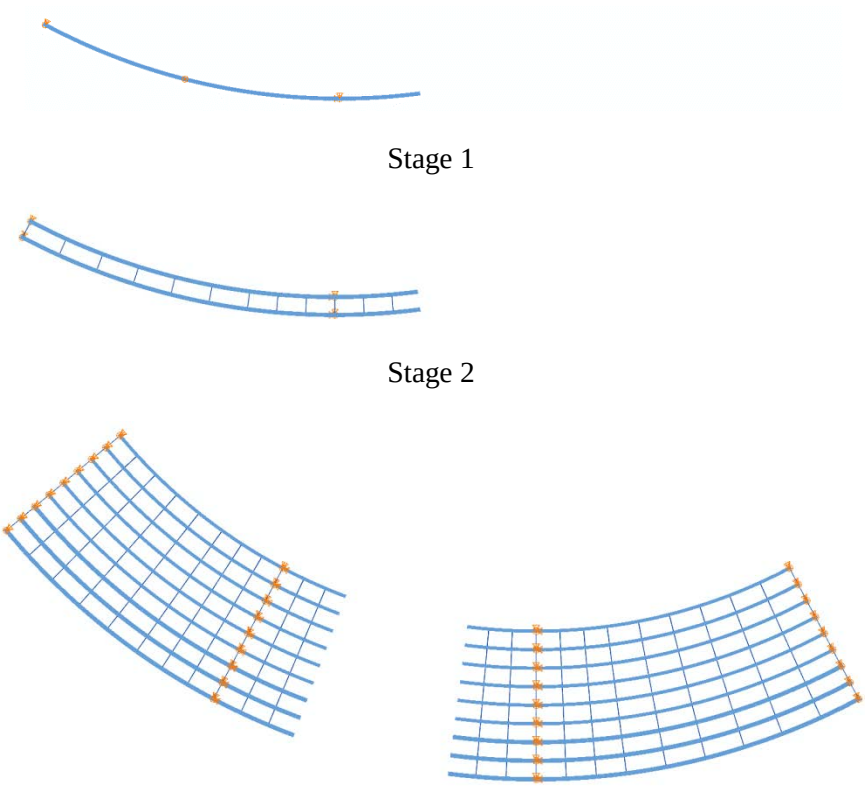

Stage 1

Stage 2

Stage 18

Fig. 1. NICCR8, Considered different analysis stages.

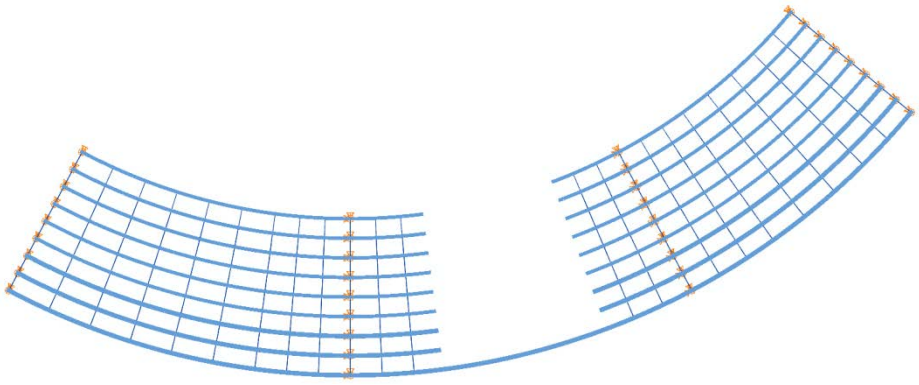

Stage 19

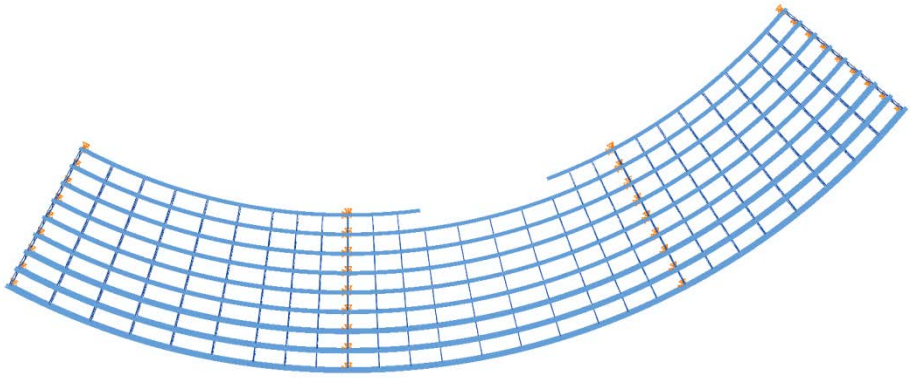

Stage 26

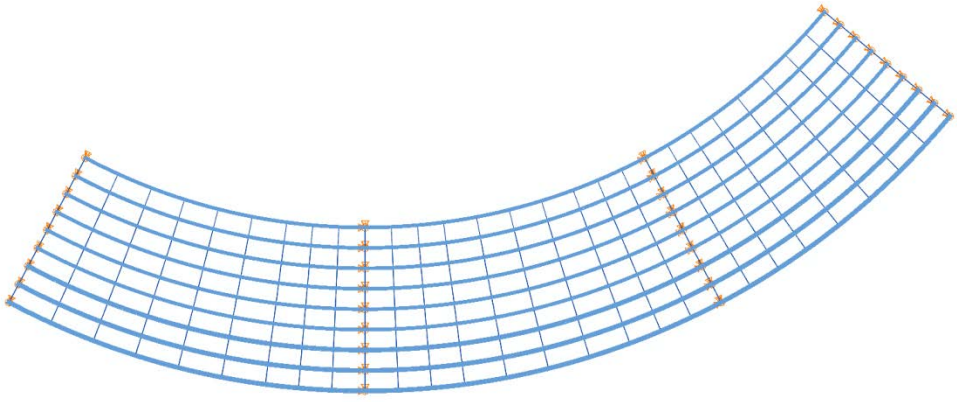

Stage 27 & 28

Fig. 1. NICCR8, Considered different analysis stages(continues).

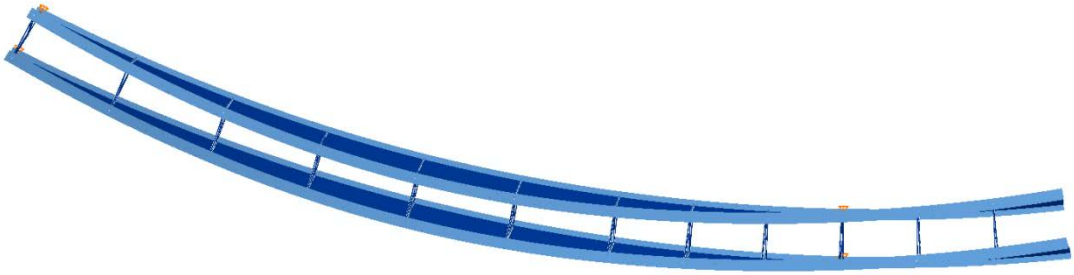

Plan View

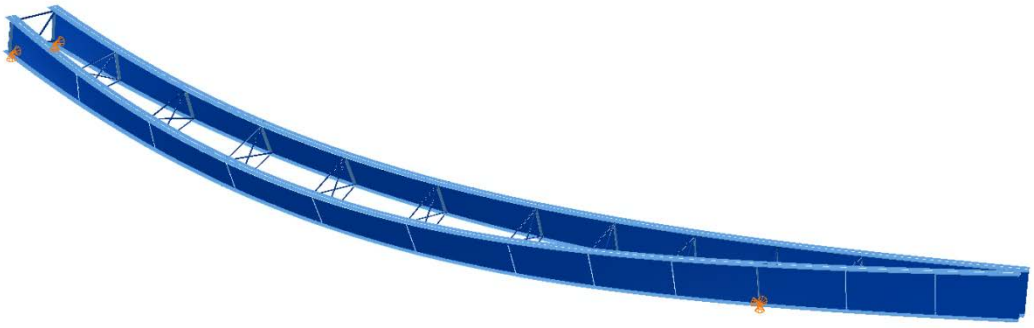

Perspective View

Fig. 2. NICCR8, Stage 2 plan and perspective deflected shapes (Magnified by 10x).

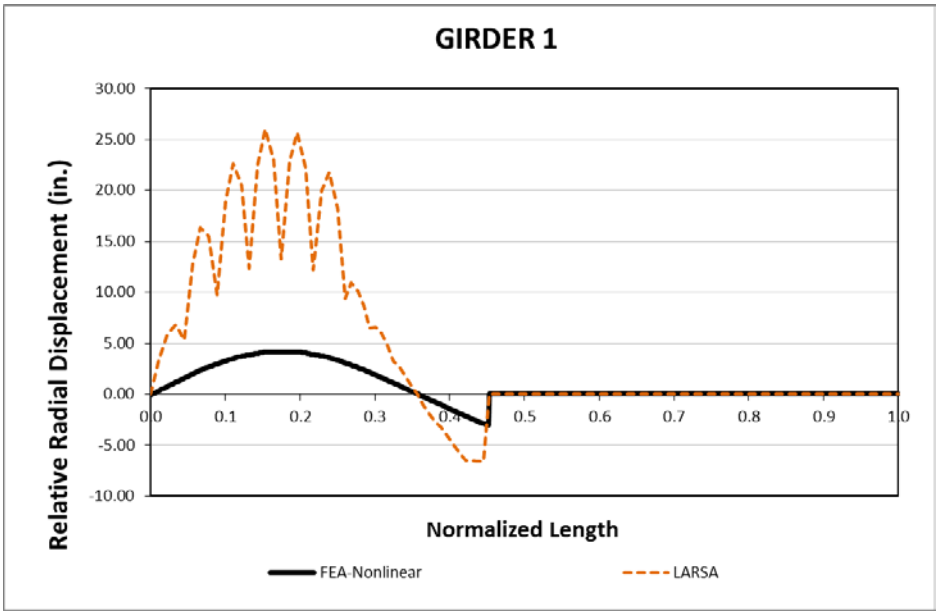

Fig. 3. NICCR8, Stage 2 Radial displacements NLF detailing.

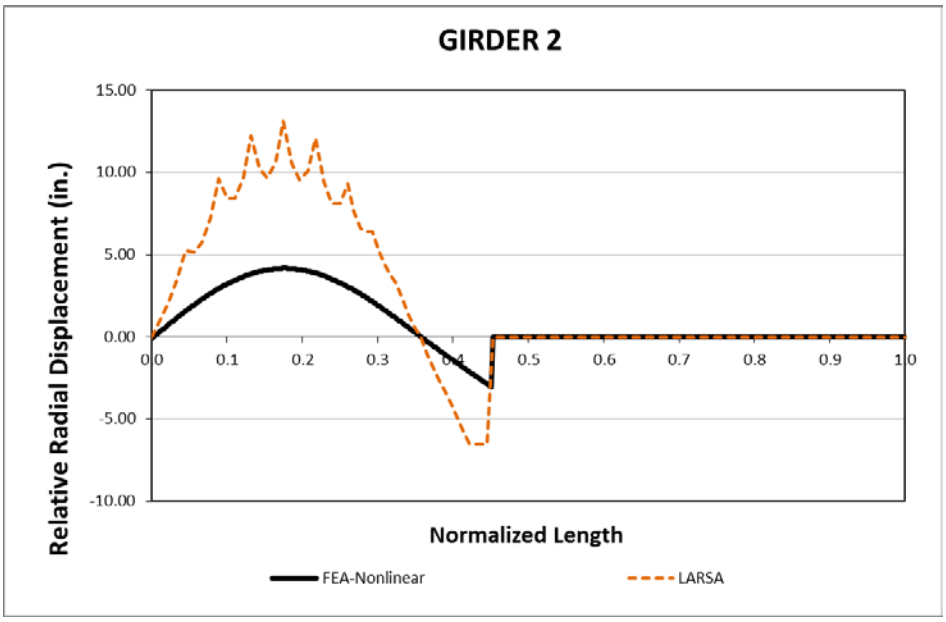

Fig. 4. NICCR8, Stage 2 radial displacements NLF detailing.

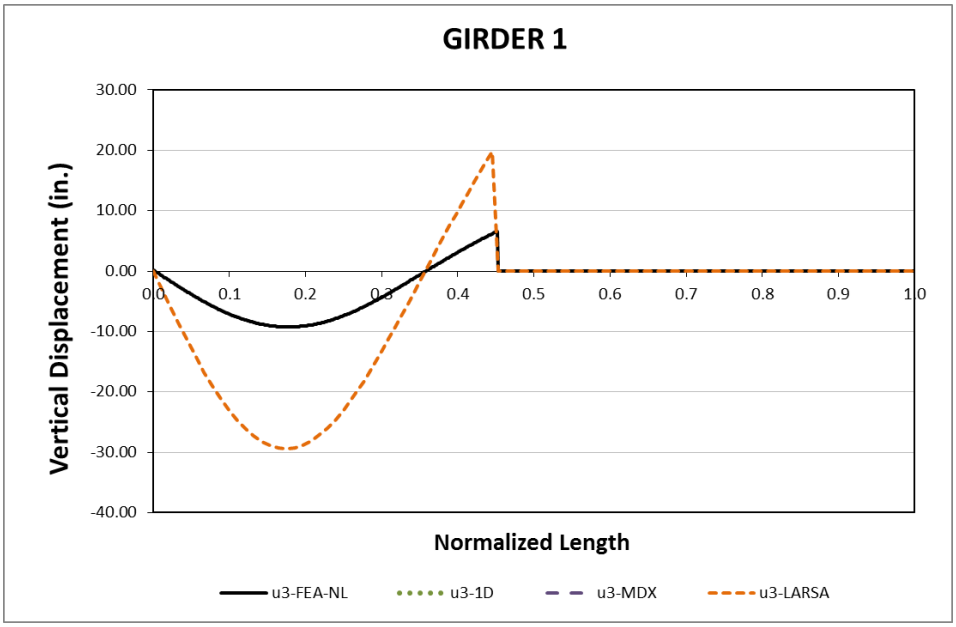

Fig. 5. NICCR8, Stage 2 vertical displacements NLF detailing.

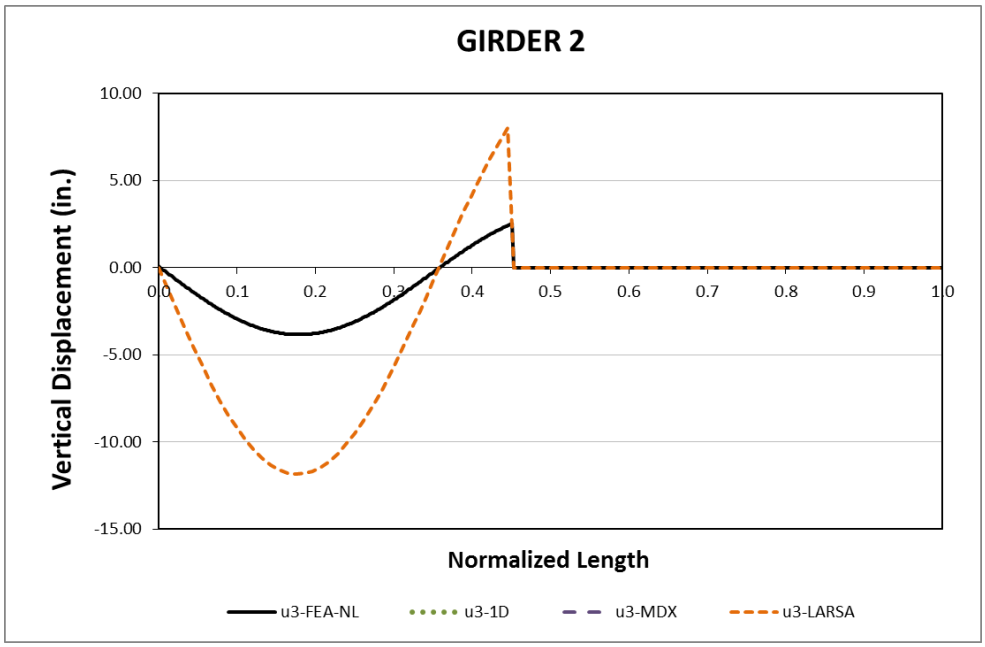

Fig. 6. NICCR8, Stage 2 vertical displacements NLF detailing.

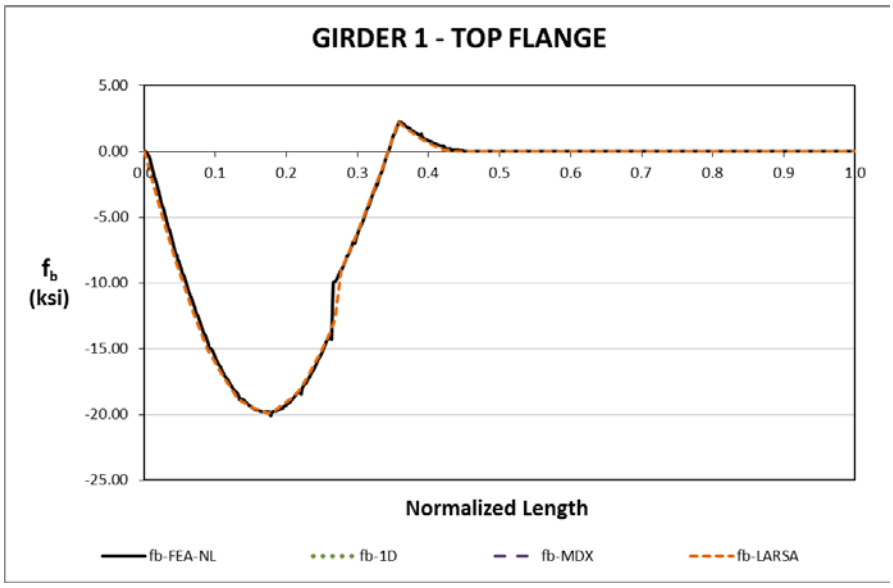

Fig. 7. NICCR8, Stage 2 major-axis bending stresses for NLF detailing.

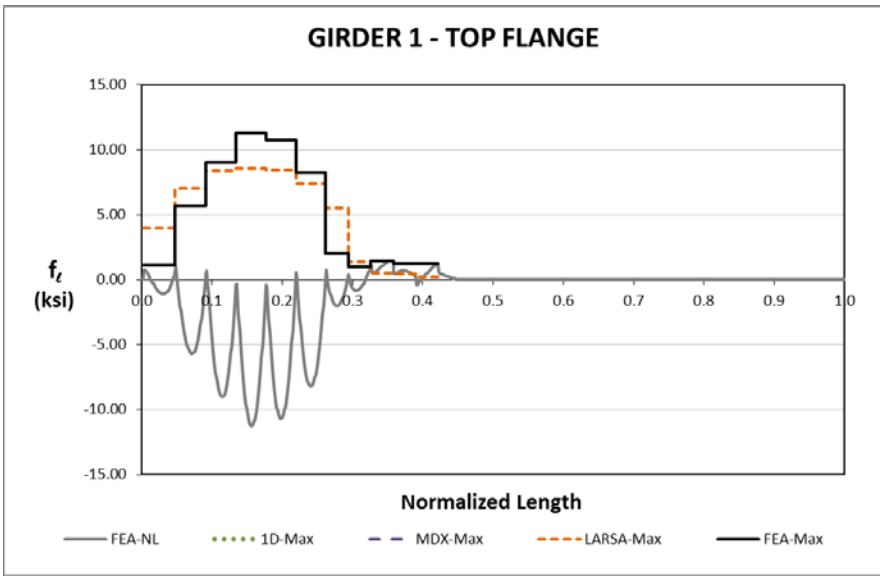

Fig. 8. NICCR8, Stage 2 flange lateral bending stresses for NLF detailing.

I5.7 NICCR12 (New, I-girder, Continuous-span, Curved, Radial supports)

Category Data:

L_1 = 350 ft, L_2 = 350 ft, L_3 = 280 ft/ R = 909 ft / w = 80 ft / $\theta_1 = 0^o$, $\theta_2 = 0^o$, / $\theta_3 = 0^o$, $\theta_4 = 0^o$/ 9 girders

Cross-Frame Detailing Method: NLF

Erection Stages Analyzed: Eight

Deck Placement Sequence: Five stages, deck thickness = 9.5 in.

Bridge Perspective & Plan Views:

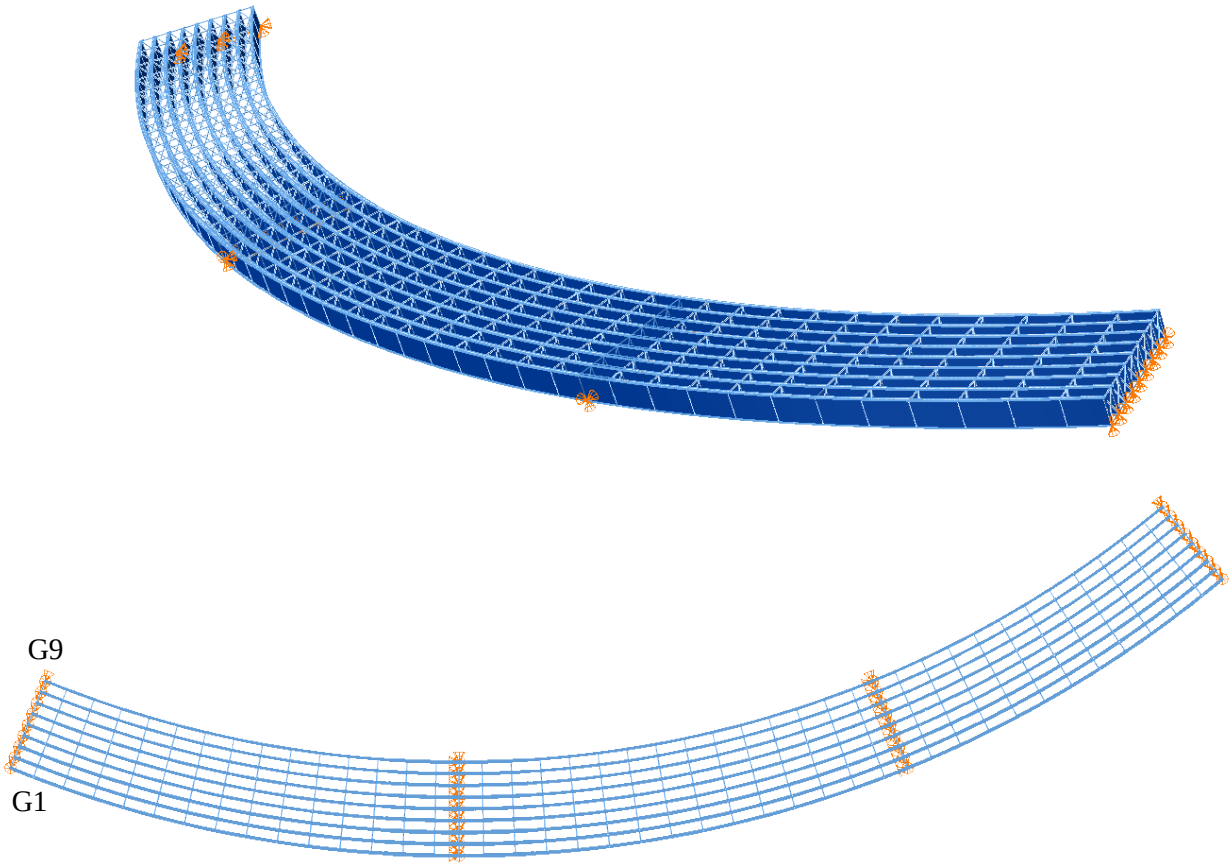

Abbreviated Analysis Results:

The erection of this bridge starts at the left end, with the placement of the first segment of girder G1. A temporary support is provided at the right end of the segment. Following the same procedure, girders G2 to G9 are placed. Next, the second segment of girder G1 is lifted and connected to the segment erected previously (Stage 10). In this operation, the girder is supported on the first interior bent, and cantilevers out from this support approximately 55 ft. A holding crane is provided at the center of the girder to limit the self-weight deflections and ensure the stability of the structure, as shown in Figure 1. In Stage 11, the second girder segment of G2 and the cross-frames of the bay G1-G2 are erected. The holding crane is removed, so the structure rests on the left abutment, the temporary supports, and the first interior bent. Subsequently, the rest of girder segments are placed to conclude the erection of Span 1, as shown in Figure 1, Stage 18. The next girder segments are erected from inside to outside. As shown in Figure 1 for Stage28, the erection concept described previously is the same, but erecting the girders from G9 to G1. Similar approaches as the discussed above are followed for the rest of the steel erection. In Stage 54, the structure has been completed, but the interior temporary supports are still in place. In Stages 55, 56, and 57 the three interior supports are removed from right to left, respectively. Finally, the structural behavior of the bridge is investigated in Stage 58 that corresponds to the total dead load condition.

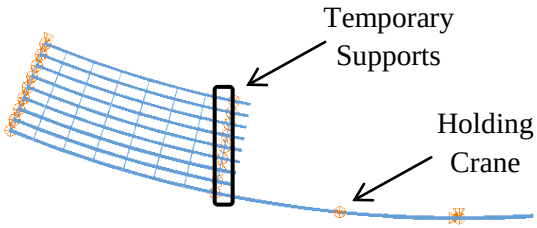

Stage 10

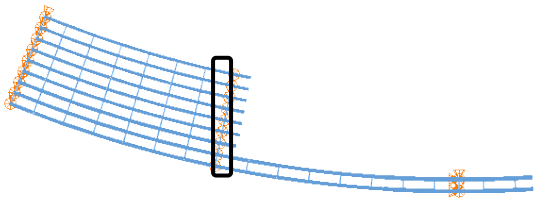

Stage 11

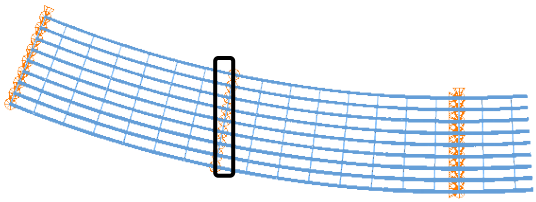

Stage 18

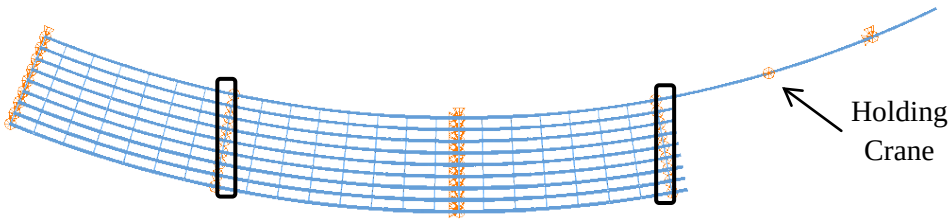

Stage 28

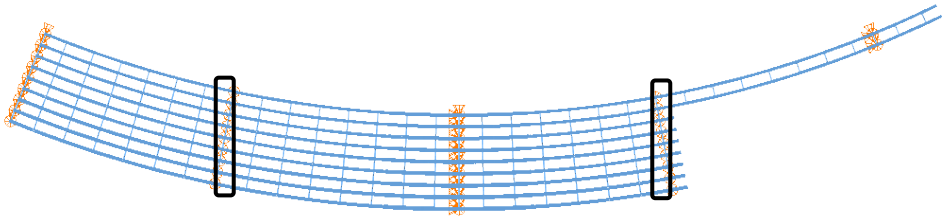

Stage 29

Fig. 1. Analyzed Construction Stages

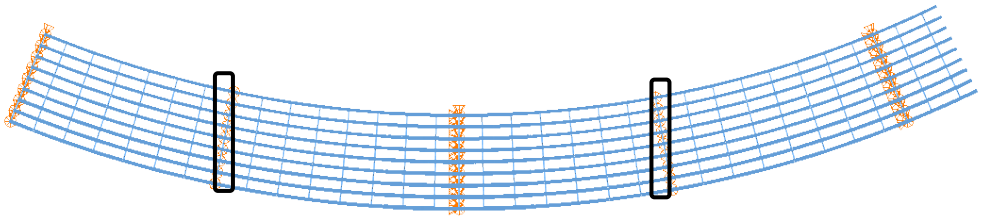

Stage 36

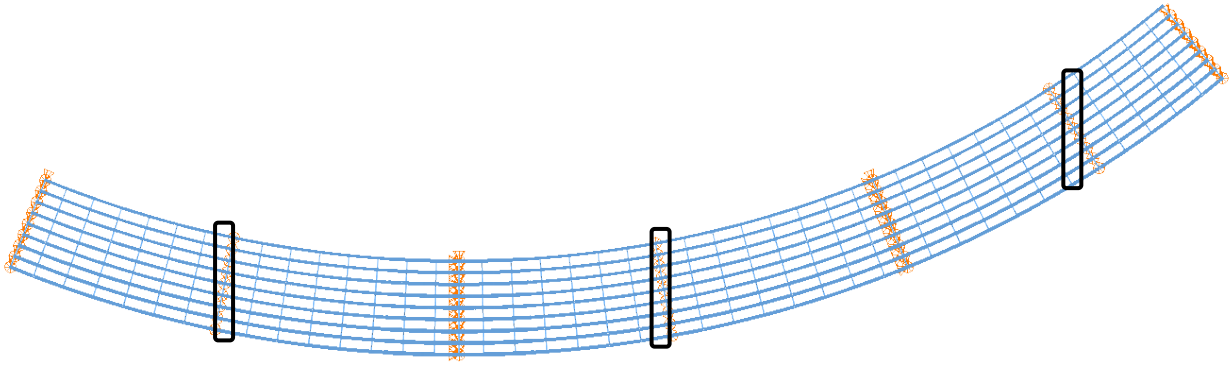

Stage 54

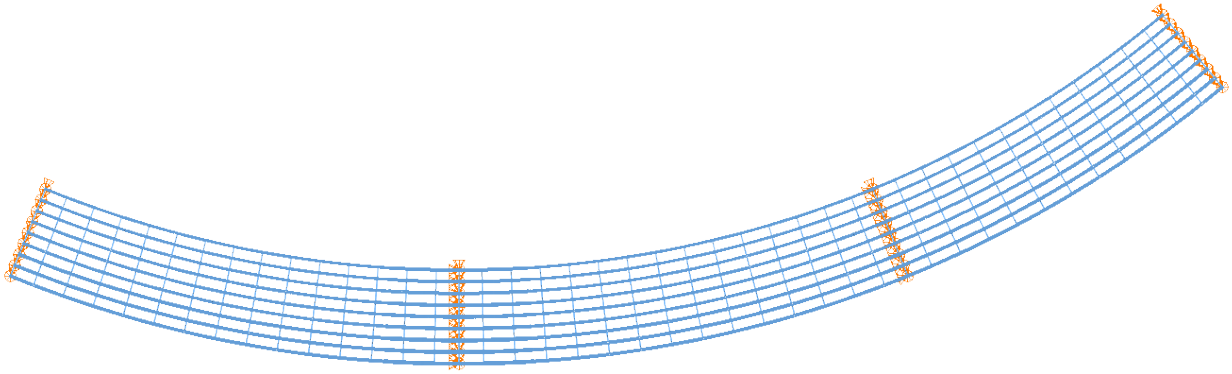

Stage 58 (TDL)

Fig. 1. Analyzed Construction Stages (Continued)

The major-axis bending response is studied first. The stress response for the top flange of the exterior girder, G1, in Stage 10 is shown in Figure 2. As shown in the figure, the 2D grid model representation captures accurately the 3D FEA prediction. In the case of the vertical displacements, the approximate

representation does not present the same level of accuracy. As shown in Figure 3, the 2D grid prediction overestimates the expected displacements. This is observation is consistent with the results obtained in from the analysis of other curved bridges. The lack of a term that considers the contribution of flange warping in the torsional stiffness of the I-girders results in misrepresentations of the actual vertical displacements. Figure 4 shows the comparison of lateral displacements predicted with each method. As shown in the figure, the lateral displacements are best predicted at the location of the cross-frames.

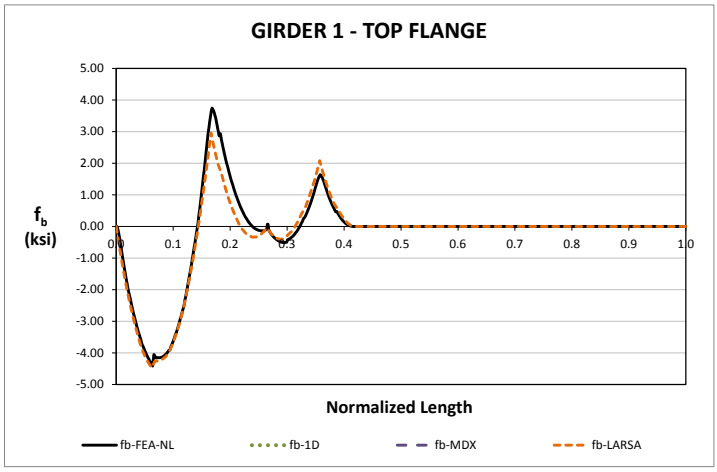

Fig. 2. Comparison of Major-Axis Bending Stresses, Stage 10

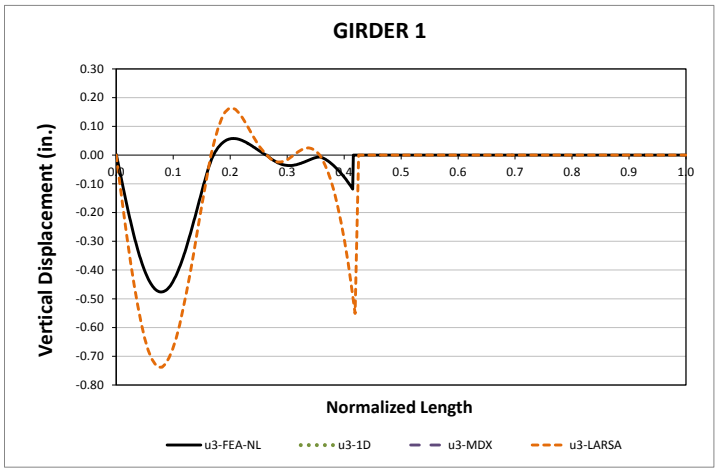

Fig. 3. Comparison of Vertical Displacements, Stage 10

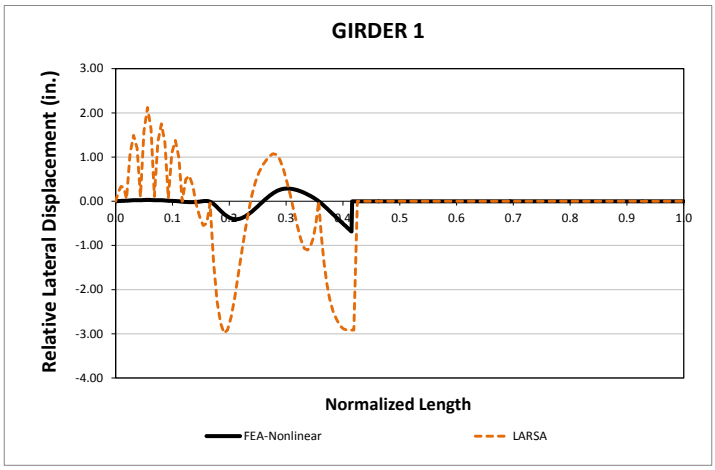

Fig. 4. Comparison of Relative Lateral Displacements, Stage 10

For the final configuration, when the total construction dead load is applied to the structure, the approximate predictions are more accurate. As shown in Figure 5, the 1D and 2D predictions are a close representation of the benchmark. In the case of the vertical displacements shown in Figure 6, the 2D grid analysis accuracy improves significantly with respect to the plot shown in Figure 3. It is believed that as the construction of the bridge progresses and more cross-frames are erected, the structure responds as an integrated system, so the dominant behavior of the individual girders observed in early stages decreases. In the case of the 1D analysis, both stresses and deflections are captured accurately for this bridge.

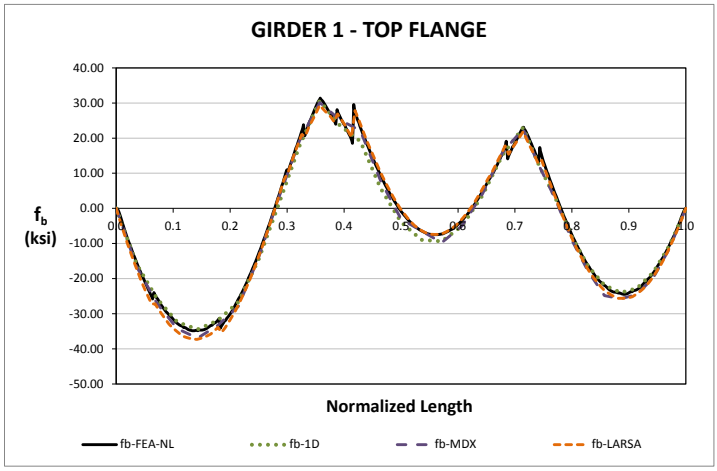

Fig. 5. Comparison of Major-axis Bending Stress, Stage 58

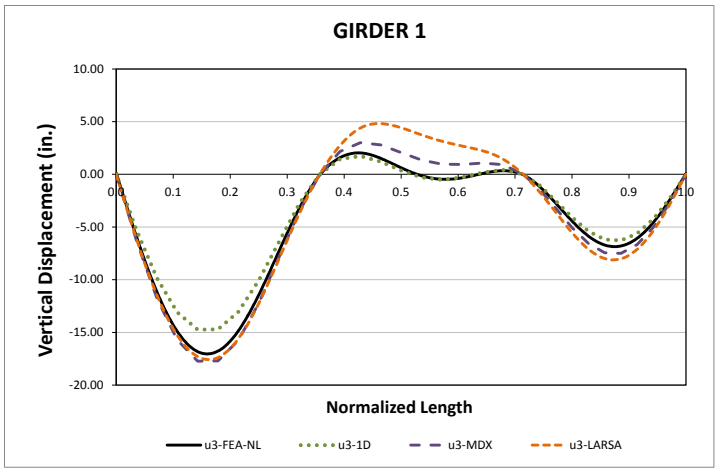

Fig. 6. Comparison of Vertical Displacement Predictions, Stage 58

The flange lateral bending response for Stage 58 is shown in Figures 7 and 8. The relative lateral displacements are accurately predicted by the 2D grid analysis at the cross-frame locations, as depicted in Figure 7. This is a typical result that is also observed in many of the curved bridges studied previously. For the prediction of the girder layover during construction, the response obtained from the 2D model could be considered valid only at the bracing points. A straight line that joins the predictions between two cross-frame positions might be sufficient to describe the response within the unbraced length.

The computation of flange lateral bending stresses based on the V-Load formulation proves to be accurate for this bridge. Figure 8 shows that the approximate predictions are consistent with the 3D FEA model predictions.

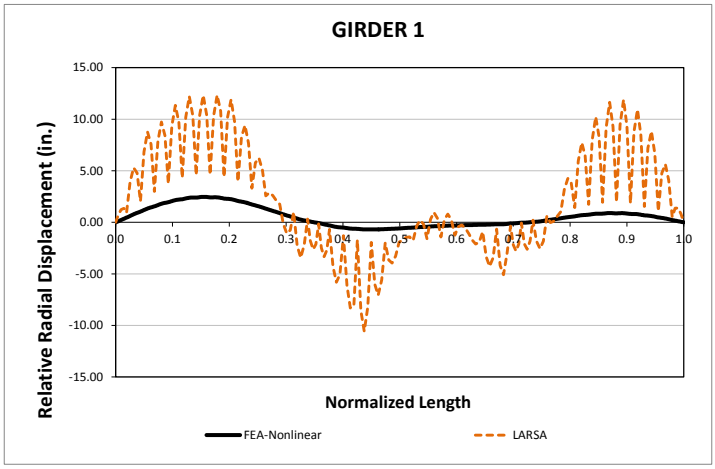

Fig. 7. Comparison of Relative Radial Displacement Predictions, Stage 58

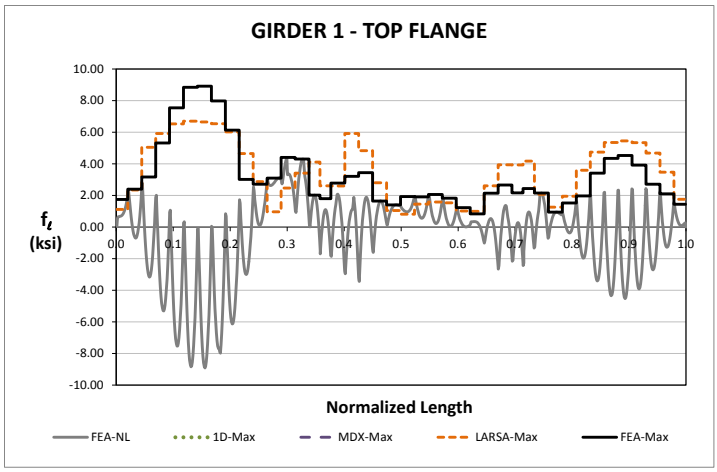

Fig. 8. Comparison of Flange Lateral Bending Stress Predictions, Stage 58

I6.1 EISCS3 (Existing, I-girder, Simple-span, Curved, Skewed supports)

Bridge Description :

SR8002 Ramp A-1, King of Prussia, PA

Category Data:

L_{as} = 153 ft / R = 279 ft / w = 35.6 ft / θ = 52.4° and 0, 6 girders

References:

Studied originally by Chavel and Earls (2003) & Chavel (2008)

Studied by Ozgur et al. (2009)

Cross-Frame Detailing Method: SDLF (see Chavel 2008 p. 48)

Erection Stages Analyzed: 5 (Analyses are performed assuming both NLF & SDLF)

Deck Placement Sequence: One stage (8 inch deck, approx. 140 cu yds concrete)

Bridge Perspective & Plan Views:

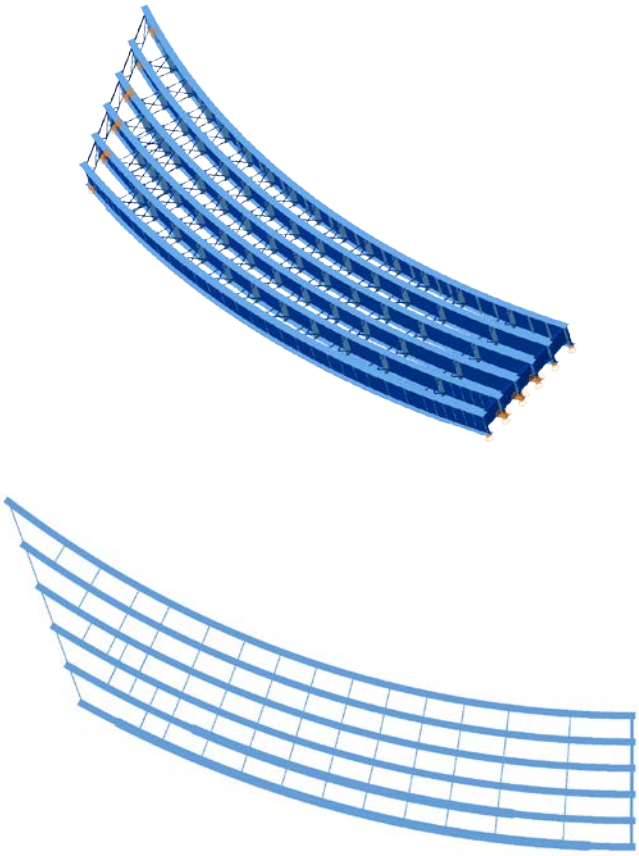

Abbreviated Analysis Results:

Figures 1 and 2 illustrate the outside girder (Girder1) and the inside girder (Girder6) vertical displacements under total dead load predicted by different analysis results. It is observed from these results that simplified analysis predictions are off from the benchmark solutions. This is mainly because the 1D and 2D solutions do not account for the warping rigidity of the I-girders. Moreover, the 1D predictions are in the opposite direction to the benchmark solutions for Girder 6 so they do not predict the system behavior correctly for this bridge. This is due to the fact that this method does not predict the correct load transfer between the girders. The problem is partly due to the combined skew and horizontal curvature effects on this bridge.

Although, the cross-frames are designed for steel dead load fit detailing (SDLF) the results are shown for no load fit detailing (NLF) to avoid any additional prediction error for the 1D and 2D analysis methods (since the 1D and 2D methods do not consider the influence of locked in stresses due to the type of cross-frame detailing). The Girder 1 relative radial displacements from the 3D-FEA and 2D LARSA solutions are compared under total dead load in Fig. 3 for NLF. One can observe from Fig. 3 that the 2D predictions are only good at the cross-frame locations, and that between the cross-frames, the behavior cannot be predicted accurately. This is the general case observed with the typical 2D grid solutions for curved bridges. Therefore, one can obtain better representation from 2D LARSA by just considering the values at the cross-frame locations.

Figure 4 provides top flange major-axis bending predictions from the different analysis methods under total dead load. Although the displacement predictions are off from each other the stress is well predicted by different analysis methods. Figure 5 provides top flange lateral bending stresses obtained from different analysis methods. In this figure the maximum values between the unbraced lengths are considered for comparison. The flange lateral bending stress values are usually derived from the major-axis bending stresses from approximate analysis methods for curved girders. It should be noted that the 2D predictions are good as long as the major-axis bending predictions are good. Also, the good accuracy of the flange lateral bending stresses is less likely at the region close to skewed bearings for simple span bridges. This is mainly because the major axis bending values are small at these regions. For instance, the maximum flange lateral bending stress is observed close to the skewed bearing for this bridge which is not concurrent with the maximum major-axis bending stress. Therefore, the 2D solutions cannot predict the effect of skew from the major-axis bending stresses when computing the flange lateral bending stresses. In general this is not a problem because usually the girders sections are designed based on the locations where the maximum major-axis bending stress is observed. Moreover, the flange lateral bending stress predictions toward the radial end are observed to be much higher than the 3D FEA predictions. This is due to the larger unbraced lengths at these locations such that these values are estimated based on the major-axis bending stress, radius of curvature and unbraced length.

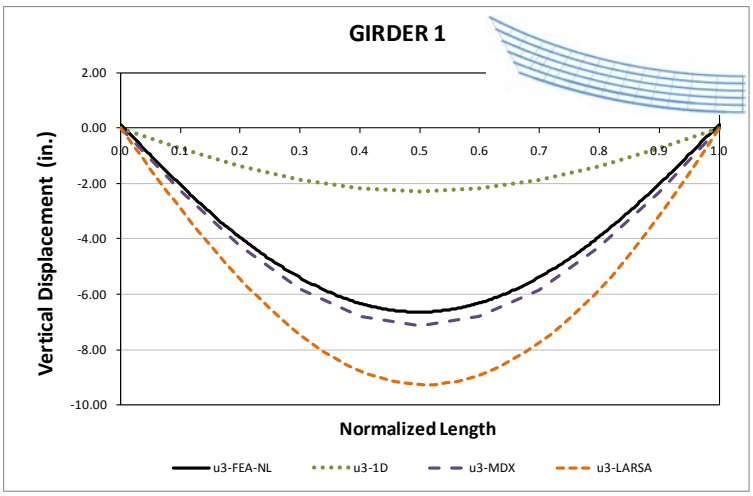

Fig. 1. EISCS3,.Vertical displacements under total dead load for NLF detailing.

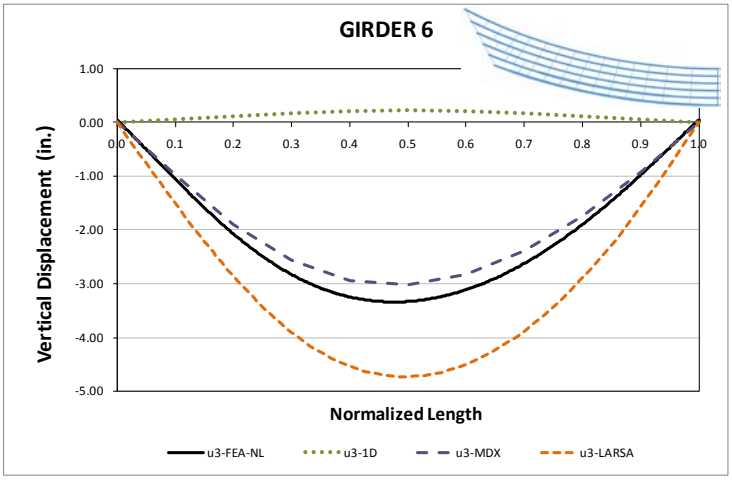

Fig. 2. EISCS3, Vertical displacements under total dead load for NLF detailing.

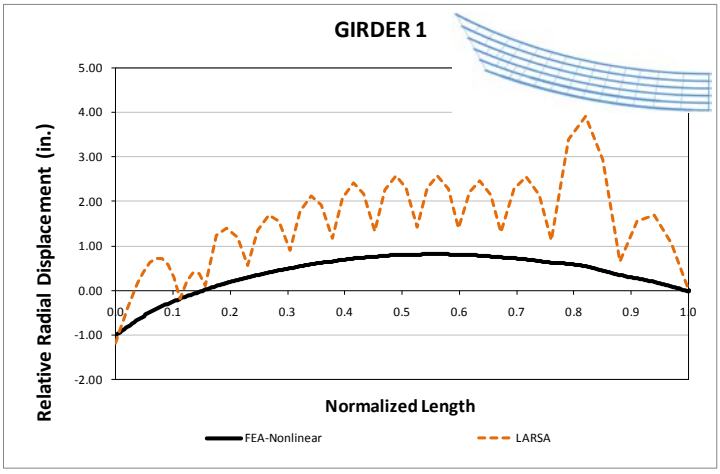

Fig. 3. EISCS3, Relative radial displacements under total dead load for NLF detailing.

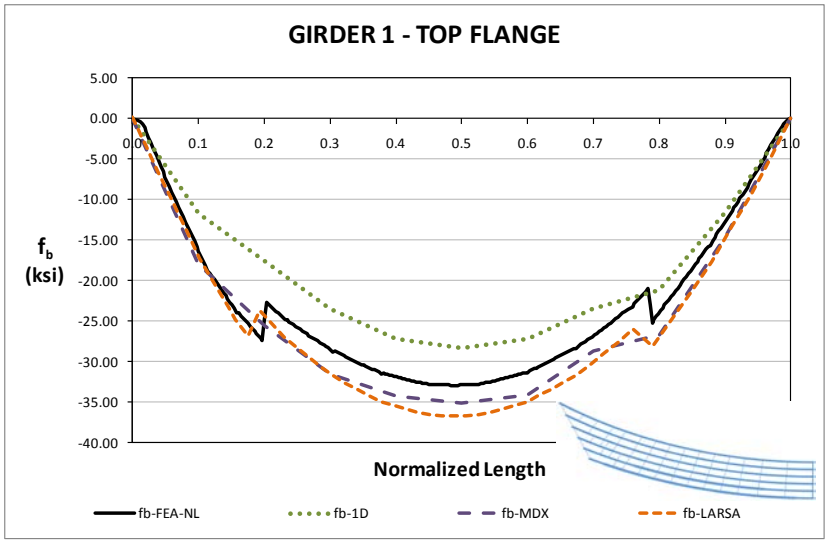

Fig. 4. EISCS3,Major-axis bending stresses under total dead load for NLF detailing.

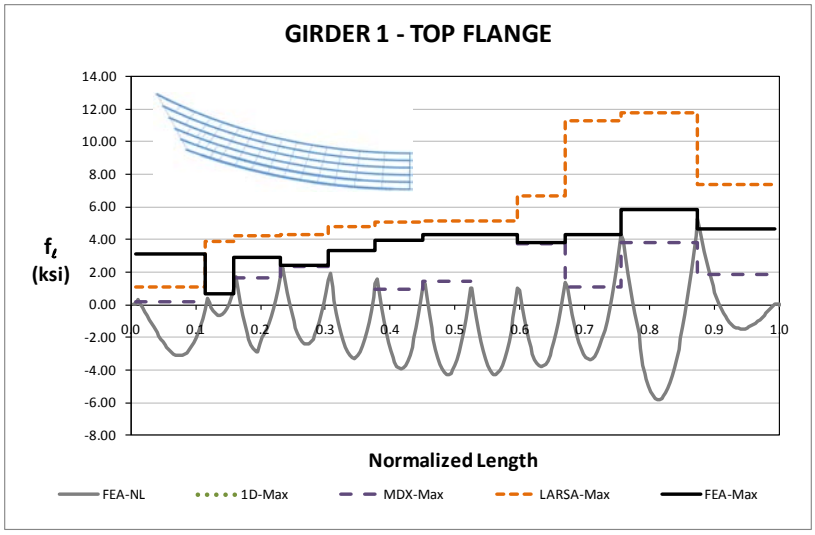

Fig. 5. EISCS3, flange lateral bending stresses under total dead load for NLF detailing.

The steel dead load cross-frame detailing method (SDLF) is used for this bridge. Usually SDLF and TDLF detailing methods may introduce additional stresses in the components due to lack of fit between cross-frames and girders that might affect the system behavior. These additional stresses are usually neglected by designers. This is believed to not present any significant problem for many bridges, but the project team expects that there is some limit at which the effect of the locked in stresses should be considered (as indicated by the AASHTO LRFD Specifications). Some stages of this bridge are selected to illustrate the effect of these additional responses. Figures 6 and 7 shows relative radial displacement of the outside girder (Girder 1) under steel dead load for no-load fit detailing (NLF) and steel dead load fit detailing (SDLF) respectively. It is observed from Fig. 7 that the girders are approximately plumb under the steel dead load. It can be seen from Figs. 6 and 7 that the LARSA 2D grid predictions will be less accurate when the bridge is designed for SDLF since they are not accounting for additional stresses due to lack of fit.

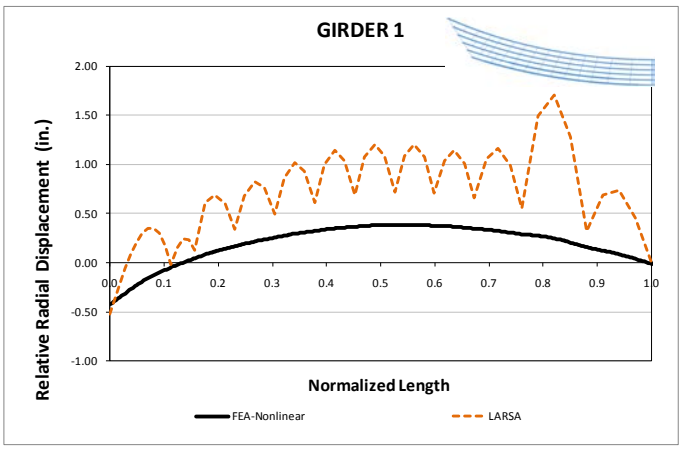

Fig. 6. EISCS3, Relative radial displacements under steel dead load for NLF detailing.

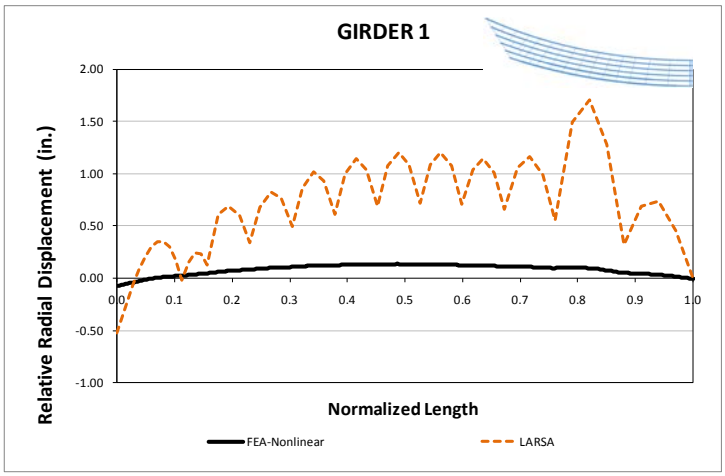

Fig. 7. EISCS3, Relative radial displacements under steel dead load for SDLF detailing.

During the construction of this bridge, a holding crane was required until the fifth girder was erected, to maintain the overall stability of the bridge system against overturning. The stage where the holding crane was released is investigated in detail. It is observed from benchmark solutions that if one runs the bridge for NLF there is an uplift (-3.44 kips) at girder 3 at the skewed bearing whereas if this bridge is run for SDLF there is no uplift at that stage. No uplift was observed in the field for this condition. Although the simplified solutions are conducted based inherenetly on the assumption of NLF, none of them captured the uplift. If this bridge were designed for NLF, some uplift uplift is expected in the field during the erection.

Conclusions:

It is observed that the accuracy of 2D analysis deflection predictions can be low due to neglecting the warping stiffness of I-girders. However, radial displacements are well predicted at the cross-frame locations for this curved bridge.

It should be noted that the 2D flange lateral bending predictions are good only when the major-axis bending predictions are good. Also, good accuracy of flange lateral bending stresses is less likely at the region close to skewed bearings for simple span bridges. This is mainly because the major axis bending values have a tendency to go to zero at these regions. Therefore, the 2D solutions cannot predict the effect of skew from the major-axis bending stresses when computing the flange lateral bending stresses. In general this is ok because usually the girder sections are designed based on locations where the maximum major-axis bending stress is observed. Moreover, significant variation in flange lateral bending stresses between the 2D and 3D analysis methods can be observed since these values are estimated based on the major-axis bending stress, radius of curvature and unbraced length.

In general, different detailing methods may introduce additional stresses in the components due to lack of fit between cross-frames and girders that might affect the system behavior. These additional stresses are usually neglected by designers. This can lead to poor prediction of the radial displacements It is observed that the reactions during erection are influenced for this bridge by the different detailing methods. Also, radial deflections cannot be predicted accurately by the simplified methods, for this bridge, since they do not account for additional stresses due to lack of fit.

I6.2 EISCS4 (Existing, I-girder, Simple-span, Curved, Skewed supports)

Bridge Description:

Stage 3 of Bridge over NC 146 (Long Shoals Road) on I-26 between Blue Ridge Parkway and SR 3495, Stage 3, Asheville, NC

Category Data:

L_1 = 252 ft / R = 2269 ft / w = 26.6 ft / θ_1 = -24.71°, θ_2 = -18.36°, 3 girders

Cross-Frame Detailing Method: NLF

Steel Erection Stages Analyzed: Four

Deck Placement Sequence: One stage

Bridge Perspective & Plan Views:

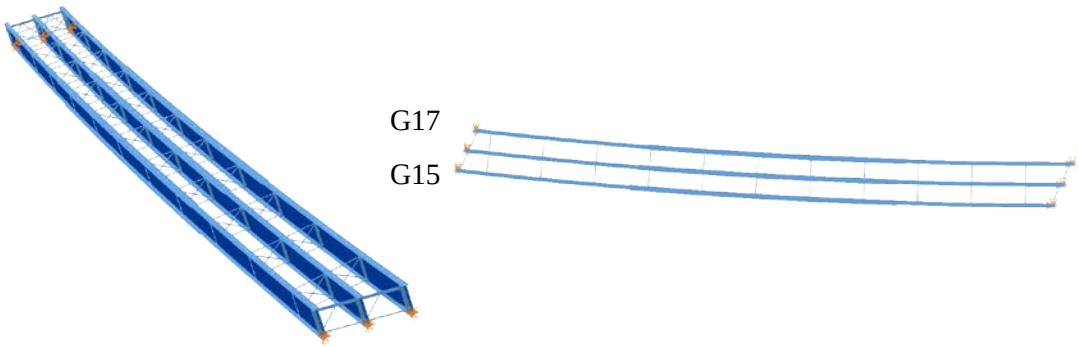

Abbreviated Analysis Results:

This bridge is a 17 I-girder bridge that was constructed in three phases. In Phase I the first eight girders were erected and the slab was placed. Subsequently, in the second phase, six additional I-girders were erected and the deck was placed. At this point 14 girders had been erected. Next, the cross-frames were inserted between the two phases and a closure pour was made and subsequently the portion of the bridge constructed in Phases 1 and 2 was opened to traffic. The next step was to construct Phase 3, which consisted of three girders (Girders 15 to 17), following the same scheme used in Phase 2. Phase 3 was independent of the other two phases until the cross-frames were to be inserted and a closure pour made between Phases 2 and 3. During the concrete placement, it was observed that the vertical deflections in the three girder unit were considerably larger than in the girders of Phase II. By the time that approximately a 70% of the concrete deck had been placed in Phase III, the difference in the top-of-slab levels between Phase II and Phase III was approximately six inches. At this point, it was decided to stop the deck placement. The bridge was potentially at a point of incipient instability.

In this report, the behavior of the three unit system erected in Phase III is studied. This structure has a relatively large span-to-width ratio. The effects of this “slenderness ratio” are studied since this is the apparent cause of the construction difficulty.

Figure 1 shows the major-axis bending and flange lateral bending stresses for the top flange of Girder 15 under the steel dead load condition (Girder 15 is the girder most distant from the center of curvature of the bridge and adjacent to Phase 2), obtained from the 3D FEA models. As shown in the plot, at the stage where all the steel has been erected, the stress levels are small. However, it is observed that substantial second-order effects are present in the structure. While the flange lateral bending stresses predicted by the geometrically linear analysis are less than about 2 ksi, the nonlinear analysis shows lateral bending stresses of 5.0 ksi at the vicinities of the left and right support. In addition, one can see that the shape of the flange lateral bending distribution has changed significantly when second-order effects are included in the analysis. The second-order flange lateral bending stresses show evidence of overall lateral bending of the entire girder between the end supports.

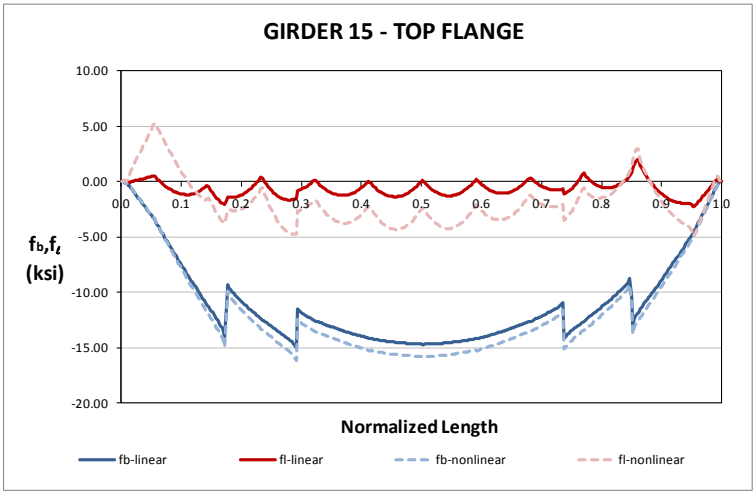

Fig. 1. EISCS4, 3D FEA stress predictions, Steel Dead Load.

Figure 2 shows the results of the lateral displacements in the same girder, under steel dead load. It is observed in this plot that a substantial lateral displacement of the girder is predicted by the nonlinear analysis. The layover of the girder, given by the difference between the lateral displacements of top and bottom flanges, respectively, is 3.1 inches at 0.48 the girder length. Although the linear analysis predicts smaller absolute lateral deflections than the nonlinear model, the predicted layover is almost the same. Finally, Figure 3 shows the vertical displacements predicted by the FEA models, for the same load condition. As shown, the difference between these steel dead load displacements from the linear and nonlinear models is negligible. The maximum deflection for the linear model is 11.8 inches and for the nonlinear model is 13.0 inches. The steel dead load camber for Girder 15 specified on the engineering drawings is 10.1 inches.

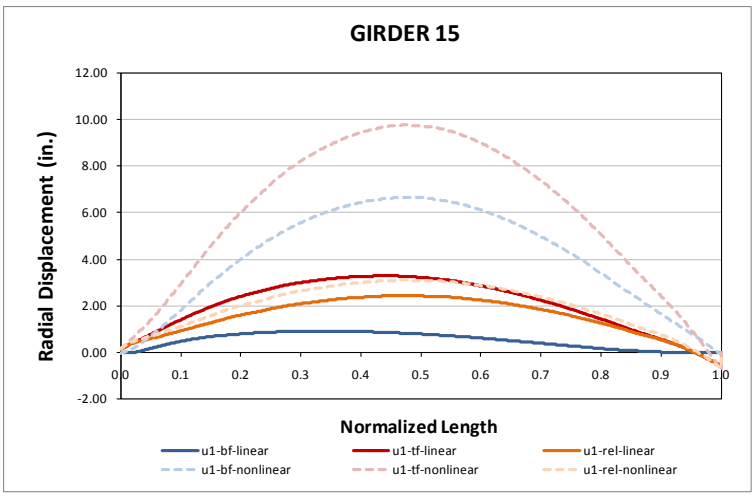

Fig. 2. EISCS4, 3D FEA lateral displacement results, Steel Dead Load

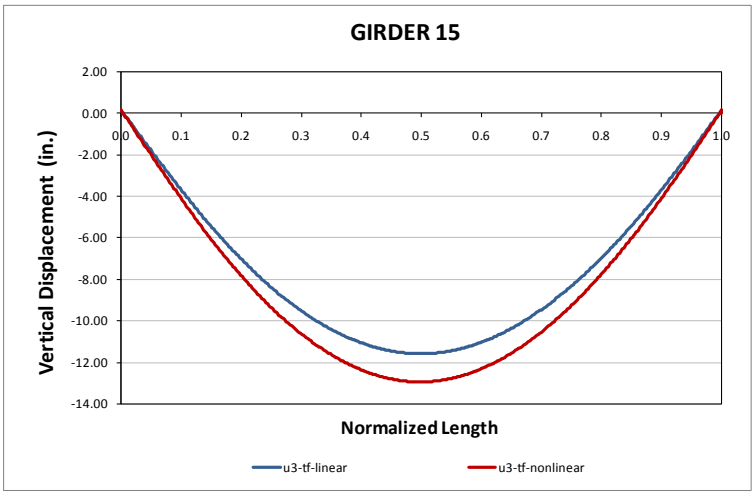

Fig. 3. EISCS4, 3D FEA vertical displacement results, Steel Dead Load

The analysis results for the total dead load condition are discussed next. Figure 4 shows the stress predictions obtained from the linear-elastic and nonlinear-elastic 3D FEA for the bottom flange of Girder G15. The figure shows that the stress levels obtained from the nonlinear analysis are above the yield limit. Obviously, this indicates that the girder will be substantially overloaded. The linear analysis does not capture this behavior. The predictions obtained from the linear analysis show that the stress levels are under the yield limit along the entire length of the girder. Similarly, the vertical deflections are dramatically underestimated by the linear analysis, as shown in Fig. 5. The nonlinear analysis predicts a maximum deflection at midspan of 213 inches, whereas the linear analysis predicts a deflection at the same point of 32 inches. The corresponding total dead load camber for Girder 15 specified on the engineering drawings (due to the steel self-weight plus the weight of the slab pour) is 27 inches.

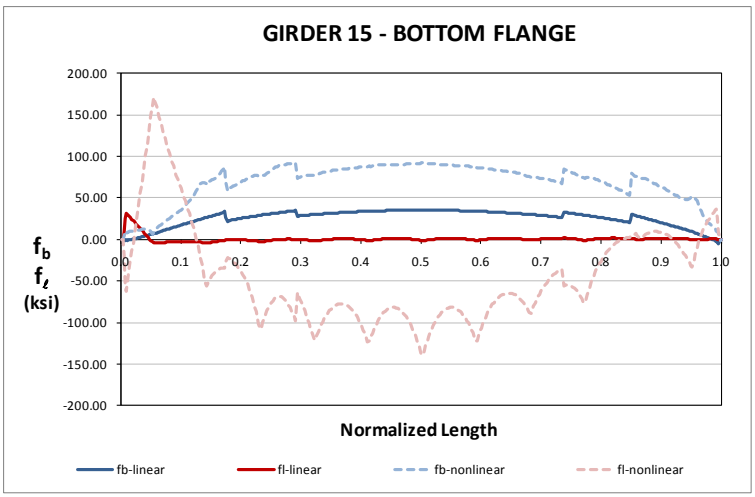

Fig. 4. EISCS4, 3D FEA stress prediction results, Total Dead Load

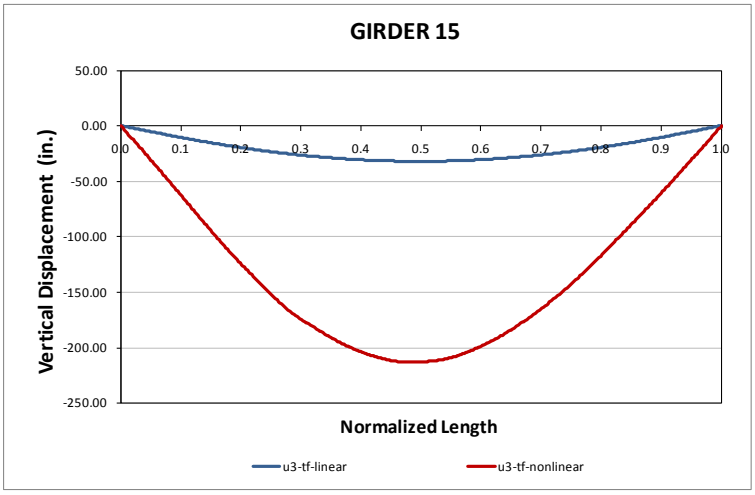

Fig. 5. EISCS4, 3D FEA vertical displacement results, Total Dead Load

A comparison of the stress and displacement results predicted by different methods of analysis is shown next. Figure 6 shows the stress responses obtained from the approximate 1D and 2D grid methods, as well as the FEA predictions discussed previously. The 1D analysis was obtained using the program Vanck, which implements the VLoad method of analysis. The MDX analysis and the Larsa analyses are 2D grid methods. As shown in the plot, the approximate methods capture accurately the response predicted by the *linear* FEA model. However, the behavior of the bridge indicated by the nonlinear response is not captured. The same observations are drawn in the case of the vertical displacements. As shown in Figure 7, the 1D and 2D analyses are able to represent the linear solution predicted by the FEA, but are not able to capture the expected nonlinear response.

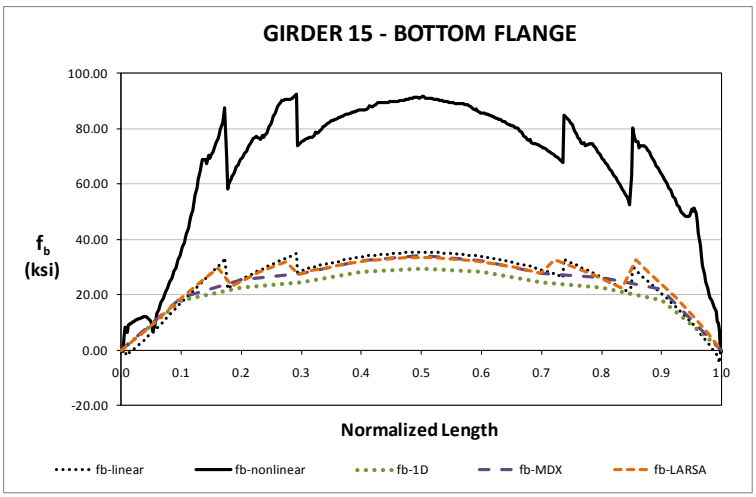

Fig. 6. EISCS4, Comparison of stress predictions, Total Dead Load

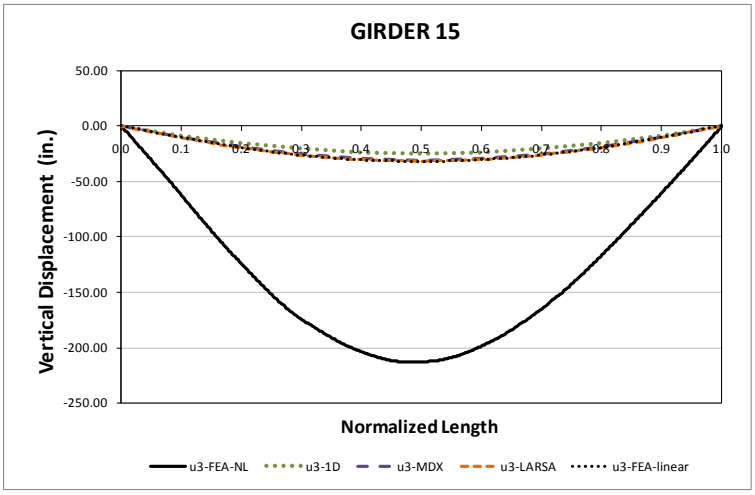

Fig. 7. EISCS4, Comparison of vertical deflection predictions, Total Dead Load

Finally, an eigenvalue analysis was conducted to determine the multiple of the steel dead load that needs to be applied to reach an unstable condition of the structure. Figure 8 shows the buckled shape of the system. The analysis predicts elastic system global buckling at 1.52 times the self-weight of the structure.

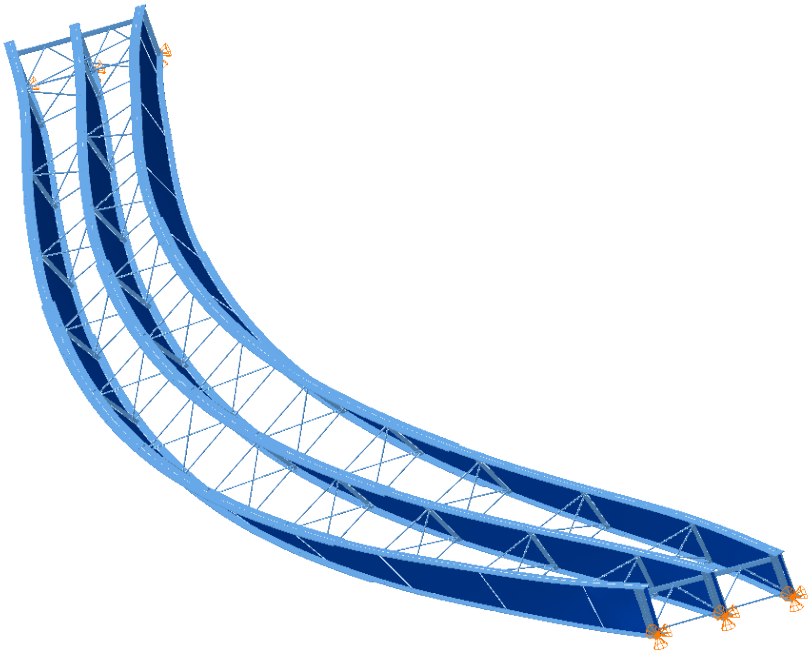

Fig. 7. EISCS4, global buckling mode at 1.52 times the Steel Dead Load

The results show that an analysis that a second order analysis is necessary to predict or anticipate the stability problem on this stage of the subject bridge. The large length-to-width of the bridge would appear to be the main factor causing this response. The comparison of results for different analysis methods show that a 1D or 2D model would be sufficient to represent the response of the bridge, as predicted by the 3D ***linear*** FEA model. The linear results obtained in these analyses match reasonably well, but are slightly larger than the corresponding camber values indicated on the engineering drawings. However, the linear analyses are not sufficient to predict the physical response of the bridge. These results indicate that stage 3 of the bridge was potentially near a state of instability when the concrete deck placement was halted.

I6.3 NISCS3 (New, I-girder, Simple-span, Curved, Skewed supports)

Category Data:

L_{as} = 150 ft / R =438 ft / w = 30 ft / θ_1 = 35.0°, θ_2 = 0°, 4 girders

Cross-Frame Detailing Method: NLF

Erection Stages Analyzed: Three

Deck Placement Sequence: One stage, deck thickness = 9.5 in.

Bridge Perspective & Plan Views:

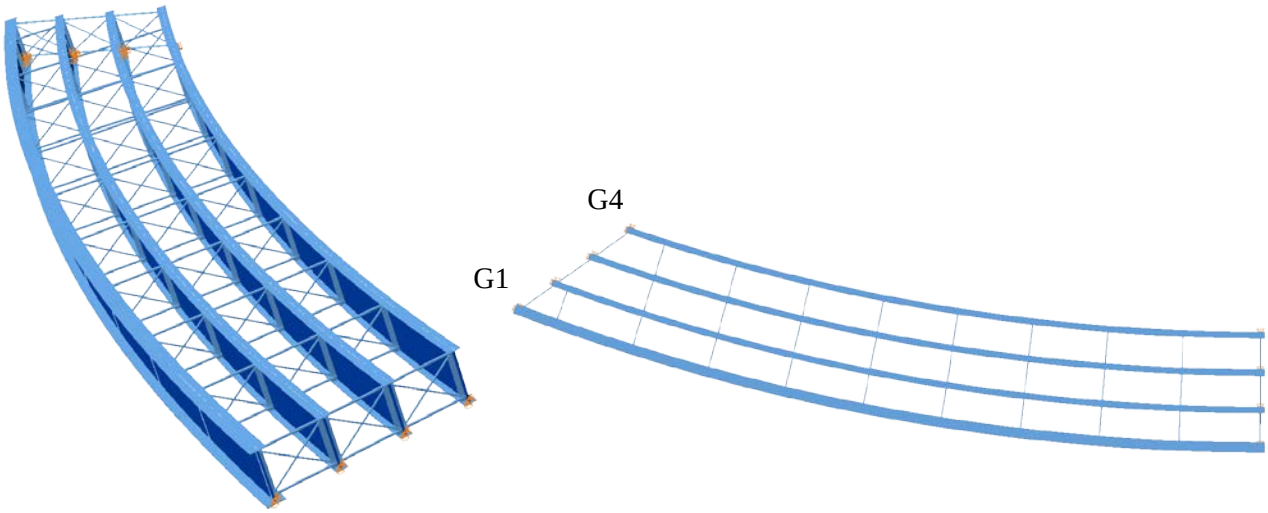

Abbreviated Analysis Results:

This bridge is a horizontally curved bridge with a skewed support at the left end and a radial support at the right end. In this bridge, the combined effects of curvature and support skew in the system performance are studied. Three stages are selected for this purpose, as shown in Figure 1. Stage 2 corresponds to the state where the first two interior girders are erected. It is considered that the two girder system is stable; therefore, no shoring towers or holding cranes are provided. Next, the behavior of the bridge is studied for Stage 3, where three girders are erected. Finally, the last studied stage corresponds to the total dead load condition. At this stage, the steel structure does not act compositely with the concrete deck. The deck is not shown for visualization purposes.

Stage 2

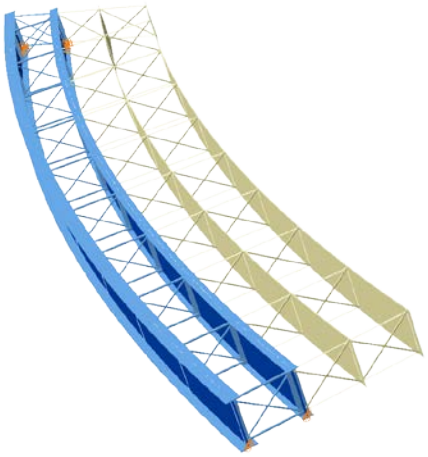

Stage 3

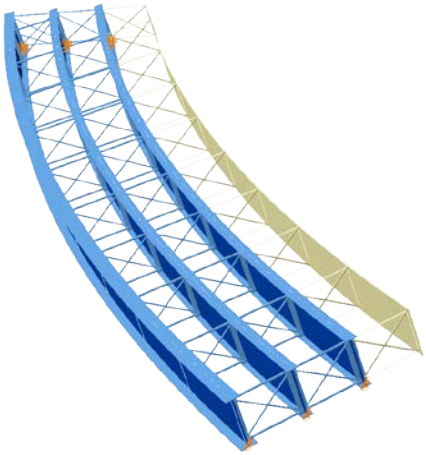

Stage 5 - TDL

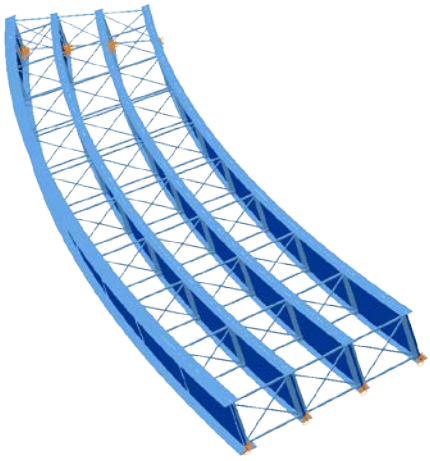

Fig. 1. NISCS 3, Studied Stages

The responses predicted by the 2D grid analysis model and the 3D benchmark are compared for the interior girder, G1, Stage 3. As shown in Figure 2, the magnitudes of the vertical displacements are not accurately captured by the approximate model. The vertical displacements are larger than the predicted by the 3D model. This trend is consistent with the observed in other curved bridges. The limitations of the approximate 2D grid analysis to represent the actual torsional behavior of an I-girder result in inaccurate representations of the vertical displacements. As a consequence, the 2D analyses predict misleading displacements that are larger than the expected.

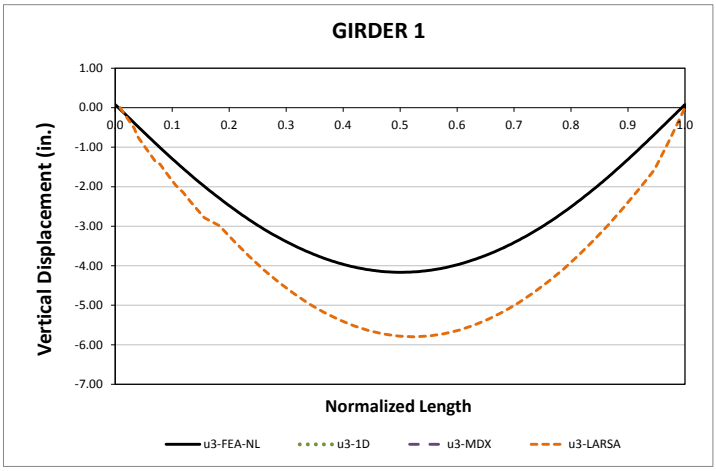

Fig. 2. Vertical Displacement Predictions, Stage 3

For the prediction of major-axis bending stresses, the 2D model captures the 3D model representation accurately. Figure 3 shows the major-axis bending stress response in the bottom flange of girder G1. As shown, the limitations of the 2D model representation do not have a severe influence in the prediction of this response. The same trend is observed for the rest of steel erection stages. The 2D grid model predictions for all the girders in both flanges match the FE model predictions as the construction of the bridge continues from the erection of the first girder segments up to the completion of the steel structure erection.

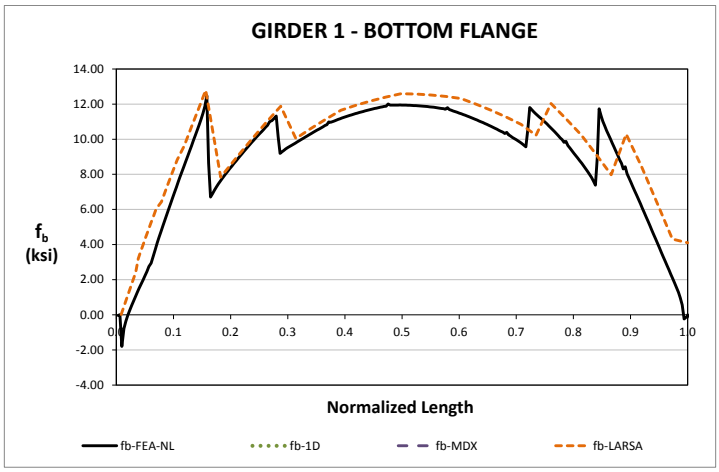

Fig. 3. Major Axis Bending Stress Predictions, Stage 3

A particular aspect of this bridge is the level of flange lateral bending stresses observed in the girders. The skew induce large stress levels, as shown in Figure 4. The plots shown in this figure correspond to linear and nonlinear elastic analyses. While in the rest of the girder, the f_ℓ stresses related to the curvature effects are relatively low, at the end support, they are significantly large.

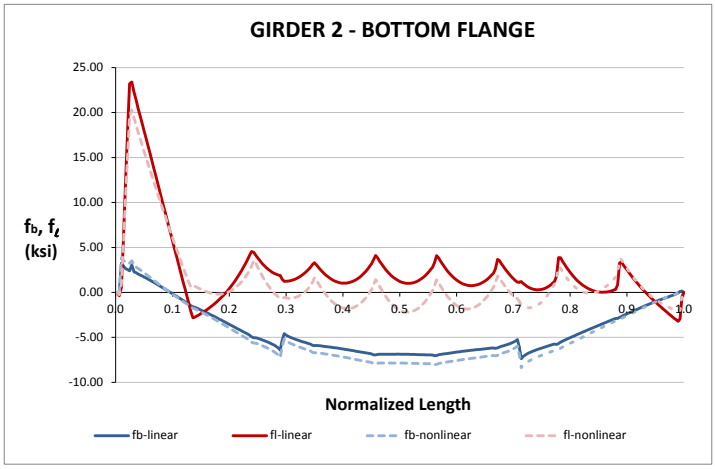

Fig. 4. Stress Predictions, Stage 2

In the 2D models, the flange lateral bending stresses are calculated according to the V-Load formula, based on the results for major-axis bending stress. As shown in Figure 5 for girder G2, Stage 2, the prediction of this response based on this formulation is relatively accurate along the girder, except at the skew region. According to these results, the simplified analysis captures only the effects of the curvature. Given that the V-Load formula has no information regarding the skew and its effects, peaks as the one shown in the figure are omitted.

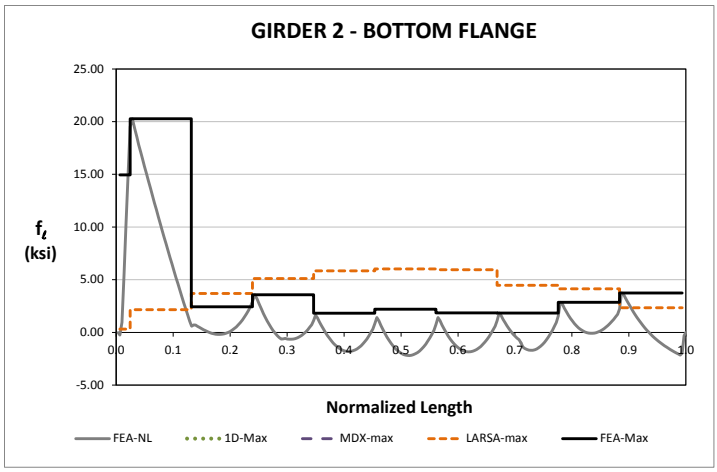

Fig. 5. Flange Lateral Bending Stress Predictions, Stage 2

The results for the total dead load condition, Stage 5, are discussed next. For the vertical displacements, shown in Figure 6, the 1D model prediction underestimates the expected displacements. In the case of the Larsa 2D grid model, the response is over predicted. The overestimation is associated to the limitations of the computational model to represent the actual behavior of an open-section thin-walled beam element. Thus, the 2D grid models do not consider the stiffness contribution that comes from the warping of the flanges. The above observations are consistent for all the girders of the bridge throughout all the construction simulation.

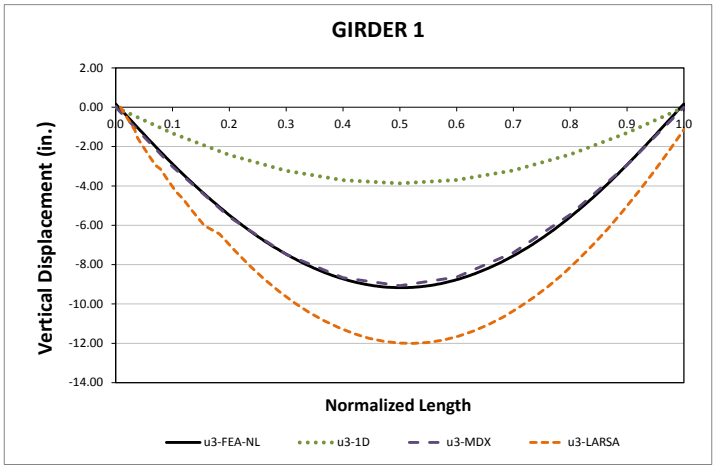

Fig. 5. Vertical Displacement Predictions, Stage 5

At the total dead load condition, Stage 9, the major-axis bending stress predictions are almost the same for all the methods. As observed for girder G1 in Figure 6, the 2D results capture the expected response, as predicted by the 3D FE model. It is apparent from a study of these predictions that the major-axis bending response is not affected as much as the displacement responses due to the limitations of the approximate methods.

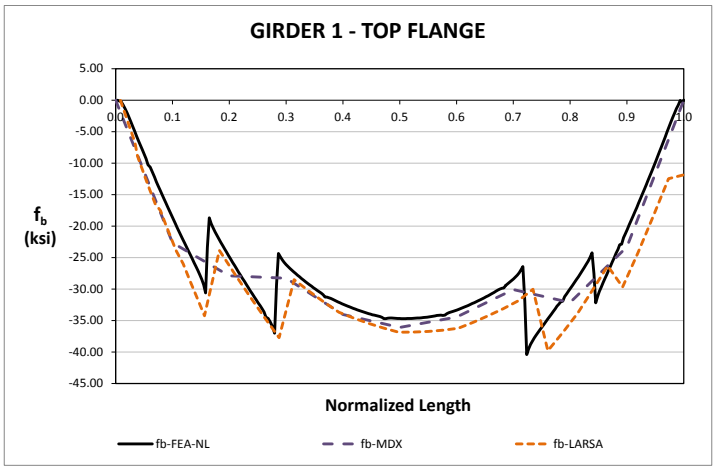

Fig. 6. Major Axis Bending Stress Predictions, Stage 9

I6.4 NISCS9 (New, I-girder, Simple-span, Curved, Skewed supports)

Category Data:

L_{as} = 150 ft / R =438 ft / w = 30 ft / θ_1 = 62.5°, θ_2 = 45.6°, 4 girders

Cross-Frame Detailing Method: NLF

Erection Stages Analyzed: Four

Deck Placement Sequence: One stage, deck thickness = 9.5 in.

Bridge Perspective & Plan Views:

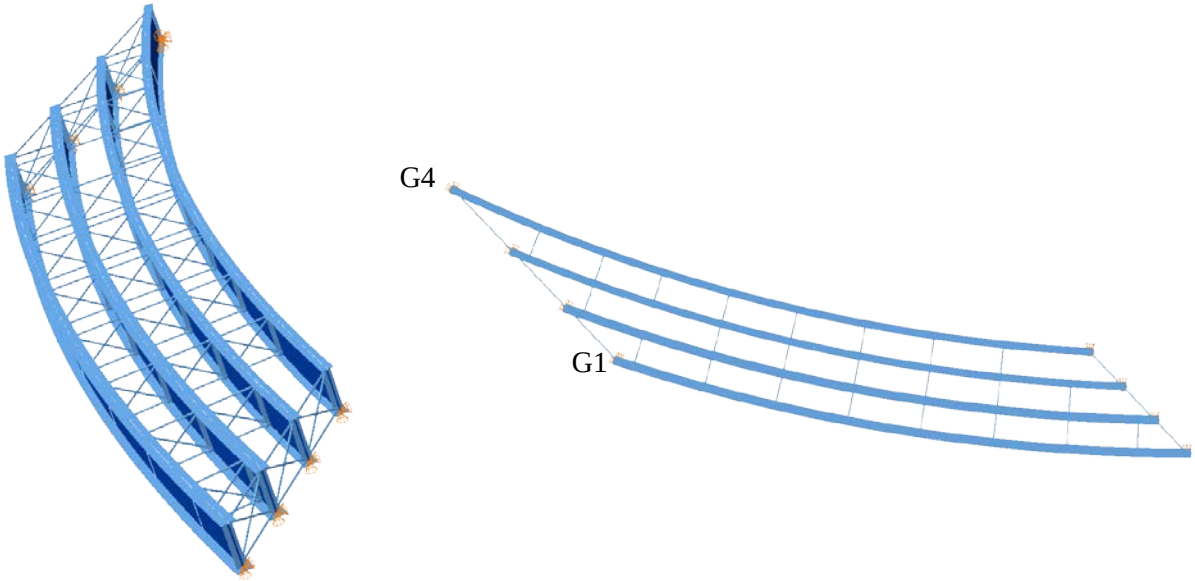

Abbreviated Analysis Results:

This bridge is a horizontally curved bridge with skewed supports. In this bridge, the combined effects of curvature and support skew in the system performance are studied. Four stages are selected for this purpose as shown in Figure 1. Stage 3 corresponds to the state where the first two interior girders are erected. Shoring towers are provided at the interior of the girders to facilitate the erection. Next, the behavior of the bridge is studied for Stage 5, where three girders are erected, and the shoring towers are still in place. In Stage 6, the towers are removed, so the girders are supported only at the location of the bearings. Finally, the last studied stage corresponds to the total dead load condition. At this stage, the steel structure does not act compositely with the concrete deck.

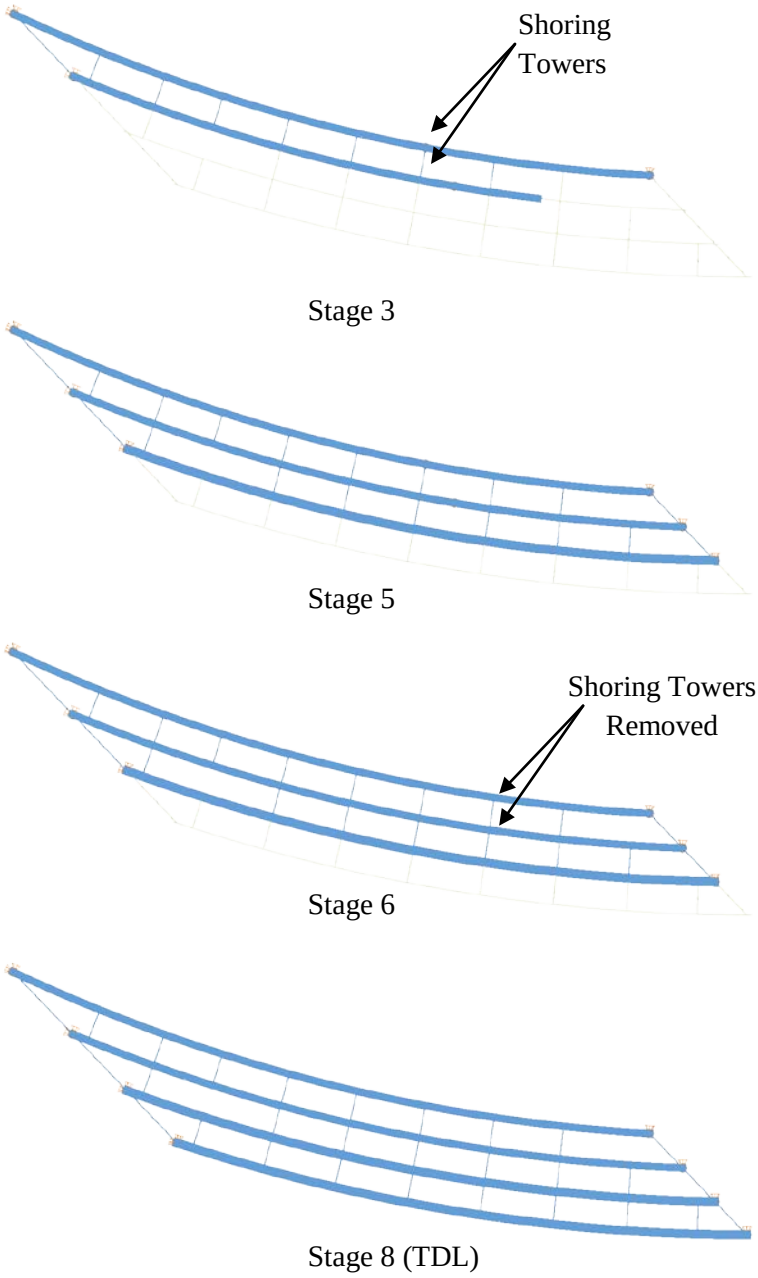

Fig. 1. NISCS 9, Studied Stages

The responses predicted by the 2D grid analysis model and the 3D benchmark are compared for the interior girder, G4, Stage 3. As shown in Figure 2, the magnitudes of the vertical displacements are not accurately captured by the approximate model. The vertical displacements are significantly larger than the predicted by the 3D model. This trend is consistent with the observed in other curved bridges. The limited model implemented in the approximate 2D grid analysis to represent the torsional stiffness of the I-girders results in inaccurate representations of the vertical displacements.

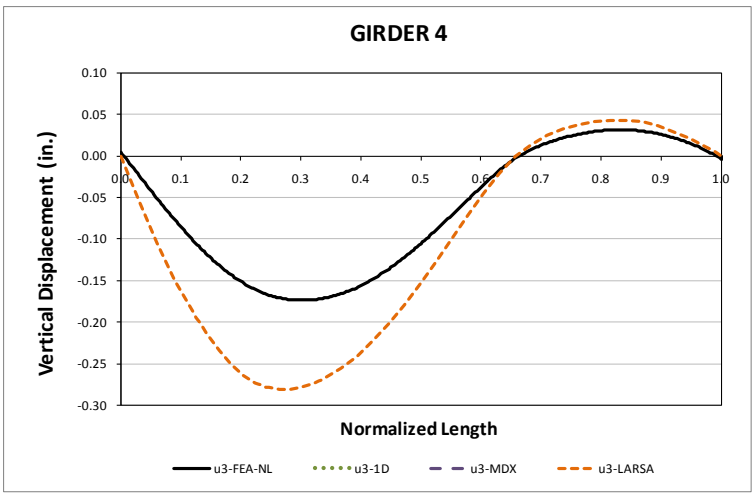

Fig. 2. Predictions on Vertical Displacements, Stage 3

For the prediction of major-axis bending stresses, the 2D model captures the 3D model representation accurately. Figure 3 shows the major-axis bending stress response in the top flange of girder G4. As shown, the limitations of the 2D model representation do not have a severe influence in the prediction of this response. The same trend is observed for the rest of steel erection stages. The 2D grid model predictions for all the girders in both flanges match the FE model predictions as the construction of the bridge continues from the erection of the first girder segments up to the completion of the steel structure erection.

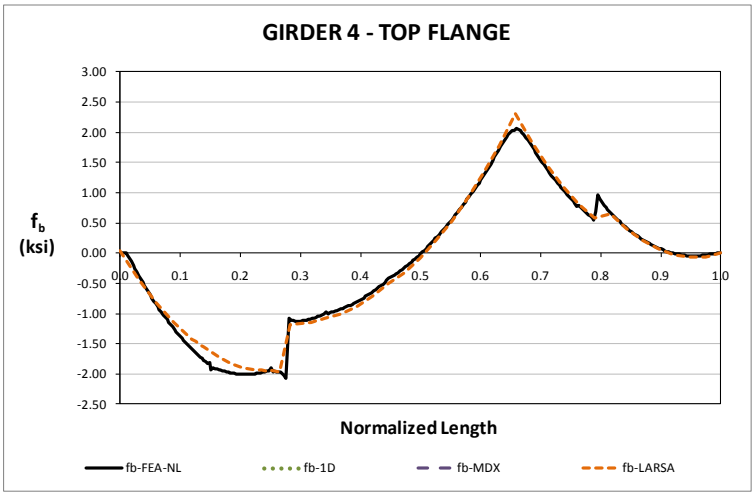

Fig. 3. Major Axis Bending Stress Predictions, Stage 3

The flange lateral bending stresses are calculated according to the V-Load formula. As shown in Figure 4 for Stage 6, the prediction of this response based on this formulation is relatively accurate. Even though for this case these stresses are small and do not deserve much attention from the design perspective, it is

observed that the prediction of the equivalent lateral load obtained from the major-axis bending response could be used to determine an upper bound limit.

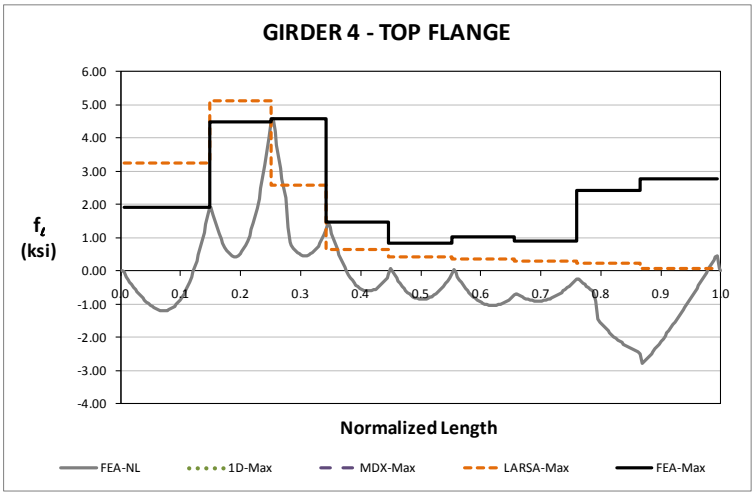

Fig. 4. Flange Lateral Bending Stress Predictions, Stage 6

The results for the total dead load condition, Stage 8, are discussed next. For the vertical displacements, shown in Figure 5, the 1D model prediction underestimates the expected displacements. In the case of the Larsa 2D grid model, the response is over predicted. The overestimation is associated to the limitations of the computational model to represent the actual behavior of an open-section thin-walled beam element. Thus, the 2D grid models do not consider the stiffness contribution that comes from the warping of the flanges. The above observations are consistent for all the girders of the bridge throughout all the construction simulation.

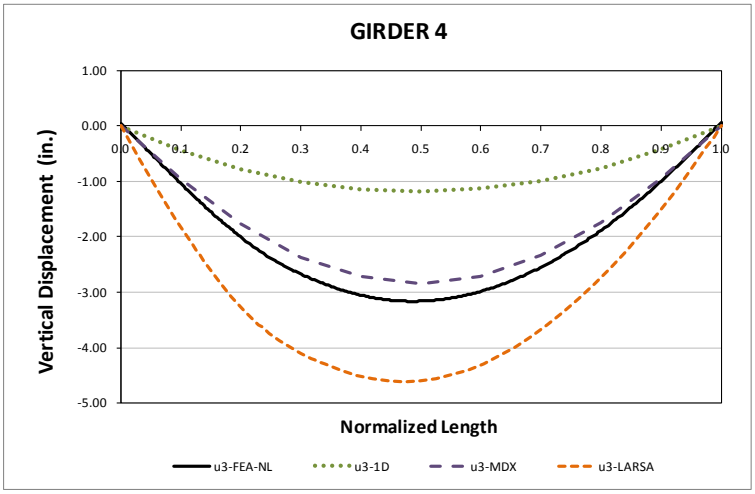

Fig. 5. Predictions on Vertical Displacements, Stage 9

At the total dead load condition, Stage 9, the major-axis bending stress predictions are almost the same for all the methods. As observed for girder G1 in Figure 6, both the 1D and 2D results capture the expected response, as predicted by the 3D FE model. It is apparent from a study of these predictions that the major-axis bending response is not affected as much as the displacement responses due to the limitations of the approximate methods.

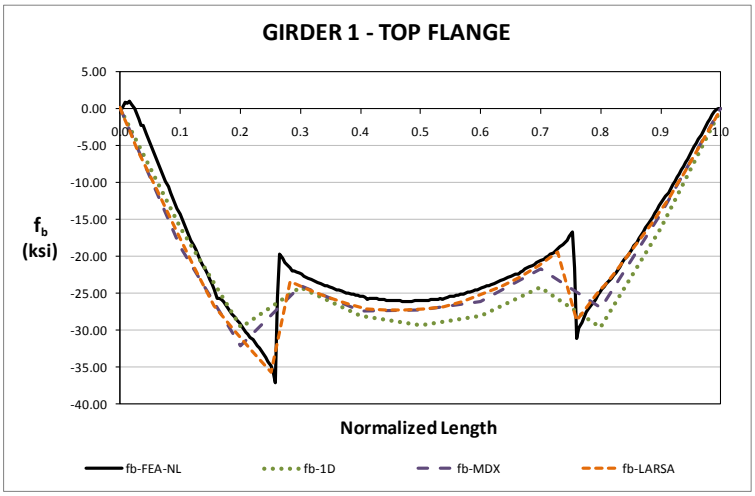

Fig. 6. Major Axis Bending Stress Predictions, Stage 9

I6.5 NISCS14 (New, I-girder, Simple-span, Curved, Skewed supports)

Category Data:

L_1 = 150 ft / R_1 = 280 ft/ w = 80 ft /θ_1 = 53.7^o, θ_2 = 0^o, 9 girders

Cross-Frame Detailing Method: NLF

Erection Stages Analyzed: 5 (Analyses are performed assuming NLF)

Deck Placement Sequence: 1 Stage

Bridge Perspective & Plan Views:

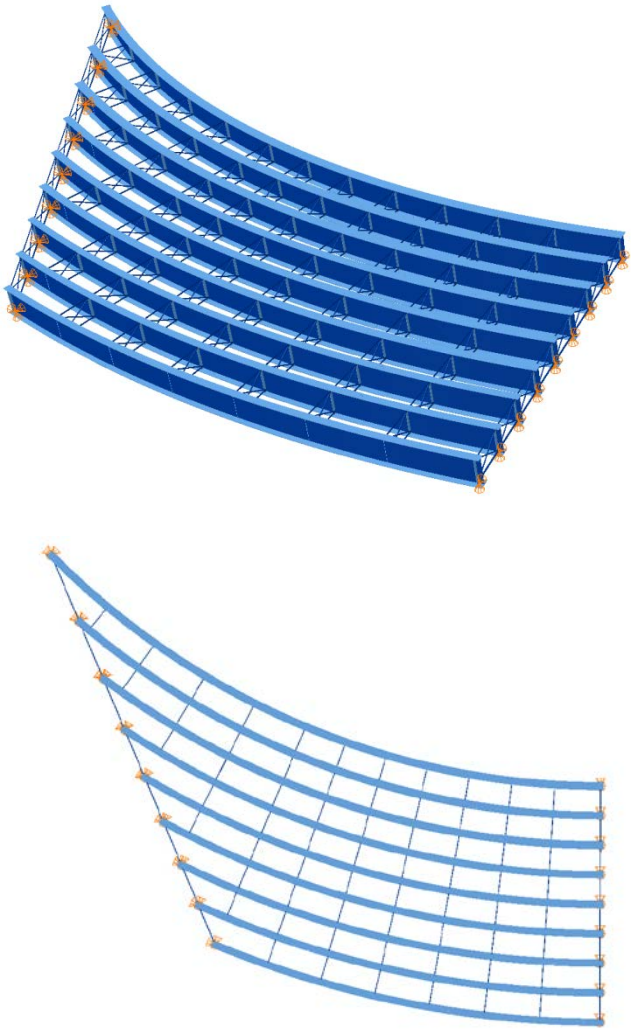

Abbreviated Analysis Results

Figure 1 shows the different analysis stages which are considered to evaluate the different analysis methods. Similar behavior is observed at the construction stages and grid analysis methods predict the stresses and the lateral displacements at the skewed bearings and cross-frame locations accurately. Furthermore, there is maximum of 2 inches difference for the vertical displacement predictions. However, this difference is not critical and can be handled in haunches.

Total dead load results are investigated in detail since this is the highest load level during construction. Figure 2 shows vertical deflection predictions under total dead load for the outside girder (Girder 1). It is observed from the results that Larsa results over predicts the deflections whereas the other methods predict close to benchmark solutions. This is believed to be due to the coarse representation of the structure for the solutions other than Larsa. Finer representation of the structure is unable to capture the warping deformations. Figure 3 shows relative radial deflection predictions under total dead load for the outside girder (Girder 1).

Similar to previous studies, the relative radial displacements are well predicted at the cross-frame locations whereas the predictions are off within the cross-frames. Figure 4 shows major-axis bending stress predictions under total dead load for the outside girder (Girder 1). The stresses are well predicted by approximate analysis methods. Figure 5 shows minor-axis bending stress predictions under total dead load for the outside girder (Girder 1). It is clear that the flange lateral bending stresses are well predicted for the positive moment regions.

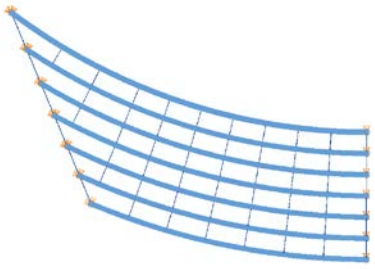

Stage 6

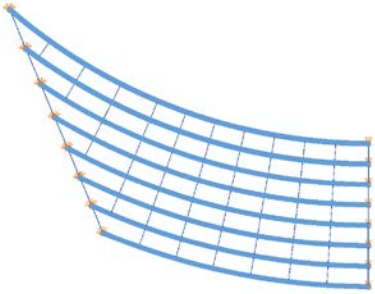

Stage 7

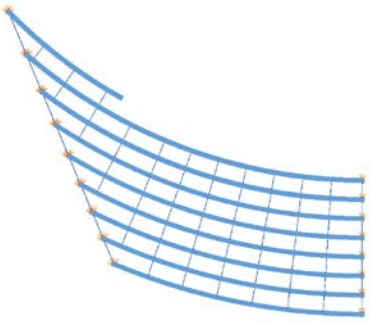

Stage 8

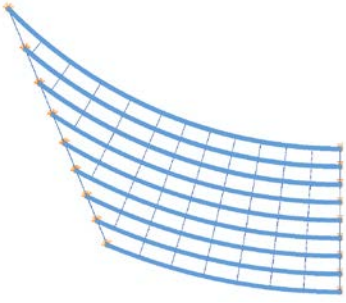

Stage 9 & 10

Fig. 1. NISCS14, Considered different analysis stages.

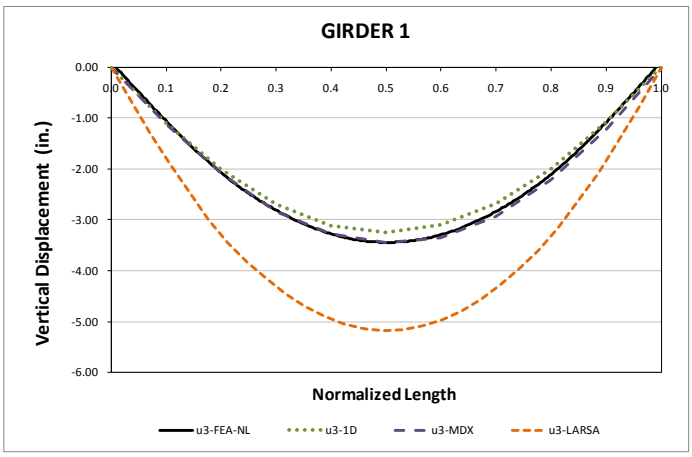

Fig. 2. NISCS14, Vertical displacements under total dead load for NLF detailing.

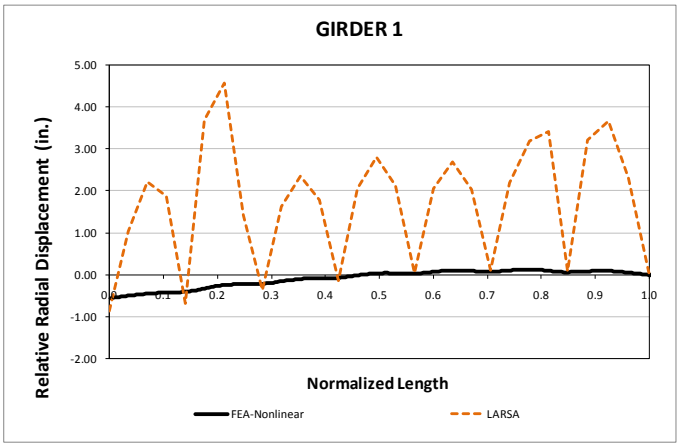

Fig. 3. NISCS14, Relative radial displacements under total dead load for NLF detailing.

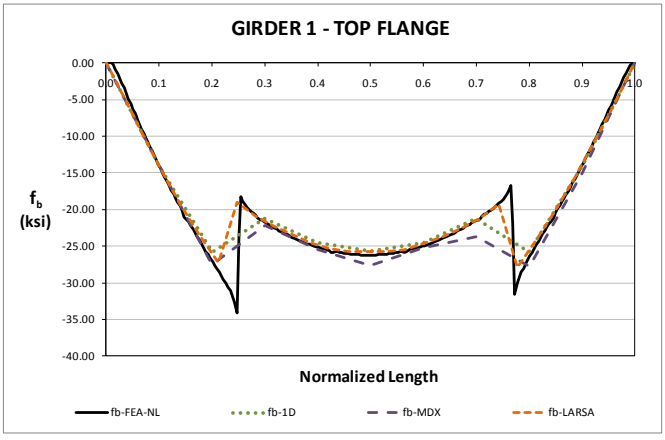

Fig. 4. NISCS14, Major-axis bending stresses under total dead load for NLF detailing.

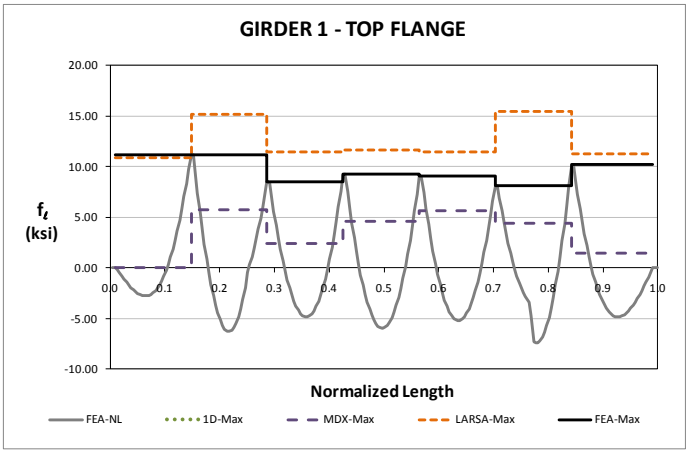

Fig. 5. NISCS14, Minor-axis bending stresses under total dead load for NLF detailing.

I6.6 NISCS15 (New, I-girder, Simple-span, Curved, Skewed supports)

Category Data:

L_1 = 150 ft / R_1 = 280 ft/ w = 80 ft /θ_1 = -35°, θ_2 = 0°, 9 girders

Cross-Frame Detailing Method: NLF

Erection Stages Analyzed: 6 (Analyses are performed assuming NLF)

Deck Placement Sequence: 1 Stage

Bridge Perspective & Plan Views:

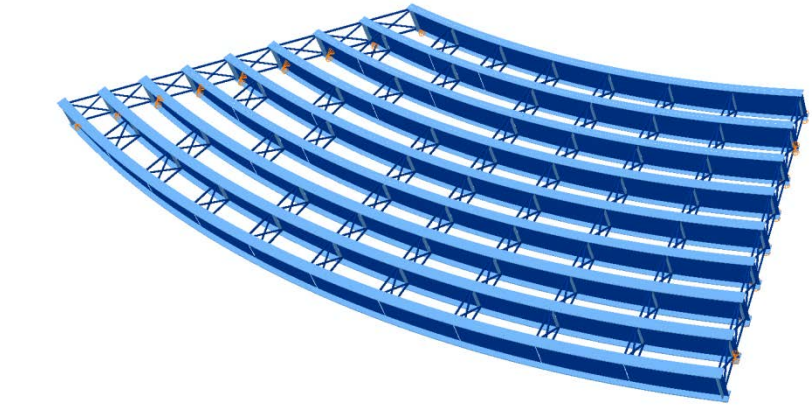

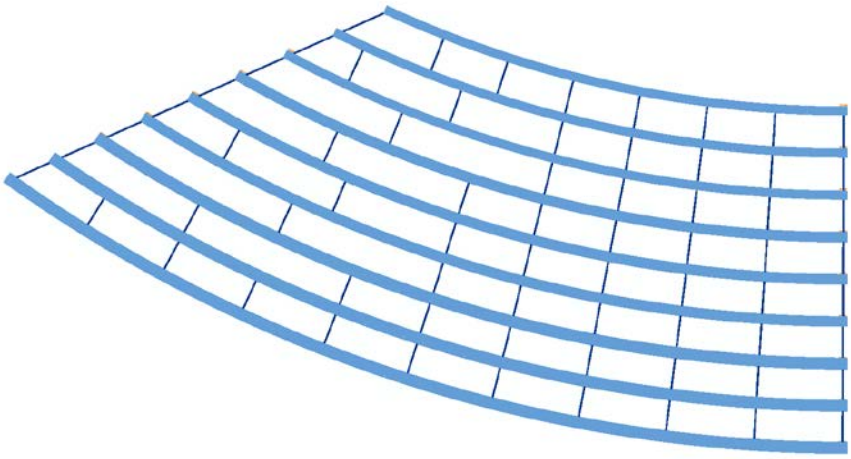

Abbreviated Analysis Results

Figure 1 shows the different analysis stages which are considered to evaluate the different analysis methods. Temporary supports are used at stages 1 through 9. It is observed that temporary supports reduce the vertical displacements significantly during the construction by keeping the girders in their cambered profiles. This may result to avoid the any fit up problems. Figure 2 shows the deflected shape of the bridge under total dead load. The deflections are magnified by fifty times. Uplift is observed at girder 9 at this stage which is not captured by other analysis methods. It is clear from Fig. 2 that the horizontal curvature and the skewed bearings both cause the layover on the same direction which increases the overall layover of the girders. However, maximum layover of the girder1 is around 2 inches which can be considered small. This might be more problematic once the span length increases. Figures 3 and 4 shows the layover of the Girders 1 and 9 under total dead load. It can be noticed from Figs. 3 and 4 that the grid analysis solutions cannot capture the layovers even at the brace points. This is due to the uplift. Figure 5 and 6 provides the vertical deflections of Girders 1 and 9 under total dead load. It should be noticed from Figs. 5 and 6 that the vertical displacement predictions cannot predicted accurately by approximate analysis methods. The reasons for this behavior are explained in the previous assessments in detail. However, it is also clear from Fig.6 that the mis-prediction is also due to the uplift of the girder which is not captured by any approximate analysis methods.

Figures 7 and 8 show the major-axis bending predictions of the Girders 1 and 9 under total dead load. It should be noted that the approximate solutions can not predict the stresses accurately. Moreover, the dense grid analysis methods can not capture the behavior on girder 9. This reasons for this behavior is explained in the previous reports. Figures 9 and 10 provide the flange lateral bending stresses for Girders 1 and 9 under total deadl load.

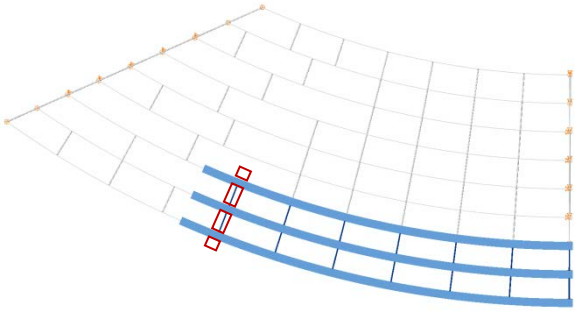

Stage 3

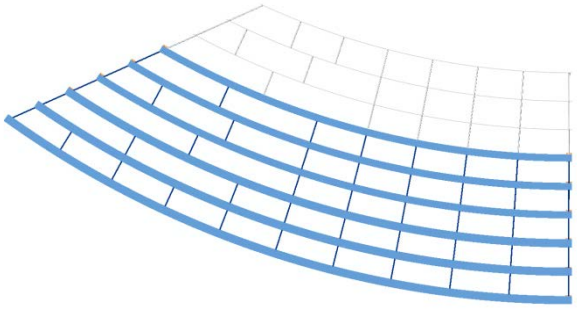

Stage 10

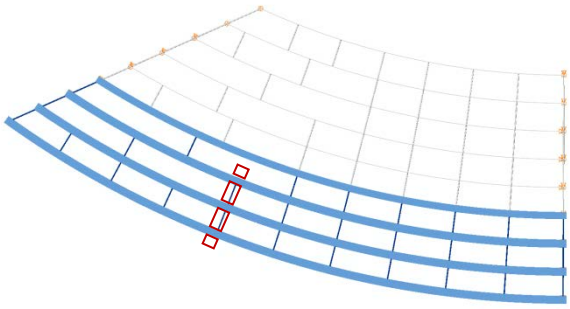

Stage 7

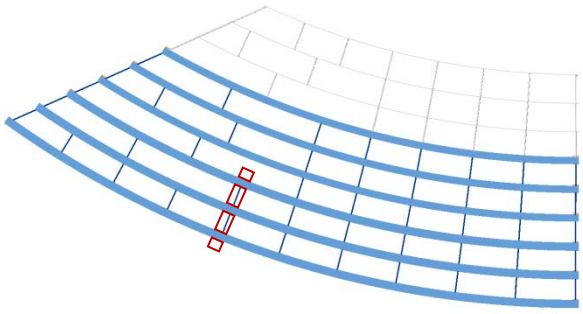

Stage 9

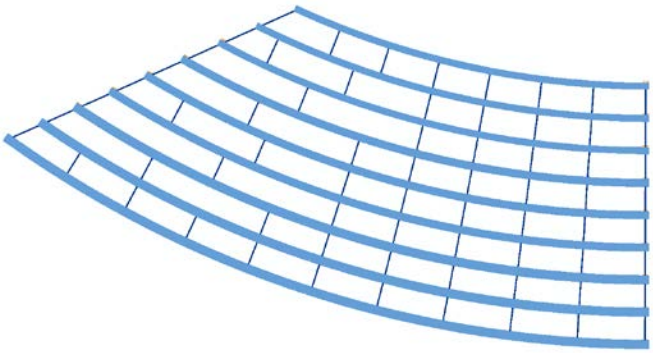

Stage 13 & 14

Fig. 1. NISCS15, Considered different analysis stages.

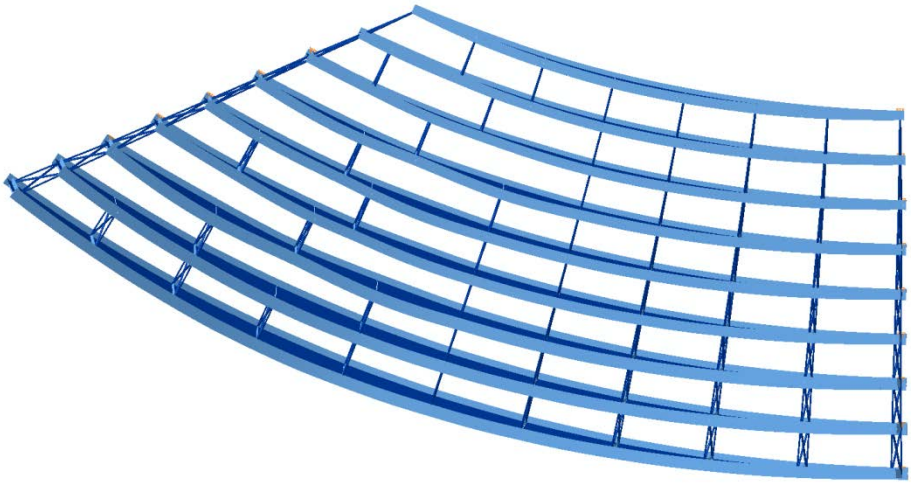

Fig. 2. NISCS15, deflected shape under total dead load, deflections are magnified by 50x.

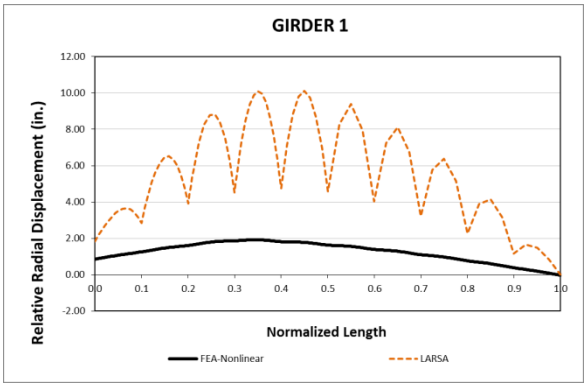

Fig. 3. NISCS15, Relative radial displacements under total dead load for NLF detailing.

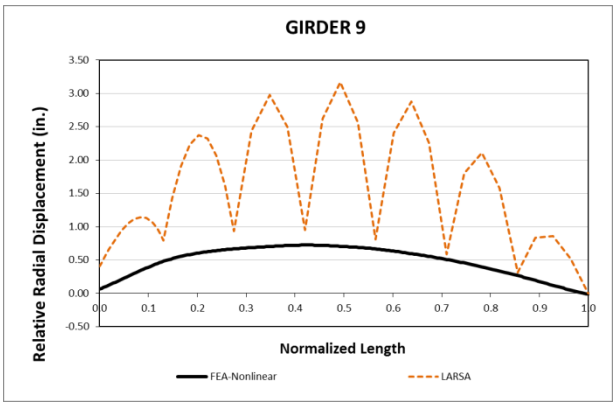

Fig. 4. NISCS15, Relative radial displacements under total dead load for NLF detailing.

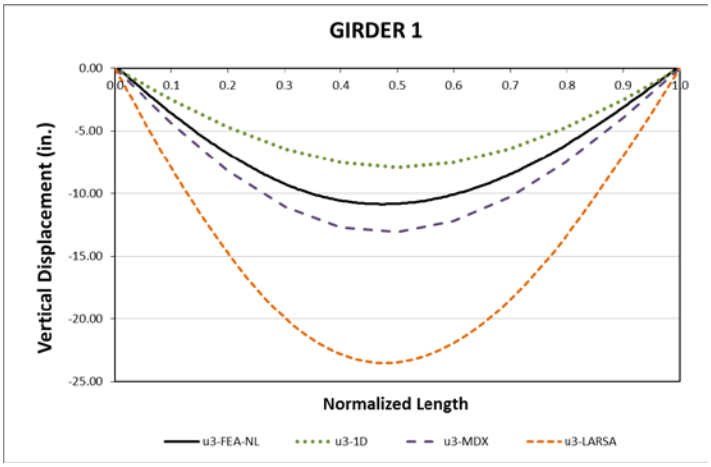

Fig. 5. NISCS15, Vertical displacements under total dead load for NLF detailing.

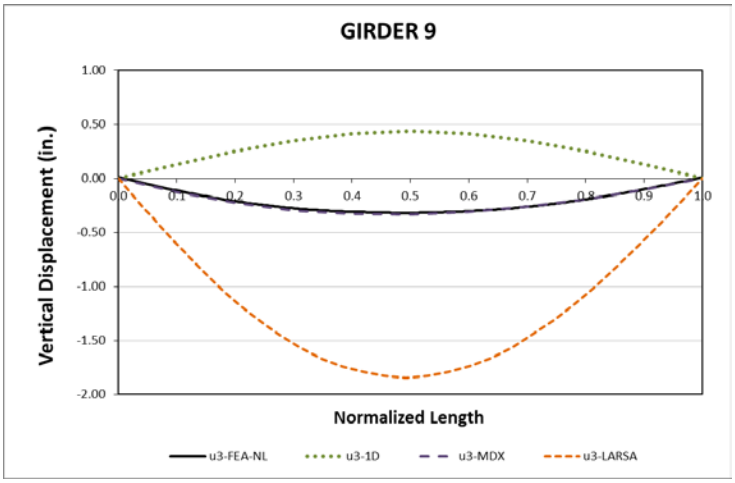

Fig. 6. NISCS15, Vertical displacements under total dead load for NLF detailing.

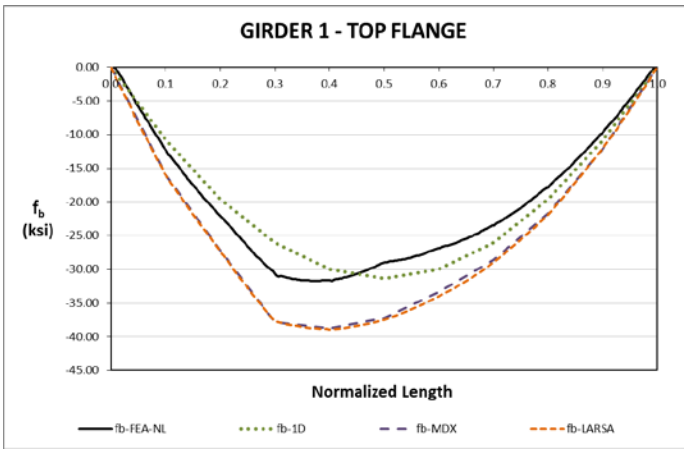

Fig. 7. NISCS15, Major-axis bending stresses under total dead load for NLF detailing.

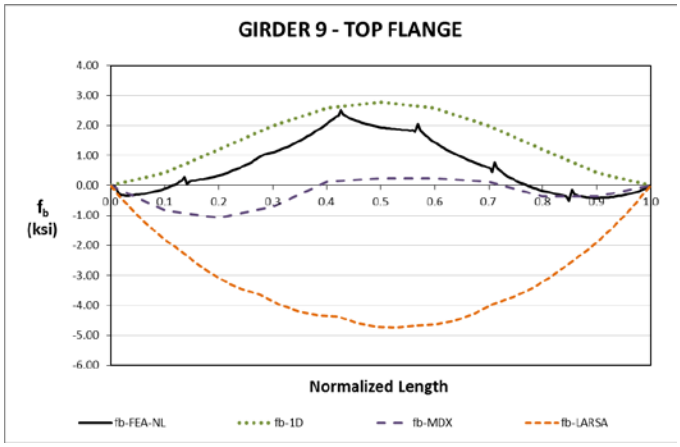

Fig. 8. NISCS15, Major-axis bending stresses under total dead load for NLF detailing.

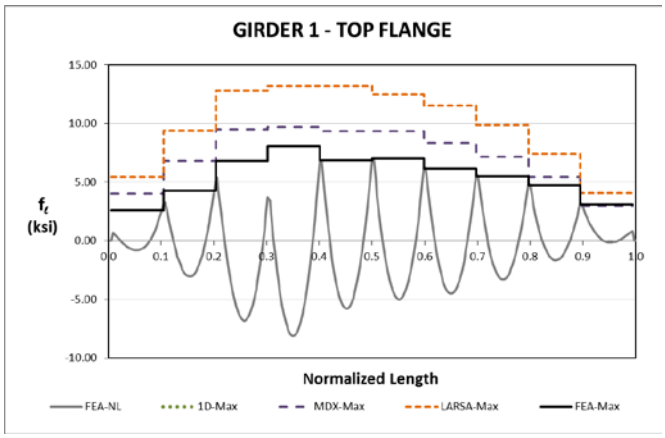

Fig. 9. NISCS15, Minor-axis bending stresses under total dead load for NLF detailing.

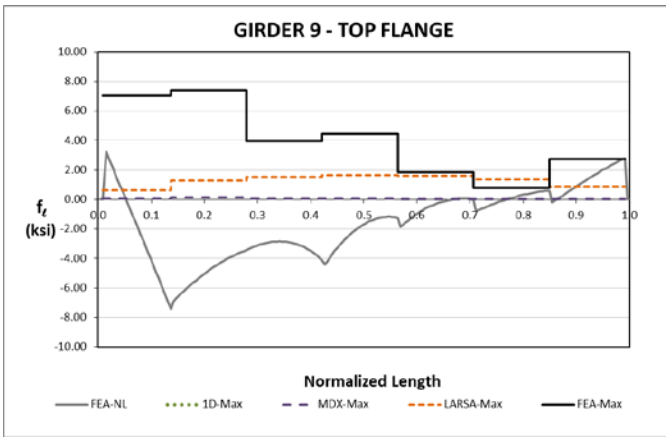

Fig. 10. NISCS15, Minor-axis bending stresses under total dead load for NLF detailing.

I6.7 NISCS37 (New, I-girder, Simple-span, Curved, Skewed supports)

Category Data:

L_1 = 300 ft / R_1 = 730 ft/ w = 80 ft /θ_1 = 35^o, θ_2 = 0^o, 9 girders

Cross-Frame Detailing Method: NLF

Erection Stages Analyzed: 4 (Analyses are performed assuming NLF)

Deck Placement Sequence: 1 Stage

Bridge Perspective & Plan Views:

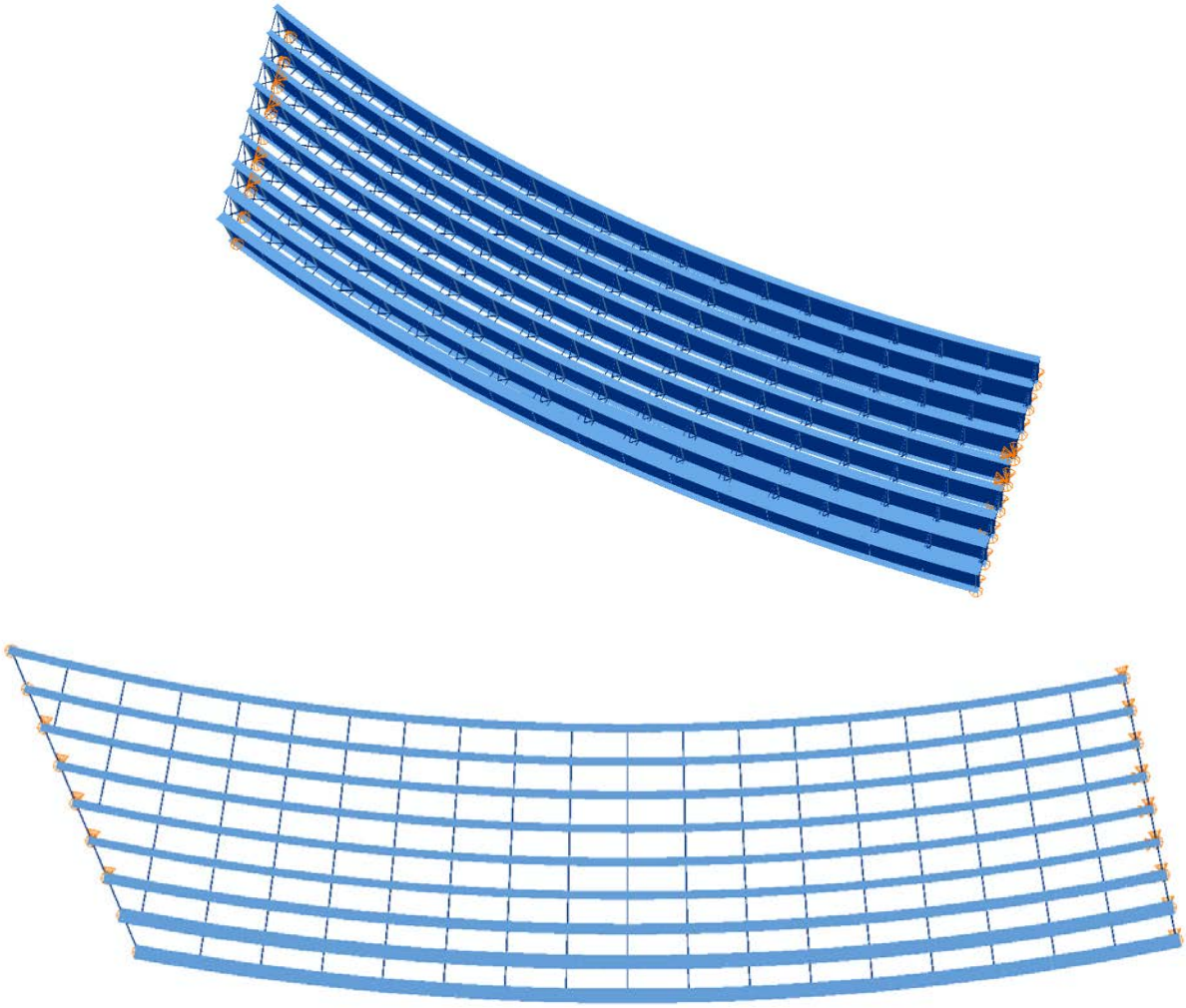

Abbreviated Analysis Results

Figure 1 shows the different analysis stages which are considered to evaluate the different analysis methods. Results from Stages 27 and 28 are investigated in detail. The only difference between these stages are the cross-frames between Girder 4 and Girder 5 are not connected yet. Therefore, the two girder assemblies act as a two different systems. These stages can be an example where one can observe fit-up problems. Figures 2 and 3 show vertical displacements of Girder 4 and 5 respectively for Stage 27. It is obvious from these figures that the deflection difference between girders 4 and 5 is huge which might result with difficulties during the placement of the cross-frames. Figures 4 and 5 provide the girder vertical displacements for Girders 4 and 5 respectively under steel dead. It should noticed from these figures that the maximum vertical deflections for Girder 5 reduced from approximately 19 inches to 5.25 inches. One way to overcome this problem is to use temporary supports during the steel erection which can control the vertical displacements during these erection stages. It should be noted that grid solution over predicts the vertical displacements in Fig. 3. As explained in the previous bridge summaries, this is mainly due to incapability of the 2D grid models to capture warping deformations between the cross-frame locations. Additionally, there is uplift observed in Stage 27 at Girders 3, 4, 6, 7, 8 and 9 by 3DFEA methods. However, grid solutions only capture uplift on Girders 3, 4, 8 and 9. As a result, the grid solutions cannot capture the global behavior of the bridge.

Figures 6 and 7 show the layover of the Girders 4 and 5 respectively for stage 27. Although the end layovers are accurately predicted by approximate analysis methods, the layovers within the span can not captured accurately by grid analysis solutions.

Figures 8 and 9 show the major-axis bending predictions of the Girders 4 and 5 respectively for Stage 27. Also Figs. 10 and 11 show the major-axis bending predictions of the Girders 4 and 5 under steel dead load. It should be noted that the approximate solutions predict the stresses accurately. It should be noted from Fig. 9 that the stress magnitudes are much higher that the values obtained from steel dead load condition.

Figures 12 and 13 illustrates the cross-frame stresses for Stages 27 and 28. It it is obvious from Figs. 12 and 13 that the cross-frame stresses are much higher for Stage 27.

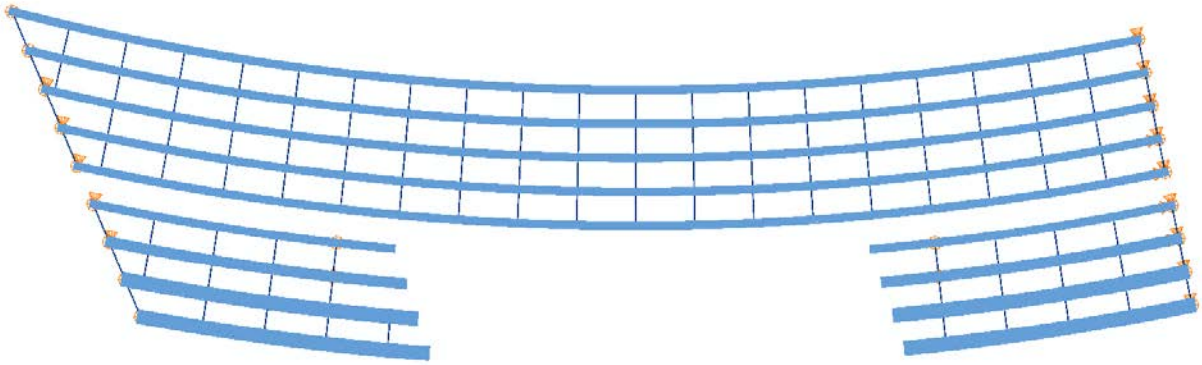

Stage 23

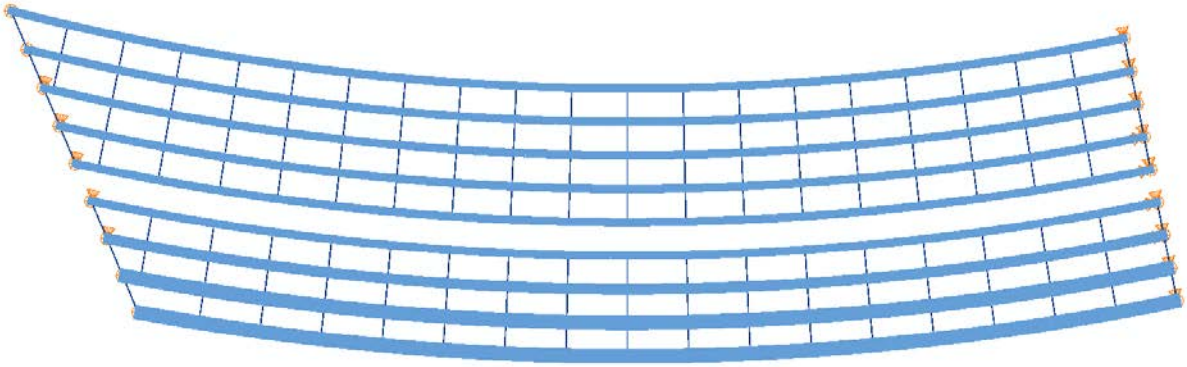

Stage 27

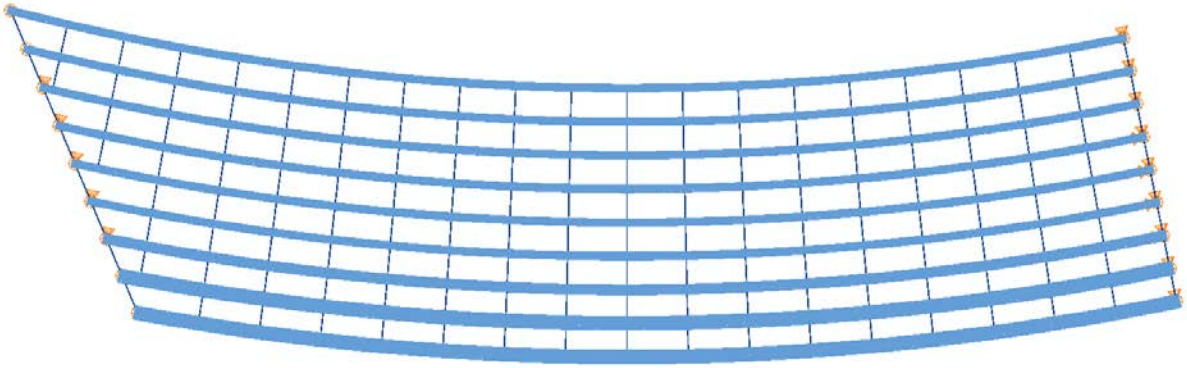

Stage 28 & 29

Fig. 1. NISCS37, Considered different analysis stages.

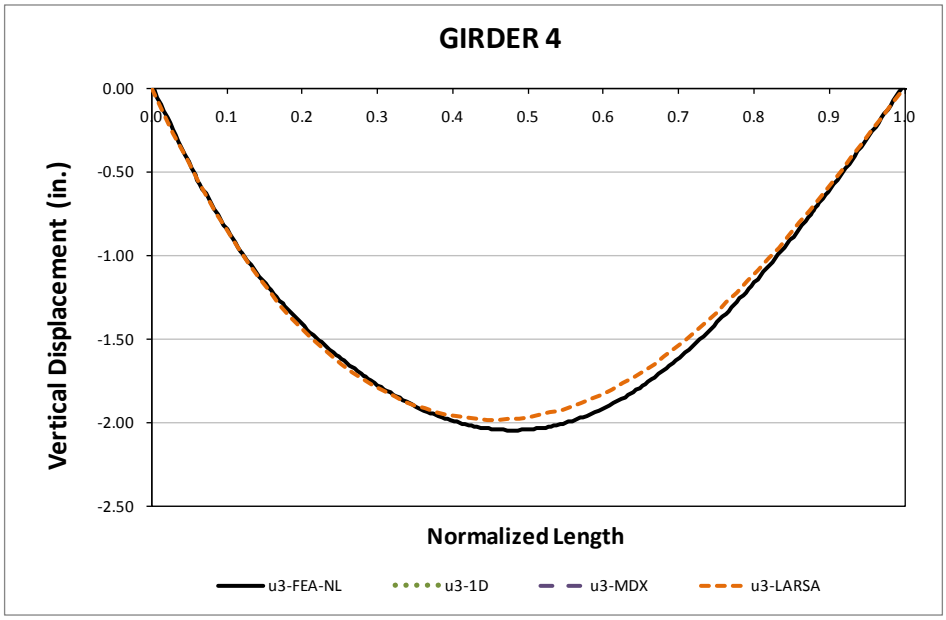

Fig. 2. NISCS37, Stage 27 Vertical displacements for NLF detailing.

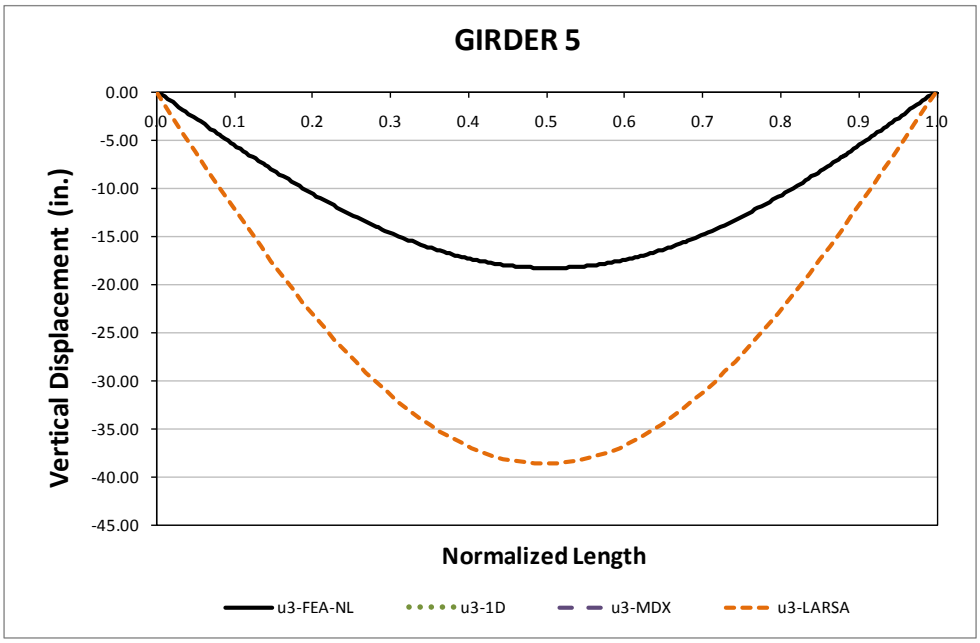

Fig. 3. NISCS37, Stage 27 Vertical displacements for NLF detailing.

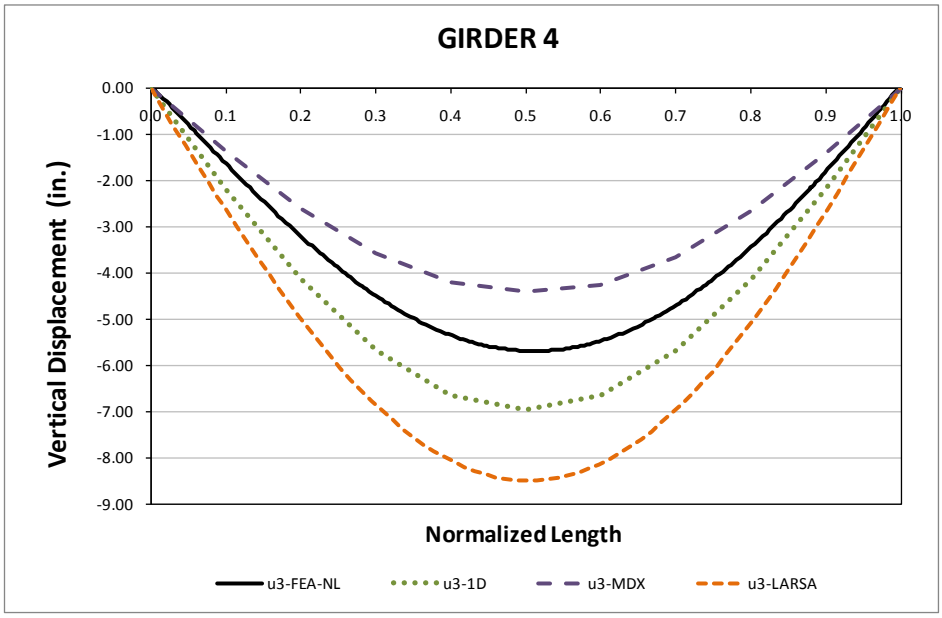

Fig. 4. NISCS37, Vertical displacements under steel dead load for NLF detailing.

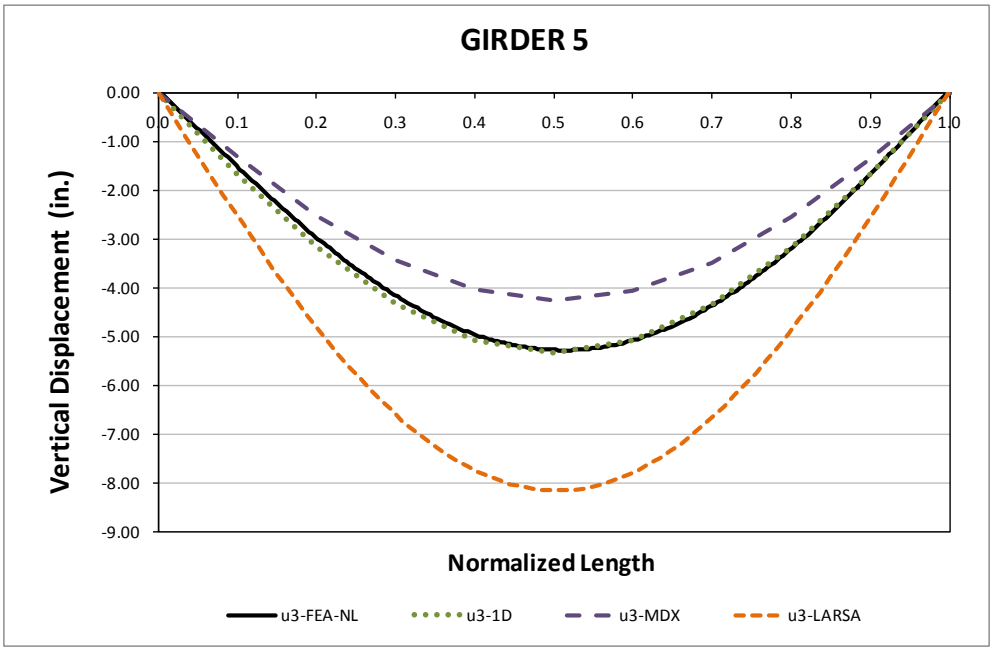

Fig. 5. NISCS37, Vertical displacements under steel dead load for NLF detailing.

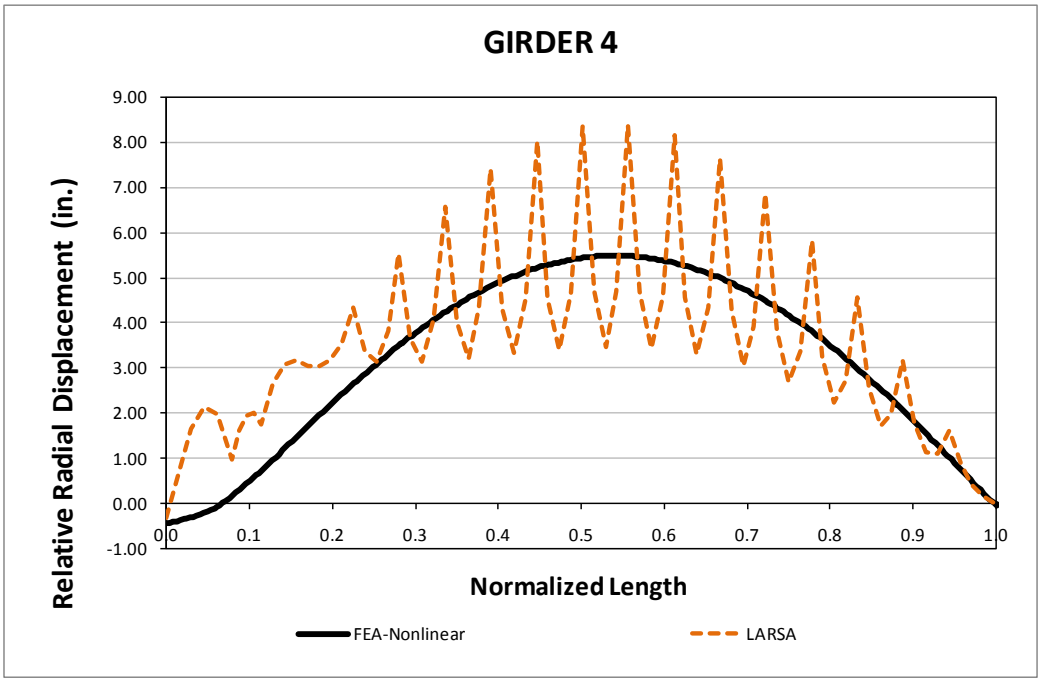

Fig. 6. NISCS37, Stage 27 Relative radial displacements for NLF detailing.

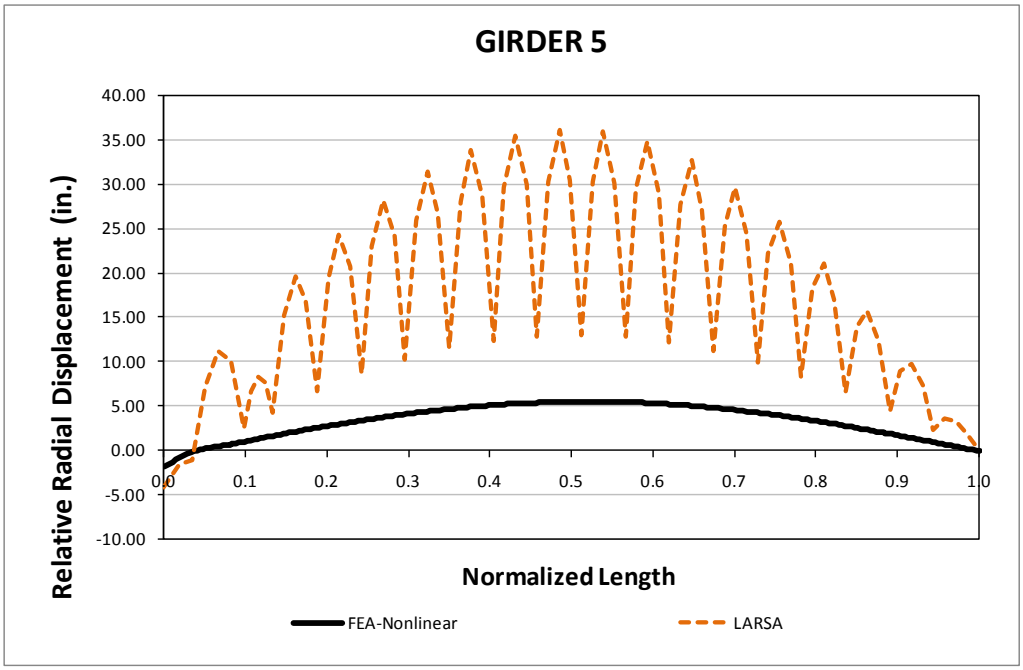

Fig. 7. NISCS37, Stage 27 Relative radial displacements for NLF detailing.

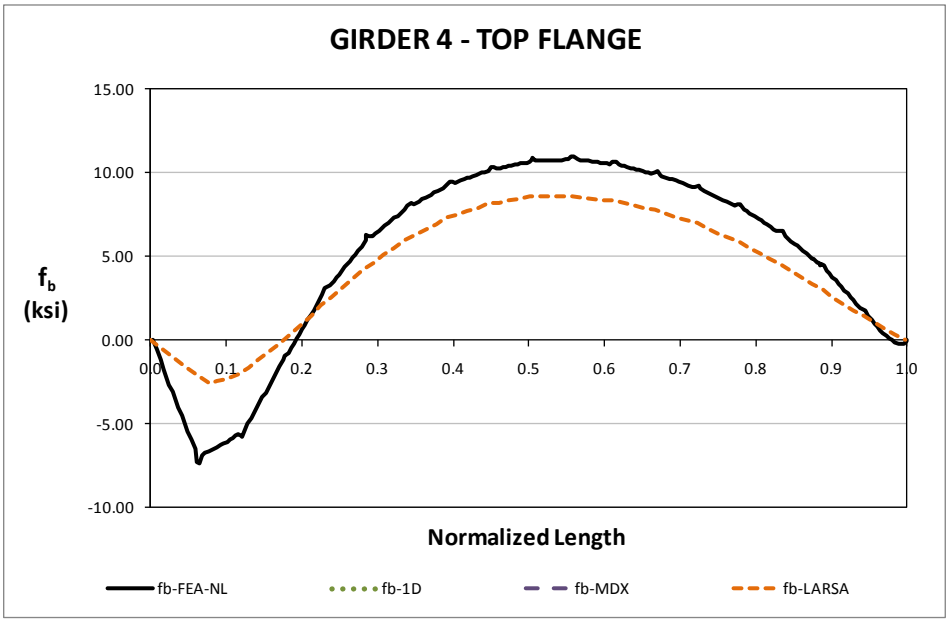

Fig. 8. NISCS37, Stage 27 Major-axis bending stresses for NLF detailing.

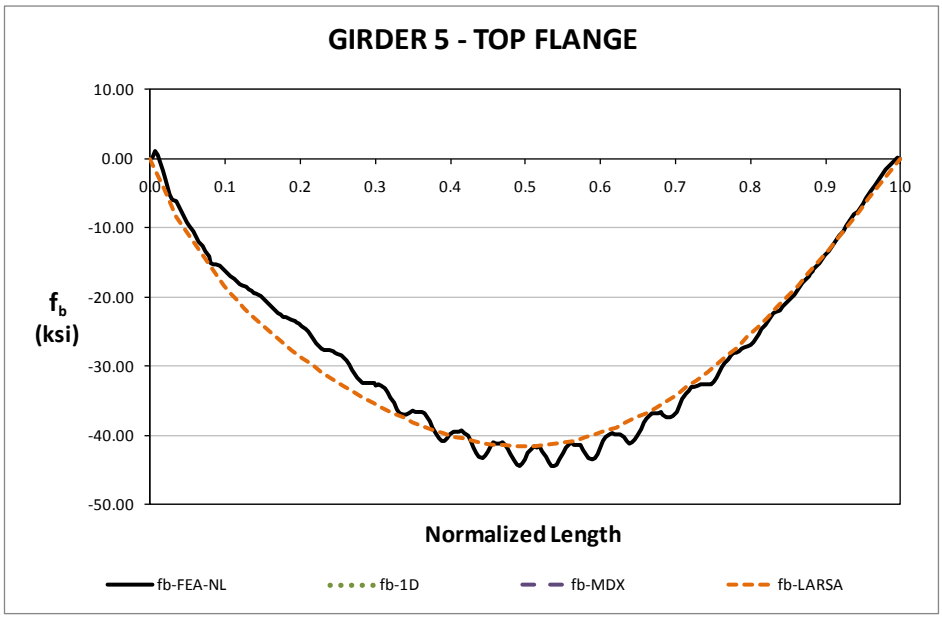

Fig. 9. NISCS37, Stage 27 Major-axis bending stresses for NLF detailing.

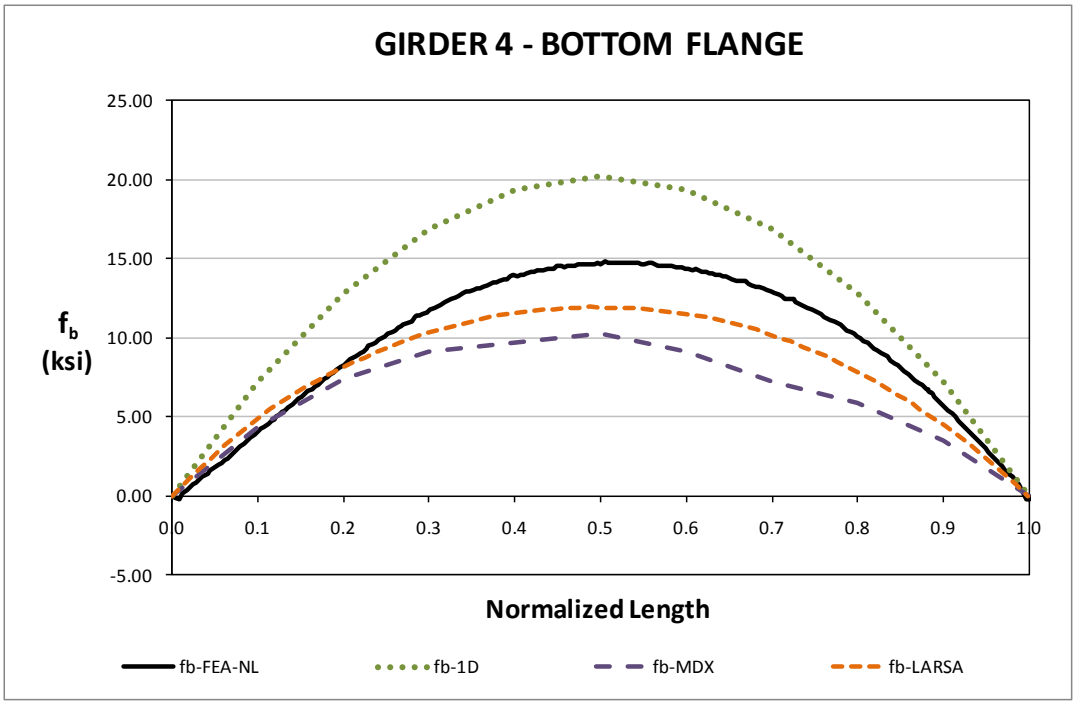

Fig. 10. NISCS37, Major-axis bending stresses under steel dead load for NLF detailing.

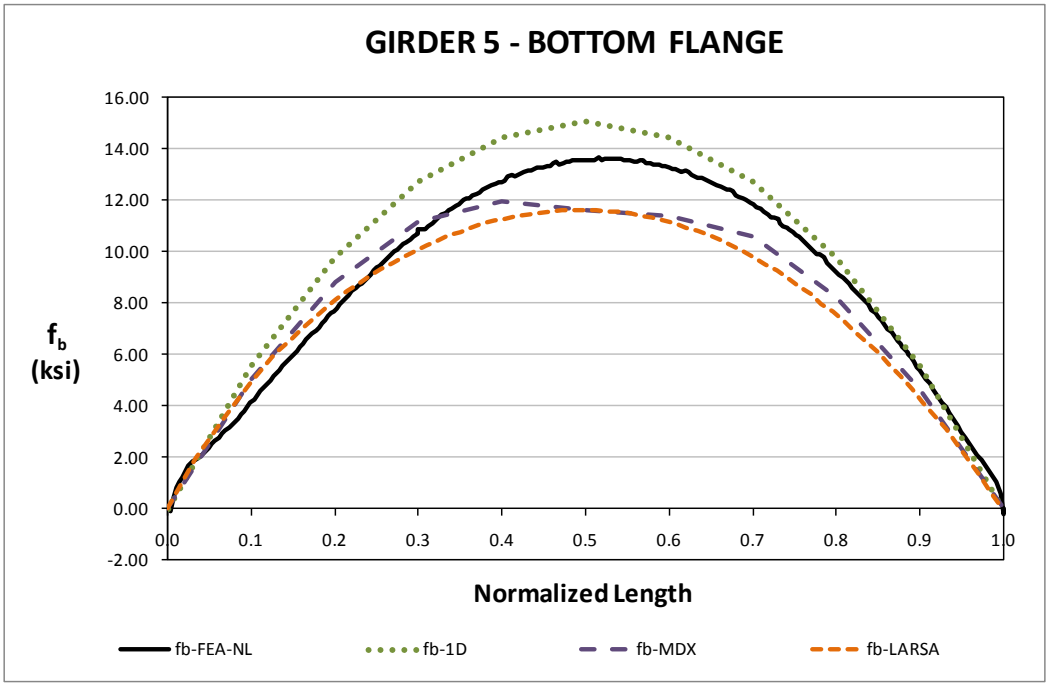

Fig. 11. NISCS37, Major-axis bending stresses under steel dead load for NLF detailing.

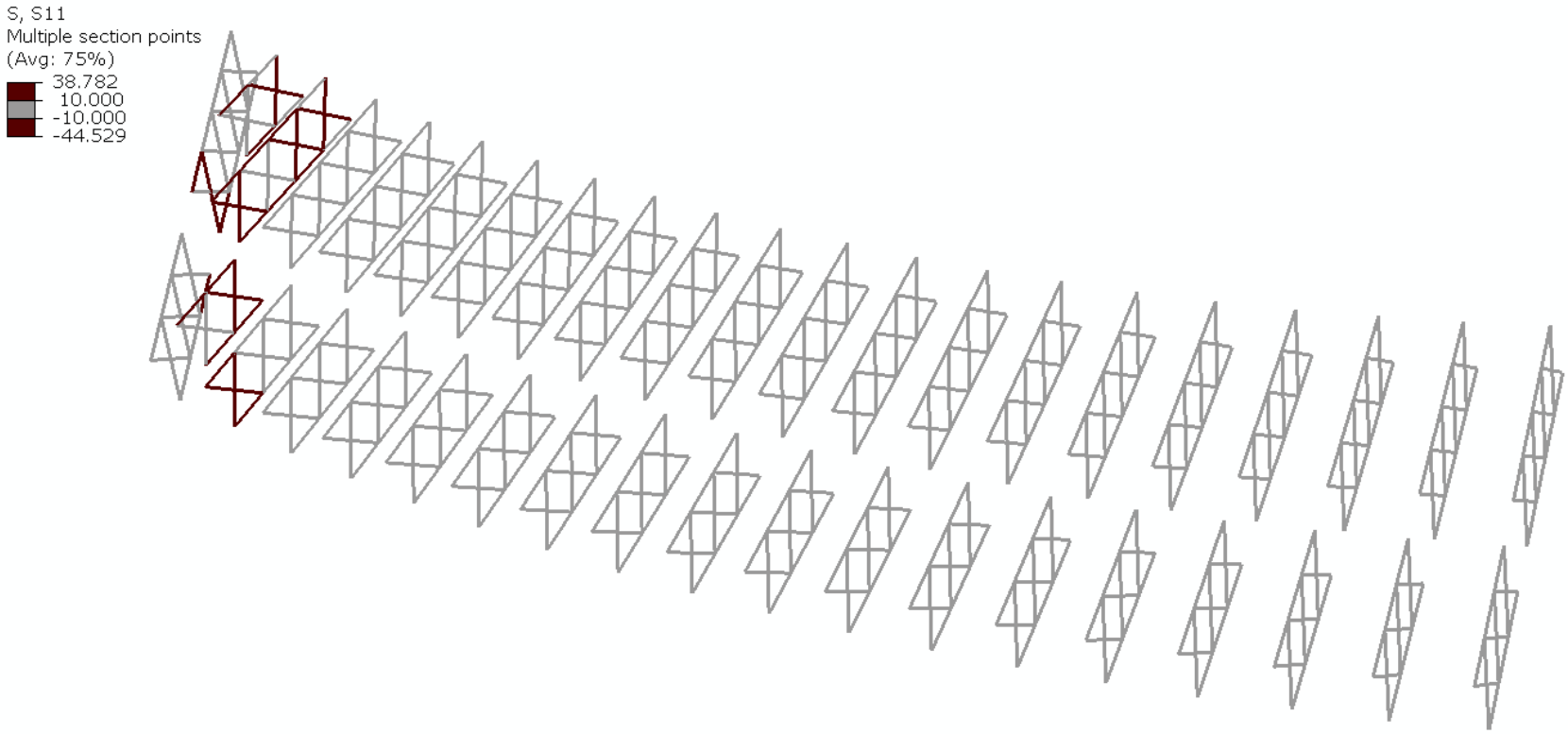

Fig. 12. NISCS37, Stage 27 cross-frame stresses for NLF detailing.

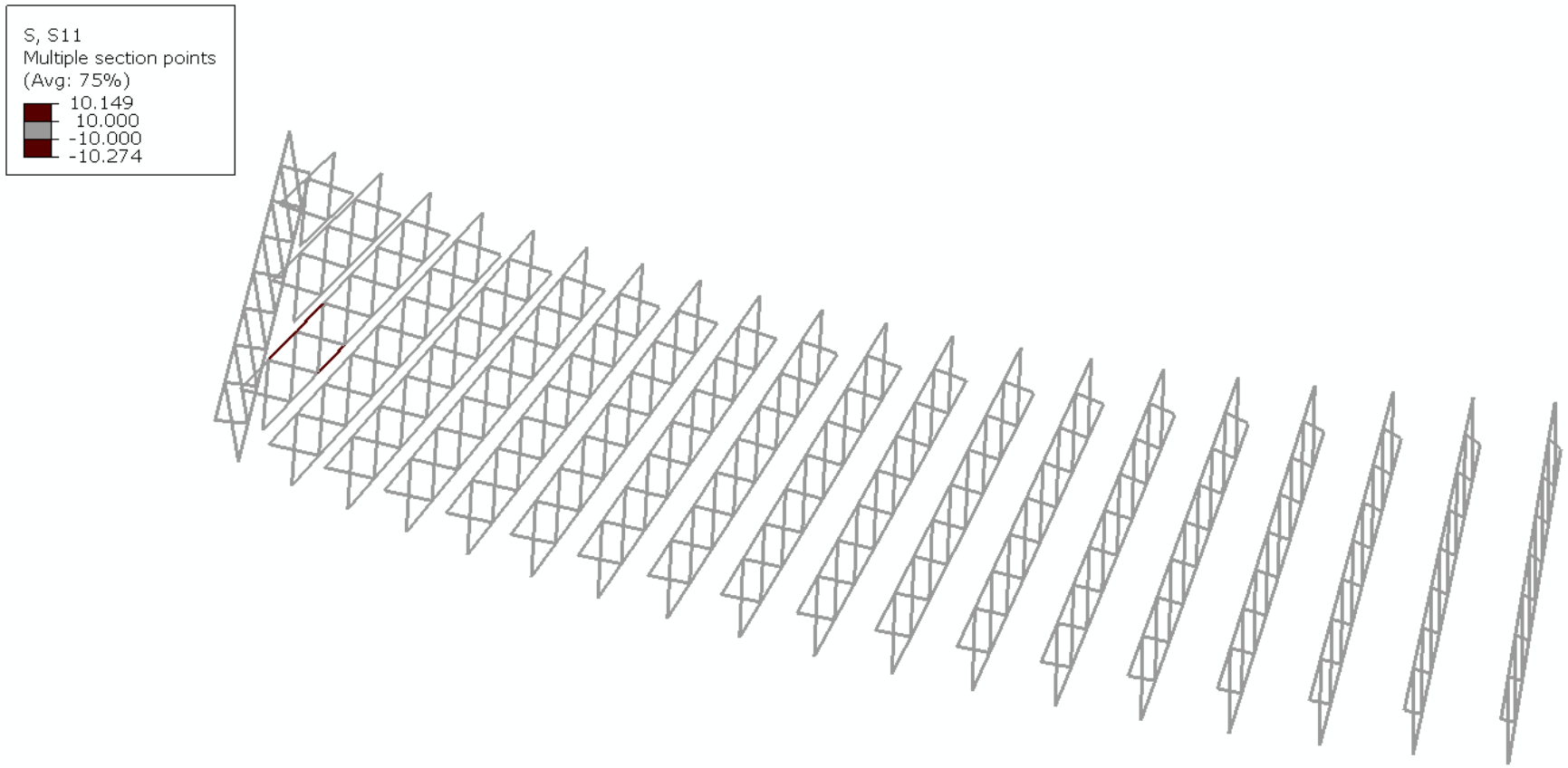

Fig. 10. NISCS37, Cross-frame stresses under steel dead load for NLF detailing.

I6.8 NISCS38 (New, I-girder, Simple-span, Curved, Skewed supports)

Category Data:

L_{as} = 300 ft / R =730 ft / w = 80 ft / θ_1 = 62.5°, θ_2 = 0°, 9 girders

Cross-Frame Detailing Method: NLF

Erection Stages Analyzed: Four

Deck Placement Sequence: One stage, deck thickness = 9.5 in.

Bridge Perspective & Plan Views:

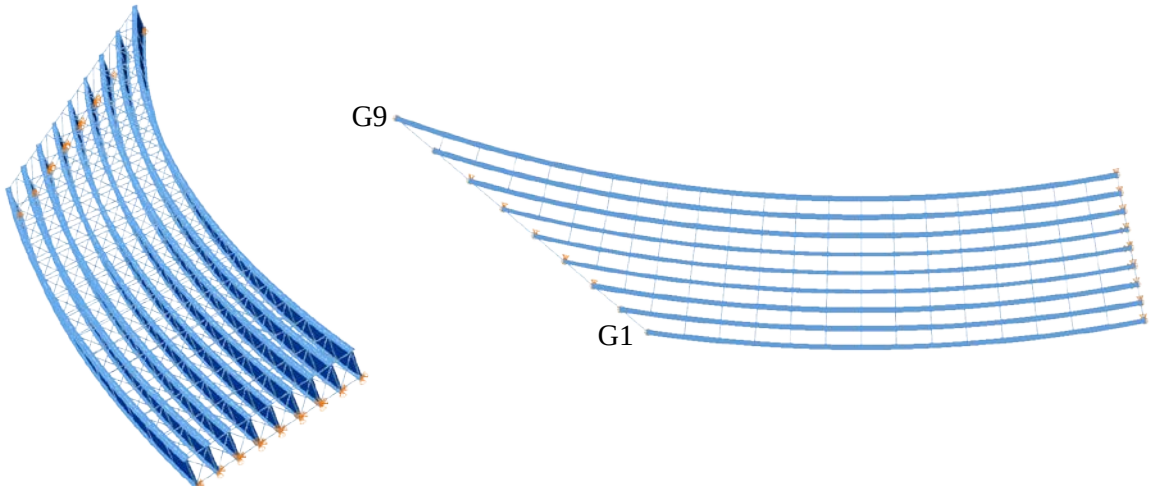

Abbreviated Analysis Results:

This bridge is a horizontally curved bridge with skewed supports. In this bridge, the combined effects of curvature and support skew in the system performance are studied. Four stages are selected for this purpose as shown in Figure 1. The first erection stage selected for the study is Stage 19. At state, girders G1 to G5 have been fully erected, and the exterior segments of girders G6 to G9 are also in place. Temporary supports are provided at the shown locations to stabilize the girders before the drop-in sections are erected. In Stage 22, all the interior segments have been erected, except the drop-in segment in girder G9. Following the erection scheme, in Stage 24 the girders are fully erected, and the shoring towers are removed, leaving the cross-frames between girders G5 and G6 as the only structural components to be erected. Finally in Stage 26, the structure behavior is studied under the total dead load condition (DC1).

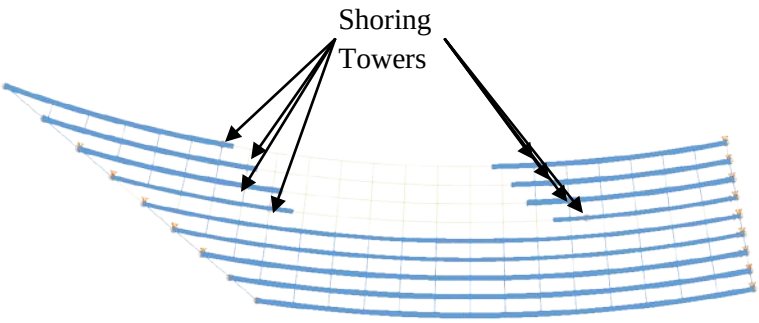

Stage 19

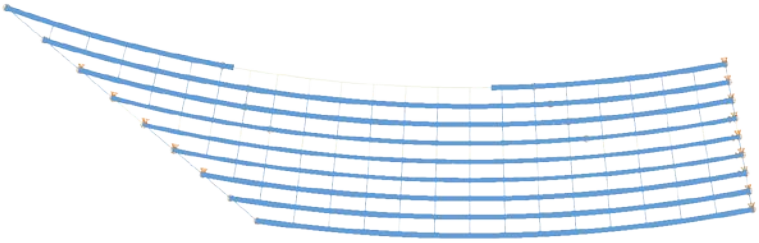

Stage 22

Shoring Towers
Removed

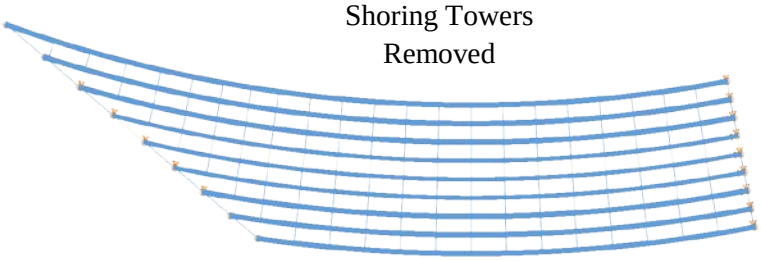

Stage 24

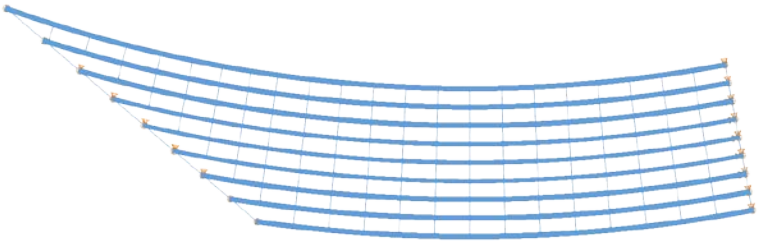

Stage 26 (TDL)

Fig. 1. NISCS 38, Studied Stages

The responses predicted by the 2D grid analysis model and the 3D benchmark are compared for the interior girder, G1, Stage 19. As shown in Figure 2, the vertical displacement predictions are not properly captured by the approximate model. The 2D grid analysis predictions are significantly larger than the predicted by the 3D model. This trend is consistent with the observed in other curved bridges, where the 2D analyses over predict the vertical displacement response. The poor torsion model implemented in the 2D grid analysis to represent the torsion stiffness of the bridge girders yields an inaccurate representation of this response.

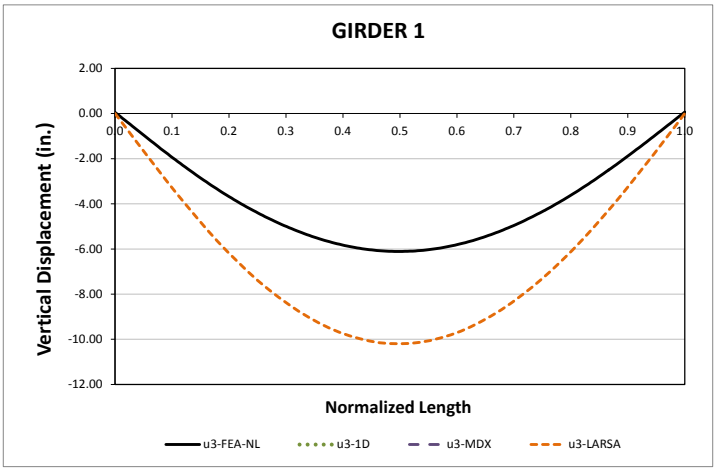

Fig. 2. Vertical Displacement Predictions, Stage 19

Figure 3 shows the comparison of lateral displacements (layover) of the same girder at Stage 19. As shown in this figure, the 2D grid analysis best predicts the expected response at the bracing points. As consistently observed in previous curved bridges, the 2D analysis is able to capture the overall rotation of the structure at the braced points, but misses the expected response within the unbraced length. This is another effect of the poor girder torsion model.

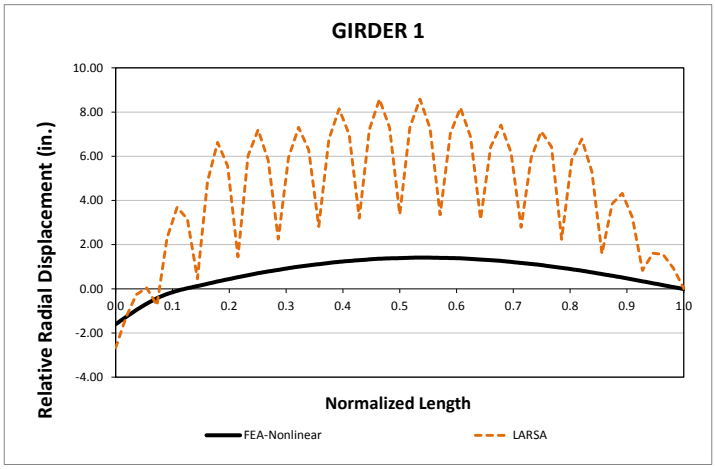

Fig. 3. Lateral Displacement Predictions, Stage 19

For the prediction of major-axis bending stresses, the 2D model captures the 3D model representation accurately. Figure 4 shows the major-axis bending stress response in the top flange of girder G2, Stage 24. As shown, the limitations of the 2D model representation do not have a severe influence in the prediction of this response. The same trend is observed for the rest of steel erection stages. The 2D grid model predictions for all the girders in both flanges match the FE model predictions as the construction of the bridge continues from the erection of the first girder segments up to the completion of the steel structure erection.

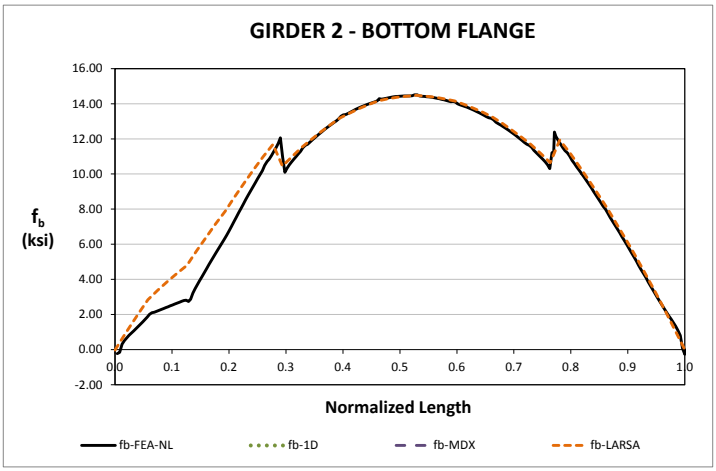

Fig. 4. Major Axis Bending Stress Predictions, Stage 24

The flange lateral bending stresses are calculated according to the V-Load formula. As shown in Figure 4 for Stage 24, the prediction of this response based on this formulation is relatively accurate, except at the location of the skew. The largest discrepancy between analyses results occurs at the left end of the girder. The peaks associated to the skew effects are not captured by the approximate response obtained from the 2D analysis, given that this method accounts only for the curvature effects.

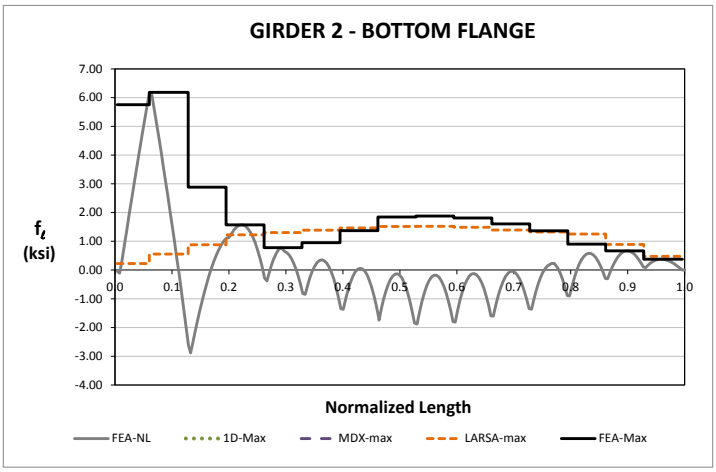

Fig. 4. Flange Lateral Bending Stress Predictions, Stage 24

Another important aspect to consider in this stage is the differential deflections between girders G5 and G6. Figures 5 and 6 show the displacement responses for these girders. From these figures, it is observed that the deflections due to the structure self-weight will be 2.60 in. in girder G5 and 32.0 in. in girder G6, at midspan. Therefore, to place the cross-frames in this bay, the erector would have to lift girder G6 approximately 30 in. This procedure, however, may be considered impractical.

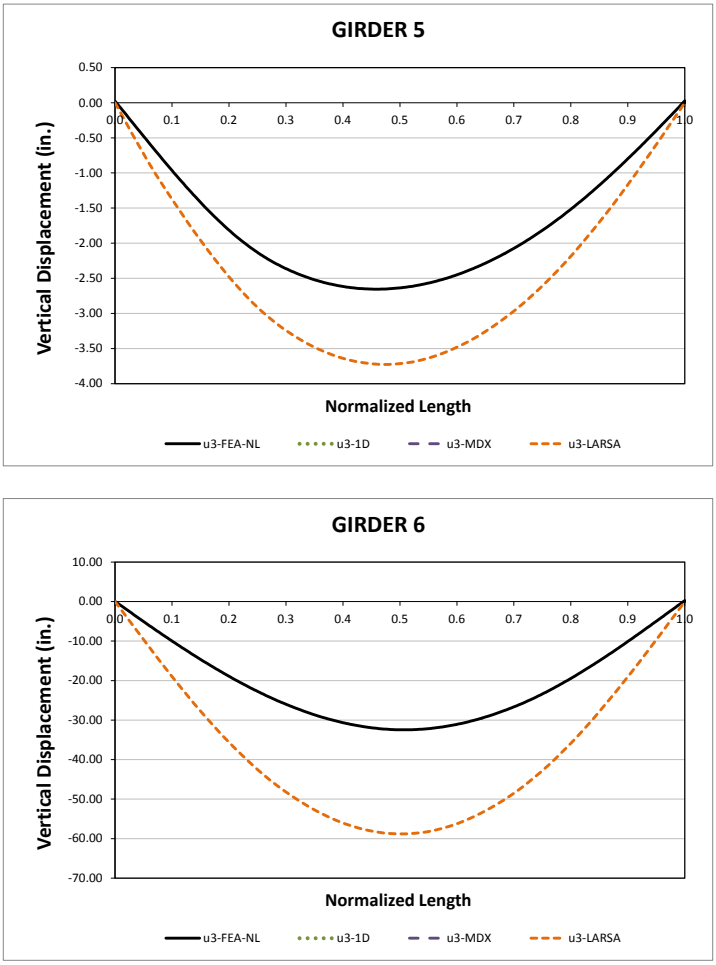

Fig. 5. Predictions on Vertical Displacements, Stage 24

The results for the total dead load condition, Stage 26, are discussed next. For the vertical displacements, shown in Figure 6, the 1D model prediction is a good representation the expected displacements. In the case of the Larsa 2D grid model, the response is over predicted. The overestimation is associated to the limitations of the computational model to represent the actual behavior of an open-section thin-walled beam element. Thus, the 2D grid models do not consider the stiffness contribution that comes from the warping of the flanges. The above observations are consistent for all the girders of the bridge throughout all the construction simulation.

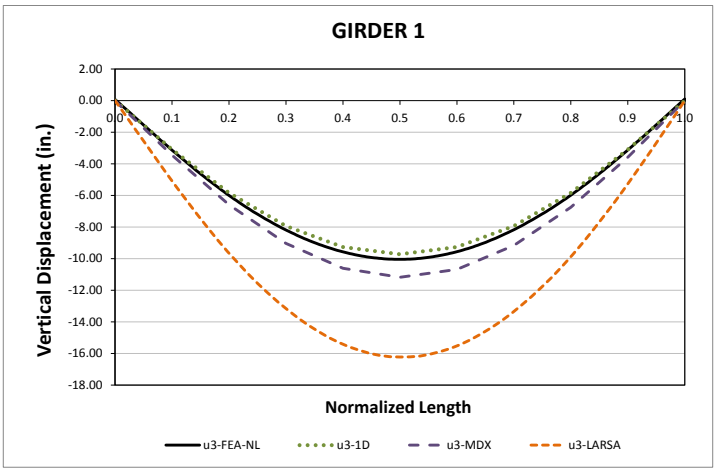

Fig. 6. Predictions on Vertical Displacements, Stage 26

At the total dead load condition, Stage 26, the major-axis bending stress predictions are almost the same for all the methods. As observed for girder G1 in Figure 7, both the 1D and 2D results capture the expected response, as predicted by the 3D FE model. It is apparent from a study of these predictions that the major-axis bending response is not affected as much as the displacement responses due to the limitations of the approximate methods.

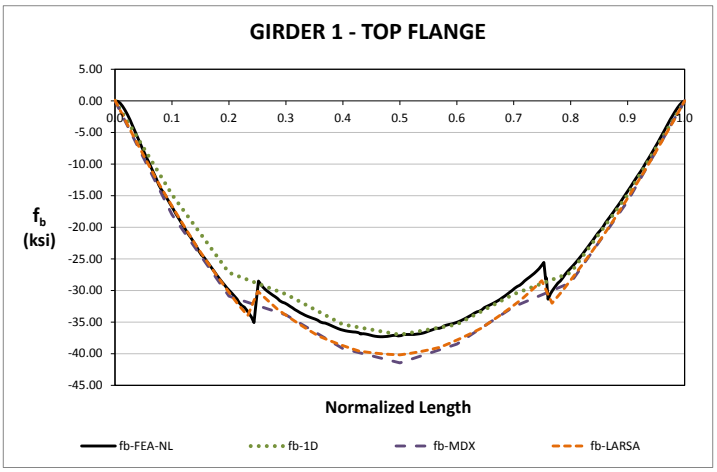

Fig. 7. Major Axis Bending Stress Predictions, Stage 26

I6.9 NISCS39 (New, I-girder, Simple-span, Curved, Skewed supports)

Category Data:

L_{as} = 300 ft / R =730 ft / w = 80 ft / θ_1 = -35°, θ_2 = 0°, 9 girders

Cross-Frame Detailing Method: NLF

Erection Stages Analyzed: Four

Deck Placement Sequence: One stage, deck thickness = 9.5 in.

Bridge Perspective & Plan Views:

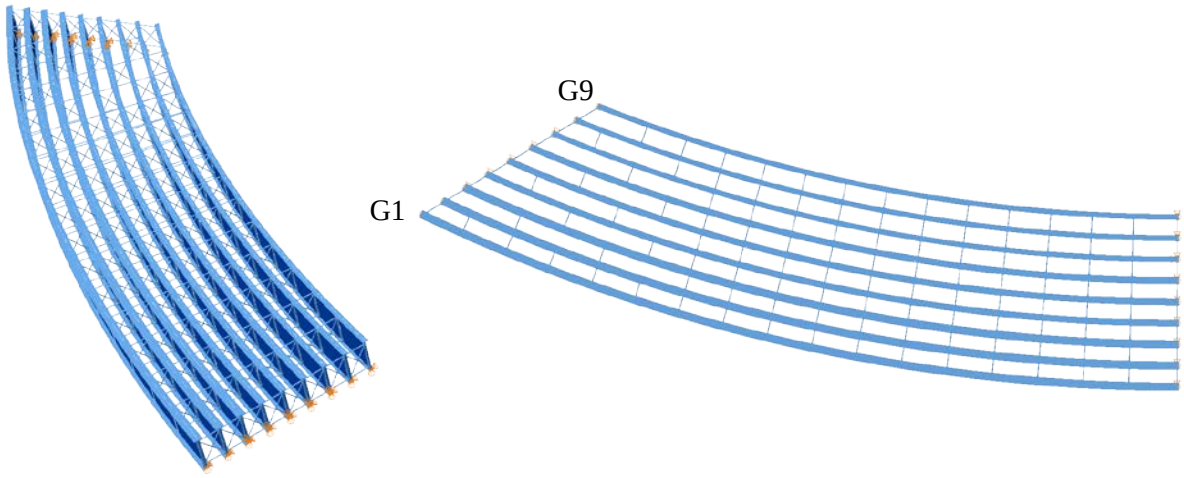

Abbreviated Analysis Results:

This bridge is horizontally curved with skewed supports. In this bridge, the combined effects of curvature and support skew in the system performance are studied. Four stages are selected for this purpose as shown in Figure 1. Due to the large span of the bridge, the erection of the girders is done in three parts. Stage 18 corresponds to the stage where the exterior segments of the nine girders are placed and supported by provisional towers. In the next step, Stage 19, the drop-in segment of girder G1 is brought to place, completing the erection of this girder. A shoring tower is provided at approximately the center of the drop-in segment to ensure the stability of the structure. In Stage 20, girder G2 is completed, and the cross-frames of the bay between girders G1 and G2 are also erected. In subsequent steps, the drop-in segments of the rest of girders and the corresponding cross-frames are connected to finish the structure. In Stage 30, the response of the bridge under the total dead load is investigated.

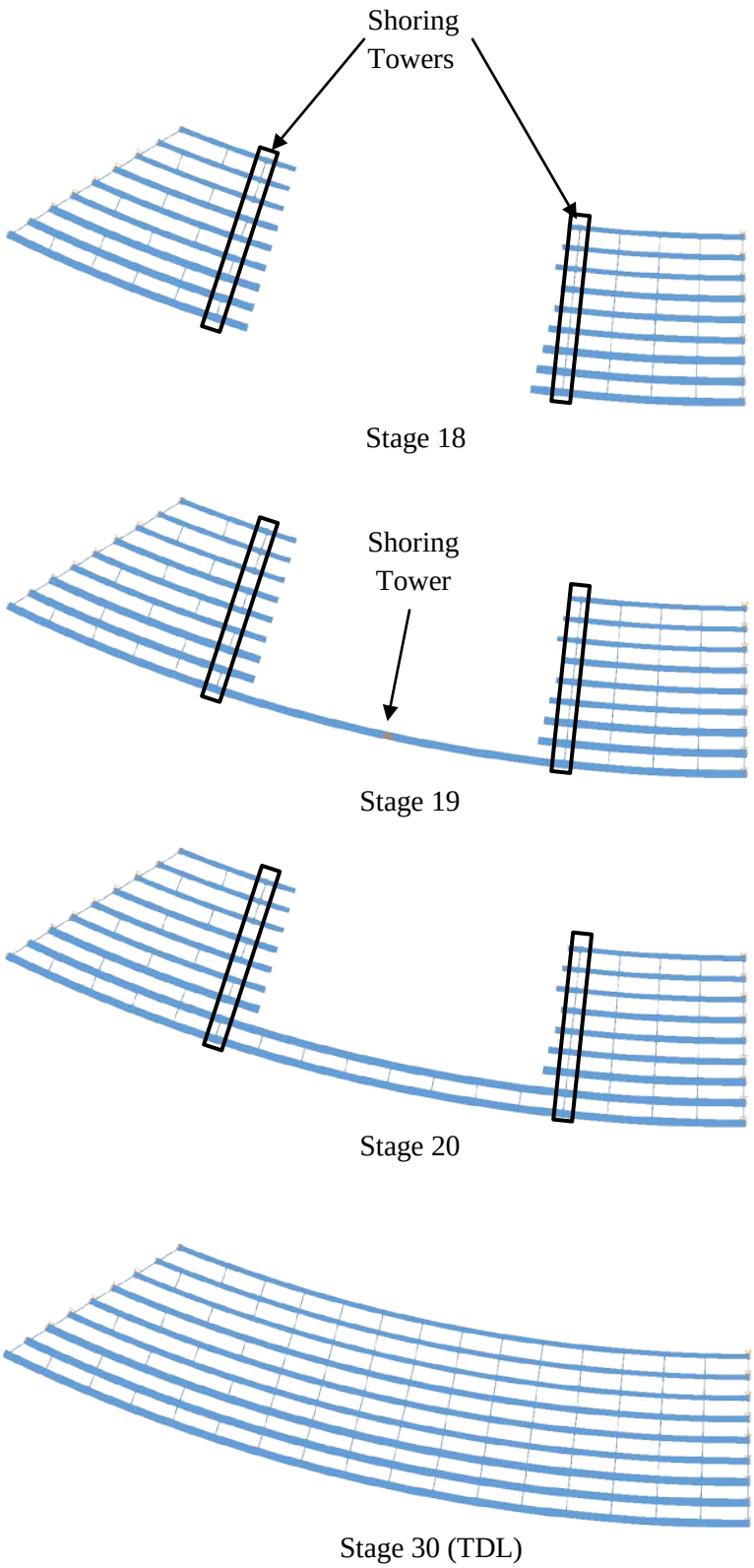

Fig. 1. NISCS 39, Studied Stages

The responses predicted by the 2D grid analysis model and the 3D benchmark are compared for the interior girder, G1, Stage 19. As shown in Figure 2, the magnitudes of the vertical displacements are over predicted. This is a consequence of the formulation used to model the torsion properties of the I-girders. As shown in this bridge, neglecting the warping contributions to the torsional stiffness of the girders can result in poor predictions of the system response.

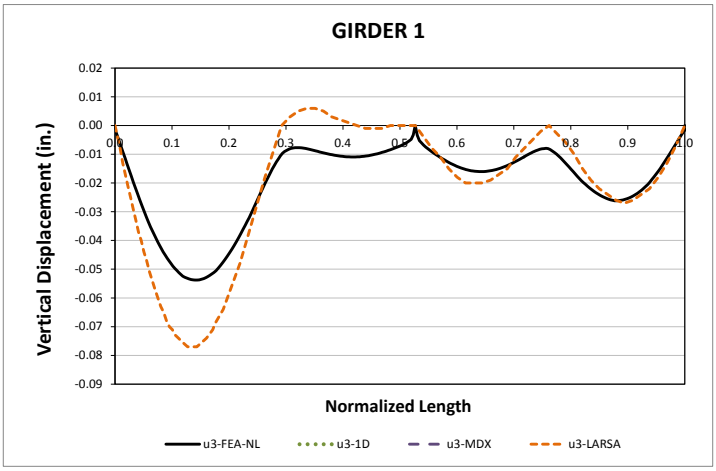

Fig. 2. Vertical Displacement Predictions, Stage 19

Figure 3 shows the comparison of the girder layovers at Stage 19. As shown in the plot, the 2D grid analysis best predicts the benchmark response at the cross-frame locations. This observation is consistent throughout the analyses conducted in curved bridges. In general, this response is properly captured at the bracing locations, but it is poorly within the unbraced length.

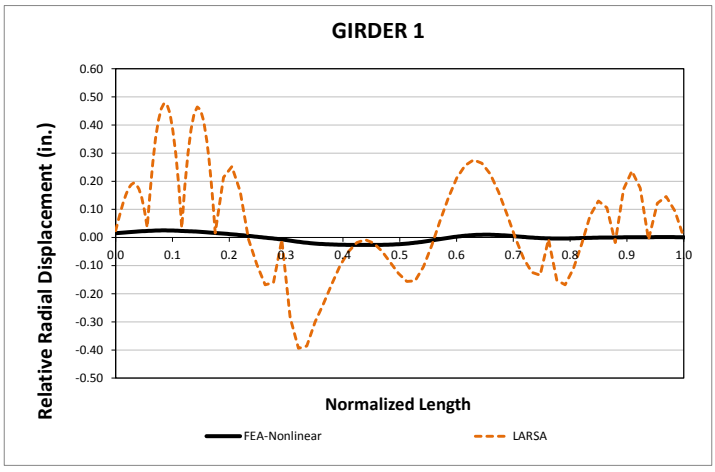

Fig. 3. Lateral Displacement Predictions, Stage 19

For the prediction of major-axis bending stresses, the 2D model captures the 3D model representation accurately. Figure 4 shows the major-axis bending stress response in the top flange of girder G1, Stage

20. As shown, the limitations of the 2D model representation do not have a severe influence in the prediction of this response. The same trend is observed for the rest of steel erection stages. The 2D grid model predictions for all the girders in both flanges match the FE model predictions as the construction of the bridge continues from the erection of the first girder segment up to the completion of the steel structure erection.

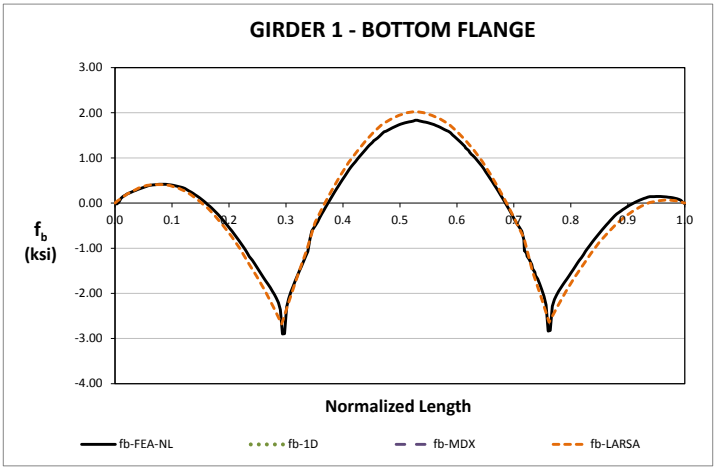

Fig. 4. Major Axis Bending Stress Predictions, Stage 20

The results for the total dead load condition, Stage 30, are discussed next. For the vertical displacements, shown in Figure 5, the 1D model prediction is a good representation the expected displacements. In the case of the LARSA 2D grid model, the response is over predicted. The overestimation is associated to the limitations of the computational model to represent the actual behavior of an open-section thin-walled beam element. Thus, the 2D grid models do not consider the stiffness contribution that comes from the warping of the flanges. The above observations are consistent for all the girders of the bridge throughout all the construction simulation.

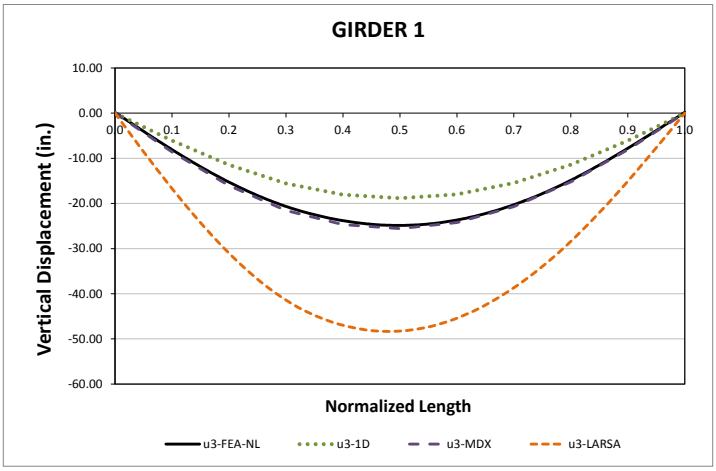

Fig. 5. Predictions on Vertical Displacements, Stage 30

At the total dead load condition, Stage 30, the major-axis bending stress predictions are almost the same for all the methods. As observed for girder G1 in Figure 7, both the 1D and 2D results capture the expected response, as predicted by the 3D FE model. It is apparent from a study of these predictions that the major-axis bending response is not affected as much as the displacement responses due to the limitations of the approximate methods.

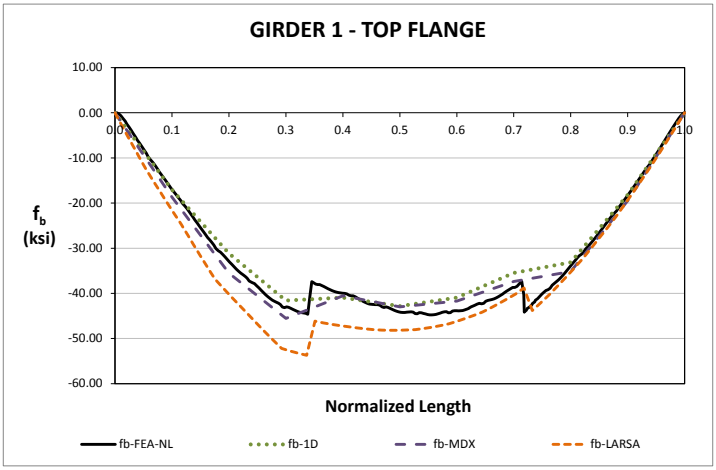

Fig. 6. Major Axis Bending Stress Predictions, Stage 30

I7.1 EICCS1 (Existing, I-girder, Continuous-span, Curved, Skewed supports)

Bridge Description:

US 31 Interchange Flyover A, Jefferson Co., AL

Category Data:

L_1 = 204 ft, L_2 = 278 ft, L_3 = 252 ft, L_4 = 185 ft / R = 757 ft / w = 40.2 ft / $\theta_1 = 0^o$, $\theta_2 = 0^o$, $\theta_3 = 32.7^o$, $\theta_4 = 0^o$, $\theta_5 = 0^o$, 5 girders

References:

Field observations documented by Osborne, 2002

Cross-Frame Detailing Method: TDLF

Steel Erection Stages Analyzed: 20

Deck Placement Sequence: 11 stages

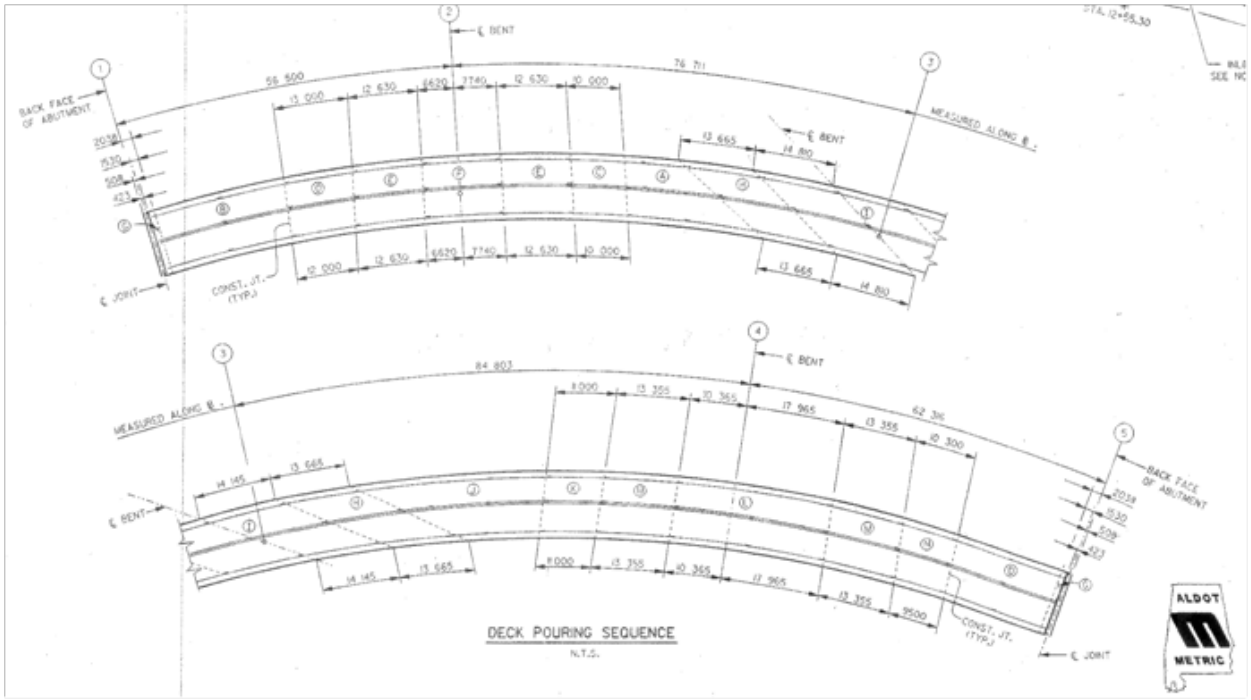

Bridge Perspective & Plan Views:

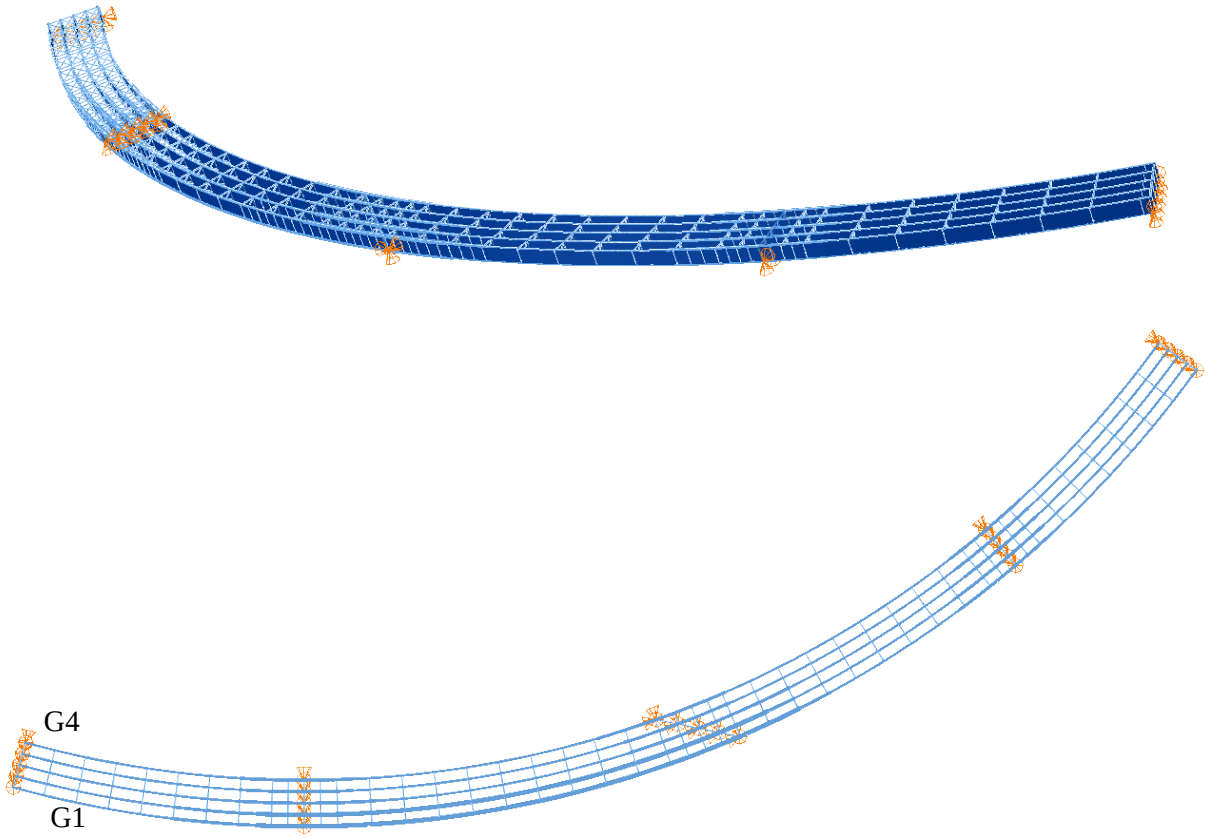

Abbreviated Analysis Results:

In this bridge, the effects of horizontal curvature, support skew, and continuity are studied. Results for three selected stages are presented in this report; they are shown in Figure 1. Stage 2 corresponds to the erection of the two first interior girders in Span 4. Stage 16, where the structure in Span 2, 3, and 4 has been erected and the interior girder of Span 1 is also in place. Finally, the condition where all the steel has been erected and the concrete poured is studied in Stage 20.

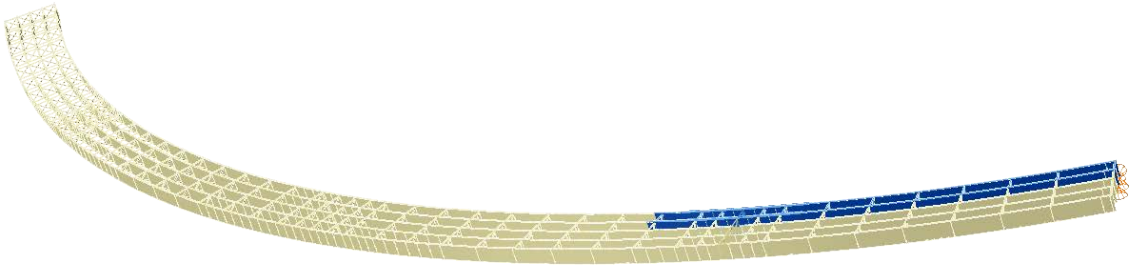

Stage 2

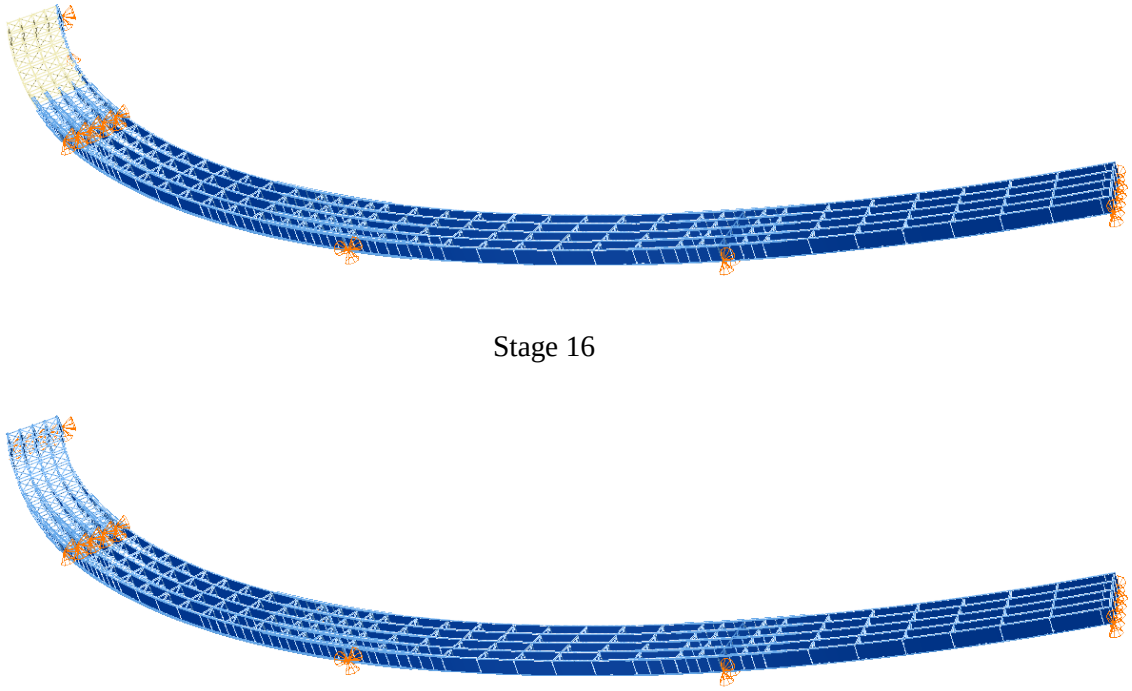

Stage 16

Stage 20

Fig. 1. EICCR1, Studied Stages

The major-axis bending predictions as predicted by the 2D grid analysis and the 3D FEA for Stage 2 are compared first. As shown in Figure 2 for girder G4, the stress responses are consistent between methods. For this response and as observed in other curved and skewed bridges, the limitations of the 2D model representation do not have a severe influence in the behavior prediction. In the case of vertical displacements, the results do not show the same correlation. As shown in Figure 3, the magnitudes of the vertical displacements are over predicted by the approximate model. This response is severely affected by the poor torsion model for the I-girders in the 2D grid computer model.

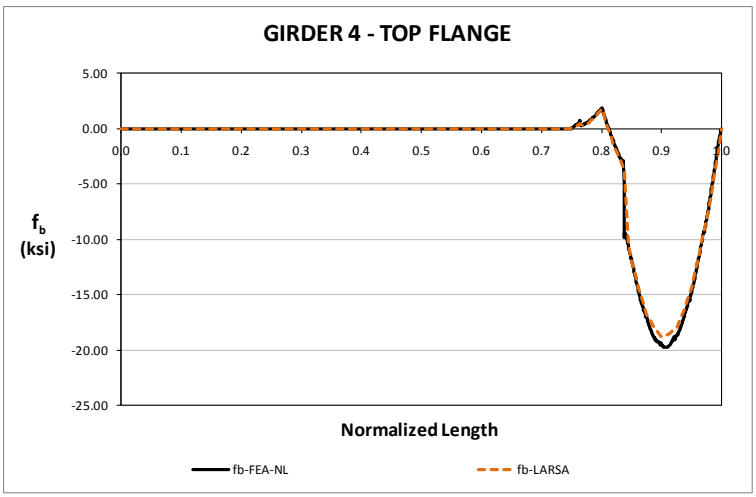

Fig. 2. Major Axis Bending Stress Predictions, Stage 2

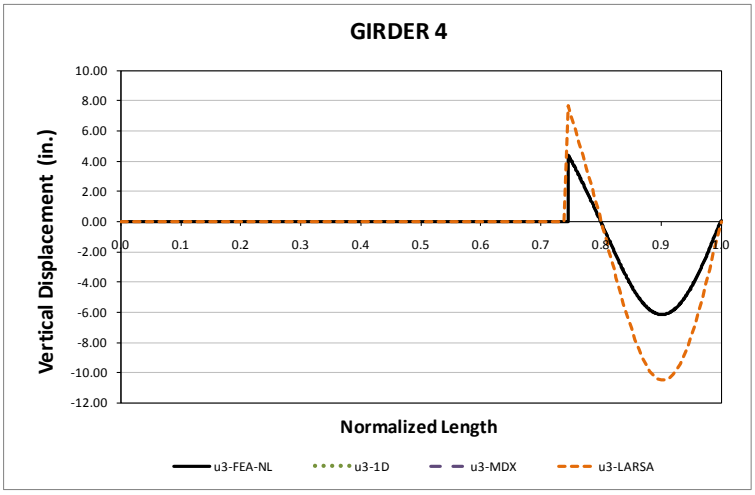

Fig. 3. Vertical Displacement Predictions, Stage 2

The flange lateral bending stresses are calculated based on the major-axis bending response, according to the V-Load formulation. Figure 4 shows the 2D model and 3D model predictions for girder G2, Stage 16. As shown in the figure, the prediction of this response based on this formulation is conservative. The stress profiles are very similar between the two methods of analysis, but the approximate method results are approximately twice the benchmark. Based on this study, it is observed that the prediction of the equivalent lateral load obtained from the major-axis bending response could be used to determine an upper bound limit.

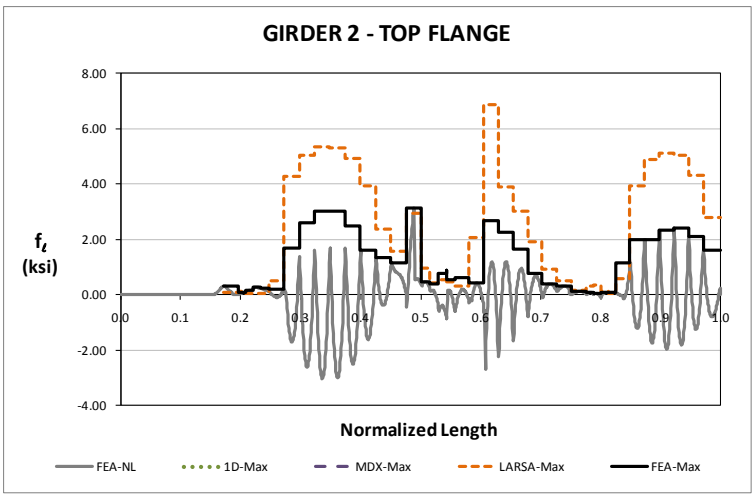

Fig. 4. Flange Lateral Bending Stress Predictions, Stage 16

The results for the total dead load condition, Stage 20, are discussed next. For the vertical displacements, shown in Figure 5, the 1D model does not capture the expected response. In Span 2, the 1D model predicts a positive deflection of the exterior girder (G5), when it actually is deflecting downward. In the case of the 2D grid models, the response is over predicted. The overestimation is associated to the limitations of the computational model to represent the actual behavior of an open-section thin-walled beam element. Thus, the 2D grid models do not consider the stiffness contribution that comes from the warping of the flanges. This limitation also affects the prediction of the girder layover, as shown in Figure 6. However, the rotation of the girder group controls over the individual rotation of the girders at the cross-frame locations, behavior that is captured by the 2D grid model. The above observations are consistent for all the girders of the bridge throughout all the construction simulation.

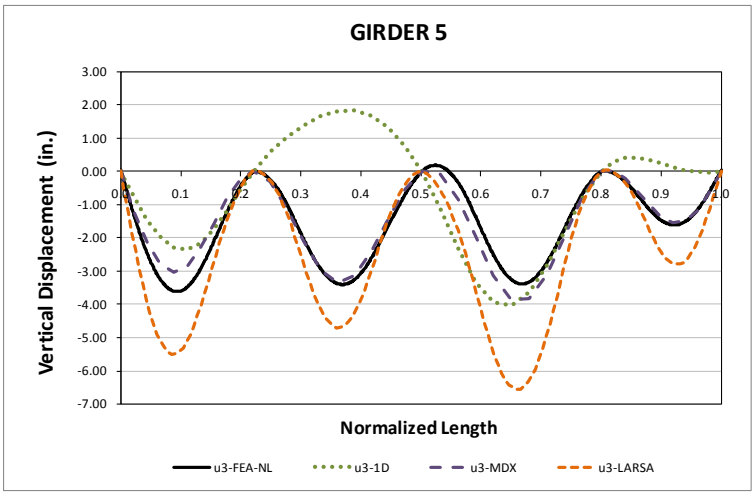

Fig. 5. Predictions on Vertical Displacements, Stage 20

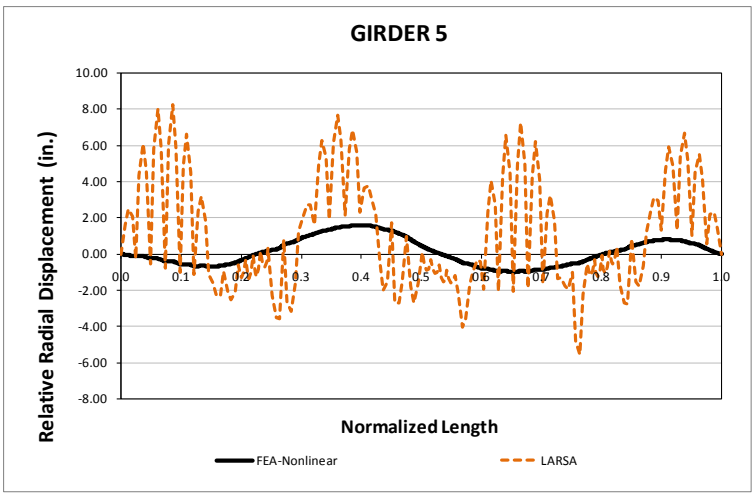

Fig. 6. Predictions on Relative Lateral Displacements, Stage 20

I7.2 EICCS10 (Existing, I-girder, Continuous-span, Curved, Skewed supports)

Bridge Description:

MN/DOT bridge No 27998, TH94 between 27th Avenue and Huron Boulevard, Minneapolis, MN

Category Data:

L_1 = 145 ft, L_2 = 150 ft / R =286 ft / w = 33.4 ft / θ_{left} = 40.1°, θ_{mid} = 34.8°, θ_{right} = -10.4°, 4 girders

References:

Field data available (Galambos et al. 1996), used by Nowak et. al (2006) in calibration of LRFD Design Specification for curved steel bridges

Cross-Frame Detailing Method: NLF

Steel Erection Stages Analyzed: Nine

Deck Placement Sequence: Two stages

Bridge Perspective & Plan Views:

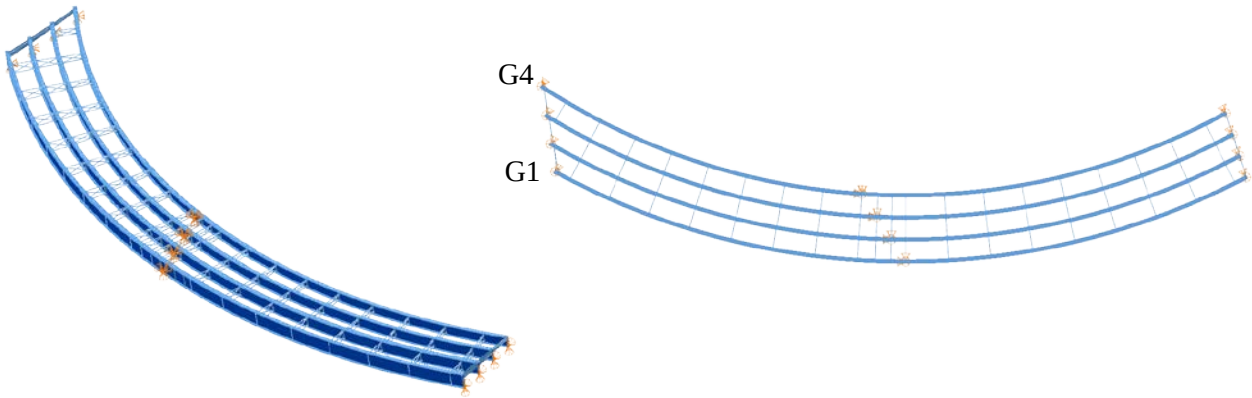

Abbreviated Analysis Results:

This bridge is a horizontally curved bridge with skewed supports. It was instrumented, and its construction monitored to observe the structural behavior of the bridge. In this bridge, the combined effects of curvature and support skew in the system performance are studied. Three stages are selected for this purpose; they are shown in Figure 1. The first corresponds to the state where the first three interior girders of Span 1 are erected. Next, the behavior of the bridge is studied for Stage 5, where the steel erection is completed for Span 1, and the exterior girder in Span 2 is in place. Finally, the last studied stage corresponds to the total dead load condition, where the bridge girders do not act compositely with the concrete deck.

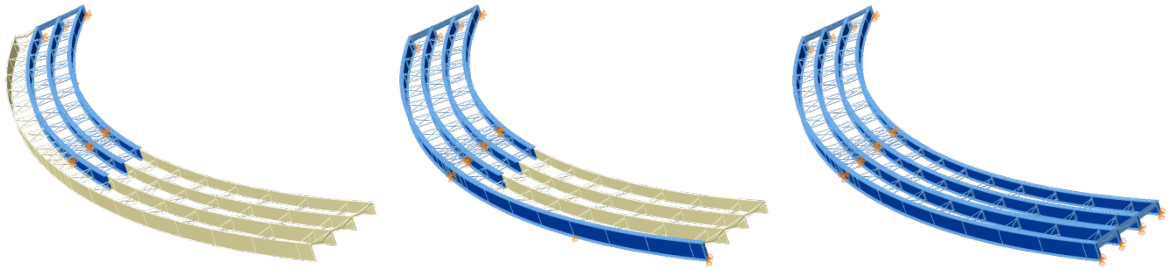

Stage 3 Stage 5 Stage 9

Fig. 1. EICCR10, Studied Stages

The responses predicted by the 2D grid analysis model and the 3D benchmark are compared for the interior girder, G4, Stage 3. As shown in Figure 2, the magnitudes of the vertical displacements are not accurately captured by the approximate model. The vertical displacements are significantly larger than the predicted by the 3D model. This trend is consistent with the observed in other curved bridges. The limitations of the approximate 2D grid analysis to represent the actual torsional behavior of an I-girder results in inaccurate representations of the vertical displacements.

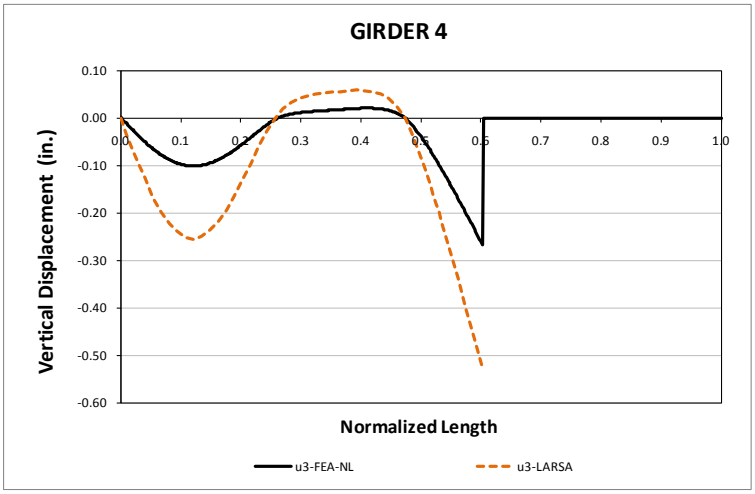

Fig. 2. Predictions on Vertical Displacements, Stage 3

For the prediction of major-axis bending stresses, the 2D model captures the 3D model prediction accurately. Figure 3 shows the major-axis bending stress response in the top flange of girder G4. As shown, the limitations of the 2D model representation do not have a severe influence in the prediction of this response. The same trend is observed for the rest of steel erection stages. The 2D grid model predictions for all the girders in both flanges match the FE model predictions as the construction of the bridge continues from the erection of the first girder segment up to the completion of the steel structure erection.

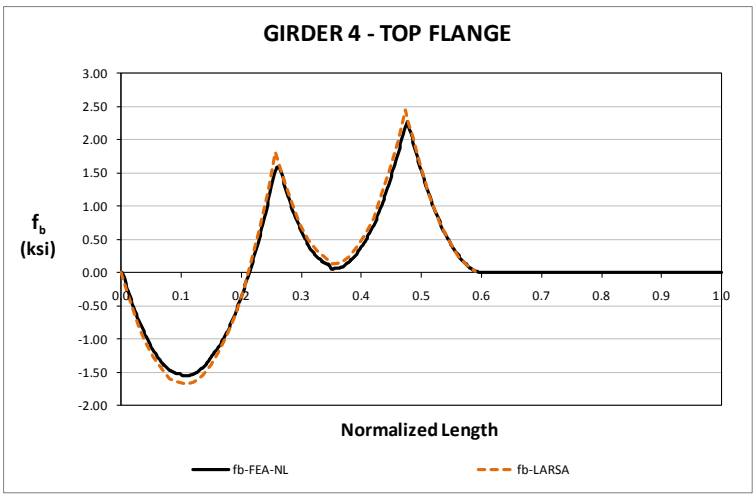

Fig. 3. Major Axis Bending Stress Predictions, Stage 3

The flange lateral bending stresses are calculated according to the V-Load formula. As shown in Figure 4 for Stage 5, the prediction of this response based on this formulation is accurate. Even though for this case these stresses are very small and do not deserve attention from the design perspective, it is observed that the prediction of the equivalent lateral load obtained from the major-axis bending response could be used to determine an upper bound limit.

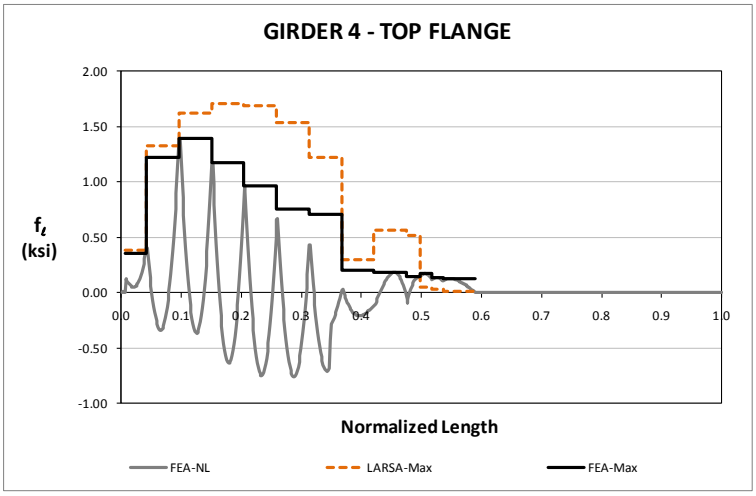

Fig. 4. Flange Lateral Bending Stress Predictions, Stage 5

The results for the total dead load condition, Stage 9, are discussed next. For the vertical displacements, shown in Figure 5, the 1D model prediction accurately represents the benchmark response. In the case of the 2D grid models, the response is over predicted. The overestimation is associated to the limitations of the computational model to represent the actual behavior of an open-section thin-walled beam element. Thus, the 2D grid models do not consider the stiffness contribution that comes from the warping of the flanges. This limitation also affects the prediction of the girder layover, as shown in Figure 6. However,

the rotation of the girder group controls over the individual rotation of the girders at the cross-frame locations, behavior that is captured by the 2D grid model. The above observations are consistent for all the girders of the bridge throughout all the construction simulation.

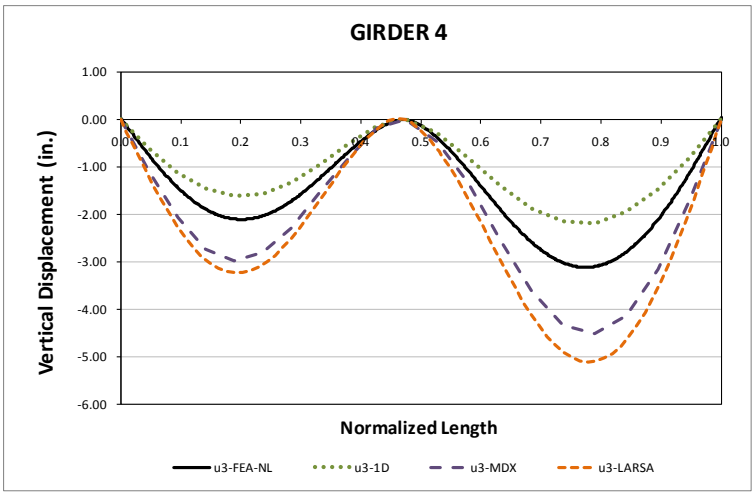

Fig. 5. Predictions on Vertical Displacements, Stage 9

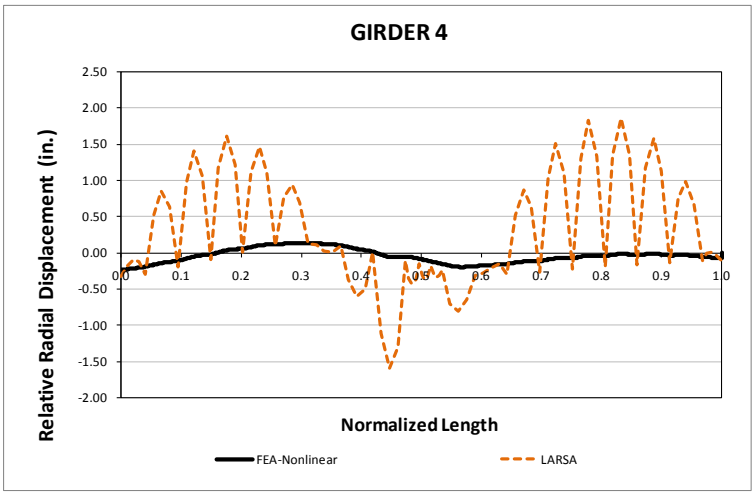

Fig. 6. Predictions on Relative Lateral Displacements, Stage 9

As for the steel erection, the major-axis bending stress predictions are almost the same for all the methods. As observed for girder G1 in Figure 7, both the 1D and 2D results capture the expected response, as predicted by the 3D FE model. It is apparent from a study of these predictions that the major-axis bending response is not affected as much as the displacement responses due to the limitations of the approximate methods. In the case of the flange lateral bending stresses shown in Figure 8, the FE model prediction shows that the response in the positive moment regions has the same behavior assumed in the derivation of the V-load formula. For these regions, the flange lateral bending stress response is maximum at about the same points where the levels of major-axis bending stress are the largest. In the

negative moment region, however, the response does not seem to follow the same trend. Therefore, the predictions obtained from the 2D analysis results are not close to the FE model predictions in this region.

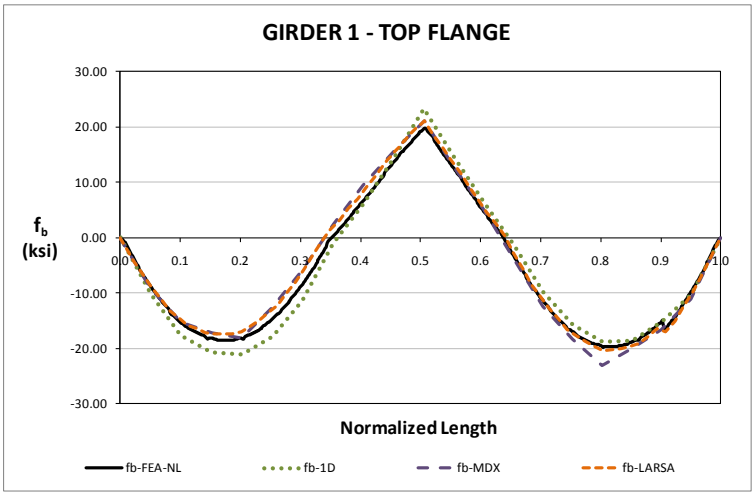

Fig. 7. Flange Lateral Bending Stress Predictions, Stage 9

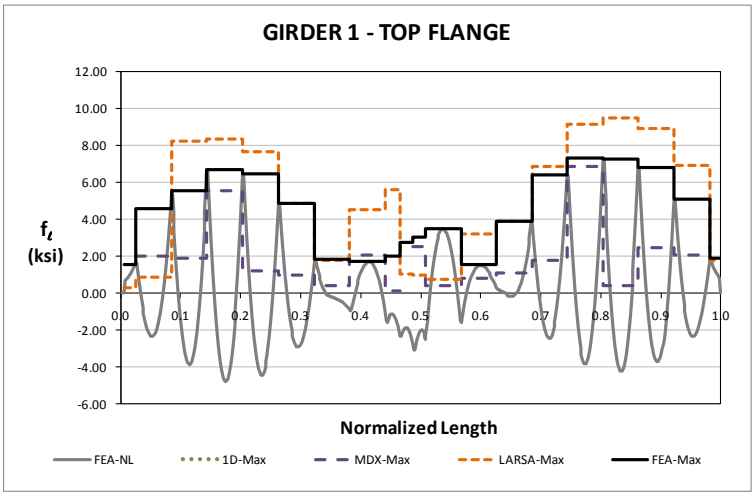

Fig. 8. Flange Lateral Bending Stress Predictions, Stage 9

I7.3 EICCS27 (Existing, I-girder, Continuous-span, Curved, Skewed supports)

Bridge Description:

SR 386 over SR 6 and Ramp F, Sumner Co, TN

Note that this bridge has chorded girders. The bridge is modeled based on the assumption of a continuous horizontal curve.

Category Data:

L_1 = 279 ft, L_2 = 224 ft, L_3 = 236 ft / R = 2546 ft / w = 88 ft / θ_1 = -53.1°, θ_2 = -59.4°, θ_3 = -64.4°, θ_4 = -69.7°, 8 girders

Cross-Frame Detailing Method: NLF

Steel Erection Stages Analyzed: 27

Deck Placement Sequence: Five stages

Bridge Perspective & Plan Views:

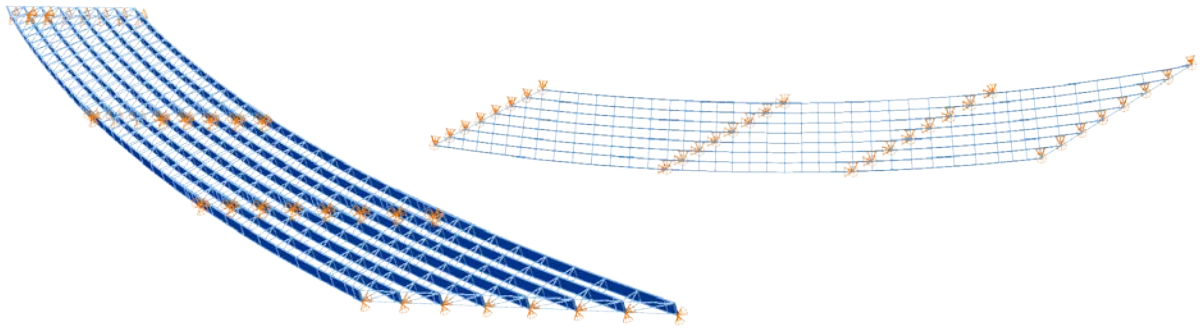

Abbreviated Analysis Results:

In this bridge, the skew and curvature effects and their interaction are studied. The three stages shown in Figure 1 are selected for this purpose. The first is Stage 2, where two girder segments of the first span are erected. The second is Stage 9, where the interior girder, G4, has been fully erected in Span 1. Finally, Stage 34 where the structure supports the total dead load in the noncomposite state is studied.

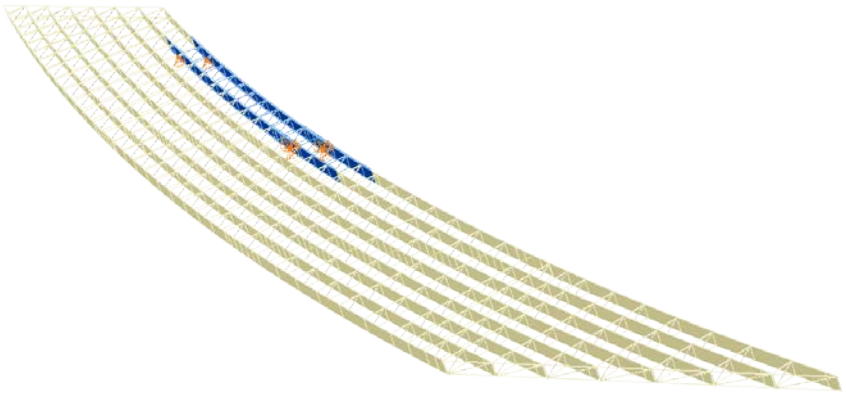

Stage 2

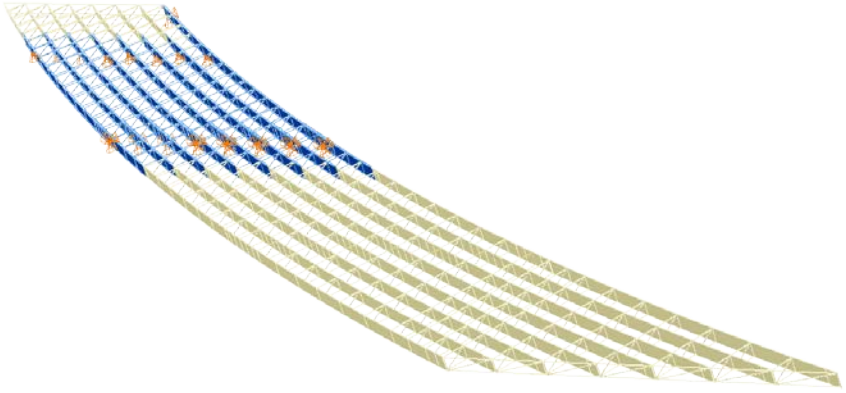

Stage 9

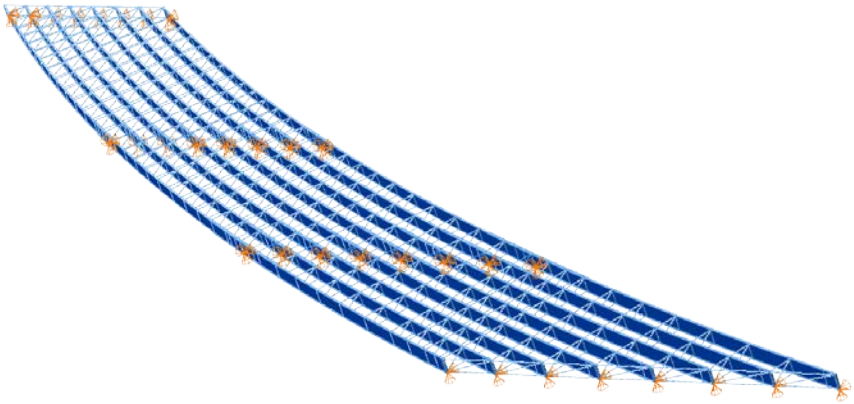

Stage 34

Fig. 1. EICCS27, Studied Stages

The responses predicted by the 2D grid analysis model and the 3D benchmark are compared for the interior girder, G8, Stage 2. As shown in Figure 2, the predictions obtained from both analyses are the same. While for other curved bridges this response is usually misrepresented by the 2D model, for this bridge it is accurate. The reason is that the radius of 2546 ft is considerable large, so the curvature does not influence the behavior of the structure severely at this Stage. Also, the relative radial displacements are accurately captured at the cross-frame points, as shown in Figure 3.

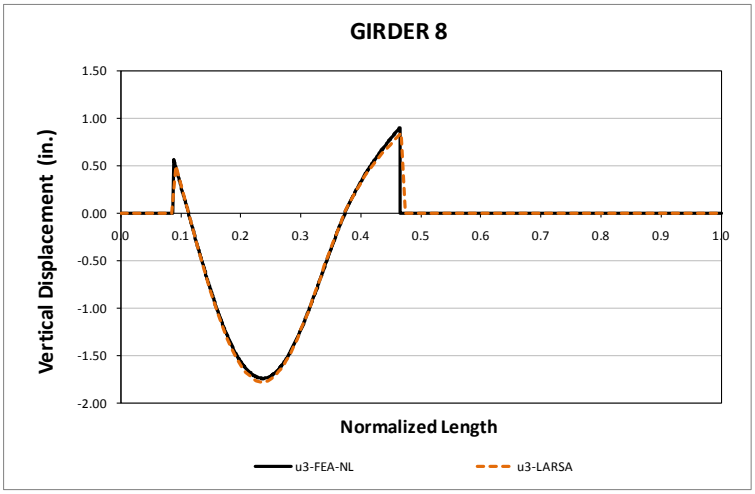

Fig. 2. Comparison of Vertical Displacement Responses, Stage 2

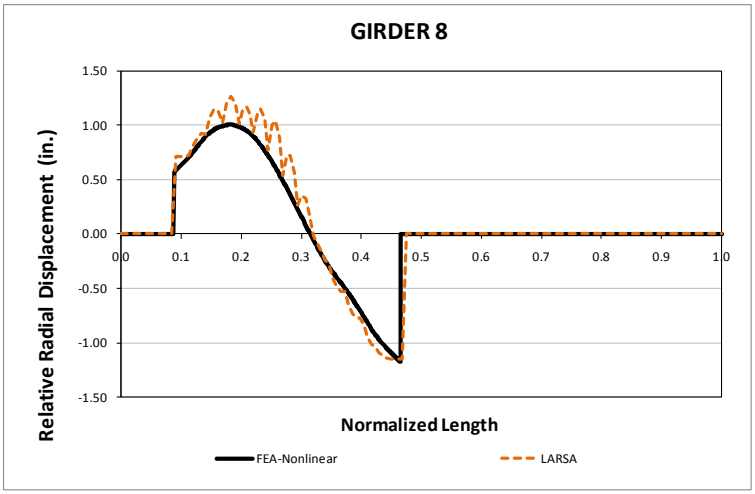

Fig. 3. Comparison of Relative Lateral Displacement Responses, Stage 2

In the case of the stress responses, the 2D model captures also the 3D model prediction accurately. Figure 4 shows the major-axis bending stress response in the top flange of the interior girder. It is observed that the limitations of the approximate analysis are minor in the prediction of this response. The same trend is observed for the rest of steel erection stages. The 2D grid model predictions for all the girders in both flanges match the FE model predictions as the construction of the bridge continues from the erection of the first girder segment up to the completion of the steel structure erection.

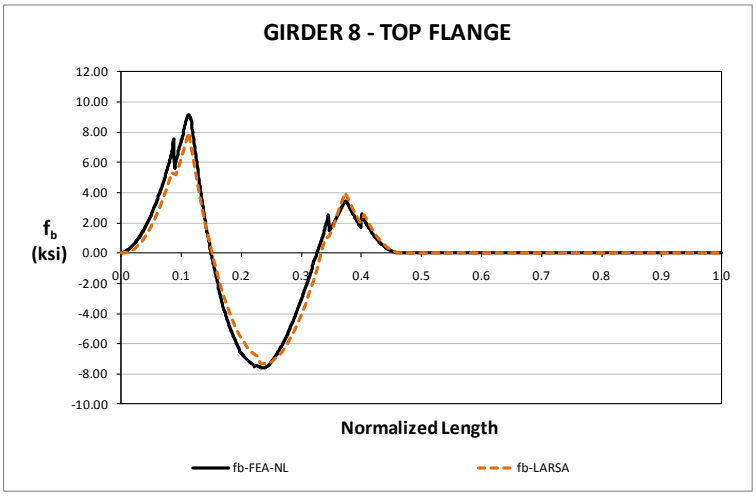

Fig. 4. Major-Axis Bending Stress Comparison for Girder G8, Stage 9

The flange lateral bending stresses are calculated according to the V-Load formula. As shown in Figure 5, the prediction of this response based on this formulation is more accurate within the positive moment region, between 0.15 and 0.33, than it is in the rest of the girder. It is observed that in other parts of the girder, the prediction based on the 2D model results is twice the expected values. The prediction of the equivalent lateral load obtained from the major-axis bending could be used to determine an upper bound limit in the prediction of this response.

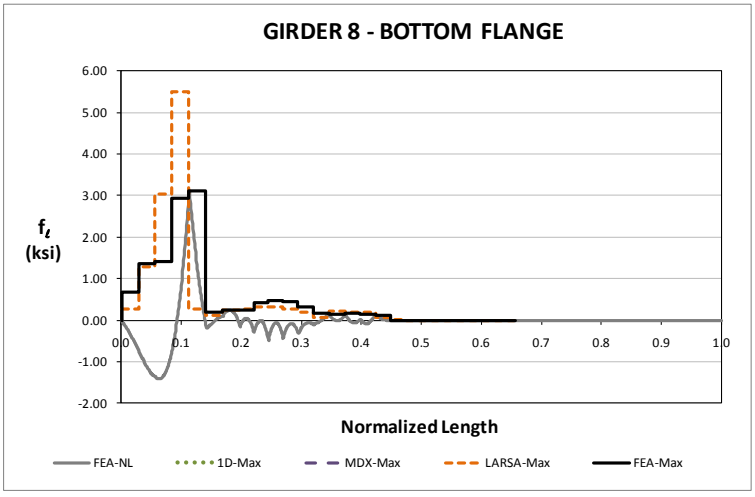

Fig. 5. Flange Lateral Bending Stress Comparison for Girder G8, Stage 9

The results for the total dead load condition are discussed next. For the vertical displacements, shown in Figure 6, the 1D model prediction accurately represents the benchmark response. In the case of the 2D grid models, the MDX response under predicts the expected displacements, while the Larsa results predict larger displacements than the benchmark. The differences between the 2D grid model results and the 3D FEA results are associated to the limitations of the computational model to represent the actual behavior of an open-section thin-walled beam element. Thus, the 2D models do not consider the stiffness contribution related to flange warping. This limitation also affects the prediction of the girder layover, as shown in Figure 7. However, the rotation of the girder group controls over the individual rotation of the girders at the cross-frame locations, behavior that is captured by the Larsa model. The above observations are consistent for all the girders of the bridge throughout all the construction simulation.

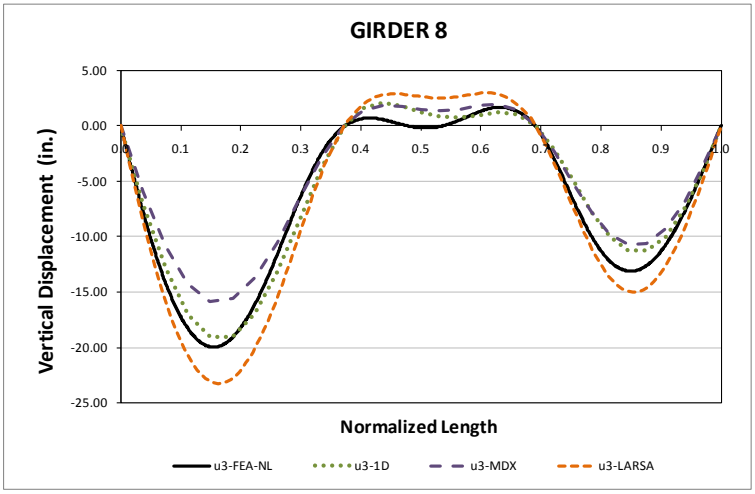

Fig. 6. Vertical Displacement Comparison for Girder G8, Stage 34

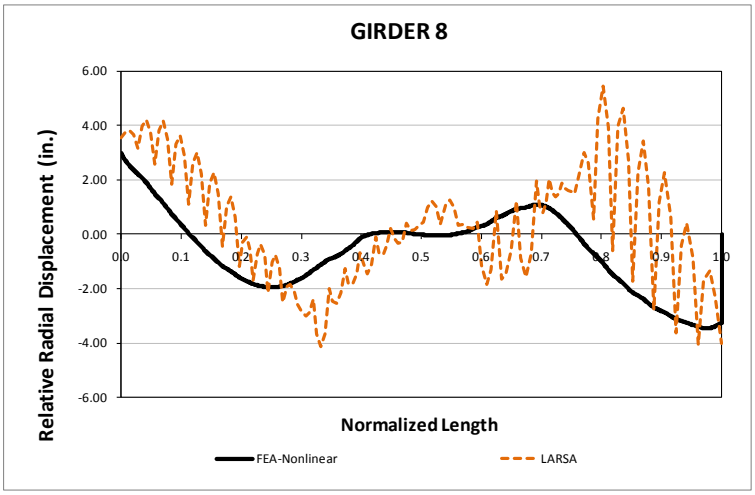

Fig. 7. Relative Lateral Displacement Comparison for Girder G8, Stage 34

I7.4 NICCS2 (New, I-girder, Continuous-span, Curved, Skewed supports)

Category Data:

L_1 = 150 ft, L_2 = 150 ft/ R = 227 ft / w =30 ft / θ_1 = 38°, θ_2 = 0°, θ_3 = 0°, 5 girders

Cross-Frame Detailing Method: NLF

Steel Erection Stages Analyzed: Five

Deck Placement Sequence: Three stages, deck thickness = 9.5 in.

Bridge Perspective & Plan Views:

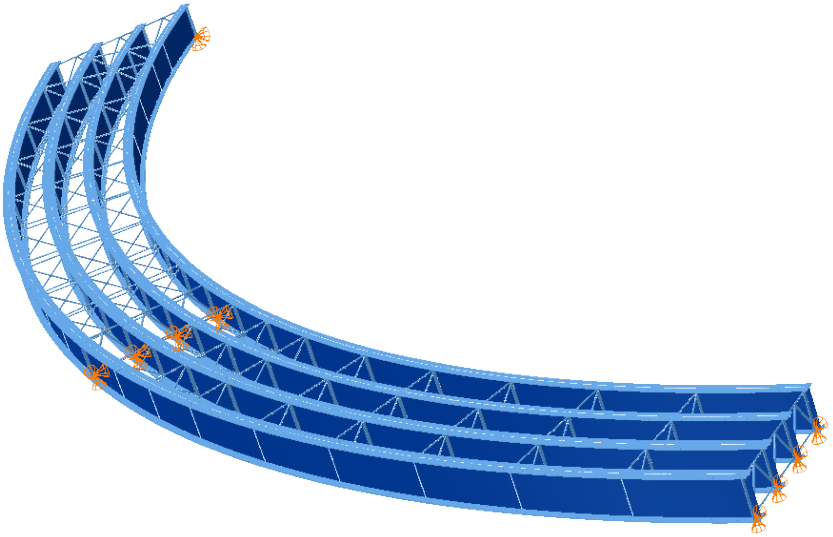

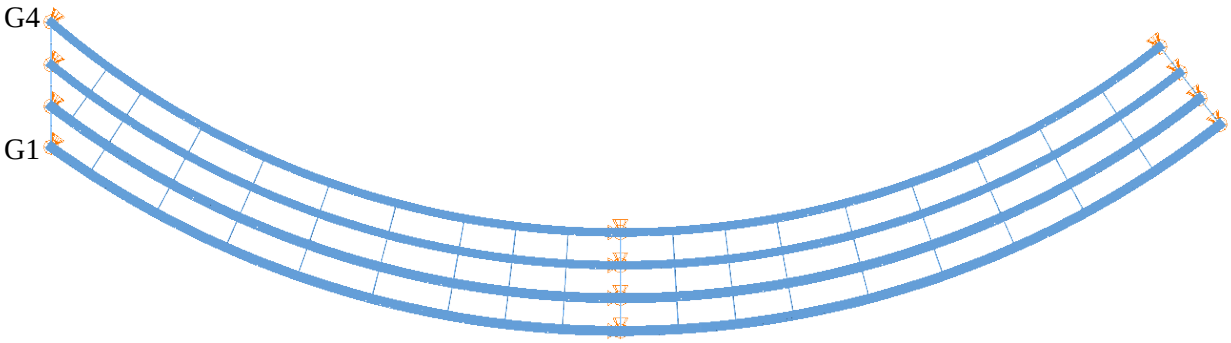

Abbreviated Analysis Results:

In this bridge, the effects of horizontal curvature, support skew, and continuity are studied. Results for the five selected stages shown in Figure 1 are presented in this report. In Stage 1, the exterior girder is erected and supported on the left and middle bearings. Additionally, a holding crane is provided at mid-span of Span 1. Next, girder G2 is placed following the same scheme, as shown in Stage 2. The holding crane is removed since the two girder system is considered to be stable without the aid of crane. In Stages 5 and 6 the erection of the exterior girders G1 and G2 is completed for both spans. In Stages 5 and 6, girders G3 and G4 are erected for Span 1, respectively. Finally, Stage 9 shows the completed structure. The load condition at this stage is total dead load, TDL.

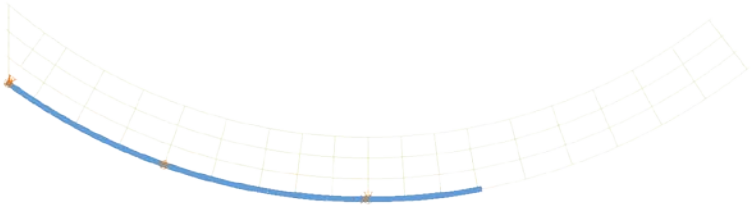

Stage 1

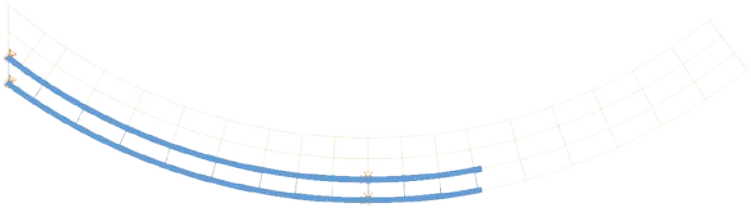

Stage 2

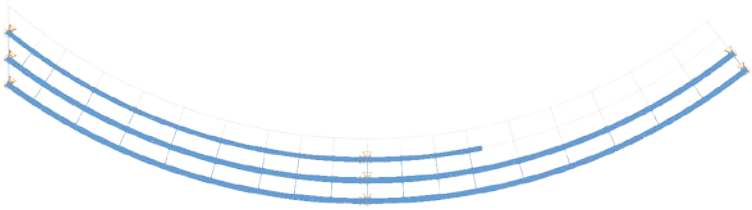

Stage 5

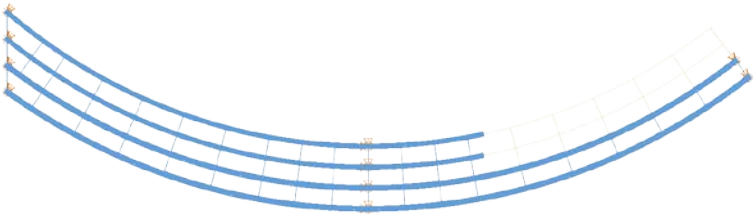

Stage 6

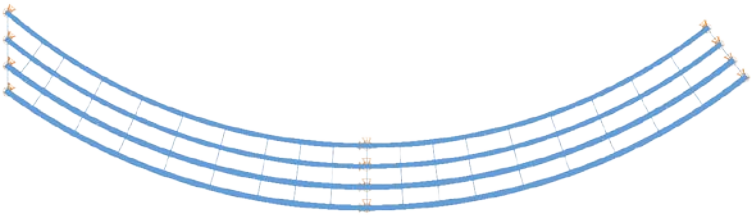

Stage 9

Fig. 1. NICCS2, Studied Stages

The major-axis bending responses as predicted by the 2D grid analysis and the 3D FEA for Stage 1 are compared first. As shown in Figure 2 for girder G1, the stress responses are consistent between methods. For this response and as observed in other curved and skewed bridges, the limitations of the 2D model representation have a minor influence in its accuracy.

In the case of vertical displacements, the results do not show the same correlation. As shown in Figure 3, the magnitudes of the vertical displacements are over predicted by the approximate model. This response is severely affected by the poor torsion model for the I-girders in the 2D grid computer model.

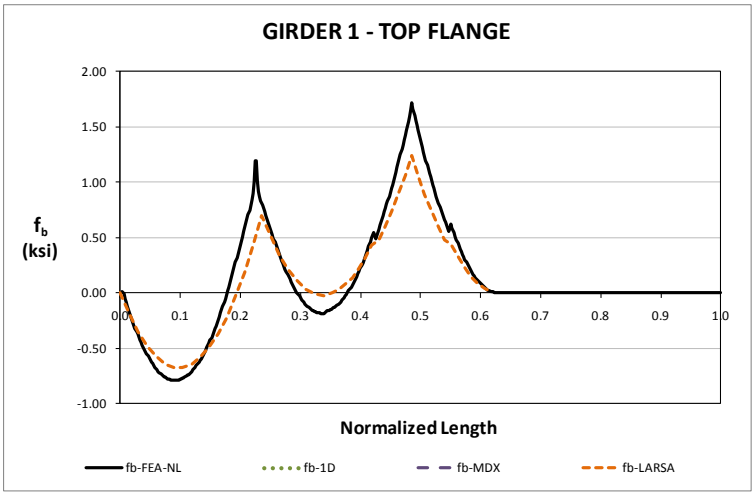

Fig. 2. Major Axis Bending Stress Predictions, Stage 1

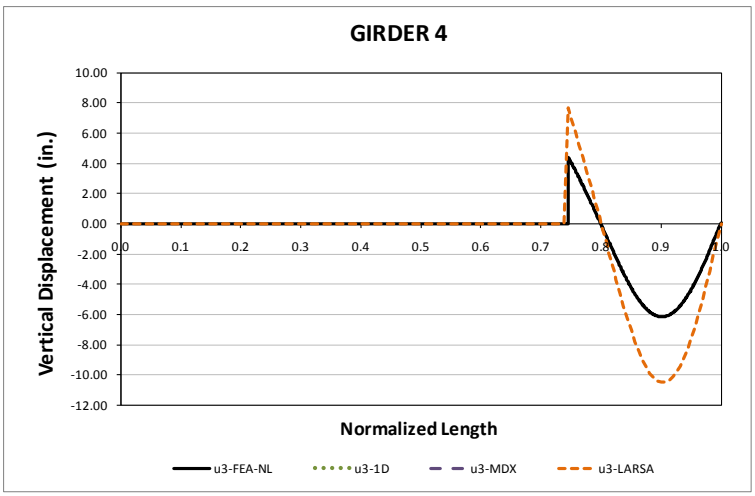

Fig. 3. Vertical Displacement Predictions, Stage 1

The flange lateral bending stresses are calculated based on the major-axis bending response, according to the V-Load method. Figure 4 shows the 2D model and 3D model predictions for girder G1, Stage 5. As shown in the figure, the prediction of this response based on this formulation is conservative. The stress profiles are very similar between the two methods of analysis, but the approximate method results are slightly higher than the benchmark. Based on this study, it is observed that the prediction of the equivalent lateral load obtained from the major-axis bending response could be used to determine an upper bound limit.

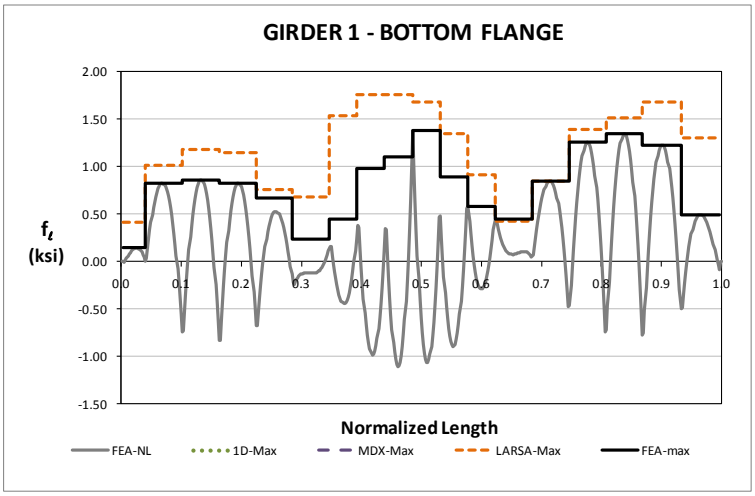

Fig. 4. Flange Lateral Bending Stress Predictions, Stage 5

The results for the total dead load condition, Stage 9, are discussed next. For the vertical displacements, shown in Figure 5, the 1D model does not capture the expected response. In the case of the 2D grid models, the response is over predicted. The overestimation is associated to the limitations of the computational model to represent the actual behavior of an open-section thin-walled beam element. Thus,

the 2D grid models do not consider the stiffness contribution that comes from the warping of the flanges. This limitation also affects the prediction of the girder layover, as shown in Figure 6. However, the rotation of the girder group controls over the individual rotation of the girders at the cross-frame locations, behavior that is captured by the 2D grid model. The above observations are consistent for all the girders of the bridge throughout all the construction simulation.

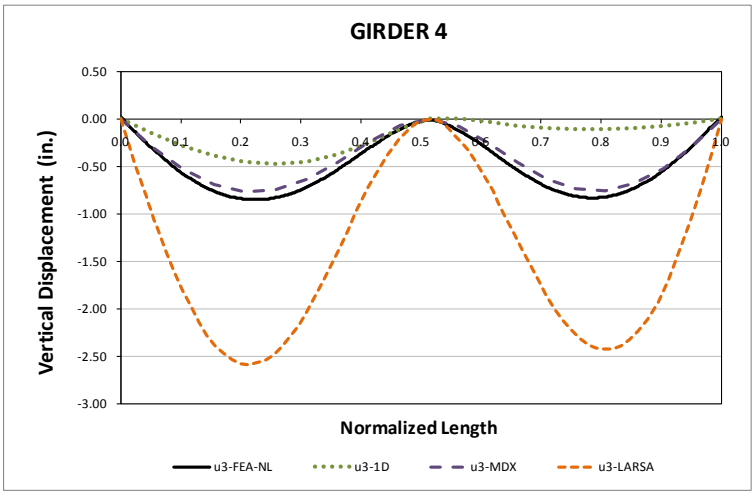

Fig. 5. Predictions on Vertical Displacements, Stage 20

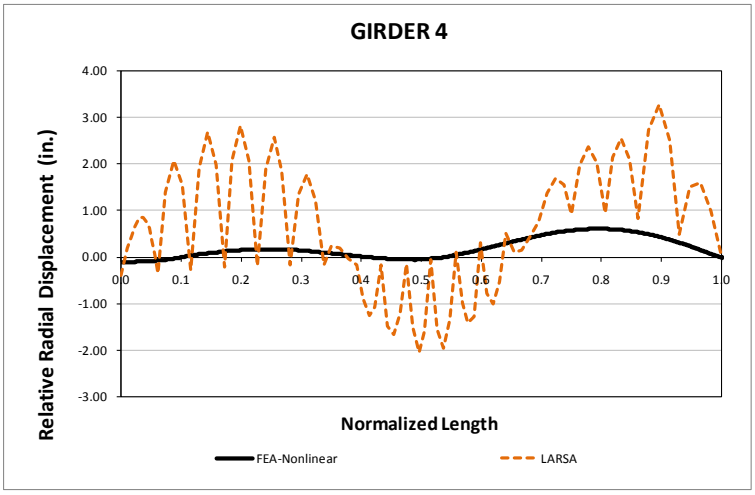

Fig. 6. Predictions on Relative Lateral Displacements, Stage 20

I7.5 NICCS3 (New, I-girder, Continuous-span, Curved, Skewed supports)

Category Data:

L_1 = 150 ft, L_2 = 150 ft / $R_{1,2}$ = 227 ft/ w = 30 ft /θ_1 = 38^o, θ_2 = 0^o, θ_3 = -38^o, 4 girders

Cross-Frame Detailing Method: NLF

Erection Stages Analyzed: 7 (Analyses are performed assuming NLF)

Deck Placement Sequence: 1 Stage

Bridge Perspective & Plan Views:

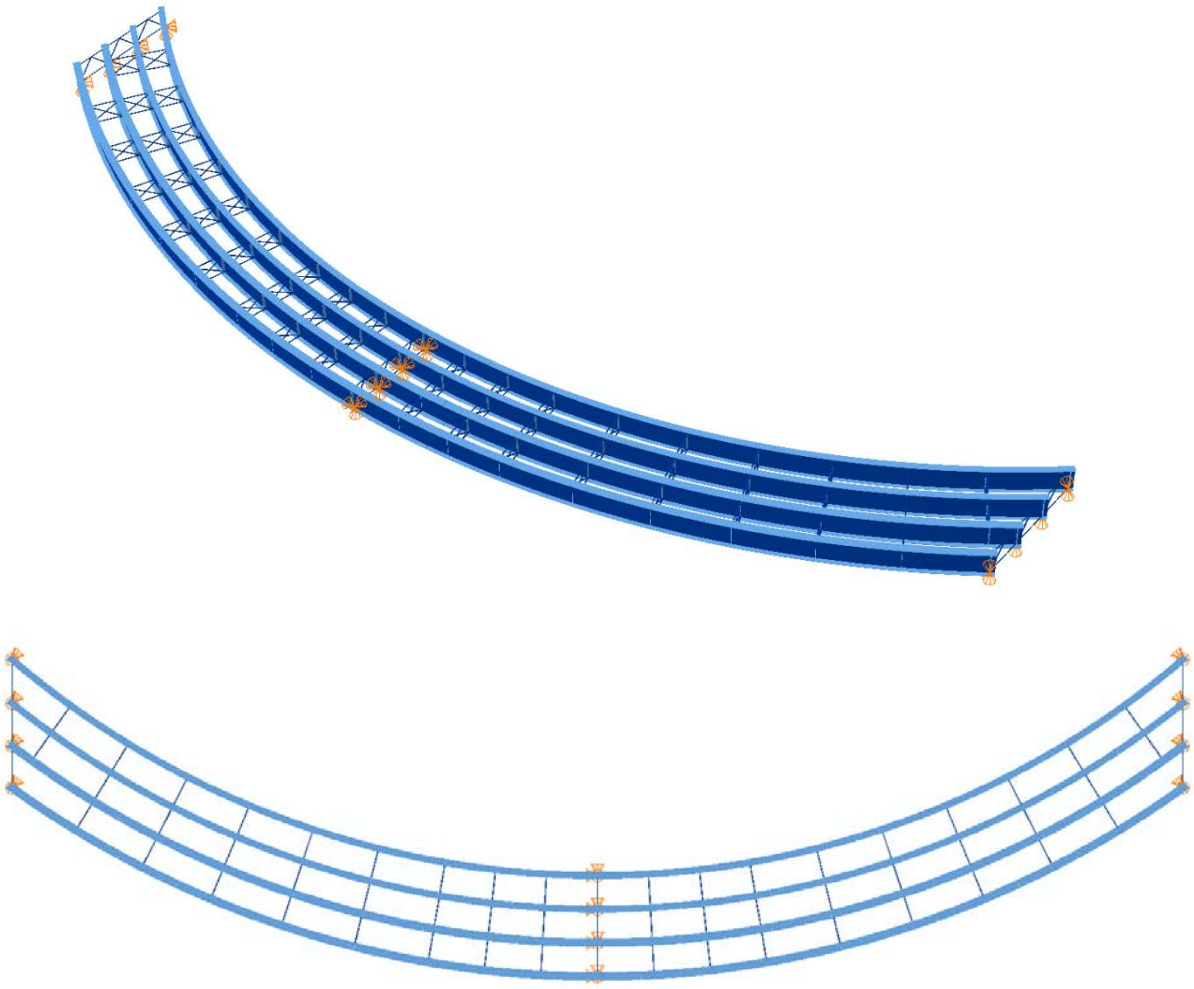

Abbreviated Analysis Results

Figure 1 shows the different analysis stages which are considered to evaluate the different analysis methods. Uplift is observed at the bearings for Stages 2, 3, 5 and 6 for girders 4, 4, 3 and 3 respectively. Uplift is also captured by Larsa results. Figure 2 shows girder 3 vertical displacement predictions for stage 2. Large displacements are observed at girder 2 for stage 2. Therefore, girder 2 is the critical for stage 2. It is obvious from the results that vertical displacements are off significantly when Larsa results are considered. This is mainly due to incapability of the 2D grid models to capture warping deformations. Figure 3 shows stage 2 radial displacement results for girder 3. Larsa could not predict the radial displacements accurately anywhere within the span. Figure 4 and 5 show stage 2 major and minor axis bending stresses for girder 3. It is clear from these figures that grid analysis methods predict the major-axis bending stresses accurately. Furthermore, the flange lateral bending stresses are estimated accurately due to accurate prediction of the major-axis bending stresses. It should be noted that for these stages there are no large unbraced lengths. Therefore flange lateral bending stresses are predicted accurately for this bridge.

Total dead load results are also investigated since this is the highest load level during construction. Figure 6 shows vertical deflection predictions under total dead load for the outside girder (Girder 1). It is observed from the results that Larsa results over predicts the deflections whereas the other methods predict close to benchmark solutions. This is due to the coarse representation of the structure for the solutions other than Larsa. Finer representation of the structure is unable to capture the warping deformations. Figure 7 shows relative radial deflection predictions under total dead load for the outside girder (Girder 1). This observation is also made in NISCS14.

Similar to previous studies, the relative radial displacements are well predicted at the cross-frame locations whereas the predictions are off within the cross-frames. Figure 8 shows major-axis bending stress predictions under total dead load for the outside girder (Girder 1). The stresses are well predicted by approximate analysis methods. Figure 9 shows minor-axis bending stress predictions under total dead load for the outside girder (Girder 1). It is clear that the flange lateral bending stresses are well predicted for the positive moment regions. However the values estimated for the negative moment regions are over conservatively predicted.

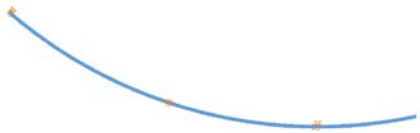

Stage 1

Stage 2

Stage 3

Stage 5

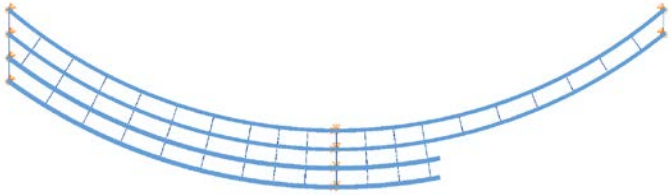

Stage 6

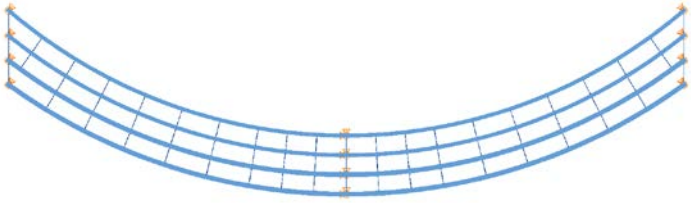

Stage 8 & 9

Fig. 1. NICCS3, Considered different analysis stages.

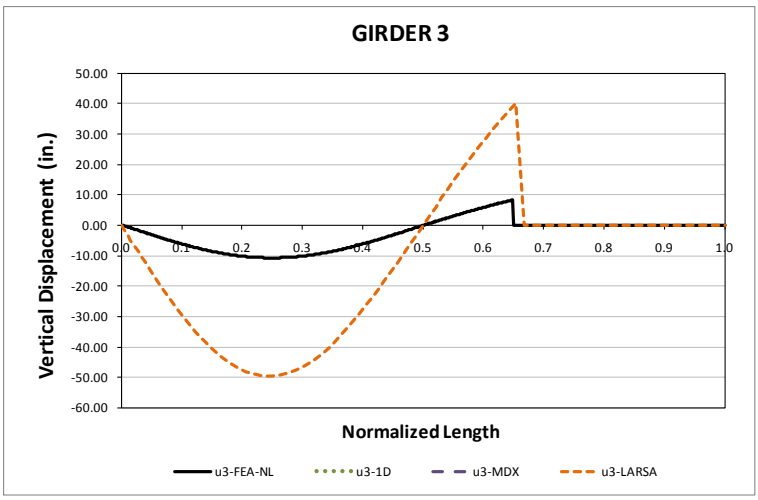

Fig. 2. NICCS3, Stage 2 vertical displacements for NLF detailing.

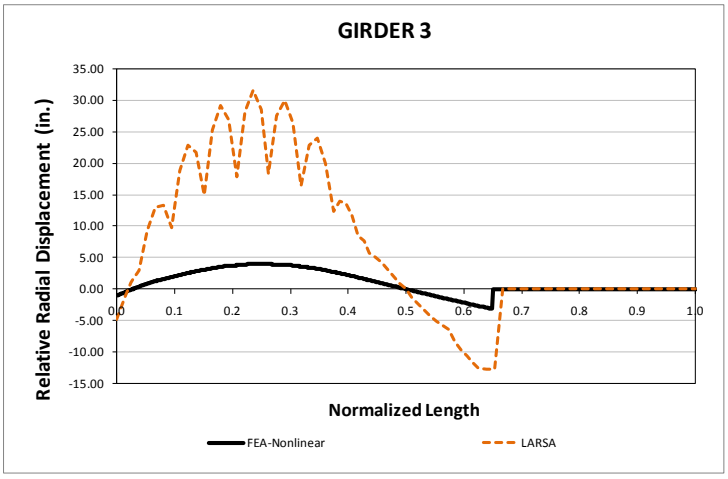

Fig. 3. NICCS3, Stage 2 relative radial displacements for NLF detailing.

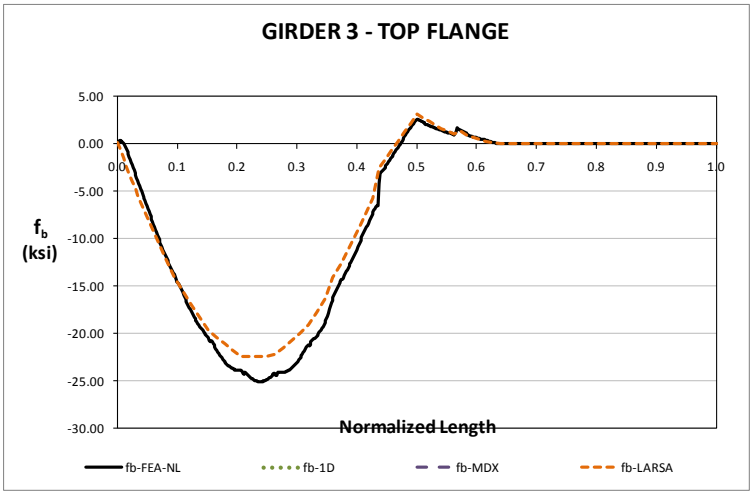

Fig. 4. NICCS3, Stage 2 major-axis bending stresses for NLF detailing.

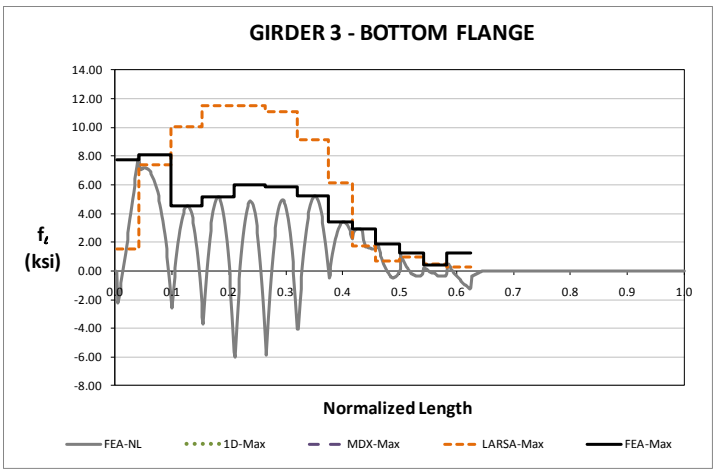

Fig. 5. NICCS3, Stage 2 minor-axis bending stresses for NLF detailing.

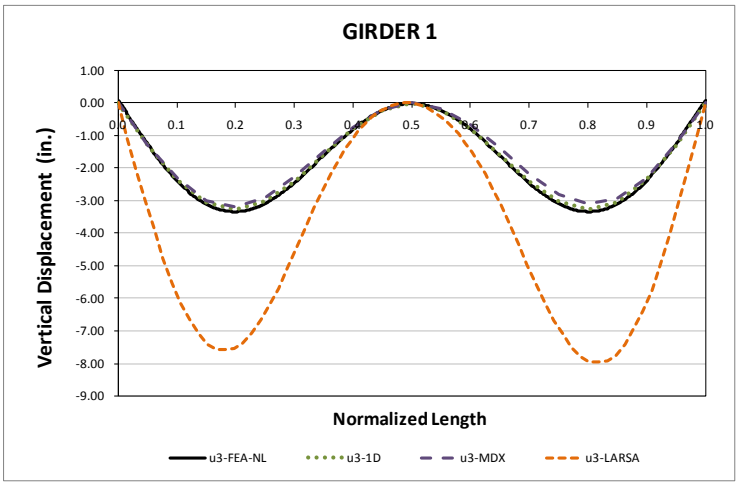

Fig. 6. NICCS3, Vertical displacements under total dead load for NLF detailing.

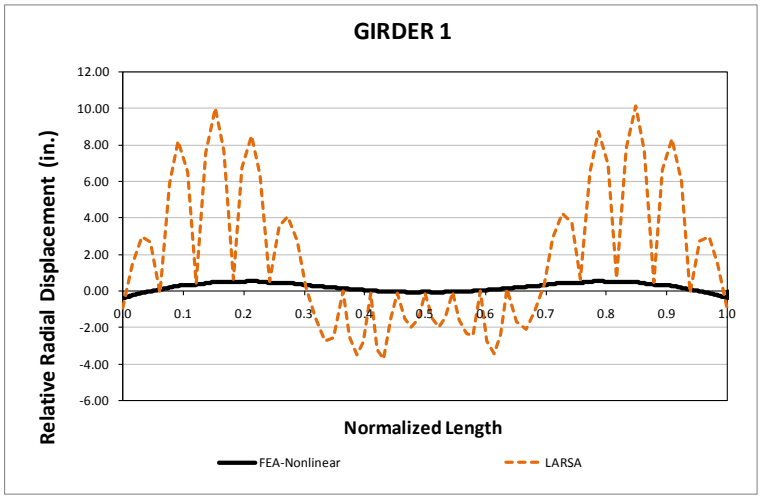

Fig. 7. NICCS3, Relative radial displacements under total dead load for NLF detailing.

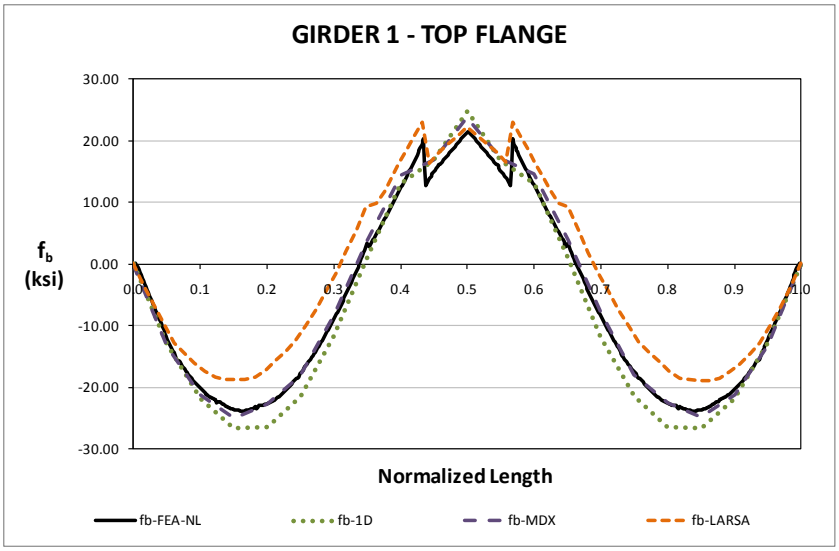

Fig. 8. NICCS3, Major-axis bending stresses under total dead load for NLF detailing.

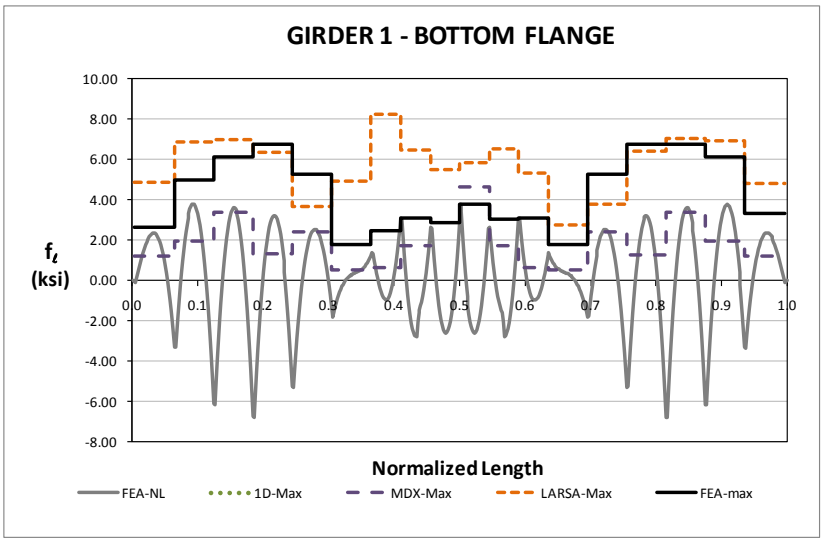

Fig. 9. NICCS3, Minor-axis bending stresses under total dead load for NLF detailing.

I7.6 NICCS9 (New, I-girder, Continuous-span, Curved, Skewed supports)

Category Data:

L_1 = 150 ft, L_2 = 150 ft / $R_{1,2}$ = 308 ft/ w = 80 ft /θ_1 = 56^o, θ_2 = 28^o, θ_3 = 0^o, 9 girders

Cross-Frame Detailing Method: NLF

Erection Stages Analyzed: 7 (Analyses are performed assuming NLF)

Deck Placement Sequence: 1 Stage

Bridge Perspective & Plan Views:

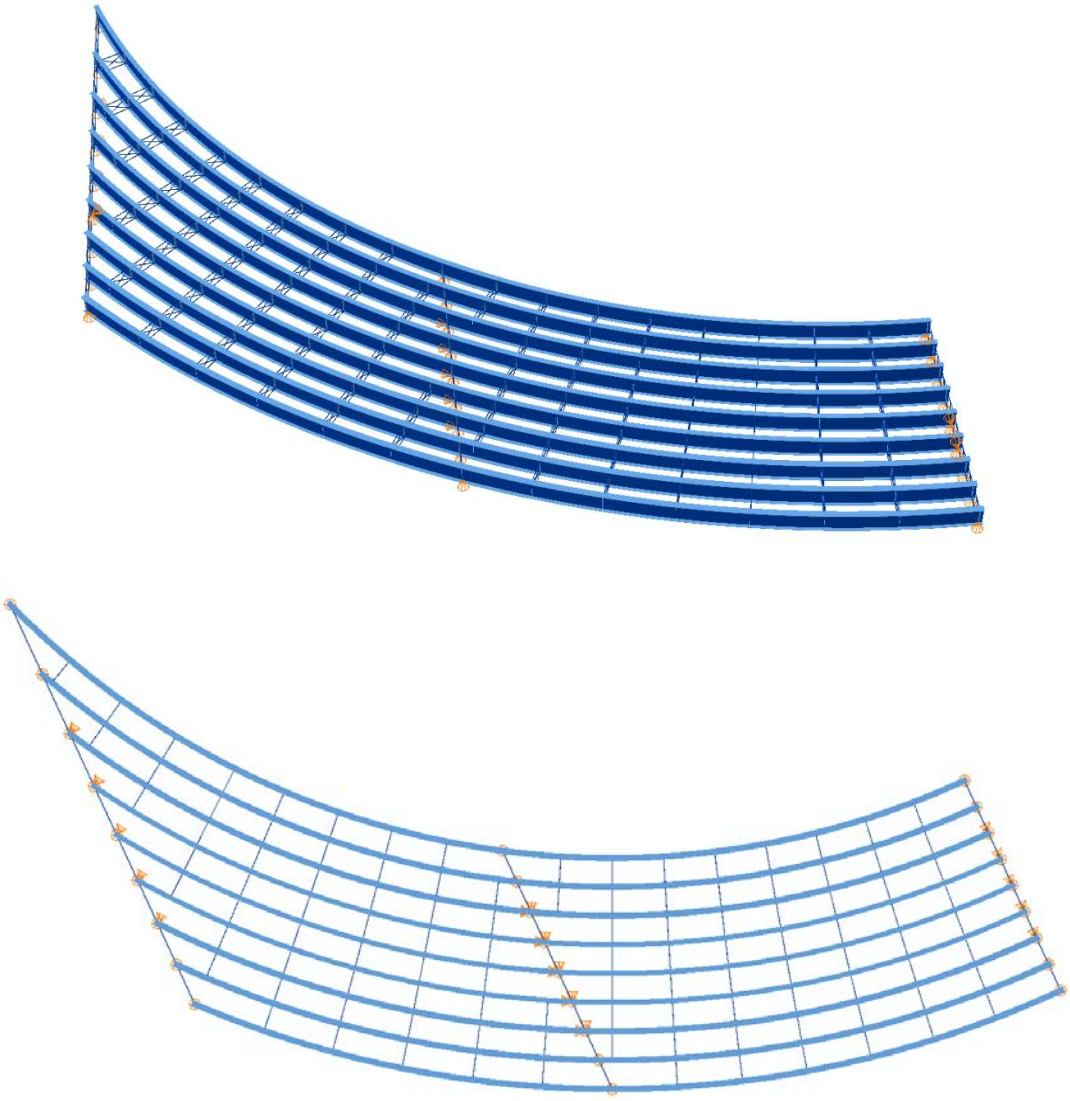

Abbreviated Analysis Results

Figure 1 shows the different analysis stages which are considered to evaluate the different analysis methods. Stage 2 results are shown here since significant observations are made from this stage. Figure 2 shows the deflected shape of Stage 2. Displacement results are magnified by 10x. It is clear from Fig.2 that two girder system is on the bearings without any additional supports. Additional to FEA linear, nonlinear solutions , coarser and refined LARSA grid solutions and 3D grid model is created and analyzed using the structural analysis program GT-SABRE (Chang and White 2008).

The difference in the refined and coarser LARSA models is that the refined model has a multiple elements between the cross-frame locations where as the coarser model has just one element between the cross-frame locations. Refined model for the LARSA grid solutions are used through the project.

GT-SABRE model enables the user to model the girders with the B14DGLW element which is a displacement-based element based on thin-walled open-section beam theory. The B14DGLW element has seven degrees of freedom per node to capture the warping effects on the member. Moreover, the diagonals of the cross-frames are modeled using T6 truss elements, which have three degrees of freedom per node. The top and bottom chords of the cross-frames are modeled with B12CW beam elements, which have 6 degrees of freedom per node. The bearing locations are modeled at the actual locations and connect to the girders with MPC's. Further information about GT-SABRE can be found in (Chang and White 2008).

An uplift of 8.5 kips is observed for G9 from the FEA solutions. All the analysis methods capture this uplift. However LARSA grid solutions have lower prediction in the reactions(4.75 kips).

Figures 3 and 4 show girder 8 and 9 relative radial displacement predictions for stage 2. The linear FEA solutions are not plotted on these figures since the predictions are same as the benchmark solution. It should be noted for Figs. 3 and 4 that layovers are way over predicted by the refined LARSA grid solutions . On the other hand, relative radial displacements are under predicted by GT-SABRE and coarse grid solutions. It is believed that the under prediction of the GTSABRE results can be due to either :, lateral shear deformation in the top and bottom flanges in the short length between the 1st intermediate cross-frames and the bearing-line cross-frames in a couple of the girders or cross-section distortion.

Figures 5 and 6 show girder 8 and 9 vertical displacement predictions for stage 2. All the solutions except the refined LARSA grid solutions predict the vertical displacements accurately. This is mainly due to incapability of the 2D grid models to capture warping deformations between the cross-frame locations. Coarser LARSA grid model does not have the elements between the brace points. As a result , it only has the predictions at the brace points which is close to the benchmark solution.

Figures 7 and 9 show girder 8 and 9 major-axis bending stress predictions for stage 2. Only GT-SABRE solutions predict the results accurately since it has the capability to capture the warping deformations. The other grid solutions could not capture the local bending effect on the skewed bearing of the girder 9. Figures 8 and 10 show girder 8 and 9 flange lateral bending stresses predicted by GT-SABRE and FEA solutions. These stresses are predicted accurately by the 3D grid solution

Figure 11 shows vertical displacements of the inside girder (girder 9) under total dead load. It should be noted from Fig. 10 that LARSA grid solutions are overestimating the vertical deflections. It is interesting

to observe that the MDX solutions provide better vertical displacement predictions. This is due to the coarser representation of the bridge. As discussed above the coarser model provides better predictions since it does not have multiple elements between the cross-frame locations.

Figure 12 shows the relative radial displacements of girder 9 under total dead load. As discussed in the previous studies the radial displacements are accurate only at the cross-frame locations. Figures 13 and 14 show the major-axis bending and the flange lateral bending stress predictions under total dead load. Figures 13 and 14 show that the approximate analysis predictions are good.

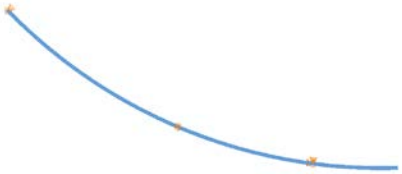

Stage 1

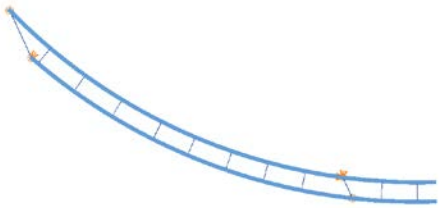

Stage 2

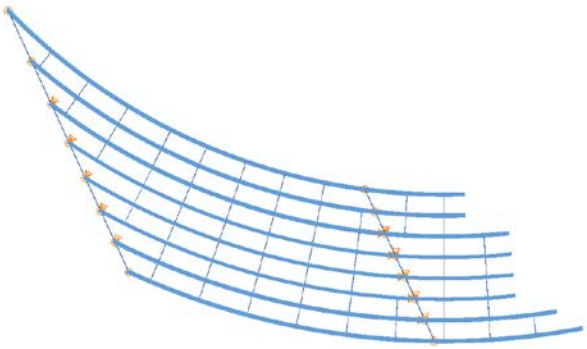

Stage 8

Fig. 1. NICCS9, Considered different analysis stages.

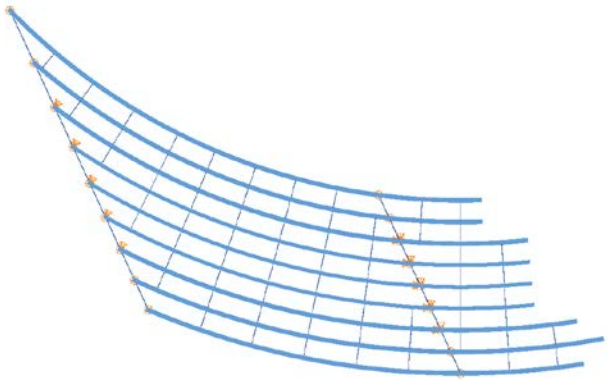

Stage 9

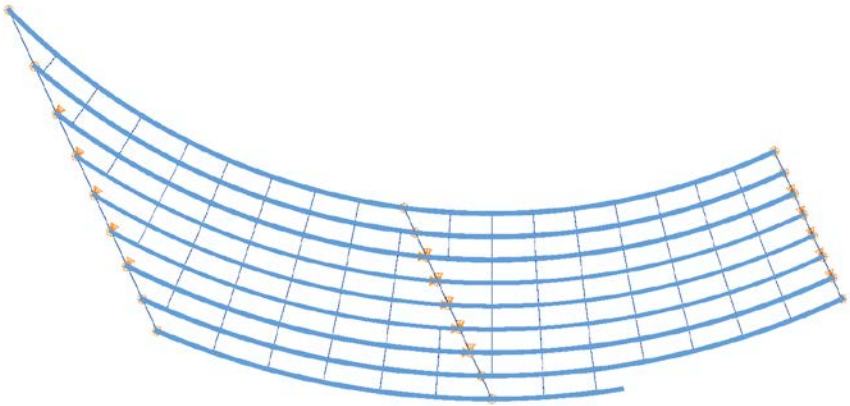

Stage 17

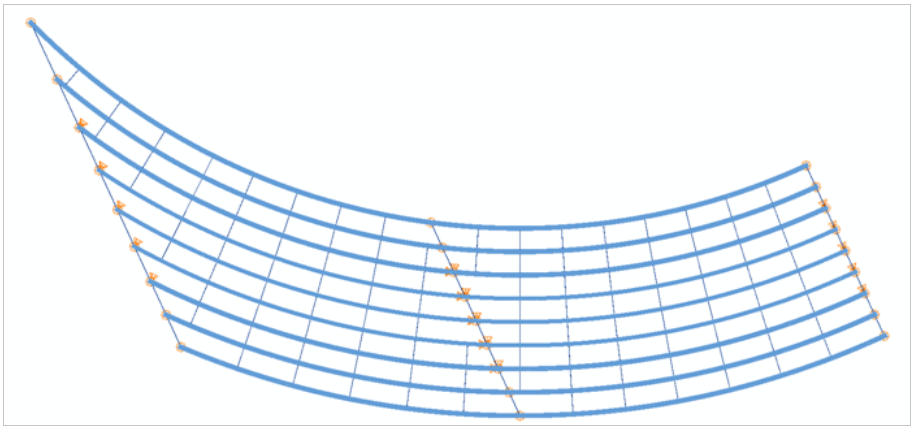

Stage 18 & 19

Fig. 1. NICCS9, Considered different analysis stages(continues).

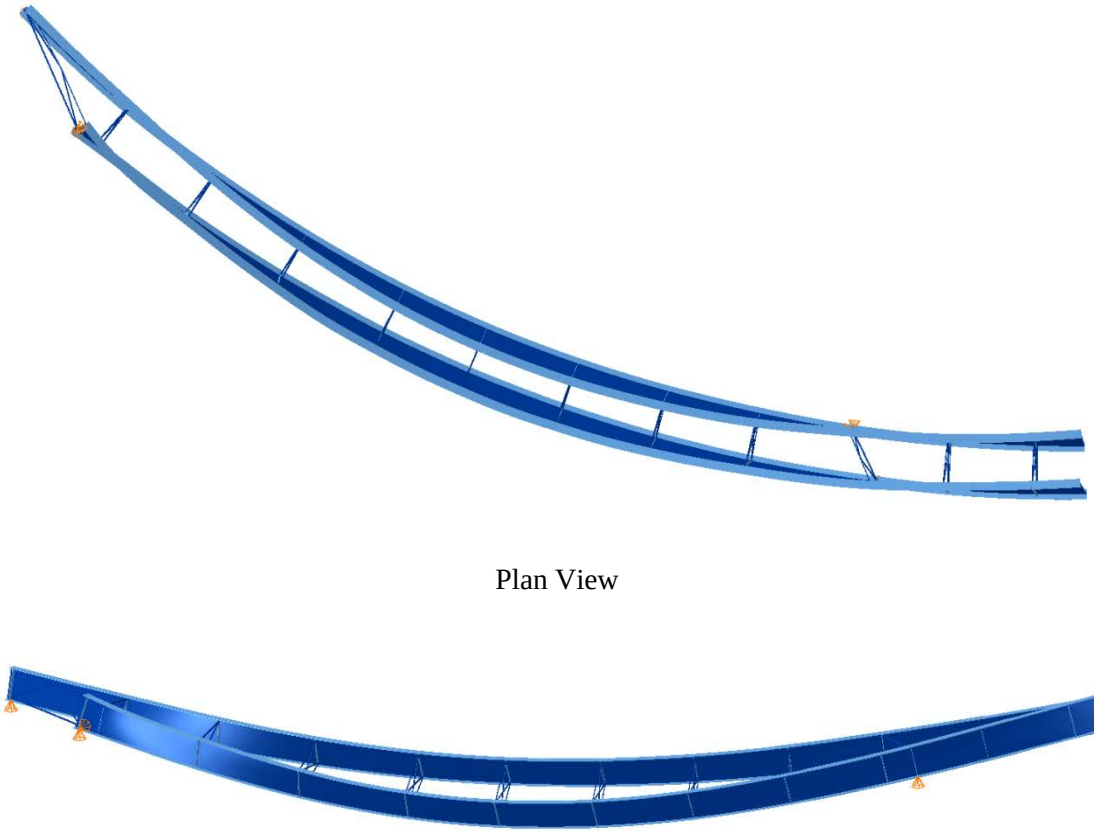

Plan View

Perspective View

Fig. 2. NICCS9, Stage 2 plan and perspective deflected shapes (Magnified by 10x).

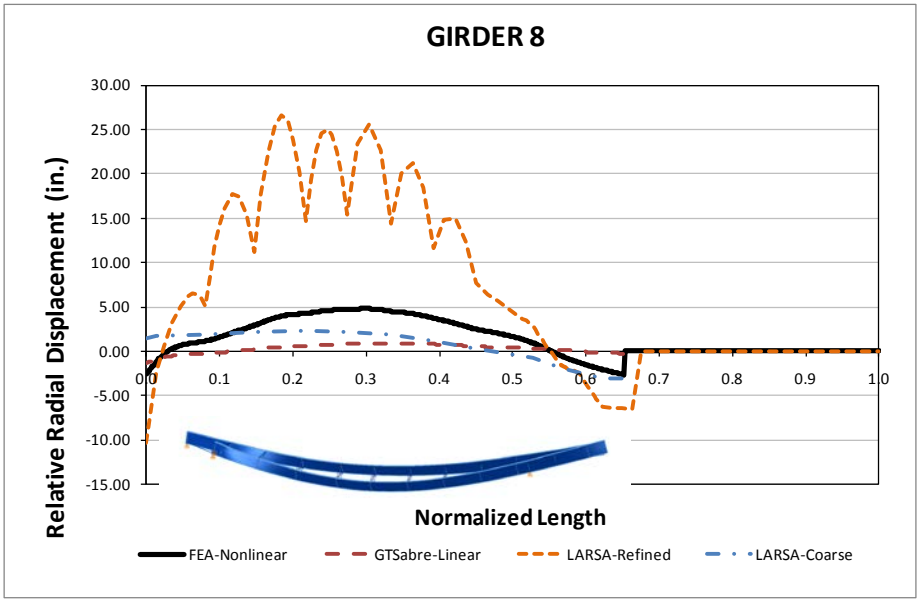

Fig. 3. NICCS9, Stage 2 Radial displacements NLF detailing.

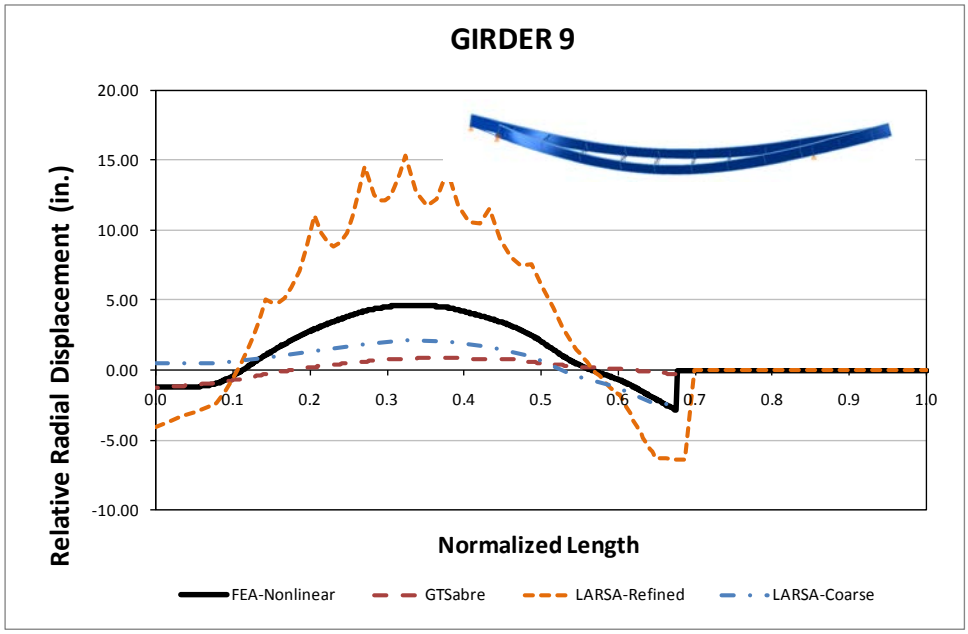

Fig. 4. NICCS9, Stage 2 radial displacements NLF detailing.

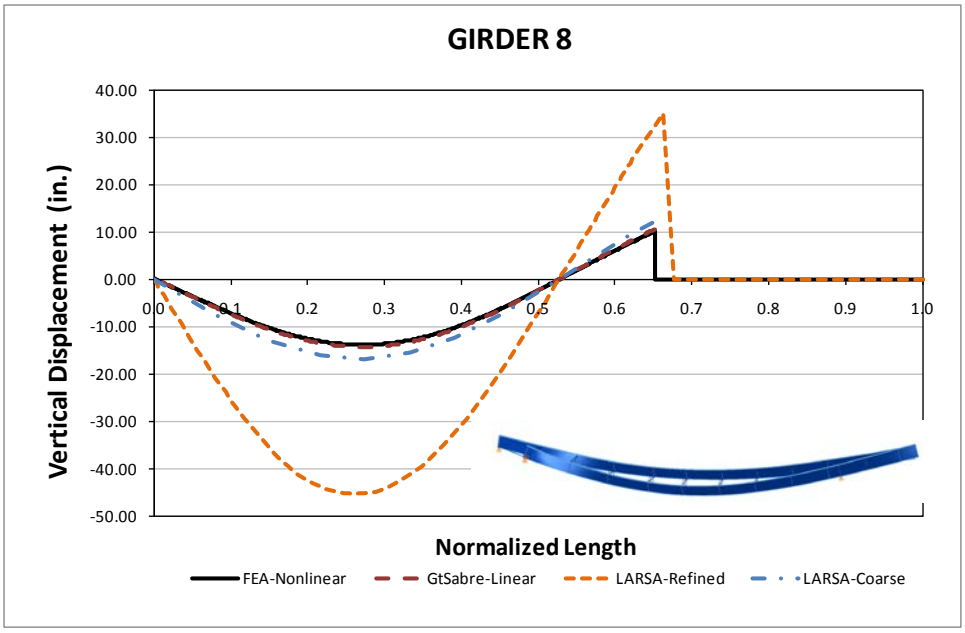

Fig. 5. NICCS9, Stage 2 vertical displacements NLF detailing.

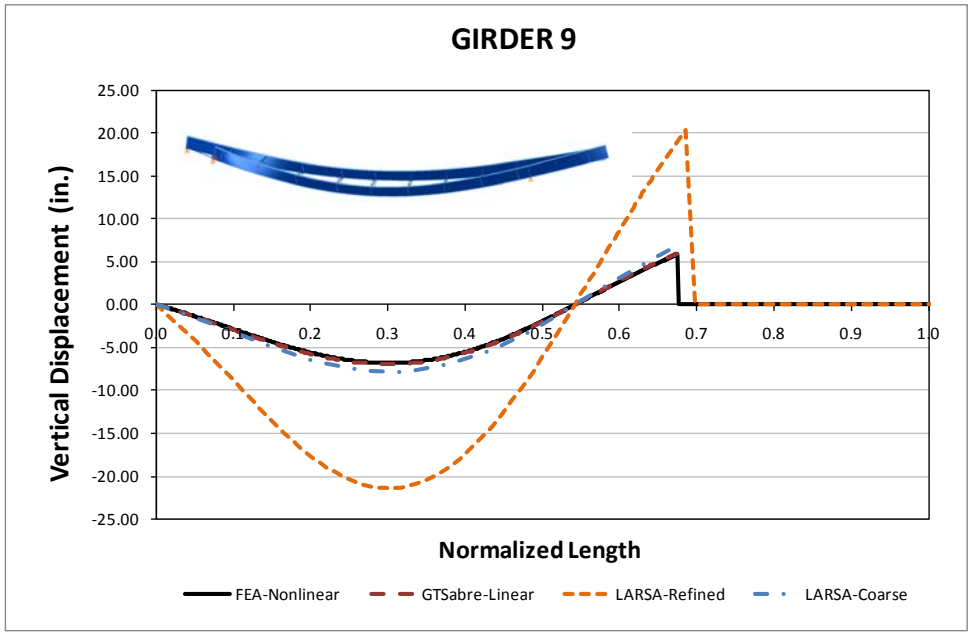

Fig. 6. NICCS9, Stage 2 vertical displacements NLF detailing.

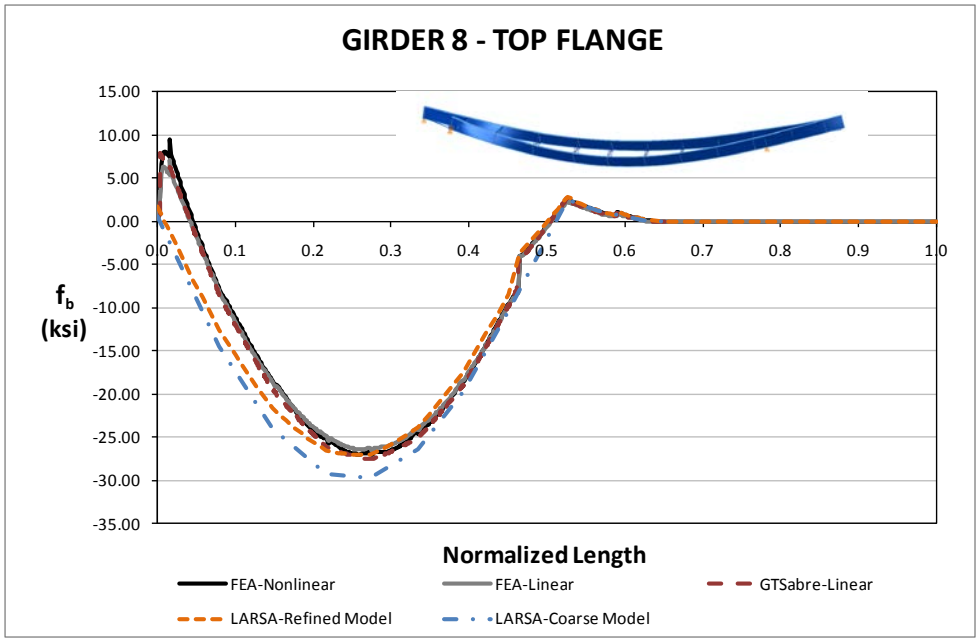

Fig. 7. NICCS9, Stage 2 major-axis bending stresses for NLF detailing.

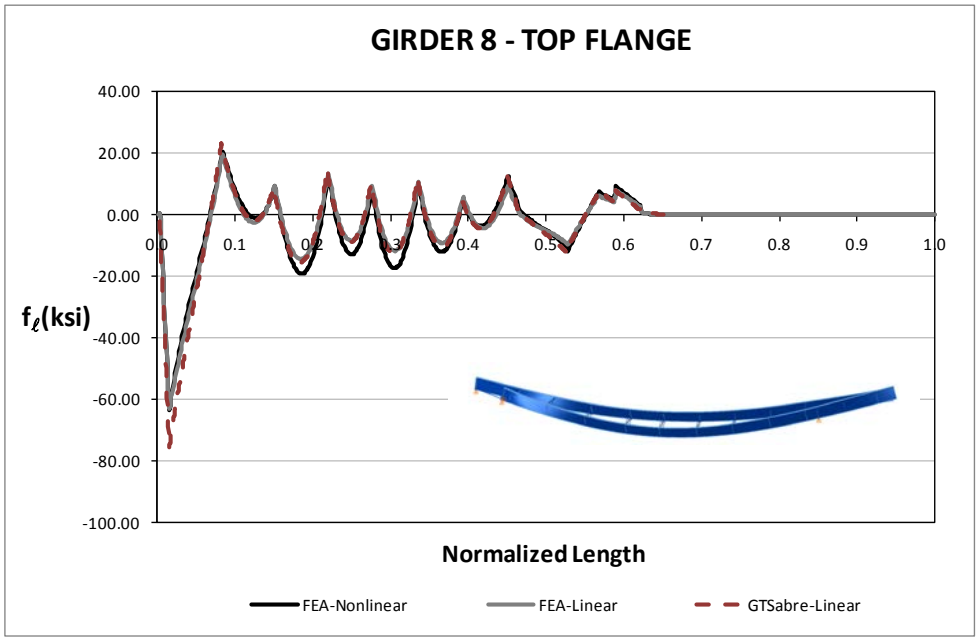

Fig. 8. NICCS9, Stage 2 flange lateral bending stresses for NLF detailing.

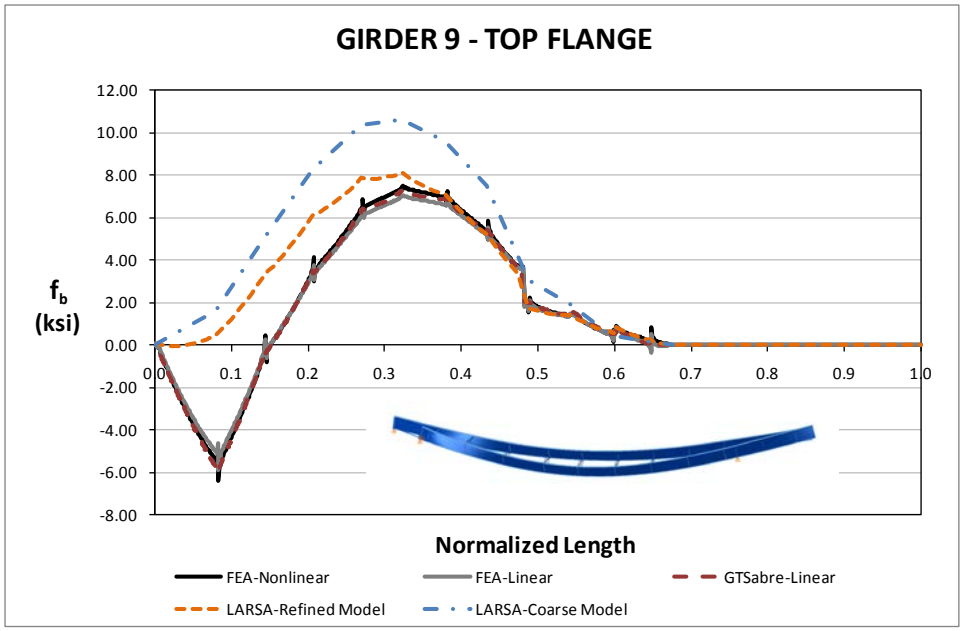

Fig. 9. NICCS9, Stage 2 major-axis bending stresses for NLF detailing.

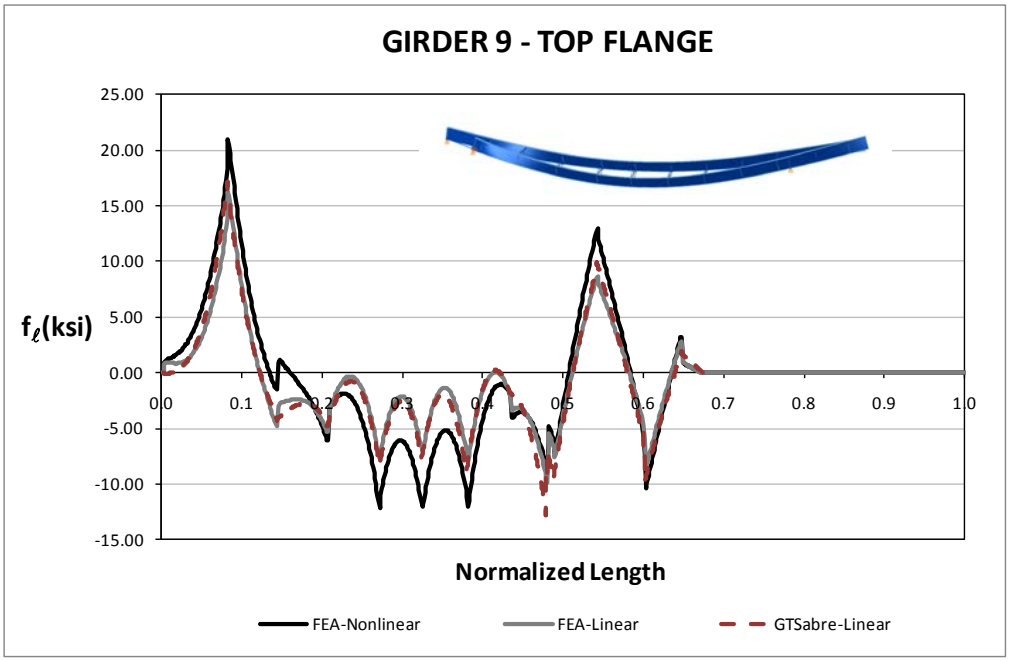

Fig. 10. NICCS9, Stage 2 flange lateral bending stresses for NLF detailing.

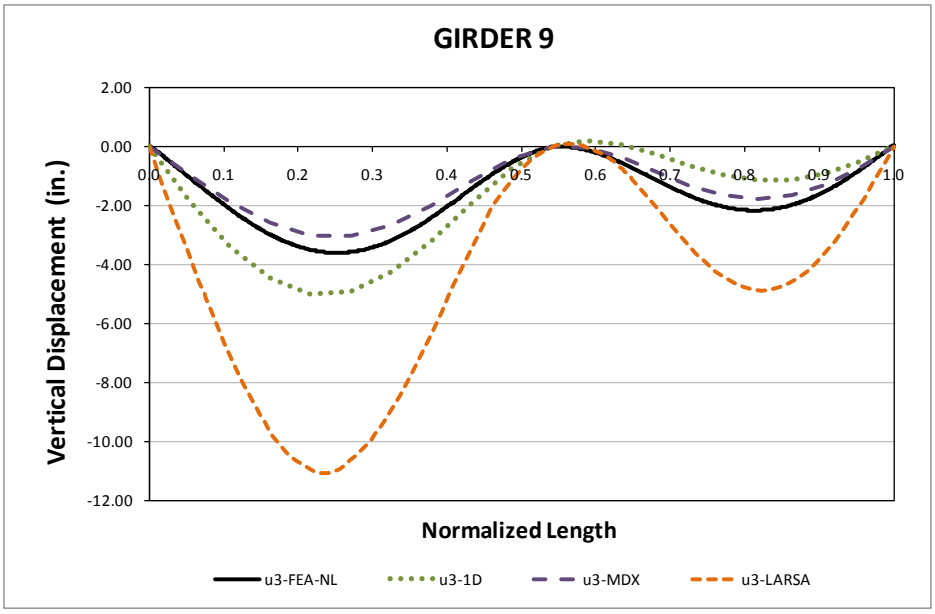

Fig. 11. NICCS9, Vertical displacements under total dead load for NLF detailing.

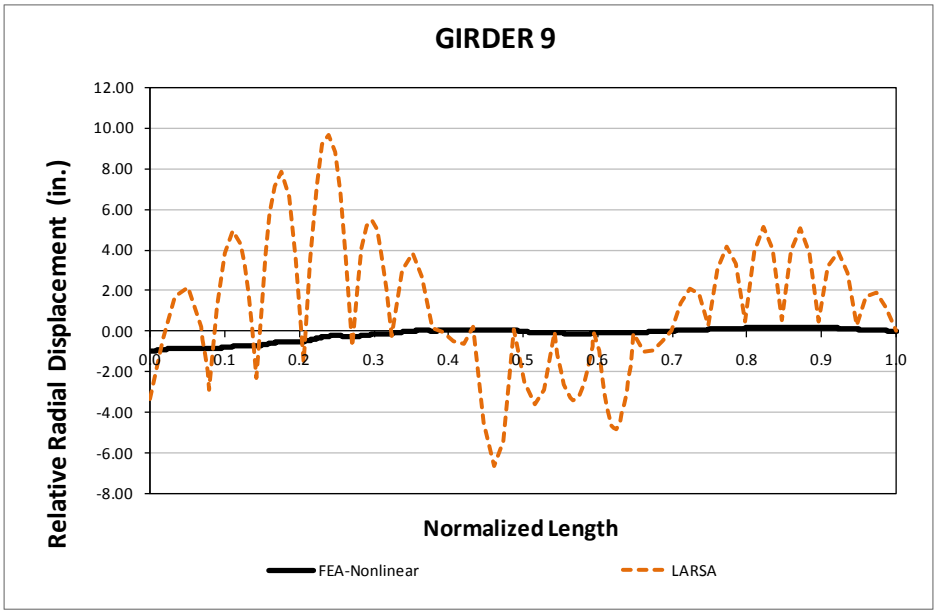

Fig. 12. NICCS9, Relative lateral displacements under total dead load for NLF detailing.

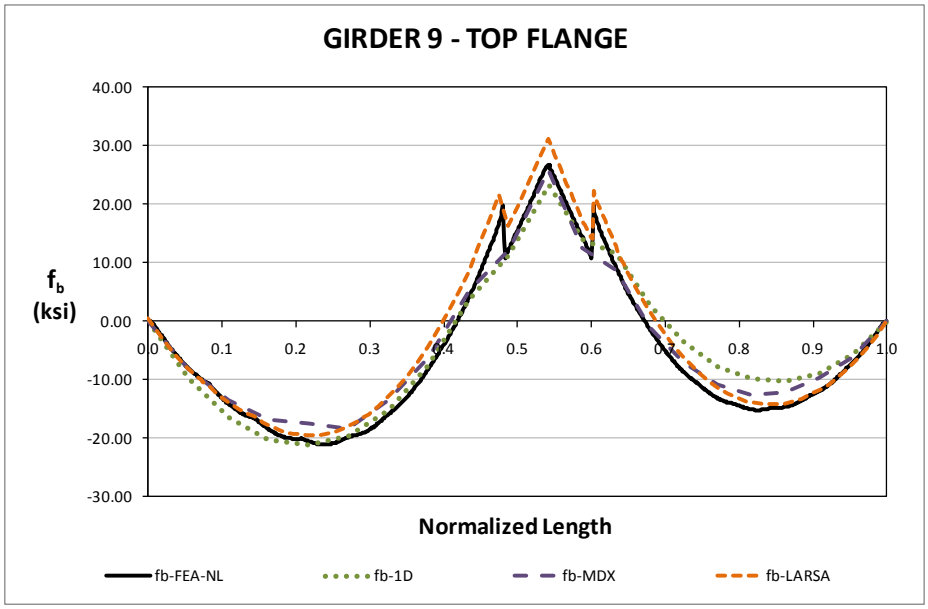

Fig. 13. NICCS9, Major-axis bending stresses under total dead load for NLF detailing.

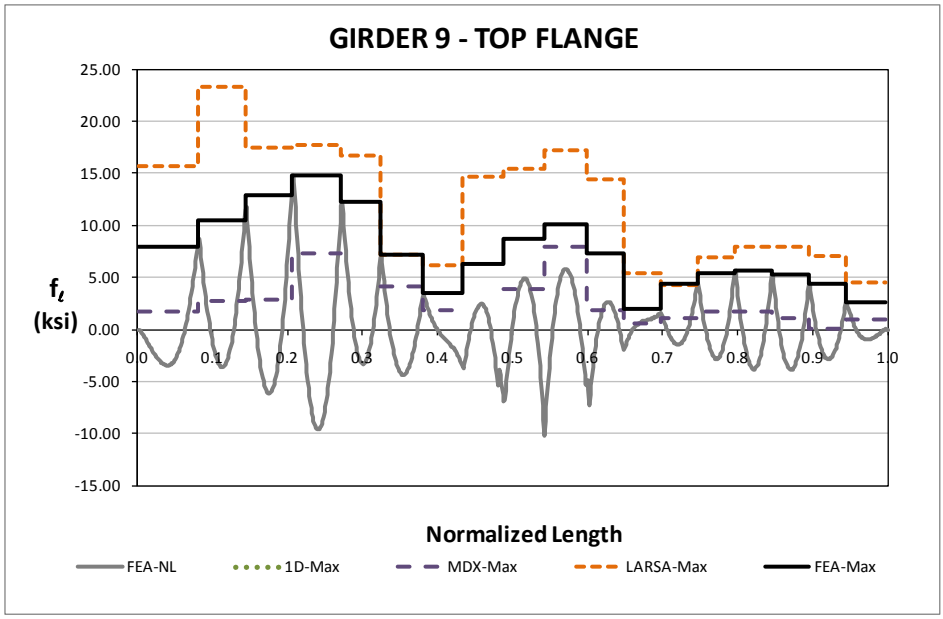

Fig. 14. NICCS9, Flange lateral bending stresses under total dead load for NLF detailing.

Conclusions:

It is observed from this bridge that neglecting the warping stiffness contributions can lead to error in the prediction of vertical displacements for 2D grid models. However, coarser LARSA grid models provide better estimates of the vertical displacements due to not having additional elements between the cross-frame locations. This provide better accuracy of the results to reduce the effect of neglecting warping contributions. however none of the 2D grid solutions can capture the relative radial and major axis-bending stresses accurately.

3D grid solutions provide accurate vertical, major-axis bending and flange lateral bending predictions . However, relative radial displacements are under predicted by 3D grid solutions. It is believed that the under prediction of the results can be due to either :, lateral shear deformation in the top and bottom flanges in the short length between the 1st intermediate cross-frames and the bearing-line cross-frames in a couple of the girders or cross-section distortion.

It is also observed from the total dead load results that refined LARSA grid solutions overestimate the displacements whereas the coarser MDX model more accurate results.

I7.7 NICCS13 (New, I-girder, Continuous-span, Curved, Skewed supports)

Category Data:

L_1 = 250 ft, L_2 = 250 ft / $R_{1,2}$ = 597 ft/ w = 30 ft /θ_1 = 47.9^o, θ_2 = 24^o, θ_3 = 0^o, 4 girders

Cross-Frame Detailing Method: NLF

Erection Stages Analyzed: 6 (Analyses are performed assuming NLF)

Deck Placement Sequence: 1 Stage

Bridge Perspective & Plan Views:

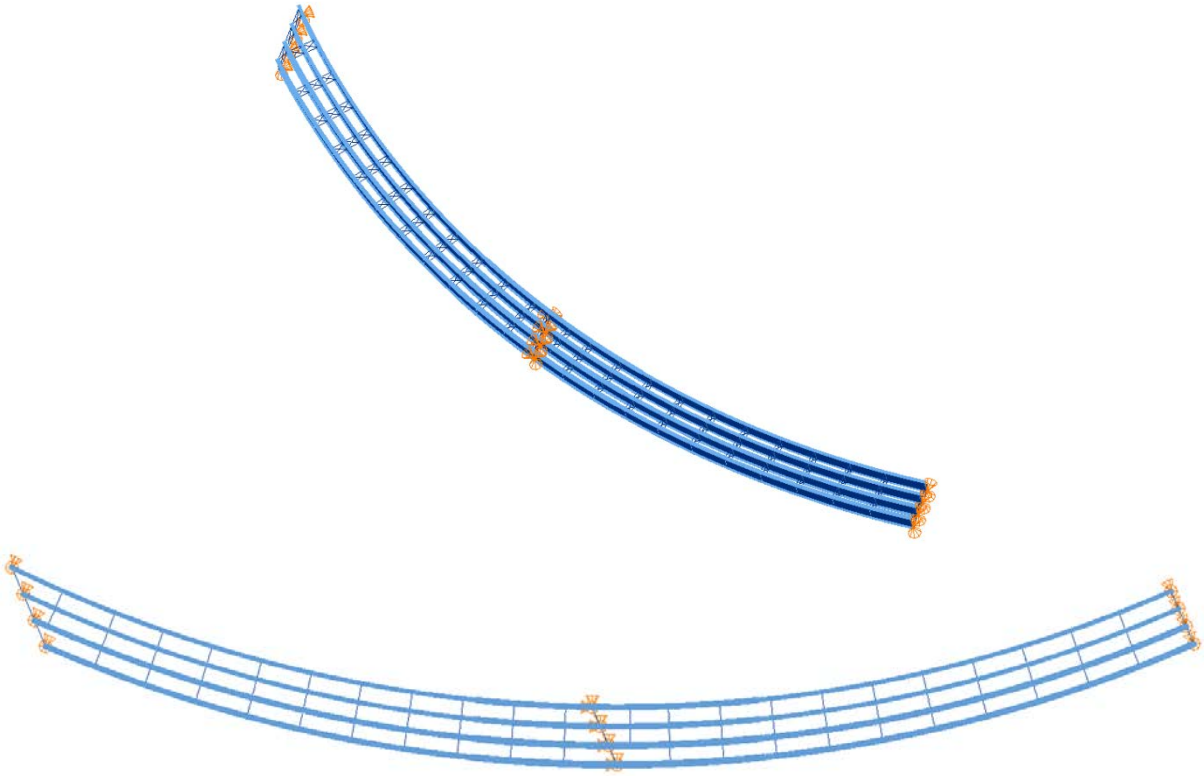

Abbreviated Analysis Results

Figure 1 shows the different analysis stages which are considered to evaluate the different analysis methods. The results from Stage 17 are provided in detail. Figure 2 shows the deflected shape of Stage 17. Displacement results are magnified by 10x. Figure 3 shows the layover of Girder 1 for Stage 17. Figure 4 provides the vertical displacements of Girder 1 for Stage 17. It is obvious from Figs. 3 and 4 that grid solutions provide over estimated predictions. The reasons for not obtaining accurate predictions for approximate analysis methods are explained in the previous summaries in detail. Figure 5 provides the girder 1 major-axis bending stresses for Stage 17. The stress predictions are predicted accurately by grid analysis solutions. Figure 6 shows girder 1 flange lateral bending stresses for Stage 17. It should be noted from this figure that the spikes close to the piers cannot predicted by grid analysis solutions since these values are derived directly from the major-axis bending stresses. Figure 6 also provides flange lateral bending stresses from linear elastic analysis. It is clear from this figure that there are some nonlinearity in the results. However this nonlinearity does not show in the vertical displacement and major-axis bending stress predictions. Figure 7 provides the flange displacements along the length of the girder 1. It can be seen from this figure that the nonlinearity is result from the overall movement of the bridge. Although the total layover is same for linear and nonlinear analyses, the top and bottom girders move differently in both analyses. This results with an increase in the flange lateral bending stresses.

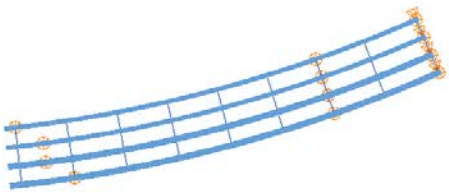

Stage 8

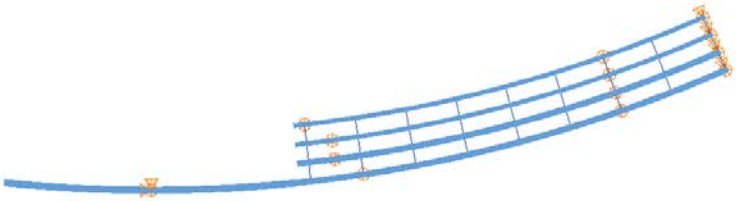

Stage 9

Stage 17

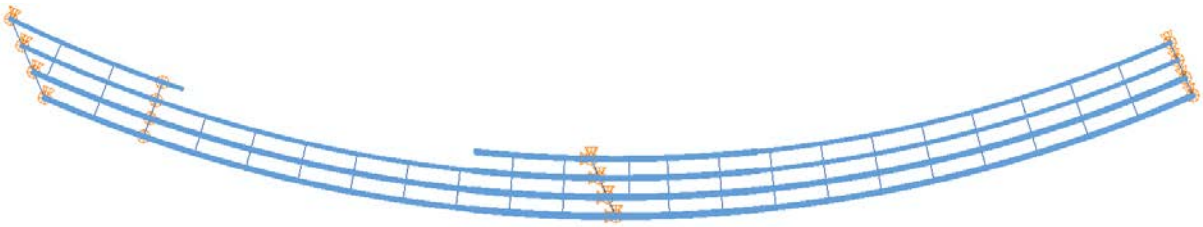

Stage 20

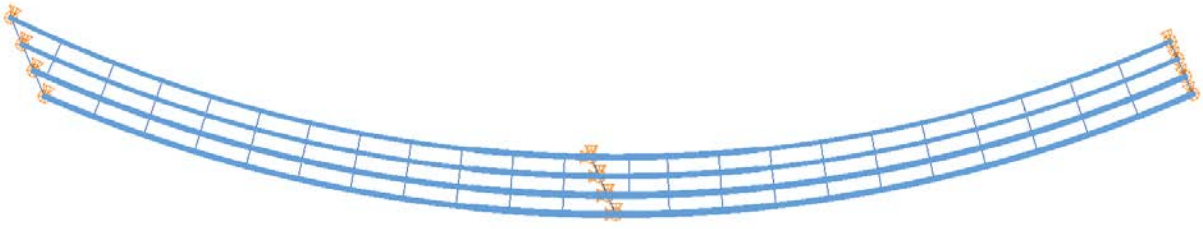

Stage 22 & 23

Fig. 1. NICCS13, Considered different analysis stages.

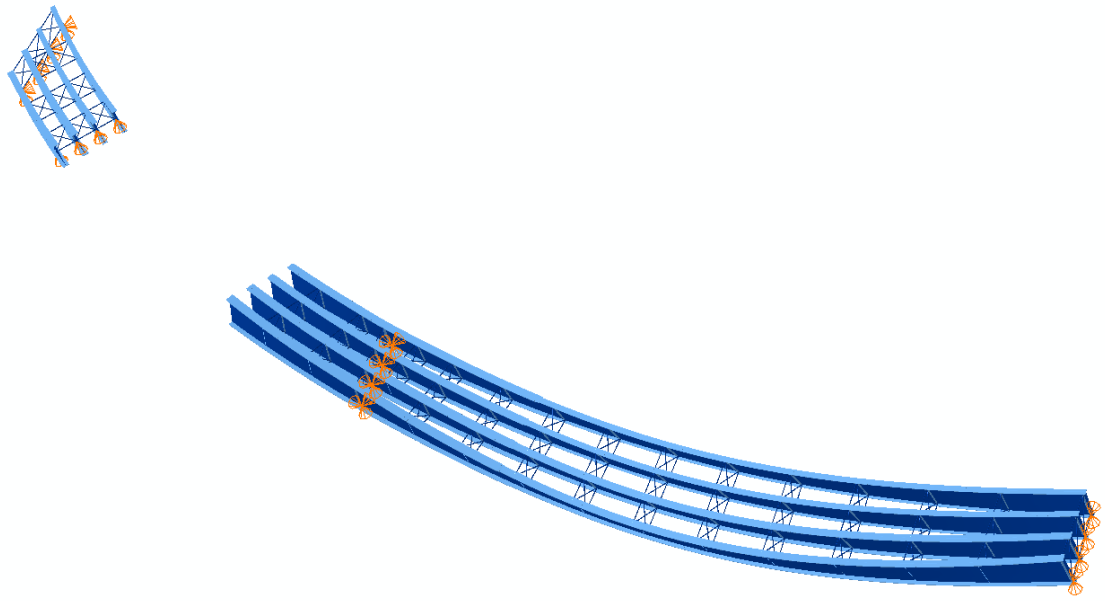

Fig. 2. NICCS13, Stage 17 deflected shape displacements are magnified by 10x.

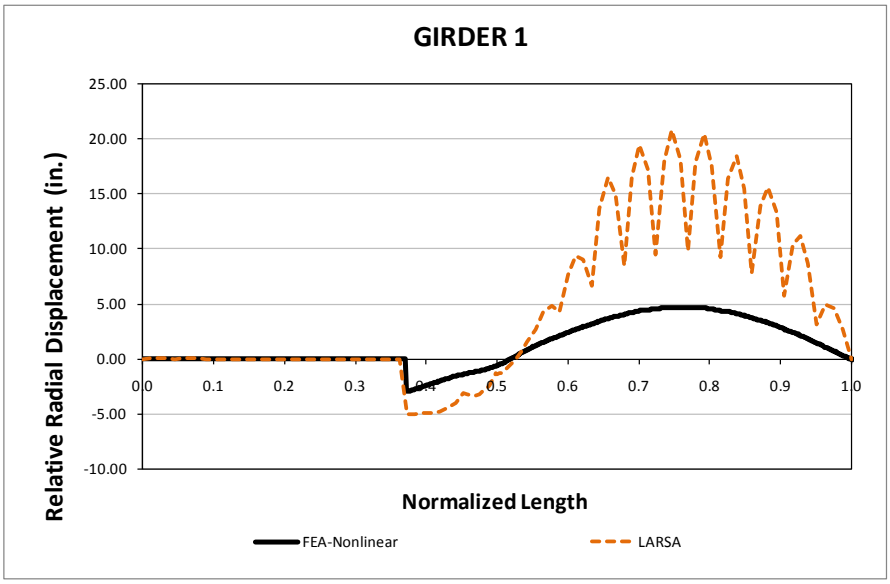

Fig. 3. NICCS13, Stage 17 Radial displacements NLF detailing.

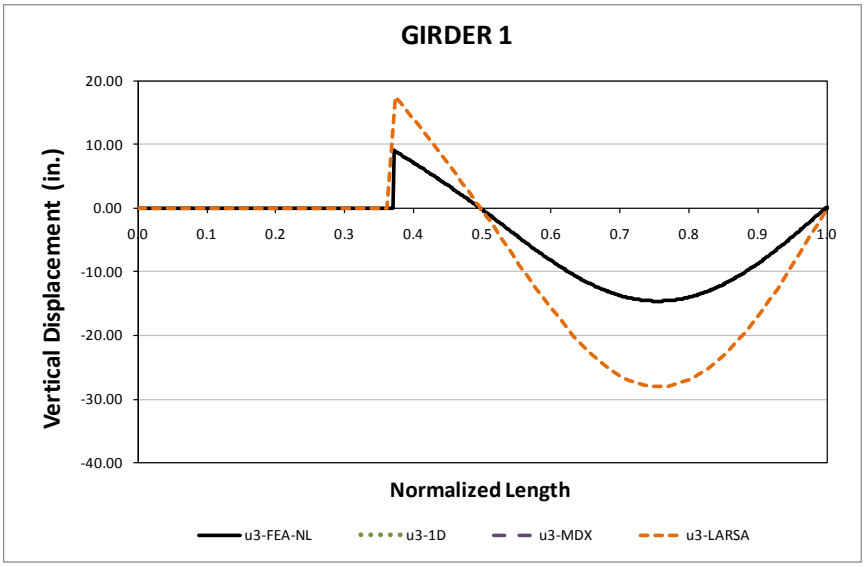

Fig. 4. NICCS13, Stage 17 vertical displacements NLF detailing.

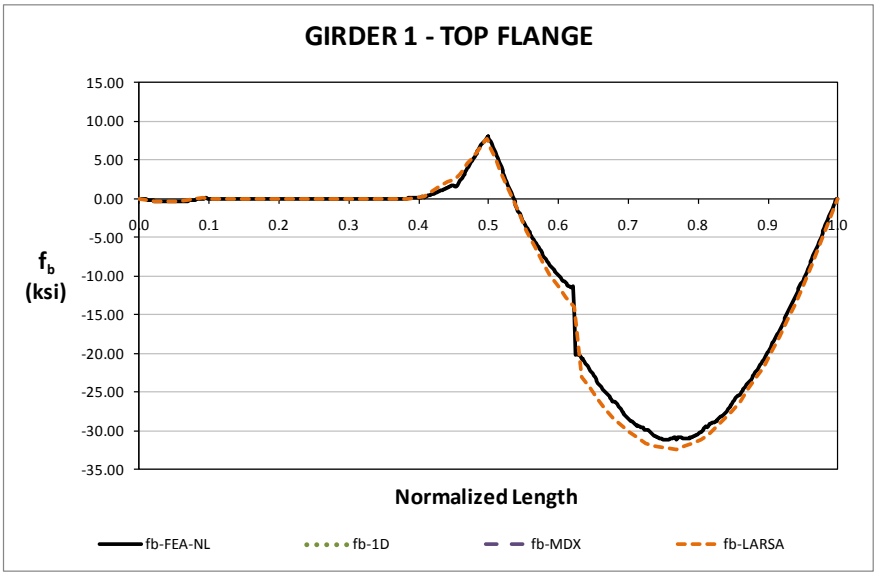

Fig. 5. NICCS13, Stage 17 major-axis bending stresses for NLF detailing.

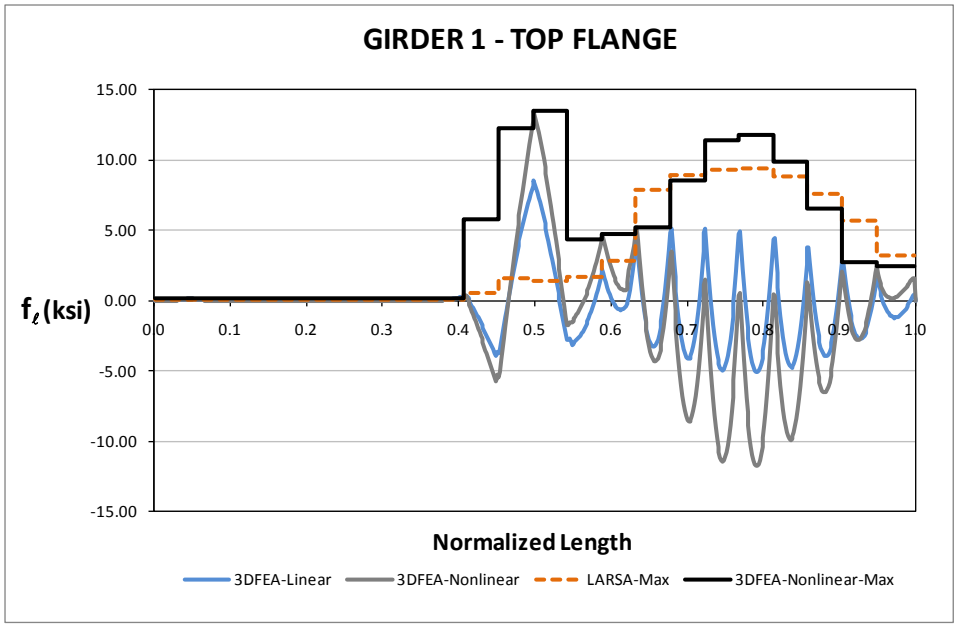

Fig. 6. NICCS13, Stage 17 flange lateral bending stresses for NLF detailing.

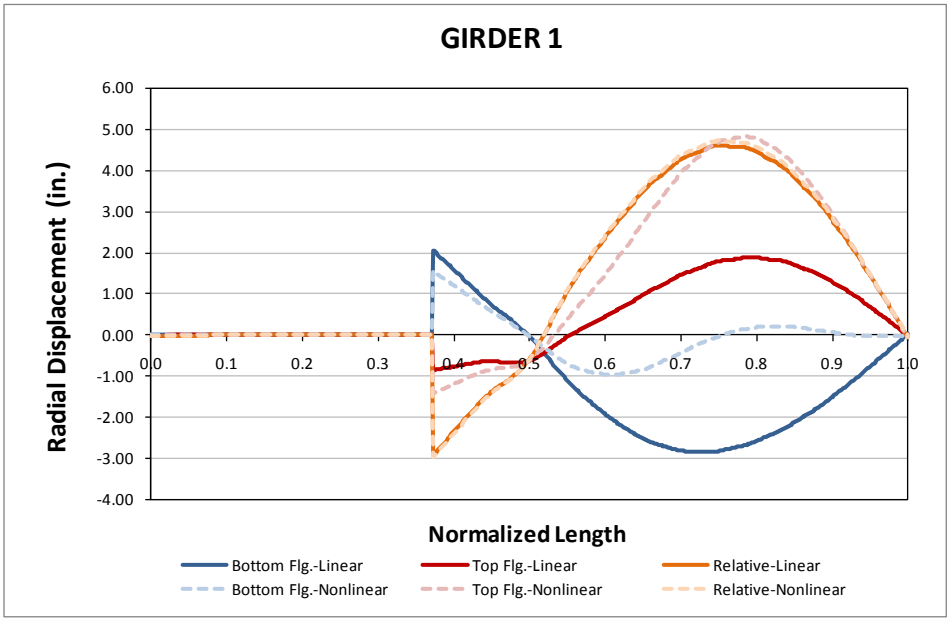

Fig. 7. NICCS13, Stage 17 Radial displacements NLF detailing.

I7.8 NICCS14 (New, I-girder, Continuous-span, Curved, Skewed supports)

Category Data:

L_1 = 250 ft, L_2 = 250 ft / $R_{1,2}$ = 597 ft/ w = 30 ft /θ_1 = 24^o, θ_2 = 0^o, θ_3 = 0^o, 4 girders

Cross-Frame Detailing Method: NLF

Erection Stages Analyzed: 6 (Analyses are performed assuming NLF)

Deck Placement Sequence: 1 Stage

Bridge Perspective & Plan Views:

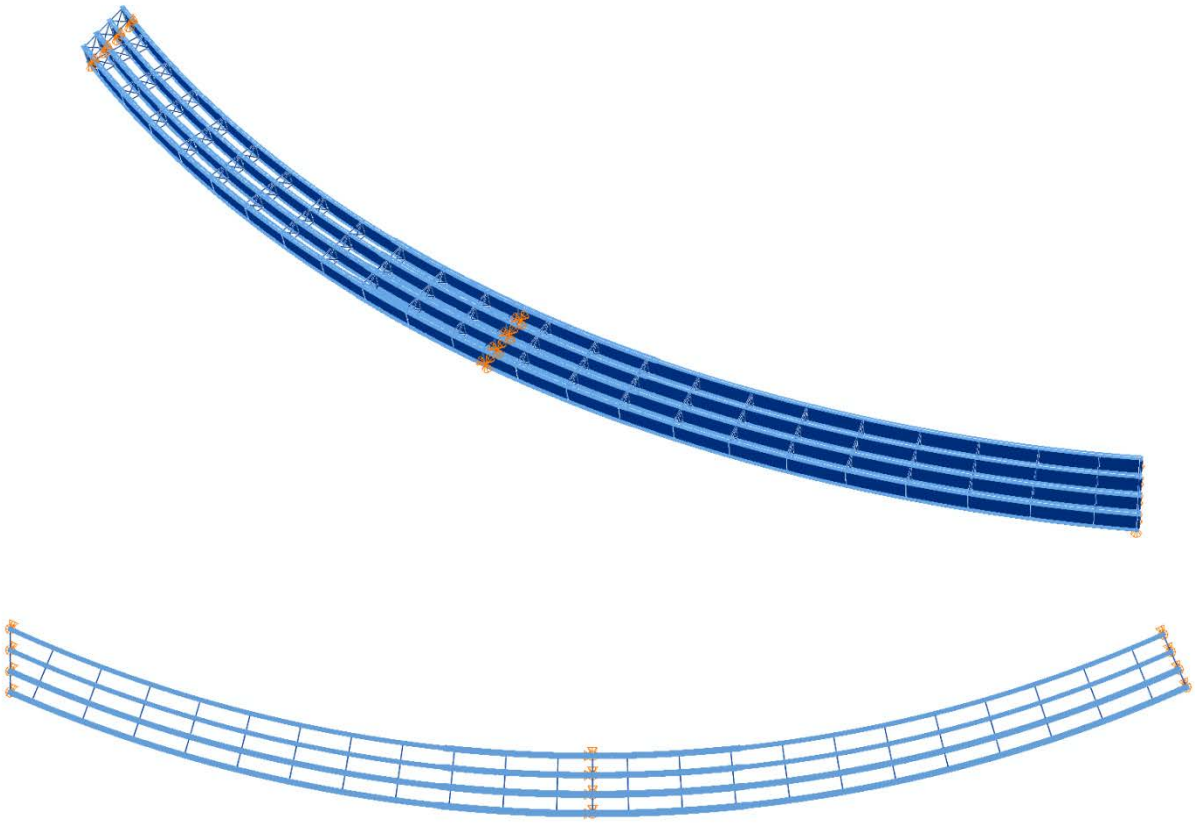

Abbreviated Analysis Results

Figure 1 shows the different analysis stages which are considered to evaluate the different analysis methods. The results from Stage 14 are provided in detail. Figure 2 shows the layover of Girder 1 for Stage 14 under total dead load. Figure 3 provides the vertical displacements of Girder 1 for Stage 14 under total dead load. It is obvious from Figs. 2 that grid solutions provide over estimated predictions between the brace points and accurate predictions at the brace points. It is also clear from Fig.3 that vertical deflections cannot predicted accurately by dense grid analysis solutions. The reasons for not obtaining accurate predictions for approximate analysis methods are explained in the previous summaries in detail. Figure 4 provides the girder 1 major-axis bending stresses for Stage 14. The stress predictions are predicted accurately by all analysis solutions. Figure 5 shows girder 1 flange lateral bending stresses for Stage 14. It should be noted from Fig. 5 that there are some nonlinearity in the results close to the mid span. However this nonlinearity does not show in the vertical displacement and major-axis bending stress predictions. The nonlinearity is result from the overall movement of the bridge which is explained in other curved bridges.

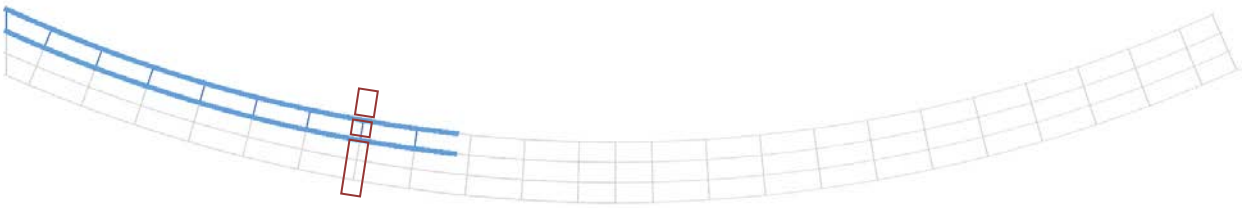

Stage 2

Stage 6

Stage 8

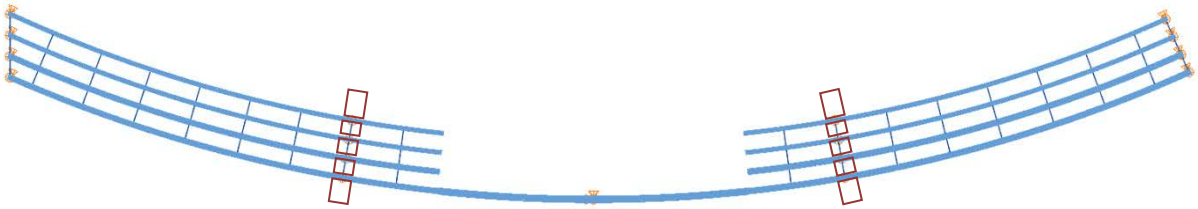

Stage 9

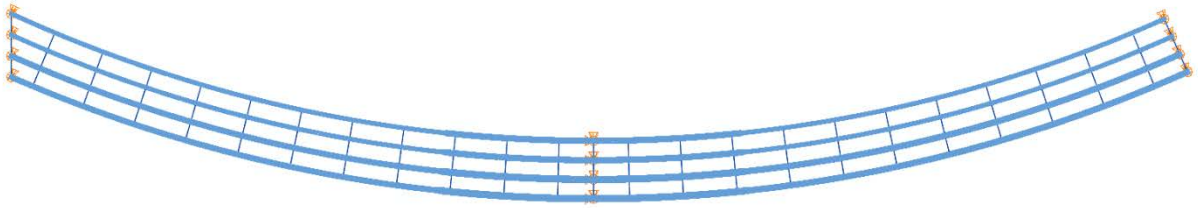

Stage 13 & 14

Fig. 1. NICCS14, Considered different analysis stages.

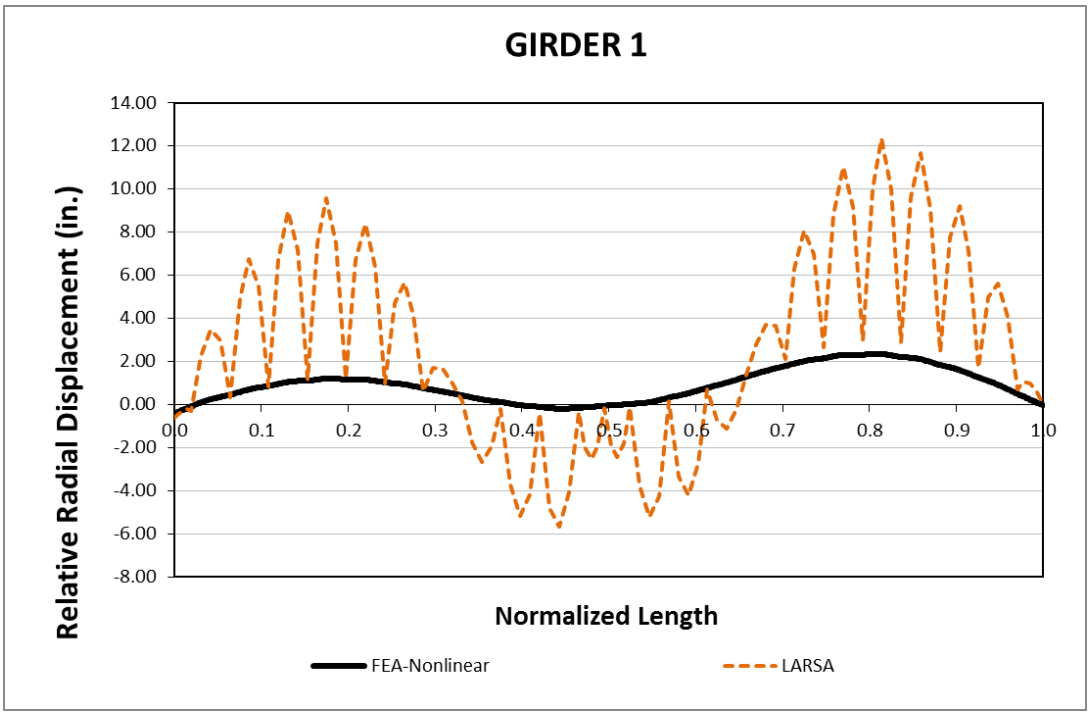

Fig. 2. NICCS14, Radial displacements NLF detailing under total dead load.

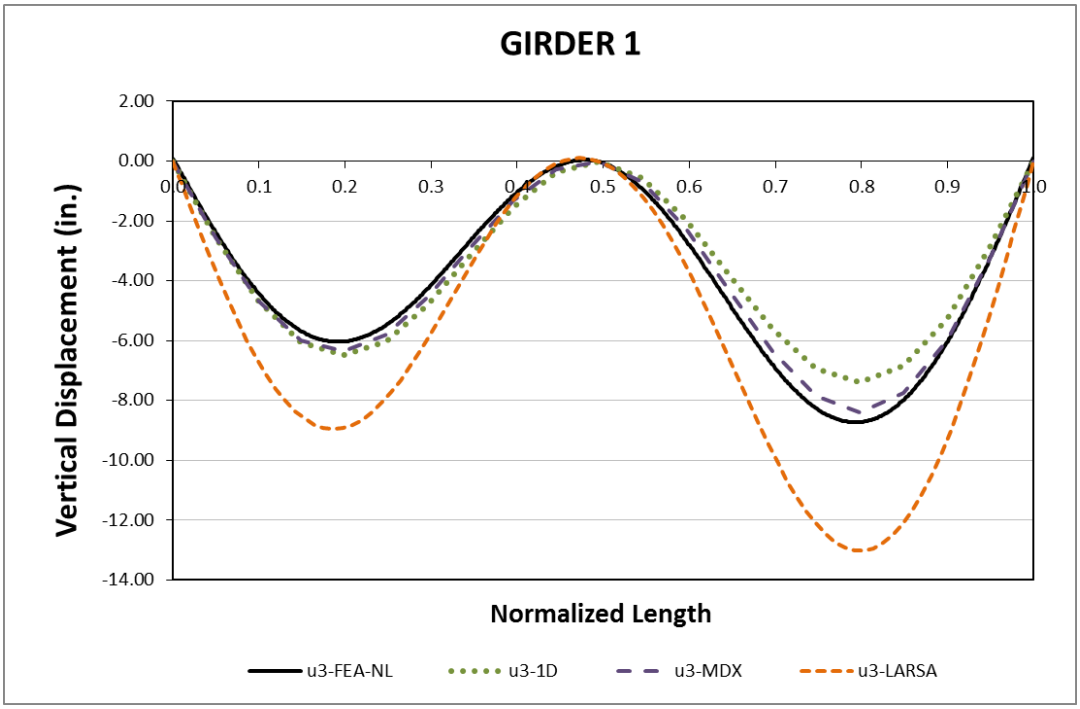

Fig. 3. NICCS14, vertical displacements NLF detailing under total dead load.

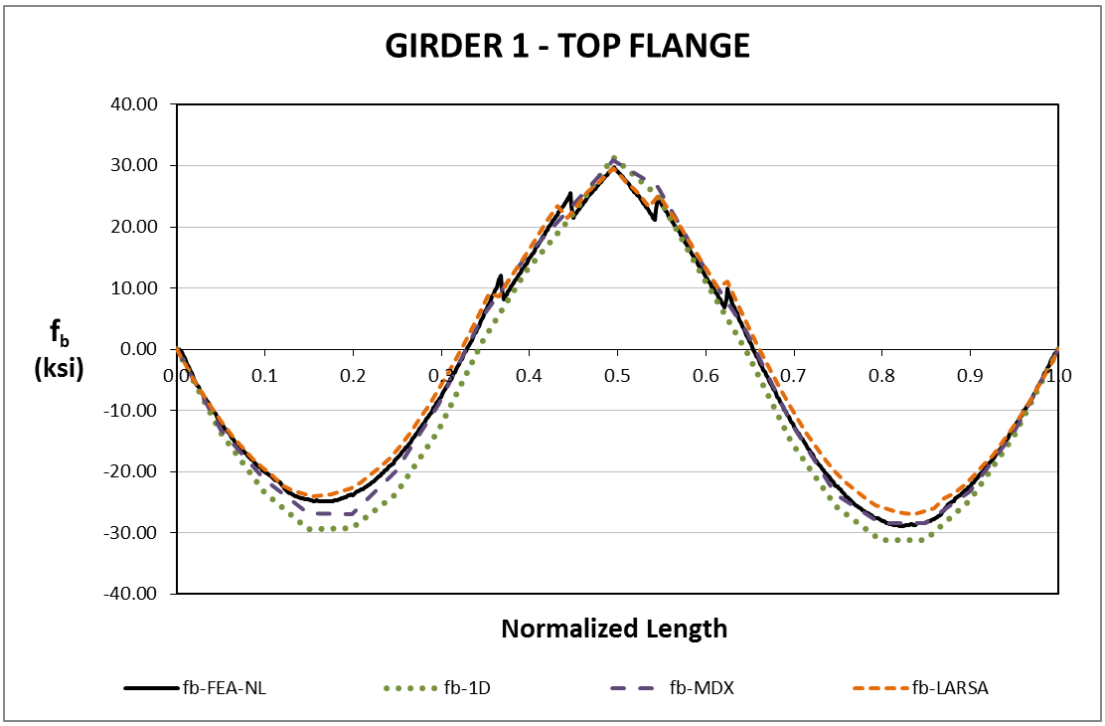

Fig. 4. NICCS14, major-axis bending stresses for NLF detailing under total dead load.

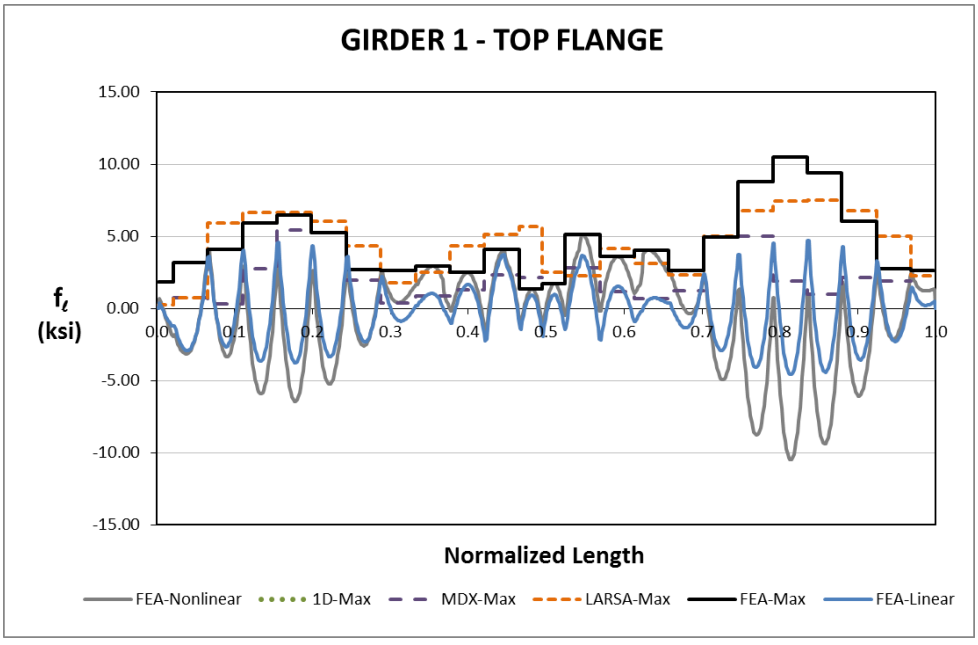

Fig. 6. NICCS14, flange lateral bending stresses for NLF detailing under total dead load.

I7.9 NICCS24 (New, I-girder, Continuous-span, Straight, Skewed supports)

Category Data:

L_1 = 350 ft, L_2 = 350 ft / R =909 ft / w = 80 ft /θ_1 = 0°, θ_2 = 22.1°, θ_3 = 0°, 9 girders

Cross-Frame Detailing Method: NLF

Erection Stages Analyzed: 7 (Analyses are performed assuming NLF)

Deck Placement Sequence: 1 Stage

Bridge Perspective & Plan Views:

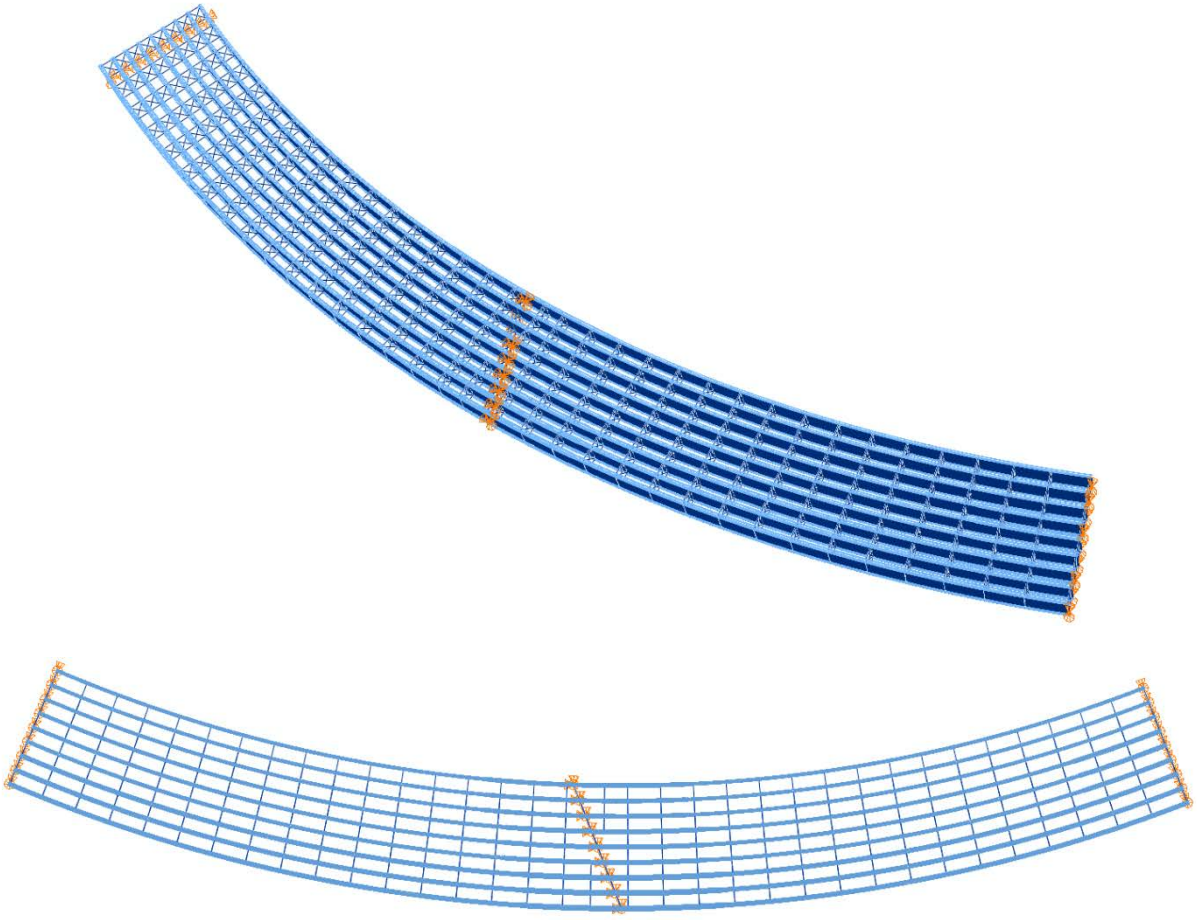

Abbreviated Analysis Results

Figure 1 shows different analysis stages which are considered to evaluate the different analysis methods. Since this bridge has two 350ft span lengths, temporary supports are used during the erection of the bridge. Figures 2, 3 and 4 provide the vertical displacements of the bottom girder (Girder 1) for Stages 46, 47 and 48 respectively. These stages are selected to show the importance of using temporary supports during the erection of the long span bridges. It is obvious from Figs. 2, 3 and 4 that the displacements tend to reduce significantly during erection due to the use of the temporary supports. Figures 4, 5 and 6 provide the layover of the Girder 1 for stages 46, 47, 48. It should be noticed that the layover of the girders are limited by the use of temporary supports. The use of the temporary supports will result with an easier erection for the long span bridges. Figures 7, 8 and 9 show the major-axis bending stresses for Stages 46, 47 and 48. It is observed from these figures that the major axis bending stresses are lower for the cases where temporary towers are used. Similar observations are made on this bridge compared to the previous bridges that are studied in terms of the analysis accuracy. Therefore, those results are not discussed here.

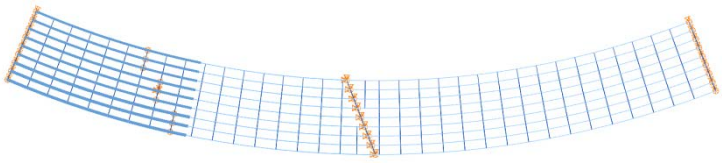

Stage 9

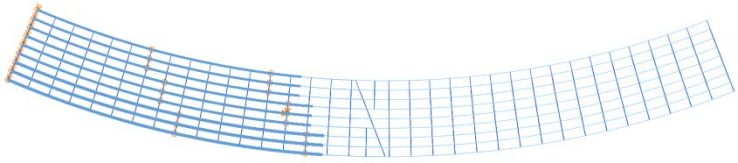

Stage 18

Stage 28

Stage 46

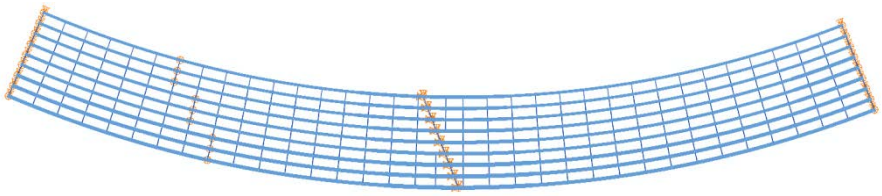

Stage 47

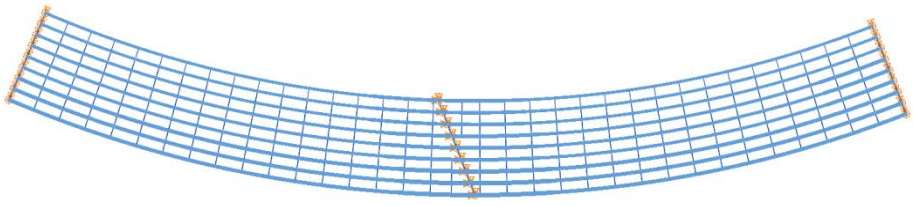

Stage 48 & 49

Fig. 1. NICCS24, Considered different analysis stages.

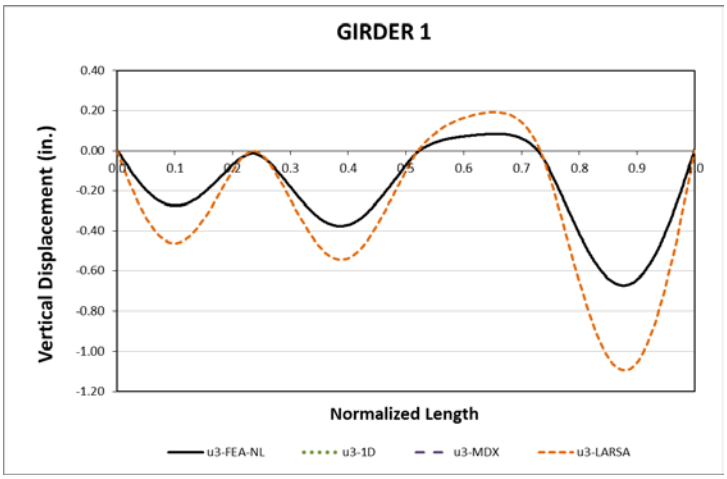

Fig. 2. NICCS24, Stage 46, Vertical displacements.

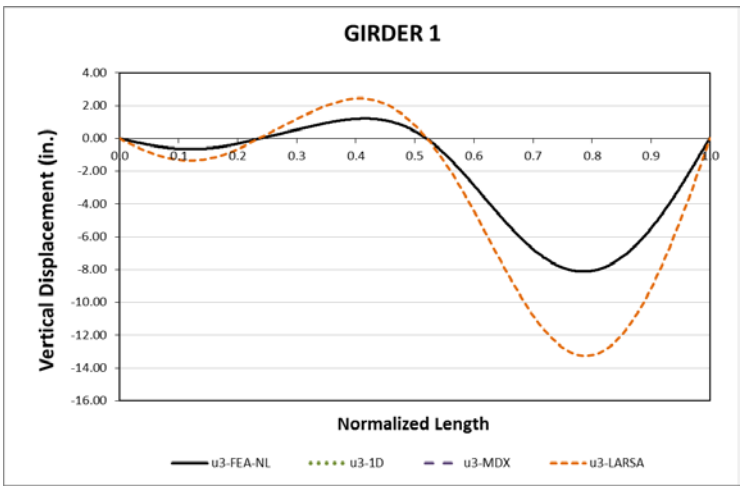

Fig. 2. NICCS24, Stage 47, Vertical displacements.

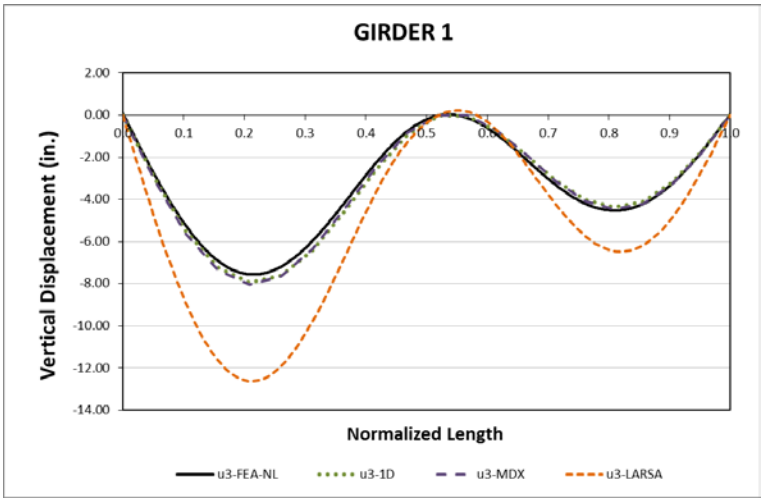

Fig. 2. NICCS24, Stage 48, Vertical displacements under steel dead load for NLF detailing.

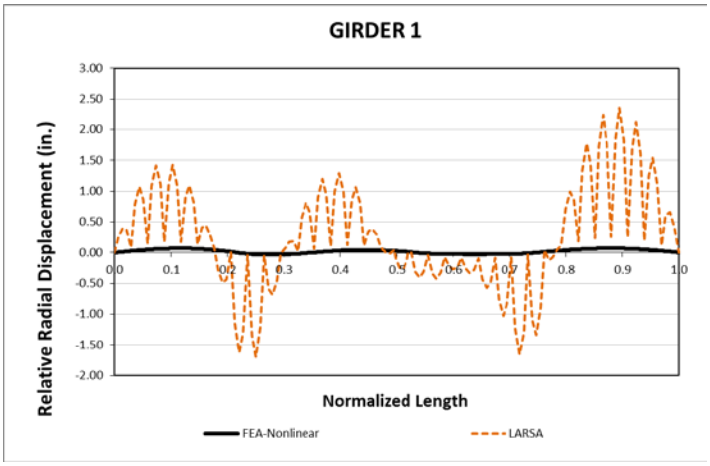

Fig. 4. NICCS24, Stage 46, Relative lateral displacements for NLF detailing.

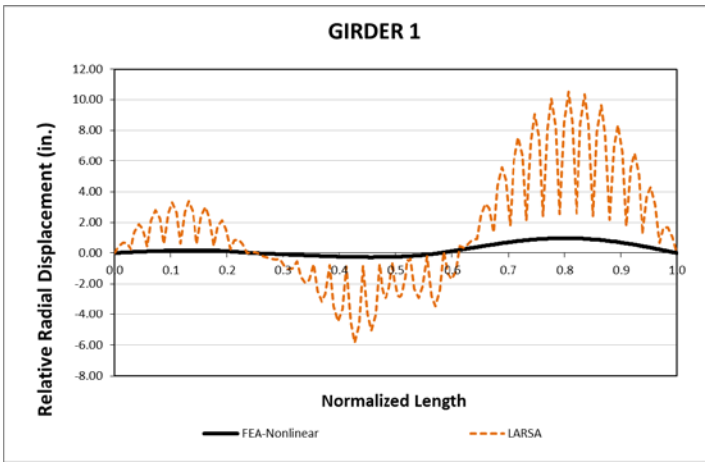

Fig. 5. NICCS24, Stage 47, Relative lateral displacements for NLF detailing.

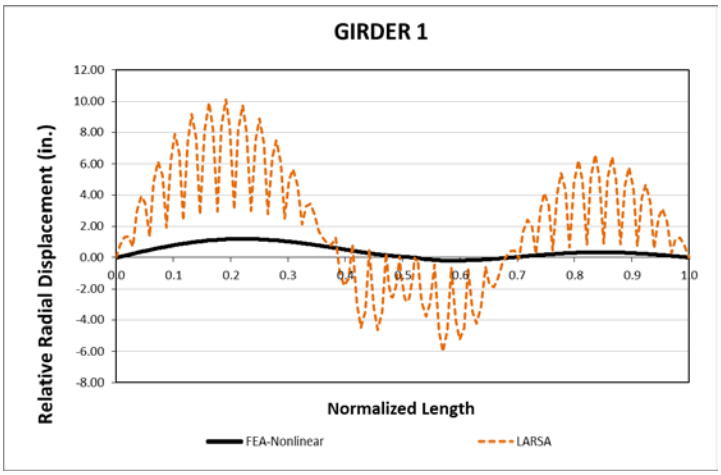

Fig. 5. NICCS24, Stage 48, Relative lateral displacements under steel dead load for NLF detailing.

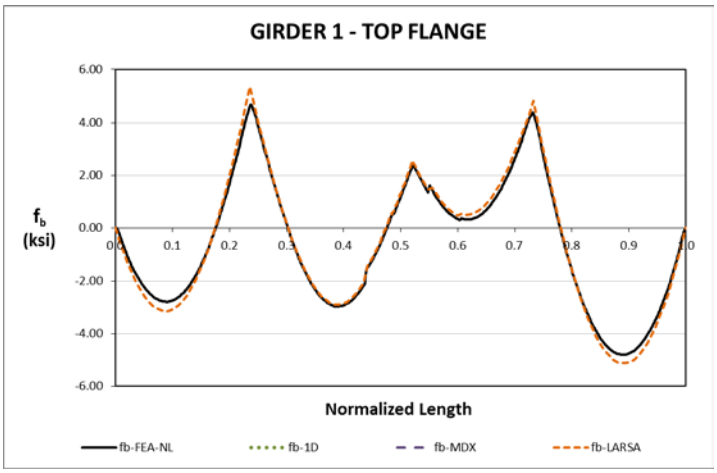

Fig. 7. NICCS24, Stage 46, Major-axis bending stresses for NLF detailing.

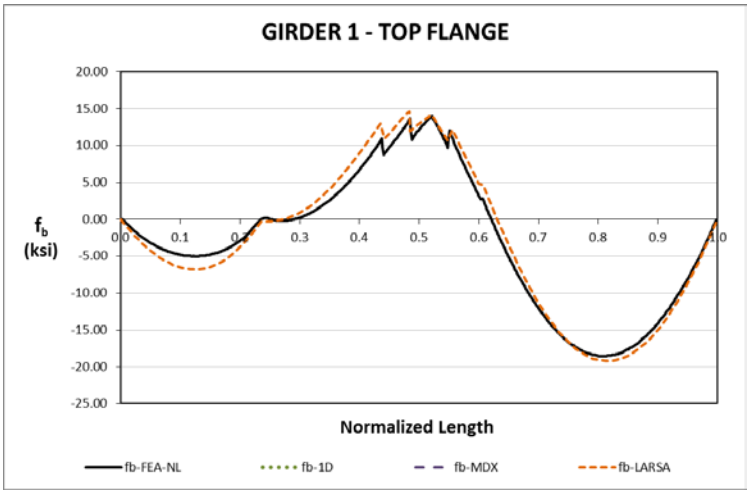

Fig. 7. NICCS24, Stage 47, Major-axis bending stresses for NLF detailing.

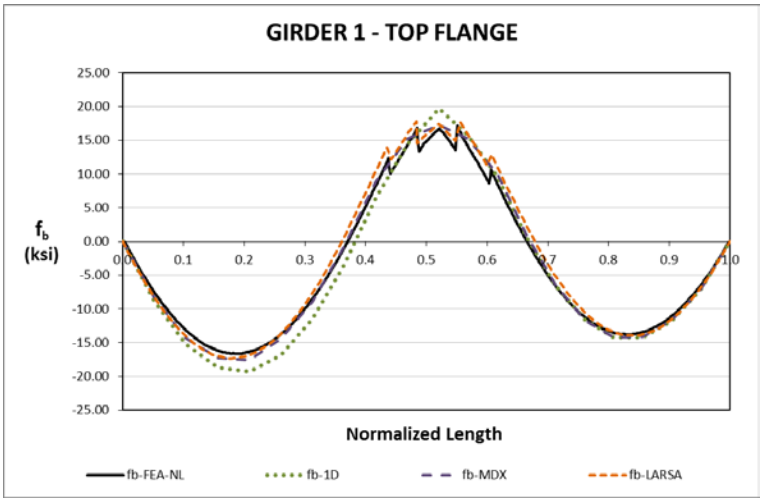

Fig. 8. NICCS24, Stage 48, Major-axis bending stresses under total steel load for NLF detailing.

I7.10 XICCS7 (eXample, I-girder, Continuous-span, Curved, Skewed supports)

Bridge Description:

Continuous curved and skewed I-girder bridge

Category Data:

L_1 = 160 ft, L_2 = 210 ft, L_3 = 160 ft / R = 700 ft / w = 40.5 ft / θ_1 = 0, θ_2 = -60, θ_3 = -60, θ_4 = 0^o, 4 girders

References:

[1] National Highway Institute (NHI), 2010, Participant Workbook, FHWA-NHI-10-086, "Load and Resistance Factored Design and Analysis of Skewed and Curved Steel Bridges."

[2] National Highway Institute (NHI), 2010, Reference Manual, FHWA-NHI-10-087, "Load and Resistance Factored Design and Analysis of Skewed and Curved Steel Bridges."

Cross-Frame Detailing Method: NLF

Steel Erection Stages Analyzed: Seven

Deck Placement Sequence: Five stages with the screed oriented in the radial direction

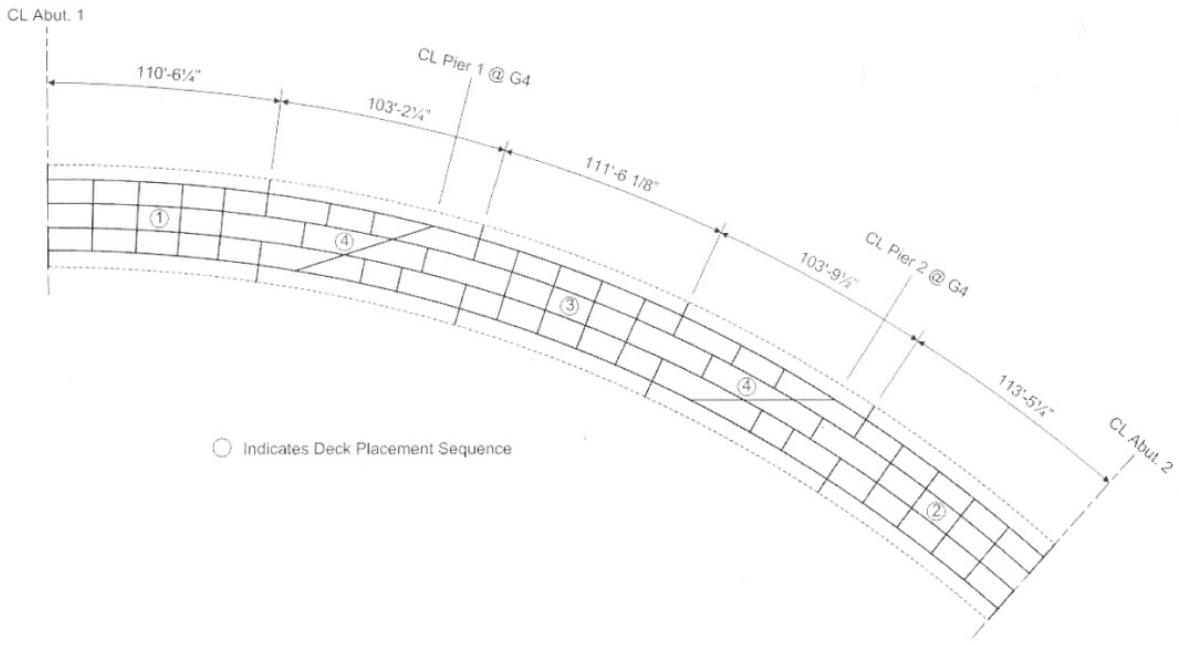

Bridge Perspective & Plan Views:

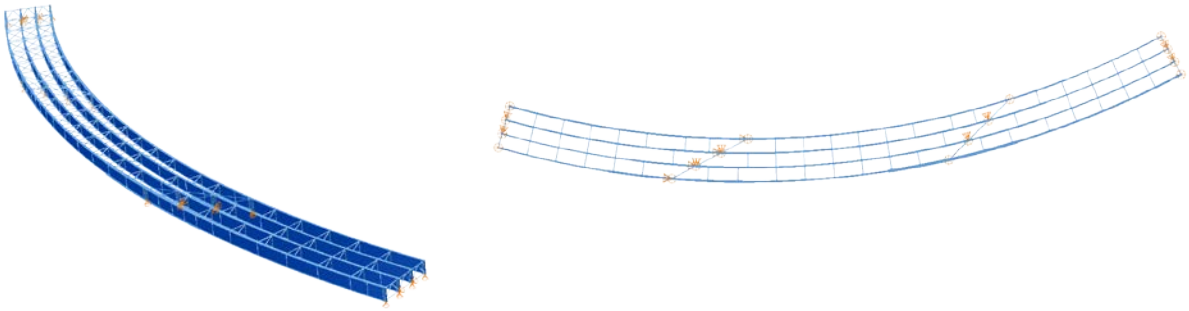

Abbreviated Analysis Results:

In this bridge, the effects of the support skew and horizontal curvature in the bridge behavior are studied. Two stages are selected for this purpose. The first is one of the initial steel erection stages, where two girders are in place, as shown in Figure 1. The second is at the total dead load, when the last segment of the deck is placed.

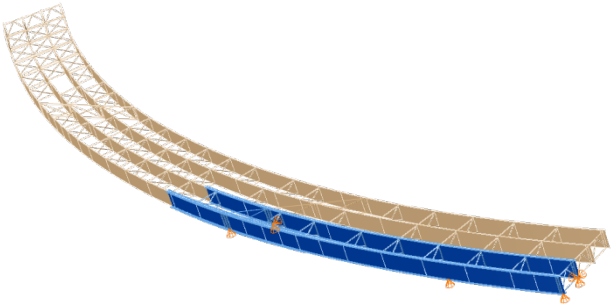

Fig. 1. XICCS7, Steel Erection – Stage 2

The responses predicted by the 2D grid analysis model and the ABAQUS 3D benchmark are compared for the exterior girder, G1, Stage 2. As shown in Figure 2.a, the magnitudes of the vertical displacements are over predicted by the approximate model. The 2D grid model is able to capture the general behavior of the girder; however, the vertical displacements are significantly larger than the predicted by the 3D model. Interestingly, the relative radial displacements are accurately predicted at the points of bracing, but overestimated within the unbraced lengths, as depicted in Figure 2.b. This trend is consistent with the observed in other curved bridges. The layover of the girder group dominates over the rotation of each individual girder, and that behavior is captured by the 2D grid model.

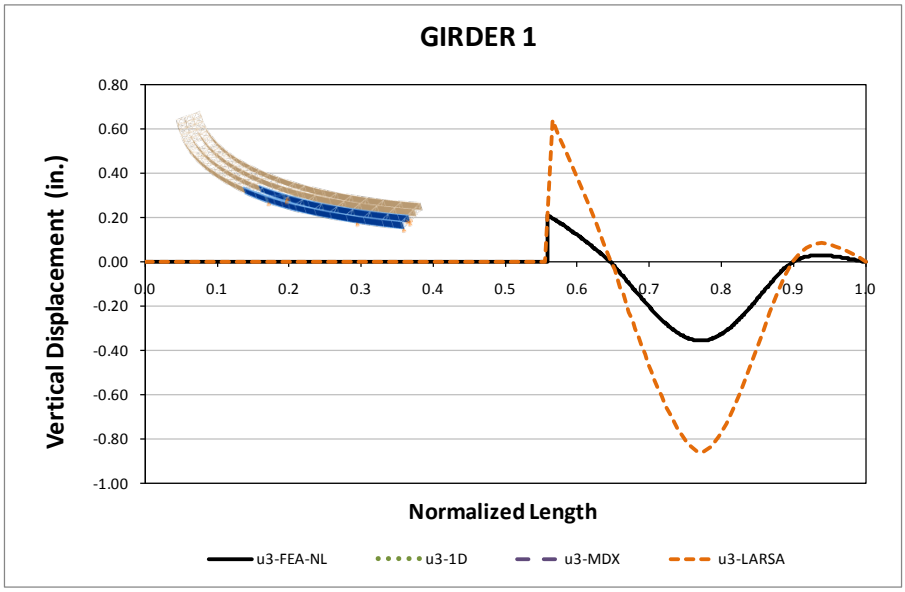

a) Vertical Displacements

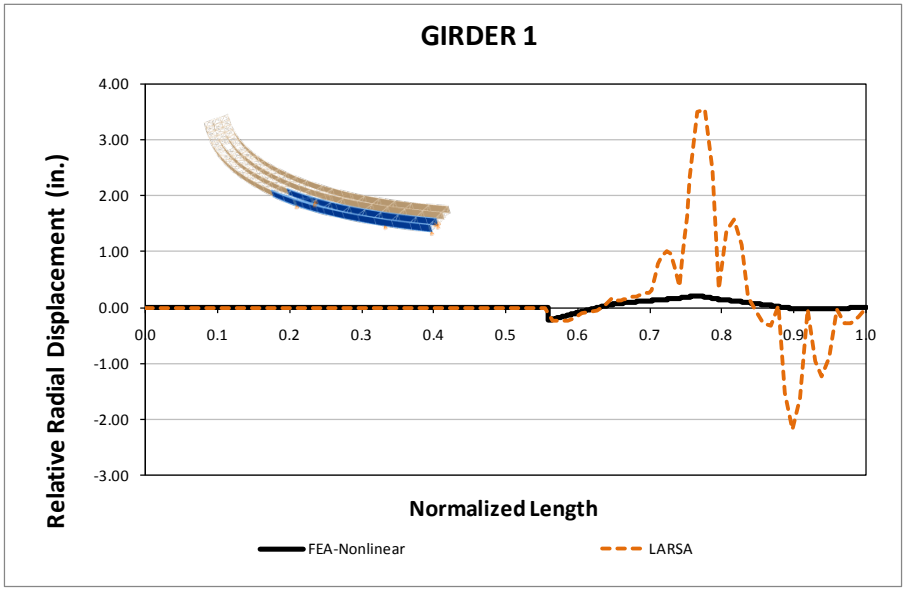

b) Relative Radial Displacements

Fig. 2. XICCS7, Comparison of Displacement Responses – Stage 2

In the case of the stress responses, the 2D model captures the 3D model prediction accurately. Figure 3 shows the major-axis bending stress response in the top flange of the exterior girder. It is observed that the limitations of the approximate analysis have a minor effect in the prediction of this response. The same trend is observed for the rest of steel erection stages. The 2D grid model predictions for all the girders in both flanges match the FE model predictions as the construction of the bridge continues from the erection of the first girder segment up to the completion of the steel structure erection.

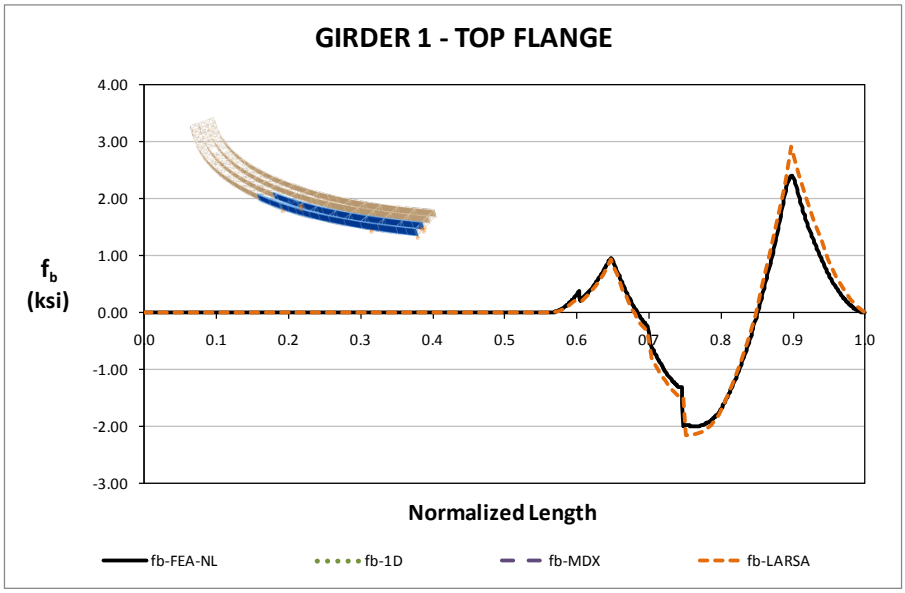

Fig. 3. XICCS7, Major-Axis Bending Stress Comparison for Girder G1 – Stage 2

The flange lateral bending stresses are calculated according to the V-Load formula at the bracing points. As shown in Figure 4, the prediction of this response based on this formulation is more accurate within the positive moment region, between 0.70 and 0.85 the girder length, than it is in the rest of the girder. Even though for this case these stresses are very small and do not deserve attention from the design perspective, it is observed that the prediction of the equivalent lateral load obtained from the major-axis bending response could be used to determine an upper bound limit in the positive moment region.

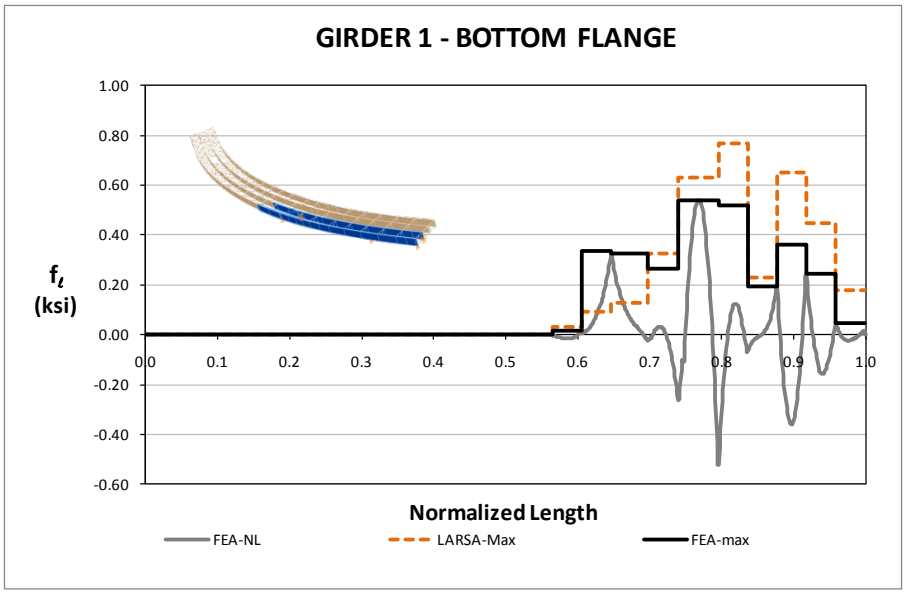

Fig. 4. XICCS7, flange lateral bending stress comparison for Girder G1 – Stage 2

The results for the total dead load condition are discussed next. For the vertical displacements, shown in Figure 5.a, the 1D model prediction accurately represents the benchmark response. In the case of the 2D grid models, the displacements obtained from the two programs are different due to the fact that the mesh density used to model the bridge in MDX is coarser that the used in Larsa . The overestimation of the Larsa model, also observed in the different steel erection stages, is associated to the limitations of the computational model to represent the actual behavior of an open-section thin-walled beam element. The grid models do not consider the stiffness contributions that result from flange warping. This limitation also affects the prediction of the girder layover, as shown in Figure 5.b. However, the rotation of the girder group controls over the individual rotation of the girders at the cross-frame locations, behavior that is captured by the Larsa model. The above observations are consistent for all the girders of the bridge throughout all the construction simulation.

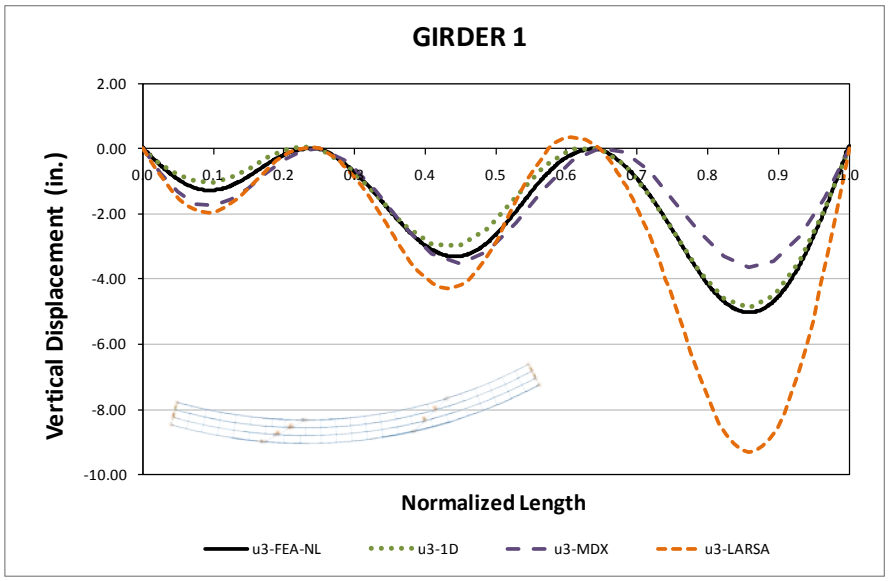

a) Vertical Displacements

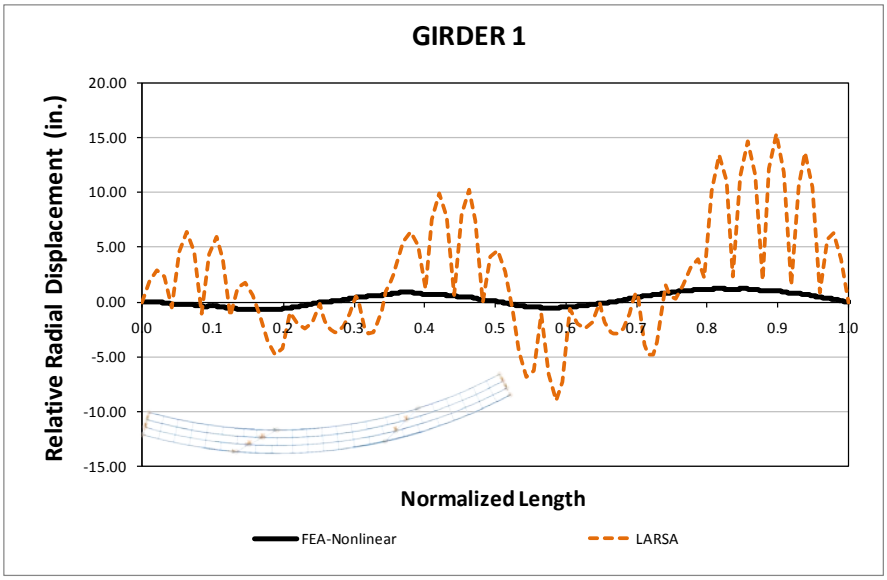

b) Relative Radial Displacements

Fig. 5. XICCS7, Comparison of Displacement Responses for the TDL Condition

As for the different construction stages, the major-axis bending stress predictions are almost the same for all the methods. As observed for girder G1 in Figure 6, both the 1D and 2D results capture the expected response, as predicted by the 3D FE model. It is apparent from a study of these predictions that the major-axis bending response is not affected as much as the displacement responses due to the limitations of the approximate methods. In the case of the flange lateral bending stresses shown in Figure 7, the FE model prediction shows that the response in the positive moment regions has the same behavior assumed in the derivation of the V-load formula. For these regions, the flange lateral bending stress response is maximum at about the same points where the major-axis bending achieves the largest values. In the negative moment region, however, the response does not seem to follow the same trend. Therefore, the predictions obtained from the 2D analysis results are not close to the FE model predictions.

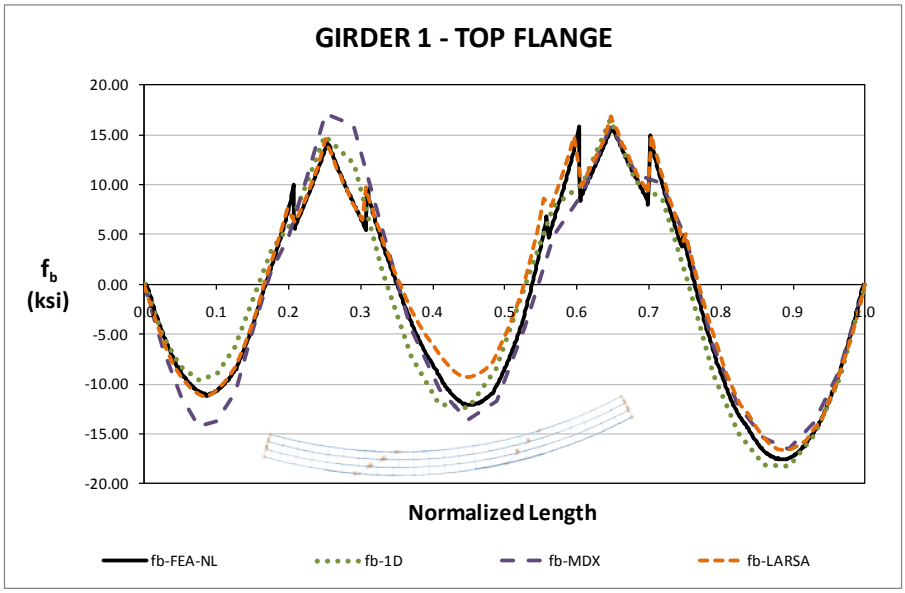

Fig. 6. XICCS7, Major-Axis Bending Stress Comparison for Girder G1 at the TDL Condition

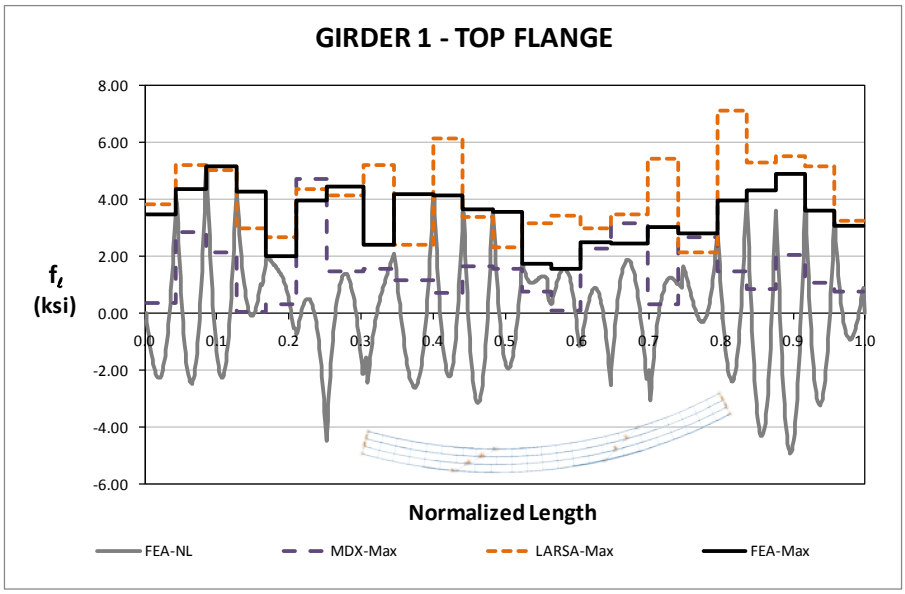

Fig. 7. XICCS7, Flange Lateral Bending Stress Comparison for Girder G1 at the TDL Condition

The results for vertical displacements from the study conducted for the NHI 2010 Course "Load and Resistance Factored Design and Analysis of Skewed and Curved Steel Bridges" and reported in references [1] and [2] are shown in Figure 8. This plot corresponds to the vertical deflections at the steel dead load condition (SDL). In Figure 8, the solid black curve corresponds to the benchmark solution. The dashed blue response represents the deflections obtained from a 1D analysis. The purple responses are obtained from a traditional 2D grid analysis, and the brown responses correspond to the obtained from a 2D plate-eccentric beam analysis (PEB). In the traditional model a medium resolution mesh was used to analyze the structure, and in the PEB model a low resolution mesh was used. Given that at this stage the

slab is not present, the predictions of both grid models should be the same. However, the mesh density affects the response, as shown in the figure. Apparently, the coarser mesh utilized in the PEB model results in better predictions than the obtained using the more refined resolution of the traditional grid model. The possible explanation for this misleading effect is discussed next.

In Figure 2.a, it is shown that the limitations of the computational 2D model to represent the actual torsional stiffness of an I-girder result in an over prediction of the vertical displacements. On the other hand, the use of a coarse mesh gives an over stiff representation of the structure that results in an under prediction of the expected displacements. Thus, when this curved bridge is analyzed using the PEB model, the effects of these two modeling considerations are overlapped, and the result is an apparent accurate estimation of the vertical displacements.

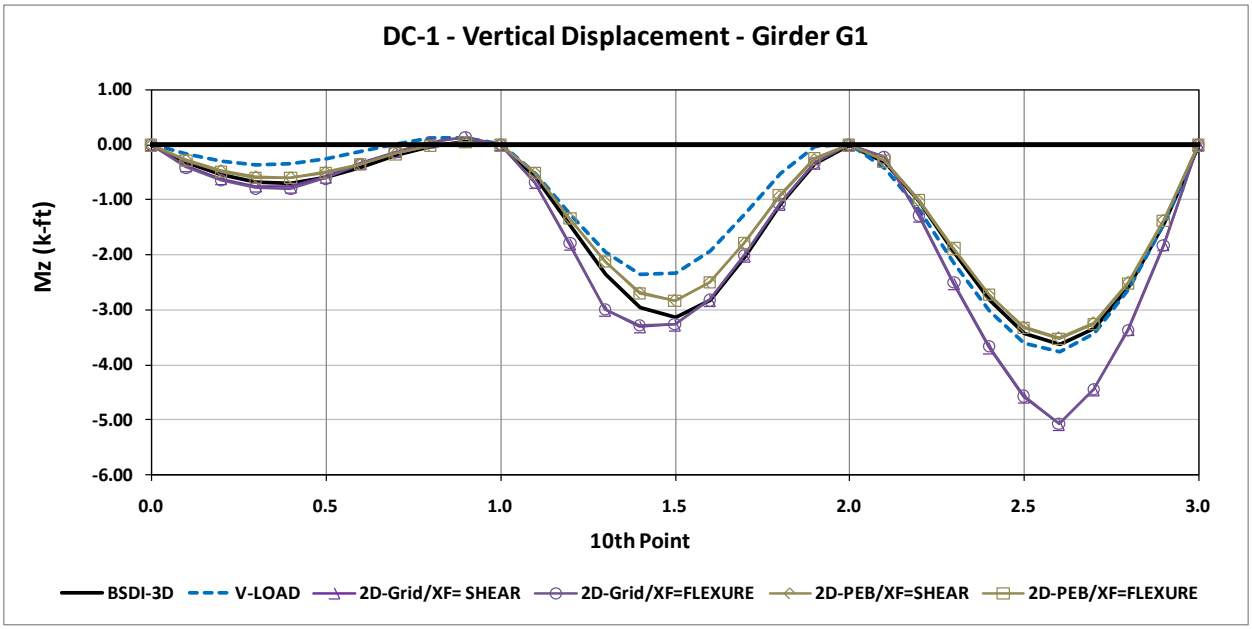

Fig. 8. XICCS7, Comparison of Displacement Responses for the SDL Condition (From References [1] and [2])

Conclusions:

The influence of curvature and the skew in the structural behavior are studied in this bridge. As observed in other curved bridges, the displacement responses are the most sensitive to the 2D grid analysis approximations. The magnitudes of the vertical displacements are over predicted due to limitations of the computational model to represent the actual torsional stiffness of the I-girders. A similar behavior is observed for the radial displacements. The stiffness contribution associated to Saint Venant's or pure torsion is considerably smaller than the contribution due to flange warping. Thus, given that the computer model is capable of modeling only the first source, the radial deflections are much larger than the expected within the unbraced lengths. However, this limitation does not contribute significantly to the overall behavior of the bridge. This is observed by looking at the accurate representation of the bridge

layover at the braced points. An accurate representation on the lateral displacements could be obtained by considering only the response at these points.

The study of the stress responses showed that for major-axis bending the response is less sensitive to the skew and curvature effects. In general, all the methods show almost the same responses. For flange lateral bending, the stress responses differ more than for the major-axis case. Apparently, the representation of these stresses as derived from the major-axis bending response works moderately well for the positive moment regions. In the negative moment regions, however, this method does not provide reliable results.

By comparing the 1D and 2D analyses, it is concluded that for this bridge, regardless its simplicity, the 1D analyses produced more accurate results that the 2D grid models. The advantage in the use of the later method is that it delivers more information about the bridge structural behavior if the above recommendations are followed to improve the results.

8.1 XTCSN3 (Example, Tub-girder, Continuous-span, Straight, No skew)

Bridge Description:

NHI Design Example for a Straight Steel Tub Girder Bridge

Category Data:

L_1 = 206 ft, L_2 = 275, L_3 = 206 ft / w = 43 ft, 2 tub-girders

References:

NHI (2007). "Load and Resistance Factor Design (LRFD) for Highway Bridge Superstructures", Design Manual, NHI Course No. 130081, 130081A-130081D, Publication No. FHWA-NHI-07-035, National Highway Institute, Federal Highway Administration, 1982 pp.

Erection Stages Analyzed: 7 steel erection stages

Deck Placement Sequence: (Analyses are performed assuming no staged deck placement).

Bridge Perspective & Plan Views:

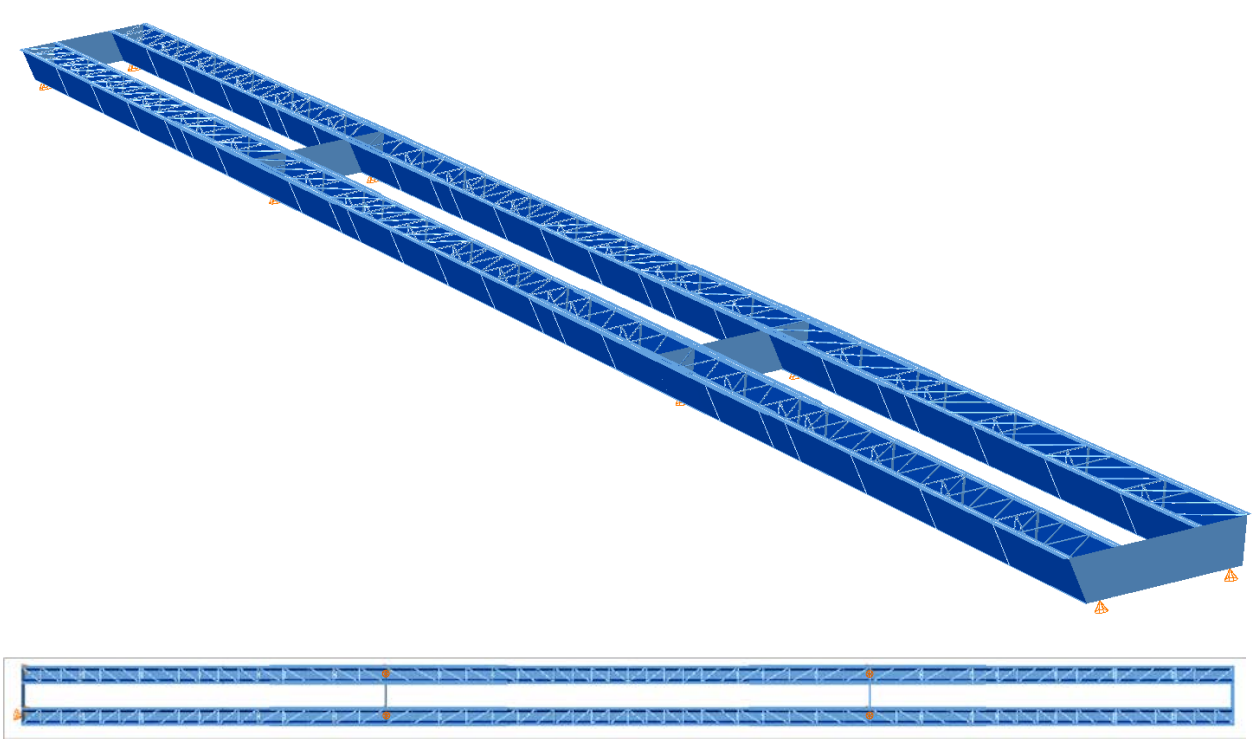

Displacement Results

Figures 1 and 2 illustrate the steel and total dead load displacements for the top flange of the exterior girder web. The results are plotted for the different methods of analysis. MDX shows a lower displacement but, as it will be seen, the stresses predictions are comparable to the other analysis. The source of error from MDX could be due to the reduced number of elements on the bridge length and in the modeling of the stiffness of the girder system.

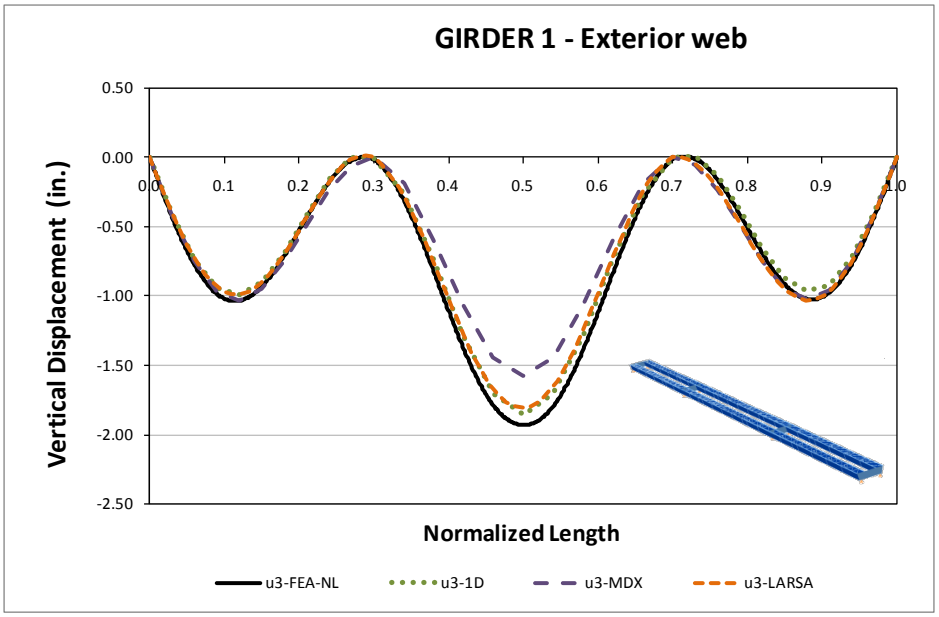

Fig. 1. Top flange vertical displacements for Girder 1 exterior web - Final Steel Dead Load

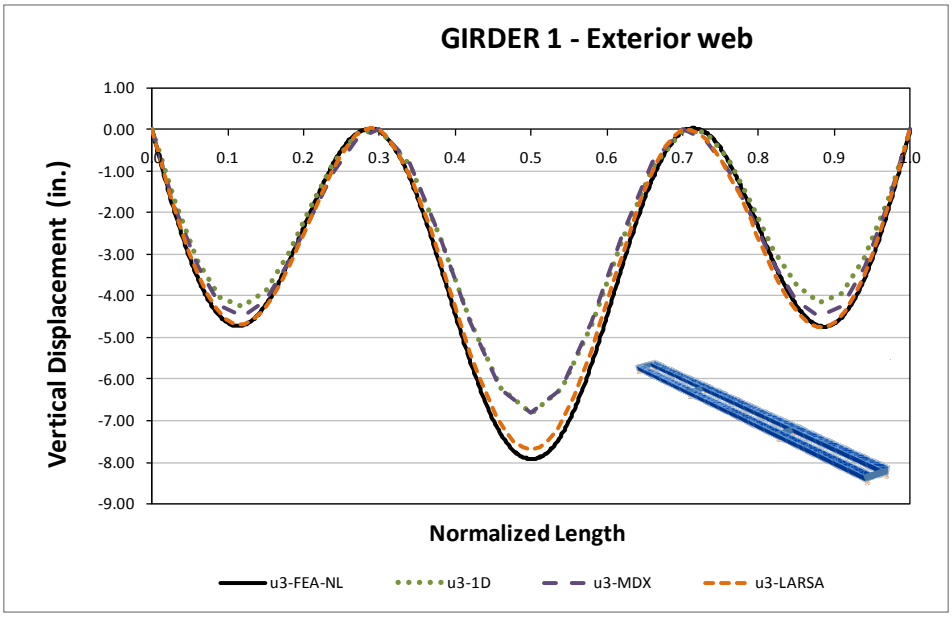

Fig. 2. Top flange vertical displacements for Girder 1 exterior web - Total Dead Load

Figure 3 illustrates the lateral displacements. The 2D grid methods predict a null lateral displacement as expected; in contrast, the 3DFEA predicts a maximum of 0.6in of lateral displacement. The lateral displacement reported in Girder 2 follow the same pattern but the sign of the displacements is reversed.

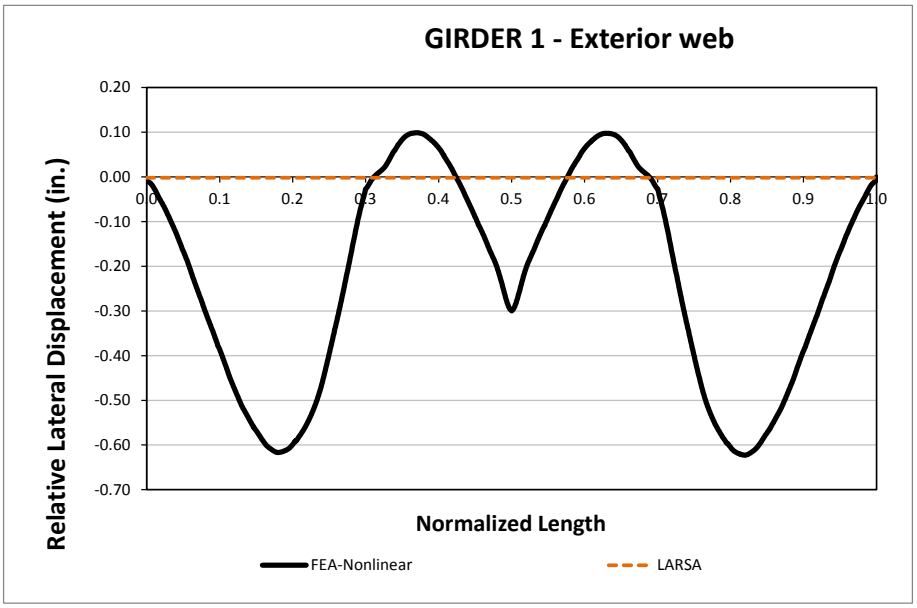

Fig. 3. Top flange relative lateral displacements for Girder 1 exterior web - Total Dead Load

Lateral displacements are not expected from the 1D or 2D analysis methods, however the interaction of the top flange lateral bracing system creates an internal moment in the system that can only be captured by the 3DFEA method. This effect will be discussed below on the TFLB section.

Bending Stress Results

Major axis bending stresses are presented in Figures 4 and 5 as predicted by different analysis methods for unfactored final steel and total dead load. Results show a good agreement in shape and magnitude as expected for the analysis of a straight case.

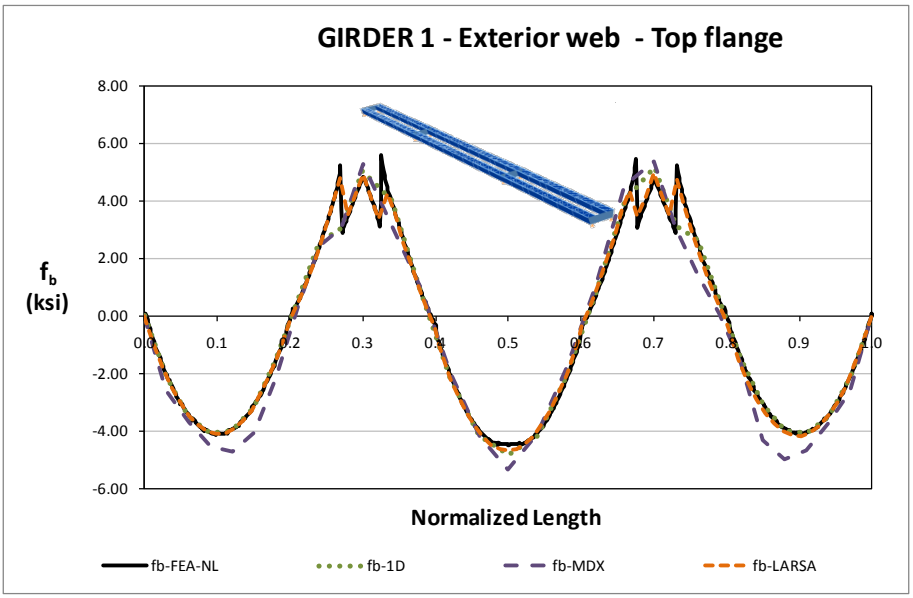

Fig. 4. Top flange major axis bending stress for Girder 1 exterior web - Final Steel Dead Load

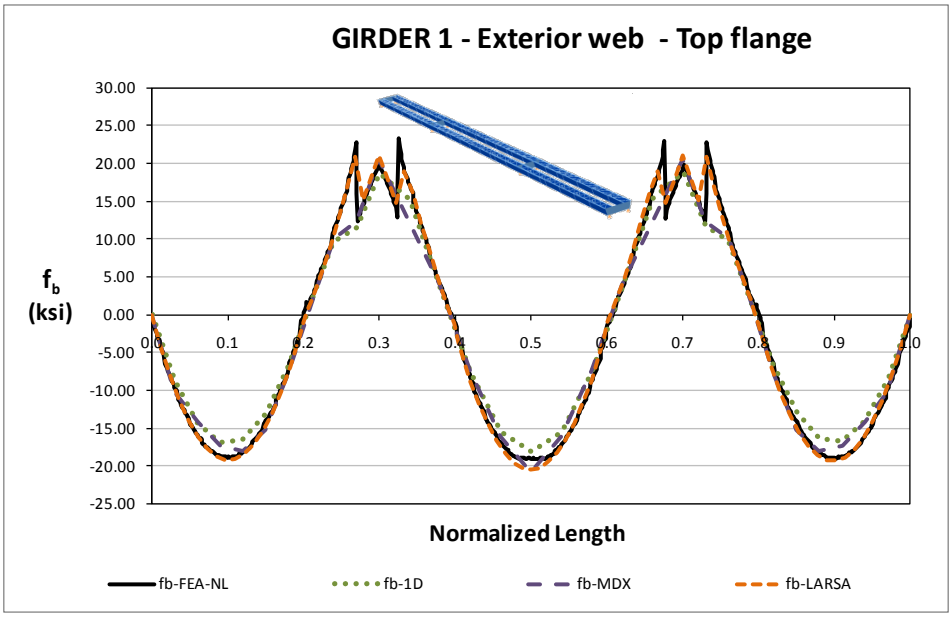

Fig. 5. Top flange major axis bending stress for Girder 1 exterior web - Total Dead Load

Figures 6 and 7 illustrate the bottom flange stresses at the web bottom flange juncture. As discussed in detail for Case XTCCR8, the 3D FEA analysis predicts a highly localized stress concentration at the interior support points, where a number of plates intersect. These stress concentrations are believed to be largely due to the local numerical approximation at these locations. The stresses one element removed from these locations are taken as the more appropriate stresses for evaluation of the simplified analysis methods.

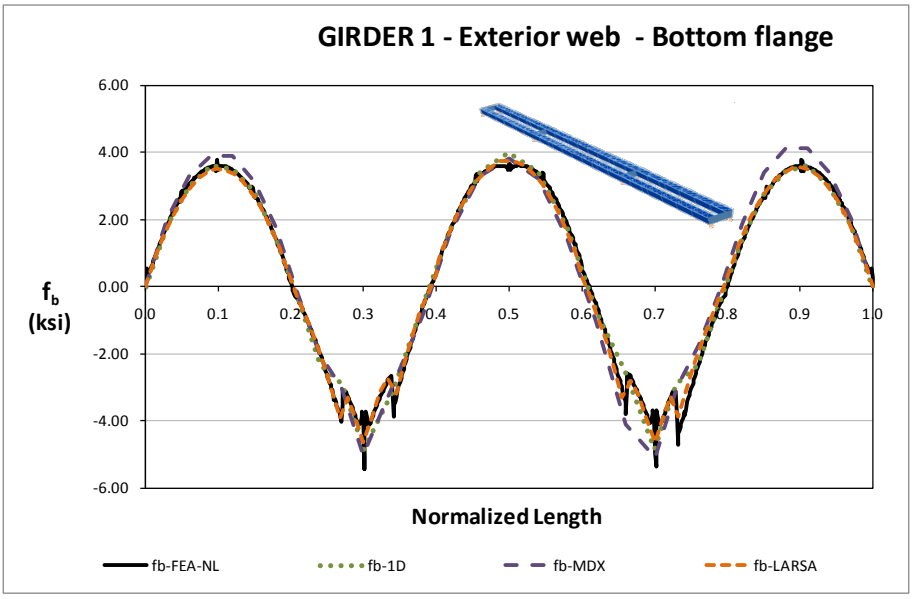

Fig. 6. Bottom flange major axis bending stress for Girder 1 exterior web - Final Steel Dead Load

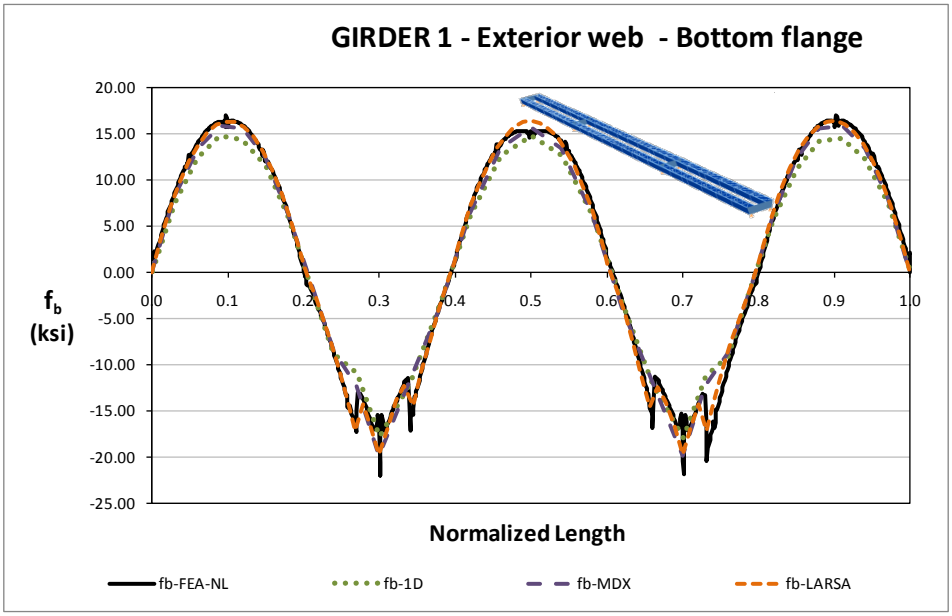

Fig. 7. Bottom flange major axis bending stress for Girder 1 exterior web - Total Dead Load

The straightness and symmetry of this study case anticipates irrelevant relative lateral displacements and lateral bending stresses, however, a 3DFEA can reveal the true interaction of the TFLB. Figure 8 sows the top flange lateral bending stresses. The stresses are small in magnitude but reflect the interaction of the top flange lateral bracing system.

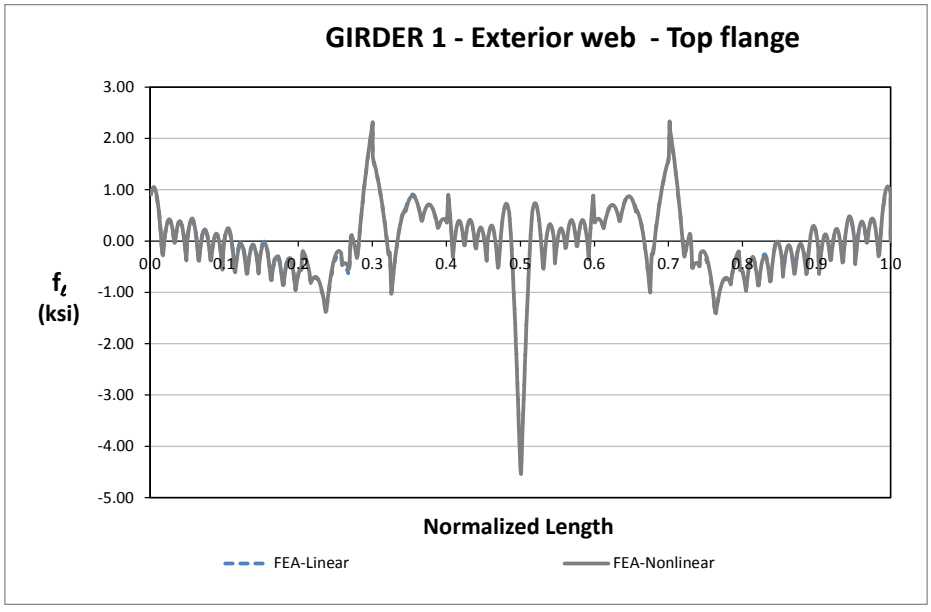

Fig. 8. Top flange lateral bending stress for Girder 1 exterior web - Total Dead Load

Top Flange Lateral Bracing Results

The TFLB diagonals and struts axial stresses are shown in Figures 9 and 10 for the total dead load condition.

The figure shows that the force on the elements, as predicted by the 2D grid method, follows the shape of the bending stress distribution. In the other hand, the 3DFEA follows a path similar to the shear force distribution. Similarly, the TFLB strut forces are mispredicted by the 2D grid methods as shown in figure 10.

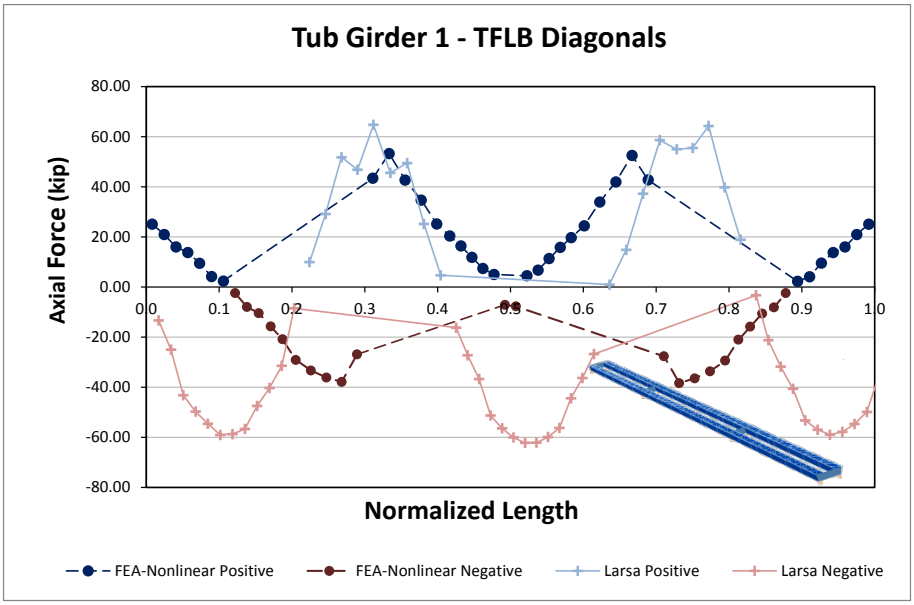

Fig. 9. Top flange lateral bracing diagonals axial forces for Girder 1 - Total Dead Load

It is not evident that a straight bridge could experience torsion, in fact at any cross section the total forces should not show a torsional force until each girder is studied independently. A 3D analysis reveals that the independent girders will be subjected to torsion caused by the top flange lateral system layout. Figure 11 shows the total torsional moment for Girder 1, the torque on Girder 2 is reversed in sign.

The TFLB elements cause the torsion and the forces on them are dependent on the torsional force they create. A 3DFEA method will be able to predict the force distribution while the 1D and 2D methods will fail under the common approach and predict forces with similar distribution as the bending stresses.

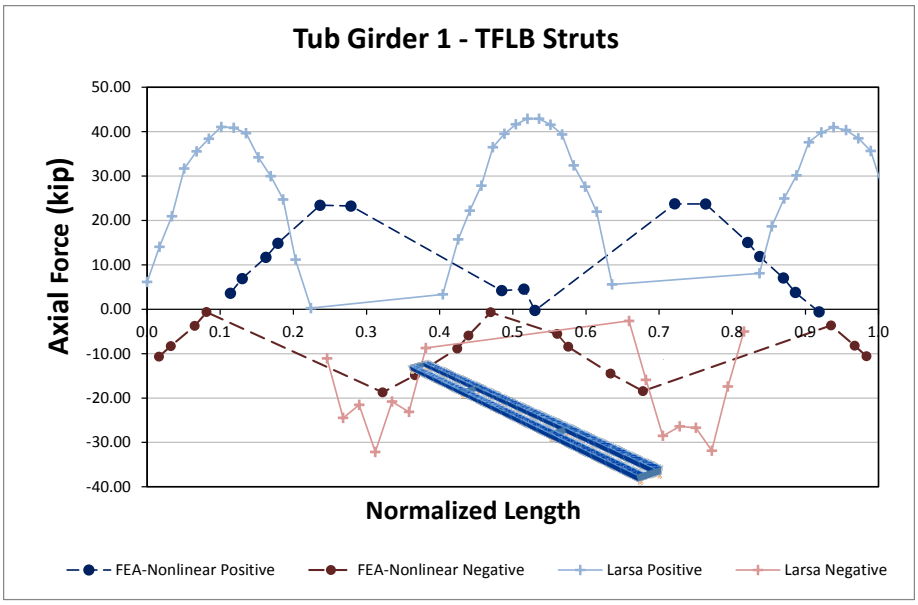

Fig. 10. Top flange lateral bracing struts axial forces for Girder 1 - Total Dead Load

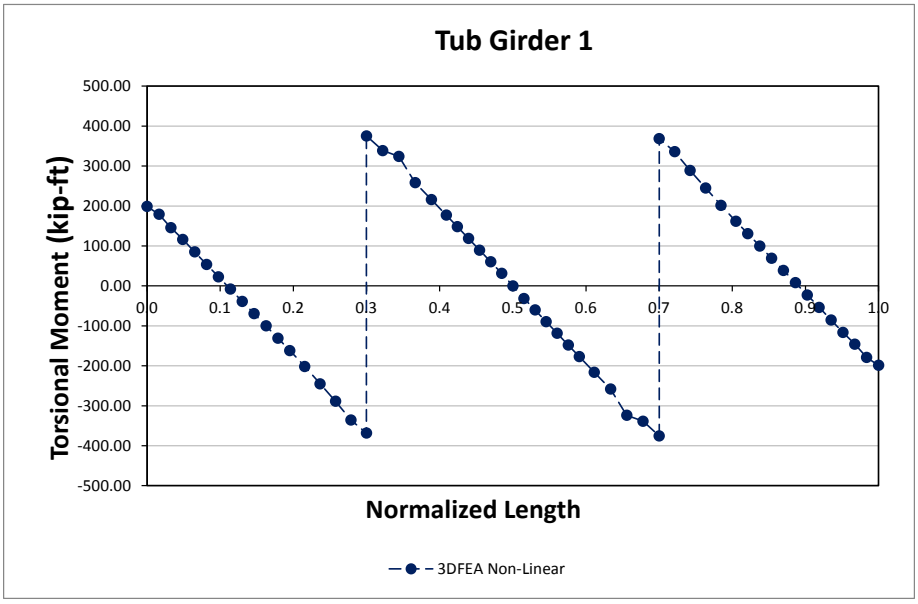

Fig. 11. Total Torsional Moment for Girder 1 - Total Dead Load

9.1 ETSSS2 (Existing, Tub-girder, Simply-supported, Straight, Skewed supports)

Bridge Description:

Sylvan Bridge over Sunset Hwy, Multnomah Co. OR

Category Data:

L_1 = 205 ft / w = 113 ft / θ=33.4°, θ=33.4°, 6 tub-girders, phased construction

References:

Provided by Oregon DOT

Erection Stages Analyzed: 6 steel erection stages

Deck Placement Sequence: 2 deck placement phases, (phased analyses are performed assuming no intermediate staged deck placement).

Bridge Perspective & Plan views (Phase1):

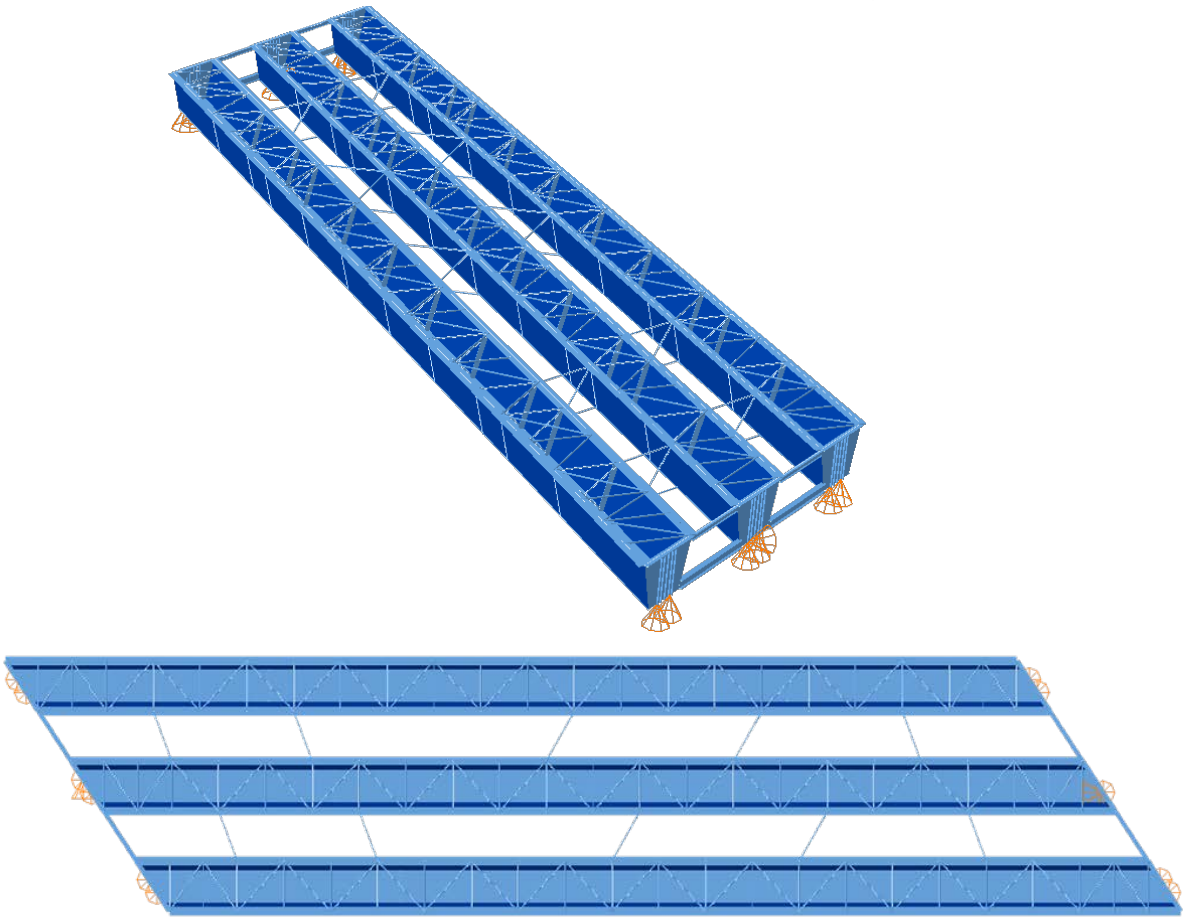

Displacement Results

The Sylvan Bridge was constructed in two phases of three tub girders each. Each phase is built independently and a closure concrete pour completes the system, for analysis purposes, the Phases 1 and 2 behave independently. The general geometry of the bridge remains practically the same but the cross-frame layout alternates. The two phases are modeled and results from construction Phase 1 are shown in

this section. The phase and girder numbering goes from bottom to top and, as in the curved bridges, the exterior web of Girder 1 corresponds to the first in the bottom.

At the bearing lines each tub is supported by a system of two elastomeric bearings. After the analysis it was found that one of the two supports had a negative vertical reaction meaning that uplift was taking place. A second analysis was run to account for this effect by removing the supports with negative vertical reactions.

Figures 1 and 2 show vertical displacements for Girder 2 under final steel and total dead load. The analysis methods predicted the response accurately for vertical displacements as expected for a simple span bridge.

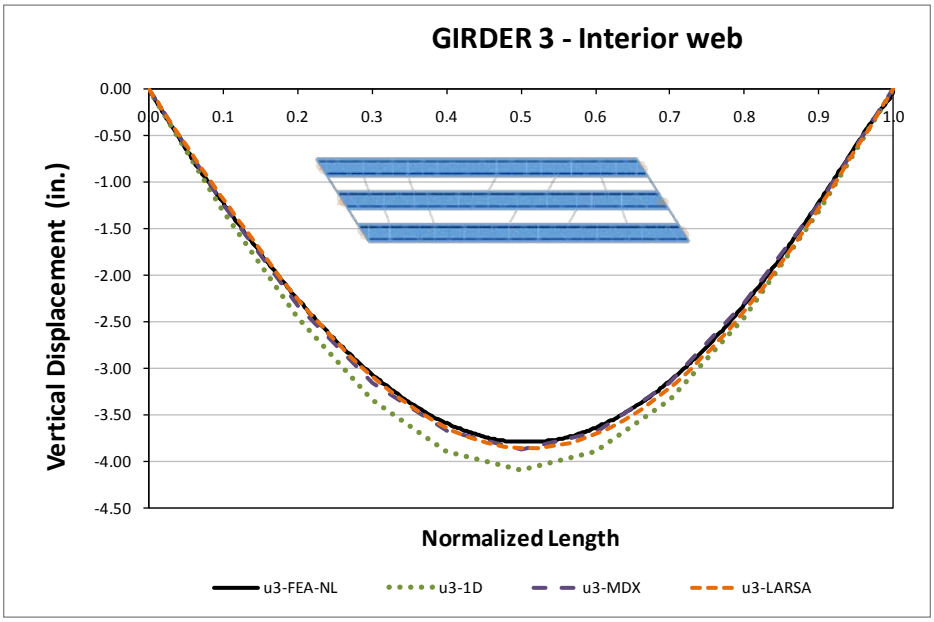

Fig. 1. Top flange vertical displacements for Girder 3 interior web - Final Steel Dead Load

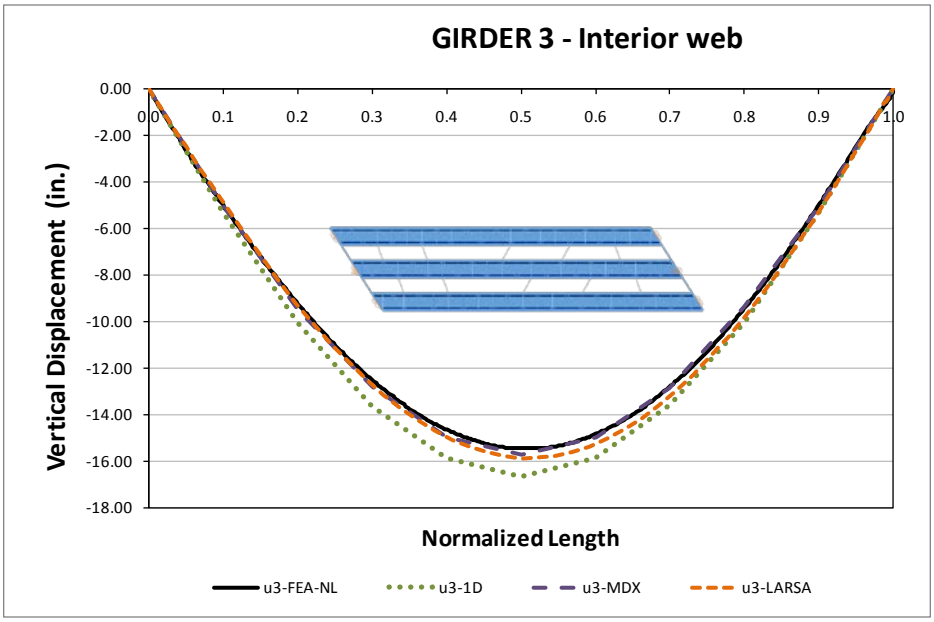

Fig. 2. Top flange vertical displacements for Girder 3 interior web - Total Dead Load

Figure 3 illustrates the lateral displacements for the girder top flange. Due to skew support configuration and to the lack of a stiffer external diaphragm system at the bearing lines the bridge experimented uplift identified by an initial displacement of about 1.7 in. The 2D analysis methods are unable to capture this effect.

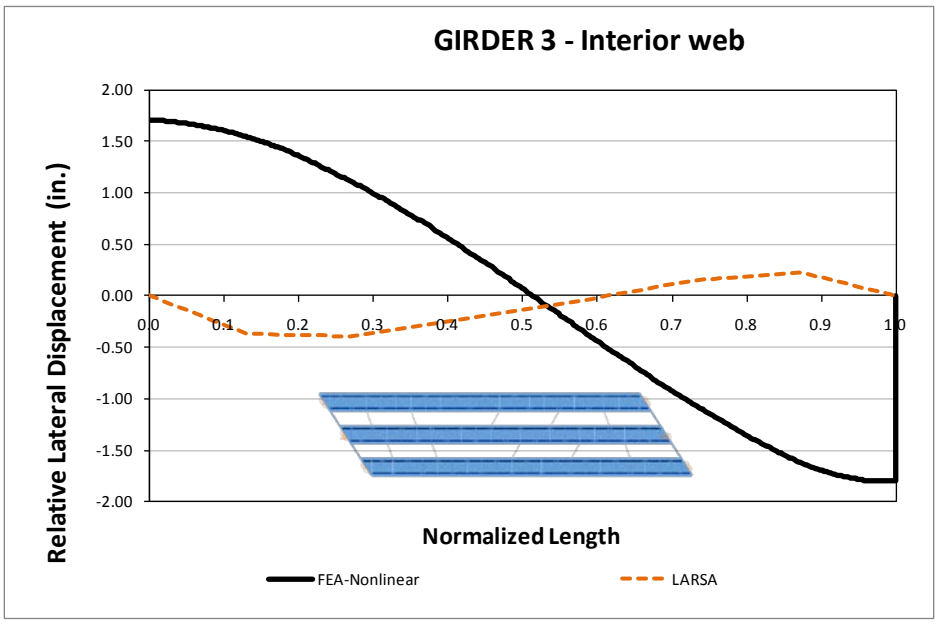

Fig. 3. Relative lateral displacements for Girder 3 interior web - Total Dead Load

Bending Stress Results

Figure 4 shows the stress distribution for the final steel dead load condition. The total dead load results are shown in Figure 5. As expected the stresses have a uniform increment between these two loading conditions. The TFLB system introduces discrete loads to the top flange resulting in a saw-toothed shape response for the bending stresses.

In Figure 6, the same results are shown for the same girder but at a different web-top flange juncture, the results show a different interaction with the TFLB system which causes a mirrored shape.

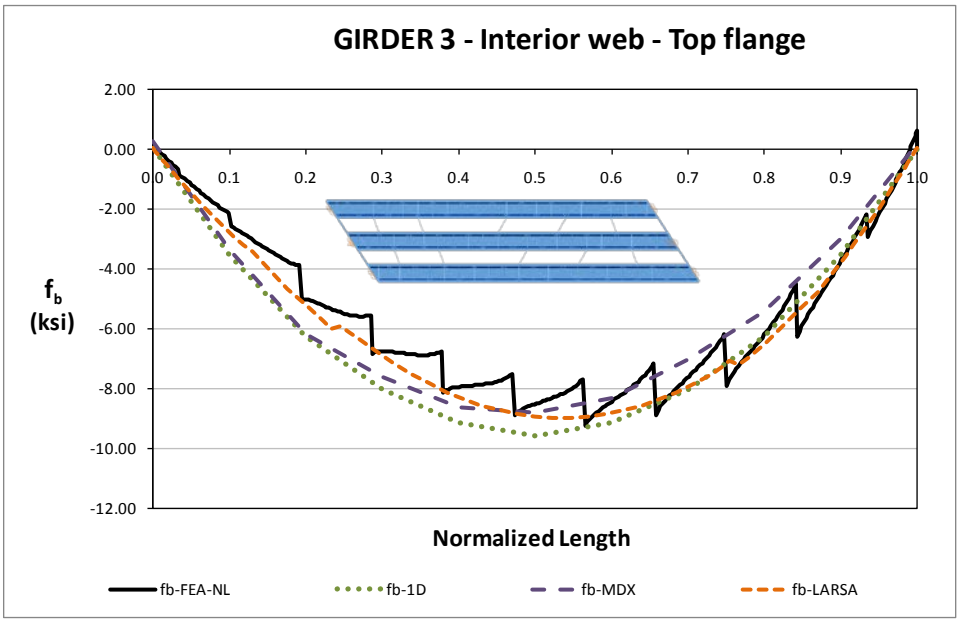

Fig. 4. Top flange major axis bending stress for Girder 3 interior web - Final Steel Dead Load

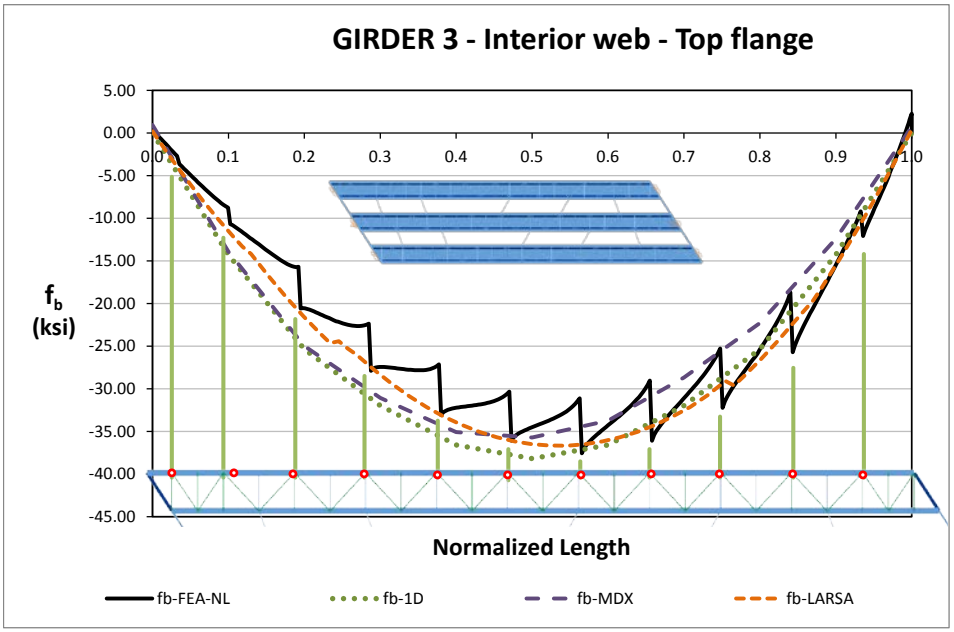

Fig. 5. Top flange major axis bending stress for Girder 3 interior web - Total Dead Load

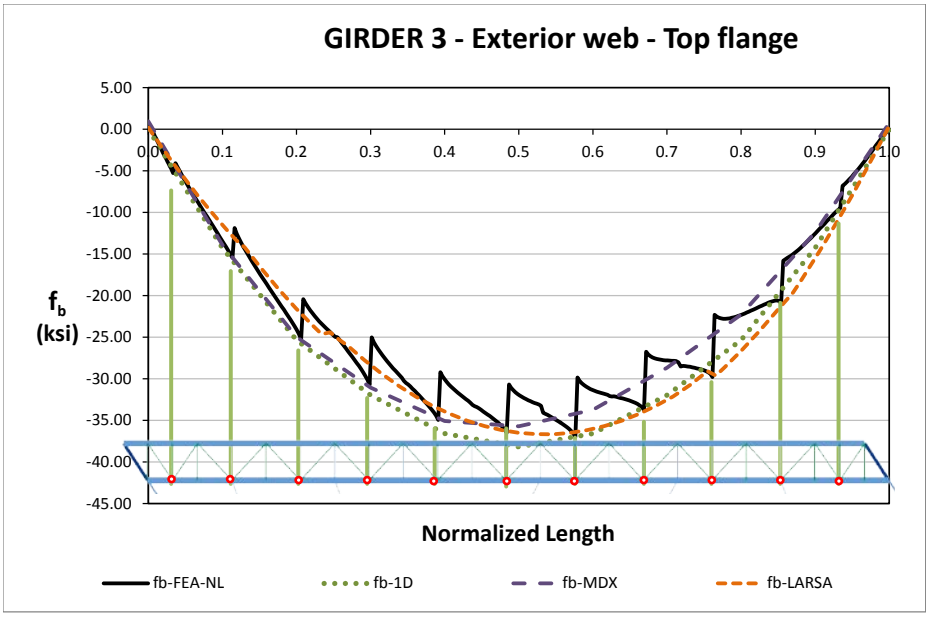

Fig. 6. Top flange major axis bending stress for Girder 3 exterior web - Total Dead Load

The top flange lateral bending stresses are presented in Figure 7 for the 3DFEA and Larsa analyses. In the majority of the cases the lateral bending stresses are overpredicted.

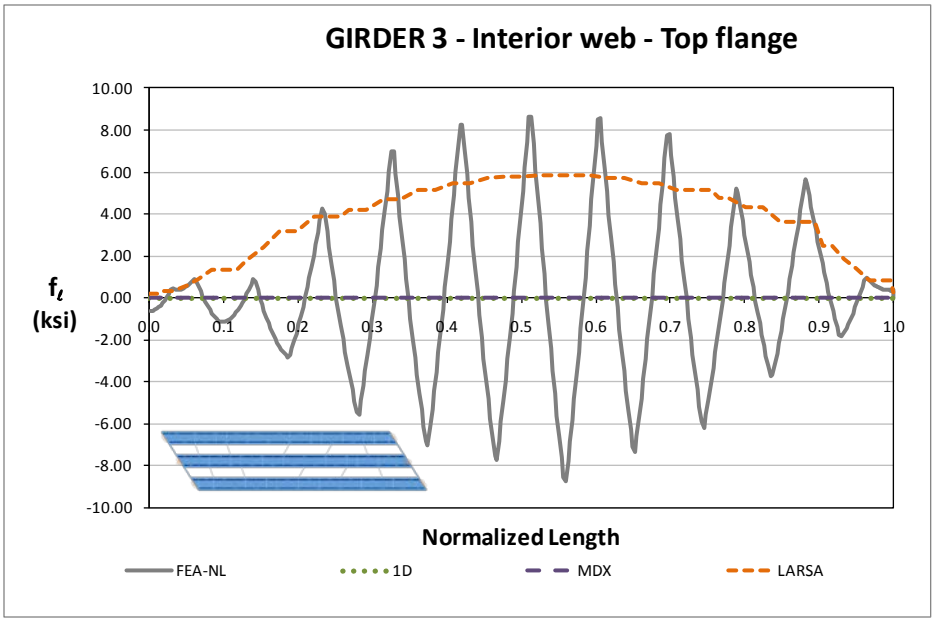

Fig. 7. Top flange lateral bending stress for Girder 3 interior web - Total Dead Load

Figure 8 shows the bottom flange stresses for total dead load, the results show a good agreement for all analysis methods. Intermittent stress jumps are reported at several points for the 3D FEA analysis; these responses are attributed to the numerical approximation at the locations where the cross frame connection plate, web and bottom flange join at a point. The stress concentration is reported only in the adjacent elements to this intersection point.

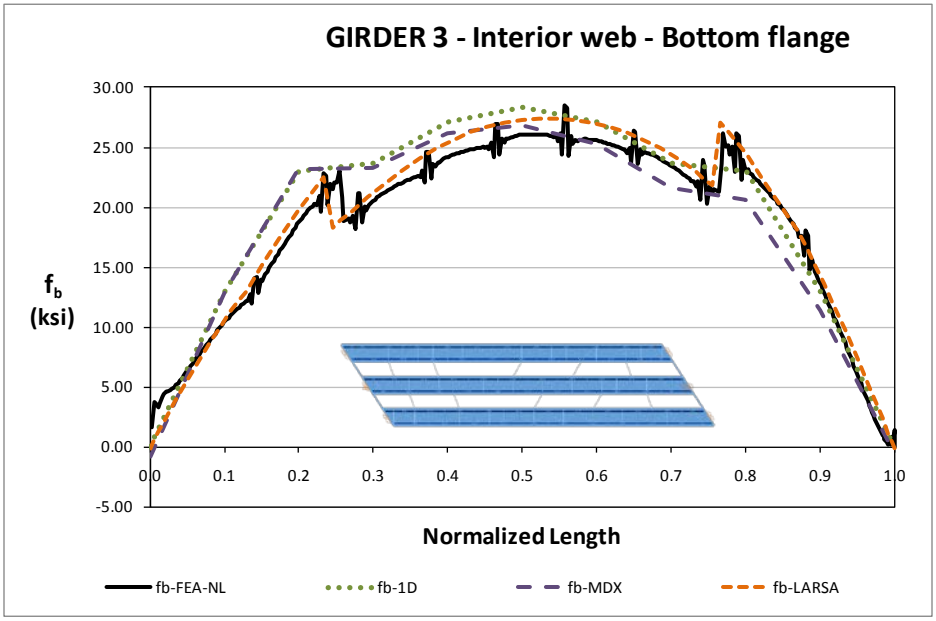

Fig. 8. Bottom flange major axis bending stress for Girder 3 interior web – Total Dead Load

Top Flange Lateral Bracing Results

Figures 9, 10 and 11 illustrate the forces in the top flange lateral bracing system diagonals for the different methods of analysis and for final steel and total dead load cases, the positive and negative results are plotted separately and joined by a line; forces are plotted at the relative position along the length. Girder 1 is located at the bottom and it is the most exterior girder while Girder 3 will be adjacent to the bridge Phase 2.

The TFLB Diagonal forces maintain an almost constant value and slightly decrease at the supports but the maximum forces tend to concentrate on the obtuse corners of the bridge. The cross sectional area of the TFLB diagonals is 8.52 in².

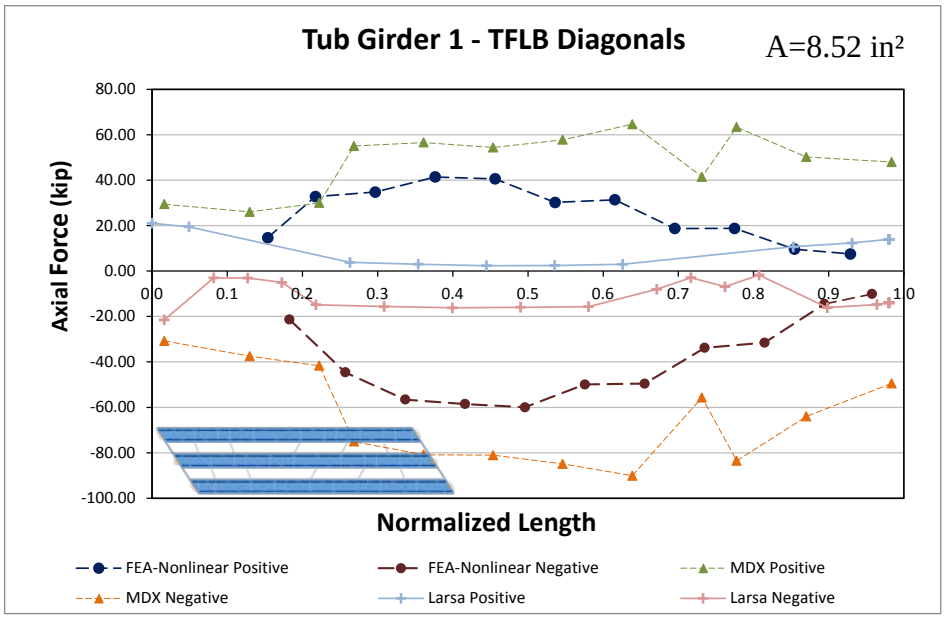

Fig. 9. Top flange lateral bracing diagonals axial force for Girder 1- Final Steel Load

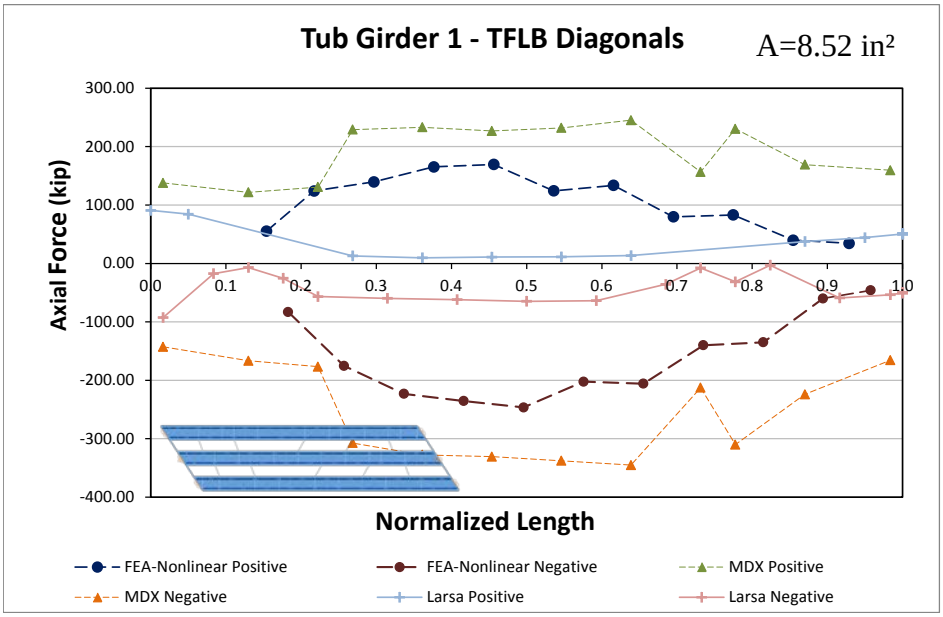

Fig. 10. Top flange lateral bracing diagonals axial forces for Girder 1- Total Dead Load

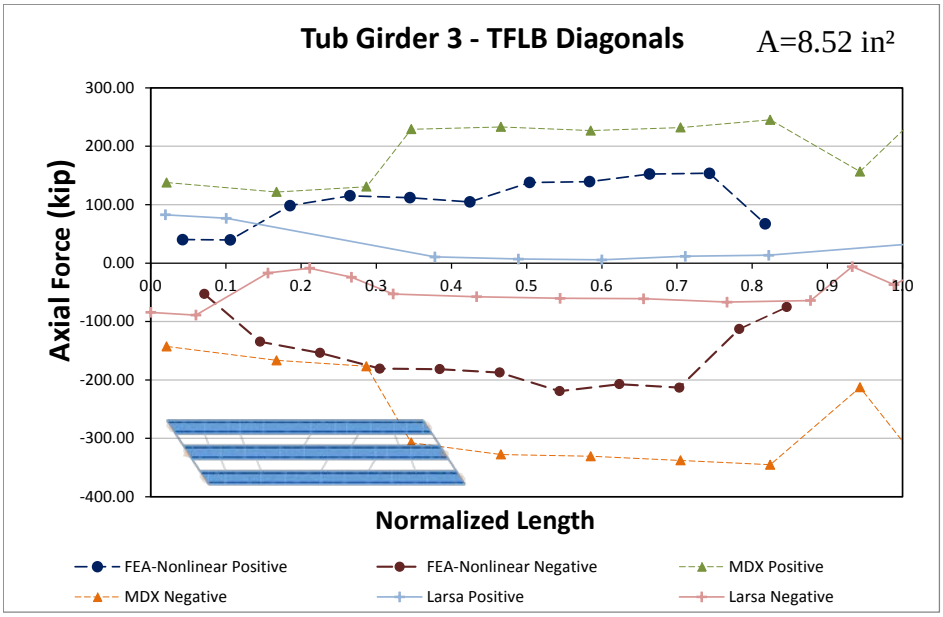

Fig. 11. Top flange lateral bracing diagonals axial forces for Girder 3- Total Dead Load

A similar effect can be seen for the TFLB Struts but the force values are lower. Figure 12 illustrate the results for strut forces for Girder 1. The cross sectional area of the TFLB struts is 8.52in² and for the 1D and 2D the CF top chords elements are plot together with an area of 3.65 in².

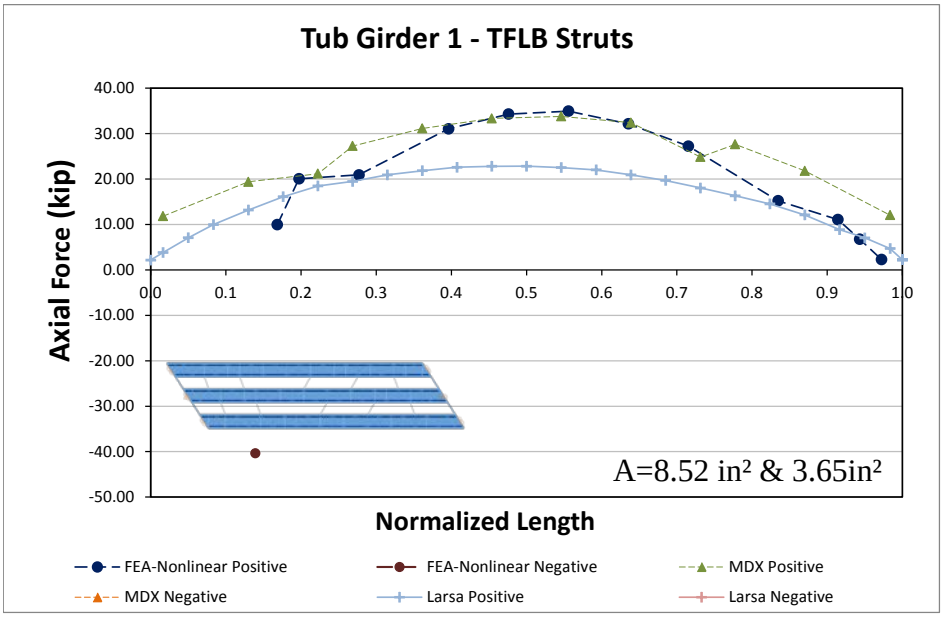

Fig. 12. Top flange lateral bracing struts axial forces for Girder 1 - Total Dead Load

Figures 13, 14 and 15 show the forces for the internal CF elements for the total dead load condition. X-type cross-frames are used at ten locations along the girder. The top chord is the most stressed element in the system as the result of the interaction with the TFLB diagonals and to the reduced area of the member. The 1D and 2D analysis methods include the internal CF top chord results in the TFLB struts.

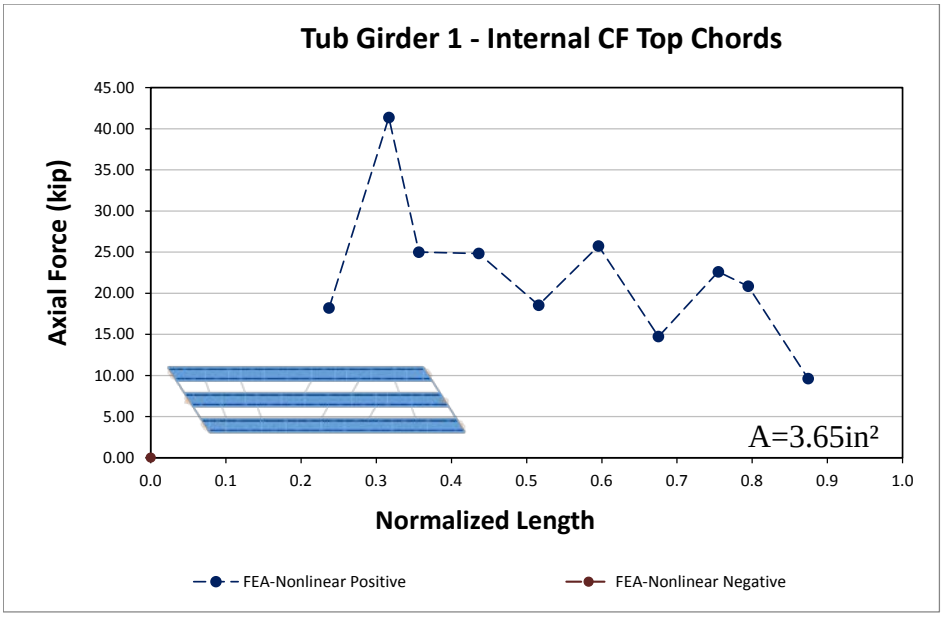

Fig. 13. Internal cross frame top chord axial forces for Girder 1 - Total Dead Load

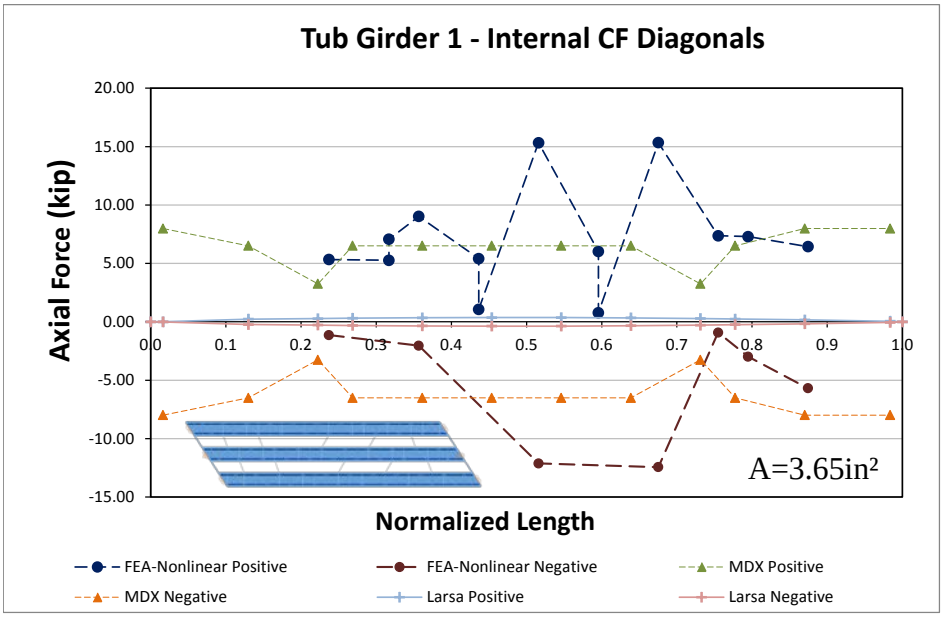

Fig. 14. Internal cross frame diagonals axial forces for Girder 1 - Total Dead Load

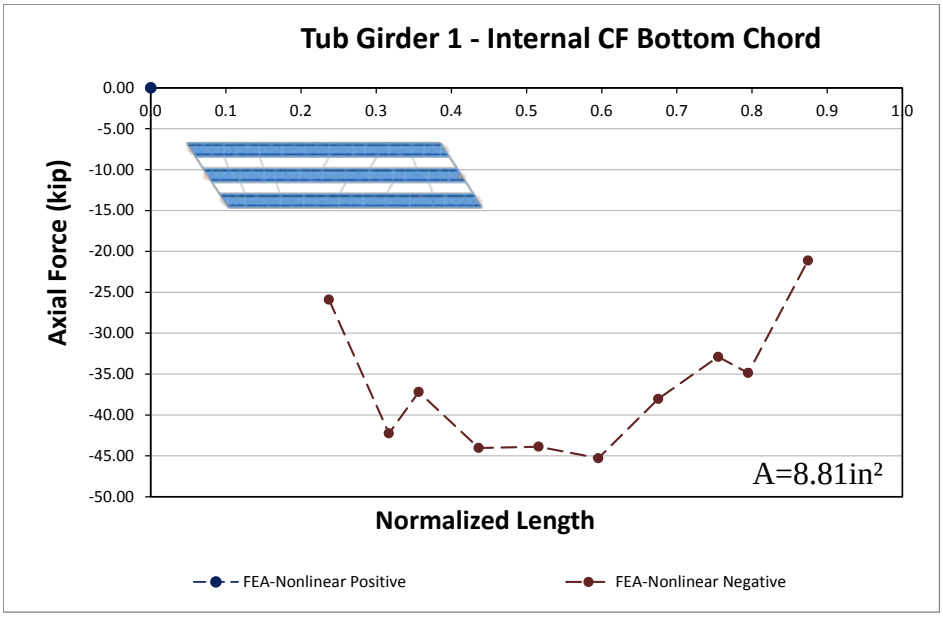

Fig. 15. Internal cross frame bottom chord axial forces for Girder 1 - Total Dead Load

9.2 NTSSS1 (New, Tub-girder, Simple-span, Straight, Skewed supports)

Bridge Description:

Category Data:

L_1 = 150 ft / w = 30 ft / θ=15°, θ=15°, 2 tub-girders

References:

Erection Stages Analyzed: 2 steel erection stages

Deck Placement Sequence: One stage, deck thickness = 9.5 in

Bridge Perspective & Plan Views:

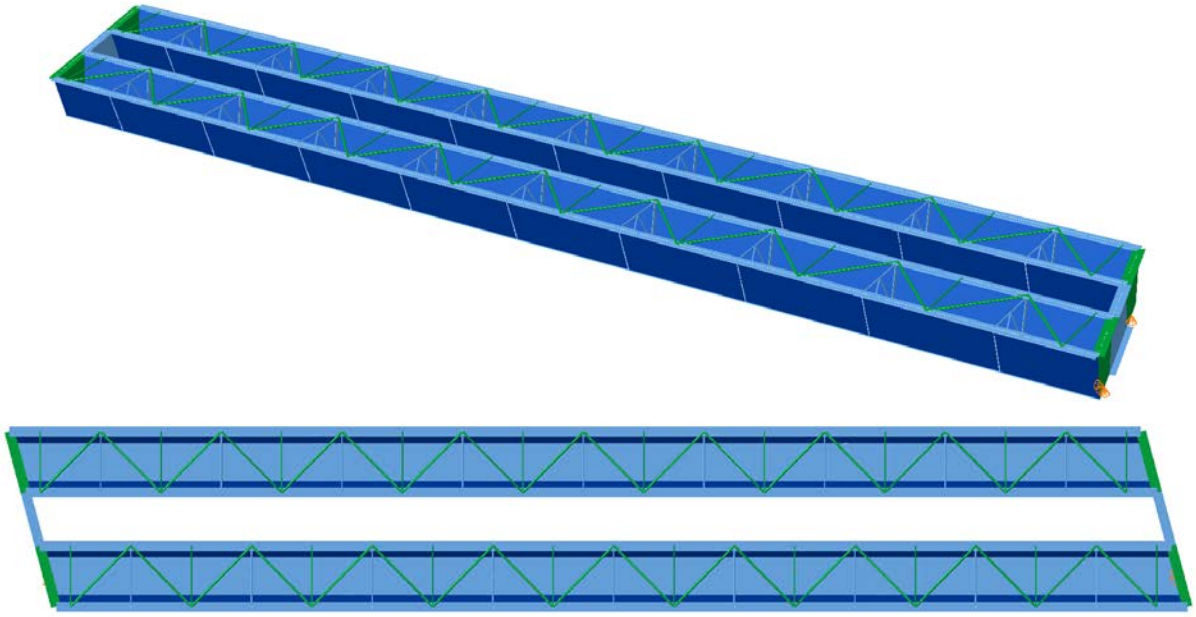

Displacement Results

Displacements and stress results are reported at the web flange juncture locations then each tub girder has four sets of results and each web has two for top flange and bottom flange. On a plan view, the girder numbering is assigned bottom to top of page, meaning that Girder 1 is always the girder at the bottom and Girder 2 is the top girder in a twin girder system. To be compatible with curved girders, webs are assigned as internal and external for each girder, meaning that for each girder the web at the bottom is the exterior and the one on top is the exterior web.

Figures 1, 2 and 3 show the evolution of the vertical displacements for the partial steel erection stage 2, final steel and total non-composite dead loads. For the partial stages the vertical displacements are plotted only for 3D FEA and 2D LARSA, all methods are shown for the final steel and total non-composite dead loads.

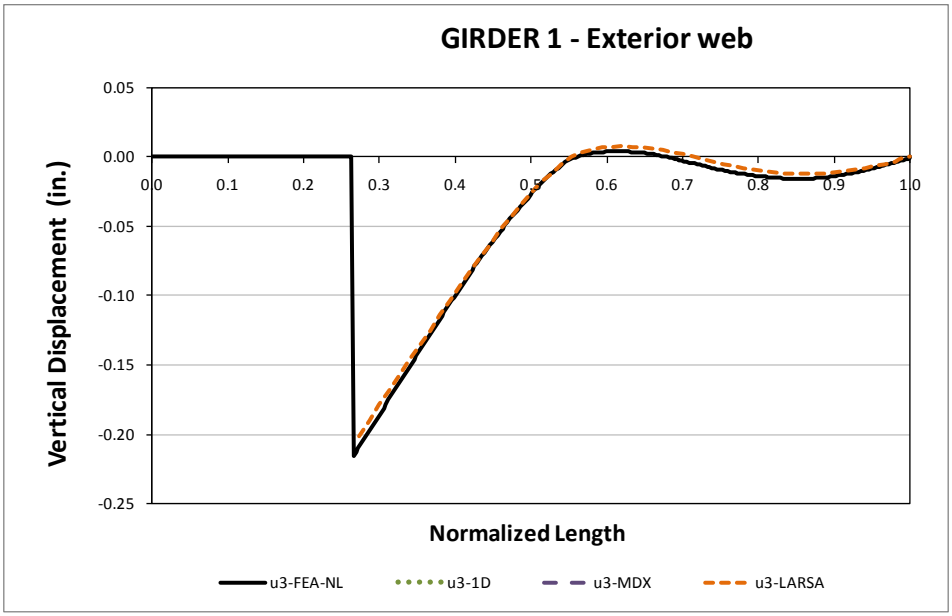

Fig. 1. Top flange vertical displacements for Girder 1 exterior web – Stage 2 Steel Dead Load

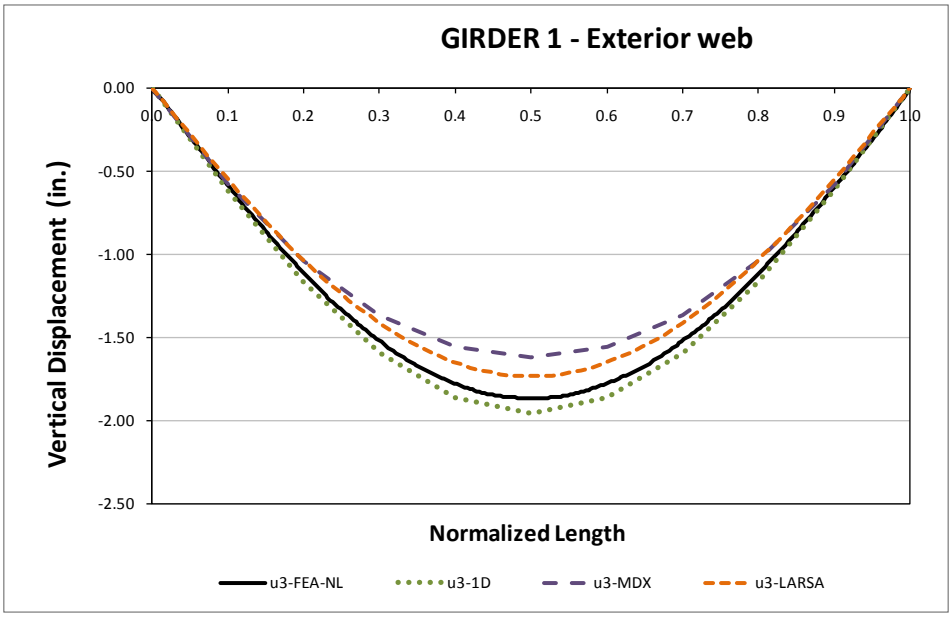

Fig. 2. Top flange vertical displacements for Girder 1 exterior web - Final Steel Dead Load

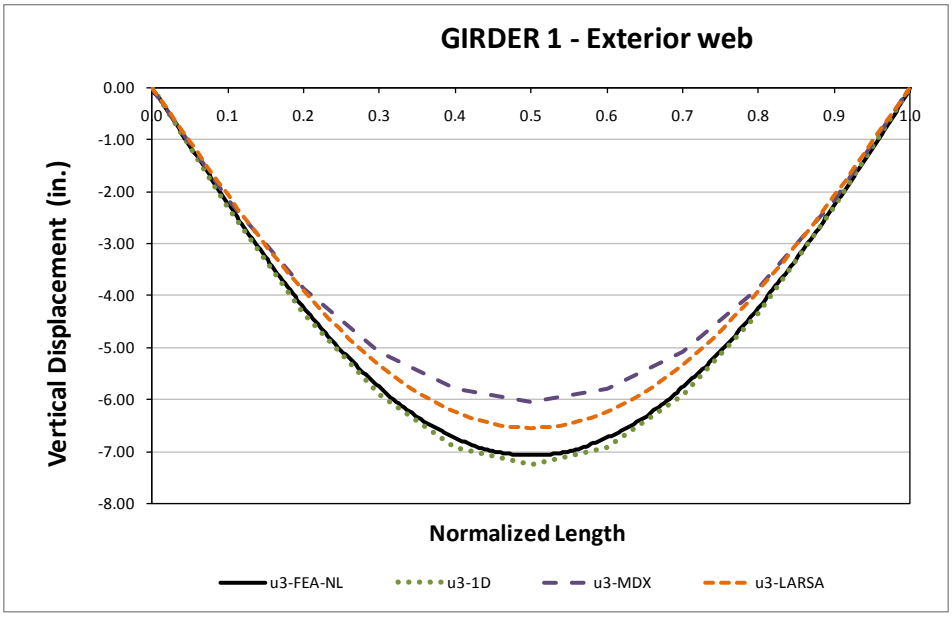

Fig. 3. Top flange vertical displacements for Girder 1 exterior web - Total Dead Load

Figure 4 illustrates the relative radial displacement between top and bottom flange junctures as a measure of lateral displacement. The 3D FEA show initial rotation as both supports ends rotate as the diaphragm plane rotates with respect to the skewed support line causing different lateral displacements on the top and bottom flanges.

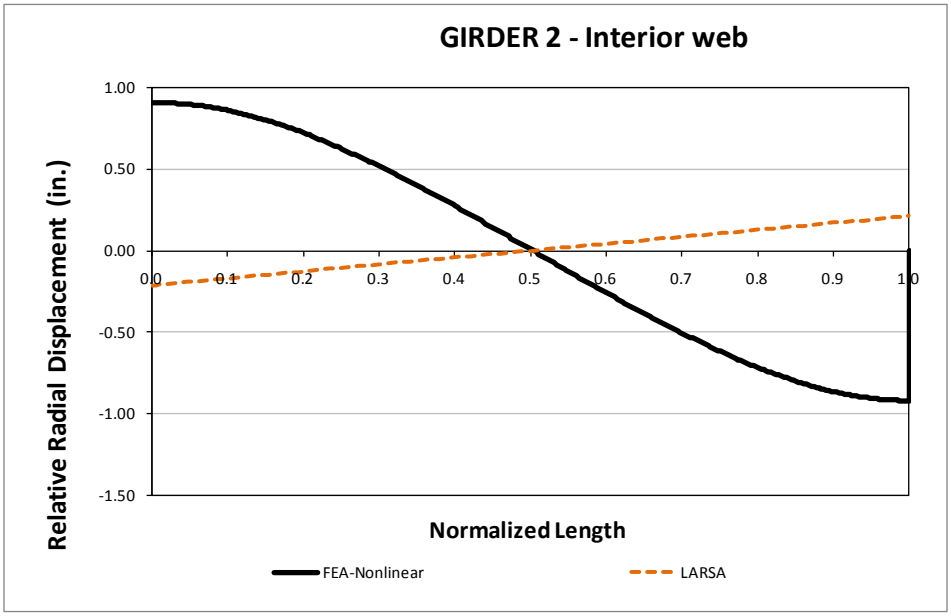

Fig. 4. Top flange relative radial displacements for Girder 2 interior web - Total Dead Load

Bending Stress Results

Major axis bending stresses are presented in Figures 5, 6 and 7 as predicted by different analysis methods for partial steel erection stage 2, final steel and total dead load stages. Results in general show a good agreement in shape and magnitude but the MDX result shows a poor prediction mainly due to the discretization size along the span length.

The local interaction of the TFLB system becomes evident in the final steel and total dead load stages. Previous to the removal of the temporal supports this interaction is negligible.

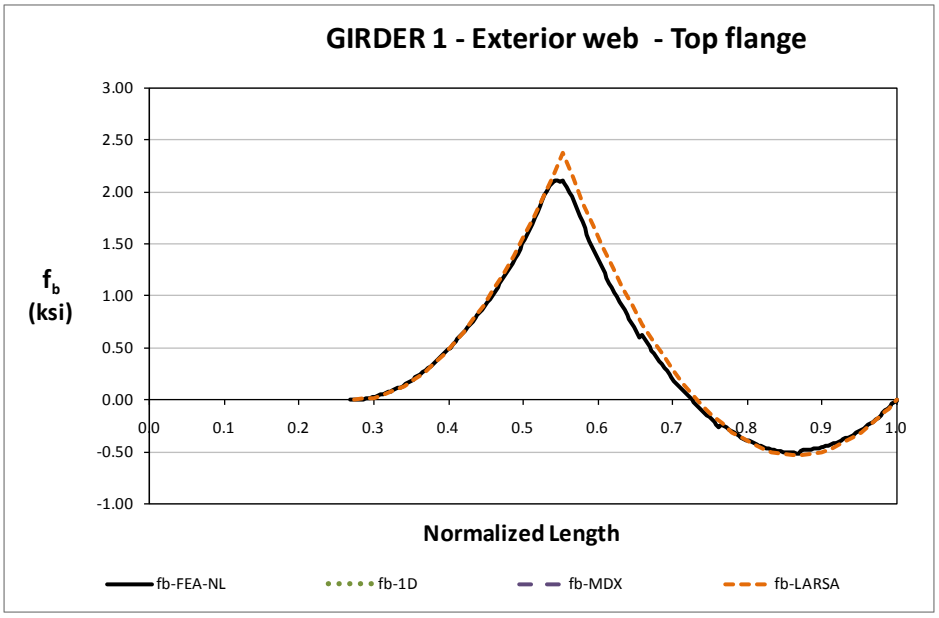

Fig. 5. Top flange major axis bending stress for Girder 1 exterior web - Stage 2 Steel Dead Load

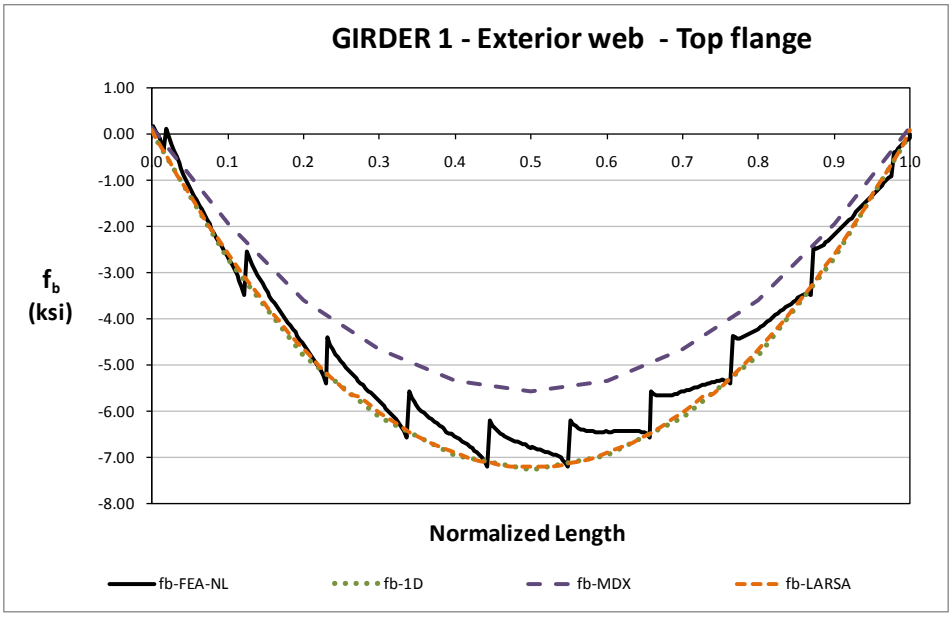

Fig. 6. Top flange major axis bending stress for Girder 1 exterior web - Final Steel Dead Load

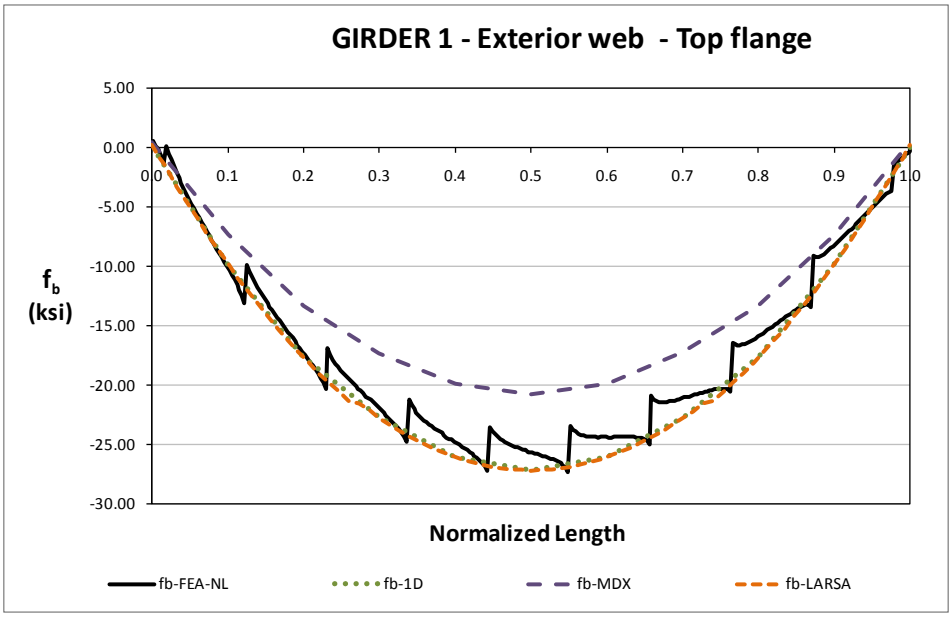

Fig. 7. Top flange major axis bending stress for Girder 1 exterior web - Total Dead Load

Figures 8, 9 and 10 illustrate the bottom flange stresses at the web bottom flange juncture. On fig. 8 the 3D FEA analysis predicts for the partial steel erection stage 2 a high localized stress concentration at the temporal support located at a point where a number of plates intersect, these stress concentrations are believed to be largely due to the numerical inaccuracies at these locations.

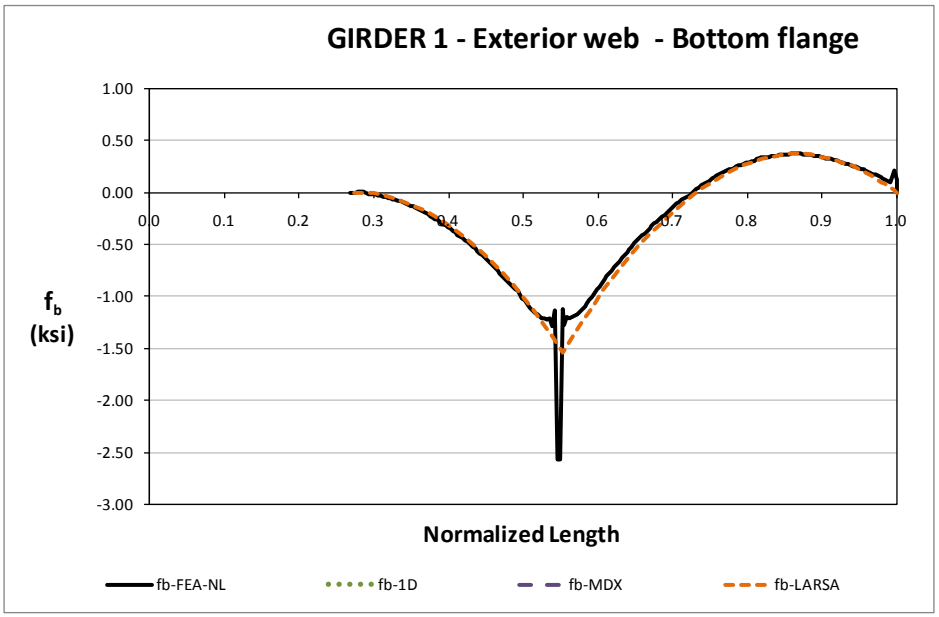

Fig. 8. Bottom flange major axis bending stress for Girder 1 exterior web - Stage 2 Steel Dead Load

Figures 9 and 10 illustrate the bottom flange stresses at the web bottom flange juncture for the final steel and total dead load cases. The stress distributions are closely predicted by all the analysis methods.

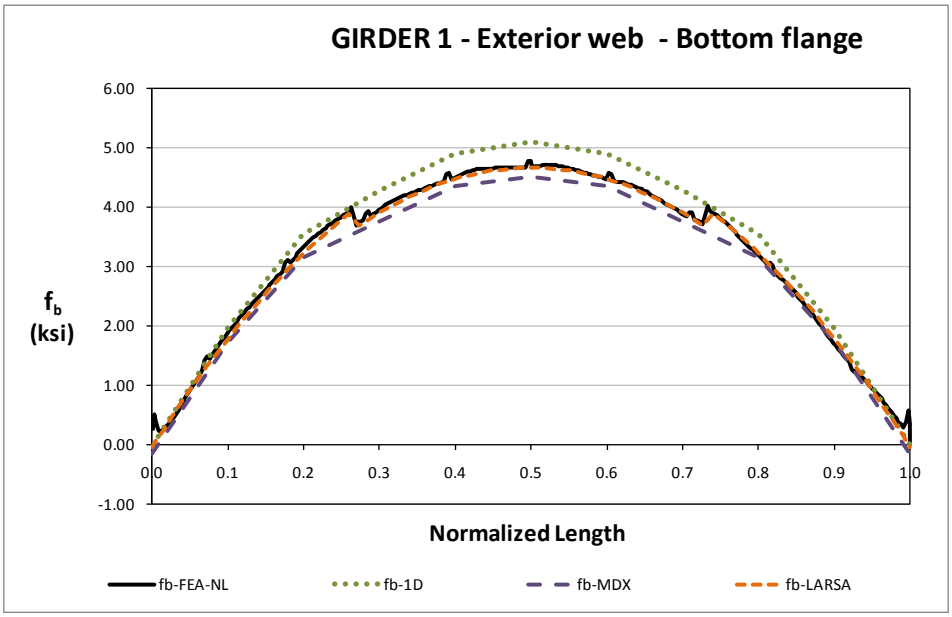

Fig. 9. Bottom flange major axis bending stress for Girder 1 exterior web - Final Steel Dead Load

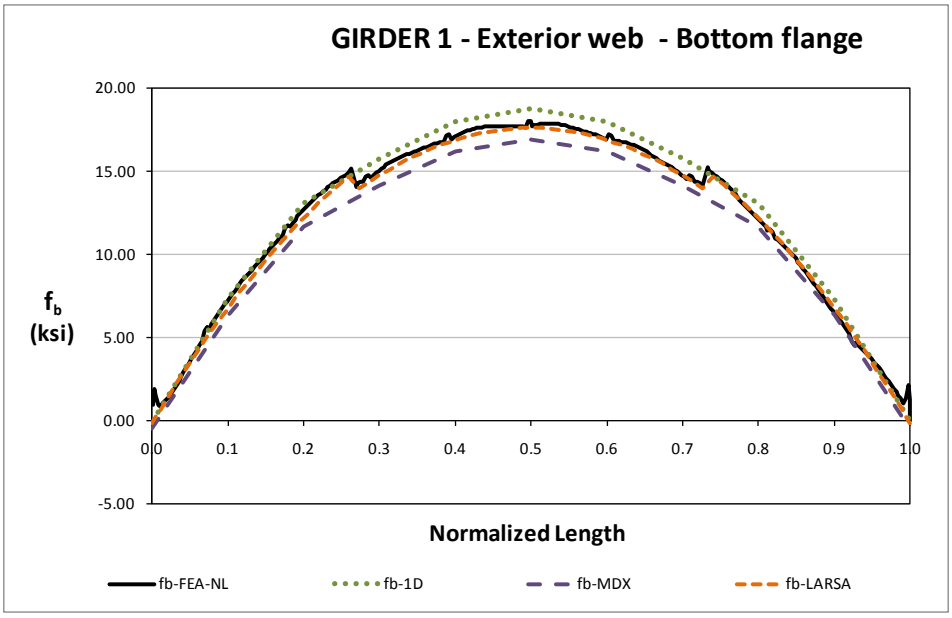

Fig. 10. Bottom flange major axis bending stress for Girder 1 exterior web - Total Dead Load

Top Flange Lateral Bracing Results

The TFLB diagonals axial forces are shown in Figures 11, 12 and 13 for the partial steel erection stage 2, final steel and total dead load condition. The TFLB system force distribution for stage 2 shows a similar shape as with the corresponding mayor axis bending stresses however, the forces reported on final steel and total dead load stages are not in agreement with their mayor axis bending stresses but correspond to a almost constant value which suggest a constant torque along the span length. This torque is caused only by the presence of skewed supports.

The cross sectional area of these elements is 10.6in² that for a maximum axial force of 50kip as reported by the 3DFEA the element experiences an axial stress of 4.7ksi on the total dead load condition. The values reported by the MDX analysis method over predict these forces.

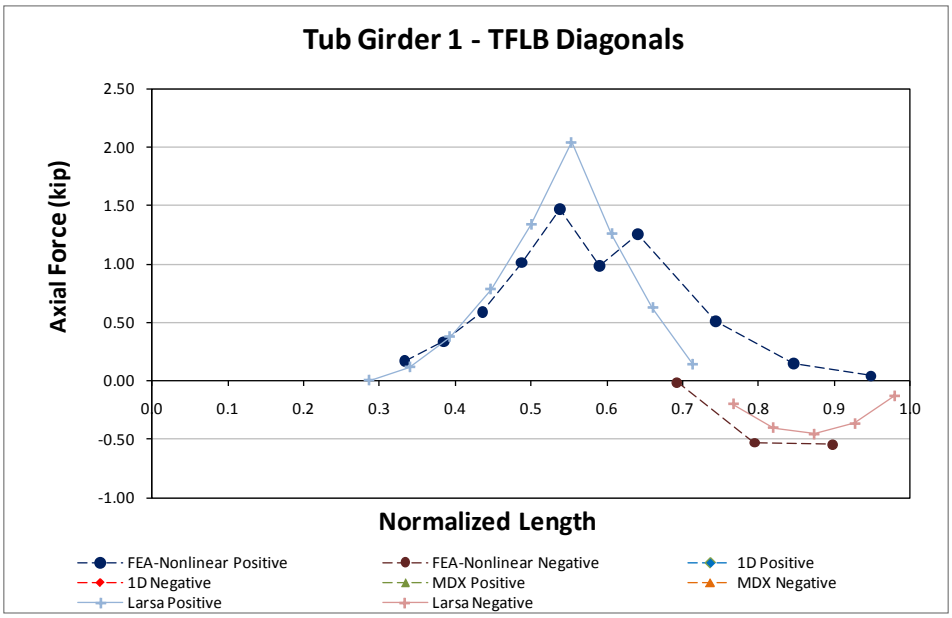

Fig. 11. Top flange lateral bracing diagonals axial forces for Girder 1 - Stage 2 Steel Dead Load

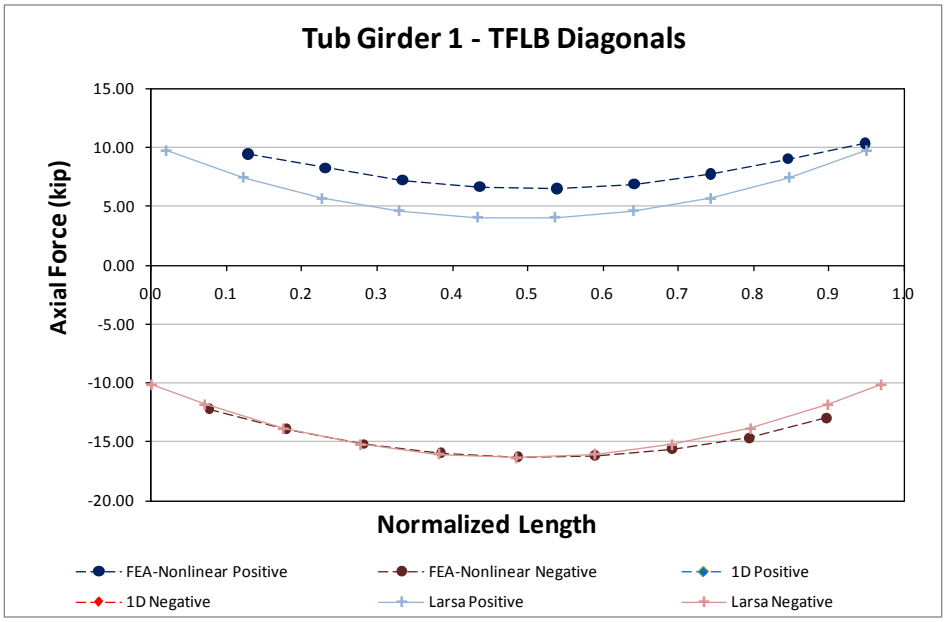

Fig. 12. Top flange lateral bracing diagonals axial forces for Girder 1 - Final Steel Dead Load

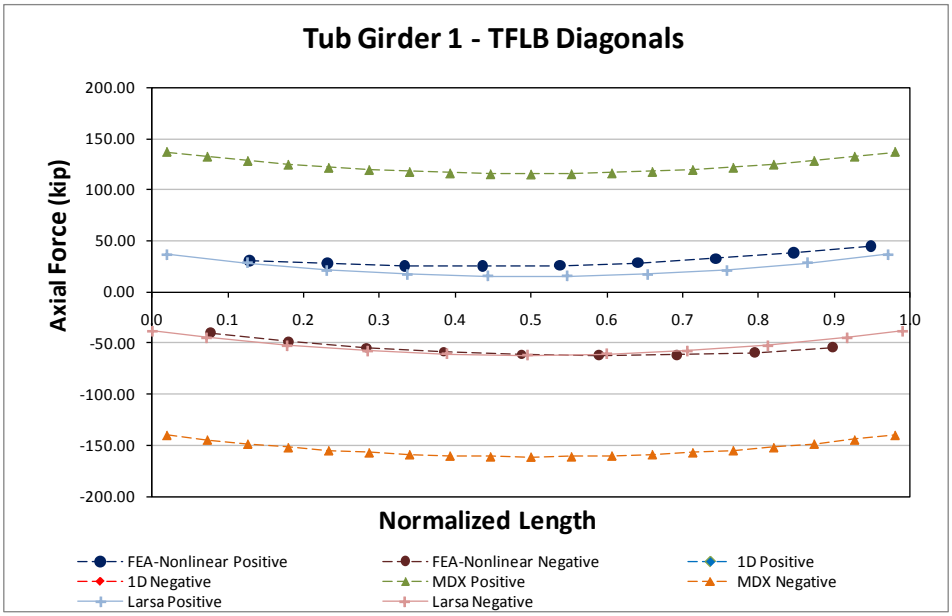

Fig. 13. Top flange lateral bracing diagonals axial forces for Girder 1 - Total Dead Load

Figure 14 shows the TFLB axial forces on the struts for the total non-composite deal load case. The area of the struts is 4.4in² which, for a maximum axial force of 20kip as reported by LARSA and MDX analyses, results on maximum axial stress of 4.5ksi. The 3DFEA reports lower values, partly because the model accommodates girder rotations which release the elements from forces.

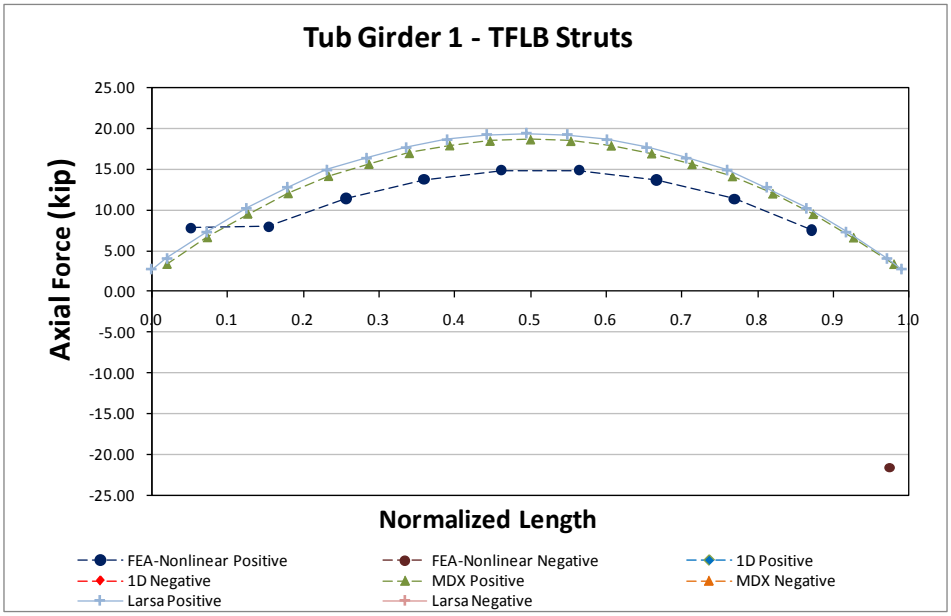

Fig. 14. Top flange lateral bracing struts axial forces for Girder 1 - Total Dead Load

9.3 NTSSS2 (New, Tub-girder, Simple-span, Straight, Skewed supports)

Bridge Description:

Category Data:

L_1 = 150 ft / w = 30 ft / θ=30°, θ=30°, 2 tub-girders

References:

Erection Stages Analyzed: 3 steel erection stages

Deck Placement Sequence: One stage, deck thickness = 9.5 in

Bridge Perspective & Plan Views:

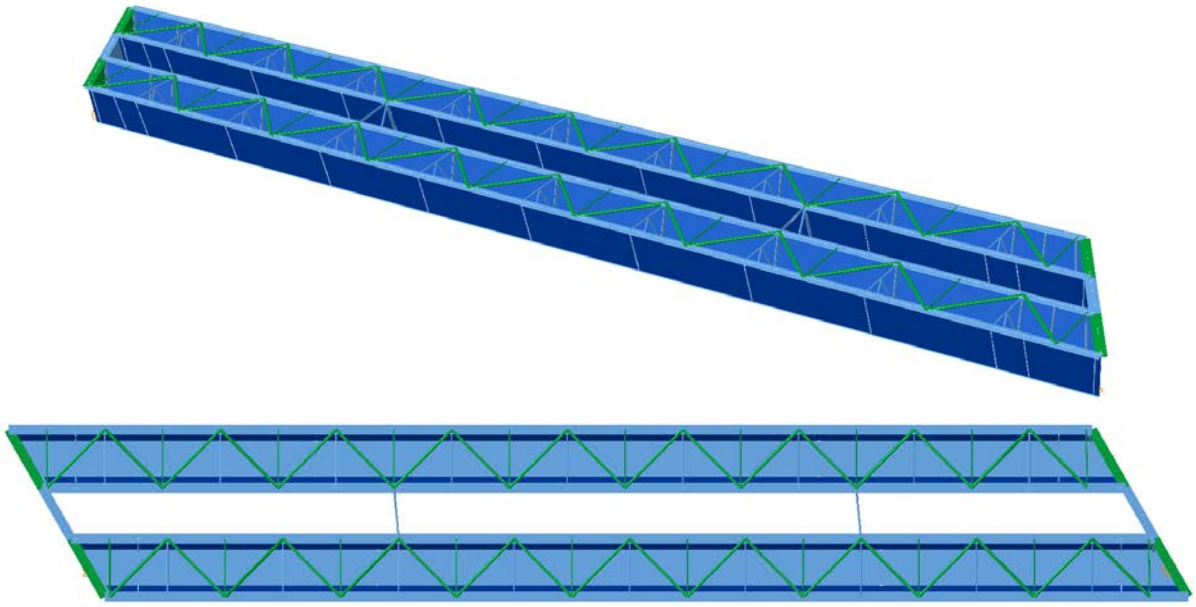

Displacement Results

Figures 1 through 4 show the partial steel erection stages 2 and 4, final steel and non-composite total dead load displacements for the top flange and the exterior web juncture of Girder 1, in other words, the top flange of the most interior web. The vertical displacements (u3) are plotted for four different methods of analysis: non-linear refined 3D FEA, 1D and using 2D analysis software MDX and LARSA. All methods show a close prediction of results, discrepancies on the results are mainly attributed to the discretization used by the analysis method leading to a system slightly stiffer when the bridge is represented by a lower number of elements along the length.

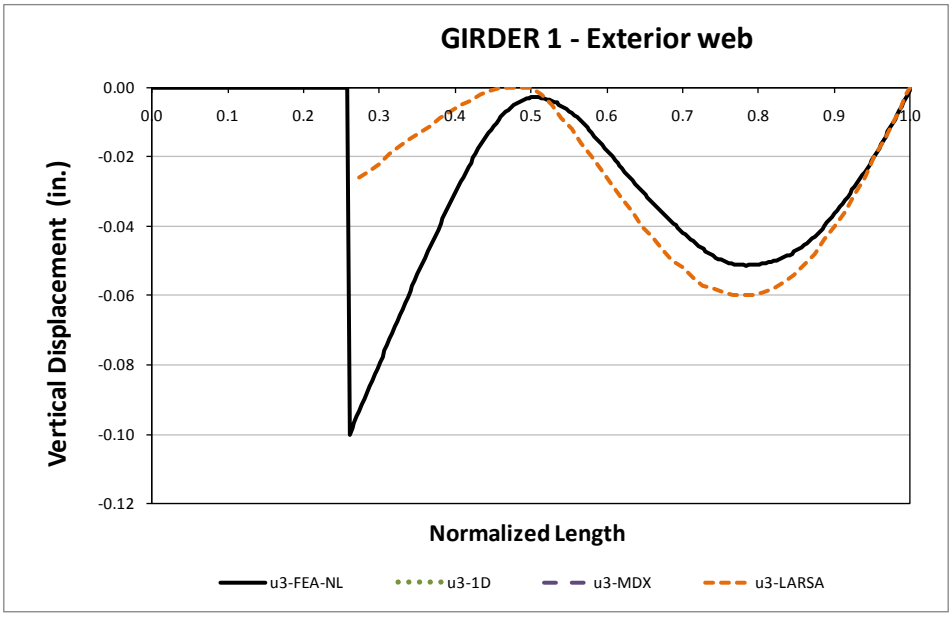

Fig. 1. Top flange vertical displacements for Girder 1 exterior web - Stage 2 Steel Dead Load

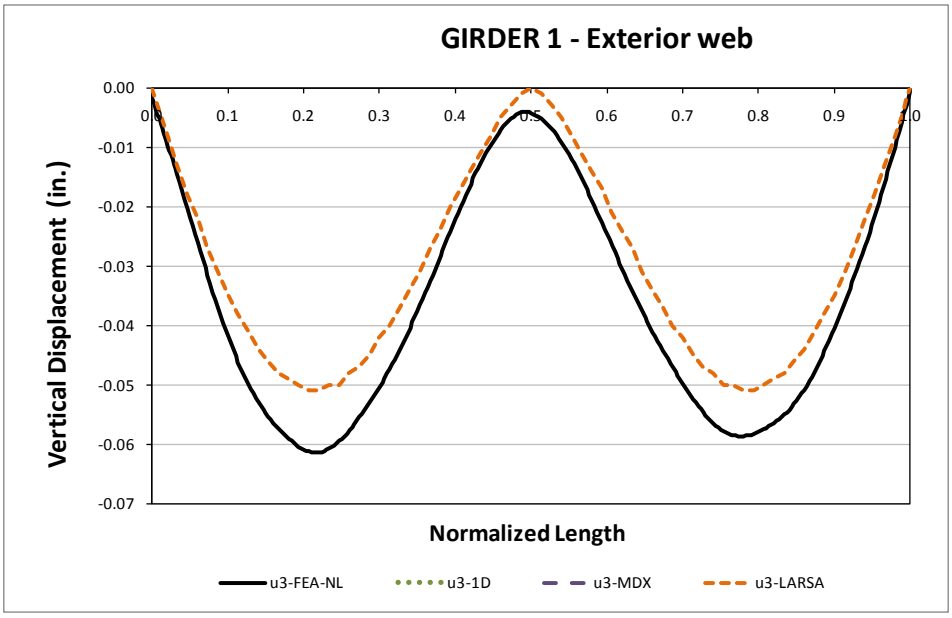

Fig. 2. Top flange vertical displacements for Girder 1 exterior web - Stage 4 Steel Dead Load

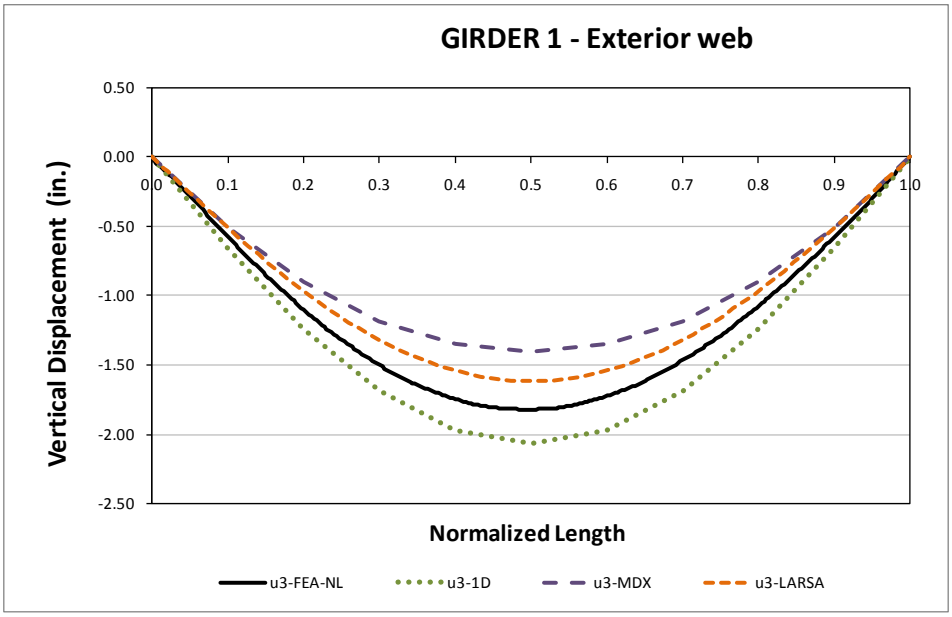

Fig. 3. Top flange vertical displacements for Girder 1 exterior web - Final Steel Dead Load

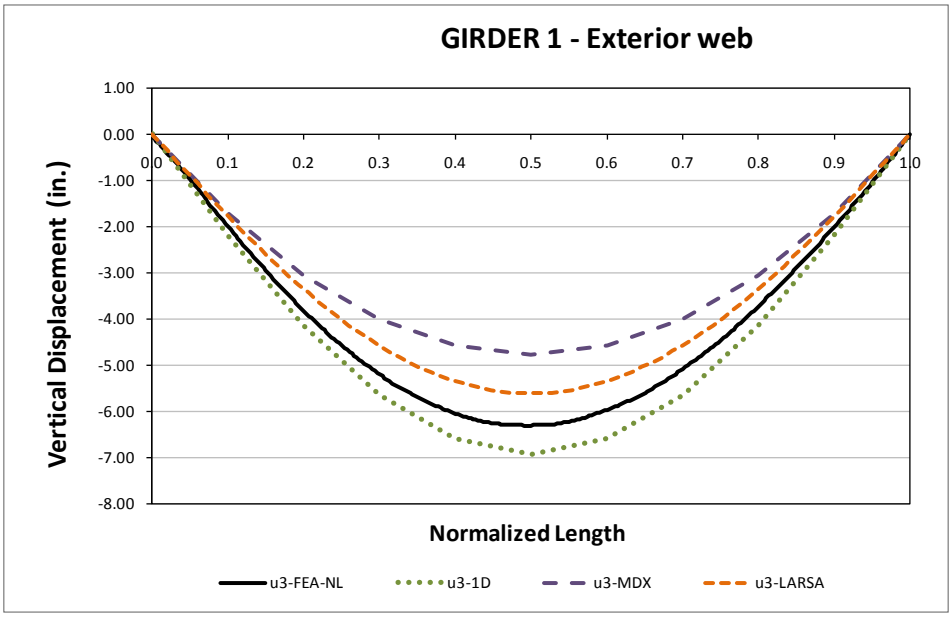

Fig. 4. Top flange vertical displacements for Girder 1 exterior web - Total Dead Load

Figure 5 illustrates the relative radial displacement between top and bottom flange junctures as a measure of lateral displacement. The 3D FEA show initial rotation as both supports ends rotate as the diaphragm plane rotates with respect to the skewed support line causing different lateral displacements on the top and bottom flanges.

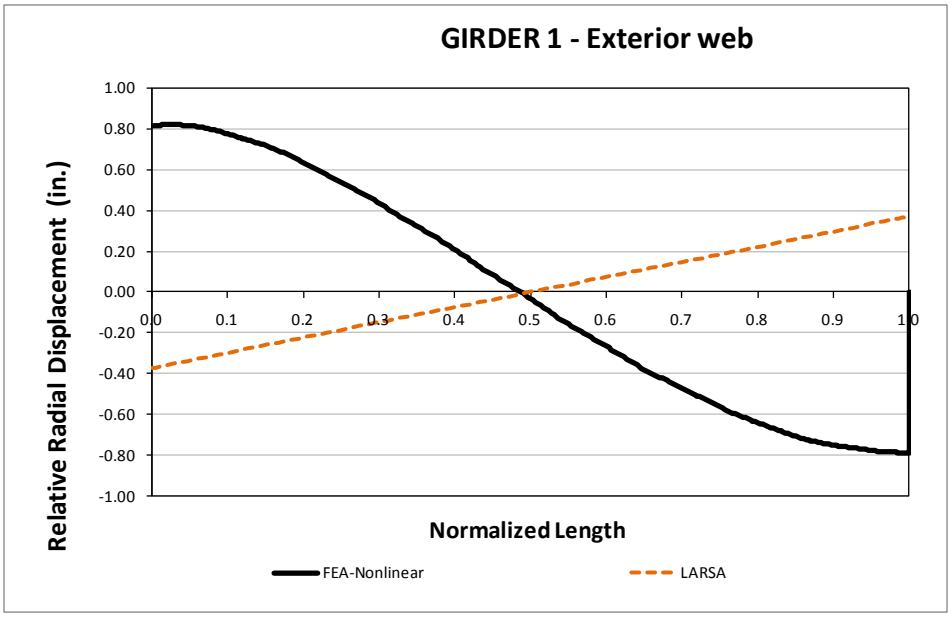

Fig. 5. Top flange relative radial displacements for Girder 1 exterior web - Total Dead Load

Bending Stress Results

Major axis bending stresses are presented in Figures 6 through 9 as predicted by different analysis methods for partial steel erection stages 2 and 4, final steel and total dead load stages. Results in general show a good agreement in shape and magnitude but the MDX result shows a poor prediction mainly due to the discretization size along the span length.

The local interaction of the TFLB system becomes evident in the final steel and total dead load stages. This interaction is lower than the one measured from the NTSSS1 case where the support skew angle was half. Previous to the removal of the temporal supports the interaction becomes noticeable as in contrast with the previous parametric case.

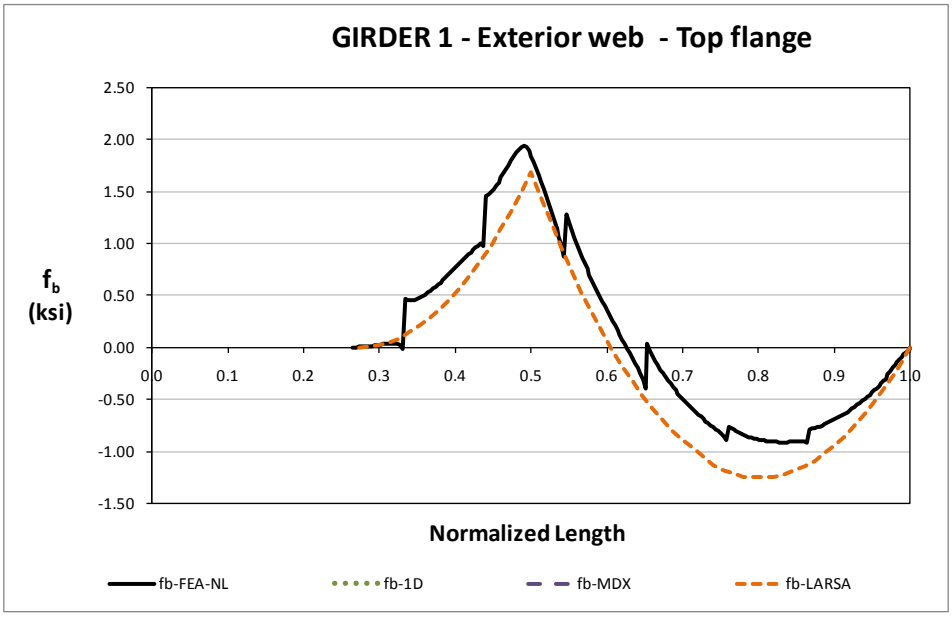

Fig. 6. Top flange major axis bending stress for Girder 1 exterior web - Stage 2 Steel Dead Load

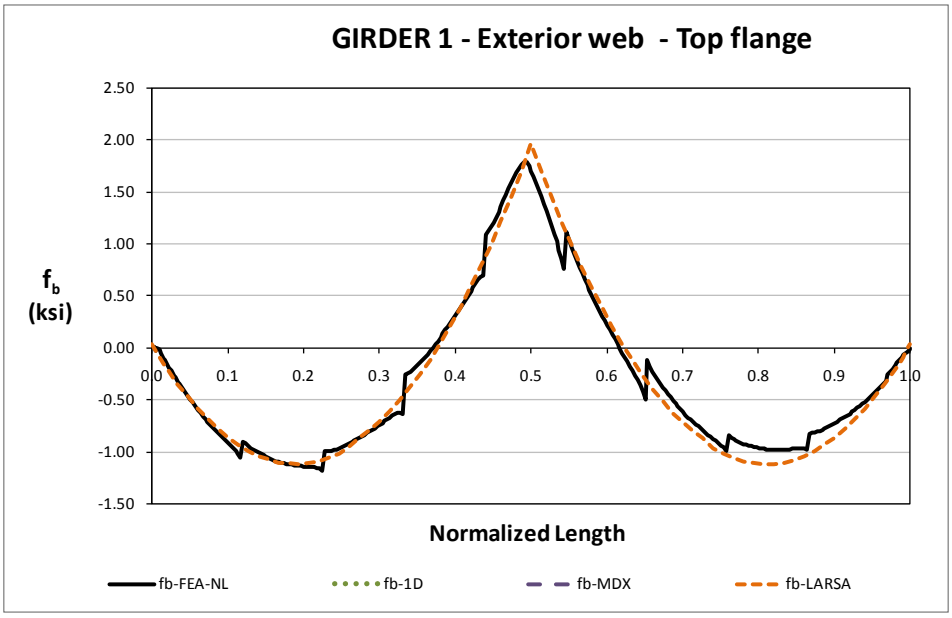

Fig. 7. Top flange major axis bending stress for Girder 1 exterior web - Stage 4 Steel Dead Load

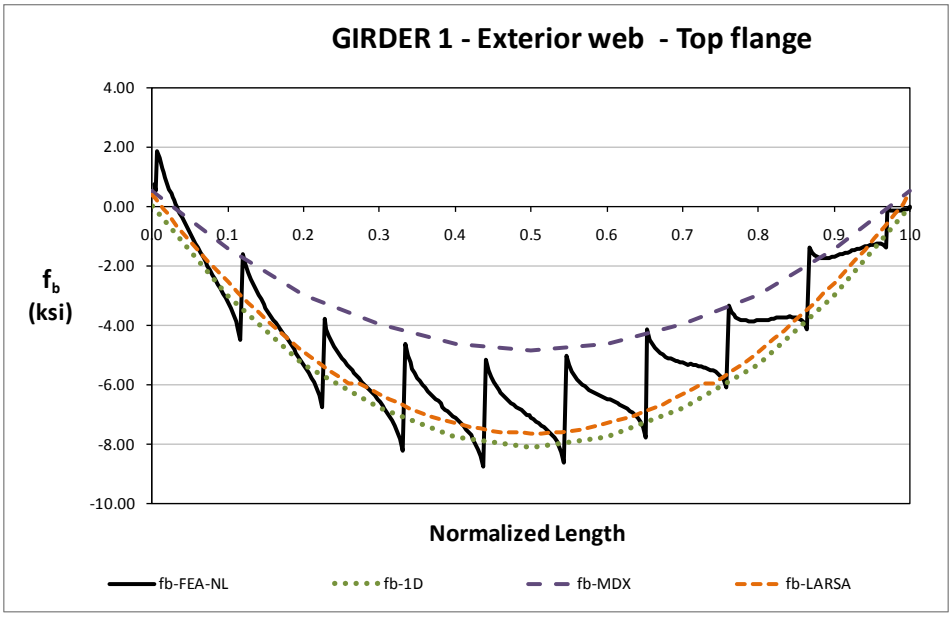

Fig. 8. Top flange major axis bending stress for Girder 1 exterior web - Final Steel Dead Load

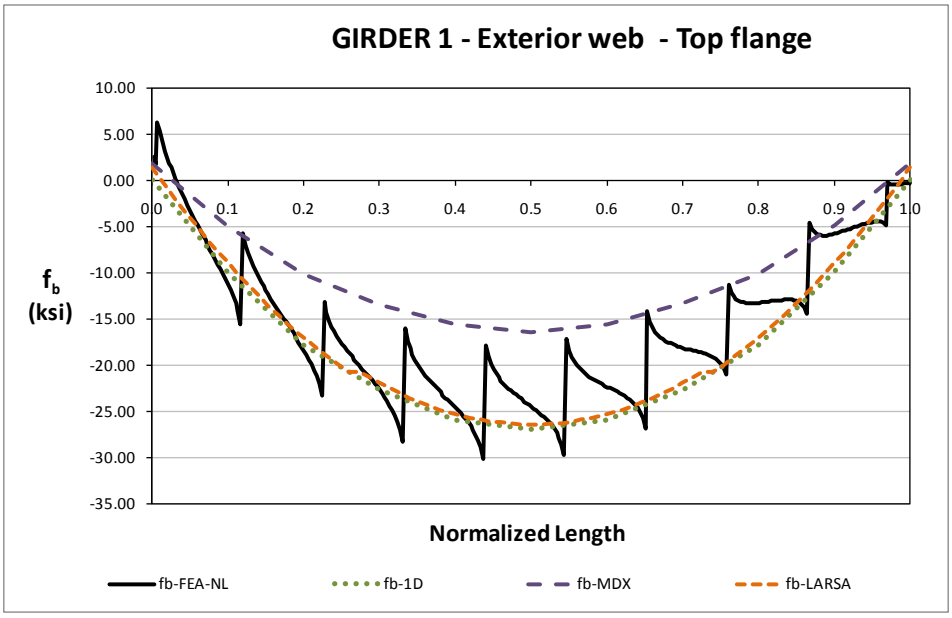

Fig. 9. Top flange major axis bending stress for Girder 1 exterior web - Total Dead Load

Figures 10, 11 and 12 illustrate the bottom flange stresses at the web bottom flange juncture. As discussed before in case NTSSS1, the 3D FEA analysis predicts a highly localized stress concentration at the temporal interior supports on stage 4.

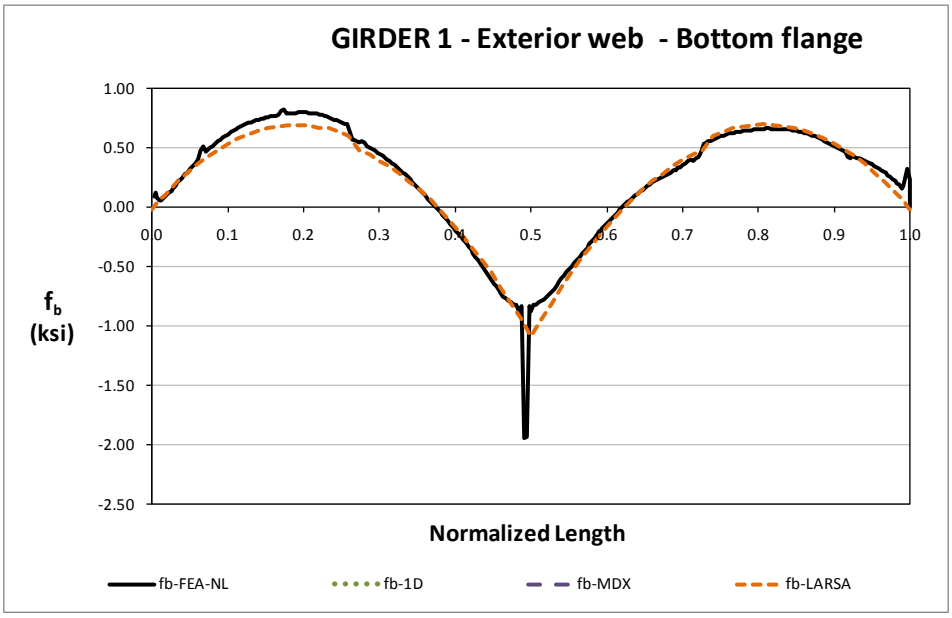

Fig. 10. Bottom flange major axis bending stress for Girder 1 exterior web - Stage 4 Steel Dead Load

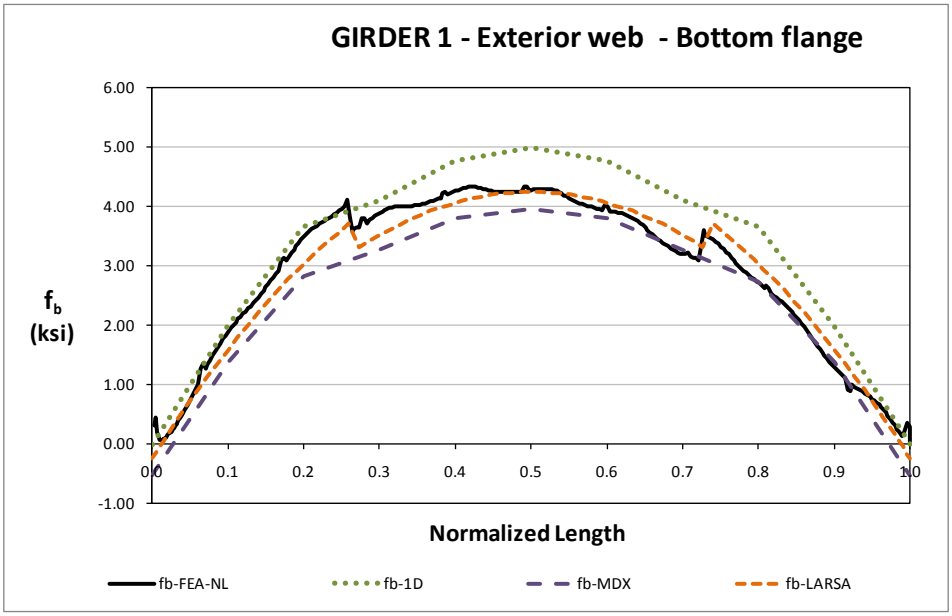

Fig. 11. Bottom flange major axis bending stress for Girder 1 exterior web - Final Steel Dead Load

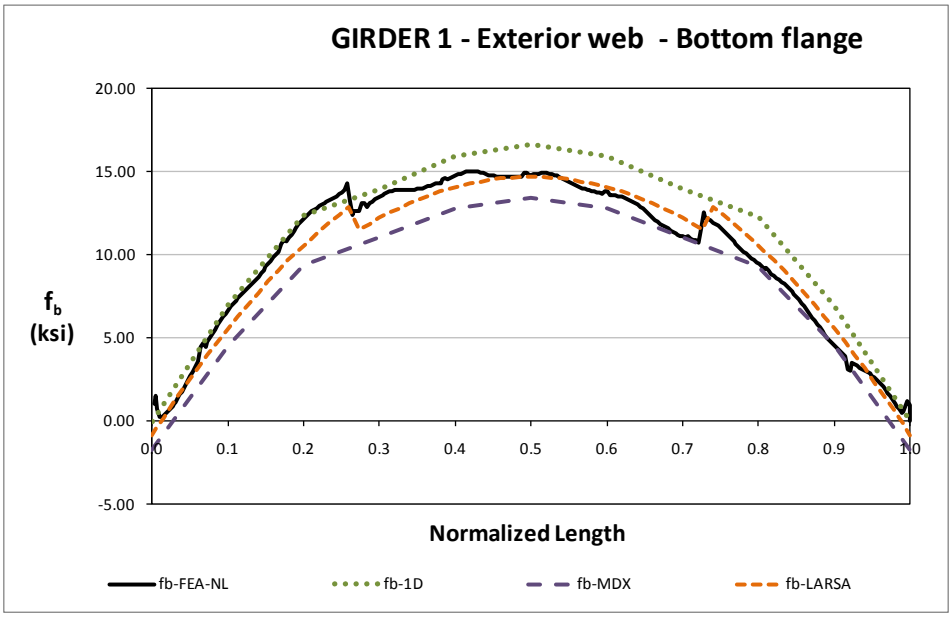

Fig. 12. Bottom flange major axis bending stress for Girder 1 exterior web - Total Dead Load

Lateral bending stress distributions are shown in figure 13, the stresses values remain half in magnitude in contrast with the major axis bending stresses reported above. It is noticeable that the skewed supports cause stresses that are already close to the maximum value reached at the center of the span.

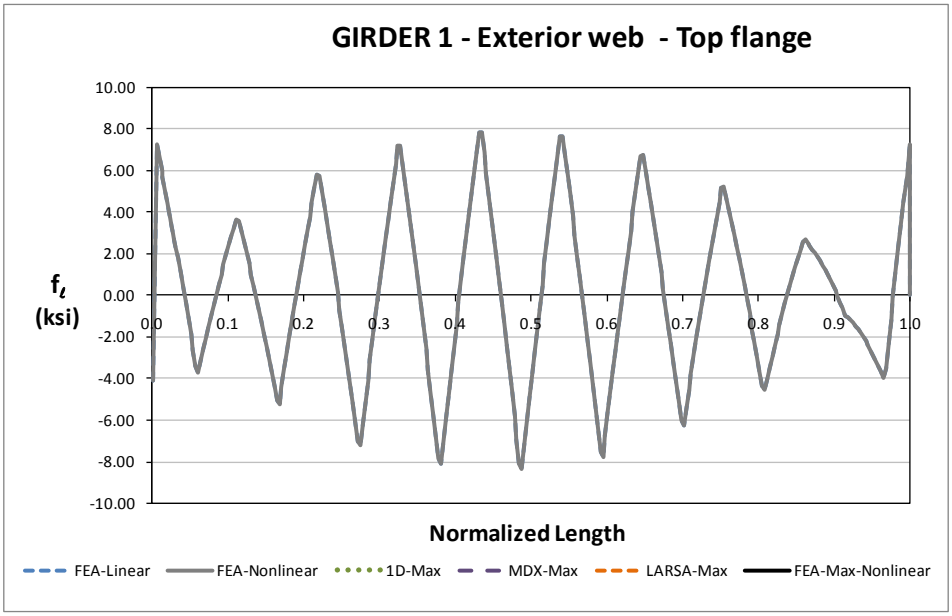

Fig. 13. Top flange lateral bending stress for Girder 1 exterior web - Total Dead Load

Top Flange Lateral Bracing Results

The TFLB diagonals axial forces are shown in Figures 14 through 17 for the partial steel erection stages 2 and 4, final steel and total dead load conditions. The TFLB system is not fully working until the system is released from the temporal supports. The cross sectional area of these elements is 20in² that for a maximum axial force of 150kip as reported by the 3DFEA the element experiences an axial stress of 7.5ksi on the total dead load condition.

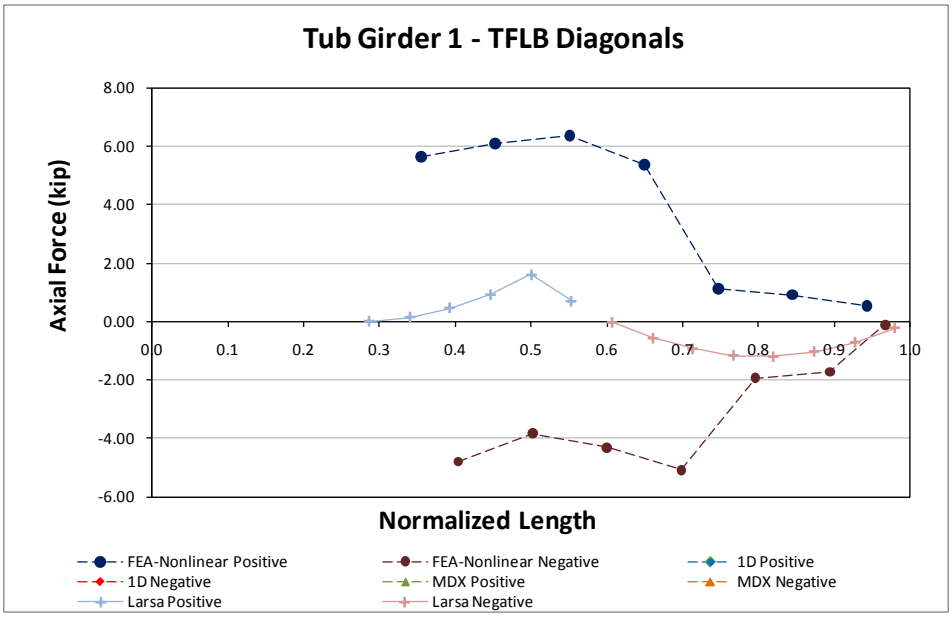

Fig. 14. Top flange lateral bracing diagonals axial forces for Girder 1 - Stage 2 Steel Dead Load

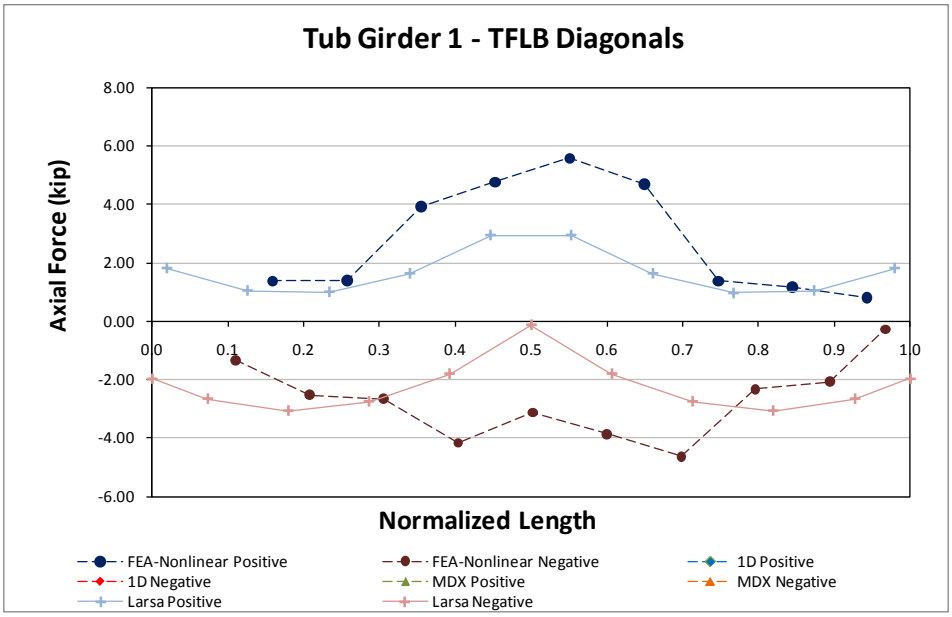

Fig. 15. Top flange lateral bracing diagonals axial forces for Girder 1 - Stage 4 Steel Dead Load

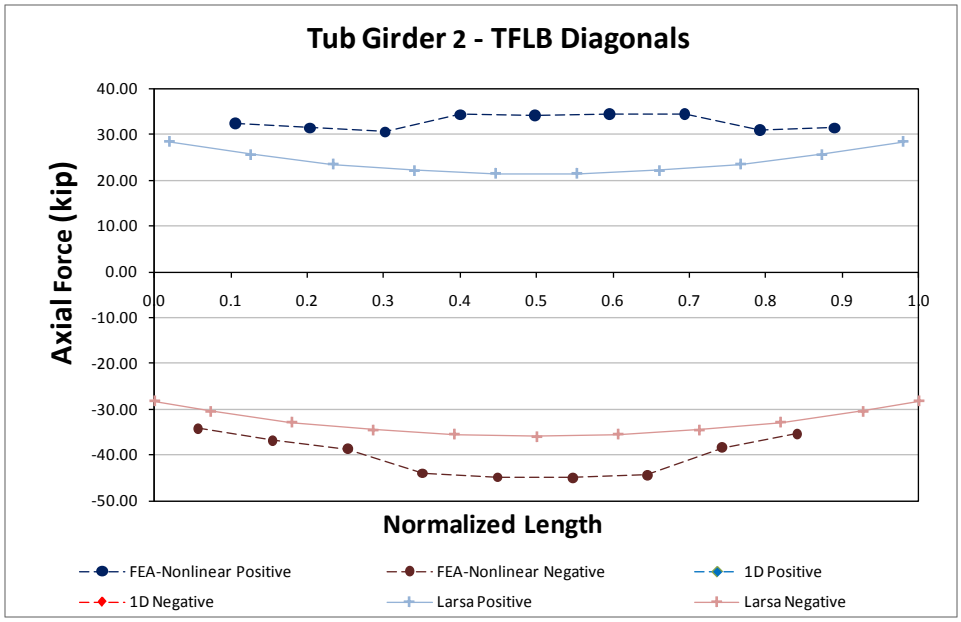

Fig. 16. Top flange lateral bracing diagonals axial forces for Girder 1 - Final Steel Dead Load

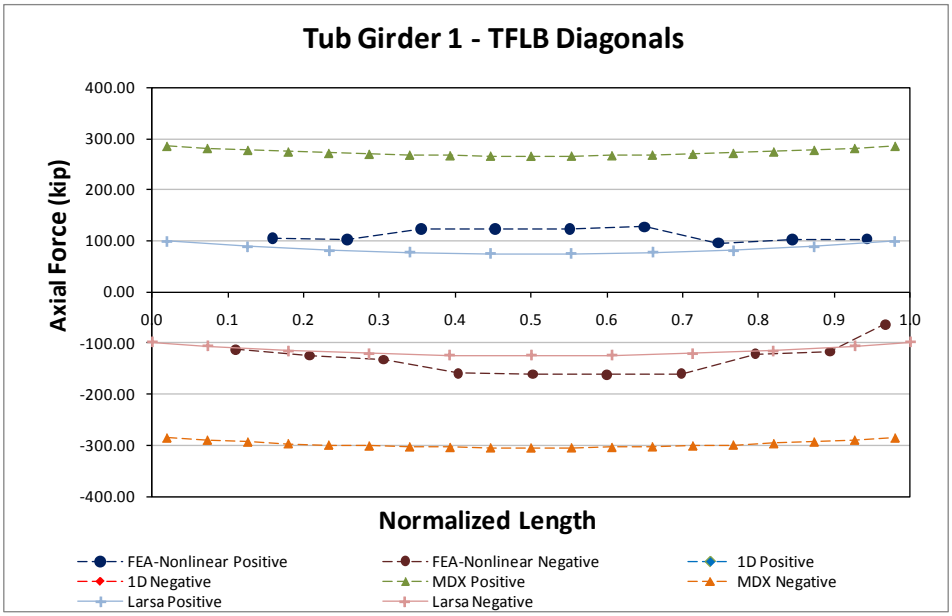

Fig. 17. Top flange lateral bracing struts axial forces for Girder 1 - Total Dead Load

Figure 18 shows the TFLB axial forces on the struts for the total non-composite deal load case. The area of the struts is 4.4in² which, for a maximum axial force of 21kip as reported by LARSA analysis, results on maximum axial stress of 4.8ksi. The 3DFEA reports lower values, partly because the model accommodates girder rotations which release the elements from forces.

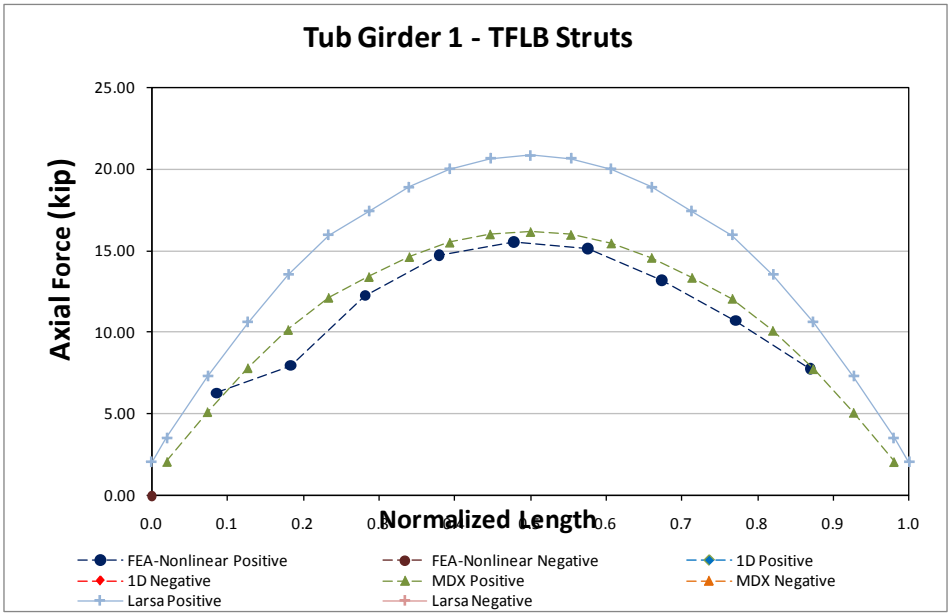

Fig. 18. Top flange lateral bracing struts axial forces for Girder 1 - Total Dead Load

When comparing with the NTSSS1 case, the forces of the TFLB diagonals and struts double as the skew angle doubles.

9.4 NTSSS4 (New, Tub-girder, Simple-span, Straight, Skewed supports)

Bridge Description:

Category Data:

L_1 = 150 ft / w = 30 ft / θ=30°, θ=-30°, 2 tub-girders

References:

Erection Stages Analyzed: 2 steel erection stages

Deck Placement Sequence: One stage, deck thickness = 9.5 in

Bridge Perspective & Plan Views:

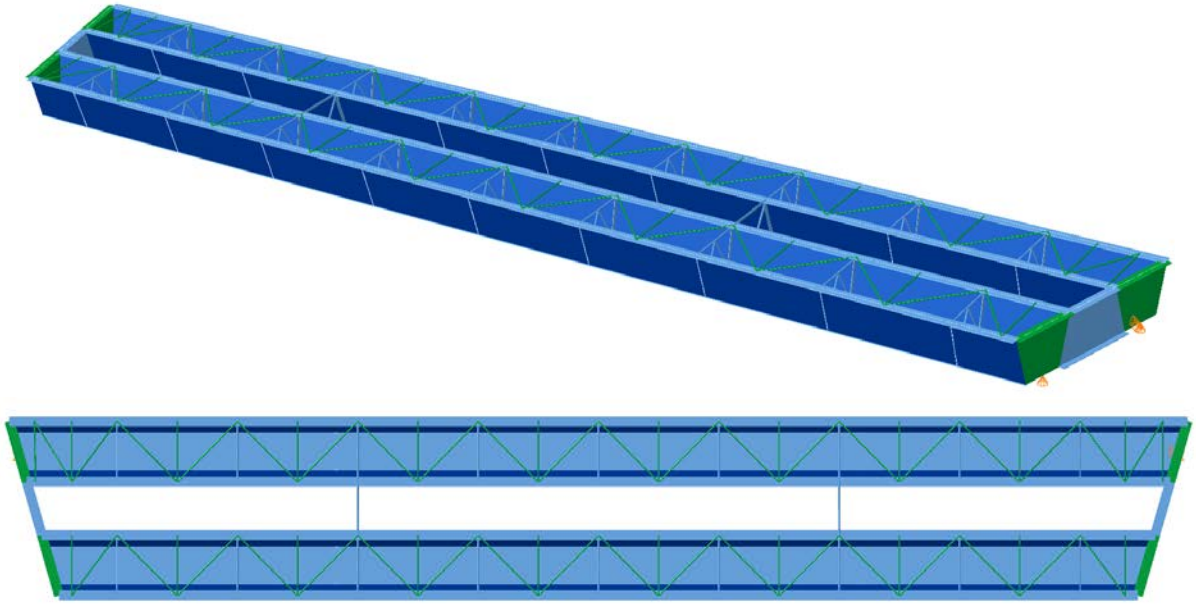

Displacement Results

In contrast with the previous two parametric cases NTSSS1 and NTSSS2 with parallel skew supports, this case has reversed skewed supports meaning that in a plan view the left support line is rotated counterclockwise while the right is clockwise.

Figures 1, 2 and 3 show the partial steel erection stage 4, final steel and non-composite total dead load displacements for the top flange and the exterior web juncture of Girder 1, in other words, the top flange of the lowest web in a plan view. The vertical displacements are plotted for four different methods of analysis: non-linear refined 3D FEA, 1D and using 2D analysis software MDX and LARSA. All methods show a close prediction of results.

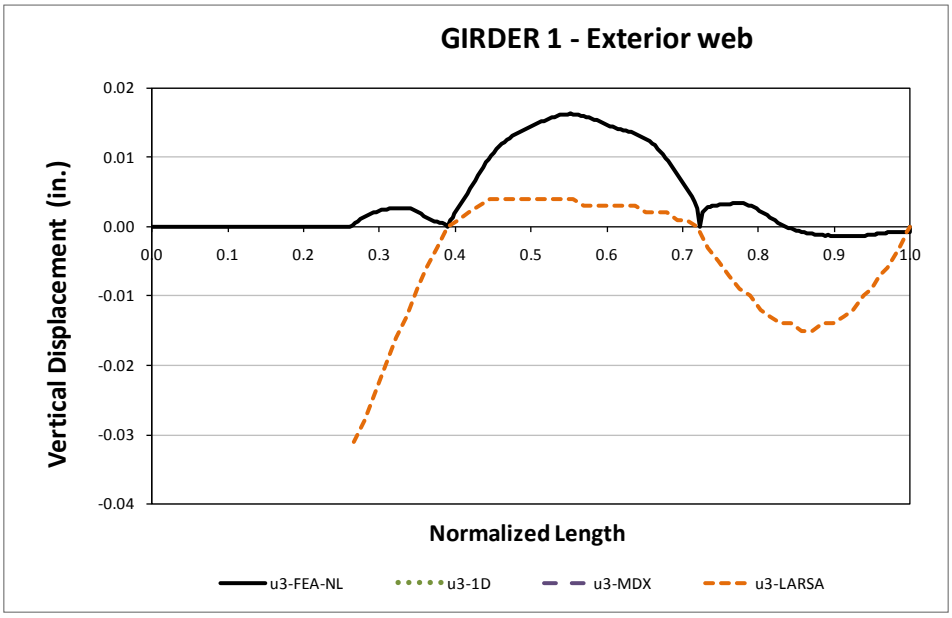

Fig. 1. Top flange vertical displacements for Girder 1 exterior web - Stage 4 Steel Dead Load

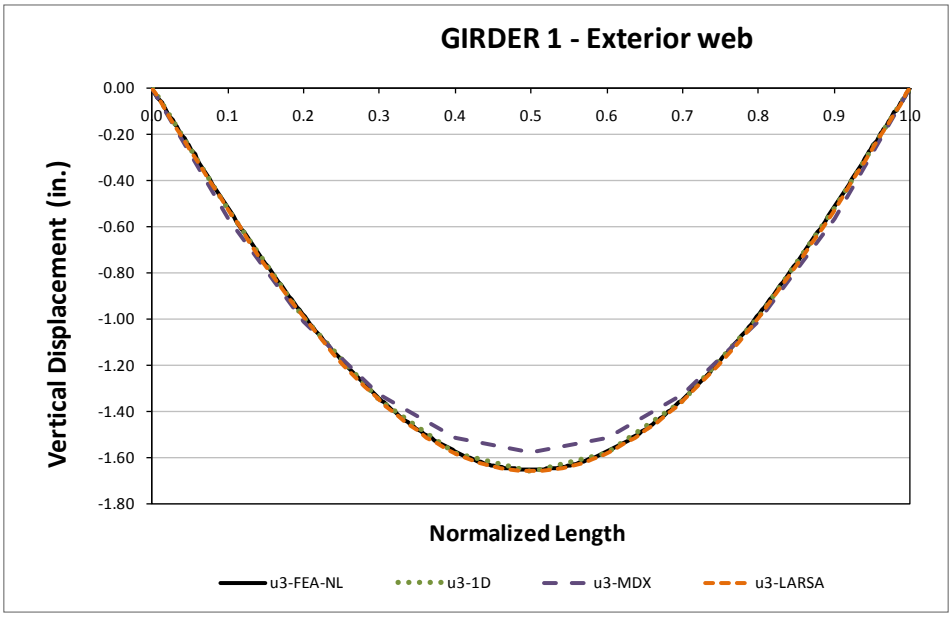

Fig. 2. Top flange vertical displacements for Girder 1 exterior web - Final Steel Dead Load

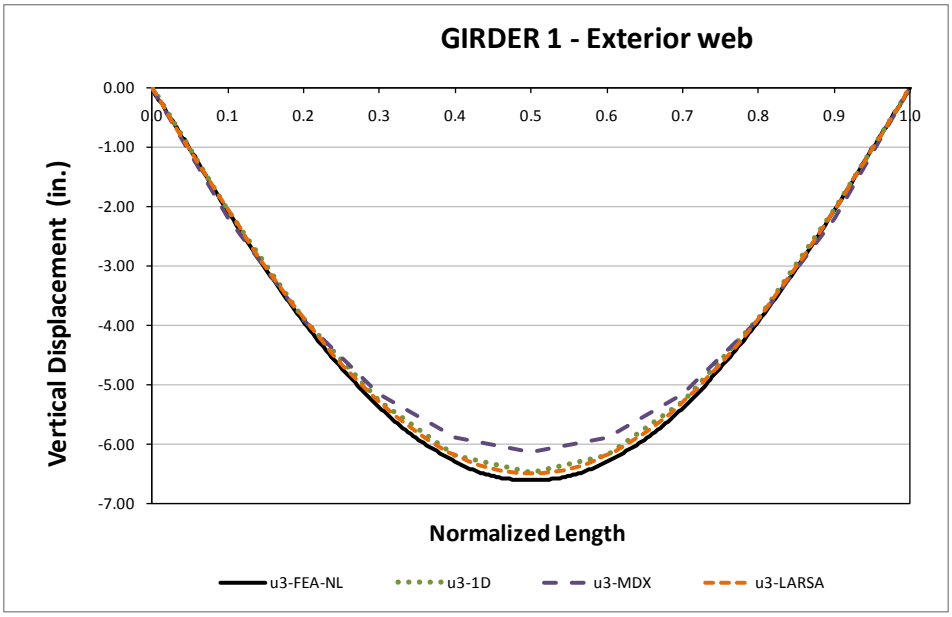

Fig. 3. Top flange vertical displacements for Girder 1 exterior web - Total Dead Load

Figure 4 illustrates the relative radial displacement between top and bottom flange junctures as a measure of lateral displacement. The 3D FEA show initial rotation as both supports ends rotate as the diaphragm plane rotates with respect to the skewed support line causing different lateral displacements on the top and bottom flanges.

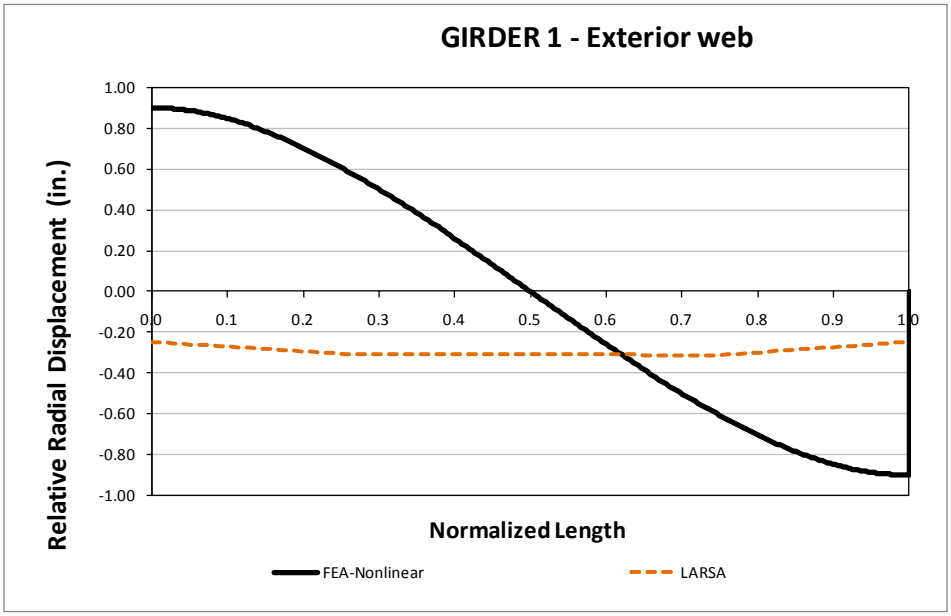

Fig. 4. Top flange relative radial displacements for Girder 1 exterior web - Total Dead Load

Bending Stress Results

Major axis bending stresses are presented in Figures 5, 6 and 7 for the partial steel erection stages 4, final steel and total dead load stages. In general results show a good agreement in shape and magnitude. Contrary to the past cases, TFLB does not have direct effect on the bending stresses.

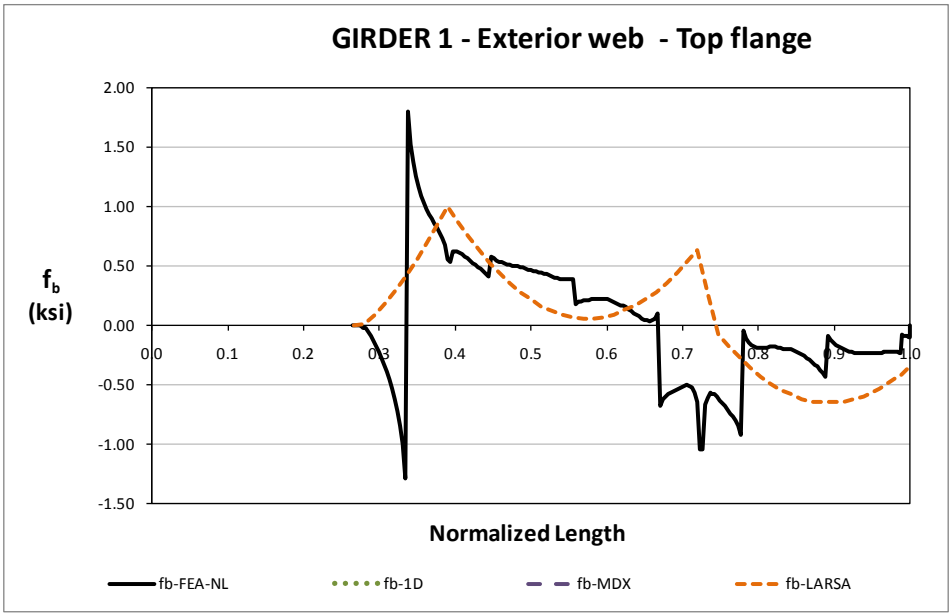

Fig. 5. Top flange major axis bending stress for Girder 1 exterior web - Stage 4 Steel Dead Load

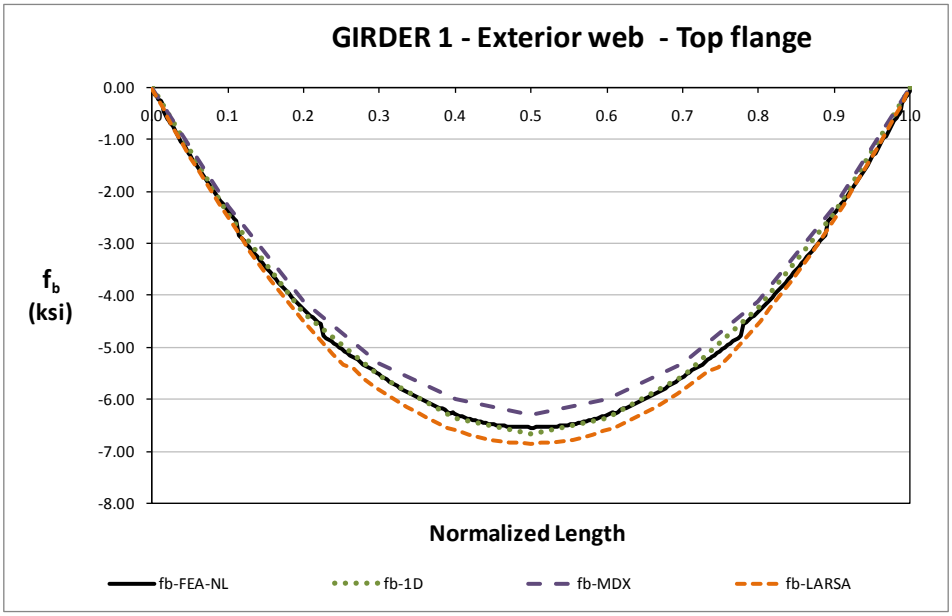

Fig. 6. Top flange major axis bending stress for Girder 1 exterior web - Final Steel Dead Load

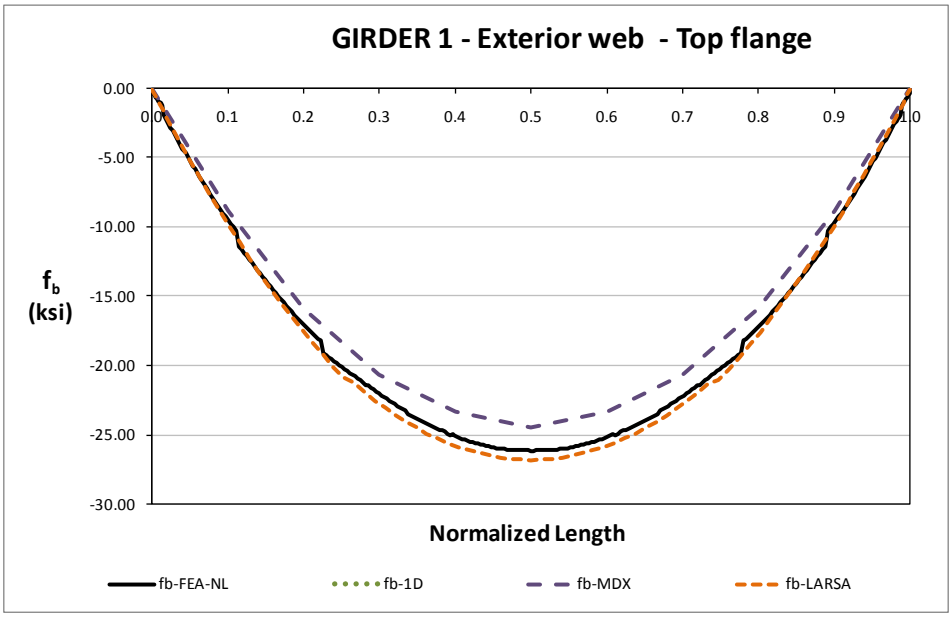

Fig. 7. Top flange major axis bending stress for Girder 1 exterior web - Total Dead Load

Figures 8, 9 and 10 illustrate evolution of the bottom flange stresses at the web bottom flange juncture for the partial steel erection stage 4, final steel and non-composite total dead load conditions.

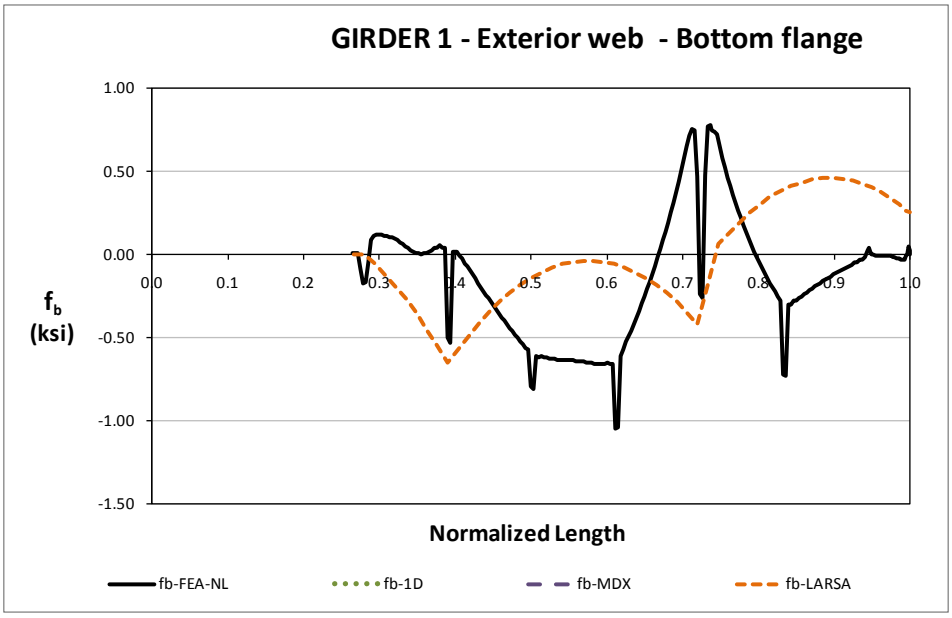

Fig. 8. Bottom flange major axis bending stress for Girder 1 exterior web - Stage 4 Steel Dead Load

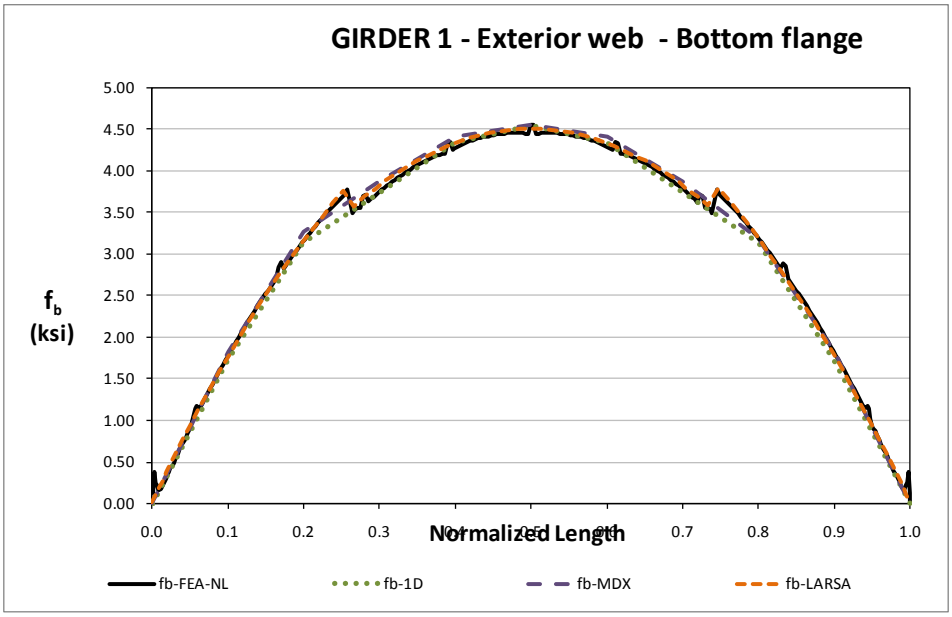

Fig. 9. Bottom flange major axis bending stress for Girder 1 exterior web - Final Steel Dead Load

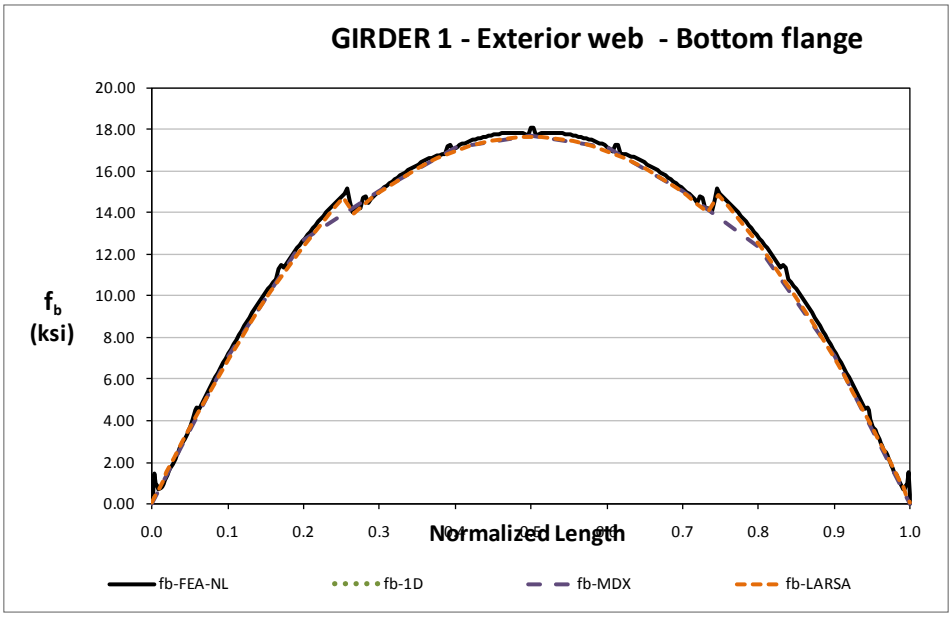

Fig. 10. Bottom flange major axis bending stress for Girder 1 exterior web - Total Dead Load

Lateral bending stress distributions are shown in figure 11, the stresses values remain half in magnitude in contrast with the major axis bending stresses reported above. It is noticeable that the skewed supports cause stresses that are already close to the maximum value reached at the center of the span.

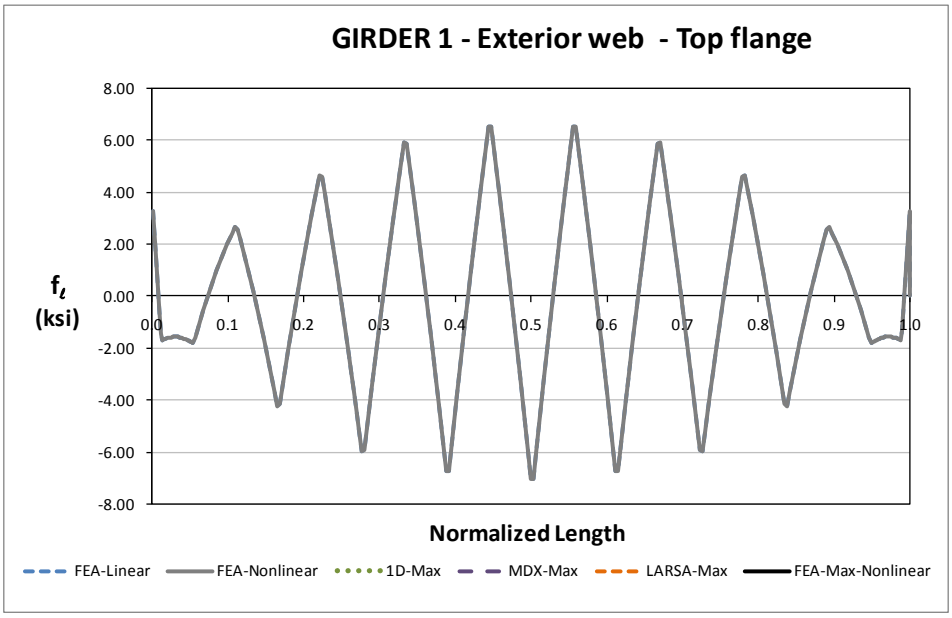

Fig. 11. Top flange lateral bending stress for Girder 1 exterior web - Total Dead Load

Top Flange Lateral Bracing Results

The TFLB diagonals axial forces are shown in Figures 12 and 13 for the final steel and total dead load conditions. The cross sectional area of these elements is 4.4in² that for a maximum axial force of 20kip as reported by the 3DFEA the element experiences an axial stress of 4.5ksi on the total dead load condition. The forces on the TFLB diagonals suggest an almost constant torque distribution along the bridge length

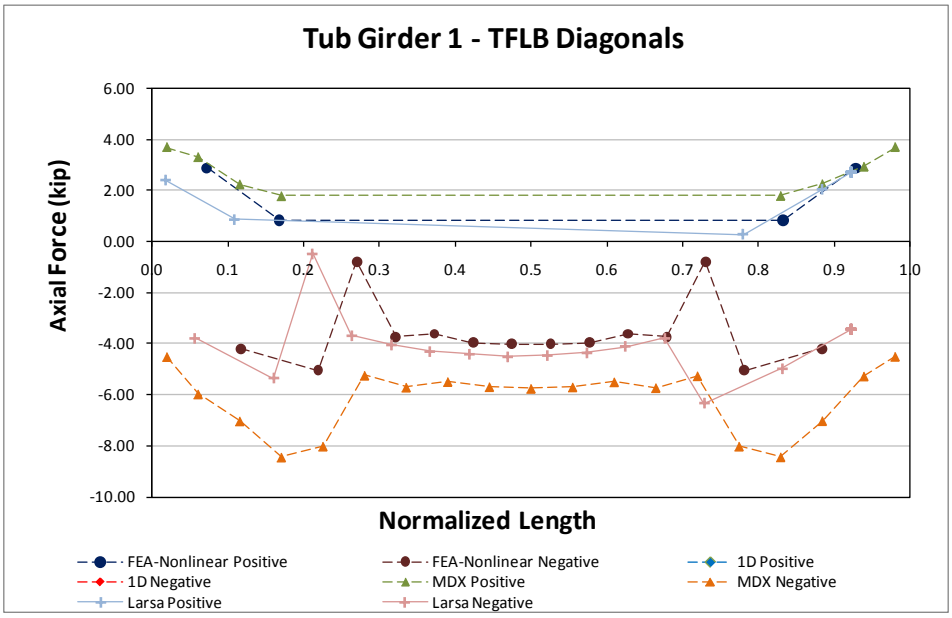

Fig. 12. Top flange lateral bracing diagonals axial forces for Girder 1 - Final Steel Dead Load

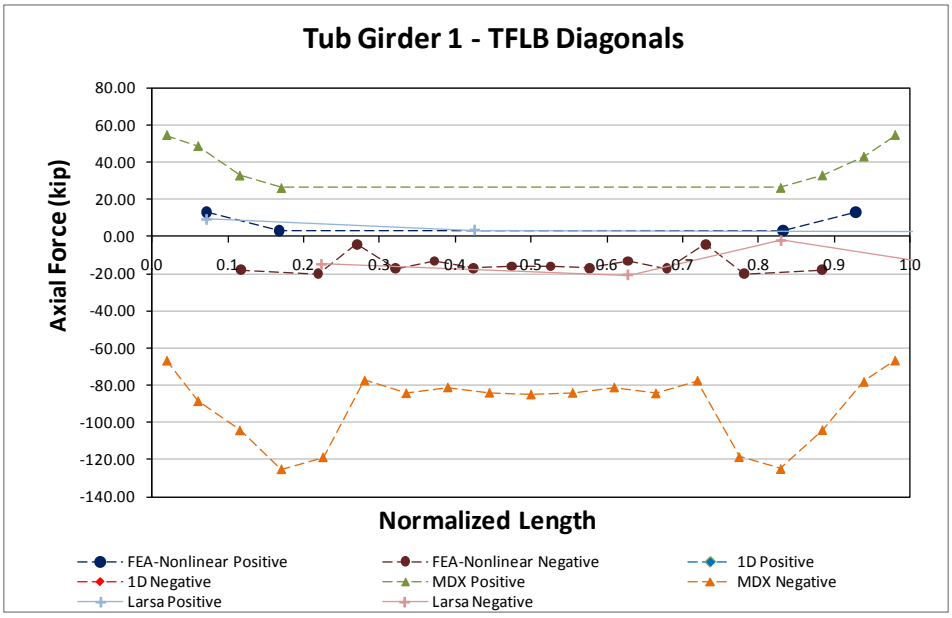

Fig. 13. Top flange lateral bracing struts axial forces for Girder 1 - Total Dead Load

Figure 14 shows the TFLB axial forces on the struts for the total non-composite deal load case. The area of the struts is 4.4in² which, for a maximum axial force of 14kip as reported by the 3D FEA analysis, results on maximum axial stress of 3.1ksi.

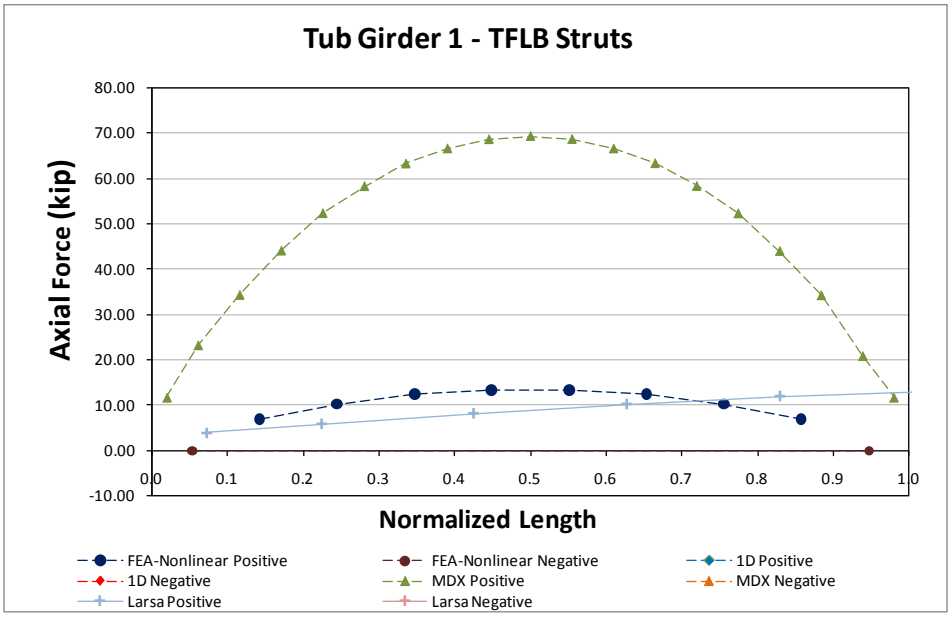

Fig. 14. Top flange lateral bracing struts axial forces for Girder 1 - Total Dead Load

Internal Cross Frame Results

Figure 15 shows the internal CF diagonal axial forces. The cross sectional area of this element is 4.4in² so that the axial forces reported correspond to a maximum axial stress of 0.6ksi.

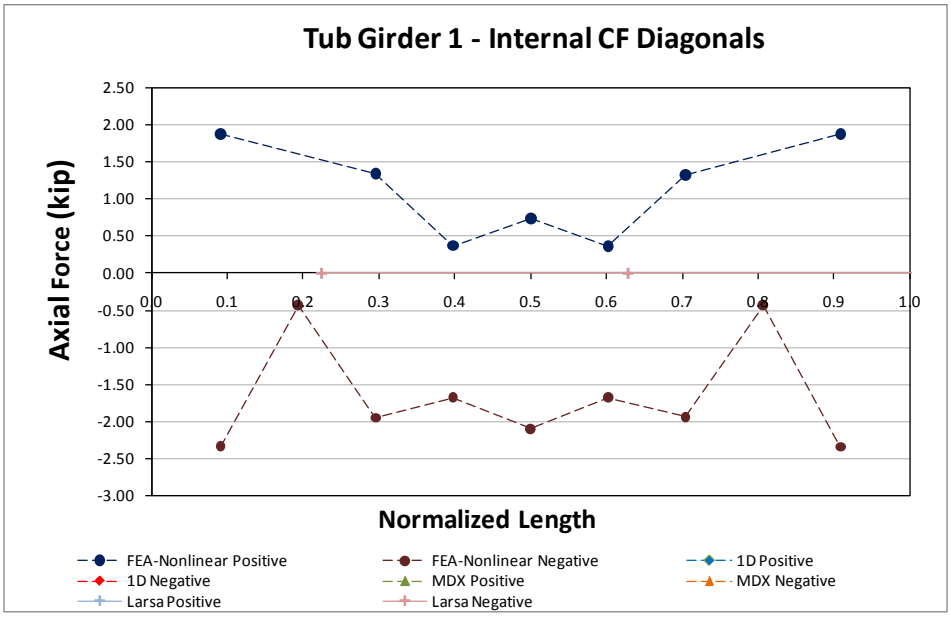

Fig. 15. Internal cross frame diagonal axial forces for Girder 1 - Total Dead Load

10.1 NTSCR1 (New, Tub-girder, Simple-span, Curved, Radial supports)

Bridge Description:

Category Data:

L_1 = 150ft / R = 400 ft / w = 30 ft, 2 tub-girders

References:

Erection Stages Analyzed: 2 steel erection stages

Deck Placement Sequence: One stage, deck thickness = 9.5 in

Bridge Perspective & Plan Views:

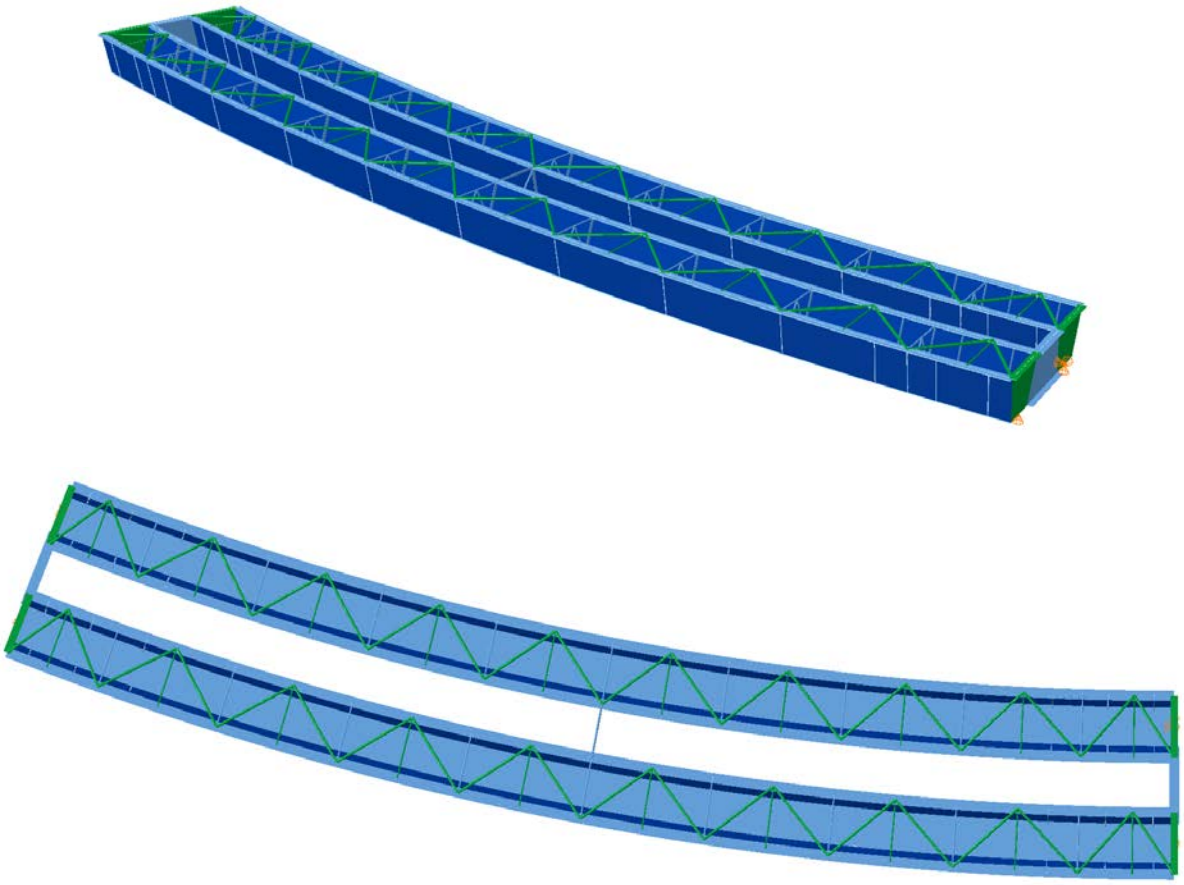

Displacement Results

Displacements and stress results are reported at the web flange juncture locations. Each tub girder has then four sets of results and each web has two for top flange and bottom flange. The girder numbering is assigned from the largest radius to the lowest, meaning that Girder 1 is always the external girder and Girder 2 is the interior girder in a twin girder system. Webs are assigned as internal and external with respect to their actual radii, meaning that the most exterior web is always on girder 1 and for a twin tub system the most interior web is located on girder 2. In a plan view the center of curvature is located above the girder leading to a concave upwards system. Straight systems follow a similar rule and will be addressed on the appropriate bridges.

Results will be shown for relevant construction stages from partial steel erection, final steel and non-composite total dead load; the non-composite total dead load condition includes the weight of steel and the concrete slab considering that concrete is on a wet condition and not providing any resistance to the system. The following figures will illustrate the results on the top and bottom web-flange juncture locations of a selected girder.

Figures 1 and 2 show the final steel and non-composite total dead load displacements for the top flange and the interior web juncture of Girder 2, in other words, the top flange of the most interior web. The vertical displacements (u3) are plotted for four different methods of analysis: non-linear refined 3D FEA, 1D and using 2D analysis software MDX and LARSA. All methods show a close prediction of results, discrepancies on the results are mainly attributed to the discretization used by the analysis method leading to a system slightly stiffer when the bridge is represented by a lower number of elements along the length.

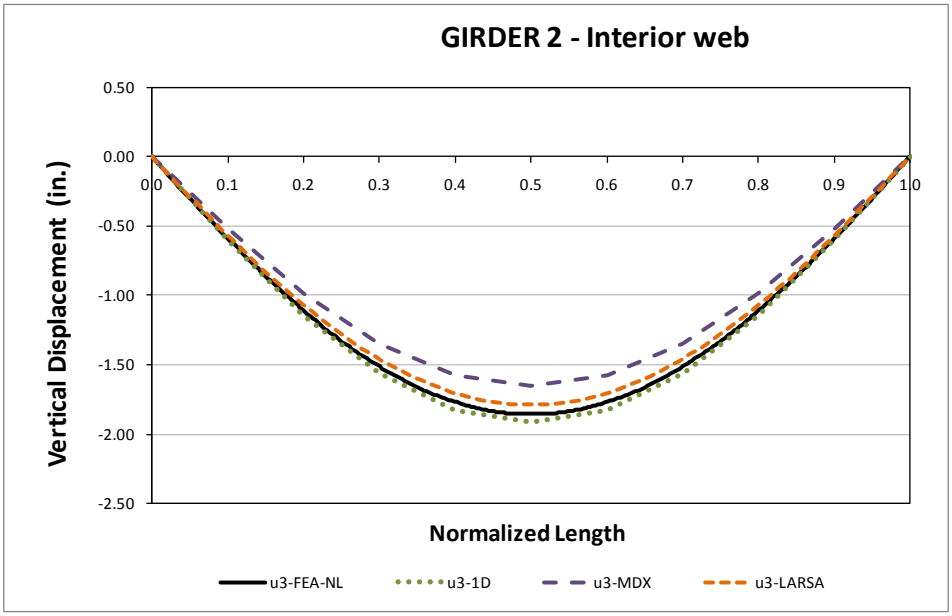

Fig. 1. Top flange vertical displacements for Girder 2 interior web - Final Steel Dead Load

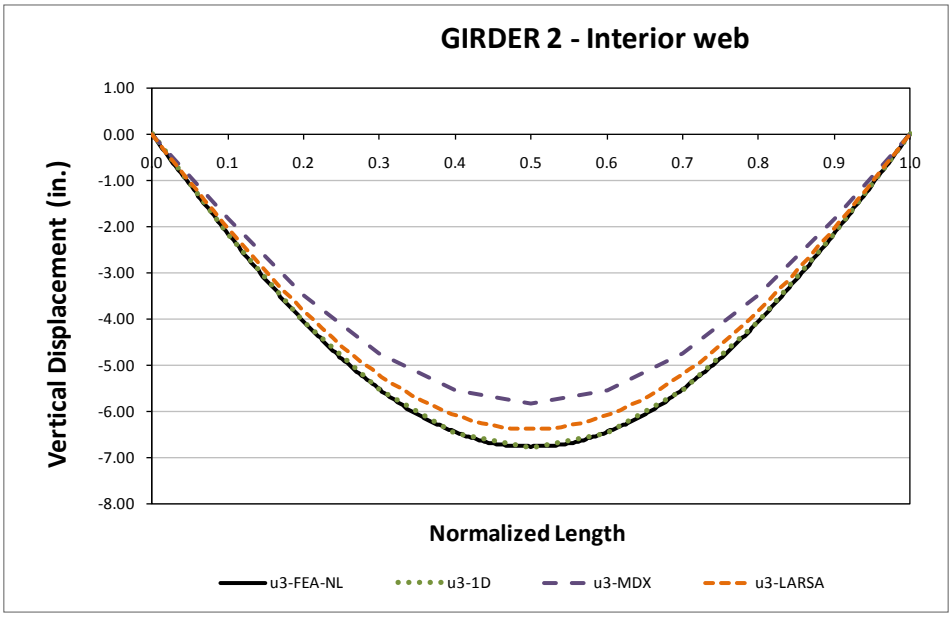

Fig. 2. Top flange vertical displacements for Girder 2 interior web - Total Dead Load

The top flange relative radial displacements are shown in fig. 3, the results are shown for the 3DFEA and LARSA models. The local variation between both methods can be attributed to the discretization of the girders at the braced points for the LARSA analysis.

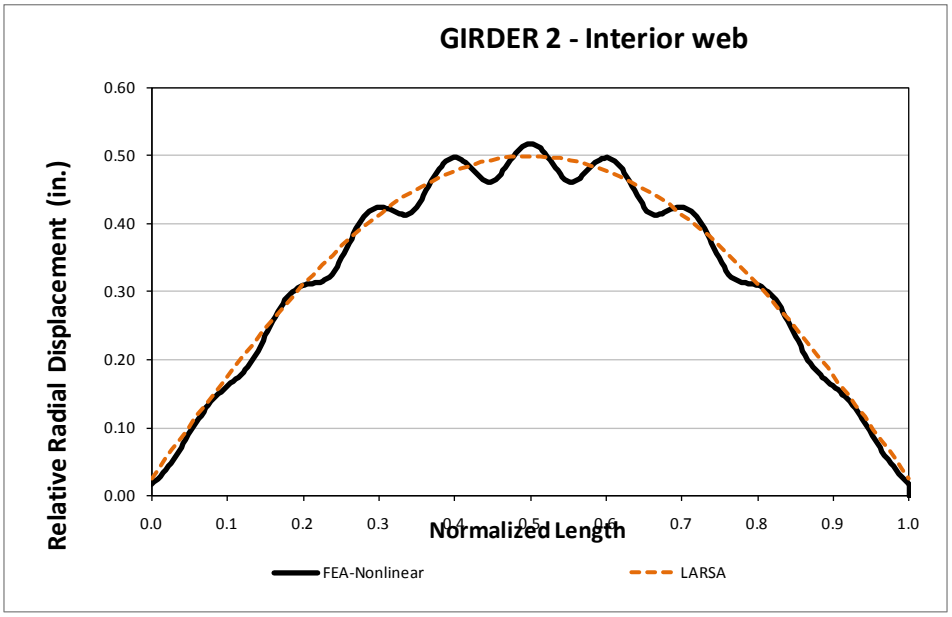

Fig. 3. Top flange relative radial displacements for Girder 2 interior web - Total Dead Load

Bending Stress Results

Major axis bending stresses for Girder 2 – Interior web are presented in Figures 4 and 5 for the final steel and total non-composite dead load construction stages as predicted by the different analysis methods. In this case, 3D results show localized effects due to the Top flange Lateral Bracing system presence. Similar results are shown on fig. 6 for the same girder but in this case for the exterior web which experiences the same localized effects but in a different distribution matching the flange bracing on that flange.

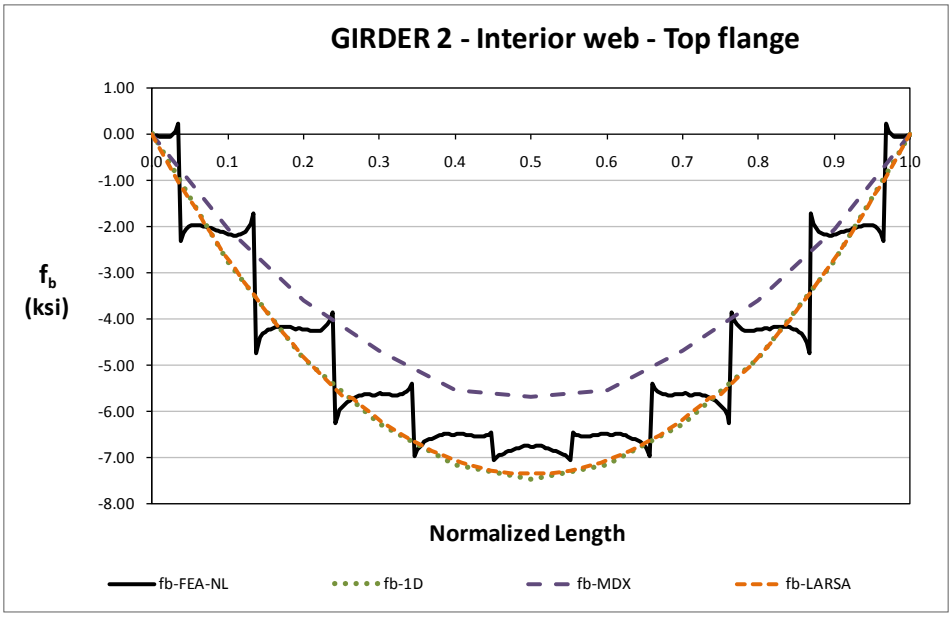

Fig. 4. Top flange major axis bending stress for Girder 2 interior web - Final Steel Dead Load

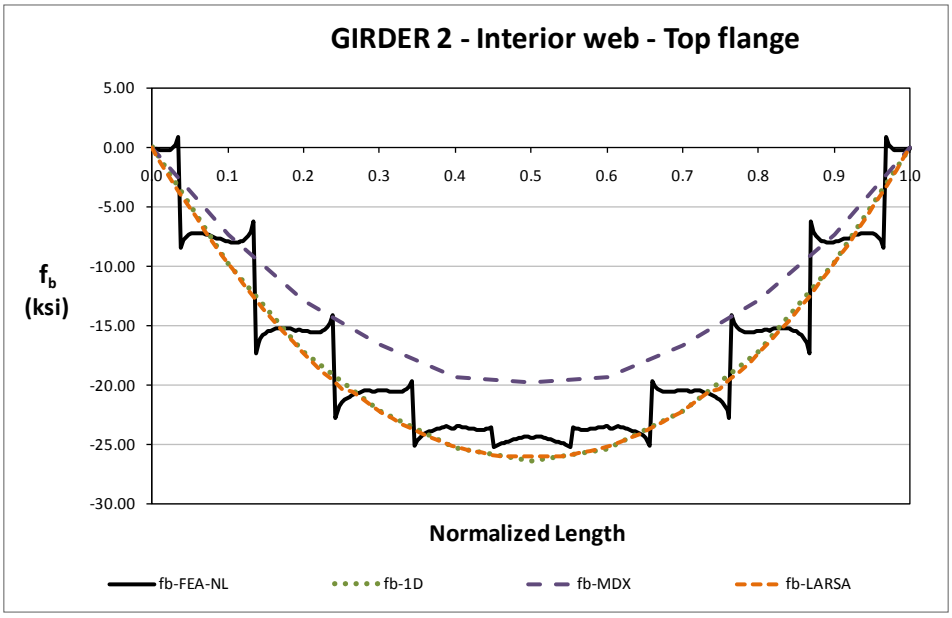

Fig. 5. Top flange major axis bending stress for Girder 2 interior web - Total Dead Load

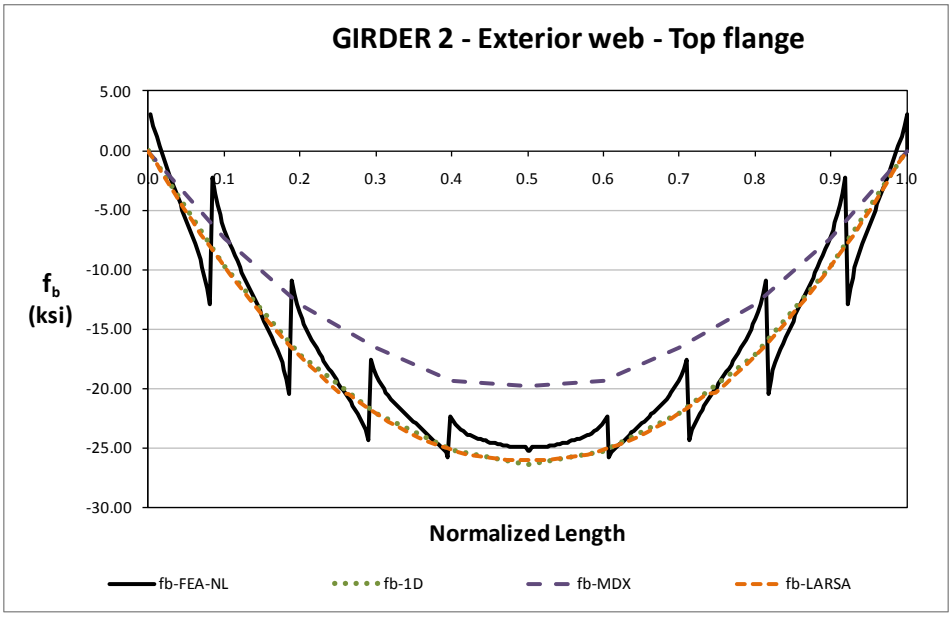

Fig. 6. Top flange major axis bending stress for Girder 2 exterior web - Total Dead Load

Figures 7 and 8 illustrate the major axis bending stresses at the web and bottom flange juncture for Girder 2 interior and exterior webs. The 3D FEA analysis predicts localized stress concentrations at the cross-frame locations in contrast as for the top flange where this happens at the TFLB locations. These stress concentrations are believed to be caused by the local interaction of the web, flange and connection plate.

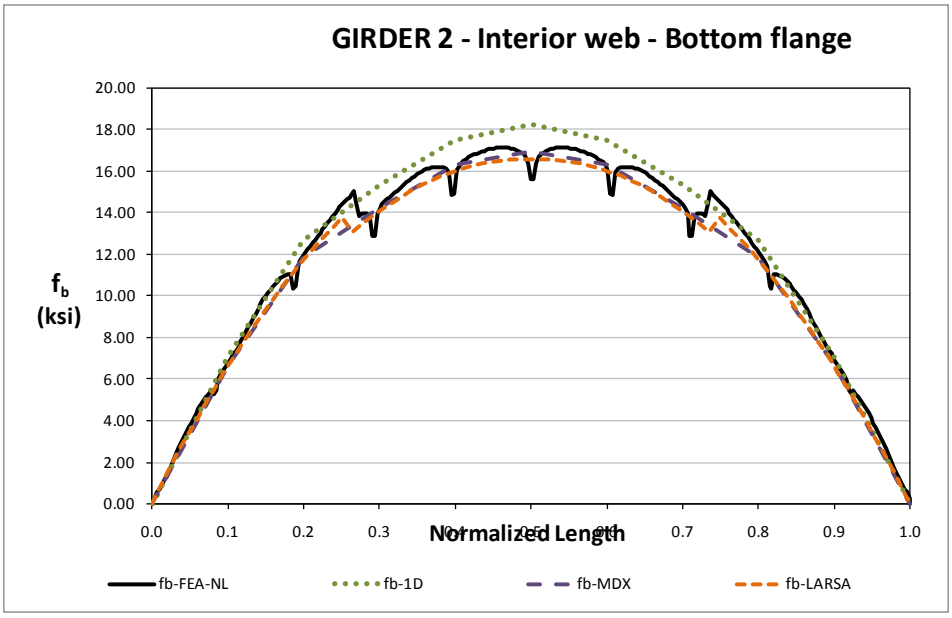

Fig. 7. Bottom flange major axis bending stress for Girder 2 interior web - Total Dead Load

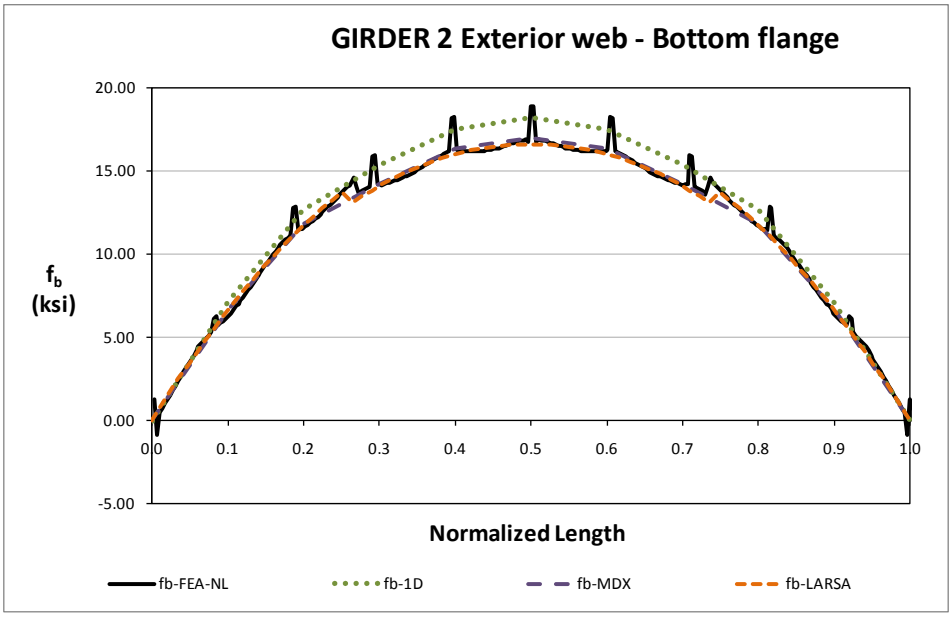

Fig. 8. Bottom flange major axis bending stress for Girder 2 exterior web - Total Dead Load

Top Flange Lateral Bracing Results

The TFLB diagonals axial forces are shown in Figures 9 and 10 for the final steel and total dead load condition. The cross sectional area of these elements is 14.1in² that for a maximum axial force of 270kip the element experiences an axial stress of 19ksi on the total dead load condition.

The forces on the TFLB diagonals match the expected torque distribution along the bridge length with maximum values at the support and vanishing at the span center. The reported axial force distribution by the different analysis methods follows the same law.

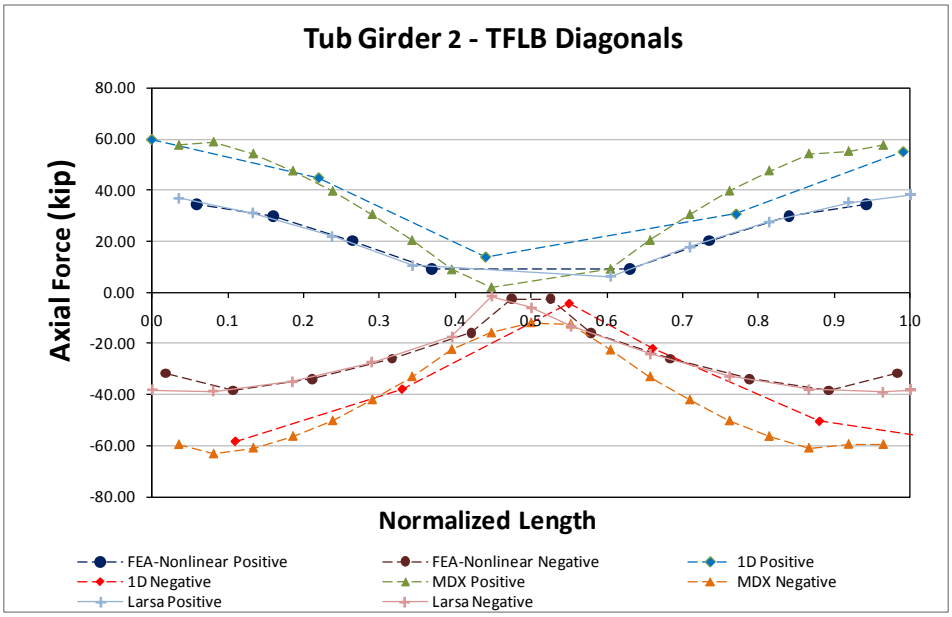

Fig. 9. Top flange lateral bracing diagonals axial forces for Girder 2 - Final Steel Dead Load

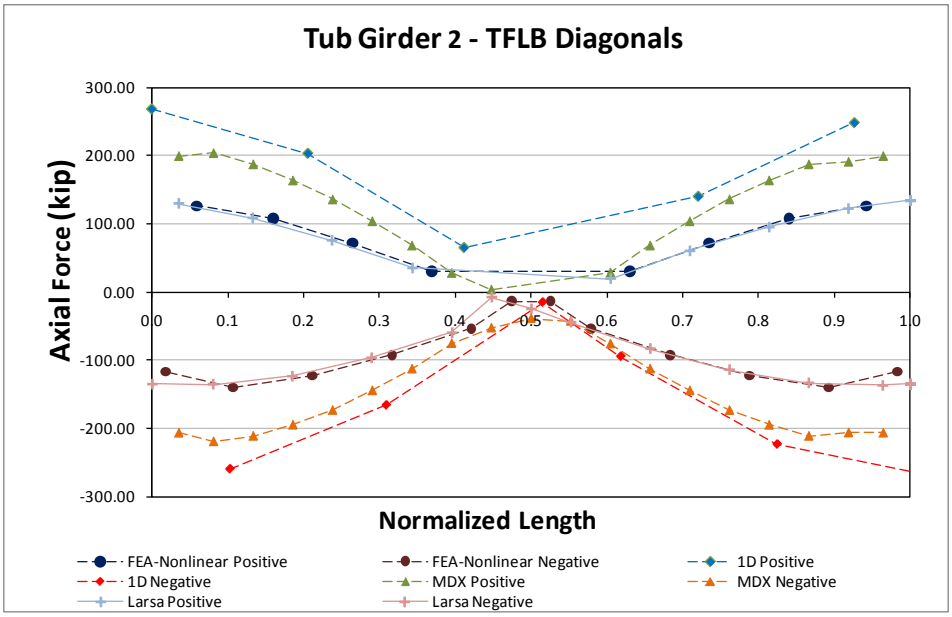

Fig. 10. Top flange lateral bracing diagonals axial forces for Girder 2 - Total Dead Load

Figure 11 shows the TFLB axial forces on the struts for the total non-composite deal load case. The area of the struts is 4.4in² which, for a maximum axial force of 25kip as reported by the 3D FEA analysis, results on maximum axial stress of 5.5ksi. As shown by Fan and Helwig (1999) the axial forces on the struts are proportional to the top flange major and minor axis bending stresses with similar distribution as those shown in fig. 11.

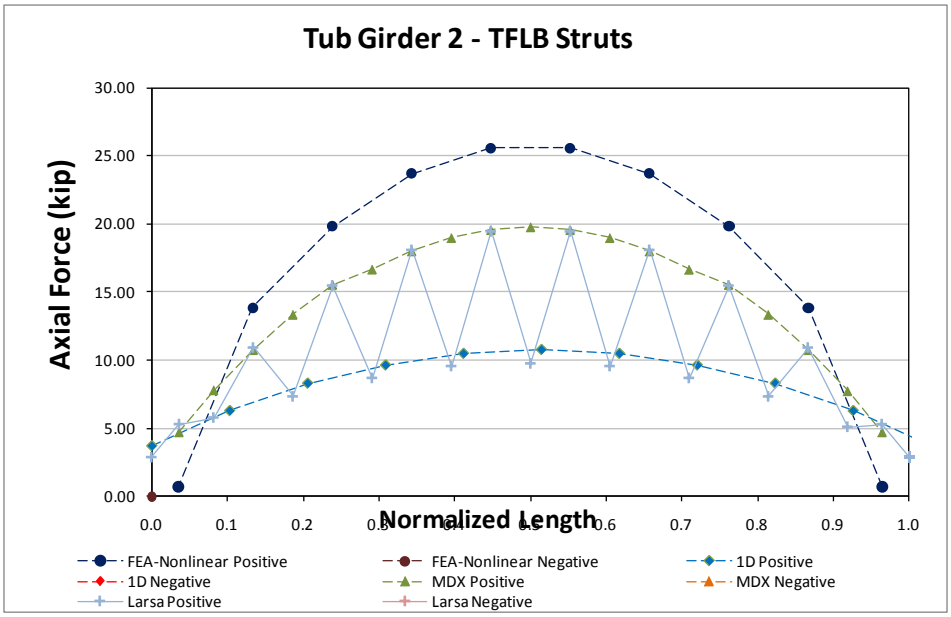

Fig. 11. Top flange lateral bracing struts axial forces for Girder 2 - Total Dead Load

Internal Cross Frame Results

Internal cross frames alternate in every other panel, these elements are composed by diagonals and top chords. Figure 12 shows the internal CF diagonal axial forces while Figure 13 shows the results for the top chord of the CF. The cross sectional area of both element types is 4.4in² so that the axial forces reported correspond to a maximum axial stress of 9.1ksi.

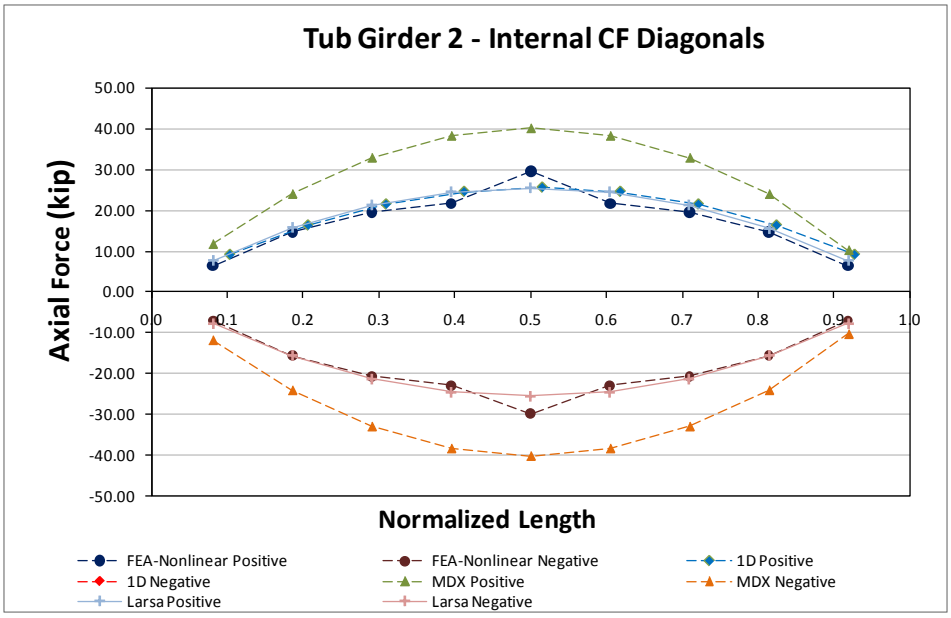

Fig. 12. Internal cross-frames diagonals axial forces for Girder 2 - Total Dead Load

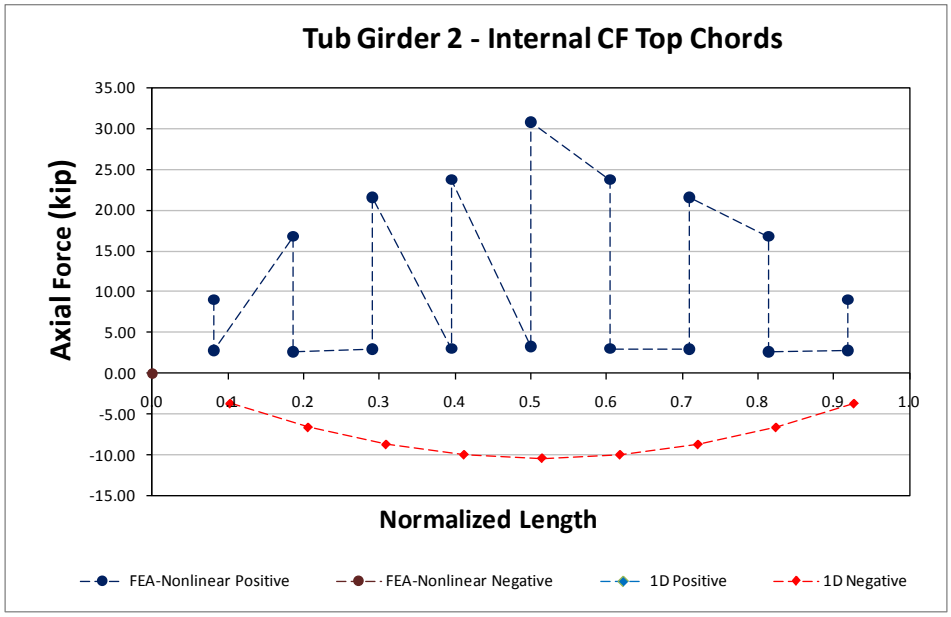

Fig. 13. Internal cross-frame top chords axial forces for Girder 2 - Total Dead Load

10.2 NTSCR2 (New, Tub-girder, Simple-span, Curved, Radial supports)

Bridge Description:

Category Data:

L_1 = 150ft / R = 600 ft / w = 30 ft, 2 tub-girders

References:

Erection Stages Analyzed: 4 steel erection stages

Deck Placement Sequence: One stage, deck thickness = 9.5 in

Bridge Perspective & Plan Views:

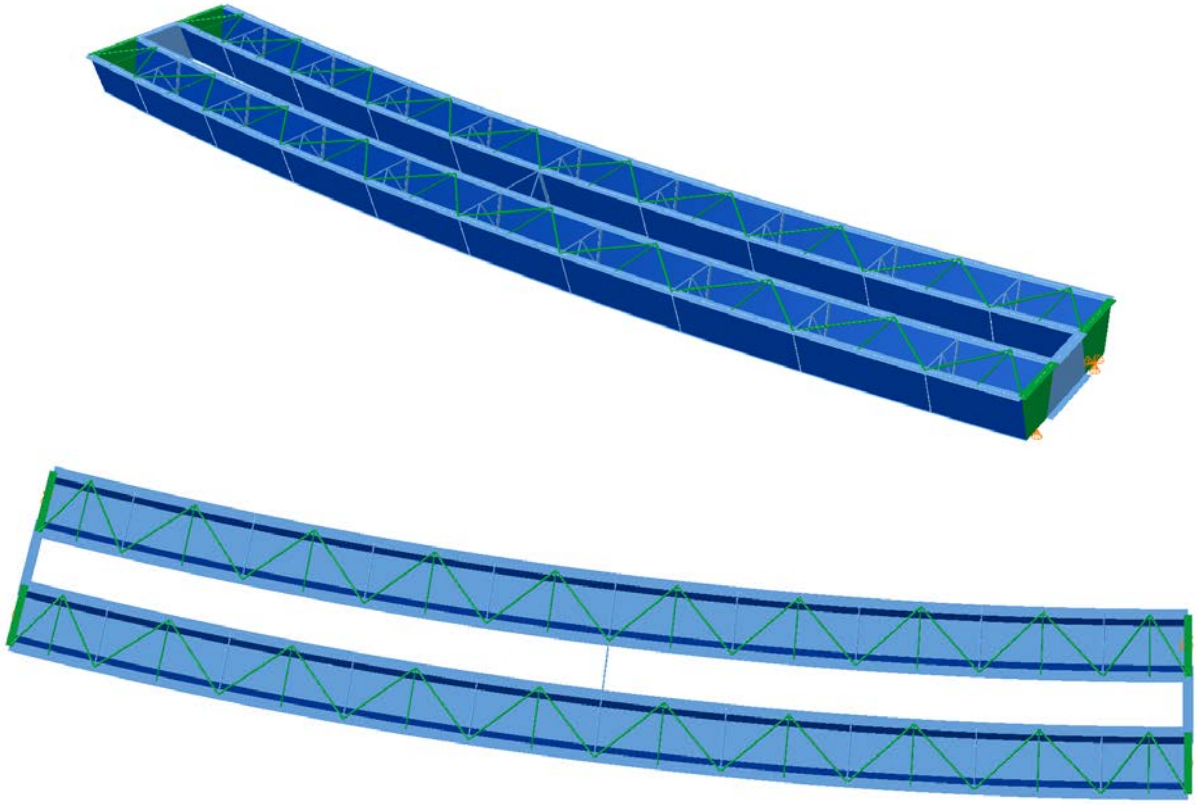

Displacement Results

Figures 1 through 4 show the evolution of the vertical displacements for the partial steel erection stages 2 and 4, final steel and total non-composite dead loads. For the partial stages the vertical displacements are plotted only for 3D FEA and 2D LARSA, all methods are shown for the final steel and total non-composite dead loads. On the partial erection stages it can be noticed that 3DFEA and LARSA results show different displacements even at the supports where vertical displacements are expected to be null, in this case, the girders are experiencing small rotations that could give a false idea of a great disagreement.

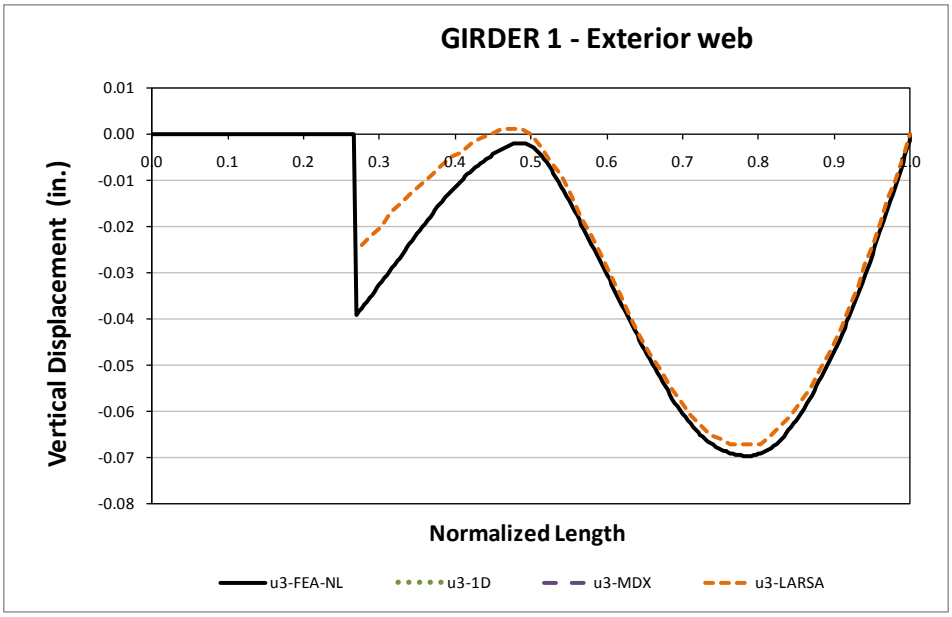

Fig. 1. Top flange vertical displacements for Girder 1 exterior web – Stage 2 Steel Dead Load

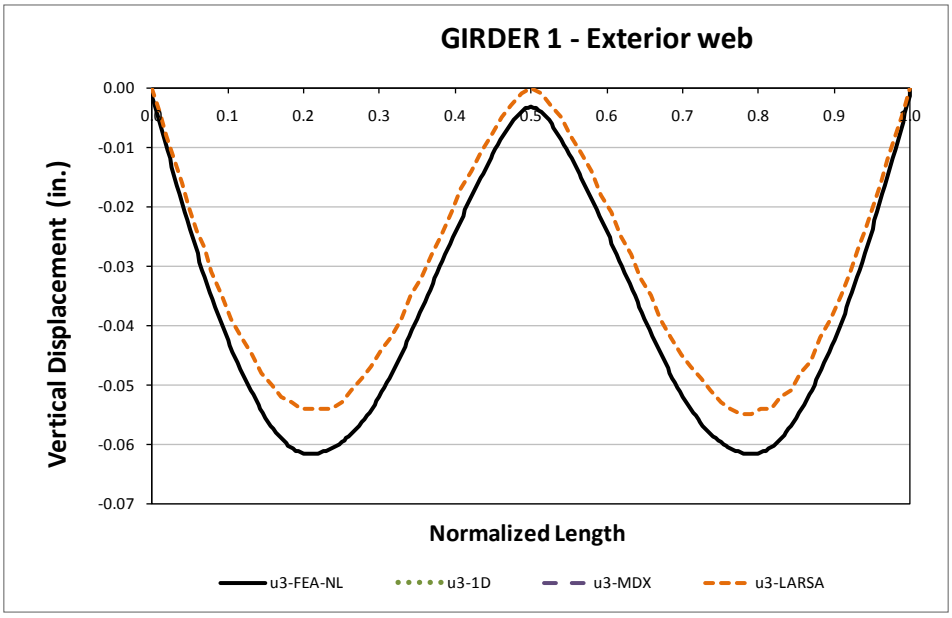

Fig. 2. Top flange vertical displacements for Girder 1 exterior web – Stage 4 Steel Dead Load

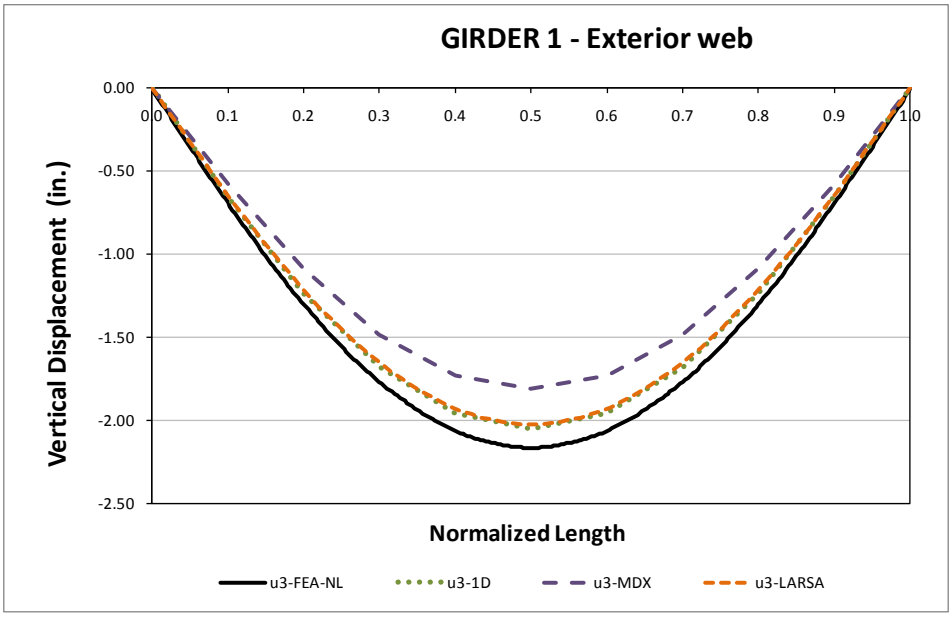

Fig. 3. Top flange vertical displacements for Girder 1 exterior web – Final Steel Dead Load

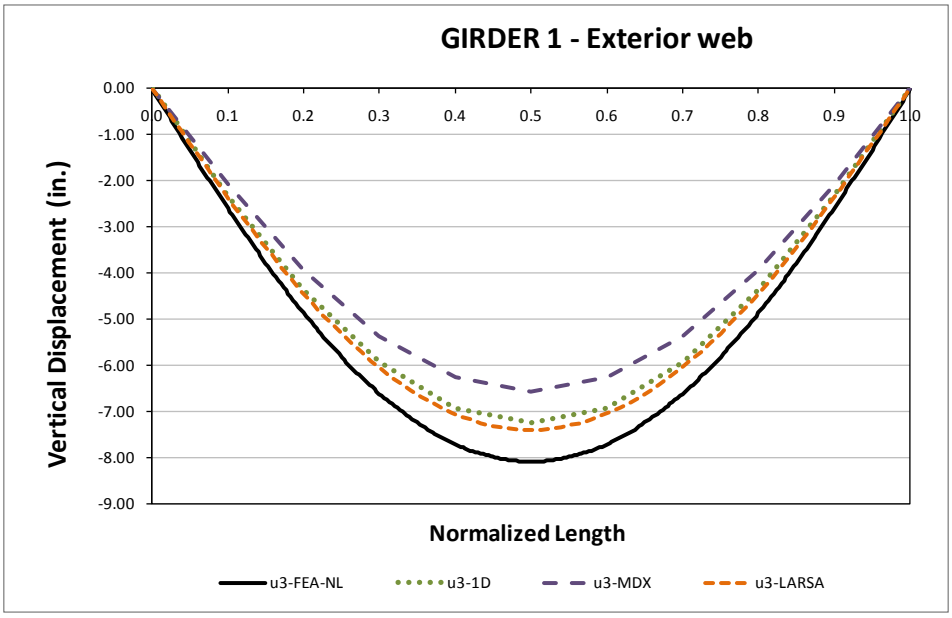

Fig. 4. Top flange vertical displacements for Girder 1 exterior web – Total Dead Load

Figure 5 illustrates the relative radial displacement between top and bottom flange junctures as a measure of lateral displacement. The values show a close approximation in the general shape while the 3D FEA shows a localized effect, mainly at the unbraced length where the flanges slightly deviate from the main shape. LARSA analysis is not capable of showing this effect due to the discretization used along the length of the girders.

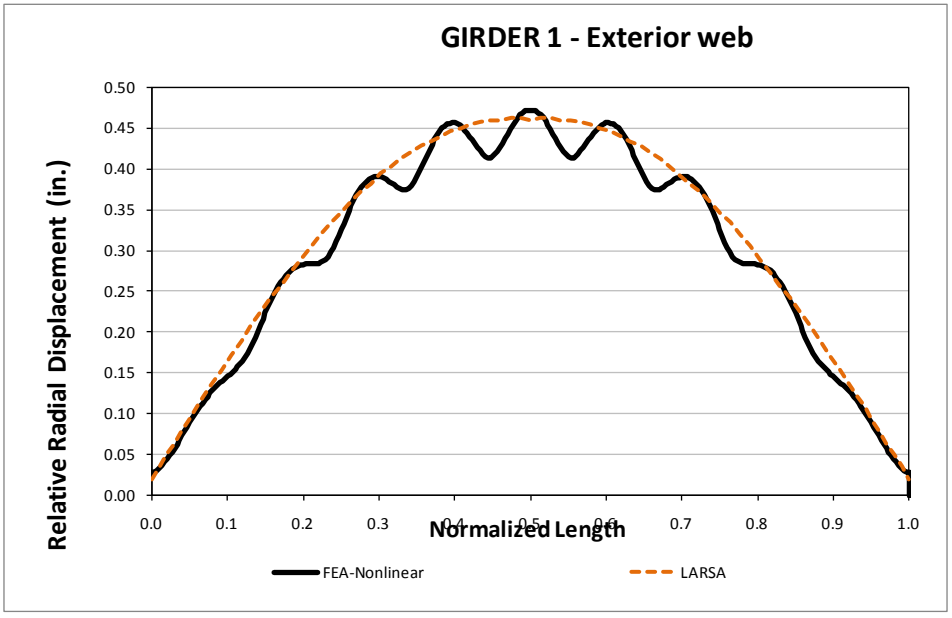

Fig. 5. Top flange relative radial displacements for Girder 1 exterior web - Total Dead Load

Bending Stress Results

Figures 6 through 9 show the evolution of the major axis bending stresses for Girder 2 – Interior Web during steel erection stages 2, 4 and final. In these stages the results are closely predicted by 1D and 2D analysis methods. For the Final Steel and Total non-composite dead load stages, the participation of the top flange lateral bracing system becomes evident in the 3DFEA methods as this system has an important effect on the bending stresses.

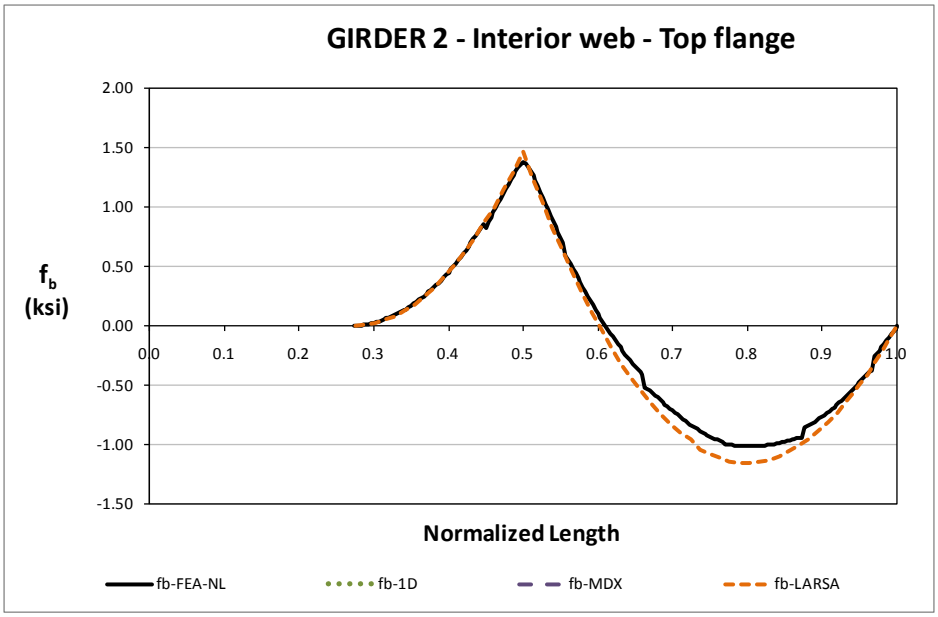

Fig. 6. Top flange major axis bending stress for Girder 2 interior web – Stage 2 Steel Dead Load

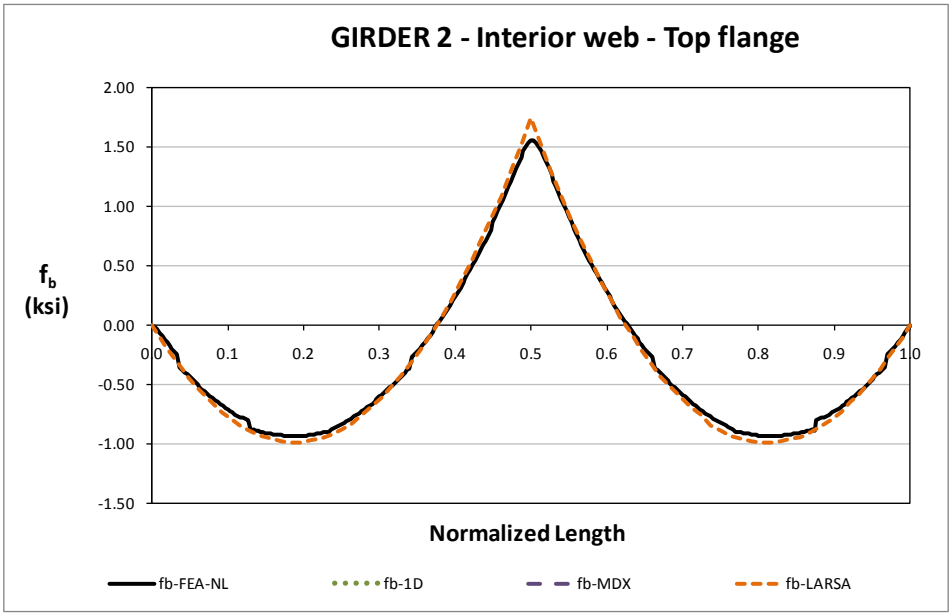

Fig. 7. Top flange major axis bending stress for Girder 2 interior web – Stage 4 Steel Dead Load

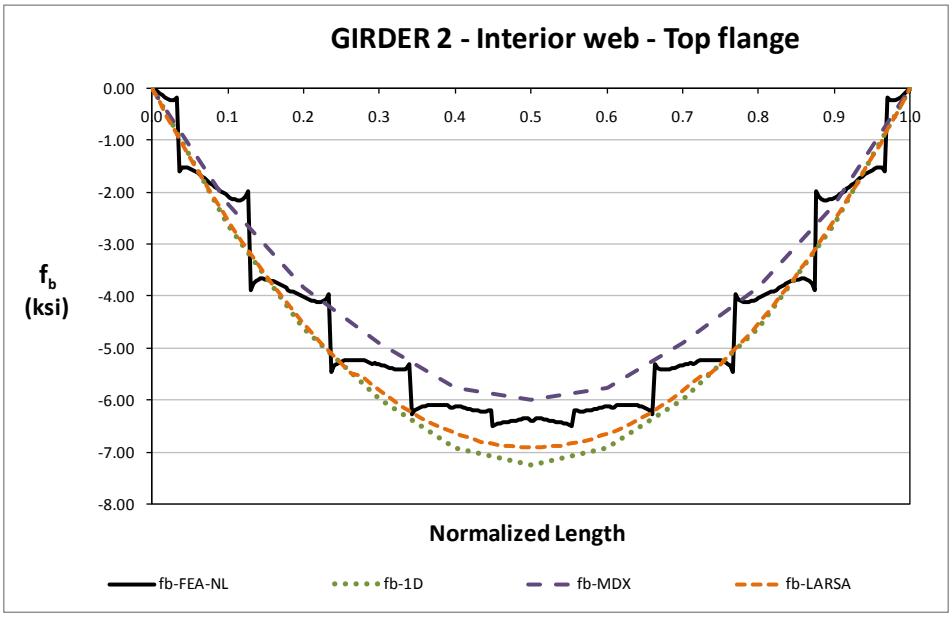

Fig. 8. Top flange major axis bending stress for Girder 2 interior web - Final Steel Dead Load

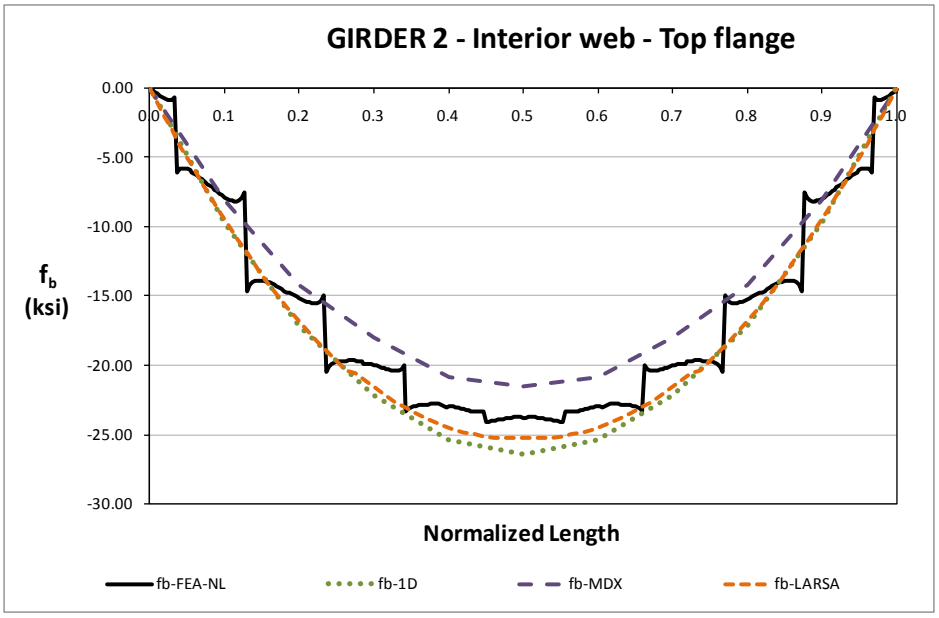

Fig. 9. Top flange major axis bending stress for Girder 2 interior web - Total Dead Load

Figure 10 illustrates results for the Girder 2 – Exterior web to show how the adjacent web in the same girder experiences the same localized effects but in a different shape that matched the position of the TFLB diagonals, the magnitude of the saw-tooth shaped stresses is inferior to the ones recorded at the NTSCR1 case mainly due to the lower curvature of this case of 600ft against 400ft and in consequence, lower torsional effects.

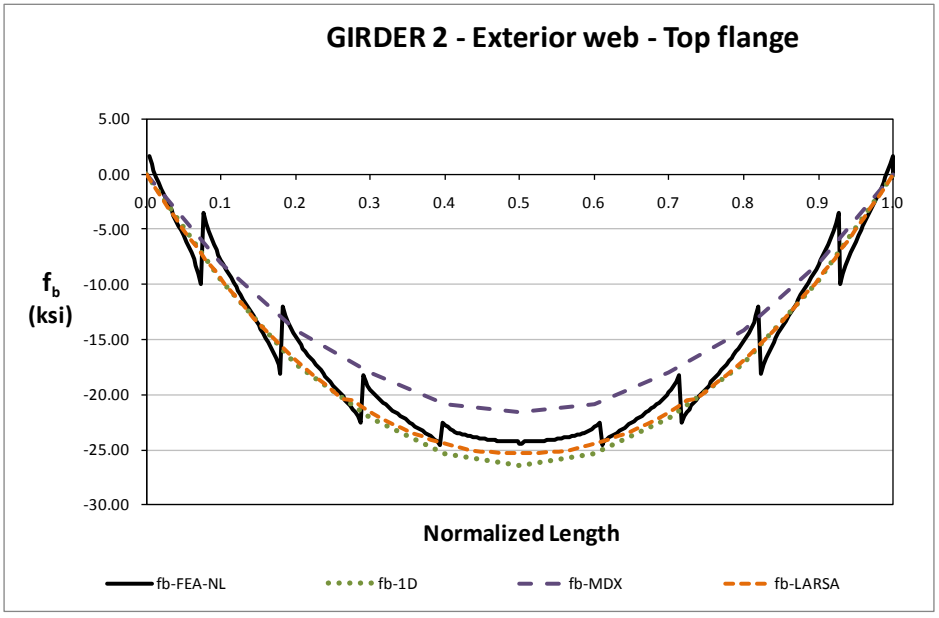

Fig. 10. Top flange major axis bending stress for Girder 2 exterior web - Total Dead Load

Figures 11 and 12 illustrate the bottom flange major axis bending stresses at the web bottom flange juncture. As seen before, some local stress concentrations are shown in the 3DFEA results at the CF locations but, as the curvature decreases so do the peaks, this can be seen when comparing with the NTSCR1 case.

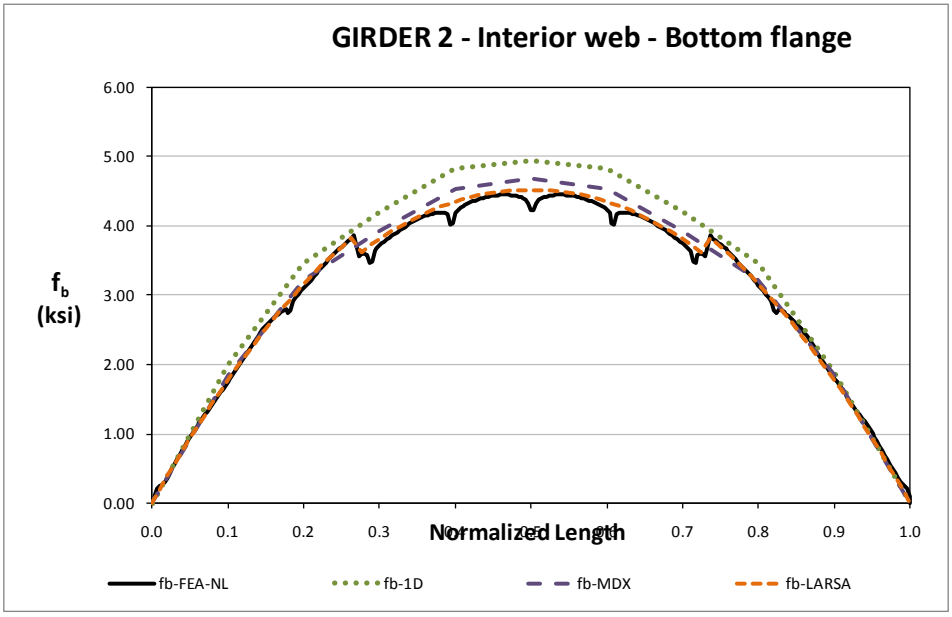

Fig. 11. Bottom flange major axis bending stress for Girder 2 interior web - Final Steel Dead Load

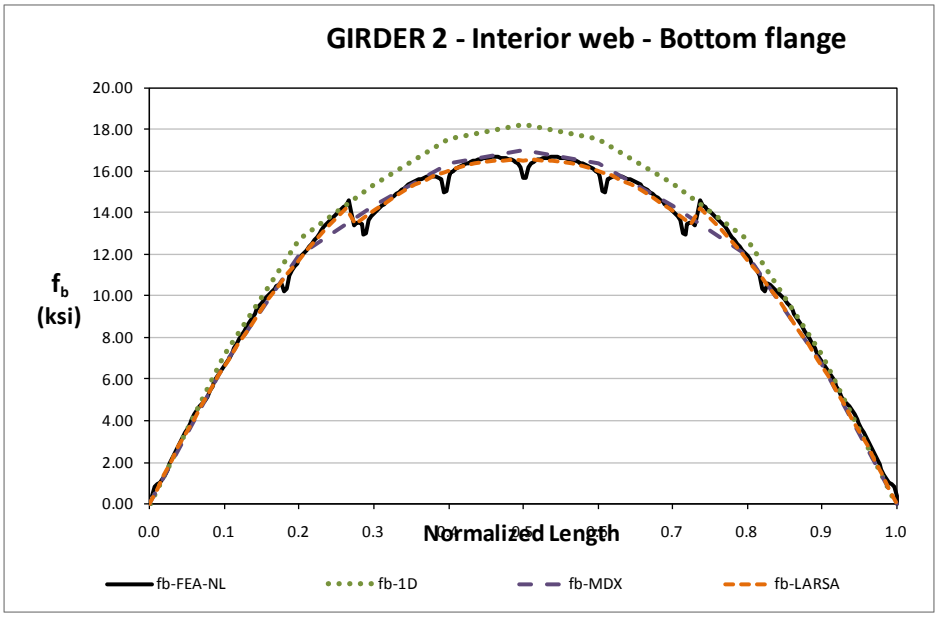

Fig. 12. Bottom flange major axis bending stress for Girder 2 interior web - Total Dead Load

Top Flange Lateral Bracing Results

The TFLB diagonals axial forces are shown in Figures 13, 14 and 15 for the steel erection stage 4, final steel and total dead load condition. The cross sectional area of these elements is 8.5in² that for a maximum axial force of 180kip the element experiences an axial stress of 21ksi on the total dead load condition.

On the partial steel erection stage 4, the torque on the bridge is low due to the temporal supports, when removed the internal forces redistribute causing axial forces on the TFLB diagonals that match the expected torque distribution along the bridge length. The reported axial force distribution by the different analysis methods follows the same law.

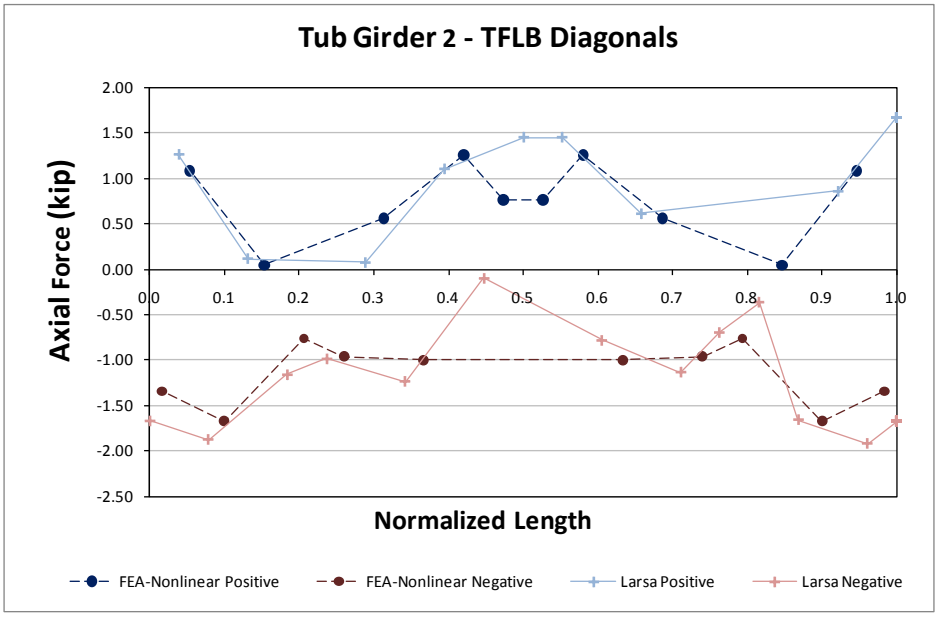

Fig. 13. Top flange lateral bracing diagonals axial forces for Girder 2 - Stage 4 Steel Dead Load

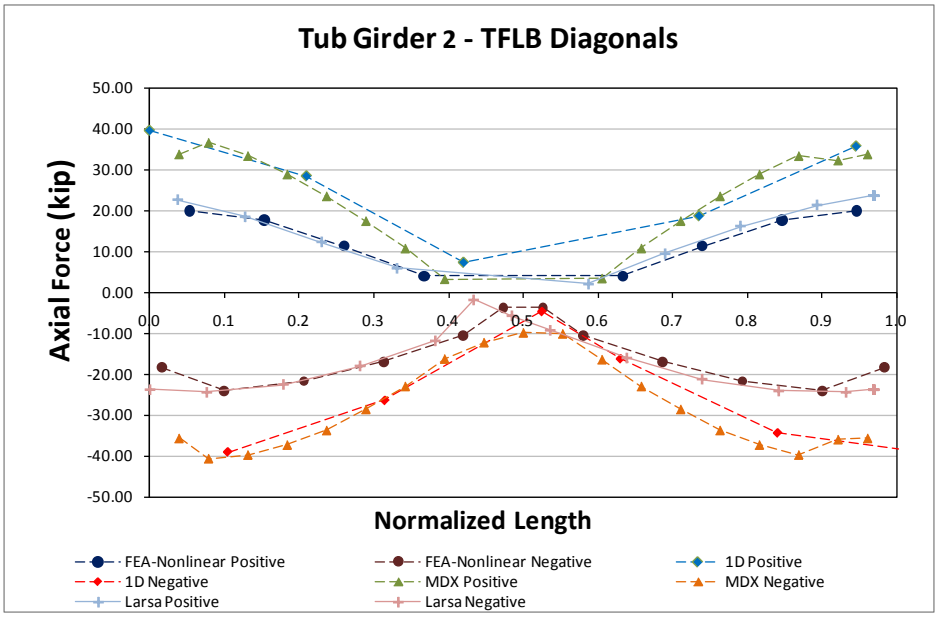

Fig. 14. Top flange lateral bracing diagonals axial forces for Girder 2 - Final Steel Dead Load

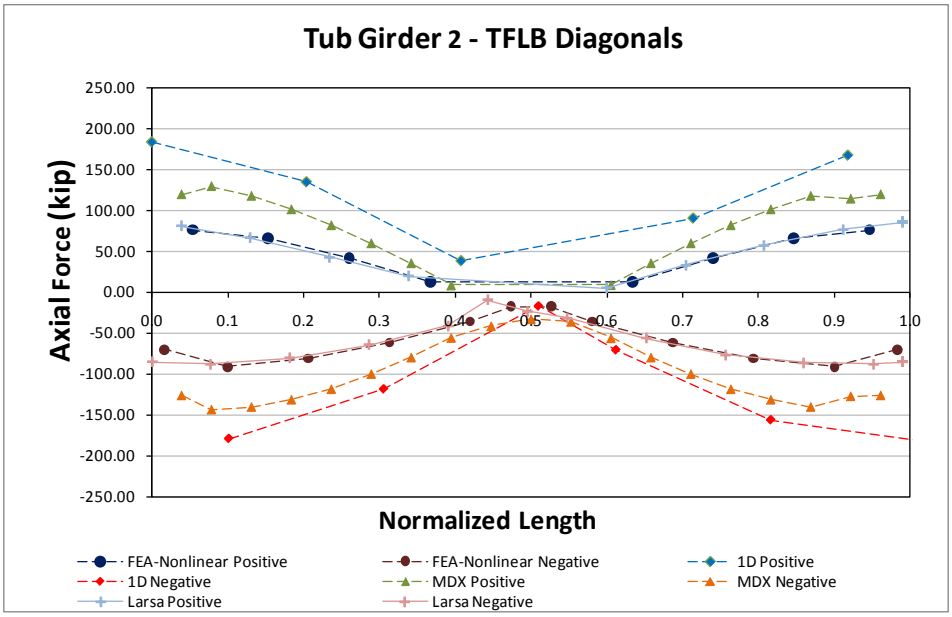

Fig. 15. Top flange lateral bracing diagonals axial forces for Girder 2 - Total Dead Load

Figure 16 shows the TFLB axial forces on the struts for the total non-composite dead load case. The area of the struts is 4.4in² which, for a maximum axial force of 20kip as reported by the 3D FEA analysis, results on maximum axial stress of 4.5ksi.

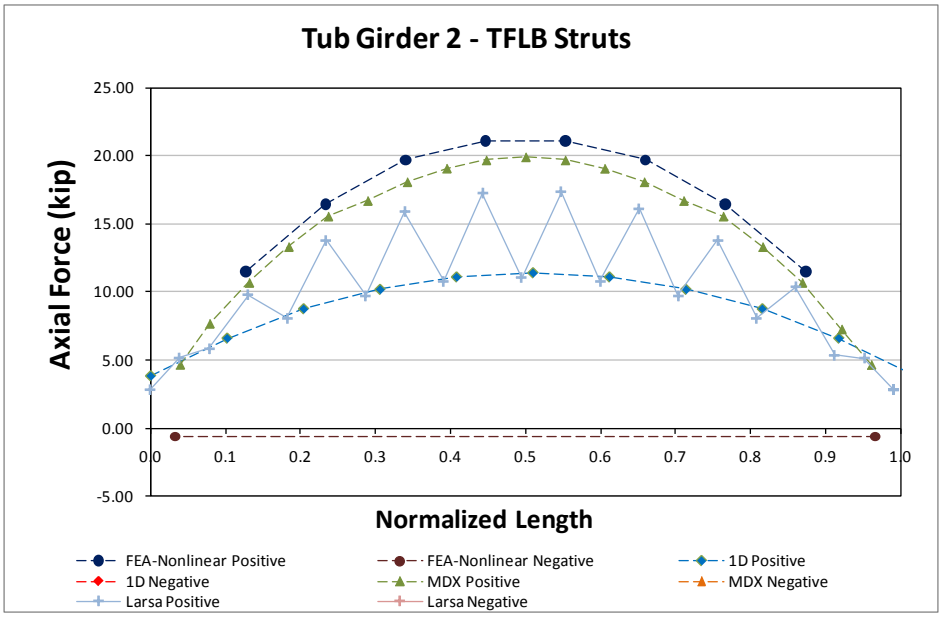

Fig. 16. Top flange lateral bracing struts axial forces for Girder 2 - Total Dead Load

Internal Cross Frame Results

Internal cross frames alternate in every other panel, these elements are composed by diagonals and top chords. Figure 17 shows the internal CF diagonal axial forces while Figure 18 shows the results for the top chord of the CF. The cross sectional area of both element types is 4.4in².

As expected, all torsional effects decrease with the curvature as it can be evidenced from the comparison with NTSCR2 case. Bending stresses remain mainly independent form the curvature and so do the displacements, for these results, the differences between the radial cases NTSCR1 and NTSCR2 are mainly caused to the bridge design.

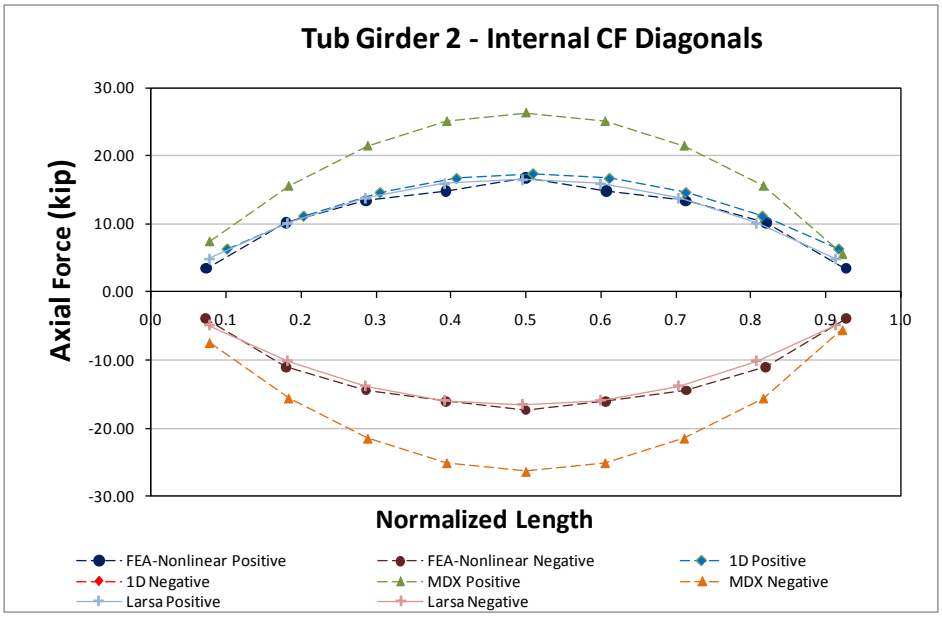

Fig. 17. Internal cross-frames diagonals axial forces for Girder 2 - Total Dead Load

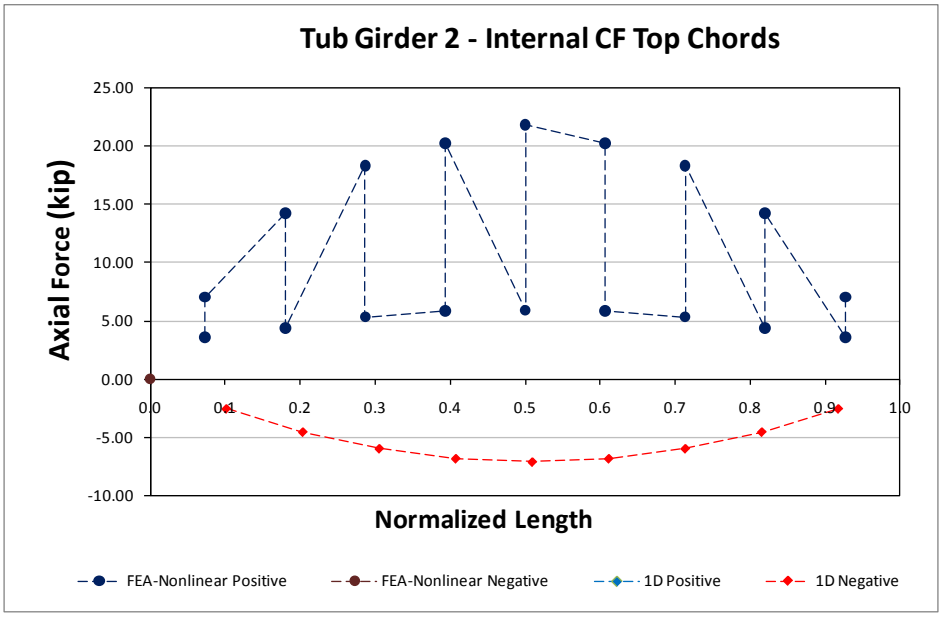

Fig. 18. Internal cross-frame top chords axial forces for Girder 2 - Total Dead Load

10.3 NTSCR5 (New, Tub-girder, Simple-span, Curved, Radial supports)

Bridge Description:

Category Data:

L_1 = 300 ft / R = 1360 ft / w = 30 ft, 2 tub-girders

Erection Stages Analyzed: 3 steel erection stages

Deck Placement Sequence: One stage, deck thickness = 9.5 in

Bridge Perspective & Plan Views:

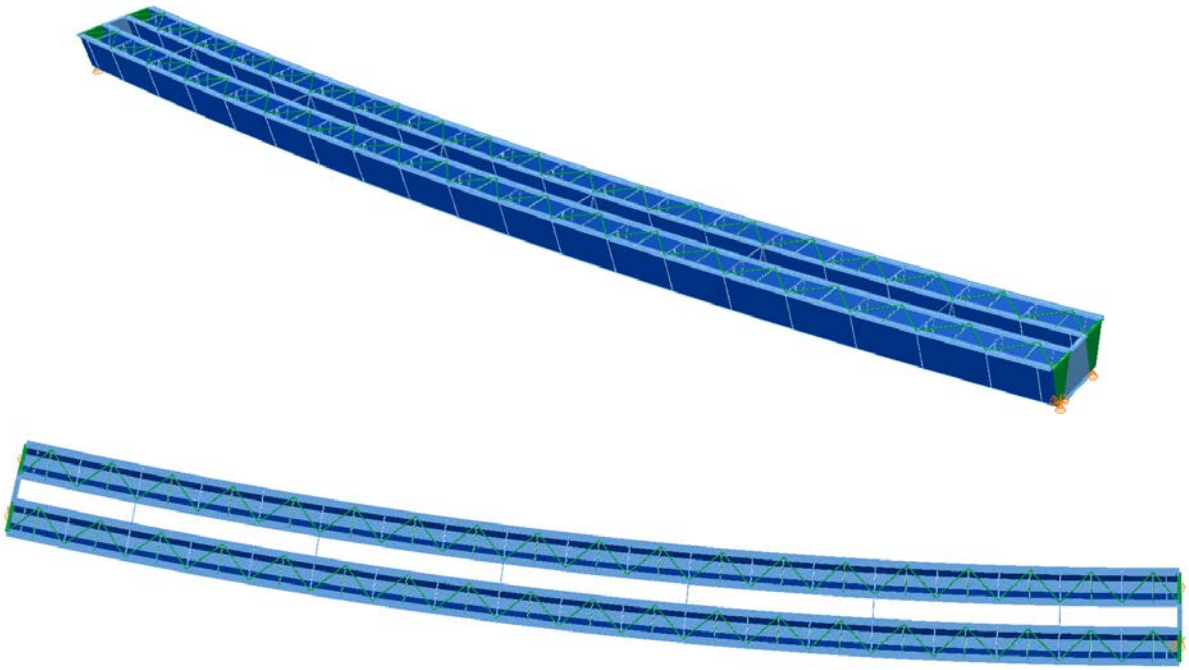

Displacement Results

Figures 1 through 5 show the evolution of the vertical displacements for the partial steel erection stages 2 and 3, final steel and total non-composite dead loads. For the partial stages the vertical displacements are plotted only for 3D FEA and 2D LARSA, all methods are shown for the final steel and total non-composite dead loads.

On the partial erection stage 2 the girder drop-in segment has not been placed while on stage 3 it is placed but the temporal supports have not been removed. On these stages the girders are experiencing small rotations but still the results agree for the 2D LARSA and the 3D FEA methods.

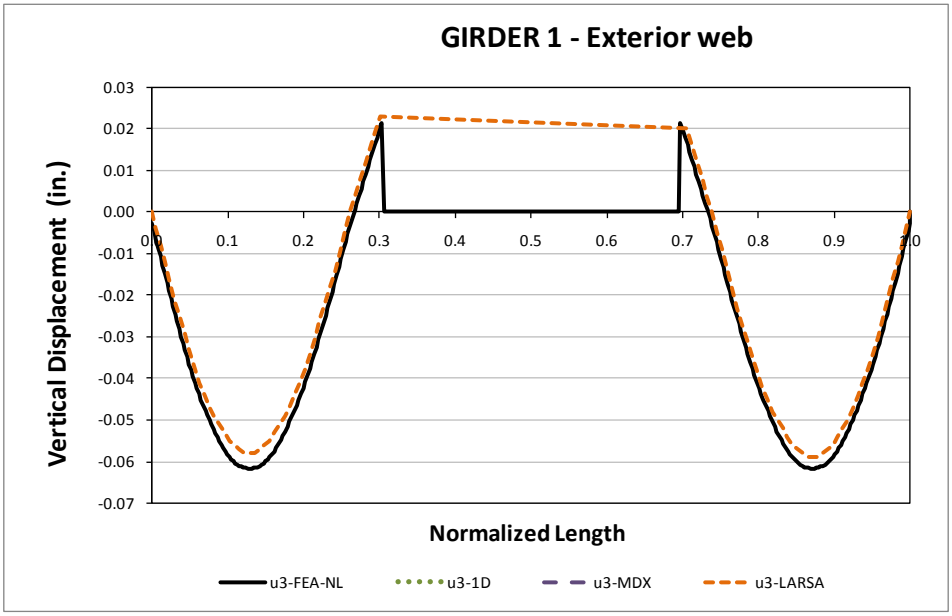

Fig. 1. Top flange vertical displacements for Girder 1 exterior web - Stage 2 Steel Dead Load

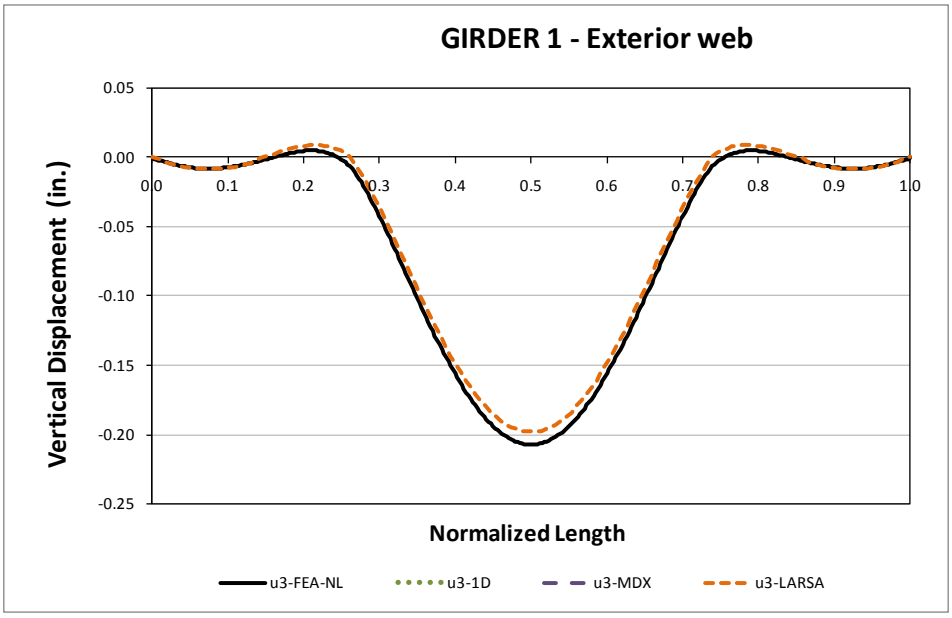

Fig. 2. Top flange vertical displacements for Girder 1 exterior web - Stage 3 Steel Dead Load

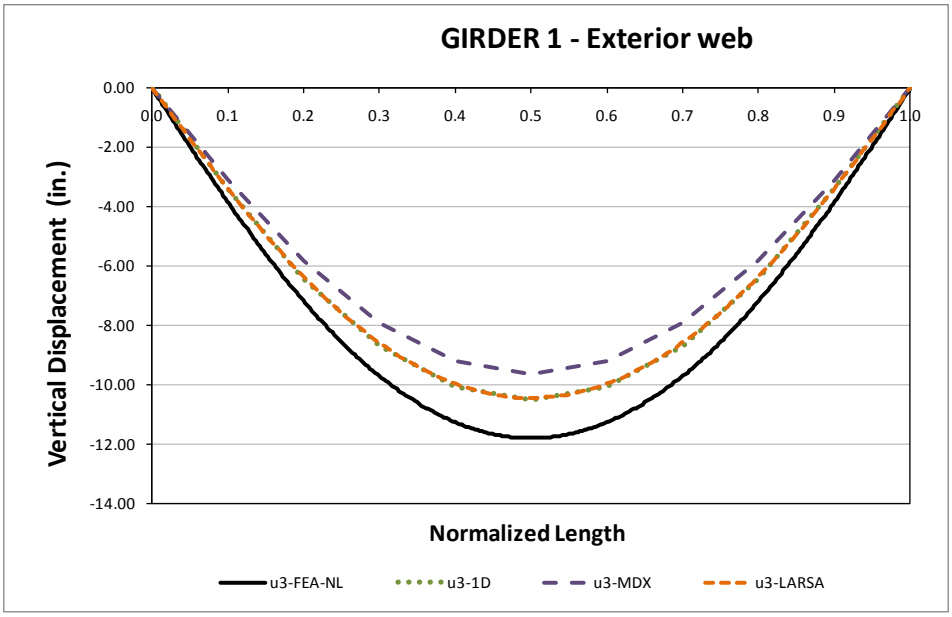

Fig. 3. Top flange vertical displacements for Girder 1 exterior web - Final Steel Dead Load

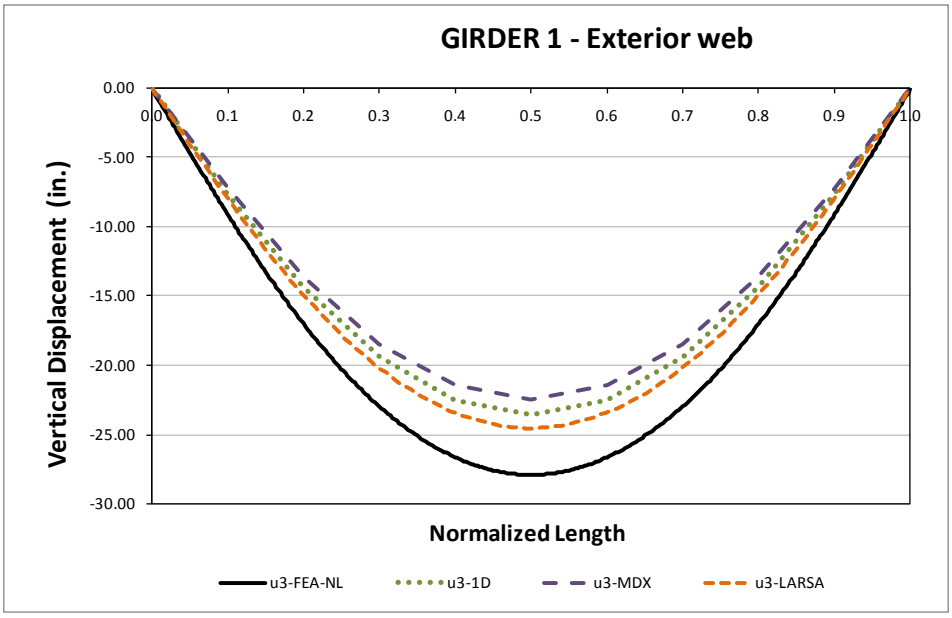

Fig. 4. Top flange vertical displacements for Girder 1 exterior web - Total Dead Load

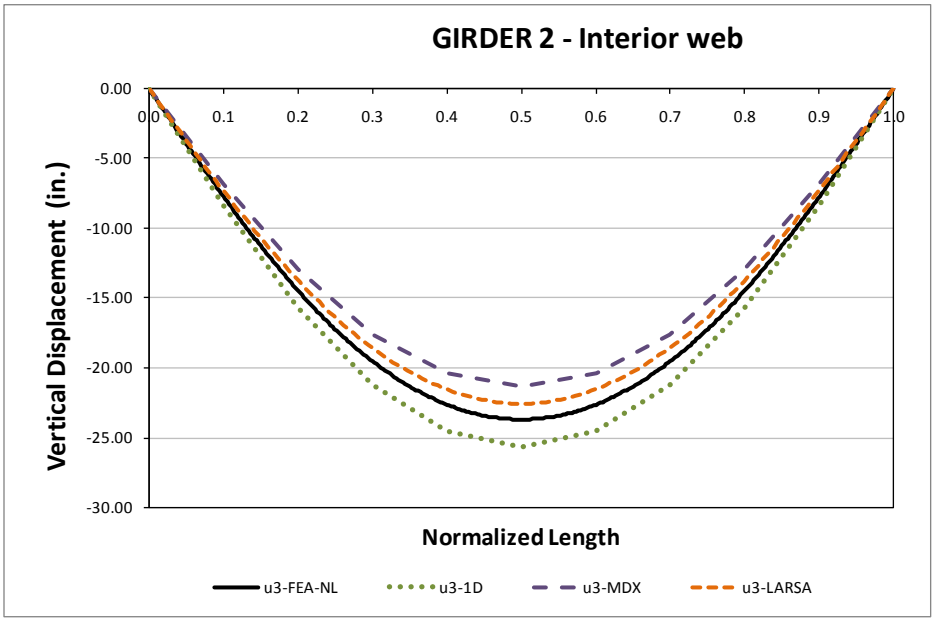

Fig. 5. Top flange vertical displacements for Girder 2 interior web - Total Dead Load

For the final steel and total dead load stages the results for the different analysis method disagree in magnitude mainly because the cross section rotation is underpredicted in the 1D and 2D analysis methods. Figure 6 illustrates the relative radial displacement between top and bottom flange junctures as a measure

of lateral displacement. It can be seen that the differences in vertical displacements shown in figures 4 and 5 for the total non-composite dead load case could be caused by the cross section rotation.

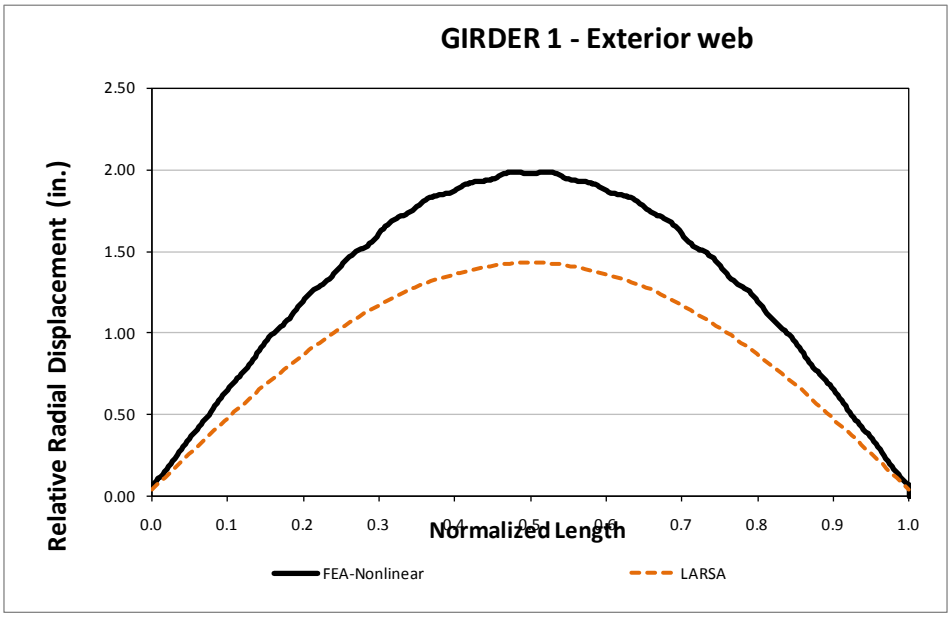

Fig. 6. Top flange relative radial displacements for Girder 1 exterior web - Total Dead Load

Bending Stress Results

Major axis bending stresses are presented in Figures 7 through 10 as predicted by different analysis methods for partial steel erection, final steel and total dead load stages. Results in general show a good agreement in shape and magnitude but the MDX result shows a poor prediction as discussed before.

The local interaction of the TFLB system is evident in the final steel and total dead load stages, previous to the removal of the temporal supports this interaction is negligible.

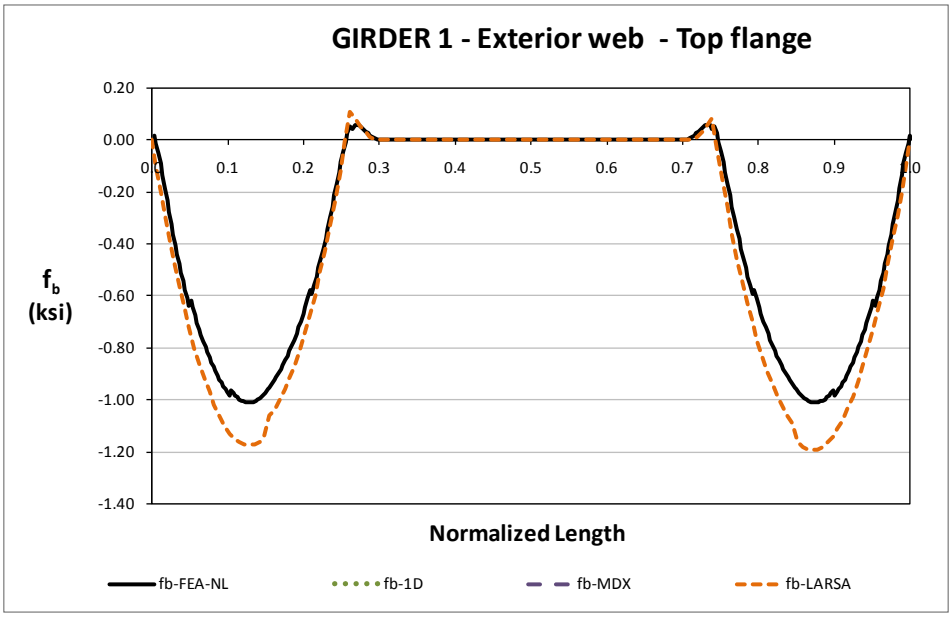

Fig. 7. Top flange major axis bending stress for Girder 1 exterior web - Stage 2 Steel Dead Load

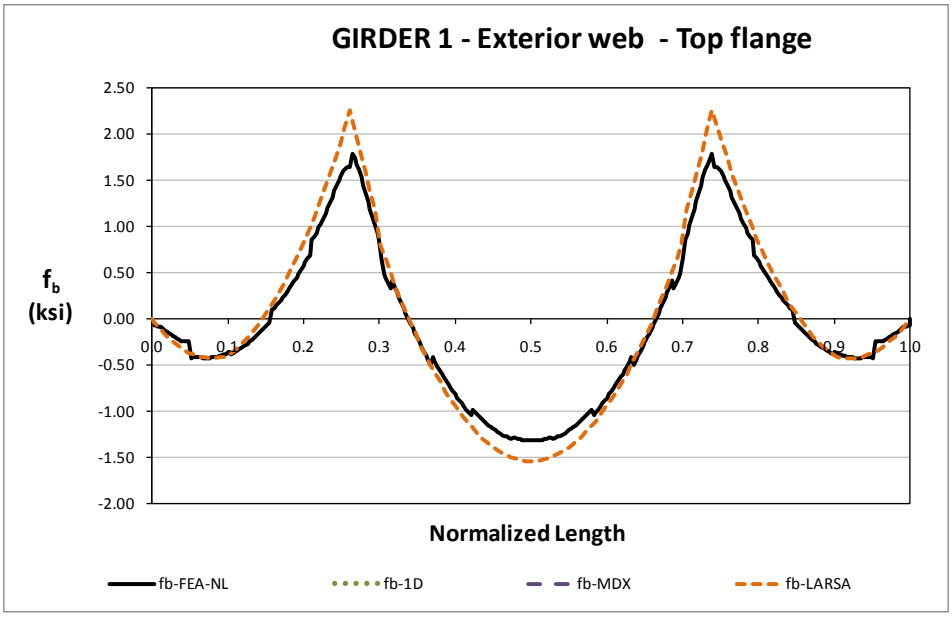

Fig. 8. Top flange major axis bending stress for Girder 1 exterior web - Stage 3 Steel Dead Load

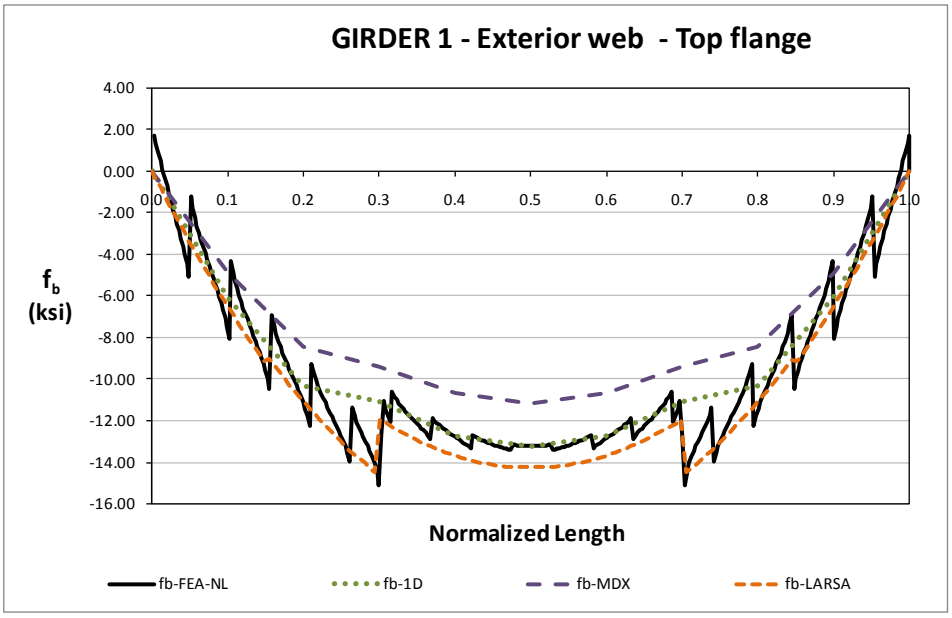

Fig. 9. Top flange major axis bending stress for Girder 1 exterior web - Final Steel Dead Load

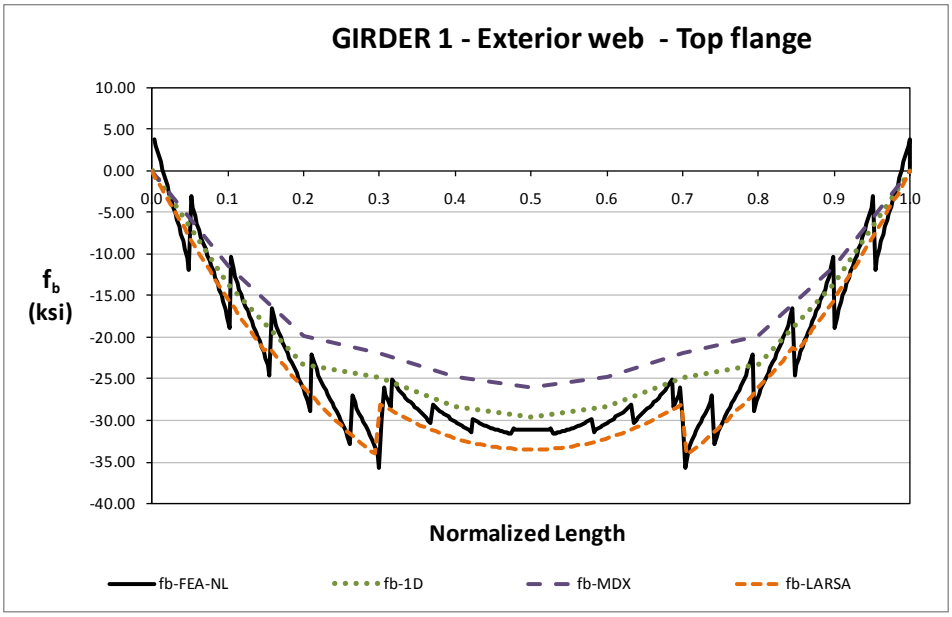

Fig. 10. Top flange major axis bending stress for Girder 1 exterior web - Total Dead Load

Figures 11 and 12 illustrate the bottom flange stresses at the web bottom flange juncture for the final steel and total dead load cases. The flanges for this design considers steel grade 70 HPS to account for the higher stress values.

As with the top flange, in the bottom flange there are local variations, these are caused by the TFLB system and the internal CF elements. In the case of the top flange the variation is found at the points where two diagonals from the TFLB coincide, for the bottom flange it happens where an internal CF is found.

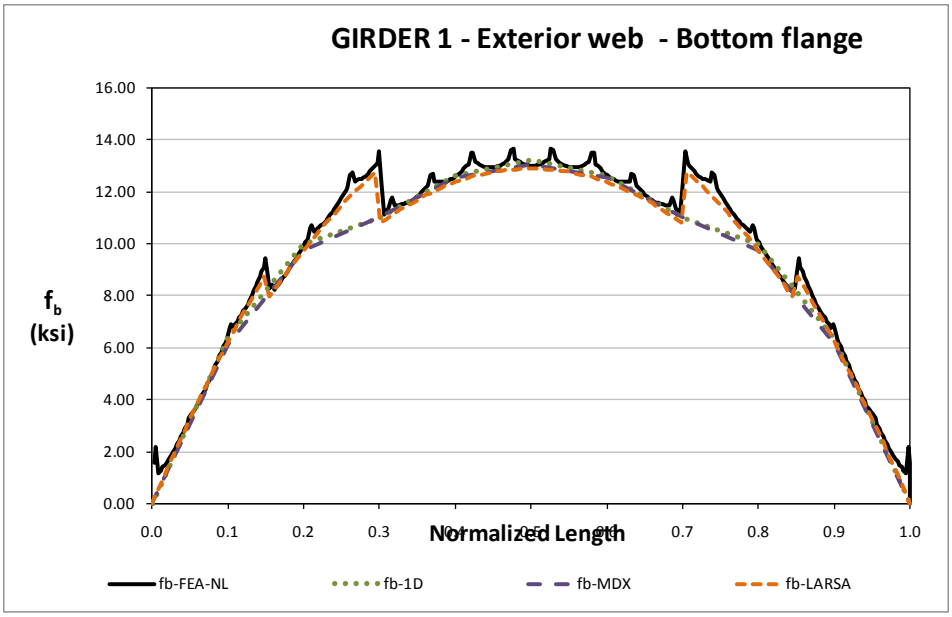

Fig. 11. Bottom flange major axis bending stress for Girder 1 exterior web - Final Steel Dead Load

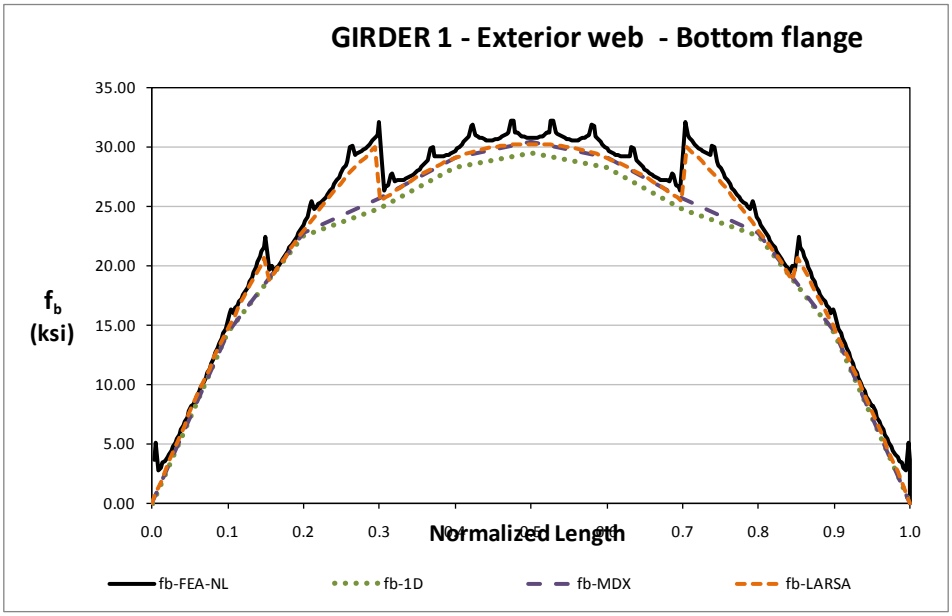

Fig. 12. Bottom flange major axis bending stress for Girder 1 exterior web - Total Dead Load

Lateral bending stress distributions are shown in figure 13, the stresses values remain low in contrast as with the major axis bending stresses reported above.

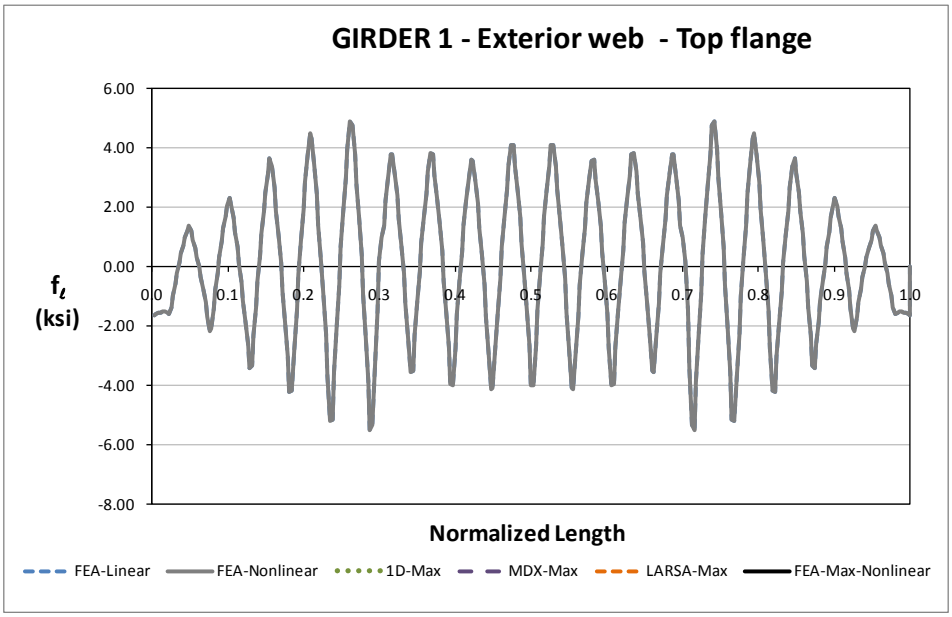

Fig. 13. Top flange lateral bending stress for Girder 1 exterior web - Total Dead Load

Top Flange Lateral Bracing Results

The TFLB diagonals axial forces are shown in Figures 14 through 17 for the partial steel erection stages 2 and 3, final steel and total dead load condition. The TFLB system is not fully working until the system is released from the temporal supports. The cross sectional area of these elements is 12.4in² that for a maximum axial force of 250kip as reported by the 3DFEA the element experiences an axial stress of 20ksi on the total dead load conditions. For the values reported by the 1D analysis methods, the element would be already yielding.

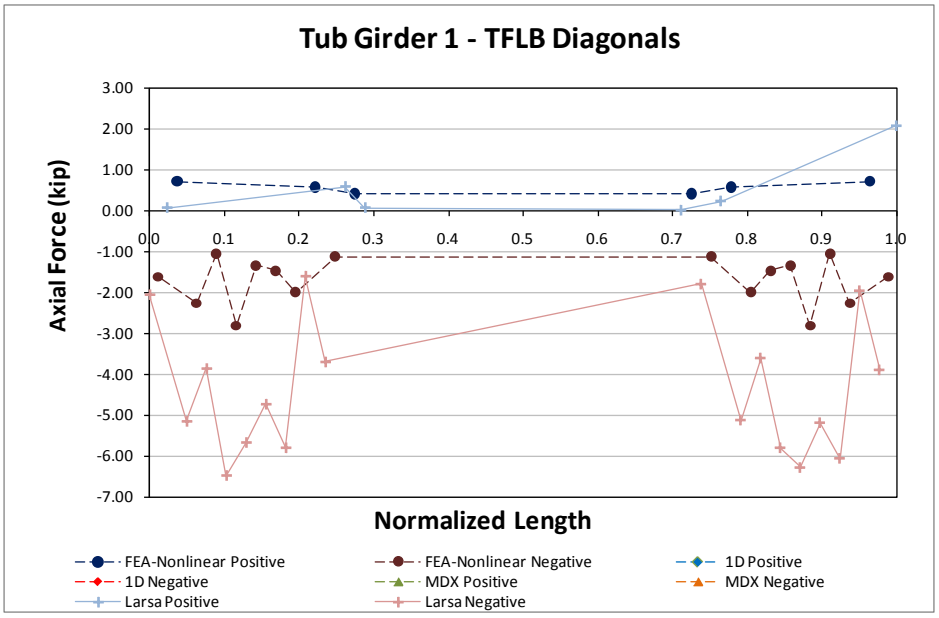

Fig. 14. Top flange lateral bracing diagonals axial forces for Girder 1 - Stage 2 Steel Dead Load

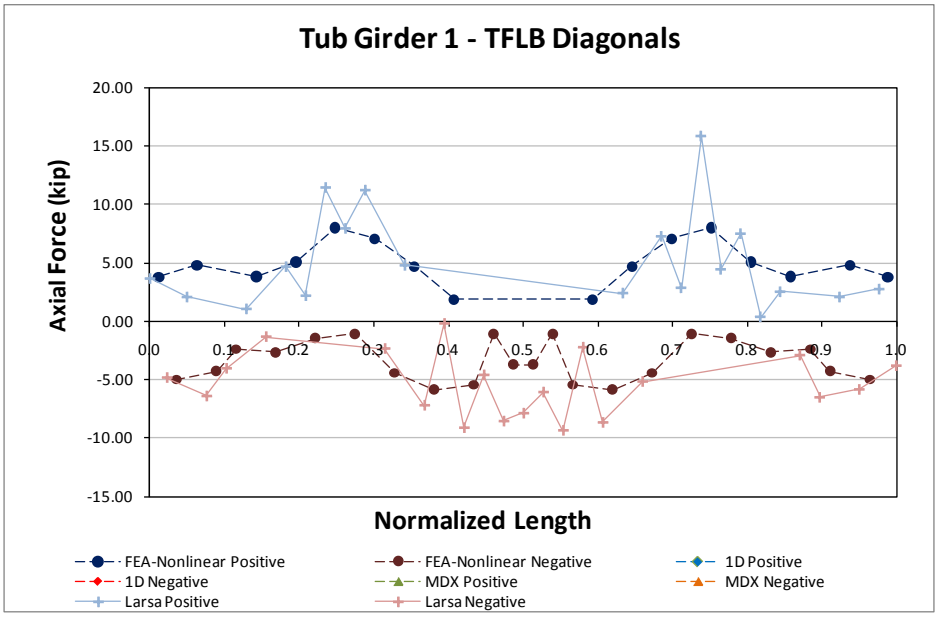

Fig. 15. Top flange lateral bracing diagonals axial forces for Girder 1 - Stage 3 Steel Dead Load

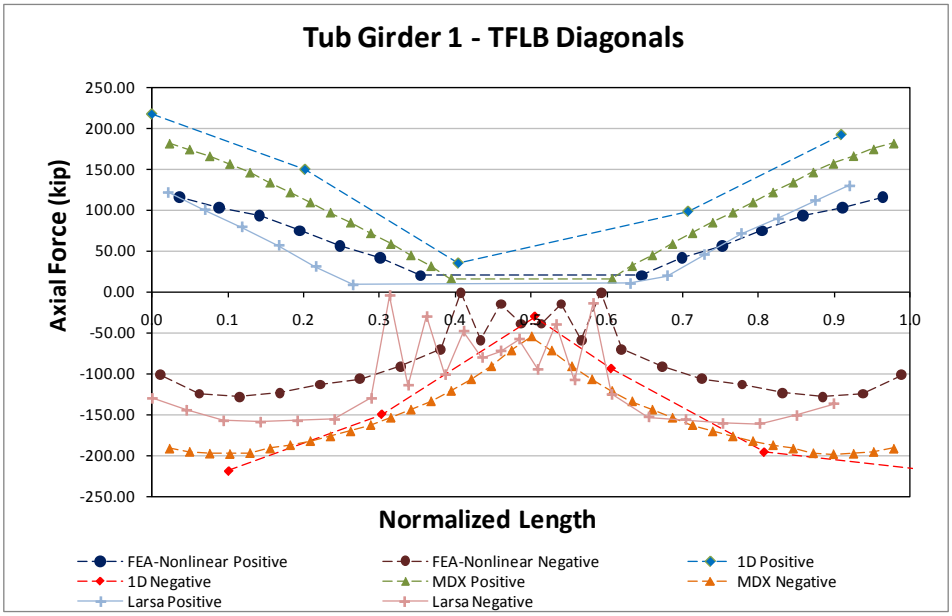

Fig. 16. Top flange lateral bracing diagonals axial forces for Girder 1 - Final Steel Dead Load

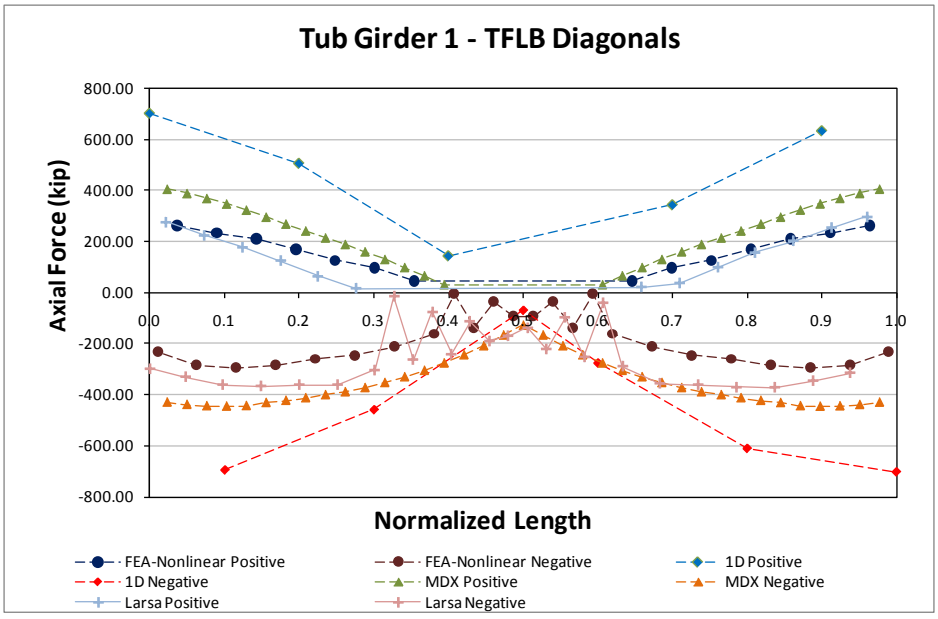

Fig. 17. Top flange lateral bracing diagonals axial forces for Girder 1 - Total Dead Load

Figure 18 shows the TFLB axial forces on the struts for the total non-composite deal load case. The area of the struts is 6.6in² which, for a maximum axial force of 120kip as reported by LARSA analysis, results

on maximum axial stress of 18ksi. The 3DFEA reports lower values, partly because the model accommodates girder rotations which release the elements from forces.

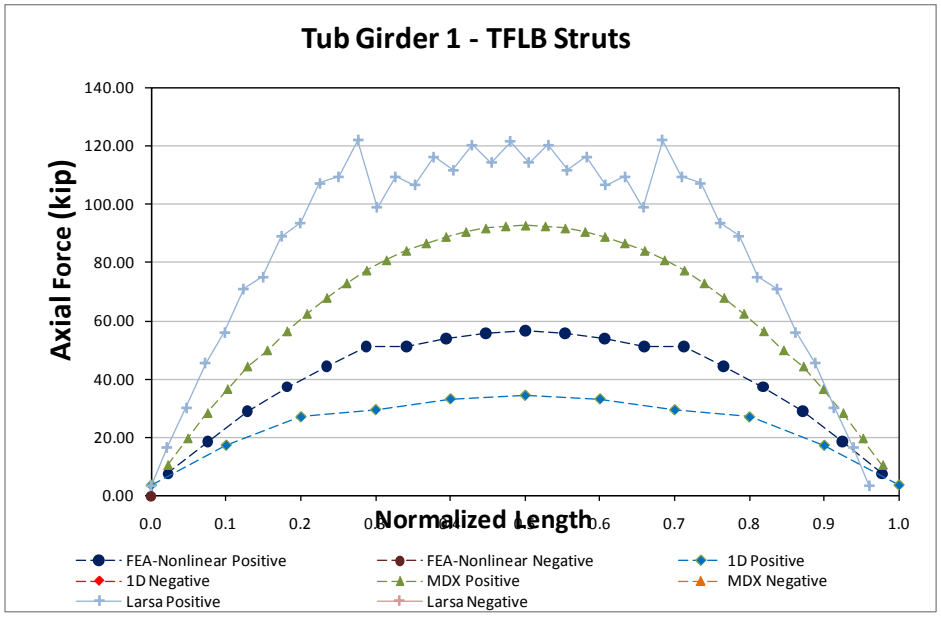

Fig. 18. Top flange lateral bracing struts axial forces for Girder 1 - Total Dead Load

Internal Cross Frame Results

Figure 19 shows the internal CF diagonal axial forces with cross sectional area of 6.6in². As expected, the torsional effects increase with the span length as it can be evidenced from the comparison with the 150ft span cases. In this case the full girder cross frame rotates more and this causes a reduction of forces in the bracing elements.

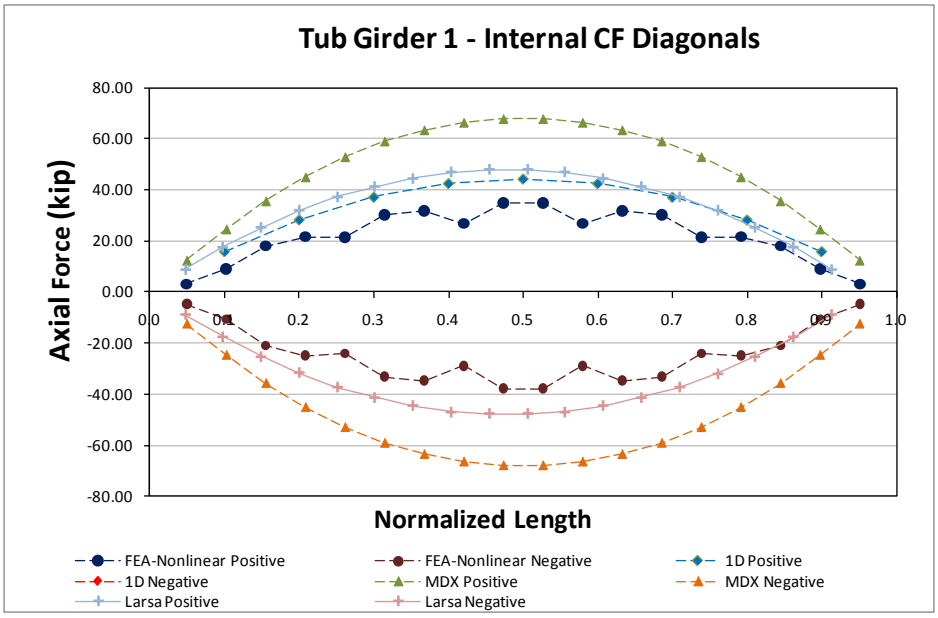

Fig. 19. Internal cross-frames diagonals axial forces for Girder 1 - Total Dead Load

11.1 ETCCR14 (Existing, Tub-girder, Continuous-span, Curved, Radial supports)

Bridge Description:

Connector EB North Beltway 8 to NB I-45, Houston, TX

Category Data:

L_1 = 189 ft, L_2 = 291 ft, L_3 = 183 ft / R = 896 ft / w = 40.8 ft, 4 tub-girders

References:

Fan, Z.F. (1999). "Field and Computational Studies of Steel Trapezoidal Box Girder Bridges," Doctoral dissertation, Civil and Environmental Engineering Department, University of Houston, 300 pp.

Erection Stages Analyzed: 5 steel erection stages

Deck Placement Sequence: 3 deck placement stages

Bridge Perspective & Plan Views:

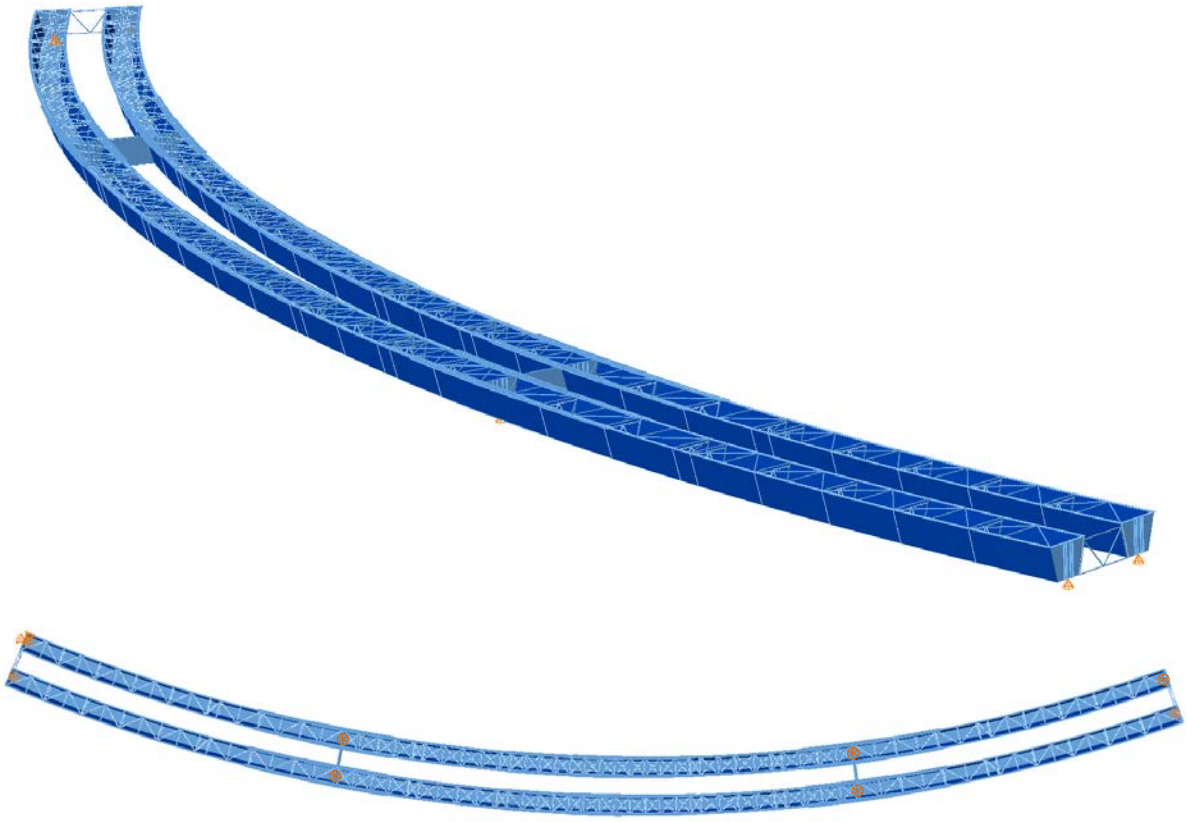

Displacement Results

The evolution of vertical displacements during the steel erection stages 2, 3 and 4 are presented on Figures 1 through 3 for the top of the web with the least radius (interior web of Girder 2).

At the end of stage 2 the tip of the cantilever girder raises up to 1.5 inches which is reduced to almost no vertical displacement when on Stage 3 as an extra segment is added to the bridge, facilitating the connection of the final drop-in segment on Stage 4.

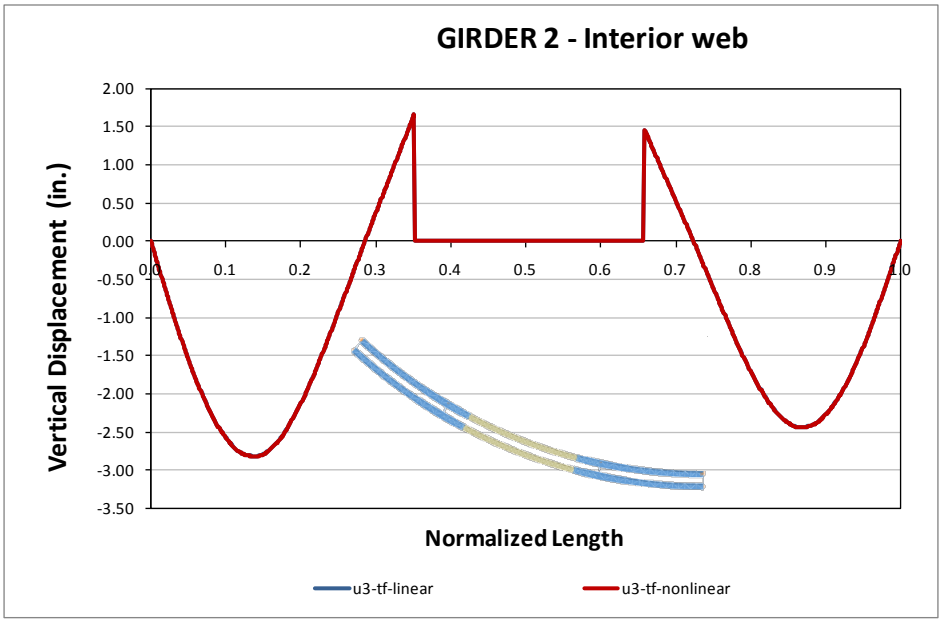

Fig. 1. Top flange vertical displacements for Girder 2 interior web - Steel Erection Stage 2

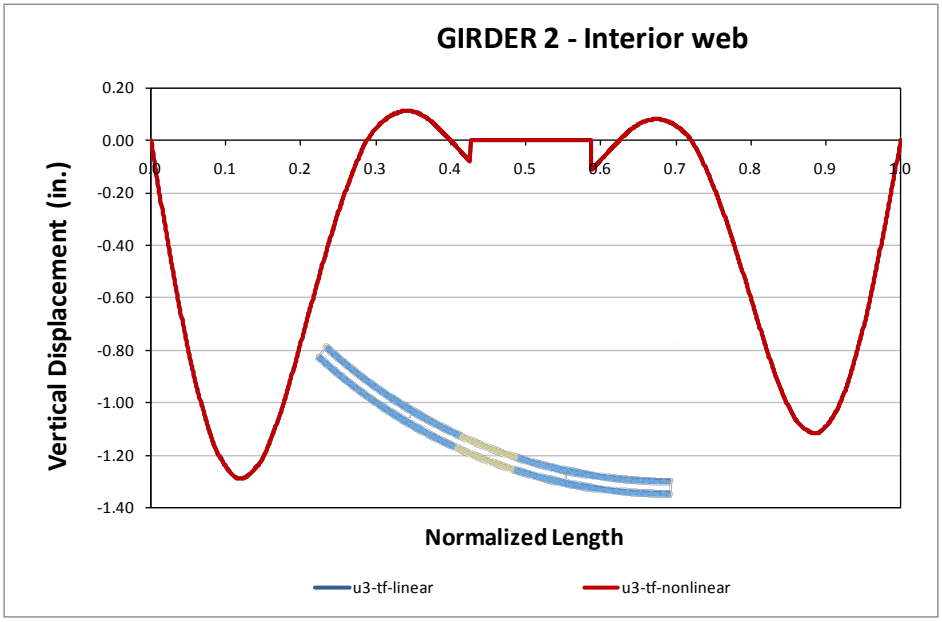

Fig. 2. Top flange vertical displacements for Girder 2 interior web - Steel Erection Stage 3

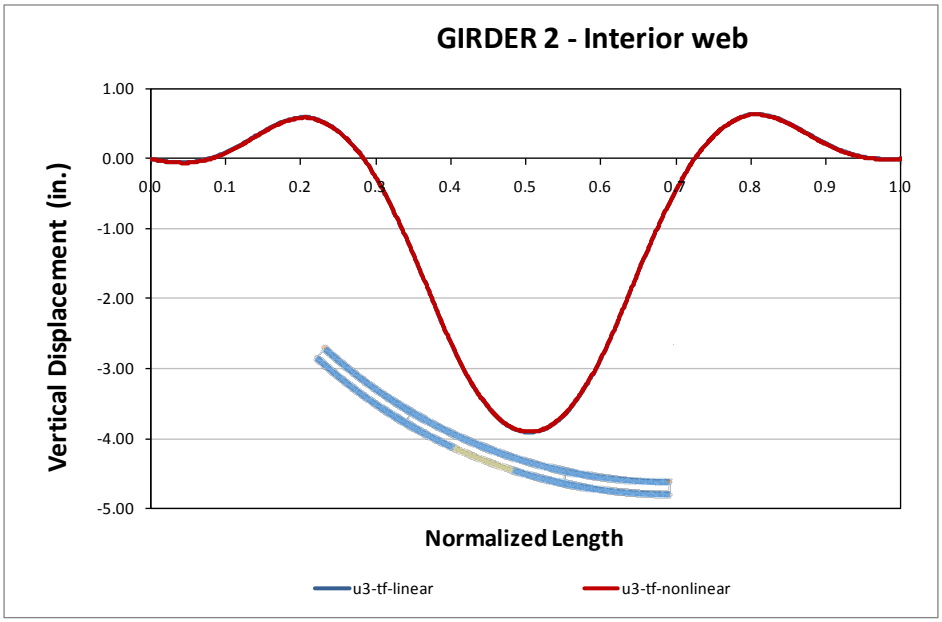

Fig. 3. Top flange vertical displacements for Girder 2 interior web - Steel Erection Stage 4

Figures 4 illustrate the results for the different methods of analysis for the final steel dead load configuration while in Figure 5 the same set of results are shown for the total dead load case: steel and concrete dead load under noncomposite action. Results show a good agreement in the evaluation of the stresses but modeling simplifications may result in over predictions for the MDX analysis method. Note that the difference between Figure 4 and 5 the results is a constant factor due to the concrete self weight as expected.

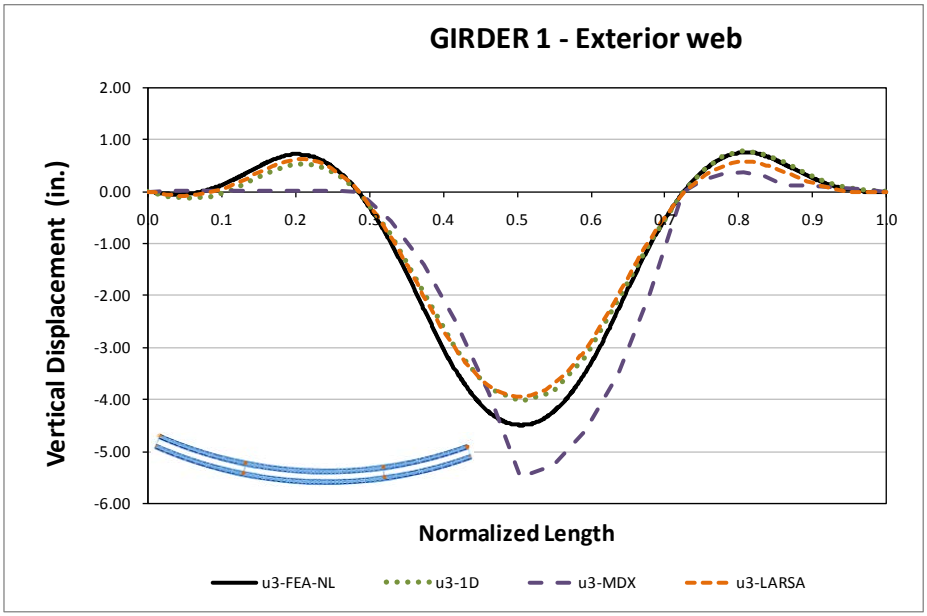

Fig. 4. Top flange vertical displacements for Girder 1 exterior web - Final Steel Dead Load

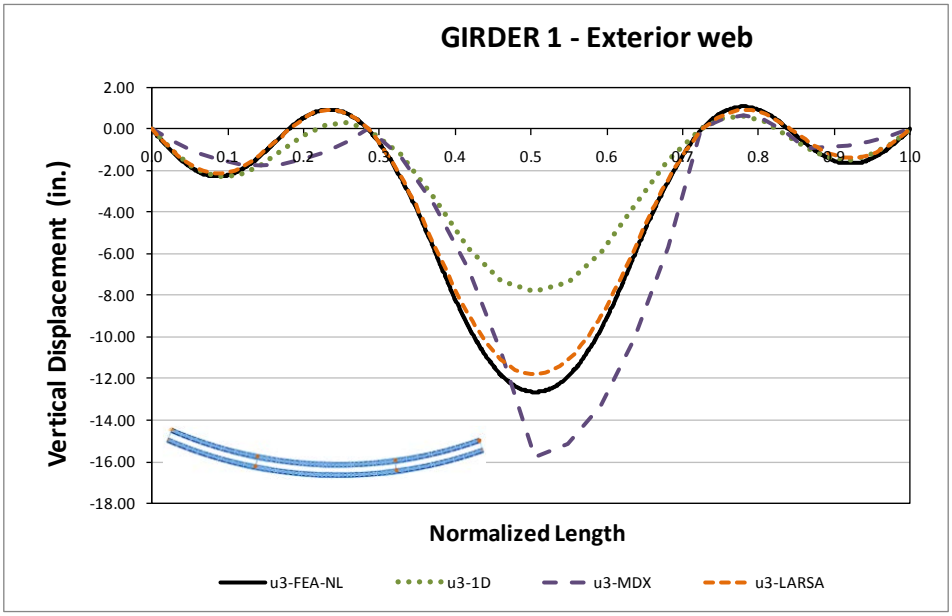

Fig. 5. Top flange vertical displacements for Girder 1 exterior web - Total Dead Load

Figure 6 shows the results for the total dead load lateral displacements under noncomposite action for Larsa and 3DFEA, limitation on the analysis capabilities of the other analysis methods limit their application in the evaluation of the lateral response of the bridge. Results between the Larsa analysis and the 3DFEA show a close agreement, missing only the behavior on the unbraced length of the bridge.

The close approximation in the central span can be caused by the continuity given by the X-type top flange lateral bracing system used.

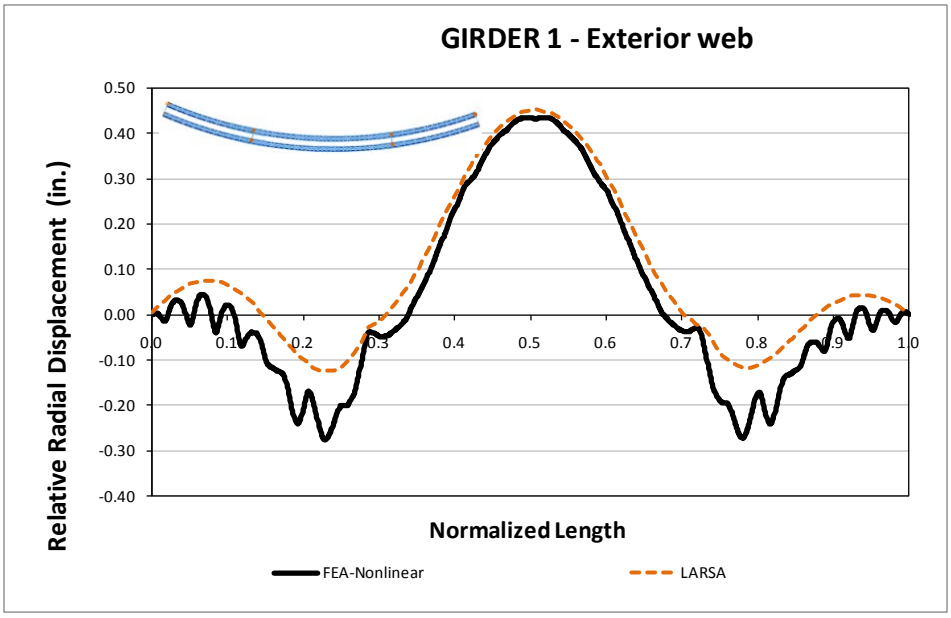

Fig. 6. Relative radial displacements for Girder 1 exterior web - Total Dead Load

The analysis methods show, in general, agreement for the displacement prediction. In the erection procedure, displacements are kept small, however, letting the system deform excessively due to the use of an inappropriate erection procedure could result on fitup problems due to the high rigidity of the system.

Bending Stress Results

Figure 7 shows the stress distribution for the final steel dead load condition while the total dead load results are shown in Figure 8, as expected the stresses have a uniform increment between these two stages.

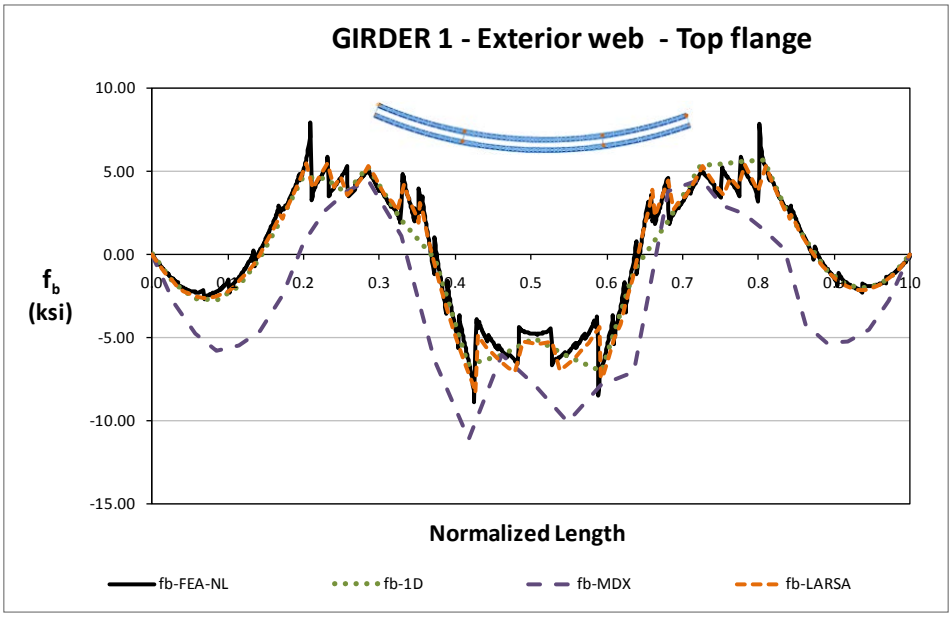

Fig. 7. Top flange major axis bending stress for Girder 1 exterior web - Final Steel Dead Load

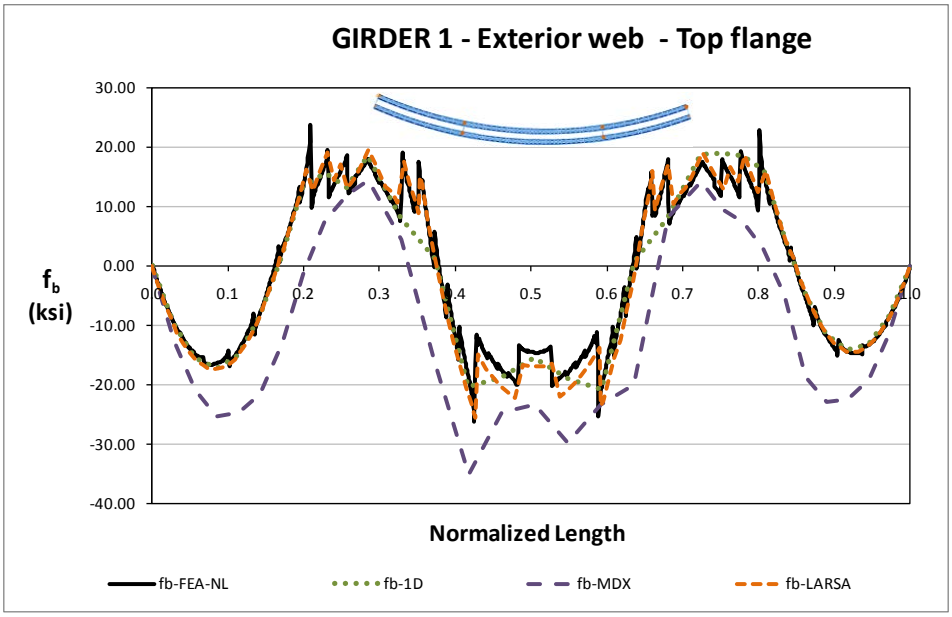

Fig. 8. Top flange major axis bending stress for Girder 1 exterior web - Total Dead Load

The total dead load results for bottom flange major axis stresses are shown in Figures 9 and top flange lateral bending stresses in Figure 10. As in the displacement section, the 1D and Larsa analysis methods show a close agreement in the bottom flange stresses prediction.

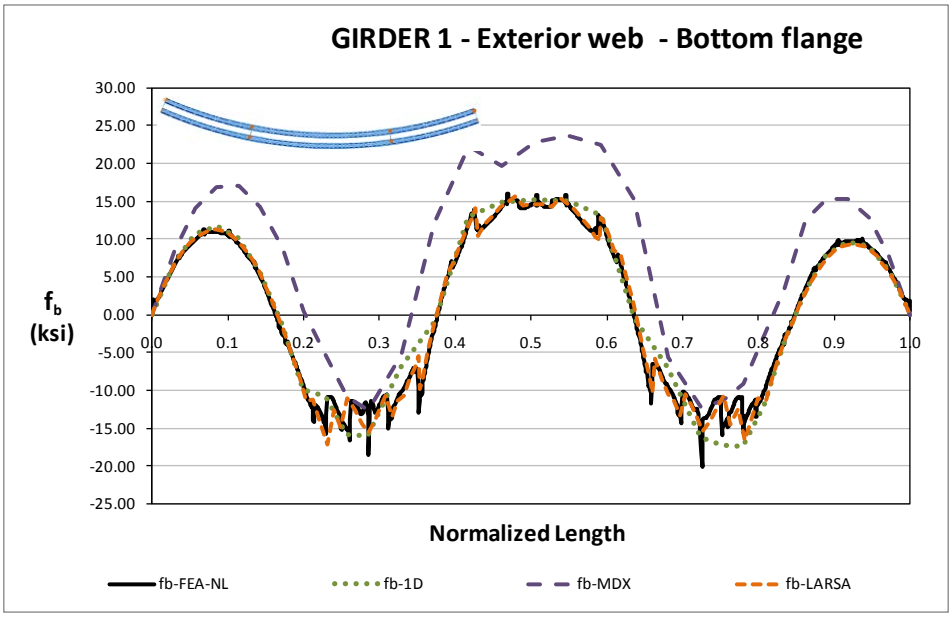

Fig. 9. Bottom flange major axis bending stress for Girder 1 exterior web – Total Dead Load

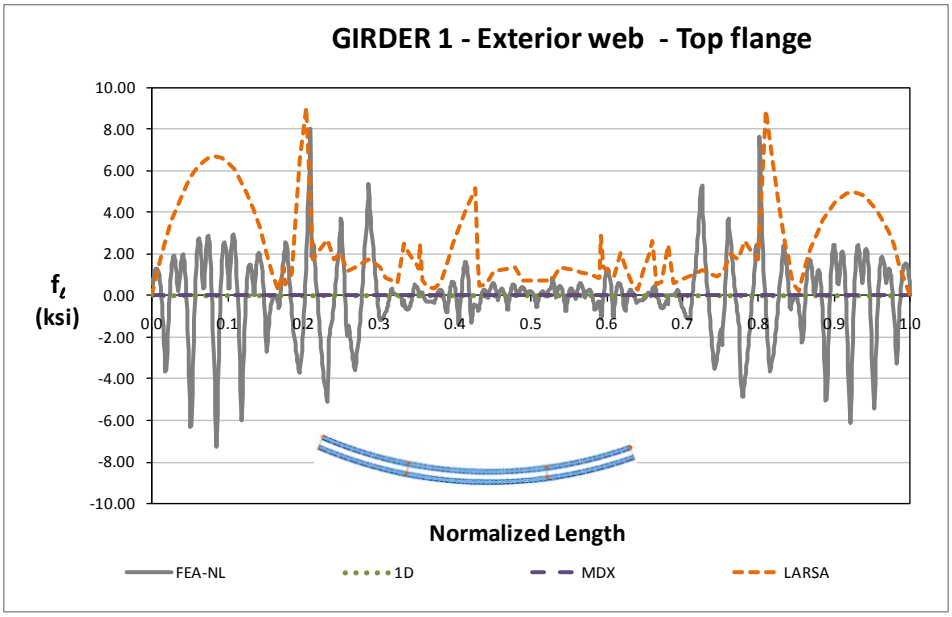

Fig. 10. Top flange lateral bending stress for Girder 1 exterior web - Total Dead Load

Top Flange Lateral Bracing Results

Figures 11 and 12 illustrate the stresses in the top flange lateral bracing system diagonals and struts, the results are presented as positive and negative stresses at the central location of the element along the length.

The higher stresses in the diagonals are recorded at the support locations and then decrease in the central span mainly due to the X-type flange lateral bracing layout. For the struts the behavior is reversed as they attract more force in the central span as every strut is taking force from two diagonals.

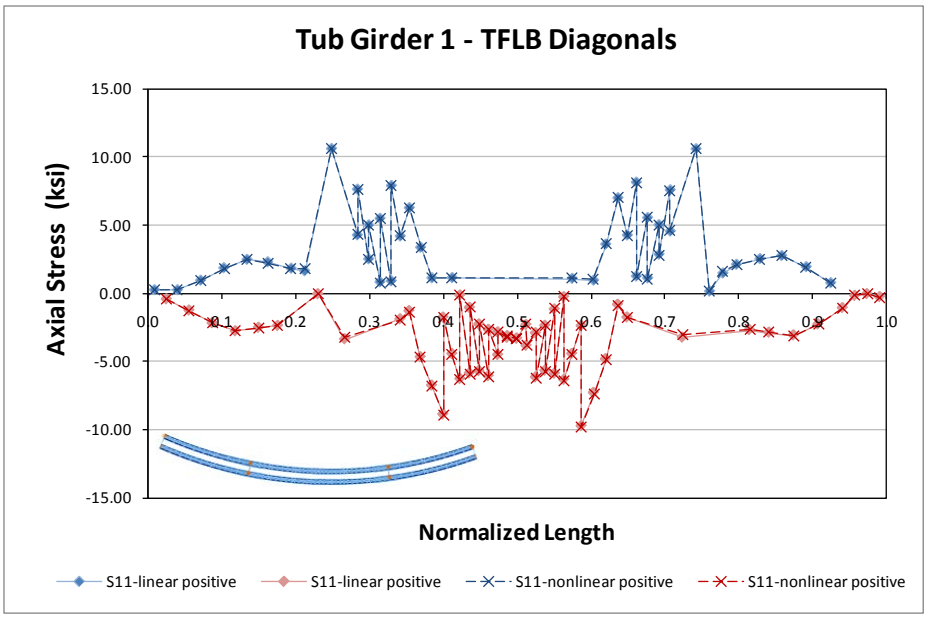

Fig. 11. Top flange lateral bracing diagonals axial stresses for Girder 1 - Total Dead Load

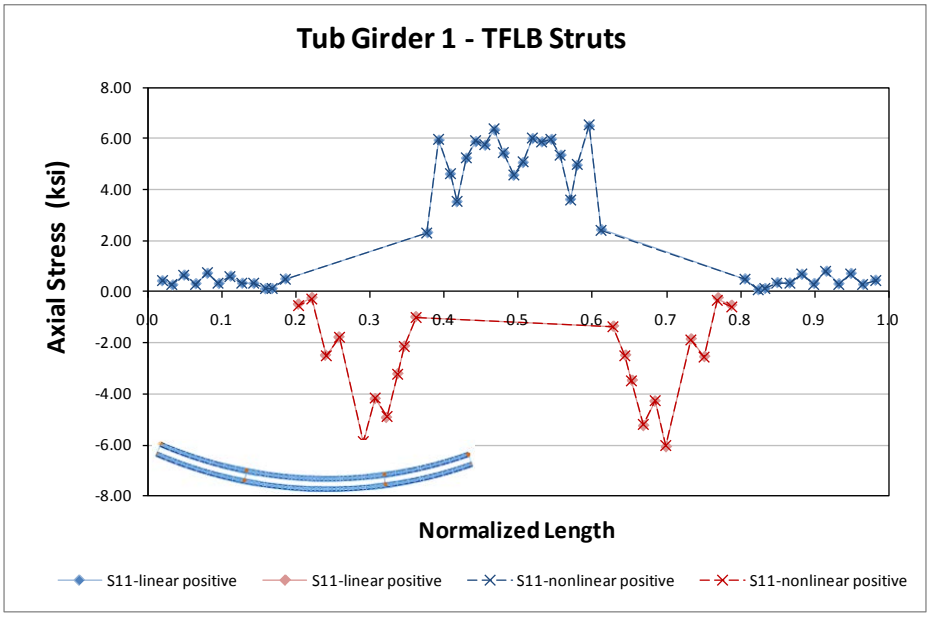

Fig. 12. Top flange lateral bracing struts axial stresses for Girder 1 - Total Dead Load

Internal Cross-Frame Results

The internal cross frame results are presented on Figures 13 and 14. This bridge uses inverted-V cross frames with and without bottom chord. The top chord stresses are plotted in Figure 13, in this case the stresses remain low due to the larger cross sectional area.

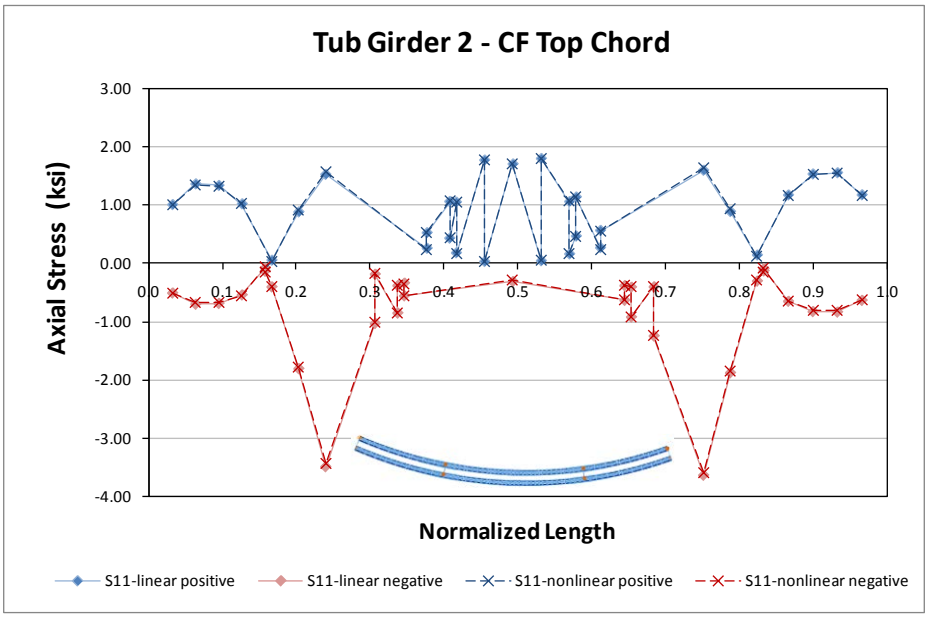

Fig. 13. Internal cross frame top chord axial stresses for Girder 1 - Total Dead Load

On Figure 14 the diagonal stresses are shown. Stresses in these elements are higher due to a smaller cross sectional area (2.4in²). Bottom chord stresses in internal cross frames are not generally higher on magnitude due to the proximity to the girder bottom flange as shown in Figure 15.

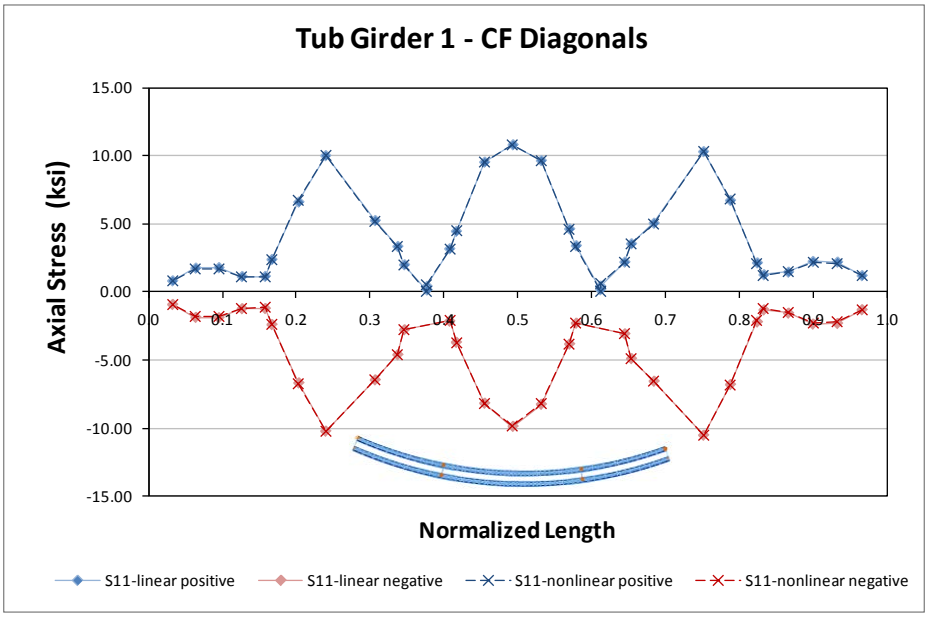

Fig. 14. Internal cross frame diagonals axial stresses for Girder 1 - Total Dead Load

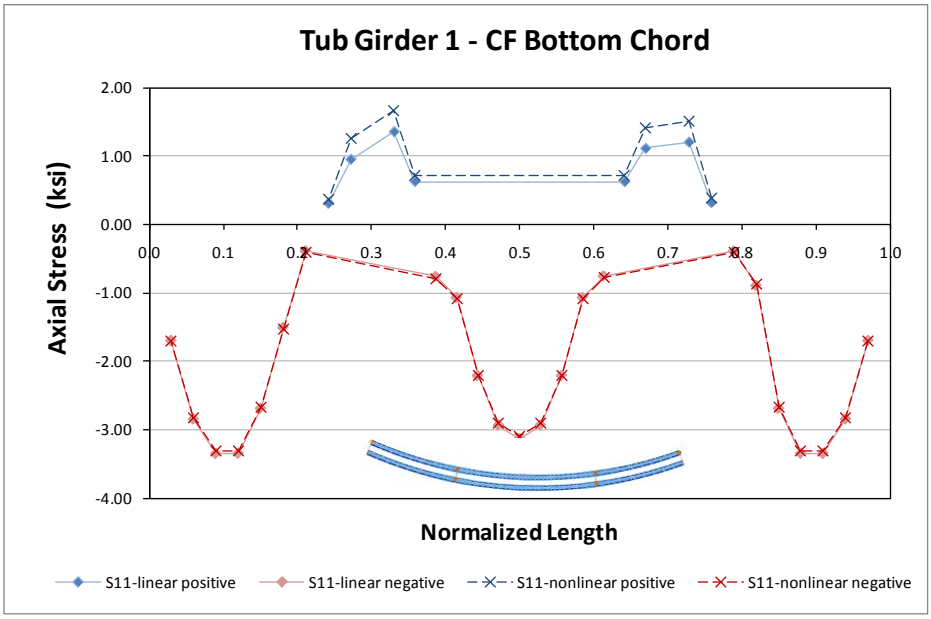

Fig. 15. Internal cross frame bottom chord axial stresses for Girder 1 - Total Dead Load

11.2 ETCCR15 (Existing, Tub-girder, Continuous-span, Curved, Radial supports)

Bridge Description:

Marquette Interchange Ramp SE, Milwaukee, WI

Category Data:

L_1 = 155ft, L_2 = 169 ft, L_3 = 232ft, L_4 = 185ft, L_5 = 185ft, L_6 = 144ft / R = 515ft, 960ft, ∞, -1904ft / w = 29.5ft, 2 tub-girders

References:

Wisconsin DOT

Erection Stages Analyzed: 9 steel erection stages

Deck Placement Sequence: (Analyses are performed assuming no staged deck placement).

Bridge Perspective & Plan views:

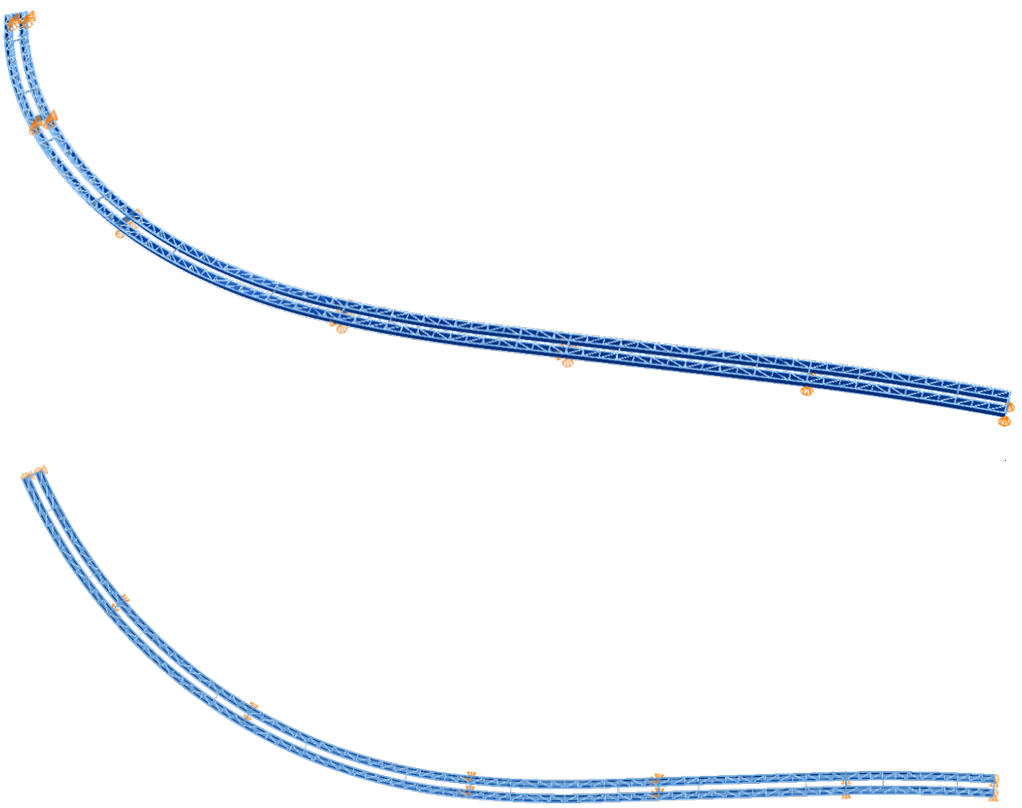

Displacement Results

The Marquette Interchange Ramp SE is a six span continuous twin girder bridge. The bridge is modeled as 4 segments of different curvature: R = 515ft, 960ft, straight and reversed 1904ft, the span lengths go from 155ft to 232ft. The bridge was designed as a continuous bridge to overcome design issues related

with the maximum height with respect to the ground level of the bridge. The results are presented left to right in conformity with the plan view presented above; the original design plans showed the layout rotated 180°.

Figure 1 illustrates the vertical displacements for the final steel dead load. The displacement reaches a maximum of 2.2in at the third (longest) span for this stage and in Figure 2 the maximum displacement reaches 6.5in for the total dead load condition.

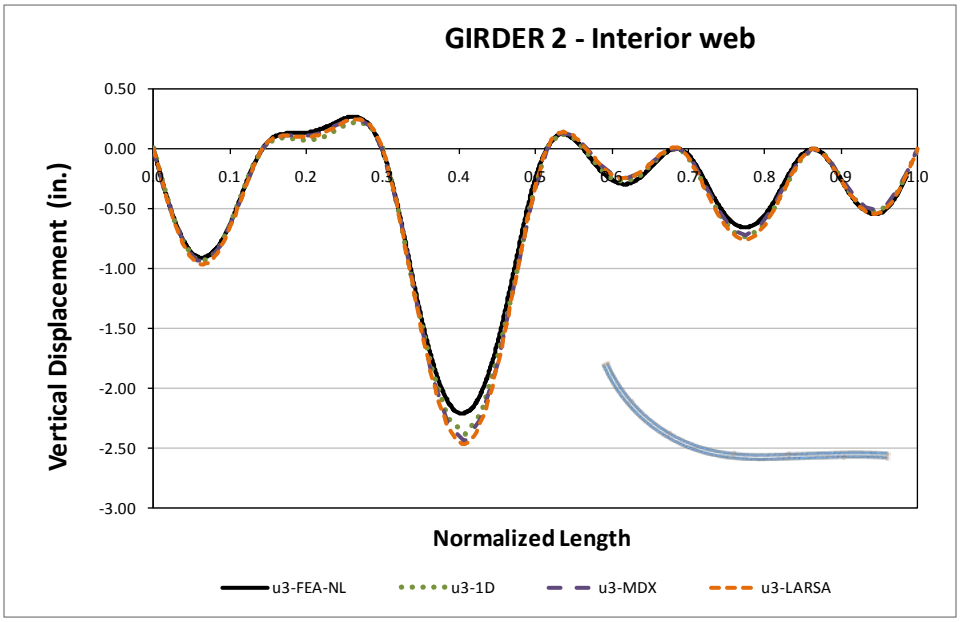

Fig. 1. Top flange vertical displacements for Girder 2 interior web - Final Steel Dead Load

Figures 2 and 3 show the vertical displacements for the two girders under total dead load. The 3DFEA results correspond to the outer and inner top flange locations. The 1D and 2D analysis methods show results for the girder centerline. A small differential displacement can be noticed between these locations, specifically at the longest span, meaning that a section rotation is taking place.

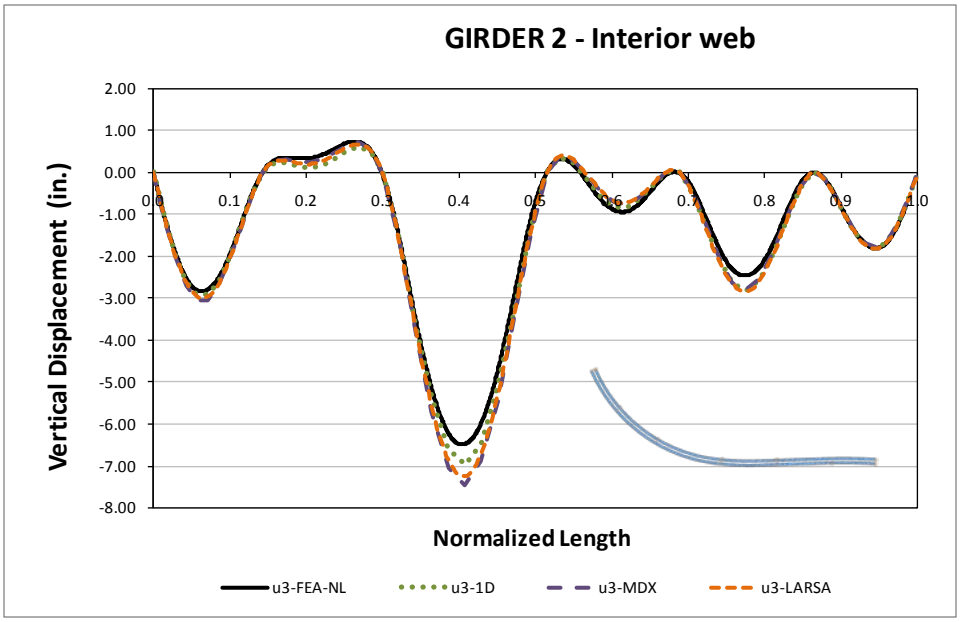

Fig. 2. Top flange vertical displacements for Girder 2 interior web - Total Dead Load

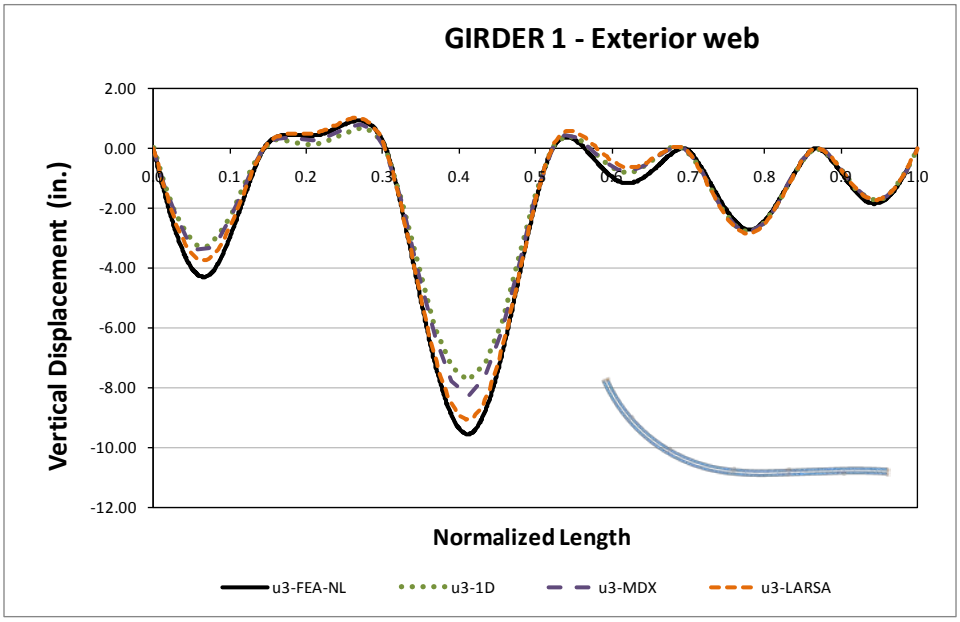

Fig. 3. Top flange vertical displacements for Girder 1 exterior web - Total Dead Load

The relative radial displacement for the final steel and total load conditions is presented on Figures 4 and 5. As identified before, the third span experiences the maximum relative displacement that can reach up to 1.2in for the total dead load. The 1D and 2D analyses also predict a similar behavior.

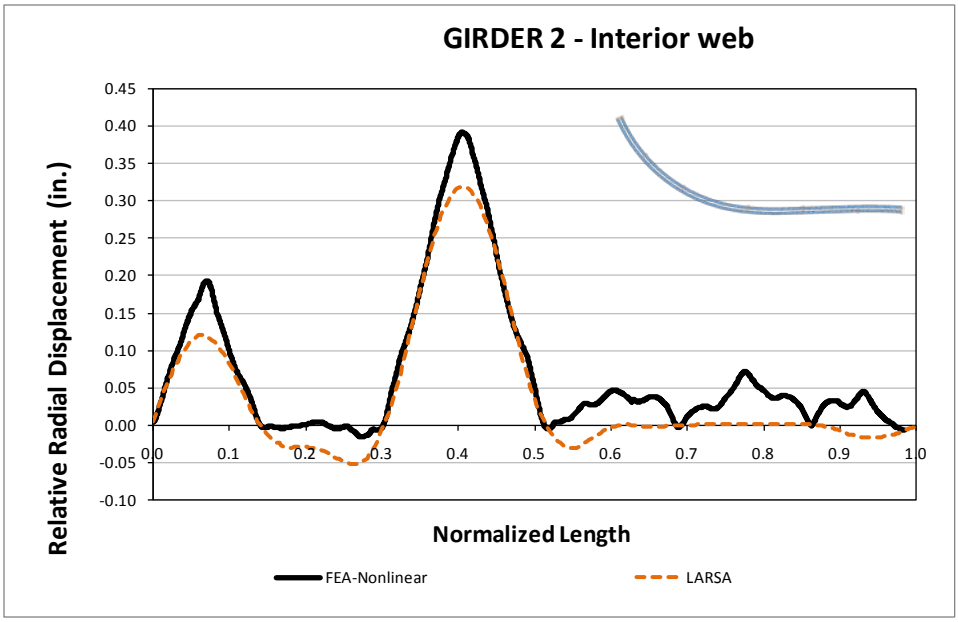

Fig. 4. Relative radial displacements for Girder 2 interior web – Final Steel Dead Load

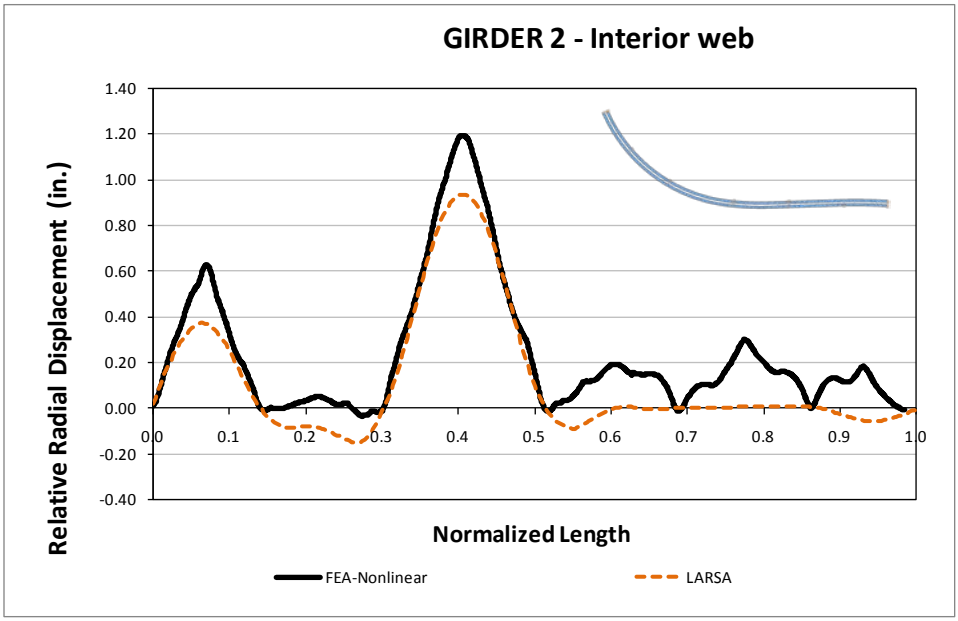

Fig. 5. Relative radial displacements for Girder 2 interior web - Total Dead Load

Bending Stress Results

The major axis bending stresses for the top and bottom flanges are shown in Figures 6 and 7 for total dead load condition. All analyses predicted the response closely as it is common for this type of results.

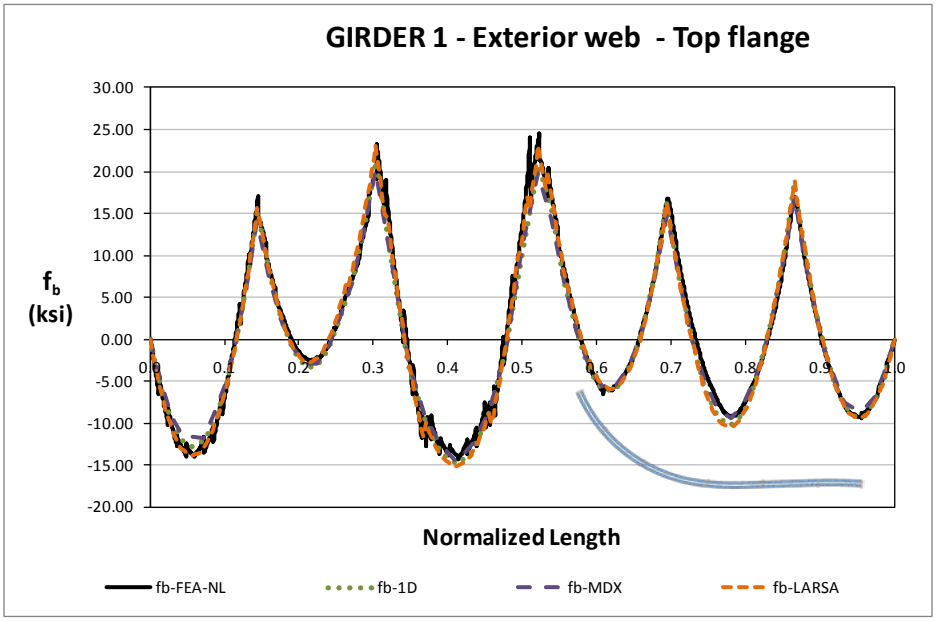

Fig. 6. Top flange major axis bending stress for Girder 1 exterior web – Total Dead Load

On Figure 7 the 3DFEA analysis show sudden changes on the bottom flange stresses. As noted before, this is caused by the interaction between 3D shell elements that coincide at this location: diaphragm, bottom flange and web plates; the nature of this localized effect is believed to be purely numerical. At support locations, a similar jump in the stress value occurs; this is the effect of the bearing plate model that it is represented as a rigid region.

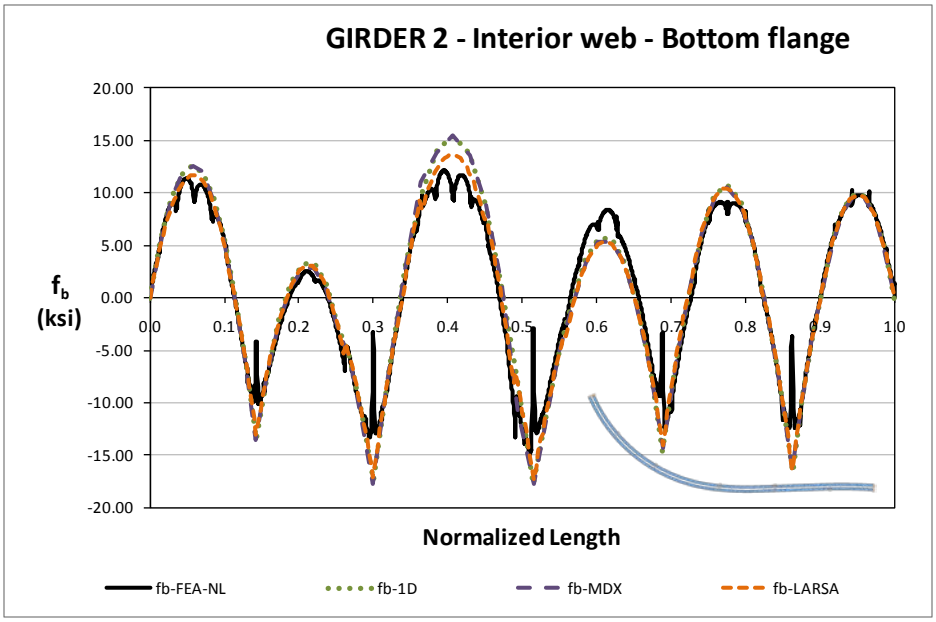

Fig. 7. Bottom flange major axis bending stress for Girder 2 interior web - Total Dead Load

Minor axis bending stresses are reported on Figure 8. Results shown correspond to the total dead load condition by using 3DFEA and Larsa analyses. Larsa bending stress values overpredict the behavior with values that are on the range of half the yielding stress, this difference is believed to be caused by the simplified analysis hypothesis and has been seen in other bridge analyses.

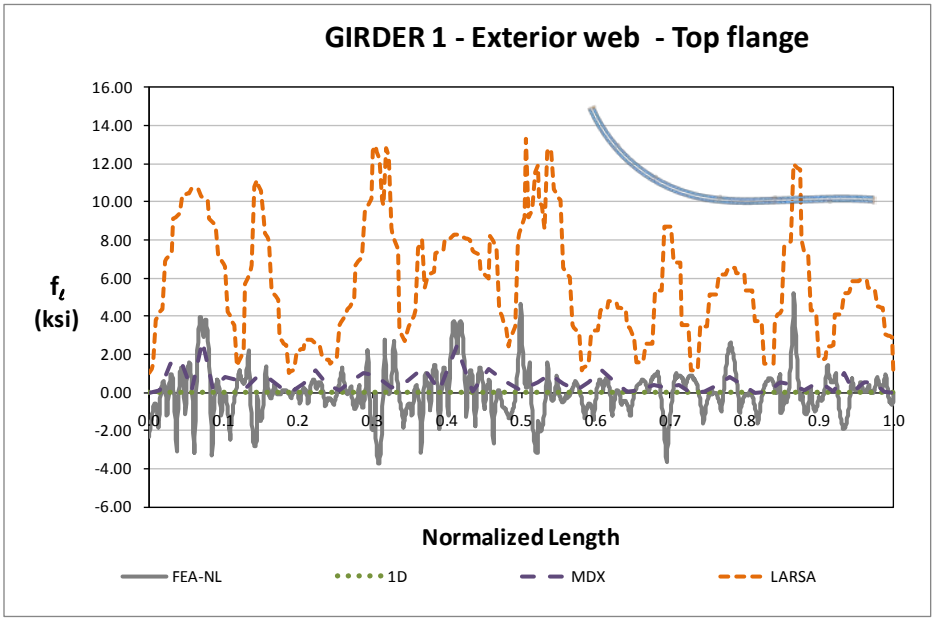

Fig. 8. Top flange lateral bending stress for Girder 1 exterior web - Total Dead Load

11.3 NTCCR1 (New, Tub-girder, Continuous-span, Curved, Radial Supports)

Bridge Description:

Category Data:

L_1 = 150 ft, L_2 = 150 ft, L_3 = 120 ft / R = 268 ft / w = 30 ft, 2 tub-girders

Erection Stages Analyzed: 6 steel erection stages

Deck Placement Sequence: Five stages, deck thickness = 9.5 in

Bridge Perspective & Plan Views:

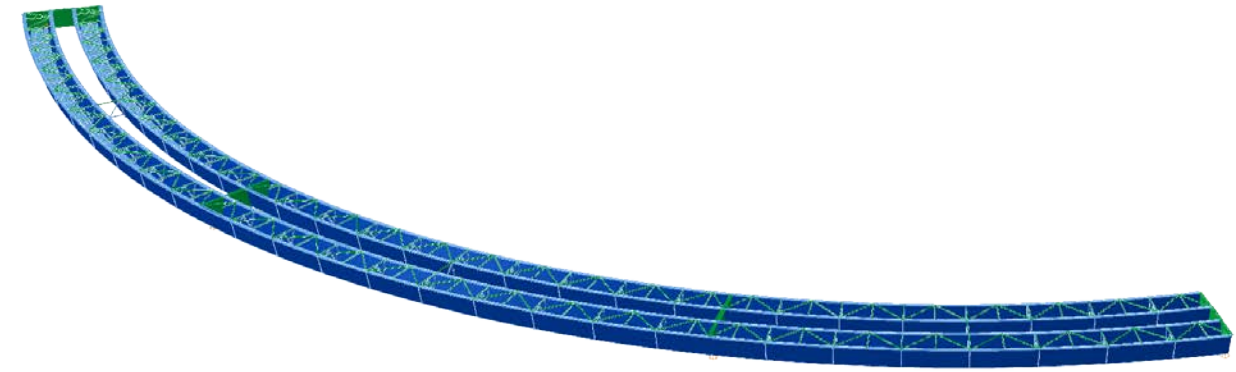

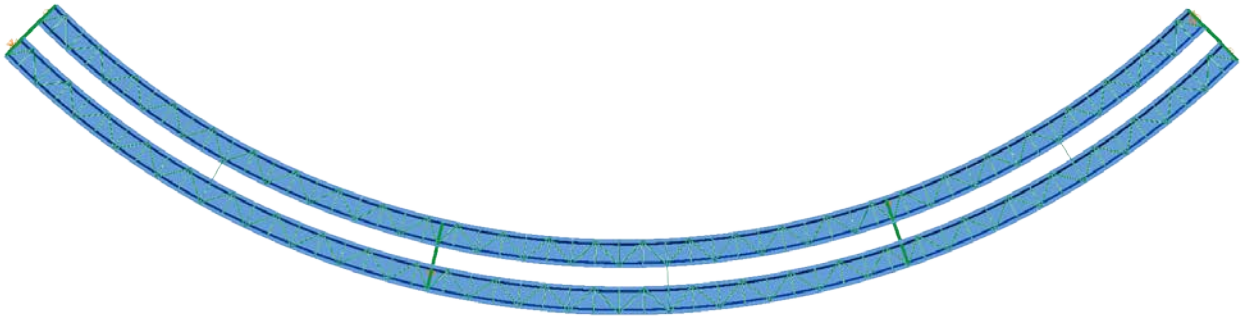

Displacement Results

Figures 1 through 4 show the evolution of the vertical displacements for the partial steel erection stages 10, 11 and final steel and total non-composite dead loads. For the partial stages the vertical displacements are plotted only for 3D FEA and 2D LARSA, all methods are shown for the final steel and total non-composite dead loads. Figure 5 shows the same set of results for total dead load but in this case the results of the interior top flange are shown.

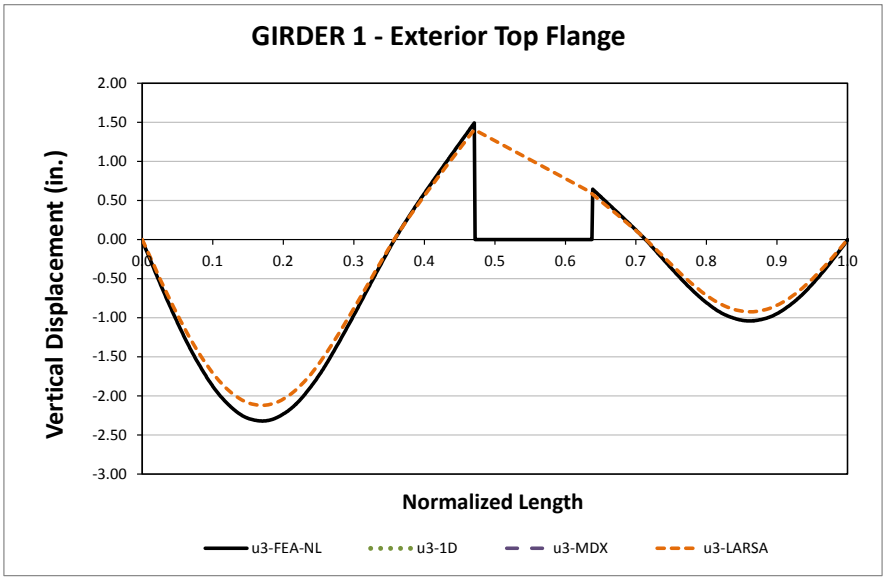

Fig. 1. Top flange vertical displacements for Girder 1 exterior flange - Stage 10 Steel Dead Load

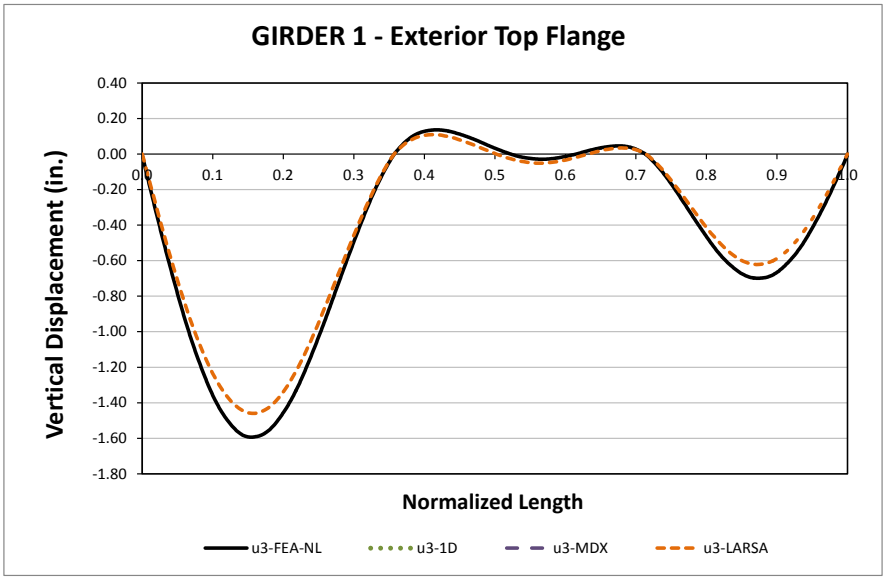

Fig. 2. Top flange vertical displacements for Girder 1 exterior flange - Stage 11 Steel Dead Load

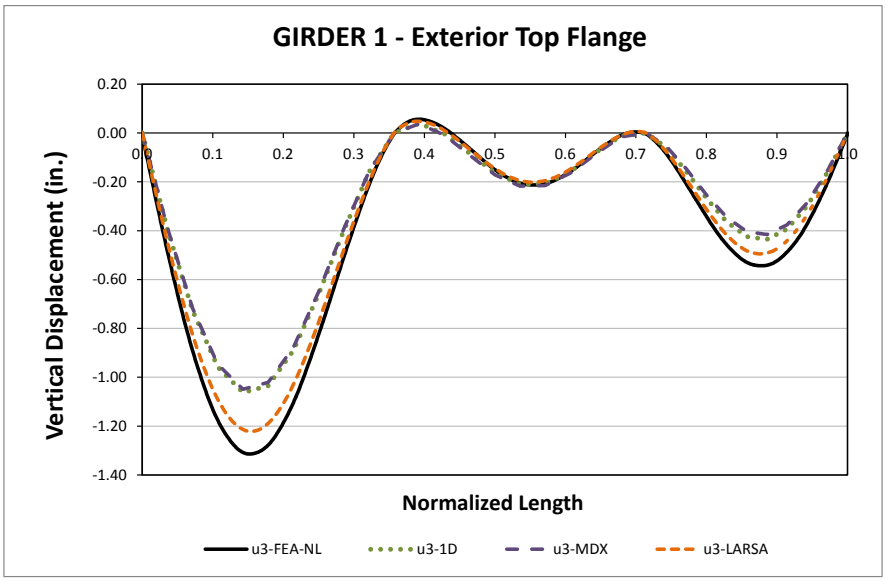

Fig. 3. Top flange vertical displacements for Girder 1 exterior flange - Final Steel Dead Load

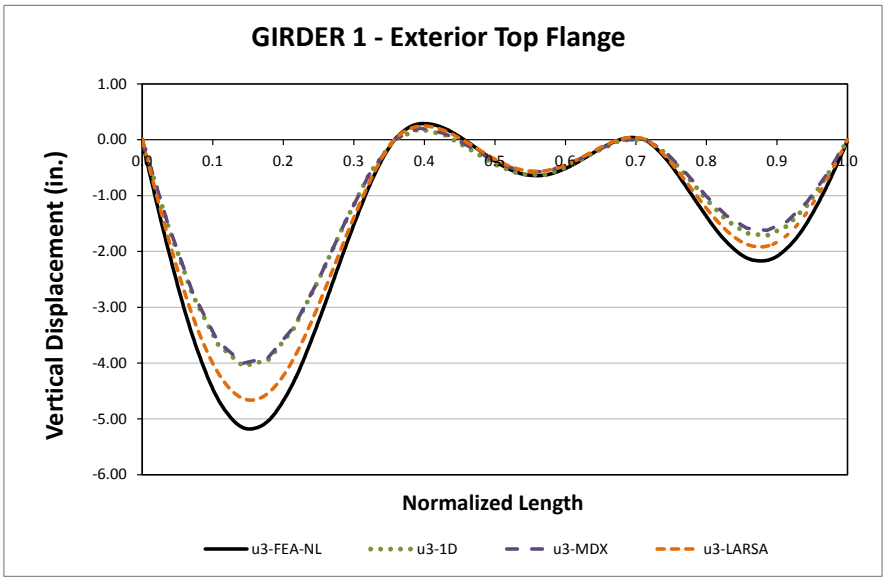

Fig. 4. Top flange vertical displacements for Girder 1 exterior flange - Total Dead Load

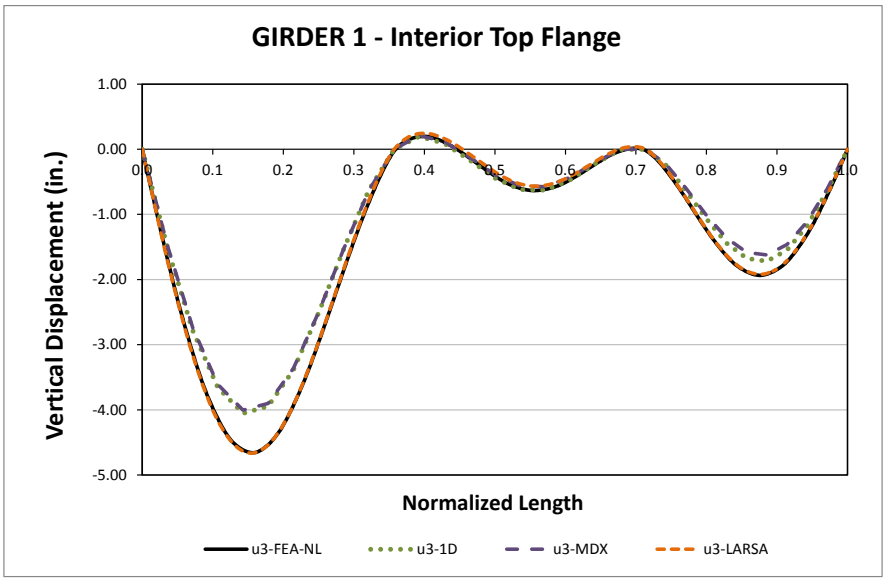

Fig. 5. Top flange vertical displacements for Girder 1 interior flange - Total Dead Load

The tub girder system experiences small vertical displacements when compared to other analyzed bridges; this is due to the short span and continuous configuration of the bridge. For these small vertical displacements, the effect of the girder twisting affects the magnitude of the vertical displacements reported by the 1D and 2D methods as shown in the previous figures. Figures 4 and 5 show the contrast between the Girder 1 exterior and interior flanges as reported by the 3DFEA method, the difference in vertical displacements shows that the girder is twisting.

Figures 6 and 7 illustrate the relative radial displacement between top and bottom flange junctures as a measure of lateral displacement for the final steel and total non-composite dead loads. This relative displacement indicates that girder twist on is occurring and that its effect on the vertical displacements is noticeable.

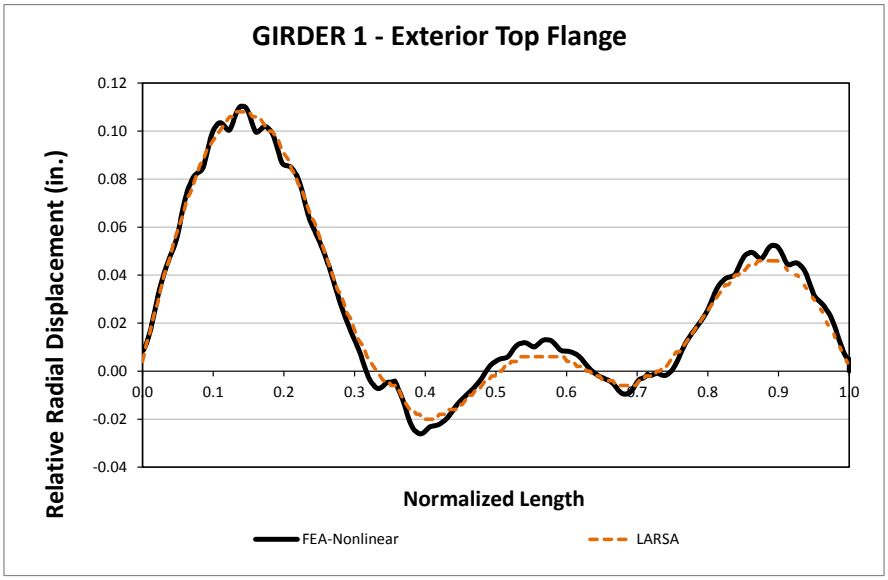

Fig. 6. Top flange relative radial displacements for Girder 1 exterior flange - Final Steel Dead Load

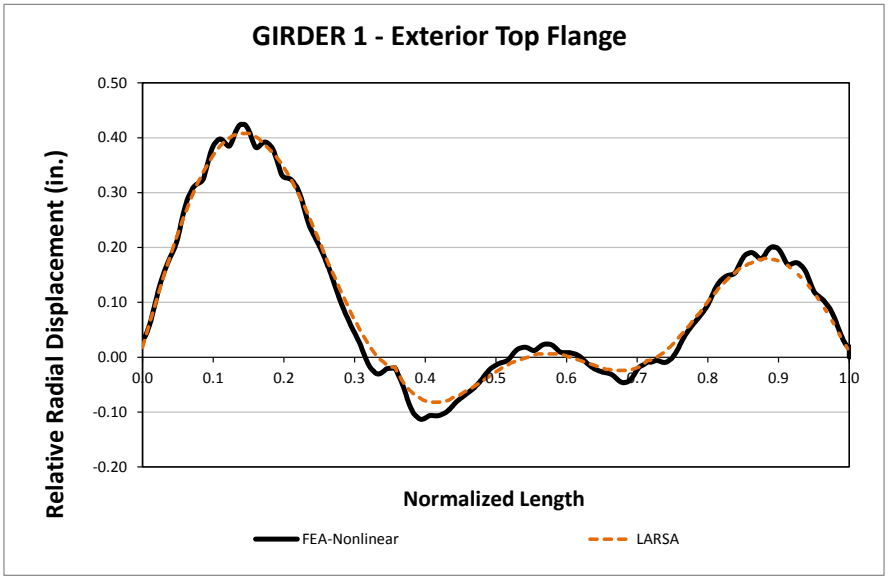

Fig. 7. Top flange relative radial displacements for Girder 1 exterior flange - Total Dead Load

Bending Stress Results

Major axis bending stresses at the top flange and web juncture are presented in Figures 8 through 11 as predicted by different analysis methods for partial steel erection, final steel and total dead load stages. Results in general show a good agreement in shape and magnitude. The local interaction of the TFLB system is evident in all stages on the 3DFEA results as the stresses curves are not smooth and exhibit a saw-tooth shape due to the TFLB system interaction.

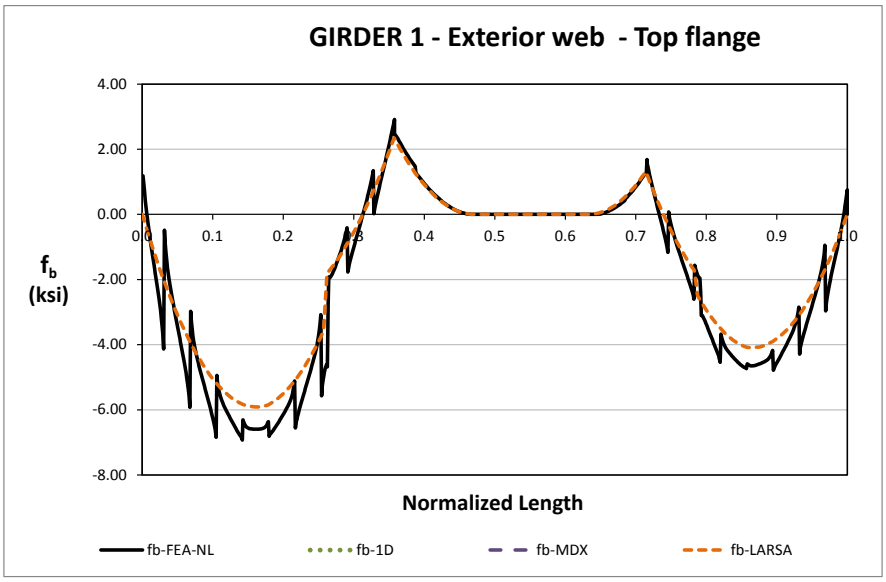

Fig. 8. Top flange major axis bending stress for Girder 1 exterior web - Stage 10 Steel Dead Load

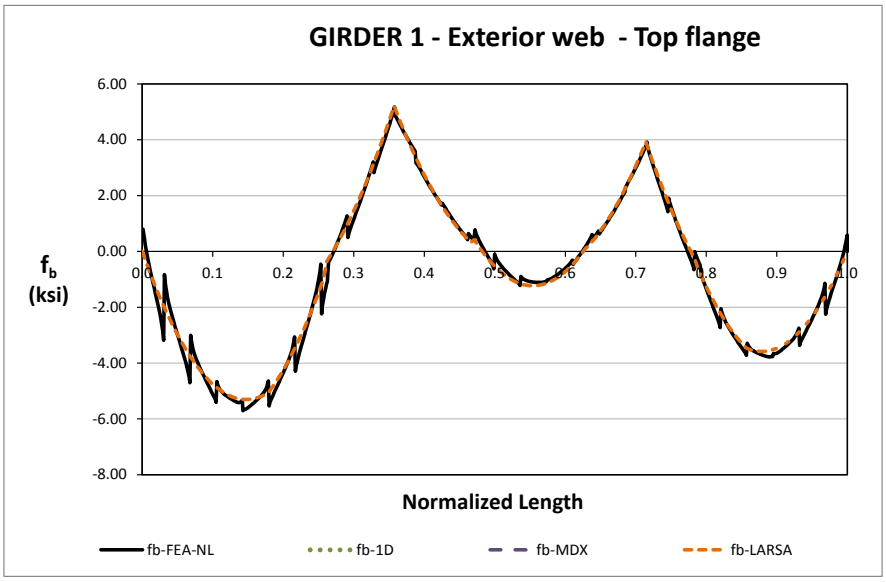

Fig. 9. Top flange major axis bending stress for Girder 1 exterior web - Stage 11 Steel Dead Load

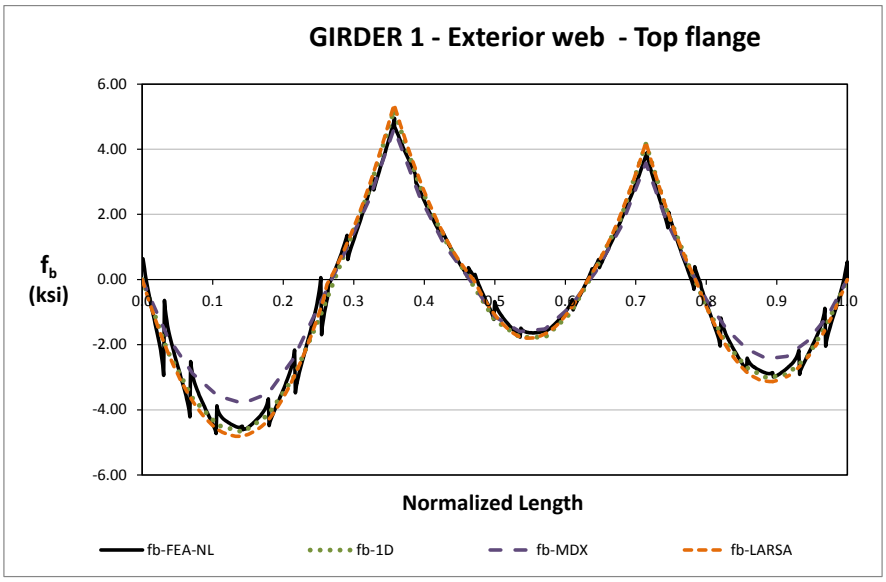

Fig. 10. Top flange major axis bending stress for Girder 1 exterior web - Final Steel Dead Load

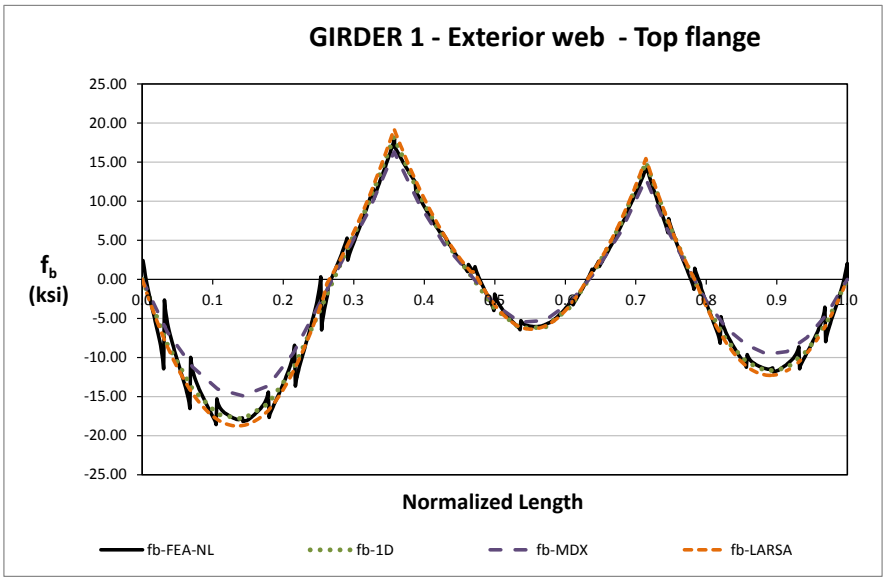

Fig. 11. Top flange major axis bending stress for Girder 1 exterior web - Total Dead Load

Figures 12 and 13 illustrate the bottom flange stresses at the bottom flange and web juncture for the final steel and total dead load cases. In the bottom flange there are small local variations caused by the internal CF elements. At the intermediate supports, the bridge stresses experiment a sudden change in value shown as spikes, this is attributed to the bearing plate model for the bridge supports. The elements surrounding the bearing points are constrained to simulate the bearing plate as a rigid zone, this modeling technique causes inaccuracies in the analytical procedure generating apparent stress concentrations.

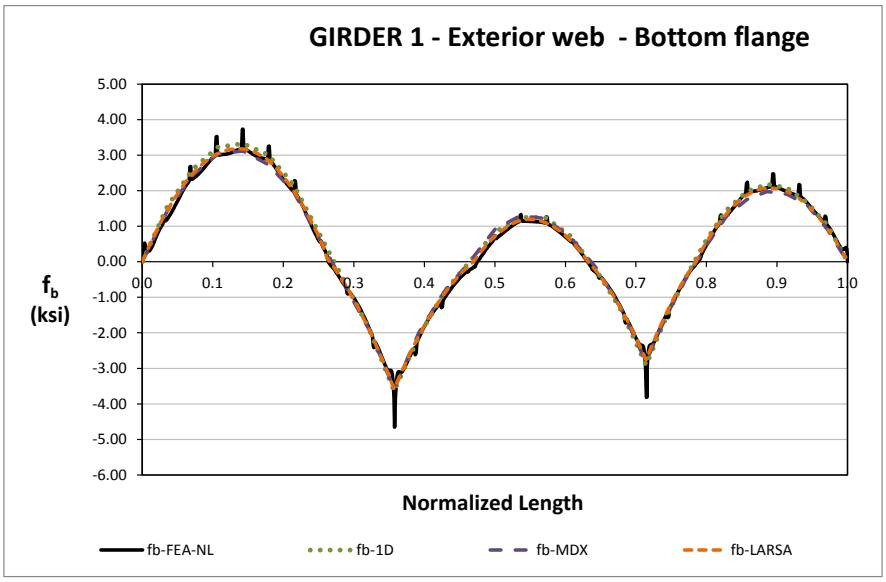

Fig. 12. Bottom flange major axis bending stress for Girder 1 exterior web - Final Steel Dead Load

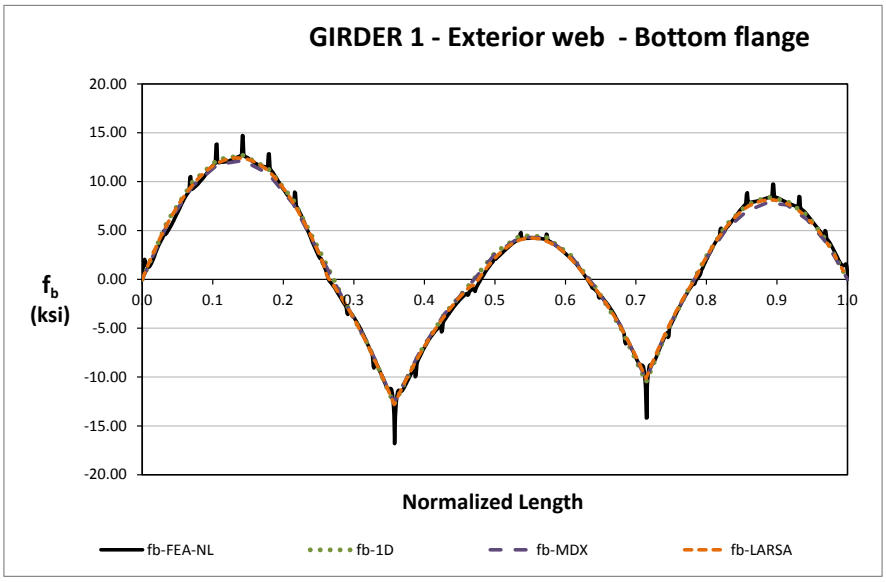

Fig. 13. Bottom flange major axis bending stress for Girder 1 exterior web - Total Dead Load

Lateral bending stress distributions is shown in fig. 14, the stresses values reported by the 3DFEA remain low in contrast as with the values reported by 1D and 2D-Larsa.

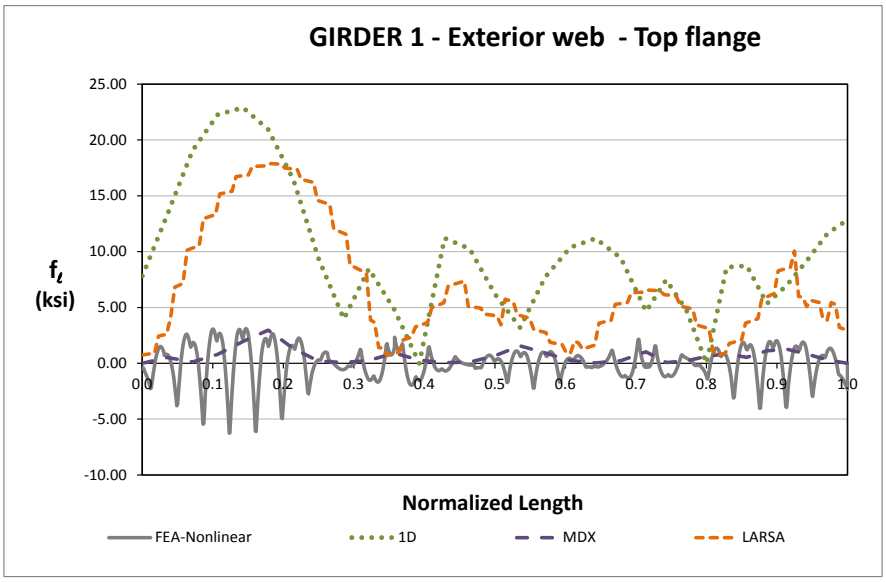

Fig. 14. Top flange lateral bending stress for Girder 1 exterior web - Total Dead Load

Top Flange Lateral Bracing Results

The TFLB diagonals axial forces are shown in Figures 15 and 16 for the final steel and total dead load condition. The cross sectional area of these elements is 10.6in² that for a maximum axial force of 30kip as reported by the 3DFEA the element experiences an axial stress of 2.8ksi on the total dead load conditions. In general, the predictions by the 1D and 2D methods are close to the 3DFEA, this behavior has been observed in radial cases as the torsional forces caused by the curvature are clearly identified in the Tub-Girder Design State of the Art.

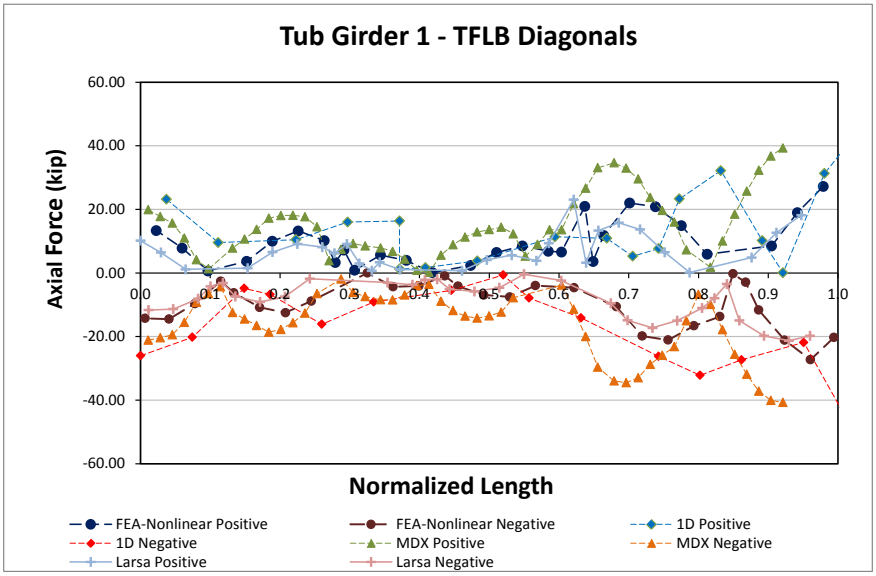

Fig. 15. Top flange lateral bracing diagonals axial forces for Girder 1 - Final Steel Dead Load

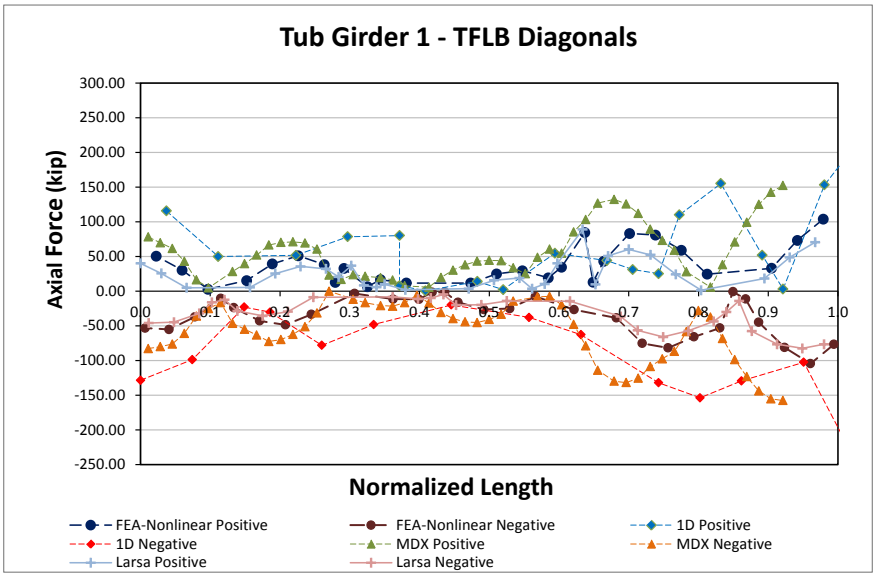

Fig. 16. Top flange lateral bracing diagonals axial forces for Girder 1 - Total Dead Load

Figure 17 shows the TFLB axial forces on the struts for the total non-composite deal load case. The area of the struts is 4.4in² which, for a maximum axial force of 25kip as reported by the 3DFEA analysis, results on maximum axial stress of 5.6ksi. The 3DFEA and 1D and 2D analyses show good predictions mainly due to the bridge short span and uniform radial geometry.

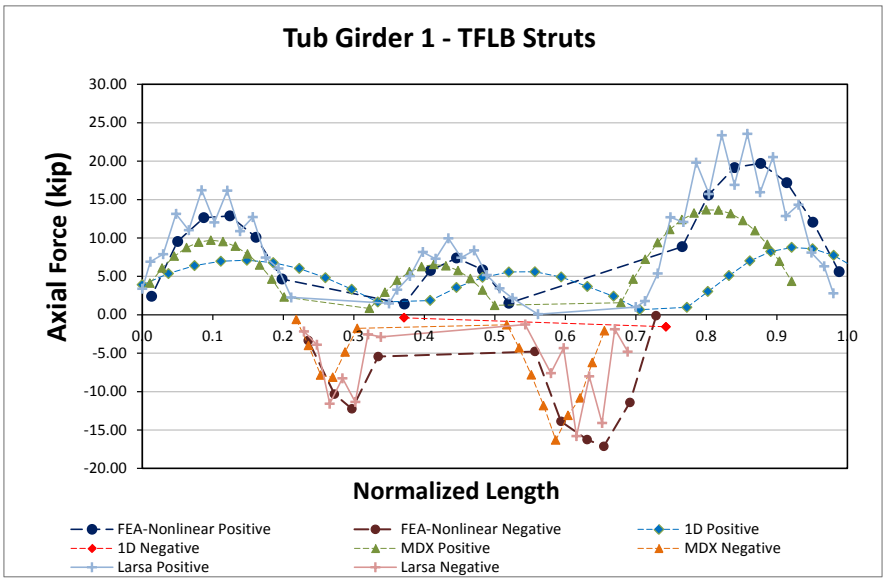

Fig. 17. Top flange lateral bracing struts axial forces for Girder 1 - Total Dead Load

Internal Cross Frame Results

Figure 18 shows the internal CF diagonal axial forces with cross sectional area of 4.4in² which for a maximum value predicted by the 3DFEA of 25kip the maximum stress is close to 6ksi. Predictions are again in the right order of magnitude for these elements.

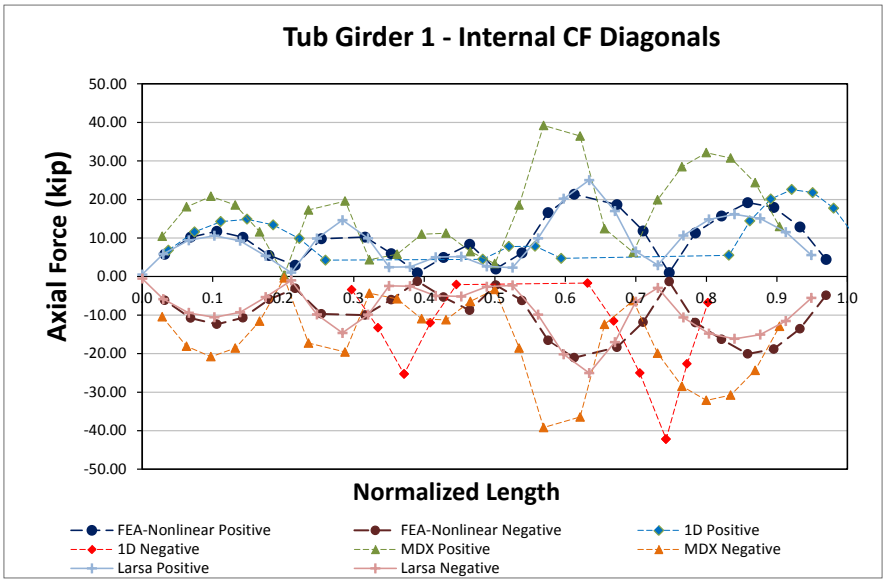

Fig. 18. Internal cross-frame diagonals axial forces for Girder 1 - Total Dead Load

11.4 NTCCR5 (New, Tub-girder, Continuous-span, Curved, Radial Supports)

Bridge Description:

Category Data:

L_1 = 350ft, L_2 = 350 ft, L_3 = 280 ft / R = 1380 ft / w = 30 ft, 2 tub-girders

References:

Erection Stages Analyzed: 7 steel erection stages

Deck Placement Sequence: Four stages, deck thickness = 9.5 in

Bridge Perspective & Plan Views:

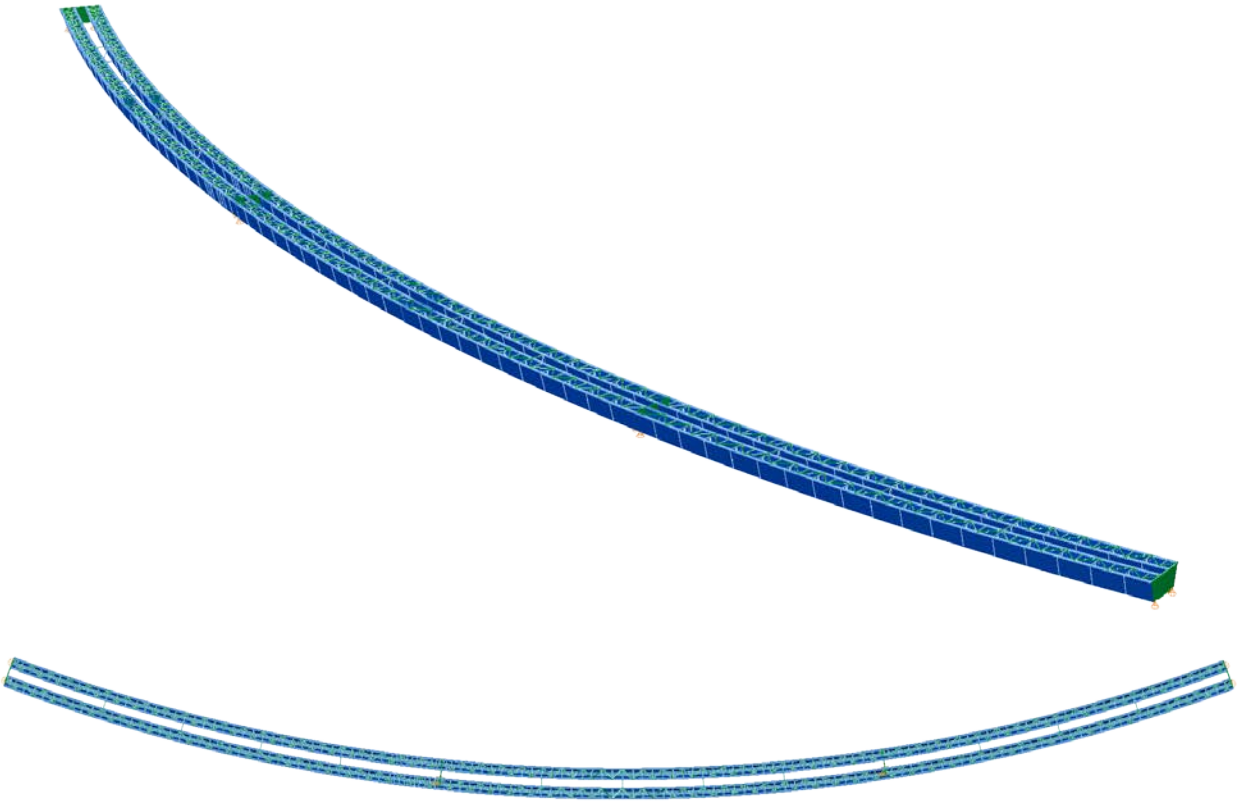

Displacement Results

Figures 1, 2 and 3 show the partial erection stage 15, the final steel and non-composite total dead load vertical displacements for the exterior top flange of Girder 1 at the web juncture. These displacements are plotted for four different methods of analysis: non-linear refined 3D FEA, 1D and using 2D analysis software MDX and LARSA. Most of the methods show a close prediction of results, discrepancies on the results are mainly attributed to the discretization used by the analysis method leading to a system slightly stiffer when the bridge is represented by a lower number of elements along the length.

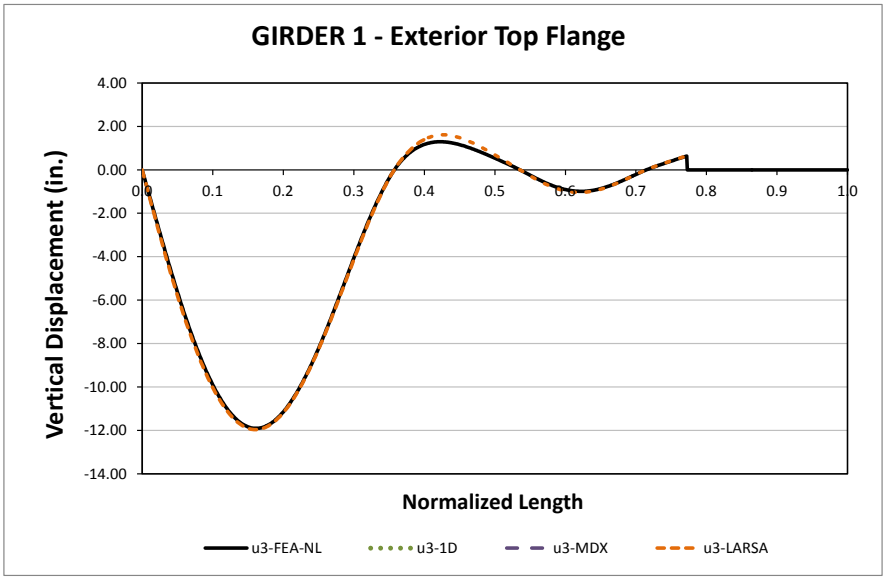

Fig. 1. Top flange vertical displacements for Girder 1 exterior flange - Stage 15 Steel Dead Load

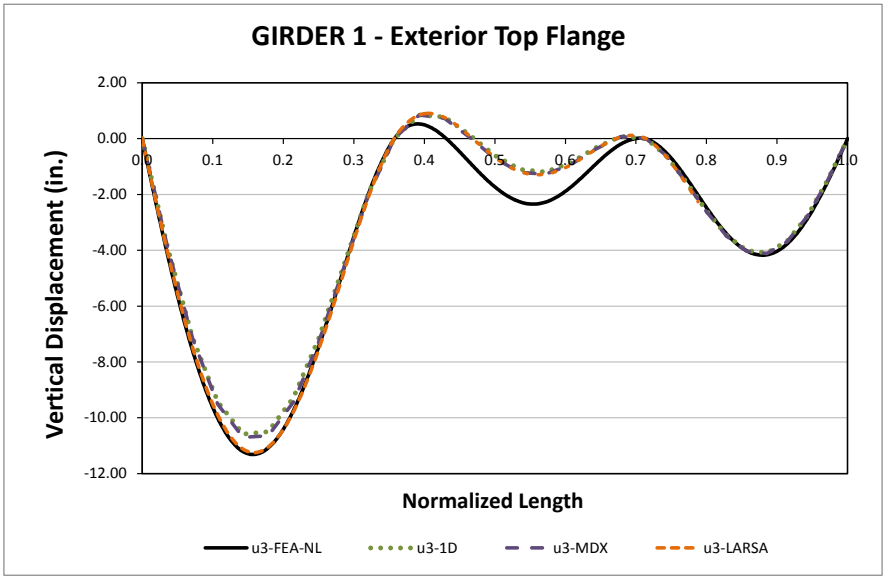

Fig. 2. Top flange vertical displacements for Girder 1 exterior flange - Final Steel Dead Load

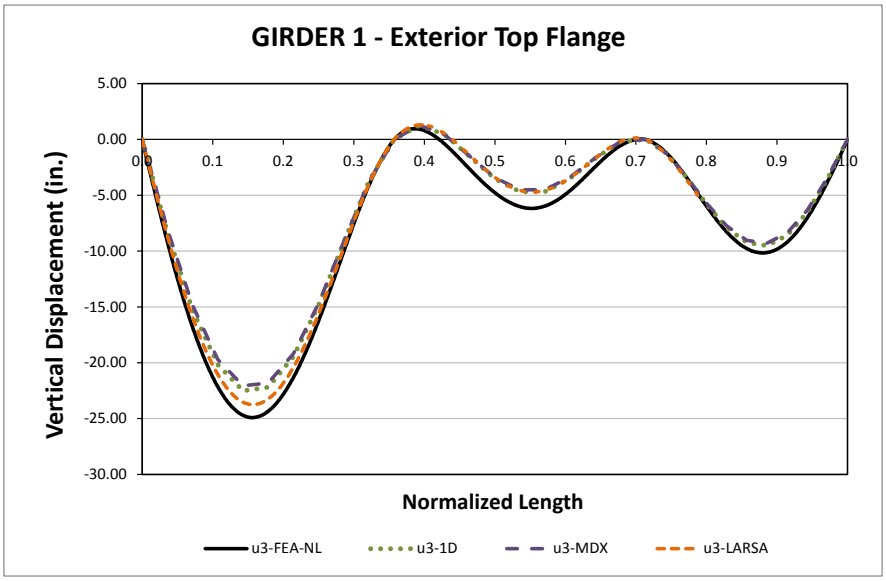

Fig. 3. Top flange vertical displacements for Girder 1 exterior flange - Total Dead Load

The top flange relative radial displacements are shown in fig. 4 for the total non-composite dead load, the results are shown for the 3DFEA and LARSA models. A small local variation on the 3DFEA is attributed to the interaction of the TFLB system. In this example the effect is not important but previous studies have shown cases where an important local increase occurs.

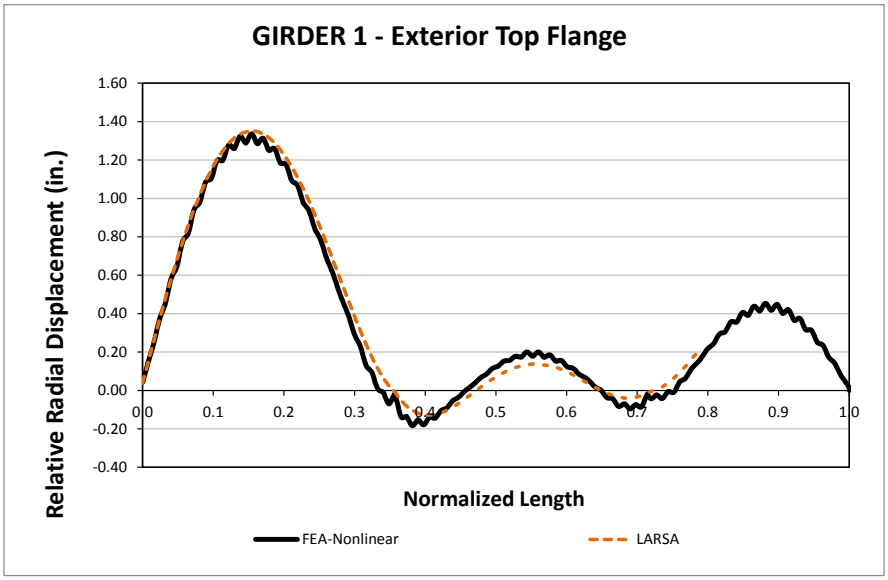

Fig. 4. Top flange relative radial displacements for Girder 1 exterior flange - Total Dead Load

Bending Stress Results

Top flange major axis bending stresses for Girder 1 at the web juncture are presented in Figures 5 and 6 for the final steel and total non-composite dead load construction stages as predicted by the different analysis methods. As reported in other bridge cases, 3D results show localized effects due to the Top flange Lateral Bracing system presence. The 1D and 2D methods predict the general shape of the stress distribution but ignore localized effects.

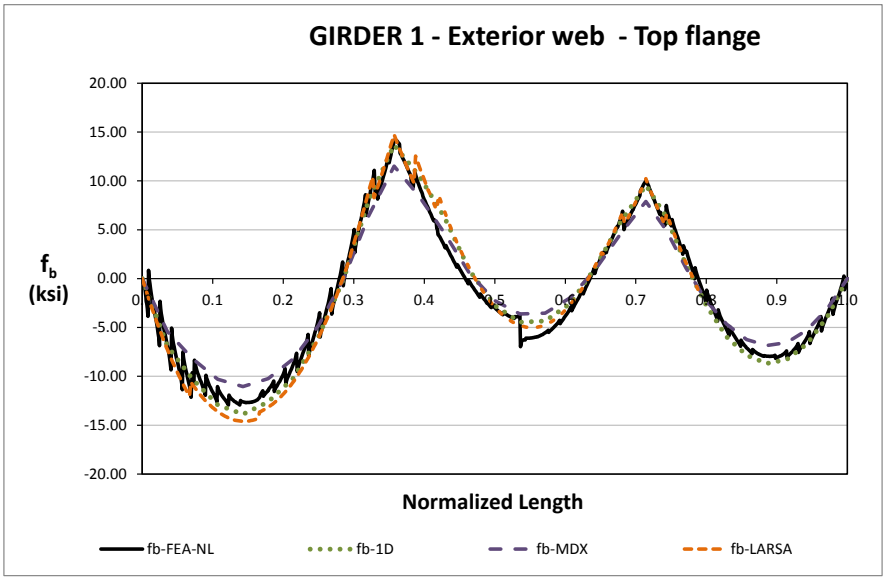

Fig. 5. Top flange major axis bending stress for Girder 1 exterior web - Final Steel Dead Load

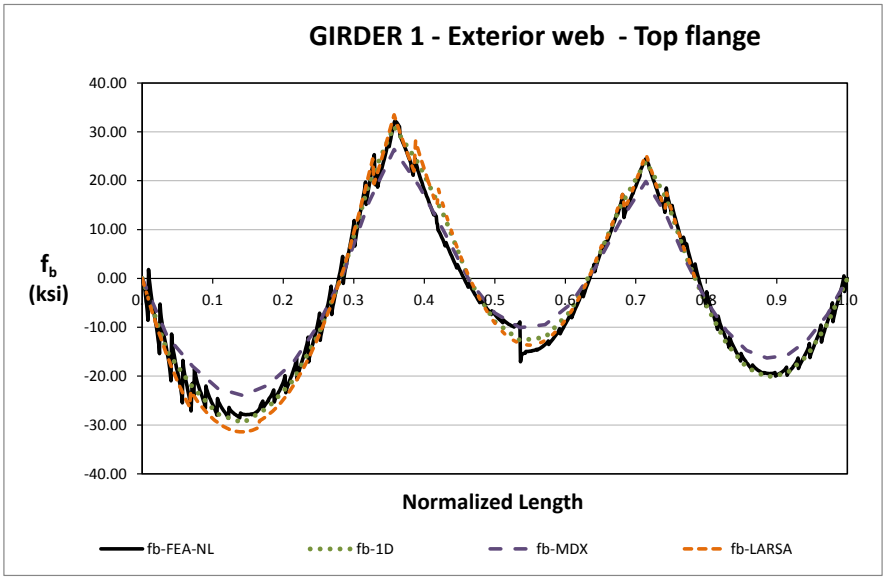

Fig. 6. Top flange major axis bending stress for Girder 1 exterior web - Total Dead Load

Figures 7 and 8 illustrate the bottom flange major axis bending stresses at the web juncture for Girder 1, results are shown for the final steel and total non-composite dead load cases. The 3DFEA analysis shows a localized stress concentration at the intermediate supports locations, as the elements surrounding the bearing points are constrained to simulate the bearing plate as a rigid zone, the analytical procedure generates apparent stress concentrations.

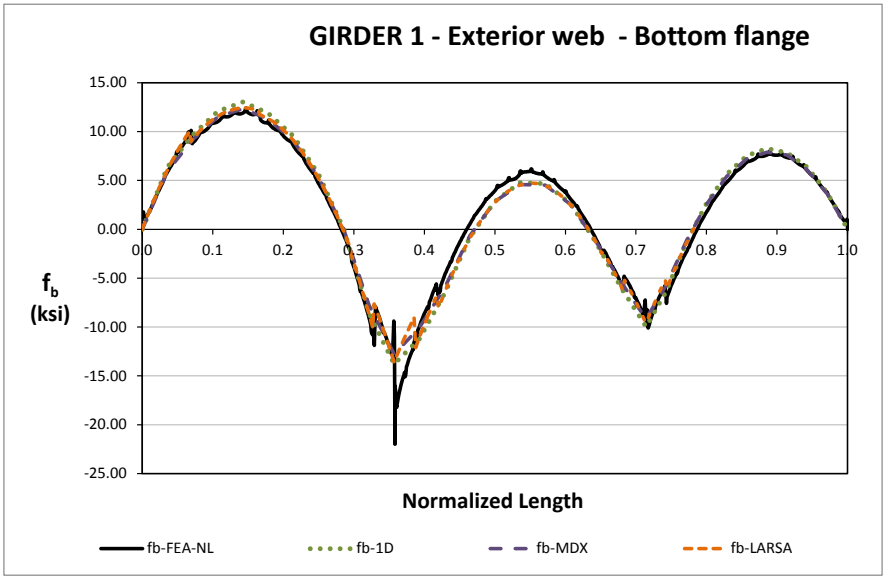

Fig. 7. Bottom flange major axis bending stress for Girder 1 exterior web – Final Steel Dead Load

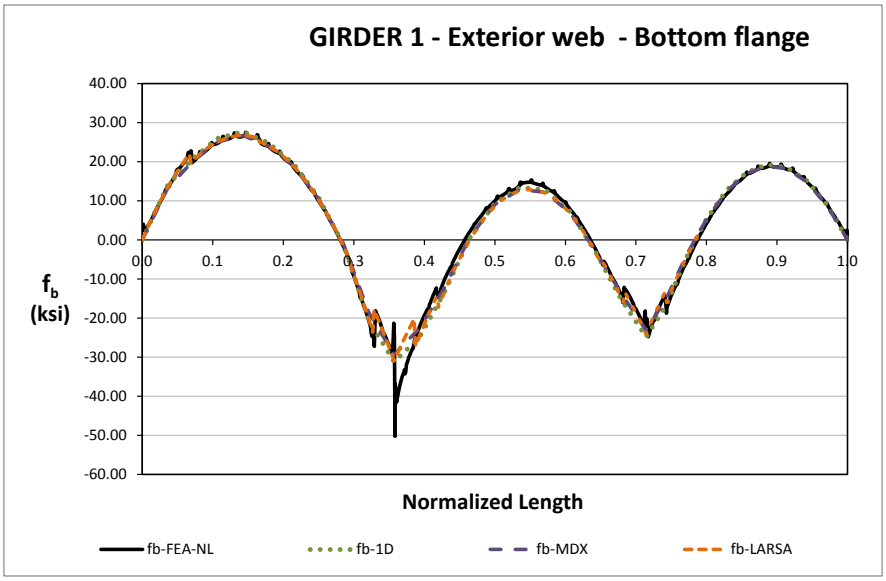

Fig. 8. Bottom flange major axis bending stress for Girder 1 exterior web - Total Dead Load

Top Flange Lateral Bracing Results

The TFLB diagonals axial forces are shown in Figures 9 and 10 for the final steel and total dead load condition. The cross sectional area of these elements is 28.1in² that for a maximum axial force of 300kip the element experiences an axial stress of 11ksi on the total dead load condition.

The forces predicted by the 1D and 2D analyses are close the 3DFEA results on both cases, this indicates that in the absence of skew, the design forces can be correctly approximated by the use of simplified expressions depending on the tub-girder major axis bending moments as recommended by Fan and Helwig (1999).

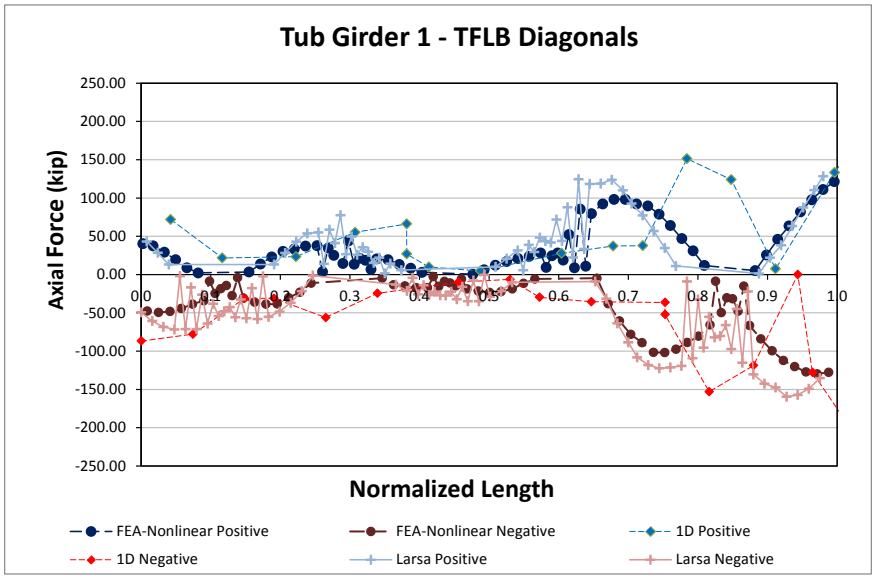

Fig. 9. Top flange lateral bracing diagonals axial forces for Girder 1 - Final Steel Dead Load

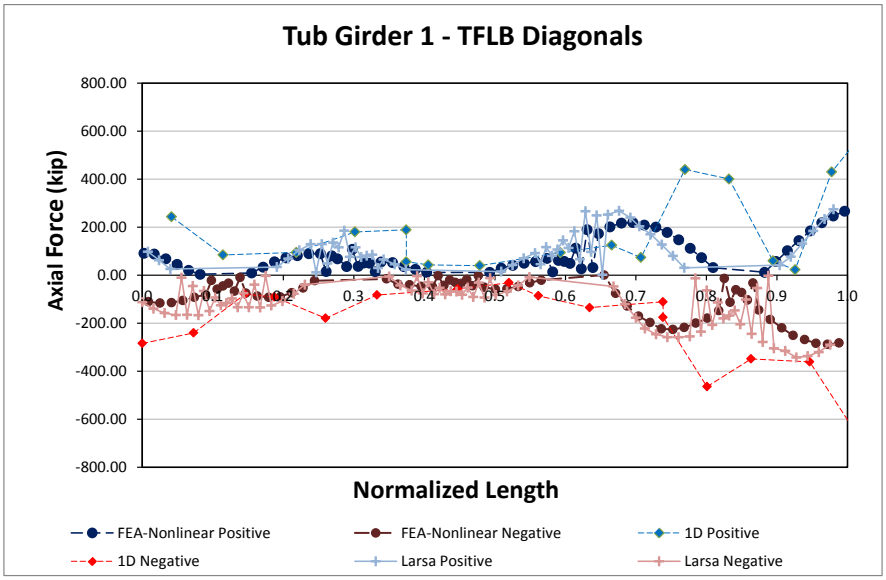

Fig. 10. Top flange lateral bracing struts axial forces for Girder 1 - Total Dead Load

Figure 11 shows the TFLB struts axial forces for the total dead load case. The area of the struts is 6.6in² which, for a maximum axial force of 75kip as reported by the 3D FEA analysis, results on maximum axial stress of 11ksi. As shown by Fan and Helwig (1999) the axial forces on the struts are proportional to the top flange major axis bending stresses, the 2D-Larsa results show the shape of the bending diagram on the predicted element forces. The 3DFEA shows a similar shape confirming this relationship, however the magnitude of the forces is in some cases is overpredicted.

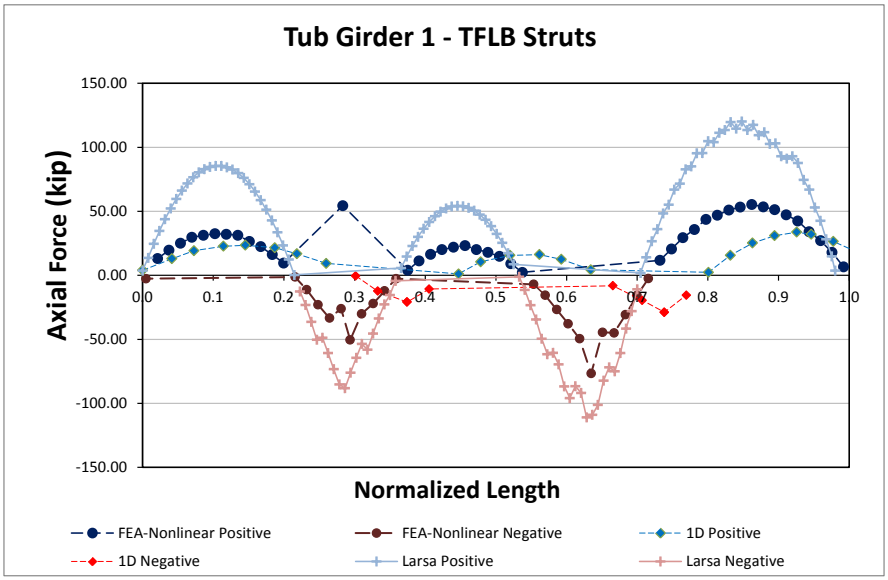

Fig. 11. Top flange lateral bracing struts axial forces for Girder 1 - Total Dead Load

Internal Cross Frame Results

Internal cross frames alternate in every other panel, these elements are composed by diagonals and top chords. Figure 12 shows the internal CF diagonal axial forces. The cross sectional area of these elements is 6.6in² so that the maximum axial force reported corresponds to an axial stress of 5ksi.

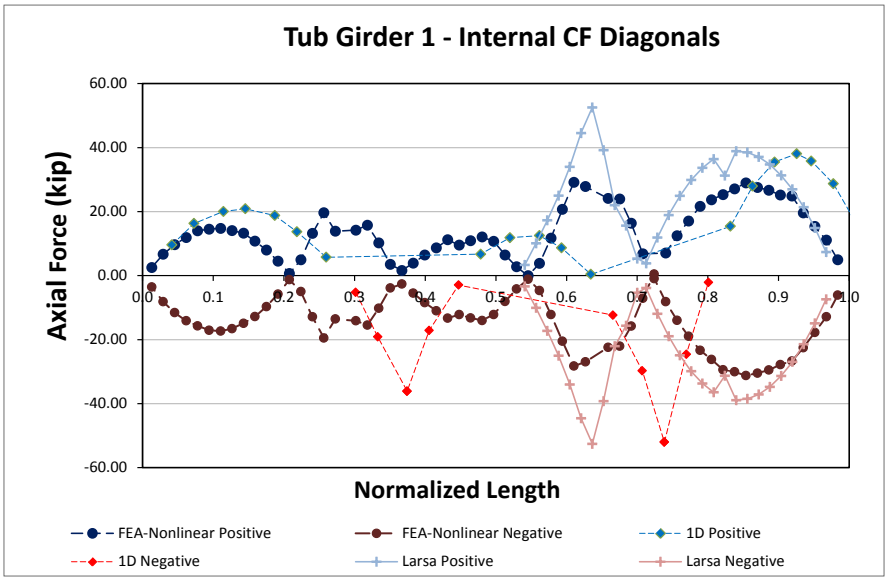

Fig. 12. Internal cross-frames diagonals axial forces for Girder 1 - Total Dead Load

11.5 XTCCR8 (Example, Tub-girder, Continuous-span, Curved, Radial supports)

Bridge Description:

NCHRP 12-52 Design Example Curved Tub-Girder Bridge

Category Data:

L_1 = 160 ft, L_2 = 210 ft, L_3 = 160 ft / R = 700 ft / w = 40.5 ft, 2 tub-girders

References:

Kulicki, J. M., Wassef, W. G., Smith, C., Johns, K. (2005) "AASHTO-LRFD Design Example Horizontally Curved Steel Box Girder Bridge," NCHRP Project No. NCHRP 12-52, National Cooperative Highway Research Program, Transportation Research Board, National Research Council, 148 pp

Erection Stages Analyzed: 6 steel erection stages

Deck Placement Sequence: (Analyses are performed assuming no staged deck placement).

Bridge Perspective & Plan Views

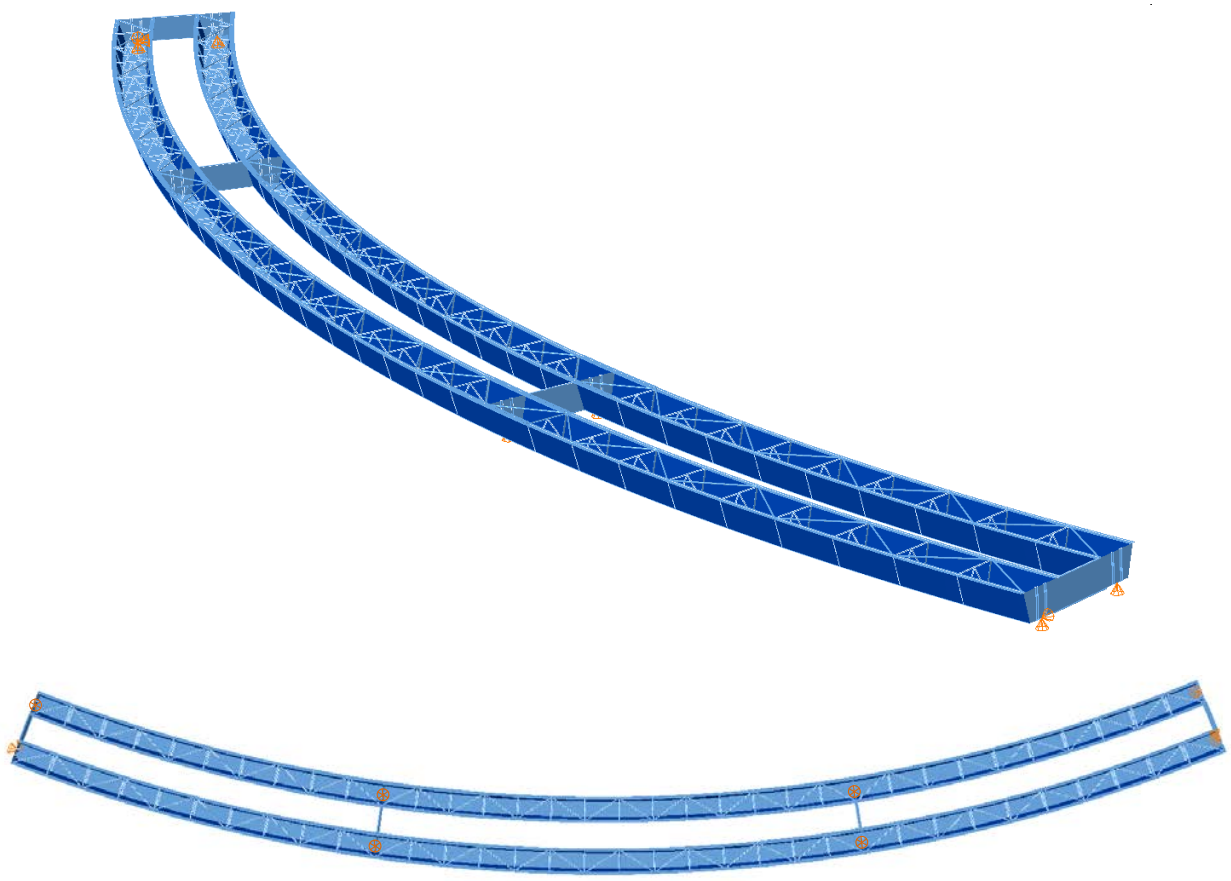

Displacement Results

Differential vertical displacements between girders can cause undesired changes in the slab thicknesses which may lead to uneven loads in the cross section and deficiencies in the composite action of the system. To evaluate the differential vertical displacements the following procedure is developed and applied to the results of the 3D-Finite Element Analysis for the final steel erection stage.

Schematic undeformed and deformed configurations of a twin tub-girder cross section are shown in Figure 1; w and **s** are the width and the tubs separation center to center. The differential displacements are represented for the expressions dd_2 and dd_3 for the webs 2 and 3; these webs are also referred as Girder 1-Interior web and Girder 2-Exterior web. The effect of rigid body motion is removed from the displacement expressions. A positive sign in the dd_2 and dd_3 expressions means that upward relative displacement in taking place.

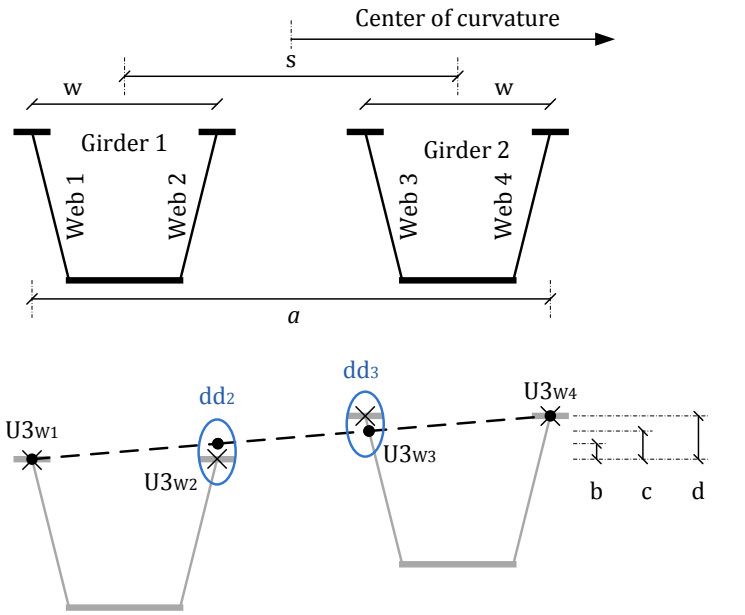

$$a = s + w; \qquad b = dw/a; \qquad c = d(a - w)/a; \qquad d = U3_{W4} - U3_{W1}$$

$$dd_2 = -(U3_{W2} - U3_{W1} - b); \qquad dd_3 = U3_{W3} - U3_{W1} - c$$

Fig. 1. Development of the relative vertical displacement expressions.

Figure 2 illustrates the results obtained for the total dead load. The results are reported for linear and nonlinear 3D-FE analysis methods. The displacements are small for this bridge, and should not pose any risk of over or under casting the concrete slab.

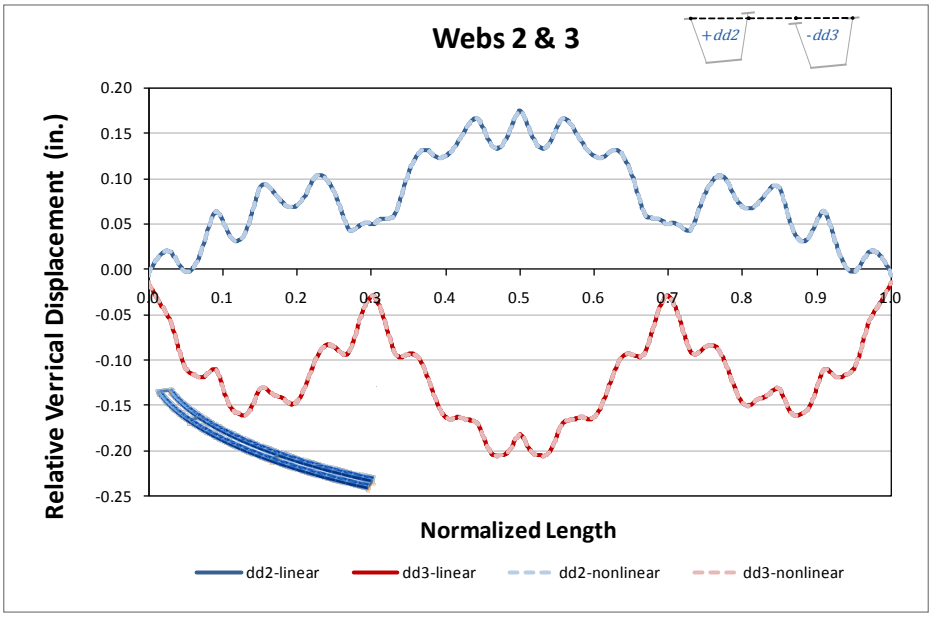

Fig. 2. Relative vertical displacements at the total dead load condition.

The vertical displacements for the different analysis methods under steel and total dead load are shown in Figures 3 and 4 for Girder 1 at the exterior web-flange juncture. The methods show a good agreement but the 1D method underpredicts the displacements for these two conditions 30% below the other methods.

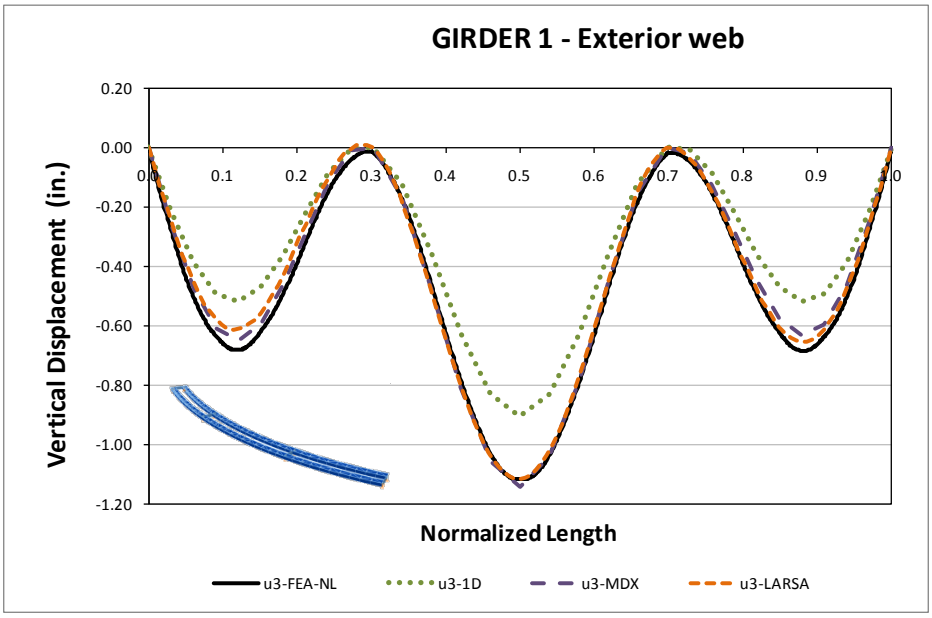

Fig. 3. Top flange vertical displacements for Girder 1 exterior web - Final Steel Dead Load

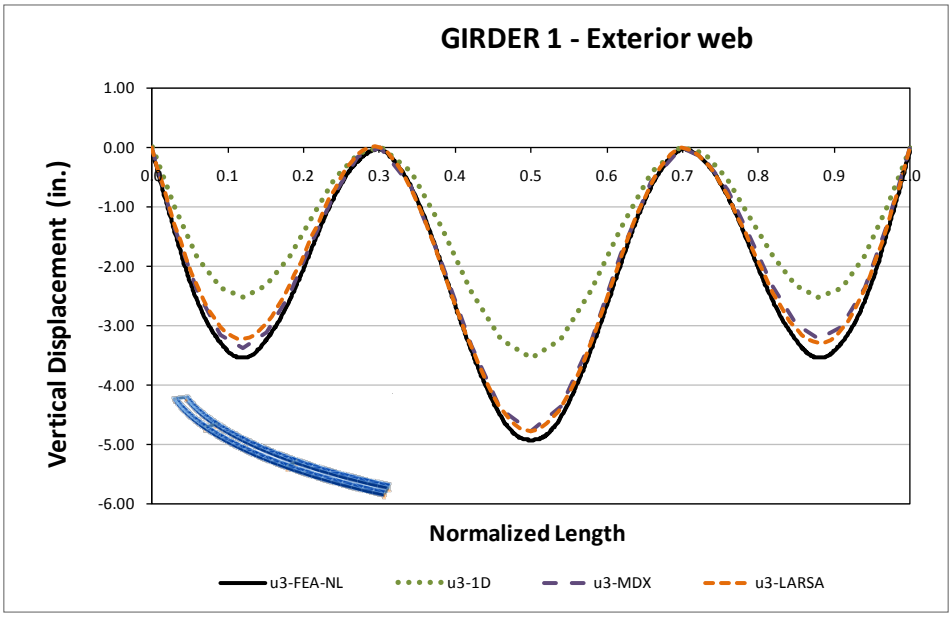

Fig. 4. Top flange vertical displacements for Girder 1 exterior web - Total Dead Load

Each girder has two bearings, each centered at 1 ft inside the adjacent bottom web-flange juncture. The 3D FEA analysis revealed that one of the twin supports experiences uplift if no tie down was used. The analysis was then corrected by removing the support with the negative reaction.

The relative rotations for the steel and total dead loads are shown in Figures 5 and 6 for the 3D FEA and the Larsa 2D grid methods. The rigid body rotation at the support is evident in the 3D FEA results, however, the relative displacement at the ends is only about 0.03 inches.

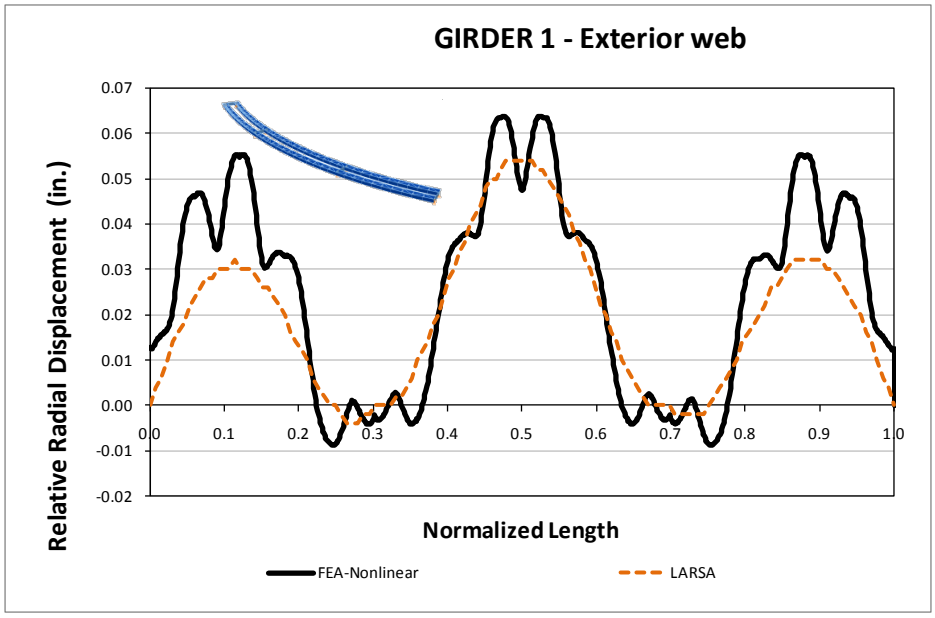

Fig. 5. Relative radial displacements for Girder 1 exterior web – Final Steel Dead Load

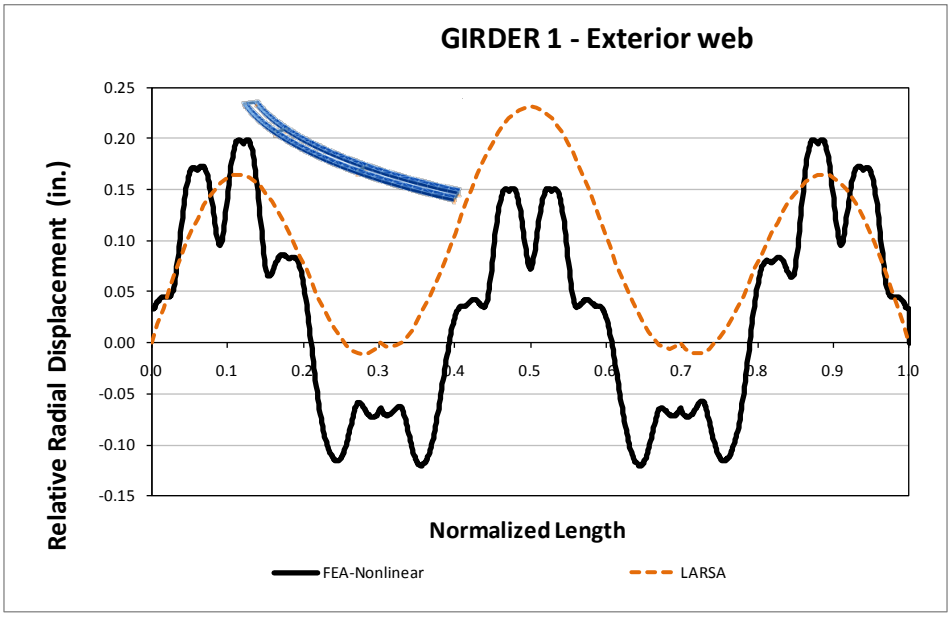

Fig. 6. Relative radial displacements for Girder 1 exterior web - Total Dead Load

Bending Stress Results

Figures 7 and 8 illustrate the results for top flange stresses for the three analysis methods. Contrary to the displacement results, the 1D method accurately predicts the major-axis bending stresses. All of the methods predict essentially the same major-axis bending stresses.

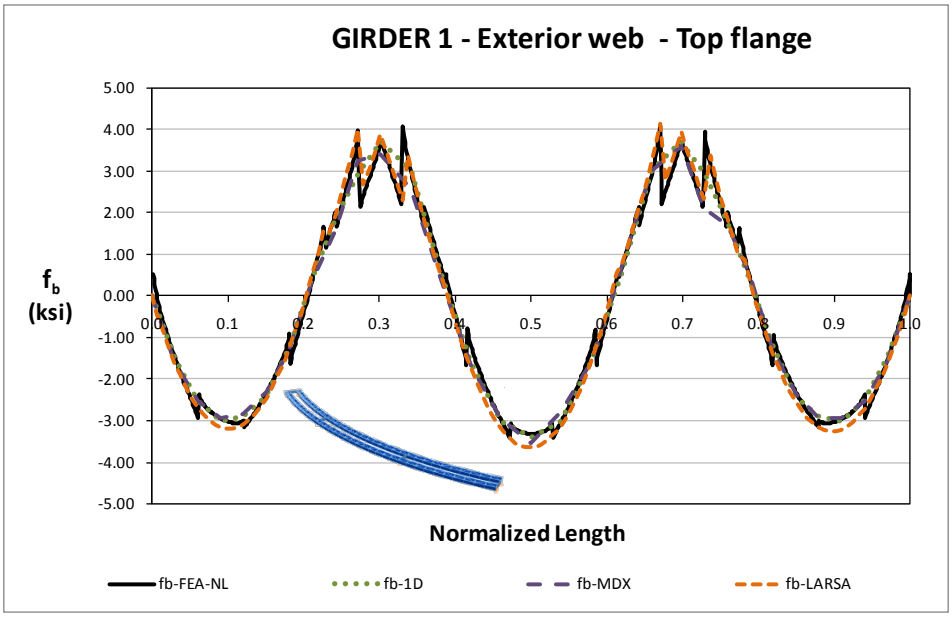

Fig. 7. Top flange major axis bending stress for Girder 1 exterior web – Final Steel Dead Load

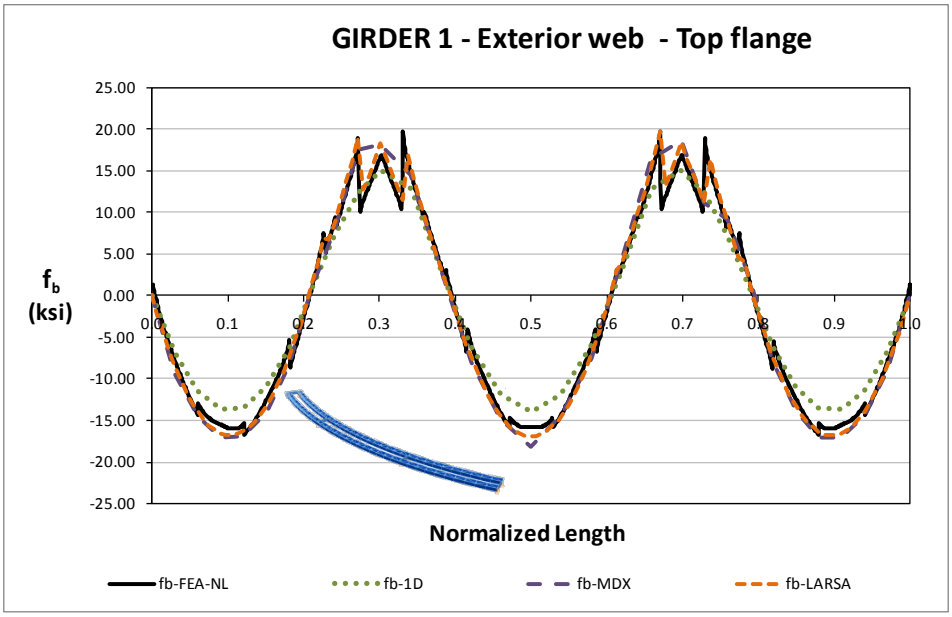

Fig. 8. Top flange major axis bending stress for Girder 1 exterior web - Total Dead Load

Figures 9 and 10 illustrate the stress results for the exterior bottom flange-web juncture of Girder 1. Highly local stress concentrations are reported at several points for the 3D FEA analysis. These local stress concentrations are particularly evident at the intermediate supports. These responses are attributed to the numerical approximation at these locations, where the cross frame or diaphragms plates, the web and bottom flanges join at a point. The stress concentration is reported only in the adjacent elements to

this intersection point. The stresses in the next element are comparable to those obtained from the simplified predictions.

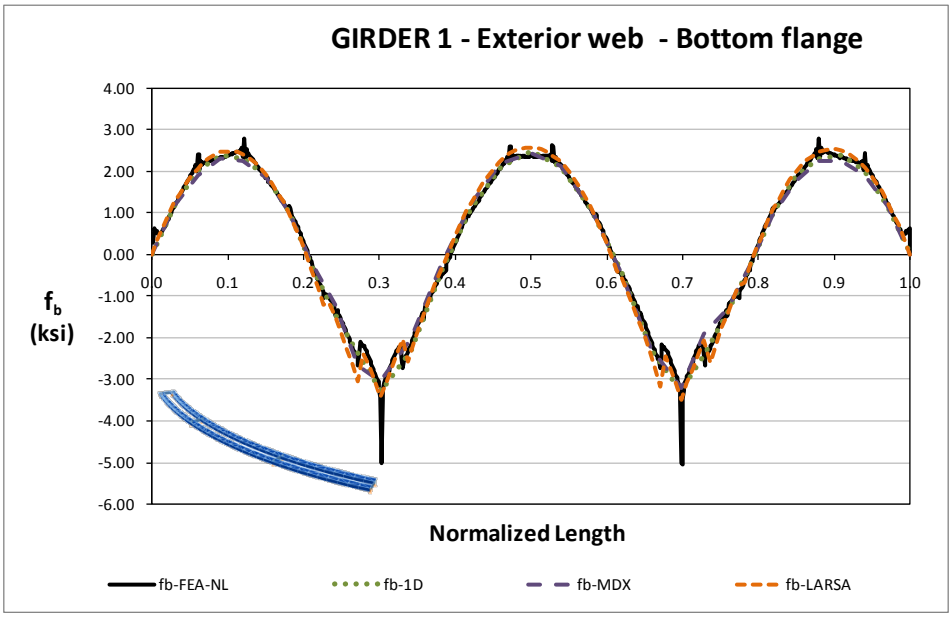

Fig. 9. Bottom flange major-axis bending stress for Girder 1 exterior web – Final Steel Dead Load

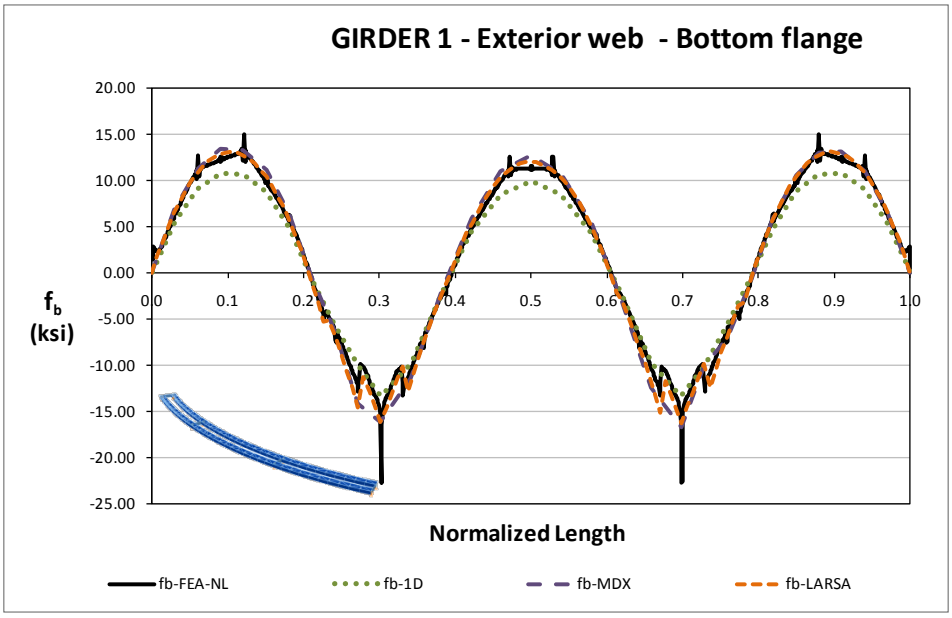

Fig. 10. Bottom flange lateral bending stress for Girder 1 exterior web - Total Dead Load

Lateral bending stresses are reported in Figures 11 and 12 for the two load conditions discussed before. The Larsa 2D grid lateral bending stress values overpredict the behavior being in the range of half the

yielding stress for the total dead load condition. This is due to the fact that these lateral bending stresses are determined using the V-load method based equation:

$$f_\ell = \frac{M_{lat\ tot}}{S_{y\ top}} \qquad M_{lat\ tot} = \frac{M_{lat}}{2} + M_{lat\ shear} + M_{lat\ bending}$$

$$\frac{M_{lat}}{2} = \frac{M_z\ {L_b}^2}{10\ R\ D}$$

$M_z = major\ axis\ bending\ moment$
$L_b = unbraced\ length$
$R = curvature\ radius$
$D = Girder\ depth$

$$M_{lat\ shear} = \frac{p}{10} s^2$$

$p = w \cdot slope$
$w = linear\ weight\ of\ girder/2$

$$M_{lat\ bending} = 2\ S_{bend} \frac{L_b}{8}$$

$S_{bend} = D_{TFLB\ bend}\ sin\alpha$
$D_{TFLB\ bend} = TFLB\ diagonal\ force$
$\alpha = TFLB\ diagonal\ angle$

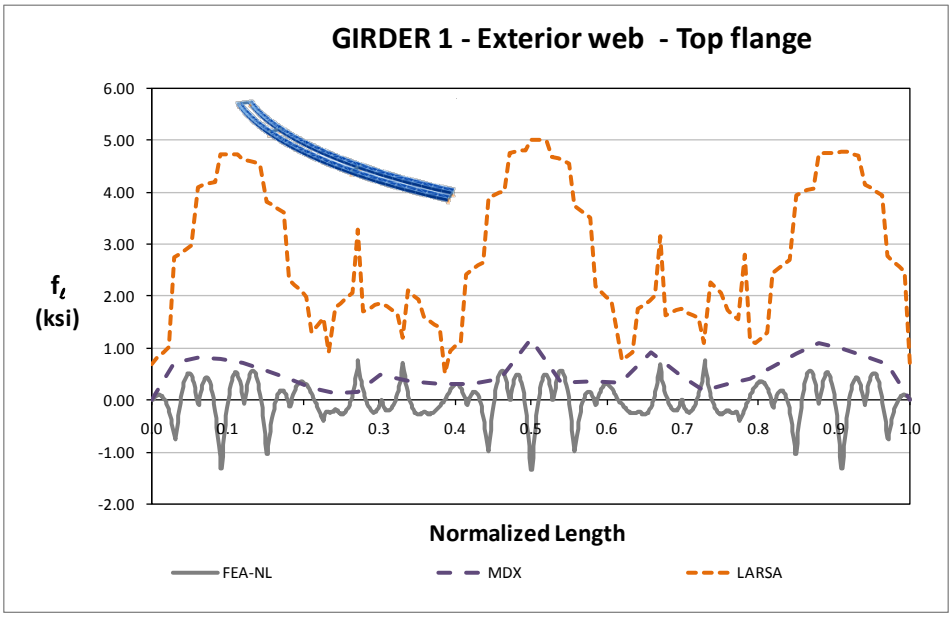

Fig. 11. Top flange lateral bending stress for Girder 1 exterior web – Final Steel Dead Load

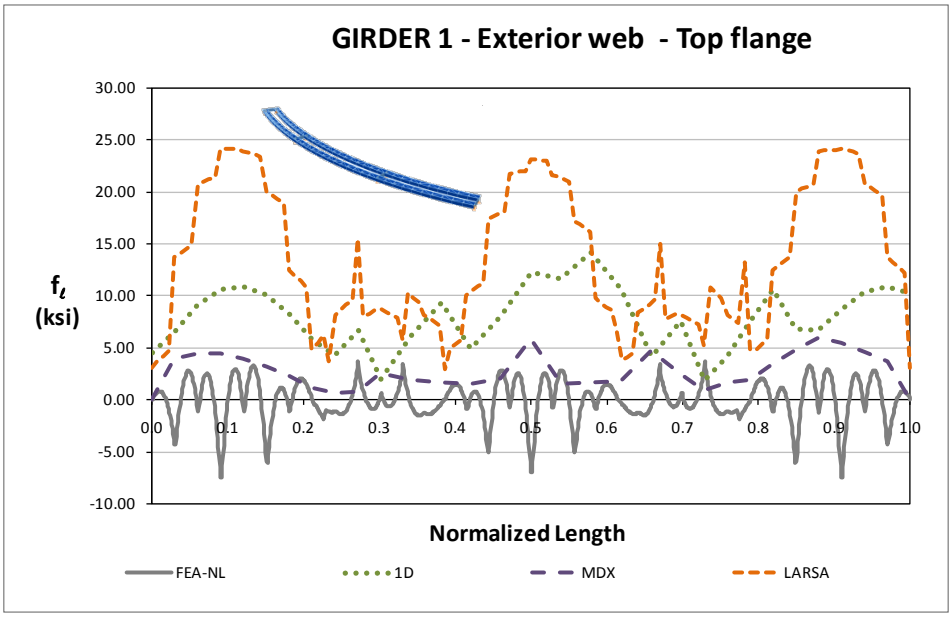

Fig. 12. Top flange lateral bending stress for Girder 1 exterior web - Total Dead Load

Top Flange Lateral Bracing Results

Results for the top flange lateral bracing system forces and internal cross frame system forces are presented as member axial stresses for each element of the system. The TFLB system is divided into Diagonals and Struts and the CF system is divided into Top Chord, Diagonals and Bottom Chord.

In this bridge, the TFLB system does not have an independent transverse Strut at the internal cross-frame locations, the CF Top Chord acts also as strut for the TFLB but it is an integral part of the CF system so it will be included in CF results. The same treatment will be given to any location in bridges where this case repeats.

Figures 12 and 13 illustrate the results for the TFLB Diagonals at the steel and total dead loads for the 3DFEA and Larsa 2D grid analysis methods. The stresses are shown in two different plots: positive and negative values. Each point represents the component's axial stress, the result is then plotted at the longitudinal location of the mid length of the component in the bridge; the lines connecting the points are used only for visual reference.

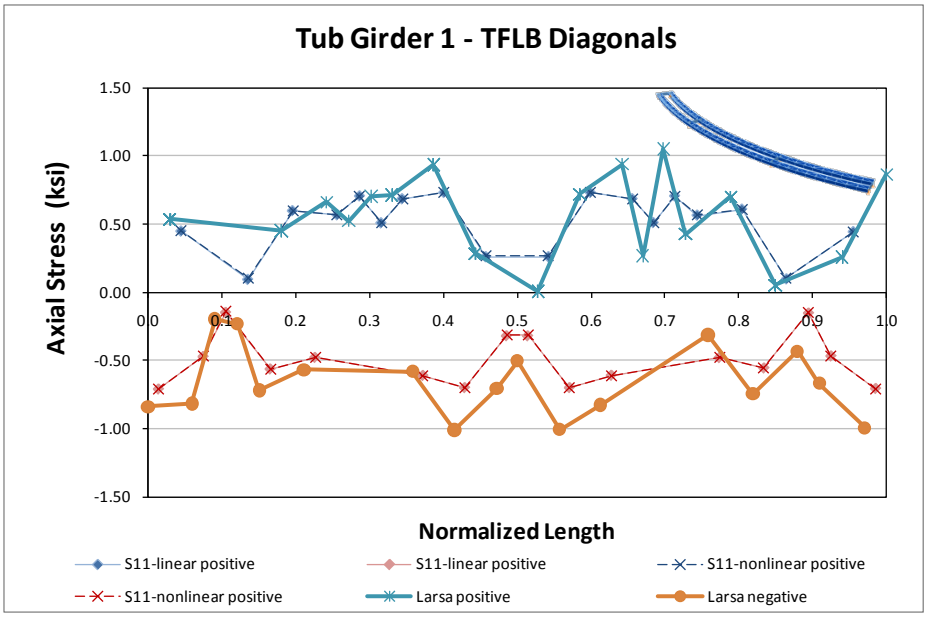

Fig. 13. Top flange lateral bracing diagonals axial stresses for Girder 1 - Final Steel Dead Load

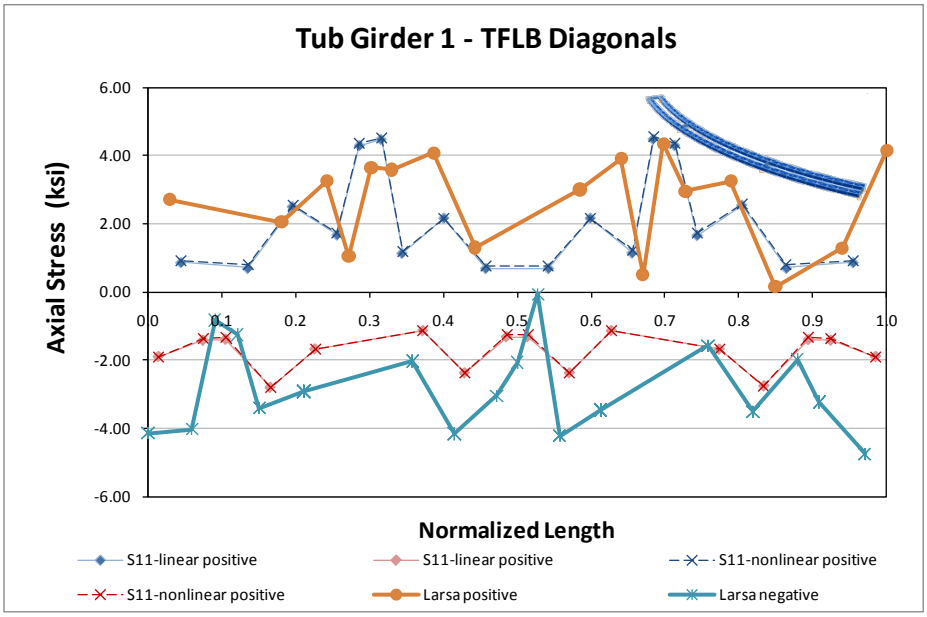

Fig. 14. Top flange lateral bracing diagonals axial stresses for Girder 1 - Total Dead Load

Internal Cross-Frame Results

Figures 15 to 20 present the results for the cross frame stresses. The results for each component are plotted separately. The study case does not have external cross frames and uses solid plate diaphragms at

the bearing lines. Solid plate diaphragms are included in the 3D FEA model. Their forces are to be evaluated subsequently.

The common practice in tub girders is to use inverted-V cross frames. In most cases the bottom chord is omitted; however, fatigue design may require the presence of this component as in this bridge.

The top chord stresses are presented on Figures 15 and 16, the diagonals on Figures 17 and 18 and finally the bottom chord on Figures 19 and 20, results are shown for steel and total dead load. Diagonal stresses are often larger due to the use of lower cross sectional area elements. Bottom chord stresses are low because the bottom flange attracts a large percentage of the transverse force.

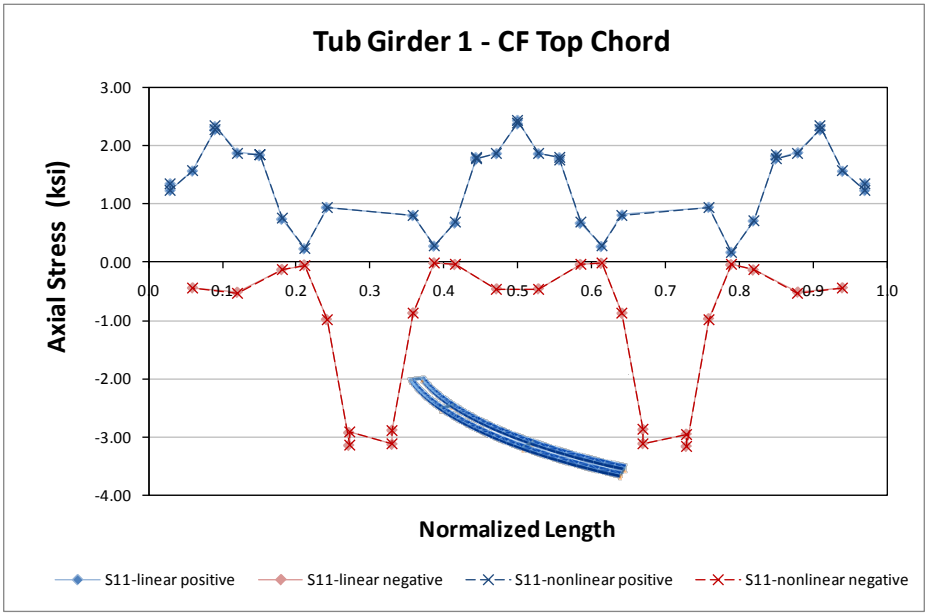

Fig. 15. Internal cross frame top chord axial stresses for Girder 1 - Final Steel Dead Load

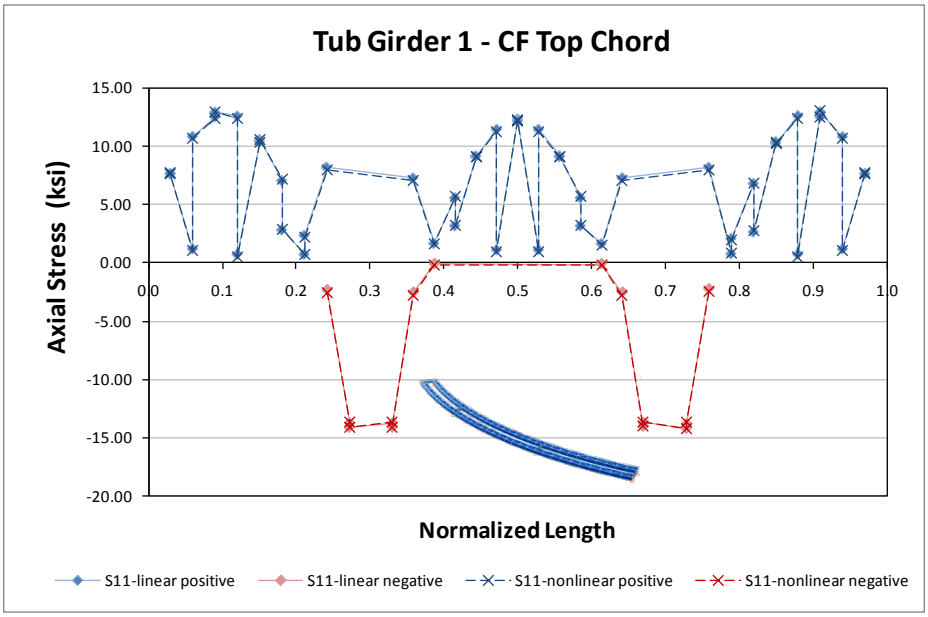

Fig. 16. Internal cross frame top chord axial stresses for Girder 1 - Total Dead Load

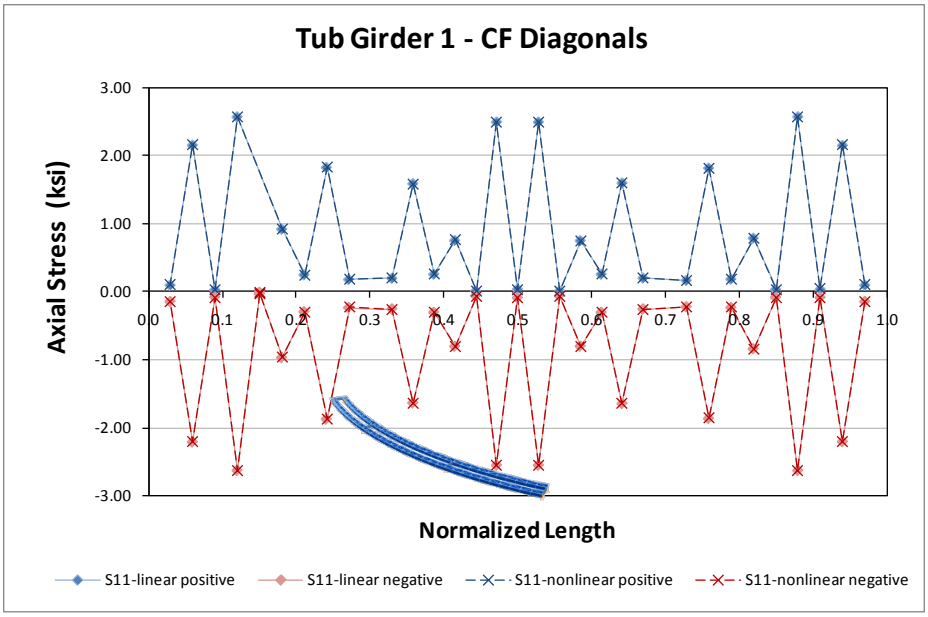

Fig. 17. Internal cross frame diagonals axial stresses for Girder 1 - Final Steel Dead Load

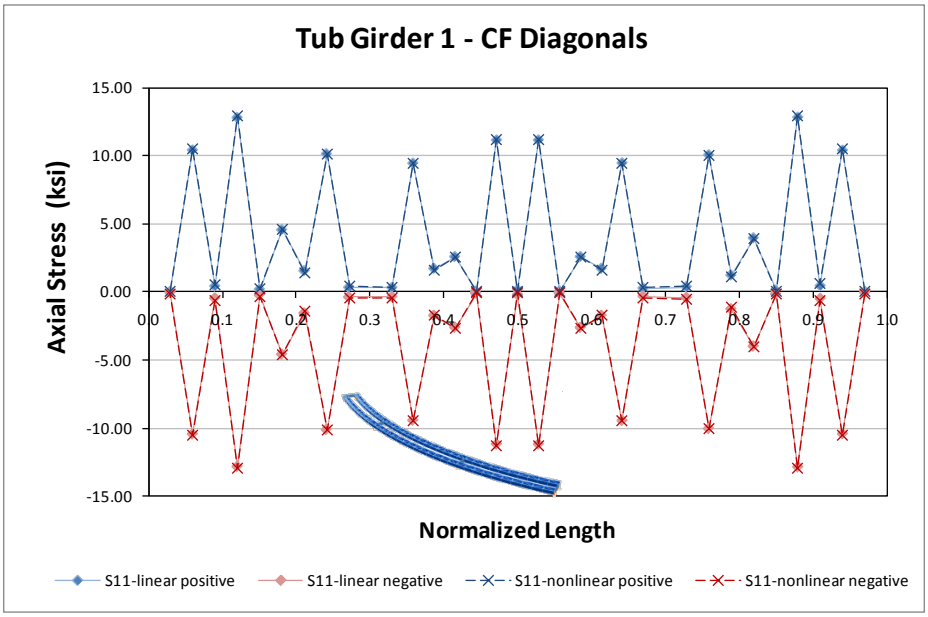

Fig. D2.1.6-18. Internal cross frame diagonals axial stresses for Girder 1 - Total Dead Load

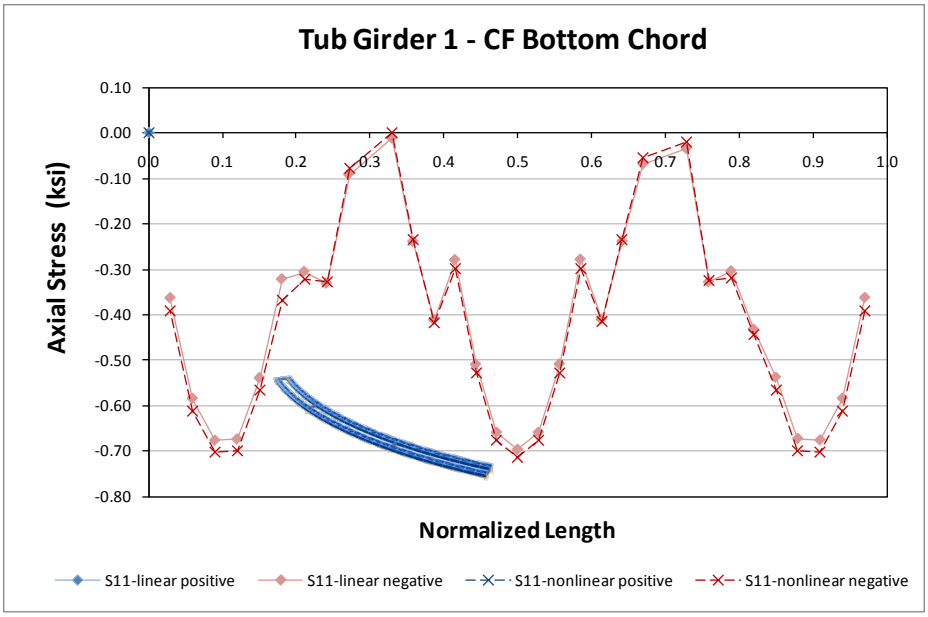

Fig. 19. Internal cross frame bottom chord axial stresses for Girder 1 - Final Steel Dead Load

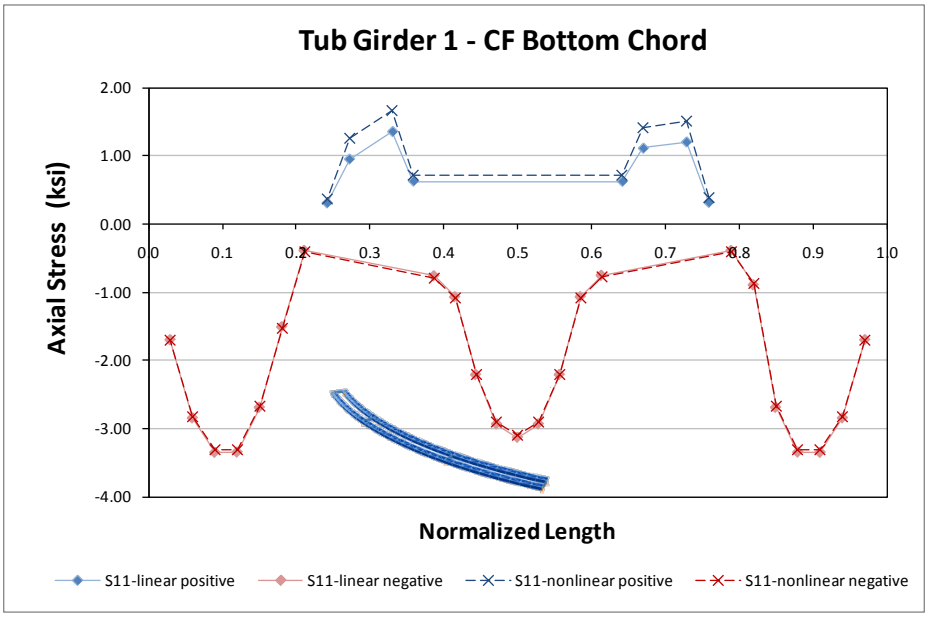

Fig. 20. Internal cross frame bottom chord axial stresses for Girder 1 - Total Dead Load

No major changes are noticed between Linear and Nonlinear analysis for any of the stresses reported

12.1 NTSCS5 (New, Tub-girder, Simple-span, Curved, Skewed supports)

Bridge Description:

Category Data:

L_1 = 150ft / R = 400 ft / w = 30 ft / θ_1 =10.7°, θ_2 =-10.7°, 2 tub-girders

References:

Erection Stages Analyzed: 2 steel erection stages

Deck Placement Sequence: One stage, deck thickness = 9.5 in

Bridge Perspective & Plan Views:

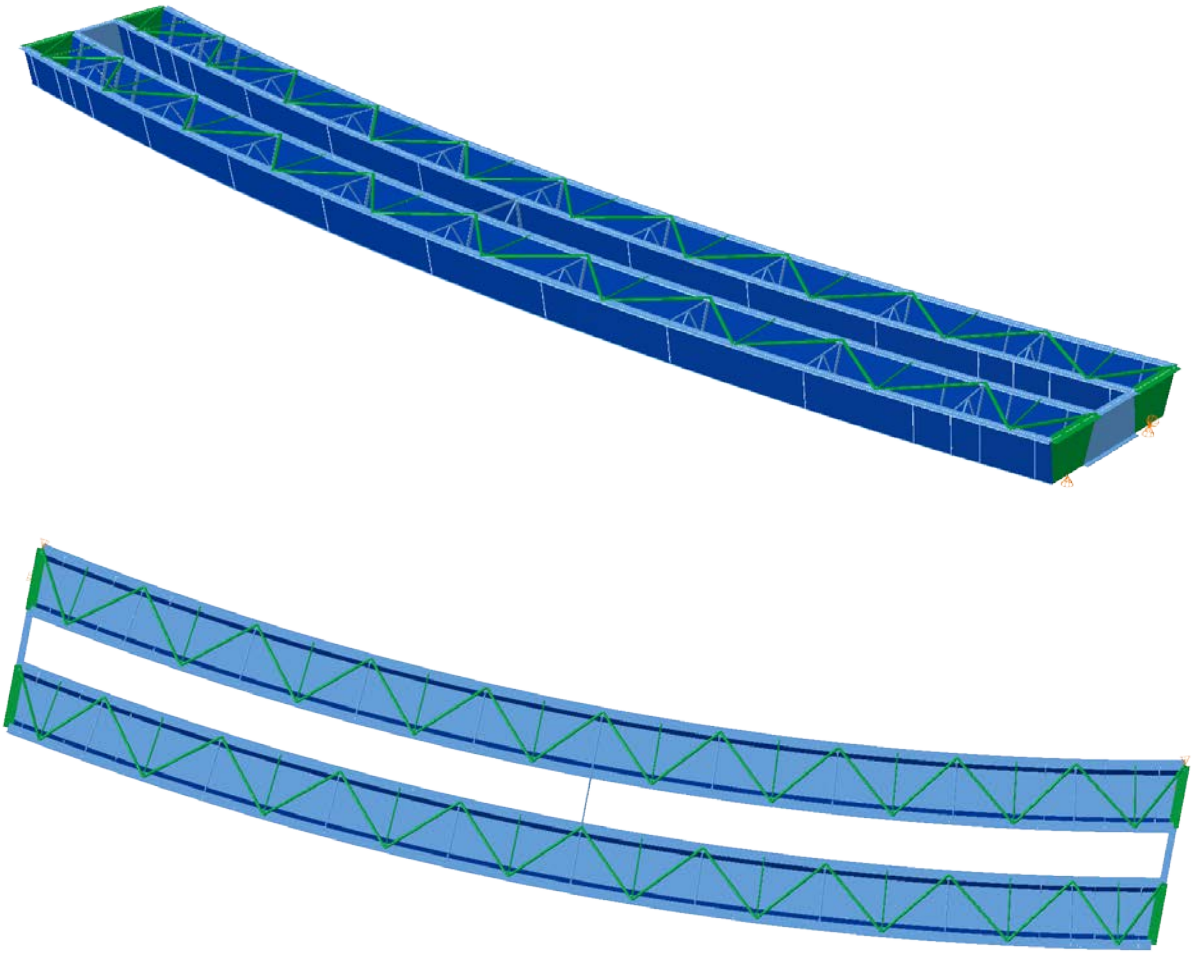

Displacement Results

Figure 1 illustrates the steel erection stages. The erection plan considers that the each girder is to be assembled at its full length on the ground and lifted to position starting with the interior girder. No intermediate temporal supports are used.

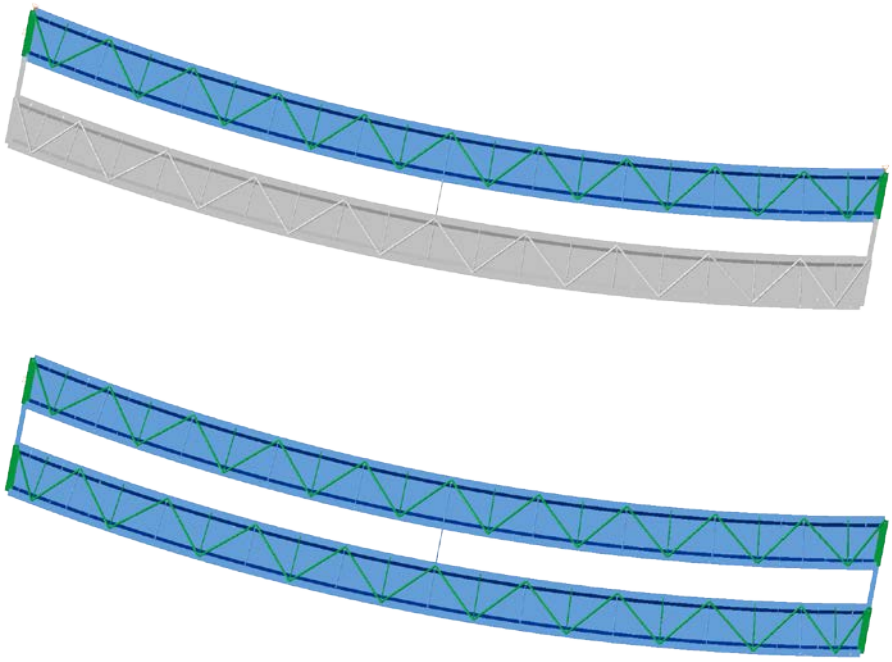

Fig. 1. Intermediate steel erection stages

Figures 2 and 3 show the final steel and non-composite total dead load vertical displacements for the top flange and the interior web juncture of Girder 2, in other words, the top flange of the most interior web. These displacements are plotted for four different methods of analysis: non-linear refined 3D FEA, 1D and using 2D analysis software MDX and LARSA. Most of the methods show a close prediction of results, discrepancies on the results are mainly attributed to the discretization used by the analysis method leading to a system slightly stiffer when the bridge is represented by a lower number of elements along the length.

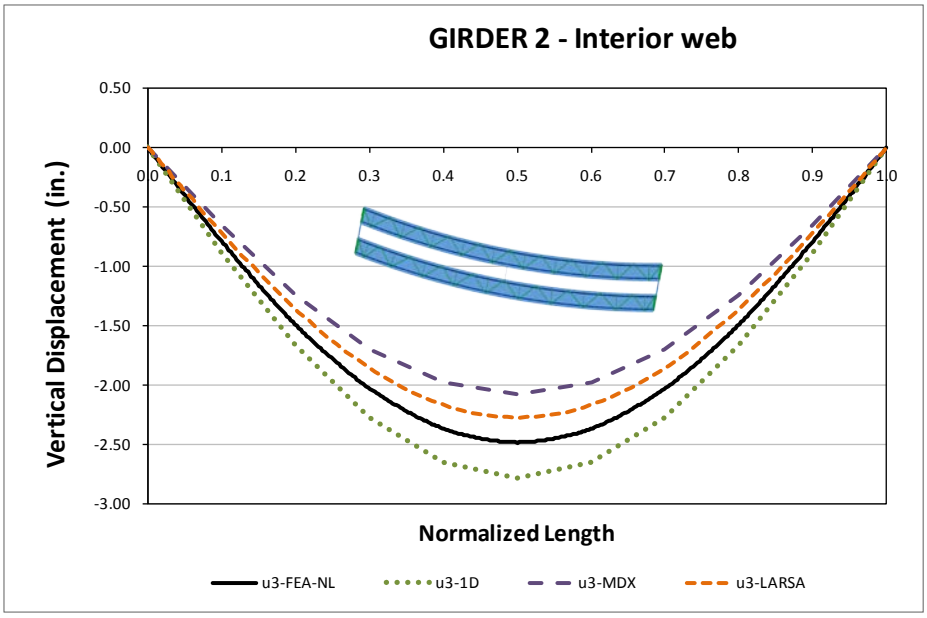

Fig. 2. Top flange vertical displacements for Girder 2 interior web - Final Steel Dead Load

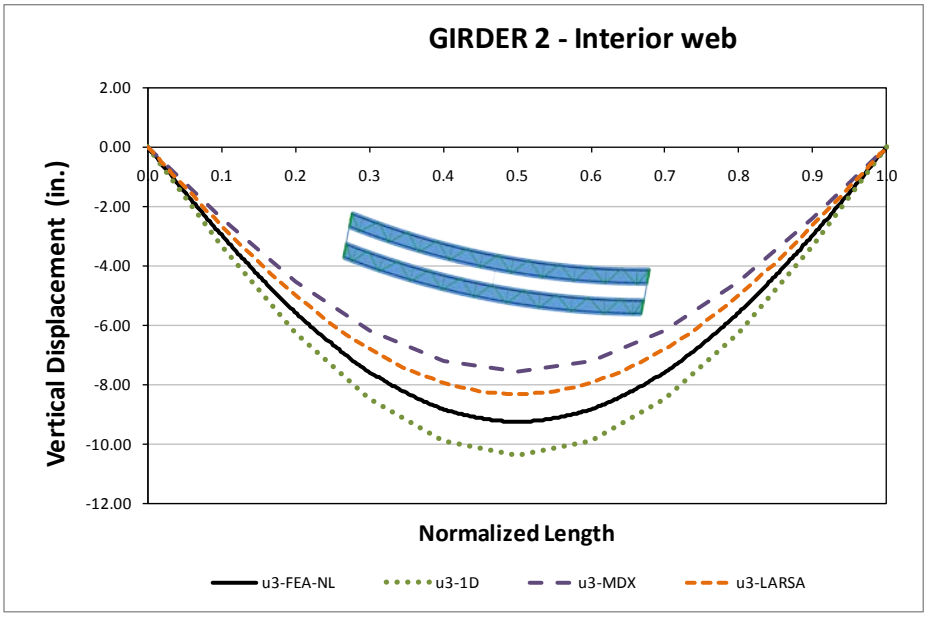

Fig. 3. Top flange vertical displacements for Girder 2 interior web - Total Dead Load

The top flange relative radial displacements are shown in fig. 4 for the total non-composite dead load, the results are shown for the 3DFEA and LARSA models. The local variation between both methods can be attributed to the discretization of the girders at the braced points for the LARSA analysis. An initial rotation is reported by both analyses at the support lines mainly due to the skew.

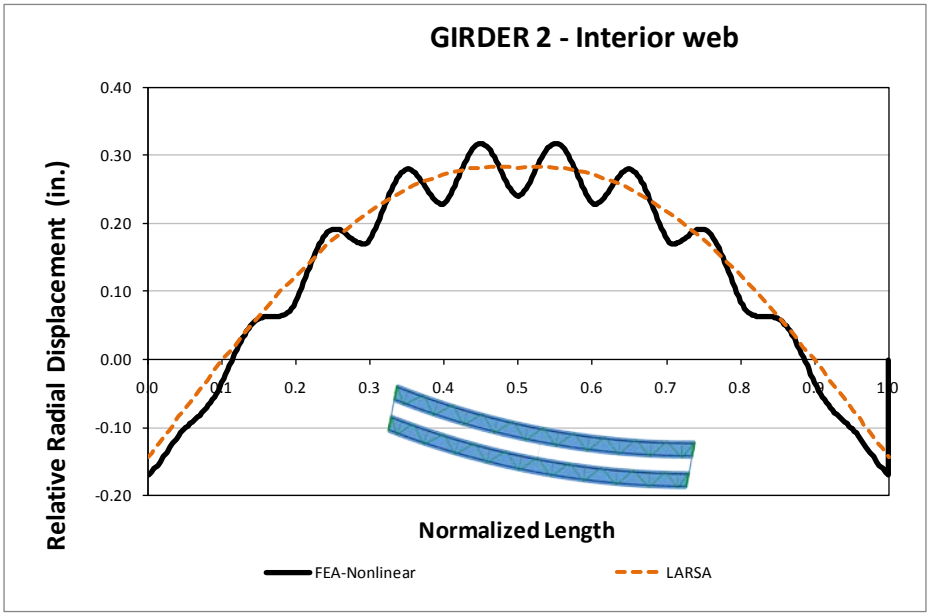

Fig. 4. Top flange relative radial displacements for Girder 2 interior web - Total Dead Load

Bending Stress Results

Major axis bending stresses for Girder 2 - Interior web are presented in Figures 5 and 6 for the final steel and total non-composite dead load construction stages as predicted by the different analysis methods. As reported in other bridge cases, 3D results show localized effects due to the Top flange Lateral Bracing system presence. Similar results are shown on fig. 7 for the same girder but in this case for the exterior web which experiences the same localized effects but in a different distribution matching the flange bracing on that flange.

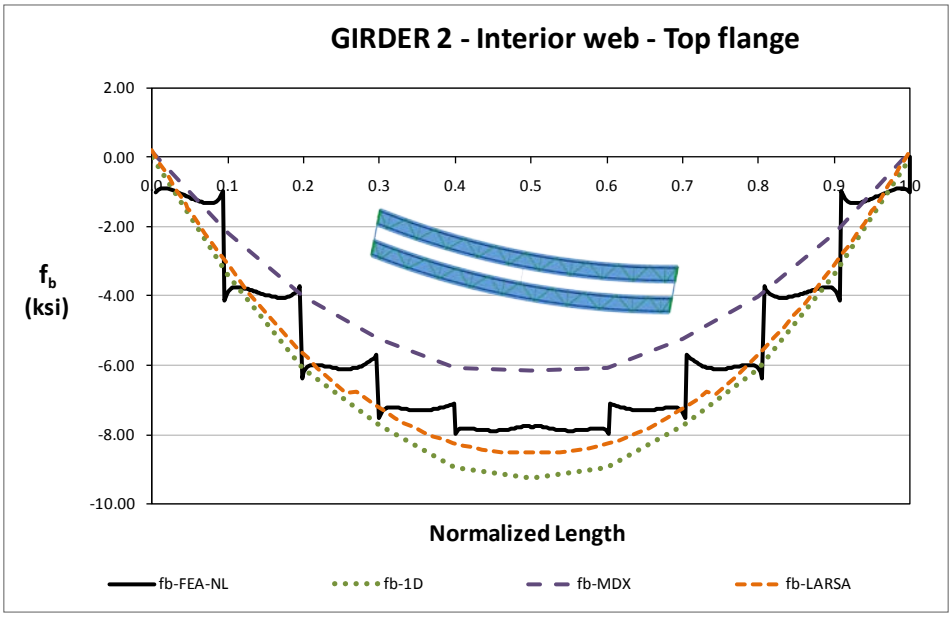

Fig. 5. Top flange major axis bending stress for Girder 2 interior web - Final Steel Dead Load

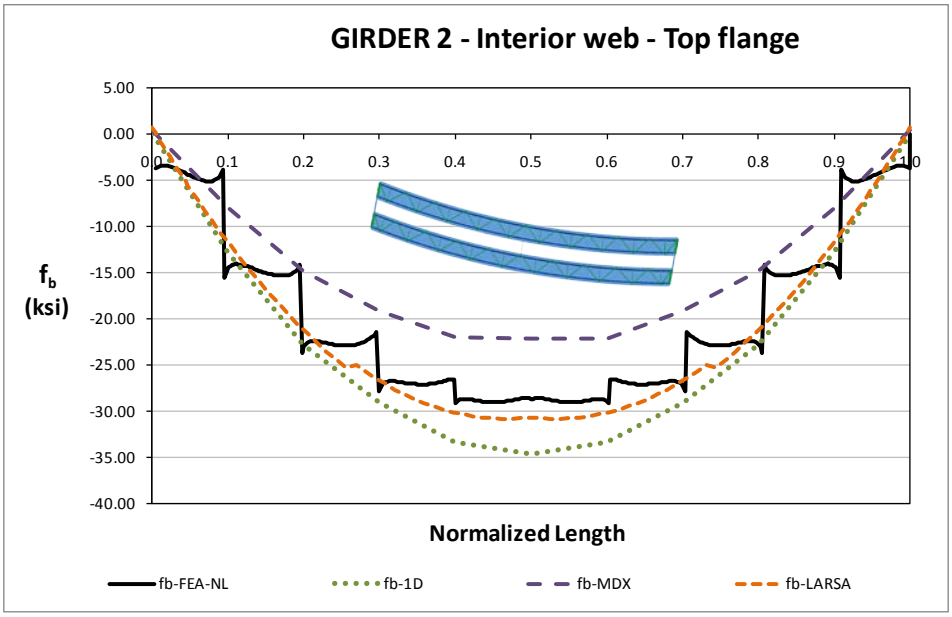

Fig. 6. Top flange major axis bending stress for Girder 2 interior web - Total Dead Load

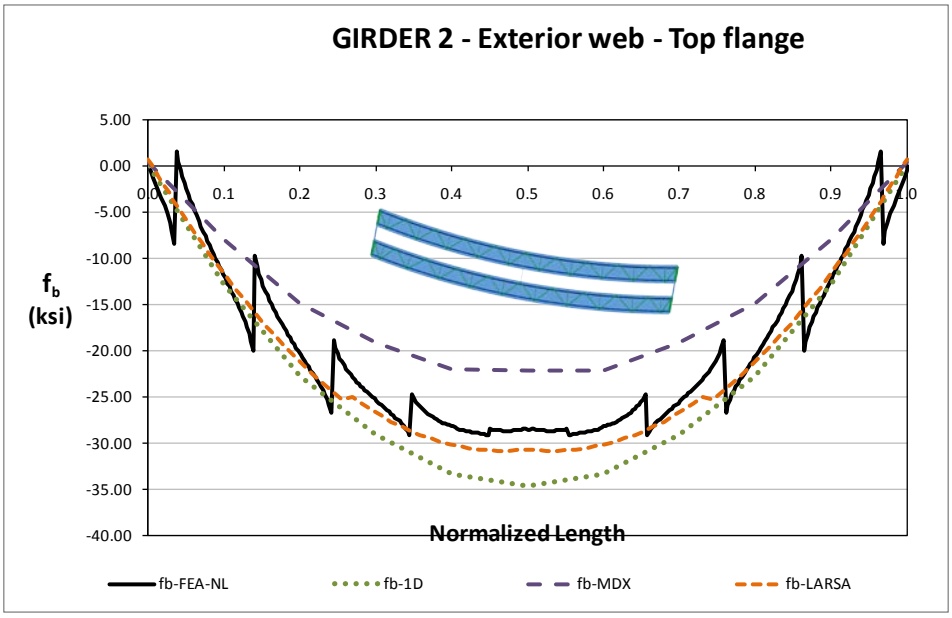

Fig. 7. Top flange major axis bending stress for Girder 2 exterior web - Total Dead Load

Figures 8 and 9 illustrate the major axis bending stresses at the web and bottom flange juncture for Girder 2 interior webs for the final steel and total non-composite dead load cases. The 3D FEA analysis predicts localized stress concentrations at the cross-frame locations in contrast as for the top flange where this happens at the TFLB locations. These stress concentrations are believed to be caused by the local interaction of the web, flange and connection plate.

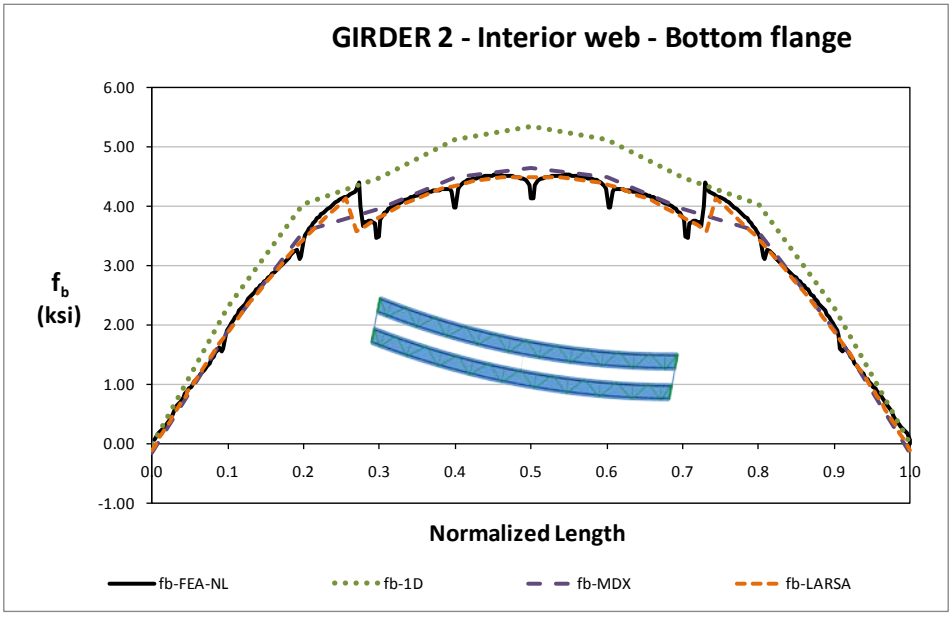

Fig. 8. Bottom flange major axis bending stress for Girder 2 interior web – Final Steel Dead Load

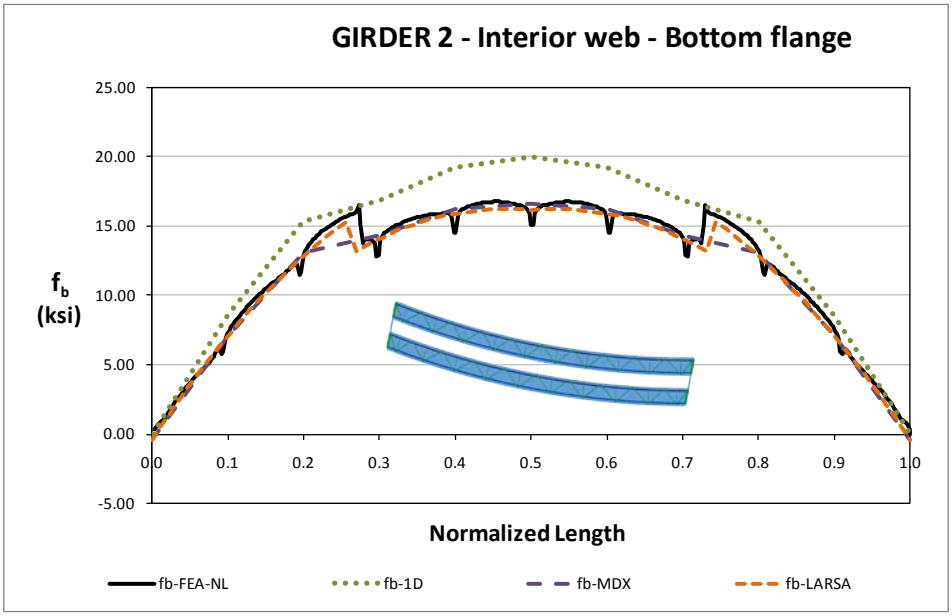

Fig. 9. Bottom flange major axis bending stress for Girder 2 interior web - Total Dead Load

Top Flange Lateral Bracing Results

The TFLB diagonals axial forces are shown in Figures 10 and 11 for the final steel and total dead load condition. The cross sectional area of these elements is 15.6in² that for a maximum axial force of 300kip the element experiences an axial stress of 19ksi on the total dead load condition.

The forces on the TFLB diagonals match the expected torque distribution along the bridge length with maximum values at the support and vanishing at the span center. The reported axial force distribution by the different analysis methods follows the same law.

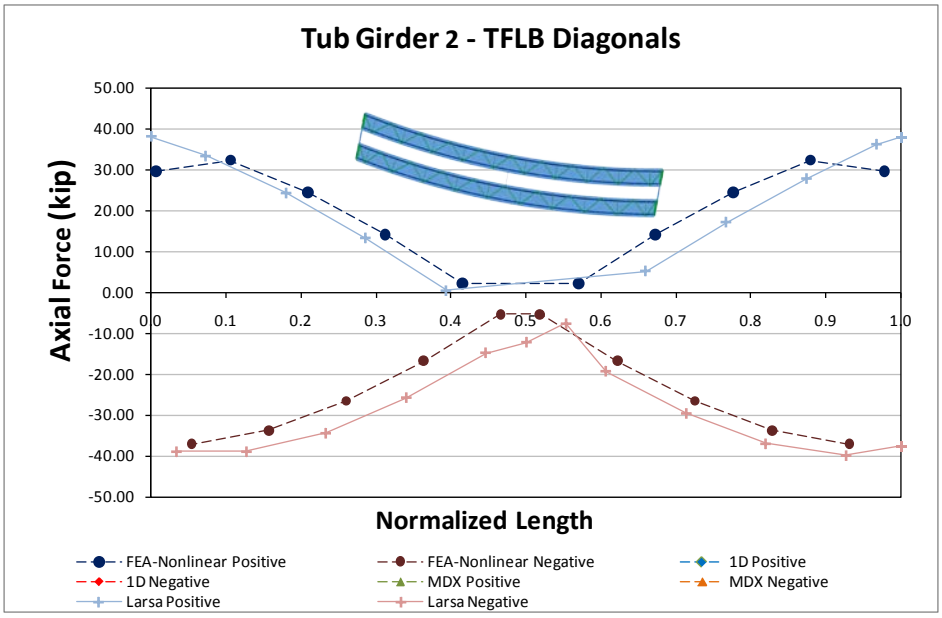

Fig. 10. Top flange lateral bracing diagonals axial forces for Girder 2 - Final Steel Dead Load

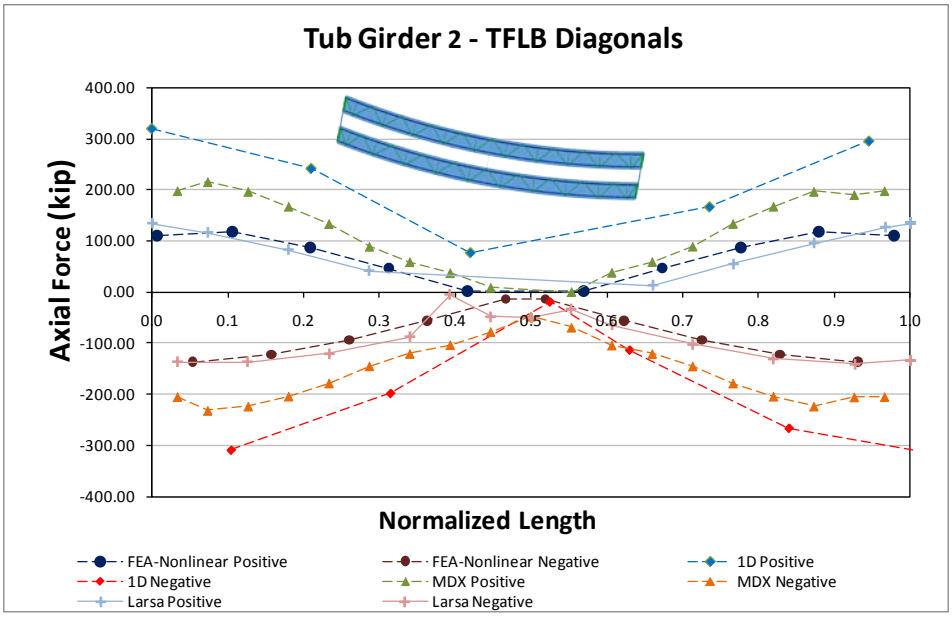

Fig. 11. Top flange lateral bracing struts axial forces for Girder 2 - Total Dead Load

Figure 12 shows the TFLB axial forces on the struts for the total non-composite deal load case. The area of the struts is 4.4in² which, for a maximum axial force of 30kip as reported by the 3D FEA analysis, results on maximum axial stress of 6.8ksi. As shown by Fan and Helwig (1999) the axial forces on the

struts are proportional to the top flange major and minor axis bending stresses with similar distribution as those shown in fig. 12.

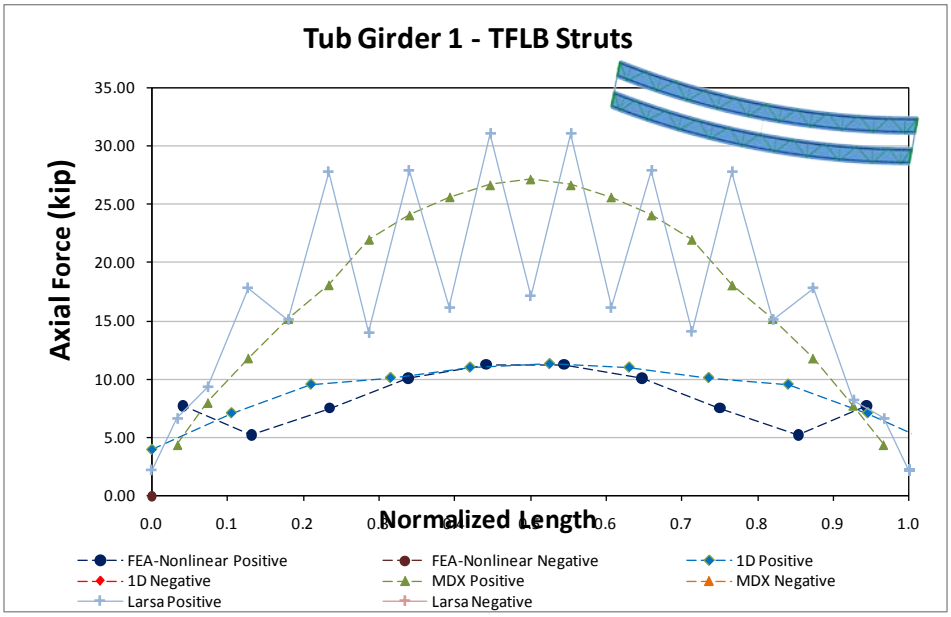

Fig. 12. Top flange lateral bracing struts axial forces for Girder 1 - Total Dead Load

Internal Cross Frame Results

Internal cross frames alternate in every other panel, these elements are composed by diagonals and top chords. Figure 13 shows the internal CF diagonal axial forces while Figure 14 shows the results for the top chord of the CF. The cross sectional area of both element types is 4.4in² so that the axial forces reported correspond to a maximum axial stress of 9.1ksi.

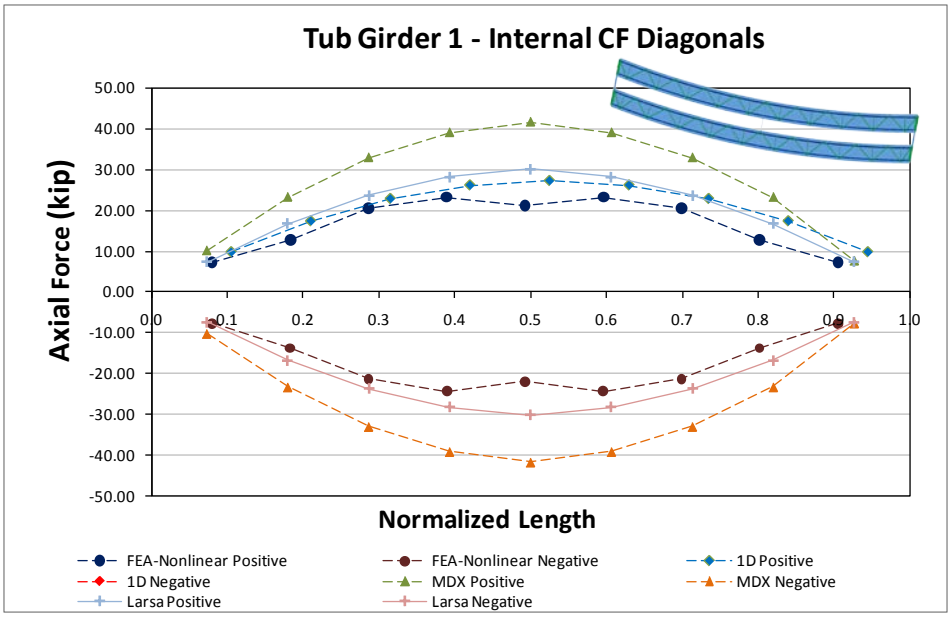

Fig. 13. Internal cross-frames diagonals axial forces for Girder 1 - Total Dead Load

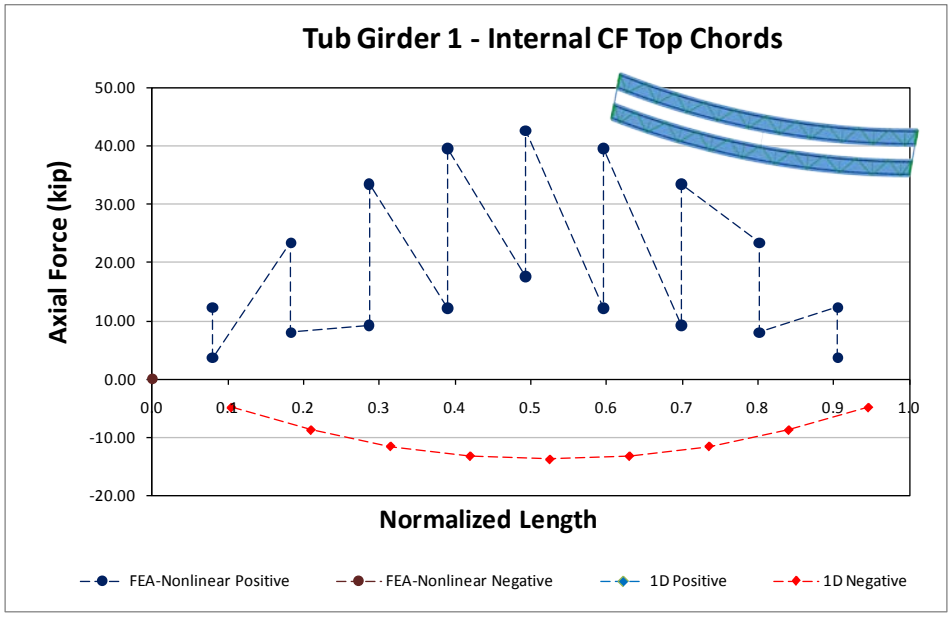

Fig. 14. Internal cross-frame top chords axial forces for Girder 1 - Total Dead Load

12.2 NTSCS29 (New, Tub-girder, Simple-span, Curved, Skewed supports)

Bridge Description:

Category Data:

L_1 = 225ft / R = 820 ft / w = 30 ft / θ_1 =15.7°, θ_2 =0°, 2 tub-girders

References:

Erection Stages Analyzed: 4 steel erection stages

Deck Placement Sequence: One stage, deck thickness = 9.5 in

Bridge Perspective & Plan Views:

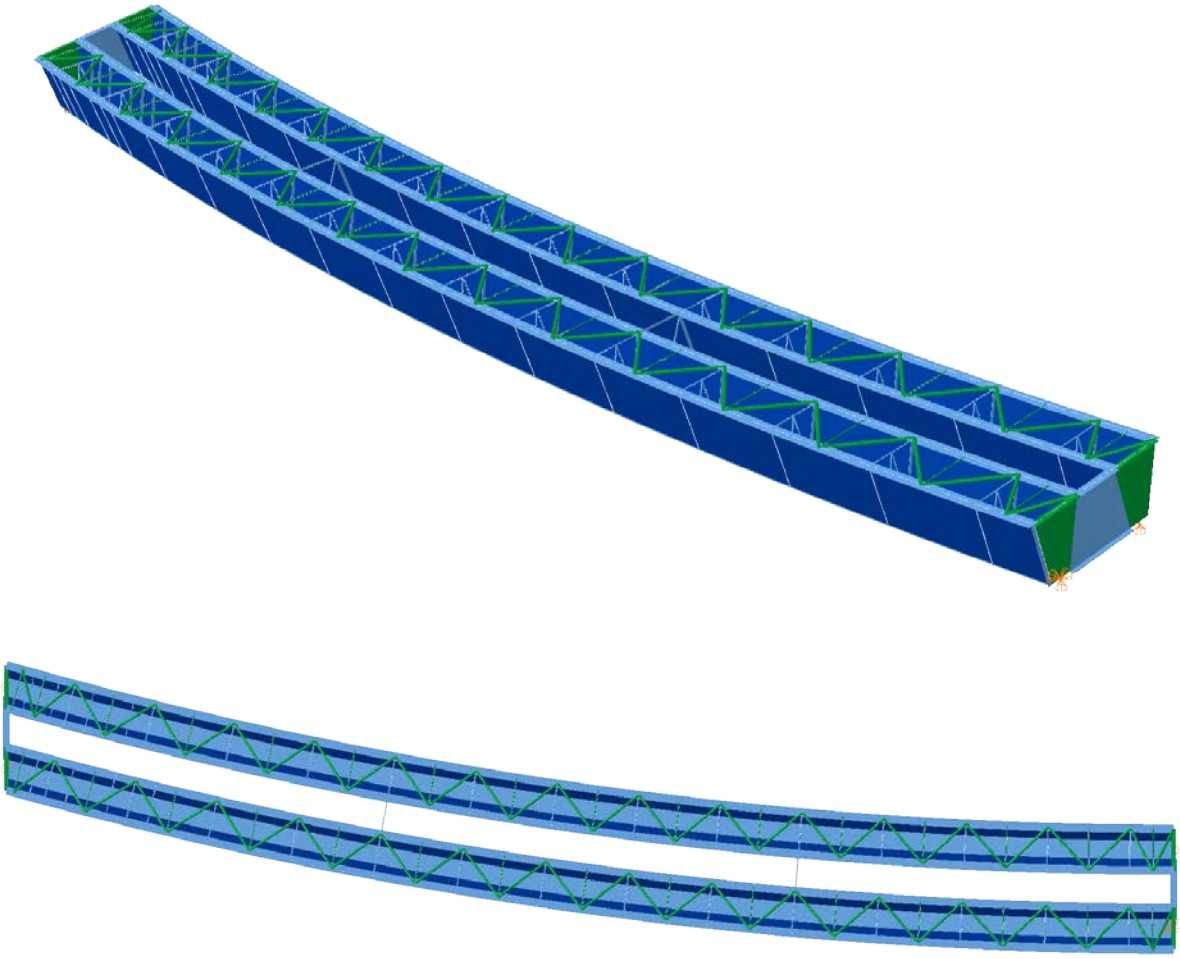

Displacement Results

Figure 1 illustrates the steel erection stages. The erection plan considers four erection stages, the first two consist on splicing two thirds of the girder lengths on the ground and lifted to position using temporal supports. The remaining stages are then added and the temporal supports are released.

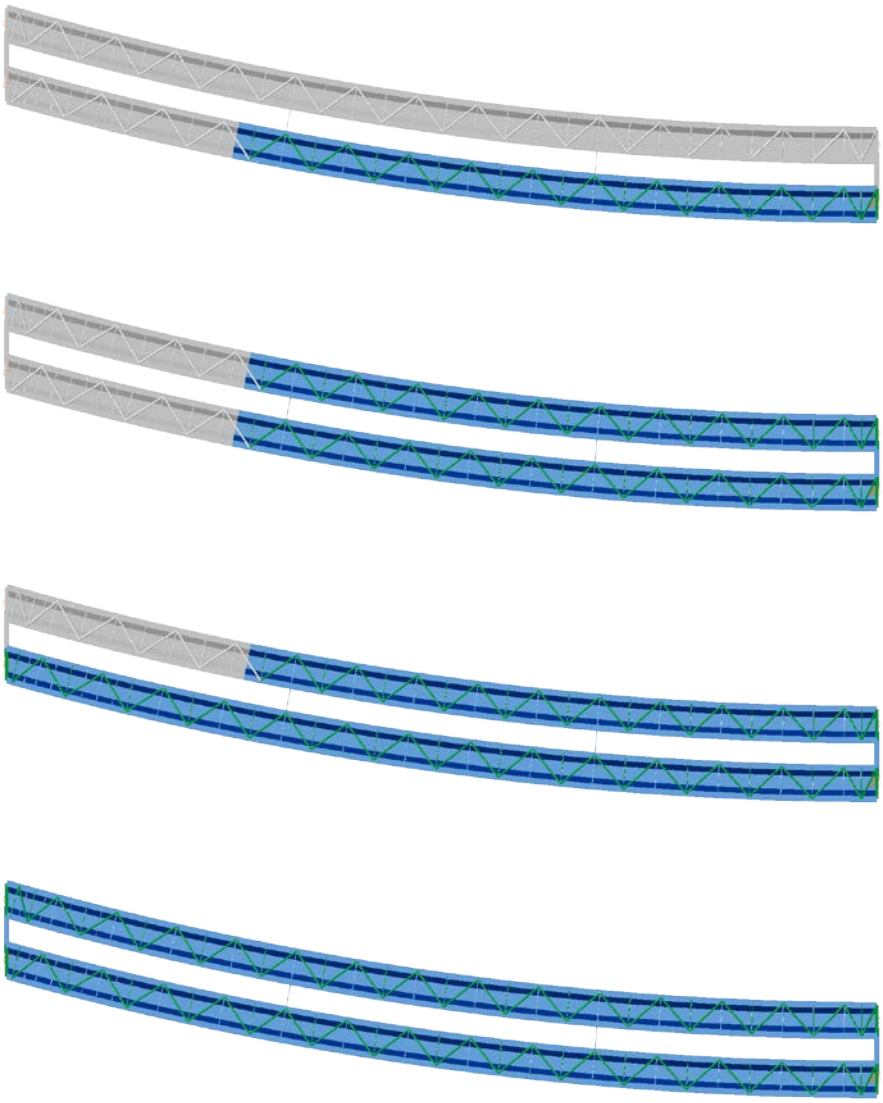

Fig. 1. Intermediate steel erection stages

Figures 2 through 5 show the evolution of the vertical displacements for the partial steel erection stages 2 and 3, final steel and total non-composite dead loads. For the partial stages the vertical displacements are plotted only for 3D FEA and 2D LARSA, all methods are shown for the final steel and total non-composite dead loads.

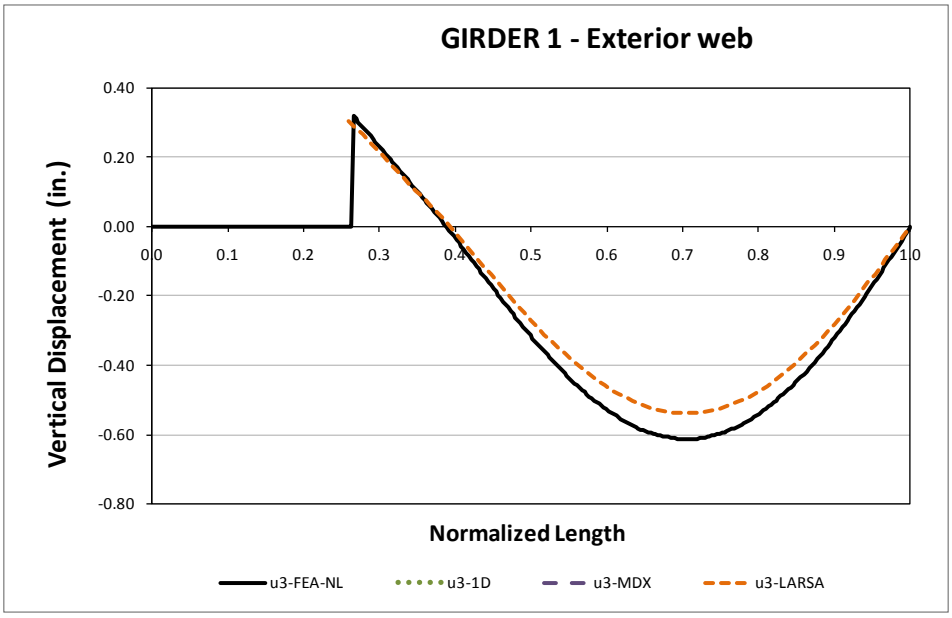

Fig. 2. Top flange vertical displacements for Girder 1 exterior web – Stage 2 Steel Dead Load

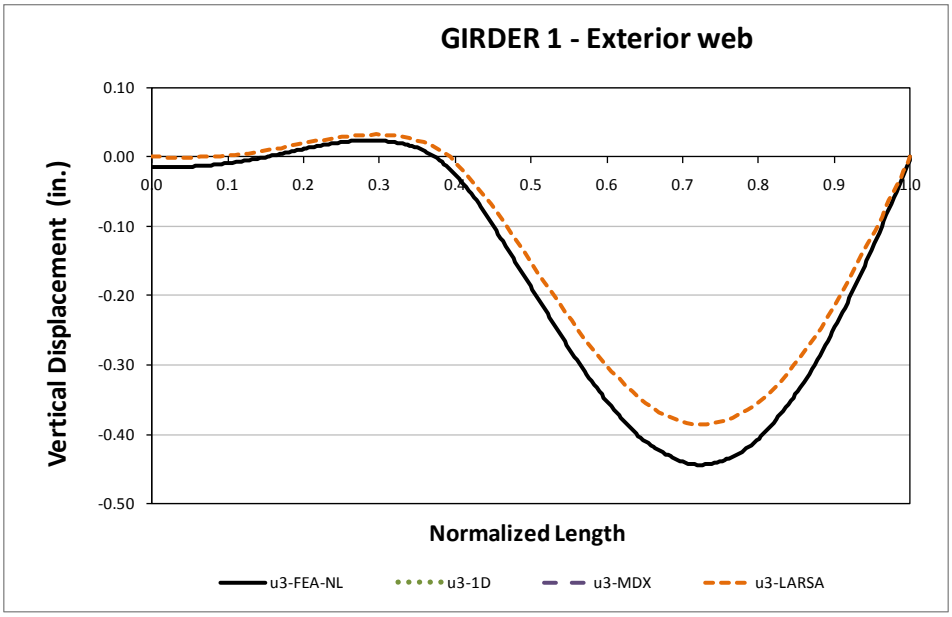

Fig. 3. Top flange vertical displacements for Girder 1 exterior web – Stage 3 Steel Dead Load

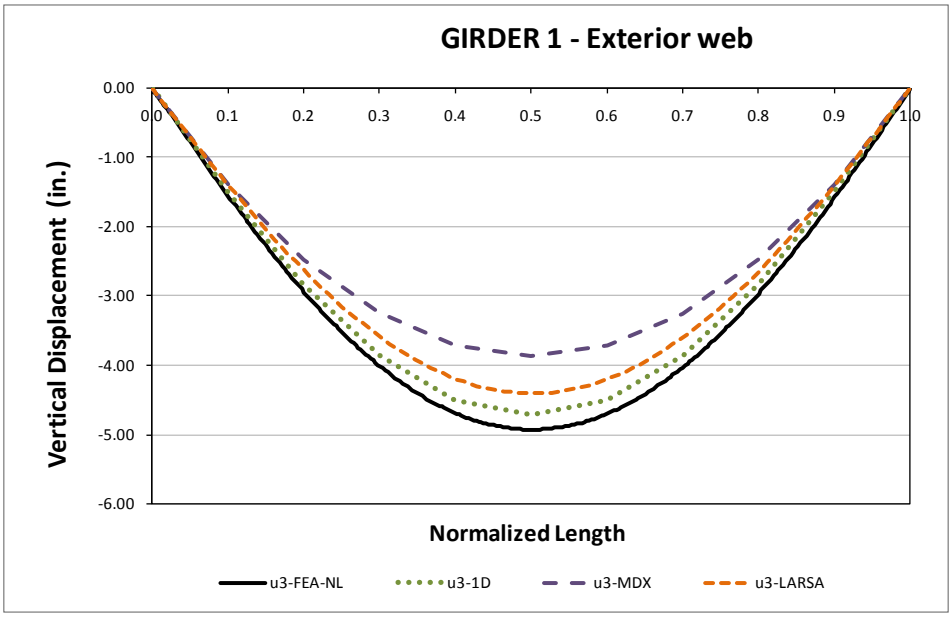

Fig. 4. Top flange vertical displacements for Girder 1 exterior web – Final Steel Dead Load

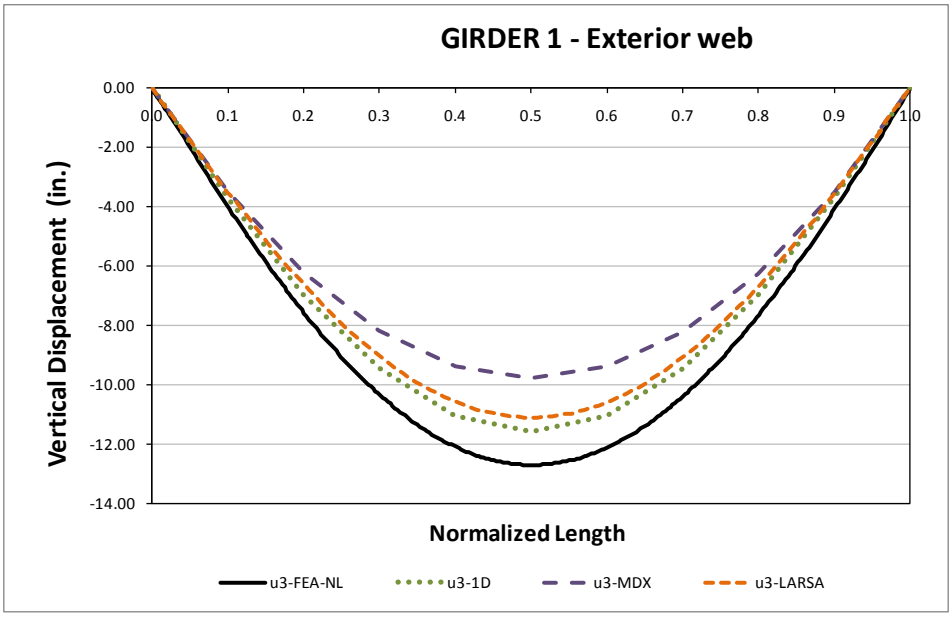

Fig. 5. Top flange vertical displacements for Girder 1 exterior web – Total Dead Load

Figure 6 illustrates the relative radial displacement between top and bottom flange junctures as a measure of lateral displacement. The values show a close approximation in the general shape while the 3D FEA shows a moderate localized effect where the flanges slightly deviate from the main shape. The results show evidence of section rotation at the left end making evident the effect of the skewed support.

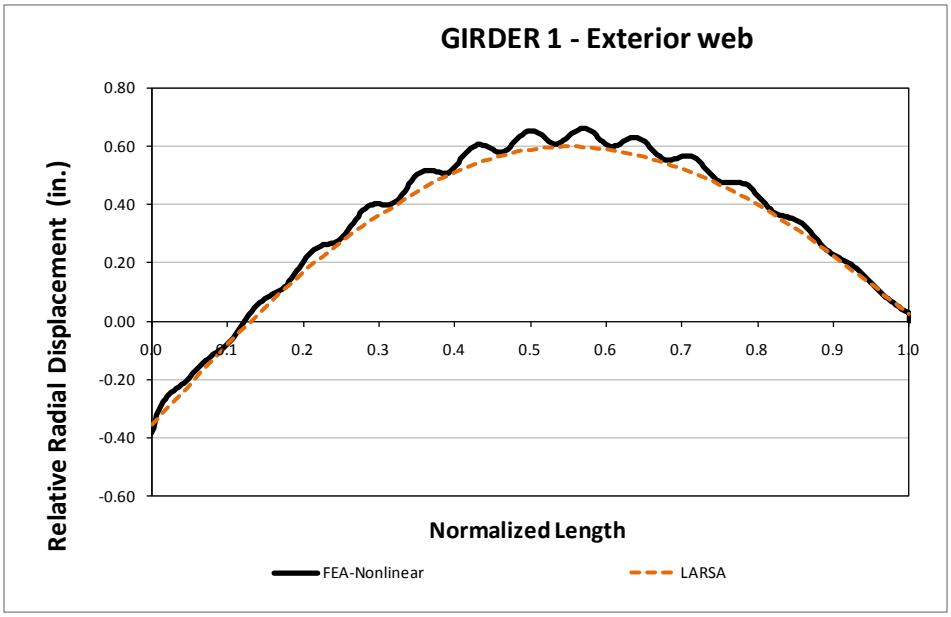

Fig. 6. Top flange relative radial displacements for Girder 1 exterior web - Total Dead Load

Bending Stress Results

Figures 7 through 10 show the evolution of the major axis bending stresses for Girder 1 - Exterior Web during steel erection stages 2, 3 and final steel and total non-composite dead load cases. In these stages the results are closely predicted by 1D and 2D analysis methods. For the Final Steel and Total non-composite dead load stages, the participation of the top flange lateral bracing system becomes evident in the 3DFEA methods as this system has an important effect on the bending stresses.

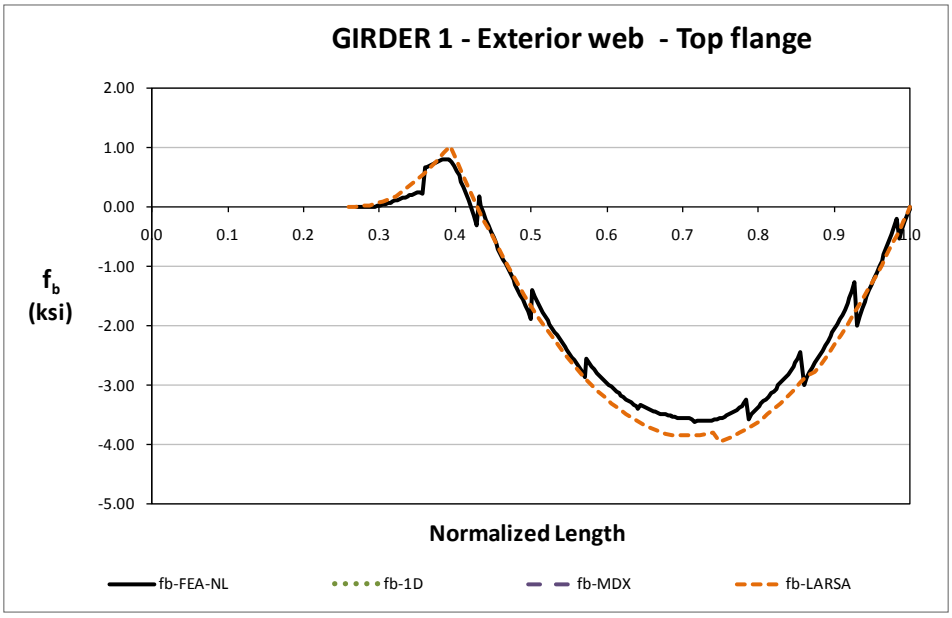

Fig. 7. Top flange major axis bending stress for Girder 1 exterior web – Stage 2 Steel Dead Load

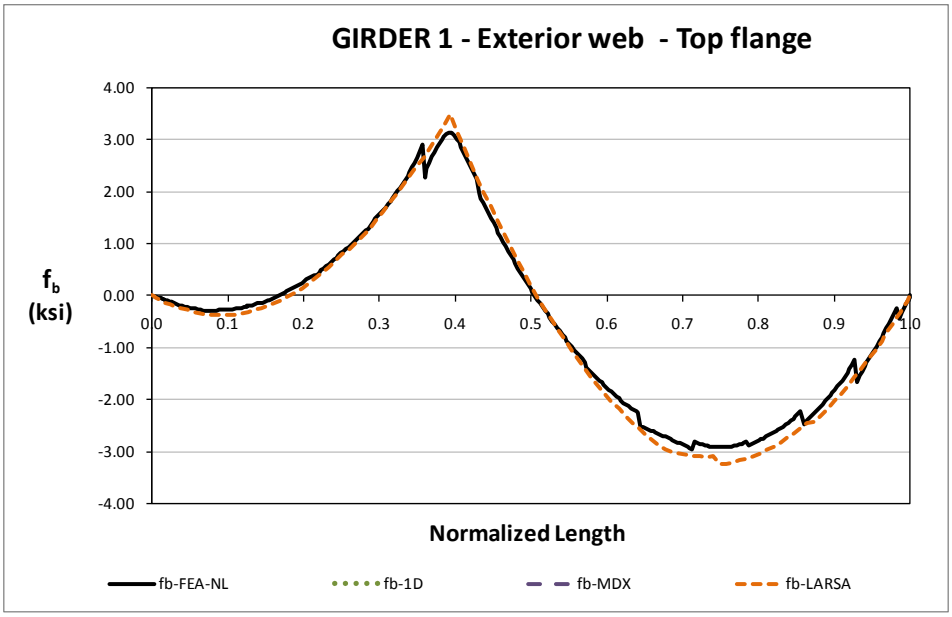

Fig. 8. Top flange major axis bending stress for Girder 1 exterior web – Stage 3 Steel Dead Load

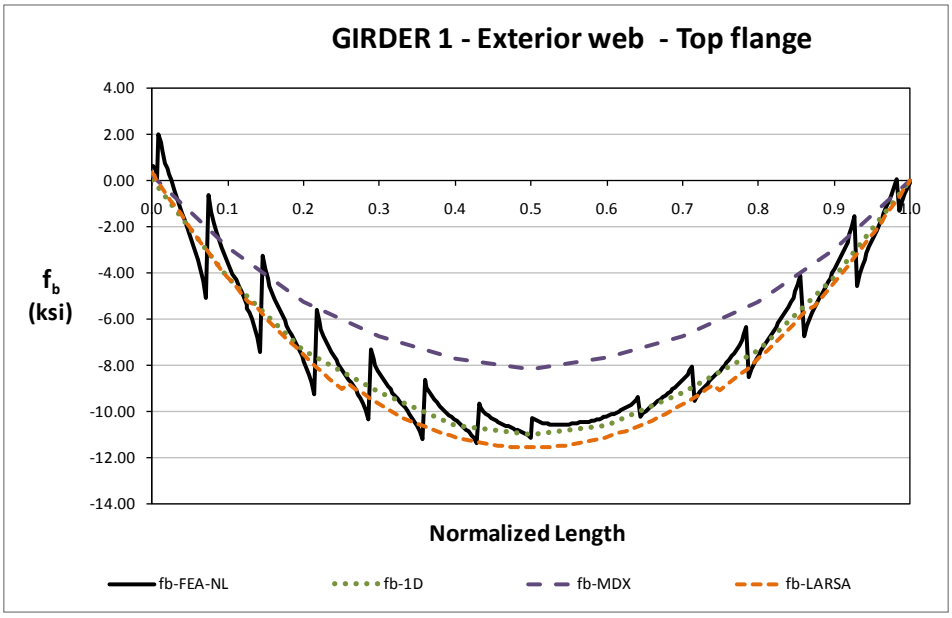

Fig. 9. Top flange major axis bending stress for Girder 1 exterior web - Final Steel Dead Load

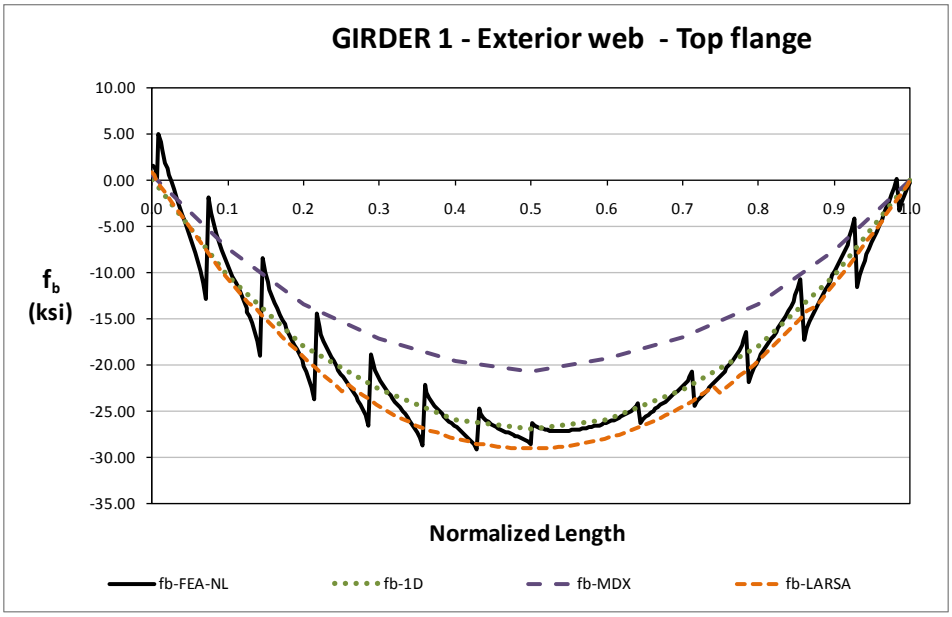

Fig. 10. Top flange major axis bending stress for Girder 1 exterior web - Total Dead Load

Figure 11 illustrates results for Girder 1 - Interior web to show how the adjacent web in the same girder experiences the same localized effects but in a different shape that matches the position of the TFLB diagonals.

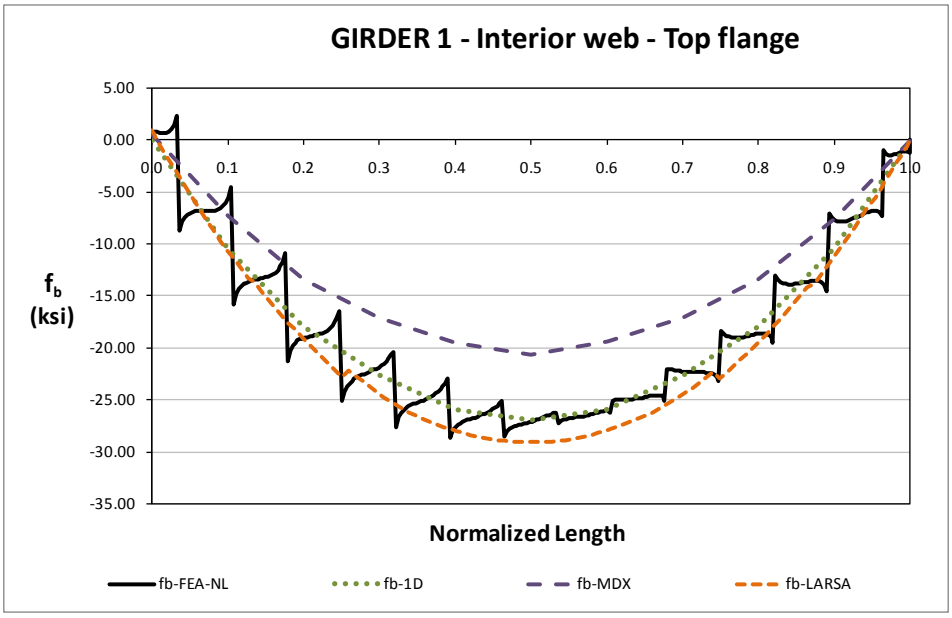

Fig. 11. Top flange major axis bending stress for Girder 1 interior web - Total Dead Load

Figures 12 and 13 illustrate the bottom flange major axis bending stresses at the web bottom flange juncture. As seen before, some local stress concentrations are shown in the 3DFEA results at the CF locations.

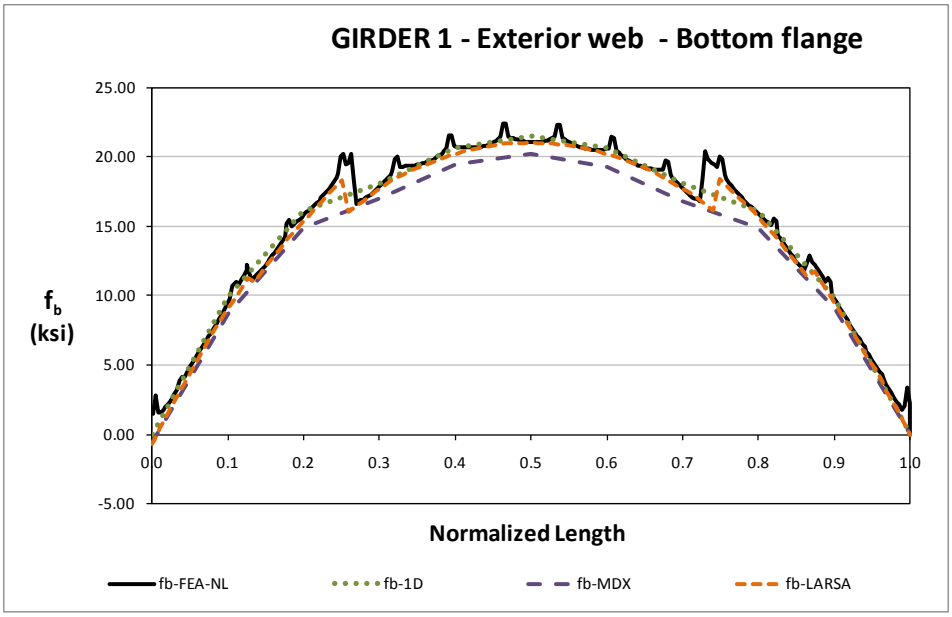

Fig. 12. Bottom flange major axis bending stress for Girder 1 exterior web - Final Steel Dead Load

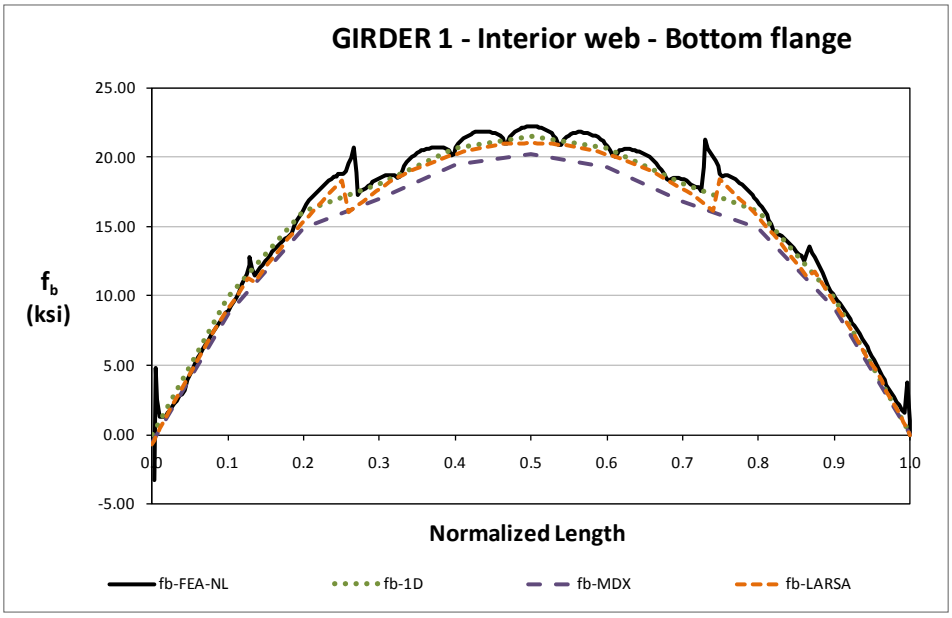

Fig. 13. Bottom flange major axis bending stress for Girder 1 interior web - Total Dead Load

Top Flange Lateral Bracing Results

The TFLB diagonals axial forces are shown in Figures 14 and 15 for the final steel and total dead load conditions. The 3DFEA method reports forces of half the values reported by the 1D and 2D analysis methods. The cross sectional area of these elements is 28.1in² that for a maximum axial force of 200kip as reported by the 3DFEA the element experiences an axial stress of 7ksi on the total dead load condition.

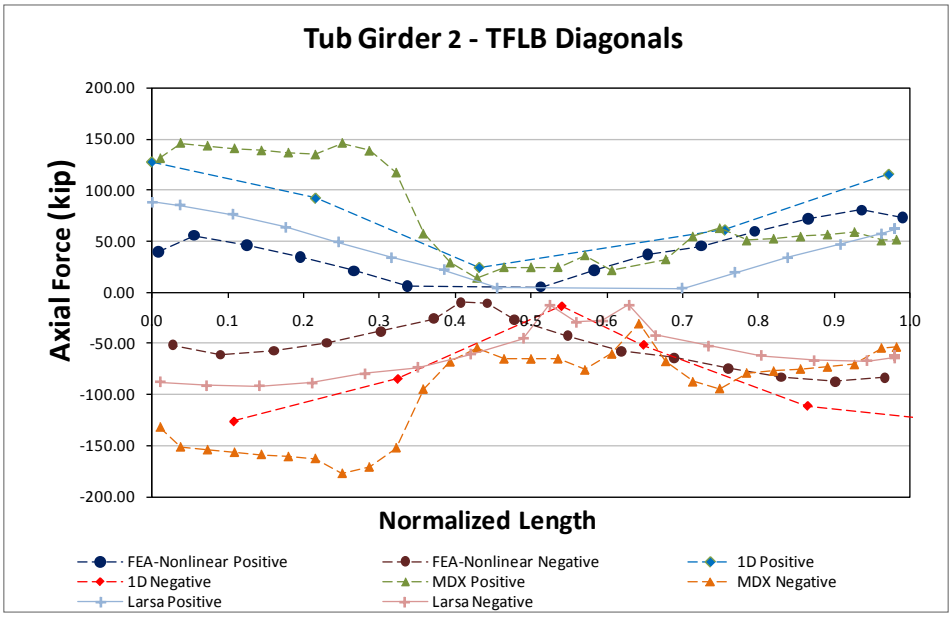

Fig. 14. Top flange lateral bracing diagonals axial forces for Girder 2 - Final Steel Dead Load

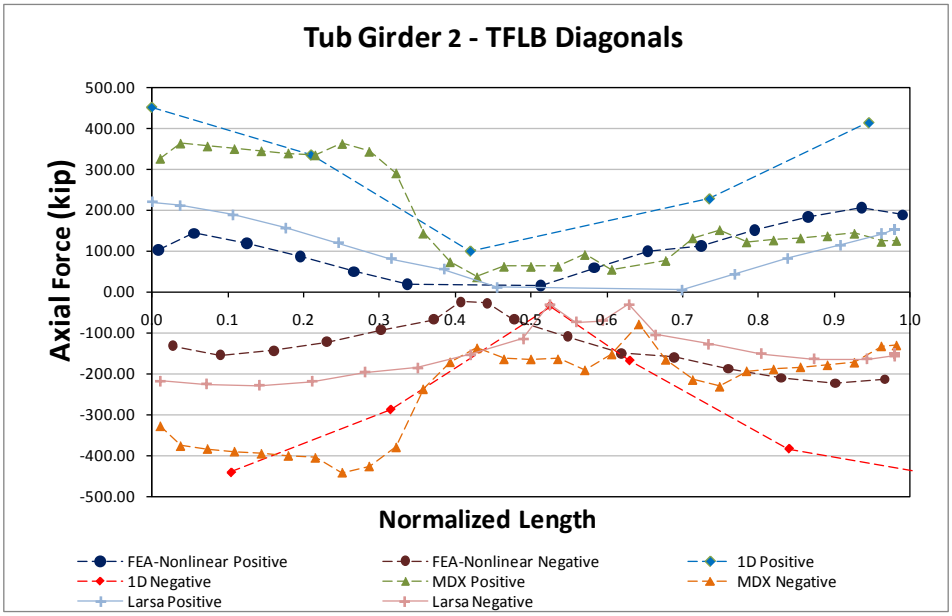

Fig. 15. Top flange lateral bracing diagonals axial forces for Girder 2 - Total Dead Load

Figure 16 and 17shows the TFLB axial forces on the struts for the final steel and total dead load conditions. The area of the struts is 4.4in² which, for a maximum axial force of 25kip as reported by the 3D FEA analysis, results on maximum axial stress of 5.7ksi. The 2D analysis methods predict a larger value for these forces.

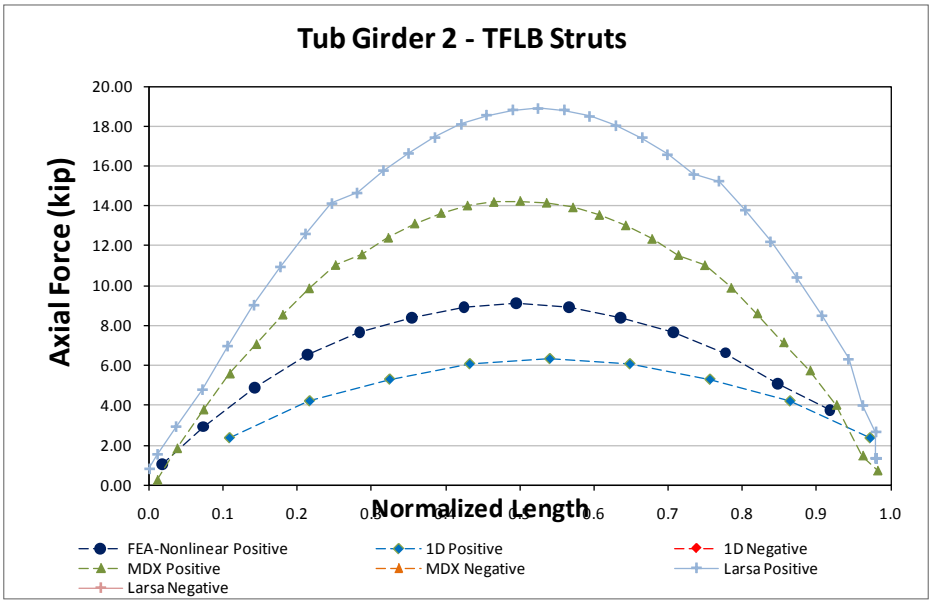

Fig. 16. Top flange lateral bracing struts axial forces for Girder 2 – Final Steel Dead Load

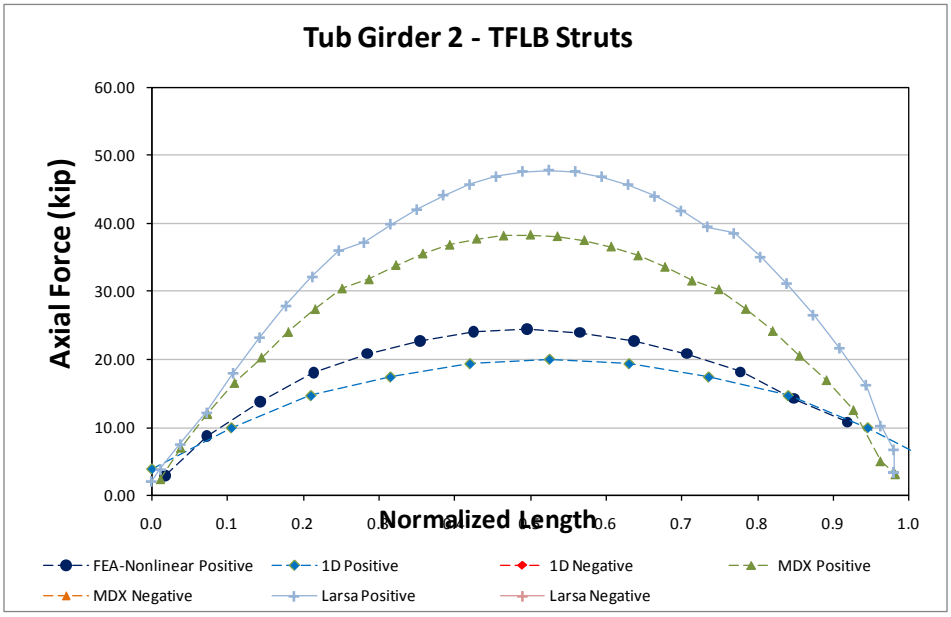

Fig. 17. Top flange lateral bracing struts axial forces for Girder 2 - Total Dead Load

Internal Cross Frame Results

Internal cross frames alternate in every other panel, these elements are composed by diagonals and top chords. Figure 18 shows the internal CF diagonal axial forces while Figure 19 shows the results for the top chord of the CF. The cross sectional area of both element types is 4.4in².

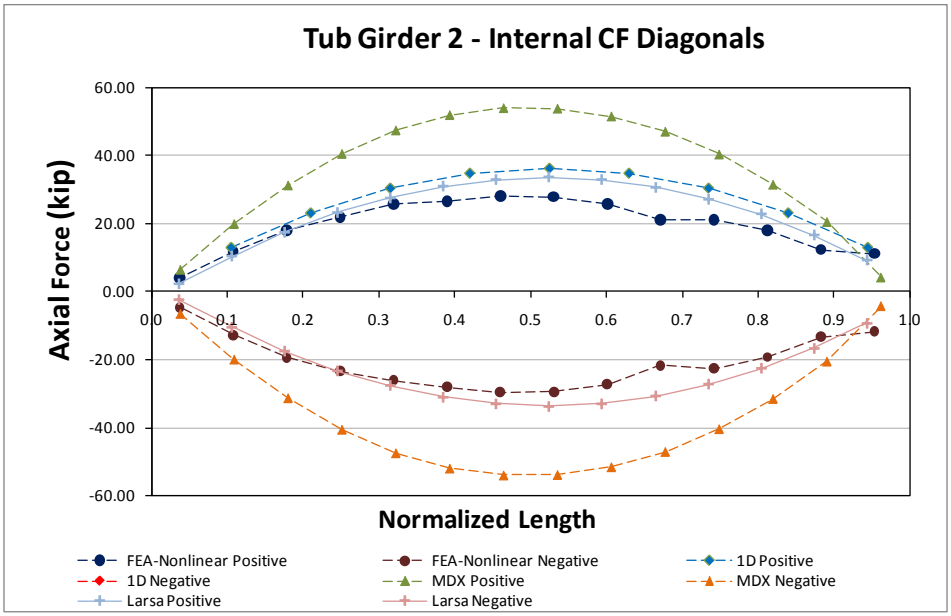

Fig. 18. Internal cross-frames diagonals axial forces for Girder 2 - Total Dead Load

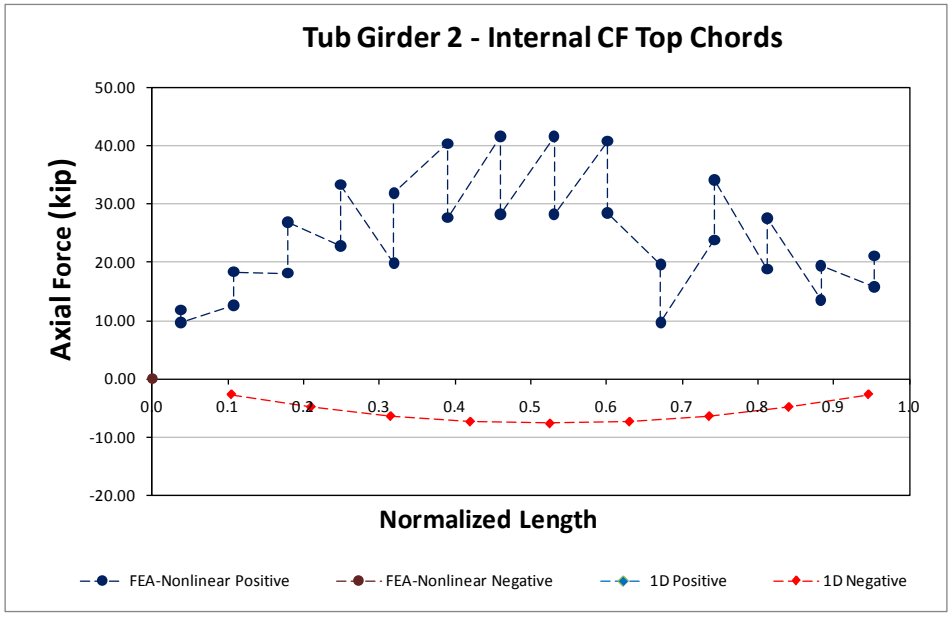

Fig. 19. Internal cross-frame top chords axial forces for Girder 2 - Total Dead Load

13.1 ETCCS5a (Existing, Tub-girder, Continuous-span, Curved, Skewed supports)

Bridge Description:

SB SR9A to EB SR202 Ramp, Duval Co., FL

Category Data:

L_1 = 183 ft, L_2 = 161 ft / R = 765 ft / w = 36.2 ft / θ_1 = 0°, θ_2 = 4.8°, θ_3 = 0°, 2 tub-girders

References:

Provided by Tensor Engineering

Erection Stages Analyzed: 6 steel erection stages and 7 parametric skew cases

Deck Placement Sequence: (Analyses are performed assuming no staged deck placement).

Bridge Perspective & Plan Views:

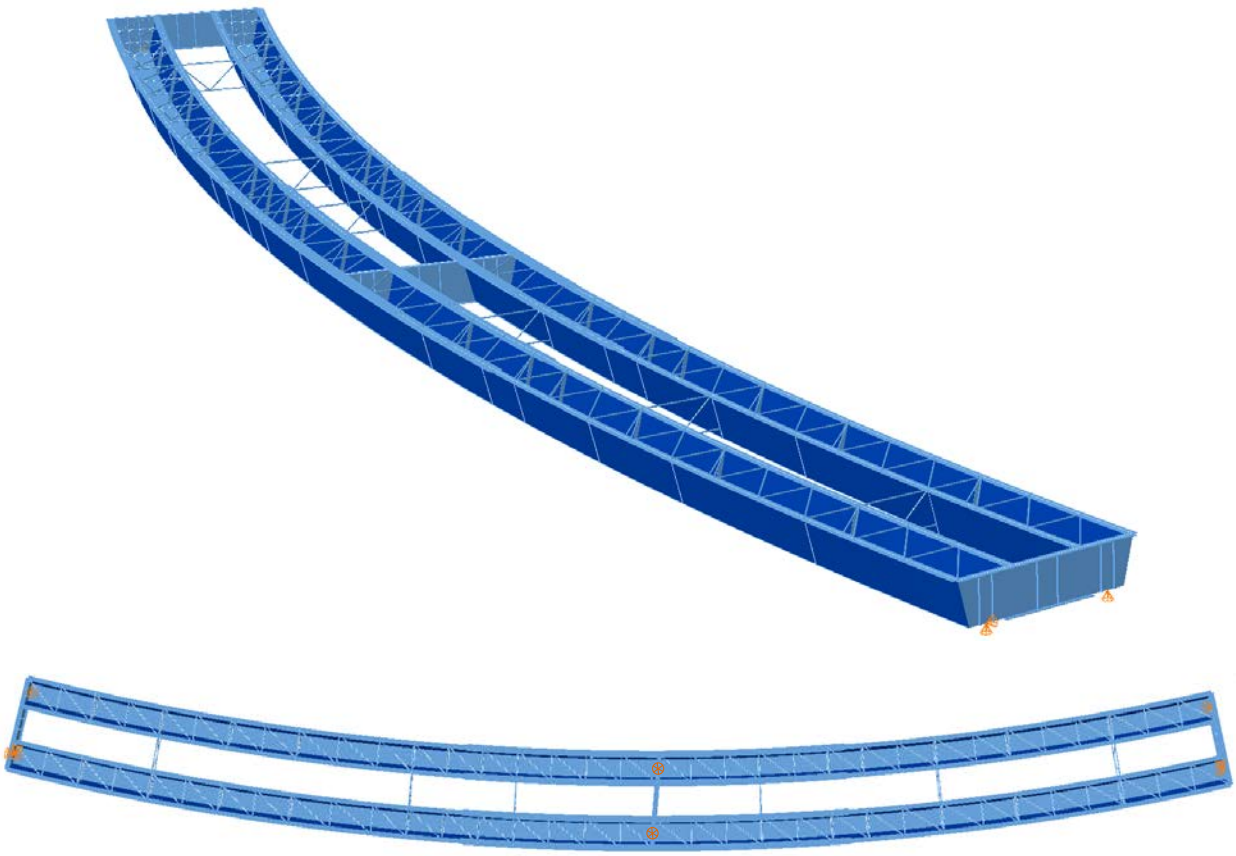

Displacement Results

Figures 1 and 2 illustrate vertical displacements predicted by different analysis methods for the most exterior and most interior flanges of the bridge under total dead load for the 3DFEA analysis method and for the girder centerline for the 1D and 2D methods.

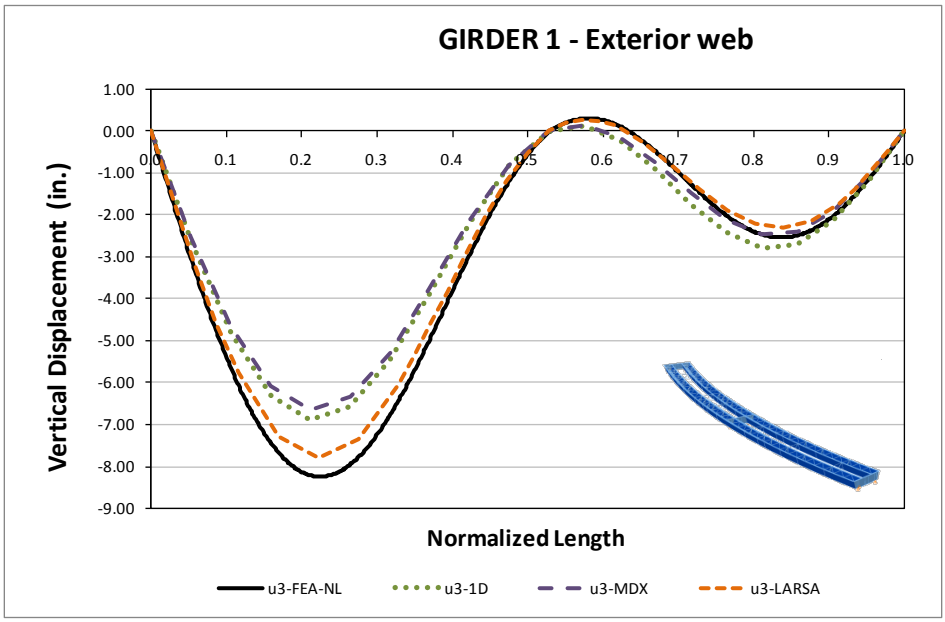

Fig. 1. Top flange vertical displacements for Girder 1 exterior web - Total Dead Load

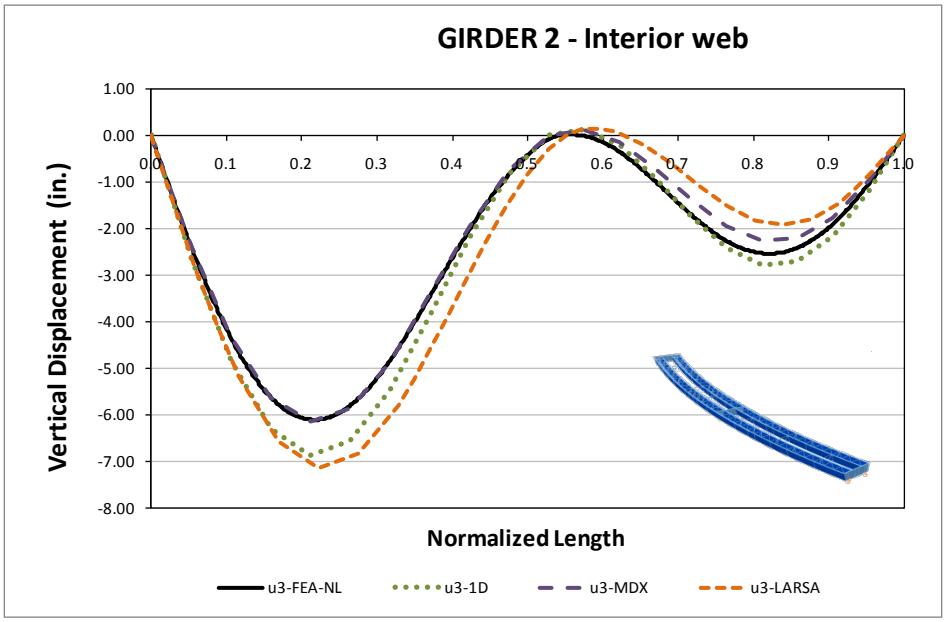

Fig. 2. Top flange vertical displacements for Girder 2 interior web - Total Dead Load

As expected, the displacements decrease as the total girder length decreases due radius change in the exterior and interior webs. Also, the span length changes due to the skewed supports. Differences in the plotted results may be caused by the modeling techniques and also due to the locations where the methods report the results.

Bending Stress Results

Figures 3 and 4 illustrate major axis bending stresses predicted by different analysis methods the top flanges for the most exterior web and most interior web for total dead load. The results from different analysis method stresses agree well in magnitude. The shape of the 3DFEA analysis reveals the interaction of the top flange lateral bracing in the normalized length 0.2 to 0.4.

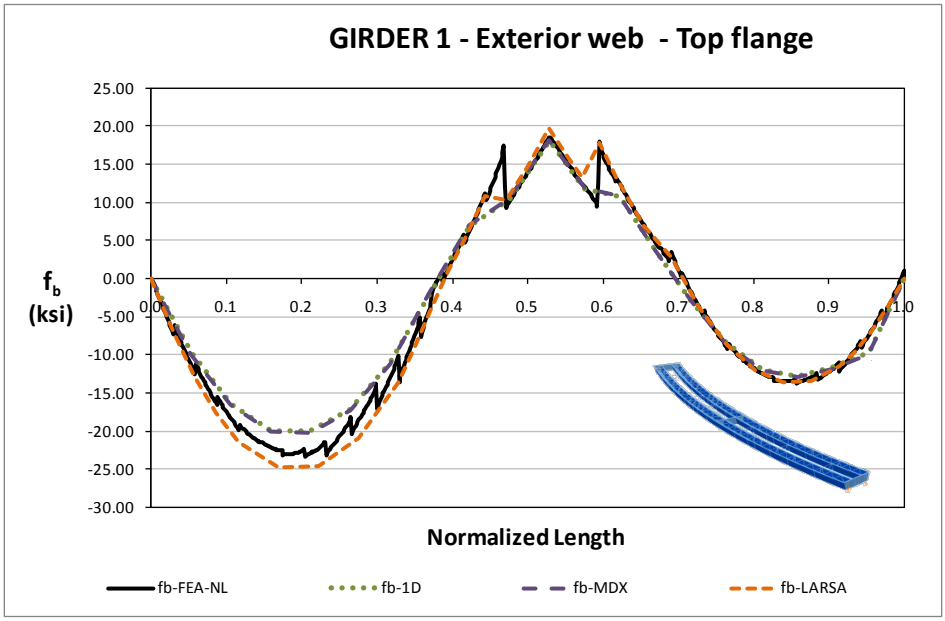

Fig. 3. Top flange major axis bending stress for Girder 1 exterior web - Total Dead Load

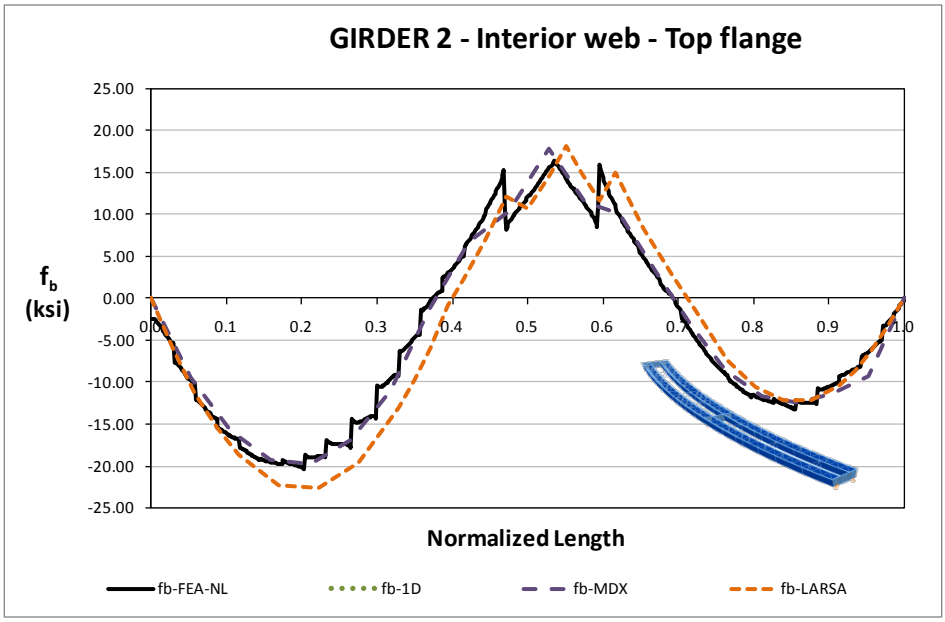

Fig. 4. Top flange major axis bending stress for Girder 2 interior web – Total Dead Load

Bottom flange stress predictions are shown in Figure 5 for total dead load. In this case, the results did not differ greatly as in the prediction of the top flange results.

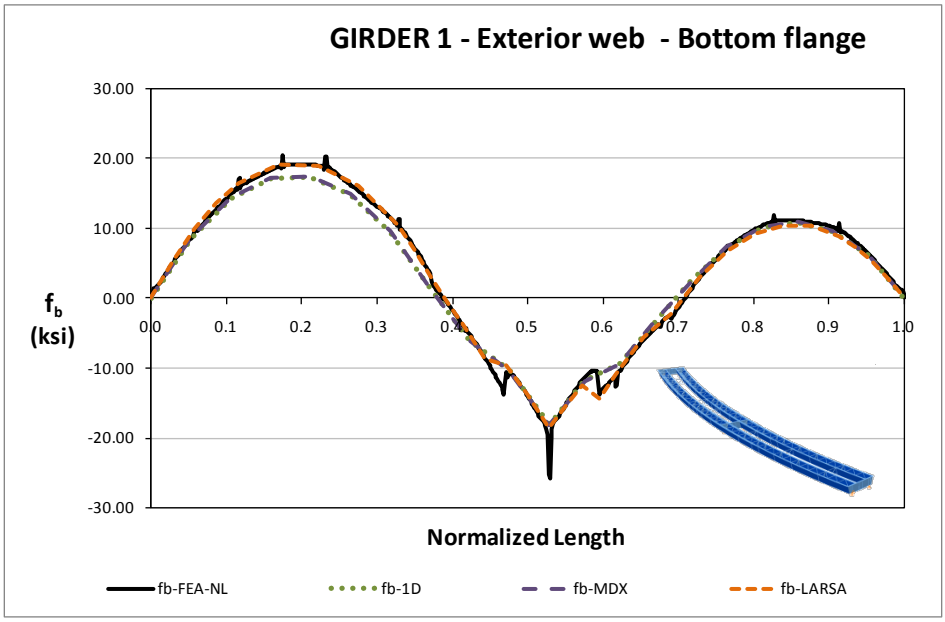

Fig. 5. Bottom flange major axis bending stress for Girder 1 exterior web – Total Dead Load

Lateral bending stresses are shown in Figure 6 for total dead load. The 1D and 2D analysis methods overpredict the response since they are based on simplified analysis. The validity of these methods is to be evaluated.

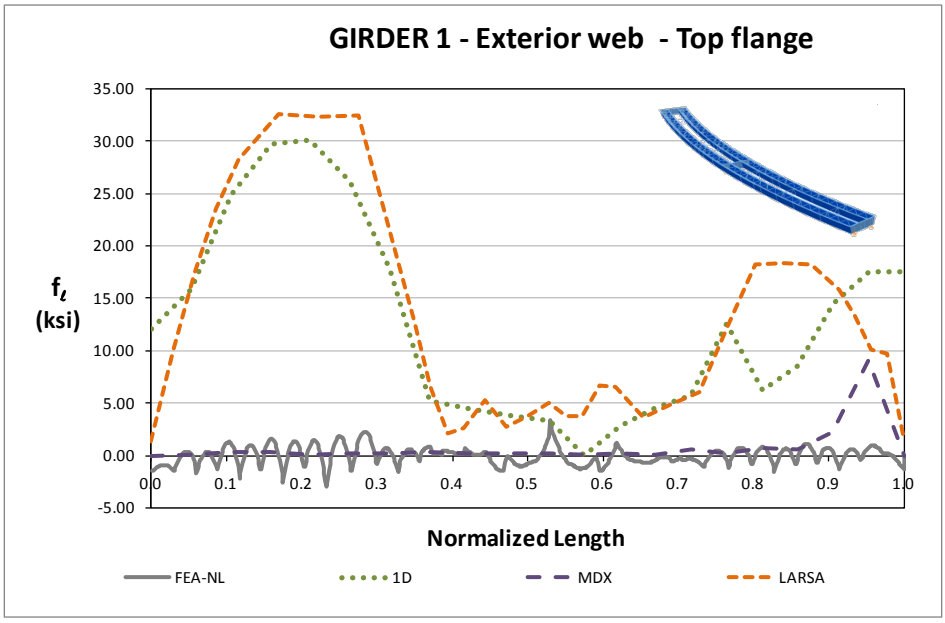

Fig. 6. Top flange lateral bending stress for Girder 1 exterior web – Total Dead Load

Top Flange Lateral Bracing Results

Figure 7 illustrate the stresses in the TFLB diagonals while in Figure 8 the results from the TFLB struts and CF Top chord are combined. The stresses reveal that in the area where the bending stresses see more local interaction, i.e. zigzag pattern, the stresses in the TFLB are lower.

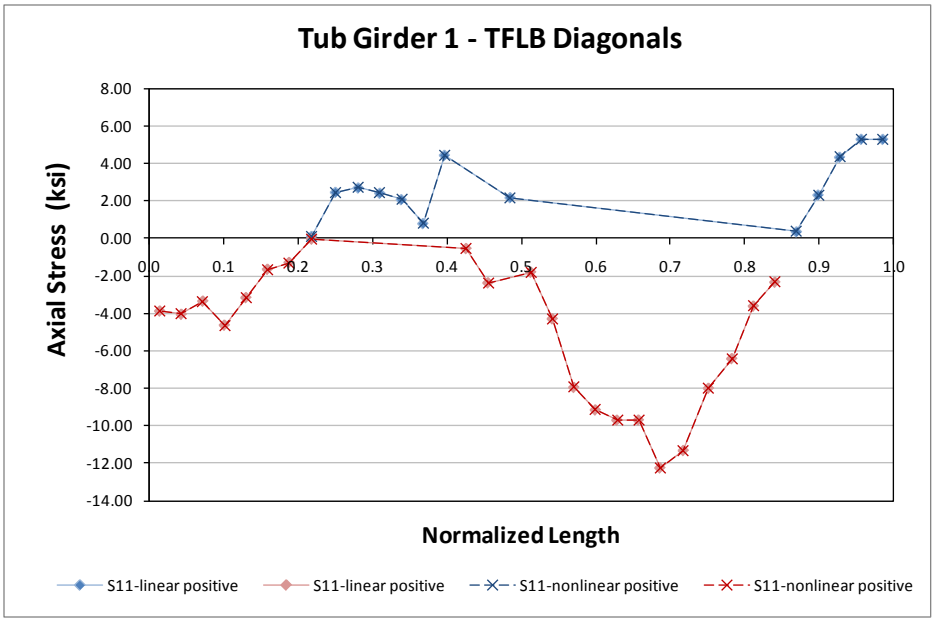

Fig. 7. Top flange lateral bracing diagonals axial stresses for Girder 1 - Total Dead Load

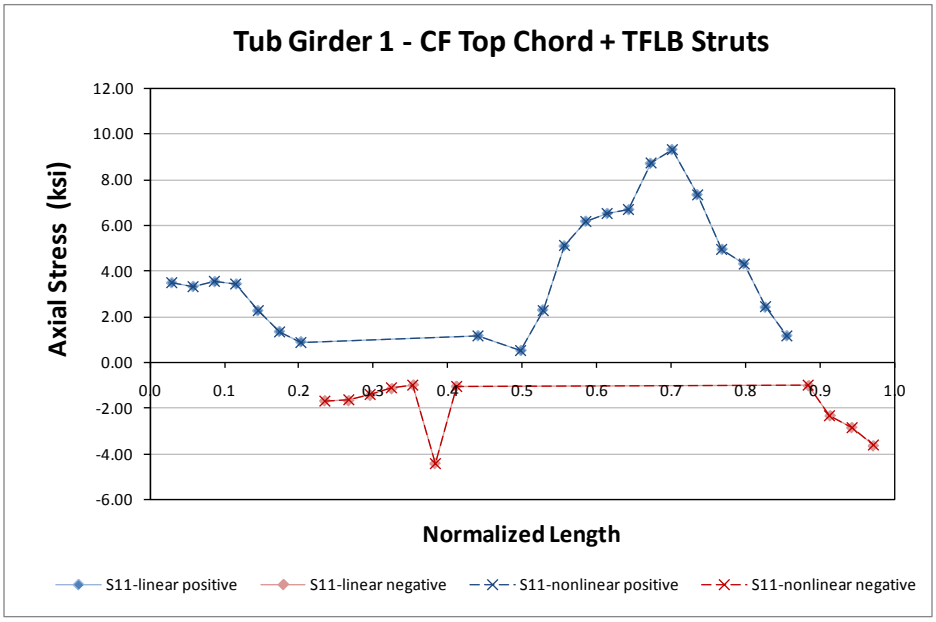

Fig. 8. CF Top chord and TFLB struts axial stresses for Girder 1 - Total Dead Load

13.2 ETCCS6 (Existing, Tub-girder, Continuous-span, Curved, Skewed supports)

Bridge Description:

Magruder Boulevard over I-64, Hampton, VA

Category Data:

L_1 = 160 ft, L_2 = 207 ft / R = 814 ft / w = 50.5 ft / θ_1 = 0°, θ_2 = 39.2°, θ_3 = 0°, 4 tub-girders

References:

Provided by Virginia DOT

Erection Stages Analyzed: Phase I: 3 steel erection stages, concrete deck dead load. Phase II: final steel erection, concrete deck load.

Deck Placement Sequence: Independent deck placement for each phase, 3 deck stages per phase

Bridge Perspective & Plan Views:

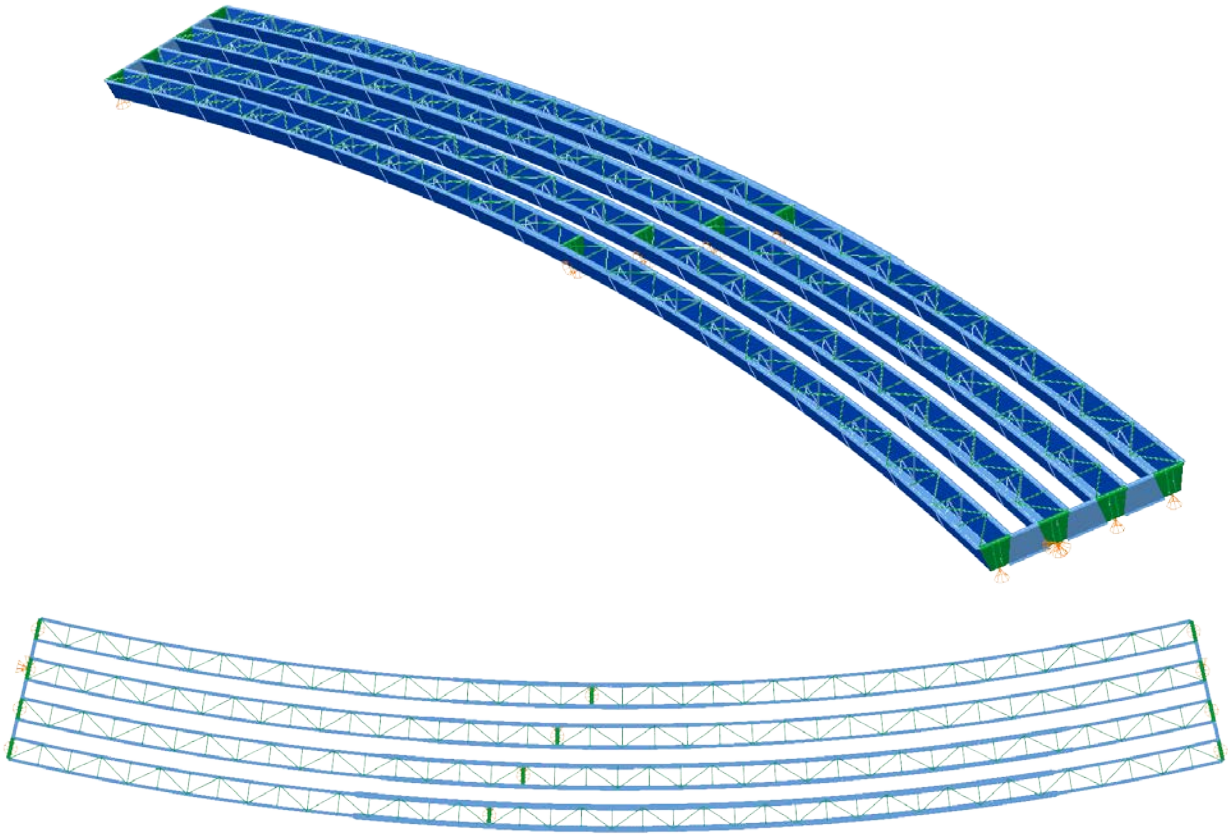

Displacements Results

The Magruder Blvd. bridge intermediate support is heavily skewed with 39° with respect to the radial line; external intermediate diaphragms were not used at these locations to interconnect the girders. The bridge was built in two independent phases: the interior girders were erected and the concrete was placed, then the two exterior girders were erected and the deck was placed, finally the phases were connected by a closure pour.

To control displacements during the erection stages, temporary supports were placed at approximately 0.4L the length of span 1 or 0.18L of the entire bridge length and were removed once the steel was completely erected in each phase. The girders were connected at the abutments by solid plate diaphragms but there were no external cross frames or diaphragms along the entire length of the bridge. At the intermediate pier there were no intermediate exterior diaphragms, internal bearing diaphragms were provided at these locations

The following figures illustrate the vertical displacements for the final steel and total non-composite dead loads for the extreme top flanges of the bridge girders. Figures 1 and 2 show the results for the most interior and most exterior top flanges for the Final Steel condition and Figures 3 and 4 show the same top flange results for the Total Dead Load, results are shown for different analysis methods, including the results reported by independent 3DFEA analysis by Wright (2002). For the 3DFEA the displacements are reported at the top flange positions while for 1D and 2D methods results are at the tub centerlines. The maximum vertical displacement across the cross section of the bridge is 3 in for the Final Steel Load and about 9 in for the Total Dead Load case, the relative vertical displacement is more than 50% of the maximum value for both load cases meaning that a the skew is impacting the displacements.

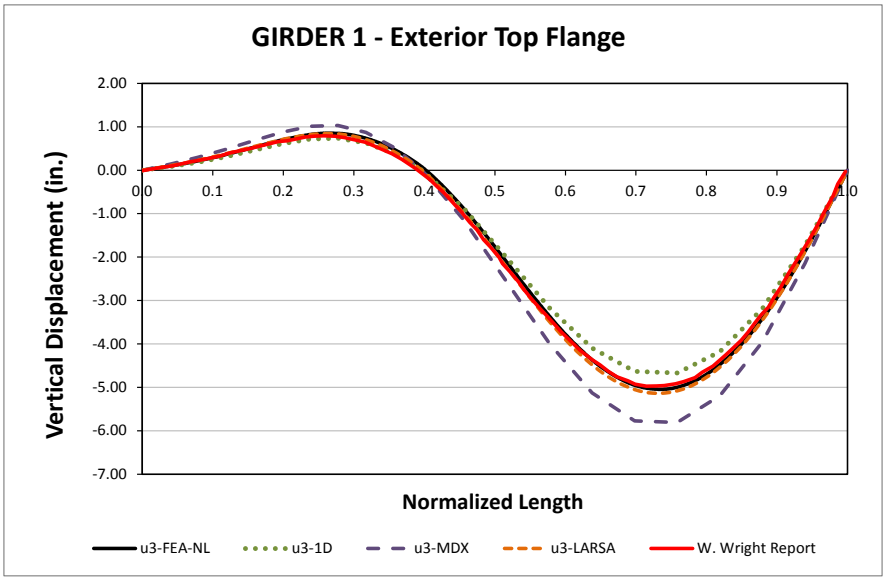

Fig. 1. Top flange vertical displacements for Girder 1 exterior web – Final Steel Dead Load

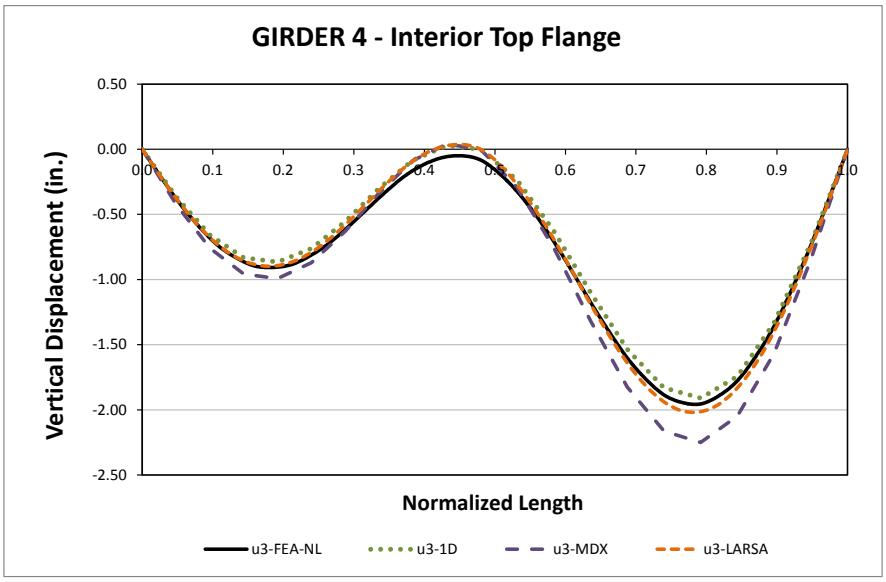

Fig. 2. Top flange vertical displacements for Girder 4 interior web – Final Steel Dead Load

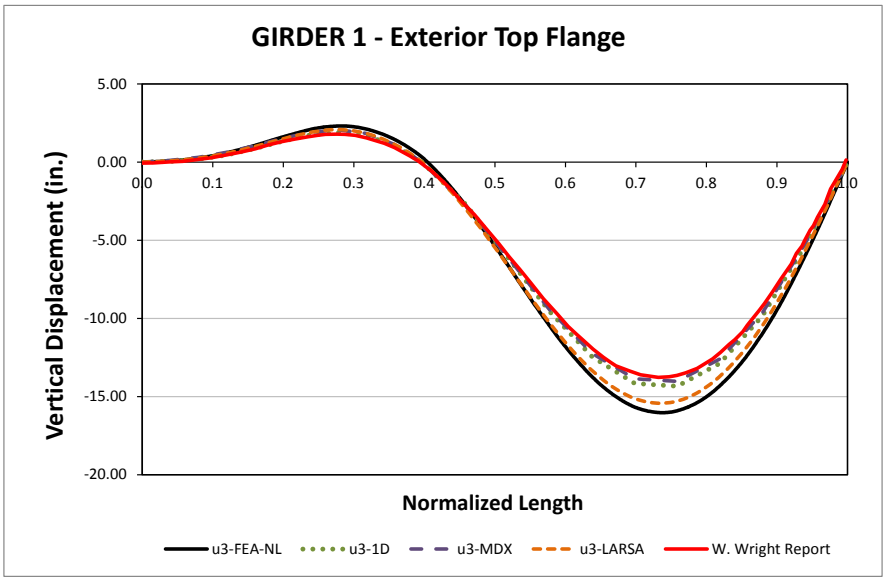

Fig. 3. Top flange vertical displacements for Girder 1 exterior web – Total Dead Load

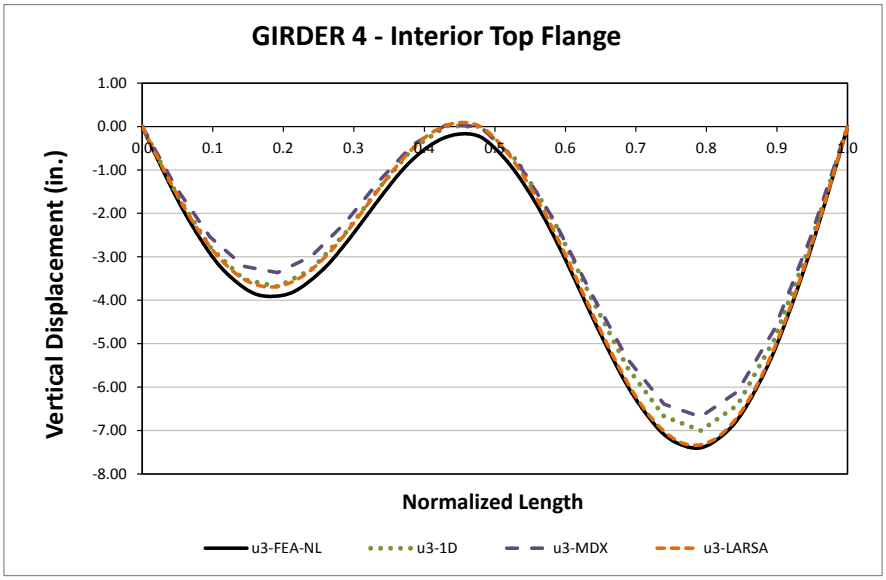

Fig. 4. Top flange vertical displacements for Girder 4 interior web – Total Dead Load

Vertical displacement predictions are accurate for the 2D-Larsa analysis and some prediction deficiencies are experienced by the 1D and 2D-MDX analyses. The differences in these analysis results are mainly caused by the discretization method used in the models as the 1D and 2D-MDX analyses use fewer elements to represent the entire bridge length.

Between the 3DFEA analyses the vertical displacement differences could be caused by the bearing modeling technique that assumes full twist restraint at the abutments and to the single girder methodology used by Wright, this effect is more noticeable for the Total Dead Load condition on fig. 3. The overhang loads on the Total Dead Load condition are included in the 3DFEA reference analysis method and directly affect the displacement prediction, these loads appear not to be included on the analyses by Wright.

Figure 5 illustrate the top flange radial displacements for the most exterior web of the bridge at the total non-composite dead load condition. The independent analysis by Wright (2002) is included in this figure; the differences seen here suggest that the bearing model technique affects the results. The top flange displacements relative to the bottom flange are shown in Figure 6, the same set of lateral displacements results from Wright show in fig. 5 are shown again in this plot for comparative purposes.

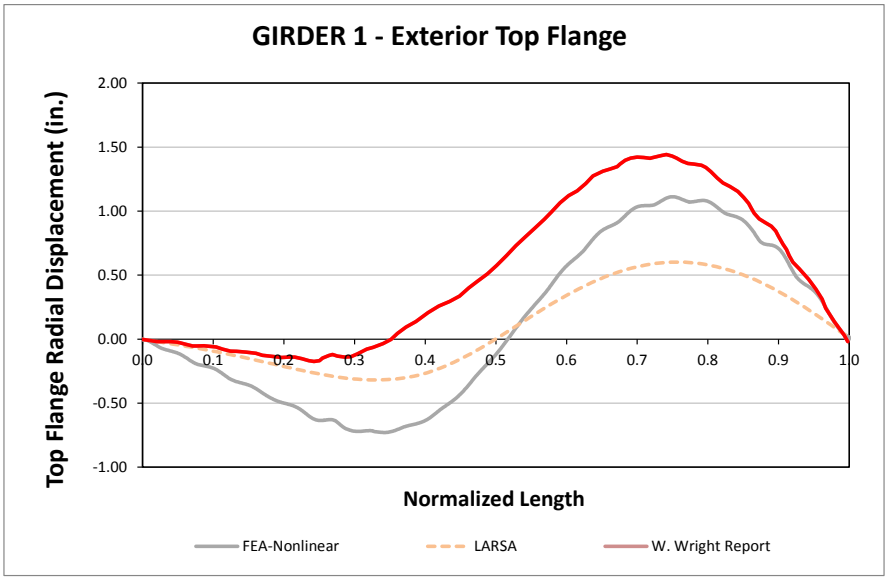

Fig. 5. Top flange radial displacements for Girder 1 exterior web - Total Dead Load

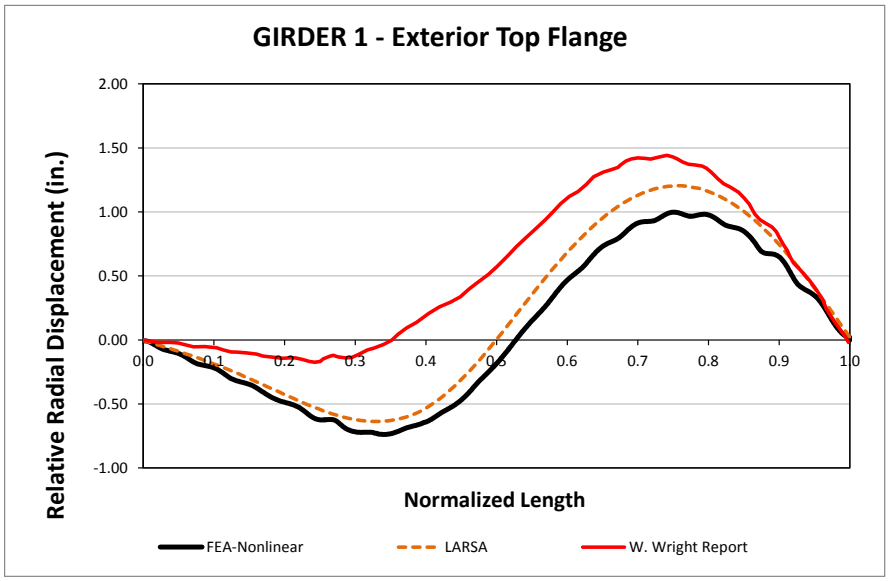

Fig. 6. Top flange radial displacements relative to the bottom flange of Girder 1 exterior web - Total Dead Load

Figure 7 illustrates the lateral results for the most interior girder, the local TFLB system interaction can be noticed in this case as the displacements curve shows small bumps following the top flange lateral bracing layout. Independent 3DFEA results for this girder are not available.

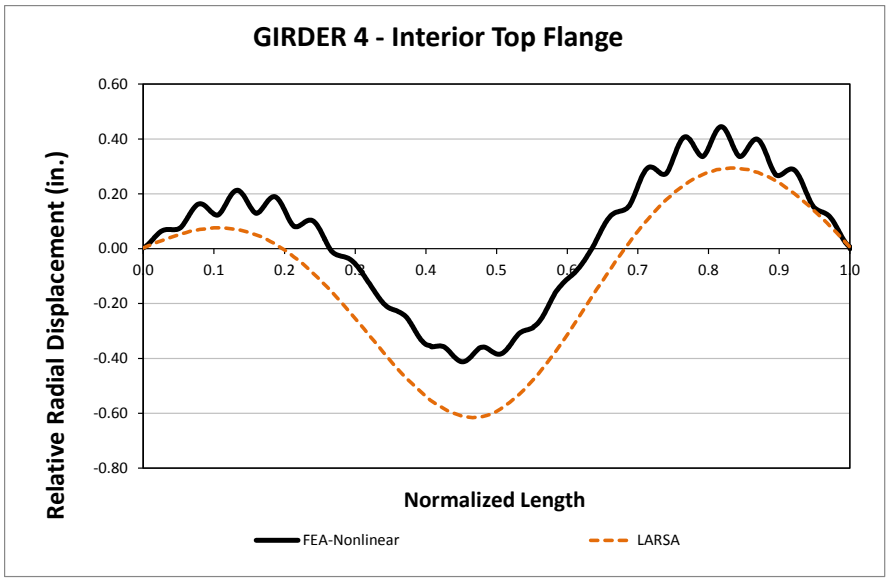

Fig. 7. Top flange radial displacements relative to the bottom flange of Girder 4 exterior web - Total Dead Load

Figure 8 illustrates the top flange vertical displacements relative to a line connecting the extreme flanges, each value reported corresponds to the six internal top flange displacements, dd2 being the most exterior and dd7 the most interior.

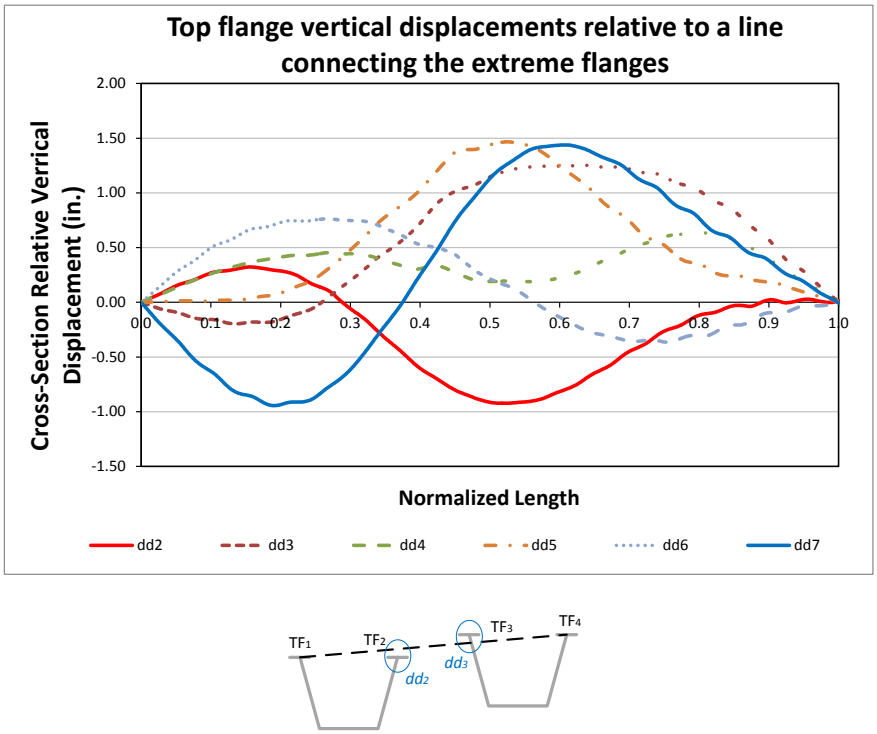

Fig. 8. Top flange relative vertical displacements - Total Dead Load

The intermediate skew induces irregular vertical cross section distortion, however the magnitude of the displacements is small and is not likely to cause concrete deck under or over run problems since these values could be easily accommodated in the girder haunches. These displacements remain small in value since the torsional stiffness of the tub-girders is high.

Figure 9 illustrates the collection of top flange vertical displacements for the total dead load condition. At the point of maximum vertical displacement the relative displacement of the first and last top flanges is close to 9in, however the entire bridge cross section is rotating and displacing rigidly as the bridge is not experiencing large cross section distortions as shown in figure 8. The differences on the vertical displacements are evidence of the length shift that the skew causes by changing the bending stiffness of the girders.

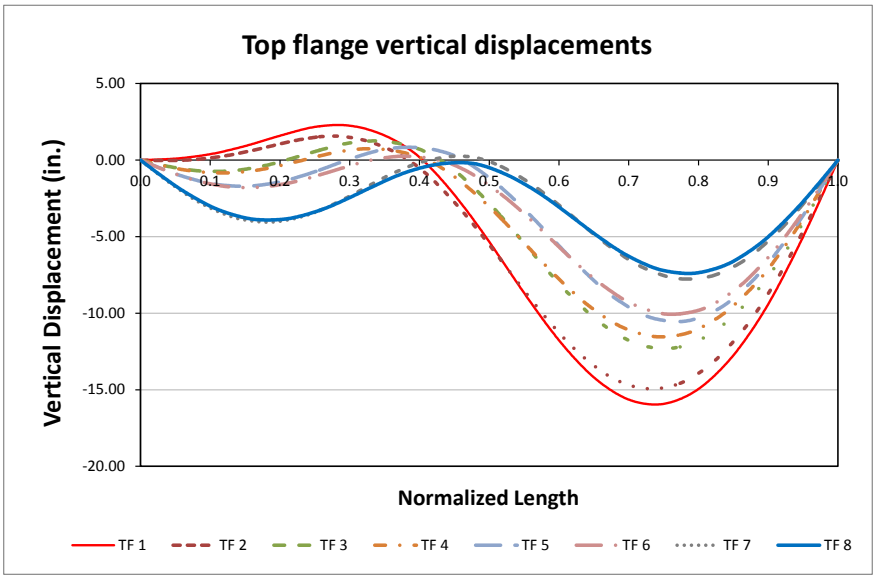

Fig. 9. Collection of top flange vertical displacements - Total Dead Load

The lack of intermediate cross frames in the length of the bridge and the lack of external diaphragm at the intermediate pier does not have a large effect on the displacements at the construction stages as these stay in low magnitude. It can be suggested that the lack of external diaphragm prevents transferring torsional loads at these girder locations, a way to show these effect would be by comparing the TFLB design forces with methods using the M/R loading procedure as the torques come only from curvature effects.

Bending Stress Results

Figures 10 and 11 show the stress distributions for the final steel and total dead load conditions for the most exterior web for the different analysis methods. The stresses show a uniform increment rising from a maximum value of 7ksi to 25ksi between these two stages.

The major axis bending stresses reported by the 3DFEA method show a saw-tooth stress pattern, these patterns are caused by the TFLB and tub-girder top flange interaction making evident that the force flow occurs in both directions. Current design expressions for 1D and 2D methods neglect that the TFLB elements transfer force back to the main plate girder system.

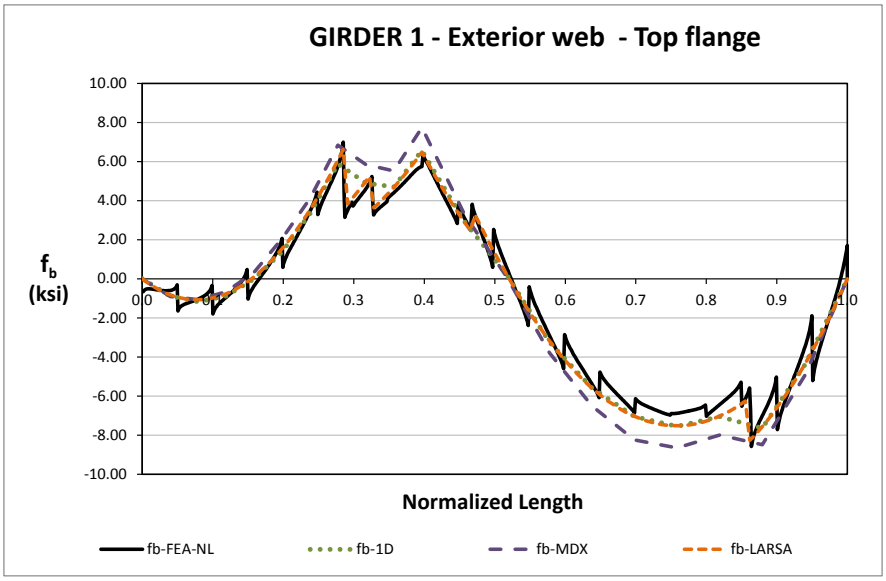

Fig. 10. Top flange major axis bending stress for Girder 1 interior web - Final Steel Dead Load

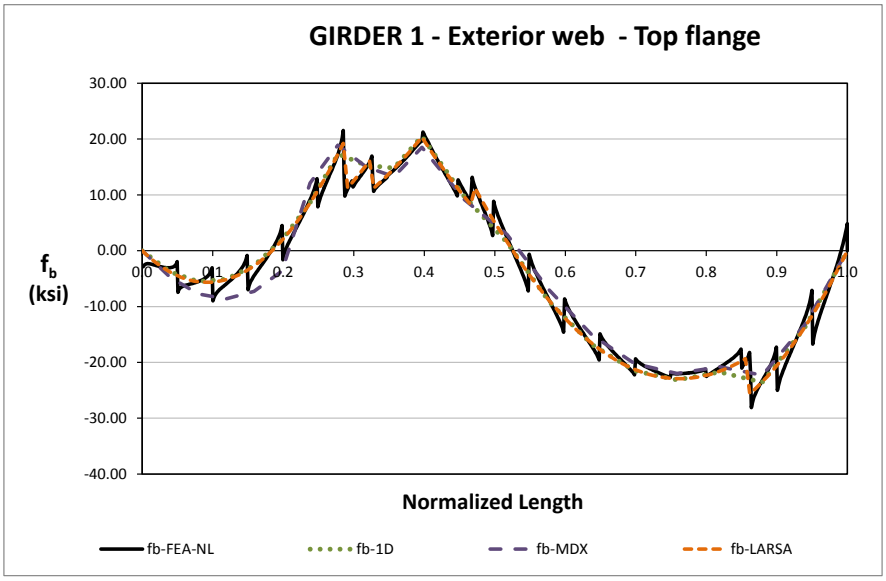

Fig. 11. Top flange major axis bending stress for Girder 1 interior web – Total Dead Load

Figure 12 shows the results for the most interior web, as expected the stresses peak moves with the support and the TFLB interaction is noticed but follows a different pattern in accordance with the points where the TFLB connects in this flange.

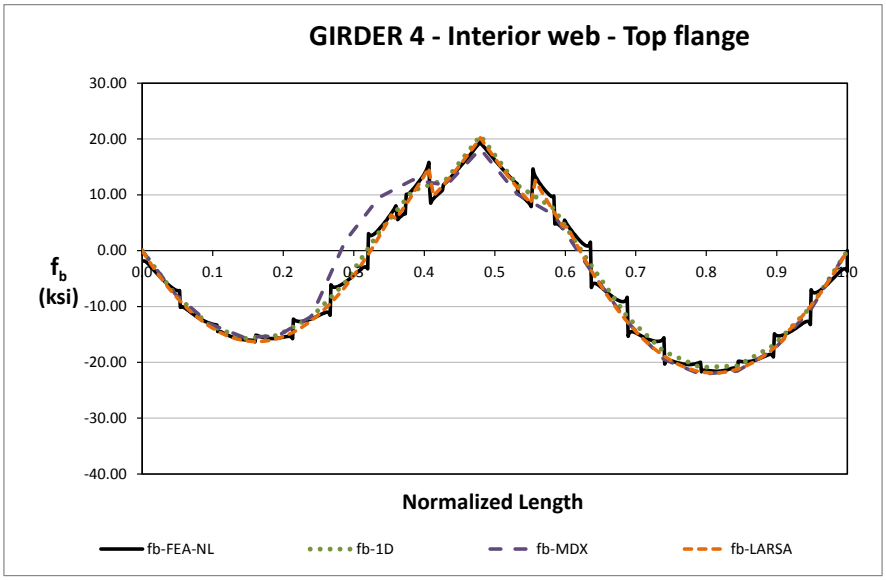

Fig. 12. Top flange major axis bending stress for Girder 4 exterior web - Total Dead Load

The bottom flange stresses are shown on Figure 13. At the intermediate supports, the bridge stresses experiment a sudden change in value, shown as a spike at around 0.4 the normalized length, this is attributed to the bearing plate model for the bridge supports. At this region, the elements surrounding the bearing points are constrained to simulate the bearing plate as a rigid zone, this modeling technique causes inaccuracies in the analytical procedure generating apparent stress concentrations.

Top flange lateral bending stresses are shown in Figure 14 for the Total Dead Load condition, the distribution of the stresses matches the TFLB layout as expected as in the major axis bending stresses sawtooths. The variability in magnitude of these stresses is mainly attributed to the change in the top flange cross sections.

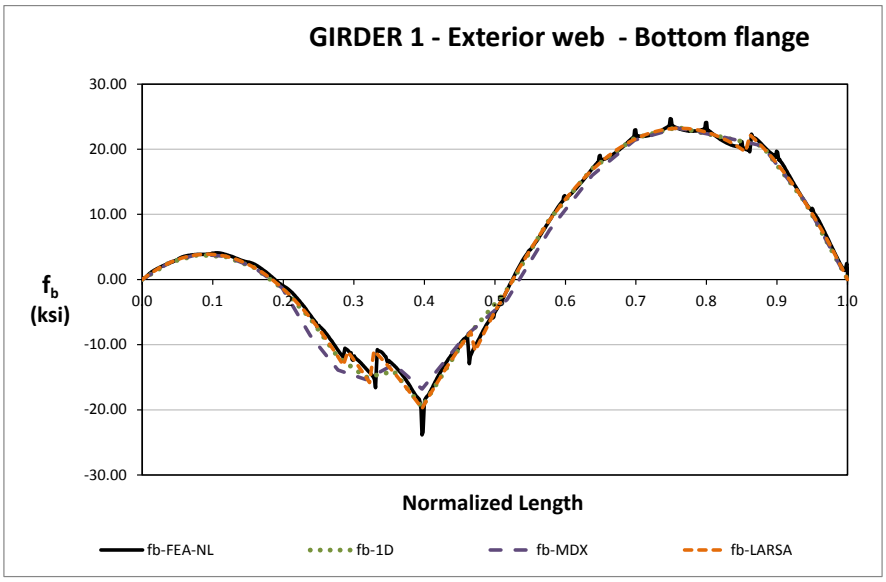

Fig. 13. Bottom flange major axis bending stress for Girder 1 exterior web – Total Dead Load

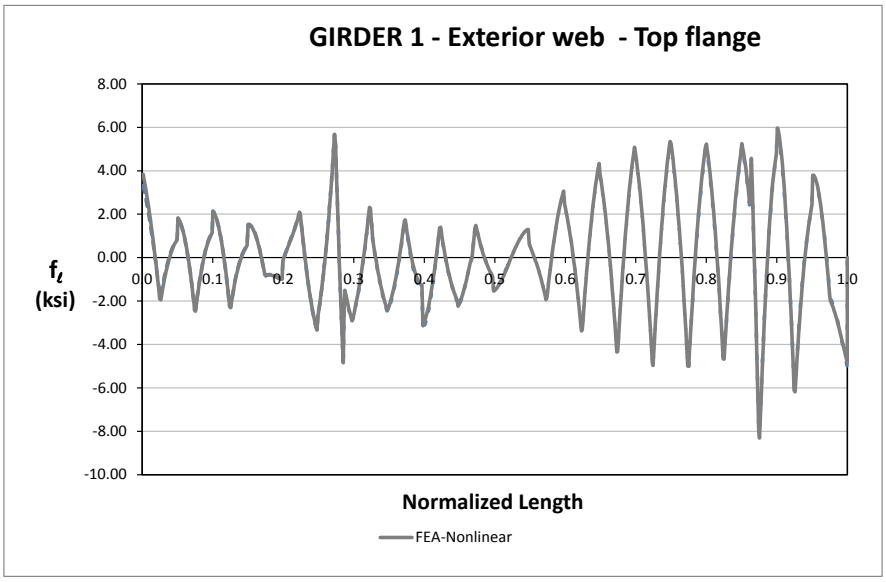

Fig. 14. Top flange lateral bending stress for Girder 1 exterior web - Total Dead Load

Top Flange Lateral Bracing Results

The TFLB Diagonals axial forces are shown in Figure 15. The forces in these elements are proportional to the torsional forces according to Fan and Helwig (1999) developments. At the intermediate support the forces reach a maximum but no rotational restraint is provided at these points to be able to generate a large torsional moment.

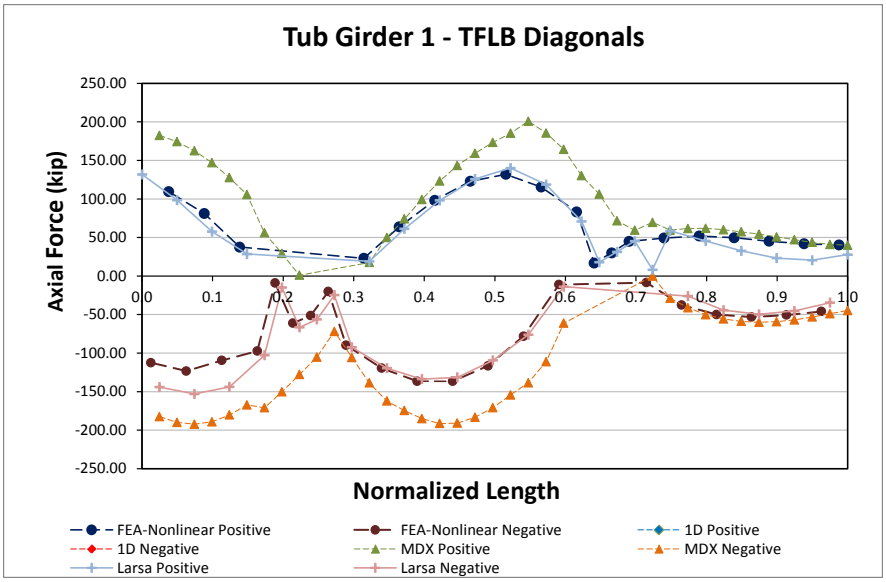

Fig. 15. Top flange lateral bracing diagonals axial forces for Girder 1 - Total Dead Load

The TFLB struts axial forces are shown in Figure 16 for the different analyses. The prediction of the behavior is accurate for the 1D and 2D-Larsa methods, 2D-MDX procedure needs a sign change at the second third of the bridge for a closer prediction. The shape of the force distribution along the length confirms the relationship with the top flange bending stresses in the bridge. The cross sectional area of both diagonals and struts is 5.6in² which results in a maximum stress value for the diagonals of 25ksi.

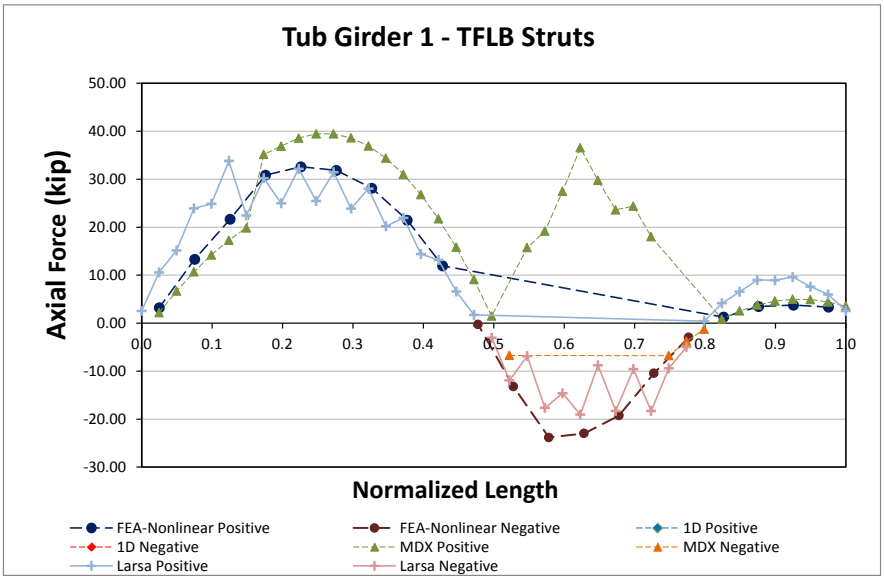

Fig. 16. Internal CF top chord and TFLB struts axial forces for Girder 1 - Total Dead Load

The 1D and 2D analyses use the M/R method to estimate the girder torsional design forces. In the case of the TFLB diagonals, the design forces major contributor is the girder torsional moment so when the forces from M/R method are close in magnitude and distribution to the 3DFEA method it can be inferred that the intermediate skewed support is not contributing to the overall girder torsional moments which suggests that the external diaphragms are the main contributors of the girder torques.

Internal Cross Frame Results

Internal cross frames alternate in every other panel, these elements are composed by diagonals and top chords. Figure 17 shows the internal CF diagonal. The cross sectional area of the diagonal is 2.5in² resulting in a maximum axial stress of 13ksi. Internal CF diagonals are mainly dependent on the M/R torsional forces according to Fan and Helwig (1999).

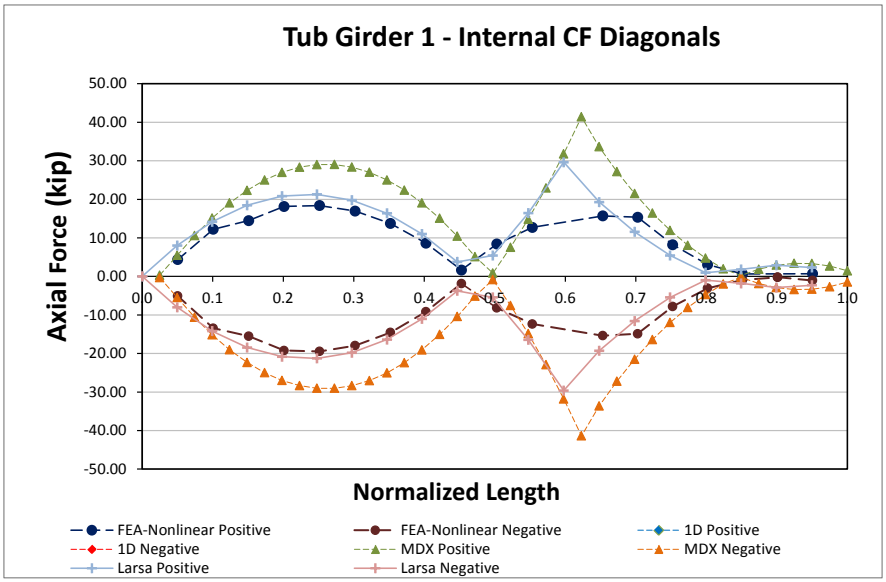

Fig. 17. Internal cross frame diagonals axial forces for Girder 1 - Total Dead Load

13.3 NTCCS22 (New, Tub-girder, Continuous-span, Curved, Skewed supports)

Bridge Description:

Category Data:

L_1 = 250 ft, L_2 = 250 ft / R = 713 ft / w = 30 ft / θ_1 =20.1°, θ_2 =0°, θ_3 =0°, 2 tub-girders

Erection Stages Analyzed: 6 steel erection stages

Deck Placement Sequence: One stage, deck thickness = 9.5 in

Bridge Perspective & Plan Views:

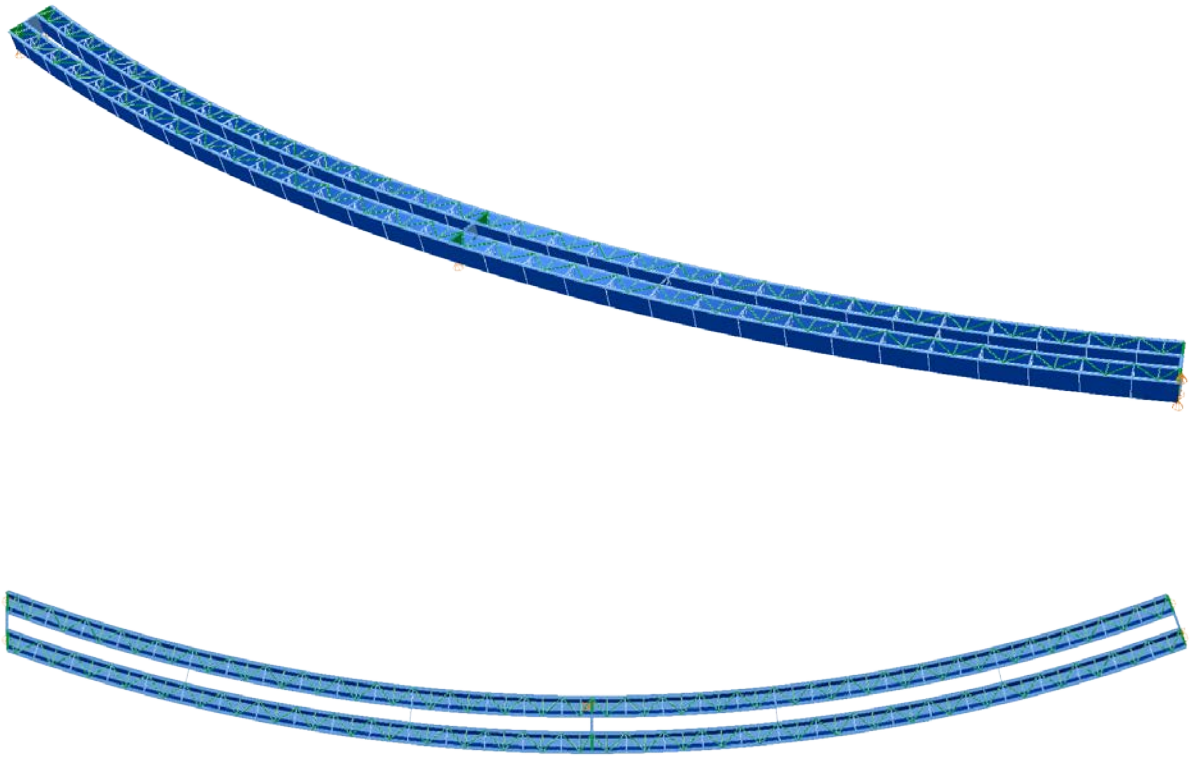

Displacement Results

Figure 1 illustrates the steel erection stages. The erection plan considers six erection stages, for the first four stages temporal supports are used.

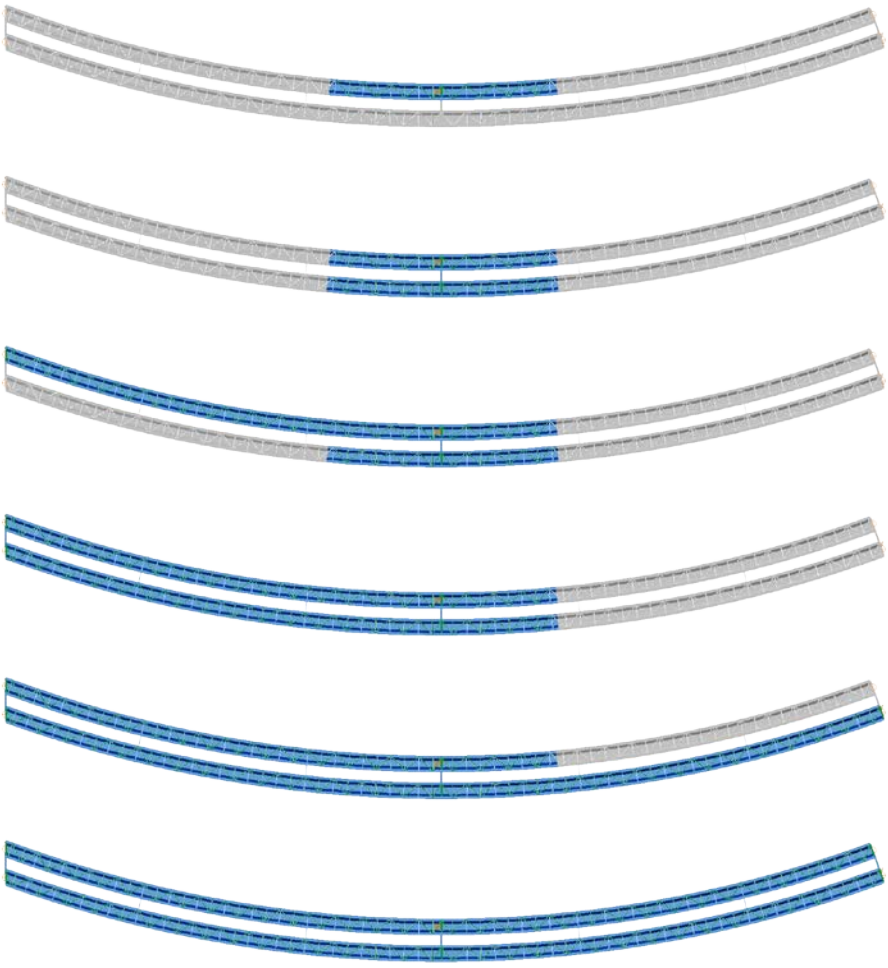

Fig. 1. Intermediate steel erection stages

Figures 2 through 6 show the evolution of the vertical displacements for the partial steel erection stages 4, 5 and 6, final steel and total non-composite dead loads. For the partial stages the vertical displacements are plotted only for 3D FEA and 2D LARSA, all methods are shown for the final steel and total non-composite dead loads.

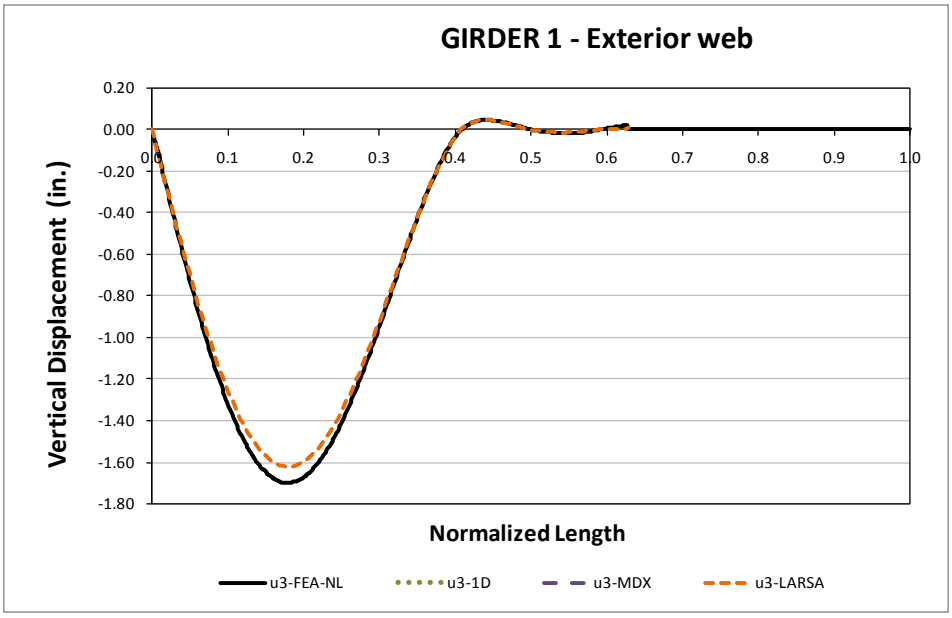

Fig. 2. Top flange vertical displacements for Girder 1 exterior web - Stage 4 Steel Dead Load

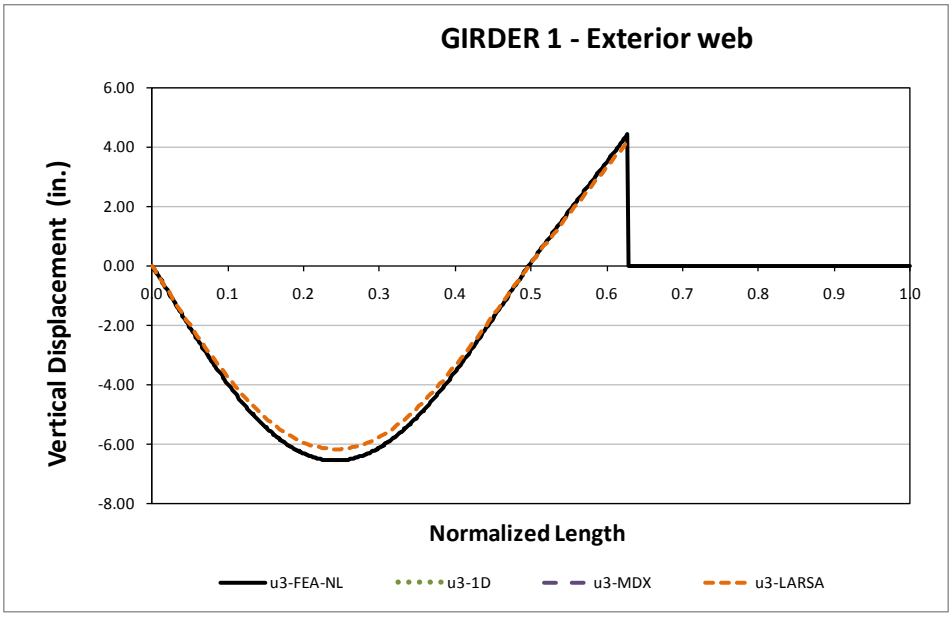

Fig. 3. Top flange vertical displacements for Girder 1 exterior web - Stage 5 Steel Dead Load

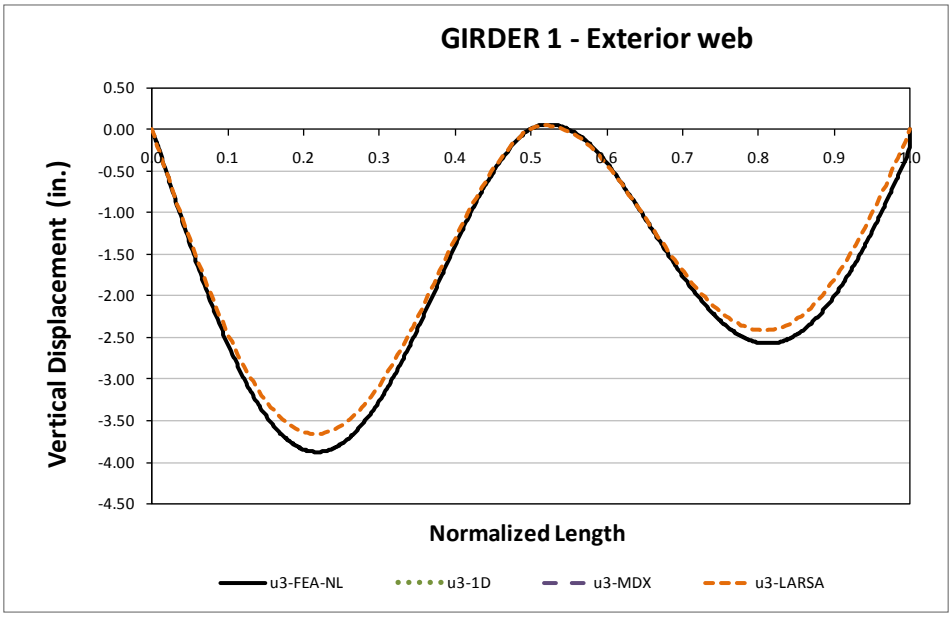

Fig. 4. Top flange vertical displacements for Girder 1 exterior web - Stage 6 Steel Dead Load

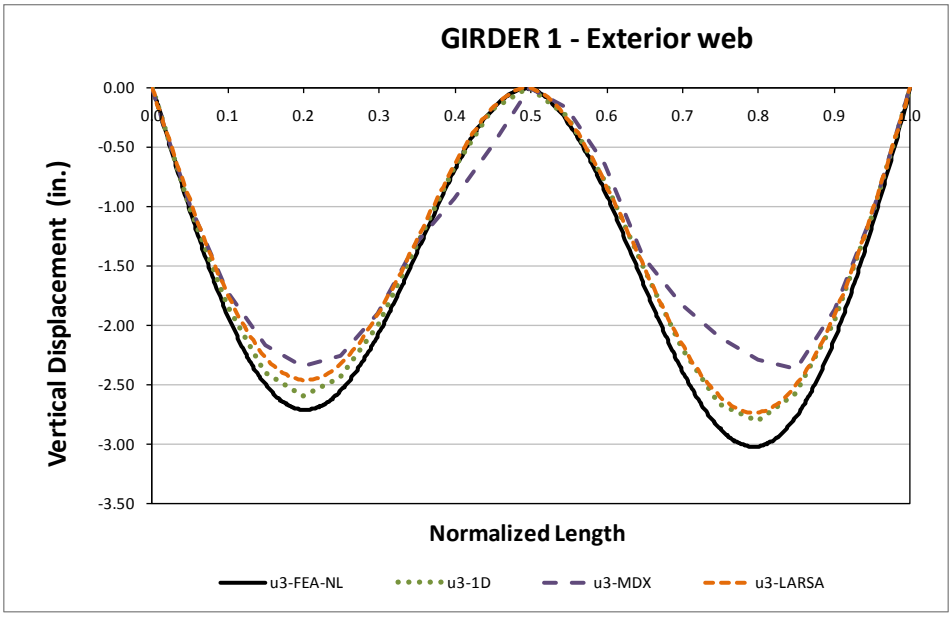

Fig. 5. Top flange vertical displacements for Girder 1 exterior web - Final Steel Dead Load

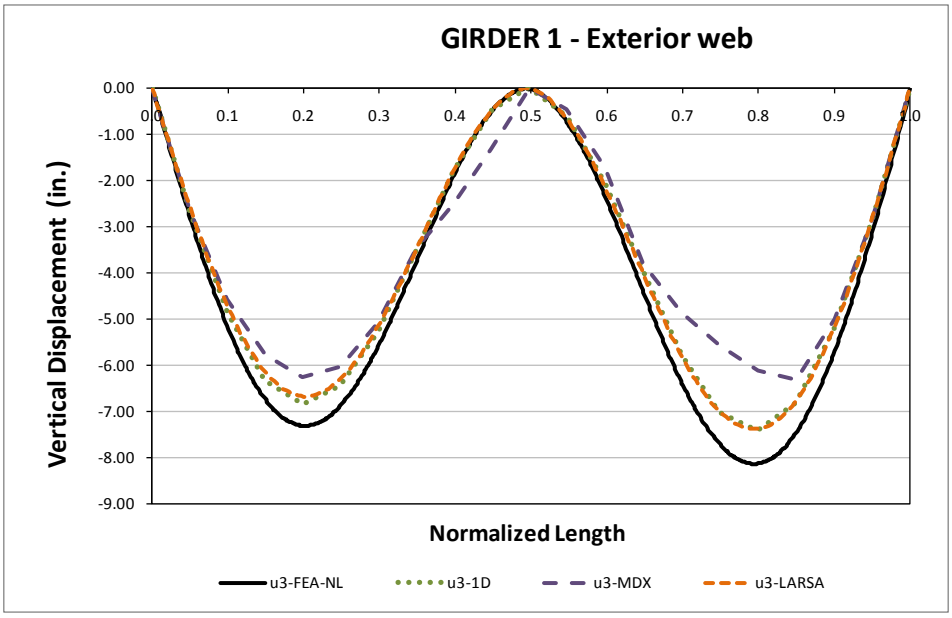

Fig. 6. Top flange vertical displacements for Girder 1 exterior web - Total Dead Load

For the final steel and total dead load stages the results for the MDX analysis method disagree in magnitude. Figures 7 and 8 illustrate the relative radial displacement between top and bottom flange junctures as a measure of lateral displacement for the final steel and total non-composite dead loads. It can be seen that the differences in vertical displacements shown in figure 6 for the total non-composite dead load case could be caused by the cross section rotation or by the extra bending stiffness that the TFLB system gives to the girders.

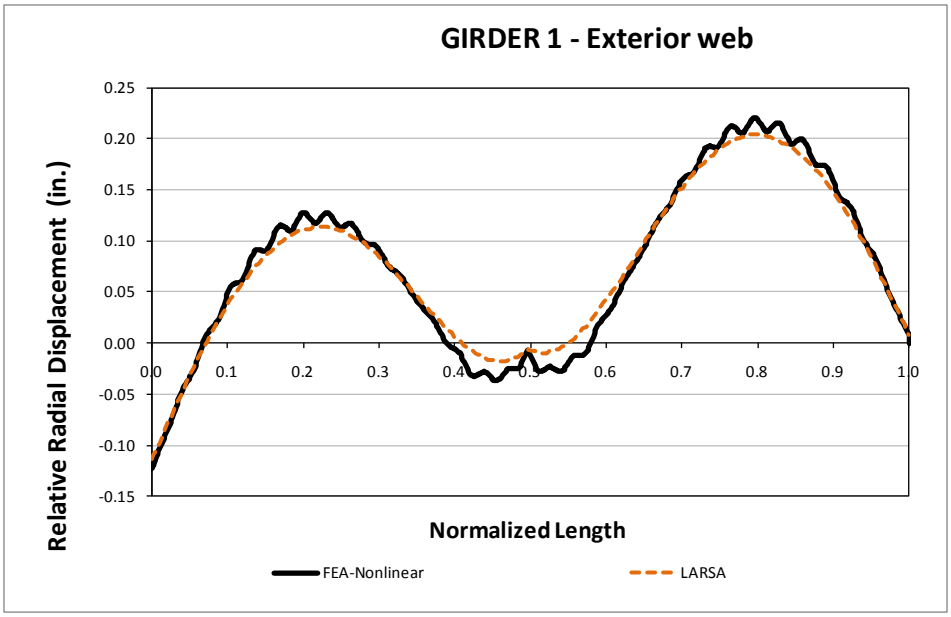

Fig. 7. Top flange relative radial displacements for Girder 1 exterior web - Final Steel Dead Load

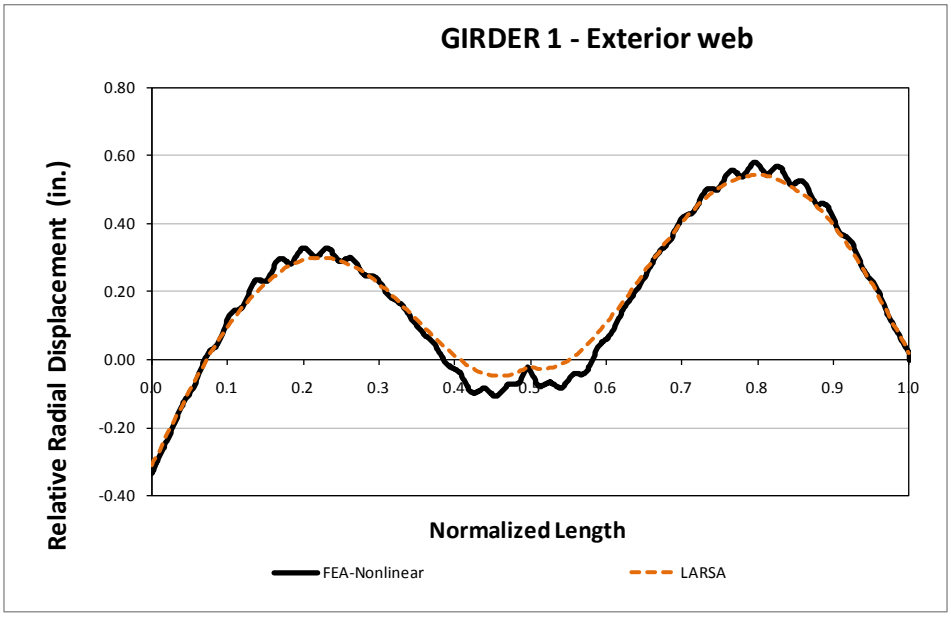

Fig. 8. Top flange relative radial displacements for Girder 1 exterior web - Total Dead Load

Bending Stress Results

Major axis bending stresses are presented in Figures 9 through 13 as predicted by different analysis methods for partial steel erection, final steel and total dead load stages. Results in general show a good

agreement in shape and magnitude. The local interaction of the TFLB system is again evident in all stages.

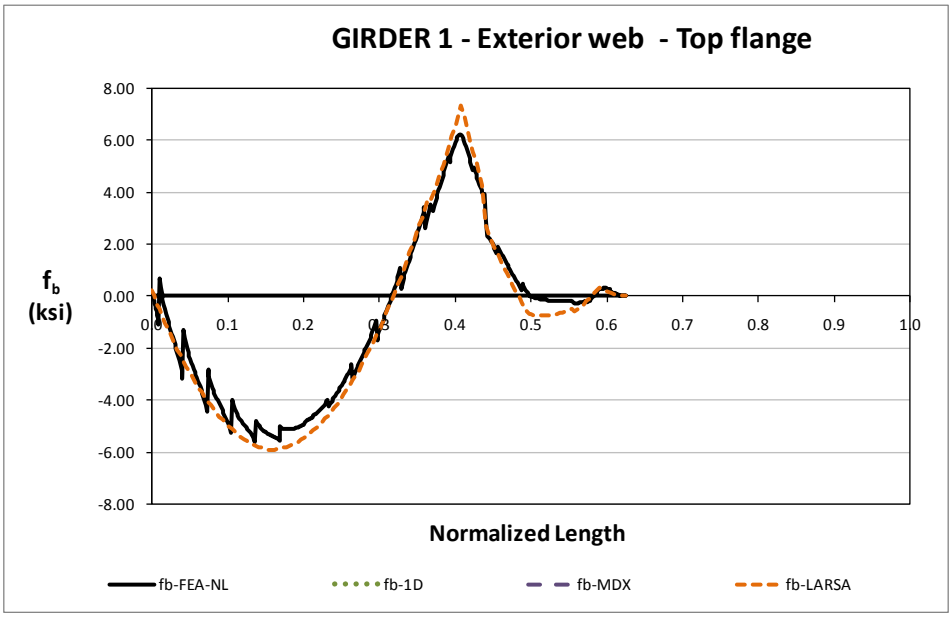

Fig. 9. Top flange major axis bending stress for Girder 1 exterior web - Stage 4 Steel Dead Load

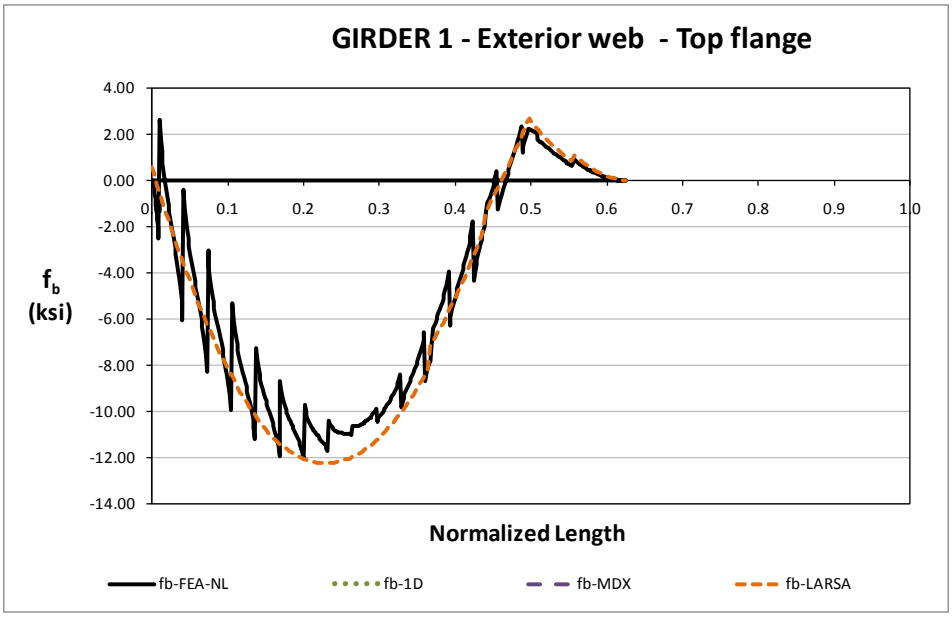

Fig. 10. Top flange major axis bending stress for Girder 1 exterior web - Stage 5 Steel Dead Load

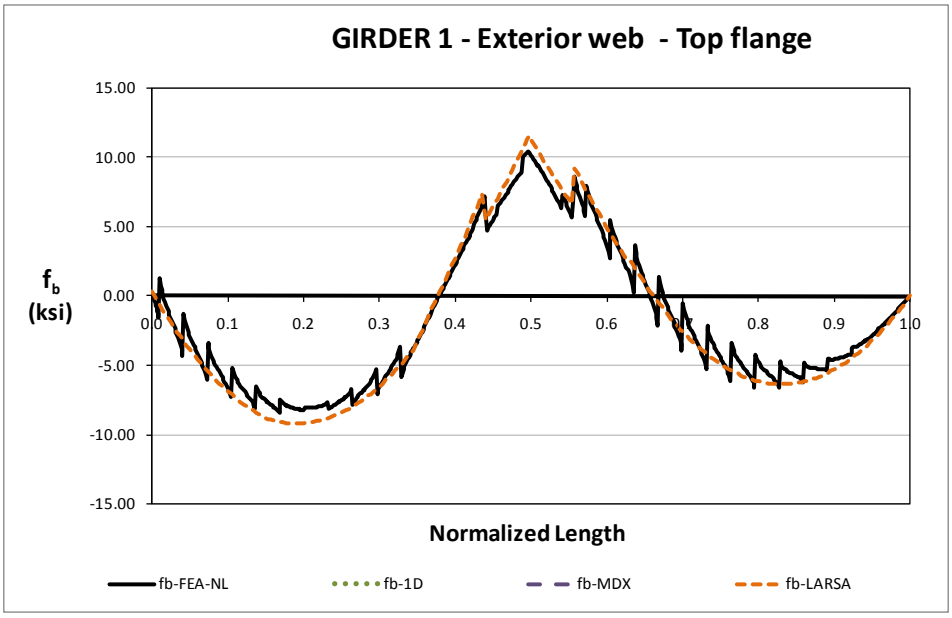

Fig. 11. Top flange major axis bending stress for Girder 1 exterior web - Stage 6 Steel Dead Load

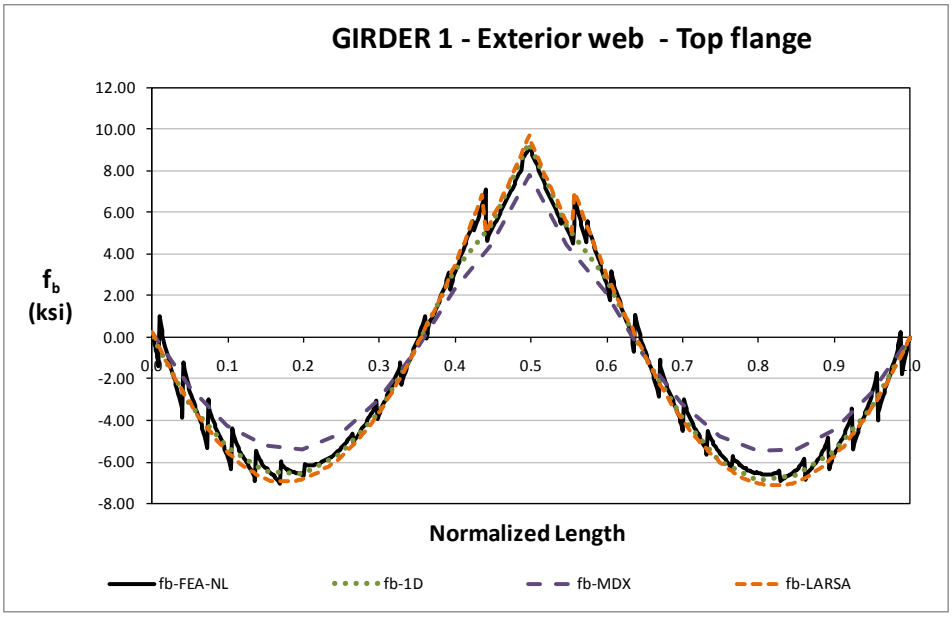

Fig. 12. Top flange major axis bending stress for Girder 1 exterior web - Final Steel Dead Load

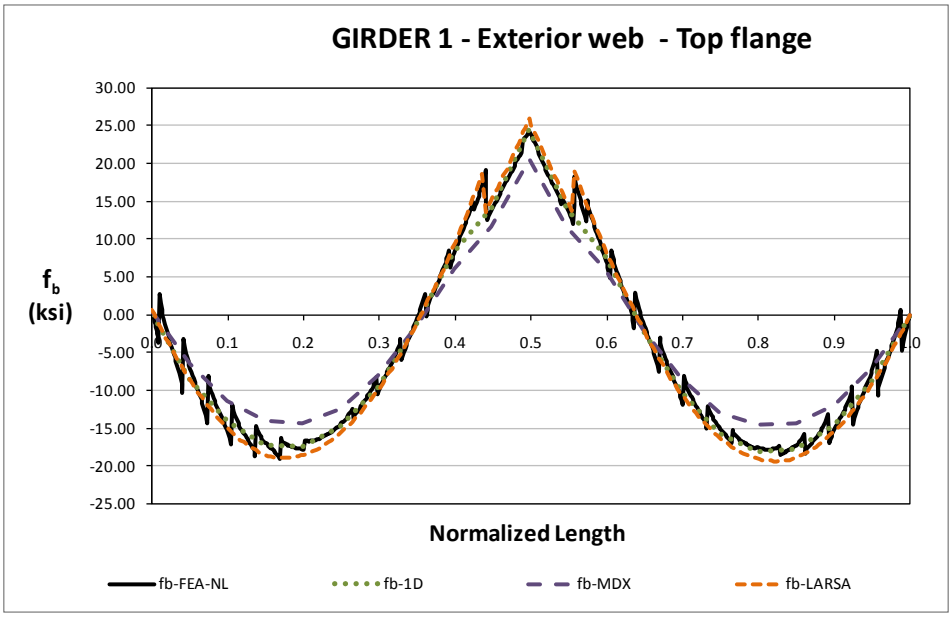

Fig. 13. Top flange major axis bending stress for Girder 1 exterior web - Total Dead Load

Figures 14 and 15 illustrate the bottom flange stresses at the web bottom flange juncture for the final steel and total dead load cases. In the bottom flange there are small local variations, these are caused by the internal CF elements.

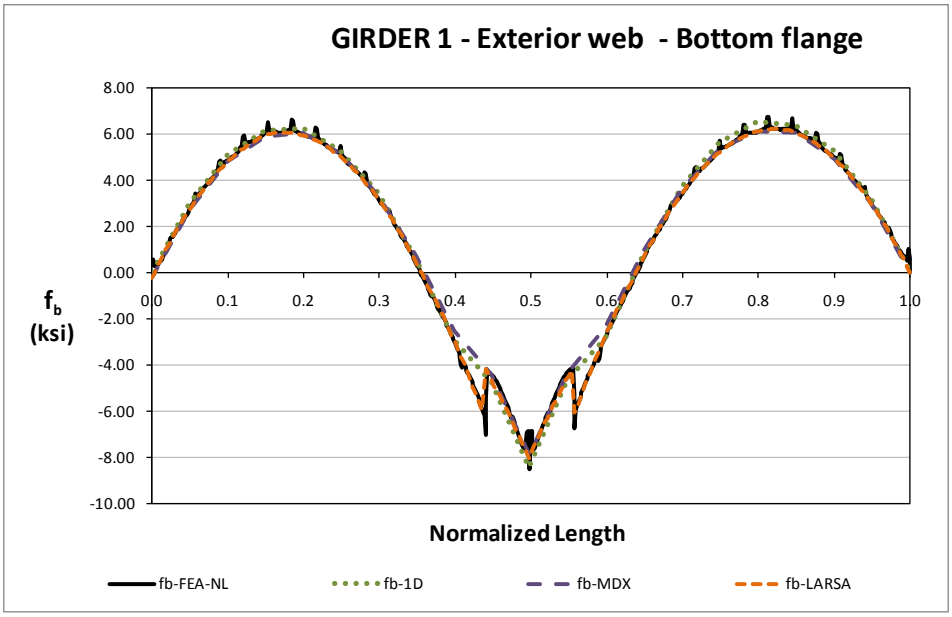

Fig. 14. Bottom flange major axis bending stress for Girder 1 exterior web - Final Steel Dead Load

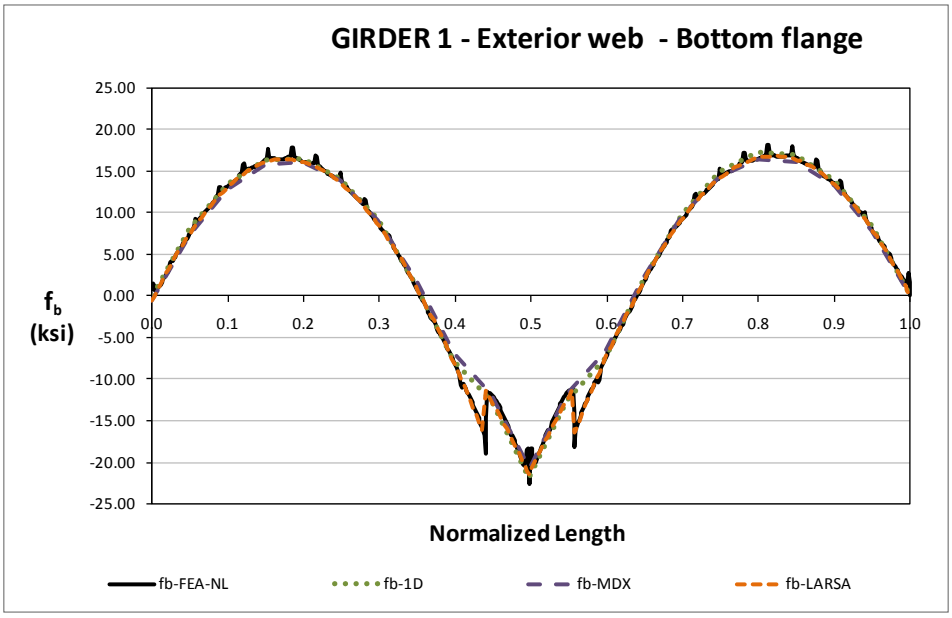

Fig. 15. Bottom flange major axis bending stress for Girder 1 exterior web - Total Dead Load

Lateral bending stress distributions are shown in figure 16, the stresses values remain low in contrast as with the major axis bending stresses reported above.

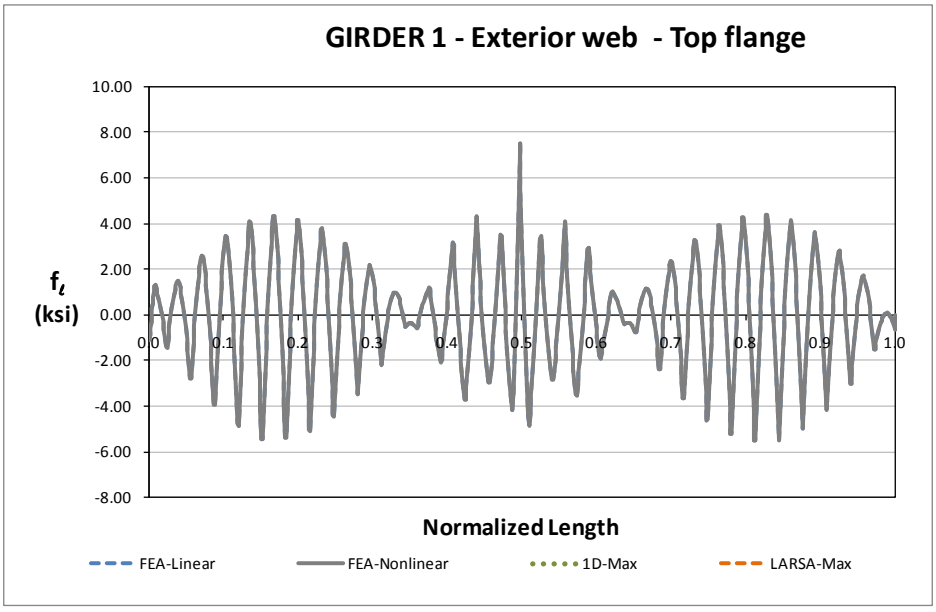

Fig. 16. Top flange lateral bending stress for Girder 1 exterior web - Total Dead Load

Top Flange Lateral Bracing Results

The TFLB diagonals axial forces are shown in Figures 17 through 18 for the final steel and total dead load condition. The cross sectional area of these elements is 21.1in² that for a maximum axial force of 150kip as reported by the 3DFEA the element experiences an axial stress of 7.1ksi on the total dead load conditions.

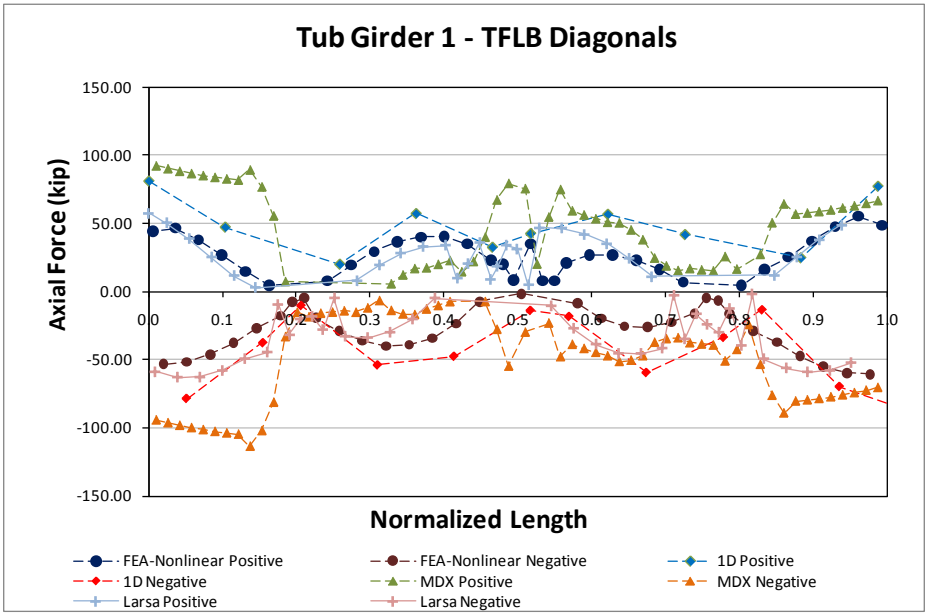

Fig. 17. Top flange lateral bracing diagonals axial forces for Girder 1 - Final Steel Dead Load

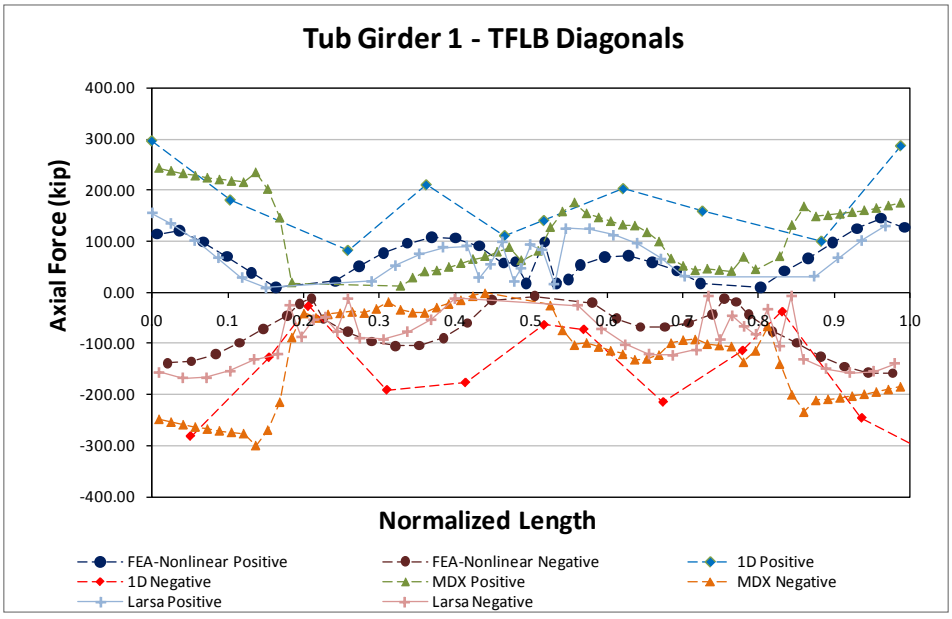

Fig. 18. Top flange lateral bracing struts axial forces for Girder 1 - Total Dead Load

Figure 19 shows the TFLB axial forces on the struts for the total non-composite deal load case. The area of the struts is 4.4in² which, for a maximum axial force of 25kip as reported by the 3DFEA analysis, results on maximum axial stress of 5.6ksi. The 3DFEA reports lower values, partly because the model accommodates girder rotations which release the elements from forces.

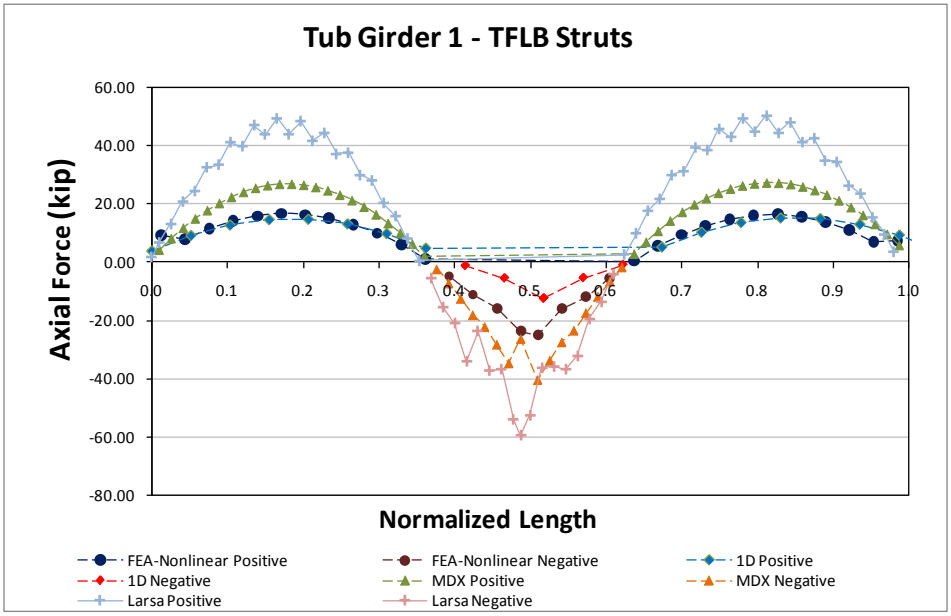

Fig. 19. Top flange lateral bracing struts axial forces for Girder 1 - Total Dead Load

Internal Cross Frame Results

Figure 20 shows the internal CF diagonal axial forces with cross sectional area of 4.4in² which for a maximum value predicted by the 3DFEA of 25kip the maximum stress is close to 6ksi. In the intermediate support a reduction of the 3DFEA predicted forces is noticeable and it can be attributed to the forces taken by the solid plate diaphragms at this position.

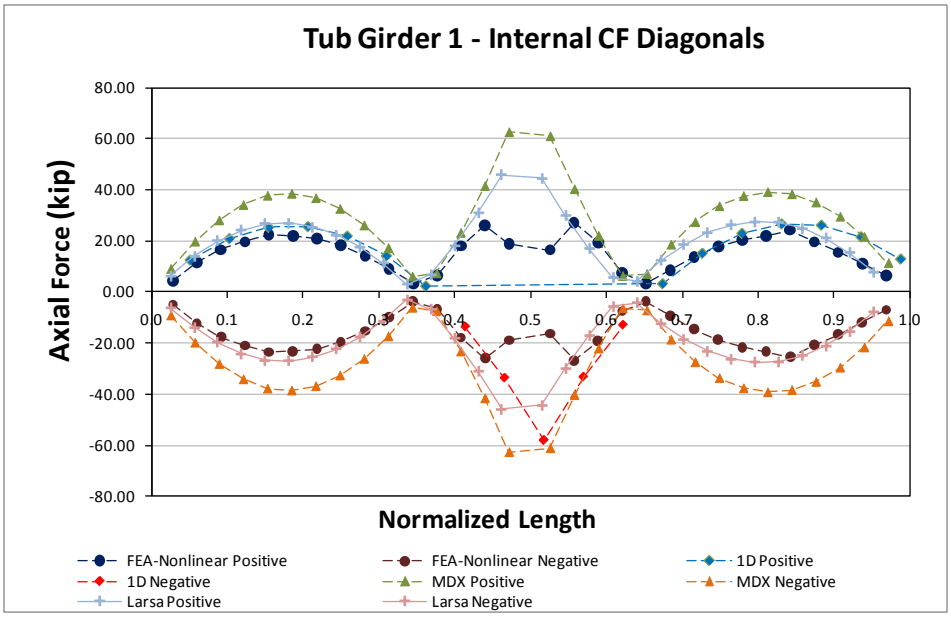

Fig. 20. Internal cross-frames diagonals axial forces for Girder 1 - Total Dead Load

NCHRP 12-79

BRIDGE DRAWINGS

(Drawings in this Appendix are in alphabetical order)

NCHRP 12-79

EICCR4

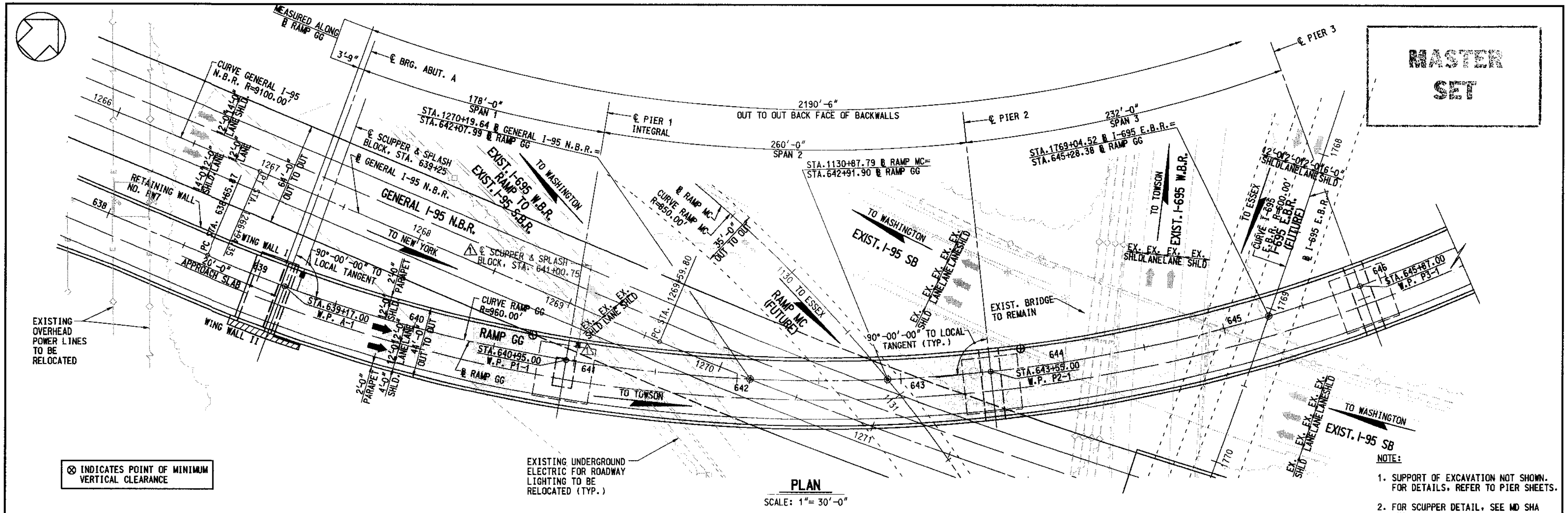

⊗ INDICATES POINT OF MINIMUM VERTICAL CLEARANCE

PLAN

SCALE: 1"= 30'-0"

NOTE:

1. SUPPORT OF EXCAVATION NOT SHOWN. FOR DETAILS, REFER TO PIER SHEETS.
2. FOR SCUPPER DETAIL, SEE MD SHA DETAIL BR-SS(0.04)-81-130.
3. FOR SPLASH BLOCK DETAIL, SEE MD SHA DETAIL NO. M(6.04)-80-119.

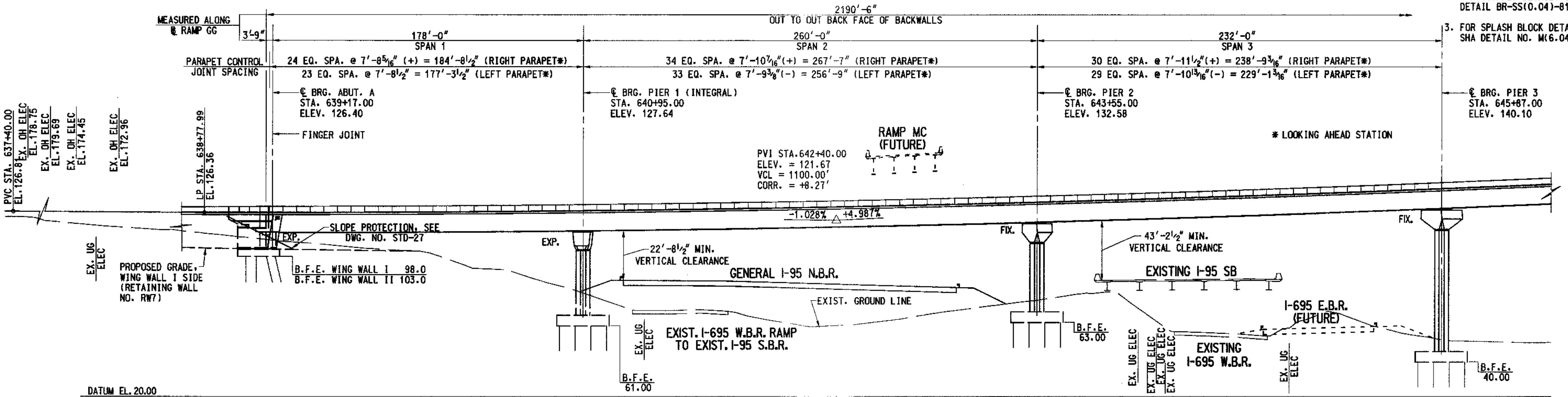

ELEVATION

SCALE: 1"= 30'-0"

JMT
JOHNSON, MIRMIRAN & THOMPSON
Engineering A Brighter Future

MARYLAND TRANSPORTATION AUTHORITY
Engineering Division

ADDENDUMS & REVISIONS

NO.	DESCRIPTION	BY	DATE
1	PIER 1 SCUPPER LOCATION REVISED	MJB	9/12/06

I-95 EXPRESS TOLL LANES : I-695 INTERCHANGE
GENERAL PURPOSE ROADWAYS AND RAMPS
JOHN F. KENNEDY MEMORIAL HIGHWAY (BALTIMORE COUNTY)
RAMP GG
GENERAL PLAN & ELEVATION I

DESIGNED BY KRM	DRAWN BY RLD	CHECKED BY MJB
CONST. REVIEW BY	DATE AUGUST, 2006	SCALE AS SHOWN

CONTRACT NO. KH-1301-000-006
DRAWING NO. S6 - 2
SHEET NO. 639 OF 1676

FILE: q:\emd\304004_I195I695_hw\cadd\struct\Ramp_GG\GG-GPE1.dgn
DATE: 9/14/2006
TIME: 1:51:58 PM

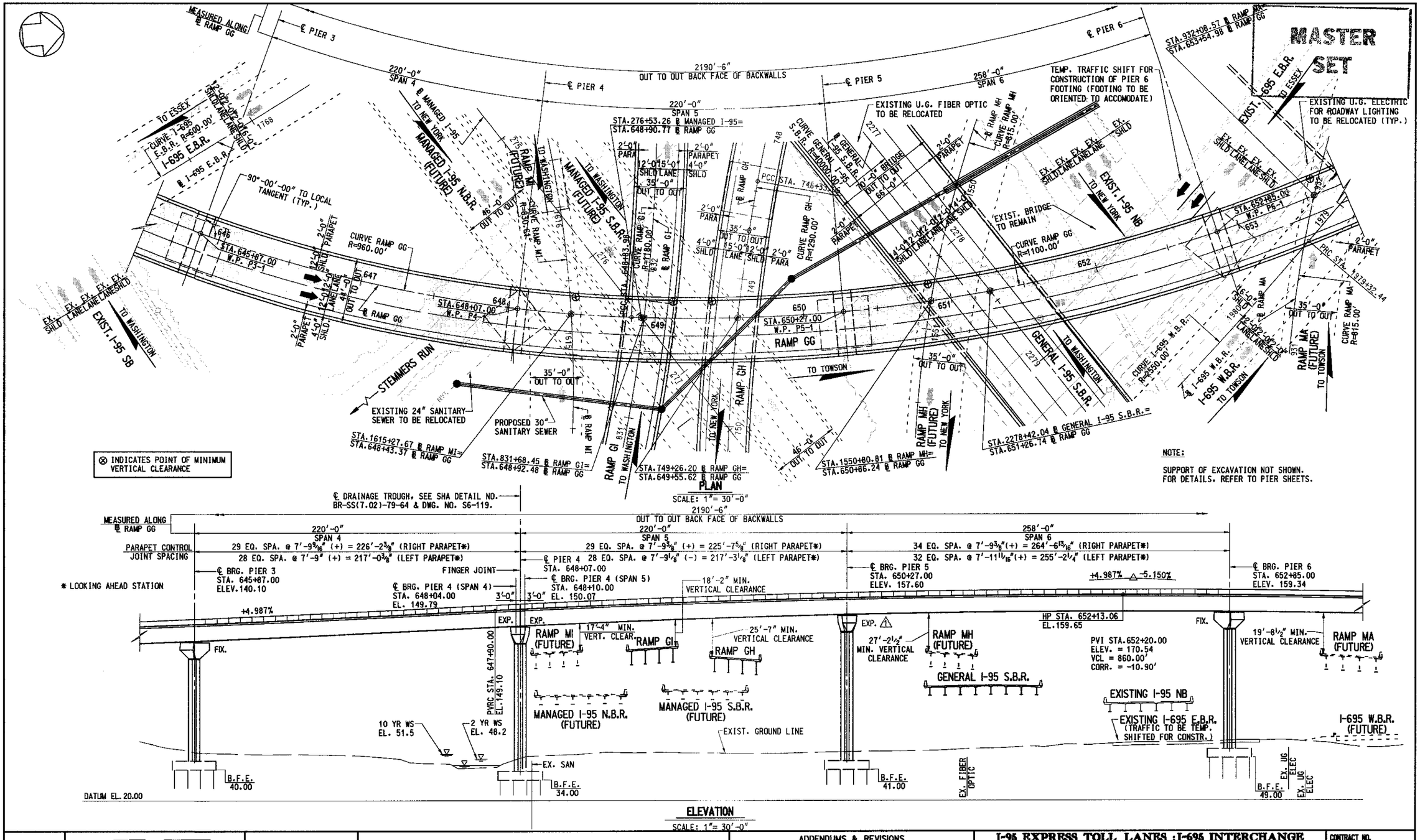

ADDENDUMS & REVISIONS			
NO.	DESCRIPTION	BY	DATE
1	CHANGED PIER 5 BEARING DESIGNATION	MJB	9/12/06

JOHNSON, MIRMIRAN & THOMPSON
Engineering A Brighter Future

MARYLAND TRANSPORTATION AUTHORITY
Engineering Division

I-95 EXPRESS TOLL LANES : I-695 INTERCHANGE GENERAL PURPOSE ROADWAYS AND RAMPS

JOHN F. KENNEDY MEMORIAL HIGHWAY (BALTIMORE COUNTY)

RAMP GG

GENERAL PLAN & ELEVATION II

DESIGNED BY KRM	DRAWN BY RLD	CHECKED BY MJB
CONST. REVIEW BY	DATE AUGUST, 2006	SCALE AS SHOWN

CONTRACT NO. KH-1301-000-006

DRAWING NO. S6 - 3

SHEET NO. 700 OF 1676

FILE: q:\smd\304004.11\956195.hw\roadd\struct\Ramp_GG\GG-GPE2.dgn
DATE: 9/14/2006
TIME: 1:16:02 PM

MASTER SET

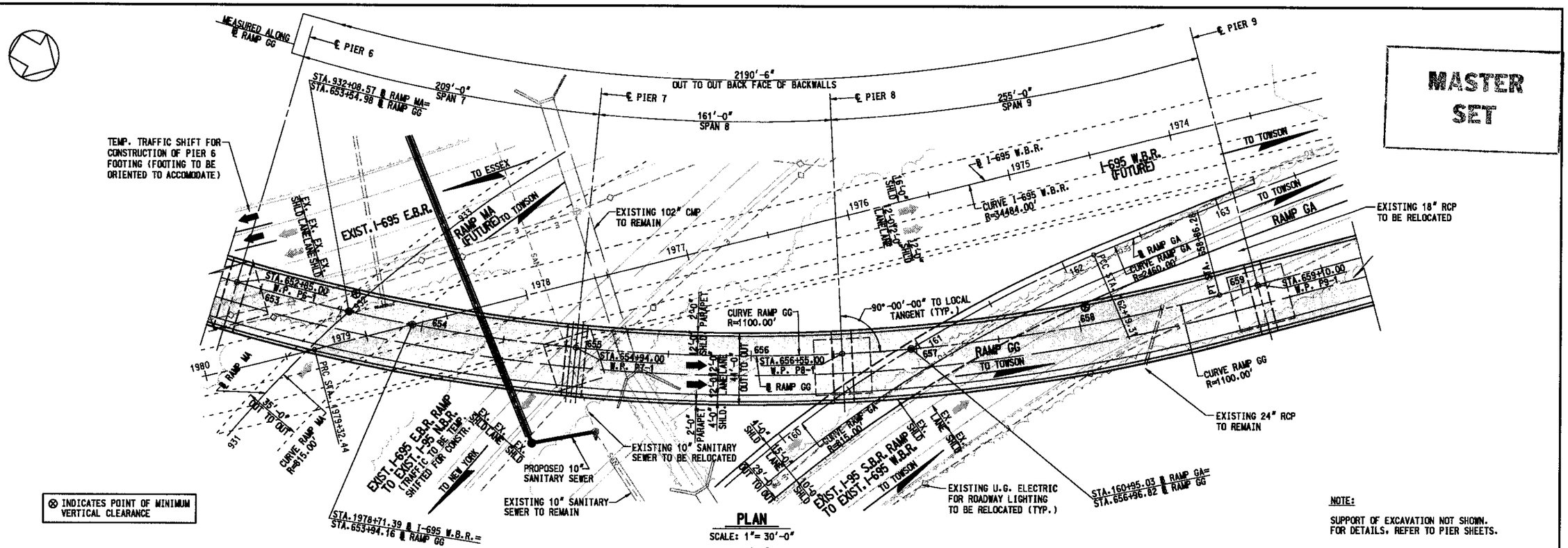

PLAN
SCALE: 1"= 30'-0"

NOTE:
SUPPORT OF EXCAVATION NOT SHOWN. FOR DETAILS, REFER TO PIER SHEETS.

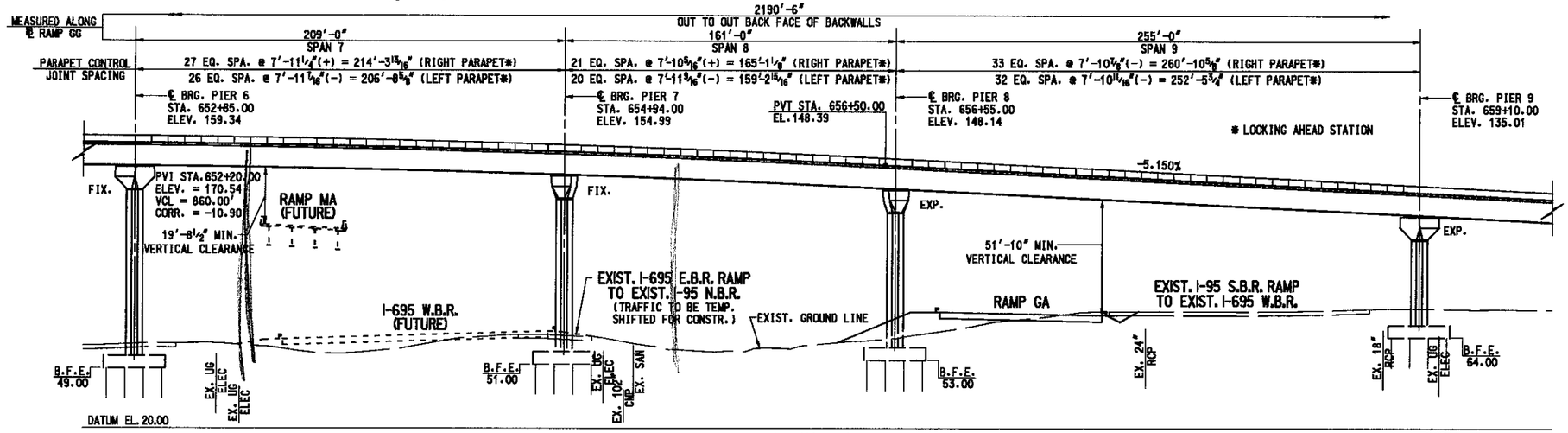

ELEVATION
SCALE: 1"= 30'-0"

JOHNSON, MIRMIRAN & THOMPSON
Engineering A Brighter Future

MARYLAND TRANSPORTATION AUTHORITY
Engineering Division

ADDENDUMS & REVISIONS

NO.	DESCRIPTION	BY	DATE

I-95 EXPRESS TOLL LANES : I-695 INTERCHANGE
GENERAL PURPOSE ROADWAYS AND RAMPS
JOHN F. KENNEDY MEMORIAL HIGHWAY (BALTIMORE COUNTY)
RAMP GG
GENERAL PLAN & ELEVATION III

DESIGNED BY KRM	DRAWN BY RLD	CHECKED BY MJB
CONST. REVIEW BY	DATE AUGUST, 2006	SCALE AS SHOWN

CONTRACT NO. KH-1301-000-006
DRAWING NO. S6 - 4
SHEET NO. 701 OF 1676

FILE: g:\smd\304004_II\95\695_hw\roads\struct\Ramp_GG\GG-GPE3.dgn
DATE: 8/4/2006
TIME: 4:03:55 AM

MASTER SET

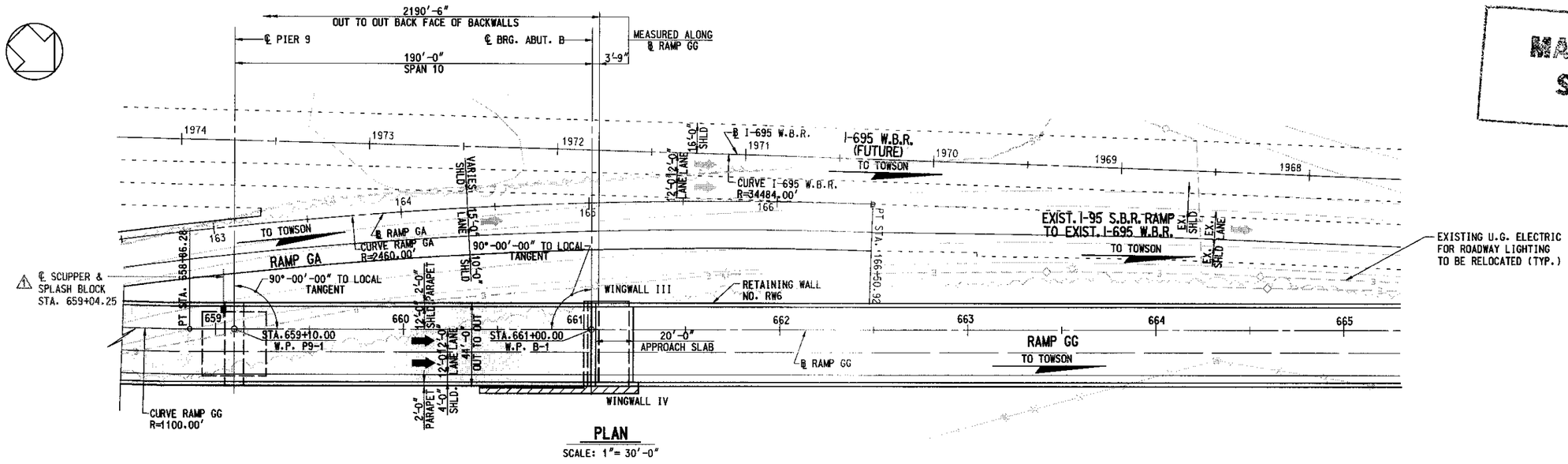

PLAN

SCALE: 1"= 30'-0"

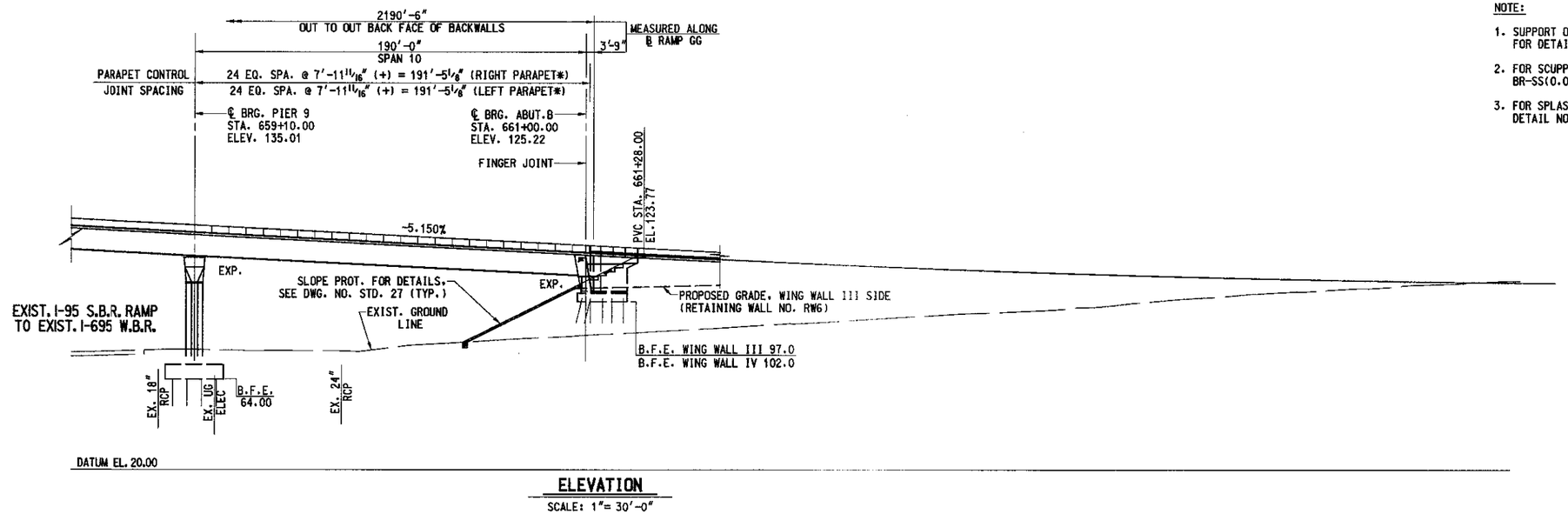

ELEVATION

SCALE: 1"= 30'-0"

NOTE:

1. SUPPORT OF EXCAVATION NOT SHOWN. FOR DETAILS, REFER TO PIER SHEETS.
2. FOR SCUPPER DETAILS, SEE MD SHA DETAIL BR-SS(0.04)-81-130.
3. FOR SPLASH BLOCK DETAIL, SEE MD SHA DETAIL NO. M(6.04)-80-119.

JOHNSON, MIRMIRAN & THOMPSON
Engineering A Brighter Future

MARYLAND TRANSPORTATION AUTHORITY
Engineering Division

ADDENDUMS & REVISIONS			
NO.	DESCRIPTION	BY	DATE
1	PIER 9 SCUPPER LOCATION REVISED	MJB	9/12/06

I-95 EXPRESS TOLL LANES : I-695 INTERCHANGE
GENERAL PURPOSE ROADWAYS AND RAMPS
JOHN F. KENNEDY MEMORIAL HIGHWAY (BALTIMORE COUNTY)
RAMP GG
GENERAL PLAN & ELEVATION IV

DESIGNED BY KRM	DRAWN BY RLD	CHECKED BY MJB
CONST. REVIEW BY	DATE AUGUST, 2006	SCALE AS SHOWN

CONTRACT NO. KH-1301-000-006
DRAWING NO. S6 - 5
SHEET NO. 702 OF 1676

FILE: q:\smd\304004_III95I695_hw\coadd\struct\Ramp_GG\GG-GPE4.dgn
DATE: 9/14/2006
TIME: 1:16:07 PM

MASTER
SET

ADDITIONAL LONGITUDINAL REINFORCING STEEL IN TOP OF DECK SLAB OVER PIERS

(SEE MD SHA DETAIL NO. BR-SS(6.30)-88-195 FOR FURTHER DETAILS)

LOCATION	L' (BACK STATIONING SPAN)	L (AHEAD STATIONING SPAN)	BAR SIZE *
PIER 1	64'-0"	55'-0"	
PIER 2	55'-0"	65'-0"	
PIER 3	65'-0"	50'-0"	
PIER 5	66'-0"	64'-0"	
PIER 6	60'-0"	56'-0"	
PIER 7	33'-0"	88'-0"	
PIER 8	73'-0"	40'-0"	
PIER 9	63'-0"	61'-0"	

* ALL BARS TO BE #5 UNLESS OTHERWISE NOTED IN THIS COLUMN

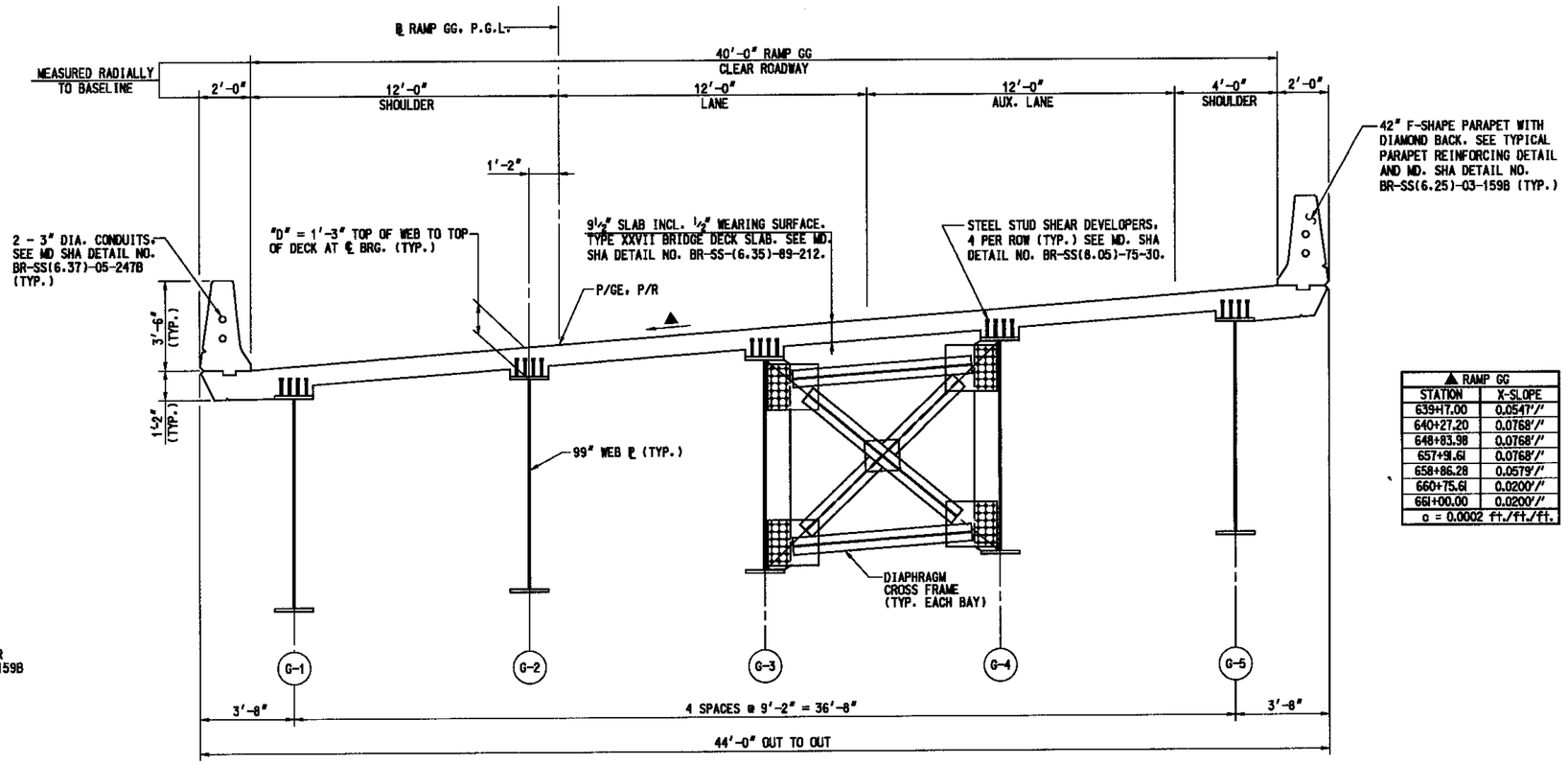

▲ RAMP GG	
STATION	X-SLOPE
639+17.00	0.0547'/'
640+27.20	0.0768'/'
648+83.98	0.0768'/'
657+91.61	0.0768'/'
658+86.28	0.0579'/'
660+75.61	0.0200'/'
661+00.00	0.0200'/'
a = 0.0002 ft./ft./ft.	

TYPICAL SECTION
SCALE: ⅜" = 1'-0"

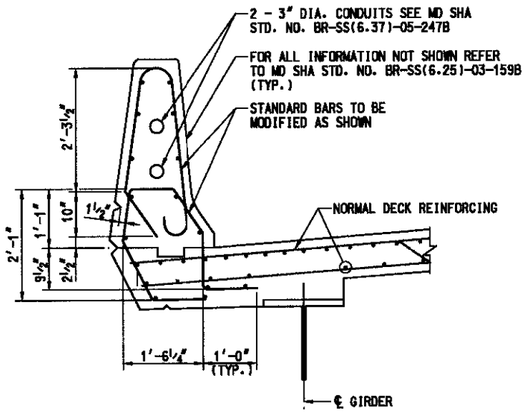

TYPICAL PARAPET REINFORCING DETAIL
SCALE: ¾" = 1'-0"

NOTES:

1. FOR DIAPHRAGM DETAILS, SEE DWG. NO. S6-105 & S6-106.
2. FOR PARAPET REVEAL DETAILS, SEE DWG. NO. STD-29.

FILE: g:\smd\304004.J1195695_hw\cadd\structure\Ramp_GG\GG-TypSect.dgn
DATE: 8/4/2006
TIME: 4:06:25 AM

JOHNSON, MIRMIRAN & THOMPSON
Engineering A Brighter Future

MARYLAND TRANSPORTATION AUTHORITY
Engineering Division

ADDENDUMS & REVISIONS			
NO.	DESCRIPTION	BY	DATE

I-95 EXPRESS TOLL LANES : I-695 INTERCHANGE
GENERAL PURPOSE ROADWAYS AND RAMPS
JOHN F. KENNEDY MEMORIAL HIGHWAY (BALTIMORE COUNTY)
RAMP GG
TYPICAL SECTION

CONTRACT NO. KH-1301-000-006
DRAWING NO. S6 - 85

DESIGNED BY TDY | DRAWN BY DJA | CHECKED BY MJB
CONST. REVIEW BY | DATE AUGUST, 2006 | SCALE AS SHOWN
SHEET NO. 782 OF 1676

MASTER SET

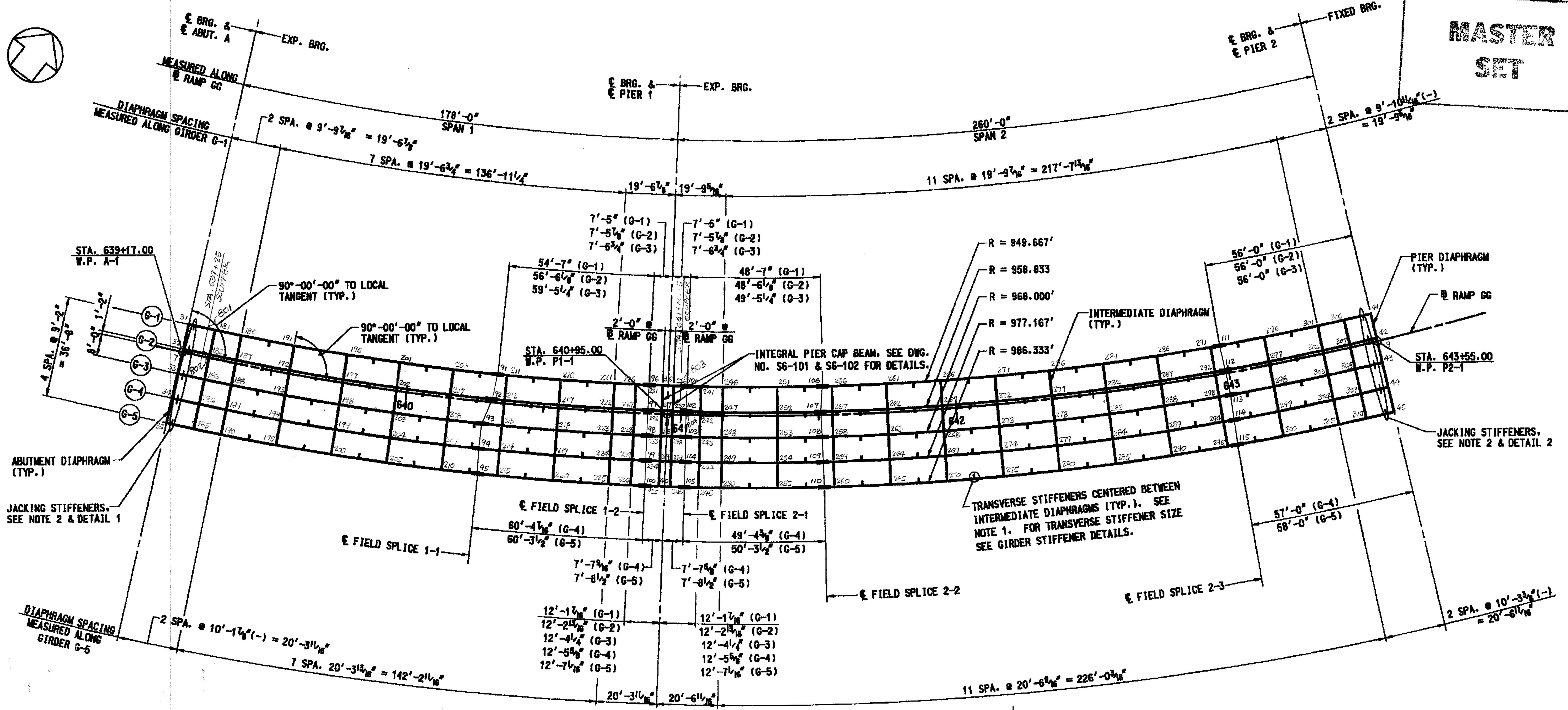

FRAMING PLAN - SPANS 1 & 2

SCALE: 1" = 20'-0"

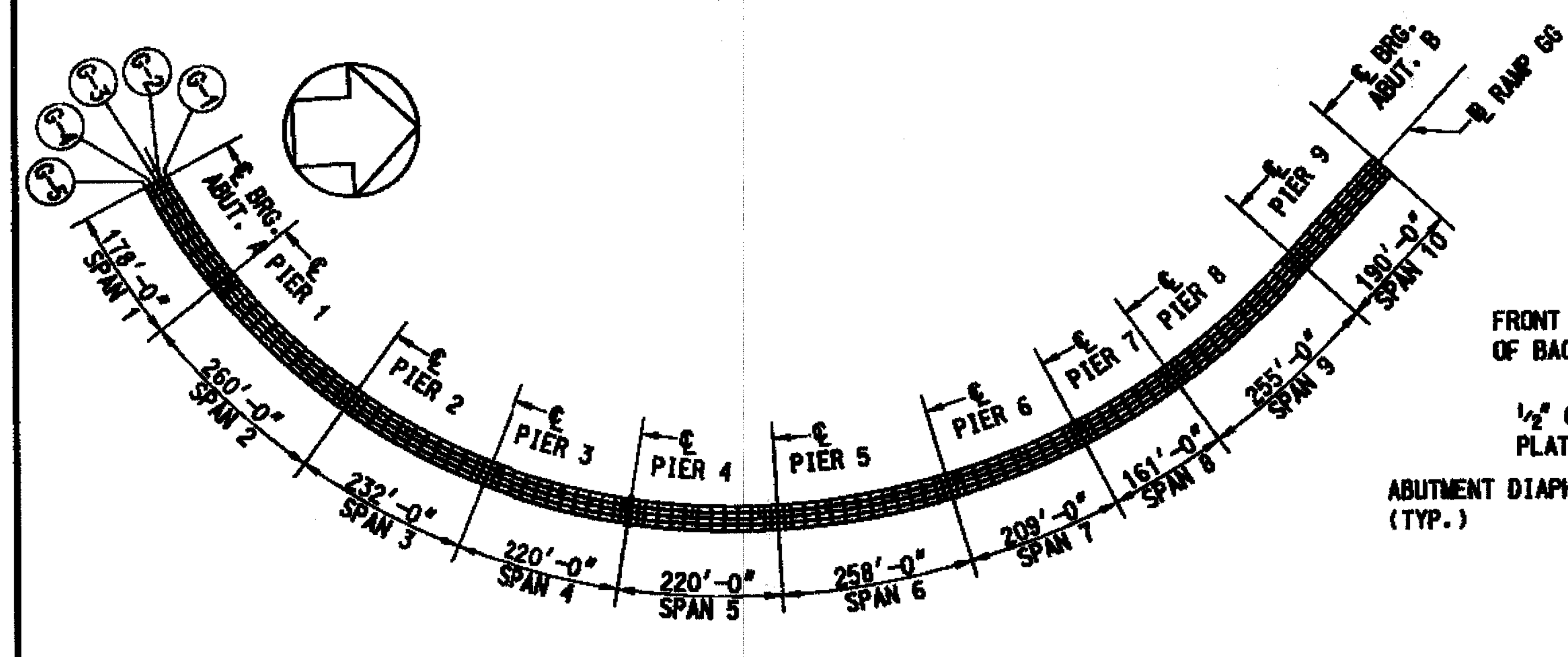

FRAMING KEY PLAN

SCALE: 1" = 200'-0"

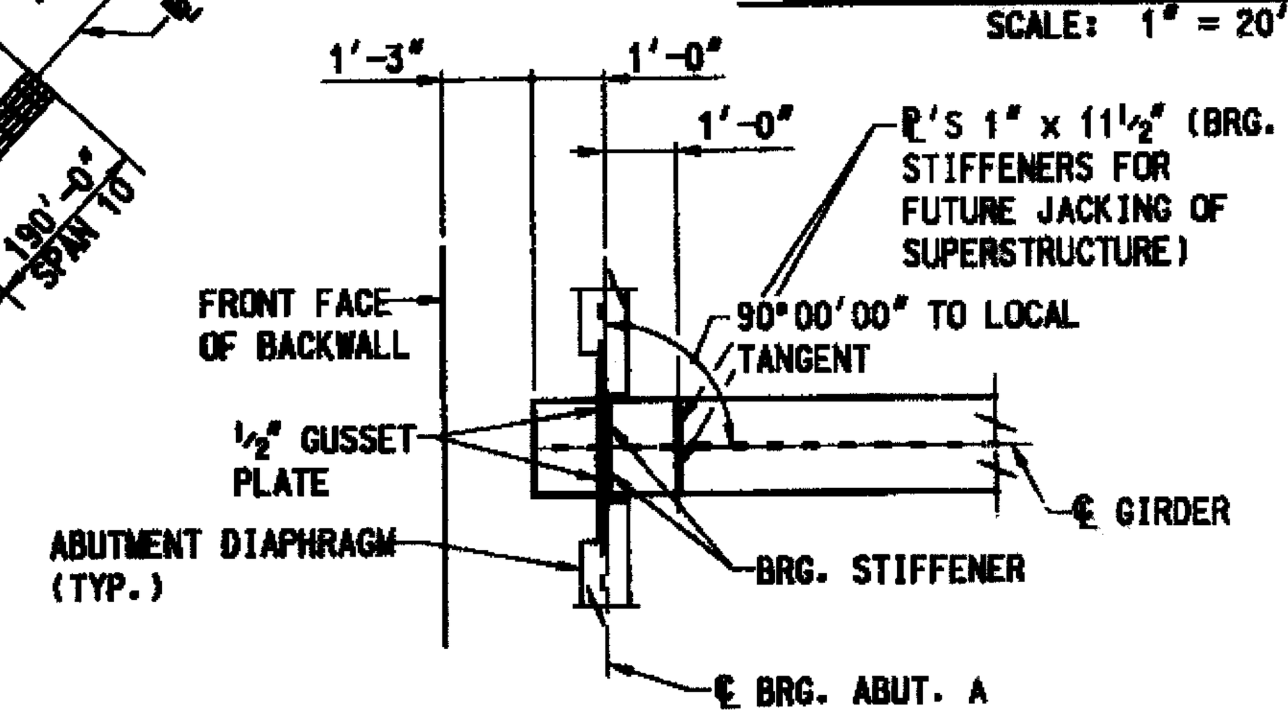

DETAIL 1

NOT TO SCALE

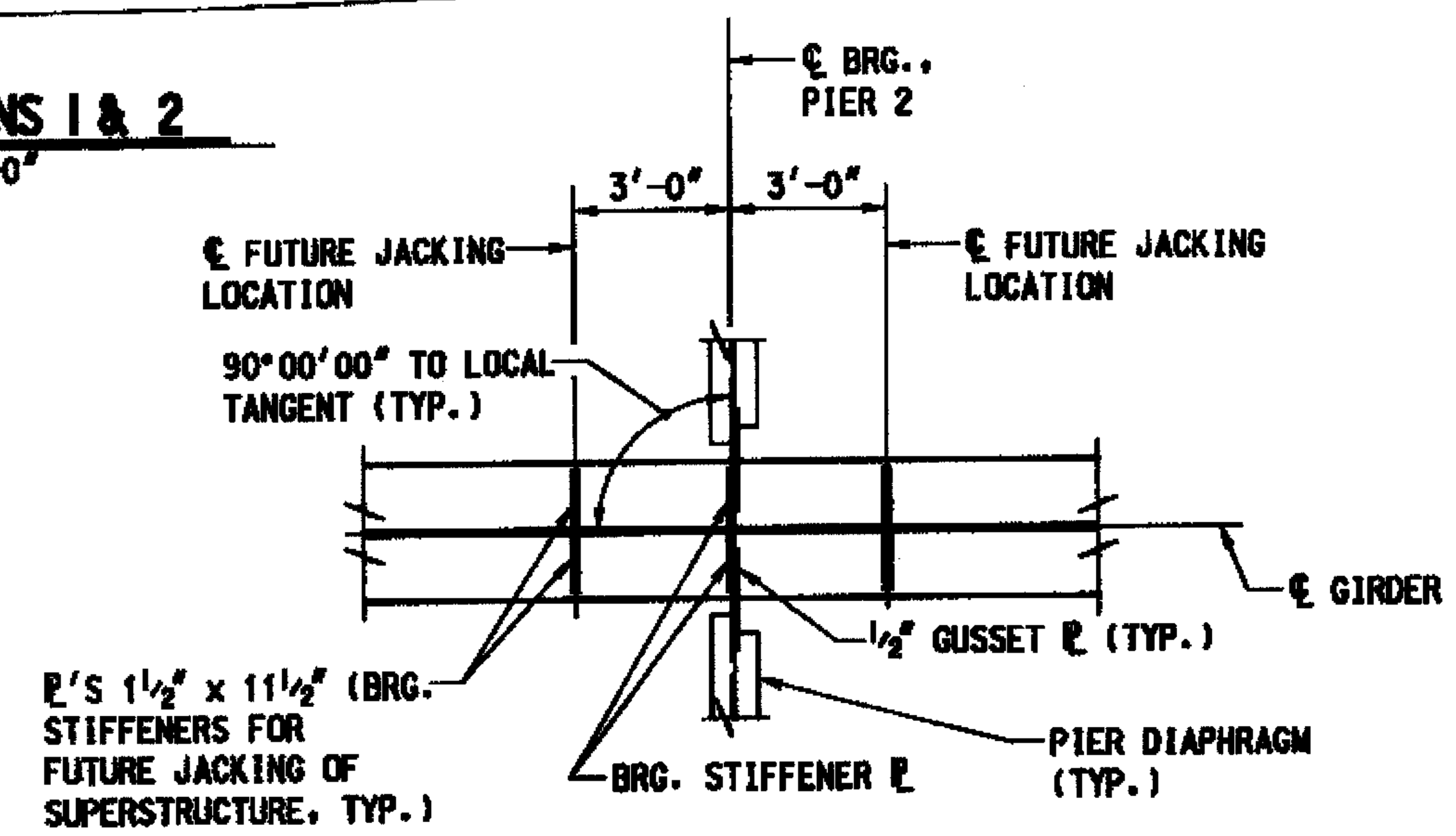

DETAIL 2

NOT TO SCALE

NOTES:

1. AT LOCATIONS WHERE TRANSVERSE STIFFENER CONFLICTS WITH FIELD SPLICE TRANSVERSE STIFFENERS SHALL BE LOCATED 1'-0" FROM EDGE OF FIELD SPLICE PLATE.

2. JACKING STIFFENERS AT ABUTMENTS AND PIER 4 LOCATED TO ACCEPT FUTURE JACKING BEAM. JACKING STIFFENERS AT ALL OTHER PIERS LOCATED TO ALLOW JACKING DIRECTLY UNDER GIRDER. SEE DETAILS 1 & 2 THIS SHEET FOR ADDITIONAL INFORMATION.

FILE: p:\amd\304004_II\951695_hw\cadd\struct\ramp-gg\GG-Framing1&2.dgn
DATE: 8/4/2006
TIME: 4:05:27 AM

JMT
JOHNSON, MIRMIRAN & THOMPSON
Engineering A Brighter Future

MARYLAND TRANSPORTATION AUTHORITY
Engineering Division

ADDENDUMS & REVISIONS			
NO.	DESCRIPTION	BY	DATE

I-95 EXPRESS TOLL LANES : I-695 INTERCHANGE
GENERAL PURPOSE ROADWAYS AND RAMPS
JOHN F. KENNEDY MEMORIAL HIGHWAY (BALTIMORE COUNTY)
RAMP GG
FRAMING PLAN - SPANS 1 & 2

DESIGNED BY TDY	DRAWN BY DJA	CHECKED BY MJB
CONST. REVIEW BY	DATE AUGUST, 2006	SCALE AS SHOWN

CONTRACT NO. KH-1301-000-006
DRAWING NO. S6 - 86
SHEET NO. 783 OF 1676

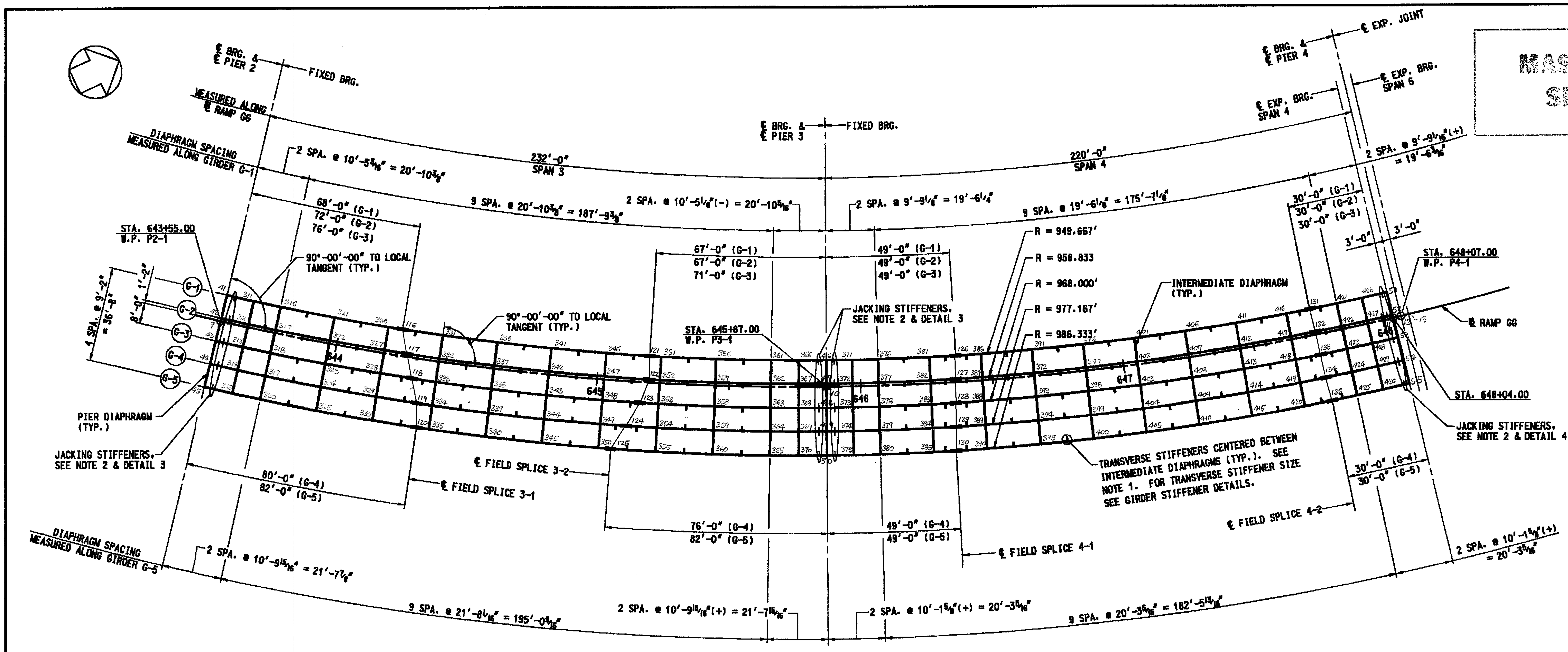

FRAMING PLAN - SPANS 3 & 4

SCALE: 1" = 20'-0"

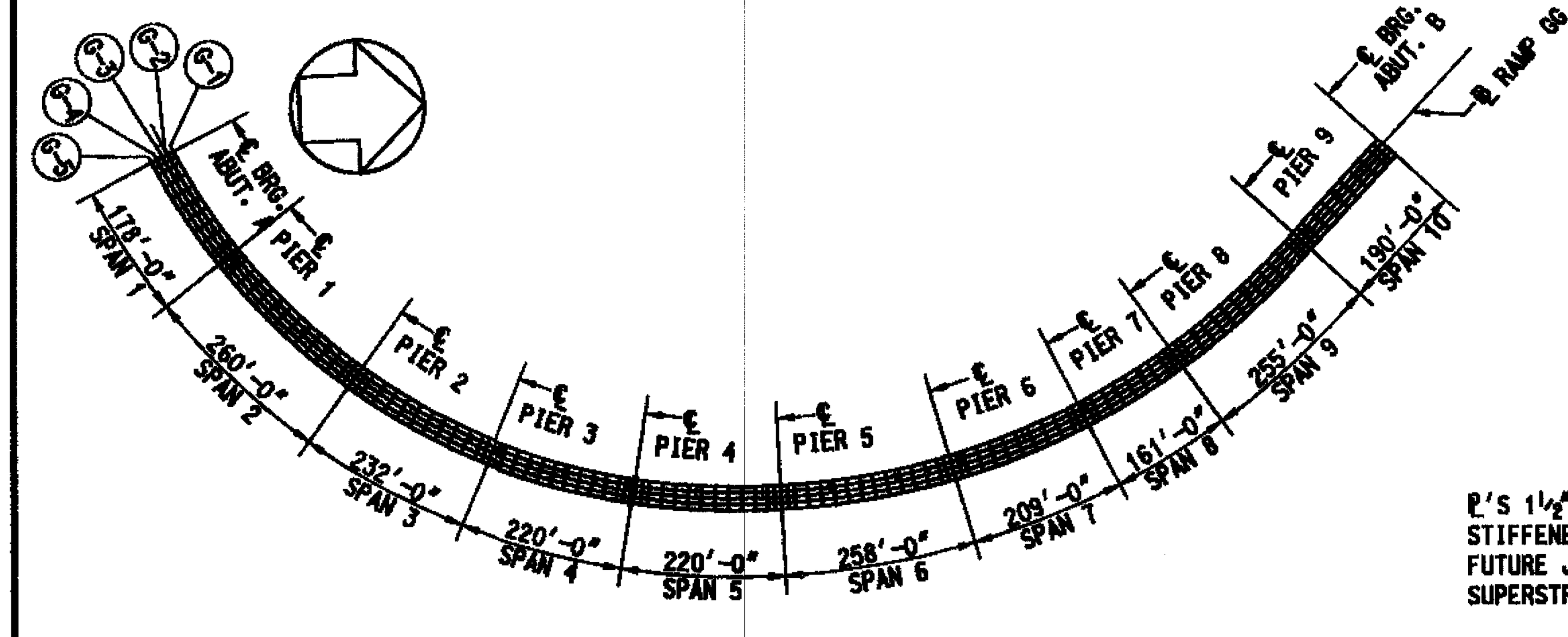

FRAMING KEY PLAN

SCALE: 1" = 200'-0"

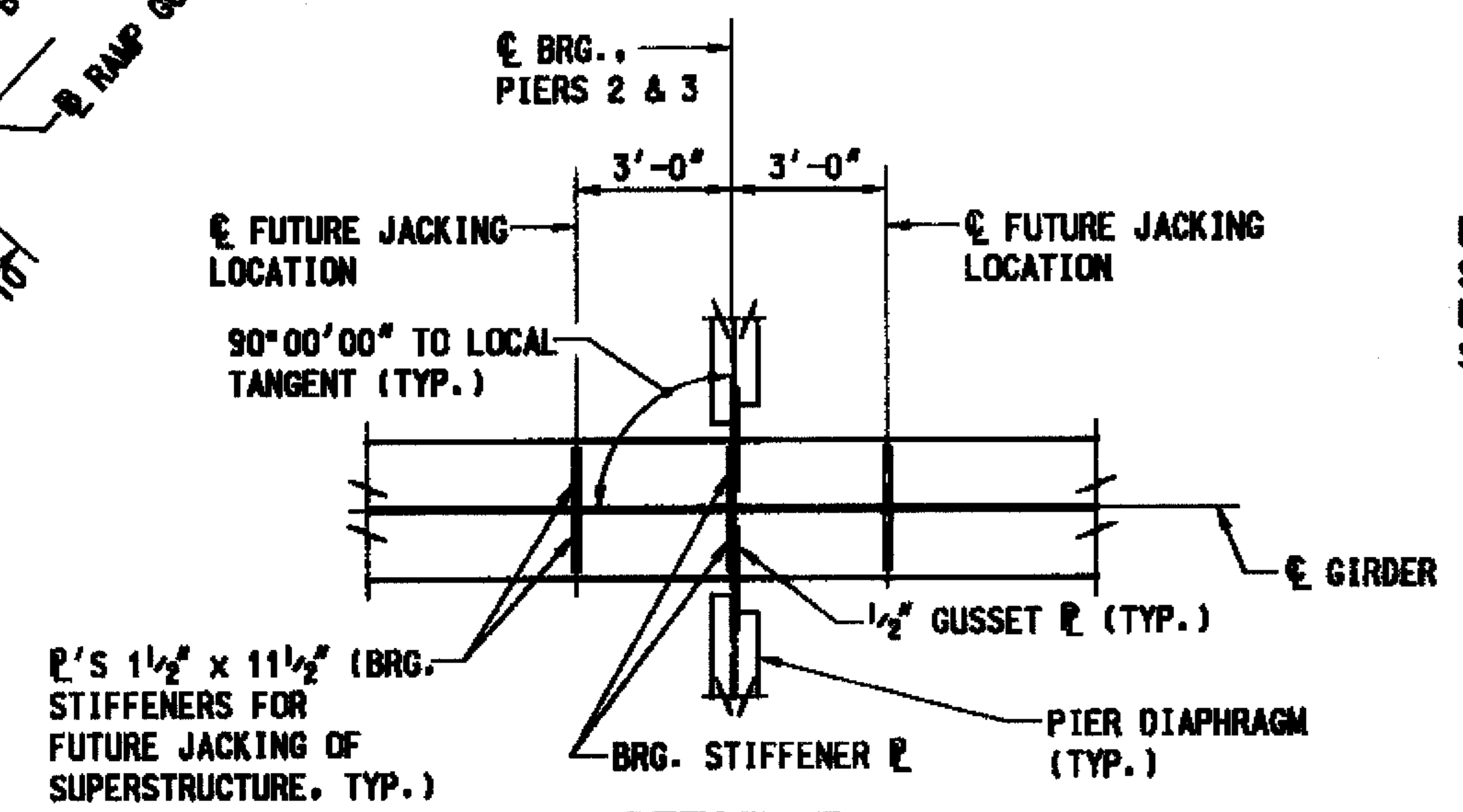

DETAIL 3

NOT TO SCALE

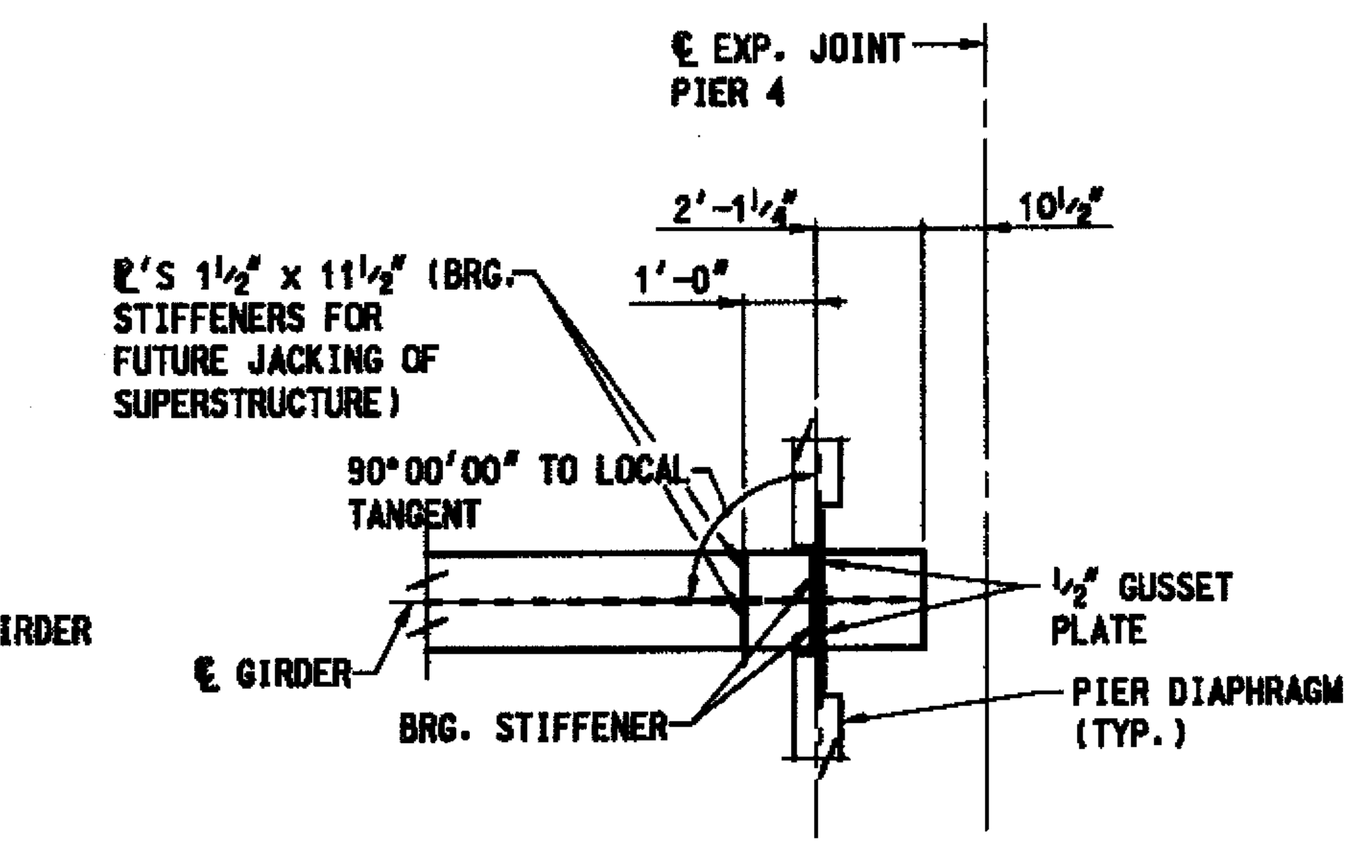

DETAIL 4

NOT TO SCALE

NOTES:

1. AT LOCATIONS WHERE TRANSVERSE STIFFENER CONFLICTS WITH FIELD SPLICE TRANSVERSE STIFFENERS SHALL BE LOCATED 1'-0" FROM EDGE OF FIELD SPLICE PLATE.
2. JACKING STIFFENERS AT ABUTMENTS AND PIER 4 LOCATED TO ACCEPT FUTURE JACKING BEAM. JACKING STIFFENERS AT ALL OTHER PIERS LOCATED TO ALLOW JACKING DIRECTLY UNDER GIRDER. SEE DETAILS 3 & 4 THIS SHEET FOR ADDITIONAL INFORMATION.

FILE: g:\wmd\304004_I1195I695_hr\cadd\struct\ramp_gg\GG-Framing3&4.dgn
DATE: 8/4/2006
TIME: 4:06:29 AM

JMT JOHNSON, MIRMIRAN & THOMPSON *Engineering A Brighter Future*

MARYLAND TRANSPORTATION AUTHORITY
Engineering Division

ADDENDUMS & REVISIONS

NO.	DESCRIPTION	BY	DATE

I-95 EXPRESS TOLL LANES : I-695 INTERCHANGE
GENERAL PURPOSE ROADWAYS AND RAMPS
JOHN F. KENNEDY MEMORIAL HIGHWAY (BALTIMORE COUNTY)
RAMP GG
FRAMING PLAN - SPANS 3 & 4

DESIGNED BY TDY	DRAWN BY DJA	CHECKED BY MJB
CONST. REVIEW BY	DATE AUGUST, 2006	SCALE AS SHOWN

CONTRACT NO. KH-1301-000-006
DRAWING NO. S6 - 87
SHEET NO. 784 OF 1676

MASTER SET

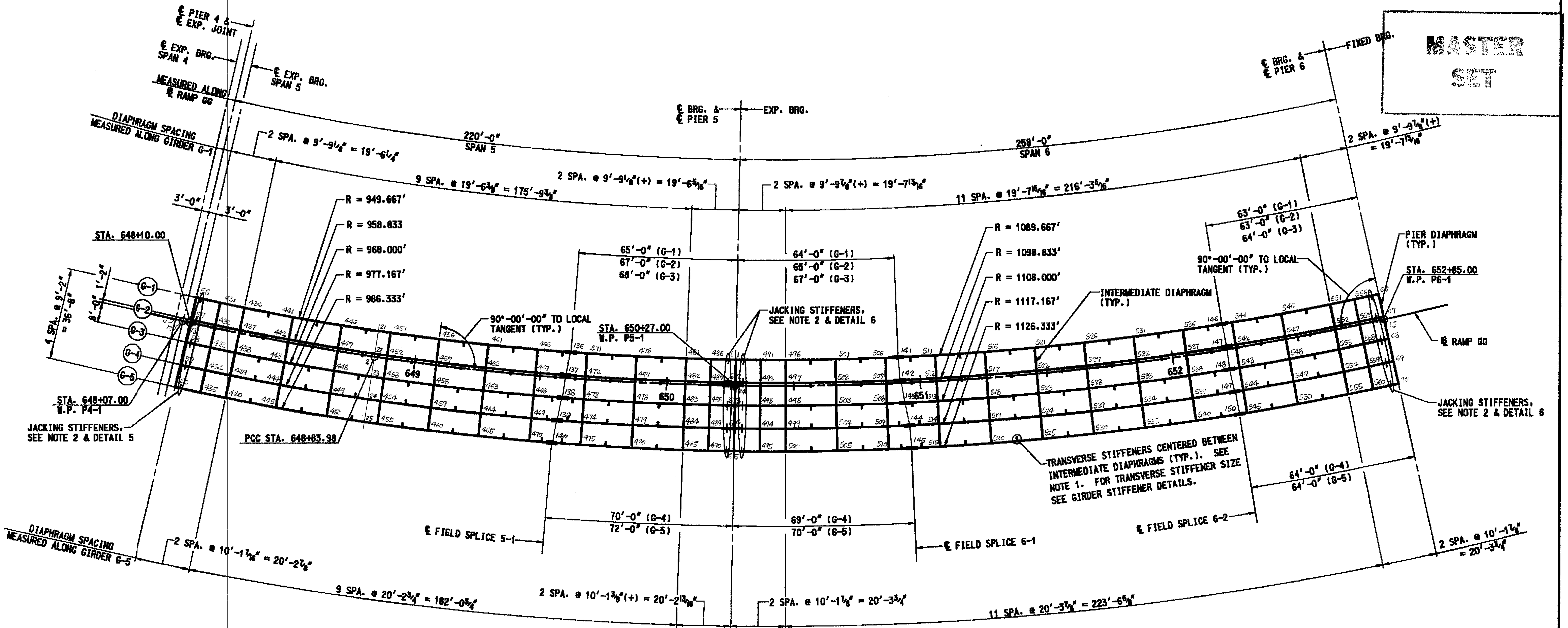

FRAMING PLAN - SPANS 5 & 6

SCALE: 1" = 20'-0"

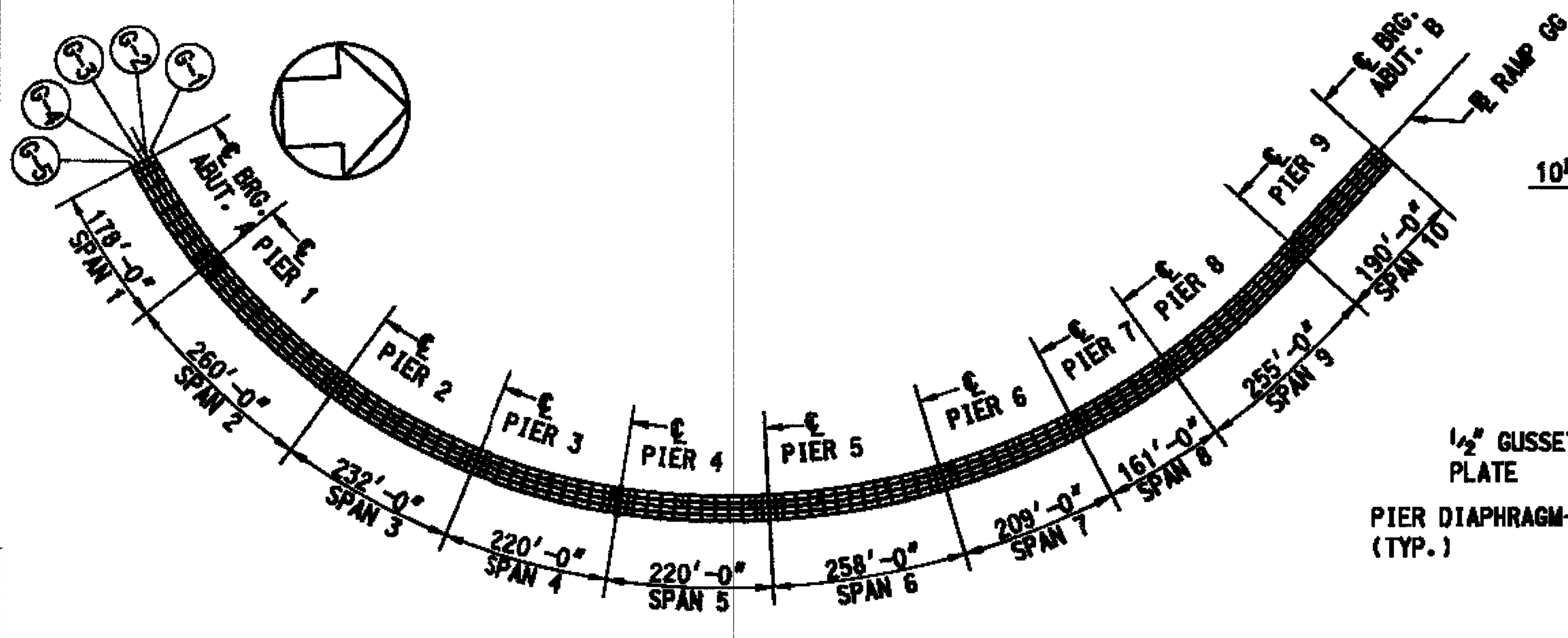

FRAMING KEY PLAN

SCALE: 1" = 200'-0"

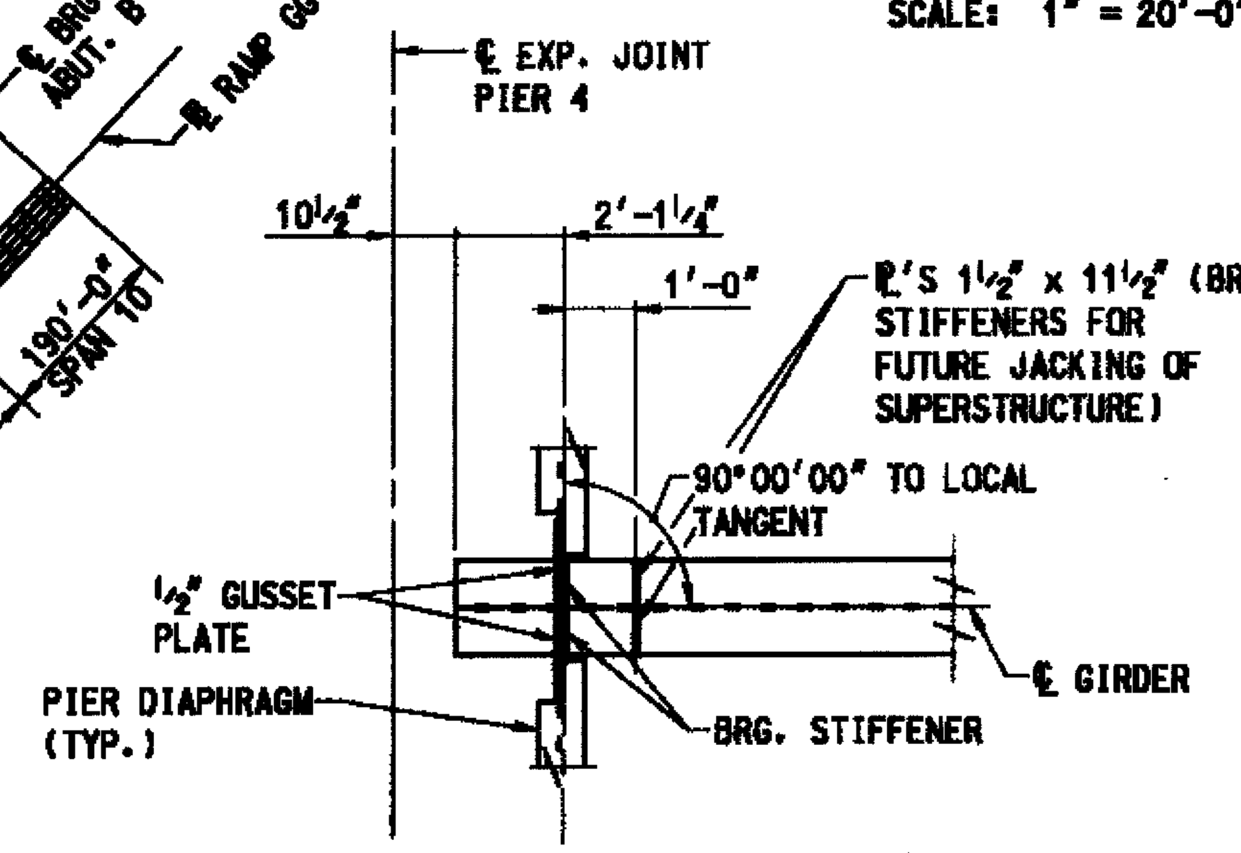

DETAIL 5

NOT TO SCALE

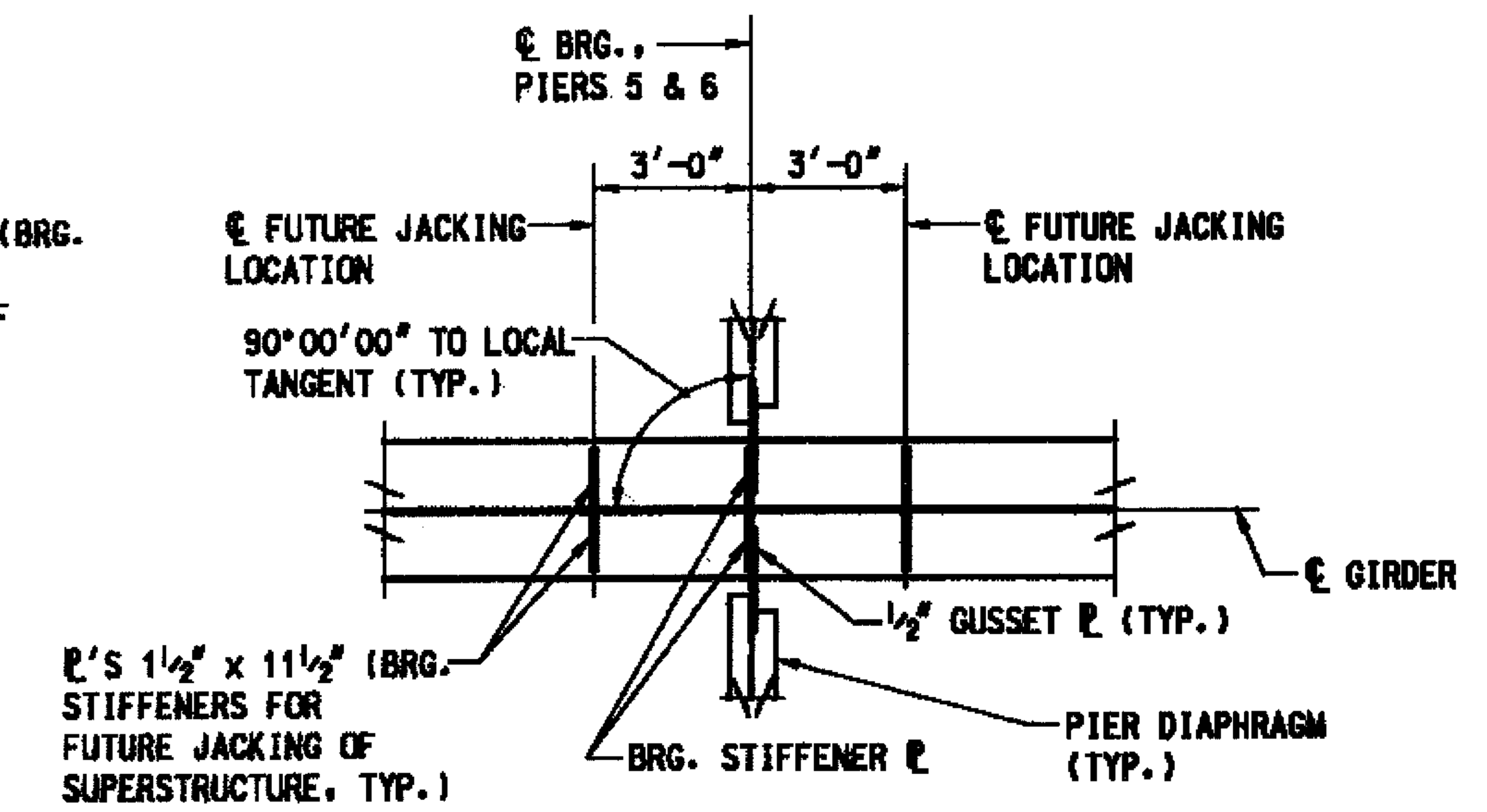

DETAIL 6

NOT TO SCALE

NOTES:

1. AT LOCATIONS WHERE TRANSVERSE STIFFENER CONFLICTS WITH FIELD SPLICE TRANSVERSE STIFFENERS SHALL BE LOCATED 1'-0" FROM EDGE OF FIELD SPLICE PLATE.
2. JACKING STIFFENERS AT ABUTMENTS AND PIER 4 LOCATED TO ACCEPT FUTURE JACKING BEAM. JACKING STIFFENERS AT ALL OTHER PIERS LOCATED TO ALLOW JACKING DIRECTLY UNDER GIRDER. SEE DETAILS 5 & 6 THIS SHEET FOR ADDITIONAL INFORMATION.

FILE: q:\emd\304004_1195695_hr\cadd\struct\ramp_gg\GG-Framing5&6.dgn
DATE: 8/4/2006
TIME: 4:06:31 AM

JMT JOHNSON, MIRMIRAN & THOMPSON *Engineering A Brighter Future*

MARYLAND TRANSPORTATION AUTHORITY *Engineering Division*

ADDENDUMS & REVISIONS			
NO.	DESCRIPTION	BY	DATE

I-95 EXPRESS TOLL LANES : I-695 INTERCHANGE
GENERAL PURPOSE ROADWAYS AND RAMPS
JOHN F. KENNEDY MEMORIAL HIGHWAY (BALTIMORE COUNTY)
RAMP GG
FRAMING PLAN - SPANS 5 & 6

DESIGNED BY TDY	DRAWN BY DJA	CHECKED BY MJB
CONST. REVIEW BY	DATE AUGUST, 2006	SCALE AS SHOWN

CONTRACT NO. KH-1301-000-006
DRAWING NO. S6 - 88
SHEET NO. 785 OF 1676

MASTER SET

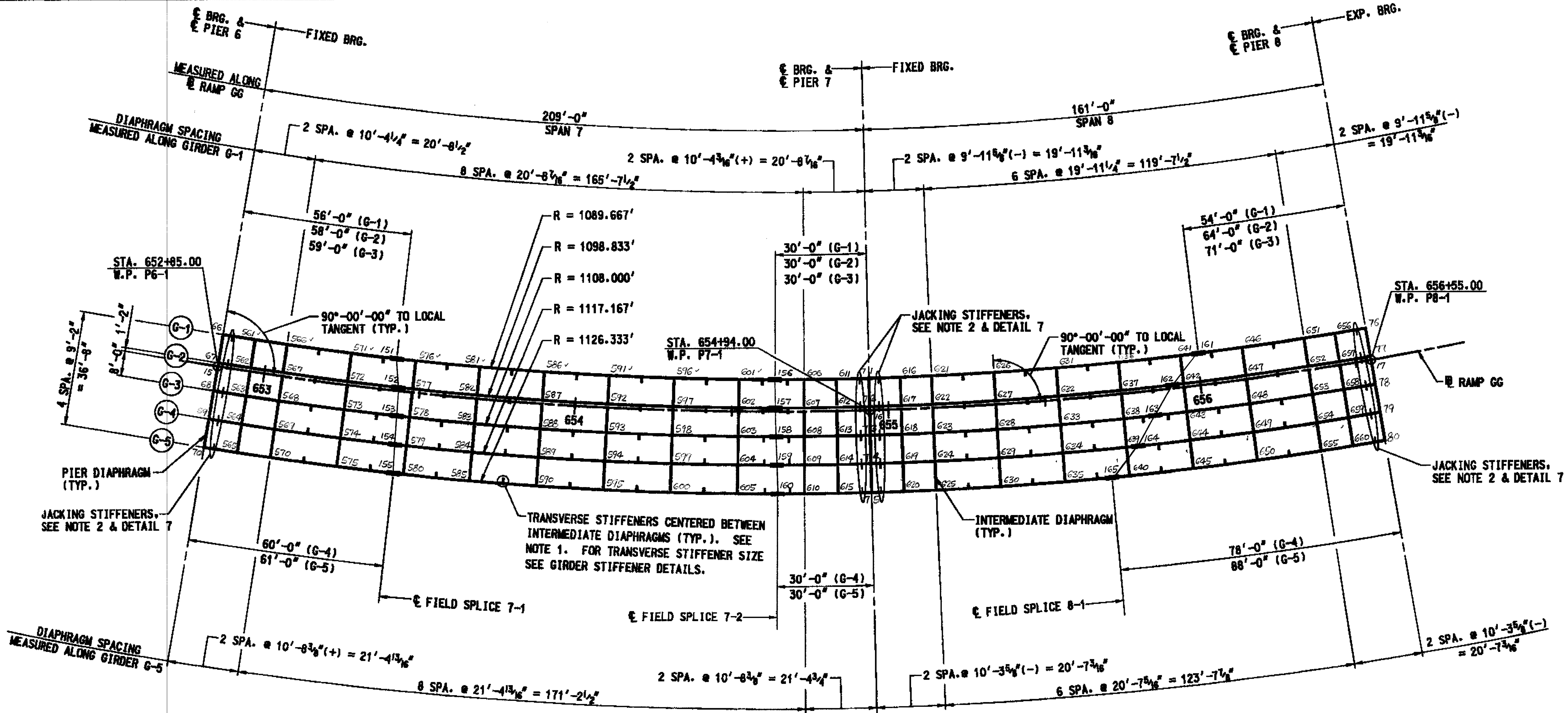

FRAMING PLAN - SPANS 7 & 8
SCALE: 1" = 20'-0"

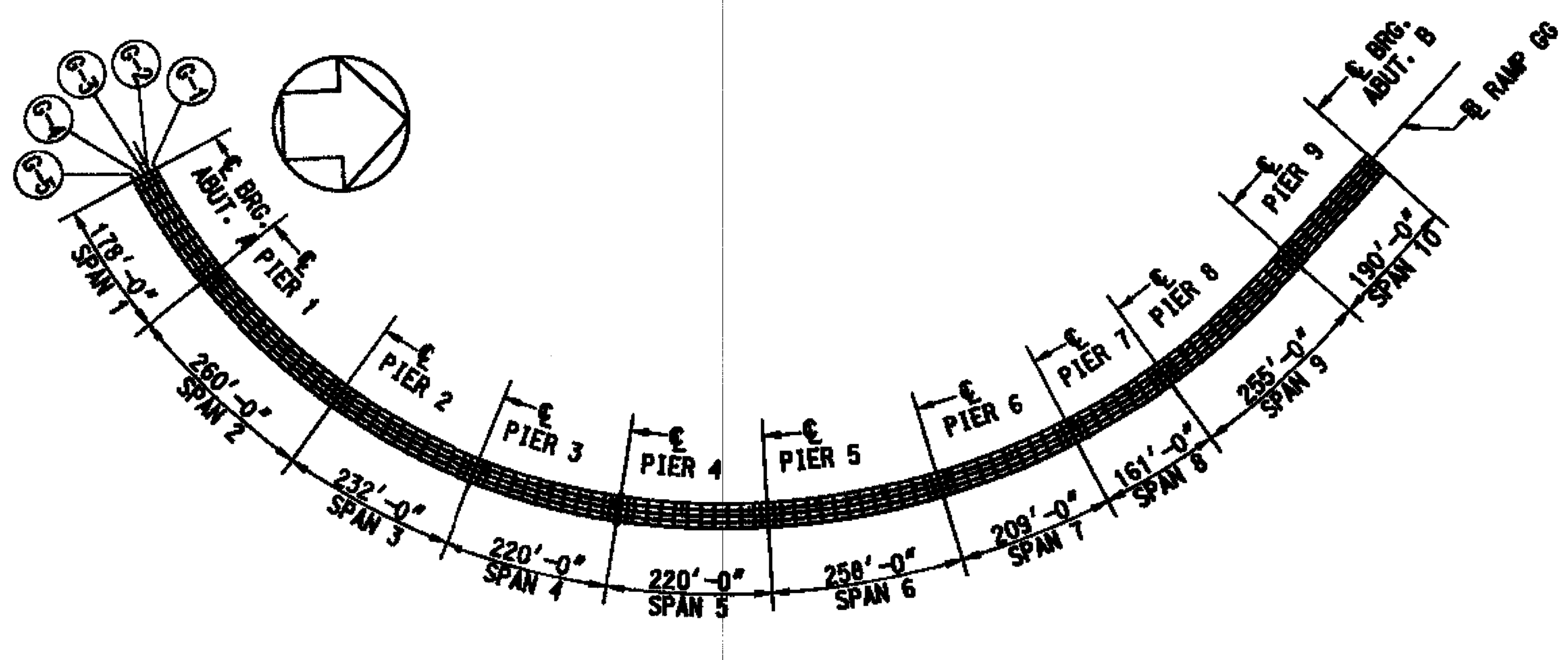

FRAMING KEY PLAN
SCALE: 1" = 200'-0"

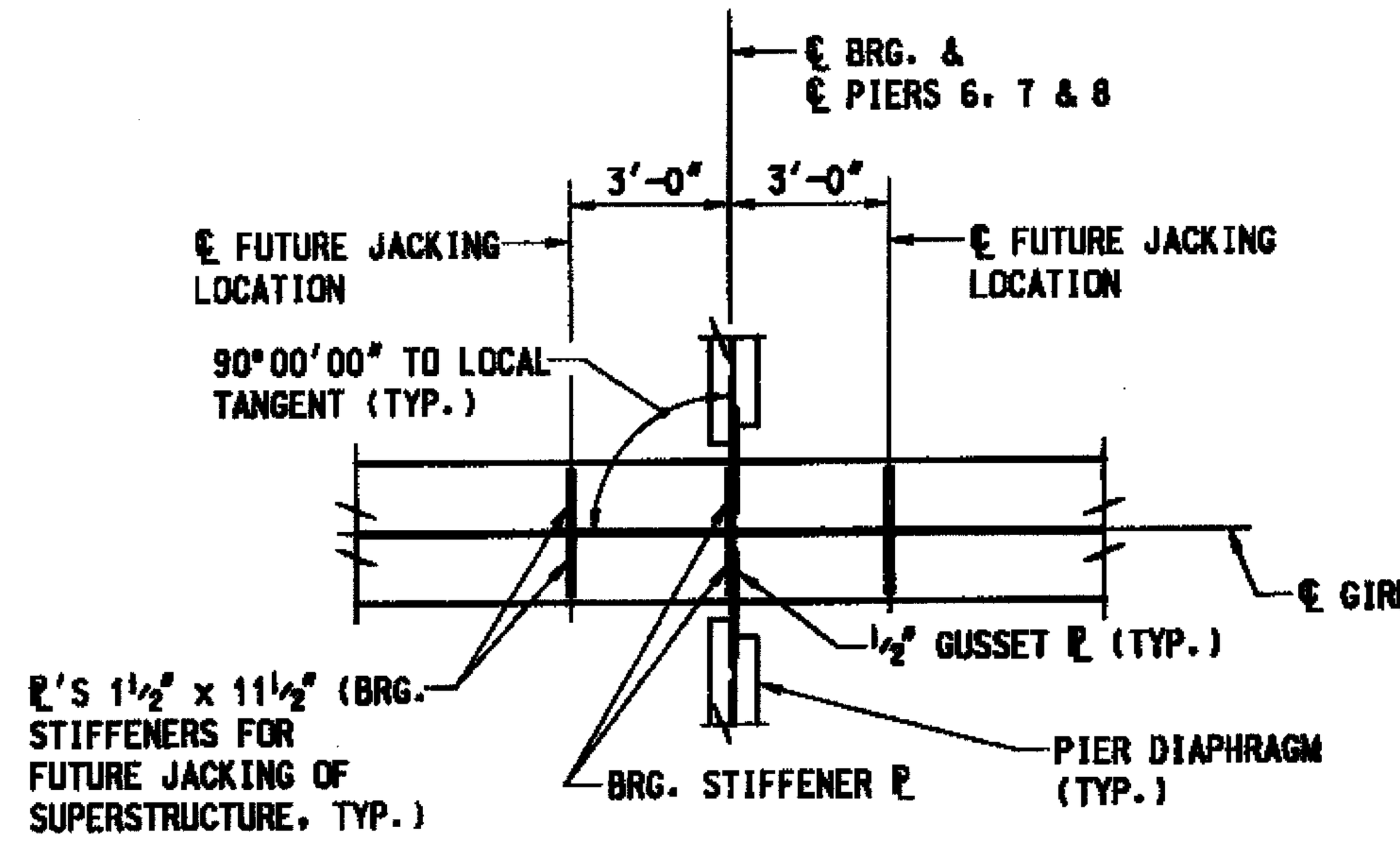

DETAIL 7
NOT TO SCALE

NOTES:

1. AT LOCATIONS WHERE TRANSVERSE STIFFENER CONFLICTS WITH FIELD SPLICE TRANSVERSE STIFFENERS SHALL BE LOCATED 1'-0" FROM EDGE OF FIELD SPLICE PLATE.
2. JACKING STIFFENERS AT ABUTMENTS AND PIER 4 LOCATED TO ACCEPT FUTURE JACKING BEAM. JACKING STIFFENERS AT ALL OTHER PIERS LOCATED TO ALLOW JACKING DIRECTLY UNDER GIRDER. SEE DETAIL 7 THIS SHEET FOR ADDITIONAL INFORMATION.

FILE: q:\enc\30400_I\I95I695_hr\cadd\struct\ramp_gg\GG-Framing7&8.dgn
DATE: 8/4/2006
TIME: 4:06:34 AM

JMT
JOHNSON, MIRMIRAN & THOMPSON
Engineering A Brighter Future

MARYLAND TRANSPORTATION AUTHORITY
Engineering Division

ADDENDUMS & REVISIONS			
NO.	DESCRIPTION	BY	DATE

I-95 EXPRESS TOLL LANES : I-695 INTERCHANGE
GENERAL PURPOSE ROADWAYS AND RAMPS
JOHN F. KENNEDY MEMORIAL HIGHWAY (BALTIMORE COUNTY)
RAMP GG
FRAMING PLAN - SPANS 7 & 8

DESIGNED BY TDY	DRAWN BY DJA	CHECKED BY MJB
CONST. REVIEW BY	DATE AUGUST, 2006	SCALE AS SHOWN

CONTRACT NO. KH-1301-000-006
DRAWING NO. S6 - 89
SHEET NO. 785 OF 1676

MASTER SET

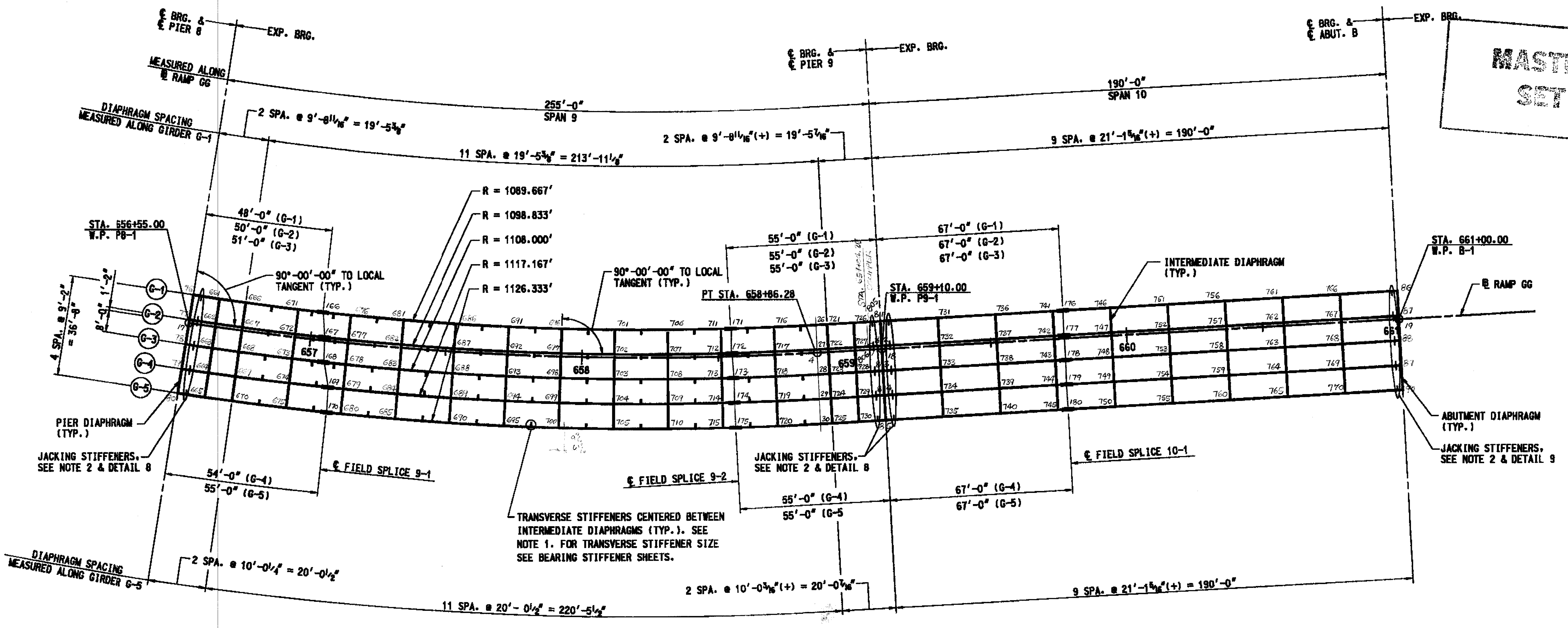

FRAMING PLAN - SPANS 9 & 10

SCALE: 1" = 20'-0"

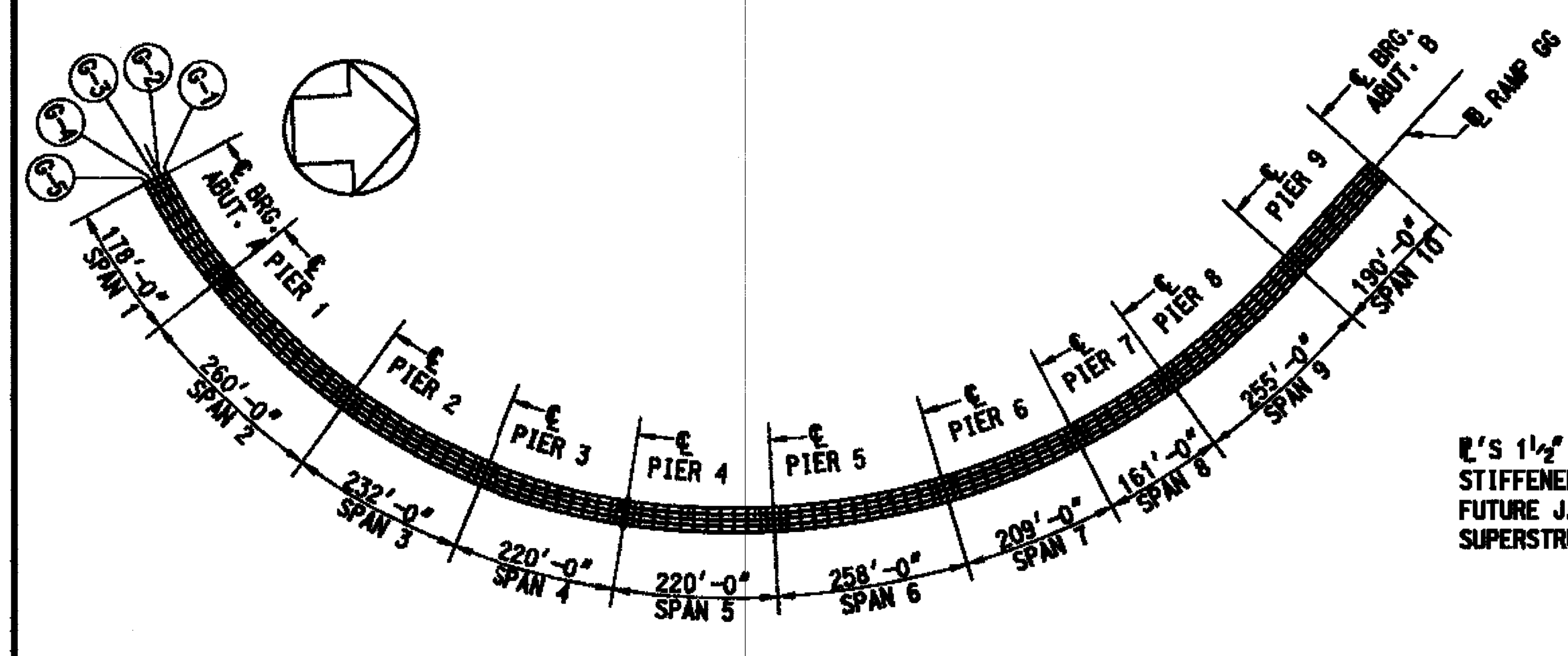

FRAMING KEY PLAN

SCALE: 1" = 200'-0"

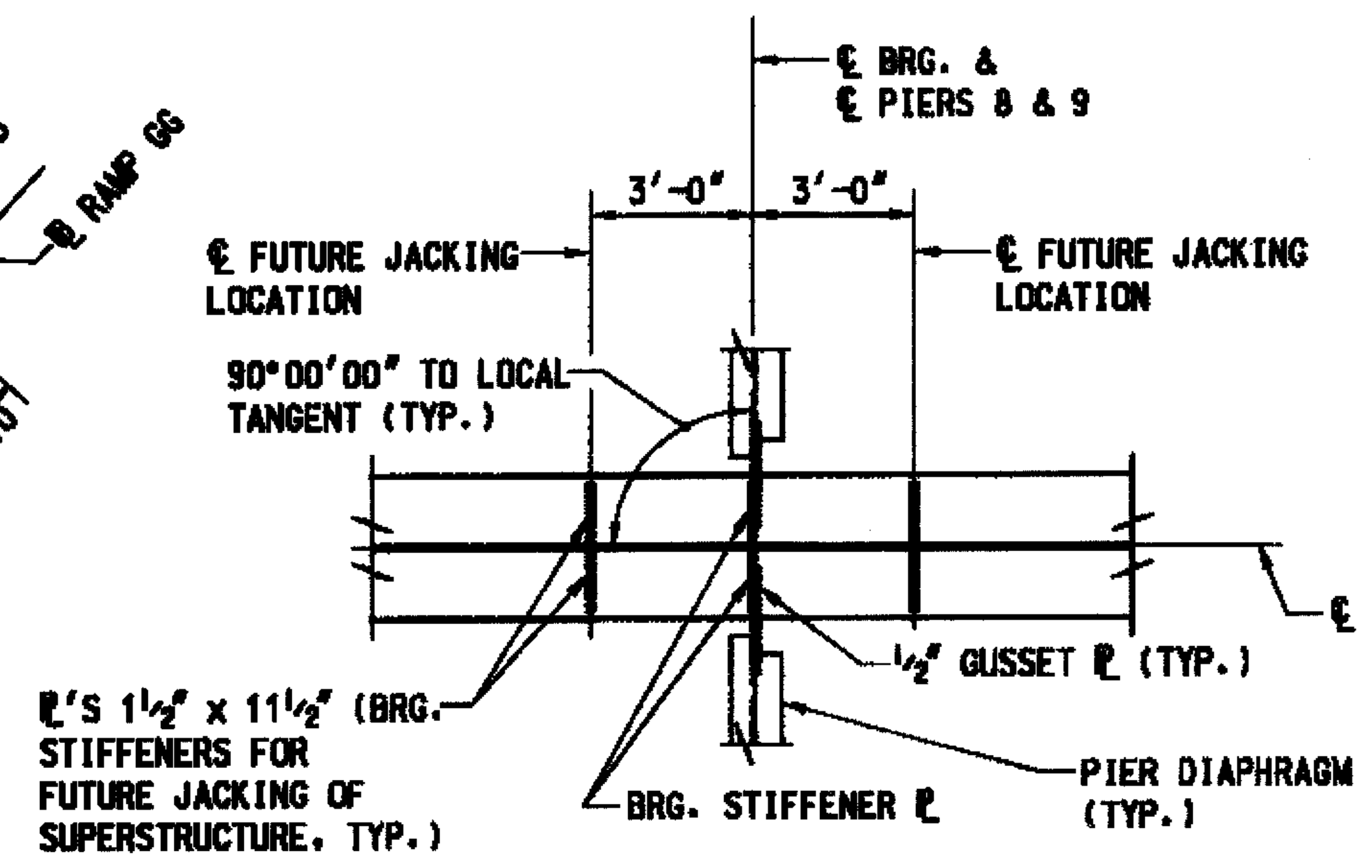

DETAIL 8

NOT TO SCALE

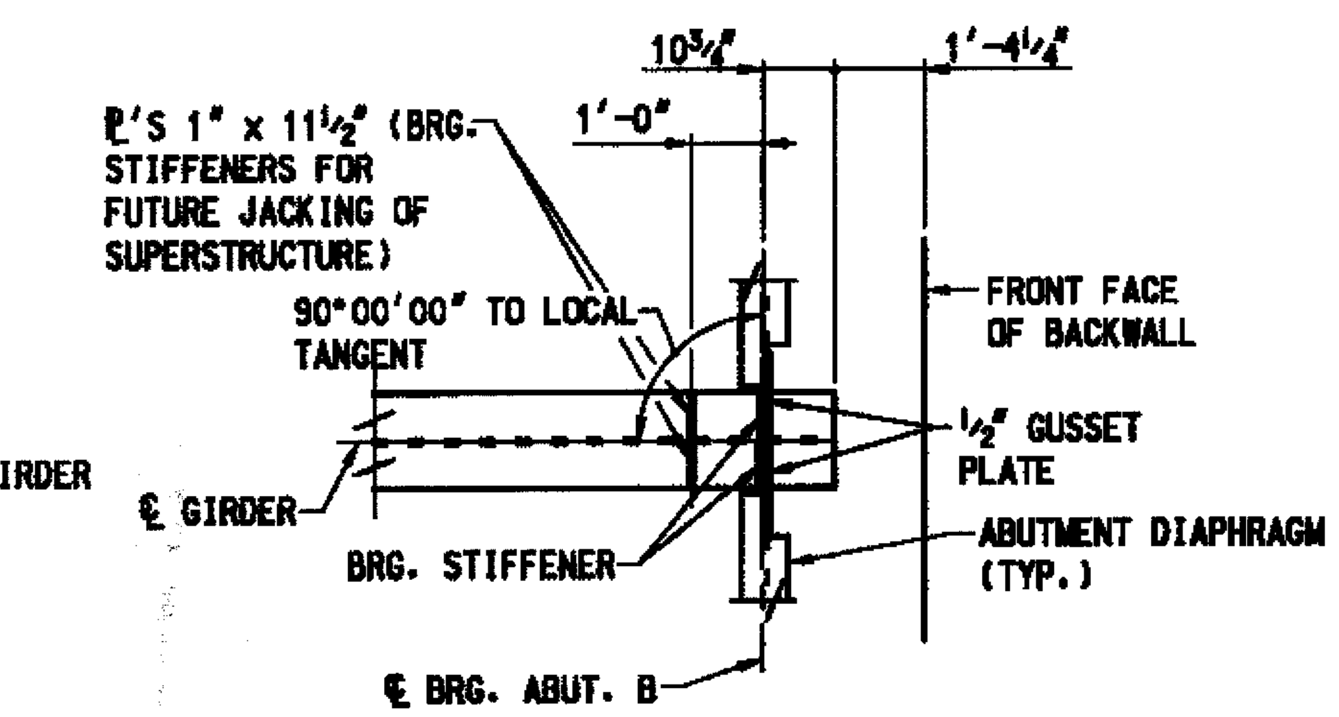

DETAIL 9

NOT TO SCALE

NOTES:

1. AT LOCATIONS WHERE TRANSVERSE STIFFENER CONFLICTS WITH FIELD SPLICE TRANSVERSE STIFFENERS SHALL BE LOCATED 1'-0" FROM EDGE OF FIELD SPLICE PLATE.
2. JACKING STIFFENERS AT ABUTMENTS AND PIER 4 LOCATED TO ACCEPT FUTURE JACKING BEAM. JACKING STIFFENERS AT ALL OTHER PIERS LOCATED TO ALLOW JACKING DIRECTLY UNDER GIRDER. SEE DETAILS 8 & 9 THIS SHEET FOR ADDITIONAL INFORMATION.

FILE: p:\emd\304004_1195695_hr\cadd\struct\ramp_gg\00-Framing9&10.dgn
DATE: 8/4/2006
TIME: 4:06:36 AM

JMT
JOHNSON, MIRMIRAN & THOMPSON
Engineering A Brighter Future

MARYLAND TRANSPORTATION AUTHORITY
Engineering Division

ADDENDUMS & REVISIONS			
NO.	DESCRIPTION	BY	DATE

I-95 EXPRESS TOLL LANES : I-695 INTERCHANGE
GENERAL PURPOSE ROADWAYS AND RAMPS
JOHN F. KENNEDY MEMORIAL HIGHWAY (BALTIMORE COUNTY)
RAMP GG
FRAMING PLAN - SPANS 9 & 10

DESIGNED BY TDY	DRAWN BY DJA	CHECKED BY MJB
CONST. REVIEW BY	DATE AUGUST, 2006	SCALE AS SHOWN

CONTRACT NO. KH-1301-000-006
DRAWING NO. S6 - 90
SHEET NO. 787 OF 1616

REVISED

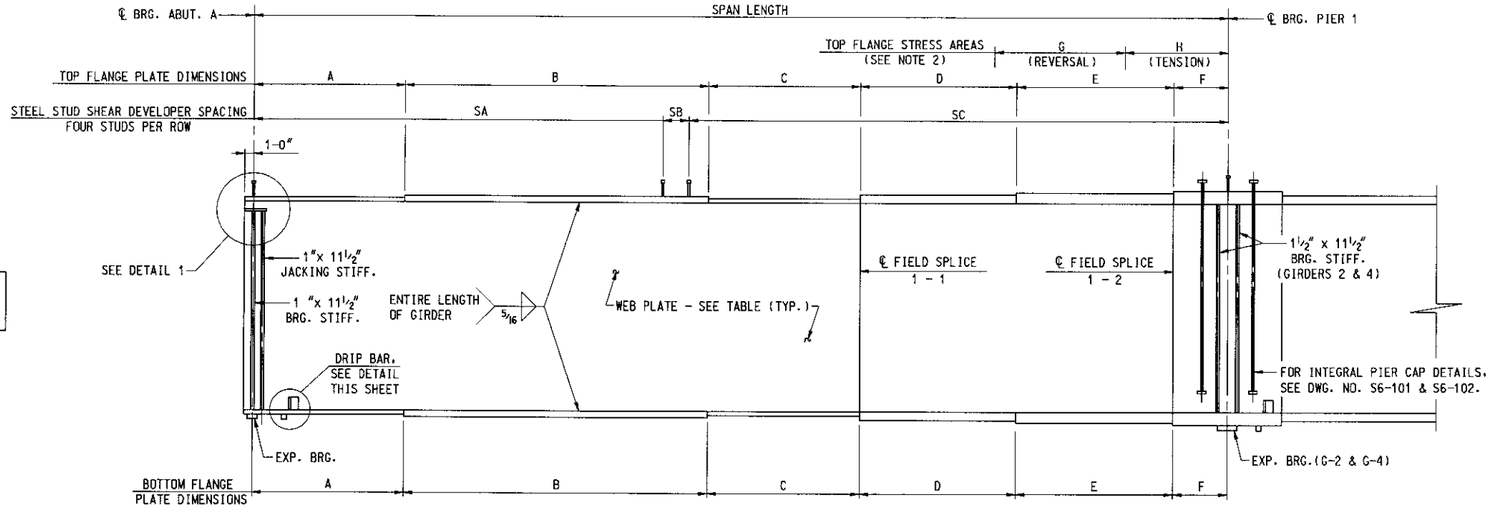

THE ESTIMATED NUMBER OF STEEL STUD SHEAR DEVELOPERS REQUIRED IS 23,888.

GIRDER ELEVATION - SPAN I
NOT TO SCALE

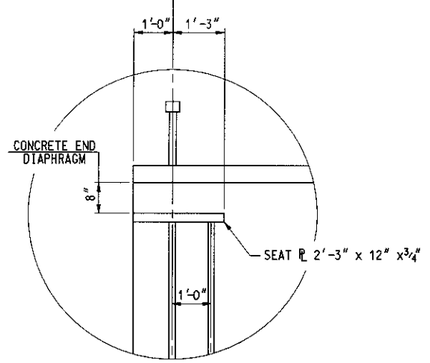

DETAIL I
NOT TO SCALE

GIRDER ELEVATION - SPAN I - DIMENSIONS

GIRDER NUMBER	SPAN LENGTH	RADIUS	PLATES	A	B	C	D	E [3]	F [3]	G	H
G-1	176'-1"	R=949.67'	TOP FLANGE	15" x 1¼" x 30'-0"	15" x 1¼" x 60'-0"	15" x 1¼" x 24'-1"	15" x 2" x 24'-7"	21" x 2½" x 30'-0"	24" x 2½" x 7'-5"	34'-2"	42'-6"
			BOTTOM FLANGE	15" x 1½" x 30'-0"	15" x 1½" x 60'-0"	15" x 1½" x 24'-1"	15" x 2" x 24'-7"	21" x 2½" x 30'-0"	24" x 2½" x 7'-5"		
			WEB	99" x ¾" x 30'-0"	99" x ¾" x 60'-0"	99" x ¾" x 24'-1"	99" x 13/16" x 24'-7"	99" x 13/16" x 30'-0"	99" x 13/16" x 7'-5"		
G-2	177'-9⅜"	R=958.83'	TOP FLANGE	15" x 1¼" x 30'-0"	15" x 1¼" x 60'-0"	15" x 1¼" x 23'-9⅜"	15" x 2" x 26'-6⅛"	21" x 2½" x 30'-0"	24" x 2½" x 7'-5⅞"	31'-1"	46'-2"
			BOTTOM FLANGE	15" x 1½" x 30'-0"	15" x 1½" x 60'-0"	15" x 1½" x 23'-9⅜"	15" x 2" x 26'-6⅛"	21" x 2½" x 30'-0"	24" x 2½" x 7'-5⅞"		
			WEB	99" x ¾" x 30'-0"	99" x ¾" x 60'-0"	99" x ¾" x 23'-9⅜"	99" x 13/16" x 26'-6⅛"	99" x 13/16" x 30'-0"	99" x 1" x 7'-5⅞"		
G-3	179'-5 13/16"	R=968.00'	TOP FLANGE	15" x 1¼" x 30'-0"	15" x 1¼" x 60'-0"	15" x 1¼" x 22'-5 13/16"	15" x 2" x 29'-5¼"	21" x 2½" x 30'-0"	21" x 2½" x 7'-6¾"	31'-0"	49'-7"
			BOTTOM FLANGE	15" x 1½" x 30'-0"	15" x 1½" x 60'-0"	15" x 1½" x 22'-5 13/16"	15" x 2" x 29'-5¼"	21" x 2½" x 30'-0"	21" x 2½" x 7'-6¾"		
			WEB	99" x ¾" x 30'-0"	99" x ¾" x 60'-0"	99" x ¾" x 22'-5 13/16"	99" x ¾" x 29'-5¼"	99" x ¾" x 30'-0"	99" x 13/16" x 7'-6¾"		
G-4	181'-2 3/16"	R=977.17'	TOP FLANGE	15" x 1¼" x 30'-0"	15" x 1¼" x 60'-0"	15" x 1¼" x 23'-2 3/16"	15" x 2" x 30'-4 7/16"	~~21"~~ x 2½" x 30'-0"	~~24"~~ x 2½" x 7'-7 9/16"	44'-11"	48'-4"
			BOTTOM FLANGE	15" x 1½" x 30'-0"	15" x 1½" x 60'-0"	15" x 1½" x 23'-2 3/16"	15" x 2" x 30'-4 7/16"	~~21"~~ x 2½" x 30'-0"	~~24"~~ x 2½" x 7'-7 9/16"		
			WEB	99" x ¾" x 30'-0"	99" x ¾" x 60'-0"	99" x ¾" x 23'-2 3/16"	99" x 13/16" x 30'-4 7/16"	99" x 13/16" x 30'-0"	99" x 1" x 7'-7 9/16"		
G-5	182'-10 9/16"	R=986.33'	TOP FLANGE	15" x 1¼" x 30'-0"	15" x 1¼" x 60'-0"	15" x 1¼" x 24'-10 9/16"	18" x 2" x 30'-3½"	26" x 2½" x 30'-0"	28" x 2½" x 7'-8½"	53'-4"	49'-0"
			BOTTOM FLANGE	15" x 1½" x 30'-0"	15" x 1½" x 60'-0"	15" x 1½" x 24'-10 9/16"	18" x 2" x 30'-3½"	26" x 2½" x 30'-0"	28" x 2½" x 7'-8½"		
			WEB	99" x ¾" x 30'-0"	99" x ¾" x 60'-0"	99" x ¾" x 24'-10 9/16"	99" x 13/16" x 30'-3½"	99" x 13/16" x 30'-0"	99" x 13/16" x 7'-8½"		

22" 30"

⅞" DIA. STEEL STUD SPACING (4 PER ROW) - SPAN I

GIRDER NUMBER	SA	SB	SC
G-1	83 SPA. @ 2'-0" = 166'-0"	11"	5 SPA. @ 1'-10" = 9'-2"
G-2	88 SPA. @ 1'-11" = 168'-8"	11 3/8"	7 SPA. @ 1'-2" = 8'-2"
G-3	80 SPA. @ 2'-0" = 160'-0"	1'-5 13/16"	9 SPA. @ 2'-0" = 18'-0"
G-4	90 SPA. @ 1'-11" = 172'-6"	1'-8 3/16"	7 SPA. @ 1'-0" = 7'-0"
G-5	24 SPA. @ 1'-8" = 40'-0"	1'-8 9/16"	77 SPA. @ 1'-10" = 141'-2"

SPLICE TYPES - SPAN I

GIRDER NUMBER	1 - 1	1 - 2
G-1	TYPE II	TYPE XIV
G-2	TYPE II	TYPE XIV
G-3	TYPE II	TYPE XIV
G-4	TYPE II	TYPE ~~XIV~~ XVI [3]
G-5	TYPE II	TYPE XV

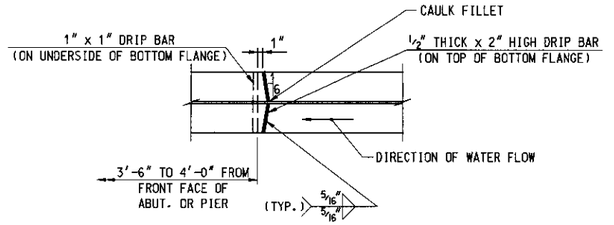

DRIP BAR DETAIL

NOTE: PLACE DRIP BAR ON HIGH SIDE OF GIRDER AT ALL ABUTMENTS AND PIERS.
NOT TO SCALE

NOTES:

1. FOR GIRDER SHOP SPLICE DETAILS, SEE STANDARD DETAIL NO. BR-SS(8.11)-85-173.
2. NO WELDING OF STAY IN PLACE DECK FORMS TO TOP FLANGE PLATE WILL BE ALLOWED IN TENSION AND STRESS REVERSAL AREAS.
3. SPACE STEEL STUD SHEAR DEVELOPERS TO MISS BOLT HEADS IN FIELD SPLICE. SEE STANDARD DETAIL NO. BR-SS(8.05)-75-30.
4. FOR CONCRETE END DIAPHRAGM AT ABUTMENTS, SEE STANDARD DETAIL NO. BR-SS(6.22)-80-120.
5. FOR TRANSVERSE STIFFENER LOCATIONS, SEE DWG. NO. S6-86.

FILE: q:\smd\304004_III95695_hw\cadd\struct\Ramp_GG\GG-SPAN1detLine3.dgn
DATE: 3/30/2007
TIME: 9:25:01 AM

JOHNSON, MIRMIRAN & THOMPSON
Engineering A Brighter Future

MARYLAND TRANSPORTATION AUTHORITY
Engineering Division

ADDENDUMS & REVISIONS

NO.	DESCRIPTION	BY	DATE
[3]	REVISED PLATE SIZES AND SPLICE TYPE	TDY	3/07

I-95 EXPRESS TOLL LANES : I-695 INTERCHANGE
GENERAL PURPOSE ROADWAYS AND RAMPS
JOHN F. KENNEDY MEMORIAL HIGHWAY (BALTIMORE COUNTY)
RAMP GG
GIRDER ELEVATION - SPAN I

CONTRACT NO. KH-1301-000-006
DRAWING NO. S6 - 91

DESIGNED BY TDY	DRAWN BY DJA	CHECKED BY MJB	SHEET NO.
CONST. REVIEW BY	DATE AUGUST, 2006	SCALE AS SHOWN	788 OF 1676

REVISED

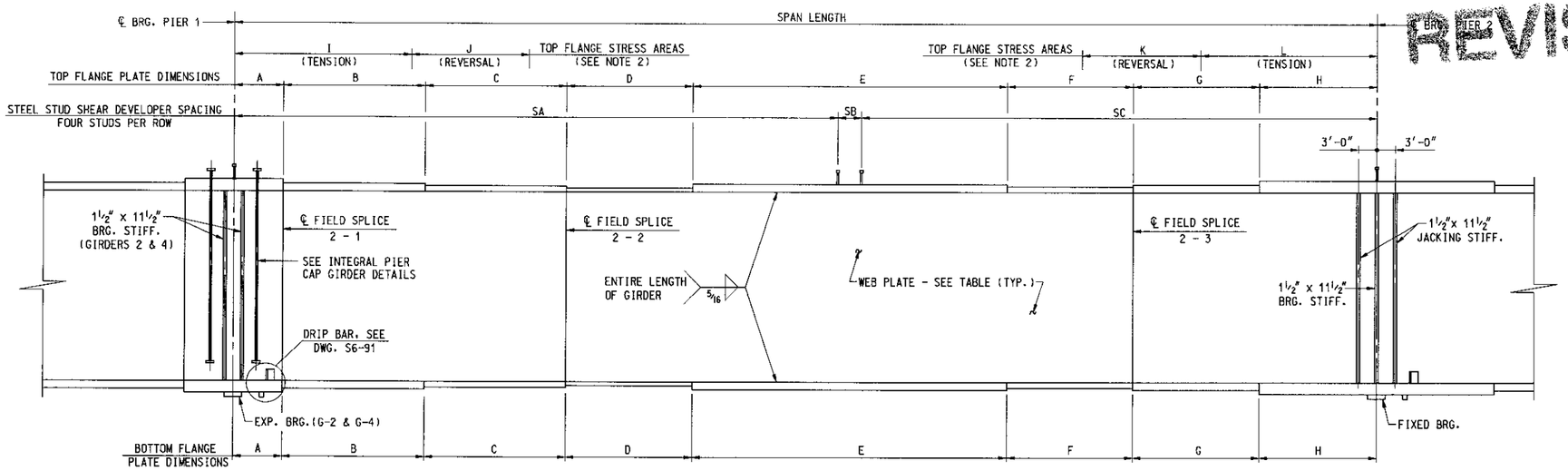

THE ESTIMATED NUMBER OF STEEL STUD SHEAR DEVELOPERS REQUIRED IS 23,888.

GIRDER ELEVATION - SPAN 2

NOT TO SCALE

GIRDER ELEVATION - SPAN 2 - DIMENSIONS

GIRDER NUMBER	SPAN LENGTH	RADIUS	PLATES	A [3]	B [3]	C	D	E	F	G	H	I	J	K	L
G-1	257'-2 7/16"	R=949.67'	TOP FLANGE	24" x 2½" x 7'-5"	21" x 2½" x 30'-0"	15" x 2" x 18'-7"	15" x 1½" x 30'-0"	15" x 1½" x 86'-0"	15" x 1½" x 29'-2 7/16"	20" x 2" x 31'-0"	24" x 2½" x 25'-0"	40'-11"	25'-1"	28'-6"	40'-3"
			BOTTOM FLANGE	24" x 2½" x 7'-5"	21" x 2½" x 30'-0"	15" x 2" x 18'-7"	18" x 2" x 30'-0"	18" x 2½" x 86'-0"	18" x 2" x 29'-2 7/16"	20" x 2" x 31'-0"	24" x 2½" x 25'-0"				
			WEB	99" x 13/16" x 7'-5"	99" x 13/16" x 30'-0"	99" x 13/16" x 18'-7"	99" x ¾" x 30'-0"	99" x ¾" x 86'-0"	99" x ¾" x 29'-2 7/16"	99" x ¾" x 31'-0"	99" x 13/16" x 25'-0"				
G-2	259'-8 3/16"	R=958.83'	TOP FLANGE	24" x 2½" x 7'-5 7/8"	21" x 2½" x 30'-0"	15" x 2" x 18'-6 1/8"	15" x 1½" x 30'-0"	15" x 1½" x 86'-0"	15" x 1½" x 31'-8 3/16"	20" x 2" x 31'-0"	24" x 2½" x 25'-0"	42'-10"	20'-2"	23'-3"	41'-9"
			BOTTOM FLANGE	24" x 2½" x 7'-5 7/8"	21" x 2½" x 30'-0"	15" x 2" x 18'-6 1/8"	18" x 2" x 30'-0"	18" x 2½" x 86'-0"	18" x 2" x 31'-8 3/16"	20" x 2" x 31'-0"	24" x 2½" x 25'-0"				
			WEB	99" x 1" x 7'-5 7/8"	99" x 13/16" x 30'-0"	99" x 13/16" x 18'-6 1/8"	99" x ¾" x 30'-0"	99" x ¾" x 86'-0"	99" x ¾" x 31'-8 3/16"	99" x ¾" x 31'-0"	99" x 13/16" x 25'-0"				
G-3	262'-2"	R=968.00'	TOP FLANGE	21" x 2½" x 7'-6¾"	21" x 2½" x 30'-0"	15" x 2" x 19'-5¼"	15" x 1½" x 30'-0"	15" x 1½" x 86'-0"	15" x 1½" x 33'-2"	20" x 2" x 31'-0"	24" x 2½" x 25'-0"	45'-0"	16'-6"	20'-1"	42'-11"
			BOTTOM FLANGE	21" x 2½" x 7'-6¾"	21" x 2½" x 30'-0"	15" x 2" x 19'-5¼"	18" x 2" x 30'-0"	18" x 2½" x 86'-0"	18" x 2" x 33'-2"	20" x 2" x 31'-0"	24" x 2½" x 25'-0"				
			WEB	99" x 13/16" x 7'-6¾"	99" x ¾" x 30'-0"	99" x ¾" x 19'-5¼"	99" x ¾" x 30'-0"	99" x ¾" x 86'-0"	99" x ¾" x 33'-2"	99" x ¾" x 31'-0"	99" x ¾" x 25'-0"				
G-4	264'-7 13/16"	R=977.17'	TOP FLANGE	~~24"~~ x 2½" x 7'-5⅞"	~~24"~~ x 2½" x 30'-0"	15" x 2" x 19'-4⅜"	15" x 1½" x 30'-0"	15" x 1½" x 86'-0"	15" x 1½" x 34'-7 13/16"	20" x 2" x 32'-0"	24" x 2½" x 25'-0"	44'-8"	21'-0"	26'-6"	40'-11"
			BOTTOM FLANGE	~~24"~~ x 2½" x 7'-5⅞"	~~21"~~ x 2½" x 30'-0"	15" x 2" x 19'-4⅜"	18" x 2" x 30'-0"	18" x 2½" x 86'-0"	18" x 2" x 34'-7 13/16"	20" x 2" x 32'-0"	24" x 2½" x 25'-0"				
			WEB	99" x 1" x 7'-5⅞"	99" x 13/16" x 30'-0"	99" x 13/16" x 19'-4⅜"	99" x ¾" x 30'-0"	99" x ¾" x 86'-0"	99" x ¾" x 34'-7 13/16"	99" x ¾" x 32'-0"	99" x 13/16" x 25'-0"				
G-5	267'-1 9/16"	R=986.33'	TOP FLANGE	28" x 2½" x 7'-8½"	26" x 2½" x 30'-0"	18" x 2" x 20'-3½"	15" x 1½" x 30'-0"	18" x 1½" x 86'-0"	15" x 1½" x 35'-1 9/16"	24" x 2" x 33'-0"	30" x 2½" x 25'-0"	45'-4"	24'-11"	32'-4"	40'-1"
			BOTTOM FLANGE	28" x 2½" x 7'-8½"	26" x 2½" x 30'-0"	18" x 2" x 20'-3½"	20" x 2" x 30'-0"	24" x 2½" x 86'-0"	24" x 2" x 35'-1 9/16"	24" x 2" x 33'-0"	30" x 2½" x 25'-0"				
			WEB	99" x 13/16" x 7'-8½"	99" x 13/16" x 30'-0"	99" x 13/16" x 20'-3½"	99" x ¾" x 30'-0"	99" x ¾" x 86'-0"	99" x ¾" x 35'-1 9/16"	99" x 13/16" x 33'-0"	99" x 13/16" x 25'-0"				

30" 22"

7/8" DIA. STEEL STUD SPACING (4 PER ROW) - SPAN 2

GIRDER NUMBER	SA	SB	SC
G-1	50 SPA. @ 1'-8" = 83'-4"	6 7/16"	104 SPA. @ 1'-8" = 173'-4"
G-2	8 SPA. @ 1'-0" = 8'-0"	1'-8 3/16"	125 SPA. @ 2'-0" = 250'-0"
G-3	10 SPA. @ 1'-11" = 19'-2"	1'-0"	121 SPA. @ 2'-0" = 242'-0"
G-4	7 SPA. @ 1'-0" = 7'-0"	9 13/16"	134 SPA. @ 1'-11" = 256'-10"
G-5	54 SPA. @ 1'-6" = 81'-0"	1'-1 9/16"	111 SPA. @ 1'-8" = 185'-0"

SPLICE TYPES - SPAN 2

GIRDER NUMBER	2 - 1	2 - 2	2 - 3
G-1	TYPE XIV	TYPE XIII	TYPE IX
G-2	TYPE XIV	TYPE XIII	TYPE IX
G-3	TYPE XIV	TYPE XIII	TYPE IX
G-4	TYPE ~~XIV~~ XVI [3]	TYPE XIII	TYPE IX
G-5	TYPE XV	TYPE X	TYPE XI

NOTES:

1. FOR GIRDER SHOP SPLICE DETAILS, SEE STANDARD DETAIL NO. BR-SS(8.11)-85-173.
2. NO WELDING OF STAY IN PLACE DECK FORMS TO TOP FLANGE PLATE WILL BE ALLOWED IN TENSION AND STRESS REVERSAL AREAS.
3. SPACE STEEL STUD SHEAR DEVELOPERS TO MISS BOLT HEADS IN FIELD SPLICE. SEE STANDARD DETAIL NO. BR-SS(8.05)-75-30.
4. FOR TRANSVERSE STIFFENER LOCATIONS, SEE DWG. NO. S6-86.

FILE: q:\smd\304004.11\951695_hw\cadd\struct\Ramp_GG\GG-SPAN2RedLine3.dgn
DATE: 3/30/2007
TIME: 9:25:03 AM

JOHNSON, MIRMIRAN & THOMPSON
Engineering A Brighter Future

MARYLAND TRANSPORTATION AUTHORITY
Engineering Division

ADDENDUMS & REVISIONS			
NO.	DESCRIPTION	BY	DATE
3	REVISED PLATE SIZES AND SPLICE TYPE	TDY	3/07

I-95 EXPRESS TOLL LANES : I-695 INTERCHANGE
GENERAL PURPOSE ROADWAYS AND RAMPS
JOHN F. KENNEDY MEMORIAL HIGHWAY (BALTIMORE COUNTY)
RAMP GG
GIRDER ELEVATION - SPAN 2

DESIGNED BY TDY	DRAWN BY DJA	CHECKED BY MJB
CONST. REVIEW BY	DATE AUGUST, 2006	SCALE AS SHOWN

CONTRACT NO. KH-1301-000-006
DRAWING NO. S6 - 92
SHEET NO. 789 OF 1676

THE ESTIMATED NUMBER OF STEEL STUD SHEAR DEVELOPERS REQUIRED IS 23,888.

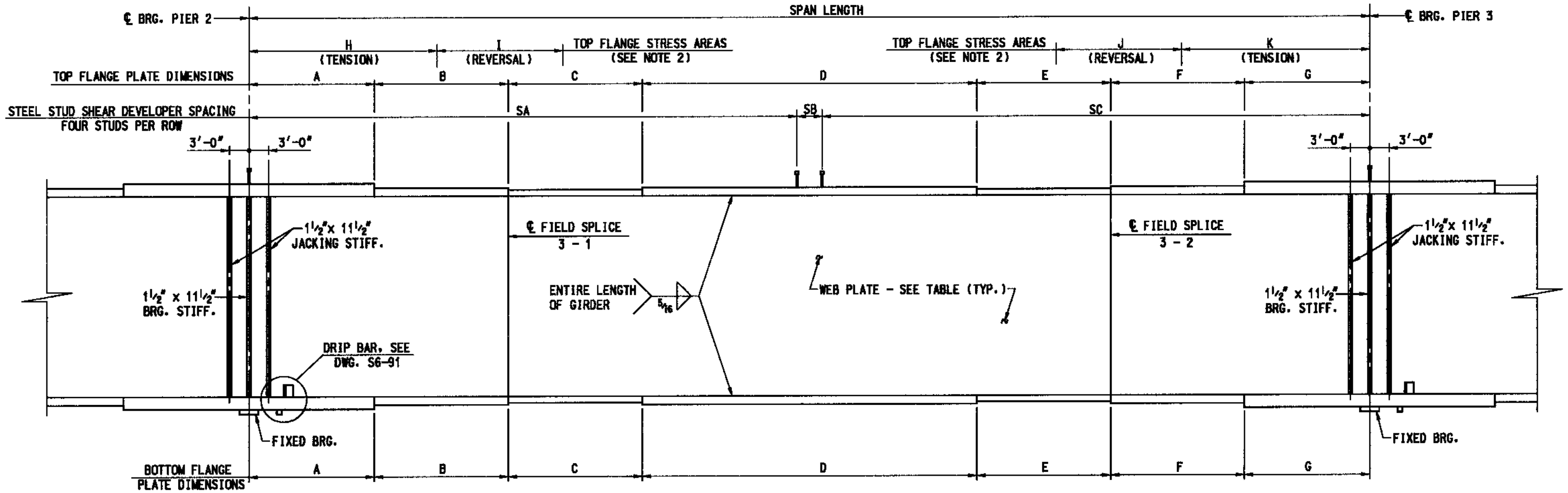

GIRDER ELEVATION - SPAN 3
NOT TO SCALE

GIRDER ELEVATION - SPAN 3 - DIMENSIONS

GIRDER NUMBER	SPAN LENGTH	RADIUS	PLATES	A	B	C	D	E	F	G	H	I	J	K
G-1	229'-6 1/16"	R=949.67'	TOP FLANGE	24" x 2 1/2" x 25'-0"	20" x 2" x 43'-0"	15" x 1 1/4" x 30'-0"	15" x 1 1/4" x 30'-0"	15" x 1 1/4" x 34'-6 1/16"	18" x 2" x 42'-0"	24" x 2 1/2" x 25'-0"	43'-9"	36'-0"	33'-2"	42'-6"
			BOTTOM FLANGE	24" x 2 1/2" x 25'-0"	20" x 2" x 43'-0"	15" x 1 1/2" x 30'-0"	15" x 1 1/2" x 30'-0"	15" x 1 1/2" x 34'-6 1/16"	18" x 2" x 42'-0"	24" x 2 1/2" x 25'-0"				
			WEB	99" x 13/16" x 25'-0"	99" x 3/4" x 43'-0"	99" x 3/4" x 30'-0"	99" x 3/4" x 30'-0"	99" x 3/4" x 34'-6 1/16"	99" x 3/4" x 42'-0"	99" x 13/16" x 25'-0"				
G-2	231'-8 5/8"	R=958.83'	TOP FLANGE	24" x 2 1/2" x 25'-0"	20" x 2" x 47'-0"	15" x 1 1/4" x 30'-0"	15" x 1 1/4" x 30'-0"	15" x 1 1/4" x 32'-8 5/8"	18" x 2" x 42'-0"	24" x 2 1/2" x 25'-0"	47'-4"	34'-6"	31'-10"	46'-9"
			BOTTOM FLANGE	24" x 2 1/2" x 25'-0"	20" x 2" x 47'-0"	15" x 1 1/2" x 30'-0"	15" x 1 1/2" x 30'-0"	15" x 1 1/2" x 32'-8 5/8"	18" x 2" x 42'-0"	24" x 2 1/2" x 25'-0"				
			WEB	99" x 13/16" x 25'-0"	99" x 3/4" x 47'-0"	99" x 3/4" x 30'-0"	99" x 3/4" x 30'-0"	99" x 3/4" x 32'-8 5/8"	99" x 3/4" x 42'-0"	99" x 3/4" x 25'-0"				
G-3	233'-11 3/16"	R=968.00'	TOP FLANGE	24" x 2 1/2" x 25'-0"	20" x 2" x 51'-0"	15" x 1 1/4" x 30'-0"	15" x 1 1/4" x 30'-0"	15" x 1 1/4" x 26'-11 3/16"	18" x 2" x 46'-0"	24" x 2 1/2" x 25'-0"	50'-8"	36'-10"	32'-9"	50'-7"
			BOTTOM FLANGE	24" x 2 1/2" x 25'-0"	20" x 2" x 51'-0"	15" x 1 1/2" x 30'-0"	15" x 1 1/2" x 30'-0"	15" x 1 1/2" x 26'-11 3/16"	18" x 2" x 46'-0"	24" x 2 1/2" x 25'-0"				
			WEB	99" x 3/4" x 25'-0"	99" x 3/4" x 51'-0"	99" x 3/4" x 30'-0"	99" x 3/4" x 30'-0"	99" x 3/4" x 26'-11 3/16"	99" x 3/4" x 46'-0"	99" x 3/4" x 25'-0"				
G-4	236'-1 13/16"	R=977.17'	TOP FLANGE	24" x 2 1/2" x 25'-0"	20" x 2" x 55'-0"	15" x 1 1/4" x 30'-0"	15" x 1 1/4" x 30'-0"	15" x 1 1/4" x 20'-1 13/16"	18" x 2" x 51'-0"	24" x 2 1/2" x 25'-0"	50'-2"	68'-0"	66'-5 13/16"	51'-6"
			BOTTOM FLANGE	24" x 2 1/2" x 25'-0"	20" x 2" x 55'-0"	15" x 1 1/2" x 30'-0"	15" x 1 1/2" x 30'-0"	15" x 1 1/2" x 20'-1 13/16"	18" x 2" x 51'-0"	24" x 2 1/2" x 25'-0"				
			WEB	99" x 13/16" x 25'-0"	99" x 3/4" x 55'-0"	99" x 3/4" x 30'-0"	99" x 3/4" x 30'-0"	99" x 3/4" x 20'-1 13/16"	99" x 3/4" x 51'-0"	99" x 13/16" x 25'-0"				
G-5	238'-4 3/8"	R=986.33'	TOP FLANGE	30" x 2 1/2" x 25'-0"	24" x 2" x 57'-0"	15" x 1 1/4" x 30'-0"	15" x 1 1/4" x 30'-0"	15" x 1 1/4" x 14'-4 3/8"	24" x 2" 57'-0"	30" x 2 1/2" x 25'-0"	50'-0"	68'-0"	67'-4 3/8"	53'-0"
			BOTTOM FLANGE	30" x 2 1/2" x 25'-0"	24" x 2" x 57'-0"	15" x 1 1/2" x 30'-0"	15" x 1 1/2" x 30'-0"	15" x 1 1/2" x 14'-4 3/8"	24" x 2" 57'-0"	30" x 2 1/2" x 25'-0"				
			WEB	99" x 13/16" x 25'-0"	99" x 3/4" x 57'-0"	99" x 3/4" x 30'-0"	99" x 3/4" x 30'-0"	99" x 3/4" x 14'-4 3/8"	99" x 3/4" x 57'-0"	99" x 13/16" x 25'-0"				

7/8" DIA. STEEL STUD SPACING (4 PER ROW) - SPAN 3

GIRDER NUMBER	SA	SB	SC
G-1	48 SPA. @ 1'-8" = 80'-0"	1'-2 1/16"	89 SPA. @ 1'-8" = 148'-4"
G-2	66 SPA. @ 2'-0" = 132'-0"	1'-8 5/8"	49 SPA. @ 2'-0" = 98'-0"
G-3	40 SPA. @ 2'-0" = 80'-0"	1'-11 13/16"	76 SPA. @ 2'-0" = 152'-0"
G-4	42 SPA. @ 1'-11" = 80'-6"	4 13/16"	81 SPA. @ 1'-11" = 155'-3"
G-5	50 SPA. @ 1'-7" = 79'-2"	10 3/8"	100 SPA. @ 1'-7" = 158'-4"

SPLICE TYPES - SPAN 3

GIRDER NUMBER	3 - 1	3 - 2
G-1	TYPE II	TYPE II
G-2	TYPE II	TYPE II
G-3	TYPE II	TYPE II
G-4	TYPE II	TYPE II
G-5	TYPE II	TYPE II

NOTES:

1. FOR GIRDER SHOP SPLICE DETAILS, SEE STANDARD DETAIL NO. BR-SS(8.11)-85-173.
2. NO WELDING OF STAY IN PLACE DECK FORMS TO TOP FLANGE PLATE WILL BE ALLOWED IN TENSION AND STRESS REVERSAL AREAS.
3. SPACE STEEL STUD SHEAR DEVELOPERS TO MISS BOLT HEADS IN FIELD SPLICE. SEE STANDARD DETAIL NO. BR-SS(8.05)-75-30.
4. FOR TRANSVERSE STIFFENER LOCATIONS, SEE DWG. NO. S6-87.

MASTER SET

FILE: q:\amd\304004_II1951695_hw\cadd\struct\ramp-gg\GG-SPAN3.dgn
DATE: 8/4/2006
TIME: 4:06:42 AM

JOHNSON, MIRMIRAN & THOMPSON
Engineering A Brighter Future

MARYLAND TRANSPORTATION AUTHORITY
Engineering Division

ADDENDUMS & REVISIONS			
NO.	DESCRIPTION	BY	DATE

I-95 EXPRESS TOLL LANES : I-695 INTERCHANGE
GENERAL PURPOSE ROADWAYS AND RAMPS
JOHN F. KENNEDY MEMORIAL HIGHWAY (BALTIMORE COUNTY)
RAMP GG
GIRDER ELEVATION - SPAN 3

DESIGNED BY TDY	DRAWN BY DJA	CHECKED BY MJB
CONST. REVIEW BY	DATE AUGUST, 2006	SCALE AS SHOWN

CONTRACT NO. KH-1301-000-006
DRAWING NO. S6 - 93
SHEET NO. 790 OF 1676

THE ESTIMATED NUMBER OF STEEL STUD SHEAR DEVELOPERS REQUIRED IS 23,888.

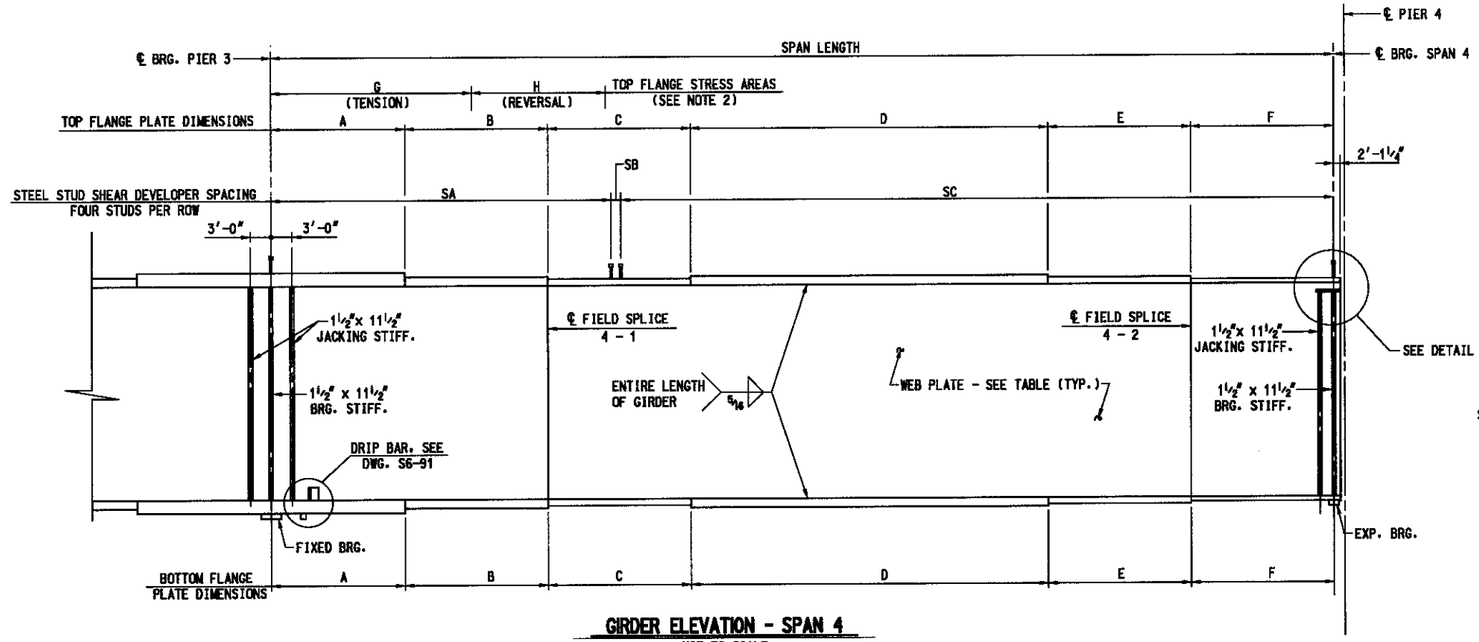

GIRDER ELEVATION - SPAN 4
NOT TO SCALE

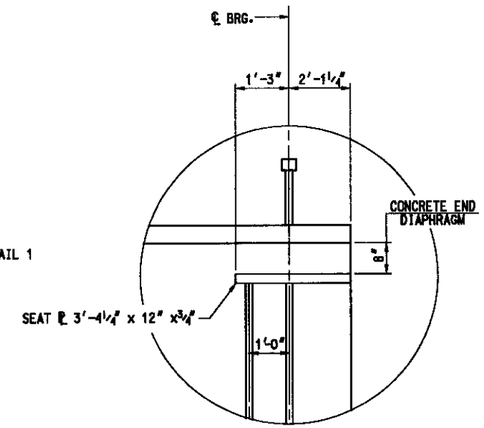

DETAIL I
NOT TO SCALE

GIRDER ELEVATION - SPAN 4 - DIMENSIONS

GIRDER NUMBER	SPAN LENGTH	RADIUS	PLATES	A	B	C	D	E	F	G	H
G-1	214'-7 9/16"	R=949.67'	TOP FLANGE	24" x 2½" x 25'-0"	18" x 2" x 24'-0"	15" x 1½" x 35'-0"	15" x 2" x 80'-0"	15" x 2" x 20'-7 9/16"	15" x 1¼" x 30'-0"	37'-8"	27'-8"
			BOTTOM FLANGE	24" x 2½" x 25'-0"	18" x 2" x 24'-0"	18" x 2" x 35'-0"	22" x 2½" x 80'-0"	18" x 2½" x 20'-7 9/16"	15" x 2" x 30'-0"		
			WEB	99" x 13/16" x 25'-0"	99" x ¾" x 24'-0"	99" x ¾" x 35'-0"	99" x ¾" x 80'-0"	99" x ¾" x 20'-7 9/16"	99" x ¾" x 30'-0"		
G-2	216'-8 13/16"	R=958.83'	TOP FLANGE	24" x 2½" x 25'-0"	18" x 2" x 24'-0"	15" x 1½" x 35'-0"	15" x 2" x 80'-0"	15" x 2" x 22'-8 13/16"	15" x 1¼" x 30'-0"	38'-8"	22'-4"
			BOTTOM FLANGE	24" x 2½" x 25'-0"	18" x 2" x 24'-0"	18" x 2" x 35'-0"	22" x 2½" x 80'-0"	18" x 2½" x 22'-8 13/16"	15" x 2" x 30'-0"		
			WEB	99" x ¾" x 25'-0"	99" x ¾" x 24'-0"	99" x ¾" x 35'-0"	99" x ¾" x 80'-0"	99" x ¾" x 22'-8 13/16"	99" x ¾" x 30'-0"		
G-3	218'-10"	R=968.00'	TOP FLANGE	24" x 2½" x 25'-0"	18" x 2" x 24'-0"	15" x 1½" x 35'-0"	15" x 2" x 80'-0"	15" x 2" x 24'-10"	15" x 1¼" x 30'-0"	39'-3"	19'-9"
			BOTTOM FLANGE	24" x 2½" x 25'-0"	18" x 2" x 24'-0"	18" x 2" x 35'-0"	22" x 2½" x 80'-0"	18" x 2½" x 24'-10"	15" x 2" x 30'-0"		
			WEB	99" x ¾" x 25'-0"	99" x ¾" x 24'-0"	99" x ¾" x 35'-0"	99" x ¾" x 80'-0"	99" x ¾" x 24'-10"	99" x ¾" x 30'-0"		
G-4	220'-11 3/16"	R=977.17'	TOP FLANGE	24" x 2½" x 25'-0"	18" x 2" x 24'-0"	15" x 1½" x 35'-0"	15" x 2" x 80'-0"	15" x 2" x 26'-11 3/16"	15" x 1¼" x 30'-0"	37'-6"	25'-8"
			BOTTOM FLANGE	24" x 2½" x 25'-0"	18" x 2" x 24'-0"	18" x 2" x 35'-0"	22" x 2½" x 80'-0"	18" x 2½" x 26'-11 3/16"	15" x 2" x 30'-0"		
			WEB	99" x 13/16" x 25'-0"	99" x ¾" x 24'-0"	99" x ¾" x 35'-0"	99" x ¾" x 80'-0"	99" x ¾" x 26'-11 3/16"	99" x ¾" x 30'-0"		
G-5	223'-0 7/16"	R=986.33'	TOP FLANGE	30" x 2½" x 25'-0"	20" x 2" x 24'-0"	15" x 1½" x 35'-0"	20" x 2" x 80'-0"	17" x 2" x 29'-0 7/16"	15" x 1¼" x 30'-0"	36'-10"	29'-6"
			BOTTOM FLANGE	30" x 2½" x 25'-0"	20" x 2" x 24'-0"	24" x 2" x 35'-0"	28" x 2½" x 80'-0"	24" x 2½" x 29'-0 7/16"	17" x 2" x 30'-0"		
			WEB	99" x 13/16" x 25'-0"	99" x 13/16" x 24'-0"	99" x ¾" x 35'-0"	99" x ¾" x 80'-0"	99" x ¾" x 29'-0 7/16"	99" x ¾" x 30'-0"		

7/8" DIA. STEEL STUD SPACING (4 PER ROW) - SPAN 4

GIRDER NUMBER	SA	SB	SC
G-1	18 SPA. @ 1'-8" = 30'-0"	7 9/16"	92 SPA. @ 2'-0" = 184'-0"
G-2	40 SPA. @ 2'-0" = 80'-0"	8 13/16"	68 SPA. @ 2'-0" = 136'-0"
G-3	40 SPA. @ 2'-0" = 80'-0"	10 "	69 SPA. @ 2'-0" = 138'-0"
G-4	40 SPA. @ 2'-0" = 80'-0"	11 3/16"	70 SPA. @ 2'-0" = 140'-0"
G-5	46 SPA. @ 1'-9" = 80'-6"	1'-7 7/16"	89 SPA. @ 1'-7" = 140'-11"

SPLICE TYPES - SPAN 4

GIRDER NUMBER	4 - 1	4 - 2
G-1	TYPE IX	TYPE V
G-2	TYPE IX	TYPE V
G-3	TYPE IX	TYPE V
G-4	TYPE IX	TYPE V
G-5	TYPE XI	TYPE VI

NOTES:

1. FOR GIRDER SHOP SPLICE DETAILS, SEE STANDARD DETAIL NO. BR-SS(8.11)-85-173.
2. NO WELDING OF STAY IN PLACE DECK FORMS TO TOP FLANGE PLATE WILL BE ALLOWED IN TENSION AND STRESS REVERSAL AREAS.
3. SPACE STEEL STUD SHEAR DEVELOPERS TO MISS BOLT HEADS IN FIELD SPLICE. SEE STANDARD DETAIL NO. BR-SS(8.05)-75-30.
4. FOR CONCRETE END DIAPHRAGM AT PIERS, SEE STANDARD DETAIL NO. BR-SS(6.22)-80-120.
5. FOR TRANSVERSE STIFFENER LOCATIONS, SEE DWG. NO. S6-87.

MASTER SET

JOHNSON, MIRMIRAN & THOMPSON
Engineering A Brighter Future

MARYLAND TRANSPORTATION AUTHORITY
Engineering Division

ADDENDUMS & REVISIONS			
NO.	DESCRIPTION	BY	DATE

I-95 EXPRESS TOLL LANES : I-695 INTERCHANGE
GENERAL PURPOSE ROADWAYS AND RAMPS
JOHN F. KENNEDY MEMORIAL HIGHWAY (BALTIMORE COUNTY)
RAMP GG
GIRDER ELEVATION - SPAN 4

CONTRACT NO. KH-1301-000-006
DRAWING NO. S6 - 94
SHEET NO. 791 OF 1676

DESIGNED BY TDY | DRAWN BY DJA | CHECKED BY MJB
CONST. REVIEW BY | DATE AUGUST, 2006 | SCALE AS SHOWN

FILE: q:\smd\304004_I195I695_hw\oddi\structr\ramp_gg\G6-SPAN4.dgn
DATE: 8/4/2006
TIME: 4:06:44 AM

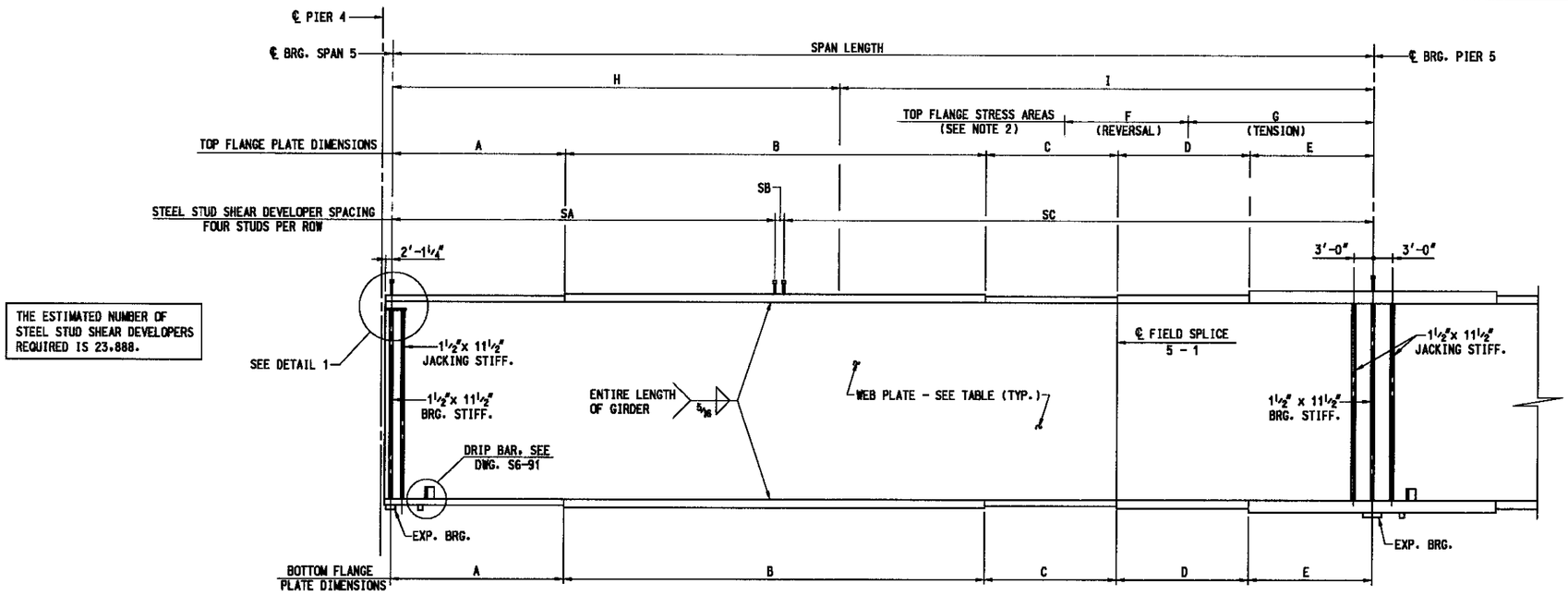

GIRDER ELEVATION - SPAN 5

NOT TO SCALE

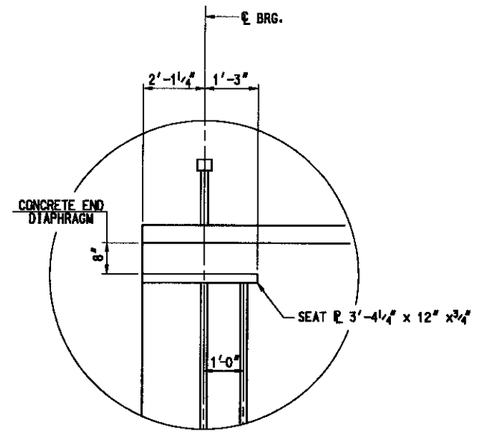

DETAIL 1

NOT TO SCALE

GIRDER ELEVATION - SPAN 5 - DIMENSIONS

GIRDER NUMBER	SPAN LENGTH	PLATES	A	B	C	D	E	F	G	H	I
G-1	214'-9 15/16"	TOP FLANGE	15" x 1 1/4" x 38'-0"	15" x 1 1/2" x 90'-0"	15" x 1 1/4" x 21'-9 15/16"	18" x 2 1/2" x 35'-0"	24" x 3" x 30'-0"	31'-3"	45'-8"	73'-1 7/8"	141'-8 1/16"
		BOTTOM FLANGE	15" x 2" x 38'-0"	18" x 2 1/2" x 90'-0"	15" x 2" x 21'-9 15/16"	18" x 2 1/2" x 35'-0"	24" x 3" x 30'-0"				
		WEB	99" x 3/4" x 38'-0"	99" x 3/4" x 90'-0"	99" x 3/4" x 21'-9 15/16"	99" x 13/16" x 35'-0"	99" x 13/16" x 30'-0"			R=949.67'	R=1089.67'
G-2	216'-9 1/16"	TOP FLANGE	15" x 1 1/4" x 38'-0"	15" x 1 1/2" x 90'-0"	15" x 1 1/4" x 21'-9 1/16"	18" x 2 1/2" x 37'-0"	24" x 3" x 30'-0"	26'-9"	48'-0"	73'-10 5/8"	142'-10 7/16"
		BOTTOM FLANGE	15" x 2" x 38'-0"	18" x 2 1/2" x 90'-0"	15" x 2" x 21'-9 1/16"	18" x 2 1/2" x 37'-0"	24" x 3" x 30'-0"				
		WEB	99" x 3/4" x 38'-0"	99" x 3/4" x 90'-0"	99" x 3/4" x 21'-9 1/16"	99" x 13/16" x 37'-0"	99" x 13/16" x 30'-0"			R=958.83'	R=1098.33'
G-3	218'-8 3/16"	TOP FLANGE	15" x 1 1/4" x 38'-0"	15" x 1 1/2" x 90'-0"	15" x 1 1/4" x 22'-8 3/16"	18" x 2 1/2" x 38'-0"	24" x 3" x 30'-0"	24'-4"	49'-10"	74'-7 7/16"	144'-0 3/4"
		BOTTOM FLANGE	15" x 2" x 38'-0"	18" x 2 1/2" x 90'-0"	15" x 2" x 22'-8 3/16"	18" x 2 1/2" x 38'-0"	24" x 3" x 30'-0"				
		WEB	99" x 3/4" x 38'-0"	99" x 3/4" x 90'-0"	99" x 3/4" x 22'-8 3/16"	99" x 13/16" x 38'-0"	99" x 13/16" x 30'-0"			R=968.00'	R=1108.00'
G-4	220'-7 5/16"	TOP FLANGE	15" x 1 1/4" x 38'-0"	15" x 1 1/2" x 90'-0"	15" x 1 1/4" x 22'-7 5/16"	18" x 2 1/2" x 40'-0"	24" x 3" x 30'-0"	32'-0"	48'-5"	75'-4 5/16"	145'-3"
		BOTTOM FLANGE	15" x 2" x 38'-0"	18" x 2 1/2" x 90'-0"	15" x 2" x 22'-7 5/16"	18" x 2 1/2" x 40'-0"	24" x 3" x 30'-0"				
		WEB	99" x 3/4" x 38'-0"	99" x 3/4" x 90'-0"	99" x 3/4" x 22'-7 5/16"	99" x 13/16" x 40'-0"	99" x 13/16" x 30'-0"			R=977.17'	R=1117.17'
G-5	222'-6 7/16"	TOP FLANGE	15" x 1 1/4" x 38'-0"	18" x 1 1/2" x 90'-0"	15" x 1 1/4" x 22'-6 7/16"	22" x 2 1/2" x 42'-0"	30" x 3" x 30'-0"	38'-0"	47'-11"	76'-1 1/8"	146'-5 5/16"
		BOTTOM FLANGE	18" x 2" x 38'-0"	24" x 2 1/2" x 90'-0"	20" x 2" x 22'-6 7/16"	22" x 2 1/2" x 42'-0"	30" x 3" x 30'-0"				
		WEB	99" x 3/4" x 38'-0"	99" x 3/4" x 90'-0"	99" x 3/4" x 22'-6 7/16"	99" x 13/16" x 42'-0"	99" x 13/16" x 30'-0"			R=986.33'	R=1126.33'

SPLICE TYPES - SPAN 5

GIRDER NUMBER	5 - 1
G-1	TYPE V
G-2	TYPE V
G-3	TYPE V
G-4	TYPE V
G-5	TYPE VII

7/8" DIA. STEEL STUD SPACING (4 PER ROW) - SPAN 5

GIRDER NUMBER	SA	SB	SC
G-1	83 SPA. @ 2'-0" = 166'-0"	1'-1 15/16"	26 SPA. @ 1'-10" = 47'-8"
G-2	26 SPA. @ 1'-10" = 47'-8"	1'-1 1/16"	84 SPA. @ 2'-0" = 168'-0"
G-3	40 SPA. @ 2'-0" = 80'-0"	8 3/16"	69 SPA. @ 2'-0" = 138'-0"
G-4	40 SPA. @ 2'-0" = 80'-0"	7 5/16"	70 SPA. @ 2'-0" = 140'-0"
G-5	24 SPA. @ 1'-6" = 40'-0"	6 7/16"	91 SPA. @ 2'-0" = 182'-0"

NOTES:

1. FOR GIRDER SHOP SPLICE DETAILS, SEE STANDARD DETAIL NO. BR-SS(8.11)-85-173.
2. NO WELDING OF STAY IN PLACE DECK FORMS TO TOP FLANGE PLATE WILL BE ALLOWED IN TENSION AND STRESS REVERSAL AREAS.
3. SPACE STEEL STUD SHEAR DEVELOPERS TO MISS BOLT HEADS IN FIELD SPLICE. SEE STANDARD DETAIL NO. BR-SS(8.05)-75-30.
4. FOR CONCRETE END DIAPHRAGM AT PIERS, SEE STANDARD DETAIL NO. BR-SS(6.22)-80-120.
5. FOR TRANSVERSE STIFFENER LOCATIONS, SEE DWG. NO. S6-88.

MASTER SET

FILE: e:\smd\304004_I1951695_hw\coddl\smruo1\ramp_gg\S6-SPAN5.dgn
DATE: 8/4/2006
TIME: 4:05:46 AM

JMT
JOHNSON, MIRMIRAN & THOMPSON
Engineering A Brighter Future

MARYLAND TRANSPORTATION AUTHORITY
Engineering Division

ADDENDUMS & REVISIONS			
NO.	DESCRIPTION	BY	DATE

I-95 EXPRESS TOLL LANES : I-695 INTERCHANGE
GENERAL PURPOSE ROADWAYS AND RAMPS
JOHN F. KENNEDY MEMORIAL HIGHWAY (BALTIMORE COUNTY)
RAMP GG
GIRDER ELEVATION - SPAN 5

DESIGNED BY TDY	DRAWN BY DJA	CHECKED BY MJB
CONST. REVIEW BY	DATE AUGUST, 2006	SCALE AS SHOWN

CONTRACT NO. KH-1301-000-006
DRAWING NO. S6 - 95
SHEET NO. 792 OF 1676

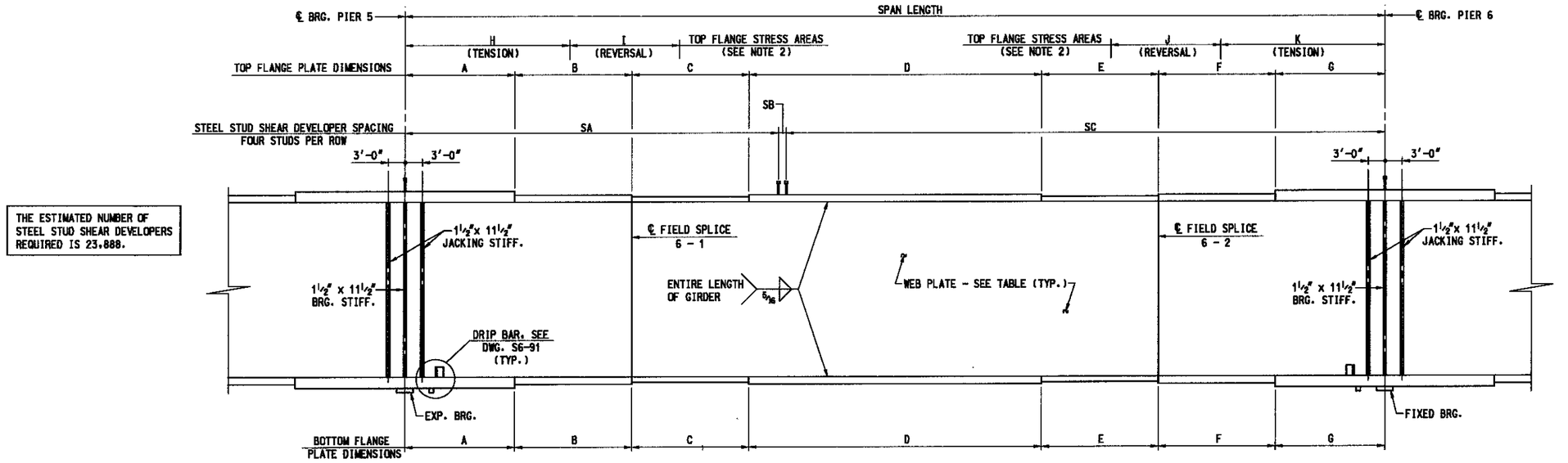

GIRDER ELEVATION - SPAN 6

NOT TO SCALE

GIRDER ELEVATION - SPAN 6 - DIMENSIONS

GIRDER NUMBER	SPAN LENGTH	RADIUS	PLATES	A	B	C	D	E	F	G	H	I	J	K
G-1	255'-6 15/16"	R=1089.67'	TOP FLANGE	24" x 3" x 30'-0"	18" x 2½" x 34'-0"	15" x 1½" x 25'-0"	15" x 1½" x 80'-0"	15" x 1½" x 23'-6 15/16"	18" x 2" x 38'-0"	24" x 2½" x 25'-0"	47'-10"	29'-4"	27'-6"	40'-8"
			BOTTOM FLANGE	24" x 3" x 30'-0"	18" x 2½" x 34'-0"	15" x 2" x 25'-0"	18" x 2" x 80'-0"	15" x 2" x 23'-6 15/16"	18" x 2" x 38'-0"	24" x 2½" x 25'-0"				
			WEB	99" x 13/16" x 30'-0"	99" x 13/16" x 34'-0"	99" x 3/4" x 25'-0"	99" x 3/4" x 80'-0"	99" x 3/4" x 23'-6 15/16"	99" x 13/16" x 38'-0"	99" x 13/16" x 25'-0"				
G-2	257'-8 11/16"	R=1098.33'	TOP FLANGE	24" x 3" x 30'-0"	18" x 2½" x 35'-0"	15" x 1½" x 25'-0"	15" x 1½" x 80'-0"	15" x 1½" x 24'-8 11/16"	18" x 2" x 38'-0"	24" x 2½" x 25'-0"	51'-3"	26'-0"	23'-4"	42'-9"
			BOTTOM FLANGE	24" x 3" x 30'-0"	18" x 2½" x 35'-0"	15" x 2" x 25'-0"	18" x 2" x 80'-0"	15" x 2" x 24'-8 11/16"	18" x 2" x 38'-0"	24" x 2½" x 25'-0"				
			WEB	99" x 13/16" x 30'-0"	99" x 13/16" x 35'-0"	99" x 3/4" x 25'-0"	99" x 3/4" x 80'-0"	99" x 3/4" x 24'-8 11/16"	99" x 3/4" x 38'-0"	99" x 3/4" x 25'-0"				
G-3	259'-10½"	R=1108.00'	TOP FLANGE	24" x 3" x 30'-0"	18" x 2½" x 37'-0"	15" x 1½" x 25'-0"	15" x 1½" x 80'-0"	15" x 1½" x 23'-10½"	18" x 2" x 39'-0"	24" x 2½" x 25'-0"	54'-8"	23'-8"	20'-5"	45'-0"
			BOTTOM FLANGE	24" x 3" x 30'-0"	18" x 2½" x 37'-0"	15" x 2" x 25'-0"	18" x 2" x 80'-0"	15" x 2" x 23'-10½"	18" x 2" x 39'-0"	24" x 2½" x 25'-0"				
			WEB	99" x 13/16" x 30'-0"	99" x 13/16" x 37'-0"	99" x 3/4" x 25'-0"	99" x 3/4" x 80'-0"	99" x 3/4" x 23'-10½"	99" x 3/4" x 39'-0"	99" x 3/4" x 25'-0"				
G-4	262'-0 5/16"	R=1117.17'	TOP FLANGE	24" x 3" x 30'-0"	18" x 2½" x 39'-0"	15" x 1½" x 25'-0"	15" x 1½" x 80'-0"	15" x 1½" x 24'-0 5/16"	18" x 2" x 39'-0"	24" x 2½" x 25'-0"	54'-11"	32'-1"	28'-2"	44'-4"
			BOTTOM FLANGE	24" x 3" x 30'-0"	18" x 2½" x 39'-0"	15" x 2" x 25'-0"	18" x 2" x 80'-0"	15" x 2" x 24'-0 5/16"	18" x 2" x 39'-0"	24" x 2½" x 25'-0"				
			WEB	99" x 13/16" x 30'-0"	99" x 13/16" x 39'-0"	99" x 3/4" x 25'-0"	99" x 3/4" x 80'-0"	99" x 3/4" x 24'-0 5/16"	99" x 13/16" x 39'-0"	99" x 13/16" x 25'-0"				
G-5	264'-2 1/8"	R=1126.33'	TOP FLANGE	30" x 3" x 30'-0"	22" x 2½" x 40'-0"	15" x 1½" x 25'-0"	18" x 1½" x 80'-0"	15" x 1½" x 25'-2 1/8"	22" x 2" x 39'-0"	30" x 2½" x 25'-0"	55'-3"	39'-6"	35'-3"	44'-2"
			BOTTOM FLANGE	30" x 3" x 30'-0"	22" x 2½" x 40'-0"	18" x 2" x 25'-0"	22" x 2" x 80'-0"	18" x 2" x 25'-2 1/8"	22" x 2" x 39'-0"	30" x 2½" x 25'-0"				
			WEB	99" x 13/16" x 30'-0"	99" x 13/16" x 40'-0"	99" x 3/4" x 25'-0"	99" x 3/4" x 80'-0"	99" x 3/4" x 25'-2 1/8"	99" x 13/16" x 39'-0"	99" x 13/16" x 25'-0"				

7/8" DIA. STEEL STUD SPACING (4 PER ROW) - SPAN 6

GIRDER NUMBER	SA	SB	SC
G-1	34 SPA. @ 1'-9" = 59'-6"	1'-9 15/16"	111 SPA. @ 1'-9" = 194'-3"
G-2	30 SPA. @ 2'-0" = 60'-0"	1'-8 11/16"	98 SPA. @ 2'-0" = 196'-0"
G-3	30 SPA. @ 2'-0" = 60'-0"	1'-10½"	99 SPA. @ 2'-0" = 198'-0"
G-4	126 SPA. @ 2'-0" = 252'-0"	10 5/16"	5 SPA. @ 1'-10" = 9'-2"
G-5	42 SPA. @ 1'-8" = 70'-0"	10 1/8"	116 SPA. @ 1'-8" = 193'-4"

SPLICE TYPES - SPAN 6

GIRDER NUMBER	6 - 1	6 - 2
G-1	TYPE VIII	TYPE VIII
G-2	TYPE VIII	TYPE VIII
G-3	TYPE VIII	TYPE VIII
G-4	TYPE VIII	TYPE VIII
G-5	TYPE IX	TYPE IX

NOTES:

1. FOR GIRDER SHOP SPLICE DETAILS, SEE STANDARD DETAIL NO. BR-SS(8.11)-85-173.
2. NO WELDING OF STAY IN PLACE DECK FORMS TO TOP FLANGE PLATE WILL BE ALLOWED IN TENSION AND STRESS REVERSAL AREAS.
3. SPACE STEEL STUD SHEAR DEVELOPERS TO MISS BOLT HEADS IN FIELD SPLICE. SEE STANDARD DETAIL NO. BR-SS(8.05)-75-30.
4. FOR TRANSVERSE STIFFENER LOCATIONS, SEE DWG. NO. S6-88.

MASTER SET

FILE: q:\amd\304004_111951695_hw\ooddistribuct\ramp_gg\GG-SPAN6.dgn
DATE: 8/4/2006
TIME: 4:06:49 AM

JOHNSON, MIRMIRAN & THOMPSON
Engineering A Brighter Future

MARYLAND TRANSPORTATION AUTHORITY
Engineering Division

ADDENDUMS & REVISIONS			
NO.	DESCRIPTION	BY	DATE

I-95 EXPRESS TOLL LANES : I-695 INTERCHANGE
GENERAL PURPOSE ROADWAYS AND RAMPS
JOHN F. KENNEDY MEMORIAL HIGHWAY (BALTIMORE COUNTY)
RAMP GG
GIRDER ELEVATION - SPAN 6

CONTRACT NO. KH-1301-000-006
DRAWING NO. S6 - 96

DESIGNED BY TDY	DRAWN BY DJA	CHECKED BY MJB	SHEET NO.
CONST. REVIEW BY	DATE AUGUST, 2006	SCALE AS SHOWN	793 OF 1676

REVISED

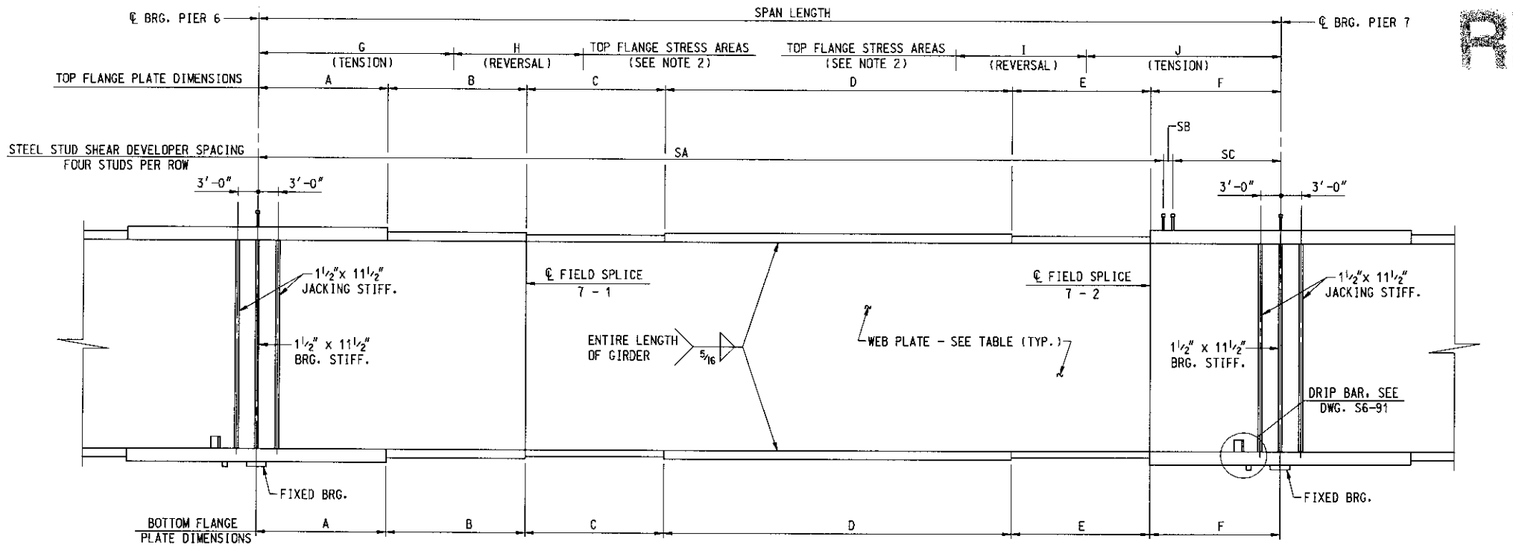

THE ESTIMATED NUMBER OF STEEL STUD SHEAR DEVELOPERS REQUIRED IS 23,888.

GIRDER ELEVATION - SPAN 7

NOT TO SCALE

GIRDER ELEVATION - SPAN 7 - DIMENSIONS

GIRDER NUMBER	SPAN LENGTH	RADIUS	PLATES	A	B	C	D	E	F [3]	G	H	I	J
G-1	207'-0 7/16"	R=1089.67'	TOP FLANGE	24" x 2 1/2" x 25'-0"	18" x 2" x 31'-0"	15" x 1 1/4" x 15'-0"	15" x 1 1/4" x 75'-0"	15" x 1 1/4" x 31'-0 7/16"	15" x 1 1/2" x 30'-0"	41'-4"	36'-2"	22'-2"	18'-9"
			BOTTOM FLANGE	24" x 2 1/2" x 25'-0"	18" x 2" x 31'-0"	15" x 1 1/2" x 15'-0"	15" x 2" x 75'-0"	15" x 1 1/2" x 31'-0 7/16"	15" x 1 1/2" x 30'-0"				
			WEB	99" x 13/16" x 25'-0"	99" x 13/16" x 31'-0"	99" x 3/4" x 15'-0"	99" x 3/4" x 75'-0"	99" x 3/4" x 31'-0 7/16"	99" x 3/4" x 30'-0"				
G-2	208'-9 5/16"	R=1098.33'	TOP FLANGE	24" x 2 1/2" x 25'-0"	18" x 2" x 33'-0"	15" x 1 1/4" x 15'-0"	15" x 1 1/4" x 75'-0"	15" x 1 1/4" x 30'-9 5/16"	15" x 1 1/2" x 30'-0"	43'-11"	30'-5"	18'-4"	19'-3"
			BOTTOM FLANGE	24" x 2 1/2" x 25'-0"	18" x 2" x 33'-0"	15" x 1 1/2" x 15'-0"	15" x 2" x 75'-0"	15" x 1 1/2" x 30'-9 5/16"	15" x 1 1/2" x 30'-0"				
			WEB	99" x 3/4" x 25'-0"	99" x 3/4" x 33'-0"	99" x 3/4" x 15'-0"	99" x 3/4" x 75'-0"	99" x 3/4" x 30'-9 5/16"	99" x 3/4" x 30'-0"				
G-3	210'-6 1/4"	R=1108.00'	TOP FLANGE	24" x 2 1/2" x 25'-0"	18" x 2" x 34'-0"	15" x 1 1/4" x 15'-0"	15" x 1 1/4" x 75'-0"	15" x 1 1/4" x 31'-6 1/4"	15" x 1 1/2" x 30'-0"	46'-1"	27'-9"	16'-8"	18'-9"
			BOTTOM FLANGE	24" x 2 1/2" x 25'-0"	18" x 2" x 34'-0"	15" x 1 1/2" x 15'-0"	15" x 2" x 75'-0"	15" x 1 1/2" x 31'-6 1/4"	15" x 1 1/2" x 30'-0"				
			WEB	99" x 3/4" x 25'-0"	99" x 3/4" x 34'-0"	99" x 3/4" x 15'-0"	99" x 3/4" x 75'-0"	99" x 3/4" x 31'-6 1/4"	99" x 3/4" x 30'-0"				
G-4	212'-3 1/8"	R=1117.17'	TOP FLANGE	24" x 2 1/2" x 25'-0"	18" x 2" x 35'-0"	15" x 1 1/4" x 15'-0"	15" x 1 1/4" x 75'-0"	15" x 1 1/4" x 32'-3 1/8"	15" x 1 1/2" x 30'-0"	44'-5"	39'-2"	22'-2"	15'-5"
			BOTTOM FLANGE	24" x 2 1/2" x 25'-0"	18" x 2" x 35'-0"	15" x 1 1/2" x 15'-0"	15" x 2" x 75'-0"	15" x 1 1/2" x 32'-3 1/8"	15" x 1 1/2" x 30'-0"				
			WEB	99" x 13/16" x 25'-0"	99" x 13/16" x 35'-0"	99" x 3/4" x 15'-0"	99" x 3/4" x 75'-0"	99" x 3/4" x 32'-3 1/8"	99" x 3/4" x 30'-0"				
G-5	214'-0 1/16"	R=1126.33'	TOP FLANGE	30" x 2 1/2" x 25'-0"	22" x 2" x 36'-0"	15" x 1 1/4" x 15'-0"	15" x 1 1/4" x 75'-0"	15" x 1 1/4" x 33'-0 1/16"	~~45"~~ x 1 1/2" x 30'-0"	43'-8"	49'-1"	28'-0"	12'-7"
			BOTTOM FLANGE	30" x 2 1/2" x 25'-0"	22" x 2" x 36'-0"	18" x 1 1/2" x 15'-0"	18" x 2" x 75'-0"	18" x 1 1/2" x 33'-0 1/16"	~~45"~~ x 1 1/2" x 30'-0"				
			WEB	99" x 13/16" x 25'-0"	99" x 13/16" x 36'-0"	99" x 3/4" x 15'-0"	99" x 3/4" x 75'-0"	99" x 3/4" x 33'-0 1/16"	99" x 13/16" x 30'-0"				

18" 13/16"

7/8" DIA. STEEL STUD SPACING (4 PER ROW) - SPAN 7

GIRDER NUMBER	SA	SB	SC
G-1	101 SPA. @ 1'-8" = 168'-4"	1'-4 7/16"	28 SPA. @ 1'-4" = 37'-4"
G-2	97 SPA. @ 1'-9" = 169'-9"	6 5/16"	22 SPA. @ 1'-9" = 38'-6"
G-3	86 SPA. @ 2'-0" = 172'-0"	1'-10 1/4"	20 SPA. @ 1'-10" = 36'-8"
G-4	94 SPA. @ 1'-10" = 172'-4"	11 1/8"	26 SPA. @ 1'-6" = 39'-0"
G-5	108 SPA. @ 1'-7" = 171'-0"	1'-0 1/16"	36 SPA. @ 1'-2" = 42'-0"

SPLICE TYPES - SPAN 7

GIRDER NUMBER	7 - 1	7 - 2
G-1	TYPE II	TYPE II
G-2	TYPE II	TYPE II
G-3	TYPE II	TYPE II
G-4	TYPE II	TYPE II
G-5	TYPE IV	TYPE ~~XII~~ IV [3]

NOTES:

1. FOR GIRDER SHOP SPLICE DETAILS, SEE STANDARD DETAIL NO. BR-SS(8.11)-85-173.
2. NO WELDING OF STAY IN PLACE DECK FORMS TO TOP FLANGE PLATE WILL BE ALLOWED IN TENSION AND STRESS REVERSAL AREAS.
3. SPACE STEEL STUD SHEAR DEVELOPERS TO MISS BOLT HEADS IN FIELD SPLICE. SEE STANDARD DETAIL NO. BR-SS(8.05)-75-30.
4. FOR TRANSVERSE STIFFENER LOCATIONS, SEE DWG. NO. S6-89.

JOHNSON, MIRMIRAN & THOMPSON
Engineering A Brighter Future

MARYLAND TRANSPORTATION AUTHORITY
Engineering Division

ADDENDUMS & REVISIONS			
NO.	DESCRIPTION	BY	DATE
[3]	REVISED PLATE SIZES	TDY	3/07

I-95 EXPRESS TOLL LANES : I-695 INTERCHANGE
GENERAL PURPOSE ROADWAYS AND RAMPS
JOHN F. KENNEDY MEMORIAL HIGHWAY (BALTIMORE COUNTY)
RAMP GG
GIRDER ELEVATION - SPAN 7

CONTRACT NO. KH-1301-000-006
DRAWING NO. S6 - 97

DESIGNED BY TDY | DRAWN BY DJA | CHECKED BY MJB
CONST. REVIEW BY | DATE AUGUST, 2006 | SCALE AS SHOWN
SHEET NO. 794 OF 1676

FILE: qp:\smd\304004.111\95695_hw\caddd\struct\Ramp_GG\GG-SPAN7redline3.dgn
DATE: 3/30/2007
TIME: 9:25:06 AM

REVISED

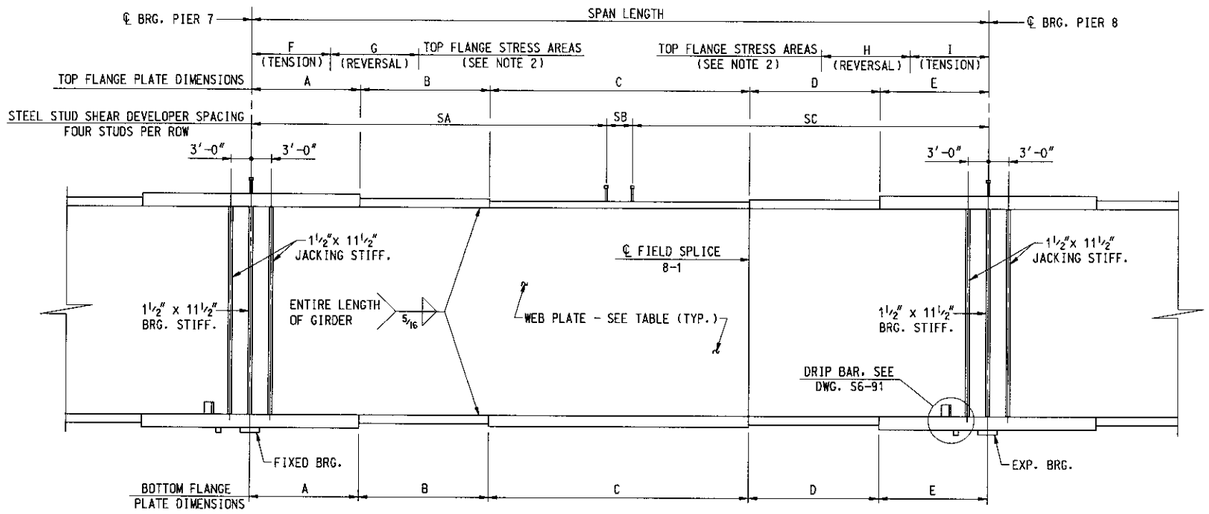

THE ESTIMATED NUMBER OF STEEL STUD SHEAR DEVELOPERS REQUIRED IS 23,888.

GIRDER ELEVATION - SPAN 8

NOT TO SCALE

GIRDER ELEVATION - SPAN 8 - DIMENSIONS

GIRDER NUMBER	SPAN LENGTH	RADIUS	PLATES	A [3]	B	C	D	E	F	G	H	I
G-1	159'-5⅞"	R=1089.67'	TOP FLANGE	15" x 1½" x 25'-0"	15" x 1½" x 15'-0"	15" x 1½" x 65'-5⅞"	15" x 2" x 29'-0"	18" x 2½" x 25'-0"	22'-5"	50'-0"	49'-5⅞"	37'-7"
			BOTTOM FLANGE	15" x 1½" x 25'-0"	15" x 1½" x 15'-0"	15" x 1½" x 65'-5⅞"	15" x 2" x 29'-0"	18" x 2½" x 25'-0"				
			WEB	99" x ¾" x 25'-0"	99" x ¾" x 15'-0"	99" x ¾" x 65'-5⅞"	99" x ¾" x 29'-0"	99" x ¾" x 25'-0"				
G-2	160'-9¹⁵⁄₁₆"	R=1098.33'	TOP FLANGE	15" x 1½" x 25'-0"	15" x 1½" x 16'-0"	15" x 1½" x 55'-9¹⁵⁄₁₆"	15" x 2" x 39'-0"	18" x 2½" x 25'-0"	25'-0"	46'-0"	46'-4¹⁵⁄₁₆"	43'-5"
			BOTTOM FLANGE	15" x 1½" x 25'-0"	15" x 1½" x 16'-0"	15" x 1½" x 55'-9¹⁵⁄₁₆"	15" x 2" x 39'-0"	18" x 2½" x 25'-0"				
			WEB	99" x ¾" x 25'-0"	99" x ¾" x 16'-0"	99" x ¾" x 55'-9¹⁵⁄₁₆"	99" x ¾" x 39'-0"	99" x ¾" x 25'-0"				
G-3	162'-2¹⁄₁₆"	R=1108.00'	TOP FLANGE	15" x 1½" x 25'-0"	15" x 1½" x 19'-0"	15" x 1½" x 47'-2¹⁄₁₆"	15" x 2" x 46'-0"	18" x 2½" x 25'-0"	27'-5"	43'-0"	42'-11¹⁄₁₆"	48'-10"
			BOTTOM FLANGE	15" x 1½" x 25'-0"	15" x 1½" x 19'-0"	15" x 1½" x 47'-2¹⁄₁₆"	15" x 2" x 46'-0"	18" x 2½" x 25'-0"				
			WEB	99" x ¾" x 25'-0"	99" x ¾" x 19'-0"	99" x ¾" x 47'-2¹⁄₁₆"	99" x ¾" x 46'-0"	99" x ¾" x 25'-0"				
G-4	163'-6⅛"	R=1117.17'	TOP FLANGE	15" x 1½" x 25'-0"	15" x 1½" x 24'-0"	15" x 1½" x 36'-6⅛"	15" x 2" x 53'-0"	18" x 2½" x 25'-0"	24'-5"	45'-0"	45'-6⅛"	48'-7"
			BOTTOM FLANGE	15" x 1½" x 25'-0"	15" x 1½" x 24'-0"	15" x 1½" x 36'-6⅛"	15" x 2" x 53'-0"	18" x 2½" x 25'-0"				
			WEB	99" x ¾" x 25'-0"	99" x ¾" x 24'-0"	99" x ¾" x 36'-6⅛"	99" x ¾" x 53'-0"	99" x ¾" x 25'-0"				
G-5	164'-10¼"	R=1126.33'	TOP FLANGE	~~15"~~ 18" x 1½" x 25'-0"	15" x 1½" x 31'-0"	15" x 1½" x 20'-10¼"	18" x 2" x 63'-0"	24" x 2½" x 25'-0"	22'-1"	47'-0"	46'-5¼"	49'-4"
			BOTTOM FLANGE	~~15"~~ 18" x 1½" x 25'-0"	15" x 1½" x 31'-0"	15" x 1½" x 20'-10¼"	18" x 2" x 63'-0"	24" x 2½" x 25'-0"				
			WEB	99" x 13⁄16" x 25'-0"	99" x ¾" x 31'-0"	99" x ¾" x 20'-10¼"	99" x ¾" x 63'-0"	99" x 13⁄16" x 25'-0"				

18" — 13⁄16"

⅞" DIA. STEEL STUD SPACING (4 PER ROW) - SPAN 8

GIRDER NUMBER	SA	SB	SC
G-1	28 SPA. @ 1'-4" = 37'-4"	5⅞"	73 SPA. @ 1'-8" = 121'-8"
G-2	20 SPA. @ 1'-9" = 35'-0"	1'-9¹⁵⁄₁₆"	62 SPA. @ 2'-0" = 124'-0"
G-3	20 SPA. @ 1'-10" = 36'-8"	1'-6¹⁄₁₆"	62 SPA. @ 2'-0" = 124'-0"
G-4	26 SPA. @ 1'-6" = 39'-0"	6¹⁄₈"	62 SPA. @ 2'-0" = 124'-0"
G-5	36 SPA. @ 1'-2" = 42'-0"	11¼"	77 SPA. @ 1'-7" = 121'-11"

SPLICE TYPES - SPAN 8

GIRDER NUMBER	8 - 1
G-1	TYPE III
G-2	TYPE III
G-3	TYPE III
G-4	TYPE III
G-5	TYPE III

NOTES:

1. FOR GIRDER SHOP SPLICE DETAILS, SEE STANDARD DETAIL NO. BR-SS(8.11)-85-173.
2. NO WELDING OF STAY IN PLACE DECK FORMS TO TOP FLANGE PLATE WILL BE ALLOWED IN TENSION AND STRESS REVERSAL AREAS.
3. SPACE STEEL STUD SHEAR DEVELOPERS TO MISS BOLT HEADS IN FIELD SPLCE. SEE STANDARD DETAIL NO. BR-SS(8.05)-75-30.
4. FOR TRANSVERSE STIFFENER LOCATIONS, SEE DWG. NO. S6-89.

FILE: qa\smd\304004.11\95\695_hw\caddd\structr\Ramp_GG\GG-SPANBRadLine3.dgn
DATE: 3/30/2007
TIME: 9:25:08 AM

JOHNSON, MIRMIRAN & THOMPSON
Engineering A Brighter Future

MARYLAND TRANSPORTATION AUTHORITY
Engineering Division

ADDENDUMS & REVISIONS			
NO.	DESCRIPTION	BY	DATE
3	REVISED PLATE SIZES	TDY	3/07

I-95 EXPRESS TOLL LANES : I-695 INTERCHANGE
GENERAL PURPOSE ROADWAYS AND RAMPS
JOHN F. KENNEDY MEMORIAL HIGHWAY (BALTIMORE COUNTY)
RAMP GG
GIRDER ELEVATION - SPAN 8

CONTRACT NO. KH-1301-000-006
DRAWING NO. S6 - 98

DESIGNED BY TDY | DRAWN BY DJA | CHECKED BY MJB
CONST. REVIEW BY | DATE AUGUST, 2006 | SCALE AS SHOWN
SHEET NO. 795 OF 1676

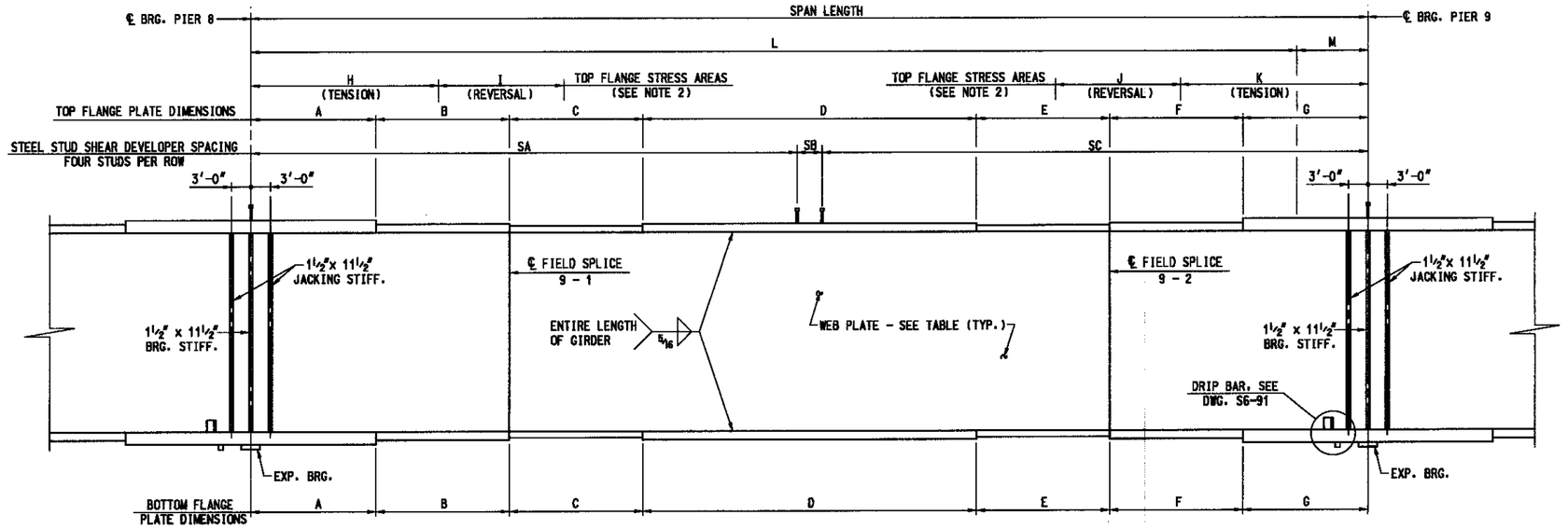

THE ESTIMATED NUMBER OF STEEL STUD SHEAR DEVELOPERS REQUIRED IS 23,888.

GIRDER ELEVATION - SPAN 9

NOT TO SCALE

GIRDER ELEVATION - SPAN 9 - DIMENSIONS

GIRDER NUMBER	SPAN LENGTH	PLATES	A	B	C	D	E	F	G	H	I	J	K	L	M
G-1	252'-9 15/16"	TOP FLANGE	18" x 2 1/2" x 25'-0"	15" x 2" x 23'-0"	15" x 1 1/2" x 24'-9 15/16"	15" x 1 1/2" x 90'-0"	15" x 1 1/2" x 35'-0"	18" x 2" x 30'-0"	24" x 2 1/2" x 25'-0"	31'-7"	20'-9"	28'-11"	44'-0"	229'-1 5/16"	23'-8 5/8"
		BOTTOM FLANGE	18" x 2 1/2" x 25'-0"	15" x 2" x 23'-0"	15" x 2" x 24'-9 15/16"	17" x 2 1/2" x 90'-0"	15" x 2" x 35'-0"	18" x 2" x 30'-0"	24" x 2 1/2" x 25'-0"					R=1089.67'	TANGENT
		WEB	99" x 3/4" x 25'-0"	99" x 3/4" x 23'-0"	99" x 3/4" x 24'-9 15/16"	99" x 3/4" x 90'-0"	99" x 3/4" x 35'-0"	99" x 3/4" x 30'-0"	99" x 13/16" x 25'-0"						
G-2	254'-9 1/16"	TOP FLANGE	18" x 2 1/2" x 25'-0"	15" x 2" x 25'-0"	15" x 1 1/2" x 24'-9 1/16"	15" x 1 1/2" x 90'-0"	15" x 1 1/2" x 35'-0"	18" x 2" x 30'-0"	24" x 2 1/2" x 25'-0"	33'-6"	16'-3"	22'-9"	45'-10"	231'-0 7/16"	23'-8 5/8"
		BOTTOM FLANGE	18" x 2 1/2" x 25'-0"	15" x 2" x 25'-0"	15" x 2" x 24'-9 1/16"	17" x 2 1/2" x 90'-0"	15" x 2" x 35'-0"	18" x 2" x 30'-0"	24" x 2 1/2" x 25'-0"					R=1098.33'	TANGENT
		WEB	99" x 3/4" x 25'-0"	99" x 3/4" x 25'-0"	99" x 3/4" x 24'-9 1/16"	99" x 3/4" x 90'-0"	99" x 3/4" x 35'-0"	99" x 3/4" x 30'-0"	99" x 3/4" x 25'-0"						
G-3	256'-8 3/16"	TOP FLANGE	18" x 2 1/2" x 25'-0"	15" x 2" x 26'-0"	15" x 1 1/2" x 25'-8 3/16"	15" x 1 1/2" x 90'-0"	15" x 1 1/2" x 35'-0"	18" x 2" x 30'-0"	24" x 2 1/2" x 25'-0"	34'-10"	13'-10"	17'-8"	47'-9"	232'-11 3/16"	23'-8 5/8"
		BOTTOM FLANGE	18" x 2 1/2" x 25'-0"	15" x 2" x 26'-0"	15" x 2" x 25'-8 3/16"	17" x 2 1/2" x 90'-0"	15" x 2" x 35'-0"	18" x 2" x 30'-0"	24" x 2 1/2" x 25'-0"					R=1108.00'	TANGENT
		WEB	99" x 3/4" x 25'-0"	99" x 3/4" x 26'-0"	99" x 3/4" x 25'-8 3/16"	99" x 3/4" x 90'-0"	99" x 3/4" x 35'-0"	99" x 3/4" x 30'-0"	99" x 3/4" x 25'-0"						
G-4	258'-7 5/16"	TOP FLANGE	18" x 2 1/2" x 25'-0"	15" x 2" x 29'-0"	15" x 1 1/2" x 24'-7 5/16"	15" x 1 1/2" x 90'-0"	15" x 1 1/2" x 35'-0"	18" x 2" x 30'-0"	24" x 2 1/2" x 25'-0"	33'-8"	18'-0"	20'-1"	47'-2"	234'-10 11/16"	23'-8 5/8"
		BOTTOM FLANGE	18" x 2 1/2" x 25'-0"	15" x 2" x 29'-0"	15" x 2" x 24'-7 5/16"	17" x 2 1/2" x 90'-0"	15" x 2" x 35'-0"	18" x 2" x 30'-0"	24" x 2 1/2" x 25'-0"					R=1117.17'	TANGENT
		WEB	99" x 3/4" x 25'-0"	99" x 3/4" x 29'-0"	99" x 3/4" x 24'-7 5/16"	99" x 3/4" x 90'-0"	99" x 3/4" x 35'-0"	99" x 3/4" x 30'-0"	99" x 13/16" x 25'-0"						
G-5	260'-6 7/16"	TOP FLANGE	24" x 2 1/2" x 25'-0"	18" x 2" x 30'-0"	15" x 1 1/2" x 25'-6 7/16"	18" x 1 1/2" x 90'-0"	15" x 1 1/2" x 35'-0"	20" x 2" x 30'-0"	30" x 2 1/2" x 25'-0"	34'-2"	20'-5"	23'-1"	46'-7"	236'-9 13/16"	23'-8 5/8"
		BOTTOM FLANGE	24" x 2 1/2" x 25'-0"	18" x 2" x 30'-0"	18" x 2" x 25'-6 7/16"	22" x 2 1/2" x 90'-0"	18" x 2" x 35'-0"	20" x 2" x 30'-0"	30" x 2 1/2" x 25'-0"					R=1126.33'	TANGENT
		WEB	99" x 15/16" x 25'-0"	99" x 3/4" x 30'-0"	99" x 3/4" x 25'-6 7/16"	99" x 3/4" x 90'-0"	99" x 3/4" x 35'-0"	99" x 3/4" x 30'-0"	99" x 13/16" x 25'-0"						

7/8" DIA. STEEL STUD SPACING (4 PER ROW) - SPAN 9

GIRDER NUMBER	SA	SB	SC
G-1	34 SPA. @ 1'-6" = 51'-0"	1'-11 15/16"	109 SPA. @ 1'-10" = 199'-10"
G-2	25 SPA. @ 2'-0" = 50'-0"	9 1/16"	102 SPA. @ 2'-0" = 204'-0"
G-3	25 SPA. @ 2'-0" = 50'-0"	8 3/16"	103 SPA. @ 2'-0" = 206'-0"
G-4	28 SPA. @ 1'-10" = 51'-4"	1'-3 5/16"	103 SPA. @ 2'-0" = 206'-0"
G-5	37 SPA. @ 1'-7" = 58'-7"	10 7/16"	127 SPA. @ 1'-7" = 201'-1"

SPLICE TYPES - SPAN 9

GIRDER NUMBER	9 - 1	9 - 2
G-1	TYPE VIII	TYPE VIII
G-2	TYPE VIII	TYPE VIII
G-3	TYPE VIII	TYPE VIII
G-4	TYPE VIII	TYPE VIII
G-5	TYPE IX	TYPE IX

NOTES:

1. FOR GIRDER SHOP SPLICE DETAILS, SEE STANDARD DETAIL NO. BR-SS(8.11)-85-173.
2. NO WELDING OF STAY IN PLACE DECK FORMS TO TOP FLANGE PLATE WILL BE ALLOWED IN TENSION AND STRESS REVERSAL AREAS.
3. SPACE STEEL STUD SHEAR DEVELOPERS TO MISS BOLT HEADS IN FIELD SPLICE. SEE STANDARD DETAIL NO. BR-SS(8.05)-75-30.
4. FOR TRANSVERSE STIFFENER LOCATIONS, SEE DWG. NO. S6-90.

MASTER SET

FILE: q:\amd\304004_I195I695_hw\cadd\struct\comp_gg\GG-SPAN9.dgn
DATE: 8/4/2006
TIME: 4:06:54 AM

JOHNSON, MIRMIRAN & THOMPSON
Engineering A Brighter Future

MARYLAND TRANSPORTATION AUTHORITY
Engineering Division

ADDENDUMS & REVISIONS

NO.	DESCRIPTION	BY	DATE

I-95 EXPRESS TOLL LANES : I-695 INTERCHANGE
GENERAL PURPOSE ROADWAYS AND RAMPS
JOHN F. KENNEDY MEMORIAL HIGHWAY (BALTIMORE COUNTY)
RAMP GG
GIRDER ELEVATION - SPAN 9

CONTRACT NO. KH-1301-000-006
DRAWING NO. S6 - 99

DESIGNED BY TDY | DRAWN BY DJA | CHECKED BY MJB
CONST. REVIEW BY | DATE AUGUST, 2006 | SCALE AS SHOWN
SHEET NO. 796 OF 1676

THE ESTIMATED NUMBER OF STEEL STUD SHEAR DEVELOPERS REQUIRED IS 23,888.

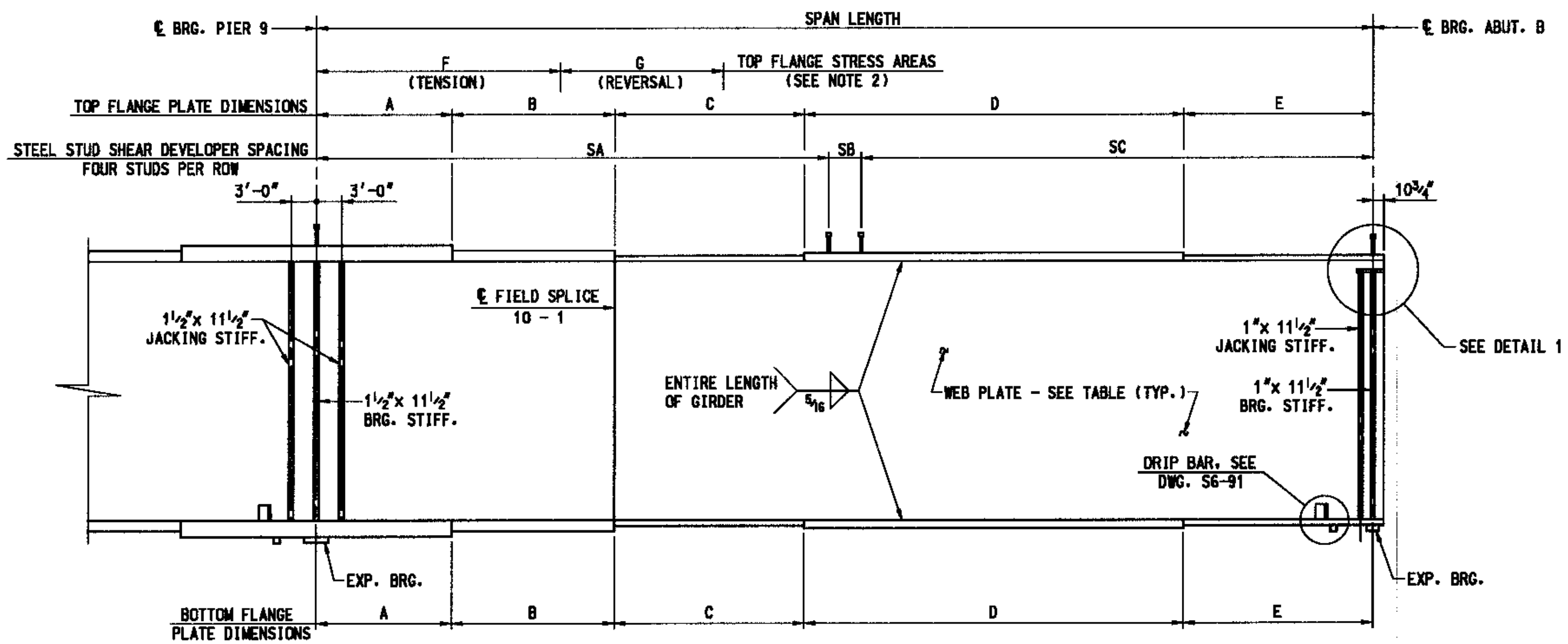

GIRDER ELEVATION - SPAN 10

NOT TO SCALE

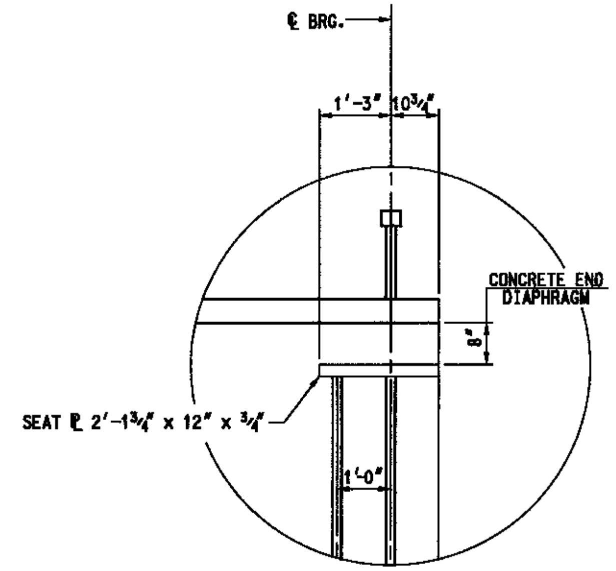

DETAIL 1

NOT TO SCALE

GIRDER ELEVATION - SPAN 10 - DIMENSIONS									
GIRDER NUMBER	SPAN LENGTH	PLATES	A	B	C	D	E	F	G
G-1	190'-0"	TOP FLANGE	24" x 2½" x 27'-0"	18" x 2" x 40'-0"	15" x 1¼" x 23'-0"	15" x 1¼" x 70'-0"	15" x 1¼" x 30'-0"	45'-4"	32'-9"
		BOTTOM FLANGE	24" x 2½" x 27'-0"	18" x 2" x 40'-0"	15" x 1¼" x 23'-0"	15" x 1¼" x 70'-0"	15" x 1¼" x 30'-0"		
		WEB	99" x 13/16" x 27'-0"	99" x ¾" x 40'-0"	99" x ¾" x 23'-0"	99" x ¾" x 70'-0"	99" x ¾" x 30'-0"		
G-2	190'-0"	TOP FLANGE	24" x 2½" x 27'-0"	18" x 2" x 40'-0"	15" x 1¼" x 23'-0"	15" x 1¼" x 70'-0"	15" x 1¼" x 30'-0"	48'-7"	29'-7"
		BOTTOM FLANGE	24" x 2½" x 27'-0"	18" x 2" x 40'-0"	15" x 1¼" x 23'-0"	15" x 1¼" x 70'-0"	15" x 1¼" x 30'-0"		
		WEB	99" x ¾" x 27'-0"	99" x ¾" x 40'-0"	99" x ¾" x 23'-0"	99" x ¾" x 70'-0"	99" x ¾" x 30'-0"		
G-3	190'-0"	TOP FLANGE	24" x 2½" x 27'-0"	18" x 2" x 40'-0"	15" x 1¼" x 23'-0"	15" x 1¼" x 70'-0"	15" x 1¼" x 30'-0"	51'-9"	28'-6"
		BOTTOM FLANGE	24" x 2½" x 27'-0"	18" x 2" x 40'-0"	15" x 1¼" x 23'-0"	15" x 1¼" x 70'-0"	15" x 1¼" x 30'-0"		
		WEB	99" x ¾" x 27'-0"	99" x ¾" x 40'-0"	99" x ¾" x 23'-0"	99" x ¾" x 70'-0"	99" x ¾" x 30'-0"		
G-4	190'-0"	TOP FLANGE	24" x 2½" x 27'-0"	18" x 2" x 40'-0"	15" x 1¼" x 23'-0"	15" x 1¼" x 70'-0"	15" x 1¼" x 30'-0"	51'-1"	38'-11"
		BOTTOM FLANGE	24" x 2½" x 27'-0"	18" x 2" x 40'-0"	15" x 1¼" x 23'-0"	15" x 1¼" x 70'-0"	15" x 1¼" x 30'-0"		
		WEB	99" x 13/16" x 27'-0"	99" x ¾" x 40'-0"	99" x ¾" x 23'-0"	99" x ¾" x 70'-0"	99" x ¾" x 30'-0"		
G-5	190'-0"	TOP FLANGE	30" x 2½" x 27'-0"	20" x 2" x 40'-0"	15" x 1¼" x 23'-0"	15" x 1¼" x 70'-0"	15" x 1¼" x 30'-0"	51'-2"	48'-4"
		BOTTOM FLANGE	30" x 2½" x 27'-0"	20" x 2" x 40'-0"	15" x 1¼" x 23'-0"	15" x 1¼" x 70'-0"	15" x 1¼" x 30'-0"		
		WEB	99" x 13/16" x 27'-0"	99" x ¾" x 40'-0"	99" x ¾" x 23'-0"	99" x ¾" x 70'-0"	99" x ¾" x 30'-0"		

⅞" DIA. STEEL STUD SPACING (4 PER ROW) - SPAN 10			
GIRDER NUMBER	SA	SB	SC
G-1	56 SPA. @ 2'-0" = 112'-0"	1'-4"	40 SPA. @ 1'-11" = 76'-8"
G-2	56 SPA. @ 2'-0" = 112'-0"	1'-4"	40 SPA. @ 1'-11" = 76'-8"
G-3	56 SPA. @ 2'-0" = 112'-0"	1'-4"	40 SPA. @ 1'-11" = 76'-8"
G-4	56 SPA. @ 2'-0" = 112'-0"	1'-4"	40 SPA. @ 1'-11" = 76'-8"
G-5	35 SPA. @ 1'-9" = 61'-3"	1'-0"	73 SPA. @ 1'-9" = 127'-9"

SPLICE TYPES - SPAN 10	
GIRDER NUMBER	10 - 1
G-1	TYPE I
G-2	TYPE I
G-3	TYPE I
G-4	TYPE I
G-5	TYPE I

NOTES:

1. FOR GIRDER SHOP SPLICE DETAILS, SEE STANDARD DETAIL NO. BR-SS(8.11)-85-173.
2. NO WELDING OF STAY IN PLACE DECK FORMS TO TOP FLANGE PLATE WILL BE ALLOWED IN TENSION AND STRESS REVERSAL AREAS.
3. SPACE STEEL STUD SHEAR DEVELOPERS TO MISS BOLT HEADS IN FIELD SPLICE. SEE STANDARD DETAIL NO. BR-SS(8.05)-75-30.
4. FOR CONCRETE END DIAPHRAGM AT ABUTMENTS, SEE STANDARD DETAIL NO. BR-SS(6.22)-80-120.

MASTER SET

JMT
JOHNSON, MIRMIRAN & THOMPSON
Engineering A Brighter Future

MARYLAND TRANSPORTATION AUTHORITY
Engineering Division

ADDENDUMS & REVISIONS			
NO.	DESCRIPTION	BY	DATE

I-95 EXPRESS TOLL LANES : I-695 INTERCHANGE
GENERAL PURPOSE ROADWAYS AND RAMPS
JOHN F. KENNEDY MEMORIAL HIGHWAY (BALTIMORE COUNTY)
RAMP GG
GIRDER ELEVATION - SPAN 10

DESIGNED BY TDY | DRAWN BY DJA | CHECKED BY MJB
CONST. REVIEW BY | DATE AUGUST, 2006 | SCALE AS SHOWN

CONTRACT NO. KH-1301-000-006
DRAWING NO. S6 - 100
SHEET NO. 797 OF 1676

DATE: 8/4/2006
TIME: 4:06:56 AM

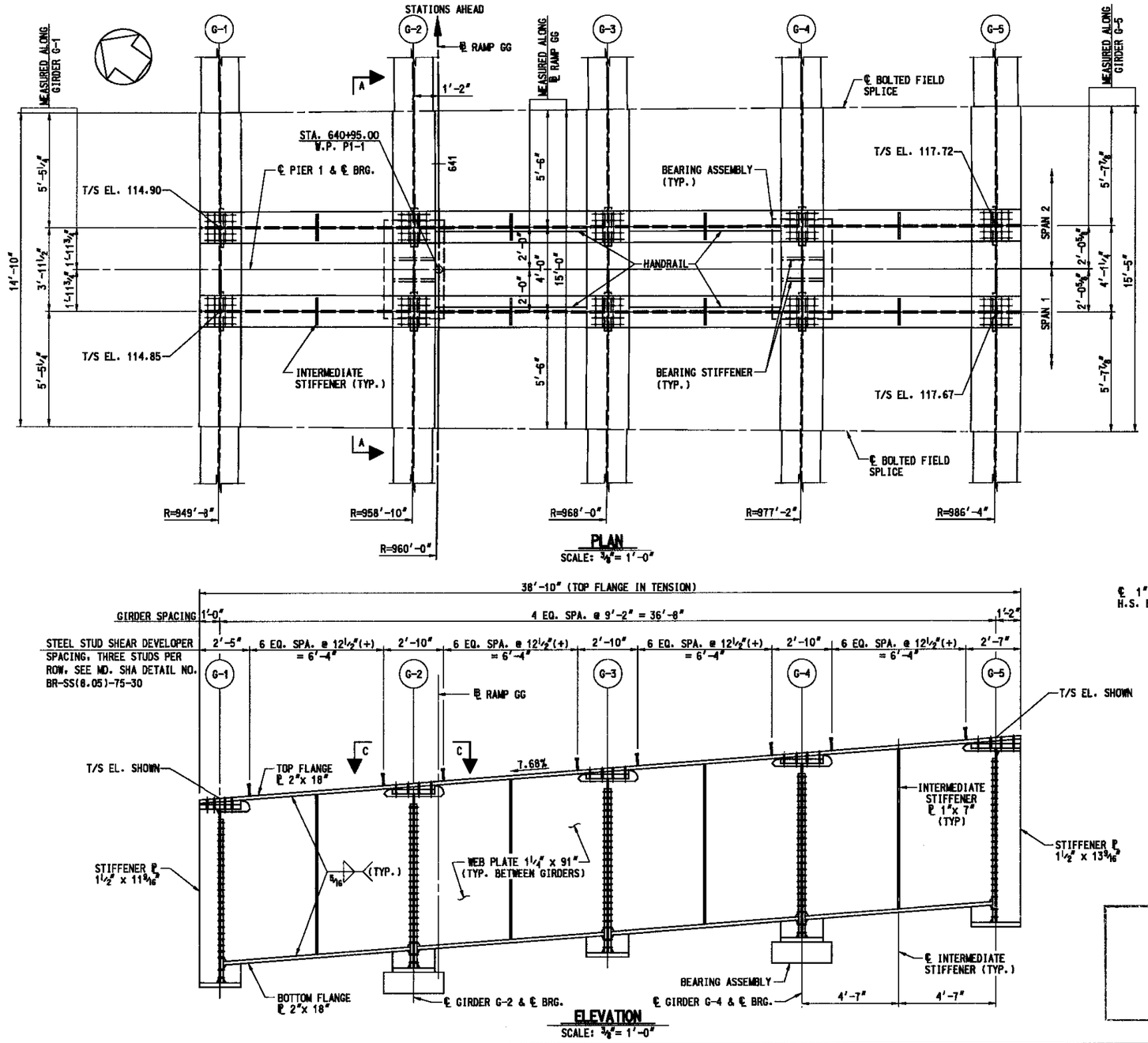

PLAN
SCALE: ⅜"= 1'-0"

ELEVATION
SCALE: ⅜"= 1'-0"

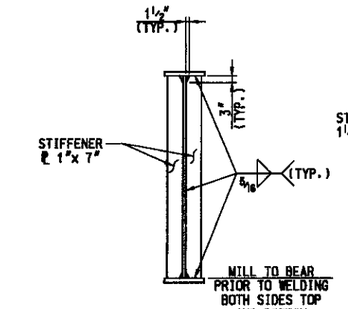

INTERMEDIATE STIFFENER DETAIL
SCALE: ⅜"= 1'-0"

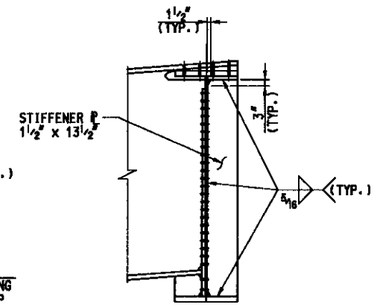

END STIFFENER DETAIL
SCALE: ⅜"= 1'-0"

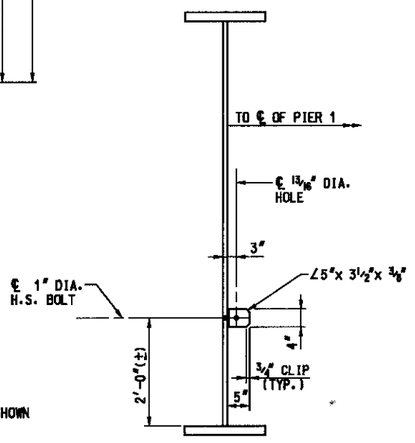

HANDRAIL CLIP ANGLE DETAIL
SCALE: ¾"= 1'-0"

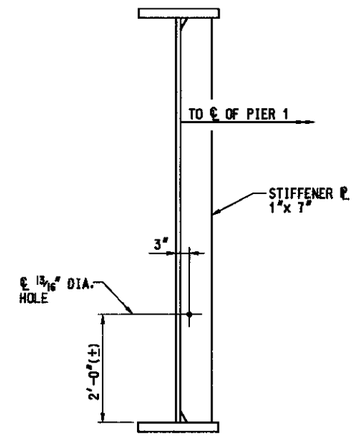

HANDRAIL AT STIFFENER DETAIL
SCALE: ¾"= 1'-0"

NOTES:

1. ALL DIMENSIONS ARE ALONG CENTERLINE OF INTEGRAL PIER CAP GIRDER AND ARE HORIZONTAL.
2. T/S DENOTES TOP OF STEEL.
3. NO WELDING OF STAY IN PLACE DECK FORMS TO TOP FLANGE PLATE WILL BE ALLOWED.
4. ALL BOLTS TO BE 1" DIA. HIGH STRENGTH BOLTS CONFORMING TO A 325, TYPE 3. ALL HOLES SHALL BE 1 13/16" DIA.
5. BOLT HEADS SHALL BE ON THE EXTERIOR FACE OF THE EXTERIOR GIRDERS AND THE BOTTOM OF THE BOTTOM FLANGES.
6. THE ENTIRE INTEGRAL PIER CAP FROM BOLTED FIELD SPLICE TO BOLTED FIELD SPLICE IS A FRACTURE CRITICAL MEMBER. ALL WELDING SHALL BE IN ACCORDANCE WITH AWS D1.5 WELDING CODE SECTION 12.

MASTER SET

FILE: q:\amd\304004_1195695_hw\oddl\structrcmp_GG\GG-Integral_Cap.dgn
DATE: 8/4/2006
TIME: 4:06:58 AM

JOHNSON, MIRMIRAN & THOMPSON
Engineering A Brighter Future

MARYLAND TRANSPORTATION AUTHORITY
Engineering Division

ADDENDUMS & REVISIONS			
NO.	DESCRIPTION	BY	DATE

I-95 EXPRESS TOLL LANES : I-695 INTERCHANGE
GENERAL PURPOSE ROADWAYS AND RAMPS
JOHN F. KENNEDY MEMORIAL HIGHWAY (BALTIMORE COUNTY)
RAMP GG
INTEGRAL PIER CAP - PLAN & ELEVATION

DESIGNED BY CLB	DRAWN BY FXT	CHECKED BY MJB	
CONST. REVIEW BY	DATE AUGUST, 2006	SCALE AS SHOWN	

CONTRACT NO. KH-1301-000-006
DRAWING NO. S6 - 101
SHEET NO. 798 OF 1676

REVISED

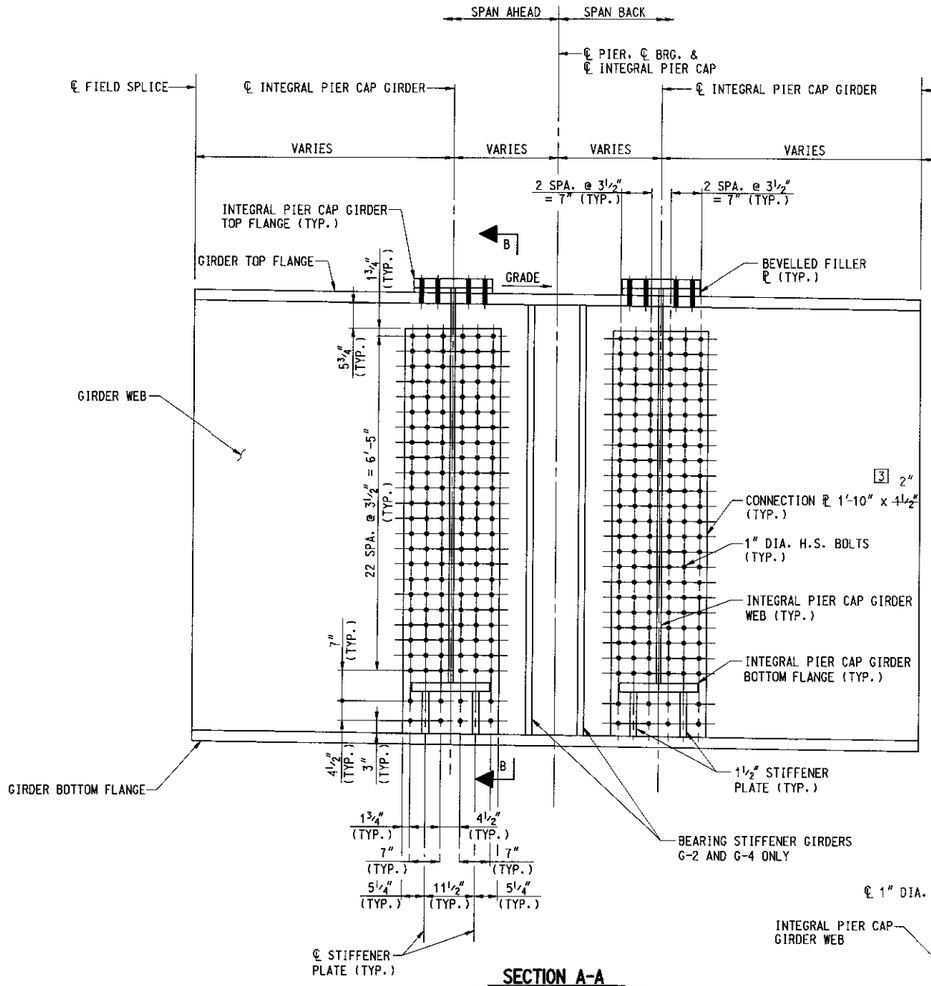

SECTION A-A
SCALE: ¾"= 1'-0"

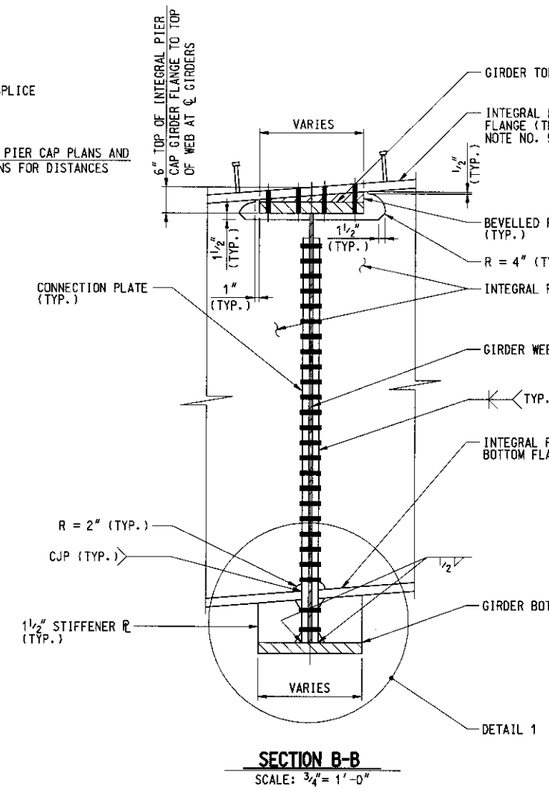

SECTION B-B
SCALE: ¾"= 1'-0"

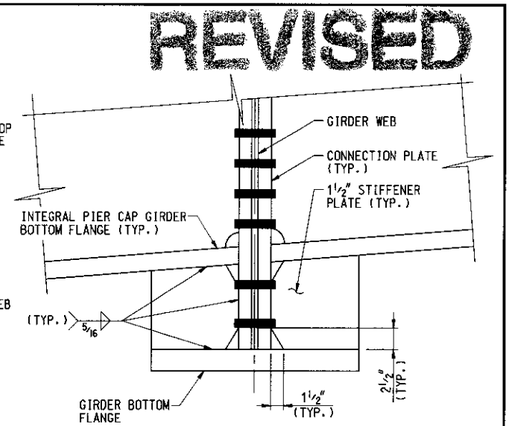

DETAIL 1
SCALE: 1½"= 1'-0"

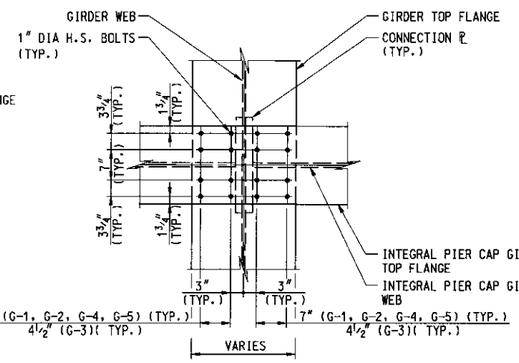

SECTION C-C
SCALE: ¾"= 1'-0"

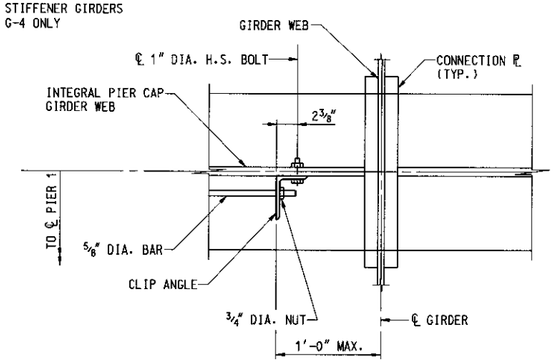

HANDRAIL PLAN AT GIRDER CONNECTION
SCALE: 1½"= 1'-0"

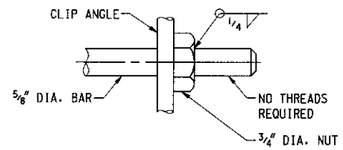

HANDRAIL END CONNECTION DETAIL
N.T.S

NOTES:

1. ALL BOLTS TO BE 1" DIA. HIGH STRENGTH BOLTS CONFORMING TO A 325, TYPE 3. ALL HOLES TO BE 1 1/16" DIA..
2. BOLTS NOT SHOWN IN SPLICE.
3. BOLT HEADS SHALL BE ON THE EXTERIOR FACE OF THE FASCIA STRINGER AND THE BOTTOM OF THE BOTTOM FLANGE.
4. FOR GIRDER FLANGE SIZES, SEE GIRDER ELEVATIONS.
5. SLOPE THE TOP FLANGES OF INTEGRAL PIER CAP GIRDERS TO MATCH GRADE.
6. FOR WELD TERMINATION DETAILS, SEE STANDARD DETAIL NO. BR-SS(8.10)-83-154.
7. CLIP STIFFENER PLATES AT CORNERS 1½" HORIZONTAL AND 2½" VERTICAL AS SHOWN.

FILE: qt:\end\3040041119511695_hw\coad\struct\Ramp_GG\GG-Integral_Cap-Det_Redline3.dgn
DATE: 3/30/2007
TIME: 9:25:40 AM

JOHNSON, MIRMIRAN & THOMPSON
Engineering A Brighter Future

MARYLAND TRANSPORTATION AUTHORITY
Engineering Division

ADDENDUMS & REVISIONS			
NO.	DESCRIPTION	BY	DATE
3	CONNECTION PLATE REVISED	MJB	3/07

I-95 EXPRESS TOLL LANES : I-695 INTERCHANGE
GENERAL PURPOSE ROADWAYS AND RAMPS
JOHN F. KENNEDY MEMORIAL HIGHWAY (BALTIMORE COUNTY)
RAMP GG
INTEGRAL PIER CAP - DETAILS

DESIGNED BY CLB	DRAWN BY FXT	CHECKED BY MJB
CONST. REVIEW BY	DATE AUGUST, 2006	SCALE AS SHOWN

CONTRACT NO. KH-1301-000-006
DRAWING NO. S6 - 102
SHEET NO. 799 OF 1676

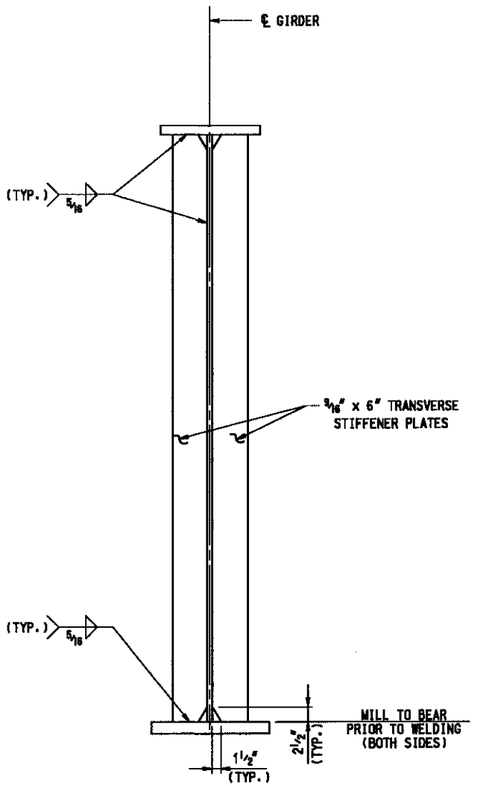

TRANSVERSE STIFFENER

SCALE: 1" = 1'-0"

(AT EITHER FLANGE WIDTH LESS THAN OR EQUAL TO 24")

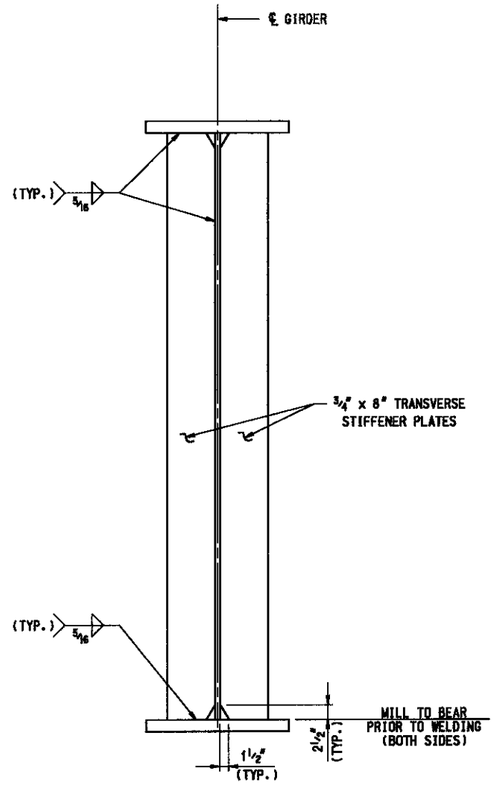

TRANSVERSE STIFFENER

SCALE: 1" = 1'-0"

(AT EITHER FLANGE WIDTH GREATER THAN 24")

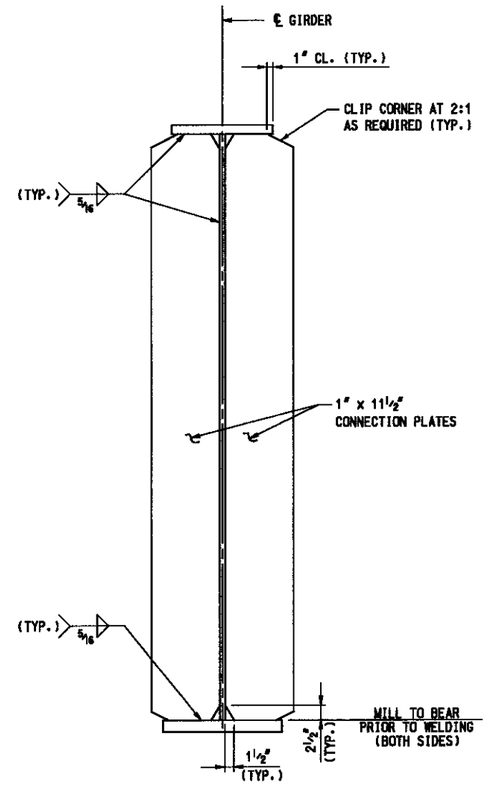

CONNECTION PLATE

SCALE: 1" = 1'-0"

MASTER SET

NOTES:

1. FOR WELD TERMINATION DETAILS, SEE STANDARD DETAIL NO. BR-SS(8.10)-83-154.
2. CLIP CONNECTION PLATES AND BEARING STIFFENERS AT CORNERS 1½" HORIZONTAL AND 2½" VERTICAL AS SHOWN.

FILE: q:\amd\304004_I195\695_hw\cadd\structr\comp_gg\GG-Brg_Stiff.dgn
DATE: 8/4/2006
TIME: 4:07:02 AM

JOHNSON, MIRMIRAN & THOMPSON
Engineering A Brighter Future

MARYLAND TRANSPORTATION AUTHORITY
Engineering Division

ADDENDUMS & REVISIONS			
NO.	DESCRIPTION	BY	DATE

I-95 EXPRESS TOLL LANES : I-695 INTERCHANGE
GENERAL PURPOSE ROADWAYS AND RAMPS
JOHN F. KENNEDY MEMORIAL HIGHWAY (BALTIMORE COUNTY)
RAMP GG
GIRDER STIFFENER DETAILS I

DESIGNED BY TDY	DRAWN BY JPB	CHECKED BY MJB	
CONST. REVIEW BY	DATE AUGUST, 2006	SCALE AS SHOWN	

CONTRACT NO. KH-1301-000-006
DRAWING NO. S6 - 103
SHEET NO. 880 OF 1676

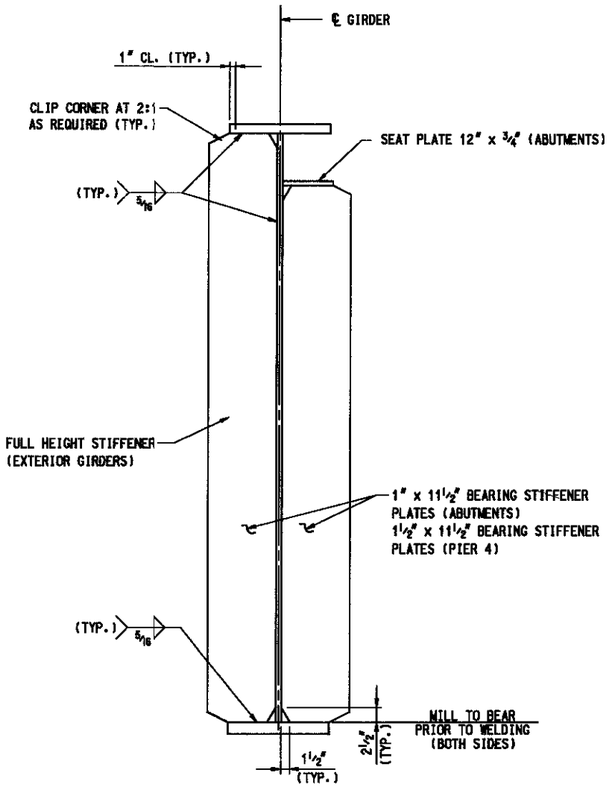

BEARING STIFFENER AND JACKING STIFFENER AT ABUTMENTS & PIER 4

SCALE: 1" = 1'-0"

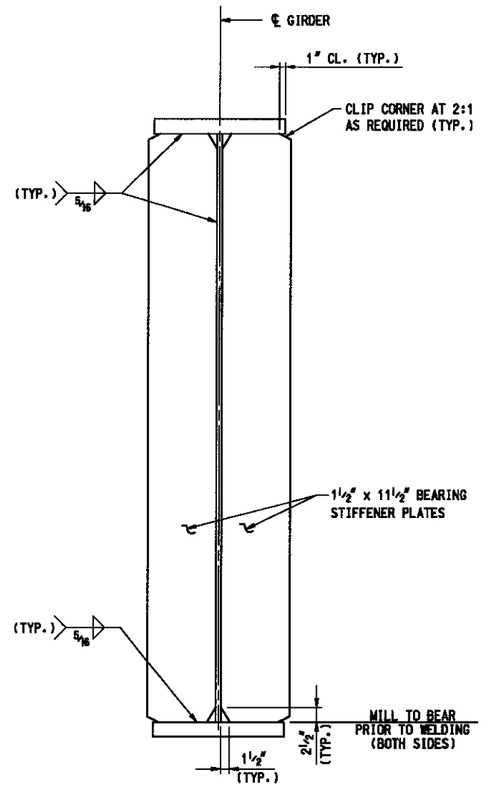

BEARING STIFFENER AND JACKING STIFFENER AT PIERS 1-3 & 5-9

SCALE: 1" = 1'-0"

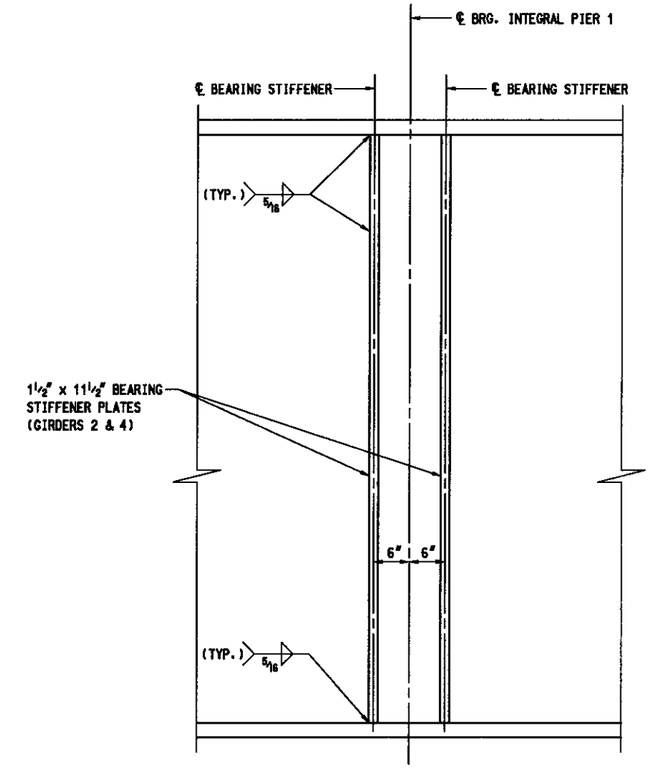

BEARING STIFFENER AT INTEGRAL PIER CAP

SCALE: 1" = 1'-0"

MASTER SET

NOTES:

1. FOR WELD TERMINATION DETAILS, SEE STANDARD DETAIL NO. BR-SS(8.10)-83-154.
2. CLIP CONNECTION PLATES AND BEARING STIFFENERS AT CORNERS 1½" HORIZONTAL AND 2½" VERTICAL AS SHOWN.

JOHNSON, MIRMIRAN & THOMPSON
Engineering A Brighter Future

MARYLAND TRANSPORTATION AUTHORITY
Engineering Division

ADDENDUMS & REVISIONS

NO.	DESCRIPTION	BY	DATE

I-95 EXPRESS TOLL LANES : I-695 INTERCHANGE
GENERAL PURPOSE ROADWAYS AND RAMPS
JOHN F. KENNEDY MEMORIAL HIGHWAY (BALTIMORE COUNTY)
RAMP GG
GIRDER STIFFENER DETAILS II

DESIGNED BY TDY	DRAWN BY JPB	CHECKED BY MJB
CONST. REVIEW BY	DATE AUGUST, 2006	SCALE AS SHOWN

CONTRACT NO. KH-1301-000-006
DRAWING NO. S6 - 104
SHEET NO. 801 OF 1676

FILE: q:\smd\304004_I1195169S_hw\cadd\struct\r\ramp_gg\GG-Brg_Stiff2.dgn
DATE: 8/4/2006
TIME: 4:07:03 AM

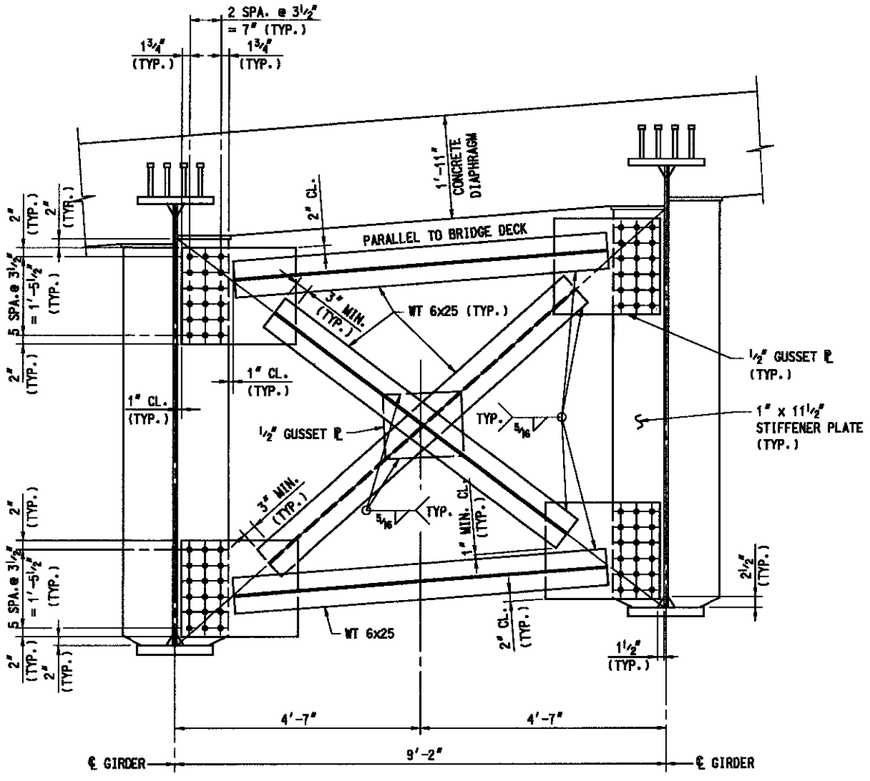

DIAPHRAGM CROSS FRAME AT ABUTMENTS AND PIER 4

SCALE: ¾" = 1'-0"

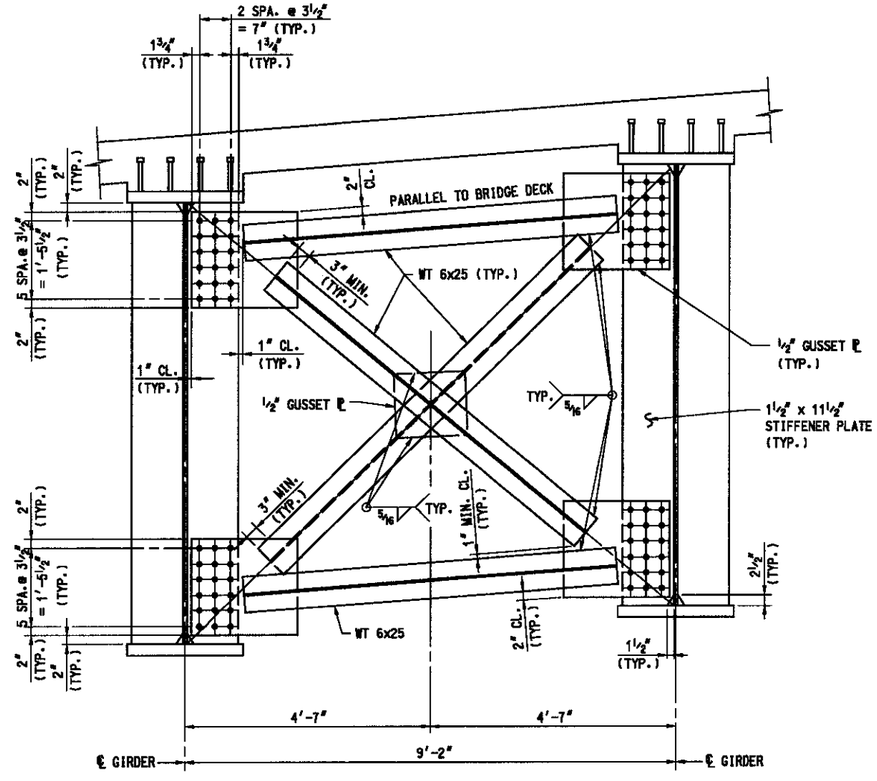

DIAPHRAGM CROSS FRAME AT PIERS

SCALE: ¾" = 1'-0"

MASTER SET

NOTES:

1. GUSSET PLATE HOLES SHALL BE 1 1/16" DIA. ALL BOLTS TO BE 1" DIA. HIGH STRENGTH BOLTS (A325).
2. ALL GUSSET PLATES TO BE ½" THICK.
3. CLIP CONNECTION PLATES AND BEARING STIFFENERS AT CORNERS 1½" HORIZONTAL AND 2½" VERTICAL, AS SHOWN.
4. FOR CONCRETE END DIAPHRAGM AT ABUTMENTS AND PIER 4, SEE STANDARD DETAIL NO. BR-SS(6.22)-80-120.

FILE: q:\ame\304004_J1195695_hw\oadd\structr\ramp_gg\G6-Diaph_1.dgn
DATE: 8/4/2006
TIME: 4:07:05 AM

JMT
JOHNSON, MIRMIRAN & THOMPSON
Engineering A Brighter Future

MARYLAND TRANSPORTATION AUTHORITY
Engineering Division

ADDENDUMS & REVISIONS			
NO.	DESCRIPTION	BY	DATE

I-95 EXPRESS TOLL LANES : I-695 INTERCHANGE
GENERAL PURPOSE ROADWAYS AND RAMPS
JOHN F. KENNEDY MEMORIAL HIGHWAY (BALTIMORE COUNTY)
RAMP GG
DIAPHRAGM DETAILS I

DESIGNED BY TDY	DRAWN BY JPB	CHECKED BY MJB	
CONST. REVIEW BY	DATE AUGUST, 2006	SCALE AS SHOWN	

CONTRACT NO. KH-1301-000-006
DRAWING NO. S6 - 105
SHEET NO. 882 OF 1676

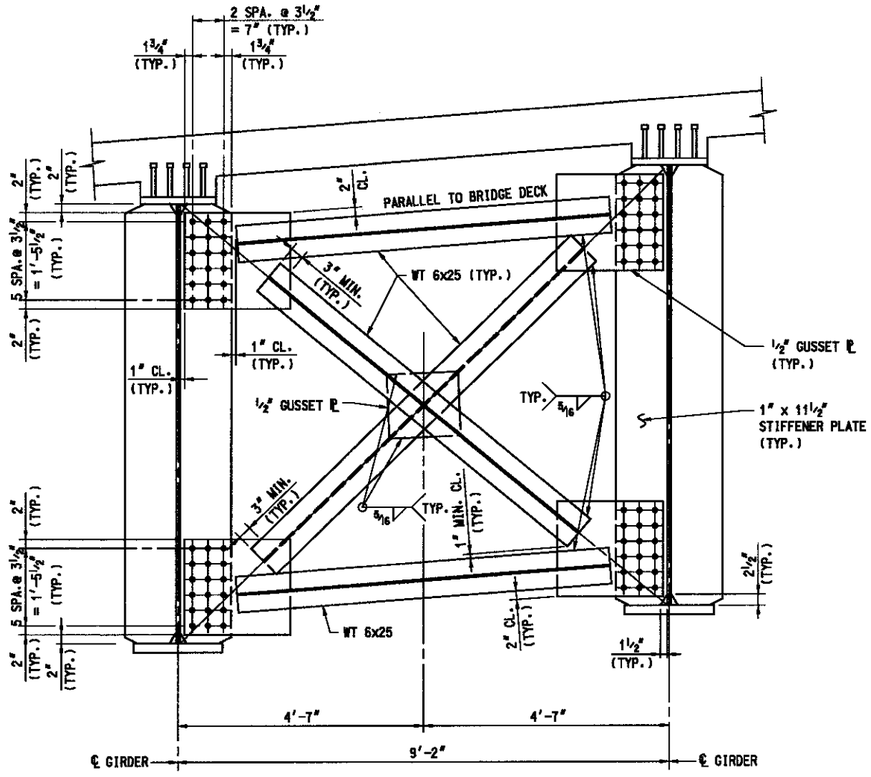

INTERMEDIATE DIAPHRAGM CROSS FRAME

SCALE: ¾" = 1'-0"

MASTER SET

NOTES:

1. GUSSET PLATE HOLES SHALL BE 1 1/16" DIA. ALL BOLTS TO BE 1" DIA. HIGH STRENGTH BOLTS (A325).
2. ALL GUSSET PLATES TO BE ½" THICK.
3. CLIP CONNECTION PLATES AND BEARING STIFFENERS AT CORNERS 1½" HORIZONTAL AND 2½" VERTICAL, AS SHOWN.

FILE: q:\amd\30400-111951695_hw\cadd\struct\ramp_gg\GG-Diaph_2.dgn
DATE: 8/4/2006
TIME: 4:07:07 AM

JOHNSON, MIRMIRAN & THOMPSON
Engineering A Brighter Future

MARYLAND TRANSPORTATION AUTHORITY
Engineering Division

ADDENDUMS & REVISIONS			
NO.	DESCRIPTION	BY	DATE

I-95 EXPRESS TOLL LANES : I-695 INTERCHANGE
GENERAL PURPOSE ROADWAYS AND RAMPS
JOHN F. KENNEDY MEMORIAL HIGHWAY (BALTIMORE COUNTY)
RAMP GG
DIAPHRAGM DETAILS II

DESIGNED BY TDY	DRAWN BY JPB	CHECKED BY MJB	
CONST. REVIEW BY	DATE AUGUST, 2006	SCALE AS SHOWN	

CONTRACT NO. KH-1301-000-006
DRAWING NO. S6 - 106
SHEET NO. 883 OF 1676

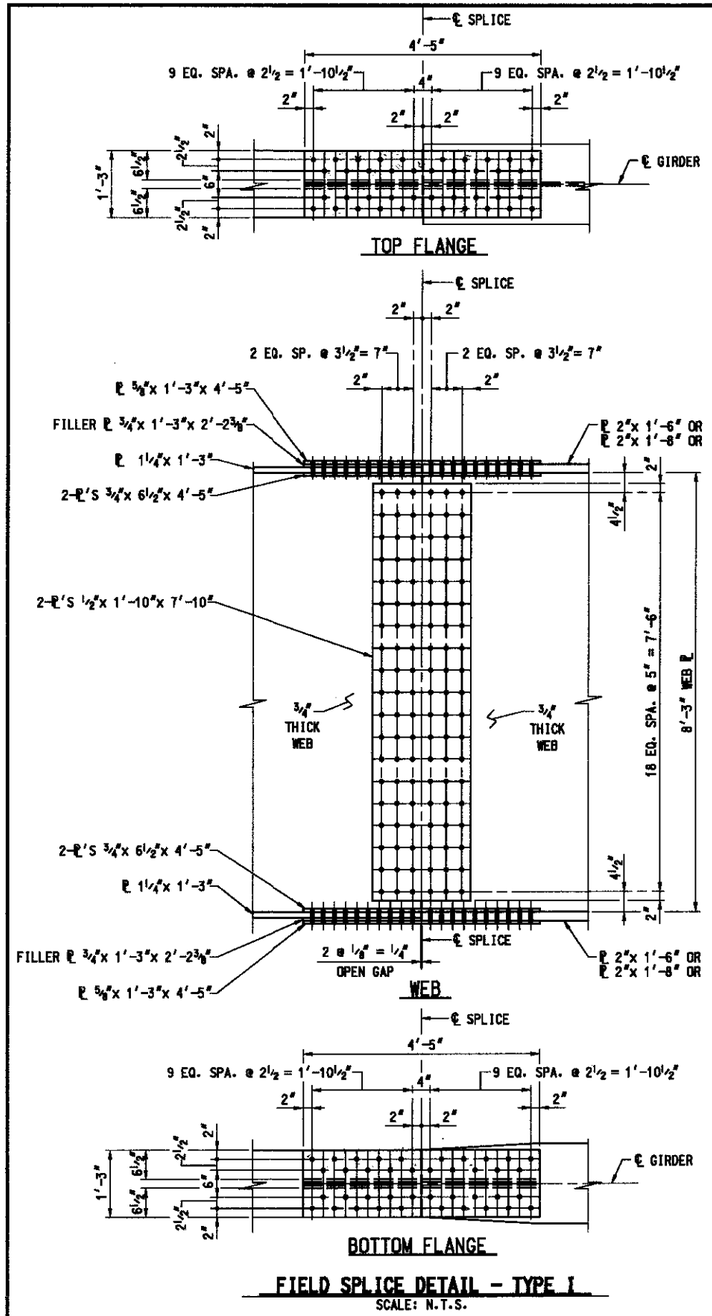

FIELD SPLICE DETAIL - TYPE I

SCALE: N.T.S.

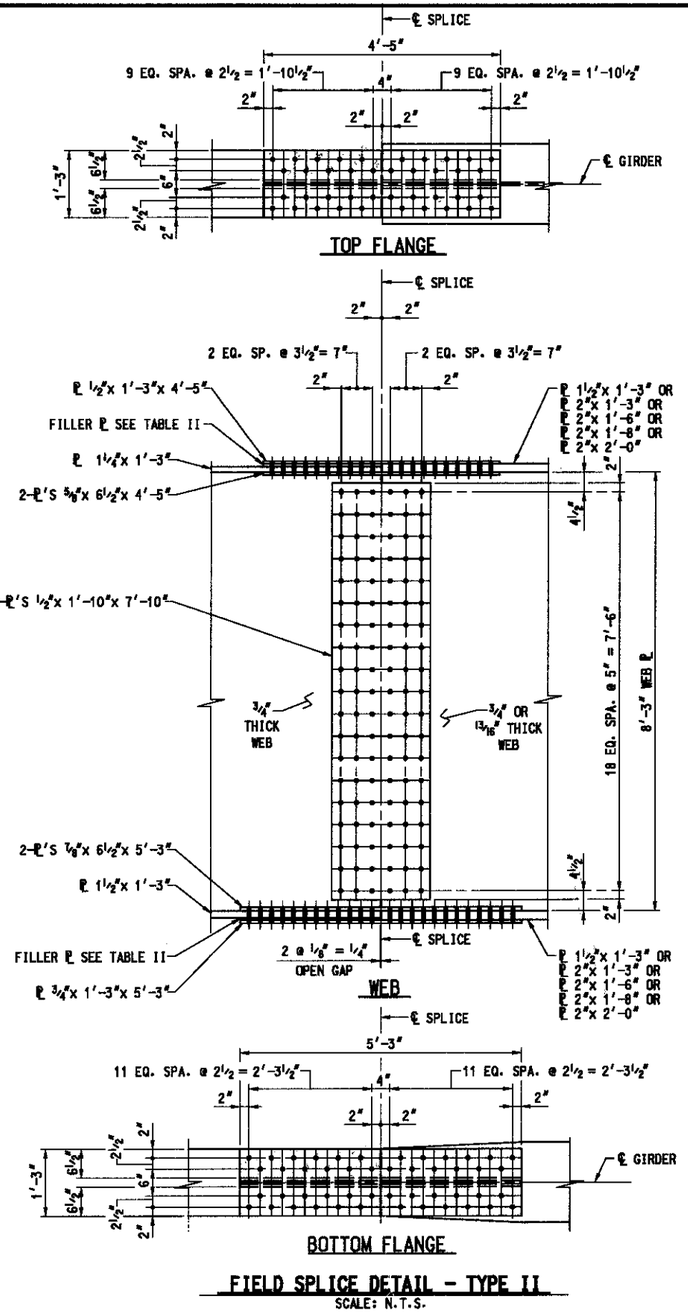

FIELD SPLICE DETAIL - TYPE II

SCALE: N.T.S.

SPLICE NOTES:

1. ALL BOLTS TO BE 1" DIA. HIGH STRENGTH BOLTS CONFORMING TO A 325, TYPE 3. ALL BOLT HOLES SHALL BE 1 1/16" DIA.
2. ON FASCIA GIRDERS THE BOLTS SHALL BE PLACED SO THAT THE BOLT HEAD IS VISIBLE ON THE OUTSIDE FACE OF WEB.
3. ALL BOLTS ON FLANGE SPLICES SHALL HAVE BOLT HEADS ON THE BOTTOM.
4. BOLTS NOT SHOWN IN SPLICE.
5. SPACE SHEAR STUDS TO MISS TOP FLANGE SPLICE BOLTS.
6. A MINIMUM OF 50 PERCENT OF THE WEB, TOP FLANGE AND BOTTOM FLANGE SPLICE BOLTS SHALL BE IN PLACE BEFORE THE GIRDER IS LEFT UNSUPPORTED.
7. WHEN FLANGE IS LARGER THAN ADJACENT FLANGE BY MORE THAN 2", THE LARGER FLANGE SHALL BE TAPERED TO THE SMALLER FLANGE WIDTH IN A DISTANCE OF ½ LENGTH OF SPLICE PLATE (BOTTOM FLANGE ONLY).
8. FIELD SPLICES SHALL BE COMPLETELY SHOP ASSEMBLED AND MATCH MARKED AFTER ALL SHOP WELDING HAS BEEN COMPLETED. CONTACT SURFACES SHALL BE FREE OF ALL OIL AND DIRT.

TYPE	LOCATION	
	GIRDER	SPLICE DESIGNATION
I	G-1	10-1
	G-2	10-1
	G-3	10-1
	G-4	10-1
	G-5	10-1
II	G-1	1-1, 3-1, 3-2, 7-1, 7-2
	G-2	1-1, 3-1, 3-2, 7-1, 7-2
	G-3	1-1, 3-1, 3-2, 7-1, 7-2
	G-4	1-1, 3-1, 3-2, 7-1, 7-2
	G-5	1-1, 3-1, 3-2

TABLE I: FILLER PLATES

GIRDER	SPLICE DESIGNATION	TOP SPLICE	BOTTOM SPLICE
G-1, G-2, G-3, G-4, G-5	1-1	¾"x 1'-3"x 2'-2⅜"	½"x 1'-3"x 2'-7⅜"
G-1, G-2, G-3, G-4, G-5	3-1	¾"x 1'-3"x 2'-2⅜"	½"x 1'-3"x 2'-7⅜"
G-1, G-2, G-3, G-4, G-5	3-2	¾"x 1'-3"x 2'-2⅜"	½"x 1'-3"x 2'-7⅜"
G-1, G-2, G-3, G-4	7-1	¾"x 1'-3"x 2'-2⅜"	½"x 1'-3"x 2'-7⅜"
G-1, G-2, G-3, G-4	7-2	¼"x 1'-3"x 2'-2⅜"	N/A

MASTER SET

FILE: q:\amd\304004.11\951695.hw\oddd\structure\ramp-gg\GG-fieldsplices.dgn
DATE: 8/4/2006
TIME: 4:07:08 AM

JOHNSON, MIRMIRAN & THOMPSON
Engineering A Brighter Future

MARYLAND TRANSPORTATION AUTHORITY
Engineering Division

ADDENDUMS & REVISIONS			
NO.	DESCRIPTION	BY	DATE

I-95 EXPRESS TOLL LANES : I-695 INTERCHANGE
GENERAL PURPOSE ROADWAYS AND RAMPS
JOHN F. KENNEDY MEMORIAL HIGHWAY (BALTIMORE COUNTY)
RAMP GG
FIELD SPLICE DETAILS - TYPE I AND TYPE II

DESIGNED BY PDR	DRAWN BY DJA	CHECKED BY MJB
CONST. REVIEW BY	DATE AUGUST, 2006	SCALE AS SHOWN

CONTRACT NO. KH-1301-000-006
DRAWING NO. S6 - 107
SHEET NO. 894 OF 1676

REVISED

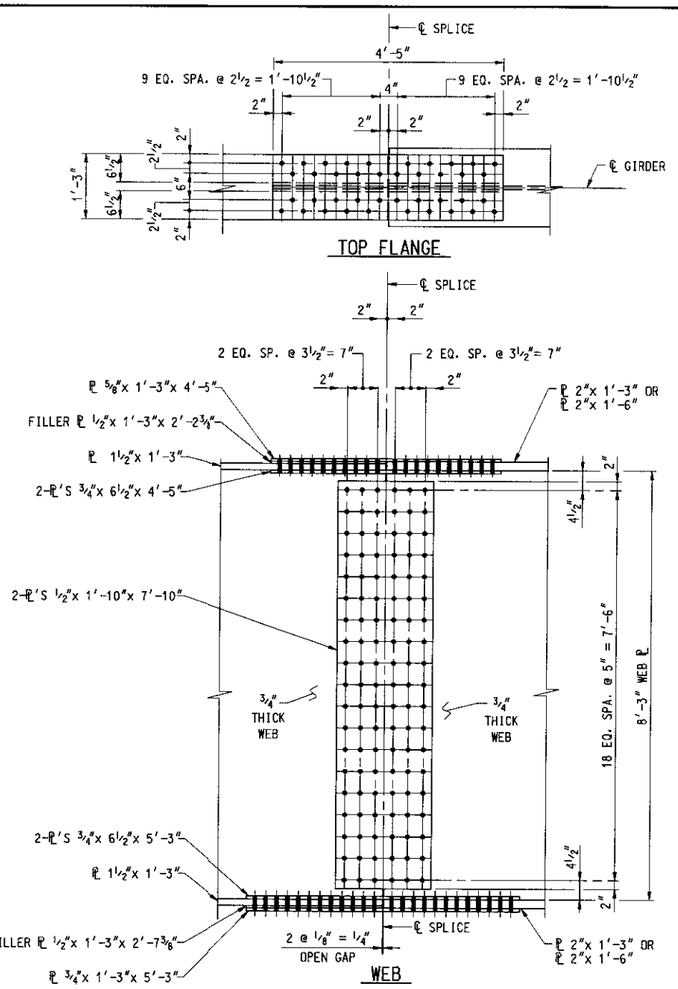

SPLICE NOTES:

1. ALL BOLTS TO BE 1" DIA. HIGH STRENGTH BOLTS CONFORMING TO A 325. TYPE 3. ALL BOLT HOLES SHALL BE 1 1/16" DIA.
2. ON FASCIA GIRDERS THE BOLTS SHALL BE PLACED SO THAT THE BOLT HEAD IS VISIBLE ON THE OUTSIDE FACE OF WEB.
3. ALL BOLTS ON FLANGE SPLICES SHALL HAVE BOLT HEADS ON THE BOTTOM.
4. BOLTS NOT SHOWN IN SPLICE.
5. SPACE SHEAR STUDS TO MISS TOP FLANGE SPLICE BOLTS.
6. A MINIMUM OF 50 PERCENT OF THE WEB, TOP FLANGE AND BOTTOM FLANGE SPLICE BOLTS SHALL BE IN PLACE BEFORE THE GIRDER IS LEFT UNSUPPORTED.
7. WHEN FLANGE IS LARGER THAN ADJACENT FLANGE BY MORE THAN 2", THE LARGER FLANGE SHALL BE TAPERED TO THE SMALLER FLANGE WIDTH IN A DISTANCE OF ½ LENGTH OF SPLICE PLATE (BOTTOM FLANGE ONLY).
8. FIELD SPLICES SHALL BE COMPLETELY SHOP ASSEMBLED AND MATCH MARKED AFTER ALL SHOP WELDING HAS BEEN COMPLETED. CONTACT SURFACES SHALL BE FREE OF ALL OIL AND DIRT.

TYPE	LOCATION	
	GIRDER	SPLICE DESIGNATION
III	G-1	8-1
	G-2	8-1
	G-3	8-1
	G-4	8-1
	G-5	8-1
IV	G-5	7-1, 7-2

3

TABLE 1: FILLER PLATES 3

GIRDER	SPLICE DESIGNATION	TOP SPLICE	BOTTOM SPLICE
G-5	7-1	¾"x 1'-3"x 2'-2 3/8"	½"x 1'-6"x 2'-0 7/8"
G-5	7-2	1¼"x 1'-3"x 2'-2 3/8"	N/A

FILE: q:\smd\304004_11951695_hw\roads\structr\Ramp_GG\GG-fieldsplice_2_Redline3.dgn
DATE: 3/30/2007
TIME: 9:25:12 AM

JOHNSON, MIRMIRAN & THOMPSON
Engineering A Brighter Future

MARYLAND TRANSPORTATION AUTHORITY
Engineering Division

ADDENDUMS & REVISIONS			
NO.	DESCRIPTION	BY	DATE
3	ADDED SPLICE 7-2	MJB	3/07

I-95 EXPRESS TOLL LANES : I-695 INTERCHANGE
GENERAL PURPOSE ROADWAYS AND RAMPS
JOHN F. KENNEDY MEMORIAL HIGHWAY (BALTIMORE COUNTY)
RAMP GG
FIELD SPLICE DETAILS - TYPE III AND TYPE IV

CONTRACT NO. KH-1301-000-006
DRAWING NO. S6 - 108
SHEET NO. 805 OF 1676

DESIGNED BY PDR | DRAWN BY DJA | CHECKED BY MJB
CONST. REVIEW BY | DATE AUGUST, 2006 | SCALE AS SHOWN

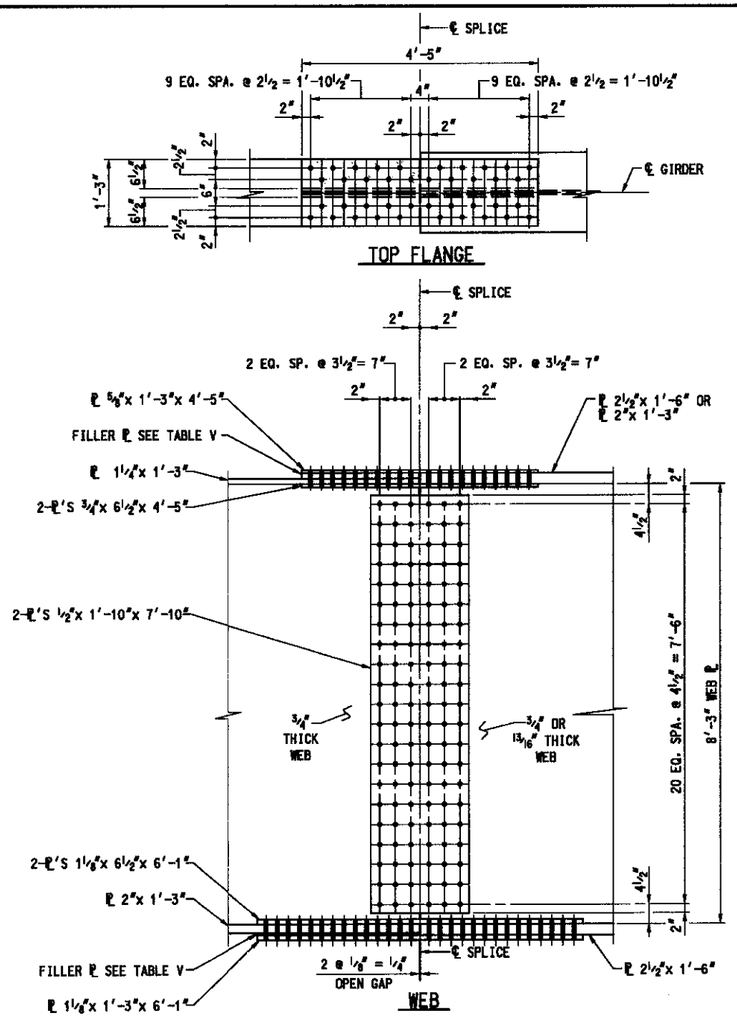

FIELD SPLICE DETAIL - TYPE V

SCALE: N.T.S.

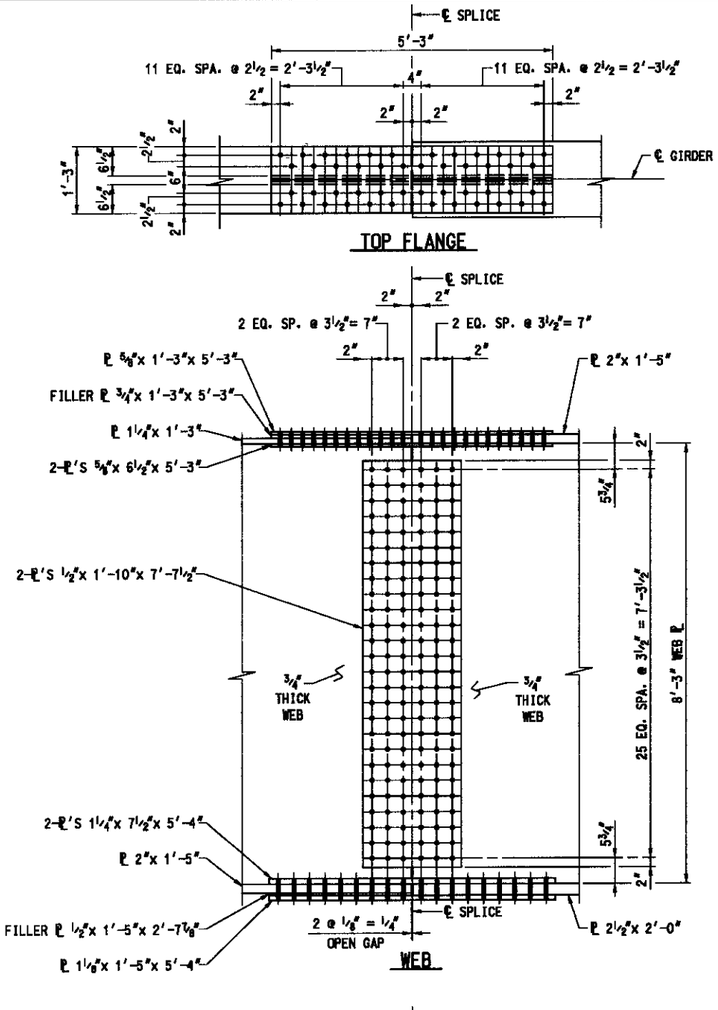

FIELD SPLICE DETAIL - TYPE VI

SCALE: N.T.S.

SPLICE NOTES:

1. ALL BOLTS TO BE 1" DIA. HIGH STRENGTH BOLTS CONFORMING TO A 325, TYPE 3. ALL BOLT HOLES SHALL BE 1 1/16" DIA.
2. ON FASCIA GIRDERS THE BOLTS SHALL BE PLACED SO THAT THE BOLT HEAD IS VISIBLE ON THE OUTSIDE FACE OF WEB.
3. ALL BOLTS ON FLANGE SPLICES SHALL HAVE BOLT HEADS ON THE BOTTOM.
4. BOLTS NOT SHOWN IN SPLICE.
5. SPACE SHEAR STUDS TO MISS TOP FLANGE SPLICE BOLTS.
6. A MINIMUM OF 50 PERCENT OF THE WEB, TOP FLANGE AND BOTTOM FLANGE SPLICE BOLTS SHALL BE IN PLACE BEFORE THE GIRDER IS LEFT UNSUPPORTED.
7. WHEN FLANGE IS LARGER THAN ADJACENT FLANGE BY MORE THAN 2", THE LARGER FLANGE SHALL BE TAPERED TO THE SMALLER FLANGE WIDTH IN A DISTANCE OF ½ LENGTH OF SPLICE PLATE (BOTTOM FLANGE ONLY).
8. FIELD SPLICES SHALL BE COMPLETELY SHOP ASSEMBLED AND MATCH MARKED AFTER ALL SHOP WELDING HAS BEEN COMPLETED. CONTACT SURFACES SHALL BE FREE OF ALL OIL AND DIRT.

TYPE	LOCATION	
	GIRDER	SPLICE DESIGNATION
V	G-1	4-2, 5-1
	G-2	4-2, 5-1
	G-3	4-2, 5-1
	G-4	4-2, 5-1
VI	G-5	4-2

TABLE V : FILLER PLATES

GIRDER	SPLICE DESIGNATION	TOP SPLICE	BOTTOM SPLICE
G-1, G-2, G-3, G-4	4-2	¾"x 1'-3"x 2'-2⅜"	½"x 1'-3"x 3'-0⅝"
G-1, G-2, G-3, G-4	5-1	1¼"x 1'-3"x 2'-2⅜"	½"x 1'-3"x 3'-0⅝"

MASTER SET

JOHNSON, MIRMIRAN & THOMPSON
Engineering A Brighter Future

MARYLAND TRANSPORTATION AUTHORITY
Engineering Division

ADDENDUMS & REVISIONS			
NO.	DESCRIPTION	BY	DATE

I-95 EXPRESS TOLL LANES : I-695 INTERCHANGE
GENERAL PURPOSE ROADWAYS AND RAMPS
JOHN F. KENNEDY MEMORIAL HIGHWAY (BALTIMORE COUNTY)
RAMP GG
FIELD SPLICE DETAILS - TYPE V AND TYPE VI

CONTRACT NO. KH-1301-000-006
DRAWING NO. S6 - 109
SHEET NO. 886 OF 1676

DESIGNED BY PDR | DRAWN BY DJA | CHECKED BY MJB
CONST. REVIEW BY | DATE AUGUST, 2006 | SCALE AS SHOWN

FILE: q:\smd\304004_I1195695_hw\ood\struct\ramp_gg\GG-fieldsplice_3.dgn
DATE: 8/4/2006
TIME: 4:07:12 AM

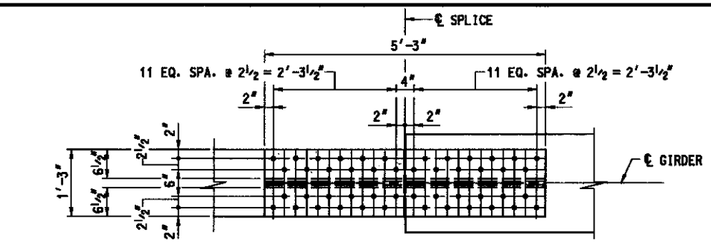

TOP FLANGE

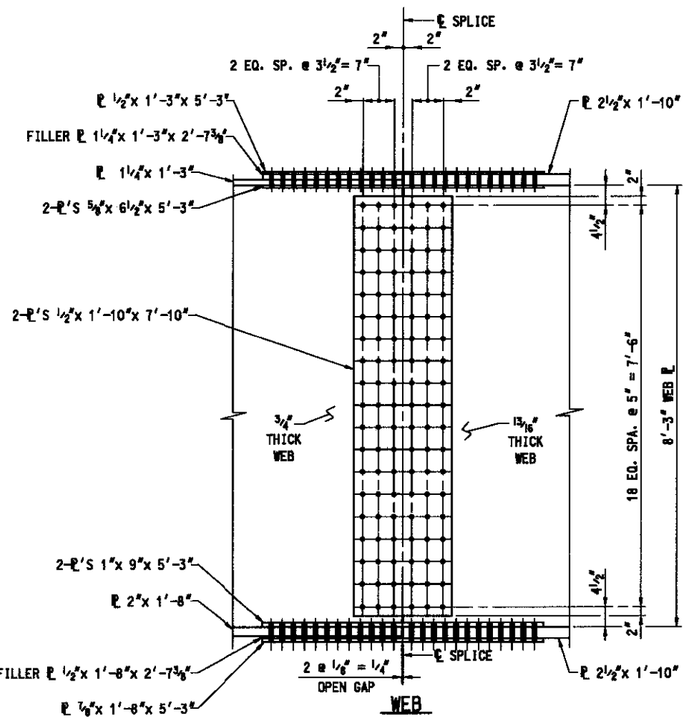

WEB

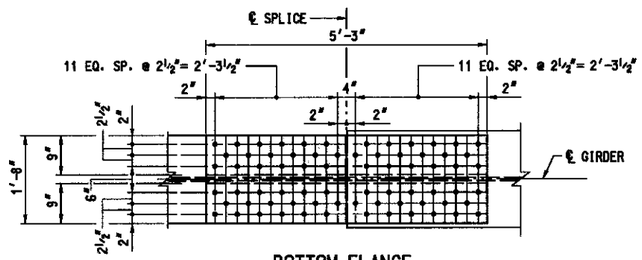

BOTTOM FLANGE

FIELD SPLICE DETAIL - TYPE VII

SCALE: N.T.S.

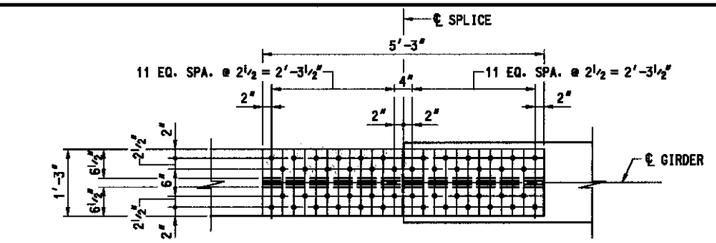

TOP FLANGE

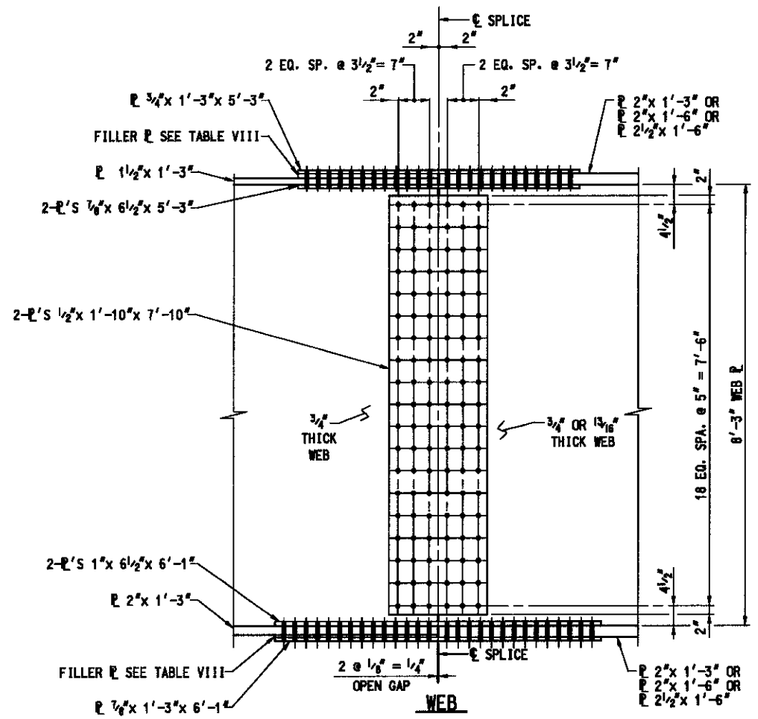

WEB

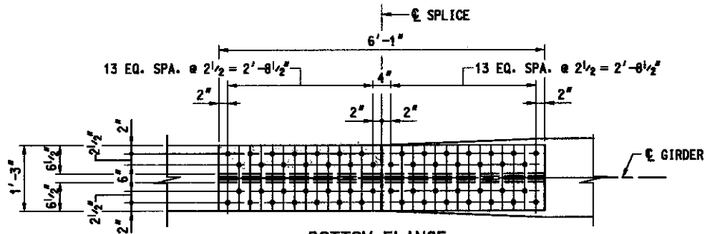

BOTTOM FLANGE

FIELD SPLICE DETAIL - TYPE VIII

SCALE: N.T.S.

SPLICE NOTES:

1. ALL BOLTS TO BE 1" DIA. HIGH STRENGTH BOLTS CONFORMING TO A 325, TYPE 3. ALL BOLT HOLES SHALL BE 1 1/16" DIA.
2. ON FASCIA GIRDERS THE BOLTS SHALL BE PLACED SO THAT THE BOLT HEAD IS VISIBLE ON THE OUTSIDE FACE OF WEB.
3. ALL BOLTS ON FLANGE SPLICES SHALL HAVE BOLT HEADS ON THE BOTTOM.
4. BOLTS NOT SHOWN IN SPLICE.
5. SPACE SHEAR STUDS TO MISS TOP FLANGE SPLICE BOLTS.
6. A MINIMUM OF 50 PERCENT OF THE WEB, TOP FLANGE AND BOTTOM FLANGE SPLICE BOLTS SHALL BE IN PLACE BEFORE THE GIRDER IS LEFT UNSUPPORTED.
7. WHEN FLANGE IS LARGER THAN ADJACENT FLANGE BY MORE THAN 2", THE LARGER FLANGE SHALL BE TAPERED TO THE SMALLER FLANGE WIDTH IN A DISTANCE OF ½ LENGTH OF SPLICE PLATE (BOTTOM FLANGE ONLY).
8. FIELD SPLICES SHALL BE COMPLETELY SHOP ASSEMBLED AND MATCH MARKED AFTER ALL SHOP WELDING HAS BEEN COMPLETED. CONTACT SURFACES SHALL BE FREE OF ALL OIL AND DIRT.

TYPE	LOCATION	
	GIRDER	SPLICE DESIGNATION
VII	G-5	5-1
VIII	G-1	6-1, 6-2, 9-1, 9-2
	G-2	6-1, 6-2, 9-1, 9-2
	G-3	6-1, 6-2, 9-1, 9-2
	G-4	6-1, 6-2, 9-1, 9-2

TABLE VIII: FILLER PLATES

GIRDER	SPLICE DESIGNATION	TOP SPLICE	BOTTOM SPLICE
G-1, G-2, G-3, G-4	6-2, 9-1, 9-2	½"x 1'-3"x 2'-7⅜"	N/A
G-1, G-2, G-3, G-4	6-1	1"x 1'-3"x 2'-7⅜"	½"x 1'-3"x 3'-0⅜"

MASTER SET

FILE: g:\smd\304004.JI1951695..hw\oddstruct\ramp_gg\GG-fieldsplice_4.dgn
DATE: 8/4/2006
TIME: 4:07:45 AM

JOHNSON, MIRMIRAN & THOMPSON
Engineering A Brighter Future

MARYLAND TRANSPORTATION AUTHORITY
Engineering Division

ADDENDUMS & REVISIONS			
NO.	DESCRIPTION	BY	DATE

I-95 EXPRESS TOLL LANES : I-695 INTERCHANGE
GENERAL PURPOSE ROADWAYS AND RAMPS
JOHN F. KENNEDY MEMORIAL HIGHWAY (BALTIMORE COUNTY)
RAMP GG
FIELD SPLICE DETAILS - TYPE VII AND TYPE VIII

CONTRACT NO. KH-1301-000-006
DRAWING NO. S6 - 110

DESIGNED BY PDR	DRAWN BY DJA	CHECKED BY MJR	SHEET NO.
CONST. REVIEW BY	DATE AUGUST, 2006	SCALE AS SHOWN	867 OF 1676

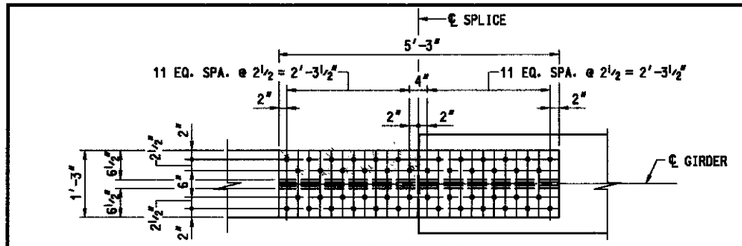

TOP FLANGE

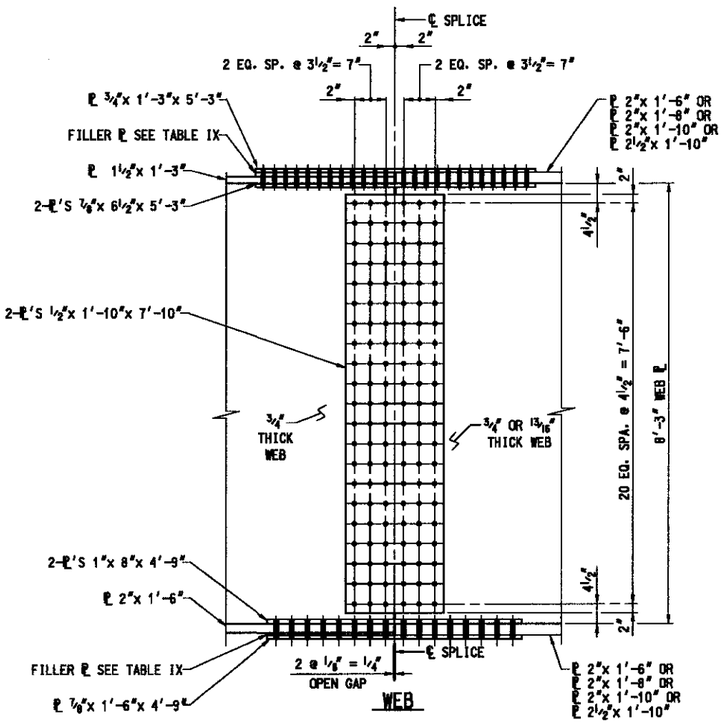

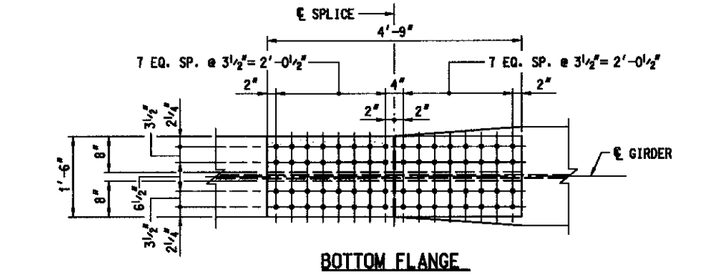

BOTTOM FLANGE

FIELD SPLICE DETAIL - TYPE IX

SCALE: N.T.S.

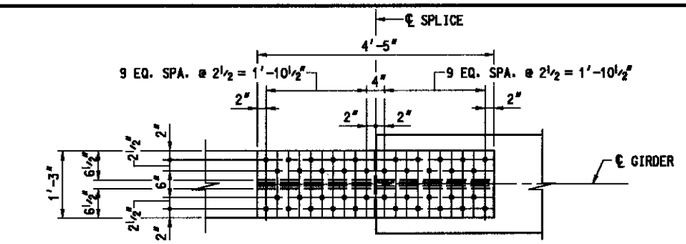

TOP FLANGE

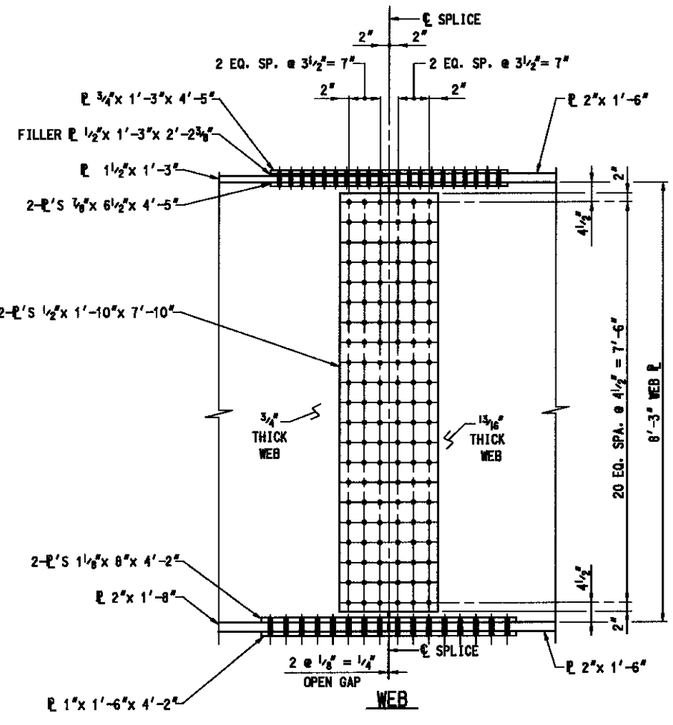

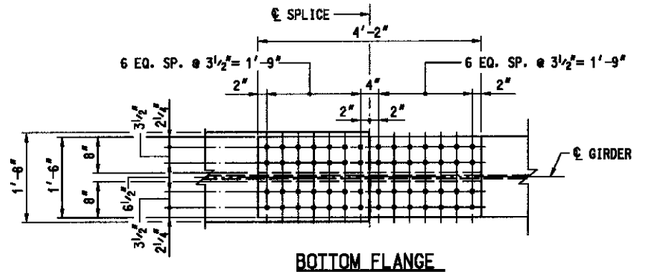

BOTTOM FLANGE

FIELD SPLICE DETAIL - TYPE X

SCALE: N.T.S.

SPLICE NOTES:

1. ALL BOLTS TO BE 1" DIA. HIGH STRENGTH BOLTS CONFORMING TO A 325, TYPE 3. ALL BOLT HOLES SHALL BE 1 1/16" DIA.
2. ON FASCIA GIRDERS THE BOLTS SHALL BE PLACED SO THAT THE BOLT HEAD IS VISIBLE ON THE OUTSIDE FACE OF WEB.
3. ALL BOLTS ON FLANGE SPLICES SHALL HAVE BOLT HEADS ON THE BOTTOM.
4. BOLTS NOT SHOWN IN SPLICE.
5. SPACE SHEAR STUDS TO MISS TOP FLANGE SPLICE BOLTS.
6. A MINIMUM OF 50 PERCENT OF THE WEB, TOP FLANGE AND BOTTOM FLANGE SPLICE BOLTS SHALL BE IN PLACE BEFORE THE GIRDER IS LEFT UNSUPPORTED.
7. WHEN FLANGE IS LARGER THAN ADJACENT FLANGE BY MORE THAN 2", THE LARGER FLANGE SHALL BE TAPERED TO THE SMALLER FLANGE WIDTH IN A DISTANCE OF ½ LENGTH OF SPLICE PLATE (BOTTOM FLANGE ONLY).
8. FIELD SPLICES SHALL BE COMPLETELY SHOP ASSEMBLED AND MATCH MARKED AFTER ALL SHOP WELDING HAS BEEN COMPLETED. CONTACT SURFACES SHALL BE FREE OF ALL OIL AND DIRT.

TYPE	LOCATION	
	GIRDER	SPLICE DESIGNATION
IX	G-1	2-3, 4-1
	G-2	2-3, 4-1
	G-3	2-3, 4-1
	G-4	2-3, 4-1
	G-5	6-1, 6-2, 9-1, 9-2
X	G-5	2-2

TABLE IX : FILLER PLATES

GIRDER	SPLICE DESIGNATION	TOP SPLICE	BOTTOM SPLICE
G-1, G-2, G-3, G-4	2-3, 4-1	½"x 1'-3"x 2'-7⅝"	N/A
G-5	6-2, 9-1, 9-2	½"x 1'-3"x 2'-7⅝"	N/A
G-5	6-1	1"x 1'-3"x 2'-7⅝"	½"x 1'-6"x 2'-4⅜"

MASTER SET

FILE: q:\smd\304004_II1951695_hw\oddfs\struct\ramp_gg\00-fieldsplice_5.dgn
DATE: 8/4/2006
TIME: 4:07:17 AM

JOHNSON, MIRMIRAN & THOMPSON
Engineering A Brighter Future

MARYLAND TRANSPORTATION AUTHORITY
Engineering Division

ADDENDUMS & REVISIONS

NO.	DESCRIPTION	BY	DATE

I-95 EXPRESS TOLL LANES : I-695 INTERCHANGE
GENERAL PURPOSE ROADWAYS AND RAMPS
JOHN F. KENNEDY MEMORIAL HIGHWAY (BALTIMORE COUNTY)
RAMP GG
FIELD SPLICE DETAILS - TYPE IX AND TYPE X

CONTRACT NO. KH-1301-000-006
DRAWING NO. S6 - 111
SHEET NO. 888 OF 1675

DESIGNED BY PDR | DRAWN BY DJA | CHECKED BY MJB
CONST. REVIEW BY | DATE AUGUST, 2006 | SCALE AS SHOWN

REVISED

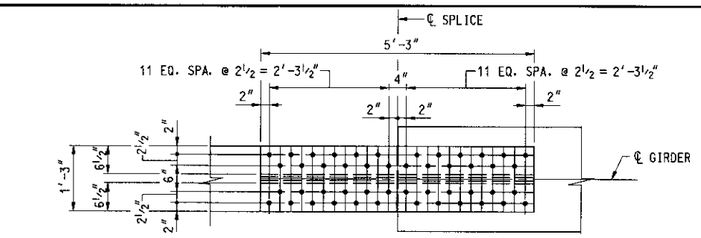

TOP FLANGE

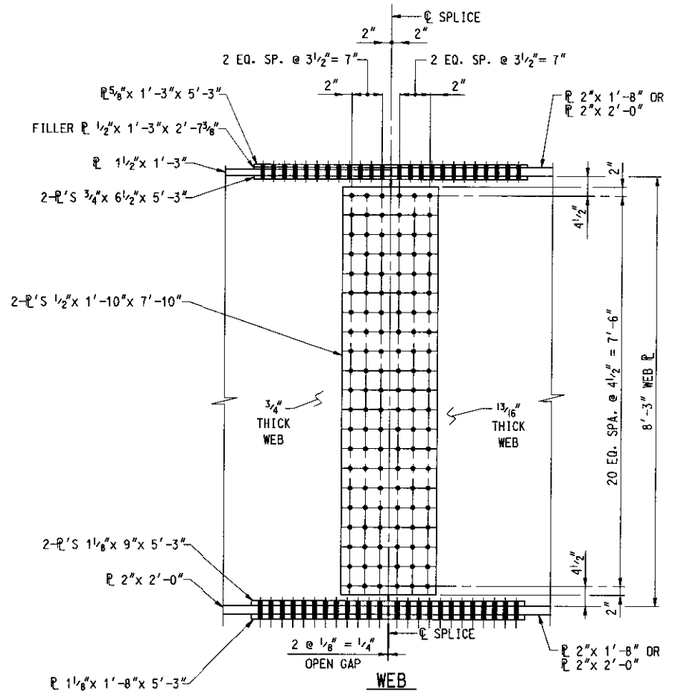

WEB

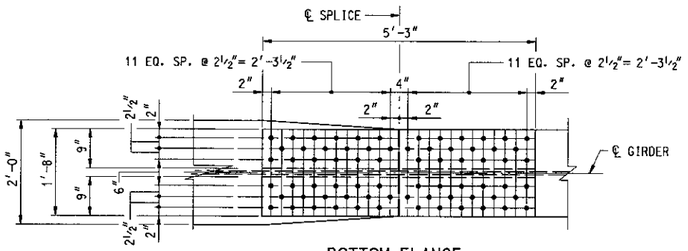

BOTTOM FLANGE

FIELD SPLICE DETAIL - TYPE XI

SCALE: N.T.S.

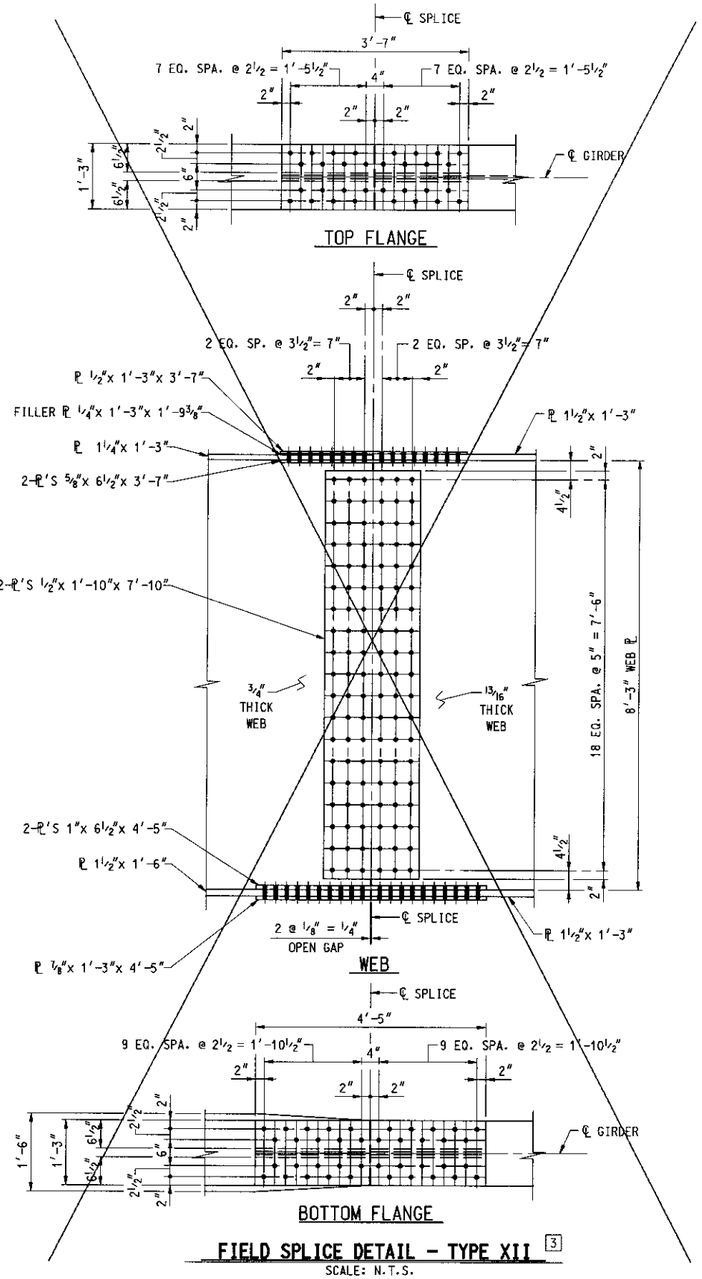

TOP FLANGE

WEB

BOTTOM FLANGE

FIELD SPLICE DETAIL - TYPE XII [3]

SCALE: N.T.S.

SPLICE NOTES:

1. ALL BOLTS TO BE 1" DIA. HIGH STRENGTH BOLTS CONFORMING TO A 325, TYPE 3. ALL BOLT HOLES SHALL BE 1 1/16" DIA.
2. ON FASCIA GIRDERS THE BOLTS SHALL BE PLACED SO THAT THE BOLT HEAD IS VISIBLE ON THE OUTSIDE FACE OF WEB.
3. ALL BOLTS ON FLANGE SPLICES SHALL HAVE BOLT HEADS ON THE BOTTOM.
4. BOLTS NOT SHOWN IN SPLICE.
5. SPACE SHEAR STUDS TO MISS TOP FLANGE SPLICE BOLTS.
6. A MINIMUM OF 50 PERCENT OF THE WEB, TOP FLANGE AND BOTTOM FLANGE SPLICE BOLTS SHALL BE IN PLACE BEFORE THE GIRDER IS LEFT UNSUPPORTED.
7. WHEN FLANGE IS LARGER THAN ADJACENT FLANGE BY MORE THAN 2", THE LARGER FLANGE SHALL BE TAPERED TO THE SMALLER FLANGE WIDTH IN A DISTANCE OF ½ LENGTH OF SPLICE PLATE (BOTTOM FLANGE ONLY).
8. FIELD SPLICES SHALL BE COMPLETELY SHOP ASSEMBLED AND MATCH MARKED AFTER ALL SHOP WELDING HAS BEEN COMPLETED. CONTACT SURFACES SHALL BE FREE OF ALL OIL AND DIRT.

TYPE	LOCATION	
	GIRDER	SPLICE DESIGNATION
XI	G-5	4-1, 2-3
~~XII~~	~~G-5~~	~~7-2~~

[3]

JOHNSON, MIRMIRAN & THOMPSON
Engineering A Brighter Future

MARYLAND TRANSPORTATION AUTHORITY
Engineering Division

ADDENDUMS & REVISIONS			
NO.	DESCRIPTION	BY	DATE
3	REMOVE TYPE XII	MJB	3/07

I-95 EXPRESS TOLL LANES : I-695 INTERCHANGE
GENERAL PURPOSE ROADWAYS AND RAMPS
JOHN F. KENNEDY MEMORIAL HIGHWAY (BALTIMORE COUNTY)
RAMP GG
FIELD SPLICE DETAILS - TYPE XI ~~AND TYPE XII~~ [3]

DESIGNED BY PDR	DRAWN BY DJA	CHECKED BY MJB
CONST. REVIEW BY	DATE AUGUST, 2006	SCALE AS SHOWN

CONTRACT NO. KH-1301-000-006
DRAWING NO. S6 - 112
SHEET NO. 809 OF 1676

FILE: G:\smd\304004_I1195695_hw\oddd\struct\Ramp_GG\GG-fieldsplice_6_Redline3.dgn
DATE: 3/30/2007
TIME: 9:25:14 AM

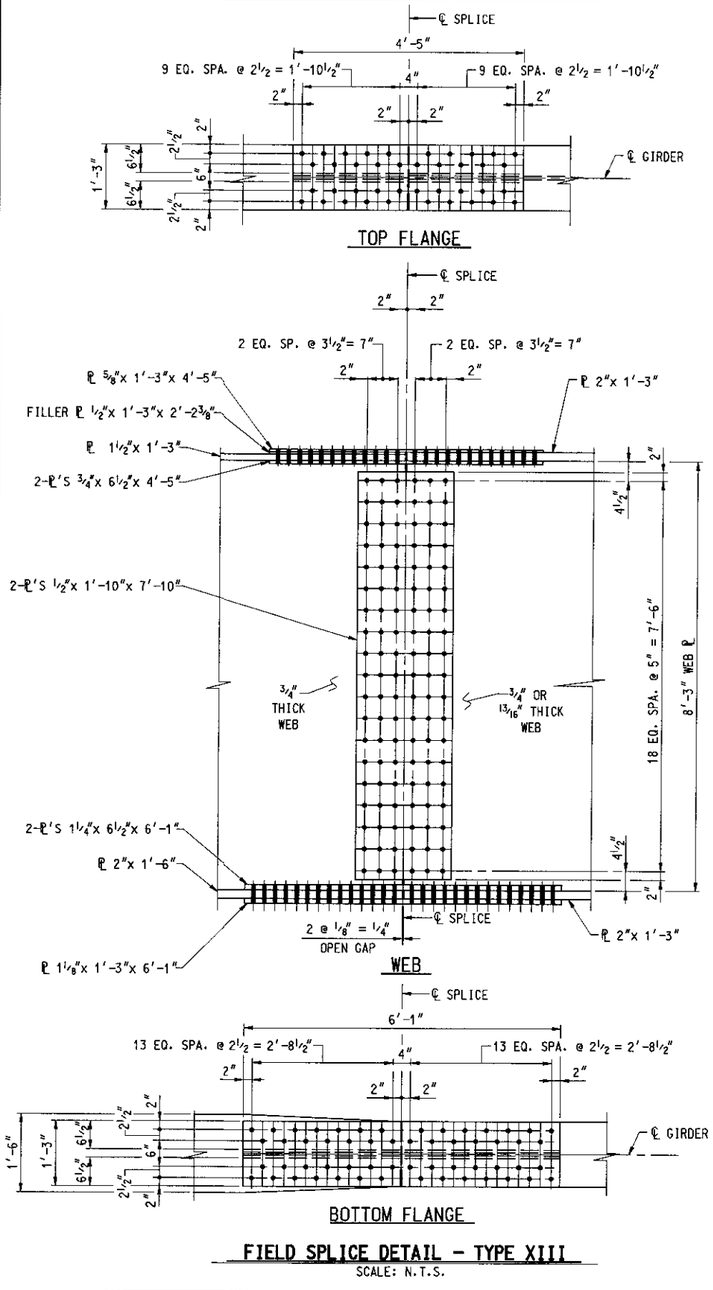

REVISED

SPLICE NOTES:

1. ALL BOLTS TO BE 1" DIA. HIGH STRENGTH BOLTS CONFORMING TO A 325, TYPE 3. ALL BOLT HOLES SHALL BE 1 1/16" DIA.
2. ON FASCIA GIRDERS THE BOLTS SHALL BE PLACED SO THAT THE BOLT HEAD IS VISIBLE ON THE OUTSIDE FACE OF WEB.
3. ALL BOLTS ON FLANGE SPLICES SHALL HAVE BOLT HEADS ON THE BOTTOM.
4. BOLTS NOT SHOWN IN SPLICE.
5. SPACE SHEAR STUDS TO MISS TOP FLANGE SPLICE BOLTS.
6. A MINIMUM OF 50 PERCENT OF THE WEB, TOP FLANGE AND BOTTOM FLANGE SPLICE BOLTS SHALL BE IN PLACE BEFORE THE GIRDER IS LEFT UNSUPPORTED.
7. WHEN FLANGE IS LARGER THAN ADJACENT FLANGE BY MORE THAN 2", THE LARGER FLANGE SHALL BE TAPERED TO THE SMALLER FLANGE WIDTH IN A DISTANCE OF 1/2 LENGTH OF SPLICE PLATE (BOTTOM FLANGE ONLY).
8. FIELD SPLICES SHALL BE COMPLETELY SHOP ASSEMBLED AND MATCH MARKED AFTER ALL SHOP WELDING HAS BEEN COMPLETED. CONTACT SURFACES SHALL BE FREE OF ALL OIL AND DIRT.

TYPE	LOCATION	
	GIRDER	SPLICE DESIGNATION
XIII	G-1	2-2
	G-2	2-2
	G-3	2-2
	G-4	2-2
XIV	G-1	1-2, 2-1
	G-2	1-2, 2-1
	G-3	1-2, 2-1
3	~~G-4~~	~~1-2, 2-1~~

FILE: q:\smd\304004_II1951695_hw\cadd\struct\Ramp_GG\GG-fieldsplice_1_Redline3.dgn
DATE: 3/30/2007
TIME: 9:25:17 AM

JOHNSON, MIRMIRAN & THOMPSON
Engineering A Brighter Future

MARYLAND TRANSPORTATION AUTHORITY
Engineering Division

ADDENDUMS & REVISIONS			
NO.	DESCRIPTION	BY	DATE
3	REMOVED G-4 FROM FIELD SPLICE TYPE XIV	MJB	3/07

I-95 EXPRESS TOLL LANES : I-695 INTERCHANGE
GENERAL PURPOSE ROADWAYS AND RAMPS
JOHN F. KENNEDY MEMORIAL HIGHWAY (BALTIMORE COUNTY)
RAMP GG
FIELD SPLICE DETAILS - TYPE XIII AND TYPE XIV

DESIGNED BY PDR	DRAWN BY DJA	CHECKED BY MJB	
CONST. REVIEW BY	DATE AUGUST, 2006	SCALE AS SHOWN	

CONTRACT NO. KH-1301-000-006
DRAWING NO. S6 - 113
SHEET NO. 810 OF 1676

REVISED

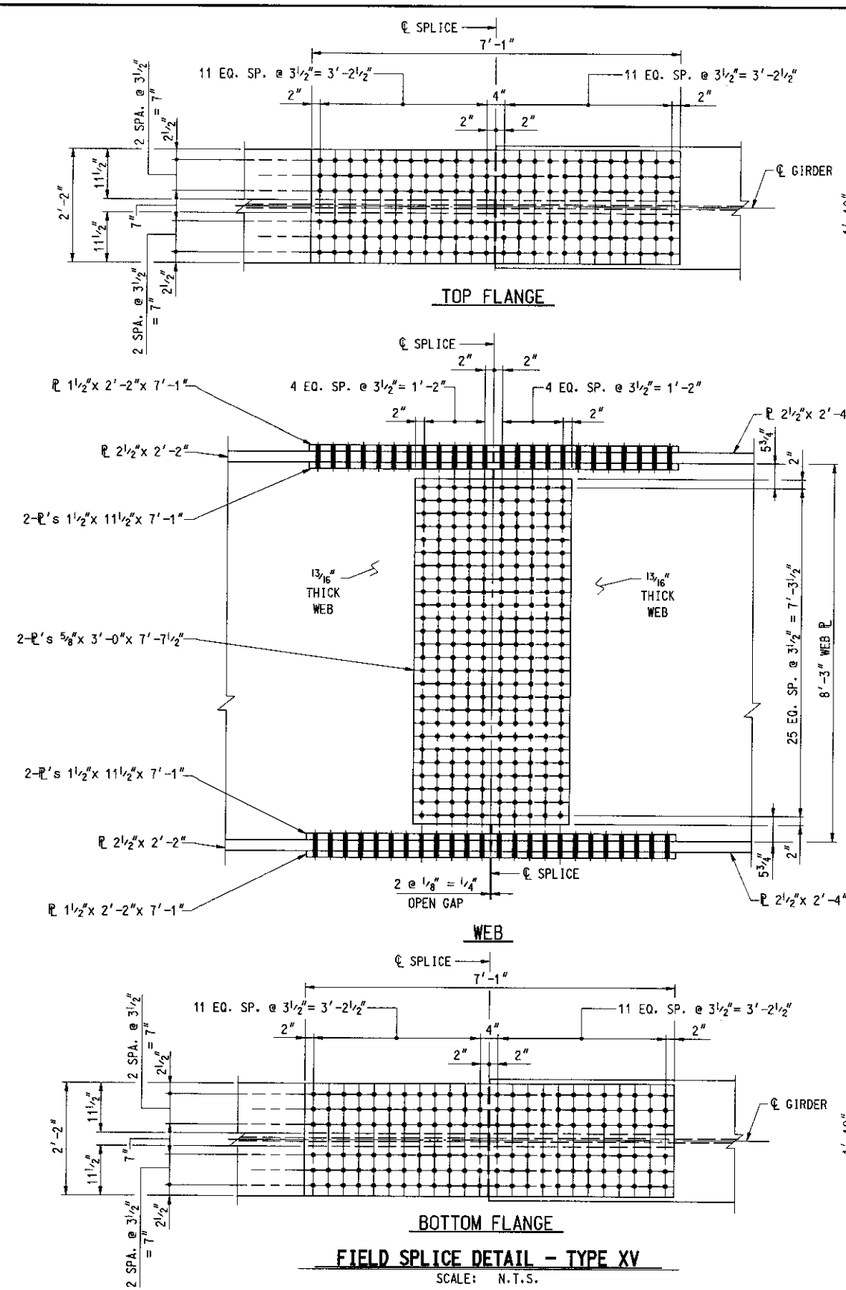

FIELD SPLICE DETAIL - TYPE XV

SCALE: N.T.S.

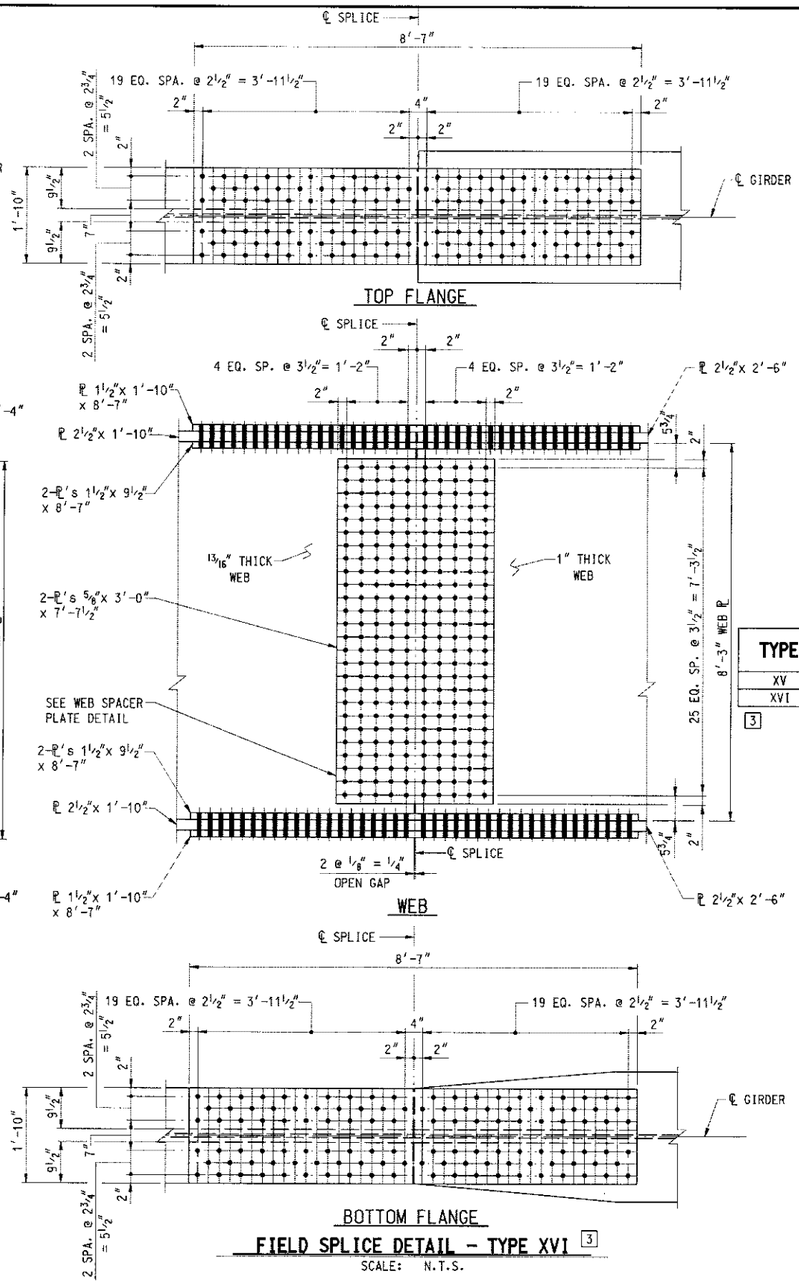

FIELD SPLICE DETAIL - TYPE XVI [3]

SCALE: N.T.S.

SPLICE NOTES:

1. ALL BOLTS TO BE 1" DIA. HIGH STRENGTH BOLTS CONFORMING TO A 325, TYPE 3. ALL BOLT HOLES SHALL BE 1 1/16" DIA.
2. ON FASCIA GIRDERS THE BOLTS SHALL BE PLACED SO THAT THE BOLT HEAD IS VISIBLE ON THE OUTSIDE FACE OF WEB.
3. ALL BOLTS ON FLANGE SPLICES SHALL HAVE BOLT HEADS ON THE BOTTOM.
4. BOLTS NOT SHOWN IN SPLICE.
5. SPACE SHEAR STUDS TO MISS TOP FLANGE SPLICE BOLTS.
6. A MINIMUM OF 50 PERCENT OF THE WEB, TOP FLANGE AND BOTTOM FLANGE SPLICE BOLTS SHALL BE IN PLACE BEFORE THE GIRDER IS LEFT UNSUPPORTED.
7. WHEN FLANGE IS LARGER THAN ADJACENT FLANGE BY MORE THAN 2", THE LARGER FLANGE SHALL BE TAPERED TO THE SMALLER FLANGE WIDTH IN A DISTANCE OF ½ LENGTH OF SPLICE PLATE (BOTTOM FLANGE ONLY).
8. FIELD SPLICES SHALL BE COMPLETELY SHOP ASSEMBLED AND MATCH MARKED AFTER ALL SHOP WELDING HAS BEEN COMPLETED. CONTACT SURFACES SHALL BE FREE OF ALL OIL AND DIRT.

TYPE	LOCATION	
	GIRDER	SPLICE DESIGNATION
XV	G-5	1-2, 2-1
XVI	G-4	1-2, 2-1

[3]

FILE: q:\smd\304004_111951695_hw\oadd\struct\Ramp_GG\GG-fieldsplice_8.Redline3.dgn
DATE: 3/30/2007
TIME: 9:25:19 AM

JOHNSON, MIRMIRAN & THOMPSON
Engineering A Brighter Future

MARYLAND TRANSPORTATION AUTHORITY
Engineering Division

ADDENDUMS & REVISIONS			
NO.	DESCRIPTION	BY	DATE
[3]	ADDED FIELD SPLICE - TYPE XVI	MJB	3/07

I-95 EXPRESS TOLL LANES : I-695 INTERCHANGE
GENERAL PURPOSE ROADWAYS AND RAMPS
JOHN F. KENNEDY MEMORIAL HIGHWAY (BALTIMORE COUNTY)
RAMP GG
FIELD SPLICE DETAILS - TYPE XV AND TYPE XVI [3]

DESIGNED BY CLB	DRAWN BY DJA	CHECKED BY MJB	
CONST. REVIEW BY	DATE AUGUST, 2006	SCALE AS SHOWN	

CONTRACT NO. KH-1301-000-006
DRAWING NO. S6 - 114
SHEET NO. 81 OF 1676

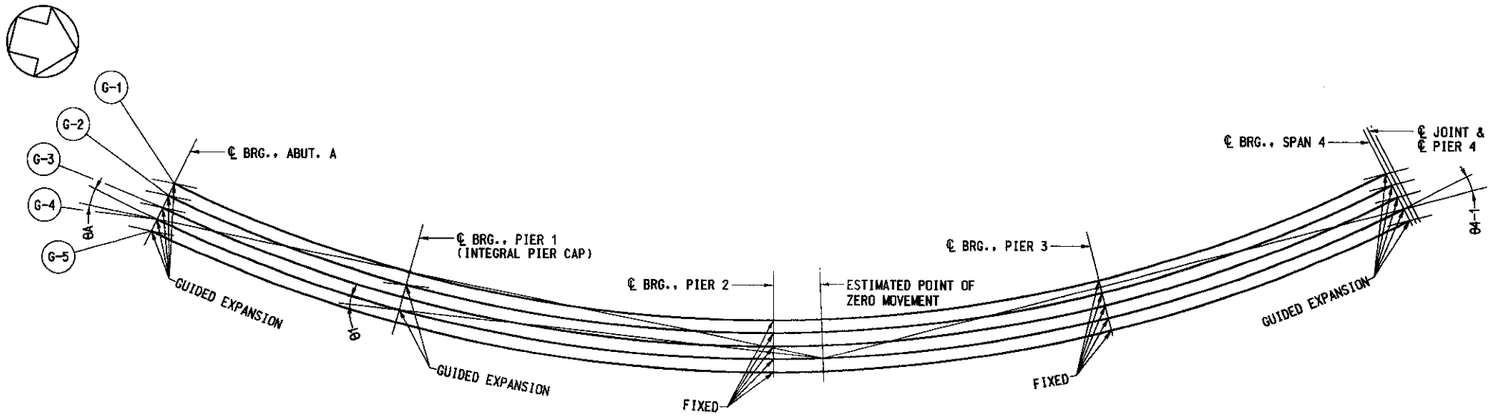

BEARING ORIENTATION PLAN - SPANS 1 THRU 4

N.T.S.

GUIDED BEARING SKEW	
θ A	-14°05′
θ 1	-08°46′
θ 4-1	12°34′

NOTE:

SKEW ANGLE MEASURED FROM ℄ GIRDER TO ℄ MOVEMENT:
+ CLOCKWISE FROM ℄ GIRDER TO ℄ MOVEMENT
- COUNTERCLOCKWISE FROM ℄ GIRDER TO ℄ MOVEMENT

⚠ NOTE:

IF THE CONCRETE BEARING PAD DIMENSIONS SHOWN ON THE PLANS CANNOT ACCOMODATE THE BEARING SIZE, THE DIMENSIONS OF THE CONCRETE BEARING PAD MAY BE MODIFIED, MAINTAINING THE MINIMUM EDGE DISTANCES SHOWN ON THE ANCHOR BOLT DETAIL. THE ENGINEER SHALL BE NOTIFIED OF ANY PROPOSED CHANGE FOR VERIFICATION AND NO ADDITIONAL COMPENSATION WILL BE ALLOWED.

ADDITIONALLY, AT EACH PIER, THE CONTRACTOR SHALL SURVEY THE TOP OF PIER CAP PRIOR TO POURING THE CONCRETE BEARING PADS TO DETERMINE IF ANY ADJUSTMENT TO THE CONCRETE BEARING PAD SIZE IS NEEDED IN ORDER TO MAINTAIN THE MINIMUM EDGE DISTANCES.

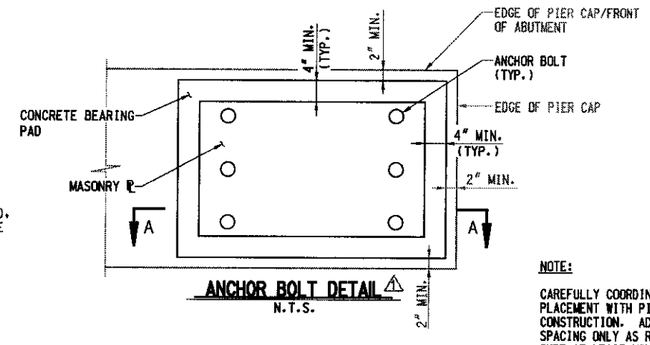

ANCHOR BOLT DETAIL ⚠

N.T.S.

NOTE:

CAREFULLY COORDINATE ANCHOR ROD / SLEEVE PLACEMENT WITH PIER CAP REINFORCING CAGE CONSTRUCTION. ADJUST STIRRUP AND TIE SPACING ONLY AS REQUIRED TO CLEAR, MAKING SURE AT LEAST MINIMUM SPACING IS MAINTAINED.

HIGH LOAD MULTI-ROTATIONAL BEARING NOTES

INSTALLATION NOTES:

1. CONTRACTOR IS RESPONSIBLE FOR ANY DISCREPANCY IN THE BEARING ELEVATIONS.
2. CONDUCT HANDLING AND INSTALLATION OF HIGH LOAD MULTI-ROTATIONAL BEARINGS IN SUCH A MANNER AS TO PROTECT THE BEARINGS. IN ADDITION, PARTICULAR ATTENTION IS TO BE GIVEN TO PROTECTING OF ALL SLIDING SURFACES OF BEARINGS AND ANY PROTECTIVE COATINGS ON BEARINGS. HIGH LOAD MULTI-ROTATIONAL BEARINGS ARE SUPPLIED WITH REQUIRED PROTECTIVE COATINGS AS NOTED IN SHOP NOTES. BEARINGS MAY NOT BE DISASSEMBLED FOR ANY FURTHER COATING APPLICATION OR COATING TOUCH-UP AT JOB SITE.
3. PROTECT THE PURE WOVEN PTFE FIBER PADS AND STAINLESS STEEL SURFACES FROM DIRT, DEBRIS, WELD SPATTER, BLASTING SAND/GRIT, GRINDING PARTICLES, PAINT, PAINT OVER SPRAY, AND ANY OTHER FOREIGN MATTER. AVOID EXPOSURE OF PTFE FIBER PADS TO DIRECT SUNLIGHT TO PREVENT ULTRA-VIOLET RAY DAMAGE TO PTFE FIBER PADS.
4. REMOVE BANDING WHICH SECURES BEARING AS A UNIT ONLY AFTER BEARING IS SET IN PLACE AND PRIOR TO POSITIONING SOLE ℄ FOR GIRDER INSTALLATION. THESE BEARINGS MAY NOT BE DISASSEMBLED AT THE JOB SITE UNDER ANY CIRCUMSTANCES WITHOUT INSPECTOR APPROVAL AND THE APPROVAL OR PRESENCE OF THE MANUFACTURER'S REPRESENTATIVE.
5. BLOCK GIRDERS AT EXPANSION BEARINGS DURING ERECTION IN ORDER TO: (a) PROTECT THE BEARINGS FROM IMPACT AND/OR ECCENTRIC LOADS, (b) STABILIZE THE GIRDER, (c) INSURE PROPER BRIDGE/GIRDER ALIGNMENT.
6. USE EDGE PROTECTORS OR NYLON SLINGS WHEN HANDLING HIGH LOAD MULTI-ROTATIONAL BEARINGS IN ORDER TO PROTECT THE PROTECTIVE COATINGS ON THE BEARINGS. TO AVOID DAMAGING PROTECTIVE COATING ON BEARINGS, DO NOT POSITION HIGH LOAD MULTI-ROTATIONAL BEARINGS BY MEANS OF STRIKING.
7. IN THE EVENT OF DAMAGE TO PROTECTIVE COATINGS, MAKE REPAIRS AS QUICKLY AS POSSIBLE IN ORDER TO AVOID MOISTURE INDUCED COATING FAILURE. PROPERLY PREPARE STEEL SURFACES IN AREA OF DAMAGED COATINGS BY REMOVING ALL LOOSE COATINGS AND RUST AND BY PROVIDING REQUIRED STEEL PROFILE FOR COATING ADHERENCE. PERFORM RECOATING WITHIN 8 HOURS OF STEEL PREPARATION.
8. WHEN WELDING SOLE PLATE TO GIRDER FLANGE, ENSURE THAT SURFACES CONTACTING PTFE SURFACES DO NOT EXCEED 250°F, TO AVOID DAMAGING THE PTFE.

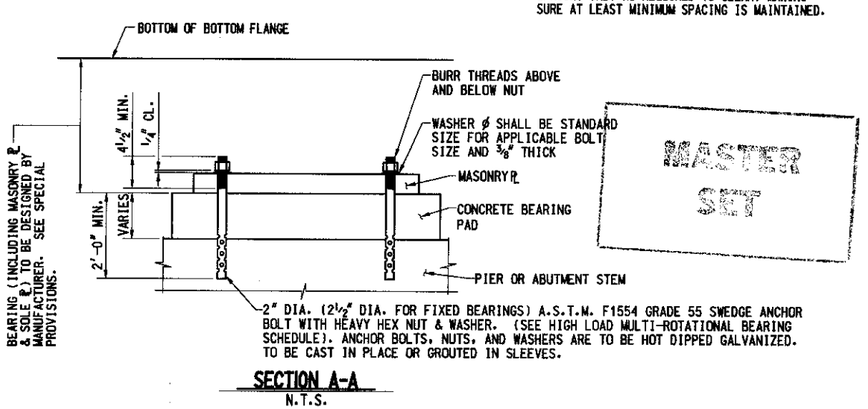

SECTION A-A

N.T.S.

MASTER SET

FILE: q:\amd\304004_1195695_hw\caddd\struct\Ramp_GG\GG-Brg_Orient.dgn
DATE: 9/14/2006
TIME: 14:24 PM

JOHNSON, MIRMIRAN & THOMPSON
Engineering A Brighter Future

MARYLAND TRANSPORTATION AUTHORITY
Engineering Division

ADDENDUMS & REVISIONS			
NO.	DESCRIPTION	BY	DATE
1	ADDED BEARING SIZE REQUIREMENTS	MJB	9/12/06

I-95 EXPRESS TOLL LANES : I-695 INTERCHANGE
GENERAL PURPOSE ROADWAYS AND RAMPS
JOHN F. KENNEDY MEMORIAL HIGHWAY (BALTIMORE COUNTY)
RAMP GG
BEARING ORIENTATION PLANS & NOTES I

DESIGNED BY TDY	DRAWN BY DJA	CHECKED BY MJB	
CONST. REVIEW BY	DATE AUGUST, 2006	SCALE AS SHOWN	

CONTRACT NO. KH-1301-000-006
DRAWING NO. S6 - 115
SHEET NO. 812 OF 1676

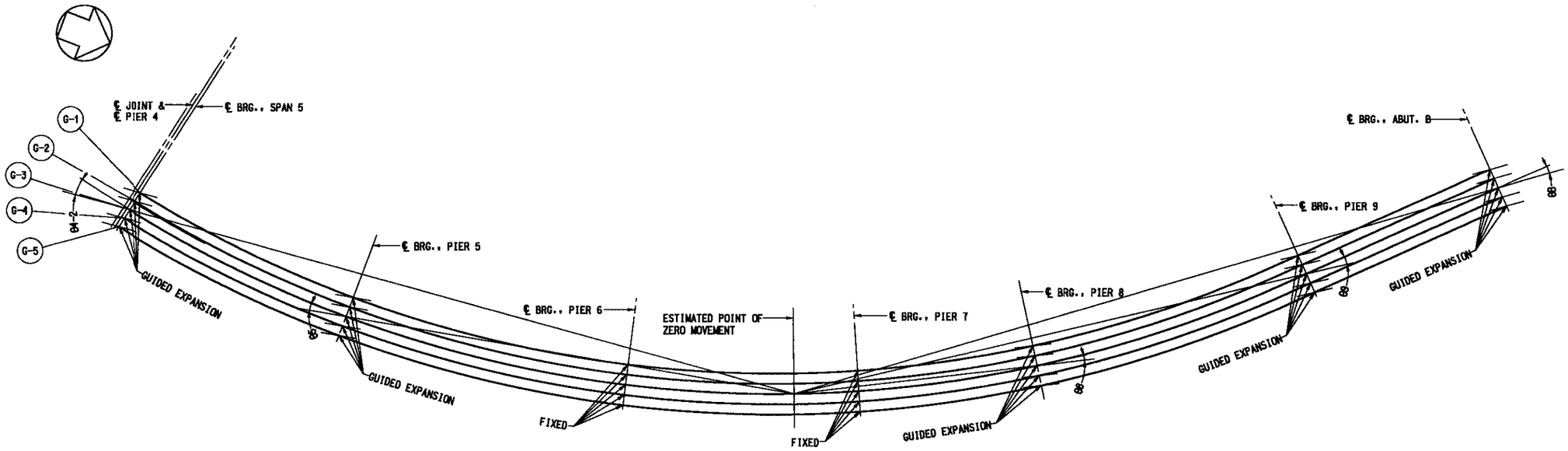

BEARING ORIENTATION PLAN - SPANS 5 THRU 10
N.T.S.

GUIDED BEARING SKEW	
θ4-2	-17°01'
θ5	-10°39'
θ8	05°42'
θ9	11°08'
θ8	07°55'

NOTE:

SKEW ANGLE MEASURED FROM ℄ GIRDER TO ℄ MOVEMENT:
+ CLOCKWISE FROM ℄ GIRDER TO ℄ MOVEMENT
- COUNTERCLOCKWISE FROM ℄ GIRDER TO ℄ MOVEMENT

MASTER SET

FILE: q:\smd\304004_II\951695_hw\cadd\struct\ramp_gg\GG-Brg_Orient2.dgn
DATE: 8/4/2006
TIME: 4:07:27 AM

JOHNSON, MIRMIRAN & THOMPSON
Engineering A Brighter Future

MARYLAND TRANSPORTATION AUTHORITY
Engineering Division

ADDENDUMS & REVISIONS			
NO.	DESCRIPTION	BY	DATE
	BEARING ORIENTATION PLANS & NOTES		

I-95 EXPRESS TOLL LANES : I-695 INTERCHANGE
GENERAL PURPOSE ROADWAYS AND RAMPS
JOHN F. KENNEDY MEMORIAL HIGHWAY (BALTIMORE COUNTY)
RAMP GG
BEARING ORIENTATION PLANS & NOTES I

DESIGNED BY TDY	DRAWN BY DJA	CHECKED BY MJB
CONST. REVIEW BY	DATE AUGUST, 2006	SCALE AS SHOWN

CONTRACT NO. KH-1301-000-006
DRAWING NO. S6 - 116
SHEET NO. 113 OF 1676

DECK POURING SEQUENCE NOTES:

1. THE CONTRACTOR SHOULD FOLLOW THE POURING SEQUENCE SHOWN ON THESE PLANS.

2. THE CONTRACTOR MUST SUBMIT EVIDENCE FOR PROVIDING A MINIMUM POUR RATE OF 50 CUBIC YARDS PER HOUR FOR ALL POURS.

3. THE POURING SEQUENCE FOR THE BRIDGE DECK SLAB SHALL BE MADE IN THE NUMBERED ORDER INDICATED. THERE MUST BE AT LEAST FORTY (40) HOURS BETWEEN THE COMPLETION OF ONE NUMBERED POUR AND THE START OF THE NEXT NUMBERED POUR, EXCEPT THAT THERE SHALL BE SIXTEEN (16) HOURS BETWEEN THE COMPLETION OF POURS NUMBERED ⑥ AND ⑦ AND BETWEEN THE COMPLETION OF POURS ⑧ AND ⑨.

4. AN ALTERNATIVE SEQUENCE FOR DECK PLACEMENT WOULD BE AS FOLLOWS:
   - POUR NOS. ① AND ② WOULD BE MADE ON THE FIRST POUR DAY USING TWO INDIVIDUAL SCREEDS, PLACING CREWS AND PUMPS.
   - POUR NOS. ③ AND ④ WOULD BE MADE A MINIMUM OF 40 HOURS AFTER THE FIRST POUR USING TWO INDIVIDUAL SCREEDS, PLACING CREWS AND PUMPS.
   - POUR NO. ⑤ WOULD BE MADE A MINIMUM OF 40 HOURS AFTER THE SECOND POUR USING ONE SCREED, PLACING CREW AND PUMP.
   - POUR NOS. ⑥ AND ⑦ WOULD BE MADE A MINIMUM OF 40 HOURS AFTER THE THIRD POUR USING TWO INDIVIDUAL SCREEDS, PLACING CREWS AND PUMPS.
   - POUR NOS. ⑧ AND ⑨ WOULD BE MADE A MINIMUM OF 40 HOURS AFTER THE FOURTH POUR USING TWO INDIVIDUAL SCREEDS, PLACING CREWS AND PUMPS.
   - POUR NO. ⑩ WOULD BE MADE A MINIMUM OF 40 HOURS AFTER THE FIFTH POUR EITHER USING ONE SCREED, PLACING CREW AND PUMP STARTING FROM POUR NO. ④ END OR USING TWO INDIVIDUAL SCREEDS, PLACING CREW AND PUMP STARTING FROM BOTH ENDS.

5. ONLY THESE TWO POURING SEQUENCES WILL BE CONSIDERED AND NO OTHER SEQUENCES WILL BE CONSIDERED FOR ANY REASON. ANY REQUEST FOR AN ALTERNATE SEQUENCE WILL BE RETURNED WITHOUT ANY CONSIDERATION.

6. CONSIDER THE POURING SEQUENCE OUTLINE ABOVE FOR SPANS 5 THROUGH 10 INDEPENDENT OF THE POURING SEQUENCE OUTLINED FOR SPANS 1 THROUGH 4 ON THE PREVIOUS SHEET.

7. FOR DECK SLAB CONSTRUCTION JOINT DETAILS, SEE MD SHA DETAIL NO. BR-SS(6.07)-77-68.

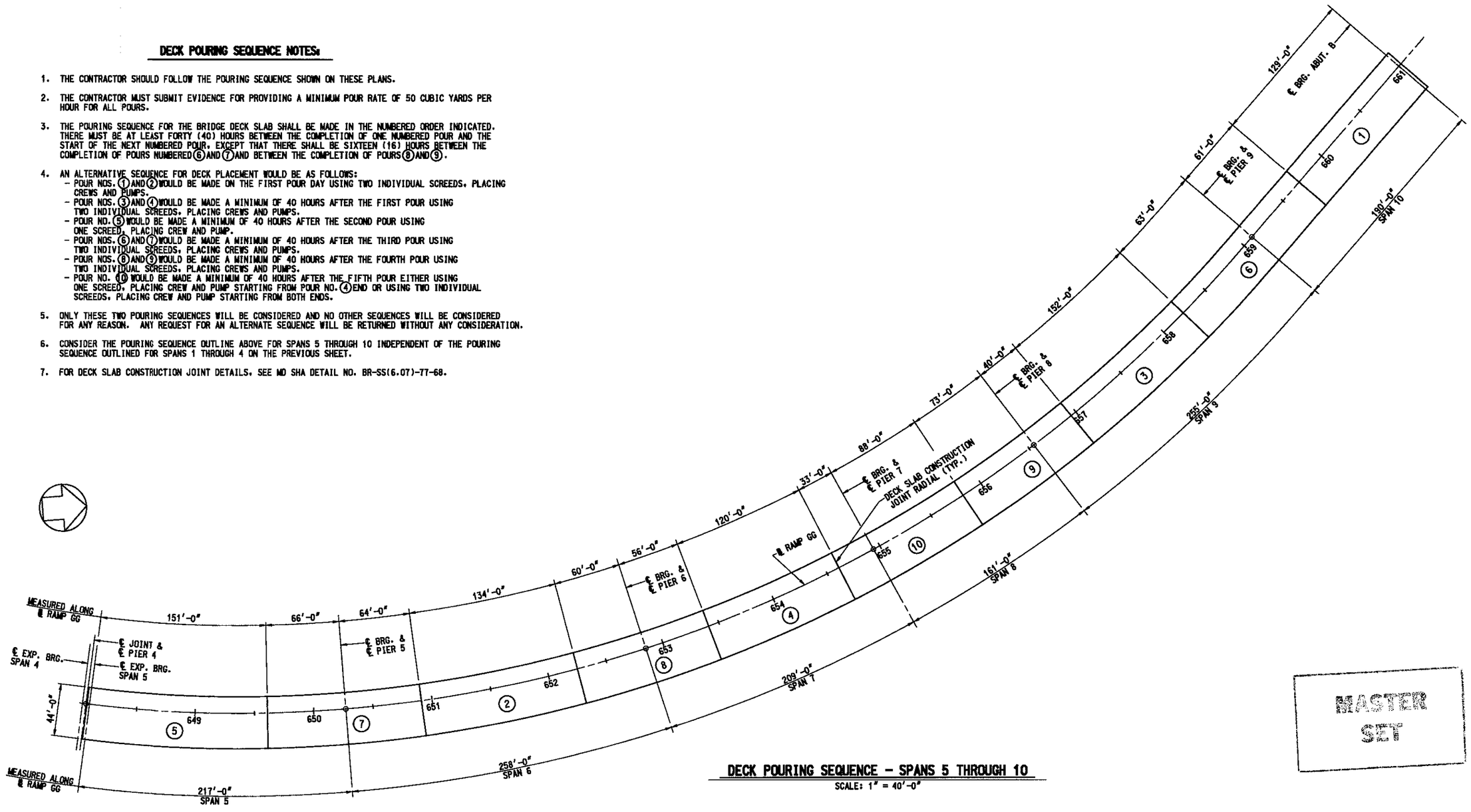

DECK POURING SEQUENCE - SPANS 5 THROUGH 10

SCALE: 1" = 40'-0"

MASTER SET

JOHNSON, MIRMIRAN & THOMPSON
Engineering A Brighter Future

MARYLAND TRANSPORTATION AUTHORITY
Engineering Division

ADDENDUMS & REVISIONS			
NO.	DESCRIPTION	BY	DATE

I-95 EXPRESS TOLL LANES : I-695 INTERCHANGE
GENERAL PURPOSE ROADWAYS AND RAMPS
JOHN F. KENNEDY MEMORIAL HIGHWAY (BALTIMORE COUNTY)
RAMP GG
DECK POURING SEQUENCE - SPANS 5 THRU 10

DESIGNED BY KRM	DRAWN BY DJA	CHECKED BY MJB	
CONST. REVIEW BY	DATE AUGUST, 2006	SCALE AS SHOWN	

CONTRACT NO. KH-1301-000-006
DRAWING NO. S6 - 126
SHEET NO. 823 OF 1676

FILE: q:\amd\304004_I195\695_hov\roads\structure\ramp_gg\06-DECKPOUR2.dgn
DATE: 8/4/2006
TIME: 4:07:54 AM

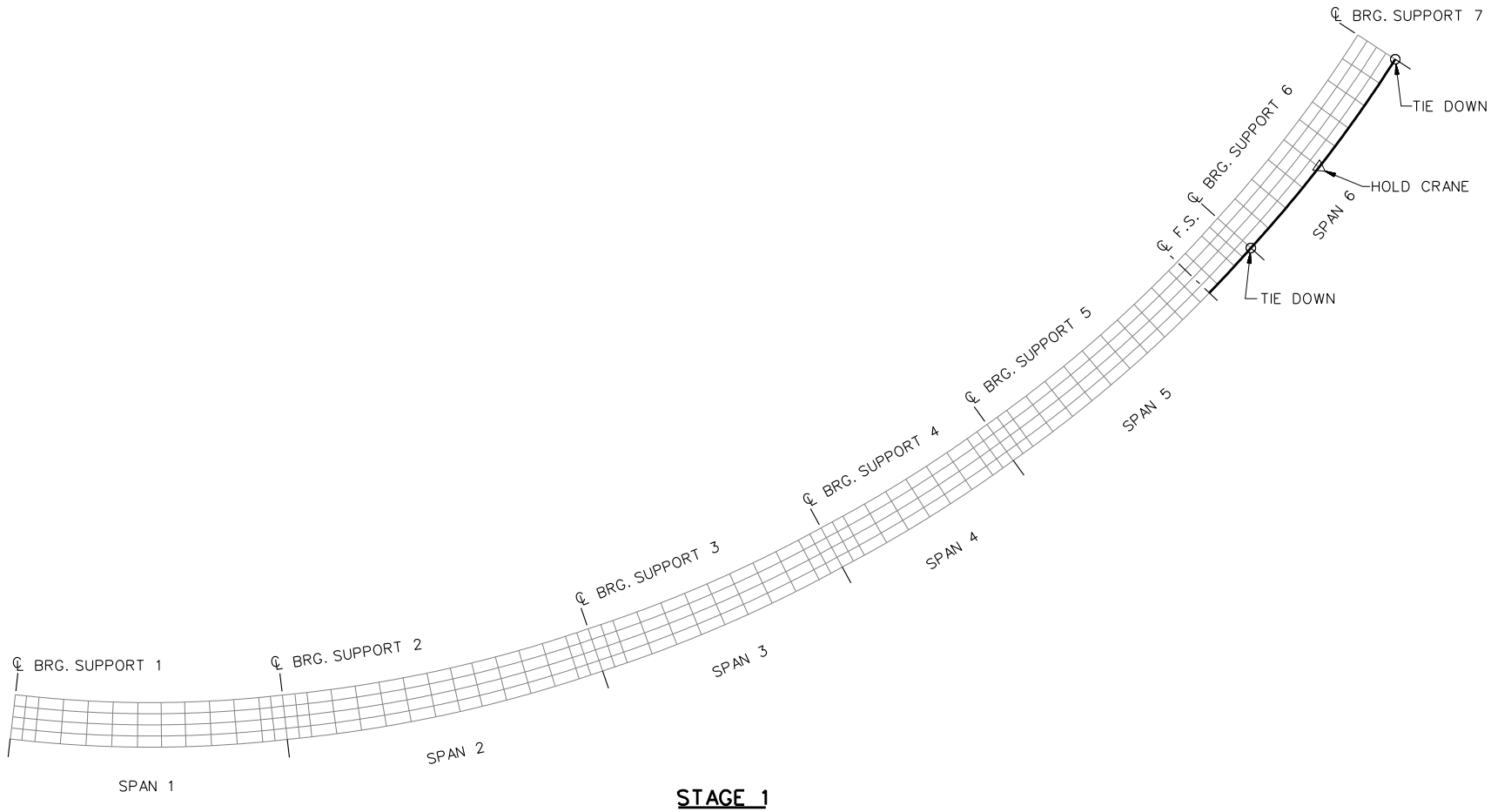

STAGE 1

LEGEND

▽ = HOLD OR LIFT CRANE

○ = TIE DOWN

□ = TEMPORARY SUPPORT STRUCTURE

NCHRP 12-79

BRIDGE EICCR4

GENERAL ERECTION PROCEDURE

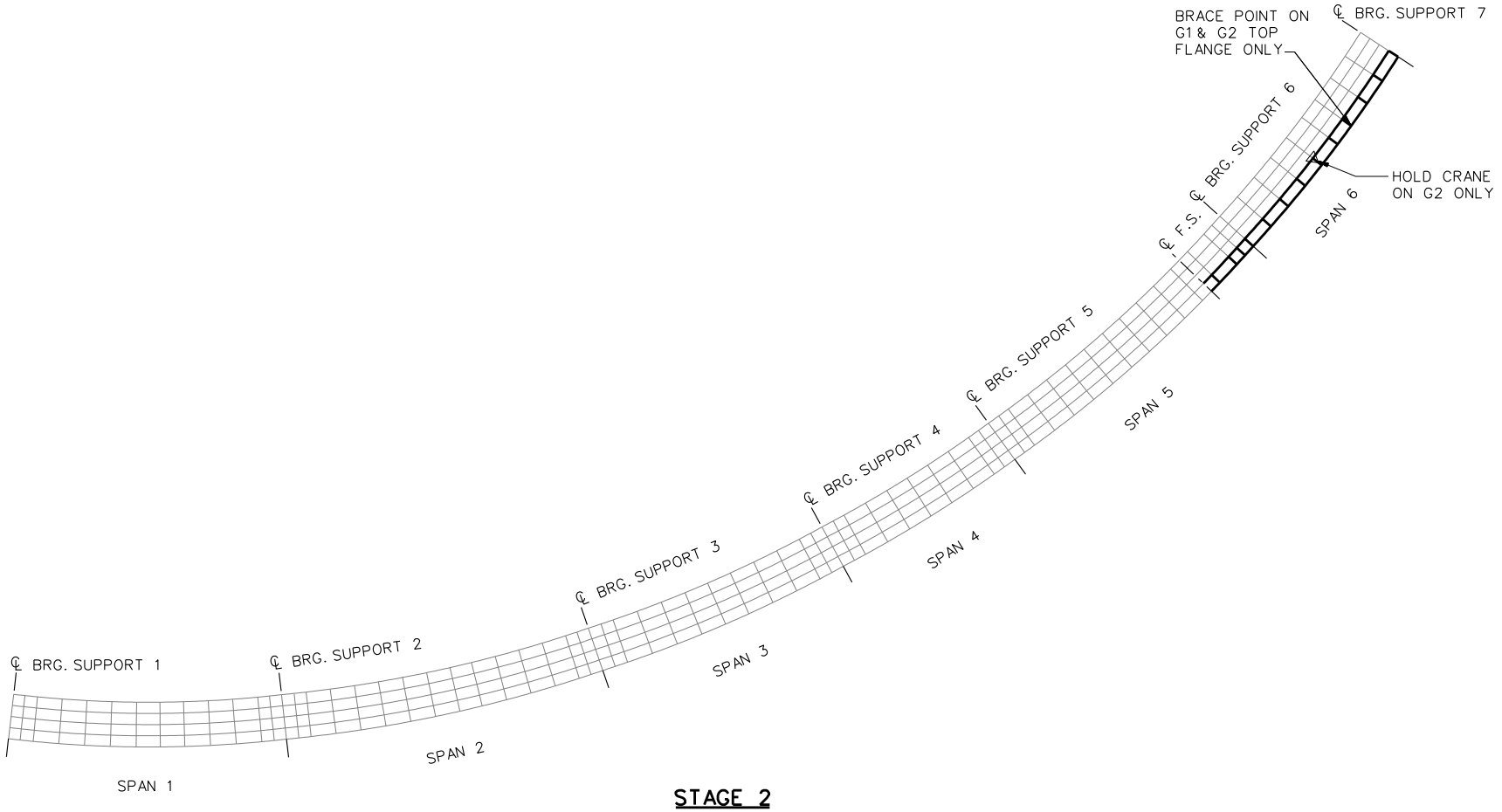

STAGE 2

LEGEND

▽ = HOLD OR LIFT CRANE

○ = TIE DOWN

□ = TEMPORARY SUPPORT STRUCTURE

NCHRP 12-79

BRIDGE EICCR4

GENERAL ERECTION PROCEDURE

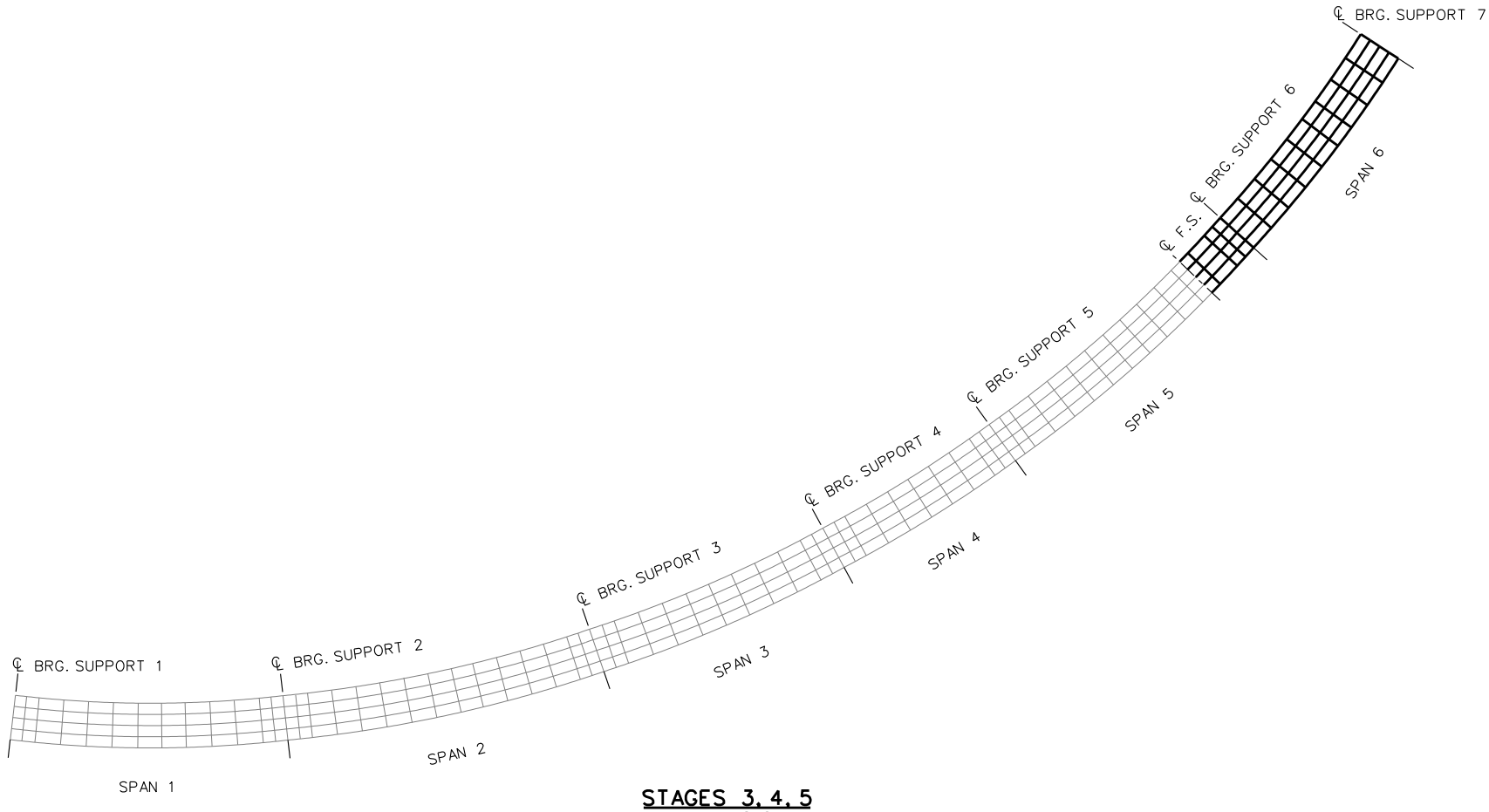

STAGES 3, 4, 5

(STAGE 5 SHOWN)
ERECT STG 3 = G3
ERECT STG 4 = G4
ERECT STG 5 = G5
NO HOLD CRANES
ANY OF ABOVE STAGES

LEGEND

▽ = HOLD OR LIFT CRANE

○ = TIE DOWN

□ = TEMPORARY SUPPORT STRUCTURE

NCHRP 12-79

BRIDGE EICCR4

GENERAL ERECTION PROCEDURE

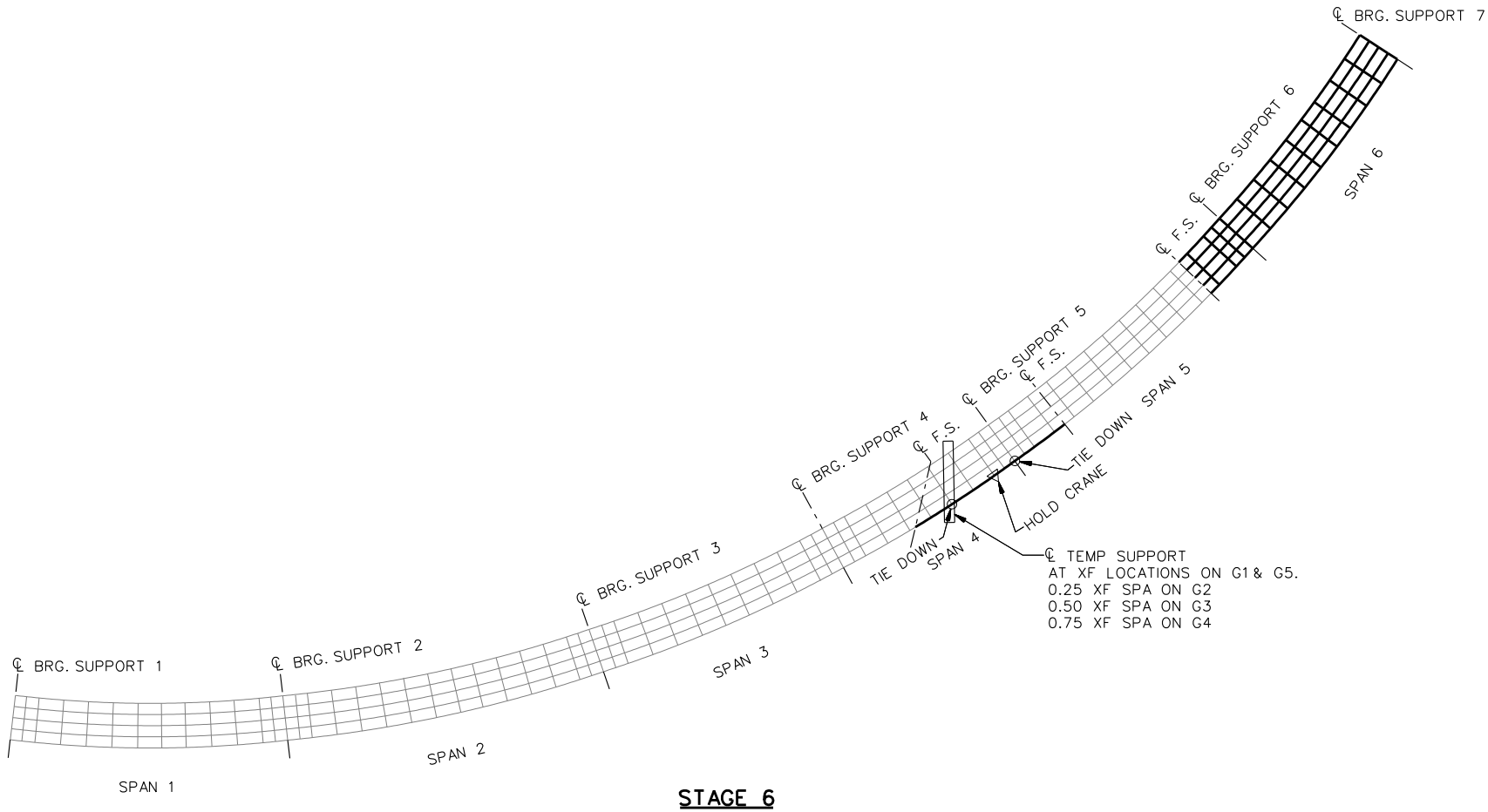

STAGE 6

LEGEND

▽ = HOLD OR LIFT CRANE

○ = TIE DOWN

□ = TEMPORARY SUPPORT STRUCTURE

NCHRP 12-79

BRIDGE EICCR4

GENERAL ERECTION PROCEDURE

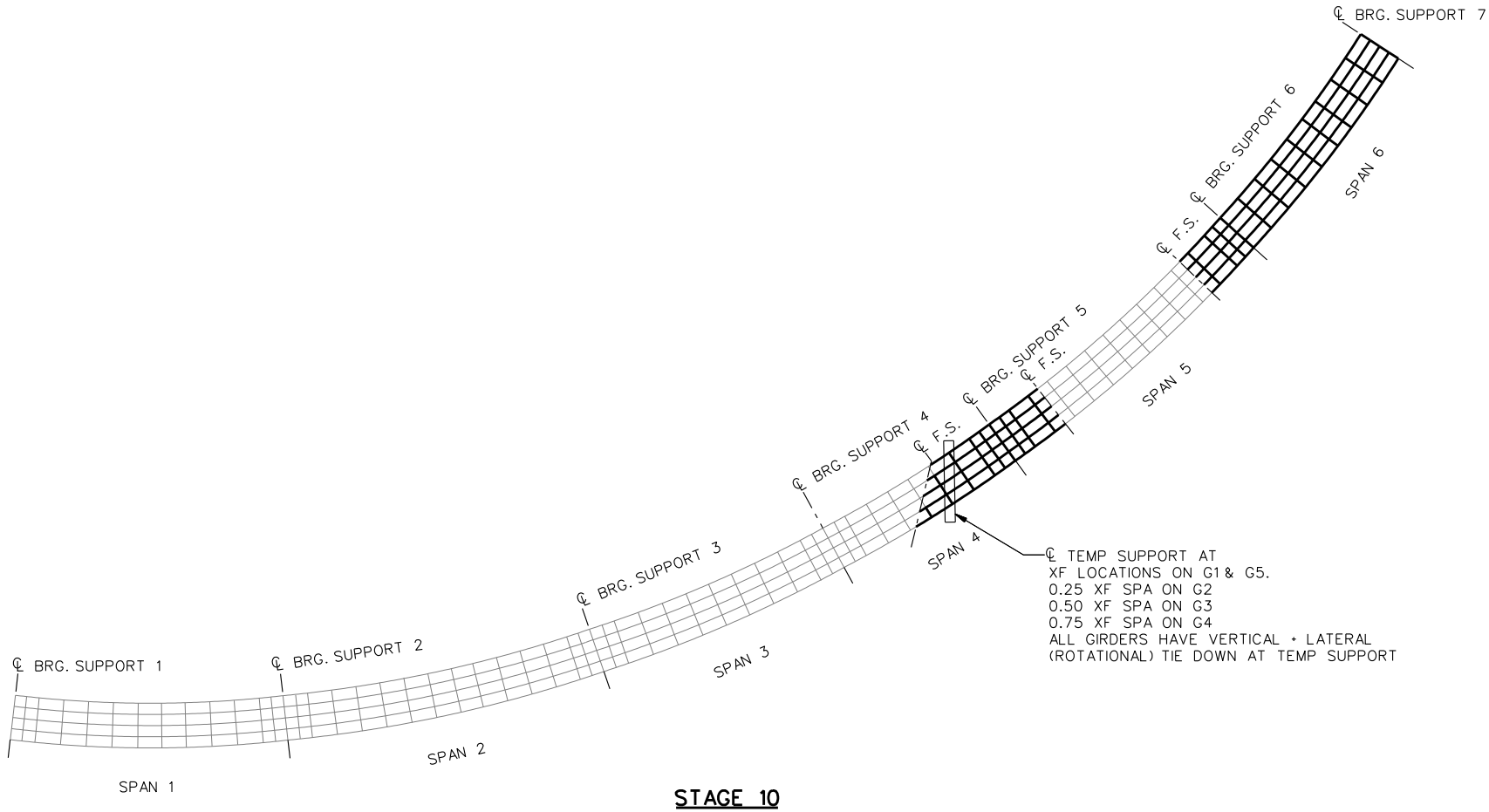

STAGE 10

LEGEND

▽ = HOLD OR LIFT CRANE

○ = TIE DOWN

□ = TEMPORARY SUPPORT STRUCTURE

NCHRP 12-79

BRIDGE EICCR4

GENERAL ERECTION PROCEDURE

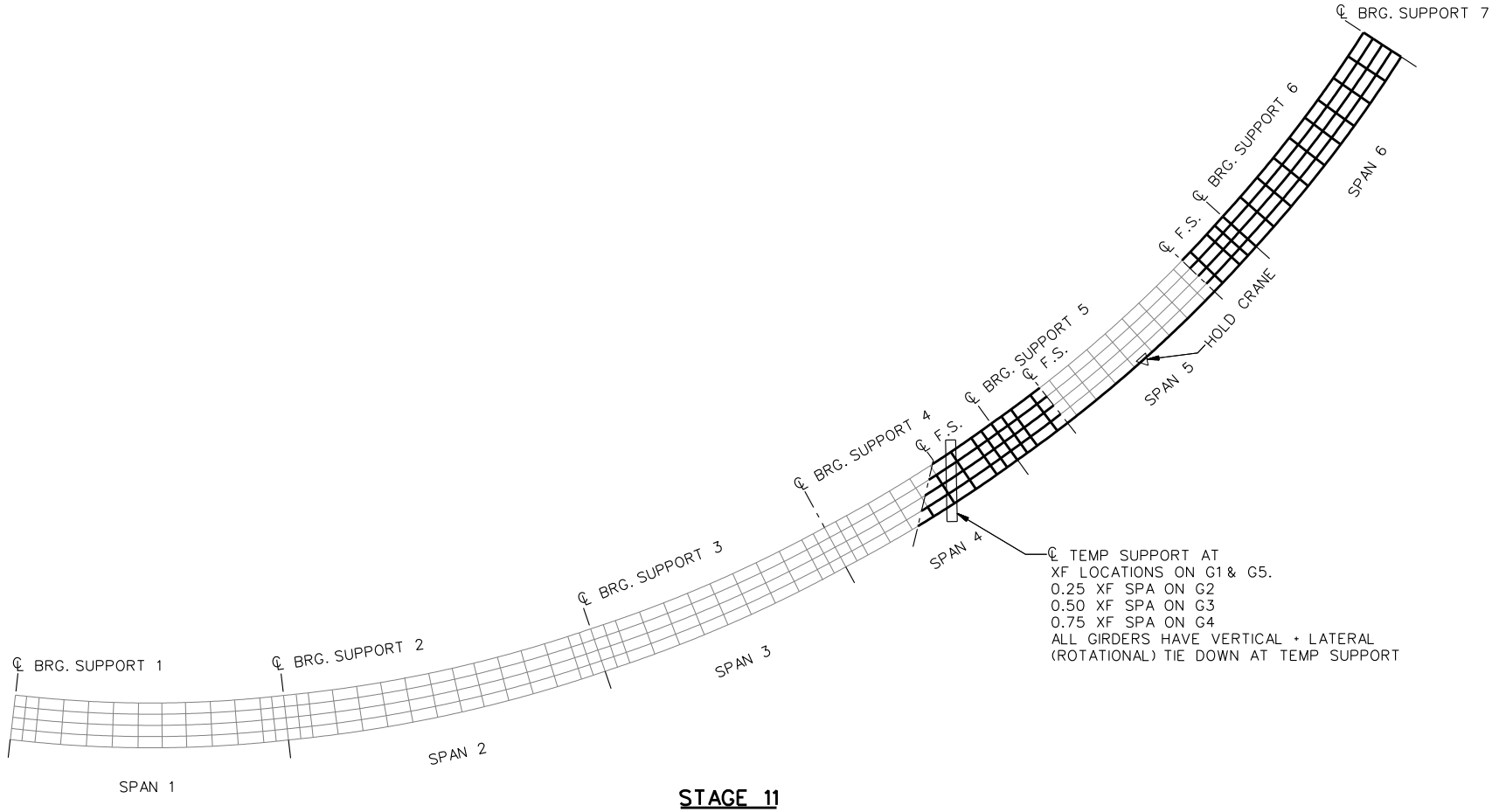

STAGE 11

LEGEND

▽ = HOLD OR LIFT CRANE

○ = TIE DOWN

□ = TEMPORARY SUPPORT STRUCTURE

NCHRP 12-79

BRIDGE EICCR4

GENERAL ERECTION PROCEDURE

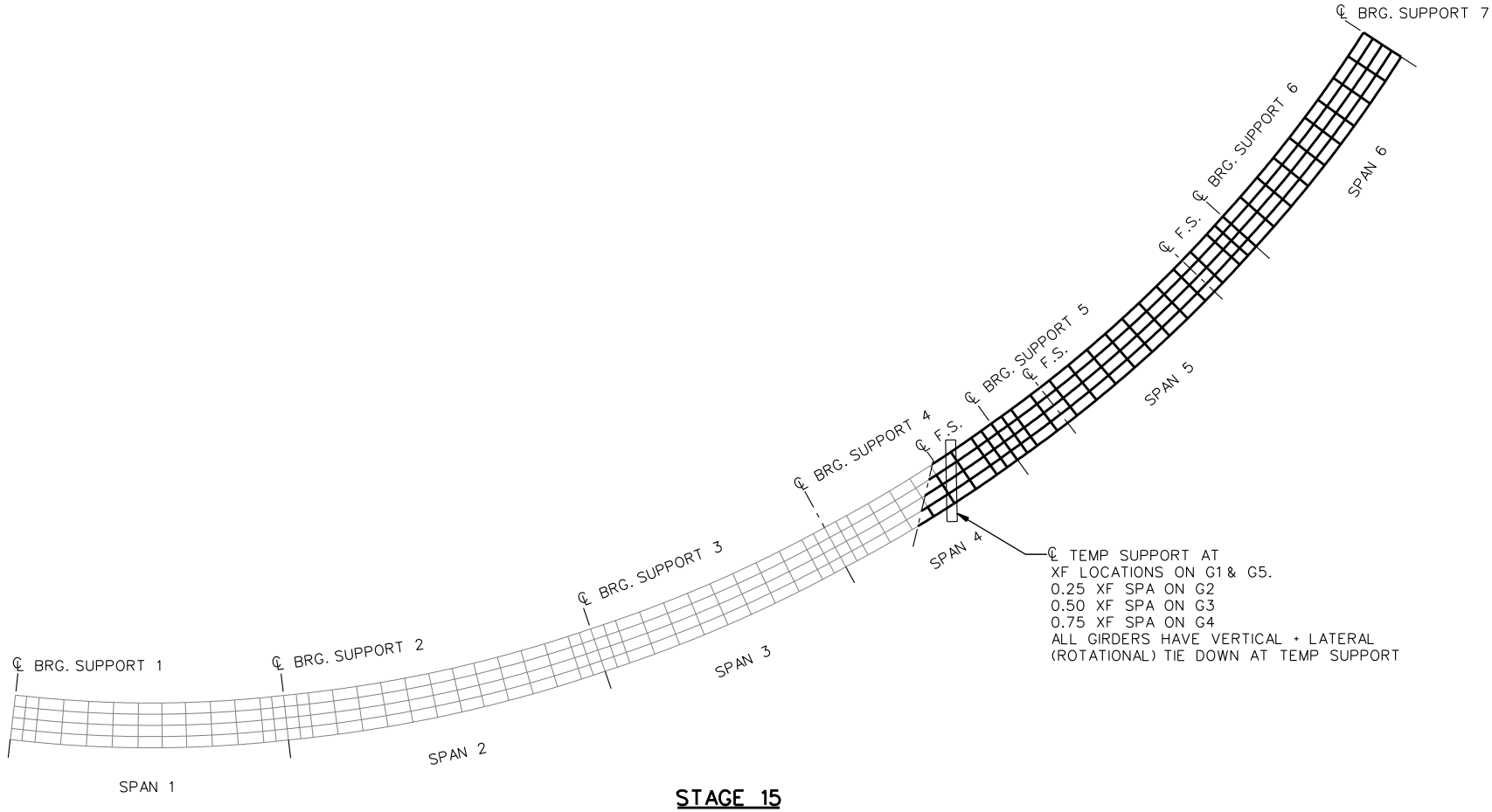

STAGE 15

LEGEND

▽ = HOLD OR LIFT CRANE

○ = TIE DOWN

□ = TEMPORARY SUPPORT STRUCTURE

NCHRP 12-79

BRIDGE EICCR4

GENERAL ERECTION PROCEDURE

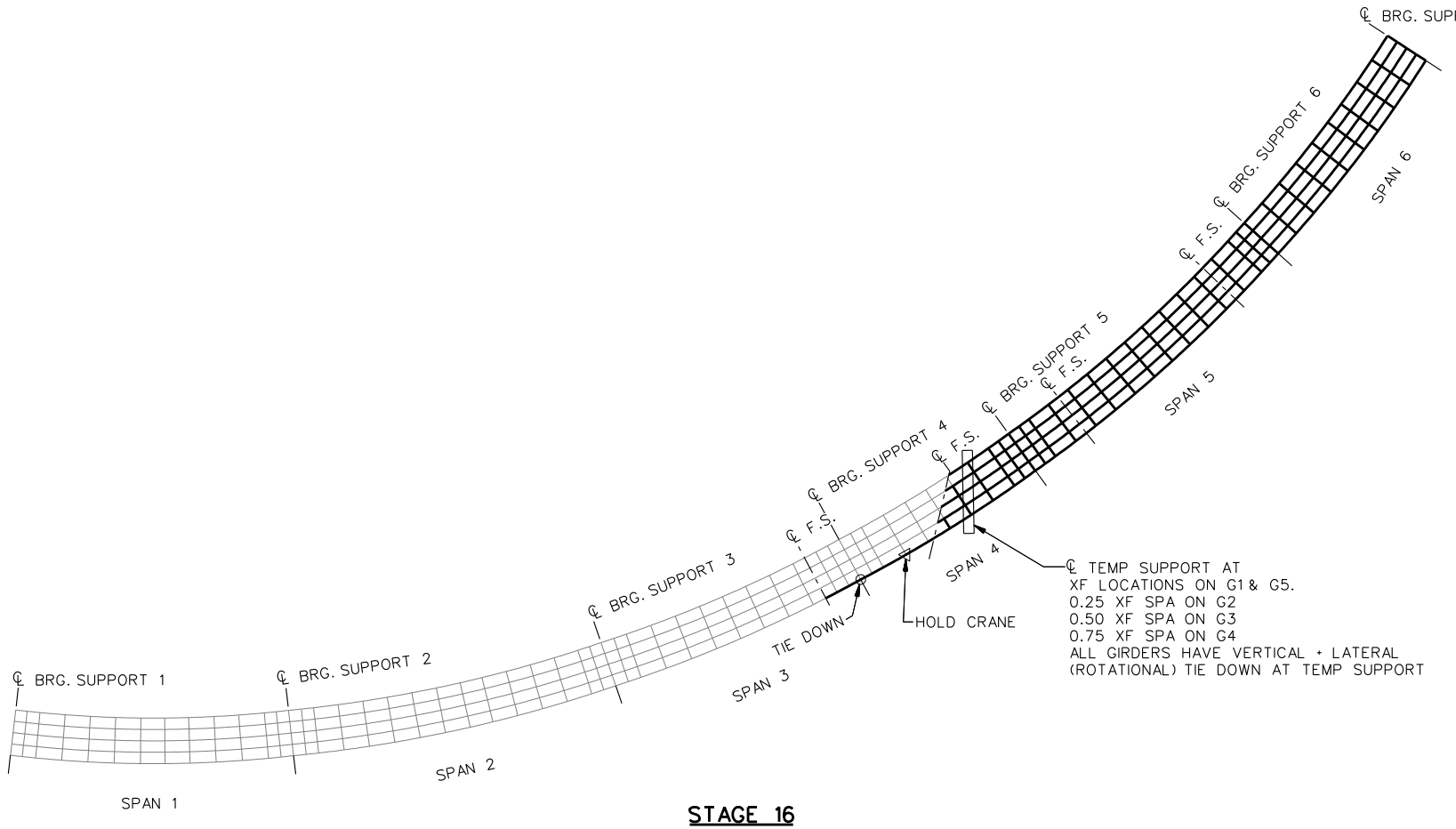

STAGE 16

LEGEND

▽ = HOLD OR LIFT CRANE

○ = TIE DOWN

□ = TEMPORARY SUPPORT STRUCTURE

NCHRP 12-79

BRIDGE EICCR4

GENERAL ERECTION PROCEDURE

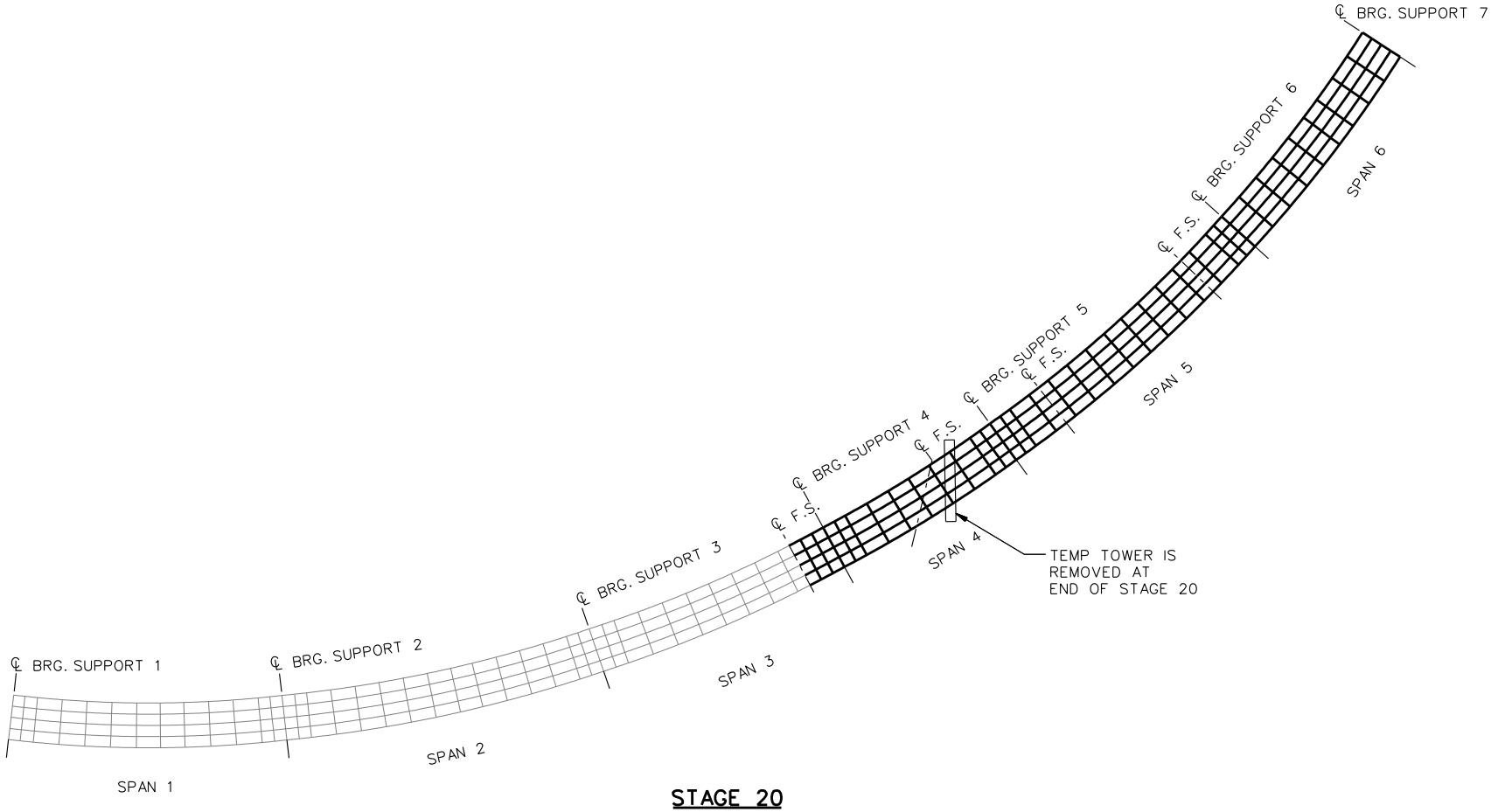

STAGE 20

LEGEND

▽ = HOLD OR LIFT CRANE

○ = TIE DOWN

□ = TEMPORARY SUPPORT STRUCTURE

NCHRP 12-79

BRIDGE EICCR4

GENERAL ERECTION PROCEDURE

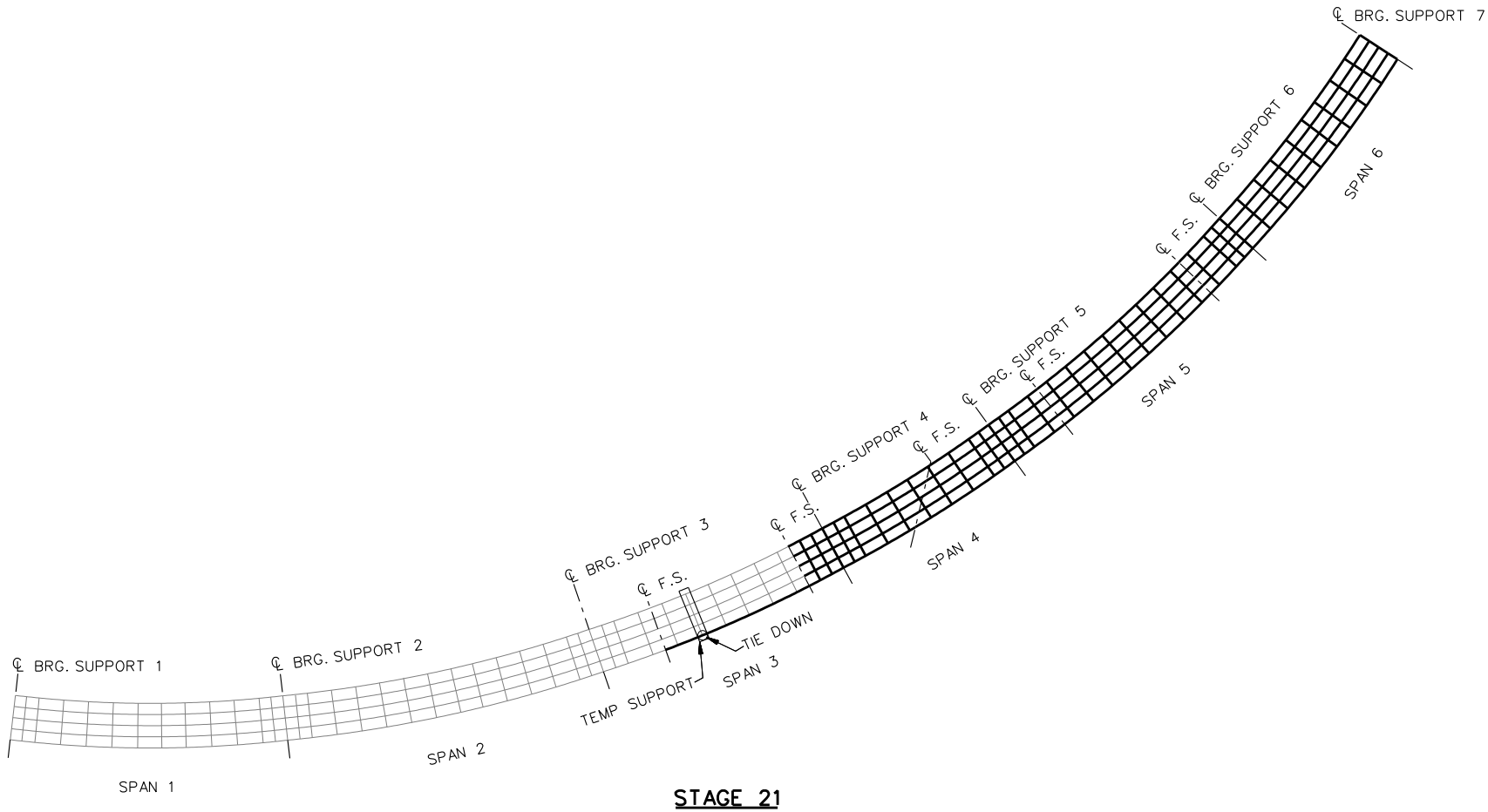

STAGE 21

LEGEND

▽ = HOLD OR LIFT CRANE

○ = TIE DOWN

□ = TEMPORARY SUPPORT STRUCTURE

NCHRP 12-79

BRIDGE EICCR4

GENERAL ERECTION PROCEDURE

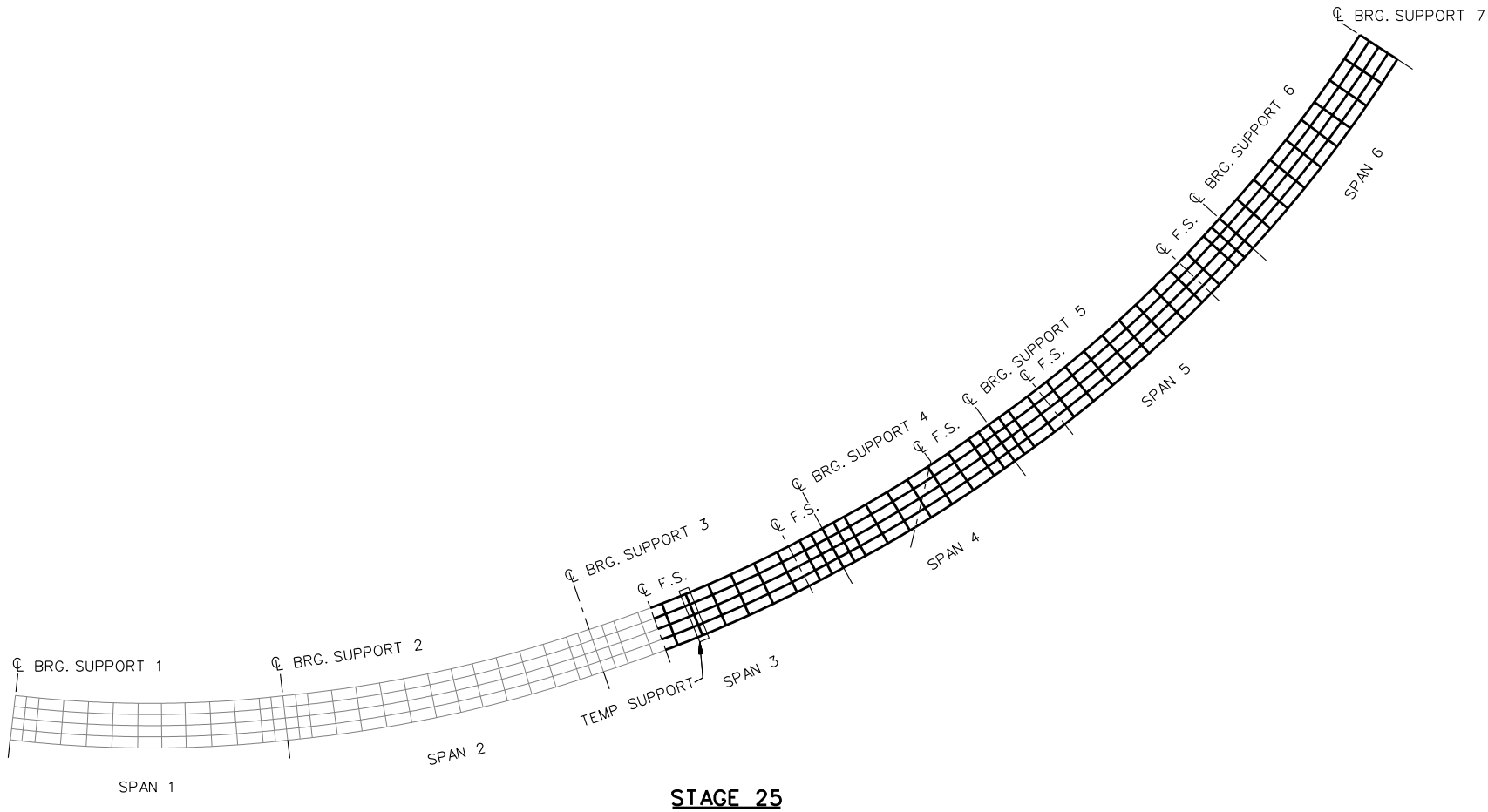

STAGE 25

LEGEND

▽ = HOLD OR LIFT CRANE

○ = TIE DOWN

□ = TEMPORARY SUPPORT STRUCTURE

NCHRP 12-79

BRIDGE EICCR4

GENERAL ERECTION PROCEDURE

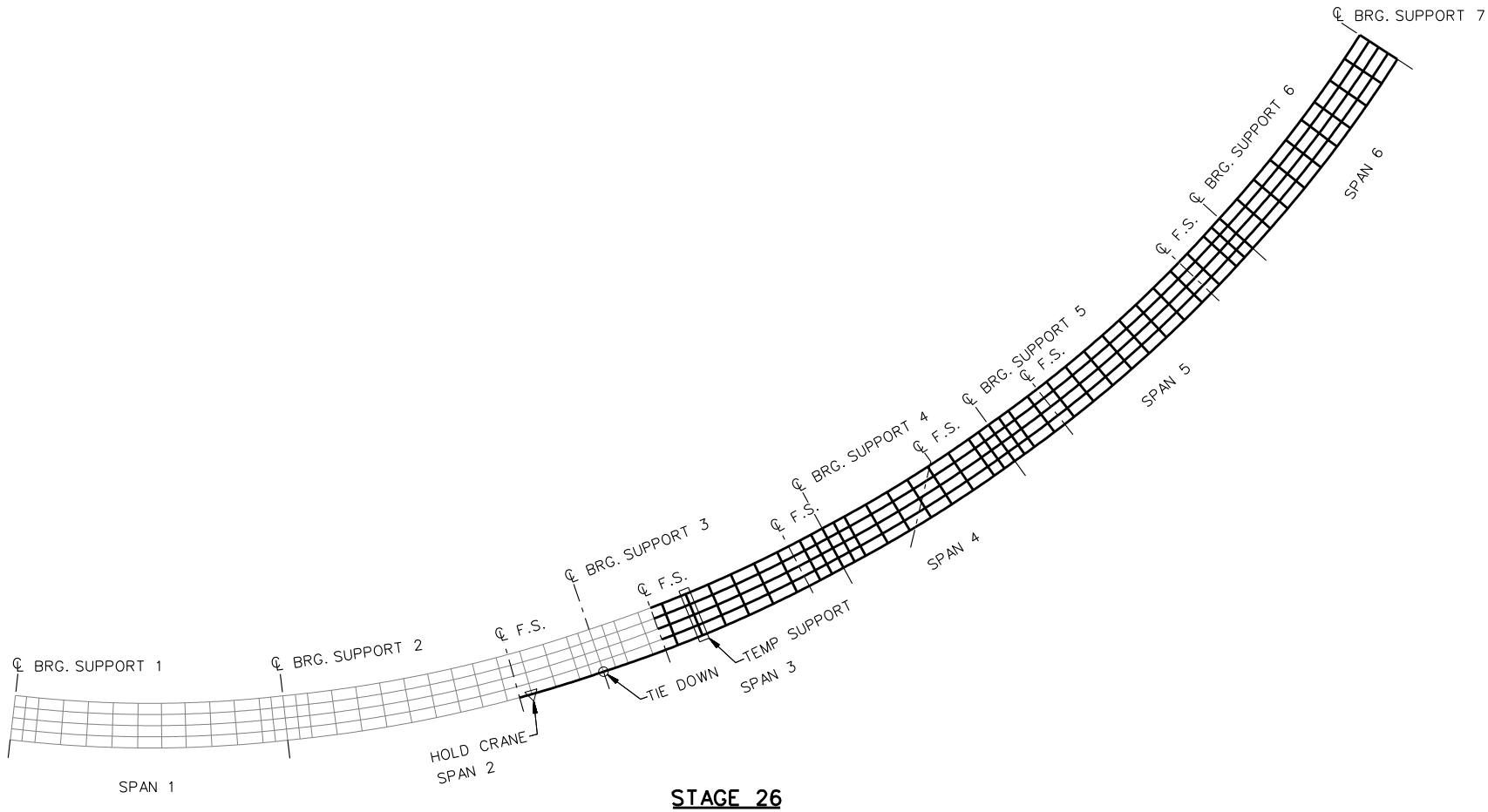

STAGE 26

LEGEND

▽ = HOLD OR LIFT CRANE

○ = TIE DOWN

□ = TEMPORARY SUPPORT STRUCTURE

NCHRP 12-79

BRIDGE EICCR4

GENERAL ERECTION PROCEDURE

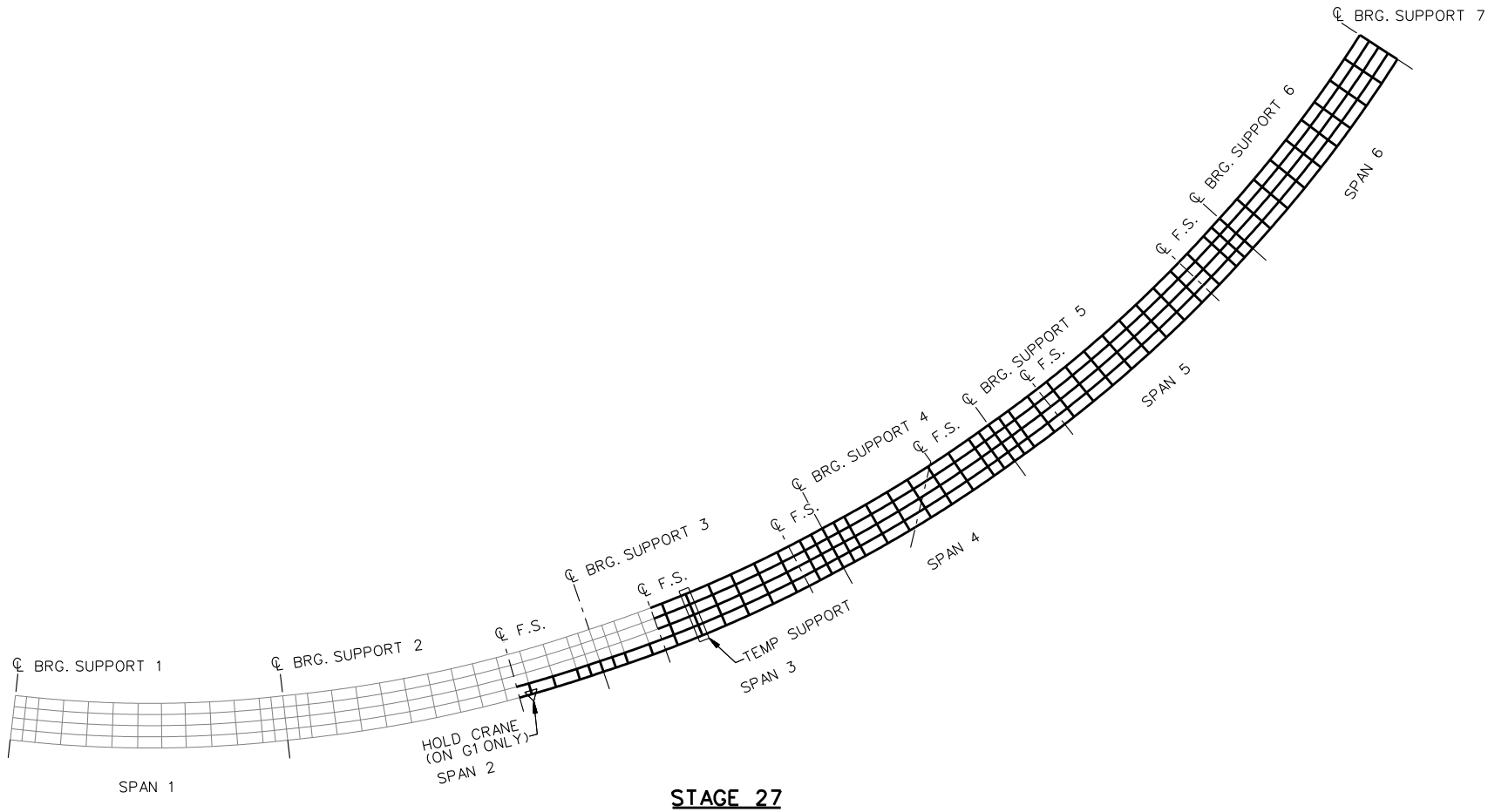

STAGE 27

LEGEND

▽ = HOLD OR LIFT CRANE

○ = TIE DOWN

□ = TEMPORARY SUPPORT STRUCTURE

NCHRP 12-79

BRIDGE EICCR4

GENERAL ERECTION PROCEDURE

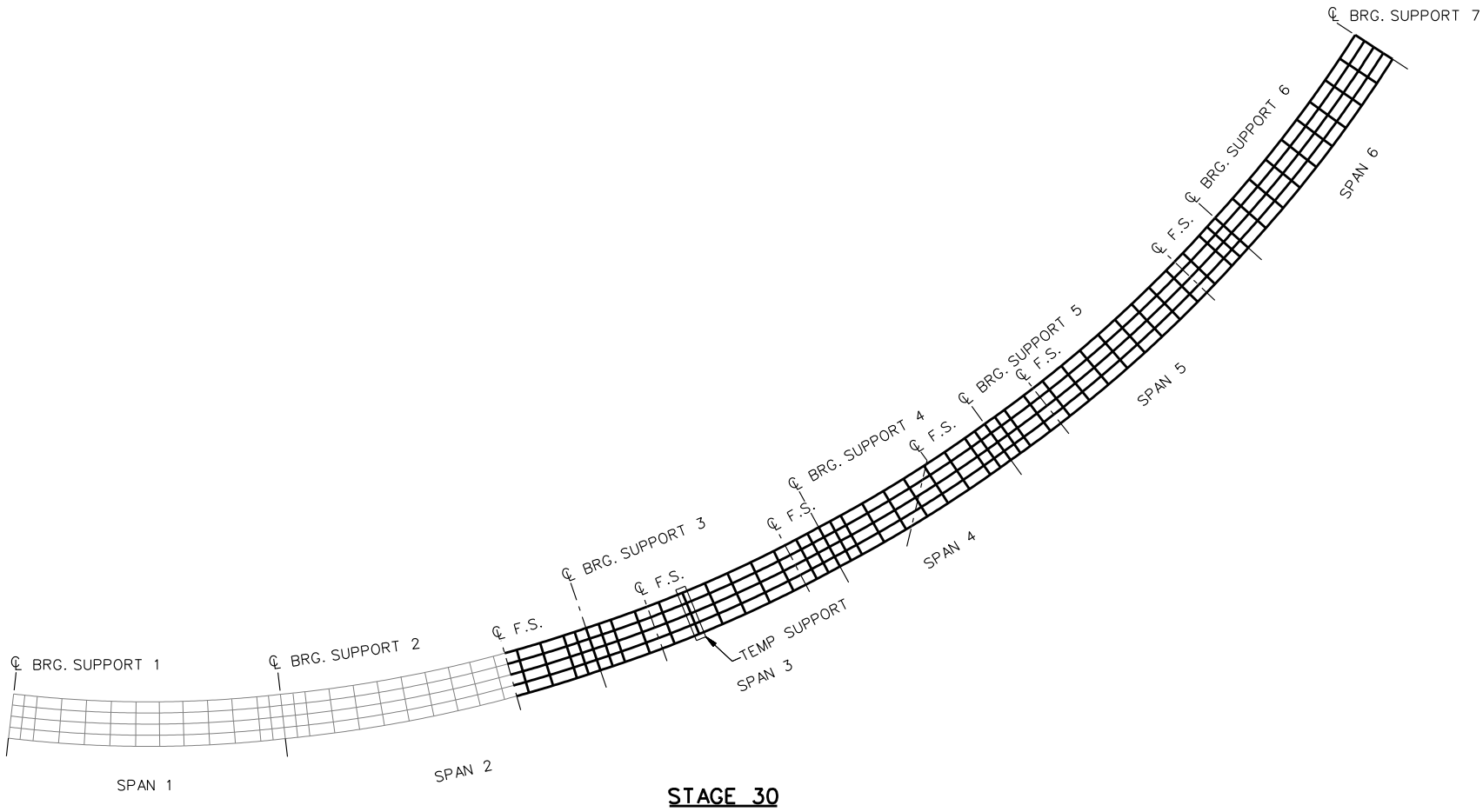

STAGE 30

LEGEND

▽ = HOLD OR LIFT CRANE

○ = TIE DOWN

□ = TEMPORARY SUPPORT STRUCTURE

NCHRP 12-79

BRIDGE EICCR4

GENERAL ERECTION PROCEDURE

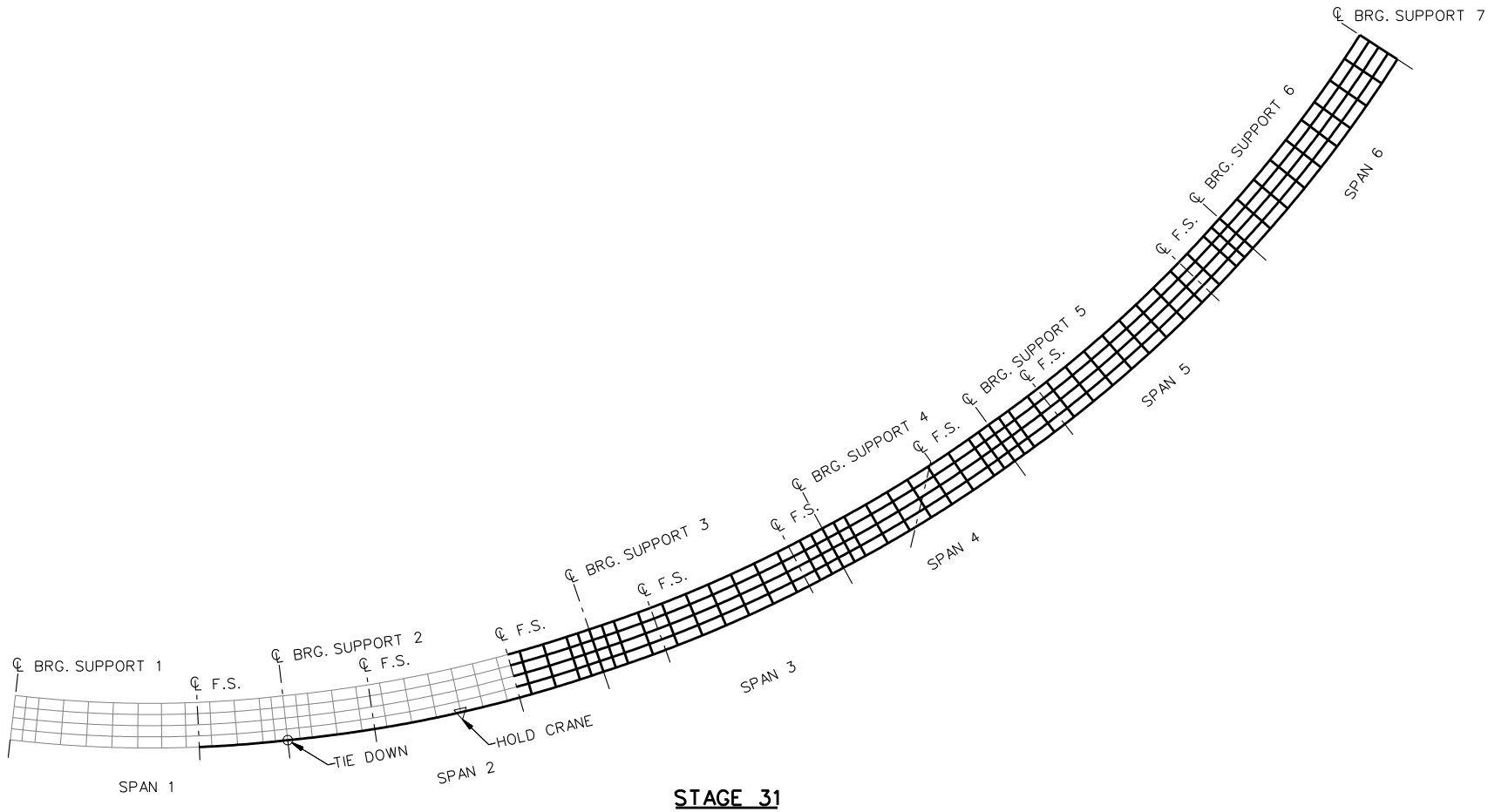

STAGE 31

LEGEND

▽ = HOLD OR LIFT CRANE

○ = TIE DOWN

□ = TEMPORARY SUPPORT STRUCTURE

NCHRP 12-79

BRIDGE EICCR4

GENERAL ERECTION PROCEDURE

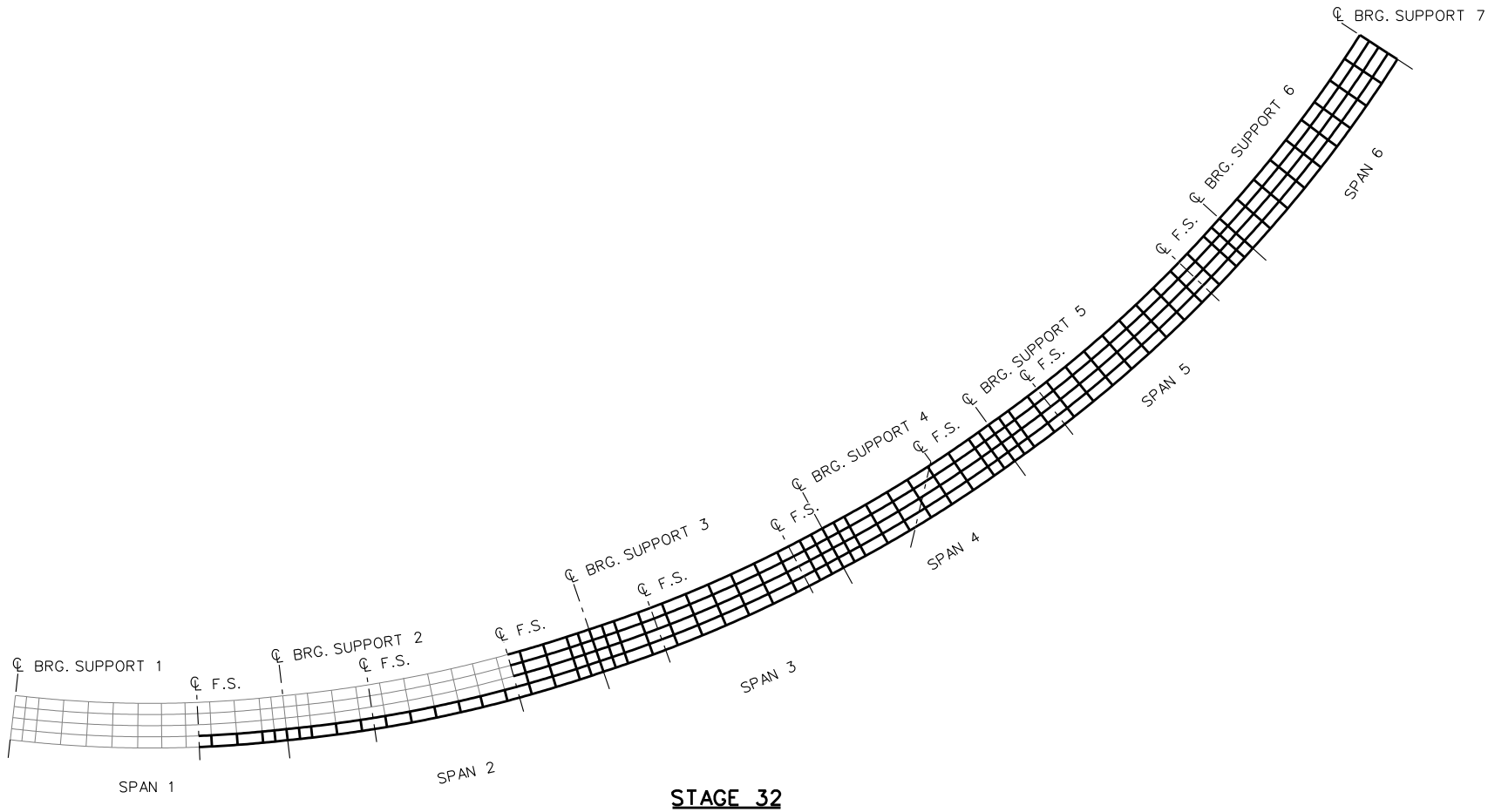

STAGE 32

LEGEND

▽ = HOLD OR LIFT CRANE

○ = TIE DOWN

□ = TEMPORARY SUPPORT STRUCTURE

NCHRP 12-79

BRIDGE EICCR4

GENERAL ERECTION PROCEDURE

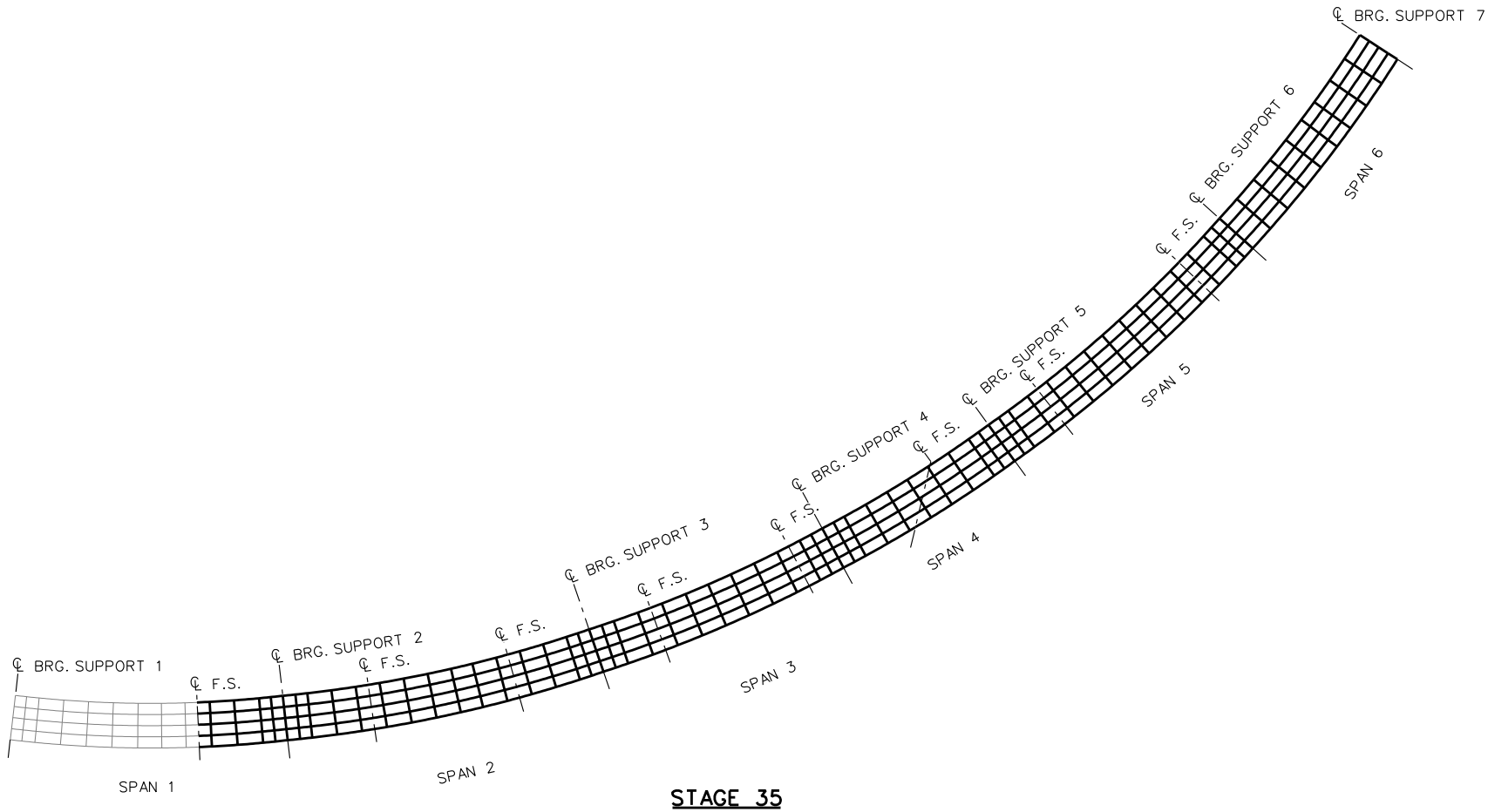

STAGE 35

LEGEND

▽ = HOLD OR LIFT CRANE

○ = TIE DOWN

□ = TEMPORARY SUPPORT STRUCTURE

NCHRP 12-79

BRIDGE EICCR4

GENERAL ERECTION PROCEDURE

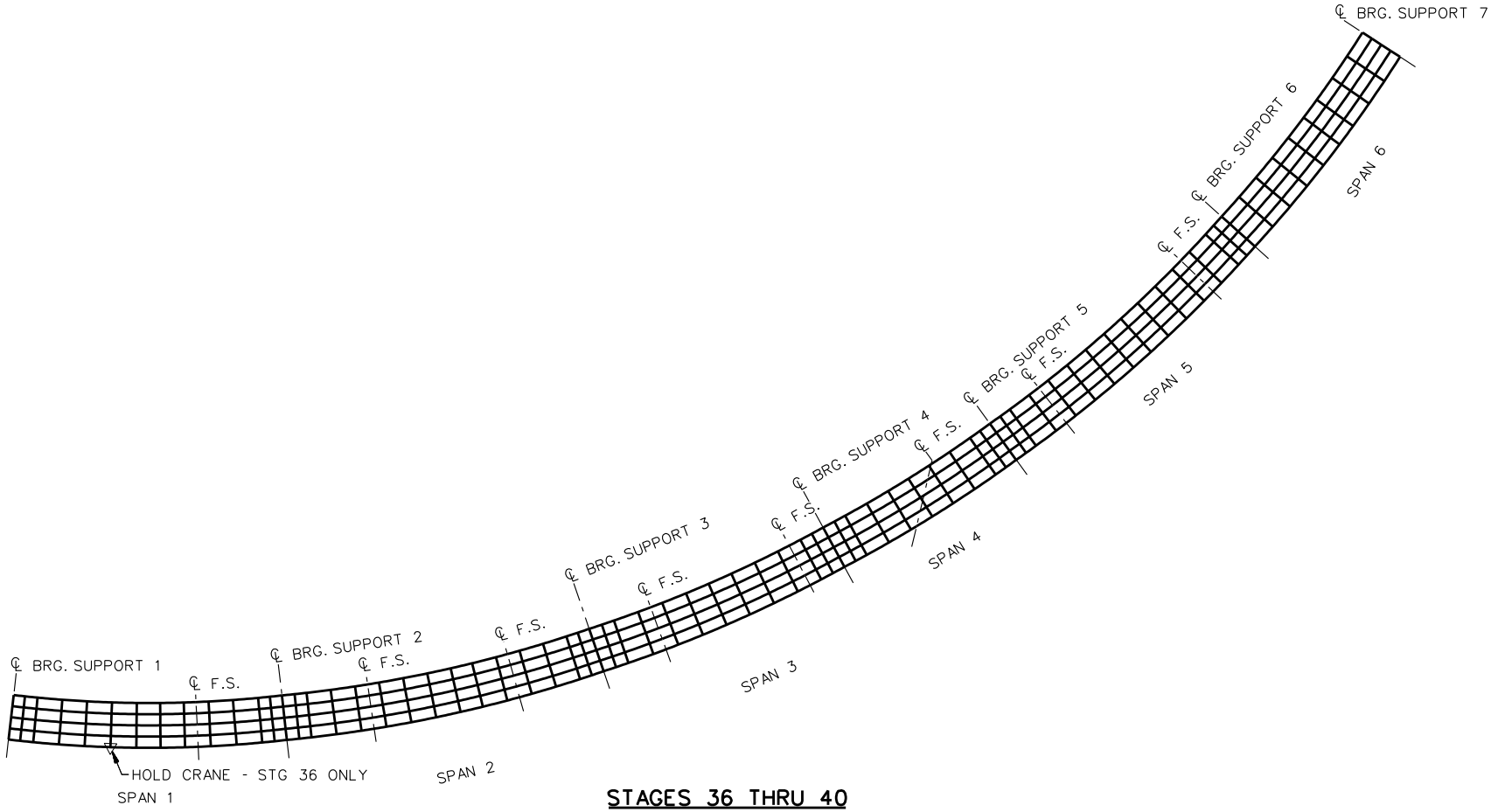

STAGES 36 THRU 40

ALL SPAN 1
STG 36 - G1
STG 37 - G2
STG 38 - G3
STG 39 - G4
STG 40 - G5

LEGEND

▽ = HOLD OR LIFT CRANE

○ = TIE DOWN

□ = TEMPORARY SUPPORT STRUCTURE

NCHRP 12-79

BRIDGE EICCR4

GENERAL ERECTION PROCEDURE

NCHRP 12-79

EICCR11

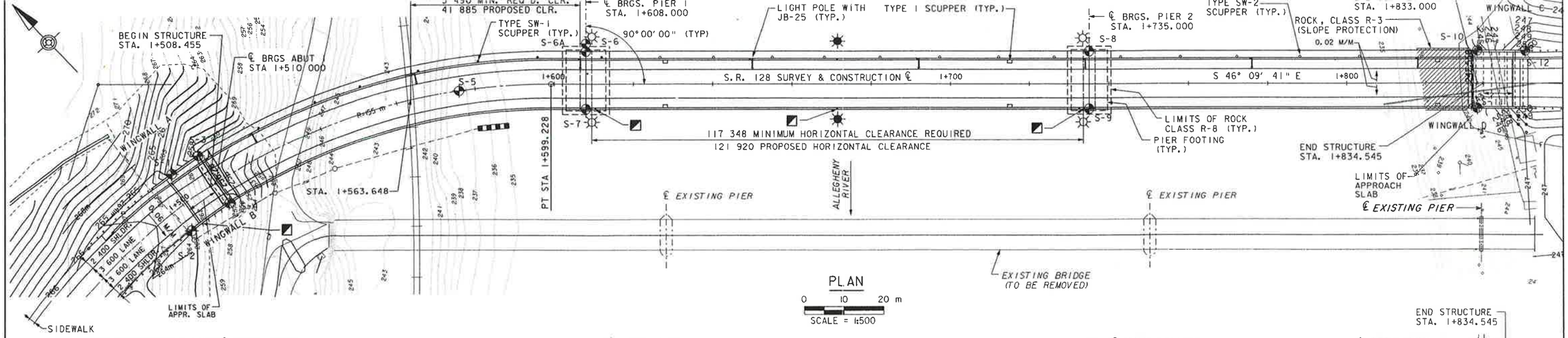

PLAN

0 10 20 m

SCALE = 1:500

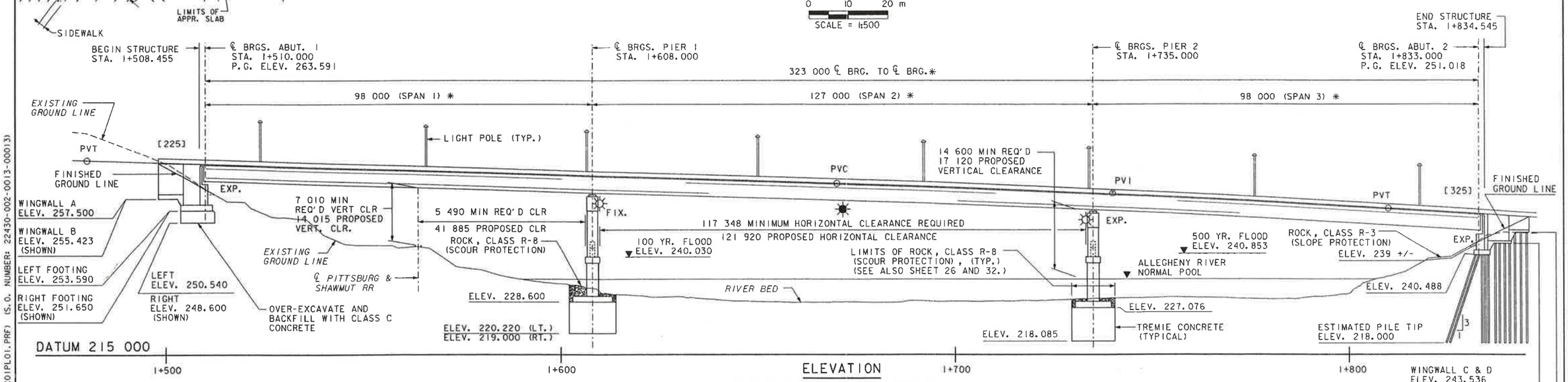

ELEVATION

* MEASURED ALONG SURVEY & CONSTRUCTION ℄

0 10 20 m

SCALE = 1:500

HORIZONTAL CURVE DATA 1

PI STA 1+516.640
PC STA 1+402.629
Δ = 72°40'22.5" RT
D = 11°16'01"
T = 114.011M
L = 196.599M
R = 155.000M
E = 37.415M
SE = 6%

HORIZONTAL CURVE DATA 2

PI STA 1+973.889
PC STA 1+855.414
Δ = 86°55'44.8" LT
D = 13°58'16"
T = 118.474M
L = 189.650M
R = 125.000M
E = 47.224M
SE = 6%

VERTICAL CURVE DATA

-3.00% Δ -5.98%

PVI = STA 1+740
ELEV 256.547
VC = 140
MO = -0.522

NOTES:

FOR INDEX OF DRAWINGS. SEE SHEET 4.

FOR GIRDER RATINGS, SEE SHEET 5.

FOR TYPICAL SECTIONS, SEE SHEET 5.

ALL STATIONS AND ELEVATIONS SHOWN ARE IN METERS. UNLESS NOTED OTHERWISE, ALL DIMENSIONS ARE IN MILLIMETERS.

FOR SCUPPER LOCATIONS, SEE DECK PLANS SHEET 84 THROUGH 88.

FOR LIGHT POLE LOCATIONS, SEE LIGHTING PLAN AND DECK PLANS.

O.H.W. DENOTES ORDINARY HIGH WATER

P.G. DENOTES PROFILE GRADE

[225] INDICATES TOOTH EXPANSION DAM MOVEMENT

EXP. DENOTES EXPANSION POT BEARING

FIX. DENOTES FIXED POT BEARING

HYDRAULIC DATA

FREQUENCY	DISCHARGE	WATER SURFACE ELEVATION	VELOCITY
100 YEAR	6088.1 CMS	240.030 M	2.62 MPS
500 YEAR	7390.7 CMS	240.853 M	2.92 MPS

DRAINAGE AREA = 23 240 km²

FLOOD OF RECORD MARCH 1913
MAGNITUDE = 7,617.2 CMS

LEGEND:

- RED NAVIGATIONAL LIGHTING
- GREEN NAVIGATIONAL LIGHTING
- JUNCTION BOX
- DRILLED CORE BORING
- SIDEWALK SCUPPER, TYPE SW-1
- SIDEWALK SCUPPER, TYPE SW-2
- DECK SCUPPER, TYPE 1
- LIGHT POLE WITH JB-25
- LIGHT POLE

DESCRIPTION	DWG. NO.	APP. DATE
CLASSIFICATION OF EARTHWORK FOR STRUCTURES	RC-11M	5-16-97
BACKFILL AT STRUCTURES	RC-12M	10-25-96
BRIDGE APPROACH SLAB	RC-23M	5-16-97
ALUMINUM PEDESTRIAN RAILING	BC-716M	1-2-96
ELECTRICAL DETAILS	BC-721M	1-2-96
LIGHTING POLE ANCHORAGE	BC-722M	1-2-96
PERMANENT METAL DECK FORMS	BC-732M	1-2-96
ANCHOR SYSTEMS	BC-734M	1-2-96
WALL CONSTRUCTION & EXPANSION JOINT DETAILS	BC-735M	1-2-96
BRIDGE PARAPET TO GUIDE RAIL TRANSITION	BC-739M	1-2-96
BRIDGE DRAINAGE	BC-751M	1-2-96
CONCRETE DECK SLAB DETAILS	BC-752M	1-2-96
STEEL GIRDER DETAILS	BC-753M	1-2-96
STEEL DIAPHRAGMS	BC-754M	1-2-96
STEEL PILE TIP REINFORCEMENTS AND SPLICES	BC-757M	1-2-96
TOOTH EXPANSION DAM	BC-762M	1-2-96

SUPPLEMENTAL DRAWINGS

Mark	Description	By	Chk'd.	App'd.	Date

REVISIONS

Designed by:	MJB
Checked by:	SDV
Drawn by:	EEM
Checked by:	MJB

PREPARED BY:
MICHAEL BAKER JR., INC.
AIRPORT OFFICE PARK, BUILDING 3
420 ROUSER ROAD
CORAOPOLIS, PENNSYLVANIA 15108

COMMONWEALTH OF PENNSYLVANIA
REGISTERED PROFESSIONAL
RONALD S. CAPP
ENGINEER
PENNSYLVANIA

Ronald S. Capp 1/19/98

COMMONWEALTH OF PENNSYLVANIA
REGISTERED PROFESSIONAL
MICHAEL J. BONKOVICH
ENGINEER 043452-R
PENNSYLVANIA

Michael J. Bonkovich 1/19/98

COMMONWEALTH OF PENNSYLVANIA
DEPARTMENT OF TRANSPORTATION

ARMSTRONG COUNTY
S.R. 0128 SEC. 013
SEG. 0250 OFFSET 0
S.R. 0128 STA. 1+671.500
OVER ALLEGHENY RIVER & PITTSBURG & SHAWMUT R.R.
3-SPAN CONTINUOUS STEEL PLATE GIRDER BRIDGE
GENERAL PLAN & ELEVATION

RECOMMENDED Scott Christie 1/26/98
BRIDGE ENGINEER

SHEET 1 OF 112 + SUPPLEMENTAL DRAWINGS

S-22234

S.O. NUMBER: 22430-002-0013-00013

J:\DESIGN\FORDCITY\FINAL\SUPER\DWG\FC01PL01.DGN 01/19/98 11:38:14 (S:\PAPERV\FC01PL01.PRF)

TAM 1/26/98
8/8/97

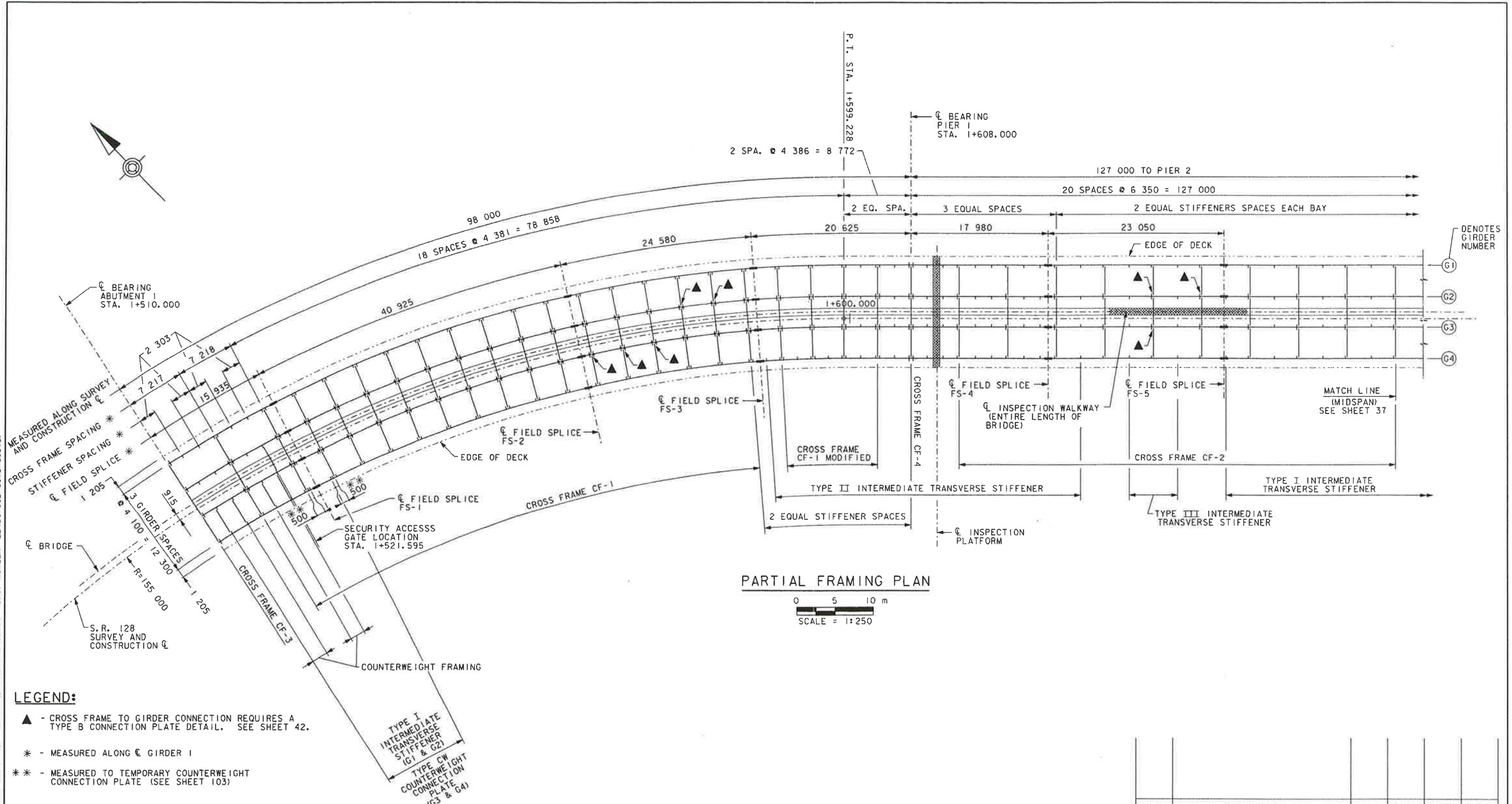

PARTIAL FRAMING PLAN

0 5 10 m

SCALE = 1:250

LEGEND:

▲ - CROSS FRAME TO GIRDER CONNECTION REQUIRES A TYPE B CONNECTION PLATE DETAIL. SEE SHEET 42.

* - MEASURED ALONG ℄ GIRDER 1

** - MEASURED TO TEMPORARY COUNTERWEIGHT CONNECTION PLATE (SEE SHEET 103)

NOTES:

FOR GENERAL NOTES, SEE SHEET 2.

FOR GIRDER ELEVATIONS, SEE SHEETS 38 THROUGH 41.

FOR MISCELLANEOUS GIRDER DETAILS, SEE SHEETS 42 AND 43.

FOR GIRDER SPLICES, SEE SHEETS 44 THROUGH 46.

FOR CROSS FRAME DETAILS, SEE SHEETS 47 THROUGH 50.

FOR COUNTERWEIGHT DETAILS, SEE SHEETS 51, 52, AND 103.

FOR SECURITY ACCESS GATE, INSPECTION WALKWAY, AND INSPECTION PLATFORM DETAILS, SEE SHEET 59 THROUGH 62.

CROSS FRAMES ARE RADIAL TO THE ℄ OF S.R. 128 WHERE REQUIRED.

UNLESS NOTED OTHERWISE, ALL CROSS FRAME TO GIRDER CONNECTIONS REQUIRE A TYPE A CONNECTION PLATE DETAIL, (SEE SHEET 42, AND LEGEND THIS SHEET -▲)

Designed by:	SDV
Checked by:	LAC
Drawn by:	EEM
Checked by:	SDV/MJB

Mark	Description	By	Chk'd.	App'd.	Date
REVISIONS					

COMMONWEALTH OF PENNSYLVANIA
DEPARTMENT OF TRANSPORTATION

ARMSTRONG COUNTY
S.R. 0128 SEC. 013
SEG. 0250 OFFSET 0
S.R. 0128 STA. 1+671.500
OVER ALLEGHENY RIVER & PITTSBURG & SHAWMUT R.R.
3-SPAN CONTINUOUS STEEL PLATE GIRDER BRIDGE
PARTIAL FRAMING PLAN - 1

COMMONWEALTH OF PENNSYLVANIA REGISTERED PROFESSIONAL MICHAEL J. BONKOVICH ENGINEER 043452-R

RECOMMENDED JAN 26 1998

SHEET 36 OF 112

S-22234

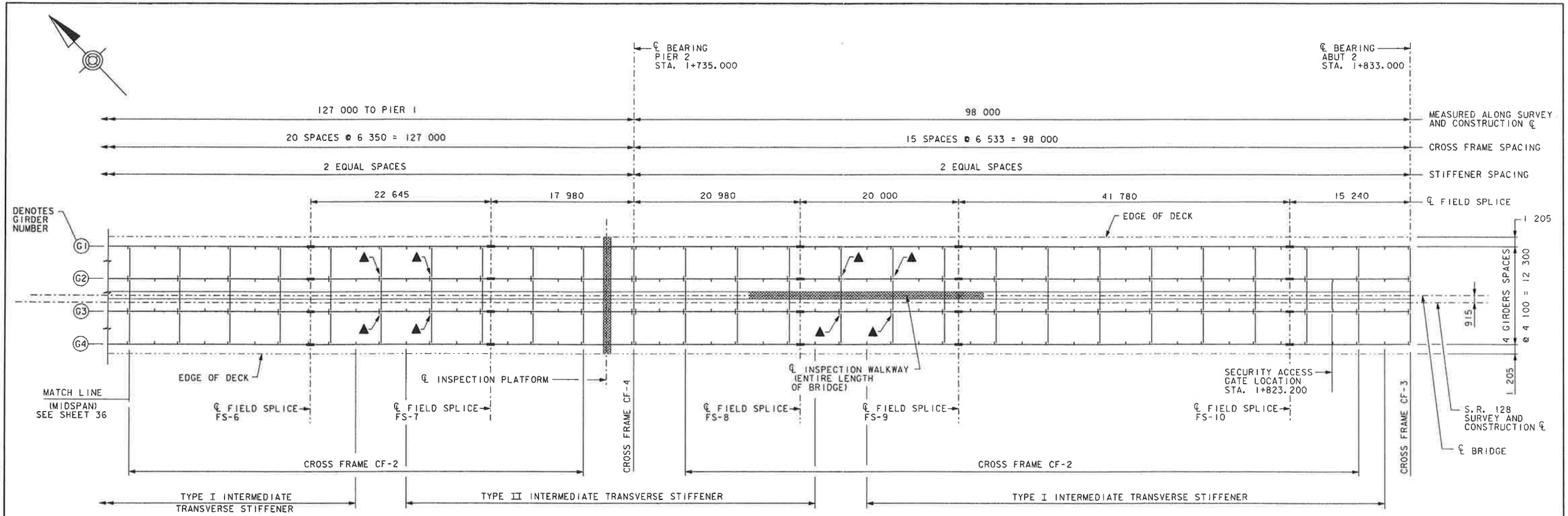

PARTIAL FRAMING PLAN

0 5 10 m
SCALE = 1:250

LEGEND:

▲ - CROSS FRAME TO GIRDER CONNECTION REQUIRES A TYPE B CONNECTION PLATE DETAIL. SEE SHEET 42.

NOTES:

FOR GENERAL NOTES, SEE SHEET 2.

FOR GIRDER ELEVATIONS, SEE SHEETS 38 THROUGH 41.

FOR MISCELLANEOUS GIRDER DETAILS, SEE SHEETS 42 AND 43.

FOR GIRDER SPLICES, SEE SHEETS 44 THROUGH 46.

FOR CROSS FRAME DETAILS, SEE SHEETS 47 THROUGH 50.

FOR COUNTERWEIGHT DETAILS, SEE SHEETS 51, 52, AND 103.

FOR SECURITY ACCESS GATE, INSPECTION WALKWAY, AND INSPECTION PLATFORM DETAILS, SEE SHEET 59 THROUGH 62.

UNLESS NOTED OTHERWISE, ALL CROSS FRAME TO GIRDER CONNECTIONS REQUIRE A TYPE A CONNECTION PLATE DETAIL, (SEE SHEET 42, AND LEGEND THIS SHEET - ▲)

Designed by:	SDV
Checked by:	LAC
Drawn by:	EEM

Mark	Description	By	Chk'd.	App'd.	Date
REVISIONS					

COMMONWEALTH OF PENNSYLVANIA
DEPARTMENT OF TRANSPORTATION

ARMSTRONG COUNTY
S.R. 0128 SEC. 013
SEG. 0250 OFFSET 0
S.R. 0128 STA. 1+671.500
OVER ALLEGHENY RIVER & PITTSBURG & SHAWMUT R.R.
3-SPAN CONTINUOUS STEEL PLATE GIRDER BRIDGE
PARTIAL FRAMING PLAN - 2

COMMONWEALTH OF PENNSYLVANIA REGISTERED PROFESSIONAL MICHAEL J. BONKOVICH ENGINEER 043452-R

RECOMMENDED JAN 26 1998

SHEET 37 OF 112

S-22234

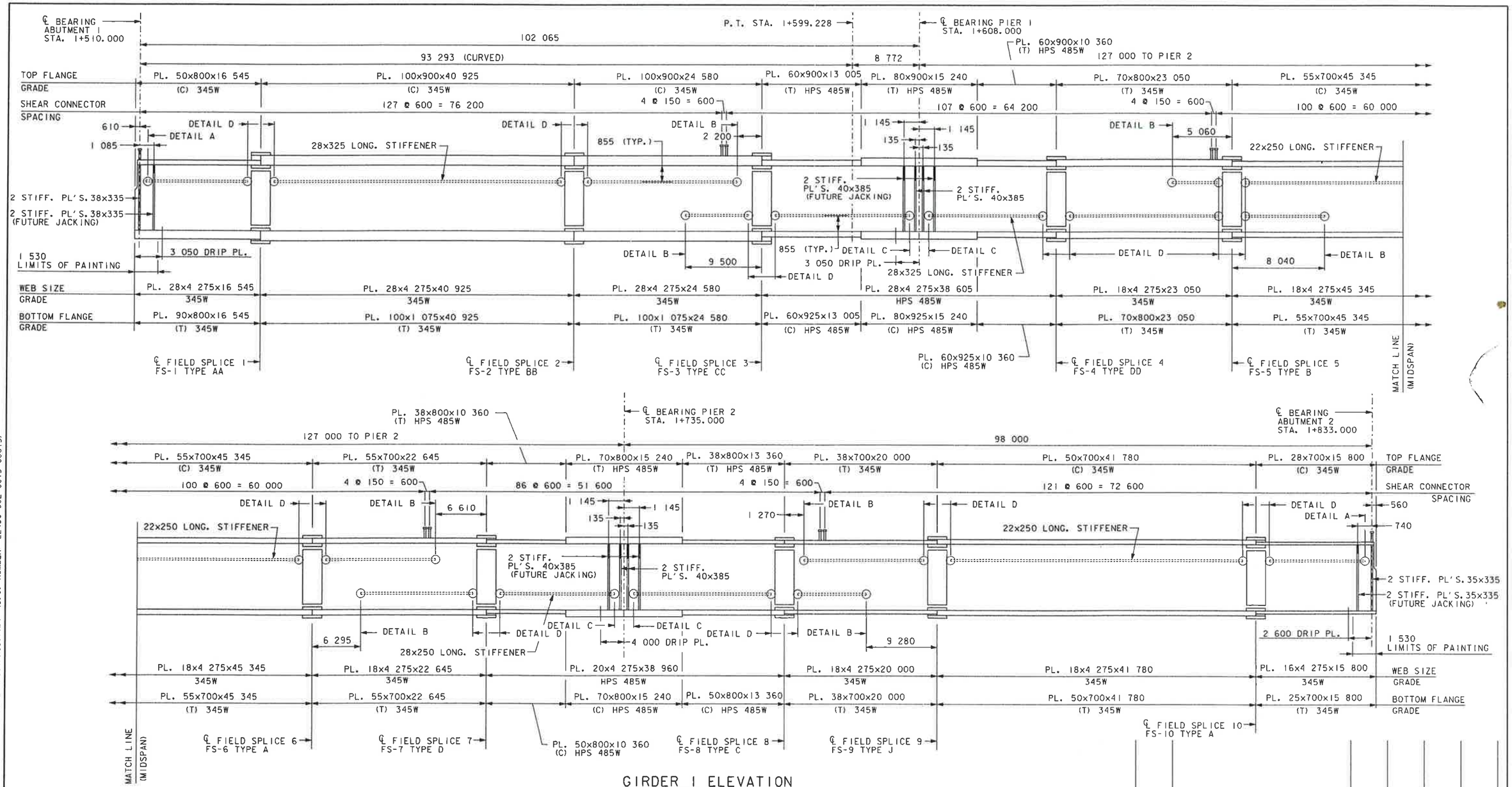

GIRDER 1 ELEVATION

NO SCALE

NOTES:

FOR GENERAL NOTES, SEE SHEET 2.

FOR FRAMING PLAN, SEE SHEETS 36 AND 37.

FOR SHEAR CONNECTOR, DRIP PLATE, AND OTHER MISCELLANEOUS GIRDER DETAILS, SEE SHEETS 42 AND 43.

FOR GIRDER SPLICES, SEE SHEETS 44 THROUGH 46.

CHARPY V-NOTCH TESTING IS REQUIRED ON ALL TENSION FLANGES, WEBS, DIAPHRAGM MEMBERS, AND SPLICE PLATES.

SHEAR CONNECTORS SHALL CONFORM TO AASHTO M169 (ASTM A108).

FOR LONGITUDINAL STIFFENER INTERSECTION DETAILS (A,B,C, AND D), SEE SHEET 43.

GIRDERS, CROSS FRAMES, STIFFENER PLATES, AND BEARINGS SHALL BE PAINTED AT THE SUPPORT LOCATIONS WITHIN THE LIMITS SHOWN.

FOR CONVENIENCE, LONGITUDINAL STIFFENERS ARE SHOWN CONTINUOUS BETWEEN SUCCESSIVE SPLICES, AND BETWEEN BEARING STIFFENERS AND SPLICES. LONGITUDINAL STIFFENERS ARE INTERRUPTED AT TYPE A CROSS FRAME CONNECTION PLATES, (SEE FRAMING PLAN, AND SHEETS 42 AND 43).

LEGEND:

(T) DENOTES TENSION FLANGE
(C) DENOTES COMPRESSION FLANGE

Mark	Description	By	Chk'd.	App'd.	Date
REVISIONS					

COMMONWEALTH OF PENNSYLVANIA
REGISTERED PROFESSIONAL
MICHAEL J. BONKOVICH
ENGINEER 043452-R
PENNSYLVANIA

COMMONWEALTH OF PENNSYLVANIA
DEPARTMENT OF TRANSPORTATION

ARMSTRONG COUNTY
S.R. 0128 SEC. 013
SEG. 0250 OFFSET 0
S.R. 0128 STA. 1+671.500
OVER ALLEGHENY RIVER & PITTSBURG & SHAWMUT R.R.
3-SPAN CONTINUOUS STEEL PLATE GIRDER BRIDGE
GIRDER 1 ELEVATION

RECOMMENDED JAN 26 1998

SHEET 38 OF 112

Designed by:	SDV
Checked by:	LAC
Drawn by:	EEM

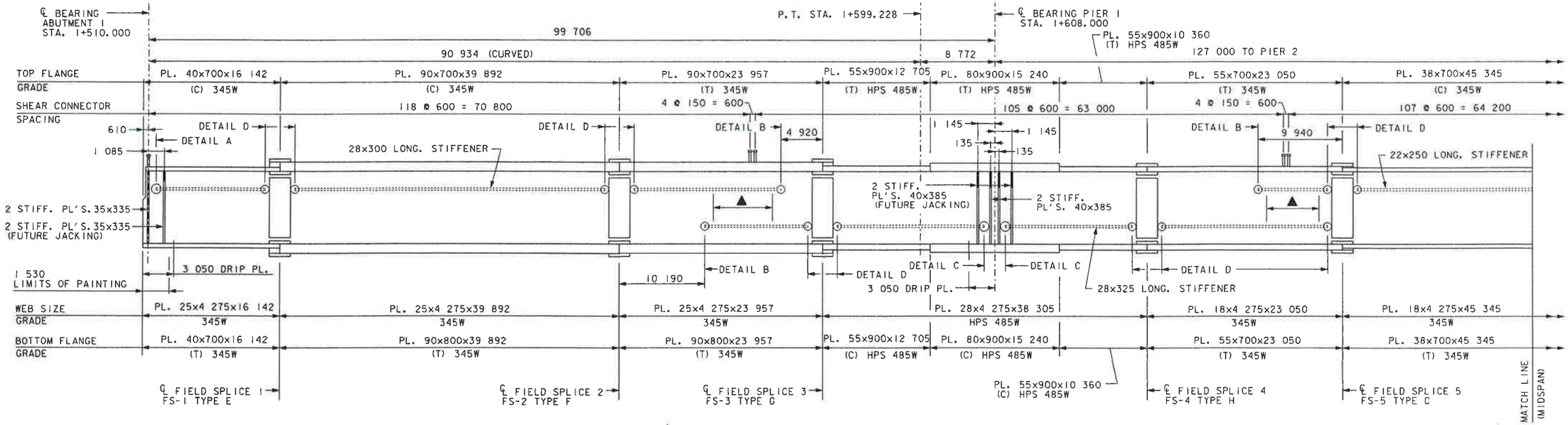

GIRDER 2 ELEVATION

NO SCALE

NOTES:

FOR GENERAL NOTES, SEE SHEET 2.

FOR FRAMING PLAN, SEE SHEETS 36 AND 37.

FOR SHEAR CONNECTOR, DRIP PLATE, AND OTHER MISCELLANEOUS GIRDER DETAILS, SEE SHEETS 42 AND 43.

FOR GIRDER SPLICES, SEE SHEETS 44 THROUGH 46.

CHARPY V-NOTCH TESTING IS REQUIRED ON ALL TENSION FLANGES, WEBS, DIAPHRAGM MEMBERS, AND SPLICE PLATES.

SHEAR CONNECTORS SHALL CONFORM TO AASHTO M169 (ASTM A108).

FOR LONGITUDINAL STIFFENER INTERSECTION DETAILS (A,B,C, AND D), SEE SHEET 43.

GIRDERS, CROSS FRAMES, STIFFENER PLATES, AND BEARINGS SHALL BE PAINTED AT THE SUPPORT LOCATIONS WITHIN THE LIMITS SHOWN.

FOR CONVENIENCE, LONGITUDINAL STIFFENERS ARE SHOWN CONTINUOUS BETWEEN SUCCESSIVE SPLICES, AND BETWEEN BEARING STIFFENERS AND SPLICES. LONGITUDINAL STIFFENERS ARE INTERRUPTED AT TYPE A CROSS FRAME CONNECTION PLATES, (SEE FRAMING PLAN, AND SHEETS 42 AND 43).

LEGEND:

(T) DENOTES TENSION FLANGE
(C) DENOTES COMPRESSION FLANGE

▲ - CROSS FRAME TO GIRDER CONNECTION IN THIS REGION REQUIRE A TYPE B CONNECTION PLATE DETAIL.

Mark	Description	By	Chk'd.	App'd.	Date
REVISIONS					

COMMONWEALTH OF PENNSYLVANIA
DEPARTMENT OF TRANSPORTATION

ARMSTRONG COUNTY
S.R. 0128 SEC. 013
SEG. 0250 OFFSET 0
S.R. 0128 STA. 1+671.500
OVER ALLEGHENY RIVER & PITTSBURG & SHAWMUT R.R.
3-SPAN CONTINUOUS STEEL PLATE GIRDER BRIDGE
GIRDER 2 ELEVATION

COMMONWEALTH OF PENNSYLVANIA REGISTERED PROFESSIONAL MICHAEL J. BONKOVICH ENGINEER 043452-R

RECOMMENDED JAN 26 1998

SHEET 39 OF 112

Designed by:	SDV
Checked by:	LAC
Drawn by:	EEM

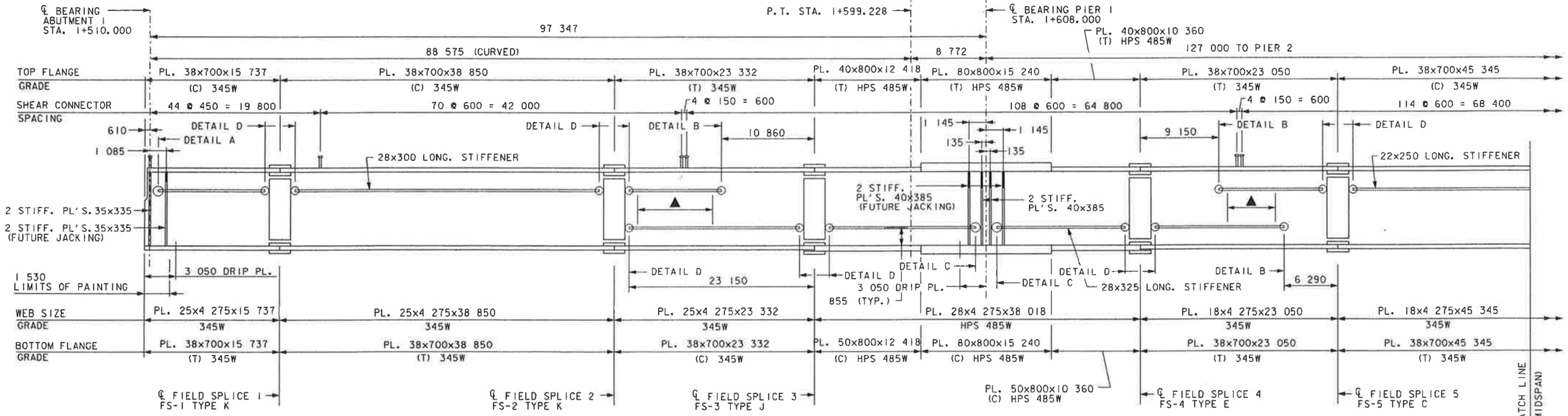

GIRDER 3 ELEVATION

NO SCALE

NOTES:

FOR GENERAL NOTES, SEE SHEET 2.

FOR FRAMING PLAN, SEE SHEETS 36 AND 37.

FOR SHEAR CONNECTOR, DRIP PLATE, AND OTHER MISCELLANEOUS GIRDER DETAILS, SEE SHEETS 42 AND 43.

FOR GIRDER SPLICES, SEE SHEETS 44 THROUGH 46.

CHARPY V-NOTCH TESTING IS REQUIRED ON ALL TENSION FLANGES, WEBS, DIAPHRAGM MEMBERS, AND SPLICE PLATES.

SHEAR CONNECTORS SHALL CONFORM TO AASHTO M169 (ASTM A108).

FOR LONGITUDINAL STIFFENER INTERSECTION DETAILS (A,B,C, AND D), SEE SHEET 43.

GIRDERS, CROSS FRAMES, STIFFENER PLATES, AND BEARINGS SHALL BE PAINTED AT THE SUPPORT LOCATIONS WITHIN THE LIMITS SHOWN.

FOR CONVENIENCE, LONGITUDINAL STIFFENERS ARE SHOWN CONTINUOUS BETWEEN SUCCESSIVE SPLICES, AND BETWEEN BEARING STIFFENERS AND SPLICES. LONGITUDINAL STIFFENERS ARE INTERRUPTED AT TYPE A CROSS FRAME CONNECTION PLATES, (SEE FRAMING PLAN, AND SHEETS 42 AND 43).

LEGEND:

(T) DENOTES TENSION FLANGE
(C) DENOTES COMPRESSION FLANGE
▲ - CROSS FRAME TO GIRDER CONNECTION IN THIS REGION REQUIRE A TYPE B CONNECTION PLATE DETAIL.

Mark	Description	By	Chk'd.	App'd.	Date
REVISIONS					

Designed by:	SDV
Checked by:	LAC
Drawn by:	EEM
Checked by:	SDV

COMMONWEALTH OF PENNSYLVANIA
DEPARTMENT OF TRANSPORTATION

ARMSTRONG COUNTY
S.R. 0128 SEC. 013
SEG. 0250 OFFSET 0
S.R. 0128 STA. 1+671.500
OVER ALLEGHENY RIVER & PITTSBURG & SHAWMUT R.R.
3-SPAN CONTINUOUS STEEL PLATE GIRDER BRIDGE
GIRDER 3 ELEVATION

COMMONWEALTH OF PENNSYLVANIA REGISTERED PROFESSIONAL MICHAEL J. BONKOVICH ENGINEER 043452-R

RECOMMENDED _____

SHEET 40 OF 112

S-22234

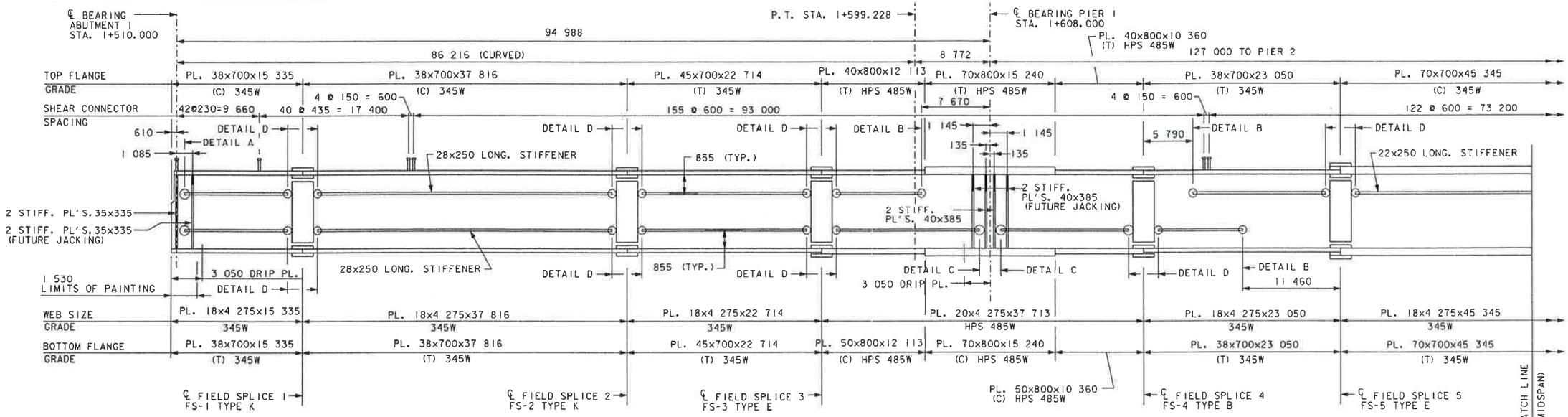

GIRDER 4 ELEVATION

NO SCALE

NOTES:

FOR GENERAL NOTES, SEE SHEET 2.

FOR FRAMING PLAN, SEE SHEETS 36 AND 37.

FOR SHEAR CONNECTOR, DRIP PLATE, AND OTHER MISCELLANEOUS GIRDER DETAILS, SEE SHEETS 42 AND 43.

FOR GIRDER SPLICES, SEE SHEETS 44 THROUGH 46.

CHARPY V-NOTCH TESTING IS REQUIRED ON ALL TENSION FLANGES, WEBS, DIAPHRAGM MEMBERS, AND SPLICE PLATES.

SHEAR CONNECTORS SHALL CONFORM TO AASHTO M169 (ASTM A108).

FOR LONGITUDINAL STIFFENER INTERSECTION DETAILS (A,B,C, AND D), SEE SHEET 43.

GIRDERS, CROSS FRAMES, STIFFENER PLATES, AND BEARINGS SHALL BE PAINTED AT THE SUPPORT LOCATIONS WITHIN THE LIMITS SHOWN.

FOR CONVENIENCE, LONGITUDINAL STIFFENERS ARE SHOWN CONTINUOUS BETWEEN SUCCESSIVE SPLICES, AND BETWEEN BEARING STIFFENERS AND SPLICES. LONGITUDINAL STIFFENERS ARE INTERRUPTED AT TYPE A CROSS FRAME CONNECTION PLATES, (SEE FRAMING PLAN, AND SHEETS 42 AND 43).

LEGEND:

(T) DENOTES TENSION FLANGE
(C) DENOTES COMPRESSION FLANGE

Mark	Description	By	Chk'd.	App'd.	Date
REVISIONS					

COMMONWEALTH OF PENNSYLVANIA
DEPARTMENT OF TRANSPORTATION

ARMSTRONG COUNTY
S.R. 0128 SEC. 013
SEG. 0250 OFFSET 0
S.R. 0128 STA. 1+671.500
OVER ALLEGHENY RIVER & PITTSBURG & SHAWMUT R.R.
3-SPAN CONTINUOUS STEEL PLATE GIRDER BRIDGE
GIRDER 4 ELEVATION

COMMONWEALTH OF PENNSYLVANIA REGISTERED PROFESSIONAL MICHAEL J. BONKOVICH ENGINEER 043452-R

RECOMMENDED JAN 26 1998

SHEET 41 OF 112

S-22234

Designed by:	SDV
Checked by:	LAC
Drawn by:	EEM

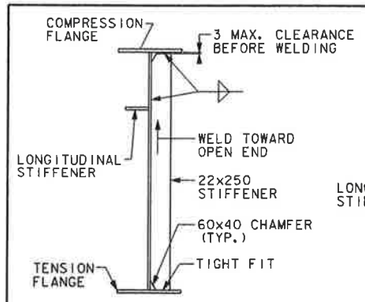

INTERMEDIATE STIFFENER TYPE I DETAIL

NO SCALE

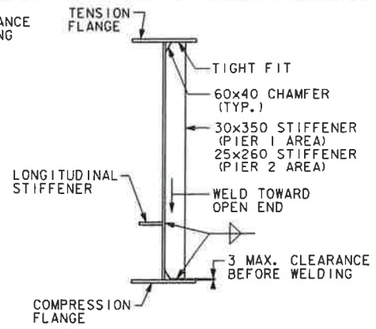

INTERMEDIATE STIFFENER TYPE II DETAIL

NO SCALE

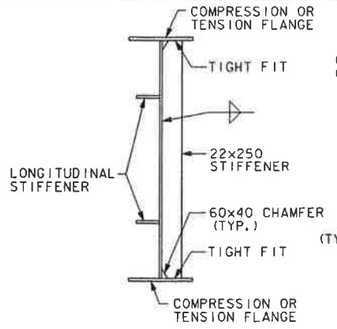

INTERMEDIATE STIFFENER TYPE III DETAIL

NO SCALE

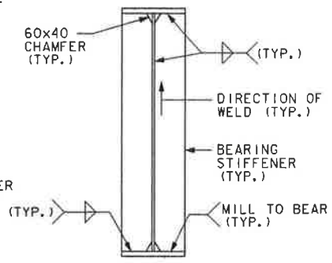

BEARING STIFFENER DETAIL

NO SCALE

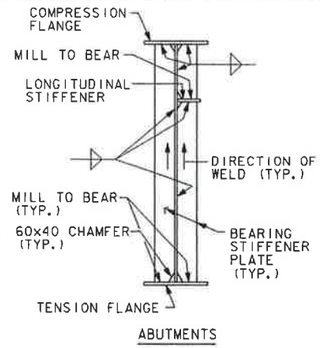

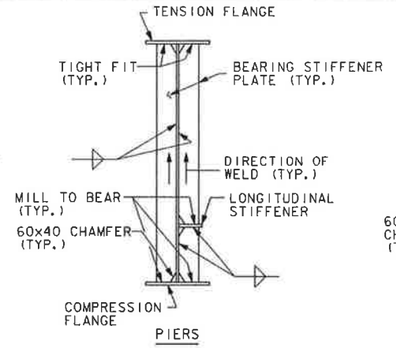

FUTURE JACKING BEARING STIFFENER DETAIL

NO SCALE

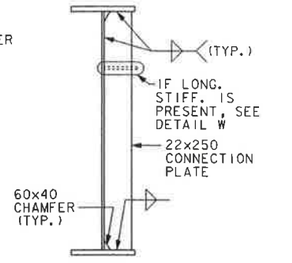

COUNTERWEIGHT CONNECTION PLATE TYPE CW DETAIL

NO SCALE

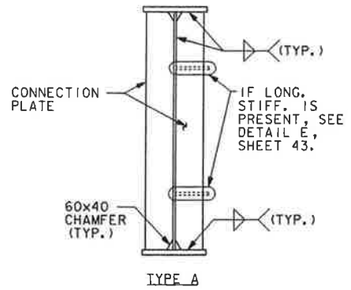

TYPE A

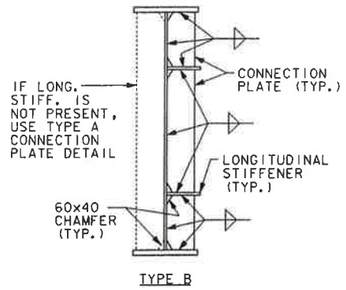

TYPE B

CROSS FRAME CONNECTION PLATE DETAIL

NO SCALE

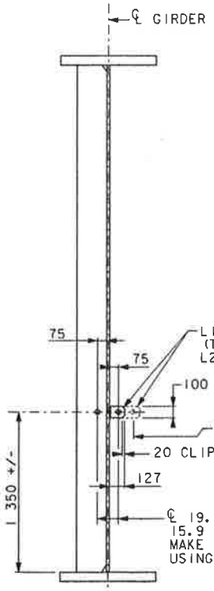

SECTION

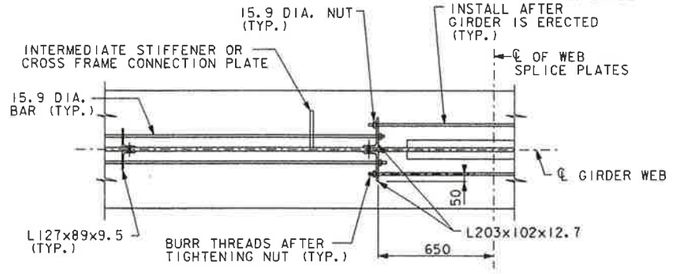

PLAN

FLANGE SPLICE PLATES NOT SHOWN FOR CLARITY.

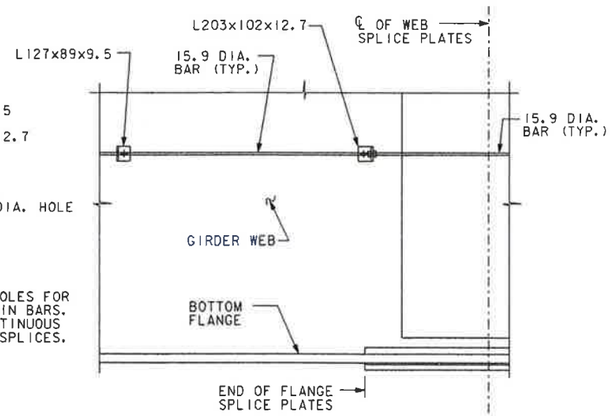

ELEVATION

HANDRAIL LOCATION DETAIL

NO SCALE

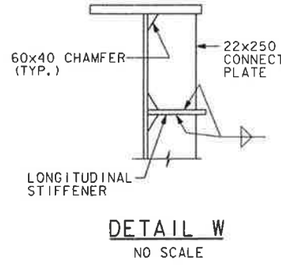

DETAIL W

NO SCALE

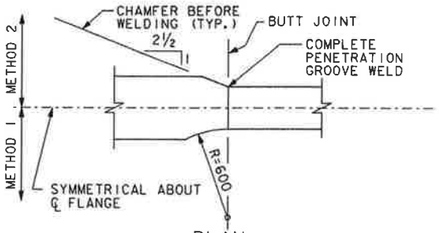

PLAN

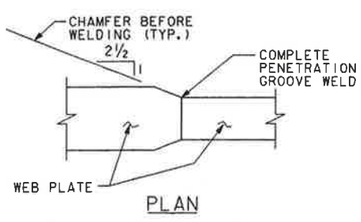

PLAN

WEB SPLICE DETAIL

NO SCALE

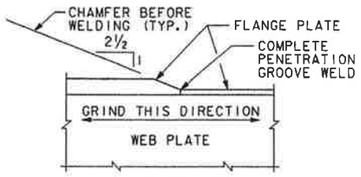

ELEVATION

FLANGE SPLICE DETAIL

NO SCALE

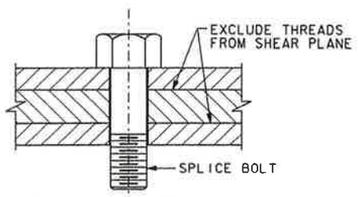

SPLICE BOLT THREAD DETAIL

NO SCALE

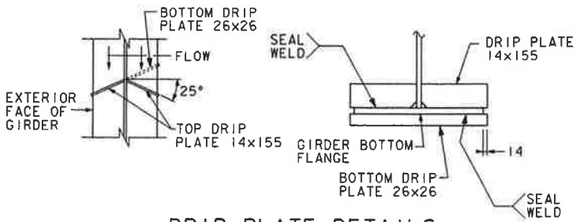

DRIP PLATE DETAILS

NO SCALE

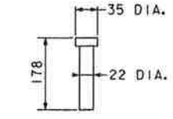

STUD DETAIL

NO SCALE

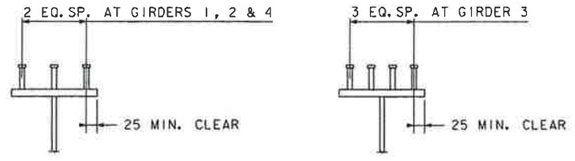

SHEAR CONNECTOR DETAIL

NO SCALE

NOTES:

FOR GENERAL NOTES, SEE SHEET 2.

FOR WEB, FLANGE AND BEARING STIFFENER PLATE SIZES, SEE SHEETS 38 THROUGH 41.

FOR CROSS FRAME DETAILS, SEE SHEETS 47 THROUGH 50.

FOR LOCATIONS OF INTERMEDIATE STIFFENERS, SEE SHEETS 36 AND 37.

HANDRAILS SHALL NOT BE PLACED ON EXTERIOR OF FASCIA GIRDERS.

FOR ADDITIONAL NOTES AND DETAILS, SEE STD. DWG. BC-753M.

DIRECTION OF WELD IN BEARING STIFFENER DETAIL IS NOT APPLICABLE IF STIFFENERS ARE FITTED WITH TACK WELDS.

FOR LOCATION OF DRIP PLATES, SEE SHEETS 38 THROUGH 41.

FOR HANDRAIL, USE CLIP ANGLES BETWEEN STIFFENERS WHEN STIFFENERS ARE SPACED AT 2 550 OR GREATER.

UNDER FULL DEAD LOAD, ALL COUNTERWEIGHT CONNECTION PLATES ARE VERTICAL TO WITHIN APPLICABLE AASHTO/AWS FABRICATION AND CONSTRUCTION TOLERANCES.

Mark	Description	By	Chk'd.	App'd.	Date
REVISIONS					

Designed by:	SDV
Checked by:	LAC
Drawn by:	CLM/EEM

COMMONWEALTH OF PENNSYLVANIA
DEPARTMENT OF TRANSPORTATION

ARMSTRONG COUNTY
S.R. 0128 SEC. 013
SEG. 0250 OFFSET 0
S.R. 0128 STA. 1+671.500
OVER ALLEGHENY RIVER & PITTSBURG & SHAWMUT R.R.
3-SPAN CONTINUOUS STEEL PLATE GIRDER BRIDGE
MISCELLANEOUS GIRDERS DETAILS - 1

COMMONWEALTH OF PENNSYLVANIA REGISTERED PROFESSIONAL MICHAEL J. BONKOVICH ENGINEER 043452-R

RECOMMENDED JAN 26 1998

SHEET 42 OF 112

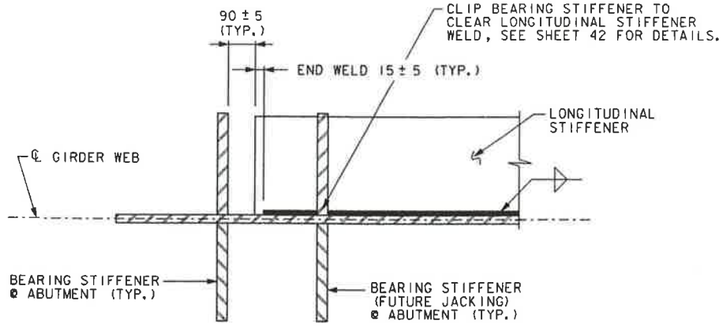

DETAIL A
NO SCALE

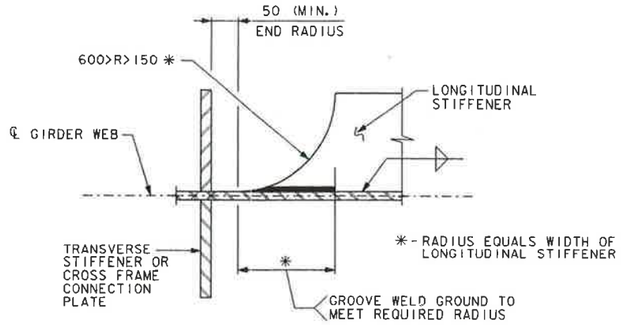

DETAIL B
(LONGITUDINAL STIFFENER TERMINUS)
NO SCALE

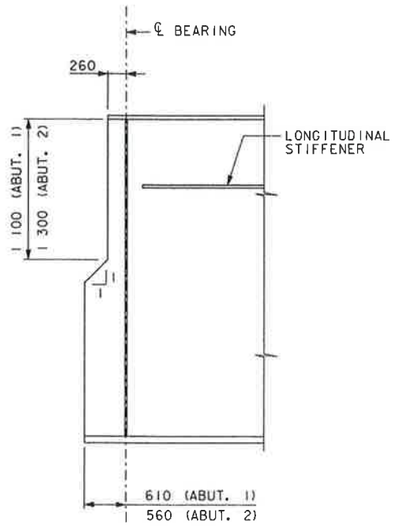

GIRDER WEB COPE
NO SCALE

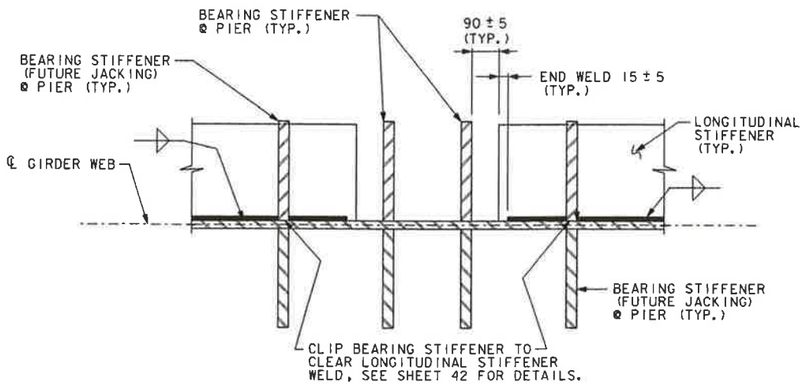

DETAIL C
NO SCALE

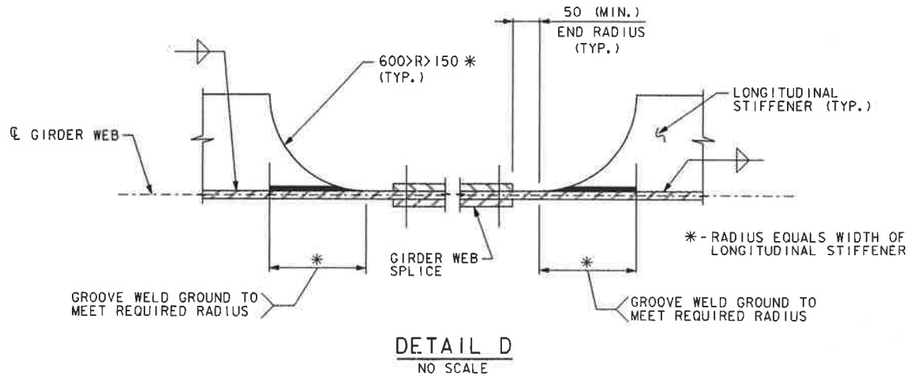

DETAIL D
NO SCALE

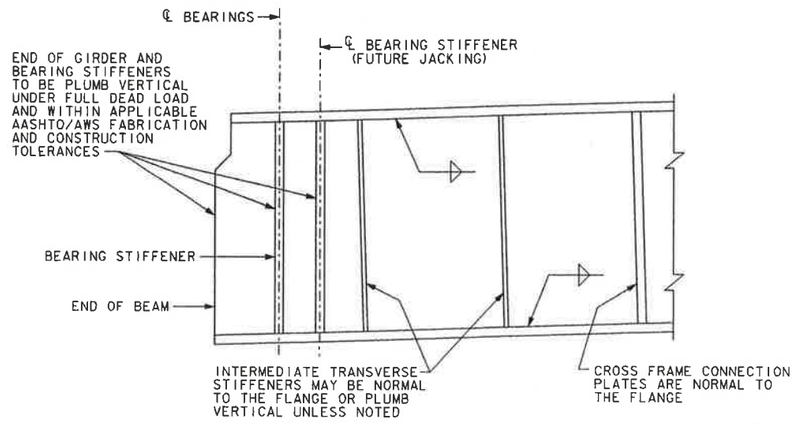

TYPICAL GIRDER DETAIL
NO SCALE

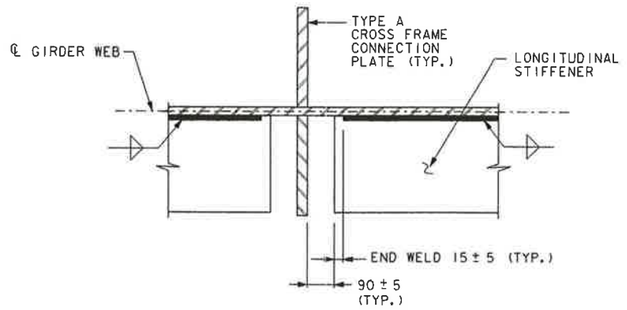

DETAIL E
NO SCALE

FILLET WELD TABLE	
THICKNESS OF THICKER PLATE JOINED	MINIMUM WELD SIZE
TO 18 INCLUSIVE	6
OVER 18	8

WELD SIZE NOT TO EXCEED THE THICKNESS OF THE THINNER PLATE JOINED MINUS 2

NOTES:

FOR GENERAL NOTES, SEE SHEET 2.

FOR WEB, FLANGE, AND BEARING STIFFENER PLATE SIZES, SEE SHEET 38 THROUGH 41.

FOR LOCATION OF DETAIL A THROUGH D, SEE SHEET 38 THROUGH 41.

FOR ADDITIONAL NOTES AND DETAILS, SEE STANDARD DRAWINGS BC-753M.

DETAIL E IS REQUIRED FOR TYPE A CROSS FRAME CONNECTION PLATE DETAILS WHEN A LONGITUDINAL STIFFENER IS PRESENT ON BOTH SIDES OF THE CROSS FRAME CONNECTION PLATE, (SEE ALSO SHEET 42).

Mark	Description	By	Chk'd.	App'd.	Date
REVISIONS					

COMMONWEALTH OF PENNSYLVANIA
DEPARTMENT OF TRANSPORTATION

ARMSTRONG COUNTY
S.R. 0128 SEC. 013
SEG. 0250 OFFSET 0
S.R. 0128 STA. 1+671.500
OVER ALLEGHENY RIVER & PITTSBURG & SHAWMUT R.R.
3-SPAN CONTINUOUS STEEL PLATE GIRDER BRIDGE
MISCELLANEOUS GIRDER DETAILS - 2

RECOMMENDED JAN 26 1999

SHEET 43 OF 112

S-22234

Designed by:	SDV
Checked by:	LAC
Drawn by:	EEM
Checked by:	SDV/MJB

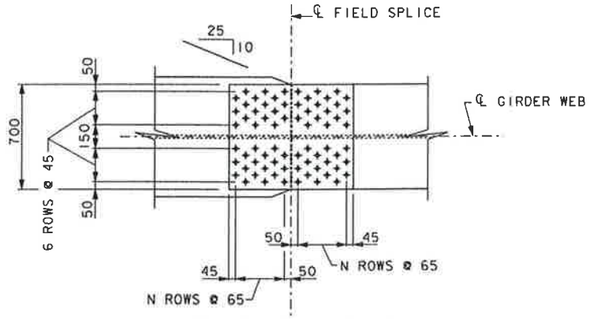

TOP FLANGE SPLICE

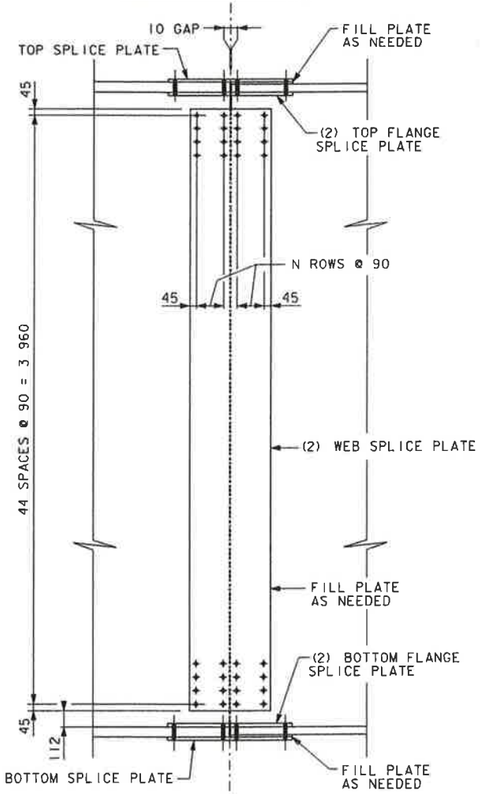

ELEVATION - FIELD SPLICE

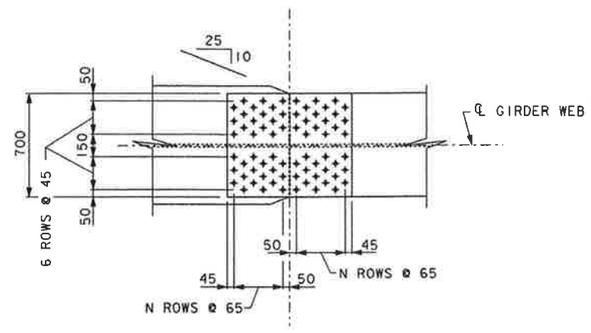

BOTTOM FLANGE SPLICE

0 500 1000 mm

SCALE = 1:20

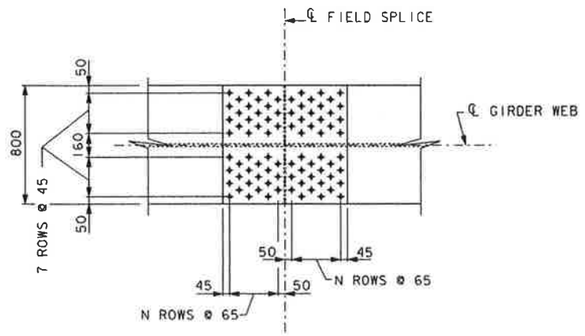

BOTTOM FLANGE SPLICE

0 500 1000 mm

SCALE = 1:20

TYPE OF SPLICE	TOP SPLICE PLATE	TOP FLANGE SPLICE PLATE	WEB SPLICE PLATE	BOTTOM FLANGE SPLICE PLATE	BOTTOM SPLICE PLATE	NUMBER (N) OF ROWS OF BOLTS PER SIDE		
						TOP SPLICE PL.	WEB SPLICE PLATE	BOTTOM SPLICE PL.
A	20 x 700 x 840	22 x 325 x 840	14 x 550 x 4 050	25 x 325 x 1 200	22 x 700 x 1 200	6	3	8
B	20 x 700 x 840	22 x 325 x 840	16 x 550 x 4 050	22 x 325 x 840	22 x 700 x 840	6	3	6
C	20 x 700 x 580	20 x 325 x 580	14 x 550 x 4 050	22 x 325 x 840	22 x 700 x 840	4	3	6
D	22 x 700 x 1 200	25 x 325 x 1 200	14 x 550 x 4 050	25 x 325 x 1 200	25 x 700 x 1 200	8	3	8
E	22 x 700 x 1 200	25 x 325 x 1 200	20 x 730 x 4 050	25 x 325 x 1 360	25 x 700 x 1 360	8	4	10
F	32 x 700 x 1 200	32 x 325 x 1 200	16 x 550 x 4 050	38 x 370 x 1 230	35 x 800 x 1 230	8	3	7
G	35 x 700 x 1 360	35 x 325 x 1 360	18 x 550 x 4 050	35 x 370 x 1 230	35 x 800 x 1 230	10	3	9
H	35 x 700 x 1 620	35 x 325 x 1 620	14 x 730 x 4 050	32 x 325 x 1 620	30 x 325 x 1 620	12	4	12
J	20 x 700 x 840	22 x 325 x 840	18 x 730 x 4 050	22 x 325 x 1 200	20 x 700 x 1 200	6	4	8
K	14 x 700 x 580	14 x 325 x 580	16 x 550 x 4 050	16 x 325 x 580	16 x 700 x 580	4	3	4

NOTES:

FOR GENERAL NOTES, SEE SHEET 2.

FOR LOCATION OF SPLICES, SEE SHEETS 36 THROUGH 41.

ALL SPLICE BOLTS SHALL BE M22 M164M, 25.4 WITH HEX NUTS AND WASHERS. THREADS EXCLUDED FROM THE SHEAR PLANE.

ALL SPLICE MATERIAL SHALL BE AASHTO M270, GRADE 345W.

FOR FLANGE SPLICE AND WEB SPLICE DETAILS, SEE SHEET 42.

CHARPY V-NOTCH ALL SPLICE PLATES , WEBS AND FLANGES.

ALL FILL PLATES LESS THAN 2mm THICK CAN BE OMITTED.

Mark	Description	By	Chk'd.	App'd.	Date
REVISIONS					

COMMONWEALTH OF PENNSYLVANIA
DEPARTMENT OF TRANSPORTATION

ARMSTRONG COUNTY
S.R. 0128 SEC. 013
SEG. 0250 OFFSET 0
S.R. 0128 STA. 1+671.500
OVER ALLEGHENY RIVER & PITTSBURG & SHAWMUT R.R.
3-SPAN CONTINUOUS STEEL PLATE GIRDER BRIDGE
GIRDER SPLICES - 1

COMMONWEALTH OF PENNSYLVANIA REGISTERED PROFESSIONAL MICHAEL J. BONKOVICH ENGINEER 043452-R

RECOMMENDED JAN 2 6 1998

SHEET 44 OF 112

S-22234

Designed by:	LAC
Checked by:	GRL
Drawn by:	EEM

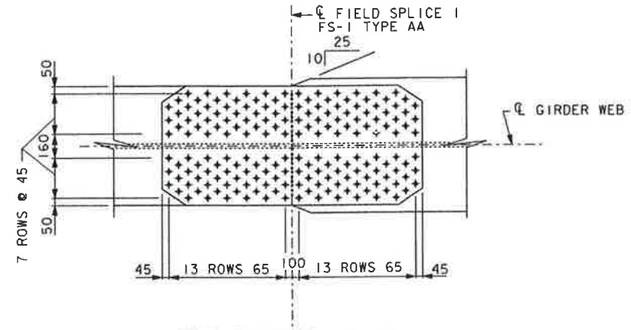

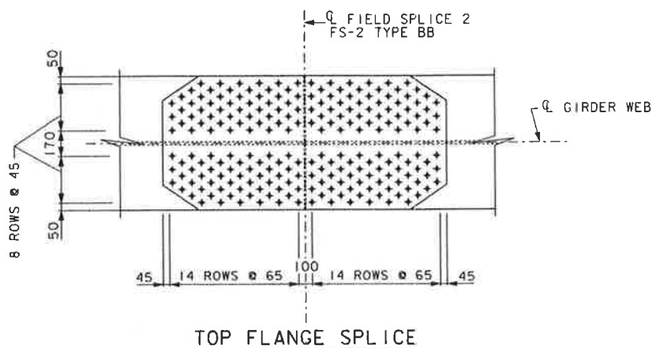

TOP FLANGE SPLICE

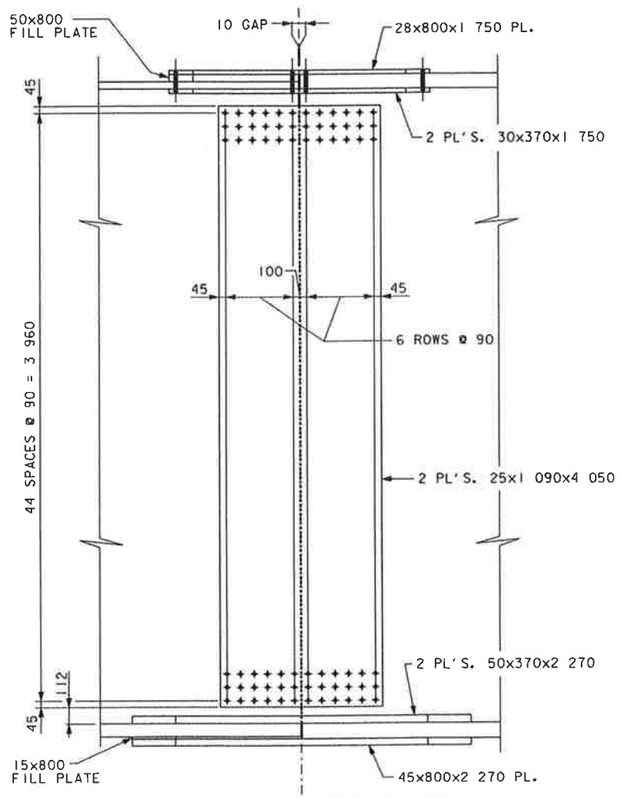

ELEVATION - FIELD SPLICE TYPE AA

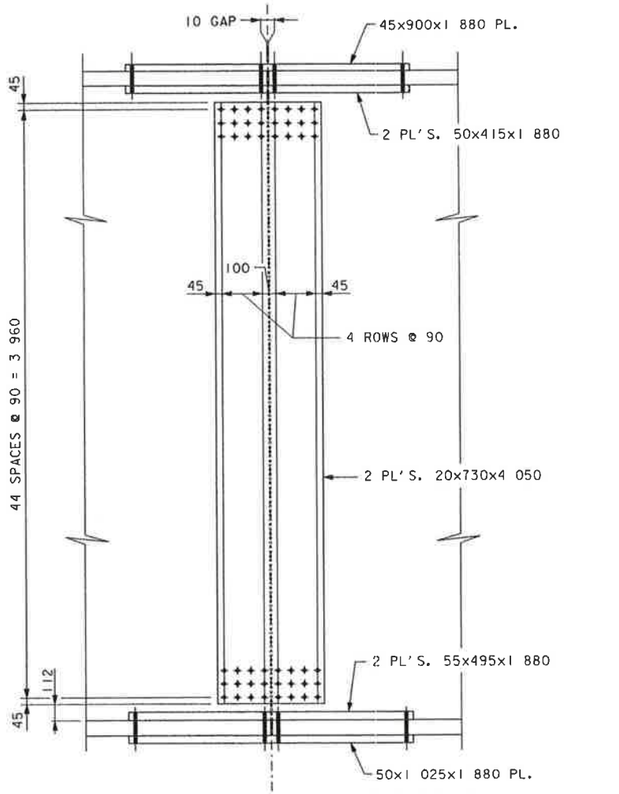

ELEVATION - FIELD SPLICE TYPE BB

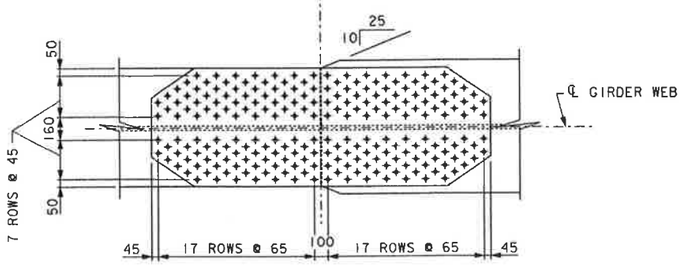

BOTTOM FLANGE SPLICE

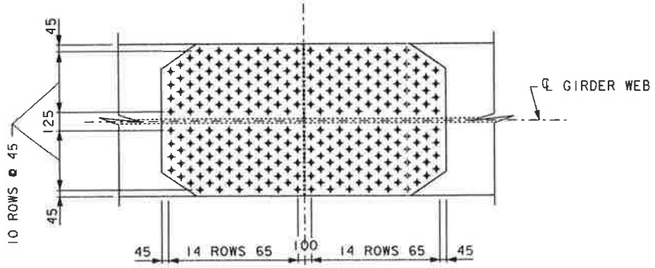

BOTTOM FLANGE SPLICE

0 500 1000 mm
SCALE = 1:20

0 500 1000 mm
SCALE = 1:20

NOTES:

FOR GENERAL NOTES, SEE SHEET 2.

FOR LOCATION OF SPLICES, SEE SHEETS 36 THROUGH 41.

ALL SPLICE BOLTS SHALL BE M22 M164M, 25.4 WITH HEX NUTS AND WASHERS. THREADS EXCLUDED FROM THE SHEAR PLANE.

ALL SPLICE MATERIAL SHALL BE AASHTO M270, GRADE 345W.

FOR FLANGE SPLICE AND WEB SPLICE DETAILS, SEE SHEET 42.

CHARPY V-NOTCH ALL SPLICE PLATES , WEBS AND FLANGES.

Mark	Description	By	Chk'd.	App'd.	Date
REVISIONS					

Designed by:	LAC
Checked by:	GRL
Drawn by:	EEM

COMMONWEALTH OF PENNSYLVANIA
DEPARTMENT OF TRANSPORTATION

ARMSTRONG COUNTY
S.R. 0128 SEC. 013
SEG. 0250 OFFSET 0
S.R. 0128 STA. 1+671.500
OVER ALLEGHENY RIVER & PITTSBURG & SHAWMUT R.R.
3-SPAN CONTINUOUS STEEL PLATE GIRDER BRIDGE
GIRDER SPLICES - 2

COMMONWEALTH OF PENNSYLVANIA REGISTERED PROFESSIONAL MICHAEL J. BONKOVICH ENGINEER 043452-R

RECOMMENDED JAN 26 1998

SHEET 45 OF 112

S-22234

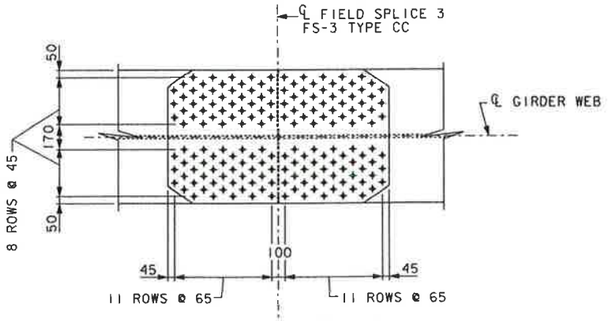

TOP FLANGE SPLICE

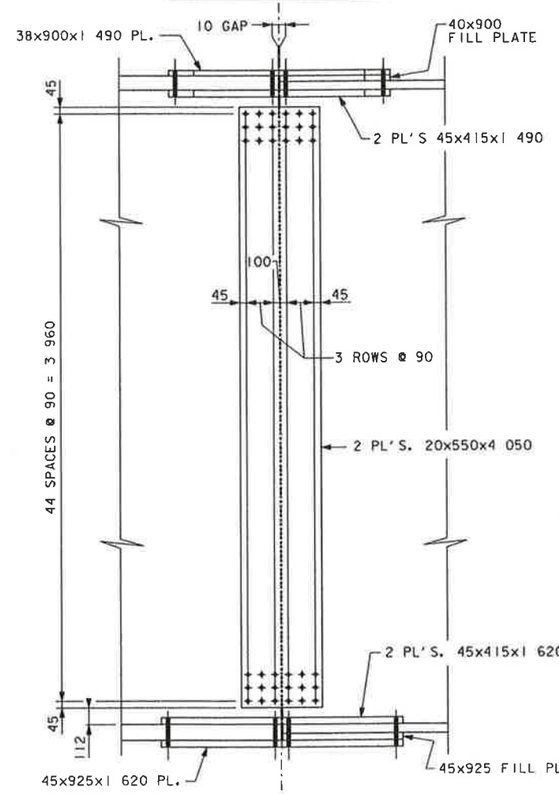

ELEVATION - FIELD SPLICE TYPE CC

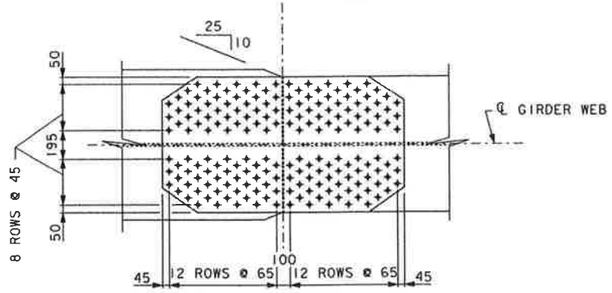

BOTTOM FLANGE SPLICE

0 500 1000 mm
SCALE = 1:20

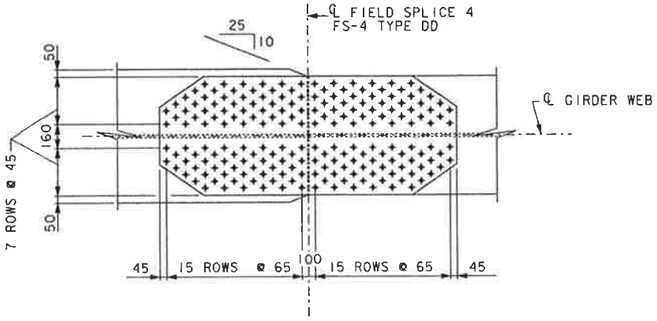

TOP FLANGE SPLICE

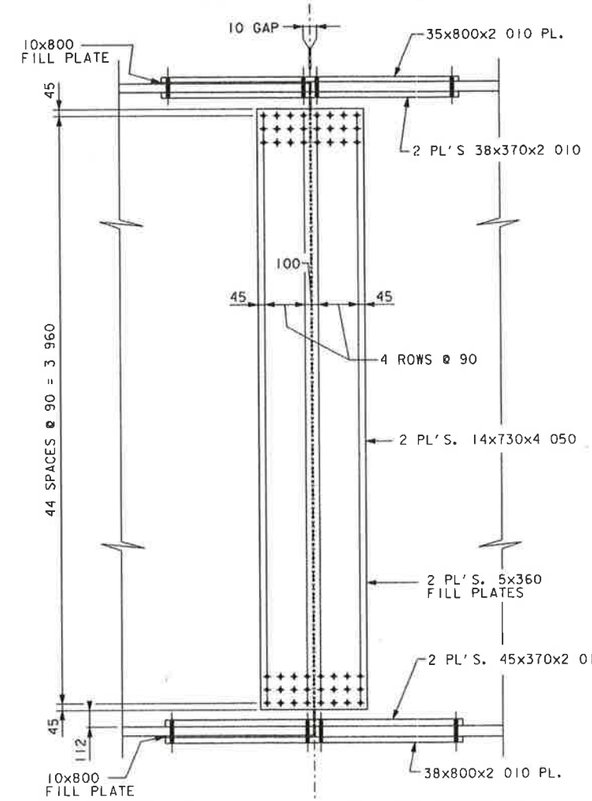

ELEVATION - FIELD SPLICE TYPE DD

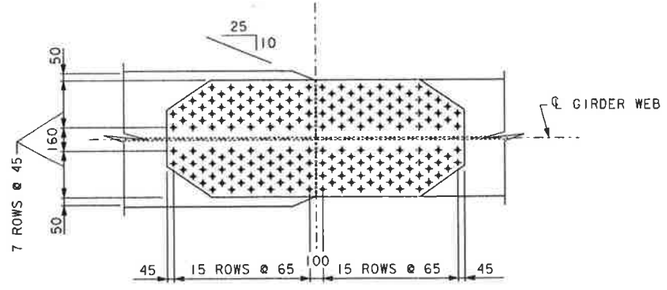

BOTTOM FLANGE SPLICE

0 500 1000 mm
SCALE = 1:20

NOTES:

FOR GENERAL NOTES, SEE SHEET 2.

FOR LOCATION OF SPLICES, SEE SHEETS 36 THROUGH 41.

ALL SPLICE BOLTS SHALL BE M22 M164M, 25.4 WITH HEX NUTS AND WASHERS. THREADS EXCLUDED FROM THE SHEAR PLANE.

ALL SPLICE MATERIAL SHALL BE AASHTO M270, GRADE 345W.

FOR FLANGE SPLICE AND WEB SPLICE DETAILS, SEE SHEET 42.

CHARPY V-NOTCH ALL SPLICE PLATES , WEBS AND FLANGES.

Mark	Description	By	Chk'd.	App'd.	Date
REVISIONS					

COMMONWEALTH OF PENNSYLVANIA
DEPARTMENT OF TRANSPORTATION

ARMSTRONG COUNTY
S.R. 0128 SEC. 013
SEG. 0250 OFFSET 0
S.R. 0128 STA. 1+671.500
OVER ALLEGHENY RIVER & PITTSBURG & SHAWMUT R.R.
3-SPAN CONTINUOUS STEEL PLATE GIRDER BRIDGE
GIRDER SPLICES - 3

COMMONWEALTH OF PENNSYLVANIA REGISTERED PROFESSIONAL MICHAEL J. BONKOVICH ENGINEER 043452-R

RECOMMENDED JAN 26 1998

SHEET 46 OF 112

S-22234

Designed by:	LAC
Checked by:	GRL
Drawn by:	EEM

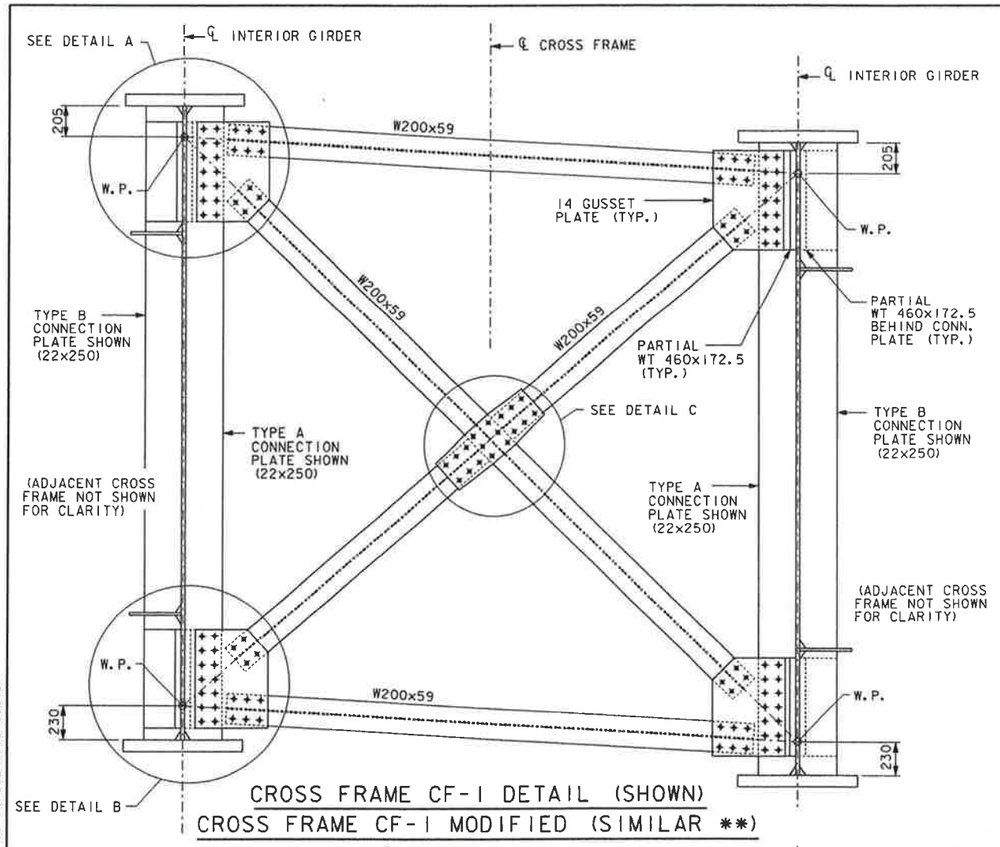

CROSS FRAME CF-1 DETAIL (SHOWN)
CROSS FRAME CF-1 MODIFIED (SIMILAR **)

0 500 1000 mm
SCALE = 1:20

** OMIT THE PARTIAL WT 460x172.5 BRACKETS. PROVIDE TWIN CONNECTION PLATES INSTEAD AT ALL GIRDER CONNECTIONS.

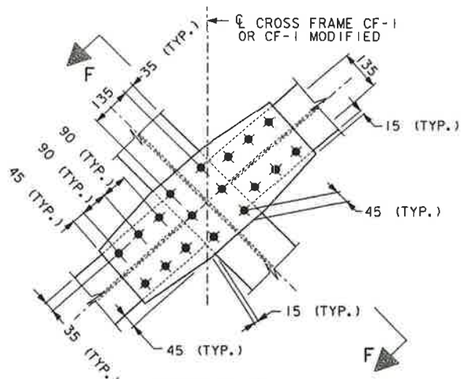

DETAIL C
0 200 400 mm
SCALE = 1:10

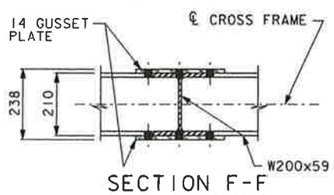

SECTION F-F
0 200 400 mm
SCALE = 1:10

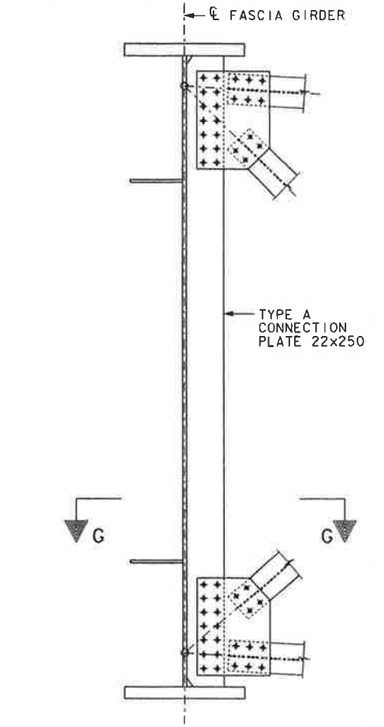

CROSS FRAME FASCIA DETAIL
0 500 1000 mm
SCALE = 1:20

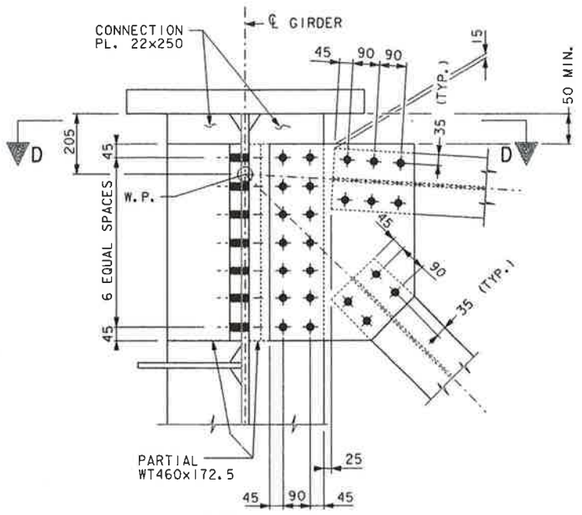

DETAIL A
0 200 400 mm
SCALE = 1:10

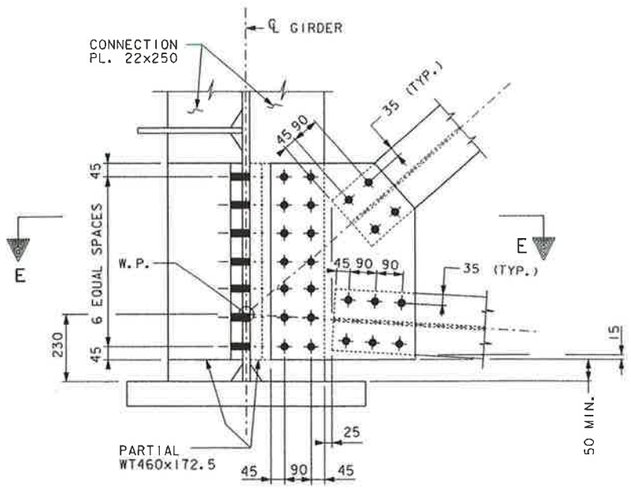

DETAIL B
0 200 400 mm
SCALE = 1:10

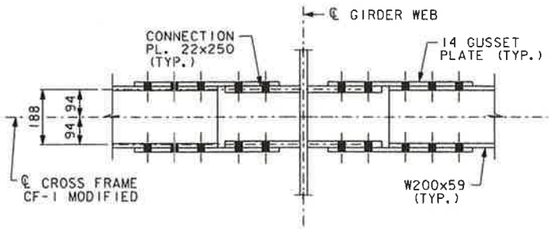

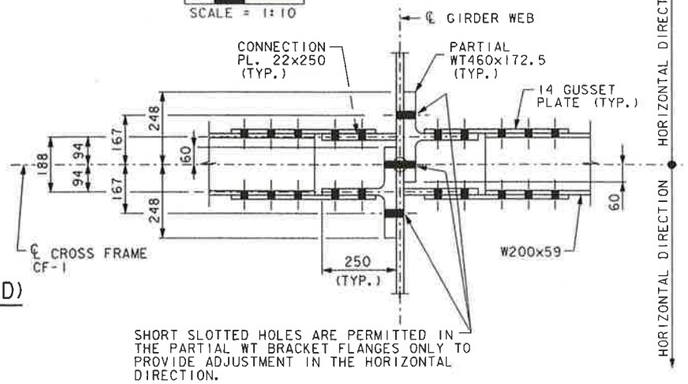

SHORT SLOTTED HOLES ARE PERMITTED IN THE PARTIAL WT BRACKET FLANGES ONLY TO PROVIDE ADJUSTMENT IN THE HORIZONTAL DIRECTION.

SECTION D-D (CROSSFRAME CF-1 MODIFIED)
(SECTION E-E SIMILAR)

0 200 400 mm
SCALE = 1:10

SECTION D-D (CROSSFRAME CF-1)
(SECTION E-E SIMILAR)

0 200 400 mm
SCALE = 1:10

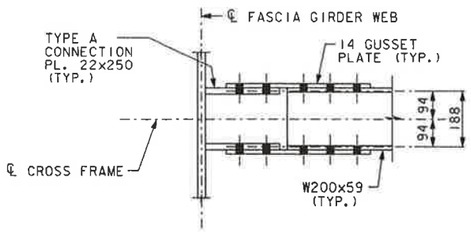

SECTION G-G
0 200 400 mm
SCALE = 1:10

NOTES:

FOR LOCATION OF CROSS FRAMES, SEE SHEETS 36 AND 37.

FOR CROSS FRAME DETAILS NOT SHOWN, SEE BC-754M.

FOR CROSS FRAME CONNECTION PLATES, SEE SHEET 42.

USE 27.0mm DIAMETER HOLES IN CONNECTION PLATES, GUSSET PLATES, BEAMS, AND WT'S, EXCEPT AS NOTED.

USE 25.4mm DIAMETER AASHTO M164 BOLTS WITH THREADS EXCLUDED FROM SHEAR PLANE.

USE THE NUMBER OF BOLTS SHOWN IN DETAILS.

ALL CROSS FRAMES MATERIAL (INCLUDING CONNECTION PLATES) SHALL BE SUBJECT TO CHARPY V-NOTCH TESTING AS PER SPECIFICATIONS.

Mark	Description	By	Chk'd.	App'd.	Date
REVISIONS					

COMMONWEALTH OF PENNSYLVANIA
DEPARTMENT OF TRANSPORTATION

ARMSTRONG COUNTY
S.R. 0128 SEC. 013
SEG. 0250 OFFSET 0
S.R. 0128 STA. 1+671.500
OVER ALLEGHENY RIVER & PITTSBURG & SHAWMUT R.R.
3-SPAN CONTINUOUS STEEL PLATE GIRDER BRIDGE
CROSS FRAME CF-1 DETAILS

RECOMMENDED JAN 26 1998

SHEET 47 OF 112

S-22234

Designed by: SDV/LAC
Checked by: MJB
Drawn by: EEM

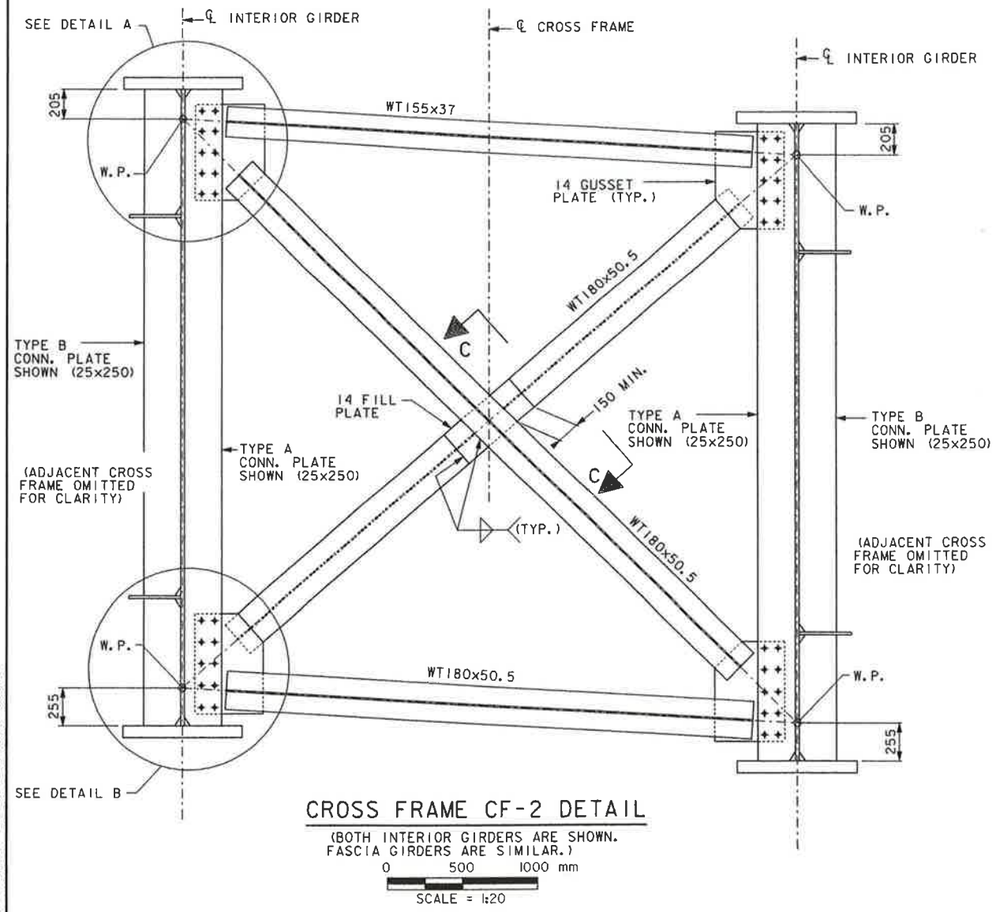

CROSS FRAME CF-2 DETAIL

(BOTH INTERIOR GIRDERS ARE SHOWN. FASCIA GIRDERS ARE SIMILAR.)

0 500 1000 mm

SCALE = 1:20

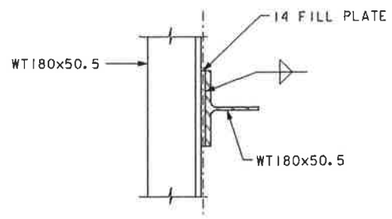

SECTION C-C

0 200 400 mm

SCALE = 1:10

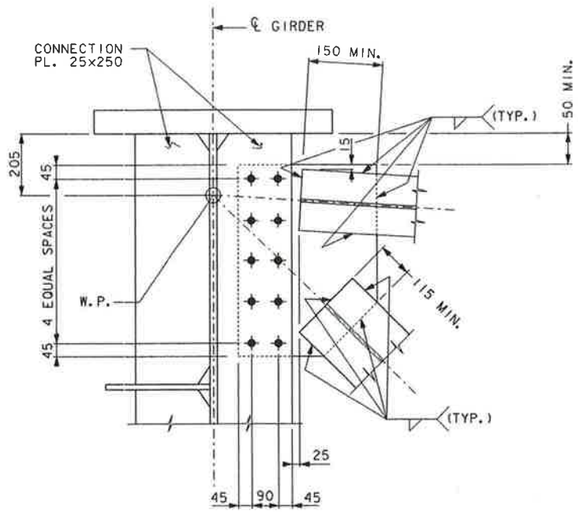

DETAIL A

0 200 400 mm

SCALE = 1:10

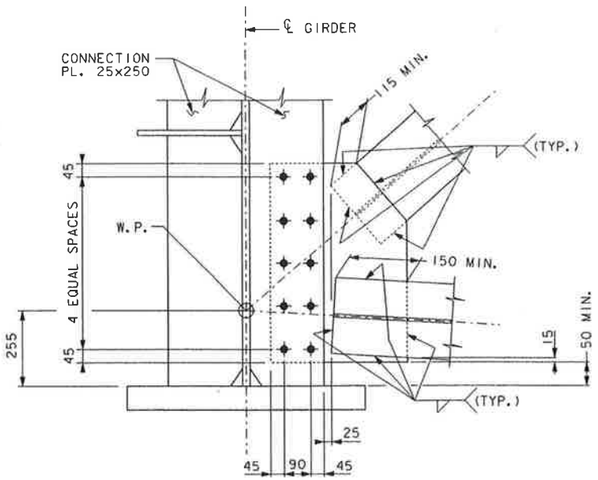

DETAIL B

0 200 400 mm

SCALE = 1:10

NOTES:

FOR LOCATION OF CROSS FRAMES, SEE SHEETS 36 AND 37.

FOR CROSS FRAME DETAILS NOT SHOWN, SEE BC-754M.

FOR CROSS FRAME CONNECTION PLATES, SEE SHEET 42.

USE 27.0mm DIAMETER HOLES IN CONNECTION PLATES, GUSSET PLATES, AND WT'S.

USE 25.4mm DIAMETER AASHTO M164 BOLTS WITH THREADS EXCLUDED FROM SHEAR PLANE.

FOR FILLET WELD SIZES SEE TABLE ON SHEET 43.

USE THE NUMBER OF BOLTS SHOWN IN DETAILS.

ALL CROSS FRAMES MATERIAL (INCLUDING CONNECTION PLATES) SHALL BE SUBJECT TO CHARPY V-NOTCH TESTING AS PER SPECIFICATIONS.

Mark	Description	By	Chk'd.	App'd.	Date
REVISIONS					

COMMONWEALTH OF PENNSYLVANIA
DEPARTMENT OF TRANSPORTATION

ARMSTRONG COUNTY
S.R. 0128 SEC. 013
SEG. 0250 OFFSET 0
S.R. 0128 STA. 1+671.500
OVER ALLEGHENY RIVER & PITTSBURG & SHAWMUT R.R.
3-SPAN CONTINUOUS STEEL PLATE GIRDER BRIDGE
CROSS FRAME CF-2 DETAILS

COMMONWEALTH OF PENNSYLVANIA REGISTERED PROFESSIONAL MICHAEL J. BONKOVICH ENGINEER 043452-R

RECOMMENDED JAN 26 1998

SHEET 48 OF 112

S-22234

Designed by:	SDV/LAC
Checked by:	MJB
Drawn by:	EEM

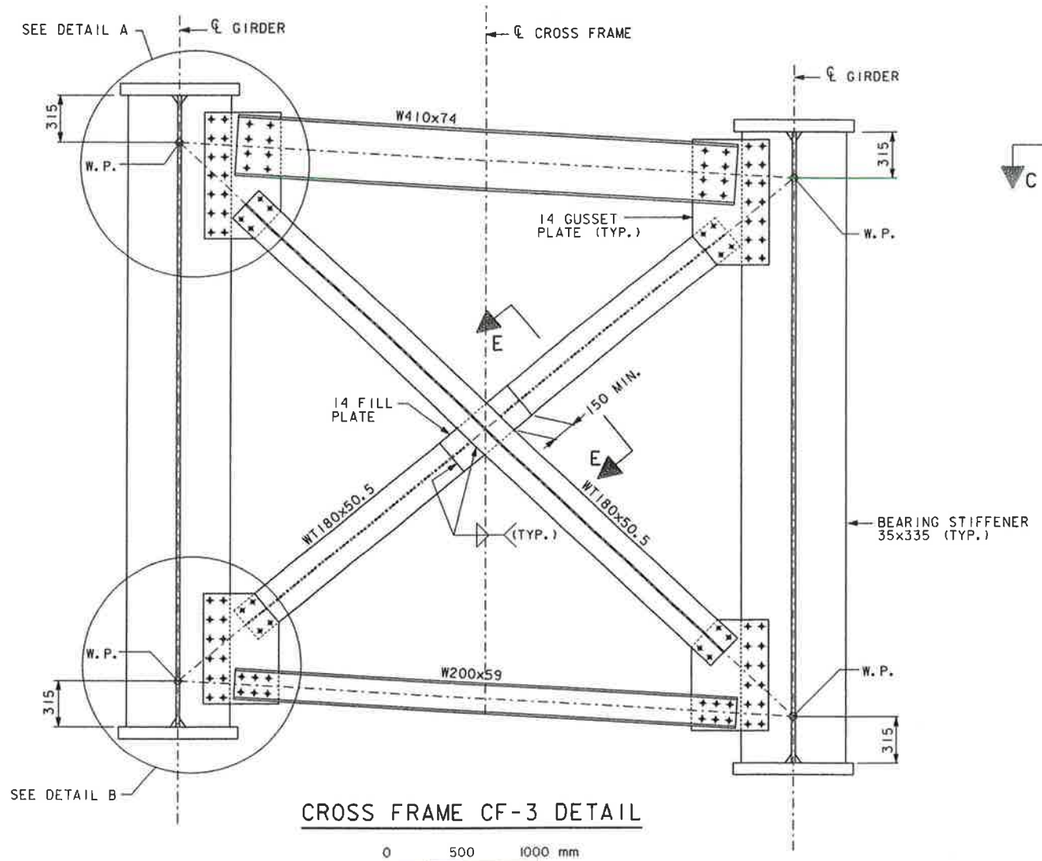

CROSS FRAME CF-3 DETAIL

0 500 1000 mm
SCALE = 1:20

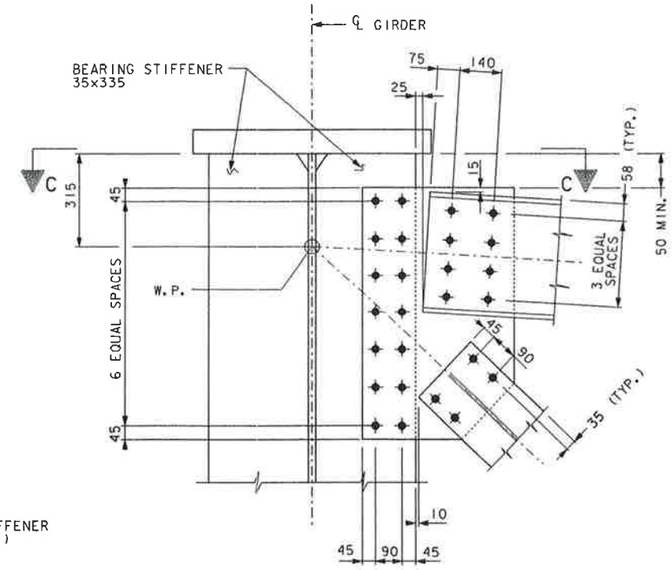

DETAIL A

0 200 400 mm
SCALE = 1:10

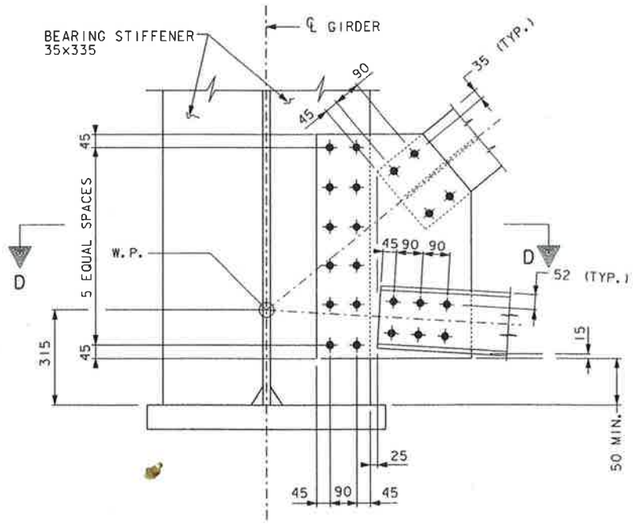

DETAIL B

0 200 400 mm
SCALE = 1:10

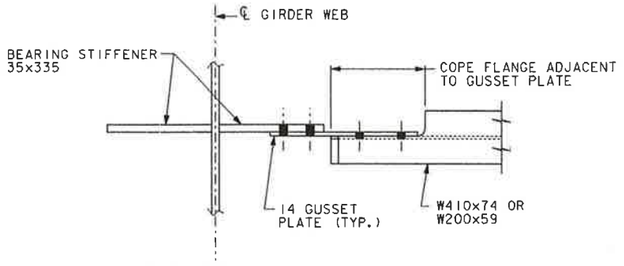

SECTION C-C
(SECTION D-D SIMILAR)

0 200 400 mm
SCALE = 1:10

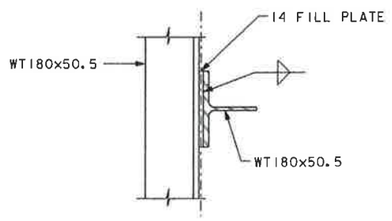

SECTION E-E

0 200 400 mm
SCALE = 1:10

NOTES:

FOR LOCATION OF CROSS FRAMES, SEE SHEETS 36 AND 37.

FOR CROSS FRAME DETAILS NOT SHOWN, SEE BC-754M.

FOR BEARING STIFFENER DETAILS, SEE SHEET 42.

USE 27.0mm DIAMETER HOLES IN BEARING STIFFENERS, GUSSET PLATES, BEAMS, AND WT'S.

USE 25.4mm DIAMETER AASHTO M164 BOLTS WITH THREADS EXCLUDED FROM SHEAR PLANE.

FOR FILLET WELD SIZES SEE TABLE ON SHEET 43.

USE THE NUMBER OF BOLTS SHOWN IN DETAILS.

ALL CROSS FRAMES MATERIAL (INCLUDING BEARING STIFFENERS) SHALL BE SUBJECT TO CHARPY V-NOTCH TESTING AS PER SPECIFICATIONS.

Mark	Description	By	Chk'd.	App'd.	Date
REVISIONS					

COMMONWEALTH OF PENNSYLVANIA
DEPARTMENT OF TRANSPORTATION

ARMSTRONG COUNTY
S.R. 0128 SEC. 013
SEG. 0250 OFFSET 0
S.R. 0128 STA. 1+671.500
OVER ALLEGHENY RIVER & PITTSBURG & SHAWMUT R.R.
3-SPAN CONTINUOUS STEEL PLATE GIRDER BRIDGE
CROSS FRAME CF-3 DETAILS

REGISTERED PROFESSIONAL ENGINEER
MICHAEL J. BONKOVICH
043452-R
COMMONWEALTH OF PENNSYLVANIA

RECOMMENDED JAN 26 1998

SHEET 49 OF 112

S-22234

Designed by:	SDV/LAC
Checked by:	MJB
Drawn by:	EEM

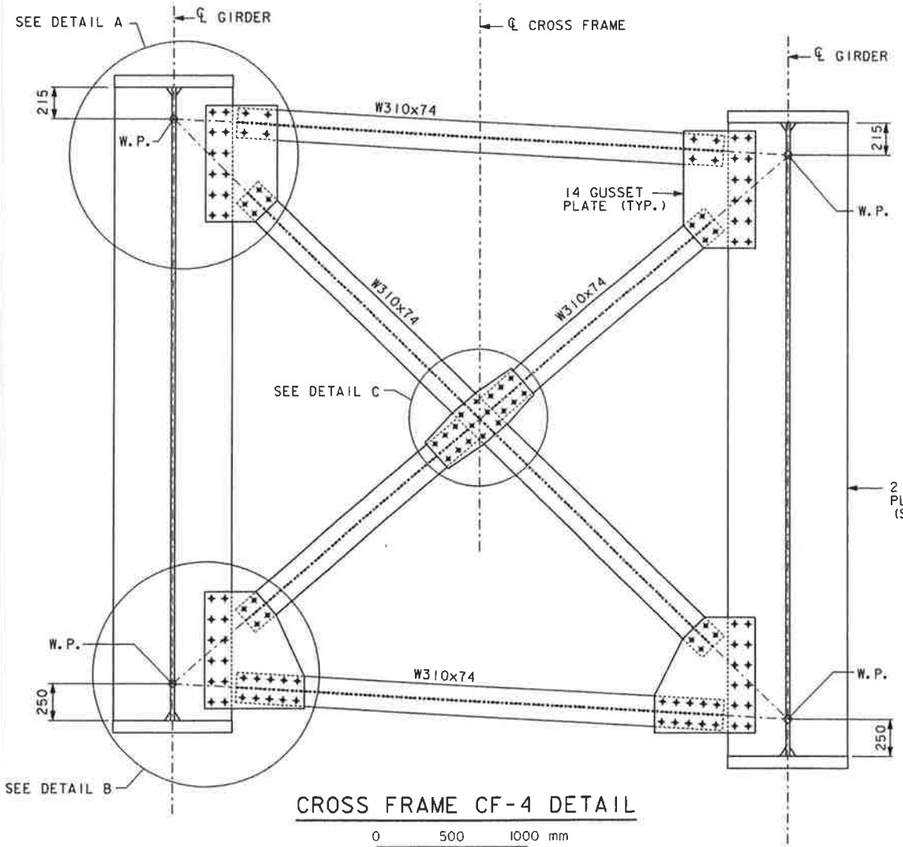

CROSS FRAME CF-4 DETAIL

0 500 1000 mm

SCALE = 1:20

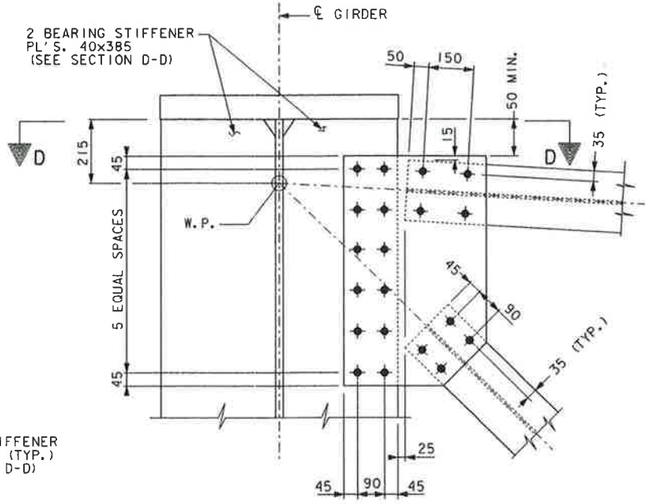

DETAIL A

0 200 400 mm

SCALE = 1:10

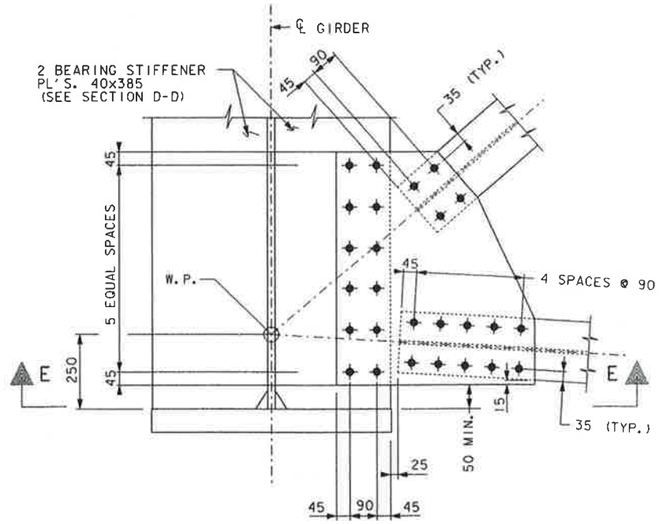

DETAIL B

0 200 400 mm

SCALE = 1:10

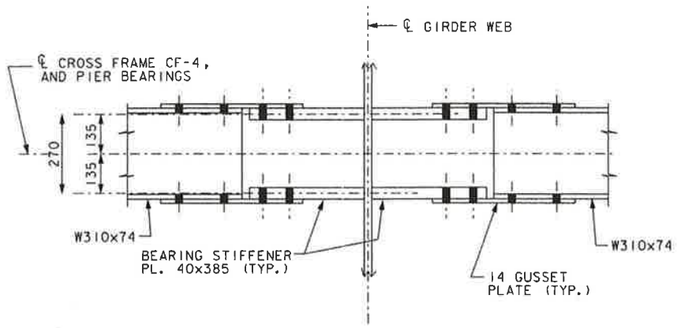

SECTION D-D
(SECTION E-E SIMILAR)

0 200 400 mm

SCALE = 1:10

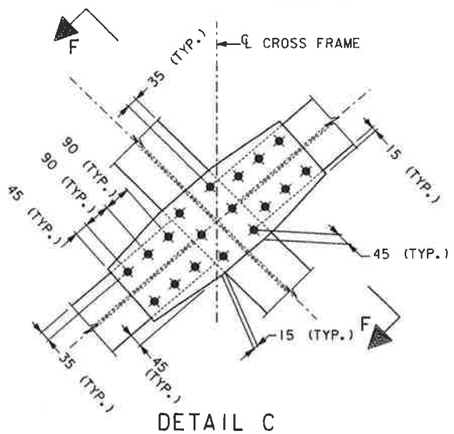

DETAIL C

0 200 400 mm

SCALE = 1:10

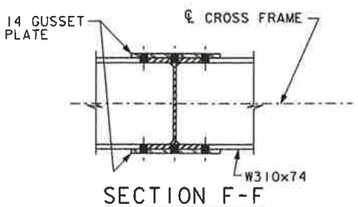

SECTION F-F

0 200 400 mm

SCALE = 1:10

NOTES:

FOR LOCATION OF CROSS FRAMES, SEE SHEETS 36 AND 37.

FOR CROSS FRAME DETAILS NOT SHOWN, SEE BC-754M.

FOR BEARING STIFFENER DETAILS, SEE SHEET 42.

USE 27.0mm DIAMETER HOLES IN BEARING STIFFENERS, GUSSET PLATES, AND CROSS FRAME MEMBERS.

USE 25.4mm DIAMETER AASHTO M164 BOLTS WITH THREADS EXCLUDED FROM SHEAR PLANE.

USE THE NUMBER OF BOLTS SHOWN IN DETAILS.

ALL CROSS FRAMES MATERIAL (INCLUDING BEARING STIFFENERS) SHALL BE SUBJECT TO CHARPY V-NOTCH TESTING AS PER SPECIFICATIONS.

Mark	Description	By	Chk'd.	App'd.	Date
REVISIONS					

Designed by:	SDV/LAC
Checked by:	MJB
Drawn by:	EEM

COMMONWEALTH OF PENNSYLVANIA
DEPARTMENT OF TRANSPORTATION

ARMSTRONG COUNTY
S.R. 0128 SEC. 013
SEG. 0250 OFFSET 0
S.R. 0128 STA. 1+671.500
OVER ALLEGHENY RIVER & PITTSBURG & SHAWMUT R.R.
3-SPAN CONTINUOUS STEEL PLATE GIRDER BRIDGE
CROSS FRAME CF-4 DETAILS

COMMONWEALTH OF PENNSYLVANIA REGISTERED PROFESSIONAL MICHAEL J. BONKOVICH ENGINEER 043452-R

RECOMMENDED JAN 26 1998

SHEET 50 OF 112

S-22234

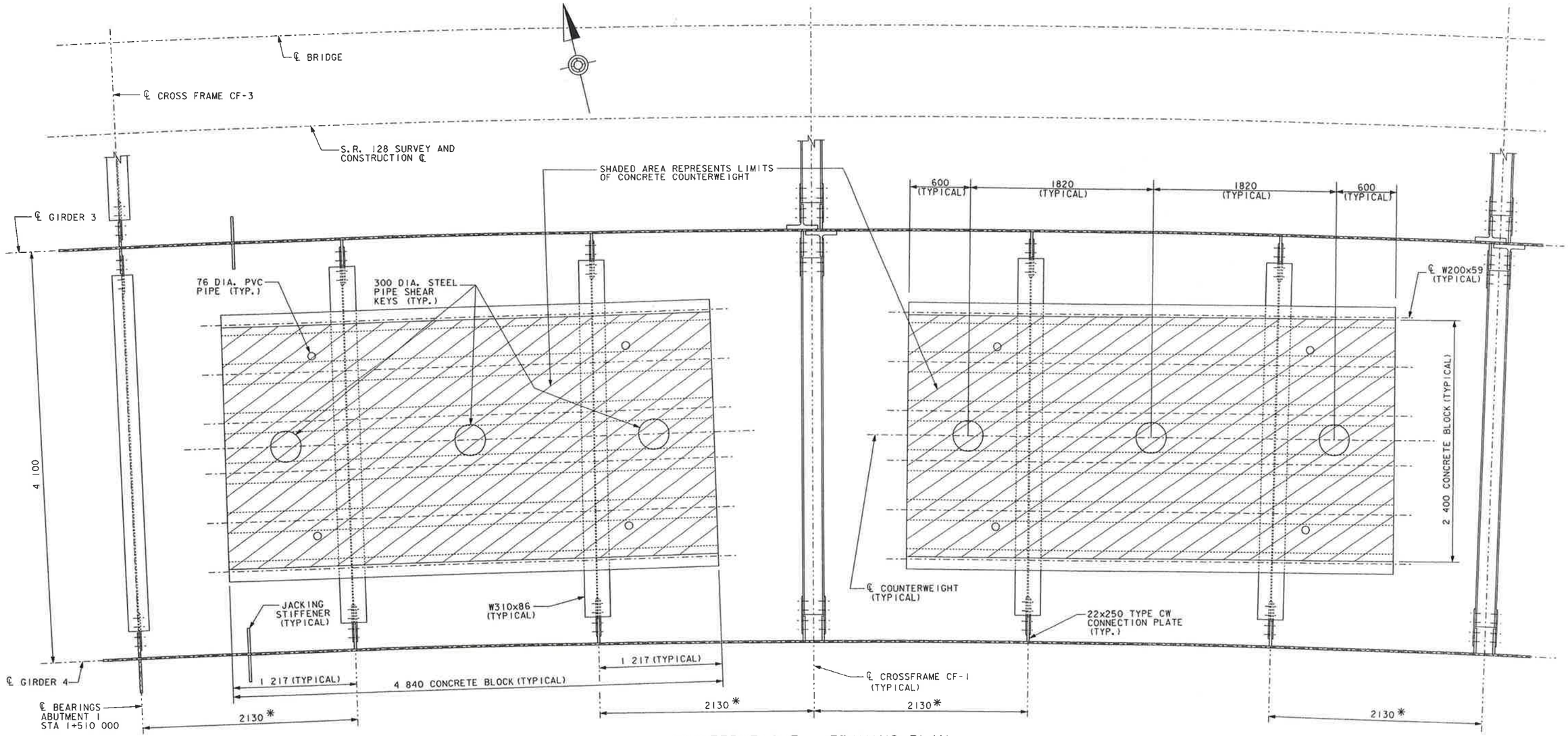

COUNTERWEIGHT - FRAMING PLAN

0 500 1000 mm

SCALE = 1:20

* MEASURED ALONG ℄ OF GIRDER 4

Mark	Description	By	Chk'd.	App'd.	Date
REVISIONS					

NOTES:

ALL COUNTERWEIGHT COMPONENTS PLACED LEVEL.

FOR CROSS SECTION OF COUNTERWEIGHT, SEE SHEET 52.

UNDER FULL DEAD LOAD, ALL COUNTERWEIGHT CONNECTION PLATES ARE VERTICAL TO WITHIN APPLICABLE AASHTO/AWS FABRICATION AND CONSTRUCTION TOLERANCES.

COMMONWEALTH OF PENNSYLVANIA
REGISTERED PROFESSIONAL
MICHAEL J. BONKOVICH
ENGINEER
043452-R
PENNSYLVANIA

COMMONWEALTH OF PENNSYLVANIA
DEPARTMENT OF TRANSPORTATION

ARMSTRONG COUNTY
S.R. 0128 SEC. 013
SEG. 0250 OFFSET 0
S.R. 0128 STA. 1+671.500
OVER ALLEGHENY RIVER & PITTSBURG & SHAWMUT R.R.
3-SPAN CONTINUOUS STEEL PLATE GIRDER BRIDGE
CONCRETE COUNTERWEIGHT PLAN

RECOMMENDED JAN 26 1998

SHEET 51 OF 112

S-22234

Designed by:	LAC
Checked by:	VN
Drawn by:	SGW

D:\DESIGN\FORDCITY\FINAL\SUPER\DWG\FC01GDOT.DGN 01/02/98 10:20:14 (S:\PAPER\FC01GDOT.PRF) (S.O. NUMBER: 22430-002-0013-000013)

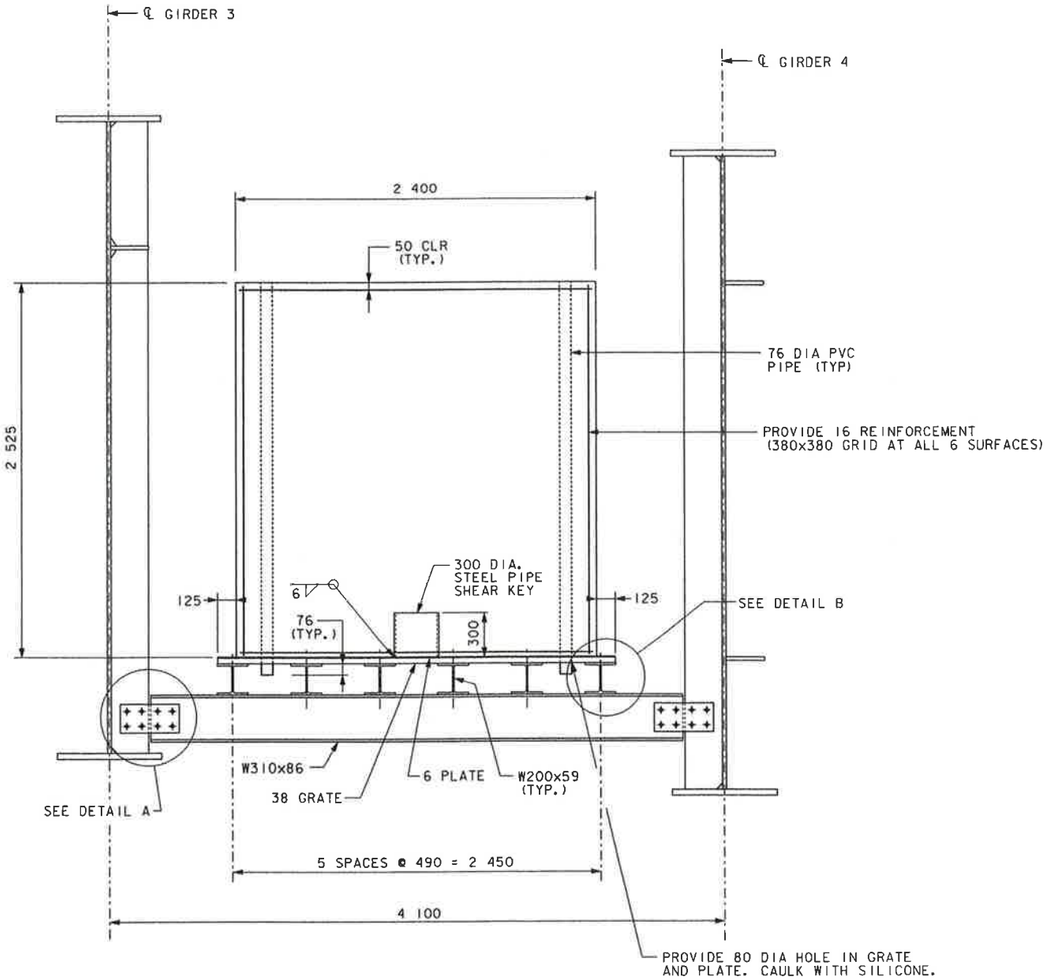

COUNTERWEIGHT - CROSS SECTION

0 500 1000 mm

SCALE = 1:20

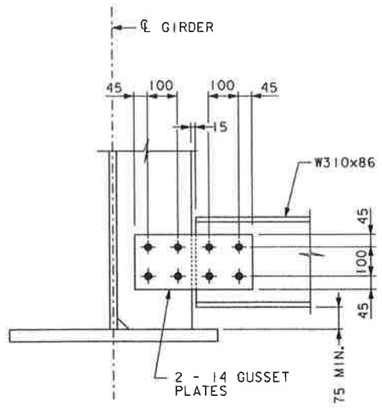

DETAIL A

0 200 400 mm

SCALE = 1:10

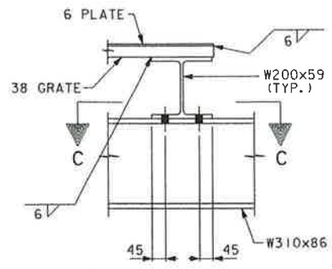

DETAIL B

0 200 400 mm

SCALE = 1:10

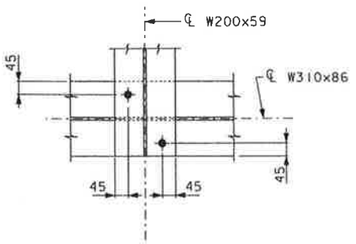

SECTION C-C

0 200 400 mm

SCALE = 1:10

NOTES:

ALL COUNTERWEIGHT COMPONENTS PLACED LEVEL.

FOR LOCATION OF COUNTERWEIGHT, SEE SHEET 36 AND 51.

USE 22.2 DIAMETER AASHTO M164 H.S. BOLTS FOR ALL COUNTERWEIGHT CONNECTIONS.

MAXIMUM WEIGHT FOR 38 GRATE IS 57.6 Kg/M².

USE CLASS A CEMENT CONCRETE FOR THE COUNTERWEIGHTS.

Mark	Description	By	Chk'd.	App'd.	Date
REVISIONS					

Designed by:	LAC
Checked by:	VN
Drawn by:	EEM

COMMONWEALTH OF PENNSYLVANIA
DEPARTMENT OF TRANSPORTATION

ARMSTRONG COUNTY
S.R. 0128 SEC. 013
SEG. 0250 OFFSET 0
S.R. 0128 STA. 1+671.500
OVER ALLEGHENY RIVER & PITTSBURG & SHAWMUT R.R.
3-SPAN CONTINUOUS STEEL PLATE GIRDER BRIDGE
CONCRETE COUNTERWEIGHT CROSS SECTION

COMMONWEALTH OF PENNSYLVANIA REGISTERED PROFESSIONAL MICHAEL J. BONKOVICH ENGINEER 043452-R

RECOMMENDED JAN 26 1998

SHEET 52 OF 112

S-22234

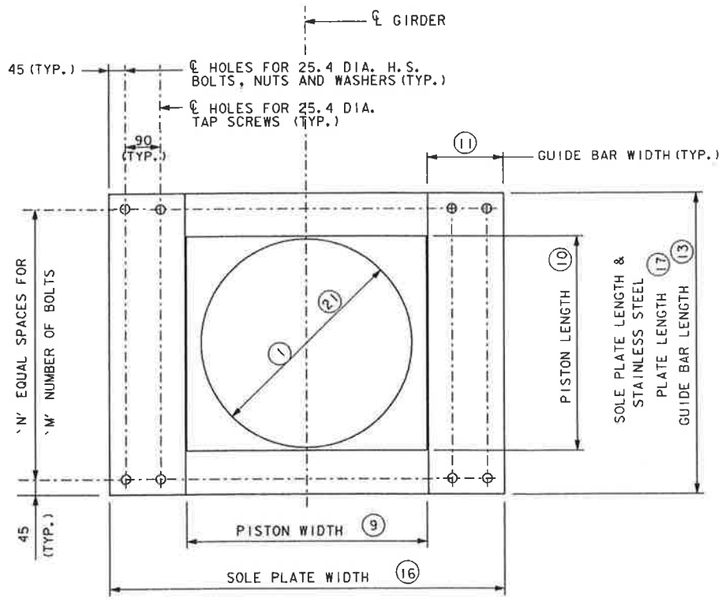

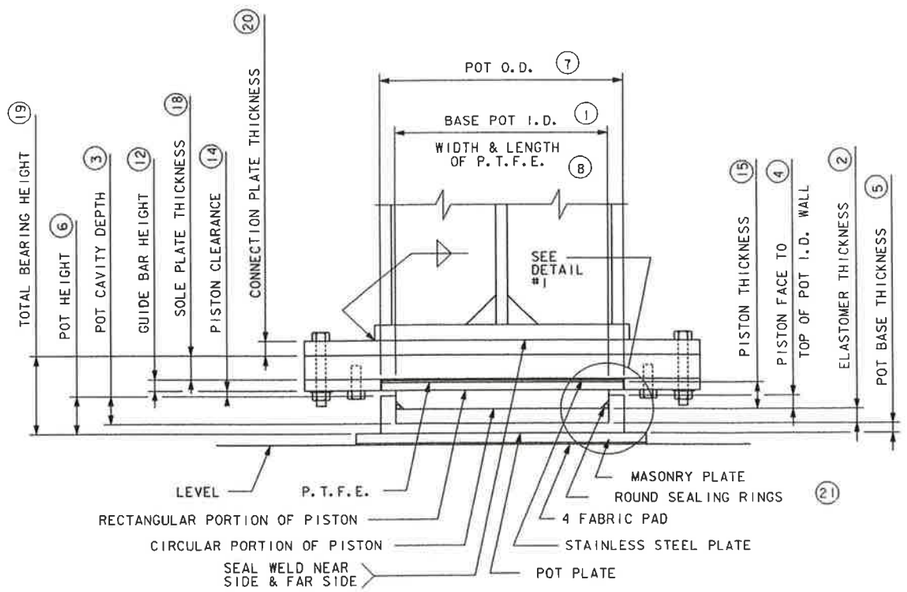

EXPANSION BEARING

NO SCALE

NOTE: GUIDED EXPANSION BEARING SHOWN.
FOR NON-GUIDED EXPANSION BEARING,
OMIT GUIDE BAR DETAILS AND TAP SCREWS.

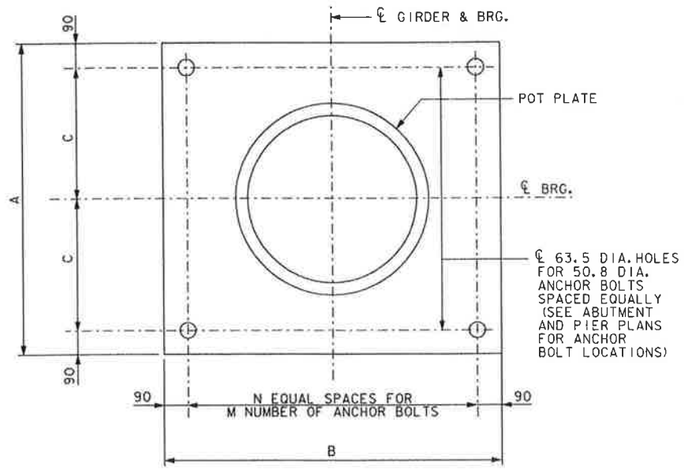

MASONRY PLATE

NO SCALE

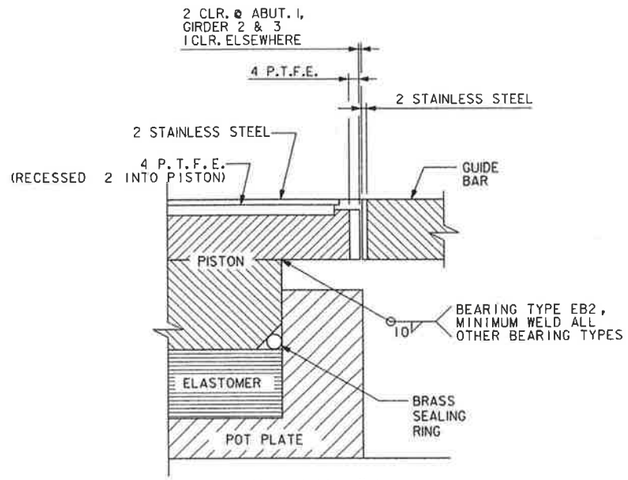

DETAIL #1

NO SCALE

NOTES:

FOR BEARING DIMENSIONS, SEE SHEET 55.
ALL WELDS ARE 8 MINIMUM UNLESS NOTED OTHERWISE.
FOR ADDITIONAL BEARING NOTES, SEE SHEET 56.
ALLOWABLE COEFFICIENT OF FRICTION IS 0.04.
USE BRASS SEALING RINGS.

Mark	Description	By	Chk'd.	App'd.	Date
REVISIONS					

COMMONWEALTH OF PENNSYLVANIA
DEPARTMENT OF TRANSPORTATION

ARMSTRONG COUNTY
S.R. 0128 SEC. 013
SEG. 0250 OFFSET 0
S.R. 0128 STA. 1+671.500
OVER ALLEGHENY RIVER & PITTSBURG & SHAWMUT R.R.
3-SPAN CONTINUOUS STEEL PLATE GIRDER BRIDGE
EXPANSION POT BEARING DETAILS

COMMONWEALTH OF PENNSYLVANIA REGISTERED PROFESSIONAL MICHAEL J. BONKOVICH ENGINEER 043452-R

RECOMMENDED JAN 26 1998

SHEET 53 OF 112

S-22234

Designed by:	KEK
Checked by:	ELR
Drawn by:	SGW

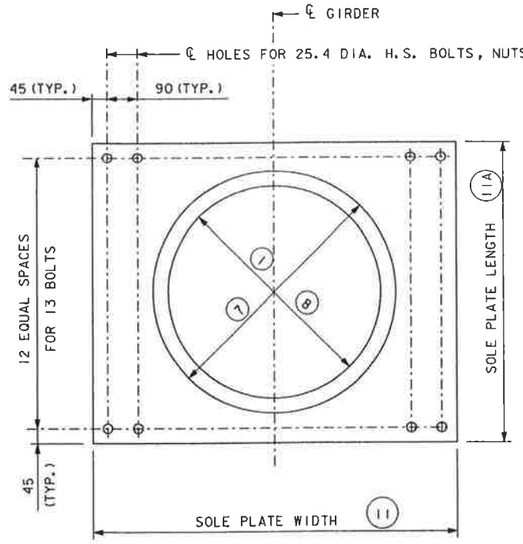

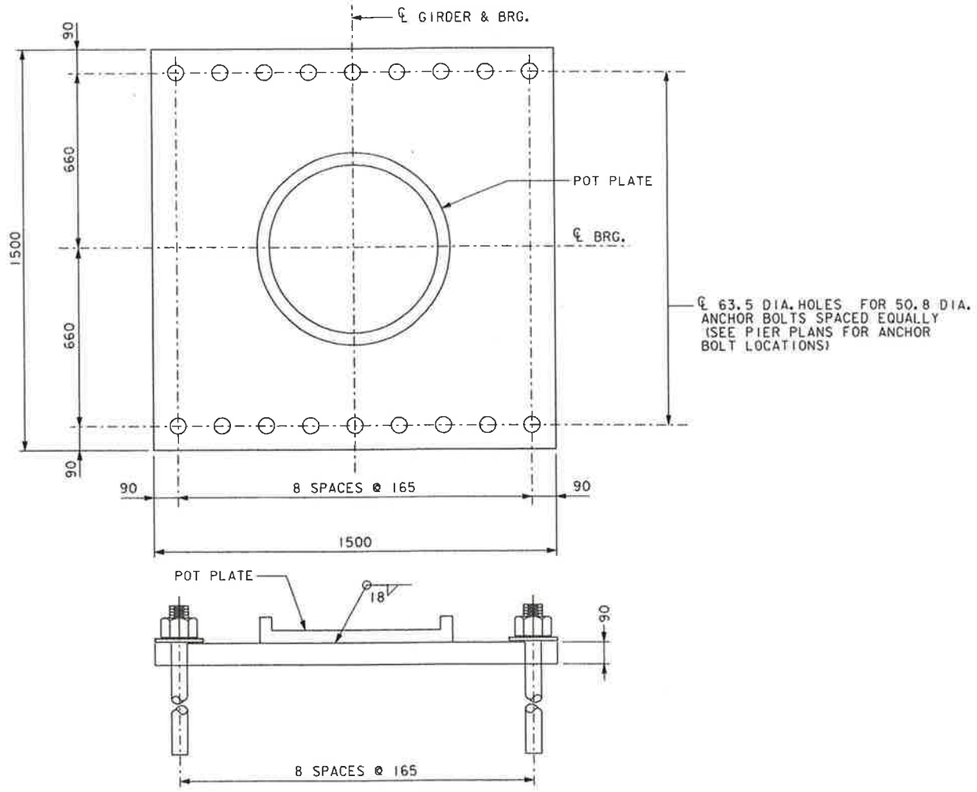

MASONRY PLATE

NO SCALE

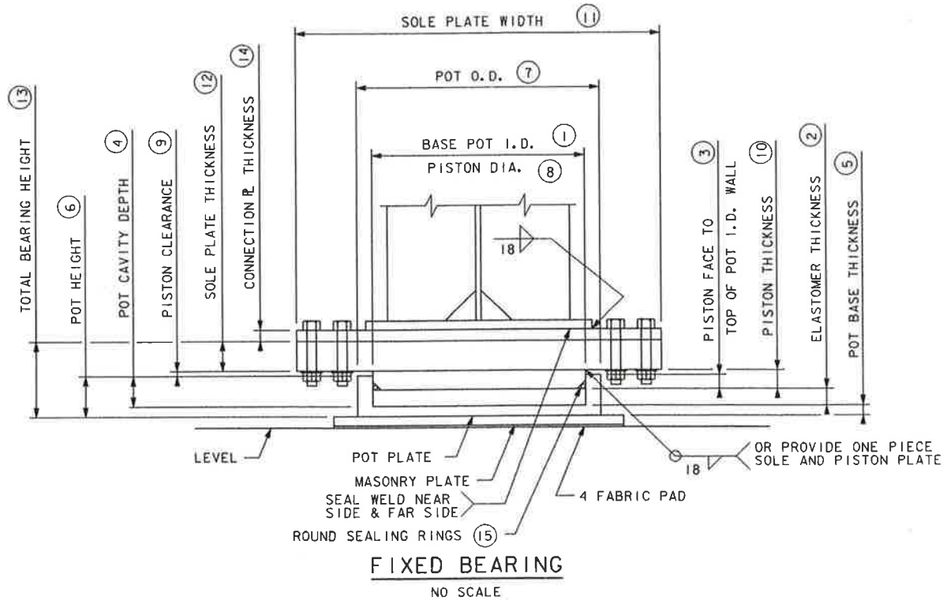

FIXED BEARING

NO SCALE

NOTES:

FOR BEARING DIMENSIONS, SEE SHEET 55.

ALL WELDS ARE 8 MINIMUM UNLESS NOTED OTHERWISE.

FOR ADDITIONAL BEARING NOTES, SEE SHEET 56.

ALLOWABLE COEFFICIENT OF FRICTION IS 0.04.

USE BRASS SEALING RINGS.

DIMENSIONS SHOWN ARE FOR BOTH BEARING TYPE FB1 AND FB2.

Mark	Description	By	Chk'd.	App'd.	Date
REVISIONS					

COMMONWEALTH OF PENNSYLVANIA
DEPARTMENT OF TRANSPORTATION

ARMSTRONG COUNTY
S.R. 0128 SEC. 013
SEG. 0250 OFFSET 0
S.R. 0128 STA. 1+671.500
OVER ALLEGHENY RIVER & PITTSBURG & SHAWMUT R.R.
3-SPAN CONTINUOUS STEEL PLATE GIRDER BRIDGE
FIXED POT BEARING DETAILS

COMMONWEALTH OF PENNSYLVANIA REGISTERED PROFESSIONAL MICHAEL J. BONKOVICH ENGINEER 043452-R

RECOMMENDED JAN 26 1998

SHEET 54 OF 112

S-22234

Designed by:	KEK
Checked by:	ELR
Drawn by:	SGW

EXPANSION BEARING DIMENSIONS

LOCATION	BEARING TYPE	VERTICAL LOAD DESIGN KN	VERTICAL LOAD CAPACITY KN	1	2	3	4	5	6	7	8	9	10	11	12	13	14	15	16	17	18	19*	20*	21	N	M	P.T.F.E. THICKNESS	STAINLESS STEEL THICKNESS	BRASS RING DIAMETER
ABUT. 1, GIRDER 1	EB1	5 645	6 160	585	70	110	40	35	145	665	585	665	665	N/A	N/A	N/A	15	90	995	915	90	289	46	585	5	6	4	2	10
ABUT. 1, GIRDER 2 & 3	EB2	2 994	3 407	435	55	90	35	25	115	510	435	510	510	185	50	815	24	105	896	815	85	274	38	435	8	9	4	2	8
ABUT. 1, GIRDER 4	EB3	2 144	2 335	360	45	80	35	30	110	435	360	435	435	N/A	N/A	N/A	15	80	890	715	70	229	36	360	4	5	4	2	8
PIER 2, ALL GIRDERS	EB4	8 309	8 571	690	85	135	50	40	175	790	690	790	790	183	50	1 070	34	130	1 170	1 070	115	374	62	690	10	11	4	2	12.5
ABUT. 2, GIRDER 1 & 4	EB5	2 429	2 669	385	50	85	35	25	110	445	385	445	445	N/A	N/A	N/A	20	80	890	815	95	254	50	385	5	6	4	2	8
ABUT. 2, GIRDER 2 & 3	EB6	2 349	2 669	385	50	85	35	25	110	445	385	445	445	216	50	815	24	105	891	815	95	279	50	385	5	6	4	2	8

* - THICKNESS AT ℄ OF BEARING

FIXED BEARING DIMENSIONS

LOCATION	BEARING TYPE	VERTICAL LOAD DESIGN KN	VERTICAL LOAD CAPACITY KN	1	2	3	4	5	6	7	8	9	10	11	11A	12	13*	14*	15	BRASS RING DIAMETER
PIER 1, GIRDER 1 & 2	FB1	9 367	9 861	740	90	60	150	40	190	835	739	20	80	1 300	1 300	125	335	85	740	12.5
PIER 1, GIRDER 3 & 4	FB2	9 367	9 861	740	90	60	150	40	190	835	739	20	80	1 170	1 170	110	320	83	740	12.5

* - THICKNESS AT ℄ OF BEARING

MASONRY PLATE DIMENSIONS

LOCATION	A	B	C	T	N	M	TOTAL NUMBER OF ANCHOR BOLTS
ABUT. 1, GIRDER 1	1 195	1 195	507.5	85	2	3	6
ABUT. 1, GIRDER 2 & 3	1 095	1 170	457.5	80	3	4	8
ABUT. 1, GIRDER 4	995	815	407.5	65	2	3	6
PIER 2, ALL GIRDERS	1 400	1 400	610	95	3	4	8
ABUT. 2, GIRDER 1 & 4	860	965	340	85	2	3	6
ABUT. 2, GIRDER 2 & 3	860	1 145	340	90	2	3	6

BEVELED CONNECTION PLATE DIMENSIONS

LOCATION	G	T1	T2
ABUT. 1, GIRDER 1	-3.00%	60	32
ABUT. 1, GIRDER 2 & 3	-3.00%	50	25
ABUT. 1, GIRDER 4	-3.00%	47	25
PIER 1, GIRDER 1 & 2	-3.00%	104	65
PIER 1, GIRDER 3 & 4	-3.00%	101	65
PIER 2, ALL GIRDERS	-4.38%	85	38
ABUT. 2, GIRDER 1 & 4	-5.98%	74	25
ABUT. 2, GIRDER 2 & 3	-5.98%	74	25

NOTES:

ALL DIMENSIONS ARE IN mm.

FOR BEARING DETAILS SEE SHEET 53 AND 54.

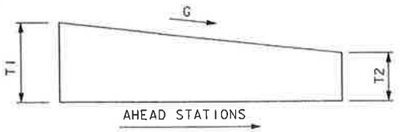

BEVELED CONNECTION PLATE DETAIL

NO SCALE

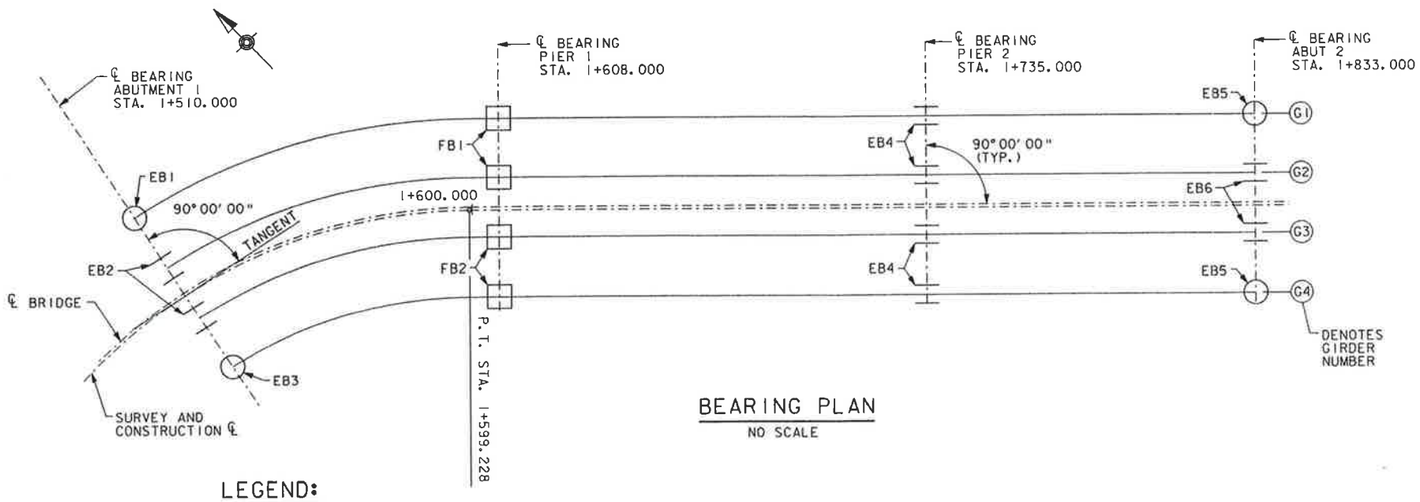

BEARING PLAN

NO SCALE

LEGEND:

- ◯ - INDICATES MULTI-ROTATIONAL NON-GUIDED EXPANSION BEARING
- □ - INDICATES MULTI-ROTATIONAL FIXED BEARING
- — - INDICATES MULTI-ROTATIONAL GUIDED EXPANSION BEARING

Designed by:	KEK
Checked by:	ELR
Drawn by:	FEM

Mark	Description	By	Chk'd.	App'd.	Date
REVISIONS					

COMMONWEALTH OF PENNSYLVANIA
DEPARTMENT OF TRANSPORTATION

ARMSTRONG COUNTY
S.R. 0128 SEC. 013
SEG. 0250 OFFSET 0
S.R. 0128 STA. 1+671.500
OVER ALLEGHENY RIVER & PITTSBURG & SHAWMUT R.R.
3-SPAN CONTINUOUS STEEL PLATE GIRDER BRIDGE
POT BEARING DETAILS - 1

COMMONWEALTH OF PENNSYLVANIA REGISTERED PROFESSIONAL MICHAEL J. BONKOVICH ENGINEER 043452-E

RECOMMENDED JAN 28 1998

SHEET 55 OF 112

S-22234

POT BEARING SCHEDULE

LOCATION	GIRDER NUMBER	BEARING DESIGN LOADS, KN SERVICE LOADS										DESIGN MOVEMENTS (mm) ***	DESIGN ROTATION (RADIANS)	GIRDER BOTTOM FLANGE UNDERSIDE ELEVATION	MAXIMUM STRESS ON TEFLON (MPa)	MAXIMUM STRESS ON ELASTOMER (MPa)	BEARING TYPE
		GROUP I				GROUP V			GROUP VII								
		VERTICAL LOAD			HORIZONTAL LOAD	VERTICAL LOAD		HORIZONTAL LOAD	VERTICAL LOAD	HORIZONTAL LOAD							
		DEAD LOAD	LL+I** MINIMUM	LL+I** MAXIMUM		DEAD LOAD	W			TRANSVERSE	LONGITUDINAL						
ABUT. 1	1	4 457*	- 387	1 188	618	4 457*	169	414	4 457*	--	--	155	0.03	259.035	16	21	EXPANSION
	2	2 366*	- 116	627	458	2 366*	169	818	2 366*	1 365	--	155	0.03	259.074	16	20	GUIDED EXPANSION
	3	1 846*	- 49	485	458	1 846*	169	818	1 846*	1 365	--	155	0.03	258.840	16	20	GUIDED EXPANSION
	4	1 628*	- 258	516	236	1 628*	169	414	1 628*	--	--	155	0.03	258.594	17	21	EXPANSION
PIER 1	1	7 606	- 552	1 761	987	7 606	374	2 936	7 606	1 678	4 261	N/A	0.03	255.997	N/A	22	FIXED
	2	7 526	- 67	1 655	987	7 526	374	2 936	7 526	1 678	4 261	N/A	0.03	256.020	N/A	22	FIXED
	3	7 237	- 165	1 855	987	7 237	374	2 936	7 237	1 678	4 261	N/A	0.03	255.830	N/A	22	FIXED
	4	5 258	- 356	1 775	987	5 258	374	2 936	5 258	1 678	4 261	N/A	0.03	255.622	N/A	22	FIXED
PIER 2	1	6 450*	- 107*	961*	858	6 450*	374	1 864	6 450*	1 357	--	180	0.03	251.328	17	22	GUIDED EXPANSION
	2	6 023	- 151	1 583	858	6 023	374	1 864	6 023	1 357	--	180	0.03	251.463	17	22	GUIDED EXPANSION
	3	6 040	- 98	1 615	858	6 040	374	1 864	6 040	1 357	--	180	0.03	251.510	17	22	GUIDED EXPANSION
	4	6 436	- 147	1 873	858	6 436	374	1 864	6 436	1 357	--	180	0.03	251.352	17	22	GUIDED EXPANSION
ABUT. 2	1	2 010*	- 76*	378*	267	2 010*	160	289	2 010*	--	--	280	0.03	246.111	16	21	EXPANSION
	2	1 721	- 102	627	267	1 721	160	738	1 721	761	--	280	0.03	246.252	16	20	GUIDED EXPANSION
	3	1 672	- 102	636	267	1 672	160	738	1 672	761	--	280	0.03	246.381	16	20	GUIDED EXPANSION
	4	1 686	- 165	743	267	1 686	160	289	1 686	--	--	280	0.03	246.370	16	21	EXPANSION

* - OCCURS DURING REDECKING.

** - FINAL LIVELOAD + IMPACT, INCLUDING SIDEWALK, UNLESS OTHERWISE NOTED.

*** - INCLUDES 25 mm ADDITIONAL MOVEMENT IN EACH DIRECTION

NOTE:
THE ABOVE FORCES ARE ACTUAL SERVICE LOADS. THE PERCENTAGE INCREASE OF THE ALLOWABLE UNIT STRESS (AS PER COLUMN 14 OF AASHTO TABLE 3.22.1A) HAS NOT BEEN FACTORED INTO THESE VALUES.

POT BEARING SCHEDULE NOTES:

1. DEAD LOAD = DL1 + DL2
2. W = WIND ON STRUCTURE
3. TEFLON AND ELASTOMER MAXIMUM ALLOWABLE STRESS = 24 MPa
4. N/A - NOT APPLICABLE
5. GROUP LOADS SHOWN IN POT BEARING SCHEDULE REPRESENT GOVERNING LOAD CASES.

POT BEARING NOTES

THESE POT BEARINGS ARE DESIGNED IN ACCORDANCE WITH THE PENNSYLVANIA DEPARTMENT OF TRANSPORTATION DESIGN MANUAL PART 4, AUGUST 1993 EDITION, (INCLUDING JANUARY 1994 AND AUGUST 1995 REVISIONS) AND 1992 AASHTO STANDARD SPECIFICATIONS FOR HIGHWAY BRIDGES INCLUDING 1993 AND 1994 AASHTO INTERIM SPECIFICATIONS.

PROVIDE MATERIALS, FABRICATE AND INSTALL THE BEARINGS IN ACCORDANCE WITH AASHTO SPECIFICATIONS AND THE 1996 EDITION FOR PUBLICATION 408M, INCLUDING SECTION 1111.

BEARINGS SHOWN ON THE DATA TABLE ON SHEET 55 SHALL BE FABRICATED USING AASHTO M270/M270M, GRADE 345 STEEL. ALTERNATE CONTRACTOR-DESIGNED BEARINGS SHALL BE FABRICATED USING AASHTO M270/M270M, GRADE 250 OR AASHTO M270/M270M, GRADE 345 STEEL.

ADJUST BEARING SEAT ELEVATIONS AS NECESSARY, BASED ON THE ACTUAL BEARING DEPTH AS SUPPLIED BY THE BEARING MANUFACTURER.

THE COEFFICIENT OF FRICTION FOR THE PTFE/ STAINLESS STEEL IS TO BE 0.04 MAXIMUM.

THE ROTATIONS INDICATED IN THE BEARING TABLE INCLUDE BOTH DEAD AND LIVE LOAD MOVEMENT.

DO NOT DISMANTLE THE BEARING UNIT DURING SHIPPING OR CONSTRUCTION UNLESS DIRECTED BY THE BEARING MANUFACTURER. PROTECT THE BEARINGS FROM DAMAGE DURING CONSTRUCTION IN ACCORDANCE WITH THE MANUFACTURER'S RECOMMENDATIONS.

PROTECT THE ELASTOMERIC AND PTFE MATERIALS FROM ANY WELDING HEAT, SPARKS AND FLASH IN ACCORDANCE WITH THE MANUFACTURER'S RECOMMENDATIONS. UNDER NO CIRCUMSTANCES SHALL THE TEMPERATURE OF THE METAL EXCEED 300°F (150°C). CONTROL THE TEMPERATURE BY WELDING PROCEDURES AND TEMPERATURE-INDICATING CRAYONS OR OTHER DEVICES APPROVED BY THE ENGINEER.

PROVIDE AASHTO M270/M270M, GRADE 345 STEEL CONNECTION AND MASONRY PLATES AS SHOWN.

PROVIDE ASTM A167 OR ASTM A240, TYPE 304 STAINLESS STEEL SHEETS. WHERE THE STAINLESS STEEL IS IN CONTACT WITH THE PTFE SHEETS, PROVIDE AN ANSI 0.4 MICRO-METERS SURFACE FINISH OR LESS.

PAINT ALL EXPOSED STEEL SURFACES INCLUDING THE UNDERSIDE OF THE POT AND MASONRY PLATES. APPLY ALL COATS OF PAINT IN THE SHOP. MASK THE BEARING BEFORE SURFACE PREPARATION AND PAINTING OF THE SUPERSTRUCTURE NEAR THE BEARING AREAS.

FOR ANCHOR BOLT DETAILS, SEE THE SUBSTRUCTURE DRAWINGS.

THE DESIGN ROTATION INCLUDES A CONSTRUCTION TOLERANCE OF 0.02 RADIANS.

IN THE CASE OF A CONTRACTOR'S ALTERNATE BEARING DESIGN:

DESIGN THE COMPLETE BEARING ASSEMBLY FOR THE LOADS, ROTATION AND MOVEMENTS SHOWN IN THE BEARING DATA TABLE. ALL LOADS SHOWN ARE SERVICE LOADS. PROVIDE A BOLTED TOP CONNECTION PLATE FOR THE LOADS, ROTATION AND MOVEMENTS GIVEN. CHECK THE GIRDER FLANGES, WEB AND BEARING STIFFENERS TO VERIFY THAT THE LOADS CAN BE TRANSFERRED FROM THE GIRDER TO THE BEARINGS WITHOUT OVERSTRESSING THE GIRDER OR BEARING STIFFENER. THE BEARING MANUFACTURER IS RESPONSIBLE FOR THE DESIGN OF ALL BEARINGS AND IS TO SUBMIT TO THE DEPARTMENT DESIGN CALCULATIONS ALONG WITH THE SHOP DRAWINGS OF THE BEARING ASSEMBLIES.

PROVIDE THE TOP BEARING (SOLE) PLATE FOR THE MOVEMENTS INDICATED IN THE BEARING DATA TABLE AND IN ACCORDANCE WITH DM-4, SECTION 19.2.1P. THE 25mm ADDITIONAL MOVEMENT IN EACH DIRECTION REQUIRED BY DM-4 IS INCLUDED IN THE VALUES OF THE BEARING DATA TABLE. BEVEL THE TOP CONNECTION OR SOLE PLATE LONGITUDINALLY AS REQUIRED TO MATCH THE ACTUAL BRIDGE GRADE. MARK THE THICKER END OF THE BEVELED PLATE CLEARLY SO THAT IT IS ERECTED CORRECTLY IN THE FIELD.

COMMONWEALTH OF PENNSYLVANIA REGISTERED PROFESSIONAL MICHAEL J. BONKOVICH ENGINEER 043452-R

Mark	Description	By	Chk'd.	App'd.	Date
REVISIONS					

COMMONWEALTH OF PENNSYLVANIA
DEPARTMENT OF TRANSPORTATION

ARMSTRONG COUNTY
S.R. 0128 SEC. 013
SEG. 0250 OFFSET 0
S.R. 0128 STA. 1+671.500
OVER ALLEGHENY RIVER & PITTSBURG & SHAWMUT R.R.
3-SPAN CONTINUOUS STEEL PLATE GIRDER BRIDGE
POT BEARING DETAILS - 2

RECOMMENDED JAN 26 1998

SHEET 56 OF 112

S-22234

Designed by:	KEK
Checked by:	ELR
Drawn by:	EEM

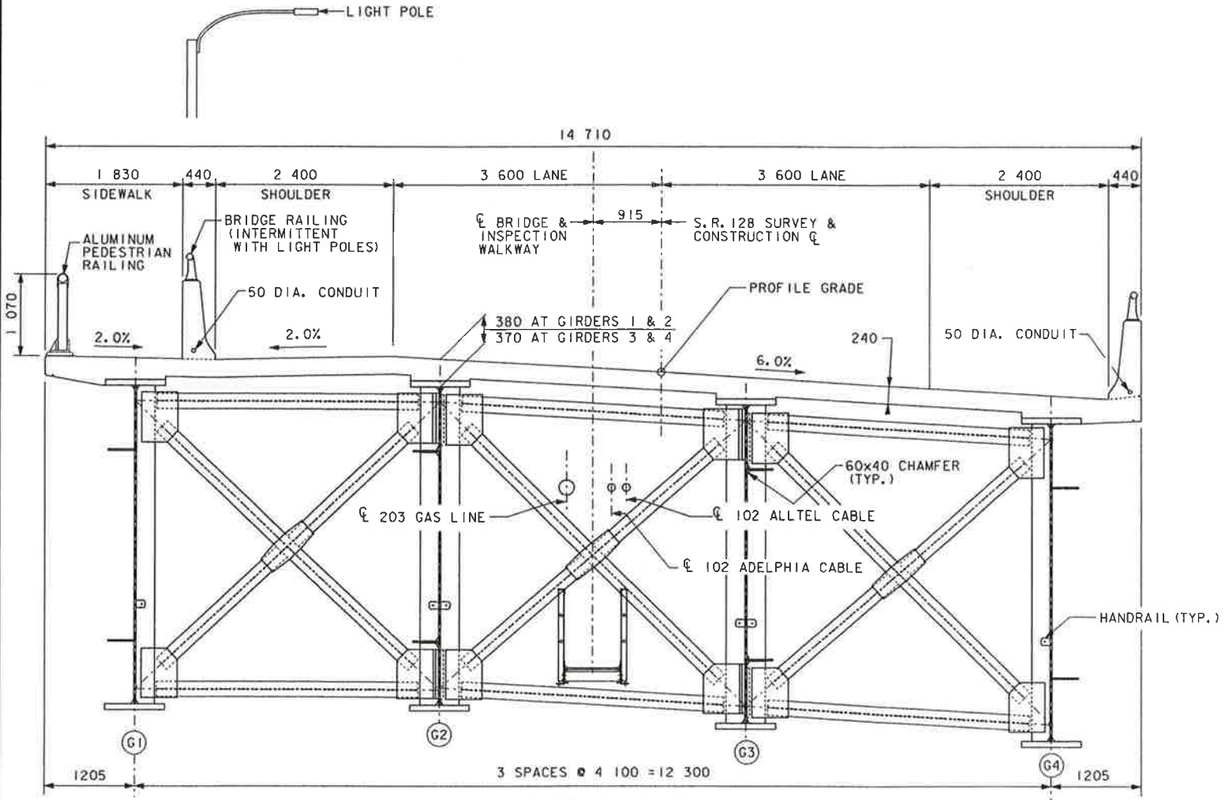

TYPICAL SUPERELEVATION SECTION

0 1000 2000 mm
SCALE = 1:40

LOOKING AHEAD STATIONS

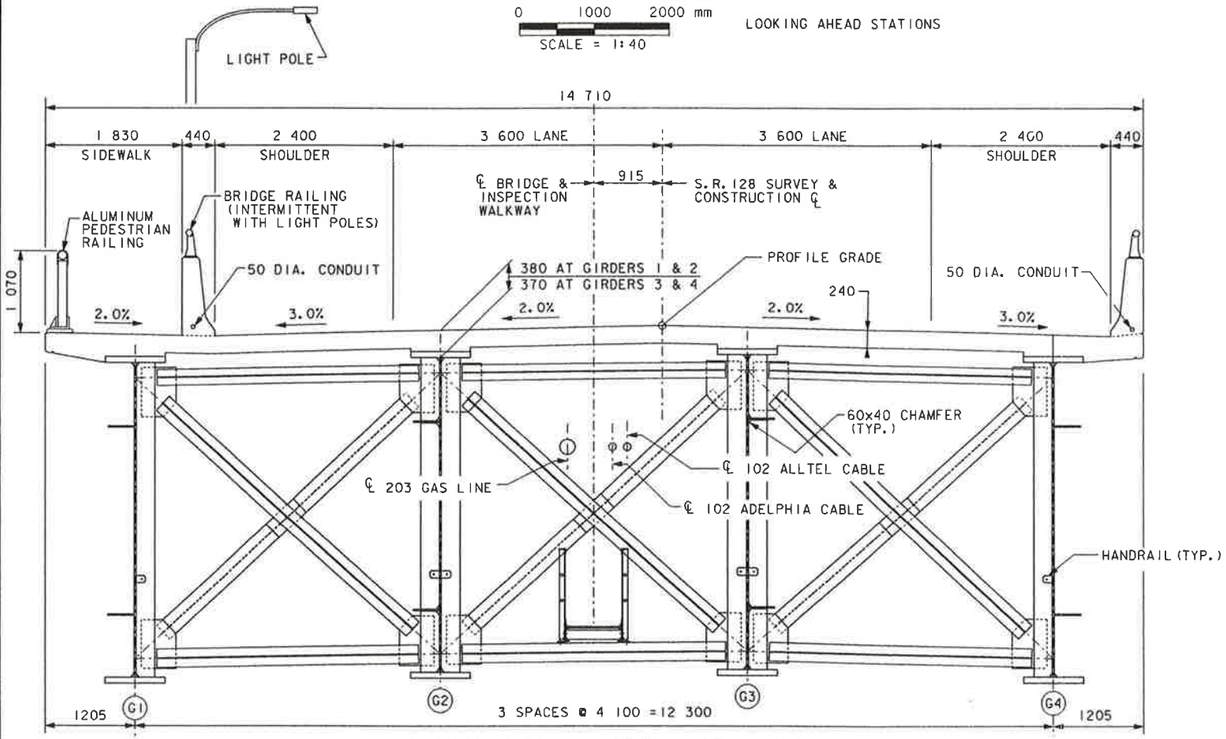

TYPICAL NORMAL CROWN SECTION

0 1000 2000 mm
SCALE = 1:40

LOOKING AHEAD STATIONS

Designed by:	MJB/LAC
Checked by:	GRL
Drawn by:	EEM
Checked by:	EDV

BRIDGE LOAD RATINGS WITH FUTURE WEARING SURFACE

		H20		HS25		ML80		P82	
		RATING FACTOR	tonne	RATING FACTOR	tonne	RATING FACTOR	tonne	RATING FACTOR	tonne
GIRDER 1	INVENTORY LEVEL	1.30	23.6	1.04	42.5	2.47	84.6	---	---
	OPERATING LEVEL	2.17	39.4	1.74	71.0	4.12	141.1	2.46	227.6
	ULTIMATE MOMENT CAPACITY	191 654.4 kN m		191 654.4 kN m		84 167.3 kN m		84 167.3 kN m	
	UTIMATE SHEAR CAPACITY	21 914.2 kN		21 914.2 kN		11 649.9 kN		11 649.9 kN	
	CONTROLLING CONDITION	FLEXURE		FLEXURE		FLEXURE		FLEXURE	
	CRITICAL LOCATION	SPAN 2, x = 000 mm		SPAN 2, x = 000 mm		SPAN 3, x = 58 802 mm		SPAN 3, x = 58 802 mm	
GIRDER 2	INVENTORY LEVEL	1.60	29.0	1.28	52.3	2.63	90.1	---	---
	OPERATING LEVEL	2.67	48.4	2.14	87.4	4.39	150.3	3.35	310.0
	ULTIMATE MOMENT CAPACITY	74 666.5 kN m		74 666.5 kN m		74 666.5 kN m		56 609.8 kN m	
	UTIMATE SHEAR CAPACITY	11 649.9 kN		11 649.9 kN		11 649.9 kN		4 323.7 kN	
	CONTROLLING CONDITION	FLEXURE		FLEXURE		FLEXURE		SHEAR	
	CRITICAL LOCATION	SPAN 3, x = 58 802 mm		SPAN 3, x = 58 802 mm		SPAN 3, x = 58 802 mm		SPAN 3, x = 98 000 mm	
GIRDER 3	INVENTORY LEVEL	1.54	27.9	1.23	50.2	2.49	85.3	---	---
	OPERATING LEVEL	2.57	46.6	2.05	83.7	4.15	142.1	3.38	312.8
	ULTIMATE MOMENT CAPACITY	79 596.1 kN m		79 596.1 kN m		79 596.1 kN m		56 609.8 kN m	
	UTIMATE SHEAR CAPACITY	11 649.9 kN		11 649.9 kN		11 649.9 kN		4 323.7 kN	
	CONTROLLING CONDITION	FLEXURE		FLEXURE		FLEXURE		SHEAR	
	CRITICAL LOCATION	SPAN 3, x = 58 802 mm		SPAN 3, x = 58 802 mm		SPAN 3, x = 58 802 mm		SPAN 3, x = 98 000 mm	
GIRDER 4	INVENTORY LEVEL	1.36	24.7	1.09	44.5	2.12	72.6	---	---
	OPERATING LEVEL	2.26	41.0	1.81	73.9	3.53	120.9	2.18	201.7
	ULTIMATE MOMENT CAPACITY	84 167.3 kN m		84 167.3 kN m		56 303.8 kN m		56 303.8 kN m	
	UTIMATE SHEAR CAPACITY	11 649.9 kN		11 649.9 kN		10 164.2 kN		10 164.2 kN	
	CONTROLLING CONDITION	FLEXURE		FLEXURE		FLEXURE		FLEXURE	
	CRITICAL LOCATION	SPAN 3, x = 58 802 mm		SPAN 3, x = 58 802 mm		SPAN 3, x = 82 760 mm		SPAN 3, x = 82 760 mm	

BRIDGE LOAD RATINGS WITHOUT FUTURE WEARING SURFACE

		H20		HS25		ML80		P82	
		RATING FACTOR	tonne	RATING FACTOR	tonne	RATING FACTOR	tonne	RATING FACTOR	tonne
GIRDER 1	INVENTORY LEVEL	1.42	25.8	1.14	46.5	2.75	94.2	---	---
	OPERATING LEVEL	2.37	43.0	1.90	77.6	4.59	157.2	2.73	252.6
	ULTIMATE MOMENT CAPACITY	191 654.4 kN m		191 654.4 kN m		84 167.3 kN m		84 167.3 kN m	
	UTIMATE SHEAR CAPACITY	21 914.2 kN		21 914.2 kN		11 649.9 kN		11 649.9 kN	
	CONTROLLING CONDITION	FLEXURE		FLEXURE		FLEXURE		FLEXURE	
	CRITICAL LOCATION	SPAN 2, x = 000 mm		SPAN 2, x = 000 mm		SPAN 3, x = 58 802 mm		SPAN 3, x = 58 802 mm	
GIRDER 2	INVENTORY LEVEL	1.78	32.3	1.42	58.0	2.84	97.3	---	---
	OPERATING LEVEL	2.96	53.7	2.37	96.8	4.73	162.0	3.58	331.3
	ULTIMATE MOMENT CAPACITY	74 666.5 kN m		74 666.5 kN m		56 609.8 kN m		56 609.8 kN m	
	UTIMATE SHEAR CAPACITY	11 649.9 kN		11 649.9 kN		4 323.7 kN		4 323.7 kN	
	CONTROLLING CONDITION	FLEXURE		FLEXURE		SHEAR		SHEAR	
	CRITICAL LOCATION	SPAN 3, x = 58 802 mm		SPAN 3, x = 58 802 mm		SPAN 3, x = 98 000 mm		SPAN 3, x = 98 000 mm	
GIRDER 3	INVENTORY LEVEL	1.69	30.7	1.35	55.1	2.74	93.8	---	---
	OPERATING LEVEL	2.82	51.2	2.26	92.3	4.56	156.2	3.61	334.0
	ULTIMATE MOMENT CAPACITY	79 596.1 kN m		79 596.1 kN m		79 596.1 kN m		56 609.8 kN m	
	UTIMATE SHEAR CAPACITY	11 649.9 kN		11 649.9 kN		11 649.9 kN		4 323.7 kN	
	CONTROLLING CONDITION	FLEXURE		FLEXURE		FLEXURE		SHEAR	
	CRITICAL LOCATION	SPAN 3, x = 58 802 mm		SPAN 3, x = 58 802 mm		SPAN 3, x = 58 802 mm		SPAN 3, x = 98 000 mm	
GIRDER 4	INVENTORY LEVEL	1.49	27.0	1.19	48.6	2.38	81.5	---	---
	OPERATING LEVEL	2.49	45.2	1.99	81.2	3.97	136.0	2.45	226.7
	ULTIMATE MOMENT CAPACITY	84 167.3 kN m		84 167.3 kN m		56 303.8 kN m		56 303.8 kN m	
	UTIMATE SHEAR CAPACITY	11 649.9 kN		11 649.9 kN		10 164.2 kN		10 164.2 kN	
	CONTROLLING CONDITION	FLEXURE		FLEXURE		FLEXURE		FLEXURE	
	CRITICAL LOCATION	SPAN 3, x = 58 802 mm		SPAN 3, x = 58 802 mm		SPAN 3, x = 82 760 mm		SPAN 3, x = 82 760 mm	

NOTES:

FOR HANDRAIL DETAILS, SEE SHEET 42.

FOR CROSS FRAME DETAILS, SEE SHEETS 47 THROUGH 50.

FOR UTILITY DETAILS, SEE SHEET 58.

FOR INSPECTION WALKWAY DETAILS, SEE SHEETS 59 THROUGH 61.

FOR ALUMINUM PEDESTRIAN RAILING DETAILS, SEE BC-716M.

FOR ALUMINUM BRIDGE RAILING DETAILS, SEE SHEET 100.

FOR RATING TABLES, X = DISTANCE MEASURED FROM BEGINNING OF SPAN INDICATED.

Mark	Description	By	Chk'd.	App'd.	Date
REVISIONS					

COMMONWEALTH OF PENNSYLVANIA
DEPARTMENT OF TRANSPORTATION

ARMSTRONG COUNTY
S.R. 0128 SEC. 013
SEG. 0250 OFFSET 0
S.R. 0128 STA. 1+671.500
OVER ALLEGHENY RIVER & PITTSBURG & SHAWMUT R.R.
3-SPAN CONTINUOUS STEEL PLATE GIRDER BRIDGE
TYPICAL SECTIONS & GIRDER RATINGS

COMMONWEALTH OF PENNSYLVANIA REGISTERED PROFESSIONAL MICHAEL J. BONKOVICH ENGINEER 043452-R

RECOMMENDED JAN 26 1998

SHEET 5 OF 112

S-22234

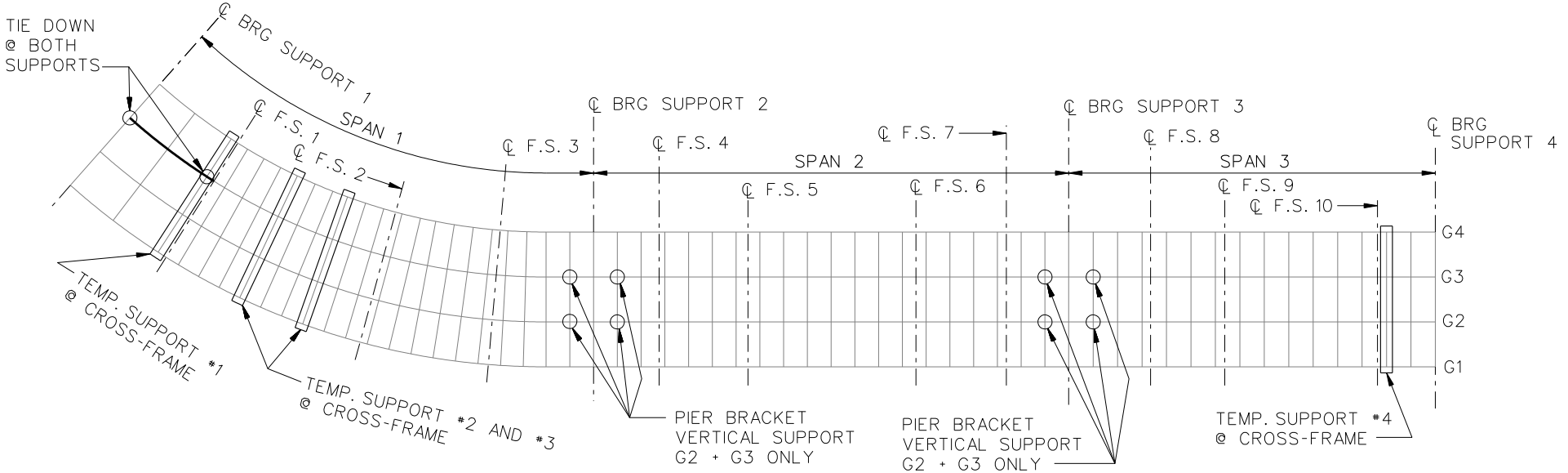

STAGE 1

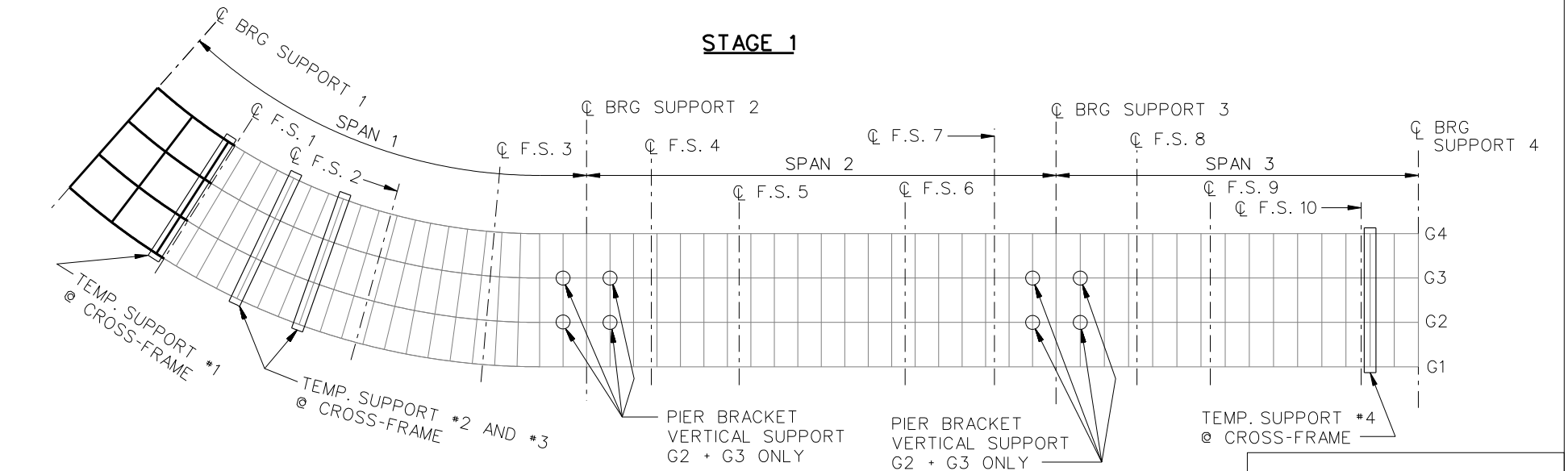

STAGE 4

LEGEND

▽ = HOLD OR LIFT CRANE

○ = TIE DOWN

□ = TEMPORARY SUPPORT STRUCTURE

NOTE:
STAGE 2 ERECT G2 SECTION
STAGE 3 ERECT G4 SECTION
STAGE 4 ERECT G1 SECTION

NCHRP 12-79

BRIDGE EICCR11

GIRDER ERECTION PROCEDURE

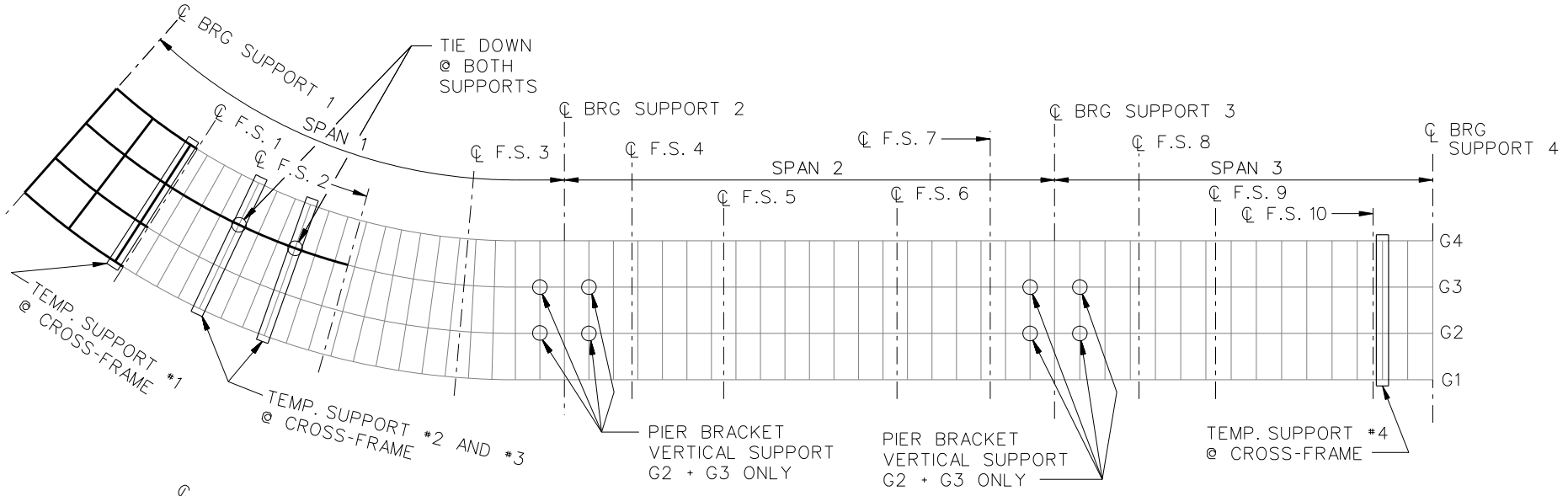

STAGE 5

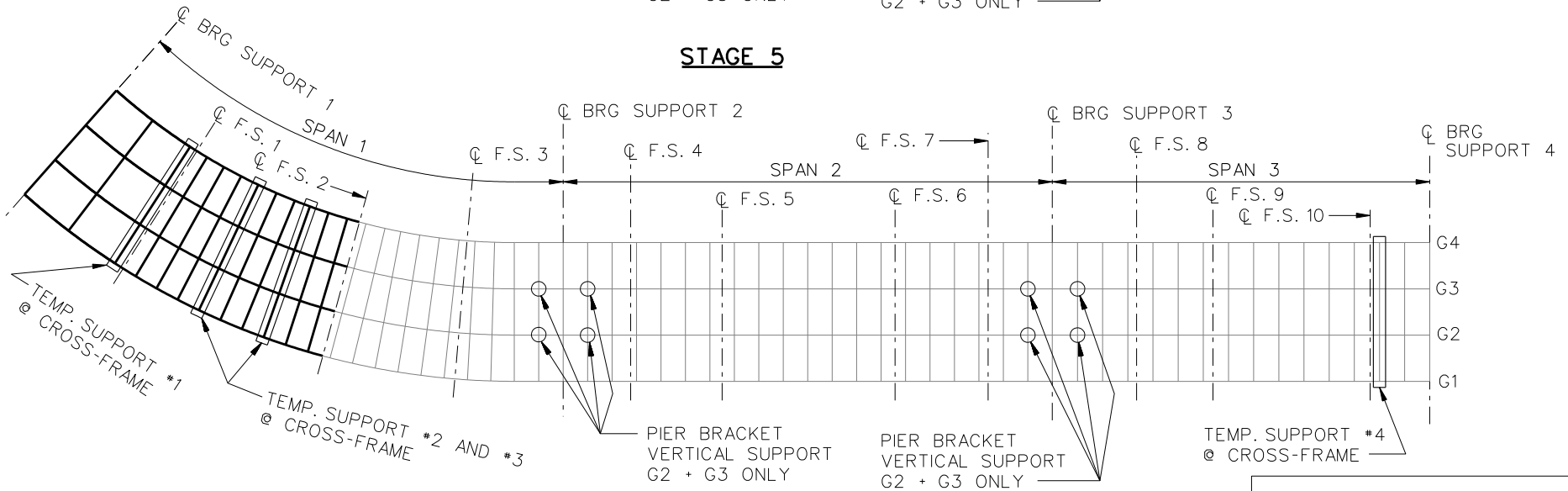

STAGE 8

LEGEND

▽ = HOLD OR LIFT CRANE

○ = TIE DOWN

□ = TEMPORARY SUPPORT STRUCTURE

NOTE:
ERECT STAGE 6 = G2 SECTION + XF'S
ERECT STAGE 7 = G4 SECTION + XF'S
ERECT STAGE 8 = G1 SECTION + XF'S

NCHRP 12-79

BRIDGE EICCR11

GIRDER ERECTION PROCEDURE

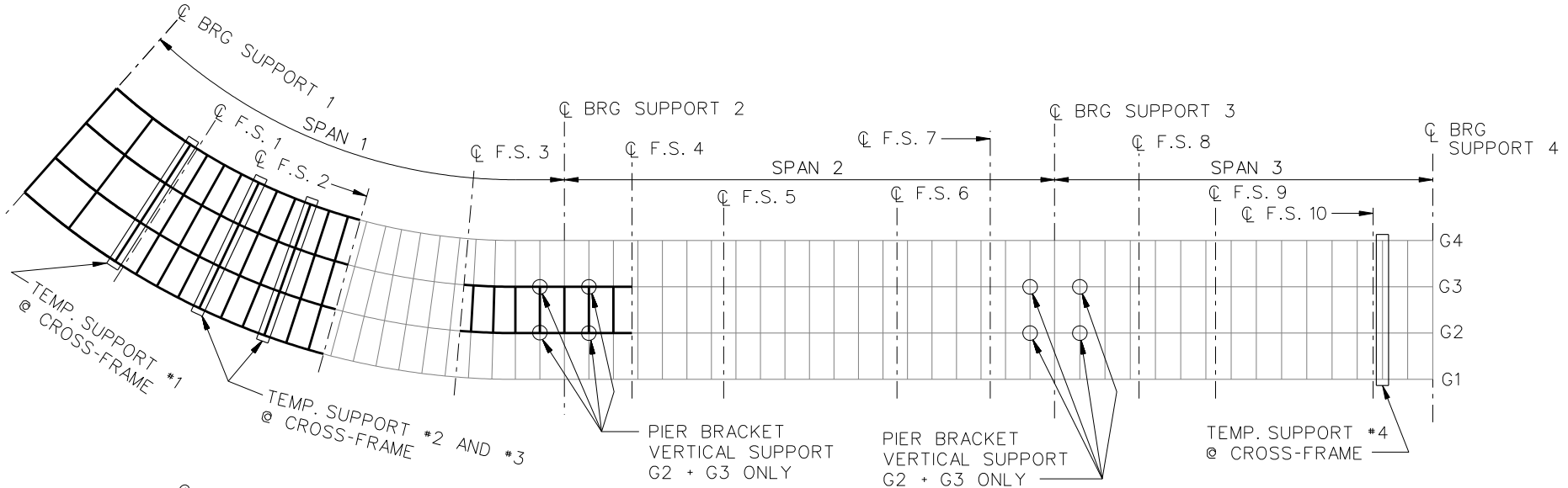

STAGE 10

NOTE:
ERECT STAGE 9 = G2 OVER SUPPORT *2
ERECT STAGE 10 = G3 OVER SUPPORT *2

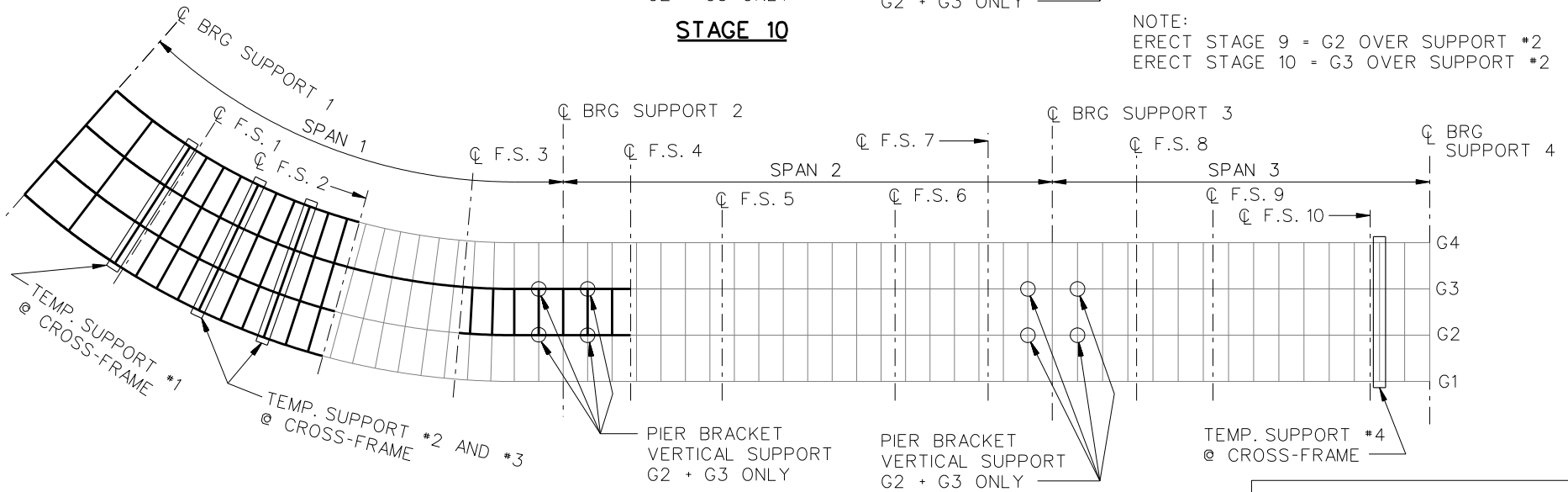

STAGE 11

LEGEND

▽ = HOLD OR LIFT CRANE

○ = TIE DOWN

□ = TEMPORARY SUPPORT STRUCTURE

NCHRP 12-79

BRIDGE EICCR11

GIRDER ERECTION PROCEDURE

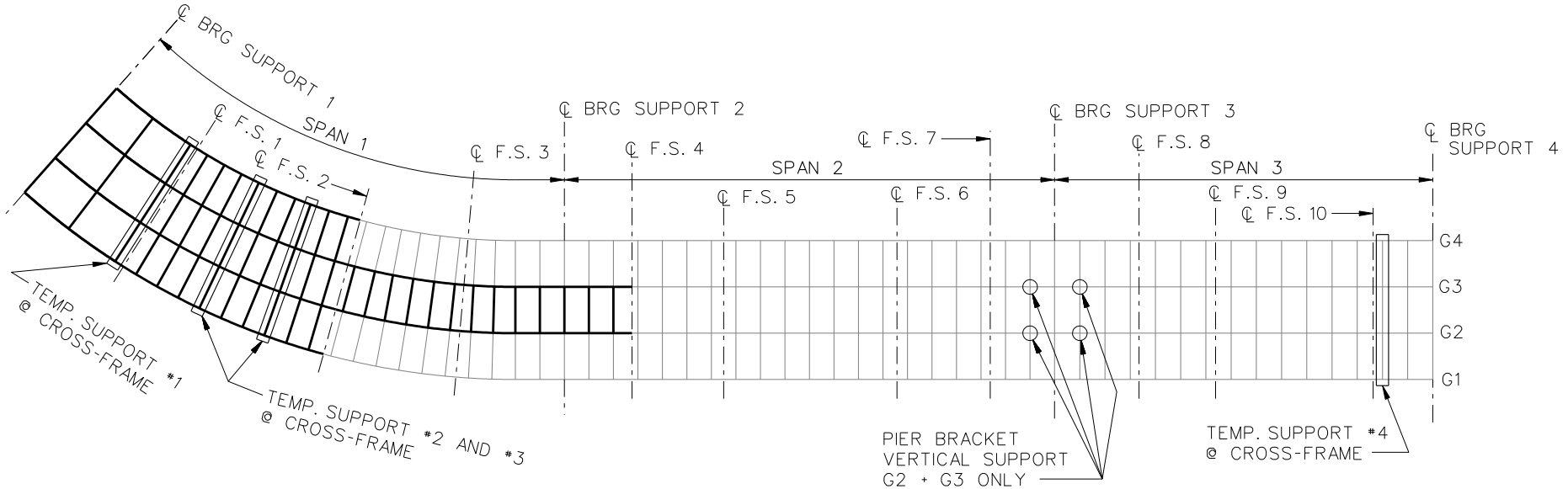

STAGE 12

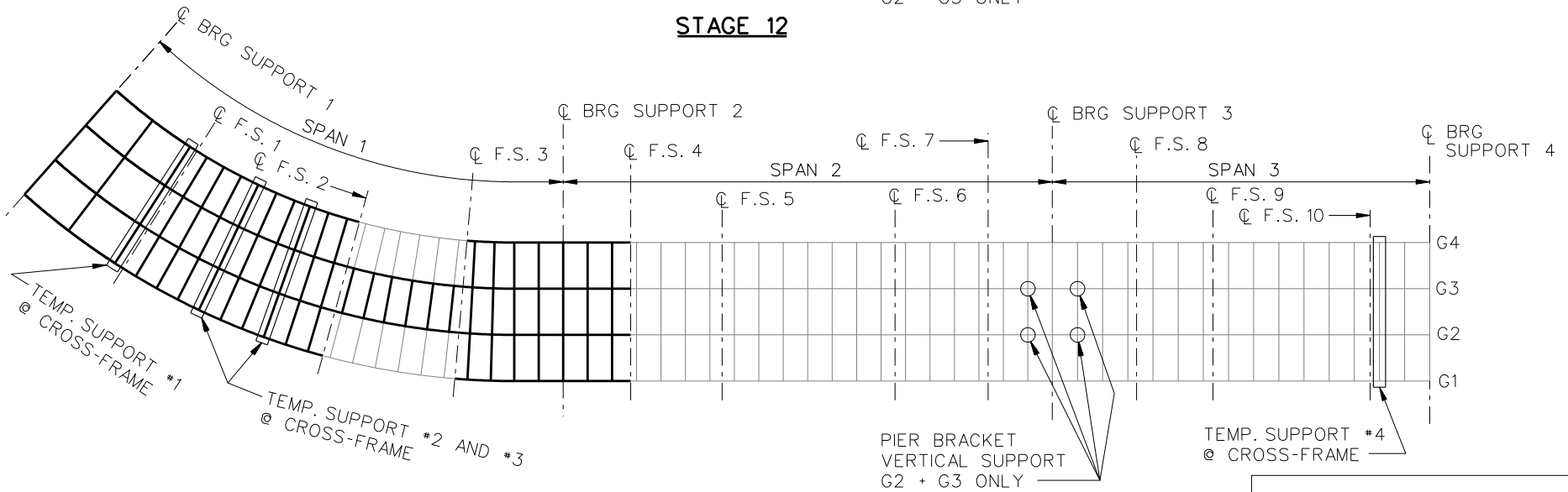

STAGE 14

LEGEND

▽ = HOLD OR LIFT CRANE

○ = TIE DOWN

□ = TEMPORARY SUPPORT STRUCTURE

NOTE:
STAGE 13 = G4 OVER SUPPORT 2
STAGE 14 = G1 OVER SUPPORT 2

NCHRP 12-79

BRIDGE EICCR11

GIRDER ERECTION PROCEDURE

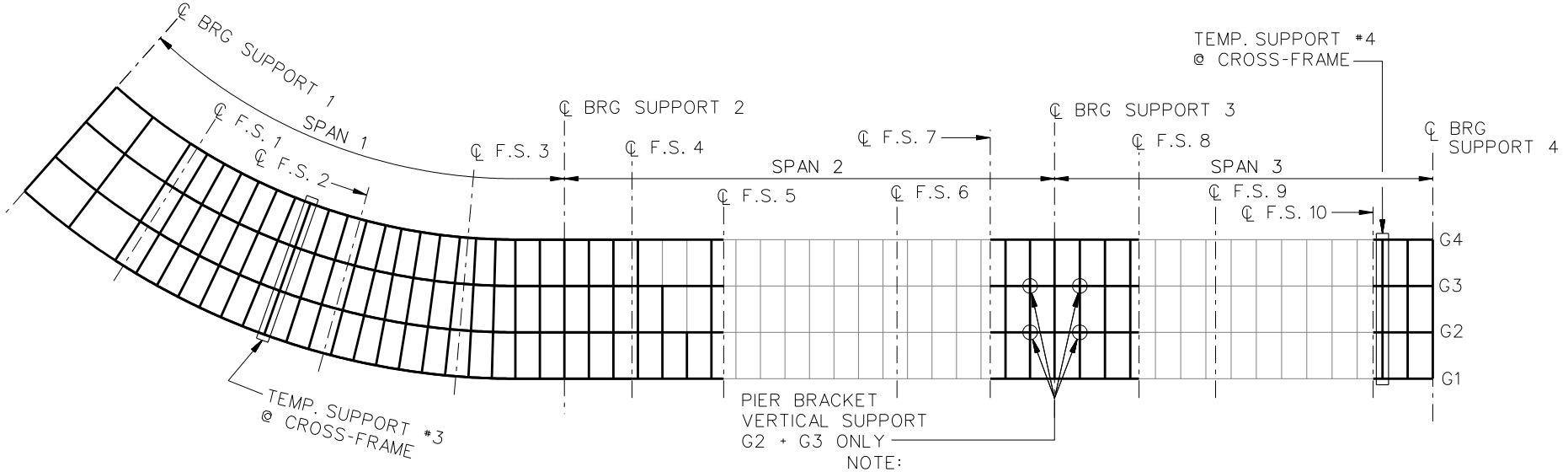

STAGE 26

NOTE:
STAGE 15 = G2 - FS #4 TO FS #5
STAGE 16 = G3 - FS #4 TO FS #5
STAGE 17 = G4 - FS #4 TO FS #5
STAGE 18 = G1 - FS #4 TO FS #5
STAGES 19 THRU 22 = FS #10 TO SUPPORT #4, ORDER = G2, G3, G4, G1
STAGES 23 THRU 26 = FS #7 TO FS #8, ORDER = G2, G3, G4, G1

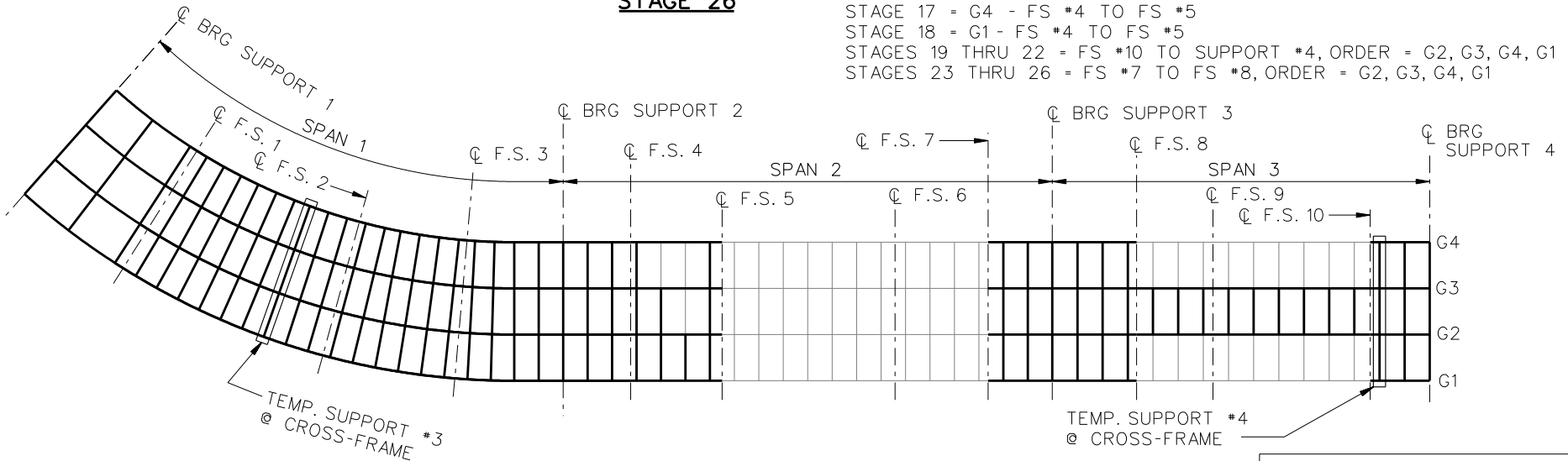

STAGE 27

LEGEND

▽ = HOLD OR LIFT CRANE

○ = TIE DOWN

□ = TEMPORARY SUPPORT STRUCTURE

NCHRP 12-79

BRIDGE EICCR11

GIRDER ERECTION PROCEDURE

SHEET 5 OF 6

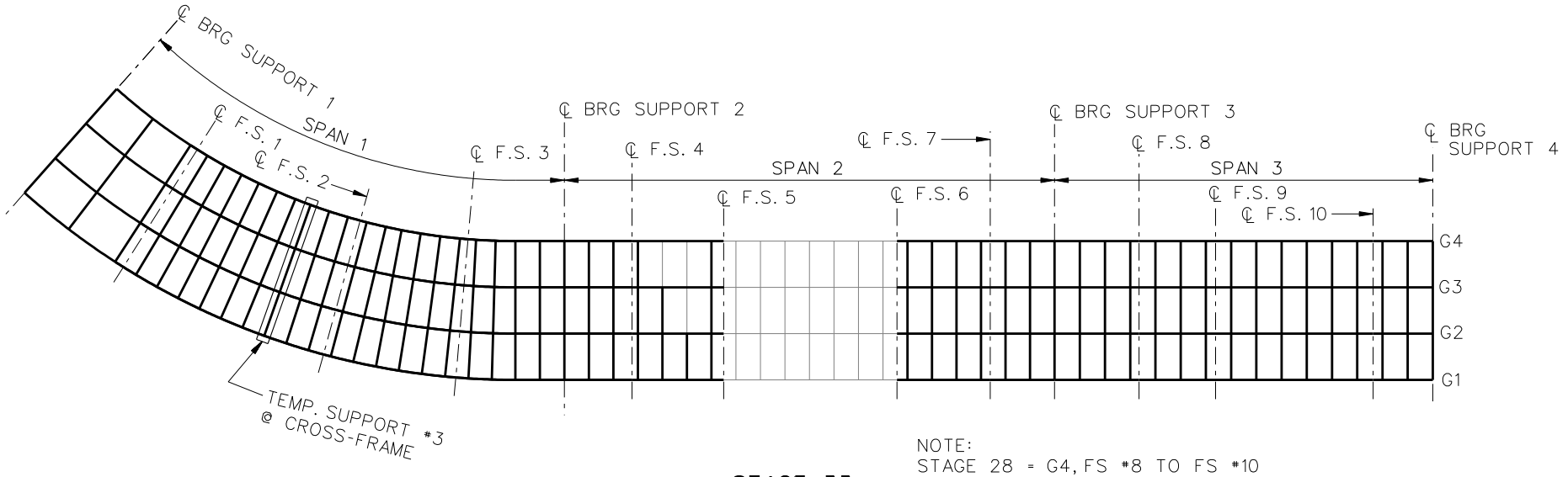

STAGE 33

NOTE:
STAGE 28 = G4, FS #8 TO FS #10
STAGE 29 = G1, FS #8 TO FS #10
STAGES 30 THRU 33 = FS #6 TO FS #7, ORDER = G2, G3, G4, G1

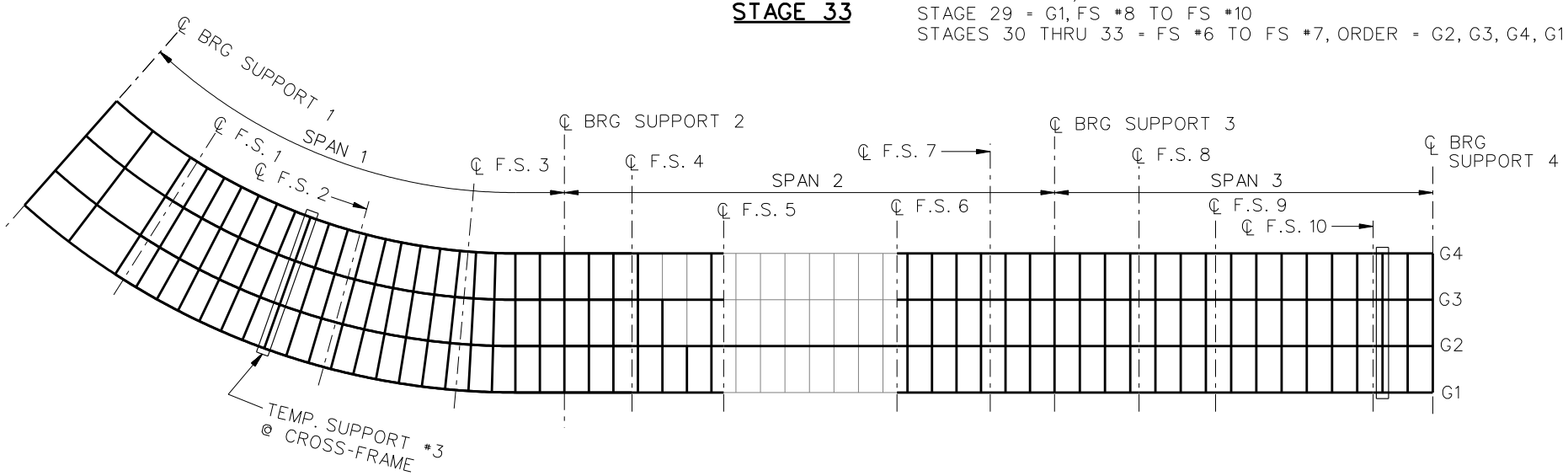

STAGE 34

NOTE:
STAGE 35 = G3 - FS #5 TO FS #6
STAGE 36 = G4 - FS #5 TO FS #6
STAGE 37 = G1 - FS #5 TO FS #6, AND
REMOVE TEMP. SUPPORT #3

LEGEND

▽ = HOLD OR LIFT CRANE

○ = TIE DOWN

□ = TEMPORARY SUPPORT STRUCTURE

NCHRP 12-79

BRIDGE EICCR11

GIRDER ERECTION PROCEDURE

SHEET 6 OF 6

NCHRP 12-79

EICCR15

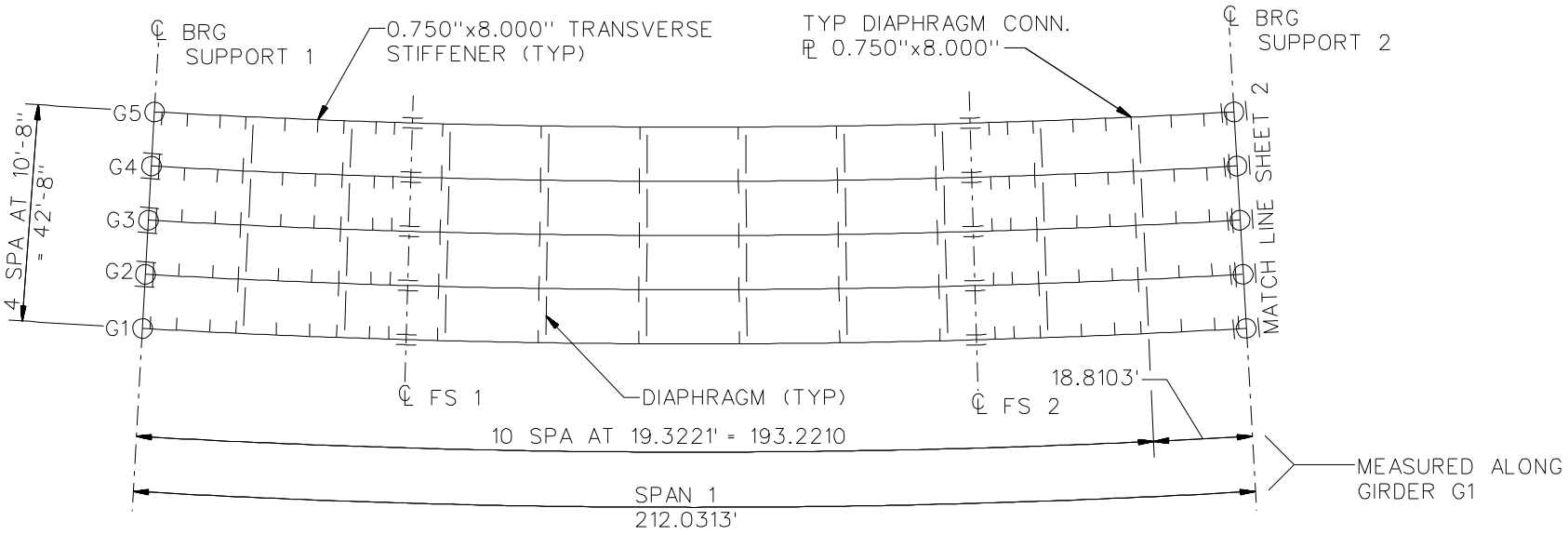

FRAMING PLAN

NOTE :

1. ALL DIMENSIONS TAKEN ALONG G1.

○ - NON-GUIDED EXPANSION POT BEARING

|○ - LONGITUDINALLY GUIDED POT BEARING

|○| - TRANSVERSELY GUIDED POT BEARING

NCHRP 12-79

BRIDGE EICCR15

FRAMING PLAN

SHEET 1 OF 11

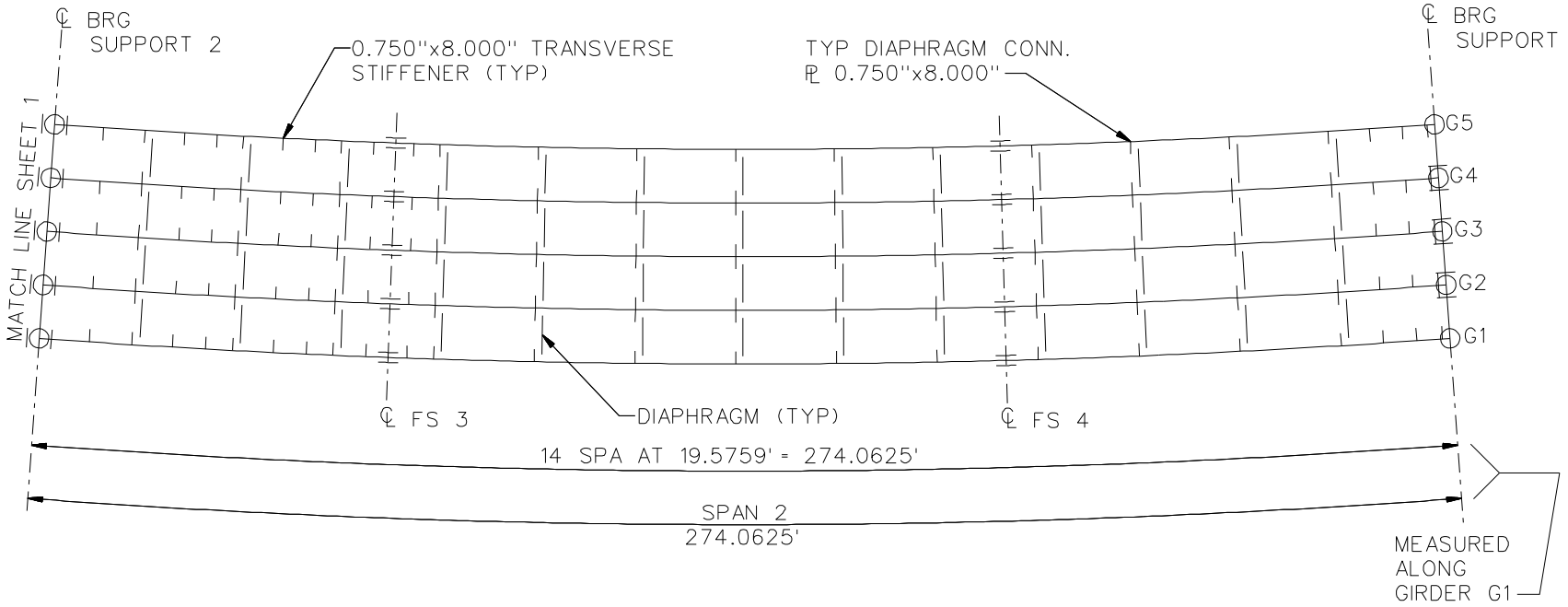

FRAMING PLAN

NOTE :

1. ALL DIMENSIONS TAKEN ALONG G1.

○ - NON-GUIDED EXPANSION POT BEARING

|○ - LONGITUDINALLY GUIDED POT BEARING

|○| - TRANSVERSELY GUIDED POT BEARING

NCHRP 12-79

BRIDGE EICCR15

FRAMING PLAN

SHEET 2 OF 11

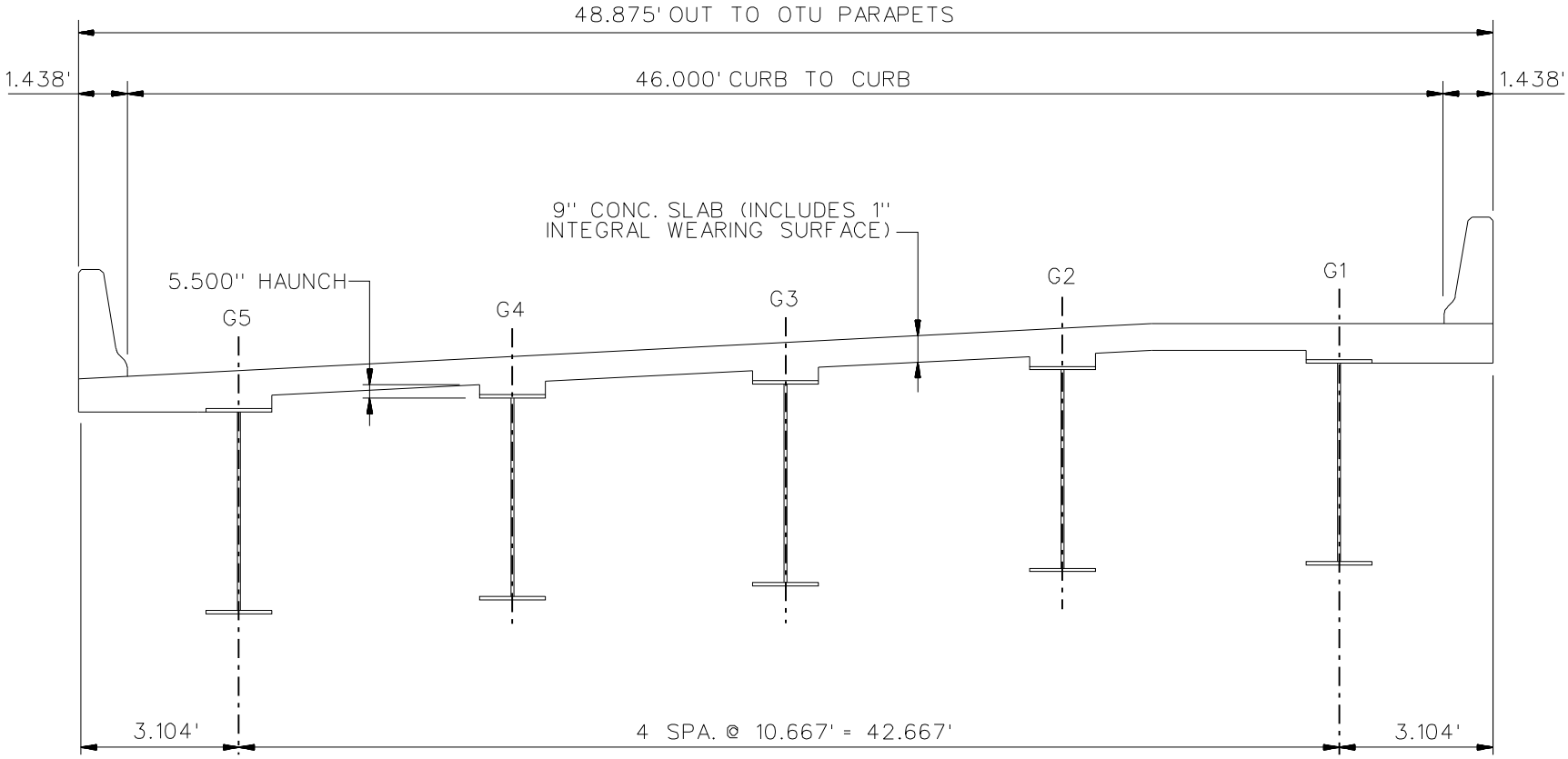

TYPICAL SECTION

NOTE:

1. CROSS-FRAMES ARE NOT SHOWN FOR CLARITY.

NCHRP 12-79

BRIDGE EICCR15

TYPICAL SECTION

SHEET 3 OF 11

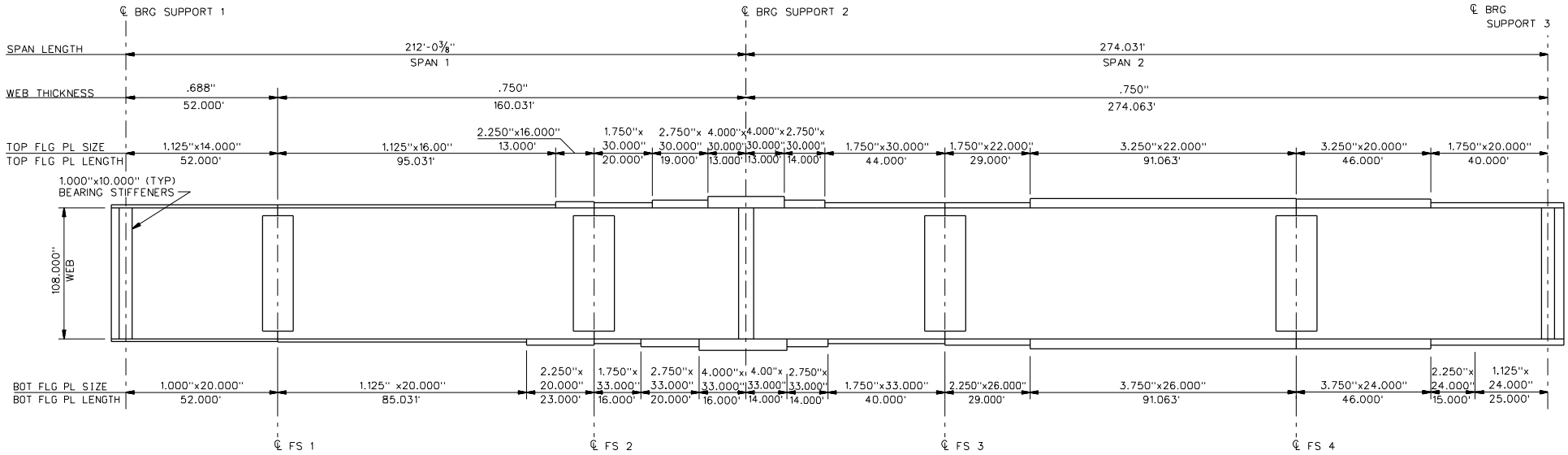

ELEVATION - GIRDER G1

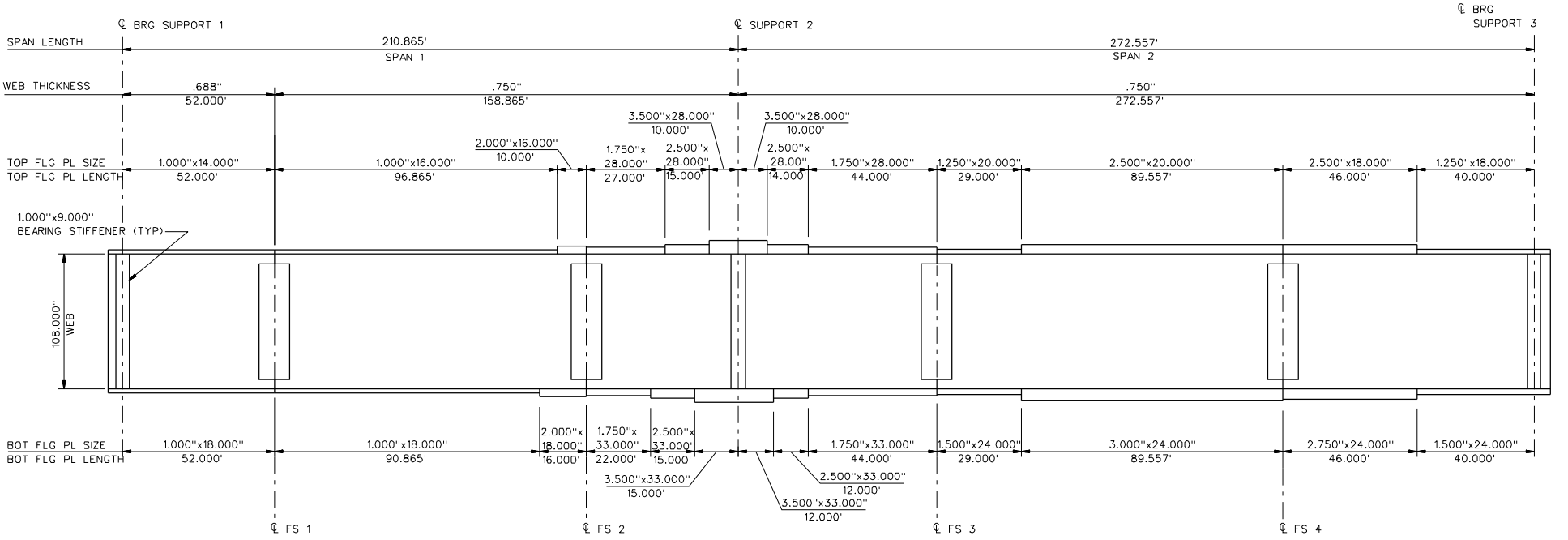

ELEVATION - GIRDER G2

NCHRP 12-79
BRIDGE EICCR15
GIRDER ELEVATIONS
SHEET 4 OF 11

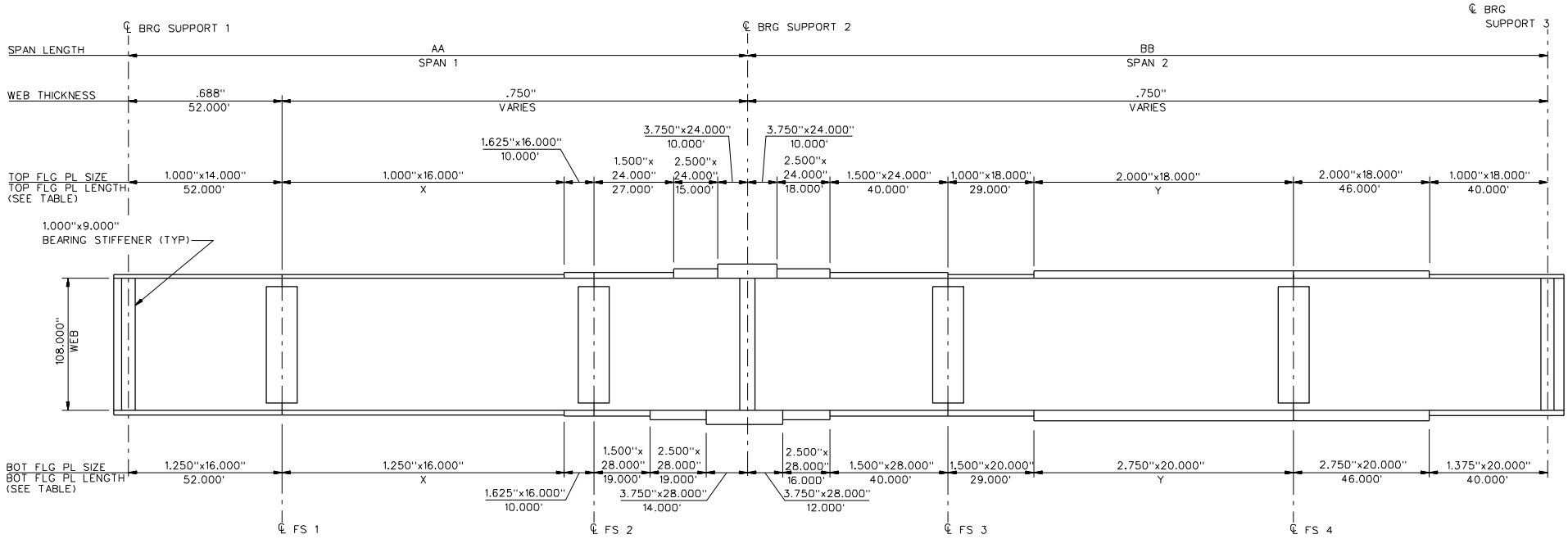

ELEVATION - GIRDERS G3, G4, AND G5

** FOR LENGTHS, SEE TABLE, THIS SHEET

GIRDER AND PLATE LENGTHS					
	AA	BB	X	Y	Z
GIRDER G3	209.703'	271.052'	95.703'	88.052'	134.052'
GIRDER G4	208.537'	269.547'	94.537'	86.547'	132.547'
GIRDER G5	207.370'	268.042'	93.370'	85.042'	131.042'

NCHRP 12-79

BRIDGE EICCR15

GIRDER ELEVATIONS

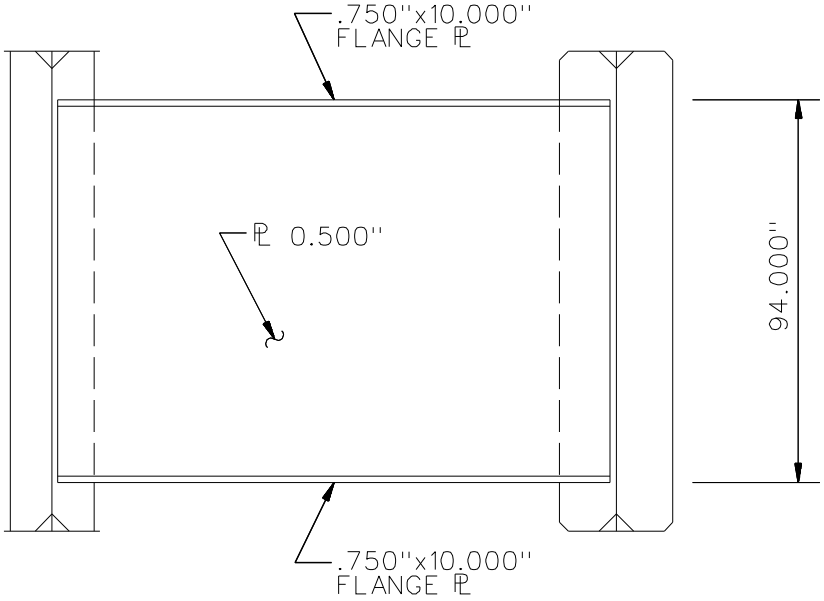

TYPICAL END DIAPHRAGM

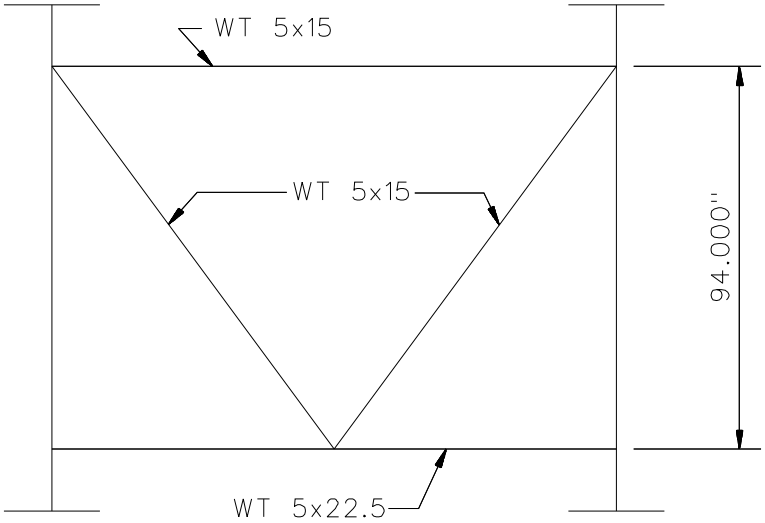

TYPICAL INTERMEDIATE DIAPHRAGM

NOTES:

1. STEEL DEAD LOAD INCREASED BY 5% FOR MDX AND LARSA MODELS; 2% FOR 3D MODEL; AND 10% FOR APPROXIMATE ANALYSIS TO ACCOUNT FOR MISC. DETAILS.

2. FORMWORK LOAD OF 10PSF IS INCLUDED IN CONCRETE DEAD LOAD.

NCHRP 12-79

BRIDGE EICCR 15

MISC. DETAILS AND NOTES

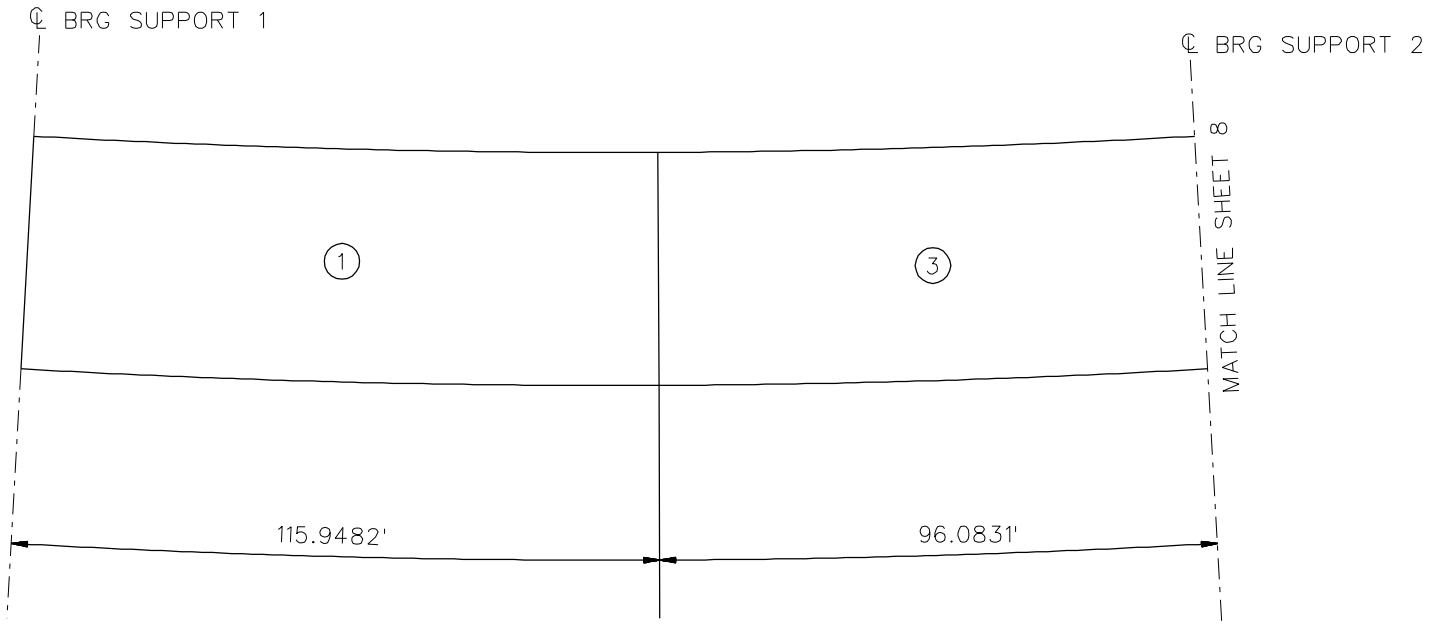

DECK PLACEMENT SEQUENCE

(MEASURED ALONG GIRDER G1)

NCHRP 12-79

BRIDGE EICCR15

DECK POURING SEQUENCE

SHEET 7 OF 11

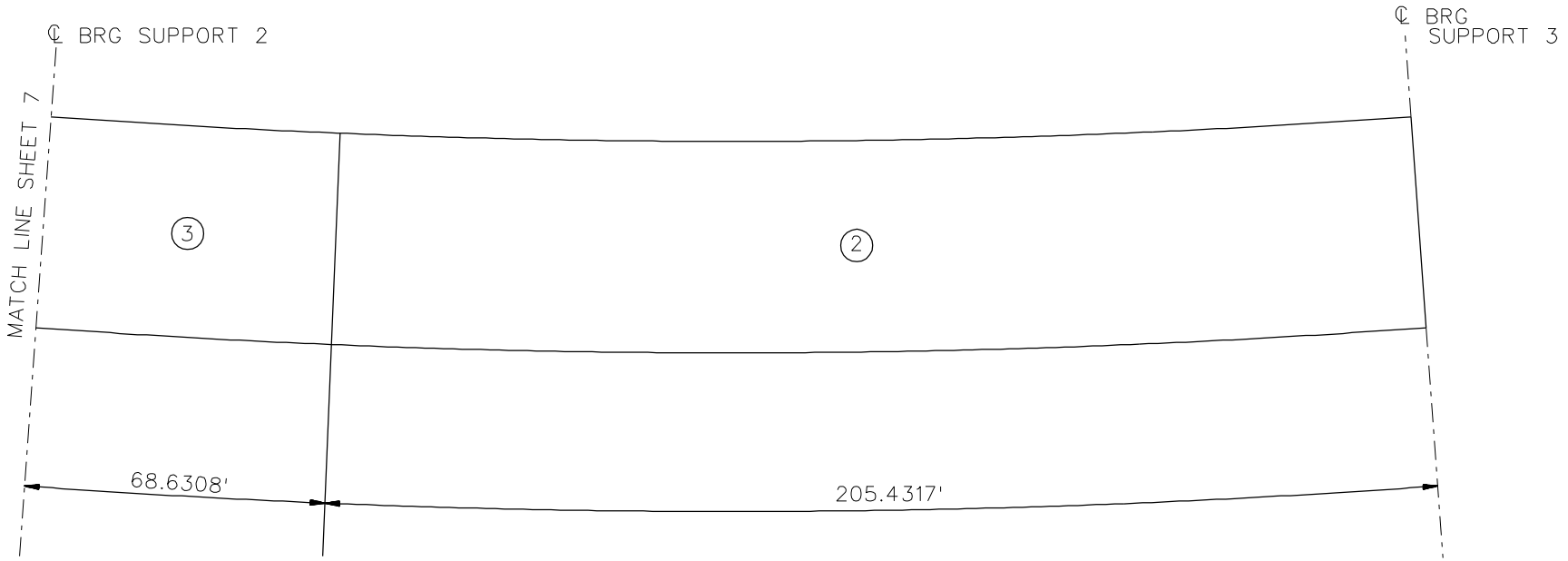

DECK PLACEMENT SEQUENCE

(MEASURED ALONG GIRDER G1)

NCHRP 12-79

BRIDGE EICCR15

DECK POURING SEQUENCE

SHEET 8 OF 11

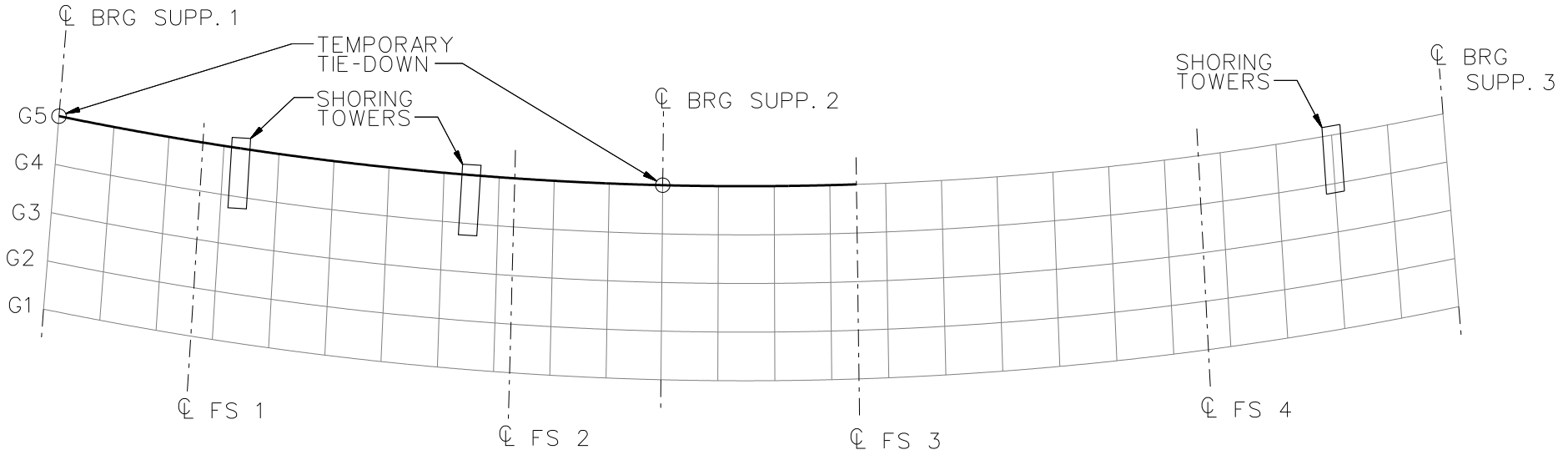

STAGE 1

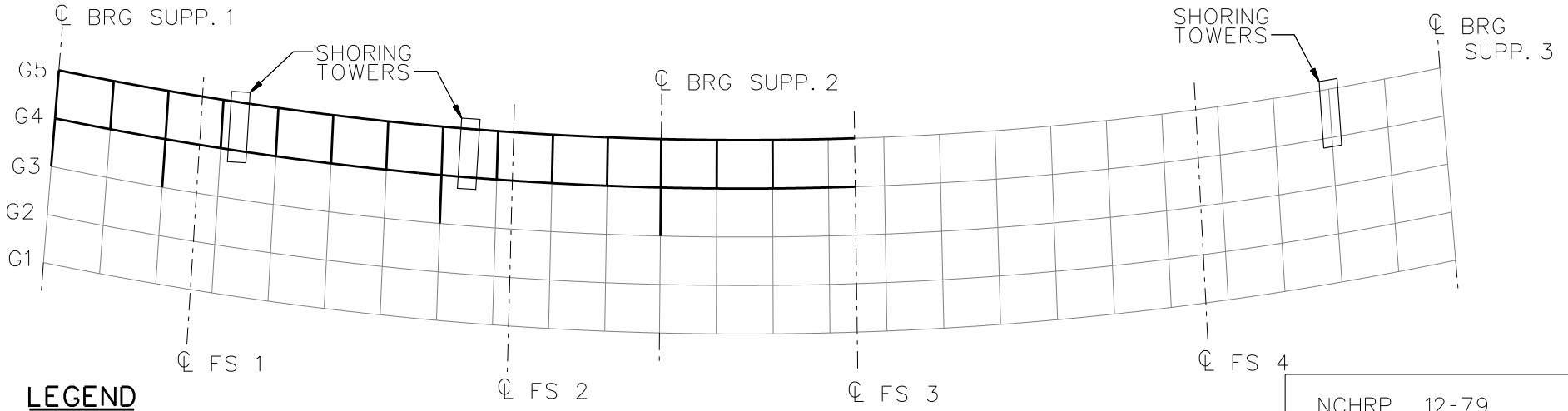

STAGE 2

LEGEND

▽ = HOLD OR LIFT CRANE

○ = TIE DOWN

□ = TEMPORARY SUPPORT STRUCTURE

NCHRP 12-79

BRIDGE EICCR15

ERECTION PROCEDURE

SHEET 9 OF 11

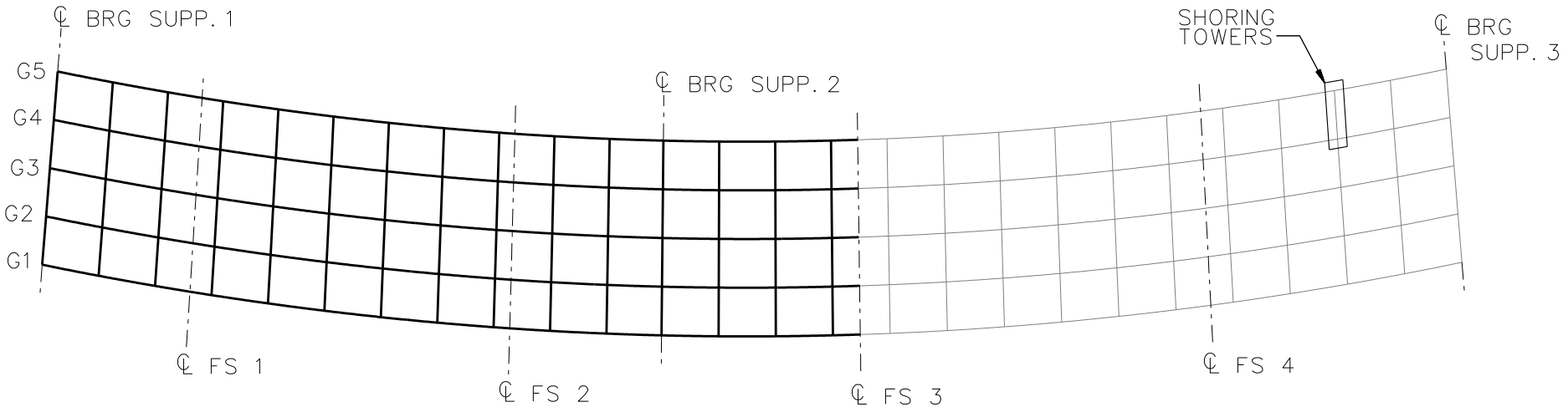

STAGE 5

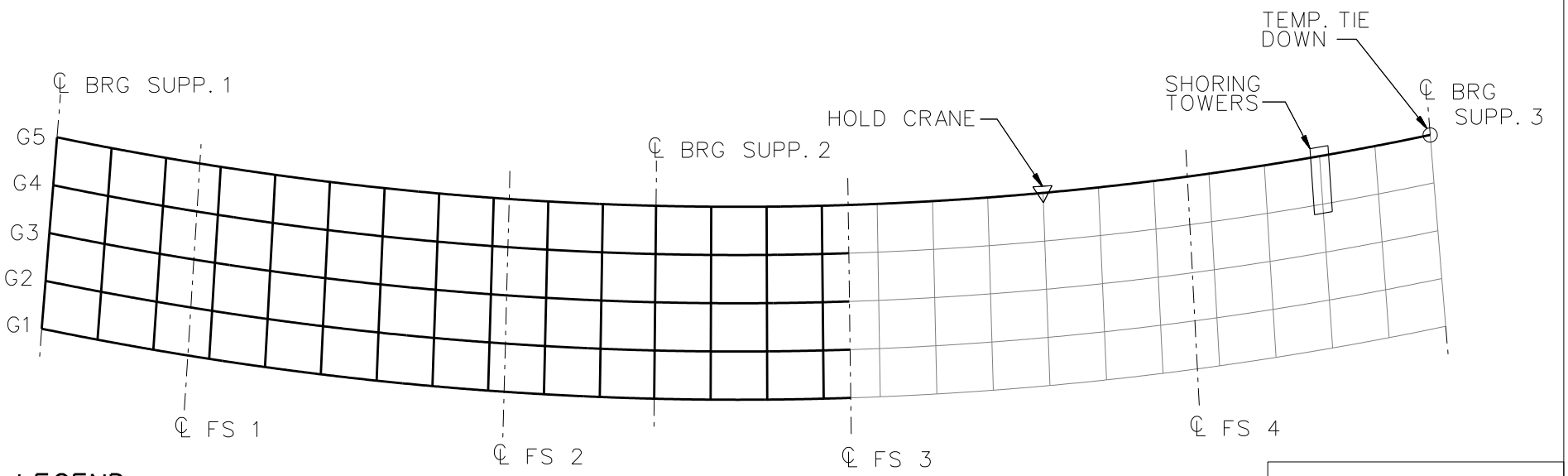

STAGE 6

LEGEND

▽ = HOLD OR LIFT CRANE

○ = TIE DOWN

□ = TEMPORARY SUPPORT STRUCTURE

NCHRP 12-79

BRIDGE EICCR15

ERECTION PROCEDURE

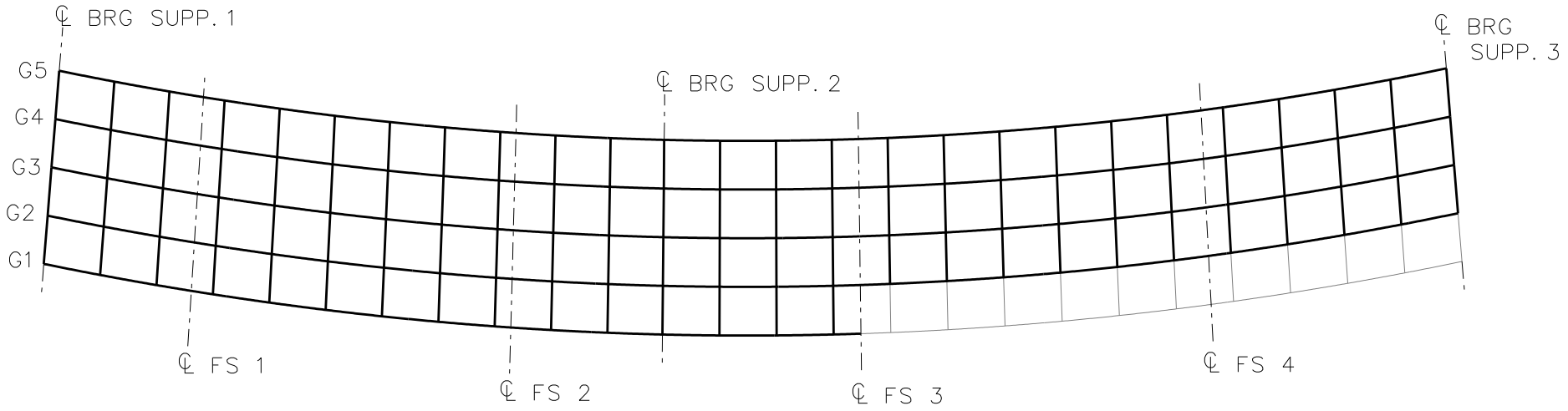

STAGE 9

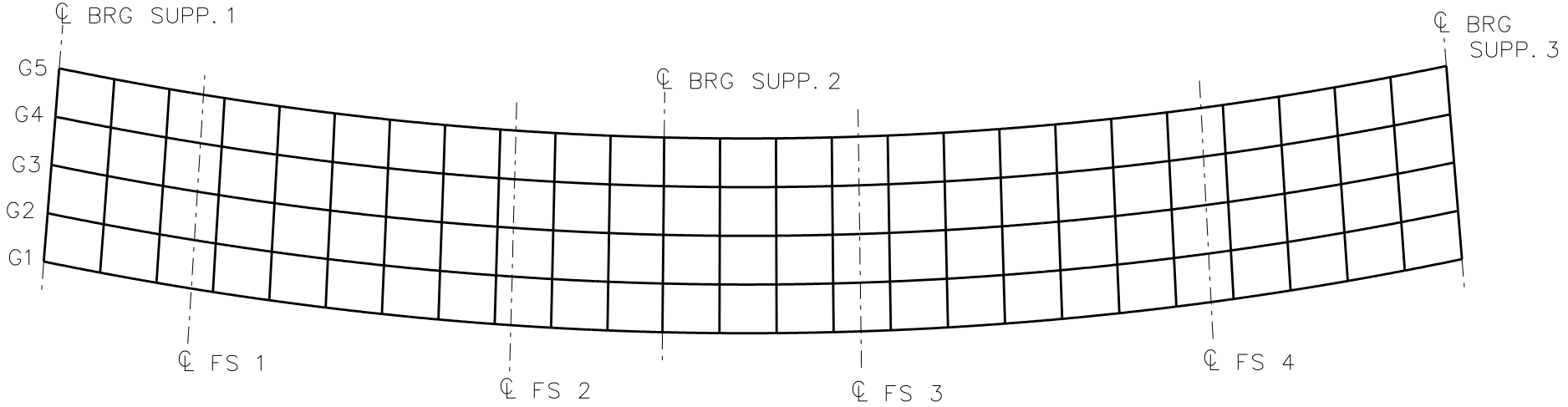

STAGE 10

LEGEND

▽ = HOLD OR LIFT CRANE

○ = TIE DOWN

□ = TEMPORARY SUPPORT STRUCTURE

NCHRP 12-79

BRIDGE EICCR15

ERECTION PROCEDURE

NCHRP 12-79

EICCR22A

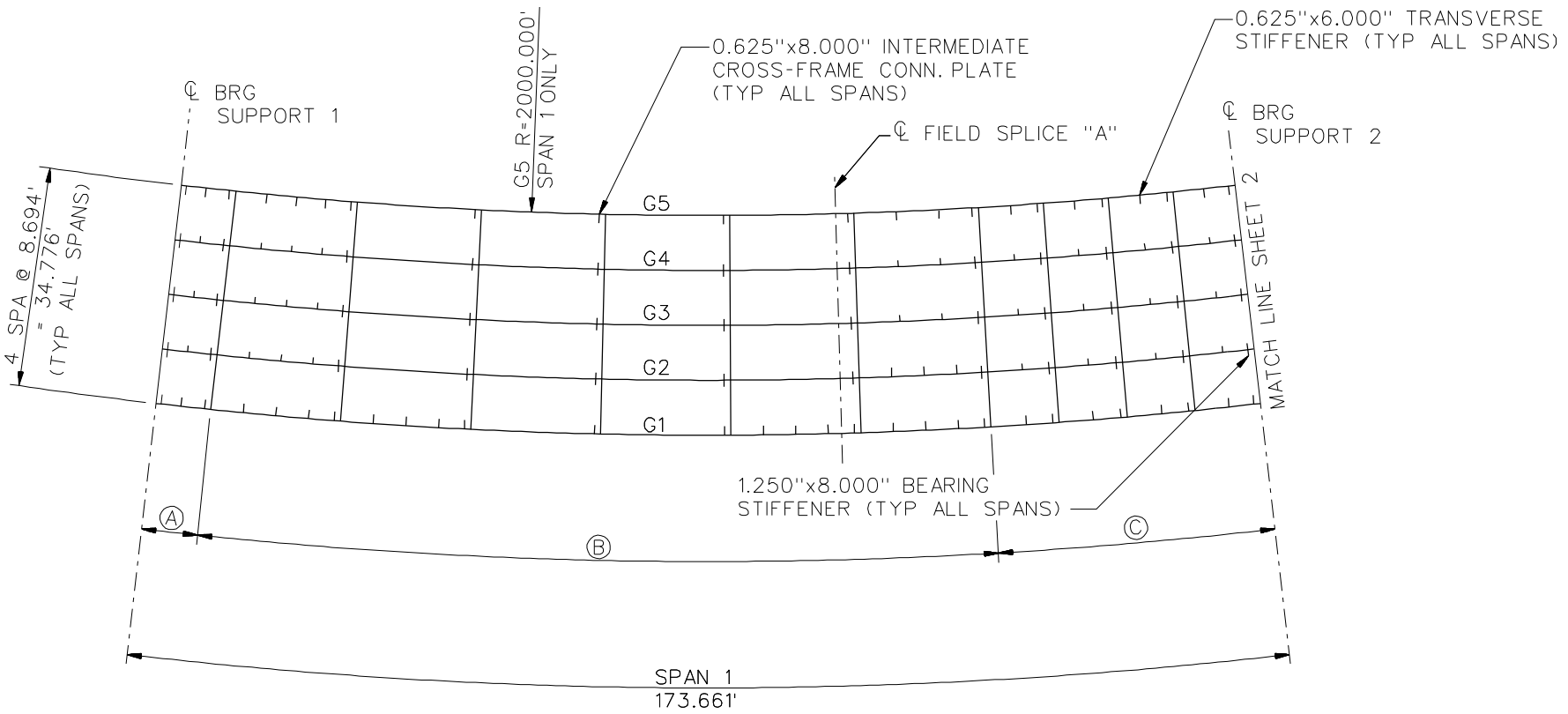

FRAMING PLAN

NOTE :

1. ALL DIMENSIONS TAKEN ALONG G1.

BEARING ARRANGEMENT

1. LONGITUDINALLY GUIDED BEARINGS ARE USED AT SUPPORTS 1 AND 9, FOR ALL GIRDERS.
2. FIXED BEARINGS ARE USED AT SUPPORTS 2 THROUGH 8, FOR ALL GIRDERS.
3. BEARING ARRANGEMENTS NOT SHOWN ON FRAMING PLAN FOR CLARITY.

CROSS-FRAME SPACING DIMENSIONS ALONG GIRDER G1	
Ⓐ	1 SPA. @ 8.694'
Ⓑ	6 SPA. @ 20.594'
Ⓒ	4 SPA. @ 10.351'

NCHRP 12-79

BRIDGE EICCR22a

FRAMING PLAN

SHEET 1 OF X

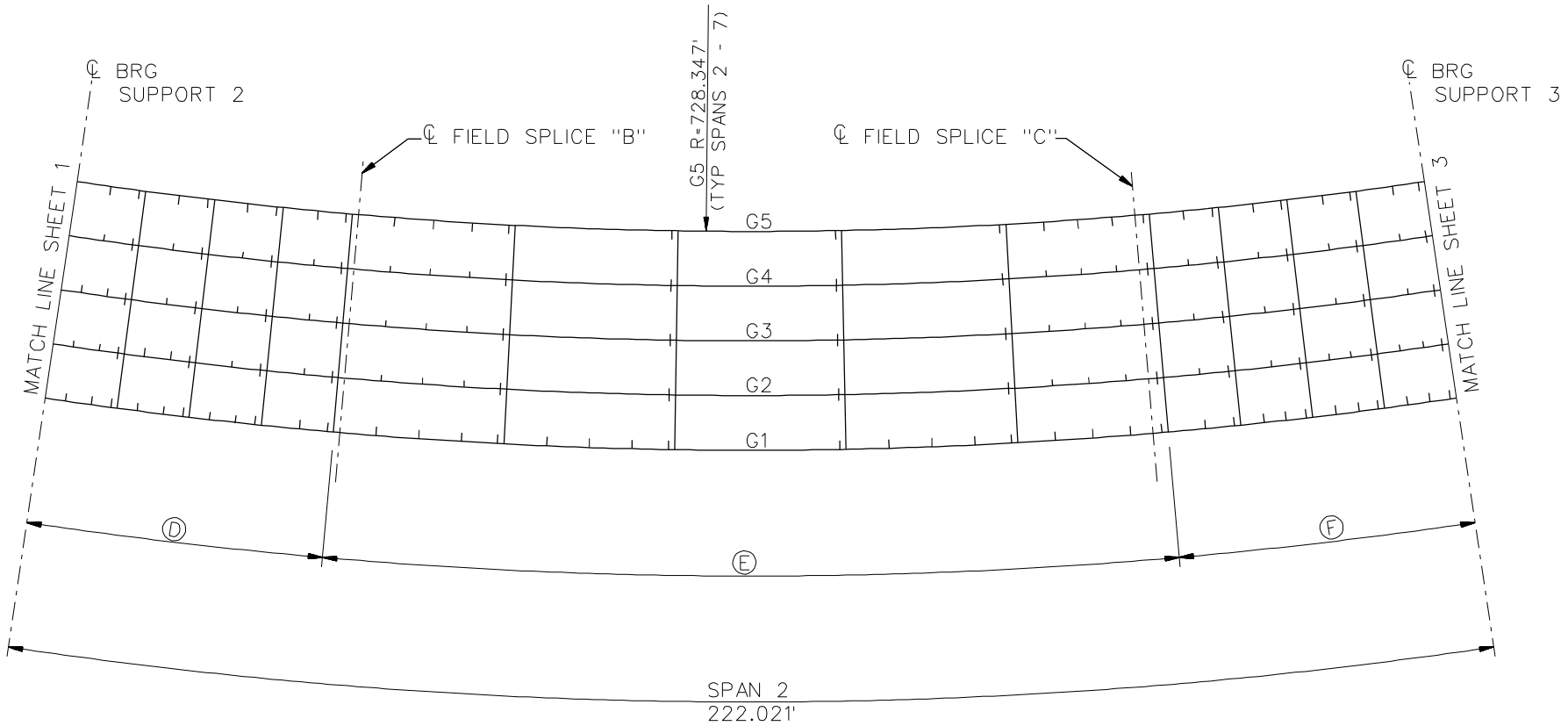

FRAMING PLAN

NOTE :

1. ALL DIMENSIONS TAKEN ALONG G1.

CROSS-FRAME SPACING DIMENSIONS ALONG GIRDER G1	
Ⓓ	4 SPA. @ 11.529'
Ⓔ	5 SPA. @ 25.958'
Ⓕ	4 SPA. @ 11.529'

NCHRP 12-79

BRIDGE EICCR22a

FRAMING PLAN

SHEET 2 OF X

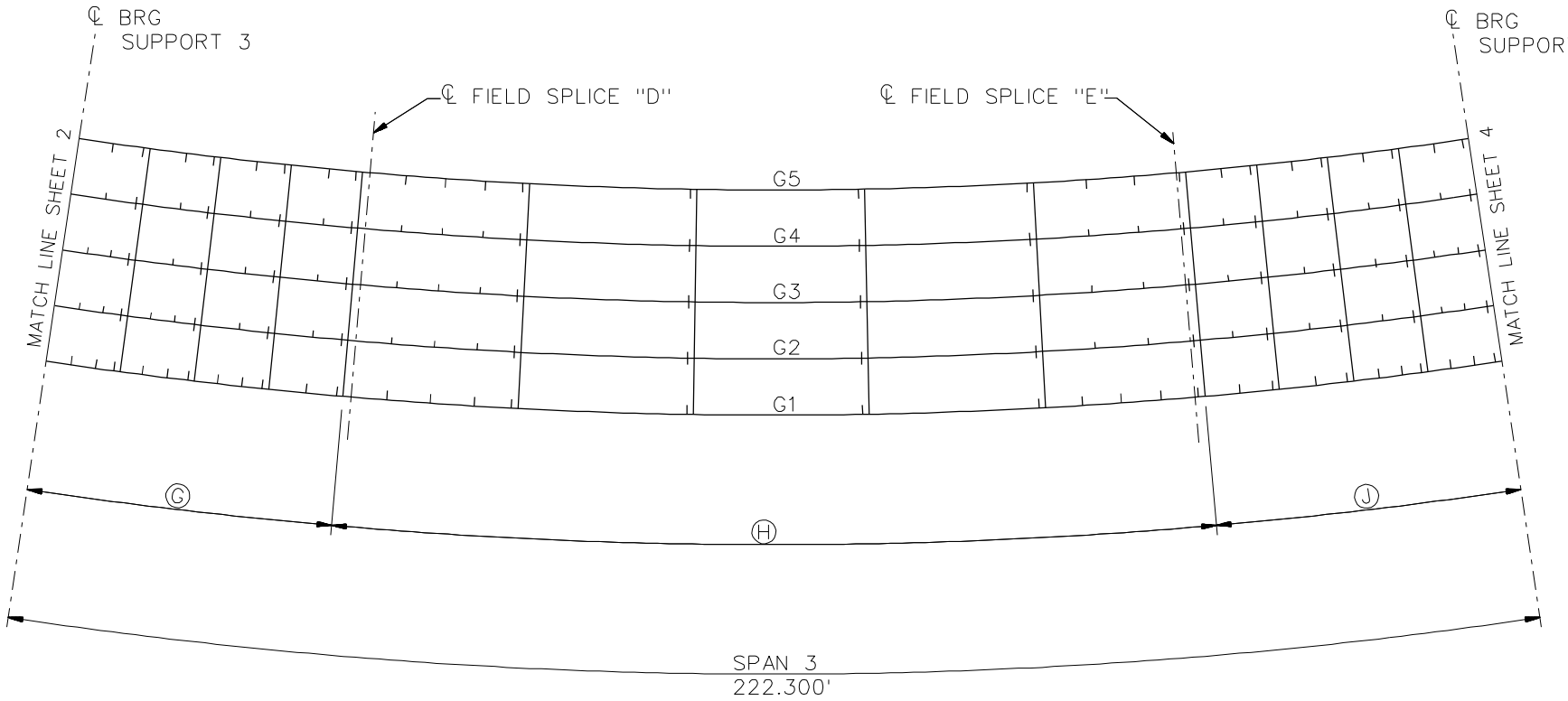

FRAMING PLAN

NOTE :

1. ALL DIMENSIONS TAKEN ALONG G1.

CROSS-FRAME SPACING DIMENSIONS ALONG GIRDER G1	
Ⓖ	4 SPA. @ 11.529'
Ⓗ	5 SPA. @ 26.014'
Ⓙ	4 SPA. @ 11.529'

NCHRP 12-79

BRIDGE EICCR22a

FRAMING PLAN

SHEET 3 OF X

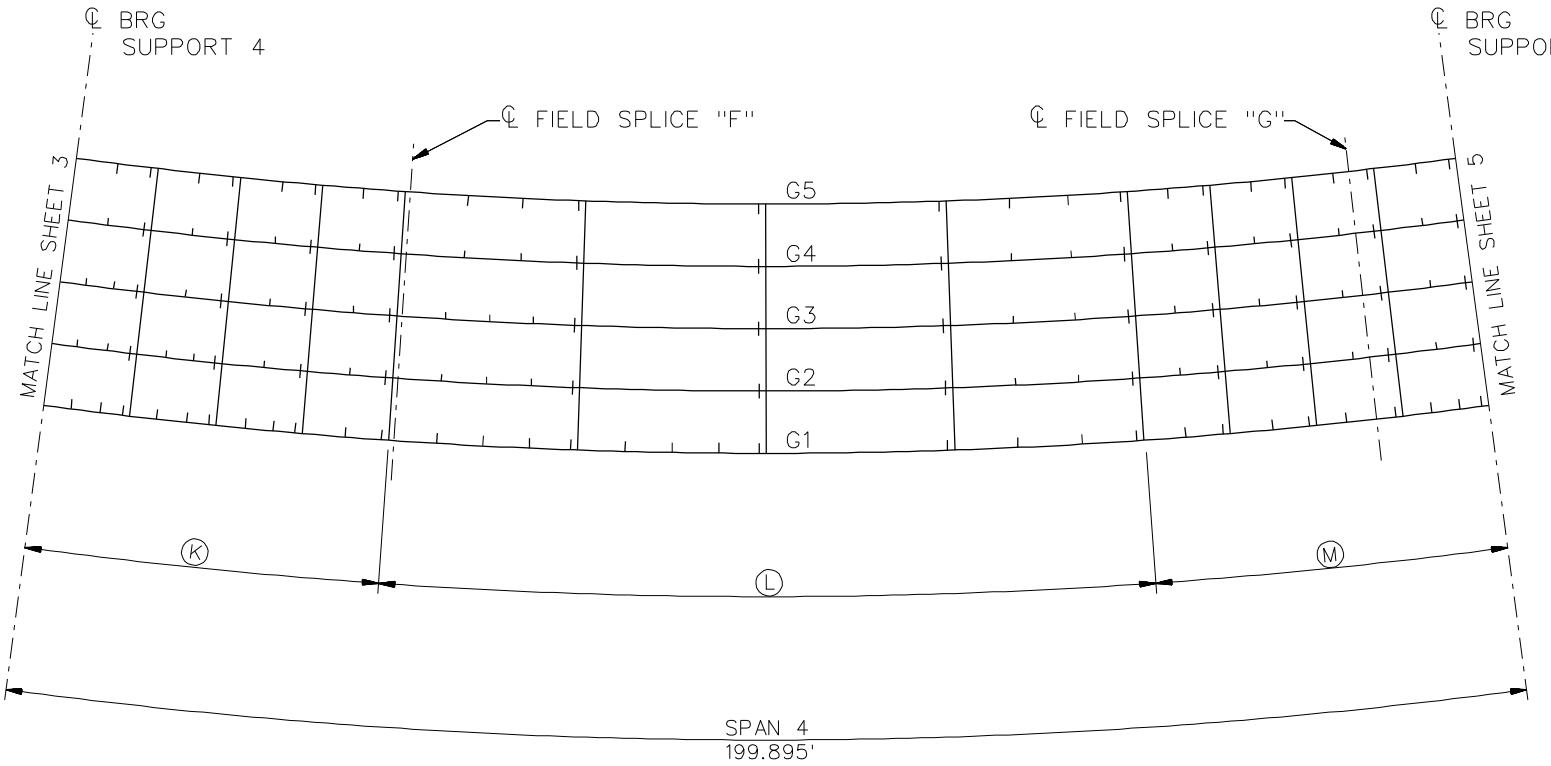

FRAMING PLAN

NOTE :

1. ALL DIMENSIONS TAKEN ALONG G1.

CROSS-FRAME SPACING DIMENSIONS ALONG GIRDER G1	
Ⓚ	4 SPA. @ 12.083'
Ⓛ	4 SPA. @ 25.807'
Ⓜ	4 SPA. @ 12.083'

NCHRP 12-79

BRIDGE EICCR22a

FRAMING PLAN

SHEET 4 OF X

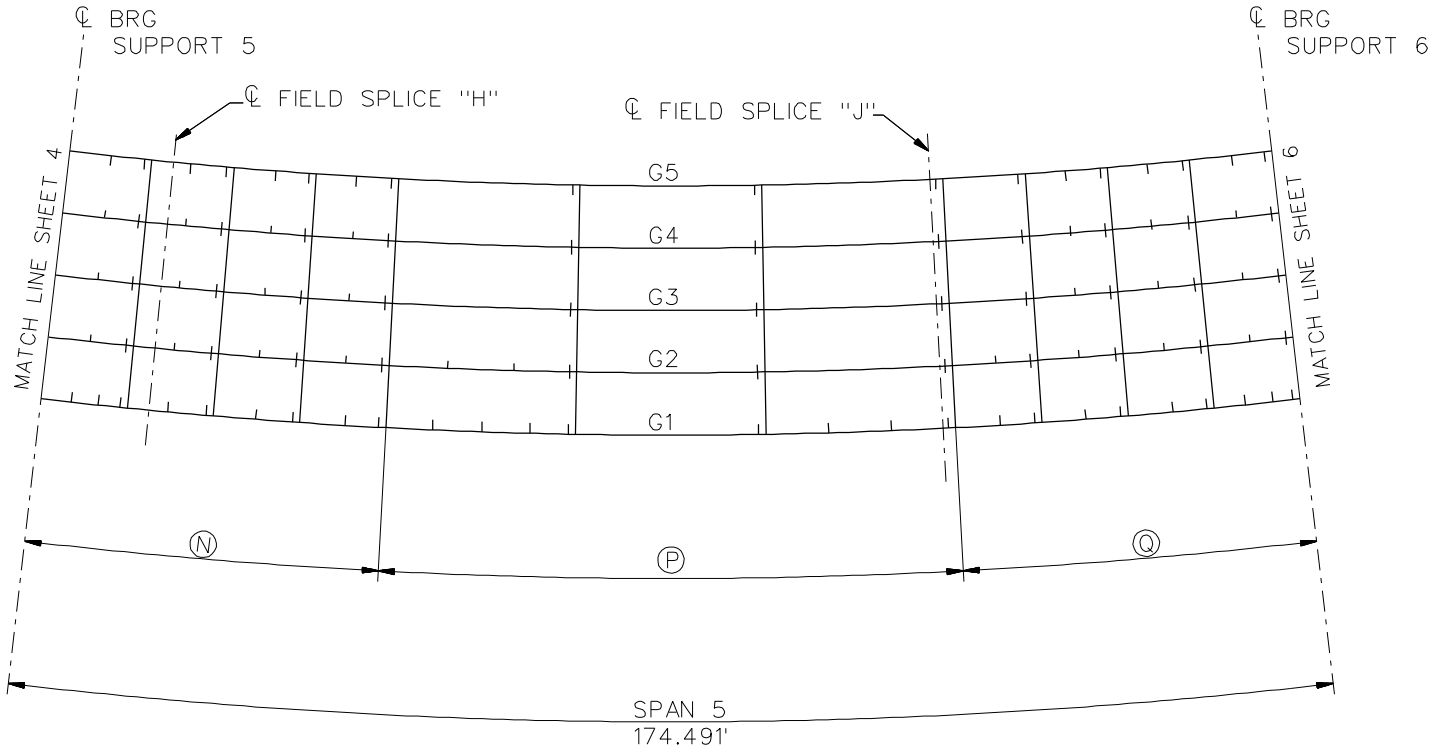

FRAMING PLAN

NOTE :

1. ALL DIMENSIONS TAKEN ALONG G1.

CROSS-FRAME SPACING DIMENSIONS ALONG GIRDER G1	
Ⓝ	4 SPA. @ 12.054'
Ⓟ	4 SPA. @ 26.020'
Ⓠ	4 SPA. @ 12.054'

NCHRP 12-79

BRIDGE EICCR22a

FRAMING PLAN

SHEET 5 OF X

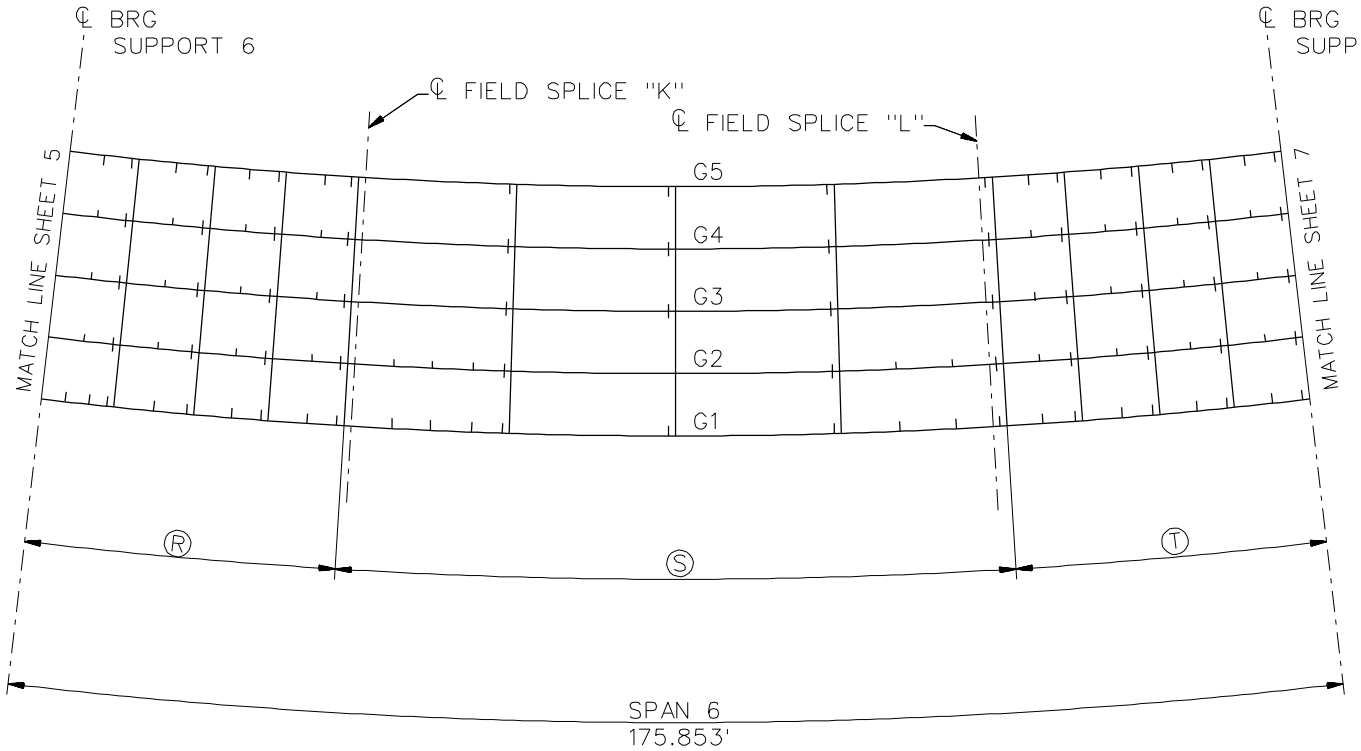

FRAMING PLAN

CROSS-FRAME SPACING DIMENSIONS ALONG GIRDER G1	
Ⓡ	4 SPA. @ 10.581'
Ⓢ	4 SPA. @ 22.802'
Ⓣ	4 SPA. @ 10.581'

NOTE :

1. ALL DIMENSIONS TAKEN ALONG G1.

NCHRP 12-79

BRIDGE EICCR22a

FRAMING PLAN

SHEET 6 OF X

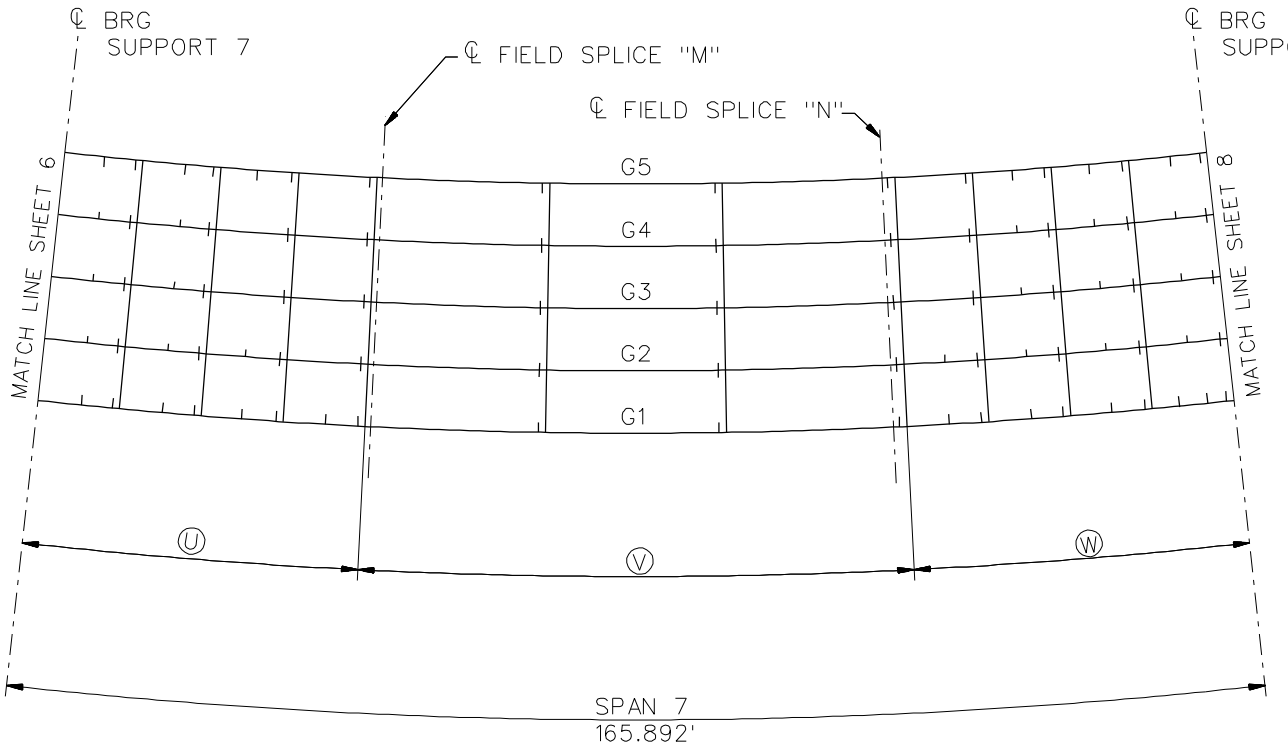

FRAMING PLAN

CROSS-FRAME SPACING DIMENSIONS ALONG GIRDER G1	
Ⓤ	4 SPA. @ 11.440'
Ⓥ	3 SPA. @ 24.790'
Ⓦ	4 SPA. @ 11.440'

NOTE :

1. ALL DIMENSIONS TAKEN ALONG G1.

NCHRP 12-79

BRIDGE EICCR22a

FRAMING PLAN

SHEET 7 OF X

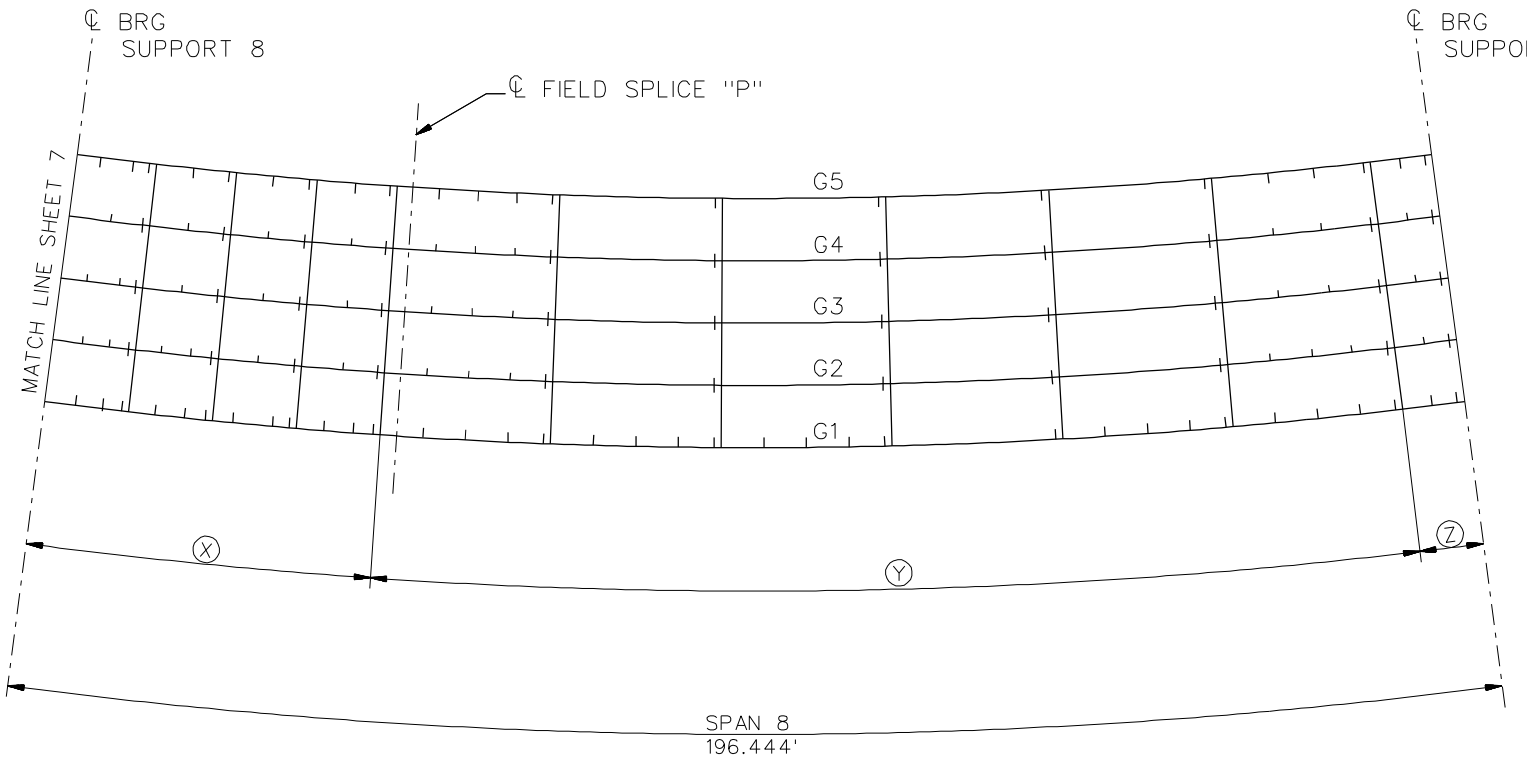

FRAMING PLAN

CROSS-FRAME SPACING DIMENSIONS ALONG GIRDER G1	
X	4 SPA. @ 11.755'
Y	6 SPA. @ 23.455'
Z	1 SPA. @ 8.694'

NOTE :

1. ALL DIMENSIONS TAKEN ALONG G1.

NCHRP 12-79

BRIDGE EICCR22a

FRAMING PLAN

SHEET 8 OF X

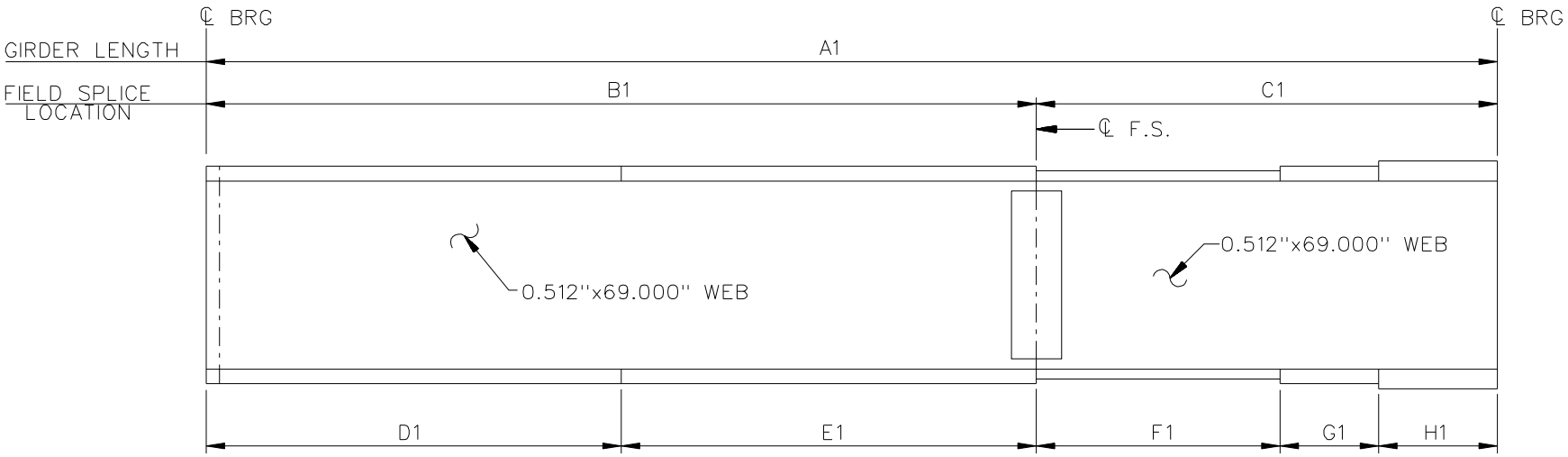

ELEVATION OF SPAN 1 GIRDERS

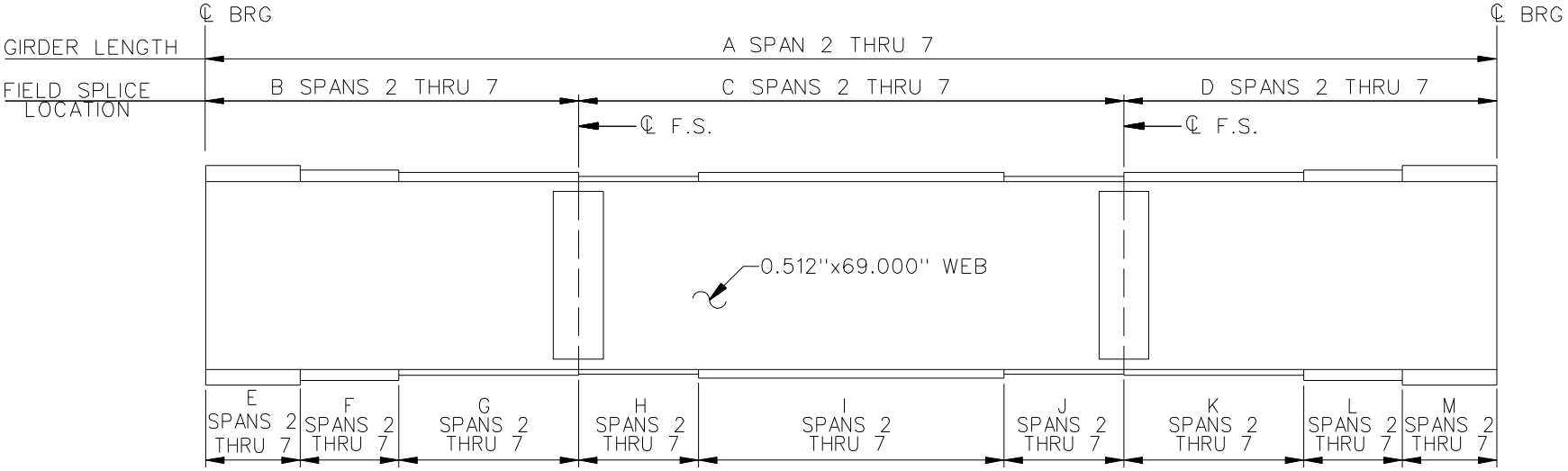

ELEVATION OF SPAN 2 THRU 7 GIRDERS

NOTE:

1. FOR DIMENSIONS AND FLANGE SIZES SEE SHEETS XX TO XX.

NCHRP 12-79

BRIDGE EICCR22a

GIRDER ELEVATIONS

SHEET 9 OF X

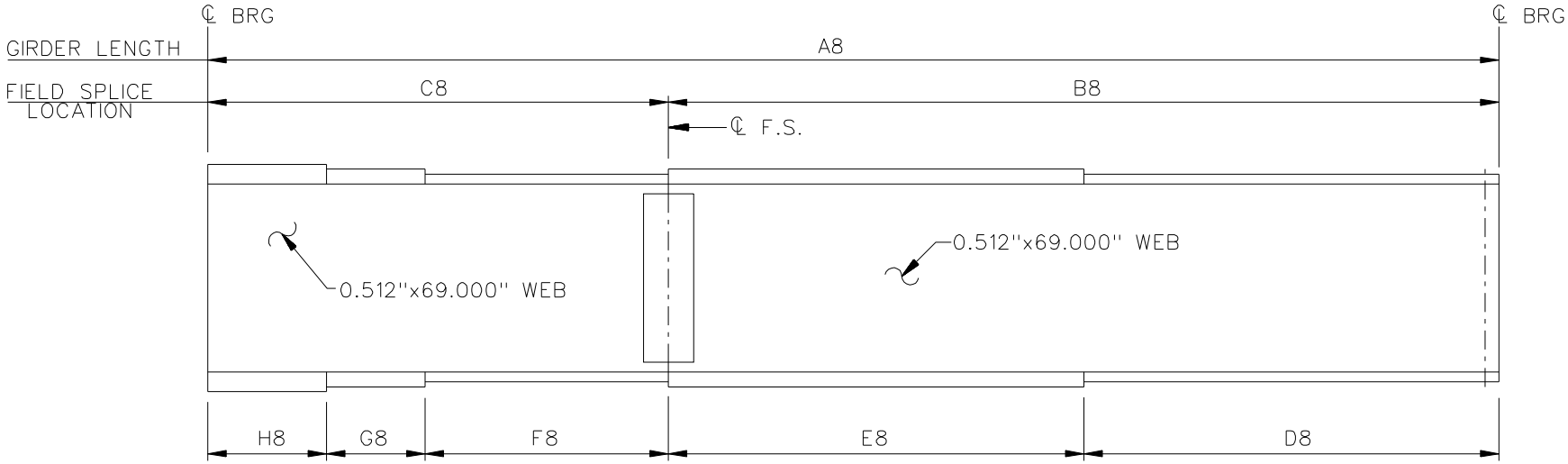

ELEVATION OF SPAN 8 GIRDERS

NOTE:

1. FOR DIMENSIONS AND FLANGE SIZES SEE SHEETS XX TO XX.

NCHRP 12-79

BRIDGE EICCR22a

GIRDER ELEVATIONS

SHEET 10 OF X

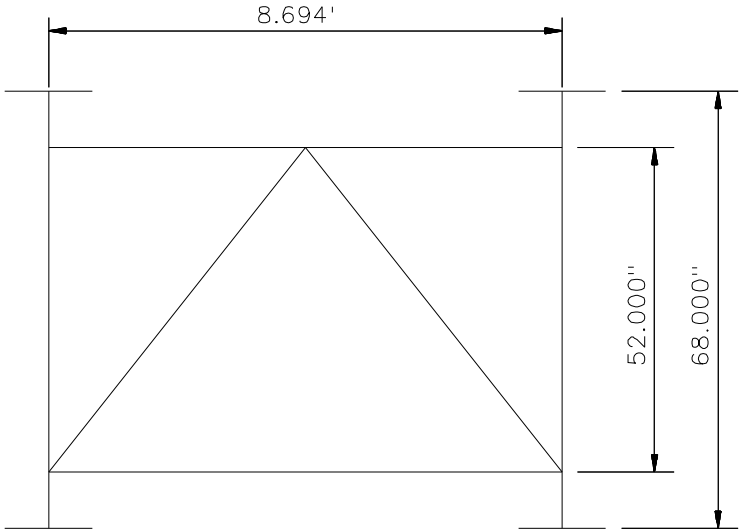

NOTE:

1. ALL CROSS FRAME MEMBERS ARE L8x6x112 (LLV).
2. GIRDER CONNECTION PLATE IS 0.625''x8.000''.

TYPICAL INTERMEDIATE CROSS FRAME

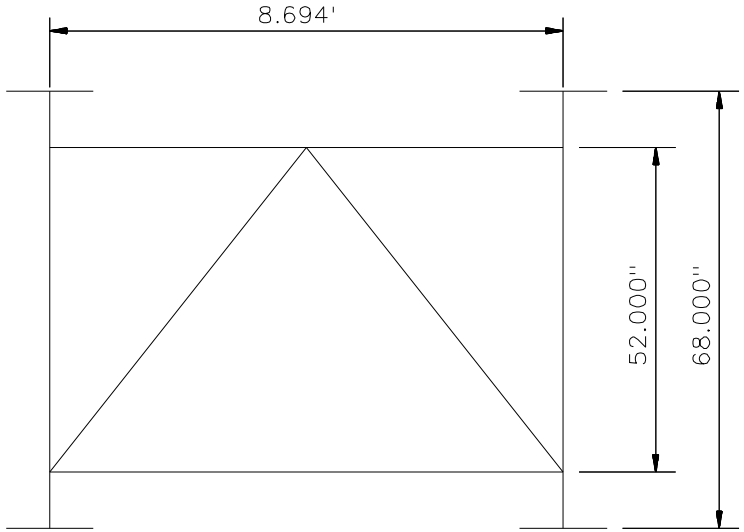

NOTE:

1. ALL CROSS FRAME MEMBERS ARE L8x6x1/2 (LLV).
2. GIRDER CONNECTION PLATE IS 1.250''x8.000''.

TYPICAL CROSS FRAME AT SUPPORT

LOADING NOTES:

1. STEEL DEAD LOAD INCREASED BY 5% (MDX AND LARSA), 10% (APPROX.), AND 2% (3D) TO ACCOUNT FOR MISC. DETAILS.
2. FORMWORK LOAD OF 10PSF IS INCLUDED IN CONCRETE DEAD LOAD.

NCHRP 12-79

BRIDGE EICCR22a

CROSS - FRAMES AND LOADING NOTES

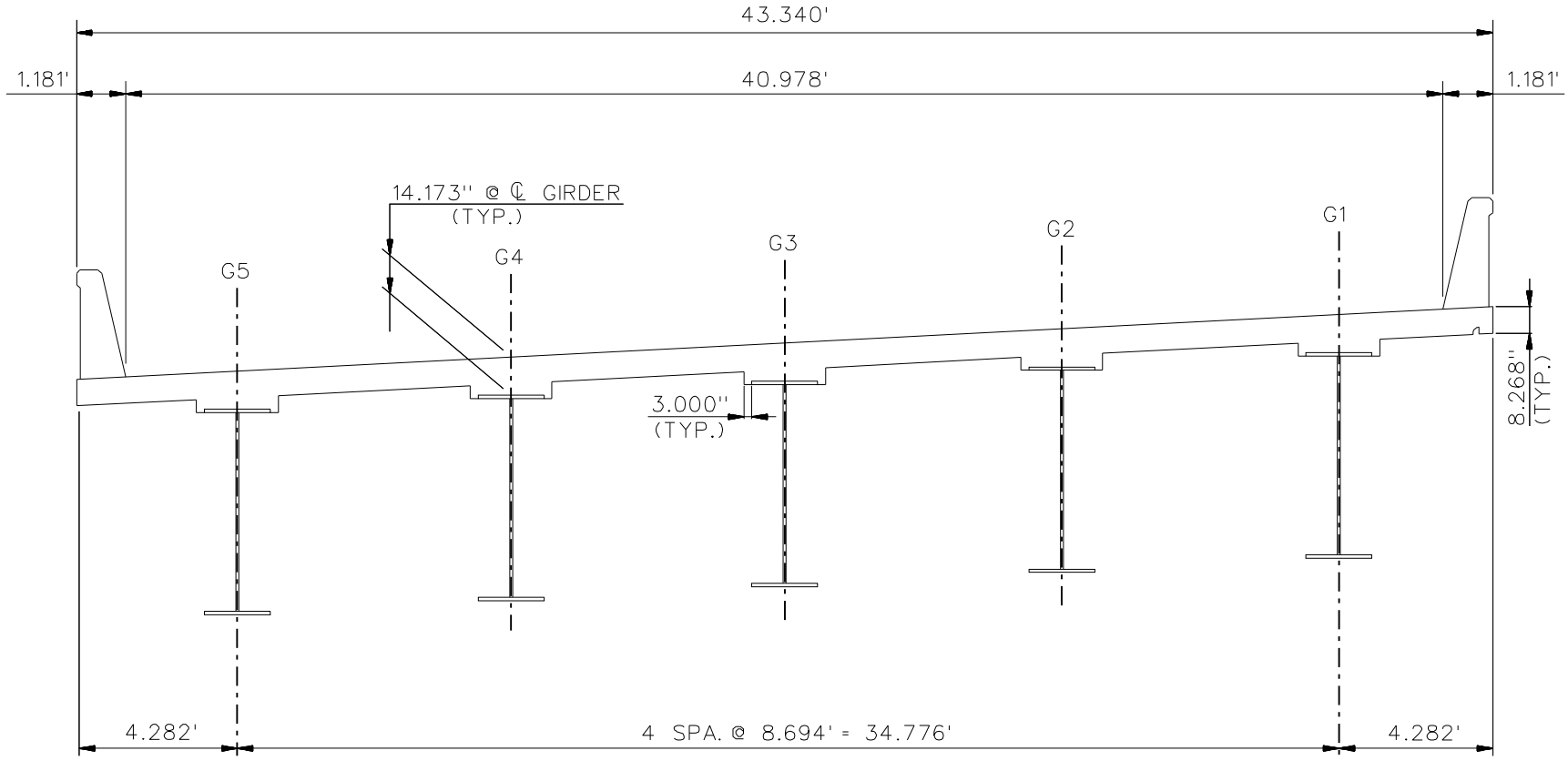

TYPICAL SECTION

NOTE:

1. CROSS-FRAMES ARE NOT SHOWN FOR CLARITY.

NCHRP 12-79

BRIDGE EICCR22a

TYPICAL SECTION

SHEET 12 OF X

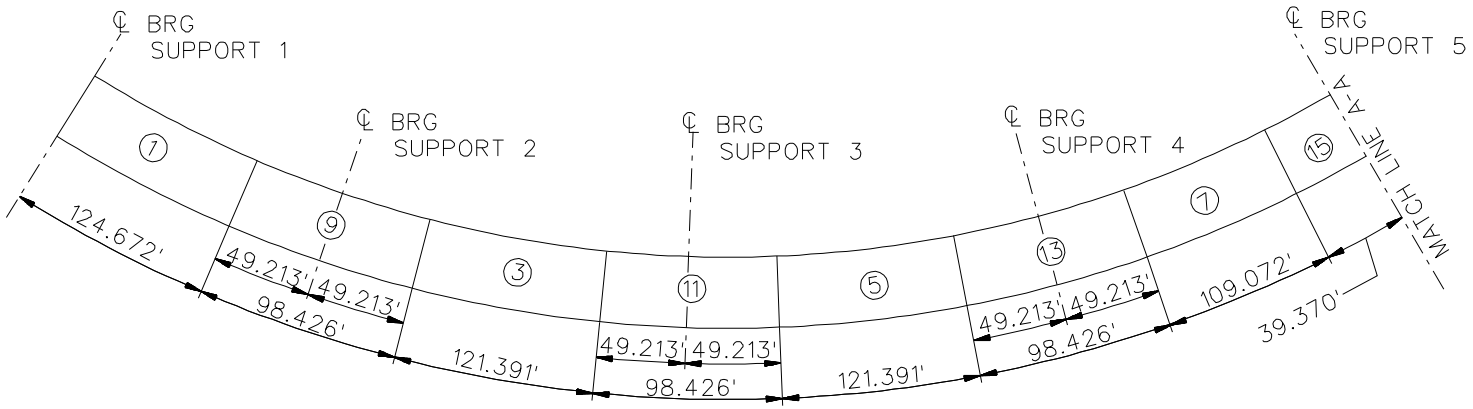

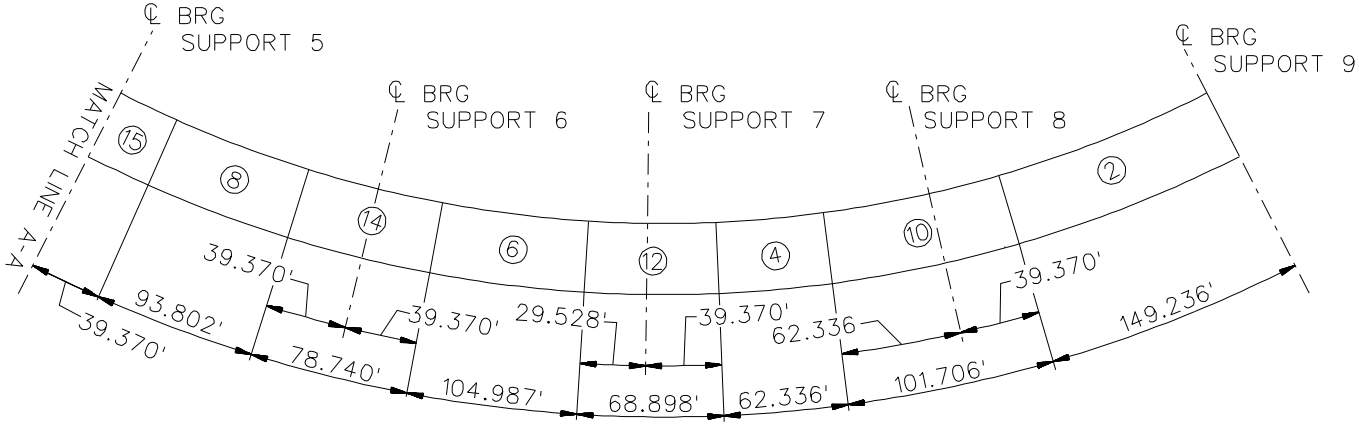

DECK POUR SEQUENCE

NCHRP 12-79

BRIDGE EICCR22a

DECK POUR SEQUENCE

SHEET 13 OF X

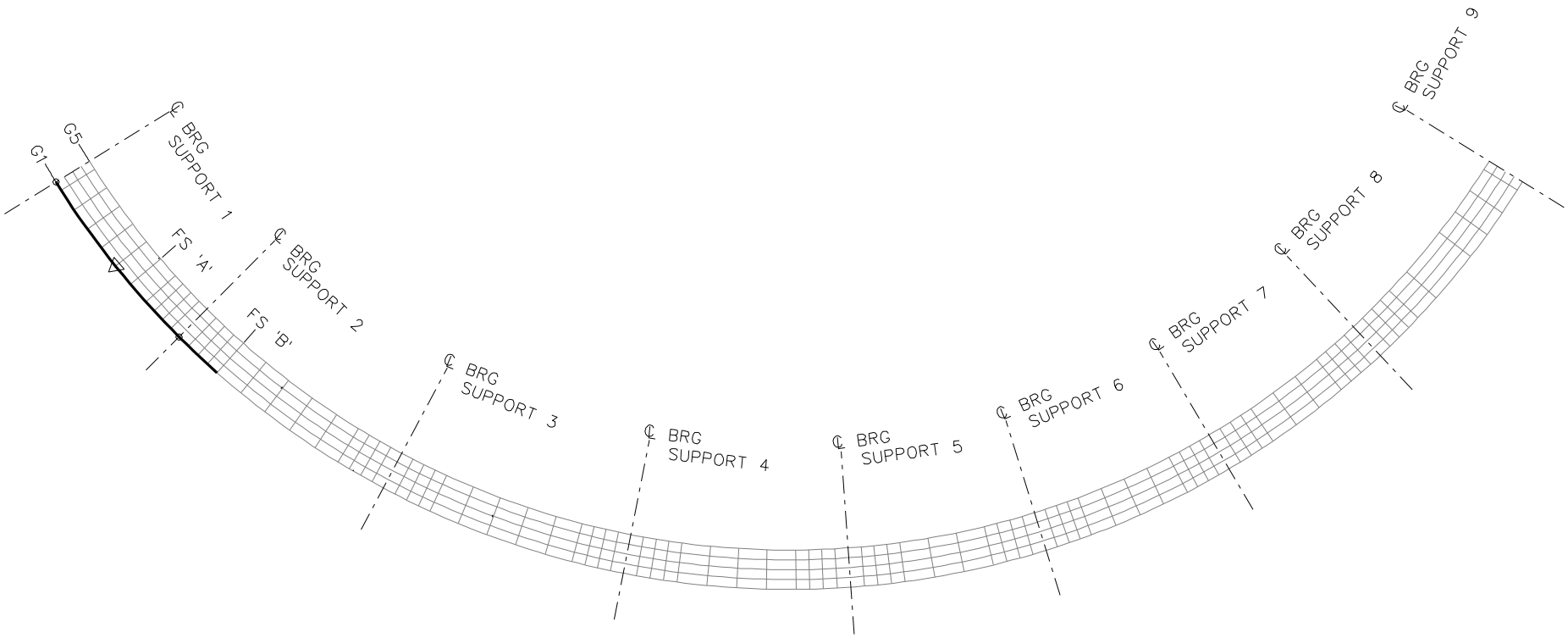

ERECTION SEQUENCE

STAGE 1-A

LEGEND

▽ = HOLD OR LIFT CRANE

○ = TIE DOWN

□ = TEMPORARY SUPPORT STRUCTURE

FS = FIELD SPLICE

NCHRP 12-79

BRIDGE EICCR22a

ERECTION SEQUENCE

SHEET 14 OF X

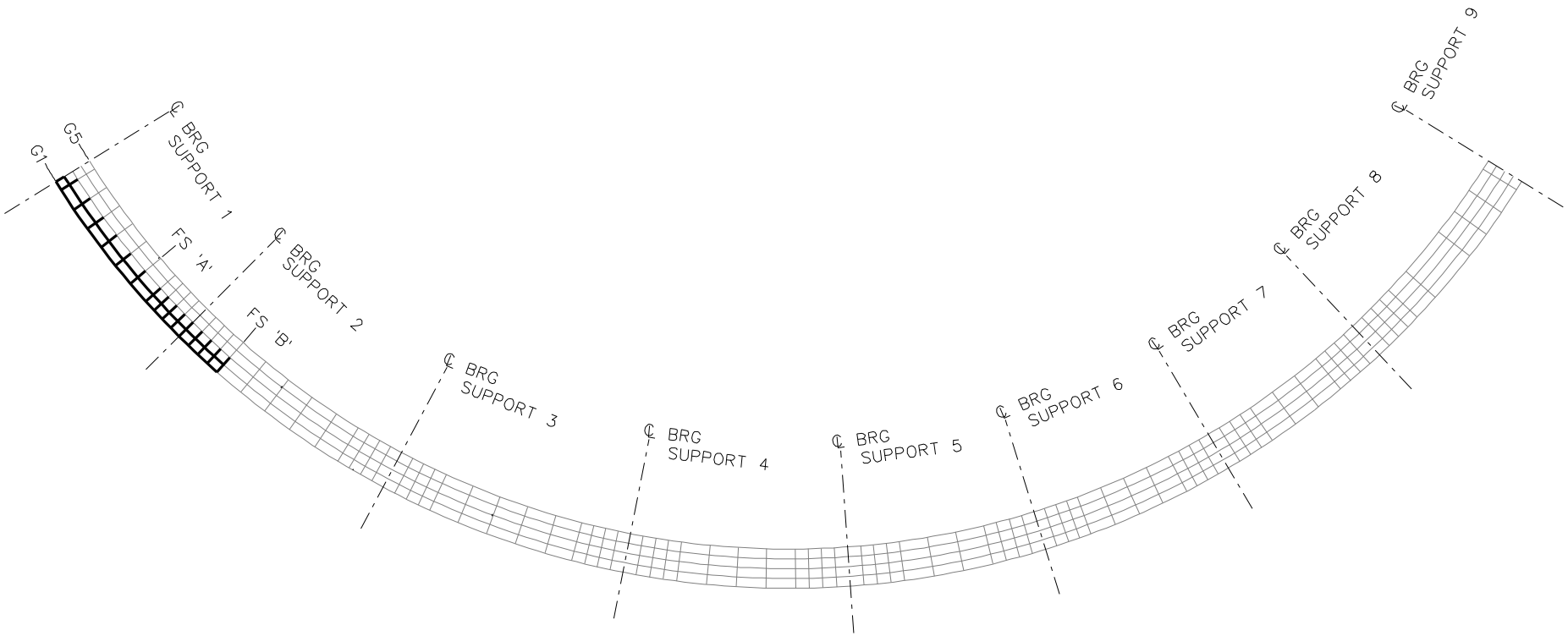

ERECTION SEQUENCE

STAGE 1-B

LEGEND

▽ = HOLD OR LIFT CRANE

○ = TIE DOWN

□ = TEMPORARY SUPPORT STRUCTURE

FS = FIELD SPLICE

NCHRP 12-79

BRIDGE EICCR22a

ERECTION SEQUENCE

SHEET 15 OF X

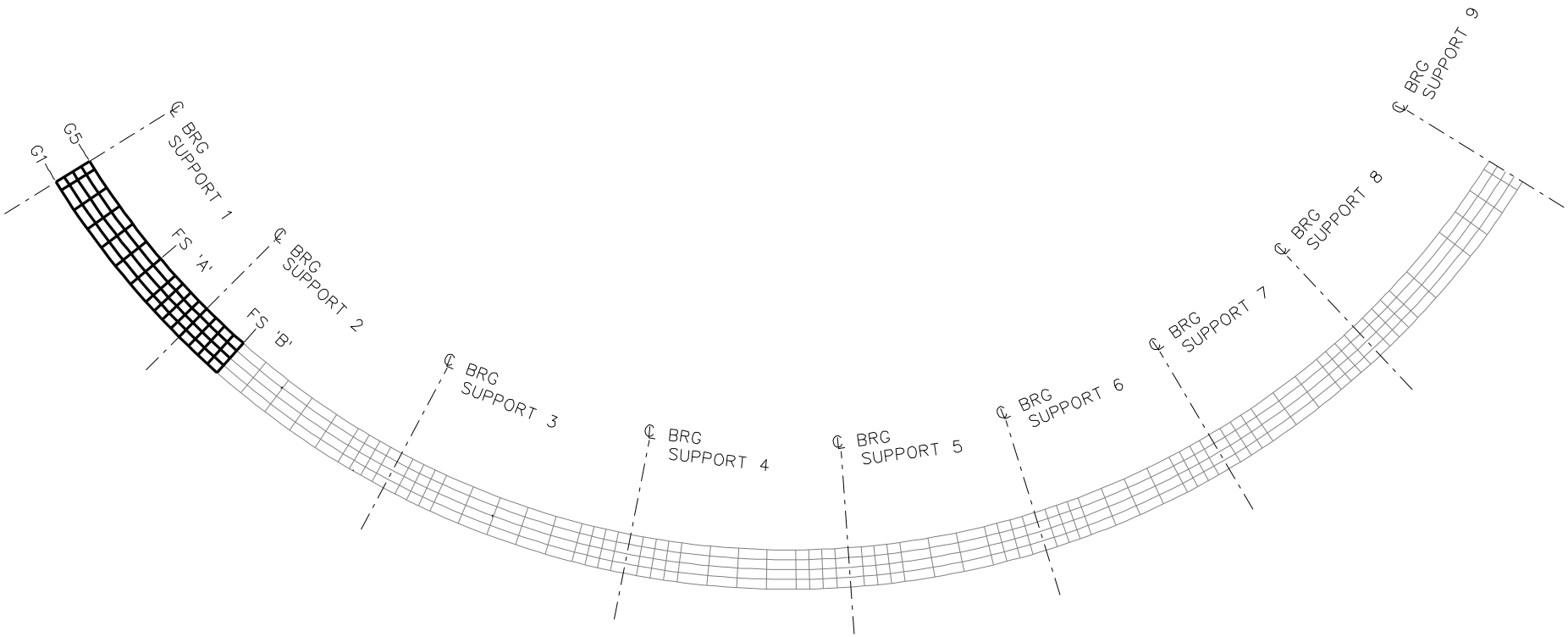

ERECTION SEQUENCE

STAGE 1-E

LEGEND

▽ = HOLD OR LIFT CRANE

○ = TIE DOWN

□ = TEMPORARY SUPPORT STRUCTURE

FS = FIELD SPLICE

NCHRP 12-79

BRIDGE EICCR22a

ERECTION SEQUENCE

SHEET 16 OF X

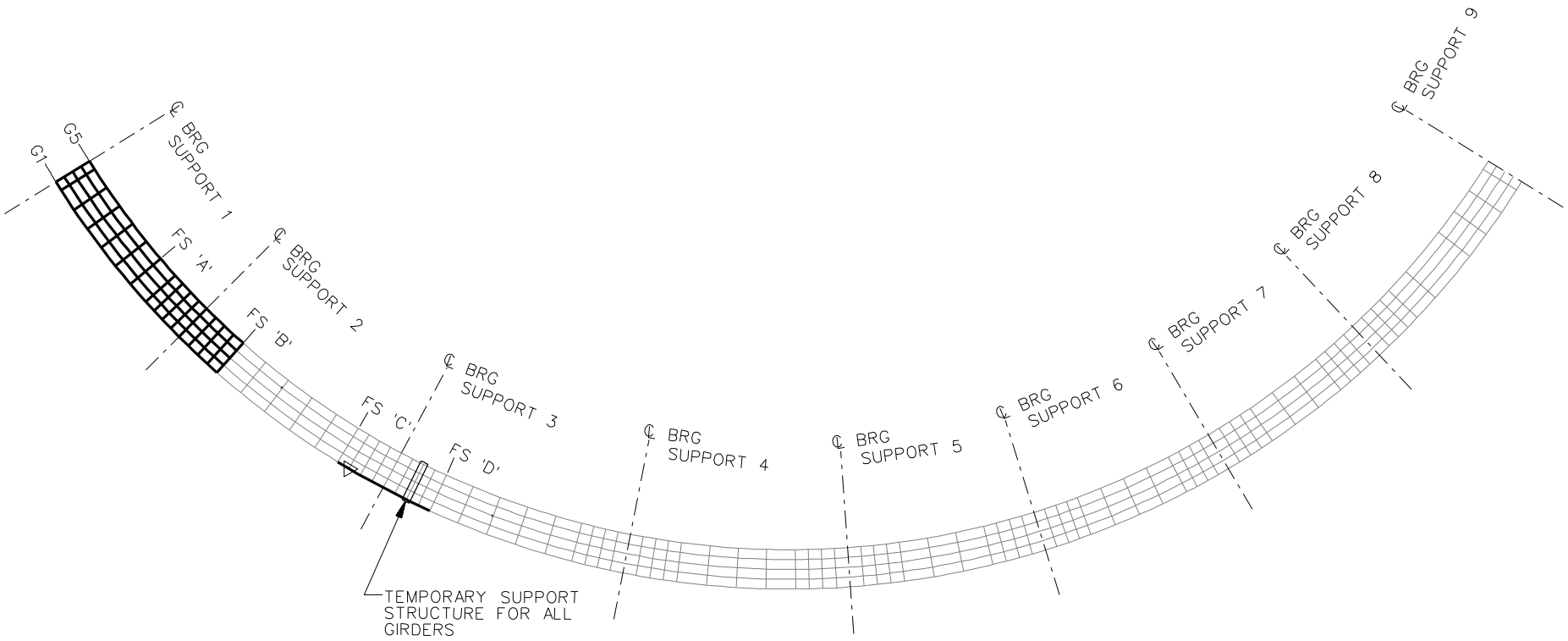

ERECTION SEQUENCE

STAGE 2-A

LEGEND

▽ = HOLD OR LIFT CRANE

○ = TIE DOWN

□ = TEMPORARY SUPPORT STRUCTURE

FS = FIELD SPLICE

NCHRP 12-79

BRIDGE EICCR22a

ERECTION SEQUENCE

SHEET 17 OF X

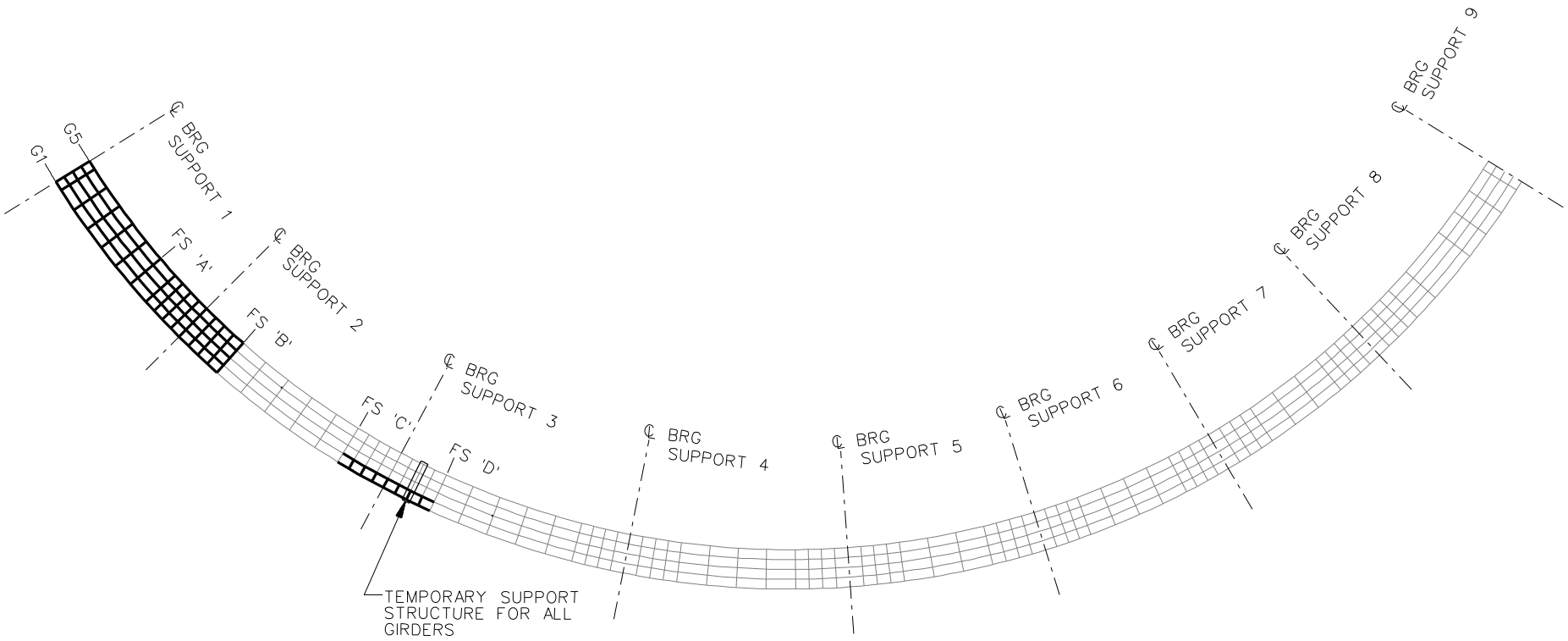

ERECTION SEQUENCE

STAGE 2-B

LEGEND

▽ = HOLD OR LIFT CRANE

○ = TIE DOWN

□ = TEMPORARY SUPPORT STRUCTURE

FS= FIELD SPLICE

NCHRP 12-79

BRIDGE EICCR22a

ERECTION SEQUENCE

SHEET 18 OF X

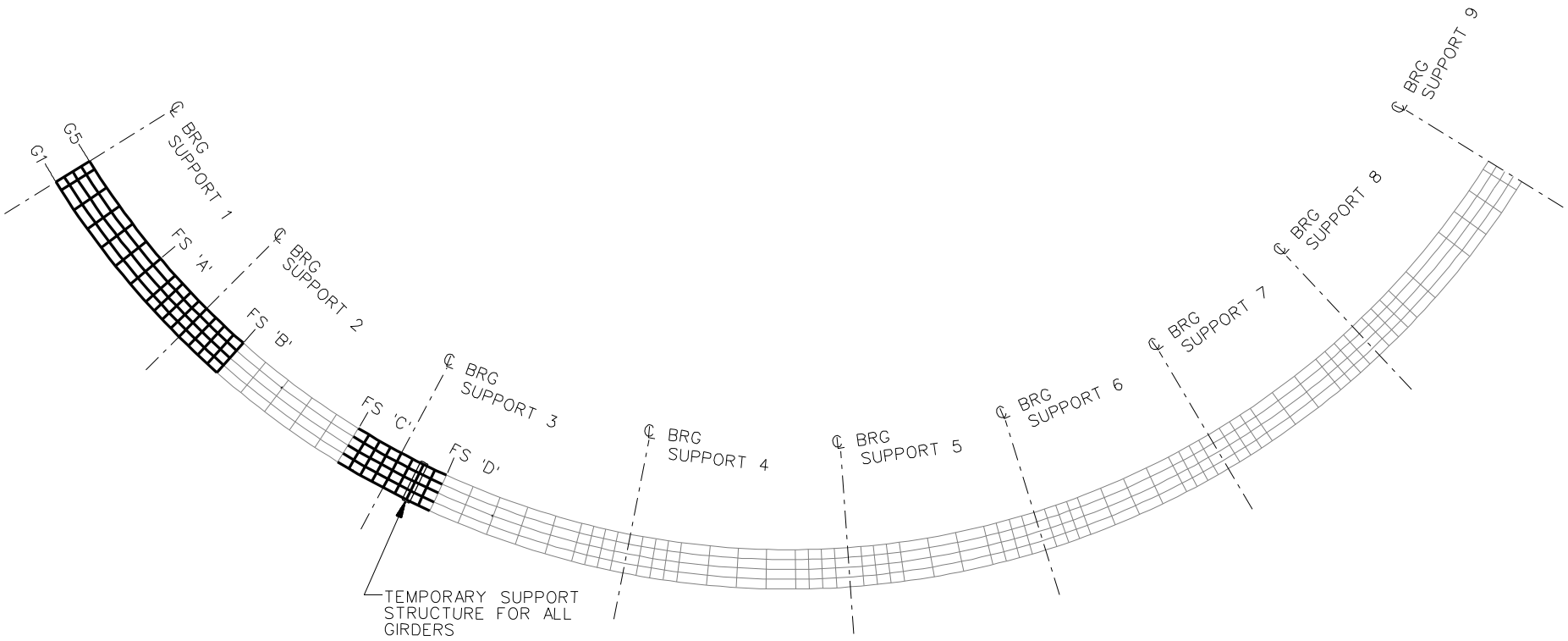

ERECTION SEQUENCE

STAGE 2-E

LEGEND

▽ = HOLD OR LIFT CRANE

○ = TIE DOWN

□ = TEMPORARY SUPPORT STRUCTURE

FS = FIELD SPLICE

NCHRP 12-79

BRIDGE EICCR22a

ERECTION SEQUENCE

SHEET 19 OF X

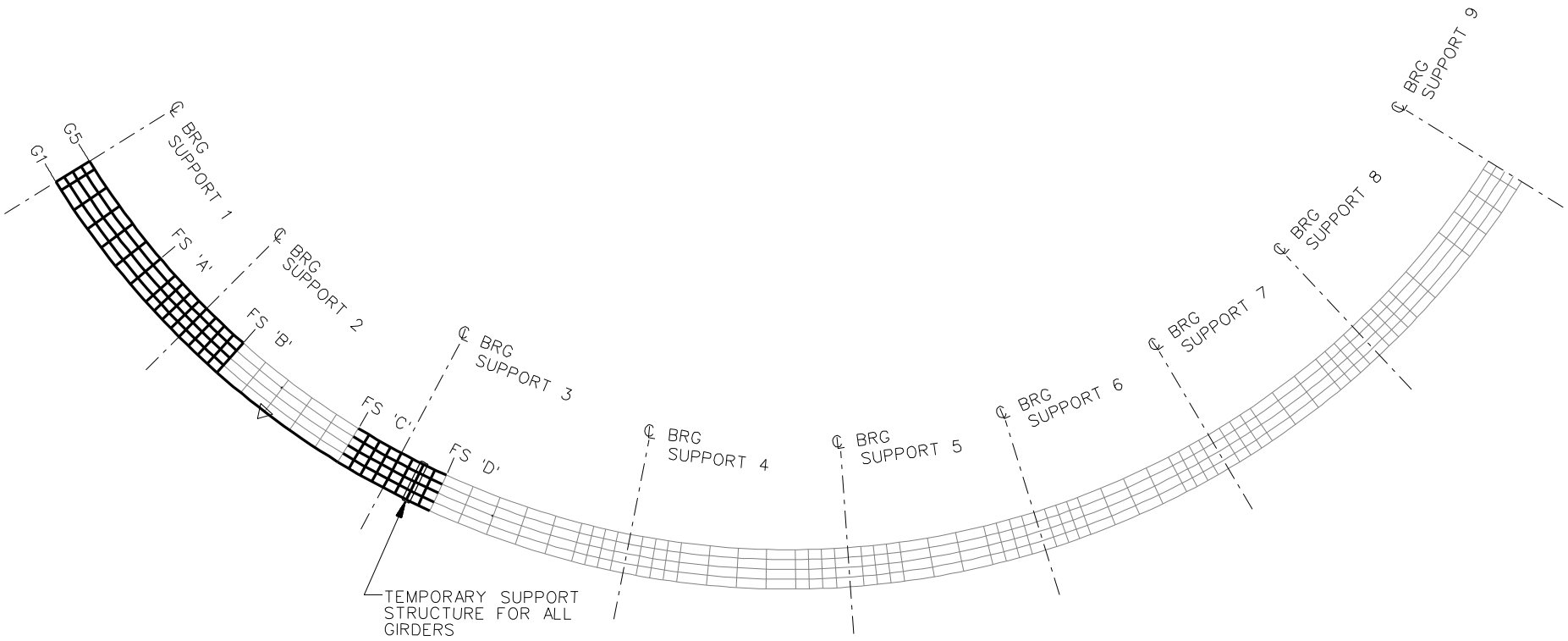

ERECTION SEQUENCE

STAGE 3-A

LEGEND

▽ = HOLD OR LIFT CRANE

○ = TIE DOWN

□ = TEMPORARY SUPPORT STRUCTURE

FS = FIELD SPLICE

NCHRP 12-79

BRIDGE EICCR22a

ERECTION SEQUENCE

SHEET 20 OF X

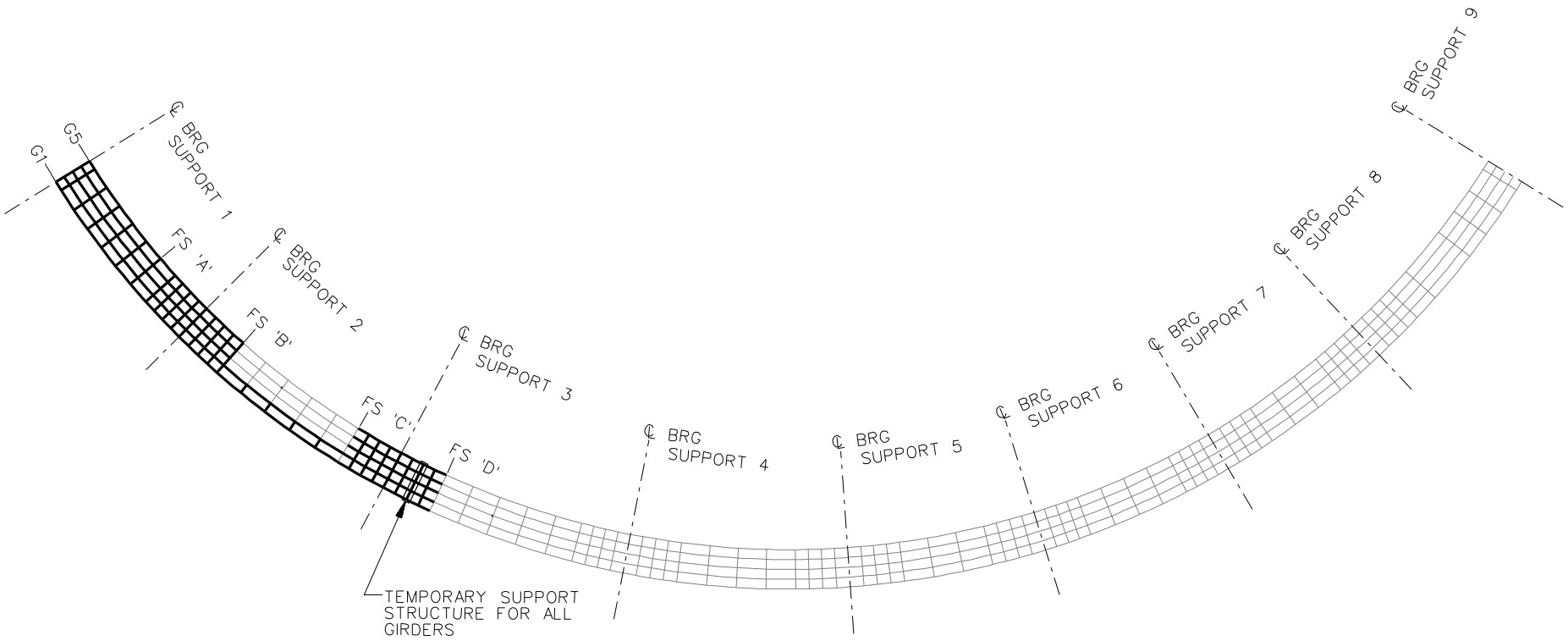

ERECTION SEQUENCE

STAGE 3-B

LEGEND

▽ = HOLD OR LIFT CRANE

○ = TIE DOWN

□ = TEMPORARY SUPPORT STRUCTURE

FS = FIELD SPLICE

NCHRP 12-79

BRIDGE EICCR22a

ERECTION SEQUENCE

SHEET 21 OF X

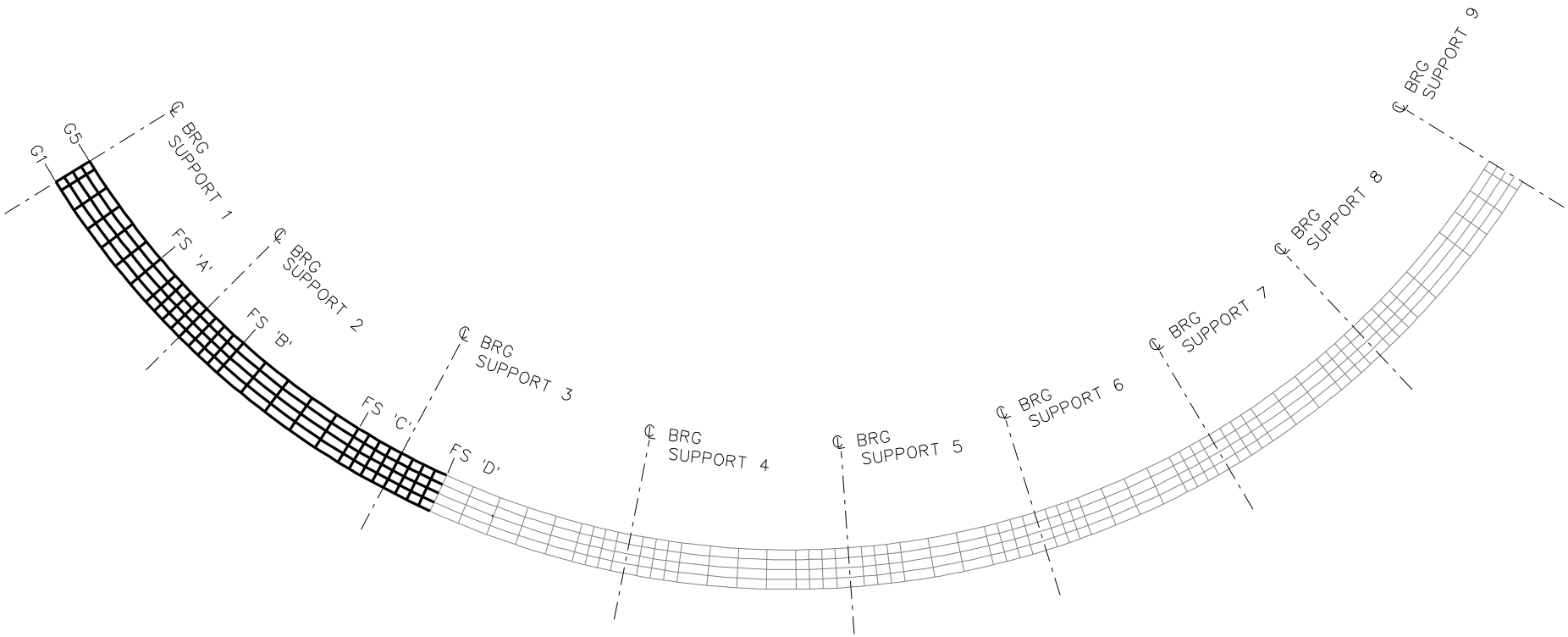

ERECTION SEQUENCE

STAGE 3-E

LEGEND

▽ = HOLD OR LIFT CRANE

○ = TIE DOWN

□ = TEMPORARY SUPPORT STRUCTURE

FS = FIELD SPLICE

NCHRP 12-79

BRIDGE EICCR22a

ERECTION SEQUENCE

SHEET 22 OF X

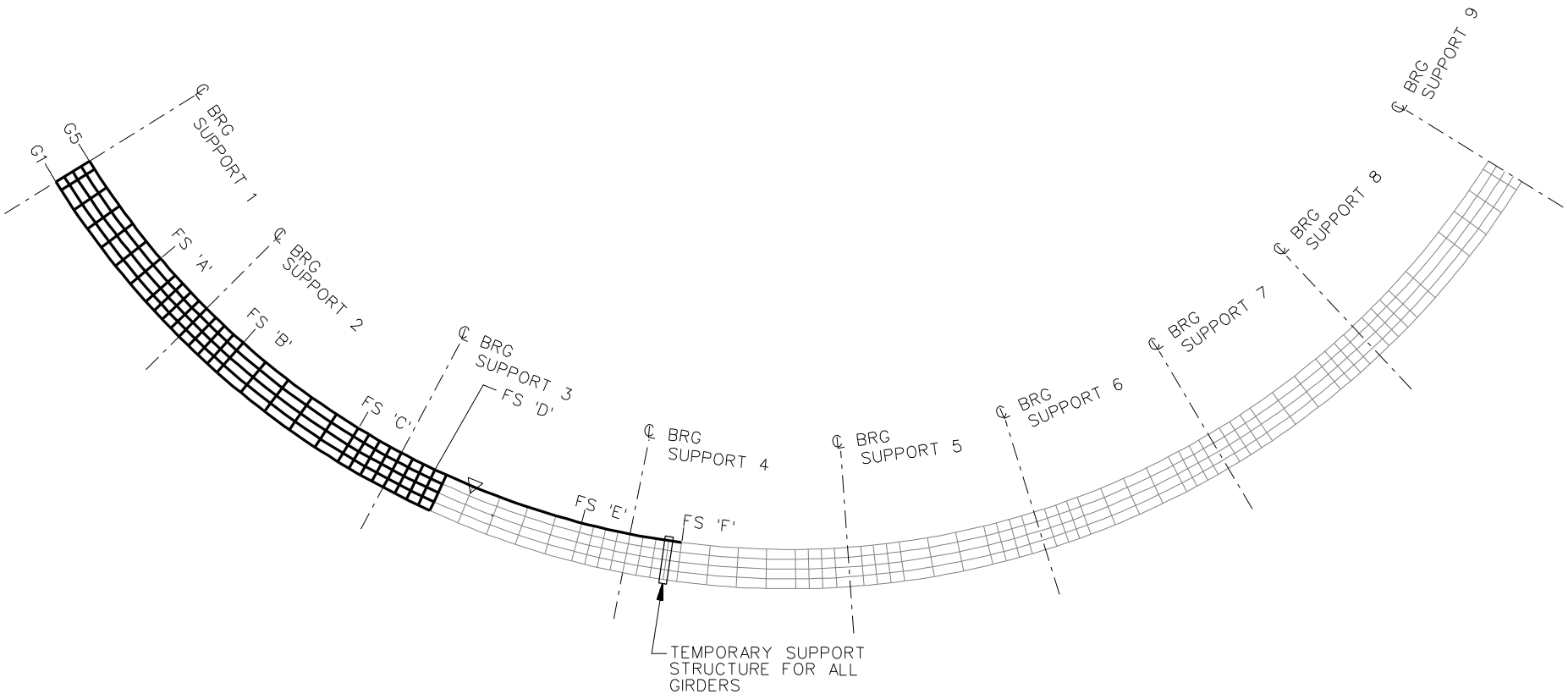

ERECTION SEQUENCE
STAGE 4-A

LEGEND

▽ = HOLD OR LIFT CRANE

○ = TIE DOWN

□ = TEMPORARY SUPPORT STRUCTURE

FS= FIELD SPLICE

NCHRP 12-79

BRIDGE EICCR22a

ERECTION SEQUENCE

SHEET 23 OF X

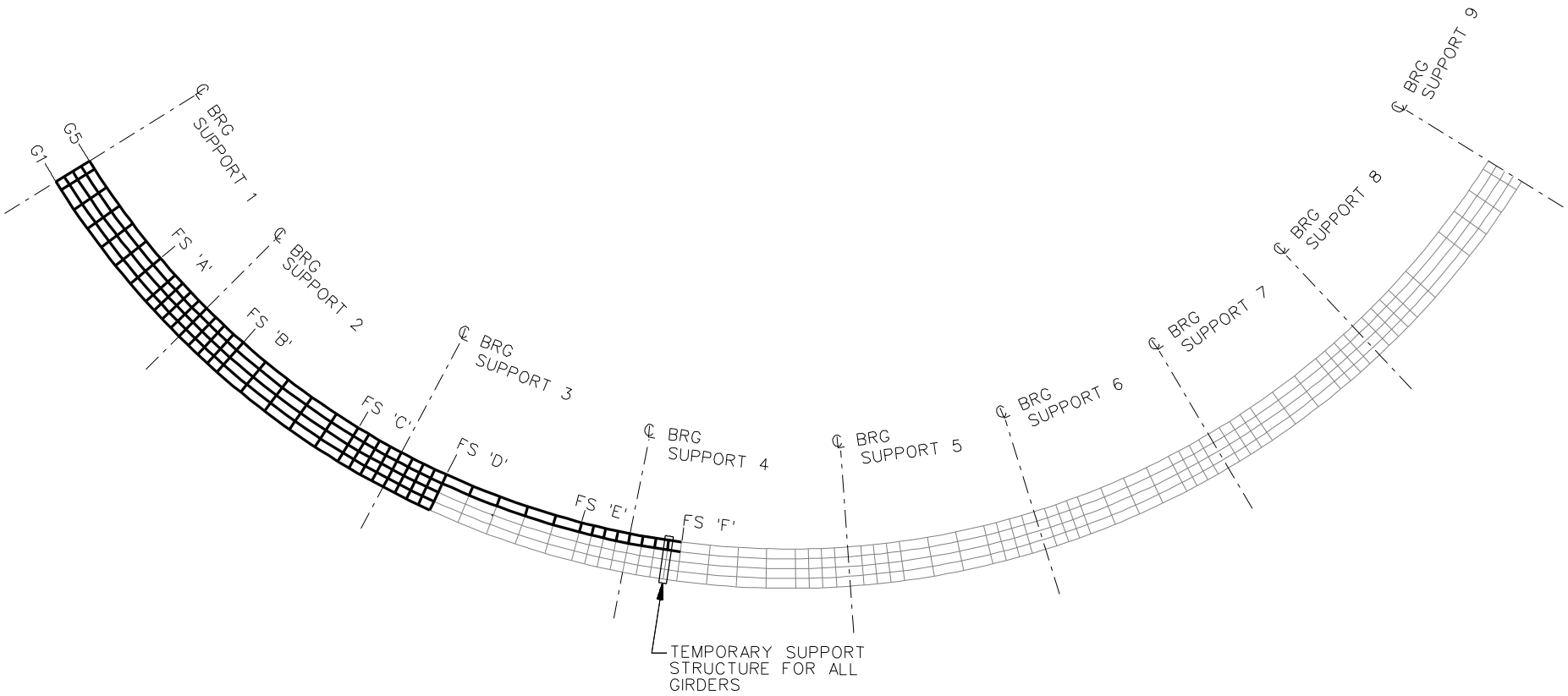

ERECTION SEQUENCE
STAGE 4-B

LEGEND

▽ = HOLD OR LIFT CRANE

○ = TIE DOWN

□ = TEMPORARY SUPPORT STRUCTURE

FS= FIELD SPLICE

NCHRP 12-79

BRIDGE EICCR22a

EECTIONR SEQUENCE

SHEET 24 OF X

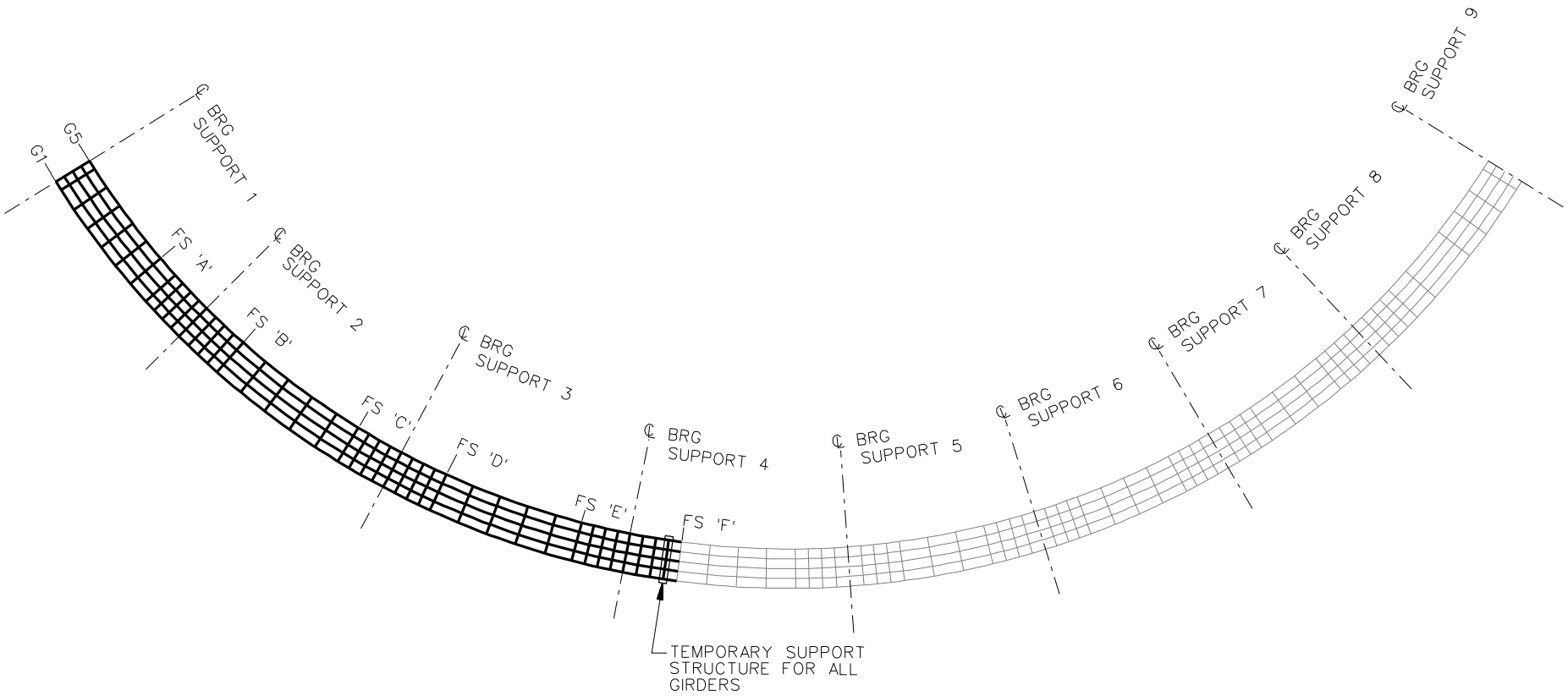

ERECTION SEQUENCE

STAGE 4-E

LEGEND

▽ = HOLD OR LIFT CRANE

○ = TIE DOWN

□ = TEMPORARY SUPPORT STRUCTURE

FS = FIELD SPLICE

NCHRP 12-79

BRIDGE EICCR22a

ERECTION SEQUENCE

SHEET 25 OF X

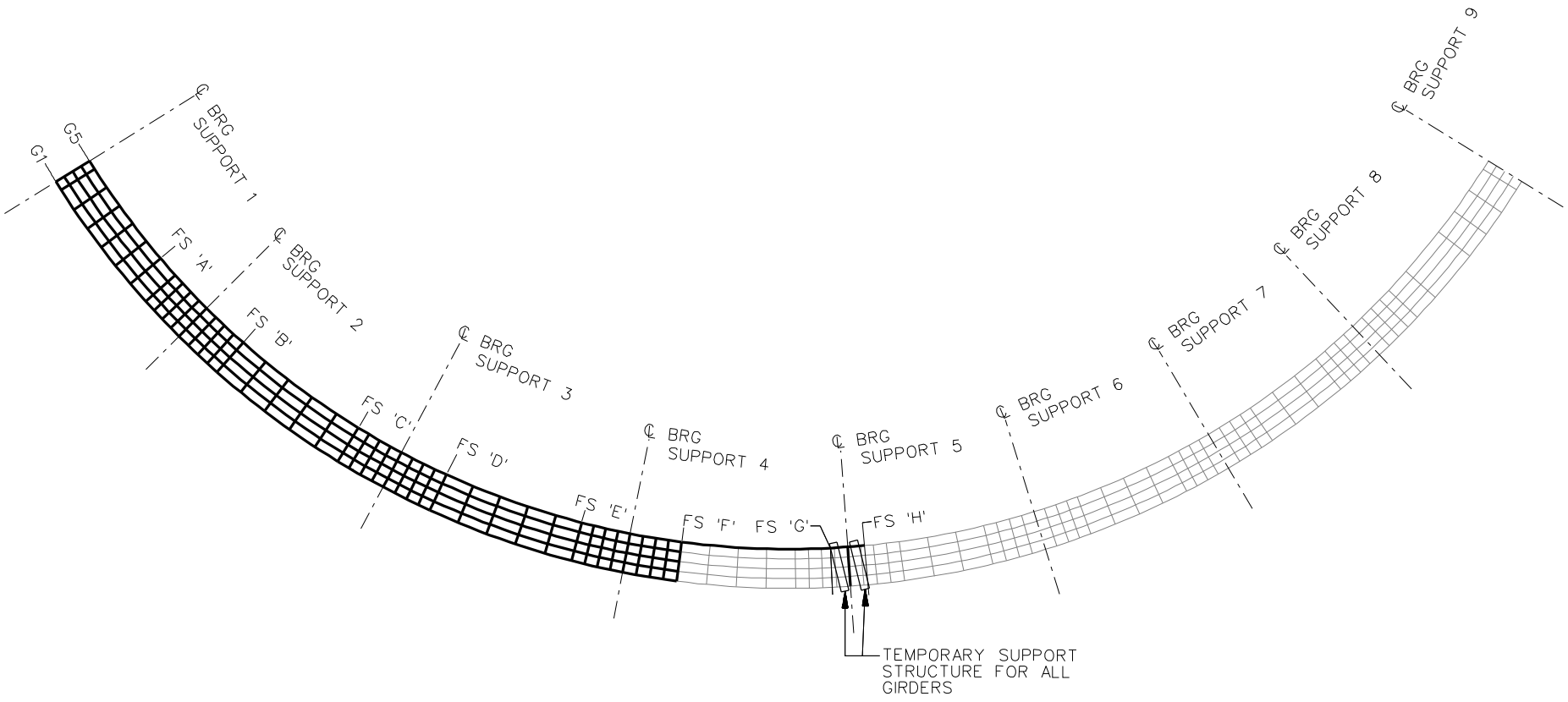

ERECTION SEQUENCE

STAGE 5-A

LEGEND

▽ = HOLD OR LIFT CRANE

○ = TIE DOWN

□ = TEMPORARY SUPPORT STRUCTURE

FS = FIELD SPLICE

NCHRP 12-79

BRIDGE EICCR22a

ERECTION SEQUENCE

SHEET 26 OF X

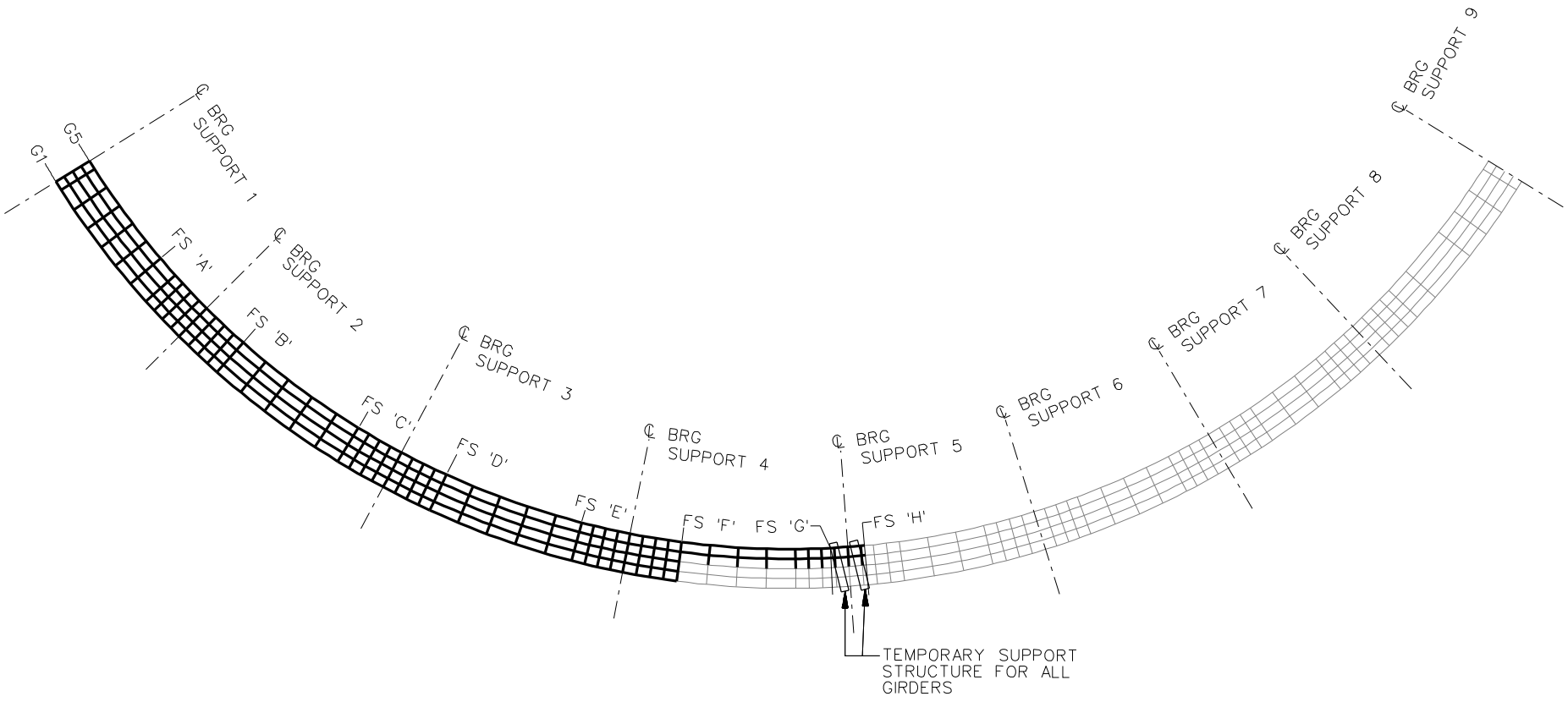

ERECTION SEQUENCE
STAGE 5-B

LEGEND

▽ = HOLD OR LIFT CRANE

○ = TIE DOWN

□ = TEMPORARY SUPPORT STRUCTURE

FS= FIELD SPLICE

NCHRP 12-79

BRIDGE EICCR22a

ERECTION SEQUENCE

SHEET 27 OF X

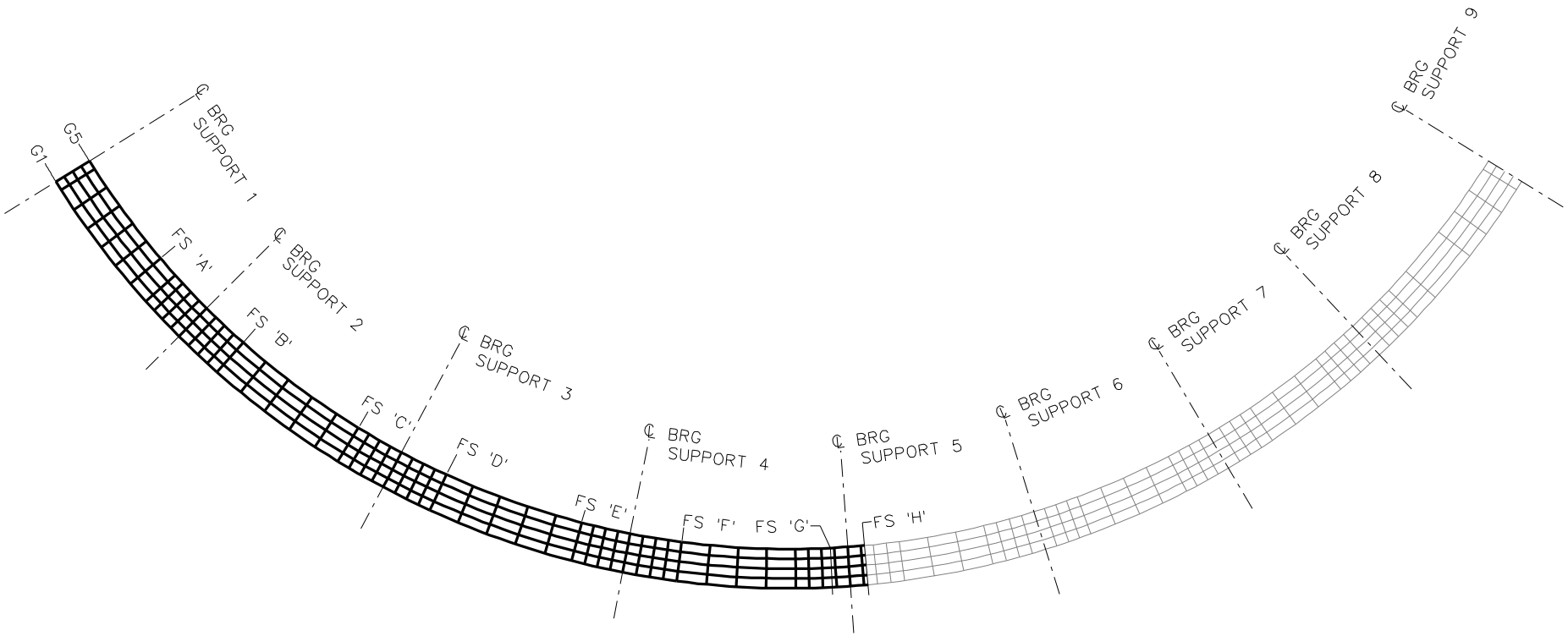

ERECTION SEQUENCE

STAGE 5-E

LEGEND

▽ = HOLD OR LIFT CRANE

○ = TIE DOWN

□ = TEMPORARY SUPPORT STRUCTURE

FS = FIELD SPLICE

NCHRP 12-79

BRIDGE EICCR22a

ERECTION SEQUENCE

SHEET 28 OF X

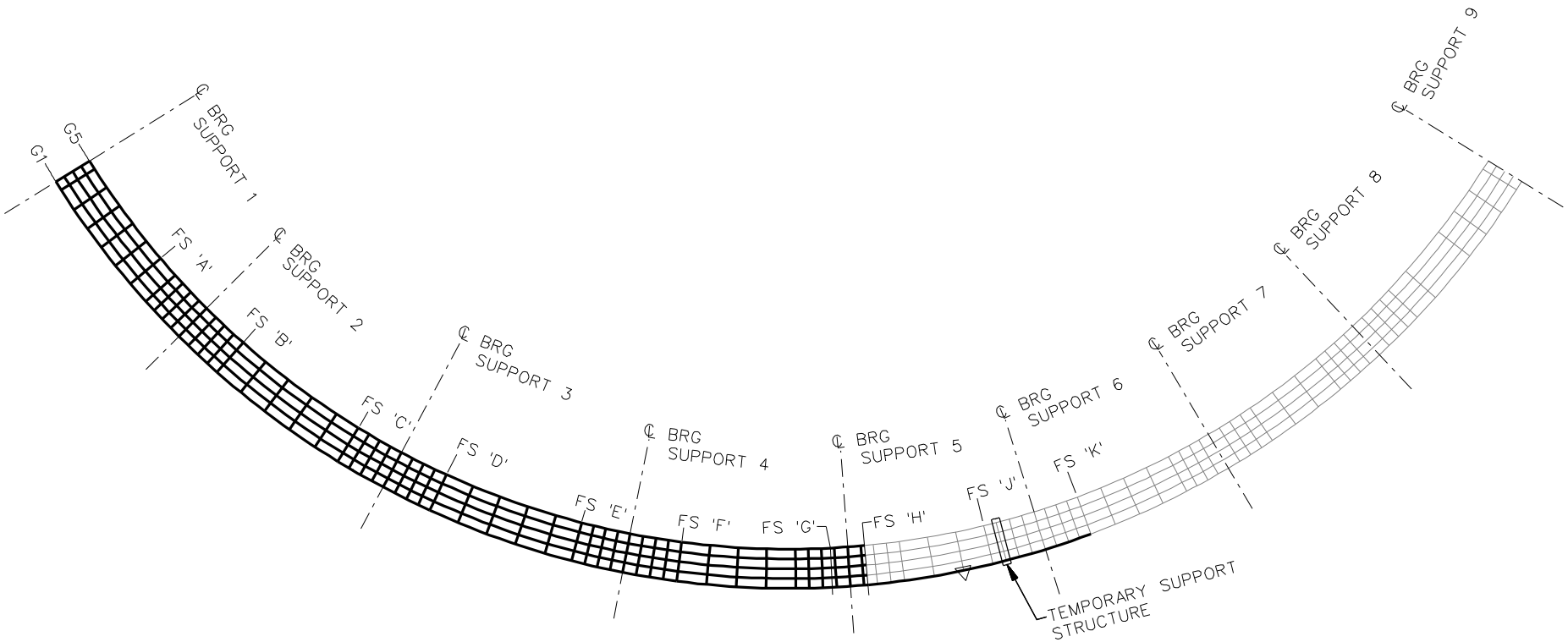

ERECTION SEQUENCE
STAGE 6-A

LEGEND

▽ = HOLD OR LIFT CRANE

○ = TIE DOWN

□ = TEMPORARY SUPPORT STRUCTURE

FS= FIELD SPLICE

NCHRP 12-79

BRIDGE EICCR22a

ERECTION SEQUENCE

SHEET 29 OF X

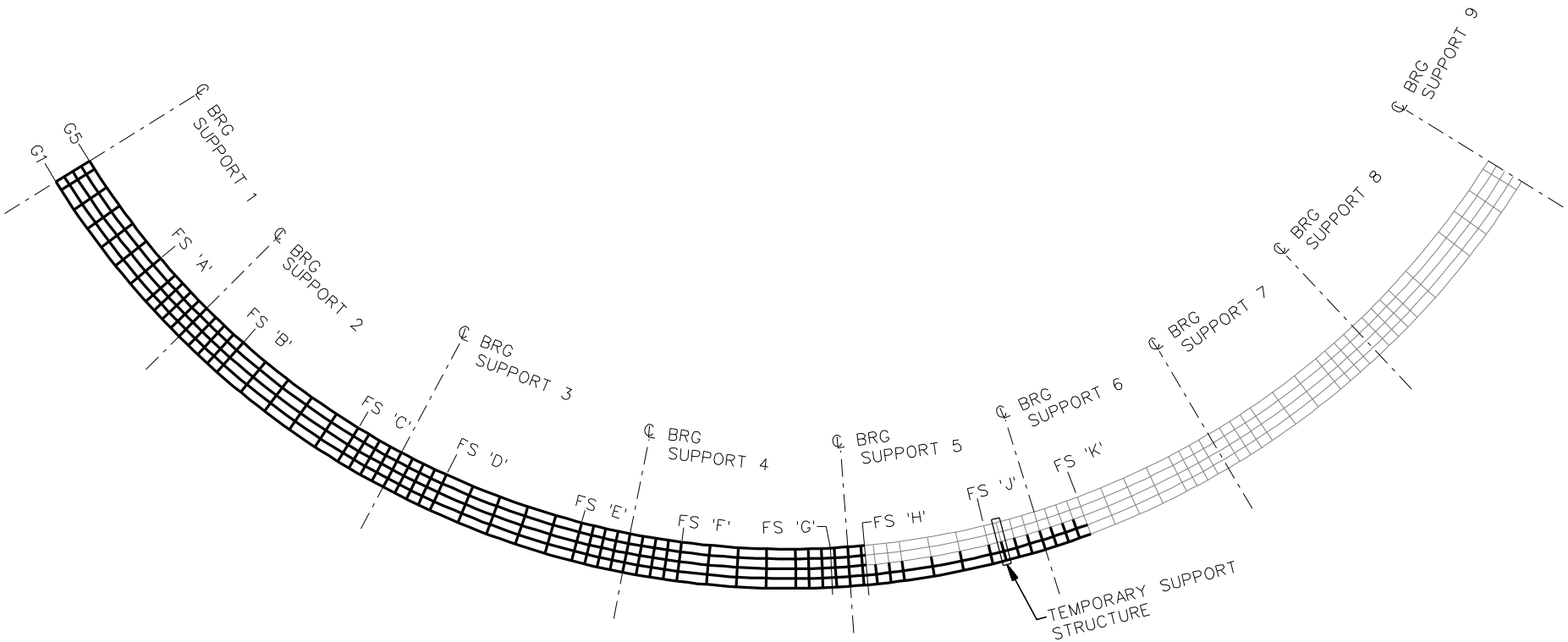

ERECTION SEQUENCE
STAGE 6-B

LEGEND

▽ = HOLD OR LIFT CRANE

○ = TIE DOWN

□ = TEMPORARY SUPPORT STRUCTURE

FS = FIELD SPLICE

NCHRP 12-79

BRIDGE EICCR22a

ERECTION SEQUENCE

SHEET 30 OF X

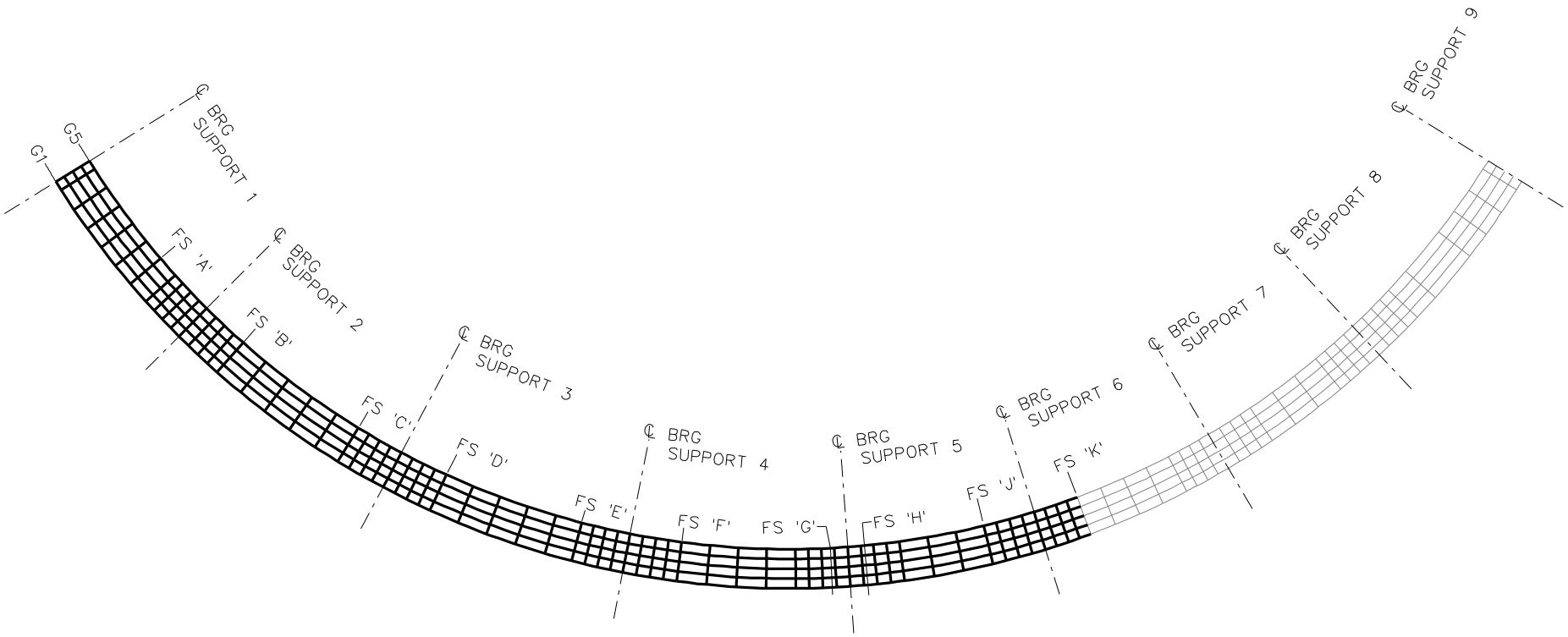

ERECTION SEQUENCE

STAGE 6-E

LEGEND

▽ = HOLD OR LIFT CRANE

○ = TIE DOWN

□ = TEMPORARY SUPPORT STRUCTURE

FS = FIELD SPLICE

NCHRP 12-79

BRIDGE EICCR22a

ERECTION SEQUENCE

SHEET 31 OF X

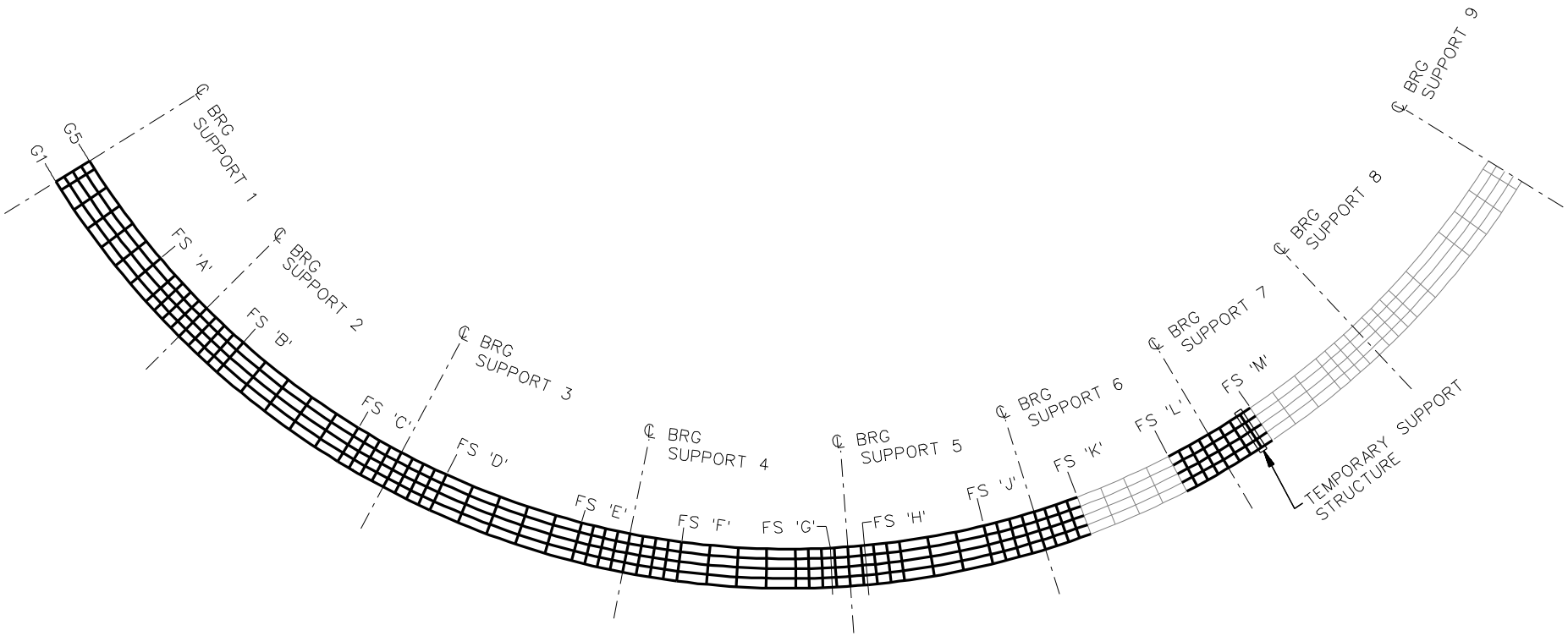

ERECTION SEQUENCE

STAGE 7-A TO E

LEGEND

▽ = HOLD OR LIFT CRANE

○ = TIE DOWN

□ = TEMPORARY SUPPORT STRUCTURE

FS= FIELD SPLICE

7-A - ERECT G5

7-B - ERECT G4 AND CROSSFRAMES BETWEEN G4 AND G5.

7-C - ERECT G3 AND CROSSFRAMES BETWEEN G3 AND G4.

7-D - ERECT G2 AND CROSSFRAMES BETWEEN G2 AND G3.

7-E - ERECT G1 AND CROSSFRAMES BETWEEN G1 AND G2.

NCHRP 12-79

BRIDGE EICCR22a

ERECTION SEQUENCE

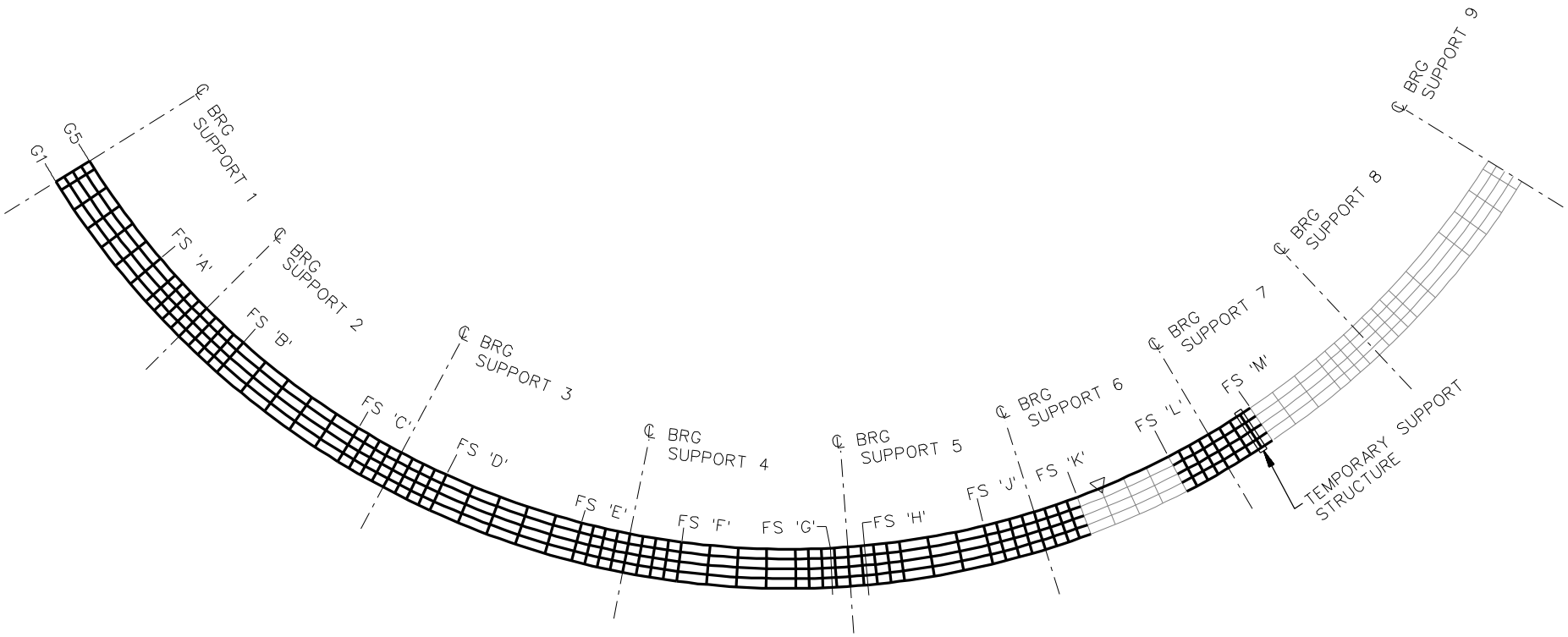

ERECTION SEQUENCE

STAGE 8-A

LEGEND

▽ = HOLD OR LIFT CRANE

○ = TIE DOWN

□ = TEMPORARY SUPPORT STRUCTURE

FS = FIELD SPLICE

NCHRP 12-79

BRIDGE EICCR22a

ERECTION SEQUENCE

SHEET 33 OF X

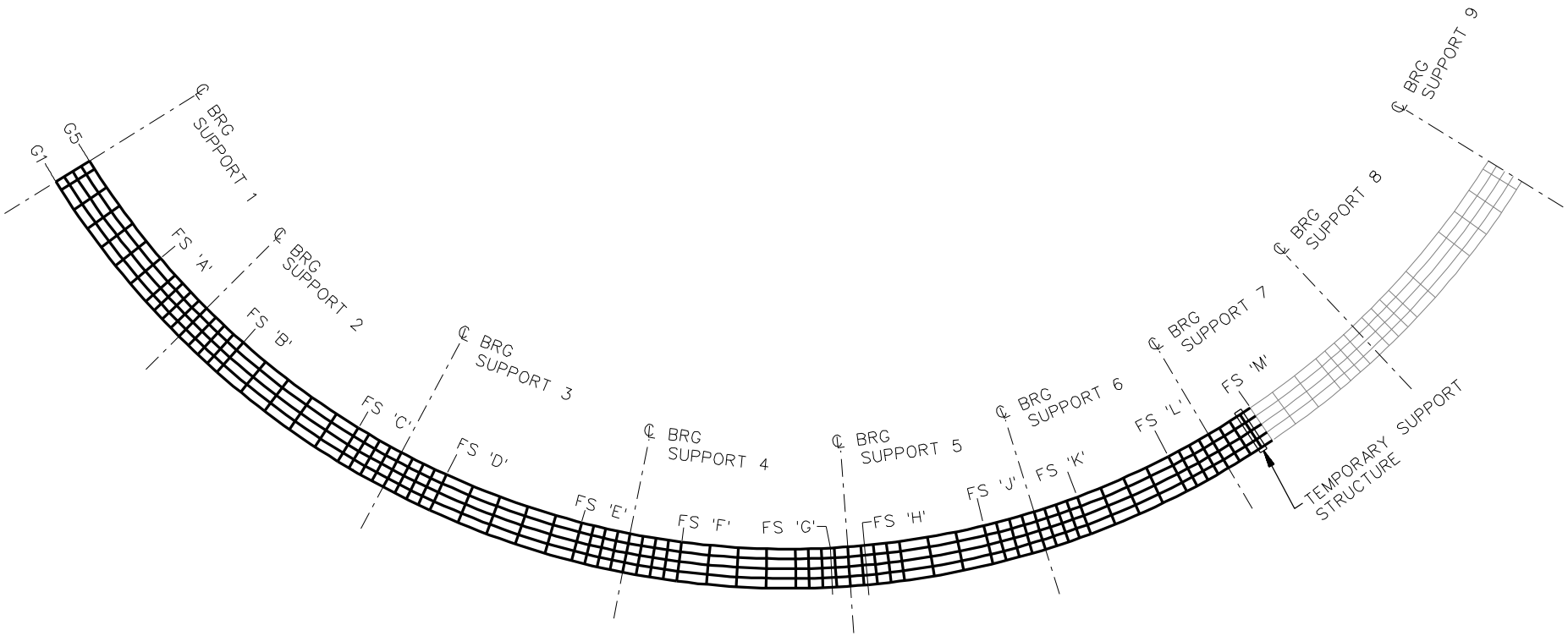

ERECTION SEQUENCE

STAGE 8-B TO 8-E

8-B - ERECT G4 AND CROSSFRAMES BETWEEN G4 AND G5.

8-C - ERECT G3 AND CROSSFRAMES BETWEEN G3 AND G4.

8-D - ERECT G2 AND CROSSFRAMES BETWEEN G2 AND G3.

8-E - ERECT G1 AND CROSSFRAMES BETWEEN G1 AND G2.

LEGEND

▽ = HOLD OR LIFT CRANE

○ = TIE DOWN

□ = TEMPORARY SUPPORT STRUCTURE

FS = FIELD SPLICE

NCHRP 12-79

BRIDGE EICCR22a

ERECTION SEQUENCE

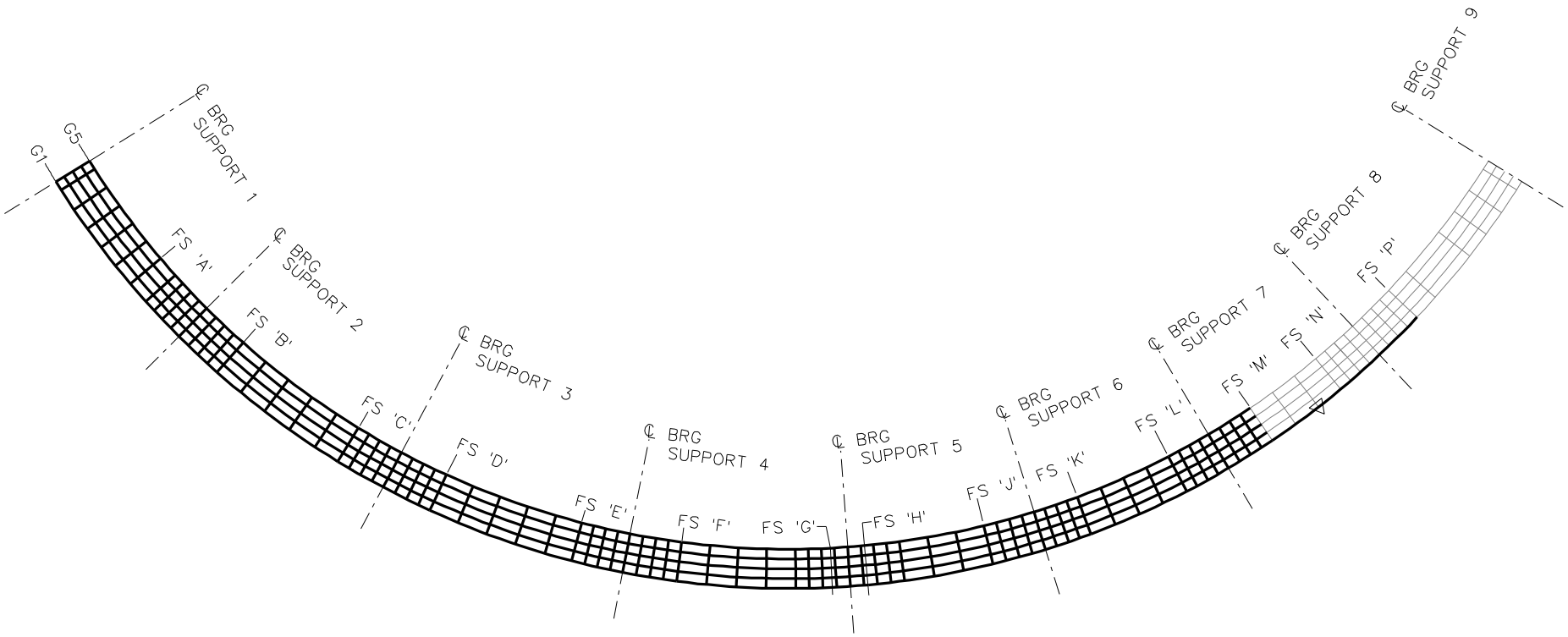

ERECTION SEQUENCE

STAGE 9-A

LEGEND

▽ = HOLD OR LIFT CRANE

○ = TIE DOWN

□ = TEMPORARY SUPPORT STRUCTURE

FS = FIELD SPLICE

NCHRP 12-79

BRIDGE EICCR22a

ERECTION SEQUENCE

SHEET 35 OF X

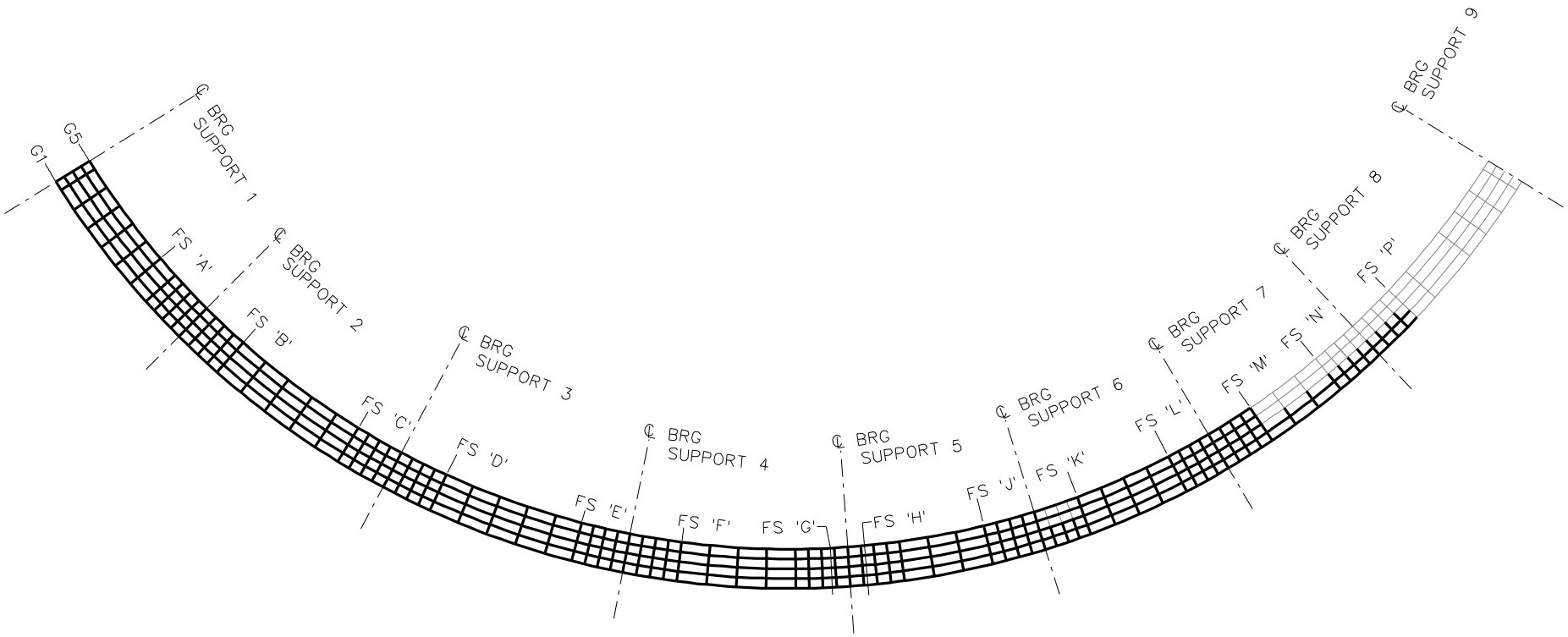

ERECTION SEQUENCE

STAGE 9-B

LEGEND

▽ = HOLD OR LIFT CRANE

○ = TIE DOWN

□ = TEMPORARY SUPPORT STRUCTURE

FS = FIELD SPLICE

NCHRP 12-79

BRIDGE EICCR22a

ERECTION SEQUENCE

SHEET 36 OF X

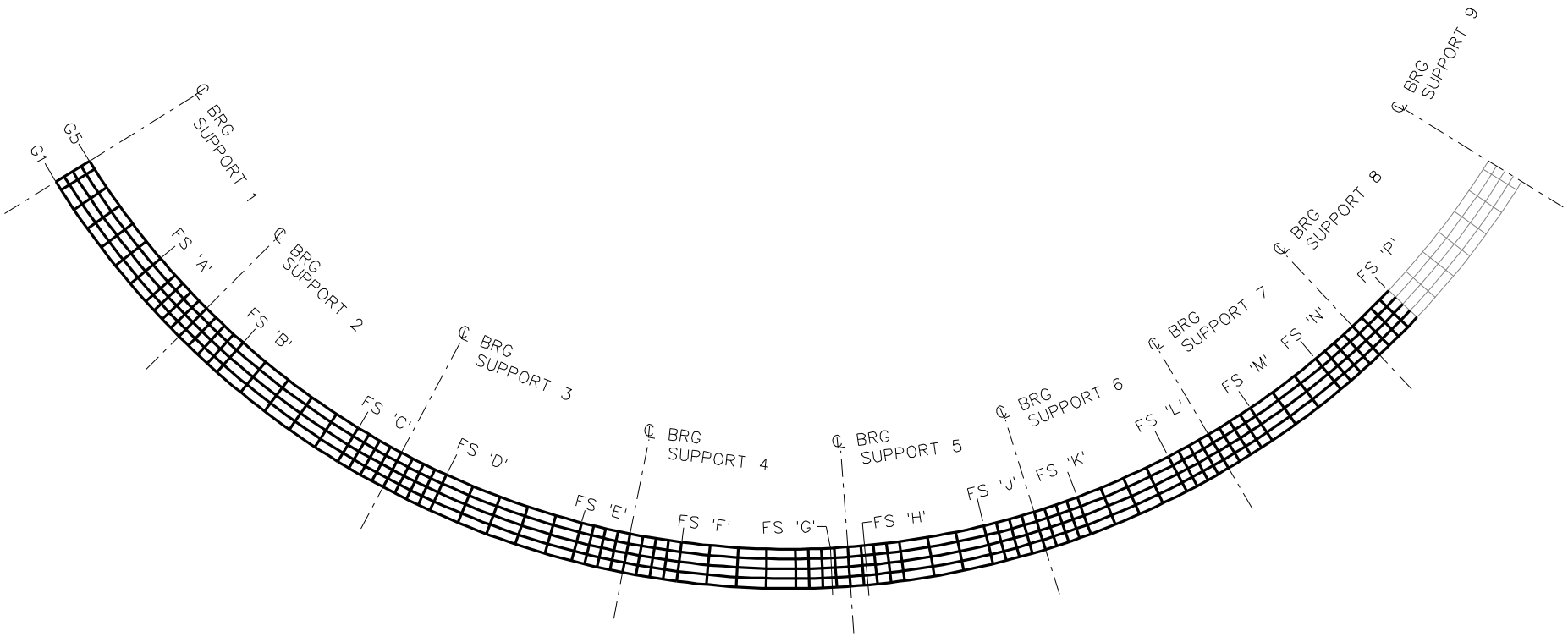

ERECTION SEQUENCE

STAGE 9-E

LEGEND

▽ = HOLD OR LIFT CRANE

○ = TIE DOWN

□ = TEMPORARY SUPPORT STRUCTURE

FS = FIELD SPLICE

NCHRP 12-79

BRIDGE EICCR22a

ERECTION SEQUENCE

SHEET 37 OF X

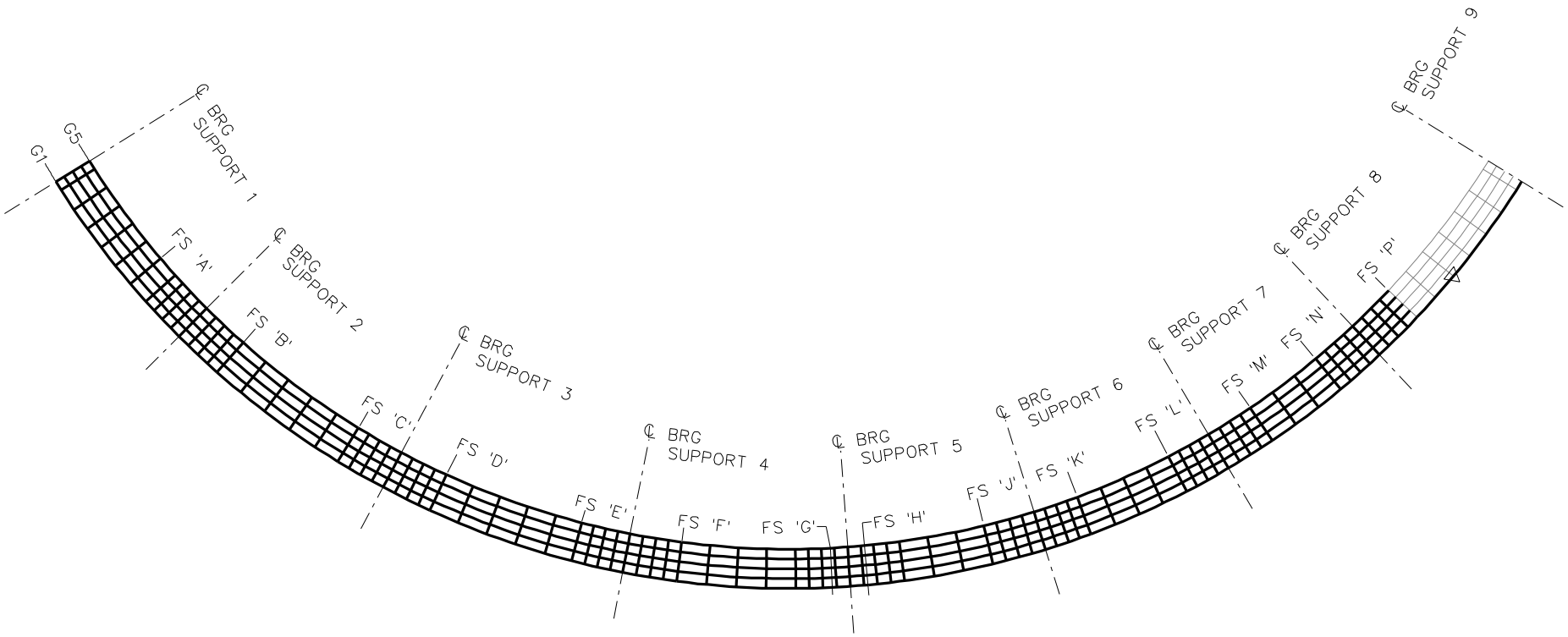

ERECTION SEQUENCE

STAGE 10-A THRU E

10-A - ERECT G1

10-B - ERECT G2 AND CROSSFRAMES BETWEEN G1 AND G2.

10-C - ERECT G3 AND CROSSFRAMES BETWEEN G2 AND G3.

10-D - ERECT G4 AND CROSSFRAMES BETWEEN G3 AND G4.

10-E - ERECT G5 AND CROSSFRAMES BETWEEN G4 AND G5.

LEGEND

▽ = HOLD OR LIFT CRANE

○ = TIE DOWN

□ = TEMPORARY SUPPORT STRUCTURE

FS = FIELD SPLICE

NCHRP 12-79

BRIDGE EICCR22a

ERECTION SEQUENCE

NCHRP 12-79

EICCS1

FHWA REG. NO.	STATE	PROJECT NUMBER	FISCAL YEAR	SHEET NO.	TOTAL SHEETS
4	ALA.	IM-459-4 (78)	2000	165	662

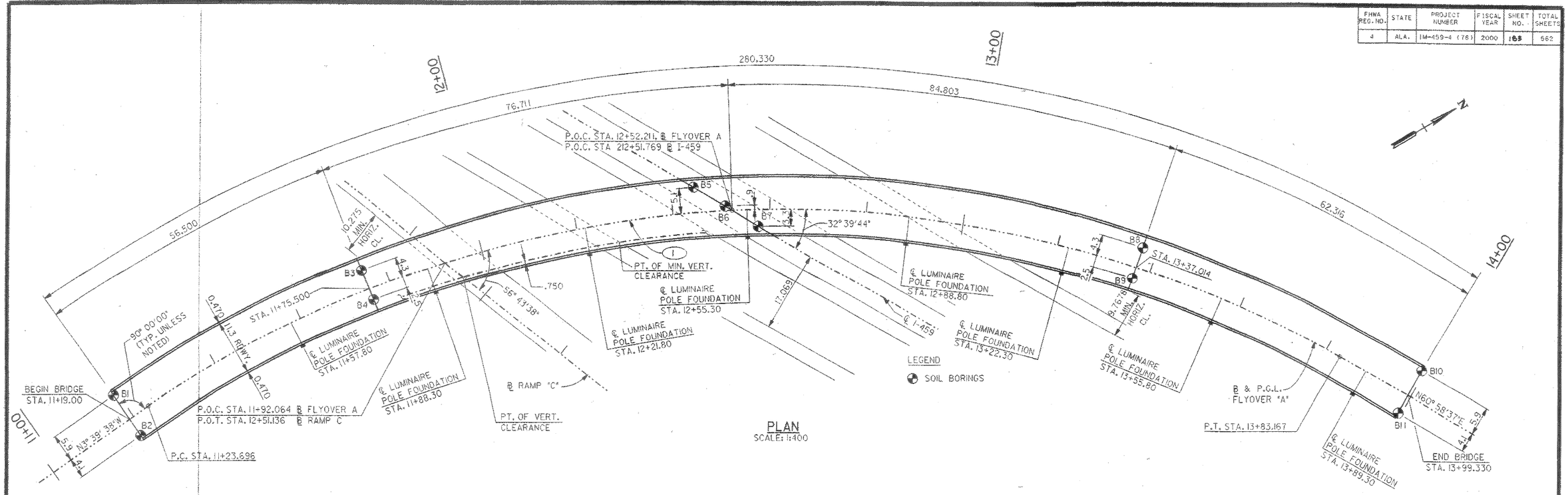

PLAN
SCALE: 1:400

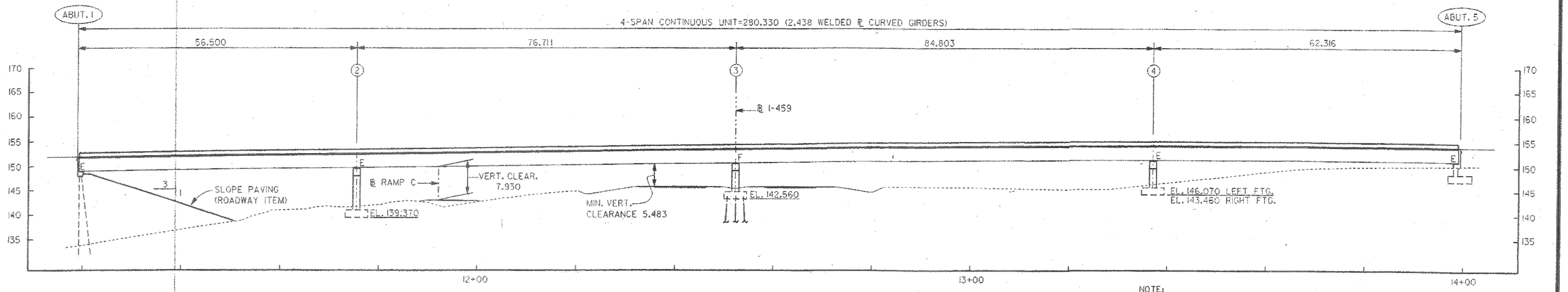

ELEVATION
SCALE: 1:400

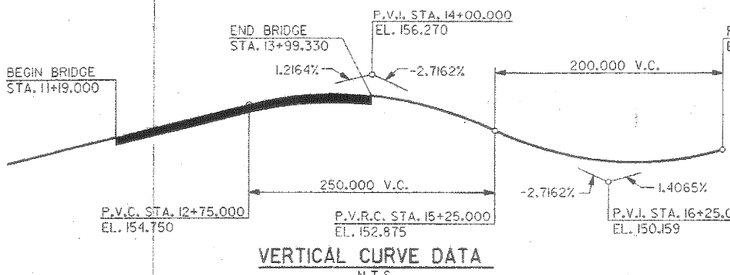

VERTICAL CURVE DATA
N.T.S.

CURVE DATA	
CURVE NO.	(1)
P.C. STA.	11+23.696
P.I. STA.	12+69.201
P.T. STA.	13+83.167
Δ	64°38'15" RT.
T	145.505
L	259.472
R	230.000

NOTE:
ALL DIMENSIONS SHOWN IN METERS UNLESS OTHERWISE NOTED.

ALABAMA DEPARTMENT OF TRANSPORTATION

BRIDGE SHEET NO. 2 OF 39

REVISIONS

DAVID VOLKERT AND ASSOCIATES, INC.
CONSULTING ENGINEERS

PROJECT IM-459-4 (78)
I-459/U.S. 31 INTERCHANGE
FLYOVER A
HOOVER, ALABAMA

GENERAL PLAN AND ELEVATION

STRUCTURAL APPROVAL:	STRUCTURAL APPROVAL: S.R.J.	QUANTITIES COMP:	DRAWN: J.W.C./ R.K.L.
ASSISTANT BRIDGE ENGINEER	DESIGNER J.T.L.	CHKD:	REINF CHKD:
BRIDGE ENGINEER	SECTION SUPERVISOR	CHKD: S.R.J.	SCALE: AS SHOWN DATE:

ALDOT METRIC

317

FHWA REG. NO.	STATE	PROJECT NUMBER	FISCAL YEAR	SHEET NO.	TOTAL SHEETS
4	ALA.	IM-459-4 (78)	2000	196	562

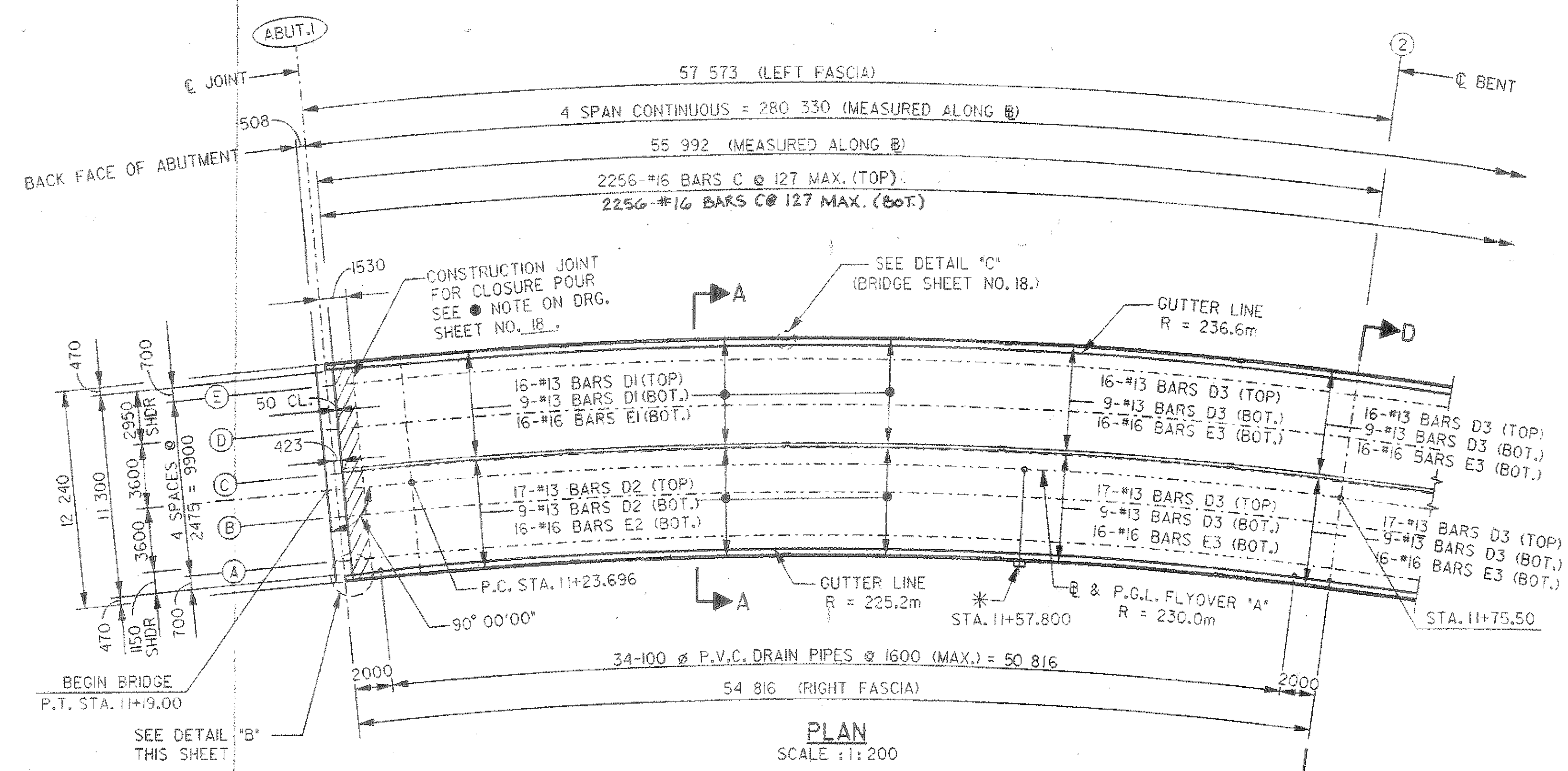

PLAN
SCALE : 1:200

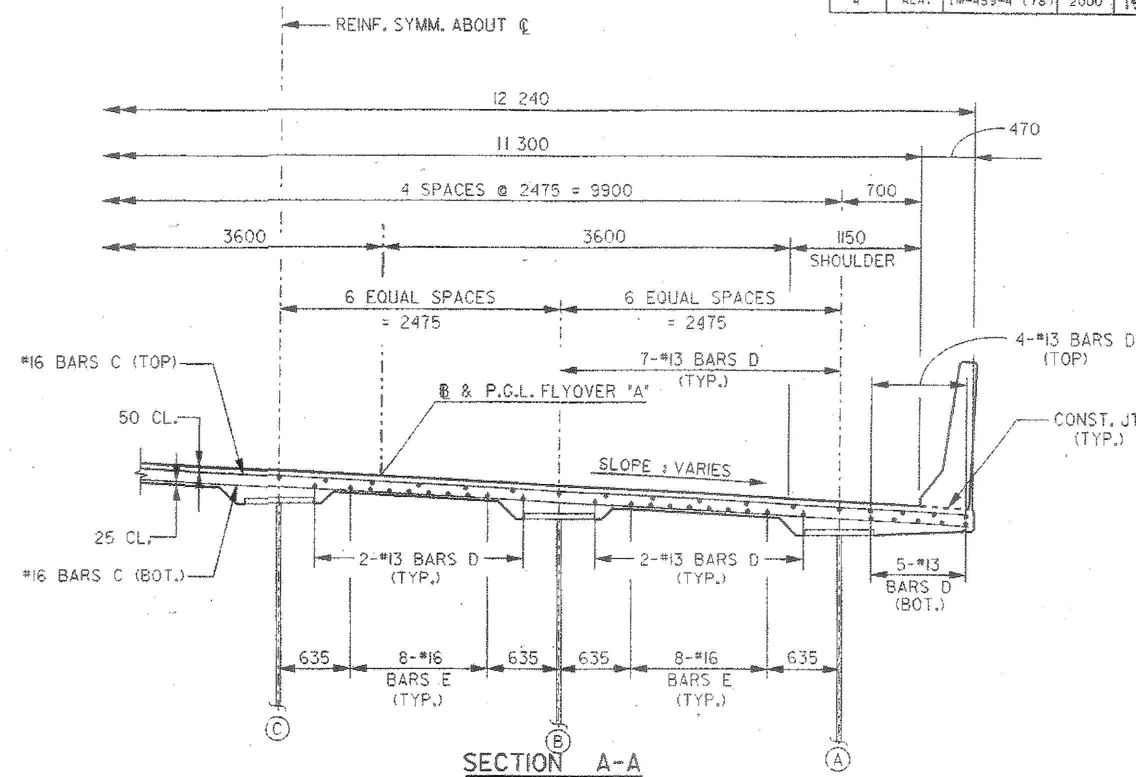

SECTION A-A
SCALE : 1:33 ⅓

NOTES :

1. FOR BILL REINFORCEMENT AND ESTIMATED QUANTITIES, SEE BRIDGE SHEET NO. 18 .
2. FOR DETAIL "C" SEE BRIDGE SHEET NO. 18 .
3. ▲ FOR BARRIER RAIL REINFORCEMENT & DETAILS, SEE BRIDGE SHEET NO. 36
4. ✳ FOR LUMINAIRE POLE FOUNDATION DETAILS AND BARS SEE BRIDGE SHEET NO. 37

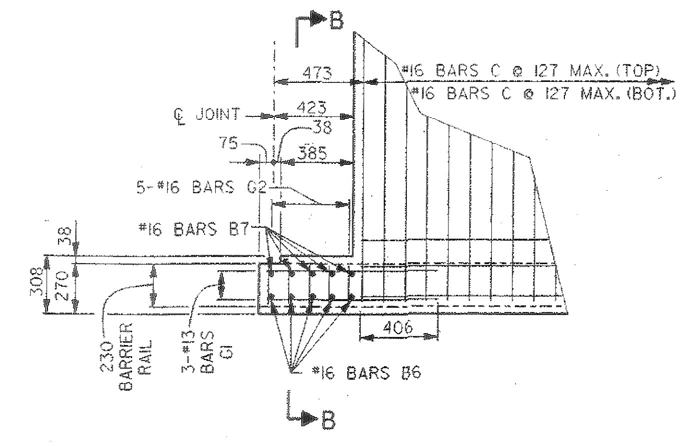

DETAIL "B"
SCALE: 1:20

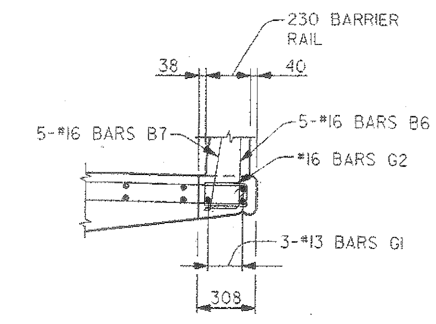

SECTION B-B
SCALE : 1:20

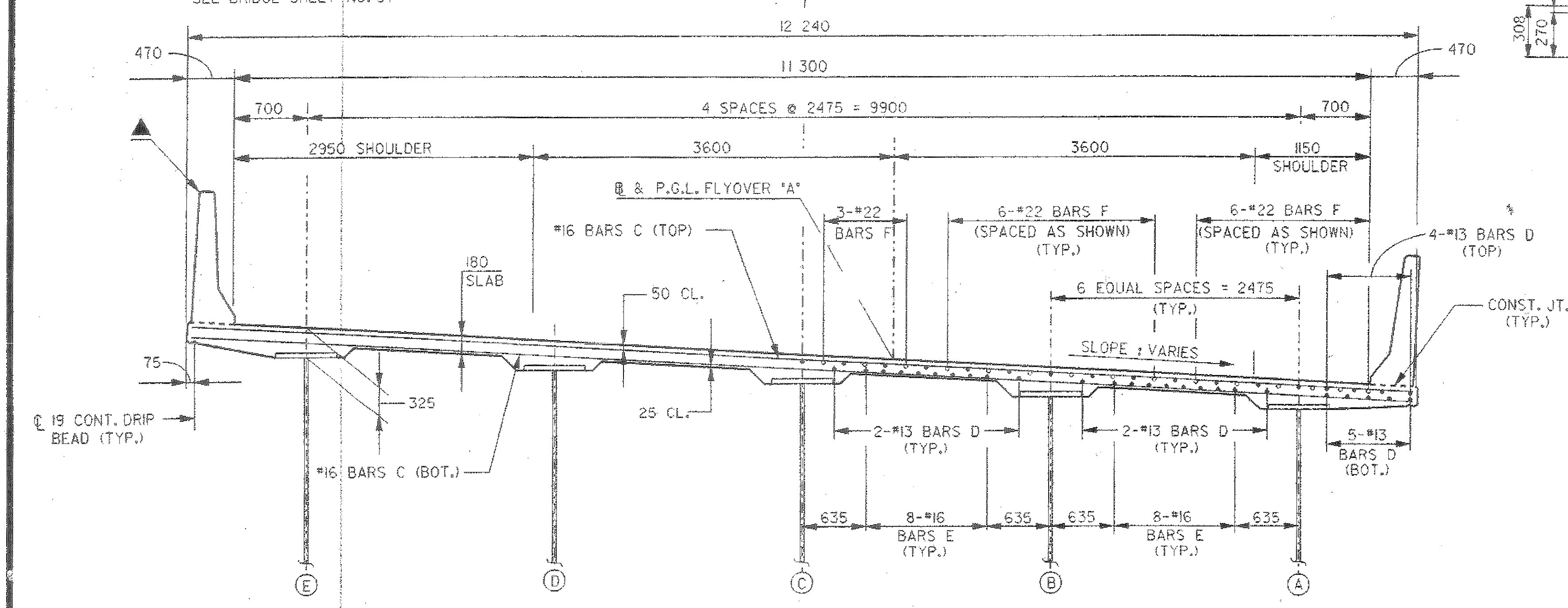

SECTION D-D
SCALE : 1:33 ⅓

NOTE:
ALL DIMENSIONS SHOWN ARE IN MILLIMETERS, UNLESS OTHERWISE NOTED.

ALABAMA DEPARTMENT OF TRANSPORTATION

BRIDGE SHEET NO. 15 OF 39

REVISIONS

DAVID VOLKERT AND ASSOCIATES, INC.
CONSULTING ENGINEERS

PROJECT IM-459-4 (78)
I-459/U.S. 31 INTERCHANGE
FLYOVER A
HOOVER, ALABAMA

DECK SLAB, SPAN 1 (SHT. 1 OF 4)

ALDOT METRIC

STRUCTURAL APPROVAL:	STRUCTURAL APPROVAL: S.R.J.	QUANTITIES	DRAWN: T.V.V.
ASSISTANT BRIDGE ENGINEER	DESIGNER J.T.L.	COMP: S.R.J.	REINF CHKD:
		CHKD:	SCALE: AS SHOWN
BRIDGE ENGINEER	SECTION SUPERVISOR	CHKD:	DATE:

User is: jamesa
21-JUN-2000 15:14
DVA GRAPHICS

818

FHWA REG. NO.	STATE	PROJECT NUMBER	FISCAL YEAR	SHEET NO.	TOTAL SHEETS
4	ALA.	IM-459-4 (78)	2000	197	562

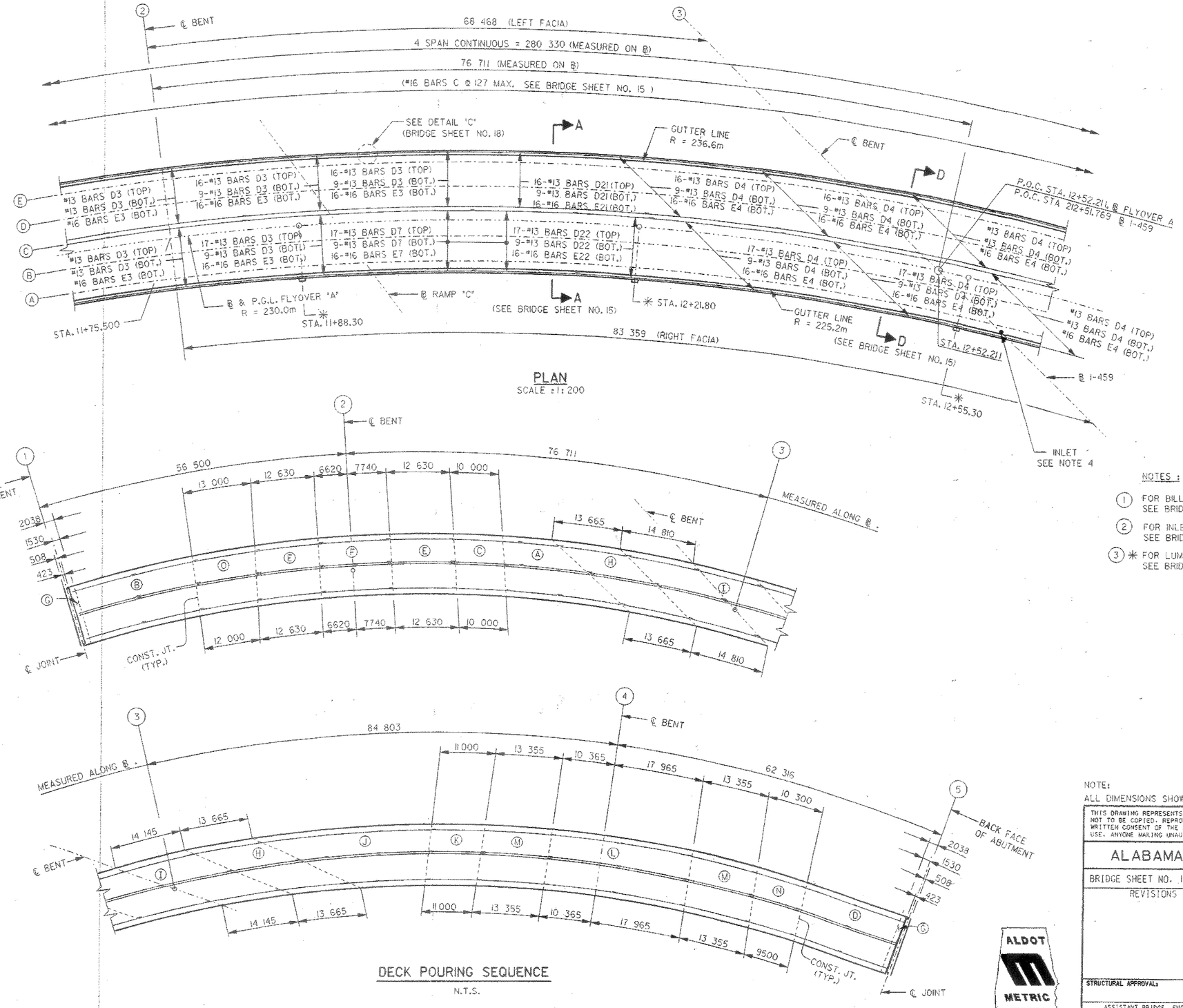

PLAN
SCALE : 1: 200

DECK POURING SEQUENCE
N.T.S.

NOTES :

1. FOR BILL OF REINFORCEMENT AND ESTIMATED QUANTITIES, SEE BRIDGE SHEET NO. 18 .
2. FOR INLET DETAILS, SEE BRIDGE SHEET NO. 35 .
3. ✳ FOR LUMINAIRE POLE FOUNDATION DETAILS AND BARS. SEE BRIDGE SHEET NO. 37.

NOTE:
ALL DIMENSIONS SHOWN ARE IN MILLIMETERS, UNLESS OTHERWISE NOTED.

ALABAMA DEPARTMENT OF TRANSPORTATION

BRIDGE SHEET NO. 16 OF 39

REVISIONS

DAVID VOLKERT AND ASSOCIATES, INC.
CONSULTING ENGINEERS

PROJECT IM-459-4 (78)
I-459/U.S. 31 INTERCHANGE
FLYOVER A
HOOVER, ALABAMA

DECK SLAB, SPAN 2 (SHT. 2 OF 4)

STRUCTURAL APPROVAL:	STRUCTURAL APPROVAL: S.R.J.	QUANTITIES COMP: S.R.J.	DRAWN: T.V.V.
ASSISTANT BRIDGE ENGINEER	DESIGNER J.T.L.	CHKD:	REINF CHKD:
BRIDGE ENGINEER	SECTION SUPERVISOR	CHKD:	SCALE: AS SHOWN
			DATE:

ALDOT METRIC

319

FHWA REG. NO.	STATE	PROJECT NUMBER	FISCAL YEAR	SHEET NO.	TOTAL SHEETS
4	ALA.	IM-459-4 (78)	2000	198	562

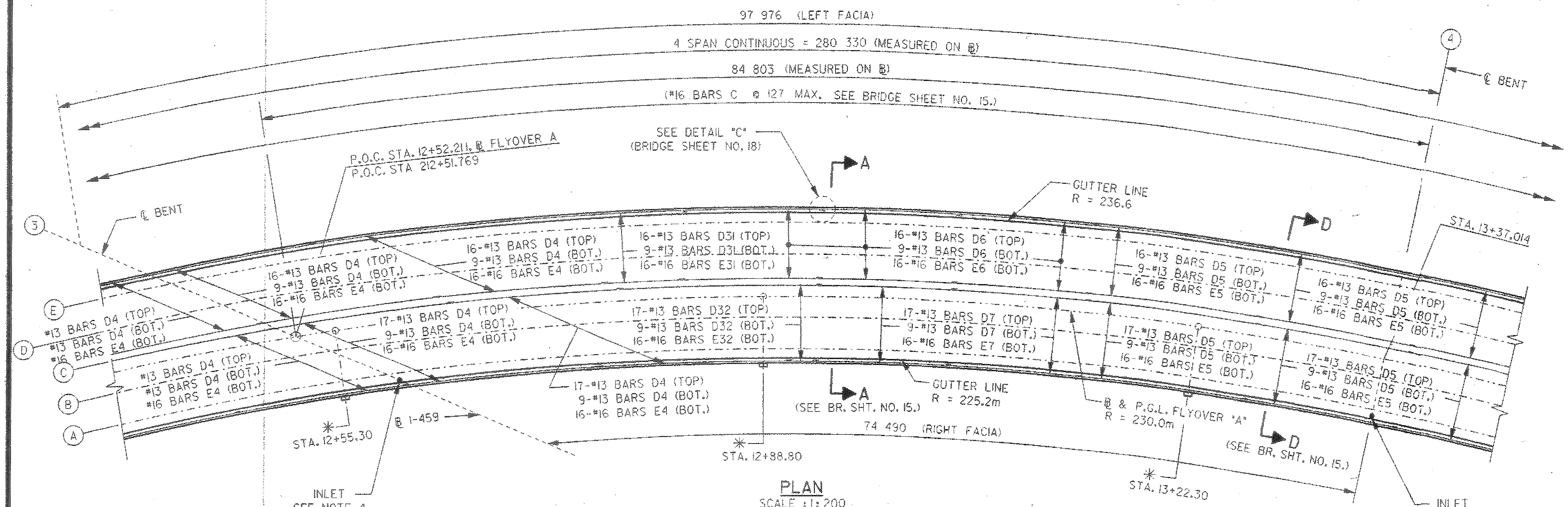

PLAN
SCALE 1:200

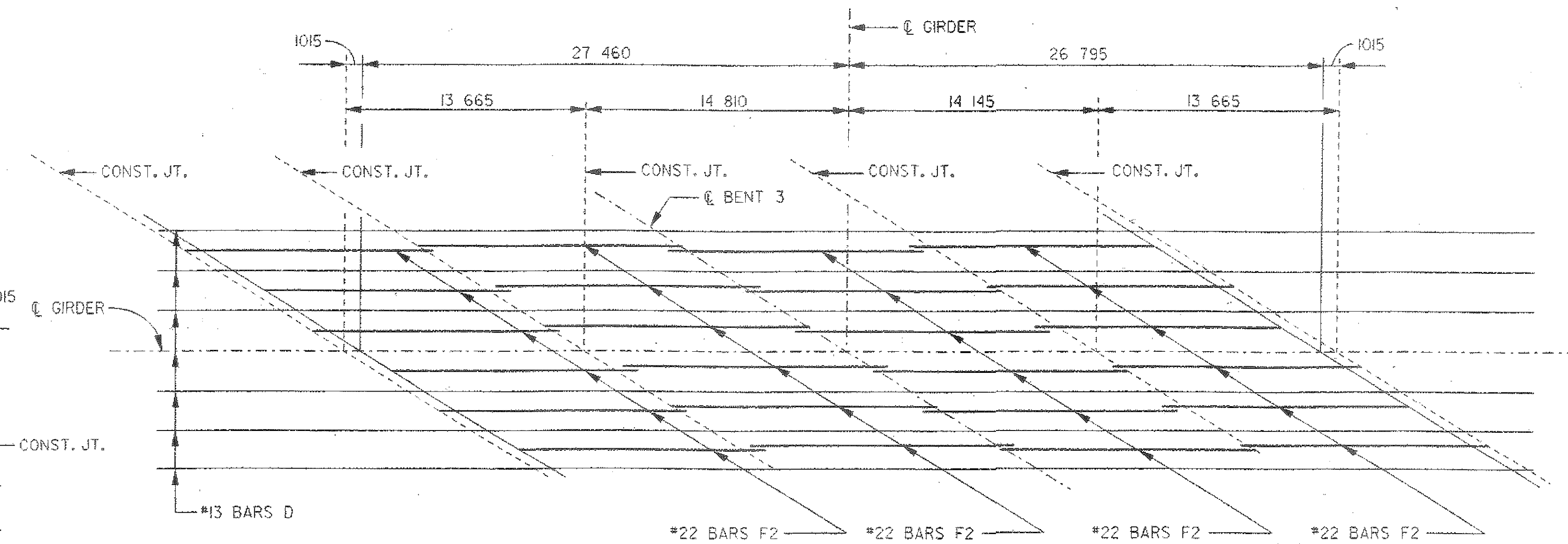

PLAN ADDITIONAL REINFORCING IN TOP OF SLAB
(AT BENT NO. 3)
(PLAN CURVE NOT SHOWN)
N.T.S.

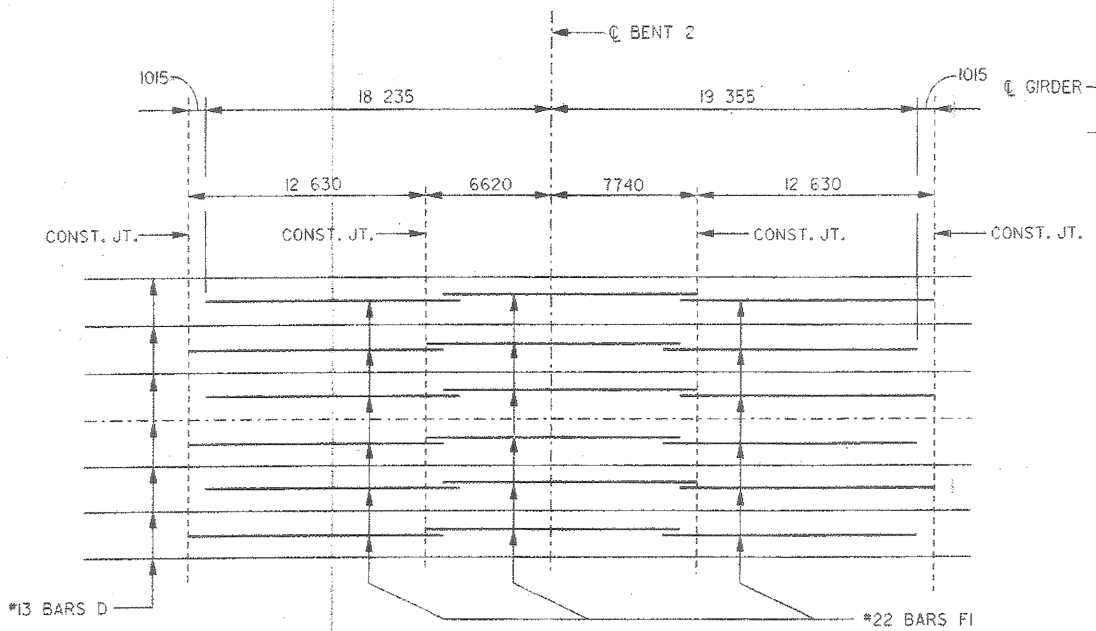

PLAN ADDITIONAL REINFORCING IN TOP OF SLAB
(AT BENT NO. 2)
(PLAN CURVE NOT SHOWN)
N.T.S.

NOTES :

1. FOR BILL OF REINFORCEMENT AND ESTIMATED QUANTITIES. SEE BRIDGE SHEET NO. 18 .
2. FOR INLET DETAILS, SEE BRIDGE SHEET NO. 35 .
3. ✳ FOR LUMINAIRE POLE FOUNDATION DETAILS AND BARS. SEE BRIDGE SHEET NO. 37.

NOTE:
ALL DIMENSIONS SHOWN ARE IN MILLIMETERS, UNLESS OTHERWISE NOTED.

ALDOT METRIC

ALABAMA DEPARTMENT OF TRANSPORTATION

BRIDGE SHEET NO. 17 OF 39

REVISIONS

DAVID VOLKERT AND ASSOCIATES, INC.
CONSULTING ENGINEERS

PROJECT IM-459-4 (78)
I-459/U.S. 31 INTERCHANGE
FLYOVER A
HOOVER, ALABAMA

DECK SLAB, SPAN 3 (SHT. 3 OF 4)

STRUCTURAL APPROVAL:
ASSISTANT BRIDGE ENGINEER
BRIDGE ENGINEER
STRUCTURAL APPROVAL: S.R.J.
DESIGNER J.T.L.
SECTION SUPERVISOR
QUANTITIES COMP: S.R.J.
CHKD:
CHKD:
DRAWN: T.V.V.
REINF CHKD:
SCALE: AS SHOWN
DATE:

FHWA REG. NO.	STATE	PROJECT NUMBER	FISCAL YEAR	SHEET NO.	TOTAL SHEETS
4	ALA.	IM-459-4 (78)	2000	199	562

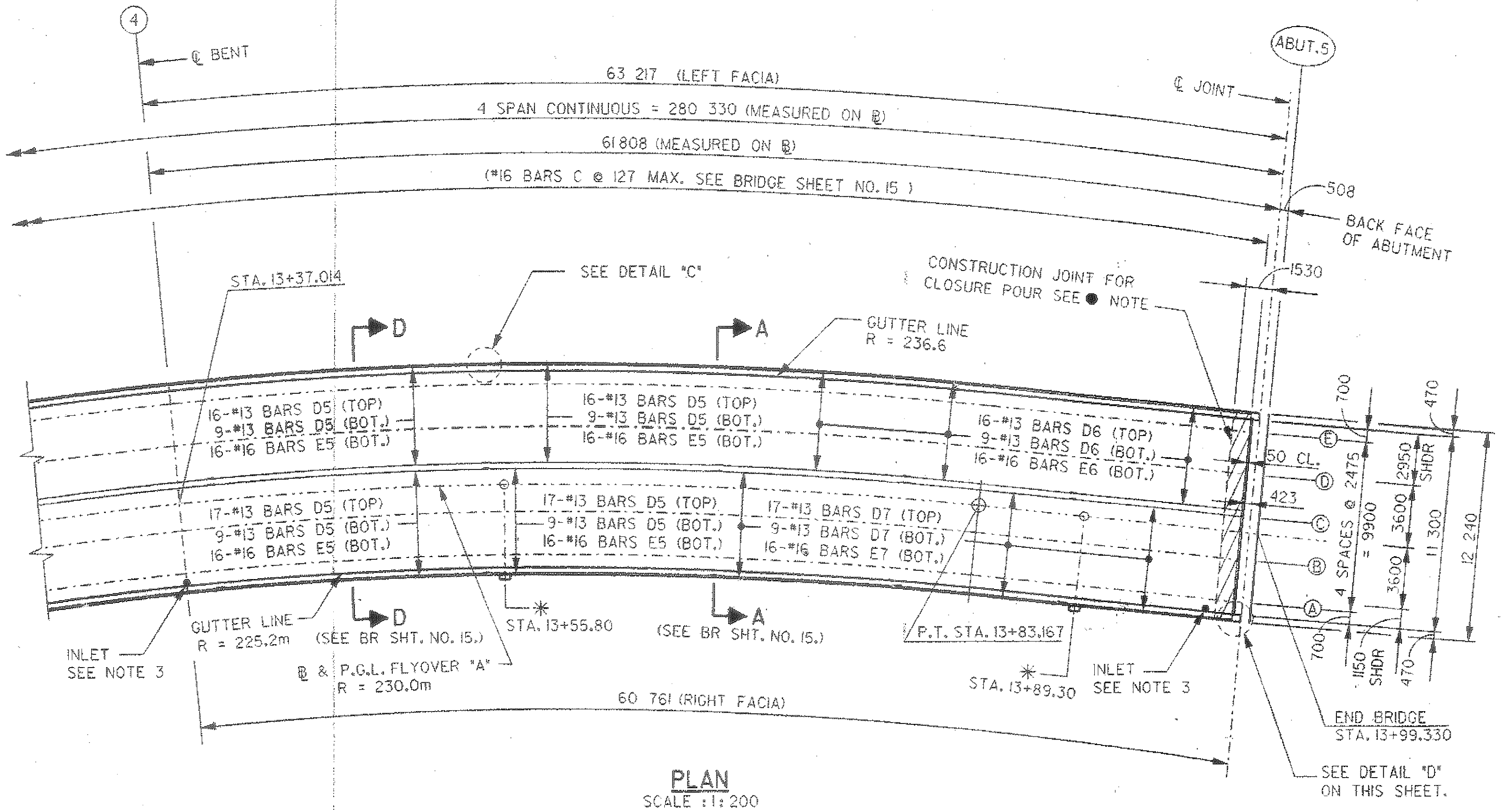

PLAN
SCALE : 1:200

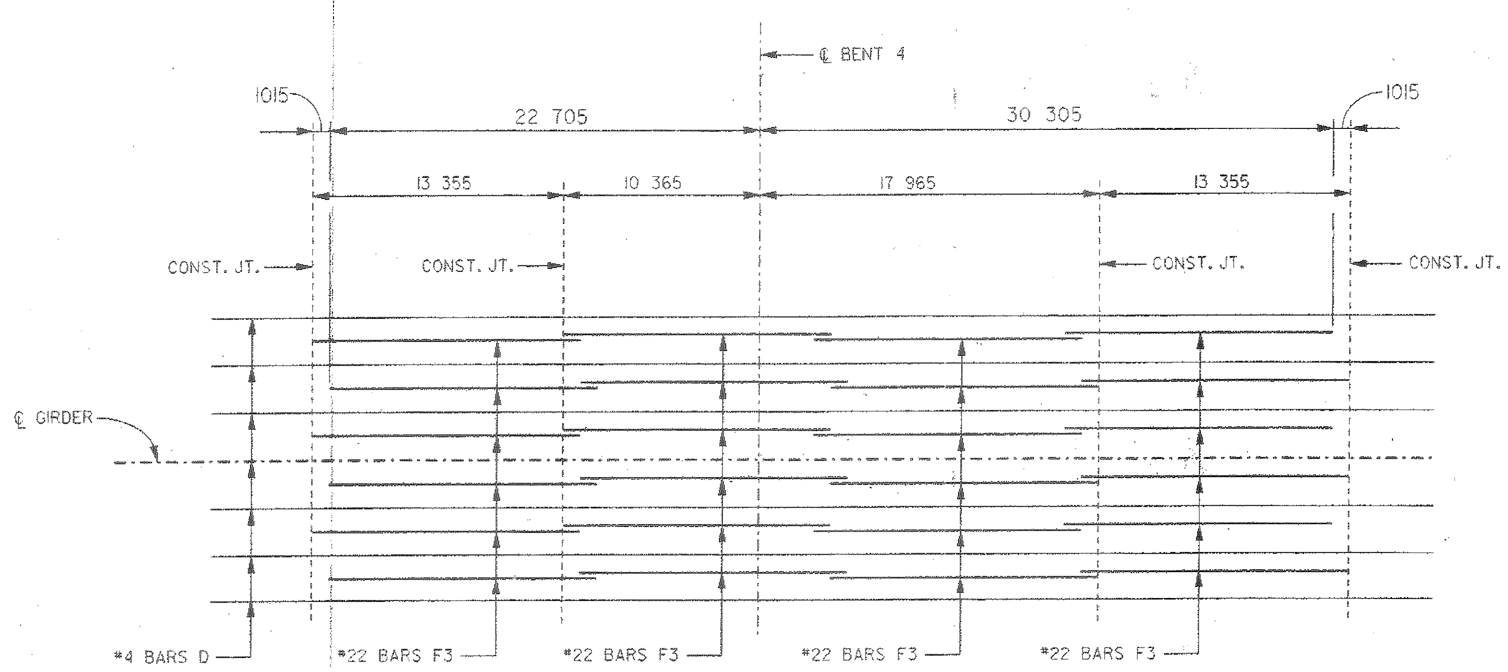

PLAN ADDITIONAL REINFORCING IN TOP OF SLAB (AT BENT NO. 4) (PLAN CURVE NOT SHOWN)
N.T.S.

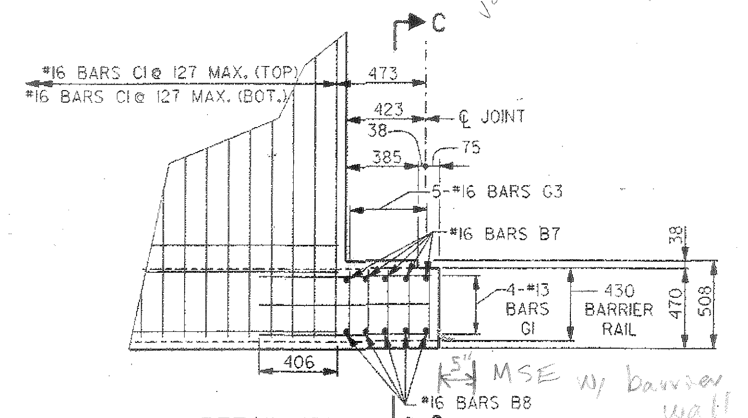

DETAIL "D"
SCALE: 1:20

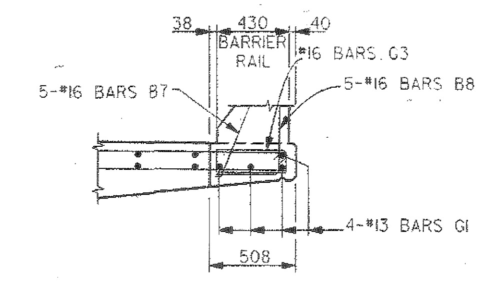

SECTION C-C
SCALE: 1:20

NOTES :

① ● NOTE :
A 1530 CLOSURE POUR IS REQUIRED AT THE ABUTMENTS TO ALLOW FOR PROPER ALIGNMENT AND PLACEMENT OF THE EXPANSION DAM. SLAB BARS TYPE D AND TYPE E AND BARRICADE BARS BL SHALL EXTEND A MINIMUM OF 35 DIAMETERS PAST CONSTRUCTION JOINT TO PROVIDE LAP FOR CLOSURE POUR REINFORCEMENT. EXPANSION DAM SHALL BE PAID FOR UNDER 508-B PAY ITEM.
FOR FINGER EXPANSION JOINT DETAILS SEE BRIDGE SHEET NO. 33 & 34.

② FOR INLET DETAILS, SEE BRIDGE SHEET NO. 35 .
STEEL REINFORCEMENT AT INLET IS INCLUDED IN ESTIMATED QUANTITIES.

③ ▲ FOR BARRIER RAIL REINFORCEMENT AND DETAILS, SEE BRIDGE SHEET NO. 36.

④ ✳ FOR LUMINAIRE POLE FOUNDATION DETAILS AND BARS, SEE BRIDGE SHEET NO. 37.

⑤ CONCRETE AND REINFORCEMENT IN BARRIER RAILS AND POLE FOUNDATIONS ARE INCLUDED IN THE ESTIMATED QUANTITIES.

⑥ BOLTS AND OTHER INSERTS AND FIXURES REQUIRED FOR LUMINAIRE POLE FOUNDATION ARE NOT INCLUDED IN THE ESTIMATED QUANTITIES.

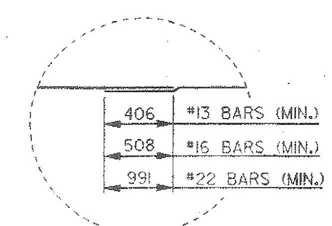

406	#13 BARS (MIN.)
508	#16 BARS (MIN.)
991	#22 BARS (MIN.)

DETAIL "C"
N.T.S.

BILL OF REINFORCEMENT

MARK	SIZE	NO.	LENGTH	LOCATION	BENDING
B1	16	4516	1170	RAIL	▲
B2	16	2260	850	RAIL	▲
B3	16	2184	1065	RAIL	▲
B4	16	32	1065	RAIL	▲
B5	16	76	1065	RAIL	▲
B6	16	10	670	RAIL	SEE DIAG.
B7	16	20	735	RAIL	SEE DIAG.
B8	16	10	820	RAIL	SEE DIAG.
BL1	13	11	▲	RAIL	▲
BL2	13	11	▲	RAIL	▲
C	16	4512	12 140	SLAB	STRAIGHT
D1	13	75	13 175	SLAB	STRAIGHT
D2	13	78	12 255	SLAB	STRAIGHT
D3	13	178	13 480	SLAB	STRAIGHT
D4	13	204	14 380	SLAB	STRAIGHT
D5	13	204	14 065	SLAB	STRAIGHT
D6	13	150	11 030	SLAB	STRAIGHT
D7	13	182	13 625	SLAB	STRAIGHT
D21	13	25	11088	SLAB	STRAIGHT
D22	13	26	11 168	SLAB	STRAIGHT
D31	13	25	8298	SLAB	STRAIGHT
D32	13	26	8395	SLAB	STRAIGHT
E1	16	48	13 275	SLAB	STRAIGHT
E2	16	48	12 360	SLAB	STRAIGHT
E3	16	112	13 550	SLAB	STRAIGHT
E4	16	128	15 330	SLAB	STRAIGHT
E5	16	128	14 145	SLAB	STRAIGHT
E6	16	96	11 135	SLAB	STRAIGHT
E7	16	112	10 725	SLAB	STRAIGHT
E21	16	16	7600 TO 15 045	SLAB	STRAIGHT
E22	16	16	7655 TO 15 700	SLAB	STRAIGHT
E31	16	16	2630 TO 14 375	SLAB	STRAIGHT
E32	16	16	2730 TO 14 470	SLAB	STRAIGHT
F1	22	90	13 495	SLAB	STRAIGHT
F2	22	120	14 535	SLAB	STRAIGHT
F3	22	120	14 225	SLAB	STRAIGHT
G1	13	14	900	SLAB	STRAIGHT
G2	16	10	1006	SLAB	STRAIGHT
G3	16	10	1306	SLAB	STRAIGHT

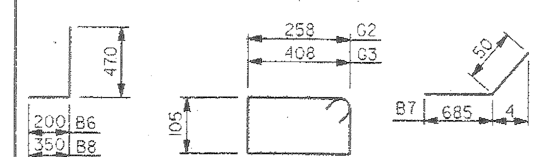

ESTIMATED QUANTITIES

ITEM	UNIT	QUANTITY
SUPERSTRUCTURE CONCRETE	m3	1080
STEEL REINFORCEMENT	kg	150 176

NOTE:
ALL DIMENSIONS SHOWN ARE IN MILLIMETERS, UNLESS OTHERWISE NOTED.

ALABAMA DEPARTMENT OF TRANSPORTATION

BRIDGE SHEET NO. 18 OF 39
REVISIONS

DAVID VOLKERT AND ASSOCIATES, INC.
CONSULTING ENGINEERS

PROJECT IM-459-4 (78)
I-459/U.S. 31 INTERCHANGE
FLYOVER A
HOOVER, ALABAMA

DECK SLAB, SPAN 4 (SHT. 4 OF 4)

ALDOT METRIC

STRUCTURAL APPROVAL:
ASSISTANT BRIDGE ENGINEER
BRIDGE ENGINEER
STRUCTURAL APPROVAL: S.R.J.
DESIGNER J.T.L.
SECTION SUPERVISOR
QUANTITIES COMP: S.R.J.
CHKD:
CHKD:
DRAWN: T.V.V./K.K.L.
REINF CHKD:
SCALE: AS SHOWN
DATE:

FHWA REG. NO.	STATE	PROJECT NUMBER	FISCAL YEAR	SHEET NO.	TOTAL SHEETS
4	ALA.	IM-459-4 (78)	2000	200	562

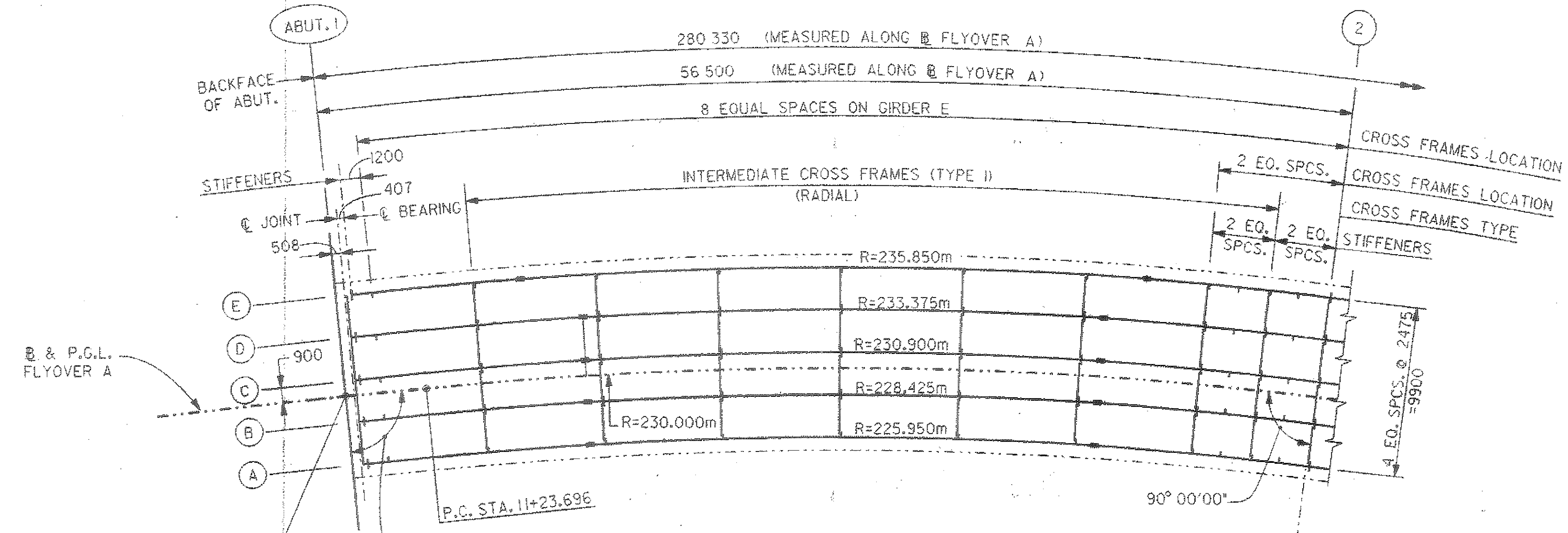

FRAMING PLAN - SPAN NO. 1
SCALE: 1:200

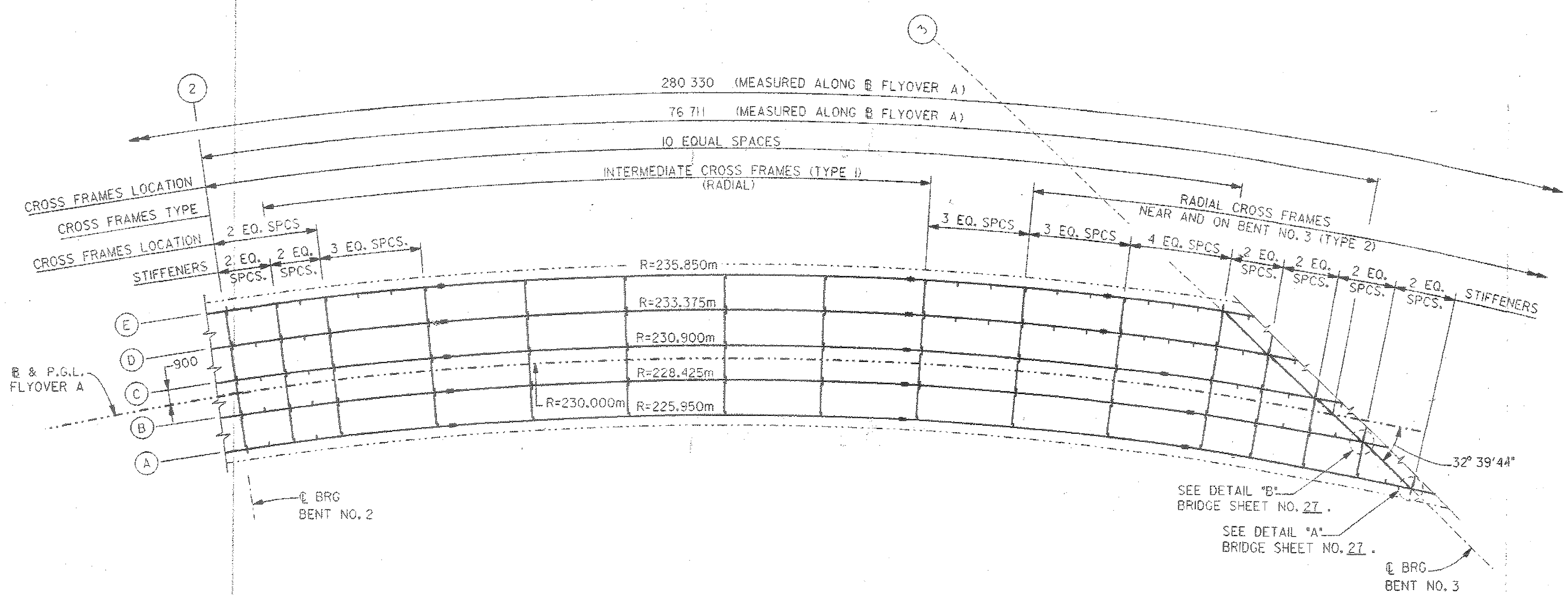

FRAMING PLAN - SPAN NO. 2
SCALE: 1:200

NOTES:

1. STRUCTURAL STEEL SHALL CONFORM TO AASHTO M270 GRADE 345.
2. GIRDERS SHALL BE CAMBERED FOR DEAD LOAD DEFLECTION AND VERTICAL CURVATURE. GIRDER WEBS SHALL BE CUT TO PROVIDE CAMBER.
3. ALL FLANGE PLATES SHALL BE UNIVERSAL MILL PLATES OR SHALL BE FLAME CUT FROM WIDER PLATES.
4. GIRDER ENDS AND BEARING STIFFENERS SHALL BE VERTICAL. ALL OTHER STIFFENERS, CROSS FRAMES, FIELD BOLTED SPLICES AND SHOP SPLICES SHALL BE PERPENDICULAR TO THE FLANGES.
5. ALL CAMBER ORDINATES ARE REFERENCED TO CHORDS BETWEEN SUPPORTS.
6. HOLES IN FIELD SPLICE CONNECTIONS SHALL BE SUB-DRILLED AND REAMED, OR DRILLED FULL SIZE WHILE ASSEMBLED.
7. SHOP CONNECTIONS SHALL BE WELDED AS SHOWN. FIELD CONNECTIONS SHALL BE BOLTED WITH M22 HIGH STRENGTH BOLTS (A325m) IN 24ø HOLES UNLESS OTHERWISE NOTED.
8. FLANGE PLATES MAY BE HEAT CUT FROM WIDER PLATES TO THE RADII SHOWN, OR GIRDERS MAY BE CURVED BY THE UPSET METHOD FOR TYPE FLANGE SECTION NOS. FS1, FS2, FS4, FS5 AND FS6. SEE NOTE ■■ ON BRIDGE SHEET NO. 25 .
9. FOR GIRDER ELEVATIONS, SEE BRIDGE SHEET NOS. 21 THRU 25 . SEE NOTE NO. 1 THRU 4 ON BRIDGE SHEET NO. 21.

NOTE:
ALL DIMENSIONS SHOWN ARE IN MILLIMETERS, WITH THE EXCEPTION OF STATIONS AND ELEVATIONS, UNLESS OTHERWISE NOTED.

ALABAMA DEPARTMENT OF TRANSPORTATION

BRIDGE SHEET NO. 19 OF 39

REVISIONS

DAVID VOLKERT AND ASSOCIATES, INC.
CONSULTING ENGINEERS

PROJECT IM-459-4 (78)
I-459/U.S. 31 INTERCHANGE
FLYOVER A
HOOVER, ALABAMA

FRAMING PLAN SPANS 1 - 4 (SHT. 1 OF 2)

STRUCTURAL APPROVAL:	STRUCTURAL APPROVAL:	QUANTITIES	DRAWN: K.K.L. T.V.V.
ASSISTANT BRIDGE ENGINEER	S.R.J. DESIGNER	COMP: S.R.J.	REINF CHKD:
	J.T.L.	CHKD:	SCALE: AS SHOWN
BRIDGE ENGINEER	SECTION SUPERVISOR	CHKD: S.R.J.	DATE:

ALDOT METRIC

322

FHWA REG. NO.	STATE	PROJECT NUMBER	FISCAL YEAR	SHEET NO.	TOTAL SHEETS
4	ALA.	IM-459-4 (78)	2000	201	562

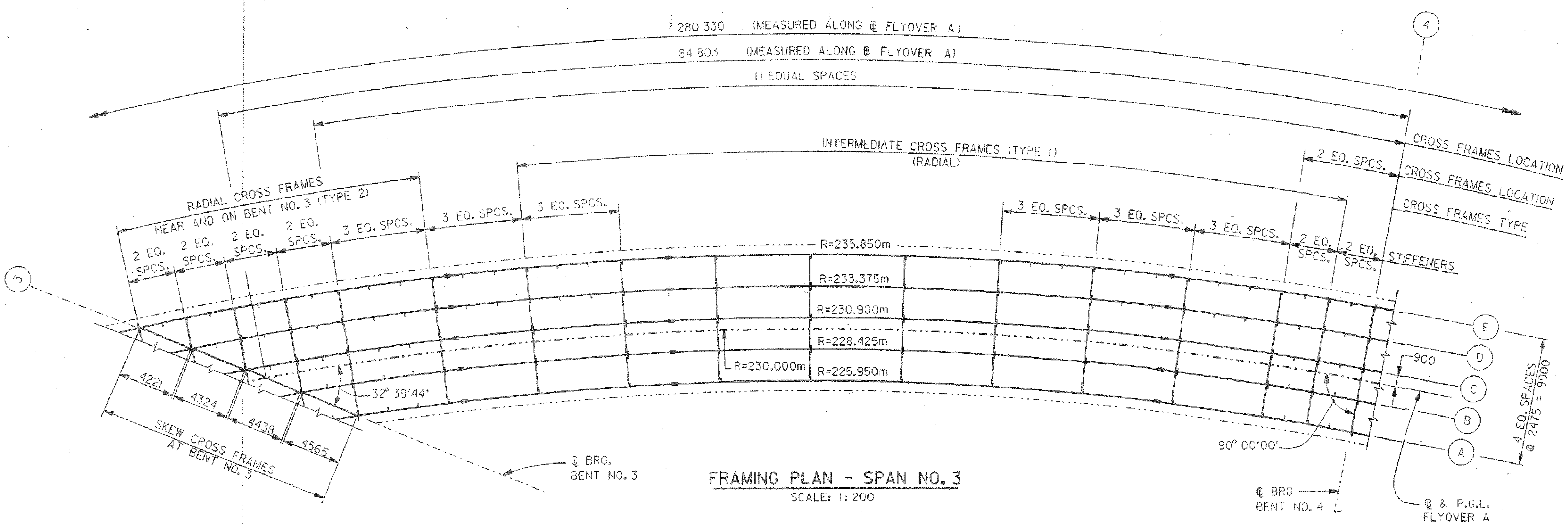

FRAMING PLAN - SPAN NO. 3

SCALE: 1:200

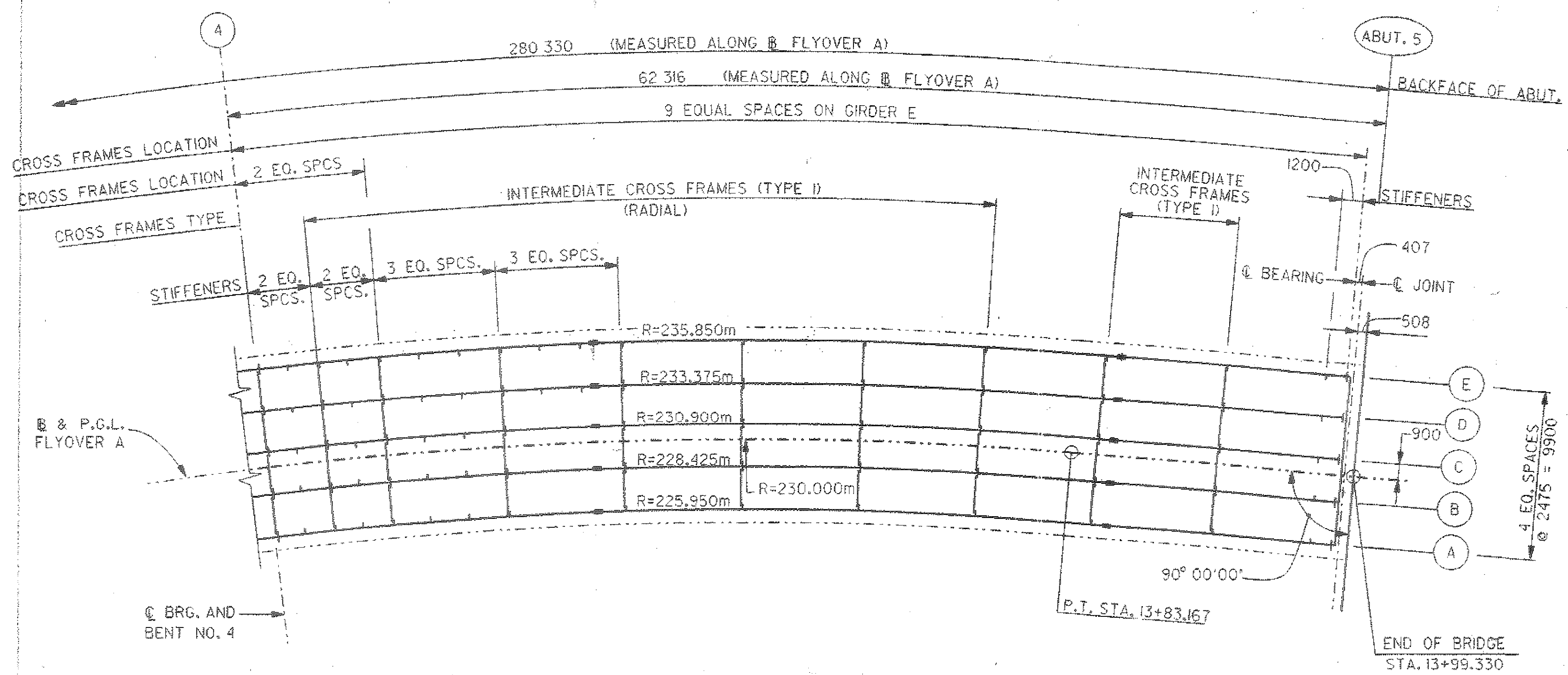

FRAMING PLAN - SPAN NO. 4

SCALE: 1:200

NOTE:
FOR GIRDER ELEVATIONS, SEE BRIDGE SHEET NOS. 21 THRU 25.
SEE NOTE NOS. 1 THRU 4 ON BRIDGE SHEET NO. 21.

NOTE:
ALL DIMENSIONS SHOWN ARE IN MILLIMETERS, WITH THE EXCEPTION OF STATIONS AND ELEVATIONS, UNLESS OTHERWISE NOTED.

ALABAMA DEPARTMENT OF TRANSPORTATION

BRIDGE SHEET NO. 20 OF 39

REVISIONS

DAVID VOLKERT AND ASSOCIATES, INC.
CONSULTING ENGINEERS

PROJECT IM-459-4 (78)
I-459/U.S. 31 INTERCHANGE
FLYOVER A
HOOVER, ALABAMA

FRAMING PLAN SPANS 1 - 4 (SHT. 2 OF 2)

ALDOT METRIC

STRUCTURAL APPROVAL:
ASSISTANT BRIDGE ENGINEER
BRIDGE ENGINEER

STRUCTURAL APPROVAL:
S.R.J. DESIGNER
J.T.L. SECTION SUPERVISOR

QUANTITIES
COMP: S.R.J.
CHKD:
CHKD: S.R.J.

DRAWN: K.K.L. T.V.V.
REINF CHKD:
SCALE: AS SHOWN
DATE:

FHWA REG. NO.	STATE	PROJECT NUMBER	FISCAL YEAR	SHEET NO.	TOTAL SHEETS
4	ALA.	IM-459-4 (78)	2000	202	562

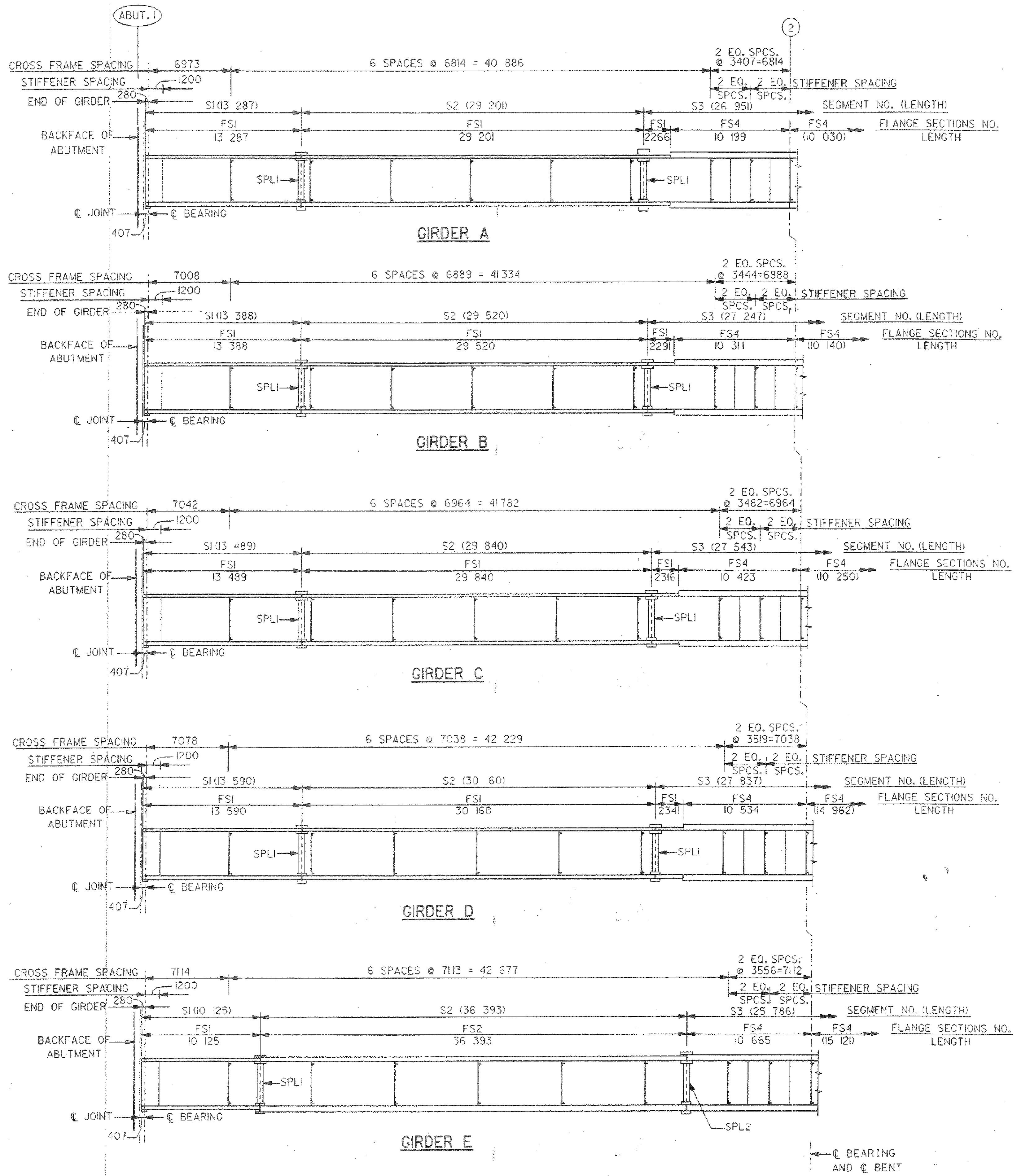

NOTE :

CHECK SAMPLE REQUIRED.
OBTAIN SAMPLE FROM TOP FLANGE PLATE, GIRDER A, END OF GIRDER IN SPAN 1.

NOTES:

1. FOR GIRDER DIMENSIONS, SEGMENTS AND FLANGE SIZES, SEE BRIDGE SHEET NO. 25

   FOR SHOP WELDED SPLICE DETAILS, SEE BRIDGE SHEET NO. 24

   FOR DETAILS OF CROSS FRAMES, SEE BRIDGE SHEET NO. 26

   FOR DETAILS OF STIFFENERS, SEE BRIDGE SHEET NO. 27

   FOR DETAILS OF FIELD SPLICES, SEE BRIDGE SHEET NO. 28

   FOR DETAILS OF SHEAR CONNECTION, SEE BRIDGE SHEET NOS. 25&26 .

   FOR DETAILS OF BEARINGS, SEE BRIDGE SHEET NO. 29 .

   FOR CAMBER DIAGRAM, SEE BRIDGE SHEET NOS. 30&31.

   FOR EXPANSION DAM DETAILS, SEE BRIDGE SHEET NOS. 33&34 .

2. SPL* INDICATES SPLICE TYPE NUMBER (*).
   F* INDICATES STIFFENERS TYPE NUMBER (*).

3. ALL INTERMEDIATE CROSS FRAMES NOT SPECIALLY MARKED ON THIS SHEET ARE TYPE I.

4. ALL INTERMEDIATE STIFFENERS, NOT SPECIALLY MARKED, ARE OF TYPE F1.

NOTE:
ALL DIMENSIONS SHOWN ARE IN MILLIMETERS, UNLESS OTHERWISE NOTED.

ALABAMA DEPARTMENT OF TRANSPORTATION

BRIDGE SHEET NO. 21 OF 39

REVISIONS

DAVID VOLKERT AND ASSOCIATES, INC.
CONSULTING ENGINEERS

PROJECT IM-459-4 (78)
I-459/U.S. 31 INTERCHANGE
FLYOVER A
HOOVER, ALABAMA

ALDOT METRIC

GIRDER ELEVATIONS, SPANS 1- 4 (SHT. 1 OF 5)

STRUCTURAL APPROVAL:
ASSISTANT BRIDGE ENGINEER
BRIDGE ENGINEER

STRUCTURAL APPROVAL:
S.R.J.
DESIGNER
J.T.A.
SECTION SUPERVISOR

QUANTITIES
COMP: S.R.J.
CHKD:
CHKD: S.R.J.

DRAWN: K.K.L. T.V.V.
REINF CHKD:
SCALE: AS SHOWN
DATE:

FHWA REG. NO.	STATE	PROJECT NUMBER	FISCAL YEAR	SHEET NO.	TOTAL SHEETS
4	ALA.	IM-459-4 (78)	2000	205	562

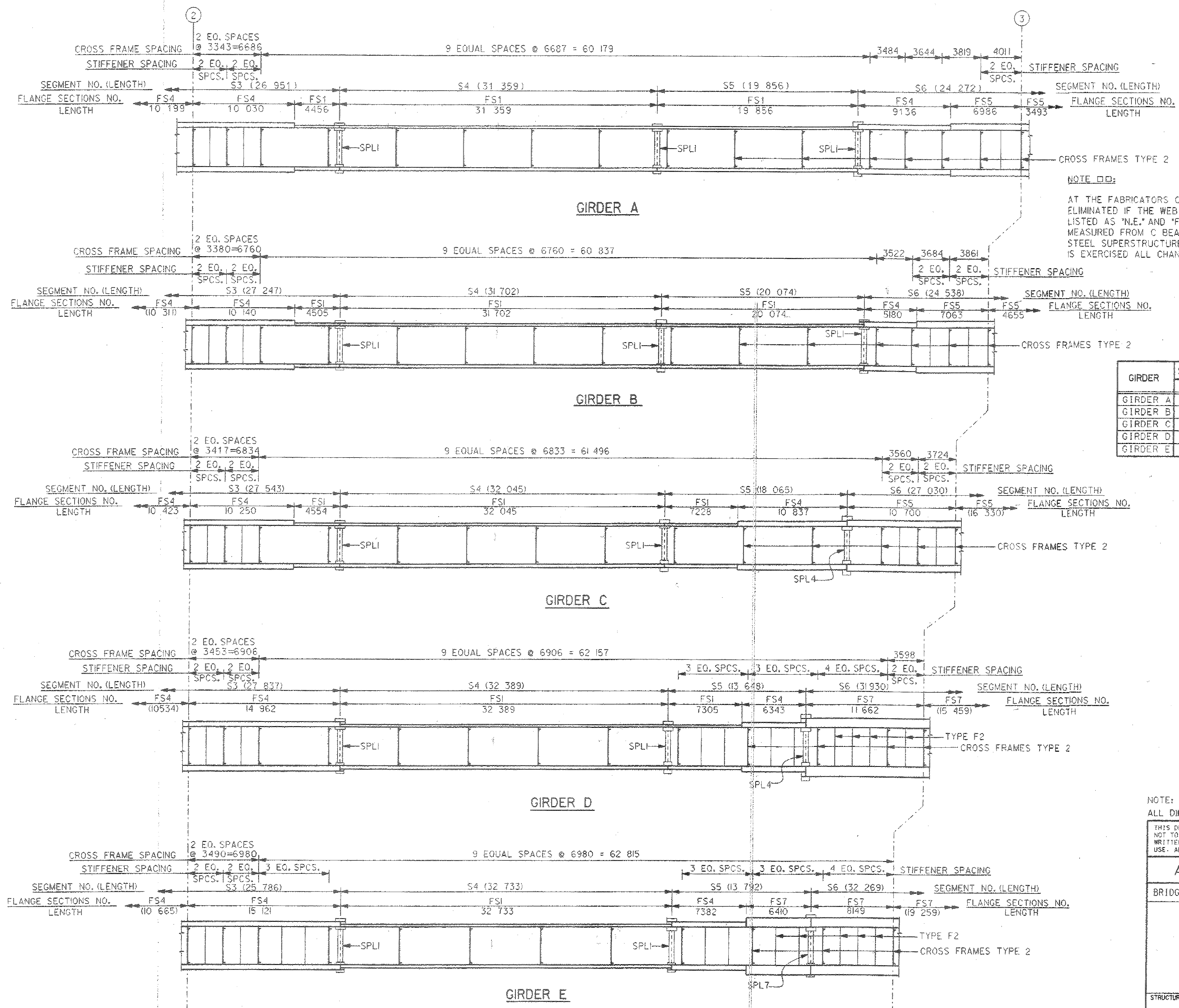

GIRDER ELEVATION - SPAN NO. 2

SCALE: 1 : 200

NOTE ☐☐:

AT THE FABRICATORS OPTION, THE INTERMEDIATE TRANSVERSE STIFFENERS MAY BE ELIMINATED IF THE WEB THICKNESS IS INCREASED TO 24mm OVER THE LENGTHS LISTED AS "N.E." AND "F.E." FOR "NEAR END" AND "FAR END" LENGTHS OF GIRDER RESPECTIVELY, MEASURED FROM ℄ BEARINGS IN SPANS NOS. 1 TO 4. ALL QUANTITIES SHOWN FOR STRUCTURAL STEEL SUPERSTRUCTURE ARE BASED ON THE THINNER WEB WITH STIFFENERS. IF THE OPTION IS EXERCISED ALL CHANGES SHALL BE SUBMITTED ON SHOP DRAWINGS FOR APPROVAL.

GIRDER	SPAN NO. 1	SPAN NO. 2		SPAN NO. 3		SPAN NO. 4
	F.E.	N.E.	F.E.	N.E.	F.E.	N.E.
GIRDER A	9100	8500	0	10 000	10 900	6700
GIRDER B	6200	6900	11 000	9800	11 800	6800
GIRDER C	7500	8700	9500	9800	12 400	3500
GIRDER D	9500	9600	20 700	23 200	29 800	13 800
GIRDER E	12 400	10 500	18 900	22 100	33 400	14 000

NOTE: SEE NOTES 1 TO 4 ON BRIDGE SHEET NO. 21.

ALDOT METRIC

NOTE:

ALL DIMENSIONS SHOWN ARE IN MILLIMETERS, UNLESS OTHERWISE NOTED.

ALABAMA DEPARTMENT OF TRANSPORTATION

BRIDGE SHEET NO. 22 OF 39

REVISIONS

DAVID VOLKERT AND ASSOCIATES, INC.
CONSULTING ENGINEERS

PROJECT IM-459-4 (78)
I-459/U.S. 31 INTERCHANGE
FLYOVER A
HOOVER, ALABAMA

GIRDER ELEVATIONS, SPANS 1 - 4 (SHT. 2 OF 5)

STRUCTURAL APPROVAL:
ASSISTANT BRIDGE ENGINEER
BRIDGE ENGINEER

STRUCTURAL APPROVAL:
S.R.J.
DESIGNER
J.T.L.
SECTION SUPERVISOR

QUANTITIES
COMP: S.R.J.
CHKD:
CHKD: S.R.J.

DRAWN: K.K.L. T.V.V.
REINF CHKD:
SCALE: AS SHOWN
DATE:

325

FHWA REG. NO.	STATE	PROJECT NUMBER	FISCAL YEAR	SHEET NO.	TOTAL SHEETS
4	ALA.	IM-459-4 (78)	2000	204	562

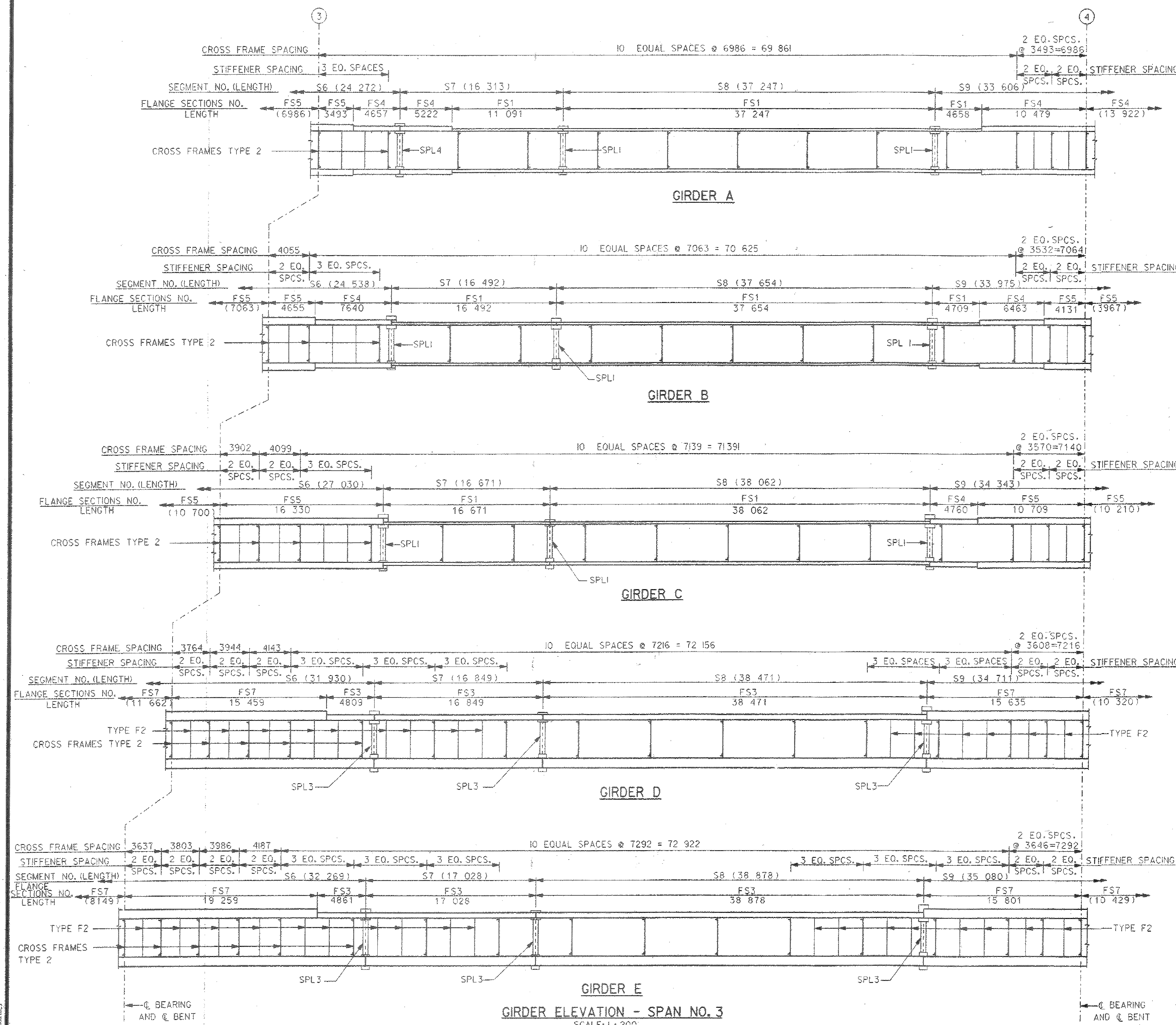

NOTE: SEE NOTES 1 TO 4 ON BRIDGE SHEET NO. 21.

NOTE:
- ALL DIMENSIONS SHOWN ARE IN MILLIMETERS, UNLESS OTHERWISE NOTED.

ALABAMA DEPARTMENT OF TRANSPORTATION

BRIDGE SHEET NO. 23 OF 39

REVISIONS

DAVID VOLKERT AND ASSOCIATES, INC.
CONSULTING ENGINEERS

PROJECT IM-459-4 (78)
I-459/U.S. 31 INTERCHANGE
FLYOVER A
HOOVER, ALABAMA

GIRDER ELEVATIONS, SPANS 1 - 4 (SHT. 3 OF 5)

STRUCTURAL APPROVAL: ASSISTANT BRIDGE ENGINEER; BRIDGE ENGINEER

STRUCTURAL APPROVAL: S.R.J. DESIGNER; J.T.L. SECTION SUPERVISOR

QUANTITIES — COMP: S.R.J.; CHKD:; CHKD: S.R.J.

DRAWN: K.K.L. T.V.V.; REINF CHKD:; SCALE: AS SHOWN; DATE:

326

FHWA REG. NO.	STATE	PROJECT NUMBER	FISCAL YEAR	SHEET NO.	TOTAL SHEETS
4	ALA.	IM-459-4 (78)	2000	205	562

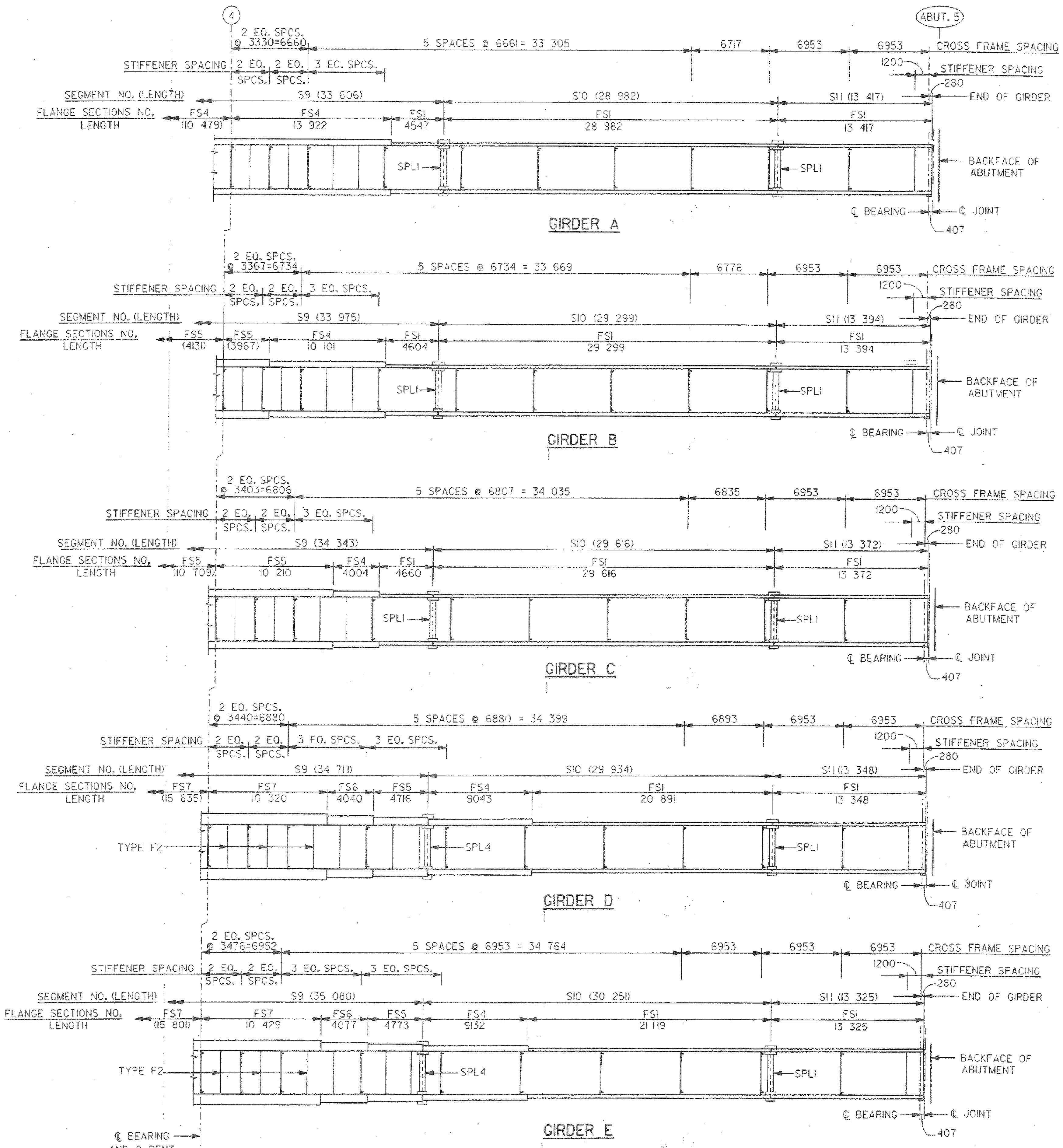

GIRDER ELEVATION - SPAN NO. 4

N.T.S.

NOTE: SEE NOTES 1 TO 4 ON BRIDGE SHEET NO. 21.

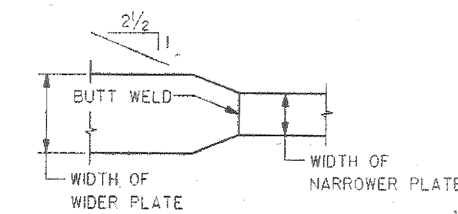

TAPERED FLANGE TRANSITION (PLAN)

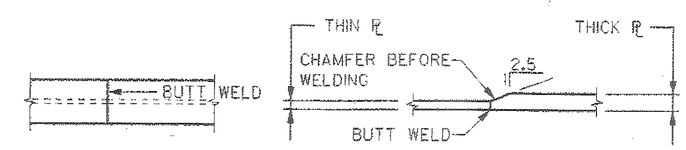

PLAN

ELEVATION

FLANGE TAPER DETAIL

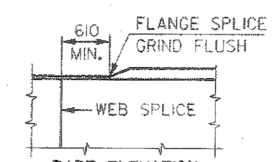

PART ELEVATION

WELDED WEB & FLANGE SPLICES

WITH APPROVAL FROM THE BRIDGE ENGINEER, WEB & FLANGE MATERIAL MAY BE SPLICED IF REQUIRED LENGTHS ARE UNOBTAINABLE. ANY SUCH SPLICE SHALL BE MADE IN THE SHOP USING AWS FULL PENETRATION SUBMERGED ARC WELDS. FLANGE AND/OR WEB SHOP SPLICES SHALL BE FULL PENETRATION BUTT WELDED USING APPROVED AWS JOINTS. THE LOCATION OF ANY SUCH SPLICE SHALL BE AT THE APPROX. ¼ AND/OR ¾ POINT OF THE REQUIRED MATERIAL LENGTHS.

SHOP WELDED SPLICE DETAILS

N.T.S.

ALDOT METRIC

NOTE:

ALL DIMENSIONS SHOWN ARE IN MILLIMETERS, UNLESS OTHERWISE NOTED.

ALABAMA DEPARTMENT OF TRANSPORTATION

BRIDGE SHEET NO. 24 OF 39

REVISIONS

DAVID VOLKERT AND ASSOCIATES, INC.
CONSULTING ENGINEERS

PROJECT IM-459-4 (78)
I-459/U.S. 31 INTERCHANGE
FLYOVER A
HOOVER, ALABAMA

GIRDER ELEVATIONS, SPANS 1 - 4 (SHT. 4 OF 5)

STRUCTURAL APPROVAL:
ASSISTANT BRIDGE ENGINEER
BRIDGE ENGINEER

STRUCTURAL APPROVAL:
S.R.J.
DESIGNER
J.T.L.
SECTION SUPERVISOR

QUANTITIES
COMP: S.R.J.
CHKD:
CHKD: S.R.J.

DRAWN: K.K.L. T.V.V.
REINF CHKD:
SCALE: AS SHOWN
DATE:

DVA GRAPHICS

327

FHWA REG. NO.	STATE	PROJECT NUMBER	FISCAL YEAR	SHEET NO.	TOTAL SHEETS
4	ALA.	IM-459-4 (78)	2000	200	562

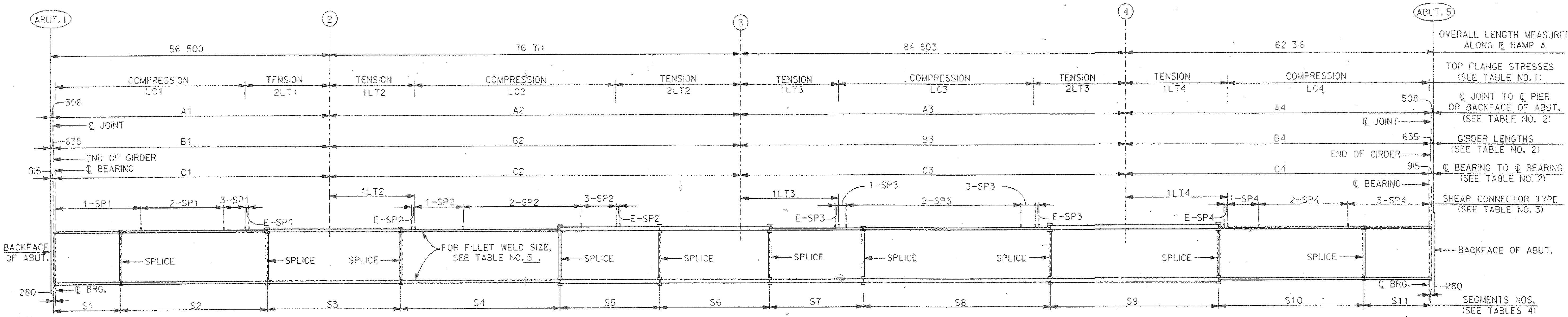

ELEVATION
N.T.S.

NOTE:
FOR LOCATION OF CROSS FRAMES AND STIFFENERS, SEE FRAMING PLAN BRIDGE SHEET. NOS. 19&20
FOR SPLICE TYPE, SEE GIRDER ELEVATION BRIDGE SHEET NOS. 21 TO 24.

TOP FLANGE STRESSES - DISTANCE "LC" AND "LT" (TABLE NO. 1)

GIRDER	SPAN NO. 1		SPAN NO. 2			SPAN NO. 3			SPAN NO. 4	
	LC1	2LT1	1LT2	LC2	2LT2	1LT3	LC3	2LT3	1LT4	LC4
GIRDER A	37 332	17 341	17 068	39 432	25 323	18 038	39 837	18 972	19 064	41 517
GIRDER B	38 429	16 801	17 495	37 874	23 294	17 875	44 833	19 036	20 786	40 292
GIRDER C	39 560	16 025	17 764	33 370	24 481	20 568	46 192	19 771	22 797	38 777
GIRDER D	40 807	14 981	18 462	30 629	23 570	22 573	48 192	20 457	26 674	35 396
GIRDER E	42 032	14 313	18 413	24 814	26 568	25 900	48 113	21 814	29 414	33 153

DIMENSIONS - A, B AND C (TABLE NO. 2)

GIRDER	A1	A2, B2, C2	A3, B3, C3	A4	B1	B4	C1	C4
GIRDER A	55 080	81 823	76 847	60 995	54 953	60 868	54 673	60 588
GIRDER B	55 637	78 664	81 744	61 492	55 510	61 365	55 230	61 085
GIRDER C	56 195	75 614	86 532	61 989	56 068	61 862	55 788	61 582
GIRDER D	56 752	72 661	91 223	62 485	56 625	62 358	56 345	62 078
GIRDER E	57 310	69 795	95 827	62 982	57 183	62 855	56 903	62 575

SHEAR CONNECTORS (TABLE NO. 3)

GIRDER	1-SP1	2-SP1	3-SP1	E-SP1	E-SP2	1-SP2	2-SP2	3-SP2	E-SP2
GIRDER A	13 SPACES @ 535 = 6955	36 SPACES @ 570 = 20 520	19 SPACES @ 550 = 10 450	5 SPACES @ 145 = 725	5 SPACES @ 145 = 725	21 SPACES @ 465 = 9765	43 SPACES @ 465 = 19 995	17 SPACES @ 600 = 10 200	5 SPACES @ 145 = 725
GIRDER B	15 SPACES @ 465 = 6975	42 SPACES @ 490 = 20 580	20 SPACES @ 540 = 10 800	5 SPACES @ 145 = 725	5 SPACES @ 145 = 725	24 SPACES @ 400 = 9600	46 SPACES @ 440 = 20 240	18 SPACES @ 455 = 8190	5 SPACES @ 145 = 725
GIRDER C	18 SPACES @ 390 = 7020	50 SPACES @ 420 = 21 000	22 SPACES @ 520 = 11 440	5 SPACES @ 145 = 725	5 SPACES @ 145 = 725	27 SPACES @ 355 = 9585	34 SPACES @ 400 = 13 600	28 SPACES @ 445 = 12 460	5 SPACES @ 145 = 725
GIRDER D	20 SPACES @ 355 = 7100	57 SPACES @ 370 = 21 090	23 SPACES @ 520 = 11 960	5 SPACES @ 145 = 725	5 SPACES @ 145 = 725	29 SPACES @ 335 = 9715	38 SPACES @ 365 = 13 870	22 SPACES @ 415 = 9130	5 SPACES @ 145 = 725
GIRDER E	21 SPACES @ 340 = 7140	63 SPACES @ 340 = 21 420	25 SPACES @ 480 = 12 000	5 SPACES @ 145 = 725	5 SPACES @ 145 = 725	33 SPACES @ 295 = 9735	43 SPACES @ 325 = 13 975	16 SPACES @ 365 = 5840	5 SPACES @ 145 = 725

GIRDER	E-SP3	1-SP3	2-SP3	3-SP3	E-SP3	E-SP4	1-SP4	2-SP4	3-SP4
GIRDER A	5 SPACES @ 145 = 725	14 SPACES @ 595 = 8330	35 SPACES @ 600 = 21 000	16 SPACES @ 595 = 9520	5 SPACES @ 145 = 725	5 SPACES @ 145 = 725	24 SPACES @ 540 = 12 960	23 SPACES @ 580 = 13 340	26 SPACES @ 535 = 13 910
GIRDER B	5 SPACES @ 145 = 725	23 SPACES @ 565 = 12 995	37 SPACES @ 575 = 21 275	17 SPACES @ 495 = 8415	5 SPACES @ 145 = 725	5 SPACES @ 145 = 725	22 SPACES @ 520 = 11 440	26 SPACES @ 520 = 13 520	30 SPACES @ 465 = 13 950
GIRDER C	5 SPACES @ 145 = 725	17 SPACES @ 465 = 7905	58 SPACES @ 490 = 28 420	18 SPACES @ 450 = 8100	5 SPACES @ 145 = 725	5 SPACES @ 145 = 725	35 SPACES @ 495 = 17 325	16 SPACES @ 425 = 6800	35 SPACES @ 395 = 13 825
GIRDER D	5 SPACES @ 145 = 725	20 SPACES @ 460 = 9200	65 SPACES @ 445 = 28 925	19 SPACES @ 405 = 7695	5 SPACES @ 145 = 725	5 SPACES @ 145 = 725	20 SPACES @ 485 = 9700	29 SPACES @ 430 = 12 470	44 SPACES @ 345 = 15 180
GIRDER E	5 SPACES @ 145 = 725	24 SPACES @ 405 = 9720	49 SPACES @ 445 = 21 805	36 SPACES @ 405 = 14 580	5 SPACES @ 145 = 725	5 SPACES @ 145 = 725	21 SPACES @ 430 = 9030	40 SPACES @ 350 = 14 000	42 SPACES @ 330 = 13 860

DETAILS OF FLANGE & FILLET WELD SIZES AT SECTIONS (TABLE NO. 5)

	TYPE FLANGE SECTIONS	TOP FLANGE			BOTTOM FLANGE		
		WIDTH	THICK.	WEB FILLET	WIDTH	THICK.	WEB FILLET
	FS1	406	25	8	559	32	8
	FS2	406	38	8	559	51	10
■■	FS3	559	57	10	838	95	13
	FS4	762	51	10	762	51	10
	FS5	762	64	10	762	64	10
	FS6	762	76	13	762	76	13
■■	FS7	1067	95	13	1067	95	13

NOTE: PLATE SIZES ARE IN MM UNITS, CONVERTED FROM "INCH" UNITS. THESE ARE NOT ROUNDED TO STANDARD METRIC PLATE SIZES TO AVOID DOUBLE ROUNDING UP. USE INCH EQUIVALENTS OR THE ROUNDED UP METRIC SIZES AS AVAILABLE.

PLATE GIRDER LENGTHS FOR SEGMENTS (TABLE NO. 4)

GIRDER	S1	S2	S3	S4	S5	S6	S7	S8	S9	S10	S11
A	13 287	29 201	26 951	31 359	19 856	24 272	16 313	37 247	33 606	28 982	13 417
B	13 388	29 520	27 247	31 702	20 074	24 538	16 492	37 654	33 975	29 299	13 394
C	13 489	29 840	27 543	32 045	18 065	27 030	16 671	38 062	34 343	29 616	13 372
D	13 590	30 160	27 837	32 389	13 648	31 930	16 849	38 471	34 711	29 934	13 348
E	10 125	36 393	25 786	32 733	13 792	32 269	17 028	38 878	35 080	30 251	13 325

WEB PLATE 18x2438 FOR ALL SEGMENTS.
FOR FLANGE SECTIONS, SEE TABLE NO. 5 AND BRIDGE SHEET NOS. 21 TO 24
SEE ALSO NOTE ■■ BELOW.

■■ NOTE:
CURVED GIRDER FLANGE PLATES MAY BE CUT FROM WIDER PLATE TO THE RADII SHOWN.
GIRDERS MAY BE CURVED BY THE HEAT-UPSET METHOD FOR TYPE FLANGE SECTION NOS. FS1, FS2, FS4, FS5 AND FS6.
FOR FLANGE SECTION NOS. FS3 AND FS7 CURVING BY HEAT-UPSET METHOD IS NOT ALLOWED.

ALDOT METRIC

NOTE:
ALL DIMENSIONS SHOWN ARE IN MILLIMETERS, UNLESS OTHERWISE NOTED.

ALABAMA DEPARTMENT OF TRANSPORTATION

BRIDGE SHEET NO. 25 OF 39
REVISIONS

DAVID VOLKERT AND ASSOCIATES, INC.
CONSULTING ENGINEERS

PROJECT IM-459-4 (78)
I-459/U.S. 31 INTERCHANGE
FLYOVER A
HOOVER, ALABAMA

GIRDER ELEVATIONS, SPANS 1 - 4 (SHT. 5 OF 5)

STRUCTURAL APPROVAL:
ASSISTANT BRIDGE ENGINEER
BRIDGE ENGINEER
STRUCTURAL APPROVAL: S.R.J.
DESIGNER J.T.L.
SECTION SUPERVISOR
QUANTITIES COMP: S.R.J. CHKD:
CHKD: S.R.J.
DRAWN: K.K.L.
REINF CHKD:
SCALE: AS SHOWN
DATE:

328

FHWA REG. NO.	STATE	PROJECT NUMBER	FISCAL YEAR	SHEET NO.	TOTAL SHEETS
4	ALA.	IM-459-4 (78)	2000	207	562

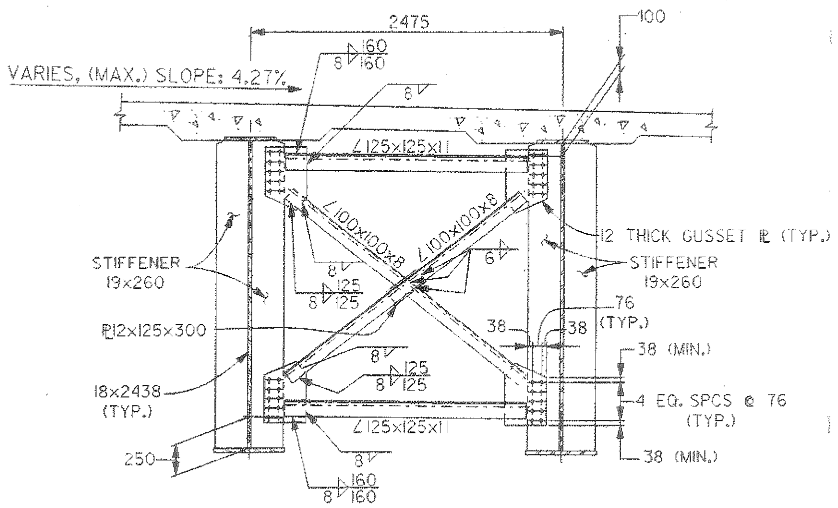

END SUPPORT CROSS FRAME AT ABUTMENT NOS. 1 AND 5
SCALE: 1:30

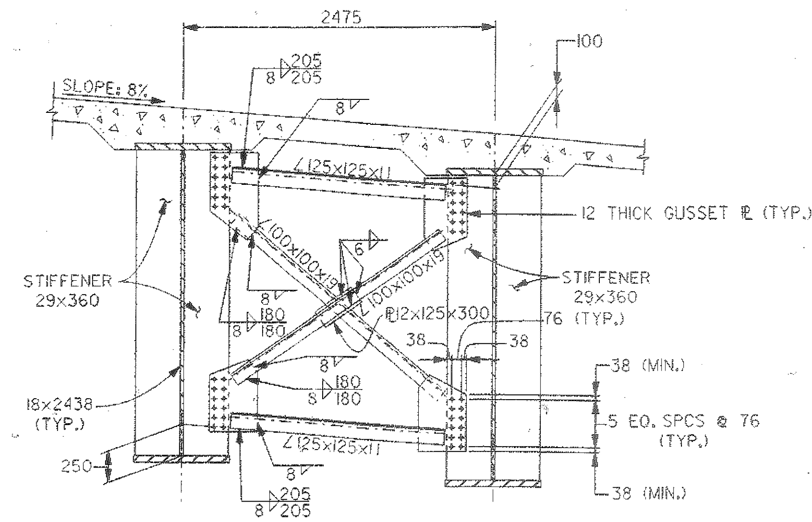

INTERIOR SUPPORT CROSS FRAME AT BENT NO. 2
SCALE: 1:30

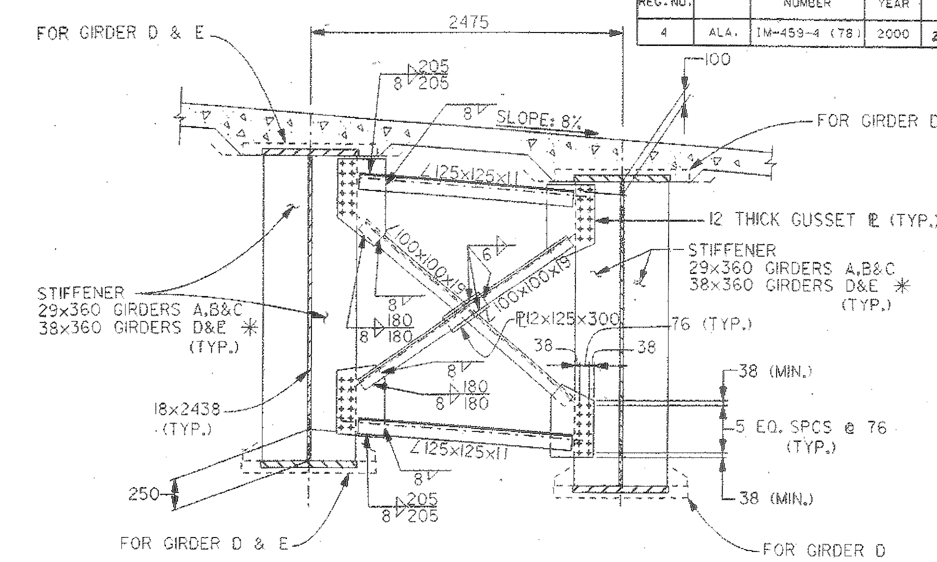

INTERIOR SUPPORT CROSS FRAME AT BENT NO. 4
SCALE: 1:30

✻ TO FIT CROSS FRAME, SEE DETAILS FOR BEARING STIFFENER ON BRIDGE SHEET NO. 27 .

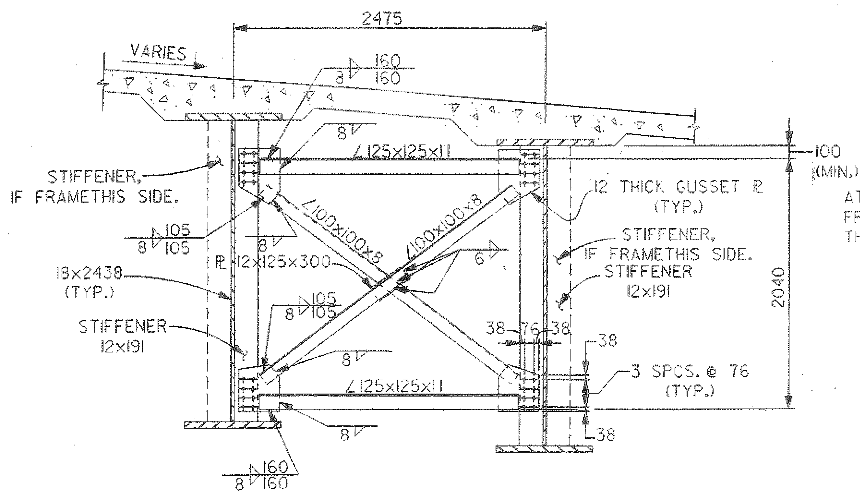

TYPICAL INTERMEDIATE CROSS FRAME TYPE 1
SCALE: 1:30

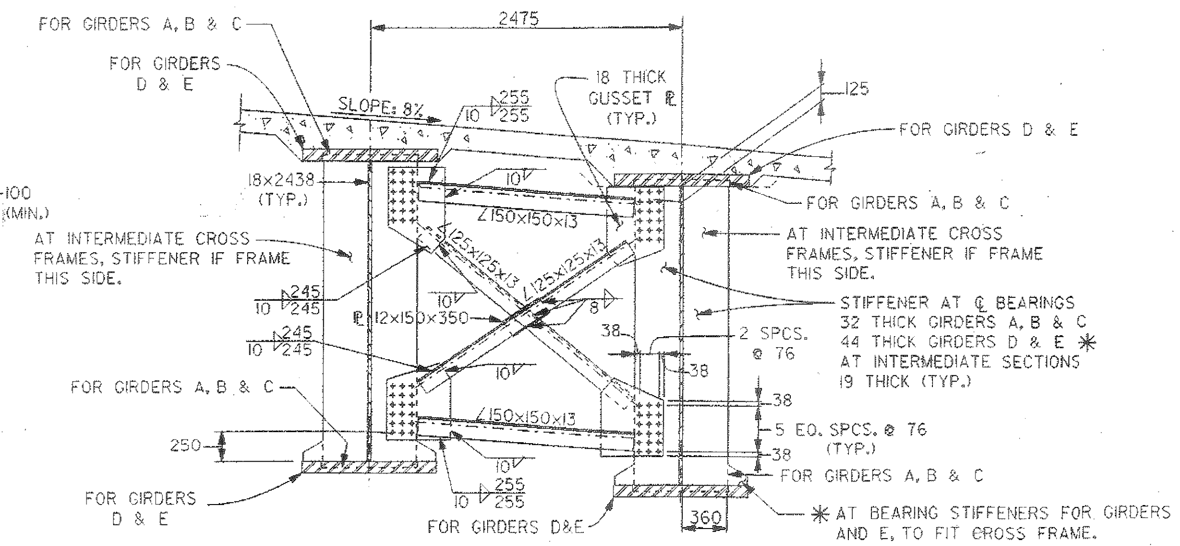

RADIAL CROSS FRAMES NEAR AND ON BENT NO. 3 (TYPE 2)
SCALE: 1:30

NOTE :

FOR LOCATION OF CROSS FRAMES AND STIFFENERS, SEE FRAMING PLAN BRIDGE SHEET NOS. 19 & 20. FOR SPLICE TYPE, SEE GIRDER ELEVATION BRIDGE SHEET NOS. 21 & 24.

PLATE AND ANGLE SIZES SHOWN ARE IN MM UNITS, CONVERTED FROM "INCH" UNITS. THESE ARE NOT ROUNDED TO STANDARD METRIC SIZES TO AVOID DOUBLE ROUNDING UP. USE INCH EQUIVALENTS OR THE METRIC SIZES AS AVAILABLE.

ALDOT METRIC

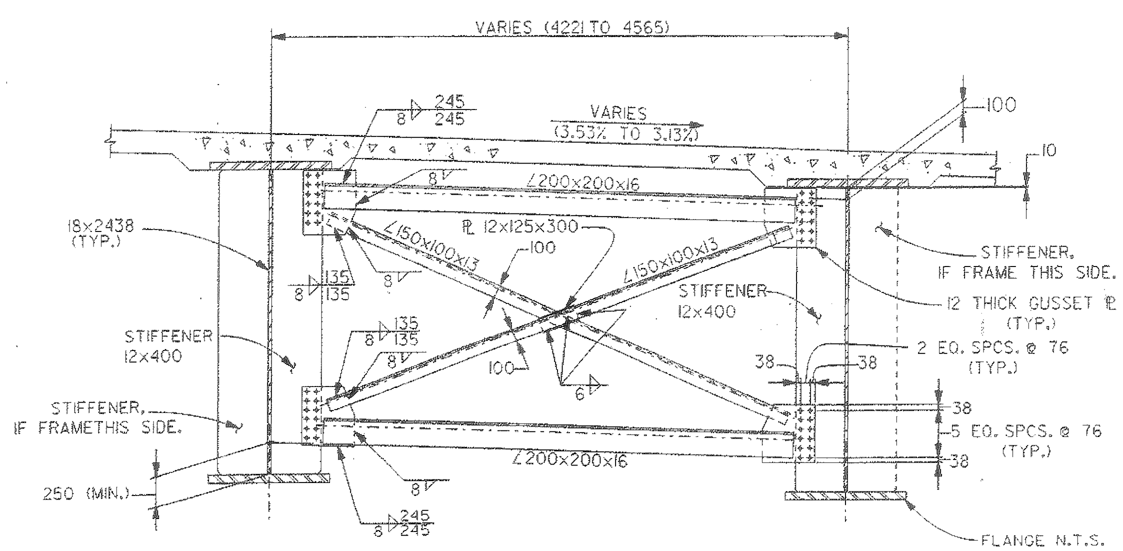

INTERIOR SUPPORT SKEW CROSS FRAME AT BENT NO. 3
SCALE: 1:30

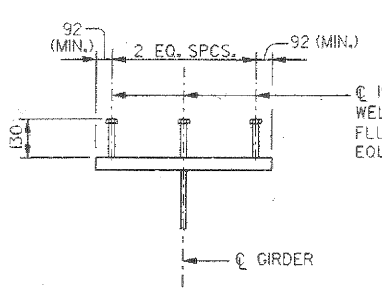

WITHIN FIELD SECTION

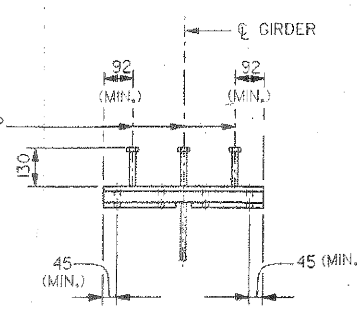

AT FIELD SPLICES

SHEAR CONNECTOR DETAILS
N.T.S.

NOTE:
ALL DIMENSIONS SHOWN ARE IN MILLIMETERS, UNLESS OTHERWISE NOTED.

ALABAMA DEPARTMENT OF TRANSPORTATION

BRIDGE SHEET NO. 26 OF 39

REVISIONS

DAVID VOLKERT AND ASSOCIATES, INC.
CONSULTING ENGINEERS

PROJECT IM-459-4 (78)
I-459/U.S. 31 INTERCHANGE
FLYOVER A
HOOVER, ALABAMA

STEEL DETAILS, SPAN 1 - 4 (SHEET 1 OF 4)

STRUCTURAL APPROVAL:	STRUCTURAL APPROVAL:	QUANTITIES	DRAWN: K.K.L.
	S.R.J.	COMP: S.R.J.	REINF CHKD:
ASSISTANT BRIDGE ENGINEER	DESIGNER	CHKD:	SCALE: AS SHOWN
	J.T.L.		
BRIDGE ENGINEER	SECTION SUPERVISOR	CHKD: S.R.J.	DATE:

User ies James
S:\projects\503800\cadd\MAP x\stfrom_det.dgn
S:\PROJECTS\PLOTFEN\dfen.tbl
S:\PROJECTS\PLOTCONFIG\w.ctb
3-JUN-2000 8:53
DVA GRAPHICS

FHWA REG. NO.	STATE	PROJECT NUMBER	FISCAL YEAR	SHEET NO.	TOTAL SHEETS
4	ALA.	IM-459-4 (78)	2000	209	562

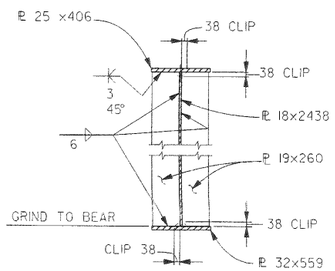

END BEARINGS STIFFENER
ABUTMENT NOS. 1 AND 5
SCALE: 1 : 20

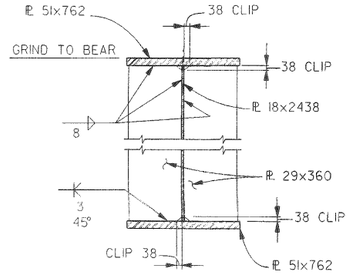

INTERIOR BEARING STIFFENER
BENT NO. 2
SCALE: 1 : 20

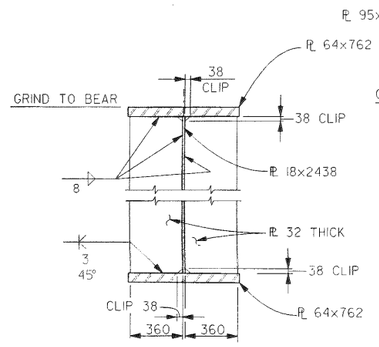

INTERIOR BEARING STIFFENER
AT BENT NO. 3 GIRDERS A, B&C
SCALE: 1 : 20

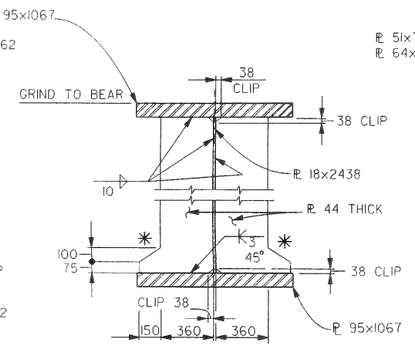

INTERIOR BEARING STIFFENER
AT BENT NO. 3 GIRDERS D&E
SCALE: 1 : 20

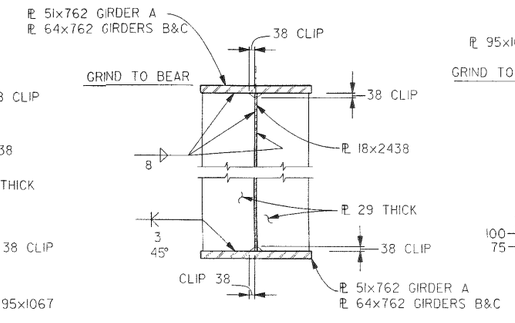

INTERIOR BEARING STIFFENER
AT BENT NO. 4 GIRDERS A, B&C
SCALE: 1 : 20

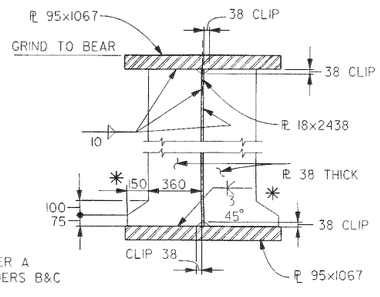

INTERIOR BEARING STIFFENER
AT BENT NO. 4 GIRDERS D&E
SCALE: 1 : 20

✱ TO FIT CROSS FRAME
FOR DETAILS OF CROSS FRAME,
SEE BRIDGE SHEET NO. 26 .

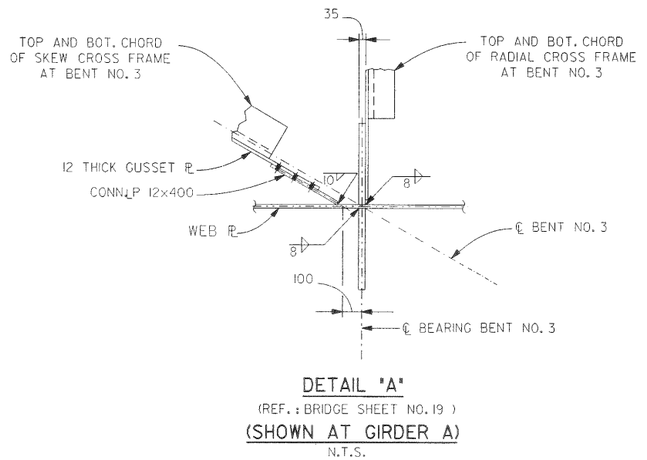

DETAIL "A"
(REF. : BRIDGE SHEET NO. 19)
(SHOWN AT GIRDER A)
N.T.S.

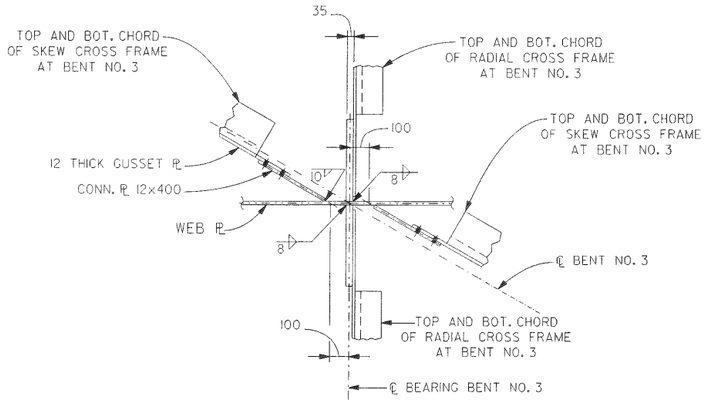

DETAIL "B"
(REF. : BRIDGE SHEET NO. 19)
(SHOWN AT GIRDER B)
N.T.S.

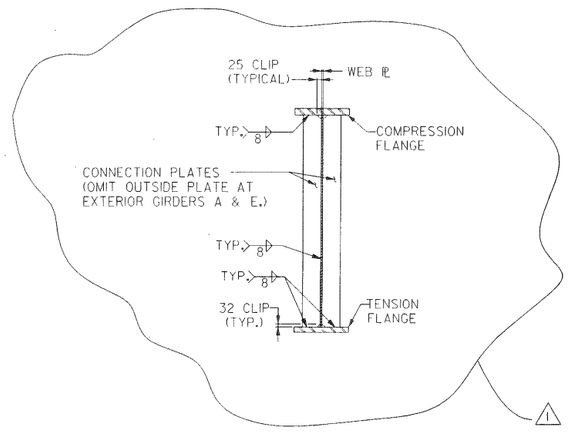

TYPICAL INTERMEDIATE CROSS FRAME CONNECTION PLATE DETAIL
N.T.S.

NOTE :
PLATE SIZES ARE IN MM UNITS. CONVERTED FROM "INCH" UNITS. THESE ARE NOT ROUNDED TO STANDARD METRIC PLATE SIZES TO AVOID DOUBLE ROUNDING UP. USE INCH EQUIVALENTS OR THE ROUNDED UP METRIC SIZES AS AVAILABLE.

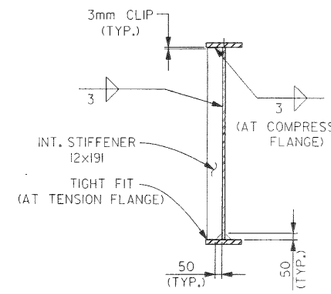

TYPE F1 TYPE F2

INTERMEDIATE STIFFENER DETAILS
N.T.S.
(SECTION DEPICTED FOR COMPRESSION FLANGE AT TOP)

NOTE:
ALL DIMENSIONS SHOWN ARE IN MILLIMETERS, UNLESS OTHERWISE NOTED.

ALABAMA DEPARTMENT OF TRANSPORTATION

BRIDGE SHEET NO. 27 OF 39

REVISIONS
1 J.T.L. INT. TRANSV. STIFF. & X-FRAME CONN. PLATE DETAILS. (9/6/00)

DAVID VOLKERT AND ASSOCIATES, INC.
CONSULTING ENGINEERS

PROJECT IM-459-4 (78)
I-459/U.S. 31 INTERCHANGE
FLYOVER A
HOOVER, ALABAMA

STEEL DETAILS, SPAN 1 - 4 (SHEET 2 OF 4)

STRUCTURAL APPROVAL:	STRUCTURAL APPROVAL: S.R.J.	QUANTITIES COMP: S.R.J.	DRAWN: K.K.L.
ASSISTANT BRIDGE ENGINEER	DESIGNER J.T.L.	CHKD:	REINF CHKD:
BRIDGE ENGINEER	SECTION SUPERVISOR	CHKD: S.R.J.	SCALE: AS SHOWN DATE:

ALDOT METRIC

User Is: lg
Si:\Projects\503800\cadd\RAMP A\stfrm_det.dgn
Model: Default
Si:\PROJECTS\PLOTVER\ldpc.pen
Si:\PROJECTS\PLOTVER\DGNFO\bw.ctb
08-SEP-2000 9:26
DVA GRAPHICS

325

FHWA REG. NO.	STATE	PROJECT NUMBER	FISCAL YEAR	SHEET NO.	TOTAL SHEETS
4	ALA.	IM-459-4 (78)	2000	208	562

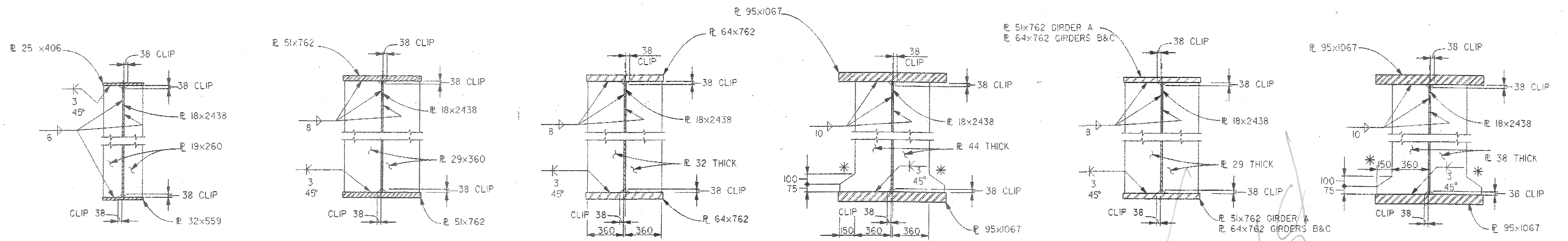

END BEARINGS STIFFENER ABUTMENT NOS. 1 AND 5
SCALE: 1 : 20

INTERIOR BEARING STIFFENER BENT NO. 2
SCALE: 1 : 20

INTERIOR BEARING STIFFENER AT BENT NO. 3 GIRDERS A, B&C
SCALE: 1 : 20

INTERIOR BEARING STIFFENER AT BENT NO. 3 GIRDERS D&E
SCALE: 1 : 20

INTERIOR BEARING STIFFENER AT BENT NO. 4 GIRDERS A, B&C
SCALE: 1 : 20

INTERIOR BEARING STIFFENER AT BENT NO. 4 GIRDERS D&E
SCALE: 1 : 20

✳ TO FIT CROSS FRAME
FOR DETAILS OF CROSS FRAME,
SEE BRIDGE SHEET NO. 26 .

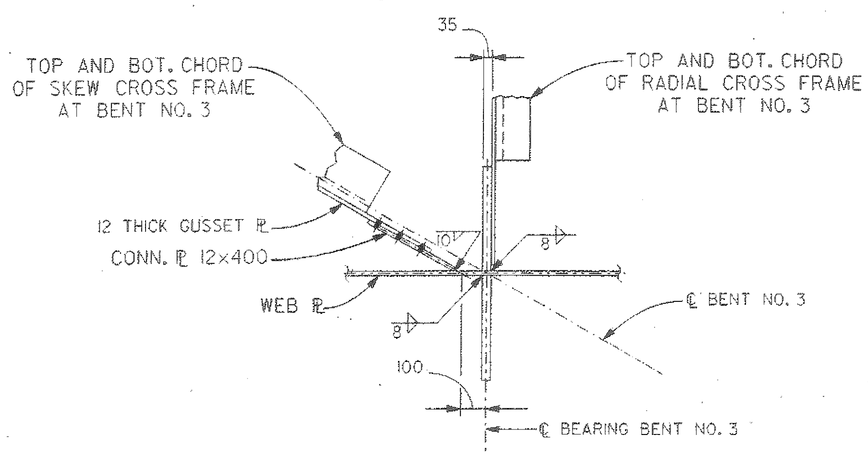

DETAIL "A"
(REF.: BRIDGE SHEET NO. 19)
(SHOWN AT GIRDER A)
N.T.S.

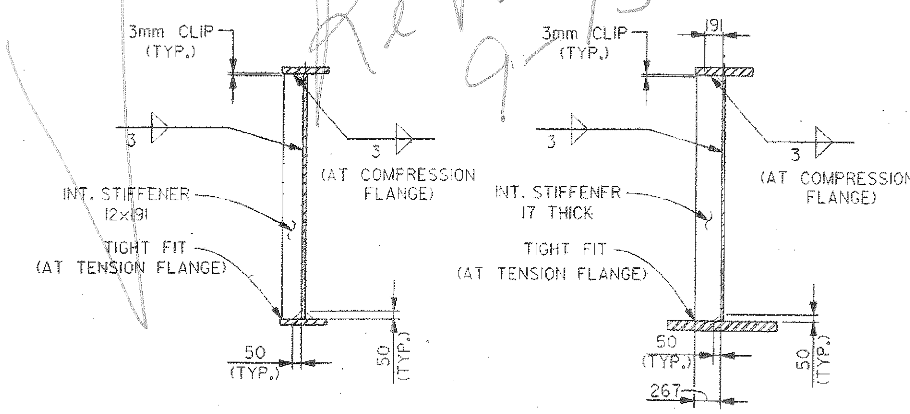

TYPE F1

TYPE F2

INTERMEDIATE STIFFENER DETAILS
N.T.S.
(SECTION DEPICTED FOR COMPRESSION FLANGE AT TOP)

Revised 9-15-00

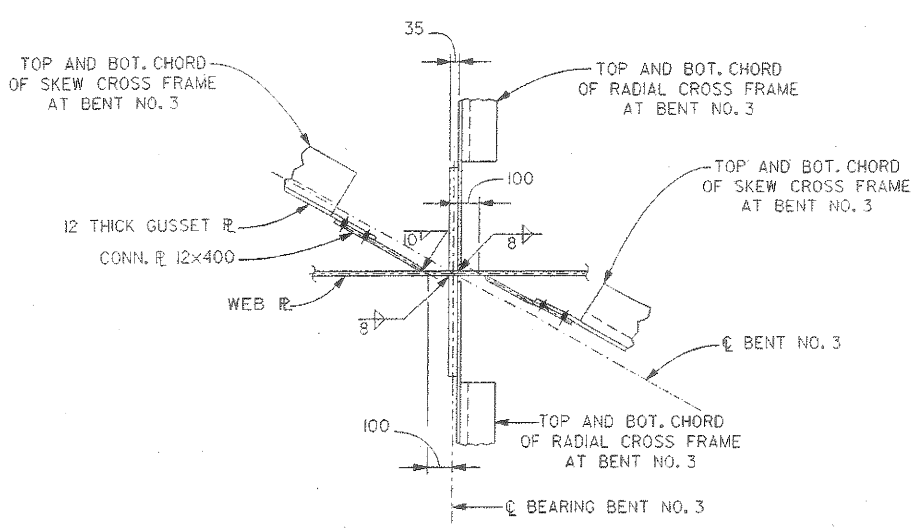

DETAIL "B"
(REF.: BRIDGE SHEET NO. 19)
(SHOWN AT GIRDER B)
N.T.S.

NOTE :
PLATE SIZES ARE IN MM UNITS, CONVERTED FROM "INCH" UNITS. THESE ARE NOT ROUNDED TO STANDARD METRIC PLATE SIZES TO AVOID DOUBLE ROUNDING UP. USE INCH EQUIVALENTS OR THE ROUNDED UP METRIC SIZES AS AVAILABLE.

NOTE:
ALL DIMENSIONS SHOWN ARE IN MILLIMETERS, UNLESS OTHERWISE NOTED.

ALABAMA DEPARTMENT OF TRANSPORTATION

BRIDGE SHEET NO. 27 OF 39
REVISIONS
Revised 9-15-00 V014

DAVID VOLKERT AND ASSOCIATES, INC.
CONSULTING ENGINEERS

PROJECT IM-459-4 (78)
I-459/U.S. 31 INTERCHANGE
FLYOVER A
HOOVER, ALABAMA

STEEL DETAILS, SPAN 1 - 4 (SHEET 2 OF 4)

ALDOT METRIC

STRUCTURAL APPROVAL:	STRUCTURAL APPROVAL:	QUANTITIES	DRAWN: K.K.L.
ASSISTANT BRIDGE ENGINEER	S.R.J. DESIGNER	COMP: S.R.J.	REINF CHKD:
BRIDGE ENGINEER	J.T.L. SECTION SUPERVISOR	CHKD:	SCALE: AS SHOWN
		CHKD: S.R.J.	DATE:

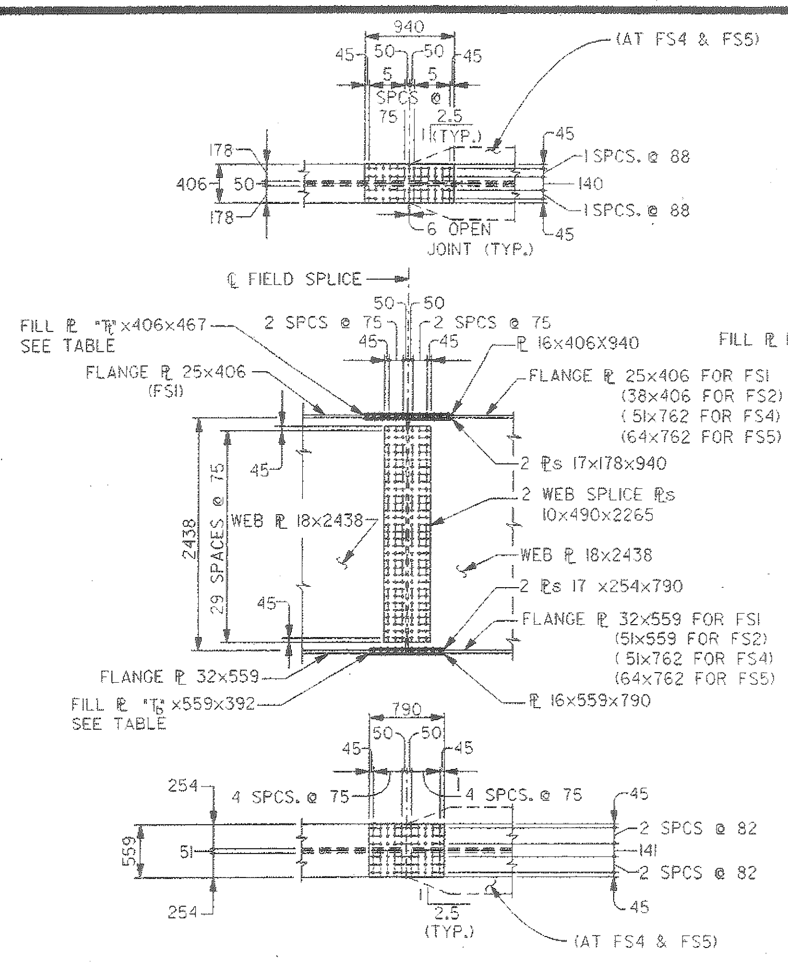

FIELD SPLICE TYPE SPL1
SCALE : 1:30

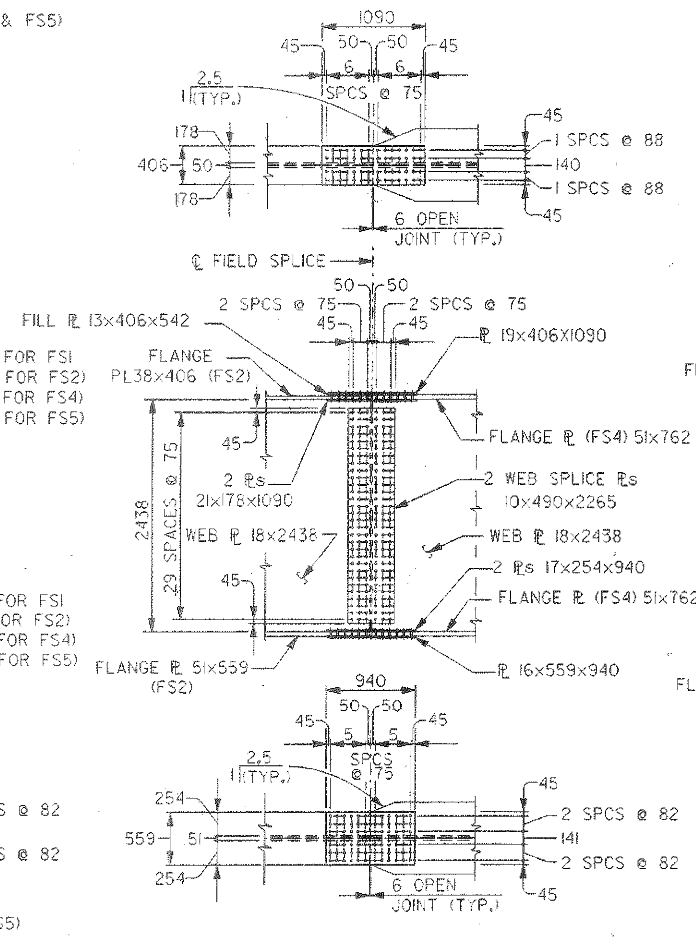

FIELD SPLICE TYPE SPL2
SCALE : 1:30

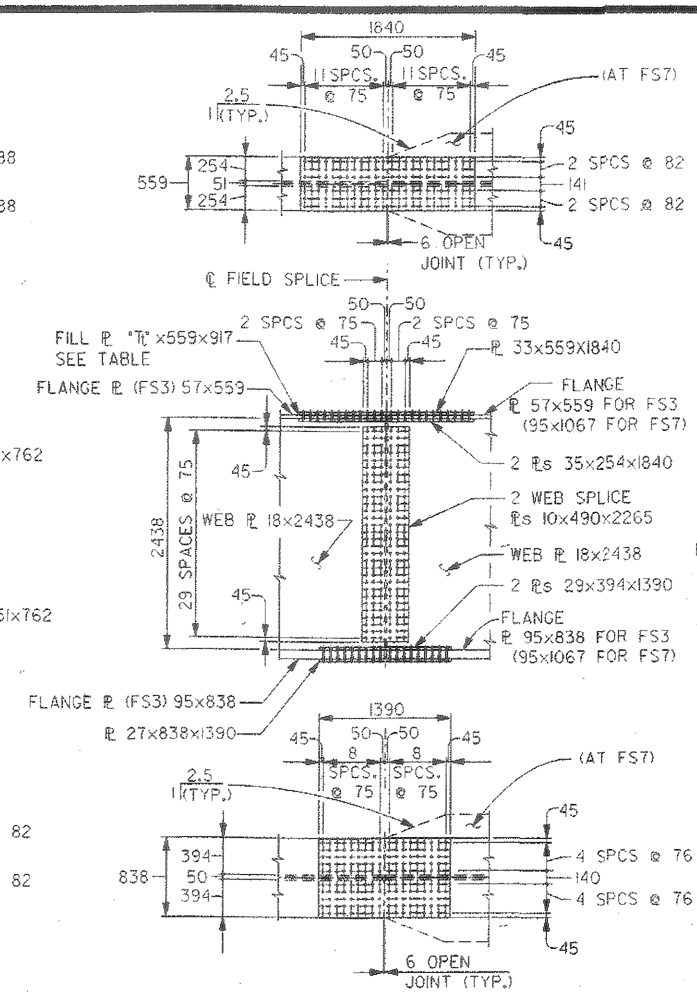

FIELD SPLICE TYPE SPL3
SCALE : 1:30

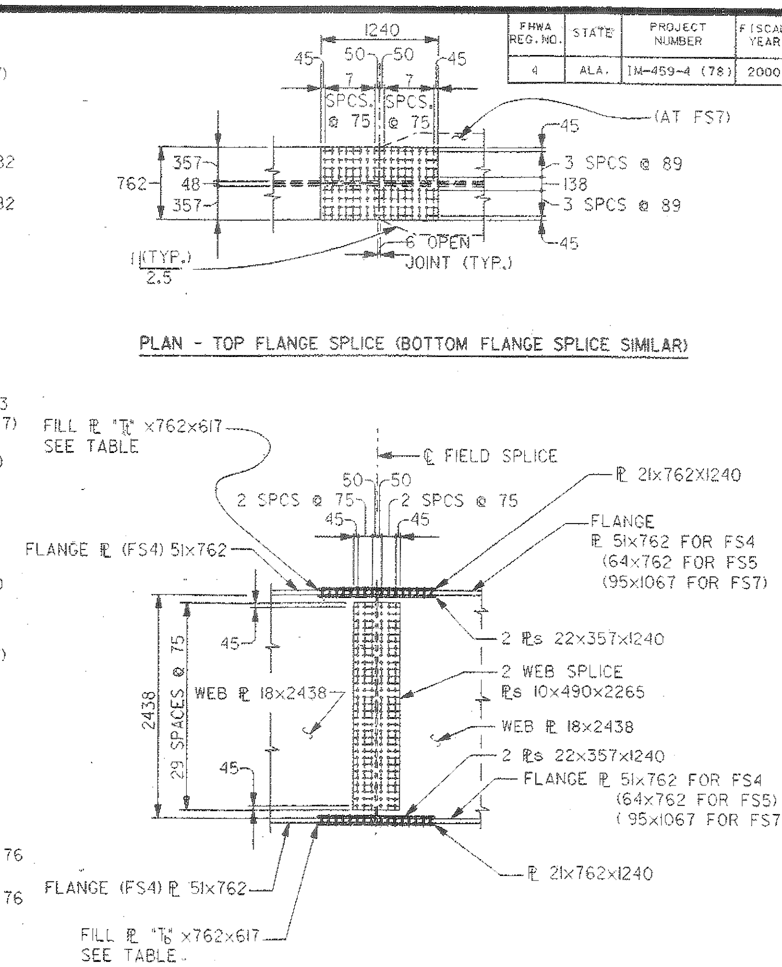

PLAN - TOP FLANGE SPLICE (BOTTOM FLANGE SPLICE SIMILAR)

FIELD SPLICE TYPE SPL4
SCALE : 1:30

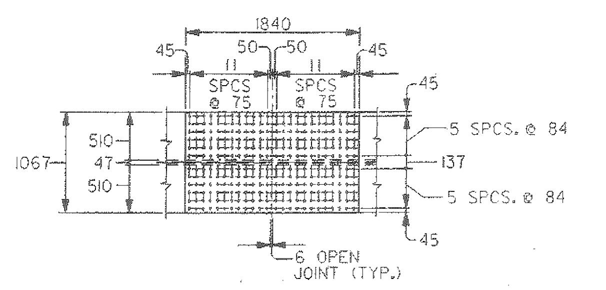

PLAN - TOP FLANGE SPLICE (BOTTOM FLANGE SPLICE SIMILAR)

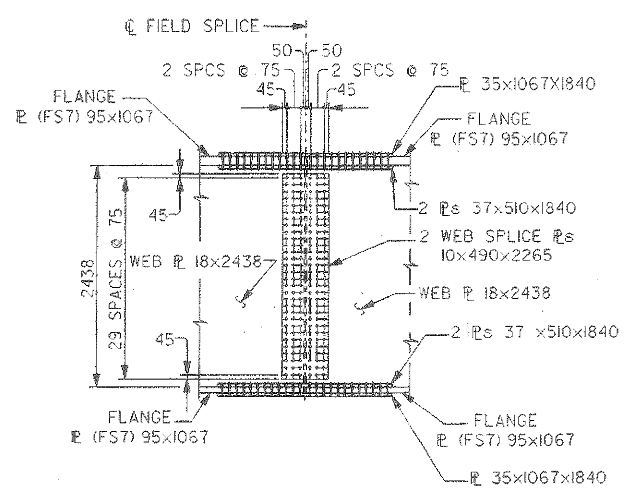

FIELD SPLICE TYPE SPL7
SCALE : 1:30

FILL ℙ THICKNESSES AT SPLICE JOINTS			
FILL FOR SPLICE TYPE	FILL ℙ "t1"	FILL ℙ "t2"	NO. OF JOINTS
SPL1 AT			
FS1 & FS2	13	19	1
FS1 & FS4	26	19	7
FS1 & FS5	39	32	1
SPL2 AT	AS SHOWN		
FS2 & FS4	(13)	——	1
SPL3 AT			
FS3 & FS7	38	——	2
SPL4 AT			
FS4 & FS5	13	13	3
FS4 & FS7	44	44	1

NOTE:
FOR LOCATION OF CROSS FRAMES AND STIFFENERS, SEE FRAMING PLAN BRIDGE SHEET NOS. 19 & 20.
FOR SPLICE TYPE, SEE GIRDER ELEVATION BRIDGE SHEET NOS. 21 & 24.

PLATE SIZES ARE IN MM UNITS, CONVERTED FROM "INCH" UNITS. THESE ARE NOT ROUNDED TO STANDARD METRIC PLATE SIZES TO AVOID DOUBLE ROUNDING UP. USE INCH EQUIVALENTS OR THE ROUNDED UP METRIC SIZES AS AVAILABLE.

ALDOT METRIC

NOTE:
ALL DIMENSIONS SHOWN ARE IN MILLIMETERS, UNLESS OTHERWISE NOTED.

ALABAMA DEPARTMENT OF TRANSPORTATION

BRIDGE SHEET NO. 28 OF 39
REVISIONS

DAVID VOLKERT AND ASSOCIATES, INC.
CONSULTING ENGINEERS

PROJECT IM-459-4 (78)
I-459/U.S. 31 INTERCHANGE
FLYOVER A
HOOVER, ALABAMA

STEEL DETAILS, SPAN 1 - 4 (SHEET 3 OF 4)

STRUCTURAL APPROVAL: | STRUCTURAL APPROVAL: S.R.J. | QUANTITIES | DRAWN: K.K.L.
ASSISTANT BRIDGE ENGINEER | DESIGNER J.T.L. | COMP: S.R.J. | REINF CHKD:
BRIDGE ENGINEER | SECTION SUPERVISOR | CHKD: S.R.J. | SCALE: AS SHOWN | DATE:

FHWA REG. NO.	STATE	PROJECT NUMBER	FISCAL YEAR	SHEET NO.	TOTAL SHEETS
4	ALA.	IM-459-4 (78)	2000	209	562

FHWA REG. NO.	STATE	PROJECT NUMBER	FISCAL YEAR	SHEET NO.	TOTAL SHEETS
4	ALA.	IM-459-4 (78)	2000	210	562

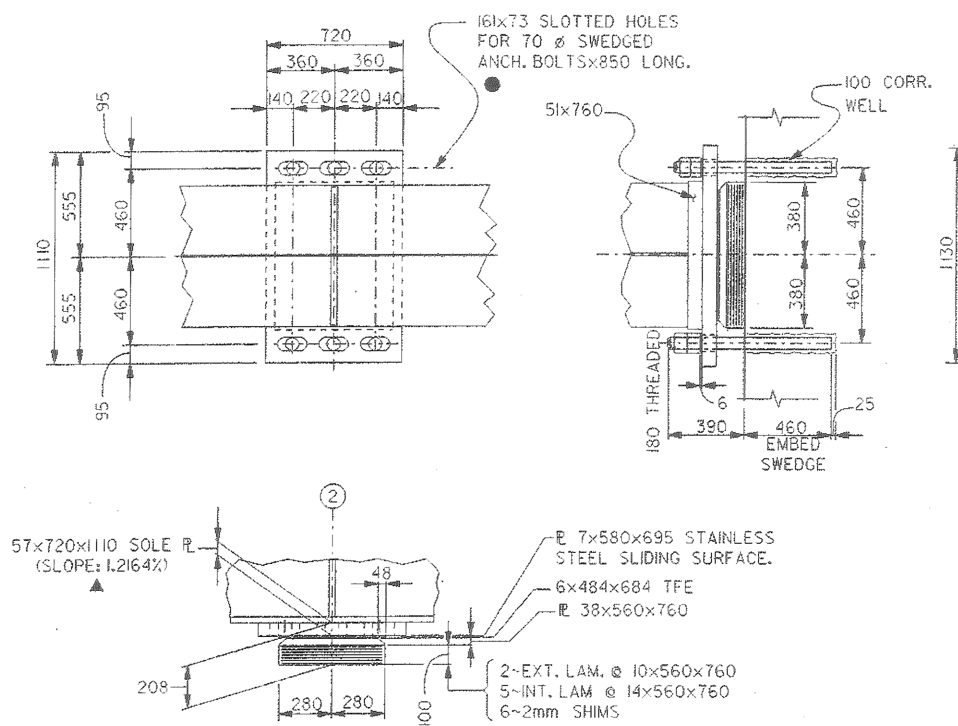

EXPANSION BEARING DETAILS BENT NO. 2

(BEARING PAD TYPE 5)

SCALE: 1 : 20

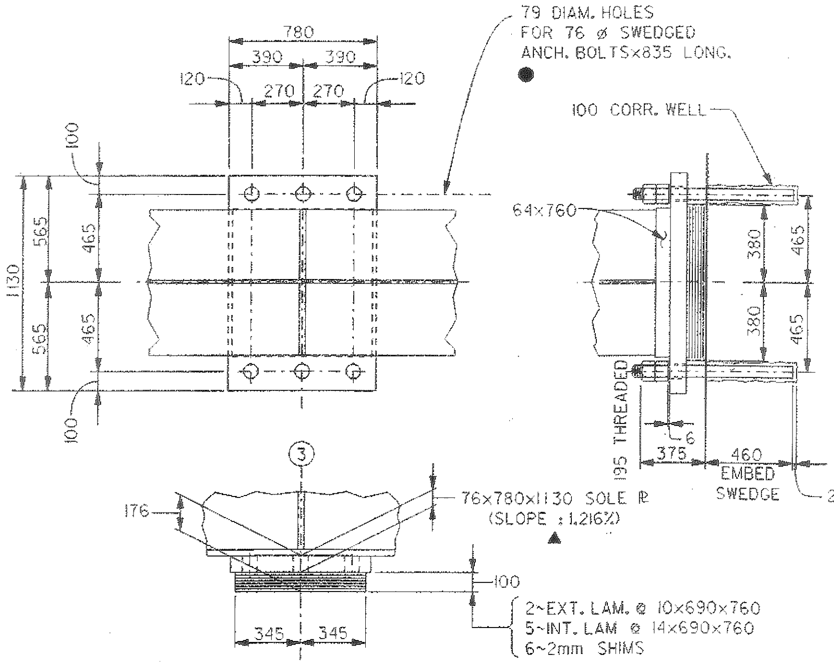

FIXED BEARING DETAILS AT BENT NO. 3 GIRDERS A,B&C

(BEARING PAD TYPE 4)

SCALE: 1 : 20

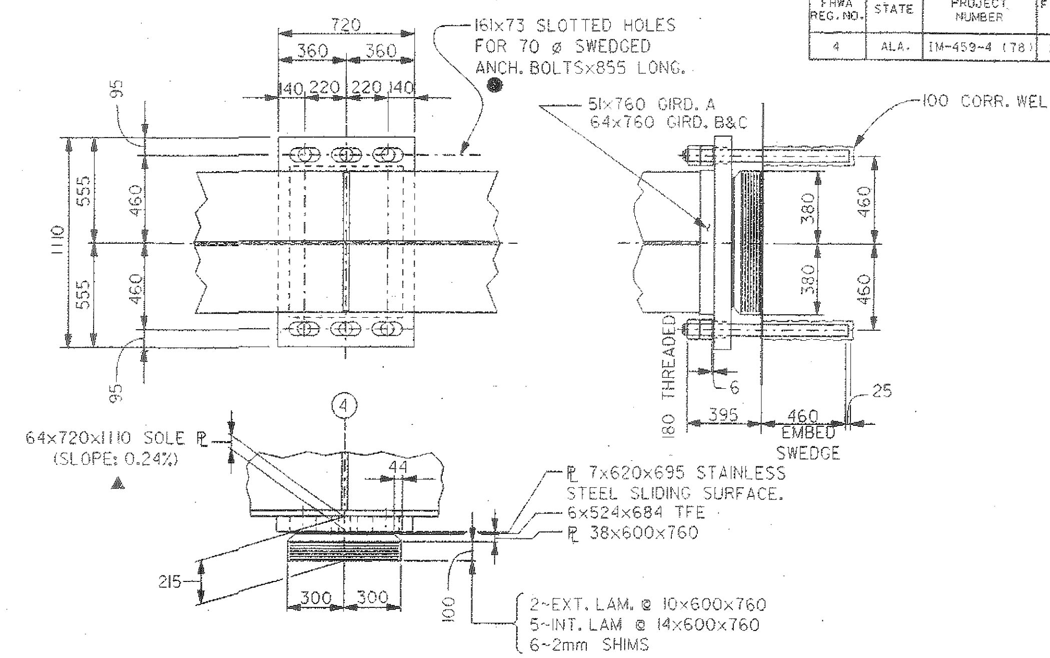

EXPANSION BEARING DETAILS AT BENT NO. 4 GIRDERS A,B&C

(BEARING PAD TYPE 5)

SCALE: 1 : 20

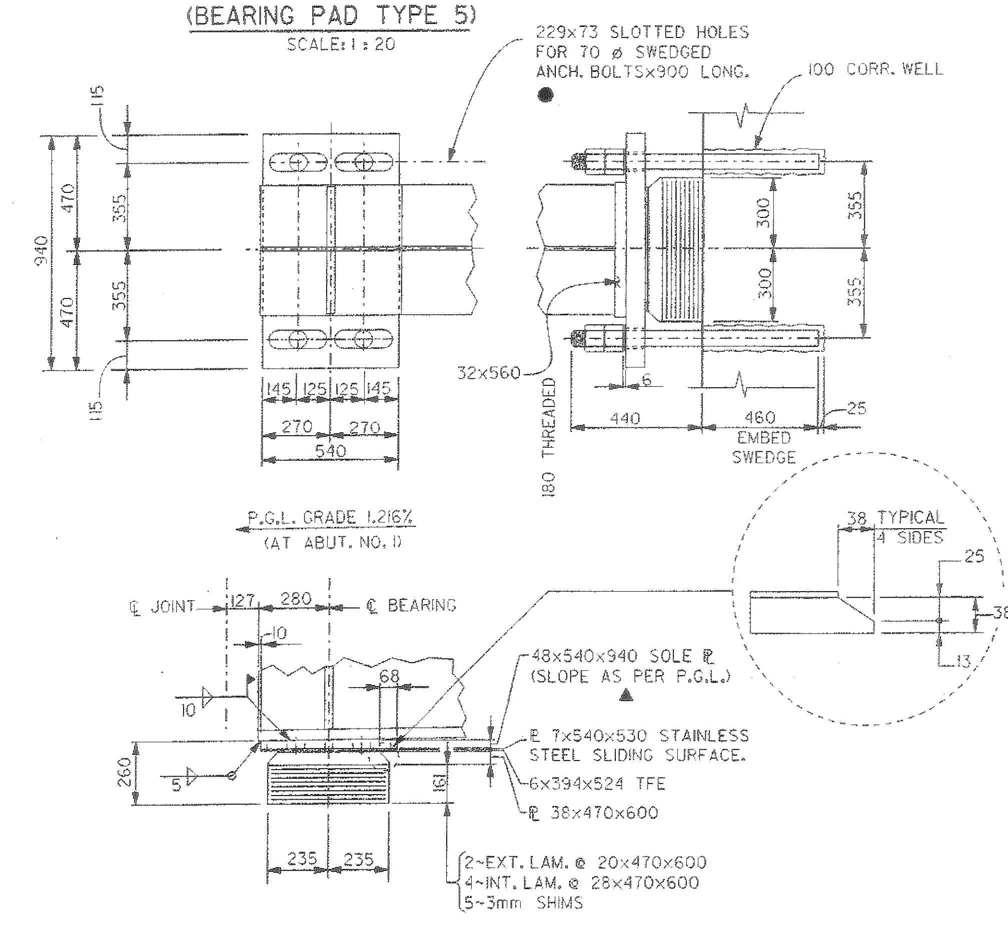

EXPANSION BEARING DETAILS AT ABUTMENTS NO. 1 AND NO. 5

(ABUTMENT NO. 1 SHOWN)

(ABUTMENT 5 IS SIMILAR WITH P.G.L. GRADE -0.726%)

(BEARING PAD TYPE 5)

SCALE: 1 : 20

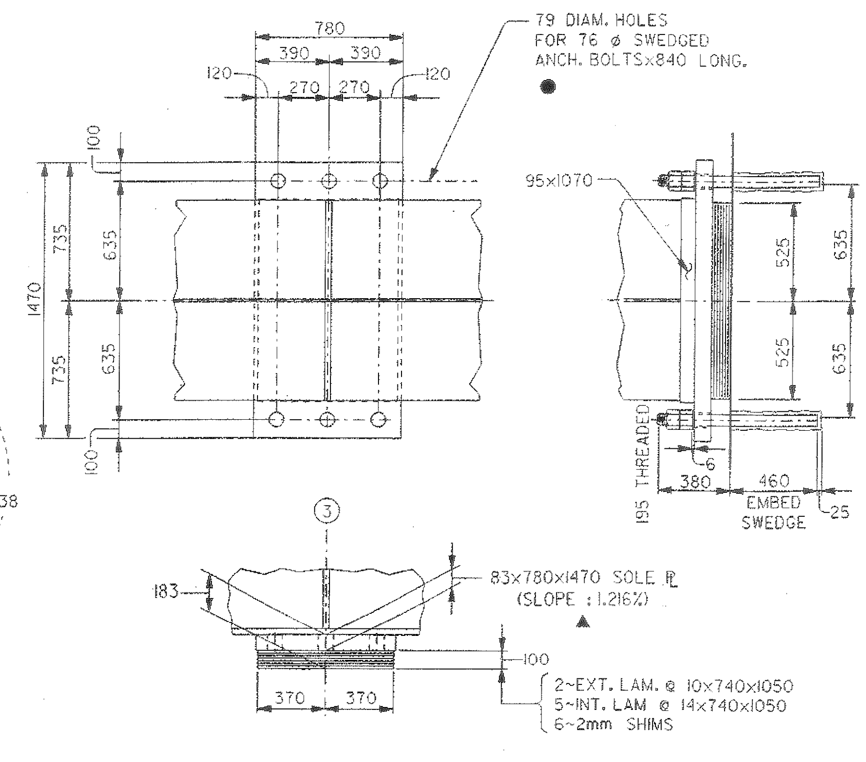

FIXED BEARING DETAILS AT BENT NO. 3 GIRDERS D&E

(BEARING PAD TYPE 4)

SCALE: 1 : 20

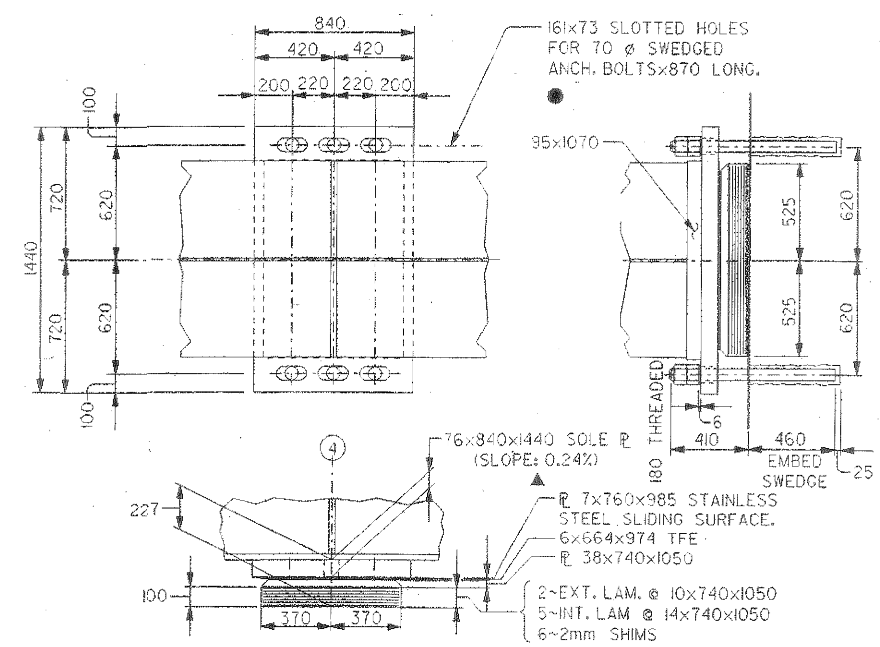

EXPANSION BEARING DETAILS AT BENT NO. 4 GIRDERS D&E

(BEARING PAD TYPE 5) SCALE: 1 : 20

NOTES :

▲ SOLE PLATES FIELD WELD TO FLANGE

● ANCHOR BOLT DETAILS SIMILAR TO THAT SHOWN ON BRIDGE SHEET NO. 10 .

NOTE :

ANCHOR BOLTS, NUTS & WASHERS ARE INCLUDED IN PAY ITEM "Kg-STRUCTURAL STEEL."

ALDOT METRIC

NOTE:

ALL DIMENSIONS SHOWN ARE IN MILLIMETERS, UNLESS OTHERWISE NOTED.

ALABAMA DEPARTMENT OF TRANSPORTATION

BRIDGE SHEET NO. 29 OF 39

REVISIONS

DAVID VOLKERT AND ASSOCIATES, INC.
CONSULTING ENGINEERS

PROJECT IM-459-4 (78)
I-459/U.S. 31 INTERCHANGE
FLYOVER A
HOOVER, ALABAMA

STEEL DETAILS, SPAN 1 - 4 (SHEET 4 OF 4)

STRUCTURAL APPROVAL:	STRUCTURAL APPROVAL:	QUANTITIES	DRAWN: K.K.L.
ASSISTANT BRIDGE ENGINEER	S.R.J. DESIGNER	COMP: S.R.J.	REINF CHKD:
BRIDGE ENGINEER	J.T.L. SECTION SUPERVISOR	CHKD:	SCALE: AS SHOWN
		CHKD: S.R.J.	DATE:

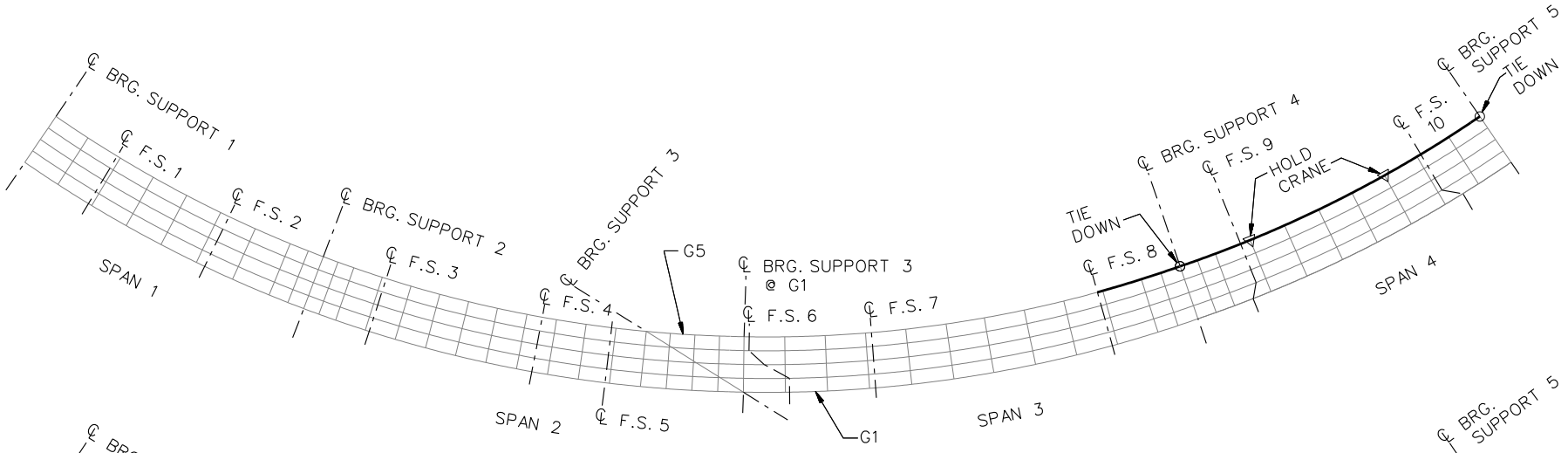

STAGE 1

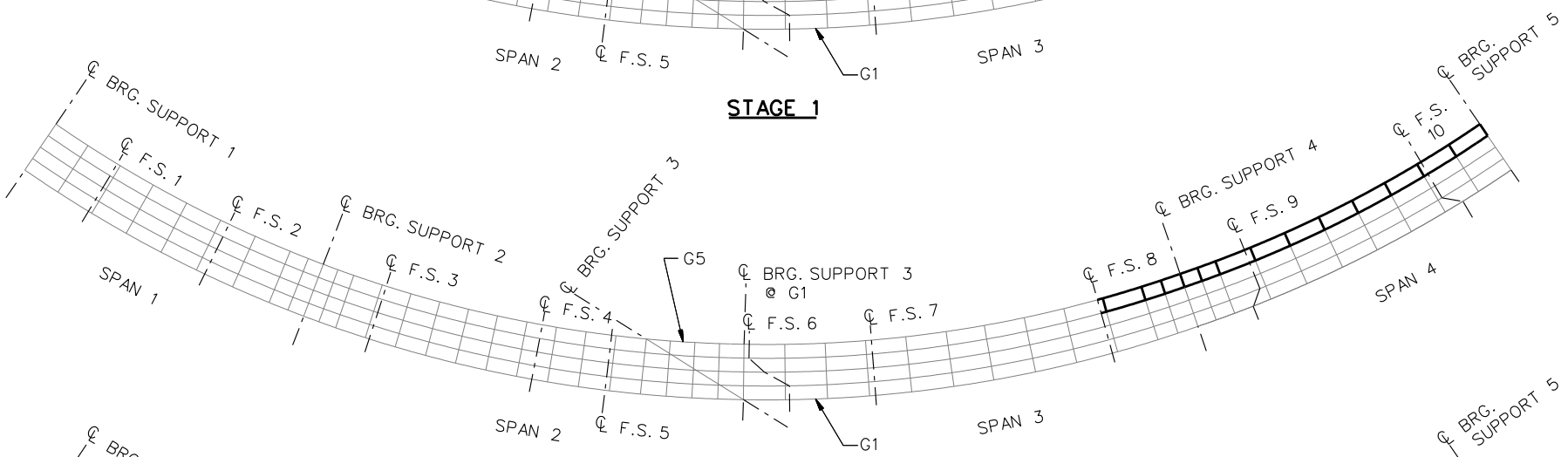

STAGE 2

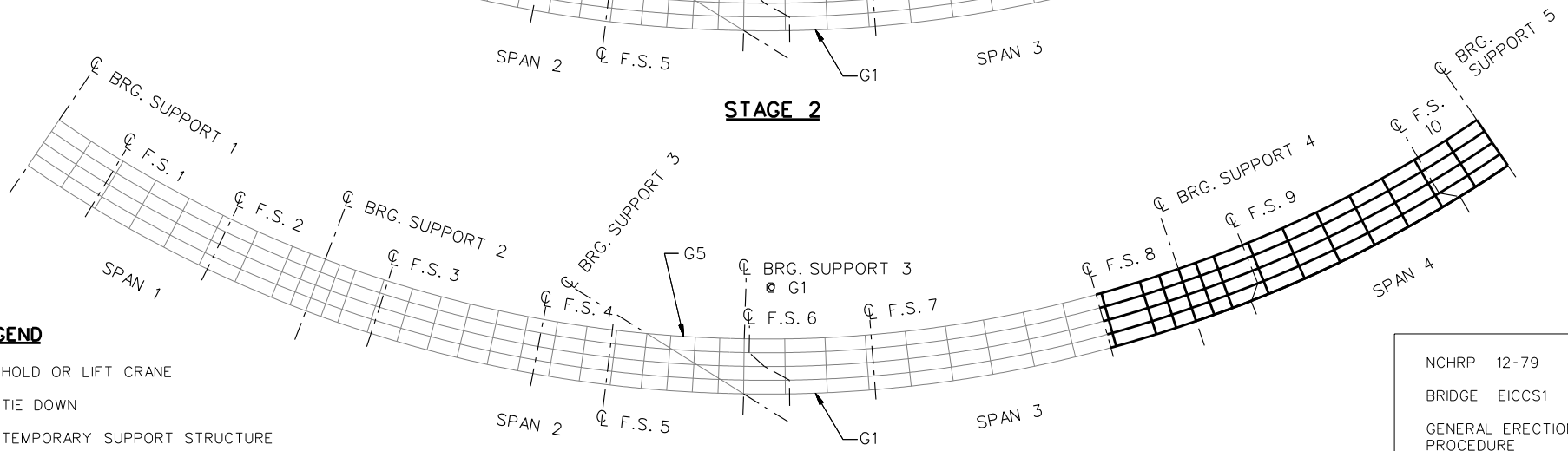

STAGE 5

LEGEND

▽ = HOLD OR LIFT CRANE

○ = TIE DOWN

□ = TEMPORARY SUPPORT STRUCTURE

NCHRP 12-79

BRIDGE EICCS1

GENERAL ERECTION PROCEDURE

SHEET 1 OF 4

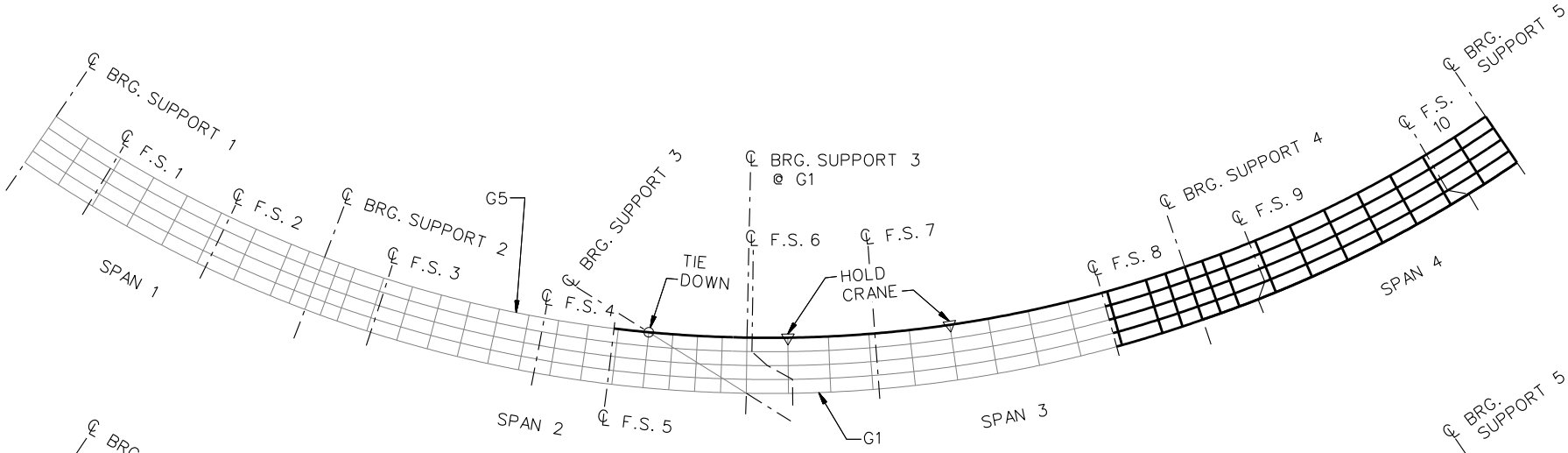

STAGE 6

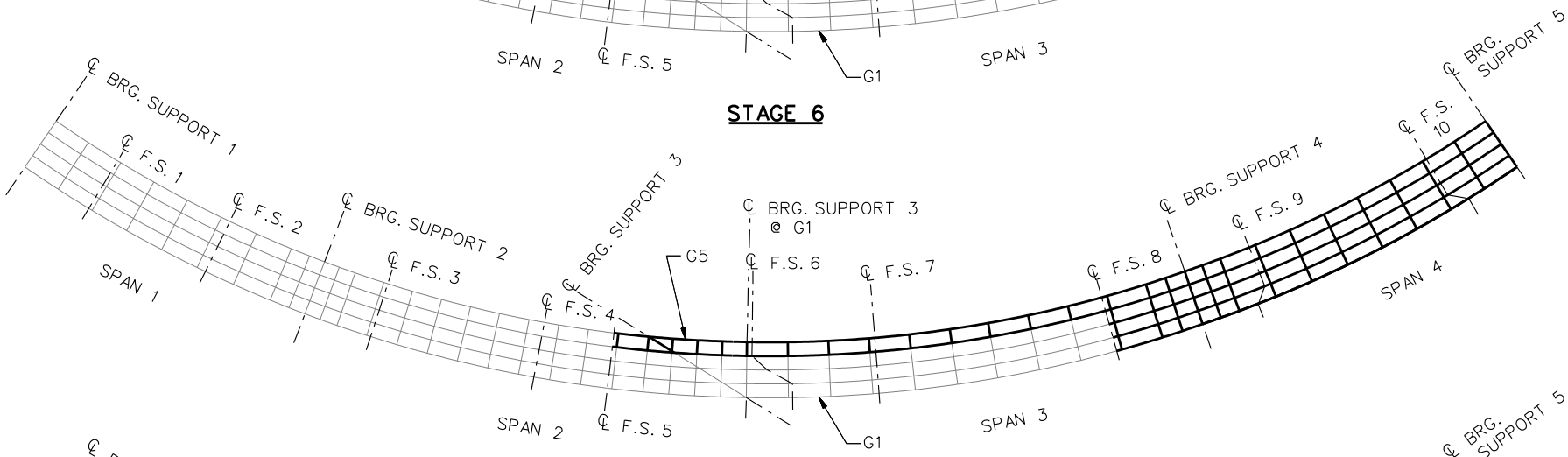

STAGE 7

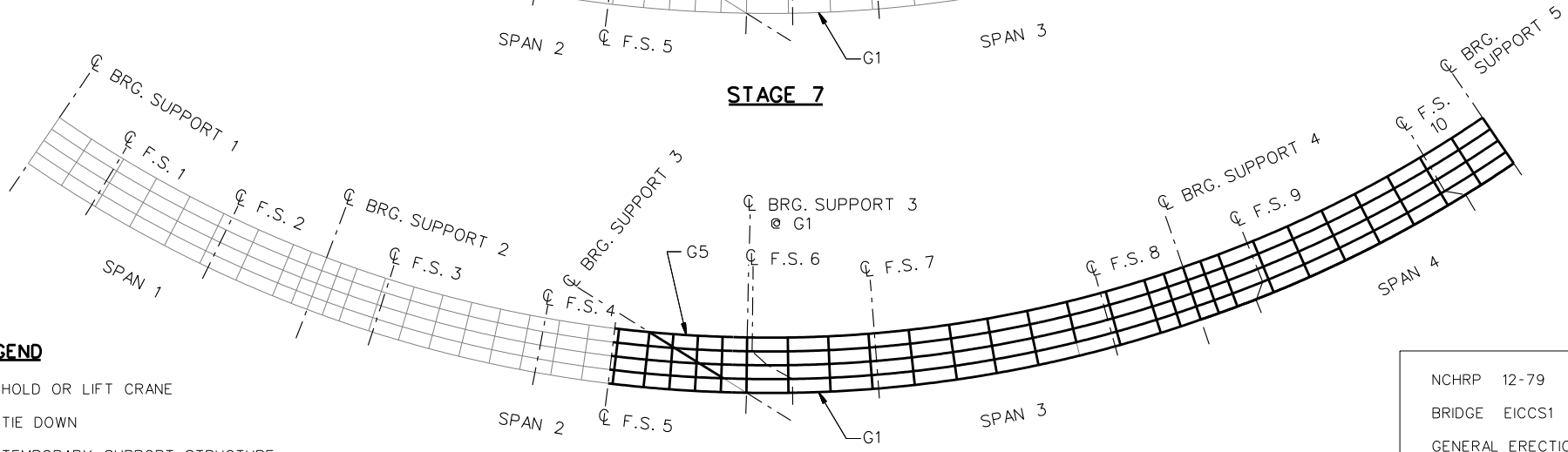

STAGE 10

LEGEND

▽ = HOLD OR LIFT CRANE

○ = TIE DOWN

□ = TEMPORARY SUPPORT STRUCTURE

NCHRP 12-79

BRIDGE EICCS1

GENERAL ERECTION PROCEDURE

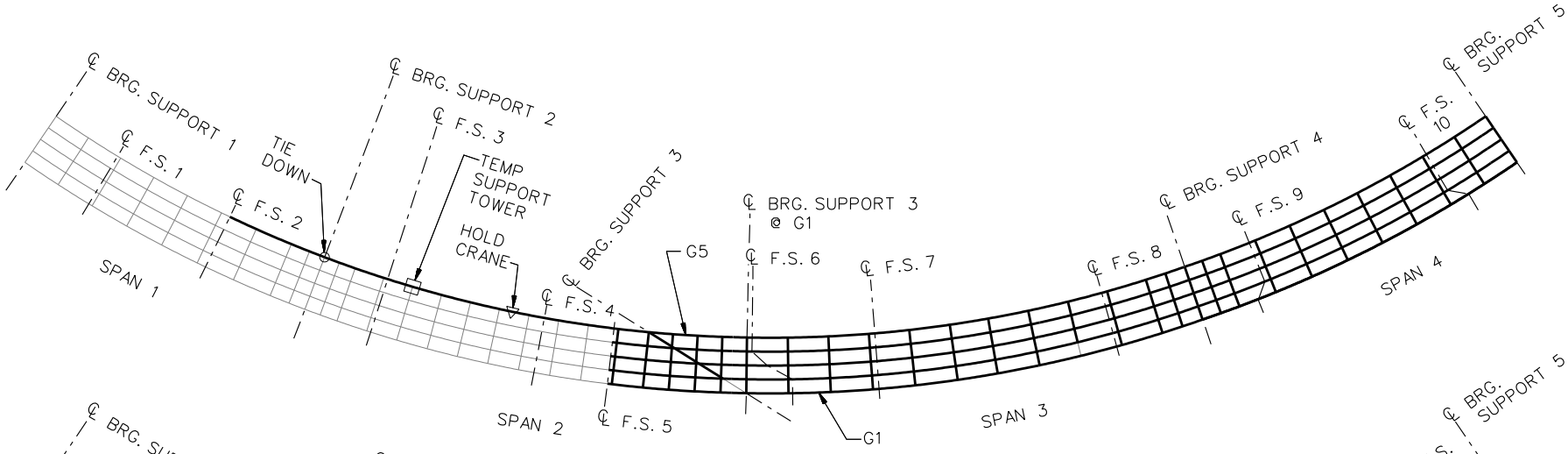

STAGE 11

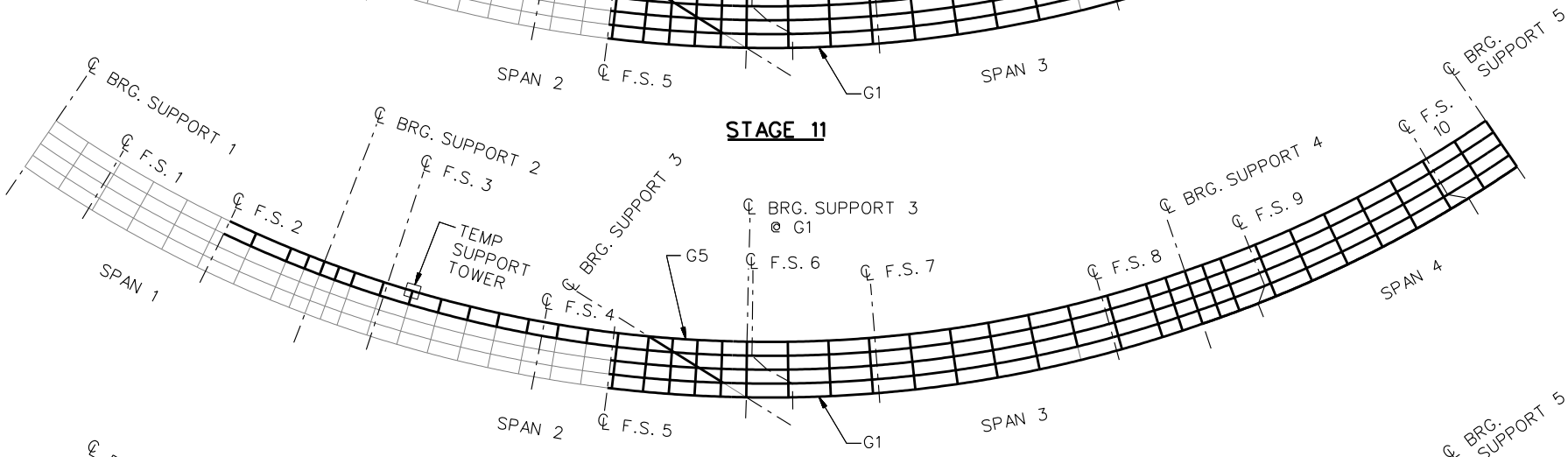

STAGE 12

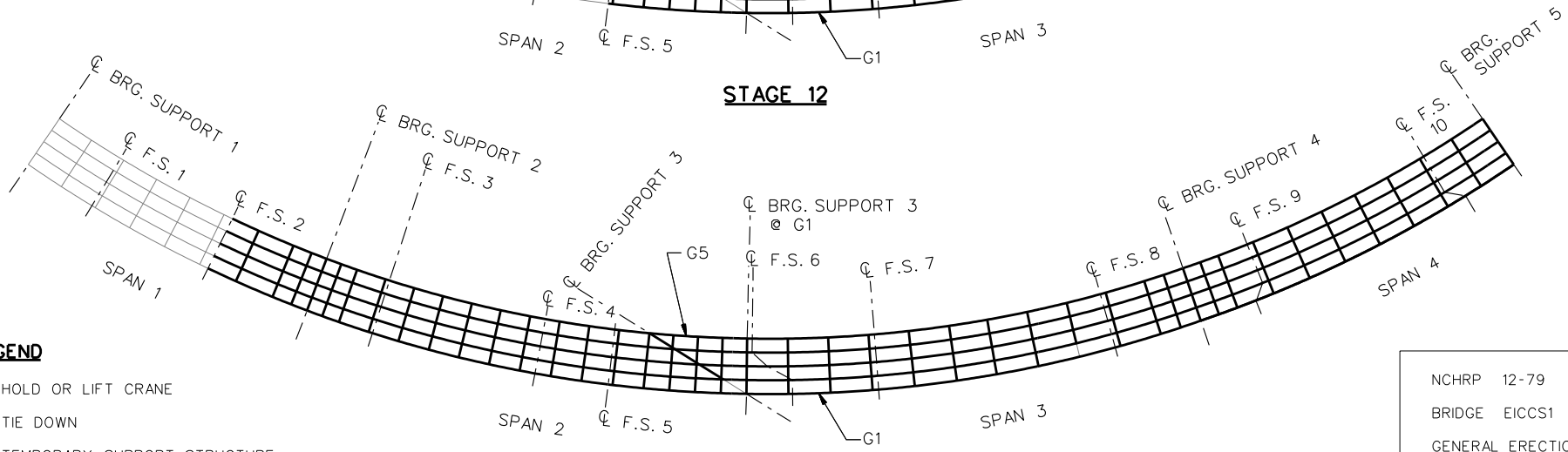

STAGE 15

LEGEND

▽ = HOLD OR LIFT CRANE

○ = TIE DOWN

□ = TEMPORARY SUPPORT STRUCTURE

NCHRP 12-79

BRIDGE EICCS1

GENERAL ERECTION PROCEDURE

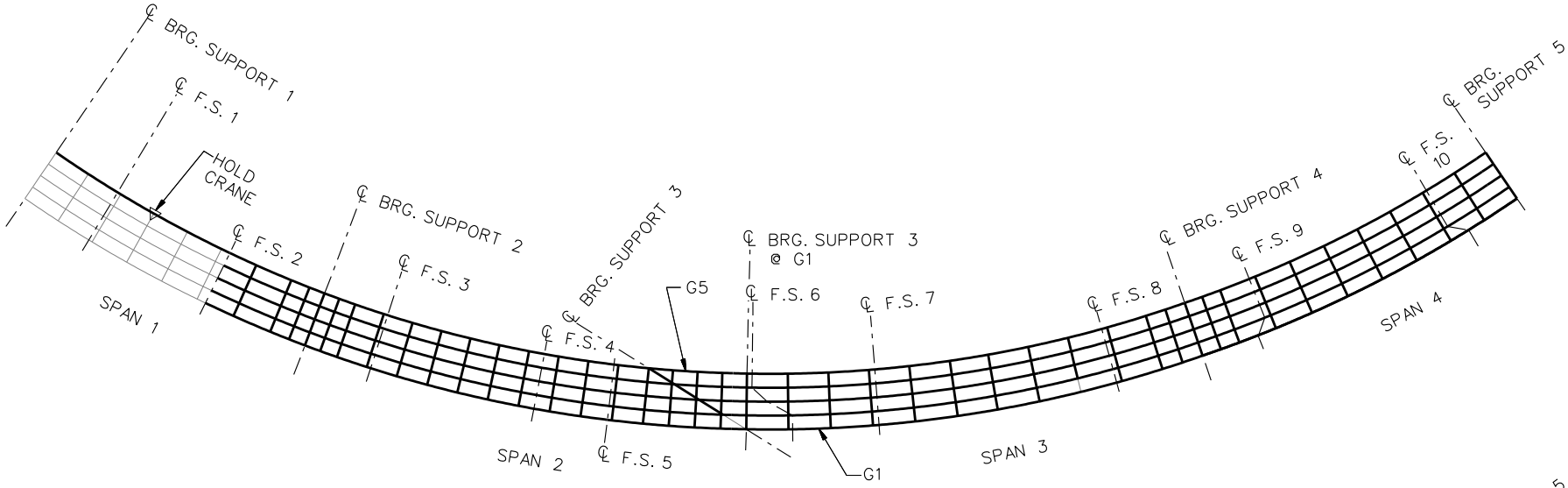

STAGE 16

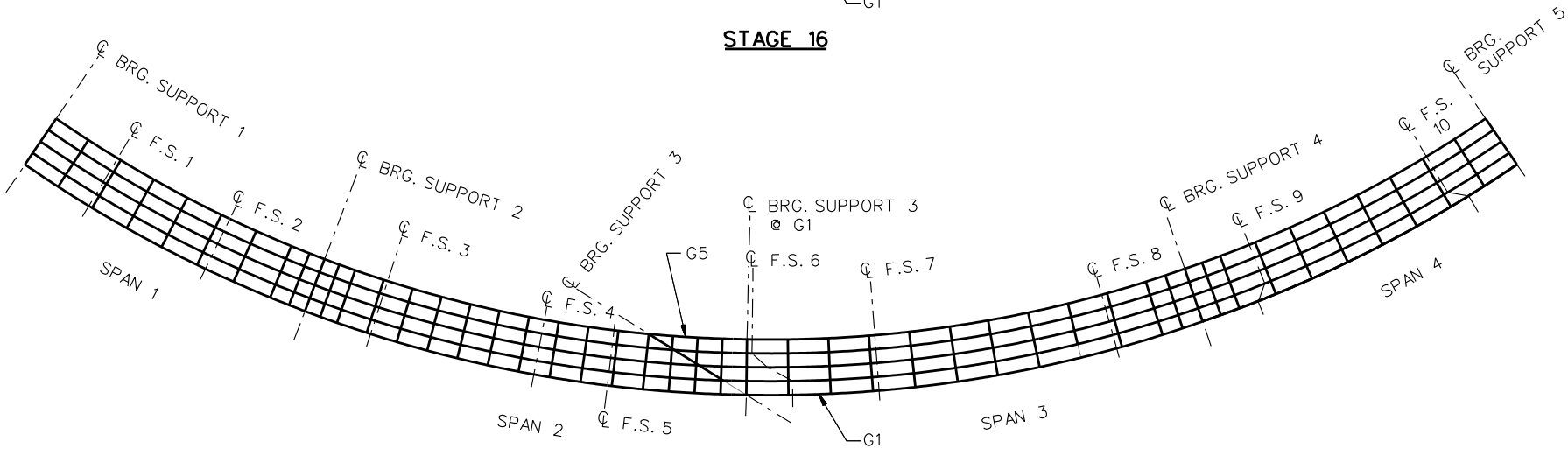

STAGE 20
COMPLETE STRUCTURE

LEGEND

▽ = HOLD OR LIFT CRANE

○ = TIE DOWN

□ = TEMPORARY SUPPORT STRUCTURE

NCHRP 12-79

BRIDGE EICCS1

GENERAL ERECTION PROCEDURE

SHEET 4 OF 4

NCHRP 12-79

EICCS10

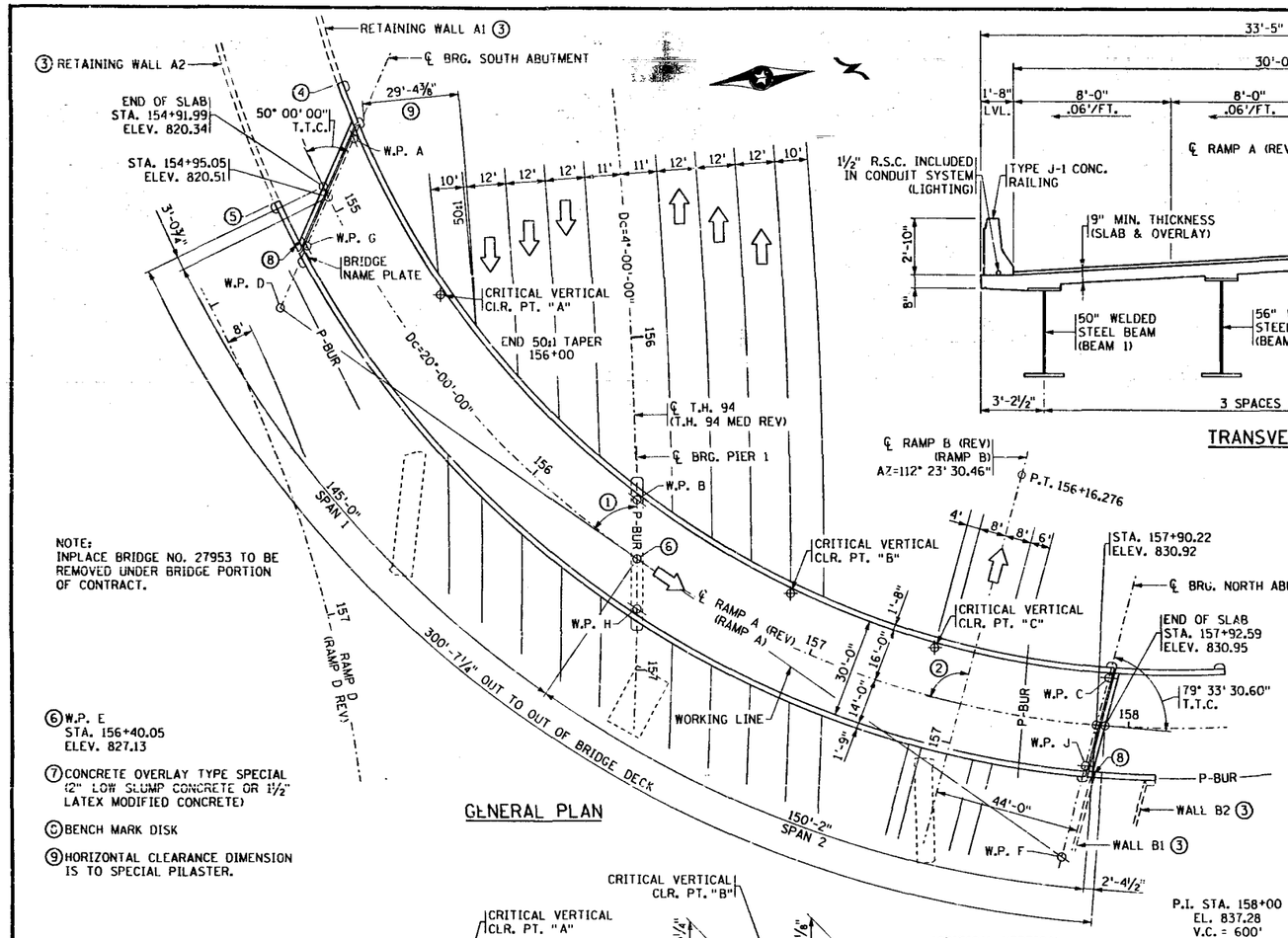

GENERAL PLAN

NOTE:
INPLACE BRIDGE NO. 27953 TO BE REMOVED UNDER BRIDGE PORTION OF CONTRACT.

⑥ W.P. E
STA. 156+40.05
ELEV. 827.13

⑦ CONCRETE OVERLAY TYPE SPECIAL (2" LOW SLUMP CONCRETE OR 1½" LATEX MODIFIED CONCRETE)

Ⓒ BENCH MARK DISK

⑨ HORIZONTAL CLEARANCE DIMENSION IS TO SPECIAL PILASTER.

TRANSVERSE SECTION

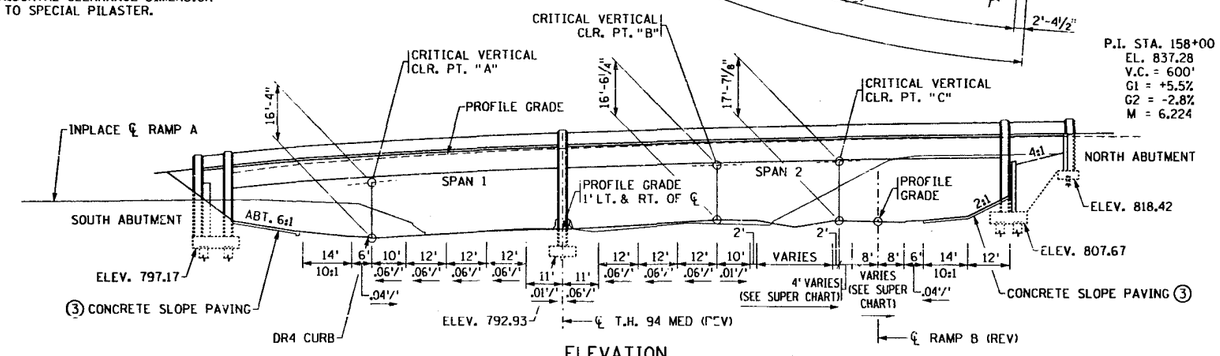

ELEVATION

① INTERSECTION ANGLE 55° 18' 25.53" T.T.C.
(INTER. ANGLE IS TYPICAL FOR ℄ PIER 1)
℄ RAMP A (REV) P.O.C. STA. 156+40.05
℄ MED. T.H. 94 (REV) P.O.T. STA. 156+66.64
X=901806.2524 Y=100142.8760

② INTERSECTION ANGLE 92° 05' 00.52" T.T.C.
℄ RAMP A (REV) P.O.C. STA. 157+48.43
℄ RAMP B (REV) P.O.T. STA. 156+87.71
X=901861.9717 Y=100235.0765

③ INCLUDED IN GRADING PORTION OF CONTRACT.

④ END RETAINING WALL A1, BEGIN WINGWALL A PT. 17.5' LT. RAMP A P.O.C. STA. 154+50.92

⑤ END RETAINING WALL A2, BEGIN WINGWALL A PT. 15.58' RT. RAMP A P.O.C. STA. 154+90.00

CONSTRUCTION NOTES

THE 1988 EDITION OF THE MINNESOTA DEPARTMENT OF TRANSPORTATION "STANDARD SPECIFICATIONS FOR CONSTRUCTION" AS AMENDED BY THE JANUARY 2,1991, SUPPLEMENTAL SPECIFICATIONS SHALL GOVERN.

BRIDGE SEAT REINFORCEMENT SHALL BE CAREFULLY PLACED TO AVOID INTERFERENCE WITH DRILLING HOLES FOR ANCHOR RODS. THE SUPERSTRUCTURE BEAMS SHALL BE ERECTED IN FINAL POSITION PRIOR TO DRILLING HOLES FOR AND PLACING ANCHOR RODS.

THE FIRST DIGIT OR THE FIRST TWO DIGITS OF EACH BAR MARK INDICATE THE BAR SIZE.

BARS MARKED WITH THE SUFFIX "E" SHALL BE EPOXY COATED.

Fed. Proj. No. IM094-3 (516)

DESIGN DATA

1992 AND CURRENT INTERIM A.A.S.H.T.O. DESIGN SPECIFICATIONS.
LOAD FACTOR DESIGN METHOD
HS 25 LIVE LOADING
DEAD LOAD INCLUDES 17 p.s.f. ALLOWANCE FOR FUTURE WEARING COURSE MODIFICATIONS.
MAXIMUM ALLOWABLE DESIGN STRESSES :
REINFORCED CONCRETE :
f'c = 4000 p.s.i. n=8
fy = 60000 p.s.i. REINFORCEMENT
STRUCTURAL STEEL :
fy = 50000 p.s.i. STRUCTURAL STEEL Mn/Dot 3309
DECK AREA 10050 SQ. FT.
5000 PROJECTED A.D.T. FOR YEAR 2012
OPERATING RATING HS 33.5

LIST OF SHEETS

I HEREBY CERTIFY THAT THIS PLAN WAS PREPARED BY ME OR UNDER MY DIRECT SUPERVISION AND THAT I AM A DULY REGISTERED PROFESSIONAL ENGINEER UNDER THE LAWS OF THE STATE OF MINNESOTA.

SIGNED James J. Hill
DATE 6-22-94 REG NO. 7315

B.M. ELEV. 823.125 (M.S.L. 1929 ADJ.)
2781AN1 STD. DISK IN SE CORNER OF BR. 27953 (RAMP A OVER 94)

AS Built.

TRUNK HIGHWAY NO. 94
MINNESOTA
DEPARTMENT OF TRANSPORTATION

Bridge No. 27998

T.H. 94 & RAMP UNDER E.B. OFF RAMP TO N. OF M. 1.6 MI. S.E. OF JCT. OF T.H. 55 & T.H. 94 IN MINNEAPOLIS

145'-150' STEEL CONTINUOUS BEAM SPANS 30'-0" ROADWAY, TYPE J-1 & J-2 BARRIERS 50° 00' 00" & 79° 33' 30.60" SKEWS

IDENTIFICATION NO. 401

GENERAL PLAN AND ELEVATION

SEC. 30 TWP. 29 N. R. 23 W.
CITY OF MINNEAPOLIS HENNEPIN COUNTY

APPROVED Donald J. Flemming 6-22-94
STATE BRIDGE ENGINEER DATE

0404.608
BLASTING (SPECIAL) *
SQ. FT.
~~9027~~ 11,177

0401.601	0452.604	0452.604	0452.602
STRUCTURE EXCAVATION	30" DIA. DRILLED SHAFT (EARTH)	30" DRILLED SHAFT (ROCK)	PILE TIP PROTECTION 12"
LUMP SUM	LIN. FT.	LIN. FT.	EACH
1	~~186.7~~ 186	~~101.9~~ 82	5

* ADDED BY ADDENDUM

SCHEDULE OF QUANTITIES FOR ENTIRE BRIDGE

ITEM NO.	2402.521	2401.501	240..501	2401.512	2404.501	2401.513	2401.513	2401.541	2401.541	2402.591	2402.595	2442.501	2401.521	2545.509	2452.511	2452.510	0478.602	0478.601	2452.520
ITEM	STRUCTURAL STEEL (3309)	STRUCTURE CONCRETE (1A43)	STRUCTURE CONCRETE (3Y43)	BRIDGE SLAB CONCRETE (3Y36)	CONCRETE OVERLAY TYPE SPECIAL	TYPE J-1 RAILING CONCRETE (3Y46)	TYPE J-2 RAILING CONCRETE (3Y46)	REINFORCE-MENT BARS	REINFORCE-MENT BARS (EPOXY COATED)	EXPANSION JOINT DEVICES TYPE 5	BEARING ASSEMBLY	REMOVE OLD BRIDGE	STRUCTURE EXCAVATION CLASS R	CONDUIT SYSTEM (LIGHTING)	STEEL H-PILING DELIVERED 12"	STEEL H-PILING DRIVEN 12"	EPOXY ZINC-RICH PAINT SYSTEM (SHOP)	EPOXY ZINC-RICH PAINT SYSTEM (FIELD)	STEEL H-TEST PILE 20 FT. LONG 12"
UNIT	POUND	CU. YD.	CU. YD.	SQ. FT.	SQ. FT.	LIN. FT.	LIN. FT.	POUND	POUND	LIN. FT.	EACH	LUMP SUM	CU. YD.	LUMP SUM	LIN. FT.	LIN. FT.	SQ. FT.	LUMP SUM	EACH
QUANTITY	596000 (P)	211 (P)	376 (P)	10047 (P)	~~9027~~ 11,177 (P)	358 (P)	332 (P)	25730 (P)	146420 (P)	74 (P)	12 (P)	1	0 ~~2~~	1	130.0 ~~60~~	121.4 ~~60~~	28000	1	1

DES. SWE DR. SWB CHK. JJH CHK. SWE 27998

Area No. 52 Job No. 914 Design Unit: JAMES J. HILL State Proj. No. 2781-27998 (T.H. 94=392) Sheet No. 1 of 73 Sheets

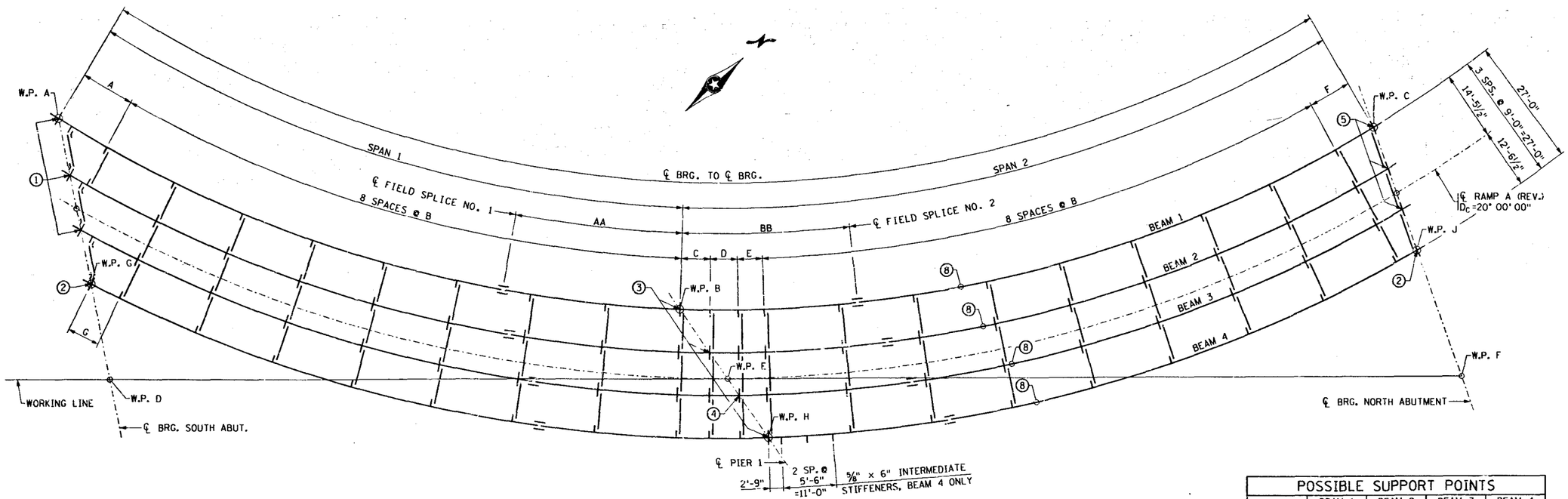

FRAMING PLAN

POSSIBLE SUPPORT POINTS				
	BEAM 1	BEAM 2	BEAM 3	BEAM 4
STATION	156+92.98	156+96.17	157+00.57	157+03.90
⑨ ELEVATION	822.72	822.85	822.93	822.78

DIAPHRAGM SPACING							
	A	B	C	D	E	F	G
℄ BEAM 1	11'-11"	16'-0"	6'-5⅝"	5'-11⅝"	5'-6⅜"	9'-5¼"	---
℄ BEAM 2	4'-1⅝"	16'-6⅜"	6'-8⅛"	6'-2"	5'-8½"	8'-0"	---
℄ BEAM 3	---	17'-0¼"	6'-10¾"	6'-4⅜"	5'-10¾"	6'-6¾"	13'-7¼"
℄ BEAM 4	---	17'-7"	7'-1¼"	6'-6¾"	6'-0⅞"	5'-1⅝"	6'-8½"

FIELD SPLICE LOCATIONS		
	AA	BB
℄ BEAM 1	38'-0"	38'-0"
℄ BEAM 2	43'-0"	38'-0"
℄ BEAM 3	44'-0"	37'-0"
℄ BEAM 4	49'-0"	39'-0"

SPAN LENGTHS			
	RADIUS	SPAN 1	SPAN 2
℄ BEAM 1	272'-0¼"	139'-10⅞"	155'-4¾"
℄ BEAM 2	281'-0¼"	143'-0⅝"	152'-1⅜"
℄ BEAM 3	290'-0¼"	146'-3⅜"	148'-11⅛"
℄ BEAM 4	299'-0¼"	149'-6⅞"	145'-10⅛"

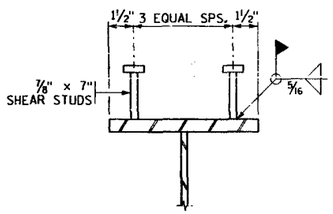

SHEAR STUD DETAIL

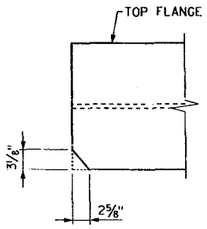

COPING DETAIL
TYPICAL AT SOUTH ABUTMENT ONLY.

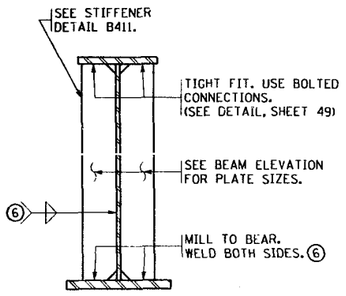

BEARING STIFFENER DETAIL
TYPICAL AT PIERS.

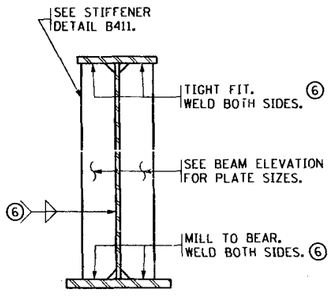

BEARING STIFFENER DETAIL
TYPICAL AT ABUTMENTS.

① VULCANIZED EXPANSION CURVED PLATE BEARING ASSEMBLY, TYPE 1

② VULCANIZED EXPANSION CURVED PLATE BEARING ASSEMBLY, TYPE 2

③ FIXED CURVED PLATE BEARING ASSEMBLY, TYPE 1

④ FIXED CURVED PLATE BEARING ASSEMBLY, TYPE 2

⑤ VULCANIZED EXPANSION CURVED PLATE BEARING ASSEMBLY, TYPE 3.

⑥ SEE SPEC. 2471.3J4b1 FOR MINIMUM SIZE OF FILLET WELD. WELD SIZE NEED NOT EXCEED ⅜" FOR INTERMEDIATE DIAPHRAGM STIFFENERS.

⑦ SEE SHEET 48 FOR INTERMEDIATE DIAPHRAGM DETAILS.

⑧ SEE POSSIBLE SUPPORT POINTS CHART FOR STATIONS AND ELEVATIONS. (UNIVERSITY OF MINNESOTA RESEARCH PROJECT)

⑨ ELEVATION OF BOTTOM OF FLANGE ABOVE MID-POINT OF T.H. 94 SHOULDER (UNLOADED POSITION).

STRUCTURAL STEEL NOTES:

ALL STRUCTURAL STEEL TO CONFORM TO MN/DOT 3309 UNLESS OTHERWISE NOTED.

BEARING STIFFENERS SHALL BE VERTICAL.

ENDS OF BEAMS SHALL BE VERTICAL.

FIELD CONNECTIONS SHALL BE MADE WITH ⅞" HIGH STRENGTH BOLTS OR ⅞" PIN BOLTS, EXCEPT AS NOTED.

SHEAR CONNECTORS TO BE INCLUDED IN WEIGHT OF STRUCTURAL STEEL MN/DOT 3309 AND CONFORM TO 3391.

FULL ASSEMBLY REAMING PER 2471.3E 1e WILL BE REQUIRED.

FOR WELDED BUTT SPLICES AND WIDTH AND THICKNESS TRANSITIONS IN FLANGES, SEE MN/DOT 2471.3J.

WEB PLATES SHALL BE FURNISHED IN AVAILABLE MILL LENGTHS WITH A MINIMUM NUMBER OF WEB SPLICES. LOCATION OF SPLICES SHALL BE SUBJECT TO THE APPROVAL OF THE ENGINEER AND SHALL BE A MINIMUM OF 1'-0" FROM STIFFENERS OR FLANGE SPLICES.

FLANGE PLATES FOR BEAMS SHALL BE CUT TO PROPER CURVATURE.

AS Built.

CERTIFIED BY James D. Hill
PROFESSIONAL ENGINEER
REG. NO. 7345 6-22-1994

TITLE: FRAMING PLAN

DES: S.W.E. | DR: S.W.B. | APPROVED: 6-22-94
CHK: M.J.L. | CHK: S.W.E.

SHEET NO. 40 OF 73 SHEETS

BRIDGE NO. 27998

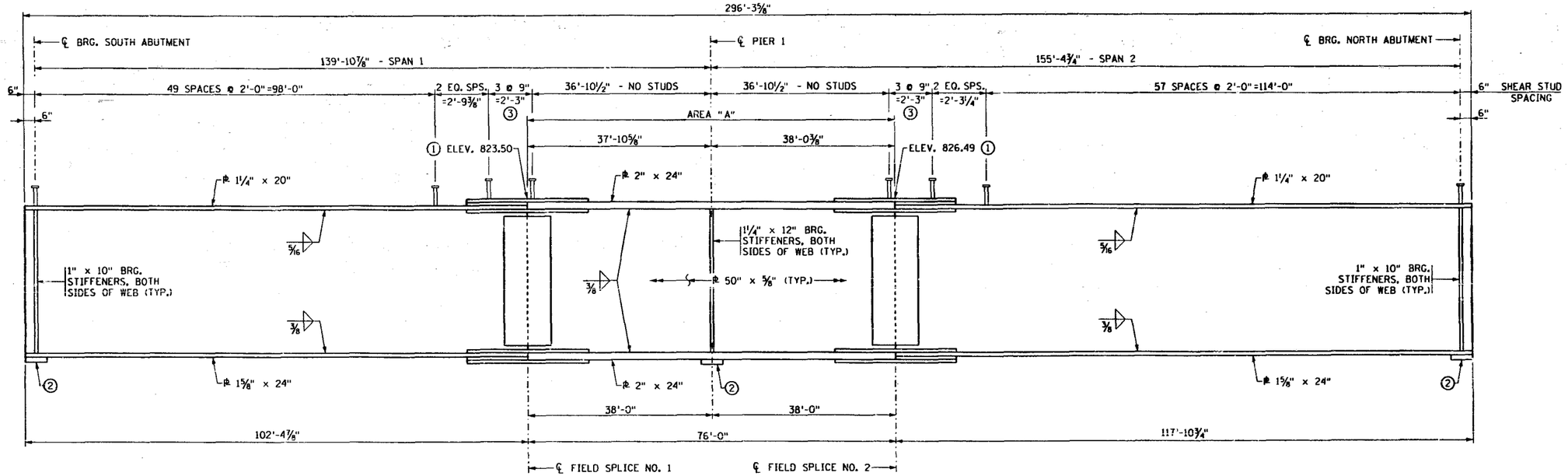

BEAM 1 ELEVATION

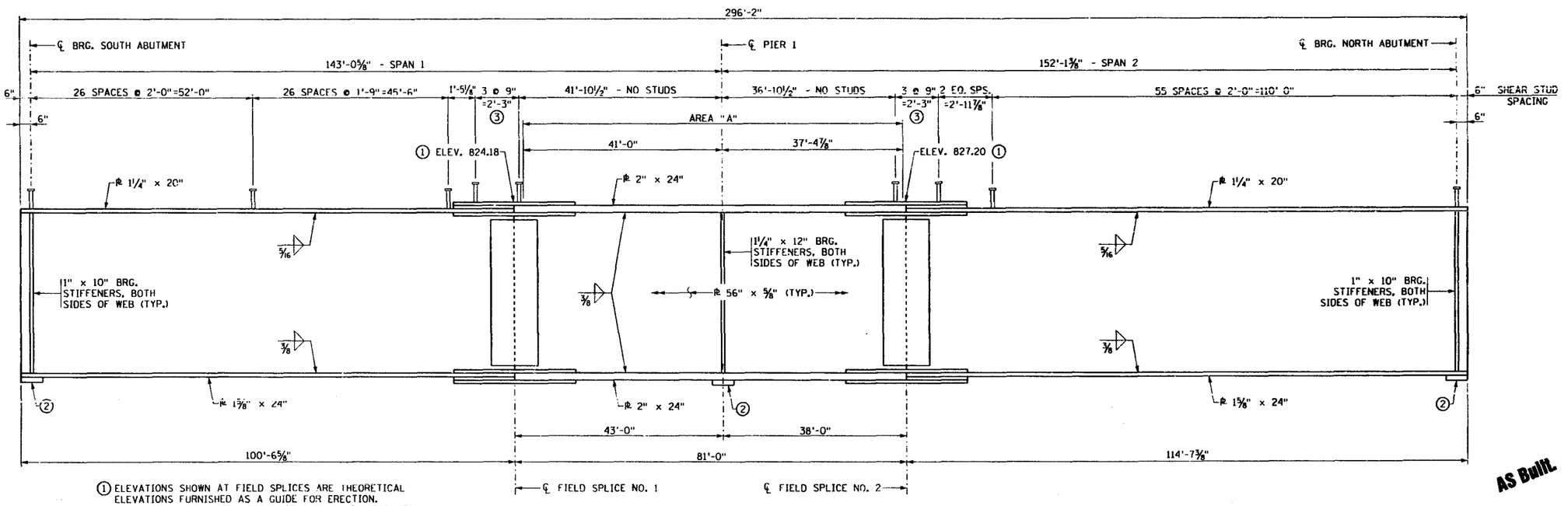

BEAM 2 ELEVATION

AS Built

① ELEVATIONS SHOWN AT FIELD SPLICES ARE THEORETICAL ELEVATIONS FURNISHED AS A GUIDE FOR ERECTION. ELEVATIONS ARE TAKEN AT TOP OF FLANGE SPLICE PLATE.

② SOLE PLATE (TYPICAL). SEE BEARING DETAILS.

③ ADJUST SHEAR STUDS TO MISS BOLTS.

CERTIFIED BY James J. Hill PROFESSIONAL ENGINEER
REG. NO. 7395 6-22-1994

TITLE: STRUCTURAL STEEL DETAILS

DES: S.W.E.	DR: S.W.B.	APPROVED: 6-22-94
CHK: M.J.L.	CHK: S.W.E.	

SHEET NO. 41 OF 73 SHEETS

BRIDGE NO. 27998

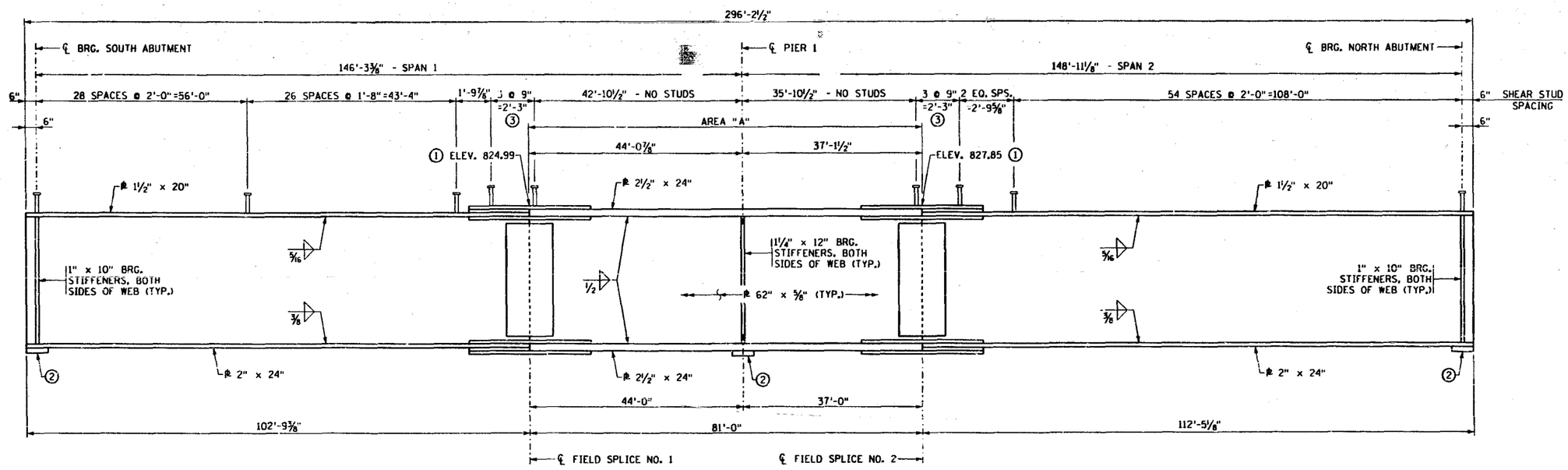

BEAM 3 ELEVATION

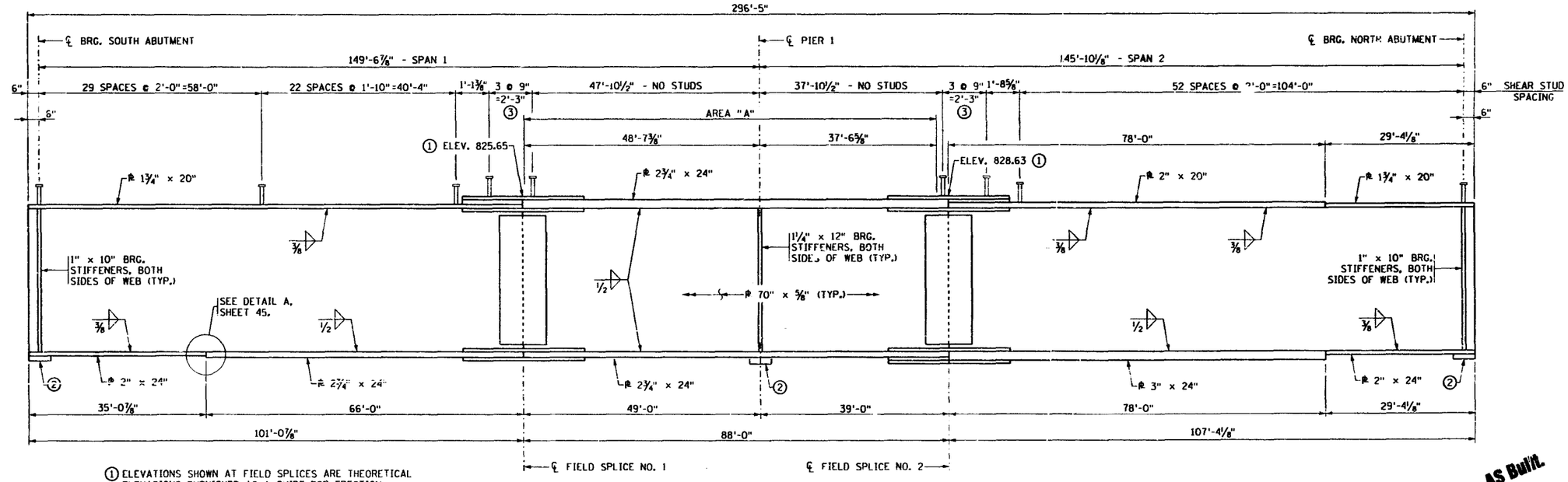

BEAM 4 ELEVATION

AS Built

① ELEVATIONS SHOWN AT FIELD SPLICES ARE THEORETICAL ELEVATIONS FURNISHED AS A GUIDE FOR ERECTION. ELEVATIONS ARE TAKEN AT TOP OF FLANGE SPLICE PLATE.

② SOLE PLATE (TYPICAL). SEE BEARING DETAILS.

③ ADJUST SHEAR STUDS TO MISS BOLTS.

CERTIFIED BY James J. Hill PROFESSIONAL ENGINEER
REG. NO. 7315 6-22-1994

TITLE: STRUCTURAL STEEL DETAILS

DES: S.W.E.	DR: S.W.B.	APPROVED: 6-22-94
CHK: M.J.L.	CHK: S.W.E.	

SHEET NO. 42 OF 73 SHEETS

BRIDGE NO. 27998

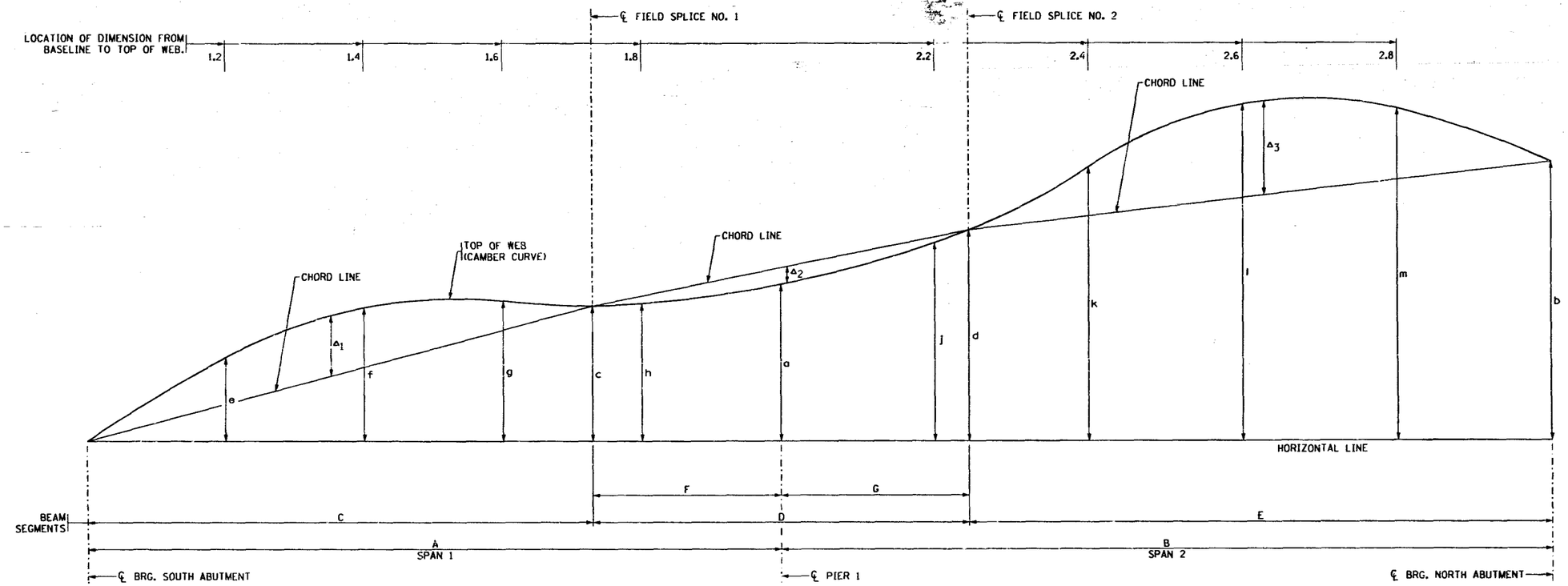

CAMBER DIAGRAM

DIMENSIONS

BEAM	A	B	C	D	E	F	G	a	b	c	d	e	f	g	h	J	k	l	m
BEAM 1	139'-10 7/16"	155'-4 3/4"	101'-10 7/8"	76'-0"	117'-4 3/4"	38'-0"	38'-0"	6'-9"	11'-0 1/2"	5'-4 5/16"	8'-4 1/4"	1'-9 3/8"	3'-4"	4'-7 1/4"	5'-8 7/16"	8'-0 1/2"	9'-2 3/4"	10'-2 13/16"	10'-9 9/16"
BEAM 2	143'-0 5/8"	152'-1 3/8"	100'-0 5/8"	81'-0"	114'-1 3/8"	43'-0"	38'-0"	6'-7 5/8"	10'-7 13/16"	5'-1 11/16"	8'-1 15/16"	1'-9 1/2"	3'-4 1/8"	4'-6 13/16"	5'-7 3/16"	7'-10 1/16"	8'-11 7/16"	9'-10 11/16"	10' 5 1/8"
BEAM 3	146'-3 3/8"	148'-11 1/8"	102'-3 3/8"	81'-0"	111'-11 1/8"	44'-0"	37'-0"	6'-5 11/16"	10'-3"	5'-0 1/4"	7'-10 5/8"	1'-9 3/4"	3'-3 9/16"	4'-5 3/4"	5'-5 3/4"	7'-7 1/8"	8'-7 3/4"	9'-6 1/4"	10'-0 3/8"
BEAM 4	149'-6 7/8"	145'-10 7/8"	100'-6 7/8"	88'-0"	106'-10 1/8"	49'-0"	39'-0"	6'-3 9/16"	9'-10 3/16"	4'-8 7/8"	7'-8 3/4"	1'-9 1/2"	3'-3 1/16"	4'-4 7/16"	5'-3 3/4"	7'-4 5/16"	8'-4 3/16"	9'-2 1/8"	9'-7 7/8"

HORIZONTAL DISTANCES MEASURED FROM LEFT END OF SPAN TO POINT SHOWN

BEAM	1.2	1.4	1.6	1.8	2.2	2.4	2.6	2.8
BEAM 1	27'-11 13/16"	55'-11 5/8"	83'-11 3/8"	111'-11 3/16"	31'-0 15/16"	62'-1 7/8"	93'-2 7/8"	124'-3 13/16"
BEAM 2	28'-7 5/16"	57'-2 5/8"	85'-10"	114'-5 5/16"	30'-5 1/16"	60'-10 1/8"	91'-3 1/4"	121'-8 5/16"
BEAM 3	29'-3 1/16"	58'-6 1/8"	87'-9 1/4"	117'-0 5/16"	29'-9 7/16"	59'-6 7/8"	89'-4 1/4"	119'-1 11/16"
BEAM 4	29'-11"	59'-9 15/16"	89'-8 15/16"	119'-7 7/8"	29'-2"	58'-4"	87'-6"	116'-8"

MAXIMUM CAMBER IN SEGMENTS

BEAM	Δ1	Δ2	Δ3
BEAM 1	4 13/16"	15/16"	7 7/16"
BEAM 2	5"	15/16"	6 7/8"
BEAM 3	5 5/16"	1 1/4"	6 3/8"
BEAM 4	5 1/2"	15/16"	5 7/8"

NOTES:

CAMBER DIAGRAM SHOWN IS FOR ALL BEAMS IN UNLOADED POSITION AND PROVIDES FOR ALL DEAD LOAD DEFLECTIONS AND RESIDUAL CAMBER.

CHORD LINES ARE STRAIGHT LINES FROM END TO END OF BEAM SEGMENTS AT TOP OF WEB.

AS Built.

CERTIFIED BY James D. Hill PROFESSIONAL ENGINEER
REG. NO. 7345 6-22-1994

TITLE: STRUCTURAL STEEL DETAILS

DES: S.W.E. DR: S.W.B. APPROVED: 6-22-94
CHK: J.J.H. CHK: S.W.E.

SHEET NO. 43 OF 73 SHEETS

BRIDGE NO. 27998

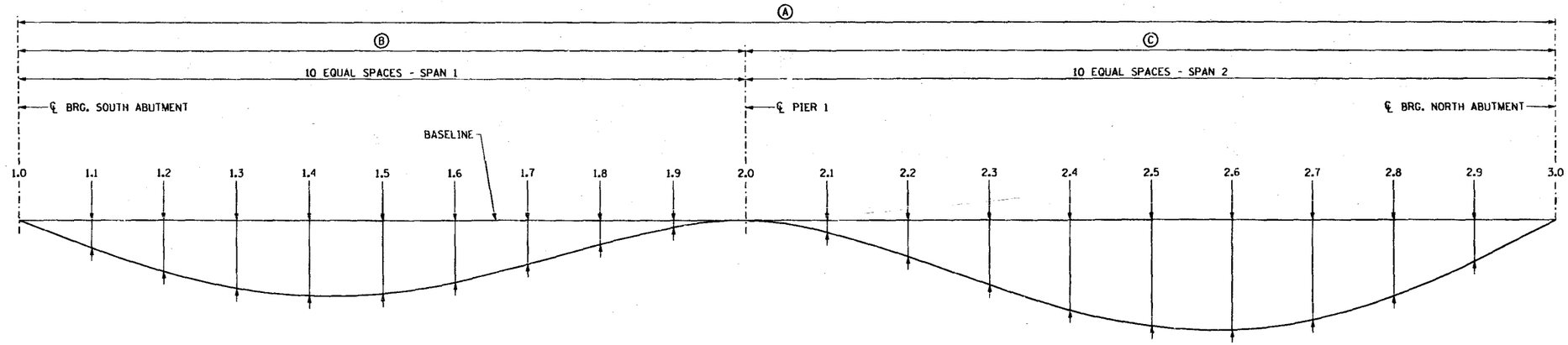

DEFLECTION DIAGRAM

BEAM DEFLECTIONS IN FEET (DEFLECTIONS DUE TO WEIGHT OF STRUCTURAL STEEL)

BEAM	Ⓐ	Ⓑ	Ⓒ	1.0	1.1	1.2	1.3	1.4	1.5	1.6	1.7	1.8	1.9	2.0	2.1	2.2	2.3	2.4	2.5	2.6	2.7	2.8	2.9	3.0
BEAM 1	295'-3⅜"	139'-10⅞"	155'-4¾"	0.0000	0.0179	0.0332	0.0439	0.0484	0.0469	0.0397	0.0282	0.0154	0.0045	0.0000	0.0076	0.0230	0.0408	0.0564	0.0661	0.0683	0.0619	0.0473	0.0258	0.0000
BEAM 2	295'-2"	143'-0⅝"	152'-1⅜"	0.0000	0.0191	0.0354	0.0465	0.0511	0.0491	0.0409	0.0285	0.0151	0.0043	0.0000	0.0079	0.0232	0.0413	0.0575	0.0678	0.0703	0.0638	0.0487	0.0265	0.0000
BEAM 3	295'-2½"	146'-3⅜"	148'-11⅛"	0.0000	0.0211	0.0391	0.0513	0.0560	0.0533	0.0439	0.0299	0.0153	0.0038	0.0000	0.0085	0.0243	0.0432	0.0600	0.0710	0.0737	0.0671	0.0512	0.0279	0.0000
BEAM 4	295'-5"	149'-6⅞"	145'-10⅛"	0.0000	0.0264	0.0479	0.0616	0.0661	0.0609	0.0482	0.0309	0.0145	0.0024	0.0000	0.0095	0.0270	0.0476	0.0666	0.0791	0.0827	0.0755	0.0582	0.0322	0.0000

BEAM DEFLECTIONS IN FEET (DEFLECTIONS DUE TO WEIGHT OF SLAB, RAILING, AND CONCRETE OVERLAY)

BEAM	Ⓐ	Ⓑ	Ⓒ	1.0	1.1	1.2	1.3	1.4	1.5	1.6	1.7	1.8	1.9	2.0	2.1	2.2	2.3	2.4	2.5	2.6	2.7	2.8	2.9	3.0
BEAM 1	295'-3⅝"	139'-10⅞"	155'-4¾"	0.0000	0.0522	0.0969	0.1283	0.1422	0.1379	0.1167	0.0828	0.0448	0.0129	0.0000	0.0227	0.0686	0.1225	0.1703	0.2003	0.2076	0.1885	0.14[illegible]	0.0785	0.0000
BEAM 2	295'-2"	143'-0⅝"	152'-1⅜"	0.0000	0.0522	0.0963	0.1262	0.1380	0.1316	0.1087	0.0746	0.0387	0.0104	0.0000	0.0225	0.0649	0.1150	0.1592	0.1874	0.1940	0.1761	0.1344	0.0734	0.0000
BEAM 3	295'-2½"	146'-3⅜"	148'-11⅛"	0.0000	0.0515	0.0948	0.1234	0.1336	0.1262	0.1028	0.0689	0.0344	0.0079	0.0000	0.0214	0.0596	0.1055	0.1455	0.1714	0.1775	0.1613	0.1233	0.0674	0.0000
BEAM 4	295'-5"	149'-6⅞"	145'-10⅛"	0.0000	0.0553	0.1003	0.1293	0.1387	0.1279	0.1010	0.0646	0.0301	0.0048	0.0000	0.0193	0.0553	0.0980	0.1373	0.1630	0.1706	0.1560	0.1204	0.0667	0.0000

NOTES:

BASELINES ARE STRAIGHT LINES FROM ℄ BEARING TO ℄ BEARING AT TOP OF WEB.

AS Built.

CERTIFIED BY James F Hall PROFESSIONAL ENGINEER
REG. NO. 7375 6-22-1994

TITLE: STRUCTURAL STEEL DETAILS

DES: S.W.E. DR: S.W.B. APPROVED: 6-22-94
CHK: J.J.H. CHK: S.W.E.

SHEET NO. 44 OF 73 SHEETS

BRIDGE NO. 27998

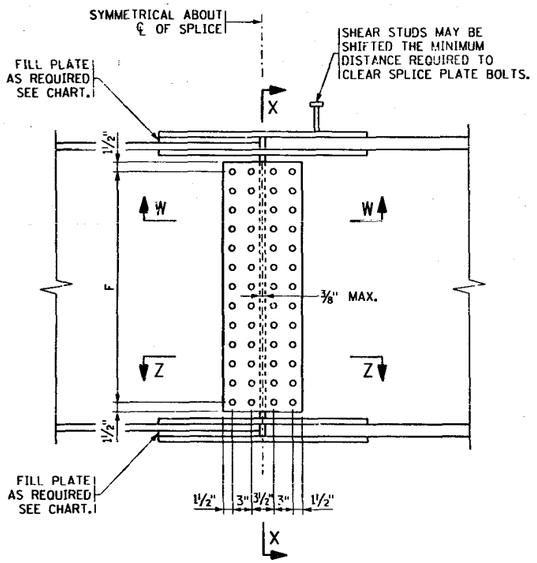

ELEVATION

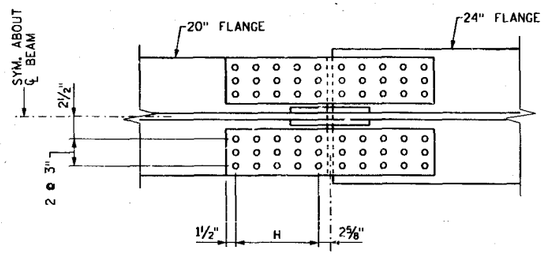

VIEW W-W

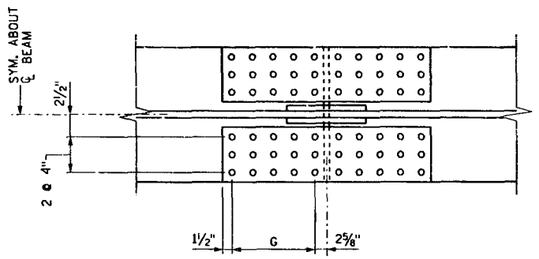

VIEW Z-Z

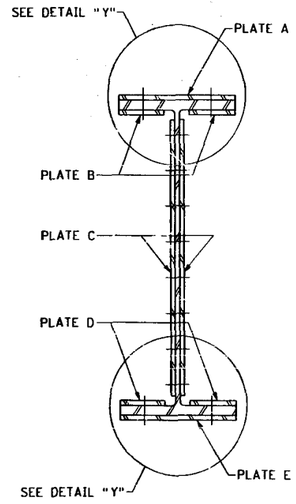

SECTION X-X

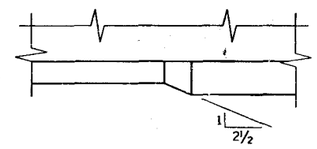

DETAIL A

SEE SHEET 42 FOR LOCATION.

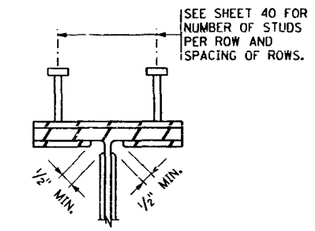

DETAIL "Y"

SPLICE PLATE CHART

BEAM	LOCATION	PLATE A	PLATE B	PLATE C	PLATE D	PLATE E	F	G	H
BEAM 1	FIELD SPLICE NO. 1	20" x ⅝" x 3'-2¼"	9" x ⅝" x 3'-2¼"	47" x 12½" x ½"	11" x ¾" x 3'-8¼"	24" x ⅝" x 3'-8¼"	16 SPS. @ 2¾"=3'-8"	6 SPS. @ 3"=1'-6"	5 SPS. @ 3"=1'-3"
BEAM 1	FIELD SPLICE NO. 2	20" x ⅝" x 3'-2¼"	9" x ⅝" x 3'-2¼"	47" x 12½" x ½"	11" x ¾" x 3'-8¼"	24" x ⅝" x 3'-8¼"	16 SPS. @ 2¾"=3'-8"	6 SPS. @ 3"=1'-6"	5 SPS. @ 3"=1'-3"
BEAM 2	FIELD SPLICE NO. 1	20" x ⅝" x 3'-2½"	9" x ⅝" x 3'-2¼"	52½" x 12½" x ½"	11" x ¾" x 3'-8¼"	24" x ⅝" x 3'-8¼"	18 SPS. @ 2¾"=4'-1½"	6 SPS. @ 3"=1'-6"	5 SPS. @ 3"=1'-3"
BEAM 2	FIELD SPLICE NO. 2	20" x ⅝" x 3'-2¼"	9" x ⅝" x 3'-2¼"	52½" x 12½" x ½"	11" x ¾" x 3'-8¼"	24" x ⅝" x 3'-8¼"	18 SPS. @ 2¾"=4'-1½"	6 SPS. @ 3"=1'-6"	5 SPS. @ 3"=1'-3"
BEAM 3	FIELD SPLICE NO. 1	20" x ⅝" x 3'-8¼"	9" x ⅞" x 3'-8¼"	58" x 12½" x ½"	11" x ¾" x 3'-8¼"	24" x ⅞" x 3'-8¼"	20 SPS. @ 2¾"=4'-7"	6 SPS. @ 3"=1'-6"	6 SPS. @ 3"=1'-6"
BEAM 3	FIELD SPLICE NO. 2	20" x ⅝" x 3'-8¼"	9" x ⅞" x 3'-8¼"	58" x 12½" x ½"	11" x ¾" x 3'-8¼"	24" x ⅞" x 3'-8¼"	20 SPS. @ 2¾"=4'-7"	6 SPS. @ 3"=1'-6"	6 SPS. @ 3"=1'-6"
BEAM 4	FIELD SPLICE NO. 1	20" x ⅞" x 4'-2¼"	9" x ⅞" x 4'-2¼"	66" x 12½" x ½"	11" x 1¼" x 4'-8¼"	24" x 1⅛" x 4'-8¼"	21 SPS. @ 3"=5'-3"	8 SPS. @ 3"=2'-0"	7 SPS. @ 3"=1'-9"
BEAM 4	FIELD SPLICE NO. 2	20" x ⅞" x 4'-2¼"	9" x 1" x 4'-2¼"	66" x 12½" x ½"	11" x 1¼" x 4'-8¼"	24" x 1⅛" x 4'-8¼"	21 SPS. @ 3"=5'-3"	8 SPS. @ 3"=2'-0"	7 SPS. @ 3"=1'-9"

FILL PLATE CHART

	BEAM 1		BEAM 2		BEAM 3		BEAM 4	
	TOP FLANGE	BOTTOM FLANGE	TOP FLANGE	BOTTOM FLANGE	TOP FLANGE	BOTTOM FLANGE	TOP FLANGE	BOTTOM FLANGE
FIELD SPLICE NO. 1	20" x ¾" x 1'-7"	24" x ⅜" x 1'-10"	20" x ¾" x 1'-7"	24" x ⅜" x 1'-10"	20" x 1" x 1'-10"	24" x ½" x 1'-10"	20" x 1" x 2'-1"	--- --- ---
FIELD SPLICE NO. 2	20" x ¾" x 1'-7"	24" x ⅜" x 1'-10"	20" x ¾" x 1'-7"	24" x ⅜" x 1'-10"	20" x 1" x 1'-10"	24" x ½" x 1'-10"	20" x ¾" x 2'-1"	24" x ¼" x 2'-4"

NOTES:

SPLICE DESIGN IS FOR STRUCTURAL STEEL SPEC. 3309.

FILL PLATES SHALL BE STRUCTURAL STEEL, MINIMUM THICKNESS 1/16".

AS Built

CERTIFIED BY James J. Hill PROFESSIONAL ENGINEER
REG. NO. 7395 6-22-1994

TITLE: STRUCTURAL STEEL DETAILS

DES: S.W.E. | DR: S.W.B. | APPROVED: 6-22-94
CHK: J.J.H. | CHK: S.W.E.

SHEET NO. 45 OF 73 SHEETS

BRIDGE NO. 27998

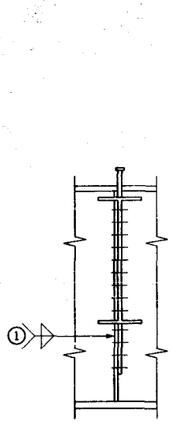

SECTION B-B

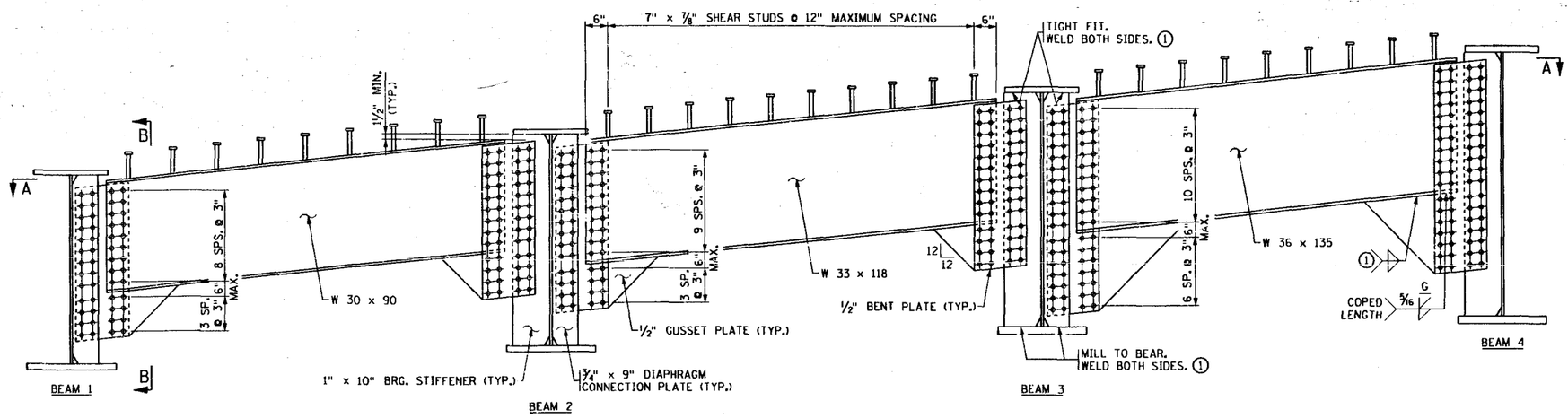

ELEVATION - SOUTH ABUTMENT END DIAPHRAGMS

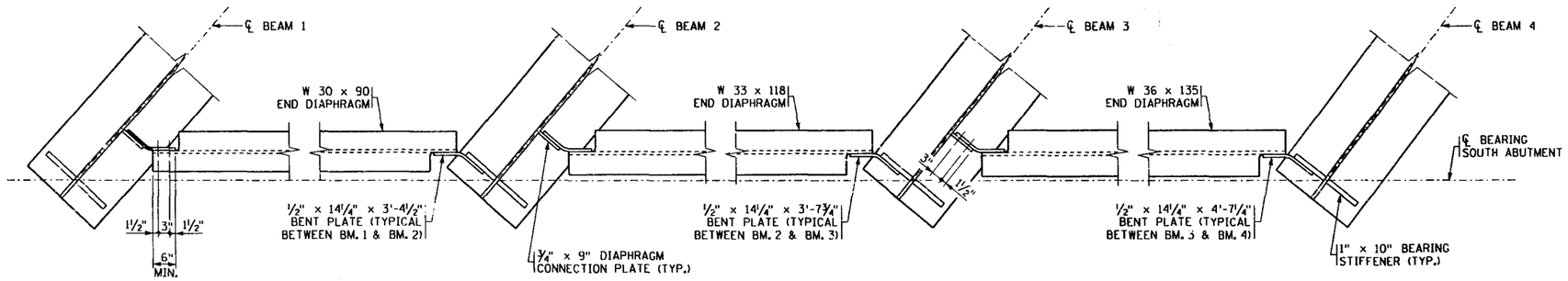

PART SECTION A-A

① SEE SPEC. 2471.3J4b1 FOR MINIMUM SIZE OF FILLET WELD.

AS Built.

CERTIFIED BY James J. Hill PROFESSIONAL ENGINEER REG. NO. 7315 6-22-1994	TITLE: STRUCTURAL STEEL DETAILS	DES: S.W.E. DR: S.W.B. APPROVED: 6-22-94 CHK: J.J.H. CHK: S.W.E.	BRIDGE NO. 27998
		SHEET NO. 46 OF 73 SHEETS	

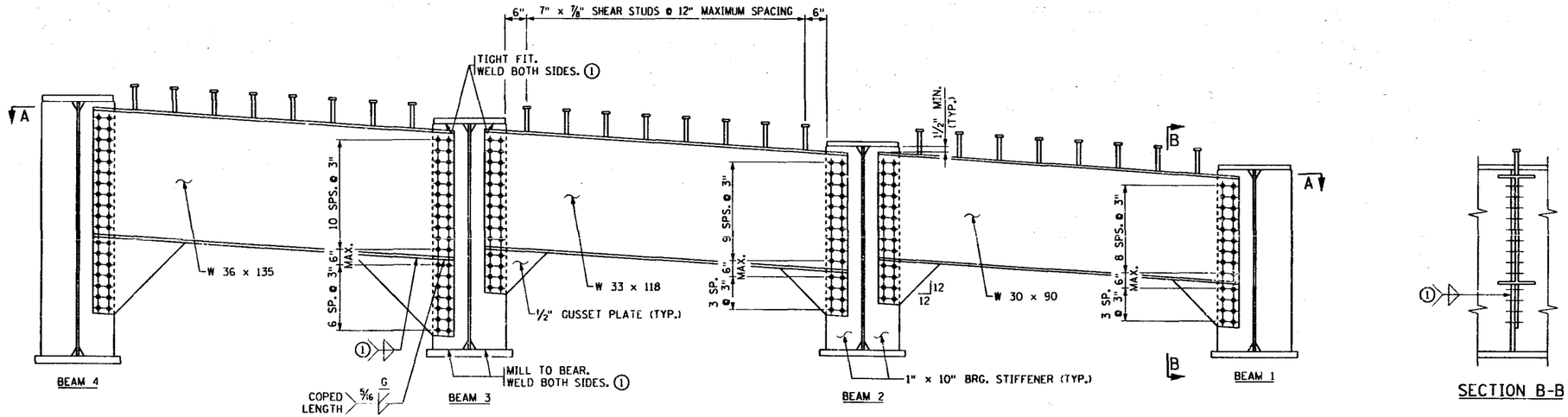

ELEVATION - NORTH ABUTMENT END DIAPHRAGMS

SECTION B-B

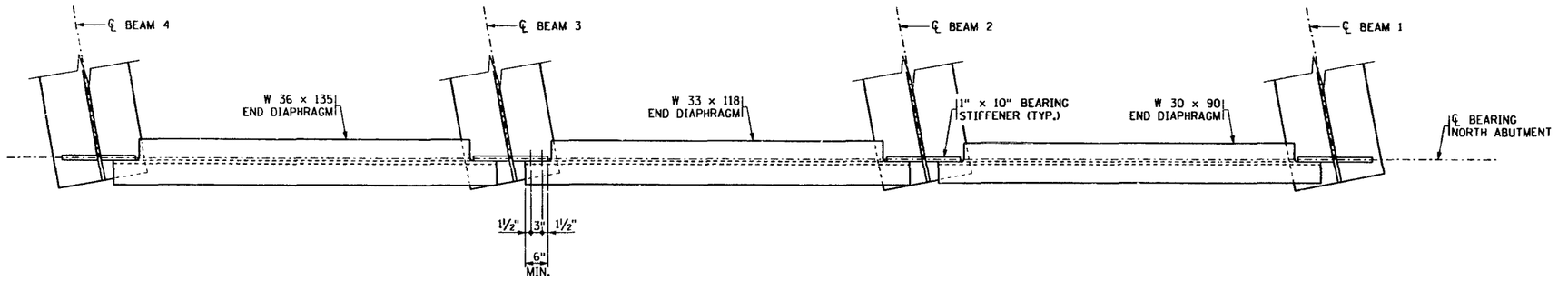

SECTION A-A

(1) SEE SPEC. 2471.3J4b1 FOR MINIMUM SIZE OF FILLET WELD.

AS Built.

CERTIFIED BY James J Hill PROFESSIONAL ENGINEER REG. NO. 7395 6-22-1994	TITLE: STRUCTURAL STEEL DETAILS	DES: S.W.E. CHK: J.J.H.	DR: S.W.B. CHK: S.W.E.	APPROVED: 6-22-94	BRIDGE NO. 27998
		SHEET NO. 47 OF 73 SHEETS			

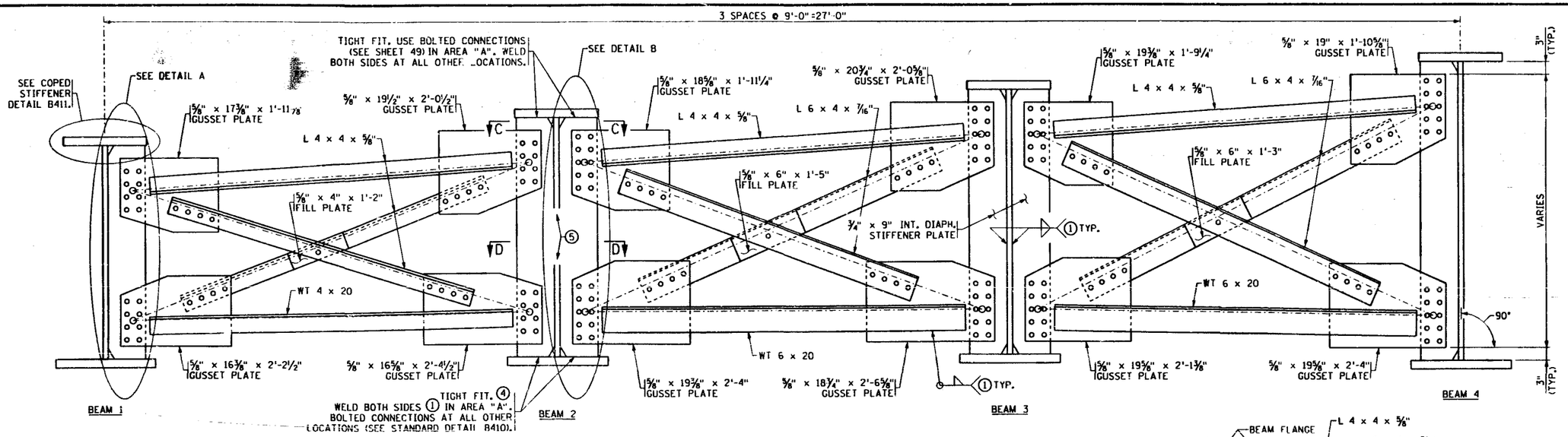

ELEVATION - INTERMEDIATE CROSS FRAME DIAPHRAGM

SEE FRAMING PLAN, SHEET 40, FOR LOCATIONS.

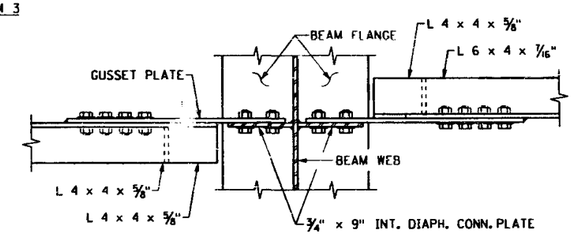

SECTION C-C

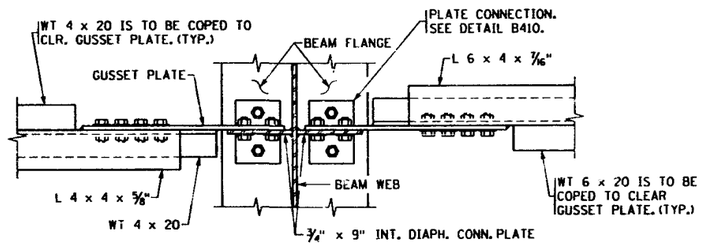

SECTION D-D

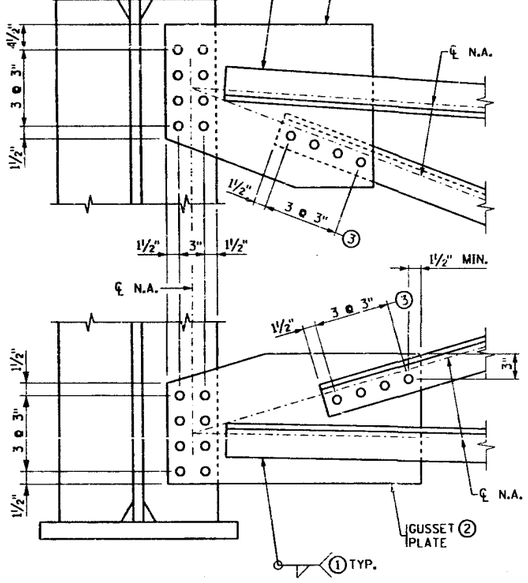

DETAIL A

TYPICAL BETWEEN BEAMS 1 & 2.

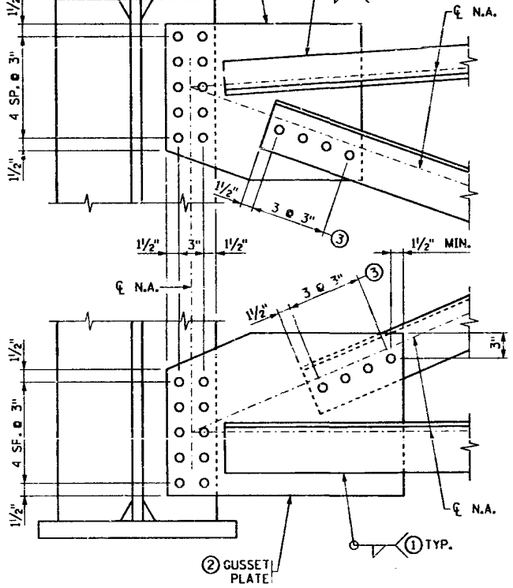

DETAIL B

TYPICAL BETWEEN BEAMS 2 & 3 AND 3 & 4.

NOTES:

ALL STEEL SHALL CONFORM TO SPEC. 3309.

① SEE SPEC. 2471.3J4b1 FOR MINIMUM SIZE OF FILLET WELD. WELD SIZE NEED NOT EXCEED 3/8" FOR INTERMEDIATE DIAPHRAGM STIFFENERS.

② BOLT HOLES IN GUSSET PLATE MAY BE FIELD DRILLED.

③ WELDING MAY BE USED IN LIEU OF BOLTS SHOWN.

④ MILL TO BEAR AT BEARING STIFFENERS.

⑤ THE CENTER OF GRAVITIES OF THE BOLT PATTERNS ARE TO BE PLACED AT THE SAME ELEVATION (TYPICAL).

⑥ THE NEUTRAL AXES OF THE DIAPHRAGM MEMBERS SHALL INTERSECT WITH THE CENTER OF GRAVITY OF THE BOLT PATTERNS.

AS Built.

CERTIFIED BY James J. Hill PROFESSIONAL ENGINEER
REG. NO. 7545 6-22-1994

TITLE: STRUCTURAL STEEL DETAILS

DES: S.W.E.	DR: S.W.B.	APPROVED: 6-22-94
CHK: J.J.H.	CHK: S.W.E.	

SHEET NO. 48 OF 73 SHEETS

BRIDGE NO. 27998

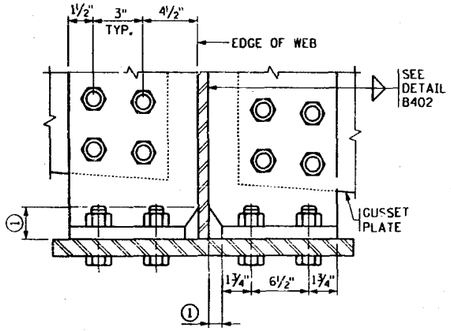

SECTION B-B
PLATE CONNECTION AT INTERMEDIATE BEAMS ⑤

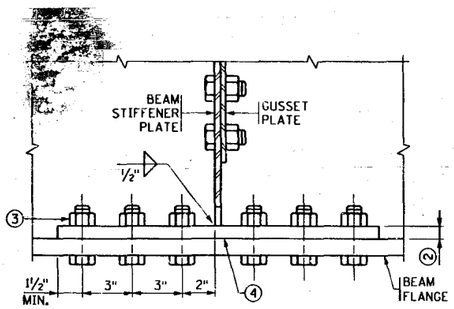

SECTION D-D
PLATE CONNECTION DETAIL

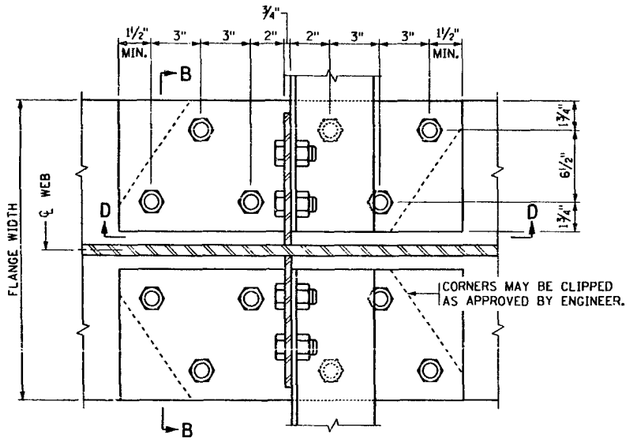

PLAN VIEW
AT INTERMEDIATE BEAMS

NOTES:

ALL STEEL SHALL CONFORM TO SPEC. 3309.

① SEE DETAIL B411.

② MINIMUM PLATE THICKNESS SHALL BE ¾".

③ BOLT PLATE TO BEAM FLANGE PRIOR TO WELDING PLATE TO BEAM STIFFENER PLATE.

④ REMOVE LOOSE SCALE AND RUST FROM CONTACT AREA AT DIAPHRAGM CONNECTION. SURFACE MUST BE FLAT AND PRIMED.

⑤ USE ON UPPER (TENSION) FLANGE WITHIN AREA "A". USE ON LOWER (TENSION) FLANGE OUTSIDE OF AREA "A".

APPROVED: DECEMBER 11, 1992 OFFICE of BRIDGES and STRUCTURES	STATE OF MINNESOTA DEPARTMENT OF TRANSPORTATION BOLTED FLANGE TO STIFFENER DETAIL FOR STEEL BEAMS		DETAIL NO. B410

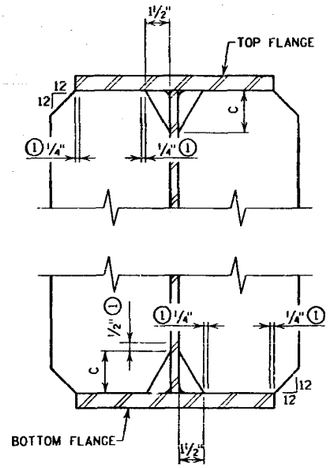

STIFFENER TO FLANGE CONNECTION

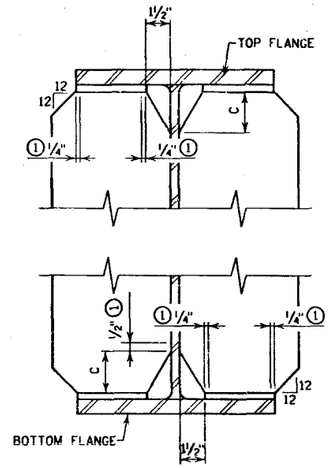

STIFFENER TO TAB PLATE CONNECTION

COPED STIFFENER DETAIL
(PLATE GIRDER OR ROLLED BEAM)

NOTES:
① DO NOT WELD IN THIS AREA.

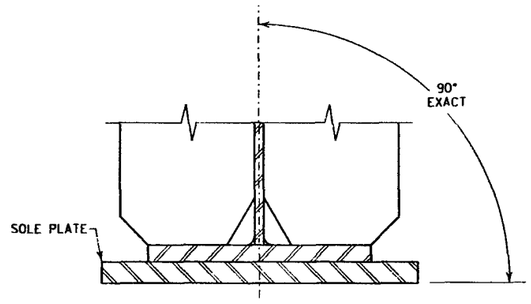

PLACING SOLE PLATE AT BEARING

TABLE	
WEB THICKNESS	DIMENSION C
½", 9/16", 5/8"	2½"
~~11/16", ¾"~~	~~3"~~

AS Built.

APPROVED: OFFICE of BRIDGES and STRUCTURES	STATE OF MINNESOTA DEPARTMENT OF TRANSPORTATION STIFFENER DETAILS FOR STEEL BEAMS	DATE: 3/17/92 DR: K.L.W. CHK:	DETAIL NO. MODIFIED B411

CERTIFIED BY James J. Hill PROFESSIONAL ENGINEER REG. NO. 7315 6-22-1994	TITLE: STRUCTURAL STEEL DETAILS	DES: S.W.E. DR: S.W.B. APPROVED: 6-22-94 CHK: J.J.H. CHK: S.W.E. SHEET NO. 49 OF 73 SHEETS	BRIDGE NO. 27998

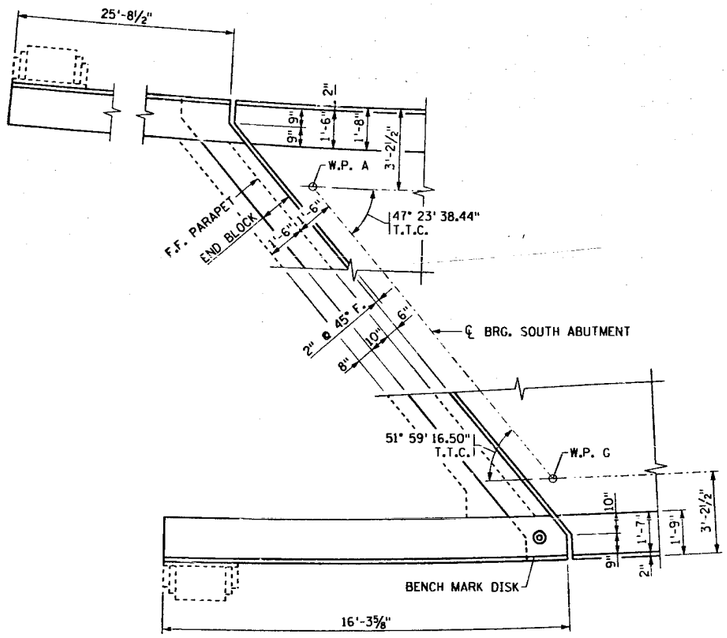

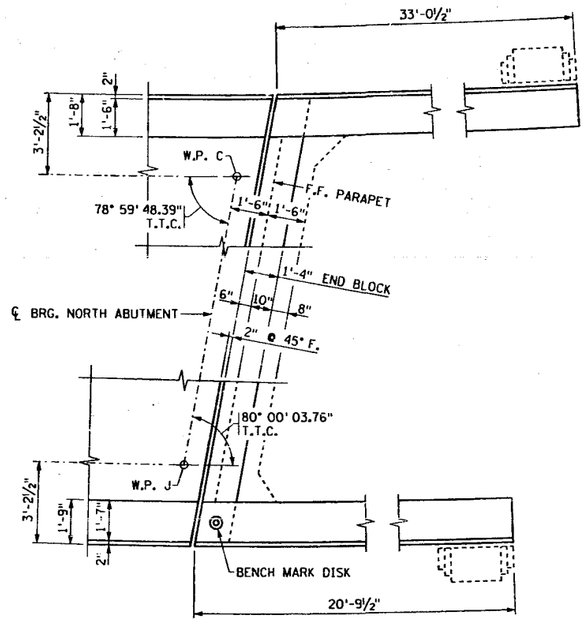

CORNER DETAILS

BILL OF REINFORCEMENT FOR SUPER.				
BAR	NO.	LENGTH	SHAPE	LOCATION
S601E	1 SERIES OF 42	6'-1" - 31'-6"	STRT.	BOTTOM TRANSVERSE
S602E	550	32'-9"	STRT.	BOTTOM TRANSVERSE
S603E	1 SERIES OF 11	3'-1" - 30'-6"	STRT.	BOTTOM TRANSVERSE
S504E	1 SERIES OF 45	24'-0" - 36'-3"	STRT.	BOTTOM LONGITUDINAL
S505E	180	60'-0"	STRT.	BOTTOM LONGITUDINAL
S506E	1 SERIES OF 45	30'-0" - 41'-6"	STRT.	BOTTOM LONGITUDINAL
S407E	1 SERIES OF 22	15'-4" - 26'-6"	STRT.	TOP LONGITUDINAL
S408E	44	40'-0"	STRT.	TOP LONGITUDINAL
S409E	66	60'-0"	STRT.	TOP LONGITUDINAL
S410E	1 SERIES OF 22	21'-0" - 32'-3"	STRT.	TOP LONGITUDINAL
S611E	1 SERIES OF 42	6'-3" - 31'-8"	STRT.	TOP TRANSVERSE
S612E	550	33'-1"	STRT.	TOP TRANSVERSE
S613E	1 SERIES OF 11	3'-3" - 30'-8"	STRT.	TOP TRANSVERSE
S514E	2	5'-2"	BENT	CORNER TIE
S515E	8	42'-8"	STRT.	TOP & BOT. TRANS. @ EXP. JT.
S516E	8	33'-7"	STRT.	TOP & BOT. TRANS. @ EXP. JT.
S617E	40	60'-0"	STRT.	TOP LONGIT. @ PIER
S418E	72	4'-4"	BENT	END BLOCK TIE
S619E	18	4'-6"	STRT.	TOP & BOT. TRANSVERSE
S520E	2	3'-2"	BENT	CORNER TIE
S621E	80	20'-6"	STRT.	TOP LONGIT. @ PIER

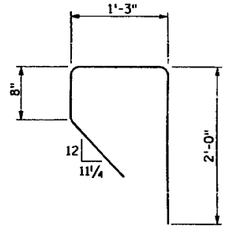

S514E

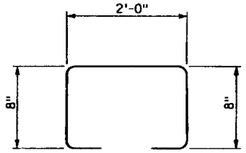

S418E

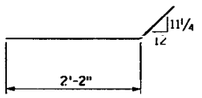

S520E

AS Built.

CERTIFIED BY James J. Hill PROFESSIONAL ENGINEER
REG. NO. 7315 6-22-1994

TITLE: SUPERSTRUCTURE DETAILS AND REINFORCEMENT

DES: S.W.E. | DR: S.W.B. | APPROVED: 6-22-94
CHK: J.J.H. | CHK: S.W.E.

SHEET NO. 50 OF 73 SHEETS

BRIDGE NO. 27998

① DIMENSIONS ARE ALONG EDGE OF DECK. BARS ARE SPACED RADIALLY ON A CURVE 2" CLEAR TO EDGE OF DECK (TOP TRANSVERSE) AND ON A CURVE 4" CLEAR TO EDGE OF DECK (BOTTOM TRANSVERSE).

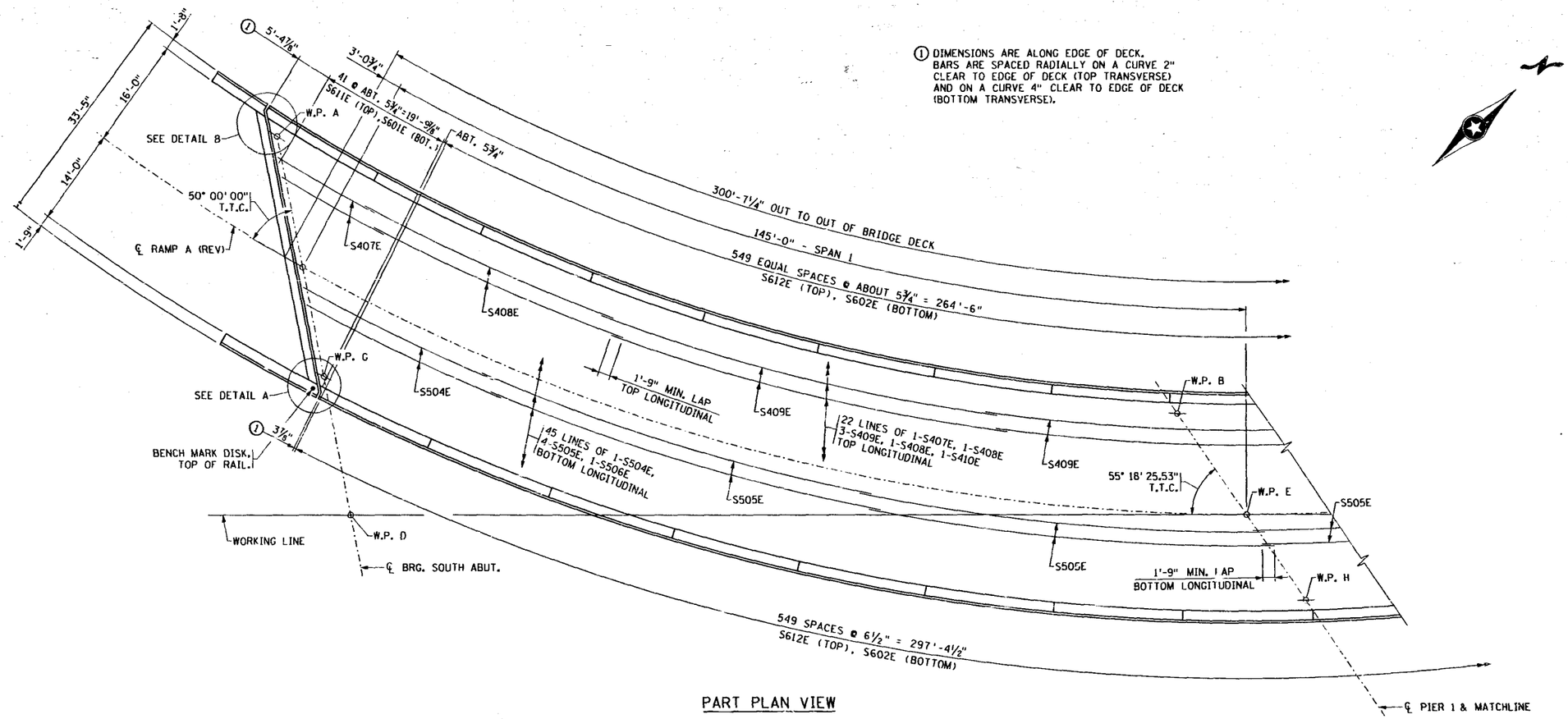

PART PLAN VIEW

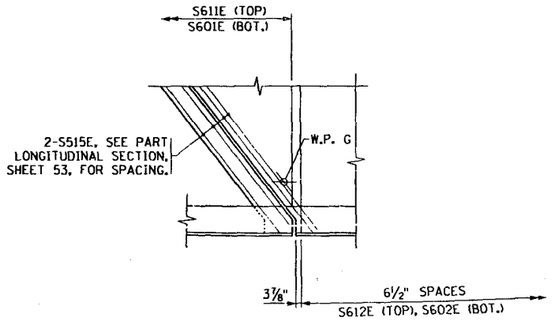

DETAIL A

SEE SHEET 50 FOR CORNER DETAILS.

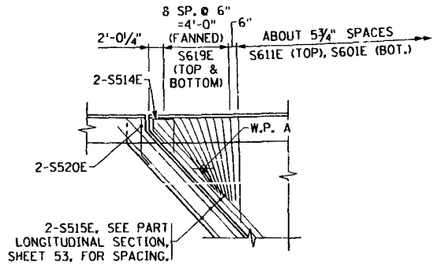

DETAIL B

SEE SHEET 50 FOR CORNER DETAILS.

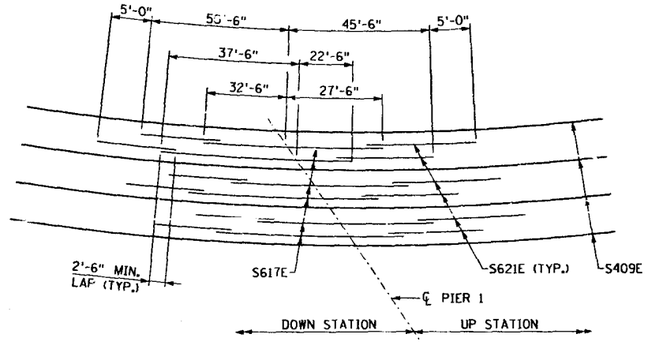

STAGGER DIAGRAM

AS Built.

CERTIFIED BY James J. Hill, PROFESSIONAL ENGINEER REG. NO. 7395 6-22-1994	TITLE: SUPERSTRUCTURE DETAILS AND REINFORCEMENT	DES: S.W.E.	DR: S.W.B.	APPROVED: 6-22-94	BRIDGE NO. 27998
		CHK: J.J.H.	CHK: R.E.H.	SHEET NO. 51 OF 73 SHEETS	

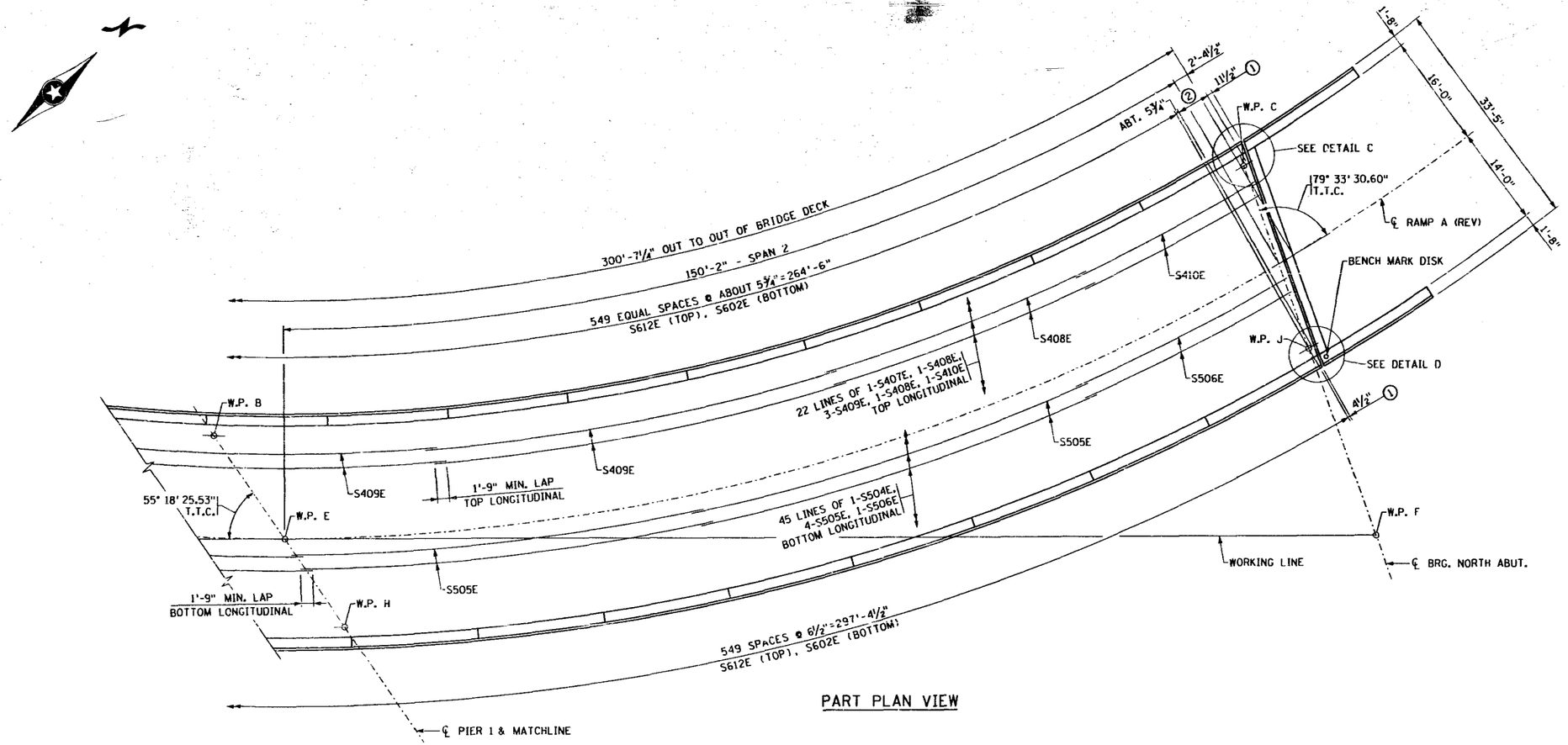

PART PLAN VIEW

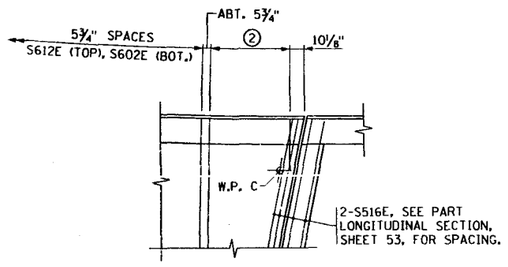

DETAIL C

SEE SHEET 50 FOR CORNER DETAILS.

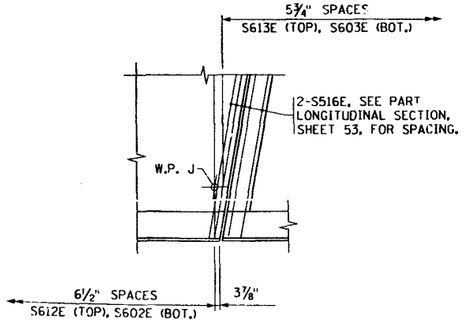

DETAIL D

SEE SHEET 50 FOR CORNER DETAILS.

① DIMENSIONS ARE ALONG EDGE OF DECK. BARS ARE SPACED RADIALLY ON A CURVE 2" CLEAR TO EDGE OF DECK (TOP TRANSVERSE) AND ON A CURVE 4" CLEAR TO EDGE OF DECK (BOTTOM TRANSVERSE).

② 10 SPACES @ ABOUT 5¾"=4'-10⅛" S613E (TOP), S603E (BOTTOM)

AS Built

CERTIFIED BY James J. Hill PROFESSIONAL ENGINEER REG. NO. 7395 6-22-1994	TITLE: SUPERSTRUCTURE DETAILS AND REINFORCEMENT	DES: S.W.E. DR: S.W.B. APPROVED: 6-22-94 CHK: J.J.H. CHK: R.E.H.	SHEET NO. 52 OF 73 SHEETS	BRIDGE NO. 27998

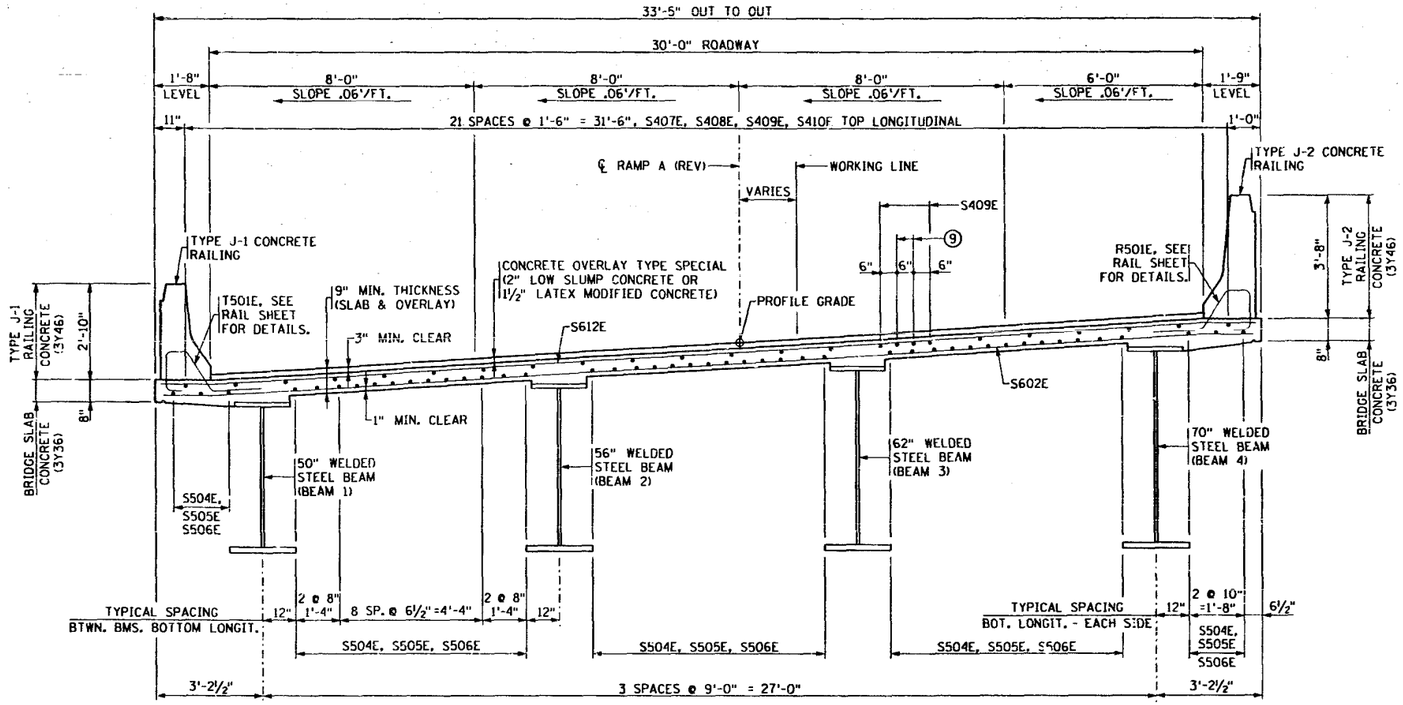

TRANSVERSE SECTION

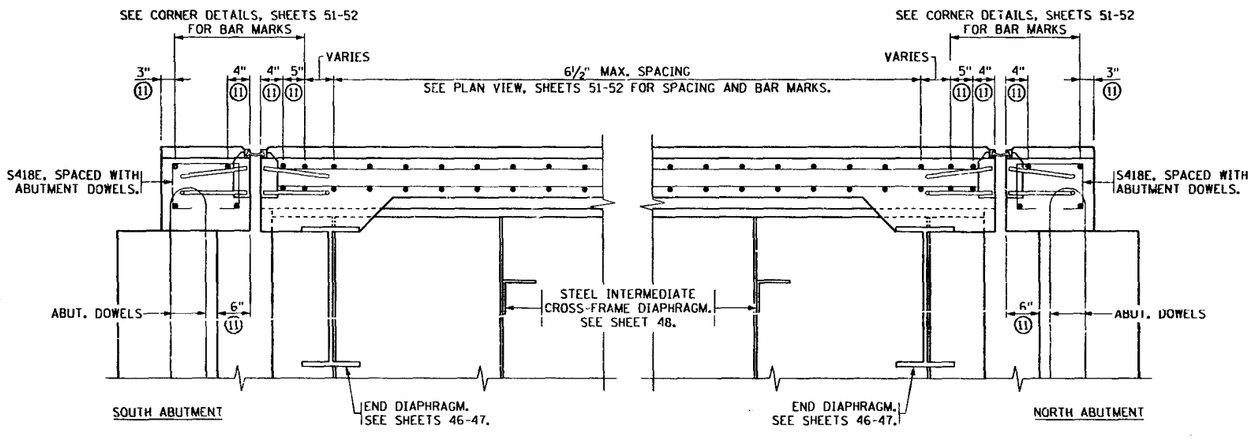

PART LONGITUDINAL SECTION

① SUMMARY OF QUANTITIES FOR SUPERSTRUCTURE		
② BRIDGE SLAB CONCRETE (3Y36)	10047	SQ. FT.
③ TYPE J-1 RAILING CONCRETE (3Y46)	358	LIN. FT.
⑫ TYPE J-2 RAILING CONCRETE (3Y46)	332	LIN. FT.
⑩ CONCRETE OVERLAY TYPE SPECIAL	9021	SQ. FT.
④ REINFORCEMENT BARS (EPOXY COATED	96030	POUND
STRUCTURAL STEEL (3309)	596000	POUND
⑤ VULCANIZED EXP. CURVED PLATE BEARING ASSEMBLY TYPE 1	3	EACH
⑤ VULCANIZED EXP. CURVED PLATE BEARING ASSEMBLY TYPE 2	2	EACH
⑤ VULCANIZED EXP. CURVED PLATE BEARING ASSEMBLY TYPE 3	3	EACH
⑤ FIXED CURVED PLATE BEARING ASSEMBLY TYPE 1	3	EACH
⑤ FIXED CURVED PLATE BEARING ASSEMBLY TYPE 2	1	EACH
⑥ BRIDGE NAME PLATE	1	UNIT
⑥⑧ 1" CORK	45	SQ. FT.
⑦ BENCH MARK DISK	2	UNIT
EXPANSION JOINT DEVICE TYPE S	74	LIN. FT.

① INCLUDES RAILING QUANTITIES.

② BRIDGE SLAB CONCRETE (3Y36) VOLUME IS APPROXIMATELY 252 CU. YD., USING LOW SLUMP CONCRETE WEARING COURSE ALTERNATE, (266 CU. YD. WITH LATEX OPTION) AND AN AVERAGE STOOL HEIGHT OF 3¼" INCHES. INCLUDES END BLOCKS.

③ TYPE J-1 RAILING CONCRETE (3Y46) VOLUME IS APPROXIMATELY 38 CU. YDS.

④ INCLUDES RAIL REINFORCEMENT.

⑤ PAYMENT FOR BEARINGS INCLUDED IN ITEM BEARING ASSEMBLY PER EACH.

⑥ TO BE INCLUDED IN PRICE BID FOR OTHER ITEMS.

⑦ STATE WILL FURNISH DISK. BEND PRONGS OUTWARD TO ANCHOR DISK IN CONCRETE. BOTTOM OF DISK TO BE PLACED FLUSH WITH CONCRETE. PAYMENT FOR PLACING TO BE INCLUDED IN PRICE BID FOR OTHER ITEMS.

⑧ FOR CONTRACTORS CONVENIENCE ONLY. SEE SPECIAL PROVISIONS.

⑨ S617E, STAGGERED OVEP PIER. SEE STAGGER DIAGRAM, SHEET 51.

⑩ CONCRETE WEARING COURSE TYPE SPECIAL VOLUME IS APPROXIMATELY 56 CU. YDS. USING LOW SLUMP CONCRETE WEARING COURSE ALTERNATE.

⑪ NORMAL TO JOINT.

⑫ TYPE J-2 RAILING CONCRETE (3Y46) VOLUME IS APPROXIMATELY 47 CU. YDS.

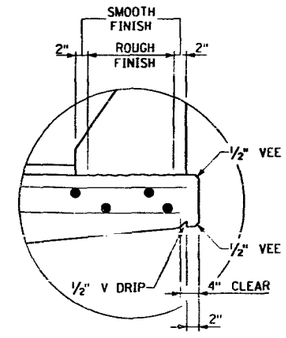

DETAIL A

AS Built

CERTIFIED BY James J. Hill PROFESSIONAL ENGINEER
REG. NO. 7395 6-22- 1994

TITLE: SUPERSTRUCTURE DETAILS AND REINFORCEMENT

DES: S.W.E	DR: S.W.B.	APPROVED: 6-22-94
CHK: J.J.H.	CHK: R.E.H.	

SHEET NO. 53 OF 73 SHEETS

BRIDGE NO. 27998

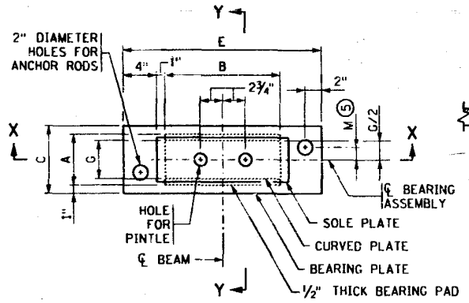

PLAN

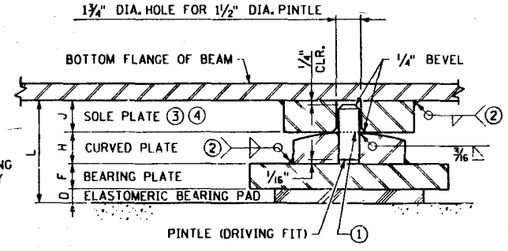

SECTION Y-Y
(ENLARGED BEARING ASSEMBLY)

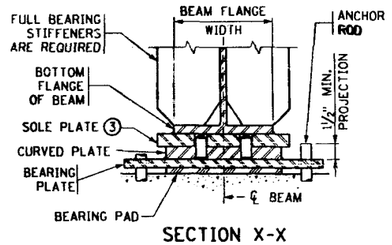

SECTION X-X

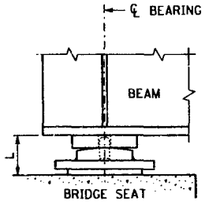

END ELEVATION
(ANCHOR RODS NOT SHOWN)

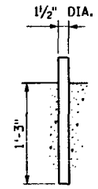

ANCHOR ROD DETAIL

TABLE

BEAM FLANGE WIDTH	LOCATION	BEARING PAD SIZE A	B	D	SHAPE FACTOR	BEARING PLATE SIZE C	E	F	CURVED PLATE SIZE G	B	H	① RAD.	SOLE PLATE SIZE WIDTH	LENG.	J ③	PINTLE DIA.	ASSY. HEIGHT L	ANCHOR ROD OFFSET M ⑤	TYPE
24"	PIER 1 BMS. 1, 2, 4	24"	22"	¾"	7.7	26"	32"	2"	12"	22"	3"	16"	14"	28"	2½"	1½"	8¼"	6"	1
24"	PIER 1 BEAM 3	26"	26"	¾"	8.7	28"	36"	2½"	12"	26"	3"	16"	14"	28"	2½"	1½"	8¾"	6"	2

NOTES:

ELASTOMERIC MATERIALS & PAD CONSTRUCTION SHALL COMPLY WITH SPEC. 3741.

ALL STEEL PLATES & ANCHOR RODS SHALL COMPLY WITH SPEC. 3309.

FOR SPANS UP TO 150 FEET, USE 1½" DIAMETER ANCHOR RODS. ABOVE 150 FOOT SPANS, DESIGN ANCHOR RODS PER AASHTO DESIGN CRITERIA.

ALL PLATES SHALL BE FLAT AFTER FABRICATION AND GALVANIZING. WELDING DISTORTION OF BEARING PLATES SHALL BE STRAIGHTENED TO WITHIN 1/16" OF FLATNESS BY MECHANICAL MEANS WITHOUT DAMAGE TO THE ZINC COATING.

PINTLES SHALL COMPLY WITH SPEC. 3309.

GALVANIZE STRUCTURAL STEEL BEARING ASSEMBLY AFTER FABRICATION PER SPEC. 3394, EXCEPT AS NOTED.

PAYMENT FOR BEARING ASSEMBLY SHALL INCLUDE ALL MATERIAL ON THIS DETAIL EXCEPT THE SOLE PLATE. THE SOLE PLATE IS INCLUDED IN THE WEIGHT OF STRUCTURAL STEEL AND SHALL BE THE SAME MATERIAL AS THE STEEL BEAMS.

① THE RADIUS OF THE CURVED PLATE SHALL BE 1'-4" MINIMUM AND 2'-0" MAXIMUM UNLESS OTHERWISE SPECIFIED IN TABLE. FINISH TO 250 MICRO. THE FINISHED THICKNESS OF THE PLATE MAY BE 1/16" LESS THAN SHOWN.

② WELDING PER SPEC. 2471.

③ WHEN THE SOLE PLATE IS TAPERED, DIMENSIONS J AND L ARE THICKNESS OF SOLE PLATE AND BEARING ASSEMBLY AT CENTERLINE OF BEARING.

④ DO NOT GALVANIZE THIS PLATE.

⑤ OFFSET MAY BE OPPOSITE OF THAT SHOWN. SEE ANCHOR ROD LAYOUT FOR DETAILS.

DESIGN DATA:
MAXIMUM HORIZONTAL LOAD IS 70 KIPS
MINIMUM SOLE PLATE THICKNESS IS 1¼ INCHES

APPROVED: JANUARY 12, 1993
OFFICE of BRIDGES and STRUCTURES

STATE OF MINNESOTA
DEPARTMENT OF TRANSPORTATION
CURVED PLATE BEARING ASSEMBLY
STEEL BEAMS
(FIXED)

REVISION 4/12/94 NKL

DETAIL NO. B354

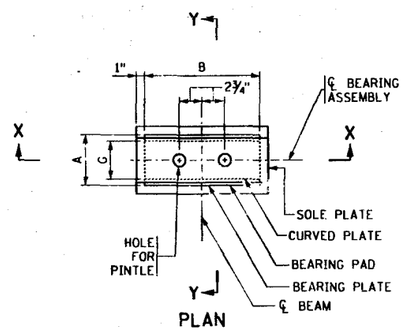

PLAN

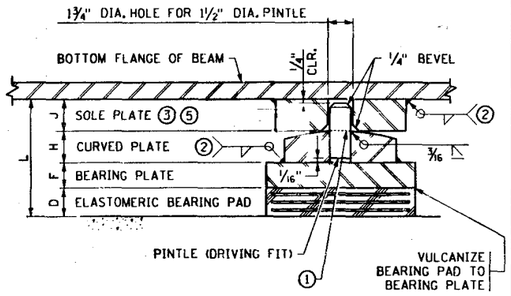

SECTION Y-Y
(ENLARGED BEARING ASSEMBLY)

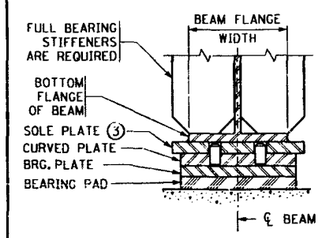

SECTION X-X

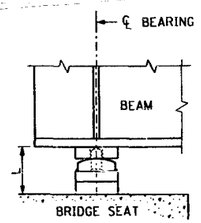

END ELEVATION

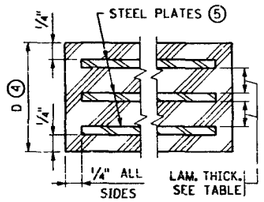

SECTION THRU BEARING PAD

TABLE

BEAM FLANGE WIDTH	BEARING PAD SIZE A	B	D	STEEL PLATES NO.	THICK.	LAMINATES NO.	THICK.	SHAPE FACTOR	BEARING PLATE SIZE A	B	F	CURVED PLATE SIZE G	B	H	① RAD.	SOLE PLATE SIZE WIDTH	LENG.	THICK. J ③	PINTLE DIA.	ASSY. HEIGHT L	TYPE	LOCATION
24"	12"	14"	4⅝"	9	⅛"	8	⅜"	8.6	12"	14"	1¼"	6"	14"	1¾"	16"	6"	28"	1"	1½"	8⅝"	1	SOUTH ABUT. BEAMS 1, 2, 3
24"	16"	20"	4 13/16"	7	3/16"	6	½"	8.9	16"	20"	1½"	3"	20"	2¼"	16"	8"	28"	1¼"	1½"	9 13/16"	2	N. & S. ABUT. BEAM 4
24"	12"	16"	4⅝"	9	⅛"	8	⅜"	9.1	12"	16"	1¼"	6"	16"	1¾"	16"	6"	28"	1"	1½"	8⅝"	3	NORTH ABUT. BEAMS 1, 2, 3

NOTES:

ELASTOMERIC MATERIALS & PAD CONSTRUCTION SHALL COMPLY WITH SPEC. 3741.

ALL STEEL PLATES SHALL COMPLY WITH SPEC. 3306.

ALL PLATES SHALL BE FLAT AFTER FABRICATION AND GALVANIZING. WELDING DISTORTION OF BEARING PLATES SHALL BE STRAIGHTENED TO WITHIN 1/16" OF FLATNESS BY MECHANICAL MEANS WITHOUT DAMAGE TO THE ZINC COATING.

PINTLES SHALL COMPLY WITH SPEC. 3309.

GALVANIZE STRUCTURAL STEEL BEARING ASSEMBLY AFTER FABRICATION PER SPEC. 3394, EXCEPT AS NOTED.

PAYMENT FOR BEARING ASSEMBLY SHALL INCLUDE ALL MATERIAL ON THIS DETAIL EXCEPT THE SOLE PLATE. THE SOLE PLATE IS INCLUDED IN THE WEIGHT OF STRUCTURAL STEEL AND SHALL BE THE SAME MATERIAL AS THE STEEL BEAMS.

① THE RADIUS OF THE CURVED PLATE SHALL BE 1'-4" MINIMUM AND 2'-0" MAXIMUM UNLESS OTHERWISE SPECIFIED IN TABLE. FINISH TO 250 MICRO. THE FINISHED THICKNESS OF THE PLATE MAY BE 1/16" LESS THAN SHOWN.

② WELDING PER SPEC. 2471.

③ WHEN THE SOLE PLATE IS TAPERED, DIMENSIONS J AND L ARE THICKNESS OF SOLE PLATE AND BEARING ASSEMBLY AT CENTERLINE OF BEARING.

④ THE TOTAL THICKNESS SHOWN INCLUDES THE STEEL PLATES.

⑤ DO NOT GALVANIZE THESE PLATES.

AS Built.

DESIGN DATA:
MAXIMUM HORIZONTAL LOAD IS 70 KIPS
MINIMUM SOLE PLATE THICKNESS IS 1¼ INCHES

APPROVED: AUGUST 4,1992
OFFICE of BRIDGES and STRUCTURES

STATE OF MINNESOTA
DEPARTMENT OF TRANSPORTATION
CURVED PLATE BEARING ASSEMBLY
STEEL BEAMS
(VULCANIZED EXPANSION)

REVISION 4/12/94 NKL

DETAIL NO. B357

CERTIFIED BY James J. Hill
PROFESSIONAL ENGINEER
REG. NO. 7595 6-22-1994

TITLE: DETAILS

DES: | DR: S.W.B. | APPROVED:
CHK: | CHK: S.W.E.

SHEET NO. 61 OF 73 SHEETS

BRIDGE NO. 27998

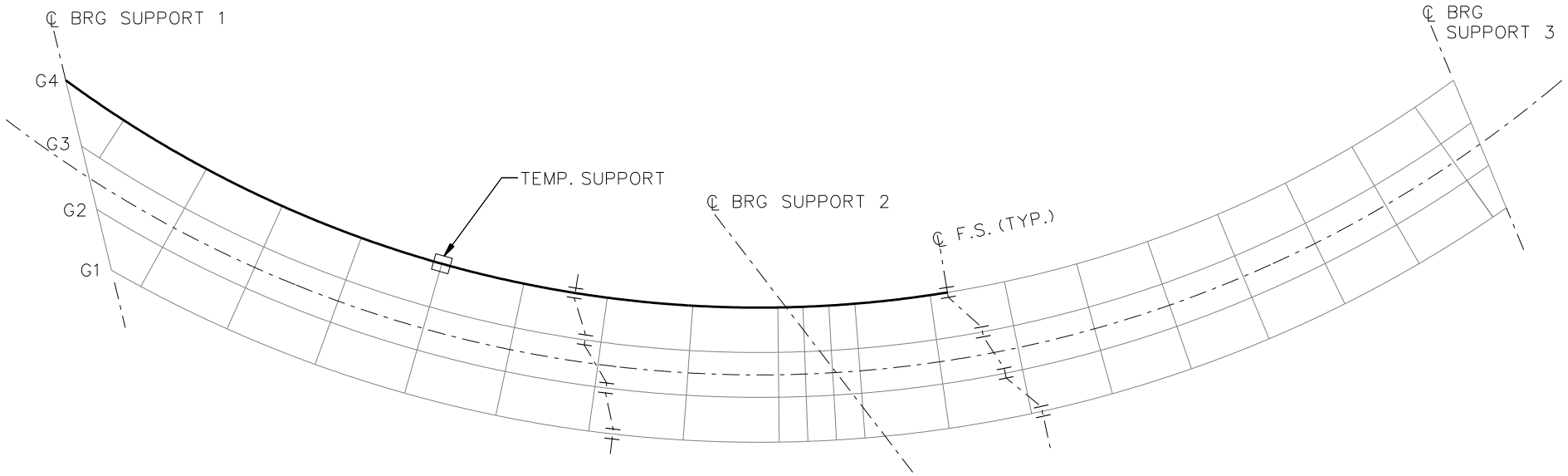

STAGE 1

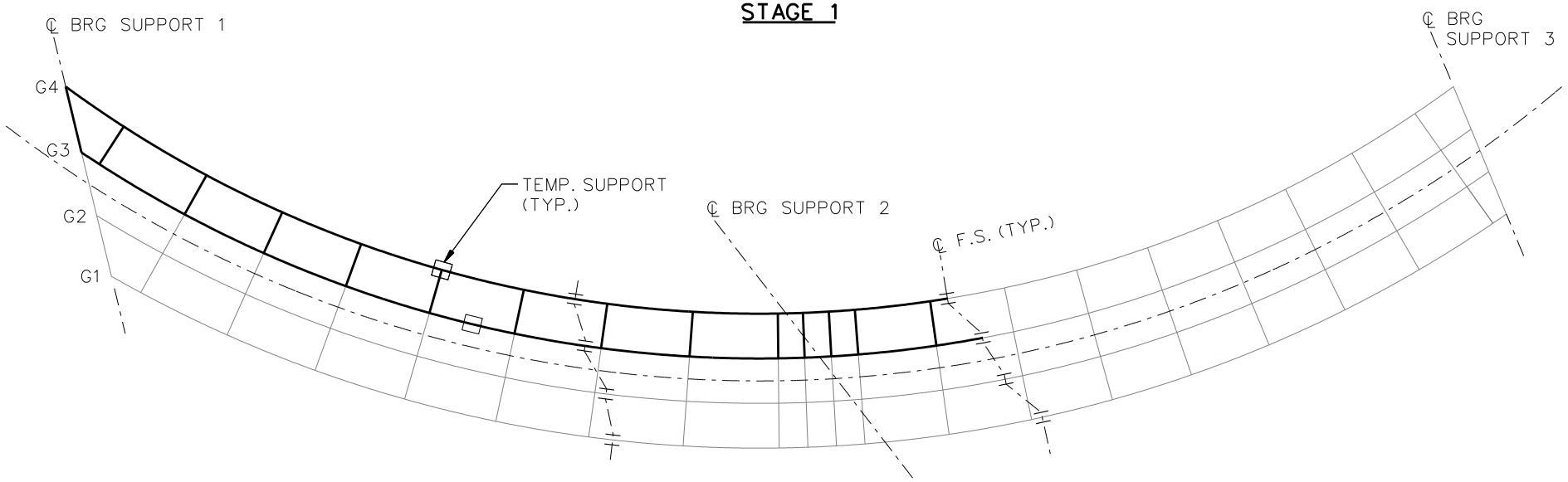

STAGE 2

LEGEND

▽ = HOLD OR LIFT CRANE

○ = TIE DOWN

□ = TEMPORARY SUPPORT STRUCTURE

NCHRP 12-79

BRIDGE EICCS10

GIRDER ERECTION PROCEDURE

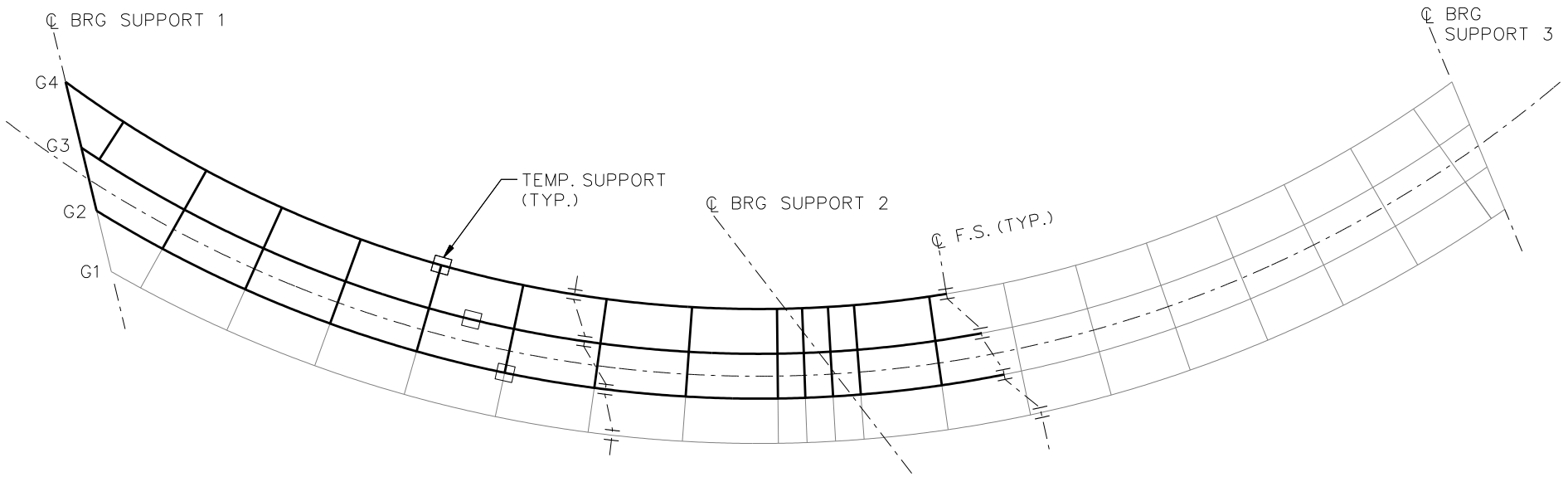

STAGE 3

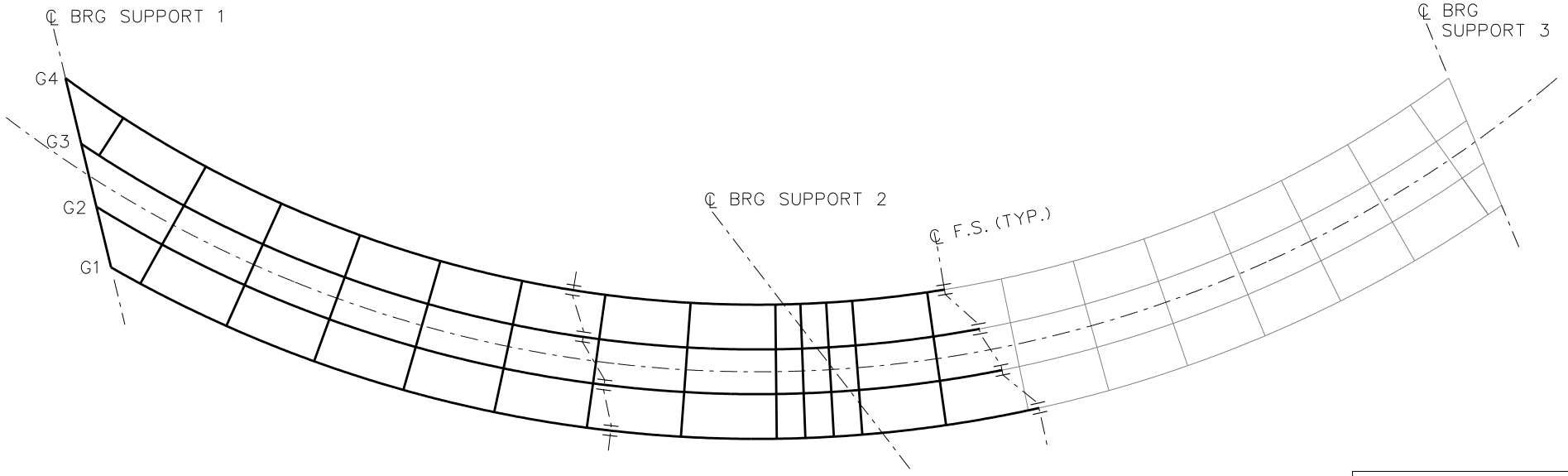

STAGE 4

LEGEND

▽ = HOLD OR LIFT CRANE

○ = TIE DOWN

□ = TEMPORARY SUPPORT STRUCTURE

NCHRP 12-79

BRIDGE EICCS10

GIRDER ERECTION PROCEDURE

SHEET 2 OF 4

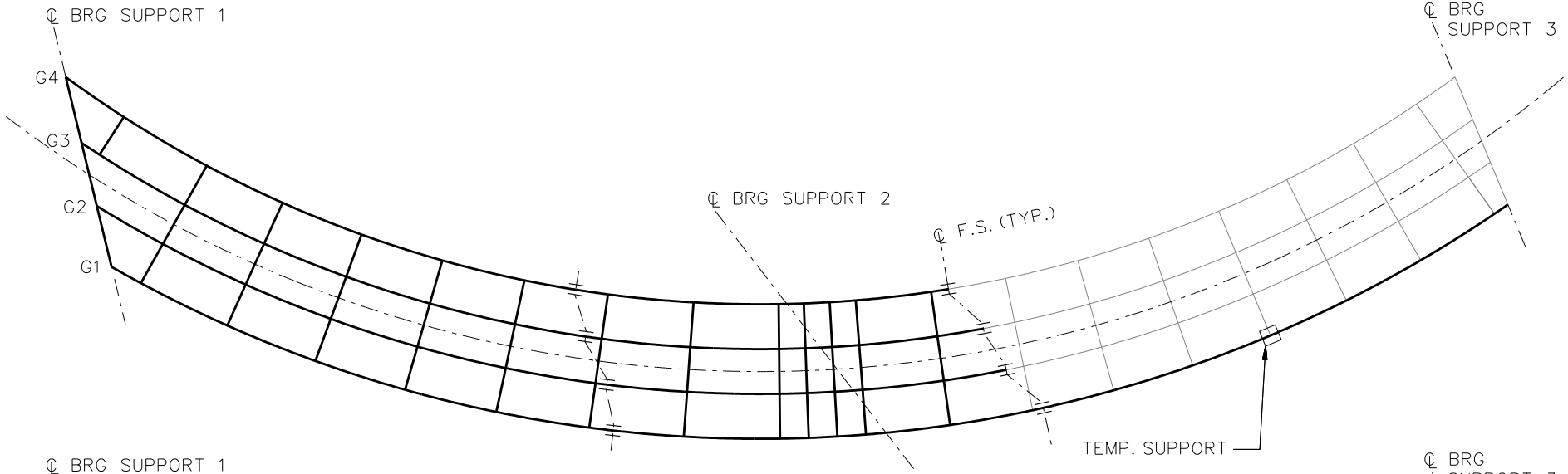

STAGE 5

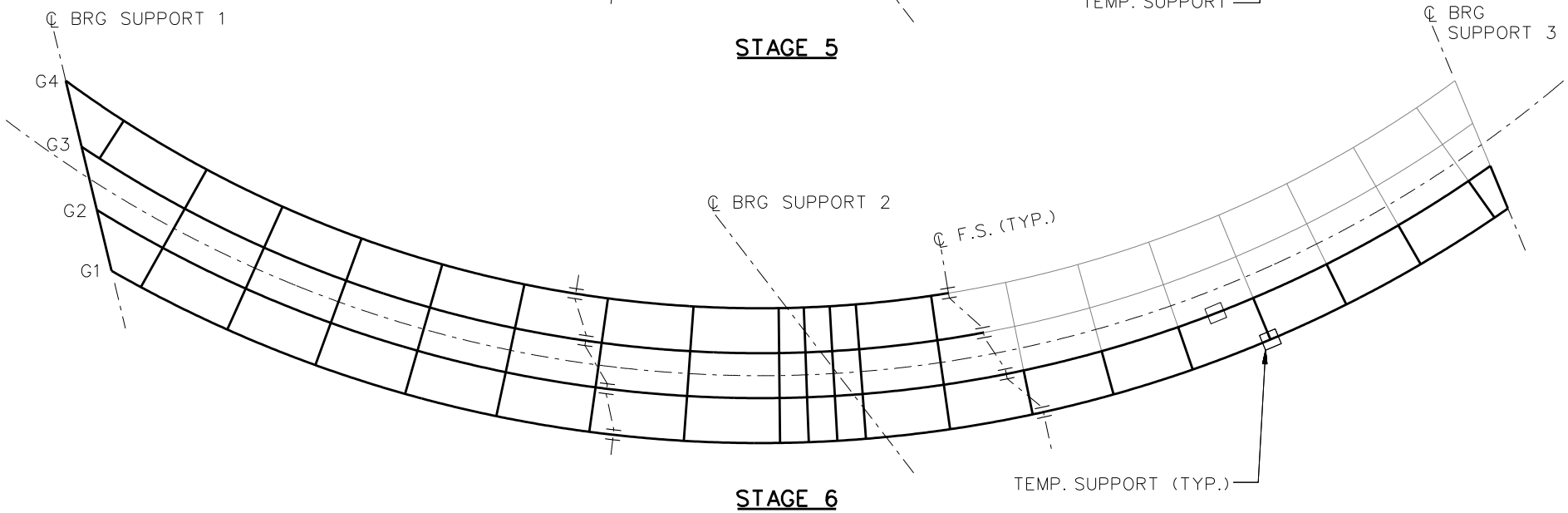

STAGE 6

LEGEND

▽ = HOLD OR LIFT CRANE

○ = TIE DOWN

□ = TEMPORARY SUPPORT STRUCTURE

NCHRP 12-79

BRIDGE EICCS10

GIRDER ERECTION PROCEDURE

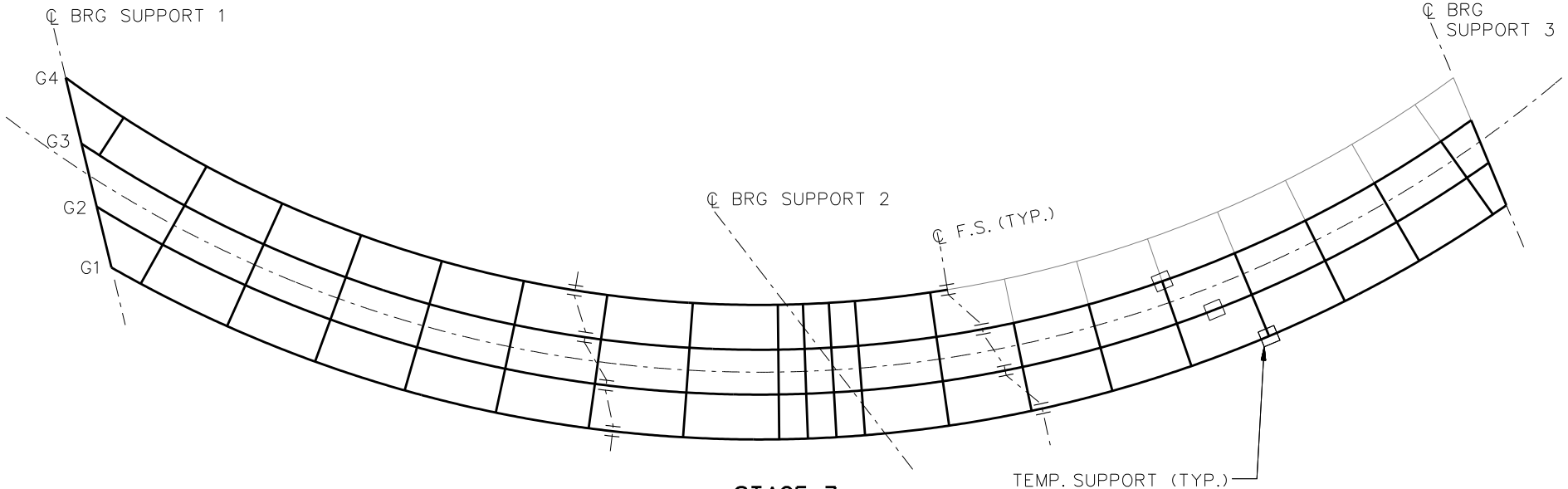

STAGE 7

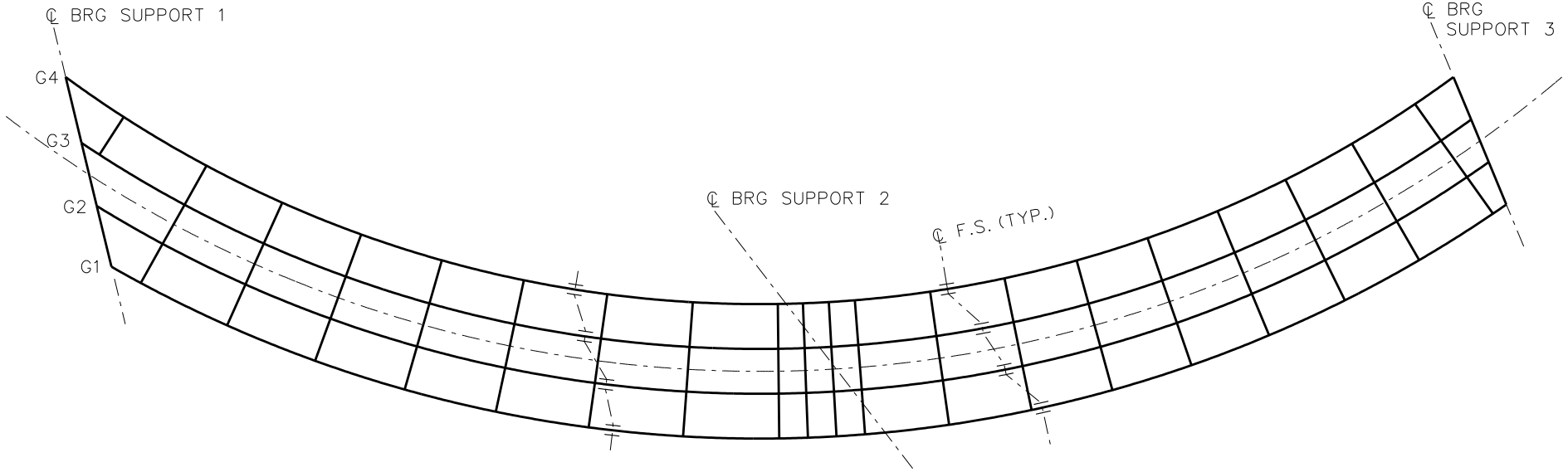

STAGE 8
(FINAL STEEL DL)

LEGEND

▽ = HOLD OR LIFT CRANE

○ = TIE DOWN

□ = TEMPORARY SUPPORT STRUCTURE

NCHRP 12-79

BRIDGE EICCS10

GIRDER ERECTION PROCEDURE

NCHRP 12-79

EICCS27

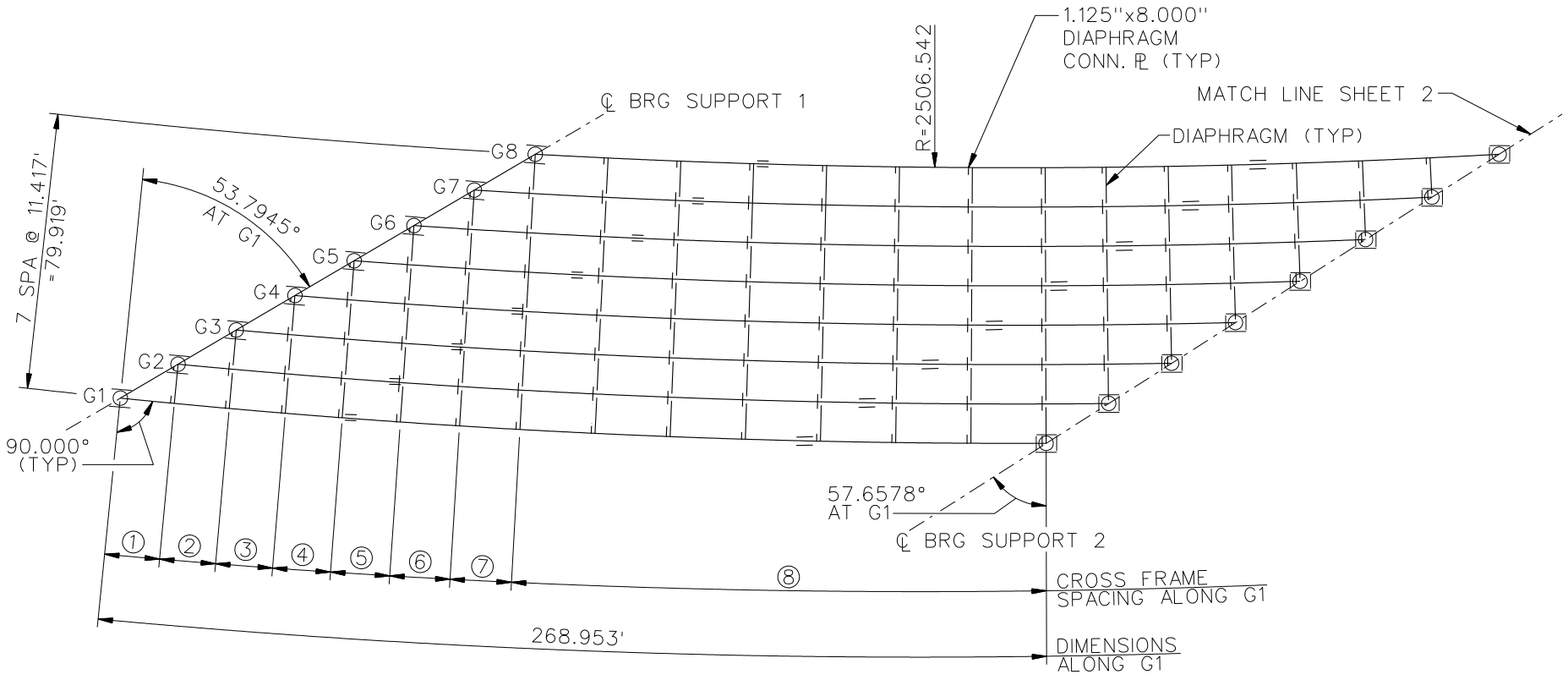

FRAMING PLAN

BEARING LEGEND

- ○ NON-GUIDED
- ○ LONGITUDINALLY GUIDED
- ○ TRANSVERSELY GUIDED
- ○ FIXED

NCHRP 12-79

BRIDGE EICCS27

FRAMING PLAN 1

SHEET 1 OF 13

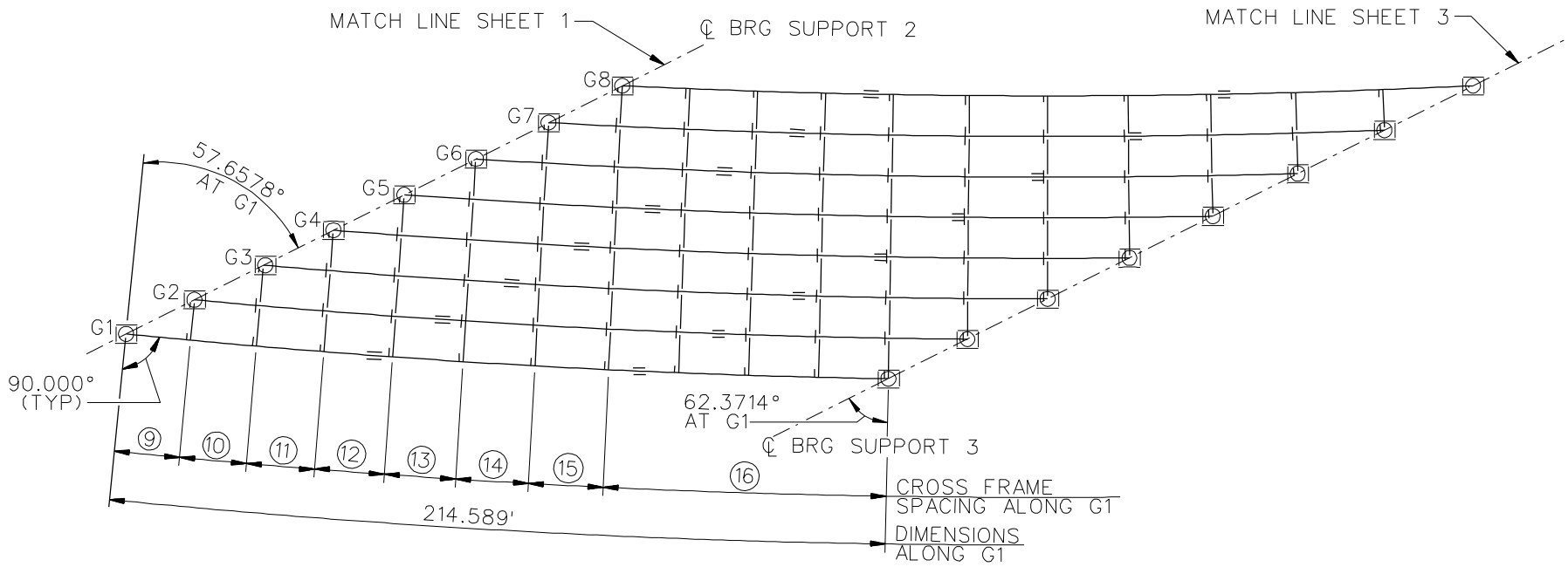

FRAMING PLAN

BEARING LEGEND

- ○ NON-GUIDED
- ○ LONGITUDINALLY GUIDED
- ○ TRANSVERSELY GUIDED
- ○ FIXED

NCHRP 12-79

BRIDGE EICCS27

FRAMING PLAN 2

SHEET 2 OF 13

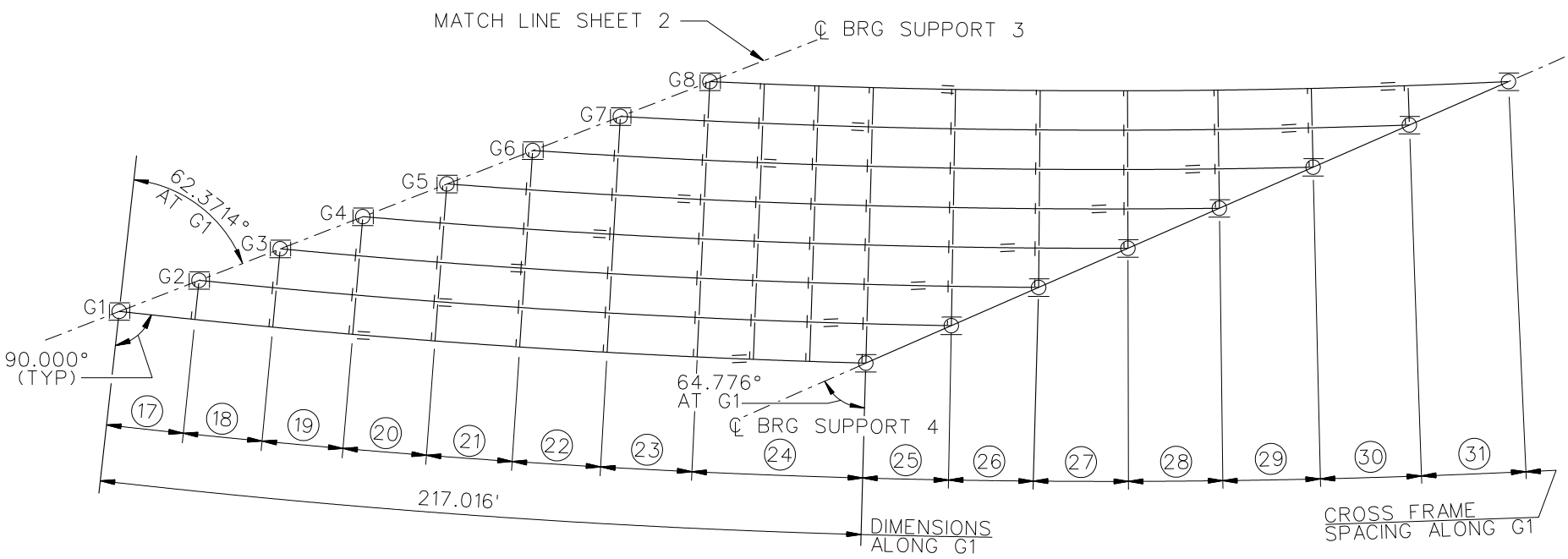

FRAMING PLAN

BEARING LEGEND

- ○ NON-GUIDED
- ⊖ LONGITUDINALLY GUIDED
- |○| TRANSVERSELY GUIDED
- ⊡ FIXED

NCHRP 12-79

BRIDGE EICCS27

FRAMING PLAN 3

SHEET 3 OF 13

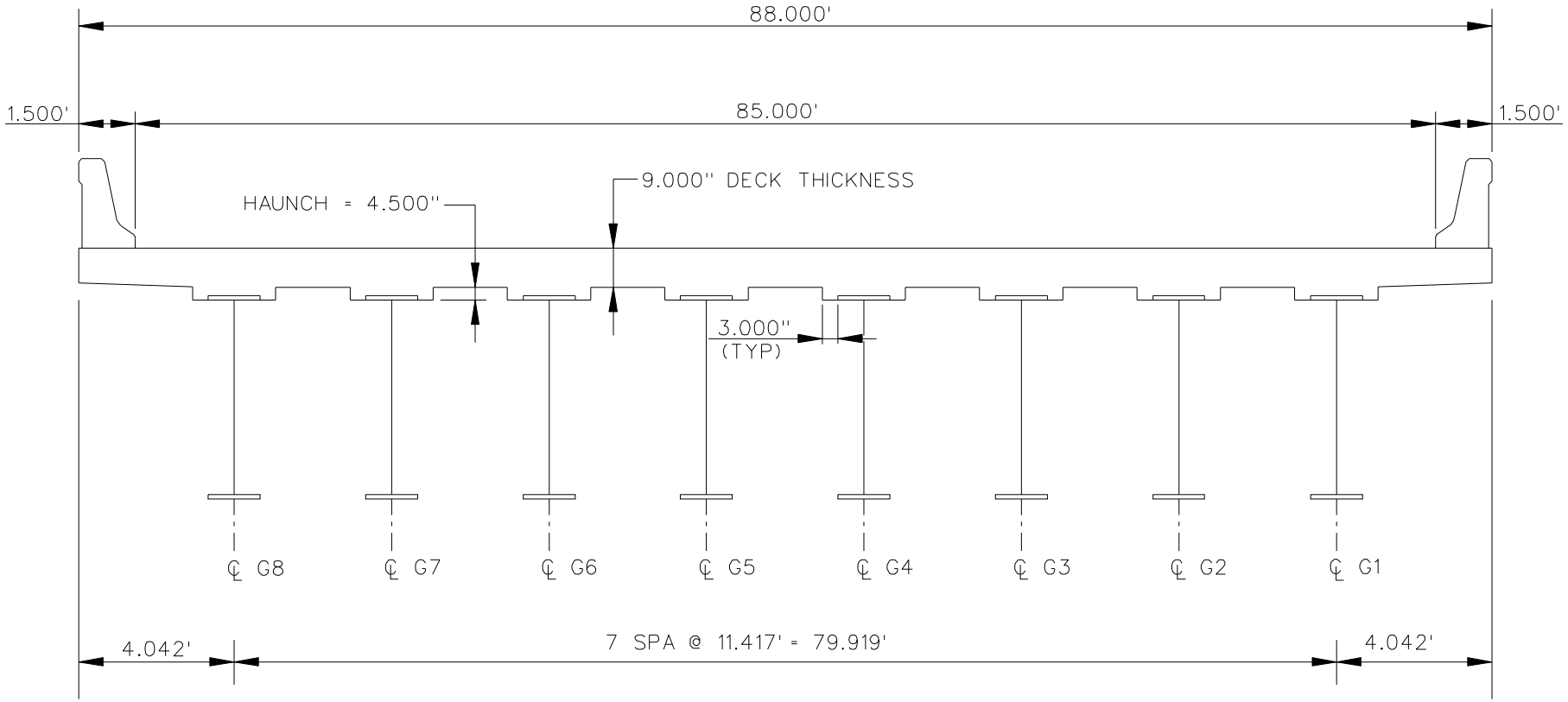

TYPICAL CROSS SECTION

NCHRP 12-79

BRIDGE EICCS27

TYPICAL SECTION

SHEET 4 OF 13

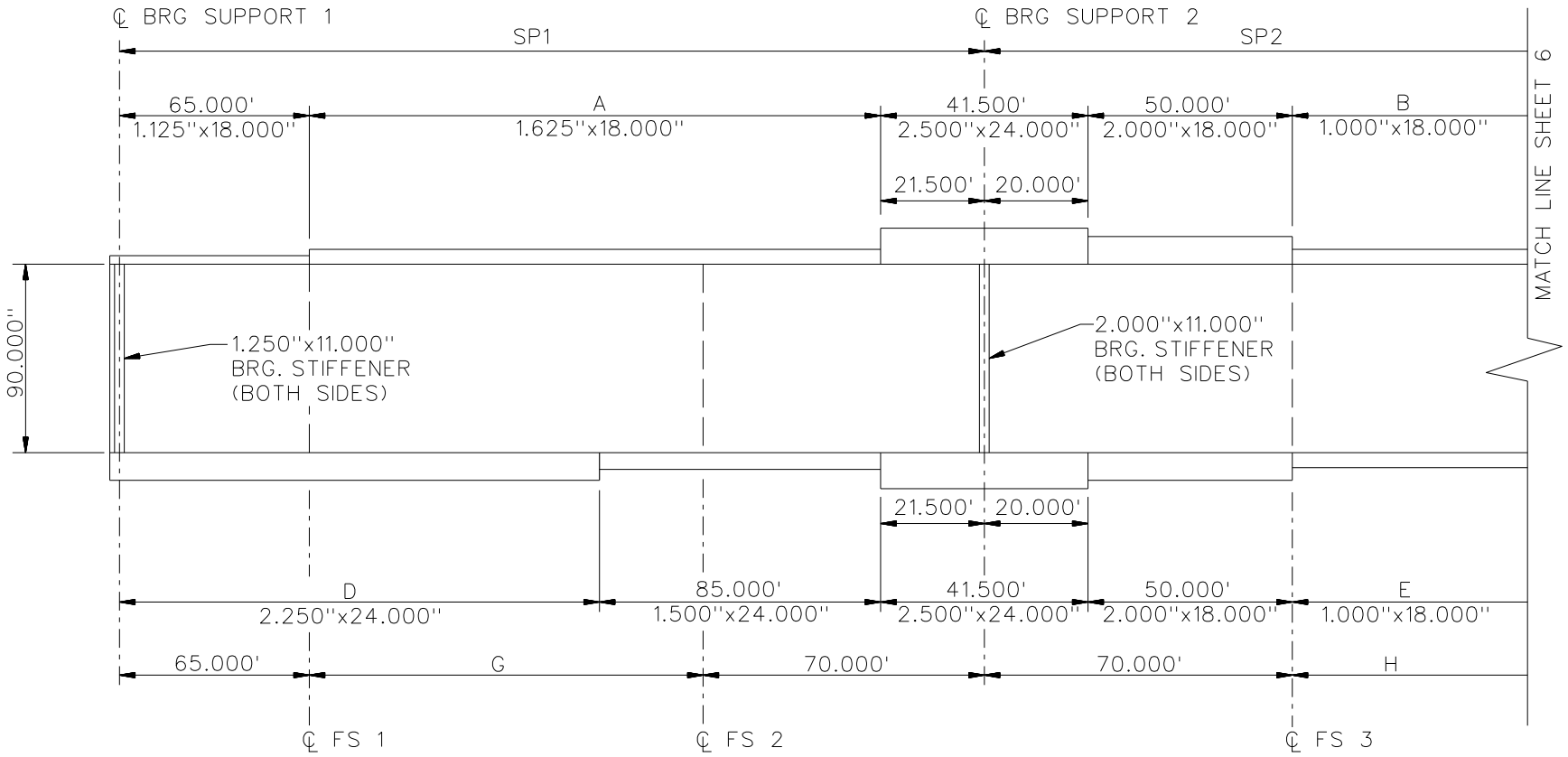

GIRDER ELEVATION

(TYP ALL GIRDERS)

NOTES:

1. WEB THICKNESS IS 0.750'' FOR ALL FIELD PIECES AND ALL GIRDERS.

NCHRP 12-79

BRIDGE EICCS27

GIRDER ELEVATIONS

SHEET 5 OF 13

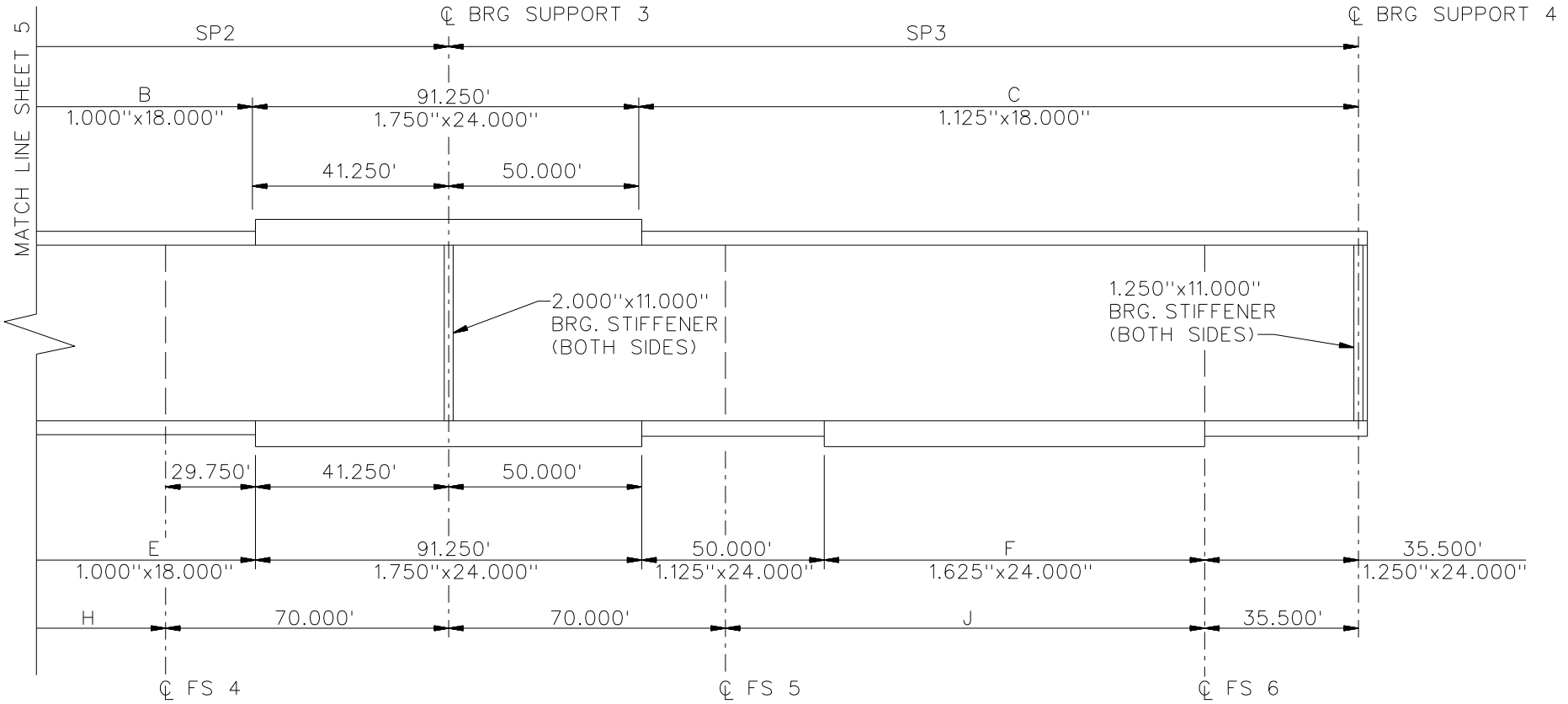

GIRDER ELEVATION

(TYP ALL GIRDERS)

NOTES:

1. WEB THICKNESS IS 0.750'' FOR ALL FIELD PIECES AND ALL GIRDERS.

NCHRP 12-79

BRIDGE EICCS27

GIRDER ELEVATIONS

SHEET 6 OF 13

	RADIUS (FT)	SPAN LENGTHS (FT)		
		SP1	SP2	SP3
G1	2586.458	268.953	214.589	217.016
G2	2575.042	270.237	217.501	218.549
G3	2563.625	271.594	220.582	220.228
G4	2552.208	273.031	223.845	222.072
G5	2540.792	274.554	227.309	224.103
G6	2529.375	276.172	230.994	226.341
G7	2517.958	277.888	234.926	228.817
G8	2506.542	279.712	239.128	231.573

SPACING #	LENGTH (FT)	SPACING #	LENGTH (FT)
1	15.731	17	22.093
2	16.007	18	22.666
3	16.292	19	23.275
4	16.585	20	23.925
5	16.892	21	24.621
6	17.213	22	25.361
7	17.542	23	26.160
8	7 SPA @ 21.813	24	3 SPA @ 16.305
9	18.207	25	24.593
10	18.585	26	25.338
11	18.973	27	26.137
12	19.380	28	27.004
13	19.808	29	27.939
14	20.255	30	28.959
15	20.725	31	30.0174
16	4 SPA @ 19.664		

	DIMENSIONS (FT)								
	A	B	C	D	E	F	G	H	J
G1	182.453	103.339	167.016	162.453	103.339	81.516	133.953	74.589	111.516
G2	183.737	106.251	168.549	163.737	106.251	83.049	135.237	77.501	113.049
G3	185.094	109.332	170.228	165.094	109.332	84.728	136.594	80.582	114.728
G4	186.531	112.595	172.072	166.531	112.595	86.572	138.031	83.845	116.572
G5	188.054	116.059	174.103	168.054	116.059	88.603	139.554	87.309	118.603
G6	189.672	119.744	176.341	169.672	119.744	90.841	141.172	90.994	120.841
G7	191.388	123.676	178.817	171.388	123.676	93.317	142.888	94.926	123.317
G8	193.212	127.878	181.573	173.212	127.878	96.073	144.712	99.128	126.073

NCHRP 12-79

BRIDGE EICCS27

DIMENSION TABLES

SHEET 7 OF 13

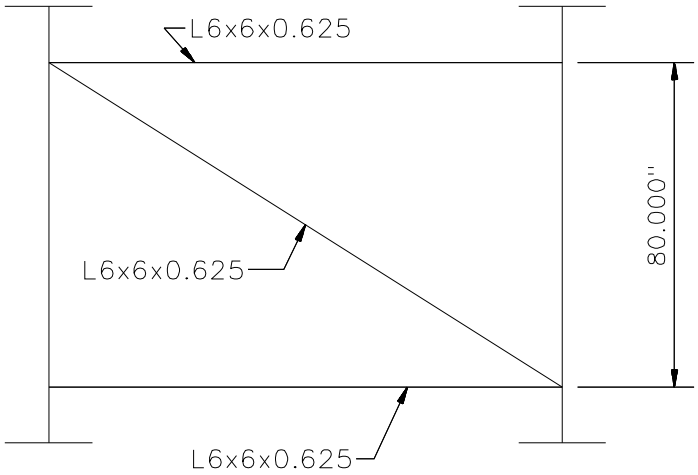

TYPICAL END AND INTERMEDIATE DIAPHRAGM

NOTES:

1. STEEL DEAD LOAD INCREASED BY 5% (MDX AND LARSA), 10% (APPROX), AND 2% (3D) TO ACCOUNT FOR MISC. DETAILS.
2. FORMWORK LOAD OF 10 PSF IS INCLUDED IN CONCRETE DEAD LOAD.
3. DIAPHRAGM MEMBER CALL-OUTS ARE IN UNITES OF INCHES.

NCHRP 12-79

BRIDGE EICCS27

MISC. DETAILS AND NOTES

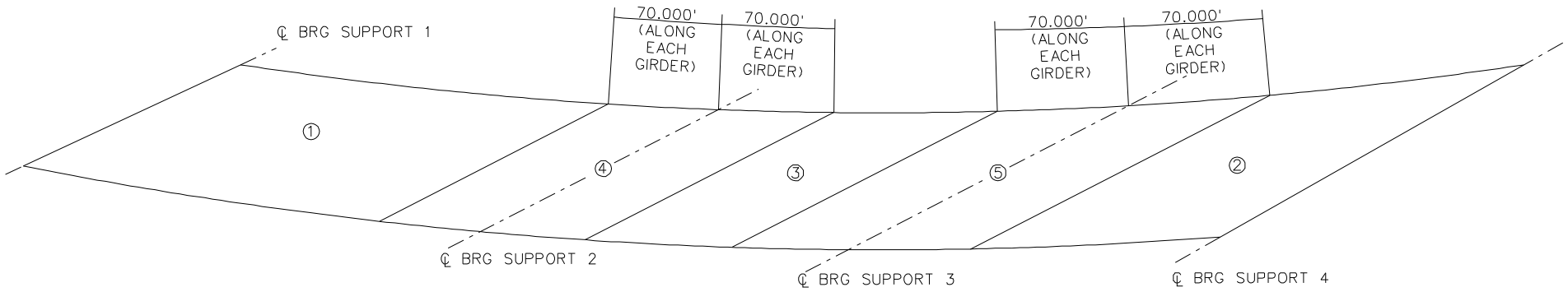

DECK POUR SEQUENCE

NCHRP 12-79

BRIDGE EICCS27

DECK POUR SEQUENCE

SHEET 9 OF 13

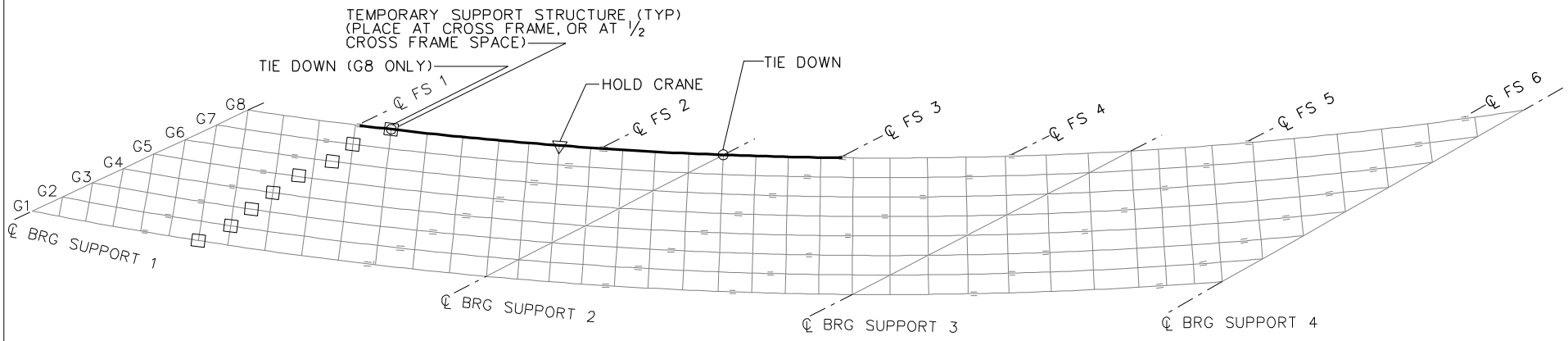

STAGE 1

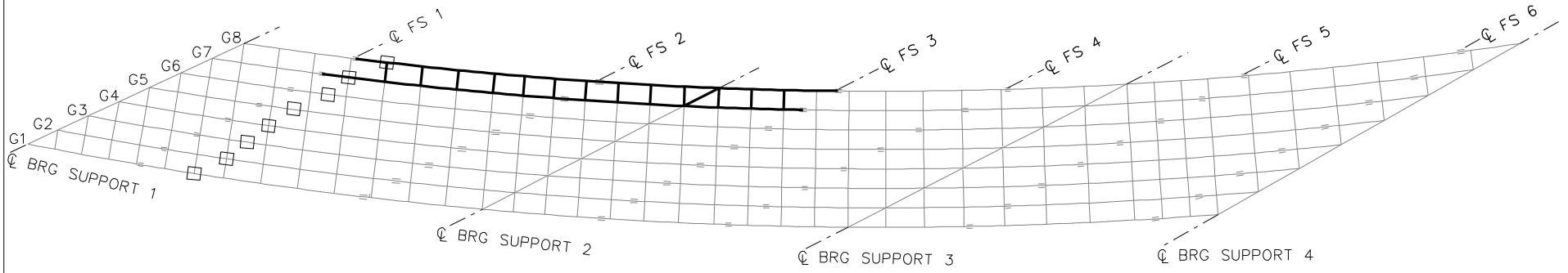

STAGE 2

LEGEND

▽ = HOLD OR LIFT CRANE

○ = TIE DOWN

□ = TEMPORARY SUPPORT STRUCTURE

NCHRP 12-79

BRIDGE EICCS27

GIRDER ERECTION PROCEDURE

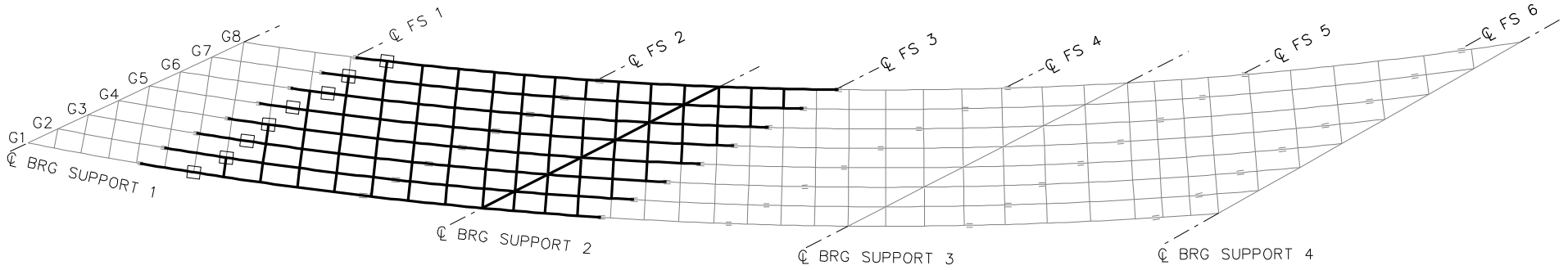

STAGE 8

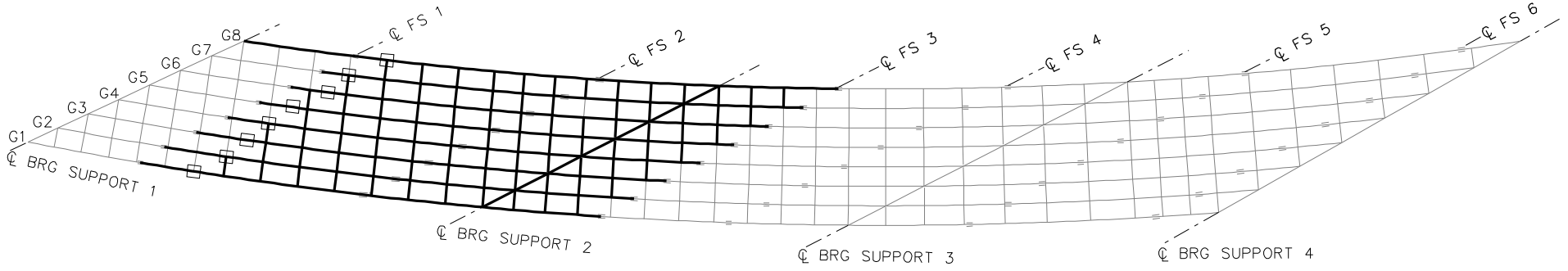

STAGE 9

ERECTION STAGES THAT FOLLOW:

10 - ERECT G7, AND CROSS FRAMES BETWEEN G7 AND G8
11 - ERECT G6 AND CROSS FRAMES
12 - ERECT G5 AND CROSS FRAMES
13 - ERECT G4 AND CROSS FRAMES
14 - ERECT G3 AND CROSS FRAMES
15 - ERECT G2 AND CROSS FRAMES
16 - ERECT G1 AND CROSS FRAMES

LEGEND

▽ = HOLD OR LIFT CRANE

○ = TIE DOWN

□ = TEMPORARY SUPPORT STRUCTURE

NCHRP 12-79

BRIDGE EICCS27

GIRDER ERECTION PROCEDURE

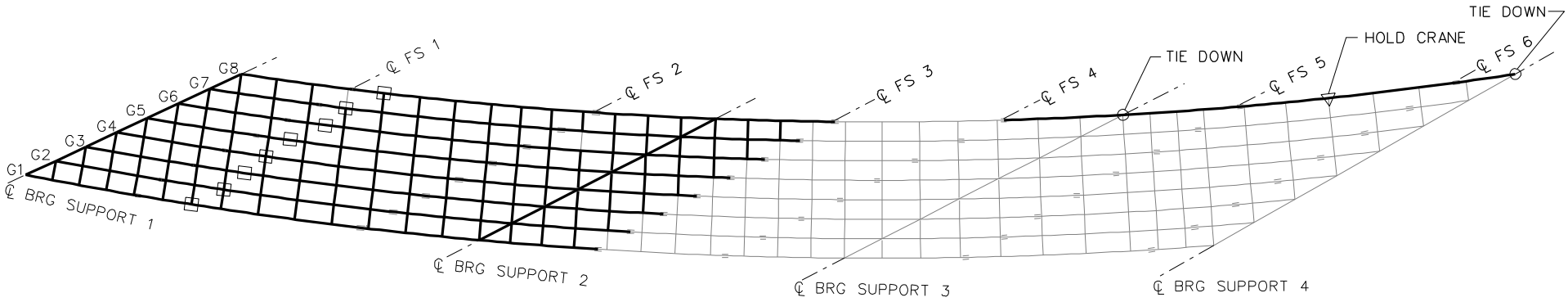

STAGE 17

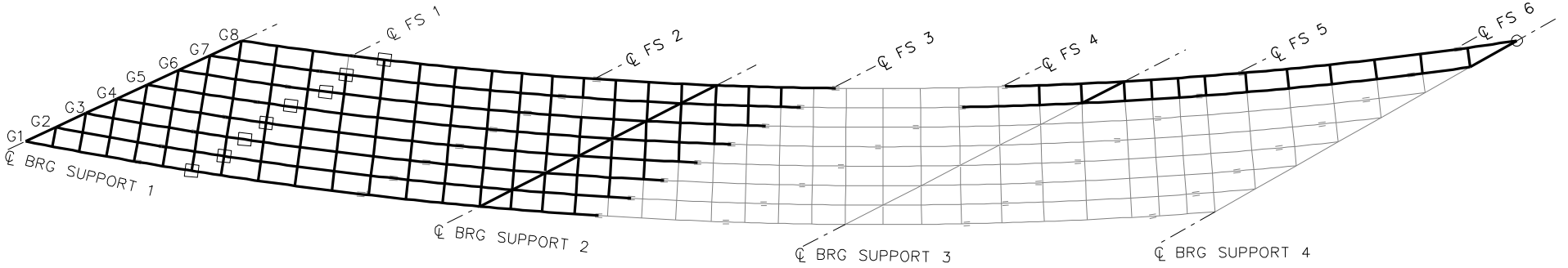

STAGE 18

ERECTION STAGES THAT FOLLOW:

19 - ERECT G6, AND CROSS FRAMES
20 - ERECT G5 AND CROSS FRAMES
21 - ERECT G4 AND CROSS FRAMES
22 - ERECT G3 AND CROSS FRAMES
23 - ERECT G2 AND CROSS FRAMES
24 - ERECT G1 AND CROSS FRAMES

LEGEND

▽ = HOLD OR LIFT CRANE

○ = TIE DOWN

□ = TEMPORARY SUPPORT STRUCTURE

NCHRP 12-79

BRIDGE EICCS27

GIRDER ERECTION PROCEDURE

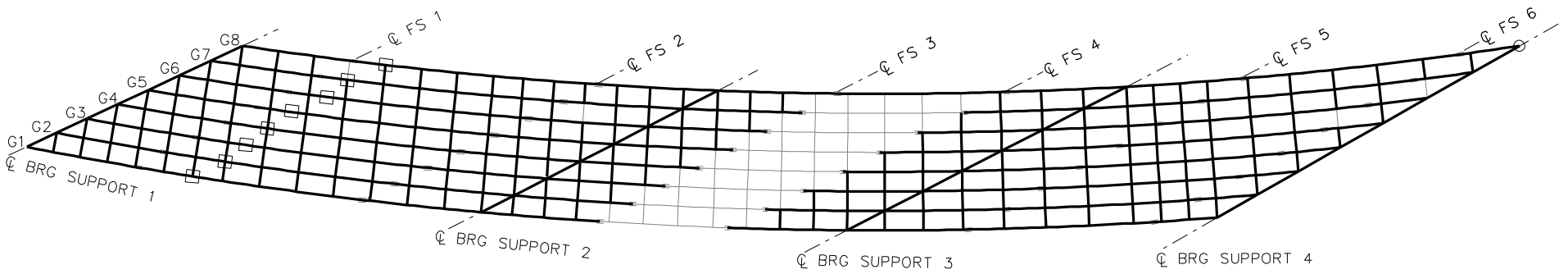

STAGE 18

ERECTION STAGES THAT FOLLOW:

26 - ERECT G7, AND CROSS FRAMES
27 - ERECT G6, AND CROSS FRAMES
28 - ERECT G5 AND CROSS FRAMES
29 - ERECT G4 AND CROSS FRAMES
30 - ERECT G3 AND CROSS FRAMES
31 - ERECT G2 AND CROSS FRAMES
32 - ERECT G1 AND CROSS FRAMES
33 - REMOVE TEMPORARY SUPPORTS

NCHRP 12-79

BRIDGE EICCS27

GIRDER ERECTION PROCEDURE

NCHRP 12-79

EICSS1

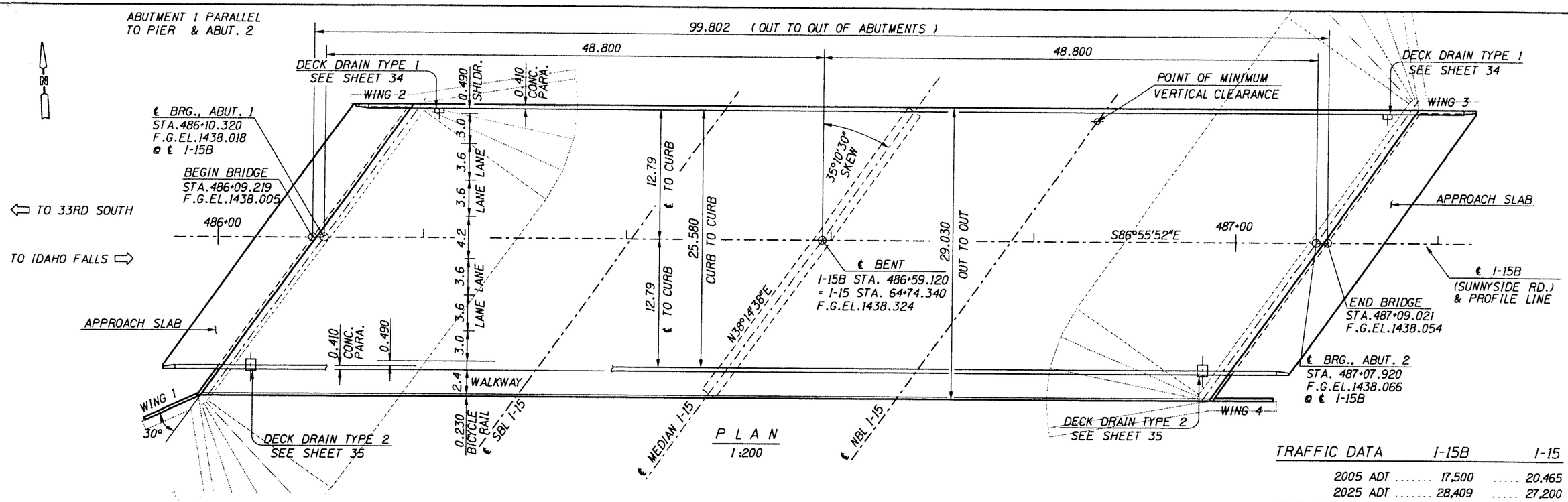

P L A N
1:200

TRAFFIC DATA	I-15B	I-15
2005 ADT	17,500	20,465
2025 ADT	28,409	27,200
2005 ADT % TRUCK	13	13
2025 ADT % TRUCK	13	13
DESIGN SPEED	90 km/h	120 km/h

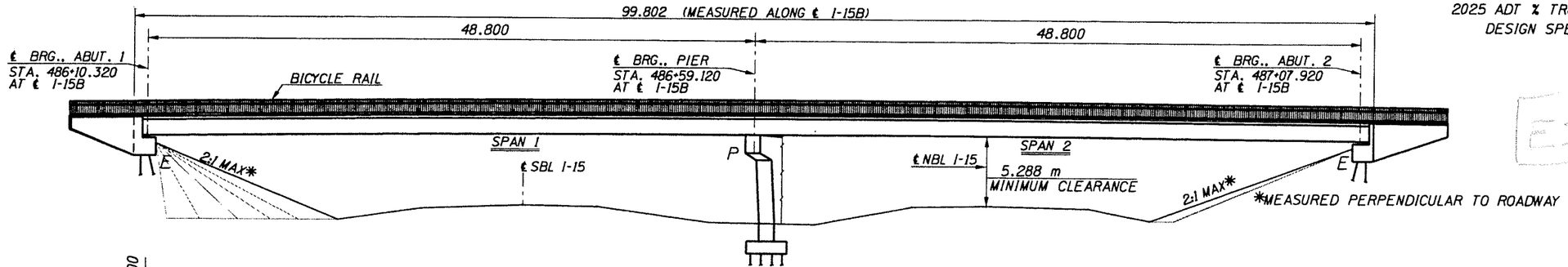

E L E V A T I O N
(VIEW ALONG RT. EDGE OF DECK)
1:200

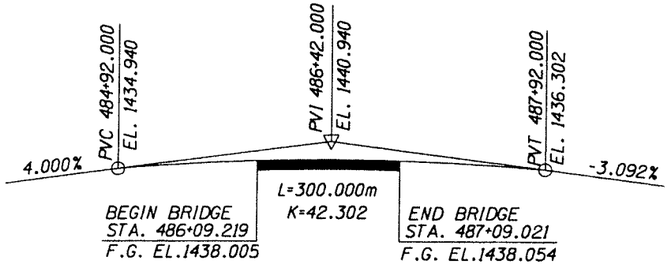

P R O F I L E D A T A
NOT TO SCALE

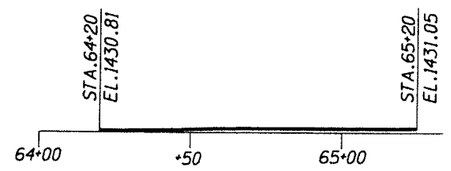

EXISTING
CENTERLINE PROFILE SBL I-15
NOT TO SCALE

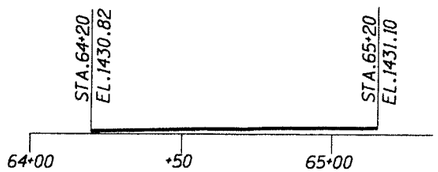

EXISTING
CENTERLINE PROFILE NBL I-15
NOT TO SCALE

ALL DIMENSIONS ARE IN METERS
UNLESS NOTED OTHERWISE.

EICSS

REVISIONS			
NO.	DATE	BY	DESCRIPTION

DESIGNED L. ZARATE
DESIGN CHECKED J. VETTER/K. CLAUSEN
DETAILED A. BASTON
DWG. CHECKED L. ZARATE
CORRECTIONS

SCALES SHOWN ARE FOR 864 mm X 559 mm PRINTS ONLY
CADD FILE NO. f:\projects\pr7771\7771br01.dgn
DRAWING DATE: 01/23/2004

ORIGINAL SIGNED BY: PROFESSIONAL ENGINEER REGISTERED 6518 STATE OF IDAHO LUIS R. ZARATE
ORIGINAL DATE SIGNED: JANUARY 23,2004
ORIGINAL STORED AT ITD BRIDGE SECTION

ORIGINAL APPROVED BY: REGISTERED PROFESSIONAL ENGINEER 4701 STATE OF IDAHO MATTHEW M. FARRAR
BRIDGE ENGINEER
DATE SIGNED: JANUARY 23,2004

IDAHO TRANSPORTATION DEPARTMENT

metric

PROJECT NO.
IM-NH-15-3(106)113

SITUATION AND LAYOUT
100 m STEEL OVERPASS
SUNNYSIDE ROAD I.C. (I-15B) OVER I-15
I-15B STA. 486+59.12 I-15 STA. 64+74.34

BRIDGE PLANS
BRIDGE INSPECTION MASTER KEY 21614
COUNTY BONNEVILLE
KEY NO. 7771
BRIDGE DRAWING NO. 15779
SHEET 1 OF 44

DESIGN NOTES

DESIGN SPECIFICATIONS

IN ACCORDANCE WITH : "AASHTO LRFD BRIDGE DESIGN SPECIFICATION" 2nd EDITION.

DESIGN PROCEDURES

DECK SLAB DESIGNED USING EMPIRICAL DESIGN METHOD. PIER DESIGNED FOR VEHICULAR COLLISION FORCE. GIRDERS DESIGNED USING MERLIN-DASH VERSION 2.2 LRFD COMPUTER PROGRAM. WING WALLS DESIGNED FOR AT-REST SOIL CONDITION.

DESIGN LOADS

PERMANENT LOADS

DC	UNIT WEIGHT OF REINFORCED CONCRETE	23.6 kN/m³
	UNIT WEIGHT OF STRUCTURAL STEEL	77.0 kN/m³
	METAL RAIL OVER PARAPET	0.245 kN/m³
	METAL DECK FORMS	0.77 kN/m²
	CONCRETE PARAPET (CONCRETE ONLY)	4.6 kN/m²
	BICYCLE RAIL	1.291 kN/m²
DW	FUTURE WEARING SURFACE	1.05 kN/m²
EV	UNIT WEIGHT OF SOIL	19.6 kPA/m
	ANGLE OF INTERNAL FRICTION, ø	34°
EH	EQUIVALENT ACTIVE FLUID PRESSURE	5.5 kPA/m
	EQUIVALENT AT REST FLUID PRESSURE	8.6 kPA/m

TRANSIENT LOADS

LL	HL-93 INCLUDING PAIR OF DESIGN TANDEMS IN NEGATIVE MOMENT REGIONS	
IM	DYNAMIC ALLOWANCE APPLIED TO TRUCK & TANDEM	
LS	LIVE LOAD SURCHARGE AT ABUTMENT	0.0 m
	LIVE LOAD SURCHARGE AT WINGWALL	0.0 m

THERMAL LOADS

TU	UNIFORM TEMPERATURE RANGE	(-)35° C TO 50° C
	BASE SETTING TEMPERATURE	16 °C

EXTREME EVENT LOADS

EQ	ACCELERATION COEFFICIENT	0.13 g
	SOIL PROFILE TYPE	I
	SEISMIC PERFORMANCE ZONE	2
CT	RAILING TEST LEVEL	TL-4
	VEHICULAR COLLISION FORCE	1800 kN

LOAD FACTORS

IN ACCORDANCE WITH ITD LRFD MANUAL

ELASTOMERIC BEARINGS

DESIGN PROCEDURE: METHOD A
GRADE: 4
DESIGN LOADS: 1,170 kN (SERVICE I)

PILE DESIGN LOADS

ABUTMENTS 1 & 2

STRENGTH LIMIT STATE (VERTICAL)
q_n = 3,060 kN/PILE
RESISTANCE FACTOR $\phi_{BEARING}$ = 0.5
ϕQn = 1,530 kN/PILE
Q max = 796 kN/PILE
Q min = -27 kN/PILE (UPLIFT)

SERVICE LIMIT STATE (LATERAL - STRONG AXIS)
DESIGN FACTOR $\phi_{LATERAL}$ = 1.00
* ϕVn = 133 kN/PILE
γV = 36 kN/PILE

* BASED ON PILE DISPLACEMENT = 6.40 mm

GENERAL NOTES

CONSTRUCTION SPECIFICATIONS

MATERIALS, CONSTRUCTION AND WORKMANSHIP SHALL BE IN ACCORDANCE WITH THE STATE OF IDAHO TRANSPORTATION DEPARTMENT, "STANDARD SPECIFICATIONS FOR HIGHWAY CONSTRUCTION", 1999 EDITION, THE PROJECT PLANS AND SUPPLEMENTAL SPECIFICATIONS UNLESS NOTED OTHERWISE.

MATERIAL

CONCRETE : DECK SLAB AND PARAPET - CLASS 27.5 AF ..... f'c = 27.5 MPa
ABUTMENTS AND WINGS - CLASS 27.5 BF ..... f'c = 27.5 MPa
METAL REINFORCEMENT : AASHTO M31, GRADE 420 ..... fy = 414 MPa
STRUCTURAL STEEL : GIRDER FLANGES & WEBS - AASHTO M270M GRADE HPS 485W ..... fy = 485 MPa
CROSS-FRAMES & STIFFENERS - AASHTO M270M GRADE 345W ..... fy = 345 MPa
IN ACCORDANCE WITH AASHTO M270M SUPPLEMENTARY REQUIREMENT S4, THE BASE METAL & WELD METAL CHARPY V-NOTCH REQUIREMENT SHALL MEET ZONE (3).
HIGH STRENGTH BOLTS : AASHTO M164 TYPE 3
CARBON STEEL BOLTS : ASTM A307
ELASTOMERIC BEARINGS: GRADE 4, 60-DUROMETER POLYISOPRENE.

PLAN DIMENSIONS AND ELEVATIONS

ALL EXPOSED EDGES OF CONCRETE SHALL BE BEVELED 20 mm UNLESS NOTED OTHERWISE.
ALL DIMENSIONS TO REINFORCING STEEL ARE TO CENTERLINE OF BAR UNLESS NOTED OTHERWISE.
CONCRETE COVER MEASURED FROM THE FACE OF THE CONCRETE TO THE FACE OF ANY REINFORCING BAR SHALL BE 50 mm, UNLESS SHOWN OTHERWISE ON THE DRAWINGS.

CONSTRUCTION

ALL REINFORCING STEEL TO BE EPOXY COATED IS DESIGNATED BY AN "E" AFTER THE BAR MARK.
CONSTRUCTION JOINTS WILL BE PERMITTED ONLY AT THE LOCATIONS SHOWN ON THE PLANS OR AS APPROVED BY THE ENGINEER.
ALL SURFACES OF THE SUBSTRUCTURE EXCEPT WINGWALLS WHICH WILL BE EXPOSED ON THE COMPLETED STRUCTURE SHALL BE PROTECTED TO PREVENT STAINING WITH PLASTIC SHEETS OR OTHER APPROVED METHODS UNTIL DECK PLACEMENT IS COMPLETED AND GIRDERS ARE BLAST CLEANED.
WELDED FABRICATION SHALL BE IN ACCORDANCE WITH ANSI/AASHTO/AWS D 1.5 AND ALL INTERIM REVISIONS PUBLISHED BY AASHTO.

INCIDENTAL ITEMS

ALL ITEMS SHOWN OR NOTED ON PLANS WHICH ARE NOT SPECIFICALLY BID ITEMS ARE CONSIDERED INCIDENTAL ITEMS. THE COST OF FURNISHING AND INSTALLING ALL INCIDENTAL ITEMS WILL NOT BE PAID FOR SEPERATELY BUT SHALL BE INCLUDED IN THE UNIT PRICE BID FOR OTHER ITEMS, UNLESS NOTED OTHERWISE.

PIER

STRENGTH LIMIT STATE (VERTICAL)
qn = 3,060 kN/PILE
RESISTANCE FACTOR $\phi_{BEARING}$ = 0.5
ϕQn = 1,530 kN/PILE
Q max = 1090 kN/PILE
Q min = 170 kN/PILE

EXTREME EVENT I LIMIT STATE (VERTICAL)
RESISTANCE FACTOR ϕ = 1.00
ϕQn (bearing) = 3,060 kN/PILE
ϕQn (uplift) = -440 kN/PILE
Q max = 1220 kN/PILE
Q min = -200 kN/PILE

SERVICE LIMIT STATE (LATERAL)
STRONG AXIS
DESIGN FACTOR $\phi_{LATERAL}$ = 1.00
* ϕVn = 1120 kN/PILE GROUP
γV = 1080 kN/PILE GROUP
WEAK AXIS
DESIGN FACTOR $\phi_{LATERAL}$ = 1.00
* ϕVn = 780 kN/PILE GROUP
γV = 130 kN/PILE GROUP

* BASED ON PILE GROUP DISPLACEMENT = 6.40 mm

REVISIONS				DESIGNED	SCALES SHOWN ARE FOR 864 mm X 559 mm PRINTS ONLY	ORIGINAL SIGNED BY:	IDAHO TRANSPORTATION DEPARTMENT	metric	DESIGN AND GENERAL NOTES	BRIDGE PLANS
NO.	DATE	BY	DESCRIPTION	L. ZARATE/R. JENSEN				PROJECT NO.	100 m STEEL OVERPASS	BRIDGE INSPECTION MASTER KEY
				DESIGN CHECKED J. VETTER/K. CLAUSEN	CADD FILE NO. f:\projects\pr7771\7771br02.dgn	ORIGINAL DATE SIGNED: JANUARY 23,2004	ORIGINAL APPROVED BY: BRIDGE ENGINEER MATTHEW M. FARRAR	IM-NH-15-3(106)113	SUNNYSIDE ROAD I.C. (I-15B) OVER I-15	COUNTY BONNEVILLE / KEY NO. 7771
				DETAILED A. BASTON	DRAWING DATE: 01/23/2004	ORIGINAL STORED AT ITD BRIDGE SECTION	ORIGINAL SIGNED ON DATE: JANUARY 23,2004		I-15B STA.486+59.12 I-15 STA.64+74.34	BRIDGE DRAWING NO. 15779 / SHEET 2 OF 44
				DWG. CHECKED L. ZARATE						
				CORRECTIONS						

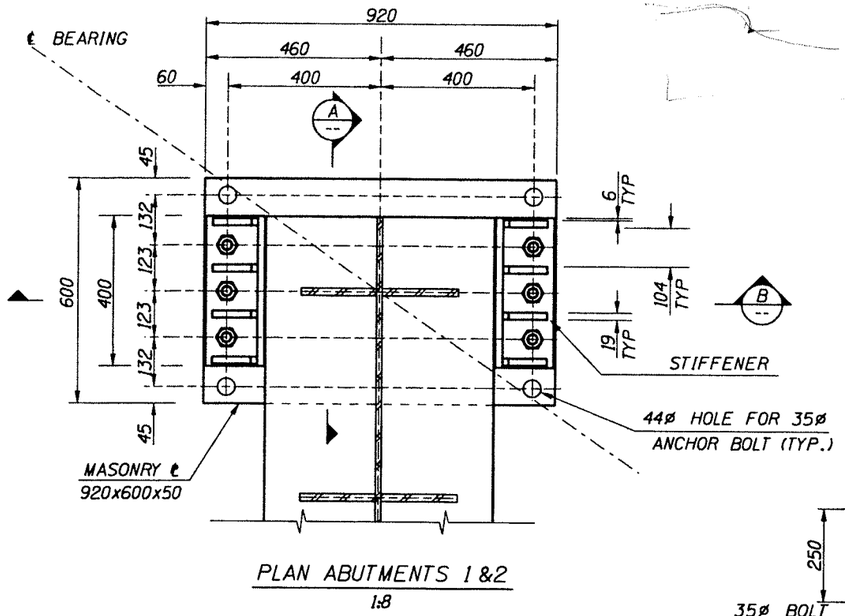

PLAN ABUTMENTS 1 &2
1:8

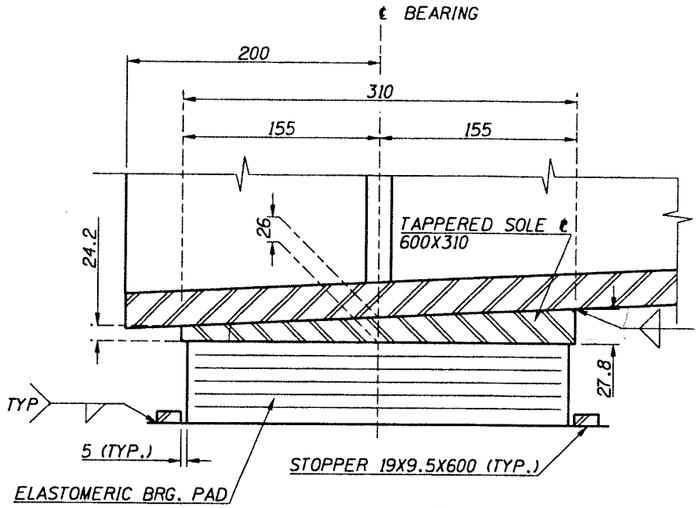

SECTION A
N.T.S.

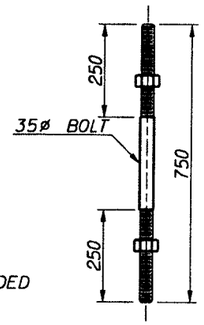

ANCHOR BOLT DETAIL
1:8

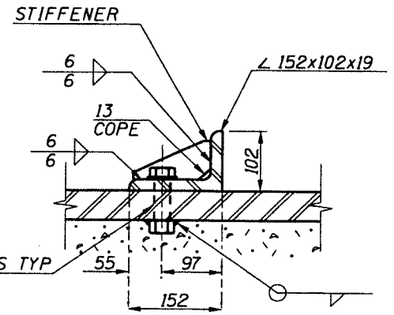

DETAIL 1
1:5

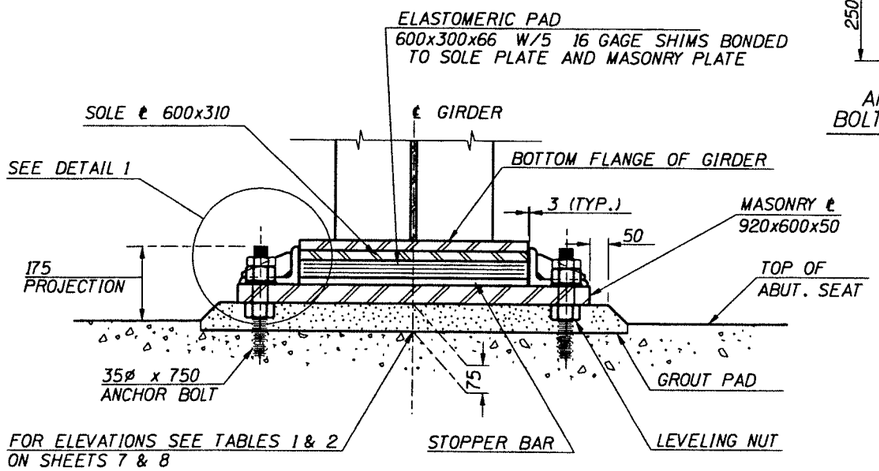

SECTION B
1:8

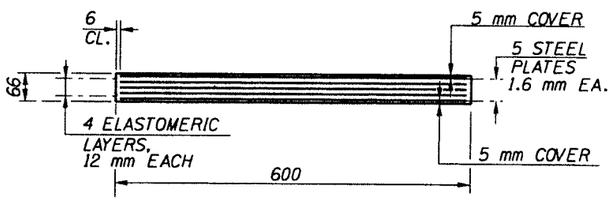

SECTION C
N.T.S.

BEARING NOTES

GENERAL

ANCHOR BOLTS & NUTS SHALL BE ASTM F-1554 GRADE 36, HOT DIP ZINC COATED.
STRUCTURAL STEEL SHALL CONFORM TO AASHTO M270M 345W.
GROUT SHALL MEET THE REQUIREMENTS OF SUBSECTION 506.03.1.2 FOR GROUT, TYPE B CLASS 1.
ALL EXPOSED METAL SURFACES, SHALL BE CLEANED AND PRIMED AT THE FABRICATION PLANT.
THE SURFACES SHALL BE PAINTED IN ACCORDANCE WITH SECTION 627. PAINT SYSTEM NO. D, EXCEPT THAT COLOR SHALL BE GRAY TO MATCH THAT OF CONCRETE.
THE COST OF FURNISHING AND INSTALLING BEARING UNITS SHALL BE INCLUDED IN THE UNIT PRICE BID FOR "S501-25F SP-BRIDGE, STEEL BRIDGE (HPS)"
SHOP DRAWINGS SHALL BE IN ACCORDANCE WITH SUBSECTION 504.01.G.

PIN BEARING

127 x 446 PIN BLOCK SHALL CONFORM TO ASTM 668 CLASS D WITH SUPPLEMENTAL REQUIREMENTS S4.
76 ø PIN SHALL CONFORM TO ASTM 668 CLASS G WITH SUPPLEMENTAL REQUIREMENTS S4.
PIN NUTS SHALL CONFORM TO AASHTO M291, GRADE DH.
CLEAN BEARING PIN AND ADJOINING SURFACES AND COAT THESE SURFACES WITH MOLUB ALLOY 369 DRY FILM LUBRICANT OR APPROVED EQUAL.
LINE DRILL UPPER AND LOWER BEARING BLOCK AFTER ASSEMBLY.
TIGHTEN PIN NUTS TO SNUG TIGHT, THEN SET 10 mm ø SOCKET HEAD SET SCREW.
UPPER TABS AND UPPER BEARING CRADLE SHALL BE WELDED TOGETHER PRIOR TO WELDING WHOLE ASSEMBLY TO SOLE PLATE.
WELD UPPER TABS AND BEARING CRADLE TO SOLE PLATE WITH ONE ALL-AROUND WELD.

EXPANSION BEARING

ELASTOMERIC PADS SHALL BE STEEL REINFORCED, MADE OF 60-DUROMETER HARDNESS ELASTOMER.
THE PADS MUST BE SHOP BONDED TO INTERMEDIATE PLATES AT THE FABRICATION PLANT.

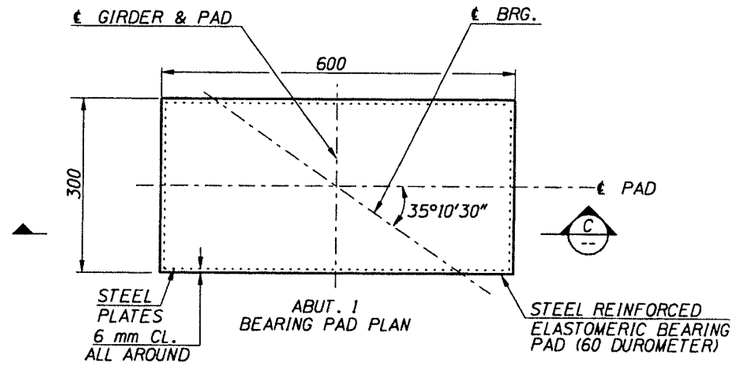

BEARING PAD PLAN
N.T.S.

ALL DIMENSIONS ARE IN MILLIMETERS UNLESS NOTED OTHERWISE

REVISIONS			
NO.	DATE	BY	DESCRIPTION

DESIGNED L. ZARATE
DESIGN CHECKED K. CLAUSEN
DETAILED A. BASTON
DWG. CHECKED L. ZARATE
CORRECTIONS G.B.

SCALES SHOWN ARE FOR 864 mm X 559 mm PRINTS ONLY
CADD FILE NO. f:\proj\projects\pr\f7771\7771br19.dgn
DRAWING DATE: 01/23/2004

ORIGINAL SIGNED BY:
PROFESSIONAL ENGINEER REGISTERED 6518 STATE OF IDAHO LUIS R. ZARATE
ORIGINAL DATE SIGNED: JANUARY 23 2004
ORIGINAL STORED AT ITD BRIDGE SECTION

IDAHO TRANSPORTATION DEPARTMENT

ORIGINAL APPROVED BY: BRIDGE ENGINEER MATTHEW M. FARRAR
ORIGINAL SIGNED ON DATE: JANUARY 23,2004

metric

PROJECT NO. NH-15-3(106)113

ABUTMENT BEARING DETAILS

100 m STEEL OVERPASS
SUNNYSIDE ROAD I.C. (I-15B) OVER I-15
I-15B STA. 486+59.12 I-15 STA. 64+74.34

BRIDGE PLANS
BRIDGE INSPECTION MASTER KEY
COUNTY BONNEVILLE
KEY NO. 7771
BRIDGE DRAWING NO. 15779
SHEET 19 OF 44

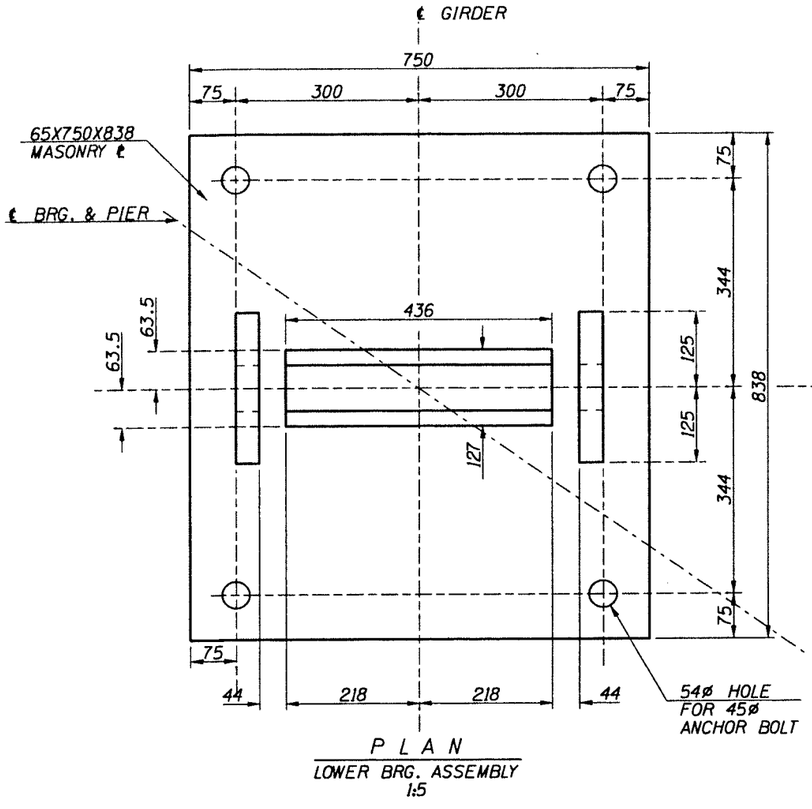

P L A N
LOWER BRG. ASSEMBLY
1:5

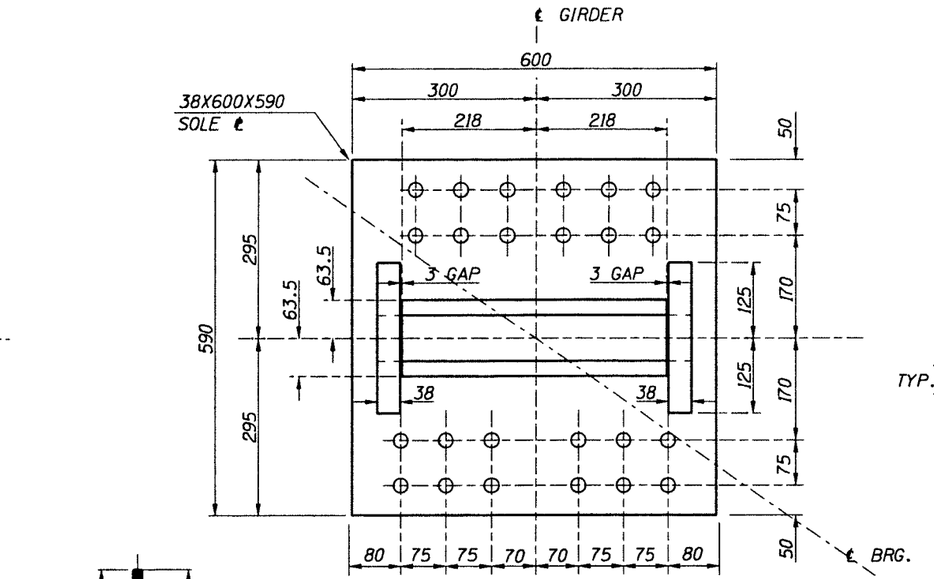

SECTION B
REFLECTED PLAN
UPPER BRG. ASSEMBLY
1:5

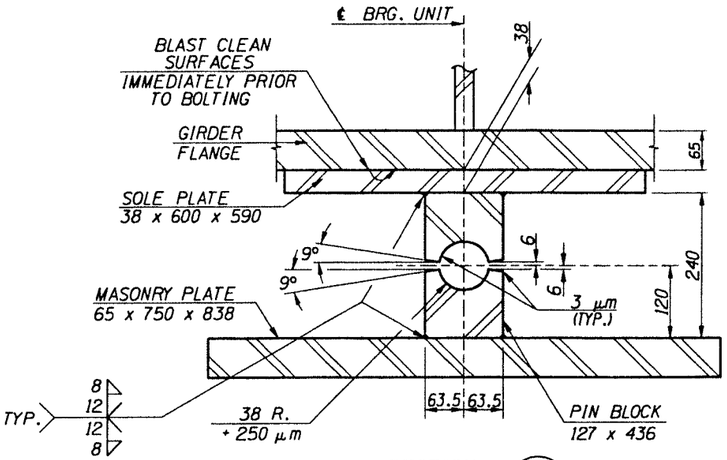

SECTION A
1:5

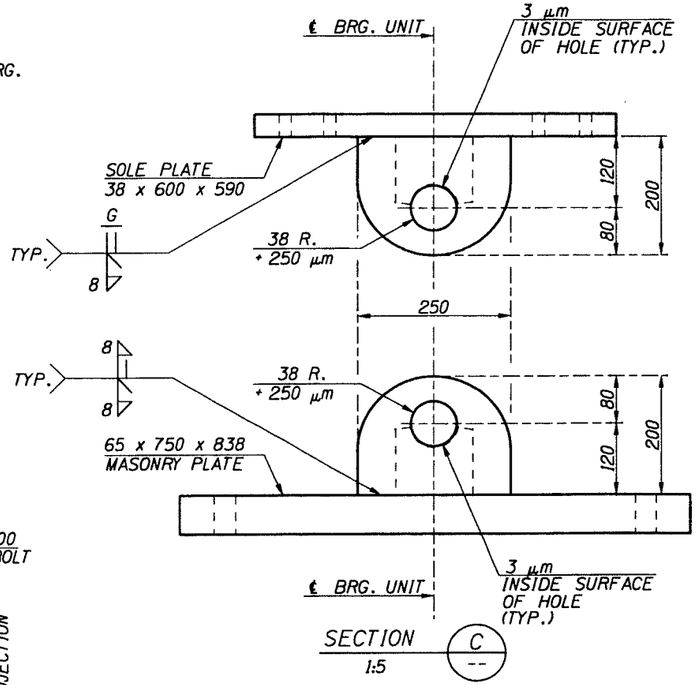

SECTION C
1:5

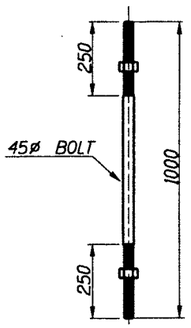

ANCHOR
BOLT DETAIL
1:10

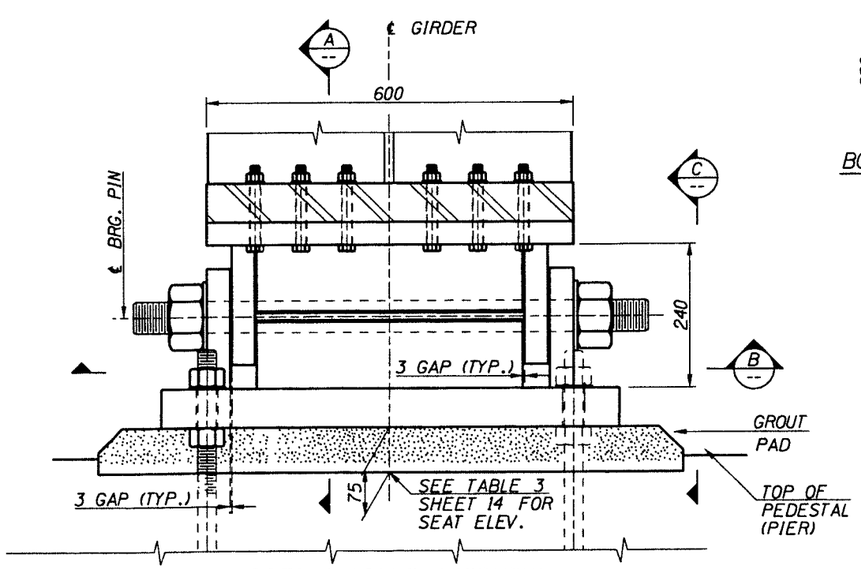

UPPER & LOWER ASSEMBLY
1:5

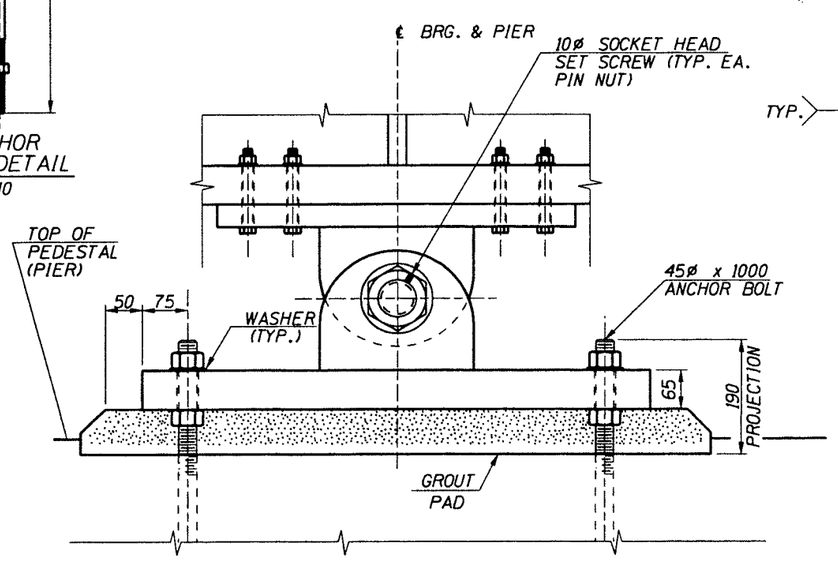

SIDE VIEW
1:5

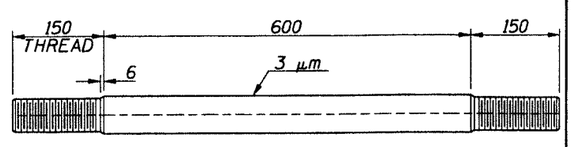

BEARING PIN DETAIL
1:5

ALL DIMENSIONS ARE IN MILLIMETERS
UNLESS NOTED OTHERWISE

REVISIONS NO.	DATE	BY	DESCRIPTION
1			
2			
3			
4			
5			

DESIGNED R. JENSEN
DESIGN CHECKED L. ZARATE
DETAILED A. BASTON
DWG. CHECKED L. ZARATE
CORRECTIONS G.B.

SCALES SHOWN ARE FOR 864mm X 559mm PRINTS ONLY
CADD FILE NO. f:\projects\pr\7771\7771br20.dgn
DRAWING DATE: 01/23/2004

ORIGINAL SIGNED BY: PROFESSIONAL ENGINEER REGISTERED 6386 STATE OF IDAHO RICHARD L. JENSEN, JR.
ORIGINAL DATE SIGNED: JANUARY 23, 2004
ORIGINAL STORED AT ITD BRIDGE SECTION

IDAHO TRANSPORTATION DEPARTMENT
ORIGINAL APPROVED BY: BRIDGE ENGINEER MATTHEW M. FARRAR
ORIGINAL SIGNED ON DATE: JANUARY 23, 2004

metric
PROJECT NO.
NH-15-3(106)113

PIER PINNED BEARING DETAILS
100 m STEEL OVERPASS
SUNNYSIDE ROAD I.C. (I-15B) OVER I-15
I-15B STA. 486+59.12 I-15 STA. 64+74.34

BRIDGE PLANS
BRIDGE INSPECTION MASTER KEY
COUNTY: BONNEVILLE
KEY NO.: 7771
BRIDGE DRAWING NO.: 15645
SHEET: 20 OF 44

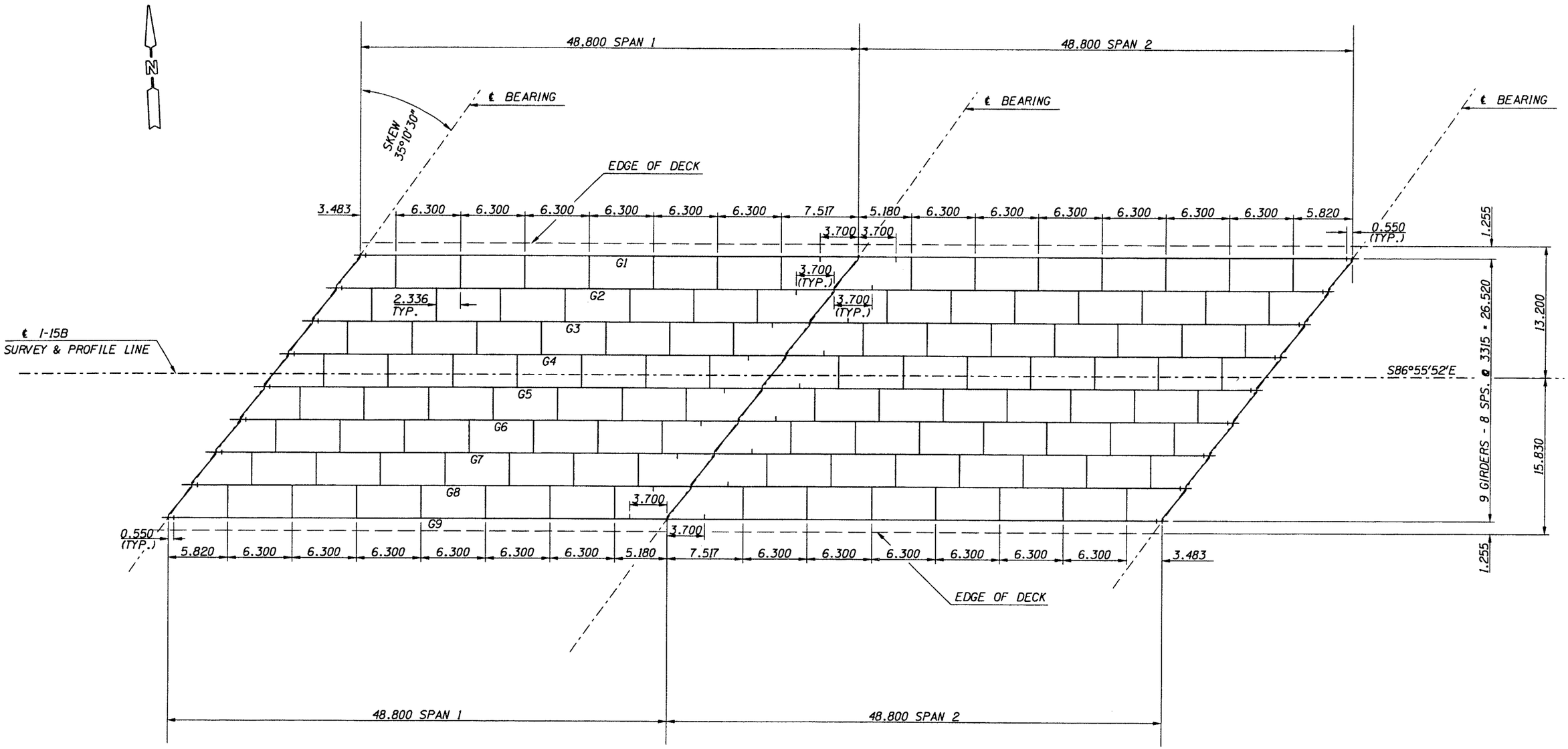

PLAN SPANS 1 & 2

1:200

ALL DIMENSIONS ARE IN METERS
UNLESS NOTED OTHERWISE

REVISIONS			
NO.	DATE	BY	DESCRIPTION

DESIGNED: L. ZARATE
DESIGN CHECKED: J. VETTER
DETAILED: A. BASTON
DWG. CHECKED: L. ZARATE
CORRECTIONS: G.B.

SCALES SHOWN ARE FOR 864 mm X 559 mm PRINTS ONLY

CADD FILE NO.
f:\projects\pr\7771\
7771br21.dgn

DRAWING DATE: 01/23/2004

ORIGINAL SIGNED BY:
PROFESSIONAL ENGINEER REGISTERED 6518 STATE OF IDAHO LUIS R. ZARATE
ORIGINAL DATE SIGNED: JANUARY 23,2004
ORIGINAL STORED AT ITD BRIDGE SECTION

IDAHO TRANSPORTATION DEPARTMENT

ORIGINAL APPROVED BY: BRIDGE ENGINEER MATTHEW M. FARRAR
ORIGINAL SIGNED ON DATE: JANUARY 23,2004

metric

PROJECT NO.
DHP-NH-6470(103)

FRAMING PLAN - SPANS 1 & 2

100 m STEEL OVERPASS
SUNNYSIDE ROAD I.C. (I-15B) OVER I-15
I-15B STA. 486+59.12 I-15 STA. 64+74.34

BRIDGE PLANS
BRIDGE INSPECTION MASTER KEY
COUNTY: BONNEVILLE
KEY NO.: 7771
BRIDGE DRAWING NO.: 15779
SHEET: 21 OF 44

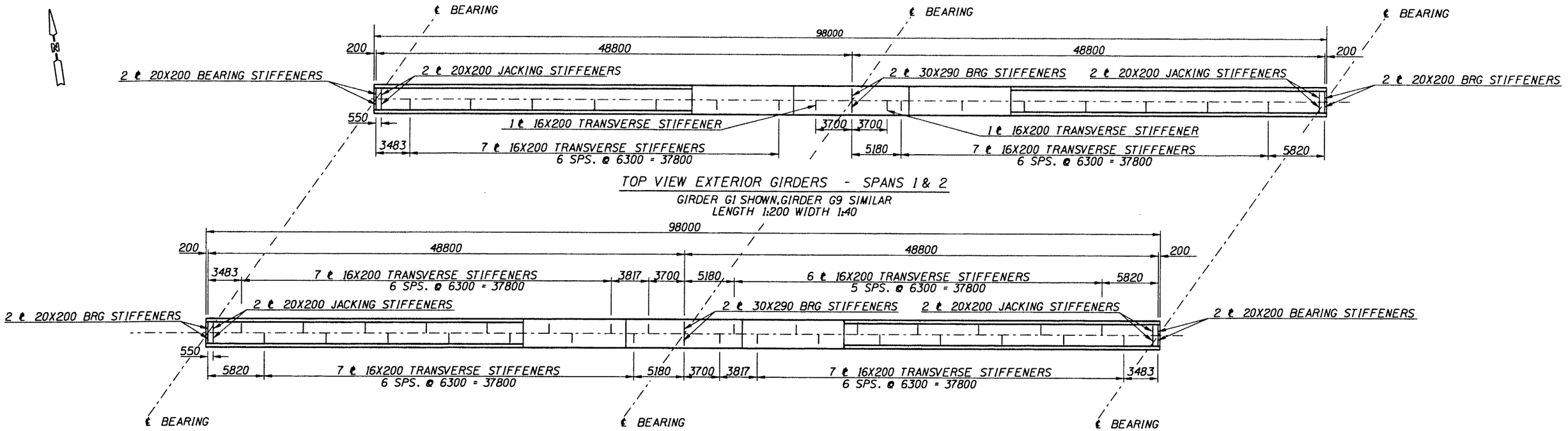

SRZ. = STRESS REVERSAL ZONE

ELEVATION GIRDERS - SPANS 1 & 2

LENGTH 1:200 HEIGHT 1:40
(STIFFENERS NOT SHOWN FOR CLARITY)

ALL DIMENSIONS ARE IN MILLIMETERS UNLESS NOTED OTHERWISE

REVISIONS			
NO.	DATE	BY	DESCRIPTION
1			
2			
3			
4			
5			

DESIGNED: L. ZARATE
DESIGN CHECKED: J. VETTER
DETAILED: A. BASTON
DWG. CHECKED: L. ZARATE
CORRECTIONS:

SCALES SHOWN ARE FOR 864 mm X 559 mm PRINTS ONLY

CADD FILE NO. f:\projects\pr17771\ 17771br22.dgn

DRAWING DATE: 01/23/2004

ORIGINAL SIGNED BY: PROFESSIONAL ENGINEER REGISTERED 6518 STATE OF IDAHO LUIS R. ZARATE

ORIGINAL DATE SIGNED: JANUARY 23,2004

ORIGINAL STORED AT ITD BRIDGE SECTION

IDAHO TRANSPORTATION DEPARTMENT

ORIGINAL APPROVED BY: BRIDGE ENGINEER MATTHEW M. FARRAR

ORIGINAL SIGNED ON DATE: JANUARY 23,2004

metric

PROJECT NO.

NH-15-3(106)113

STEEL GIRDER DETAILS

100 m STEEL OVERPASS
SUNNYSIDE ROAD I.C. (I-15B) OVER I-15
I-15B STA. 486+59.12 I-15 STA. 64+74.34

BRIDGE PLANS

BRIDGE INSPECTION MASTER KEY

COUNTY: BONNEVILLE
KEY NO.: 7771
BRIDGE DRAWING NO.: 15779
SHEET: 22 OF 44

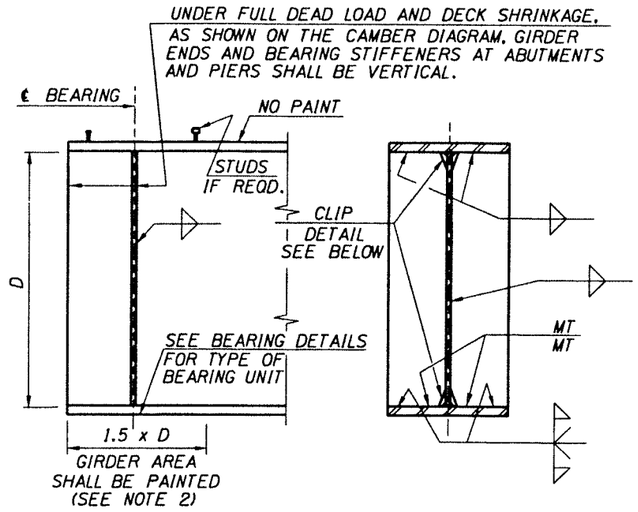

GIRDER END DETAILS

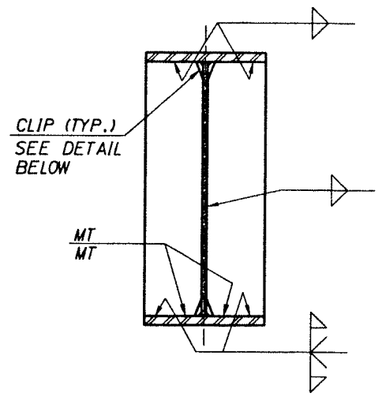

CONTINUOUS SUPPORT DETAILS

INTERMEDIATE STIFFENERS SHALL BE NORMAL TO TOP FLANGE UNLESS OTHERWISE SPECIFIED. PLACE INTERMEDIATE STIFFENERS ON ONE SIDE ONLY.

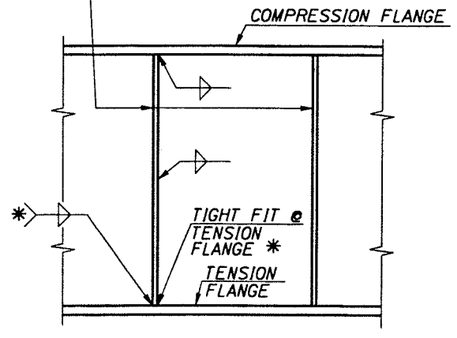

* WELD INTERMEDIATE STIFFENER TO TENSION FLANGE ONLY WHERE LATERAL BRACING DIAPHRAGMS OR CROSS FRAMES ARE ATTACHED TO STIFFENERS. TIGHT FIT AT TENSION FLANGE AT ALL OTHER LOCATIONS.

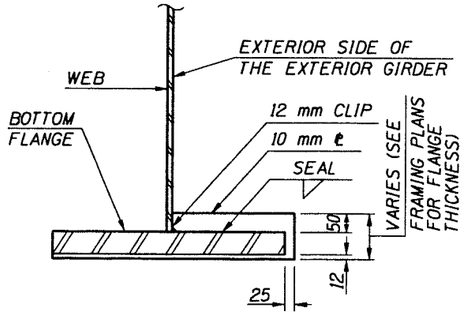

BOLTED FIELD SPLICES SHALL BE NORMAL TO TOP FLANGE UNLESS SPECIFIED OTHERWISE.

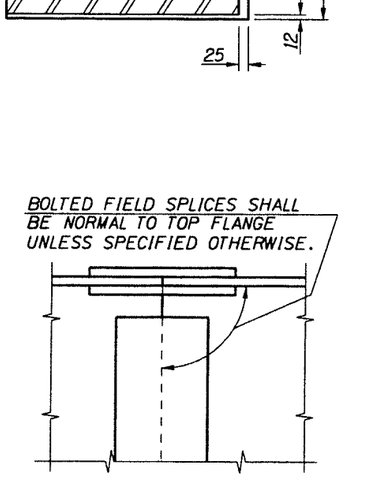

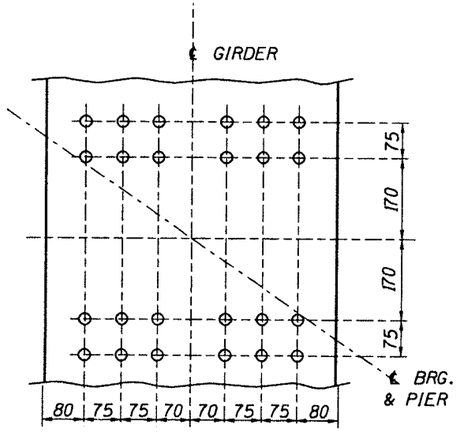

GENERAL STEEL NOTES

1. STRUCTURAL STEEL FOR GIRDER FLANGES & WEBS SHALL CONFORM TO AASHTO M270M GRADE HPS 485W. ALL OTHER STRUCUTRAL STEEL SHALL CONFORM TO AASHTO SPECIFICATION M270M GRADE 345W UNLESS OTHERWISE NOTED ON THE PLANS.
2. AT DECK EXPANSION JOINTS, PAINT THE BEARING UNITS, END CROSS FRAMES, AND END OF EACH GIRDER (EXCEPT FOR THE TOP OF THE TOP FLANGE AND BOLTED FAYING SURFACES) WITHIN A HORIZONTAL DISTANCE OF 1.5 x GIRDER DEPTH FROM DECK EXPANSION JOINTS. THEY SHALL BE PAINTED IN THE FABRICATION SHOP IN ACCORDANCE WITH ITD STANDARD SPECIFICATION FOR PAINT SYSTEM D, EXCEPT TOPCOAT COLOR SHALL BE 20122 (FEDERAL STANDARD NUMBER 595). THE CONTRACTOR SHALL REPAIR ALL PAINTED AREAS THAT MAY BE DAMAGED DURING CONSTRUCTION.
3. ALL FIELD SPLICES SHALL BE SLIP - CRITICAL JOINTS WITH CLASS B SURFACE CONDITIONS MADE WITH 7/8" ø HIGH STRENGTH BOLTS. ALL CONTACT SURFACES OF THE FIELD SPLICES SHALL BE FIELD INSPECTED IMMEDIATELY PRIOR TO ASSEMBLY TO ENSURE THAT THE SURFACES ARE FREE OF ALL MILL SCALE, DIRT, ROAD OIL, AND OTHER FOREIGN MATERIAL.
4. STEEL GIRDER SUPERSTRUCTURE ERECTION SHALL BE COMPLETE BEFORE PLACING FORMS.
5. UNLESS OTHERWISE SHOWN ALL BOLTS SHALL CONFORM TO A-325 TYPE 3.
6. NO WELDING SHALL BE PERMITTED IN THE TENSION OR STRESS REVERSAL ZONES OF THE GIRDERS EXCEPT AS SHOWN ON THE PLANS.
7. IF THE PLATE THICKNESS FOR PARALLEL GROOVE WELD EXCEEDS THE PREQUALIFIED THICKNESS LISTED IN D1.5 THEN SINGLE V GROOVE WELD SHALL BE SUBSTITUTED.
8. IF A BOLT SIZE IS NOT SHOWN, IT SHALL BE ASSUMED TO BE 7/8" ø HIGH STRENGTH BOLTS, AND ALL BOLT HOLES SHALL BE STANDARD UNLESS NOTED.

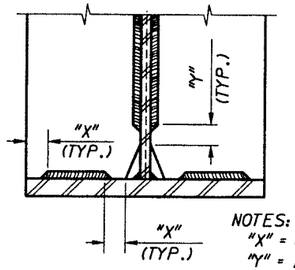

NOTES:
"X" = 6 ±3
"Y" = 12 ±6

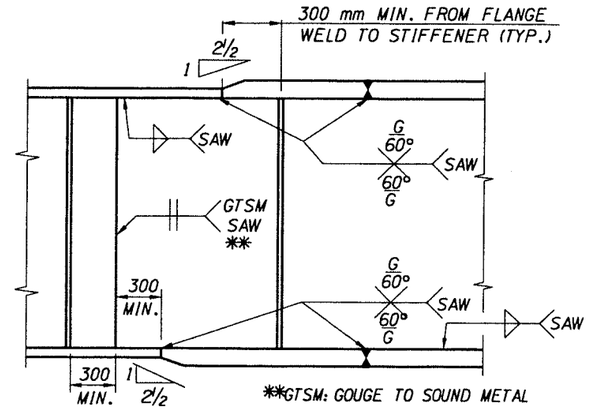

**GTSM: GOUGE TO SOUND METAL

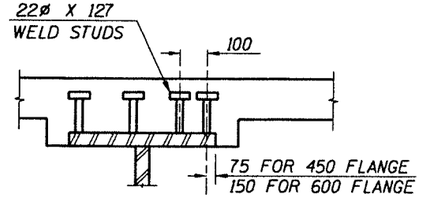

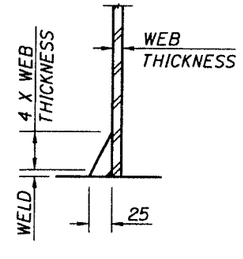

REVISIONS			
NO.	DATE	BY	DESCRIPTION

DESIGNED L. ZARATE
DESIGN CHECKED J. VETTER
DETAILED DICK JENSEN
DWG. CHECKED L. ZARATE
CORRECTIONS

SCALES SHOWN ARE FOR 864mm X 559mm PRINTS ONLY

CADD FILE NO. f:\projects\pr17771\ 17771br23.dgn

DRAWING DATE: 01/23/2004

ORIGINAL SIGNED BY: PROFESSIONAL ENGINEER REGISTERED 6518 STATE OF IDAHO LUIS R. ZARATE

ORIGINAL DATE SIGNED: JANUARY 23,2004

ORIGINAL STORED AT ITD BRIDGE SECTION

IDAHO TRANSPORTATION DEPARTMENT

ORIGINAL APPROVED BY: BRIDGE ENGINEER MATTHEW M. FARRAR

ORIGINAL SIGNED ON DATE: JANUARY 23,2004

metric

PROJECT NO.

NH-15-3-(106)113

GIRDER FABRICATION DETAILS

100 m STEEL OVERPASS
SUNNYSIDE ROAD I.C. (I-15B) OVER I-15
I-15B STA. 486+59.12 I-15 STA. 64+74.34

BRIDGE PLANS

BRIDGE INSPECTION MASTER KEY

COUNTY	KEY NO.
BONNEVILLE	7771
BRIDGE DRAWING NO. 15779	SHEET 23 OF 44

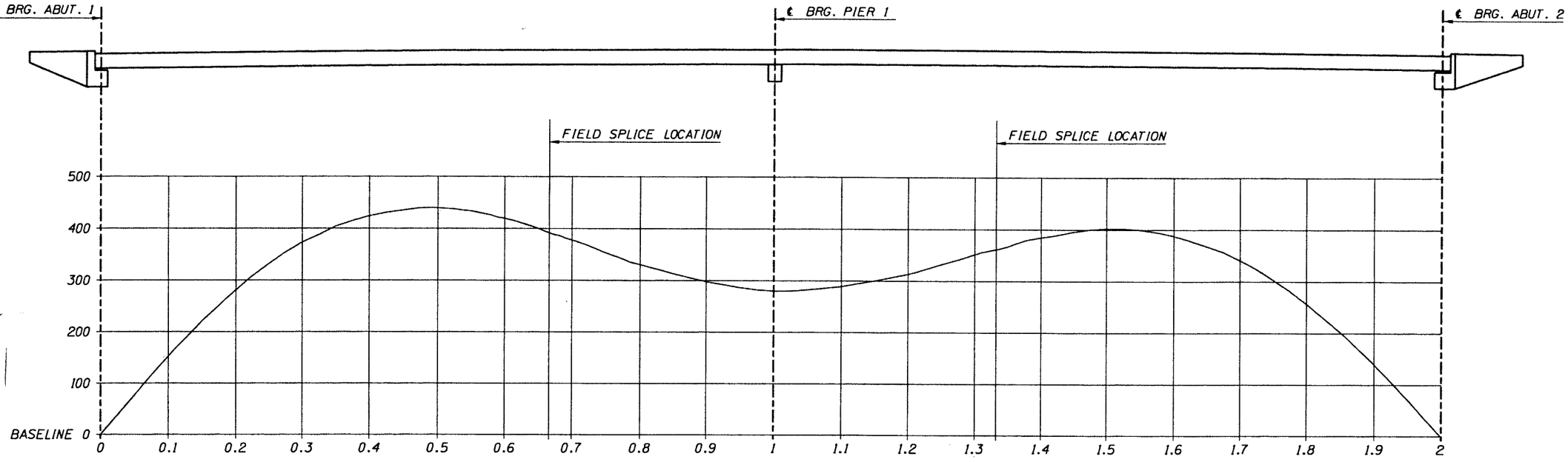

	ABUT 1	SPAN 1						FIELD SPLICE				PIER 1	SPAN 2				FIELD SPLICE							ABUT 2
	0	0.1	0.2	0.3	0.4	0.5	0.6	0.664	0.7	0.8	0.9	1	1.1	1.2	1.3	1.336	1.4	1.5	1.6	1.7	1.8	1.9	2
GIRDER DL	0	14	26	33	35	33	26	20	17	8	2	0	2	8	17	20	26	33	35	33	26	14	0
SLAB DL *	0	68	125	162	176	165	134	106	90	46	15	0	6	28	63	76	99	128	140	132	103	57	0
SHRINKAGE	0	10	15	16	15	12	9	7	5	2	1	0	1	2	5	7	9	12	15	16	15	10	0
COMPOSITE DL	0	7	14	17	19	18	14	11	10	5	1	0	1	5	10	11	14	18	19	17	14	7	0
TOTAL DL DEFLECTION	0	99	179	229	245	228	183	145	122	62	19	0	10	44	95	114	148	191	210	199	157	88	0
		95	153	196	210	195	157		105	54	17												
VERTICAL CURVE	0	53	101	144	180	211	236	249	256	270	279	281	279	270	256	249	236	211	180	144	101	53	0
TOTAL WEB CAMBER	0	152	280	373	425	439	419	393	378	332	298	281	289	314	351	363	384	402	390	343	258	141	0

* NOT SYMMETRICAL BECAUSE IT IS BASED ON A 2 PART DECK PLACEMENT SEQUENCE

GIRDER G1 - THROUGH G9 WEB CAMBER DATA

SPAN 1 & 2

ALL DIMENSIONS ARE IN MILLIMETERS
UNLESS NOTED OTHERWISE

REVISIONS			
NO.	DATE	BY	DESCRIPTION
1			
2			
3			
4			
5			

DESIGNED: L. ZARATE
DESIGN CHECKED: J. VETTER
DETAILED: A. BASTON
DWG. CHECKED: L. ZARATE
CORRECTIONS:

SCALES SHOWN ARE FOR 864mm X 559mm PRINTS ONLY

CADD FILE NO.
f:\projects\pr\7771\7771br24.dgn

DRAWING DATE: 01/23/2004

ORIGINAL SIGNED BY:
PROFESSIONAL ENGINEER REGISTERED 6518 STATE OF IDAHO LUIS R. ZARATE
ORIGINAL DATE SIGNED: JANUARY 23,2004
ORIGINAL STORED AT ITD BRIDGE SECTION

IDAHO TRANSPORTATION DEPARTMENT

ORIGINAL APPROVED BY; BRIDGE ENGINEER MATTHEW M. FARRAR
ORIGINAL SIGNED ON DATE: JANUARY 23,2004

metric

PROJECT NO.
NH-15-3-(106)113

GIRDER CAMBER DETAILS
100 m STEEL OVERPASS
SUNNYSIDE ROAD I.C. (I-15B) OVER I-15
I-15B STA. 486+59.12 I-15 STA. 64+74.34

BRIDGE PLANS
BRIDGE INSPECTION MASTER KEY
COUNTY: BONNEVILLE
KEY NO.: 7771
BRIDGE DRAWING NO.: 15779
SHEET: 24 OF 44

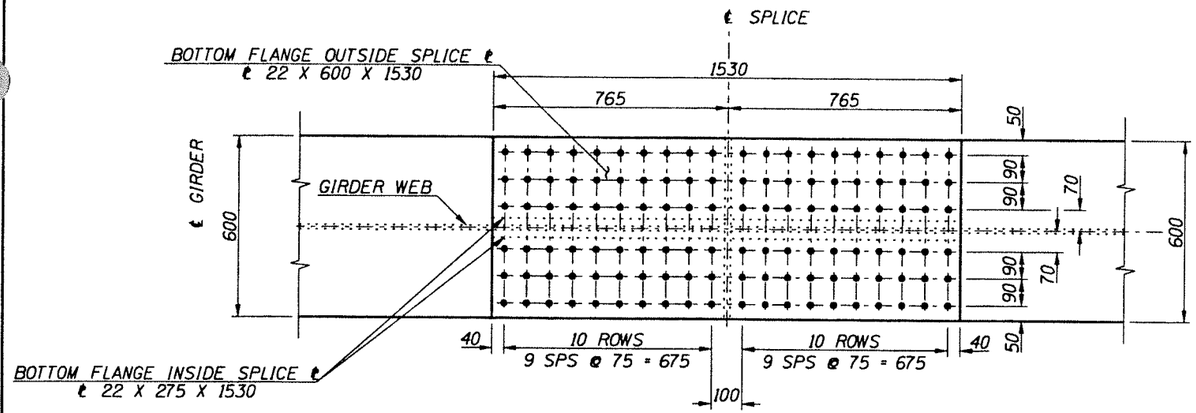

PLAN - BOTTOM FLANGE (G1 AND G9)

1:10

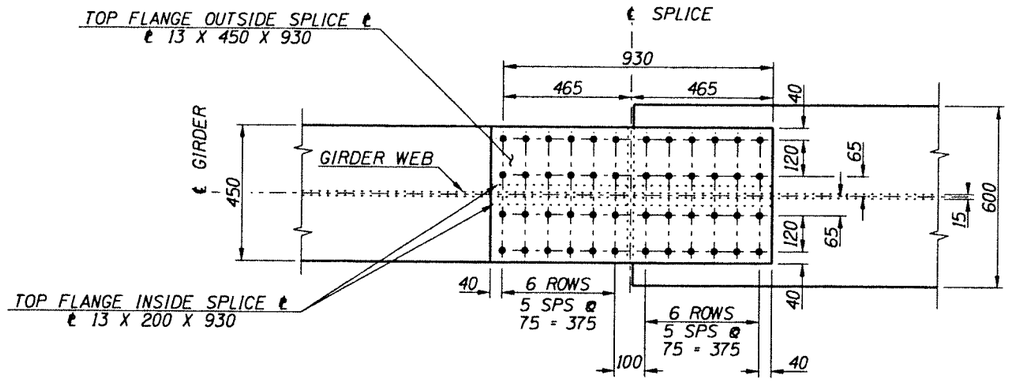

PLAN - TOP FLANGE (G1 THROUGH G9)

1:10

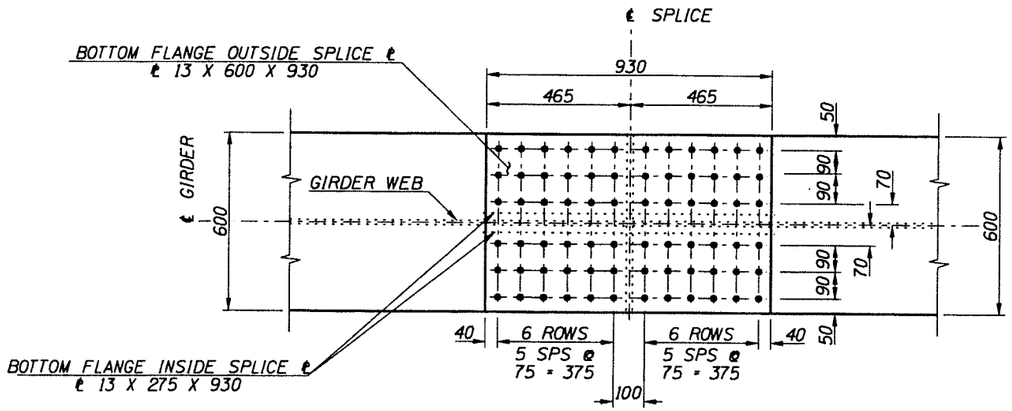

PLAN - BOTTOM FLANGE (G2 THROUGH G8)

1:10

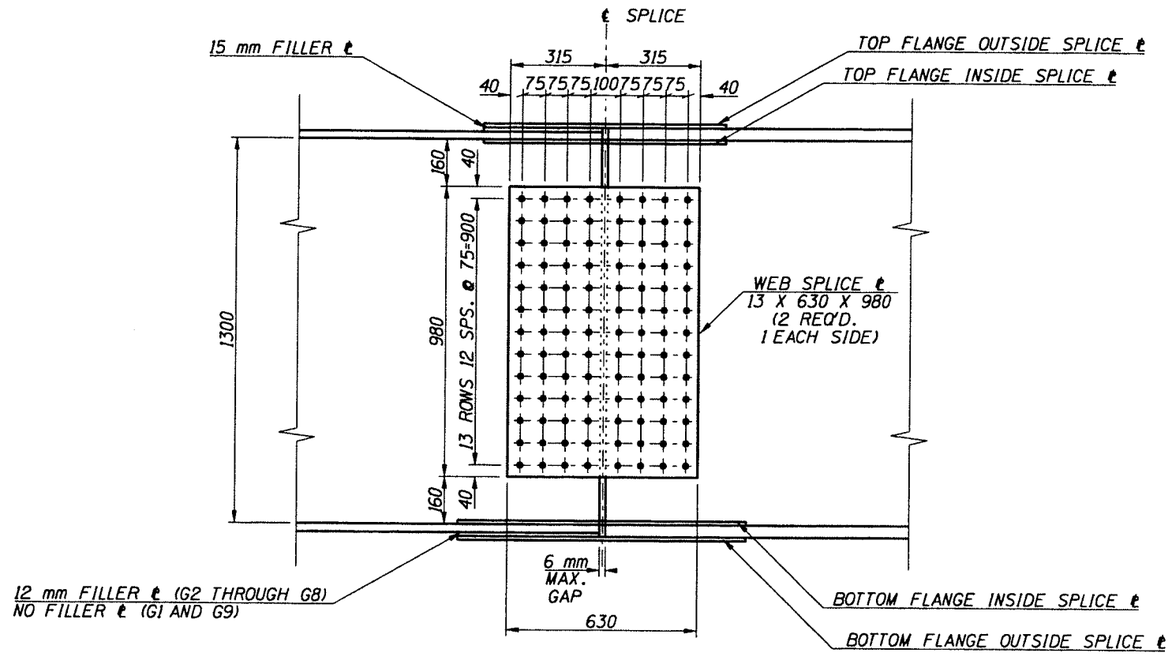

ELEVATION - WEB FIELD SPLICE (G1 THROUGH G9)

1:10

ALL DIMENSIONS ARE IN MILLIMETERS
UNLESS NOTED OTHERWISE

REVISIONS			
NO.	DATE	BY	DESCRIPTION
1			
2			
3			
4			
5			

DESIGNED: L. ZARATE
DESIGN CHECKED:
DETAILED: A. BASTON
DWG. CHECKED:
CORRECTIONS:

SCALES SHOWN ARE FOR 864 mm X 559 mm PRINTS ONLY

CADD FILE NO.
f:\projects\pr7771\7771br25.dgn

DRAWING DATE:
01/23/2004

ORIGINAL SIGNED BY:
PROFESSIONAL ENGINEER REGISTERED 6518 STATE OF IDAHO LUIS R. ZARATE
ORIGINAL DATE SIGNED: JANUARY 23,2004
ORIGINAL STORED AT ITD BRIDGE SECTION

IDAHO TRANSPORTATION DEPARTMENT

ORIGINAL APPROVED BY:
BRIDGE ENGINEER MATTHEW M. FARRAR
ORIGINAL SIGNED ON DATE: JANUARY 23,2004

metric

PROJECT NO.
NH-15-3(106)113

FIELD SPLICE DETAILS

100 m STEEL OVERPASS
SUNNYSIDE ROAD I.C. (I-15B) OVER I-15
I-15B STA. 486+59.12 I-15 STA. 64+74.34

BRIDGE PLANS

BRIDGE INSPECTION MASTER KEY

COUNTY	KEY NO.
BONNEVILLE	7771
BRIDGE DRAWING NO. 15779	SHEET 25 OF 44

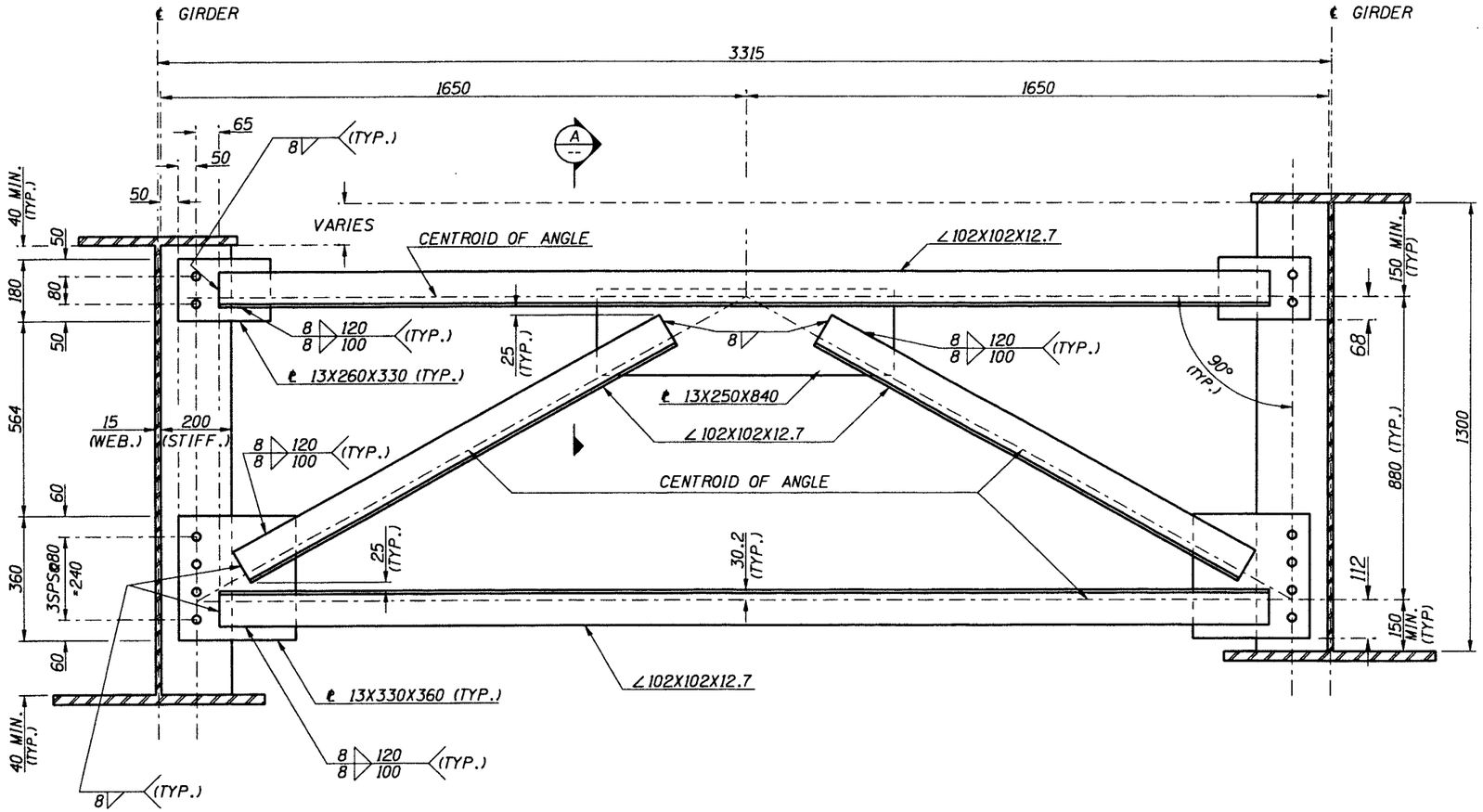

INTERMEDIATE CROSS FRAME
1:8

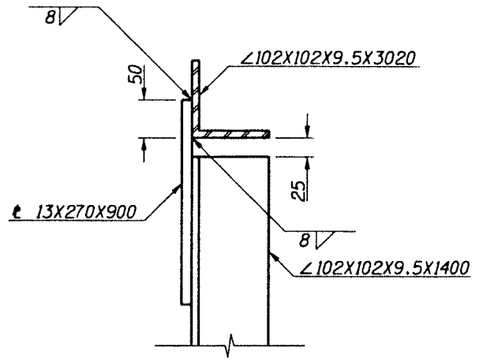

SECTION A
1:4

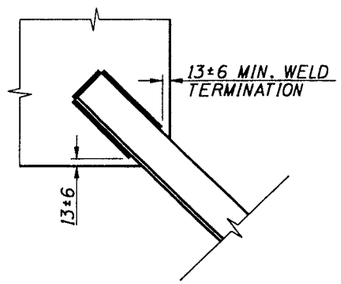

TYPICAL WELD DETAIL
1:8

ALL DIMENSIONS ARE IN MILLIMETERS
UNLESS NOTED OTHERWISE

REVISIONS NO.	DATE	BY	DESCRIPTION
1			
2			
3			
4			
5			

DESIGNED: L. ZARATE
DESIGN CHECKED: J. VETTER
DETAILED: A. BASTON
DWG. CHECKED: L. ZARATE
CORRECTIONS:

SCALES SHOWN ARE FOR 864 mm X 559 mm PRINTS ONLY

CADD FILE NO. f:\projects\pr\7771\7771br26.dgn

DRAWING DATE: 01/23/2004

ORIGINAL SIGNED BY: PROFESSIONAL ENGINEER REGISTERED 6518 STATE OF IDAHO LUIS R. ZARATE

ORIGINAL DATE SIGNED: JANUARY 23,2004

ORIGINAL STORED AT ITD BRIDGE SECTION

IDAHO TRANSPORTATION DEPARTMENT

ORIGINAL APPROVED BY: BRIDGE ENGINEER MATTHEW M. FARRAR

ORIGINAL SIGNED ON DATE: JANUARY 23,2004

metric

PROJECT NO.

NH-15-3(106)113

INTERMEDIATE CROSS-FRAME DETAILS

100 m STEEL OVERPASS
SUNNYSIDE ROAD I.C. (I-15B) OVER I-15
I-15B STA. 486+59.12 I-15 STA. 64+74.34

BRIDGE PLANS

BRIDGE INSPECTION MASTER KEY

COUNTY: BONNEVILLE
KEY NO.: 7771

BRIDGE DRAWING NO.: 15779
SHEET: 26 OF 44

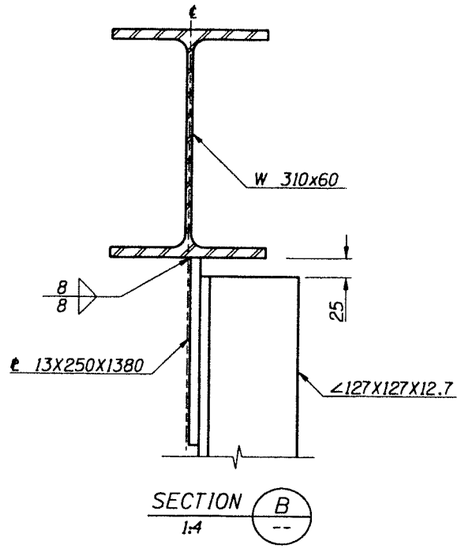

SECTION B
1:4

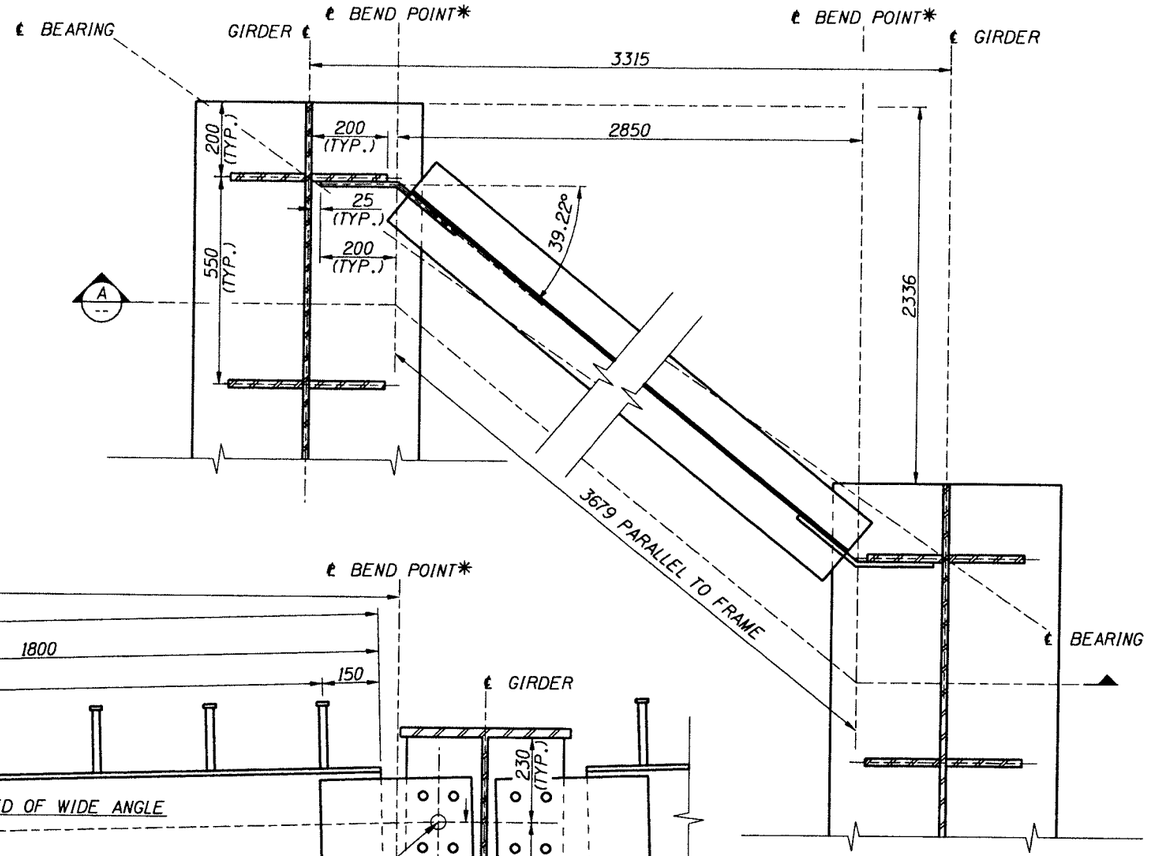

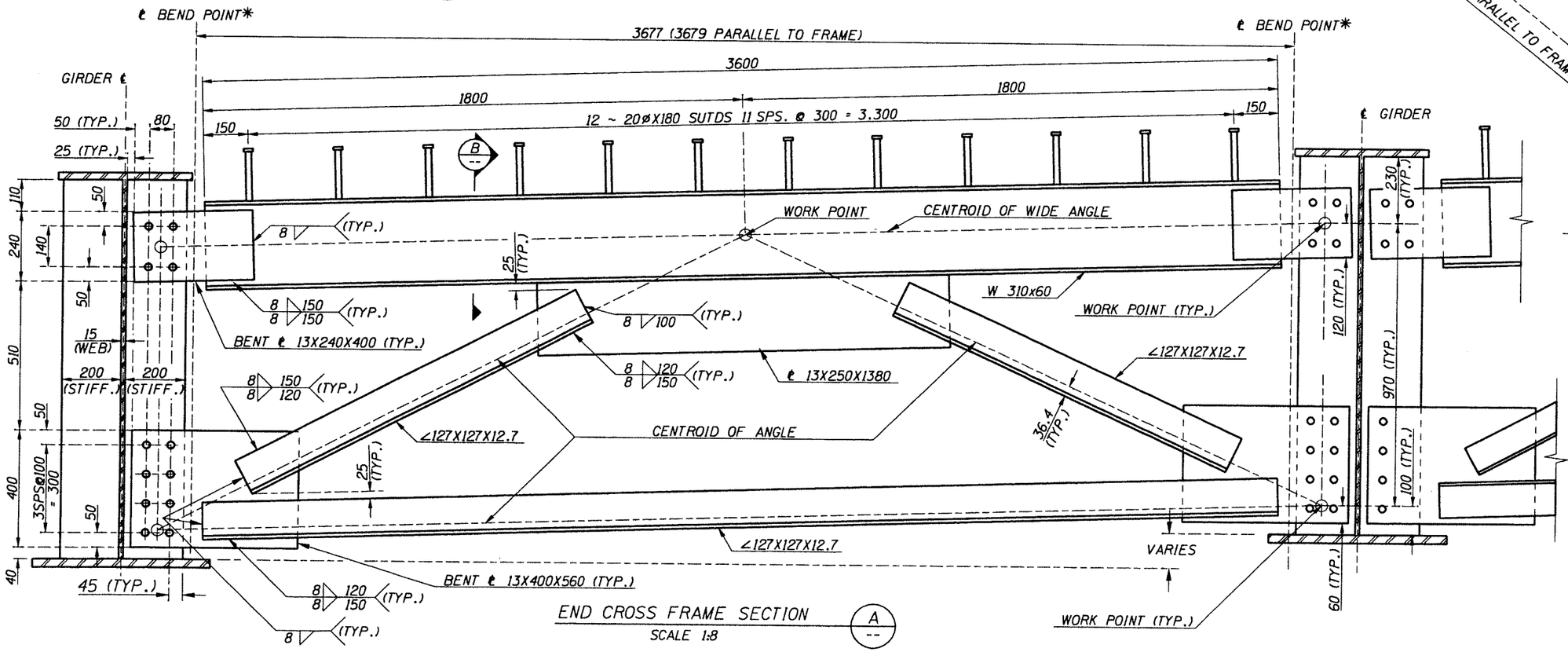

END CROSS FRAME SECTION
SCALE 1:8

A

END CROSS FRAME PLAN VIEW
SCALE 1:8

* ℄ BEND POINT MEASURED @ INSIDE OF BEND

ALL DIMENSIONS ARE IN MILLIMETERS
UNLESS NOTED OTHERWISE

REVISIONS			
NO.	DATE	BY	DESCRIPTION
1			
2			
3			
4			
5			

DESIGNED L. ZARATE
DESIGN CHECKED J. VETTER
DETAILED A. BASTON
DWG. CHECKED L. ZARATE
CORRECTIONS

SCALES SHOWN ARE FOR 864 mm X 559 mm PRINTS ONLY
CADD FILE NO. f:\projects\pr7771\7771br27.dgn
DRAWING DATE: 01/23/2004

ORIGINAL SIGNED BY:
PROFESSIONAL ENGINEER REGISTERED 6518 STATE OF IDAHO LUIS R. ZARATE
ORIGINAL DATE SIGNED: JANUARY 23,2004
ORIGINAL STORED AT ITD BRIDGE SECTION

IDAHO TRANSPORTATION DEPARTMENT

ORIGINAL APPROVED BY: BRIDGE ENGINEER MATTHEW M. FARRAR
ORIGINAL SIGNED ON DATE: JANUARY 23,2004

metric

PROJECT NO.
NH-15-3(106)113

END CROSS FRAME DETAILS

100 m STEEL OVERPASS
SUNNYSIDE ROAD I.C. (I-15B) OVER I-15
I-15B STA. 486+59.12 I-15 STA. 64+74.34

BRIDGE PLANS
BRIDGE INSPECTION MASTER KEY
COUNTY BONNEVILLE
KEY NO. 7771
BRIDGE DRAWING NO. 15779
SHEET 27 OF 44

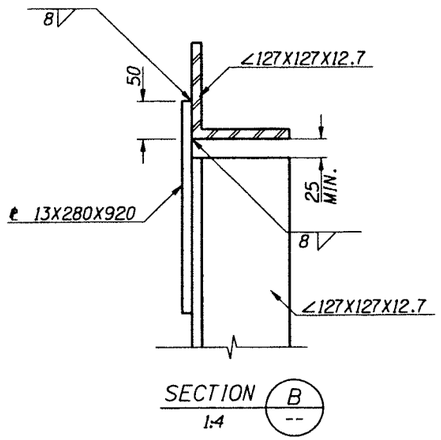

SECTION B
1:4

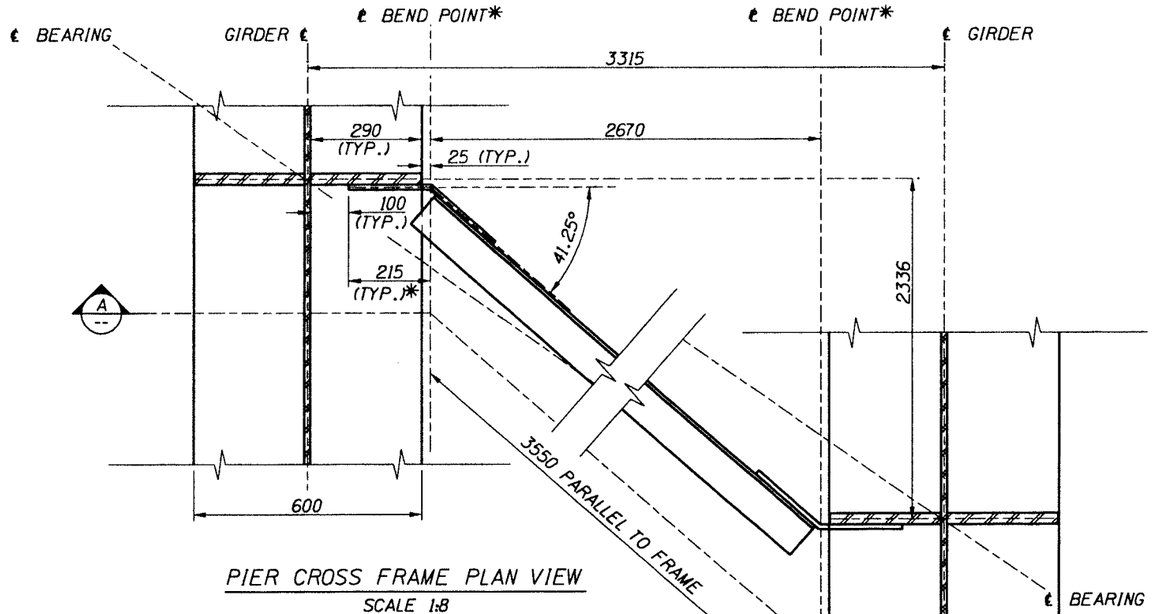

PIER CROSS FRAME PLAN VIEW
SCALE 1:8

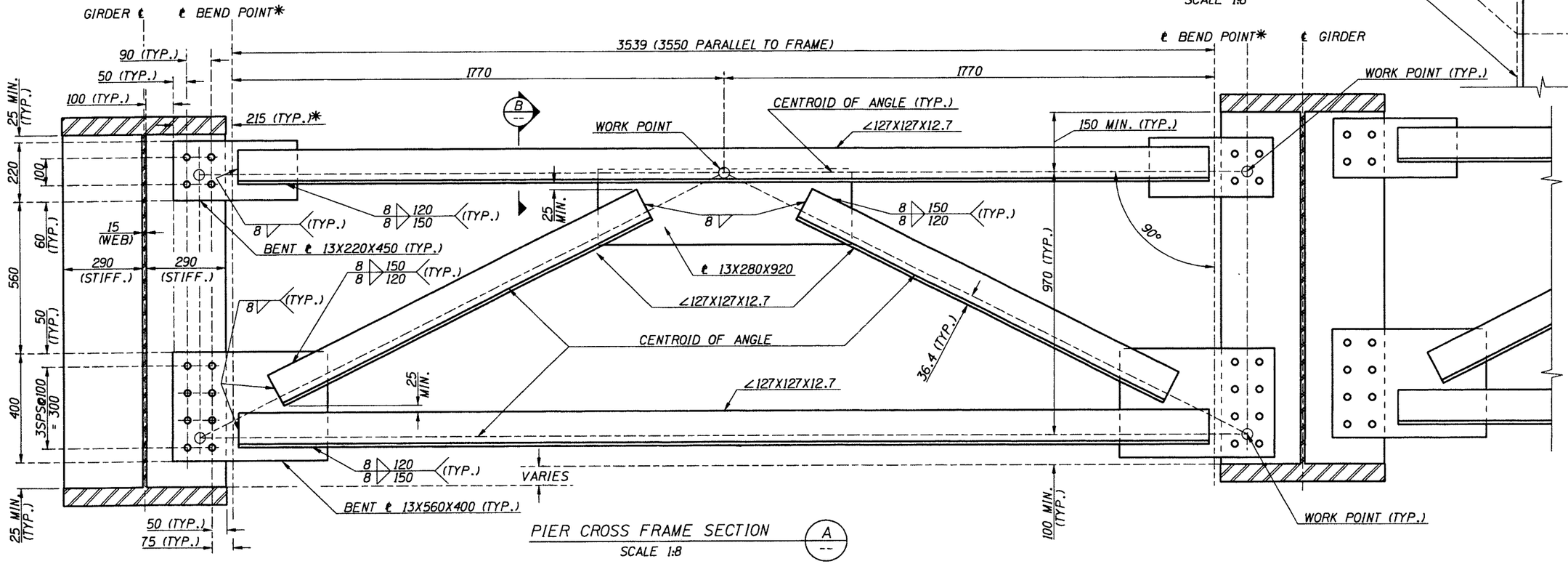

PIER CROSS FRAME SECTION
SCALE 1:8

A

* ℄ BEND POINT MEASURED @ INSIDE OF BEND

ALL DIMENSIONS ARE IN MILLIMETERS
UNLESS NOTED OTHERWISE

REVISIONS			
NO.	DATE	BY	DESCRIPTION

DESIGNED L. ZARATE
DESIGN CHECKED J. VETTER
DETAILED A. BASTON
DWG. CHECKED L. ZARATE
CORRECTIONS

SCALES SHOWN ARE FOR 864 mm X 559 mm PRINTS ONLY
CADD FILE NO. f:\projects\pr7771\7771br28.dgn
DRAWING DATE: 01/23/2004

ORIGINAL SIGNED BY: PROFESSIONAL ENGINEER REGISTERED 6518 STATE OF IDAHO LUIS R. ZARATE
ORIGINAL DATE SIGNED: JANUARY 23,2004
ORIGINAL STORED AT ITD BRIDGE SECTION

IDAHO TRANSPORTATION DEPARTMENT
ORIGINAL APPROVED BY: BRIDGE ENGINEER MATTHEW M. FARRAR
ORIGINAL SIGNED ON DATE: JANUARY 23,2004

metric
PROJECT NO.
NH-15-3(106)113

PIER CROSS FRAME DETAILS

100 m STEEL OVERPASS
SUNNYSIDE ROAD I.C. (I-15B) OVER I-15
I-15B STA. 486+59.12 I-15 STA. 64+74.34

BRIDGE PLANS
BRIDGE INSPECTION MASTER KEY
COUNTY BONNEVILLE
KEY NO. 7771
BRIDGE DRAWING NO. 15779
SHEET 28 OF 44

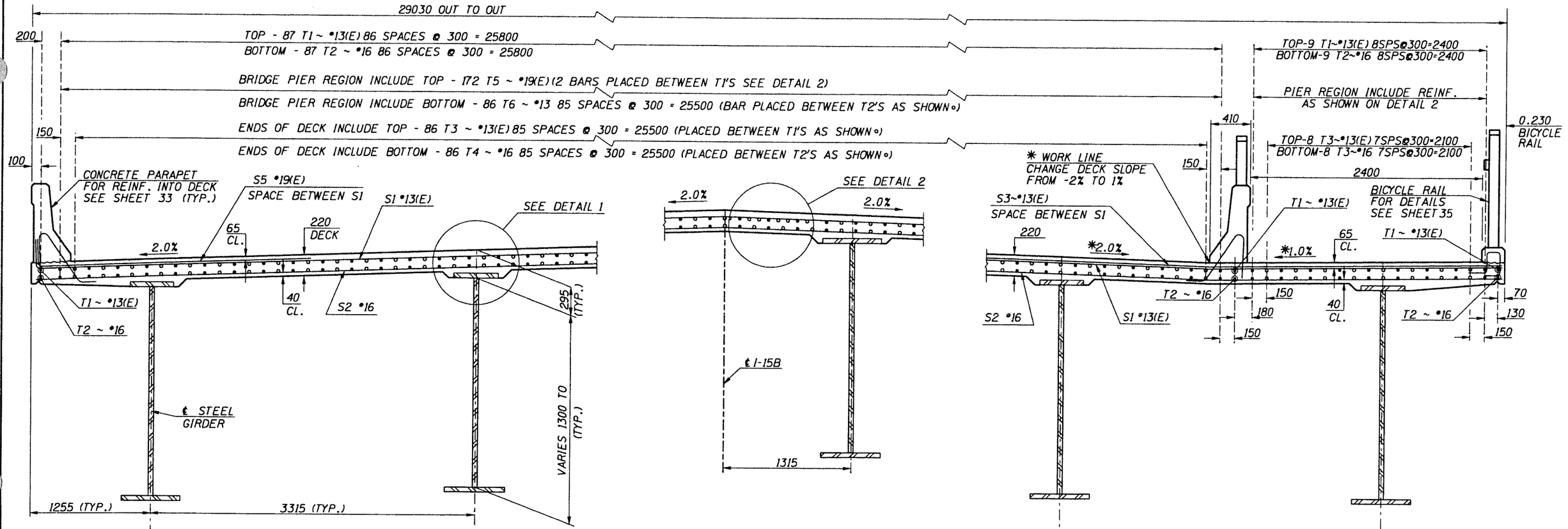

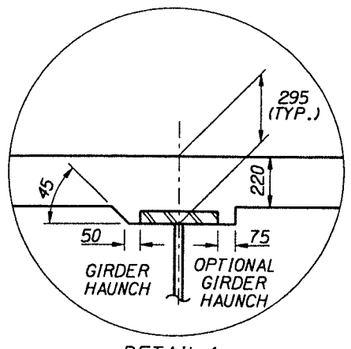

DETAIL 1
NTS

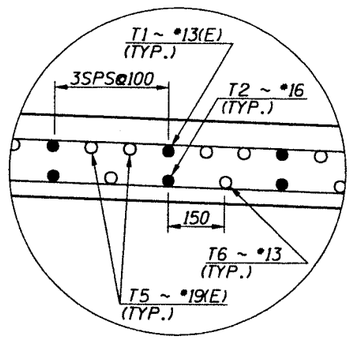

DETAIL 2
TYPICAL LONGITUDINAL
RIENFORCEMENT OVER
PIER REGION
NTS

NOTES :

PERMANENT METAL DECK SLAB FORMS MAY BE USED AT THE CONTRACTOR'S OPTION. MAXIMUM ADDITIONAL WEIGHT OF PERMANENT METAL DECK SLAB FORMS AND ADDITIONAL WEIGHT OF CONCRETE IN THE FLUTES SHALL NOT EXCEED 766 Pa.

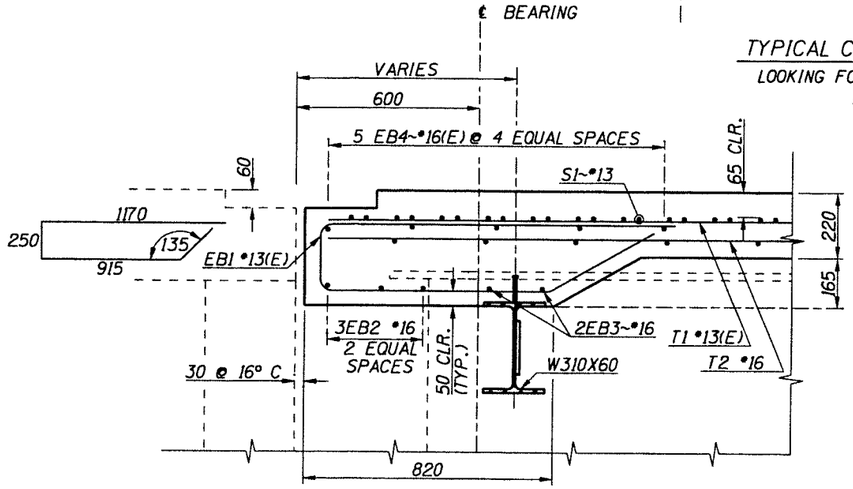

SECTION A
1:10
30

TYPICAL CROSS SECTION
LOOKING FORWARD STATION
1:20

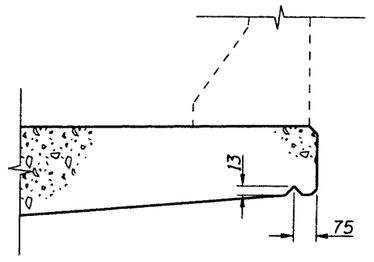

DRIP V-GROVE DETAIL
TYPICAL
NTS

ALL DIMENSIONS ARE IN MILLIMETERS
UNLESS NOTED OTHERWISE

REVISIONS			
NO.	DATE	BY	DESCRIPTION

DESIGNED L. ZARATE
DESIGN CHECKED J. VETTER
DETAILED A. BASTON
DWG. CHECKED L. ZARATE
CORRECTIONS

SCALES SHOWN ARE FOR 864mm X 559mm PRINTS ONLY
CADD FILE NO. f:\project\pr1777\777tbr29.dgn
DRAWING DATE: 01/23/2004

ORIGINAL SIGNED BY:
PROFESSIONAL ENGINEER REGISTERED 6518 STATE OF IDAHO LUIS R. ZARATE
ORIGINAL DATE SIGNED: JANUARY 23,2004
ORIGINAL STORED AT ITD BRIDGE SECTION

IDAHO TRANSPORTATION DEPARTMENT

ORIGINAL APPROVED BY:
BRIDGE ENGINEER MATTHEW M. FARRAR ORIGINAL SIGNED ON DATE: JANUARY 23,2004

metric

PROJECT NO.
NH-15-3(106)113

DECK TYPICAL SECTION

100 m STEEL OVERPASS
SUNNYSIDE ROAD I.C. (I-15B) OVER I-15
I-15B STA. 486+59.12 I-15 STA. 64+74.34

BRIDGE PLANS

BRIDGE INSPECTION MASTER KEY

COUNTY	KEY NO.
BONNEVILLE	7771
BRIDGE DRAWING NO.	SHEET
15779	29 OF 44

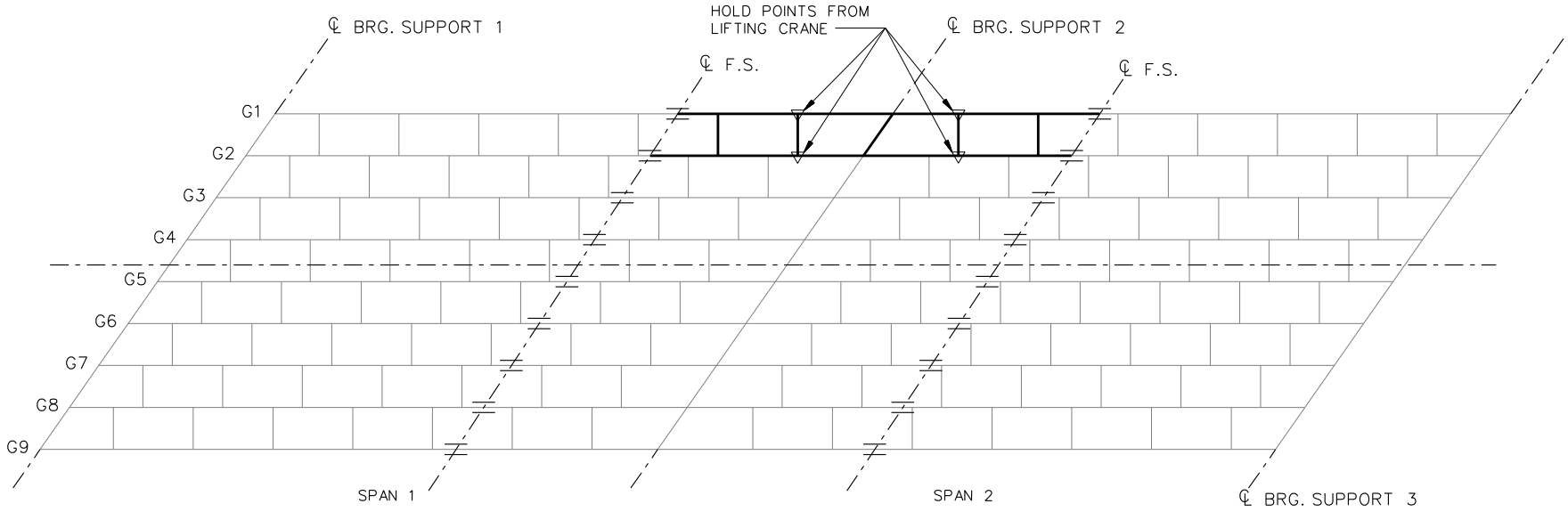

STAGE 1

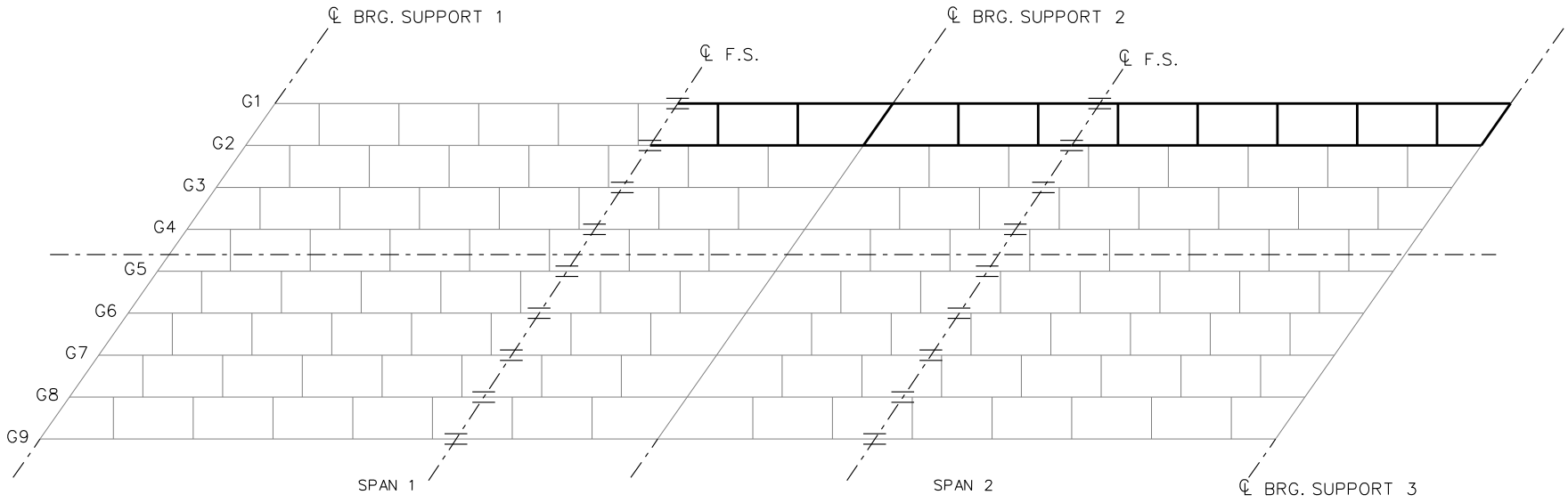

STAGE 2

LEGEND

▽ = HOLD OR LIFT CRANE

○ = TIE DOWN

□ = TEMPORARY SUPPORT STRUCTURE

NCHRP 12-79

BRIDGE EICSS1

GIRDER ERECTION PROCEDURE

SHEET 1 OF 3

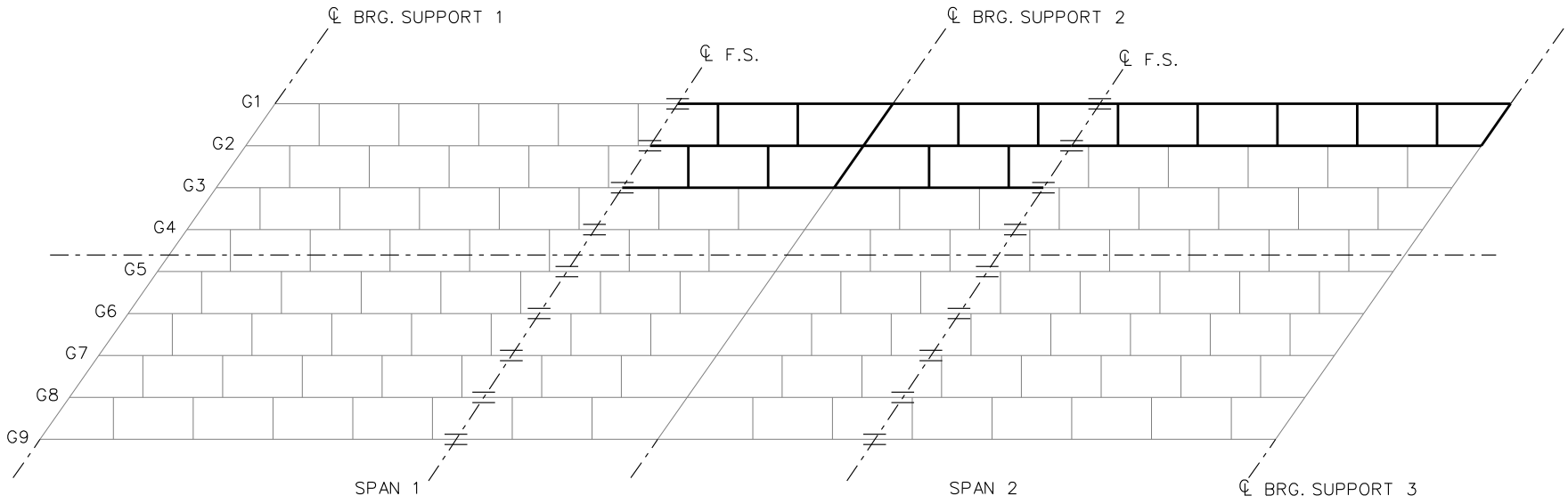

STAGE 3

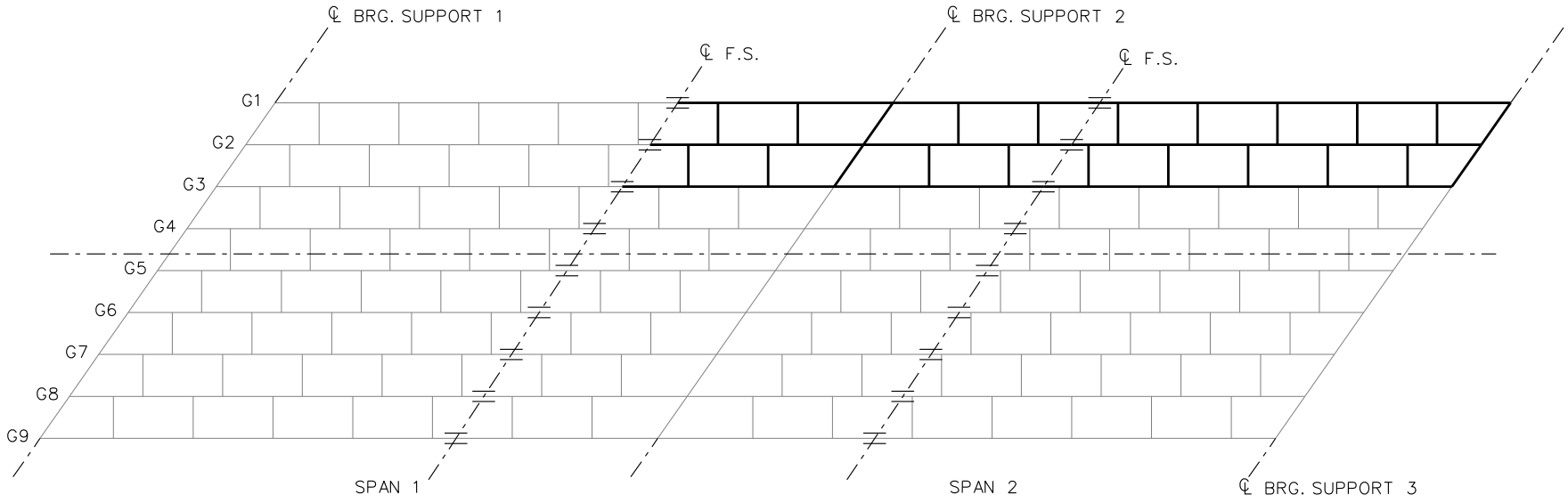

STAGE 4

LEGEND

▽ = HOLD OR LIFT CRANE

○ = TIE DOWN

□ = TEMPORARY SUPPORT STRUCTURE

NCHRP 12-79

BRIDGE EICSS1

GIRDER ERECTION PROCEDURE

SHEET 2 OF 3

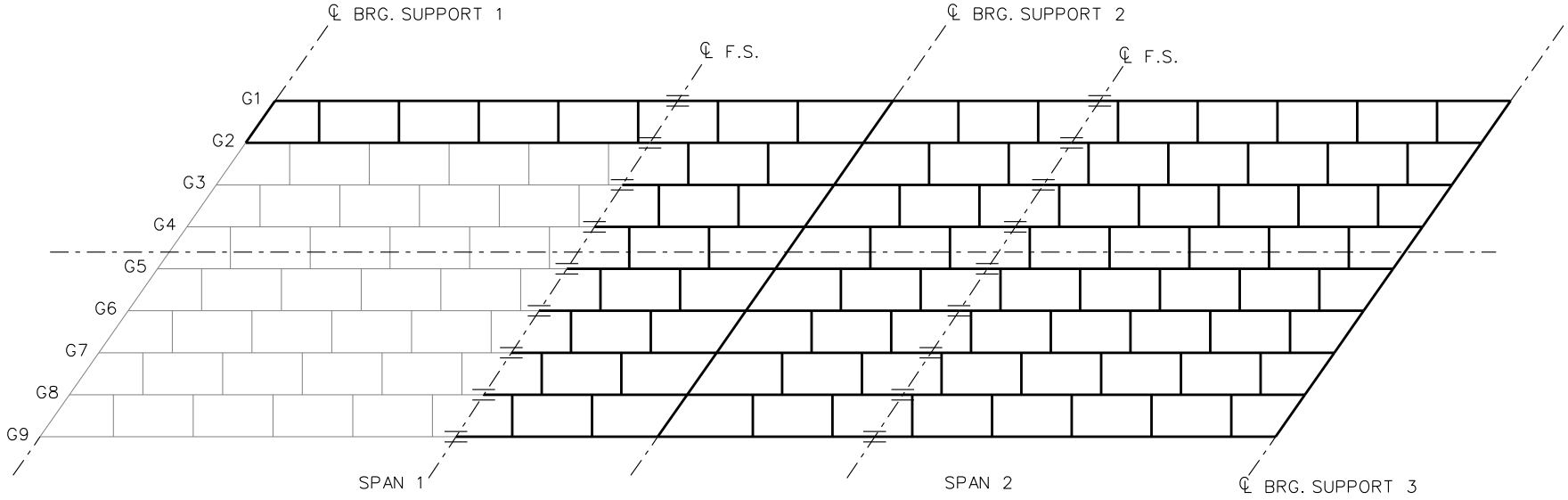

STAGE 17

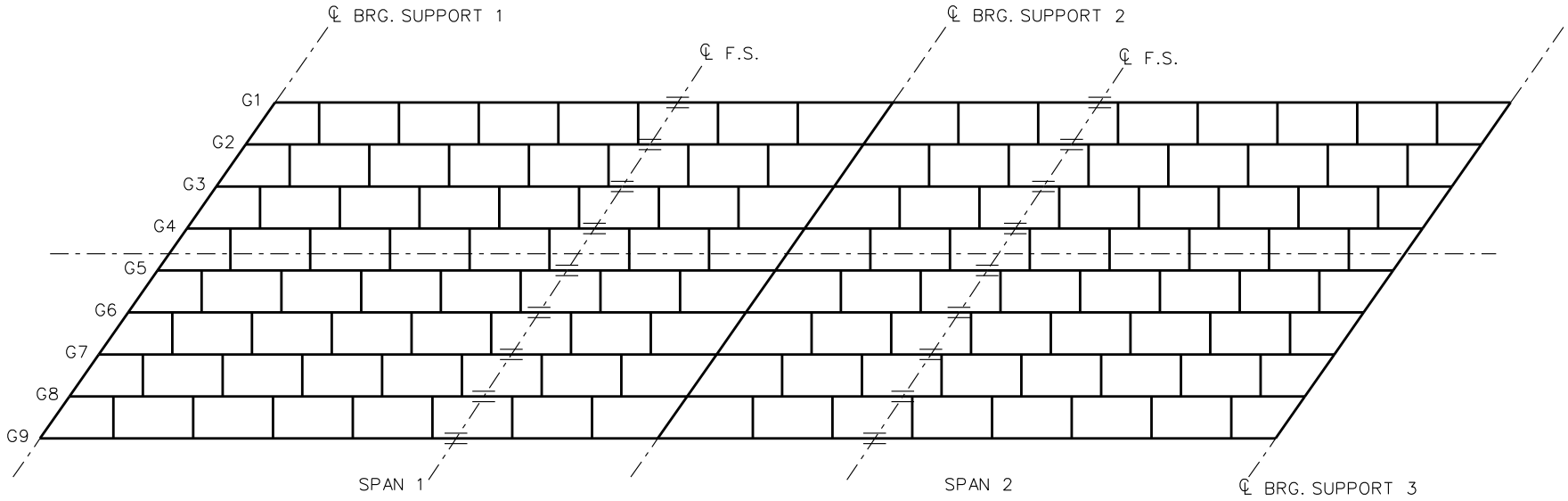

STAGE 24

LEGEND

▽ = HOLD OR LIFT CRANE

○ = TIE DOWN

□ = TEMPORARY SUPPORT STRUCTURE

NCHRP 12-79

BRIDGE EICSS1

GIRDER ERECTION PROCEDURE

SHEET 3 OF 3

NCHRP 12-79

EICSS2

BENCH MARK NO. 691, STA. 567+56.577 103.35 RT. SET RR SPK N. SIDE P. POLE NE QUAD E. 19TH & WALKER ELEV. 251.587

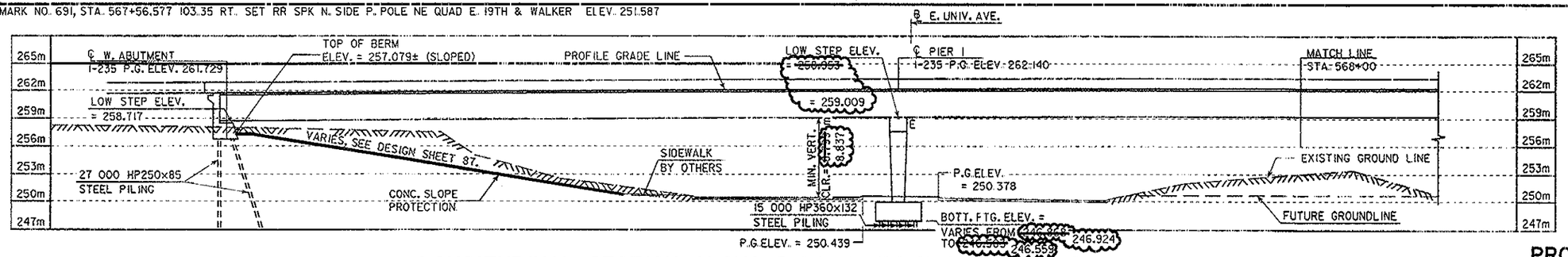

LONGITUDINAL SECTION ALONG P.G.L. I-235 EAST BOUND ROADWAY

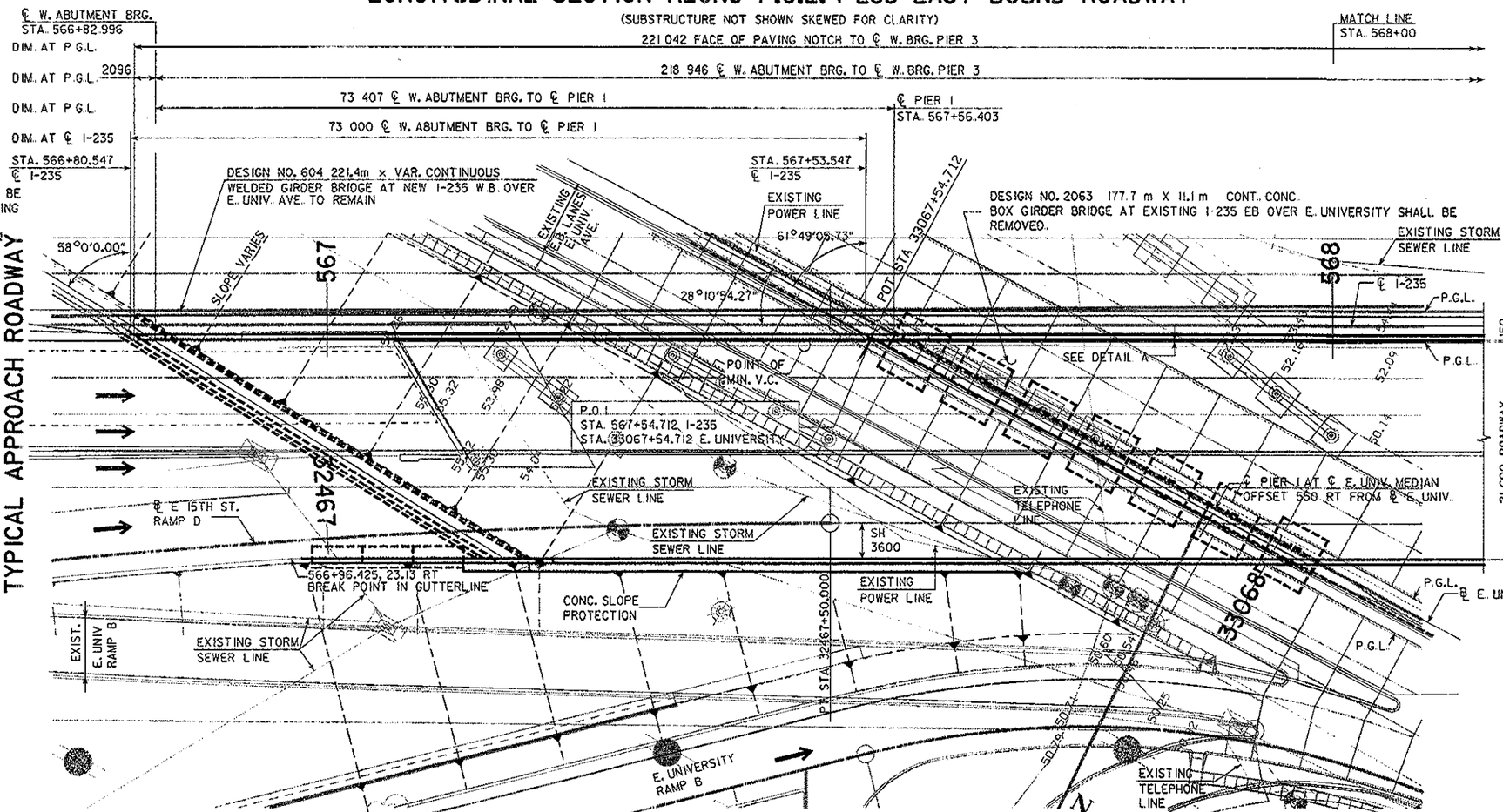

SITUATION PLAN

EXISTING TRAFFIC TO BE MAINTAINED ON EXISTING WEST BOUND BRIDGE DURING CONSTRUCTION

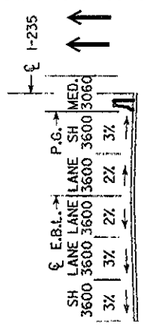

NOTES:
ALL DIMENSIONS ARE IN MILLIMETERS (mm) UNLESS OTHERWISE NOTED OR SHOWN.
ALL ELEVATIONS ON THESE PLANS SHOWN IN METERS.
ADD 200 METERS TO ALL SPOT ELEVATIONS.
FOR LIGHT POLE AND CONDUIT LAYOUT DETAILS, SEE DESIGN SHEET 82.
FOR DECK DRAIN LOCATIONS, SEE DESIGN SHEET 62.
CONCRETE SLOPE PROTECTION FOR EB AND WB BRIDGES INCLUDED IN THIS DESIGN.
FOR DEMOLITION DETAILS, SEE DESIGN SHEET 90.
FOR RELOCATION OF EXISTING UTILITIES SEE UTILITY RELOCATION PLANS.

REVISED 9-10-04: REVISED PIER ELEVATIONS & VERTICAL CLEARANCE

MINIMUM VERTICAL CLEARANCE (UNIVERSITY AVE)
OVERHEAD STATION=567+44.031
OVERHEAD ELEVATION=262.101 (2.105 m RT)
DEPTH OF SUPERSTRUCTURE=~~2.891 m~~ 2.853
UNDERPASS STATION=33067+46.295
UNDERPASS ELEVATION=250.411 (6.900 m RT)
MINIMUM VERTICAL CLEARANCE=~~6.799 m~~ 8.837

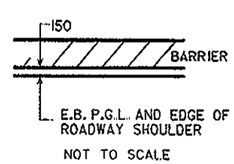

NOT TO SCALE

DETAIL A

PROPOSED GRADE ON I-235

G1 = +0.5996 % G2 = -2.0536 %

PI STA 568+90
PI ELEV 262.970
VC = 320 m

PROPOSED GRADE ON E. 15TH ST. RAMP D ℄

PROFILE GRADE ENDS AT
STATION 32466+39.309, ELEV. 261.077

CURVE DATA RAMP E15D

Δ = 9°0'0.00" (RT)
T = 62.961 m
L = 125.664 m
E = 2.474 m
R = 800.000 m

PROPOSED GRADE ON E. UNIVERSITY AVE.

G1 = -0.8500 % G2 = -6.0000 %

PI STA 33068+80
PI ELEV 249.362
VC = 160 m

TRAFFIC ESTIMATE

I-235 A.D.T. = 48,500 VPD (1996)
A.D.T. = 74,100 VPD (2025)
8% TRUCKS

LOCATION

I-235 EB OVER E. UNIVERSITY AVE.
T 79 N R 24 W
SECTION 36
SAYLOR TOWNSHIP AND
T 78 N R 24 W
SECTION 2
LEE TOWNSHIP
POLK COUNTY
CITY OF DES MOINES

FHWA #: 04292I
MAINT. #: 7710.6R235

DESIGN FOR VARIABLE SKEW (R.A.)

218.946 m x 21.6 m CONTINUOUS WELDED GIRDER BRIDGE

VARIABLE END SPANS VARIABLE CENTER SPAN

SITUATION PLAN

STA. 567+54.712 I-235 = STA. 33067+54.712 E. UNIV. AVE. JAN. 2004

POLK COUNTY

IOWA DEPARTMENT OF TRANSPORTATION - HIGHWAY DIVISION

DESIGN SHEET NO. 3 OF 90 FILE NO. 29554 DESIGN NO. 705

DESIGNED BY HRH CHECKED BY NAM
DETAILED BY NMB CADD FILE h770705.s03

POLK COUNTY | PROJECT NUMBER | SHEET NUMBER 4

PLOTTED: 09-SEP-2004 14:37 wgregory K:\b36630\705\DRAWINGS\ZPLOT_B03.dgn
PLOTTED: 09-SEP-2004 14:37 wgregory K:\b36630\705\DRAWINGS\ZPLOT_B03.dgn

BENCH MARK NO. 691, STA. 567+56.577 103.35 RT. SET RR SPK N. SIDE P POLE NE QUAD E. 19TH & WALKER ELEV. 251.587

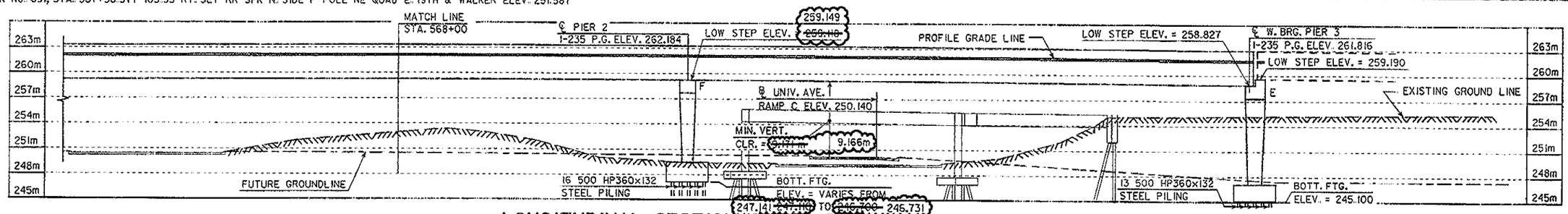

LONGITUDINAL SECTION ALONG P.G.L. I-235 EAST BOUND ROADWAY

(SUBSTRUCTURE NOT SHOWN SKEWED FOR CLARITY)

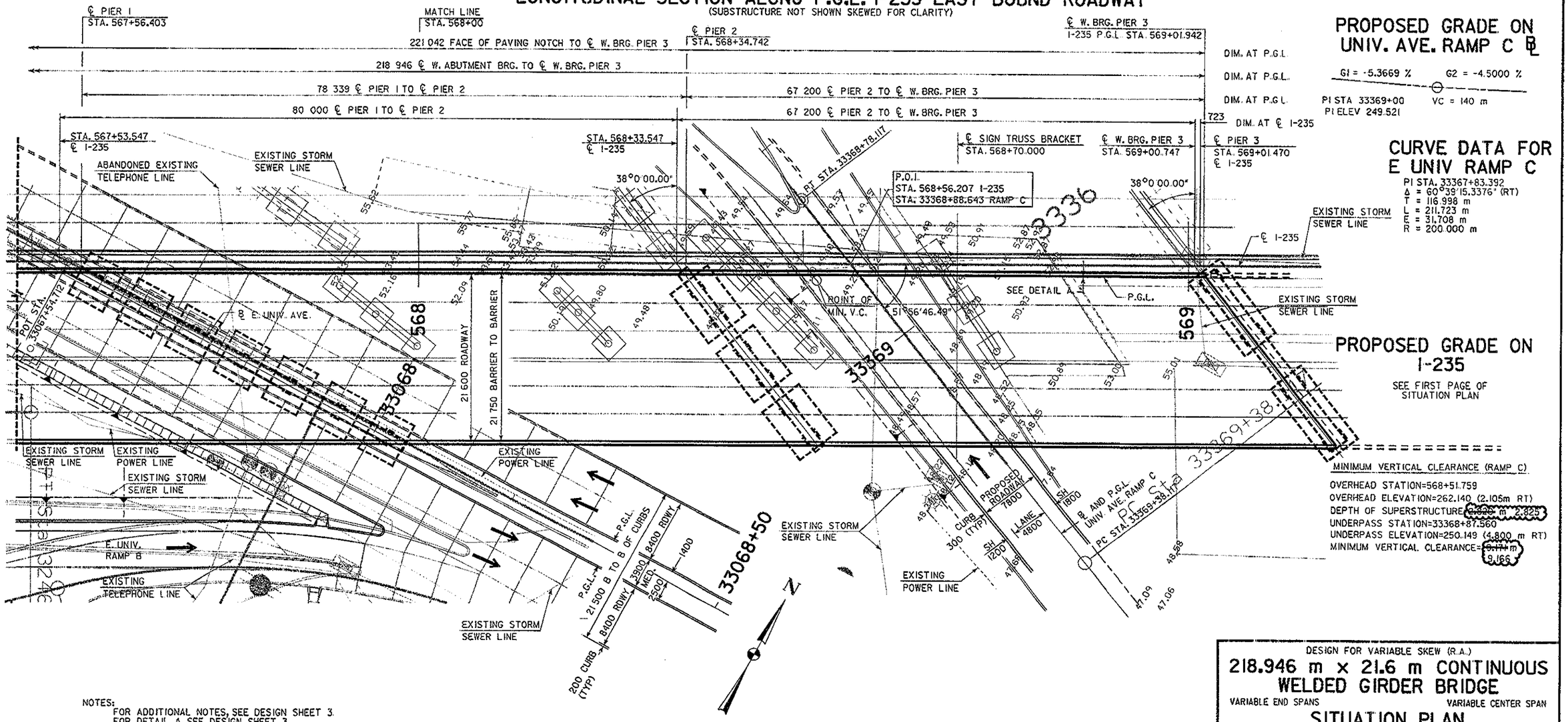

PROPOSED GRADE ON UNIV. AVE. RAMP C ℄

G1 = -5.3669 % G2 = -4.5000 %

PI STA 33369+00 VC = 140 m

PI ELEV 249.521

CURVE DATA FOR E UNIV RAMP C

PI STA. 33367+83.392
Δ = 60°39'15.3376" (RT)
T = 116.998 m
L = 211.723 m
E = 31.708 m
R = 200.000 m

PROPOSED GRADE ON I-235

SEE FIRST PAGE OF SITUATION PLAN

MINIMUM VERTICAL CLEARANCE (RAMP C)

OVERHEAD STATION=568+51.759
OVERHEAD ELEVATION=262.140 (2.105m RT)
DEPTH OF SUPERSTRUCTURE ~~2.939 m~~ 2.825
UNDERPASS STATION=33368+87.560
UNDERPASS ELEVATION=250.149 (4.800 m RT)
MINIMUM VERTICAL CLEARANCE= ~~9.777 m~~ 9.166

NOTES:
FOR ADDITIONAL NOTES, SEE DESIGN SHEET 3.
FOR DETAIL A, SEE DESIGN SHEET 3.

SITUATION PLAN

REVISED 9-10-04: REVISED PIER ELEVATIONS & VERTICAL CLEARANCE

DESIGN FOR VARIABLE SKEW (R.A.)

218.946 m x 21.6 m CONTINUOUS WELDED GIRDER BRIDGE

VARIABLE END SPANS VARIABLE CENTER SPAN

SITUATION PLAN

STA. 567+54.712 I-235 = STA. 33067+54.712 E. UNIV. AVE. JAN. 2004

POLK COUNTY

IOWA DEPARTMENT OF TRANSPORTATION - HIGHWAY DIVISION

DESIGN SHEET NO. 4 OF 90 FILE NO. 29554 DESIGN NO. 705

DESIGNED BY HRH CHECKED BY NAM
DETAILED BY NMB CADD FILE h770705.s04

POLK COUNTY PROJECT NUMBER SHEET NUMBER 5

PLOTTED: 09-SEP-2004 14:37 WGREGORY University Ave\366301\705\DRAWINGS\ZPLOT_B04.dgn
PLOTTED: 09-SEP-2004 14:37 WGREGORY K:\b366301\705\DRAWINGS\ZPLOT_B04.dgn

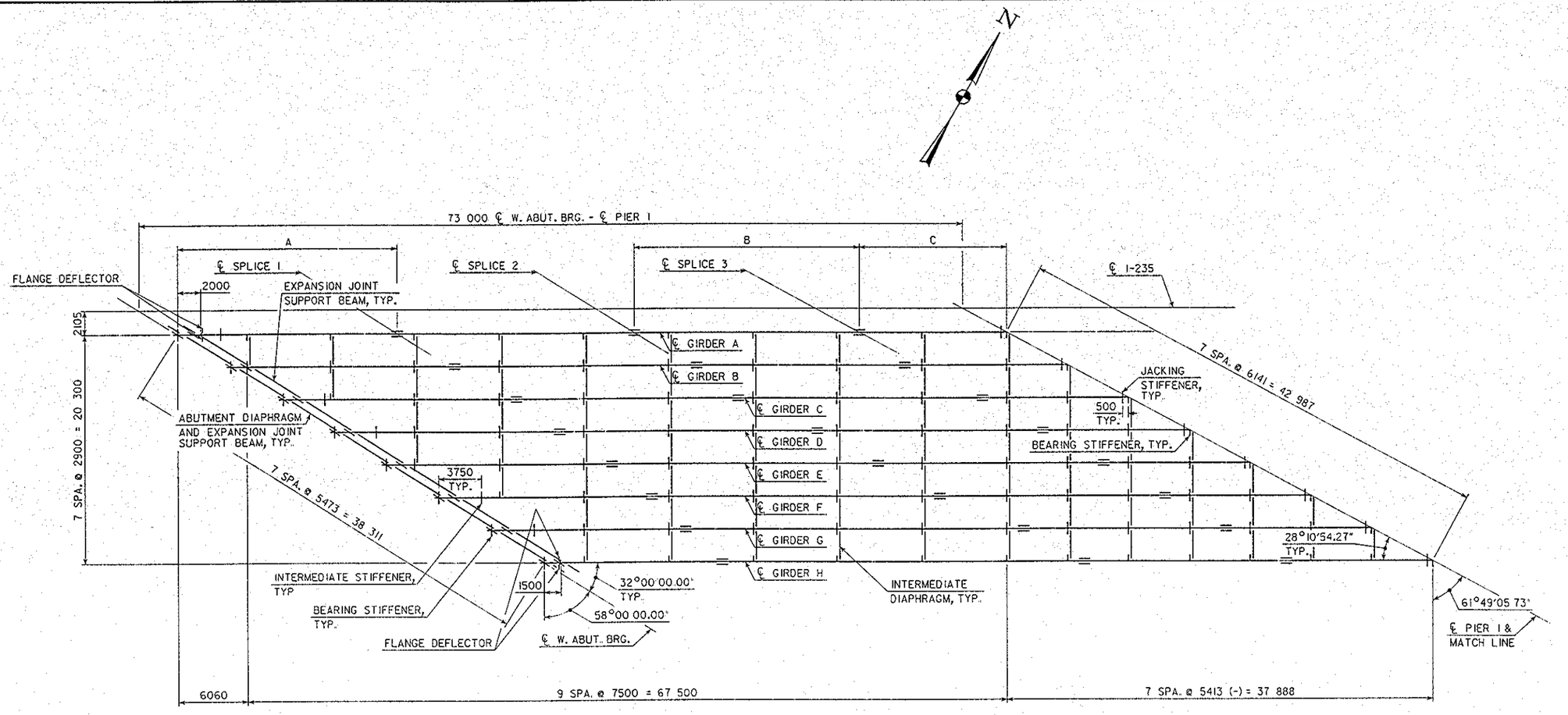

FRAMING PLAN - SPAN 1

TABLE OF DIMENSIONS			
GIRDER	A	B	C
A	19 560	20 000	13 000
B	20 000	18 600	14 400
C	20 778	21 825	13 000
D	20 000	20 000	13 000
E	20 000	20 000	13 000
F	18 855	20 000	13 000
G	17 214	17 975	13 000
H	15 800	17 975	13 000

NOTES:
FOR DIAPHRAGM DETAILS, SEE DESIGN SHEETS 31 AND 32.
FOR GIRDER DETAILS, SEE DESIGN SHEETS 27 THRU 30.
FOR SUPERSTRUCTURE NOTES, SEE DESIGN SHEET 32.
FOR STEEL DETAILS, SEE DESIGN SHEETS 48 THRU 50.
FOR EXPANSION JOINT DETAILS, SEE DESIGN SHEETS 70 THRU 75.
FOR CAMBER DIAGRAMS, SEE DESIGN SHEETS 37 THRU 46.

DESIGN FOR VARIABLE SKEW (R.A.)

218.946 m x 21.6 m CONTINUOUS WELDED GIRDER BRIDGE

VARIABLE END SPANS VARIABLE CENTER SPAN

SUPERSTRUCTURE DETAILS

STA. 567+54.712 I-235 = STA. 33067+54.712 E UNIV. AVE. JAN. 2004

POLK COUNTY

IOWA DEPARTMENT OF TRANSPORTATION - HIGHWAY DIVISION

DESIGN SHEET NO. 24 OF 90 FILE NO. 29554 DESIGN NO. 705

DESIGNED BY MJT CHECKED BY MJT/HRH
DETAILED BY DAL CADD FILE h770705.s24

POLK COUNTY | PROJECT NUMBER | SHEET NUMBER 25

PLOTTED: DLINENBERGER
PLOTTED: 13-MAY-2004 14:38
K:\D36630\705\DRAWINGS\ZPLOT_B21.dgn
University Ave 836630

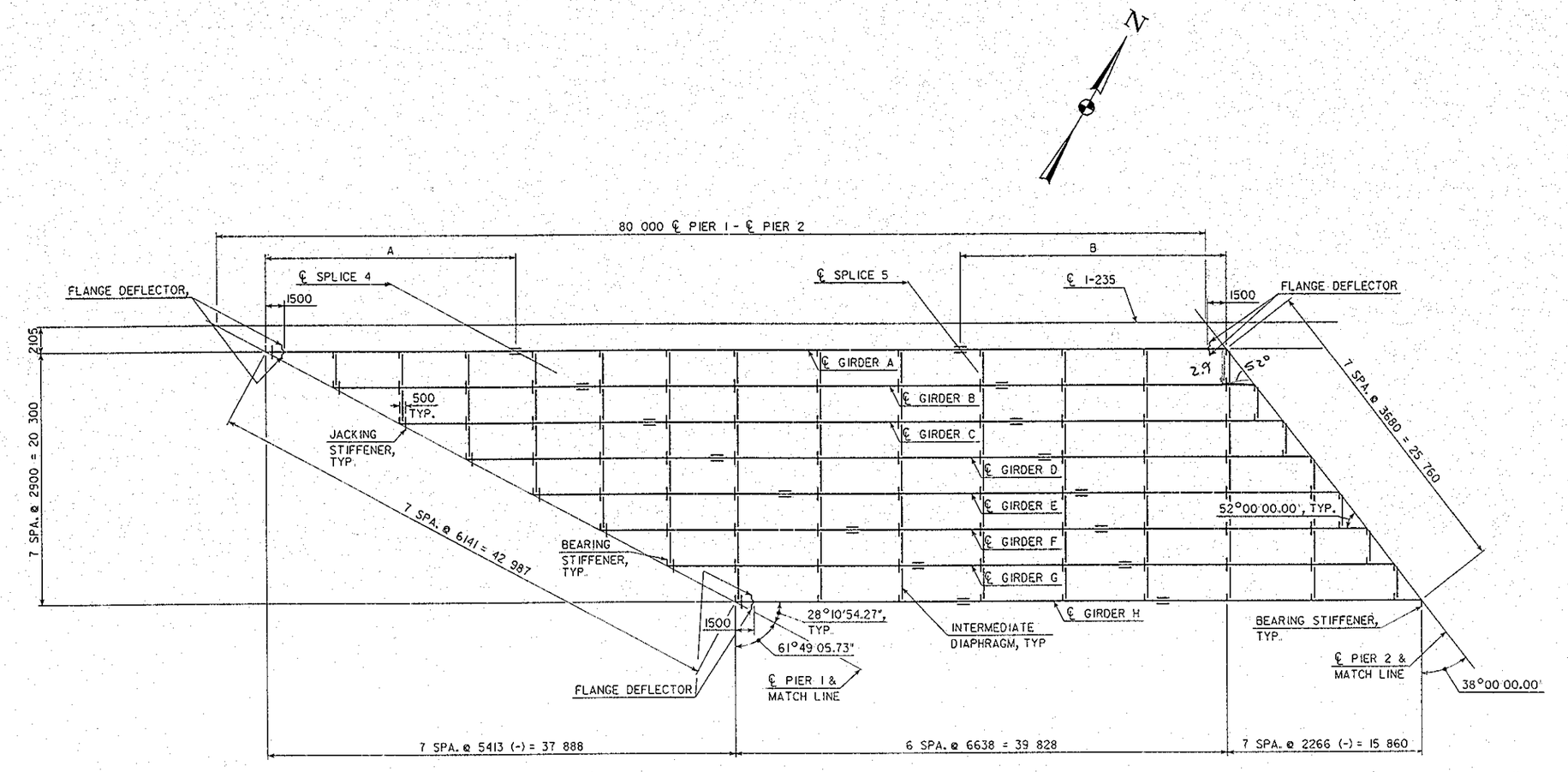

FRAMING PLAN - SPAN 2

$\tan 52° = \frac{2.9}{A}$ $A = 2\,266$ m

TABLE OF DIMENSIONS		
GIRDER	A	B
A	20 250	21 500
B	20 250	20 400
C	20 250	21 500
D	20 250	21 500
E	20 250	20 800
F	20 250	21 500
G	20 250	21 800
H	18 500	21 000

NOTES:
FOR DIAPHRAGM DETAILS, SEE DESIGN SHEETS 31 AND 32.
FOR GIRDER DETAILS, SEE DESIGN SHEETS 27 THRU 30
FOR SUPERSTRUCTURE NOTES, SEE DESIGN SHEET 32.
FOR STEEL DETAILS, SEE DESIGN SHEETS 48 THRU 50.
FOR CAMBER DIAGRAMS, SEE DESIGN SHEETS 37 THRU 46

DESIGN FOR VARIABLE SKEW (R.A.)

218.946 m x 21.6 m CONTINUOUS WELDED GIRDER BRIDGE

VARIABLE END SPANS — VARIABLE CENTER SPAN

SUPERSTRUCTURE DETAILS

STA 567+54.712 I-235 = STA. 33067+54.712 E. UNIV. AVE. JAN. 2004

POLK COUNTY

IOWA DEPARTMENT OF TRANSPORTATION - HIGHWAY DIVISION

DESIGN SHEET NO. 25 OF 90 FILE NO. 29554 DESIGN NO. 705

DESIGNED BY MJT CHECKED BY MJT/HRH
DETAILED BY DAL CADD FILE h770705.s25

POLK COUNTY | PROJECT NUMBER | SHEET NUMBER 26

PLOTTED: DLINENBERGER
PLOTTED: 13-MAY-2004 14:38
University Ave 936630
K:\b936301705\DRAWINGS\ZPLOT_822.dgn

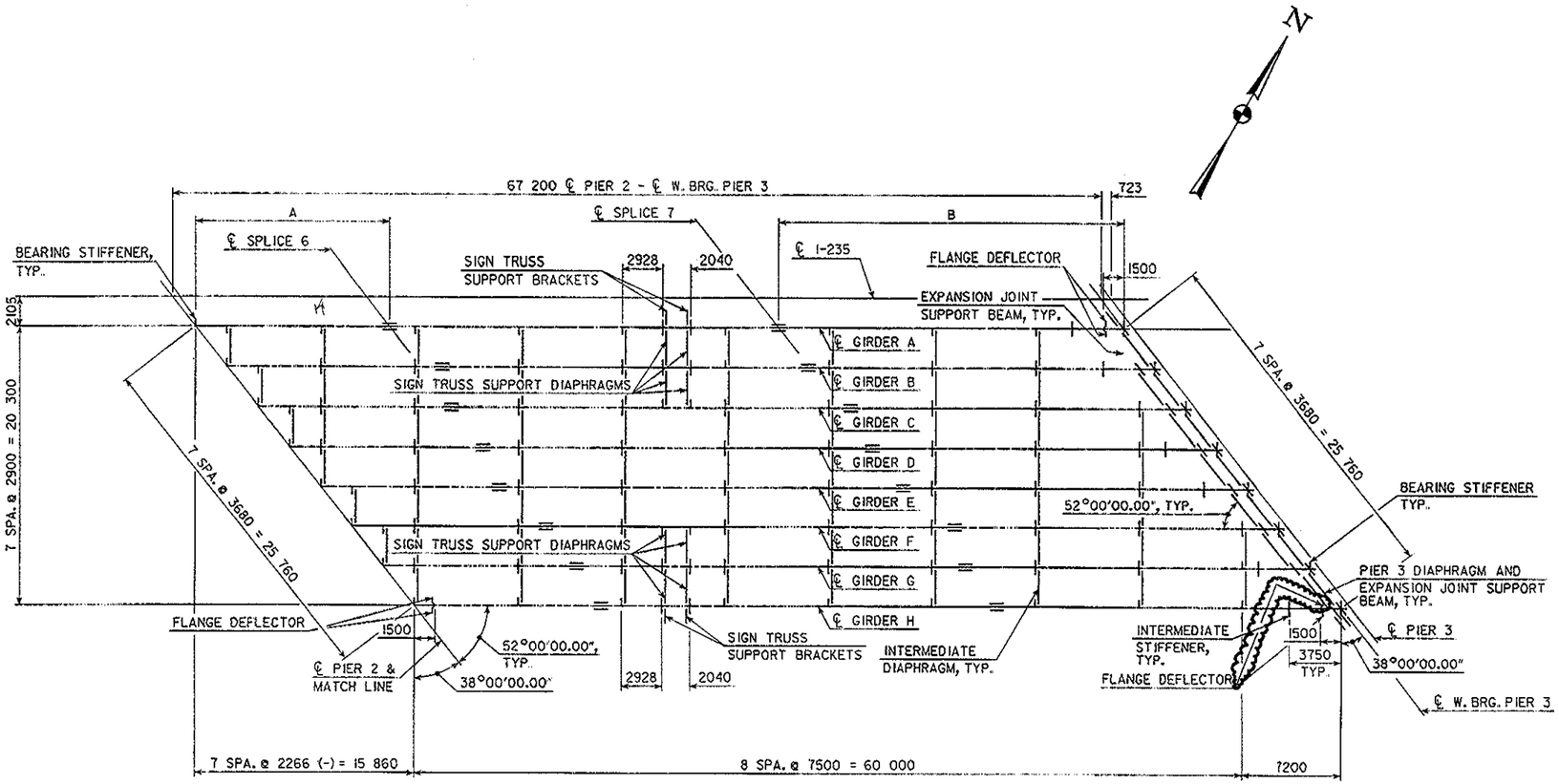

FRAMING PLAN - SPAN 3

TABLE OF DIMENSIONS

GIRDER	A	B
A	14 000	25 000
B	15 600	25 100
C	14 000	24 300
D	14 000	25 000
E	12 900	25 000
F	14 000	23 500
G	14 000	25 000
H	13 500	25 000

NOTES:
FOR DIAPHRAGM DETAILS, SEE DESIGN SHEETS 31 AND 32.
FOR GIRDER DETAILS, SEE DESIGN SHEETS 27 THRU 30.
FOR SUPERSTRUCTURE NOTES, SEE DESIGN SHEET 32.
FOR STEEL DETAILS, SEE DESIGN SHEETS 48 THRU 50.
FOR EXPANSION JOINT DETAILS, SEE DESIGN SHEETS 70 THRU 75.
FOR SIGN TRUSS DETAILS, SEE DESIGN SHEET 51.
FOR CAMBER DIAGRAMS, SEE DESIGN SHEETS 37 THRU 46.

REVISED 9-10-04: ADDED FLANGE DEFLECTOR.

DESIGN FOR VARIABLE SKEW (R.A.)

218.946 m x 21.6 m CONTINUOUS WELDED GIRDER BRIDGE

VARIABLE END SPANS — VARIABLE CENTER SPAN

SUPERSTRUCTURE DETAILS

STA. 567+54.712 I-235 = STA. 33067+54.712 E. UNIV. AVE. JAN. 2004

POLK COUNTY

IOWA DEPARTMENT OF TRANSPORTATION - HIGHWAY DIVISION

DESIGN SHEET NO. 26 OF 90 FILE NO. 29554 DESIGN NO. 705

DESIGNED BY MJT CHECKED BY MJT/HRH
DETAILED BY DAL CADD FILE h770705.s26

POLK COUNTY | PROJECT NUMBER | SHEET NUMBER 27

09-SEP-2004 14:39 vgregory K:\b36630\705\DRAWINGS\ZPLOT_823.dgn

PLOTTED: 09-SEP-2004 14:39 vgregory
PLOTTED: K:\b36630\705\DRAWINGS\ZPLOT_823.dgn
universityAve836630

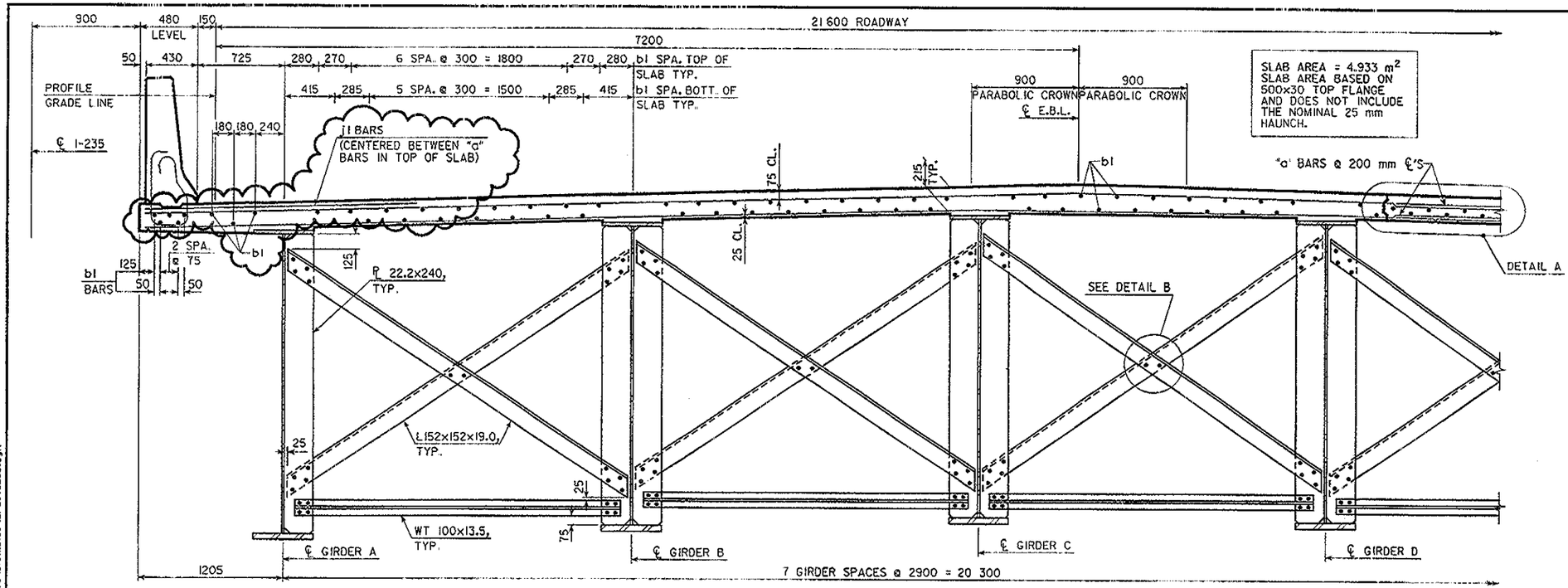

PART SECTION NEAR INTERMEDIATE DIAPHRAGM

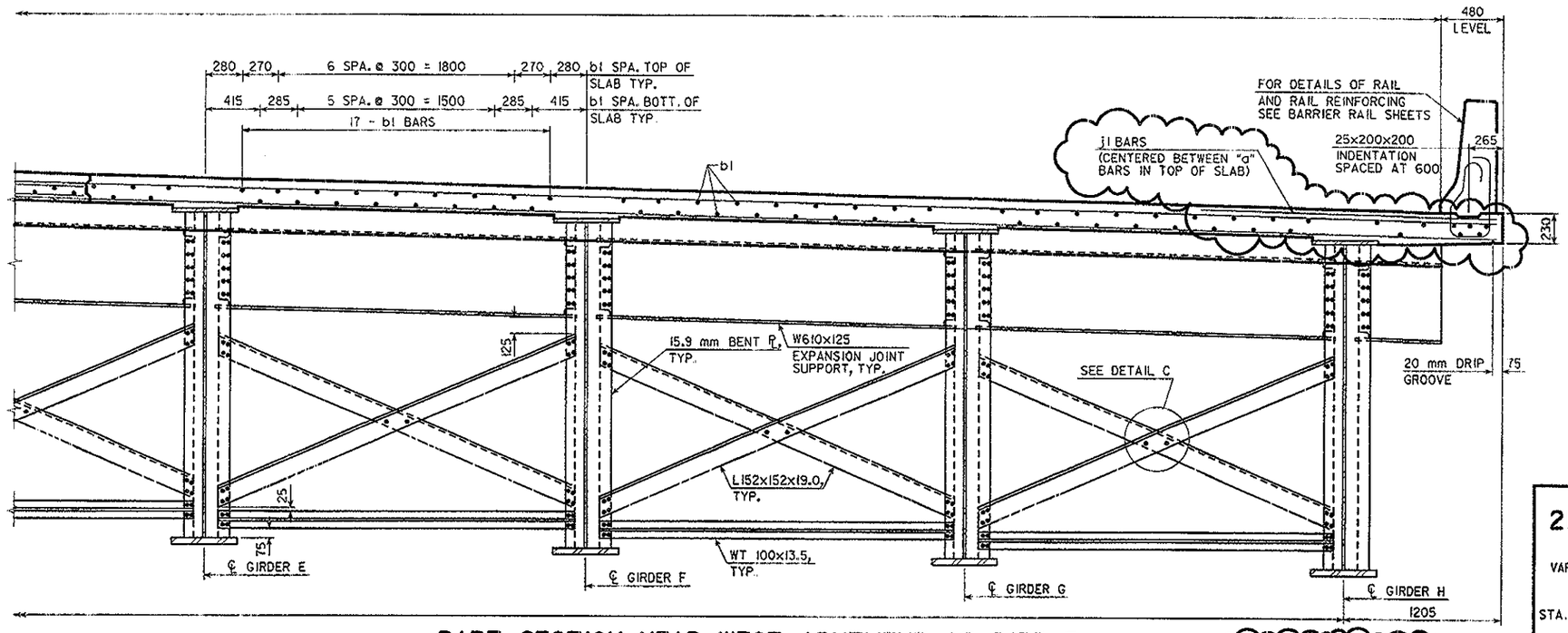

PART SECTION NEAR WEST ABUTMENT OR PIER 3

BEARING STIFFENERS NOT SHOWN FOR CLARITY

REVISED 9-10-04: ADDED j1 BARS

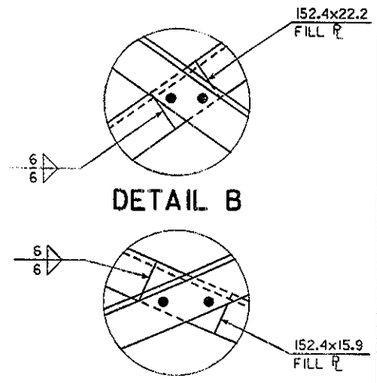

NOTES:
FOR ADDITIONAL STIFFENER AND WELDING DETAILS, SEE DESIGN SHEET 48.
FOR SUPERSTRUCTURE NOTES AND MISCELLANEOUS DETAILS, SEE DESIGN SHEET 32.
FOR DETAIL A SEE DESIGN SHEET 32.
FOR EXPANSION JOINT SUPPORT, SEE DESIGN SHEETS 70 THRU 72.

DESIGN FOR VARIABLE SKEW (R.A.)

218.946 m x 21.6 m CONTINUOUS WELDED GIRDER BRIDGE

VARIABLE END SPANS — VARIABLE CENTER SPAN

SUPERSTRUCTURE DETAILS

STA. 567+54.712 I-235 = STA. 33067+54.712 E. UNIV. AVE. JAN. 2004

POLK COUNTY

IOWA DEPARTMENT OF TRANSPORTATION - HIGHWAY DIVISION

DESIGN SHEET NO. 31 OF 90 FILE NO. 29554 DESIGN NO. 705

DESIGNED BY MJT CHECKED BY NAM
DETAILED BY DAL CADD FILE h770705.s31

POLK COUNTY | PROJECT NUMBER | SHEET NUMBER 32

09-SEP-2004 14:40 vgregory K:\b36630\705\DRAWINGS\ZPLOT_833.dgn

PLOTTED: 09-SEP-2004 14:40 VGREGORY
K:\b36630\705\DRAWINGS\ZPLOT_833.dgn
University Ave

Wayne's Cell Phone
515 291-9290

SUPERSTRUCTURE NOTES:

THE FLOOR SLAB AS SHOWN INCLUDES 13 mm INTEGRAL WEARING SURFACE.

FORMS FOR THE SLAB AND BARRIER RAIL ARE TO BE SUPPORTED BY THE GIRDERS.

CLEAR DISTANCE FROM FACE OF CONCRETE TO NEAR REINFORCING BAR SHALL BE 50 mm UNLESS OTHERWISE NOTED OR SHOWN.

TOP TRANSVERSE REINFORCING STEEL IS TO BE PARALLEL TO AND 75 mm CLEAR BELOW TOP OF SLAB. BOTTOM TRANSVERSE REINFORCING STEEL IS TO BE PARALLEL TO AND 25 mm CLEAR ABOVE BOTTOM OF SLAB. TOP AND BOTTOM REINFORCING STEEL IS TO BE SUPPORTED BY INDIVIDUAL EPOXY COATED METAL BAR CHAIRS SPACED AT NO MORE THAN 900 mm CENTERS LONGITUDINALLY AND TRANSVERSELY, OR BY CONTINUOUS ROWS OF EPOXY COATED METAL BAR HIGH CHAIRS OR SLAB BOLSTERS SPACED 1200 mm APART.

ALL REINFORCING BARS ARE TO BE EPOXY COATED.

ALL FIELD CONNECTIONS ARE TO BE BOLTED USING "HIGH STRENGTH BOLTS". UNLESS OTHERWISE NOTED, ALL OPEN HOLES ARE TO BE 24 mmϕ AND ALL BOLTS ARE TO BE 22.2 mmϕ.

BOTTOM FLANGES ARE TO BE PERPENDICULAR TO WEBS AT THE REACTION POINTS.

FILL ℄ THICKNESSES SHOWN ON PLANS ARE BASED ON NOMINAL GIRDER DIMENSIONS. THESE THICKNESSES ARE TO BE VERIFIED OR ADJUSTED DURING FABRICATION TO SECURE A CLOSE FIT. EACH FILL PLATE SHALL FIT TO THE NEAREST 2 mm IN THICKNESS AND SINGLE PLATES ARE REQUIRED AT EACH FILL LOCATION. GIRDERS ARE TO BE TRULY SQUARE AT SPLICE POINTS WITH FLANGES PERPENDICULAR TO WEBS.

THE DESIGN DRAWINGS INDICATE AWS PREQUALIFIED WELDED JOINTS. ALTERNATE JOINT DETAILS MAY BE SUBMITTED FOR APPROVAL.

MAGNETIC PARTICLE INSPECTION OF WELDS, IN ACCORDANCE WITH THE STANDARD SPECIFICATIONS, WILL BE REQUIRED.

BRACING IN CLOSURE POUR BAY SHALL BE INSTALLED AFTER THE TWO ADJACENT SLABS ARE POURED AND PRIOR TO PLACING THE CLOSURE POUR. THE BOLT HOLES SHALL BE FIELD DRILLED IN THE CROSS BRACING MEMBERS TO PROVIDE ALLOWANCES FOR FIT UP OF DIAPHRAGMS.

IN ADDITION TO THE REQUIREMENTS OF 4152 OF THE STANDARD SPECIFICATIONS CHARPY V-NOTCH REQUIREMENTS SHALL ALSO APPLY TO THE STIFFENERS CONNECTING THE EXPANSION JOINT SUPPORT BEAM TO THE GIRDERS AT ALL EXPANSION JOINT LOCATIONS AND THE CONNECTION PLATES, DIAPHRAGMS AND SUPPORT BRACKETS FOR THE SIGN TRUSS.

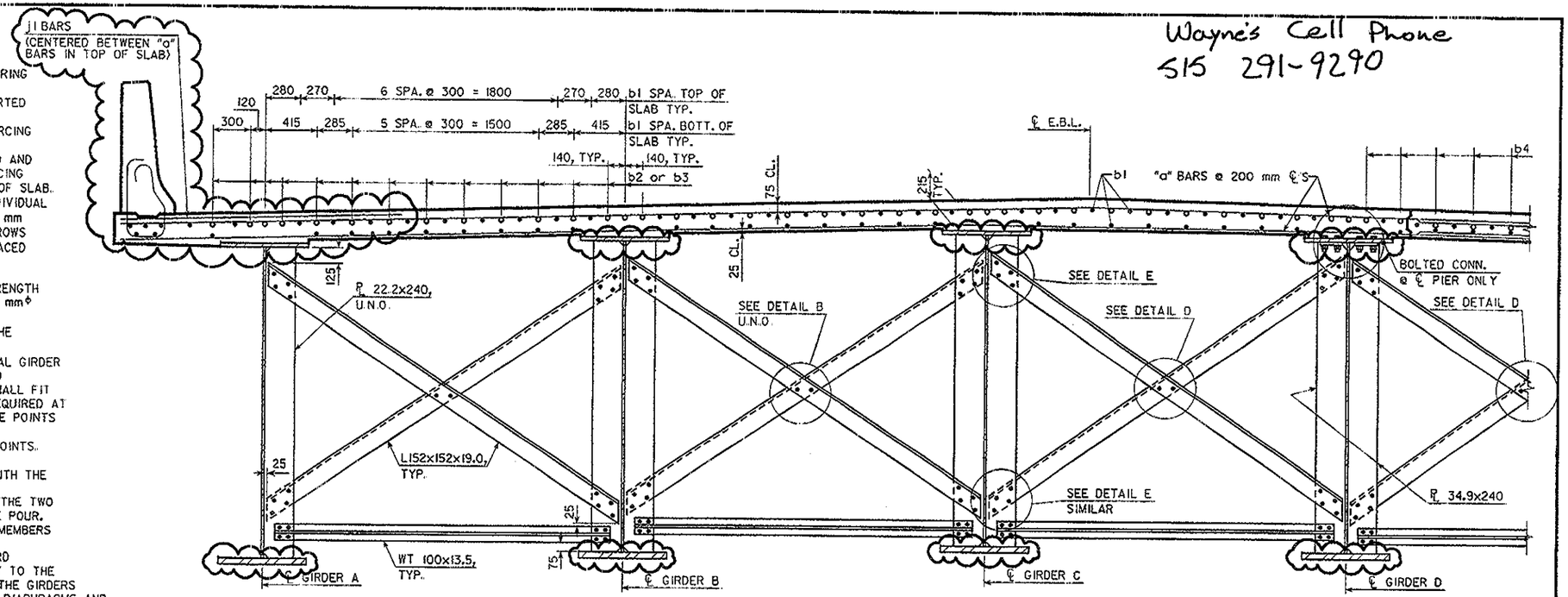

PART SECTION NEAR PIER

(SECTION CUT WHERE GIRDER D IS AT ℄ PIER)

WEATHERING STEEL NOTES:

ALL STRUCTURAL STEEL, EXCEPT AS NOTED, SHALL CONFORM TO ASTM A709M GRADE 345W. THE MINIMUM YIELD POINT FOR GRADE 345W STRUCTURAL STEEL IS 345 MPa FOR PLATES 100 mm AND UNDER IN THICKNESS, AND ALL STRUCTURAL SHAPES. THE GRADE 345W STEEL IS A WEATHERING STEEL AND IS TO REMAIN UNPAINTED, EXCEPT AS NOTED IN THESE PLANS AND IN 2408.30 OF THE STANDARD SPECIFICATIONS.

FLANGE DEFLECTORS AS DETAILED ON DESIGN SHEET 48 ARE TO BE GRADE 250 OR 345W. FLOOR DRAINS INCLUDING PLATES WELDED TO THE DRAIN FOR DRAIN SUPPORT ARE TO BE GRADE 250 STEEL.

ALL PIECES COMPRISING THE ABUTMENT AND PIER BEARINGS SHALL COMPLY WITH THE REQUIREMENTS AS STATED IN THE NOTES ON DESIGN SHEETS 52 THRU 55.

SHEAR STUDS ARE TO BE OF AN APPROVED TYPE LISTED IN MATERIALS I.M. 453.10, APPENDIX A.

THE FINISH ON FLOOR DRAINS, BEARINGS, FLANGE DEFLECTORS AND WEATHERING STEEL SHALL BE IN ACCORDANCE WITH THE PLAN NOTES AND STANDARD SPECIFICATIONS.

THE GRADE 345W STEEL FOR THE WEBS OF THE EXTERIOR GIRDERS OF THE BRIDGE SHALL BE OF THE SAME TYPE AND FROM THE SAME PRODUCER.

BOLTS FOR USE WITH WEATHERING STEEL SHALL BE A325 TYPE III WITH A563 GRADE DH3 NUTS AND F436 TYPE III WASHERS.

BOLTS USED TO SPLICE GIRDER SECTIONS ARE TO BE INSTALLED SUCH THAT NUTS ARE ON THE INSIDE FACE OF THE GIRDER WEBS FOR THE EXTERIOR GIRDERS, AND ON THE TOP OF BOTH TOP AND BOTTOM FLANGES OF ALL THE GIRDERS.

THE STEEL SHALL BE KEPT FREE OF OIL, GREASE, DIRT, CRAYON OR CHALK MARKS, CONCRETE SPATTER AND ANY OTHER FOREIGN MATTER THAT MAY AFFECT THE NATURAL OXIDATION OF THE STEEL. ANY FOREIGN MATTER REMAINING ON THE STEEL AFTER COMPLETION OF BRIDGE CONSTRUCTION SHALL BE REMOVED BY THE BRIDGE CONTRACTOR AS DIRECTED BY THE ENGINEER. THE RESULTANT SURFACE SHALL BE FREE OF ALL VISIBLE RESIDUES. ALL COSTS ASSOCIATED WITH CLEANING STEEL SURFACES SHALL BE BORNE BY THE BRIDGE CONTRACTOR.

SEAL MATERIAL FOR CAULKING SHALL BE NEUTRAL CURE AND NON SAG SILICONE. THREE PRODUCTS MEETING THESE CRITERIA ARE DOW 888, CSL342 AND CRAFCO-ROADSAVER SILICONE JOINT SEALANT.

TO ENSURE UNIFORM WEATHERING, ALL UNPAINTED AREAS OF OUTSIDE SURFACES OF THE FASCIA GIRDERS SHALL RECEIVE, AFTER BLASTING, AT LEAST THREE UNIFORM APPLICATIONS OF WATER MIST WITH A 24 HOUR INTERVAL BETWEEN APPLICATIONS. EACH APPLICATION SHALL BE APPLIED ON DRY SURFACES. THE WATER MIST APPLICATION SHALL BE PERFORMED WITHIN 48 HOURS AFTER THE PAINTED SURFACES HAVE BEEN PROPERLY CURED. ALL WATER MIST APPLICATIONS SHALL BE WITNESSED BY A REPRESENTATIVE OF THE CONTRACTING AUTHORITY.

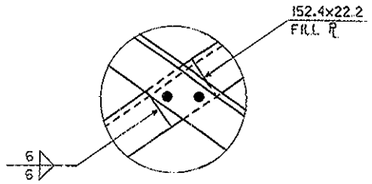

DETAIL B

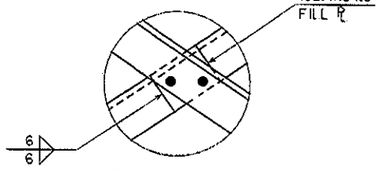

DETAIL D

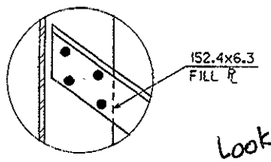

DETAIL E

Looking East

300 mm to South

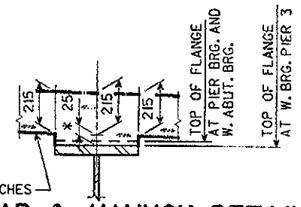

TYP. SLAB & HAUNCH DETAIL

* THE HAUNCH DIMENSION SHOWN IS THE NOMINAL HAUNCH DIMENSION NEAR THE WEST BEARING AT PIER 3. FOR THE SLAB THICKNESS OVER THE GIRDER AT ANY LOCATION THE NOMINAL HAUNCH DIMENSION IS TO BE DECREASED BY THE ADDITIONAL FLANGE THICKNESS AT THAT POINT AND INCREASED OR DECREASED BY THE AMOUNT INDICATED ON THE "HAUNCH THICKENING DIAGRAM" SHOWN ON DES. SHTS. 37 THRU 46 AND MAY BE ADDITIONALLY INCREASED OR DECREASED TO COMPENSATE FOR CONSTRUCTION INACCURACIES. THE MAXIMUM HAUNCH ALLOWED IS 50 mm AND THE MINIMUM HAUNCH ALLOWED IS 0.

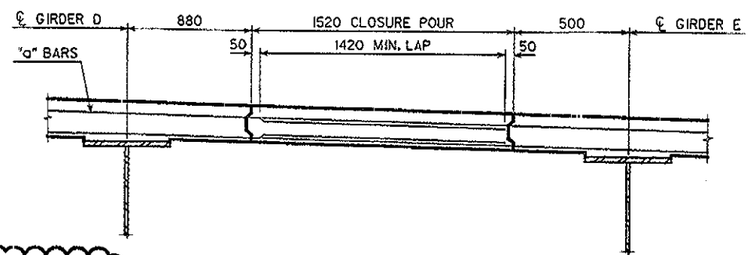

DETAIL A

NOTES:
FOR ADDITIONAL STIFFENER AND WELDING DETAILS, SEE DESIGN SHEET 48.
FOR LOCATION OF DETAIL A, SEE DESIGN SHEET 31.
U.N.O. DENOTES UNLESS NOTED OTHERWISE.

REINFORCING BAR SIZE

MARK	SIZE
a	22
b	19
e	22

REVISED 9-10-04: ADDED j1 BARS & CHANGED FLANGE SIZES

DESIGN FOR VARIABLE SKEW (R.A.)

218.946 m x 21.6 m CONTINUOUS WELDED GIRDER BRIDGE

VARIABLE END SPANS — VARIABLE CENTER SPAN

SUPERSTRUCTURE DETAILS

STA. 567+54.712 I-235 = STA. 33067+54.712 E. UNIV. AVE. JAN. 2004

POLK COUNTY

IOWA DEPARTMENT OF TRANSPORTATION - HIGHWAY DIVISION

DESIGN SHEET NO. 32 OF 90 FILE NO. 29554 DESIGN NO. 705

DESIGNED BY MJT CHECKED BY NAM
DETAILED BY DAL CADD FILE h770705.s32

POLK COUNTY | PROJECT NUMBER | SHEET NUMBER 33

09-SEP-2004 14:40 wgregory K:\b36630\705\DRAWINGS\ZPLOT.B35.dgn

PLOTTED: 09-SEP-2004 14:40
PLOTTED BY: WGREGORY
K:\b36630\705\DRAWINGS\ZPLOT.B35.dgn
University Ave

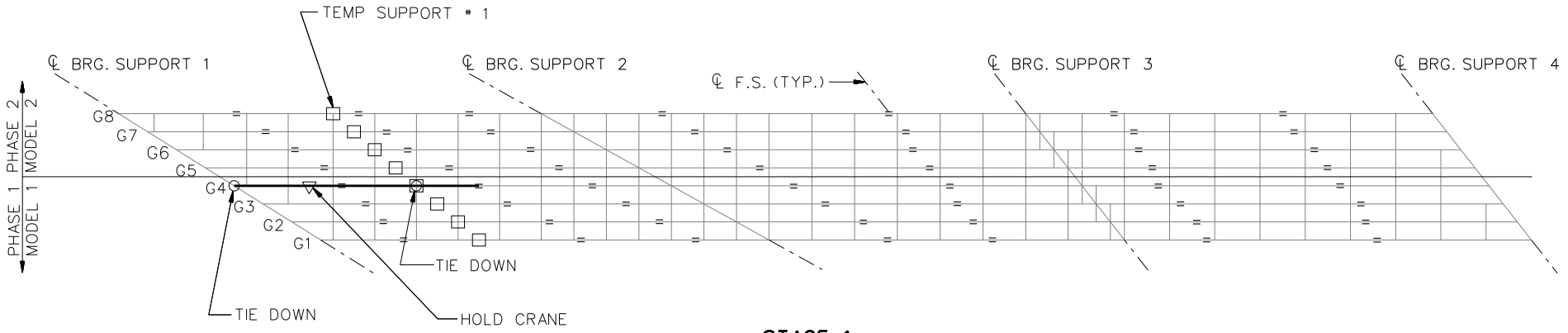

STAGE 1

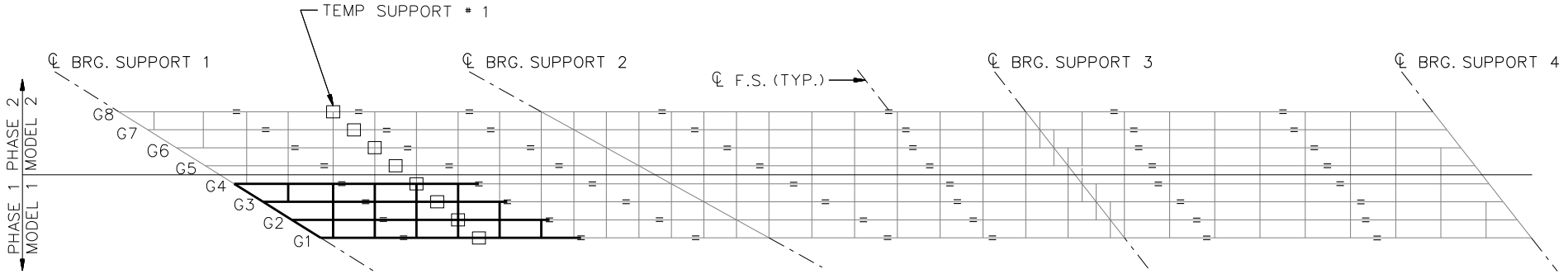

STAGE 4

LEGEND

▽ = HOLD OR LIFT CRANE

○ = TIE DOWN

□ = TEMPORARY SUPPORT STRUCTURE

NOTE:

ERECTION IS SHOWN FOR MODEL 1 ONLY (PHASE 1).
MODEL 2 (PHASE 2) WILL FOLLOW SIMILAR PROCEDURE.

NCHRP 12-79

BRIDGE EICSS2

GENERAL ERECTION PROCEDURE

SHEET 1 OF 4

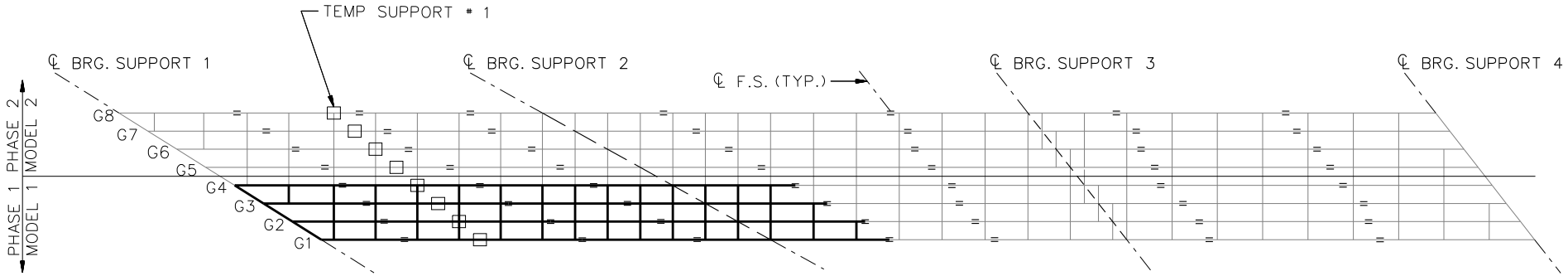

STAGE 8

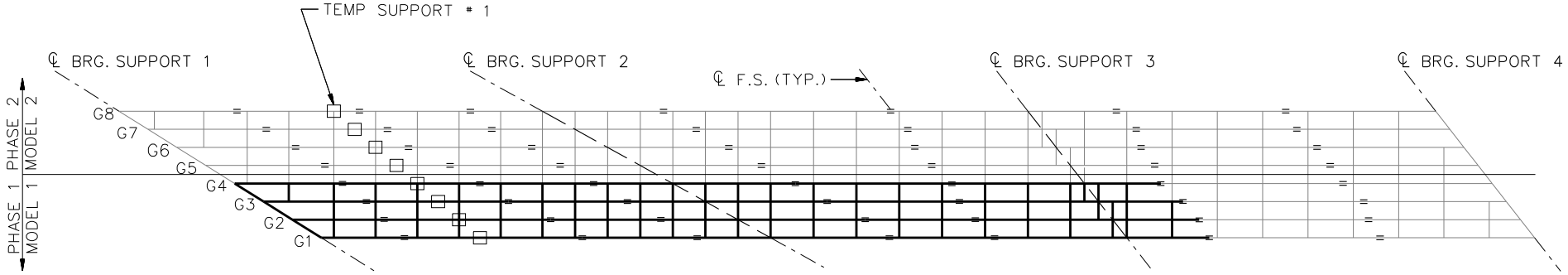

STAGE 12

LEGEND

▽ = HOLD OR LIFT CRANE

○ = TIE DOWN

□ = TEMPORARY SUPPORT STRUCTURE

NOTE:

ERECTION IS SHOWN FOR MODEL 1 ONLY (PHASE 1).
MODEL 2 (PHASE 2) WILL FOLLOW SIMILAR PROCEDURE.

NCHRP 12-79

BRIDGE EICSS2

GENERAL ERECTION PROCEDURE

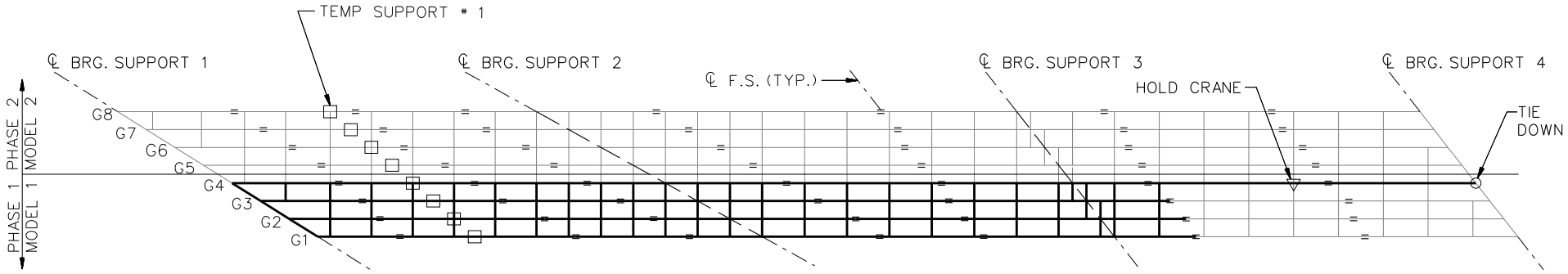

STAGE 13

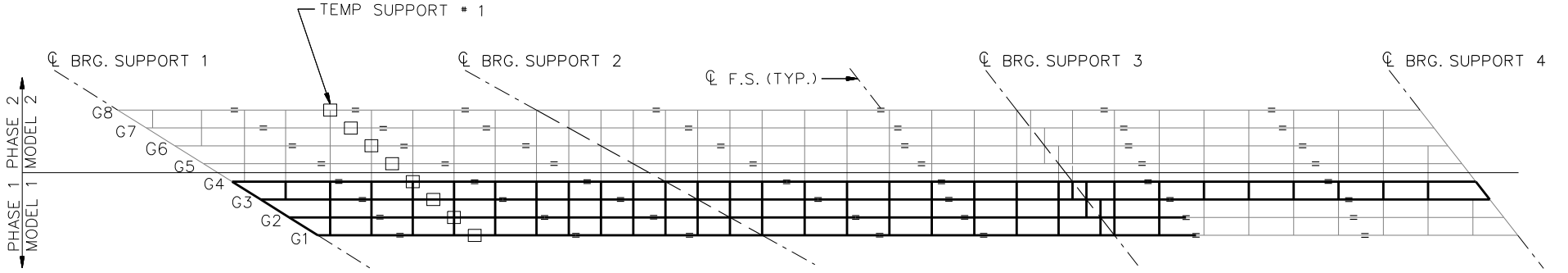

STAGE 14

LEGEND

▽ = HOLD OR LIFT CRANE

○ = TIE DOWN

□ = TEMPORARY SUPPORT STRUCTURE

NOTE:

ERECTION IS SHOWN FOR MODEL 1 ONLY (PHASE 1).
MODEL 2 (PHASE 2) WILL FOLLOW SIMILAR PROCEDURE.

NCHRP 12-79

BRIDGE EICSS2

GENERAL ERECTION PROCEDURE

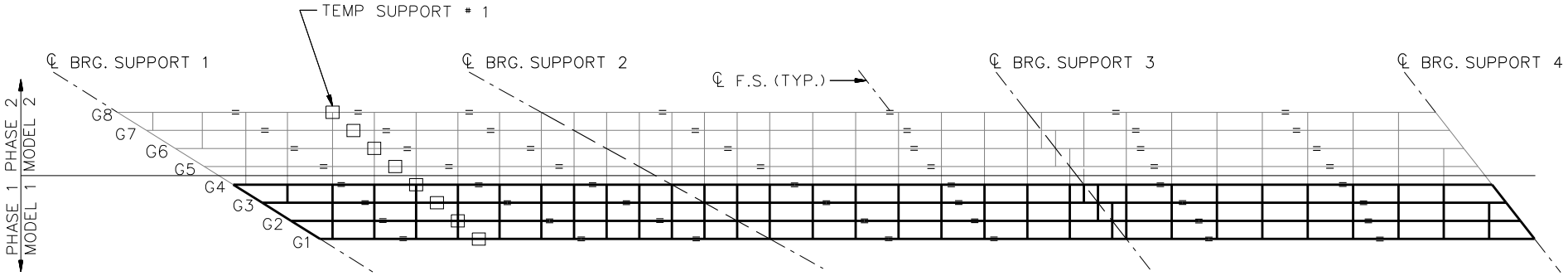

STAGE 16

LEGEND

▽ = HOLD OR LIFT CRANE

○ = TIE DOWN

□ = TEMPORARY SUPPORT STRUCTURE

NOTE:

ERECTION IS SHOWN FOR MODEL 1 ONLY (PHASE 1).
MODEL 2 (PHASE 2) WILL FOLLOW SIMILAR PROCEDURE.

NCHRP 12-79

BRIDGE EICSS2

GENERAL ERECTION PROCEDURE

SHEET 4 OF 4

NCHRP 12-79

EICSS12

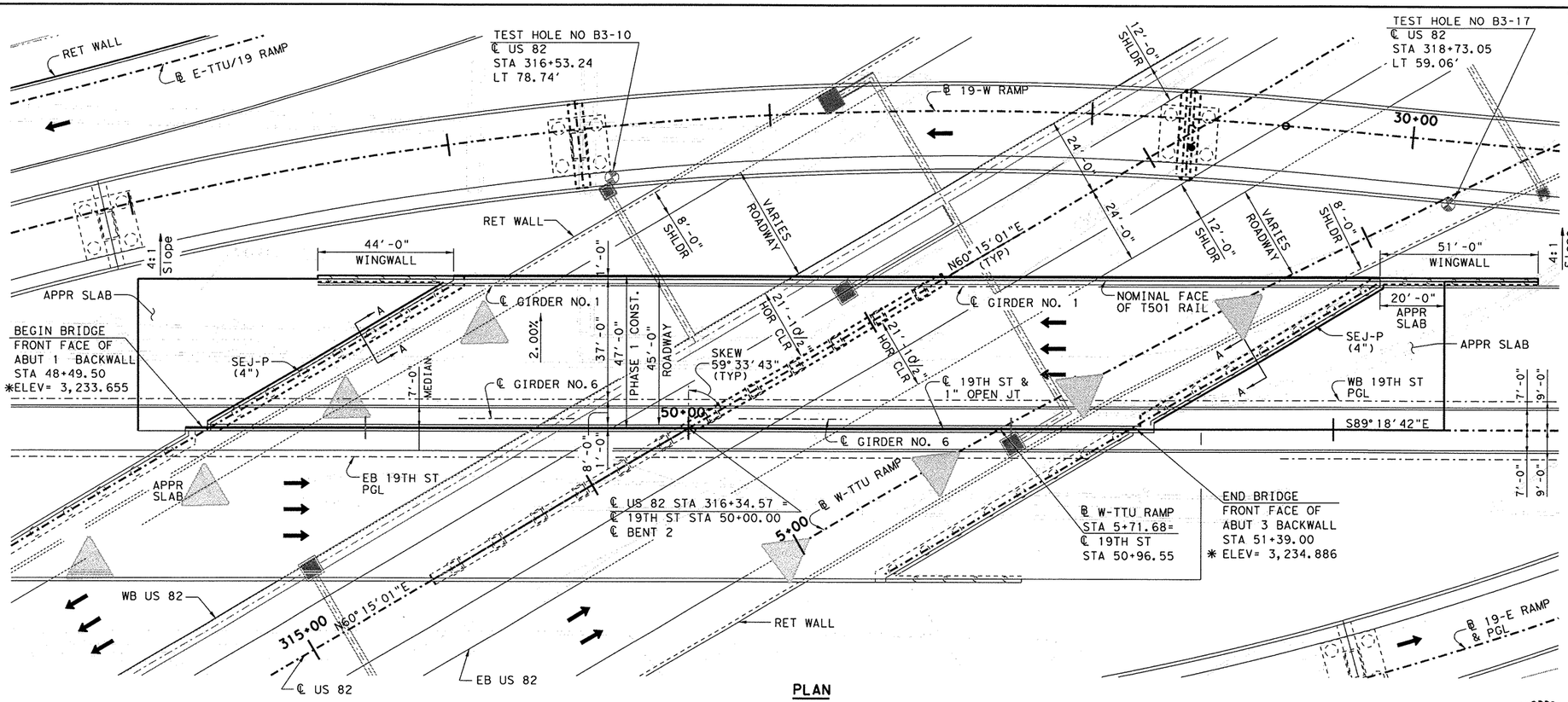

PLAN

DESIGN SPEED :	30 MPH
FUNCT CLASS :	URBAN LOCAL
ADT :	12,900/YR2000 ADT, 22,600/YR2020 ADT
PERM STR NO :	05-150-0-0380-01-045

NOTES:
1. ALL DIMENSIONS ARE IN FEET UNLESS SHOWN OTHERWISE.
2. SECTION A-A SEE SHEET 3 OF 3.
3. THE USE OF PRECAST PANEL IS NOT ALLOWED IN THIS BRIDGE.
4. ALL BENT AND ABUTMENT SHALL HAVE THE SAME BEARING.

* ELEVATION SHOWN IS AT ℄ OF 19TH STREET.

△ UNDERPASS ILLUMINATE

VERTICAL CLEARANCES ARE CONTROLLED BY THE EB STRUCTURE. SEE US 82 MAINLANE UNDERPASS AT 19TH STREET EB BRIDGE LAYOUT FOR LOCATION OF THE POINT OF MINIMUM VERTICAL CLEARANCE AND THE CALCULATED VERTICAL CLEARANCE.

STATE OF TEXAS
JOHN S. BEARD
92743
LICENSED PROFESSIONAL ENGINEER
9-10-2004

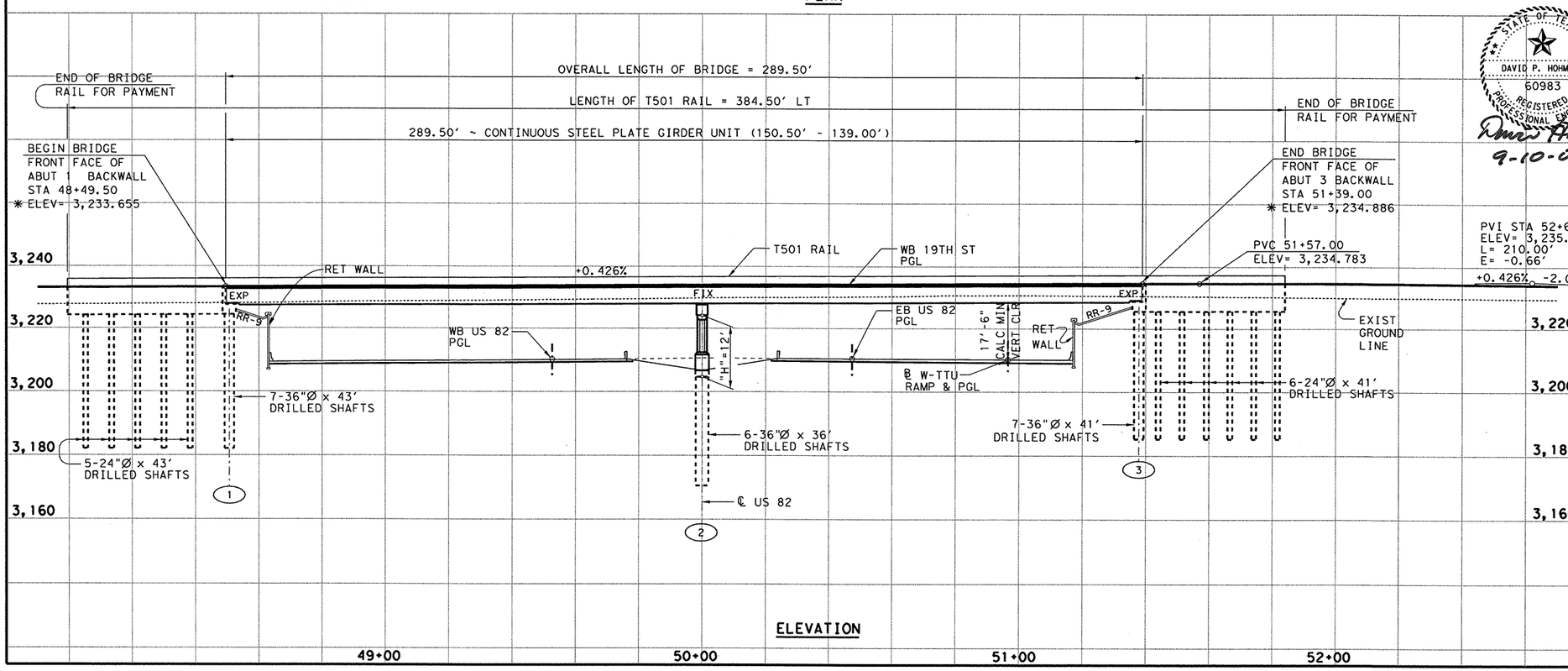

ELEVATION

STATE OF TEXAS
DAVID P. HOHMANN
60983
REGISTERED PROFESSIONAL ENGINEER
9-10-04

SCALE 0 20 40

STATE OF TEXAS
FLOYD A. MARTINEZ
82224
REGISTERED PROFESSIONAL ENGINEER
9.15.04

THE HORIZONTAL AND VERTICAL GEOMETRICAL DESIGN HAS BEEN DESIGNED BY ME OR UNDER MY RESPONSIBLE SUPERVISION.

HS 20 LOADING

No.	Revision	By	Date

STRUCTURAL ENGINEERING ASSOCIATES, INC.
CONSULTING ENGINEERS SAN ANTONIO . TEXAS

HNTB ARCHITECTS ENGINEERS PLANNERS
The HNTB Companies

 Texas Department of Transportation

U.S. 82 EAST-WEST FREEWAY

U.S. 82 MAINLANE UNDERPASS AT 19TH STREET WB BRIDGE LAYOUT

SHEET 1 OF 3

		FED.ROAD DIV. NO.	STATE	FEDERAL AID PROJECT NO.	SHEET NO.
Designed:	MC		TEXAS	~~NHP 55(1)~~	1465
Checked:	DAR	STATE DIST. NO.	COUNTY	CONTROL NO. / SECTION NO. / JOB NO.	HIGHWAY NO.
Drawn:	CSW	5	LUBBOCK	0380 / 01 / 064	US 82
Checked:	JCC				

DGN: MR
DATE:
DWG:
Ck: MR

PATH:
COMMENTS:
82191y01.dgn

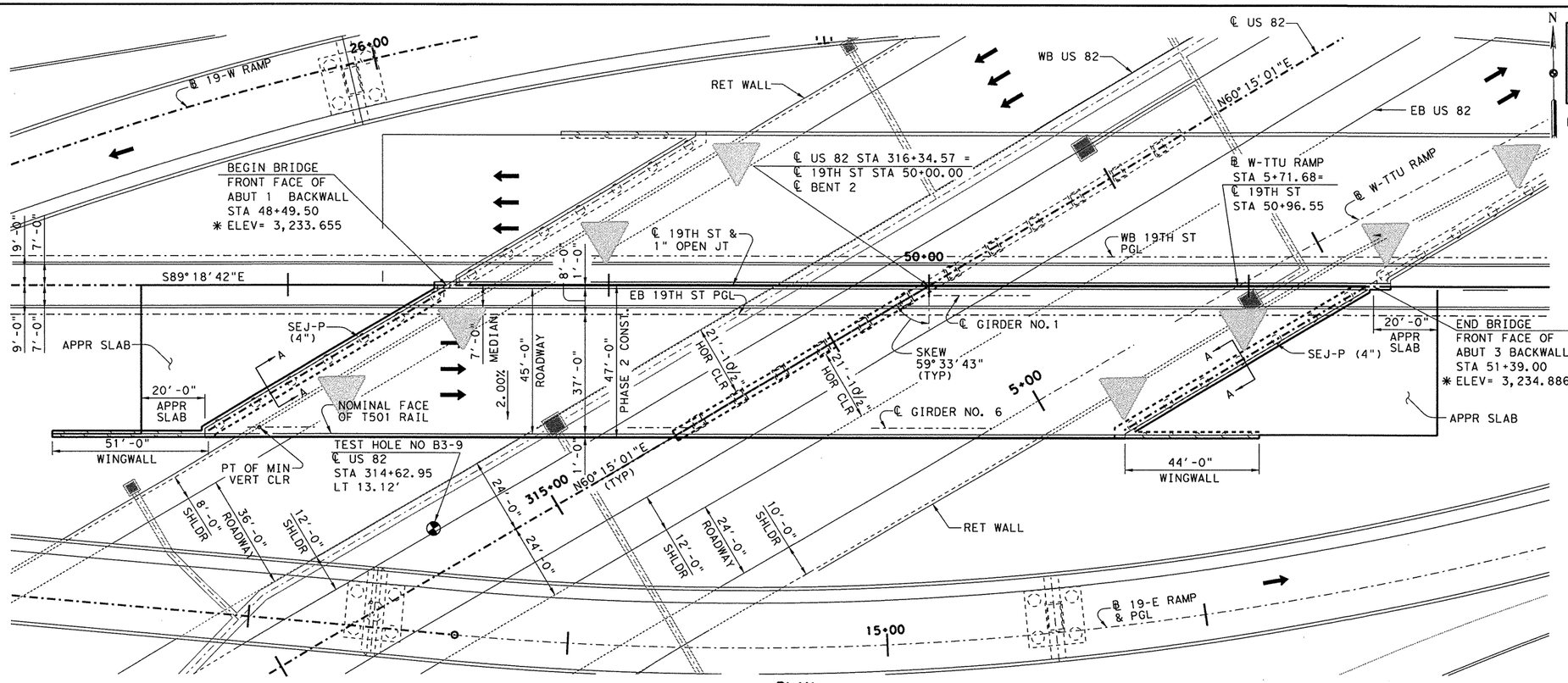

PLAN

DESIGN SPEED :	30 MPH
FUNCT CLASS :	URBAN LOCAL
ADT :	15,700/YR2000 ADT, 27,500/YR2020 ADT
PERM STR NO :	05-152-0-0380-01-042

NOTES:

1. ALL DIMENSIONS ARE IN FEET UNLESS SHOWN OTHERWISE.
2. SECTION A-A SEE SHEET 3 OF 3.
3. THE USE OF PRECAST PANEL IS NOT ALLOWED IN THIS BRIDGE.
4. ALL BENT AND ABUTMENT SHALL HAVE THE SAME BEARING.

* ELEVATION SHOWN IS AT ℄ OF 19TH STREET.

△ UNDERPASS ILLUMINATE

STATE OF TEXAS
DAVID P. HOHMANN
60983
REGISTERED PROFESSIONAL ENGINEER
9-10-04

STATE OF TEXAS
JOHN S. BEARD
92743
LICENSED PROFESSIONAL ENGINEER
9-10-2004

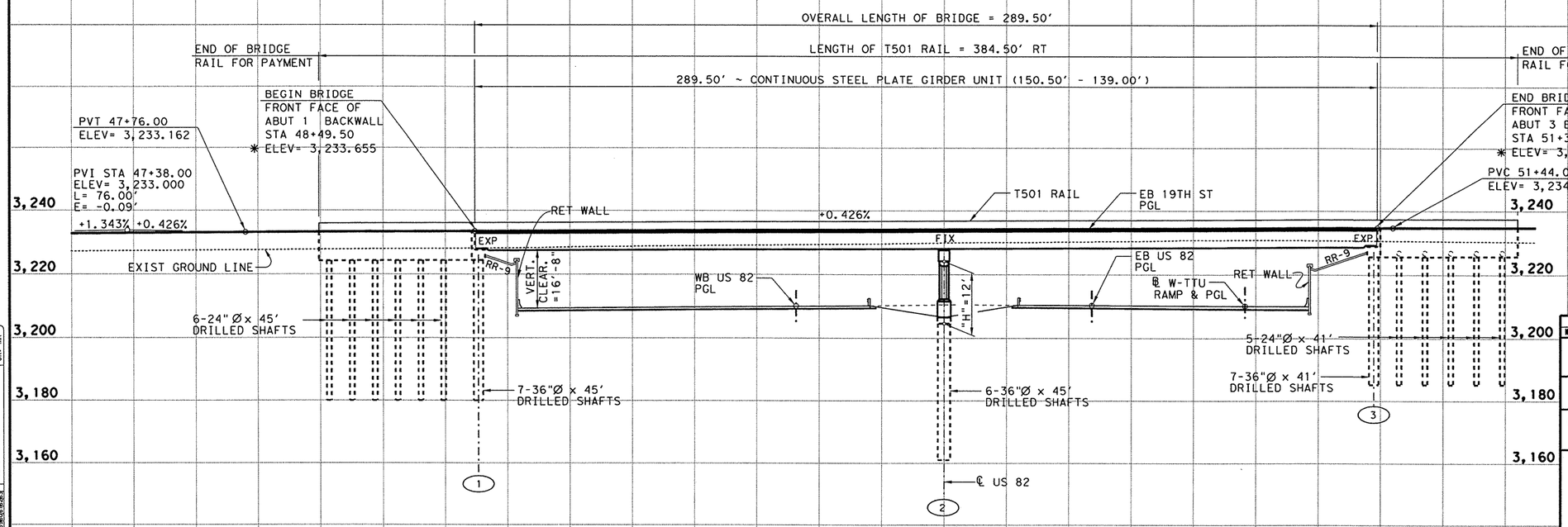

ELEVATION

SCALE 0 20 40

STATE OF TEXAS
FLOYD A. MARTINEZ
82224
REGISTERED PROFESSIONAL ENGINEER
Floyd A. Martinez 9.15.04

THE HORIZONTAL AND VERTICAL GEOMETRICAL DESIGN HAS BEEN DESIGNED BY ME OR UNDER MY RESPONSIBLE SUPERVISION.

HS20 LOADING

No.	Revision	By	Date

STRUCTURAL ENGINEERING ASSOCIATES, INC.
CONSULTING ENGINEERS SAN ANTONIO, TEXAS

HNTB ARCHITECTS ENGINEERS PLANNERS
The HNTB Companies

U.S. 82 EAST-WEST FREEWAY

U.S. 82 MAINLANE UNDERPASS AT 19TH STREET EB BRIDGE LAYOUT

SHEET 2 OF 3

		FED. ROAD DIV. NO.	STATE	FEDERAL AID PROJECT NO.	SHEET NO.
Designed:	MC		TEXAS	NH 56(1)	1466
Checked:	DAR				
Drawn:	CSW	STATE DIST. NO.	COUNTY	CONTROL NO. / SECTION NO. / JOB NO.	HIGHWAY NO.
Checked:	JCC	5	LUBBOCK	0380 / 01 / 064	US 82

DGN: MR
DW:
CK'D: MR

PATH:
COMMENTS: 6218y01.dgn

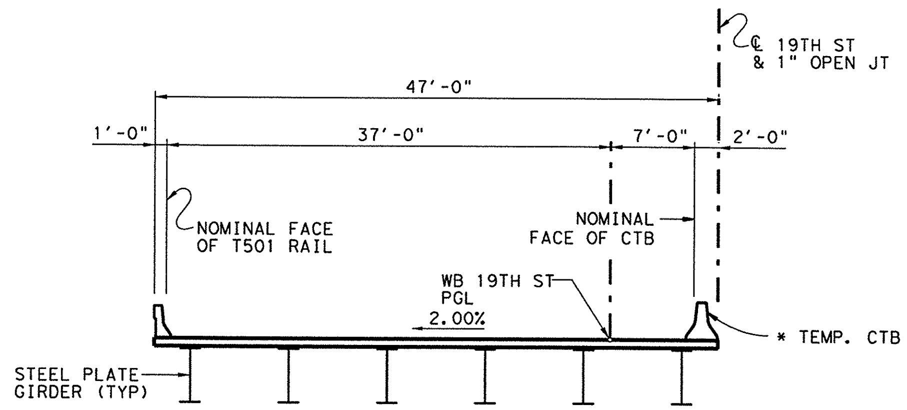

PHASE 1

* See Traffic Control Plans
for CTB quantities.

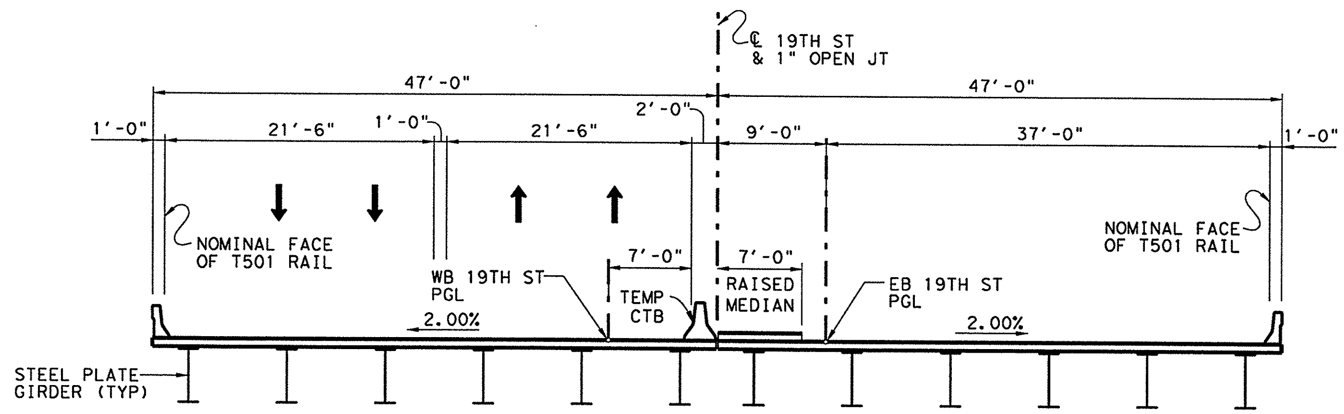

PHASE 2

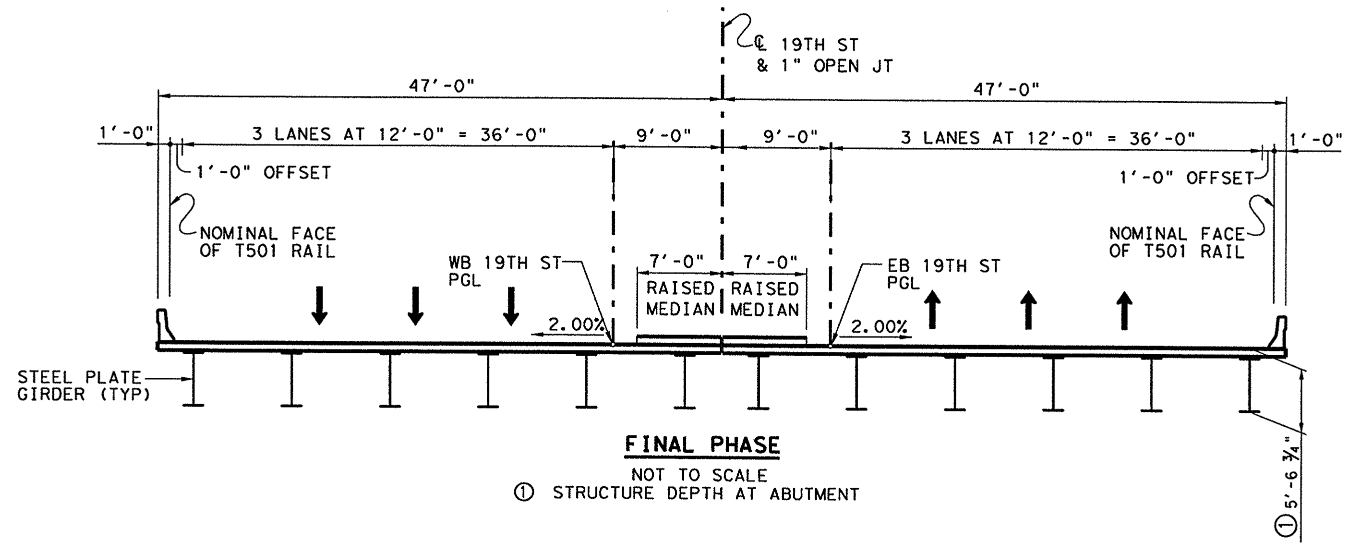

FINAL PHASE

NOT TO SCALE
① STRUCTURE DEPTH AT ABUTMENT

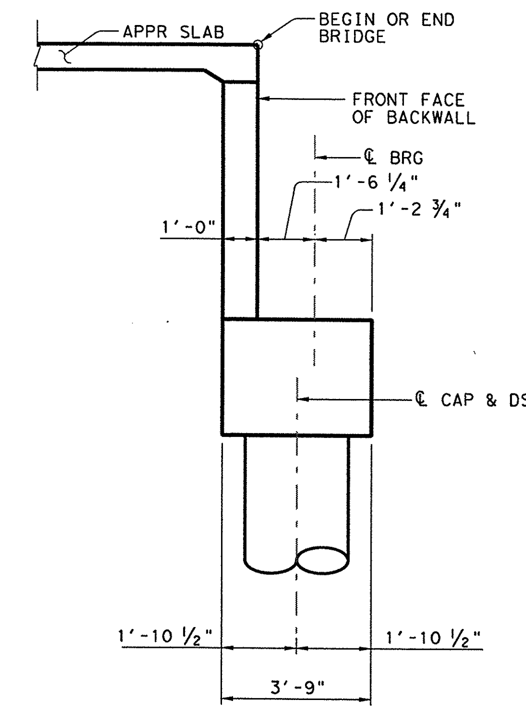

SECTION A-A

NOT TO SCALE

NOTES:
SECTION A-A DIMENSIONS ARE IN FEET.
WIDER ABUT CAP IS USED TO ACCOMODATE
BEARING PLATE IN SEVERE SKEW ANGLE.
CAP DIMENSIONS ASSUME PLACEMENT OF SE5
END EXPANSION BEARING.
CAP DIMENSIONS SHOULD BE ADJUSTED
IF DIFFERENT SIZED BEARING IS USED.

STATE OF TEXAS
DAVID P. HOHMANN
60983
REGISTERED PROFESSIONAL ENGINEER
9-7-04

STATE OF TEXAS
FLOYD A. MARTINEZ
82224
REGISTERED PROFESSIONAL ENGINEER
9.15.04

THE HORIZONTAL AND VERTICAL GEOMETRICAL
DESIGN HAS BEEN DESIGNED BY ME OR UNDER
MY RESPONSIBLE SUPERVISION.

HS 20 LOADING

No.	Revision	By	Date

STRUCTURAL ENGINEERING ASSOCIATES, INC.
CONSULTING ENGINEERS SAN ANTONIO, TEXAS

HNTB ARCHITECTS ENGINEERS PLANNERS
The HNTB Companies

U.S. 82 EAST-WEST FREEWAY

U.S. 82 MAINLANE UNDERPASS AT 19TH STREET PHASE CONSTRUCTION

SHEET 3 OF 3

Designed: JCC	FED. ROAD DIV. NO.	STATE	FEDERAL AID PROJECT NO.				SHEET NO.
Checked: DAR		TEXAS	~~HP 55(1)~~				1467
Drawn: CSW	STATE DIST. NO.	COUNTY	CONTROL NO.	SECTION NO.	JOB NO.		HIGHWAY NO.
Checked: JCC	5	LUBBOCK	0380	01	064		US 82

LEVELS DISPLAYED
PATH:
COMMENTS:
62191y01.dgn
DN: MR
CK:
DW:
CK: MR

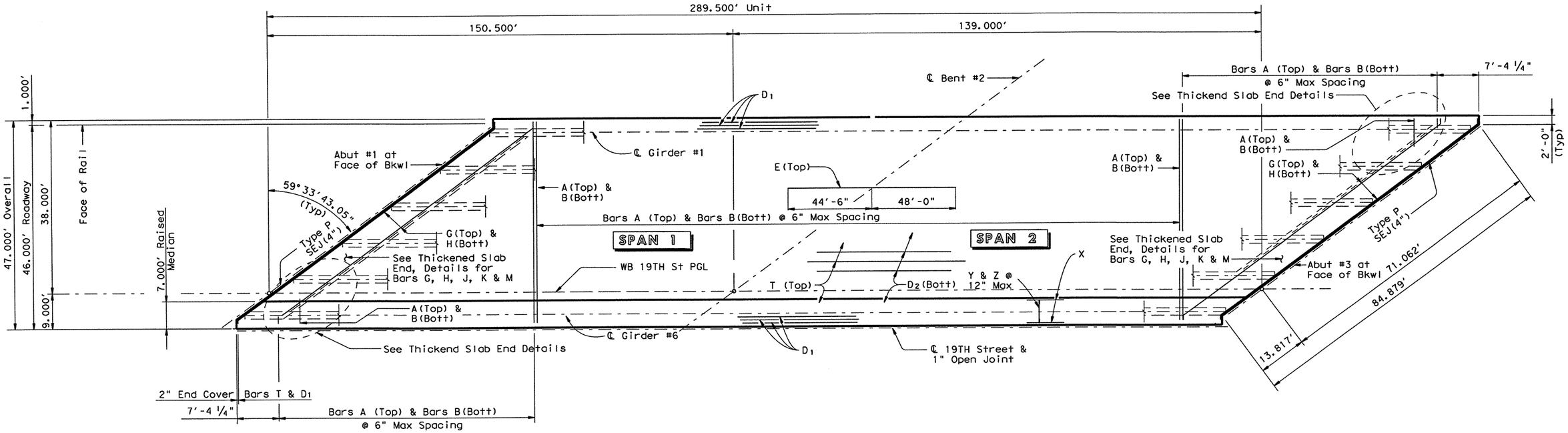

PLAN

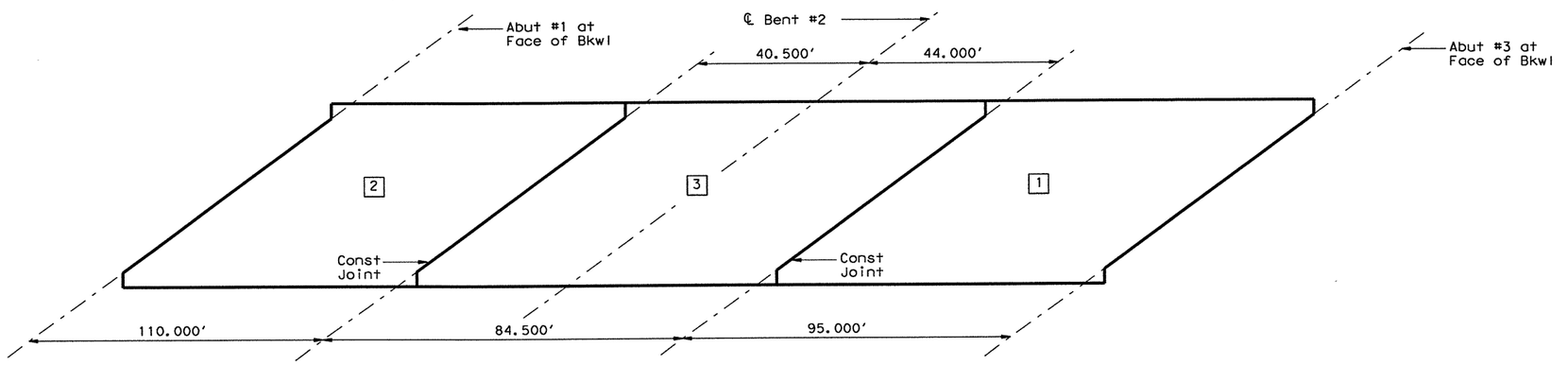

CONCRETE PLACEMENT SEQUENCE

(CONTINUOUS PLACEMENT SHALL NOT BE PERMITTED)

Deposit concrete parallel to skew so that all girders are loaded uniformly along their length.

GENERAL NOTES:

Designed according to AASHTO 1996 Standard and current Interim Specifications.

See Thickened Slab End Details sheet for details not shown.

See PMDF(S) standard sheet for details and quantity adjustments if this option is used.

Prestressed concrete panels shall not be permitted.

All reinforcing steel shall be Grade 60 and concrete strength f'c = 4,000 psi.

See Type P SEJ(4") Standard sheet for details and weights of Type P SEJ(4") to be placed with slab.

All Reinforcing shall be Epoxy Coated. Class "S" concrete for Slab shall include 0.0325 LBS of 100% virgin polypropylene fabrillated fibers per cubic foot. Approved fibers shall be as listed in the Contract and as approved by the Engineer.

Bar laps, where required, shall be as follows:
Epoxy Coated ~ #4 = 2'-1"
~ #5 = 2'-7"
~ #6 = 3'-1"

HS20 LOADING

SHEET 1 OF 6

STATE OF TEXAS
DAVID P. HOHMANN
60983
REGISTERED PROFESSIONAL ENGINEER
9-7-04

Texas Department of Transportation
Bridge Division

289.50' CONTINUOUS PLATE GIRDER UNIT
(SPANS 1 & 2)
US 82 ML UNDERPASS AT 19TH STREET WB

FILE: 6219sp01.dgn	DN: MR	CK: TCS	DW: WMB	CK: MR
©TxDOT JAN 2004	DISTRICT	FEDERAL AID PROJECT		SHEET
REVISIONS	05	[redacted]		1480
	COUNTY	CONTROL	SECT	JOB	HIGHWAY
	LUBBOCK	0380	01	064	US82

LEVELS DISPLAYED
1 2 3 4 5 6 7 8 9 10 11 12 13 14 15 16
17 18 19 20 21 22 23 24 25 26 27 28 29 30 31 32
33 34 35 36 37 38 39 40 41 42 43 44 45 46 47 48
49 50 51 52 53 54 55 56 57 58 59 60 61 62 63
PATH:

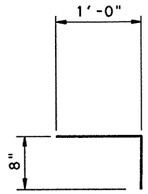

BARS Z

BAR TABLE	
Bar	Size
A	#5
B	#5
D	#5
E	#6
G	#5
H	#5
J	#5
K	#5
M	#5
T	#4
X	#4
Y	#4
Z	#4

TABLE OF ESTIMATED QUANITITIES

Span	Reinforced Concrete Slab	(1) Reinf Steel *	Class "S" Conc (HPC) *	(2) Median Class "S" Conc (HPC) *	Structural Steel (HS)
No.	SF	Lb	CY	CY	Lb
1	7074	49518	186.4	19.5	
2	6533	45731	172.2	18.0	
Total	13607	95249	358.6	37.5	587000

(1) Reinforcing Steel weight is calculated using an approximate factor of 7.0 Lbs/SF.

(2) Median Concrete quantites are subsidiary to slab.

* Quantities shown for Contractor's information only.

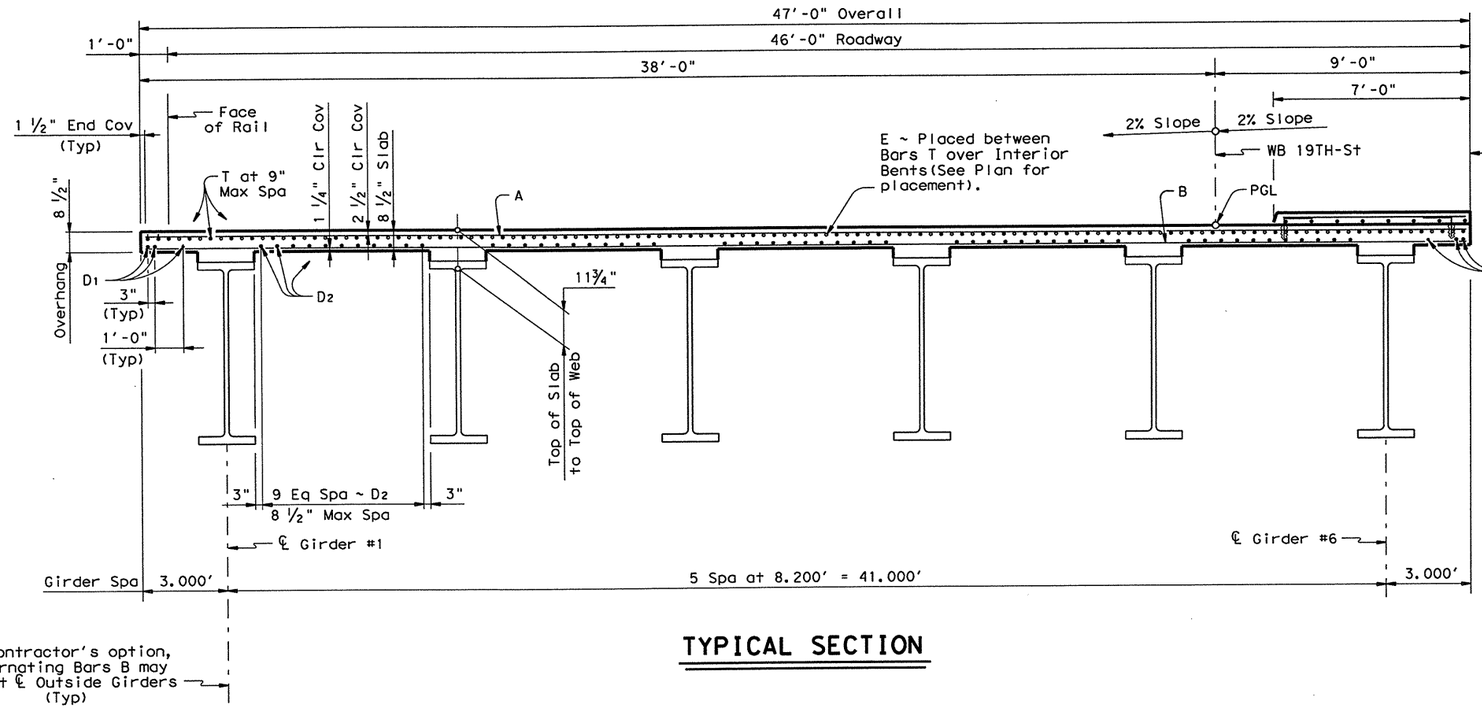

TYPICAL SECTION

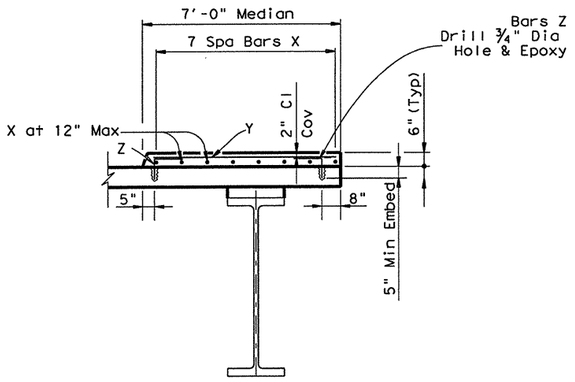

TYPICAL MEDIAN SECTION

SIDEWALK NOTES:

Installation of sidewalk and/or median dowels shall be in accordance with Item 420.11(9). The holes for dowels shall be drilled with rotary (coring) type drilling equipment. Percussion (star) or masonry drill type drilling equipment shall not be used. Holes must be wire brushed and then cleaned with compressed air which shall have no oil or water in suspension. The holes shall be clean and dry prior to placing adhesive and anchors. The Anchoring adhesive shall be Type III Class A as specified in DMS-6100 and shall be applied per manufacturer's instructions.

STATE OF TEXAS
THOMAS C. STOUT
84829
LICENSED PROFESSIONAL ENGINEER

Thomas C. Stout

9-24-04

HS20 LOADING

Texas Department of Transportation
Bridge Division

289.50' CONTINUOUS PLATE GIRDER UNIT
(SPANS 1 & 2)
US 82 ML UNDERPASS AT 19TH STREET WB

FILE: 6219sp01.dgn	DN: MR	CK: TCS	DW: WMB	CK: MR
©TxDOT JAN 2004	DISTRICT	FEDERAL AID PROJECT		SHEET
REVISIONS	05	~~NH-56(1)~~		1481
	COUNTY	CONTROL	SECT	JOB	HIGHWAY
	LUBBOCK	0380	01	064	US82

LEVELS DISPLAYED
1 2 3 4 5 6 7 8 9 10 11 12 13 14 15 16 17 18 19 20 21 22 23 24 25 26 27 28 29 30 31 32 33 34 35 36 37 38 39 40 41 42 43 44 45 46 47 48 49 50 51 52 53 54 55 56 57 58 59 60 61 62 63

PATH:

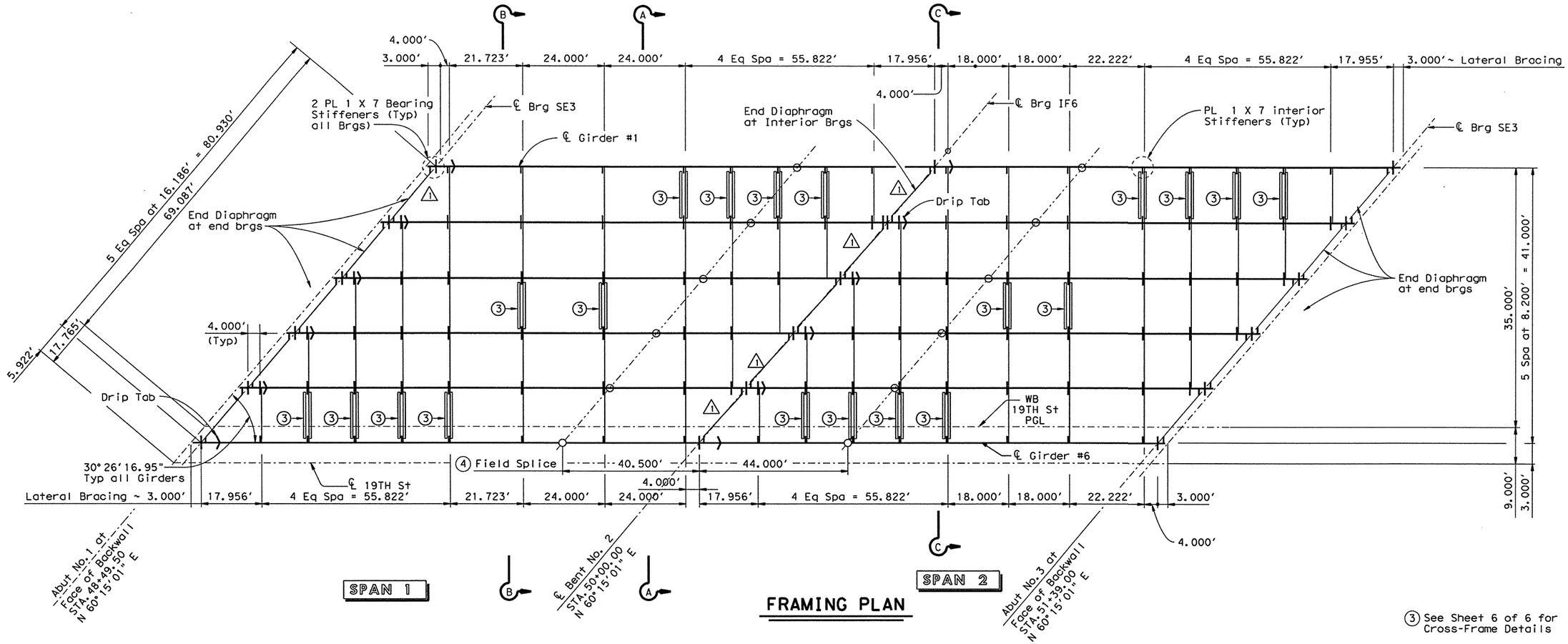

FRAMING PLAN

③ See Sheet 6 of 6 for Cross-Frame Details

④ Measured along ℄ of Girder

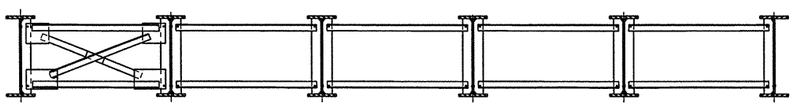

SECTION A-A

(Lean on bracing system)

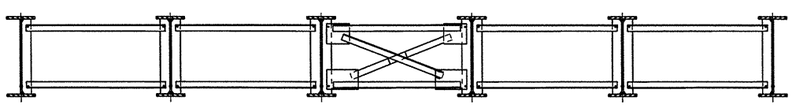

SECTION B-B

(Lean on bracing system)

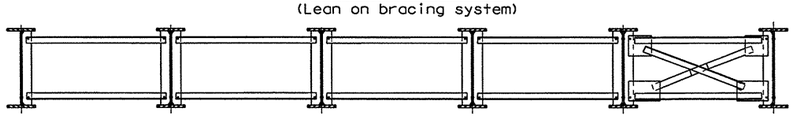

SECTION C-C

(Lean on bracing system)

(For Details not shown see sheet 4 of 6 for Lean on Bracing details)

⚠ Girder Placement Sequence:

The bolts fastened on the struts are structural bolts. The structural and erection bolts must be tightened in accordance with Item 447 "Structural Bolting" before hanging paired girders or before releasing cranes for single girders.

Crane cables must remain in tension during girder placement until End Diaphragms are attached and bolted.

End Diaphragms should be positioned and bolted after the placement of each pair or individual girder before placing another girder or pair of girders.

The girder placement sequence does not release the contractor from the responsibility of submitting girder erection plans to the Engineer of record. Girder erection plans must be submitted to the Engineer.

The contractor may reverse the girder placement sequence as stated below; however, the erection sequence must begin with the exterior girders.

1. Field splices in span one shall be completed before lifting girders to supports.
2. All end diaphragms, cross-frames, and struts shall be positioned and bolted between girders 5 and 6.
3. Girders 5 and 6 shall be lifted and placed as a paired unit.
4. All end diaphragms, cross-frames, and struts shall be positioned and bolted between girders 3 and 4.
5. Lift and place girders 3 and 4 as a paired unit.
6. Position and bolt the end diaphragm and a minimum of every other pair of struts between girders 4 and 5.
7. All end diaphragms, cross-frames, and struts shall be positioned between girders 1 and 2.
8. Lift and place girders 1 and 2 as a paired unit.
9. Position and bolt end diaphragms and a minimum of every other pair of struts between girders 2 and 3.
10. Once the first span of girders has been placed successfully, the contractor may begin lifting and placing the final girder sections. The lifting and placement of the final sections must follow the same steps and sequence explained above.

⚠ REVISED 11-24-04 VN

STATE OF TEXAS
DAVID P. HOHMANN
60983
REGISTERED PROFESSIONAL ENGINEER
11-17-04

HS20 LOADING SHEET 3 OF 6

Texas Department of Transportation
Bridge Division

289.50' CONTINUOUS PLATE GIRDER UNIT
(SPANS 1 & 2)
US 82 ML UNDERPASS AT 19TH STREET WB

FILE: 6219sp01.dgn	DN: MR	CK: TCS	DW: WMB	CK: MR	
©TxDOT JAN 2004	DISTRICT	FEDERAL AID PROJECT			SHEET
REVISIONS	05	HP 55(1)			14B2
⚠1 11/10/04	COUNTY		CONTROL	SECT	JOB	HIGHWAY
	LUBBOCK		0380	01	064	US82

LEVELS DISPLAYED 1 2 3 4 5 6 7 8 9 10 11 12 13 14 15 16
PATH: 1 2 3 4 5 6 7 8 9 10 11 12 13 14 15 16 17 18 19 20 21 22 23 24 25 26 27 28 29 30 31 32 33 34 35 36 37 38 39 40 41 42 43 44 45 46 47 48 49 50 51 52 53 54 55 56 57 58 59 60 61 62 63

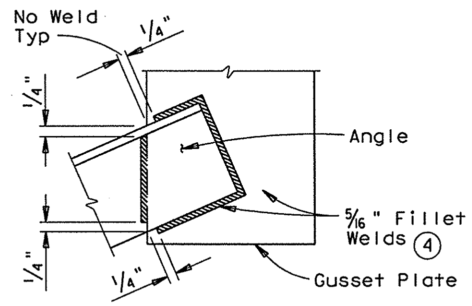

WELD DETAIL - CROSS FRAMES AND END DIAPHRAGM

(At Lean on Bracing Systems)

(4) Total length of fillet weld shall be 1'-10" min ⚠1

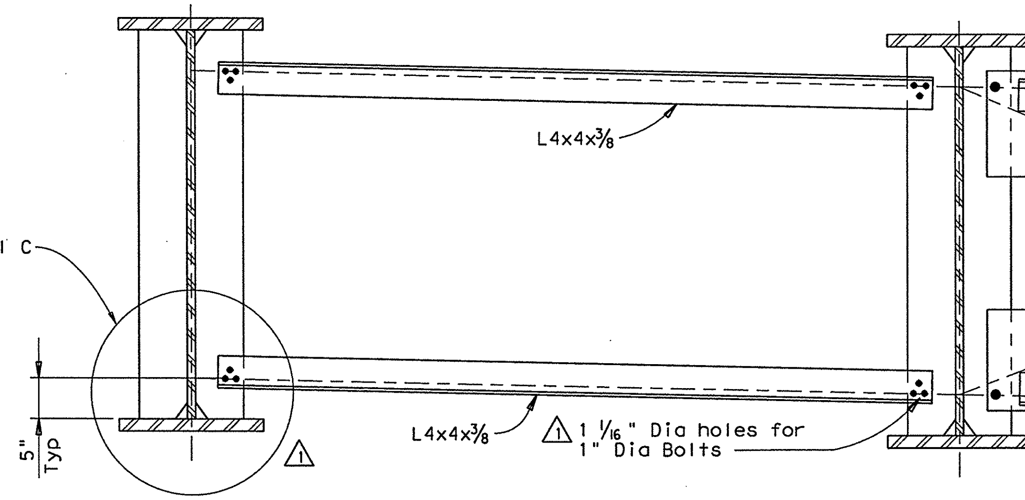

⚠ **PAIR OF STRUTS**

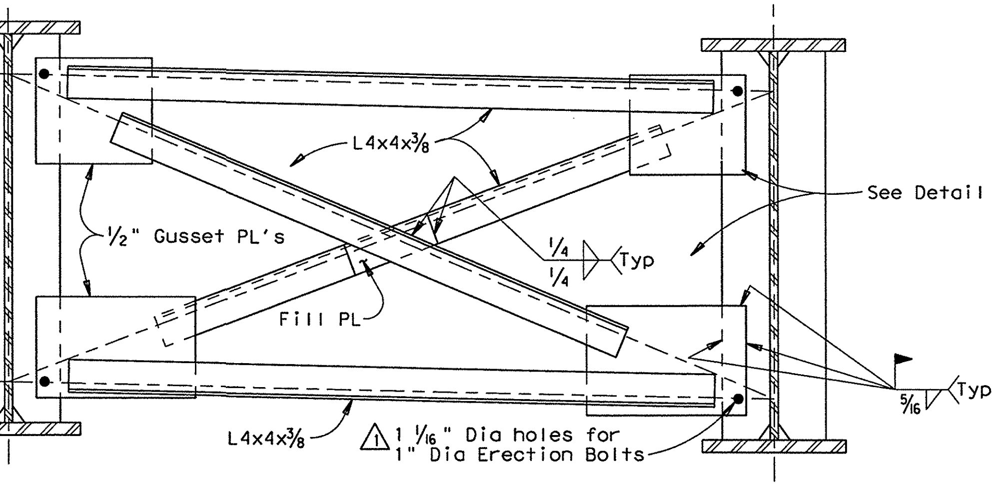

(3) **CROSS-FRAMES**

LEAN ON BRACING SYSTEM DETAILS

Lean on Bracing system shall be used at all locations except along ℄ Bearing of Abutments and Interior Bent.

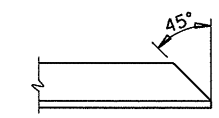

Clip outstanding leg of all angles on diaphragms & cross frames

CLIP DETAIL

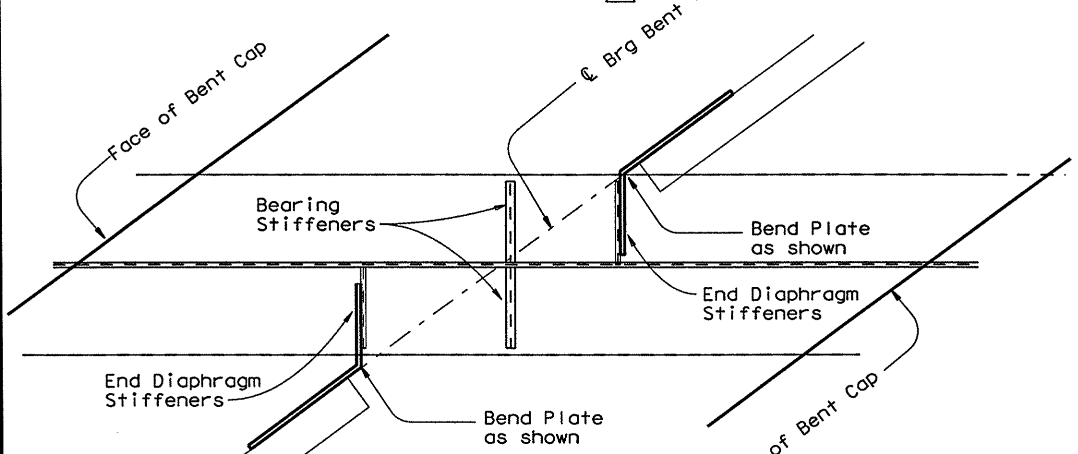

DETAIL B

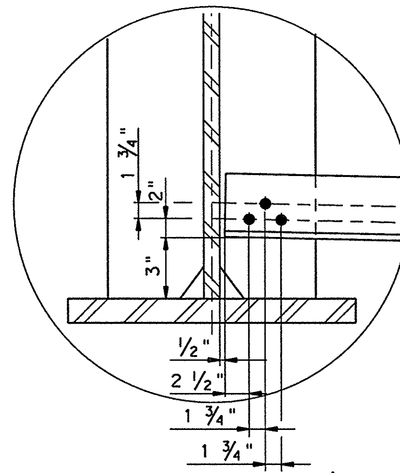

DETAIL C ⚠

(5) Interior diaphragms are perpendicular or radial to girders unless shown otherwise on span details. Interior Diaphragms at Interior bearings are parallel to the skew unless shown otherwise on span details.

(6) The designer shall ensure that the forces in the Cross-Frames and End diaphragms members and connections, obtained by rational analysis, do not exceed allowables.

See SPGD Standard for details not shown. ⚠

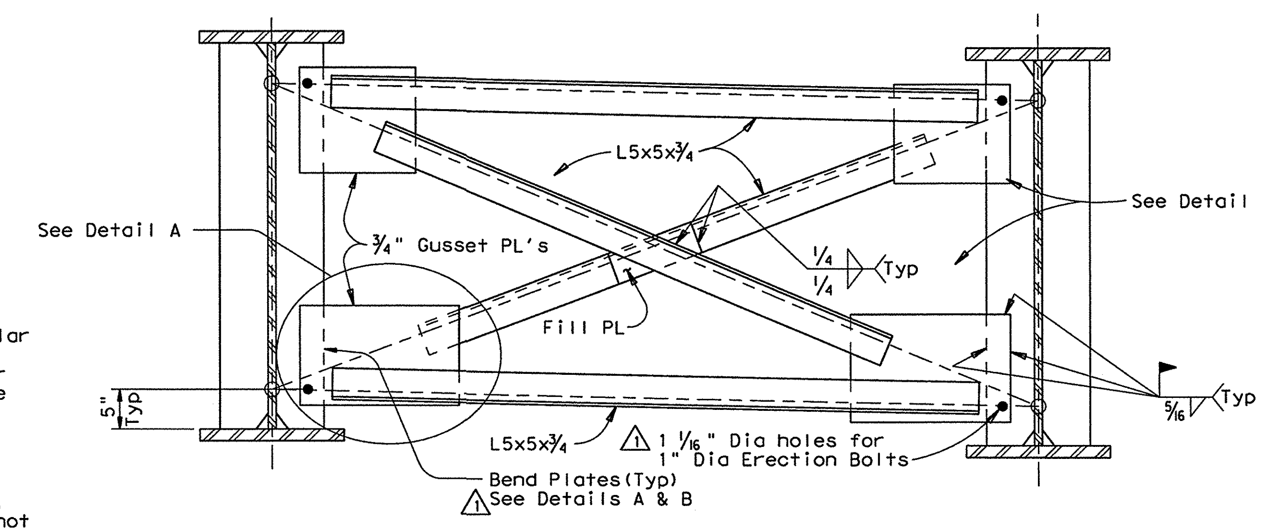

END DIAPHRAGM (5) (6)

(At Abutments & Bent only)

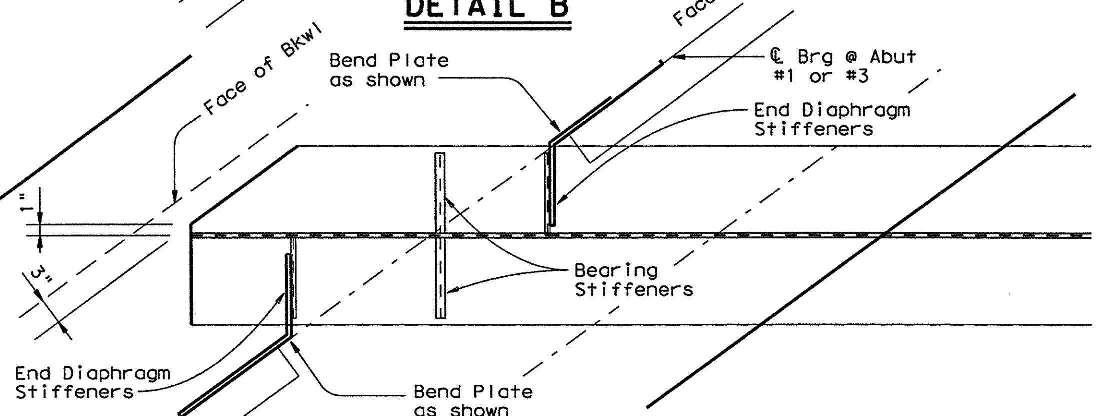

DETAIL A

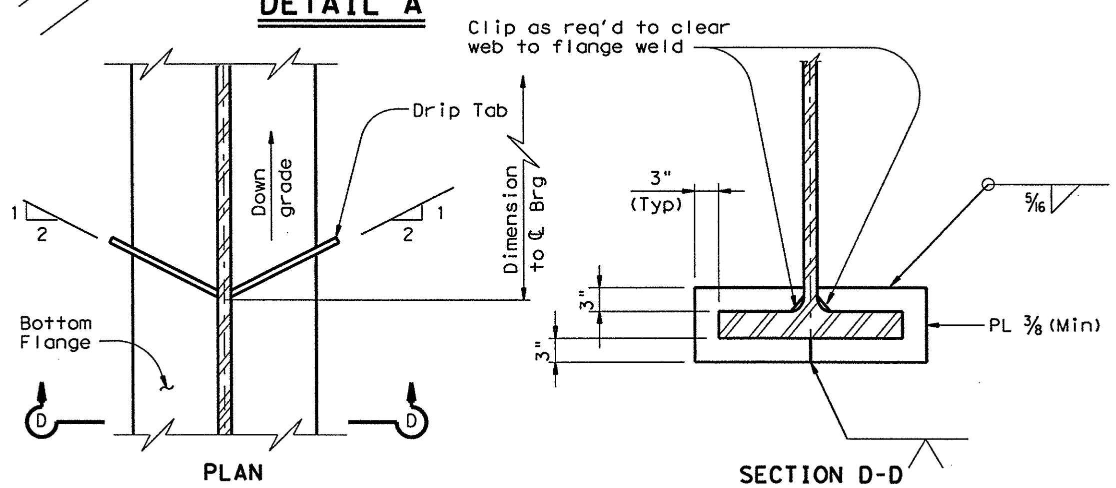

Drip Tab, where indicated on the girder framing plan, shall be located 8'-0" from the ℄ Bent measured along ℄ girder.

DRIP TAB DETAILS

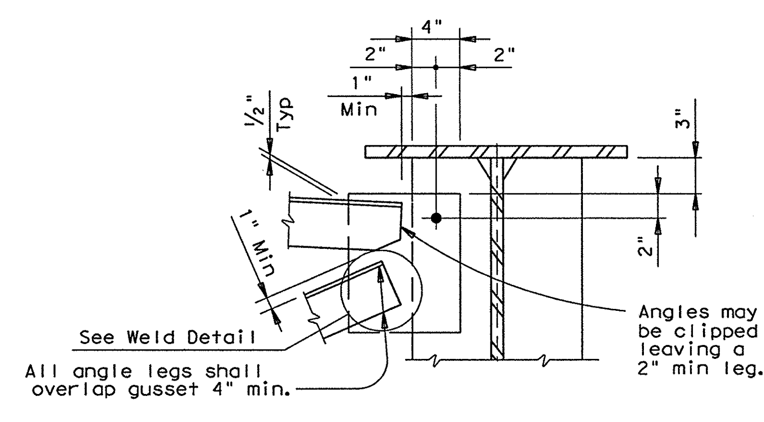

DETAIL E

⚠ REVISED 11-24-04 VN

STATE OF TEXAS
DAVID P. HOHMANN
60983
REGISTERED PROFESSIONAL ENGINEER
David Hohmann
11-18-04

HS20 LOADING

SHEET 4 OF 6

Texas Department of Transportation
Bridge Division

289.50' CONTINUOUS PLATE GIRDER UNIT
(SPANS 1 & 2)
US 82 ML UNDERPASS AT 19TH STREET WB

FILE: 6219sp01.dgn	DN: MR	CK: TCS	DW: WMB	CK: MR
©TxDOT JAN 2004	DISTRICT	FEDERAL AID PROJECT		SHEET
REVISIONS	05	HP 55(1)		1483
⚠1 11/10/04	COUNTY	CONTROL	SECT	JOB / HIGHWAY
	LUBBOCK	0380	01	064 / US82

LEVELS DISPLAYED ACC:

1	2	3	4	5	6	7	8	9	10	11	12	13	14	15	16
17	18	19	20	21	22	23	24	25	26	27	28	29	30	31	32
33	34	35	36	37	38	39	40	41	42	43	44	45	46	47	48
49	50	51	52	53	54	55	56	57	58	59	60	61	62	63	

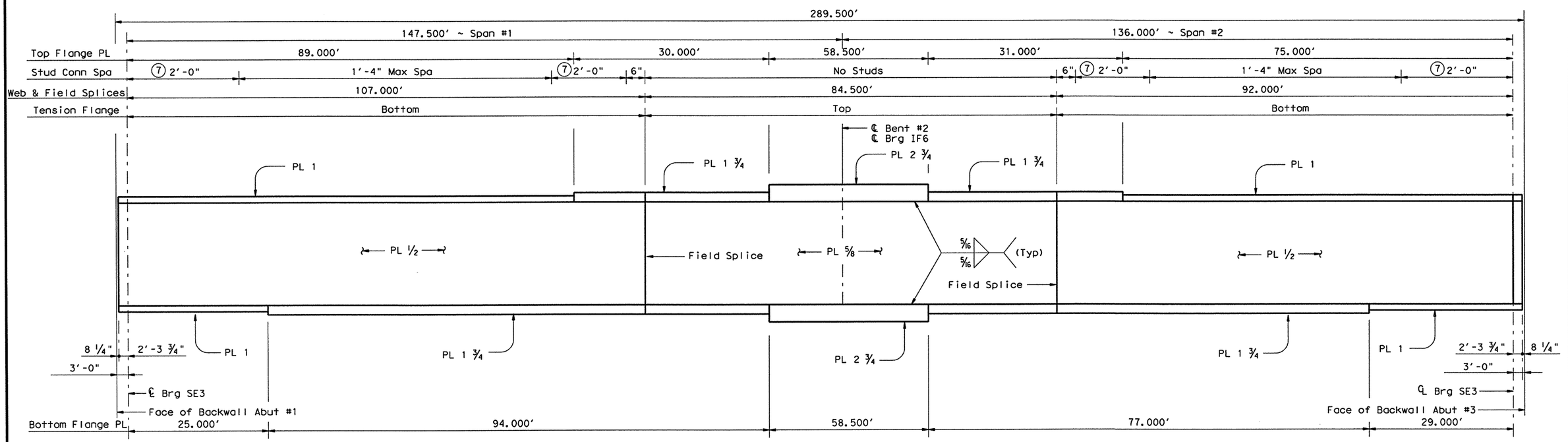

All Web Plates are 54" deep.

All Flange Plates are 18" wide.

STEEL GIRDER FABRICATION NOTES:

All structural steel, including connection plates and diaphragms, shall conform to the requirements of A709 Grade 50 W and shall be paid for at the unit price bid for "Structural Steel-HS".

Girders tension flanges and webs are classified as tension components and shall conform to Item 442.3(1).

Field splices shall be made by full penetration groove welds.

Except at changes in section, shop or field flange and web splices in plate girders may be located as desirable to optimize plate lengths and erection procedures, except that splices will not be allowed where a 40' or less unspliced length would suffice, neither will tension flange splices be allowed within 0.05S either side of interior bearings, within 0.10S either side of the centerlines of the interior span, nor within the range between 0.30S and 0.50S from the end bearings. (S=length c.c. Bearing of Span in which the splice is made.)

Flange and Web Splices shall be made by full penetration groove welds in accordance with the Item 441, "Steel Structures".

All dimensions shown in Girder Elevations are Horizontal.

Bolted Field Splice shall not be permitted on this structure.

HS20 LOADING

LEVELS DISPLAYED
1 2 3 4 5 6 7 8 9 10 11 12 13 14 15 16
17 18 19 20 21 22 23 24 25 26 27 28 29 30 31 32
33 34 35 36 37 38 39 40 41 42 43 44 45 46 47 48
49 50 51 52 53 54 55 56 57 58 59 60 61 62 63
PATH:

STATE OF TEXAS
DAVID P. HOHMANN
60983
REGISTERED
PROFESSIONAL ENGINEER

9-7-04

Texas Department of Transportation
Bridge Division

289.50' CONTINUOUS PLATE GIRDER UNIT
(SPANS 1 & 2)
US 82 ML UNDERPASS AT 19TH STREET WB

FILE: 6219sp01.dgn	DN: MR	CK: TCS	DW: WMB	CK: MR
©TxDOT JAN 2004	DISTRICT	FEDERAL AID PROJECT		SHEET
REVISIONS	05	~~NH 55(11)~~		104
	COUNTY	CONTROL	SECT	JOB	HIGHWAY
	LUBBOCK	0380	01	064	US82

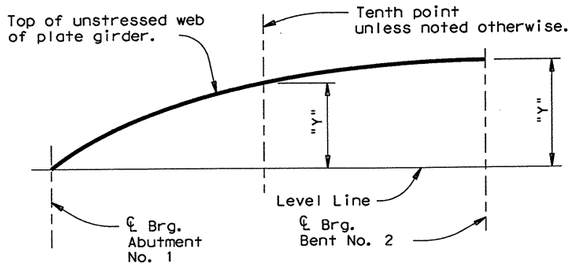

WEB CUTTING DIAGRAM

Note: Web may be cut on straight lines between ordinates shown or to a smooth curve at the Fabricator's option. Ordinates shown include total dead load deflection and vertical curve corrections.

CAMBER DIAGRAM TABLE

"Y" values in feet

LOCATION		GIRDER #1	#2	#3	#4	#5	#6
SPAN #1	0	0.000	0.000	0.000	0.000	0.000	0.000
	1	0.190	0.190	0.190	0.195	0.195	0.195
	2	0.354	0.354	0.354	0.363	0.363	0.363
	3	0.483	0.483	0.483	0.496	0.495	0.496
	4	0.571	0.571	0.571	0.583	0.583	0.583
	5	0.618	0.618	0.618	0.629	0.629	0.629
	6	0.628	0.628	0.628	0.638	0.638	0.638
	7	0.616	0.615	0.616	0.623	0.623	0.623
	FS	0.611	0.611	0.611	0.618	0.617	0.618
	8	0.601	0.601	0.601	0.605	0.605	0.605
	9	0.600	0.600	0.600	0.602	0.602	0.602
	10	0.628	0.628	0.628	0.628	0.628	0.628
SPAN #2	11	0.688	0.688	0.688	0.688	0.688	0.688
	12	0.768	0.768	0.768	0.770	0.769	0.770
	13	0.861	0.861	0.861	0.865	0.864	0.865
	FS	0.884	0.884	0.884	0.887	0.887	0.887
	14	0.957	0.957	0.957	0.961	0.961	0.961
	15	1.047	1.047	1.047	1.052	1.052	1.052
	16	1.120	1.120	1.120	1.125	1.125	1.125
	17	1.162	1.172	1.172	1.178	1.178	1.178
	18	1.160	1.193	1.203	1.208	1.208	1.208
	19	1.115	1.170	1.202	1.214	1.214	1.214
	20	1.033	1.111	1.166	1.198	1.207	1.207

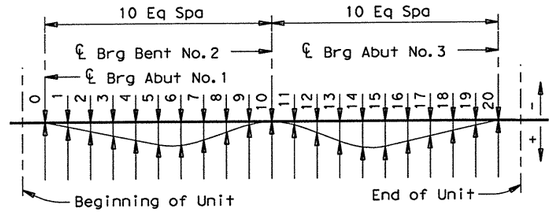

DEAD LOAD DEFLECTION DIAGRAM

FS = Field Splice

TABLE OF DEAD LOAD DEFLECTIONS

Location		Girder (Values in Ft) Deflections due to cast-in-place concrete only ALL				Total dead load deflections (including steel) 1-3	4-6		
SPAN 1	0	0.000				0.000	0.000		
	1	0.089				0.127	0.132		
	2	0.161				0.228	0.237		
	3	0.208				0.295	0.307		
	4	0.225				0.320	0.332		
	5	0.213				0.304	0.315		
	6	0.175				0.251	0.261		
	7	0.123				0.176	0.183		
	FS	0.109				0.156	0.162		
	8	0.069				0.099	0.103		
	9	0.025				0.035	0.037		
	10	0.000				0.000	0.000		
SPAN 2	11	0.000				0.002	0.002		
	12	0.015				0.025	0.026		
	13	0.039				0.060	0.063		
	FS	0.045				0.069	0.072		
	14	0.065				0.098	0.102		
	15	0.087				0.130	0.135		
	16	0.098				0.145	0.150		
	17	0.095				0.139	0.145		
	18	0.077				0.112	0.117		
	19	0.043				0.063	0.065		
	20	0.000				0.000	0.000		

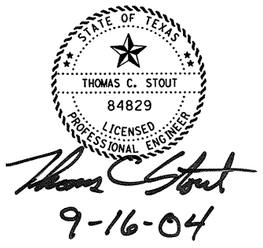

HS20 LOADING SHEET 6 OF 6

Texas Department of Transportation
Bridge Division

289.50' CONTINUOUS PLATE GIRDER UNIT
(SPANS 1 & 2)
US 82 ML UNDERPASS AT 19TH STREET WB

FILE: 6219sp01.dgn	DN: MR	CK: TCS	DW: WMB	CK: MR
©TxDOT JAN 2004	DISTRICT	FEDERAL AID PROJECT		SHEET
REVISIONS	05	~~HP 95(17)~~		1985
	COUNTY	CONTROL	SECT	JOB	HIGHWAY
	LUBBOCK	0380	01	064	US82

LEVELS DISPLAYED
1 2 3 4 5 6 7 8 9 10 11 12 13 14 15 16 17 18 19 20 21 22 23 24 25 26 27 28 29 30 31 32 33 34 35 36 37 38 39 40 41 42 43 44 45 46 47 48 49 50 51 52 53 54 55 56 57 58 59 60 61 62 63
PATH:

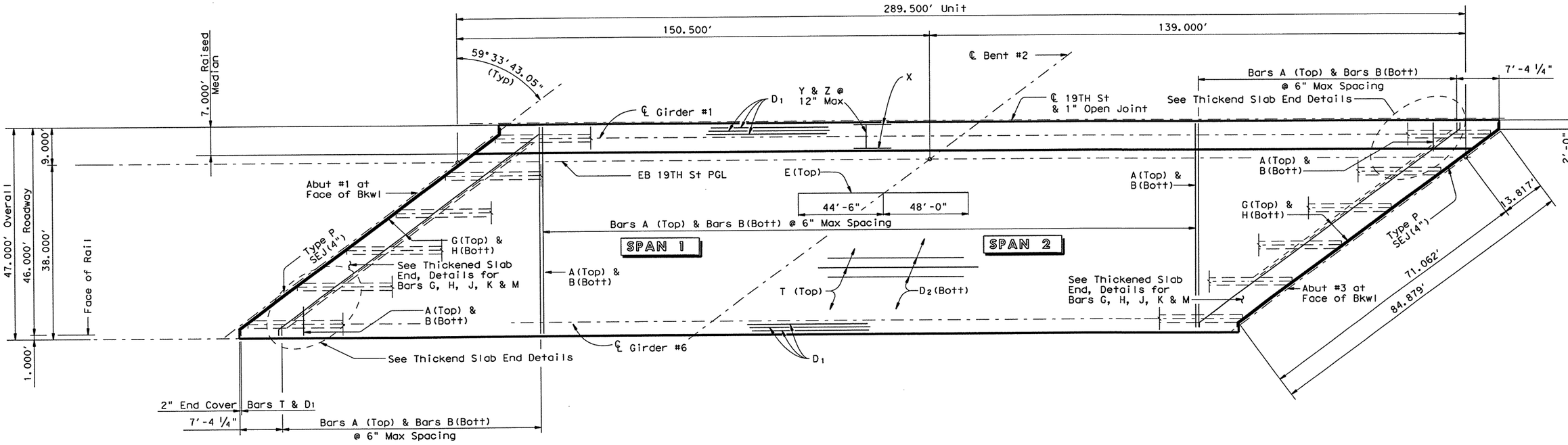

PLAN

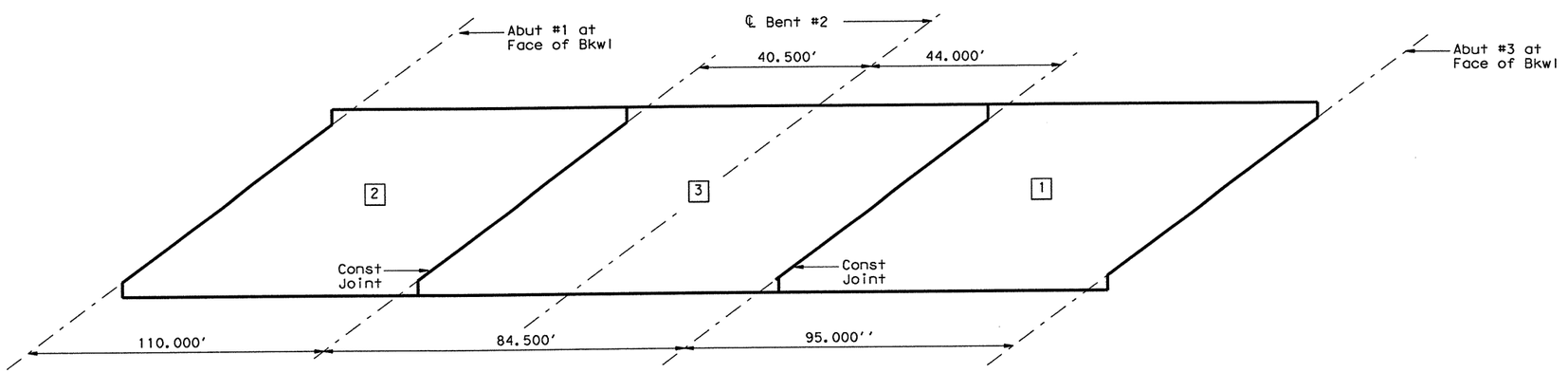

Deposit concrete parallel to skew so that all girders are loaded uniformly along their length.

CONCRETE PLACEMENT SEQUENCE

(CONTINUOUS PLACEMENT SHALL NOT BE PERMITTED)

GENERAL NOTES:

Designed according to AASHTO 1996 Standard and current Interim Specifications.

See Thickened Slab End Details sheet for details not shown.

See PMDF(S) standard sheet for details and quantity adjustments if this option is used.

Prestressed concrete panels shall not be permitted.

All reinforcing steel shall be Grade 60 and concrete strength f'c = 4,000 psi.

See Type P SEJ(4") Standard sheet for details and weights of Type P SEJ(4") to be placed with slab.

All Reinforcing shall be Epoxy Coated. Class "S" concrete for Slab shall include 0.0325 LBS of 100% virgin polypropylene fabrillated fibers per cubic foot. Approved fibers shall be as listed in the Contract and as approved by the Engineer.

Bar laps, where required, shall be as follows:
Epoxy Coated ~ #4 = 2'-1"
~ #5 = 2'-7"
~ #6 = 3'-1"

HS20 LOADING

STATE OF TEXAS
DAVID P. HOHMANN
60983
REGISTERED PROFESSIONAL ENGINEER
9-7-04

Texas Department of Transportation
Bridge Division

289.50' CONTINUOUS PLATE GIRDER UNIT
(SPANS 1 & 2)
US 82 ML UNDERPASS AT 19TH STREET EB

FILE: 6218sp01.dgn	DN: MR	CK: TCS	DW: WMB	CK: MR
©TxDOT JAN 2004	DISTRICT	FEDERAL AID PROJECT		SHEET
REVISIONS	05	[redacted]		1497
	COUNTY	CONTROL	SECT	JOB	HIGHWAY
	LUBBOCK	0380	01	064	US82

LEVELS DISPLAYED
PATH:

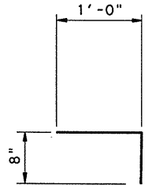

BARS Z

BAR TABLE

Bar	Size
A	#5
B	#5
D	#5
E	#6
G	#5
H	#5
J	#5
K	#5
M	#5
T	#4
X	#4
Y	#4
Z	#4

TABLE OF ESTIMATED QUANITITIES

Span	Reinforced Concrete Slab	(1) Reinf Steel *	Class "S" Conc (HPC) *	(2) Median Class "S" Conc (HPC) *	Structural Steel (HS)
No.	SF	Lb	CY	CY	Lb
1	7074	49518	186.4	19.5	
2	6533	45731	172.2	18.0	
Total	13607	95249	358.6	37.5	587000

(1) Reinforcing Steel weight is calculated using an approximate factor of 7.0 Lbs/SF.

(2) Median Concrete quantites are subsidiary to slab.

* Quantities shown for Contractor's information only.

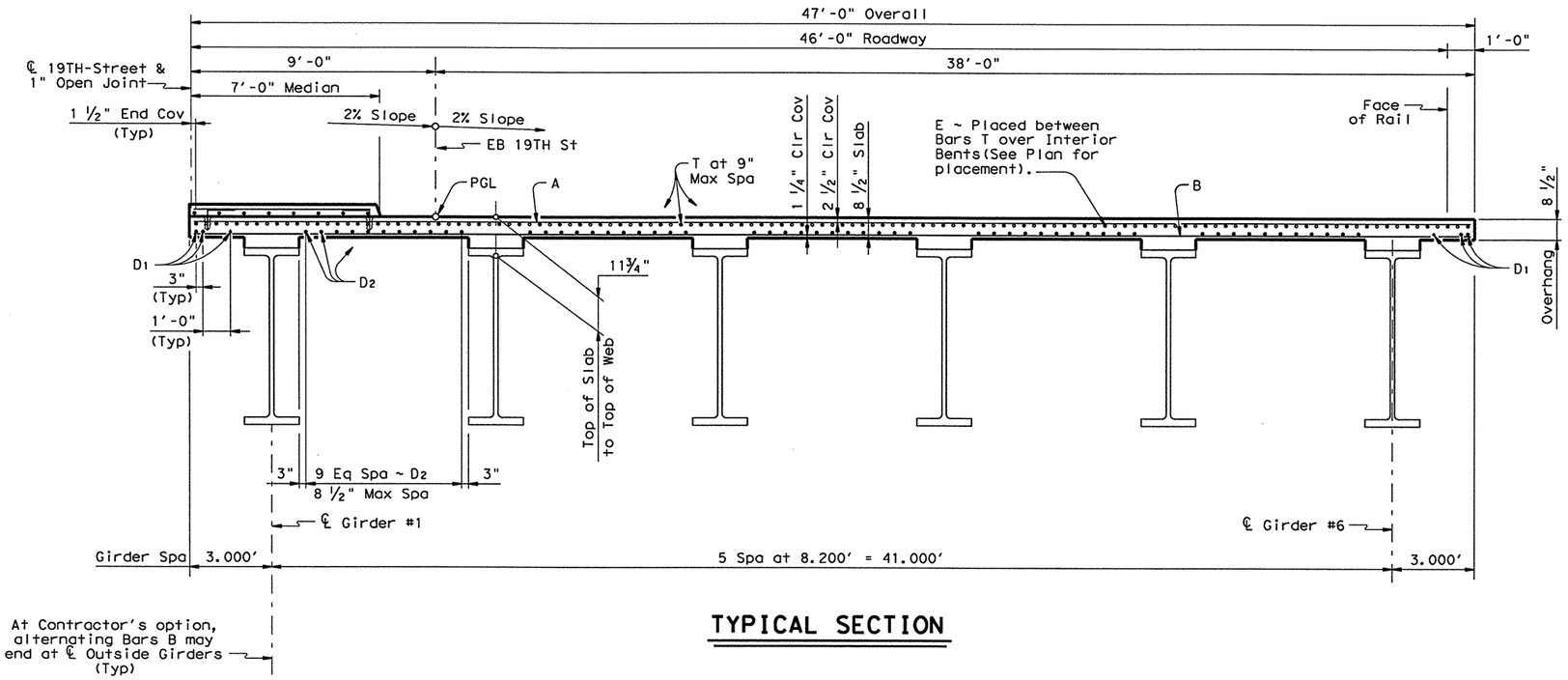

TYPICAL SECTION

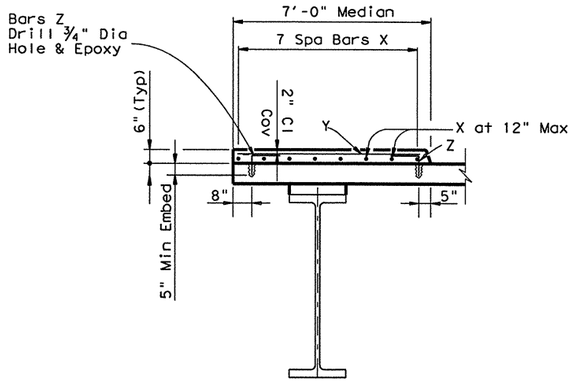

TYPICAL MEDIAN SECTION

SIDEWALK NOTES:

Installation of sidewalk and/or median dowels shall be in accordance with Item 420.11(9). The holes for dowels shall be drilled with rotary (coring) type drilling equipment. Percussion (star) or masonry drill type drilling equipment shall not be used. Holes must be wire brushed and then cleaned with compressed air which shall have no oil or water in suspension. The holes shall be clean and dry prior to placing adhesive and anchors. The Anchoring adhesive shall be Type III Class A as specified in DMS-6100 and shall be applied per manufacturer's instructions.

STATE OF TEXAS
THOMAS C. STOUT
84829
LICENSED PROFESSIONAL ENGINEER

9-24-04

HS20 LOADING

SHEET 2 OF 6

Texas Department of Transportation
Bridge Division

289.50' CONTINUOUS PLATE GIRDER UNIT
(SPANS 1 & 2)
US 82 ML UNDERPASS AT 19TH STREET EB

FILE: 6218sp01.dgn	DN: MR	CK: TCS	DW: WMB	CK: MR			
©TxDOT JAN 2004	DISTRICT	FEDERAL AID PROJECT			SHEET		
REVISIONS	05	~~HP-55(4)~~			1498		
	COUNTY		CONTROL	SECT	JOB	HIGHWAY	
	LUBBOCK		0380	01	064	US82	

LEVELS DISPLAYED
1 2 3 4 5 6 7 8 9 10 11 12 31 41 51 6
7 71 81 91 02 12 22 32 42 52 62 72 82 93 03 13 2
83 84 35 53 63 73 83 94 04 14 24 34 44 54 64 74 8
95 05 15 25 35 45 55 65 75 85 96 06 16 26 3

PATH:

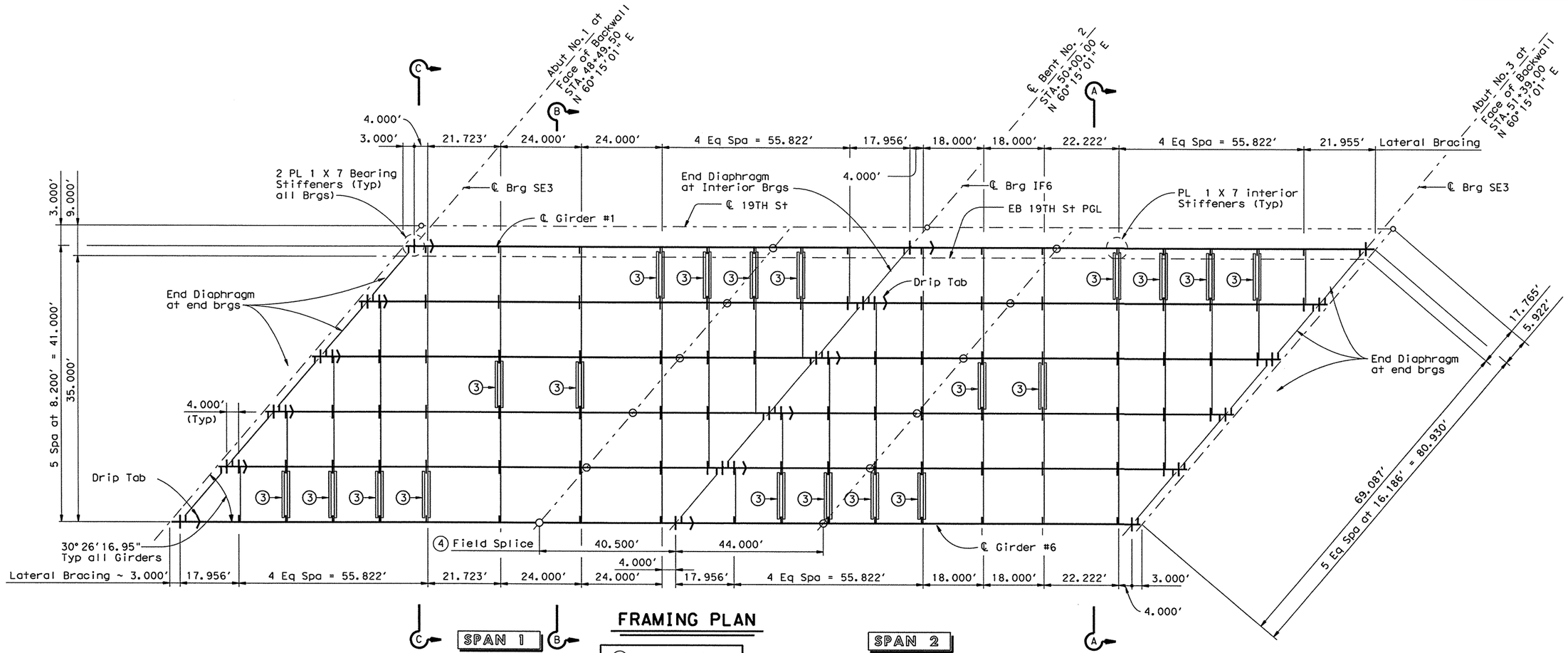

FRAMING PLAN

④ Measured along ℄ of Girder

③ See Sheet 6 of 6 for Cross-Frame Details

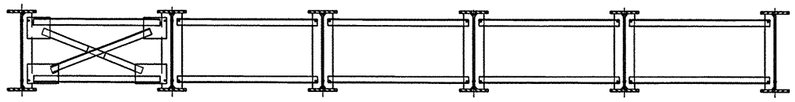

SECTION A-A

(Lean on bracing system)

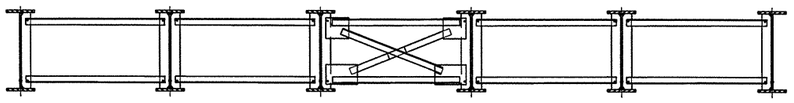

SECTION B-B

(Lean on bracing system)

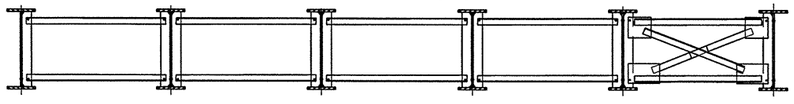

SECTION C-C

(Lean on bracing system)

(For Details not shown see sheet 4 of 6 for Lean on Bracing details)

⚠ Girder Placement Sequence:

The bolts fastened on the struts are structural bolts. The structural and erection bolts must be tightened in accordance with Item 447 "Structural Bolting" before hanging paired girders or before releasing cranes for single girders.

Crane cables must remain in tension during girder placement until End Diaphragms are attached and bolted.

End Diaphragms should be positioned and bolted after the placement of each pair or individual girder before placing another girder or pair of girders.

The girder placement sequence does not release the contractor from the responsibility of submitting girder erection plans to the Engineer of record. Girder erection plans must be submitted to the Engineer.

The contractor may reverse the girder placement sequence as stated below; however, the erection sequence must begin with the exterior girders.

1. Field splices in span one shall be completed before lifting girders to supports.
2. All end diaphragms, cross-frames, and struts shall be positioned and bolted between girders 5 and 6.
3. Girders 5 and 6 shall be lifted and placed as a paired unit.
4. All end diaphragms, cross-frames, and struts shall be positioned and bolted between girders 3 and 4.
5. Lift and place girders 3 and 4 as a paired unit.
6. Position and bolt the end diaphragm and a minimum of every other pair of struts between girders 4 and 5.
7. All end diaphragms, cross-frames, and struts shall be positioned between girders 1 and 2.
8. Lift and place girders 1 and 2 as a paired unit.
9. Position and bolt end diaphragms and a minimum of every other pair of struts between girders 2 and 3.
10. Once the first span of girders has been placed successfully, the contractor may begin lifting and placing the final girder sections. The lifting and placement of the final sections must follow the same steps and sequence explained above.

⚠ REVISED 11-24-04 VN

STATE OF TEXAS
DAVID P. HOHMANN
60983
REGISTERED PROFESSIONAL ENGINEER
11-17-04

HS20 LOADING

SHEET 3 OF 6

Texas Department of Transportation
Bridge Division

289.50' CONTINUOUS PLATE GIRDER UNIT
(SPANS 1 & 2)
US 82 ML UNDERPASS AT 19TH STREET EB

FILE: 6218sp01.dgn	DN: MR	CK: TCS	DW: WMB	CK: MR
©TxDOT JAN 2004	DISTRICT	FEDERAL AID PROJECT		SHEET
REVISIONS	05	HP 55(1)		1499
⚠ 11/10/04	COUNTY	CONTROL	SECT	JOB	HIGHWAY
	LUBBOCK	0380	01	064	US82

LEVELS DISPLAYED
1 2 3 4 5 6 7 8 9 10 11 12 13 14 15 16 17 18 19 20 21 22 23 24 25 26 27 28 29 30 31 32 33 34 35 36 37 38 39 40 41 42 43 44 45 46 47 48 49 50 51 52 53 54 55 56 57 58 59 60 61 62 63 64 65 66 67 68

PATH:

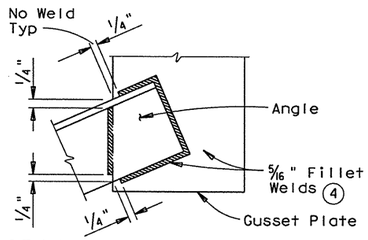

WELD DETAIL - CROSS FRAMES AND END DIAPHRAGM

(At Lean on Bracing Systems)

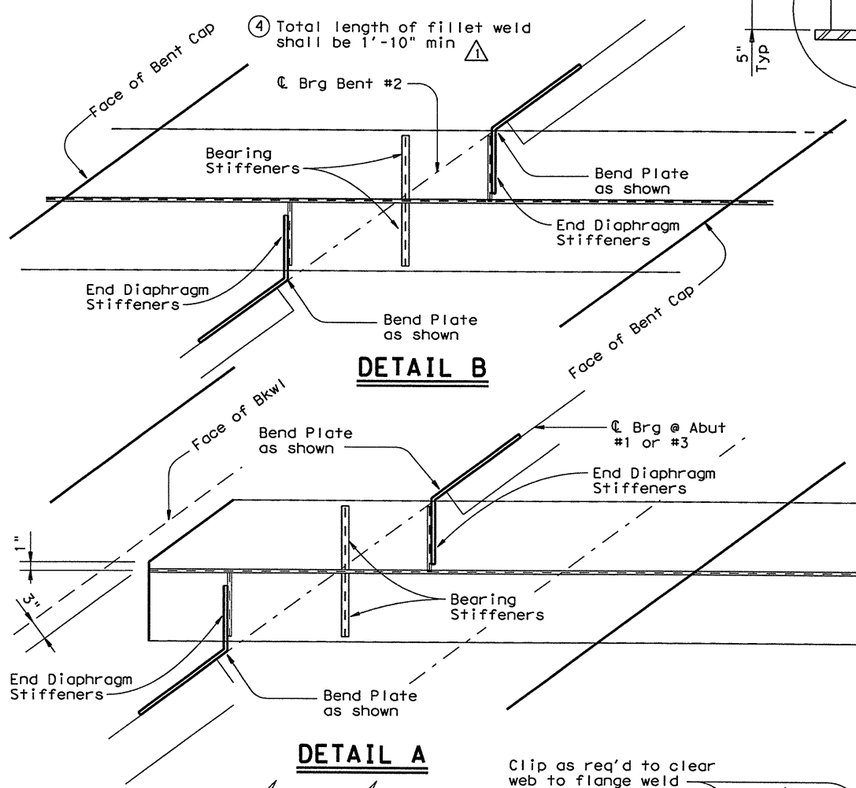

DETAIL B

DETAIL A

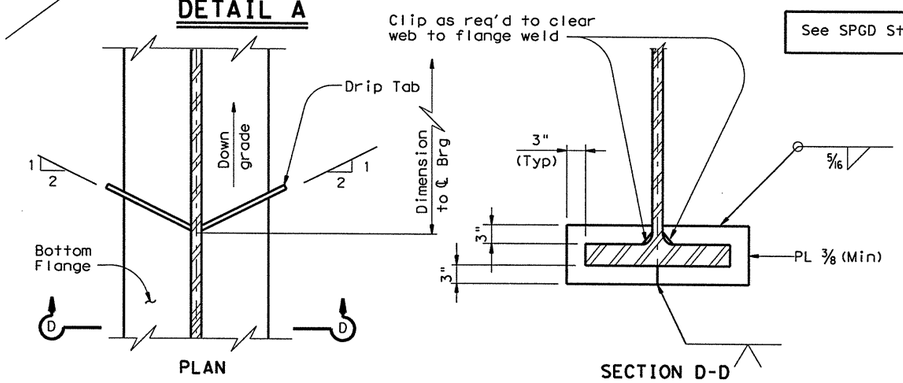

Drip Tab, where indicated on the girder framing plan, shall be located 8'-0" from the ℄ Bent measured along ℄ girder.

DRIP TAB DETAILS

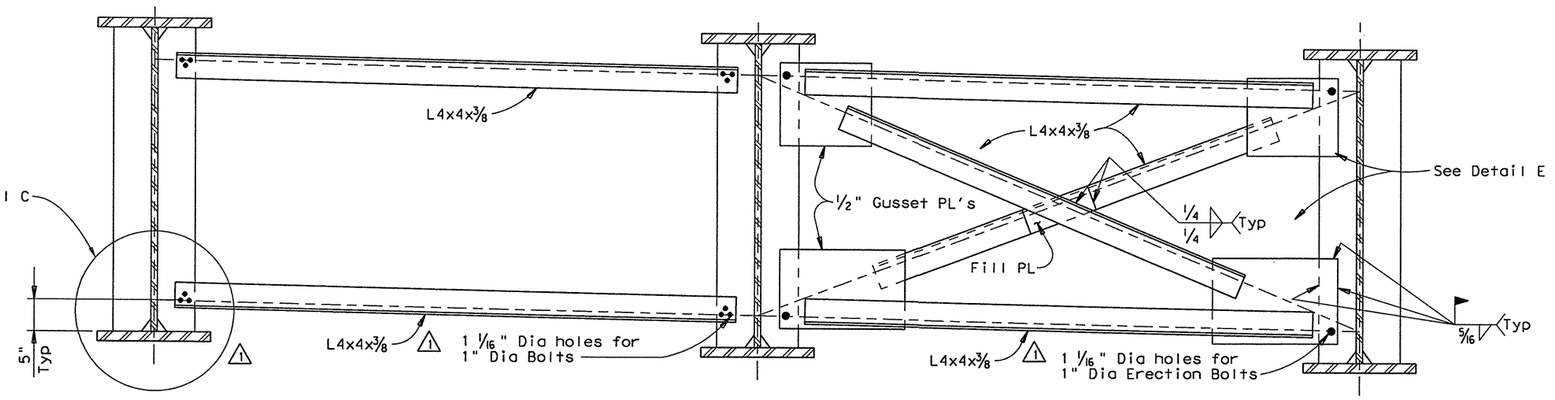

(1) PAIR OF STRUTS

(3) CROSS-FRAMES

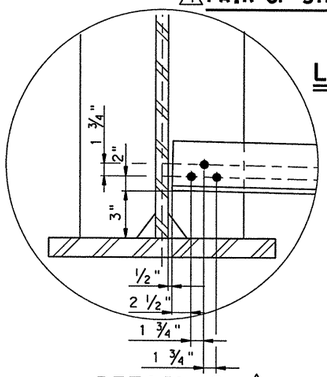

DETAIL C (1)

LEAN ON BRACING SYSTEM DETAILS

Lean on Bracing system shall be used at all locations except along ℄ Bearing of Abutments and Interior Bent.

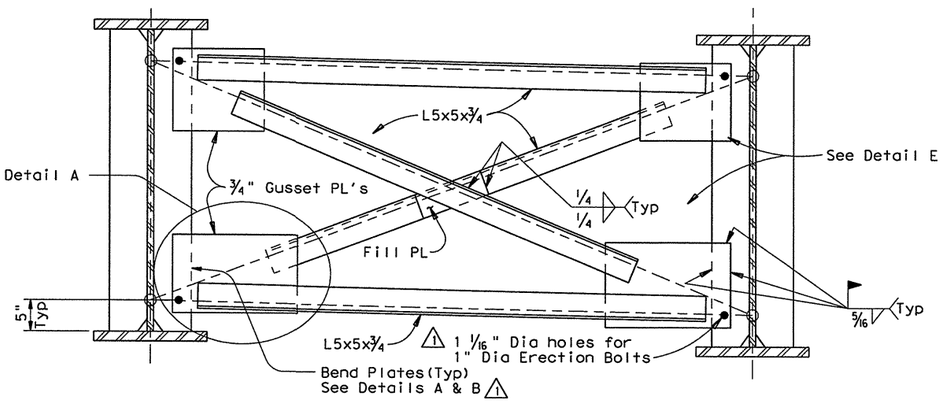

END DIAPHRAGM (5) (6)

(At Abutments & Bent only)

(5) Interior diaphragms are perpendicular or radial to girders unless shown otherwise on span details. Interior Diaphragms at Interior bearings are parallel to the skew unless shown otherwise on span details.

(6) The designer shall ensure that the forces in the Cross-Frames and End diaphragms members and connections, obtained by rational analysis, do not exceed allowables.

See SPGD Standard for details not shown. (1)

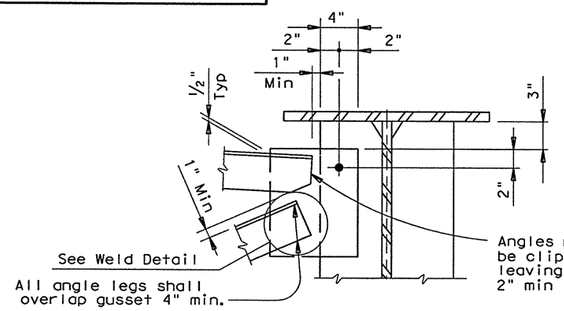

DETAIL E

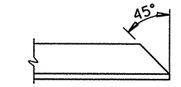

Clip outstanding leg of all angles on diaphragms & cross frames

CLIP DETAIL

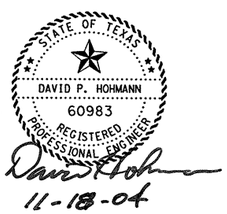

HS20 LOADING

SHEET 4 OF 6

Texas Department of Transportation
Bridge Division

289.50' CONTINUOUS PLATE GIRDER UNIT
(SPANS 1 & 2)
US 82 ML UNDERPASS AT 19TH STREET EB

FILE: 6218sp01.dgn	DN: MR	CK: TCS	DW: WMB	CK: MR
©TxDOT JAN 2004	DISTRICT	FEDERAL AID PROJECT		SHEET
REVISIONS	05	HP 55(1)		1500
(1) 11/10/04	COUNTY	CONTROL	SECT	JOB	HIGHWAY
	LUBBOCK	0380	01	064	US82

LEVELS DISPLAYED ACC:
1 2 3 4 5 6 7 8 9 10 11 12 13 14 15 16
17 18 19 20 21 22 23 24 25 26 27 28 29 30 31 32
33 34 35 36 37 38 39 40 41 42 43 44 45 46 47 48
49 50 51 52 53 54 55 56 57 58 59 60 61 62 63

(1) REVISED 11-24-04 VN

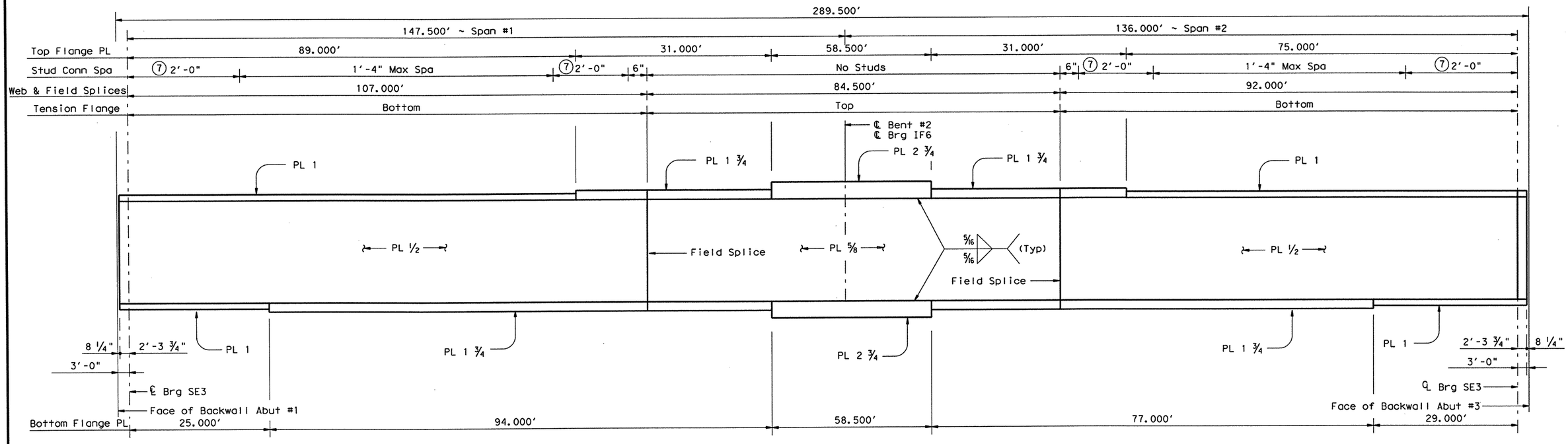

All Web Plates are 54" deep.

All Flange Plates are 18" wide.

STEEL GIRDER FABRICATION NOTES:

All structural steel, including connection plates and diaphragms, shall conform to the requirements of A709 Grade 50 W and shall be paid for at the unit price bid for "Structural Steel-HS".

Girders tension flanges and webs are classified as tension components and shall conform to Item 442.3(1).

Field splices shall be made by full penetration groove welds.

Except at changes in section, shop or field flange and web splices in plate girders may be located as desirable to optimize plate lengths and erection procedures, except that splices will not be allowed where a 40' or less unspliced length would suffice, neither will tension flange splices be allowed within 0.05S either side of interior bearings, within 0.10S either side of the centerlines of the interior span, nor within the range between 0.30S and 0.50S from the end bearings. (S=length c.c. Bearing of Span in which the splice is made.)

Flange and Web Splices shall be made by full penetration groove welds in accordance with the Item 441, "Steel Structures".

All dimensions shown in Girder Elevations are Horizontal.

Bolted Field Splice shall not be permitted on this structure.

HS20 LOADING

STATE OF TEXAS
DAVID P. HOHMANN
60983
REGISTERED PROFESSIONAL ENGINEER

9-7-04

Texas Department of Transportation
Bridge Division

289.50' CONTINUOUS PLATE GIRDER UNIT
(SPANS 1 & 2)
US 82 ML UNDERPASS AT 19TH STREET EB

FILE: 6218sp01.dgn	DN: MR	CK: TCS	DW: WMB	CK: MR
©TxDOT JAN 2004	DISTRICT	FEDERAL AID PROJECT		SHEET
REVISIONS	05	~~HP 5514~~		150

COUNTY	CONTROL	SECT	JOB	HIGHWAY
LUBBOCK	0380	01	064	US82

LEVELS DISPLAYED
1 2 3 4 5 6 7 8 9 10 11 12 13 14 15 16
17 18 19 20 21 22 23 24 25 26 27 28 29 30 31 32
33 34 35 36 37 38 39 40 41 42 43 44 45 46 47 48
49 50 51 52 53 54 55 56 57 58 59 60 61 62 63

PATH:

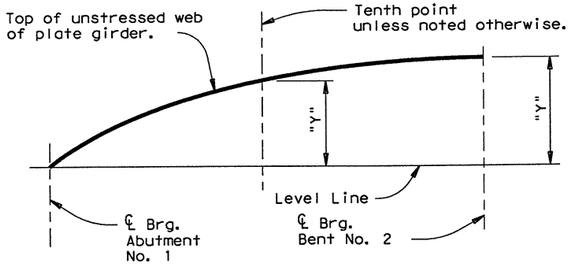

WEB CUTTING DIAGRAM

Note: Web may be cut on straight lines between ordinates shown or to a smooth curve at the Fabricator's option. Ordinates shown include total dead load deflection and vertical curve corrections.

CAMBER DIAGRAM TABLE

"Y" values in feet

LOCATION		GIRDER #1	#2	#3	#4	#5	#6
SPAN #1	0	0.000	0.000	0.000	0.000	0.000	0.000
	1	0.195	0.195	0.195	0.190	0.190	0.190
	2	0.363	0.363	0.363	0.354	0.354	0.354
	3	0.496	0.496	0.496	0.484	0.484	0.484
	4	0.583	0.583	0.583	0.571	0.571	0.571
	5	0.629	0.629	0.629	0.618	0.618	0.618
	6	0.638	0.638	0.638	0.628	0.628	0.628
	7	0.623	0.623	0.623	0.616	0.616	0.616
	FS	0.617	0.618	0.617	0.612	0.611	0.612
	8	0.605	0.605	0.605	0.601	0.601	0.601
	9	0.602	0.602	0.602	0.600	0.600	0.600
	10	0.628	0.628	0.628	0.628	0.628	0.628
SPAN #2	11	0.688	0.688	0.688	0.688	0.688	0.688
	12	0.770	0.770	0.770	0.769	0.769	0.769
	13	0.865	0.865	0.865	0.862	0.862	0.862
	FS	0.887	0.887	0.887	0.884	0.884	0.884
	14	0.961	0.961	0.961	0.957	0.957	0.957
	15	1.052	1.052	1.052	1.047	1.047	1.047
	16	1.125	1.125	1.125	1.120	1.120	1.120
	17	1.178	1.178	1.178	1.172	1.172	1.172
	18	1.208	1.208	1.208	1.203	1.203	1.203
	19	1.214	1.214	1.214	1.212	1.212	1.212
	20	1.207	1.207	1.207	1.207	1.207	1.207

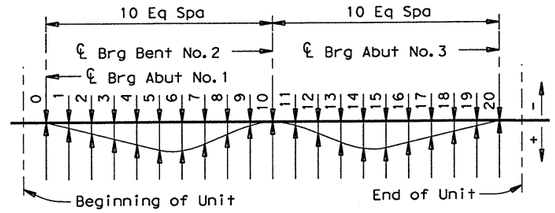

DEAD LOAD DEFLECTION DIAGRAM

FS = Field Splice

TABLE OF DEAD LOAD DEFLECTIONS

Location		Girder (Values in Ft) Deflections due to cast-in-place concrete only ALL				Total dead load deflections (including steel) 1-3	4-6		
SPAN 1	0	0.000				0.000	0.000		
	1	0.089				0.132	0.127		
	2	0.161				0.237	0.228		
	3	0.208				0.307	0.295		
	4	0.225				0.332	0.320		
	5	0.213				0.315	0.304		
	6	0.175				0.261	0.251		
	7	0.123				0.183	0.176		
	FS	0.109				0.162	0.156		
	8	0.069				0.103	0.099		
	9	0.025				0.037	0.035		
	10	0.000				0.000	0.000		
SPAN 2	11	0.000				0.002	0.002		
	12	0.015				0.026	0.025		
	13	0.039				0.063	0.060		
	FS	0.045				0.072	0.069		
	14	0.065				0.102	0.098		
	15	0.087				0.135	0.130		
	16	0.098				0.150	0.145		
	17	0.095				0.145	0.139		
	18	0.077				0.177	0.112		
	19	0.043				0.065	0.063		
	20	0.000				0.000	0.000		

LEVELS DISPLAYED
1 2 3 4 5 6 7 8 9 10 11 12 13 14 15 16
17 18 19 20 21 22 23 24 25 26 27 28 29 30 31 32
33 34 35 36 37 38 39 40 41 42 43 44 45 46 47 48
49 50 51 52 53 54 55 56 57 58 59 60 61 62 63 64
PATH:

HS20 LOADING SHEET 6 OF 6

Texas Department of Transportation
Bridge Division

289.50' CONTINUOUS PLATE GIRDER UNIT
(SPANS 1 & 2)
US 82 ML UNDERPASS AT 19TH STREET EB

STATE OF TEXAS
THOMAS C. STOUT
84829
LICENSED PROFESSIONAL ENGINEER
9-16-04

FILE: 6218sp01.dgn	DN: MR	CK: TCS	DW: WMB	CK: MR
©TxDOT JAN 2004	DISTRICT	FEDERAL AID PROJECT		SHEET
REVISIONS	05	HP FF(1)		1502
	COUNTY	CONTROL	SECT	JOB	HIGHWAY
	LUBBOCK	0380	01	064	US82

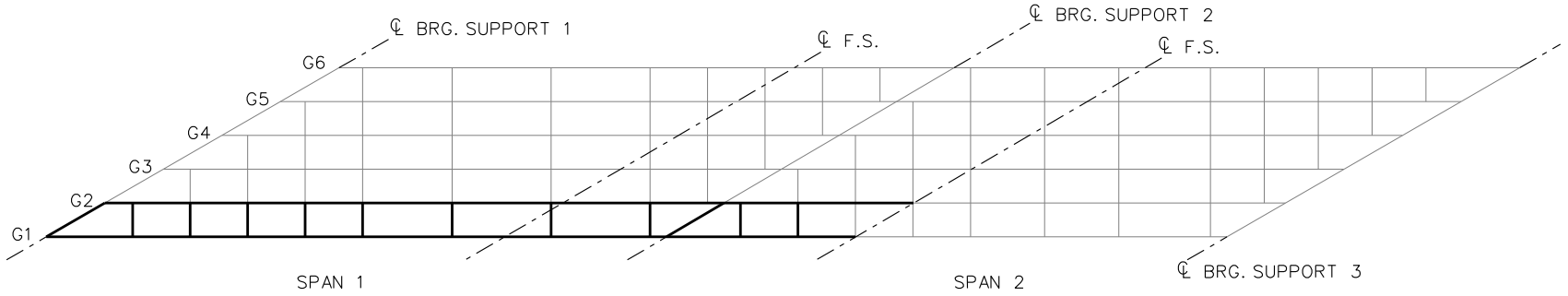

STAGE 1

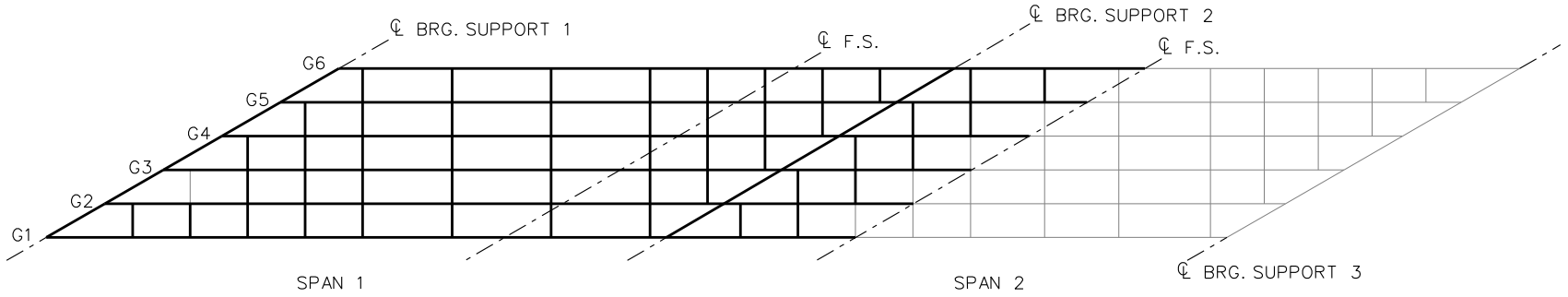

STAGE 3

LEGEND

▽ = HOLD OR LIFT CRANE

○ = TIE DOWN

□ = TEMPORARY SUPPORT STRUCTURE

NOTE:

GIRDERS ARE ERECTED IN PAIRS.

NCHRP 12-79

BRIDGE EICSS12

GENERAL ERECTION PROCEDURE

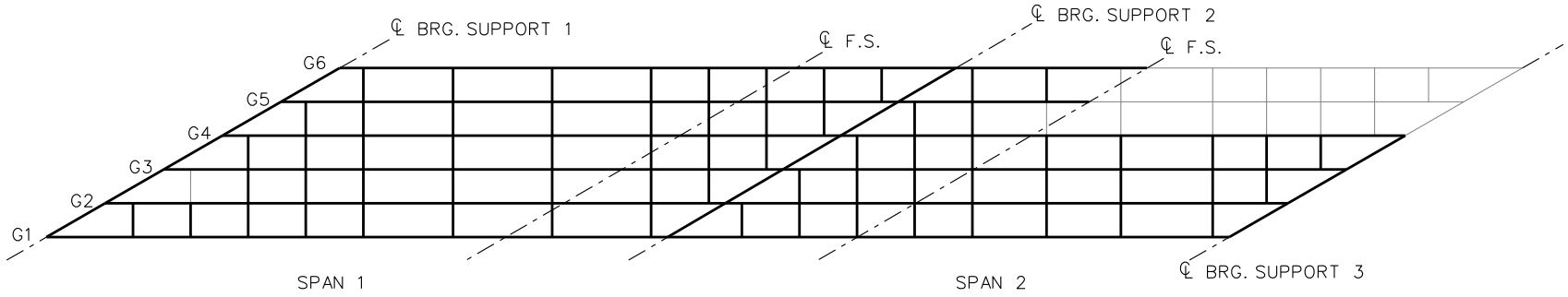

STAGE 5

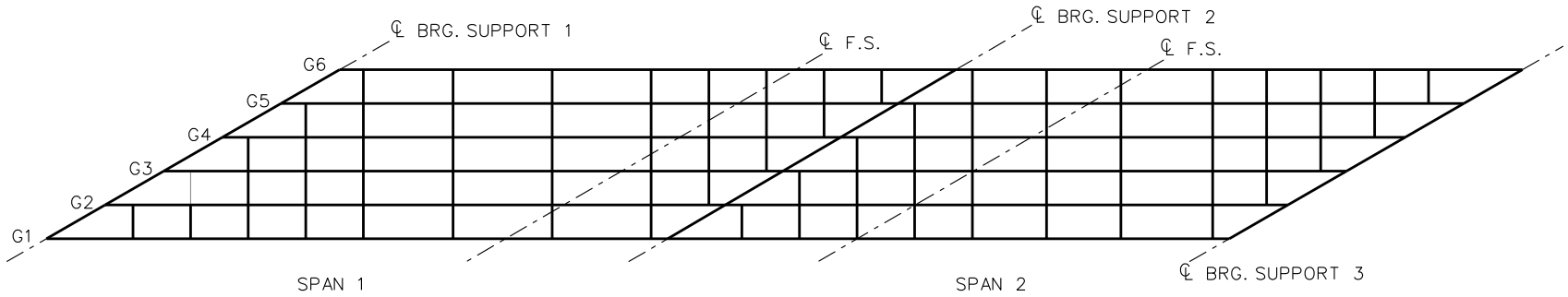

STAGE 6

LEGEND

▽ = HOLD OR LIFT CRANE

○ = TIE DOWN

□ = TEMPORARY SUPPORT STRUCTURE

NOTE:

GIRDERS ARE ERECTED IN PAIRS.

NCHRP 12-79

BRIDGE EICSS12

GENERAL ERECTION PROCEDURE

SHEET 2 OF 2

NCHRP 12-79

EISCR1

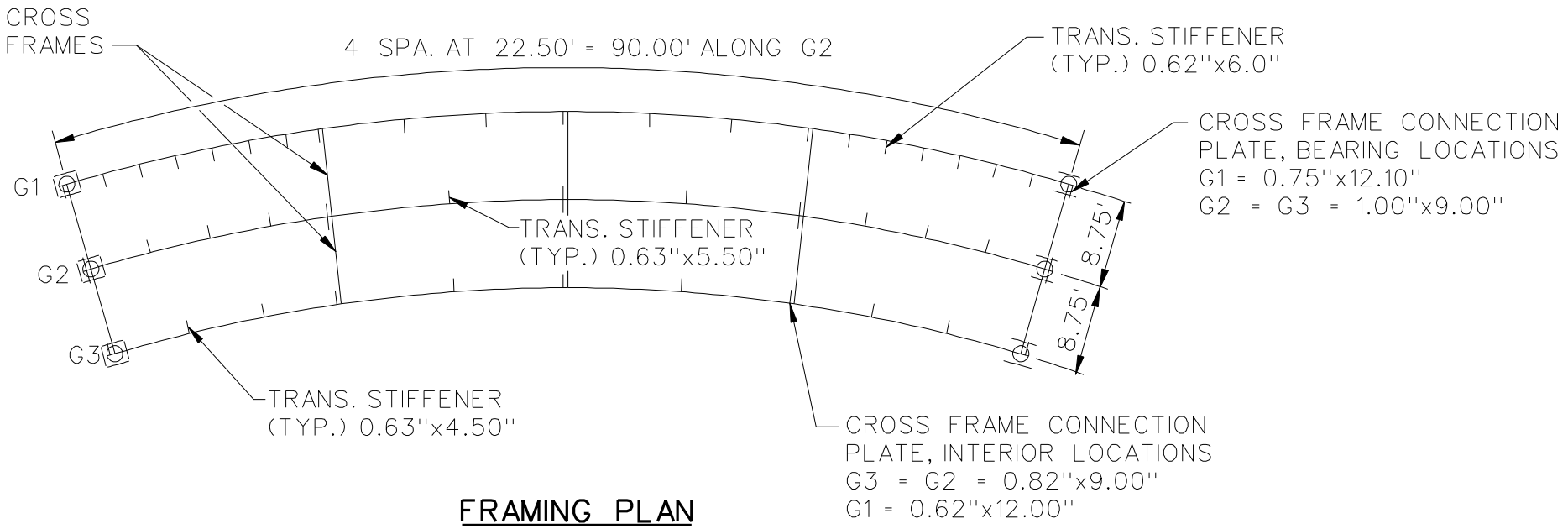

FRAMING PLAN

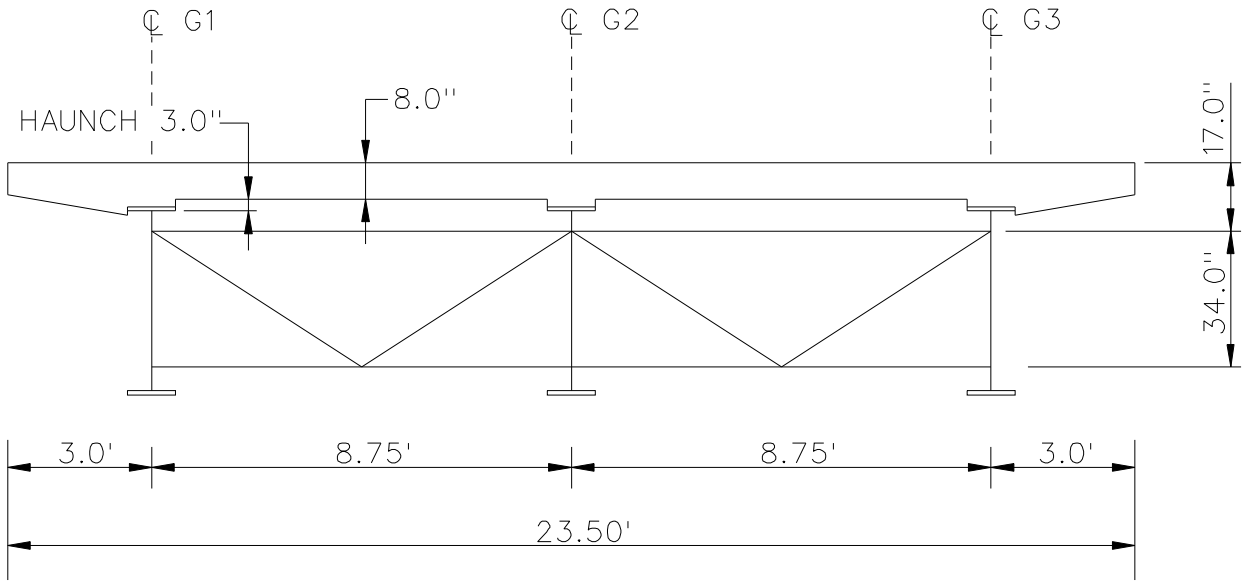

CROSS - SECTION

BEARING LEGEND

- ○ NON-GUIDED
- ⎸○⎸ LONGITUDINALLY GUIDED
- |○| TRANSVERSELY GUIDED
- ⎸○⎸ FIXED

NCHRP 12-79

BRIDGE EISCR1

FRAMING PLAN AND CROSS-SECTION

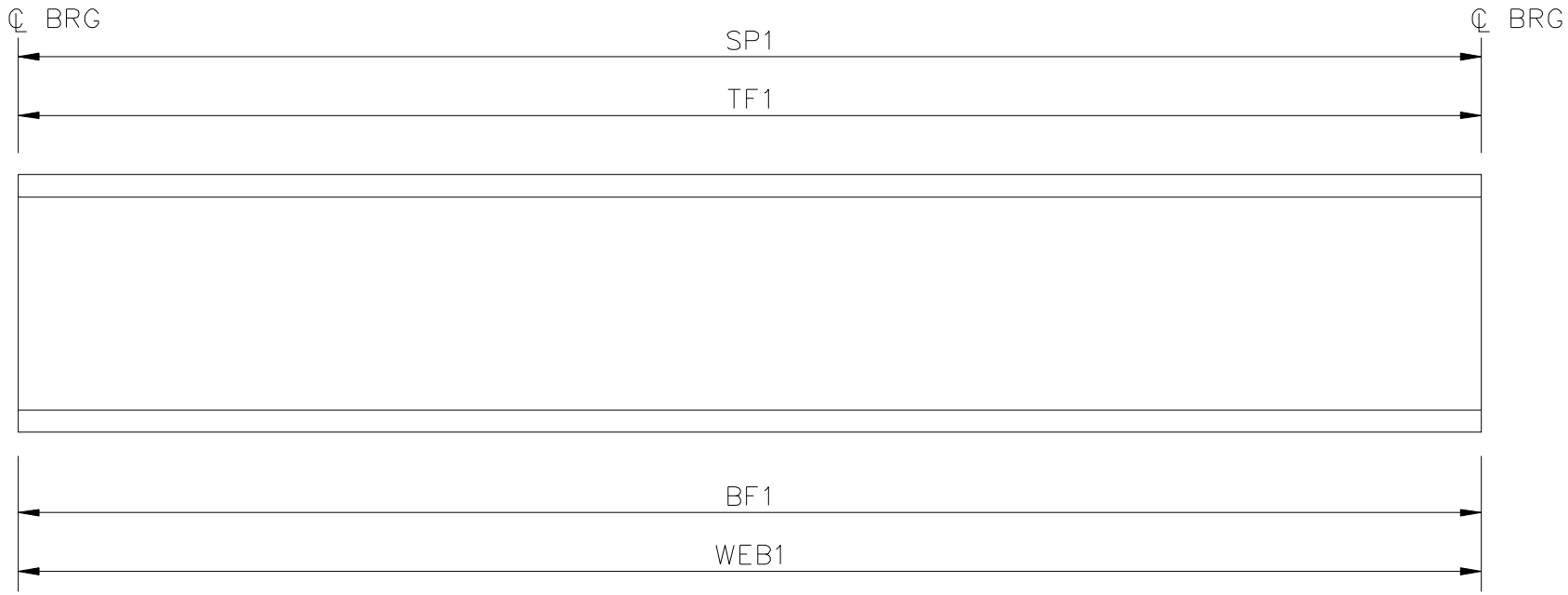

GIRDER	SP1	TF1	BF1	WEB1
G1	86.0625'	0.833'' x 12.2''	0.886'' x 17.3''	0.331'' x 48.0''
G2	90.0000'	0.877'' x 14.2''	1.000'' x 22.2''	0.323: x 48.0''
G3	93.9375'	1.000'' x 24.2''	1.389'' x 24.2''	0.362'' x 48.0''

NCHRP 12-79

BRIDGE EISCR1

GIRDER ELEVATION

SHEET 2 OF 4

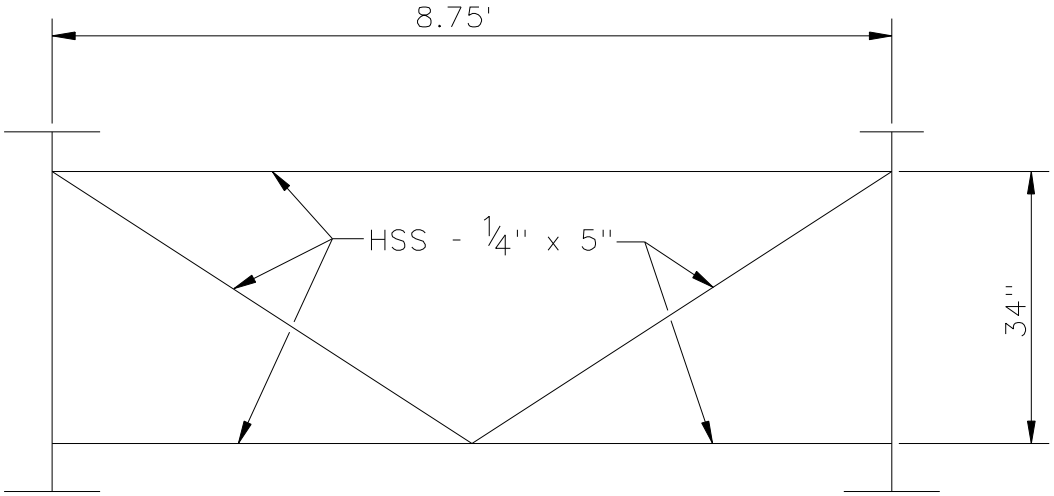

TYPICAL CROSS - FRAME

NOTES:

1. STEEL DEAD LOAD INCREASED BY 5% TO ACCOUNT FOR MISC. DETAILS.
2. FORMWORK LOAD OF 10PSF IS INCLUDED IN CONCRETE DEAD LOAD.

NCHRP 12-79

BRIDGE EISCR1

MISC. DETAILS AND NOTES

SHEET 3 OF 4

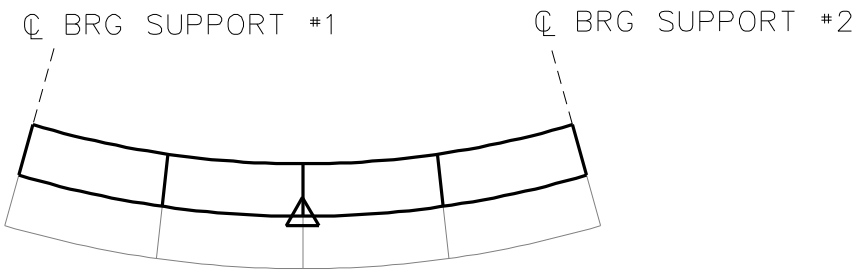

STAGE 1

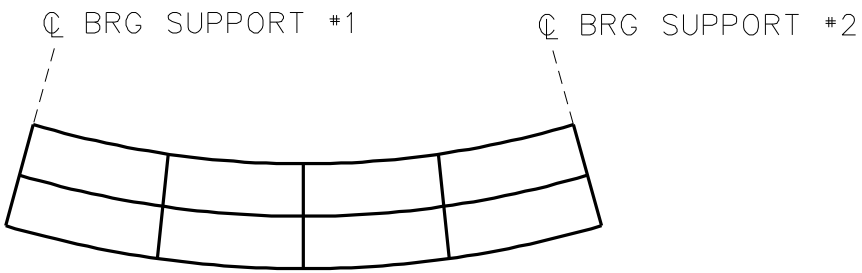

STAGE 2

LEGEND

△ = HOLD OR LIFT CRANE

○ = TIE DOWN

□ = TEMPORARY SUPPORT STRUCTURE

NCHRP 12-79

BRIDGE EISCR1

GENERAL ERECTION PROCEDURE

NCHRP 12-79

EISCS3

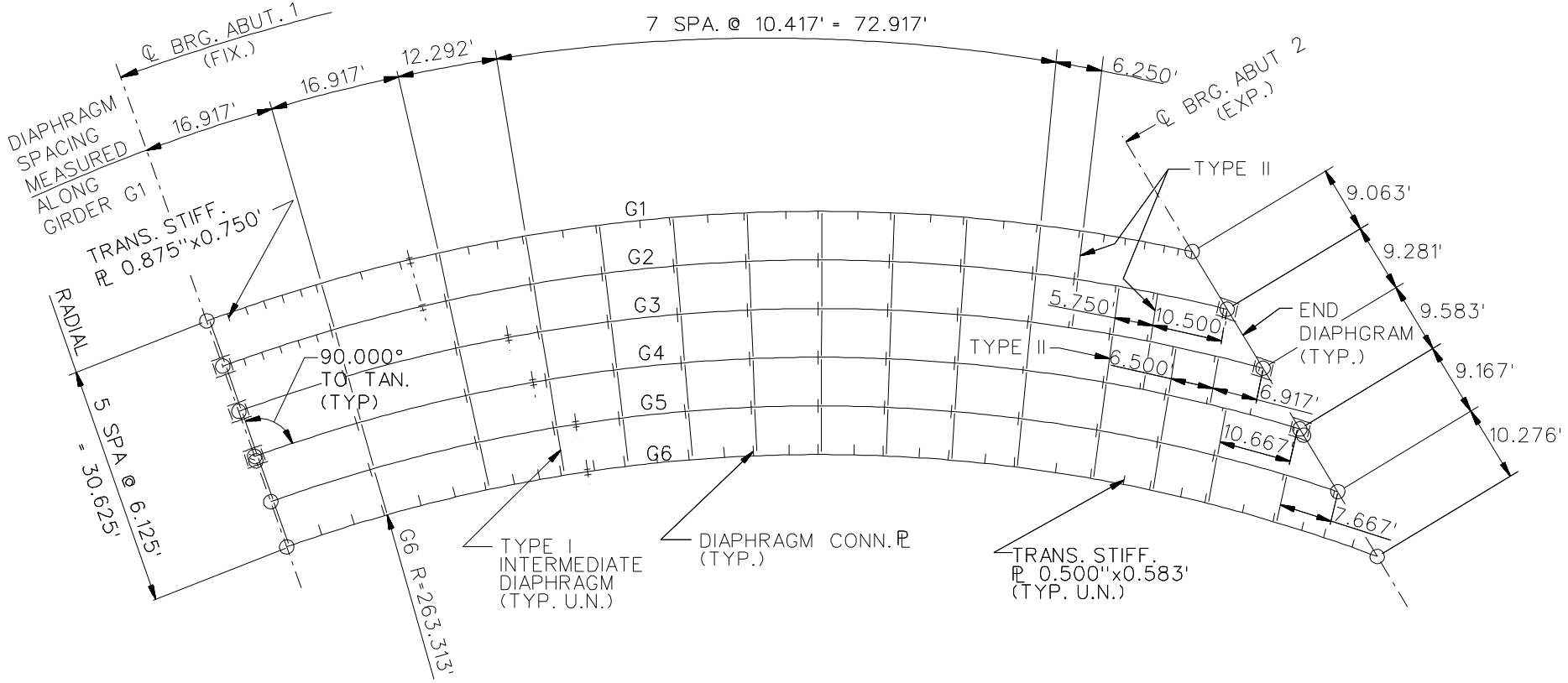

FRAMING PLAN

BEARING LEGEND

○ NON-GUIDED

⎓○ LONGITUDINALLY GUIDED

|○| TRANSVERSELY GUIDED

|⎓○⎓| FIXED

NCHRP 12-79

BRIDGE EISCS3

FRAMING PLAN

SHEET 1 OF 5

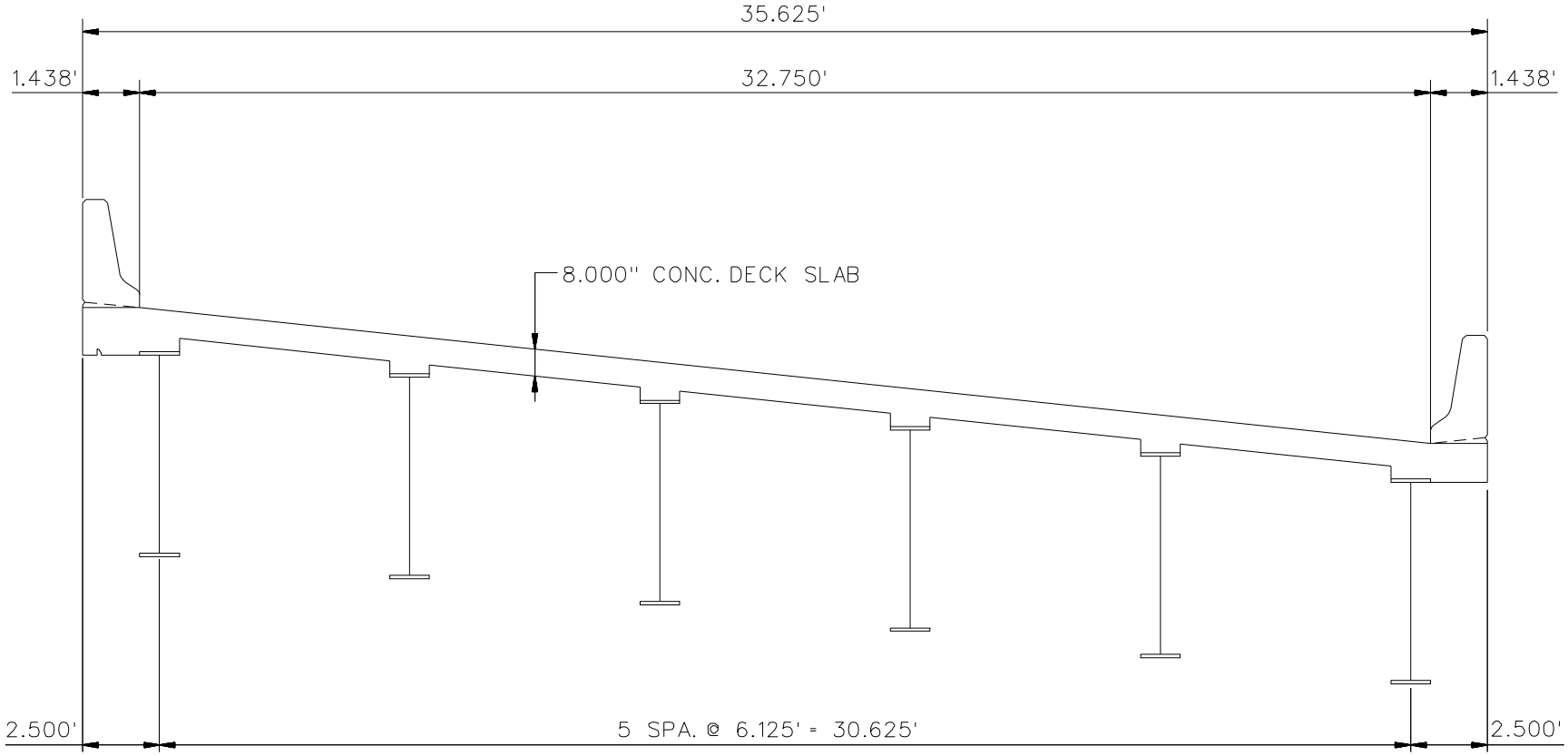

TYPICAL SECTION

NCHRP 12-79

BRIDGE EISCS3

CROSS-SECTION

SHEET 2 OF 5

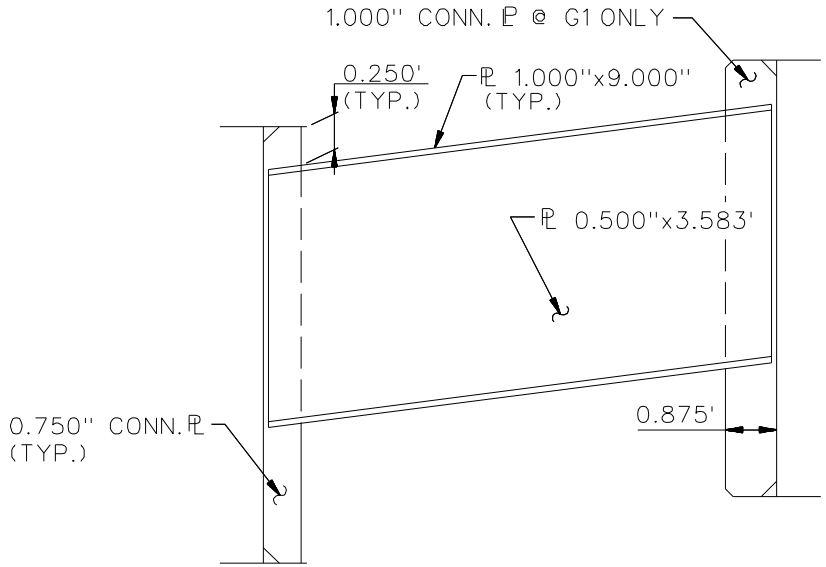

END DIAPHGRAM @ ABUT. 1

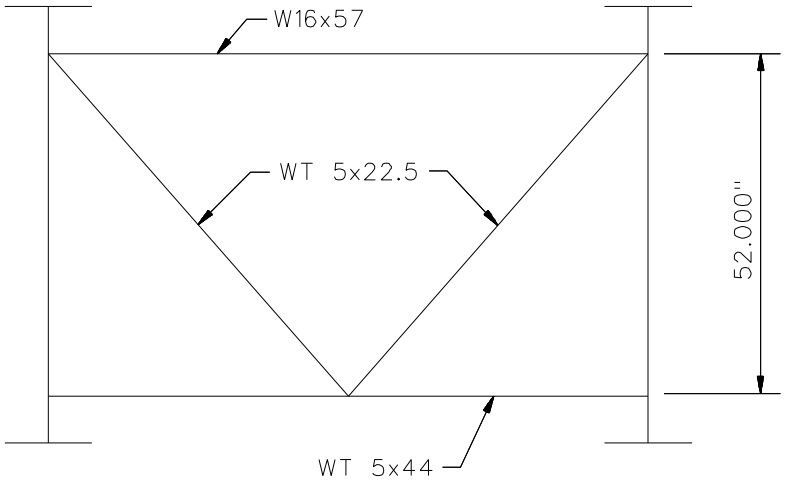

END DIAPHGRAM @ ABUT. 2

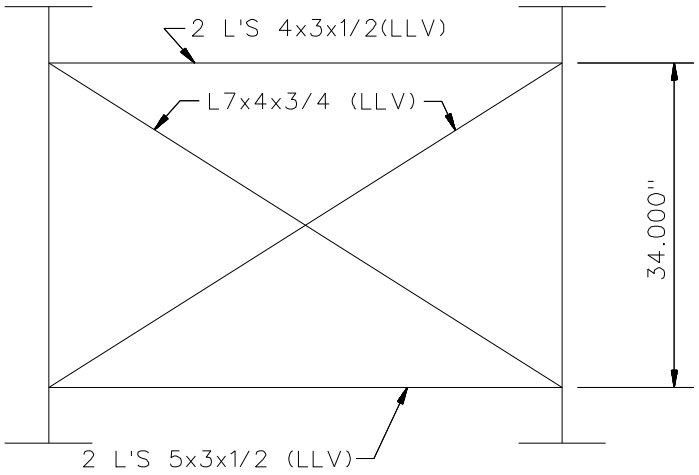

INTERMEDIATE DIAPHRAGM - TYPE I

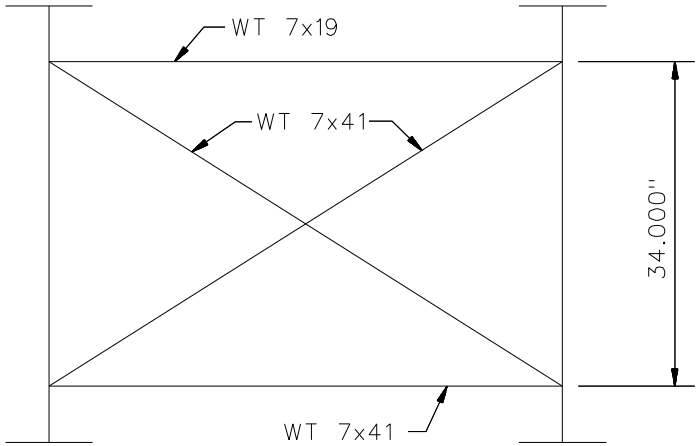

INTERMEDIATE DIAPHRAGM - TYPE II

NCHRP 12-79

BRIDGE EISCS3

MISC. DETAILS

SHEET 3 OF 5

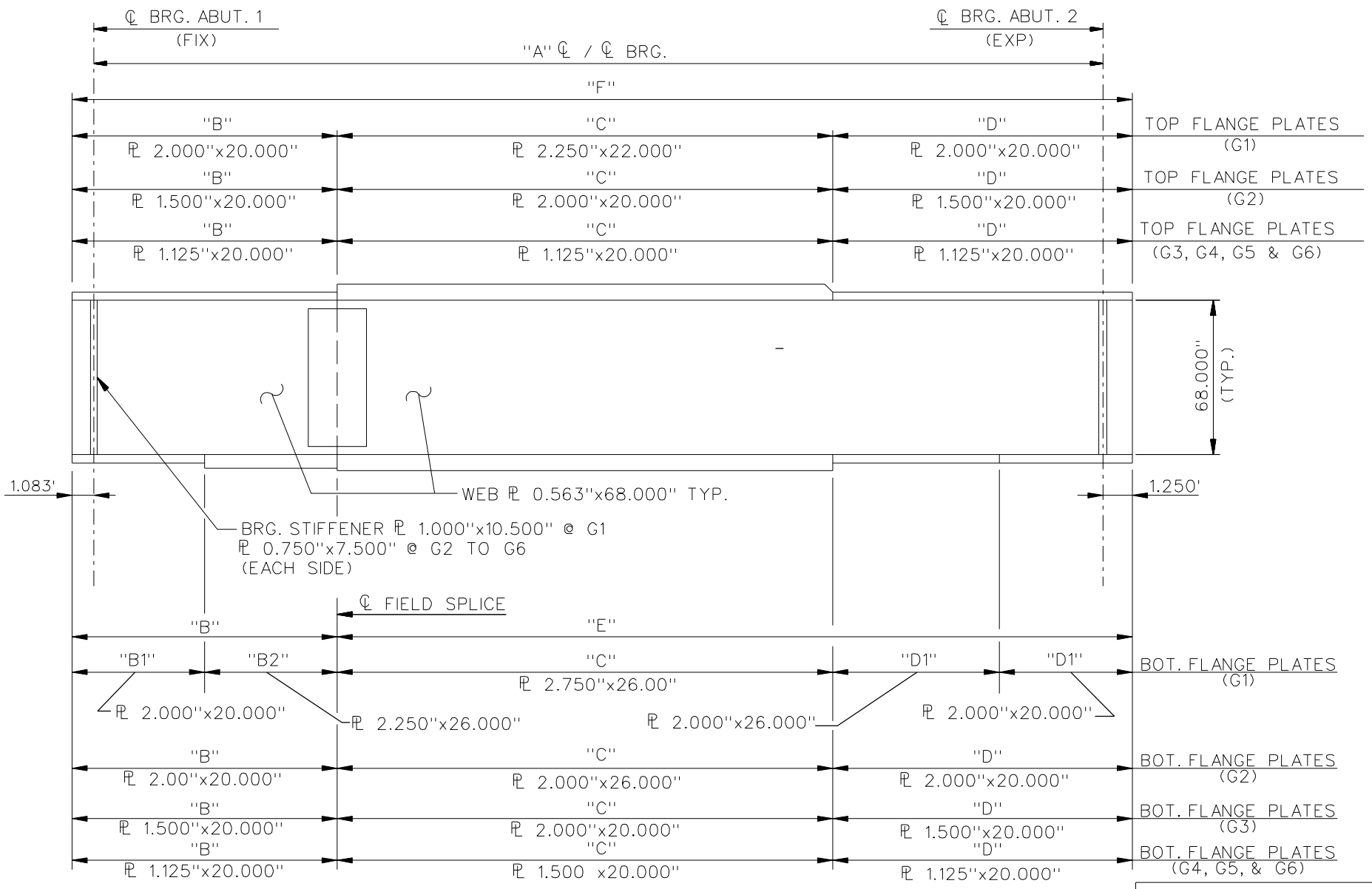

TABLE OF GIRDER DIMENSIONS

GIRDER	DIM. "A"	DIM. "B"	DIM. "B1"	DIM. "B2"	DIM. "C"	DIM. "D"	DIM. "D1"	DIM. "D1"	DIM. "E"	DIM. "F"
G1	141.208'	30.917'	11.000'	19.917'	84.167'	28.458'	18.458'	10.000'	112.625'	143.542'
G2	144.865'	30.250'	———	———	83.417'	33.531'	———	———	116.948'	147.198'
G3	148.698'	39.333'	———	———	73.333'	38.365'	———	———	111.698'	151.031'
G4	152.760'	40.833'	———	———	74.333'	39.927'	———	———	114.260'	155.094'
G5	157.073'	46.917'	———	———	68.333'	44.156'	———	———	112.490'	159.406'
G6	161.708'	46.417'	———	———	69.250'	48.375'	———	———	117.625'	164.042'

NCHRP 12-79

BRIDGE EISCS3

GIRDER ELEVATION

SHEET 4 OF 5

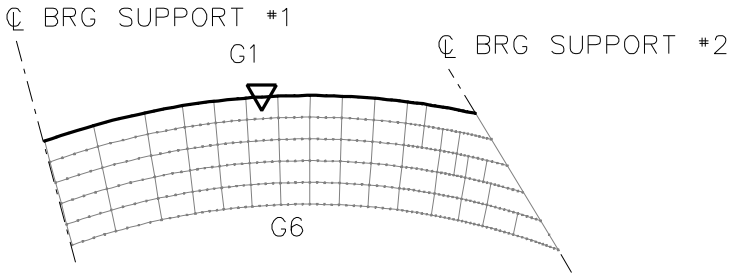

STAGE 1

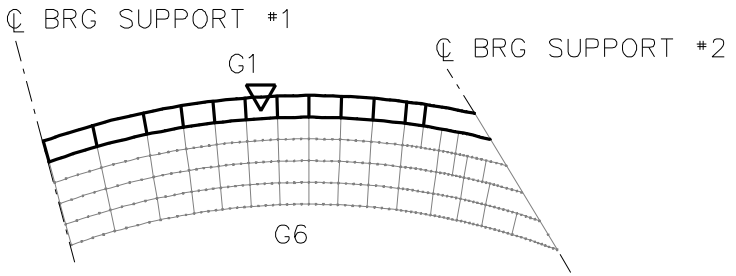

STAGE 2

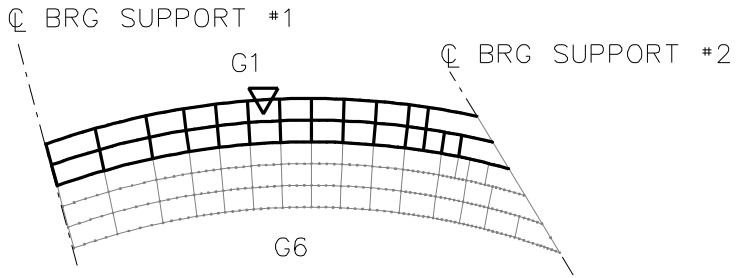

STAGE 3

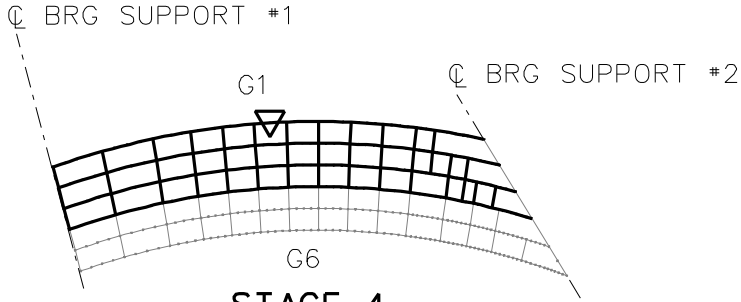

STAGE 4

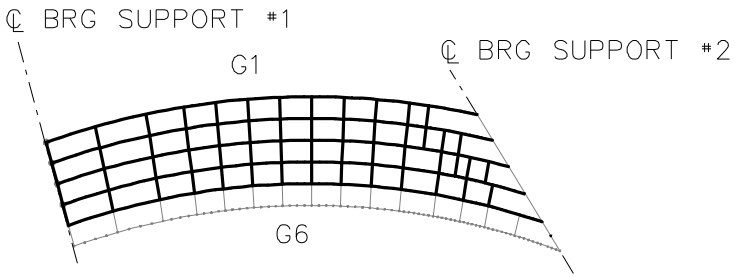

STAGE 5

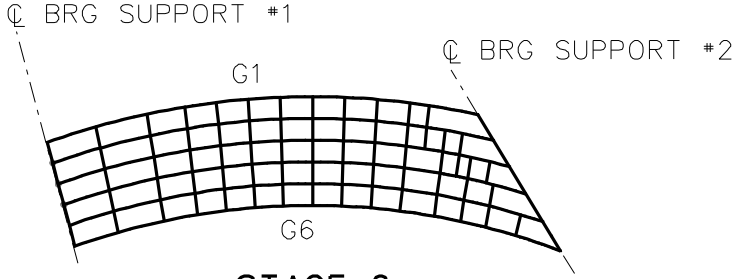

STAGE 6

LEGEND

▽ = HOLD OR LIFT CRANE

○ = TIE DOWN

□ = TEMPORARY SUPPORT STRUCTURE

NCHRP 12-79

BRIDGE EISCS3

GENERAL ERECTION PROCEDURE

SHEET 5 OF 5

NCHRP 12-79

EISCS4

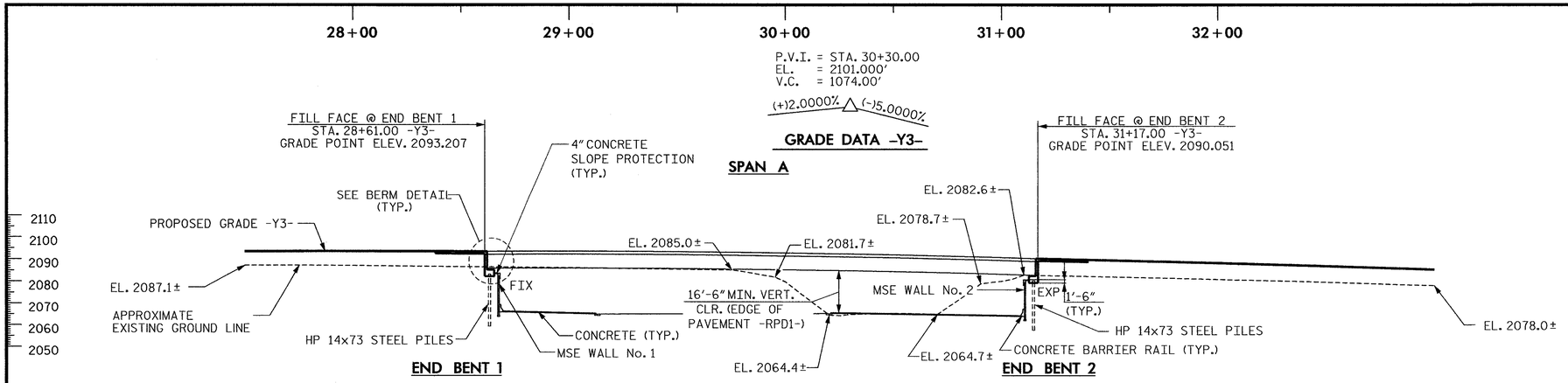

SECTION ALONG -Y3-

(END BENTS ON SECTION AT RIGHT ANGLES TO ℄ END BENTS)

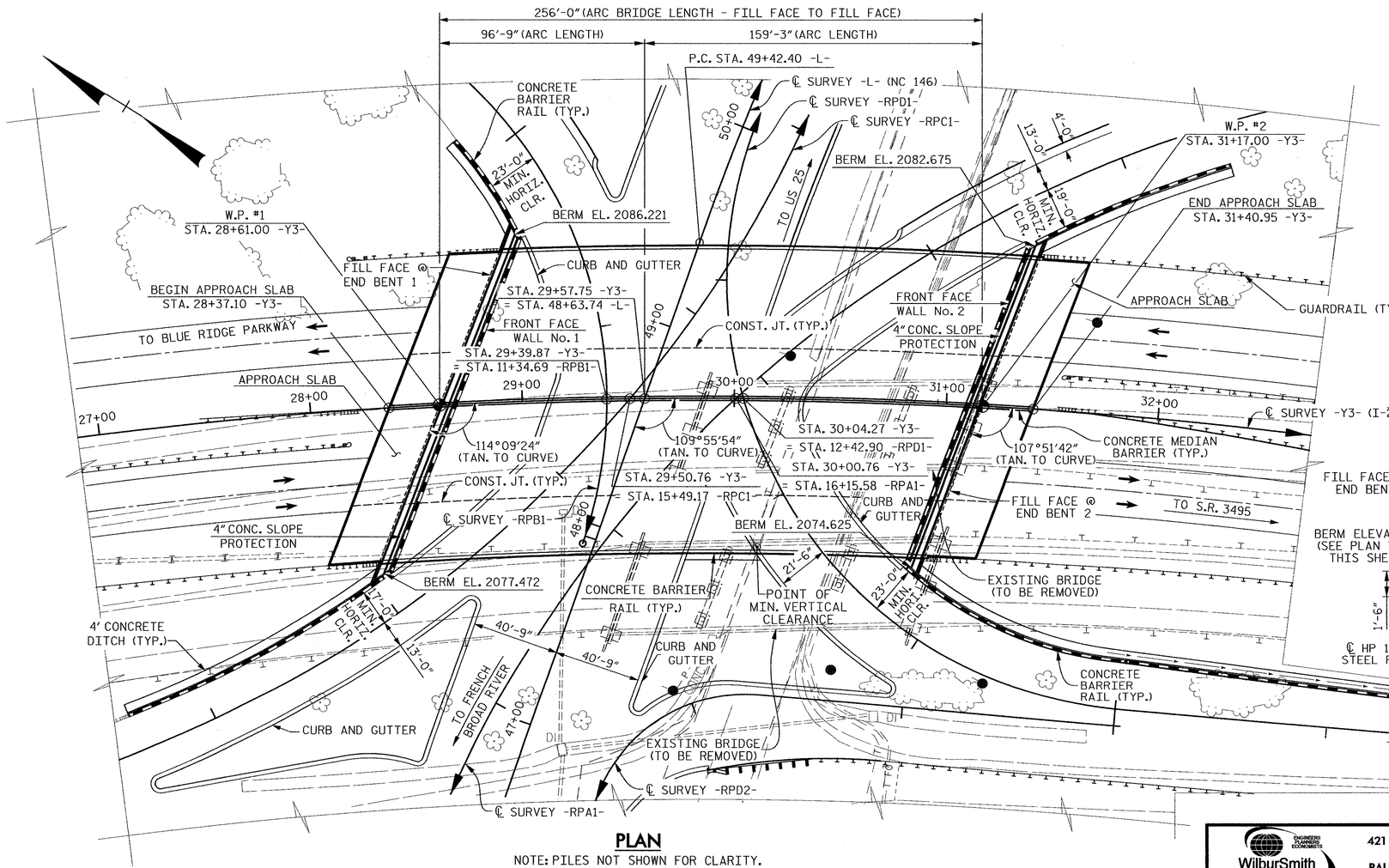

PLAN

NOTE: PILES NOT SHOWN FOR CLARITY.

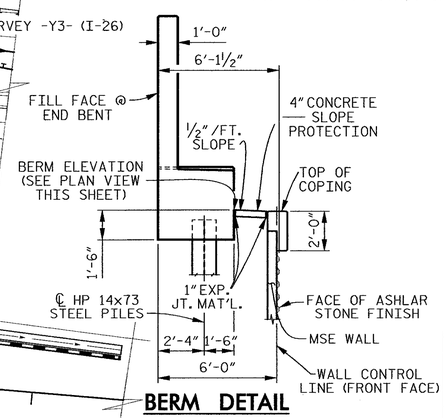

BERM DETAIL

GENERAL NOTES

ASSUMED LIVE LOAD = HS20 OR ALTERNATE LOADING, EXCEPT THAT THE GIRDERS HAVE BEEN DESIGNED FOR HS25 TRUCK LOAD.

FOR HORIZONTAL CURVE AND GRADE DATA, SEE SHEET 4 OF 4.

FOR OTHER DESIGN DATA AND GENERAL NOTES, SEE "STANDARD NOTES" SHEET.

FOR EROSION CONTROL MEASURES SEE EROSION CONTROL PLANS.

THIS BRIDGE HAS BEEN DESIGNED BY THE STRENGTH DESIGN METHOD AS SPECIFIED IN AASHTO STANDARD SPECIFICATIONS.

REMOVABLE FORMS MAY BE USED IN LIEU OF METAL STAY-IN- PLACE FORMS IN ACCORDANCE WITH ARTICLE 420-3 OF THE STANDARD SPECIFICATIONS.

AFTER SERVING AS TEMPORARY STRUCTURES THE EXISTING I-26 EAST-BOUND AND WESTBOUND LANE BRIDGES SHALL BE REMOVED.

FOR MAINTENANCE AND PROTECTION OF TRAFFIC BENEATH PROPOSED STRUCTURE, SEE SPECIAL PROVISIONS.

THE CLASS AA CONCRETE IN THE BRIDGE DECK SHALL CONTAIN FLY ASH OR GROUND GRANULATED BLAST FURNACE SLAG AT THE SUBSTITUTION RATE SPECIFIED IN ARTICLE 1024-1 AND IN ACCORDANCE WITH ARTICLES 1024-5 AND 1024-6 OF THE STANDARD SPECIFICATIONS.

THIS BRIDGE HAS BEEN DESIGNED IN ACCORDANCE WITH THE REQUIREMENTS OF THE AASHTO STANDARD SPECIFICATIONS FOR SEISMIC DESIGN OF HIGHWAY BRIDGES FOR SEISMIC PERFORMANCE CATEGORY B.

TEMPORARY SHORING WILL BE REQUIRED. SEE SPECIAL PROVISIONS FOR TEMPORARY SHORING.

THE CONTRACTOR SHALL PROVIDE INDEPENDENT ASSURANCE SAMPLES OF REINFORCING STEEL AS FOLLOWS: FOR PROJECTS REQUIRING UP TO 400 TONS OF REINFORCING STEEL, ONE 30 INCH SAMPLE OF EACH SIZE BAR USED, AND FOR PROJECTS REQUIRING OVER 400 TONS OF REINFORCING STEEL, TWO 30 INCH SAMPLES OF EACH SIZE BAR USED. THE BARS FROM WHICH THE SAMPLES ARE TAKEN MUST THEN BE SPLICED WITH REPLACEMENT BARS OF THE SIZE AND LENGTH OF THE SAMPLE, PLUS A MINIMUM LAP SPLICE OF THIRTY BAR DIAMETERS.

INASMUCH AS THE PAINT SYSTEM ON THE EXISTING STRUCTURAL STEEL CONTAINS LEAD, THE CONTRACTOR'S ATTENTION IS DIRECTED TO ARTICLE 107-1 OF THE STANDARD SPECIFICATIONS.

NEEDLE BEAMS WILL NOT BE ALLOWED UNLESS OTHERWISE CALLED FOR ON THE PLANS OR APPROVED BY THE ENGINEER.

FOR SUBMITTAL OF WORKING DRAWINGS, SEE SPECIAL PROVISIONS.

FOR FALSEWORK AND FORMWORK, SEE SPECIAL PROVISIONS.

FOR CRANE SAFETY, SEE SPECIAL PROVISIONS.

FOR FALSEWORK AND FORMWORK OVER OR ADJACENT TO TRAFFIC, SEE SPECIAL PROVISIONS.

ALL REINFORCING STEEL SHALL BE GRADE 60.

FOR GROUT FOR STRUCTURES, SEE SPECIAL PROVISIONS.

RELEASE FOR CONSTRUCTION
DATE: 5-30-08

PROJECT NO. R-2813B

BUNCOMBE COUNTY

STATION: 48+63.74 -L- P.O.T. = 29+57.75 -Y3- P.O.C.

SHEET 1 OF 4 REPLACES BRIDGE No. 113 AND 114

STATE OF NORTH CAROLINA
DEPARTMENT OF TRANSPORTATION
RALEIGH

GENERAL DRAWING

BRIDGE OVER NC 146 (LONG SHOALS ROAD) ON I-26 BETWEEN BLUE RIDGE PARKWAY AND SR 3495

WilburSmith ASSOCIATES
ENGINEERS PLANNERS ECONOMISTS
421 Fayetteville Street
Suite 1303
RALEIGH, N. C. 27601

DRAWN BY : K.E. LOFTON DATE : 5-08
CHECKED BY : T.M. HARRIS DATE : 5-08

DWG. No. S-81

NORTH CAROLINA PROFESSIONAL SEAL 19299 ENGINEER THOMAS M. HARRIS
5-30-08

REVISIONS						SHEET NO.
No.	BY:	DATE:	No.	BY:	DATE:	
1			3			TOTAL SHEETS
2			4			

s:\NCDOT\R2813B\Design\I-26 Bridge\RFC\R2813B_SD_001_01.dgn
5/30/2008

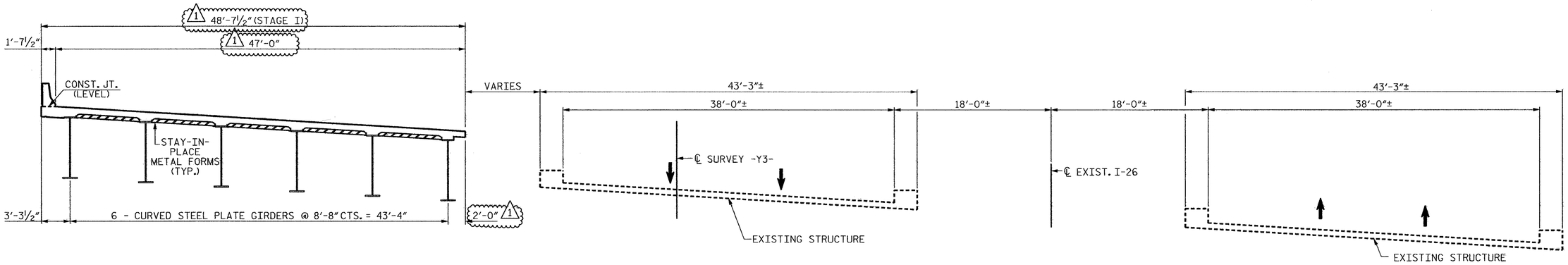

STAGE I

NOTE: HORIZONTAL DIMENSIONS ARE RADIAL TO ℄ SURVEY -Y3- OR ℄ EXIST. I-26.

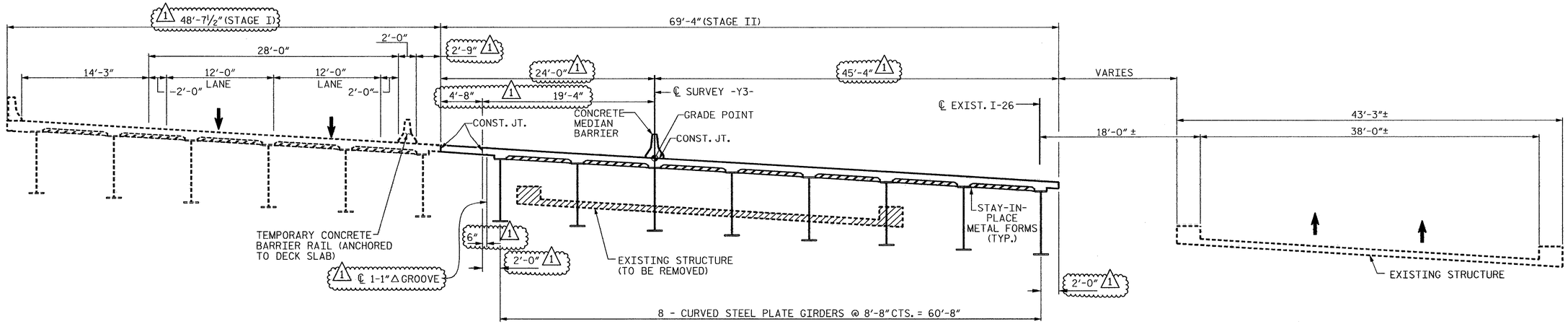

STAGE II

NOTE: HORIZONTAL DIMENSIONS ARE RADIAL TO ℄ SURVEY -Y3- OR ℄ EXIST. I-26.

1 REVISED DECK CONSTRUCTION JOINT LOCATIONS.

PROJECT NO. R-2813B

BUNCOMBE COUNTY

STATION: 48+63.74 -L- P.O.T.

SHEET 1 OF 2

RELEASE FOR CONSTRUCTION
DATE: 3/12/08

STATE OF NORTH CAROLINA
DEPARTMENT OF TRANSPORTATION
RALEIGH

CONSTRUCTION SEQUENCE

WilburSmith ASSOCIATES
ENGINEERS PLANNERS ECONOMISTS
421 Fayetteville Street
Suite 1303
RALEIGH, N. C. 27601

DRAWN BY : K.E. LOFTON DATE : 3-08
CHECKED BY : T.M. HARRIS DATE : 3-08
DWG. No. S-85.1

NORTH CAROLINA PROFESSIONAL SEAL 19299 ENGINEER THOMAS M. HARRIS
3-12-08

REVISIONS						SHEET NO.
No.	BY:	DATE:	No.	BY:	DATE:	
1	LOFTON	3-12-08	3			TOTAL SHEETS
2			4			

S:\NCDOT\R2813B\Design\I-26 Bridge\RFC\R2813B_SD_STAGECONST_REV1.01.dgn
3/12/2008

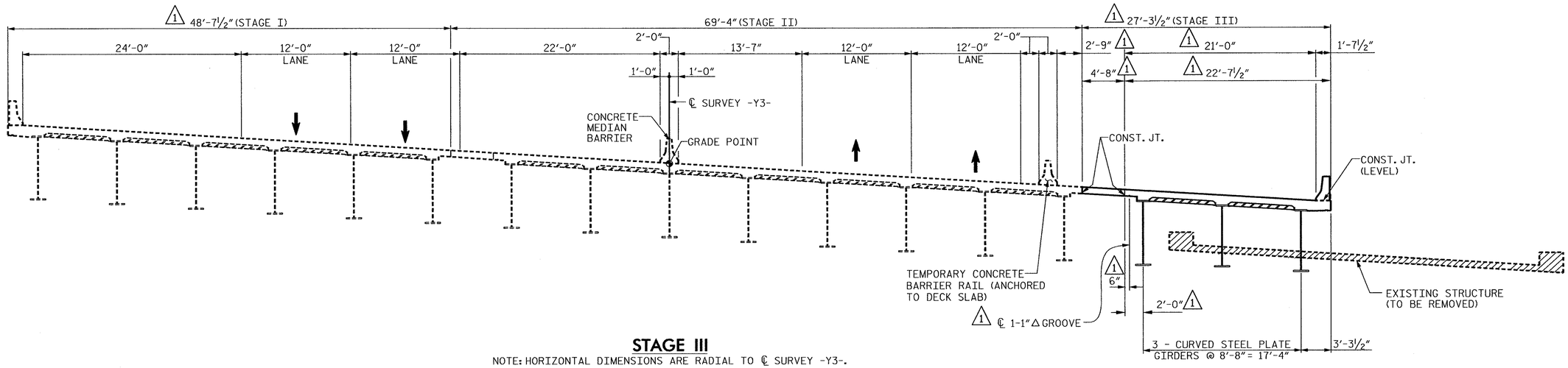

STAGE III

NOTE: HORIZONTAL DIMENSIONS ARE RADIAL TO ℄ SURVEY -Y3-.

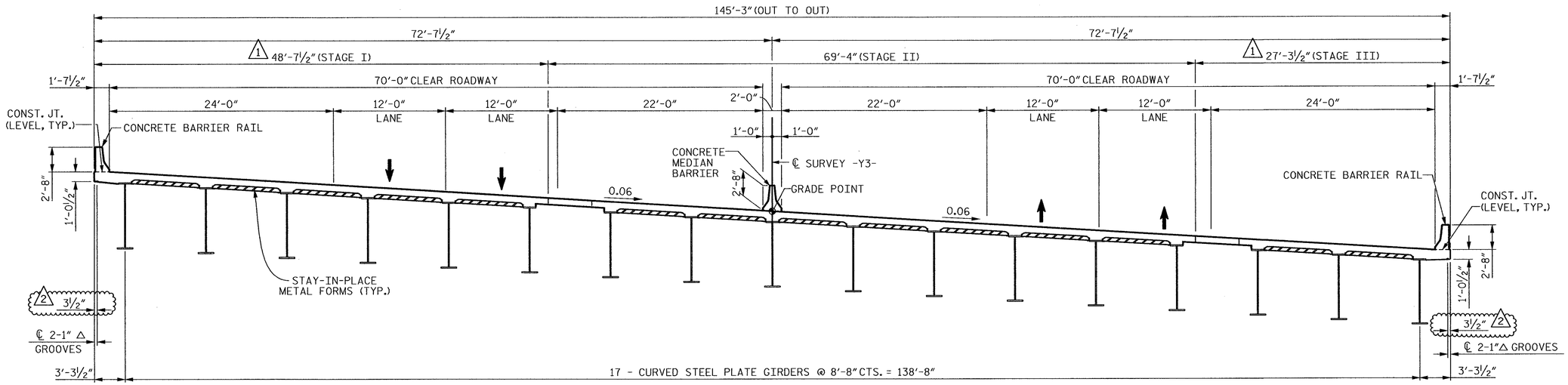

TYPICAL SECTION

NOTE: HORIZONTAL DIMENSIONS ARE RADIAL TO ℄ SURVEY -Y3-.

2 REVISED LOCATION OF 2 -1" △ GROOVES IN OVERHANGS.

1 REVISED DECK CONSTRUCTION JOINT LOCATIONS.

PROJECT NO. R-2813B

BUNCOMBE COUNTY

STATION: 48+63.74 -L- P.O.T.

SHEET 2 OF 2

RELEASE FOR CONSTRUCTION
DATE: 5-30-08

STATE OF NORTH CAROLINA
DEPARTMENT OF TRANSPORTATION
RALEIGH

CONSTRUCTION SEQUENCE

WilburSmith ASSOCIATES — ENGINEERS PLANNERS ECONOMISTS
421 Fayetteville Street
Suite 1303
RALEIGH, N. C. 27601

DRAWN BY : K.E. LOFTON DATE : 3-08
CHECKED BY : T.M. HARRIS DATE : 3-08

DWG. No. S-86.2

NORTH CAROLINA PROFESSIONAL SEAL 19299 ENGINEER THOMAS M. HARRIS
5-30-08

REVISIONS						SHEET NO.
No.	BY:	DATE:	No.	BY:	DATE:	
1	LOFTON	3-12-08	3			TOTAL SHEETS
2	LOFTON	5-30-08	4			

S:\NCDOT\R2813B\Design\I-26 Bridge\RFC\R2813B_SD_STAGECONST_REV2_02.dgn
5/30/2008

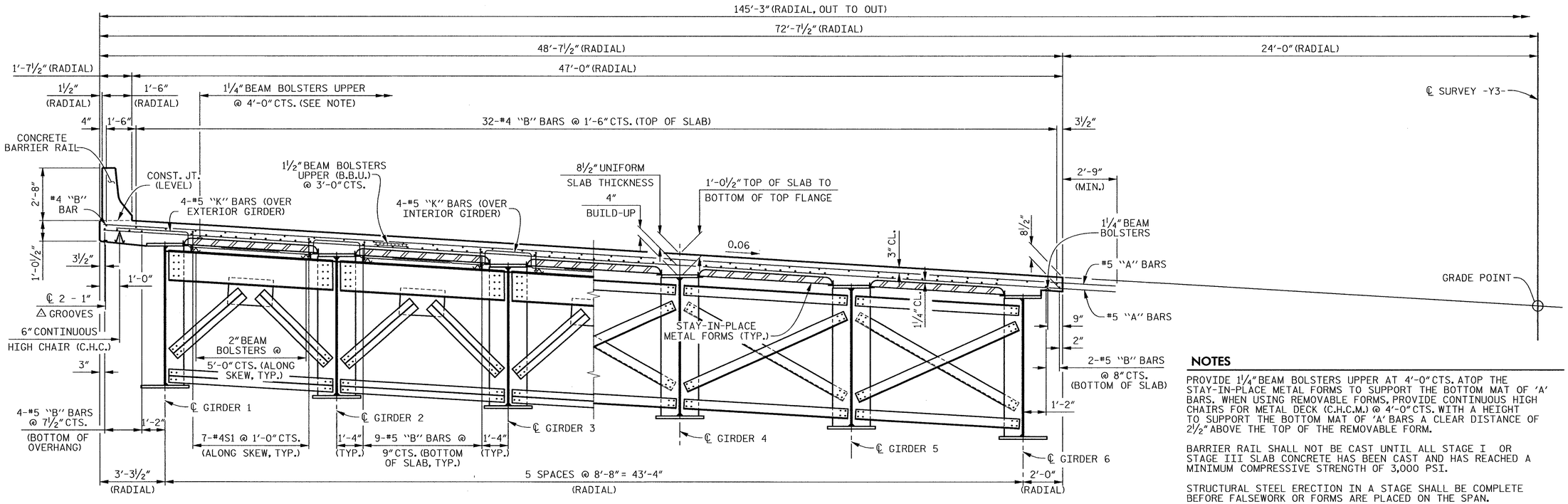

HALF SECTION SHOWING END BENT CROSSFRAMES

HALF SECTION SHOWING INTERMEDIATE CROSSFRAMES

TYPICAL SECTION – STAGE I

NOTES

PROVIDE 1¼" BEAM BOLSTERS UPPER AT 4'-0" CTS. ATOP THE STAY-IN-PLACE METAL FORMS TO SUPPORT THE BOTTOM MAT OF 'A' BARS. WHEN USING REMOVABLE FORMS, PROVIDE CONTINUOUS HIGH CHAIRS FOR METAL DECK (C.H.C.M.) @ 4'-0" CTS. WITH A HEIGHT TO SUPPORT THE BOTTOM MAT OF 'A' BARS A CLEAR DISTANCE OF 2½" ABOVE THE TOP OF THE REMOVABLE FORM.

BARRIER RAIL SHALL NOT BE CAST UNTIL ALL STAGE I OR STAGE III SLAB CONCRETE HAS BEEN CAST AND HAS REACHED A MINIMUM COMPRESSIVE STRENGTH OF 3,000 PSI.

STRUCTURAL STEEL ERECTION IN A STAGE SHALL BE COMPLETE BEFORE FALSEWORK OR FORMS ARE PLACED ON THE SPAN.

THE CONTRACTOR MAY, WHEN NECESSARY, PROPOSE A SCHEME FOR AVOIDING INTERFERENCE BETWEEN STAY-IN-PLACE METAL FORM SUPPORTS OR FORMS AND BEAM/GIRDER STIFFENERS OR CONNECTOR PLATES. THE PROPOSAL SHALL BE INDICATED, AS APPROPRIATE, ON EITHER THE STEEL WORKING DRAWINGS OR THE STAY-IN-PLACE METAL FORM WORKING DRAWINGS.

PREVIOUSLY CAST CONCRETE IN A STAGE SHALL HAVE ATTAINED A MINIMUM COMPRESSIVE STRENGTH OF 3,000 PSI BEFORE ADDITIONAL CONCRETE IS CAST.

MEDIAN BARRIER SHALL NOT BE CAST UNTIL ALL STAGE II SLAB CONCRETE HAS REACHED A MINIMUM COMPRESSIVE STRENGTH OF 3,000 PSI.

PROJECT NO. R-2813B

BUNCOMBE COUNTY

STATION: 48+63.74 -L- P.O.T.

RELEASE FOR CONSTRUCTION
DATE: 5-30-08

WilburSmith ASSOCIATES
421 Fayetteville Street
Suite 1303
RALEIGH, N. C. 27601

DRAWN BY : K.E. LOFTON DATE : 5-08
CHECKED BY : T.M. HARRIS DATE : 5-08

DWG. No. S-87

NORTH CAROLINA PROFESSIONAL SEAL 19299 ENGINEER THOMAS M. HARRIS
5-30-08

STATE OF NORTH CAROLINA
DEPARTMENT OF TRANSPORTATION
RALEIGH

SUPERSTRUCTURE

TYPICAL SECTION
STAGE I

REVISIONS						SHEET NO.
No.	BY:	DATE:	No.	BY:	DATE:	
1			3			TOTAL SHEETS
2			4			

s:\NCDOT\R2813B\Design\T-26 Bridge\RFC\R2813B_SD_TS_01.dgn
5/30/2008

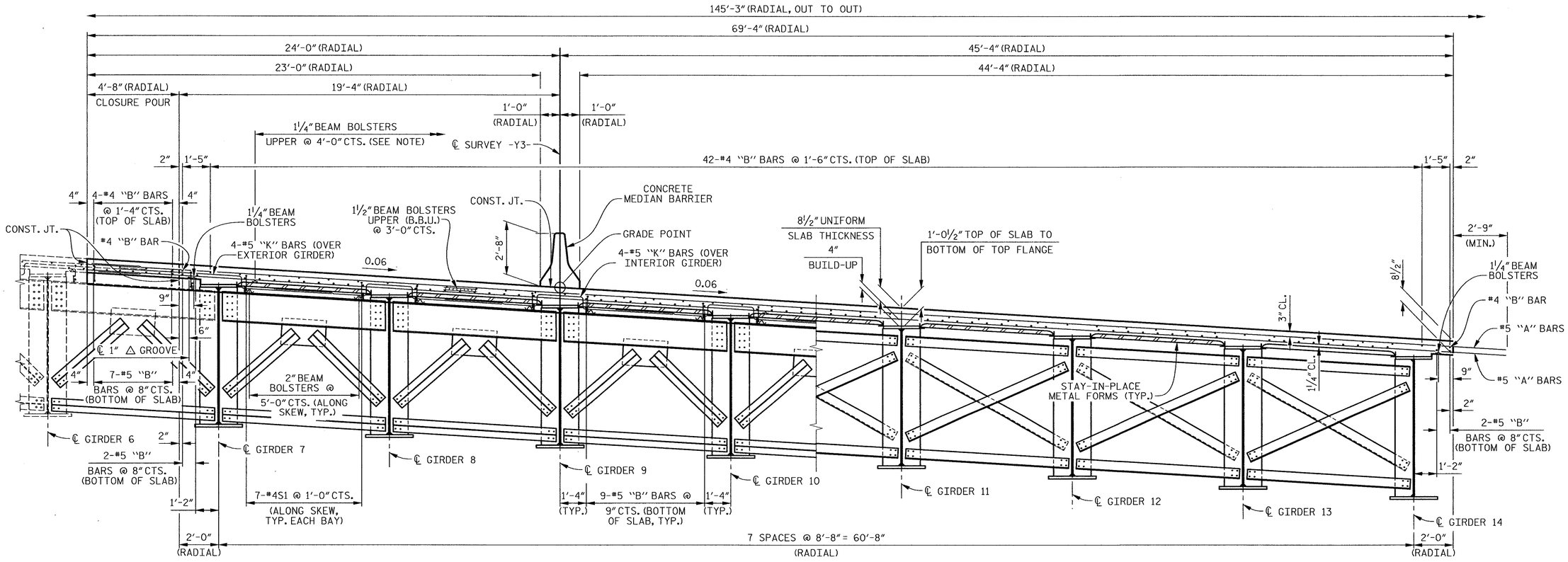

HALF SECTION SHOWING END BENT CROSSFRAMES

HALF SECTION SHOWING INTERMEDIATE CROSSFRAMES

TYPICAL SECTION – STAGE II

NOTES

FOR CLOSURE POUR DETAILS, SEE "TYPICAL SECTION STAGE III" SHEET.

FOR NOTES, SEE "TYPICAL SECTION - STAGE I" SHEET.

PROJECT NO. R-2813B

BUNCOMBE COUNTY

STATION: 48+63.74 -L- P.O.T.

RELEASE FOR CONSTRUCTION

DATE: 5-30-08

STATE OF NORTH CAROLINA
DEPARTMENT OF TRANSPORTATION
RALEIGH

SUPERSTRUCTURE

TYPICAL SECTION
STAGE II

WilburSmith ASSOCIATES — ENGINEERS PLANNERS ECONOMISTS
421 Fayetteville Street
Suite 1303
RALEIGH, N. C. 27601

DRAWN BY : K.E. LOFTON DATE : 5-08
CHECKED BY : T.M. HARRIS DATE : 5-08

DWG. No. S-88

NORTH CAROLINA PROFESSIONAL SEAL 19293 ENGINEER THOMAS M. HARRIS
5-30-08

REVISIONS						SHEET NO.
No.	BY:	DATE:	No.	BY:	DATE:	
1			3			TOTAL SHEETS
2			4			

s:\NCDOT\R2813B\Design\I-26 Bridge\RFC\R2813B_SD_TS_02.dgn
5/30/2008

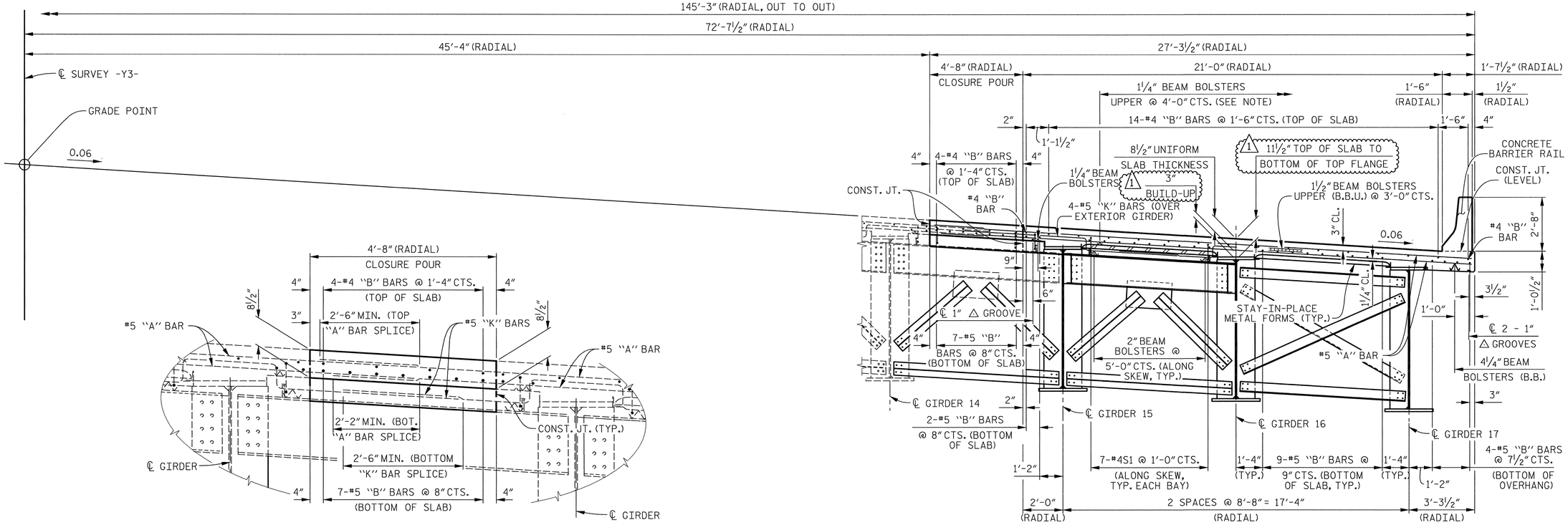

HALF SECTION SHOWING END BENT CROSSFRAMES

HALF SECTION SHOWING INTERMEDIATE CROSSFRAMES

END BENT CROSSFRAMES

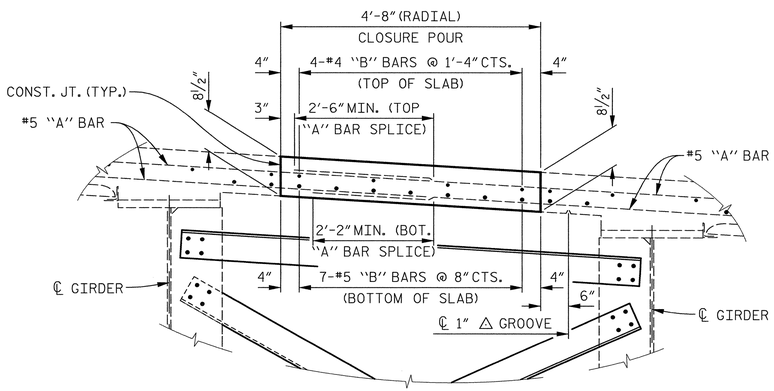

INTERMEDIATE CROSSFRAMES

CLOSURE POUR DETAILS

TYPICAL SECTION – STAGE III

NOTES

FOR NOTES, SEE "TYPICAL SECTION - STAGE I" SHEET.

OVERHANG FALSEWORK SHALL BE APPLIED TO GIRDER 17 BEFORE GIRDER 15.

1 REVISED BUILD-UP HEIGHT

PROJECT NO. R-2813B

BUNCOMBE COUNTY

STATION: 48+63.74 -L- P.O.T.

RELEASE FOR CONSTRUCTION
DATE: 1/9/09

WilburSmith ASSOCIATES
ENGINEERS PLANNERS ECONOMISTS
421 Fayetteville Street
Suite 1303
RALEIGH, N. C. 27601

DRAWN BY : K.E. LOFTON DATE :
CHECKED BY : T.M. HARRIS DATE :

DWG. No. S-89.1

NORTH CAROLINA PROFESSIONAL SEAL 19299 ENGINEER THOMAS M. HARRIS
1/9/09

STATE OF NORTH CAROLINA
DEPARTMENT OF TRANSPORTATION
RALEIGH

SUPERSTRUCTURE

TYPICAL SECTION
STAGE III

REVISIONS						SHEET NO.
No.	BY:	DATE:	No.	BY:	DATE:	
1	LOFTON	1-9-09	3			TOTAL SHEETS
2			4			

s:\ncdot\r2813b\design\r-26 bridge\RFC\R2813B_SD_TS_REV1_03.dgn
1/9/2009

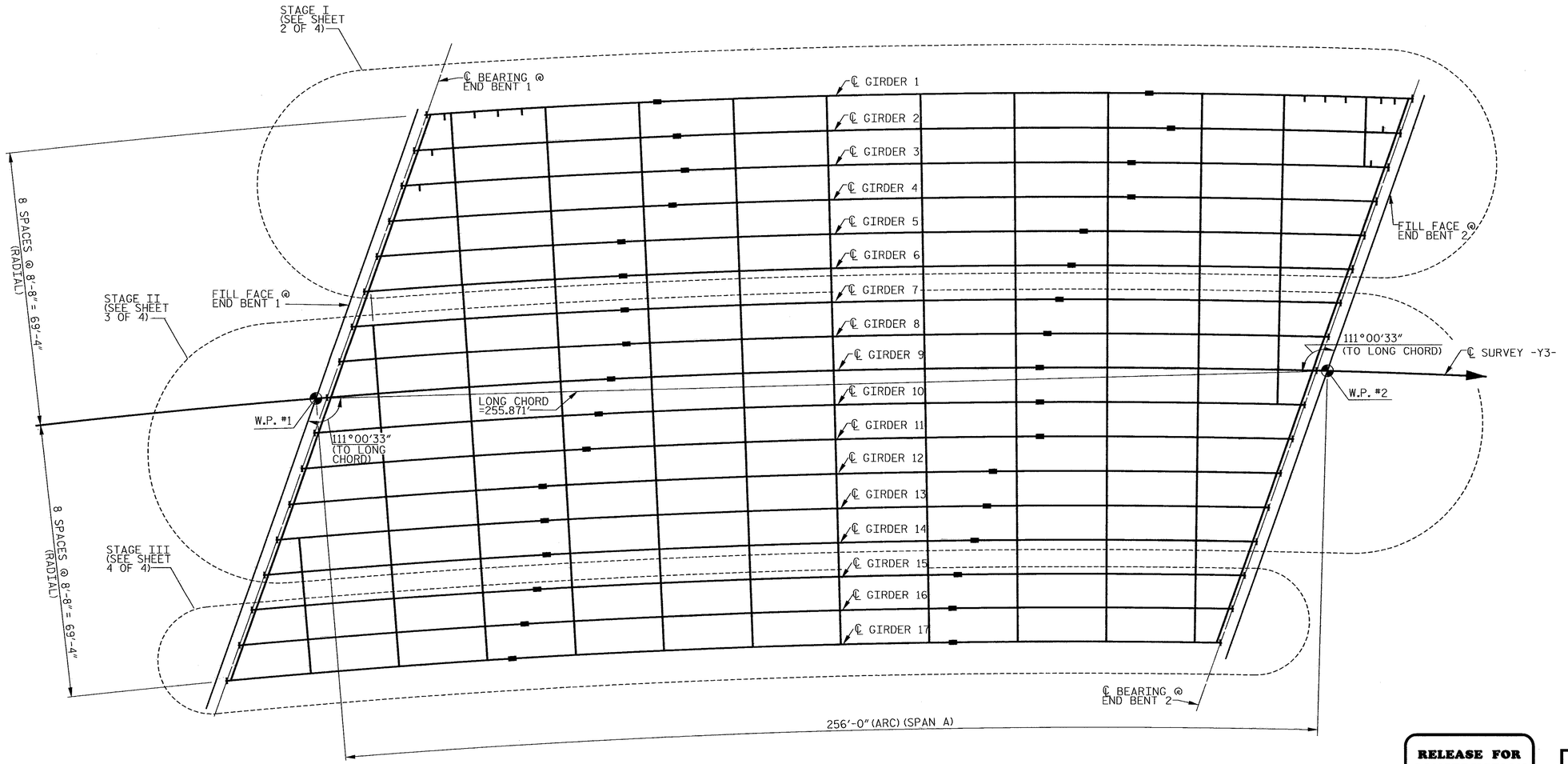

FRAMING PLAN – GENERAL

PROJECT NO. R-2813B

BUNCOMBE COUNTY

STATION: 48+63.74 -L- P.O.T.

SHEET 1 OF 4

RELEASE FOR CONSTRUCTION

DATE: 2/22/08

STATE OF NORTH CAROLINA
DEPARTMENT OF TRANSPORTATION
RALEIGH

SUPERSTRUCTURE

FRAMING PLAN – GENERAL

WilburSmith ASSOCIATES
ENGINEERS PLANNERS ECONOMISTS
421 Fayetteville Street
Suite 1303
RALEIGH, N. C. 27601

DRAWN BY : K.E. LOFTON DATE : 9-07
CHECKED BY : T.M. HARRIS DATE : 9-07

DWG. No. S-99

NORTH CAROLINA PROFESSIONAL SEAL 19299 ENGINEER THOMAS M. HARRIS
2-22-08

REVISIONS						SHEET NO.
No.	BY:	DATE:	No.	BY:	DATE:	
1			3			TOTAL SHEETS
2			4			

s:\NCDOT\R2813\Design\1-26 Bridge\RFC\R2813B_SD_FP_01.dgn
2/21/2008

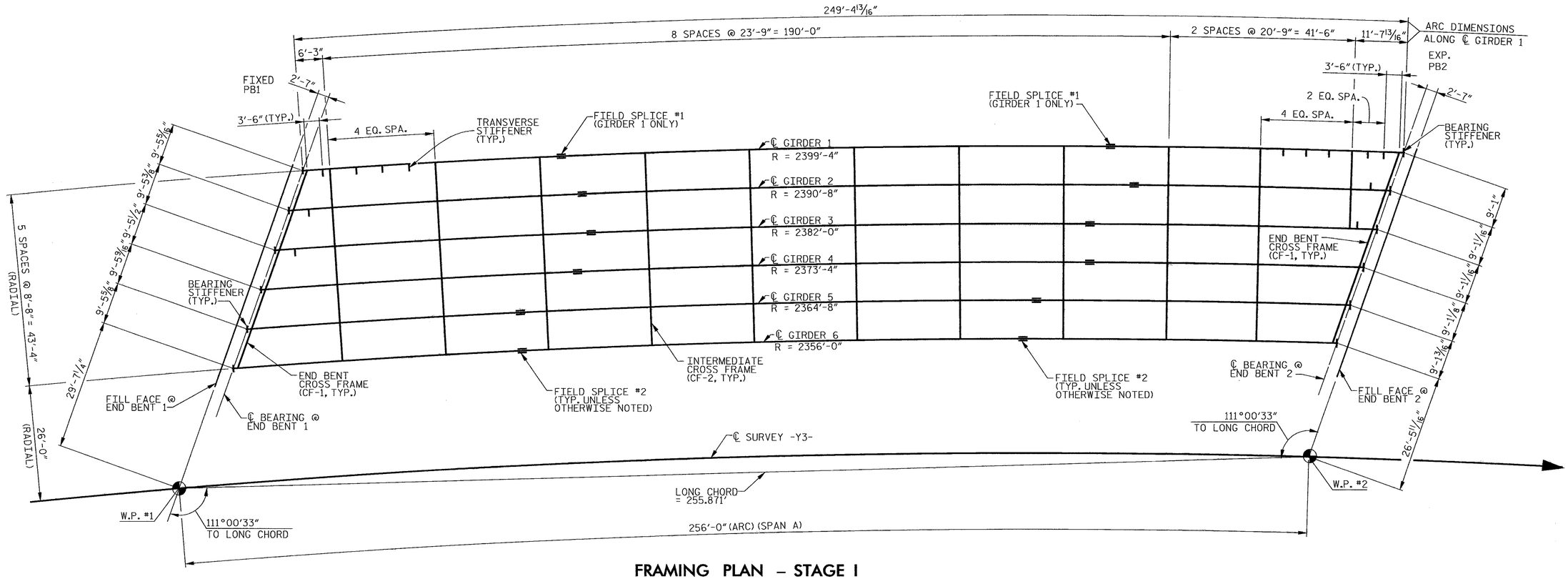

FRAMING PLAN – STAGE 1

NOTES

ALL INTERMEDIATE CROSS FRAMES ARE RADIAL TO ℄ SURVEY -Y3-.

ALL DIMENSIONS SHOWN ARE HORIZONTAL.

CONNECTOR PLATES NOT SHOWN FOR CLARITY.

STRUCTURAL STEEL NOTES;

STRUCTURAL STEEL FOR GIRDER WEBS, FLANGES, TRANSVERSE STIFFENERS, AND SPLICE PLATES SHALL BE AASHTO M270 GRADE HPS70W AND PAINTED IN ACCORDANCE WITH SYSTEM 4 OF ARTICLE 442-7 OF THE STANDARD SPECIFICATIONS.

ALL OTHER STRUCTURAL STEEL SHALL BE AASHTO M270 GRADE 50W AND PAINTED IN ACCORDANCE WITH SYSTEM 4 OF ARTICLE 442-7 OF THE STANDARD SPECIFICATIONS, UNLESS OTHERWISE NOTED ON PLANS.

ALL DIMENSIONS SHOWN ARE HORIZONTAL OR VERTICAL, UNLESS OTHERWISE NOTED.

TENSION ON THE AASHTO M164 BOLTS SHALL BE CALIBRATED USING DIRECT TENSION INDICATOR WASHERS IN ACCORDANCE WITH ARTICLE 440-10 OF THE STANDARD SPECIFICATIONS.

ALL CROSSFRAME CONNECTIONS SHALL BE 7/8"DIAMETER HIGH STRENGTH BOLTS.

ALL FIELD SPLICE CONNECTIONS SHALL BE 1"DIAMETER HIGH STRENGTH BOLTS.

FOR HIGH STRENGTH BOLTS, SEE SPECIAL PROVISIONS.

CONNECTOR PLATES SHALL BE PLACED NORMAL TO FLANGES AND WEB AT INTERMEDIATE CROSS FRAME LOCATIONS.

ENDS OF GIRDERS SHALL BE PLUMB.

FOR SUBMITTAL OF WORKING DRAWINGS, SEE SPECIAL PROVISIONS.

BEARING STIFFENERS SHALL BE PLACED NORMAL TO WEB OF THE GIRDER AND SHALL BE PLUMB.

FOR HIGH PERFORMANCE STEEL, THE FABRICATOR MAY USE A THERMO-MECHANICAL CONTROLLED PROCESS (TMCP) ON PLATE SIZES UP TO 2 INCHES IN THICKNESS.

FOR HIGH PERFORMANCE STEEL, SEE SPECIAL PROVISIONS.

SHOP SPLICES ARE PERMITTED TO LIMIT THE MAXIMUM REQUIRED FLANGE PIECE LENGTHS TO 60 FEET AND WEB PIECE LENGTHS TO 45 FEET. PERMITTED FLANGE AND WEB SHOP SPLICES SHALL NOT BE LOCATED WITHIN 15 FEET OF MAXIMUM DEAD LOAD DEFLECTION. KEEP 2 FEET MINIMUM BETWEEN WEB AND FLANGE SHOP SPLICES. KEEP 6"MINIMUM BETWEEN CONNECTOR PLATE WELDS OR TRANSVERSE STIFFENER WELDS AND WEB OR FLANGE SHOP SPLICES.

SHEAR STUDS ON GIRDERS MAY BE SHIFTED UP TO 1"IF NECESSARY TO CLEAR FLANGE SPLICE WELD.

CHARPY V-NOTCH TESTS ARE REQUIRED FOR ALL BOTTOM FLANGE PLATES, ALL WEB PLATES, ALL BOTTOM FLANGE SPLICE PLATES AND ALL WEB SPLICE PLATES. SEE ARTICLE 1072-9 OF THE STANDARD SPECIFICATIONS.

FOR CHARPY V-NOTCH TEST, SEE SPECIAL PROVISIONS.

CHARPY V-NOTCH TEST REQUIRED ON CROSSFRAME MEMBERS, SEE SPECIAL PROVISIONS.

FOR SHIPPING STEEL STRUCTURAL MEMBERS, SEE SPECIAL PROVISIONS.

THE CONTRACTOR SHALL MAINTAIN STABILITY OF CURVED GIRDERS UNTIL ALL FIELD SPLICES AND CROSS FRAME CONNECTIONS HAVE BEEN COMPLETED. THE CONTRACTOR'S ATTENTION IS CALLED TO THE LARGE GIRDER DEFLECTIONS AND MOVEMENTS.

FOR FALSEWORK AND FORMWORK, SEE SPECIAL PROVISIONS.

STRUCTURAL STEEL ERECTION SHALL BE COMPLETE BEFORE FALSEWORK OR FORMS ARE PLACED ON EACH STAGE OF CONSTRUCTION.

INTERMEDIATE CROSS FRAMES CF-3 SHALL NOT BE ATTACHED TO GIRDER 6 OR GIRDER 7 UNTIL POUR 6 HAS REACHED A COMPRESSIVE STRENGTH OF 3000 PSI.

INTERMEDIATE CROSS FRAMES CF-3 SHALL NOT BE ATTACHED TO GIRDER 14 OR GIRDER 15 UNTIL POUR 9 HAS REACHED A COMPRESSIVE STRENGTH OF 3000 PSI.

THE DIAGONAL AND CHORD LENGTHS FOR EACH INTERMEDIATE CROSSFRAME CF-3 SHALL BE DETERMINED BY THE FABRICATOR USING THE DEAD LOAD DEFLECTIONS CALCULATED FOR THE ADJACENT GIRDERS AT THE TIME OF INSTALLATION.

CURVATURE OF STEEL GIRDERS MAY BE ACCOMPLISHED BY CUTTING PLATES OR BY HEAT TREATING TO THE REQUIRED RADIUS. HEAT CURVING OF GIRDERS IS ALLOWED. FOR HEAT CURVING OF GIRDERS, SEE SPECIAL PROVISIONS.

RELEASE FOR CONSTRUCTION
DATE: 2/22/08

PROJECT NO. R-2813B
BUNCOMBE COUNTY
STATION: 48+63.74 -L- P.O.T.
SHEET 2 OF 4

STATE OF NORTH CAROLINA
DEPARTMENT OF TRANSPORTATION
RALEIGH

SUPERSTRUCTURE

FRAMING PLAN – STAGE 1

WilburSmith ASSOCIATES
ENGINEERS PLANNERS ECONOMISTS
421 Fayetteville Street
Suite 1303
RALEIGH, N. C. 27601

DRAWN BY : K.E. LOFTON DATE : 9-07
CHECKED BY : T.M. HARRIS DATE : 9-07
DWG. No. S-100

NORTH CAROLINA PROFESSIONAL SEAL 19299 ENGINEER THOMAS M. HARRIS
2-22-08

REVISIONS						SHEET NO.
No.	BY:	DATE:	No.	BY:	DATE:	
1			3			TOTAL SHEETS
2			4			

s:\NCDOT\R2813B\Design\I-26 Bridge\RFC\R2813B_SD_FP_02.dgn
2/21/2008

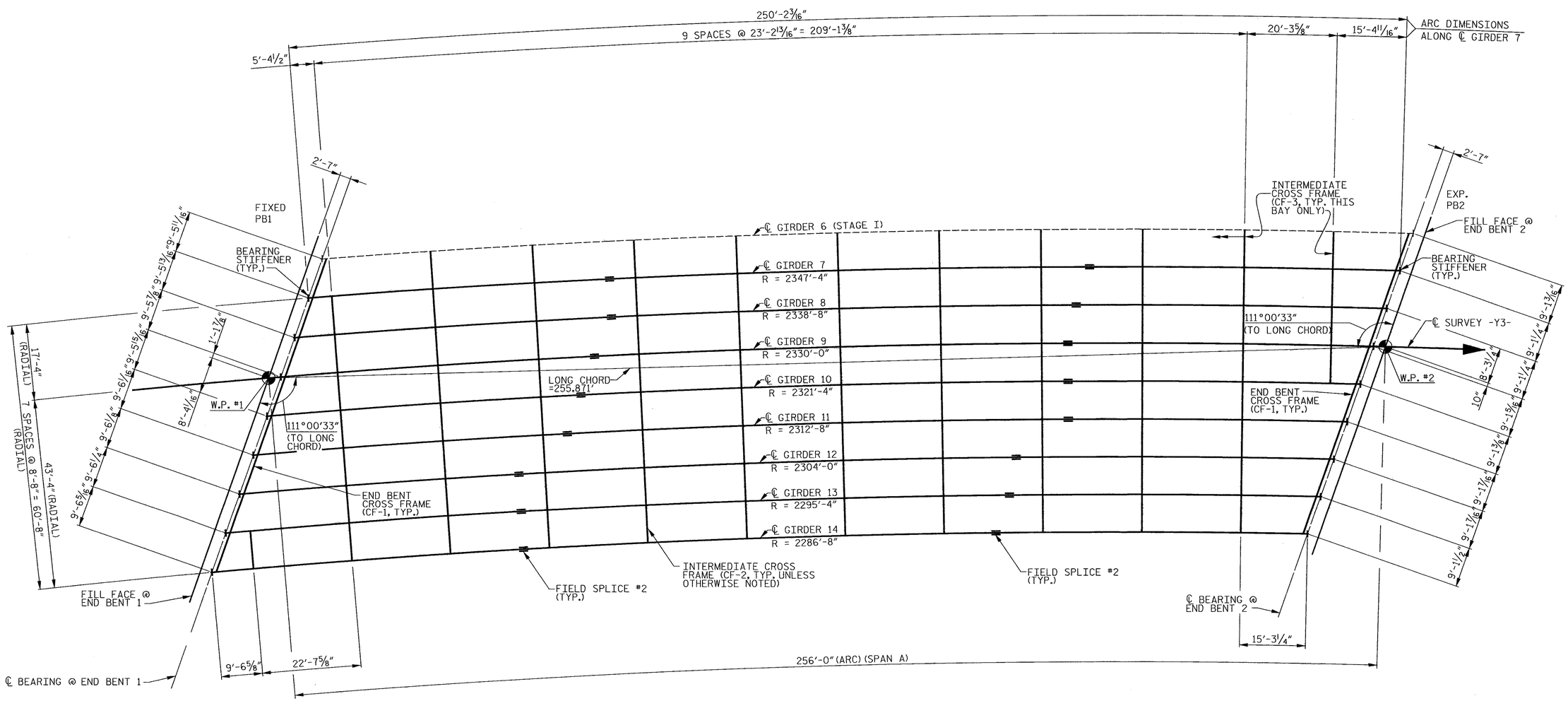

FRAMING PLAN – STAGE II

FOR NOTES, SEE SHEET 2 OF 4

PROJECT NO. R-2813B

BUNCOMBE COUNTY

STATION: 48+63.74 -L- P.O.T. –

SHEET 3 OF 4

RELEASE FOR CONSTRUCTION

DATE: 2/22/08

STATE OF NORTH CAROLINA
DEPARTMENT OF TRANSPORTATION
RALEIGH

SUPERSTRUCTURE

FRAMING PLAN – STAGE II

WilburSmith ASSOCIATES ENGINEERS PLANNERS ECONOMISTS
421 Fayetteville Street
Suite 1303
RALEIGH, N. C. 27601

NORTH CAROLINA PROFESSIONAL SEAL 19299 ENGINEER THOMAS M. HARRIS
2-22-08

DRAWN BY : K.E. LOFTON	DATE : 9-07	DWG. No. S-101
CHECKED BY : T.M. HARRIS	DATE : 9-07	

REVISIONS						SHEET NO.
No.	BY:	DATE:	No.	BY:	DATE:	
1			3			TOTAL SHEETS
2			4			

s:\NCDOT\R2813B\Design\I-26 Bridge\RFC\R2813B_SD_FP_03.dgn
2/21/2008

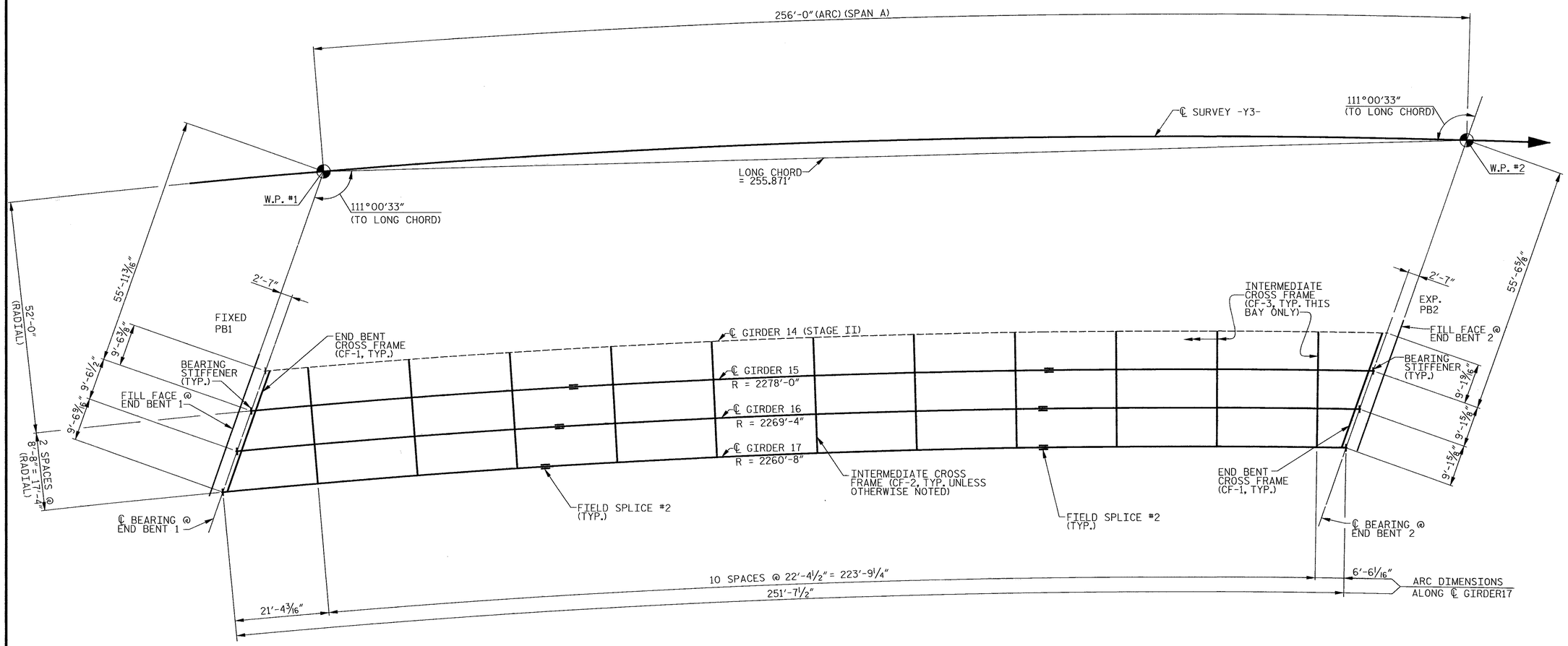

FRAMING PLAN – STAGE III

FOR NOTES, SEE SHEET 2 OF 4

PROJECT NO. R-2813B

BUNCOMBE COUNTY

STATION: 48+63.74 -L- P.O.T.

RELEASE FOR CONSTRUCTION

DATE: 2/22/08

STATE OF NORTH CAROLINA
DEPARTMENT OF TRANSPORTATION
RALEIGH

SUPERSTRUCTURE

FRAMING PLAN – STAGE III

WilburSmith ASSOCIATES
ENGINEERS PLANNERS ECONOMISTS
421 Fayetteville Street
Suite 1303
RALEIGH, N. C. 27601

DRAWN BY : K.E. LOFTON DATE : 9-07
CHECKED BY : T.M. HARRIS DATE : 9-07

DWG. No. S-102

NORTH CAROLINA PROFESSIONAL SEAL 19299 ENGINEER THOMAS M. HARRIS
2-22-08

REVISIONS						SHEET NO.
No.	BY:	DATE:	No.	BY:	DATE:	
1			3			TOTAL SHEETS
2			4			

s:\NCDOT\R2813B\Design\I-26 Bridge\RFC\R2813B_SD_FP_04.dgn
2/21/2008

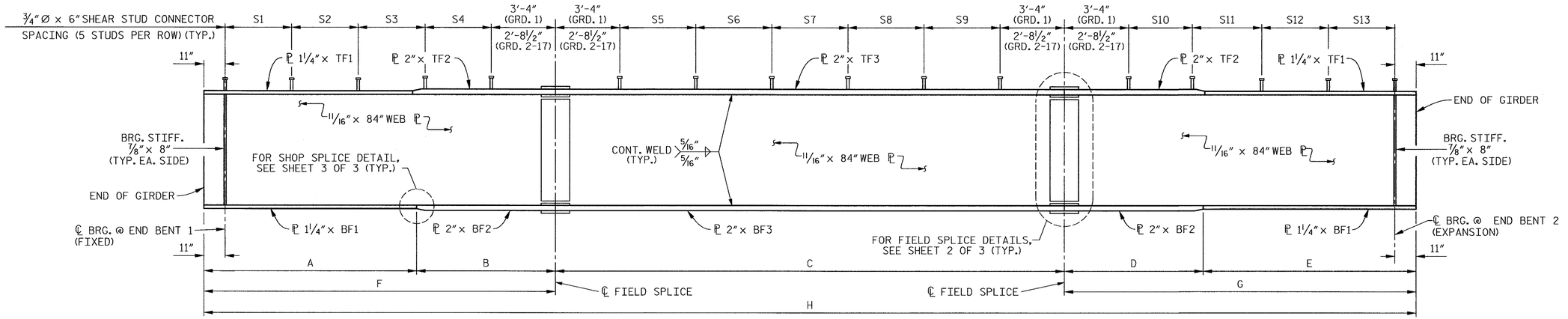

GIRDER ELEVATION

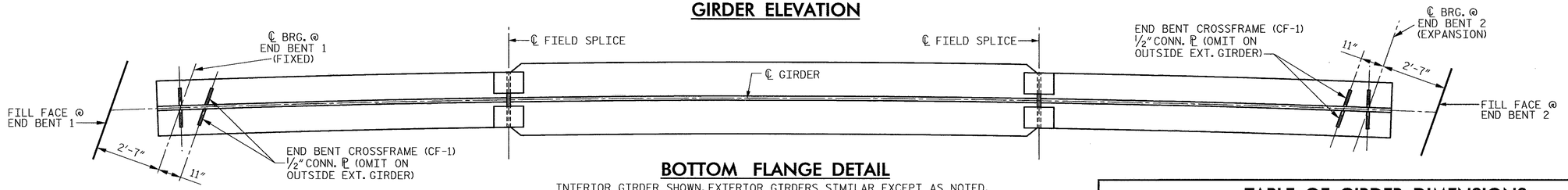

BOTTOM FLANGE DETAIL

INTERIOR GIRDER SHOWN, EXTERIOR GIRDERS SIMILAR EXCEPT AS NOTED.

TRANSVERSE STIFFENERS AND CONNECTOR PLATES FOR INTERMEDIATE CROSSFRAMES NOT SHOWN FOR CLARITY.

SHEAR STUD CONNECTOR SPACING

GIRDER No.	S1	S2	S3	S4	S5	S6	S7	S8	S9	S10	S11	S12	S13	* TOTAL No. OF STUDS
1	6"	63 SPA. @ 8"	12 SPA. @ 1'-0"	7¼"	16 SPA. @ 1'-4"	9 11/16"	49 SPA. @ 1'-6"	9¾"	16 SPA. @ 1'-4"	1'-1⅛"	28 SPA. @ 1'-0"	40 SPA. @ 10"	9"	1,215
2	8"	58 SPA. @ 10"	14 SPA. @ 1'-0"	10"	15 SPA. @ 1'-2"	10 1/16"	62 SPA. @ 1'-4"	10 1/16"	15 SPA. @ 1'-2"	11 3/16"	13 SPA. @ 1'-0"	49 SPA. @ 10"	9"	1,225
3	8"	52 SPA. @ 10"	24 SPA. @ 1'-0"	10 3/16"	17 SPA. @ 1'-0"	10 3/16"	54 SPA. @ 1'-4"	10⅛"	17 SPA. @ 1'-0"	1'- 0"	28 SPA. @ 1'-0"	39 SPA. @ 10"	8 5/16"	1,250
4	8"	48 SPA. @ 10"	27 SPA. @ 1'-0"	1'-3⅛"	15 SPA. @ 1'-2"	6½"	56 SPA. @ 1'-4"	6½"	15 SPA. @ 1'-2"	1'-0¼"	25 SPA. @ 1'-0"	39 SPA. @ 10"	9	1,220
5	8"	53 SPA. @ 10"	14 SPA. @ 1'-0"	5"	14 SPA. @ 1'-2"	9¾"	58 SPA. @ 1'-4"	9 11/16"	14 SPA. @ 1'-2"	11½"	22 SPA. @ 1'-2"	49 SPA. @ 10"	9"	1,215
6	5"	87 SPA. @ 6"	37 SPA. @ 6"	5"	22 SPA. @ 9"	9¼"	98 SPA. @ 9"	9 5/16"	22 SPA. @ 9"	8"	44 SPA. @ 8"	91 SPA. @ 5"	5"	2,100
7	9"	40 SPA. @ 10"	27 SPA. @ 1'-2"	10"	25 SPA. @ 1'-2"	7⅜"	30 SPA. @ 1'-6"	7 1/16"	25 SPA. @ 1'-2"	1'-3⅜"	25 SPA. @ 1'-4"	33 SPA. @ 1'-0"	9"	1,120
8	8"	35 SPA. @ 1'-0"	29 SPA. @ 1'-2"	6"	18 SPA. @ 1'-4"	1'-2 3/16"	38 SPA. @ 1'-4"	1'-2½"	18 SPA. @ 1'-4"	4¾"	25 SPA. @ 1'-4"	29 SPA. @ 1'-2"	10"	1,055
9	8"	39 SPA. @ 1'-0"	24 SPA. @ 1'-2"	1'-6"	19 SPA. @ 1'-4"	11 1/16"	38 SPA. @ 1'-4"	11 1/16"	19 SPA. @ 1'-4"	1'-6⅜"	24 SPA. @ 1'-4"	33 SPA. @ 1'-0"	9"	1,075
10	8"	42 SPA. @ 1'-0"	22 SPA. @ 1'-2"	10 3/16"	17 SPA. @ 1'-2"	8"	49 SPA. @ 1'-4"	8"	17 SPA. @ 1'-2"	1'-5 9/16"	21 SPA. @ 1'-4"	34 SPA. @ 1'-0"	9"	1,105
11	8"	45 SPA. @ 1'-0"	19 SPA. @ 1'-2"	1'-5 3/16"	15 SPA. @ 1'-2"	6 15/16"	55 SPA. @ 1'-4"	6 15/16"	15 SPA. @ 1'-2"	1'-7 13/16"	23 SPA. @ 1'-2"	32 SPA. @ 1'-0"	8"	1,115
12	8"	45 SPA. @ 1'-0"	13 SPA. @ 1'-2"	7"	5 SPA. @ 1'-2"	1'-11 1/16"	71 SPA. @ 1'-4"	1'-11 1/16"	5 SPA. @ 1'-2"	1'-5 1/16"	35 SPA. @ 1'-2"	27 SPA. @ 1'-0"	9"	1,100
13	8"	51 SPA. @ 10"	21 SPA. @ 1'-0"	11¼"	6 SPA. @ 1'-2"	11¼"	68 SPA. @ 1'-4"	11 3/16"	6 SPA. @ 1'-2"	11⅝"	35 SPA. @ 1'-2"	26 SPA. @ 1'-0"	9"	1,160
14	8"	41 SPA. @ 10"	33 SPA. @ 1'-0"	10 15/16"	25 SPA. @ 1'-2"	1'-0 1/16"	32 SPA. @ 1'-4"	1'- 0 1/16"	25 SPA. @ 1'-2"	1'-2"	22 SPA. @ 1'-2"	41 SPA. @ 1'-0"	9"	1,190
15	8"	51 SPA. @ 10"	22 SPA. @ 1'-2"	7 11/16"	29 SPA. @ 1'-2"	8 1/16"	25 SPA. @ 1'-4"	8⅜"	29 SPA. @ 1'-2"	1'-2 3/8"	22 SPA. @ 1'-2"	41 SPA. @ 1'-0"	9"	1,190
16	8"	51 SPA. @ 10"	22 SPA. @ 1'-2"	8 5/16"	25 SPA. @ 1'-4"	10 1/16"	26 SPA. @ 1'-4"	10"	25 SPA. @ 1'-4"	1'-5 5/16"	28 SPA. @ 1'-2"	40 SPA. @ 10"	8"	1,180
17	8"	45 SPA. @ 1'-0"	20 SPA. @ 1'-2"	6 15/16"	23 SPA. @ 1'-6"	1'-4 9/16"	23 SPA. @ 1'-6"	1'-4 9/16"	23 SPA. @ 1'-6"	10 7/16"	20 SPA. @ 1'-4"	44 SPA. @ 10"	9"	1,085
														20,600

*TOTAL INCLUDES SHEAR CONNECTORS ON TOP FLANGE SPLICE PLATES

TABLE OF GIRDER DIMENSIONS

GIRDER No.	A	B	C	D	E	F	G	H
1	34'-2"	25'-2 1/4"	124'-5 7/16"	26'-10 5/16"	40'-6 13/16"	59'-4 1/4"	67'-5 1/8"	251'-2 13/16"
2	42'-11 3/8"	24'-6 1/8"	124'-9 1/8"	18'-6 11/16"	40'-7"	67'-5 1/2"	59'-11 11/16"	251'-4 5/16"
3	42'-11 5/8"	29'-6 1/16"	113'-1 5/16"	25'-3 5/16"	40'-7 1/8"	72'-6 1/16"	65'-10 1/16"	251'-5 13/16"
4	43'-0"	29'-6 5/8"	116'-2"	22'-3 7/16"	40'-7 5/16"	72'-6 5/8"	62'-10 3/4"	251'-7 3/8"
5	43'-0 5/16"	19'-10 3/16"	117'-0 7/16"	31'-2 1/2"	40'-7 1/2"	62'-10 1/2"	71'-10"	251'-8 5/16"
6	43'-0 11/16"	23'-4 13/16"	113'-5 9/16"	31'-3 13/16"	40'-7 11/16"	66'-5 1/2"	71'-11 1/2"	251'-10 9/16"
7	43'-1"	26'-11 1/2"	109'-11 13/16"	31'-4"	40'-7 7/8"	70'-0 1/2"	71'-11 7/8"	252'-0 3/16"
8	43'-1 3/8"	30'-6 1/8"	106'-6 1/16"	31'-4 1/8"	40'-8 1/8"	73'-7 1/2"	72'-0 1/4"	252'-1 13/16"
9	43'-1 3/4"	29'-7 3/4"	108'-7 1/8"	30'-2 9/16"	40'-8 5/16"	72'-9 1/2"	70'-10 7/8"	252'-3 1/2"
10	43'-2 1/16"	29'-8"	111'-9"	27'-1 5/8"	40'-8 7/16"	72'-10 1/16"	67'-10 1/16"	252'-5 1/8"
11	43'-2 7/16"	29'-8 1/4"	114'-10 7/8"	24'-0 5/8"	40'-8 11/16"	72'-10 11/16"	64'-9 9/16"	252'-6 7/8"
12	43'-2 13/16"	21'-9 11/16"	114'-0 3/8"	32'-10 13/16"	40'-8 7/8"	65'-0 1/2"	73'-7 11/16"	252'-8 9/16"
13	43'-3 3/16"	25'-5 9/16"	111'-11 7/16"	31'-5"	40'-9 1/8"	68'-8 3/4"	72'-2 1/8"	252'-10 5/16"
14	43'-3 9/16"	29'-0 1/8"	108'-5 1/8"	31'-5 3/16"	40'-9 5/16"	72'-4 7/16"	72'-2 1/2"	253'-0 1/16"
15	43'-4"	29'-9 3/16"	107'-9 13/16"	31'-5 3/8"	40'-9 1/2"	73'-1 3/16"	72'-2 7/8"	253'-1 7/8"
16	43'-4 3/8"	29'-9 7/16"	108'-5 1/16"	30'-11 1/16"	40'-9 3/4"	73'-1 13/16"	71'-8 13/16"	253'-3 11/16"
17	43'-4 3/4"	29'-9 11/16"	111'-8 1/8"	28'-7 1/16"	39'-11 7/8"	73'-2 7/16"	68'-6 15/16"	253'-5 1/2"

NOTE: DIMENSIONS ARE ARC LENGTHS ALONG ℄ GIRDER

TABLE OF PLATE SIZES

GIRDER No.	TF1	TF2	TF3	BF1	BF2	BF3
1	20"	20"	28"	26"	26"	38"
2	18"	18"	24"	22"	22"	32"
3 THRU 17	18"	18"	24"	22"	22"	28"

PROJECT NO. R-2813B

BUNCOMBE COUNTY

STATION: 48+63.74 -L- P.O.T.

SHEET 1 OF 3

RELEASE FOR CONSTRUCTION
DATE: 2/22/08

STATE OF NORTH CAROLINA
DEPARTMENT OF TRANSPORTATION
RALEIGH

SUPERSTRUCTURE

STEEL PLATE GIRDER

WilburSmith ASSOCIATES (ENGINEERS PLANNERS ECONOMISTS)
421 Fayetteville Street
Suite 1303
RALEIGH, N. C. 27601

DRAWN BY : K.E. LOFTON DATE : 9-07
CHECKED BY : T.M. HARRIS DATE : 9-07

DWG. No. S-103

NORTH CAROLINA PROFESSIONAL SEAL 19299 ENGINEER THOMAS M. HARRIS
2-22-08

REVISIONS						SHEET NO.
No.	BY:	DATE:	No.	BY:	DATE:	
1			3			TOTAL SHEETS
2			4			

s:\NCDOT\R2813B\Design\I-26 Bridge\RFC\R2813B_SD_SSD_01.dgn
2/21/2008

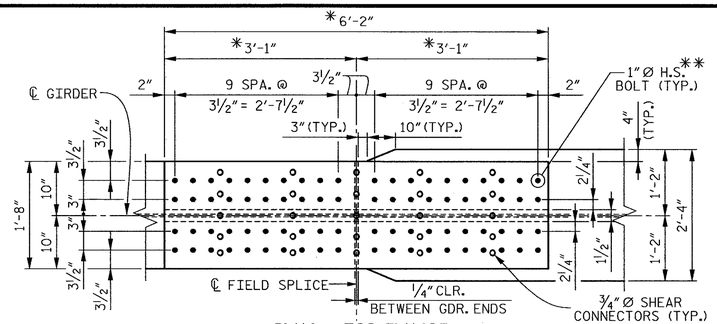

PLAN – TOP FLANGE
(TOP OF TOP FLANGE)

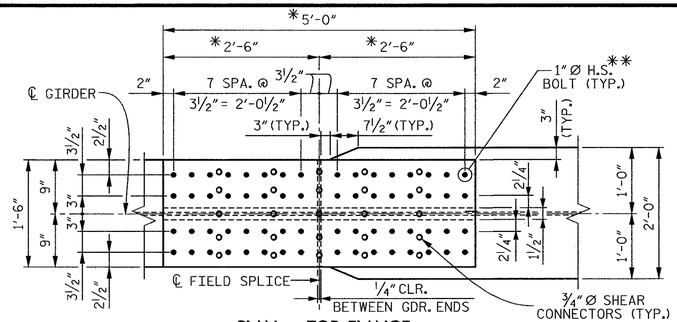

PLAN – TOP FLANGE
(TOP OF TOP FLANGE)

NOTES

* ARC DIMENSION ALONG INSIDE EDGE OF PLATE.

** ALL BOLTS IN WEB AND FLANGE SPLICES SHALL BE 1"Ø H.S. BOLTS. BOLT THREADS SHALL BE EXCLUDED FROM ALL SHEAR PLANES. AN ADDITIONAL HARDENED WASHER MAY BE REQUIRED TO ALLOW FULL TIGHTENING OF BOLT AND TO PREVENT THE NUT FROM JAMMING INTO THE THREAD RUNOUT.

SHEAR CONNECTORS ARE TO BE SHOP WELDED ON TOP OF THE SPLICE PLATE BEFORE FIELD ASSEMBLY.

FOR LOCATION OF FIELD SPLICES, SEE FRAMING PLANS.

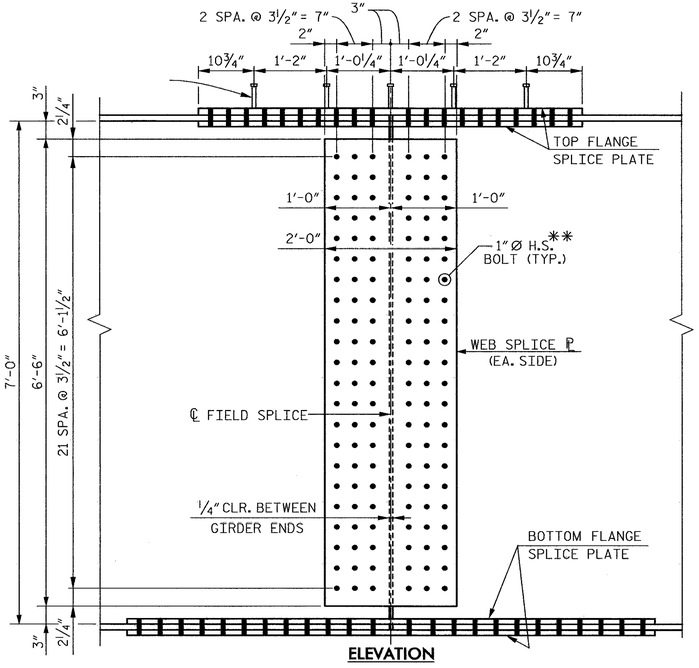

ELEVATION

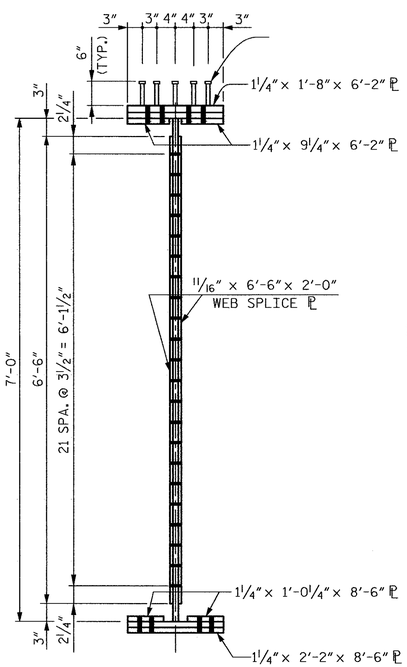

SECTION THRU GIRDER AT FIELD SPLICE #1

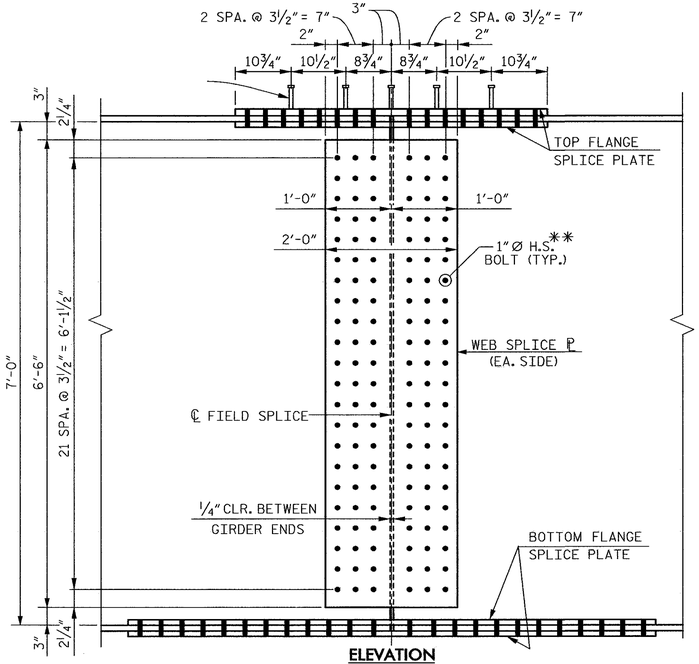

ELEVATION

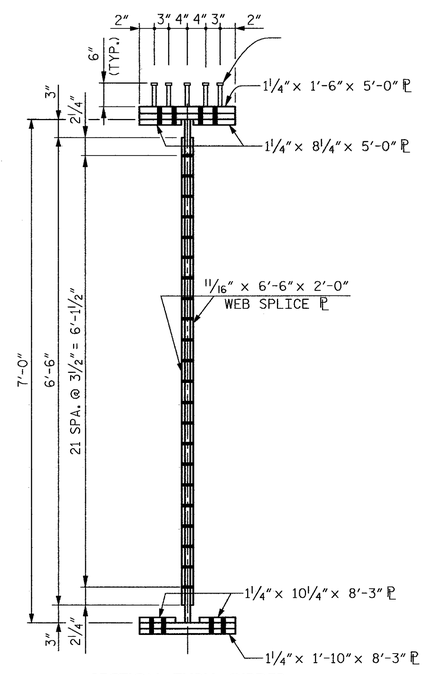

SECTION THRU GIRDER AT FIELD SPLICE #2

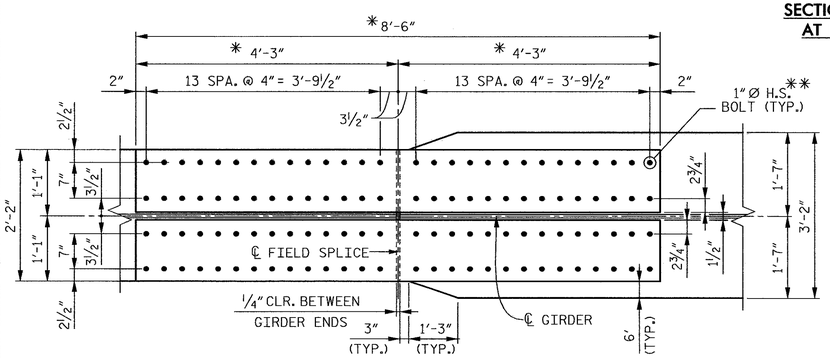

PLAN – BOTTOM FLANGE
(TOP OF BOT. FLANGE)

FIELD SPLICE #1 DETAILS
TOTAL NUMBER OF BOLTS = 324

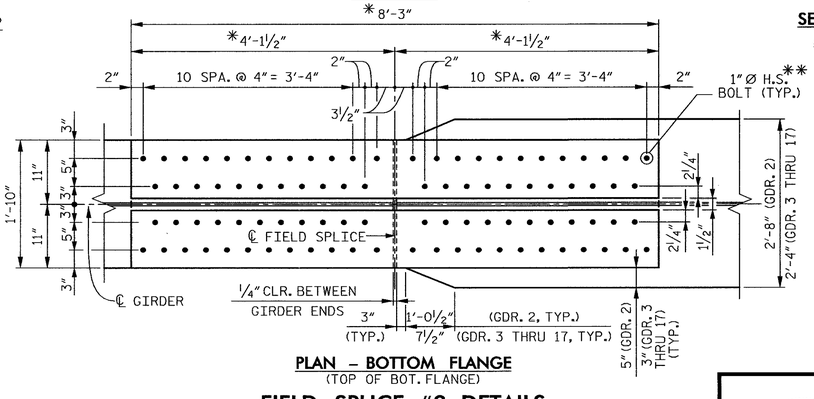

PLAN – BOTTOM FLANGE
(TOP OF BOT. FLANGE)

FIELD SPLICE #2 DETAILS
TOTAL NUMBER OF BOLTS = 288

RELEASE FOR CONSTRUCTION
DATE: 2/22/08

PROJECT NO. R-2813B
BUNCOMBE COUNTY
STATION: 48+63.74 -L- P.O.T.
SHEET 2 OF 3

STATE OF NORTH CAROLINA
DEPARTMENT OF TRANSPORTATION
RALEIGH

SUPERSTRUCTURE

BOLTED FIELD SPLICE

WilburSmith ASSOCIATES
ENGINEERS PLANNERS ECONOMISTS
421 Fayetteville Street
Suite 1303
RALEIGH, N. C. 27601

DRAWN BY : K.E. LOFTON DATE : 9-07
CHECKED BY : T.M. HARRIS DATE : 9-07
DWG. No. S-104

NORTH CAROLINA PROFESSIONAL SEAL 19299 ENGINEER THOMAS M. HARRIS
2-22-08

REVISIONS						SHEET NO.
No.	BY:	DATE:	No.	BY:	DATE:	
1			3			TOTAL SHEETS
2			4			

s:\NCDOT\R2813B\Design\I-26 Bridge\NFC\R2813B_SD_SSD_02.dgn
2/21/2008

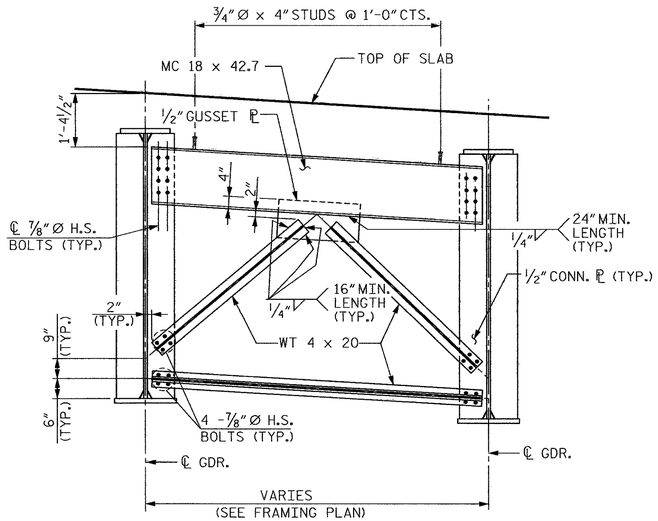

END BENT CROSSFRAME CF–1

(ADJACENT CROSS FRAMES NOT SHOWN FOR CLARITY)

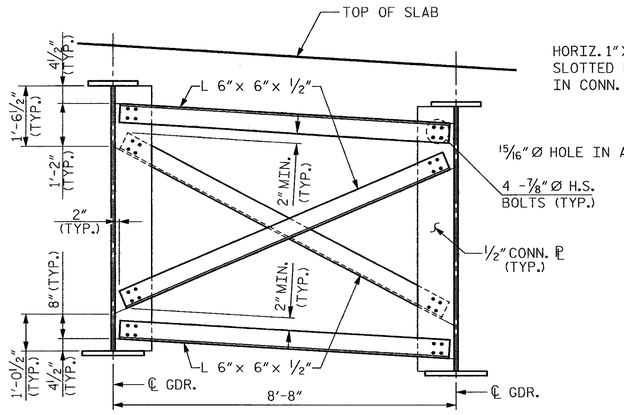

INTERMEDIATE CROSSFRAME CF–2

(ADJACENT CROSS FRAMES NOT SHOWN FOR CLARITY)

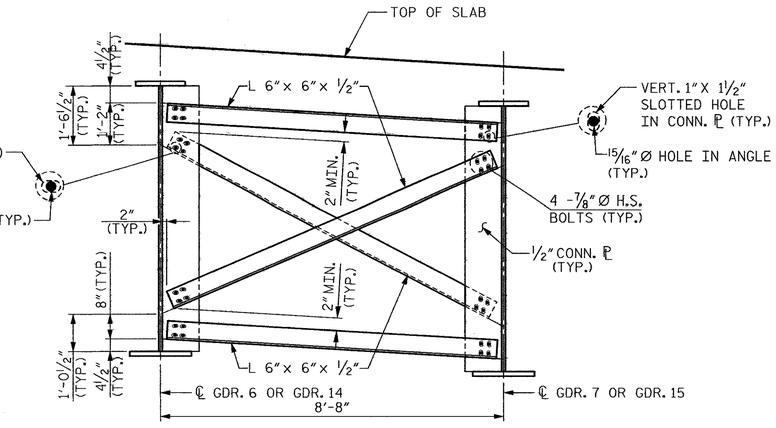

INTERMEDIATE CROSSFRAME CF–3

(ADJACENT CROSS FRAMES NOT SHOWN FOR CLARITY)

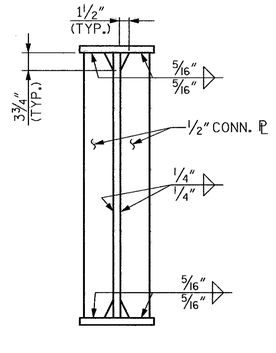

END BENT CROSSFRAME CONNECTOR PLATE

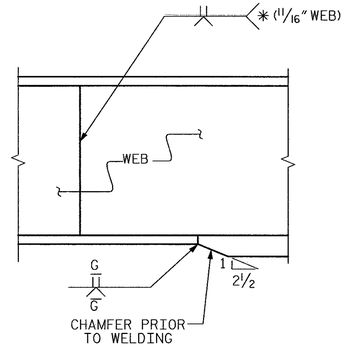

SHOP SPLICE DETAIL

* GRIND SMOOTH AND FLUSH ON OUTER FACE OF EXTERIOR GIRDERS

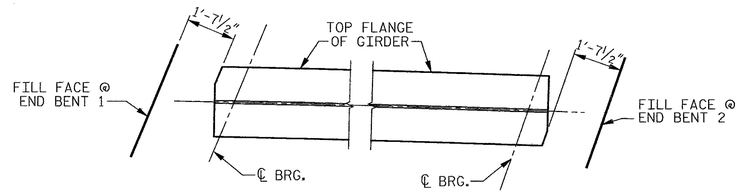

TOP FLANGE CLIP DETAIL

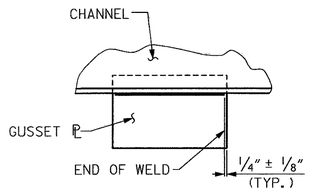

TYPICAL GUSSET PLATE CONNECTION

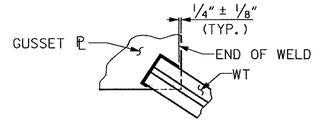

TYPICAL `TEE' TO GUSSET PLATE CONNECTION

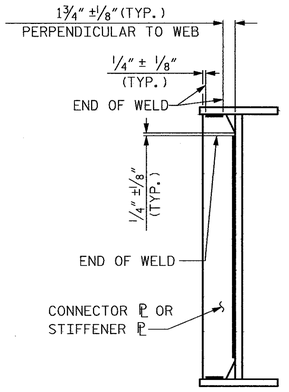

TYPICAL STIFFENER OR CONNECTOR PLATE CONNECTIONS

WELD TERMINATION DETAILS

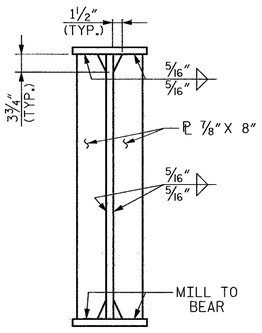

END BENT BEARING STIFFENER

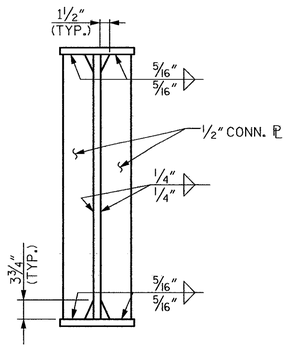

INTERMEDIATE CROSSFRAME CONNECTOR PLATE

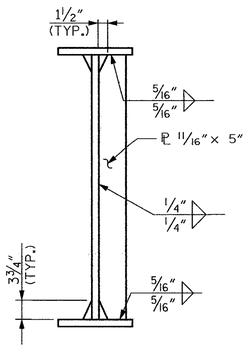

TRANSVERSE STIFFENER

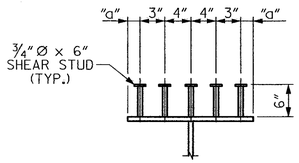

ON GIRDER

GDRS. 6, 7, 14 & 15

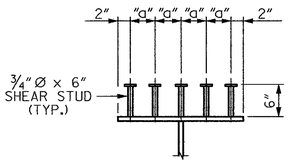

ON GIRDER

GDRS. 1-5, 8-13, 16 & 17

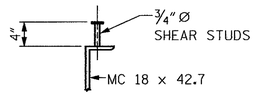

ON CHANNEL

SHEAR STUD DETAILS

SHEAR STUD TRANSVERSE SPACING "a"				
FLANGE WIDTH	18"	20"	24"	28"
GDRS. 1-5, 8-13, 16 & 17	3 1/2"	4"	5"	6"
GDRS. 6, 7, 14 & 15	2"	—	5"	—

RELEASE FOR CONSTRUCTION
DATE: 2/22/08

PROJECT NO. R-2813B
BUNCOMBE COUNTY
STATION: 48+63.74 -L- P.O.T.
SHEET 3 OF 3

STATE OF NORTH CAROLINA
DEPARTMENT OF TRANSPORTATION
RALEIGH

SUPERSTRUCTURE

CROSS FRAME & MISC. GIRDER DETAILS

WilburSmith ASSOCIATES
ENGINEERS PLANNERS ECONOMISTS
421 Fayetteville Street
Suite 1303
RALEIGH, N. C. 27601

DRAWN BY : K.E. LOFTON DATE : 9-07
CHECKED BY : T.M. HARRIS DATE : 9-07
DWG. No. S-105

NORTH CAROLINA PROFESSIONAL SEAL 19299 ENGINEER THOMAS M. HARRIS
2-22-08

REVISIONS						SHEET NO.
No.	BY:	DATE:	No.	BY:	DATE:	
1			3			TOTAL SHEETS
2			4			

a:\NDOT\R2813B\Design\I-26 Bridge\RFC\R2813B_SD_SS01_03.dgn
2/21/2008

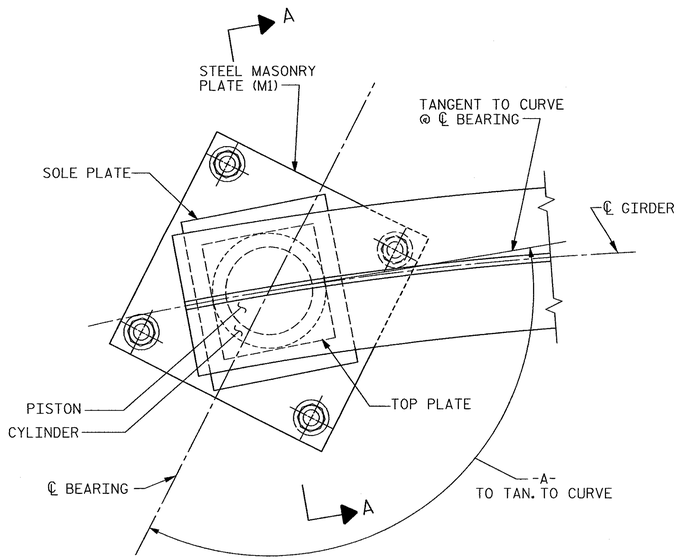

PLAN AT END BENT 1

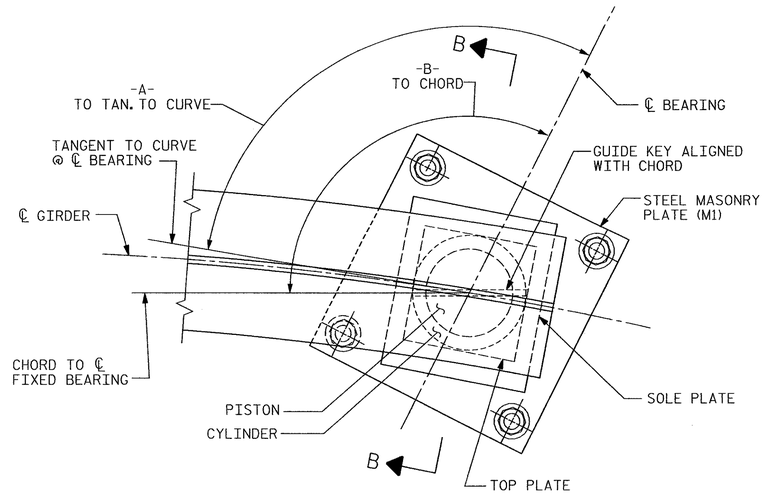

PLAN AT END BENT 2

NOTES

FOR POT BEARINGS, SEE SPECIAL PROVISIONS.

AT ALL POINTS OF SUPPORT NUTS FOR ANCHOR BOLTS SHALL BE TIGHTENED FINGER TIGHT AND GIVEN AN ADDITIONAL 1/4 TURN. THE THREAD OF THE NUT AND BOLT SHALL THEN BE BURRED WITH A SHARP POINTED TOOL.

WHEN WELDING THE SOLE PLATE TO THE GIRDER, USE TEMPERATURE INDICATING WAX PENS, OR OTHER SUITABLE MEANS, TO ENSURE THAT THE TEMPERATURE OF THE BEARING DOES NOT EXCEED 250°F TEMPERATURES ABOVE THIS MAY DAMAGE THE TFE OR ELASTOMER.

AFTER BEARING ASSEMBLY IS IN PLACE AND ANCHOR BOLTS HAVE BEEN FINALLY POSITIONED. THEY SHALL BE GROUTED IN PLACE AS SHOWN.

THE CLOSURE PLATE, GROUT PIPE AND STANDARD PIPE FOR THIS ASSEMBLY NEED NOT BE GALVANIZED.

SOLE PLATES SHOULD BE WELDED TO BEAM FLANGES AND ANCHOR BOLTS SHOULD BE GROUTED BEFORE FALSEWORK IS PLACED.

ALL SURFACES OF BEARING PLATES SHALL BE SMOOTH AND STRAIGHT.

FOR THERMAL SPRAYED COATINGS (METALLIZATION), SEE SPECIAL PROVISIONS.

BEARINGS SHALL HAVE A MINIMUM ROTATIONAL CAPACITY OF 0.03 RADIANS.

FOR OPTIONAL DISC BEARINGS, SEE SPECIAL PROVISIONS.

TABLE OF ANGLES

GIRDER No.	END BENT 1	END BENT 2	
	-A-	-A-	-B-
1	113°20′ 57″	107°23′ 36″	110°22′ 17″
2	113°26′ 20″	107°27′ 31″	110°26′ 55″
3	113°31′ 45″	107°31′ 27″	110°31′ 36″
4	113°37′ 13″	107°35′ 25″	110°36′ 19″
5	113°42′ 44″	107°39′ 24″	110°41′ 4″
6	113°48′ 17″	107°43′ 26″	110°45′ 52″
7	113°53′ 53″	107°47′ 29″	110°50′ 41″
8	113°59′ 32″	107°51′ 35″	110°55′ 33″
9	114°5′ 14″	107°55′ 42″	111°0′ 28″
10	114°10′ 58″	107°59′ 51″	110°5′ 25″
11	114°16′ 45″	108°4′ 2″	111°10′ 24″
12	114°22′ 35″	108°8′ 16″	111°15′ 25″
13	114°28′ 28″	108°12′ 31″	111°20′ 30″
14	114°34′ 24″	108°16′ 48″	111°25′ 36″
15	114°40′ 23″	108°21′ 7″	111°30′ 45″
16	114°46′ 25″	108°25′ 29″	111°35′ 57″
17	114°52′ 31″	108°29′ 52″	111°41′ 11″

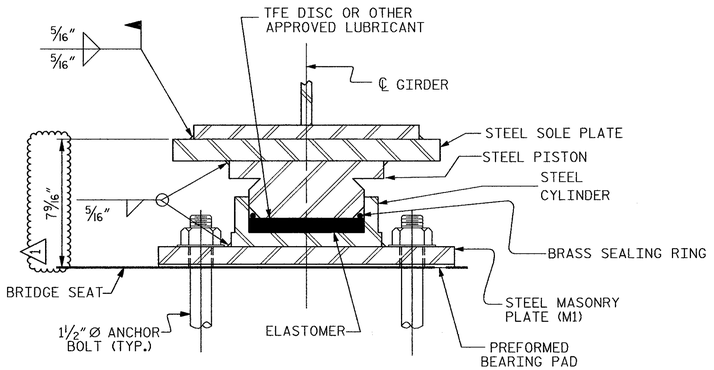

SECTION A–A

PB1, FIXED

(17 REQ'D.)

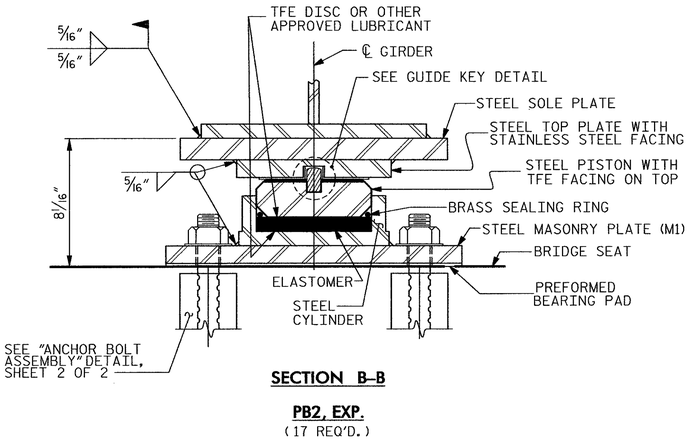

SECTION B–B

PB2, EXP.

(17 REQ'D.)

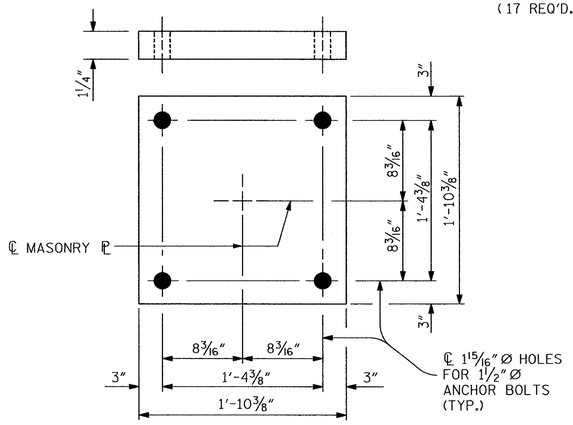

PLAN

M1 (34 REQ'D.)

MASONRY PLATE DETAILS

POT BEARING DETAILS

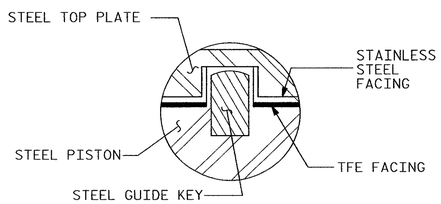

GUIDE KEY DETAIL

1 INCREASED HEIGHT OF FIXED BEARING.

RELEASE FOR CONSTRUCTION
DATE: 5-30-08

PROJECT NO. R-2813B
BUNCOMBE COUNTY
STATION: 48+63.74 -L- P.O.T.
SHEET 1 OF 2

STATE OF NORTH CAROLINA
DEPARTMENT OF TRANSPORTATION
RALEIGH
STANDARD
POT BEARING DETAILS

WilburSmith ASSOCIATES ENGINEERS PLANNERS ECONOMISTS
421 Fayetteville Street
Suite 1303
RALEIGH, N. C. 27601

DRAWN BY : K.E. LOFTON DATE : 9-07
CHECKED BY : T.M. HARRIS DATE : 9-07
DWG. No. S-106.1

NORTH CAROLINA PROFESSIONAL SEAL 19299 ENGINEER THOMAS M. HARRIS
5-30-08

No.	BY:	DATE:	No.	BY:	DATE:
1	LOFTON	5-30-08	3		
2			4		

REVISIONS

SHEET NO.

TOTAL SHEETS

ASSEMBLED BY : K.E. LOFTON DATE : 9/07
CHECKED BY : T.M. HARRIS DATE : 9/07
DRAWN BY : RWW 8/99
CHECKED BY : LES 8/99

REV. 10/17/00	RWW/LES
REV. 7/10/01	LES/RDR
REV. 5/7/03	RWW/JTE

srvncdot\r2813b\design\r26 bridge\r60\r2813B_SD_PBRG_REV1_01.dgn
5/30/2008

PB1.STD

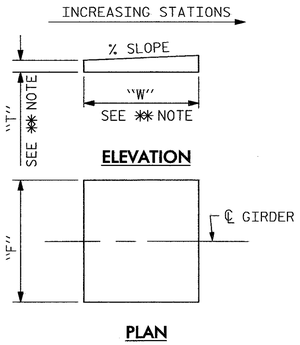

✳✳ NOTE:
DIMENSIONS "W" AND "T" ARE TO BE DETERMINED BY THE MANUFACTURER.

SOLE PLATE DETAILS

GIRDER No.	END BENT 1		END BENT 2	
	"F"	% SLOPE	"F"	% SLOPE
1	2'-4"	-0.60%	2'-4"	-2.10%
2 THRU 6	2'-0"	-0.55%	2'-0"	-2.00%
7 THRU 14	2'-0"	-0.40%	2'-0"	-2.00%
15 THRU 17	2'-0"	-0.25%	2'-0"	-2.00%

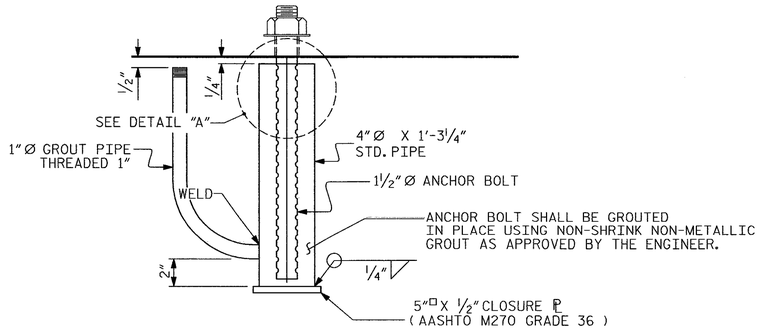

ANCHOR BOLT ASSEMBLY

(END BENT 2)

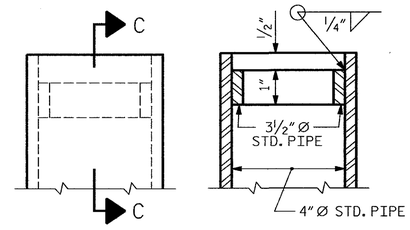

SECTION C–C

DETAIL "A"

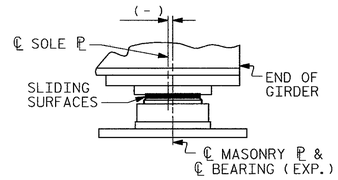

TABLE FOR PLATE SETTING DATA (EXPANSION POT BEARINGS)				
TEMPERATURE AT TIME OF SETTING	30° F	60° F	90° F	✳
END BENT 2	-5/8"	0	+5/8"	- 1 7/8"

✳ CORRECTION FOR END ROTATION DUE TO WEIGHT OF SLAB AND COMPOSITE DEAD LOAD.

TEMPERATURE SETTING DETAIL

TABLE FOR LOADS AND MOVEMENTS						
BEARING	LOCATION	VERTICAL LOAD (KIPS)			LATERAL LOAD (KIPS)	TOTAL MOVEMENT (INCHES)
		DEAD	LIVE	TOTAL		
PB1 (FIXED)	EB1	370	130	500	50	0
PB2 (EXP.)	EB2	370	130	500	50	2 9/16"

PROJECT NO. R-2813B

BUNCOMBE COUNTY

STATION: 48+63.74 -L- P.O.T.

SHEET 2 OF 2

RELEASE FOR CONSTRUCTION
DATE: 2/22/08

STATE OF NORTH CAROLINA
DEPARTMENT OF TRANSPORTATION
RALEIGH

STANDARD

POT BEARING DETAILS

WilburSmith ASSOCIATES
421 Fayetteville Street
Suite 1303
RALEIGH, N. C. 27601

DRAWN BY : K.E. LOFTON DATE : 9-07
CHECKED BY : T.M. HARRIS DATE : 9-07

DWG. No. S-107

NORTH CAROLINA PROFESSIONAL SEAL 19299 ENGINEER THOMAS M. HARRIS
2-22-08

REVISIONS						SHEET NO.
No.	BY:	DATE:	No.	BY:	DATE:	
1			3			TOTAL SHEETS
2			4			

ASSEMBLED BY : K.E. LOFTON DATE : 9/07
CHECKED BY : T.M. HARRIS DATE : 9/07

DRAWN BY : RWW 8/99
CHECKED BY : LES 8/99

REV. 10/17/00	RWW/LES
REV. 7/10/01	LES/RDR
REV. 5/7/03	RWW/JTE

s:\ncdot\r-2813b\design\i-26 bridge\VFC\R2813B_SD_PB01_02.dgn
2/21/2008

PB1.STD

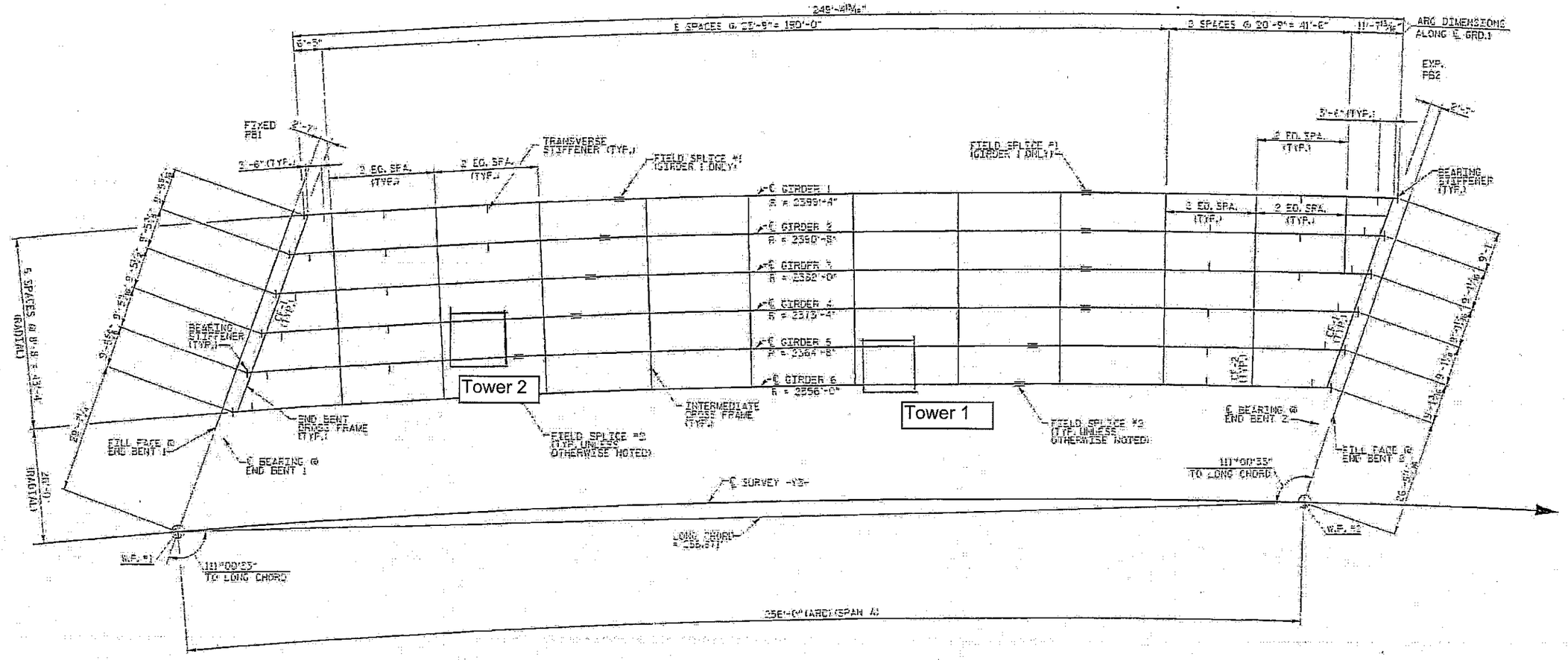

FRAMING PLAN – STAGE I

NOTES

ALL INTERMEDIATE CROSS FRAMES ARE RADIAL TO ℄ SURVEY -Y5-.

ALL DIMENSIONS SHOWN ARE HORIZONTAL.

CONNECTOR PLATES NOT SHOWN FOR CLARITY.

STRUCTURAL STEEL NOTES:

ALL STRUCTURAL STEEL SHALL BE AASHTO M270 GRADE 50W AND PAINTED IN ACCORDANCE WITH SYSTEM 4 OF ARTICLE 442-4 OF THE STANDARD SPECIFICATIONS, UNLESS OTHERWISE NOTED ON PLANS.

ALL DIMENSIONS SHOWN ARE HORIZONTAL OR VERTICAL, UNLESS OTHERWISE NOTED.

TENSION ON THE AASHTO M164 BOLTS SHALL BE CALIBRATED USING DIRECT TENSION INDICATOR WASHERS IN ACCORDANCE WITH ARTICLE 440-10 OF THE STANDARD SPECIFICATIONS.

ALL CROSS FRAME CONNECTIONS TO BE ⅞" DIA. HIGH STRENGTH BOLTS UNLESS OTHERWISE NOTED.

ALL FIELD SPLICE CONNECTIONS TO BE 1" DIA. HIGH STRENGTH BOLTS UNLESS OTHERWISE NOTED.

CONNECTOR PLATES ARE TO BE PLACED NORMAL TO FLANGES AND WEB AT INTERMEDIATE CROSS FRAME LOCATIONS.

ENDS OF GIRDERS BE PLUMB.

BEARING STIFFENERS ARE TO BE PLACED NORMAL TO WEB OF THE GIRDER AND SHALL BE PLUMB.

STRUCTURAL STEEL FOR GIRDER WEBS, FLANGES, TRANSVERSE STIFFENERS, END SPLICE PLATES SHALL BE AASHTO M270 GRADE HPS 70W AND PAINTED IN ACCORDANCE WITH SYSTEM 4 OF ARTICLE 442-4 OF THE STANDARD SPECIFICATIONS.

FOR HIGH PERFORMANCE STEEL, THE FABRICATOR MAY USE A THERMO-MECHANICAL CONTROLLED PROCESS (TMCP) ON PLATE SIZES UP TO 2 INCHES IN THICKNESS.

FOR HIGH PERFORMANCE STEEL, SEE SPECIAL PROVISIONS.

SHOP SPLICES ARE PERMITTED TO LIMIT THE MAXIMUM REQUIRED FLANGE PIECE LENGTHS TO 60 FEET AND WEB PIECE LENGTHS TO 45 FEET. PERMITTED FLANGE AND WEB SHOP SPLICES SHALL NOT BE LOCATED WITHIN 15 FEET OF MAXIMUM DEAD LOAD DEFLECTION, NOR 5 FEET MINIMUM BETWEEN WEB AND FLANGE SHOP SPLICES. KEEP 6" MINIMUM BETWEEN CONNECTOR PLATE WELDS OR TRANSVERSE STIFFENER WELDS AND WEB OR FLANGE SHOP SPLICES.

SHEAR STUDS ON GIRDERS MAY BE SHIFTED UP TO 1" IF NECESSARY TO CLEAR FLANGE SPLICE WELD.

CHARPY V-NOTCH TESTS ARE REQUIRED FOR ALL BOTTOM FLANGE PLATES, ALL WEB PLATES, ALL BOTTOM FLANGE SPLICE PLATES AND ALL WEB SPLICE PLATES. IF A PERMITTED SHOP FLANGE SPLICE IS NOT USED, CHARPY V-NOTCH TESTS WILL BE REQUIRED FOR THE ENTIRE FLANGE PLATE. FOR CHARPY V-NOTCH TESTS, SEE ARTICLE 1072-9 OF THE STANDARD SPECIFICATIONS.

FOR CHARPY V-NOTCH TEST, SEE SPECIAL PROVISIONS.

THE CONTRACTOR SHALL MAINTAIN STABILITY OF CURVED GIRDERS UNTIL ALL FIELD SPLICES AND CROSS FRAME CONNECTOR PLATES HAVE BEEN COMPLETED.

PROJECT NO. R-2813B

BUNCOMBE COUNTY

STATION: 48+63.74 -L- P.O.T.

SHEET 2 OF 4

STATE OF NORTH CAROLINA
DEPARTMENT OF TRANSPORTATION
RALEIGH

SUPERSTRUCTURE

FRAMING PLAN – STAGE I

WilburSmith ASSOCIATES
421 Fayetteville Street
Suite 1303
RALEIGH, N. C. 27601

DRAWN BY : E.M. HASSALL DATE : 2/07
CHECKED BY : T.M. HARRIS DATE : 2/07
DWG. NO. 18

PRELIMINARY PLANS
NOT TO BE USED FOR CONSTRUCTION

REVISIONS						SHEET NO.
NO.	BY:	DATE:	NO.	BY:	DATE:	
1			3			TOTAL SHEETS
2			4			

NCHRP 12-79

EISSS3

15+30 15+40 15+50 15+60 15+70 15+80 15+90 16+00 16+10 16+20 16+30 16+40

$$$$$$$SYSTIME$$$$$
$$$$$$$$$$$$$$$$$$$$$$DGN$$$$$$$$$$$$$$$$$$$$$$$$$
$$$$USERNAME$$$$

56 54 52 50 48 46 44 42

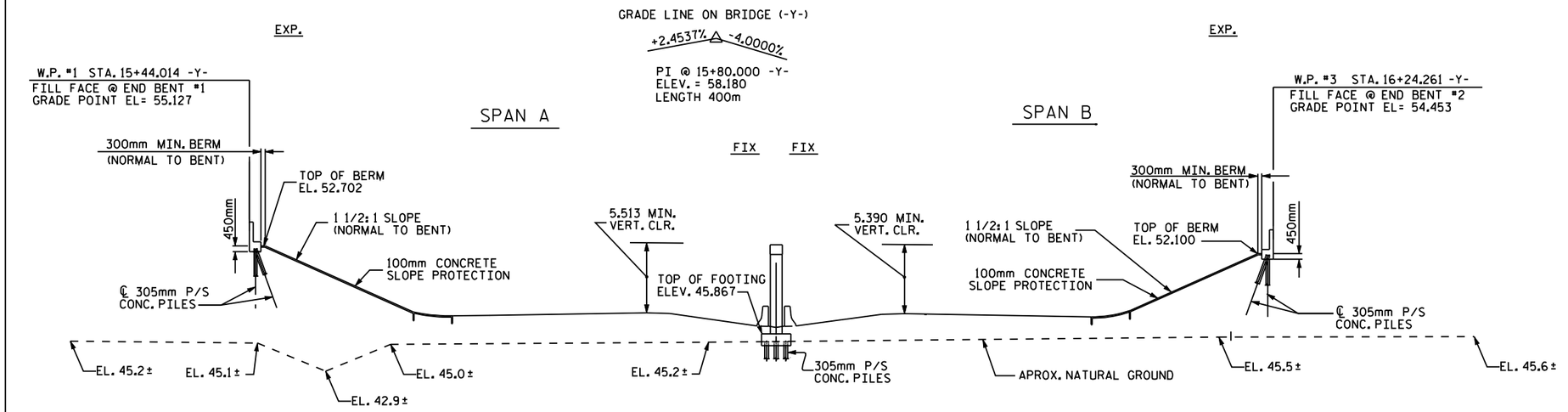

NOTES

FOR NOTES, SEE SHEET 4 OF 4.

SECTION ALONG ℄ -Y-

SECTION AT END BENTS AND INT. BENT ARE TAKEN AT RIGHT ANGLES

HORIZ. CURVE DATA (-Y-)

PIs STA. 14+76.976		PI STA. 16+40.304	
θs =	0°-47'-16.1"	△ =	14°-28'-08.2" (RT.)
Ls =	33.000	L =	303.037
LT =	22.000	T =	152.329
ST =	11.000	R =	1200.000
SE =	0.041		

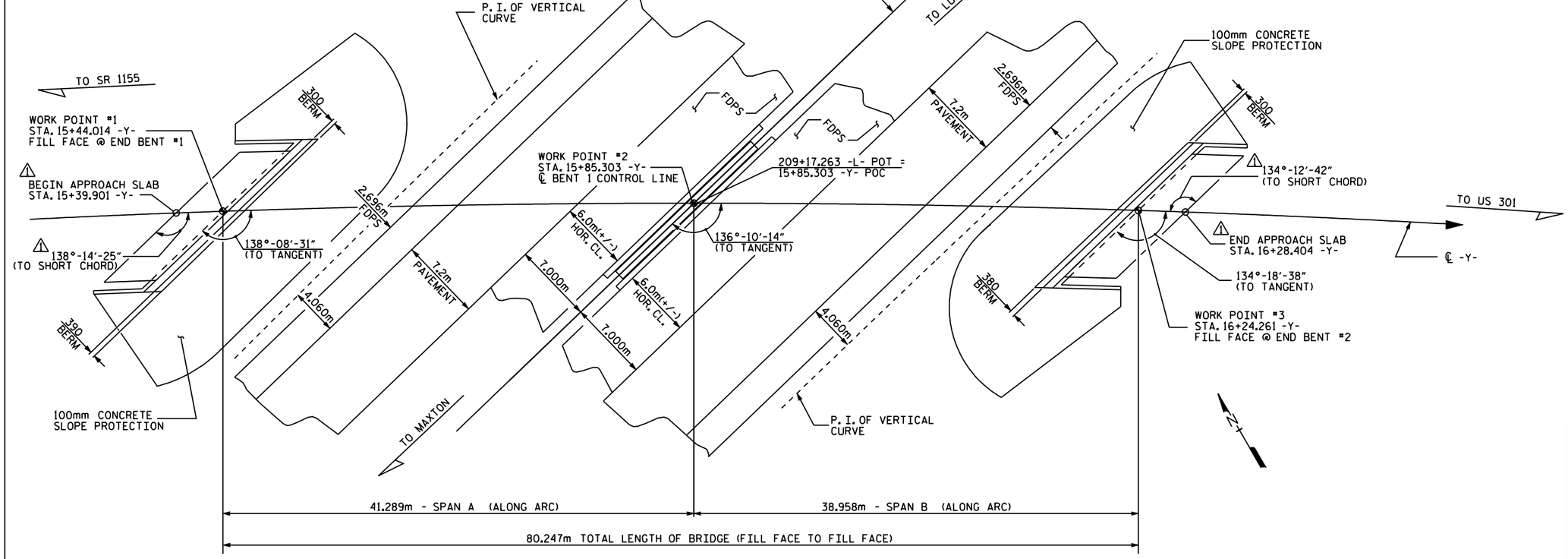

PLAN

FOOTINGS AND PILES NOT SHOWN

⚠ REVISION #1: MODIFIED SHAPE OF APPROACH SLABS
BY: DRA 10/23/06 CK. BY: WFP 10/24/06

DRAWN BY : D.R. ANDERSON DATE : 5-7-03
CHECKED BY : T.A. WALTER DATE : 8-19-03

PROJECT NO. R-513BB
ROBESON COUNTY
STATION: 209+17.263 -L-
15+85.303 -Y-
SHEET 1 OF 4 BRIDGE NO. 483

STATE OF NORTH CAROLINA
DEPARTMENT OF TRANSPORTATION
RALEIGH

GENERAL DRAWING

FOR BRIDGE ON SR 1003
(CHICKEN ROAD) OVER US74
BETWEEN SR 1155 & SR 1161

REVISIONS						SHEET NO.
NO.	BY:	DATE:	NO.	BY:	DATE:	S-32
1	DRA	10/23/06	3			TOTAL SHEETS
2			4			312

STR. 2

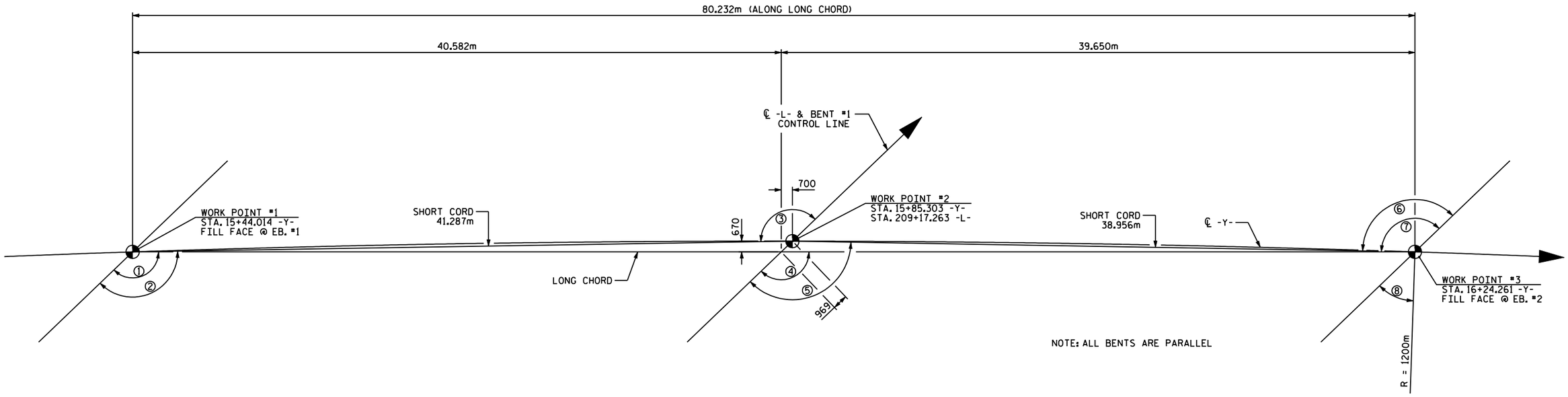

NOTE: ALL BENTS ARE PARALLEL

LONG CHORD LAYOUT

ANGLES

① = 136°13'35"
② = 137°09'23"
③ = 137°09'23"
④ = 136°13'35"
⑤ = 135°14'26"
⑥ = 135°14'26"
⑦ = 136°13'35"
⑧ = 44°18'40"

PROJECT NO. R-513BB
ROBESON COUNTY
STATION: 209+17.263 -L-

SHEET 3 OF 4

STATE OF NORTH CAROLINA
DEPARTMENT OF TRANSPORTATION
RALEIGH

LONG CHORD LAYOUT

REVISIONS						SHEET NO.
NO.	BY:	DATE:	NO.	BY:	DATE:	S-3
1			3			TOTAL SHEETS
2			4			

DRAWN BY : W.K. FISCHER DATE : 1/8/04
CHECKED BY : N.O. TRAN DATE : 1/9/04

$$$$$$SYSTIME$$$$$
$$$$$$$$$$$$$$$$$$$$$$$$$DGN$$$$$$$$$$$$$$$$$$$$$$$$
$$$$USERNAME$$$$

STR #2

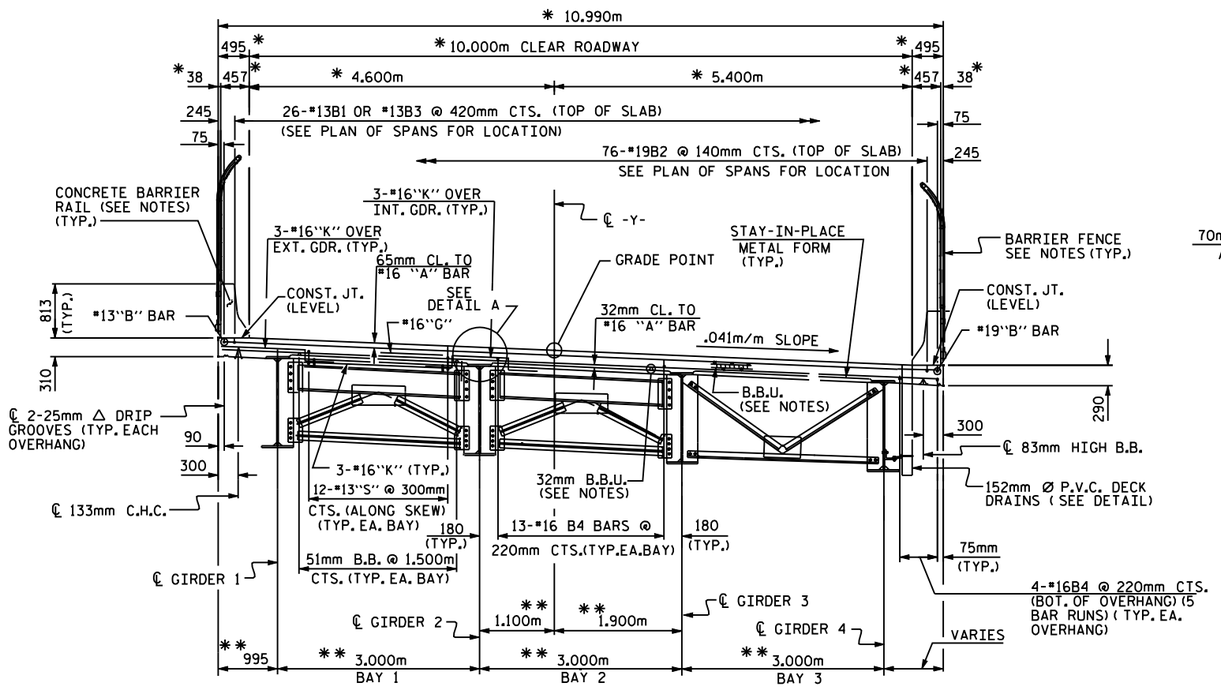

PART SECTION
SHOWING END BENT DIAPHRAGMS
(BENT DIAPHRAGMS SIMILAR)

PART SECTION
SHOWING INTERMEDIATE DIAPHRAGMS

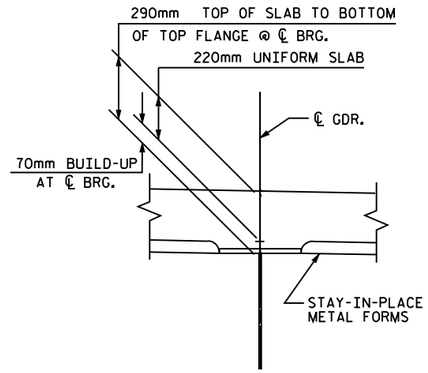

DETAIL A

NOTES

PROVIDE 32mm HIGH BEAM BOLSTERS UPPER AT 1.2m CTS. ATOP THE METAL STAY-IN-PLACE FORMS TO SUPPORT THE BOTTOM MAT OF 'A' BARS. WHEN USING REMOVABLE FORMS, PROVIDE CONTINUOUS HIGH CHAIRS FOR METAL DECK (C.H.C.M.) @ 1.2m CTS. WITH A HEIGHT TO SUPPORT THE BOTTOM MAT OF 'A' BARS A CLEAR DISTANCE OF 65mm ABOVE THE TOP OF THE REMOVABLE FORM.

FOR CONCRETE BARRIER RAIL REINFORCING STEEL AND DETAILS, SEE "CONCRETE BARRIER RAIL" SHEET.

METAL STAY-IN-PLACE FORMS SHALL NOT BE WELDED TO BEAM OR GIRDER FLANGES IN THE ZONES REQUIRING CHARPY V-NOTCH TEST. SEE STRUCTURAL STEEL DETAIL SHEETS.

PREVIOUSLY CAST CONCRETE IN A SIMPLE SPAN SHALL HAVE ATTAINED A MINIMUM COMPRESSIVE STRENGTH OF 20.7 MPa BEFORE ADDITIONAL CONCRETE IS CAST IN THE UNIT.

#16"G" BAR MAY BE SHIFTED SLIGHTLY, AS NECESSARY, TO CLEAR REINFORCING STEEL AND STIRRUPS.

THE CONTRACTOR MAY, WHEN NECESSARY, PROPOSE A SCHEME FOR AVOIDING INTERFERENCE BETWEEN METAL STAY-IN-PLACE FORM SUPPORTS OR FORMS AND BEAM/GIRDER STIFFENERS OR CONNECTOR PLATES. THE PROPOSAL SHALL BE INDICATED, AS APPROPRIATE, ON EITHER THE STEEL WORKING DRAWINGS OR THE METAL STAY-IN- PLACE FORM WORKING DRAWINGS.

57mm HIGH B.B.U. LOCATED BETWEEN TOP & BOTTOM MATS OF REINFORCING STEEL AT THE #13 "B" BAR (TOP BAR) LOCATION ONLY, SEE PLAN OF SPANS.

51mm HIGH B.B.U. LOCATED BETWEEN TOP & BOTTOM MATS OF REINFORCING STEEL AT THE #19 "B" BAR (TOP BAR) LOCATION ONLY, SEE PLAN OF SPANS.

FOR BARRIER FENCE DETAILS, SEE "BRIDGE MOUNTED CHAIN LINK FENCE" SHEET.

1 FOR EVAZOTE JOINT SEALS, SEE SPECIAL PROVISIONS.

1 THE NOMINAL UNCOMPRESSED SEAL WIDTH OF THE EVAZOTE JOINT SEAL SHALL BE 64mm.

1 FOR ELASTOMERIC CONCRETE, SEE SPECIAL PROVISIONS.

TYPICAL SECTION

* RADIAL DIMENSION
** RADIAL THRU WORKPOINT

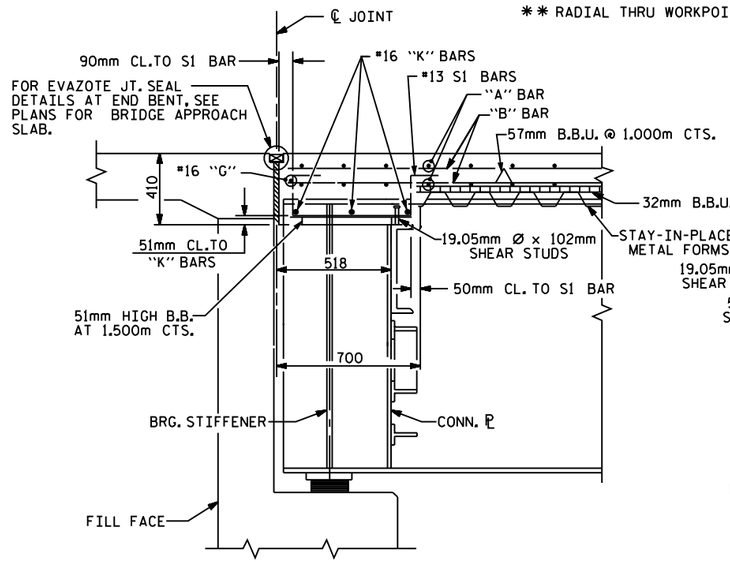

SECTION THRU END BENT DIAPHRAGM
NORMAL TO CAP

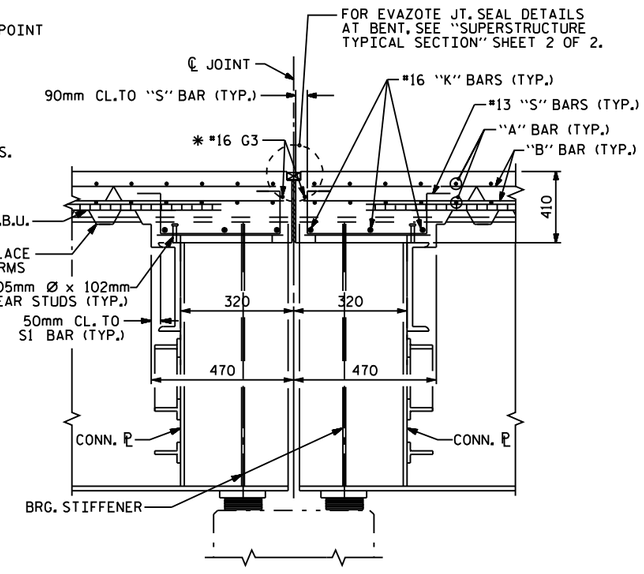

1 SECTION THRU BENT DIAPHRAGM

* #16 G3 BAR MAY BE SHIFTED SLIGHTLY, AS NECESSARY, TO CLEAR DIAPHRAGM AND REINFORCING STEEL.

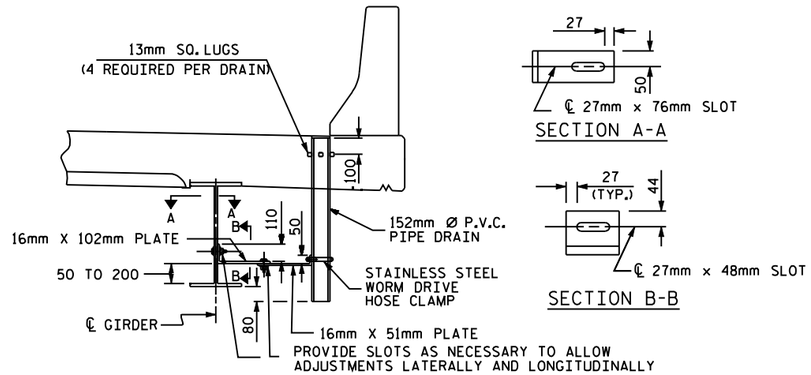

DRAIN CONNECTOR DETAIL

COUPLING IN DRAIN PIPE WILL BE PERMITTED AS APPROVED BY THE ENGINEER.

TOP OF FLOOR DRAINS TO BE SET 10mm BELOW SURFACE OF SLAB.

4-13mm SQ. LUGS TO BE GLUED TO THE P.V.C. PLASTIC PIPE AT EQUAL SPACES AROUND THE PIPE DRAIN APPROXIMATELY 100mm FROM THE TOP OF THE PIPE.

BOLT SIZE TO BE SAME AS DIAPHRAGM AND CROSSFRAME CONNECTIONS. STAINLESS STEEL WORM HOSE CLAMP SHALL BE COMMERCIAL QUALITY.

PVC DECK DRAINS SHALL BE PAINTED WITH TWO COATS OF BROWN PRIMER MEETING THE REQUIREMENTS OF ARTICLE 1080-12 OF THE STANDARD SPECIFICATIONS. EACH COAT SHALL BE 2 DRY MILS (0.050mm) THICK. DECK DRAINS SHALL BE ROUGHENED PRIOR TO PAINTING. NO SEPARATE PAYMENT SHALL BE MADE FOR PAINTING PVC DECK DRAINS AS THIS IS CONSIDERED INCIDENTAL TO THE PAY ITEM FOR REINFORCED CONCRETE DECK SLAB.

THE 152mm Ø PVC PLASTIC PIPE AND FITTINGS SHALL BE SCHEDULE 40 AND CONFORM TO ASTM D1785.

1 REV. NO 1 - ADDED EVAZOTE JOINT AT BENT 1. CONCRETE DIAPHRAGM, ELASTOMERIC CONCRETE, AND ADDITIONAL REINFORCING STEEL ARE ADDED AS A RESULT.
DRAWN BY: T.A.H. 1/24/07
CHECKED BY: W.F.P. 1/24/07

M56S2D FOR 1:20 SCALE

DRAWN BY : N. O. TRAN DATE : 7/23/03
CHECKED BY : M. A. ALLEN DATE : 7/23/03

PROJECT NO. R-513BB
ROBESON COUNTY
STATION: 209+17.263 -L-
SHEET 1 OF 2 1

STATE OF NORTH CAROLINA
DEPARTMENT OF TRANSPORTATION
RALEIGH

SUPERSTRUCTURE
TYPICAL SECTION

REVISIONS						SHEET NO.
NO.	BY:	DATE:	NO.	BY:	DATE:	S-
1	TAH	1/24/07	3			TOTAL SHEETS
2			4			

STR 2

$$$$$$$SYSTIME$$$$$
$$$$$$$$$$$$$$$$$$$$$$$$DGN$$$$$$$$$$$$$$$$$$$$$$$$
$$$$USERNAME$$$$$

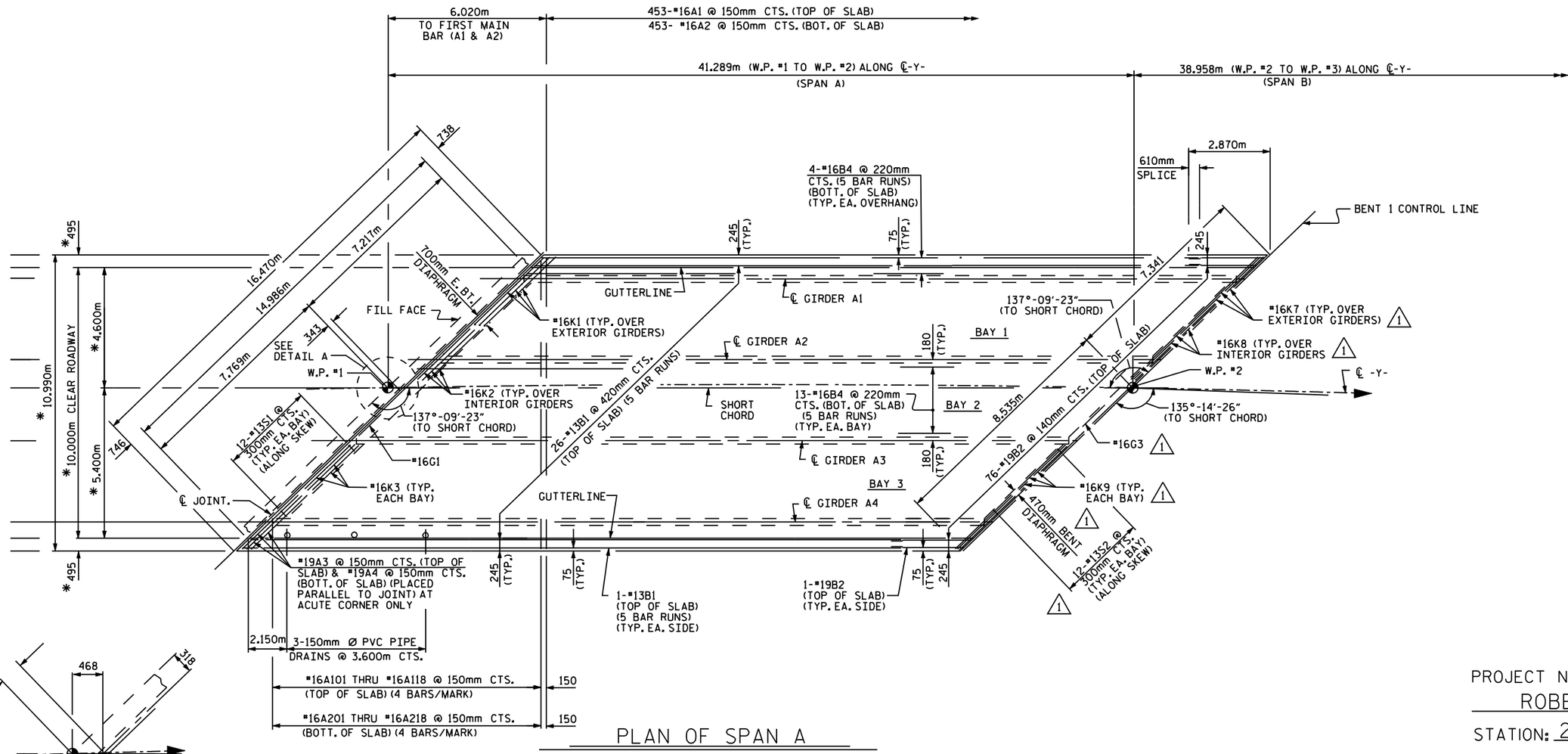

PLAN OF SPAN A

NOTES : BARRIER RAIL NOT SHOWN FOR CLARITY.

✱ RADIAL DIMENSION

1 CUT "A", B2, B4 BARS AS NECESSARY TO AVOID EVAZOTE JOINT.

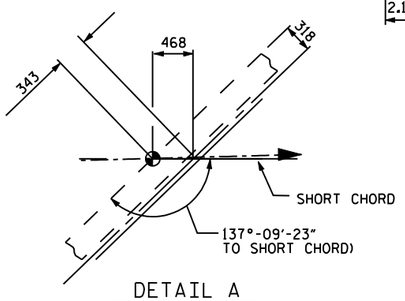

DETAIL A

1 REV. NO 1 - ADDED EVAZOTE JOINT AT BENT 1.
DIAPHRAGM MODIFIED AT BENT 1.
REMOVED TRANS. CONST. JT.
DRAWN BY: T.A.H. 1/24/07
CHECKED BY: W.F.P. 1/24/07

DRAWN BY : N. Q. TRAN DATE : 7-27-03
CHECKED BY : M. A. ALLEN DATE : 2-04

PROJECT NO. R-513BB
ROBESON COUNTY
STATION: 209+17.263 -L-

SHEET 1 OF 2

STATE OF NORTH CAROLINA
DEPARTMENT OF TRANSPORTATION
RALEIGH

SUPERSTRUCTURE
PLAN OF SPANS

REVISIONS						SHEET NO.
NO.	BY:	DATE:	NO.	BY:	DATE:	
1	TAH	1/24/07	3			TOTAL SHEETS
2			4			

STR 2

$$$$$$$SYSTIME$$$$$
$$$$$$$$$$$$$$$$$$$$$$$$DGN$$$$$$$$$$$$$$$$$$$$$$$$
$$$$USERNAME$$$$$

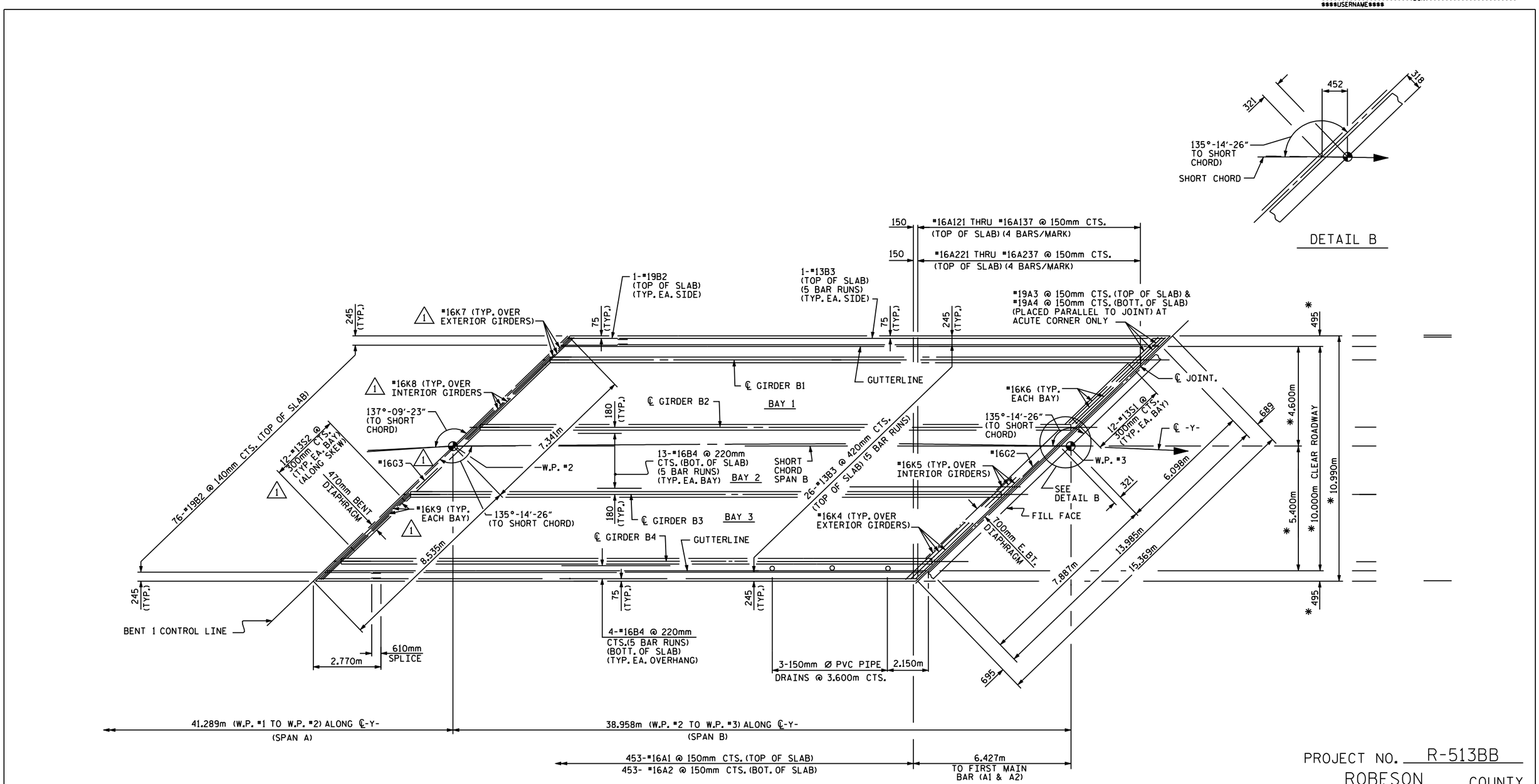

PLAN OF SPAN B

NOTES : BARRIER RAIL NOT SHOWN FOR CLARITY.

* RADIAL DIMENSION

1 CUT "A", B2, B4 BARS AS NECESSARY TO AVOID EVAZOTE JOINT.

PROJECT NO. R-513BB

ROBESON COUNTY

STATION: 209+17.263 -L-

SHEET 2 OF 2

STATE OF NORTH CAROLINA
DEPARTMENT OF TRANSPORTATION
RALEIGH

SUPERSTRUCTURE PLAN OF SPANS

REVISIONS						SHEET NO.
NO.	BY:	DATE:	NO.	BY:	DATE:	
1	TAH	1/24/07	3			TOTAL SHEETS
2			4			

1 REV. NO 1 - ADDED EVAZOTE JOINT AT BENT 1.
DIAPHRAGM MODIFIED AT BENT 1.
REMOVED TRANS. CONST. JT.
DRAWN BY: T.A.H. 1/24/07
CHECKED BY: W.F.P. 1/24/07

DRAWN BY : N. Q. TRAN DATE : 7-27-03
CHECKED BY : M. A. ALLEN DATE : 2-04

STR 2

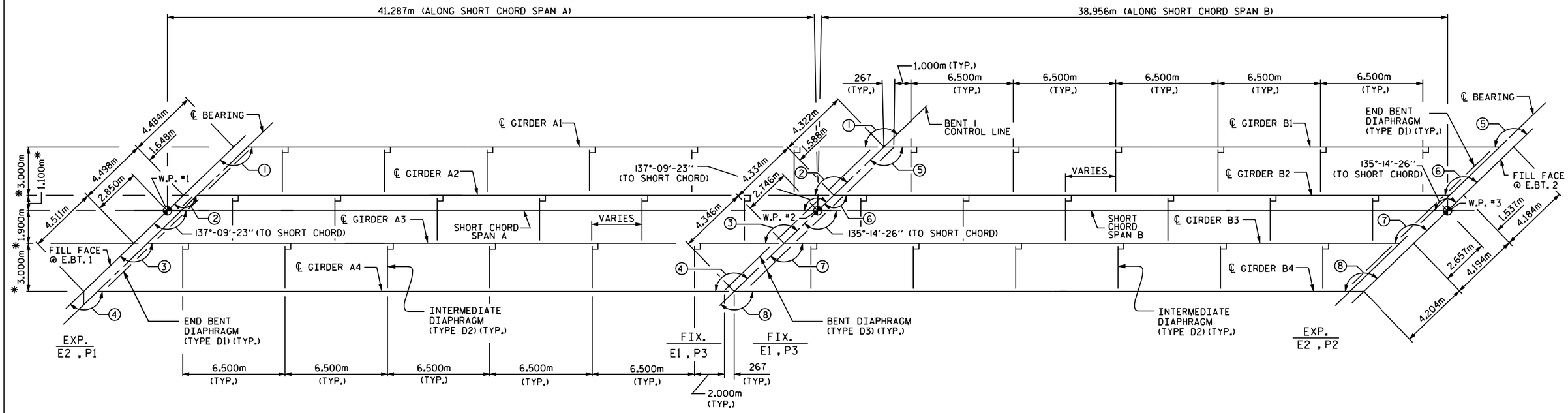

✱ RADIAL DIMENSION

SKEW ANGLES				
	SPAN A		SPAN B	
GIRDER #1	①	136°-56'-46"	⑤	135°-02'-39"
GIRDER #2	②	137°-05'-59"	⑥	135°-11'-16"
GIRDER #3	③	137°-15'-16"	⑦	135°-19'-56"
GIRDER #4	④	137°-24'-37"	⑧	135°-28'-41"

PROJECT NO. R-513BB

ROBESON COUNTY

STATION: 209+17.263 -L-

STATE OF NORTH CAROLINA
DEPARTMENT OF TRANSPORTATION
RALEIGH

SUPERSTRUCTURE

FRAMING PLAN SPANS A & B

REVISIONS						SHEET NO.
NO.	BY:	DATE:	NO.	BY:	DATE:	S-9
1			3			TOTAL SHEETS
2			4			

DRAWN BY : N. Q. TRAN DATE : 7-30-03
CHECKED BY : M. A. ALLEN DATE : 2-04

STR #2

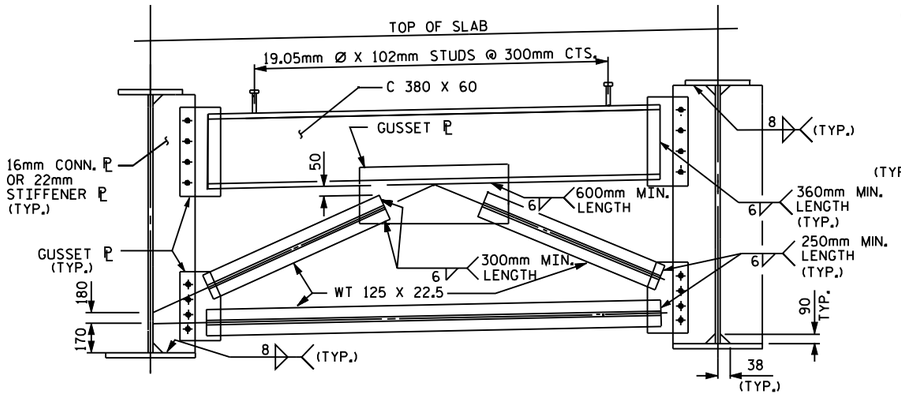

TYPICAL END BENT DIAPHRAGM (D1)

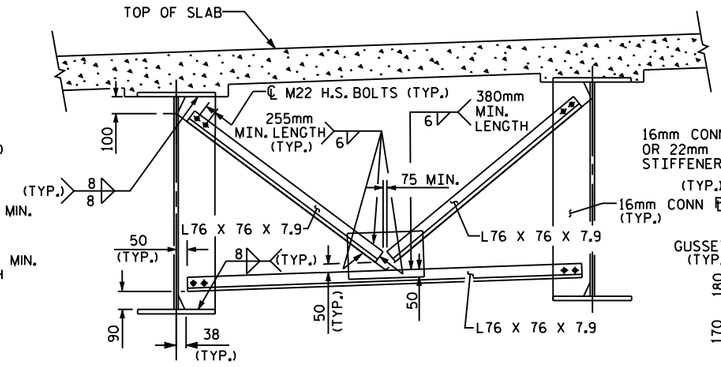

TYPICAL INTERMEDIATE DIAPHRAGM (D2)

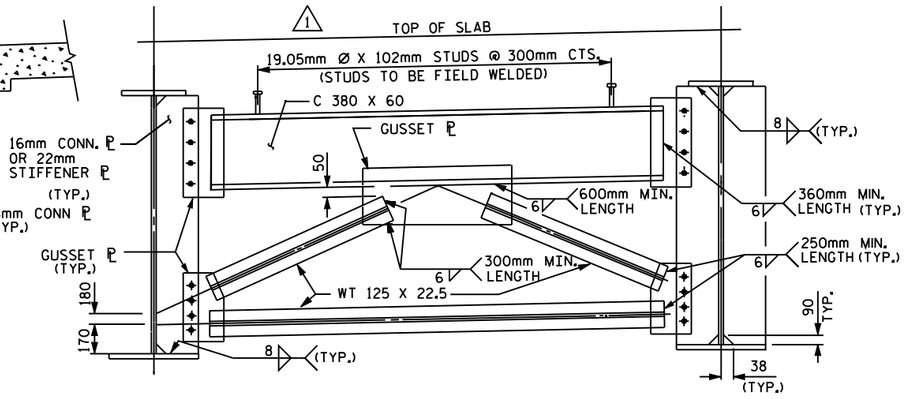

TYPICAL BENT DIAPHRAGM (D3)

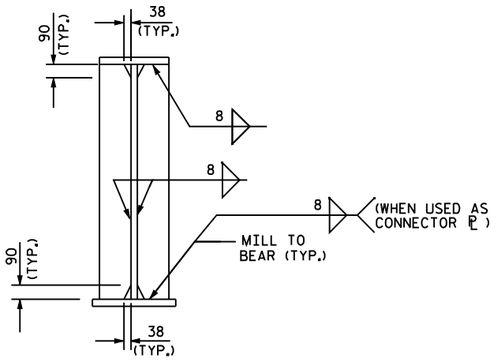

BEARING STIFFENER

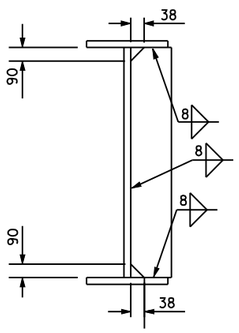

CONNECTOR PLATE

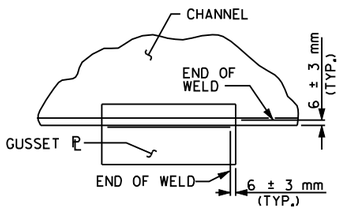

TYPICAL GUSSET PLATE CONNECTION

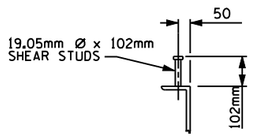

SHEAR STUD DETAILS

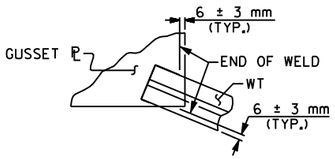

TYPICAL "TEE" TO GUSSET PLATE CONNECTION

WELD TERMINATION DETAILS

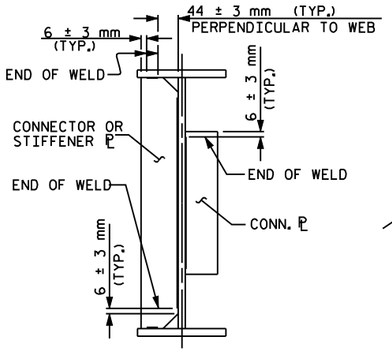

TYPICAL STIFFENER OR CONNECTOR PLATE CONNECTIONS

NOTES

1. ALL STRUCTURAL STEEL SHALL BE AASHTO M270 GRADE 345W STEEL AND PAINTED IN ACCORDANCE WITH SYSTEM 4 OF ARTICLE 442-7 OF THE STANDARD SPECIFICATIONS UNLESS OTHERWISE NOTED ON THE PLANS.
2. ALL DIMENSIONS SHOWN ARE HORIZONTAL OR VERTICAL, UNLESS OTHERWISE NOTED.
3. ALL FIELD CONNECTIONS TO BE 22.23mm DIA. HIGH STRENGTH BOLTS UNLESS OTHERWISE NOTED.
4. TENSION ON THE AASHTO M164 BOLTS SHALL BE CALIBRATED USING DIRECT TENSION INDICATOR WASHERS IN ACCORDANCE WITH ARTICLE 440-10 OF THE STANDARD SPECIFICATIONS.
5. BEARING STIFFENERS ARE TO BE PLACED NORMAL TO THE WEB OF THE GIRDER AT END BENTS 1 & 2, BENT 1 AND SHALL BE PLUMB.
6. AT ALL POINTS OF SUPPORT IN SPANS A-B, NUTS FOR ANCHOR BOLTS SHALL BE TIGHTENED FINGER TIGHT AND GIVEN AN ADDITIONAL 1/4 TURN. THE THREAD OF THE NUT AND BOLT SHALL THEN BE BURRED WITH A SHARP POINTED TOOL.
7. SHOP SPLICES ARE PERMITTED TO LIMIT THE MAXIMUM REQUIRED FLANGE PIECE LENGTHS TO 18 METERS AND WEB PIECE LENGTHS TO 14 METERS. PERMITTED FLANGE AND WEB SHOP SPLICES SHALL NOT BE LOCATED WITHIN 4.5 METERS OF MAXIMUM DEAD LOAD DEFLECTION (NOR WITHIN 4.5 METERS OF INTERMEDIATE BEARINGS OF CONTINUOUS UNITS). KEEP 600mm MINIMUM BETWEEN WEB AND FLANGE SHOP SPLICES. KEEP 150mm MINIMUM BETWEEN CONNECTOR PLATE OR TRANSVERSE STIFFENER WELDS AND WEB OR FLANGE SHOP SPLICES.
8. STUDS ON GIRDERS MAY BE SHIFTED UP TO 25mm IF NECESSARY TO CLEAR FLANGE SPLICE WELD.
9. ENDS OF GIRDERS SHALL BE PLUMB.
10. A CHARPY V-NOTCH TEST IS REQUIRED FOR WEB PLATES, BOTTOM FLANGE PLATES, BOTTOM FLANGE SPLICE PLATES AND WEB SPLICE PLATES (IF USED) FOR ALL GIRDERS IN SPANS A & B.

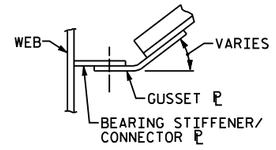

PLAN

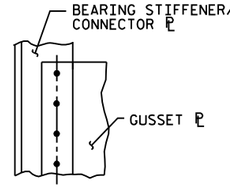

ELEVATION

GUSSET ℄ DETAILS

PROJECT NO. R-513BB

ROBESON COUNTY

STATION: 209+17.263 -L-

SHEET 3 OF 3

STATE OF NORTH CAROLINA
DEPARTMENT OF TRANSPORTATION
RALEIGH

SUPERSTRUCTURE
STRUCTURAL STEEL DETAILS

REVISIONS						SHEET NO.
NO.	BY:	DATE:	NO.	BY:	DATE:	
1	TAH	1/24/07	3			TOTAL SHEETS
2			4			

1 REV. NO 1 - ADDED EVAZOTE JOINT AT BENT 1. DIAPHRAGM AT BENT 1 MODIFIED TO INCUDED STUDS.
DRAWN BY: T.A.H. 1/24/07
CHECKED BY: D.A. 1/24/07

DRAWN BY : N. Q. TRAN DATE : 7/30/03
CHECKED BY : M. A. ALLEN DATE : 2-04

STR. #2

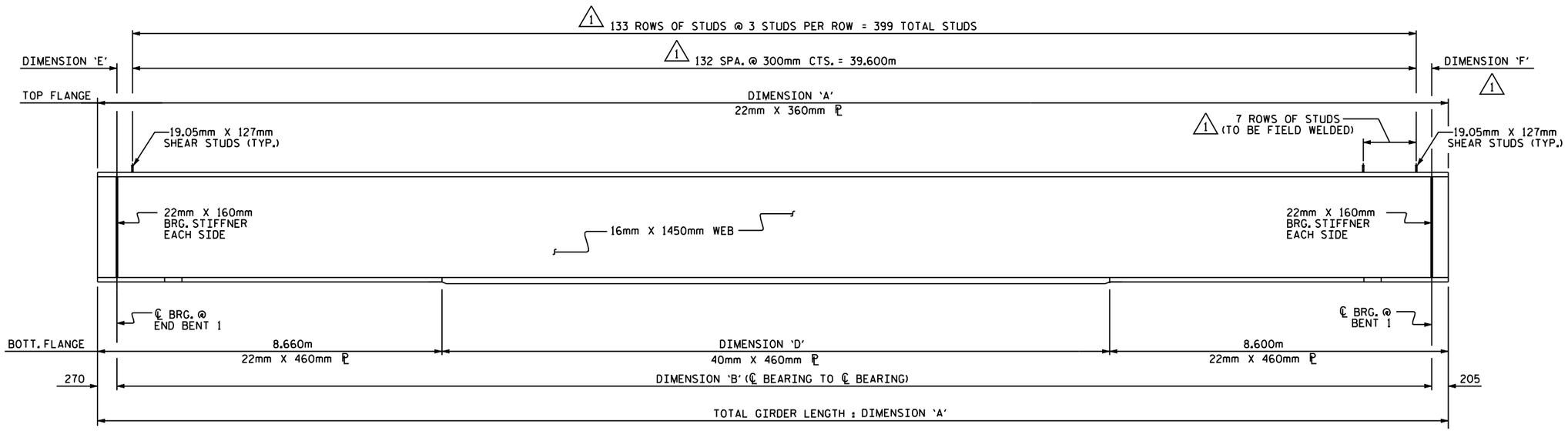

GIRDER ELEVATION

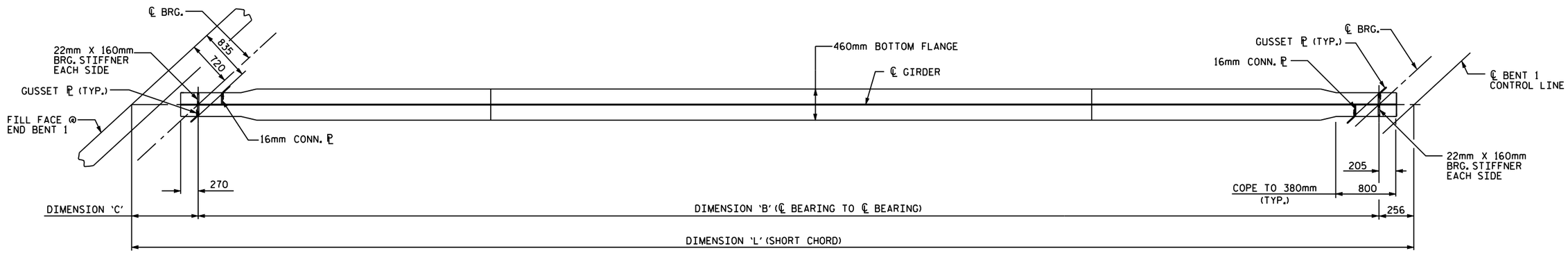

BOTTOM FLANGE DETAIL

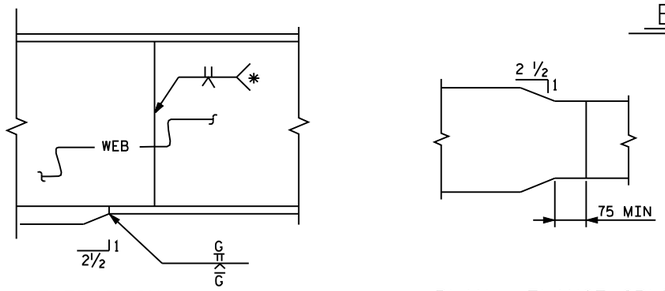

TYPICAL FLANGE BUTT JOINT

* GRIND SMOOTH AND FLUSH ON OUTER FACE OF EXTERIOR GIRDERS

DIMENSIONS 1							
GRD. NO.	L	A	B	C	D	E	F
A1	41.125	40.289	39.814	1.055	23.029	0.119	0.095
A2	41.243	40.405	39.930	1.058	23.145	0.235	0.095
A3	41.363	40.522	40.047	1.061	23.262	0.352	0.095
A4	41.486	40.641	40.166	1.064	23.381	0.471	0.095

1 REV. NO 1 - REMOVED ROOFING FELT AND ADDED SHEAR STUDS
DRAWN BY: T.A.H. 1/24/07
CHECKED BY: W.F.P. 1/24/07

DRAWN BY : N. Q. TRAN DATE : 7/30/03
CHECKED BY : M. A. ALLEN DATE : 2-04

PROJECT NO. R-513BB
ROBESON COUNTY
STATION: 209+17.263 -L-

SHEET 1 OF 3

STATE OF NORTH CAROLINA
DEPARTMENT OF TRANSPORTATION
RALEIGH

SUPERSTRUCTURE
STRUCTURAL STEEL DETAILS
SPAN ''A''

NORTH CAROLINA PROFESSIONAL SEAL 16301 ENGINEER WING HSIUNG FANG

REVISIONS						SHEET NO.
NO.	BY:	DATE:	NO.	BY:	DATE:	S-10
1	TAH	1/24/07	3			TOTAL SHEETS
2			4			

STR. #2

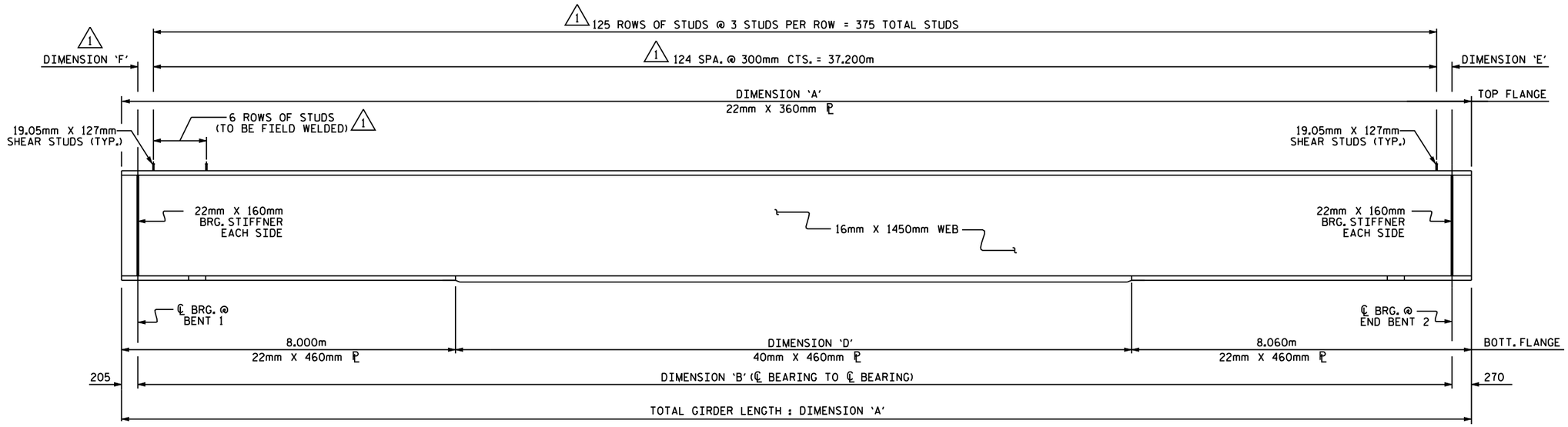

GIRDER ELEVATION

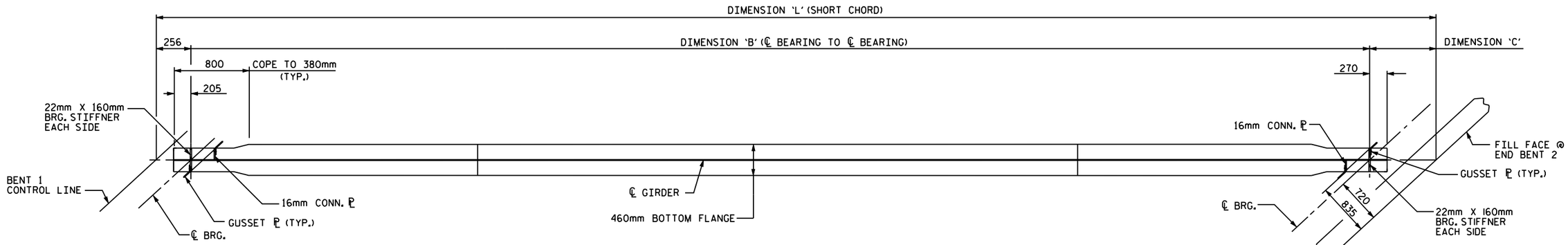

BOTTOM FLANGE DETAIL

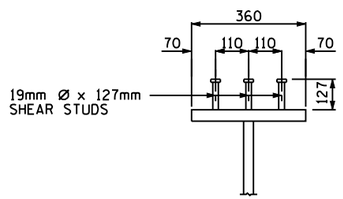

SHEAR STUD DETAIL

DIMENSIONS 1							
GRD. NO.	L	A	B	C	D	E	F
B1	38.821	38.022	37.547	1.019	21.962	0.052	0.295
B2	38.920	38.117	37.642	1.022	22.057	0.147	0.295
B3	39.019	38.214	37.739	1.024	22.154	0.244	0.295
B4	39.120	38.312	37.837	1.027	22.252	0.342	0.295

1 REV. NO 1 - REMOVED ROOFING FELT AND ADDED SHEAR STUDS
DRAWN BY: T.A.H. 1/24/07
CHECKED BY: W.F.P. 1/24/07

DRAWN BY : N. O. TRAN DATE : 7/30/03
CHECKED BY : M. A. ALLEN DATE : 2-04

PROJECT NO. R-513BB
ROBESON COUNTY
STATION: 209+17.263 -L-

SHEET 2 OF 3

STATE OF NORTH CAROLINA
DEPARTMENT OF TRANSPORTATION
RALEIGH

SUPERSTRUCTURE
STRUCTURAL STEEL DETAILS
SPAN ''B''

NORTH CAROLINA PROFESSIONAL SEAL 16301 ENGINEER TING HSIUNG FANG

REVISIONS						SHEET NO.
NO.	BY:	DATE:	NO.	BY:	DATE:	S-11
1	TAH	1/24/07	3			TOTAL SHEETS
2			4			

STR. #2

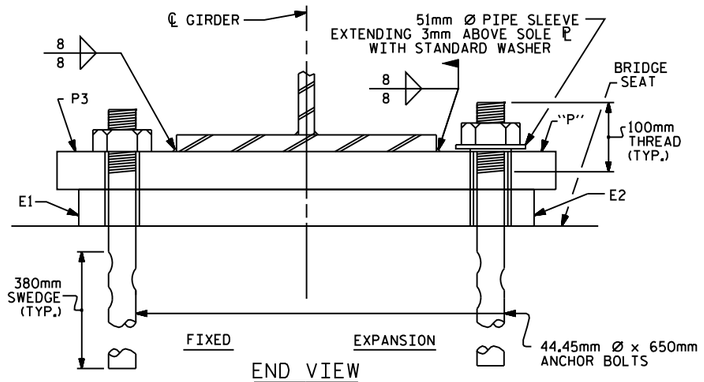

END VIEW

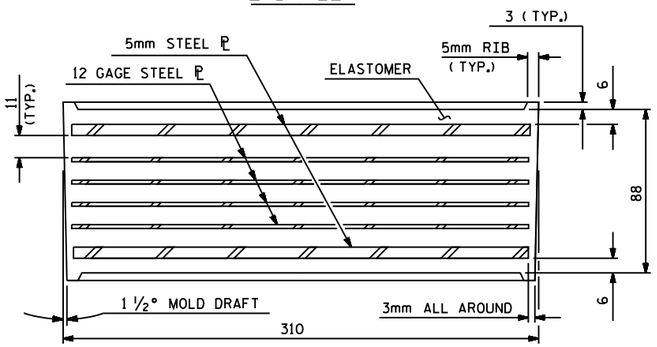

TYPICAL SECTION OF ELASTOMERIC BEARING

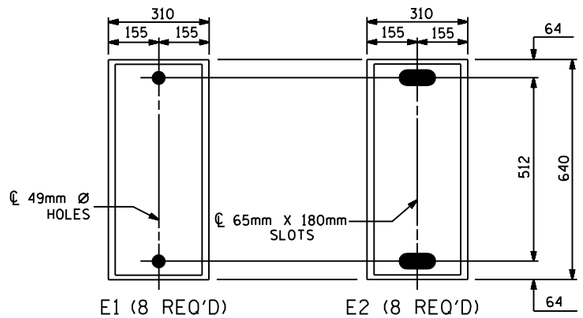

PLAN VIEW OF ELASTOMERIC BEARING

TYPE V

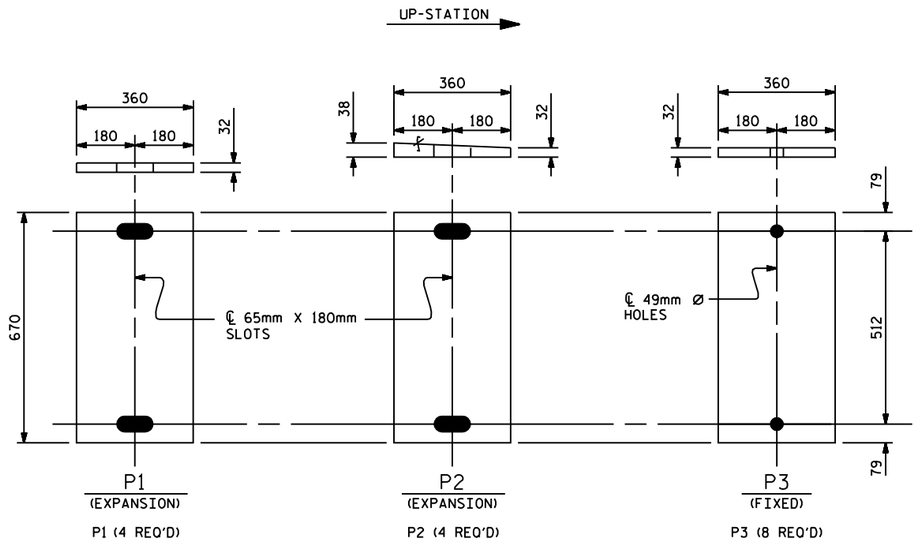

SOLE PLATE DETAILS ("P")

NOTES

FOR ELASTOMERIC BEARINGS, SEE SPECIAL PROVISIONS.

AT ALL FIXED POINTS OF SUPPORT, NUTS FOR ANCHOR BOLTS ARE TO BE TIGHTENED FINGER TIGHT AND THEN BACKED OFF ½ TURN. THE THREAD OF THE NUT AND BOLT SHALL THEN BE BURRED WITH A SHARP POINTED TOOL.

THE 51mm Ø PIPE SLEEVE SHALL BE CUT FROM SCHEDULE 40 PVC PLASTIC PIPE. THE PVC PLASTIC PIPE SHALL MEET THE REQUIREMENTS OF ASTM D1785.

THE PAYMENT FOR THE PIPE SLEEVES SHALL BE INCLUDED IN THE SEVERAL PAY ITEMS.

FOR AASHTO M270 GRADE 345W STRUCTURAL STEEL, SOLE PLATE SHALL BE AASHTO M270 GRADE 345W AND SHALL NOT BE GALVANIZED, ANCHOR BOLTS AND NUTS SHALL BE GALVANIZED IN ACCORDANCE WITH THE STANDARD SPECIFICATIONS.

ANCHOR BOLTS SHALL MEET THE REQUIREMENTS OF ASTM A449. NUTS SHALL MEET THE REQUIREMENTS OF AASHTO M291M-12 OR AASHTO M292M-2H. WASHERS SHALL MEET THE REQUIREMENTS OF AASHTO M293M. SHOP DRAWINGS ARE NOT REQUIRED FOR ANCHOR BOLTS, NUTS AND WASHERS. SHOP INSPECTION IS REQUIRED.

WHEN FIELD WELDING THE SOLE PLATE TO THE GIRDER FLANGE, USE TEMPERATURE INDICATING WAX PENS, OR OTHER SUITABLE MEANS, TO ENSURE THAT THE TEMPERATURE OF THE SOLE PLATE DOES NOT EXCEED 149°C. TEMPERATURES ABOVE THIS MAY DAMAGE THE ELASTOMER.

ALL SURFACES OF BEARING PLATES SHALL BE SMOOTH AND STRAIGHT.

—LOAD RATINGS—	
	MAX.D.L.+ L.L.
TYPE V	943 kN

PROJECT NO. R-513BB

ROBESON COUNTY

STATION: 209+17.263 -L-

ASSEMBLED BY : N. O. TRAN	DATE : 12/1/03				
CHECKED BY : M.A. ALLEN	DATE : 2/04				
DRAWN BY : EEM 10/95	REV. 7/17/98	RWW/LES			
CHECKED BY : PEK 10/95	REV. 8/16/99	MAB/LES			
	REV. 10/17/00	RWW/LES			

USE .0014 X SCALE FOR PE SEAL

STATE OF NORTH CAROLINA
DEPARTMENT OF TRANSPORTATION
RALEIGH

STANDARD

SUPERSTRUCTURE ELASTOMERIC BEARING DETAILS

REVISIONS						SHEET NO.
NO.	BY:	DATE:	NO.	BY:	DATE:	S-13
1			3			TOTAL SHEETS
2			4			

STR. 2 STD. NO. EB2SM

$$$$$$SYSTIME$$$$$
$$$$$$$$$$$$$$$$$$$$$$$$$$DGN$$$$$$$$$$$$$$$$$$$$$$$$$$
$$$$USERNAME$$$$

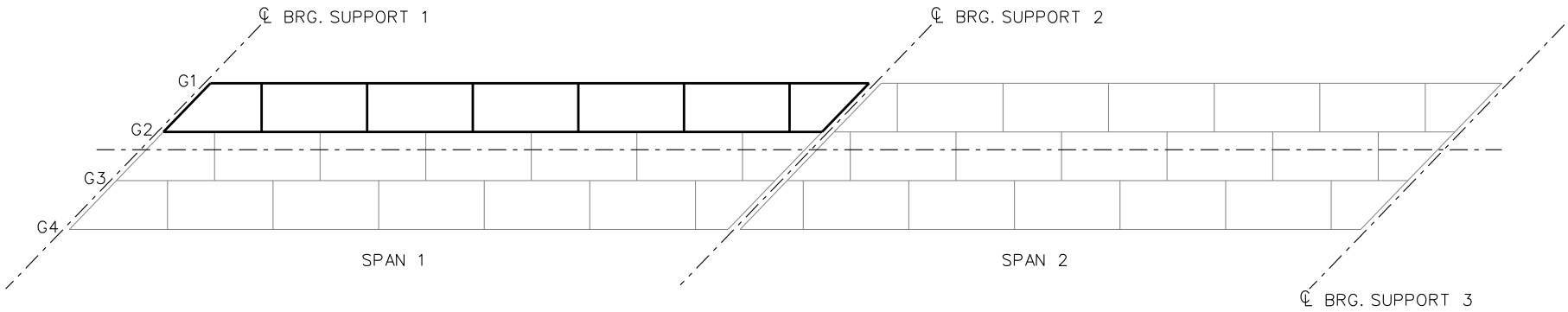

STAGE 1

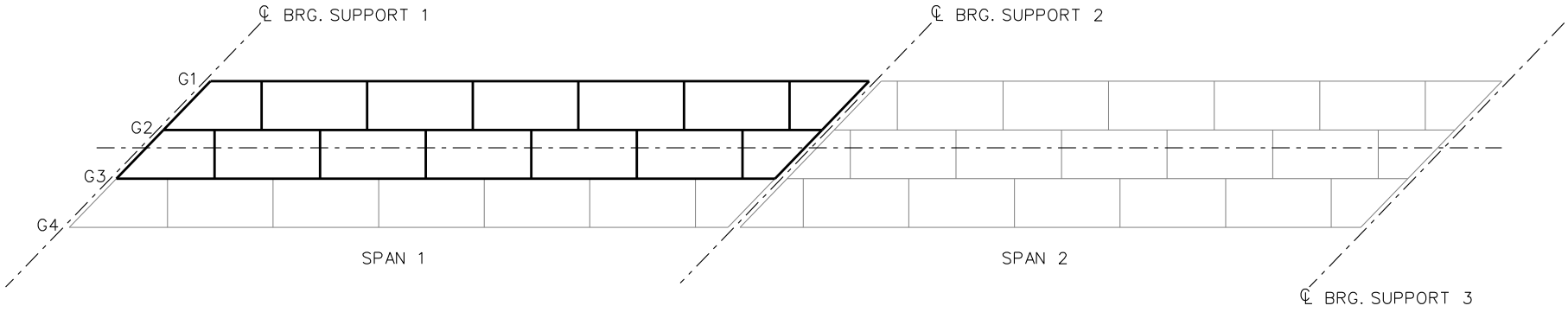

STAGE 2

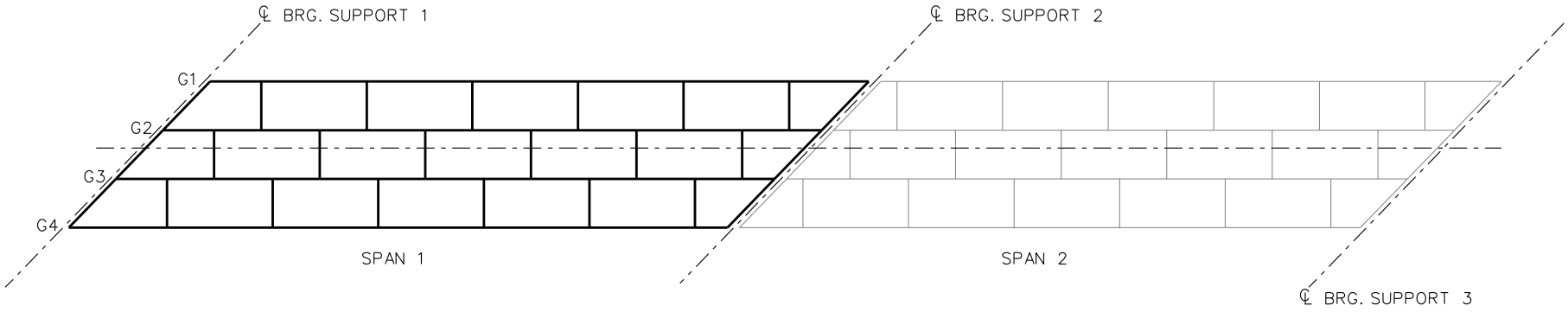

STAGE 3

LEGEND

▽ = HOLD OR LIFT CRANE

○ = TIE DOWN

□ = TEMPORARY SUPPORT STRUCTURE

NCHRP 12-79

BRIDGE EISSS3

GIRDER ERECTION PROCEDURE

SHEET 1 OF 1

NCHRP 12-79

EISSS5

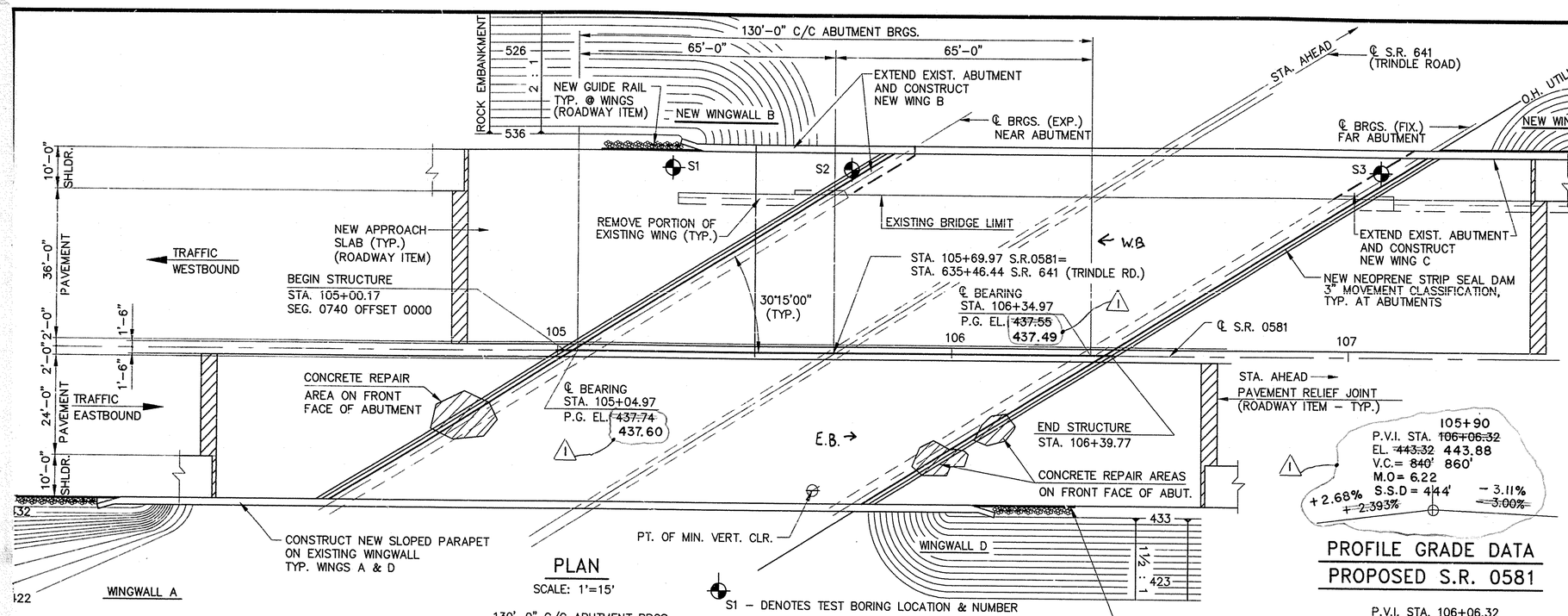

PLAN

SCALE: 1"=15'

S1 - DENOTES TEST BORING LOCATION & NUMBER

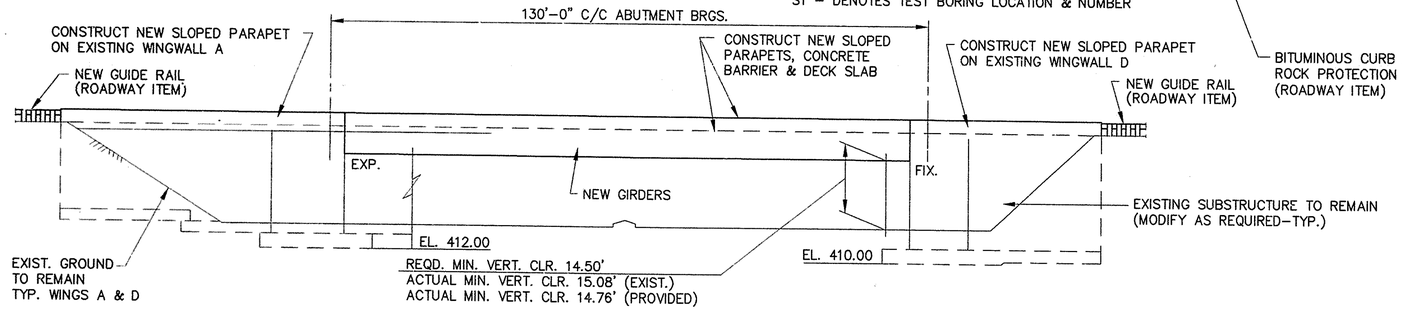

ELEVATION

SCALE: 1"=15'

PROFILE GRADE DATA PROPOSED S.R. 0581

P.V.I. STA. 106+06.32
EL. 442.57
V.C.= 840'
+ 2.393% - 3.00%

PROFILE GRADE DATA EXISTING S.R. 0581

INDEX OF DRAWINGS

BRIDGE LOAD RATINGS - PROPOSED

ADTT = 5664 (1993)

LOAD CONFIGURATION CRITICAL LOCATION (SPAN/TENTH)	EASTBOUND MAIN GIRDERS H 1.5	HS 1.5	ML 1.5	P 1.2	WESTBOUND MAIN GIRDERS H 1.5	HS 1.5	ML 1.5	P 1.5
IR	30.9	52.3	49.6	61.2	30.8	52.2	49.5	62.8
OR	51.5	87.2	82.7	102.1	51.4	87.0	82.5	104.7
SHEAR STRENGTH (K)	417.9	417.9	417.9	464.6	317.8	317.8	317.8	317.8
MAX. MOMENT STRENGTH (K-FT)	13,094.7	13,094.7	13,094.7	8,715.4	11,395.3	11,395.3	11,395.3	11,395.3
SERVICE MOM'T STRENGTH (K-FT)	12,440.0	12,440.0	12,440.0	8,279.7	10,825.5	10,825.5	10,825.5	10,825.5

NOTES:
1. THE LOAD FACTOR METHOD WAS UTILIZED TO OBTAIN THE ABOVE RATINGS.
2. AASHTO LIVE LOAD DISTRIBUTION FACTORS WERE USED FOR RATINGS.
3. FUTURE WEARING SURFACE HAS BEEN INCLUDED IN THE RATING COMPUTATIONS.
4. RATINGS ARE IN TONS.
5. * INDICATES ESTIMATED TRAFFIC COUNT.

NOTES:
- FOR GENERAL NOTES, SEE SHEET NO. 2
- FOR TYPICAL SECTIONS, SEE SHEET NO. 3

Mark	Description	By	Chk'd.	App'd.	Date
1	CHANGE IN ELEVATION	G.B.B	REM	RHK	3-2-94

REVISIONS

DESIGNED: J.E.L.	DRAWN: R.J.C.	CHECKED: R.M.H.

PREPARED BY
ERDMAN, ANTHONY, ASSOCIATES
3 CROSSGATE DRIVE
MECHANICSBURG, PENNSYLVANIA
May 6, 1993

DESCRIPTION	DWG. NO.	APP. DATE
STRUCTURE MOUNTED GUIDE RAIL AND CONCRETE BARRIER	BC-738	11-15-89
STEEL DIAPHRAGMS FOR STEEL BEAM/GIRDER STRUCTURES	BC-754	6-1-91
STEEL GIRDER DETAILS	BC-753	6-1-91
NEOPRENE STRIP SEAL DAM	BC-767	5-3-89
CONCRETE DECK SLAB DETAILS	BC-752	1-20-89
BRIDGE PARAPET TO GUIDE RAIL TRANSITION	BC-339	9-3-91
PERMANENT METAL DECK FORMS	BC-732	1-20-89
CLASSIFICATION OF EARTHWORK FOR STRUCTURES	RC-11	6-30-90
BACKFILL AT STRUCTURES	RC-12	3-30-92
WALL CONSTR. & EXPANSION JOINT DETAILS	BC-735	1-20-89
REINFORCEMENT BAR FABRICATION DETAILS	BC-736	6-1-91
ANCHOR SYSTEMS	BC-734	11-15-89

SUPPLEMENTAL DRAWINGS

Commonwealth of Pennsylvania
DEPARTMENT OF TRANSPORTATION
BUREAU OF DESIGN

CUMBERLAND COUNTY
S.R. 0581, SECTION A01
SEG.0740 OFFSET 0000
S.R. 0581 STA. 105+69.97 OVER S.R. 641
SINGLE SPAN COMPOSITE STEEL MULTI GIRDER BRIDGE
REHABILITION AND WIDENING
GENERAL PLAN & RATINGS

RECOMMENDED MAY 13 1993
M. G. Patel NU
CHIEF BRIDGE ENGINEER

SHEET 1 OF 21 + SUPPLEMENTAL DRAWINGS

S-20590

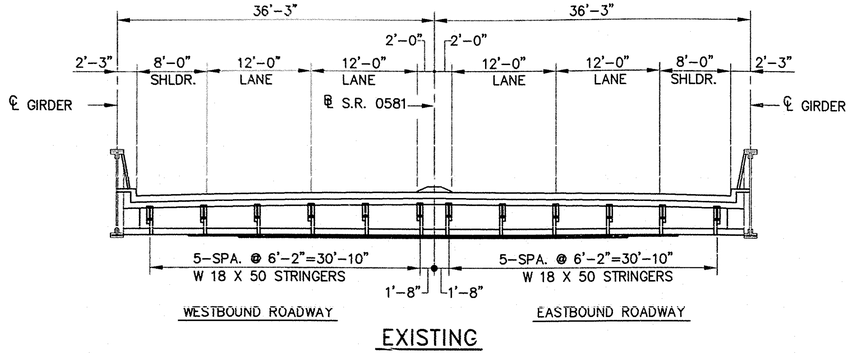

EXISTING

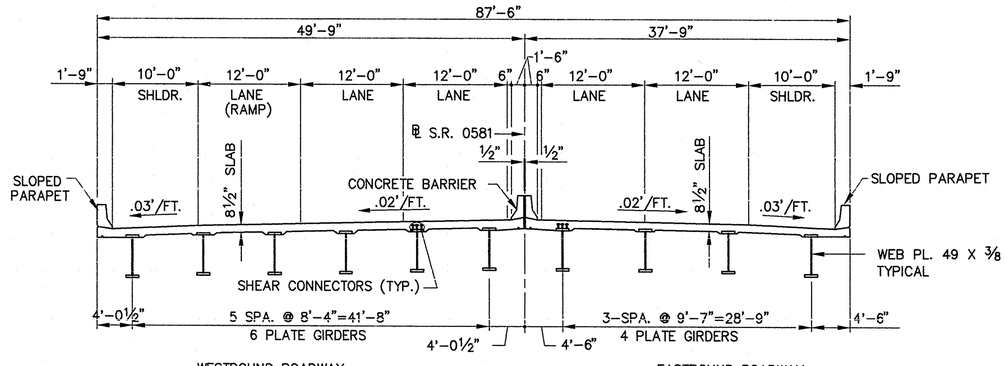

COMPLETED BRIDGE

SCALE: 1/8"=1'-0"

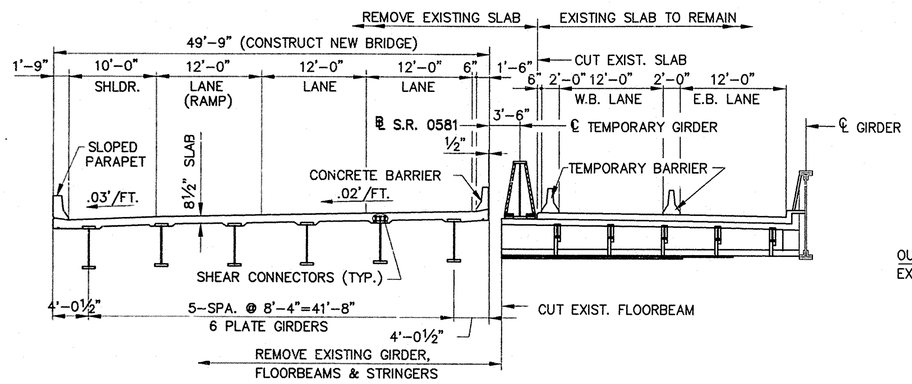

STAGE 1 CONSTRUCTION

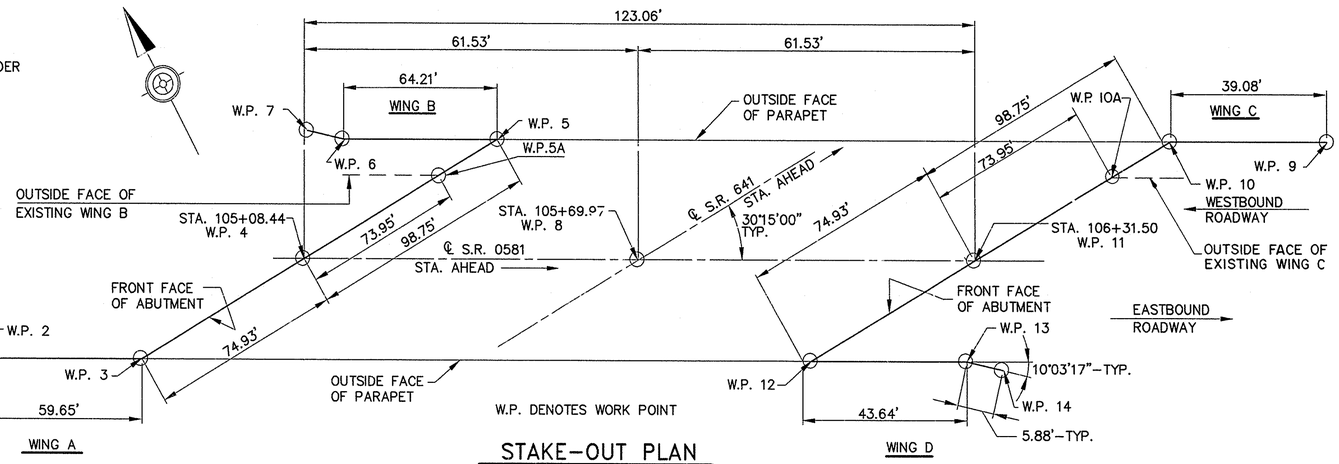

STAKE-OUT PLAN

SCALE: NONE

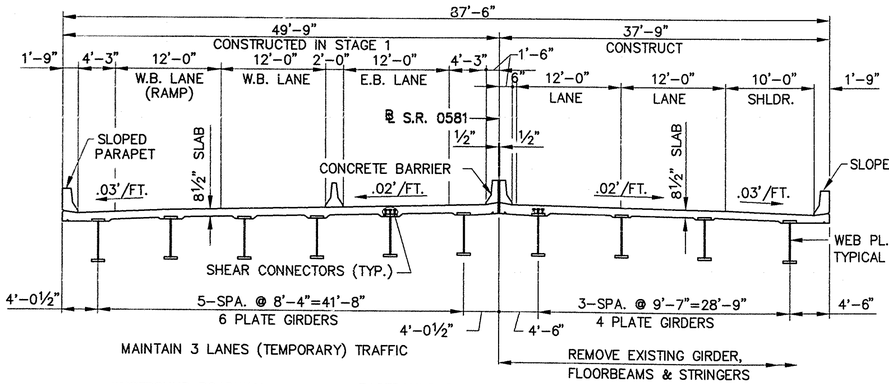

STAGE 2 CONSTRUCTION

TYPICAL DECK SECTIONS

SCALE: 1/8"=1'-0"

GENERAL CONSTRUCTION SEQUENCE

STAGE 1

1. INSTALL TEMPORARY BARRIERS AND DIVERT TRAFFIC TO SOUTH SIDE OF EXISTING BRIDGE.
2. REMOVE PORTION OF EXISTING DECK AS REQUIRED TO ALLOW SETTING TEMPORARY GIRDER IN PLACE.
3. CONSTRUCT PEDESTALS AND SET TEMPORARY GIRDER IN PLACE.
4. REMOVE BALANCE OF DECK ON NORTH SIDE OF BRIDGE.
* 5. ATTACH EXISTING FLOORBEAMS TO NEW TEMPORARY GIRDER.
6. CUT FLOORBEAMS AND REMOVE (NORTH SIDE) STRINGERS, FLOORBEAMS AND GIRDER.
7. CONSTRUCT NORTHERN HALF OF NEW BRIDGE.

STAGE 2

8. INSTALL TEMPORARY BARRIERS AND DIVERT TRAFFIC TO NORTH SIDE OF NEW BRIDGE.
9. REMOVE SOUTH HALF OF EXISTING BRIDGE.
10. CONSTRUCT SOUTHERN HALF OF NEW BRIDGE.

* DO NOT ATTACH EXISTING FLOORBEAMS TO TEMPORARY GIRDER UNTIL THE DECK SLAB & STRINGERS ON THE NORTH SIDE OF THE EXISTING BRIDGE HAS BEEN REMOVED.

Mark	Description	By	Chk'd.	App'd.	Date
REVISIONS					

Commonwealth of Pennsylvania
DEPARTMENT OF TRANSPORTATION
BUREAU OF DESIGN

CUMBERLAND COUNTY
S.R. 0581, SECTION A01
SEG. 0740 OFFSET 0000
S.R. 0581 STA. 105+69.97 OVER S.R. 641
SINGLE SPAN COMPOSITE STEEL MULTI GIRDER BRIDGE
REHABILITATION AND WIDENING

STAKE OUT PLAN AND DECK SECTIONS

RECOMMENDED MAY 13 1993

SHEET 3 OF 21

S-20590

DESIGNED: J.E.L. | DRAWN: R.J.C. | CHECKED: R.M.H.

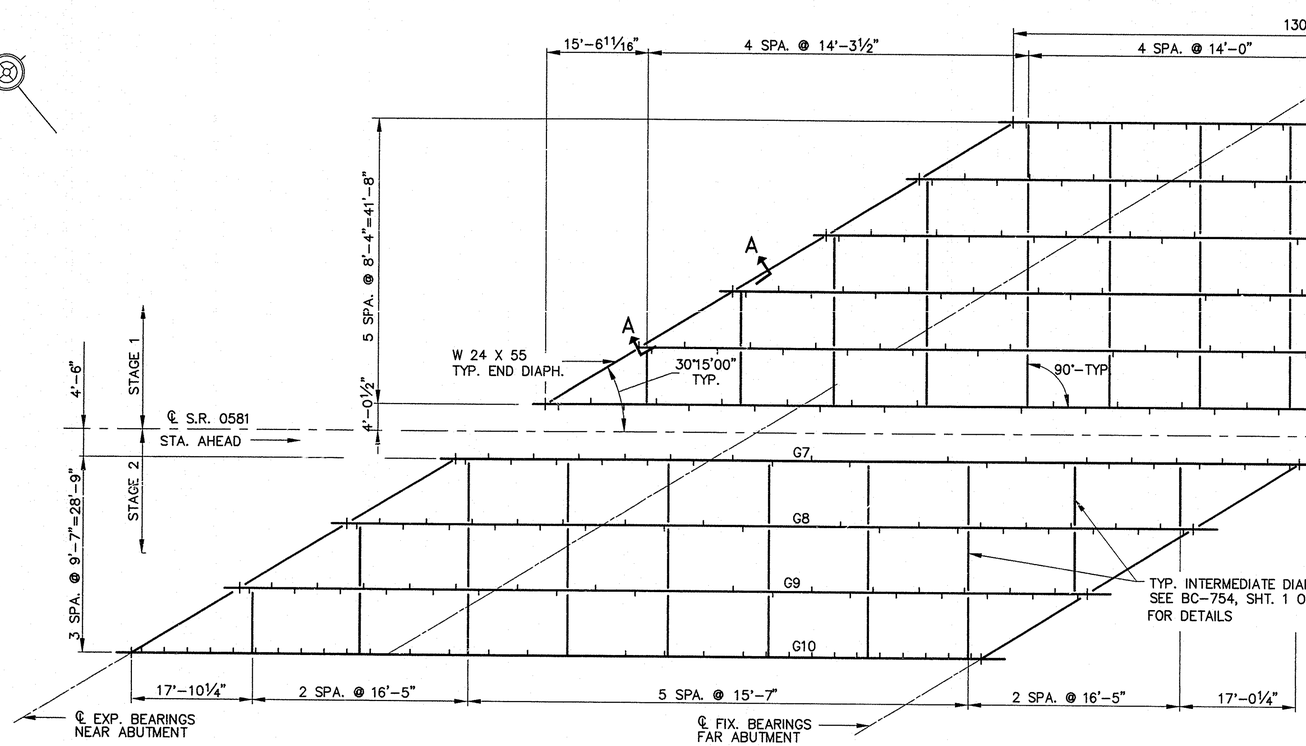

NEW FRAMING PLAN

SCALE: 3/32" = 1'-0"

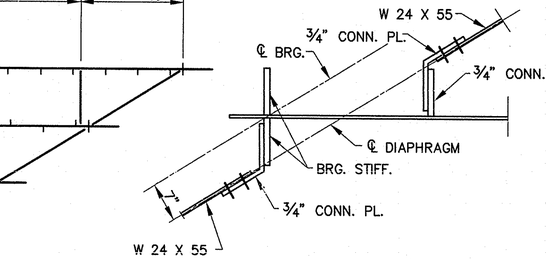

SECTION B-B

SCALE: 1" = 1'-0"

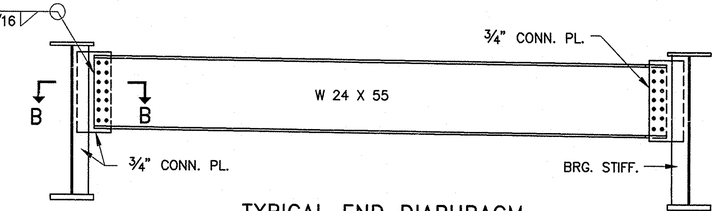

TYPICAL END DIAPHRAGM VIEW A-A

SCALE: 1/2" = 1'-0"

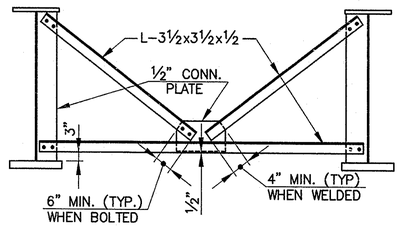

TYPICAL INTERMEDIATE DIAPHRAGM

SCALE: 1/2" = 1'-0"

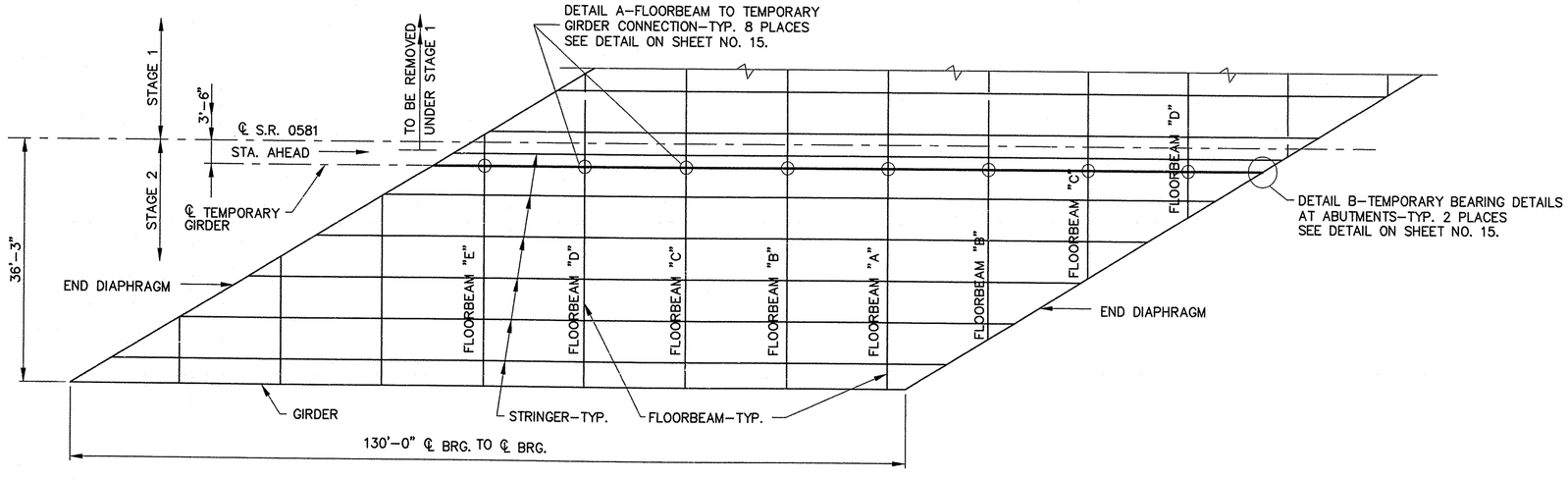

PARTIAL EXISTING FRAMING PLAN

SCALE: 3/32" = 1'-0"

- FOR GENERAL NOTES, SEE SHEET NO. 2.
- FOR ADDITIONAL DETAILS, SEE SHEET NO. 17 & 18.
- FOR DETAIL A, SEE SHEET NO. 15.
- FOR DETAIL B, SEE SHEET NO. 15.
- FOR ADDITIONAL DIAPHRAGM DETAILS, SEE BC-754.

Mark	Description	By	Chk'd.	App'd.	Date
REVISIONS					

Commonwealth of Pennsylvania
DEPARTMENT OF TRANSPORTATION
BUREAU OF DESIGN

CUMBERLAND COUNTY
S.R. 0581, SECTION A01
SEG. 0740 OFFSET 0000
S.R. 0581 STA. 105+69.97 OVER S.R. 641

SINGLE SPAN COMPOSITE STEEL MULTI GIRDER BRIDGE

FRAMING PLAN

RECOMMENDED MAY 13 1993

SHEET 16 OF 21

S-20590

DESIGNED: J.E.L.	DRAWN: R.J.C.	CHECKED: J.E.L.

DATE: 5/12/1993
DRAWING FILE:S2532FR

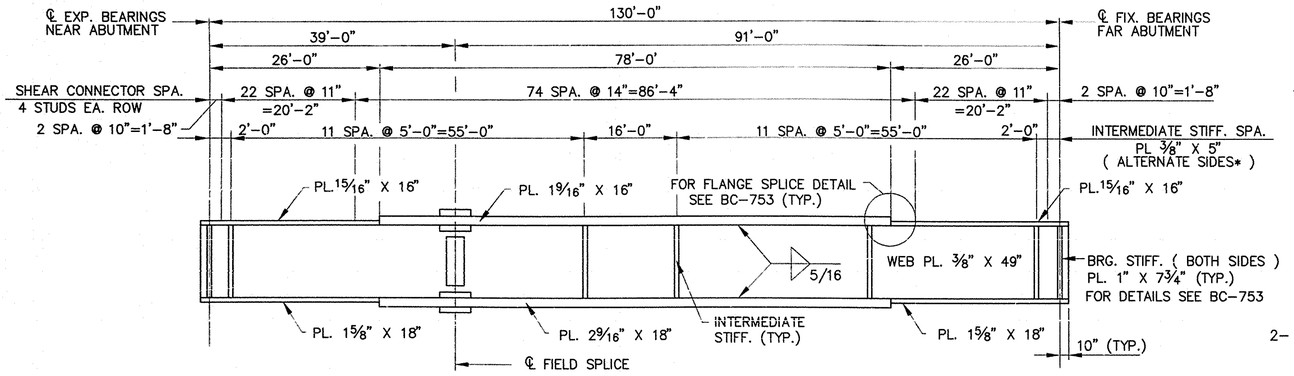

TYPICAL GIRDER ELEVATION–G1 TO G6

NOT TO SCALE

* PLACE ALL TRANSVERSE STIFFENERS ON INSIDE FACE OF FASCIA GIRDERS.

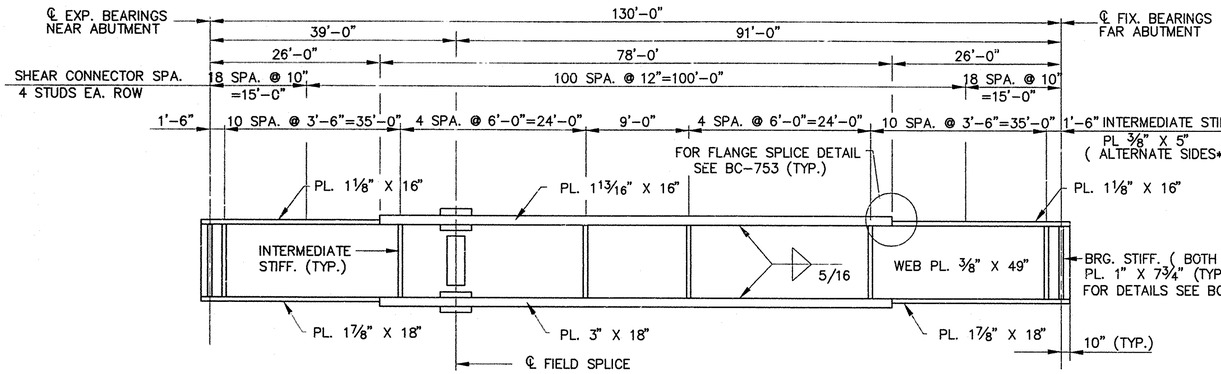

TYPICAL GIRDER ELEVATION–G7 TO G10

NOT TO SCALE

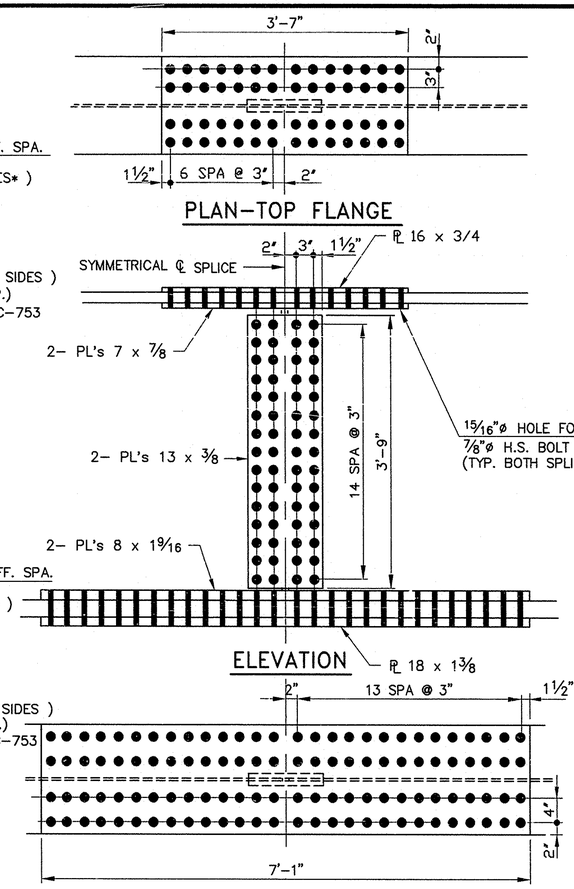

FIELD SPLICE–G7 TO G10

SCALE: 1"= 1'–0"

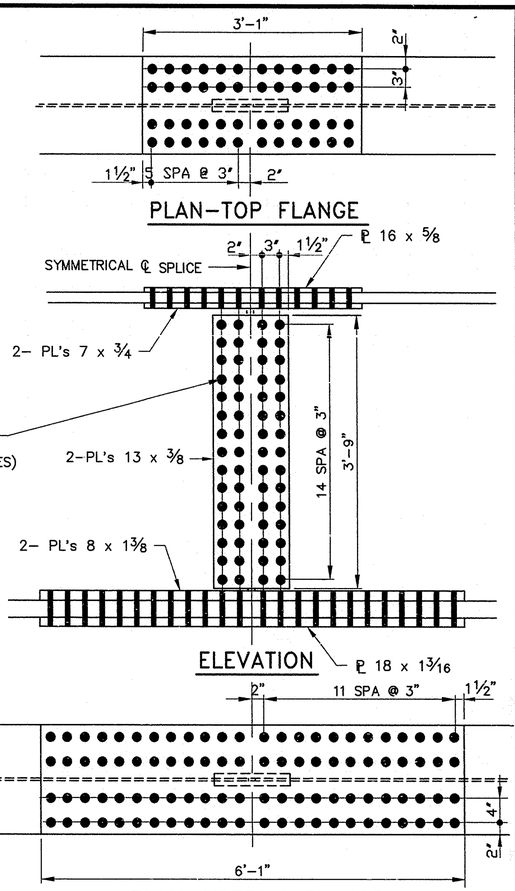

FIELD SPLICE–G1 TO G6

SCALE: 1"= 1'–0"

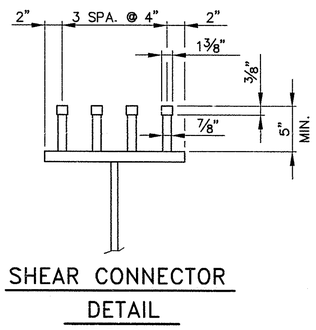

SHEAR CONNECTOR DETAIL

NOT TO SCALE

CAMBER (INCHES)

CAMBER DUE TO		POINT .1	.2	.3 & F.S.	.4	.5	.6	.7	.8	.9
STEEL	G1 TO G6	0.44	0.82	1.09	1.26	1.31	1.26	1.09	0.82	0.44
	G7 TO G10	0.43	0.80	1.07	1.23	1.28	1.23	1.07	0.80	0.43
CONCRETE	G1 TO G6	1.76	3.26	4.35	5.00	5.20	5.00	4.35	3.26	1.76
	G7 TO G10	1.72	3.19	4.25	4.89	5.08	4.89	4.25	3.19	1.72
SUPER. DEAD LOAD	G1 TO G6	0.17	0.32	0.43	0.50	0.52	0.50	0.43	0.32	0.17
	G7 TO G10	0.19	0.36	0.48	0.55	0.58	0.55	0.48	0.36	0.19
VERTICAL CURVE	G1 TO G6	0.59	1.04	1.37	1.56	1.63	1.56	1.37	1.04	0.59
	G7 TO G10	0.59	1.04	1.37	1.56	1.63	1.56	1.37	1.04	0.59
TOTAL	G1 TO G6	2.96	5.44	7.24	8.31	8.65	8.31	7.24	5.44	2.96
	G7 TO G10	2.93	5.39	7.17	8.23	8.56	8.23	7.17	5.39	2.93

- FOR GENERAL NOTES, SEE SHEET NO. 2.
- FOR ADDITIONAL DETAILS, SEE SHEET NO. 16 & 18.
- FOR ADDITIONAL DIAPHRAGM DETAILS, SEE BC–753.
- FOR SHEAR CONNECTOR DETAILS, SEE BC–753.
- GIRDER FLANGES, WEBS AND SPLICE PLATES ARE AASHTO M270–GRADE 50 (ASTM 2572).

Mark	Description	By	Chk'd.	App'd.	Date
REVISIONS					

Commonwealth of Pennsylvania
DEPARTMENT OF TRANSPORTATION
BUREAU OF DESIGN

CUMBERLAND COUNTY
S.R. 0581, SECTION A01
SEG. 0740 OFFSET 0000
S.R. 0581 STA. 105+69.97 OVER S.R. 641

SINGLE SPAN COMPOSITE STEEL MULTI GIRDER BRIDGE

GIRDER DETAILS

RECOMMENDED MAY 13 1993

SHEET 17 OF 21

S–20590

DESIGNED: J.E.L. | DRAWN: R.J.C. | CHECKED: J.E.L.

DATE: 5/5/1993
DRAWING FILE:S2532BM

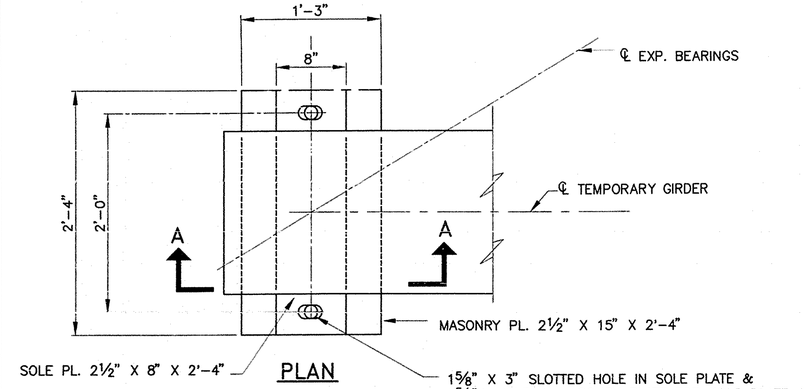

PLAN

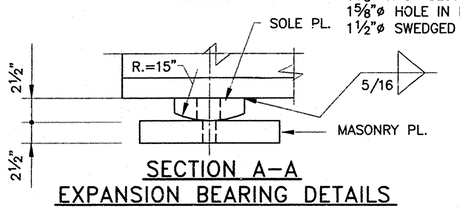

SECTION A–A
EXPANSION BEARING DETAILS

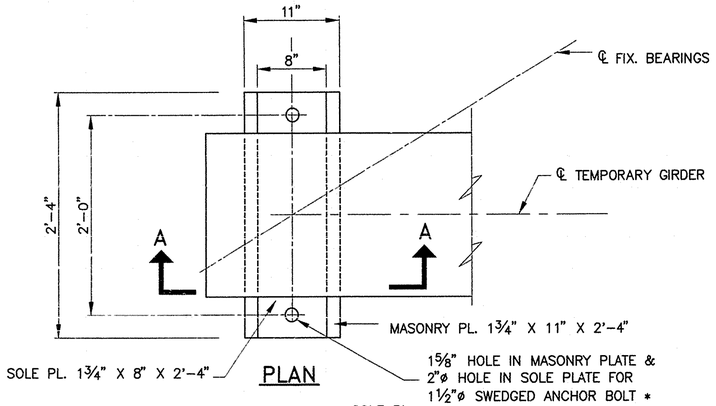

PLAN

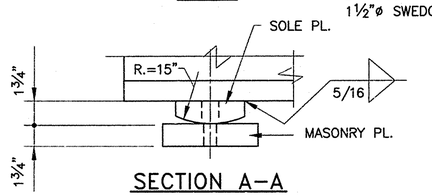

SECTION A–A
FIXED BEARING DETAILS

TEMPORARY GIRDER BEARING DETAILS

SCALE: 1½"= 1'-0"

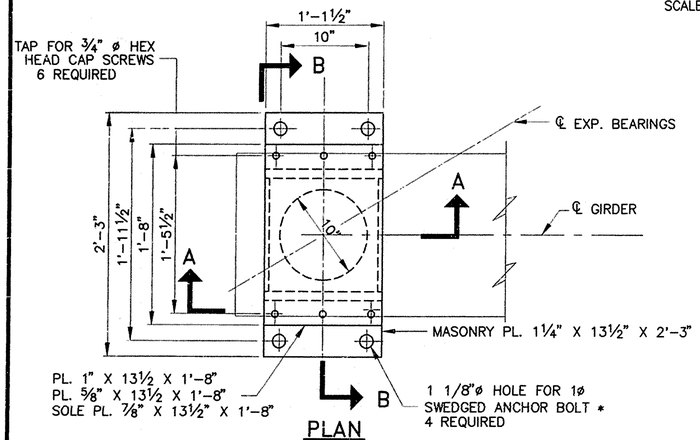

PLAN

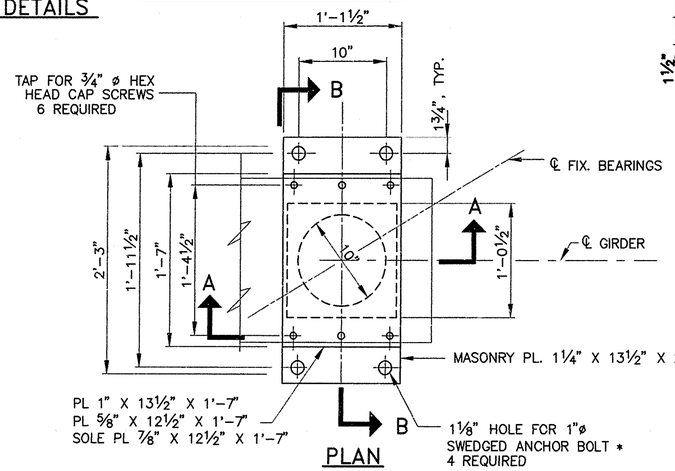

PLAN

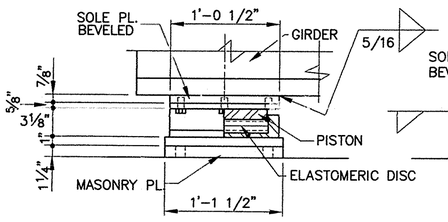

SECTION A–A

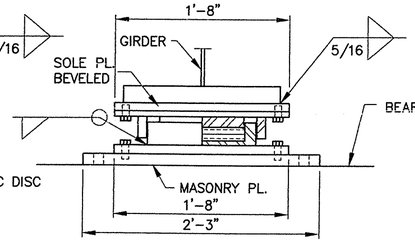

SECTION B–B

EXPANSION BEARING DETAILS

SCALE: 1½"= 1'-0"

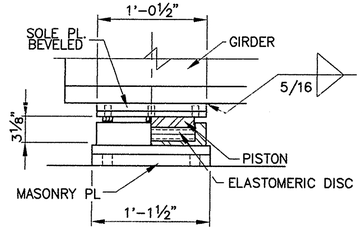

SECTION A–A

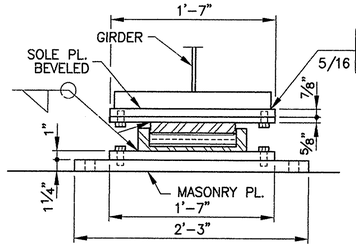

SECTION B–B

FIXED BEARING DETAILS

SCALE: 1½"= 1'-0"

SPHERICAL BEARINGS

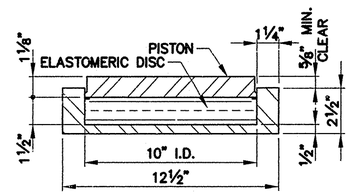

POT DETAIL

SCALE: 3"= 1'-0"

BEARING SCHEDULE

	G7–G10	G1–G6
MAXIMUM VERTICAL LOAD	257 KIPS	276 KIPS
MINIMUM VERTICAL LOAD	84 KIPS	49 KIPS
HORIZONTAL LOADS:		
GROUP I	0.0 KIPS	0.0 KIPS
GROUP II	32.1 KIPS	32.1 KIPS
GROUP III	26.8 KIPS	30.5 KIPS
GROUP IV	9.4 KIPS	12.2 KIPS
GROUP V	37.1 KIPS	38.9 KIPS
GROUP VI	34.9 KIPS	41.5 KIPS
GROUP VII	101.1 KIPS	135.3 KIPS
MINIMUM DESIGN ROTATIONS: (RADIANS)	0.045	0.045
ANTICIPATED MOVEMENTS:		
LONGITUDINAL	1.22 INCHES	1.22 INCHES
TRANSVERSE	0 INCHES	0 INCHES
NUMBER OF BEARINGS:		
FIXED	4 EACH	6 EACH
GUIDED EXPANSION	4 EACH	6 EACH
ALLOWABLE STEEL PLATE PRESSURE	29 KSI	29 KSI
ALLOWABLE CONCRETE PRESSURE	0.9 KSI	0.9 KSI
ANCHORAGE REQUIREMENTS	SEE CONTRACT DRAWINGS	
GRADES, BEVELS & SLOPES	SEE SEPARATE TABLE	
ALLOWABLE COEFFICIENT OF FRICTION OF SLIDE SURFACES	0.08	0.08

PAINT ALL EXPOSED STRUCTURAL STEEL PLATES WITH THE SAME PAINT SYSTEM AS THE MAIN BRIDGE MEMBERS.

		NEAR ABUT.	FAR ABUT.
BEVELS FOR SOLE PLATES POT BEARINGS	G1	0.00	–0.01
	G2	0.00	–0.01
	G3	0.00	–0.01
	G4	0.00	–0.01
	G5	0.00	–0.01
	G6	0.00	–0.01
	G7	0.00	0.00
	G8	0.00	0.00
	G9	0.01	0.00
	G10	0.01	0.00

+ BEVEL=UPWARD, LOOKING AHEAD STATION
– BEVEL=DOWWARD, LOOKING AHEAD STATION
THICKNESS OF SOLE PLATE WILL BE ¾" AT ℄ BEARINGS

• FOR GENERAL NOTES, SEE SHEET NO. 2.
* SWEDGED ANCHOR BOLTS WILL BE EMBEDED 1'–4" INTO CONCRETE. BOLTS WILL HAVE 1–HEAVY HEX HEAD NUT & PLATE WASHER.

Mark	Description	By	Chk'd.	App'd.	Date

REVISIONS

Commonwealth of Pennsylvania
DEPARTMENT OF TRANSPORTATION
BUREAU OF DESIGN

CUMBERLAND COUNTY
S.R. 0581, SECTION A01
SEG. 0740 OFFSET 0000
S.R. 0581 STA. 105+69.97 OVER S.R. 641
SINGLE SPAN COMPOSITE STEEL MULTI GIRDER BRIDGE
BEARINGS

RECOMMENDED MAY 13 1993

SHEET 18 OF 21

S– 20590

DESIGNED: J.E.L. | DRAWN: R.J.C. | CHECKED: J.E.L.

DRAWING FILE: S2532BRG

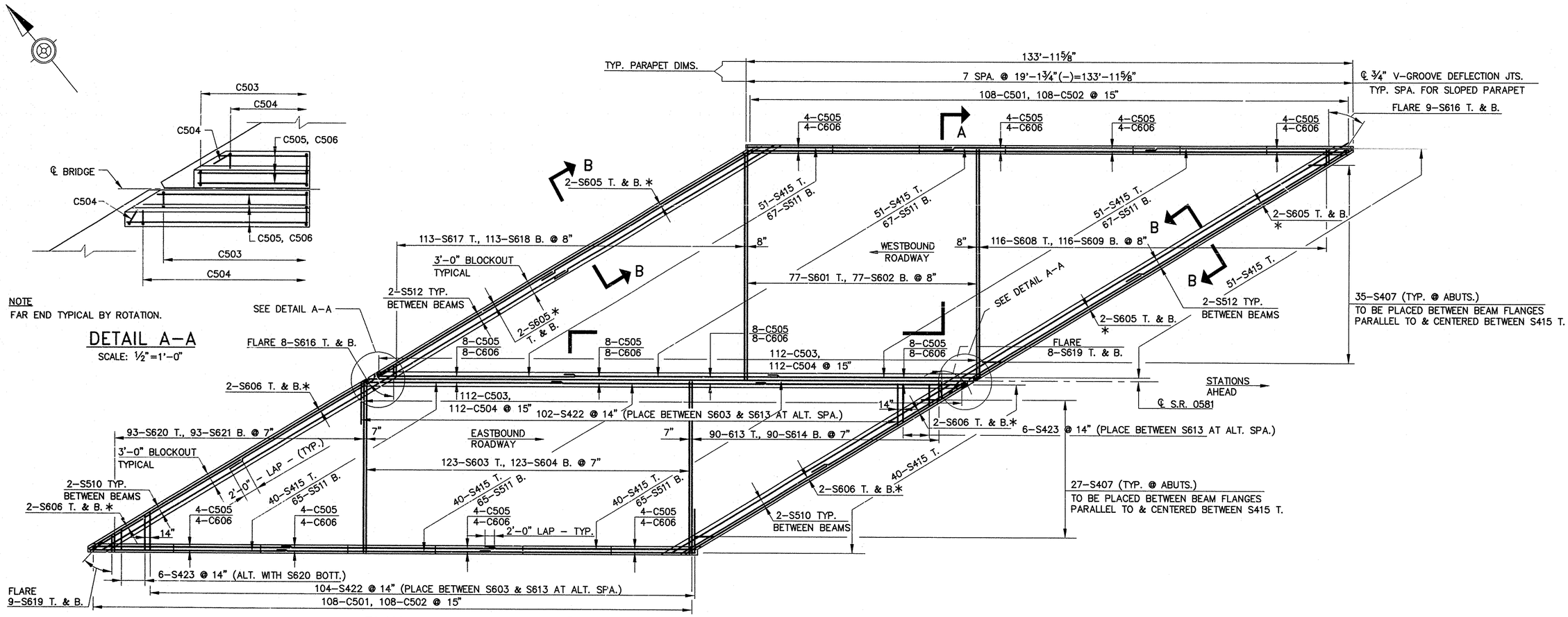

NOTE
FAR END TYPICAL BY ROTATION.

DETAIL A-A
SCALE: ½"=1'-0"

PLAN
SCALE: 3/32"= 1'-0"

* TIE TO TOP & BOTTOM STUDS-TYP.

DECK ELEVATIONS - E.B. LANES

STATION	GUTTER 0'-6" LEFT	PROFILE GRADE	EDGE OF LANE 24' RIGHT	GUTTER 34'-0" RIGHT
104+50	437.36	437.35	436.87	436.57
104+60	437.42	437.41	436.93	436.63
104+70	437.48	437.47	436.99	436.69
104+80	437.54	437.53	437.05	436.75
104+90	437.59	437.58	437.10	436.80
105+00	437.63	437.62	437.14	436.84
105+10	437.66	437.65	437.17	436.87
105+20	437.69	437.68	437.20	436.90
105+30	437.71	437.70	437.22	436.92
105+40	437.73	437.72	437.24	436.94
105+50	437.74	437.73	437.25	436.95
105+60	437.74	437.73	437.25	436.95
105+70	437.74	437.73	437.25	436.95
105+80	437.73	437.71	437.23	436.93
105+90	437.71	437.70	437.22	436.92

DECK ELEVATIONS - W.B. LANES

STATION	GUTTER 46' LEFT	EDGE OF LANE 36' LEFT	PROFILE GRADE	GUTTER 0'-6" RIGHT
105+20	436.66	436.96	437.68	437.69
105+30	436.68	436.98	437.70	437.71
105+40	436.70	437.00	437.72	437.73
105+50	436.71	437.01	437.73	437.74
105+60	436.71	437.01	437.73	437.74
105+70	436.71	437.01	437.73	437.74
105+80	436.70	436.99	437.71	437.73
105+90	436.68	436.98	437.70	437.71
106+00	436.66	436.96	437.68	437.69
106+10	436.63	436.93	437.65	437.66
106+20	436.59	436.89	437.61	437.62
106+30	436.55	436.85	437.57	437.58
106+40	436.50	436.80	437.52	437.53
106+50	436.44	436.74	437.46	437.47
106+60	436.38	436.68	437.40	437.41
106+70	436.31	436.61	437.33	437.34
106+80	436.24	436.54	437.26	437.27
106+90	436.16	436.46	437.18	437.19
107+00	436.07	436.37	437.09	437.10
107+10	435.98	436.28	437.00	437.01

(1) FOR REVISED DECK ELEVATION TABLES SEE SHEETS 8 AND 13.

NOTES:
- FOR GENERAL NOTES, SEE SHEET NO. 2.
- FOR SECTION A-A, SEE SHEET NO. 20.
- FOR SECTION B-B , SEE SHEET NO. 20.
- FOR REINFORCING BAR SCHEDULE, SEE SHEET NO. 20.
- REINFORCING BARS AT ABUTMENTS TYPICAL .

Mark	Description	By	Chk'd.	App'd.	Date
1	CHANGE IN ELEVATION	G.B.B	R E M	RHK	3-2-94

REVISIONS

Commonwealth of Pennsylvania
DEPARTMENT OF TRANSPORTATION
BUREAU OF DESIGN

CUMBERLAND COUNTY
S.R. 0581, SECTION A01
SEG. 0740 OFFSET 0000
S.R. 0581 STA. 105+69.97 OVER S.R. 641

SINGLE SPAN COMPOSITE STEEL MULTI GIRDER BRIDGE

DECK SLAB PLAN

RECOMMENDED _____

SHEET 19 OF 21

S-20590

DESIGNED: J.E.L. | DRAWN: R.J.C. | CHECKED: J.E.L.

DATE: 5/14/1993
DRAWING FILE:S2532DS

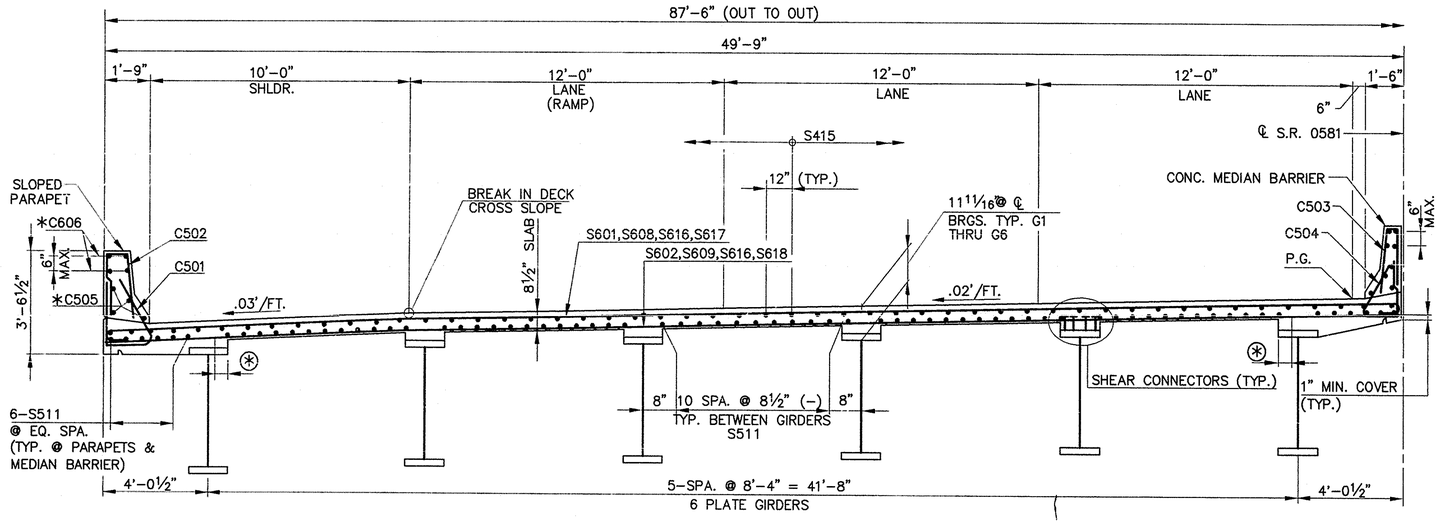

* REBARS SHOWN ARE TYPICAL FOR SLOPED PARAPET AND BARRIER.

⊛ EXTEND ALTERNATE BOTTOM BARS (S602, S604) A MIMUMUM OF 6" OVER FLANGE OF THE FASCIA BEAM,

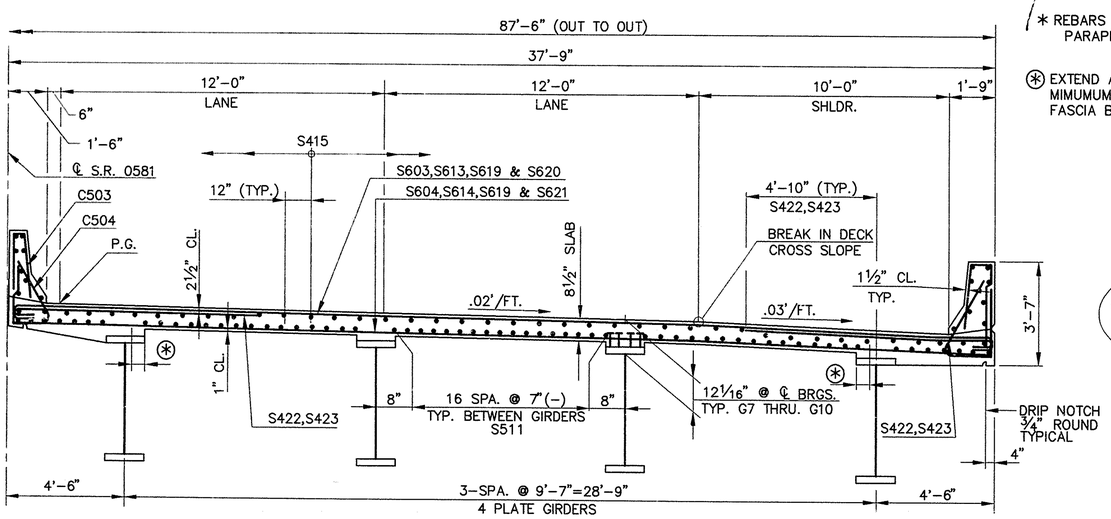

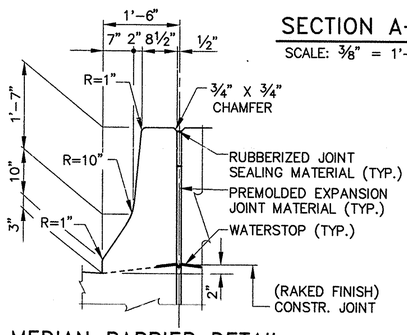

SECTION A-A
SCALE: ⅜" = 1'-0"

MEDIAN BARRIER DETAIL
SCALE: ¾"=1'-0"

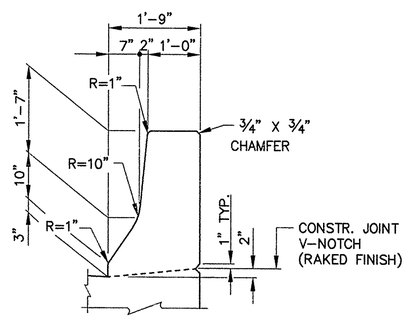

SLOPED PARAPET DETAIL
SCALE: ¾"=1'-0"

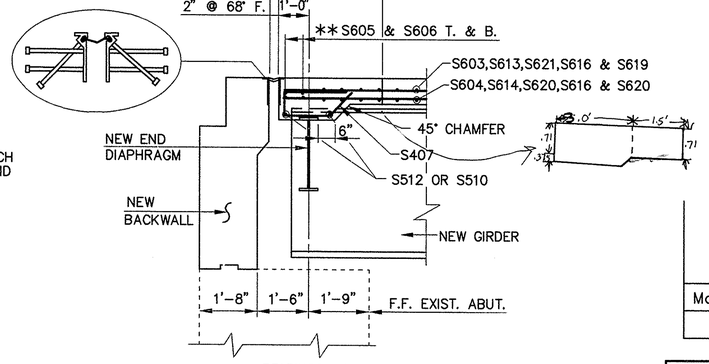

BEARINGS NOT SHOWN
HORIZONTAL DIMENSIONS SHOWN ARE NORMAL TO ℄ BRG.
** TIE TO TOP & BOTTOM STUDS - (TYP.)

SECTION B-B
SCALE: ½"=1'-0"

REINFORCING BAR SCHEDULE

MARK	SIZE	LENGTH	NO.	TYPE	A	B	C	D	REMARKS
S601	6	50'-9"	77	4	8"	49'-5"			
S602	6	45'-6"	77	STR.					
S603	6	38'-9"	123	4	8"	37'-5"			
S604	6	33'-1"	123	STR.					
S605	6	50'-6"	16	STR.					
S606	6	37'-6"	16	STR.					
S407	4	4'-9"	124	1	9"	1'-4"	11"	1'-9"	K=6"
S608	6	5'-5⅛" TO 49'-9"	116	5	8"	4'-9⅛" TO 49'-1"			1 EA., VARY BY 4⅝"
S609	6	4'-9⅛" TO 49'-1"	116	STR					1 EA., VARY BY 4⅝"
S510	5	18'-4"	12	STR.					
S511	5	46'-0"	396	STR.					
S512	5	15'-10"	20	STR.					
S613	6	6'-0½" TO 36'-8"	90	5	8"	5'-4½" TO 36'-0"			1 EA., VARY BY 4⅛"
S614	6	5'-4½" TO 36'-0"	90	STR					1 EA., VARY BY 4⅛"
S415	4	34'-9"	364	STR.					
S616	6	4'-5"	34	STR.					
S617	6	5'-6" TO 48'-8"	113	5	8"	4'-10" TO 48'-0"			1 EA., VARY BY 4⅝"
S618	6	4'-10" TO 48'-0"	113	STR.					1 EA., VARY BY 4⅝"
S619	6	5'-0"	34	STR.					
S620	6	6'-1½" TO 37'-9"	94	5	8"	5'-5½" TO 37'-1"			1 EA., VARY BY 4⅛"
S621	6	5'-5½" TO 37'-1"	94	STR.					1 EA., VARY BY 4⅛"
S422	4	9'-8"	206	5	6"	9'-2"			
S423	4	5'-6¾" TO 9'-0"	12	5	6"	5'-0¾" TO 8'-6"			2 EA., VARY BY 8¼"
C501	5	7'-0"	216	27	2'-6"	1'-4"	7½"	2'-6½"	K=1'-2", R=3"
C502	5	5'-5"	216	7	2'-3½"	9"	2'-4½"		K=3"
C503	5	5'-2"	224	7	2'-3½"	6"	2'-4½"		K=3"
C504	5	6'-9"	224	27	2'-6"	1'-1"	7½"	2'-6½"	K=1'-2", R=3"
C505	5	34'-7"	64	STR.					
C606	6	35'-0"	64	STR.					

NOTE:
- REINFORCEMENT BAR SCHEDULE FOR INFORMATION ONLY VERIFY PRIOR TO BIDDING OR FABRICATION.
- ALL BARS WILL BE EPOXY COATED.

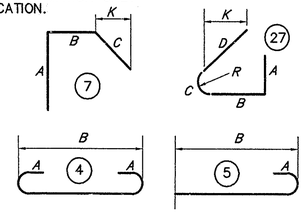

NOTES
- FOR GENERAL NOTES, SEE SHEET NO. 2.
- FOR NEOPRENE STRIP SEAL DAM DETAILS, SEE BC-767.
- FOR MODIFIED DEFLECTION JOINT DETAILS IN PARAPET, SEE BC-752.
- FOR PERMANENT METAL DECK FORM DETAILS, SEE BC-732.
- FOR LOCATION OF SECTION A-A, & B-B SEE SHEET NO. 19.
- FOR WATERSTOP AND JOINT SEALING MATERIALS IN MEDIAN BARRIER SEE BC-738.

Mark	Description	By	Chk'd.	App'd.	Date
REVISIONS					

Commonwealth of Pennsylvania
DEPARTMENT OF TRANSPORTATION
BUREAU OF DESIGN

CUMBERLAND COUNTY
S.R. 0581, SECTION A01
SEG. 0740 OFFSET 0000
S.R. 0581 STA. 105+69.97 OVER S.R. 641
SINGLE SPAN COMPOSITE STEEL MULTI GIRDER BRIDGE

SUPERSTRUCTURE DETAILS

RECOMMENDED _____

SHEET 20 OF 21

S-20590

DESIGNED: J.E.L.	DRAWN: R.J.C.	CHECKED: J.E.L.

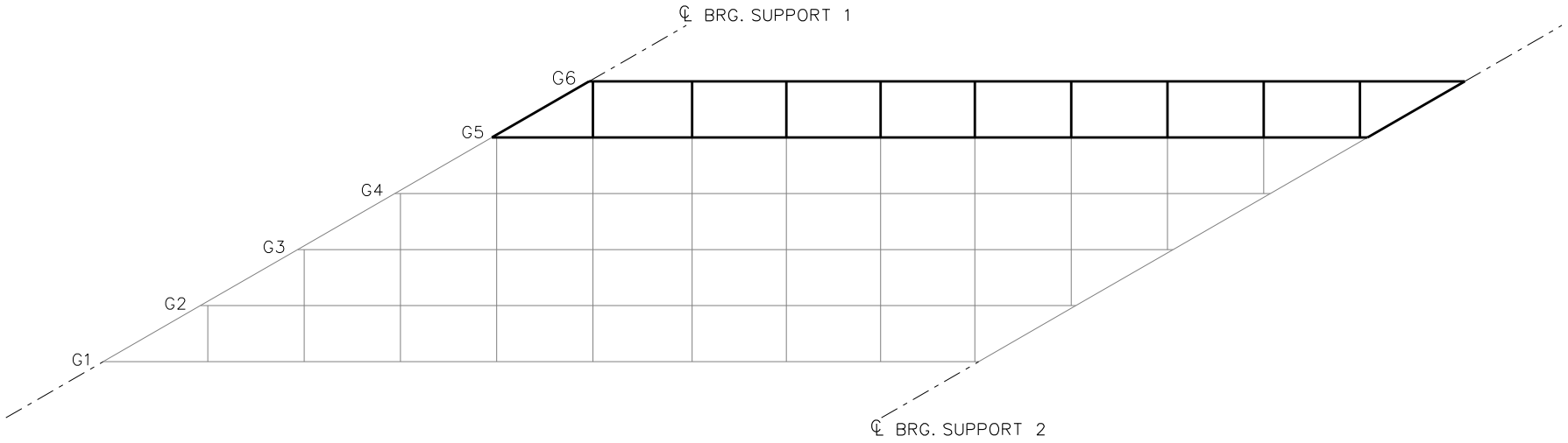

STAGE 1

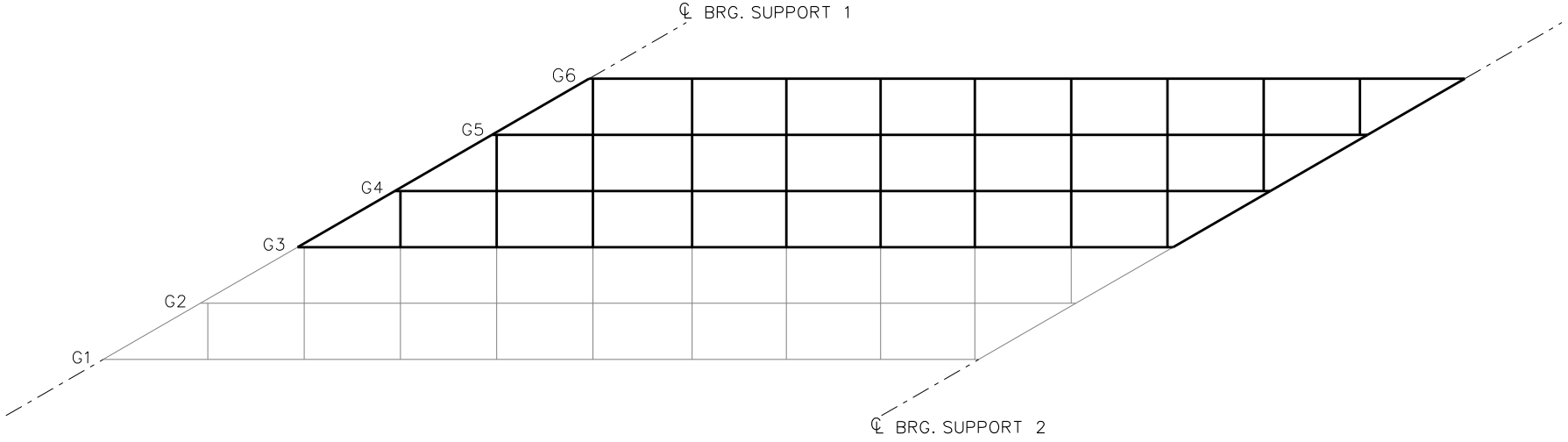

STAGE 2

LEGEND

▽ = HOLD OR LIFT CRANE

○ = TIE DOWN

□ = TEMPORARY SUPPORT STRUCTURE

NCHRP 12-79

BRIDGE EISSS5

GENERAL ERECTION PROCEDURE

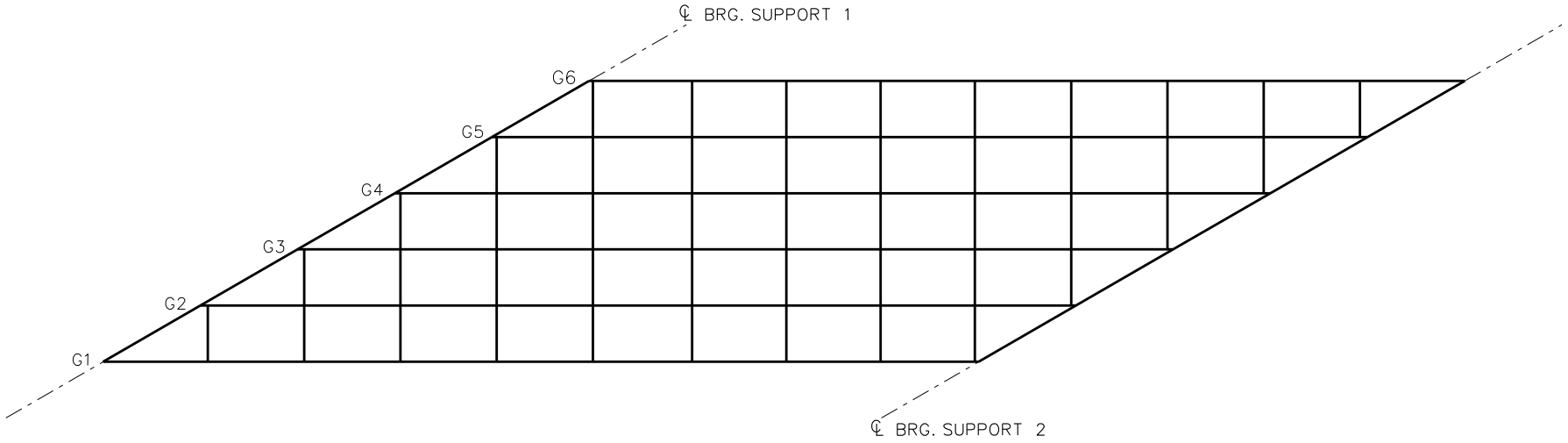

STAGE 3

LEGEND

▽ = HOLD OR LIFT CRANE

○ = TIE DOWN

□ = TEMPORARY SUPPORT STRUCTURE

NCHRP 12-79

BRIDGE EISSS5

GENERAL ERECTION PROCEDURE

SHEET 2 OF 2

NCHRP 12-79

ETCCR14

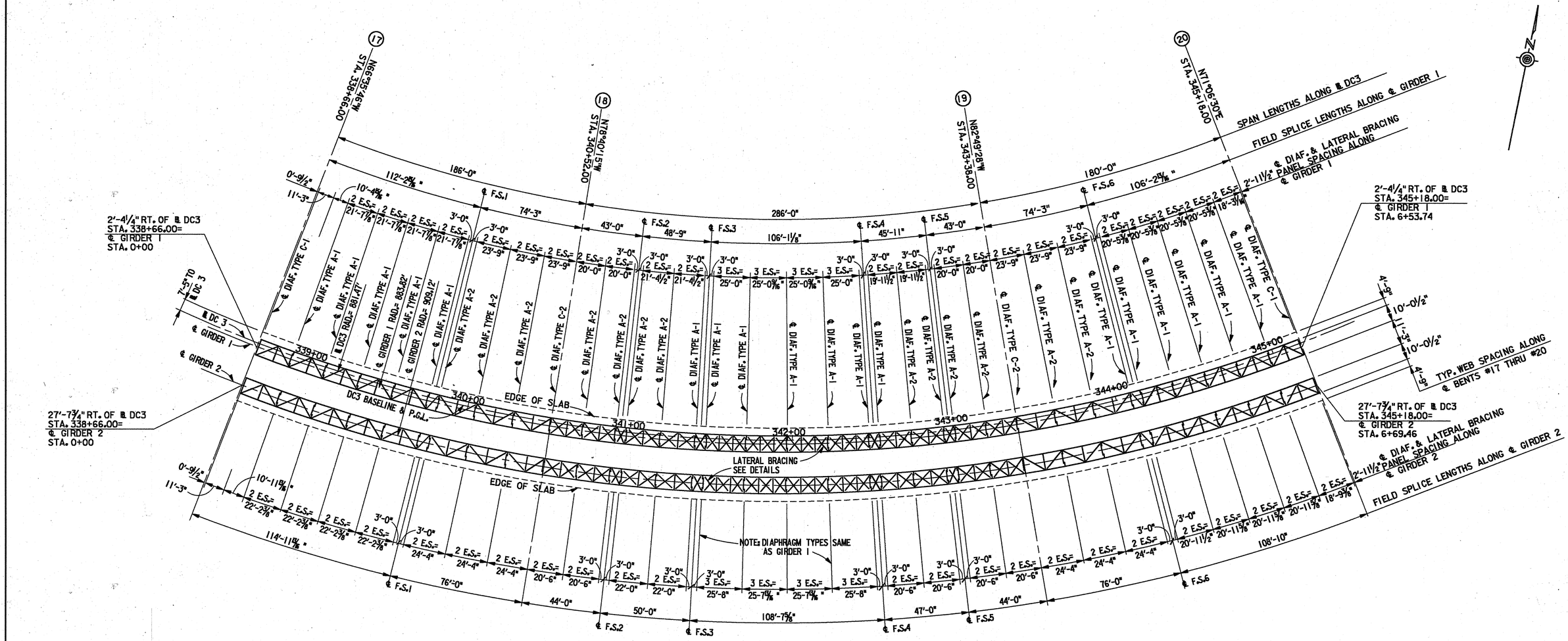

FRAMING PLAN DC3 UNIT D GIRDERS 1 & 2

1"=30'-0"

ESTIMATED QUANTITIES UNIT D		
STRUCTURAL STEEL (HS)	LBS.	1,261,536
STRUCTURAL STEEL (HYC)	LBS.	168,086

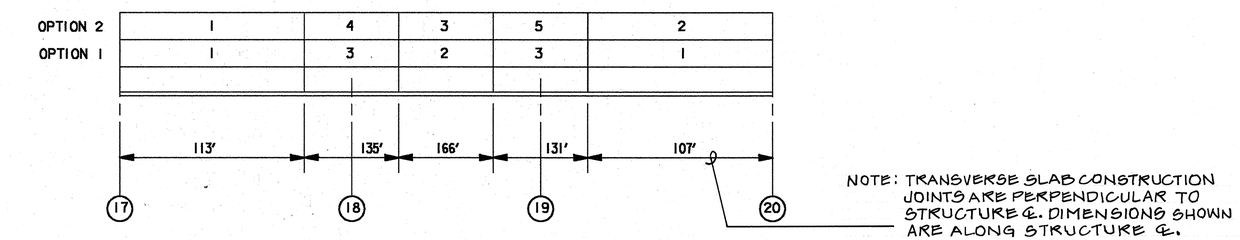

SLAB POUR SEQUENCE DIAGRAM

NOTE: TRANSVERSE SLAB CONSTRUCTION JOINTS ARE PERPENDICULAR TO STRUCTURE ℄. DIMENSIONS SHOWN ARE ALONG STRUCTURE ℄.

REVISED 1-15-93

STATE OF TEXAS
WALLY R. BURNS
44162
REGISTERED PROFESSIONAL ENGINEER
11/5/92

ALTERNATE DESIGN STEEL GIRDER FRAMING PLAN

FED. RD. DIV. NO.	STATE	FEDERAL PROJECT NO.				SHEET NO.
6	TEXAS	NH93 (14)				1559
STATE DIST. NO.	COUNTY	CONT.	SECT.	JOB		HWY. NO.
12	HARRIS	0110	06	102		IH 45

Design Filename: /usr/projhctra/407/bx43fp01.dgn
Plotted on: 04-DEC-1992

AD-76-0

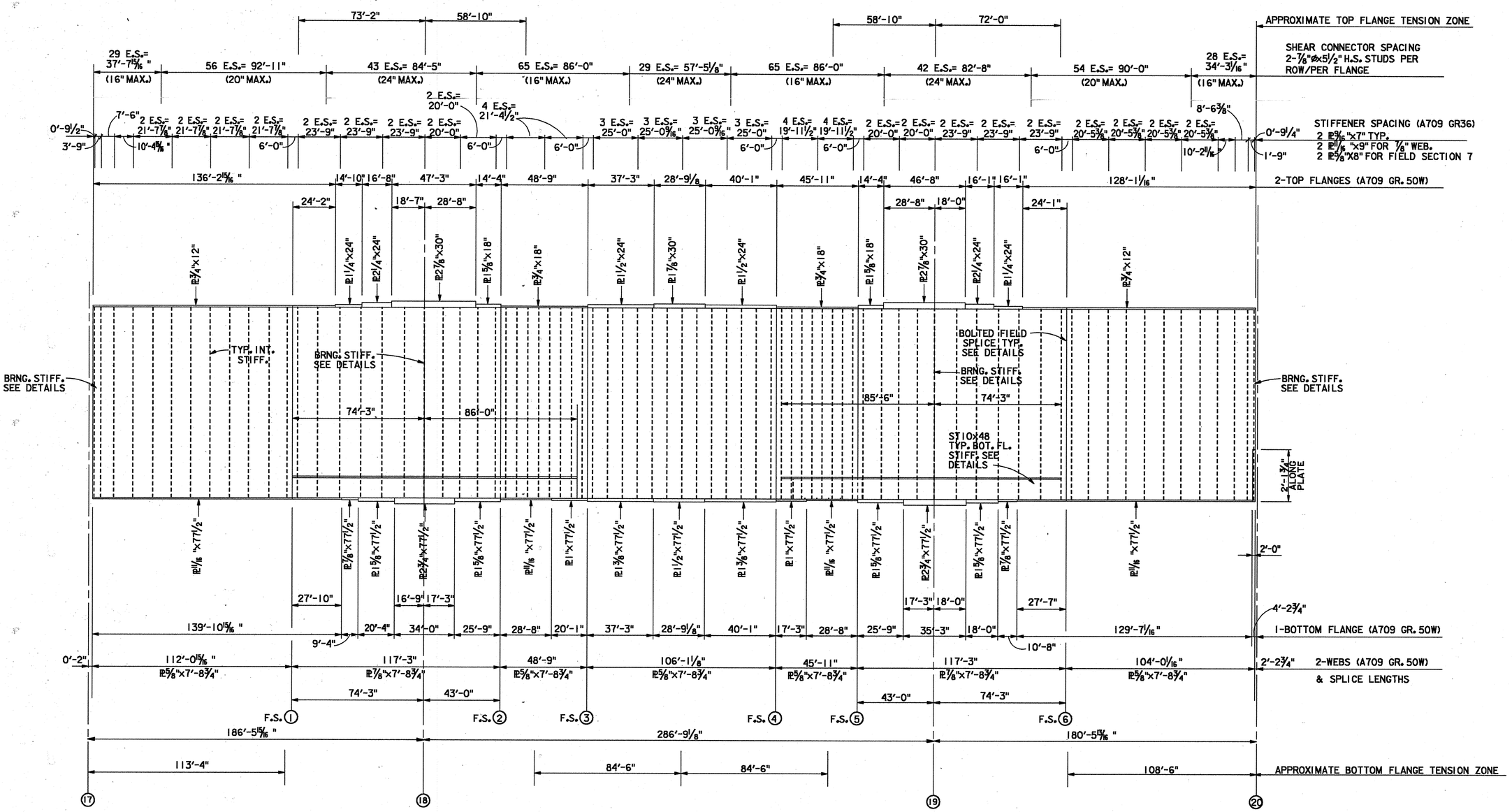

GIRDER ELEVATION DC3 UNIT D GIRDER 1

SCALE: 1"=30'-0" HORIZ.
1/2"=1'-0" VERT.

NOTE:
1. ALL DIMENSIONS ALONG ℄ OF GIRDER.
2. PROTIONS OF TOP AND BOTTOM FLANGES AND ADJACENT HALF OF WEB IN TENSION ZONE ARE FRACTURE CRITICAL
3. OPTIONAL SHOP SPLICES SHALL NOT BE LOCATED WITHIN 12 FT. EITHER SIDE OF INTERIOR BEARINGS, WITHIN 18 FT. EITHER SIDE OF ℄ OF INTERIOR SPAN NOR WITHIN A ZONE STARTING A DISTANCE OF 60FT. AND EXTENDING TO 118 FT. MEASURED FROM THE END BEARINGS OF EXTERIOR SPANS.

STATE OF TEXAS
WALLY R. BURNS
44162
REGISTERED PROFESSIONAL ENGINEER
11/3/92

REVISED 1-15-93 REVISED 1-6-93

ALTERNATE DESIGN STEEL GIRDER ELEVATION

FED. RD. DIV. NO.	STATE	FEDERAL PROJECT NO.				SHEET NO.
6	TEXAS	NH 93 (14)				1561
STATE DIST. NO.	COUNTY	CONT.	SECT.	JOB	HWY. NO.	
12	HARRIS	0110	06	102	IH 45	

Design Filename: /hou2/hctra/407dc3/tx43sg07.dgn
Plotted on: 04-DEC-1992

AD-76-0

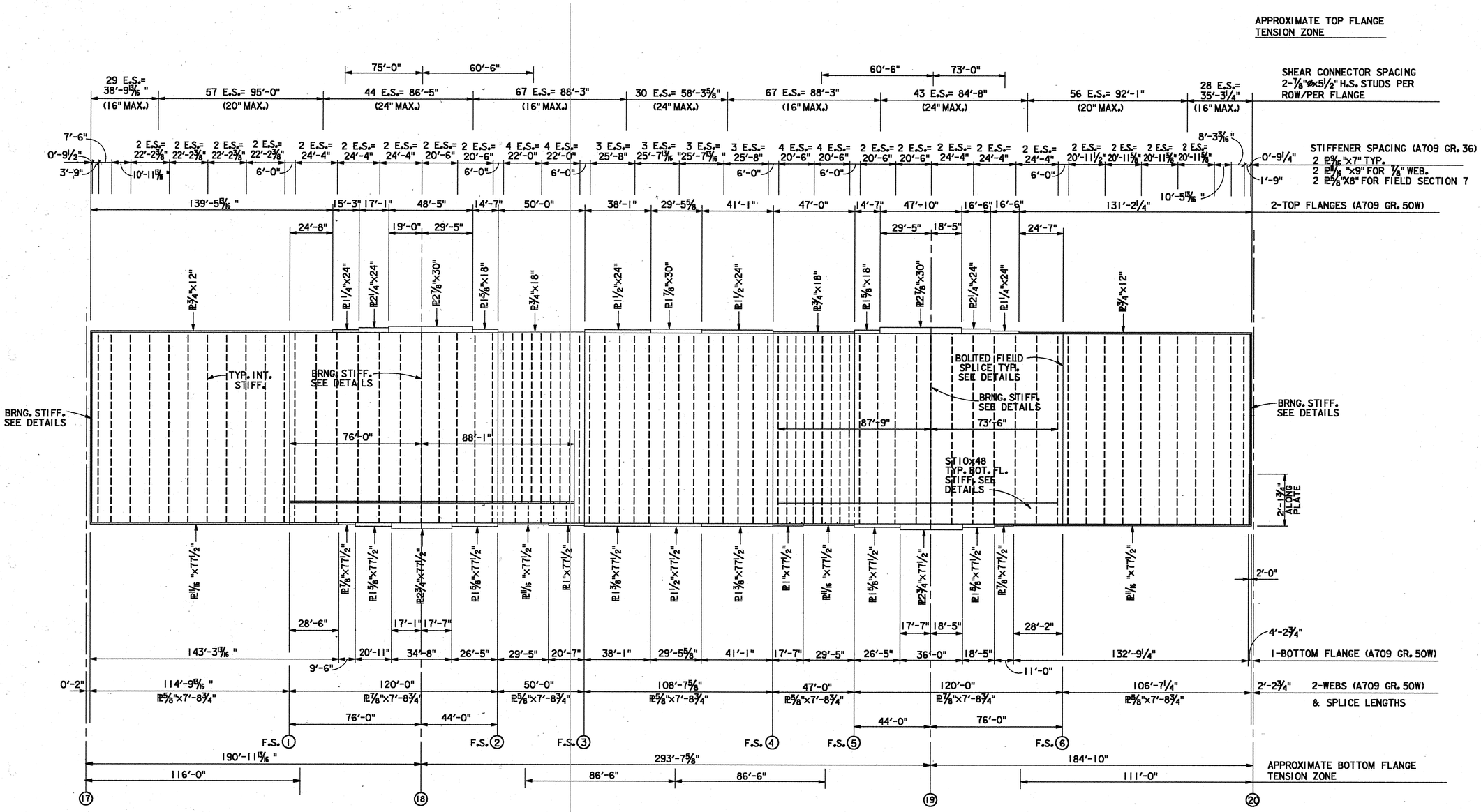

NOTE: ALL DIMENSIONS ALONG ℄ OF GIRDER.

GIRDER ELEVATION DC3 UNIT D GIRDER 2

SCALE: 1"=30'-0" HORIZ.
1/2"=1'-0" VERT.

NOTES:

1. ALL DIMENSIONS ARE ALONG ℄ GIRDER.
2. PORTIONS OF TOP AND BOTTOM FLANGES AND ADJACENT HALF OF WEB IN TENSION ZONE ARE FRACTURE CRITICAL.
3. OPTIONAL SHOP SPLICES SHALL NOT BE LOCATED WITHIN 12 FT. EITHER SIDE OF INTERIOR BEARINGS, WITHIN 18 FT. EITHER SIDE OF ℄ OF INTERIOR SPAN NOR WITHIN A ZONE STARTING A DISTANCE OF 60FT. AND EXTENDING TO 118 FT. MEASURED FROM THE END BEARINGS OF EXTERIOR SPANS.

STATE OF TEXAS
WALLY R. BURNS
44162
REGISTERED PROFESSIONAL ENGINEER
11/9/92

REVISED 1-15-93 REVISED 1-6-93

ALTERNATE DESIGN STEEL GIRDER ELEVATION

FED. RD. DIV. NO.	STATE	FEDERAL PROJECT NO.				SHEET NO.
6	TEXAS	NH 93 (14)				1561A
STATE DIST. NO.	COUNTY	CONT.	SECT.	JOB		HWY. NO.
12	HARRIS	0110	06	102		IH 45

Design Filename: /hou2/hctra/407dc3/6x43sg06.dgn
Plotted on: 04-DEC-1992

AD-76-0

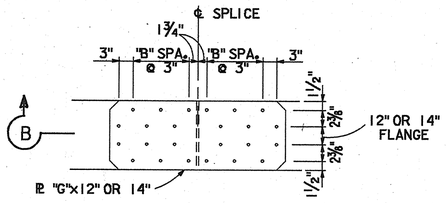

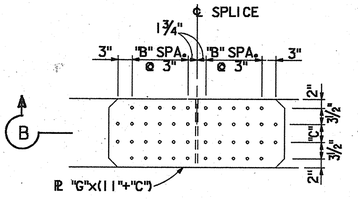

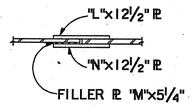

SECTION B-B

1½" = 1'-0"

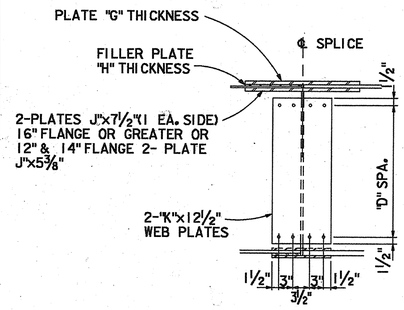

WEB SPLICE
TYPE A (TYP)

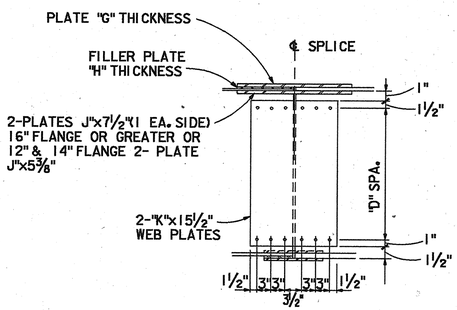

WEB SPLICE
TYPE B

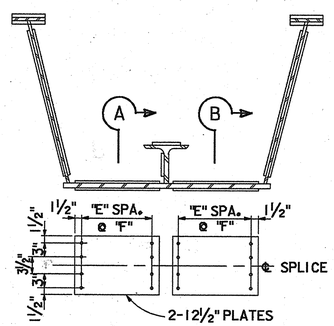

BOTTOM FLANGE SPLICE
TYPE A (TYP)

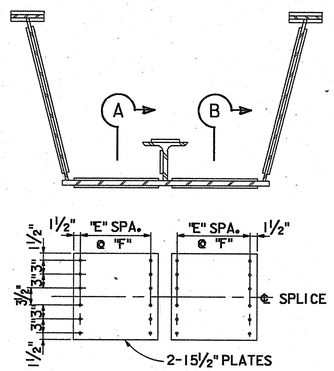

BOTTOM FLANGE SPLICE
TYPE B

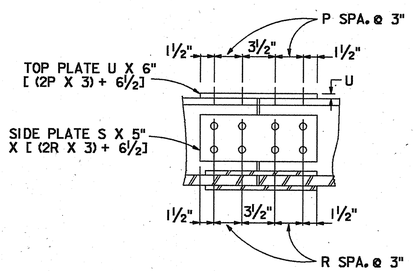

SECTION A-A

1½" = 1'-0"

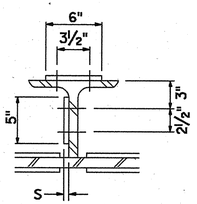

NOTE: ALL BOLT HOLES SHALL BE 15/16" ø FOR ¾" ø ASTM A325 BOLTS

DC3 SPLICE TABLE

UNIT	SPLICE	BOLT SPACING					PLATE THICKNESS							LONGITUDINAL STIFFENER			
		TOP		WEB	BOTTOM		TOP FLANGE			WEB	BOTTOM FLANGE			TOP PLATE		SIDE PLATE	
		B	C	D	E	F	G	H	J	K	L	M	N	BOLT SPACING P	PLATE THICKNESS U	BOLT SPACING R	PLATE THICKNESS S
A	1 & 4	2	-	20*	10	3½	¾	⅞	9/16	½	7/16	0	7/16	3	5/8	3	5/8
	2 & 3	2	-	17	7	5	½	0	5/8	5/8	7/16	0	7/16	3	5/8	3	5/8
D	1 & 6	2	-	29	8	4	5/8	0	¾	½	7/16	0	7/16	7	1 3/16	7	1 3/16
	2 & 5	3	7	27*	11	3¼	9/16	⅞	11/16	7/16	½	5/16	7/16	13	1 3/16	1	1 3/16
	3 & 4	4	7	27*	9	3½	9/16	¾	11/16	7/16	5/8	⅜	9/16	-	-	-	-
I	1	2	-	20	6	4¼	5/8	0	5/8	7/16	7/16	0	7/16	4	11/16	3	11/16
	2	2	-	20	4	4½	7/16	⅜	9/16	7/16	7/16	0	7/16	4	13/16	4	13/16
	3	2	-	20	4	3¾	7/16	⅜	9/16	7/16	7/16	0	7/16	5	⅞	5	⅞
	4	2	-	17	3	4¼	¾	¼	5/8	7/16	7/16	0	7/16	6	15/16	5	15/16

NOTES:
1. ALL BOLTS HOLES SHALL BE 1"ø FOR ⅞"ø ASTM A325 TYPE 3 BOLTS.
2. ~~TENSION INDICATOR WASHERS SHALL BE USED AT ALL CONNECTIONS. TENSION INDICATOR BOLTS MAY BE USED IN LIEU OF TENSION INDICATOR WASHERS. LOAD INDICATOR WASHERS SHALL BE EPOXY COATED.~~
3. ALL SPLICE TYPE A EXCEPT AS NOTED WITH AN "*" USE TYPE B AT THE SPLICES NOTED WITH AN "*".

STATE OF TEXAS
WALLY R. BURNS
44162
REGISTERED PROFESSIONAL ENGINEER
11/11/92

ALTERNATE DESIGN SPLICE DETAILS DC 3 (ALT. DSGN.)

SHEET 1 OF 1

FED. RD. DIV. NO.	STATE	FEDERAL PROJECT NO.				SHEET NO.
6	TEXAS	NH 93 (14)				1562
STATE DIST. NO.	COUNTY		CONT.	SECT.	JOB	HWY. NO.
12	HARRIS		0110	06	102	IH 45

AD-76-0

Design Filename: /hou2hctra/407dc3tx3std01.dgn
Plotted on: 11-NOV-1992

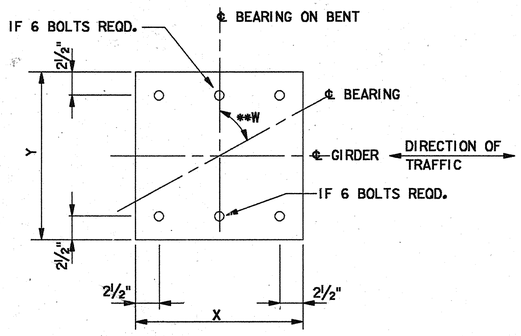

MASONRY PLATE PLAN

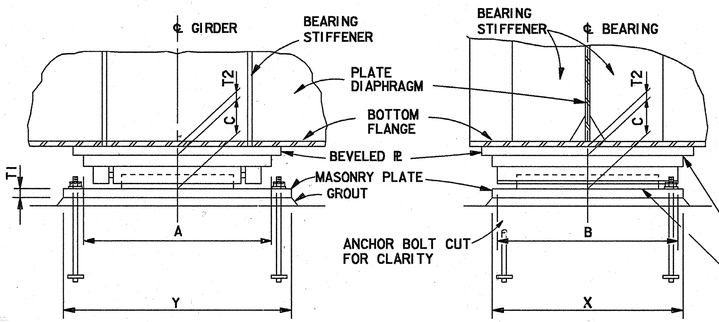

EXPANSION BEARING (PMG DESIGNATION)

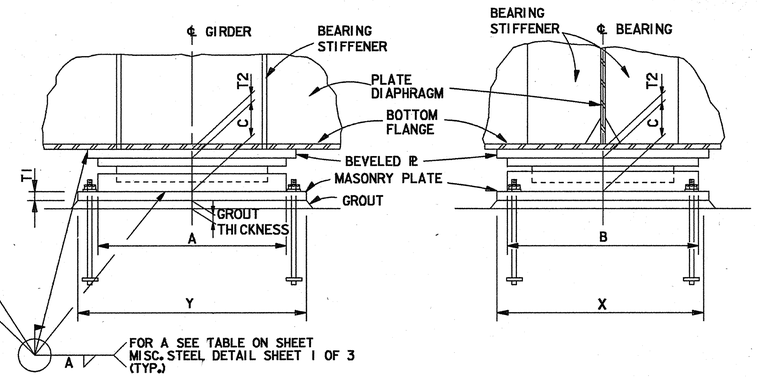

FIXED BEARING (PF DESIGNATION)

Bent No	Bearing Selection Designation*	A in	B in	C in	Bevel Pl. Thk. (T2) in	Movement in	Lat. Load kips	Long. Load kips	Masonry Plate X x Y x T1 in in in	Anchor Bolt No. Type	Grout in	Remark
9b	PMG300	15.62	14.87	3.12	1.000	3.11	8.86	8.36	14 x 24 x 1 5/8	4 7/8" x 1'-9"	4.750	2 required each beam
10	PMG1100	27.00	25.25	4.93	1.125	1.56	35.42	37.45	24 x 36 x 2 5/8	4 1 3/8" x 2'-3"	1.500	
11	PF1100	22.00	22.00	4.05	0.875	0.00	35.42	48.05	24 x 31 x 1 7/8	4 1 1/2" x 2'-6"	1.500	
12a	PMG500	19.37	17.75	3.66	1.125	1.56	17.71	16.53	17 x 28 x 2 1/8	4 1" x 2'-3"	1.500	
12b	PMG400	17.62	16.37	3.37	1.125	1.38	15.74	14.72	16 x 26 x 2	4 7/8" x 1'-9"	3.000	
13	PF1300	24.00	24.00	4.37	1.625	0.00	37.39	57.35	26 x 33 x 1 7/8	4 1 ½" x 2'-3"	1.750	CHANGED TO 1½" ϕ BOLT
14	PMG1300	29.25	27.00	5.36	1.875	1.90	37.39	41.35	38 x 38 x 2 7/8	~~4 1 3/8" x 2'-3"~~	2.000	SEE BENT DWG. FOR DETAIL
15a	PMG400	17.62	16.75	3.37	1.500	3.28	15.74	14.72	16 x 26 x 2	4 7/8" x 1'-9"	2.000	
15b	PMG500	19.37	17.75	3.66	1.500	1.75	19.93	18.67	17 x 28 x 2 1/4	4 1" x 2'-3"	1.625	
16	PF1600	26.62	26.62	4.71	1.750	0.00	39.85	29.03	29 x 36 x 2 7/8	6 1 3/8" x 2'-3"	1.875	
17a	PMG500	19.37	17.75	3.66	1.500	1.75	19.93	18.67	17 x 28 x 2 1/4	4 1" x 2'-3"	1.625	
17b	PMG400	17.62	16.37	3.37	1.500	1.61	18.30	16.24	16 x 26 x 2	4 1" x 2'-3"	1.500	
18	PF1700	27.37	27.37	4.87	1.875	0.00	46.44	81.88	30 x 37 x 2	6 1 1/2" x 2'-6"	2.000	
19	PMG1700	33.12	30.12	6.11	2.125	2.47	45.85	71.40	42 x 42 x 3		2.250	SEE BENT DWG. FOR DETAIL
20a	PMG400	17.62	17.50	3.37	--->	4.09	17.71	15.70	16 x 26 x 2	4 1" X 2'-3"	4.260	-->1.125 (1) & 1.0 (2)
36b	PMG300	15.62	14.75	3.12	1.000	1.44	10.94	10.91	17 x 24 x 1 3/4	4 7/8" x 1'-9"	2.875	1 required for beam #1
36b	PMG200	13.25	12.87	2.87	1.000	1.44	5.47	5.46	12 x 24 x 1 3/4	4 7/8" x 1'-9"	1.500	2 required for each beam #2 & #3
37	PF3500	39.37	39.37	6.80	0.750	0.00	39.00	36.00	44 x 49 x 2		1.500	SEE BENT DWG.
38	PMG1000	27.00	25.25	4.93	1.250	2.02	26.85	30.69	24 x 36 x 2 1/2	4 1 1/4" x 2'-3"	1.500	
39a	PMG300	15.62	15.30	3.12	1.000	3.54	11.50	10.67	14 x 24 x 1 7/8	4 7/8" x 1'-9"	1.500	

NOTES:

1. ALL STRUCTURAL STEEL SHALL BE ASTM A709 GR 50W UNLESS SHOWN OTHERWISE.
2. ALL ANCHOR BOLTS SHALL BE ASTM A-193 B-7 WITH HEX NUTS A-194 GRADE 2H AND WASHERS A588 STD.
3. CONCRETE FOR BENT SHALL BE CLASS H, fc'=5000 psi.
4. PROVIDE BEVELED PLATE TO MATCH SLOPE OF GIRDER.
5. BOLT PROJECTION= (T1) + (GROUT) + (2 x BOLT DIA.)

* BEARING SEATS AND MASONRY PLATE SIZE ARE BASED ON D.S. BROWN BEARING ASSEMBLIES. ADJUST BEARING SEAT ELEVATIONS, TOP OF BENT AND TOP OF COLUMN ELEVATIONS IF A DIFFERENT SUPPLIER IS SELECTED. ADJUST MASONRY PLATE SIZE AND BEARING SEAT ELEV. IF NEEDED. OTHER ACCEPTABLE MFG'S. ARE DIXEN AND CON-SERV., INC.

** W= SEE BEARING ELEVATION SHEET (90° TYP.)

REVISED 1-6-93, 1-15-93

ALTERNATE DESIGN
DC 3
BELTWAY 8 / WESTBOUND TO IH 45 / SOUTHBOUND BEARING DETAILS

STATE OF TEXAS
WALLY R. BURNS
44162
REGISTERED PROFESSIONAL ENGINEER

11/10/92

REVISED 8/30/94

FED. RD. DIV. NO.	STATE	FEDERAL PROJECT NO.				SHEET NO.
6	TEXAS	NH 93 (14)				1563
STATE DIST. NO.	COUNTY	CONT.	SECT.	JOB	HWY. NO.	
12	HARRIS	0110	06	102	IH 45	

Design Filename: /hou2hctra/407dc3/bx443br01.dgn
Plotted on: 10-NOV-1992

AD-76-0

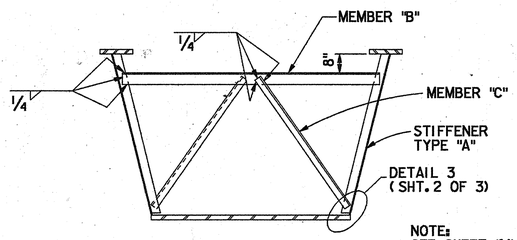

TYPE "A1" (POSITIVE MOMENT)

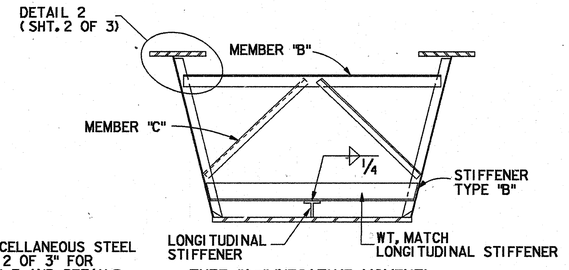

TYPE "A2" (NEGATIVE MOMENT)

NOTE:
SEE SHEET "MISCELLANEOUS STEEL DETAILS SHEET 2 OF 3" FOR DETAILS 2 THRU 3 AND DETAILS FOR STIFFENERS TYPE "A" & "B"

INTERMEDIATE DIAFRAM "A"

3/8" = 1'-0"

INTERMEDIATE DIAFRAM "A"			
BRIDGE	SPAN	MEMBER "B"	MEMBER "C"
DC3	9-11, 24-25, 33-40	L4 X 4 X 5/16	L3 X 3 X 5/16
DC3	12, 14, 17, 19	L5 X 5 X 3/8	L4 X 4 X 5/16
DC3	13, 15, 16	WT 6 X 29	L4 X 4 X 5/16
DC3	18	WT 7 X 41	L4 X 4 X 5/16
DC4	1-8, 12-14, 22-25	L4 X 4 X 5/16	L3 X 3 X 5/16
DC4	16-20	WT 6 X 29	L4 X 4 X 5/16
DC4	21	L5 X 5 X 3/8	L4 X 4 X 5/16
DC8	2-4	L4 X 4 X 5/16	L3 X 3 X 5/16
DC8	8-11	L3 1/2 X 3 1/2 X 1/4	L3 X 3 X 1/4
IASML@GREENS	1-3	L4X4X5/16	L3X3X5/16

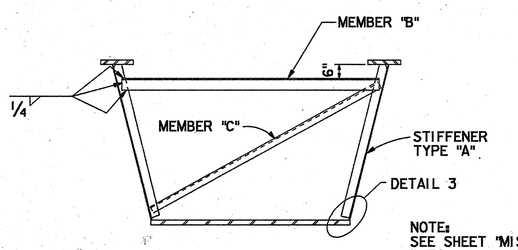

TYPE "B1" (POSITIVE MOMENT)

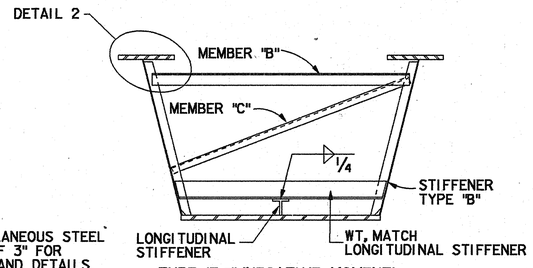

TYPE "B2" (NEGATIVE MOMENT)

NOTE:
SEE SHEET "MISCELLANEOUS STEEL DETAILS SHEET 2 OF 3" FOR DETAILS 2 THRU 3 AND DETAILS FOR STIFFENERS TYPE "A" & "B"

INTERMEDIATE DIAFRAM "B"

3/8" = 1'-0"

INTERMEDIATE DIAFRAM "B"			
BRIDGE	SPAN	MEMBER "B"	MEMBER "C"
DC3	20-23, 26-29, 30-32	L3 1/2 X 3 1/2 X 5/16	L4 X 4 X 5/16
DC4	9-11	L3 1/2 X 3 1/2 X 5/16	L4 X 4 X 5/16
DC4	15	L4 X 4 X 5/16	L4 X 4 X 5/16
DC8	5, 6	L5 X 5 X 3/8	L4 X 4 X 5/16
DC8	7	L3 1/2 X 3 1/2 X 5/16	L4 X 4 X 5/16

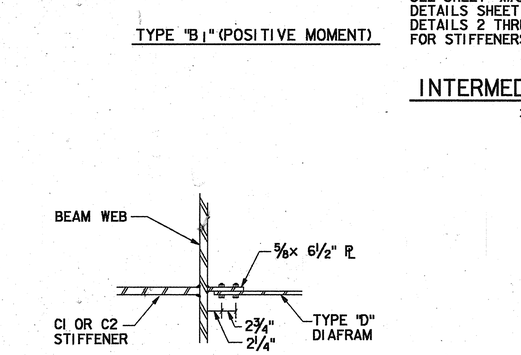

DIAFRAM "D"

Type "D" diaframs are required between steel girders at the ℄ of the following bents —
I45 over Greens Rd. bents 2, 3, 4
DC3 bents 10, 11, 13, 14, 16, 18, 19, 21, 27, 28, 32, 34, 35, 37, 38, 40
DC4 bents 4, 6, 7, 8, 10, 11, 13, 14, 17, 18, 20, 21, 25
DC8 bents 3, 4, 7, 9, 10, 11
DC3 alternate bents 10, 11, 13, 14, 16, 18, 19, 38
DC4 alternate bents 4, 23, 24, 26, 27
DC8 alternate bent 8

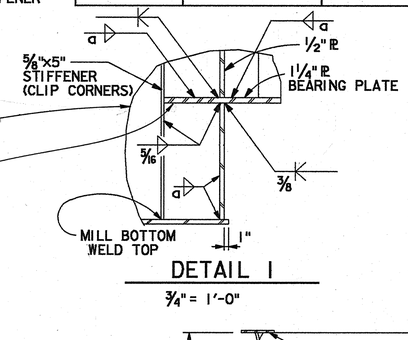

DETAIL 1

3/4" = 1'-0"

WELD TABLE	
PLATE THICKNESS	a
≤ 1/2	3/16
1/2 ≤ t ≤ 3/4	1/4
1/2 ≤ t ≤ 3/4	5/16
1 1/2 ≤ t ≤ 2 1/4	3/8
2 1/2 ≤ t ≤ 4	1/2

END BOX BEAM SECTION

3/8" = 1'-0"

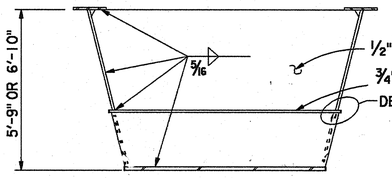

SECTION B-B

3/8" = 1'-0"

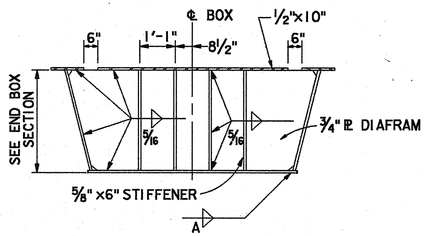

SECTION C-C

3/8" = 1'-0"

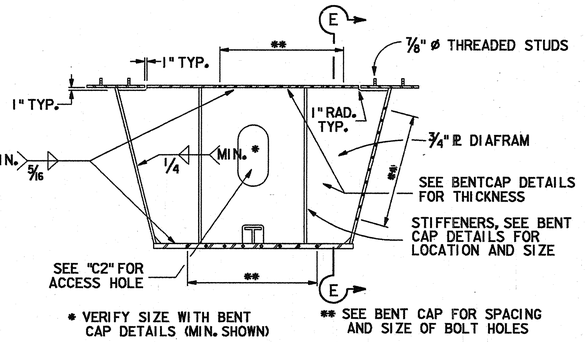

* VERIFY SIZE WITH BENT CAP DETAILS (MIN. SHOWN)

** SEE BENT CAP FOR SPACING AND SIZE OF BOLT HOLES

INTERIOR BENT DIAFRAM "C3" (PASS THRU BENTS)

3/8" = 1'-0"

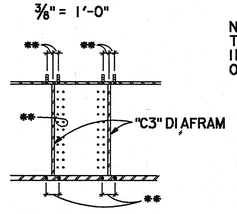

SECTION E-E

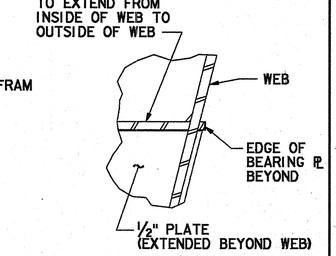

DETAIL 2

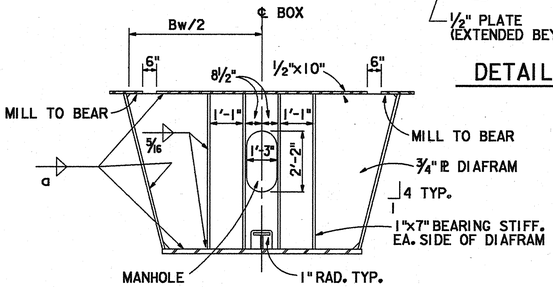

INTERIOR BENT DIAFRAM "C2"

3/8" = 1'-0"

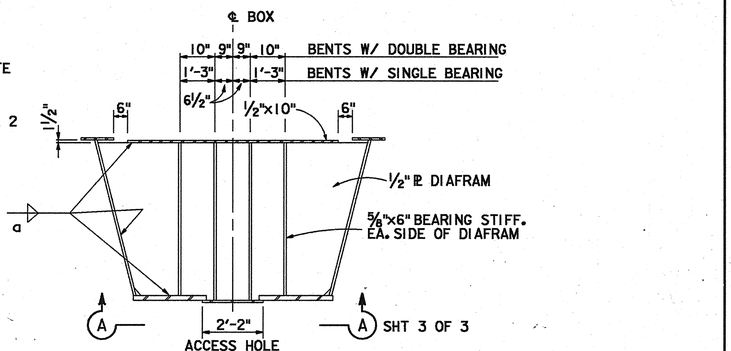

END DIAFRAM "C1"

3/8" = 1'-0"

MISCELLANEOUS STEEL DETAILS

SHEET 1 OF 3

REVISED 2-12-93

FED. RD. DIV. NO.	STATE	FEDERAL PROJECT NO.				SHEET NO.
6	TEXAS	NH 93 (14)				1372
STATE DIST. NO.	COUNTY		CONT.	SECT.	JOB	HWY. NO.
12	HARRIS		0110	06	102	IH 45

STATE OF TEXAS
WALLY R. BURNS
44162
REGISTERED PROFESSIONAL ENGINEER
10/11/92

REVISED 1-6-93

Design Filename: /hou2/hctra448hc448stdt.dgn
Plotted on: 07-OCT-1992

AD-76-0

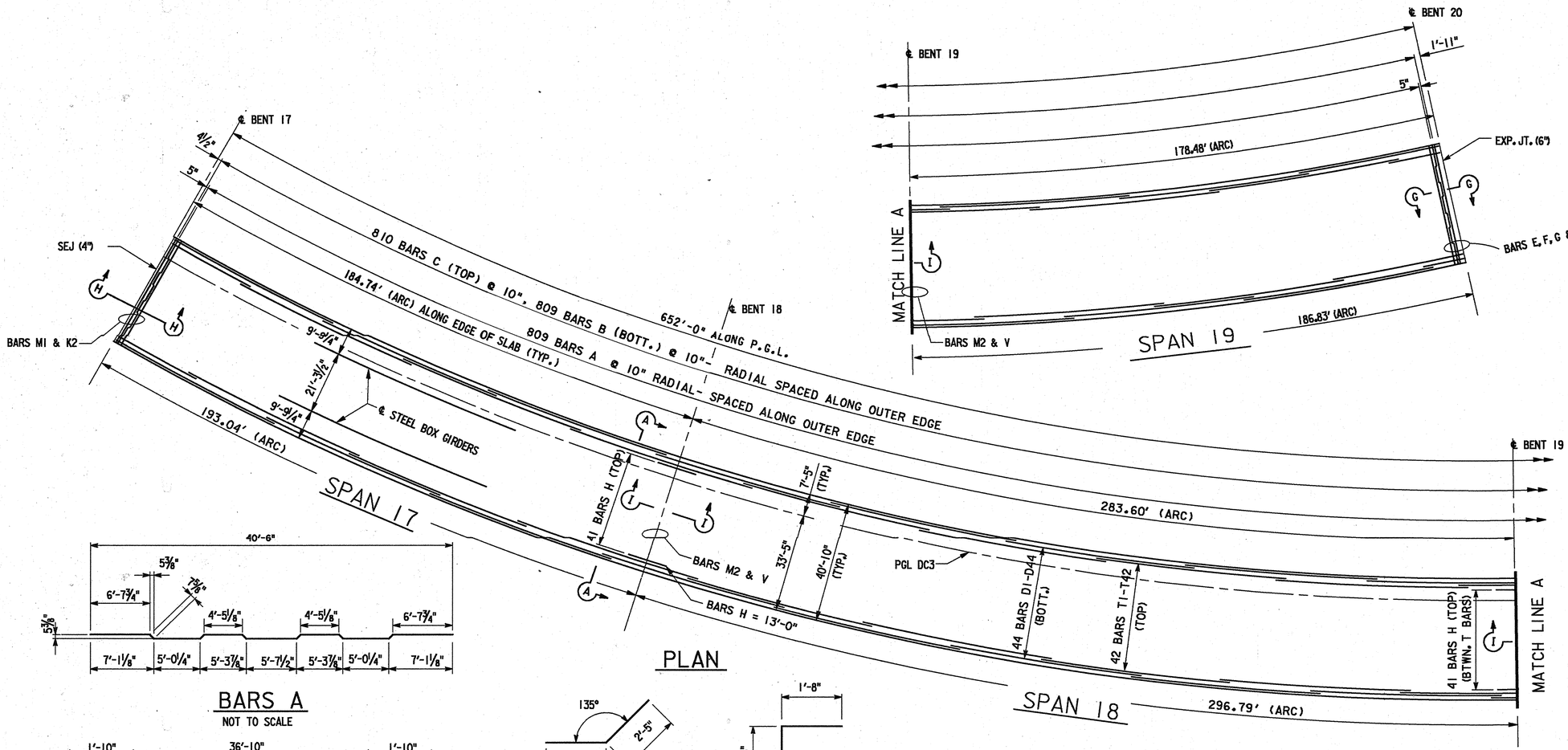

BARS A
NOT TO SCALE

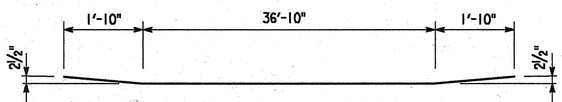

BARS B
NOT TO SCALE

BARS K
NOT TO SCALE

BARS E
NOT TO SCALE

TABLE OF SPAN UNIT 7 ESTIMATED QUANTITIES				
BAR	No.	SIZE	LENGTH	WEIGHT
A	809	5	41'-8"	35,161
B	809	5	40'-6"	34,173
C	810	5	40'-6"	34,216
(1)(5) D1-D46	46	5	676'-3"	32,445
E	39	5	3'-4"	135
F	39	5	2'-5"	98
G	39	5	4'-3"	173
H	82	6	13'-0"	1,601
K2	39	4	2'-8"	70
M1	11	5	37'-8"	432
M2	4	5	32'-0"	134
(2)(5) T1-T44	44	4	673'-6"	12,706
V	34	4	2'-8"	61
(3) REINFORCING STEEL			LB.	158,495
(3) CLASS "S" CONC.			C.Y.	915
CONC. SURF. TREAT.			S.Y.	2793
T 501 RAIL			L.F.	1,236
T 502 RAIL			L.F.	87.2
(4) EXP. JOINT (6")			L.F.	38.6
REINF. CONC. SLAB			S.F.	27015

(1) INCLUDES 11-1'-6" (MIN.) SPLICES
(2) INCLUDES 11-1'-3" (MIN.) SPLICES
(3) FOR CONTRACTORS INFORMATION ONLY
(4) ONE COMPLETE EXP. JOINT (6")
(5) USE ALTERNATE SPLICE LOCATION

NOTE :
SEE SLAB DETAIL SHEETS FOR SECTIONS, BARS & BAR DETAILS NOT SHOWN.

GENERAL NOTE:
DESIGN Fc = 1200 psi
MINIMUM RATE OF CONCRETE PLACEMENT SHALL BE 30 L.F. PER HOUR IF CONTINUOUS PLACEMENT IS USED FOR THE SLAB. SEE BLOCKING DIAGRAMS FOR DEAD LOAD DEFLECTIONS DUE TO SLAB. PERMANENT METAL DECK FORMS ONLY WILL BE ALLOWED THIS UNIT.
REINF. GRADE 60

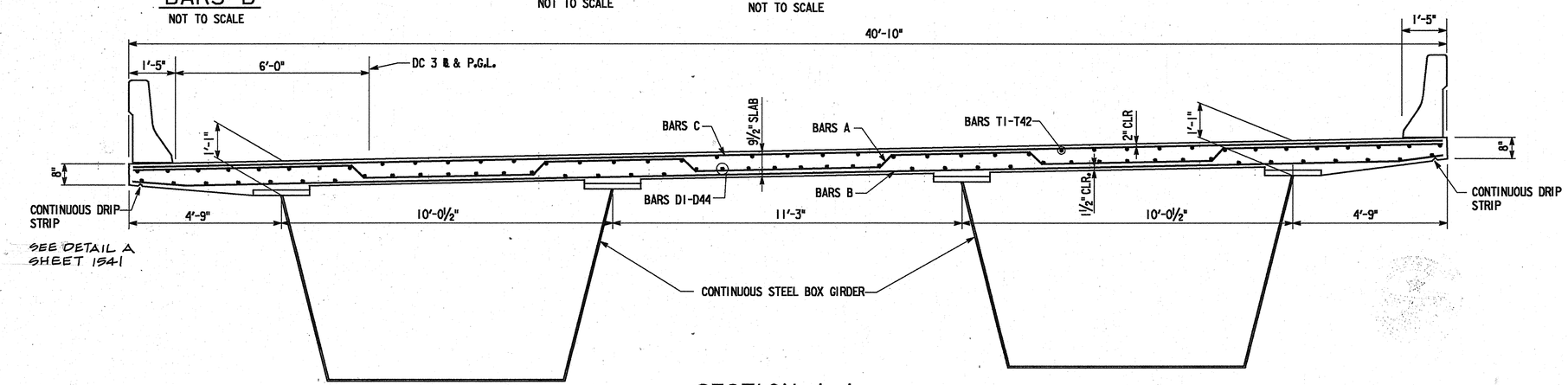

SECTION A-A
½"=1'-0"

ALTERNATE DESIGN

DC 3
SLAB UNIT #7

STATE OF TEXAS
WALLY R. BURNS
44162
REGISTERED PROFESSIONAL ENGINEER
11/10/92
REVISED 2-12-93

FED. RD. DIV. NO.	STATE	FEDERAL PROJECT NO.				SHEET NO.
6	TEXAS	NH 93 (14)				1534
STATE DIST. NO.	COUNTY	CONT.	SECT.	JOB	HWY. NO.	
12	HARRIS	0110	06	102	IH 45	

Design Filename: /hou2hctra/407dc3/tx43sd07.dgn
Plotted on: 09-NOV-1992

AD-76-0

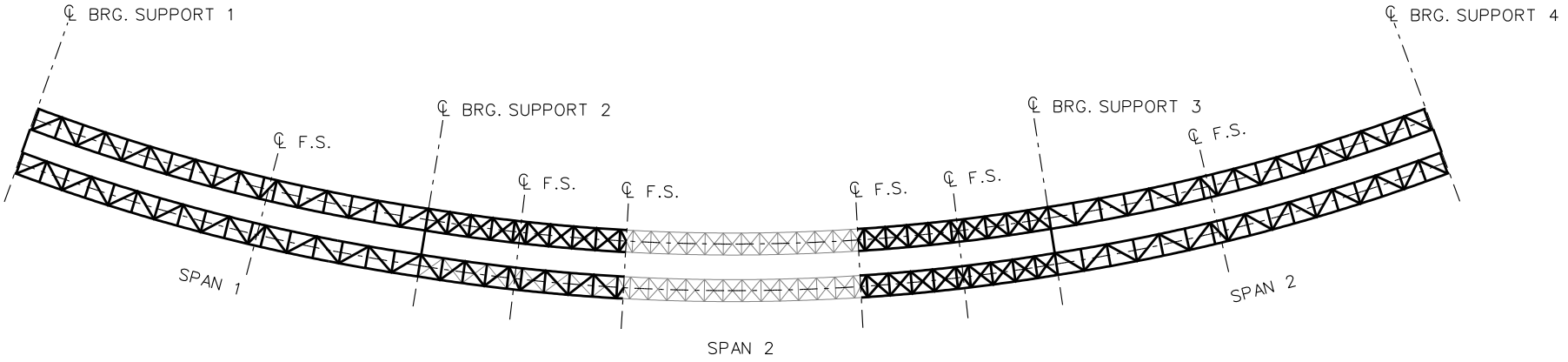

STAGE 4

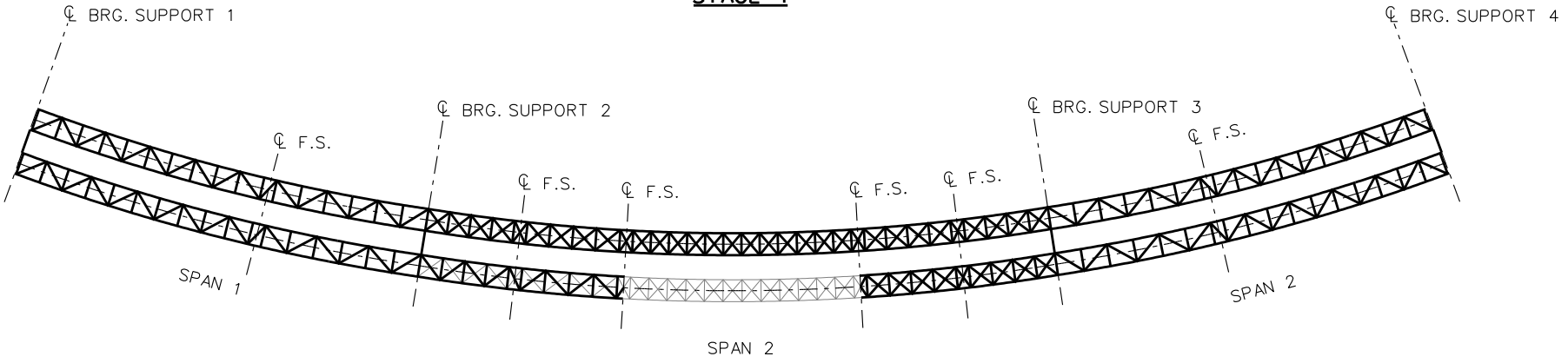

STAGE 5

LEGEND

▽ = HOLD OR LIFT CRANE

○ = TIE DOWN

□ = TEMPORARY SUPPORT STRUCTURE

NCHRP 12-79

BRIDGE ETCCR14

GIRDER ERECTION PROCEDURE

SHEET 1 OF 1

NCHRP 12-79

ETCCR15

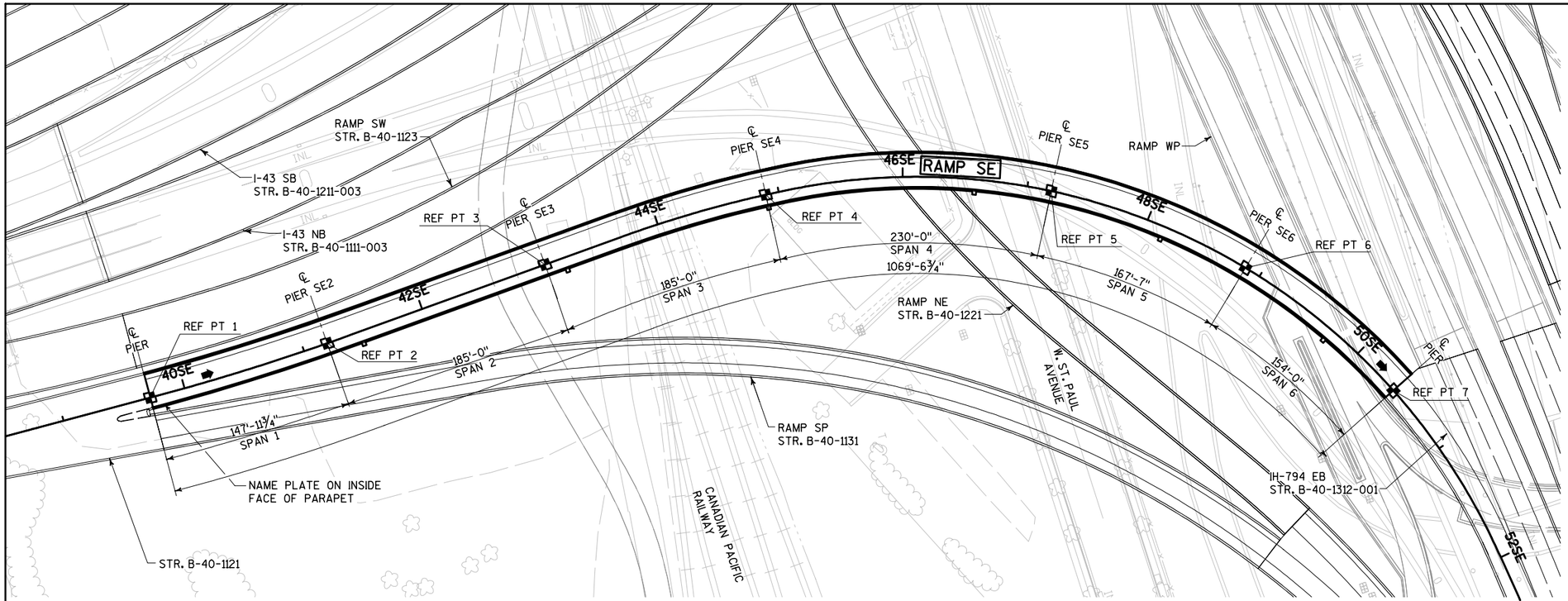

PLAN

RAMP SE: 6 SPAN CURVED STEEL BOX GIRDER
ALL PIERS ARE NORMAL OR RADIAL TO ℄ SE
DIMENSIONS SHOWN ARE ALONG ℄ SE

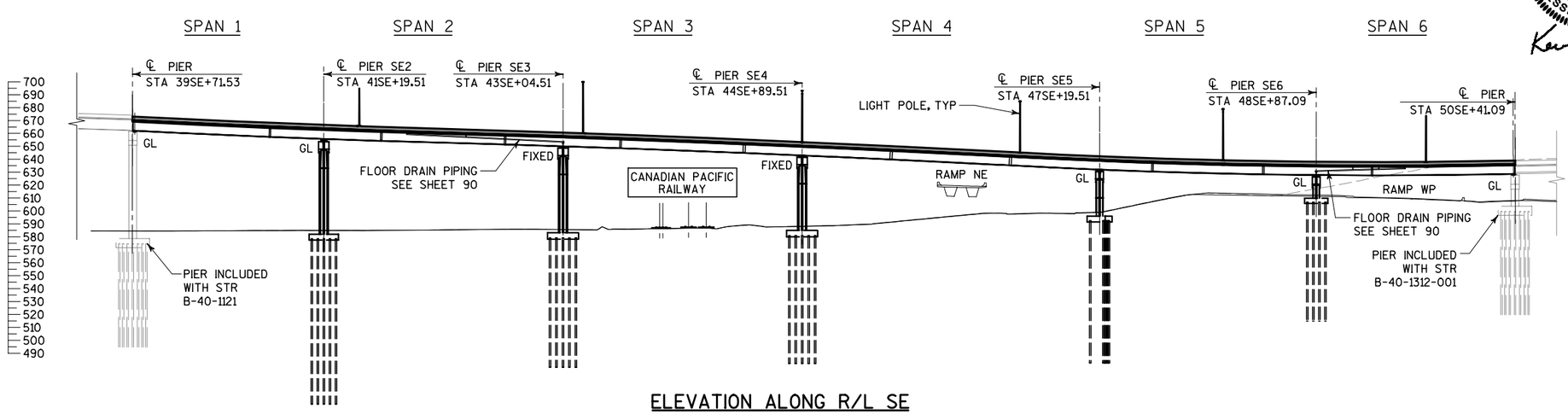

ELEVATION ALONG R/L SE

3/30/05

KEVIN G. WILLIS
E-35247
MILWAUKEE, WI
WISCONSIN PROFESSIONAL ENGINEER

Kevin Willis

STATE PROJECT NUMBER

1060-05-75

LEGEND

GL: UNIDIRECTIONAL BEARINGS

FIXED: FIXED BEARINGS

GEOMETRY REFERENCE POINTS. SEE SHEET 3 FOR COORDINATES.

DIRECTION OF TRAVEL

NOTES

1. SEE SHEET 3 FOR REFERENCE LINE LAYOUT AND ASSOCIATED GEOMETRY REFERENCE POINT LOCATIONS.
2. SEE SHEET 4 FOR GENERAL NOTES.
3. SEE SHEETS 6 TO 8 FOR VERTICAL AND HORIZONTAL CLEARANCES.
4. SEE SHEET 9 FOR LOCATION OF SUBSURFACE INVESTIGATION BOREHOLES.
5. SEE SHEET 18 FOR FOUNDATION LAYOUT AND ESTIMATED PILE LENGTHS.
6. SEE SHEET 73 FOR STATIONING OF LIGHT POLE BASES.

WISDOT BRIDGE OFFICE CONTACT:

PHIL CIHA - DISTRICT 2
(262) 548-8742

CONSULTANT CONTACT (MTP):

KEVIN WILLIS - CH2M HILL
(414) 272-2426

Milwaukee Transportation Partners LLC

NO.	DATE	REVISION	BY

WISDOT
BUREAU OF STRUCTURES

STRUCTURE B-40-1122

MARQUETTE INTERCHANGE - RAMP SE

COUNTY: MILWAUKEE		~~TOWN~~/CITY/~~VILLAGE~~: MILWAUKEE	
DESIGN SPEC.: AASHTO 2002		LOAD: HS-25	CONST. SPEC.: 2004
DESIGNED BY: KGW	DESIGN CK'D.: RCA	DRAWN BY: ADH	PLANS CK'D.: KGW

APPROVED: G. H. Anderson — CHIEF STRUCTURAL DESIGN ENGINEER — 4-30-05 DATE

GENERAL PLAN AND ELEVATION

SHEET 1 OF 109

MAR 22 2005

8

STATE PROJECT NUMBER
1060-05-75

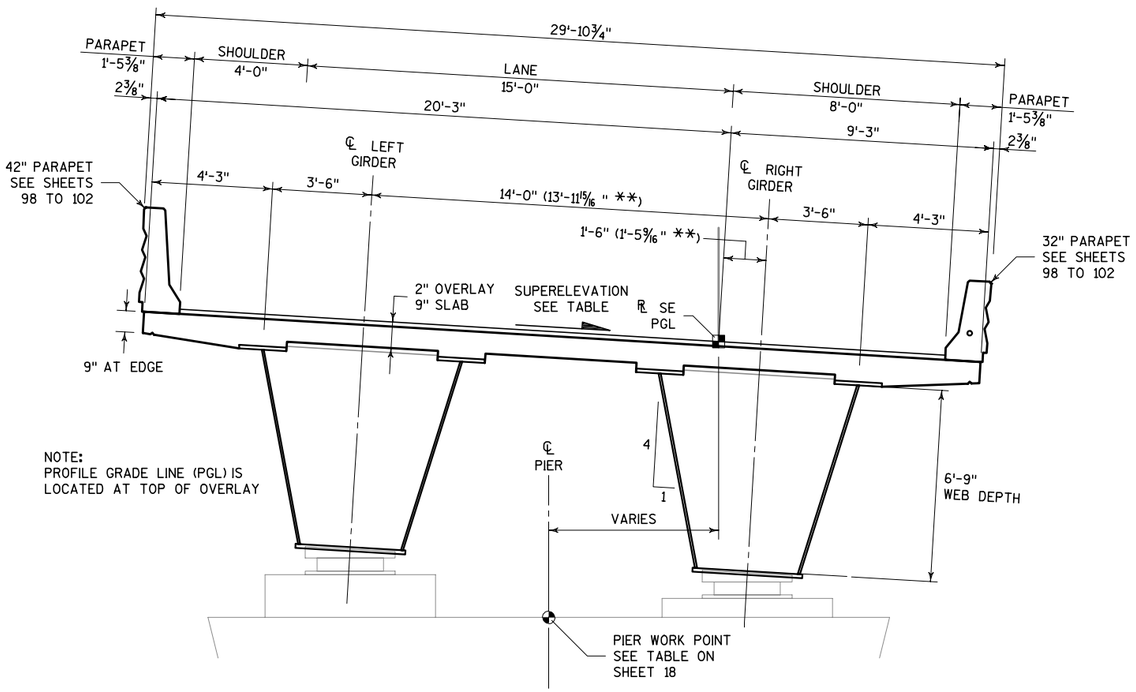

TYPICAL DECK SECTION

GEOMETRY REFERENCE POINTS							
POINT	STATION	EASTING	NORTHING	ELEV'N	BEARING	SUPER (%)	GRADE (%)
RP 1	39SE+71.53	602607.83	297451.54	671.12	N 3°37'47" E	3.53	-5.00
RP 2	41SE+19.51	602611.71	297599.44	664.67	N 0°42'50" W	3.94	-3.55
RP 3	43SE+04.51	602607.54	297784.39	659.24	N 1°19'40" W	-1.38	-3.14
RP 4	44SE+89.51	602610.89	297969.19	652.31	N 5°55'26" E	-6.00	-4.35
RP 5	47SE+19.51	602680.79	298186.31	641.32	N 30°44'06" E	-6.00	-4.15
RP 6	48SE+87.09	602788.38	298313.81	637.07	N 49°35'16" E	-6.00	-0.93
RP 7	50SE+41.09	602918.83	298394.54	637.92	N 66°54'46" E	-4.45	2.03

R/L HORIZONTAL ALIGNMENT							
LOC'N	STATION	EASTING	NORTHING	BEARING	RADIUS	ARC LENGTH	DEFL'N ANGLE DELTA
PT	27SE+65.33	602531.47	296247.76	N 3°37'47" E			
PC	39SE+74.72	602608.03	297454.73	N 3°37'47" E			
PI	40SE+57.40	602613.27	297537.25		1909.86	165.26	4°57'28" L
PT	41SE+39.98	602611.35	297619.90	N 1°19'40" W			
PC	43SE+68.65	602606.05	297848.51	N 1°19'40" W			
PI	44SE+39.34	602604.41	297919.19		954.93	141.13	8°28'04" R
PCC	45SE+09.78	602613.20	297989.34	N 7°08'25" E			
PI	49SE+05.55	602662.39	298382.04		509.30	672.90	75°42'04" R
PCC	51SE+82.68	603055.08	298431.36	N 82°50'29" E			

R/L VERTICAL PROFILE								
LOC'N	STATION	ELEV'N	GRADE AHEAD (%)	SEGMENT LENGTH	VPI		MAX/MIN POINT	
					STATION	ELEV'N	STATION	ELEV'N
VPT	37SE+55.00	681.95	-5.000	235.00				
VPC	39SE+90.00	670.20	-5.000	220.00	41SE+00.00	664.70	44SE+35.37	659.07
VPRC	42SE+10.00	661.92	-2.530	380.00	44SE+00.00	657.11	38SE+20.77	666.84
VPT	45SE+90.00	647.61	-5.000	85.00				
VPC	46SE+75.00	643.36	-5.000	420.00	48SE+85.00	632.86	49SE+35.38	636.85
VPT	50SE+95.00	639.30	3.065	5.00				

SUPERELEVATION	
STATION	SUPER (%)*
38SE+10.00	-2.00
40SE+00.00	4.50
41SE+00.00	4.50
44SE+65.00	-6.00
49SE+75.00	-6.00
50SE+42.03	-4.43

* POSITIVE SUPERELEVATION MEANS RIGHT EDGE OF DECK IS HIGHER WHEN LOOKING IN THE DIR'N OF INCREASING STATION.

SUPERELEVATION VARIES LINEARLY BETWEEN THE TABULATED VALUES.

** DENOTES ALTERNATIVE HORIZONTAL DIMENSIONS CALCULATED BASED ON AN AVERAGE SUPERELEVATION OF -2.89%

HORIZONTAL DIMENSIONS ARE GIVEN BETWEEN THE REFERENCE LINE AT FINISHED TOP OF DECK ELEVATION AND THE TOP FLANGE GIRDER CENTERLINE WORKPOINTS AS IDENTIFIED ON SHEET 46.

CONTRACTOR MAY ELECT TO DETAIL AND FABRICATE STEEL GIRDERS BASED ON EITHER THE SLOPED DIMENSIONS OR THE ALTERNATIVE HORIZONTAL DIMENSIONS.

ALL OTHER DIMENSIONS SHALL REMAIN UNMODIFIED AND TAKEN ALONG THE SLOPE AS SHOWN.

NO.	DATE	REVISION	BY

STATE OF WISCONSIN
DEPARTMENT OF TRANSPORTATION
STRUCTURES DESIGN SECTION

STRUCTURE B-40-1122

CONST. SPEC.	DRAWN BY	PLANS CK'D.
2004	KGW	RSR

TYPICAL SECTION AND LAYOUT DATA

SHEET 3 OF 109

MAR 22 2005

8

STATE PROJECT NUMBER
1060-05-75

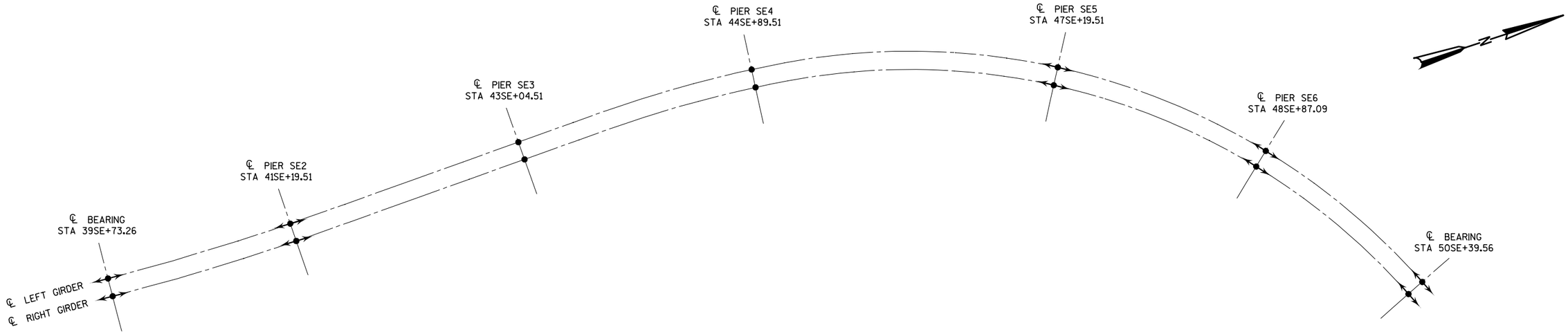

BEARING MARK	BEARING TYPE	BEARING ℄ DIRECTION	SKEW ANGLE 'SK'	GIRDER ELEV'N AT ℄	PEDESTAL ELEV'N	DEAD LOAD (KIPS)	TOTAL LOAD (KIPS)	HORIZ FORCES		MVMT RANGE		SHIM PLATE THICKNESS					NOMINAL BEARING DIMENSIONS						ANCHOR BOLTS	BOLT ARR'T
								TRANS (KIPS)	LONG (KIPS)	TRANS (IN)	LONG (IN)	LL (IN)	RL (IN)	LH (IN)	RH (IN)	CC (IN)	A (IN)	B (IN)	C (IN)	D (IN)	E (IN)	H (IN)		
SE1L	GUIDED	N 3°37'47" E	0°	662.52	661.88	210	360	40			5"	2 7/16"	3 1/4"	1"	1 7/8"	2 1/8"	24"	26"	24"	20"	1 1/2"	5 1/2"	4 - 1"ϕ	A
SE1R				663.02	662.39	240	400	40			5"	2 5/16"	3 1/8"	1"	1 7/8"	2 1/16"	24"	26"	24"	20"	1 1/2"	5 1/2"	4 - 1"ϕ	
SE2L	GUIDED	N 2°17'10" E	3°00' LHF	656.08	655.31	780	1140	40			3 3/8"	2 1/8"	3 3/16"	1"	2 3/8"	2 1/4"	36"	36"	36"	36"	1 1/2"	7"	4 - 1"ϕ	B
SE2R				656.63	655.85	760	1100	40			3 3/8"	2 1/4"	3 11/16"	1"	2 3/8"	2 5/16"	36"	36"	36"	36"	1 1/2"	7"	4 - 1"ϕ	
SE3L	FIXED	N 1°19'40" W	N/A	651.31	650.58	720	1100	75	110			2 1/2"	2"	1 1/2"	1"	1 3/4"	36"	36"	36"	36"	1 1/2"	7"	4 - 1 1/2"ϕ	B
SE3R				651.12	650.38	700	1050	75	50			2 5/8"	2 3/16"	1 1/2"	1"	1 13/16"	36"	36"	36"	36"	1 1/2"	7"	4 - 1 1/2"ϕ	
SE4L	FIXED	N 5°55'26" E	N/A	644.93	644.10	940	1380	105	175			4 13/16"	2 5/8"	3 1/4"	1"	2 15/16"	38"	38"	38"	38"	1 1/2"	7"	4 - 1 3/4"ϕ	B
SE4R				644.09	643.26	880	1280	105	80			4 7/8"	2 11/16"	3 1/4"	1"	2 15/16"	38"	38"	38"	38"	1 1/2"	7"	4 - 1 3/4"ϕ	
SE5L	GUIDED	N 32°14'06" E	1°30' LHF	633.96	633.13	820	1240	115			3 1/8"	4 3/4"	2 9/16"	3 1/4"	1"	2 7/8"	38"	38"	38"	38"	1 1/2"	7"	4 - 1 1/4"ϕ	B
SE5R				633.12	632.29	890	1290	115			3"	4 3/4"	2 9/16"	3 1/4"	1"	2 7/8"	38"	38"	38"	38"	1 1/2"	7"	4 - 1 1/4"ϕ	
SE6L	GUIDED	N 51°05'16" E	1°30' LHF	629.75	628.98	710	1070	55			5"	3 7/16"	1 5/16"	3 1/8"	1"	2 3/16"	36"	36"	36"	36"	1 1/2"	7"	4 - 1"ϕ	B
SE6R				628.91	628.15	710	1050	55			4 7/8"	3 7/16"	1 5/16"	3 1/8"	1"	2 3/16"	36"	36"	36"	36"	1 1/2"	7"	4 - 1"ϕ	
SE7L	GUIDED	N 66°54'46" E	0°	630.40	629.70	360	580	35			6 3/4"	2 1/4"	1"	2 3/4"	1 1/2"	1 7/8"	28"	30"	28"	24"	1 1/2"	6 1/2"	4 - 1"ϕ	A
SE7R				629.77	629.07	160	300	35			6 5/8"	2 1/4"	1"	2 1/8"	1 5/8"	1 15/16"	28"	30"	28"	24"	1 1/2"	6 1/2"	4 - 1"ϕ	

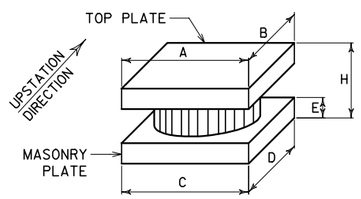

BEARING DIMENSION KEY

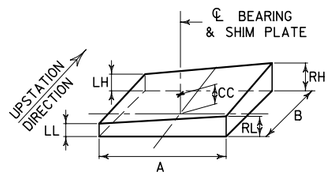

SHIM PLATE DIMENSION KEY

BEARING LEGEND

◆—▶ MULTIROTATIONAL UNIDIRECTIONAL (GUIDED)

● MULTIROTATIONAL FIXED

ARROWHEADS DENOTE MOVEMENT DIRECTIONS.

NOTES

1. SEE SHEET 44 FOR TYPICAL BEARING DETAILS
2. BEARING DIMENSIONS SHOWN ARE NOMINAL VALUES ONLY AND WILL VARY WITH THE SELECTED MANUFACTURER.
   MAKE ALL NECESSARY ADJUSTMENTS TO DIMENSIONS AND ELEVATIONS AS REQUIRED TO INCORPORATE THE SPECIFIC BEARINGS SELECTED.
3. ALL FORCES SPECIFIED ARE SERVICE (UNFACTORED) FORCES INCORPORATING AASHTO-SPECIFIED REDUCTIONS FOR ALLOWABLE OVERSTRESS WHERE APPLICABLE.
4. HORIZONTAL FORCES SPECIFIED IN THE TABLE ARE THE EXPECTED APPLIED FORCES. DESIGN BEARINGS FOR THESE VALUES OR 10 PERCENT OF THE VERTICAL DEAD LOAD, WHICHEVER IS LARGER.
5. 'RHF' (RIGHT HAND FORWARD) DENOTES A COUNTER-CLOCKWISE ROTATION WHEN VIEWED FROM ABOVE. 'LHF' (LEFT HAND FORWARD) DENOTES A CLOCKWISE ROTATION WHEN VIEWED FROM ABOVE.

NO.	DATE	REVISION	BY

STATE OF WISCONSIN
DEPARTMENT OF TRANSPORTATION
STRUCTURES DESIGN SECTION

STRUCTURE B-40-1122

CONST. SPEC.	DRAWN BY	PLANS CK'D.
2004	KGW	RSR

BEARING LAYOUT

SHEET 43 OF 109

MAR 22 2005

8

STATE PROJECT NUMBER
1060-05-75

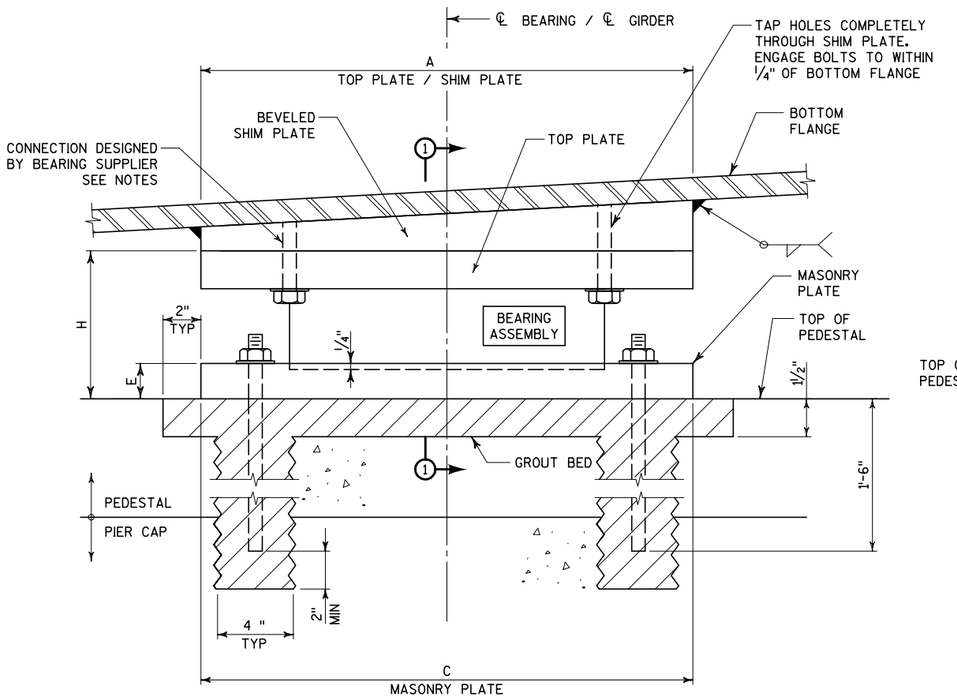

FRONT ELEVATION

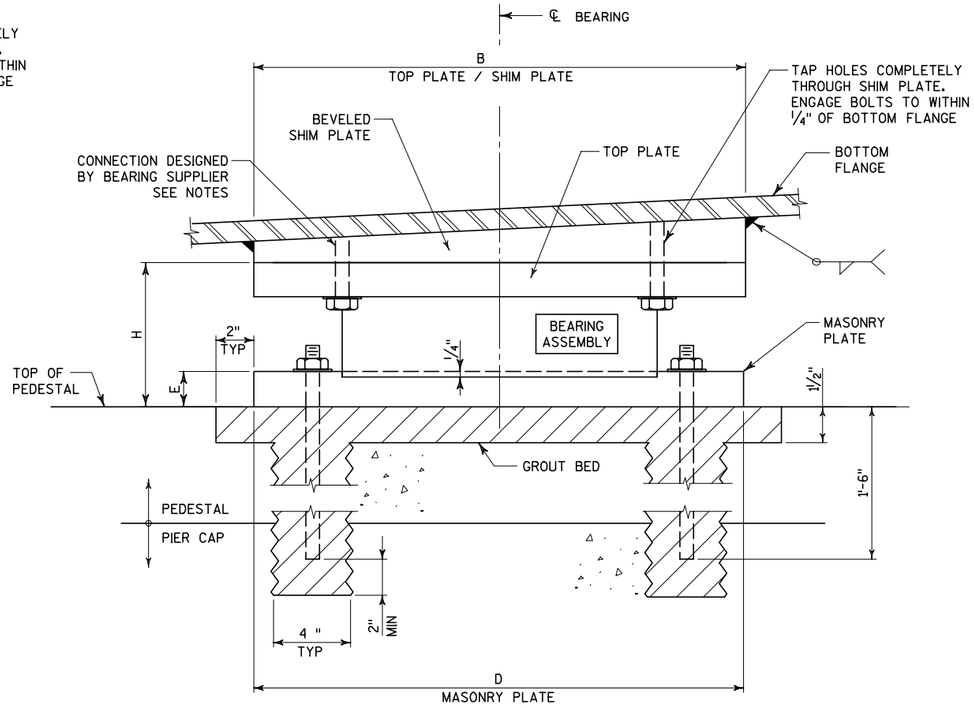

SECTION 1-1

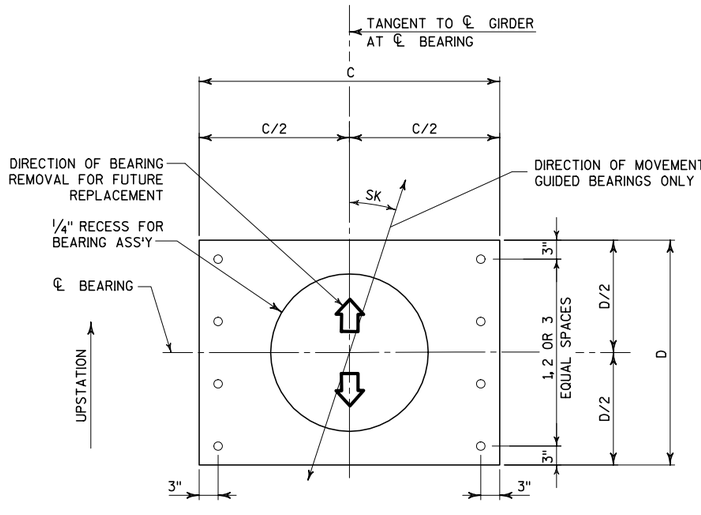

PLAN - MASONRY PLATE
ANCHOR BOLT ARRANGEMENT A

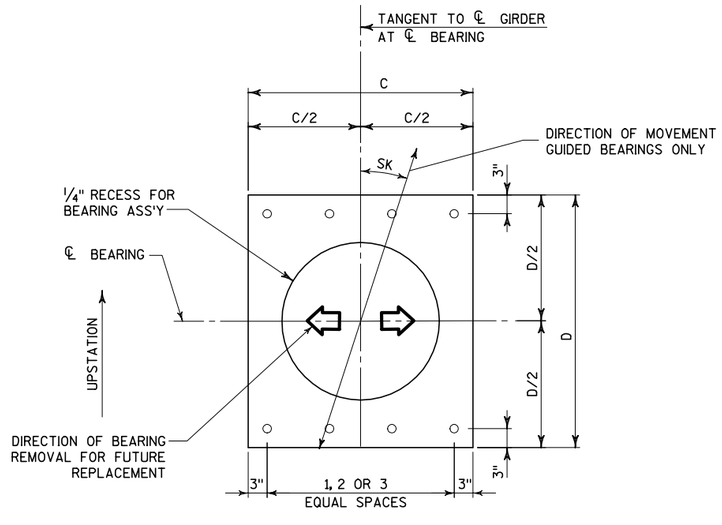

PLAN - MASONRY PLATE
ANCHOR BOLT ARRANGEMENT B

NOTES

1. SEE SHEET 43 FOR BEARING LAYOUT AND LOCATION-SPECIFIC DIMENSIONS.
2. SEE SHEET 45 FOR BEARING REPLACEMENT JACKING PADS.
3. DESIGN BOLTED CONNECTION BETWEEN TOP PLATE AND SHIM PLATE FOR A MINIMUM OF 1.25 TIMES THE COMBINED SPECIFIED HORIZONTAL LOADS.

   ARRANGE CONNECTION TO ENSURE ALL BOLTS CAN BE REMOVED WITHOUT INTERFERENCE FROM ANCHOR BOLTS OR OTHER OBSTRUCTIONS AFTER BEARING IS INSTALLED.

   TAPPED HOLE ARRANGEMENT SHOWN MAY BE REPLACED BY BOLTING DOWNWARD THROUGH THE GIRDER BOTTOM FLANGE USING BEVELED WASHER PLATES BELOW BOLT HEADS.

   HOLES IN TOP PLATE MAY BE SLOTTED OR OVERSIZED AS REQUIRED TO FACILITATE STEEL ERECTION. IF OVERSIZE OR SLOTTED HOLES ARE USED, THE CONNECTION SHALL BE DESIGNED AS SLIP-RESISTANT.

   NOTE THAT SPECIFIED BEARING LOADS ARE INTENDED FOR WORKING STRESS DESIGN AND ALREADY INCLUDE THE OVERSTRESS PERCENTAGE FROM COLUMN 14 OF TABLE 3.22.1A OF AASHTO STANDARD SPECIFICATIONS - NO FURTHER REDUCTION IS PERMITTED.
4. SKEW ANGLE SHOWN IS LEFT HAND FORWARD (LHF) - SKEW ANGLES THAT ARE RIGHT HAND FORWARD (RHF) WILL BE OPPOSITE TO THAT SHOWN.
5. GROUT SHALL BE HIGH MODULUS FLOWABLE EPOXY RESIN GROUT, SIKADUR 42 GROUT-PAK OR ACCEPTED EQUAL.
6. FOR PAYMENT PURPOSES, GROUTING MATERIALS AND INSTALLATION ARE CONSIDERED INCIDENTAL TO THE PAY ITEM FOR THE BEARING ASSEMBLY.
7. HOLES IN MASONRY PLATE SHALL BE A MAXIMUM OF 1/8" LARGER THAN THE SPECIFIED ANCHOR BOLT DIAMETER.
8. TOP PLATE, SHIM PLATE AND MASONRY PLATES ARE ALIGNED WITH THE GIRDER AND/OR THE PIER BELOW, EVEN FOR GUIDED BEARINGS WITH A NON-ZERO SKEW ANGLE. ONLY THE MOVEMENT DIRECTION VARIES AS SHOWN.
9. TOP PLATE THICKNESS TO BE SELECTED BY THE BEARING DESIGNER. MINIMUM 1".
10. MASONRY PLATE THICKNESS TO BE CONFIRMED BY THE BEARING DESIGNER AND INCREASED IF REQUIRED. NO REDUCTION PERMITTED.
11. ANCHOR BOLTS SHALL BE IN ACCORDANCE WITH ASTM F1554 (GRADE 105) AND HOT-DIP GALVANIZED IN ACCORDANCE WITH AASHTO M232.
12. BEARINGS SHALL BE DESIGNED TO PERMIT REPLACEMENT BY JACKING THE BRIDGE A MAXIMUM OF 1/2".

NO.	DATE	REVISION	BY

STATE OF WISCONSIN
DEPARTMENT OF TRANSPORTATION
STRUCTURES DESIGN SECTION

STRUCTURE B-40-1122

CONST. SPEC.	2004	DRAWN BY	KGW	PLANS CK'D.	RSR

BEARING DETAILS

SHEET 44 OF 109

MAR 22 2005

8

FILE NAME: C:\KPLOT\00044.dgn PEN TABLE: \\mtp\FinalDgn\config\plot\pentbls\bridge.pen Date: 23-MAR-2005 07:03 Plotted by: kwillis

STATE PROJECT NUMBER
1060-05-75

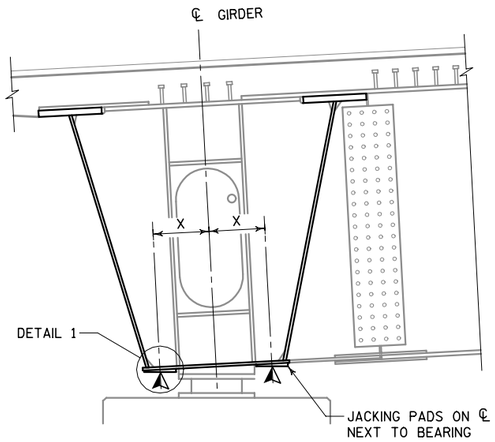

DETAIL A - SECTION AT ℄ PIER

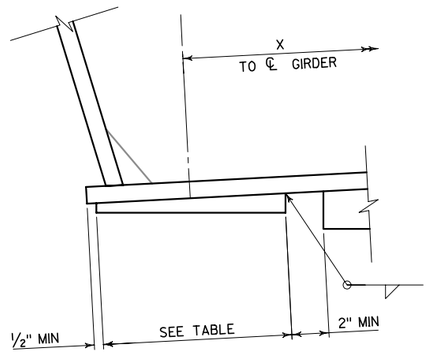

DETAIL 1
NOT TO SCALE

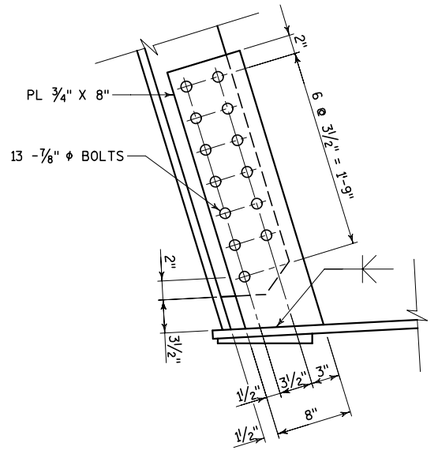

DETAIL 4
NOT TO SCALE

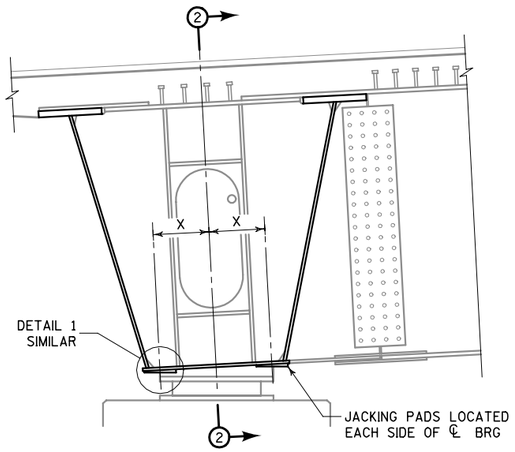

DETAIL B - SECTION AT ℄ PIER

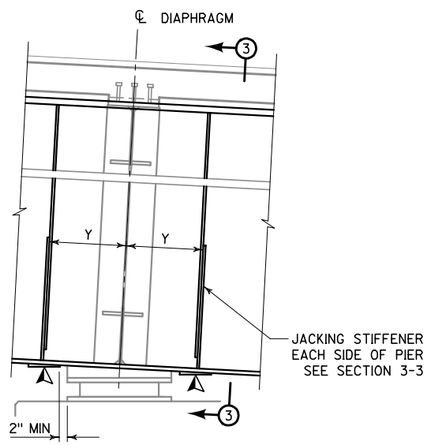

SECTION 2-2

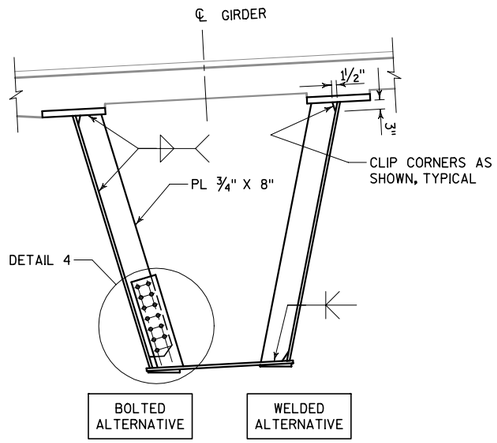

SECTION 3-3

LOCATION	DETAIL TYPE	NUMBER OF PADS	JACKING PAD DIMENSIONS							OFFSET 'X'	OFFSET 'Y'	MIN. JACK FORCE (KIP)
			WID (IN)	LEN (IN)	LL (IN)	RL (IN)	LH (IN)	RH (IN)	CC (IN)			
PIER SE1	A	2	9"	16"	1 5/16"	1 5/8"	½"	13/16 "	1 1/16"	1'-6 1/4"		120
PIER SE2	B	4	10"	10"	⅞"	1 ¼"	½"	⅞"	⅞"	1'-5 3/4"	2'-0"	216
PIER SE3	B	4	10"	10"	15/16 "	13/16 "	5/8"	½"	¾"	1'-5 3/4"	2'-0"	200
PIER SE4	B	4	10"	10"	1 9/16"	15/16 "	1 1/8"	½"	1"	1'-5 3/4"	2'-1"	264
PIER SE5	B	4	10"	10"	1 ½"	15/16 "	1 1/8"	½"	1"	1'-5 3/4"	2'-1"	248
PIER SE6	B	4	10"	10"	1 3/16"	9/16 "	1 1/8"	½"	⅞"	1'-5 3/4"	2'-0"	200
PIER SE7	A	2	7"	16"	13/16 "	½"	1 1/8"	13/16 "	13/16 "	1'-7 1/4"		184

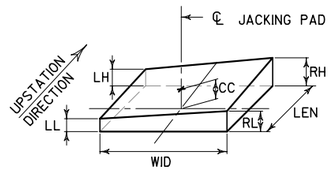

JACKING PAD DIMENSION KEY

LEGEND

▲ SUGGESTED JACKING LOCATIONS FOR FUTURE BEARING REPLACEMENT.

NOTES

1. THIS DRAWING SHOWS DETAILS AND LOCATION OF JACKING PADS AND ADDITIONAL WEB STIFFENERS REQUIRED FOR FUTURE BEARING REPLACEMENT.
2. JACKING PAD DIMENSIONS AND LOCATIONS ARE BASED ON THE MINIMUM CLEARANCES SHOWN AND THE NOMINAL BEARING DIMENSIONS GIVEN ON SHEET 43. MAKE ADJUSTMENTS AS REQUIRED TO ACCOMMODATE ACTUAL BEARINGS SUPPLIED.
3. JACKING PADS ARE PROVIDED TO GIVE A JACKING SURFACE THAT IS APPROXIMATELY LEVEL AND TO ENSURE THAT JACKING LOADS ARE APPLIED TO THE CORRECT LOCATION.

   ADDITIONAL MEASURES SHALL BE TAKEN TO CORRECT FOR ANY UNINTENDED SLOPE AND TO ENSURE THAT JACKS ARE POSITIVELY HELD IN POSITION ON THE JACKING PADS.
4. ESTIMATED JACKING FORCES ARE GIVEN AT EACH PAD AND ARE BASED ON DEAD LOAD REACTIONS ONLY - NO LIVE LOAD IS INCLUDED AND NO ADDITIONAL ALLOWANCES HAVE BEEN MADE.

   THESE FORCES MUST BE INCREASED TO ALLOW FOR JACK FRICTION AND OTHER FACTORS. RECOMMENDED MINIMUM JACK CAPACITY IS 2 TIMES THE TABULATED VALUES.
5. FORCES AND RECOMMENDATIONS ARE PROVIDED FOR INFORMATION ONLY AND MUST BE VERIFIED BY THE ENGINEER RESPONSIBLE FOR JACKING OPERATIONS.
6. JACKING PROVISIONS HAVE BEEN DESIGNED ASSUMING THAT THE STRUCTURE IS CLOSED TO TRAFFIC AT ALL TIMES THAT THE STRUCTURE IS NOT RESTING ON THE PERMANENT BEARINGS.
7. CONTROL JACKS TO ENSURE THAT FORCES APPLIED TO ALL JACKING PADS AT A SINGLE BEARING LOCATION ARE APPROXIMATELY EQUAL.

   IF THIS REQUIREMENT IS NOT MET, A COMPLETE ANALYSIS OF THE PIER DIAPHRAGM SYSTEM WILL BE REQUIRED IN ORDER TO ACCOUNT FOR THE REDISTRIBUTION OF FORCES WITHIN THE SYSTEM.

NO.	DATE	REVISION	BY

STATE OF WISCONSIN
DEPARTMENT OF TRANSPORTATION
STRUCTURES DESIGN SECTION

STRUCTURE B-40-1122

CONST. SPEC.	2004	DRAWN BY	KGW	PLANS CK'D.	RSR

JACKING PROVISIONS

SHEET 45 OF 109

MAR 22 2005

8

FILE NAME: C:\KPLOT\00045.dgn PEN TABLE: \\mtp\FinalDgn\config\plot\pentbls\bridge.pen Date: 23-MAR-2005 07:03 Plotted by: kwillis

STATE PROJECT NUMBER
1060-05-75

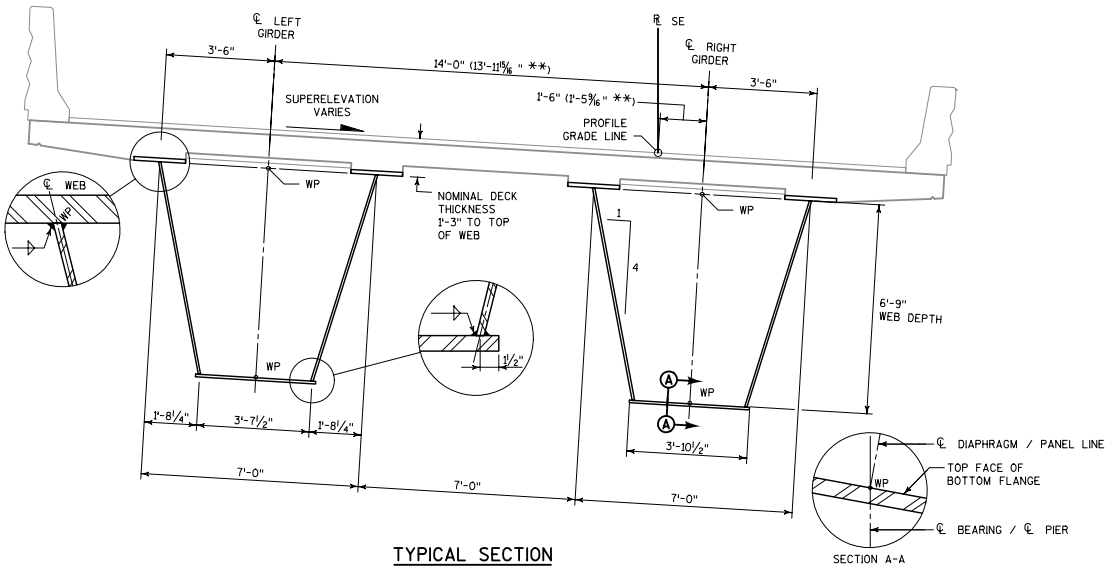

TYPICAL SECTION

LOOKING UPSTATION

LOCATION	STATION	TOP OF ERECTED STEEL (TES)			
		LEFT GIRDER		RIGHT GIRDER	
		LEFT WEB	RIGHT WEB	LEFT WEB	RIGHT WEB
CL BEARING PIER SE1	39SE+73.26	669.30	669.56	669.81	670.06
FIELD SPLICE #1	40SE+77.97	664.47	664.78	665.09	665.40
CL PIER SE2	41SE+19.51	662.87	663.15	663.42	663.70
FIELD SPLICE #2	41SE+64.14	661.78	661.96	662.14	662.32
FIELD SPLICE #3	42SE+59.82	659.61	659.60	659.59	659.58
CL PIER SE3	43SE+04.51	658.29	658.19	658.10	658.00
FIELD SPLICE #4	43SE+49.14	657.10	656.91	656.71	656.53
FIELD SPLICE #5	44SE+44.82	653.90	653.52	653.14	652.76
CL PIER SE4	44SE+89.51	652.14	651.72	651.30	650.88
FIELD SPLICE #6	45SE+58.41	649.58	649.13	648.64	648.19
FIELD SPLICE #7	46SE+50.65	645.02	644.57	644.07	643.63
CL PIER SE5	47SE+19.51	641.14	640.72	640.30	639.88
FIELD SPLICE #8	47SE+60.42	639.57	639.15	638.74	638.32
FIELD SPLICE #9	48SE+46.18	637.41	636.99	636.58	636.16
CL PIER SE6	48SE+87.09	636.87	636.45	636.03	635.61
FIELD SPLICE #10	49SE+30.22	636.89	636.46	636.01	635.58
CL BEARING PIER SE7	50SE+39.56	637.45	637.14	636.82	636.51

NOTES

1. ENSURE THE STABILITY OF ALL COMPONENTS DURING FABRICATION, HANDLING, TRANSPORTATION AND ERECTION UNTIL THE STRUCTURAL STEEL IS IN FINAL POSITION WITH ALL PERMANENT BRACING, CONNECTIONS AND SUPPORTS IN PLACE AND THE CONCRETE IN THE DECK HAS REACHED THE SPECIFIED DESIGN STRENGTH.

   DESIGN AND USE TEMPORARY CROSS FRAMES, SUPPORTS, BRACES OR WHATEVER OTHER MEANS AND METHODS DEEMED NECESSARY.
2. CARRY OUT DESIGN CALCULATIONS AS REQUIRED TO VERIFY MATERIAL STRESSES AND SUPPORT FORCES (INCLUDING UPLIFT) DURING ALL STAGES OF ERECTION AS REQUIRED BY AASHTO SPECIFICATIONS.
3. CAMBER DIAGRAMS HAVE BEEN DEVELOPED ASSUMING THAT ALL SLAB WEIGHT IS APPLIED TO A NON-COMPOSITE STRUCTURE. VERIFY THE VALIDITY OF THIS ASSUMPTION BASED ON THE SELECTED POUR SEQUENCE. ADJUST CAMBER TABLES AS NECESSARY FOR ANY EXPECTED VARIATIONS EXCEEDING .04' (½").
4. CAMBER GIRDERS TO THE VALUES SHOWN ON SHEETS 64 TO 72, AFTER INCORPORATING ANY REQUIRED ADJUSTMENTS FOR THE SELECTED POUR SEQUENCE.
5. TOP OF ERECTED STEEL ELEVATION INCLUDES DEFLECTIONS DUE TO SELF WEIGHT OF STEEL AND STAY-IN-PLACE METAL FORMWORK ONLY. ELEVATIONS ARE GIVEN AT CENTERLINE OF TOP FLANGE OR TOP FLANGE SPLICE PLATE, AS APPLICABLE.
6. BASED ON A DETAILED STUDY OF THE REDUNDANCY OF THIS STRUCTURE, THERE ARE NO ELEMENTS TO BE OFFICIALLY CLASSIFIED AS FRACTURE CRITICAL MEMBERS (FCM).
7. STEEL FABRICATION AND TESTING STANDARDS SHALL BE THE SAME AS IF TOP AND BOTTOM GIRDER FLANGES (WITHIN TENSION ZONES) AND ALL WEB PLATES WERE CLASSIFIED AS FRACTURE CRITICAL MEMBERS (FCM).

MINIMUM FILLET WELD SIZE:

THICKNESS OF THICKER PART JOINED	MINIMUM WELD SIZE
T <= ½"	3/16"
½" < T <= ¾"	¼"
¾" < T <= 1½"	5/16"
1½" < T <= 2¼"	3/8"
T > 2¼"	½"

1. MINIMUM WELD SIZES SHOWN SHALL BE USED WHEN A SIZE IS NOT OTHERWISE SPECIFIED OR SHOWN.
2. WELD SIZE SHALL NOT EXCEED THE THICKNESS OF THE THINNER PART BEING JOINED.
3. FOR ALL WELDS 5/16" OR LARGER, THE MINIMUM PASS SIZE SHALL BE 5/16".

** DENOTES ALTERNATIVE HORIZONTAL DIMENSIONS CALCULATED BASED ON AN AVERAGE SUPERELEVATION OF -2.89%

HORIZONTAL DIMENSIONS ARE GIVEN BETWEEN THE REFERENCE LINE AT FINISHED TOP OF DECK ELEVATION AND THE TOP FLANGE GIRDER CENTERLINE WORKPOINTS AS SHOWN.

CONTRACTOR MAY ELECT TO DETAIL AND FABRICATE STEEL GIRDERS BASED ON EITHER THE SLOPED DIMENSIONS OR THE ALTERNATIVE HORIZONTAL DIMENSIONS.

ALL OTHER DIMENSIONS SHALL REMAIN UNMODIFIED AND TAKEN ALONG THE SLOPE AS SHOWN.

ADDENDUM #2
REV SHT 1951
07/15/05

NO.	DATE	REVISION	BY

STATE OF WISCONSIN
DEPARTMENT OF TRANSPORTATION
STRUCTURES DESIGN SECTION

STRUCTURE B-40-1122

CONST. SPEC.	2004	DRAWN BY	KGW	PLANS CK'D.	RSR

GIRDER SECTION & ELEVATIONS

SHEET 46 OF 109

1951

JUL 07 2005

8

STATE PROJECT NUMBER
1060-05-75

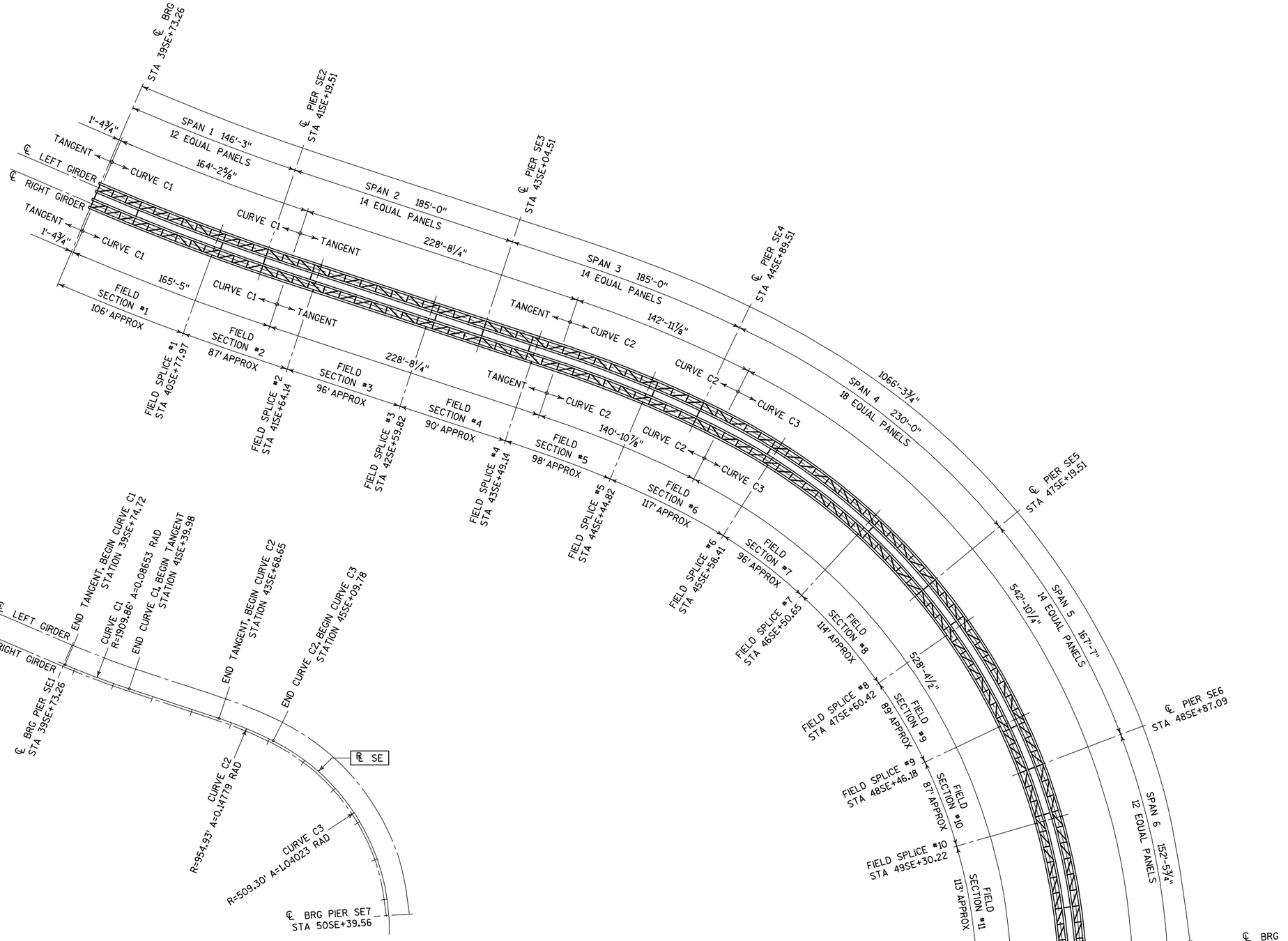

PLAN LAYOUT SKETCH

NOT TO SCALE

NOTES

1. ALL DIMENSIONS SHOWN ARE ASSUMED TO BE MEASURED AT 70°F.
2. SPAN AND UNIT LENGTHS SHOWN ARE MEASURED HORIZONTALLY ALONG THE VERTICAL PLANE DEFINED BY THE REFERENCE LINE.
3. FIELD SECTION LENGTHS ARE MEASURED ALONG THE OUTSIDE EDGE OF THE LONGEST TOP FLANGE AND ARE ROUNDED UP TO THE NEXT EVEN FOOT.
4. CURVE LENGTHS SHOWN ARE MEASURED HORIZONTALLY ALONG THE VERTICAL PLANE DEFINED BY THE CENTERLINE OF LEFT OR RIGHT GIRDER AS APPLICABLE. SEE SHEET 46 FOR LOCATION OF CENTERLINE GIRDER WORK POINTS.
5. RELOCATION OF FIELD SPLICES MAY BE ACCEPTED BUT WILL REQUIRE REDESIGN BY THE CONTRACTOR AND ACCEPTANCE BY THE ENGINEER. ADDITIONAL FIELD SPLICES WILL NOT BE ACCEPTED.
6. ADDITIONAL SHOP SPLICES MAY BE ADDED IF REQUIRED TO SUIT AVAILABLE MATERIAL LENGTHS. THE NUMBER AND LOCATION OF ADDITIONAL SPLICES IS SUBJECT TO ACCEPTANCE BY THE ENGINEER.

NO.	DATE	REVISION	BY

STATE OF WISCONSIN
DEPARTMENT OF TRANSPORTATION
STRUCTURES DESIGN SECTION

STRUCTURE B-40-1122

CONST. SPEC.	2004	DRAWN BY	KGW	PLANS CK'D.	RSR

FRAMING PLAN

SHEET 47 OF 109

MAR 22 2005

8

FILE NAME: C:\KPLOT\00047.dgn PEN TABLE: \\mtp\FinalDgn\config\plot\pentbls\bridge.pen Date: 23-MAR-2005 07:05 Plotted by: kwills

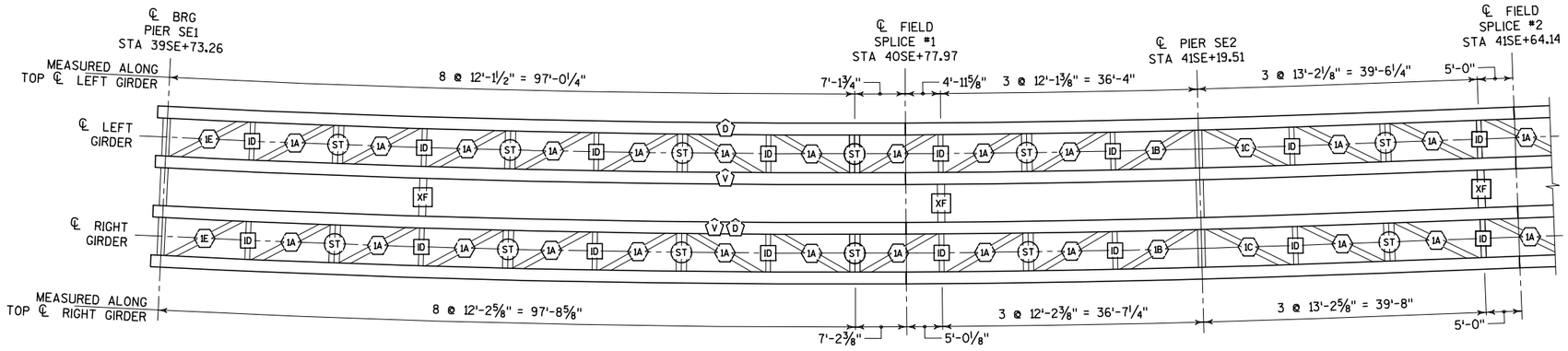

GIRDER PLAN

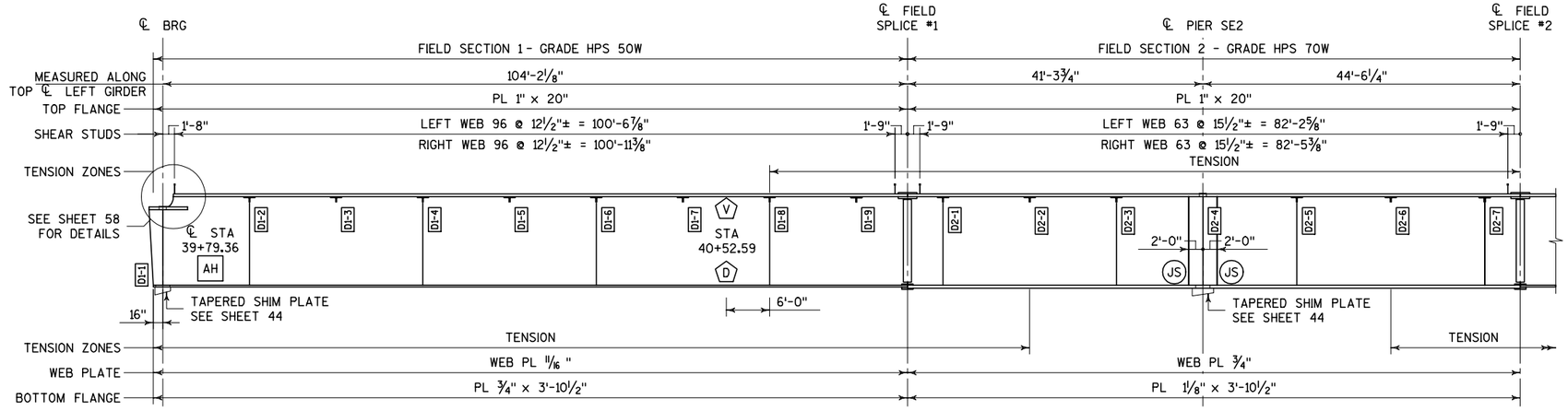

LEFT GIRDER INTERIOR ELEVATION

VERTICAL SCALE EXAGGERATED

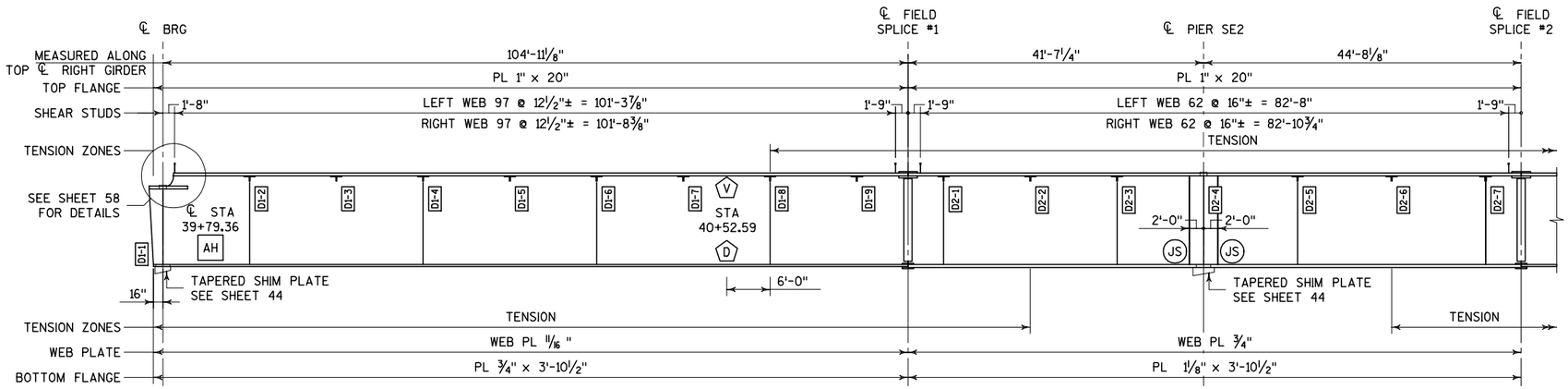

RIGHT GIRDER INTERIOR ELEVATION

VERTICAL SCALE EXAGGERATED

LEGEND

- ID — INTERNAL DIAPHRAGM LOCATION. SEE SHEET 59
- ST — TRANSVERSE STRUT LOCATION. SEE SHEET 59
- XF — EXTERIOR CROSS FRAME LOCATION. SEE SHEET 60
- 1A — LATERAL BRACING MARK NUMBER. SEE SHEET 61
- D — BOTTOM FLANGE DRAIN HOLE LOCATION. SEE DETAIL ON SHEET 63
- V — WEB PLATE VENT HOLE LOCATION. SEE DETAIL ON SHEET 63
- AH — BOTTOM FLANGE ACCESS HATCH LOCATION. SEE DETAIL ON SHEET 62
- D1-8 — DIAPHRAGM LOCATION NUMBER
- JS — JACKING STIFFENER LOCATION. SEE DETAIL ON SHEET 45

NOTES

1. STATIONS SHOWN FOR DIAPHRAGM AND STRUT LOCATIONS REFER TO THE BOTTOM FLANGE WORKPOINT. SEE DETAIL ON SHEET 46.
2. SEE SHEET 57 FOR TYPICAL CROSS FRAMES AND DIAPHRAGMS AT INTERIOR PIERS SE2, SE3, SE4, SE5 AND SE6.
3. SEE SHEET 58 FOR CROSS FRAMES AND DIAPHRAGMS AT END PIERS SE1 AND SE7.
4. SEE SHEET 63 FOR MISCELLANEOUS GIRDER DETAILS.
5. SEE SHEETS 65 AND 66 FOR CAMBER REQUIREMENTS.
6. SEE SHOP SPLICE DETAIL ON SHEET 63 FOR OFFSET REQUIREMENTS TO AVOID CONFLICT WITH DIAPHRAGM CONNECTIONS.
7. ALL SHEAR STUDS ARE ⅞" ϕ BY 6" LONG. EACH POSITION SHOWN REPRESENTS 3 STUDS ON EACH GIRDER FLANGE, LOCATED 3" FROM EDGES OF FLANGE AND EQUALLY SPACED BETWEEN. SEE DETAIL ON SHEET 63.
8. 'TENSION' DENOTES ZONES OF TOP AND BOTTOM FLANGES ASSUMED TO CARRY TENSILE STRESS IN THE COMPLETED STRUCTURE.
9. STEEL GRADE FOR WEBS AND FLANGES SHALL BE AS FOLLOWS:

   FIELD SECTION 1: HPS 50W

   FIELD SECTION 2: HPS 70W

   STEEL GRADE FOR PIER AND INTERMEDIATE DIAPHRAGMS LOCATED WITHIN THESE FIELD SECTIONS SHALL BE THE SAME.
10. SEE SHEET 60 FOR STEEL GRADE FOR EXTERIOR CROSS FRAMES. ALL OTHER STEEL (INCLUDING ROLLED SHAPES) SHALL BE GRADE 50.

NO.	DATE	REVISION	BY

STATE OF WISCONSIN
DEPARTMENT OF TRANSPORTATION
STRUCTURES DESIGN SECTION

STRUCTURE B-40-1122

CONST. SPEC.	DRAWN BY	PLANS CK'D.
2004	KGW	RSR

GIRDER PLAN & ELEVATION: FIELD SECTIONS 1 & 2

SHEET 48 OF 109

MAR 22 2005

8

STATE PROJECT NUMBER

1060-05-75

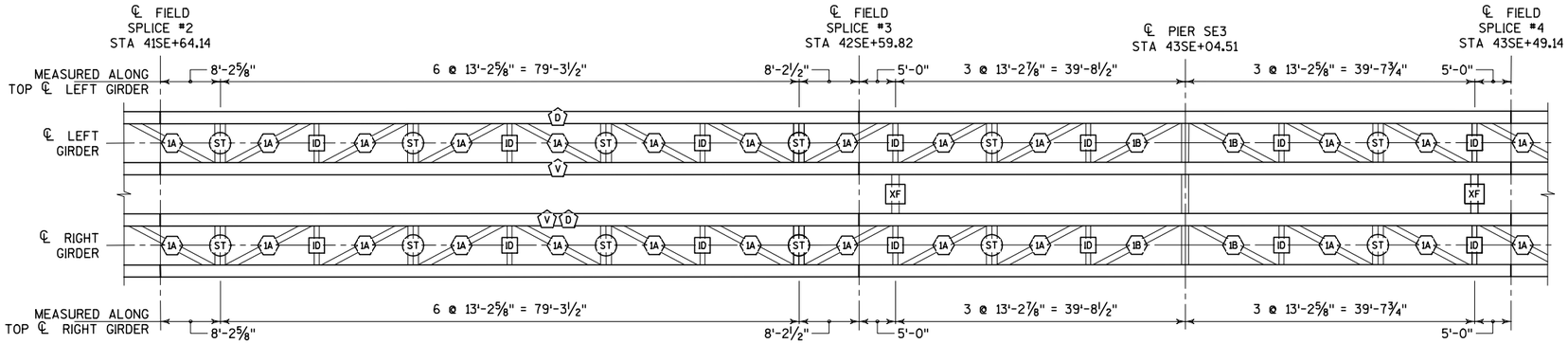

GIRDER PLAN

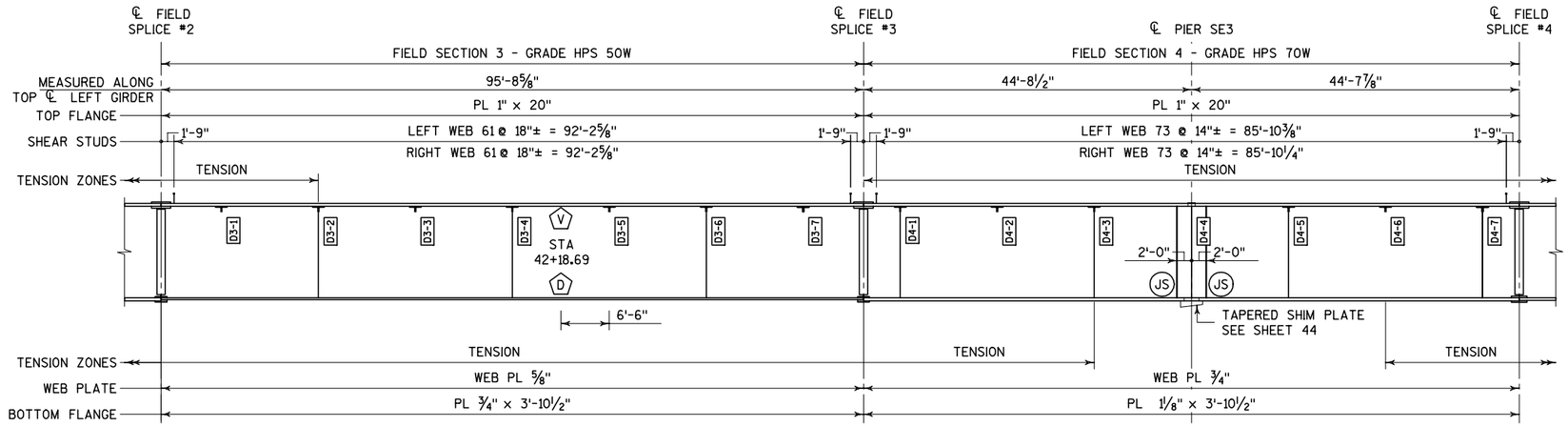

LEFT GIRDER INTERIOR ELEVATION

VERTICAL SCALE EXAGGERATED

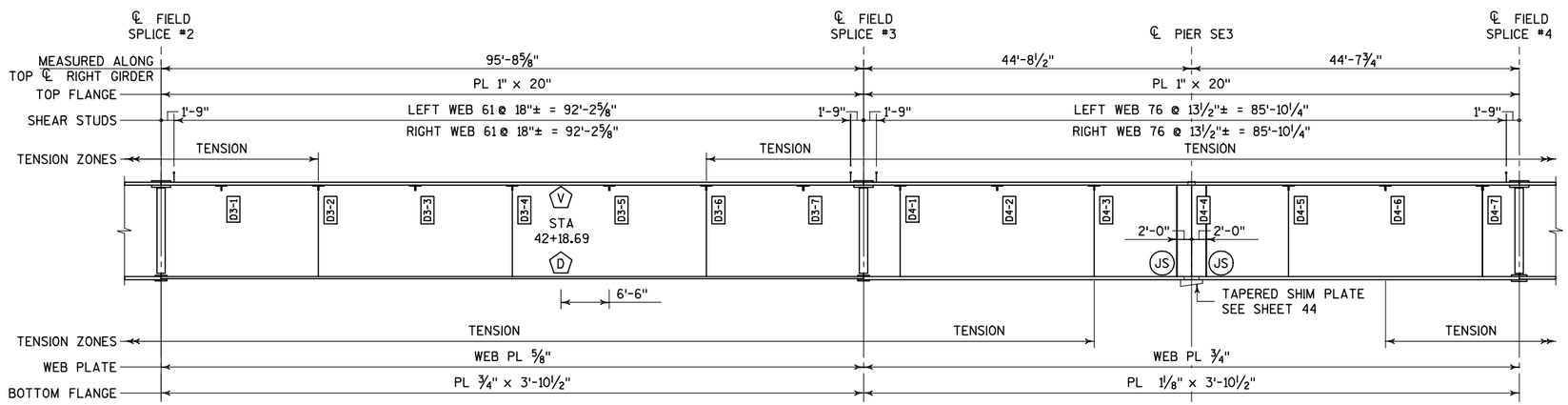

RIGHT GIRDER INTERIOR ELEVATION

VERTICAL SCALE EXAGGERATED

LEGEND

- ID — INTERNAL DIAPHRAGM LOCATION. SEE SHEET 59
- ST — TRANSVERSE STRUT LOCATION. SEE SHEET 59
- XF — EXTERIOR CROSS FRAME LOCATION. SEE SHEET 60
- 1A — LATERAL BRACING MARK NUMBER. SEE SHEET 61
- D — BOTTOM FLANGE DRAIN HOLE LOCATION. SEE DETAIL ON SHEET 63
- V — WEB PLATE VENT HOLE LOCATION. SEE DETAIL ON SHEET 63
- AH — BOTTOM FLANGE ACCESS HATCH LOCATION. SEE DETAIL ON SHEET 62
- D1-8 — DIAPHRAGM LOCATION NUMBER
- JS — JACKING STIFFENER LOCATION. SEE DETAIL ON SHEET 45

NOTES

1. STATIONS SHOWN FOR DIAPHRAGM AND STRUT LOCATIONS REFER TO THE BOTTOM FLANGE WORKPOINT. SEE DETAIL ON SHEET 46.
2. SEE SHEET 57 FOR TYPICAL CROSS FRAMES AND DIAPHRAGMS AT INTERIOR PIERS SE2, SE3, SE4, SE5 AND SE6.
3. SEE SHEET 58 FOR CROSS FRAMES AND DIAPHRAGMS AT END PIERS SE1 AND SE7.
4. SEE SHEET 63 FOR MISCELLANEOUS GIRDER DETAILS.
5. SEE SHEETS 66 AND 67 FOR CAMBER REQUIREMENTS.
6. SEE SHOP SPLICE DETAIL ON SHEET 63 FOR OFFSET REQUIREMENTS TO AVOID CONFLICT WITH DIAPHRAGM CONNECTIONS.
7. ALL SHEAR STUDS ARE 7/8" ϕ BY 6" LONG. EACH POSITION SHOWN REPRESENTS 3 STUDS ON EACH GIRDER FLANGE, LOCATED 3" FROM EDGES OF FLANGE AND EQUALLY SPACED BETWEEN. SEE DETAIL ON SHEET 63.
8. 'TENSION' DENOTES ZONES OF TOP AND BOTTOM FLANGES ASSUMED TO CARRY TENSILE STRESS IN THE COMPLETED STRUCTURE.
9. STEEL GRADE FOR WEBS AND FLANGES SHALL BE AS FOLLOWS:

   FIELD SECTION 3: HPS 50W

   FIELD SECTION 4: HPS 70W

   STEEL GRADE FOR PIER AND INTERMEDIATE DIAPHRAGMS LOCATED WITHIN THESE FIELD SECTIONS SHALL BE THE SAME.
10. SEE SHEET 60 FOR STEEL GRADE FOR EXTERIOR CROSS FRAMES. ALL OTHER STEEL (INCLUDING ROLLED SHAPES) SHALL BE GRADE 50.

NO.	DATE	REVISION	BY

STATE OF WISCONSIN
DEPARTMENT OF TRANSPORTATION
STRUCTURES DESIGN SECTION

STRUCTURE B-40-1122

CONST. SPEC.	DRAWN BY	PLANS CK'D.
2004	KGW	RSR

GIRDER PLAN & ELEVATION: FIELD SECTIONS 3 & 4

SHEET 49 OF 109

MAR 22 2005

8

FILE NAME: C:\KPLOT\00049.dgn PEN TABLE: \\mtp\FinalDgn\config\plot\pentbls\bridge.pen Date: 23-MAR-2005 07:06 Plotted by: kwills

STATE PROJECT NUMBER

1060-05-75

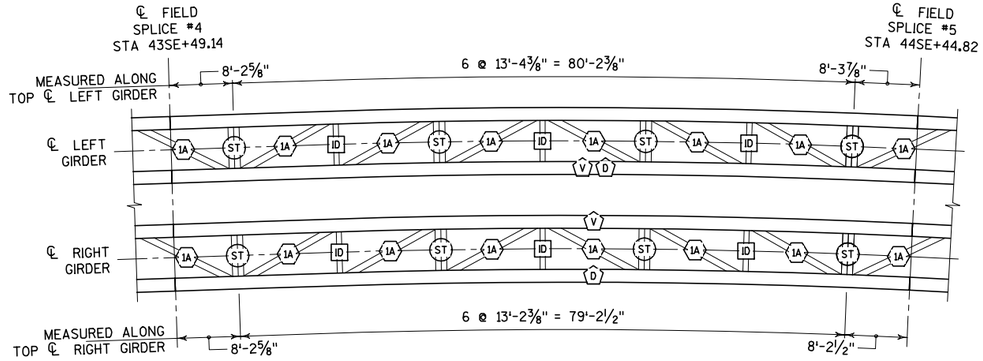

GIRDER PLAN

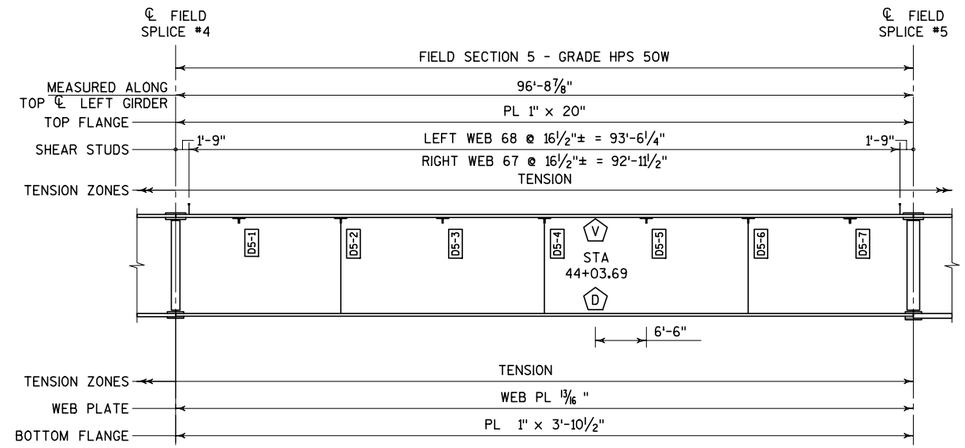

LEFT GIRDER INTERIOR ELEVATION

VERTICAL SCALE EXAGGERATED

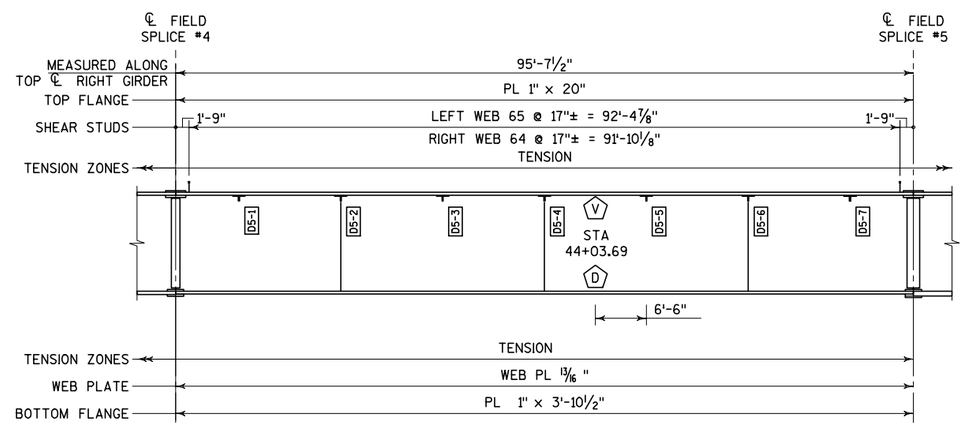

RIGHT GIRDER INTERIOR ELEVATION

VERTICAL SCALE EXAGGERATED

LEGEND

ID	INTERNAL DIAPHRAGM LOCATION. SEE SHEET 59
ST	TRANSVERSE STRUT LOCATION. SEE SHEET 59
XF	EXTERIOR CROSS FRAME LOCATION. SEE SHEET 60
1A	LATERAL BRACING MARK NUMBER. SEE SHEET 61
D	BOTTOM FLANGE DRAIN HOLE LOCATION. SEE DETAIL ON SHEET 63
V	WEB PLATE VENT HOLE LOCATION. SEE DETAIL ON SHEET 63
AH	BOTTOM FLANGE ACCESS HATCH LOCATION. SEE DETAIL ON SHEET 62
D1-8	DIAPHRAGM LOCATION NUMBER
JS	JACKING STIFFENER LOCATION. SEE DETAIL ON SHEET 45

NOTES

1. STATIONS SHOWN FOR DIAPHRAGM AND STRUT LOCATIONS REFER TO THE BOTTOM FLANGE WORKPOINT. SEE DETAIL ON SHEET 46.
2. SEE SHEET 57 FOR TYPICAL CROSS FRAMES AND DIAPHRAGMS AT INTERIOR PIERS SE2, SE3, SE4, SE5 AND SE6.
3. SEE SHEET 58 FOR CROSS FRAMES AND DIAPHRAGMS AT END PIERS SE1 AND SE7.
4. SEE SHEET 63 FOR MISCELLANEOUS GIRDER DETAILS.
5. SEE SHEET 67 FOR CAMBER REQUIREMENTS.
6. SEE SHOP SPLICE DETAIL ON SHEET 63 FOR OFFSET REQUIREMENTS TO AVOID CONFLICT WITH DIAPHRAGM CONNECTIONS.
7. ALL SHEAR STUDS ARE ⅞" ϕ BY 6" LONG. EACH POSITION SHOWN REPRESENTS 3 STUDS ON EACH GIRDER FLANGE, LOCATED 3" FROM EDGES OF FLANGE AND EQUALLY SPACED BETWEEN. SEE DETAIL ON SHEET 63.
8. 'TENSION' DENOTES ZONES OF TOP AND BOTTOM FLANGES ASSUMED TO CARRY TENSILE STRESS IN THE COMPLETED STRUCTURE.
9. STEEL GRADE FOR WEBS AND FLANGES SHALL BE AS FOLLOWS:

   FIELD SECTION 5: HPS 50W

   STEEL GRADE FOR PIER AND INTERMEDIATE DIAPHRAGMS LOCATED WITHIN THESE FIELD SECTIONS SHALL BE THE SAME.
10. SEE SHEET 60 FOR STEEL GRADE FOR EXTERIOR CROSS FRAMES. ALL OTHER STEEL (INCLUDING ROLLED SHAPES) SHALL BE GRADE 50.

NO.	DATE	REVISION	BY

STATE OF WISCONSIN
DEPARTMENT OF TRANSPORTATION
STRUCTURES DESIGN SECTION

STRUCTURE B-40-1122

CONST. SPEC.	DRAWN BY	PLANS CK'D.
2004	KGW	RSR

GIRDER PLAN & ELEVATION: FIELD SECTION 5

SHEET 50 OF 109

MAR 22 2005

8

STATE PROJECT NUMBER
1060-05-75

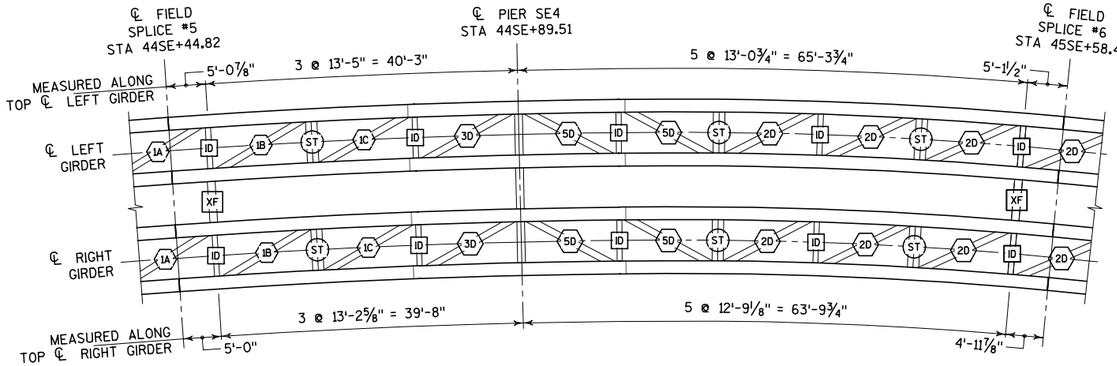

GIRDER PLAN

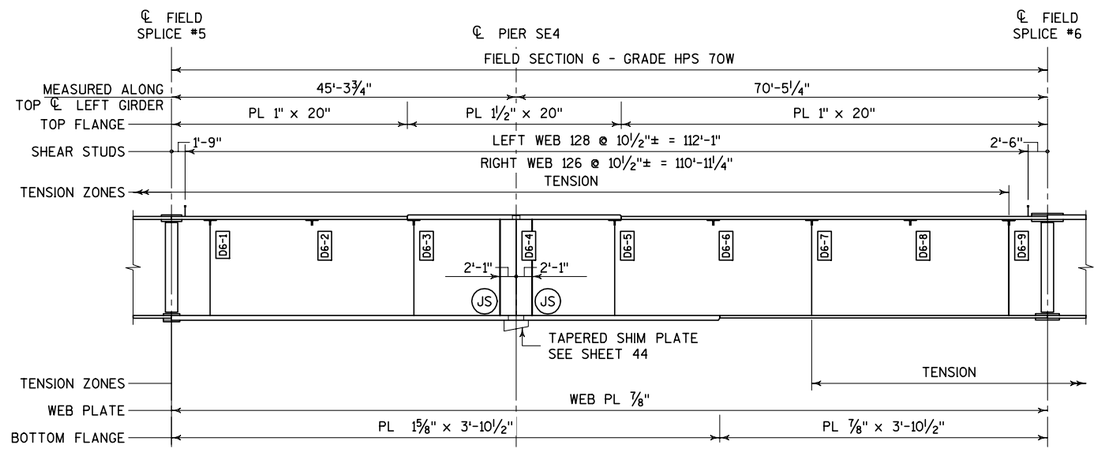

LEFT GIRDER INTERIOR ELEVATION

VERTICAL SCALE EXAGGERATED

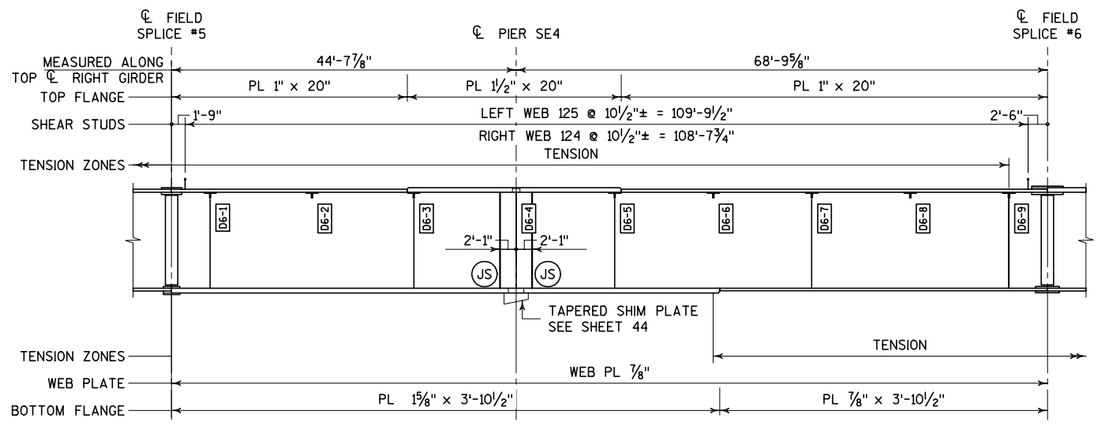

RIGHT GIRDER INTERIOR ELEVATION

VERTICAL SCALE EXAGGERATED

LEGEND

ID	INTERNAL DIAPHRAGM LOCATION. SEE SHEET 59
ST	TRANSVERSE STRUT LOCATION. SEE SHEET 59
XF	EXTERIOR CROSS FRAME LOCATION. SEE SHEET 60
1A	LATERAL BRACING MARK NUMBER. SEE SHEET 61
D	BOTTOM FLANGE DRAIN HOLE LOCATION. SEE DETAIL ON SHEET 63
V	WEB PLATE VENT HOLE LOCATION. SEE DETAIL ON SHEET 63
AH	BOTTOM FLANGE ACCESS HATCH LOCATION. SEE DETAIL ON SHEET 62
D1-8	DIAPHRAGM LOCATION NUMBER
JS	JACKING STIFFENER LOCATION. SEE DETAIL ON SHEET 45

NOTES

1. STATIONS SHOWN FOR DIAPHRAGM AND STRUT LOCATIONS REFER TO THE BOTTOM FLANGE WORKPOINT. SEE DETAIL ON SHEET 46.
2. SEE SHEET 57 FOR TYPICAL CROSS FRAMES AND DIAPHRAGMS AT INTERIOR PIERS SE2, SE3, SE4, SE5 AND SE6.
3. SEE SHEET 58 FOR CROSS FRAMES AND DIAPHRAGMS AT END PIERS SE1 AND SE7.
4. SEE SHEET 63 FOR MISCELLANEOUS GIRDER DETAILS.
5. SEE SHEET 68 FOR CAMBER REQUIREMENTS.
6. SEE SHOP SPLICE DETAIL ON SHEET 63 FOR OFFSET REQUIREMENTS TO AVOID CONFLICT WITH DIAPHRAGM CONNECTIONS.
7. ALL SHEAR STUDS ARE 7/8" ϕ BY 6" LONG. EACH POSITION SHOWN REPRESENTS 3 STUDS ON EACH GIRDER FLANGE, LOCATED 3" FROM EDGES OF FLANGE AND EQUALLY SPACED BETWEEN. SEE DETAIL ON SHEET 63.
8. 'TENSION' DENOTES ZONES OF TOP AND BOTTOM FLANGES ASSUMED TO CARRY TENSILE STRESS IN THE COMPLETED STRUCTURE.
9. STEEL GRADE FOR WEBS AND FLANGES SHALL BE AS FOLLOWS:

   FIELD SECTION 6: HPS 70W

   STEEL GRADE FOR PIER AND INTERMEDIATE DIAPHRAGMS LOCATED WITHIN THESE FIELD SECTIONS SHALL BE THE SAME.
10. SEE SHEET 60 FOR STEEL GRADE FOR EXTERIOR CROSS FRAMES. ALL OTHER STEEL (INCLUDING ROLLED SHAPES) SHALL BE GRADE 50.

NO.	DATE	REVISION	BY

STATE OF WISCONSIN
DEPARTMENT OF TRANSPORTATION
STRUCTURES DESIGN SECTION

STRUCTURE B-40-1122

CONST. SPEC.	DRAWN BY	PLANS CK'D.
2004	KGW	RSR

GIRDER PLAN & ELEVATION: FIELD SECTION 6

SHEET 51 OF 109

MAR 22 2005

8

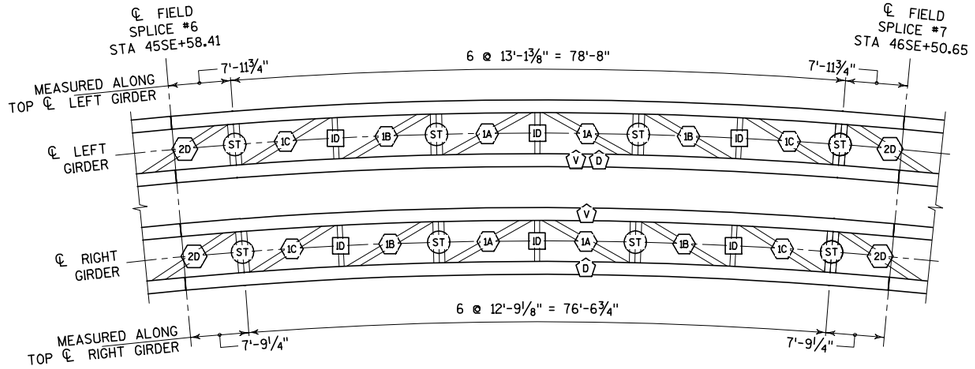

GIRDER PLAN

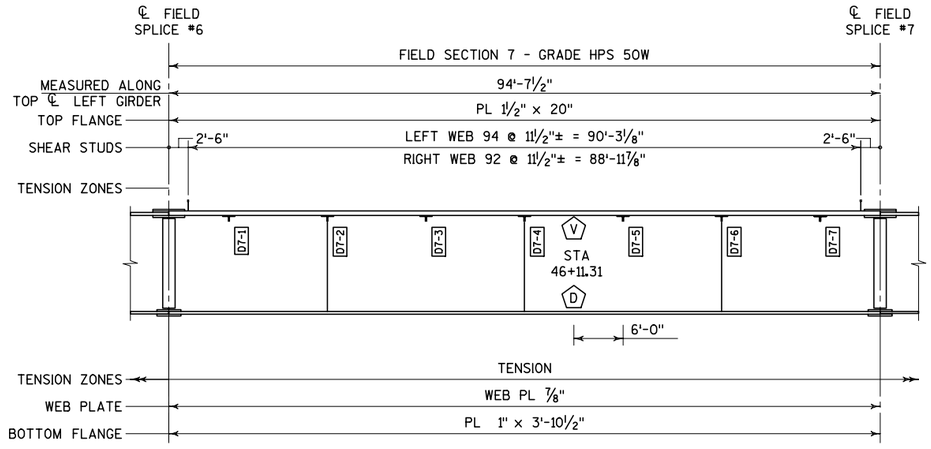

LEFT GIRDER INTERIOR ELEVATION

VERTICAL SCALE EXAGGERATED

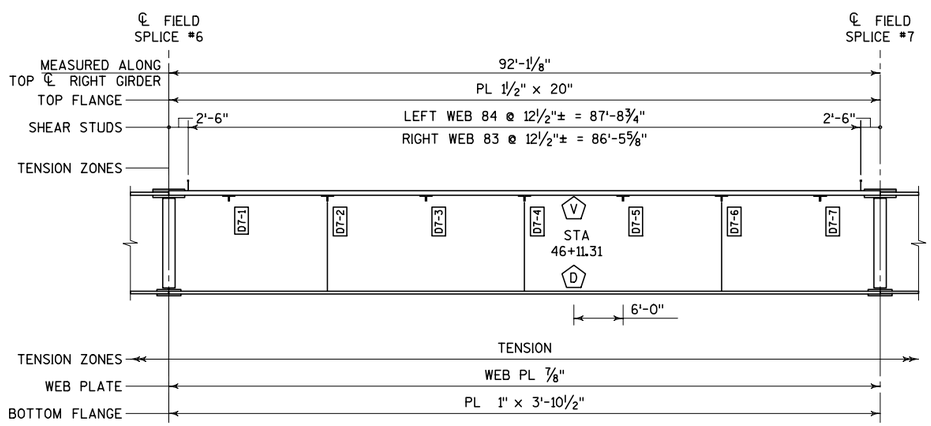

RIGHT GIRDER INTERIOR ELEVATION

VERTICAL SCALE EXAGGERATED

LEGEND

- ID — INTERNAL DIAPHRAGM LOCATION. SEE SHEET 59
- ST — TRANSVERSE STRUT LOCATION. SEE SHEET 59
- XF — EXTERIOR CROSS FRAME LOCATION. SEE SHEET 60
- 1A — LATERAL BRACING MARK NUMBER. SEE SHEET 61
- D — BOTTOM FLANGE DRAIN HOLE LOCATION. SEE DETAIL ON SHEET 63
- V — WEB PLATE VENT HOLE LOCATION. SEE DETAIL ON SHEET 63
- AH — BOTTOM FLANGE ACCESS HATCH LOCATION. SEE DETAIL ON SHEET 62
- D1-8 — DIAPHRAGM LOCATION NUMBER
- JS — JACKING STIFFENER LOCATION. SEE DETAIL ON SHEET 45

NOTES

1. STATIONS SHOWN FOR DIAPHRAGM AND STRUT LOCATIONS REFER TO THE BOTTOM FLANGE WORKPOINT. SEE DETAIL ON SHEET 46.
2. SEE SHEET 57 FOR TYPICAL CROSS FRAMES AND DIAPHRAGMS AT INTERIOR PIERS SE2, SE3, SE4, SE5 AND SE6.
3. SEE SHEET 58 FOR CROSS FRAMES AND DIAPHRAGMS AT END PIERS SE1 AND SE7.
4. SEE SHEET 63 FOR MISCELLANEOUS GIRDER DETAILS.
5. SEE SHEET 69 FOR CAMBER REQUIREMENTS.
6. SEE SHOP SPLICE DETAIL ON SHEET 63 FOR OFFSET REQUIREMENTS TO AVOID CONFLICT WITH DIAPHRAGM CONNECTIONS.
7. ALL SHEAR STUDS ARE ⅞" ϕ BY 6" LONG. EACH POSITION SHOWN REPRESENTS 3 STUDS ON EACH GIRDER FLANGE, LOCATED 3" FROM EDGES OF FLANGE AND EQUALLY SPACED BETWEEN. SEE DETAIL ON SHEET 63.
8. 'TENSION' DENOTES ZONES OF TOP AND BOTTOM FLANGES ASSUMED TO CARRY TENSILE STRESS IN THE COMPLETED STRUCTURE.
9. STEEL GRADE FOR WEBS AND FLANGES SHALL BE AS FOLLOWS:

   FIELD SECTION 7: HPS 50W

   STEEL GRADE FOR PIER AND INTERMEDIATE DIAPHRAGMS LOCATED WITHIN THESE FIELD SECTIONS SHALL BE THE SAME.
10. SEE SHEET 60 FOR STEEL GRADE FOR EXTERIOR CROSS FRAMES. ALL OTHER STEEL (INCLUDING ROLLED SHAPES) SHALL BE GRADE 50.

NO.	DATE	REVISION	BY

STATE PROJECT NUMBER

1060-05-75

STATE OF WISCONSIN
DEPARTMENT OF TRANSPORTATION
STRUCTURES DESIGN SECTION

STRUCTURE B-40-1122

CONST. SPEC.	DRAWN BY	PLANS CK'D.
2004	KGW	RSR

GIRDER PLAN & ELEVATION: FIELD SECTION 7

SHEET 52 OF 109

MAR 22 2005

8

FILE NAME: C:\KPLOT\00052.dgn PEN TABLE: \\mtp\FinalDgn\config\plot\pentbls\bridge.pen Date: 23-MAR-2005 07:08 Plotted by: kwillis

STATE PROJECT NUMBER
1060-05-75

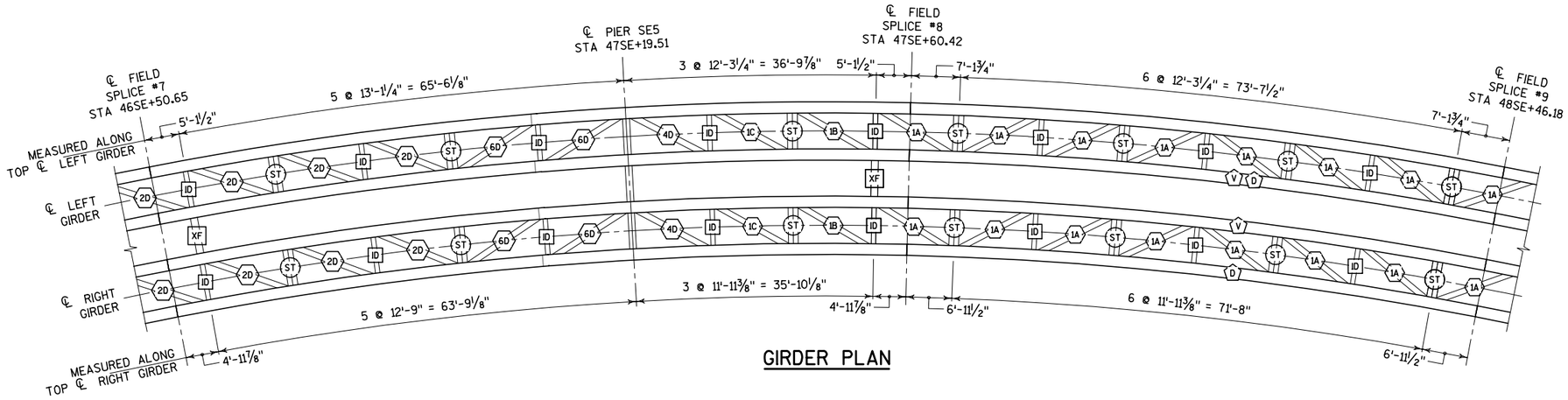

GIRDER PLAN

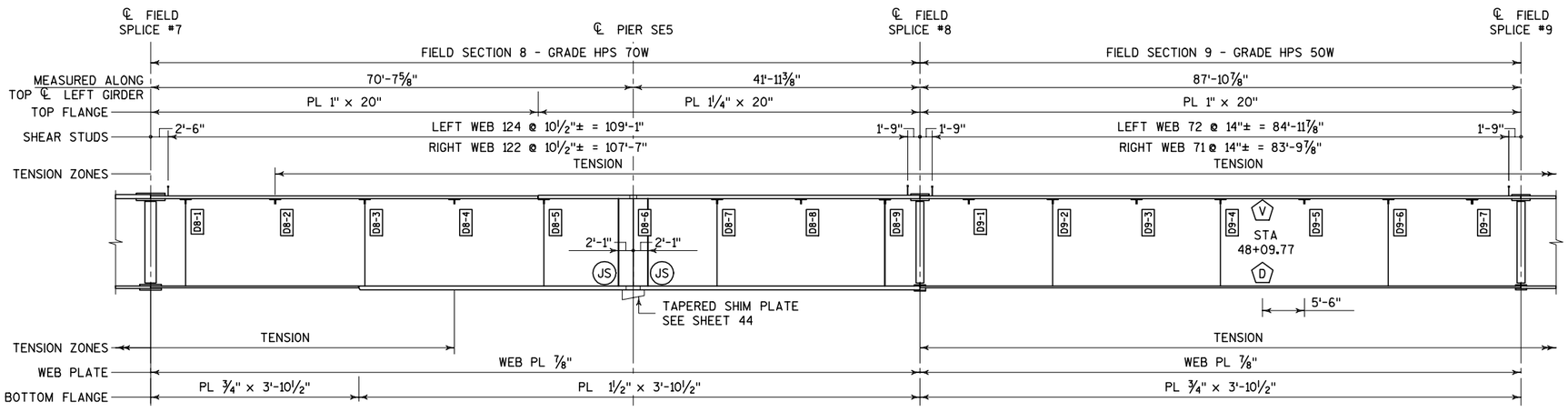

LEFT GIRDER INTERIOR ELEVATION

VERTICAL SCALE EXAGGERATED

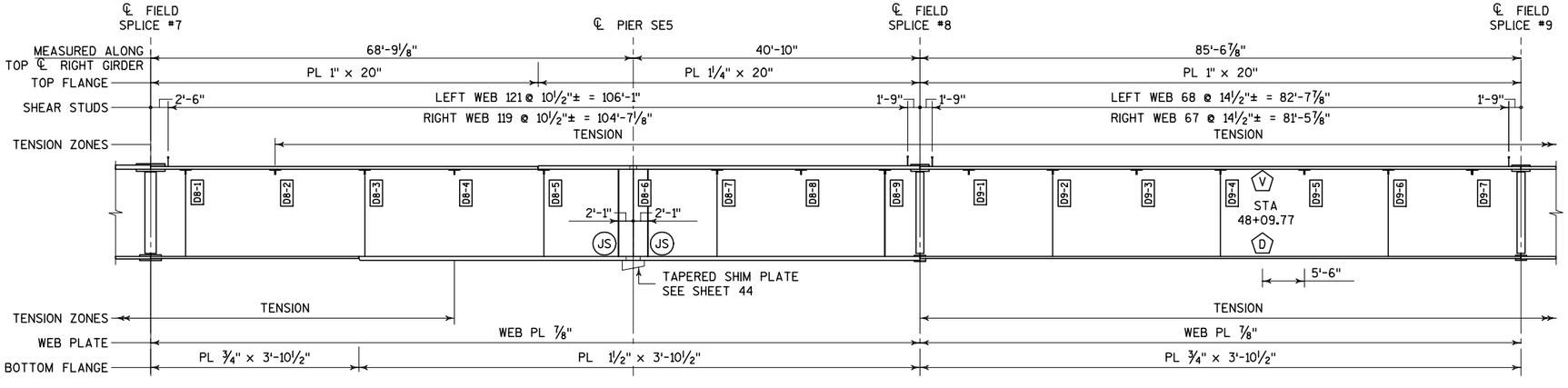

RIGHT GIRDER INTERIOR ELEVATION

VERTICAL SCALE EXAGGERATED

LEGEND

- ID — INTERNAL DIAPHRAGM LOCATION. SEE SHEET 59
- ST — TRANSVERSE STRUT LOCATION. SEE SHEET 59
- XF — EXTERIOR CROSS FRAME LOCATION. SEE SHEET 60
- 1A — LATERAL BRACING MARK NUMBER. SEE SHEET 61
- D — BOTTOM FLANGE DRAIN HOLE LOCATION. SEE DETAIL ON SHEET 63
- V — WEB PLATE VENT HOLE LOCATION. SEE DETAIL ON SHEET 63
- AH — BOTTOM FLANGE ACCESS HATCH LOCATION. SEE DETAIL ON SHEET 62
- D1-8 — DIAPHRAGM LOCATION NUMBER
- JS — JACKING STIFFENER LOCATION. SEE DETAIL ON SHEET 45

NOTES

1. STATIONS SHOWN FOR DIAPHRAGM AND STRUT LOCATIONS REFER TO THE BOTTOM FLANGE WORKPOINT. SEE DETAIL ON SHEET 46.
2. SEE SHEET 57 FOR TYPICAL CROSS FRAMES AND DIAPHRAGMS AT INTERIOR PIERS SE2, SE3, SE4, SE5 AND SE6.
3. SEE SHEET 58 FOR CROSS FRAMES AND DIAPHRAGMS AT END PIERS SE1 AND SE7.
4. SEE SHEET 63 FOR MISCELLANEOUS GIRDER DETAILS.
5. SEE SHEETS 70 AND 71 FOR CAMBER REQUIREMENTS.
6. SEE SHOP SPLICE DETAIL ON SHEET 63 FOR OFFSET REQUIREMENTS TO AVOID CONFLICT WITH DIAPHRAGM CONNECTIONS.
7. ALL SHEAR STUDS ARE ⅞" ϕ BY 6" LONG. EACH POSITION SHOWN REPRESENTS 3 STUDS ON EACH GIRDER FLANGE, LOCATED 3" FROM EDGES OF FLANGE AND EQUALLY SPACED BETWEEN. SEE DETAIL ON SHEET 63.
8. 'TENSION' DENOTES ZONES OF TOP AND BOTTOM FLANGES ASSUMED TO CARRY TENSILE STRESS IN THE COMPLETED STRUCTURE.
9. STEEL GRADE FOR WEBS AND FLANGES SHALL BE AS FOLLOWS:

   FIELD SECTION 8: HPS 70W

   FIELD SECTION 9: HPS 50W

   STEEL GRADE FOR PIER AND INTERMEDIATE DIAPHRAGMS LOCATED WITHIN THESE FIELD SECTIONS SHALL BE THE SAME.
10. SEE SHEET 60 FOR STEEL GRADE FOR EXTERIOR CROSS FRAMES. ALL OTHER STEEL (INCLUDING ROLLED SHAPES) SHALL BE GRADE 50.

8

NO.	DATE	REVISION	BY

STATE OF WISCONSIN
DEPARTMENT OF TRANSPORTATION
STRUCTURES DESIGN SECTION

STRUCTURE B-40-1122

CONST. SPEC.	DRAWN BY	PLANS CK'D.
2004	KGW	RSR

GIRDER PLAN & ELEVATION: FIELD SECTIONS 8 & 9

SHEET 53 OF 109

MAR 22 2005

STATE PROJECT NUMBER
1060-05-75

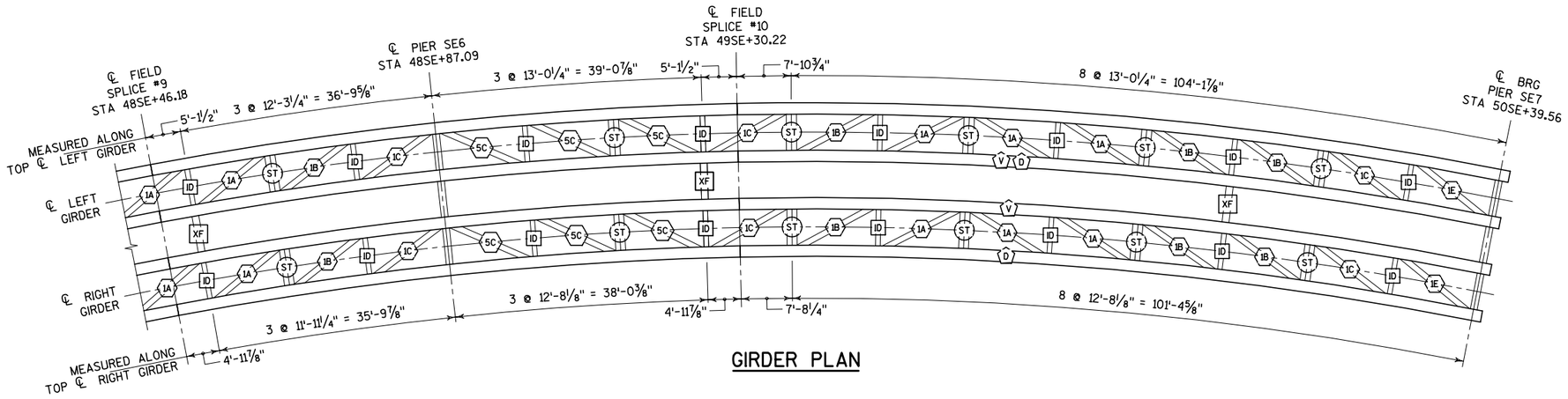

GIRDER PLAN

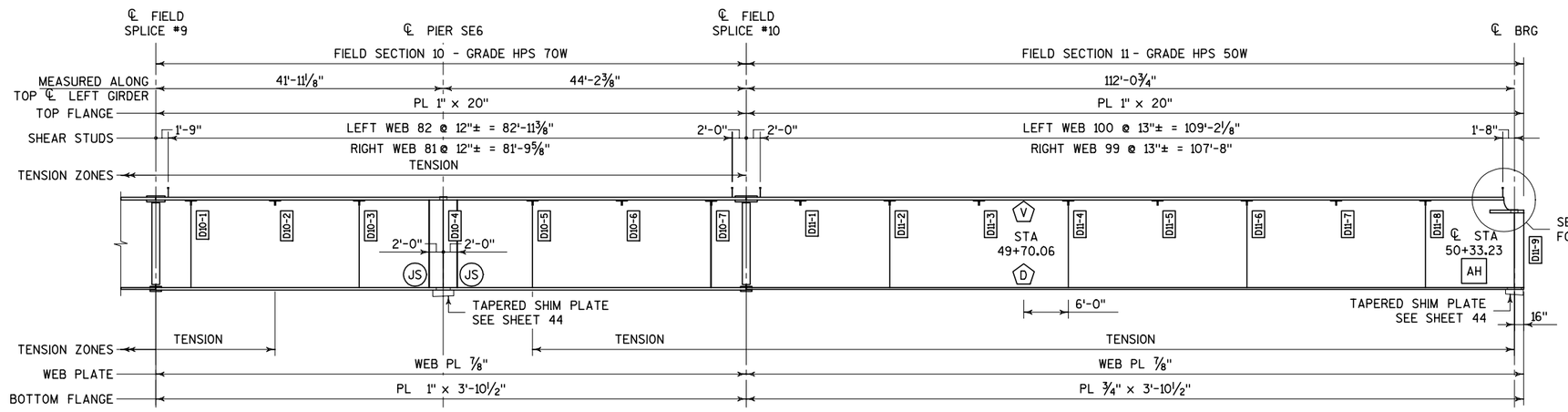

LEFT GIRDER INTERIOR ELEVATION

VERTICAL SCALE EXAGGERATED

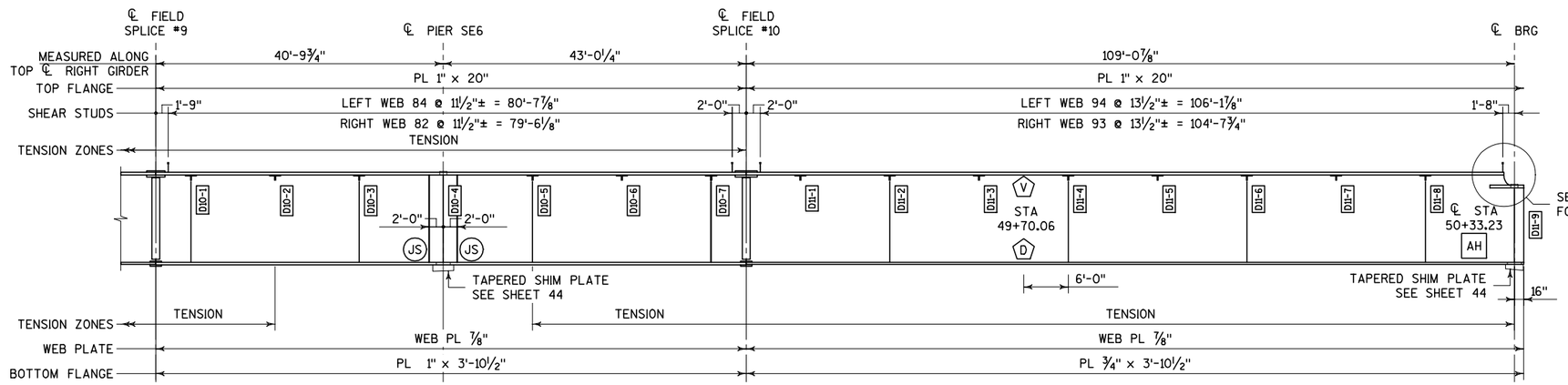

RIGHT GIRDER INTERIOR ELEVATION

VERTICAL SCALE EXAGGERATED

LEGEND

- [ID] INTERNAL DIAPHRAGM LOCATION. SEE SHEET 59
- (ST) TRANSVERSE STRUT LOCATION. SEE SHEET 59
- [XF] EXTERIOR CROSS FRAME LOCATION. SEE SHEET 60
- ⟨1A⟩ LATERAL BRACING MARK NUMBER. SEE SHEET 61
- ⟨D⟩ BOTTOM FLANGE DRAIN HOLE LOCATION. SEE DETAIL ON SHEET 63
- ⟨V⟩ WEB PLATE VENT HOLE LOCATION. SEE DETAIL ON SHEET 63
- [AH] BOTTOM FLANGE ACCESS HATCH LOCATION. SEE DETAIL ON SHEET 62
- [D1-8] DIAPHRAGM LOCATION NUMBER
- (JS) JACKING STIFFENER LOCATION. SEE DETAIL ON SHEET 45

NOTES

1. STATIONS SHOWN FOR DIAPHRAGM AND STRUT LOCATIONS REFER TO THE BOTTOM FLANGE WORKPOINT. SEE DETAIL ON SHEET 46.
2. SEE SHEET 57 FOR TYPICAL CROSS FRAMES AND DIAPHRAGMS AT INTERIOR PIERS SE2, SE3, SE4, SE5 AND SE6.
3. SEE SHEET 58 FOR CROSS FRAMES AND DIAPHRAGMS AT END PIERS SE1 AND SE7.
4. SEE SHEET 63 FOR MISCELLANEOUS GIRDER DETAILS.
5. SEE SHEETS 71 AND 72 FOR CAMBER REQUIREMENTS.
6. SEE SHOP SPLICE DETAIL ON SHEET 63 FOR OFFSET REQUIREMENTS TO AVOID CONFLICT WITH DIAPHRAGM CONNECTIONS.
7. ALL SHEAR STUDS ARE ⅞" ϕ BY 6" LONG. EACH POSITION SHOWN REPRESENTS 3 STUDS ON EACH GIRDER FLANGE, LOCATED 3" FROM EDGES OF FLANGE AND EQUALLY SPACED BETWEEN. SEE DETAIL ON SHEET 63.
8. 'TENSION' DENOTES ZONES OF TOP AND BOTTOM FLANGES ASSUMED TO CARRY TENSILE STRESS IN THE COMPLETED STRUCTURE.
9. STEEL GRADE FOR WEBS AND FLANGES SHALL BE AS FOLLOWS:

   FIELD SECTION 10: HPS 70W

   FIELD SECTION 11: HPS 50W

   STEEL GRADE FOR PIER AND INTERMEDIATE DIAPHRAGMS LOCATED WITHIN THESE FIELD SECTIONS SHALL BE THE SAME.
10. SEE SHEET 60 FOR STEEL GRADE FOR EXTERIOR CROSS FRAMES. ALL OTHER STEEL (INCLUDING ROLLED SHAPES) SHALL BE GRADE 50.

NO.	DATE	REVISION	BY

STATE OF WISCONSIN
DEPARTMENT OF TRANSPORTATION
STRUCTURES DESIGN SECTION

STRUCTURE B-40-1122

CONST. SPEC.	DRAWN BY	PLANS CK'D.
2004	KGW	RSR

GIRDER PLAN & ELEVATION: FIELD SECTIONS 10 & 11

SHEET 54 OF 109

MAR 22 2005

8

FILE NAME: C:\KPLOT\00054.dgn PEN TABLE: \\mtp\FinalDgn\config\plot\pentbls\bridge.pen Date: 23-MAR-2005 07:09 Plotted by: kwills

STATE PROJECT NUMBER
1060-05-75

TYPICAL TOP FLANGE CONNECTION

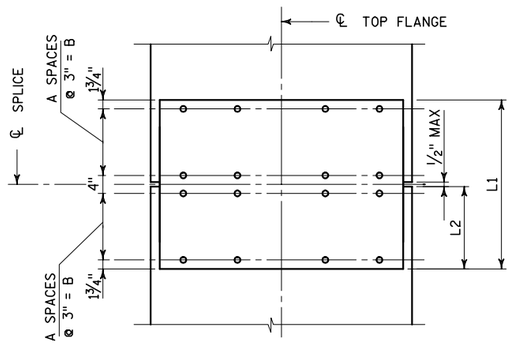

PLAN

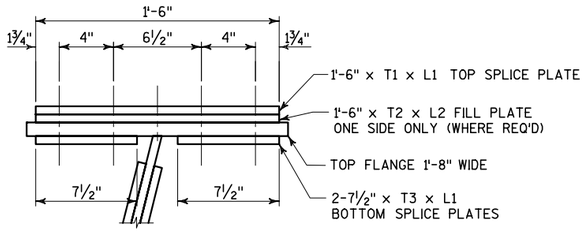

SECTION

TYPICAL BOTTOM FLANGE CONNECTION

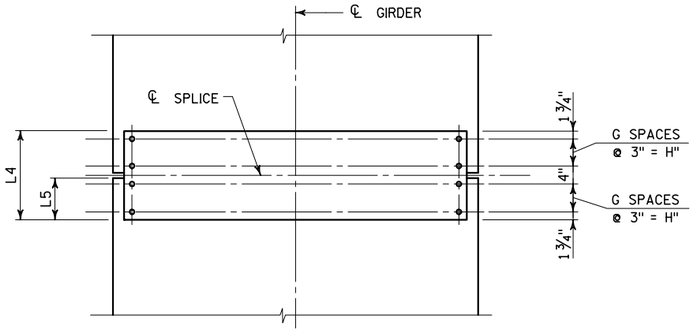

PLAN

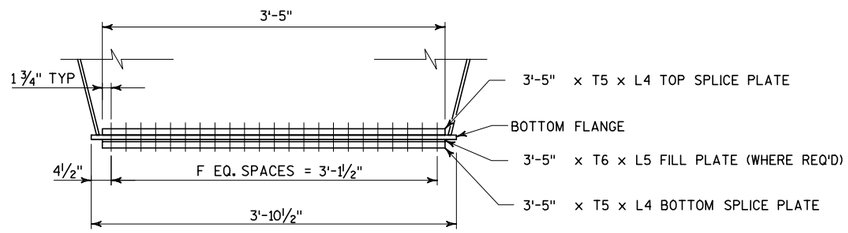

SECTION

TYPICAL WEB CONNECTION

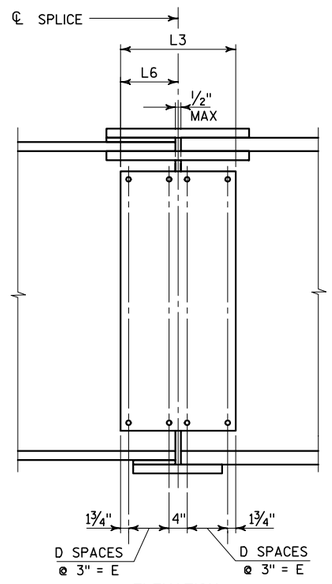

ELEVATION

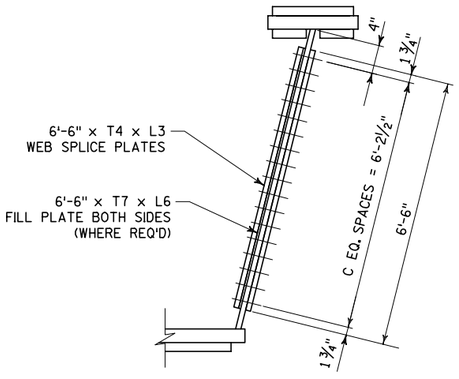

SECTION

NOTES

1. SEE SHEET 56 FOR VARIABLE DIMENSIONS AND SPACINGS DEFINED ON THIS SHEET.
2. ALL BOLTS SHOWN ARE ⅞" DIAMETER ASTM A325 TYPE 1.
3. ALL HOLES SHALL BE STANDARD DIAMETER - NO OVERSIZE HOLES.
4. ALL CONNECTIONS SHALL BE FABRICATED AND ASSEMBLED AS SLIP-CRITICAL CONNECTIONS.
5. ALL SPLICE PLATES SHALL BE GRADE HPS 70W.

8

NO.	DATE	REVISION	BY

STATE OF WISCONSIN
DEPARTMENT OF TRANSPORTATION
STRUCTURES DESIGN SECTION

STRUCTURE B-40-1122

CONST. SPEC.	2004	DRAWN BY	KGW	PLANS CK'D.	RSR

TYPICAL FIELD SPLICE LAYOUTS

SHEET 55 OF 109

MAR 22 2005

FILE NAME: C:\KPLOT\00055.dgn PEN TABLE: \\mtp\FinalDgn\config\plot\penthls\bridge.pen Date: 23-MAR-2005 07:10 Plotted by: kwillis

STATE PROJECT NUMBER
1060-05-75

FIELD SPLICE NUMBER	STATION	TOP FLANGE SPLICE							WEB SPLICE							BOTTOM FLANGE SPLICE						
		T1	T2	T3	L1	L2	A	B	T4	T7	L3	L6	C	D	E	T5	T6	L4	L5	F	G	H
1	40SE+77.97	1/2"		3/4"	2'-7 1/2"		4	1'-0"	3/8"		1'-1 1/2"		19	1	3"	3/8"	3/8"	1'-7 1/2"	9 1/2"	11	2	6"
2	41SE+64.14	1/2"		3/4"	2'-7 1/2"		4	1'-0"	3/8"	1/8"	1'-1 1/2"	6 1/2"	24	1	3"	3/8"	3/8"	1'-7 1/2"	9 1/2"	11	2	6"
3	42SE+59.82	1/2"		3/4"	2'-7 1/2"		4	1'-0"	3/8"	1/8"	1'-1 1/2"	6 1/2"	19	1	3"	3/8"	3/8"	1'-7 1/2"	9 1/2"	11	2	6"
4	43SE+49.14	1/2"		3/4"	2'-7 1/2"		4	1'-0"	3/8"		1'-1 1/2"		24	1	3"	1/2"	1/8"	2'-1 1/2"	1'-0 1/2"	11	3	9"
5	44SE+44.82	1/2"		3/4"	2'-7 1/2"		4	1'-0"	3/8"		1'-7 1/2"		19	2	6"	1/2"	5/8"	2'-1 1/2"	1'-0 1/2"	11	3	9"
6	45SE+58.41	1/2"	1/2"	3/4"	4'-1 1/2"	2'-0 1/2"	7	1'-9"	1/2"		1'-7 1/2"		19	2	6"	1/2"	1/8"	3'-1 1/2"	1'-6 1/2"	10	5	1'-3"
7	46SE+50.65	1/2"	1/2"	3/4"	4'-1 1/2"	2'-0 1/2"	7	1'-9"	1/2"		1'-7 1/2"		19	2	6"	1/2"	1/4"	3'-1 1/2"	1'-6 1/2"	10	5	1'-3"
8	47SE+60.42	1/2"	1/4"	3/4"	2'-7 1/2"	1'-3 1/2"	4	1'-0"	1/2"		1'-1 1/2"		24	1	3"	3/8"	3/4"	1'-7 1/2"	9 1/2"	12	2	6"
9	48SE+46.18	1/2"		3/4"	2'-7 1/2"		4	1'-0"	1/2"		1'-1 1/2"		24	1	3"	3/8"	1/4"	1'-7 1/2"	9 1/2"	11	2	6"
10	49SE+30.22	1/2"		3/4"	3'-1 1/2"		5	1'-3"	1/2"		1'-1 1/2"		24	1	3"	3/8"	1/4"	1'-7 1/2"	9 1/2"	11	2	6"

NOTES

1. SEE SHEET 55 FOR TYPICAL FIELD SPLICE LAYOUTS THAT DEFINE THE CONTENTS OF THIS TABLE.
2. ALL BOLTS IN GIRDER SPLICES ARE 7/8" DIAMETER ASTM A325 TYPE 1.
3. ALL HOLES SHALL BE STANDARD DIAMETER - NO OVERSIZE HOLES.
4. ALL CONNECTIONS SHALL BE FABRICATED AND ASSEMBLED AS SLIP-CRITICAL CONNECTIONS.
5. ALL SPLICE PLATES SHALL BE GRADE HPS 70W.

8

NO.	DATE	REVISION	BY

STATE OF WISCONSIN
DEPARTMENT OF TRANSPORTATION
STRUCTURES DESIGN SECTION

STRUCTURE B-40-1122

CONST. SPEC.	2004	DRAWN BY	KGW	PLANS CK'D.	RSR

FIELD SPLICE TABLE

SHEET 56 OF 109

MAR 22 2005

STATE PROJECT NUMBER
1060-05-75

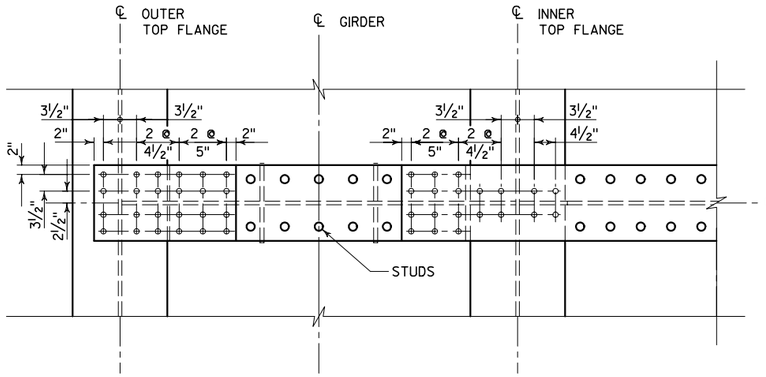

PLAN
VIEWED NORMAL TO DECK SURFACE

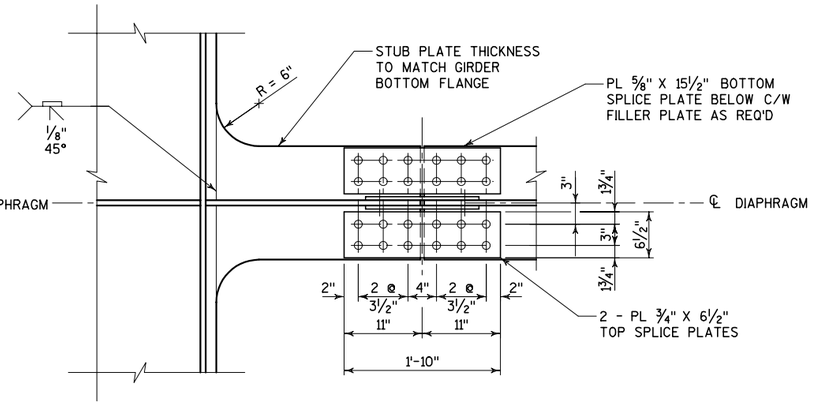

SECTION 3-3
NOT TO SCALE

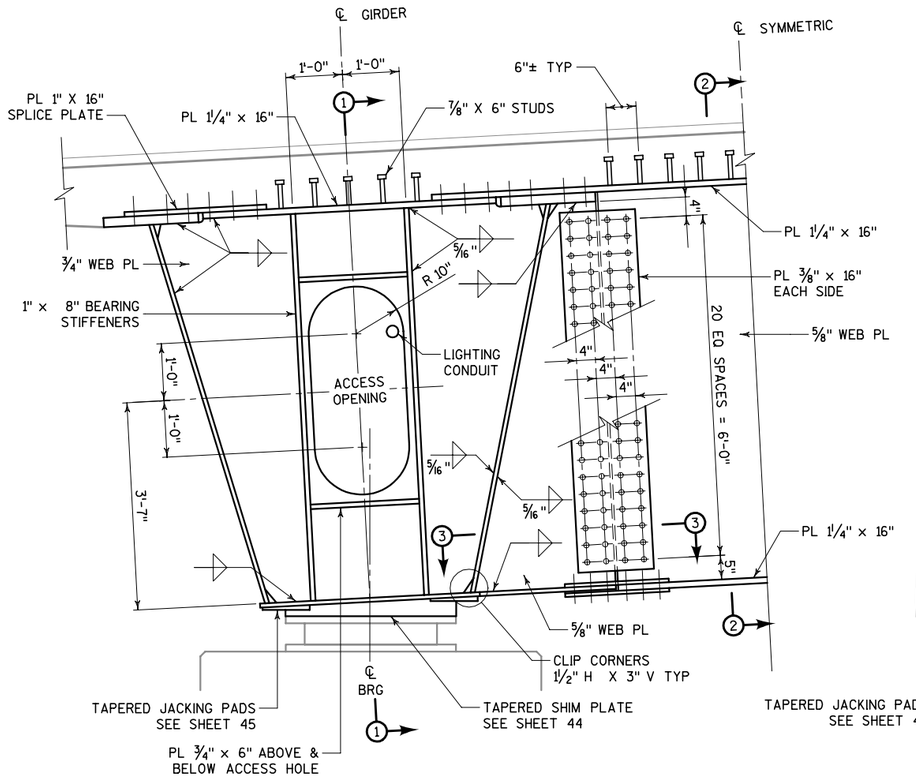

ELEVATION

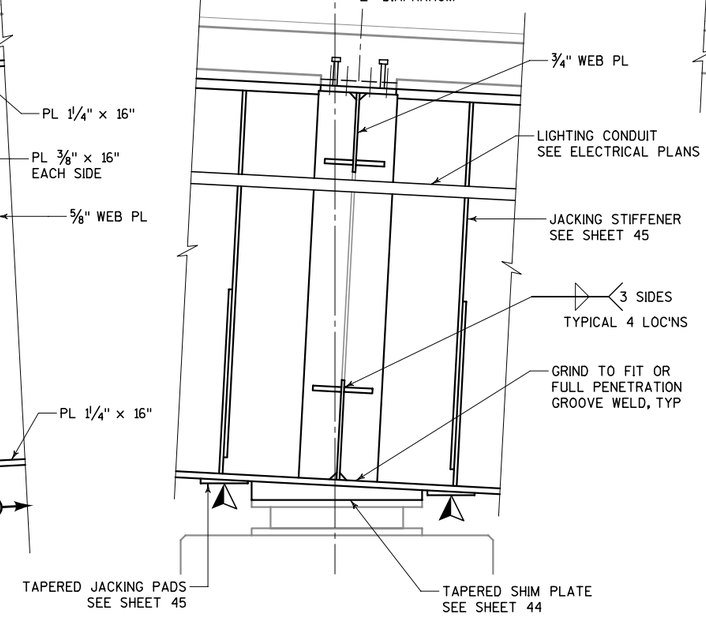

SECTION 1-1

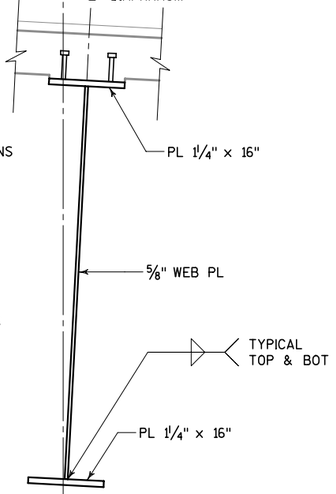

SECTION 2-2

LEGEND

⚠ SUGGESTED JACKING LOCATIONS FOR FUTURE BEARING REPLACEMENT. SEE SHEET 45 FOR DETAILS.

NOTES

1. SEE SHEET 46 FOR DETAIL DEFINING WORKPOINT BETWEEN DIAPHRAGM AND BEARING CENTERLINES.
2. ALL BOLTS IN PIER DIAPHRAGMS ARE 1" DIAMETER ASTM A325 TYPE 1.
3. DIAPHRAGMS AND CROSS FRAMES ARE ALIGNED NORMAL TO THE GIRDER UNLESS OTHERWISE NOTED.
4. THIS DRAWING SHOWS TYPICAL DIAPHRAGM DETAILS FOR ONE SPECIFIC GRADE AND SUPERELEVATION. GRADE AND SUPERELEVATION VARY BETWEEN PIER LOCATIONS.
5. ADJACENT LATERAL BRACING CONNECTIONS ARE NOT SHOWN FOR CLARITY. SEE SHEETS 47 AND 61 FOR BRACING LAYOUT AND CONNECTION DETAILS.

NO.	DATE	REVISION	BY

STATE OF WISCONSIN
DEPARTMENT OF TRANSPORTATION
STRUCTURES DESIGN SECTION

STRUCTURE B-40-1122

CONST. SPEC.	DRAWN BY	PLANS CK'D.
2004	KGW	RSR

INTERIOR PIER DIAPHRAGMS

SHEET 57 OF 109

MAR 22 2005

8

STATE PROJECT NUMBER
1060-05-75

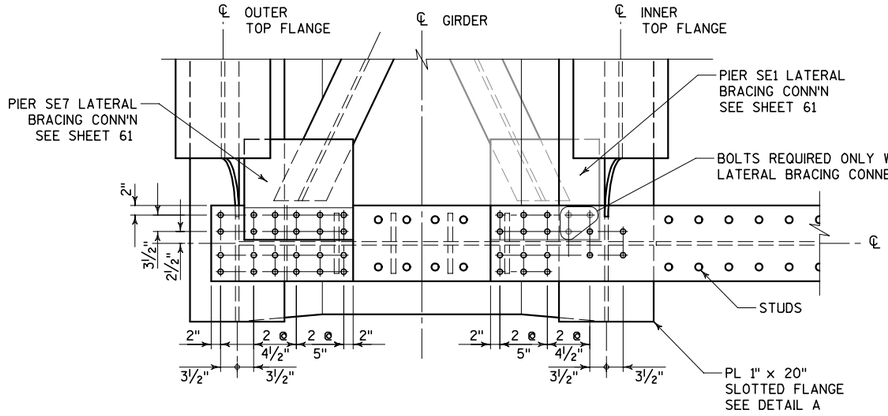

PLAN
VIEWED NORMAL TO DECK SURFACE

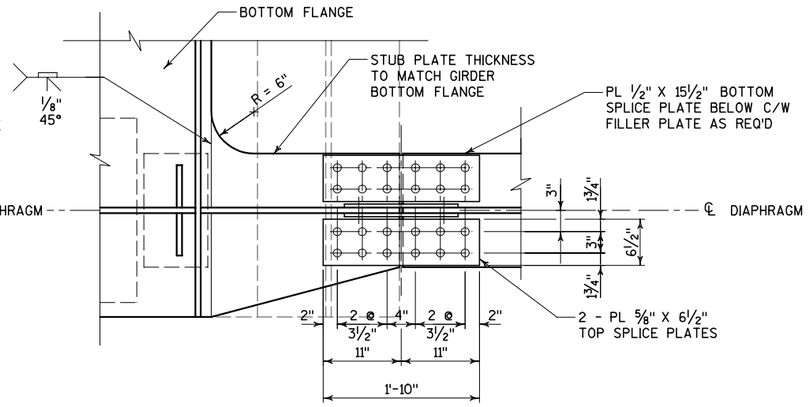

SECTION 3-3
NOT TO SCALE

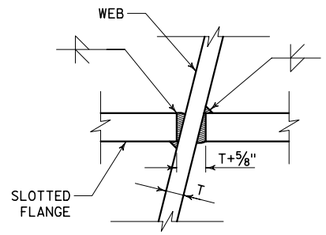

DETAIL A
NOT TO SCALE

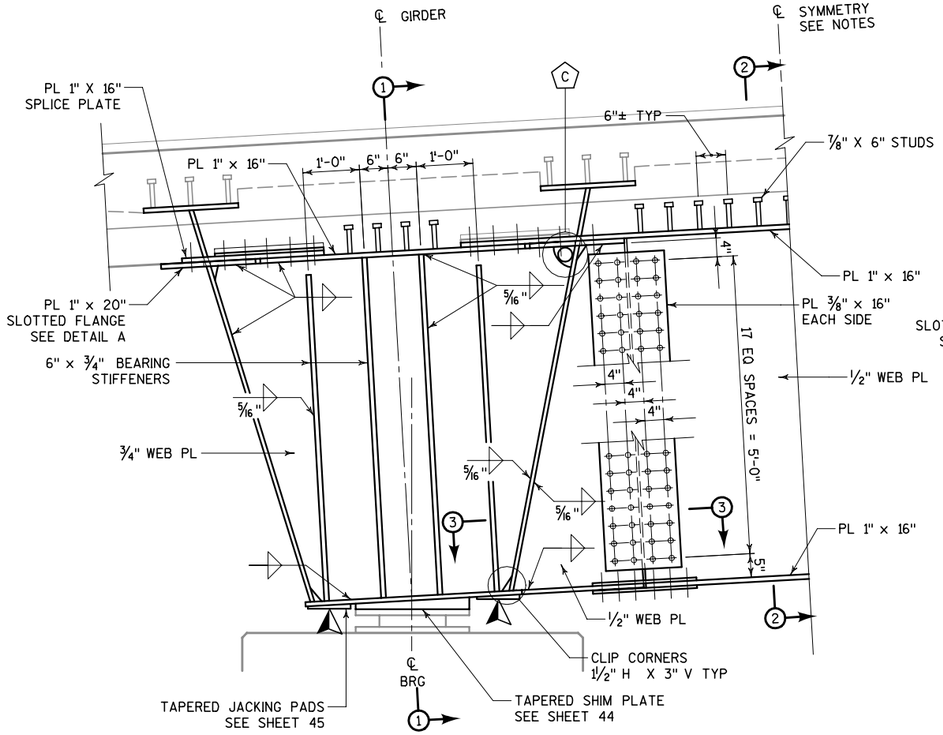

ELEVATION

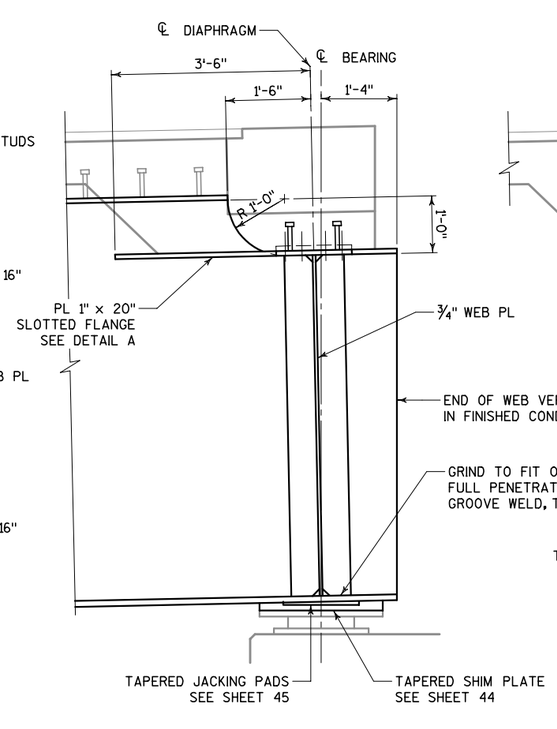

SECTION 1-1

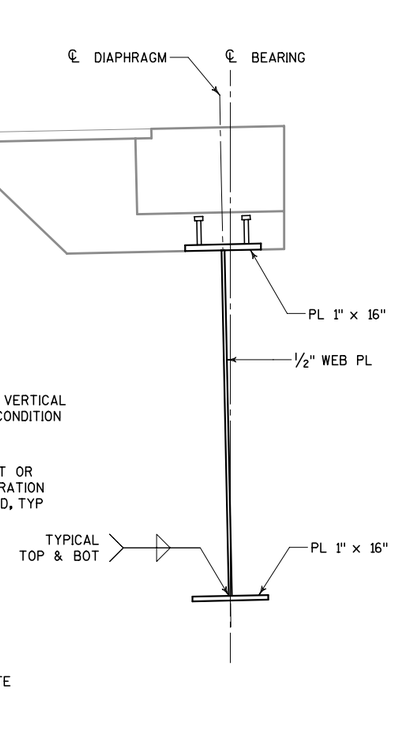

SECTION 2-2

LEGEND

- SUGGESTED JACKING LOCATIONS FOR FUTURE BEARING REPLACEMENT. SEE SHEET 45 FOR DETAILS.
- (C) PROVIDE 5" RADIUS CORNER OPENING TO PASS LIGHTING CONDUIT AS SHOWN. SEE LIGHTING PLANS FOR REQUIRED LOCATIONS.
  FIELD WELD ½" X 6" X 6" COVER PLATE TO SEAL ANY OPENINGS PROVIDED WHERE NO CONDUIT IS TO BE INSTALLED.

NOTES

1. SEE SHEET 46 FOR DETAIL DEFINING WORKPOINT BETWEEN DIAPHRAGM AND BEARING CENTERLINES.
2. ALL BOLTS IN PIER DIAPHRAGMS ARE 1" DIAMETER ASTM A325 TYPE 1.
3. DIAPHRAGMS AND CROSS FRAMES ARE ALIGNED NORMAL TO THE GIRDER UNLESS OTHERWISE NOTED.
4. THIS DRAWING SHOWS TYPICAL DIAPHRAGM DETAILS FOR ONE SPECIFIC GRADE AND SUPERELEVATION. GRADE AND SUPERELEVATION VARY BETWEEN PIER LOCATIONS.
5. DIAPHRAGM IS SYMMETRIC ABOUT THE INDICATED LINE WITH THE EXCEPTION OF LATERAL BRACING DIRECTION.

8

NO.	DATE	REVISION	BY

STATE OF WISCONSIN
DEPARTMENT OF TRANSPORTATION
STRUCTURES DESIGN SECTION

STRUCTURE B-40-1122

CONST. SPEC.	DRAWN BY	PLANS CK'D.
2004	KGW	RSR

END PIER DIAPHRAGMS

SHEET 58 OF 109

MAR 22 2005

FILE NAME: C:\KPLOT\00058.dgn PEN TABLE: \\mtp\FinalDgn\config\plot\pentbls\bridge.pen Date: 23-MAR-2005 07:11 Plotted by: kwills

STATE PROJECT NUMBER
1060-05-75

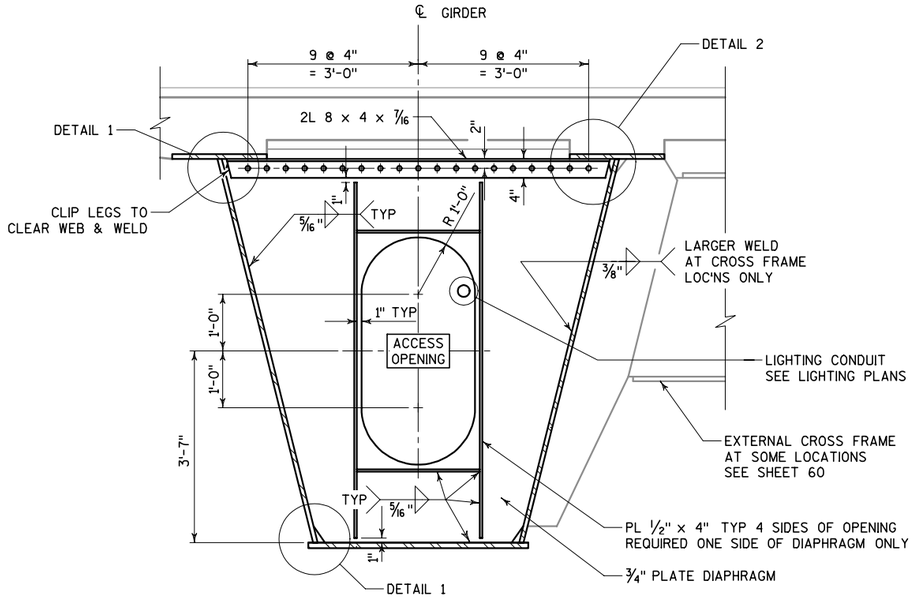

TYPICAL SECTION AT DIAPHRAGM

NOT TO SCALE

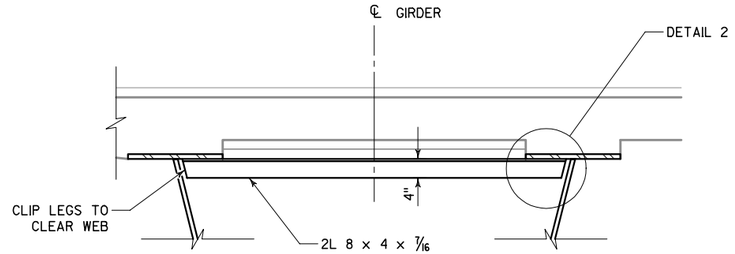

TYPICAL SECTION AT STRUT

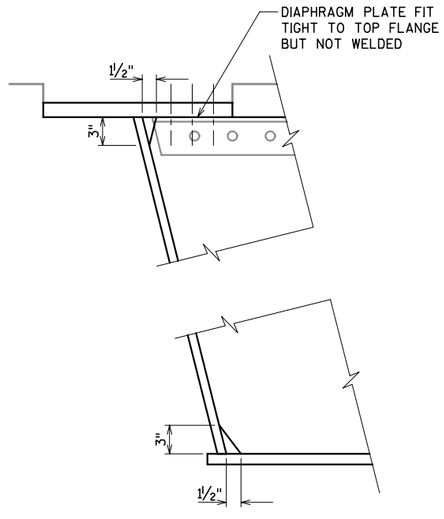

DETAIL 1

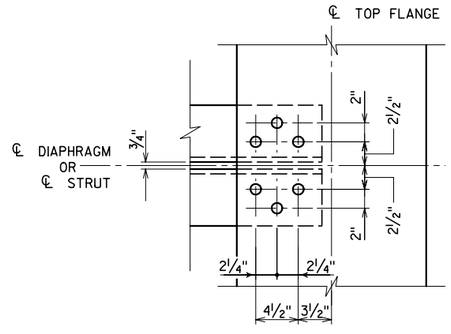

PLAN VIEW

DETAIL 2

NOTES

1. BOLTS CONNECTING STRUTS TO TOP FLANGE ARE 1" DIAMETER ASTM A325 TYPE 1.
2. BOLTS CONNECTING DIAPHRAGM WEB PLATES TO DOUBLE ANGLE TOP STRUTS ARE 7/8" DIAMETER ASTM A325 TYPE 1.
3. DIAPHRAGMS AND STRUTS ARE ALIGNED NORMAL TO THE GIRDER UNLESS OTHERWISE NOTED.

NO.	DATE	REVISION	BY

STATE OF WISCONSIN
DEPARTMENT OF TRANSPORTATION
STRUCTURES DESIGN SECTION

STRUCTURE B-40-1122

CONST. SPEC.	DRAWN BY	PLANS CK'D.
2004	KGW	RSR

INTERMEDIATE DIAPHRAGMS AND STRUTS

SHEET 59 OF 109

MAR 22 2005

8

STATE PROJECT NUMBER
1060-05-75

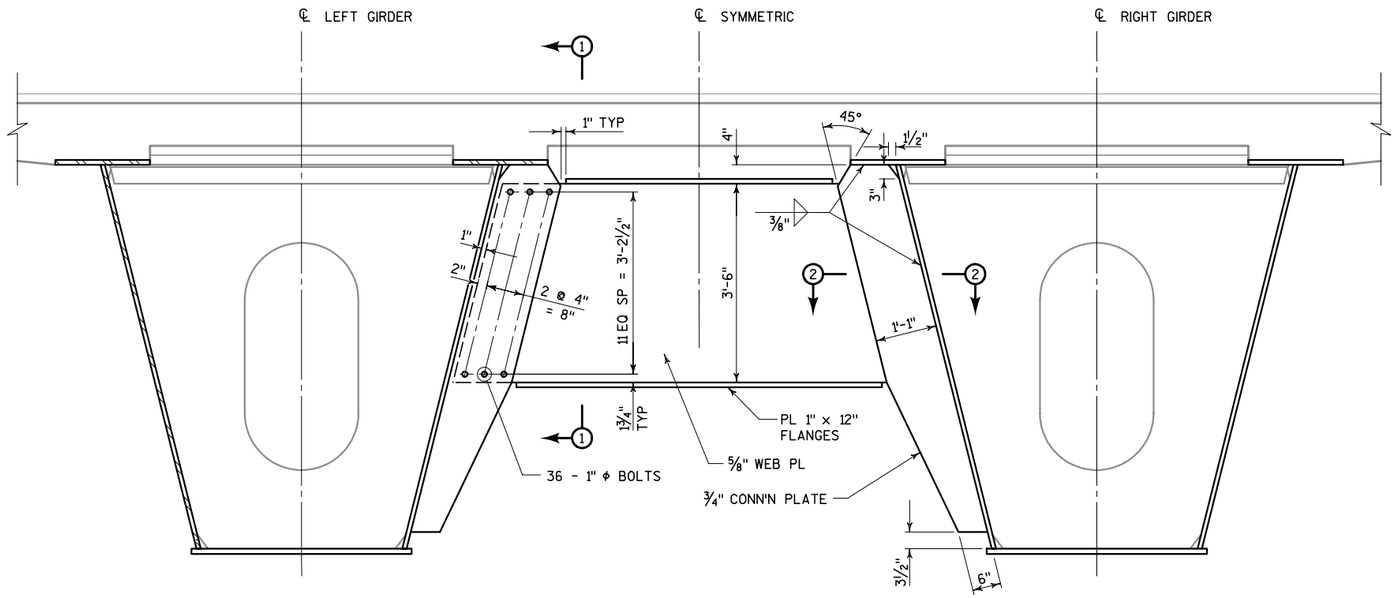

ELEVATION

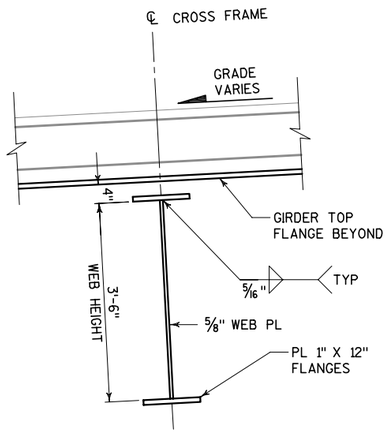

SECTION 1-1

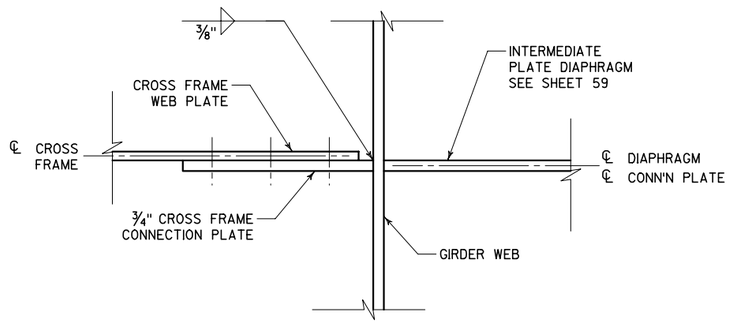

SECTION 2-2

NOT TO SCALE

NOTES

1. ALL BOLTS CONNECTING CROSS FRAMES ARE 1" DIAMETER ASTM A325 TYPE 1.
2. ALL HOLES SHALL BE STANDARD DIAMETER - NO OVERSIZE HOLES.
3. ALL CONNECTIONS SHALL BE FABRICATED AND ASSEMBLED AS SLIP-CRITICAL CONNECTIONS.
4. CROSS FRAME WEBS AND FLANGES SHALL BE GRADE HPS 70W.
5. STEEL GRADE FOR CONNECTION PLATES SHALL MATCH THE BOX GIRDER STEEL GRADE AT THE CROSS FRAME LOCATION.
6. CROSS FRAMES ARE ALIGNED NORMAL TO THE GIRDERS.
7. CONNECTION PLATES SHALL BE LOCATED DIRECTLY IN LINE WITH THE CORRESPONDING PLATE DIAPHRAGM LOCATED INSIDE THE BOX.

8

NO.	DATE	REVISION	BY

STATE OF WISCONSIN
DEPARTMENT OF TRANSPORTATION
STRUCTURES DESIGN SECTION

STRUCTURE B-40-1122

CONST. SPEC.	2004	DRAWN BY	KGW	PLANS CK'D.	RSR

EXTERIOR CROSS FRAMES

SHEET 60 OF 109

MAR 22 2005

FILE NAME: C:\KPLOT\00060.dgn PEN TABLE: \\mtp\FinalDgn\config\plot\pentbls\bridge.pen Date: 23-MAR-2005 07:13 Plotted by: kwillis

STATE PROJECT NUMBER
1060-05-75

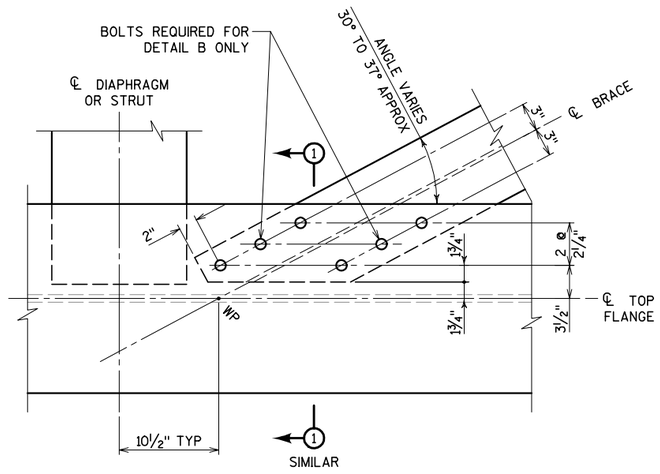

DETAIL A

4 BOLT CONNECTION

DETAIL B

6 BOLT CONNECTION

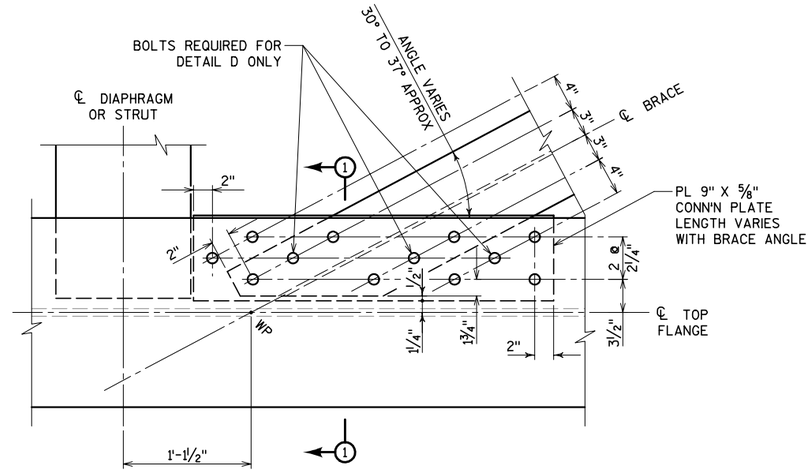

DETAIL C

9 BOLT CONNECTION

DETAIL D

12 BOLT CONNECTION

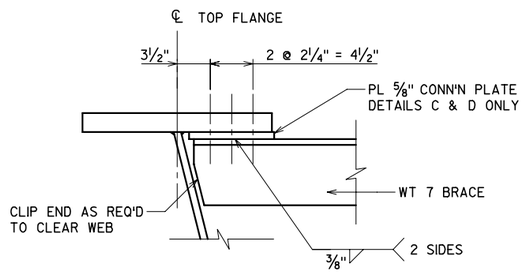

SECTION 1-1

SECTION MARKS

THE FIRST DIGIT OF THE LATERAL BRACING MARK NUMBER IDENTIFIES THE SECTION AS FOLLOWS:

1	WT 7 X 30.5
2	WT 8 X 33.5
3	WT 7 X 37.0
4	WT 8 X 38.5
5	WT 8 X 44.5
6	WT 8 X 50.0

THE SECOND CHARACTER OF THE LATERAL BRACING MARK NUMBER IDENTIFIES THE END CONNECTION DETAIL TO BE USED AND RELATES DIRECTLY TO DETAILS A THRU E AS GIVEN ON THIS SHEET.

NOTES

1. ALL BOLTS CONNECTING LATERAL BRACING MEMBER ARE 1" DIAMETER ASTM A325 TYPE 1.
2. DETAILS ON THIS SHEET SHOW TYPICAL DIMENSIONS ONLY AND WILL HAVE TO BE MIRRORED OR REVERSED AS REQUIRED.
3. DETAIL E IS SHOWN AT AN EXTERIOR WEB LOCATION. AT INTERIOR WEB LOCATIONS THE LATERAL BRACING CONNECTION IS IDENTICAL AND THE DIAPHRAGM BELOW IS SIMILAR. SEE SHEET 58.

   SEE FRAMING AND GIRDER PLANS ON SHEETS 47 TO 54 FOR CORRECT ALIGNMENT OF ALL LATERAL BRACE MEMBERS.
4. SEE SHEET 57 FOR TYPICAL INTERIOR PIER DIAPHRAGM DETAILS AND CONNECTIONS.
5. SEE SHEET 58 FOR END PIER DIAPHRAGM DETAILS AND CONNECTIONS.
6. SEE SHEET 59 FOR INTERMEDIATE DIAPHRAGM CONNECTION DETAILS.

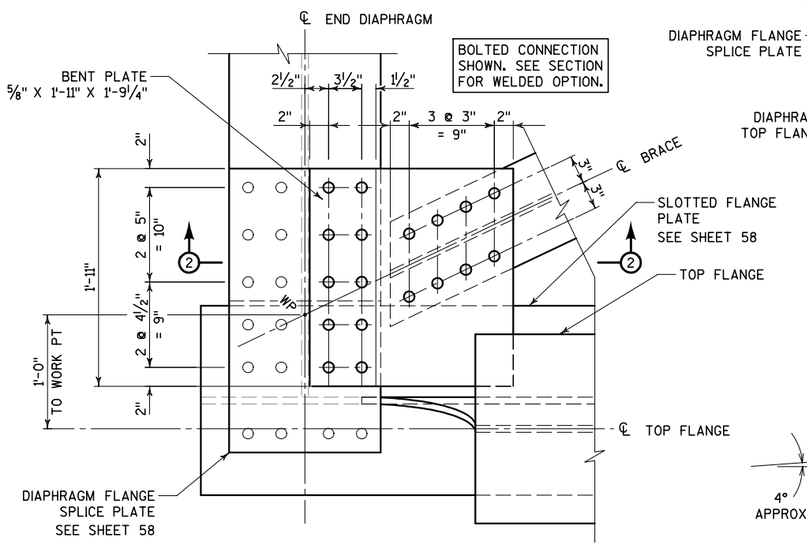

DETAIL E

AT END DIAPHRAGM

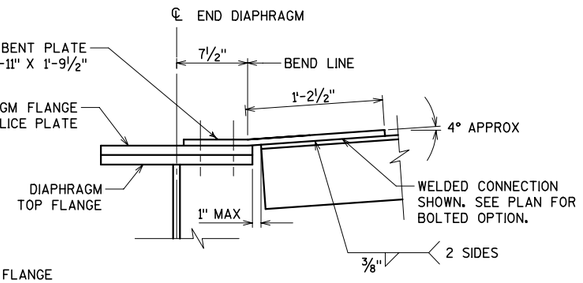

SECTION 2-2

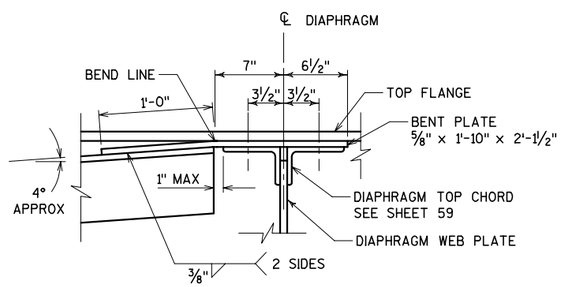

SECTION 3-3

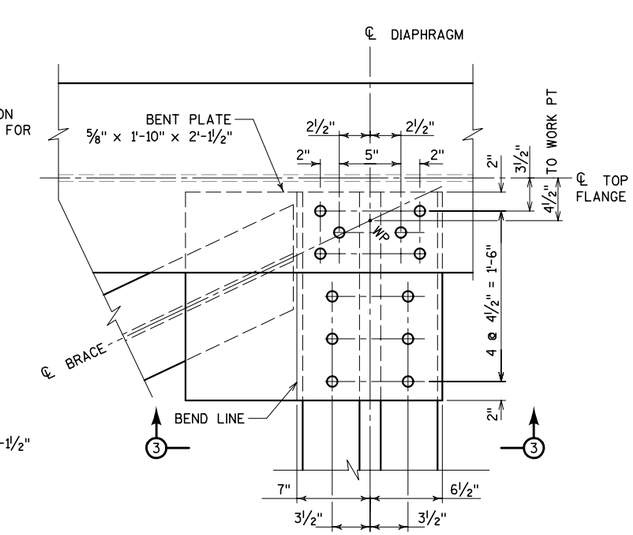

DETAIL E

AT FIRST INTERMEDIATE DIAPHRAGM

NO.	DATE	REVISION	BY

STATE OF WISCONSIN
DEPARTMENT OF TRANSPORTATION
STRUCTURES DESIGN SECTION

STRUCTURE B-40-1122

CONST. SPEC.	DRAWN BY	PLANS CK'D.
2004	KGW	RSR

LATERAL BRACING DETAILS

SHEET 61 OF 109

MAR 22 2005

8

STATE PROJECT NUMBER
1060-05-75

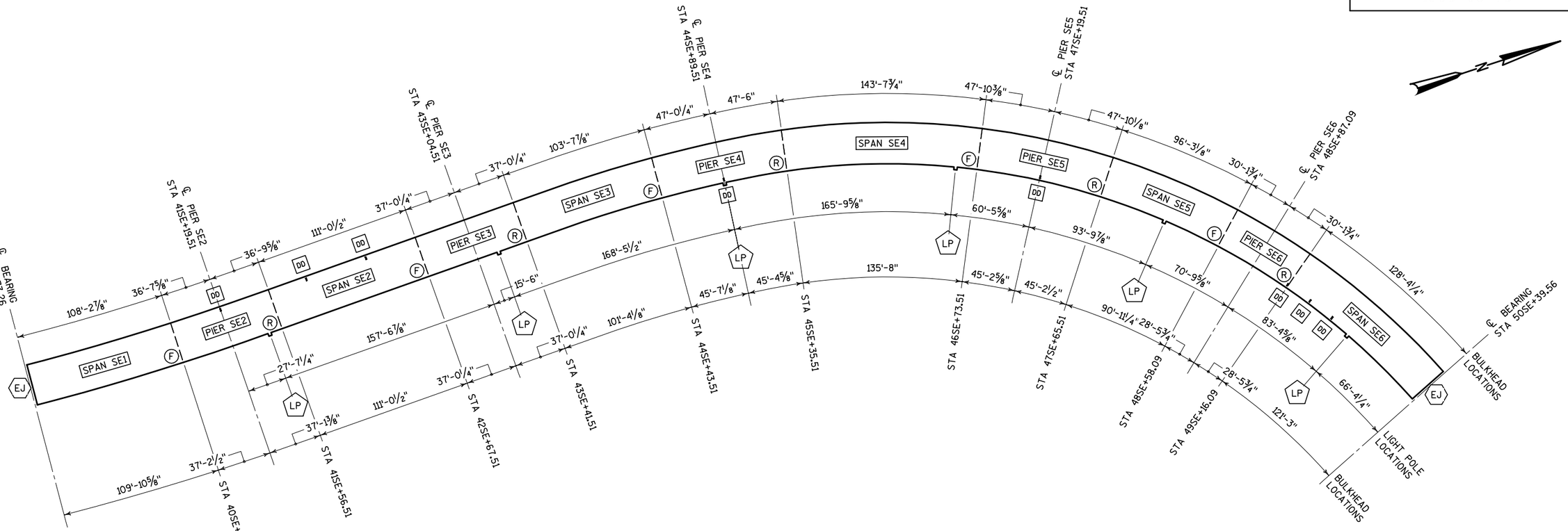

NOTES

1. SEE SHEET 4 FOR GENERAL NOTES.
2. SEE ELECTRICAL DRAWINGS FOR DETAILS OF LIGHTING REQUIREMENTS INSIDE THE BOX GIRDERS, WHICH MAY INCLUDE ANCHORS TO BE CAST INTO THE DECK SLAB.
3. SEE SHEETS 91 TO 95 FOR BLOCKOUTS AND OTHER DETAILS REQUIRED AT EXPANSION JOINT LOCATIONS.
4. DIMENSIONS ON THIS DRAWING ARE MEASURED ALONG THE ACTUAL PROFILE OF THE FINISHED EDGE OF DECK SLAB.
5. THE CONTRACTOR IS RESPONSIBLE FOR SCHEDULING AND COORDINATING DECK POURS TO BEST SUIT THE MEANS AND METHODS AVAILABLE TO HIM, SUBJECT TO THE FOLLOWING RESTRICTIONS.
6. CONTRACTOR MAY PLACE THE DECK CONTINUOUSLY FROM EITHER END OF THE STRUCTURE PROVIDED THAT ALL OTHER REQUIREMENTS ARE MET. IF MORE THAN ONE POUR IS REQUIRED, BULKHEADS BETWEEN POURS SHALL BE POSITIONED AT THE LOCATIONS IDENTIFIED ON THIS PLAN - SEE LEGEND.
7. CONTROL POUR SEQUENCE AND PLACEMENT RATE TO ENSURE THAT BEFORE THE CONCRETE IN ANY 'PIER' AREA REACHES THE INITIAL SET CONDITION, THE CONCRETE IN BOTH ADJACENT 'SPAN' AREAS IS ALREADY BE IN PLACE.
8. PREVENT UPLIFT AT ALL BEARING LOCATIONS. NOTE THAT ANY POUR SEQUENCE THAT REQUIRES POURING THE FIRST INTERIOR SPAN BEFORE THE ADJACENT END SPAN (SUCH AS THE END-TO-END SEQUENCES REFERRED TO ABOVE) WILL RESULT IN UPLIFT FORCES AT THE EXPANSION END BEARINGS THAT WILL HAVE TO BE ACCOUNTED FOR.
9. DEPOSIT FRESH CONCRETE FIRST IN THE AREA BETWEEN THE GIRDERS FOLLOWED BY THE OVERHANG AREA TO THE INSIDE OF THE CURVE AND THEN BY THE OVERHANG AREA TO THE OUTSIDE OF THE CURVE.
10. CONTROL THE PLACEMENT TO ENSURE THAT THE FURTHEST PROGRESS OF FRESH CONCRETE VARIES BY NO MORE THAN 10 FEET ACROSS THE WIDTH OF THE DECK.
11. PREVIOUSLY PLACED DECK CONCRETE MUST HAVE ATTAINED A MINIMUM COMPRESSIVE STRENGTH OF 3000 PSI BEFORE THE AREAS IMMEDIATELY ADJACENT MAY BE PLACED.
12. FOLLOW PROCEDURES OUTLINED IN THE SPECIAL PROVISIONS FOR PROMPTLY FOGGING, COVERING AND CURING FRESHLY PLACED CONCRETE.
13. FIVE DIFFERENT ZONES HAVE BEEN DEFINED FOR THE BOTTOM LONGITUDINAL REINFORCEMENT. THESE ZONES ARE DESCRIBED BELOW AND ARE ALSO SHOWN IN THE TYPICAL DECK SECTIONS.

    L - OVERHANG AREA OUTSIDE THE LEFT GIRDER

    LG - OVER THE LEFT GIRDER

    C - BETWEEN THE LEFT AND RIGHT GIRDERS

    RG - OVER THE RIGHT GIRDER

    R - OVERHANG AREA OUTSIDE THE RIGHT GIRDER
14. STAY-IN-PLACE METAL FORMS WILL ONLY BE PERMITTED INSIDE THE BOX GIRDERS - THE OVERHANGS AND THE ZONE BETWEEN THE GIRDERS SHALL USE CONVENTIONAL TEMPORARY FORMS.
15. THE USE OF STAY-IN-PLACE METAL FORMS IS OPTIONAL - CONVENTIONAL FORMWORK MAY BE USED INSIDE THE BOXES BUT MUST BE COMPLETELY REMOVED.
16. DESIGN CONNECTION BETWEEN STAY-IN-PLACE METAL FORMS AND GIRDER FLANGES TO PROVIDE ADJUSTMENT OF VERTICAL POSITION BASED ON THE ACTUAL HAUNCH HEIGHT REQUIRED. WELDED DETAILS SHALL BE FATIGUE STRESS CATEGORY C OR BETTER.
17. TOP OF STAY-IN-PLACE METAL FORMS SHALL BE ALIGNED WITH THE UNDERSIDE OF THE 9" DECK SLAB AS SHOWN IN THE SECTIONS ON SHEET 74.
18. PRECAST CONCRETE DECK PLANKS WILL NOT BE ACCEPTED IN PLACE OF STAY-IN-PLACE METAL FORMS.

DECK FEATURE SUMMARY

STATION	FEATURE	SIDE	DETAIL SHEETS
41SE+19.51	FLOOR DRAIN	LEFT	88-89
41SE+47.00	LIGHT POLE	RIGHT	105-106
41SE+84.51	FLOOR DRAIN	LEFT	88-89
42SE+29.51	FLOOR DRAIN	LEFT	88-89
43SE+20.00	LIGHT POLE	RIGHT	105-106
44SE+89.51	LIGHT POLE	RIGHT	105-106
44SE+89.51	FLOOR DRAIN	RIGHT	88-89
46SE+58.00	LIGHT POLE	RIGHT	105-106
47SE+19.51	FLOOR DRAIN	RIGHT	88-89
48SE+15.00	LIGHT POLE	RIGHT	105-106
49SE+15.38	FLOOR DRAIN	RIGHT	88-89
49SE+35.38	FLOOR DRAIN	RIGHT	88-89
49SE+55.38	FLOOR DRAIN	RIGHT	88-89
49SE+72.00	LIGHT POLE	RIGHT	105-106

LEGEND

- (F) PERMITTED BULKHEAD LOCATIONS FOR DECK POURS PROCEEDING IN THE FORWARD (INCREASING STATION) DIRECTION. SEE SHEET 87 FOR BULKHEAD DETAILS.
- (R) PERMITTED BULKHEAD LOCATIONS FOR DECK POURS PROCEEDING IN THE REVERSE (DECREASING STATION) DIRECTION. SEE SHEET 87 FOR BULKHEAD DETAILS.
- [PIER SE2] POUR AREA IDENTIFIERS.
- (EJ) EXPANSION JOINT LOCATION.
- [DD] FLOOR DRAIN LOCATION.
- (LP) LIGHT POLE MOUNTING LOCATION.

NO.	DATE	REVISION	BY

STATE OF WISCONSIN
DEPARTMENT OF TRANSPORTATION
STRUCTURES DESIGN SECTION

STRUCTURE B-40-1122

CONST. SPEC.	2004	DRAWN BY	KGW	PLANS CK'D.	RSR

DECK LAYOUT

SHEET 73 OF 109

APR 18 2005

8

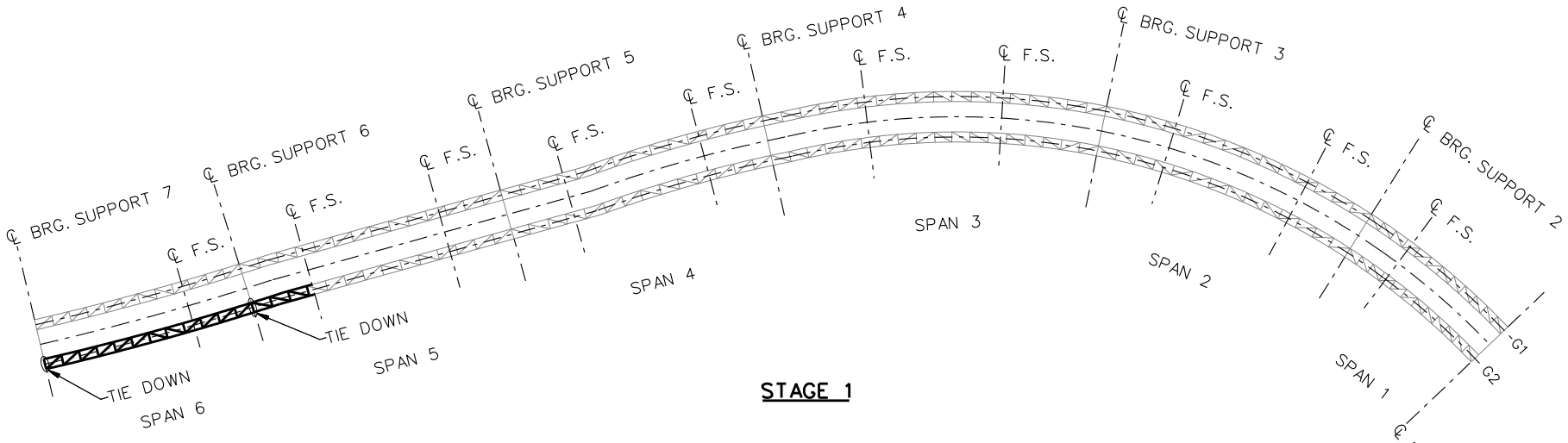

STAGE 1

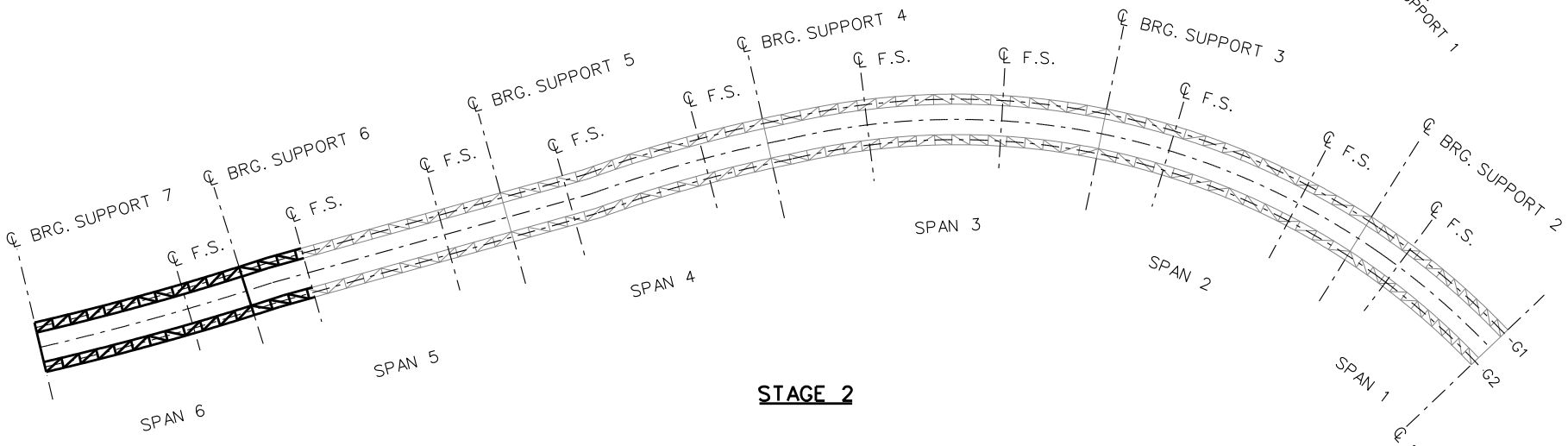

STAGE 2

LEGEND

▽ = HOLD OR LIFT CRANE

○ = TIE DOWN

□ = TEMPORARY SUPPORT STRUCTURE

NCHRP 12-79

BRIDGE ETCCR15

GENERAL ERECTION PROCEDURE

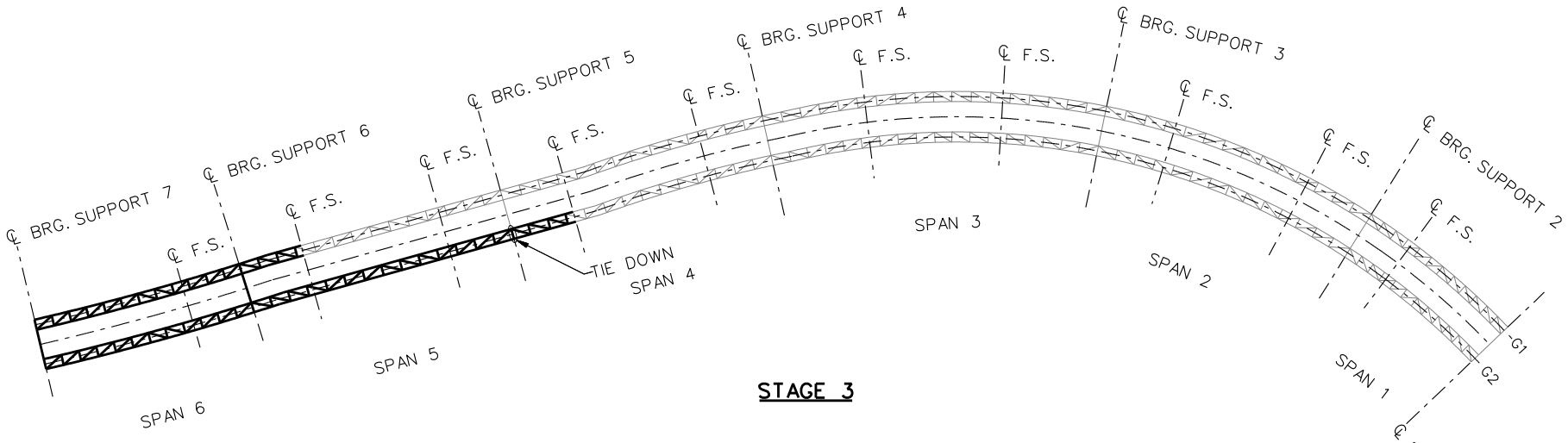

STAGE 3

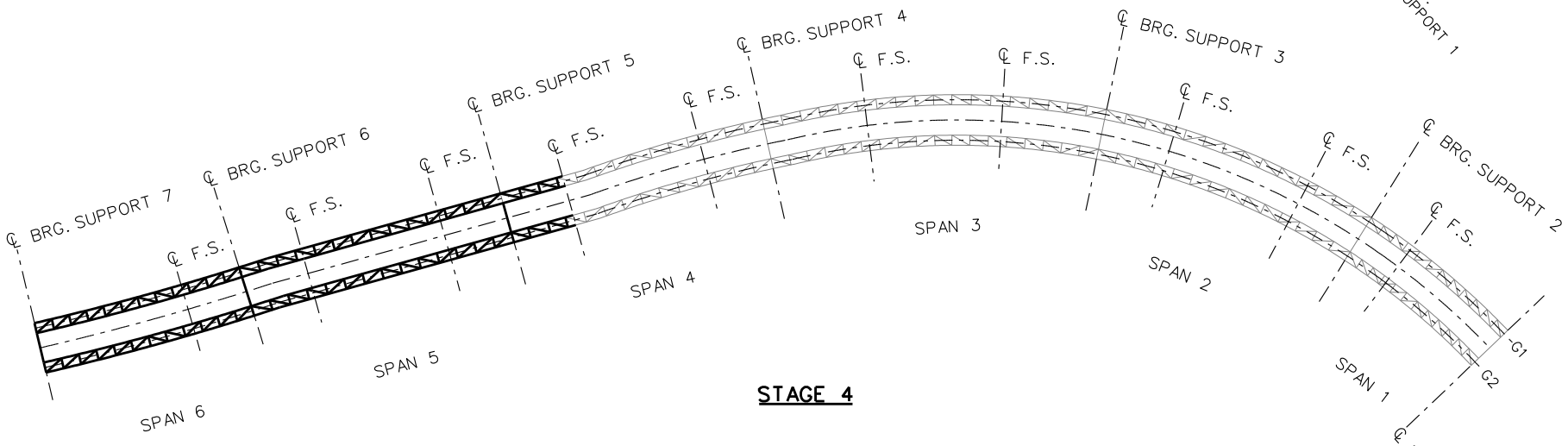

STAGE 4

LEGEND

▽ = HOLD OR LIFT CRANE

○ = TIE DOWN

□ = TEMPORARY SUPPORT STRUCTURE

NCHRP 12-79

BRIDGE ETCCR15

GENERAL ERECTION PROCEDURE

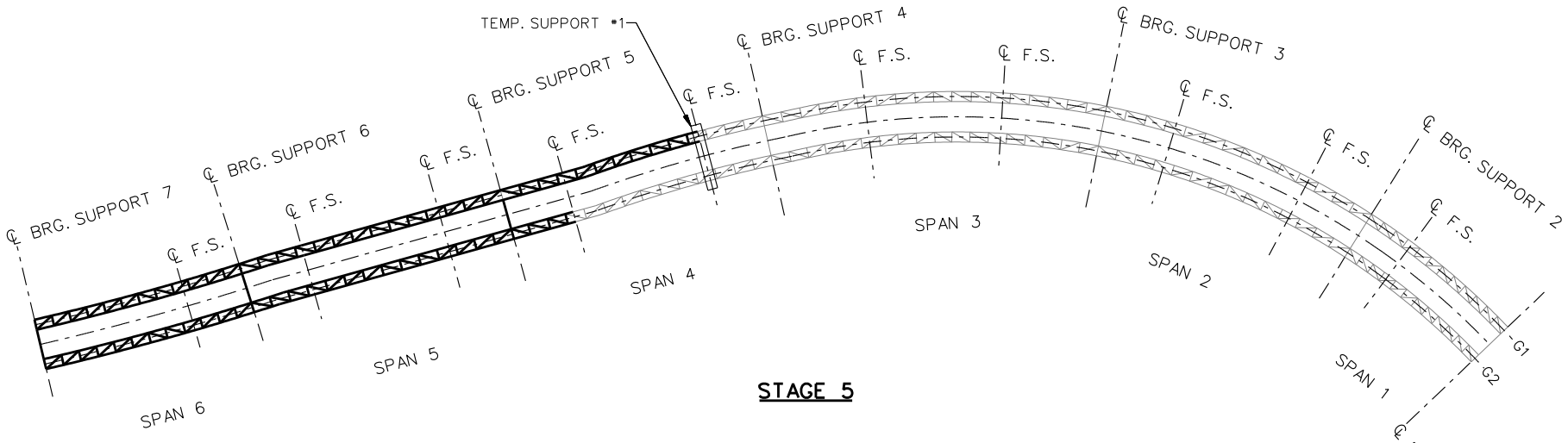

STAGE 5

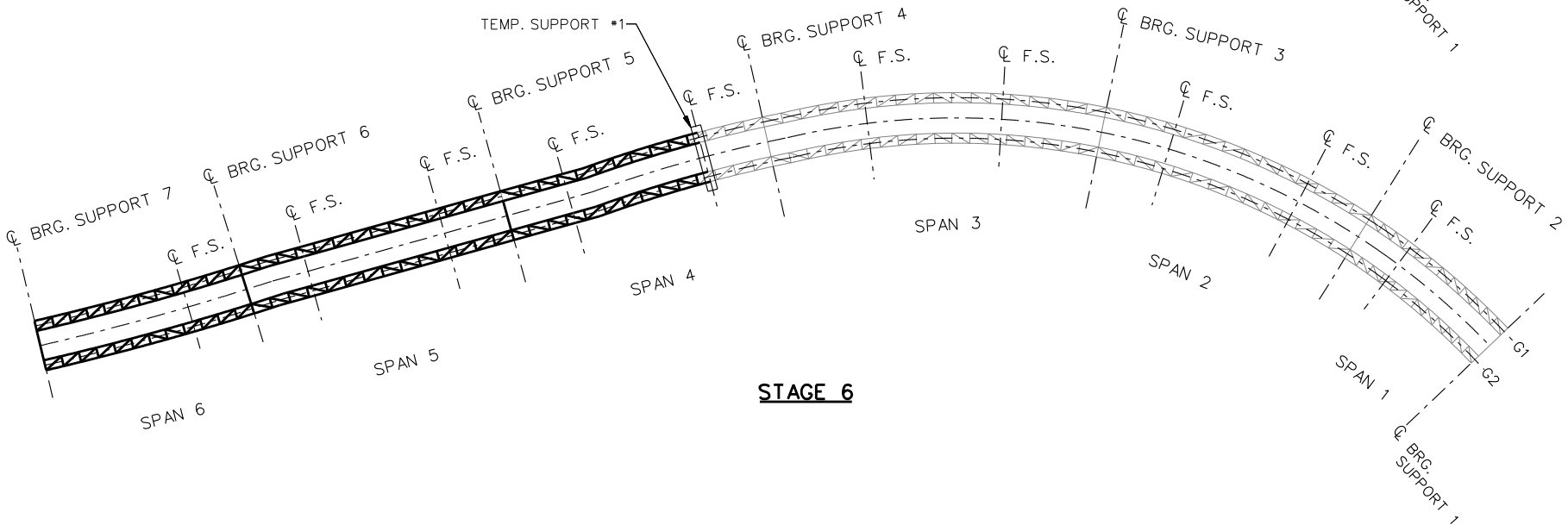

STAGE 6

LEGEND

▽ = HOLD OR LIFT CRANE

○ = TIE DOWN

□ = TEMPORARY SUPPORT STRUCTURE

NCHRP 12-79

BRIDGE ETCCR15

GENERAL ERECTION PROCEDURE

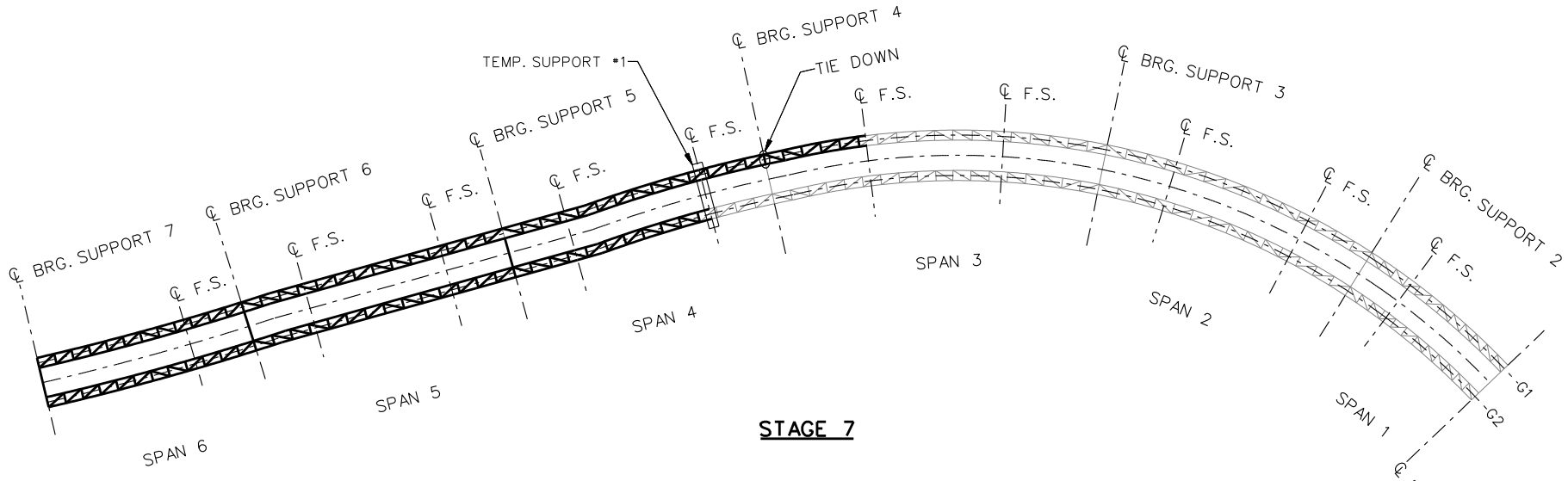

STAGE 7

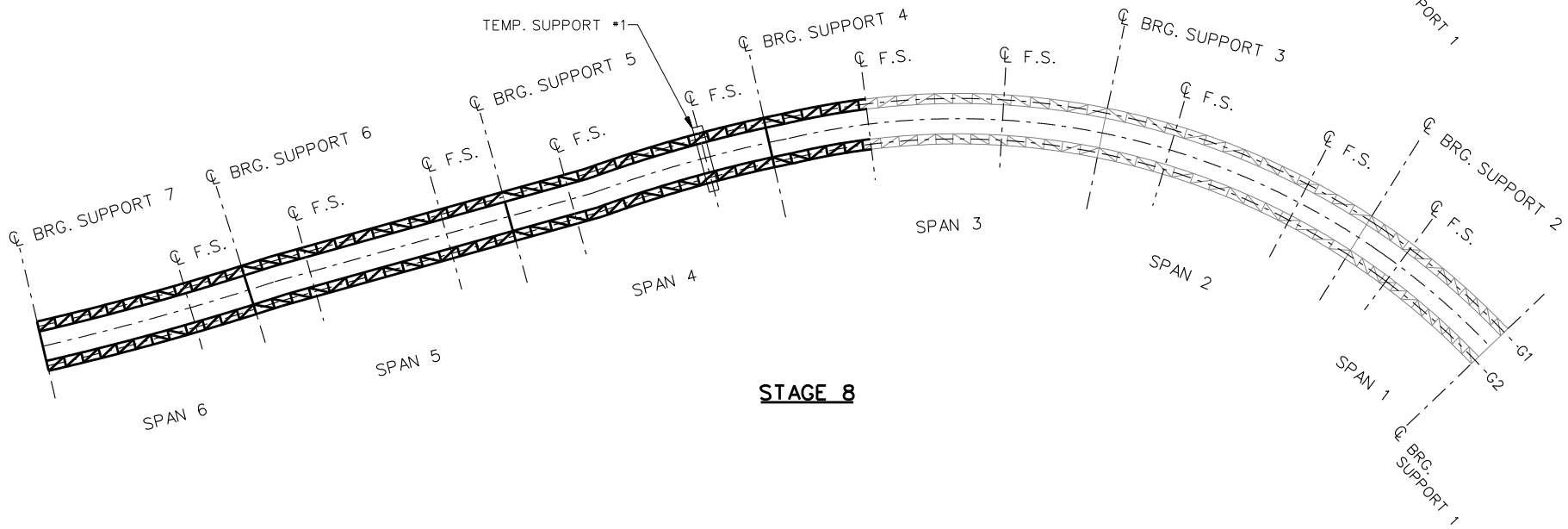

STAGE 8

LEGEND

▽ = HOLD OR LIFT CRANE

○ = TIE DOWN

□ = TEMPORARY SUPPORT STRUCTURE

NCHRP 12-79

BRIDGE ETCCR15

GENERAL ERECTION PROCEDURE

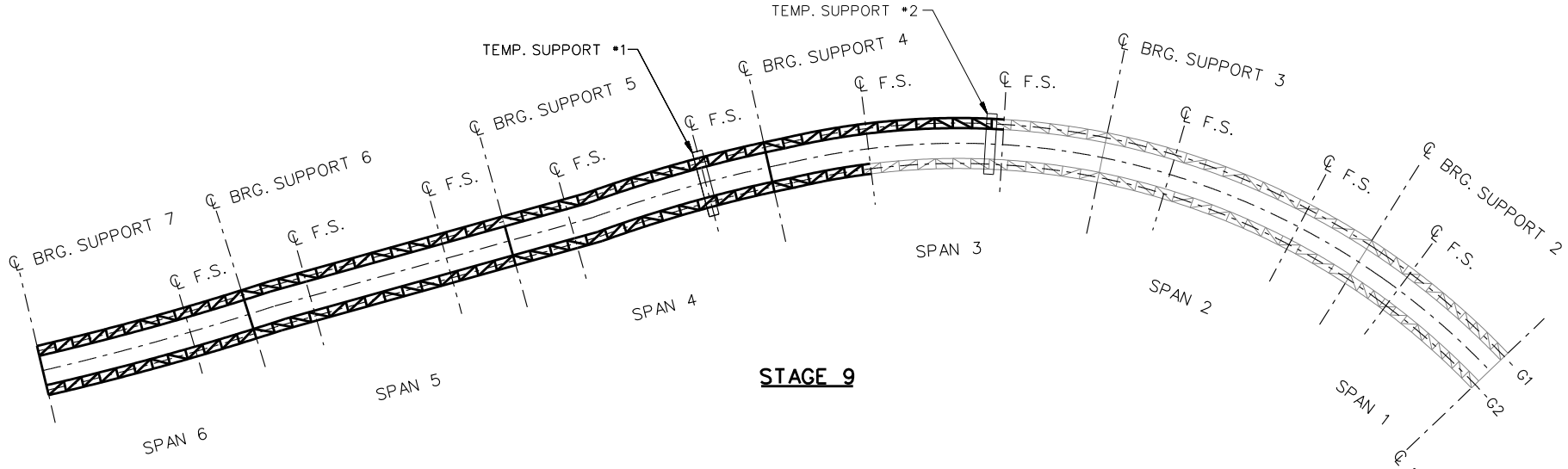

STAGE 9

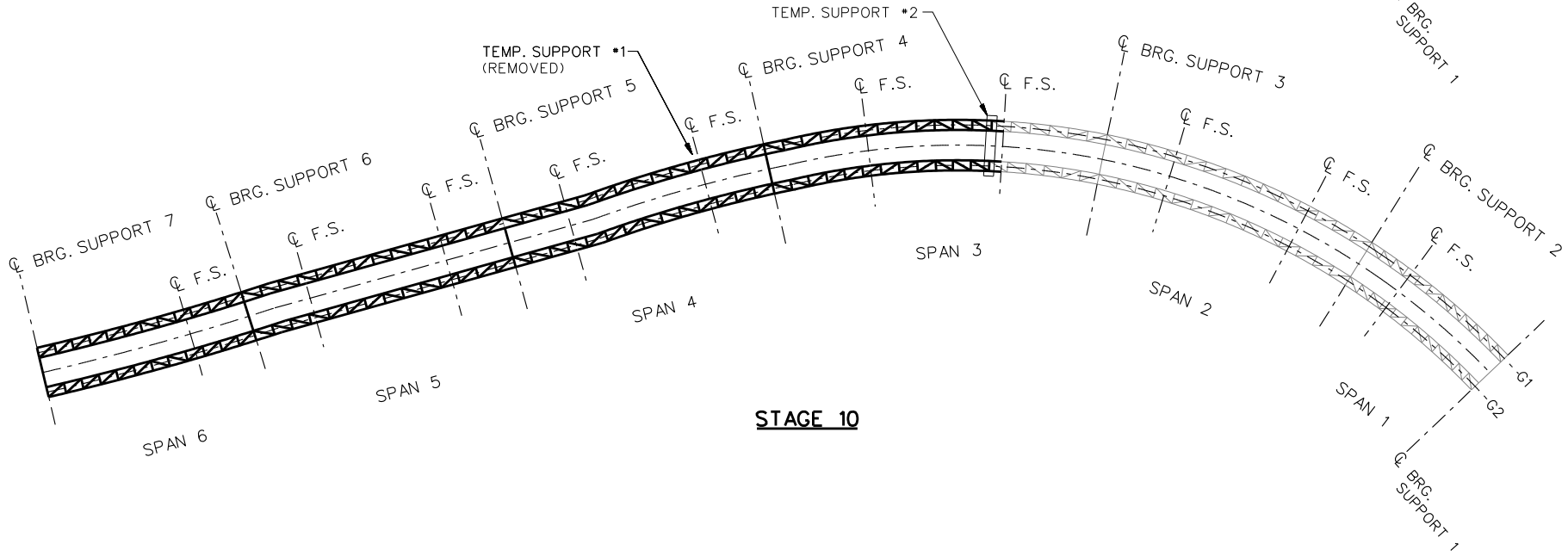

STAGE 10

LEGEND

▽ = HOLD OR LIFT CRANE

○ = TIE DOWN

□ = TEMPORARY SUPPORT STRUCTURE

NCHRP 12-79

BRIDGE ETCCR15

GENERAL ERECTION PROCEDURE

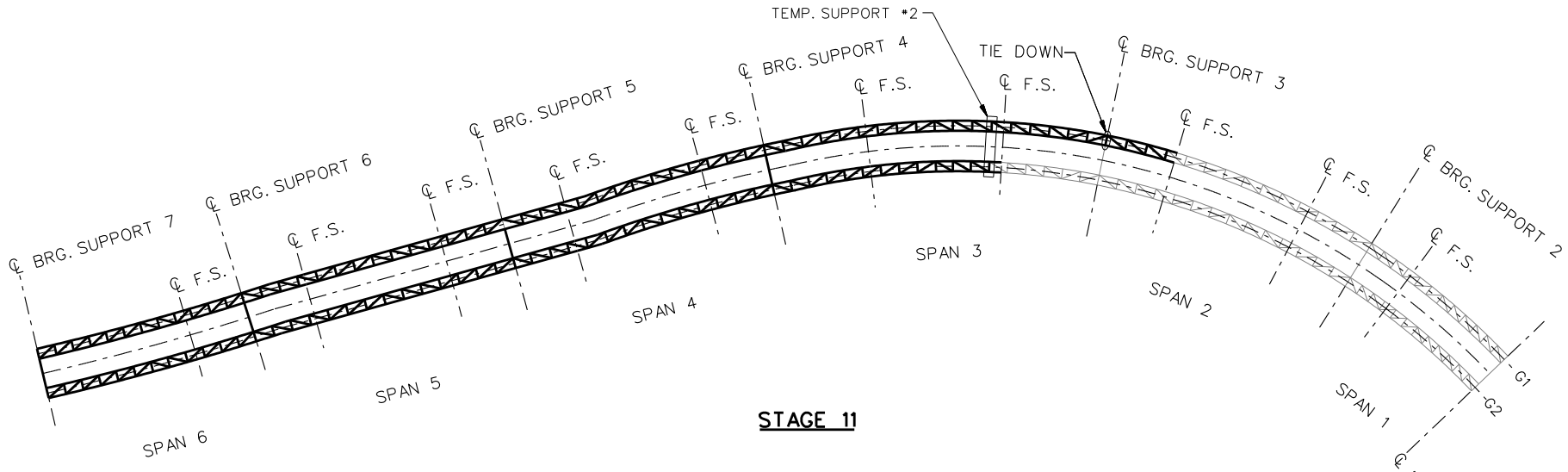

STAGE 11

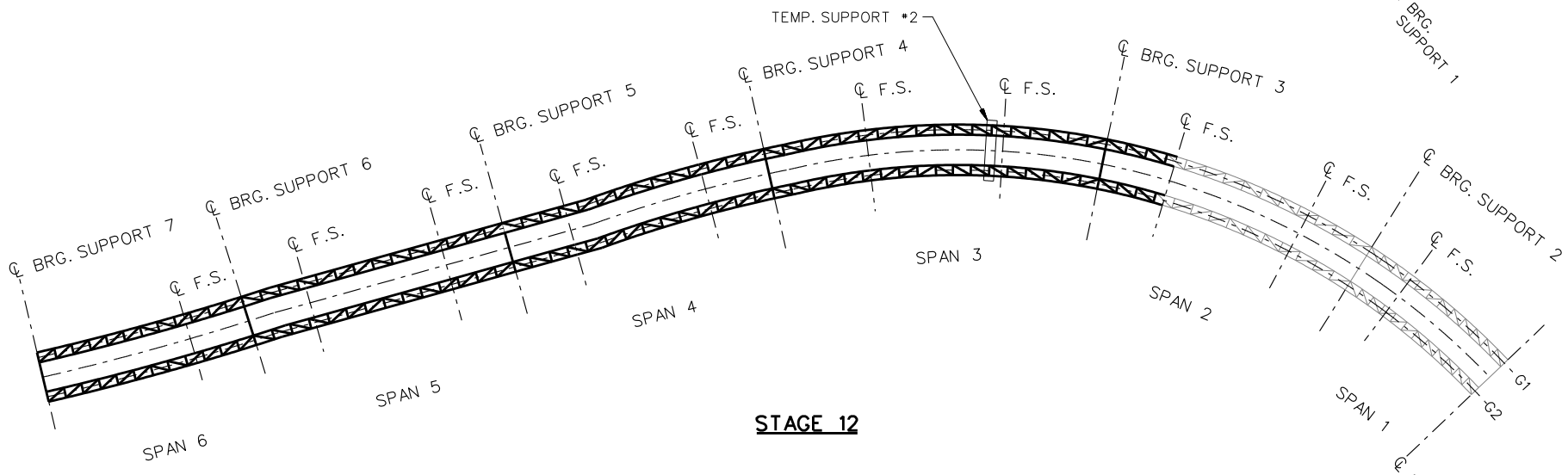

STAGE 12

LEGEND

▽ = HOLD OR LIFT CRANE

○ = TIE DOWN

□ = TEMPORARY SUPPORT STRUCTURE

NCHRP 12-79

BRIDGE ETCCR15

GENERAL ERECTION PROCEDURE

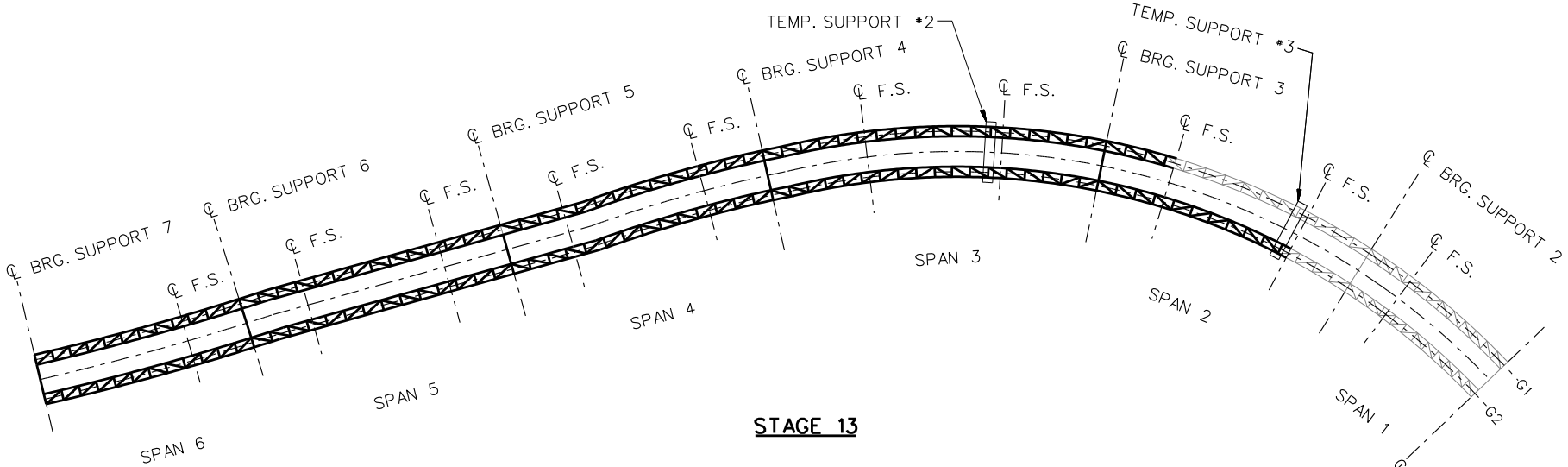

STAGE 13

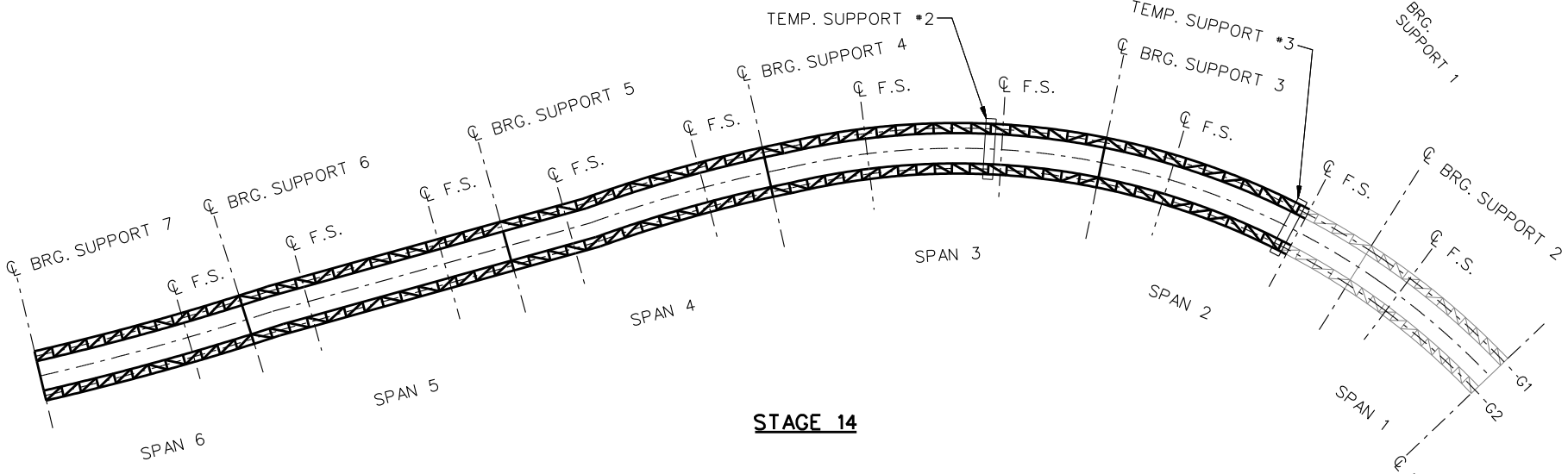

STAGE 14

LEGEND

▽ = HOLD OR LIFT CRANE

○ = TIE DOWN

□ = TEMPORARY SUPPORT STRUCTURE

NCHRP 12-79

BRIDGE ETCCR15

GENERAL ERECTION PROCEDURE

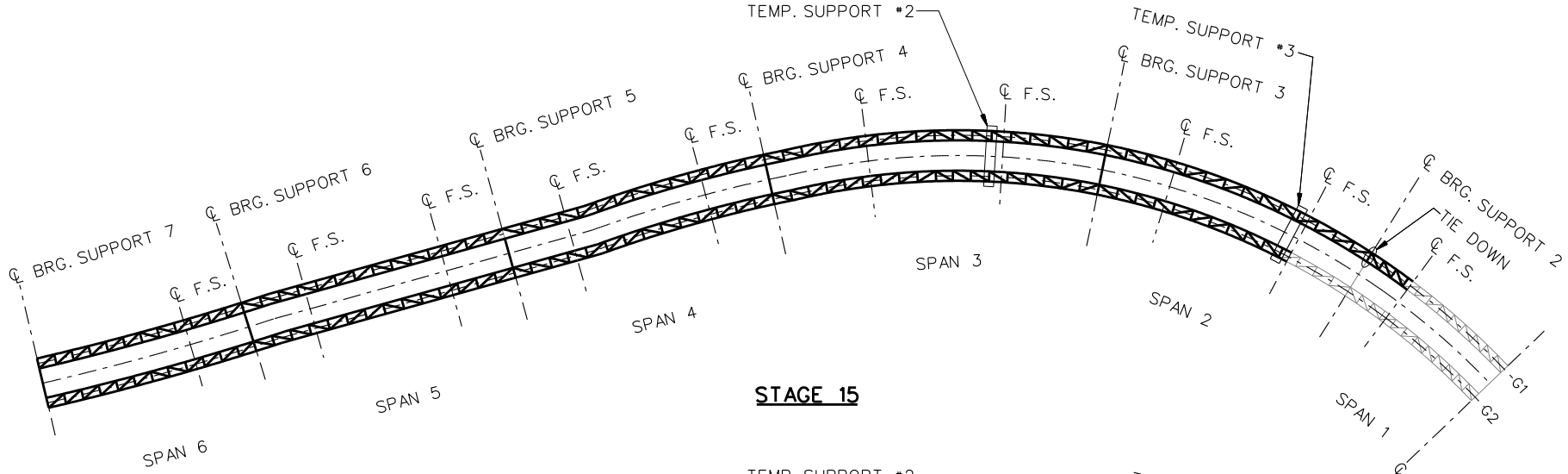

STAGE 15

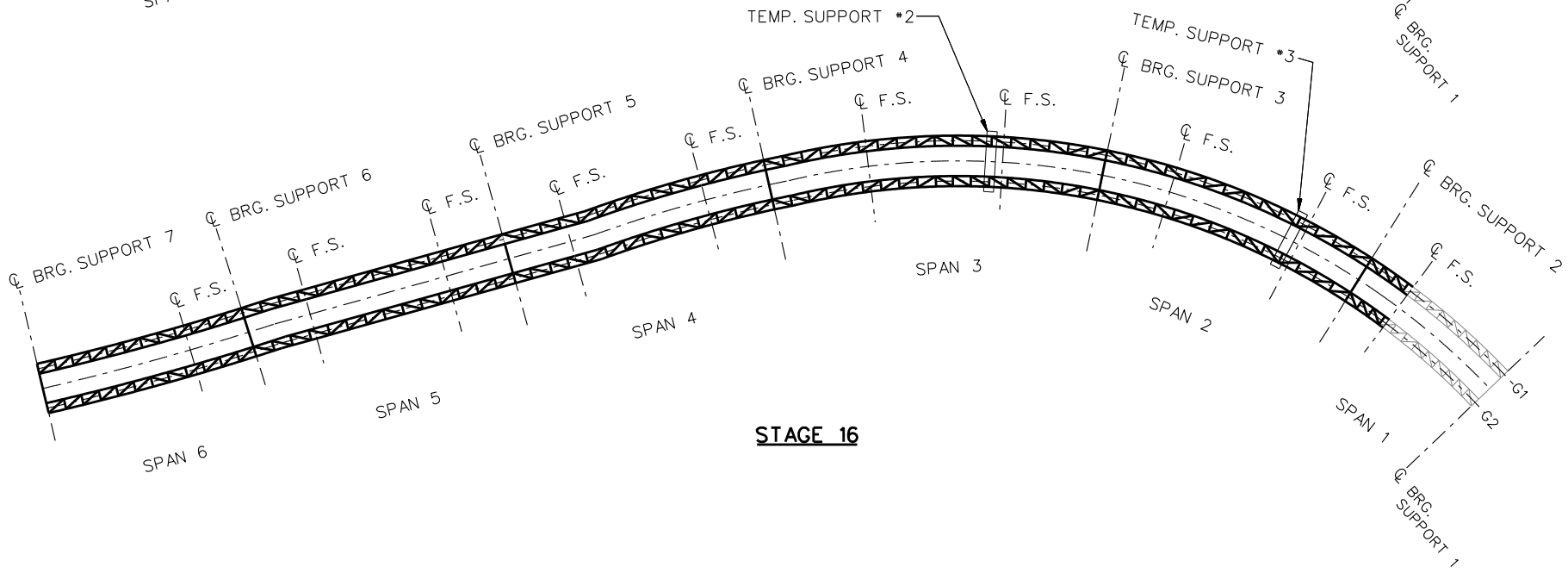

STAGE 16

LEGEND

▽ = HOLD OR LIFT CRANE

○ = TIE DOWN

□ = TEMPORARY SUPPORT STRUCTURE

NCHRP 12-79

BRIDGE ETCCR15

GENERAL ERECTION PROCEDURE

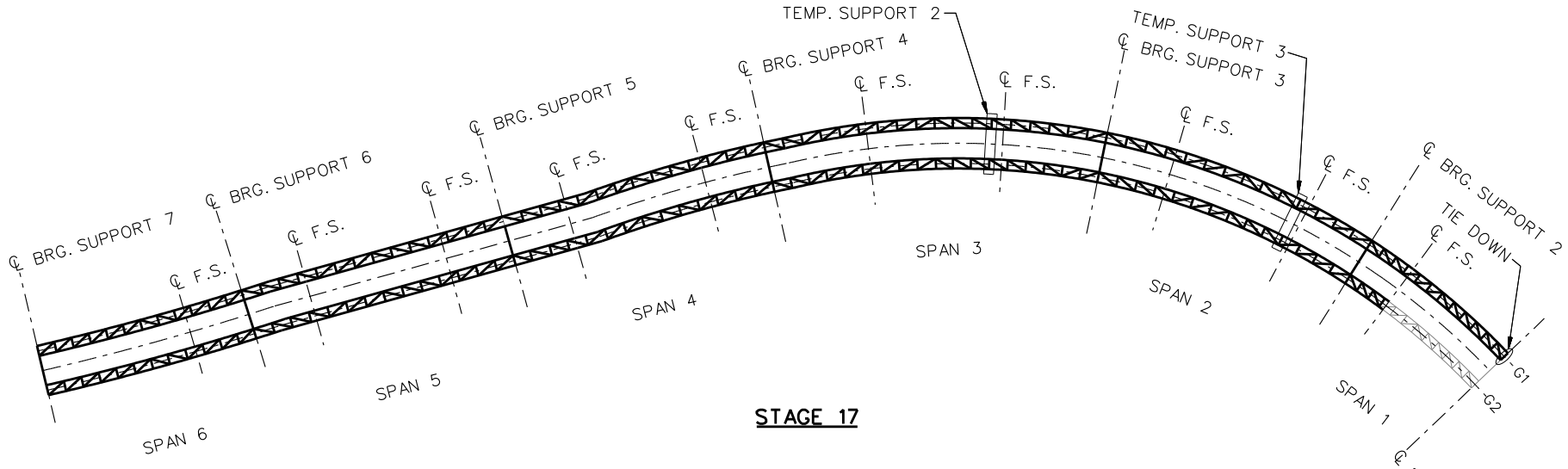

STAGE 17

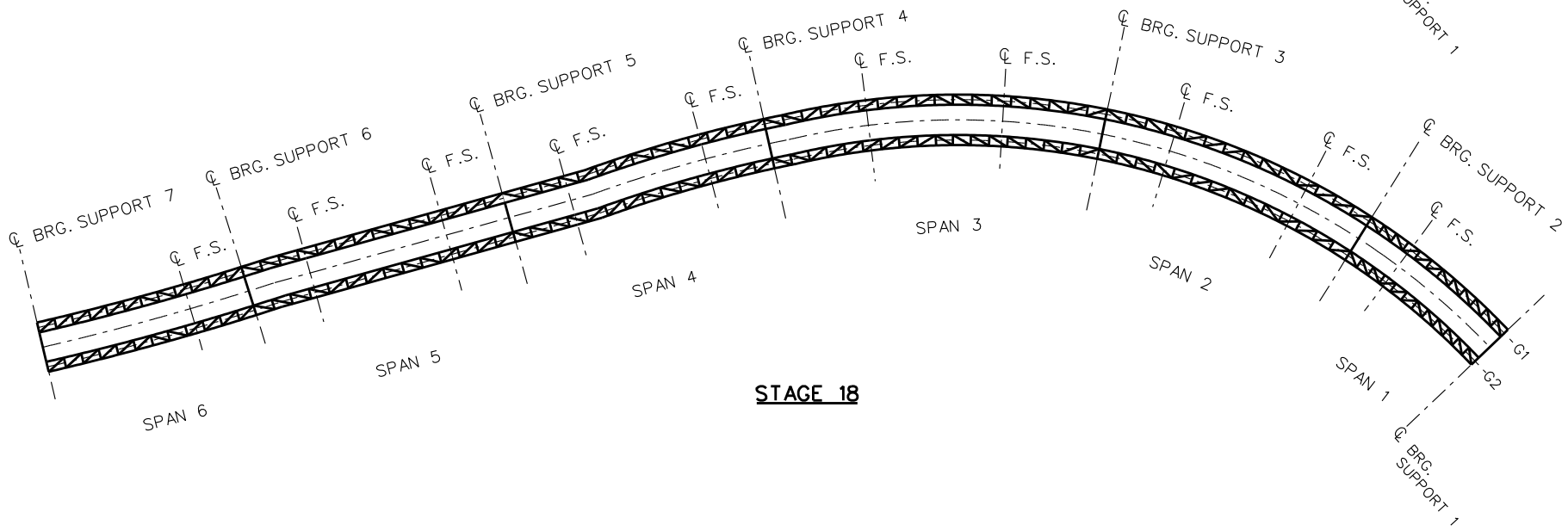

STAGE 18

LEGEND

▽ = HOLD OR LIFT CRANE

○ = TIE DOWN

□ = TEMPORARY SUPPORT STRUCTURE

NCHRP 12-79

BRIDGE ETCCR15

GENERAL ERECTION PROCEDURE

SHEET 9 OF 9

NCHRP 12-79

ETCCS5A

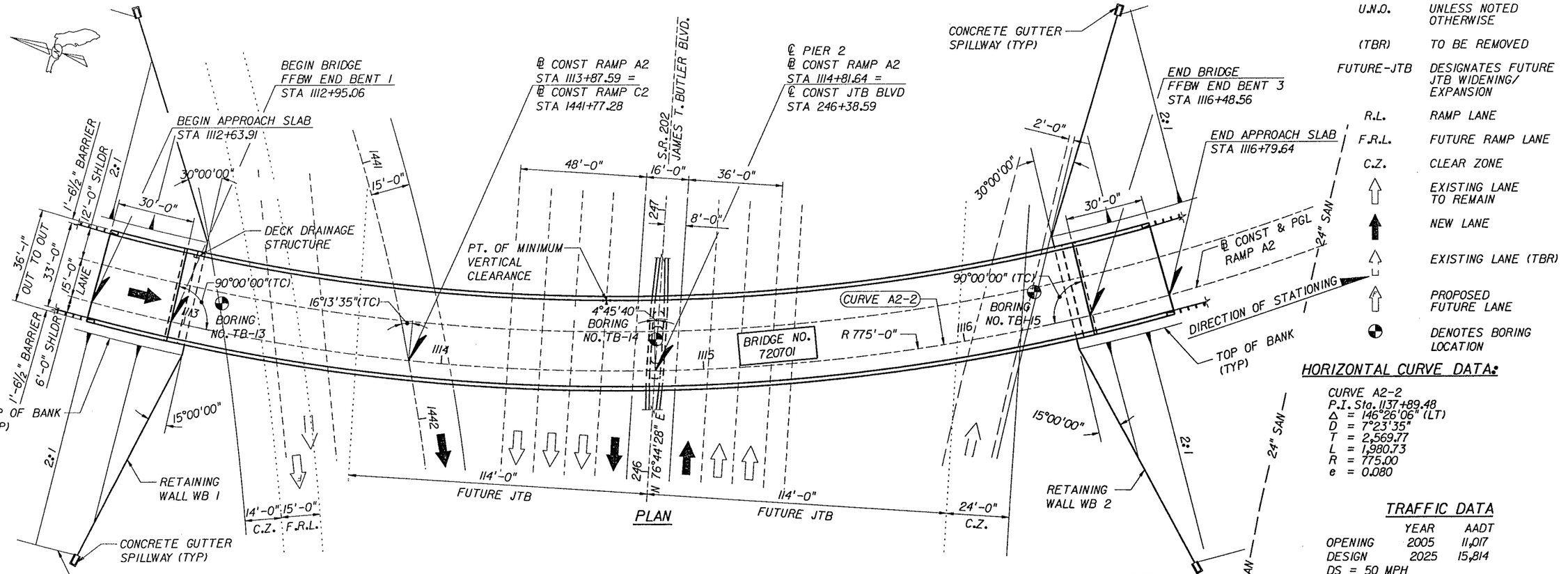

LEGEND:

U.N.O.	UNLESS NOTED OTHERWISE
(TBR)	TO BE REMOVED
FUTURE-JTB	DESIGNATES FUTURE JTB WIDENING/ EXPANSION
R.L.	RAMP LANE
F.R.L.	FUTURE RAMP LANE
C.Z.	CLEAR ZONE
⇧	EXISTING LANE TO REMAIN
⬆	NEW LANE
⇧	EXISTING LANE (TBR)
⇧	PROPOSED FUTURE LANE
◐	DENOTES BORING LOCATION

HORIZONTAL CURVE DATA:

CURVE A2-2
P.I. Sta. 1137+89.48
Δ = 146°26'06" (LT)
D = 7°23'35"
T = 2,569.77
L = 1,980.73
R = 775.00
e = 0.080

TRAFFIC DATA

	YEAR	AADT
OPENING	2005	11,017
DESIGN	2025	15,814

DS = 50 MPH
K = 9.00% d = 57% T = 4%

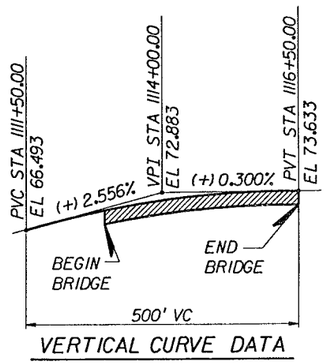

VERTICAL CURVE DATA

POINT	VERTICAL CLEARANCE
①	17'- 7½"
②	18'- 0¾"
③	20'-10⅝"
④	19'-6⅞"
⑤	19'-6¼"

NOTES:

DIMENSIONS SHOWN NORMAL TO ROADWAY FEATURES UNDER OVERPASS, U.N.O..

MSE NOT SHOWN FOR CLARITY

STEEL ALTERNATIVE - BRIDGE NO. 720701

REVISIONS					
DATE	BY	DESCRIPTION	DATE	BY	DESCRIPTION

	NAMES	DATES
DRAWN BY	ISO	02-04
CHECKED BY	WSO	02-04
DESIGNED BY	CPG	02-04
CHECKED BY	WSO	02-04
APPROVED BY	W. ODEH	

ENGINEER OF RECORD:
LOCHNER C.A. 894
H. W. LOCHNER, INC.
CONSULTING ENGINEERS AND PLANNERS
13577 FEATHER SOUND DRIVE SUITE 600
CLEARWATER, FLORIDA 33762
WAZIL S. ODEH, P.E. NO. 53920

FLORIDA DEPARTMENT OF TRANSPORTATION

ROAD NO.	COUNTY	FINANCIAL PROJECT ID
9A	DUVAL	209278-1-52-01

SHEET TITLE: GENERAL PLAN AND ELEVATION

PROJECT NAME: SR 9A & SR 202 (JAMES T. BUTLER) INTERCHANGE RAMP A2 OVER RAMP C2 AND J.T.B.

SHEET NO. B-2

h:\data\structures\projects\209278-1-52-01\sr9a_steel option\SIGNED&SEALED\720701\plans\planelev701.dgn

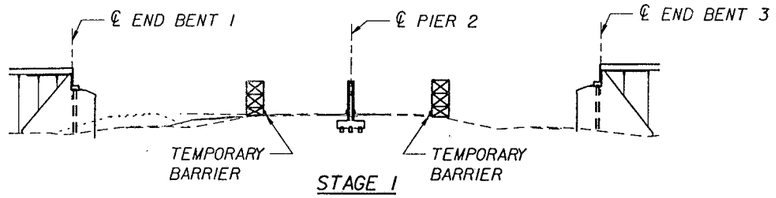

STAGE 1

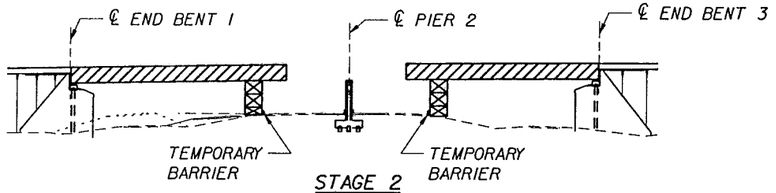

STAGE 2

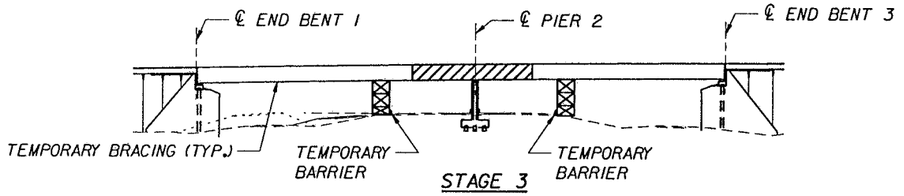

STAGE 3

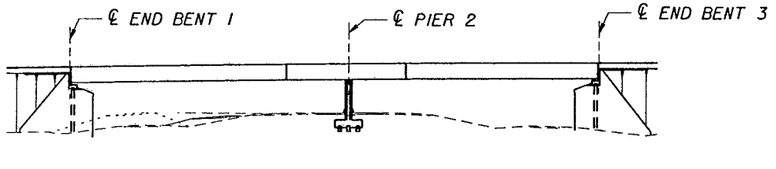

STAGE 4

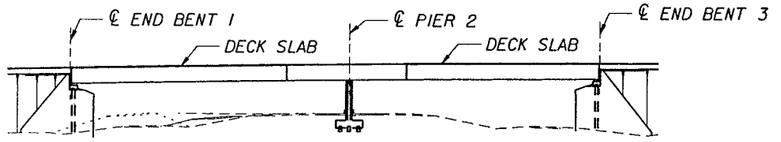

STAGE 5

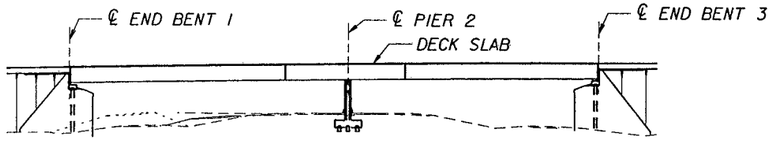

STAGE 6

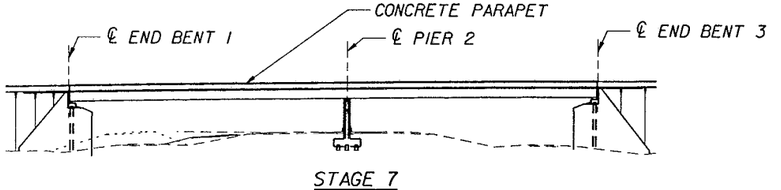

STAGE 7

CONSTRUCTION SEQUENCE

A. BEAM ERECTION

STAGE 1:

1. CONSTRUCT END BENTS, PIER FOOTINGS, AND COLUMNS, SURROUNDING MSE WALLS AND EMBANKMENTS.
2. CONSTRUCT ERECTION TOWERS AND FALSEWORK. PROTECT ERECTION TOWERS WITH TEMPORARY BARRIERS. SEE NOTE 1.

STAGE 2:

1. ERECT END BENT GIRDER SECTIONS.

STAGE 3:

1. PLACE REMAINING PIER GIRDER SECTIONS.

STAGE 4:

1. REMOVE ERECTION TOWERS AND TEMPORARY BARRIER.

B. DECK POURS

STAGE 5:

1. PLACE POSITIVE MOMENT DECK POURS FOLLOWING POURING SEQUENCE ON SHEET B-20. SEE NOTE 3.

STAGE 6:

1. PLACE REMAINING DECK POURS.

STAGE 7:

1. CAST CONCRETE PARAPETS.

NOTES:

1. ERECTION TOWERS SHALL BE DESIGNED BY A FLORIDA P.E., CALCULATIONS AND DRAWINGS SHALL BE SUBMITTED FOR APPROVAL.
2. GIRDERS SHALL BE SUPPORTED TEMPORARILY ON THE ERECTION TOWERS BY A NEOPRENE BEARING PAD.
3. CONTRACTOR IS RESPONSIBLE FOR THE TEMPORARY STABILITY OF THE STRUCTURE AND SHALL ENGAGE THE SERVICES OF A SPECIALTY ENGINEER TO DEVELOPE A DETAILED ERECTION SEQUENCE AND TO VERIFY THE ADEQUACY OF THE STRUCTURE TO RESIST THE ACTUAL COMPENSATION LOADS.
4. ERECTION STEPS SHOWN ARE A SCHEMATIC REPRESENTATION OF THE ASSUMPTIONS MADE FOR DESIGN. CONTRACTOR SHALL COORDINATE CONSTRUCTION DETAILS WITH THE MAINTENANCE OF TRAFFIC REQUIREMENTS SHOWN IN THE ROADWAY PLANS.
5. A SEQUENCE OF CONSTRUCTION, CONFORMING TO THE PLANS FOR THE MAINTENANCE OF TRAFFIC DURING CONSTRUCTION, IS SHOWN ON THIS SHEET. CHANGES IN SEQUENCE ARE PERMISSIBLE, BUT WILL REQUIRE STRUCTURAL ANALYSIS BY THE CONTRACTOR'S SPECIALTY ENGINEER, AND THEY SHALL BE REVIEWED AND APPROVED BY THE ENGINEER. GIRDER DEFLECTIONS AND CAMBERED ELEVATIONS SHALL BE COMPUTED BY THE CONTRACTOR AND REVIEWED BY THE ENGINEER. FABRICATION OF STEEL BOXES SHALL NOT COMMENCE UNTIL THE SHOP DRAWINGS HAVE BEEN APPROVED BY THE ENGINEER.

02/04/04

STEEL ALTERNATIVE - BRIDGE NO. 720701

h:\data\structures\projects\209278-1-52-01\sr9a steel option\SIGNED&SEALED\720701\plans\constseq.dgn

REVISIONS

DATE	BY	DESCRIPTION	DATE	BY	DESCRIPTION

	NAMES	DATES
DRAWN BY	BDV	02-04
CHECKED BY	WSO	02-04
DESIGNED BY	CPG	02-04
CHECKED BY	WSO	02-04
APPROVED BY	W. ODEH	

ENGINEER OF RECORD:
LOCHNER C.A. 894
H. W. LOCHNER, INC.
CONSULTING ENGINEERS AND PLANNERS
15577 FEATHER SOUND DRIVE SUITE 600
CLEARWATER, FLORIDA 33762
WAEL S. ODEH, P.E. NO. 53720

FLORIDA DEPARTMENT OF TRANSPORTATION

ROAD NO.	COUNTY	FINANCIAL PROJECT ID
9A	DUVAL	209278-1-52-01

SHEET TITLE: ERECTION SEQUENCE

PROJECT NAME: SR 9A & SR 202 (JAMES T. BUTLER) INTERCHANGE RAMP A2 OVER RAMP C2 AND J.T.B.

SHEET NO. B-3

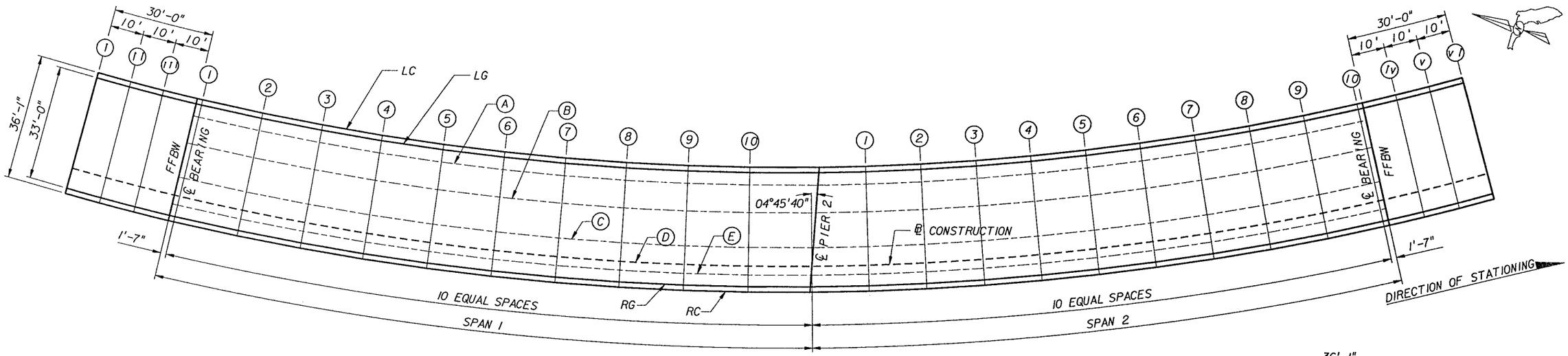

NOTES:

1. Ⓐ CL WEB BOX B LT — LC LEFT COPING
   Ⓑ CL WEB BOX B RT — LG LEFT GUTTER
   Ⓒ CL WEB BOX A LT — RC RIGHT COPING
   Ⓓ BL CONST & PGL — RG RIGHT GUTTER
   Ⓔ CL WEB BOX A RT
2. BACK BENT IS THE FFBW OR ℄ OF PIER AT THE BEGINNING OF THE SPAN AND AHEAD BENT IS THE FFBW OR ℄ OF PIER AT THE END OF THE SPAN.
3. ELEVATIONS GIVEN ARE TOP OF SLAB ELEVATIONS AT COPING LINES, GUTTER LINES, PROFILE LINE AND CENTER LINES OF BEAM WEBS.

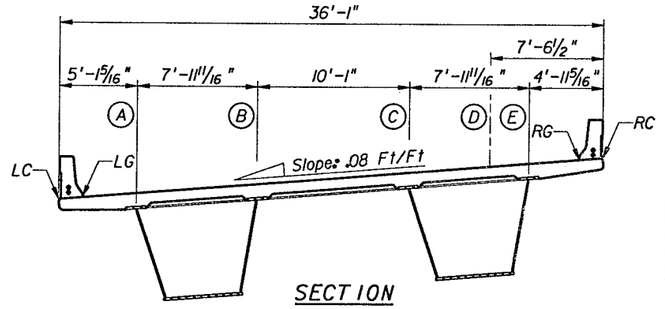

SECTION

SPAN NO. 1

LOCATION \ T-LINES & BENTS	I	II	III	BACK BENT	(1)	2	3	4	5	6	7	8	9	10	AHEAD BENT
LT COPING	66.828	67.038	67.243	67.443	67.474	67.816	68.143	68.455	68.751	69.032	69.297	69.547	69.782	70.001	70.231
LT GUTTER	66.952	67.161	67.366	67.566	67.597	67.939	68.266	68.578	68.874	69.155	69.421	69.671	69.906	70.125	70.353
CL WEB BOX B LT	N/A	N/A	N/A	67.851	67.882	68.224	68.552	68.863	69.160	69.441	69.706	69.956	70.191	70.410	70.635
CL WEB BOX B RT	N/A	N/A	N/A	68.489	68.520	68.862	69.189	69.501	69.798	70.079	70.344	70.594	70.829	71.048	71.266
CL WEB BOX A LT	N/A	N/A	N/A	69.296	69.326	69.669	69.996	70.308	70.604	70.885	71.151	71.401	71.635	71.855	72.063
BL CONST	69.112	69.321	69.526	69.726	69.756	70.099	70.426	70.738	71.034	71.315	71.581	71.831	72.066	72.285	72.489
CL WEB BOX A RT	N/A	N/A	N/A	69.934	69.964	70.307	70.634	70.946	71.242	71.523	71.789	72.039	72.273	72.493	72.694
RT GUTTER	69.592	69.801	70.006	70.206	70.236	70.579	70.906	71.218	71.514	71.795	72.061	72.311	72.546	72.765	72.963
RT COPING	69.715	69.925	70.129	70.329	70.359	70.702	71.029	71.341	71.638	71.919	72.184	72.434	72.669	72.888	73.085

SPAN NO. 2

LOCATION \ T-LINES & BENTS	BACK BENT	1	2	3	4	5	6	7	8	9	(10)	AHEAD BENT	Iv	v	v I
LT COPING	70.231	70.374	70.531	70.675	70.807	70.927	71.034	71.129	71.212	71.282	71.340	71.345	71.376	71.408	71.439
LT GUTTER	70.353	70.497	70.654	70.799	70.931	71.050	71.158	71.253	71.335	71.406	71.464	71.469	71.500	71.531	71.562
CL WEB BOX B LT	70.635	70.783	70.940	71.084	71.216	71.336	71.443	71.538	71.621	71.691	71.749	71.754	N/A	N/A	N/A
CL WEB BOX B RT	71.266	71.421	71.578	71.722	71.854	71.974	72.081	72.176	72.259	72.329	72.387	72.392	N/A	N/A	N/A
CL WEB BOX A LT	72.063	72.227	72.384	72.529	72.661	72.780	72.888	72.983	73.065	73.136	73.194	73.199	N/A	N/A	N/A
BL CONST	72.488	72.657	72.814	72.959	73.091	73.210	73.318	73.413	73.495	73.566	73.624	73.629	73.660	73.691	73.722
CL WEB BOX A RT	72.694	72.865	73.022	73.166	73.298	73.418	73.526	73.621	73.703	73.774	73.832	73.837	N/A	N/A	N/A
RT GUTTER	72.963	73.137	73.294	73.439	73.571	73.690	73.798	73.893	73.975	74.046	74.104	74.109	74.140	74.171	74.202
RT COPING	73.085	73.261	73.418	73.562	73.694	73.814	73.921	74.016	74.099	74.169	74.227	74.232	74.263	74.294	74.325

02/04/04

STEEL ALTERNATIVE - BRIDGE NO. 720701

REVISIONS

DATE	BY	DESCRIPTION	DATE	BY	DESCRIPTION

	NAMES	DATES
DRAWN BY	ISO	02-04
CHECKED BY	CPG	02-04
DESIGNED BY	CPG	02-04
CHECKED BY	WSO	02-04
APPROVED BY	W. ODEH	

ENGINEER OF RECORD:
LOCHNER C.A. 854
H. W. LOCHNER, INC.
CONSULTING ENGINEERS AND PLANNERS
15577 FEATHER SOUND DRIVE SUITE 600
CLEARWATER, FLORIDA 33762
WAEL S. ODEH, P.E. NO. 55220

FLORIDA DEPARTMENT OF TRANSPORTATION

ROAD NO.	COUNTY	FINANCIAL PROJECT ID
9A	DUVAL	209278-1-52-01

SHEET TITLE: FINISH GRADE ELEVATIONS

PROJECT NAME: SR 9A & SR 202 (JAMES T. BUTLER) INTERCHANGE RAMP A2 OVER RAMP C2 AND J.T.B.

SHEET NO. B-15

h:\data\structures\projects\209278-1-52-01\sr9a steel option\SIGNED&SEALED\720701\plans\finish grel01.dgn

DIRECTION OF STATIONING

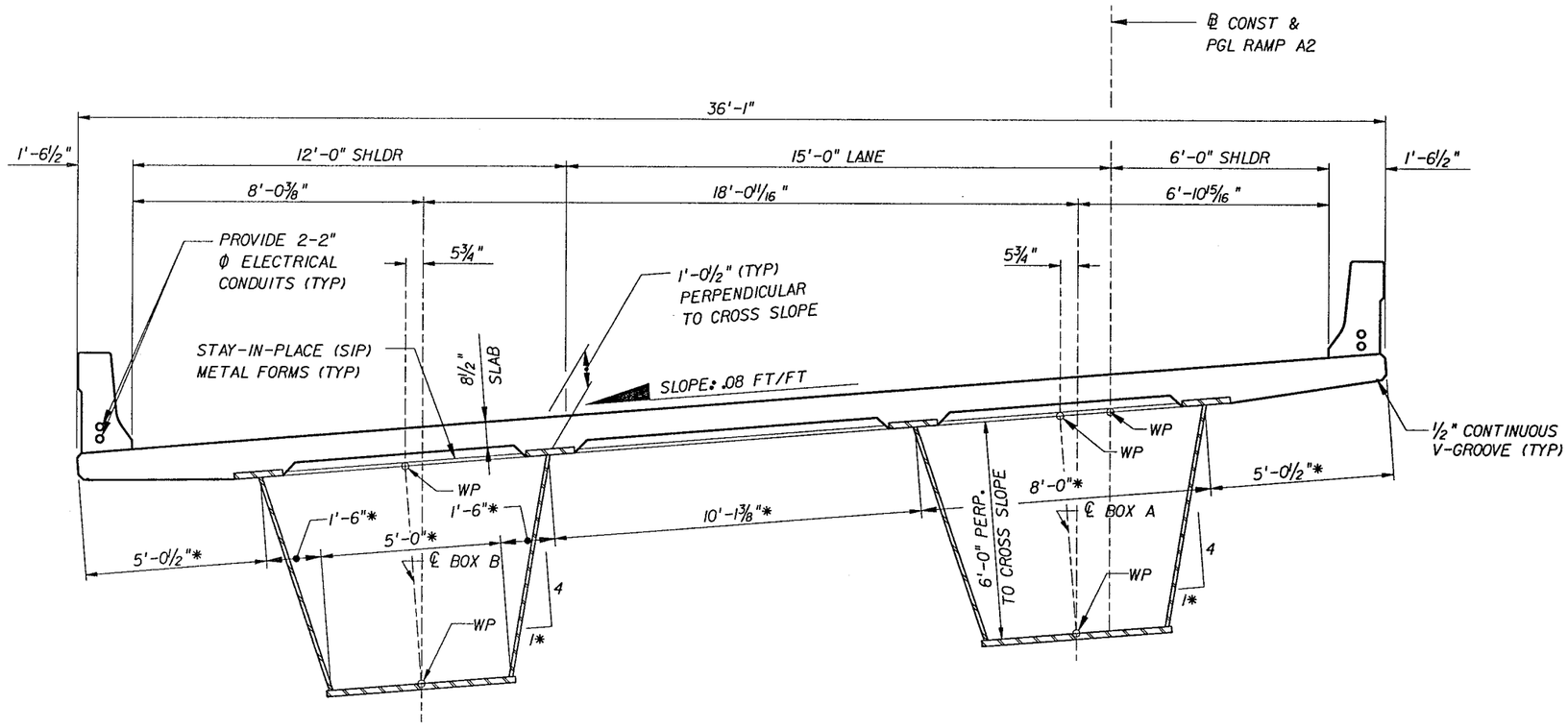

TYPICAL SECTION

NOTES:

1. * DENOTES DIMENSIONS ALONG CROSS SLOPE.

STEEL ALTERNATIVE - BRIDGE NO.720701

REVISIONS					
DATE	BY	DESCRIPTION	DATE	BY	DESCRIPTION

	NAMES	DATES
DRAWN BY	BDV	02-04
CHECKED BY	CPG	02-04
DESIGNED BY	CPG	02-04
CHECKED BY	WSO	02-04
APPROVED BY	W. ODEH	

ENGINEER OF RECORD.
LOCHNER C.A. 894
H. W. LOCHNER, INC.
CONSULTING ENGINEERS AND PLANNERS
13577 FEATHER SOUND DRIVE SUITE 600
CLEARWATER, FLORIDA 33762
WAEL S. ODEH, P.E. NO. 53950

FLORIDA DEPARTMENT OF TRANSPORTATION

ROAD NO.	COUNTY	FINANCIAL PROJECT ID
9A	DUVAL	209278-1-52-01

SHEET TITLE: TYPICAL SECTION (Sheet 1 of 2)

PROJECT NAME: SR 9A & SR 202 (JAMES T. BUTLER) INTERCHANGE RAMP A2 OVER RAMP C2 AND J.T.B.

SHEET NO. B-16

h:\data\structures\projects\209278-1-52-01\sr9a steel option\SIGNED&SEALED\720701\plans\typical section.dgn

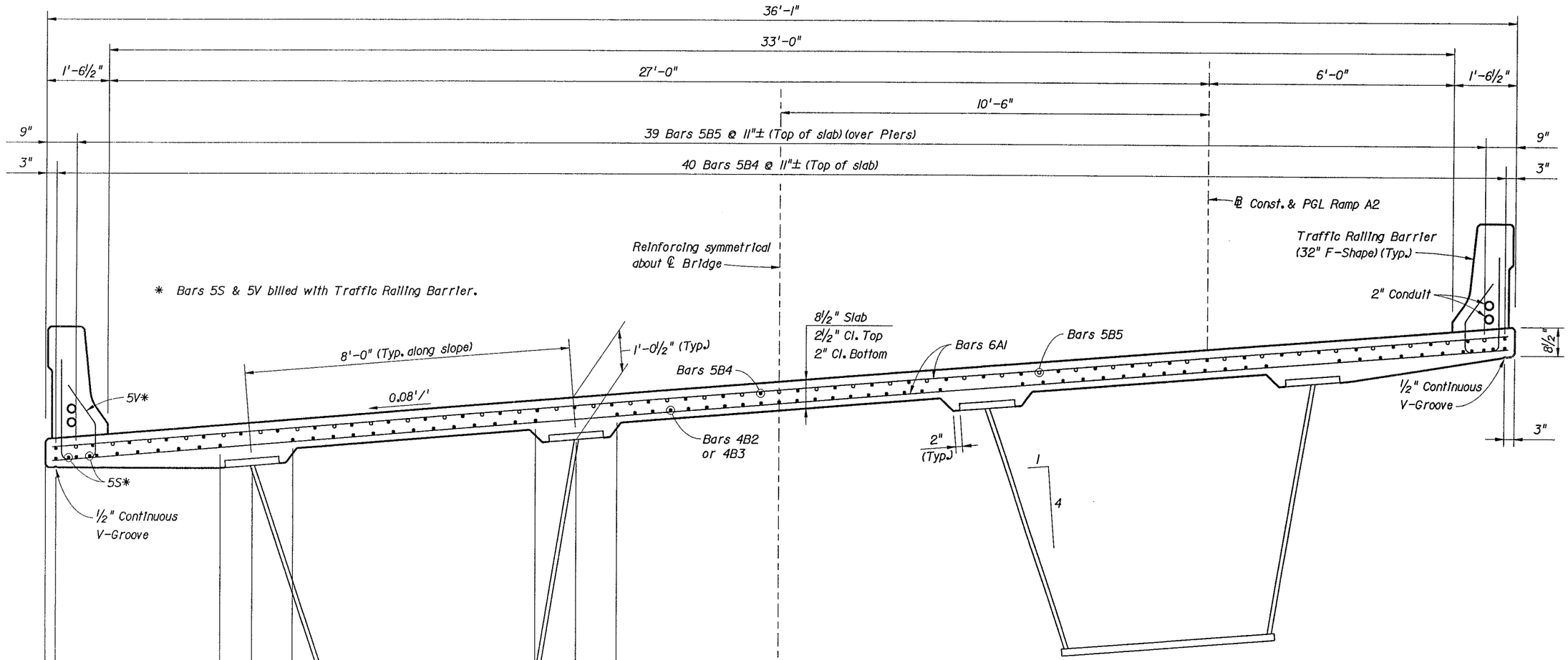

TYPICAL SECTION THRU SUPERSTRUCTURE

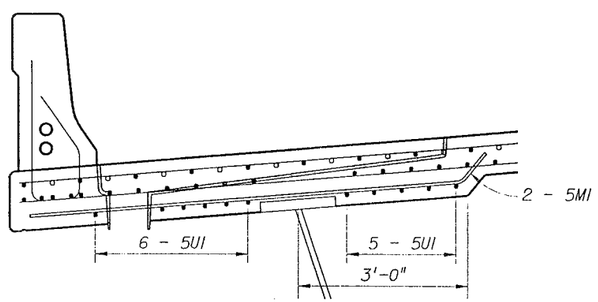

DECK SECTION AT DRAIN INLET - END BENT 1

ESTIMATED QUANTITIES		
ITEM	UNIT	QUANTITY
Class II Concrete (Superstructure)	CY	384.28
Reinforcing Steel (Superstructure)	LB	112992

CONCRETE QUANTITY BREAKDOWN

Pour 1	144.58 CY
Pour 2	113.06 CY
Pour 3	126.64 CY

NOTES:

1. For Reinforcing Bar List see sheet B-39.
2. For pour locations, see Slab Pouring Sequence & Superstructure Details.

STEEL ALTERNATIVE - BRIDGE NO. 720701

Ronald E. Rainey
11-26-03

REVISIONS

DATE	BY	DESCRIPTION	DATE	BY	DESCRIPTION

	NAMES	DATE
DRAWN BY	J.M.B.	8/03
CHECKED BY	R.K.	9/03
DESIGNED BY	M.D.M.	9/03
CHECKED BY	D.E.R.	9/03
APPROVED BY	R.D. Story	

ENGINEER OF RECORD:
ECDriver
A CORPORATION
7119 Beech Ridge Trail
Tallahassee, Florida 32312-5075
Certificate of Authorization 00003838
Donald E. Rainey, P.E.
P.E. No. 40643

FLORIDA DEPARTMENT OF TRANSPORTATION

ROAD NO.	COUNTY	FINANCIAL PROJECT ID
9A	DUVAL	209278-1-52-01

SHEET TITLE: TYPICAL SECTION (Sheet 2 of 2)

PROJECT NAME: S.R. 9A & S.R. 202 (JAMES T. BUTLER) INTERCHANGE RAMP A2 OVER RAMP C2 AND J.T.B. BLVD.

SHEET NO. B-17

E.C. Driver I:\209278\structN720701\TypicalSection.dgn 28-JAN-2004 13:39

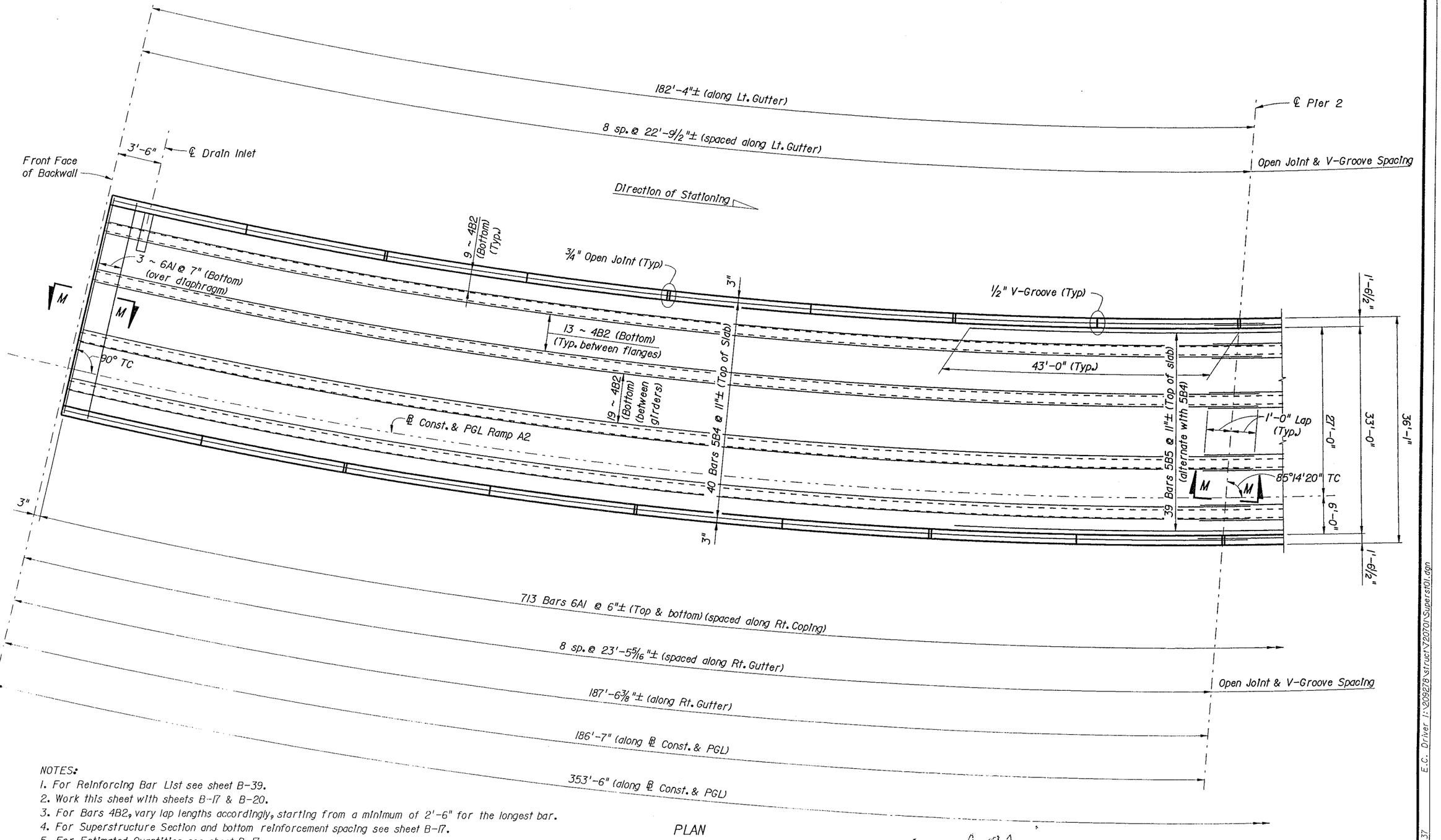

PLAN

NOTES:

1. For Reinforcing Bar List see sheet B-39.
2. Work this sheet with sheets B-17 & B-20.
3. For Bars 4B2, vary lap lengths accordingly, starting from a minimum of 2'-6" for the longest bar.
4. For Superstructure Section and bottom reinforcement spacing see sheet B-17.
5. For Estimated Quantities see sheet B-17.
6. For Section M-M see sheet B-20.
7. For construction joint locations and pouring sequence see sheet B-20.
8. Alternate splice locations for Bars 5B5.

Ronald E Rainey
1/29/04

STEEL ALTERNATIVE - BRIDGE NO. 720701

REVISIONS					
DATE	BY	DESCRIPTION	DATE	BY	DESCRIPTION

	NAMES	DATES
DRAWN BY	MDM	8/03
CHECKED BY	RK	9/03
DESIGNED BY	MDM	9/03
CHECKED BY	DER	9/03
APPROVED BY	R.D. Story	

ENGINEER OF RECORD:
ECDriver
7119 Beech Ridge Trail
Tallahassee, Florida 32312-5075
Certificate of Authorization 00003838
Donald E. Rainey, P.E.
P.E. No. 40645

FLORIDA DEPARTMENT OF TRANSPORTATION

ROAD NO.	COUNTY	FINANCIAL PROJECT ID
9A	DUVAL	209278-1-52-01

SHEET TITLE: SUPERSTRUCTURE SPAN 1

PROJECT NAME: S.R. 9A & S.R. 202 (JAMES T. BUTLER) INTERCHANGE RAMP A2 OVER RAMP C2 AND J.T.B. BLVD.

SHEET NO. B-18

E.C. Driver I:\209278\struct\720701\Superstr01.dgn 28-JAN-2004 13:37

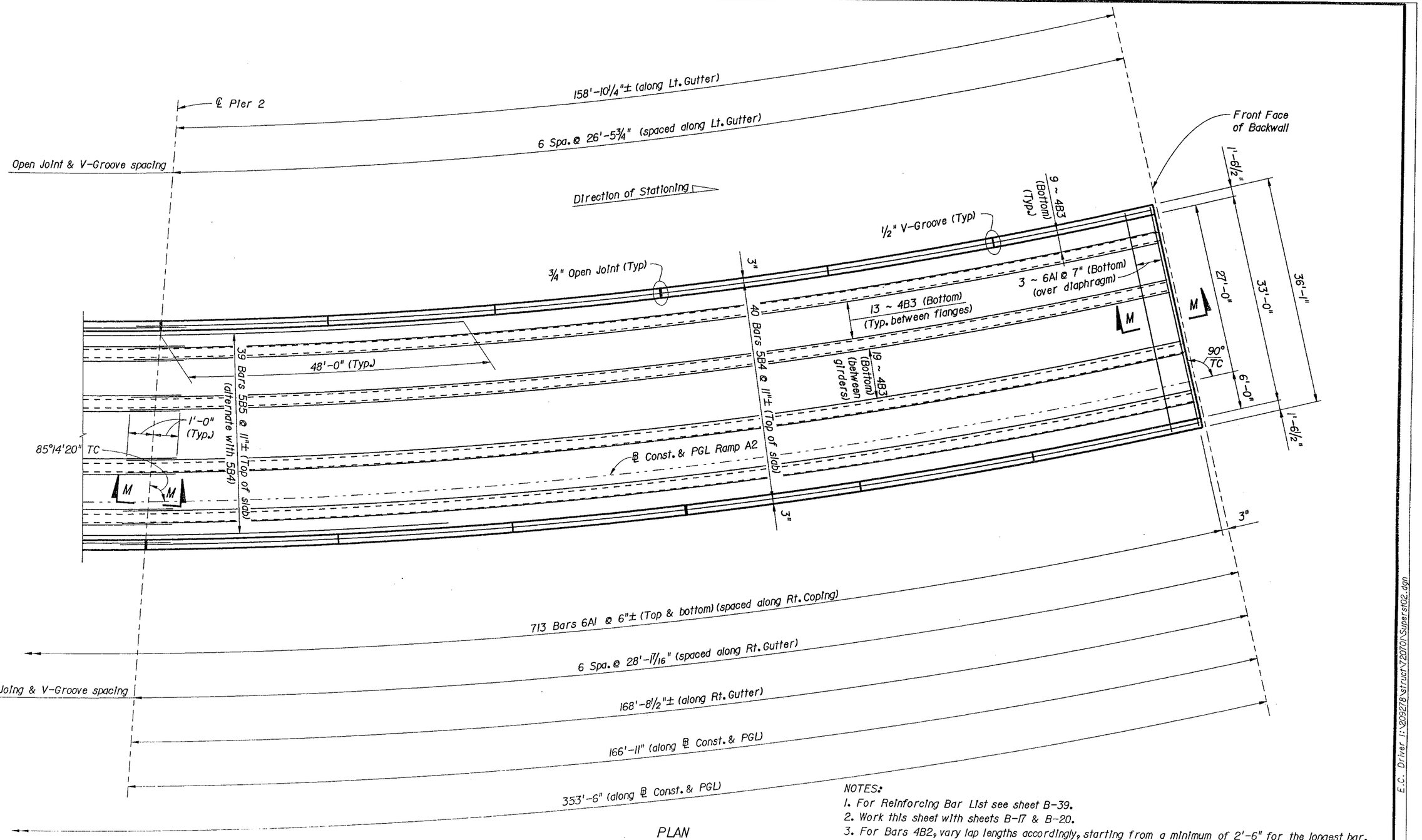

PLAN

Ronald E Rainey
1/21/04

NOTES:
1. For Reinforcing Bar List see sheet B-39.
2. Work this sheet with sheets B-17 & B-20.
3. For Bars 4B2, vary lap lengths accordingly, starting from a minimum of 2'-6" for the longest bar.
4. For Superstructure Section and bottom reinforcement spacing see sheet B-17.
5. For Estimated Quantities see sheet B-17.
6. For Section M-M see sheet B-20.
7. For construction joint locations and pouring sequence see sheet B-20.
8. Alternate splice locations for Bars 5B5.

STEEL ALTERNATIVE - BRIDGE NO. 720701

REVISIONS					
DATE	BY	DESCRIPTION	DATE	BY	DESCRIPTION

	NAMES	DATES
DRAWN BY	JMB	8/03
CHECKED BY	MDM	8/03
DESIGNED BY	MDM	7/03
CHECKED BY	DER	8/03
APPROVED BY	R.D. Story	

ENGINEER OF RECORD:
ECDriver
7119 Beech Ridge Trail
Tallahassee, Florida 32312-5075
Certificate of Authorization 00003838
Donald E. Rainey, P.E.
P.E. No. 40645

FLORIDA DEPARTMENT OF TRANSPORTATION

ROAD NO.	COUNTY	FINANCIAL PROJECT ID
9A	DUVAL	209278-1-52-01

SHEET TITLE: SUPERSTRUCTURE SPAN 2

PROJECT NAME: S.R. 9A & S.R. 202 (JAMES T. BUTLER) INTERCHANGE RAMP A2 OVER RAMP C2 AND J.T.B. BLVD.

SHEET NO. B-19

FIELD WELD
Do not weld to nor permit weld splatter on supporting Steel Girders, Diaphragms, Bracing, etc. Electrical grounding to structural steel is prohibited. See Section 400-5.7 of the Specifications for Field Welding of S.I.P. Forms in place and painting of the top flange (Typ.).

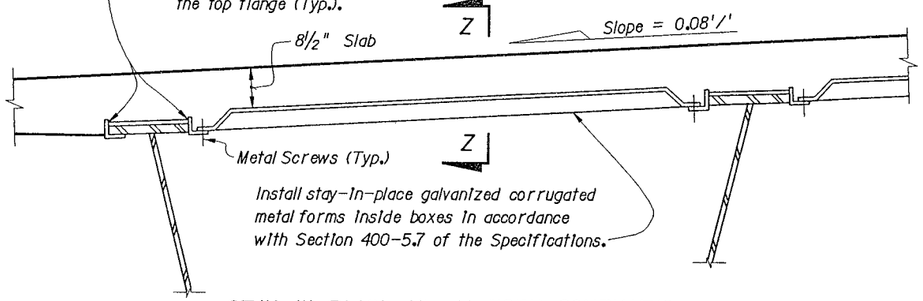

STAY-IN-PLACE METAL FORM SCHEMATIC
(NO WELDING TO FLANGE PERMITTED)

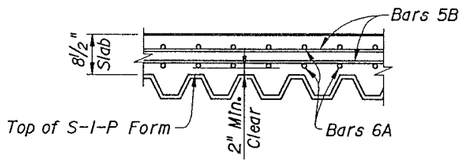

SECTION Z-Z

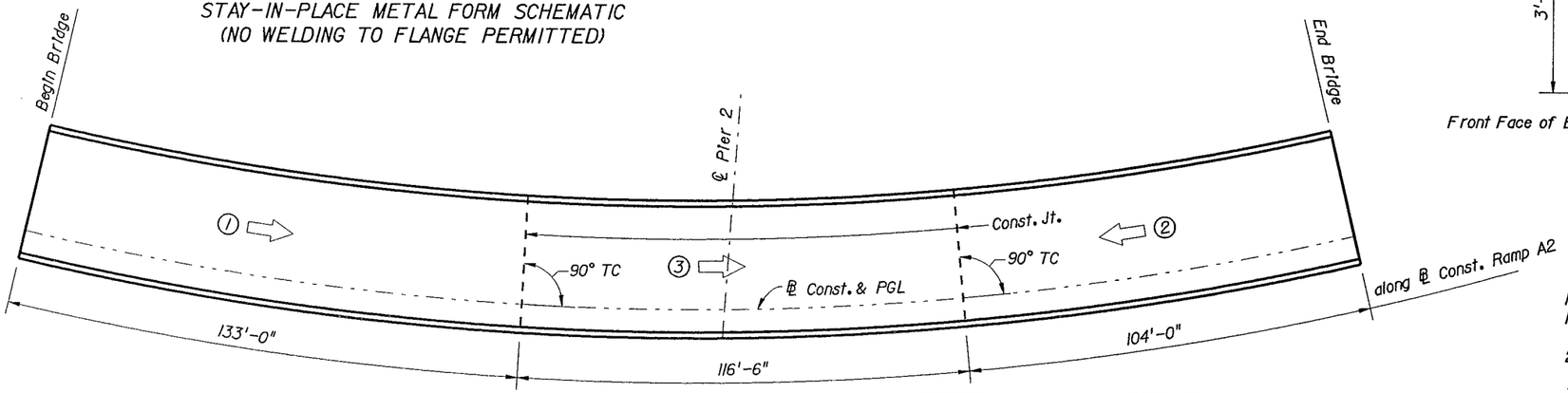

SLAB POURING SEQUENCE
(2 Span Continuous Unit)

LEGEND:
① = Pour number
⇦ = Direction of pour

NOTE: For concrete quantity breakdown, see Typical Section.

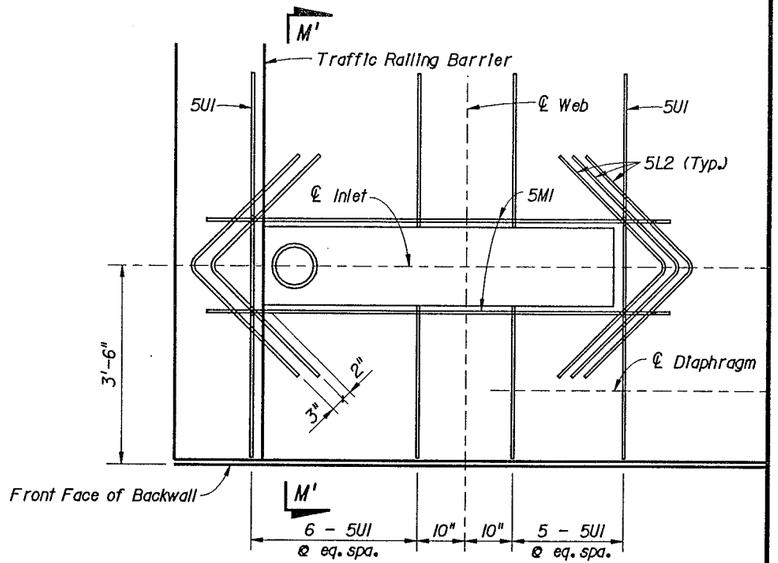

PLAN VIEW AT DRAIN INLET

NOTE: Cut Bar 5B & 4B to clear drain where shifting of bars is not practical.

NOTES:
1. No unit shall be placed adjacent to a previously placed unit that is not a minimum of 72 hours old.
2. After placement of the first unit, succeeding placements shall begin at the end away from and proceed toward the most previously placed unit.
3. The Contractor may submit for approval a revised casting sequence. The submittal shall include structural analysis by the specialty engineer reflecting the new casting sequence and its effect on the camber diagram. The revision shall be in conformance with Chapter 28 of the Plans Preparation Manual.

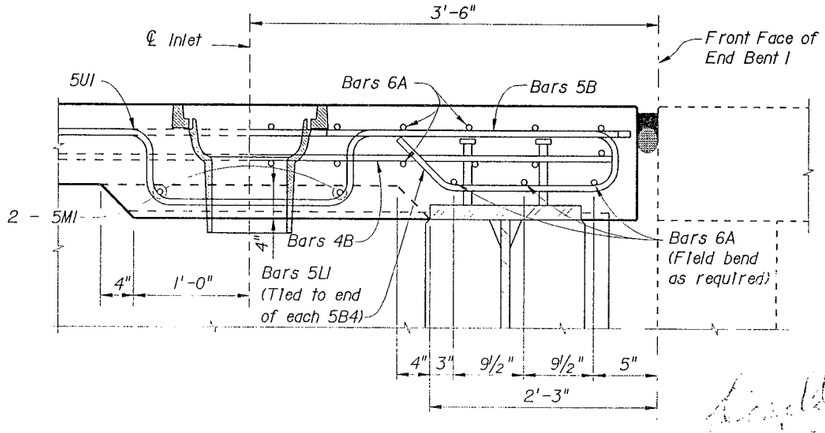

SECTION M'-M' (END BENT 1)

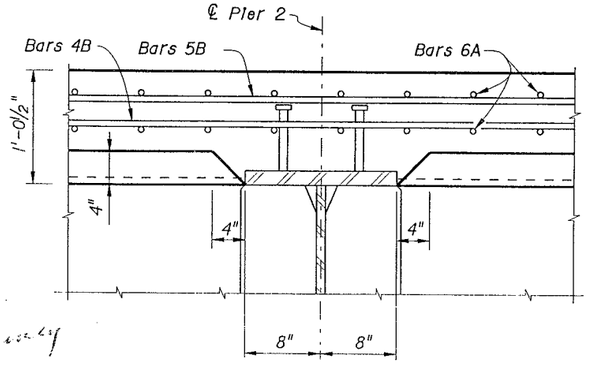

SECTION M-M
(PIER 2)

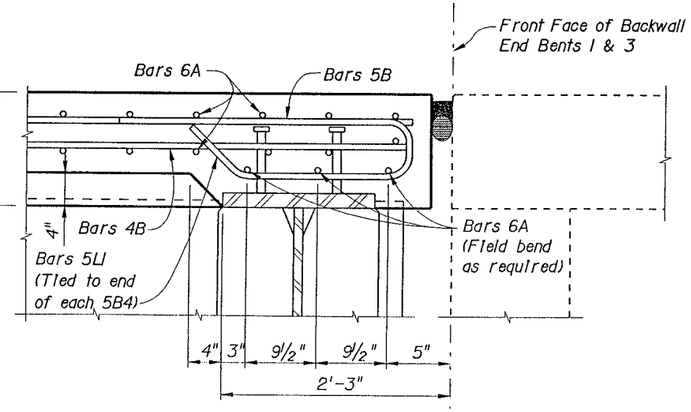

SECTION M-M (END BENTS 1 & 3)
STEEL ALTERNATIVE - BRIDGE NO. 720701

REVISIONS					
DATE	BY	DESCRIPTION	DATE	BY	DESCRIPTION

	NAMES	DATES
DRAWN BY	J.M.B.	9/03
CHECKED BY	R.K.	9/03
DESIGNED BY	R.K.	9/03
CHECKED BY	D.E.R.	10/03
APPROVED BY	R.D. Story	

ENGINEER OF RECORD:
ECDriver
7119 Beech Ridge Trail
Tallahassee, Florida 32312-5075
Certificate of Authorization 00003838
Donald E. Rainey, P.E.
P.E. No. 40645

FLORIDA DEPARTMENT OF TRANSPORTATION

ROAD NO.	COUNTY	FINANCIAL PROJECT ID
9A	DUVAL	209278-1-52-01

SHEET TITLE: SLAB POURING SEQUENCE & SUPERSTRUCTURE DETAILS

PROJECT NAME: S.R. 9A & S.R. 202 (JAMES T. BUTLER) INTERCHANGE RAMP A2 OVER RAMP C2 AND J.T.B. BLVD.

SHEET NO. B-20

E.C. Driver I:\209278\struct\720701\SuperstDet01.dgn 28-JAN-2004 13:55

Camber Diagram

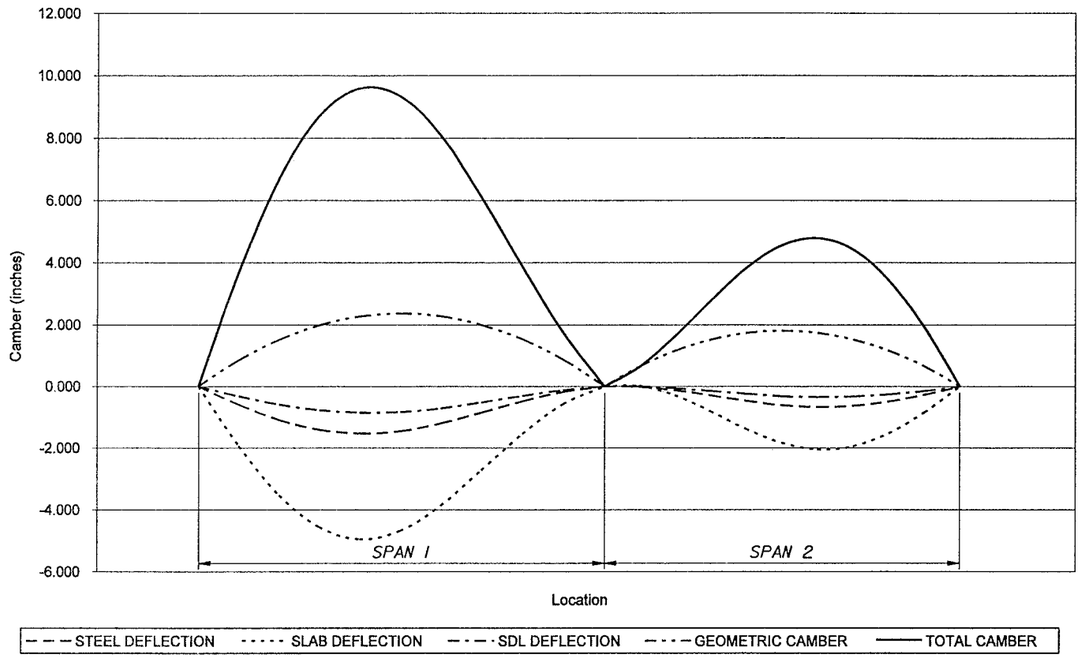

BOX B

CENTERLINE OF WEB BOX B LT

	SPAN 1											
ITEM	B BENT	0.0	0.1	0.2	0.3	0.4	0.5	0.6	0.7	0.8	0.9	1.0
STEEL (IN.)	N/A	0.000	-0.600	-1.090	-1.410	-1.530	-1.450	-1.200	-0.850	-0.480	-0.180	0.000
SLAB (IN.)	N/A	0.000	-1.940	-3.540	-4.570	-4.950	-4.680	-3.870	-2.720	-1.540	-0.580	0.000
SDL (IN.)	N/A	0.000	-0.320	-0.590	-0.770	-0.850	-0.830	-0.710	-0.520	-0.310	-0.120	0.000
TOTAL (IN.)	N/A	0.000	-2.860	-5.220	-6.750	-7.330	-6.960	-5.780	-4.090	-2.330	-0.880	0.000
VERTICAL CURVE (IN.)	N/A	0.000	0.850	1.512	1.985	2.270	2.366	2.273	1.992	1.523	0.864	0.000
REQUIRED CAMBER (IN.)	N/A	0.000	3.710	6.732	8.735	9.600	9.326	8.053	6.082	3.853	1.744	0.000

SPAN 2											
0.0	0.1	0.2	0.3	0.4	0.5	0.6	0.7	0.8	0.9	1.0	A BENT
0.000	-0.010	-0.120	-0.290	-0.470	-0.610	-0.670	-0.630	-0.490	-0.270	0.000	N/A
0.000	0.020	-0.290	-0.810	-1.380	-1.830	-2.040	-1.940	-1.520	-0.840	0.000	N/A
0.000	0.000	-0.060	-0.150	-0.240	-0.320	-0.350	-0.330	-0.260	-0.150	0.000	N/A
0.000	0.010	-0.470	-1.250	-2.090	-2.760	-3.060	-2.900	-2.270	-1.260	0.000	N/A
											N/A
0.000	0.638	1.147	1.511	1.730	1.804	1.733	1.517	1.156	0.650	0.000	N/A
0.000	0.628	1.617	2.761	3.820	4.564	4.793	4.417	3.426	1.910	0.000	N/A

BOX B

CENTERLINE OF WEB BOX B RT

	SPAN 1											
ITEM	B BENT	0.0	0.1	0.2	0.3	0.4	0.5	0.6	0.7	0.8	0.9	1.0
STEEL (IN.)	N/A	0.000	-0.630	-1.150	-1.500	-1.630	-1.550	-1.290	-0.920	-0.520	-0.200	0.000
SLAB (IN.)	N/A	0.000	-2.030	-3.720	-4.840	-5.270	-4.990	-4.150	-2.950	-1.680	-0.630	0.000
SDL (IN.)	N/A	0.000	-0.310	-0.570	-0.750	-0.830	-0.800	-0.680	-0.500	-0.290	-0.110	0.000
TOTAL (IN.)	N/A	0.000	-2.970	-5.440	-7.090	-7.730	-7.340	-6.120	-4.370	-2.490	-0.940	0.000
VERTICAL CURVE (IN.)	N/A	0.000	0.847	1.505	1.975	2.256	2.348	2.252	1.968	1.495	0.833	0.000
REQUIRED CAMBER (IN.)	N/A	0.000	3.817	6.945	9.065	9.986	9.688	8.372	6.338	3.985	1.773	0.000

SPAN 2											
0.0	0.1	0.2	0.3	0.4	0.5	0.6	0.7	0.8	0.9	1.0	A BENT
0.000	0.000	-0.100	-0.270	-0.460	-0.610	-0.680	-0.640	-0.500	-0.280	0.000	N/A
0.000	0.060	-0.210	-0.720	-1.300	-1.790	-2.030	-1.950	-1.540	-0.850	0.000	N/A
0.000	0.010	-0.040	-0.120	-0.220	-0.290	-0.320	-0.310	-0.240	-0.130	0.000	N/A
0.000	0.070	-0.350	-1.110	-1.980	-2.690	-3.030	-2.900	-2.280	-1.260	0.000	N/A
											N/A
0.000	0.666	1.172	1.533	1.749	1.820	1.746	1.527	1.163	0.654	0.000	N/A
0.000	0.596	1.522	2.643	3.729	4.510	4.776	4.427	3.443	1.914	0.000	N/A

Wael S. Odeh 02/04/04

STEEL ALTERNATIVE - BRIDGE NO. 720701

h:\data\structures\projects\209278-1-52-01\sr9a steel option\SIGNED&SEALED\720701\plans\camber701.dgn

REVISIONS					
DATE	BY	DESCRIPTION	DATE	BY	DESCRIPTION

	NAMES	DATES
DRAWN BY	DMC	02-04
CHECKED BY	CPG	02-04
DESIGNED BY	CPG	02-04
CHECKED BY	WSO	02-04
APPROVED BY	W. ODEH	

ENGINEER OF RECORD:
LOCHNER C.A. 874
H. W. LOCHNER, INC.
CONSULTING ENGINEERS AND PLANNERS
13577 FEATHER SOUND DRIVE SUITE 600
CLEARWATER, FLORIDA 33762
WAEL S. ODEH, P.E. NO. 53920

FLORIDA DEPARTMENT OF TRANSPORTATION

ROAD NO.	COUNTY	FINANCIAL PROJECT ID
9A	DUVAL	209278-1-52-01

SHEET TITLE:
CAMBER DIAGRAM (1 OF 2)

PROJECT NAME:
SR 9A & SR 202 (JAMES T. BUTLER) INTERCHANGE
RAMP A2 OVER RAMP C2 AND J.T.B.

SHEET NO.
B-21

Camber Diagram

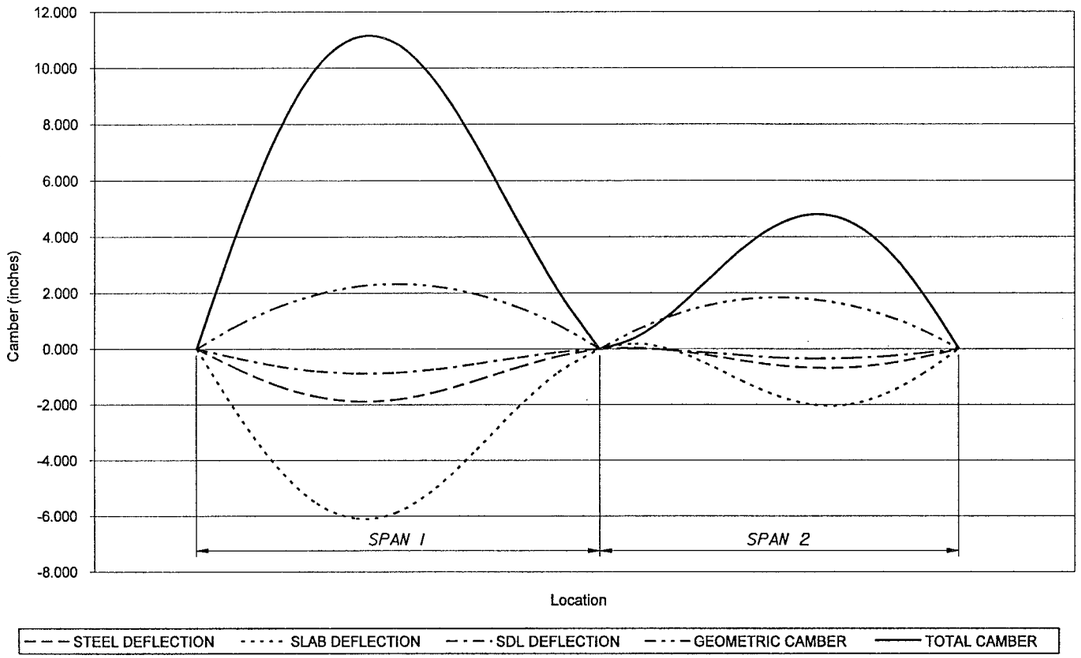

BOX A

CENTERLINE OF WEB BOX A LT

	SPAN 1											
ITEM	B BENT	0.0	0.1	0.2	0.3	0.4	0.5	0.6	0.7	0.8	0.9	1.0
STEEL (IN.)	N/A	0.000	-0.710	-1.310	-1.710	-1.880	-1.820	-1.540	-1.120	-0.660	-0.260	0.000
SLAB (IN.)	N/A	0.000	-2.310	-4.240	-5.550	-6.090	-5.880	-4.980	-3.610	-2.120	-0.840	0.000
SDL (IN.)	N/A	0.000	-0.330	-0.610	-0.800	-0.880	-0.850	-0.730	-0.530	-0.310	-0.120	0.010
TOTAL (IN.)	N/A	0.000	-3.350	-6.160	-8.060	-8.850	-8.550	-7.250	-5.260	-3.090	-1.220	0.010
VERTICAL CURVE (IN.)	N/A	0.000	0.836	1.487	1.953	2.233	2.327	2.236	1.960	1.498	0.850	0.000
REQUIRED CAMBER (IN.)	N/A	0.000	4.186	7.647	10.013	11.083	10.877	9.486	7.220	4.588	2.070	-0.010

SPAN 2											
0.0	0.1	0.2	0.3	0.4	0.5	0.6	0.7	0.8	0.9	1.0	A BENT
0.000	0.040	-0.040	-0.210	-0.420	-0.590	-0.680	-0.660	-0.530	-0.290	0.000	N/A
0.000	0.190	-0.010	-0.530	-1.150	-1.700	-2.010	-1.990	-1.600	-0.890	0.000	N/A
0.010	0.020	-0.040	-0.130	-0.230	-0.310	-0.350	-0.330	-0.260	-0.140	0.000	N/A
0.010	0.250	-0.090	-0.870	-1.800	-2.600	-3.040	-2.980	-2.390	-1.320	0.000	N/A
											N/A
0.000	0.652	1.170	1.541	1.764	1.840	1.767	1.547	1.179	0.663	0.000	N/A
-0.010	0.402	1.260	2.411	3.564	4.440	4.807	4.527	3.569	1.983	0.000	N/A

BOX A

CENTERLINE OF WEB BOX A RT

	SPAN 1											
ITEM	B BENT	0.0	0.1	0.2	0.3	0.4	0.5	0.6	0.7	0.8	0.9	1.0
STEEL (IN.)	N/A	0.000	-0.740	-1.370	-1.800	-1.990	-1.920	-1.640	-1.200	-0.710	-0.280	0.000
SLAB (IN.)	N/A	0.000	-2.400	-4.430	-5.830	-6.440	-6.220	-5.290	-3.870	-2.280	-0.910	0.000
SDL (IN.)	N/A	0.000	-0.350	-0.650	-0.850	-0.940	-0.910	-0.780	-0.580	-0.340	-0.140	-0.010
TOTAL (IN.)	N/A	0.000	-3.490	-6.450	-8.480	-9.370	-9.050	-7.710	-5.650	-3.330	-1.330	-0.010
VERTICAL CURVE (IN.)	N/A	0.000	0.834	1.481	1.943	2.220	2.311	2.217	1.937	1.471	0.820	0.000
REQUIRED CAMBER (IN.)	N/A	0.000	4.324	7.931	10.423	11.590	11.361	9.927	7.587	4.801	2.150	0.010

SPAN 2											
0.0	0.1	0.2	0.3	0.4	0.5	0.6	0.7	0.8	0.9	1.0	A BENT
0.000	0.060	-0.020	-0.190	-0.390	-0.580	-0.680	-0.670	-0.540	-0.300	0.000	N/A
0.000	0.240	0.070	-0.430	-1.070	-1.650	-2.000	-2.000	-1.630	-0.910	0.000	N/A
-0.010	-0.010	-0.060	-0.160	-0.270	-0.350	-0.390	-0.370	-0.290	-0.170	0.000	N/A
-0.010	0.290	-0.010	-0.780	-1.730	-2.580	-3.070	-3.040	-2.460	-1.380	0.000	N/A
											N/A
0.000	0.678	1.194	1.562	1.783	1.855	1.780	1.557	1.186	0.667	0.000	N/A
0.010	0.388	1.204	2.342	3.513	4.435	4.850	4.597	3.646	2.047	0.000	N/A

2/04/04

STEEL ALTERNATIVE - BRIDGE NO. 720701

REVISIONS					
DATE	BY	DESCRIPTION	DATE	BY	DESCRIPTION

	NAMES	DATES
DRAWN BY	DMC	02-04
CHECKED BY	CPG	02-04
DESIGNED BY	CPG	02-04
CHECKED BY	WSO	02-04
APPROVED BY	W. ODEH	

ENGINEER OF RECORD:
LOCHNER C.A. 894
H. W. LOCHNER, INC.
CONSULTING ENGINEERS AND PLANNERS
13577 FEATHER SOUND DRIVE SUITE 600
CLEARWATER, FLORIDA 33762
WAEL S. ODEH, P.E. NO. 53920

FLORIDA DEPARTMENT OF TRANSPORTATION

ROAD NO.	COUNTY	FINANCIAL PROJECT ID
9A	DUVAL	209278-1-52-01

SHEET TITLE:
CAMBER DIAGRAM (2 OF 2)

PROJECT NAME:
SR 9A & SR 202 (JAMES T. BUTLER) INTERCHANGE
RAMP A2 OVER RAMP C2 AND J.T.B.

SHEET NO.
B-22

h:\data\structures\projects\209278-1-52-01\sr9a steel option\SIGNED&SEALED\720701\plans\camber701.dgn

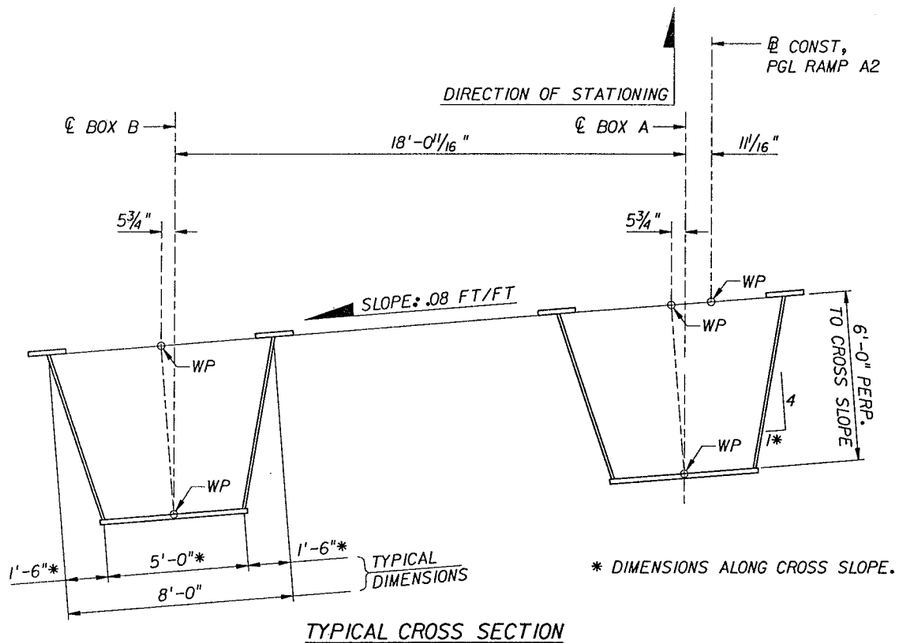

* DIMENSIONS ALONG CROSS SLOPE.

TYPICAL CROSS SECTION

NOTES FOR STRUCTURAL STEEL BOXES

1. STRUTS AND CROSS FRAMES ARE RADIAL TO CENTER LINE OF BOX A, WHEREAS DIAPHRAGMS ARE ALONG CENTER LINE OF SUPPORTS.
2. ALL LONGITUDINAL AND TRANSVERSE DIMENSIONS ARE IN A HORIZONTAL PLANE, UNLESS OTHERWISE NOTED OR SHOWN.
3. DIMENSIONS FOR STRESS REVERSIBLE AND TENSION REGIONS ARE ALONG ℄ BOXES.
4. FOR DETAILS OF WELDING FOR THE FOLLOWING ITEMS, SEE SHEET B-32.
   - B. FLANGE TRANSITION
   - C. WEB SHOP SPLICE
   - D. FLANGE TO WEB WELD (TOP AND BOTTOM)
5. FOR INTERNAL CROSS FRAMES, EXTERNAL CROSS FRAMES AND DETAILS, SEE SHEETS B-30 AND B-31.
6. FOR END BENT AND PIER DIAPHRAGMS, SEE SHEETS B-26 THRU B-29.
7. FOR DETAIL OF 2" DRAIN HOLES ON LOW SIDE OF EACH BOX, SEE SHEET B-32.
8. FOR ACCESS OPENING DETAILS, SEE SHEET A-19.
9. FOR ACCESS DOOR DETAILS, SEE SHEET A-23.
10. FOR DETAILS OF SHEAR CONNECTORS AND WIDTH TRANSITION OF FLANGE, SEE SHEET B-32.
11. FOR FIELD SPLICE DETAILS, SEE SHEET B-33.
12. ALL BOX GIRDER FLANGES AND WEBS, DIAPHRAGMS, BEARING STIFFENERS, SPLICE PLATES, AND ALL OTHER COMPONENTS INCLUDING TEMPORARY CROSS FRAMES AND INTERNAL CROSS FRAMES SHALL BE ASTM A709 GRADE 50 STEEL UNLESS NOTED OTHERWISE.
13. ▲ DENOTES TENSION MEMBERS WHICH SHALL MEET MINIMUM CHARPY V-NOTCH REQUIREMENTS OF ASTM A709-01 (S83), TABLE S1.2 (ZONE 1).
    ▲▲ DENOTES TENSION MEMBERS WHICH ARE DESIGNATED AS FRACTURE CRITICAL AND WHICH SHALL MEET MINIMUM CHARPY V-NOTCH REQUIREMENTS OF ASTM A709-01 (S84). TABLE S1.3 (ZONE 1). GIRDER SPLICE PLATES, LONGITUDINAL STIFFENERS, BOTTOM FLANGE PLATES AND WEB PLATES IN THE POSITIVE MOMENT REGION SHALL ALSO MEET THIS REQUIREMENT. FABRICATION AND TESTING OF FRACTURE CRITICAL MEMBERS SHALL MEET THE REQUIREMENTS OF 1978 EDITION OF AASHTO "GUIDE SPECIFICATIONS FOR FRACTURE CRITICAL NON-REDUNDANT STEEL BRIDGE MEMBERS "AND APPROVED REVISIONS THROUGH 1991.
14. ■ DENOTES STRESS REVERSIBLE REGION
    □ DENOTES TENSION IN BOTTOM FLANGE
    △ DENOTES TENSION IN TOP FLANGE
15. FOR LAYOUT AND DETAILS OF POWER RECEPTACLES INSIDE THE BOXES, SEE HIGHWAY LIGHTING PLANS.
16. CROSS- FRAMES (INSIDE BOX GIRDERS) AND TOP LATERAL BRACING SHALL BE INSTALLED PRIOR TO SHIPPING AND ERECTING THE GIRDERS.
17. SEE GENERAL NOTES ON SHEET A-4 FOR STRUCTURAL MATERIALS, CONNECTIONS WELDING, PAINTING, ETC.
18. ALL BOLT CONNECTIONS SHALL BE MADE WITH A.S.T.M. A-325 HIGH STRENGTH BOLTS (SLIP CRITICAL BOLT CONNECTIONS). THE SPLICE CONNECTION SHALL BE MADE WITH 7/8" Ø HIGH STRENGTH BOLTS AND ALL OTHER CONNECTIONS SHALL BE MADE AS INDICATED ON THE PLANS.
19. ALL PARTS OF EACH FIELD SPLICE SHALL BE COMPLETELY SHOP ASSEMBLED TAKING INTO ACCOUNT THEIR RELATIVE POSITION IN THE FINISHED STRUCTURE DUE TO GRADE AND CAMBER.
20. GENERAL REAMING OF THE HOLES FOR EACH FIELD SPLICE SHALL BE REQUIRED WHILE ALL PARTS FOR EACH SPLICE ARE COMPLETELY SHOP ASSEMBLED IN THE CORRECT POSITION.
21. ALL DIAPHRAGMS AT BEARINGS SHALL BE PLACED TO BE VERTICAL AFTER DEAD LOAD DEFLECTIONS.
22. SHIFT SHEAR CONNECTORS TO CLEAR AS REQUIRED.
23. CONTRACTOR SHALL COORDINATE THE HANDLING AND ERECTION OF EACH BOX GIRDER DURING CONSTRUCTION. LIFTING POINTS SHALL BE DETERMIND BY THE CONTRACTOR AND SHALL BE LOCATED SUCH THAT THE STEEL MEMBER IS STABLE AND WILL NOT BE OVER STRESSED.
24. FOR WELDING REQUIREMENTS OF, BEARING STIFFENERS, CROSS FRAME MEMBERS AND SHOP SPLICES OF WEB AND FLANGE PLATES, SEE SHEETS B-26 THRU B-32.

Wael Odeh 02/04/04

STEEL ALTERNATIVE - BRIDGE NO. 720701

REVISIONS					
DATE	BY	DESCRIPTION	DATE	BY	DESCRIPTION

	NAMES	DATES
DRAWN BY	ISO	02-04
CHECKED BY	CPG	02-04
DESIGNED BY	CPG	02-04
CHECKED BY	WSO	02-04
APPROVED BY	W. ODEH	

ENGINEER OF RECORD:
LOCHNER C.A. 894
H. W. LOCHNER, INC.
CONSULTING ENGINEERS AND PLANNERS
13577 FEATHER SOUND DRIVE SUITE 600
CLEARWATER, FLORIDA 33762
WAEL S. ODEH, P.E. NO. 53920

FLORIDA DEPARTMENT OF TRANSPORTATION

ROAD NO.	COUNTY	FINANCIAL PROJECT ID
9A	DUVAL	209278-1-52-01

SHEET TITLE: FRAMING PLAN (1 OF 3)

PROJECT NAME: SR 9A & SR 202 (JAMES T. BUTLER) INTERCHANGE RAMP A2 OVER RAMP C2 AND J.T.B.

SHEET NO. B-23

h:\data\structures\projects\209278-1-52-01\sr9a steel option\SIGNED&SEALED\720701plans\framingplan1.dgn

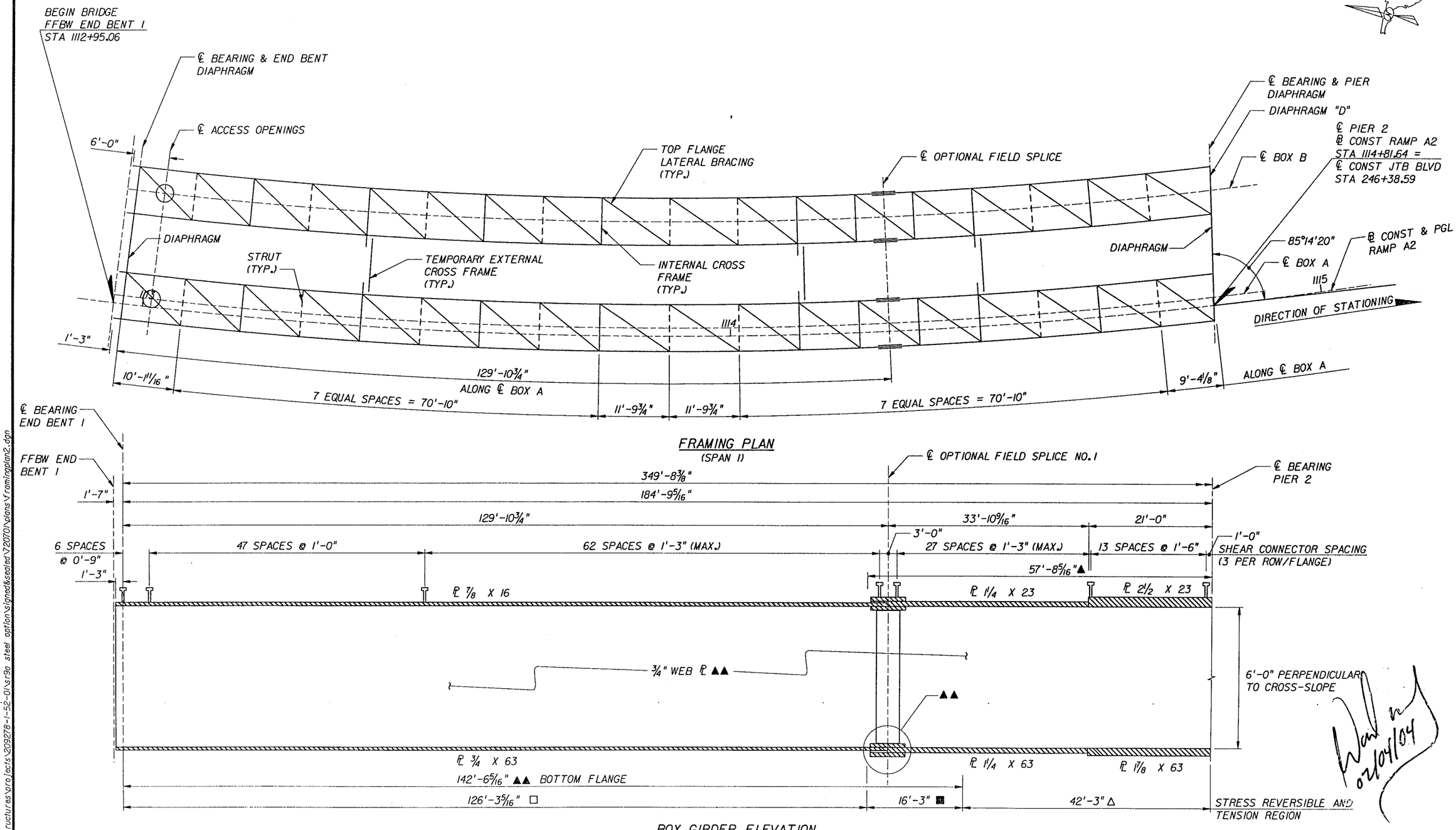

FRAMING PLAN
(SPAN 1)

BOX GIRDER ELEVATION
(SPAN 1)
(DIMENSIONS ALONG ℄ BOX A)

Wael Odeh 02/04/04

h:\data\structures\projects\209278-1-52-01\sr9a steel option\signed&sealed\720701\plans\framingplan2.dgn

STEEL ALTERNATIVE - BRIDGE NO. 720701

REVISIONS					
DATE	BY	DESCRIPTION	DATE	BY	DESCRIPTION

	NAMES	DATES
DRAWN BY	ISO	02-04
CHECKED BY	CPG	02-04
DESIGNED BY	CPG	02-04
CHECKED BY	WSO	02-04
APPROVED BY	W. ODEH	

ENGINEER OF RECORD:
LOCHNER C.A. 894
H. W. LOCHNER, INC.
CONSULTING ENGINEERS AND PLANNERS
13577 FEATHER SOUND DRIVE SUITE 600
CLEARWATER, FLORIDA 33762
WAEL S. ODEH, P.E. NO. 53920

FLORIDA DEPARTMENT OF TRANSPORTATION

ROAD NO.	COUNTY	FINANCIAL PROJECT ID
9A	DUVAL	209278-1-52-01

SHEET TITLE:
FRAMING PLAN (2 OF 3)
(SPAN 1)

PROJECT NAME:
SR 9A & SR 202 (JAMES T. BUTLER) INTERCHANGE
RAMP A2 OVER RAMP C2 AND J.T.B.

SHEET NO.
B-24

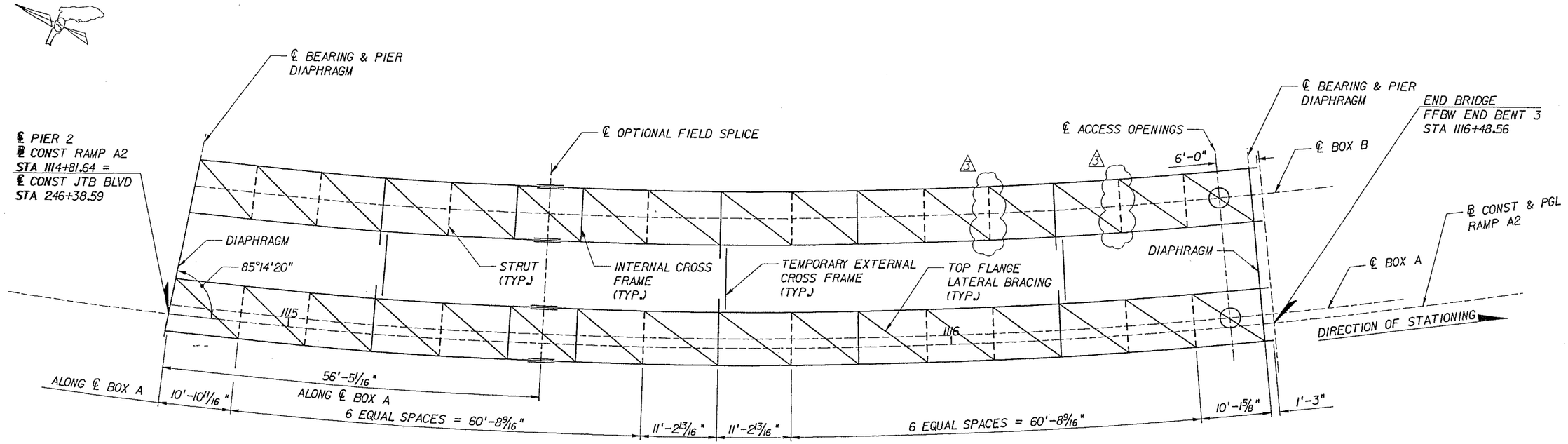

FRAMING PLAN
(SPAN 2)

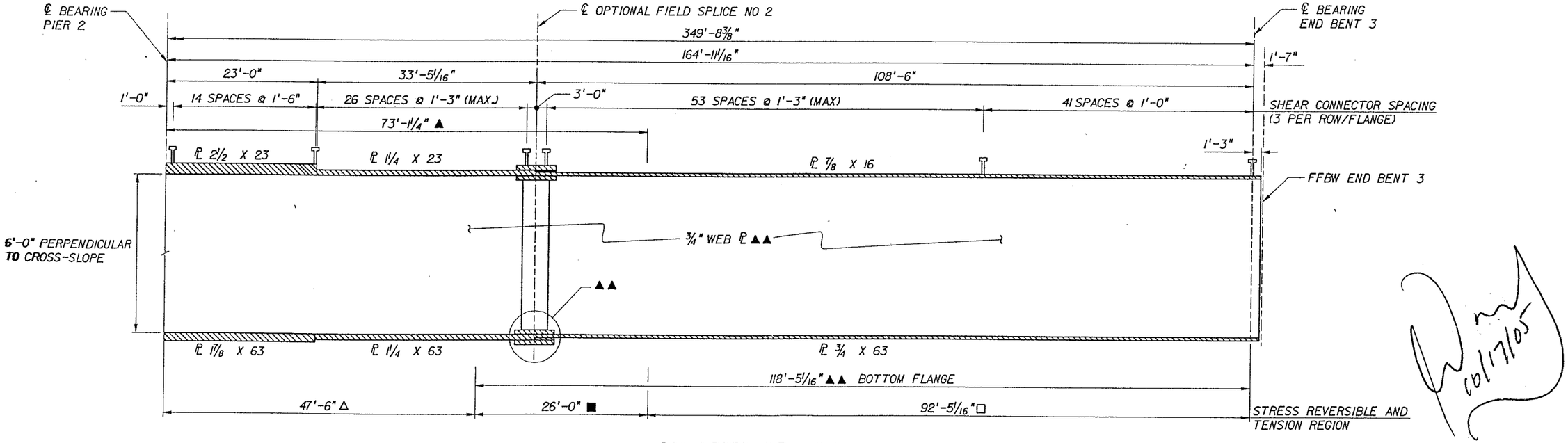

BOX GIRDER ELEVATION
(SPAN 2)
(DIMENSIONS ALONG ℄ BOX A)

10/17/05

H:\Design\D2\2026_SR9A post\209278_steel - As Built\struct\Y20701\Plans\Framing Plan3.dgn

REVISIONS

DATE	BY	DESCRIPTION	DATE	BY	DESCRIPTION
10/17/05	WSO	3 CHANGED X-BRACING TO STRUTS			

	NAMES	DATES
DRAWN BY	ISO	02-04
CHECKED BY	CPG	02-04
DESIGNED BY	CPG	02-04
CHECKED BY	WSO	02-04
APPROVED BY	W. ODEH	

ENGINEER OF RECORD:
LOCHNER C.A. 894
H. W. LOCHNER, INC.
CONSULTING ENGINEERS AND PLANNERS
12577 FEATHER SOUND DRIVE SUITE 600
CLEARWATER, FLORIDA 33762
WAEL A. ODEH, P.E. NO. 59920

FLORIDA DEPARTMENT OF TRANSPORTATION

ROAD NO.	COUNTY	FINANCIAL PROJECT ID
9A	DUVAL	209278-1-52-01

STEEL ALTERNATIVE - BRIDGE NO.720701

SHEET TITLE: FRAMING PLAN (3 OF 3) (SPAN 2)

PROJECT NAME: SR 9A & SR 202 (JAMES T. BUTLER) INTERCHANGE RAMP A2 OVER RAMP C2 AND J.T.B.

SHEET NO. B-25

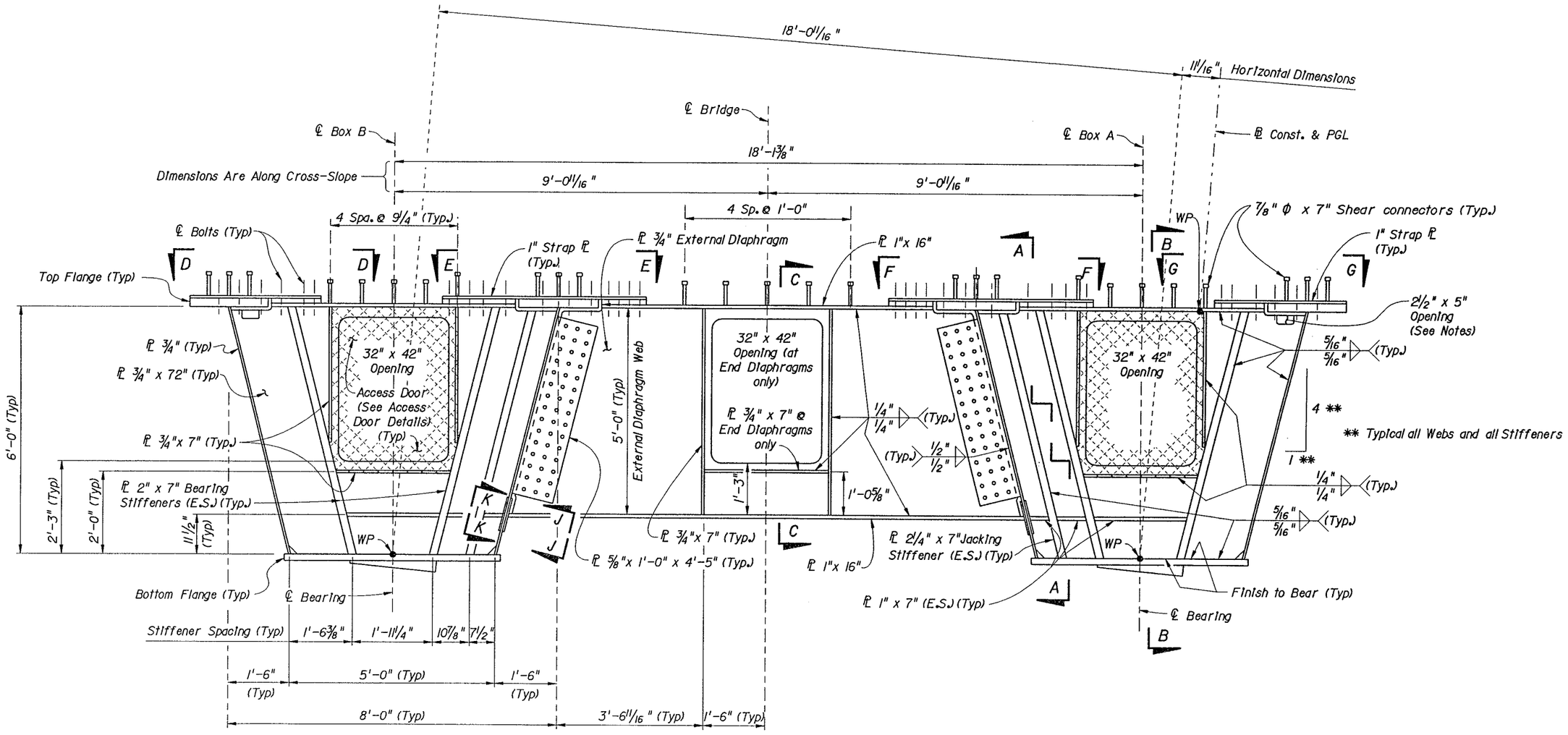

DIAPHRAGM ELEVATION

Notes:
Transverse dimensions are measured along bottom of the top flange and top of bottom flange.

The 2 1/2" x 5" opening in the interior Diaphragms is required for Maintenance Box Lighting Conduit (Typical Box A and B)

NOTES:
1. For Sections A-A, B-B and C-C see Diaphragm Detail Sheet 1 of 3.
2. For Strap Plate Connections, Views D-D, E-E, F-F & G-G, see Diaphragm Details Sheet 2 of 3.
3. For Sections J-J and K-K see Diaphragm Detail Sheet 3 of 3.
4. External diaphragm opening and 3/4" x 7" horizontal stiffener at end diphragms only.

Donald E. Rainey
11/29/04

STEEL ALTERNATIVE - BRIDGE NO. 720701

REVISIONS					
DATE	BY	DESCRIPTION	DATE	BY	DESCRIPTION

	NAMES	DATES
DRAWN BY	RCC	9/03
CHECKED BY	RK	9/03
DESIGNED BY	RK	9/03
CHECKED BY	MDM	10/03
APPROVED BY	R.D. Story	

ENGINEER OF RECORD:
ECDriver
7119 Beech Ridge Trail
Tallahassee, Florida 32312-5075
Certificate of Authorization 00003838
Donald E. Rainey, P.E.
P.E. No. 40645

FLORIDA DEPARTMENT OF TRANSPORTATION

ROAD NO.	COUNTY	FINANCIAL PROJECT ID
9A	DUVAL	209278-1-52-01

SHEET TITLE: DIAPHRAGMS

PROJECT NAME: S.R. 9A & S.R. 202 (JAMES T. BUTLER) INTERCHANGE RAMP A2 OVER RAMP C2 AND J.T.B. BLVD.

SHEET NO. B-26

E.C. Driver I:\209278\struct\720701\diaphragmdet01.dgn 28-JAN-2004 13:33

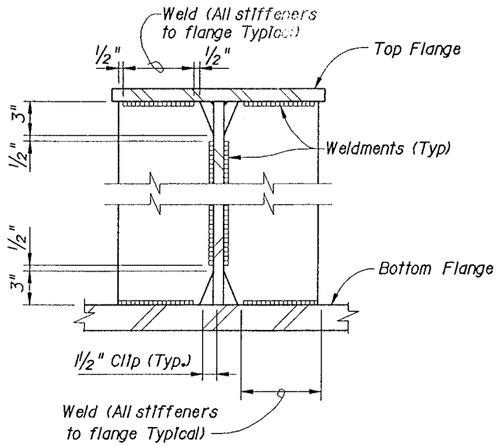

STIFFENER WELD TERMINATION DETAIL

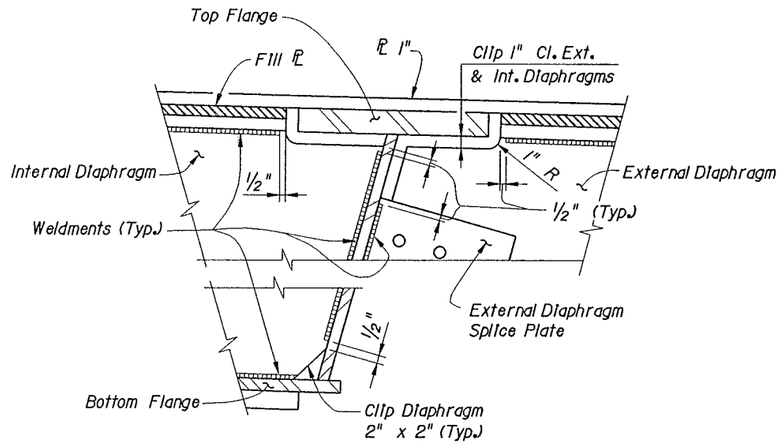

DIAPHRAGM WELD TERMINATION DETAIL
(Bolt and Shear Stud locations not shown for clarity)

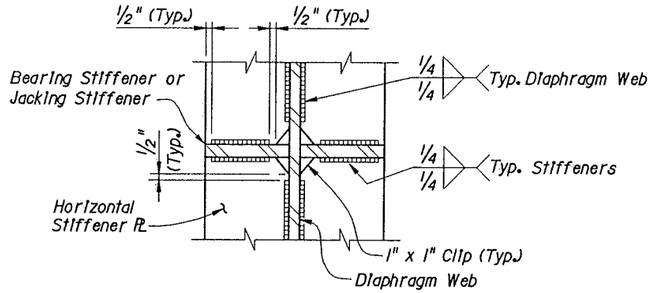

SECTION N-N

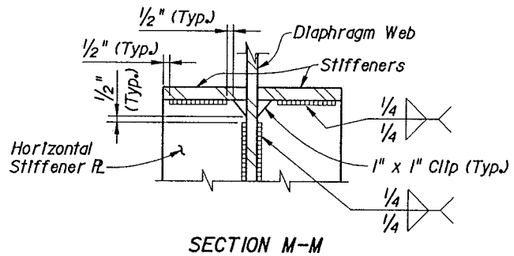

SECTION M-M
(External Diaphragm Similar)

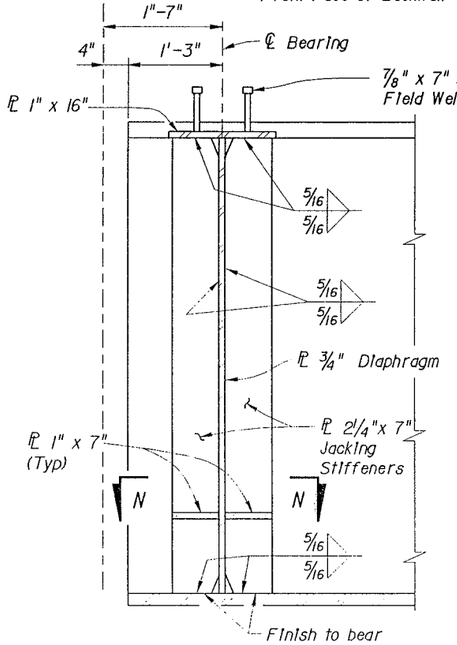

SECTION A-A
(@ END BENTS)

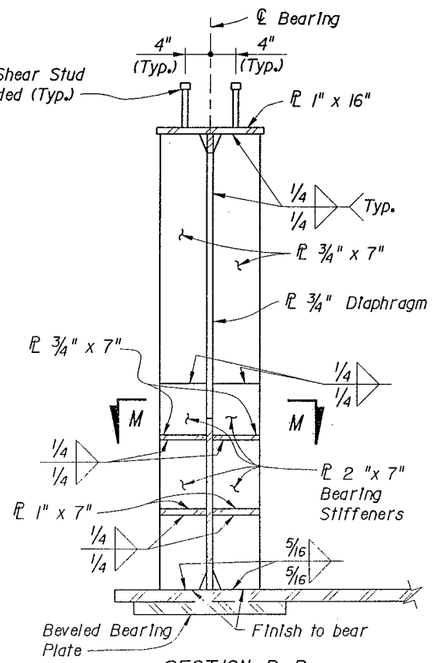

SECTION B-B
(@ END BENTS)

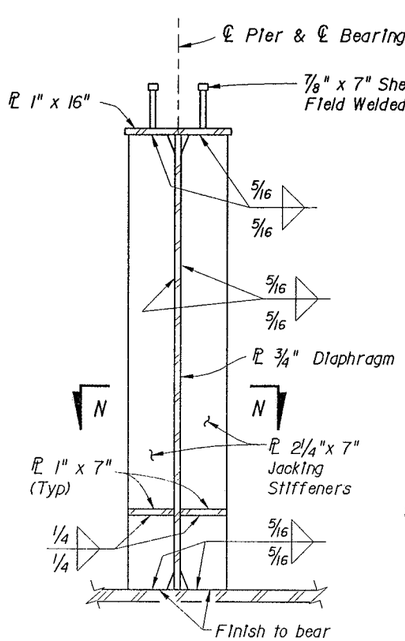

SECTION A-A
(@ PIER 2)

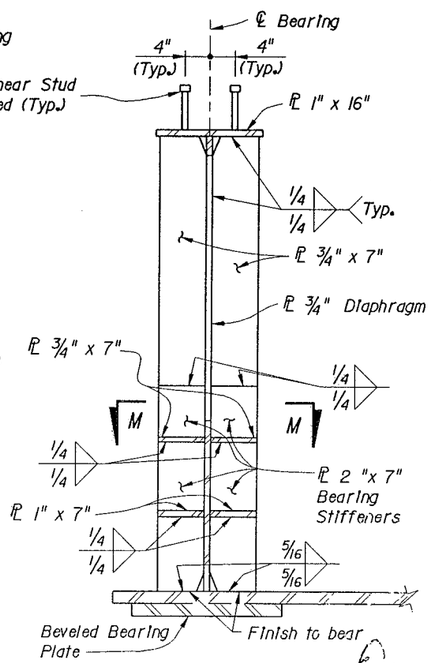

SECTION B-B
(@ PIER 2)

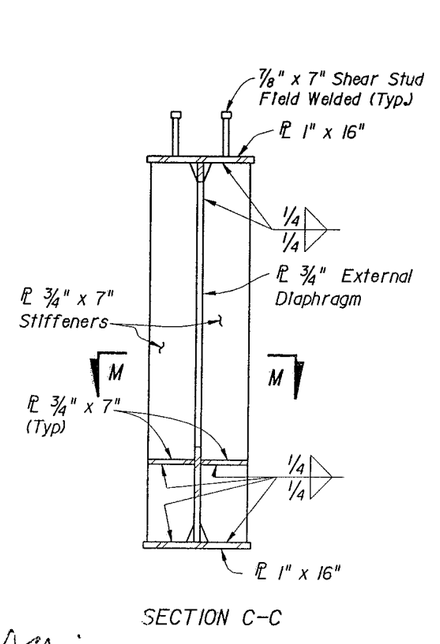

SECTION C-C

Ronald E Rainey
1/29/04

STEEL ALTERNATIVE - BRIDGE NO. 720701

REVISIONS					
DATE	BY	DESCRIPTION	DATE	BY	DESCRIPTION

	NAMES	DATES
DRAWN BY	RCC	9/03
CHECKED BY	RK	9/03
DESIGNED BY	RK	9/03
CHECKED BY	MDM	10/03
APPROVED BY	R.D. Story	

ENGINEER OF RECORD:
EcoDriver
7119 Beech Ridge Trail
Tallahassee, Florida 32312-5075
Certificate of Authorization 00003838
Donald E. Rainey, P.E.
P.E. No. 40645

FLORIDA DEPARTMENT OF TRANSPORTATION

ROAD NO.	COUNTY	FINANCIAL PROJECT ID
9A	DUVAL	209278-1-52-01

SHEET TITLE: DIAPHRAGM DETAILS (SHEET 1 OF 3)

PROJECT NAME: S.R. 9A & S.R. 202 (JAMES T. BUTLER) INTERCHANGE RAMP A2 OVER RAMP C2 AND J.T.B. BLVD.

SHEET NO. B-27

28-JAN-2004 13:33 E.C. Driver I:\209278\struct\720701\diaphragmdet02.dgn

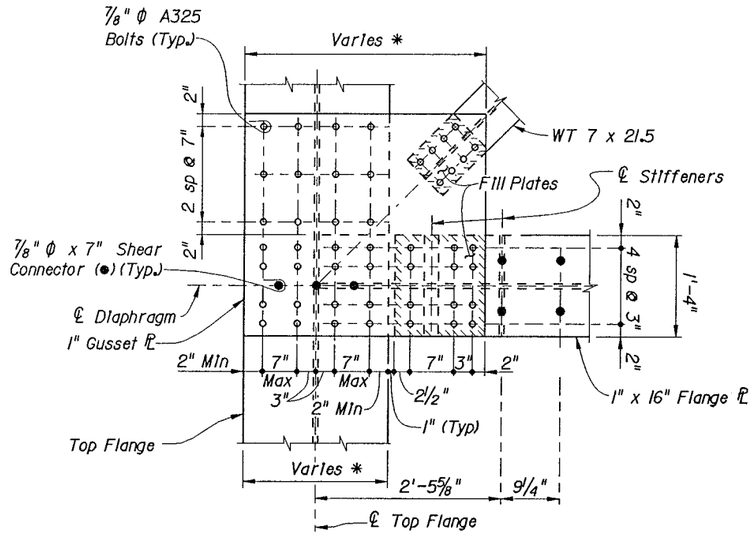

VIEW D-D
(OUTER STRAP PLATE CONNECTION
WITH LATERAL BRACING)

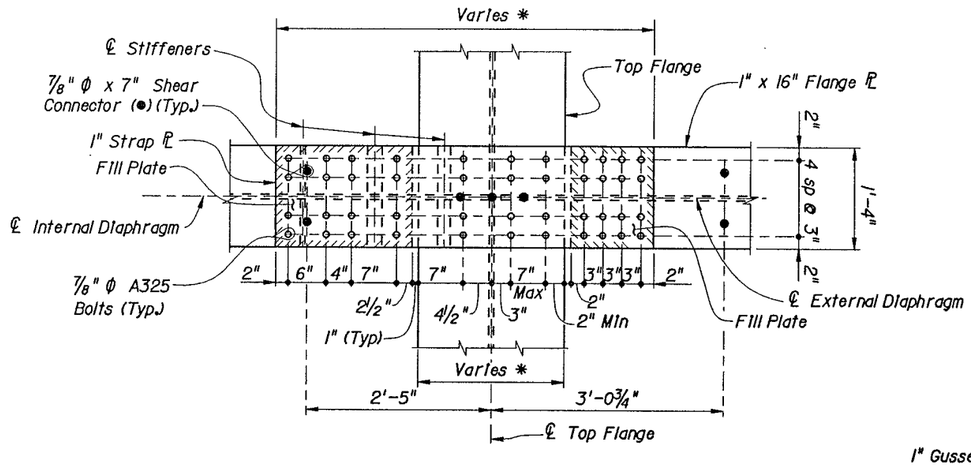

VIEW E-E
(INNER STRAP PLATE CONNECTION
WITH NO LATERAL BRACING)

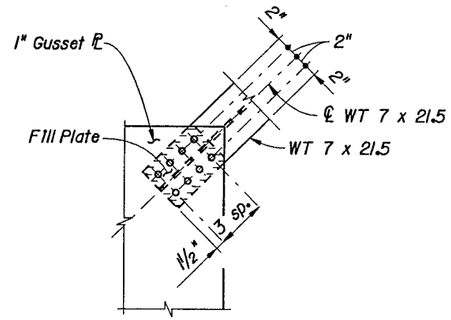

LATERAL BRACING (WT 7 X 21.5)
CONNECTION DETAIL

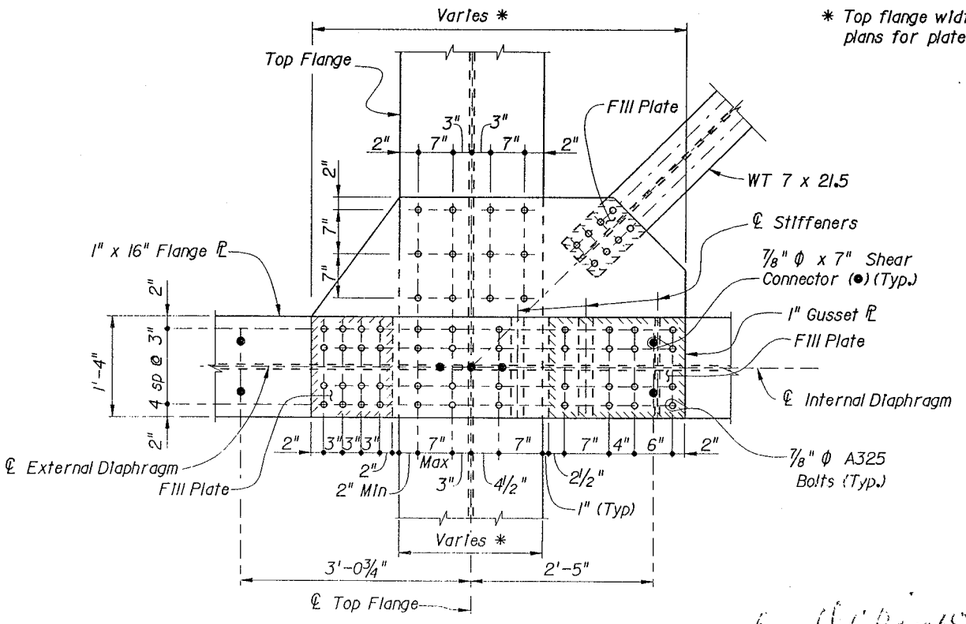

VIEW F-F
(INNER STRAP PLATE CONNECTION
WITH LATERAL BRACING)

* Top flange width varies. See framing plans for plate size and locations.

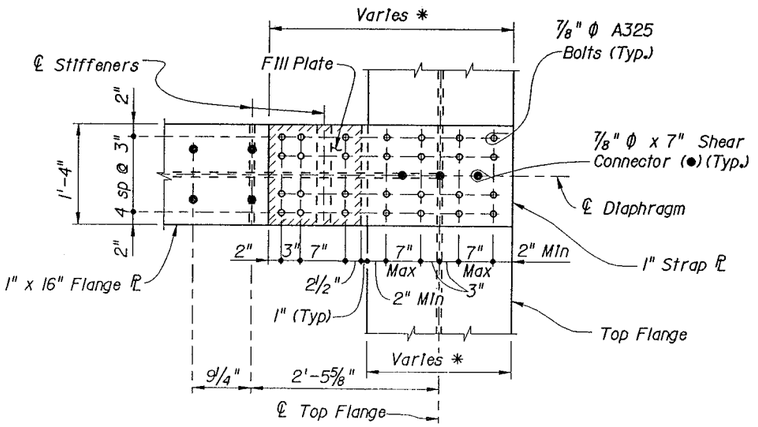

VIEW G-G
(OUTER STRAP PLATE CONNECTION
WITH NO LATERAL BRACING)

STEEL ALTERNATIVE - BRIDGE NO. 720701

REVISIONS					
DATE	BY	DESCRIPTION	DATE	BY	DESCRIPTION

	NAMES	DATES
DRAWN BY	RCC	9/03
CHECKED BY	RK	9/03
DESIGNED BY	RK	9/03
CHECKED BY	MDM	10/03
APPROVED BY	R.D. Story	

ENGINEER OF RECORD:
EC Driver
7119 Beech Ridge Trail
Tallahassee, Florida 32312-5075
Certificate of Authorization 00003838
Donald E. Rainey, P.E.
P.E. No. 40645

FLORIDA DEPARTMENT OF TRANSPORTATION

ROAD NO.	COUNTY	FINANCIAL PROJECT ID
9A	DUVAL	209278-1-52-01

SHEET TITLE: DIAPHRAGM DETAILS (SHEET 2 OF 3)

PROJECT NAME: S.R. 9A & S.R. 202 (JAMES T. BUTLER) INTERCHANGE RAMP A2 OVER RAMP C2 AND J.T.B. BLVD.

SHEET NO. B-28

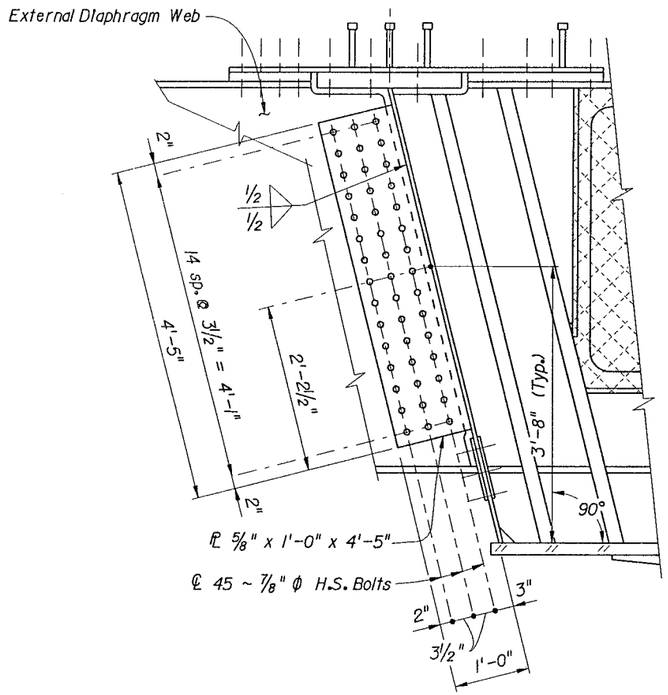

EXTERNAL DIAPHRAGM CONNECTOR PLATE DETAIL

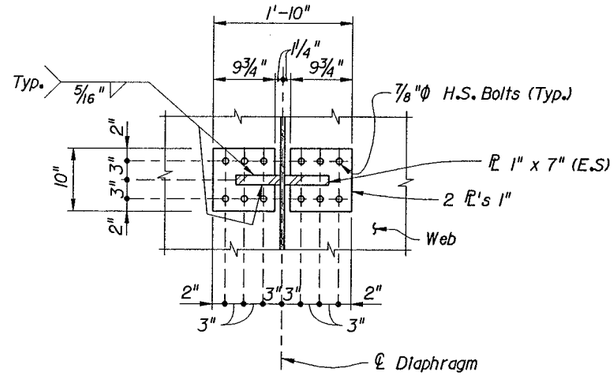

SECTION K-K

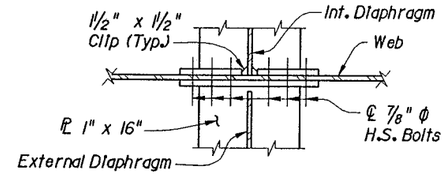

SECTION L-L

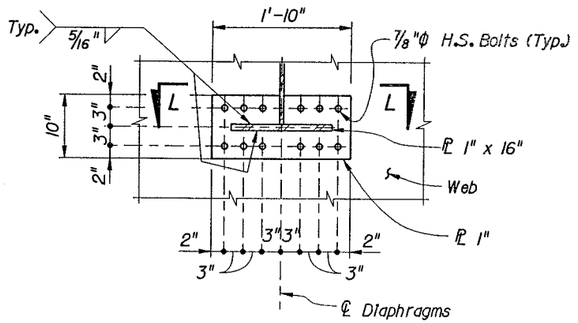

SECTION J-J

NOTES:
For location of Sections K-K & J-J see Diaphragm Sheet.

Donald E Rainey
1/29/04

STEEL ALTERNATIVE - BRIDGE NO. 720701

REVISIONS					
DATE	BY	DESCRIPTION	DATE	BY	DESCRIPTION

	NAMES	DATES
DRAWN BY	RCC	9/03
CHECKED BY	RK	9/03
DESIGNED BY	RK	9/03
CHECKED BY	MDM	10/03
APPROVED BY	R.D. Story	

ENGINEER OF RECORD:
ECDriver
7119 Beech Ridge Trail
Tallahassee, Florida 32312-5075
Certificate of Authorization 00003838
Donald E. Rainey, P.E.
P.E. No. 40645

FLORIDA DEPARTMENT OF TRANSPORTATION

ROAD NO.	COUNTY	FINANCIAL PROJECT ID
9A	DUVAL	209278-1-52-01

SHEET TITLE: DIAPHRAGM DETAILS (SHEET 3 OF 3)

PROJECT NAME: S.R. 9A & S.R. 202 (JAMES T. BUTLER) INTERCHANGE RAMP A2 OVER RAMP C2 AND J.T.B. BLVD.

SHEET NO. B-29

28-JAN-2004 13:34 E:\C. Driver I:\209278\struct\720701\diaphragmdet04.dgn

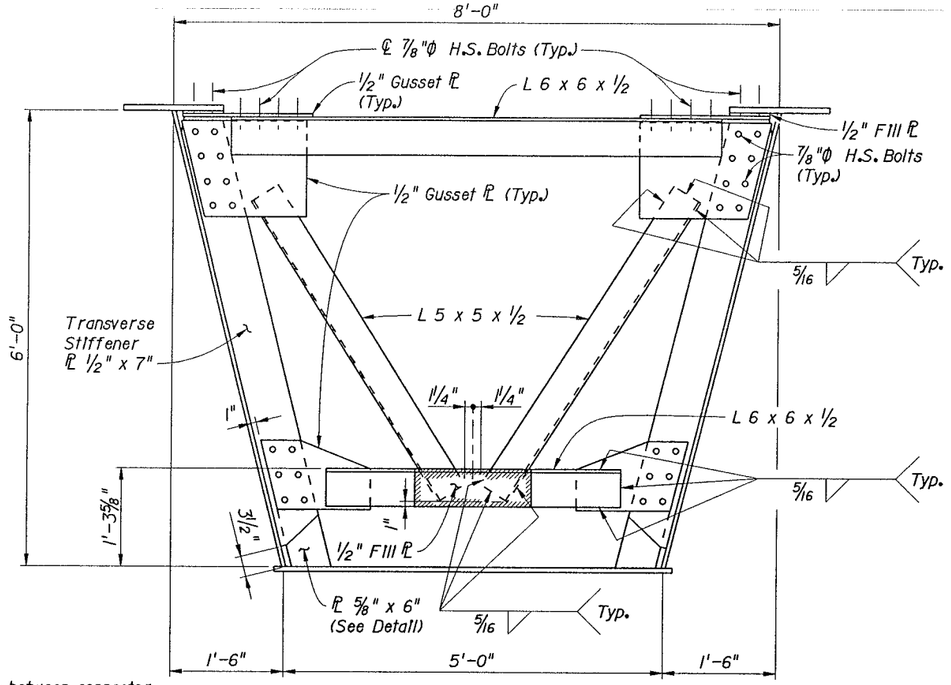

CROSS FRAME

NOTE:
The contact surfaces between connector plate & flanges shall be free of oil and bolts shall be properly torqued prior to stiffener fillet weld.

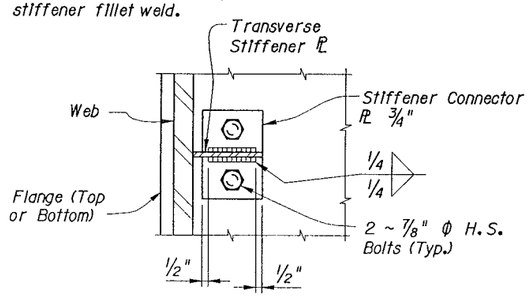

SECTION T-T
(TOP FLANGE SIMILAR)

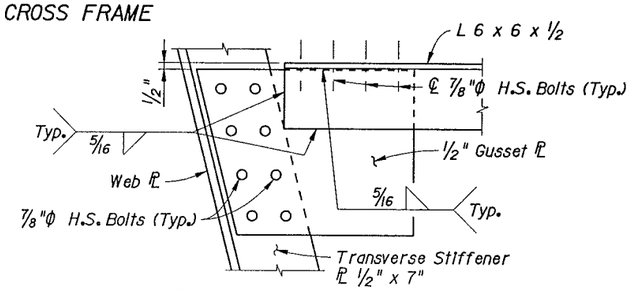

TOP GUSSET PLATE & TOP MEMBER
CONNECTION DETAIL

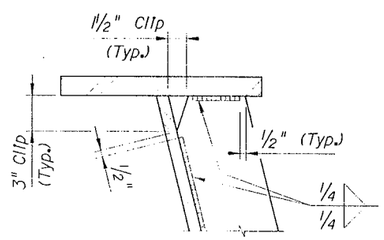

TRANSVERSE STIFFENER TOP FLANGE
DETAIL AT CROSS FRAMES

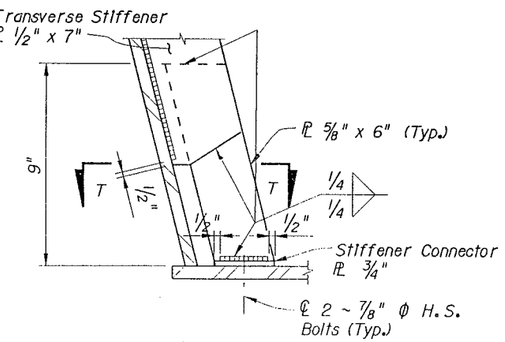

TRANSVERSE STIFFENER BOTTOM FLANGE DETAIL
(STRESS REVERSAL REGION AND BOTTOM
FLANGE IN TENSION REGION)

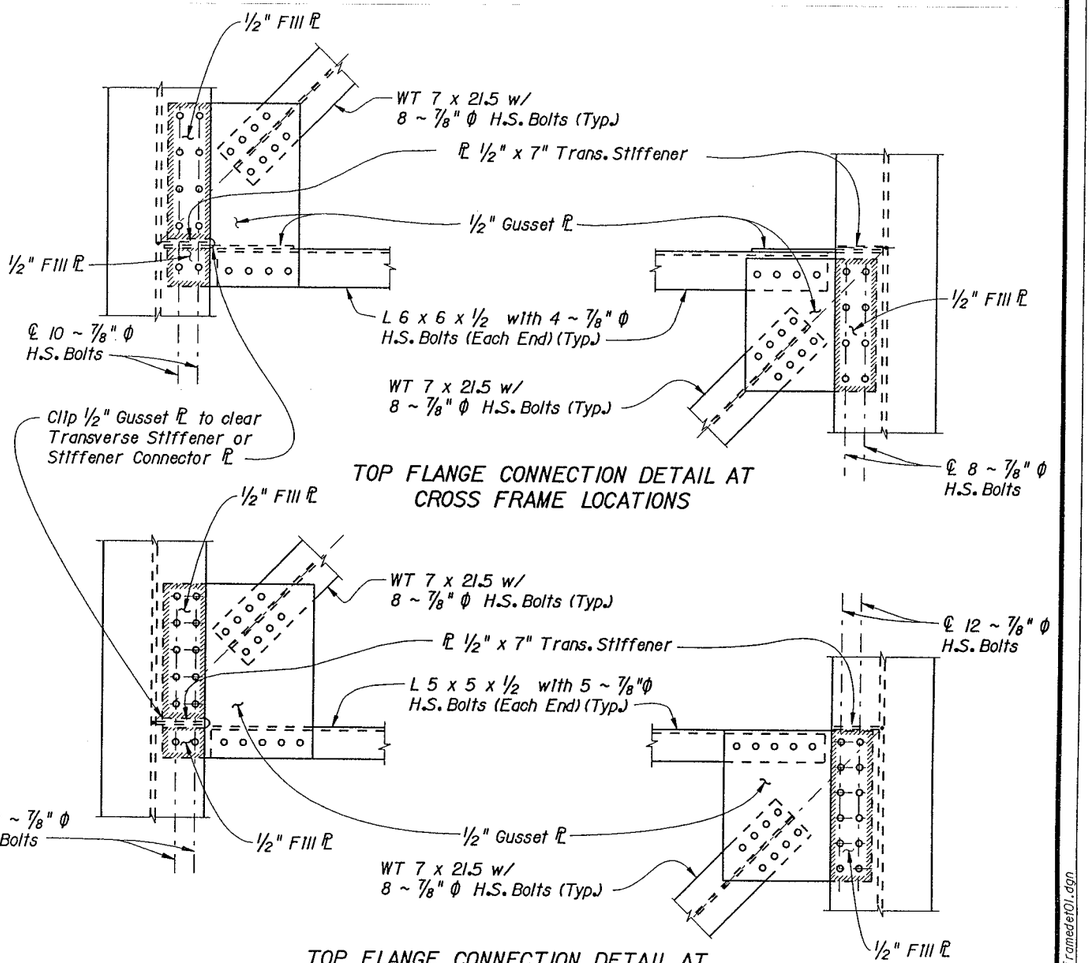

TOP FLANGE CONNECTION DETAIL AT
CROSS FRAME LOCATIONS

TOP FLANGE CONNECTION DETAIL AT
L 5 x 5 x 1/2 STRUT LOCATIONS

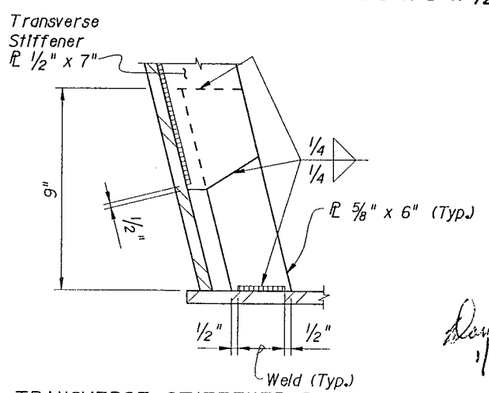

TRANSVERSE STIFFENER BOTTOM FLANGE DETAIL
(TOP FLANGE IN TENSION REGION WITH
BOTTOM FLANGE IN COMPRESSION REGION)

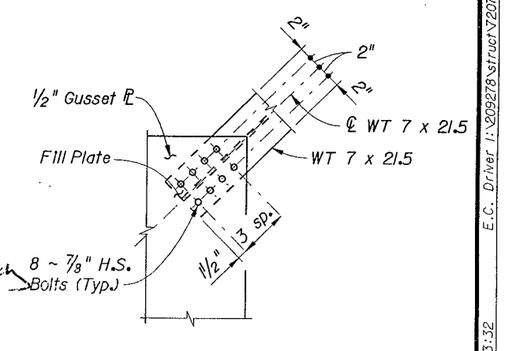

LATERAL BRACING (WT 7 X 21.5)
CONNECTION DETAIL
STEEL ALTERNATIVE - BRIDGE NO.720701

1/29/04

REVISIONS					
DATE	BY	DESCRIPTION	DATE	BY	DESCRIPTION

	NAMES	DATES
DRAWN BY	M.D.M.	8-03
CHECKED BY	R.C.C	10-03
DESIGNED BY	M.D.M.	8-03
CHECKED BY	R.C.C	10-03
APPROVED BY	R.D. Story	

ENGINEER OF RECORD:
ECDriver
7119 Beech Ridge Trail
Tallahassee, Florida 32312-5075
Certificate of Authorization 00003838
Donald E. Rainey, P.E.
P.E. No. 40645

FLORIDA DEPARTMENT OF TRANSPORTATION

ROAD NO.	COUNTY	FINANCIAL PROJECT ID
9A	DUVAL	209278-1-52-01

SHEET TITLE: STRUCTURAL STEEL DETAILS (SHEET 1 OF 3)

PROJECT NAME: S.R. 9A & S.R. 202 (JAMES T. BUTLER) INTERCHANGE RAMP A2 OVER RAMP C2 AND J.T.B. BLVD.

SHEET NO. B-30

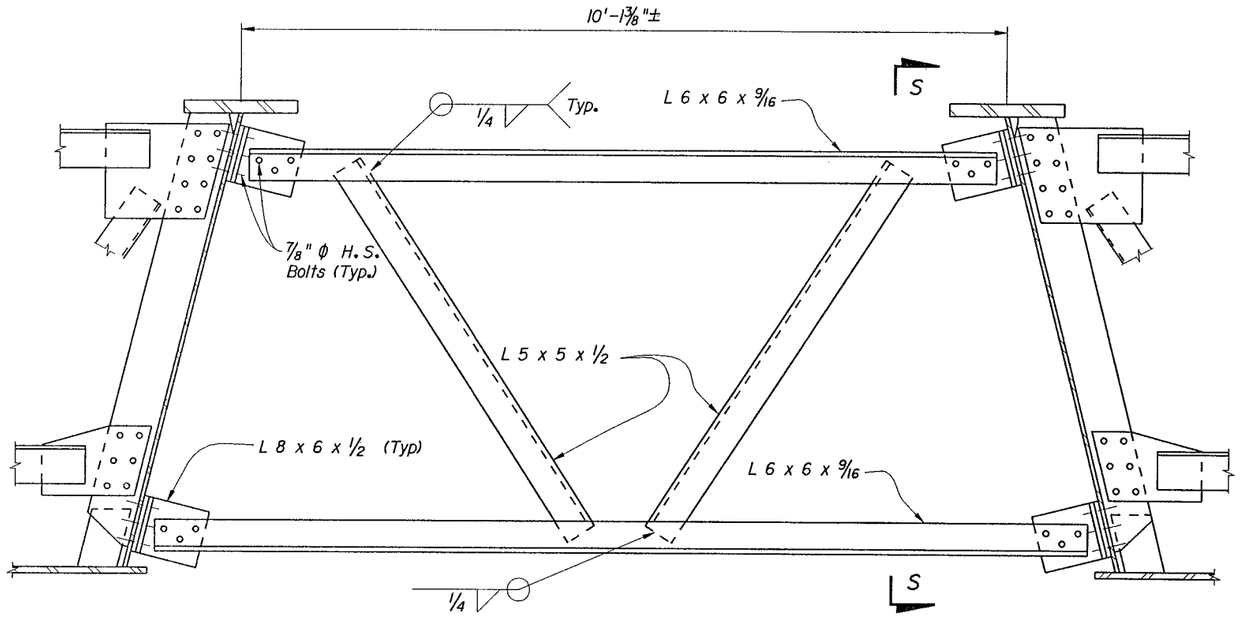

TEMPORARY EXTERNAL CROSS FRAME
(To be removed after the concrete deck is constructed)

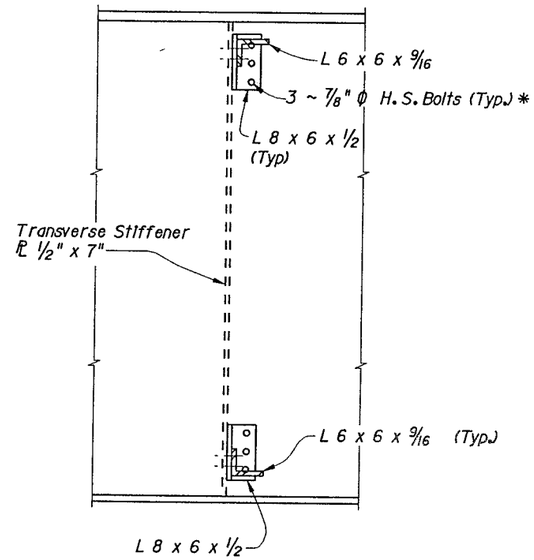

SECTION S-S

* L 8 x 6 x ½ Is to be removed and the ⅞" ϕ H.S. Bolts reinserted In the holes and tightened after the external cross frame Is removed. Slot holes In 6" leg of angle along axis of angle.

Donald E. Rainey
2004

STEEL ALTERNATIVE - BRIDGE NO. 720701

REVISIONS					
DATE	BY	DESCRIPTION	DATE	BY	DESCRIPTION

	NAMES	DATES
DRAWN BY	M.D.M.	8-03
CHECKED BY	R.C.C	10-03
DESIGNED BY	M.D.M.	8-03
CHECKED BY	R.C.C	10-03
APPROVED BY	R.D. Story	

ENGINEER OF RECORD:
ECDriver
7119 Beech Ridge Trail
Tallahassee, Florida 32312-5075
Certificate of Authorization 00003838
Donald E. Rainey, P.E.
P.E. No. 40645

FLORIDA DEPARTMENT OF TRANSPORTATION

ROAD NO.	COUNTY	FINANCIAL PROJECT ID
9A	DUVAL	209278-1-52-01

SHEET TITLE: STRUCTURAL STEEL DETAILS (SHEET 2 OF 3)

PROJECT NAME: S.R. 9A & S.R. 202 (JAMES T. BUTLER) INTERCHANGE RAMP A2 OVER RAMP C2 AND J.T.B. BLVD.

SHEET NO. B-31

E.C. Driver I:\209278\struct\720701\crossframedet01.dgn 13:33 28-JAN-2004

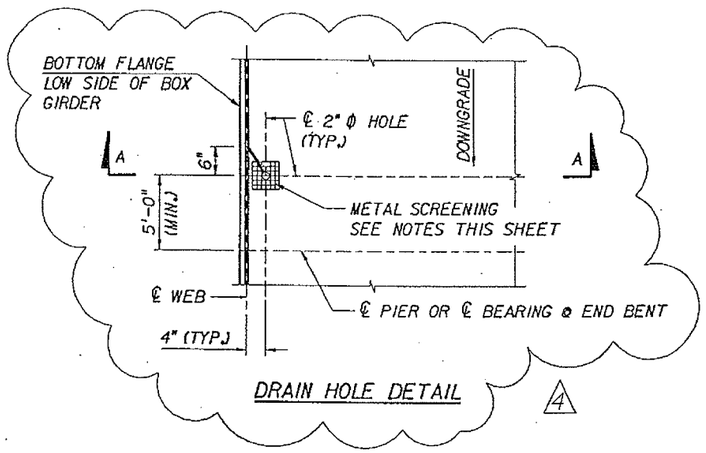

DRAIN HOLE DETAIL

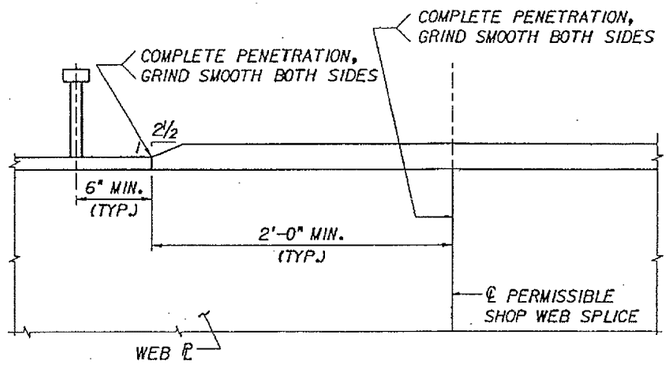

TYPICAL SHOP SPLICE DETAILS

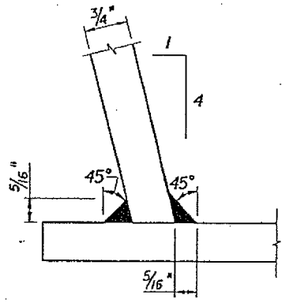

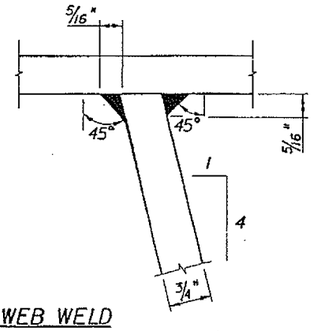

DETAIL OF FLANGE TO WEB WELD

(COMPLETE PENETRATION GROOVE WELDS MAY BE USED AT THE CONTRACTOR'S OPTION)

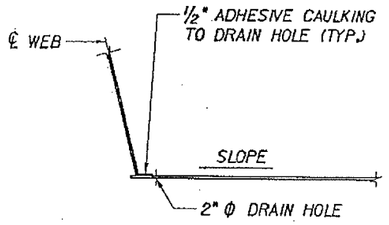

SECTION A-A

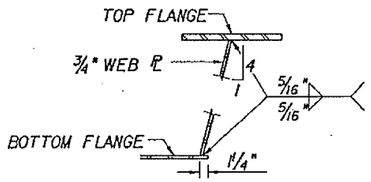

FLANGE TO WEB WELDS

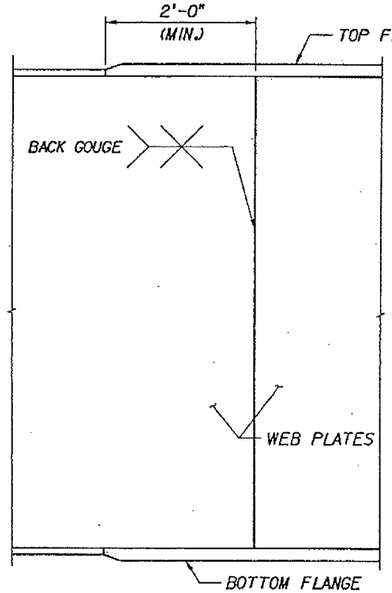

ELEVATION - SHOP WEB SPLICE DETAIL

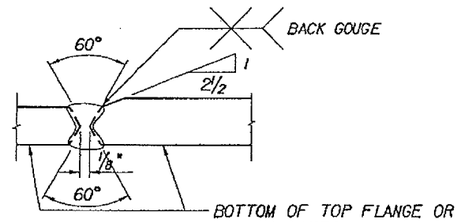

SECTION - FLANGE WELD SPLICE DETAIL

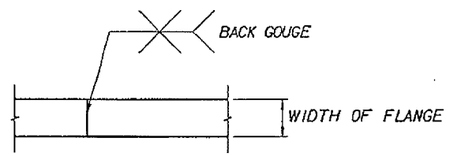

PLAN - FLANGE SPLICE

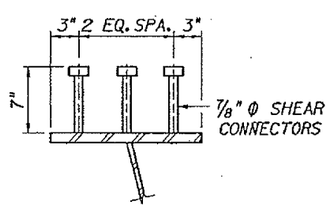

SHEAR CONNECTOR DETAIL

(TYP. ALL GIRDERS)

SEE GIRDER ELEVATIONS FOR NUMBER REQ'D AND LOCATION

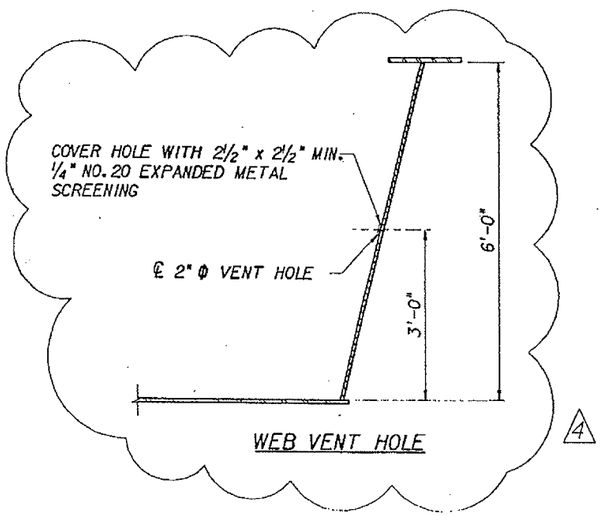

WEB VENT HOLE

4

4 VENT HOLE & DRAIN HOLE NOTES:

1. PLACE VENT HOLES AND DRAIN HOLES AT 50'-0" MAXIMUM SPACING. VENT HOLES TO BE LOCATED 25'-0" MINIMUM AND DRAIN HOLES AT 5'-0" MINIMUM FROM ℄ PIER/FFBW.
2. COVER VENT HOLES AND DRAIN HOLES WITH 20 GAGE GALVANIZED WELDED METAL SCREENING (1/4" OPENING). TACK WELD TO GIRDER WEBS/FLANGES.

SHOP SPLICES

Christopher P. Lochner
2/3/2006

STEEL ALTERNATIVE - BRIDGE NO. 720701

H:\Design\02\2026_SR9A post\209278_steel - As Built\struct\720701\Plans\Superstruct.dgn

REVISIONS					
DATE	BY	DESCRIPTION	DATE	BY	DESCRIPTION
2/3/06	WSO	REV. DRAIN HOLE DTL. ADDED NOTES. 4			

	NAME	DATE
DRAWN BY	ISO	02-04
CHECKED BY	CPG	02-04
DESIGNED BY	WSO	02-04
CHECKED BY	CPG	02-04
APPROVED BY	W. ODEH	

ENGINEER OF RECORD:
LOCHNER C.A. 894
H. W. LOCHNER, INC.
CONSULTING ENGINEERS AND PLANNERS
13577 FEATHER SOUND DRIVE SUITE 600
CLEARWATER, FLORIDA 33762
WAEL S. ODEH, P.E. NO. 53920

FLORIDA DEPARTMENT OF TRANSPORTATION

ROAD NO.	COUNTY	FINANCIAL PROJECT ID
9A	DUVAL	209278-1-52-01

SHEET TITLE: STRUCTURAL STEEL DETAILS (SHEET 3 OF 3)

PROJECT NAME: SR 9A & SR 202 (JAMES T. BUTLER) INTERCHANGE RAMP A2 OVER RAMP C2 AND J.T.B.

SHEET NO. B-32

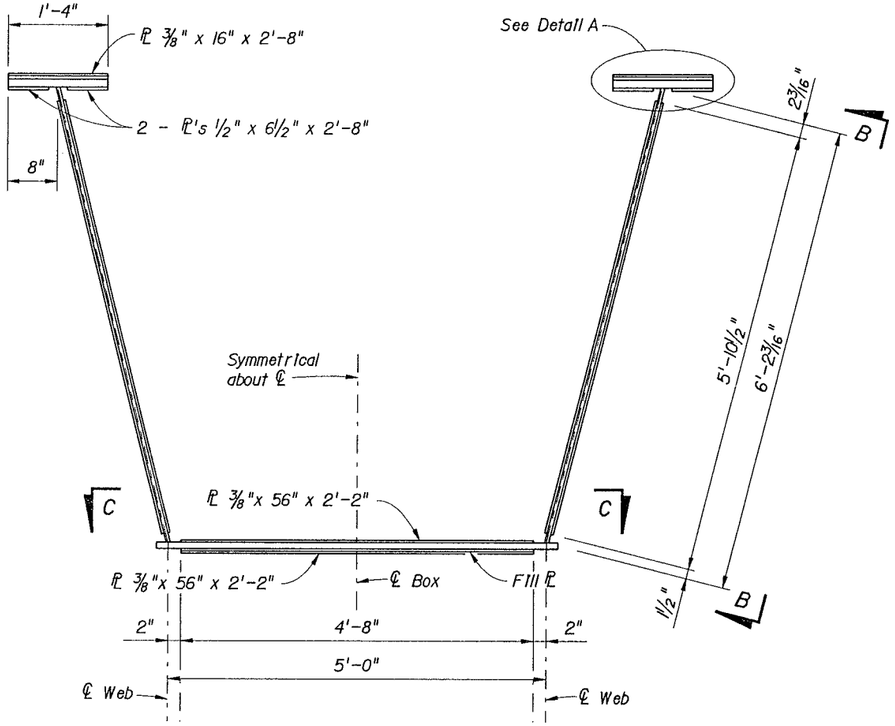

CROSS SECTION THROUGH GIRDER

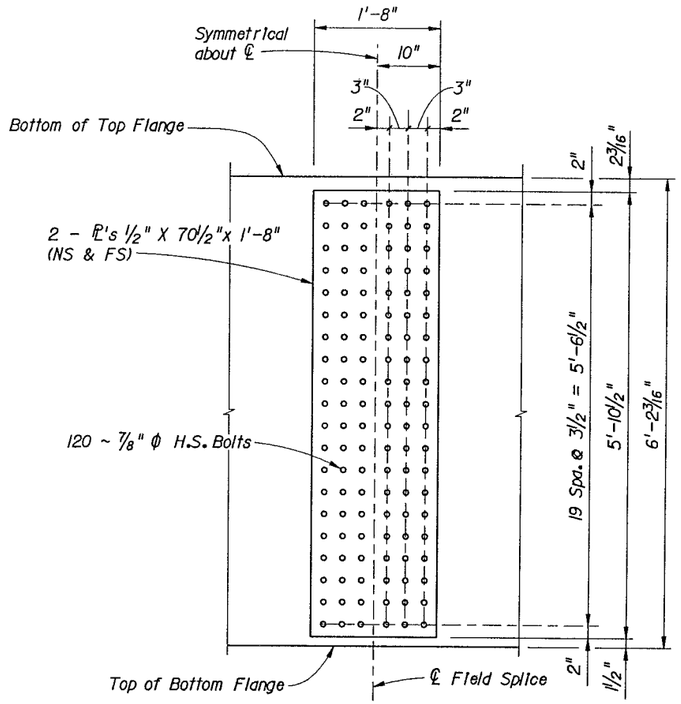

VIEW B-B
(Flange not shown)

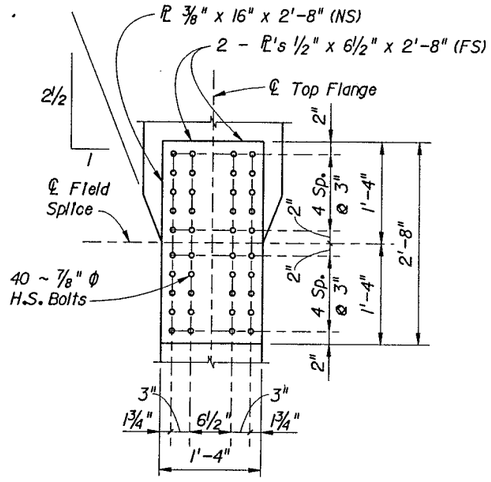

VIEW A-A

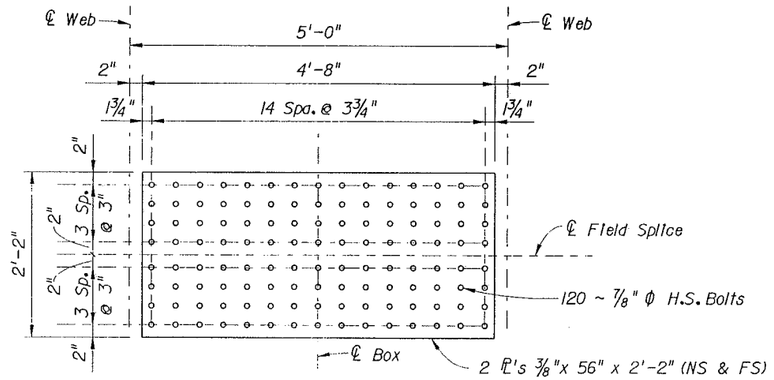

VIEW C-C
(Webs not shown)

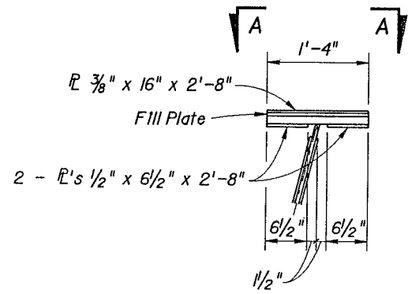

DETAIL A

* TABLE OF SPLICE FILL PLATES		
FIELD SPLICE NO.	TOP FLANGE	BOTTOM FLANGE
All	3/8" x 16" x 1'-3 3/8"	1/2" x 56" x 1'-0 1/8"

* Equivalent Commercial Grade Steel may be substituted for fill plate material.

NOTES:

All Field Splice Bolts shall be 7/8" ϕ High Strength Bolts. ASTM A-325 friction type.

(NS) denotes Near Side and
(FS) denotes Far Side.

Donald E. Rainey
1/29/04

STEEL ALTERNATIVE - BRIDGE NO. 720701

REVISIONS					
DATE	BY	DESCRIPTION	DATE	BY	DESCRIPTION

	NAMES	DATES
DRAWN BY	J.M.B.	8/03
CHECKED BY	D.E.R.	10/03
DESIGNED BY	D.E.R.	8/03
CHECKED BY	R.K.	10/03
APPROVED BY	R.D. Story	

ENGINEER OF RECORD:
ECDriver & Associates
7119 Beech Ridge Trail
Tallahassee, Florida 32312-5075
Certificate of Authorization 00003838
Donald E. Rainey, P.E.
P.E. No. 40645

FLORIDA DEPARTMENT OF TRANSPORTATION

ROAD NO.	COUNTY	FINANCIAL PROJECT ID
9A	DUVAL	209278-1-52-01

SHEET TITLE: FIELD SPLICES

PROJECT NAME: S.R. 9A & S.R. 202 (JAMES T. BUTLER) INTERCHANGE RAMP A2 OVER RAMP C2 AND J.T.B. BLVD.

SHEET NO. B-33

E.C. Driver I:\209278\struct\720701\Splice01.dgn 29-JAN-2004 08:32

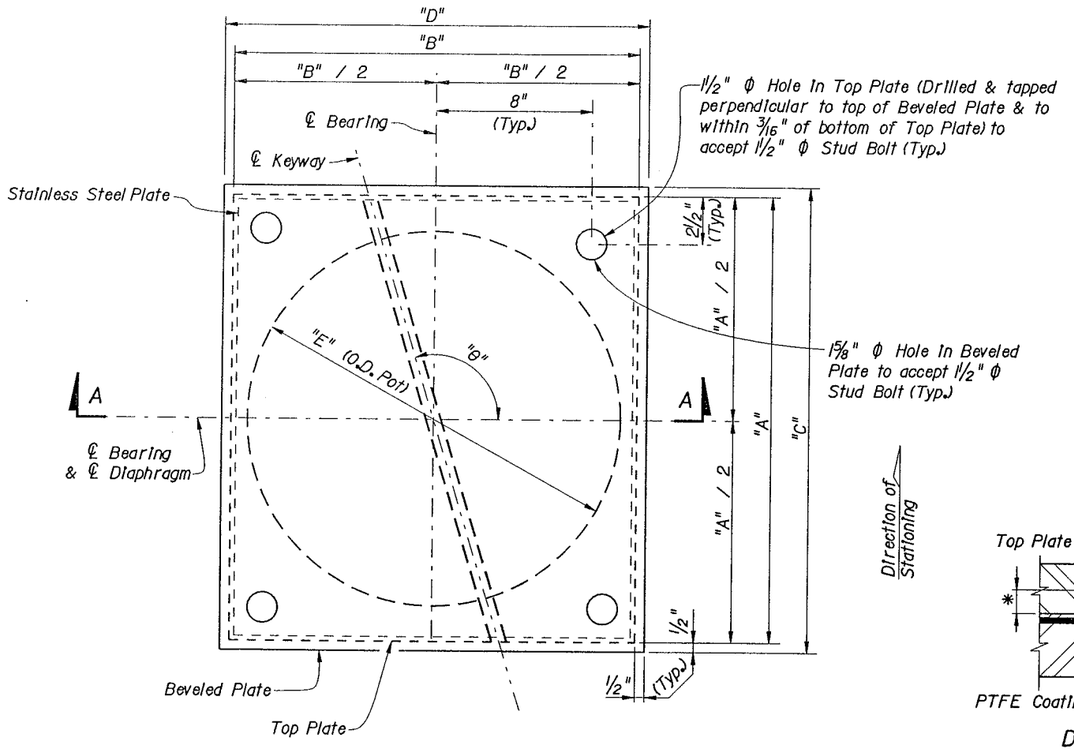

PLAN VIEW EXPANSION BEARING TYPE "E"

(Masonry Plate and Anchor Bolts not shown for clarity)

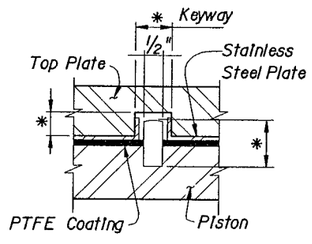

DETAIL X

*Dimension by Manufacturer's recommendation

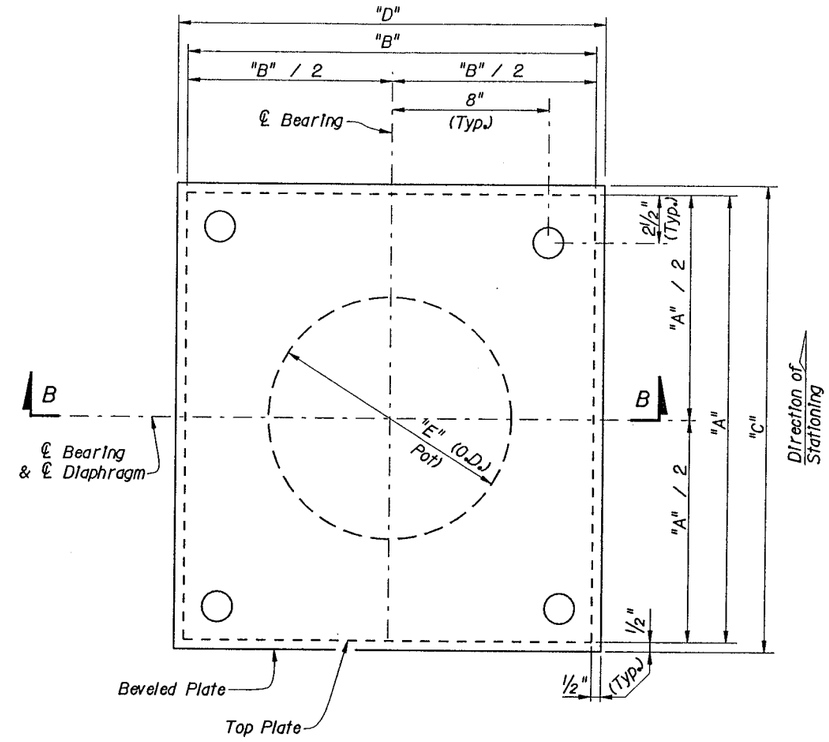

PLAN VIEW FIXED BEARING TYPE "F"

(Masonry Plate and Anchor Bolts not shown for clarity)

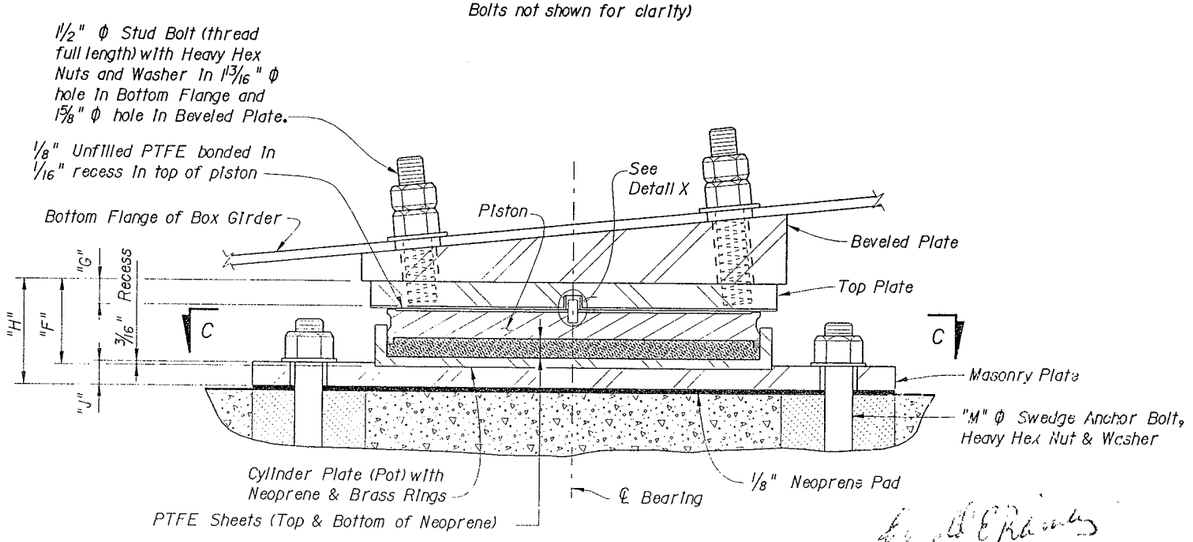

SECTION A-A

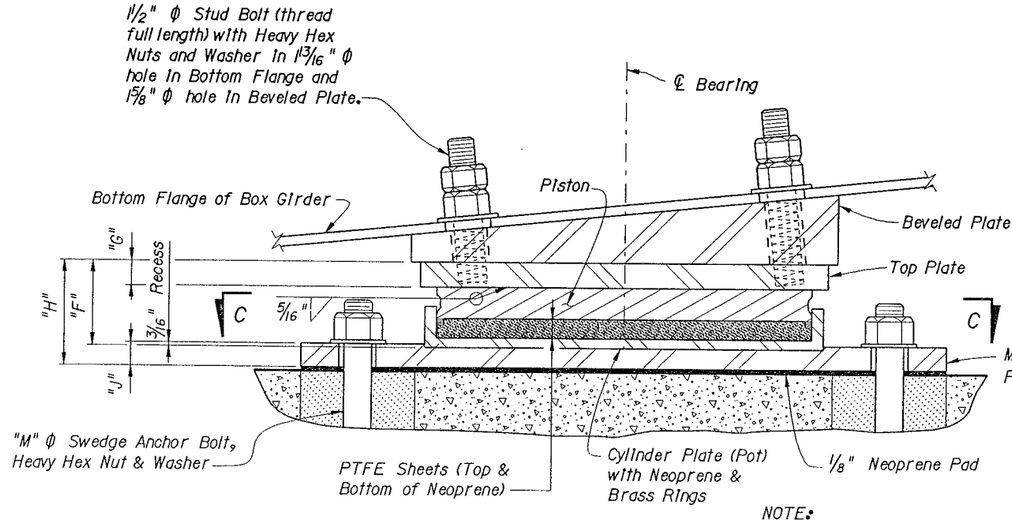

For View C-C see Pot Bearing Details Sheet 2 of 2.

SECTION B-B

NOTE:
For Beveled Plate dimensions see Sheet No. B-36.

STEEL ALTERNATIVE - BRIDGE NO. 720701

REVISIONS					
DATE	BY	DESCRIPTION	DATE	BY	DESCRIPTION

	NAME	DATE
DRAWN BY	RCC	10/03
CHECKED BY	DER	10/03
DESIGNED BY	RCC	10/03
CHECKED BY	DER	10/03
APPROVED BY	R.D. Story	

ENGINEER OF RECORD:
ECDriver
7119 Beech Ridge Trail
Tallahassee, Florida 32312-5075
Certificate of Authorization 00003838
Donald E. Rainey, P.E.
P.E. No. 40645

FLORIDA DEPARTMENT OF TRANSPORTATION

ROAD NO.	COUNTY	FINANCIAL PROJECT ID
9A	DUVAL	209278-1-52-01

SHEET TITLE: POT BEARING DETAILS (SHEET 1 OF 2)

PROJECT NAME: S.R. 9A & S.R. 202 (JAMES T. BUTLER) INTERCHANGE RAMP A2 OVER RAMP C2 AND J.T.B. BLVD.

SHEET NO. B-34

E.C. Driver I:\209278\struct\20701\PotBearings01.dgn 28-JAN-2004 13:36

BEARING NOTES:

1. Pot bearings shall be fabricated, tested and installed in accordance with Section 461 of the specifications. The Manufacturer shall submit certified copies of bearing load test reports and shop drawings to the Engineer for review. Material certificates for neoprene, steel, TFE and adhesives shall also be submitted.
2. Stud Bolts shall be ASTM A-325. Swedge Anchor Bolts shall be ASTM A-307 and shall be galvanized in accordance with Section 962-7 of the Specifications.
3. Pot bearing assemblies shall be of ASTM A 709-90 Grade 50W steel (unless otherwise noted) and exterior surfaces shall be painted with three coats of aluminum color inorganic zinc rich paint conforming to the Specifications.
4. Neoprene for pot bearings shall be of Grade 50 Durometer hardness. Neoprene thickness shall not be less than 1/15 of the inside pot diameter.
5. Should the heights of fabricated bearing assemblies differ from those indicated, the bearing elevations of end bents and piers shall be adjusted to account for the variation.
6. Unfilled PTFE shall be recessed into Backing Plate. Design coefficient of friction equals 0.04. Bonded side to be factory etched.
7. Stainless steel sheet shall be ASTM A-240 Type 316. Attachment and finish shall conform to the Specifications. Minimum Brinell hardness shall be 125. Brass retainer rings shall be ASTM B-36.
8. a. Blockout form material shall be removed and hole shall be free of debris prior to grouting. The blockouts shall be grouted with a non-shrink cementitious grout conforming to Section 934 of the Specifications.
   b. Blockouts shall not be grouted until the entire Box Girder Unit (Boxes "A" & "B") is in place and properly aligned.
   c. Payment for grout & any incidental items shall be included in the Contract Unit Price for Class IV Concrete (Mass Substructure).
9. Attach upper and lower bearing components and beveled plate with temporary metal clips to avoid separation in the field. For fabrication and installation purposes, the direction of stationing, and intended locations of the bearing assembly shall be clearly marked on each individual assembly. For example Pier 2, Unit 1, Box B.
10. If a pot diameter less than dimension "E" is used, the thickness of the top plate (dimension "G") and the beveled plate must be increased. Contractor shall submit calculations determining the required thickness. Calculations shall be signed and sealed by an Engineer registered in the state of Florida.

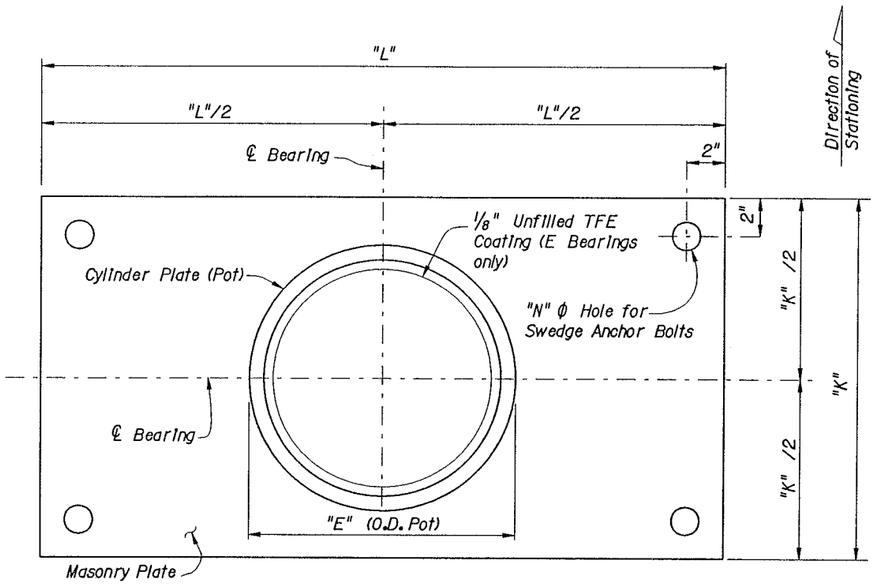

SECTION C-C

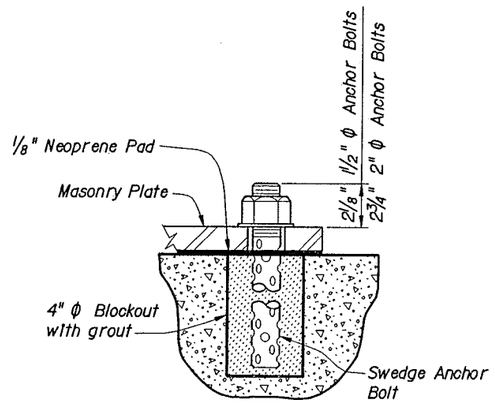

ANCHOR BOLT PLACEMENT DETAIL

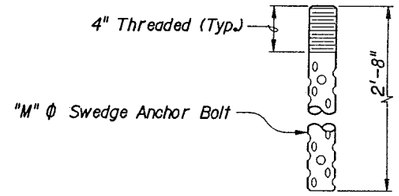

SWEDGE ANCHOR BOLT DETAIL

BEARING LOCATION	BEARING TYPE	NO. OF BEARINGS REQUIRED	DESIGN LOAD (KIPS)	DESIGN LATERAL LOAD (KIPS)	DESIGN DEAD LOAD (KIPS)	DESIGN LIVE LOAD (KIPS)	DESIGN ROTATION (RADIANS)	△ DESIGN MOVEMENT ± EACH DIRECTION (INCHES)	θ (DEGREES) BOX B	θ (DEGREES) BOX A	DIMENSIONS (INCHES)												
											A	B	C	D	E	F	G	H	J	K	L	M	N
END BENT 1	E	2	480	60.6	303	177	0.03	0.57	97°01'01"	96°57'30"	23	27	24	28	21.00	6.68	2.08	8.50	2.00	25	36	1 1/2"	1 3/4"
PIER 2	F	2	1257	185.4	927	330	0.03	-N/A-	-N/A-	-N/A-	27	27	28	28	25.75	6.53	1.50	8.59	2.25	30	36	2"	2 1/4"
END BENT 3	E	2	408	48.2	241	167	0.03	0.51	83°49'47"	83°46'26"	21	27	22	28	19.63	6.92	2.30	8.98	2.25	24	36	1 1/2"	1 3/4"

Donald E Rainey
1/28/04

STEEL ALTERNATIVE - BRIDGE NO. 720701

REVISIONS					
DATE	BY	DESCRIPTION	DATE	BY	DESCRIPTION

	NAMES	DATES
DRAWN BY	RCC	10-03
CHECKED BY	DER	10-03
DESIGNED BY	RCC	10-03
CHECKED BY	DER	10-03
APPROVED BY	R.D. Story	

ENGINEER OF RECORD:
ECDriver
A Subsidiary
7119 Beech Ridge Trail
Tallahassee, Florida 32312-5075
Certificate of Authorization 00003838
Donald E. Rainey, P.E.
P.E. No. 40645

FLORIDA DEPARTMENT OF TRANSPORTATION

ROAD NO.	COUNTY	FINANCIAL PROJECT ID
9A	DUVAL	209278-1-52-01

SHEET TITLE: POT BEARING DETAILS (SHEET 2 OF 2)

PROJECT NAME: S.R. 9A & S.R. 202 (JAMES T. BUTLER) INTERCHANGE RAMP A2 OVER RAMP C2 AND J.T.B. BLVD.

SHEET NO. B-35

E.C. Driver I:\209278\struct\20701\PotBearings02.dgn 28-JAN-2004 13:36

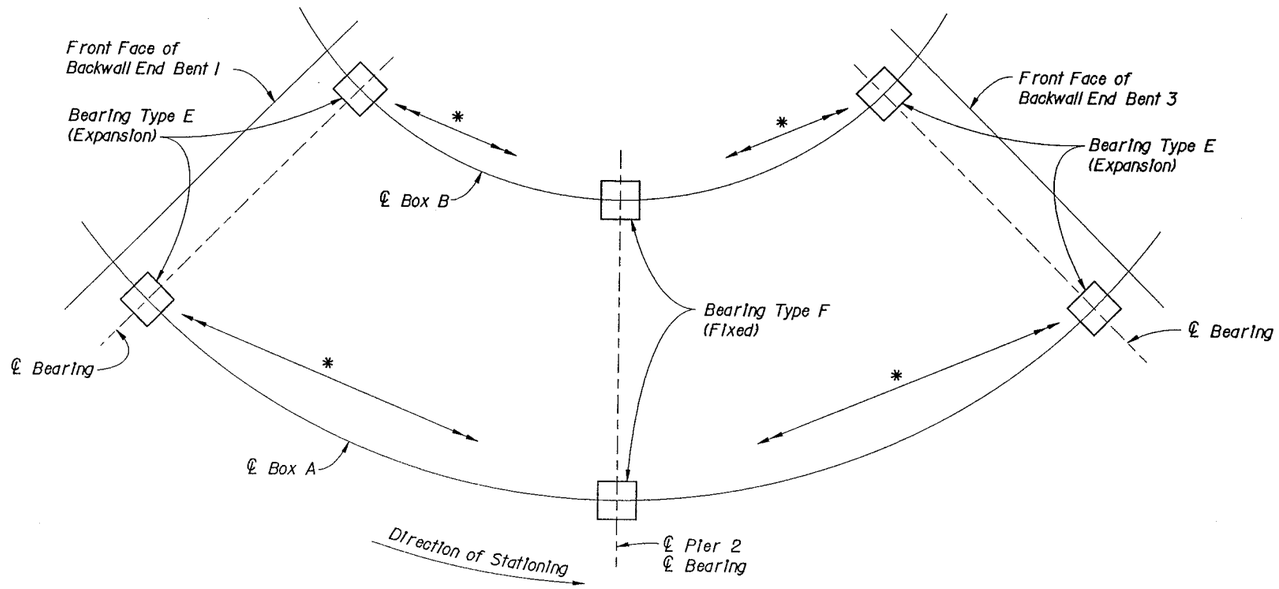

* Indicates direction of movement for guided expansion bearings. Movement is along chord between expansion bearing and fixed bearing.

SCHEMATIC SHOWING BEARING LOCATION AND TYPE

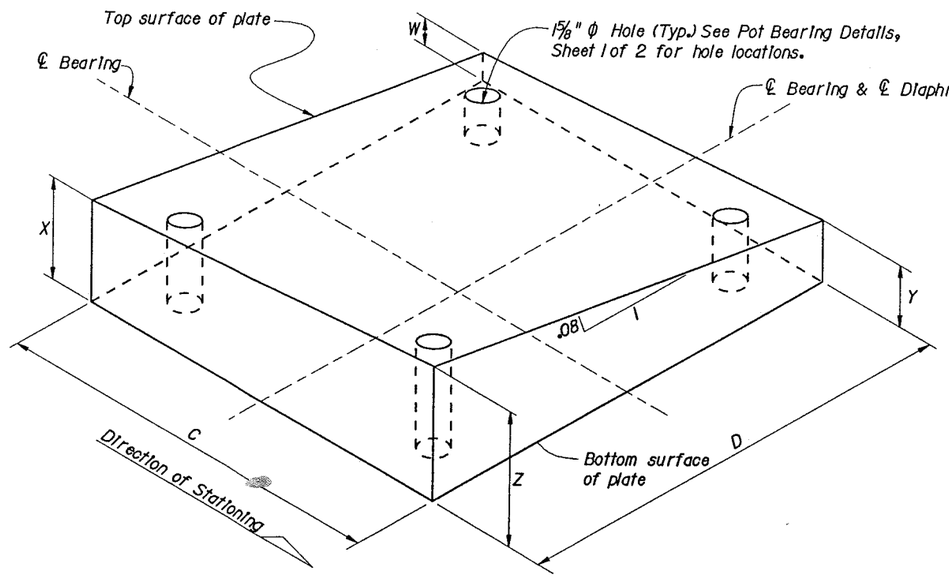

BEVELED PLATE ISOMETRIC VIEW

BEVELED PLATE TABLE OF DIMENSIONS							
LOCATION		DIMENSIONS					
		W	X	Y	Z	C	D
END BENT 1	Box B	2.08	4.32	2.38	4.62	24.00	28.00
	Box A	2.08	4.32	2.37	4.61		
PIER 2	Box B	1.50	3.74	1.70	3.94	28.00	28.00
	Box A	1.50	3.74	1.69	3.93		
END BENT 3	Box B	2.30	4.54	2.34	4.58	22.00	28.00
	Box A	2.30	4.54	2.34	4.58		

NOTE: All dimensions in Table are in inches.

BEVELED PLATE NOTES

1. For fabrication and installation purposes, the direction of stationing, top & bottom surfaces and intended locations of the beveled plates shall be clearly marked on each individual beveled plate. For example: Pier No. 2, Unit 1, Box B.
2. Extreme care shall be taken to insure the beveled plates are installed in their correct locations and in the correct direction.

Donald E Rainey 1/20/04

STEEL ALTERNATIVE - BRIDGE NO. 720701

REVISIONS					
DATE	BY	DESCRIPTION	DATE	BY	DESCRIPTION

	NAMES	DATES
DRAWN BY	RCC	10/03
CHECKED BY	DER	10/03
DESIGNED BY	RCC	10/03
CHECKED BY	DER	10/03
APPROVED BY	R.D. Story	

ENGINEER OF RECORD:
ECDriver
7119 Beech Ridge Trail
Tallahassee, Florida 32312-5075
Certificate of Authorization 00003838
Donald E. Rainey, P.E.
P.E. No. 40645

FLORIDA DEPARTMENT OF TRANSPORTATION

ROAD NO.	COUNTY	FINANCIAL PROJECT ID
9A	DUVAL	209278-1-52-01

SHEET TITLE: BEVELED PLATE DETAILS

PROJECT NAME: S.R. 9A & S.R. 202 (JAMES T. BUTLER) INTERCHANGE RAMP A2 OVER RAMP C2 AND J.T.B. BLVD.

SHEET NO. B-36

E.C. Driver I:\209278\Struct\720701\beveled plate.dgn 28-JAN-2004 13:31

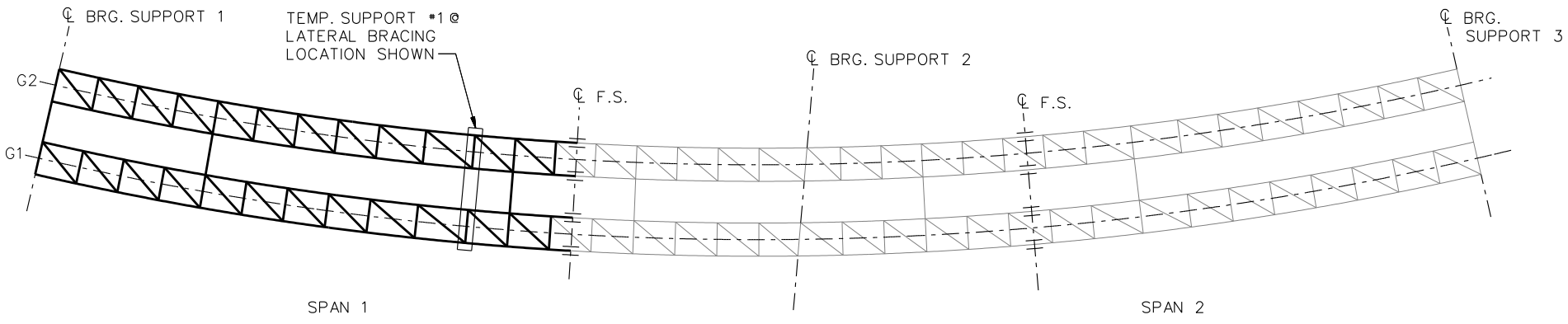

STAGE 2

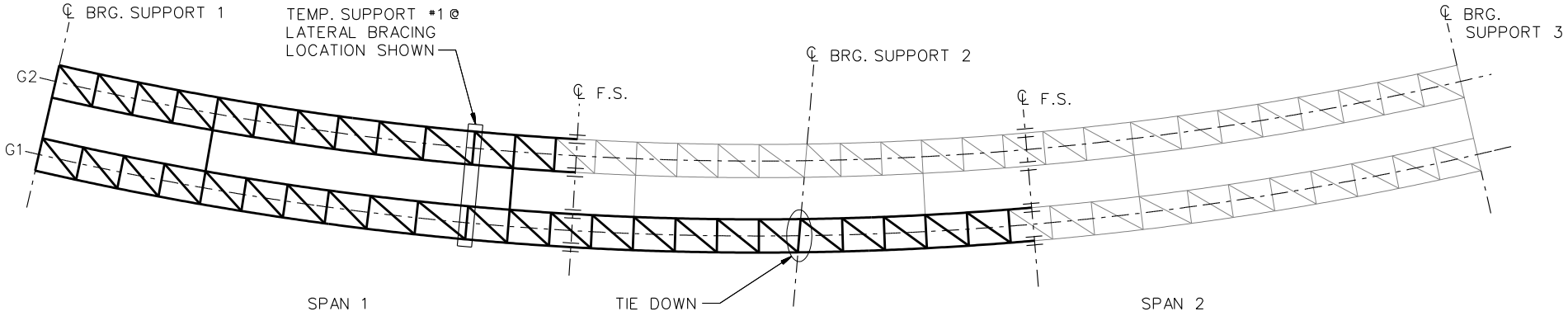

STAGE 3

LEGEND

▽ = HOLD OR LIFT CRANE

○ = TIE DOWN

□ = TEMPORARY SUPPORT STRUCTURE

NCHRP 12-79

BRIDGE ETCCS5a

GENERAL ERECTION PROCEDURE

SHEET 1 OF 2

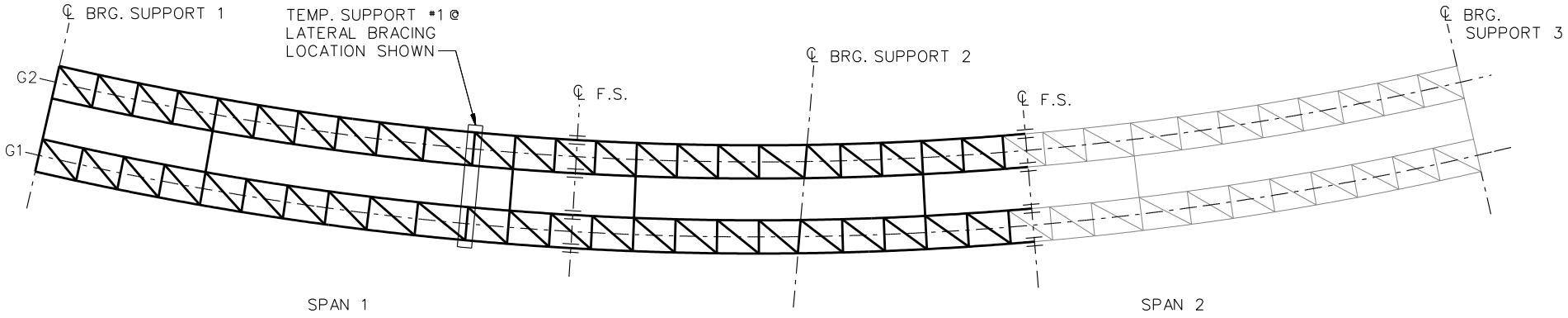

STAGE 4

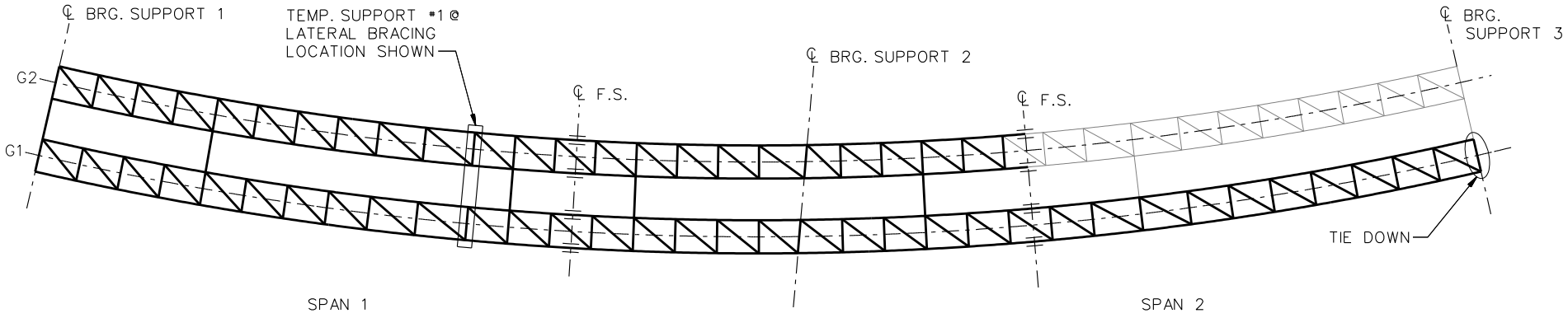

STAGE 5

LEGEND

▽ = HOLD OR LIFT CRANE

○ = TIE DOWN

□ = TEMPORARY SUPPORT STRUCTURE

NCHRP 12-79

BRIDGE ETCCS5a

GENERAL ERECTION PROCEDURE

SHEET 2 OF 2

NCHRP 12-79

ETCCS6

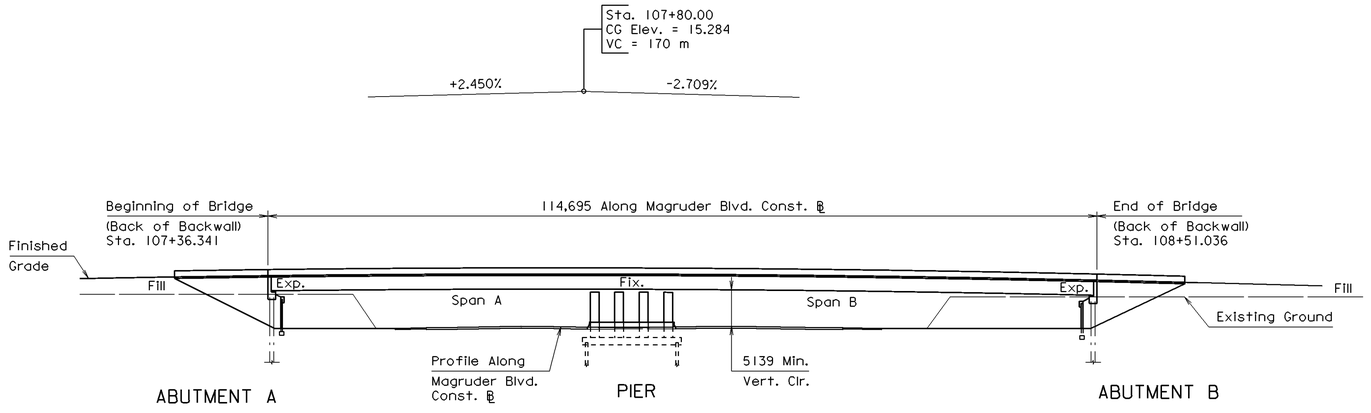

ELEVATION
Scale 1:400

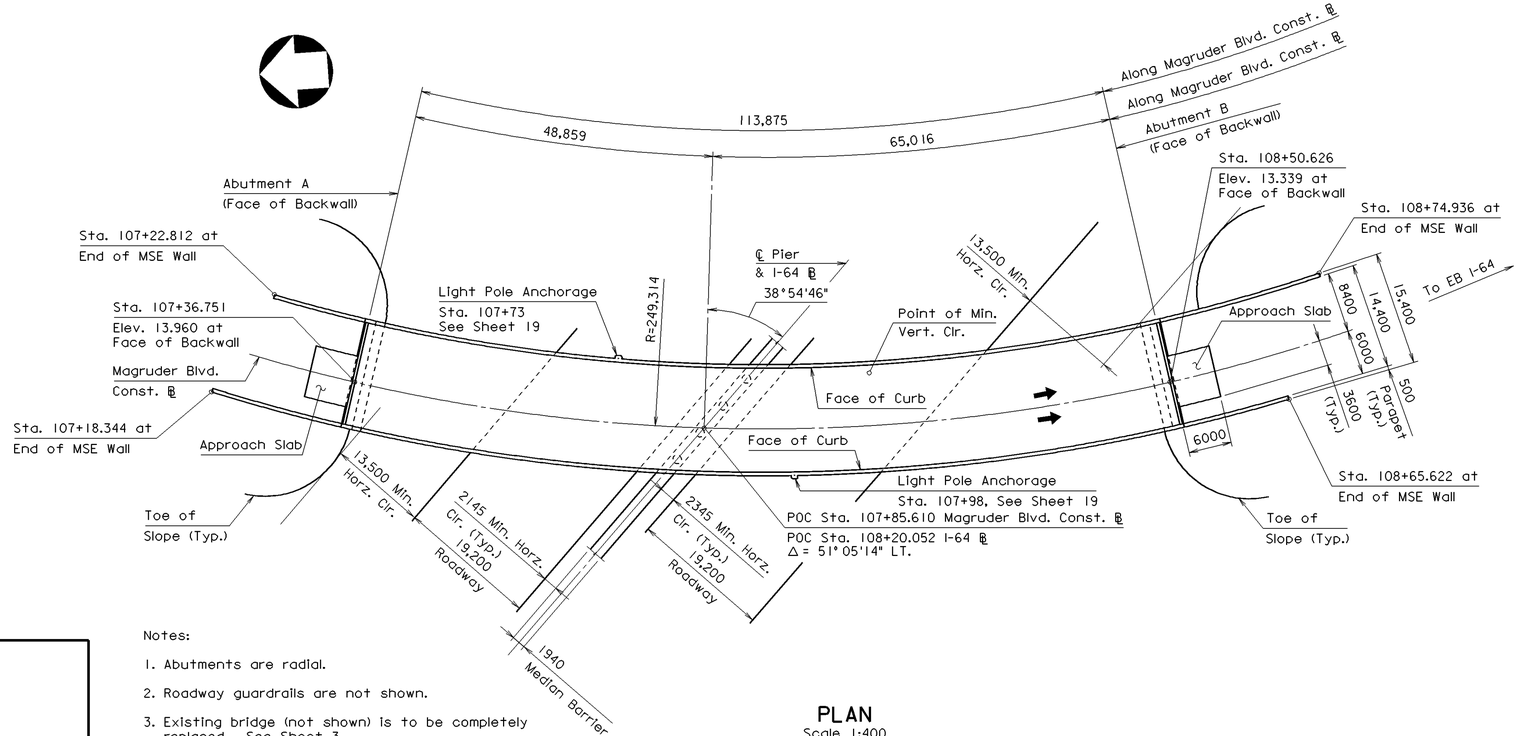

PLAN
Scale 1:400

Notes:

1. Abutments are radial.
2. Roadway guardrails are not shown.
3. Existing bridge (not shown) is to be completely replaced. See Sheet 3.
4. The Contractor shall protect, relocate, and/or remove existing utilities attached to the existing bridge as directed by the Engineer. The cost for this work will be considered incidental to other bid items for this project.
5. Grading in the vicinity of the bridge shall be coordinated with the roadway plans.

FHWA REGION	STATE	FEDERAL AID ROUTE	FEDERAL AID PROJECT	STATE ROUTE	STATE PROJECT (FO)	SHEET NO.
3	VA.	64	AC-NH-064-3(436)	64	0064-114-114, PE-101, B622	18(1)

FHWA Construction and Scour Codes: X771-SN

PPMS No. 17368

400
403

GENERAL NOTE:

Width: 14,400 mm face-to-face of curbs.

Span layout: 48,859 - 65,016 mm continuous steel box girder spans.

Capacity: MS18 loading and alternate military loading.

Specifications:

Construction:	Virginia Department of Transportation Metric Road and Bridge Specifications, 1997.
Design:	AASHTO Standard Specifications for Highway Bridges, 1989; 1990 and 1991 Interim Specifications; and VDOT Modifications.
Standards:	Virginia Department of Transportation Road and Bridge Standards, 1996.

These plans are incomplete unless accompanied by the Supplemental Specifications and Special Provisions included in the contract documents.

Design loading includes 1.0 kN/m^2 allowance for construction tolerances and construction methods.

The use of prestressed deck panels as stay-in-place forms will not be permitted.

⚠ Structural steel for girder ~~webs and~~ flanges, including splice plates ~~and filler plates~~, shall be ASTM A709M ~~Grade 345W or~~ Grade HPS485W, ~~as noted.~~ All other structural steel, including girder webs, diaphragms, cross frames, stiffeners, connector plates, and bearings including sole plates, shall be ASTM A709M Grade 345W. The structural steel shall be painted in the following areas when these areas are within 3 meters of a deck joint: diaphragms, cross frames, stiffeners, connector plates, and girder webs and flanges. In addition, the entire outside surface of the fascia girders shall be painted, and the entire inside surface of all girders shall be painted. All remaining structural steel shall be unpainted, except as required by Section 407 of the Specifications.

Exterior finish paint color for superstructure steel shall be brown, 595-20059. Interior finish paint color for box girders shall be white, 595-37875. The white paint shall conform to System B in accordance with Section 411, and may be applied in the shop and/or field. A single-coat or two-coat white paint system may be used, subject to approval by the Engineer.

Girders shall be curved by cutting the top flanges to proper curvature or by heat curving, and by cutting the bottom flanges to proper curvature.

Concrete in prestressed piles shall be Class 35. Concrete in superstructure including parapets shall be Class 30; in substructure, Class 25.

Deformed reinforcing bars shall conform to ASTM A615M and shall have a yield strength of 420 MPa. All reinforcing bar dimensions on the detailed drawings are to centers of bars except where otherwise noted and are subject to fabrication and construction tolerances.

Piles in abutments have a design capacity of 356 kN per pile.
Piles in pier have a design capacity of 712 kN per pile.

Bridge No. of existing bridge is 1818. Plan No. is 151-25.

The existing structure is designated a Type B structure in accordance with Sec. 411.

Structural approach slabs are not included in the bridge contract.

B.M.: Control Station ID 228, PK Nail with aerial target located approximately 2.3 m south of guardrail and 24 m east of Magruder Overpass on the shoulder of I-64 W.B.L.
VDOT Project Coordinates: X (East) 3,686,335.995, Y (North) 1,081,816.638. Elev. 5.923 m.

All dimensions are shown in millimeters (mm) unless otherwise noted. All stations and elevations are shown in meters (m). Symbol ø = diameter.

All dimensions affected by the geometry and/or location of the existing bridge shall be verified in the field by the Contractor prior to any construction, and prior to ordering or fabrication of materials.

COMMONWEALTH OF VIRGINIA
DEPARTMENT OF TRANSPORTATION

PROPOSED BRIDGE REPLACEMENT ON MAGRUDER BOULEVARD OVER I-64
CITY OF HAMPTON - 1.7 km W. OF US RTE. 258 INTERCHANGE
PROJECT 0064-114-114, PE-101, B622

⚠	Note revised	3-13-01
No.	Description	Date

REVISIONS

For Table of Revisions, see Sheet 2.

VDOT METRIC

Recommended for Approval: _____
State Structure and Bridge Engineer

Approved: _____
Chief Engineer

277-31

Date: September 10, 2000 Sheet 1 of 33

B27731001a 000112 011303

Alvi Associates, Inc.
CONSULTING ENGINEERS
BALTIMORE, MARYLAND

COORDINATED:	MMA
SUPERVISED:	IAA
DESIGNED:	IAA/WIS
DRAWN:	WIS/SLP
CHECKED:	FDS/PPN

FHWA REGION	STATE	FEDERAL AID		STATE		SHEET NO.
		ROUTE	PROJECT	ROUTE	PROJECT (FO)	
3	VA.	64	AC-NH-064-3(436)	64	0064-114-114, PE-101, B622	18(2)

ESTIMATED QUANTITIES

Location		Concrete ** m³ ⚠ Class 25	Concrete ** m³ ⚠ Class 30	Reinforcing Steel kg	Epoxy Coated Reinforcing Steel kg	Structural Steel High-Strength Plate Girders Grade 345W kg * ⚠	Structural Steel High-Strength Plate Girders Grade HPS485W kg * ⚠	Concrete Filled Steel Pipe Pile 356 mm m	Prestressed Concrete Pile 400 mm m	Driving Test for 356 mm Pipe Pile m	Driving Test for 400 mm Prestressed Concrete Pile m	Dynamic Pile Test Ea	Structure Excavation m³ ⊗	Concrete Parapet ** ⚠ m ⊗	Bridge Deck Grooving m² ⊗	Elastomeric Expansion Dam 0-51 mm m ⊗	Elastomeric Expansion Dam 51-76 mm m ⊗	Pipe Underdrain 150 mm m	Retaining Structure (MSE Walls) m²
Superstructure		———	404.7	———	110,830 ⊗	~~486,400~~ 289,180	197,220	———	———	———	———	———	———	230	1640	16	16	———	———
Abutment A	Neat	73.9	———	———	5940	———	———	404	———	23	———	1	137	———	———	———	———	36	285
Pier	Neat	31.9	———	3365	———	———	———	———	———	———	———	———	———	———	———	———	———	———	———
	Footing	111.5	———	13,005	———	———	———	———	399	———	18	1	225	———	———	———	———	———	———
Abutment B	Neat	73.9	———	———	6050	———	———	365		16	———	1	144	———	———	———	———	36	310
Total		291.2	404.7	16,370	122,820	~~486,400~~ 289,180	197,220	769	399	39	18	3	506	230	1640	16	16	72	595

Mobilization - Lump Sum

Construction Surveying - Lump Sum

Dismantle and Remove Existing Structure (Str. No. 1818) - Lump Sum

* Lump Sum

⚠ ** Low permeability concrete shall be used for the construction of the entire bridge.

⊗ Denotes items to be paid for on the basis of plan quantities in accordance with current Road and Bridge Standards.

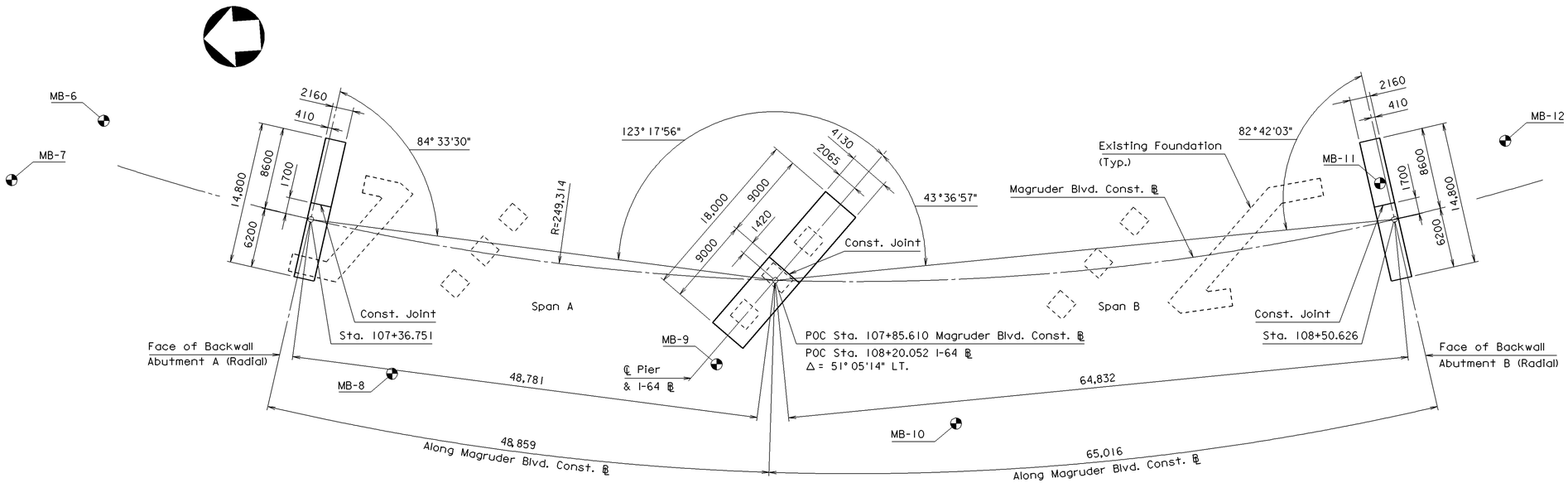

BRIDGE AND SUBSTRUCTURE LAYOUT

Scale 1:250

Denotes boring location. For boring logs, see Sheets 30 and 31.

Notes:

1. Existing and proposed piles not shown.
2. Indicated locations of existing foundations are approximate and subject to field verification by the Contractor. Existing foundations shall be removed, and existing piles shall be removed as applicable to 1.0 meter below finished grade or bottom of proposed footing.
3. This layout is to be used only for the purpose of locating footings of abutments and pier. For details of neatwork, see abutment and pier sheets.

INDEX OF SHEETS

Rev No.	Sheets Revised	Date
3	3, 4, 5, 6, 7 & 10	10-24-01
2	7, 9, 10, 23, & 24	7-05-01
1	1, 2 & 12	3-13-01

TABLE OF REVISIONS

No.	Description	Date
1	Note & quant. added	3-13-01

Revisions

COMMONWEALTH OF VIRGINIA
DEPARTMENT OF TRANSPORTATION

STRUCTURE AND BRIDGE DIVISION

ESTIMATED QUANTITIES
SUBSTRUCTURE LAYOUT
INDEX OF SHEETS

Designed: IAA/WIS	Date	Plan No.	Sheet No.
Drawn: WIS/SLP	Sept. 2000	277-31	2 of 33
Checked: FDS/PPN			

B27731002c 000112 010313 010507

FHWA REGION	STATE	FEDERAL AID		STATE		SHEET NO.
		ROUTE	PROJECT	ROUTE	PROJECT	
3	VA.			64	0064-114-114, PE-101, B622	18(3)

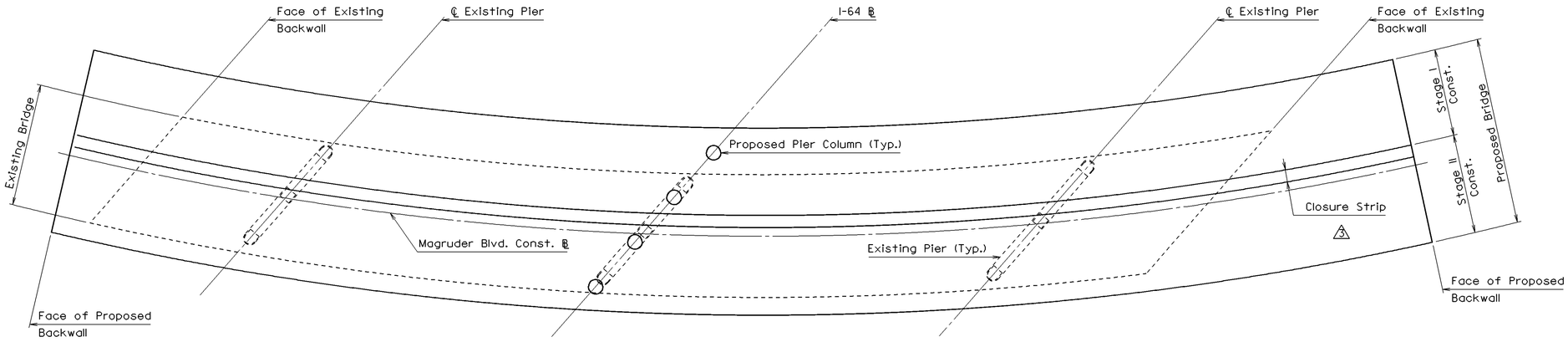

Note: Foundations are not shown. See Sheet 2.

BRIDGE PLAN
Scale 1:200

Notes:

The Contractor shall develop and submit a detailed steel erection and overall bridge construction sequence for approval by the Engineer prior to construction of this bridge, including prior to ordering or fabrication of materials. The erection/construction sequence shall provide details of demolition of the existing bridge, removal and/or relocation of attached existing utilities, temporary supports, blocking, equipment placement and types, traffic control plan, supporting calculations, sequence and schedule of operations, etc. The following requirements shall be met:

1. The bridge construction sequence shall be coordinated with the roadway construction sequence.

2. Girders shall not be erected over traffic.

3. Traffic may be closed on I-64 and Magruder Boulevard only between 1:30 AM and 4:00 AM. However, no closure period may exceed 60 minutes, and the duration between closure periods shall be at least 20 minutes. In addition, traffic may be closed in only one direction during a closure period.

4. Traffic may not be closed in the PM before or the AM after the following holiday periods: New Years Day, Easter Day and the day before, Memorial Day, Independence Day, Labor Day, Thanksgiving Day and the day after, and Christmas Day. A holiday period will include Saturday and Sunday if a holiday falls on either a Monday or Friday.

5. Traffic will be permitted to pass under an erected girder field section only if the section is fully stable and supported at three or more locations. The existing bridge piers and/or additional temporary supports may be used for this purpose. In either case, the Contractor shall submit calculations which demonstrate the structural adequacy of all supports.

6. All structural steel within a construction stage (see Sheet 4 for staging) shall be fully erected and connected as a system prior to placement of any deck slab concrete.

7. At the Contractor's option, temporary supports may be used for construction of this bridge. The construction steps may be as follows:

   a. Provide temporary supports, including bearings and foundations, for support of the girders prior to erection. The existing piers and/or additional temporary supports may be used for this purpose.

   b. Place deck slab concrete while the temporary supports are in place.

   c. Remove the temporary supports after the deck slab concrete has cured.

8. A longitudinal deck closure strip, between Stages I and II (see Sheet 4), will be permitted, subject to approval of the Contractor's proposed details by the Engineer.

9. Based on the erection/construction sequence selected by the Contractor and approved by the Engineer, the Contractor shall submit: deck pouring sequence; deck stresses; girder deflections, cambers, torques, moments, shears, and stresses; diaphragm and bracing forces and stresses; all supporting calculations and computer input/output files, for approval by the Engineer prior to fabrication of any structural steel. If temporary supports are provided during deck pouring, the calculations shall address all deflections and stresses resulting from long-term concrete creep, as well as required revisions to shear stud spacing.

10. In order to address differential settlements due to staged construction, MSE walls shall have a temporary wire face and a permanent concrete face. The concrete face shall match the appearance of other MSE walls used in the project.

11. All costs associated with complying with the above requirements will be considered incidental to other bid items for this project.

VDOT METRIC

No.	Description	Date
3	Added closure strip	10-24-01

Revisions

COMMONWEALTH OF VIRGINIA
DEPARTMENT OF TRANSPORTATION

STRUCTURE AND BRIDGE DIVISION

CONSTRUCTION SEQUENCE - I

Designed: IAA/WIS	Date	Plan No.	Sheet No.
Drawn: WIS/SLP	Sept. 2000	277-31	3 of 33
Checked: FDS/PPN			

B27731003c 012410 000112

FHWA REGION	STATE	FEDERAL AID		STATE		SHEET NO.
		ROUTE	PROJECT	ROUTE	PROJECT	
3	VA.			64	0064-114-114, PE-101, B622	18(4)

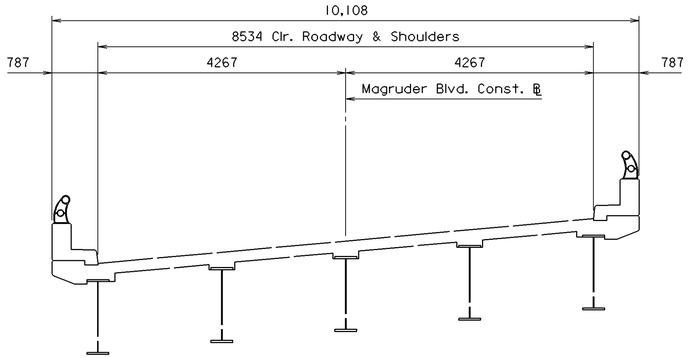

EXISTING TRANSVERSE SECTION
Scale 1:50

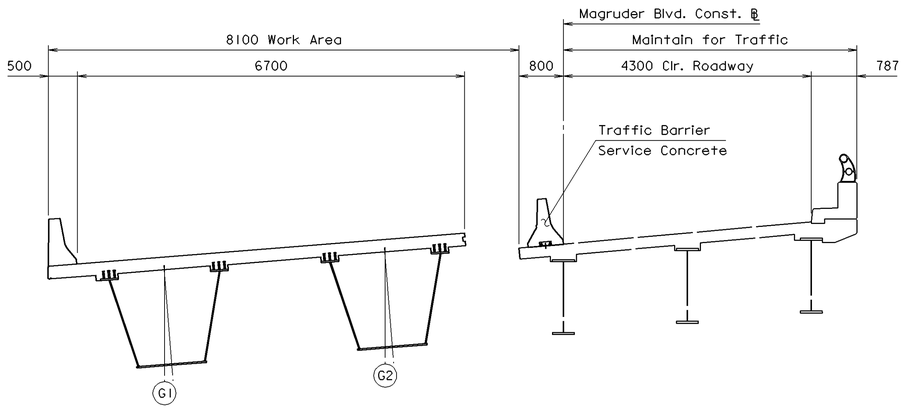

STAGE I - TRANSVERSE SECTION
Scale 1:50

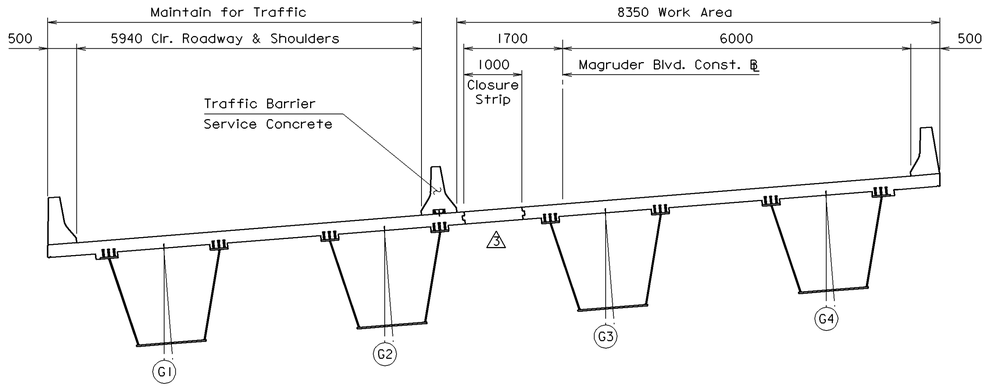

STAGE II - TRANSVERSE SECTION
Scale 1:50

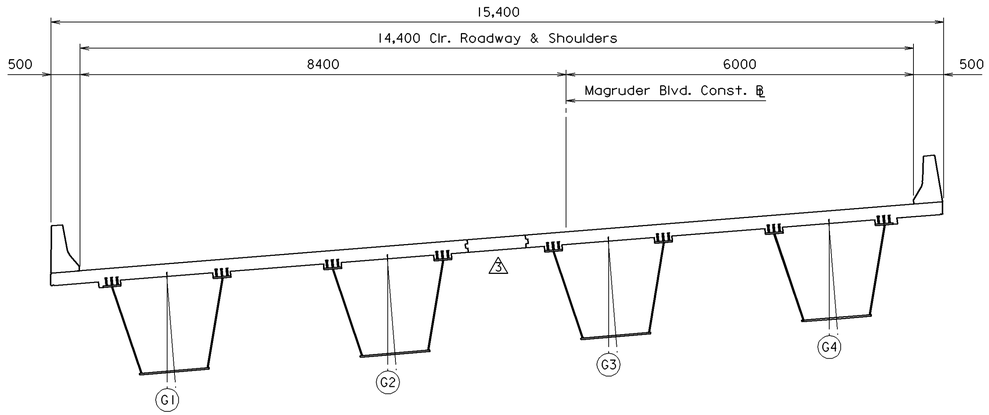

PROPOSED TRANSVERSE SECTION
Scale 1:50

Notes:

1. Traffic Barrier Service Concrete is not included in the Bridge Contract.
2. All dimensions on this sheet are approximate.
3. For additional construction sequence information, see roadway plans and Sheet 3.

VDOT METRIC

No.	Description	Date
3	Added closure strip	10-24-01

Revisions

COMMONWEALTH OF VIRGINIA
DEPARTMENT OF TRANSPORTATION

STRUCTURE AND BRIDGE DIVISION

CONSTRUCTION SEQUENCE - 2

Designed: IAA/WIS	Date	Plan No.	Sheet No.
Drawn: WIS/SLP	Sept. 2000	277-31	4 of 33
Checked: FDS/PPN			

B27731004c 012410 000112

FHWA REGION	STATE	FEDERAL AID		STATE		SHEET NO.
		ROUTE	PROJECT	ROUTE	PROJECT	
3	VA.			64	0064-114-114, PE-101, B622	18(5)

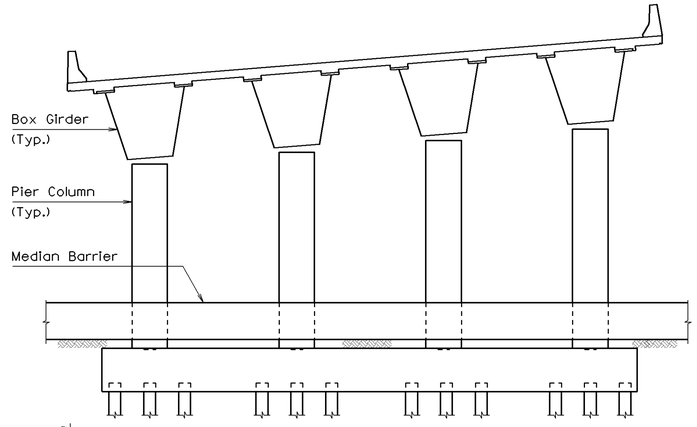

SCHEMATIC TYPICAL SECTION AT PIER
Not to Scale

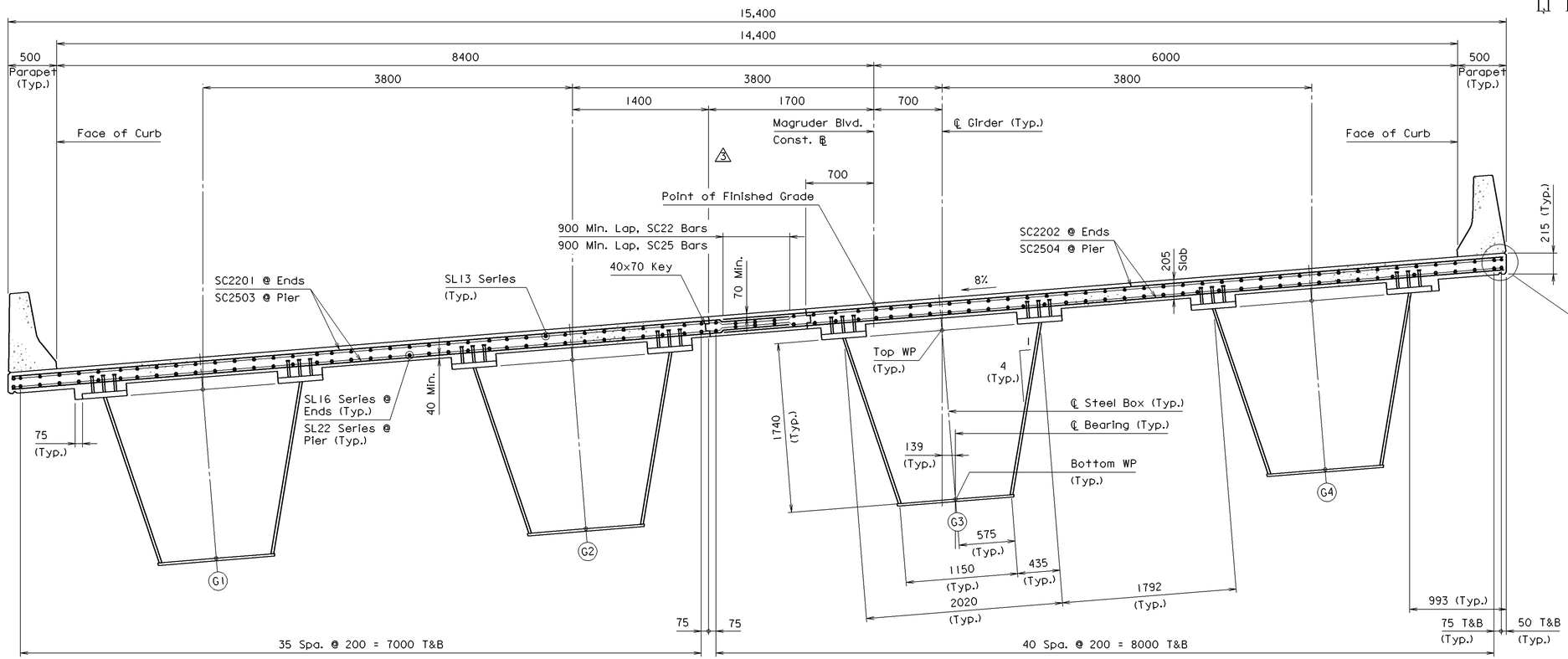

TRANSVERSE SECTION
Scale 1:25

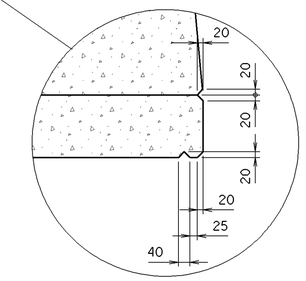

DRIP GROOVE DETAIL
Not to Scale

Notes:

1. All SC bars shall be radial.
2. All SL bars shall be field-curved to be concentric with Magruder Boulevard Construction ℄.
3. Location of bottom SL bars shall be adjusted to clear shear studs.
4. In locations where reinforcement is spliced between construction stages, the Contractor may provide mechanical splices instead of the lap splices shown, subject to the approval of the Engineer and without additional compensation.

VDOT METRIC

No.	Description	Date
3	Added const. joint	10-24-01

Revisions

COMMONWEALTH OF VIRGINIA
DEPARTMENT OF TRANSPORTATION

STRUCTURE AND BRIDGE DIVISION

TRANSVERSE SECTION

Designed: IAA/WIS	Date	Plan No.	Sheet No.
Drawn: WIS/SLP	Sept. 2000	277-31	5 of 33
Checked: FDS/PPN			

B27731005c 012410 000112

FHWA REGION	STATE	FEDERAL AID		STATE		SHEET NO.
		ROUTE	PROJECT	ROUTE	PROJECT	
3	VA.			64	0064-114-114, PE-101, B622	18(6)

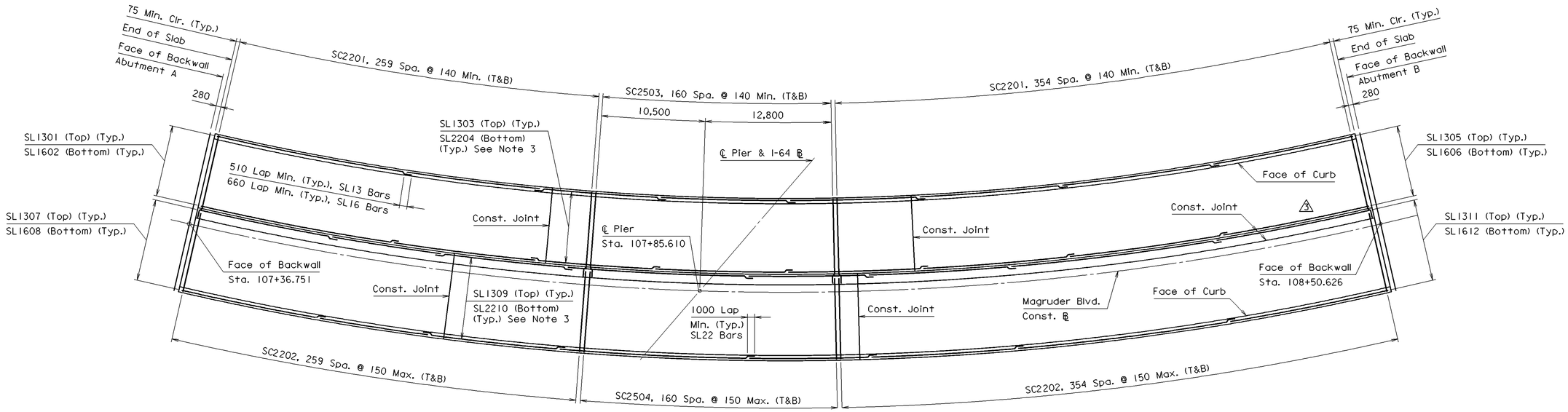

SLAB PLAN
Scale 1:200

Notes:

1. SC bars next to ends of slab and radial construction joints shall have 75 mm clear cover from end of slab.
2. Reinforcing steel shall be adjusted as required to clear shear studs.
3. SL1303, SL2204, SL1309, and SL2210 Bars are located in deck slab pours over the pier. These pours are numbered 3 and 6 in the Deck Slab Concrete Placement Schedule on Sheet 7.
4. In locations where reinforcement is spliced between construction stages, the Contractor may provide mechanical splices instead of the lap splices shown, subject to the approval of the Engineer and without additional compensation.

B27731006c 012401 000112

VDOT METRIC

No.	Description	Date
3	Added const. joint	10-24-01

Revisions

COMMONWEALTH OF VIRGINIA
DEPARTMENT OF TRANSPORTATION

STRUCTURE AND BRIDGE DIVISION

DECK SLAB PLAN

Designed: IAA/WIS	Date	Plan No.	Sheet No.
Drawn: WIS/SLP	Sept. 2000	277-31	6 of 33
Checked: FDS/PPN			

FHWA REGION	STATE	FEDERAL AID		STATE		SHEET NO.
		ROUTE	PROJECT	ROUTE	PROJECT	
3	VA.			64	0064-114-114, PE-101, B622	18(8)

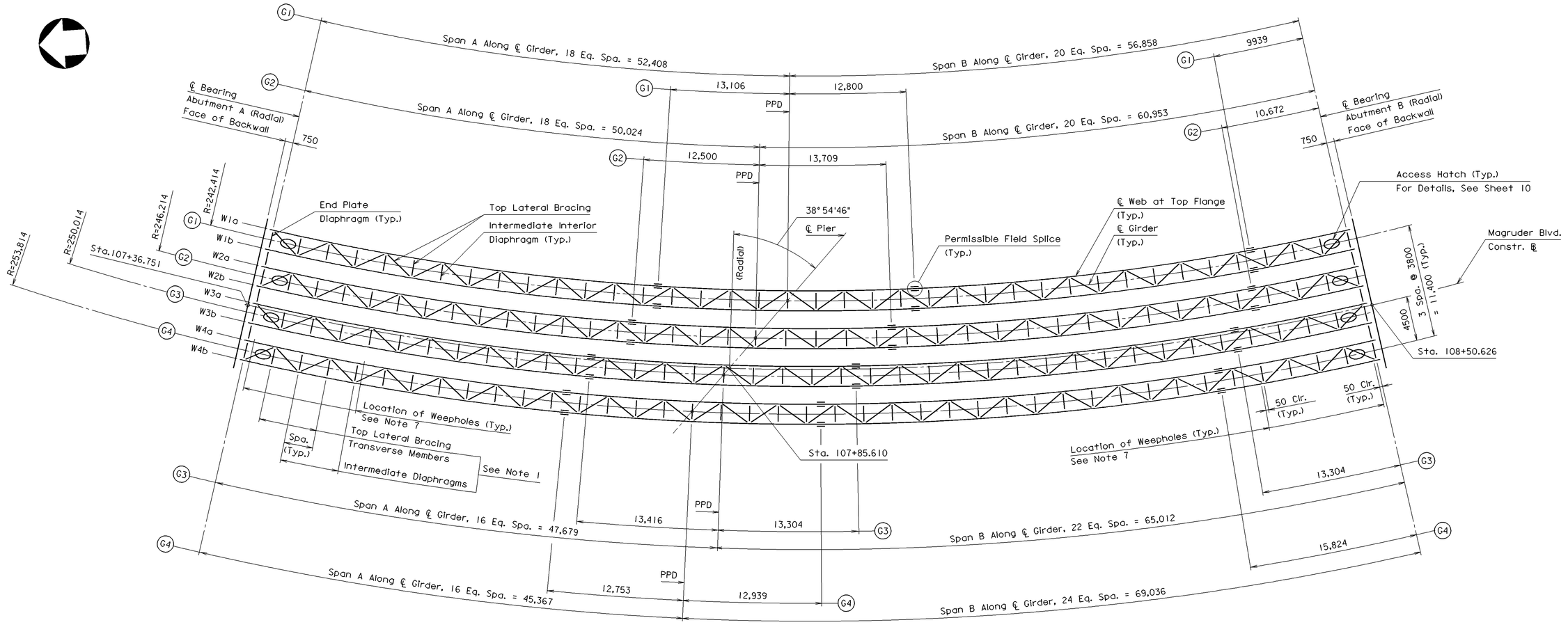

FRAMING PLAN
Scale 1:200

Notes:

1. Top Lateral Bracing Transverse Members shall alternate with Intermediate Diaphragms along both spans between End Plate Diaphragms at abutments and Pier Plate Diaphragms.
2. All cross frames shall be radial to baseline.
3. All girders shall be concentric to baseline.
4. Face of backwall is parallel to centerline bearings.
5. Web lines are shown at top of web.
6. See lighting plans for box girder interior lighting.
7. Weepholes shall be located inside box girders near end plate diaphragms and near every other intermediate diaphragm. For additional weephole requirements, see Typical Box Girder Section on Sheet 9.

Key:

PPD - Pier Plate Diaphragm

W1a - ℄ Web at Top of Web (e.g., Girder 1, Web a)

B27731008 000112

VDOT METRIC

No.	Description	Date
	Revisions	

COMMONWEALTH OF VIRGINIA
DEPARTMENT OF TRANSPORTATION

STRUCTURE AND BRIDGE DIVISION

FRAMING PLAN

Designed: IAA/WIS	Date	Plan No.	Sheet No.
Drawn: WIS/SLP	Sept. 2000	277-31	8 of 33
Checked: FDS/PPN			

FHWA REGION	STATE	FEDERAL AID		STATE		SHEET NO.
		ROUTE	PROJECT	ROUTE	PROJECT	
3	VA.			64	0064-114-114, PE-101, B622	18(9)

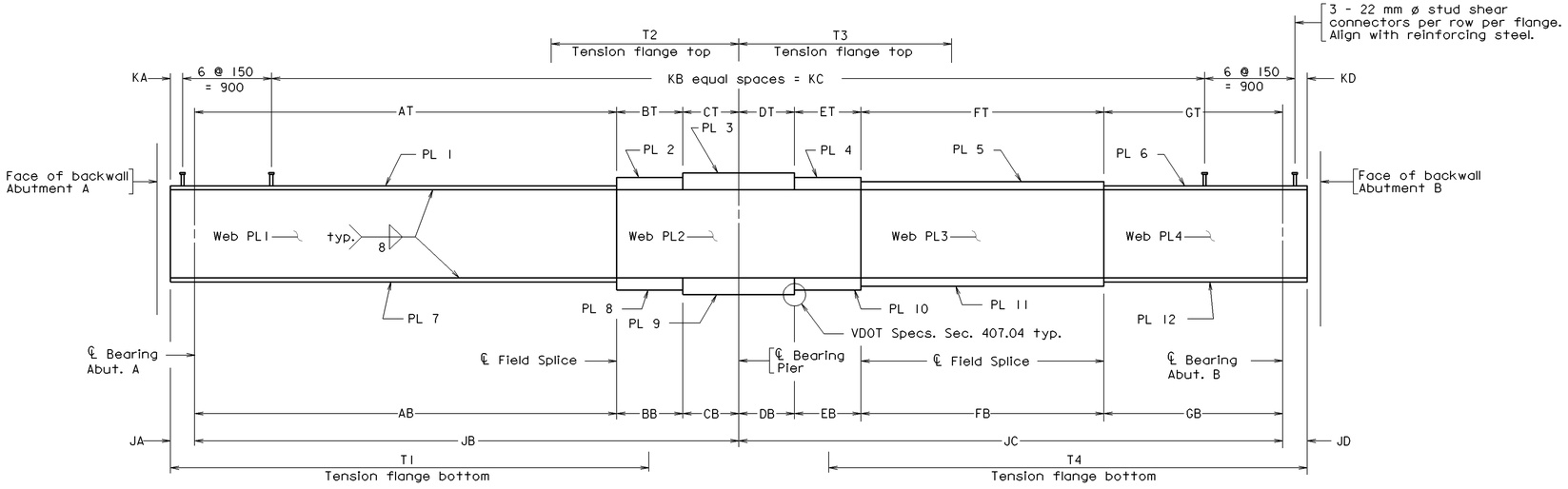

GIRDER ELEVATION

PLATE DIMENSION TABLE

Girder	Web PL1	Web PL2	Web PL3	Web PL4	PL 1	PL 2	PL 3	PL 4	PL 5	PL 6	PL 7	PL 8	PL 9	PL 10	PL 11	PL 12
G1	14x1740	18x1740	16x1740	16x1740	20x375	25x475	50x475	25x475	20x375	20x375	20x1226	25x1226	45x1226	25x1226	20x1226	20x1226
G2	14x1740	18x1740	16x1740	16x1740	20x375	25x475	50x475	25x475	20x375	20x375	22x1226	25x1226	45x1226	25x1226	20x1226	20x1226
G3	14x1740	18x1740	16x1740	16x1740	20x375	28x525	50x525	28x525	28x525	20x375	22x1226	28x1226	45x1226	28x1226	25x1226	20x1226
G4	14x1740	18x1740	16x1740	18x1740	20x375	30x625	50x625	30x625	30x625	30x375	28x1226	32~~30~~x1226	55x1226	32x1226	30x1226	25x1226

Note:

Web plate heights given in the Plate Dimension Table are projected dimensions as shown in the Typical Box Girder Section on this sheet. The fabricated web plate size shall be adjusted to account for slope of web.

GIRDER DIMENSION TABLE

Girder	AB	AT	BB	BT	CB	CT	DB	DT	EB	ET	FB	FT	GB	GT
G1	39,302	39,302	5106	5106	8000	8000	8000	8000	4800	4800	34,119	34,119	9939	9939
G2	37,524	37,524	4500	4500	8000	8000	8000	8000	5709	5709	36,572	36,572	10,672	10,672
G3	34,263	34,263	5416	5416	8000	8000	8000	8000	5304	5304	38,404	38,404	13,304	13,304
G4	32,614	32,614	5228~~4753~~	4753	7525~~8000~~	8000	7525~~8000~~	8000	5414~~4939~~	4939	40,273	40,273	15,824	15,824

GIRDER MOMENT, SHEAR, REACTION, AND STRESS TABLE

Girder	Span	Location	Moment (kN-m)	Shear (kN)	Reaction (kN)	Top Flange Stress (MPa)	Bottom Flange Stress (MPa)	Web Stress (MPa)
G1	A	Abutment A	0	1,031.52	1,031.52	0	0	21.9
	A	4/10 Point	7,833.40	279.36	-	-125.5	139.3	14.4
	-	Pier 1	-22,896.03	2,035.13	3,804.48	223.4	-218.2	36.6
	B	6/10 Point	11,199.21	303.11	-	-194.9	196.3	9.24
	B	Abutment B	0	1,013.77	1,013.77	0	0	24.8
G2	A	Abutment A	0	1,021.25	1,021.25	0	0	21.9
	A	4/10 Point	6,348.50	386.53	-	-92.6	105.5	12.6
	-	Pier 1	-22,703.77	1,861.00	3,631.96	223.2	-216.0	32.3
	B	6/10 Point	12,244.27	221.46	-	-231.7	218.6	8.68
	B	Abutment B	0	1,353.78	1,353.78	0	0	29.6
G3	A	Abutment A	0	942.49	942.49	0	0	19.1
	A	4/10 Point	5,042.97	410.24	-	-67.5	84.3	12.4
	-	Pier 1	-23,746.62	2,092.67	3,788.38	217.1	-224.2	40.9
	B	6/10 Point	15,371.79	195.60	-	-182.5	223.5	9.18
	B	Abutment B	0	1,020.82	1,020.82	0	0	37.6
G4	A	Abutment A	0	733.54	733.54	0	0	18.8
	A	4/10 Point	4,247.54	444.23	-	-35.3	58.5	12.9
	-	Pier 1	-27,327.84	2,223.88	3,976.62	213.0	-218.7	45.4
	B	6/10 Point	19,068.61	164.42	-	-193.8	242.8	6.92
	B	Abutment B	0	2,163.45	2,163.45	0	0	40.3

Note: Structural steel in flanges and flange splice plates shall be ASTM A709M Grade HPS485W. All other structural steel shall be ASTM A709M Grade 345W.

GIRDER DIMENSION TABLE

Girder	JA	JB	JC	JD	KA	KB	KC	KD	Radius
G1	350	52,408	56,858	350	75	178	108,016	75	242,414
G2	350	50,024	60,953	350	75	180	109,727	75	246,214
G3	350	47,679	65,012	350	75	183	111,441	75	250,014
G4	350	45,367	69,036	350	75	186	113,153	75	253,814

TENSION FLANGES

Girder	T1	T2	T3	T4
G1	35,150	18,350	16,500	42,100
G2	31,050	20,550	16,500	45,750
G3	27,200	21,950	15,600	50,700
G4	22,700	25,450	15,900	54,550

Notes:

For spacing of intermediate diaphragm connector PL's, see Framing Plan, Sheet 8.

For bolted splice details, see Sheet 10.

The top and bottom flanges as shown in Girder Elevation, the web, and all splice plates are areas of tensile stress for Charpy V-Notch impact requirements.

Fabrication of Grade HPS485W steel shall be in accordance with the Road and Bridge Specifications and the latest edition of the "Guide for Highway Bridge Fabrication with HPS70W (HPS485W) Steel". Where these two criteria differ, the "Guide for Highway Bridge Fabrication with HPS70W (HPS485W) Steel" shall be used.

All flange and web plate lengths indicated on this sheet are nominal lengths measured along the ℄ girder. Fabricated length and geometry for each plate shall be adjusted to account for actual girder geometry.

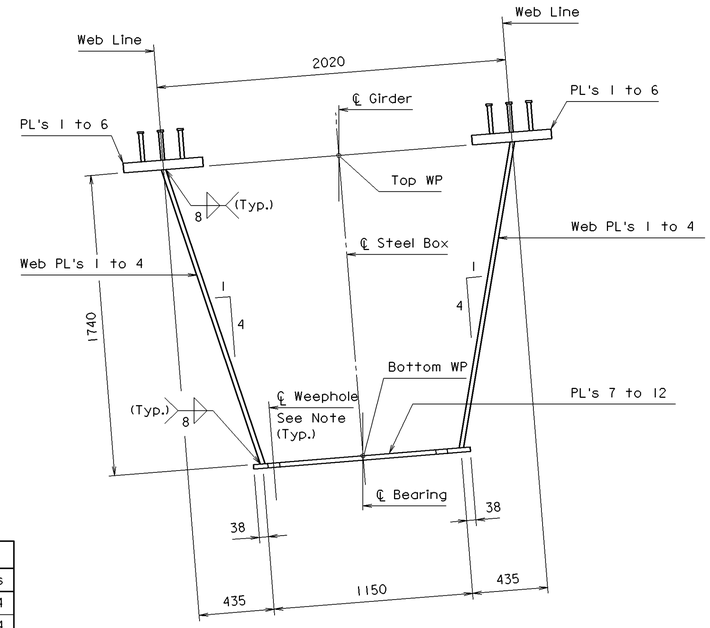

Note: Weepholes shall be 38 mm diameter and located 12 mm clear of the inside face of the web plates and on both sides of the box girder. For additional weephole requirements, see Framing Plan, Sheet 8.

TYPICAL BOX GIRDER SECTION

No.	Description	Date
	Revisions	
2	Revised dimensions	7-05-01

COMMONWEALTH OF VIRGINIA
DEPARTMENT OF TRANSPORTATION
STRUCTURE AND BRIDGE DIVISION

GIRDER DETAILS

Designed: IAA/WIS	Date	Plan No.	Sheet No.
Drawn: WIS/SLP	Sept. 2000	277-31	9 of 33
Checked: FDS/PPN			

VDOT METRIC

B27731009b 010507 000112

FHWA REGION	STATE	FEDERAL AID		STATE		SHEET NO.
		ROUTE	PROJECT	ROUTE	PROJECT	
3	VA.			64	0064-114-114, PE-101, B622	18(11)

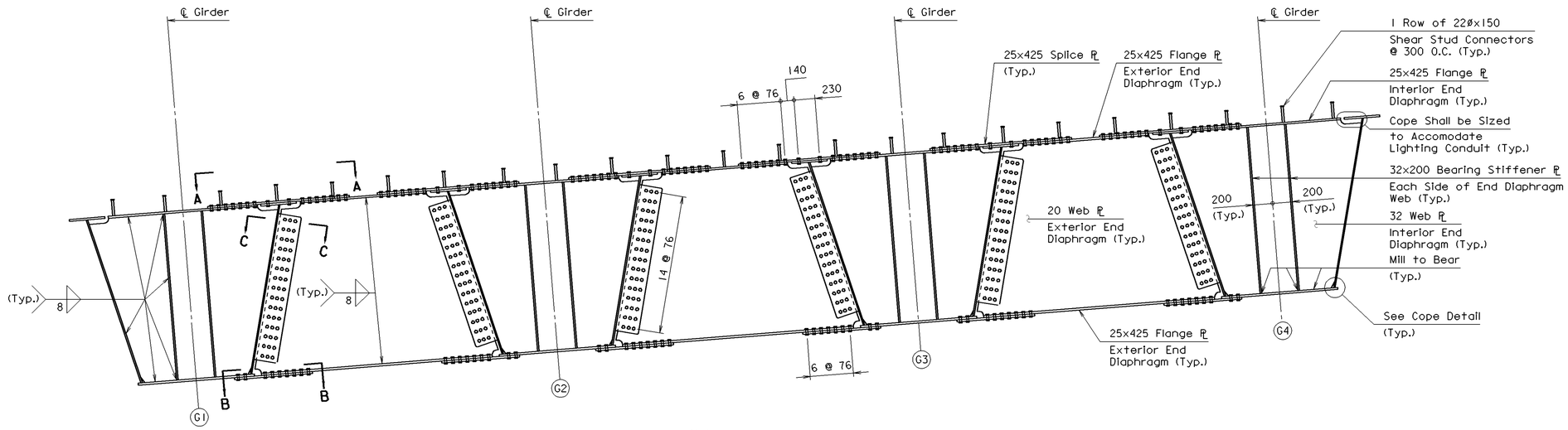

Note:

All bolt spacings are typical.

END PLATE DIAPHRAGM AT ABUTMENTS
Scale 1:25

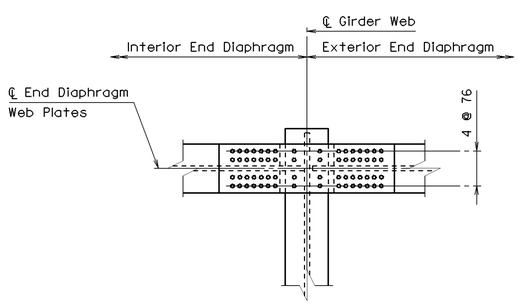

VIEW A-A
Scale 1:25

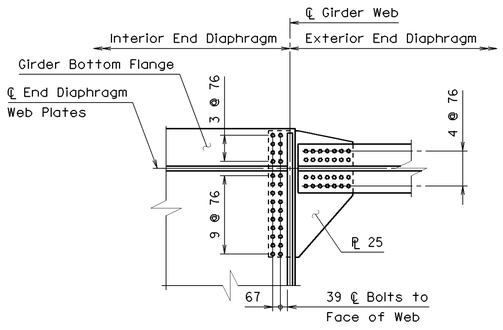

SECTION B-B
Scale 1:25

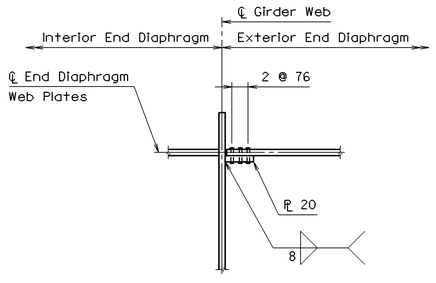

SECTION C-C
Scale 1:25

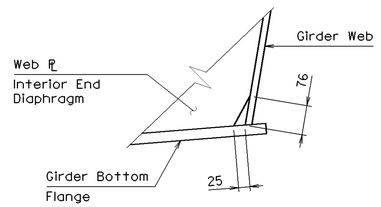

COPE DETAIL
Scale 1:25

VDOT METRIC

No.	Description	Date
	Revisions	

COMMONWEALTH OF VIRGINIA
DEPARTMENT OF TRANSPORTATION

STRUCTURE AND BRIDGE DIVISION

DIAPHRAGM DETAILS

Designed: IAA/WIS	Date	Plan No.	Sheet No.
Drawn: WIS/SLP	Sept. 2000	277-31	11 of 33
Checked: FDS/PPN			

B27731011 000112

FHWA REGION	STATE	FEDERAL AID		STATE		SHEET NO.
		ROUTE	PROJECT	ROUTE	PROJECT	
3	VA.			64	0064-114-114, PE-101, B622	18(12)

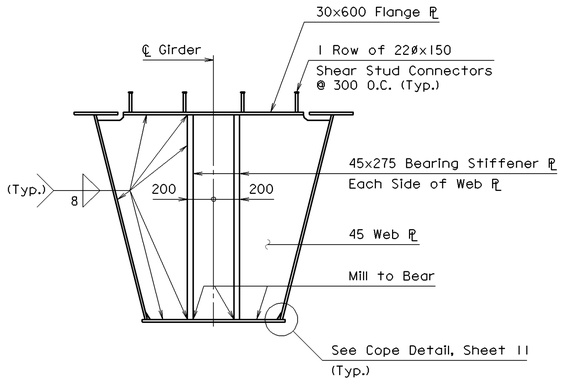

PIER PLATE DIAPHRAGM
Scale 1:25

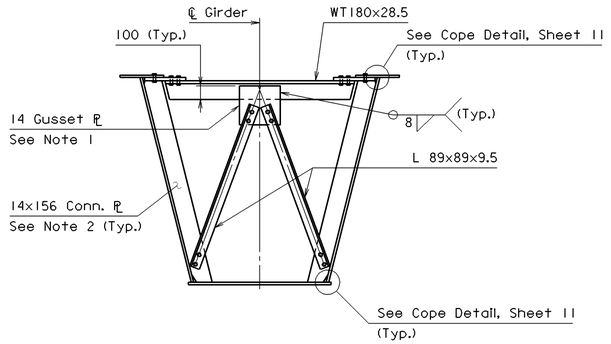

BOLTED OPTION

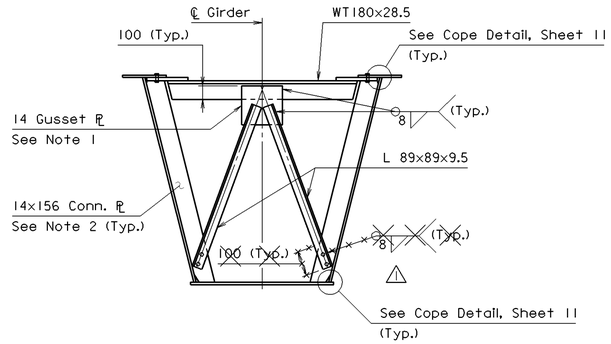

WELDED OPTION

Notes:

1. Size plate to accomodate attachment for lighting conduit.
2. Connection Plates shall be welded to the girder webs and top/bottom flanges with 8 mm welds on both sides. See Detail A.

INTERMEDIATE INTERIOR DIAPHRAGM
Scale 1:25

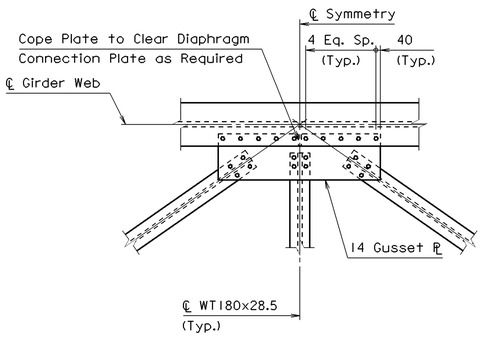

BOLTED OPTION

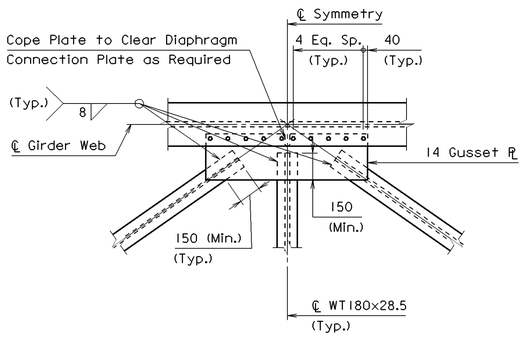

WELDED OPTION

TOP LATERAL BRACING CONNECTION AT DIAGONALS
Scale 1:25

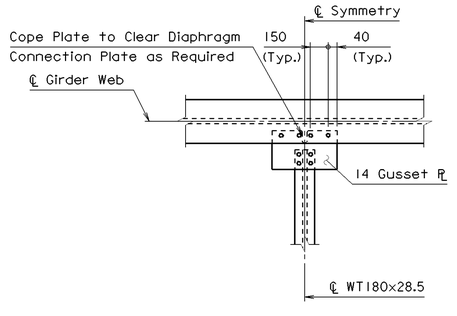

BOLTED OPTION

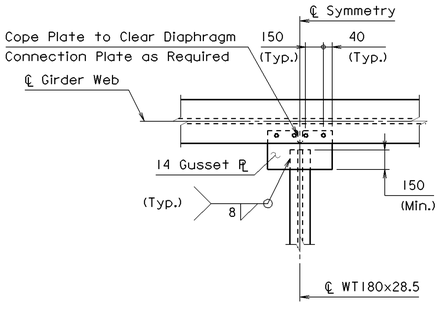

WELDED OPTION

TOP LATERAL BRACING CONNECTION BETWEEN DIAGONALS
Scale 1:25

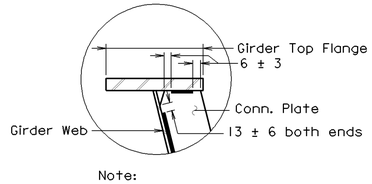

Note:

Top flange shown.
Bottom flange similar.

DETAIL A

No.	Description	Date
	Revisions	
1	Revised connection	3-13-01

COMMONWEALTH OF VIRGINIA
DEPARTMENT OF TRANSPORTATION

STRUCTURE AND BRIDGE DIVISION

DIAPHRAGM DETAILS

Designed: IAA/WIS	Date	Plan No.	Sheet No.
Drawn: WIS/SLP	Sept. 2000	277-31	12 of 33
Checked: FDS/PPN			

011303
B27731012a 000112

FHWA REGION	STATE	FEDERAL AID		STATE		SHEET NO.
		ROUTE	PROJECT	ROUTE	PROJECT	
3	VA.			64	0064-114-114, PE-101, B622	18(15)

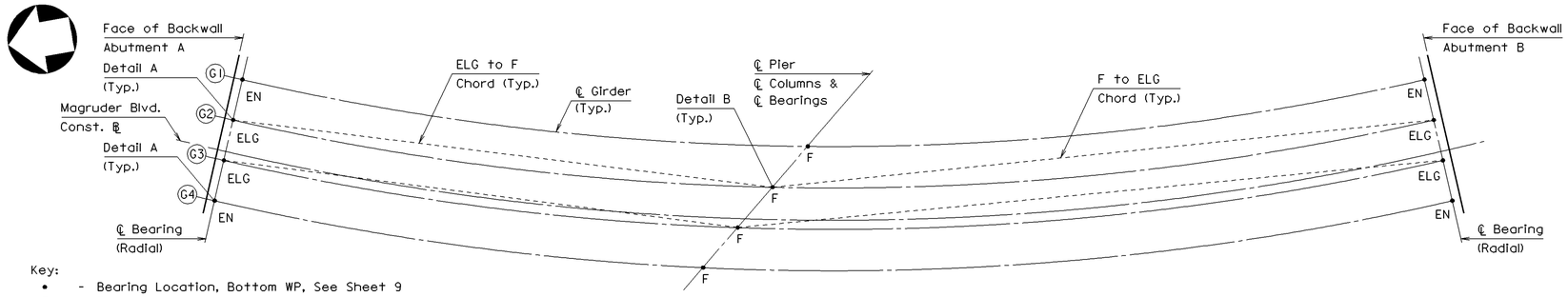

Key:

- • - Bearing Location, Bottom WP, See Sheet 9
- F - Fixed Bearing
- ELG - Expansion Bearing, Longitudinally Guided and Aligned Along Chord
- EN - Expansion Bearing, Nonguided

PLAN
BEARING ORIENTATION AND LOCATION
Not to Scale

Notes:

1. For dimensions 'A', 'L', and Grade %, see Sheet 16.
2. Bevel all sole plates for Grade % and 8% (Radial) Cross Slope. Minimum sole plate thickness is 20 mm. Plates shall not be painted on the surface in contact with the elastomeric bearing.

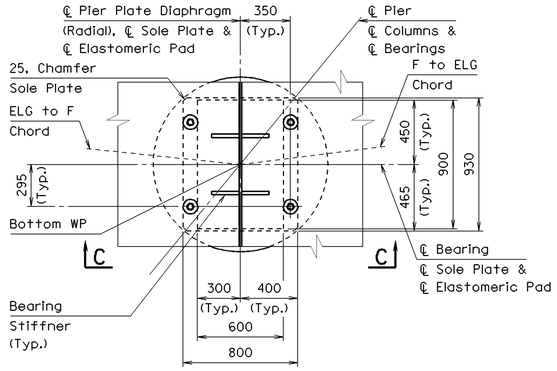

Note: Hole in sole plate for anchor bolt shall be 54 Ø.

DETAIL B - PLAN

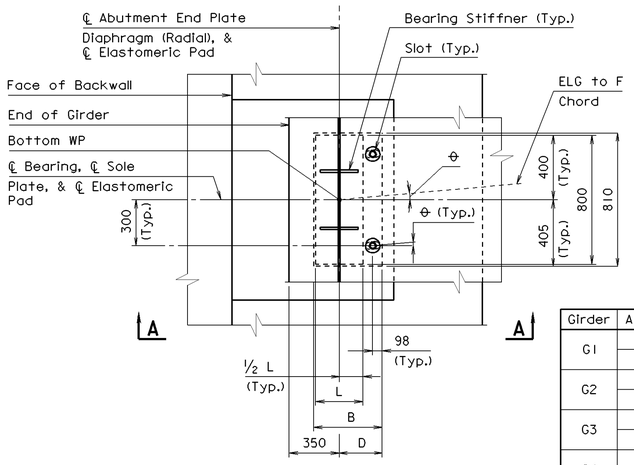

Girder	Abutment	B	D	Slot	θ
G1	A	475	310	65x95	6° 10'43"
	B	580	363	65x95	6° 44'02"
G2	A	475	310	50x95	5° 48'26"
	B	580	363	50x95	7° 06'20"
G3	A	475	310	50x95	5° 27'02"
	B	580	363	50x95	7° 27'44"
G4	A	475	310	65x95	5° 06'29"
	B	580	363	65x95	7° 48'17"

DETAIL A - PLAN

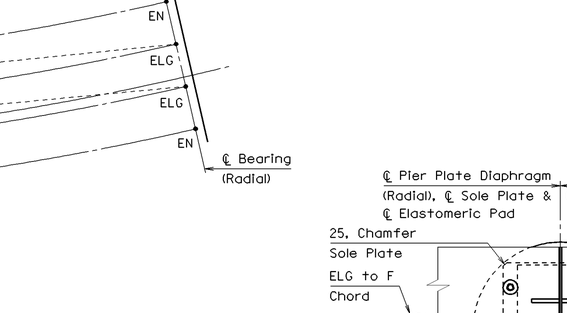

SECTION C-C
(Perpendicular to ℄ Girder)

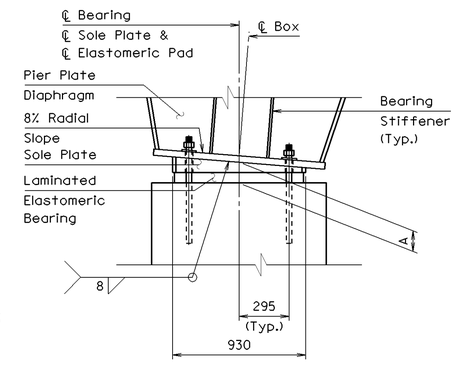

SECTION D-D
(Perpendicular to Radial Pier Plate Diaphragm)

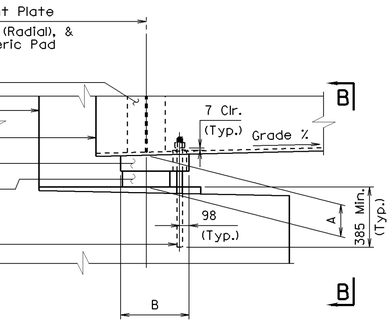

SECTION A-A
(Perpendicular to ℄ Girder)

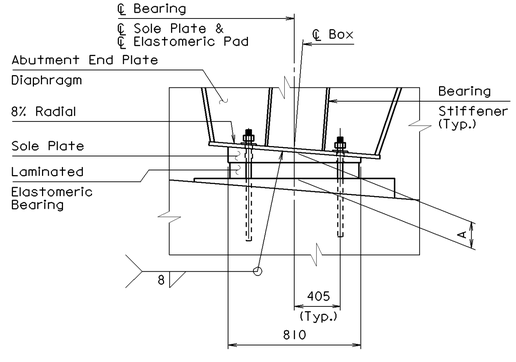

SECTION B-B
(Perpendicular to ℄ Bearing)

EXPANSION BEARING DETAILS AT ABUTMENTS
(Abutment A Shown, Abutment B Opposite Hand)
Not to Scale

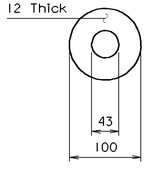

WASHER DETAIL
Not to Scale

FIXED BEARING DETAILS AT PIER
Not to Scale

No.	Description	Date
Revisions		

COMMONWEALTH OF VIRGINIA
DEPARTMENT OF TRANSPORTATION
STRUCTURE AND BRIDGE DIVISION

BEARING DETAILS

Designed: IAA/WIS	Date	Plan No.	Sheet No.
Drawn: WIS/SLP	Sept. 2000	277-31	15 of 33
Checked: FDS/PPN			

B27731015 000112

FHWA REGION	STATE	FEDERAL AID		STATE		SHEET NO.
		ROUTE	PROJECT	ROUTE	PROJECT	
3	VA.			64	0064-114-114, PE-101, B622	18(16)

Notes:

1. Material: Elastomer - 50 durometer hardness.
   Shim - ASTM A36M or A570M mild steel.
2. Elastomeric bearings shall be molded as a single unit.
3. See Sheet 15 for additional information.

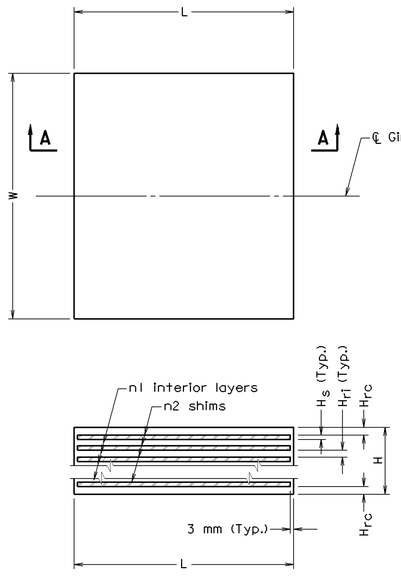

SECTION A-A
LAMINATED ELASTOMERIC BEARING

Girder	Location	A	Laminated Elastomeric Bearing						Grade %	Total Load (kN)
			W	L	H	H_{rc}	n1 @ H_{rl}	n2 @ H_s		
G1	Abut. A	162	800	300	100	6	5 @ 14	6 @ 3	1.160	975
	Pier 1	218	900	600	159	6	9 @ 13	10 @ 3	-0.430	3717
	Abut. B	198	800	405	133	11	6 @ 15	7 @ 3	-2.250	957
G2	Abut. A	162	800	300	100	6	5 @ 14	6 @ 3	1.160	967
	Pier 1	218	900	600	159	6	9 @ 13	10 @ 3	-0.358	3561
	Abut. B	198	800	405	133	9	7 @ 13	8 @ 3	-2.250	1289
G3	Abut. A	157	800	300	95	10	4 @ 15	5 @ 3	1.160	892
	Pier 1	218	900	600	159	6	9 @ 13	10 @ 3	-0.287	3715
	Abut. B	198	800	405	133	11	6 @ 15	7 @ 3	-2.250	965
G4	Abut. A	167	800	300	105	15	4 @ 15	5 @ 3	1.160	686
	Pier 1	218	900	600	159	6	9 @ 13	10 @ 3	-0.217	3903
	Abut. B	198	800	405	133	9	7 @ 13	8 @ 3	-2.250	2069

B27731016 000112

VDOT METRIC

No.	Description	Date
	Revisions	

COMMONWEALTH OF VIRGINIA
DEPARTMENT OF TRANSPORTATION

STRUCTURE AND BRIDGE DIVISION

BEARING DETAILS

Designed: IAA/WIS	Date	Plan No.	Sheet No.
Drawn: WIS/SLP	Sept. 2000	277-31	16 of 33
Checked: FDS/PPN			

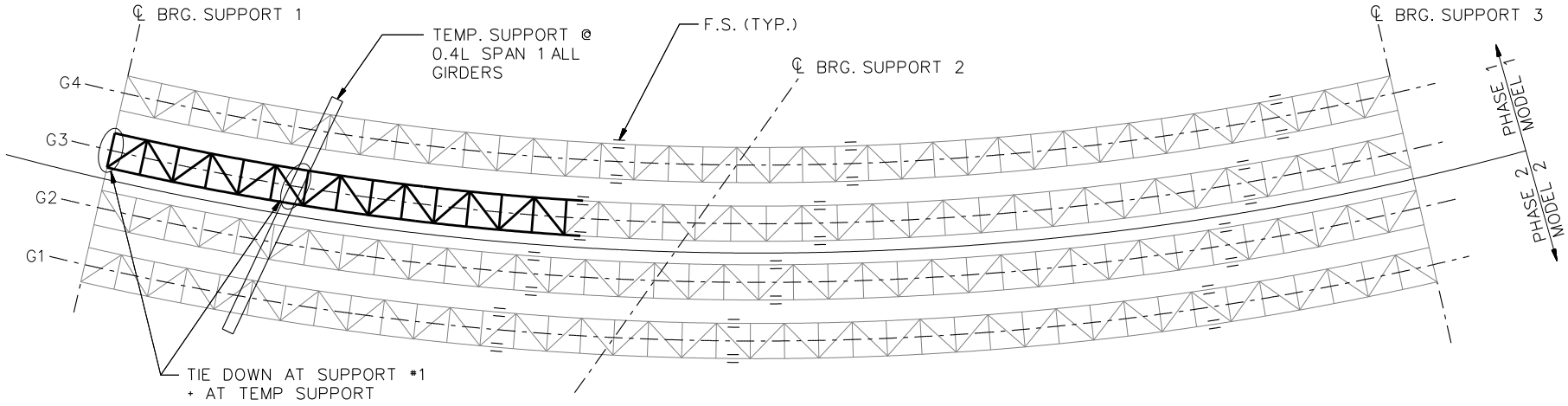

STAGE 1

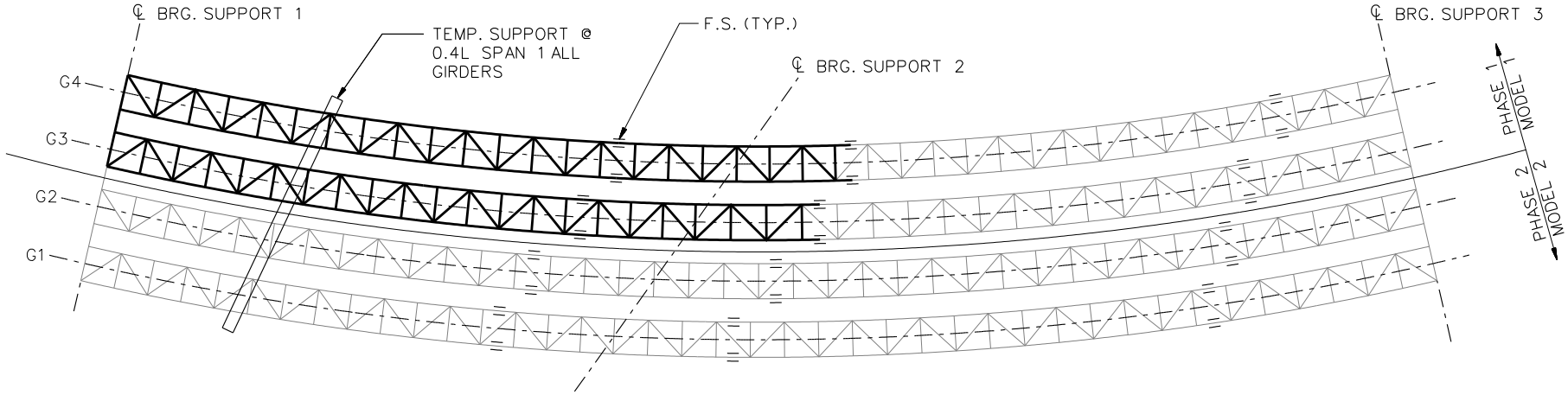

STAGE 4

LEGEND

▽ = HOLD OR LIFT CRANE

○ = TIE DOWN

□ = TEMPORARY SUPPORT STRUCTURE

NOTE:
ERECTION PROCEDURE IS SHOWN FOR PHASE 1 ONLY.
PHASE 2 WILL FOLLOW SIMILAR PROCEDURE.

NCHRP 12-79

BRIDGE ETCCS6

GENERAL ERECTION PROCEDURE

SHEET 1 OF 2

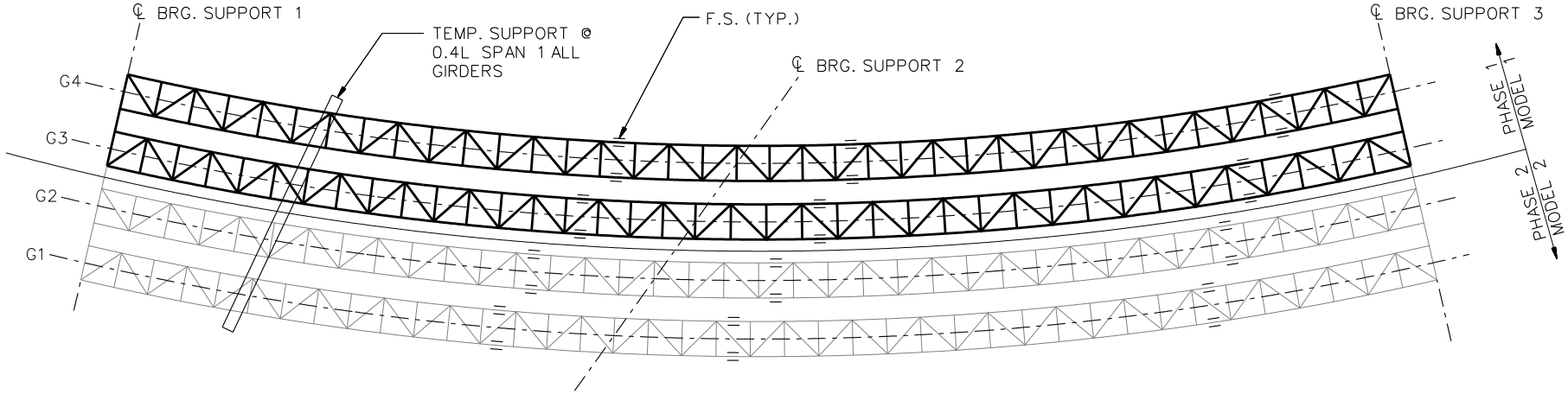

STAGE 6

LEGEND

▽ = HOLD OR LIFT CRANE

○ = TIE DOWN

□ = TEMPORARY SUPPORT STRUCTURE

NOTE:
ERECTION PROCEDURE IS SHOWN FOR PHASE 1 ONLY.
PHASE 2 WILL FOLLOW SIMILAR PROCEDURE.

NCHRP 12-79

BRIDGE ETCCS6

GENERAL ERECTION PROCEDURE

SHEET 2 OF 2

NCHRP 12-79

ETSSS2

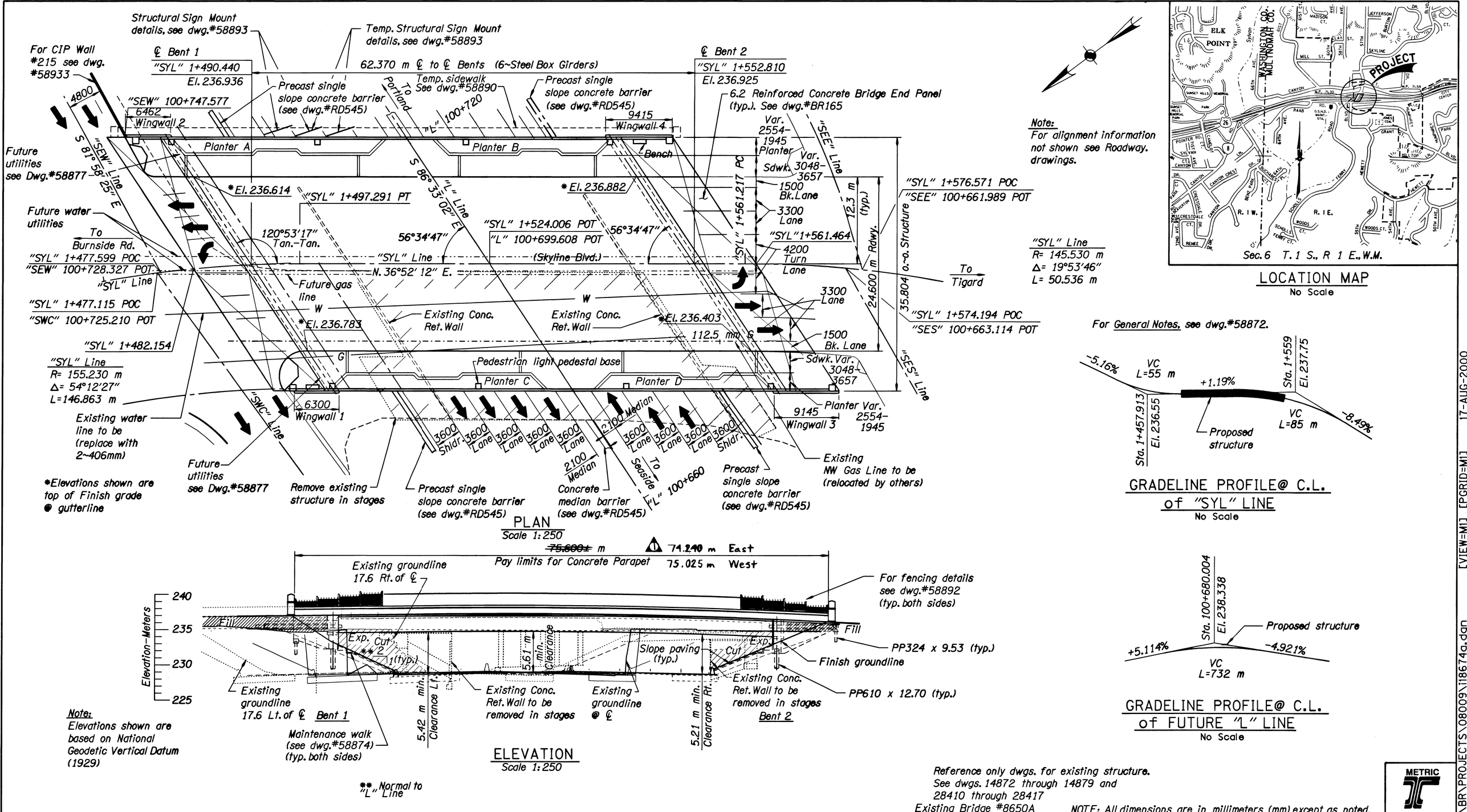

Reference only dwgs. for existing structure.
See dwgs. 14872 through 14879 and 28410 through 28417
Existing Bridge #8650A

NOTE: All dimensions are in millimeters (mm) except as noted.

METRIC

	DATE	REVISION	BY
1	9-28-00	Changed as Noted	HS

DRAFTED: E. Leon
CHECKED: Mark Lusby
REVIEWED: In-Tae Lee

DESIGNER — REGISTERED PROFESSIONAL ENGINEER 17910 OREGON JULY 25, 1995 HORMOZ SERADJ — EXPIRES: 6/30/2002

BRIDGE ENGINEER — REGISTERED PROFESSIONAL ENGINEER 13,368 OREGON JULY 17, 1998 MARK E. HINOTA — EXPIRES: 6/30/01

OREGON DEPARTMENT OF TRANSPORTATION
BRIDGE ENGINEERING SECTION

ACCOMPANIED BY DWGS. 58871 through 58894, 59114
BR115, BR165, BR200, BR241, BR240, RD500, RD545

BRIDGE NO. 18674
DATE 17-AUG-2000
CALC. BOOK 4833

SYLVAN BRIDGE O'XING SUNSET HWY.
CAMELOT INTCHGE.- SYLVAN INTCHGE.
(PHASE 2) SECTION
SUNSET HWY.#47 (MP 71.32) MULTNOMAH CO.
PLAN and ELEVATION

FEDERAL HIGHWAY ADMINISTRATION — REGION 10 — OREGON DIVISION
PROJECT NUMBER

SHEET 1 OF 25
DRAWING NO. 58870

17-AUG-2000 [VIEW=M1] [PGRID=M1] NT7440b(ejl)£:\usr\BR\PROJECTS\08009\i18674a.dgn

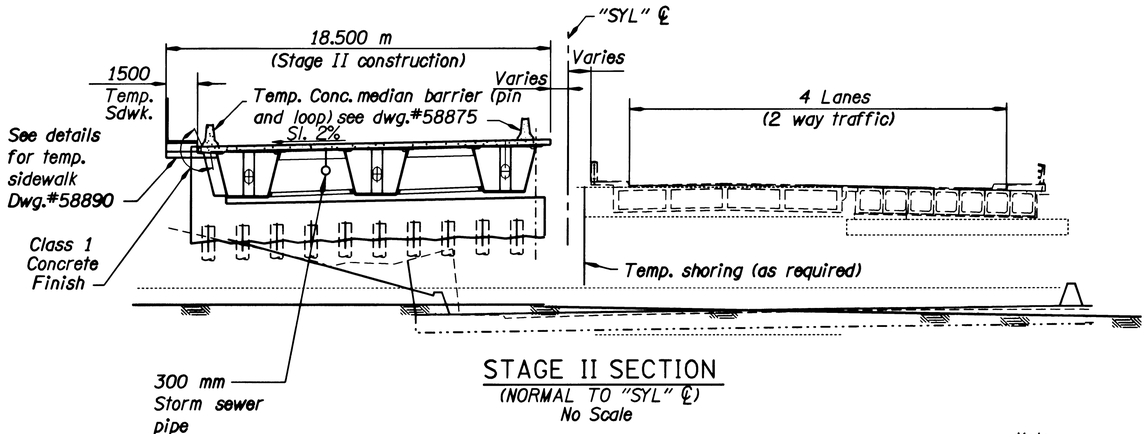

STAGE II SECTION
(NORMAL TO "SYL" ℄)
No Scale

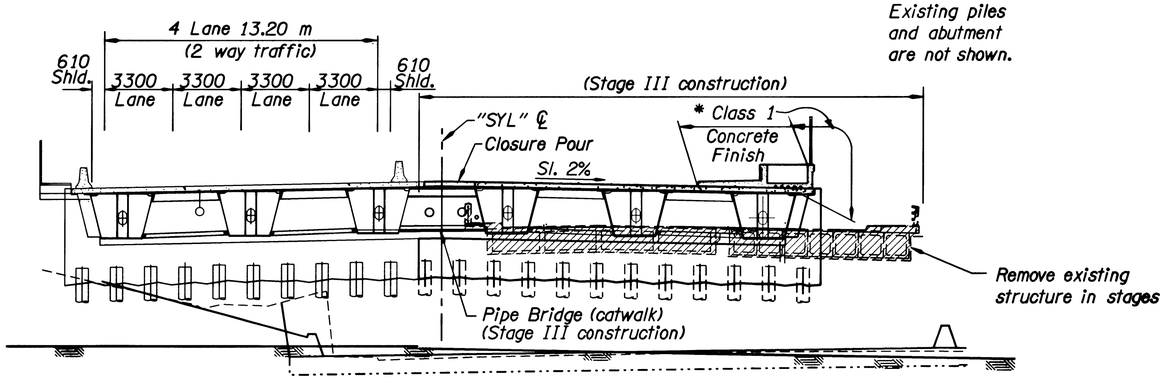

Note: Existing piles and abutment are not shown.

STAGE III SECTION
(NORMAL TO "SYL" ℄)
No Scale

*General finish 300mm under soil line in planter

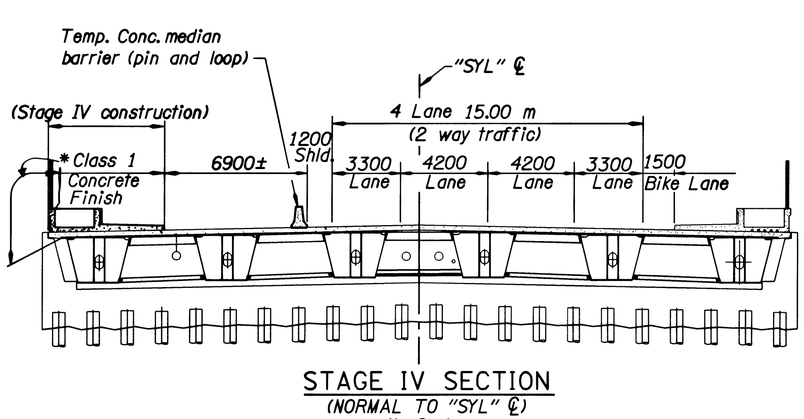

STAGE IV SECTION
(NORMAL TO "SYL" ℄)
No Scale

GENERAL NOTES

Provide all materials and perform all work according to the 1996 Standard Specifications for Highway Construction of the ODOT and the 1998 Supplemental Standard Specifications of the Oregon Department of Transportation.
Bridge is designed for HL-93 loading with an allowance of 1.2 kN/m^2 for future wearing surface.
Concrete deck is designed using the empirical method for isotropic reinforcing of the Ontario highway Bridge Design Code.
Seismic design is in accodance with the AASHTO Division I-A, Seeismic Design, "Standard Specifications
Seismic design of Highway Bridge". The site peak bedrock acceleration coefficient (A) is 0.18 g and the assumed site coefficient (S) is 1.0.
Provide all reinforcing steel according to ASTM Specification A706M, or AASHTO M31M (ASTM A615M), Grade 420. (Provide field bent reinforcing steel according to ASTM Specification A706M).
The following splice lengths shall be used unless shown otherwise:

Bar Size		10	13	16	19	22	25	29	32	36	43	57
Splice Length (mm)	Uncoated	300	325	425	600	825	1075	1350	1700	2100	Not Permitted	
	Epoxy Coated	400	450	600	850	1150	1500	1900	2400	2950	Not Permitted	

Splice reinforcing steel at alternate bars, staggered at least one splice length or as far as possible, unless shown otherwise.
Support the btm. mat reinforcing steel from the forms with precast mortar blocks at 900 mm max. centers each way
Support the top mat of reinforcing steel from the btm. mat of reinforcing steel with reinforcing bar supports by Dayton Superior Co. (SBU, BBU, or CHCUO or approved equal at 900 mm max. centers.
Epoxy coat reinforcing steel in the upper portion of the deck and bridge end panels. This includes top longitudinal bars, top transverse bars and all bars extending from the Bridge End Panel or deck into the sidewalk, curb, or parapet.
Place bars 50 mm clear of the nearest face of concrete unless shown otherwise.
Provide Class 30-19.0 mm concrete in deck.
All other concrete shall be Class 25-37.5 or 19.0.

Piling at Bents 1 and 2 shall be PP610 x 12.7 conforming to ASTM A252 Grade 3 driven open-end to an ultimate capacity of 4780 kN.
Pile tip elevations for mininum pile penetration shall be 224.0 and 223.0 meters for Bent 1 and 2 respectively.
Pile capacities will be determined by gate equation analysis. The factor of safety for the applied structure loads is 2.5.
Piling in wingwall shall be PP324 x 9.53 conforming to ASTM A252 Grade 3 driven open-end to an ultimate capacity of 2190 kN.
Pile tip elevations for mininum pile penetration shall be 224.0 and 223.0 meters for Bent 1 and 2 respectively.
Pile capacities will be determined by gate equation analysis. The factor of safety for the applied structure loads is 3.

Construction Sequence

STAGE I

1. See Traffic Control Plans Dwgs.

STAGE II

1. Install median barrier (pin and loop) on Sunset Hwy. and redirect traffic on Sunset Hwy.
2. Construct shoring as required.
3. Excavate end bents and drive piles.
4. Construct bents (including wingwalls).
5. Place steel box girders.
6. Construct end beams, Hilfiker wire walls (or approved equal), deck and temporary sidewalk.
7. Complete backfill.
8. Construct Stage II end panels.
9. Place median barriers (pin and loop). For Stage III construction per dwgs.

STAGE III

1. Redirect traffic to Stage II construction.
2. Remove existing structure as directed by the engineer.
4. Construct bents (including wingwalls).
5. Place steel box girders.
6. Construct end wall, Hilfiker wire wall (or approved equal), and deck.
7. Construct the pipe bridge (catwalk).
8. Complete backfill.
9. Pour deck closure pour.
10. Construct Stage III end panel, sidewalk and planters.
11. Relocate concrete median barrier and redirecting traffic to Stage IV construction.

STAGE IV

1. Remove temporary sidewalk.
2. Construct sidewalk and planters.
3. Remove concrete median barrier.

STAGE V

1. Install temporary signs.

Note: See Traffic Control Plan for all phases of staging.

NOTE: All dimensions are in millimeters (mm) except as noted.

METRIC

△	DATE	REVISION	BY

DRAFTED: E. Leon
CHECKED: Mark Lusby
REVIEWED: In-Tae Lee

DESIGNER
REGISTERED PROFESSIONAL ENGINEER 17910 OREGON JULY 25, 1995 HORMOZ SERADJ
EXPIRES: 6/30/2002

OREGON DEPARTMENT OF TRANSPORTATION
BRIDGE ENGINEERING SECTION

BRIDGE NO. 18674
DATE 17-AUG-2000
CALC. BOOK 4833

SYLVAN BRIDGE O'XING SUNSET HWY.

STAGE CONSTRUCTION SECTIONS

SHEET 3 OF 25
DRAWING NO. 58872

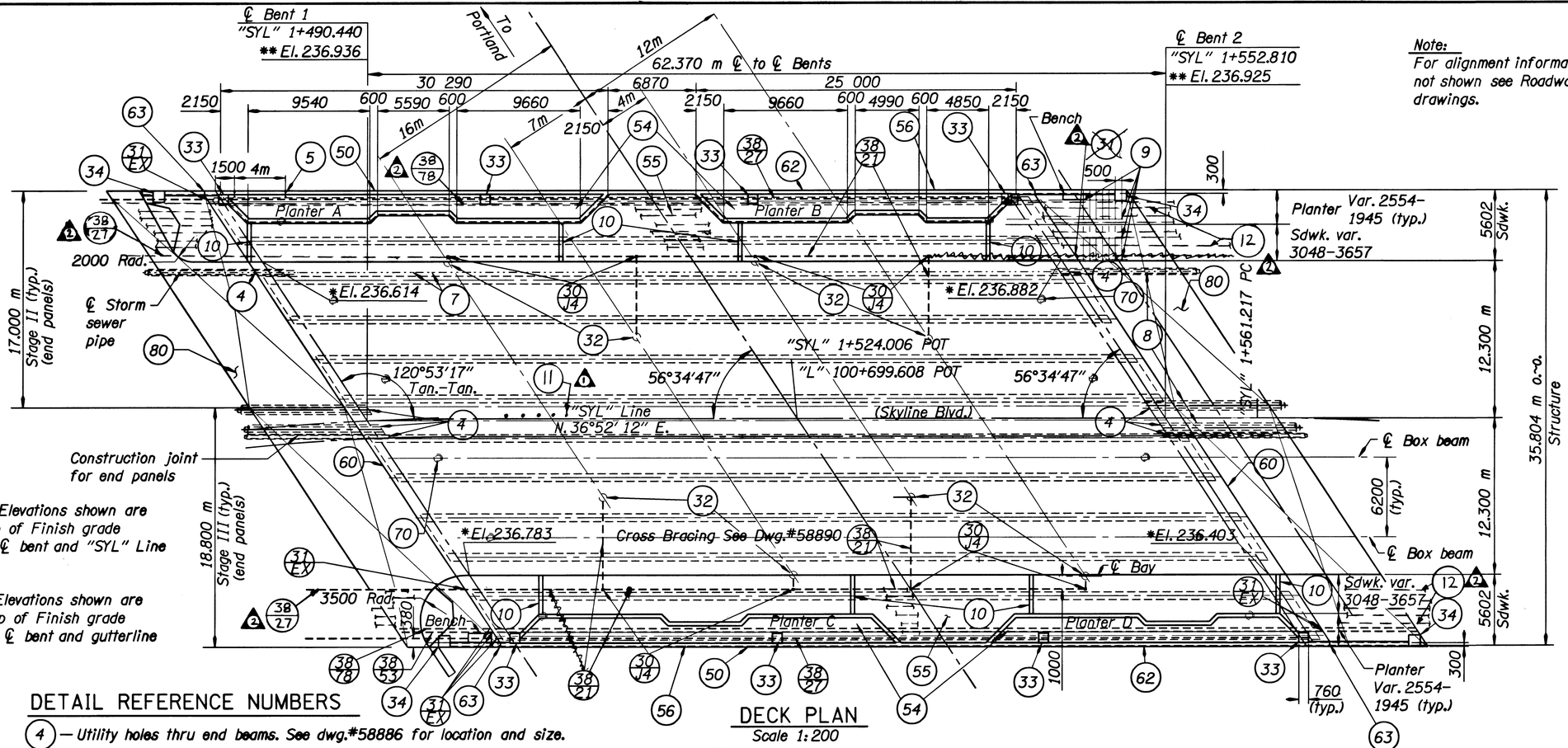

**Elevations shown are top of Finish grade @ ℄ bent and "SYL" Line

*Elevations shown are top of Finish grade @ ℄ bent and gutterline

DECK PLAN
Scale 1:200

Note: For alignment information not shown see Roadway. drawings.

Note: For electrical and illumination for details not shown see I-0741 and I-0740

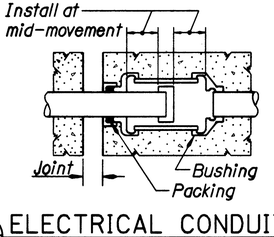

(31 EX) ELECTRICAL CONDUIT EXPANSION JOINT
No Scale

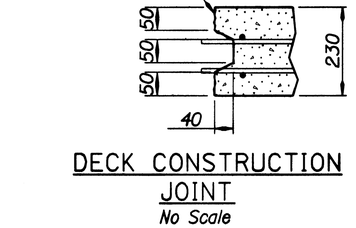

DECK CONSTRUCTION JOINT
No Scale

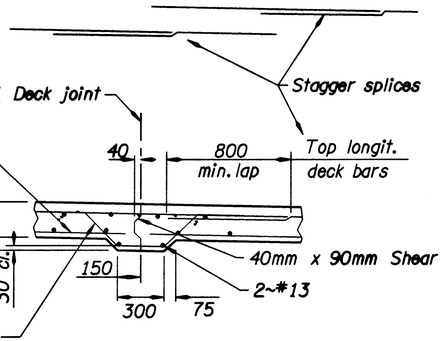

TRANSVERSE DECK JOINT DETAIL
No Scale

DETAIL REFERENCE NUMBERS

(4) — Utility holes thru end beams. See dwg.#58886 for location and size.

(5) — Dayton/Richmond (Ferrule Type) F-57 or approved equal Structural Concrete inserts (Hot-dip Galv.). 22.2 mm dia., series, see dwg.#58890 for layout.

(6) — Dayton/Richmond (Ferrule Type) F-57 or approved equal Structural Concrete inserts (Hot-dip Galv.). 19.0 mm dia., series @ 3000 mm±, or an approved equal for utility hangers. (for storm sewer).

(7) — Dayton/Richmond (Ferrule Type) F-57 or approved equal Structural Concrete inserts (Hot-dip Galv.). 22.2 mm dia., series @ 3000 mm±, or an approved equal for storm sewer hangers.

(8) — Place concrete culvert pipe under RC approach panel at each utility hole, both ends of bridge (concrete culvert pipe ID = 750 mm dia. for water, 350 mm dia. for gas, ~~500~~ mm dia. for storm sewer). Extend from hole in structure to a point 5 m minimum beyond the end of the approach panel. An oversize hole (25 mm larger diameter than the pipe) should be formed into the backwall or end beam. When the pipe is installed, the void around the pipe should be filled with a compressible material. See Special Provisions 00545.

△1 525

(9) — Resin bonded anchors @ 500 mm± see dwg.#58877

(10) — Planter drain 300 mm width see dwg.#R2

(30/J4) — Install 102mmx102mmx102mm galv. cast iron juction box w/gasketed galv. steel cover see dwg.#58856

(31/EX) — Electrical conduit expansion joint (see detail this sheet).

(32) — Under deck luminar

△1 *** Use Steel Pipe culvert for water pipe

(33) — Luminaire pole base, See dwg.#59114 and #R6 for details.

(34) — Bridge end pilaster, See dwg.#R8 for details.

(38/21) — 21 mm galvanized steel electrical conduit.

(38/27) — 27 mm galvanized steel electrical conduit.

(38/53) — 53 mm galvanized steel electrical conduit.

(38/78) — 78 mm galvanized steel electrical conduit.

(50) — Concrete Bridge Rail, See dwg.#58877 for details.

(54) — Concrete planter, see dwg.#59114 for details.

(55) — Sidewalk (See dwg.#58877 and R2 to R6).

(56) — Protective fencing (See dwg.#58892).

(60) — Expansion Joint at bents 1 and 2, see dwg.#58886 for details.

(62) — Scoring joints in parapet and planters wall where shown, equal spaces, 4600 mm max. centers., see dwg.#BR200.

(63) — Exp. joint in parapet, see dwg.#BR200.

(70) — Access holes at each end of each steel box, see dwg.#58879 and #58882.

(80) — 6200 mm Reinforced Concrete Bridge End Panel at end bents 1 and 2, see dwg. #BR165

△1 (11) — Dayton/Richmond (Ferrule Type) F-57 or approved equal structural concrete inserts (Hot-dip Galv.) 22.20mm dia., series @ 1500mm

△2 (12) Utility holes See dwg.# 58877

NOTE: All dimensions are in millimeters (mm) except as noted.

METRIC

△	DATE	REVISION	BY
1	9/28/00	Added detail reference item + Note	DHM
2	10-18-00	Added Conduit and show Utilities	EdL

DRAFTED: E. Leon
CHECKED: Mark Lusby
REVIEWED: In-Tae Lee

DESIGNER
REGISTERED PROFESSIONAL ENGINEER 17990 OREGON JULY 25, 1995 HORMOZ SERAJI
EXPIRES: 6/30/2002

OREGON DEPARTMENT OF TRANSPORTATION
BRIDGE ENGINEERING SECTION

BRIDGE NO. 18674
DATE 23-AUG-2000
CALC. BOOK 4833

SYLVAN BRIDGE O'XING SUNSET HWY.

DECK PLAN

SHEET 7 OF 25
DRAWING NO. 58876

23-AUG-2000

[PGRID=C1] [VIEW=C1] NE7400Dz(e)10: \usr\BR\PROJECTS\08009\i18674a2.dgn

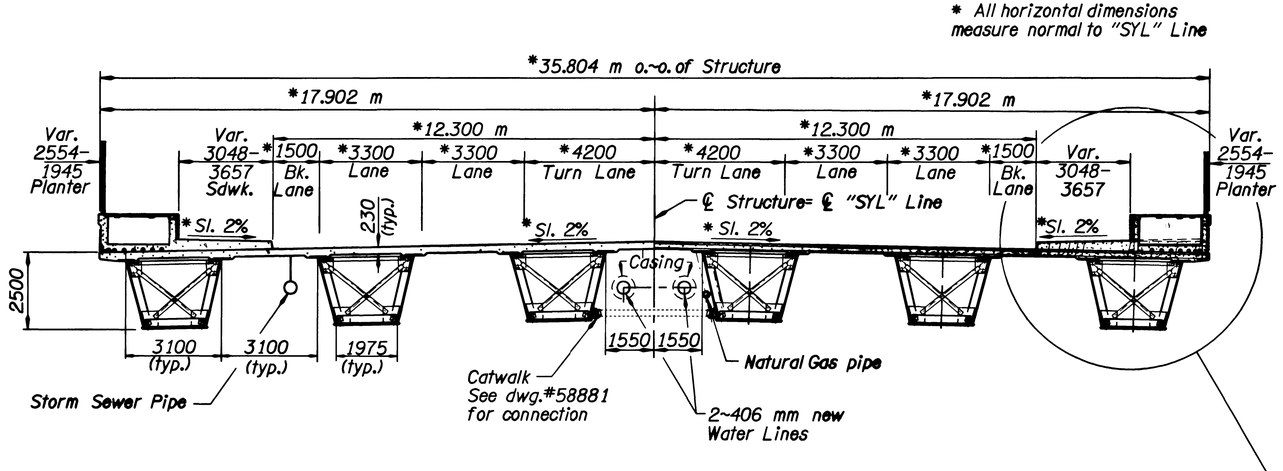

TYPICAL DECK SECTION

Scale 1:100

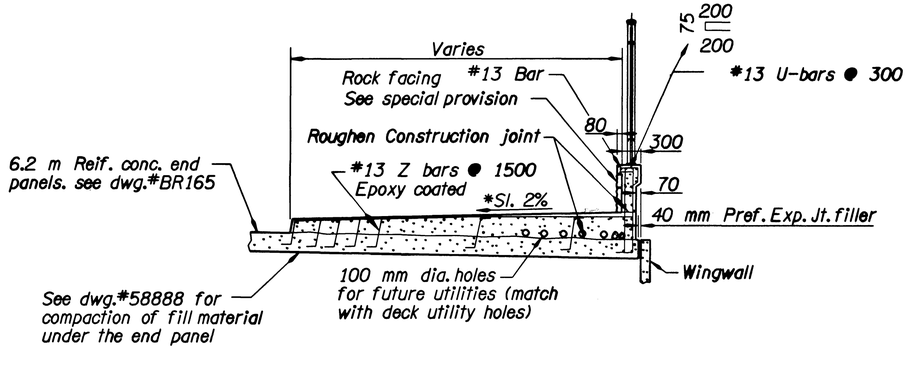

TYPICAL END PANEL and SIDEWALK SECTION

Scale 1:50

TRANSVERSE DECK STEEL

*#16 Straight bars @ 140 mm max. ctr. Top and bottom. Place normal to Box Girders. Top bars epoxy coated.

LONGITUDINAL DECK STEEL

*#13 longitudinal bars, top of deck at 250 mm ctrs. (epoxy coated).

*#16 Longitudinal bars bottom of deck @ 250 mm. See dwg.#58886 for end beam steel connection.

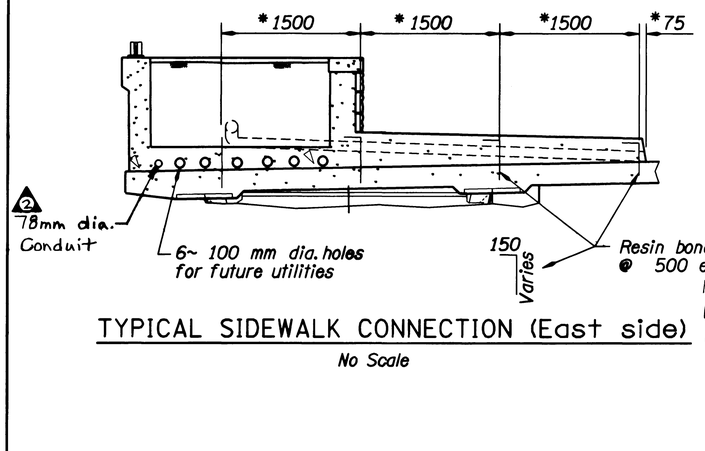

TYPICAL SIDEWALK CONNECTION (East side)

No Scale

Note: Expose top deck reinforcement at locations of resin bonded anchors before drilling holes.

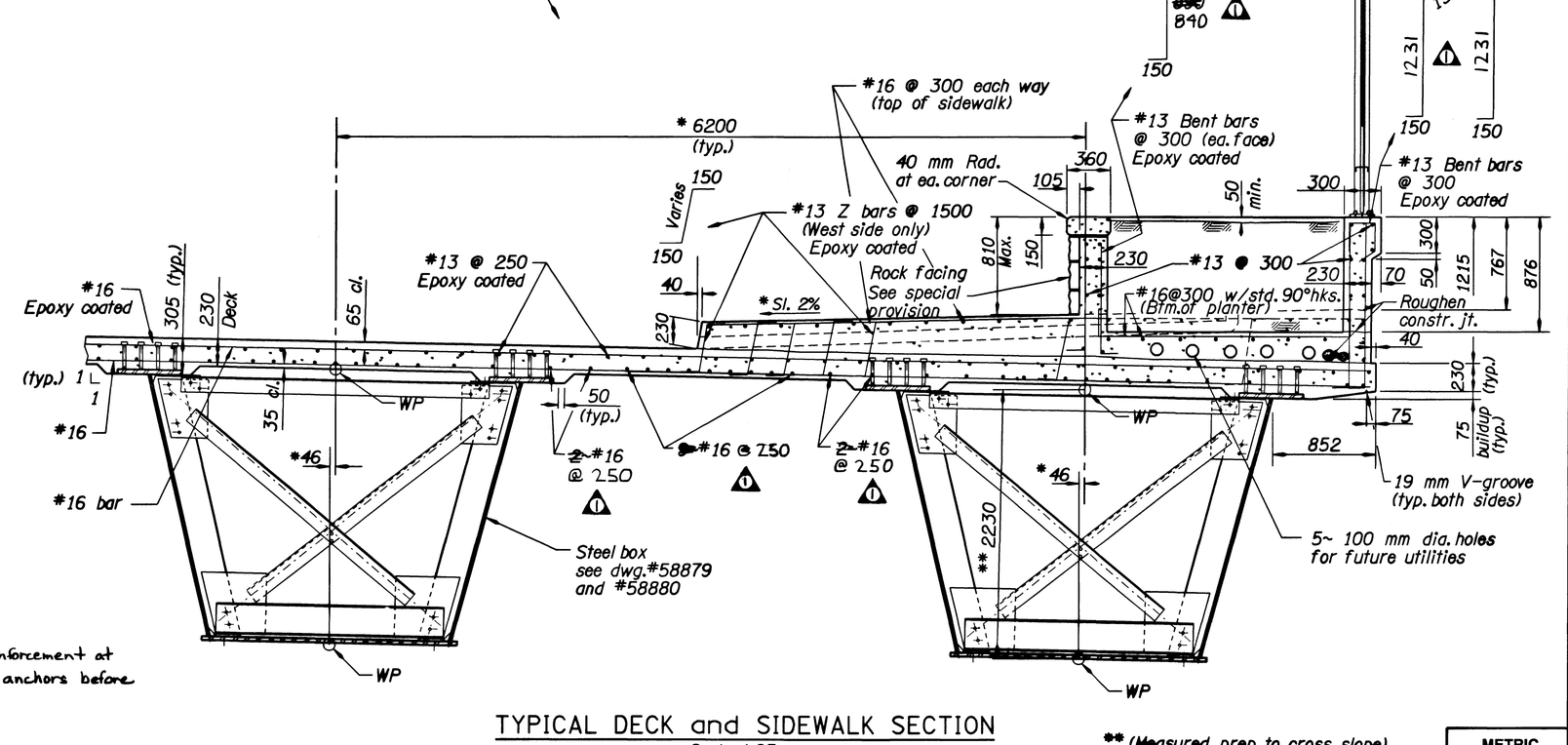

TYPICAL DECK and SIDEWALK SECTION

Scale 1:25

** (Measured prep. to cross slope)

NOTE: All dimensions are in millimeters (mm) except as noted.

	DATE	REVISION	BY
1	9-28-00	Changed as noted	HS
2	10-18-00	Added 78mm dia Conduit	HS

DRAFTED: E. Leon
CHECKED: Mark Lusby
REVIEWED: In-Tae Lee

DESIGNER
REGISTERED PROFESSIONAL ENGINEER 17910 OREGON JULY 25, 1995 HORMOZ SERADJ
EXPIRES: 6/30/2002

OREGON DEPARTMENT OF TRANSPORTATION
BRIDGE ENGINEERING SECTION

BRIDGE NO. 18674
DATE 17-AUG-2000
CALC. BOOK 4833

SYLVAN BRIDGE O'XING SUNSET HWY.

DECK SECTION

METRIC

SHEET 8 OF 25

DRAWING NO. 58877

17-AUG-2000 [VIEW=D1] [PGRID=D1] N7440b(ej):[C:\usr\BR\PROJECTS\08009\i18674a.dgn

STEEL FABRICATION NOTES

1. All dimensions shall be checked and verified befored fabrication.
2. All longitudinal dimensions are on a horizonal line - adjust for slope.
3. All stiffeners and beam ends are to be vertical in final erected postion.
4. Additional web and/or compression flange weld splices will be permited at locations approved by the engineer.
5. Web thickness shown may be increased up to 1.6 mm.
6. All structural steel shall be in accordance with ASTM A709, Grade HPS-485W, except that stiffeners are AASHTO M270M Grade 345W (ASTM A709M, Grade 345W), unless shown otherwise. ~~and~~ rolled shapes ⚠1
   Maximum ultimate design stresses are as follows:

	Grade 250	Grade 345	Grade HPS-485W
Tension	250 MPa	345 MPa	485 MPa
Shear	83 MPa	114 MPa	162 MPa
Bearing	200 MPa	276 MPa	388 MPa

7. Stop all stiffeners fillet welds 6 mm clear of caps.
8. Welding on Bridge Members shall comply with the "Bridge Welding Code", AWS D1.5, as modified in th specical provisions. The welding of incidental structures shall comply with the "Structual Welding Code-Steel", AWS D1.1.
9. All groove welds are CJP welds unless indicated otherwise.
10. ** Indicates check sample required from flange plates so marked. See Std. Spec.

Erection Note:

The contractor detailed erection scheme shall be submitted to the engineer in accordance with the Special Provisions.

Contractor may connect three segments of each box girder together in the shop, if the contractor could obtain required permits to haul the full lenght of the box beam to the location of Sylvan Bridge, haul and errect each box beam in one segment, in such a case one cross frame might be eliminated.

STEEL GENERAL NOTES:

All members subject to tension, as designed on the plans, shall be receive ~~C~~h Carpy V-Notch impact testing in accordance with ASTM A709M and Supplemental Requirements S83 or S84 as noted below:

a. Redundant members, as designated on the plans, shall be tested in accordance with Table S1.2 (Zone 2) of ASTM A709M(S83).

⚠1 ~~b. Non redundant members, as designated on the plans, shall be tested in accordance with Table S1.2 (Zone 2) of ASTM A709M(S84). Field splice plates are designated Fracture Critical and non redundant~~

⚠1 All structural steel for box girders and box girder framing, cross bracing, etc., shall ~~C~~c be fabricated by a certified shop meeting the requirements of AISC Category ~~M~~Br certification. ~~with AISC Fracture Critical endorsement~~. Shop drawings are required for all structural steel.

Welding shall be in accordance with the "ANSI/AASHTO/AWS D1.5-96 Bridge Welding Code". Welds requiring non-destructive testing shall be radiographically inspected, except where the geometry of the weld will not permit satisfactory information to be secured for verification of the weld quality. When such geometrical conditions exist, other inspection procedures or combinations of procedures such as ultrasonic inspection, dye penetration inspection, and/or magna flux inspection may be required.

⚠1 ~~All members designated as Fracture Critical shall be fabricated in accordance with Chapter 12 of the ANSI/AASHTO/AWS Bridge Welding Code D1.5-96.~~

All bolted connections shall be made with 22 diameter high strength friction type bolts in accordance with AASHTO Specification M164M, ASTM Specification A325M unless shown otherwise. All bolted connections are considered slip critical. Where possible, only the heads of bolts shall be exposed to view. Bolt spacing shall be 75 mm and bolt edge distance shall be 38 mm minimum unless noted otherwise. Connection surfaces shall be blast cleaned at time of assembly.

Bolts shall be Type 3 conforming to AASHTO M164M (ASTM A325M).
Nuts shall be AASHTO M291M (ASTM A563M).
Washers shall be AASHTO M293M, ASTM F436M use type 3 washers.

Provide structural steel according to (AASHTO) or (ASTM) Specifications in according with plan details
Provide high-strength fasteners including washers.
Tighten high-strength fasteners using the Turn-of-Nut Tightening methods.
See the special Provisions for detailed coating and tightening requirements.

Shear connectors shall conform to Section 7.3, Type B of the ANSI/AASHTO/AWS Bridge Welding Code D1.5-96.

⚠1 ~~Coat exterior of boxes, as shown, and exterior of end diaphragm, in accordance with the Specifications. The finish coat on the exterior of the box girders shall conform to Federal Color Standard most closely matching steel rusted shade. Submit rusted shade color to engineer for approval. Coat~~ inside surfaces of boxes (bottom flange, webs, end diaphragm) with ~~white~~ Silvery grey prime coat.

⚠1 ~~All high strength fasteners shall be installed with mechanically galvanized direct tension indicator washer meeting the requirements of ASTM F959 and the special provisions.~~

NOTE: All dimensions are in millimeters (mm) except as noted.

METRIC

	DATE	REVISION	BY
⚠1	9-28-00	Changed as Noted	HS

DRAFTED: E. Leon
CHECKED: Mark Lusby
REVIEWED: In-Tae Lee

DESIGNER
REGISTERED PROFESSIONAL ENGINEER 17910 OREGON JULY 25, 1995 HORMOZ SERADJ
EXPIRES: 6/30/2002

OREGON DEPARTMENT OF TRANSPORTATION
BRIDGE ENGINEERING SECTION

BRIDGE NO. 18674
DATE 17-AUG-2000
CALC. BOOK 4833

SYLVAN BRIDGE O'XING SUNSET HWY.

STEEL BOX FLANGE and GENERAL NOTES

SHEET 9 OF 25
DRAWING NO. 58878

17-AUG-2000
[VIEW=C2] [PGRID=C2]
NE7400bz(e)[0]: \usr\BR\PROJECTS\08009\i18674a2.dgn

~~2000 Exterior Paint Limits~~

~~Denotes tension members which are designated non-redundant for the Charpy V-Notch Impact Test requirement. Web plates connecting to non-redundant flanges shall be considered non-redundant.~~ (Denotes Fracture Critical Members).

38 x 530 — Top Flange Size

719 | 35 @ 300 = 10 500 | 20 @ 450 = 9000 | 600 mm max. | 20 @ 450 = 9000 | 35 @ 300 = 10 500 | 719 — Shear Connector Spacing

Transverse Stiffeners (typ.)

16 Web | 16 Web | 16 Web

2 additional Shear Connectors @ 240± mm (typ.)

22.23 x 2115 | 31.75 x 2115 | 22.23 x 2115 — Bottom Flange Size

719 | 15 233 | 32 000 | 15 233 | 719 — Field Splice Spacing

2 @ 2100 = 4200 | 4 Spcs. @ 2890 = 11 560 | 5 Spaces @ 5780 mm = 28 900 mm | 4 Spcs. @ 2890 = 11 560 | 2 @ 2100 = 4200 — Transverse Stiffeners Spacing

2 @ 2100 = 4200 | 18 @ 2890 = 52 020 | 2 @ 2100 = 4200 — Lateral Bracing Spacing

2046 | 7092 | 5780 | 2890 | 5 Spaces @ 5780 mm = 28 900 mm | 2890 | 5780 | 7092 | 1023 — Cross Frame Spacing

℄ Brg. 1 — ℄ Brg. 2

℄ Web 1 — ℄ Web 2 — ℄ Web 3 — ℄ Web 4 — ℄ Web 5 — ℄ Web 6 — ℄ Web 7 — ℄ Web 8

℄ Steel Box

610 mm dia. Access Holes (Bottom, typ.)

Additional Transverse Stiffener (typ. as shown).

600* typ. | 3000 typ. | 600* typ. | 1023 | 1023

*Add 25.4 mm for 25.4 mm x 400 mm steel plate, see dwg. no. 58887 for details.

6200

Bearing Diaphragm and Stiffeners, see dwg. no. 58887 (typ.).

Additional crossframes for catwalk 10 locations (See Dwg.* 58880)

Temporary Exterior Cross Frame Bracing (typ.).

Beam Seat for Pipe Bridge (Catwalk) typ.

3100 | 3100 | 6200 = 12 400 — 2 Spaces @

4572 | 7277.1 | 7962.9 | 7620 | 7620 | 7620 | 7948.4 | 7291.6 | 4558

"SYL" Line N. 36°52'12" E.

56°34'47"

"SYL" Line
R= 155.230 m
Δ = 54°12'27"
L = 146.863 m

151

120°53'17" tan. – tan.

Temporary Exterior Cross Frame Bracing (typ. between steel boxes except as shown).

62.370 m ctr. to ctr. Bents (measured along "SYL" Line)

Bent 1 "SYL" 1+490.440 m | "SYL" 1+497.291 PT | Bent 2 "SYL" 1+552.810 m

Note: Webs 9 thru 12 not shown, similar as indicated.

PARTIAL PLAN: BOX FRAMING

Scale: 1 : 100

NOTE: All dimensions are in millimeters (mm) except as noted.

METRIC

	DATE	REVISION	BY
1	9-28-00	Corrections Made	H S

DRAFTED: Tom Hernandez
CHECKED: Mark Lusby
REVIEWED: In-Tae Lee

DESIGNER
REGISTERED PROFESSIONAL ENGINEER 17910 OREGON JULY 25, 1995 HORMOZ SERADJ
EXPIRES: 6/30/2002

OREGON DEPARTMENT OF TRANSPORTATION
BRIDGE ENGINEERING SECTION

BRIDGE NO. 18674
DATE 17-AUG-2000
CALC. BOOK 4833

SYLVAN BRIDGE O'XING SUNSET HWY.

FRAMING DETAILS

SHEET 10 OF 25
DRAWING NO. 58879

17-AUG-2000 [VIEW=D1] [PGRID=D1]

c:\usr\br\projects\08009\b18674a3.dgn

NT7430c(TH):

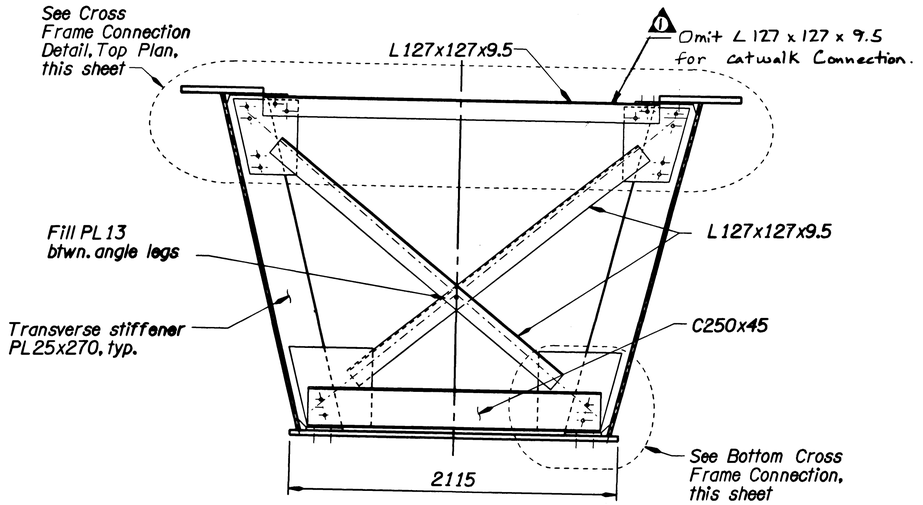

CROSS FRAME DETAIL

Scale 1:20

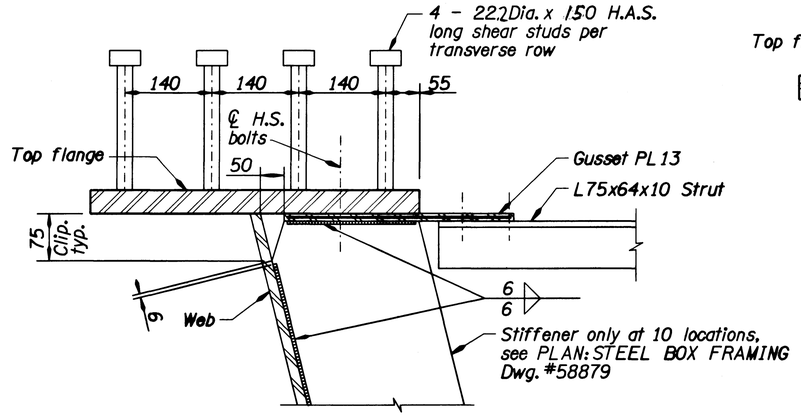

ELEVATION

TOP STRUT CONNECTION DETAIL

Scale 1:5

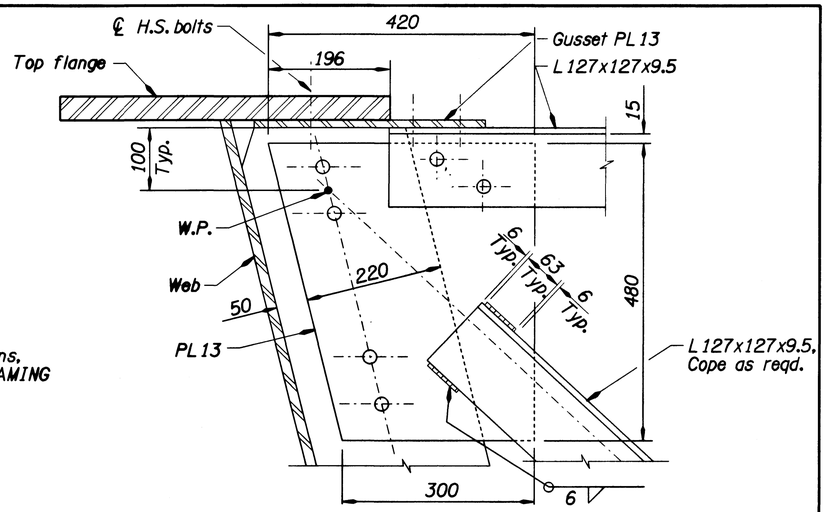

ELEVATION

TOP CROSS FRAME CONNECTION DETAIL

Scale 1:5

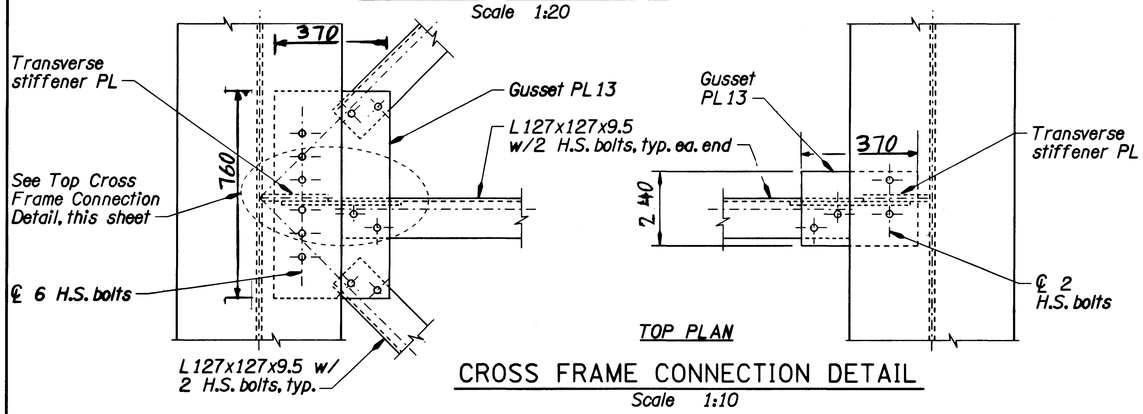

TOP PLAN

CROSS FRAME CONNECTION DETAIL

Scale 1:10

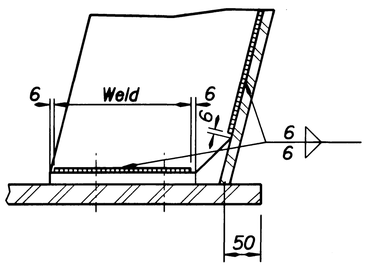

TOP STRUT CONNECTION DETAIL

Scale 1:5

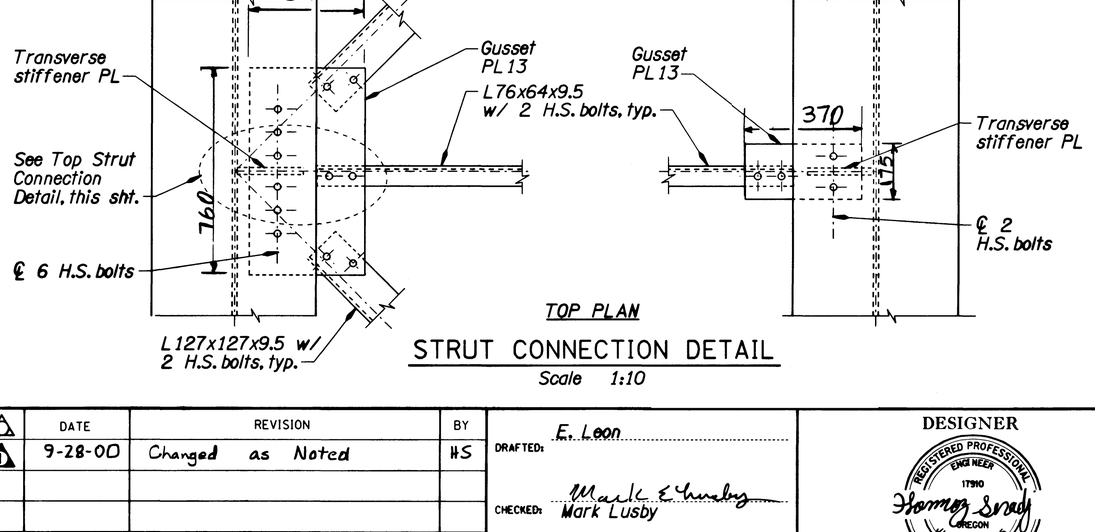

TOP PLAN

STRUT CONNECTION DETAIL

Scale 1:10

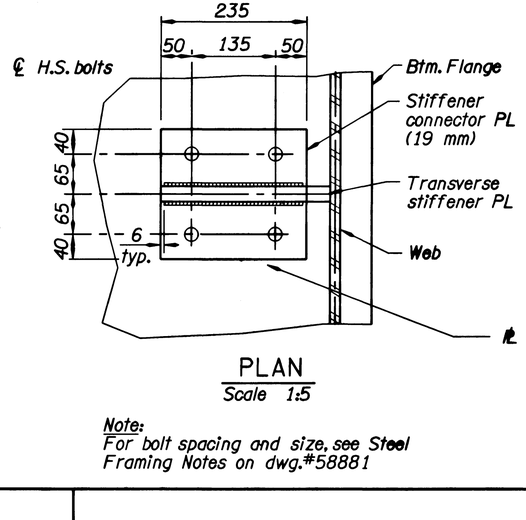

PLAN

Scale 1:5

Note:
For bolt spacing and size, see Steel Framing Notes on dwg.#58881

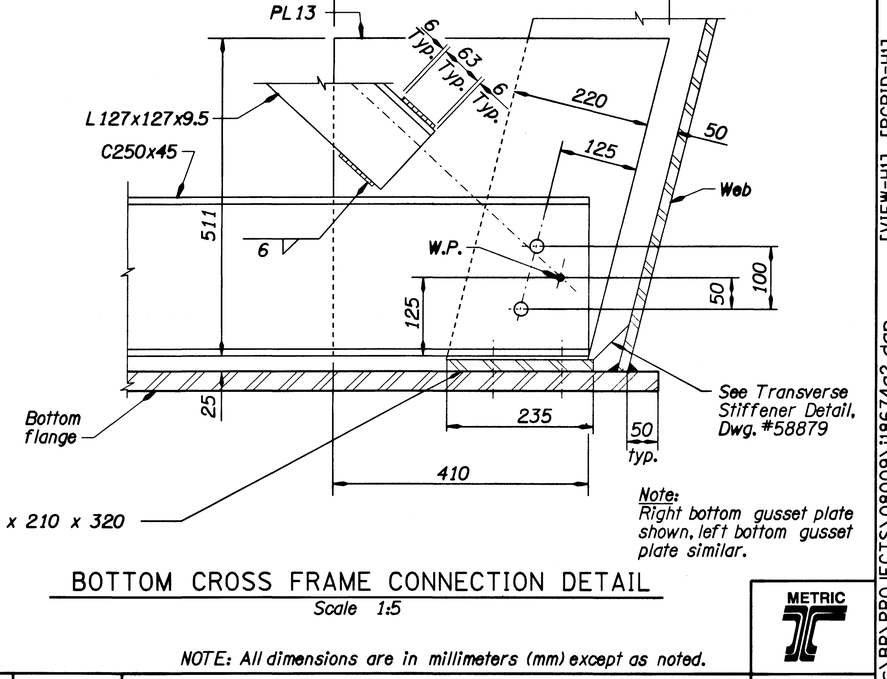

Note:
Right bottom gusset plate shown, left bottom gusset plate similar.

BOTTOM CROSS FRAME CONNECTION DETAIL

Scale 1:5

NOTE: All dimensions are in millimeters (mm) except as noted.

METRIC

	DATE	REVISION	BY
1	9-28-00	Changed as Noted	HS

DRAFTED: E. Leon
CHECKED: Mark Lusby
REVIEWED: In-Tae Lee

DESIGNER
REGISTERED PROFESSIONAL ENGINEER 17910 OREGON JULY 25, 1995 HORMOZ SERADJ
EXPIRES: 6/30/2002

OREGON DEPARTMENT OF TRANSPORTATION
BRIDGE ENGINEERING SECTION

BRIDGE NO. 18674
DATE 17-AUG-2000
CALC. BOOK 4833

SYLVAN BRIDGE O'XING SUNSET HWY.

STEEL CONNECTIONS DETAILS

SHEET 11 OF 25
DRAWING NO. 58880

17-AUG-2000

[VIEW=H1] [PGRID=H1]
NE7400dz(ejl) C:\usr\BR\PROJECTS\08009\i18674a2.dgn

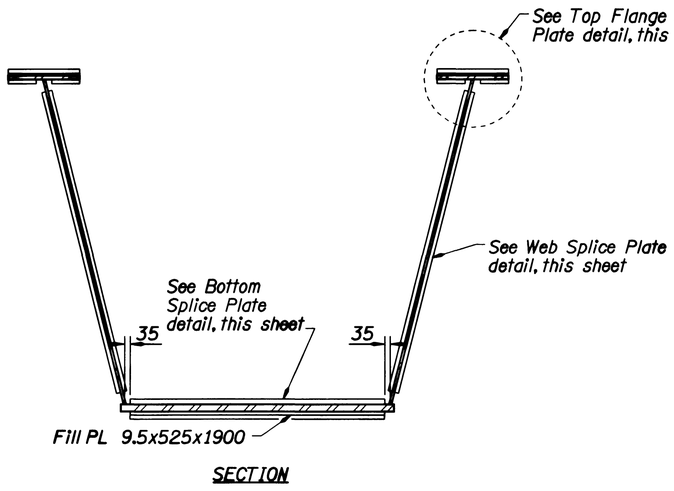

SECTION

CROSS FRAME DETAIL

Scale 1: 20

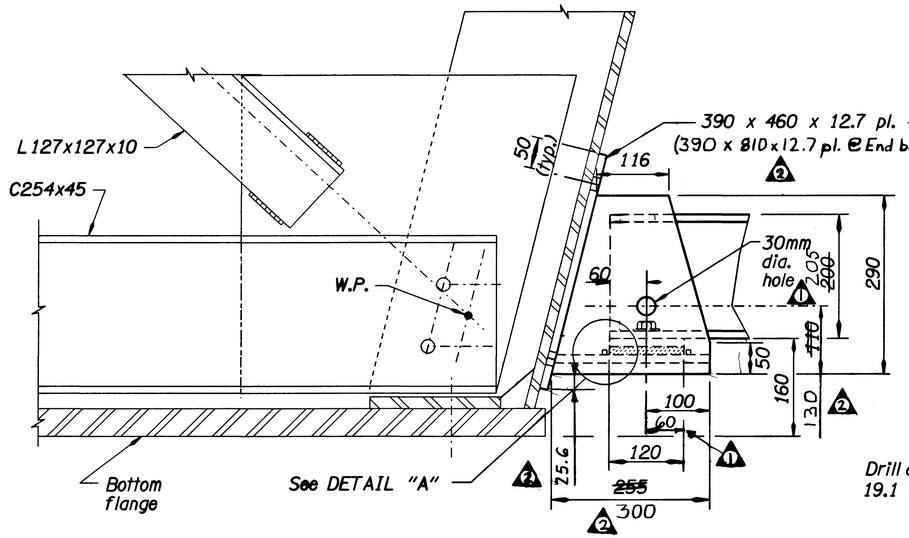

CATWALK CONNECTION DETAIL

2 No Scale ~~1:5~~

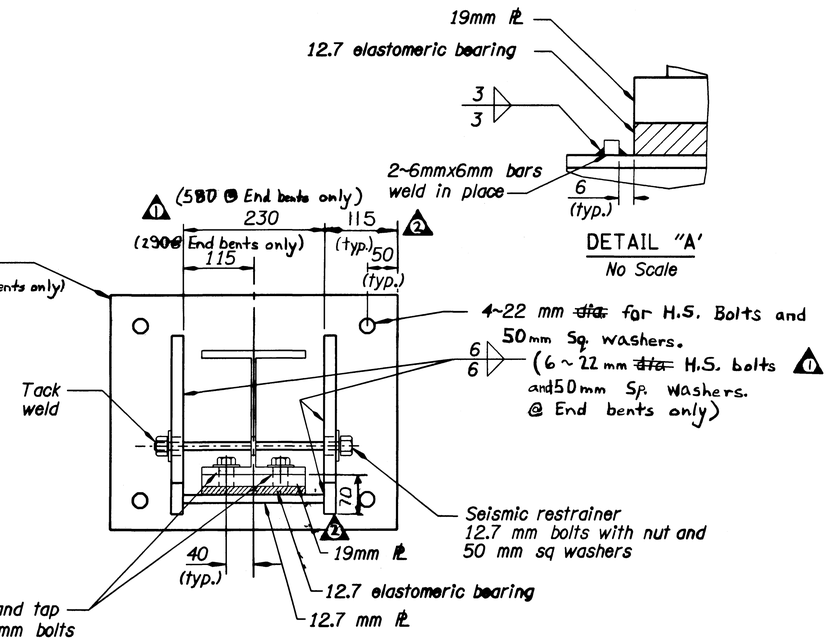

DETAIL "A"

No Scale

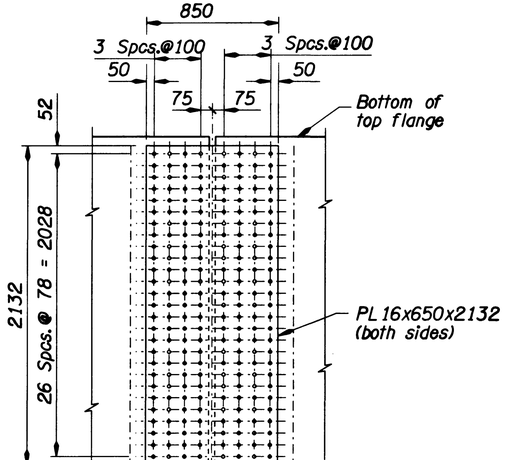

WEB SPLICE PLATE

No Scale

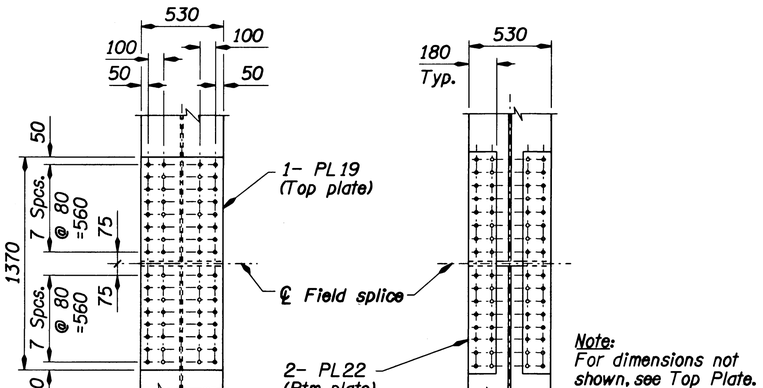

TOP FLANGE SPLICE PLATE

No Scale

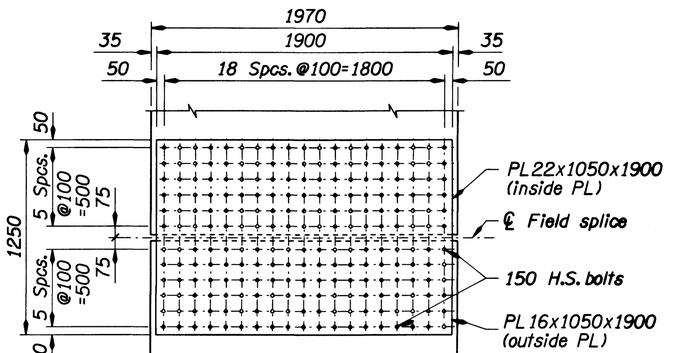

BOTTOM FLANGE SPLICE PLATE

No Scale

NOTE: All dimensions are in millimeters (mm) except as noted.

METRIC

	DATE	REVISION	BY
1	9-28-00	Changed as Noted	HS
2	10-18-00	Add dimensions	HS

DRAFTED: E. Leon

CHECKED: Mark Lusby

REVIEWED: In-Tae Lee

DESIGNER

REGISTERED PROFESSIONAL ENGINEER 17910 OREGON JULY 25, 1995 HORMOZ SERADJ

EXPIRES: 6/30/2002

OREGON DEPARTMENT OF TRANSPORTATION
BRIDGE ENGINEERING SECTION

BRIDGE NO. 18674

DATE 17-AUG-2000

CALC. BOOK 4833

SYLVAN BRIDGE O'XING SUNSET HWY.

CONNECTION DETAILS

SHEET 12 OF 25

DRAWING NO. 58881

17-AUG-2000

[VIEW=H2] [PGRID=H2]

NE7400bz1e]0:\usr\BR\PROJECTS\08009\118674d2.dgn

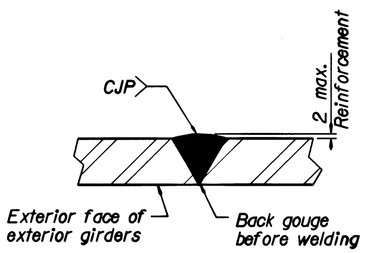

EQUAL THICKNESS WEBS

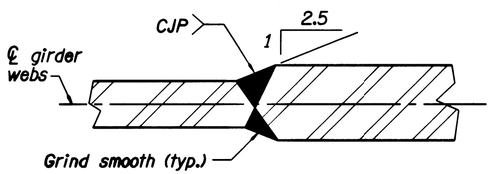

UNEQUAL THICKNESS WEBS

SHOP WEB SPLICES
No Scale

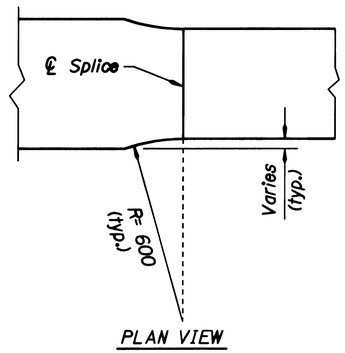

PLAN VIEW

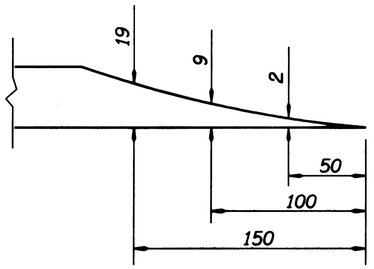

DETAIL OF CUT

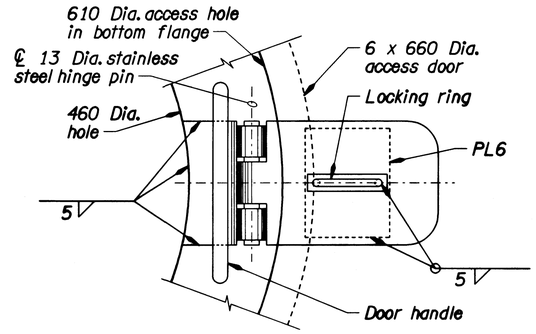

SECTION B-B

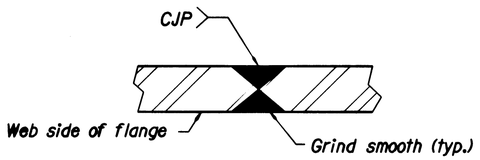

FLANGE SPLICE OF EQUAL THICKNESS

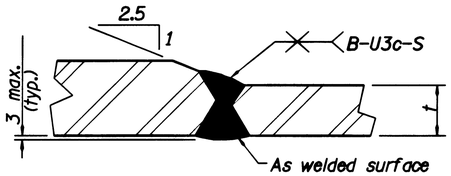

COMMPRESSION FLANGE SPLICE

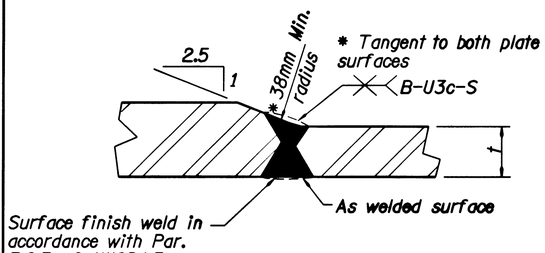

TENSION FLANGE SPLICE

SHOP FLANGE SPLICES
No Scale

FLANGE TRANSITION DETAIL
No Scale

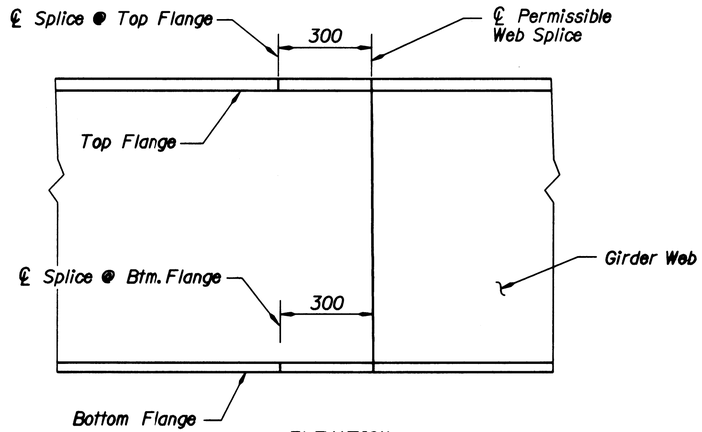

ELEVATION

SHOP WEB SPLICE
No Scale

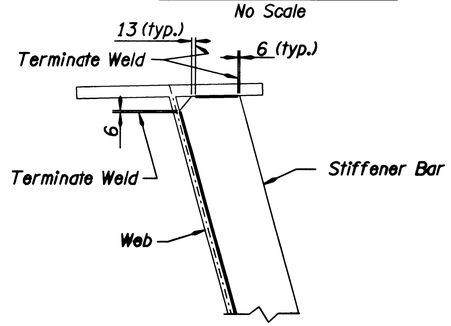

WELD TERMINATION DETAIL
No Scale

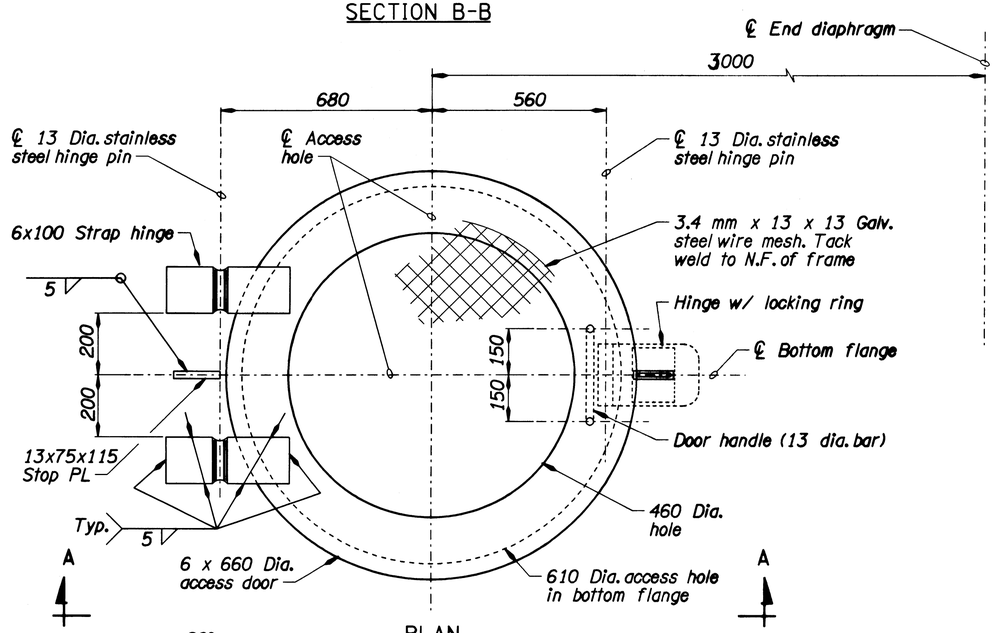

PLAN

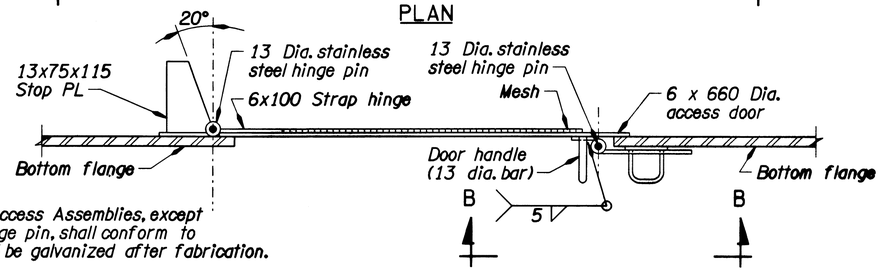

SECTION A-A

Notes:

1. *All structural steel material in Access Assemblies, except 13 diameter stainless steel hinge pin, shall conform to ASTM A36M, Gr. 250 and shall be galvanized after fabrication.*
2. *All exposed edges of plates and opening shall be ground smooth.*
3. *Stainless steel hinge pin shall conform to ASTM A276M or equivalent.*

ACCESS OPENING DETAILS
Scale : 1:5

NOTE: All dimensions are in millimeters (mm) except as noted.

△	DATE	REVISION	BY

DRAFTED: E. Leon Lynn J. Boge
CHECKED: Mark Lusby
REVIEWED: In-Tae Lee

DESIGNER
REGISTERED PROFESSIONAL ENGINEER 17910 OREGON JULY 25, 1995 HORMOZ SERADJ
EXPIRES: 6/30/2002

OREGON DEPARTMENT OF TRANSPORTATION
BRIDGE ENGINEERING SECTION

BRIDGE NO. 18674
DATE 31-JUL-2000
CALC. BOOK 4833

SYLVAN BRIDGE O'XING SUNSET HWY.

ACCESS HOLE AND GIRDER DETAILS

SHEET 13 OF 25
DRAWING NO. 58882

METRIC

31-JUL-2000
[PGRID=J11 [VIEW=J11 NE7400bz(ej0: \usr\BR\projects\Kn08009\n18674.dgn

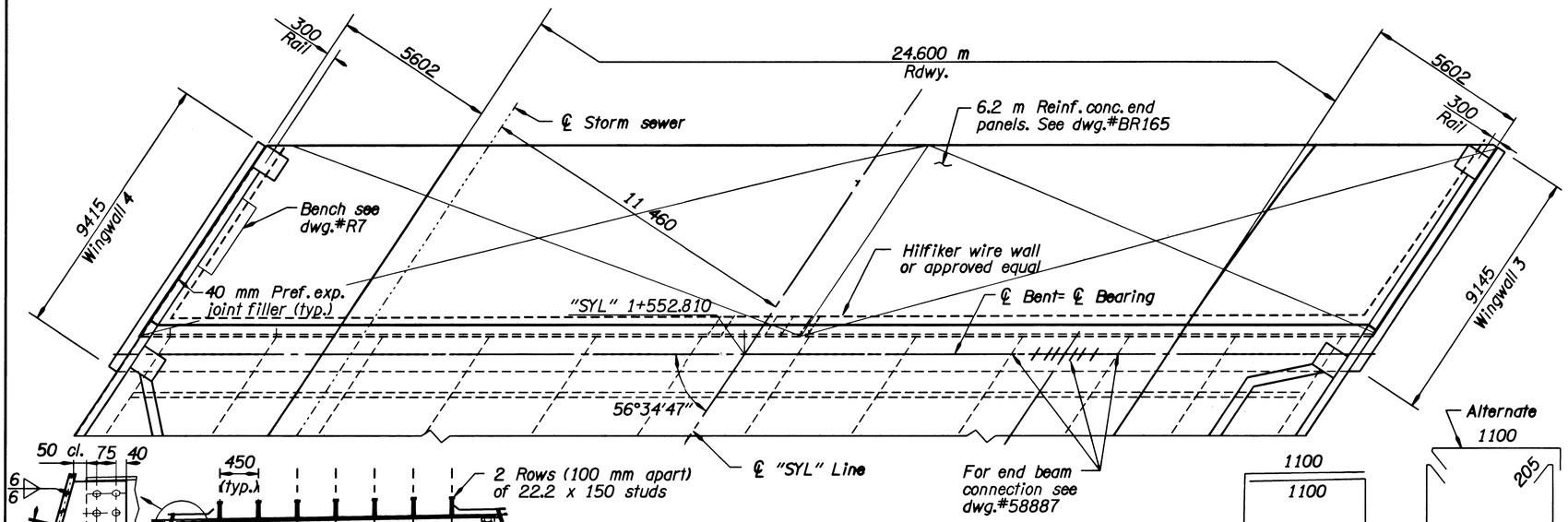

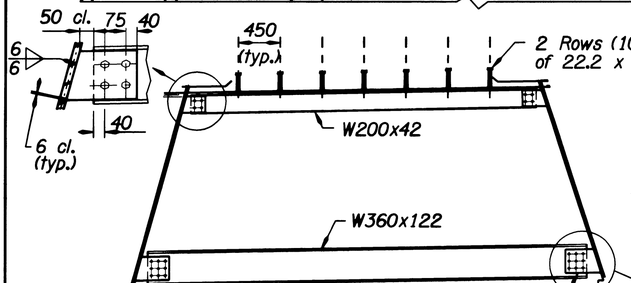

Note: Place diaphragm between each box girder at each end bent. (ten places)

ELEVATION: Diaphragm

No Scale

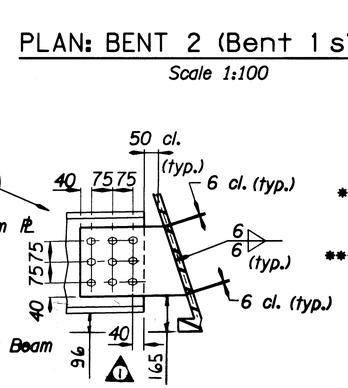

PLAN: BENT 2 (Bent 1 similar)

Scale 1:100

NOTE:

*Measured normal to "SYL" Line

**For gravel bed aggregate see Special Provisions 01090.12

***4~#13 x 800 mm bolster bars, equally spaced

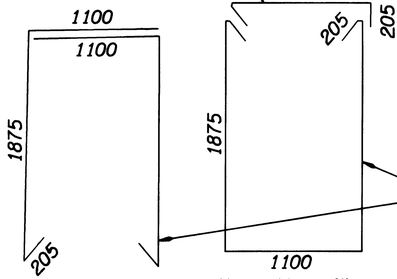

150 Slope paving w/light broom finish see dwg.#58874 and #BR115

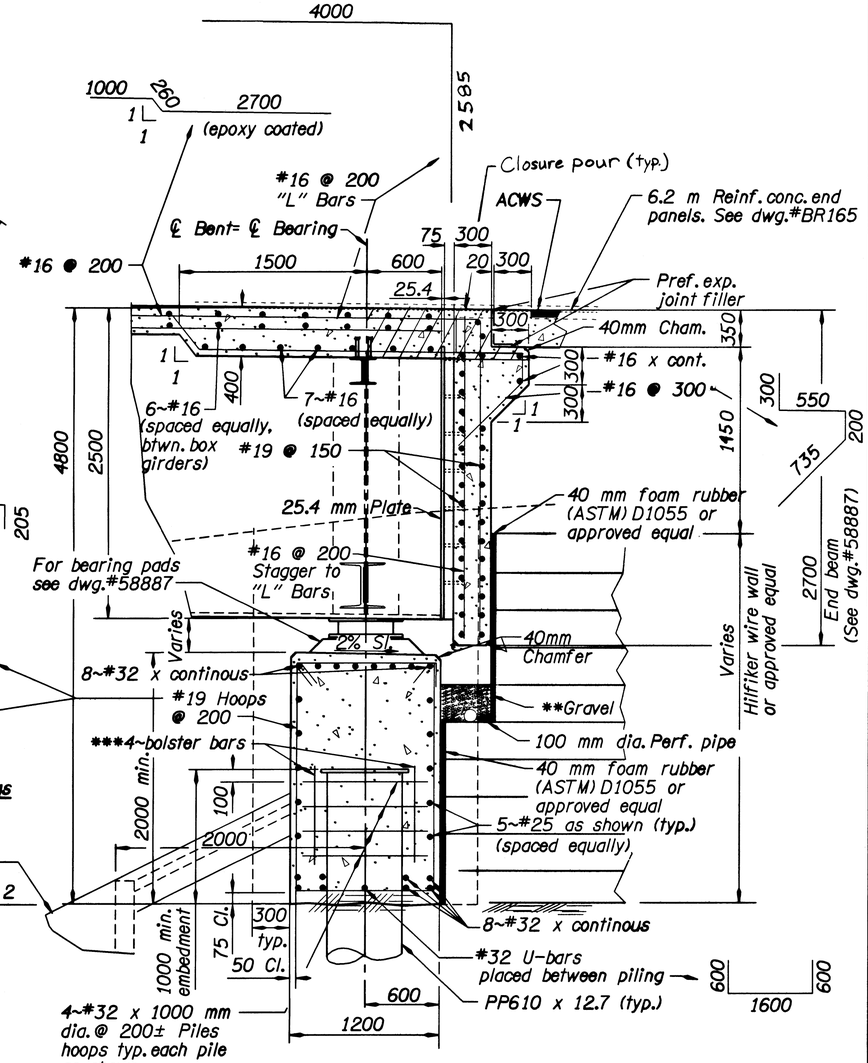

BENT 2 SECTION AA (Bt. 1 sim.)

Scale 1:25

ELEVATION: BENT 2 (Bent 1 similar)

Scale 1:100

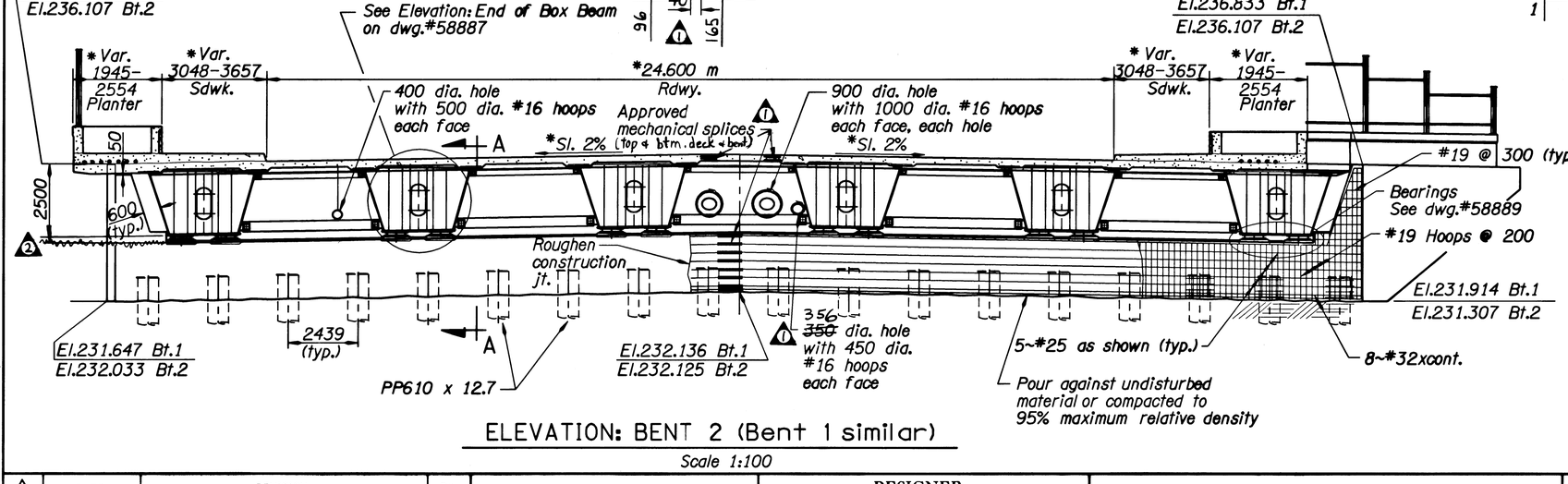

NOTE: All dimensions are in millimeters (mm) except as noted.

METRIC

	DATE	REVISION	BY
2	10-18-00	Fixed dimension	EJL
1	9-28-00	Added Changed dimensions	EJL

DRAFTED: E. Leon

CHECKED: Mark Lusby

REVIEWED: In-Tae Lee

DESIGNER

REGISTERED PROFESSIONAL ENGINEER 17910 OREGON JULY 25, 1995 HORMOZ SERADJ

EXPIRES: 6/30/2002

OREGON DEPARTMENT OF TRANSPORTATION
BRIDGE ENGINEERING SECTION

BRIDGE NO. 18674

DATE 17-AUG-2000

CALC. BOOK 4833

SYLVAN BRIDGE O'XING SUNSET HWY.

BENT 2 (Bent 1 Similar)

SHEET 17 OF 25

DRAWING NO. 58886

17-AUG-2000

[VIEW=D1] [PGRID=D1]

NET400bzejl: \usr\BR\PROJECTS\08009\118674a2.dgn

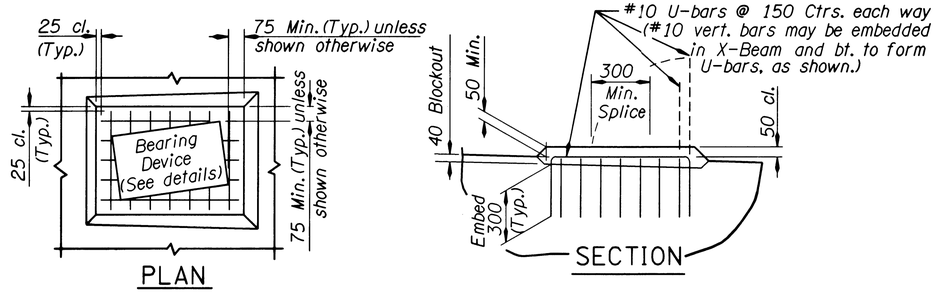

TYP. CONC. PAD
No Scale

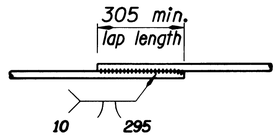

WELDED SPLICE
See Note A

Note - A:

Use ASTM A706M reinforcing steel.

Weld reinforcing steel splices according to ANSI/AWS D 1.4-79 "Structural Welding Code Reinforcing Steel"

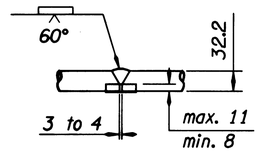

ALTERNATE WELD SPLICE
No Scale

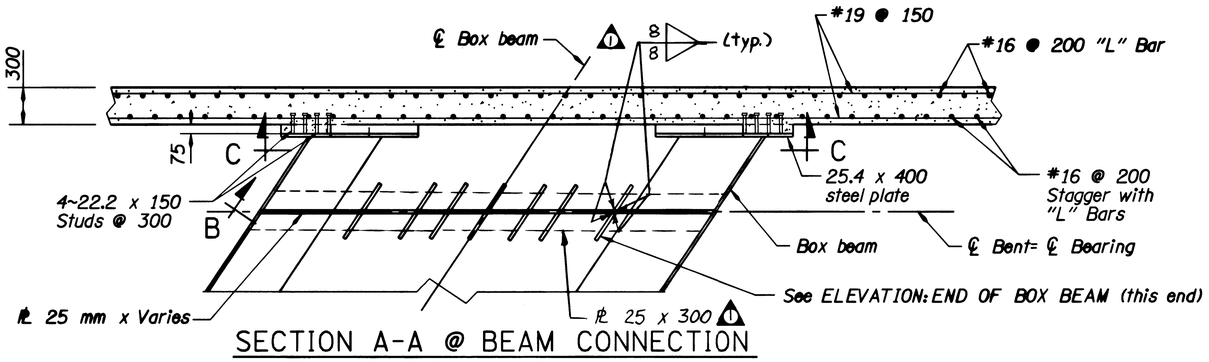

SECTION A-A @ BEAM CONNECTION
Scale 1:25

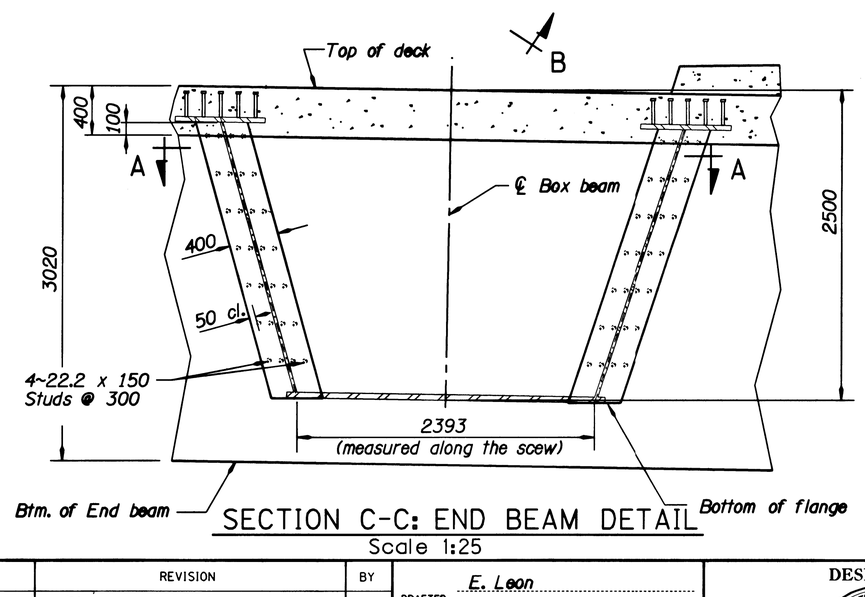

SECTION C-C: END BEAM DETAIL
Scale 1:25

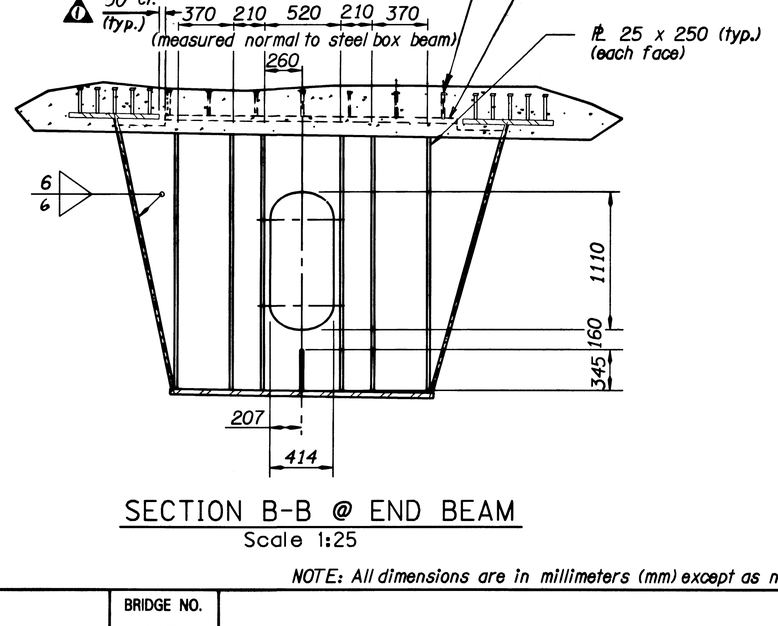

SECTION B-B @ END BEAM
Scale 1:25

NOTE: All dimensions are in millimeters (mm) except as noted.

METRIC

	DATE	REVISION	BY
1	9-28-00	Changed as Noted	H.S.

DRAFTED: E. Leon
CHECKED: Mark Lusby
REVIEWED: In-Tae Lee

DESIGNER
REGISTERED PROFESSIONAL ENGINEER 17910 OREGON JULY 25, 1995 HORMOZ SERADJ
EXPIRES: 6/30/2001

OREGON DEPARTMENT OF TRANSPORTATION
BRIDGE ENGINEERING SECTION

BRIDGE NO. 18674
DATE 17-AUG-2000
CALC. BOOK 4833

SYLVAN BRIDGE O'XING SUNSET HWY.

BENT 2 (Bent 1 Similar)

SHEET 18 OF 25
DRAWING NO. 58887

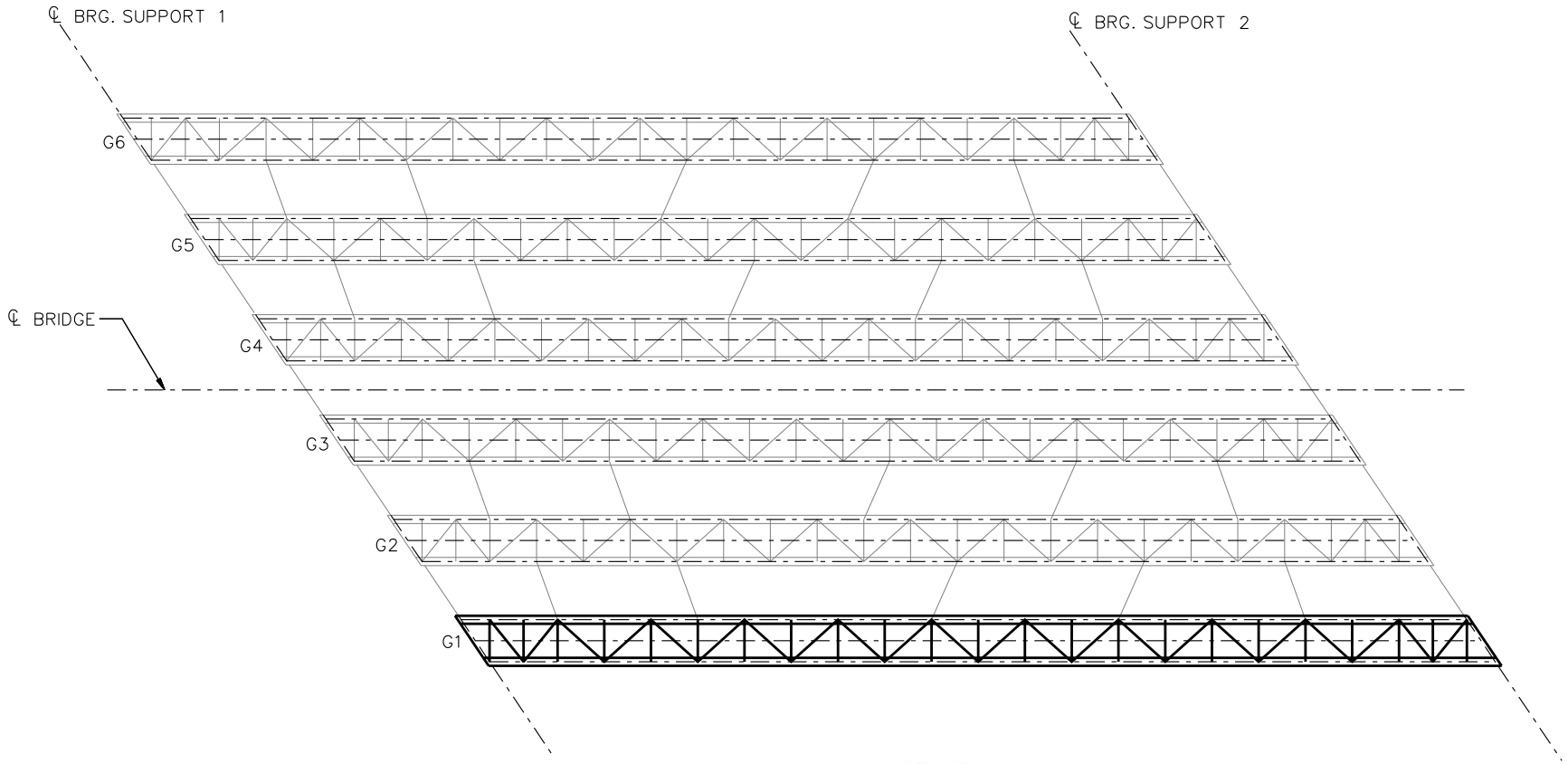

STAGE 1

LEGEND

▽ = HOLD OR LIFT CRANE

○ = TIE DOWN

□ = TEMPORARY SUPPORT STRUCTURE

NCHRP 12-79

BRIDGE ETSSS2

GIRDER ERECTION PROCEDURE

SHEET 1 OF 6

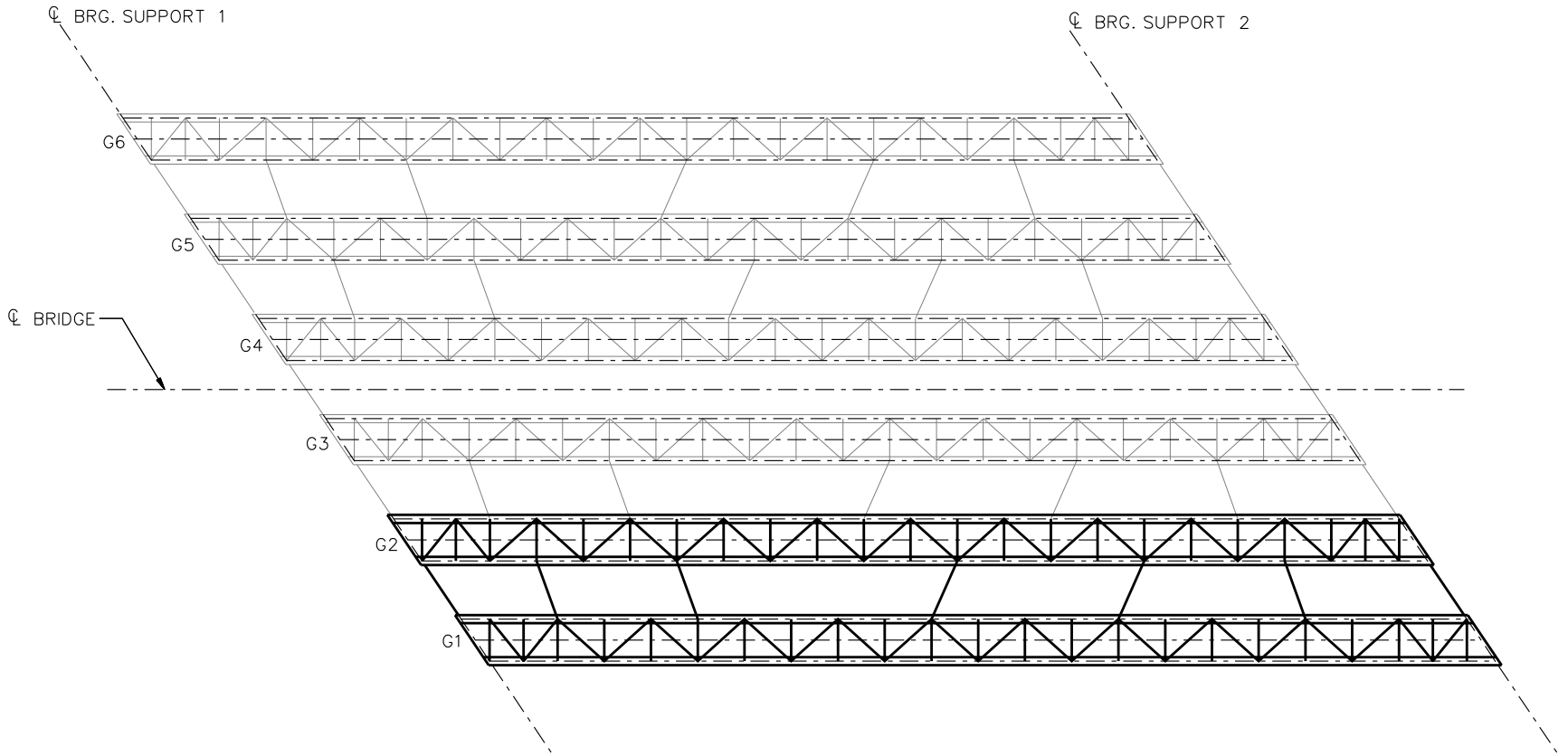

STAGE 2

LEGEND

▽ = HOLD OR LIFT CRANE

○ = TIE DOWN

□ = TEMPORARY SUPPORT STRUCTURE

NCHRP 12-79

BRIDGE ETSSS2

GENERAL ERECTION PROCEDURE

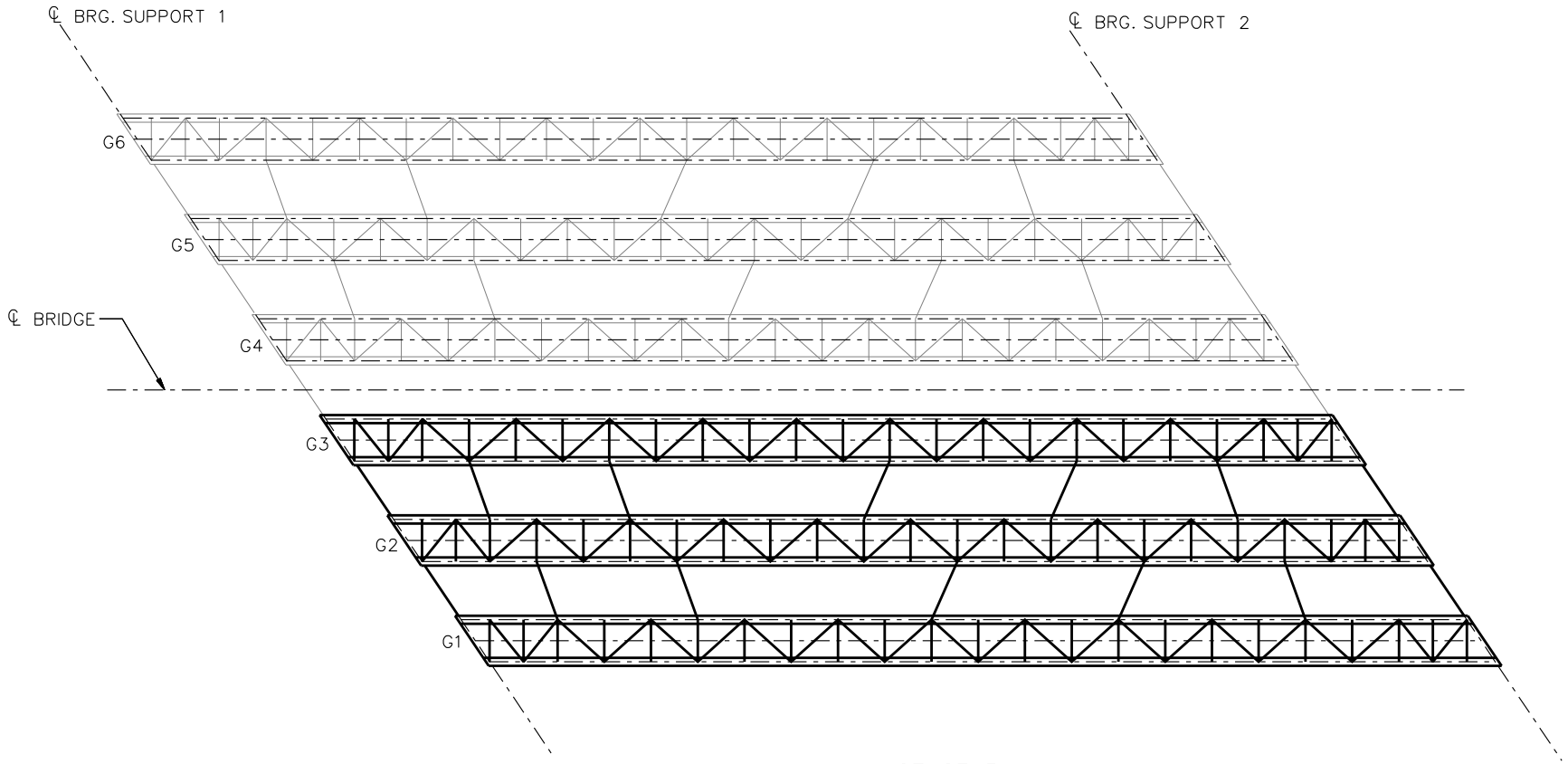

STAGE 3

STAGE 4

CONCRETE DECK PLACED ON G1 THRU G3

LEGEND

▽ = HOLD OR LIFT CRANE

○ = TIE DOWN

□ = TEMPORARY SUPPORT STRUCTURE

NCHRP 12-79

BRIDGE ETSSS2

GENERAL ERECTION PROCEDURE

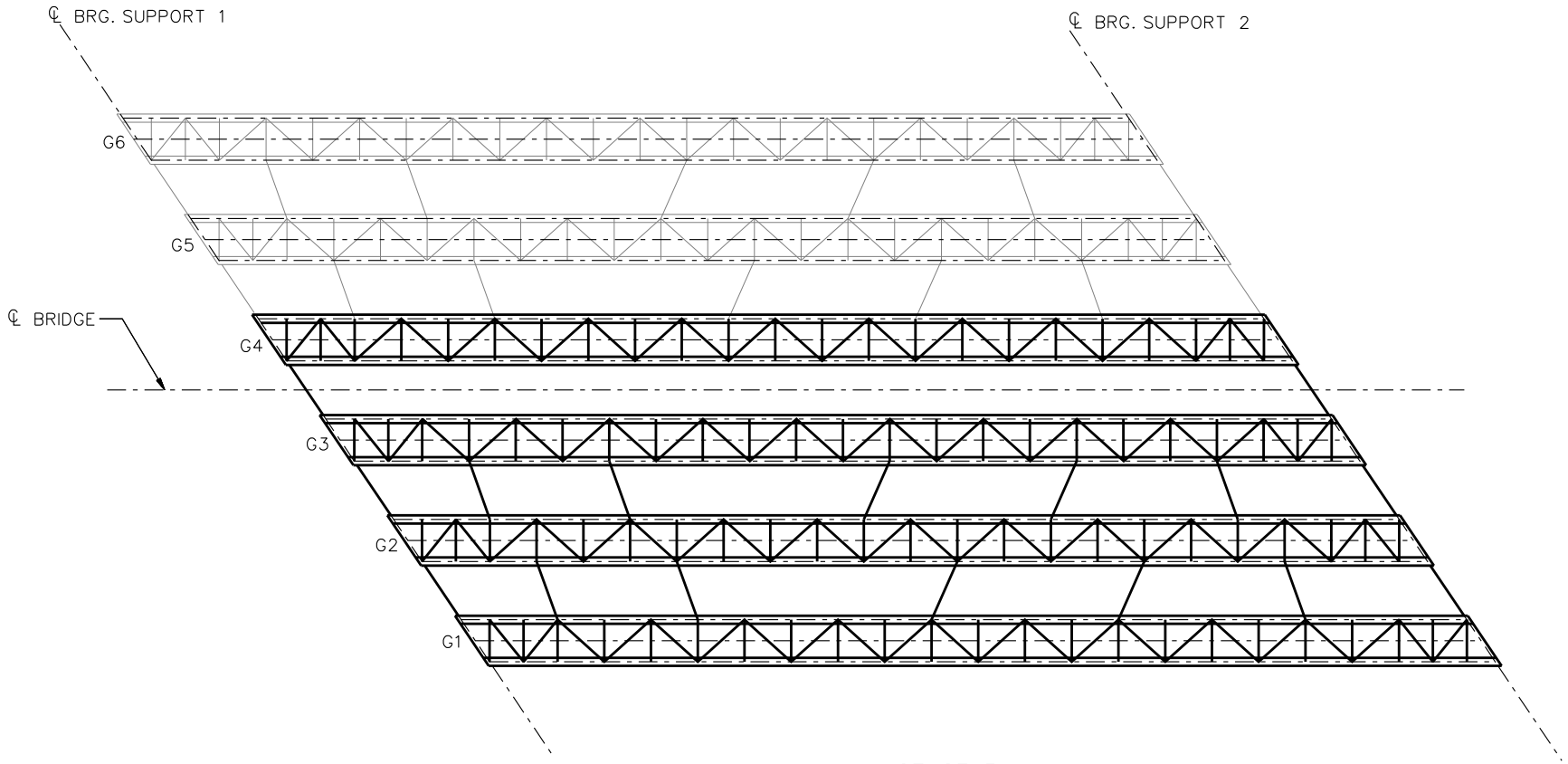

STAGE 5

LEGEND

▽ = HOLD OR LIFT CRANE

○ = TIE DOWN

□ = TEMPORARY SUPPORT STRUCTURE

NCHRP 12-79

BRIDGE ETSSS2

GENERAL ERECTION PROCEDURE

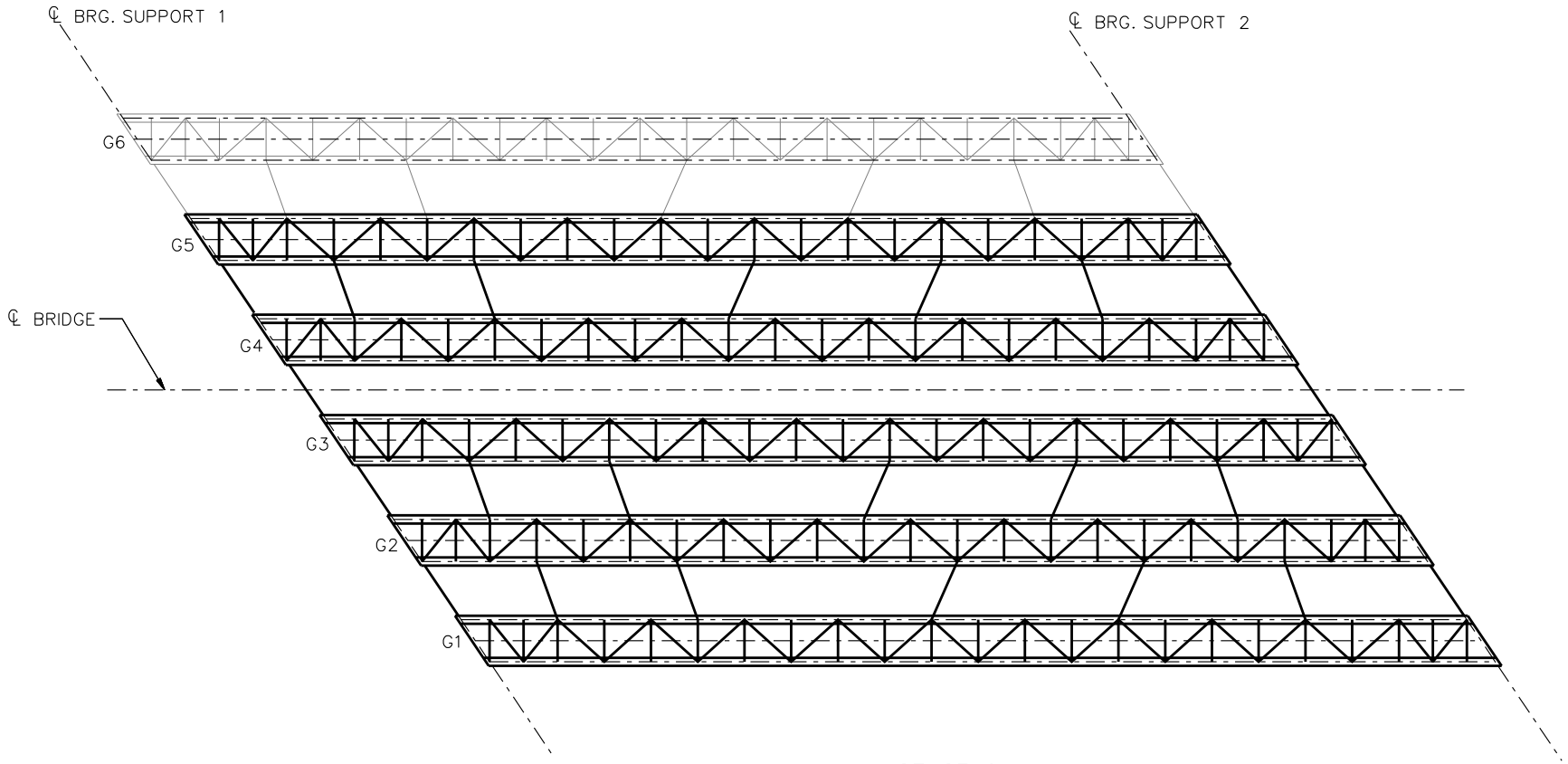

STAGE 6

LEGEND

▽ = HOLD OR LIFT CRANE

○ = TIE DOWN

□ = TEMPORARY SUPPORT STRUCTURE

NCHRP 12-79

BRIDGE ETSSS2

GENERAL ERECTION PROCEDURE

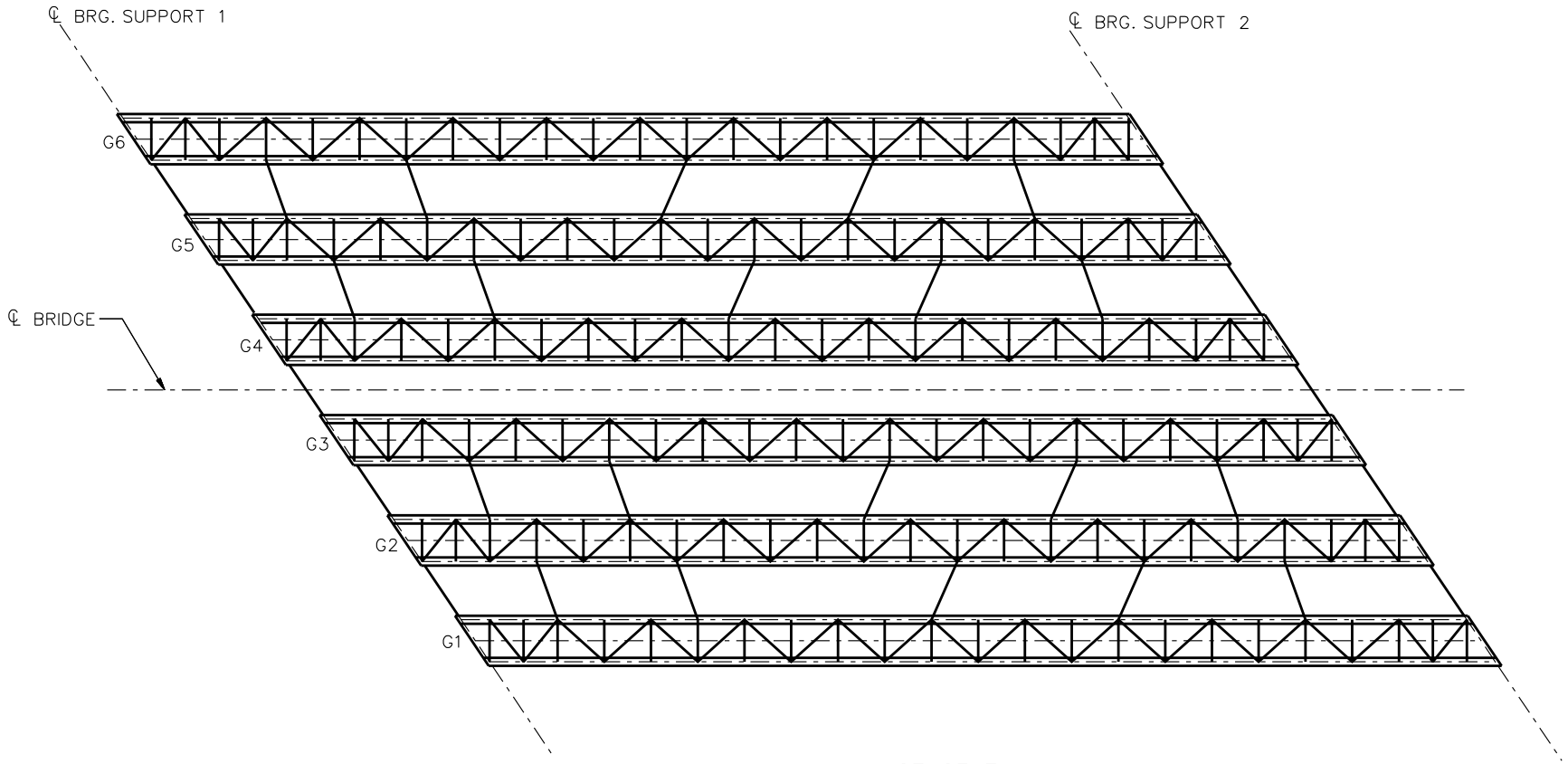

STAGE 7

STAGE 8

CONCRETE DECK PLACED ON G4 THRU G6

STAGE 9

CONNECT CROSSFRAMES BETWEEN G3 & G4
AND DECK CLOSURE POUR

LEGEND

▽ = HOLD OR LIFT CRANE

○ = TIE DOWN

□ = TEMPORARY SUPPORT STRUCTURE

NCHRP 12-79

BRIDGE ETSSS2

GENERAL ERECTION PROCEDURE

NCHRP 12-79

NICCR1

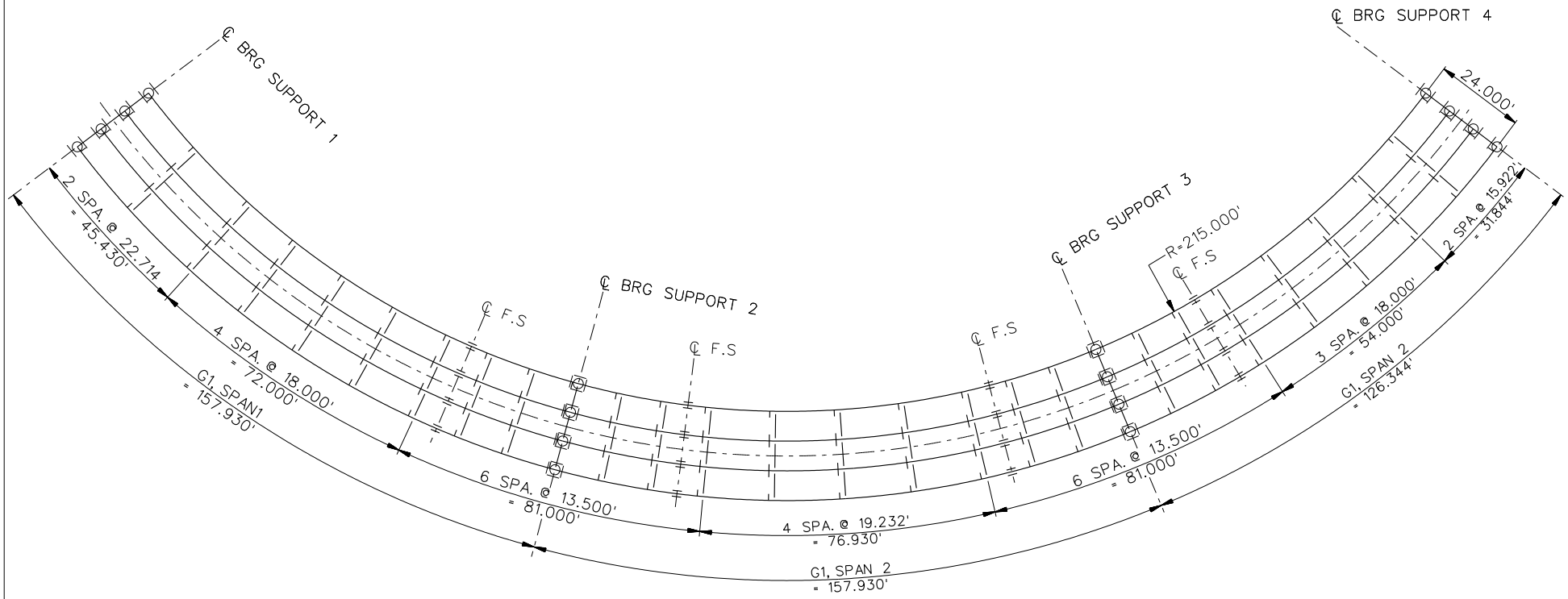

FRAMING PLAN

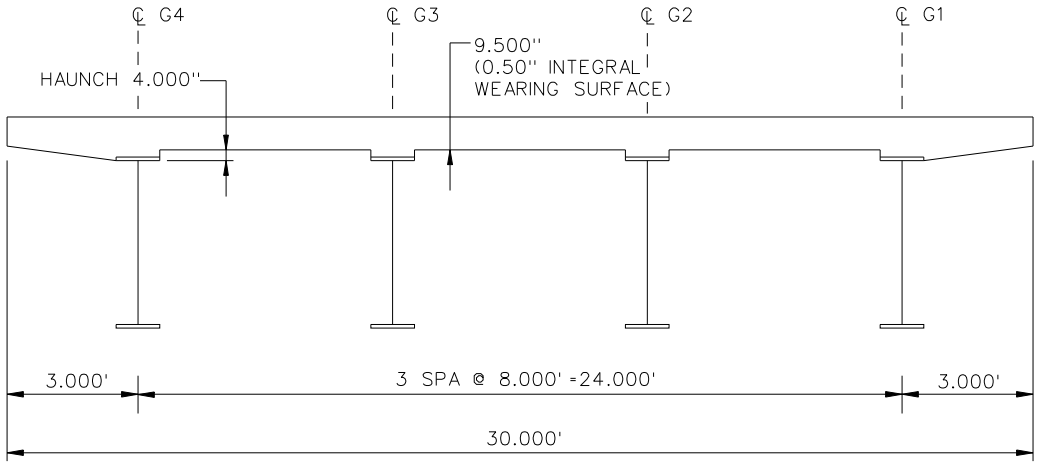

CROSS - SECTION

(DIAPHRAGMS NOT SHOWN)

BEARING LEGEND

- ○ NON-GUIDED
- O LONGITUDINALLY GUIDED
- |O| TRANSVERSELY GUIDED
- |O| FIXED

NCHRP 12-79

BRIDGE NICCR1

FRAMING PLAN AND CROSS-SECTION

SHEET 1 OF 12

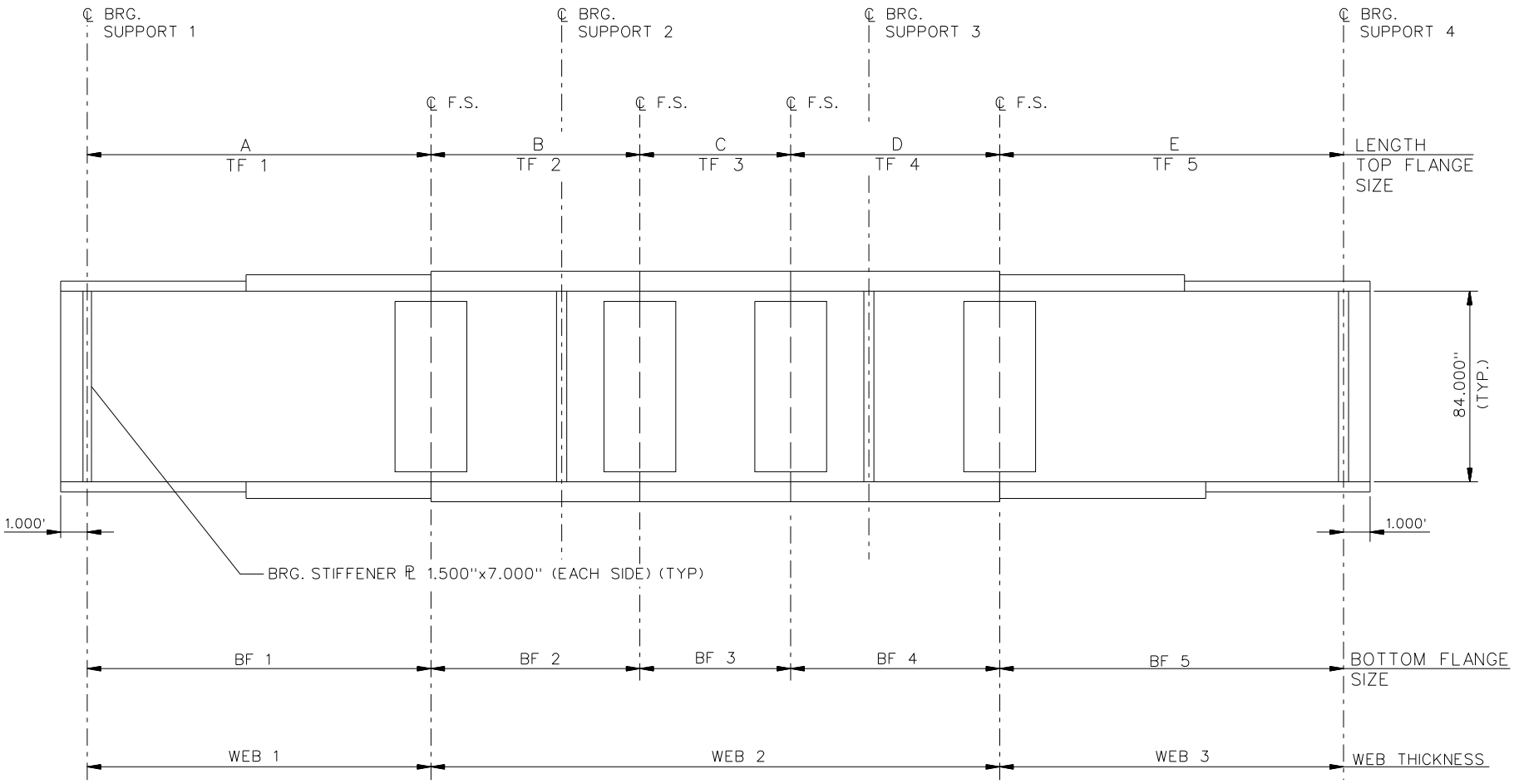

NOTE :

1. SEE TABLES ON SHEET 3 FOR GIRDER ELEVATION DIMENSIONS AND PLATE SIZES.

2. ALL GIRDERS, WEB 1 = WEB 2 = WEB 3 = 0.750".

NCHRP 12-79

BRIDGE NICCR1

GIRDER ELEVATION

SHEET 2 OF 12

	GIRDER PLATE LENGTHS ✳			
LENGTH	G1	G2	G3	G4
A	122.930	117.643	112.357	107.070
B	75.000	75.000	75.000	75.000
C	90.430	85.143	79.875	74.570
D	70.000	70.000	70.000	70.000
E	83.844	79.615	75.385	71.156

✳ ALL DIMENSIONS ARE IN FEET.

	GIRDER FLANGE DIMENSIONS ✳✳							
TOP	G1		G2		G3		G4	
FLANGE	BF	TF	BF	TF	BF	TF	BF	TF
TF1	30.000	1.500	30.000	1.500	26.000	1.250	26.000	1.750
TF2	30.000	2.000	30.000	2.000	26.000	1.250	26.000	1.250
TF3	30.000	1.500	30.000	1.500	26.000	1.250	26.000	1.250
TF4	30.000	2.000	30.000	2.000	26.000	1.250	26.000	1.250
TF5	30.000	1.500	30.000	1.500	26.000	1.250	26.000	1.250

✳✳ ALL DIMENSIONS ARE IN INCHES.

	GIRDER FLANGE DIMENSIONS ✳✳							
BOTTOM	G1		G2		G3		G4	
FLANGE	BF	TF	BF	TF	BF	TF	BF	TF
BF1	30.000	1.500	30.000	1.500	26.000	1.250	26.000	1.750
BF2	30.000	2.000	30.000	2.000	26.000	1.250	26.000	1.250
BF3	30.000	1.500	30.000	1.500	26.000	1.250	26.000	1.250
BF4	30.000	2.000	30.000	2.000	26.000	1.250	26.000	1.250
BF5	30.000	1.500	30.000	1.500	26.000	1.250	26.000	1.250

✳✳ ALL DIMENSIONS ARE IN INCHES.

NCHRP 12-79

BRIDGE NICCR1

GIRDER ELEVATION TABLES

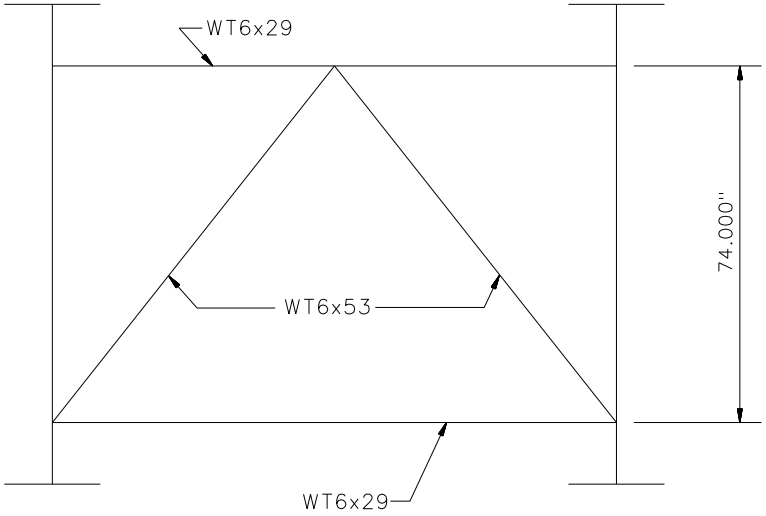

TYPICAL DIAPHRAGM AT SUPPORTS

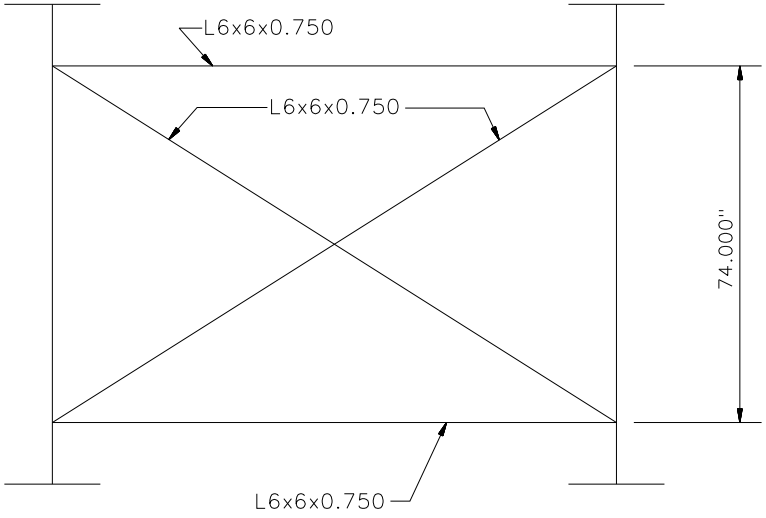

TYPICAL INTERMEDIATE DIAPHRAGM

NOTES:

1. STEEL DEAD LOAD INCREASED BY 5% FOR MDX AND LARSA MODELS; 2% FOR 3D MODEL; AND 10% FOR APPROXIMATE ANALYSIS TO ACCOUNT FOR MISC. DETAILS.

2. FORMWORK LOAD OF 10PSF IS INCLUDED IN CONCRETE DEAD LOAD.

3. ADDITIONAL DESIGN PARAMETERS:
   A. 1.500' PARAPET WIDTH BOTH SIDES.
   B. 700 LB/FT UNIFORM LOAD ASSUMED FOR PARAPET WEIGHT.
   C. ROADWAY WIDTH = 26.500'.
   D. NUMBER OF DESIGN LANES = 2.
   E. HL93 LIVE LOAD.
   F. DESIGN SPEED = 35 MPH.

4. DIAPHRAGM MEMBER CALL-OUTS ARE IN UNITS OF INCHES.

NCHRP 12-79

BRIDGE NICCR1

MISC. DETAILS AND NOTES

SHEET 4 OF 12

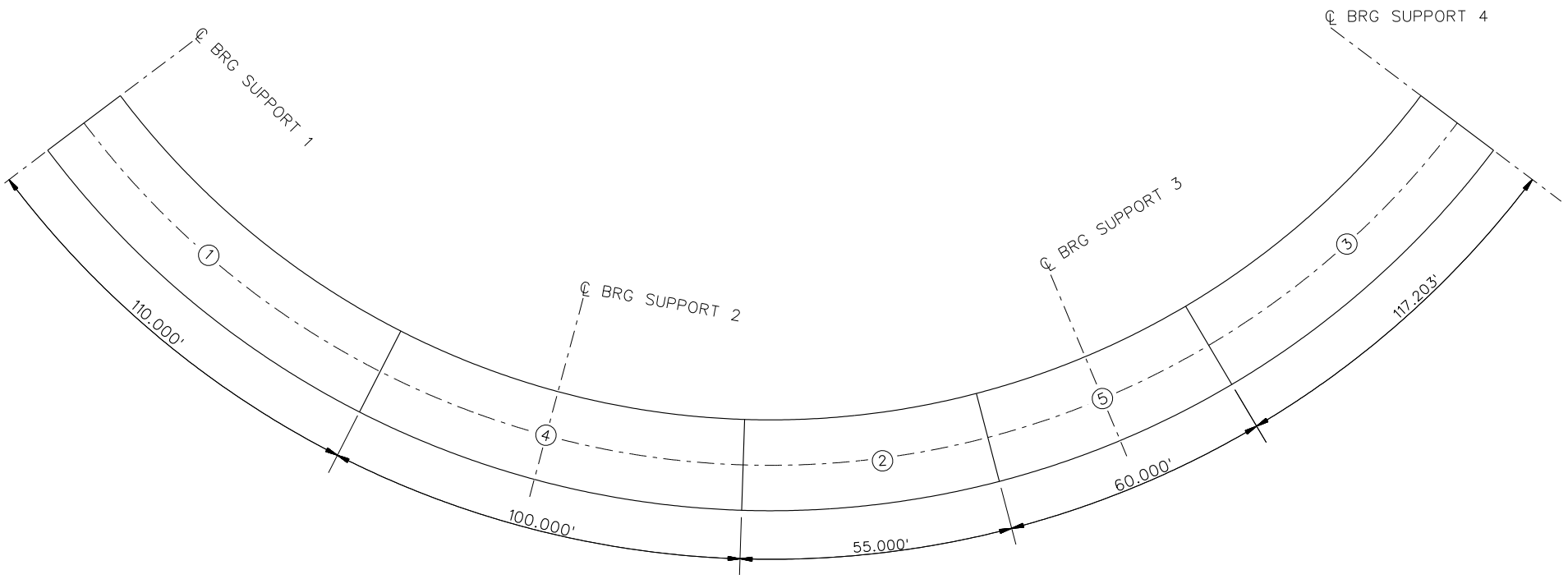

DECK POURING SEQUENCE

NOTE :
MEASURED ALONG G1

NCHRP 12-79

BRIDGE NICCR1

DECK POURING SEQUENCE

SHEET 5 OF 12

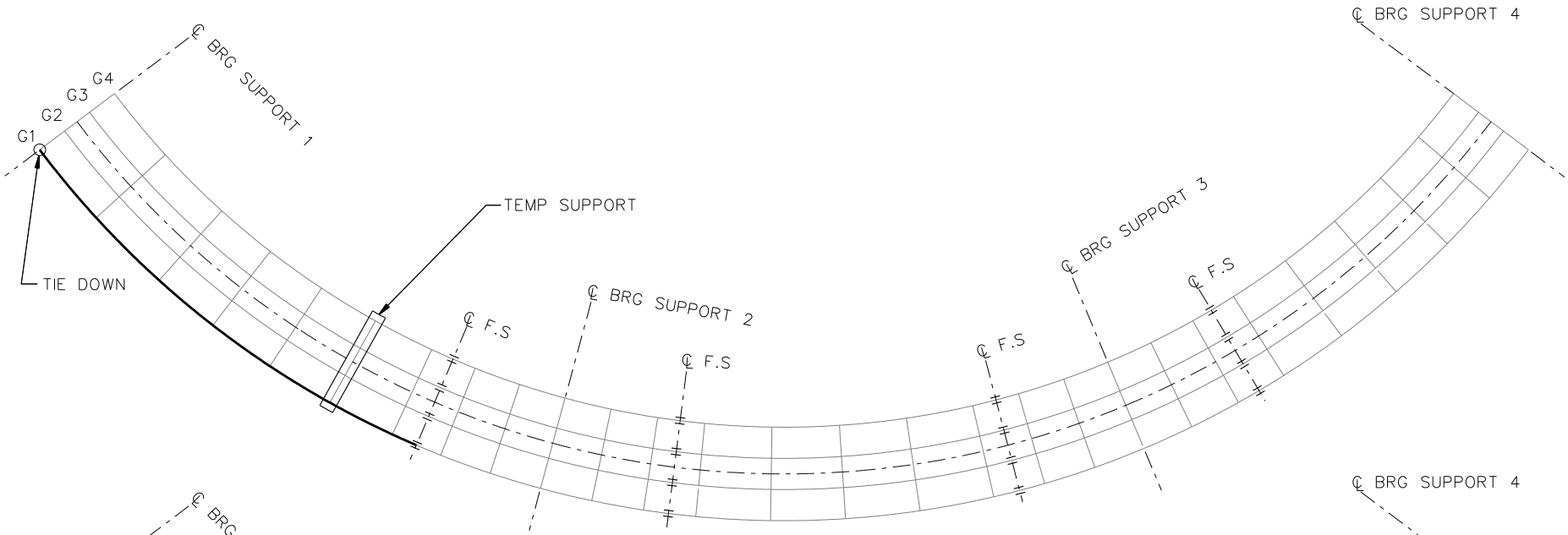

STAGE 1

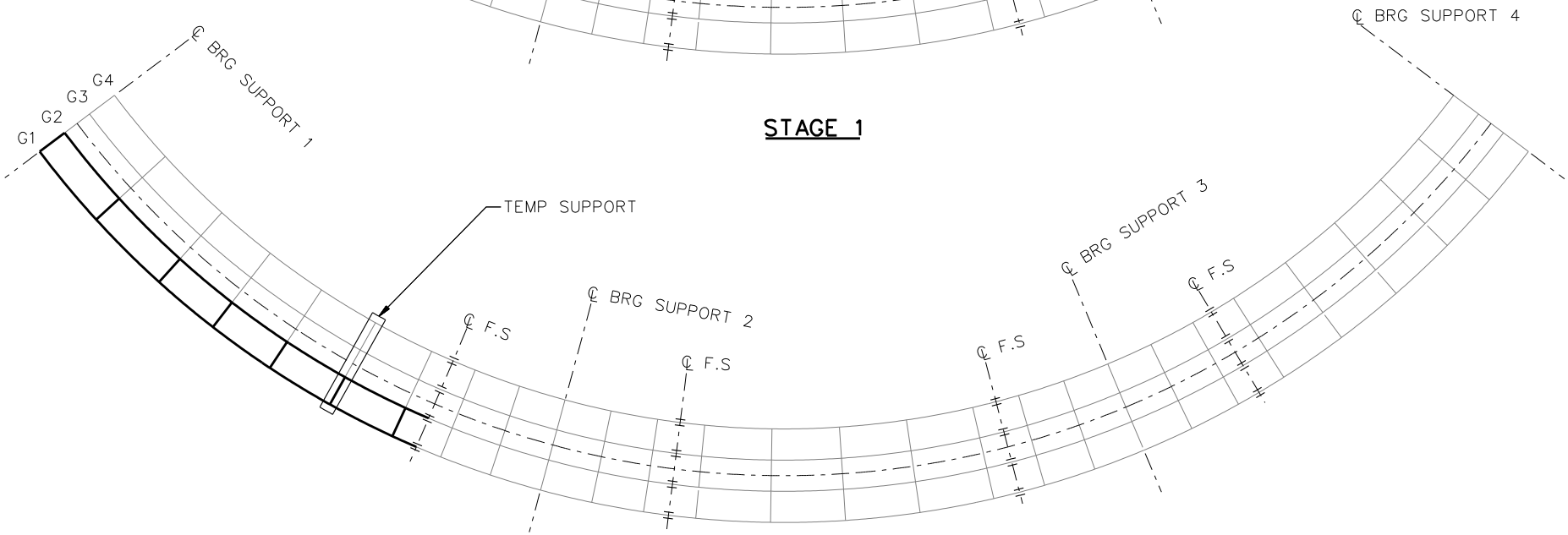

STAGE 2

LEGEND

▽ = HOLD OR LIFT CRANE

○ = TIE DOWN

□ = TEMPORARY SUPPORT STRUCTURE

NCHRP 12-79

BRIDGE NICCR1

GENERAL ERECTION PROCEDURE

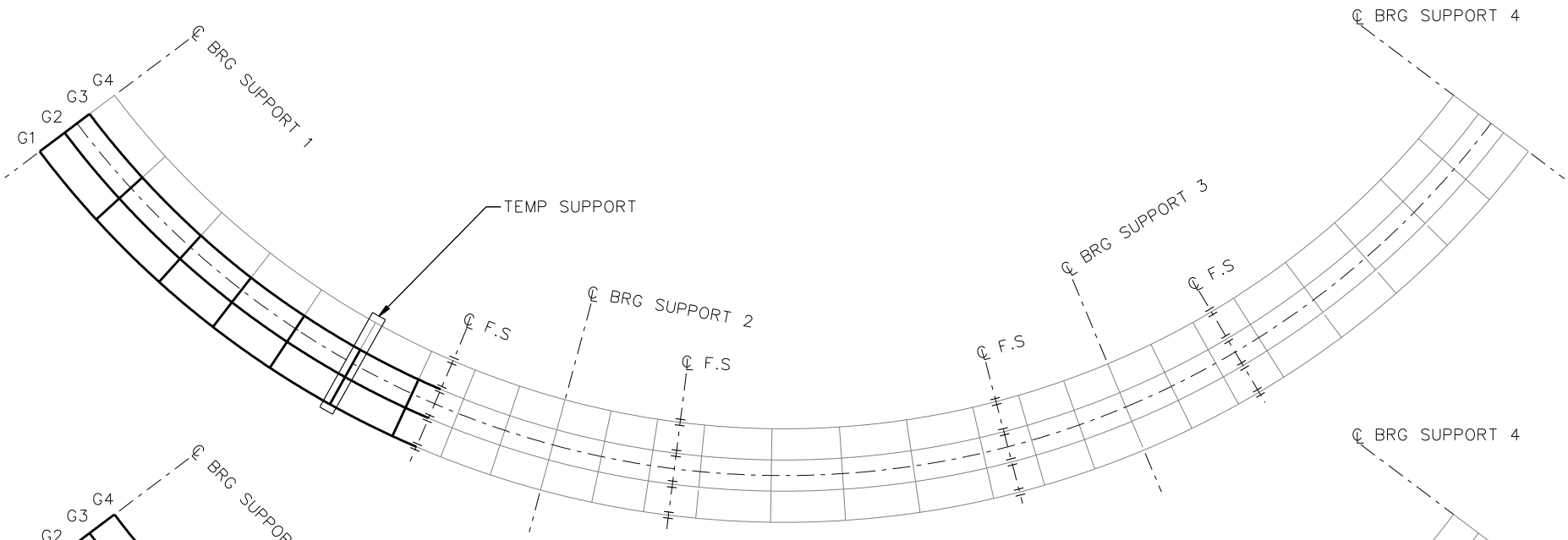

STAGE 3

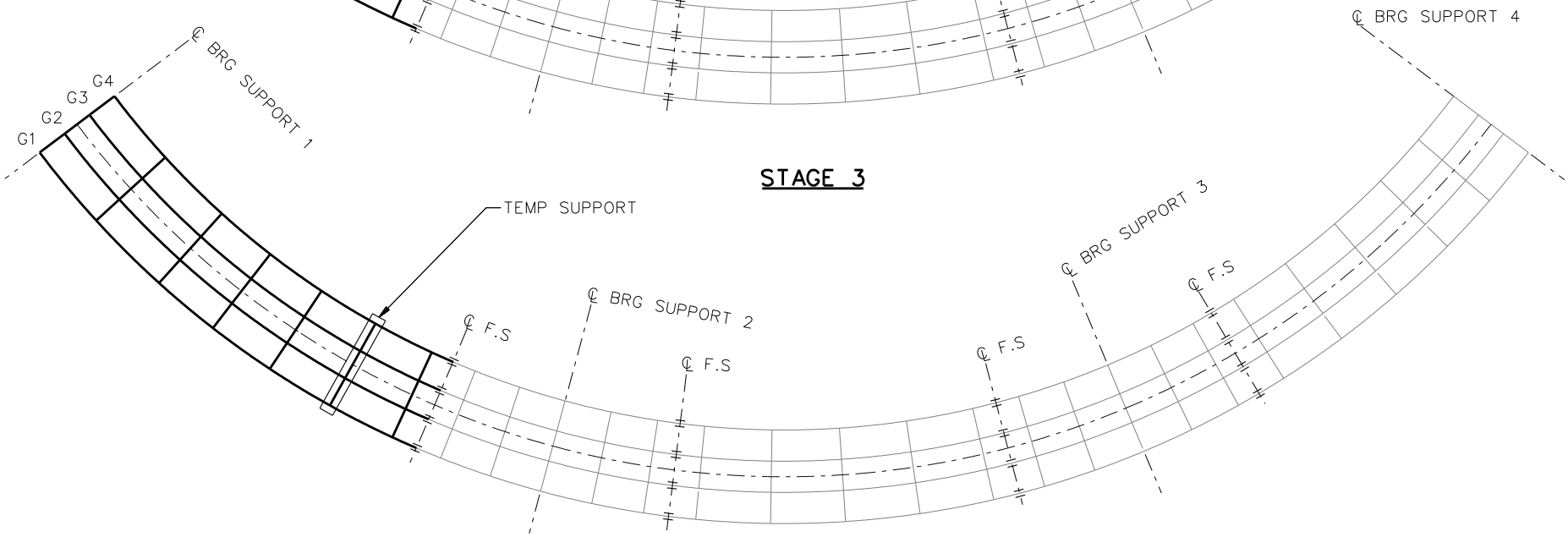

STAGE 4

LEGEND

▽ = HOLD OR LIFT CRANE

○ = TIE DOWN

□ = TEMPORARY SUPPORT STRUCTURE

NCHRP 12-79

BRIDGE NICCR1

GENERAL ERECTION PROCEDURE

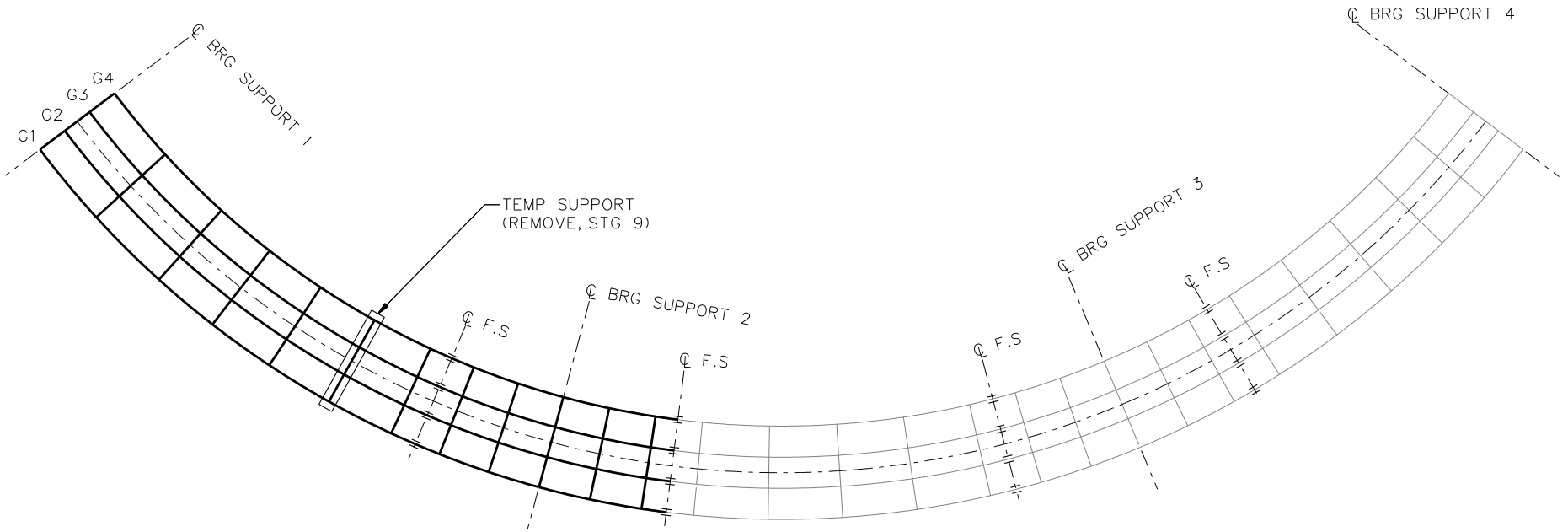

STAGE 5-8

STG 5 = G1
STG 6 = G2
STG 7 = G3
STG 8 = G4

STAGE 9

REMOVE TEMP SUPPORT

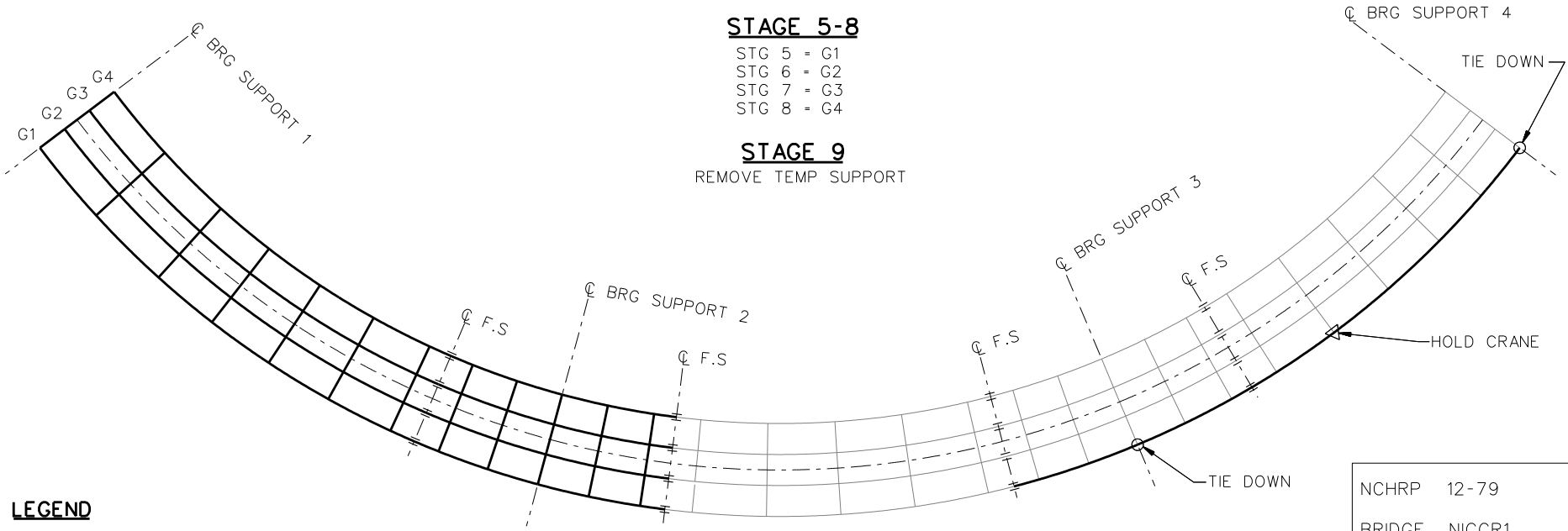

STAGE 10

LEGEND

▽ = HOLD OR LIFT CRANE

○ = TIE DOWN

□ = TEMPORARY SUPPORT STRUCTURE

NCHRP 12-79

BRIDGE NICCR1

GENERAL ERECTION PROCEDURE

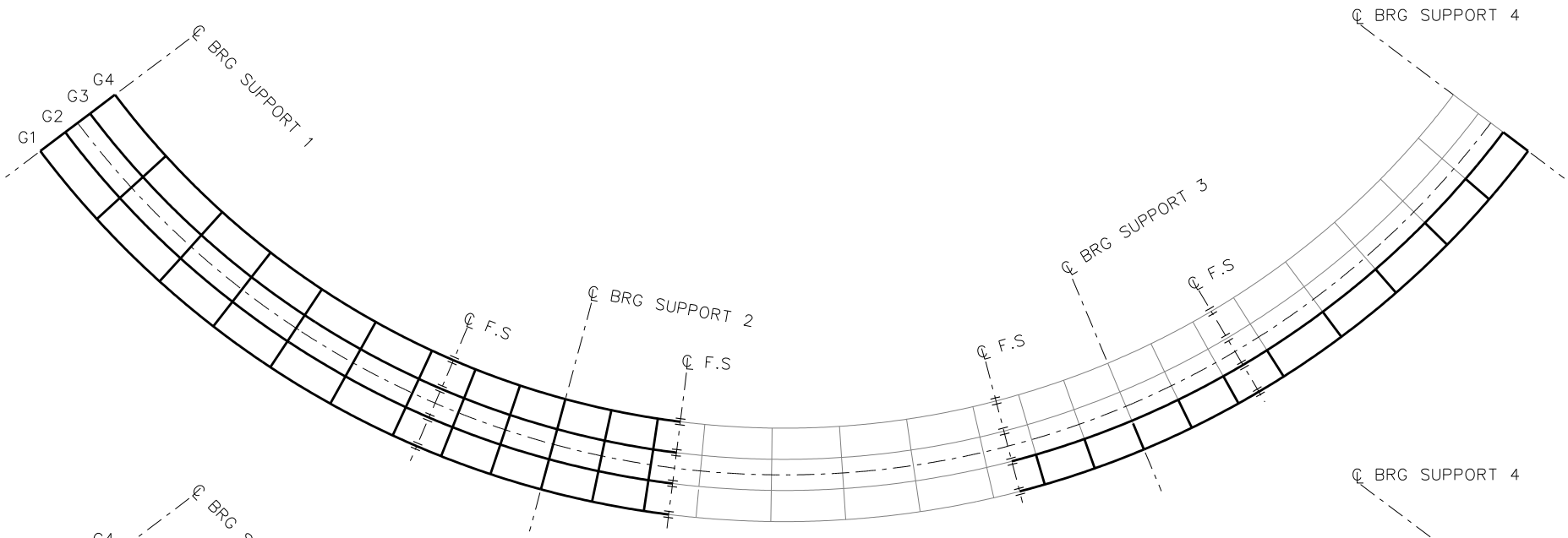

STAGE 11

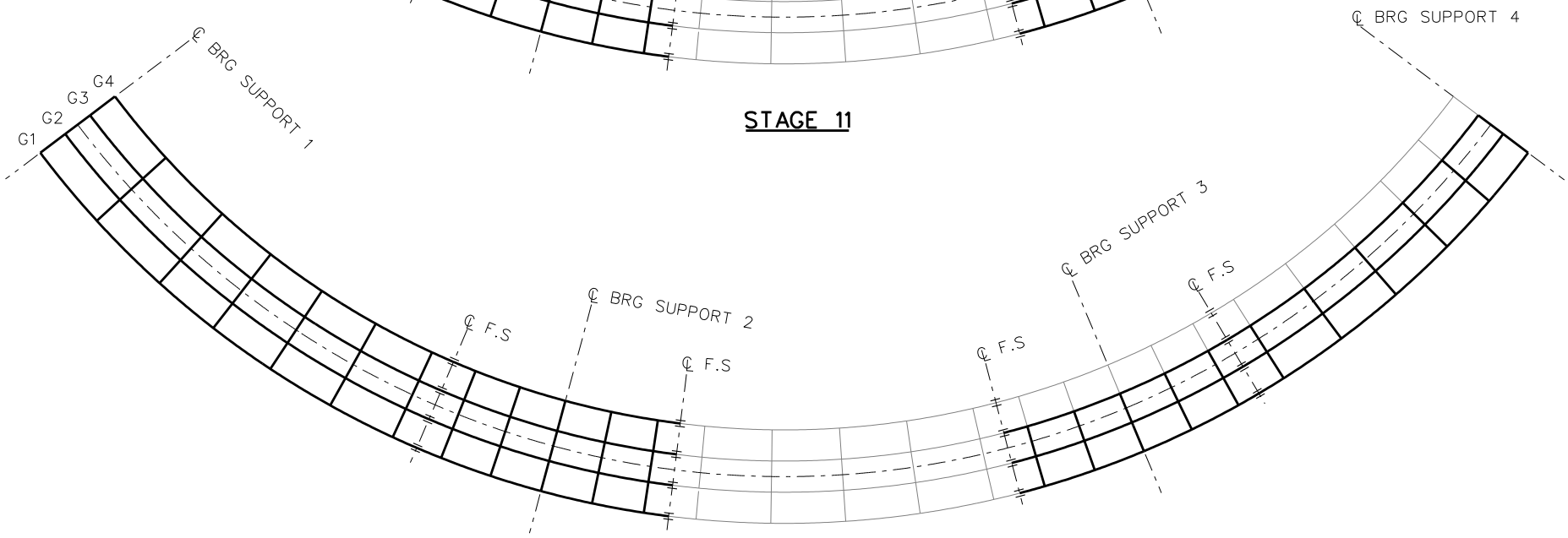

STAGE 12

LEGEND

▽ = HOLD OR LIFT CRANE

○ = TIE DOWN

□ = TEMPORARY SUPPORT STRUCTURE

NCHRP 12-79

BRIDGE NICCR1

GENERAL ERECTION PROCEDURE

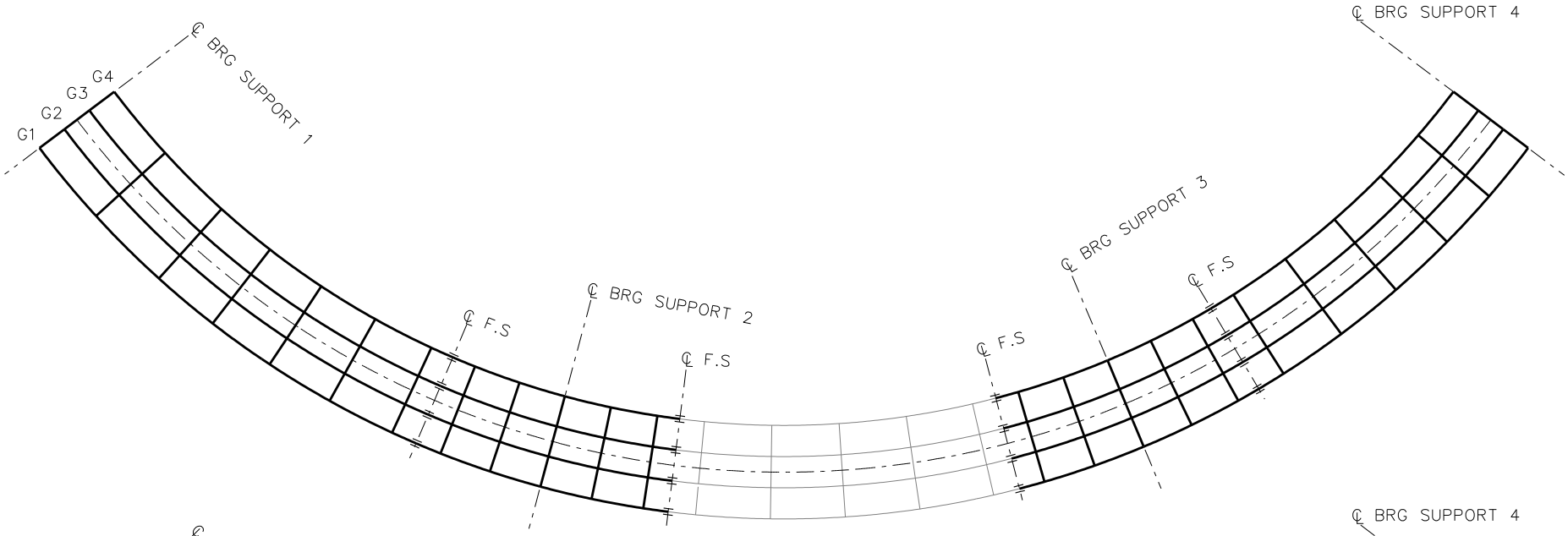

STAGE 13

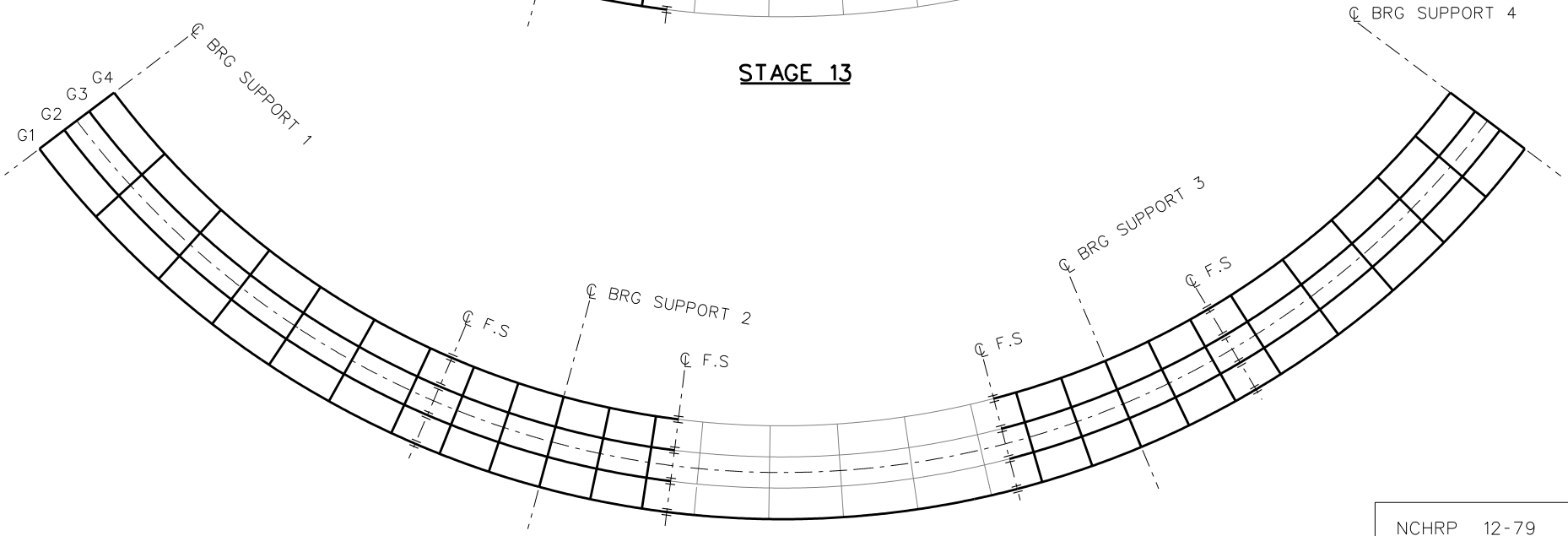

STAGE 14

LEGEND

▽ = HOLD OR LIFT CRANE

○ = TIE DOWN

□ = TEMPORARY SUPPORT STRUCTURE

NCHRP 12-79

BRIDGE NICCR1

GENERAL ERECTION PROCEDURE

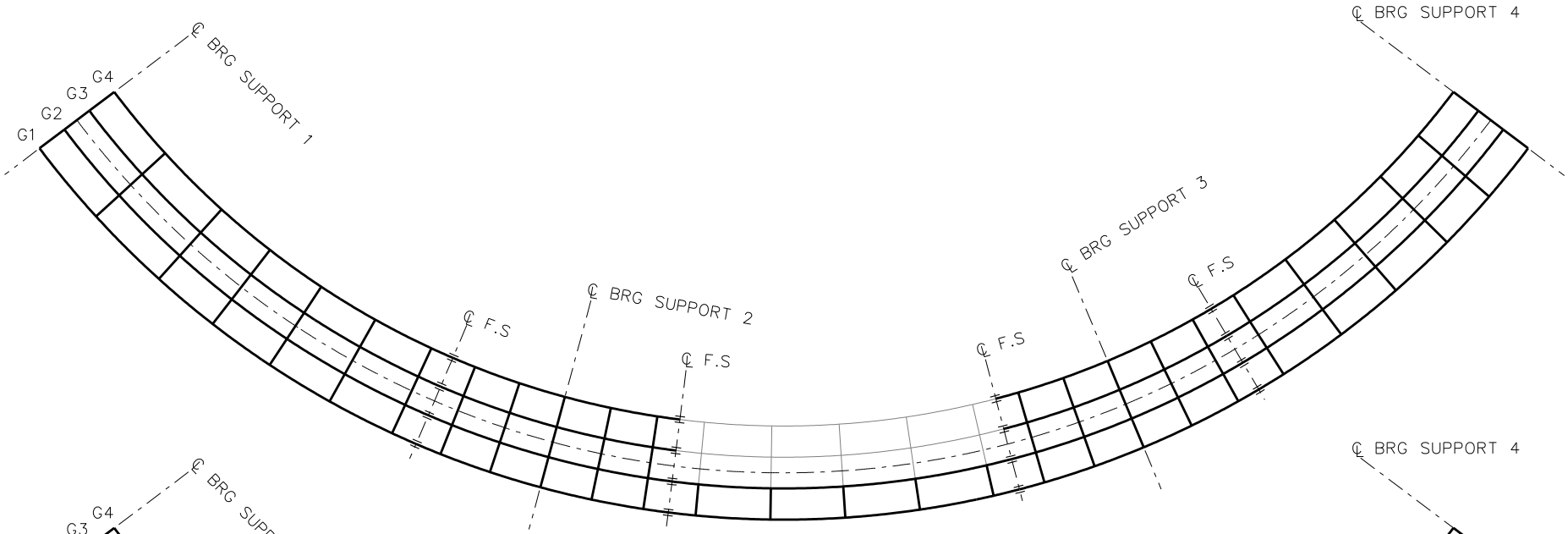

STAGE 15

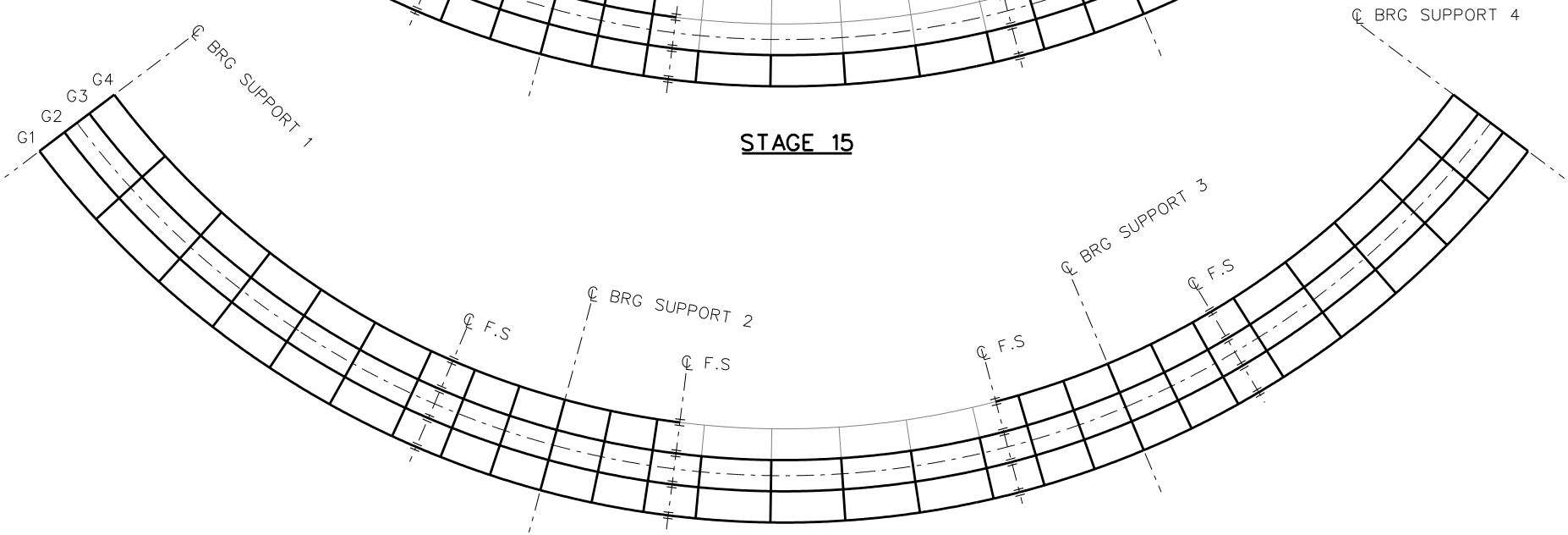

STAGE 16

LEGEND

▽ = HOLD OR LIFT CRANE

○ = TIE DOWN

□ = TEMPORARY SUPPORT STRUCTURE

NCHRP 12-79

BRIDGE NICCR1

GENERAL ERECTION PROCEDURE

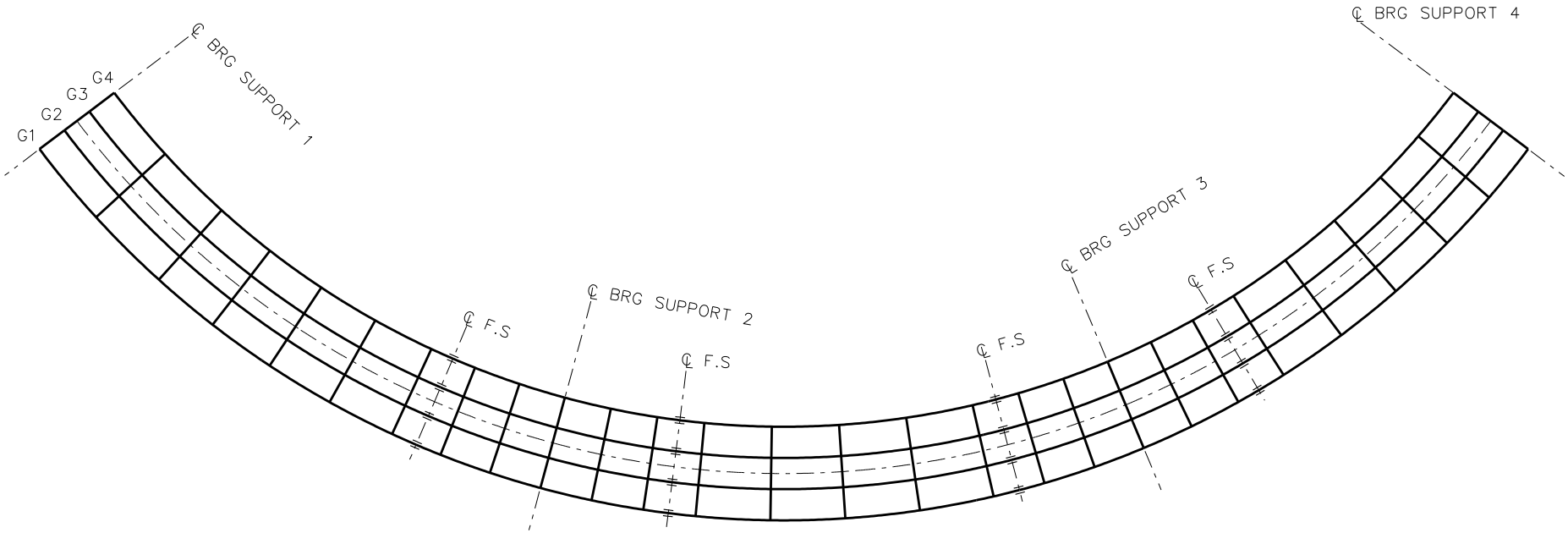

STAGE 17

LEGEND

▽ = HOLD OR LIFT CRANE

○ = TIE DOWN

□ = TEMPORARY SUPPORT STRUCTURE

NCHRP 12-79

BRIDGE NICCR1

GENERAL ERECTION PROCEDURE

NCHRP 12-79

NICCR8

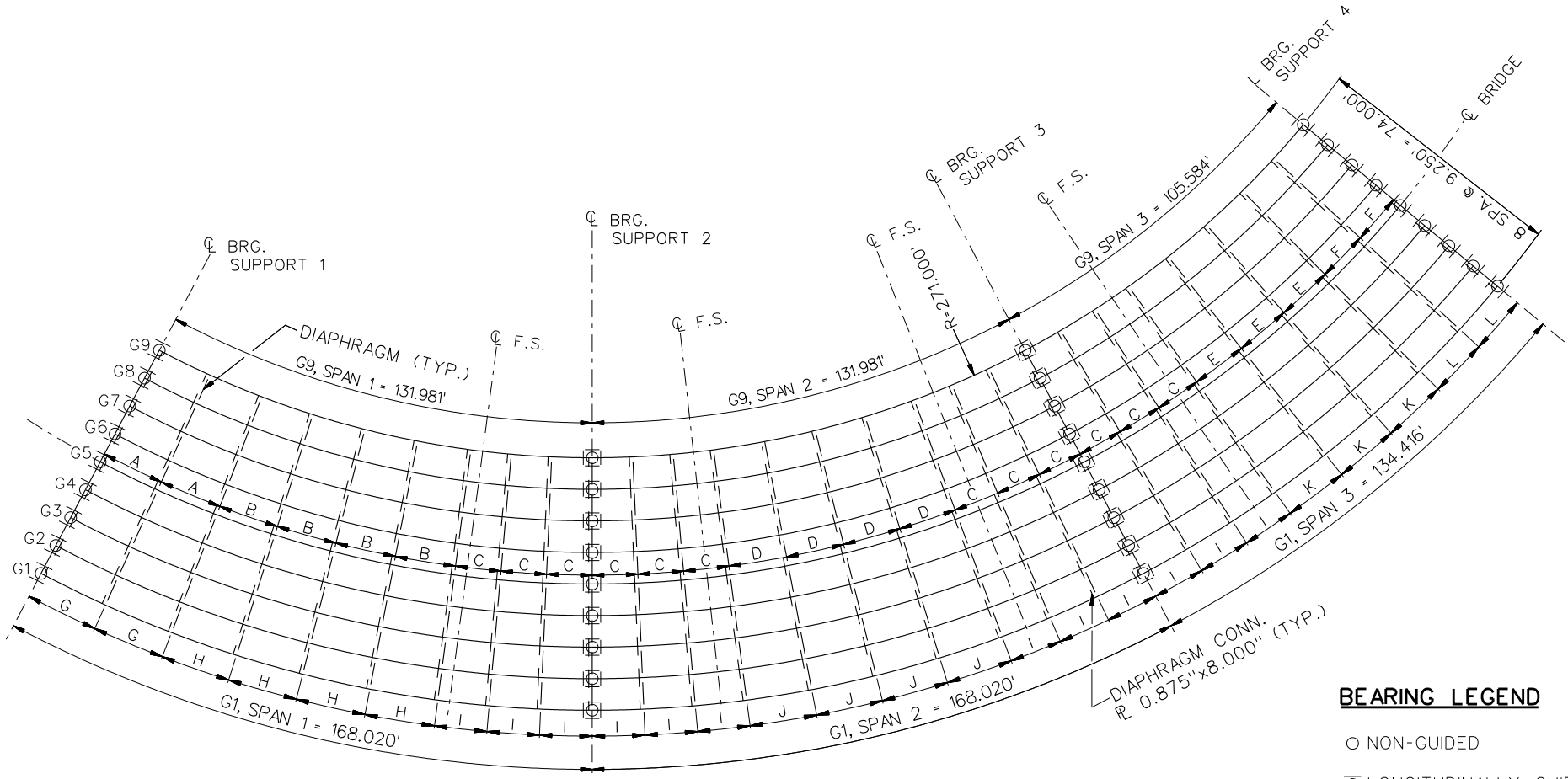

FRAMING PLAN

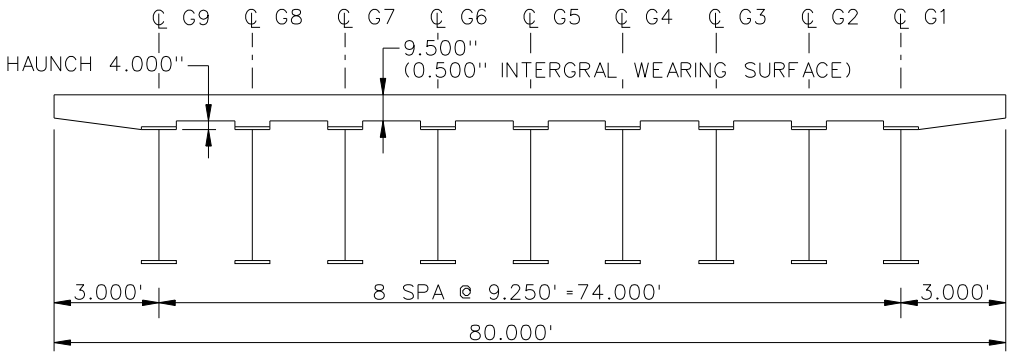

CROSS - SECTION

(DIAPHRAGMS NOT SHOWN)

CROSS FRAME SPACING @ G1	
G	21.002'
H	20.162'
I	15.122'
J	19.322'
K	18.482'
L	16.802'

CROSS FRAME SPACING @ G5	
A	18.750'
B	18.000'
C	13.500'
D	17.250'
E	16.500'
F	15.000'

BEARING LEGEND

- ○ NON-GUIDED
- ⊟ LONGITUDINALLY GUIDED
- |○| TRANSVERSELY GUIDED
- |⊟| FIXED

NCHRP 12-79

BRIDGE NICCR8

FRAMING PLAN AND CROSS-SECTION

SHEET 1 OF 10

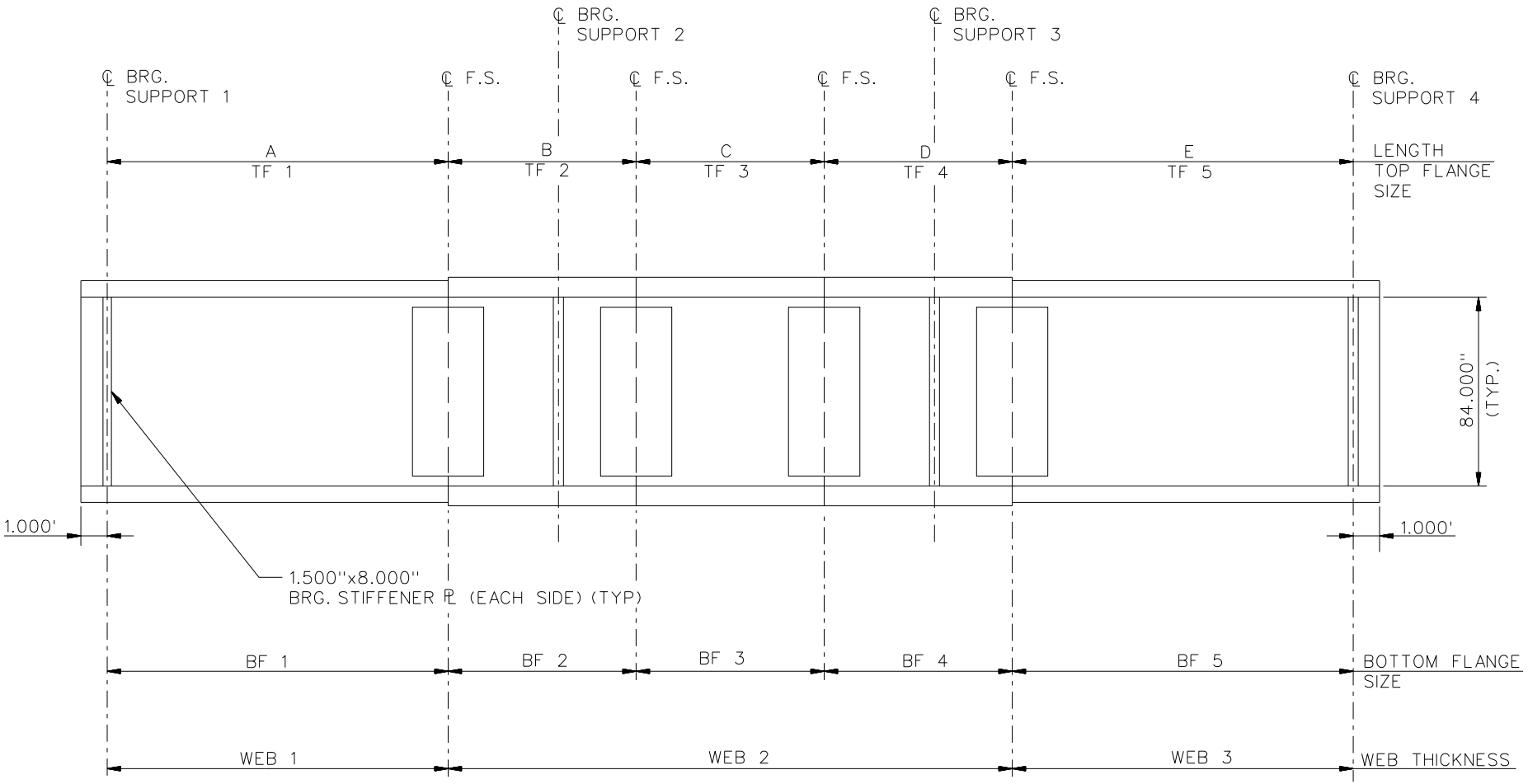

NOTES:

1. SEE TABLES ON SHEET 3 FOR GIRDER ELEVATION DIMENSIONS AND PLATE SIZES.

2. ALL GIRDERS, WEB 1 = WEB 2 = WEB 3 = 0.750"

NCHRP 12-79

BRIDGE NICCR8

GIRDER ELEVATION

SHEET 2 OF 10

	GIRDER PLATE LENGTHS ✳								
LENGTH	G1	G2	G3	G4	G5	G6	G7	G8	G9
A	128.019	123.515	119.010	114.505	110.000	105.495	100.990	96.485	91.981
B	80.000	80.000	80.000	80.000	80.000	80.000	80.000	80.000	80.000
C	88.019	83.515	79.000	74.505	70.000	65.495	60.990	56.485	51.981
D	70.000	70.000	70.000	70.000	70.000	70.000	70.000	70.000	70.000
E	104.416	100.812	97.208	93.604	90.000	86.396	82.792	79.188	75.585

✳ ALL DIMENSIONS ARE IN FEET.

	GIRDER FLANGE DIMENSIONS ✳✳					
TOP	G1, G2, G3		G4, G5, G6		G7, G8, G9	
FLANGE	BF	TF	BF	TF	BF	TF
TF1	26.000	1.250	20.000	1.000	20.000	0.875
TF2	26.000	1.750	20.000	1.250	20.000	1.000
TF3	26.000	1.250	20.000	1.000	20.000	0.875
TF4	26.000	1.250	20.000	1.250	20.000	1.000
TF5	26.000	1.250	20.000	1.000	20.000	0.875

✳✳ ALL DIMENSIONS ARE IN INCHES.

	GIRDER FLANGE DIMENSIONS ✳✳					
BOTTOM	G1, G2, G3		G4, G5, G6		G7, G8, G9	
FLANGE	BF	TF	BF	TF	BF	TF
BF1	26.000	1.250	20.000	1.000	20.000	0.875
BF2	26.000	1.750	20.000	1.250	20.000	1.000
BF3	26.000	1.250	20.000	1.000	20.000	0.875
BF4	26.000	1.250	20.000	1.250	20.000	1.000
BF5	26.000	1.250	20.000	1.000	20.000	0.875

✳✳ ALL DIMENSIONS ARE IN INCHES.

NCHRP 12-79

BRIDGE NICCR8

GIRDER ELEVATION TABLES

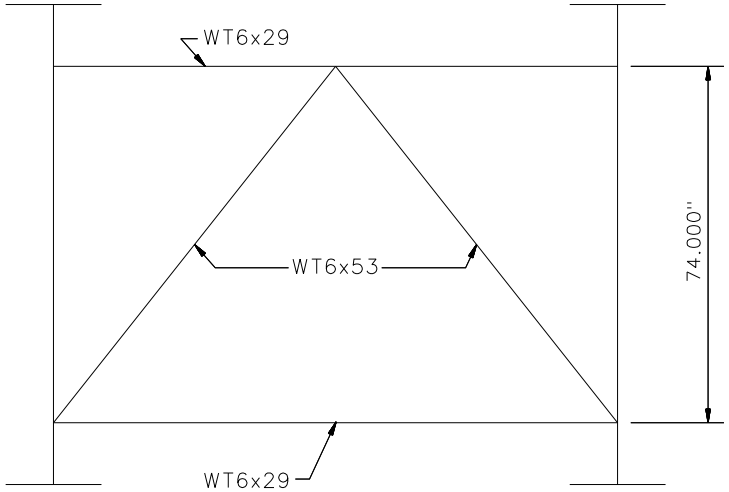

TYPICAL DIAPHRAGM

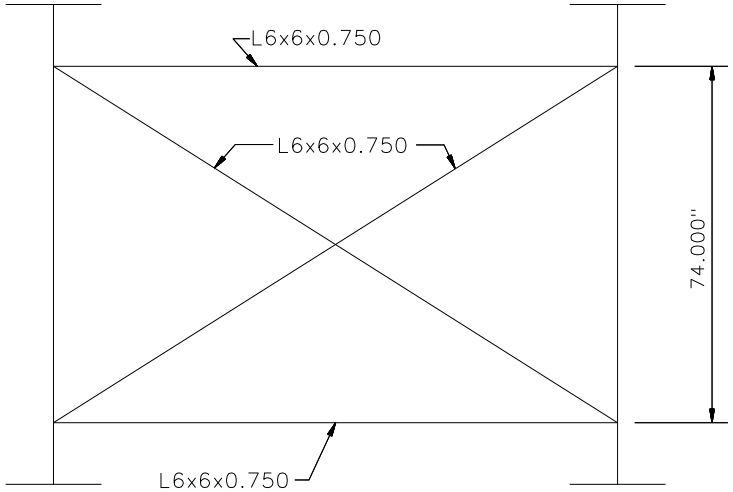

TYPICAL INTERMEDIATE DIAPHRAGM

NOTES:

1. STEEL DEAD LOAD INCREASED BY 5% FOR MDX AND LARSA MODELS; 2% FOR 3D MODEL; AND 10% FOR APPROXIMATE ANALYSIS TO ACCOUNT FOR MISC. DETAILS.

2. FORMWORK LOAD OF 10PSF IS INCLUDED IN CONCRETE DEAD LOAD.

3. ADDITIONAL DESIGN PARAMETERS:
   A. 1.500' PARAPET WIDTH BOTH SIDES.
   B. 700 LB/FT UNIFORM LOAD ASSUMED FOR PARAPET WEIGHT.
   C. ROADWAY WIDTH = 76.500'.
   D. NUMBER OF DESIGN LANES = 6.
   E. HL93 LIVE LOAD.
   F. DESIGN SPEED = 35 MPH.

4. DIAPHRAGM MEMBER CALL-OUTS ARE IN ENGLISH UNITS.

NCHRP 12-79

BRIDGE NICCR8

MISC. DETAILS AND NOTES

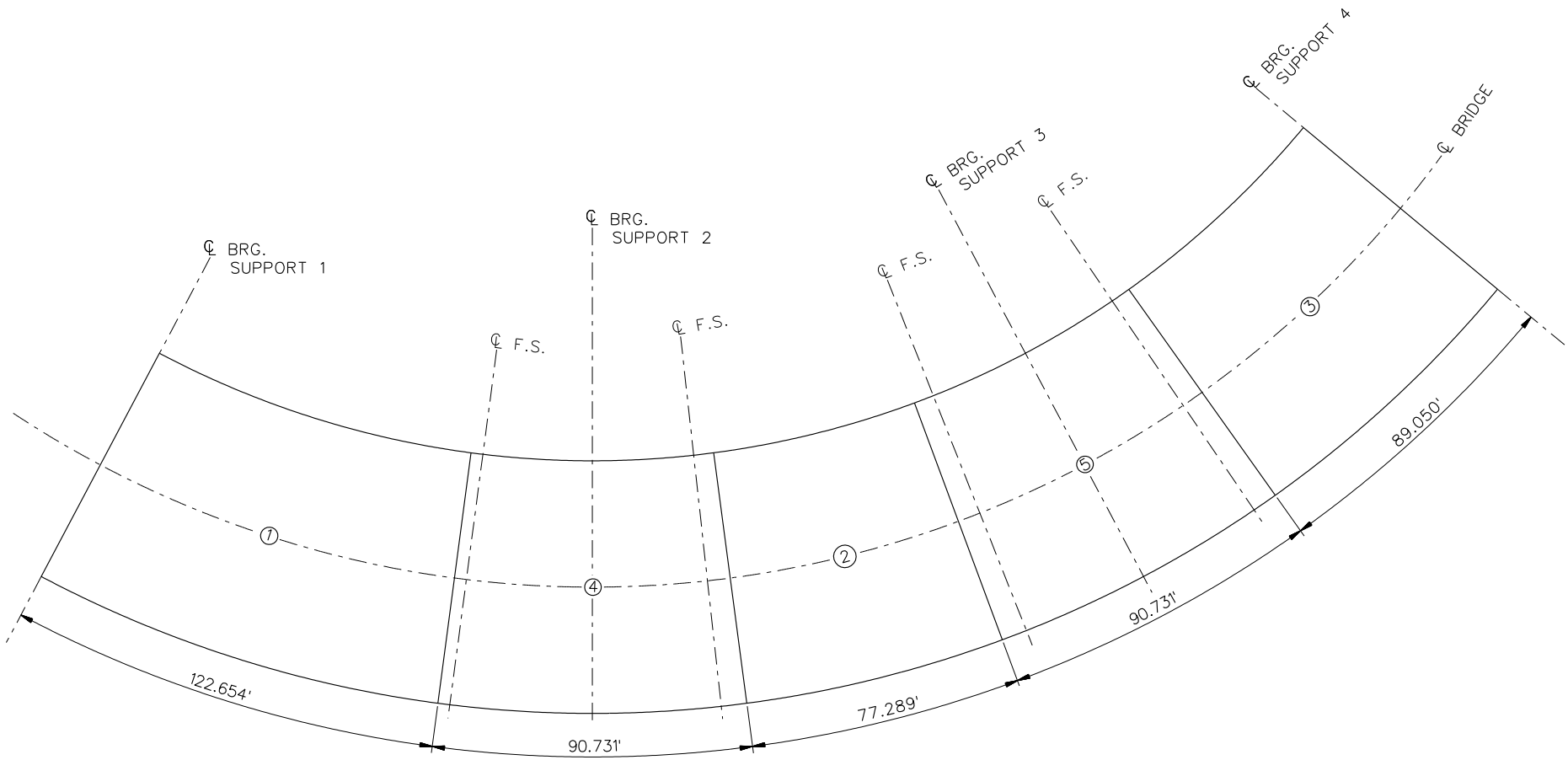

DECK POURING SEQUENCE

NOTE:

1. DECK POUR LENGTHS ARE MEASURED ALONG ℄ G1.

NCHRP 12-79

BRIDGE NICCR8

DECK POURING SEQUENCE

SHEET 5 OF 10

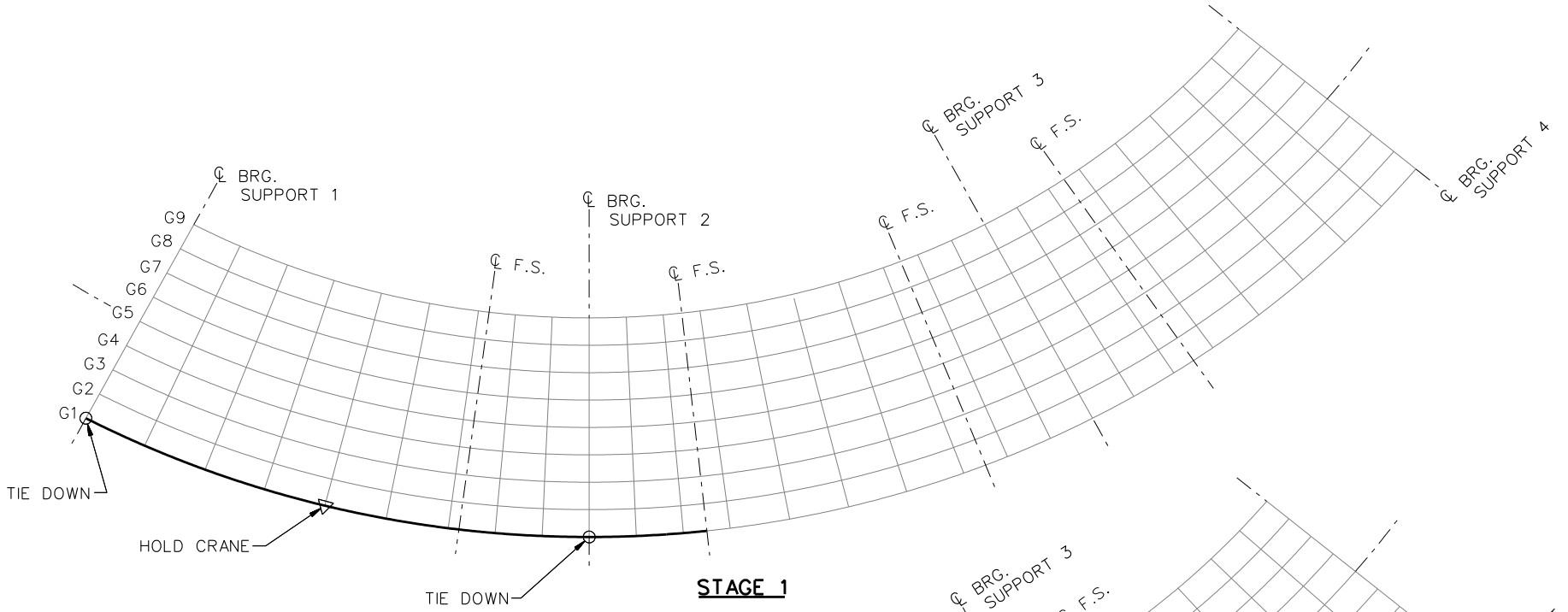

STAGE 1

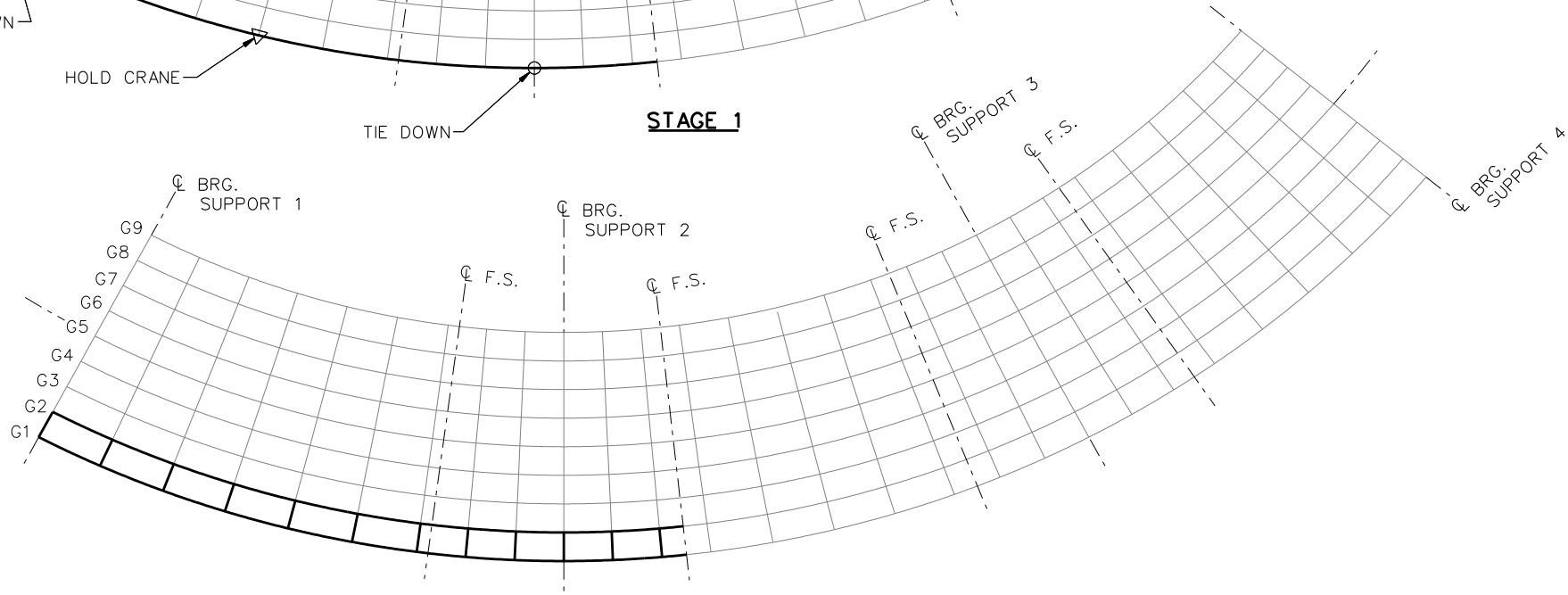

STAGE 2

LEGEND

▽ = HOLD OR LIFT CRANE

○ = TIE DOWN

□ = TEMPORARY SUPPORT STRUCTURE

NCHRP 12-79

BRIDGE NICCR8

GENERAL ERECTION PROCEDURE

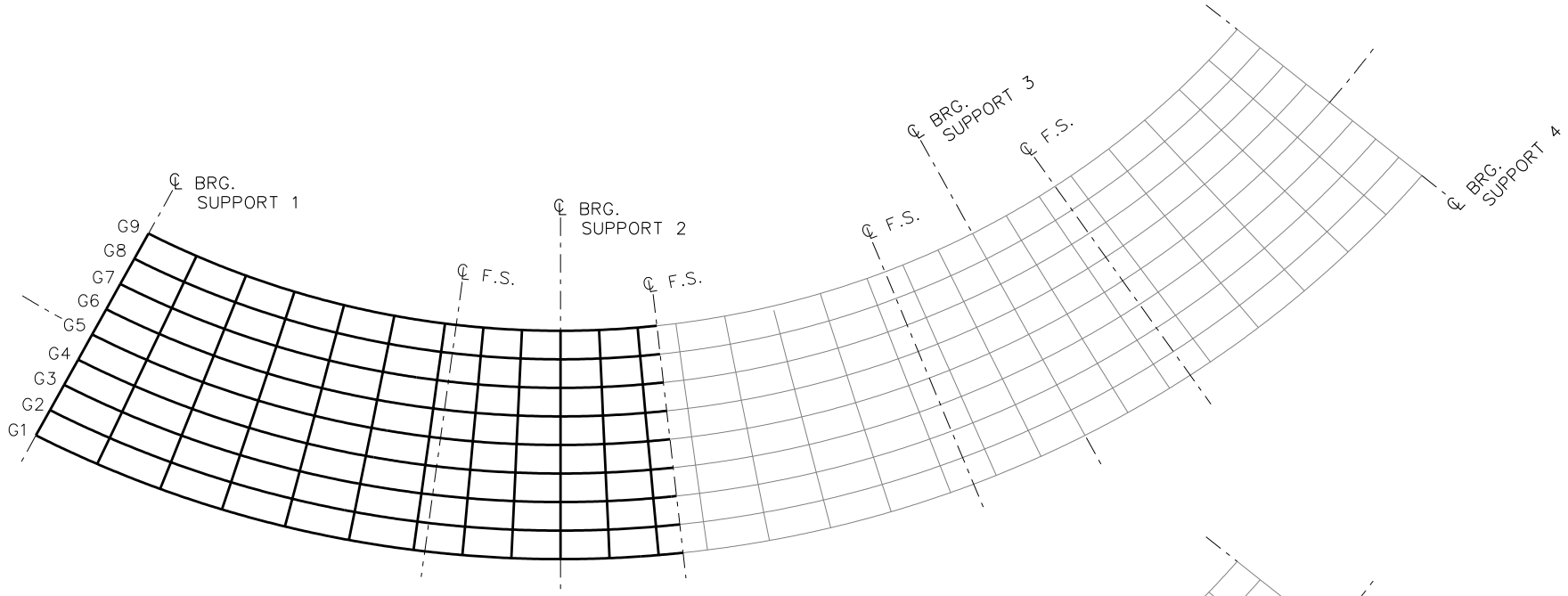

STAGES 3 THRU 9

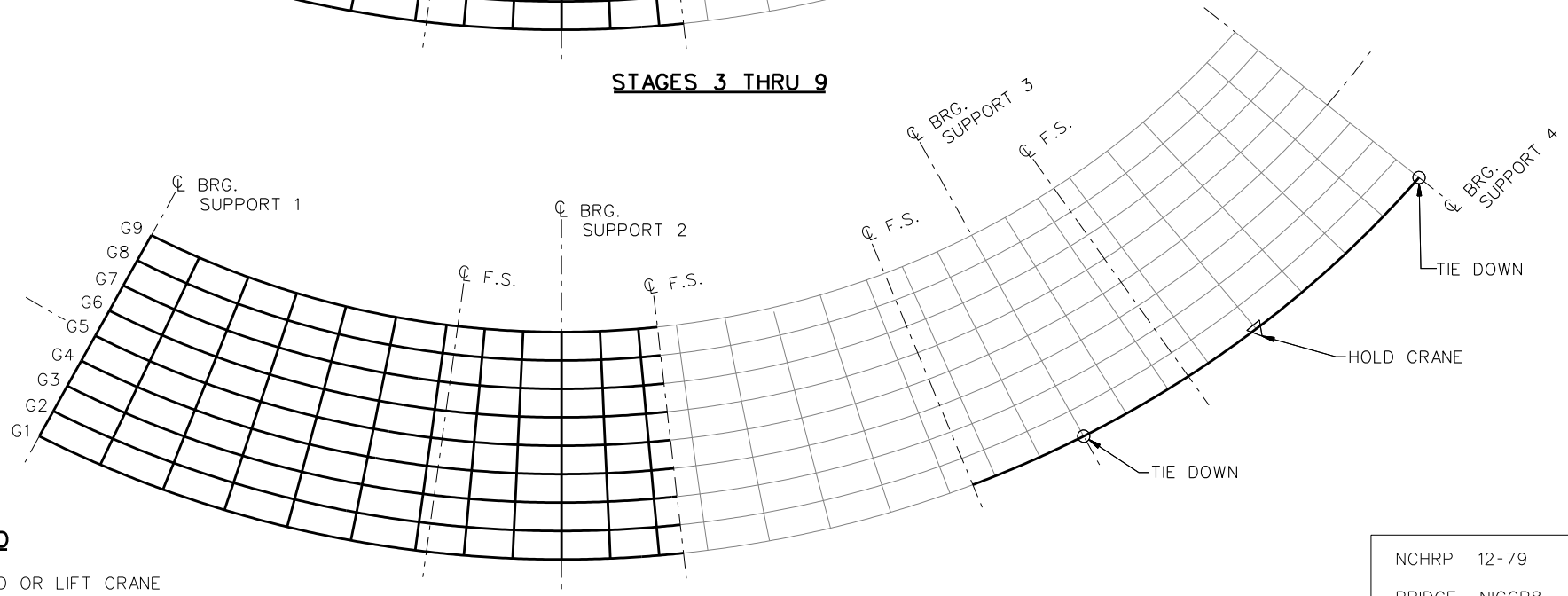

STAGE 10

LEGEND

▽ = HOLD OR LIFT CRANE

○ = TIE DOWN

□ = TEMPORARY SUPPORT STRUCTURE

NCHRP 12-79

BRIDGE NICCR8

GENERAL ERECTION PROCEDURE

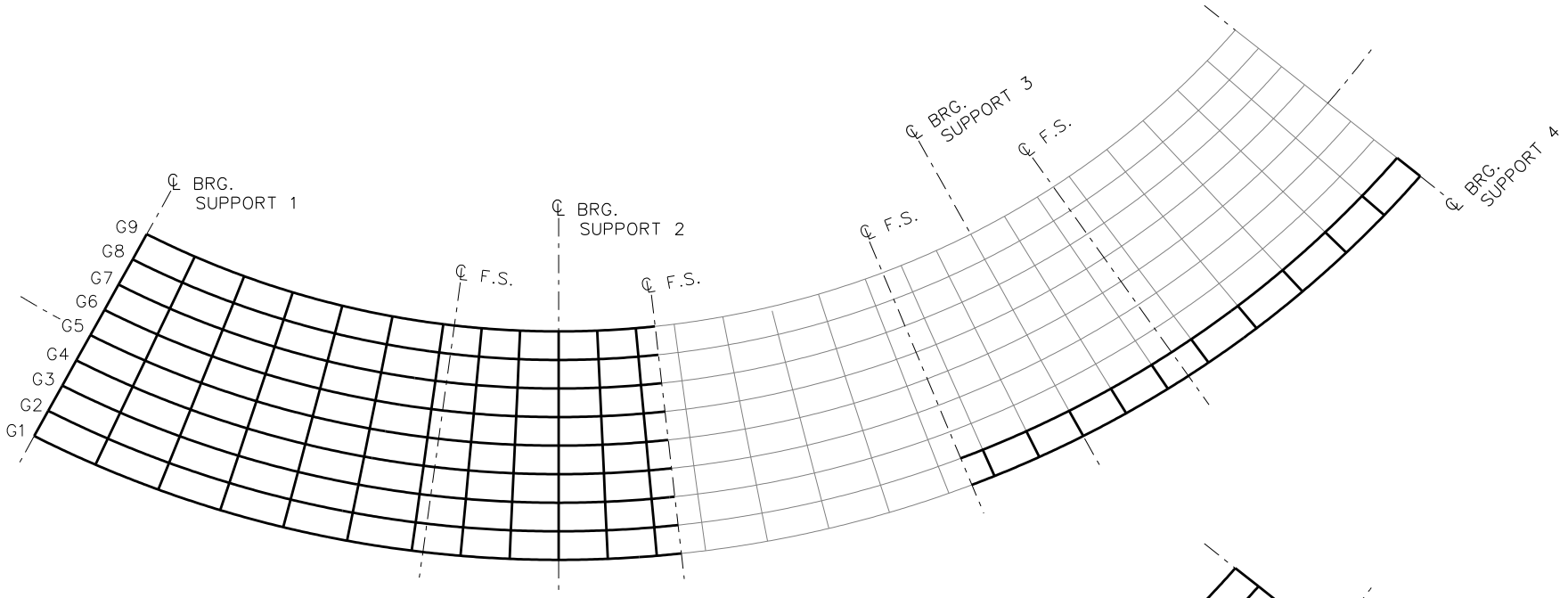

STAGE 11

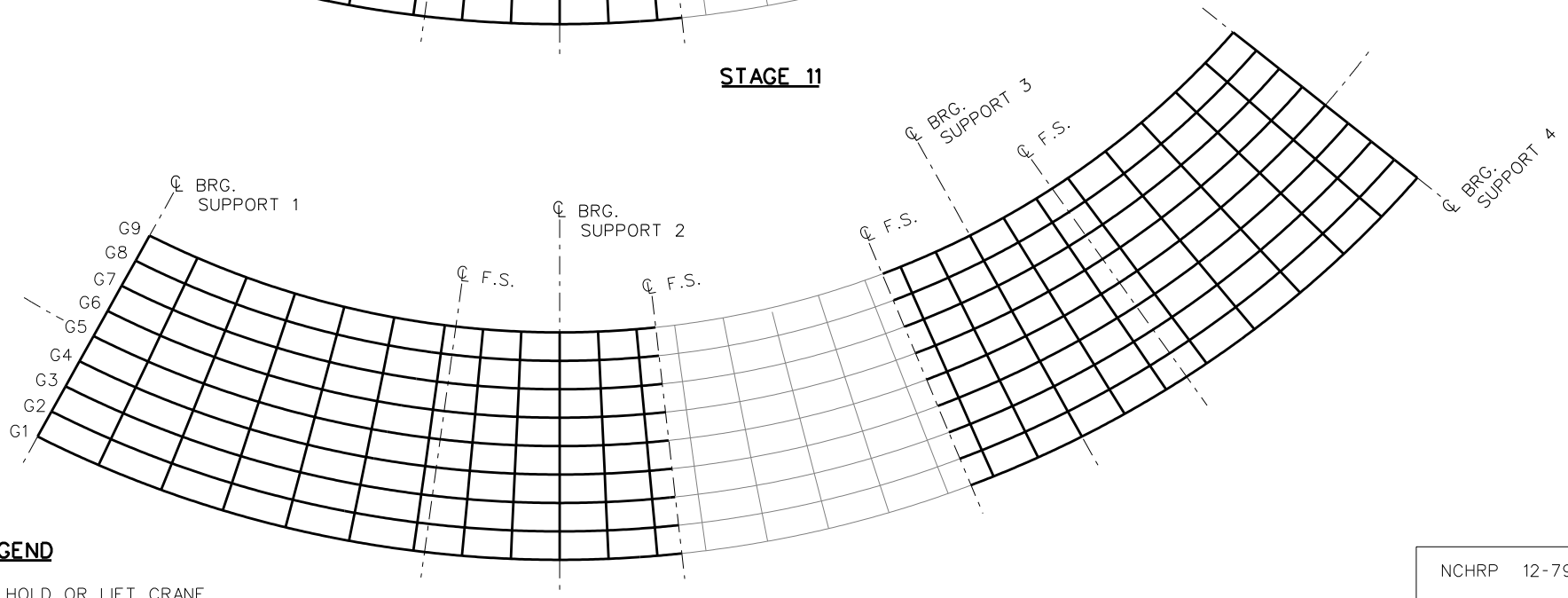

STAGES 12 THRU 18

LEGEND

▽ = HOLD OR LIFT CRANE

○ = TIE DOWN

□ = TEMPORARY SUPPORT STRUCTURE

NCHRP 12-79

BRIDGE NICCR8

GENERAL ERECTION PROCEDURE

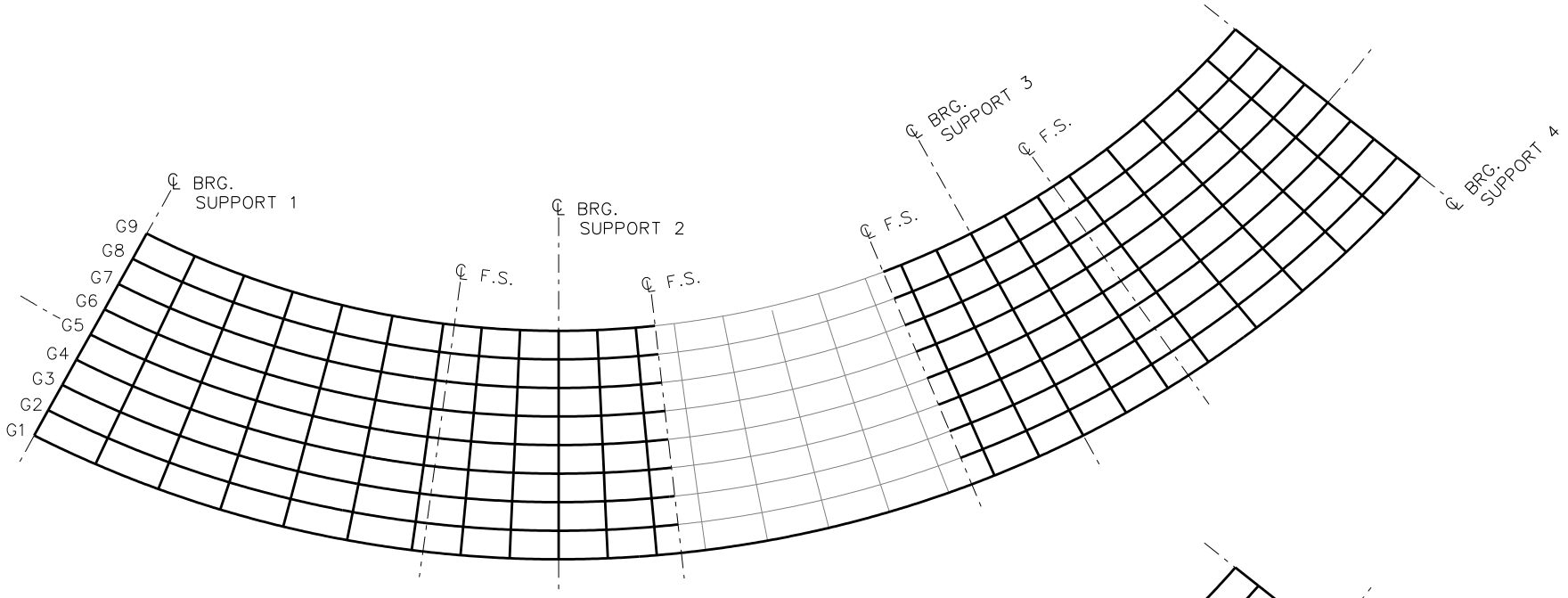

STAGE 19

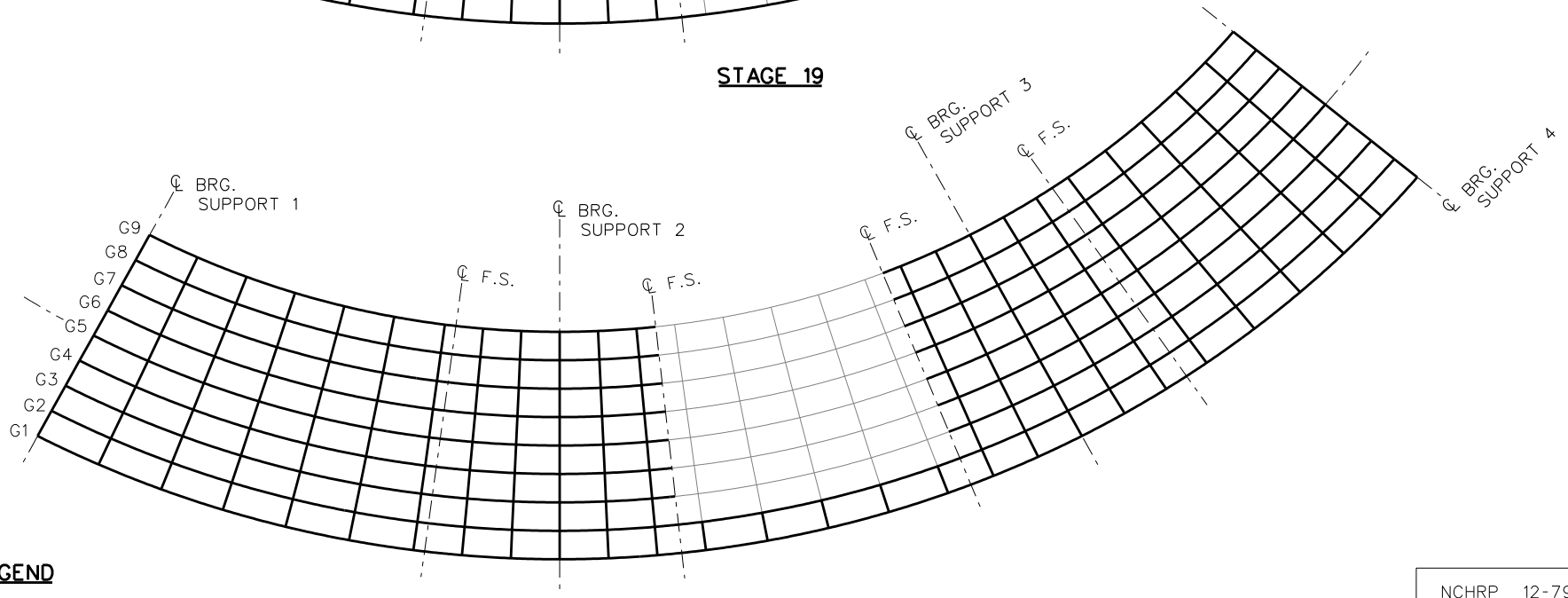

STAGE 20

LEGEND

▽ = HOLD OR LIFT CRANE

○ = TIE DOWN

□ = TEMPORARY SUPPORT STRUCTURE

NCHRP 12-79

BRIDGE NICCR8

GENERAL ERECTION PROCEDURE

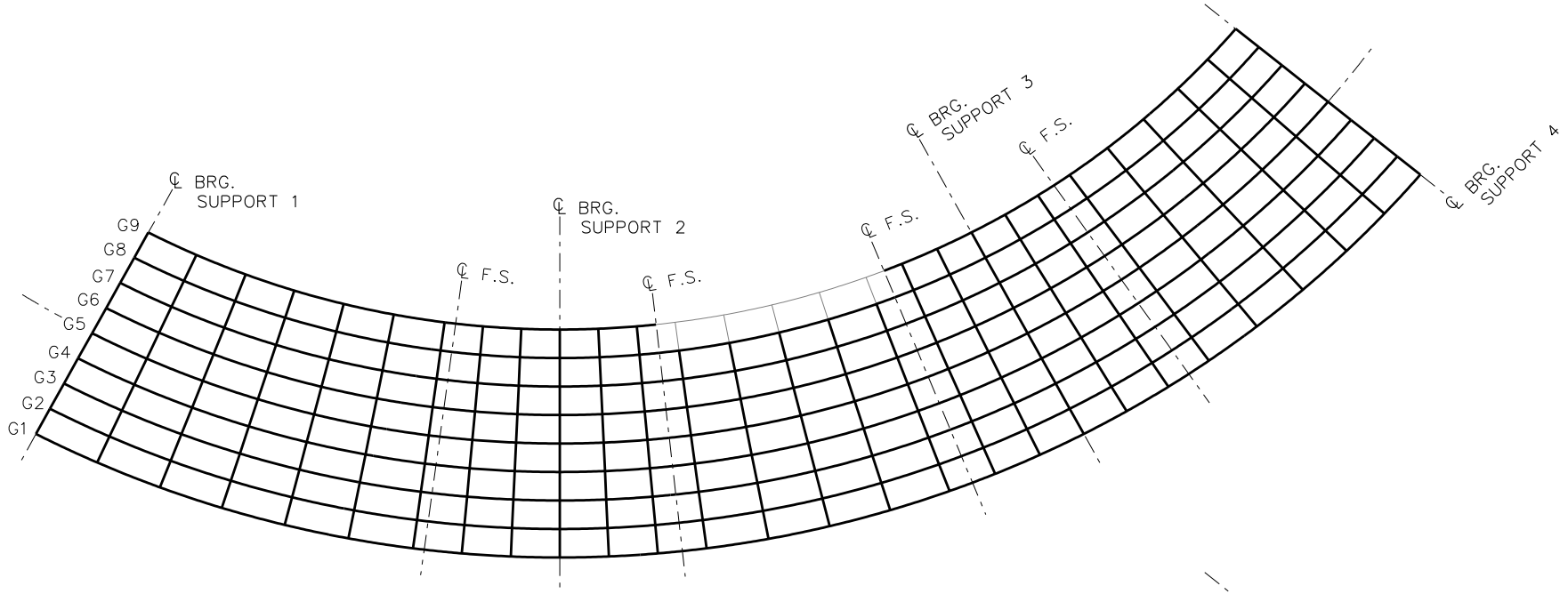

STAGES 21 THRU 26

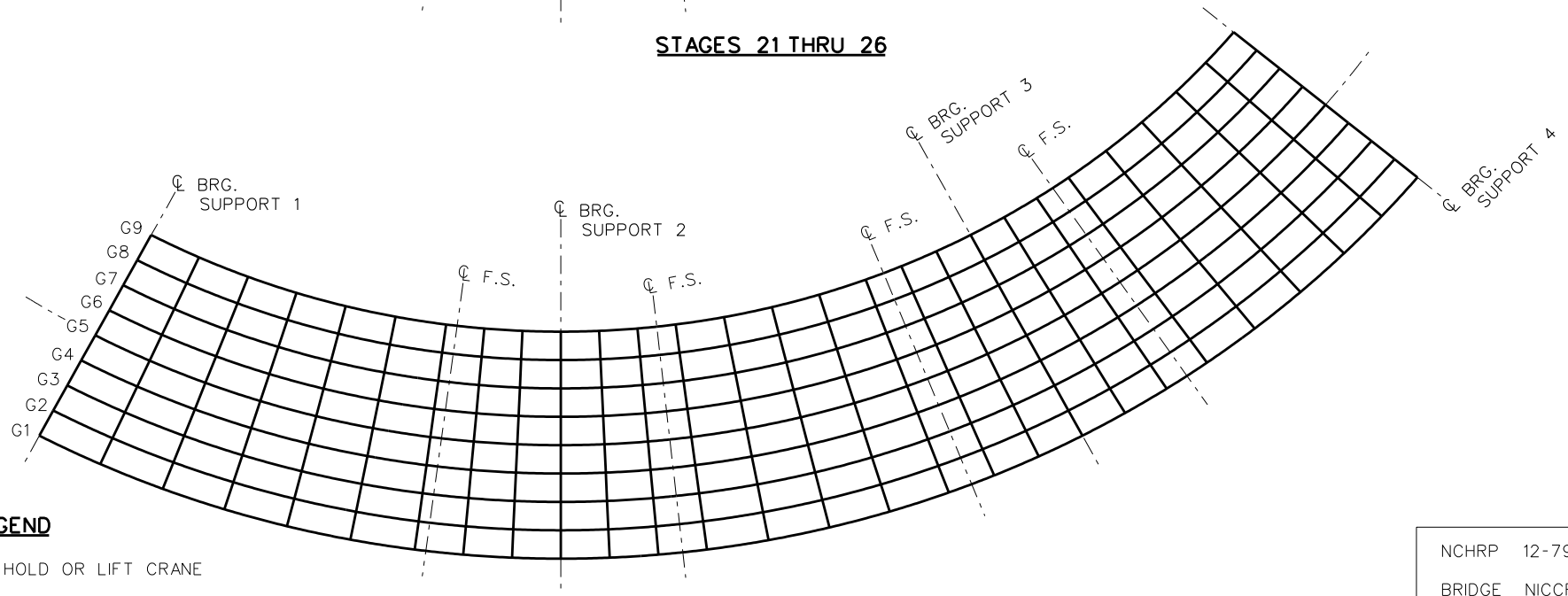

STAGE 27

LEGEND

▽ = HOLD OR LIFT CRANE

○ = TIE DOWN

□ = TEMPORARY SUPPORT STRUCTURE

NCHRP 12-79

BRIDGE NICCR8

GENERAL ERECTION PROCEDURE

SHEET 10 OF 10

NCHRP 12-79

NICCR12

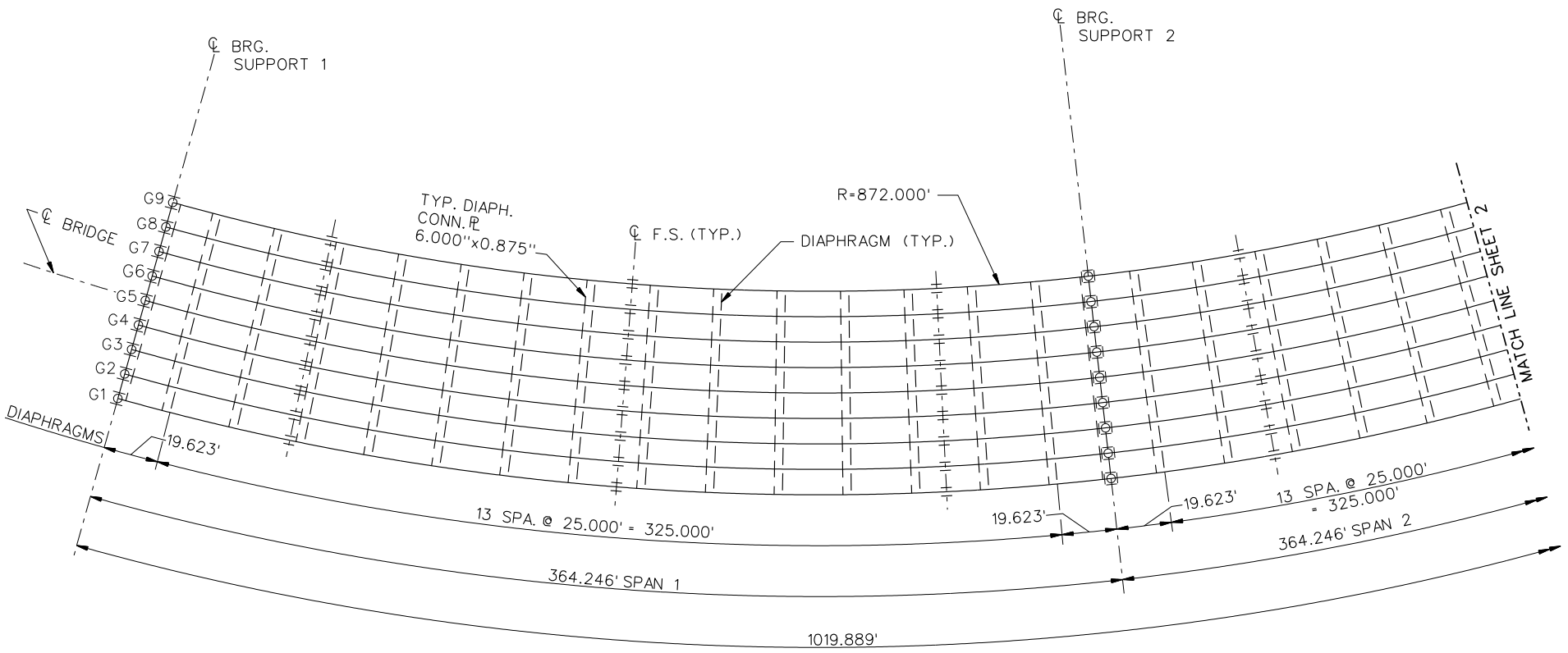

FRAMING PLAN

NOTE :

NO INT. TRANSV. STIFFS.
BRG. STIFFENERS = 12.000"x2.000"

BEARING LEGEND

- ○ NON-GUIDED
- ⊙ LONGITUDINALLY GUIDED
- |○| TRANSVERSELY GUIDED
- |⊙| FIXED

NCHRP 12-79

BRIDGE NICCR12

FRAMING PLAN AND CROSS-SECTION

SHEET 1 OF 16

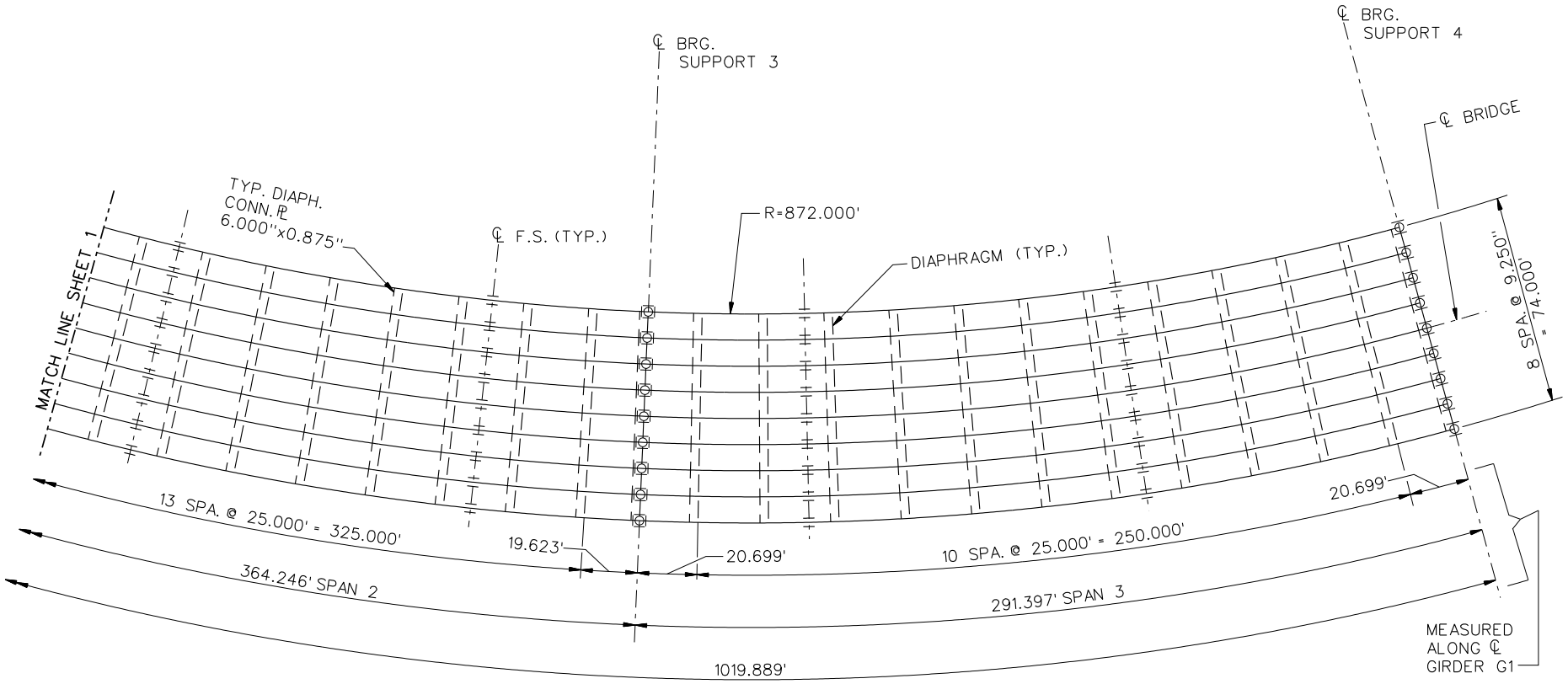

FRAMING PLAN

NOTE :

NO INT. TRANSV. STIFFS.
BRG. STIFFENERS = 12.000"x2.000"

BEARING LEGEND

- ○ NON-GUIDED
- ⊙ LONGITUDINALLY GUIDED
- |○| TRANSVERSELY GUIDED
- |⊙| FIXED

NCHRP 12-79

BRIDGE NICCR12

FRAMING PLAN AND CROSS-SECTION

SHEET 2 OF 16

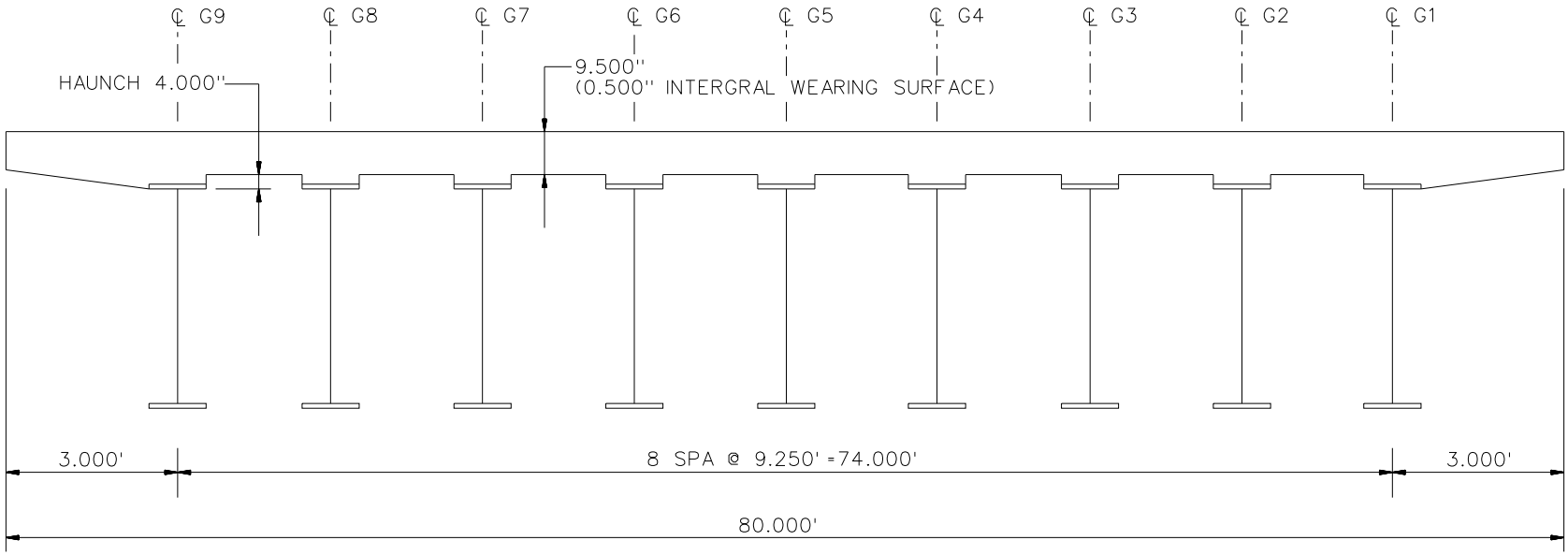

CROSS - SECTION

(DIAPHRAGMS NOT SHOWN)

NCHRP 12-79

BRIDGE NICCR12

CROSS-SECTION

SHEET 3 OF 16

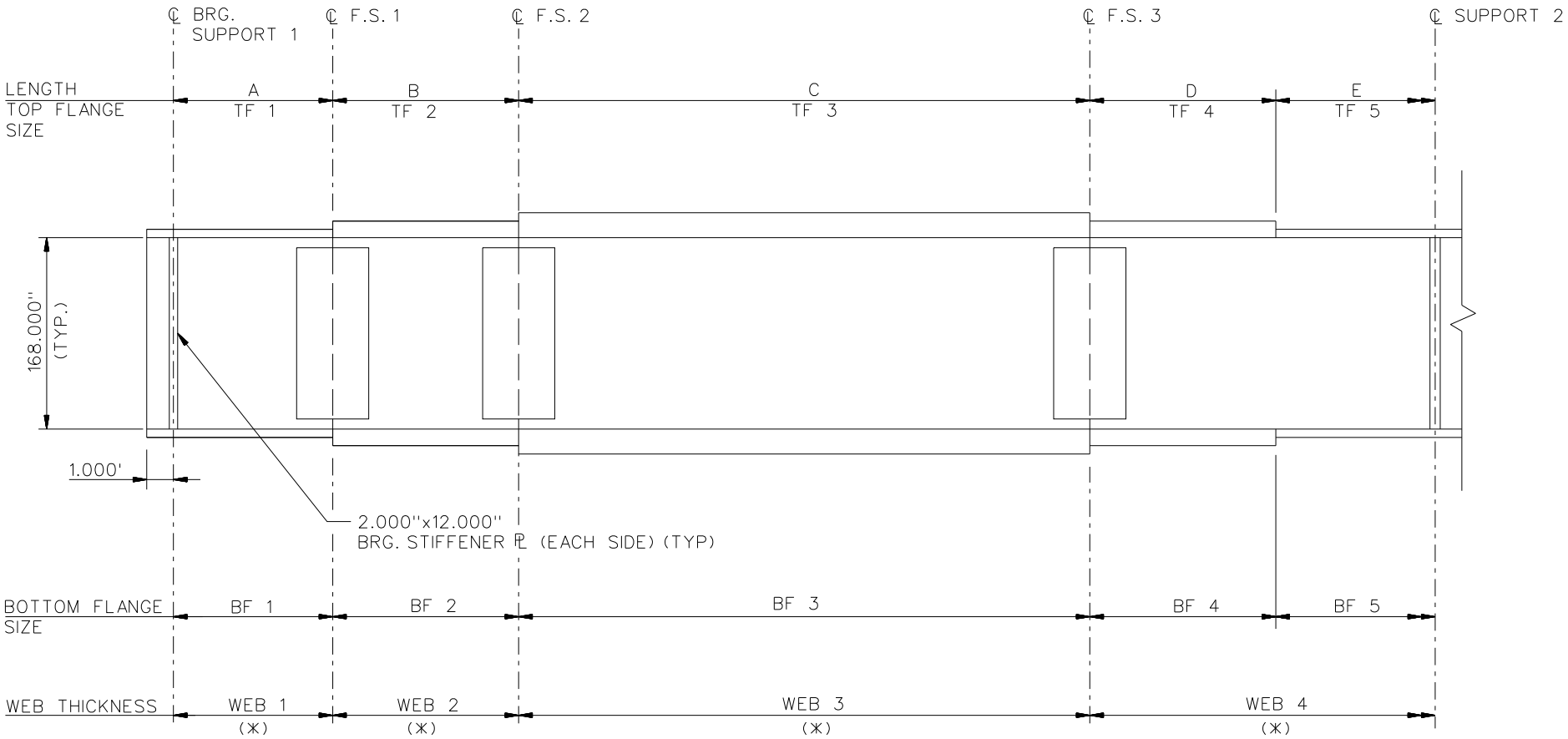

"E", "TF 5", "BF 5", INCLUDES LEFT AND RIGHT OF SUPPORT 2

NOTES:

SEE TABLES ON SHEETS 7, 8 AND 9 FOR GIRDER ELEVATION DIMENSIONS AND PLATE SIZES.

(*) G1, G2, G3, WEB 1 = WEB 2 = WEB 3 = 1.125", WEB 4 = 1.250"
G4, G5, G6, WEB 1 = WEB 2 = WEB 3 = 1.125", WEB 4 = 1.250"
G7, G8, G9, WEB 1 = WEB 2 = WEB 3 = WEB 4 = 1.125"

NCHRP 12-79

BRIDGE NICCR12

GIRDER ELEVATION SPAN 1

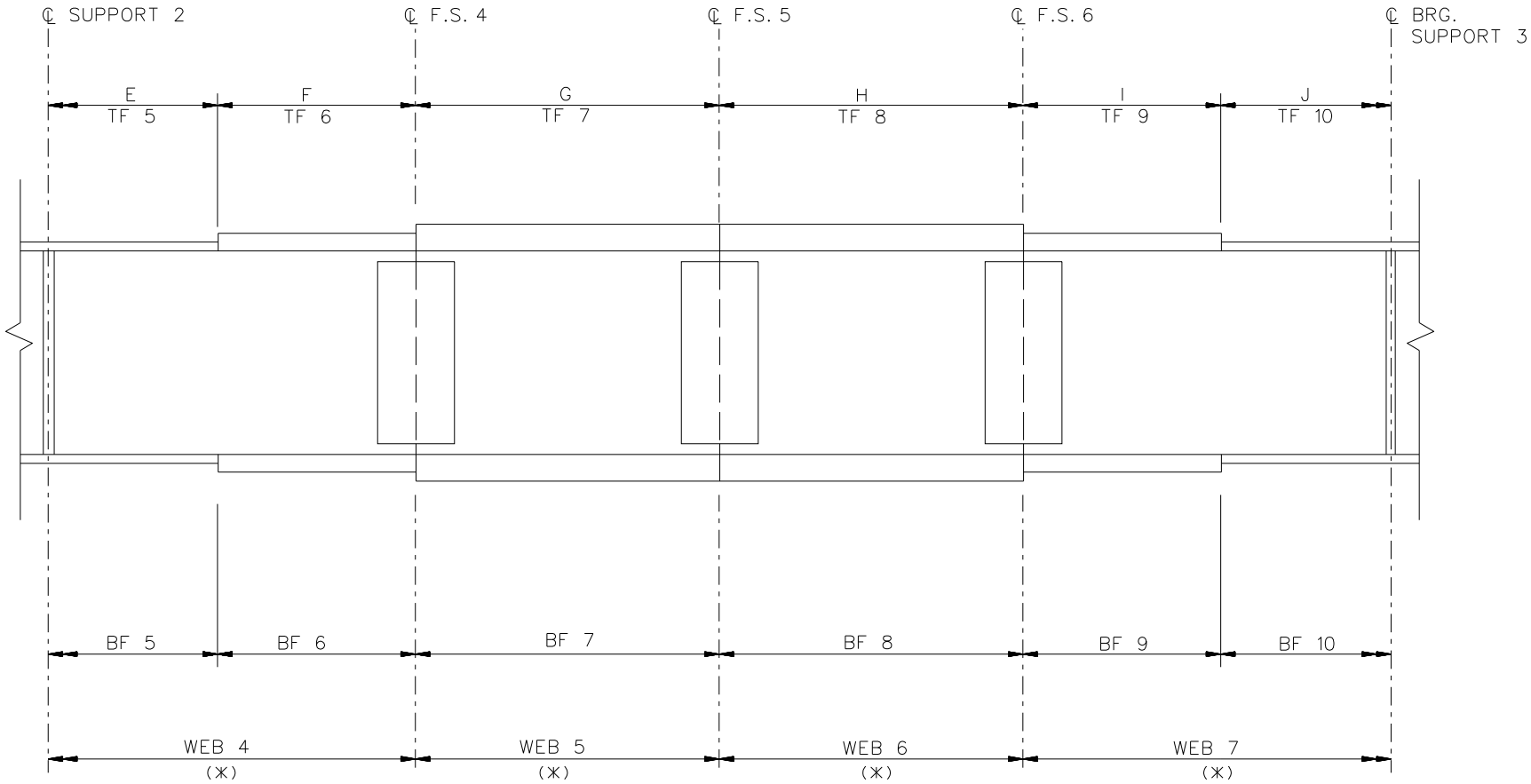

"E", "TF 5", "BF 5", "WEB 4" INCLUDES LEFT AND RIGHT OF SUPPORT 2
"J", 'TF10", "BF10", "WEB 7" INCLUDES LEFT AND RIGHT OF SUPPORT 3

NOTES:

SEE TABLES ON SHEETS 7, 8 AND 9 FOR GIRDER ELEVATION DIMENSIONS AND PLATE SIZES.

(*) G1, G2, G3, WEB 4 = WEB 7 = 1.250", WEB 5 = WEB 6 = 1.125"
G4, G5, G6, WEB 4 = 1.250", WEB 5 = WEB 6 = WEB 7 = 1.125"
G7, G8, G9, WEB 4 = WEB 5 = WEB 6 = WEB 7 = 1.125"

NCHRP 12-79

BRIDGE NICCR12

GIRDER ELEVATION
SPAN 2

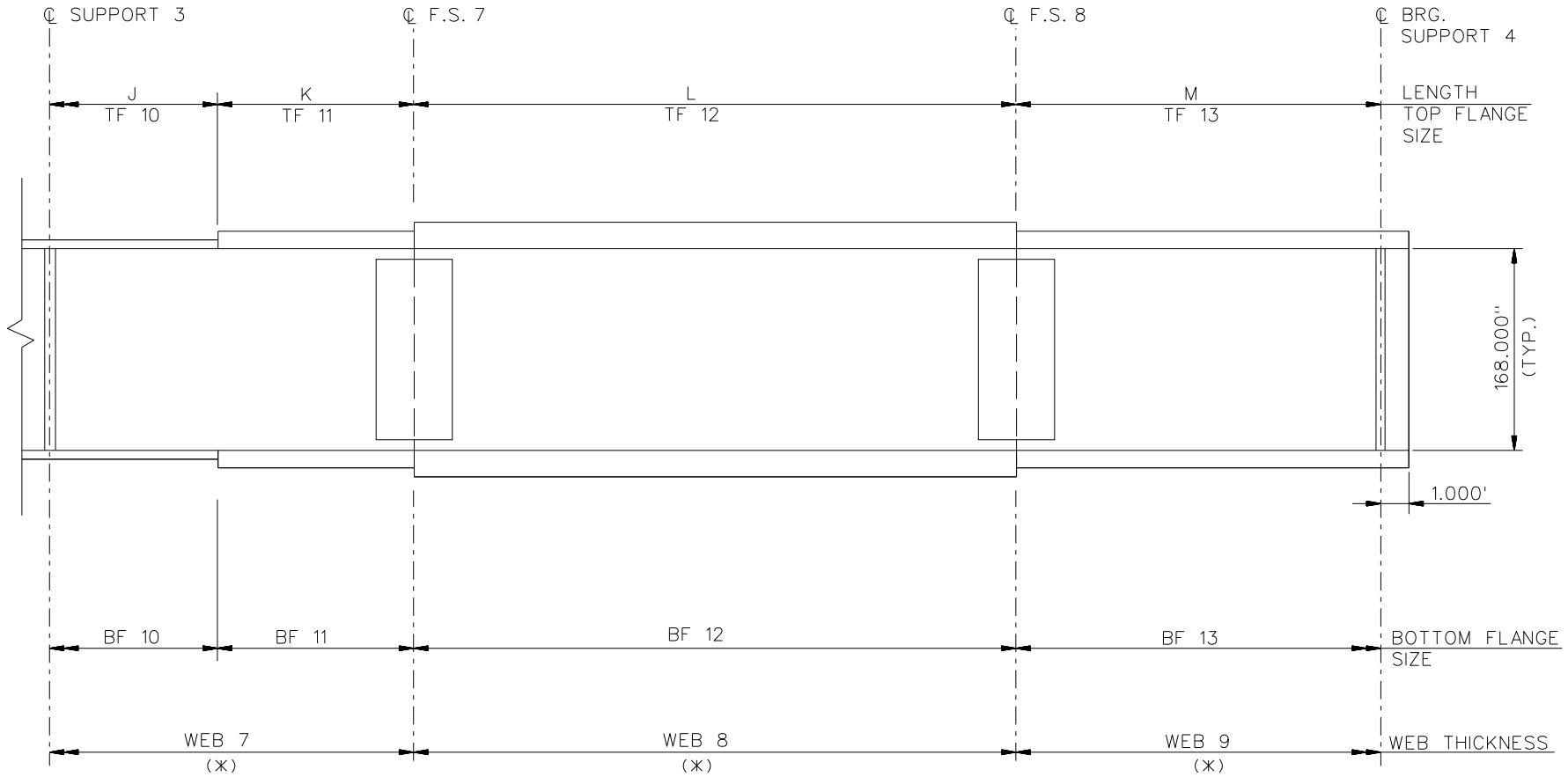

"J", 'TF10", "BF10", "WEB 7" INCLUDES LEFT AND RIGHT OF SUPPORT 3

NOTES:

SEE TABLES ON SHEETS 7, 8 AND 9 FOR GIRDER ELEVATION DIMENSIONS AND PLATE SIZES.

(*) G1, G2, G3, WEB 7 = 1.250", WEB 8 = WEB 9 = 1.125"
G4, G5, G6, WEB 7 = WEB 8 = WEB 9 = 1.125"
G7, G8, G9, WEB 7 = WEB 8 = WEB 9 = 1.125"

NCHRP 12-79

BRIDGE NICCR12

GIRDER ELEVATION
SPAN 3

	GIRDER PLATE LENGTHS ✳								
LENGTH	G1	G2	G3	G4	G5	G6	G7	G8	G9
A	64.246	63.618	62.990	62.362	61.734	61.105	60.477	59.849	59.221
B	120.000	118.827	117.653	116.480	115.307	114.133	112.960	111.786	110.613
C	120.000	118.827	117.653	116.480	115.307	114.133	112.960	111.786	110.613
D	30.000	29.707	29.413	29.120	28.827	28.533	28.240	27.947	27.653
E	60.000	59.413	58.827	58.240	57.653	57.067	56.480	55.893	55.307

✳ ALL DIMENSIONS ARE IN FEET.

	GIRDER FLANGE DIMENSIONS ✳✳					
TOP	G1, G2, G3		G4, G5, G6		G7, G8, G9	
FLANGE	BF	TF	BF	TF	BF	TF
TF1	36.000	2.250	32.000	1.750	30.000	1.500
TF2	36.000	2.500	32.000	1.750	30.000	1.500
TF3	36.000	2.250	32.000	1.750	30.000	1.500
TF4	42.000	2.250	38.000	1.750	36.000	1.500
TF5	42.000	2.750	38.000	2.250	36.000	2.000

✳✳ ALL DIMENSIONS ARE IN INCHES.

	GIRDER FLANGE DIMENSIONS ✳✳					
BOTTOM	G1, G2, G3		G4, G5, G6		G7, G8, G9	
FLANGE	BF	TF	BF	TF	BF	TF
BF1	36.000	2.500	32.000	2.000	30.000	1.750
BF2	36.000	2.750	32.000	2.000	30.000	1.750
BF3	36.000	2.500	32.000	2.000	30.000	1.750
BF4	42.000	2.500	38.000	2.000	36.000	1.750
BF5	42.000	3.000	38.000	2.500	36.000	2.250

✳✳ ALL DIMENSIONS ARE IN INCHES.

NCHRP 12-79

BRIDGE NICCR12

GIRDER ELEVATION TABLES SPAN 1

	GIRDER PLATE LENGTHS ✳								
LENGTH	G1	G2	G3	G4	G5	G6	G7	G8	G9
F	30.000	29.707	29.413	29.120	28.827	28.533	28.240	27.947	27.653
G	122.123	120.929	119.735	118.541	117.347	116.153	114.958	113.764	112.570
H	122.123	120.929	119.735	118.541	117.347	116.153	114.958	113.764	112.570
I	30.000	29.707	29.413	29.120	28.827	28.533	28.240	27.947	27.653
J	60.000	59.413	58.827	58.240	57.653	57.067	56.480	55.893	55.307

✳ ALL DIMENSIONS ARE IN FEET.

	GIRDER FLANGE DIMENSIONS ✳✳					
TOP	G1, G2, G3		G4, G5, G6		G7, G8, G9	
FLANGE	BF	TF	BF	TF	BF	TF
TF6	42.000	2.250	38.000	1.750	36.000	1.500
TF7	36.000	1.500	32.000	1.500	30.000	1.500
TF8	36.000	1.500	32.000	1.500	30.000	1.500
TF9	36.000	1.500	32.000	1.500	30.000	1.500
TF10	36.000	2.250	32.000	2.000	30.000	1.750

✳✳ ALL DIMENSIONS ARE IN INCHES.

	GIRDER FLANGE DIMENSIONS ✳✳					
BOTTOM	G1, G2, G3		G4, G5, G6		G7, G8, G9	
FLANGE	BF	TF	BF	TF	BF	TF
BF6	42.000	2.500	38.000	2.000	36.000	1.750
BF7	36.000	1.750	32.000	1.500	30.000	1.500
BF8	36.000	1.750	32.000	1.500	30.000	1.500
BF9	36.000	1.750	32.000	1.500	30.000	1.500
BF10	36.000	2.500	32.000	2.250	30.000	2.000

✳✳ ALL DIMENSIONS ARE IN INCHES.

NCHRP 12-79

BRIDGE NICCR12

GIRDER ELEVATION TABLES SPAN 2

	GIRDER PLATE LENGTHS ✳								
LENGTH	G1	G2	G3	G4	G5	G6	G7	G8	G9
K	30.000	29.707	29.413	29.120	28.827	28.533	28.240	27.947	27.653
L	120.000	118.827	117.653	116.480	115.307	114.133	112.960	111.786	110.613
M	111.397	110.308	109.219	108.129	107.040	105.951	104.862	103.772	102.683

✳ ALL DIMENSIONS ARE IN FEET.

	GIRDER FLANGE DIMENSIONS ✳✳					
TOP FLANGE	G1, G2, G3		G4, G5, G6		G7, G8, G9	
	BF	TF	BF	TF	BF	TF
TF11	36.000	1.500	32.000	1.500	30.000	1.500
TF12	36.000	1.500	32.000	1.500	30.000	1.500
TF13	30.000	1.500	32.000	1.500	30.000	1.500

✳✳ ALL DIMENSIONS ARE IN INCHES.

	GIRDER FLANGE DIMENSIONS ✳✳					
BOTTOM FLANGE	G1, G2, G3		G4, G5, G6		G7, G8, G9	
	BF	TF	BF	TF	BF	TF
BF11	36.000	1.750	32.000	1.500	30.000	1.500
BF12	36.000	1.750	32.000	1.500	30.000	1.500
BF13	36.000	1.750	32.000	1.500	30.000	1.500

✳✳ ALL DIMENSIONS ARE IN INCHES.

NCHRP 12-79

BRIDGE NICCR12

GIRDER ELEVATION TABLES SPAN 3

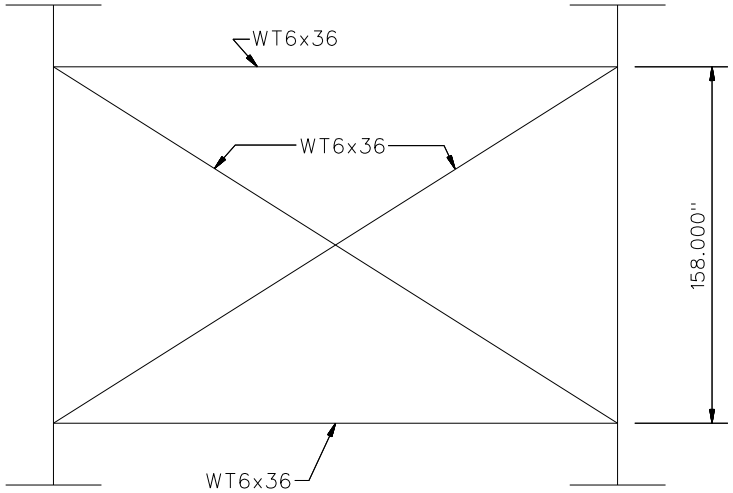

TYPICAL SUPPORT DIAPHRAGMS AND INTERMEDIATE DIAPHRAGMS

NOTES:

1. STEEL DEAD LOAD INCREASED BY 5% FOR MDX AND LARSA MODELS; 2% FOR 3D MODEL; AND 10% FOR APPROXIMATE ANALYSIS TO ACCOUNT FOR MISC. DETAILS.

2. FORMWORK LOAD OF 10PSF IS INCLUDED IN CONCRETE DEAD LOAD.

3. ADDITIONAL DESIGN PARAMETERS:
   A. 1.500' PARAPET WIDTH BOTH SIDES.
   B. 700 LB/FT UNIFORM LOAD ASSUMED FOR PARAPET WEIGHT.
   C. ROADWAY WIDTH = 76.500'.
   D. NUMBER OF DESIGN LANES = 6.
   E. HL93 LIVE LOAD.
   F. DESIGN SPEED = 35 MPH.

4. DIAPHRAGM MEMBER CALL-OUTS ARE IN ENGLISH UNITS.

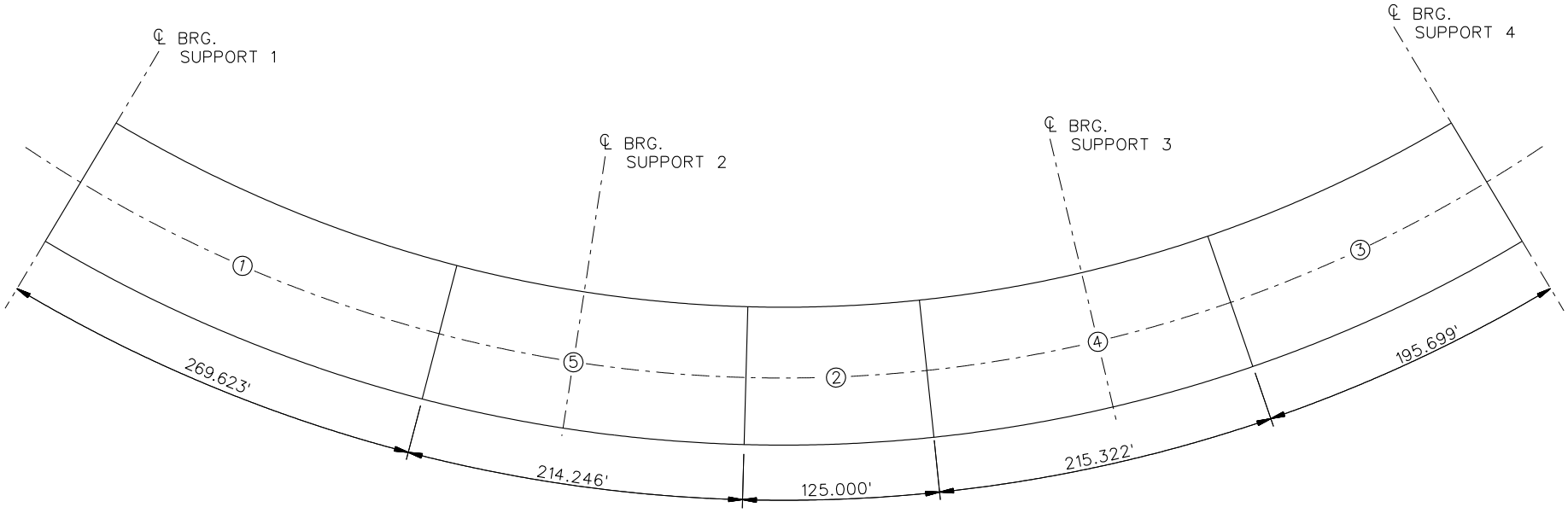

DECK POURING SEQUENCE

NCHRP 12-79

BRIDGE NICCR12

DECK POURING SEQUENCE

SHEET 11 OF 16

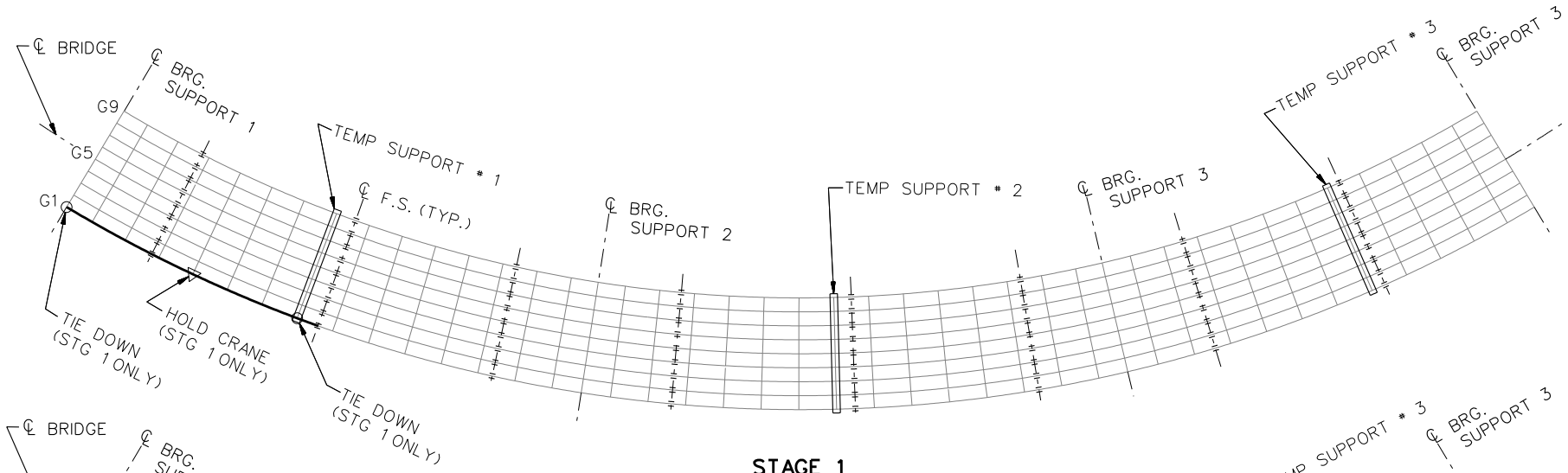

STAGE 1

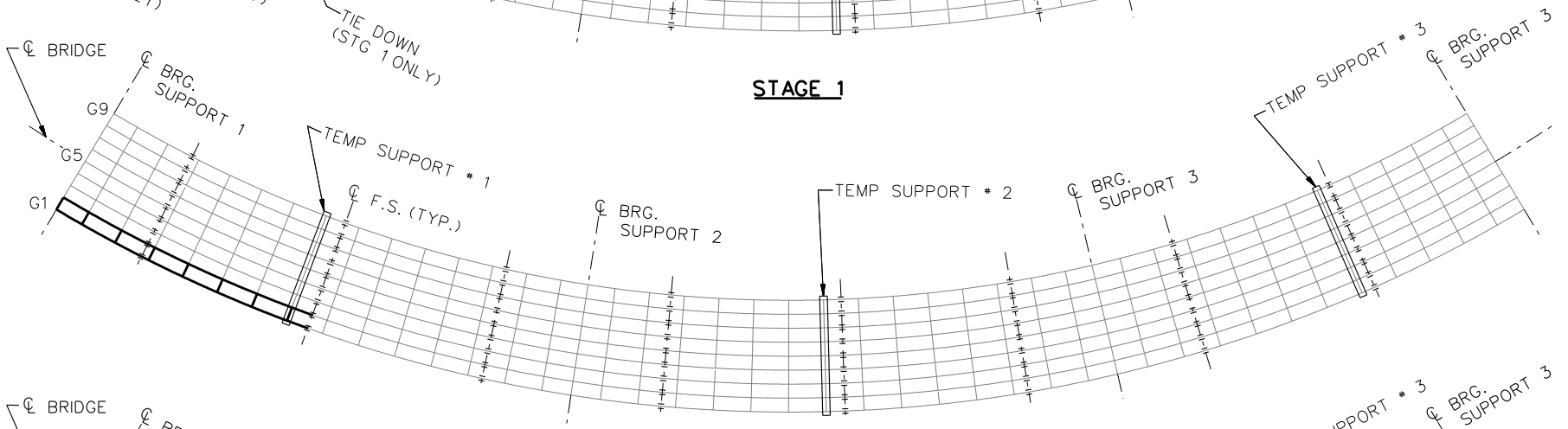

STAGE 2

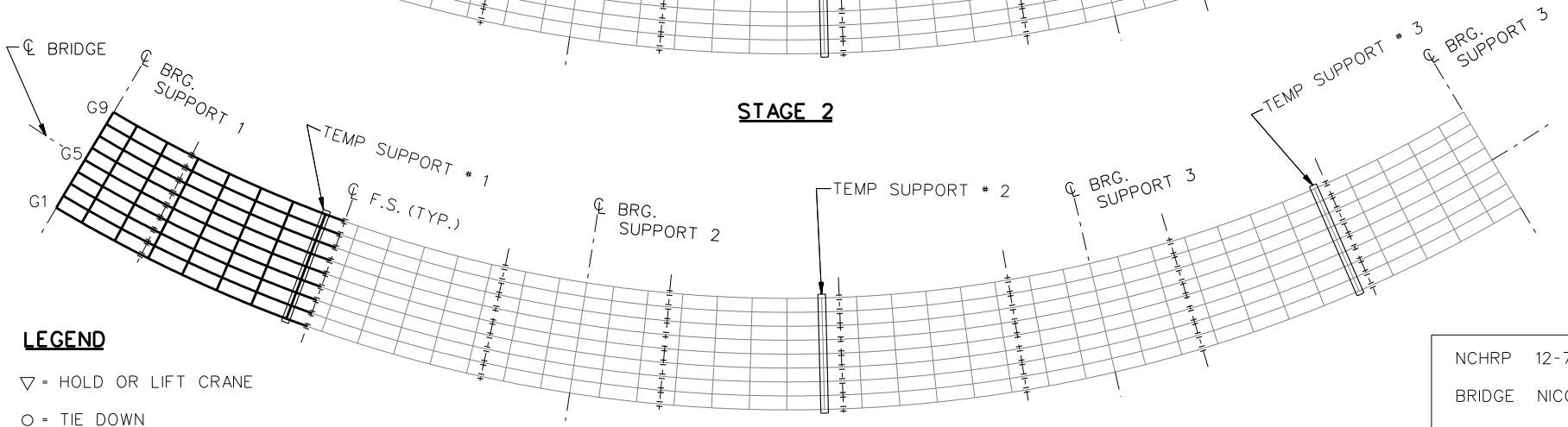

STAGES 3 THRU 9

LEGEND

▽ = HOLD OR LIFT CRANE

○ = TIE DOWN

□ = TEMPORARY SUPPORT STRUCTURE

NCHRP 12-79

BRIDGE NICCR12

GENERAL ERECTION PROCEDURE

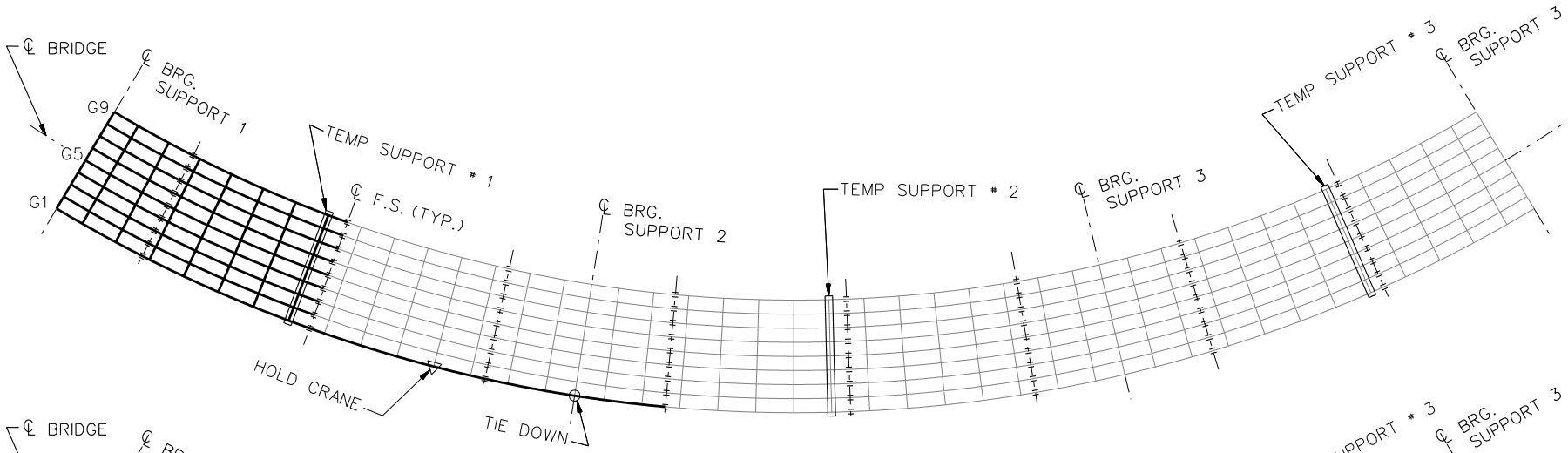

STAGE 10

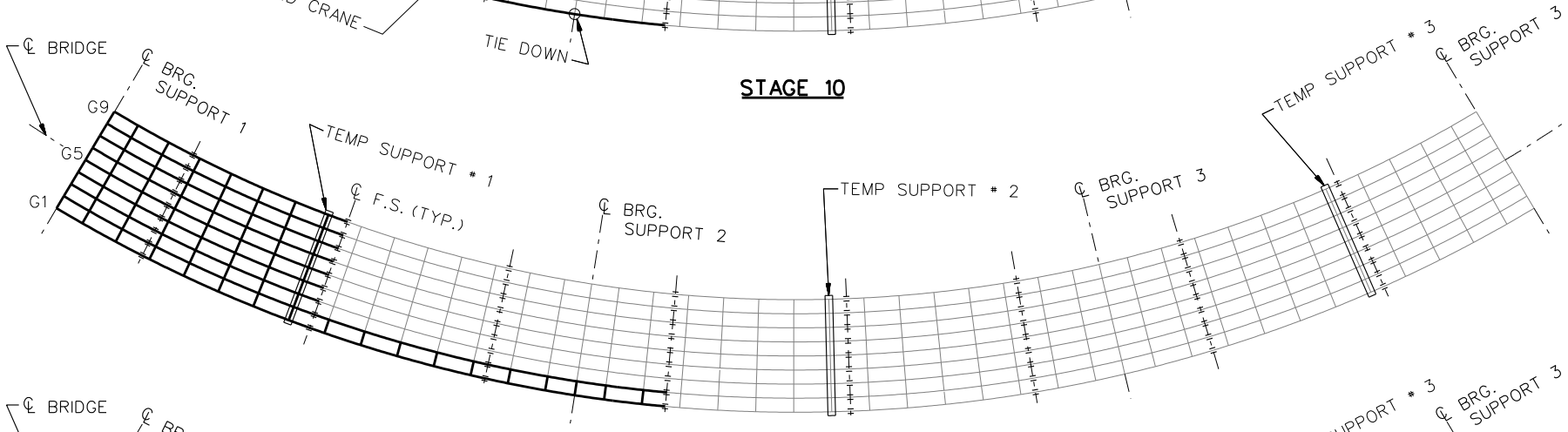

STAGE 11

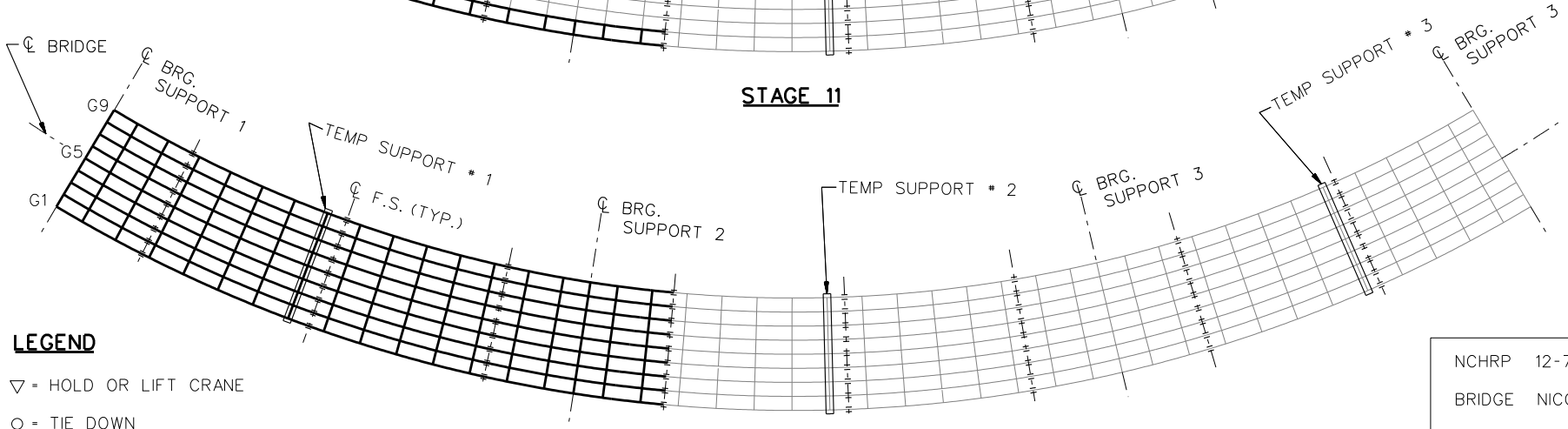

STAGES 12 THRU 18

LEGEND

▽ = HOLD OR LIFT CRANE

○ = TIE DOWN

□ = TEMPORARY SUPPORT STRUCTURE

NCHRP 12-79

BRIDGE NICCR12

GENERAL ERECTION PROCEDURE

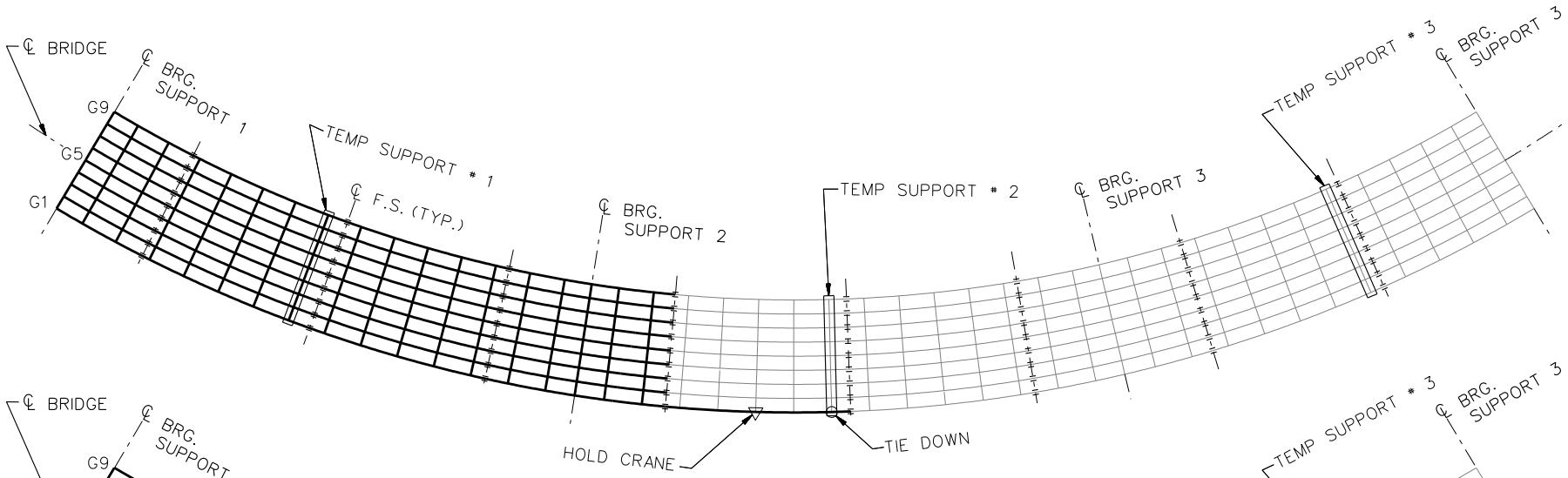

STAGE 19

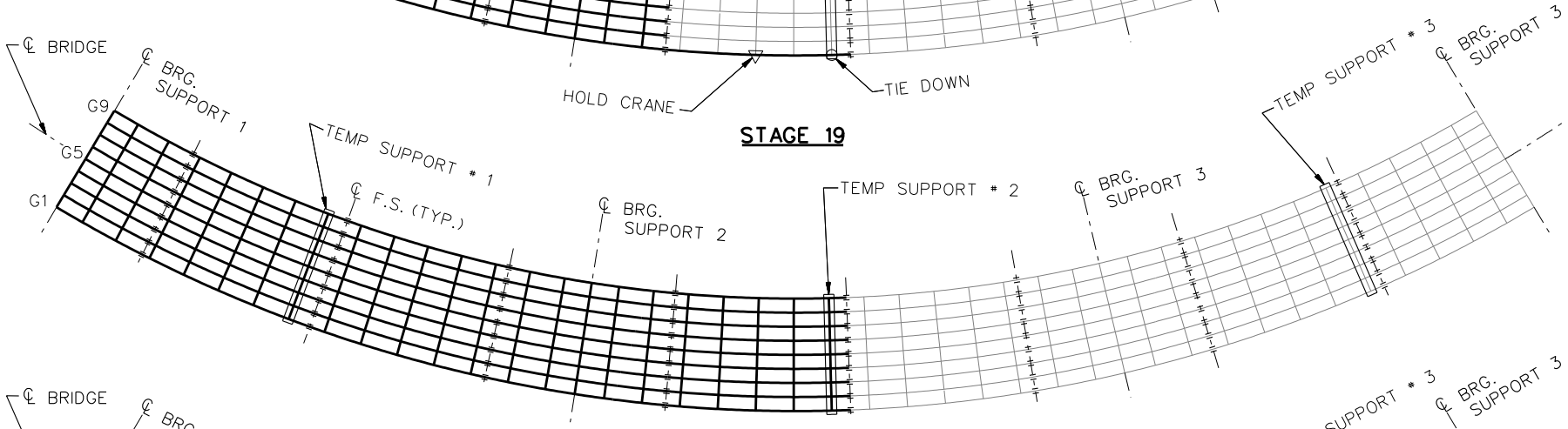

STAGES 20 THRU 27

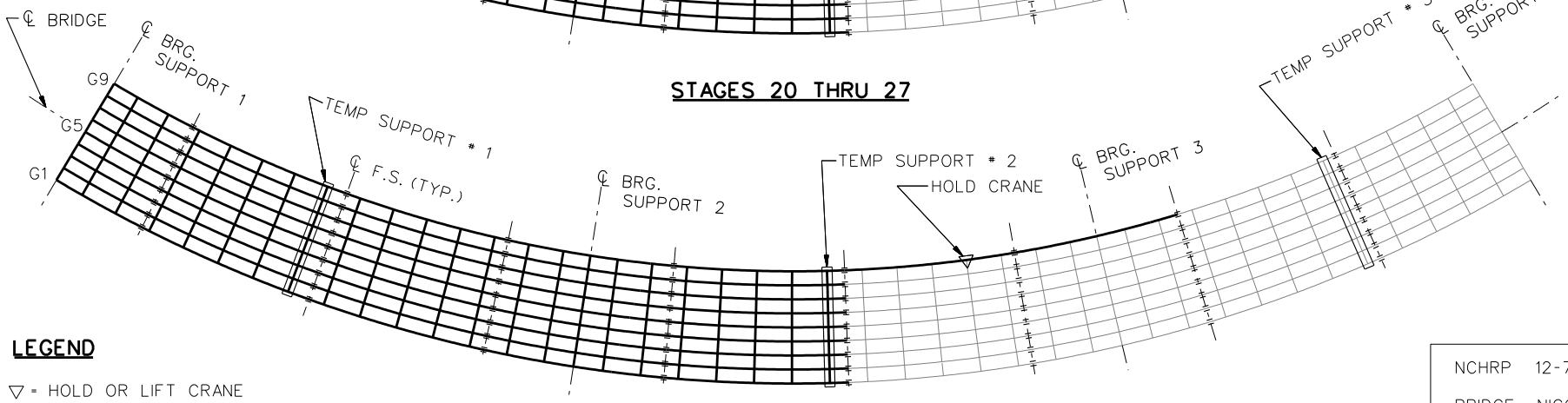

STAGES 28

LEGEND

▽ = HOLD OR LIFT CRANE

○ = TIE DOWN

□ = TEMPORARY SUPPORT STRUCTURE

NCHRP 12-79

BRIDGE NICCR12

GENERAL ERECTION PROCEDURE

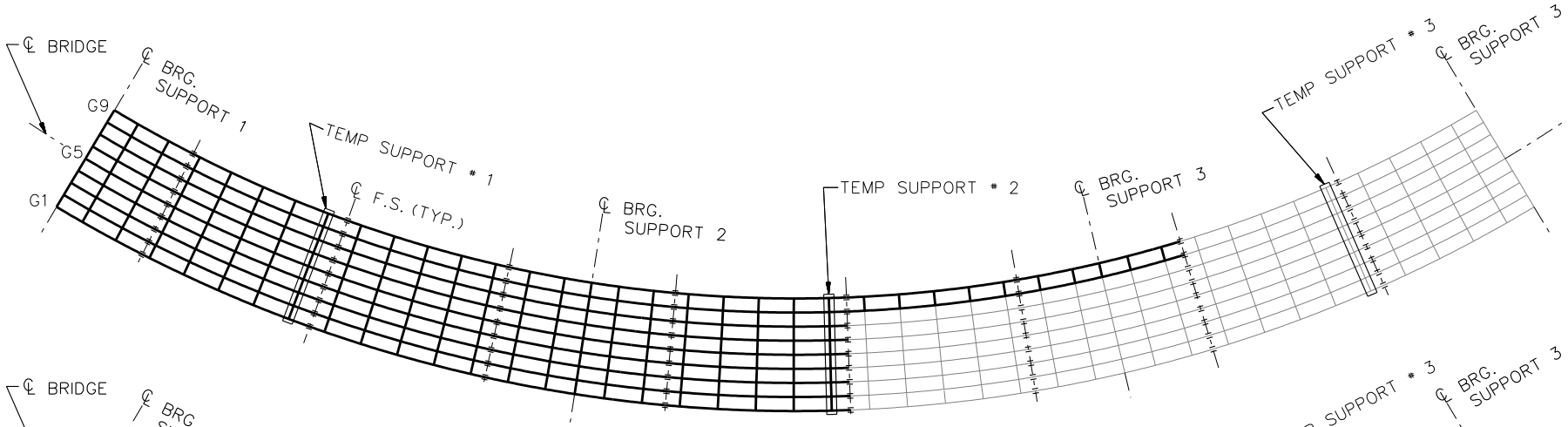

STAGE 29

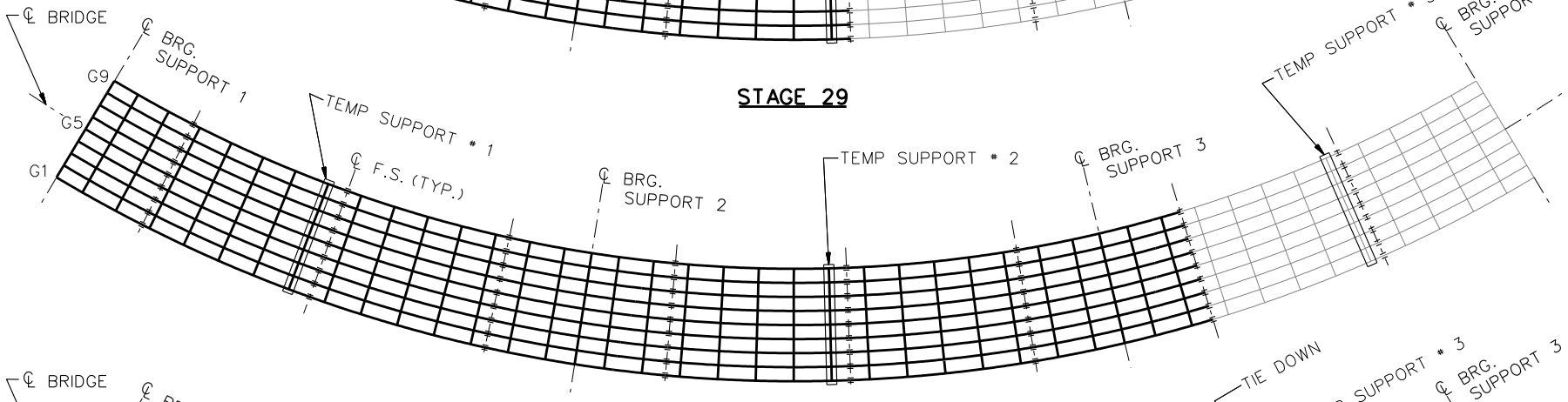

STAGES 30 THRU 36

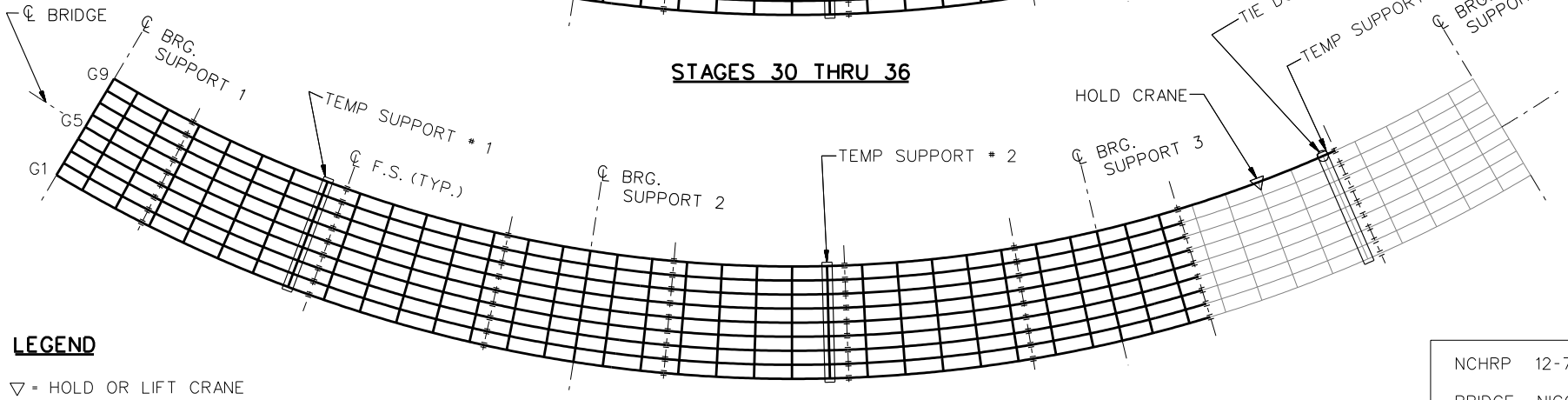

STAGE 37

LEGEND

▽ = HOLD OR LIFT CRANE

○ = TIE DOWN

□ = TEMPORARY SUPPORT STRUCTURE

NCHRP 12-79

BRIDGE NICCR12

GENERAL ERECTION PROCEDURE

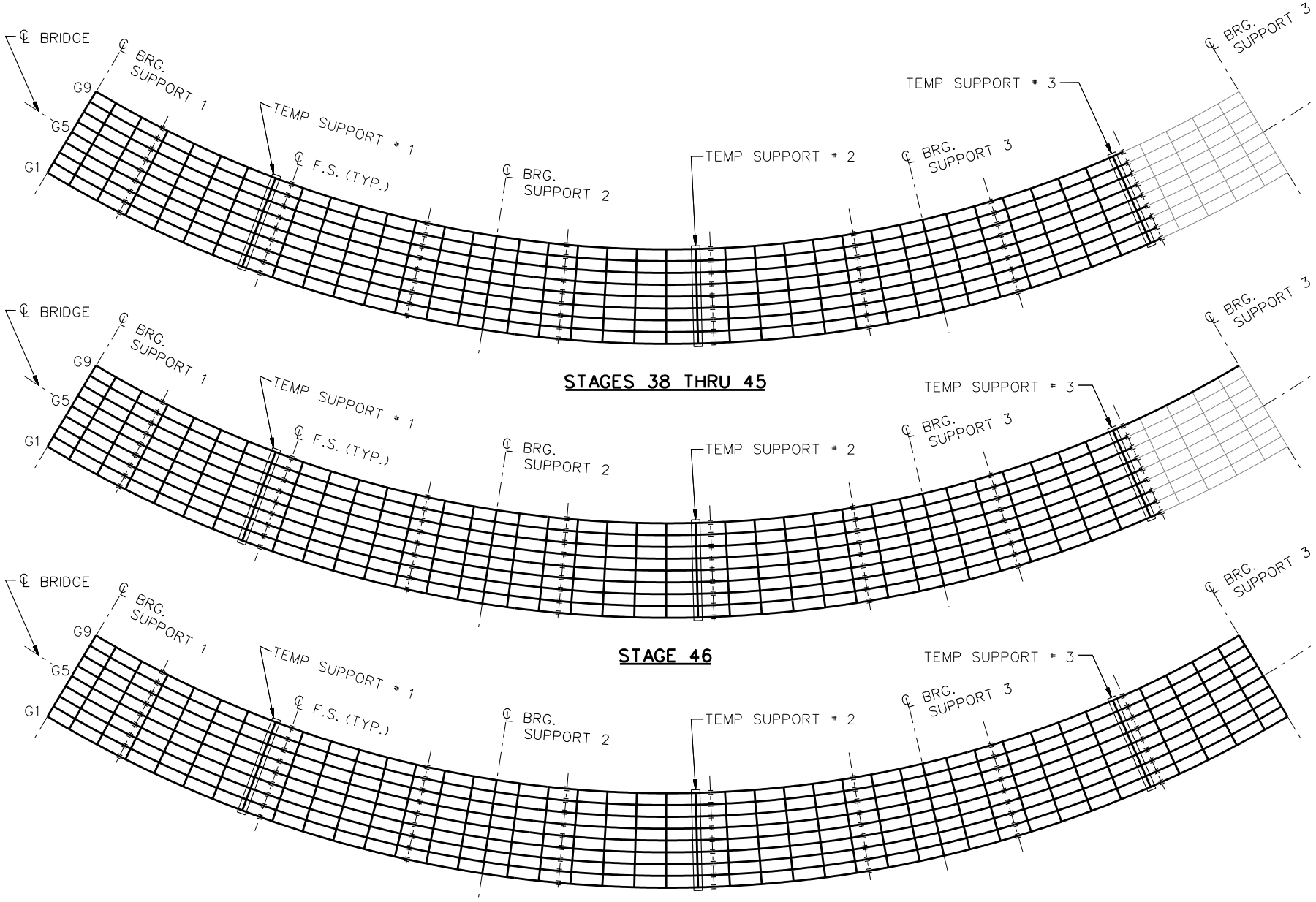

LEGEND

▽ = HOLD OR LIFT CRANE

○ = TIE DOWN

□ = TEMPORARY SUPPORT STRUCTURE

STAGE 55
REMOVE TEMP SUPPORT *3

STAGE 56
REMOVE TEMP SUPPORT * 2

STAGE 57
REMOVE TEMP SUPPORT * 1

NCHRP 12-79

BRIDGE NICCR12

GENERAL ERECTION PROCEDURE

NCHRP 12-79

NICCS2

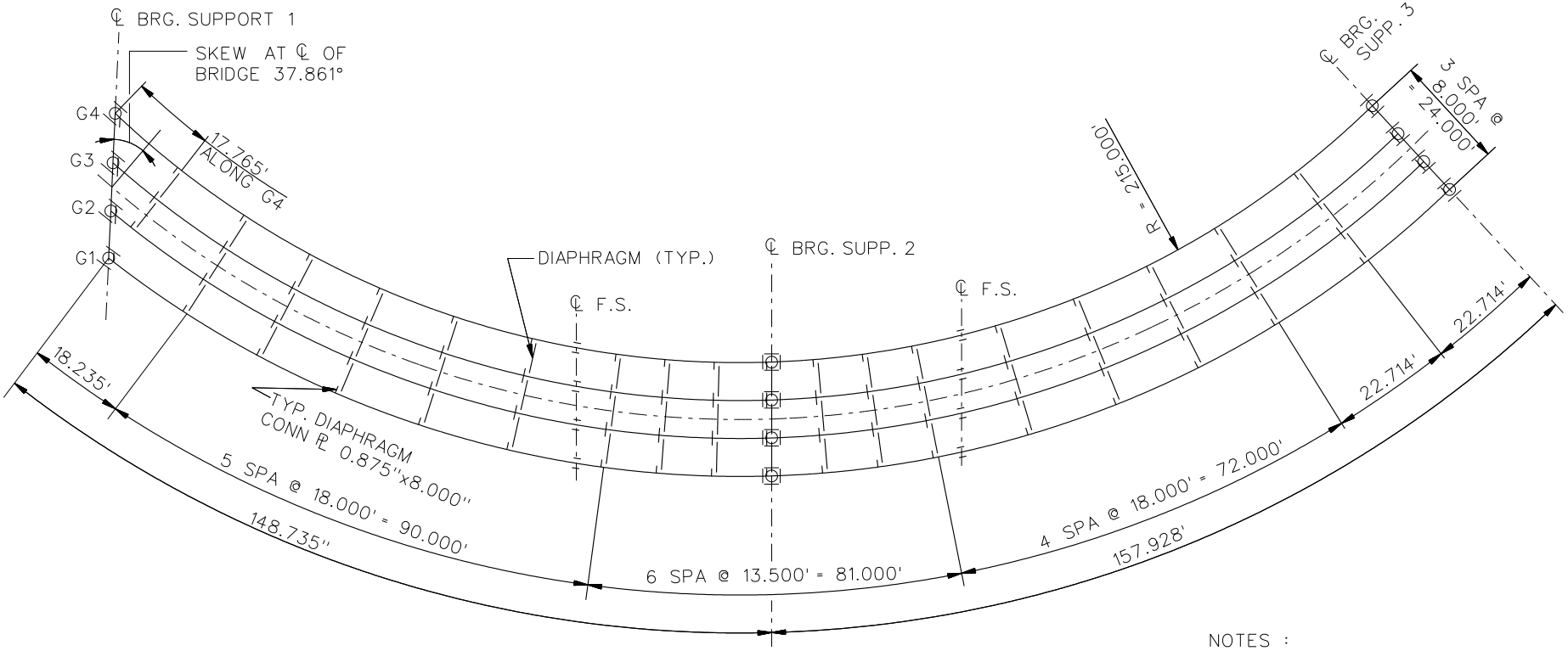

FRAMING PLAN

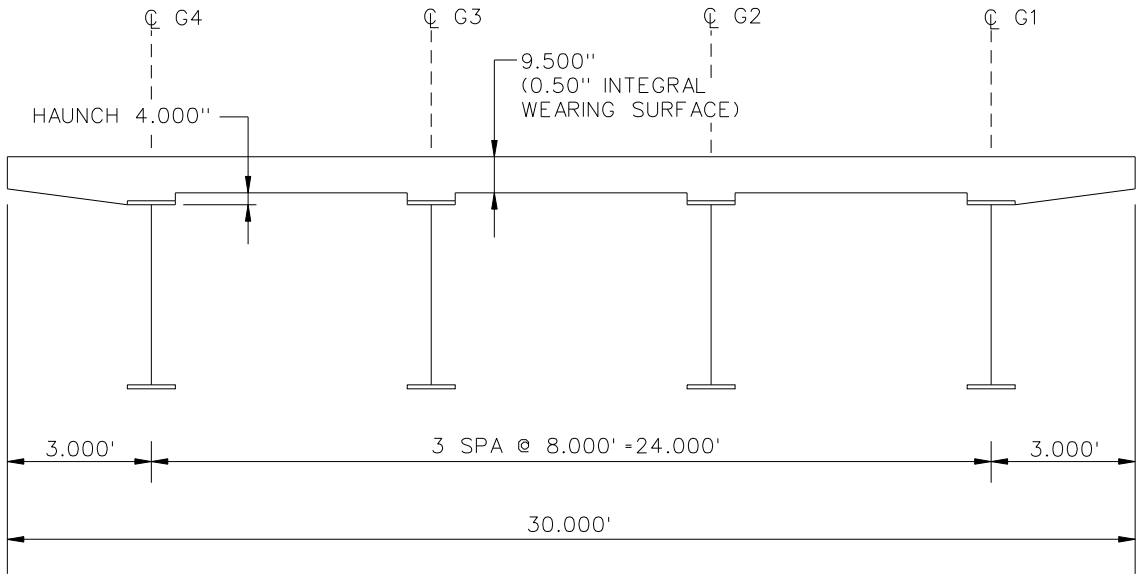

CROSS - SECTION

(DIAPHRAGMS NOT SHOWN)

NOTES :

1. ALL DIMENSIONS MEASURED ALONG G1, U.N.O.

BEARING LEGEND

○ NON-GUIDED

⊙ LONGITUDINALLY GUIDED

|○| TRANSVERSELY GUIDED

|⊙| FIXED

NCHRP 12-79

BRIDGE NICCS2

FRAMING PLAN AND CROSS-SECTION

SHEET 1 OF 9

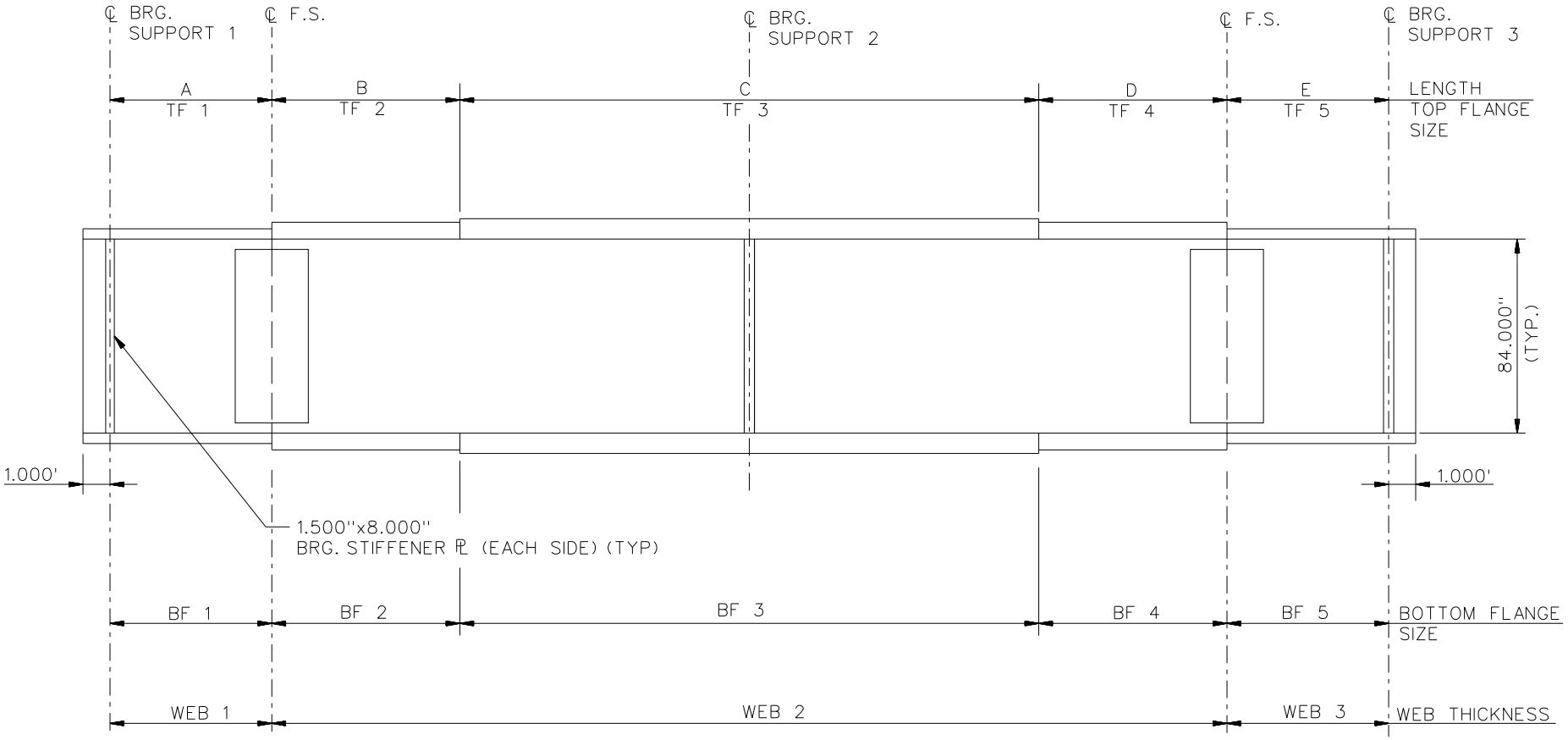

NOTES:

1. SEE TABLES ON SHEET 3 FOR GIRDER ELEVATION DIMENSIONS AND PLATE SIZES.

2. ALL GIRDERS, WEB 1 = WEB 2 = WEB 3 = 0.750"

NCHRP 12-79

BRIDGE NICCS2

GIRDER ELEVATION

SHEET 2 OF 9

	GIRDER PLATE LENGTHS ✳			
LENGTH	G1	G2	G3	G4
A	103.736	104.550	105.483	106.565
B	25.000	25.000	25.000	25.000
C	40.000	40.000	40.000	40.000
D	25.000	25.000	25.000	25.000
E	112.929	107.643	102.357	97.070

✳ ALL DIMENSIONS ARE IN FEET.

	GIRDER FLANGE DIMENSIONS ✳✳							
TOP	G1		G2		G3		G4	
FLANGE	BF	TF	BF	TF	BF	TF	BF	TF
TF1	30.000	1.750	30.000	1.750	26.000	1.250	26.000	1.250
TF2	30.000	2.000	30.000	2.000	26.000	1.250	26.000	1.250
TF3	30.000	2.500	30.000	2.500	26.000	2.000	26.000	2.000
TF4	30.000	2.000	30.000	2.000	26.000	1.250	26.000	1.250
TF5	30.000	1.750	30.000	1.750	26.000	1.250	26.000	1.250

✳✳ ALL DIMENSIONS ARE IN INCHES.

	GIRDER FLANGE DIMENSIONS ✳✳							
BOTTOM	G1		G2		G3		G4	
FLANGE	BF	TF	BF	TF	BF	TF	BF	TF
BF1	30.000	2.500	30.000	2.500	26.000	1.500	26.000	1.500
BF2	30.000	2.500	30.000	2.500	26.000	1.500	26.000	1.500
BF3	30.000	2.500	30.000	2.500	26.000	2.000	26.000	2.000
BF4	30.000	2.500	30.000	2.500	26.000	1.500	26.000	1.500
BF5	30.000	2.500	30.000	2.500	26.000	1.500	26.000	1.500

✳✳ ALL DIMENSIONS ARE IN INCHES.

NCHRP 12-79

BRIDGE NICCS2

GIRDER ELEVATION TABLES

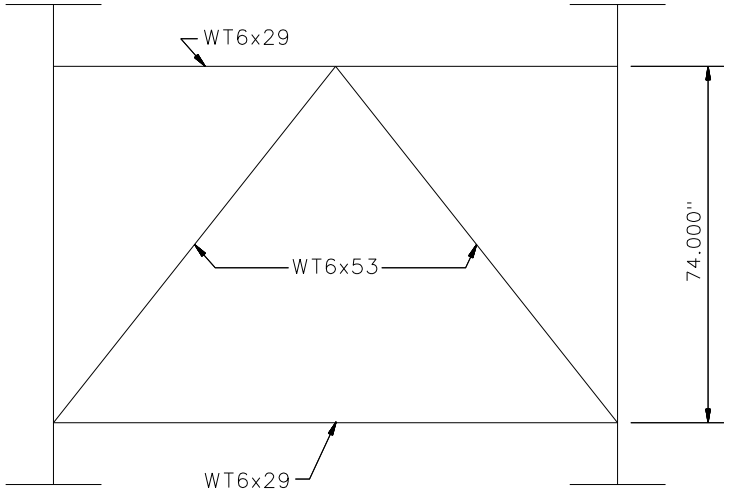

TYPICAL DIAPHRAGM AT SUPPORTS

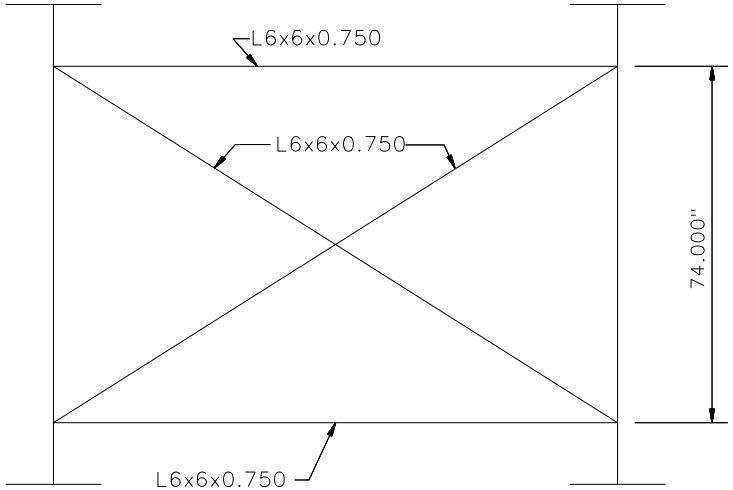

TYPICAL INTERMEDIATE DIAPHRAGM

NOTES:

1. STEEL DEAD LOAD INCREASED BY 5% FOR MDX AND LARSA MODELS; 2% FOR 3D MODEL; AND 10% FOR APPROXIMATE ANALYSIS TO ACCOUNT FOR MISC. DETAILS.

2. FORMWORK LOAD OF 10PSF IS INCLUDED IN CONCRETE DEAD LOAD.

3. ADDITIONAL DESIGN PARAMETERS:
   A. 1.500' PARAPET WIDTH BOTH SIDES.
   B. 700 LB/FT UNIFORM LOAD ASSUMED FOR PARAPET WEIGHT.
   C. ROADWAY WIDTH = 26.500'.
   D. NUMBER OF DESIGN LANES = 2.
   E. HL93 LIVE LOAD.
   F. DESIGN SPEED = 35 MPH.

4. DIAPHRAGM MEMBER CALL-OUTS ARE IN ENGLISH UNITS.

NCHRP 12-79

BRIDGE NICCS2

MISC. DETAILS AND NOTES

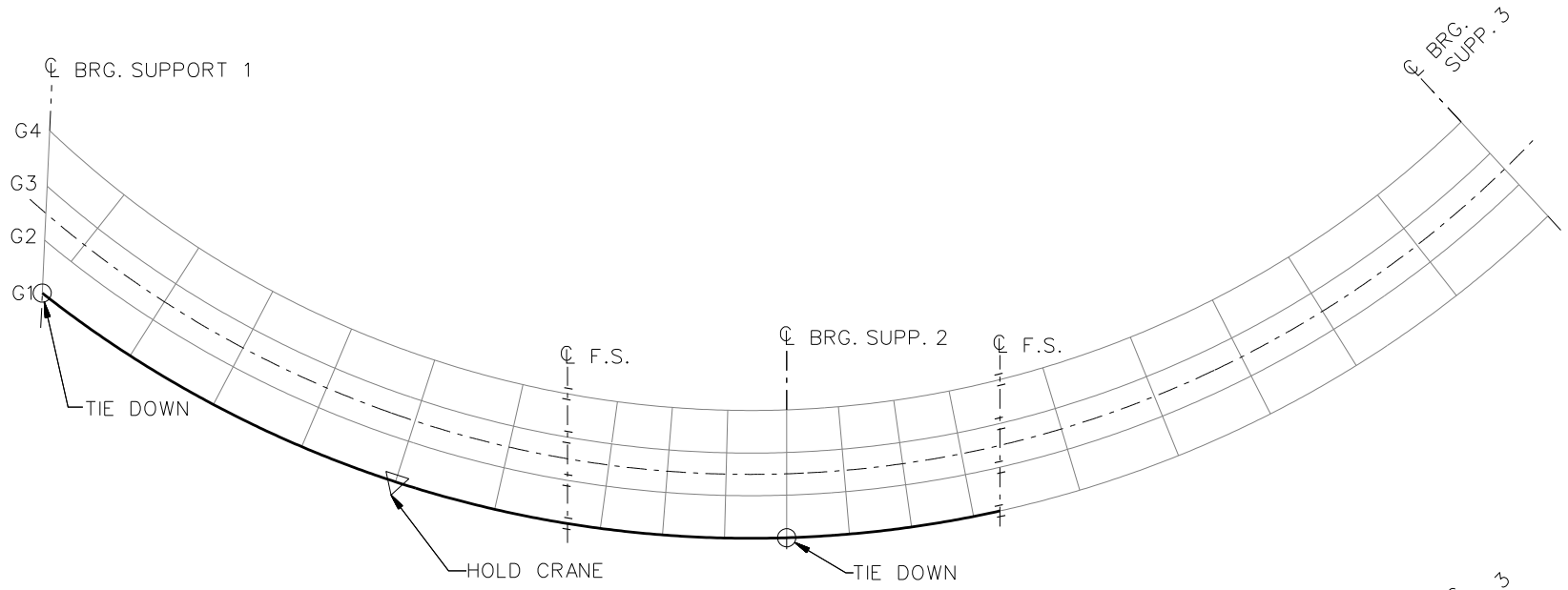

STAGE 1

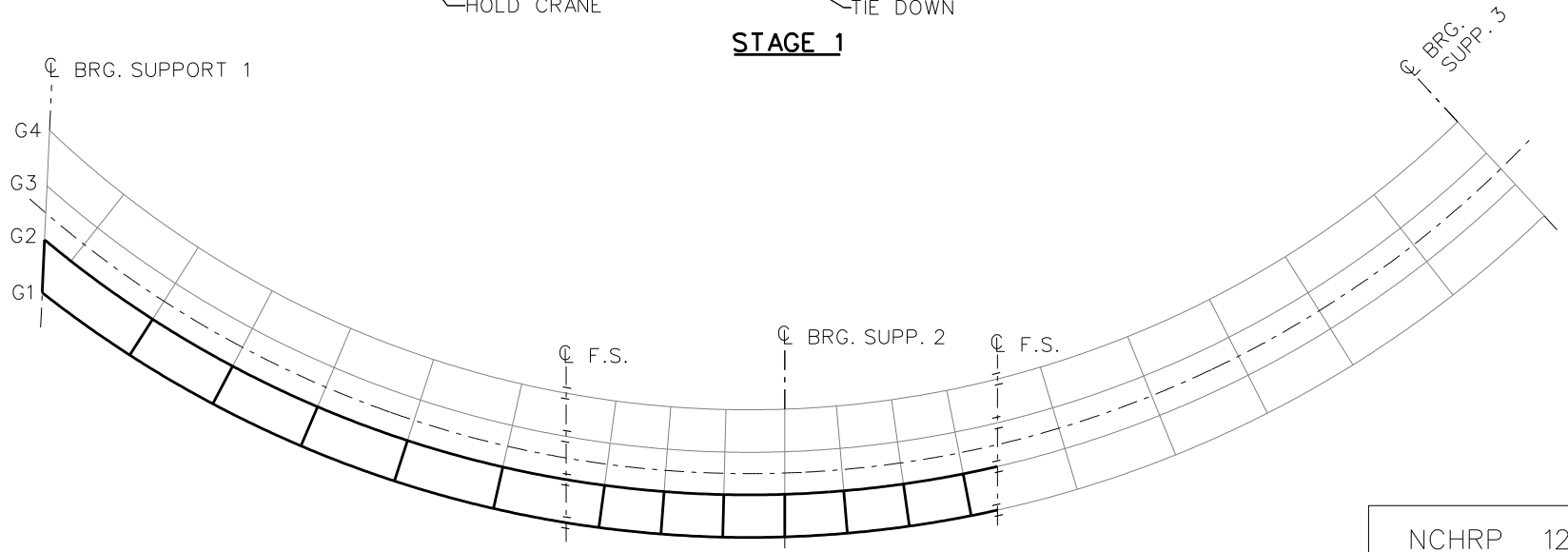

STAGE 2

LEGEND

▽ = HOLD OR LIFT CRANE

○ = TIE DOWN

□ = TEMPORARY SUPPORT STRUCTURE

NCHRP 12-79

BRIDGE NICCS2

GENERAL ERECTION PROCEDURE

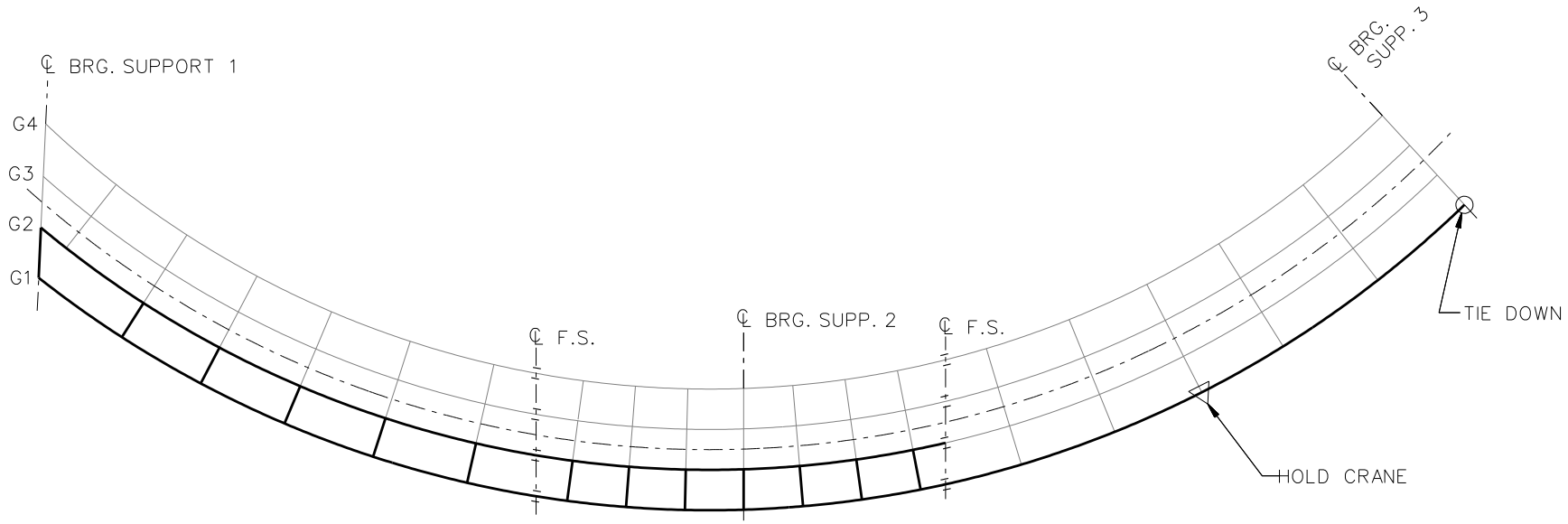

STAGE 3

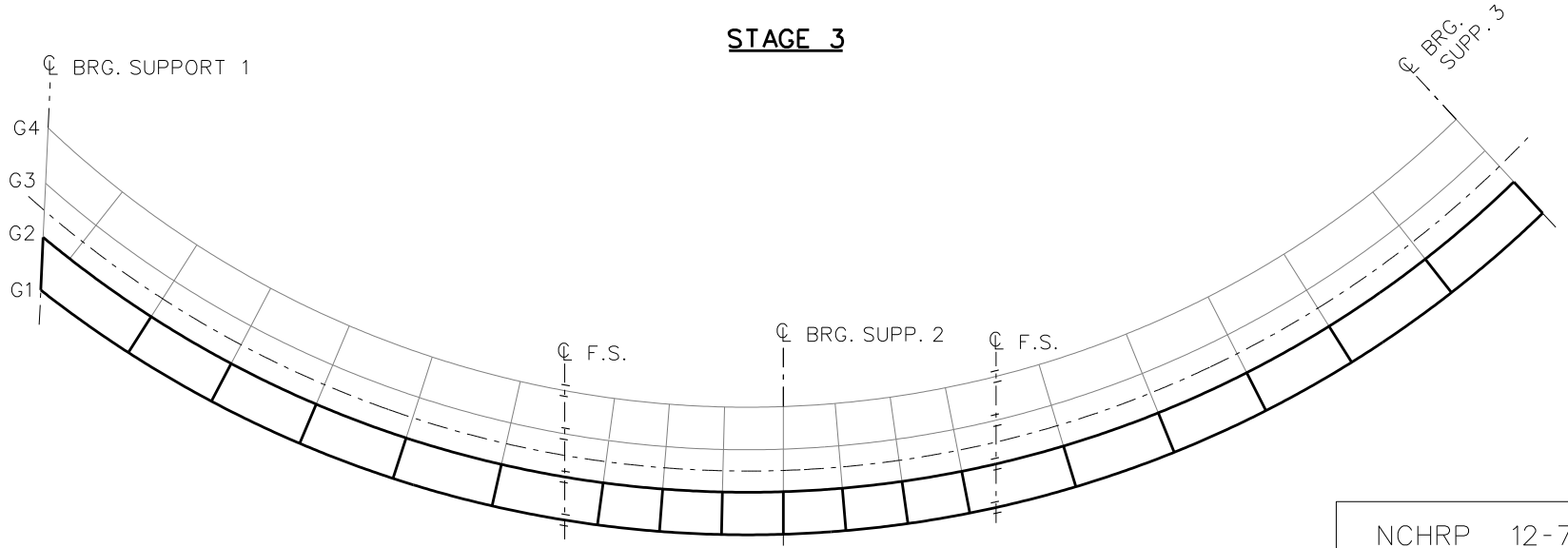

STAGE 4

LEGEND

▽ = HOLD OR LIFT CRANE

○ = TIE DOWN

□ = TEMPORARY SUPPORT STRUCTURE

NCHRP 12-79

BRIDGE NICCS2

GENERAL ERECTION PROCEDURE

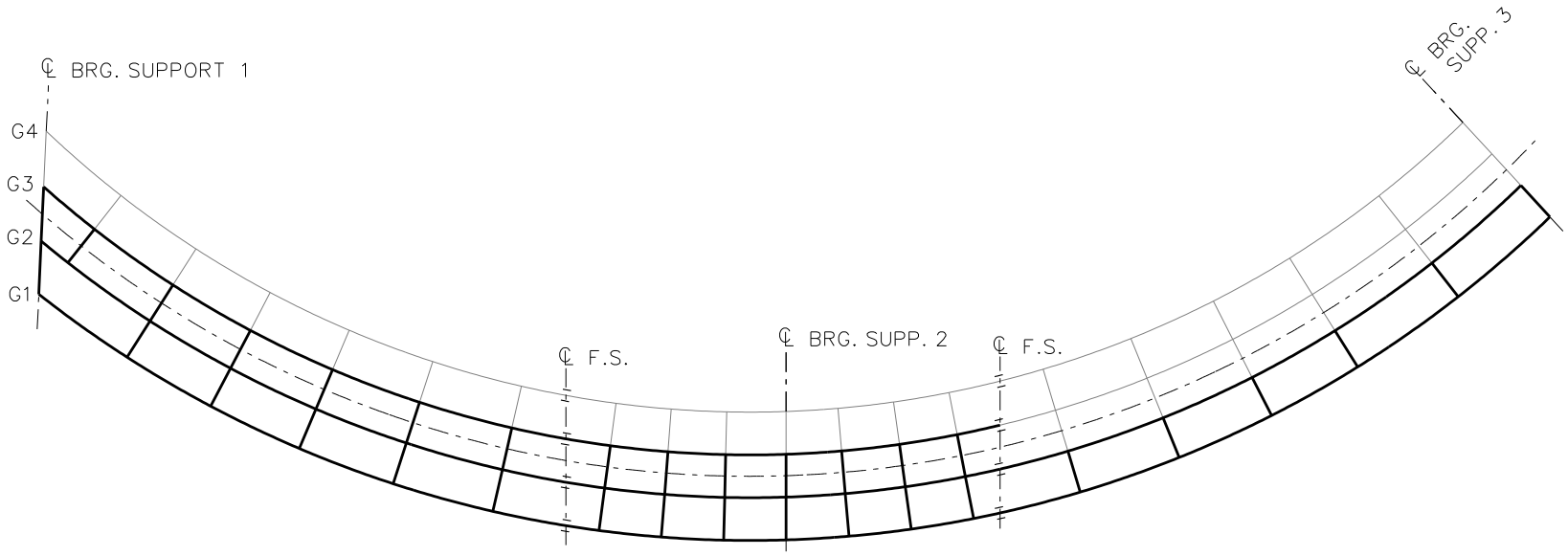

STAGE 5

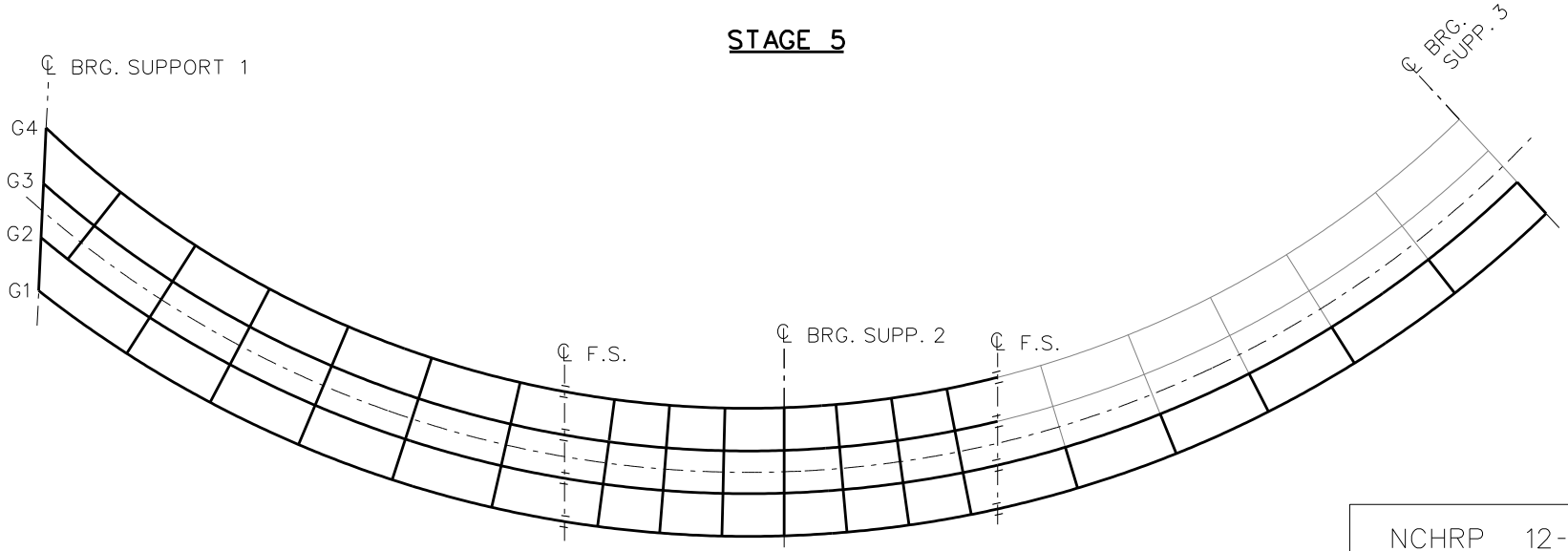

STAGE 6

LEGEND

▽ = HOLD OR LIFT CRANE

○ = TIE DOWN

□ = TEMPORARY SUPPORT STRUCTURE

NCHRP 12-79

BRIDGE NICCS2

GENERAL ERECTION PROCEDURE

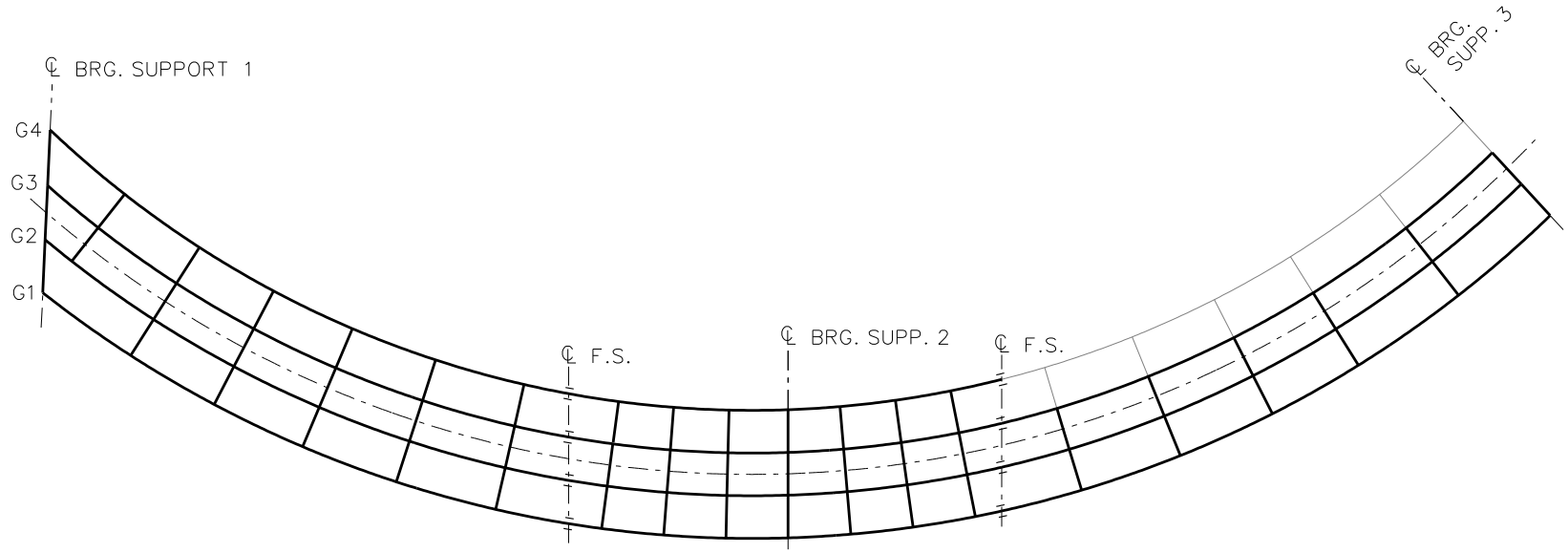

STAGE 7

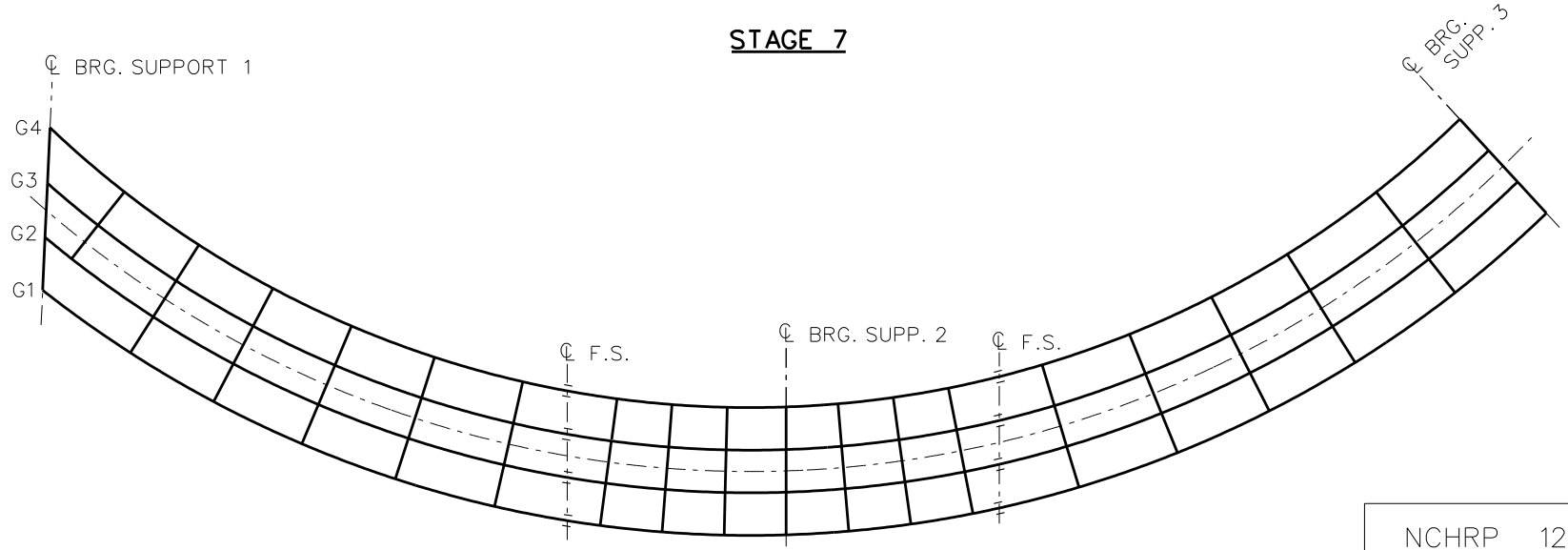

STAGE 8

LEGEND

▽ = HOLD OR LIFT CRANE

○ = TIE DOWN

□ = TEMPORARY SUPPORT STRUCTURE

NCHRP 12-79

BRIDGE NICCS2

GENERAL ERECTION PROCEDURE

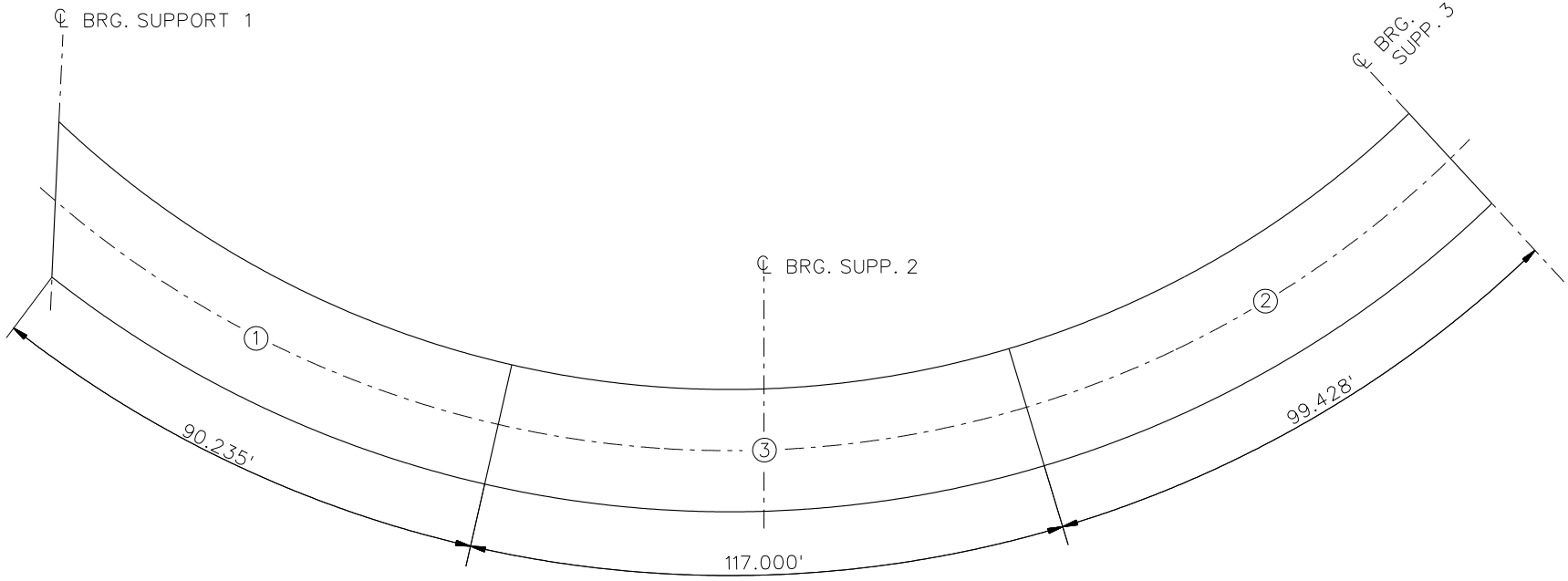

DECK POURING SEQUENCE

NOTES :

1. DECK POUR LENGTHS ARE MEASURED ALONG G1.

NCHRP 12-79

BRIDGE NICCS2

DECK POURING SEQUENCE

SHEET 9 OF 9

NCHRP 12-79

NICCS3

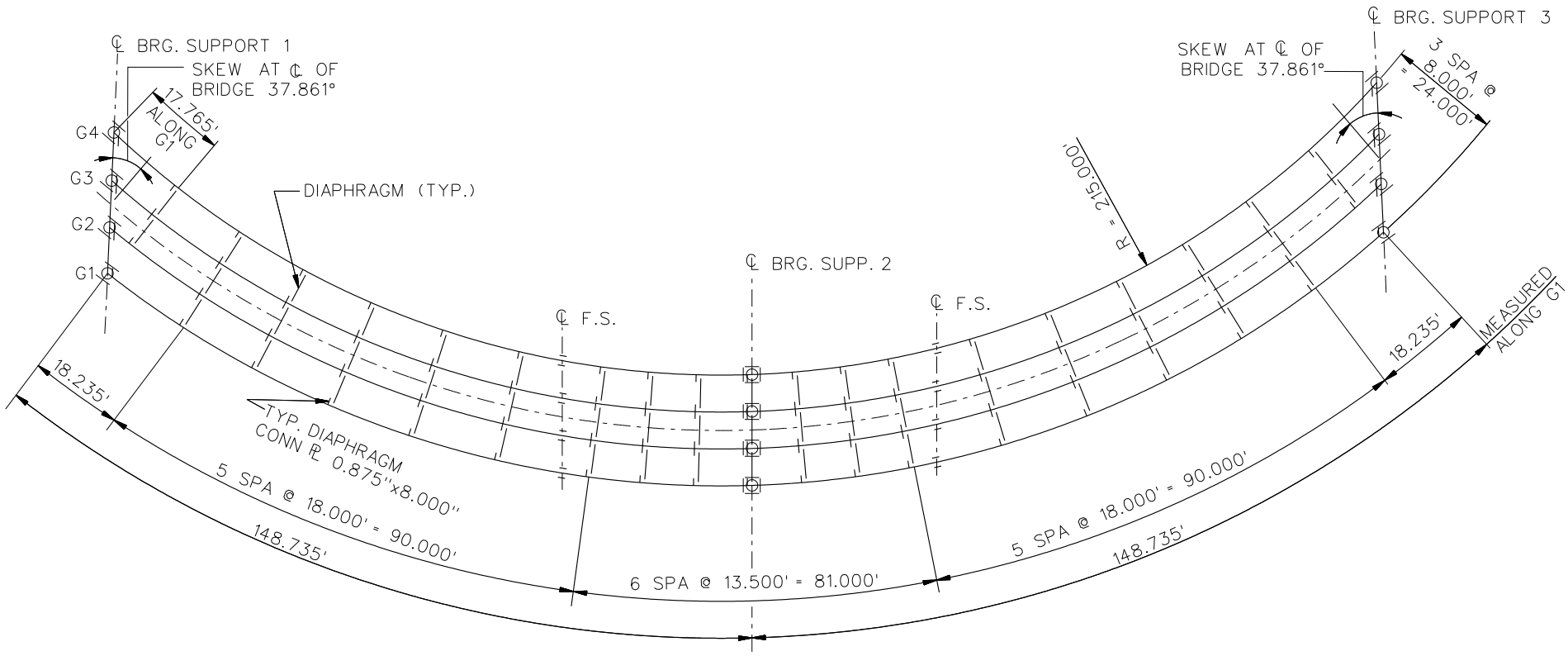

FRAMING PLAN

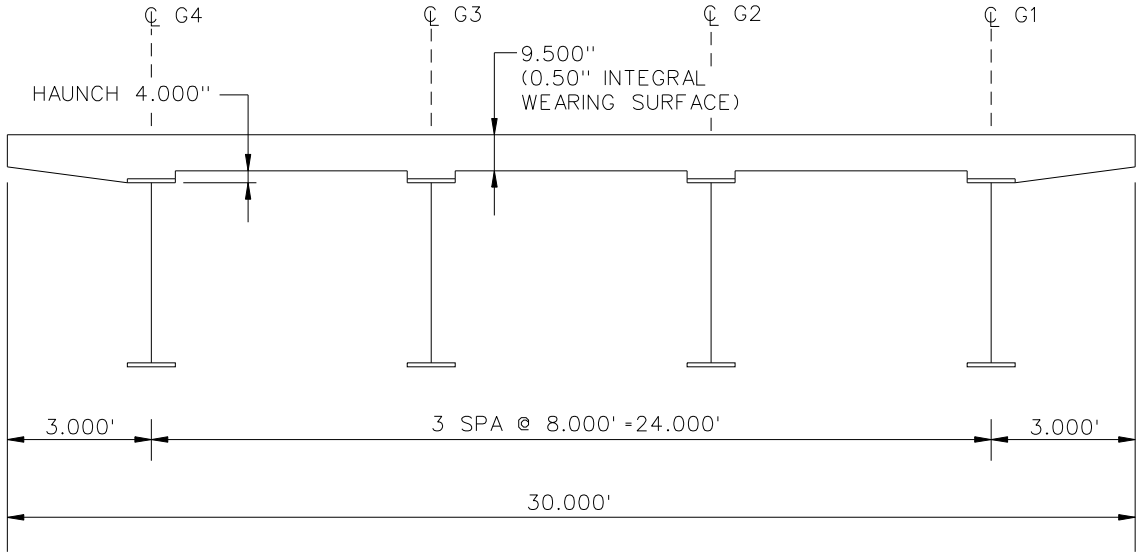

CROSS - SECTION

(DIAPHRAGMS NOT SHOWN)

BEARING LEGEND

- ○ NON-GUIDED
- ⊼○ LONGITUDINALLY GUIDED
- |○| TRANSVERSELY GUIDED
- |○⊼ FIXED

NCHRP 12-79

BRIDGE NICCS3

FRAMING PLAN AND CROSS-SECTION

SHEET 1 OF 9

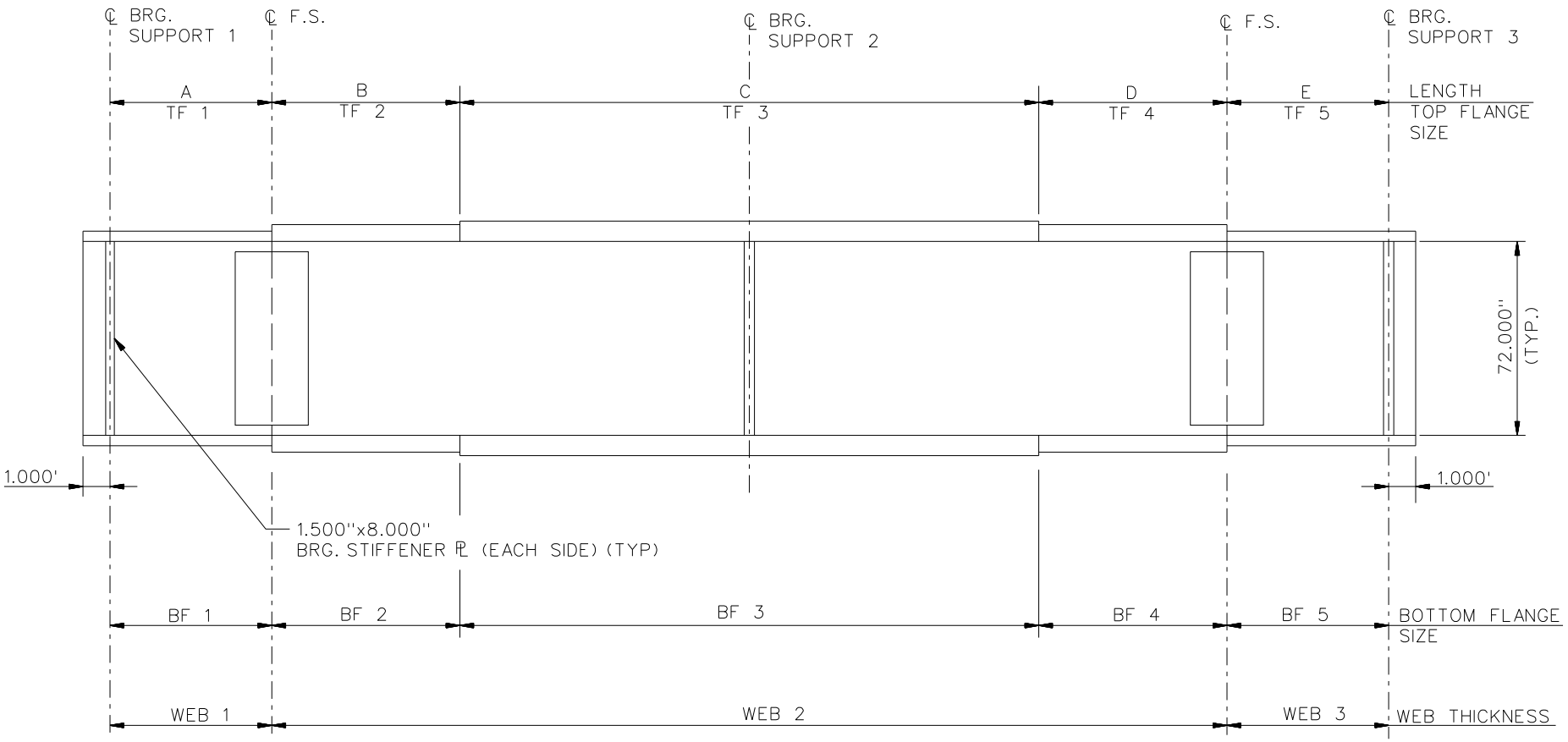

NOTES:

1. SEE TABLES ON SHEET 3 FOR GIRDER ELEVATION DIMENSIONS AND PLATE SIZES.

2. ALL GIRDERS, WEB 1 = WEB 3 = 0.625", WEB 2 = 0.750"

NCHRP 12-79

BRIDGE NICCS3

GIRDER ELEVATION

SHEET 2 OF 9

	GIRDER PLATE LENGTHS ✳			
LENGTH	G1	G2	G3	G4
A	103.736	104.550	105.483	106.565
B	25.000	25.000	25.000	25.000
C	40.000	40.000	40.000	40.000
D	25.000	25.000	25.000	25.000
E	103.736	104.550	105.483	106.565

✳ ALL DIMENSIONS ARE IN FEET.

	GIRDER FLANGE DIMENSIONS ✳✳							
TOP	G1		G2		G3		G4	
FLANGE	BF	TF	BF	TF	BF	TF	BF	TF
TF1	24.000	1.000	24.000	1.000	20.000	1.000	20.000	1.000
TF2	24.000	1.500	24.000	1.500	20.000	1.000	20.000	1.000
TF3	24.000	2.500	24.000	2.500	20.000	2.000	20.000	2.000
TF4	24.000	1.500	24.000	1.500	20.000	1.000	20.000	1.000
TF5	24.000	1.000	24.000	1.000	20.000	1.000	20.000	1.000

✳✳ ALL DIMENSIONS ARE IN INCHES.

	GIRDER FLANGE DIMENSIONS ✳✳							
BOTTOM	G1		G2		G3		G4	
FLANGE	BF	TF	BF	TF	BF	TF	BF	TF
BF1	24.000	1.500	24.000	1.500	20.000	1.250	20.000	1.250
BF2	24.000	1.500	24.000	1.500	20.000	1.250	20.000	1.250
BF3	24.000	2.500	24.000	2.500	20.000	2.000	20.000	2.000
BF4	24.000	1.500	24.000	1.500	20.000	1.250	20.000	1.250
BF5	24.000	1.500	24.000	1.500	20.000	1.250	20.000	1.250

✳✳ ALL DIMENSIONS ARE IN INCHES.

NCHRP 12-79

BRIDGE NICCS3

GIRDER ELEVATION TABLES

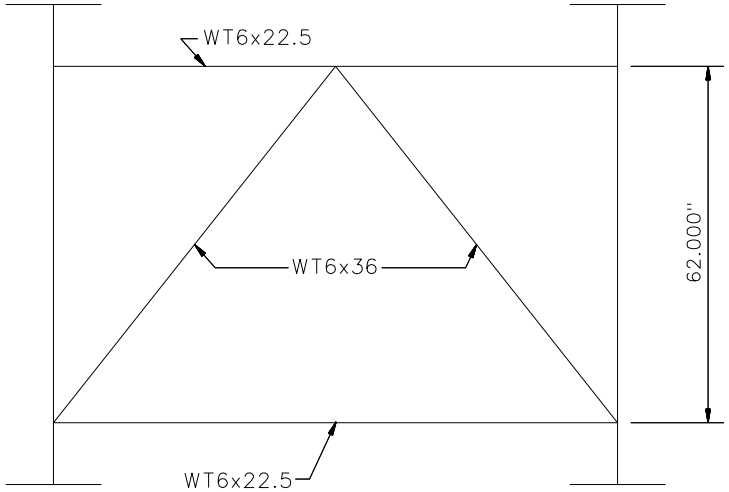

TYPICAL DIAPHRAGM AT SUPPORTS

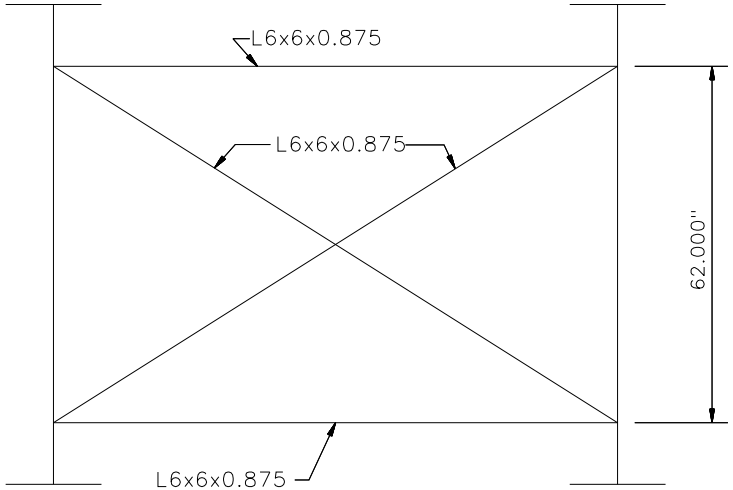

TYPICAL INTERMEDIATE DIAPHRAGM

NOTES:

1. STEEL DEAD LOAD INCREASED BY 5% FOR MDX AND LARSA MODELS; 2% FOR 3D MODEL; AND 10% FOR APPROXIMATE ANALYSIS TO ACCOUNT FOR MISC. DETAILS.

2. FORMWORK LOAD OF 10PSF IS INCLUDED IN CONCRETE DEAD LOAD.

3. ADDITIONAL DESIGN PARAMETERS:
   A. 1.500' PARAPET WIDTH BOTH SIDES.
   B. 700 LB/FT UNIFORM LOAD ASSUMED FOR PARAPET WEIGHT.
   C. ROADWAY WIDTH = 26.500'.
   D. NUMBER OF DESIGN LANES = 2.
   E. HL93 LIVE LOAD.
   F. DESIGN SPEED = 35 MPH.

4. DIAPHRAGM MEMBER CALL-OUTS ARE IN ENGLISH UNITS.

NCHRP 12-79

BRIDGE NICCS3

MISC. DETAILS AND NOTES

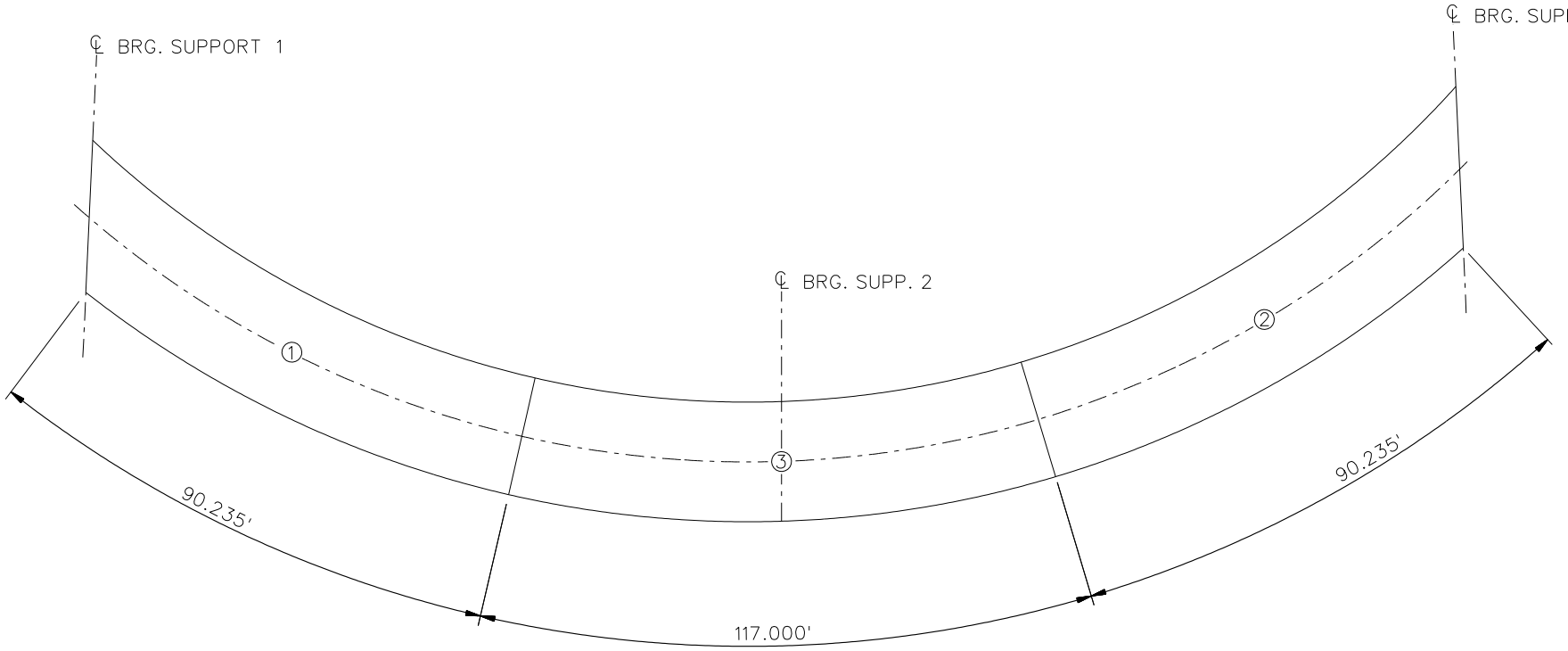

DECK POURING SEQUENCE

NOTES:

1. DECK POUR LENGTHS ARE MEASURED ALONG GIRDER G1.

NCHRP 12-79

BRIDGE NICCS3

DECK POURING SEQUENCE

SHEET 5 OF 9

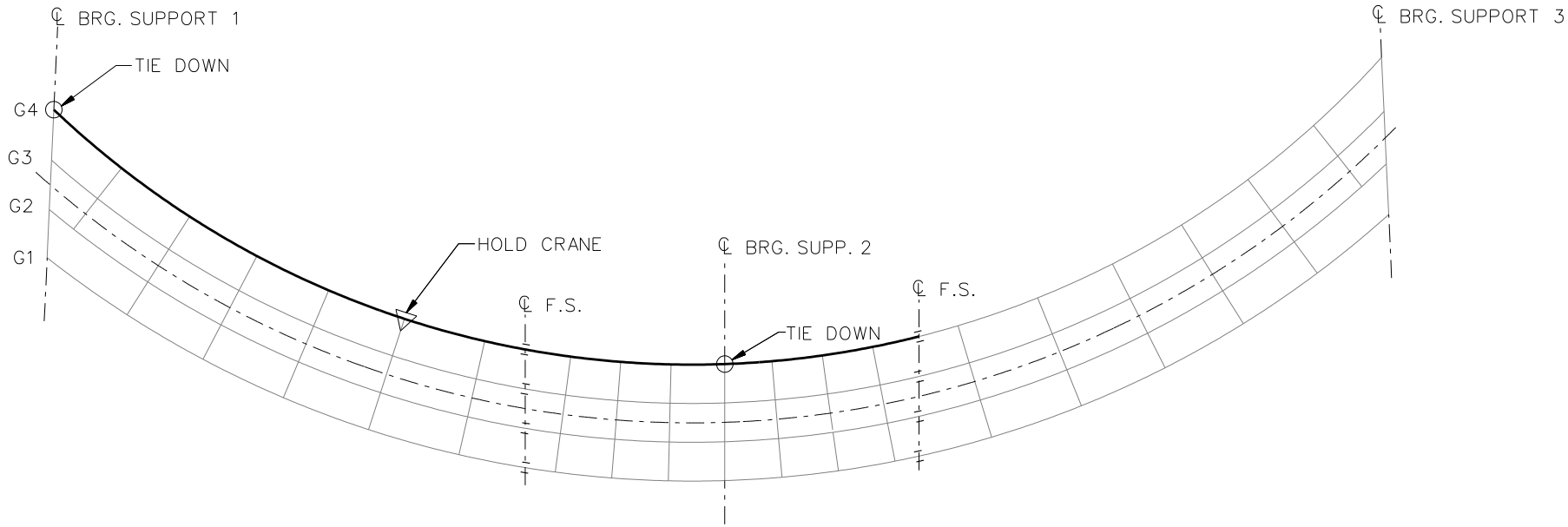

STAGE 1

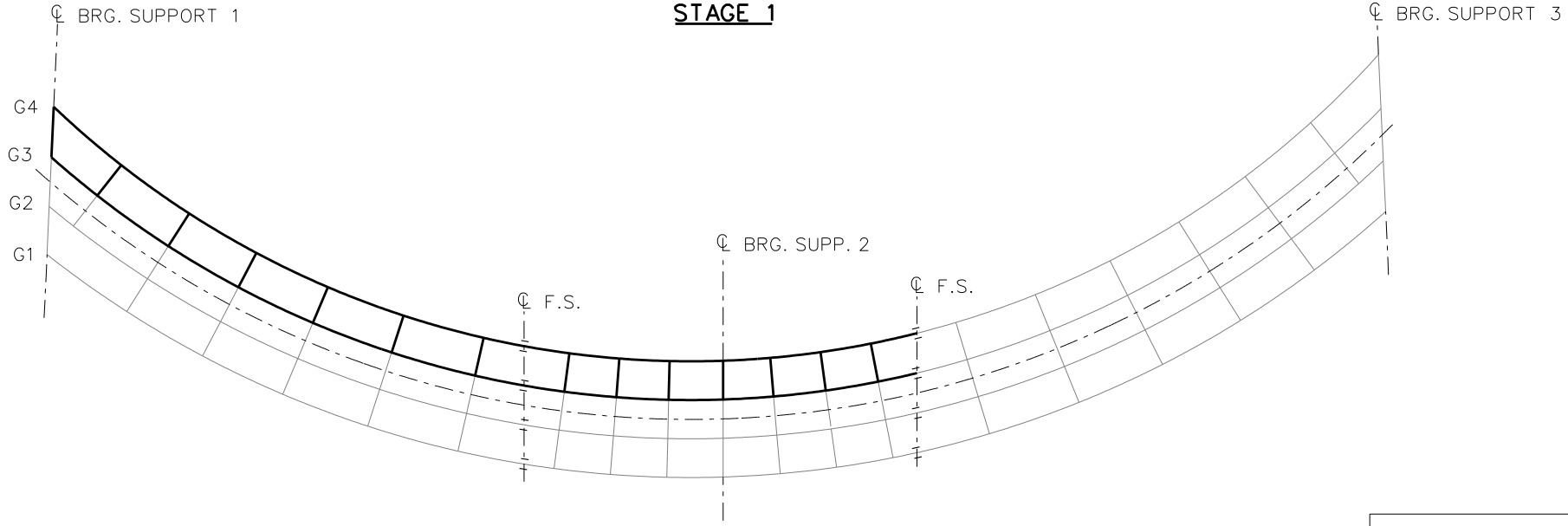

STAGE 2

LEGEND

▽ = HOLD OR LIFT CRANE

○ = TIE DOWN

□ = TEMPORARY SUPPORT STRUCTURE

NCHRP 12-79

BRIDGE NICCS3

GENERAL ERECTION PROCEDURE

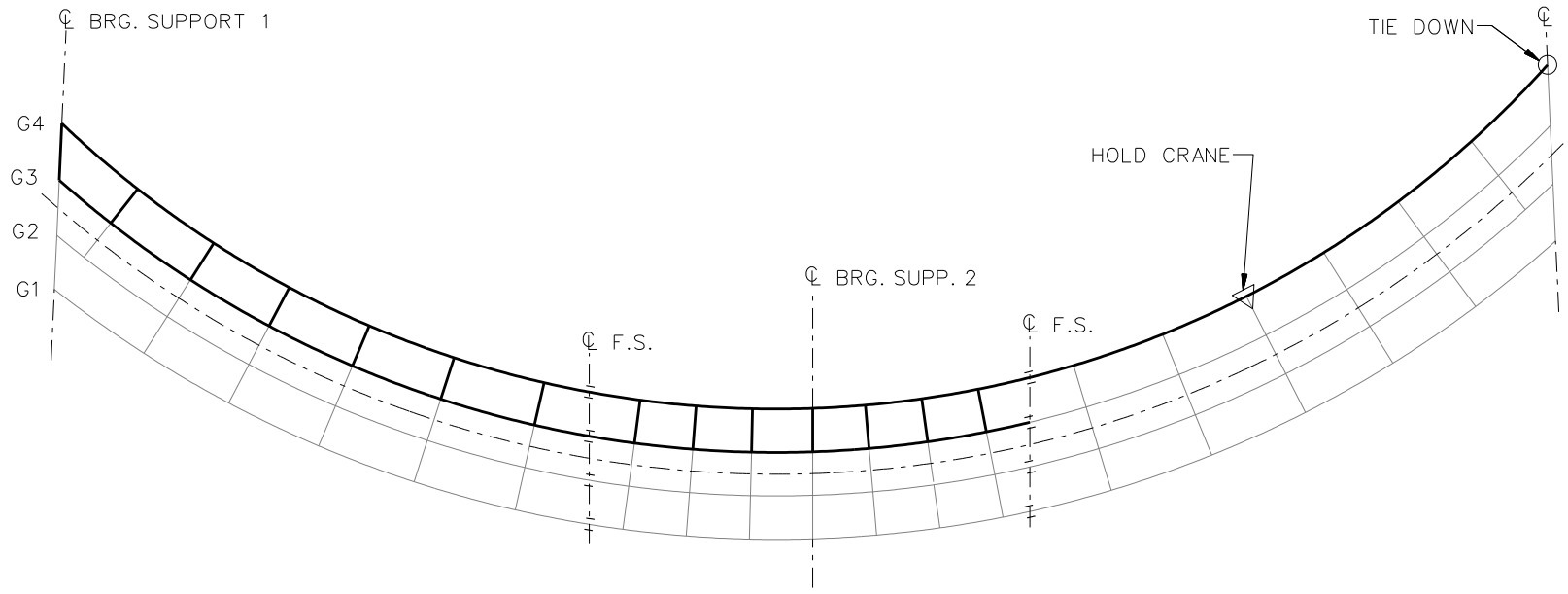

STAGE 3

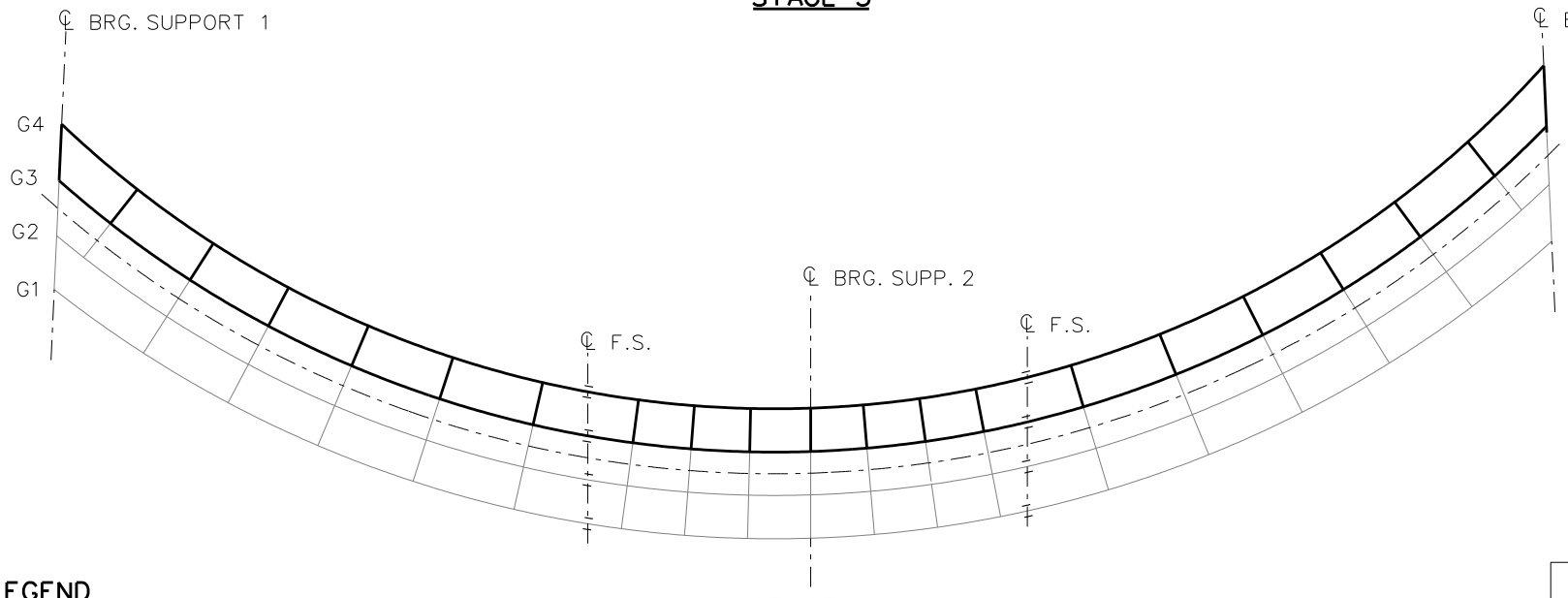

STAGE 4

LEGEND

▽ = HOLD OR LIFT CRANE

○ = TIE DOWN

□ = TEMPORARY SUPPORT STRUCTURE

NCHRP 12-79

BRIDGE NICCS3

GENERAL ERECTION PROCEDURE

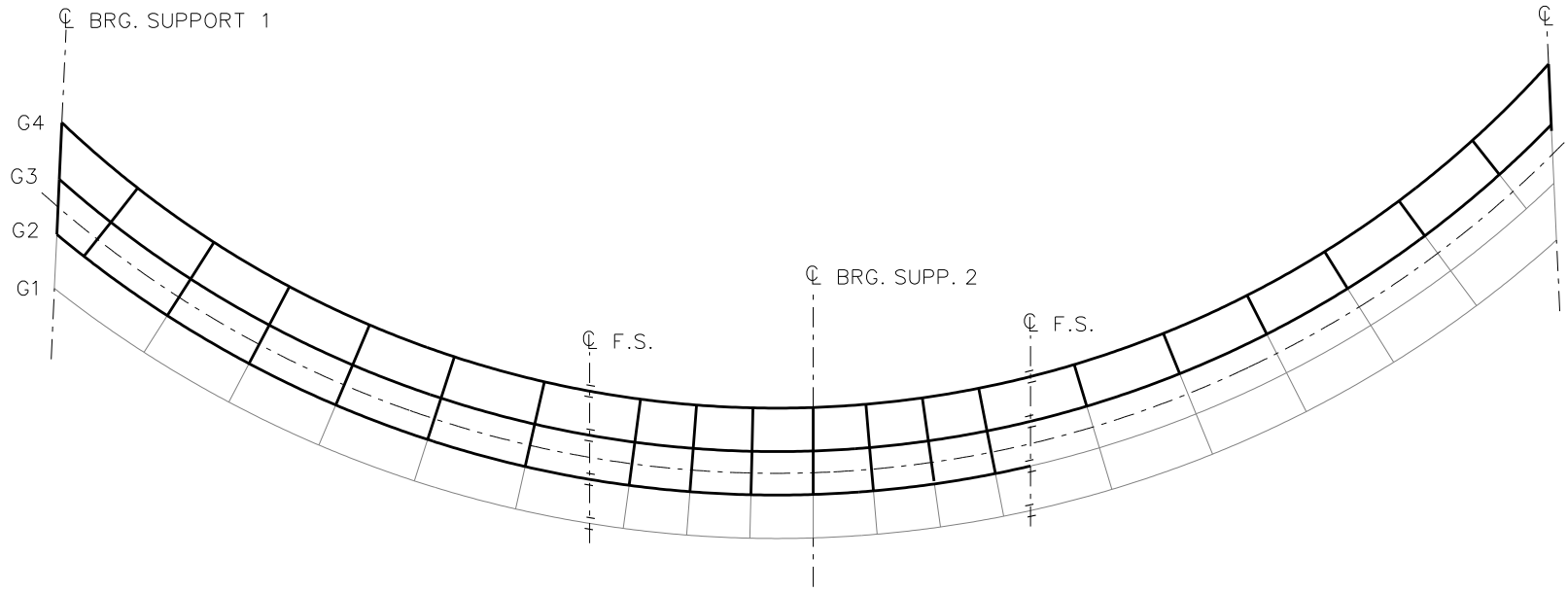

STAGE 5

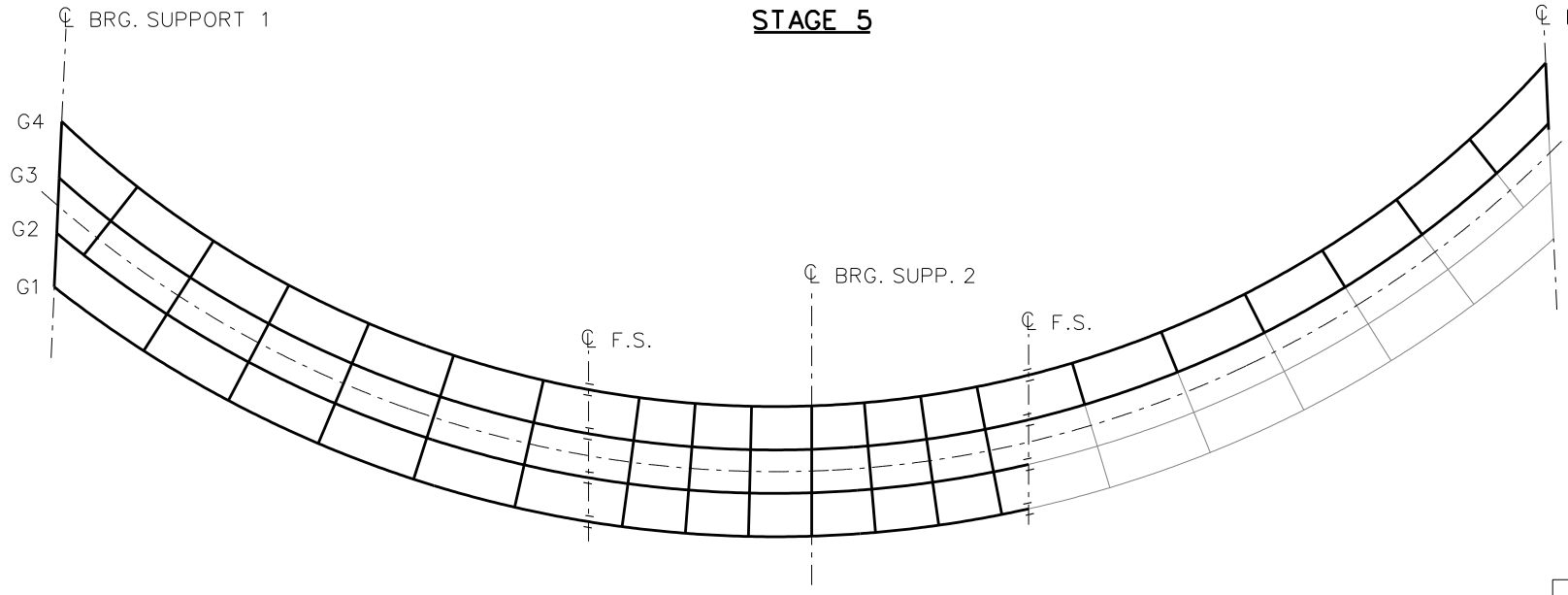

STAGE 6

LEGEND

▽ = HOLD OR LIFT CRANE

○ = TIE DOWN

□ = TEMPORARY SUPPORT STRUCTURE

NCHRP 12-79

BRIDGE NICCS3

GENERAL ERECTION PROCEDURE

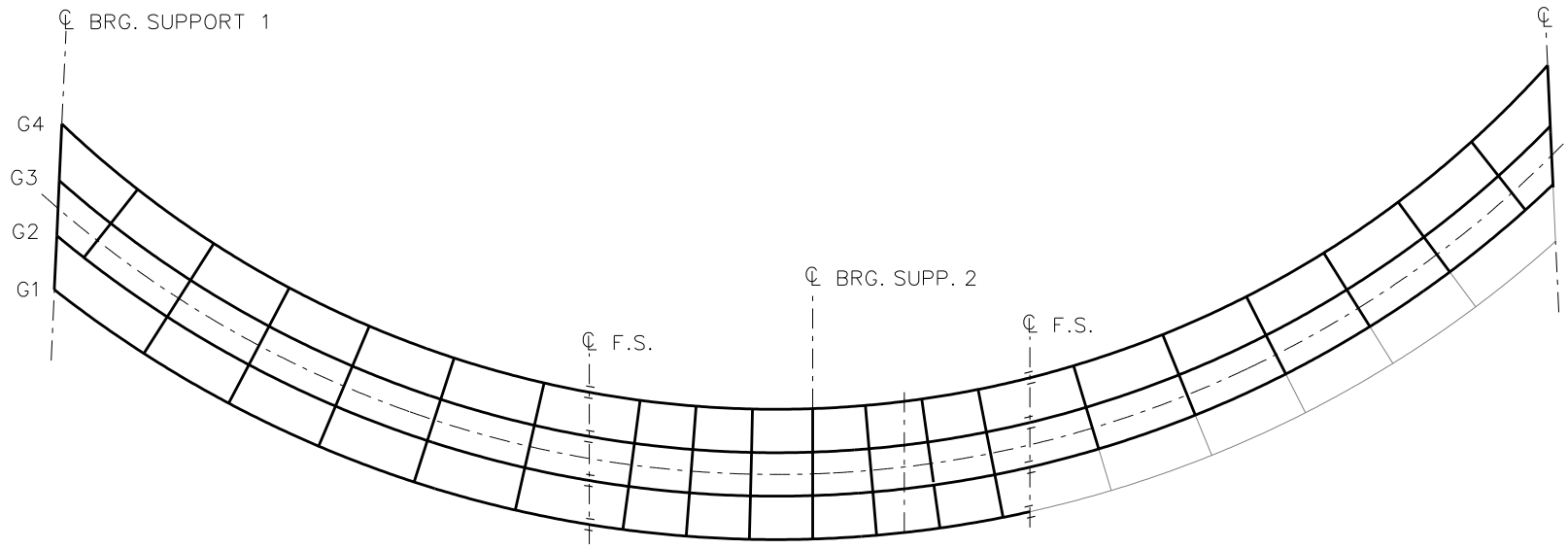

STAGE 7

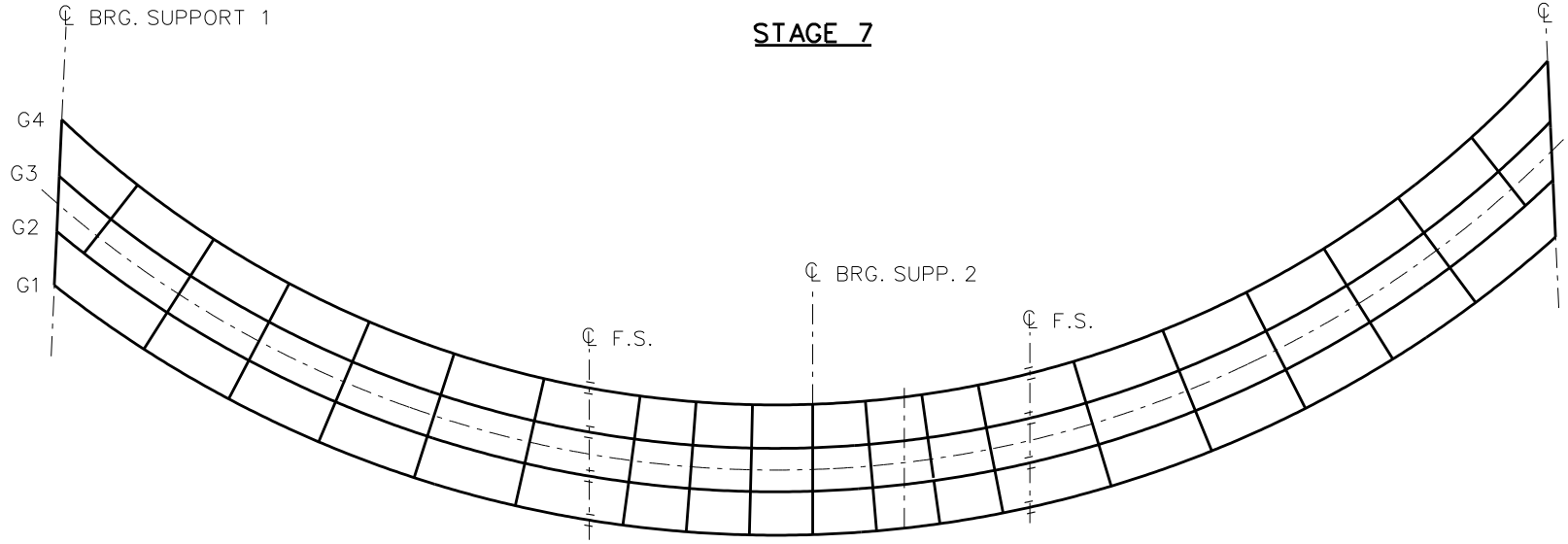

STAGE 8

LEGEND

▽ = HOLD OR LIFT CRANE

○ = TIE DOWN

□ = TEMPORARY SUPPORT STRUCTURE

NCHRP 12-79

BRIDGE NICCS3

GENERAL ERECTION PROCEDURE

NCHRP 12-79

NICCS9

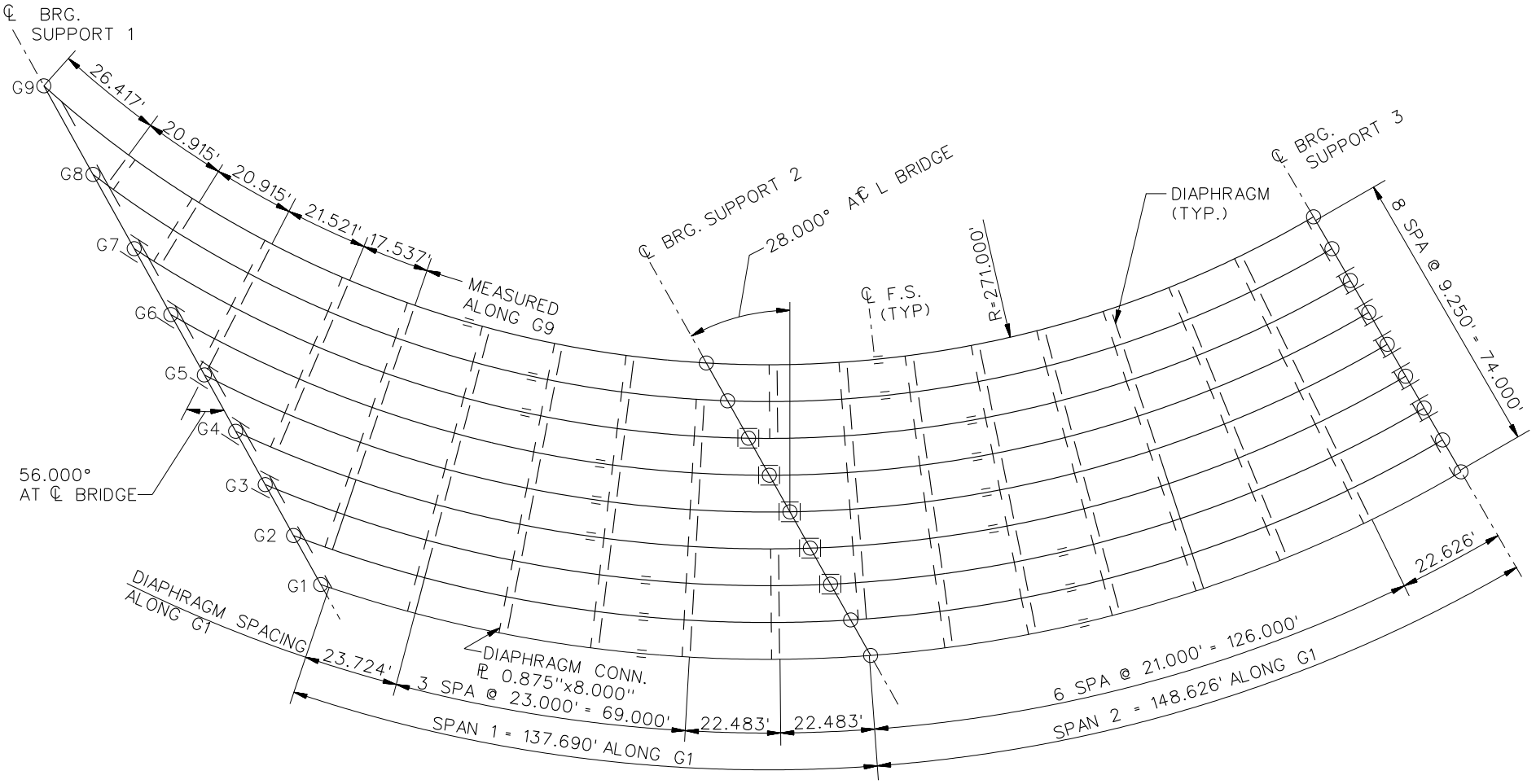

FRAMING PLAN

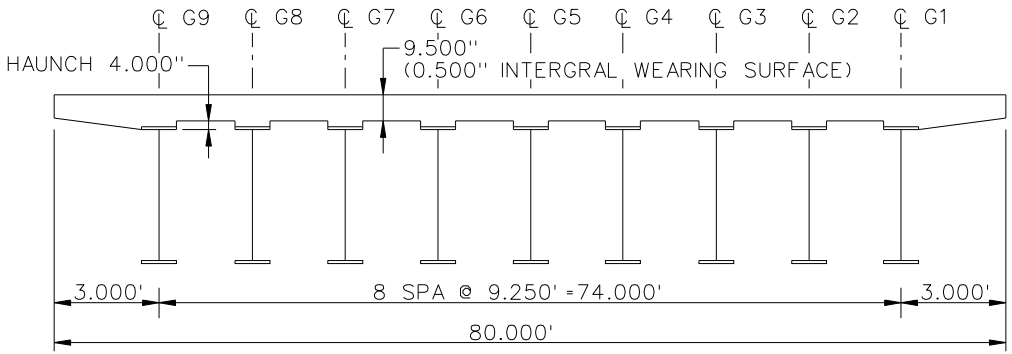

CROSS - SECTION

(DIAPHRAGMS NOT SHOWN)

BEARING LEGEND

- ○ NON-GUIDED
- ⊽○ LONGITUDINALLY GUIDED
- |○| TRANSVERSELY GUIDED
- |◎| FIXED

NCHRP 12-79

BRIDGE NICCS9

FRAMING PLAN AND CROSS-SECTION

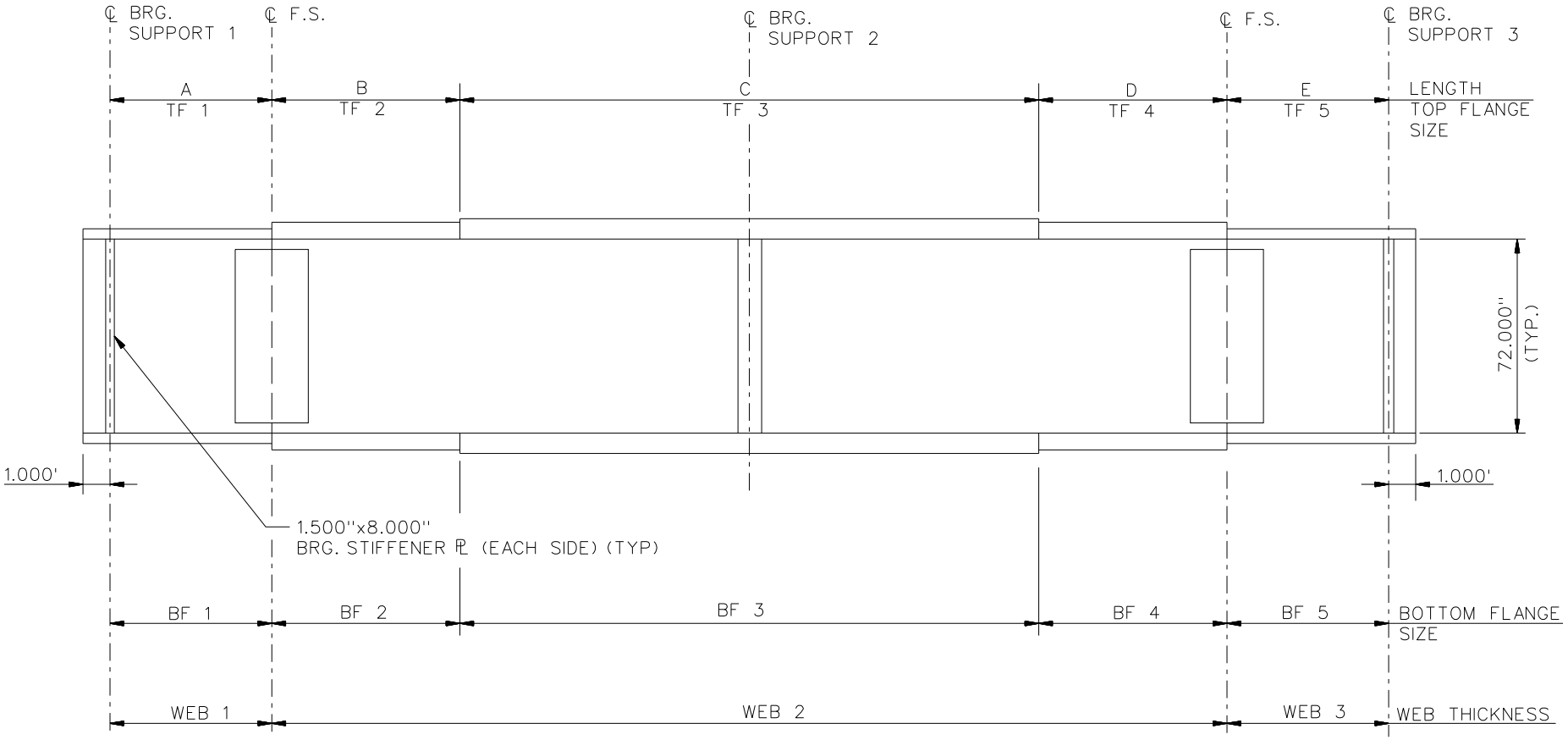

NOTES:

1. SEE TABLES ON SHEET 3 FOR GIRDER ELEVATION DIMENSIONS AND PLATE SIZES.

2. ALL GIRDERS, WEB 1 = WEB 2 = WEB 3 = 0.750"

NCHRP 12-79

BRIDGE NICCS9

GIRDER ELEVATION

SHEET 2 OF 8

	GIRDER PLATE LENGTHS ✳								
LENGTH	G1	G2	G3	G4	G5	G6	G7	G8	G9
A	80.000	88.213	96.838	90.000	100.292	111.501	105.000	120.111	120.000
B	37.690	31.860	26.003	36.100	29.708	23.275	35.804	28.658	40.140
C	40.000	40.000	40.000	40.000	40.000	40.000	40.000	40.000	40.000
D	33.625	36.471	39.343	24.606	28.062	31.559	35.104	20.134	24.417
E	95.000	92.453	89.906	105.000	101.938	98.877	95.815	111.326	107.651

✳ ALL DIMENSIONS ARE IN FEET.

	GIRDER FLANGE DIMENSIONS ✳✳					
TOP	G1, G2, G3		G4, G5, G6		G7, G8, G9	
FLANGE	BF	TF	BF	TF	BF	TF
TF1	24.000	1.000	20.000	1.000	20.000	1.000
TF2	24.000	1.500	20.000	1.000	20.000	1.000
TF3	24.000	2.500	20.000	2.000	20.000	2.000
TF4	24.000	1.500	20.000	1.000	20.000	1.000
TF5	24.000	1.000	20.000	1.000	20.000	1.000

✳✳ ALL DIMENSIONS ARE IN INCHES.

	GIRDER FLANGE DIMENSIONS ✳✳					
BOTTOM	G1, G2, G3		G4, G5, G6		G7, G8, G9	
FLANGE	BF	TF	BF	TF	BF	TF
BF1	24.000	1.500	20.000	1.250	24.000	1.500
BF2	24.000	1.500	20.000	1.250	24.000	1.500
BF3	24.000	2.750	20.000	2.000	24.000	2.500
BF4	24.000	1.500	20.000	1.250	24.000	1.500
BF5	24.000	1.750	20.000	1.250	24.000	1.500

✳✳ ALL DIMENSIONS ARE IN INCHES.

NCHRP 12-79

BRIDGE NICCS9

GIRDER ELEVATION TABLES

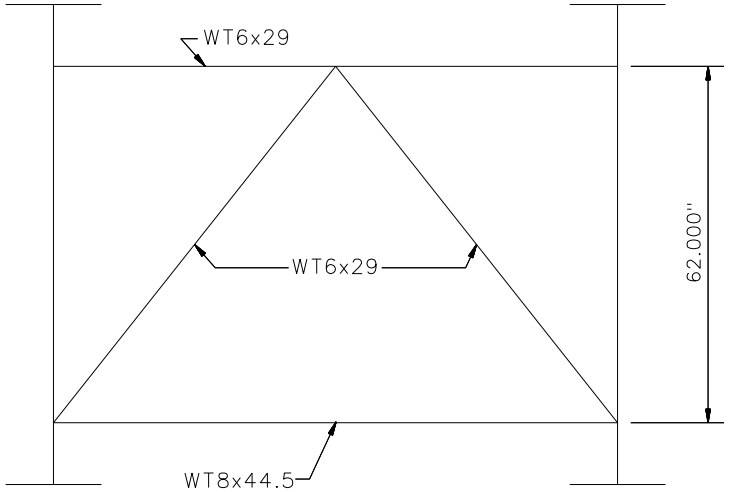

TYPICAL DIAPHRAGM AT SUPPORTS

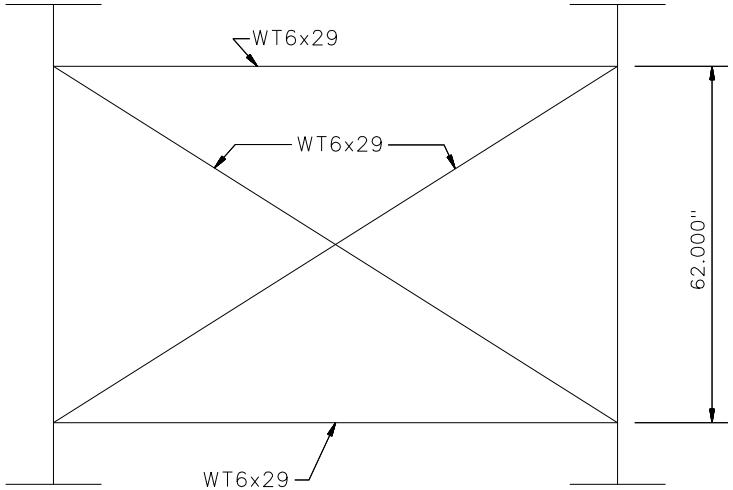

TYPICAL INTERMEDIATE DIAPHRAGM

NOTES:

1. STEEL DEAD LOAD INCREASED BY 5% FOR MDX AND LARSA MODELS; 2% FOR 3D MODEL; AND 10% FOR APPROXIMATE ANALYSIS TO ACCOUNT FOR MISC. DETAILS.

2. FORMWORK LOAD OF 10PSF IS INCLUDED IN CONCRETE DEAD LOAD.

3. ADDITIONAL DESIGN PARAMETERS:
   A. 1.500' PARAPET WIDTH BOTH SIDES.
   B. 700 LB/FT UNIFORM LOAD ASSUMED FOR PARAPET WEIGHT.
   C. ROADWAY WIDTH = 77.000'.
   D. NUMBER OF DESIGN LANES = 6.
   E. HL93 LIVE LOAD.
   F. DESIGN SPEED = 35 MPH.

4. DIAPHRAGM MEMBER CALL-OUTS ARE IN ENGLISH UNITS.

NCHRP 12-79

BRIDGE NICCS9

MISC. DETAILS AND NOTES

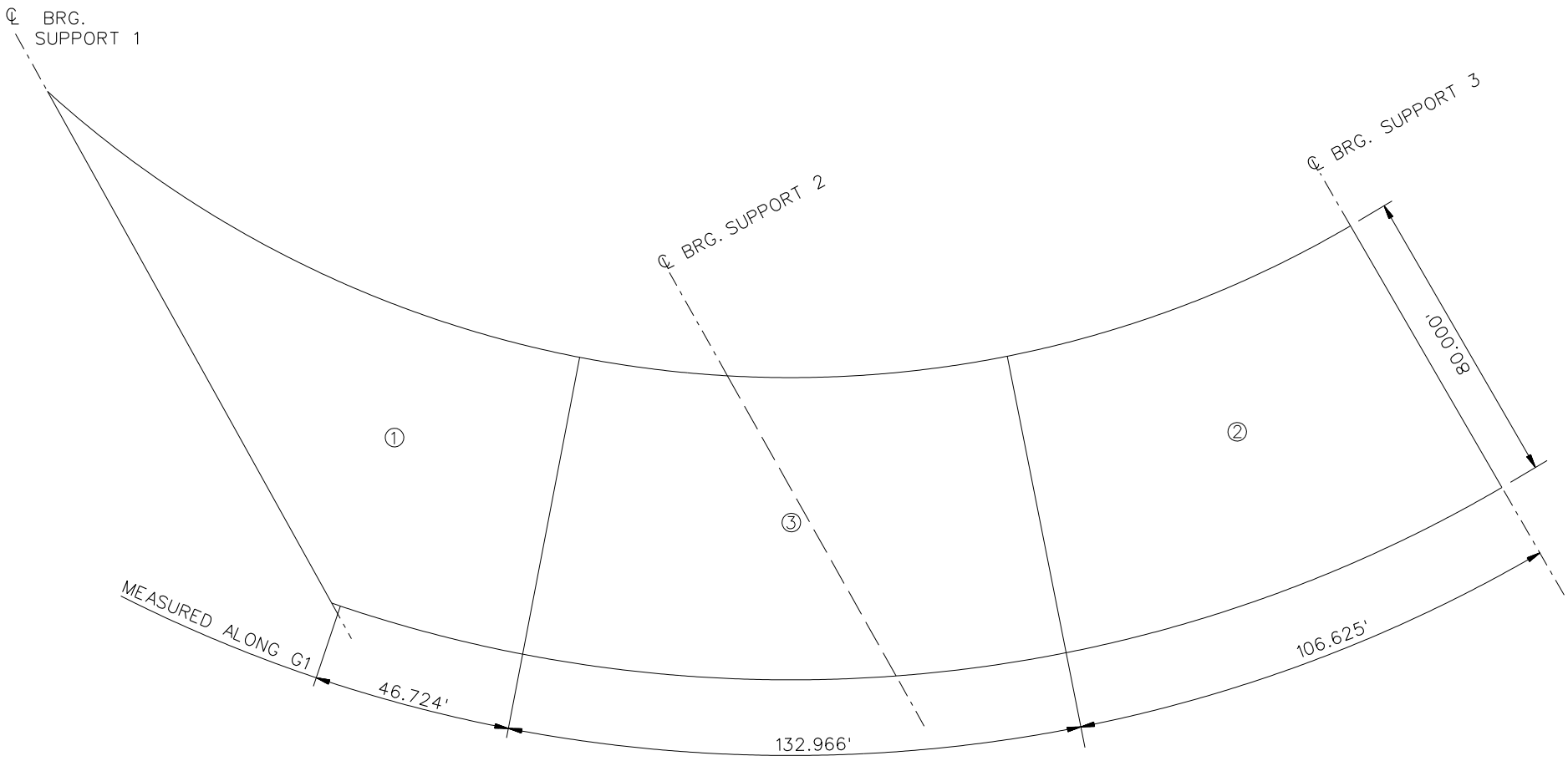

DECK POURING SEQUENCE

NCHRP 12-79

BRIDGE NICCS9

DECK POURING SEQUENCE

SHEET 5 OF 8

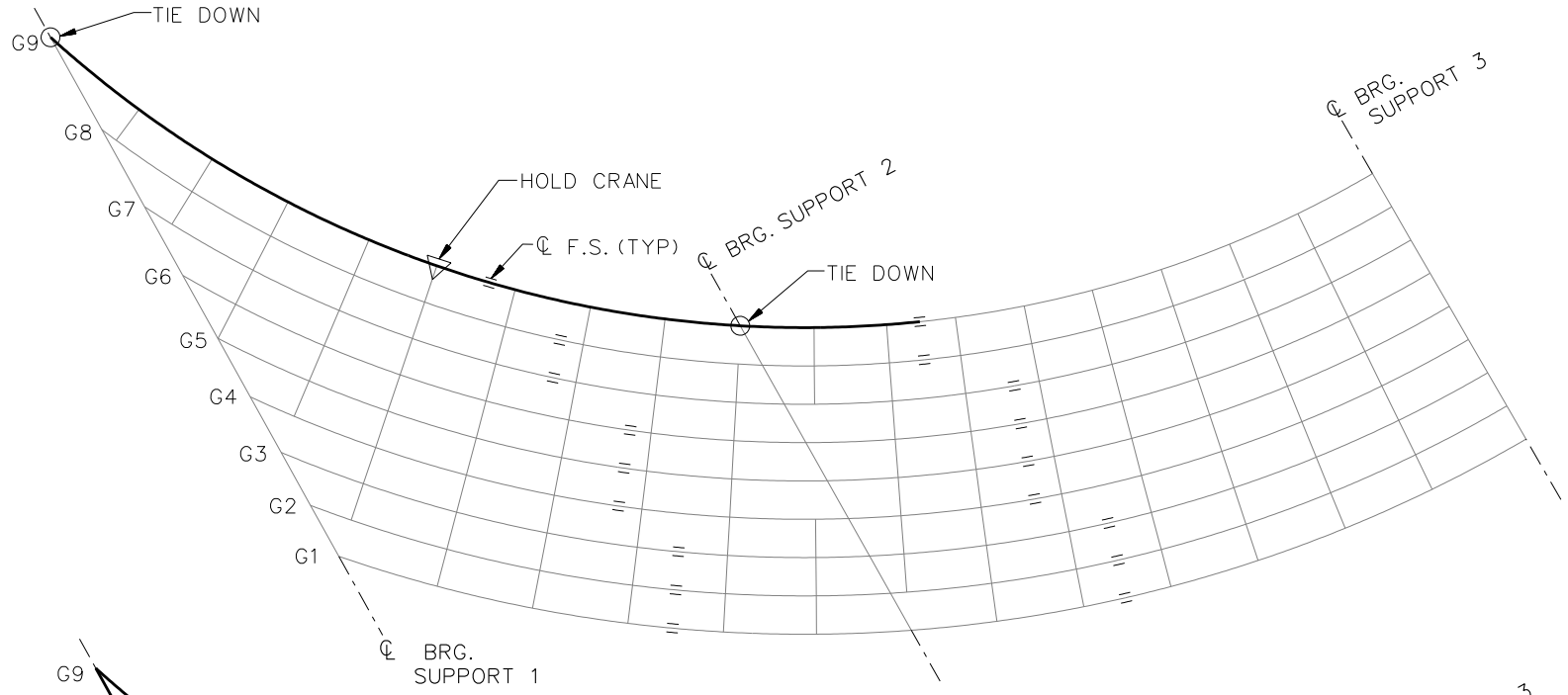

STAGE 1

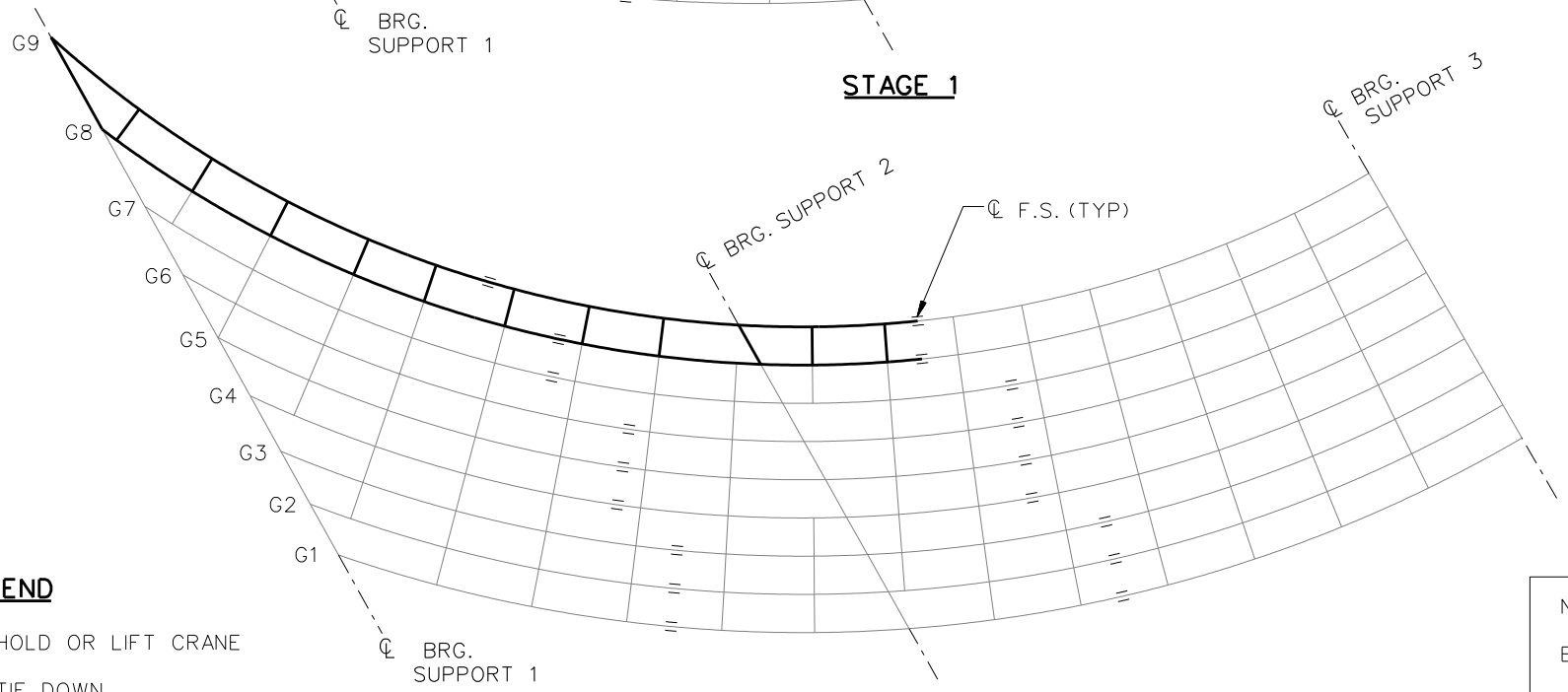

STAGE 2

LEGEND

▽ = HOLD OR LIFT CRANE

○ = TIE DOWN

□ = TEMPORARY SUPPORT STRUCTURE

NCHRP 12-79

BRIDGE NICCS9

GENERAL ERECTION PROCEDURE

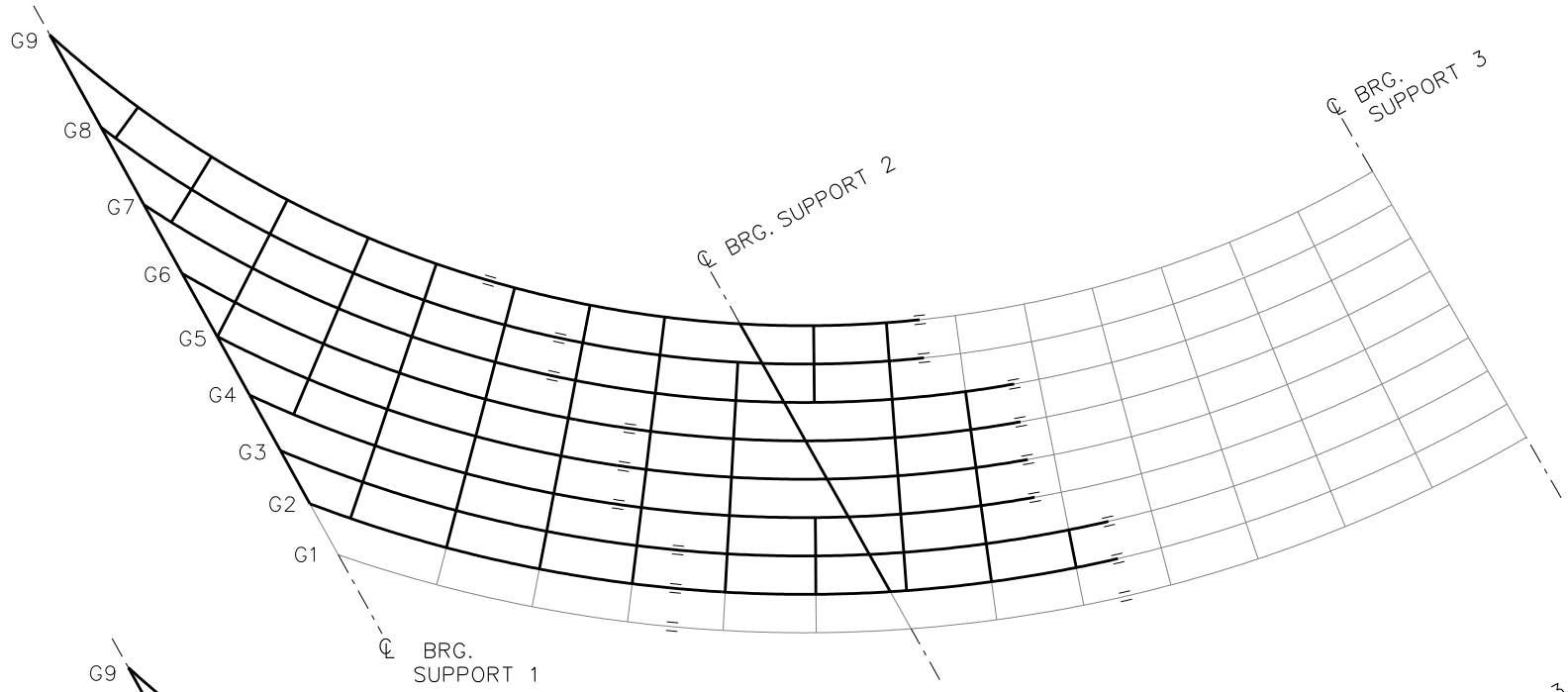

STAGE 8

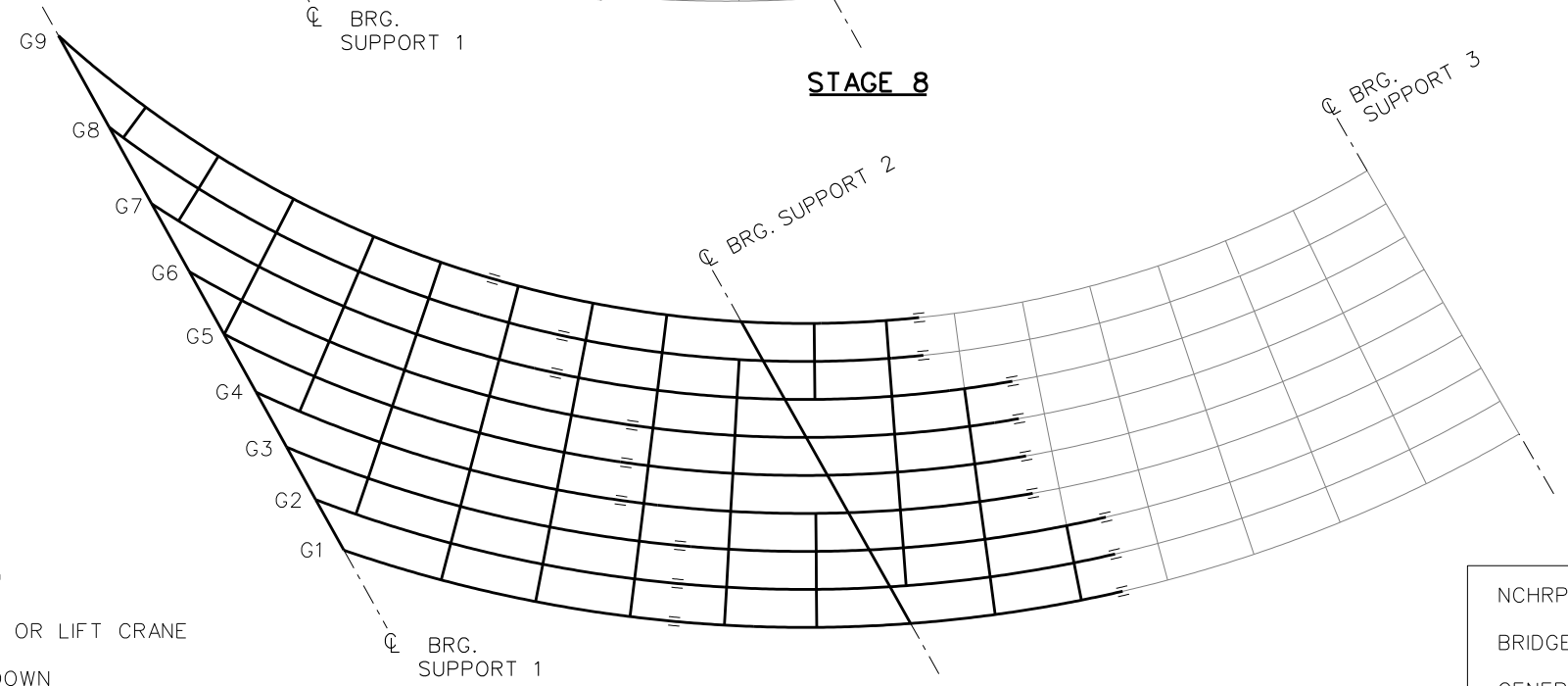

STAGE 9

LEGEND

▽ = HOLD OR LIFT CRANE

○ = TIE DOWN

□ = TEMPORARY SUPPORT STRUCTURE

NCHRP 12-79

BRIDGE NICCS9

GENERAL ERECTION PROCEDURE

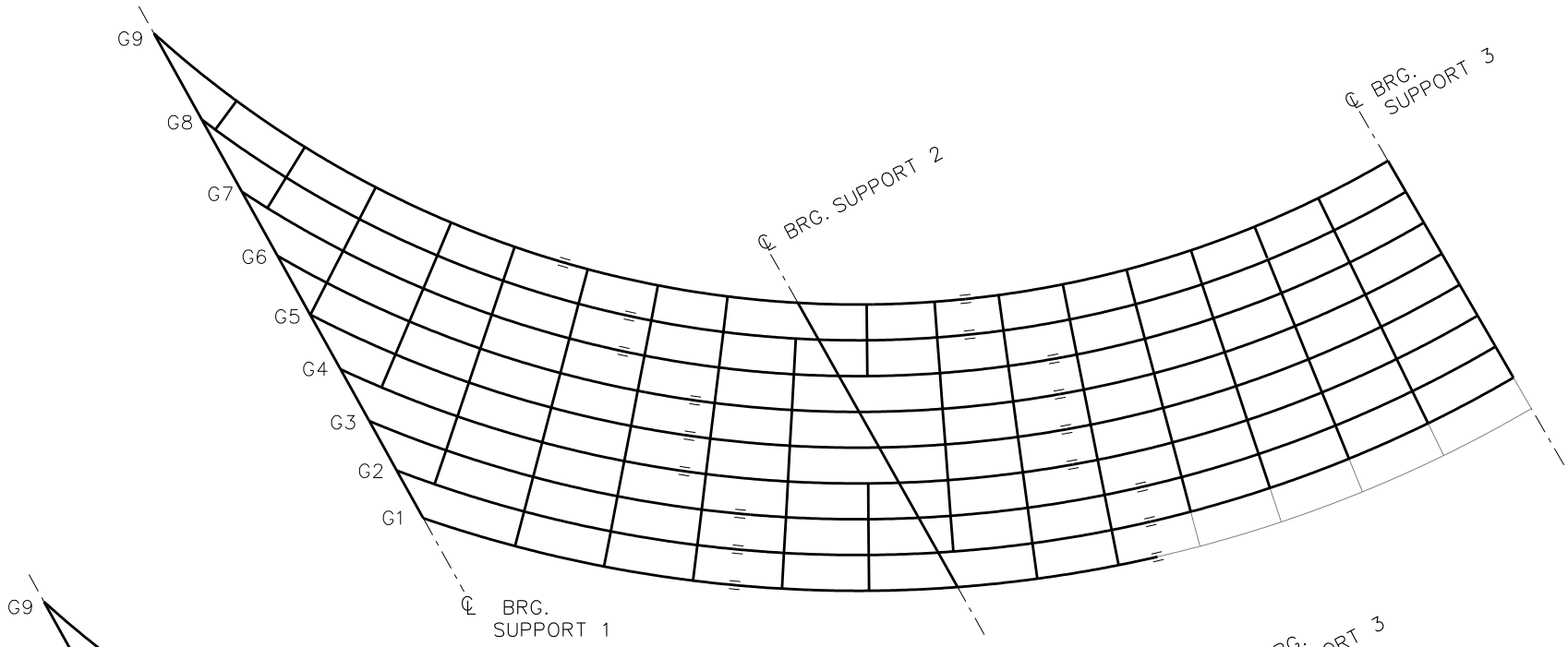

STAGE 17

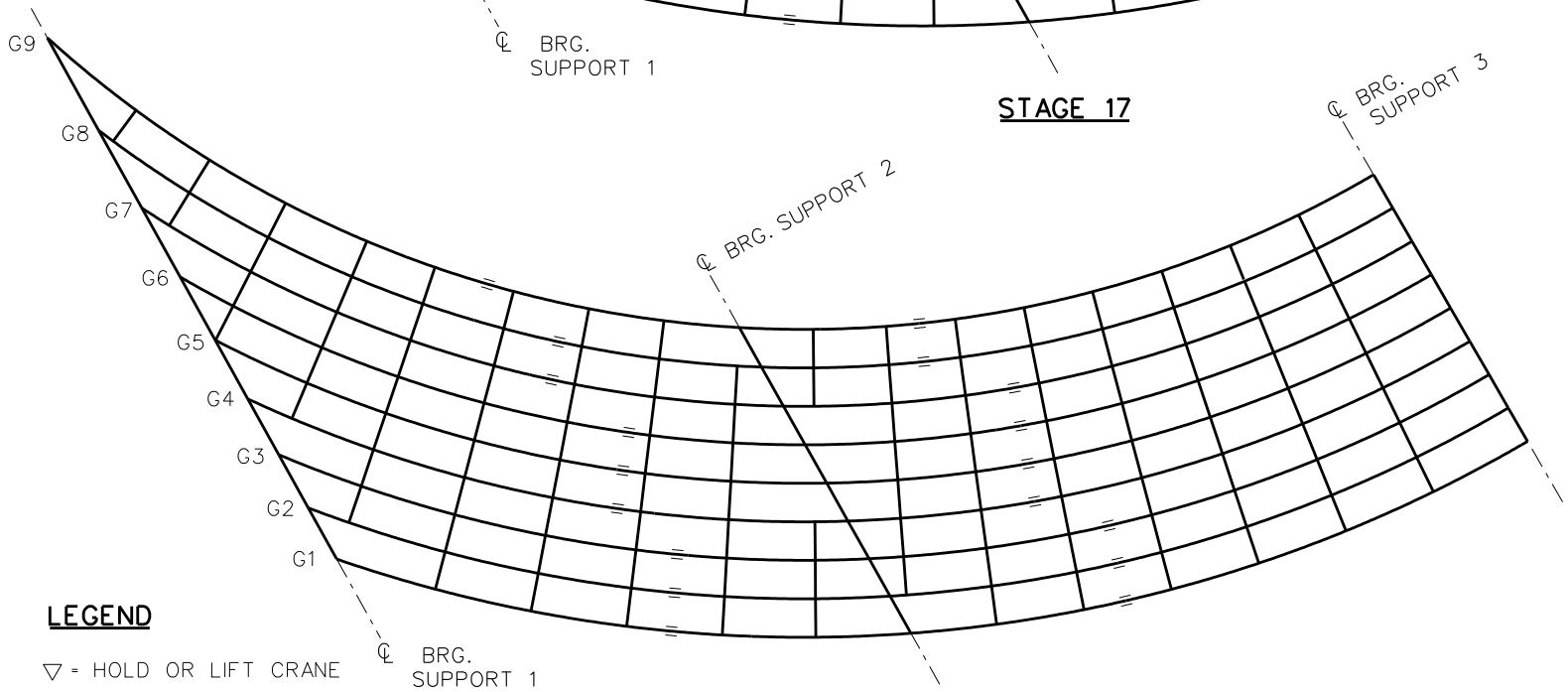

STAGE 18

LEGEND

▽ = HOLD OR LIFT CRANE

○ = TIE DOWN

□ = TEMPORARY SUPPORT STRUCTURE

NCHRP 12-79

BRIDGE NICCS9

GENERAL ERECTION PROCEDURE

NCHRP 12-79

NICCS13

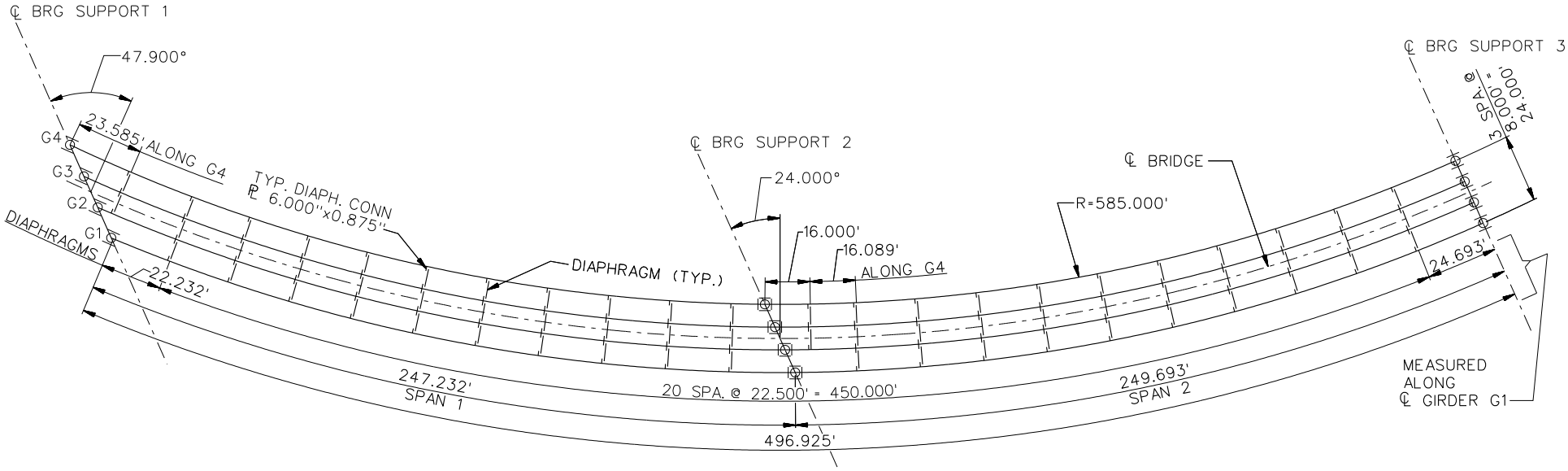

FRAMING PLAN

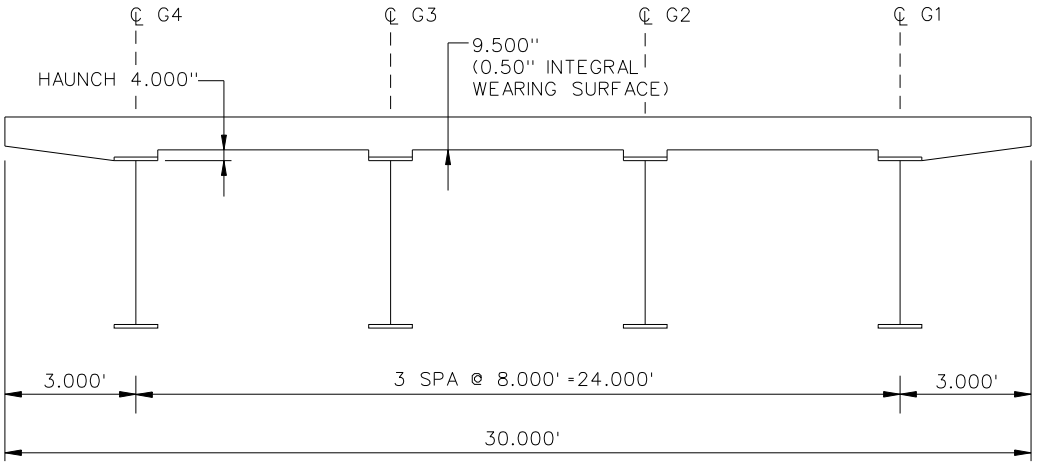

CROSS - SECTION

(DIAPHRAGMS NOT SHOWN)

BEARING LEGEND

- ○ NON-GUIDED
- ⊼○ LONGITUDINALLY GUIDED
- |○| TRANSVERSELY GUIDED
- |⊼○| FIXED

NCHRP 12-79

BRIDGE NICCS13

FRAMING PLAN AND CROSS-SECTION

SHEET 1 OF 9

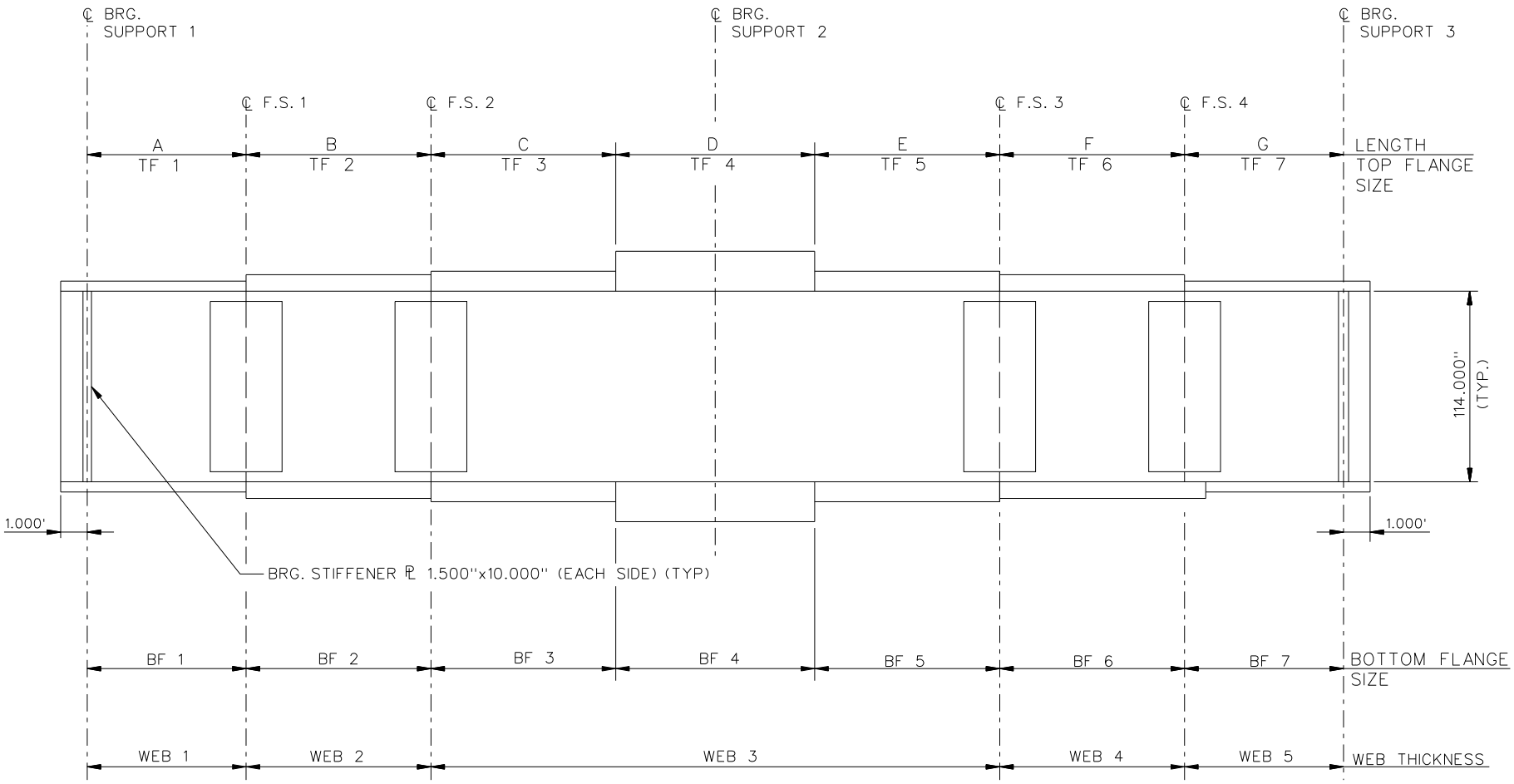

NOTE :

1. SEE TABLES ON SHEET 3 FOR GIRDER ELEVATION DIMENSIONS AND PLATE SIZES.

2. ALL GIRDERS, WEB 1 = WEB 2 = WEB 4 = WEB 5 = 0.875".
   WEB 3 = 1.000".

NCHRP 12-79

BRIDGE NICCS13

GIRDER ELEVATION

SHEET 2 OF 9

	GIRDER PLATE LENGTHS ✳			
LENGTH	G1	G2	G3	G4
A	54.732	62.557	70.520	78.636
B	130.000	128.292	126.584	124.877
C	37.500	37.008	36.515	36.023
D	50.000	49.343	48.686	48.029
E	37.500	37.007	36.515	36.022
F	130.000	128.292	126.585	124.877
G	57.193	56.442	55.690	54.939

✳ ALL DIMENSIONS ARE IN FEET.

	GIRDER FLANGE DIMENSIONS ✳✳							
TOP	G1		G2		G3		G4	
FLANGE	BF	TF	BF	TF	BF	TF	BF	TF
TF1	30.000	1.500	30.000	1.500	24.000	1.000	24.000	1.000
TF2	30.000	1.500	30.000	1.500	24.000	1.000	24.000	1.000
TF3	36.000	2.250	36.000	2.250	32.000	1.500	32.000	1.500
TF4	36.000	2.750	36.000	2.750	32.000	2.500	32.000	2.500
TF5	36.000	2.250	36.000	2.250	32.000	1.500	32.000	1.500
TF6	30.000	1.500	30.000	1.500	24.000	1.000	24.000	1.000
TF7	30.000	1.500	30.000	1.500	24.000	1.000	24.000	1.000

✳✳ ALL DIMENSIONS ARE IN INCHES.

	GIRDER FLANGE DIMENSIONS ✳✳							
BOTTOM	G1		G2		G3		G4	
FLANGE	BF	TF	BF	TF	BF	TF	BF	TF
BF1	30.000	1.750	30.000	1.750	24.000	1.000	24.000	1.000
BF2	30.000	1.750	30.000	1.750	24.000	1.000	24.000	1.000
BF3	36.000	2.250	36.000	2.250	32.000	2.000	32.000	2.000
BF4	36.000	3.000	36.000	3.000	32.000	2.500	32.000	2.500
BF5	36.000	2.250	36.000	2.250	32.000	2.000	32.000	2.000
BF6	32.000	2.250	32.000	2.250	24.000	1.000	24.000	1.000
BF7	32.000	2.000	32.000	2.000	24.000	1.000	24.000	1.000

✳✳ ALL DIMENSIONS ARE IN INCHES.

NCHRP 12-79

BRIDGE NICCS13

GIRDER ELEVATION TABLES

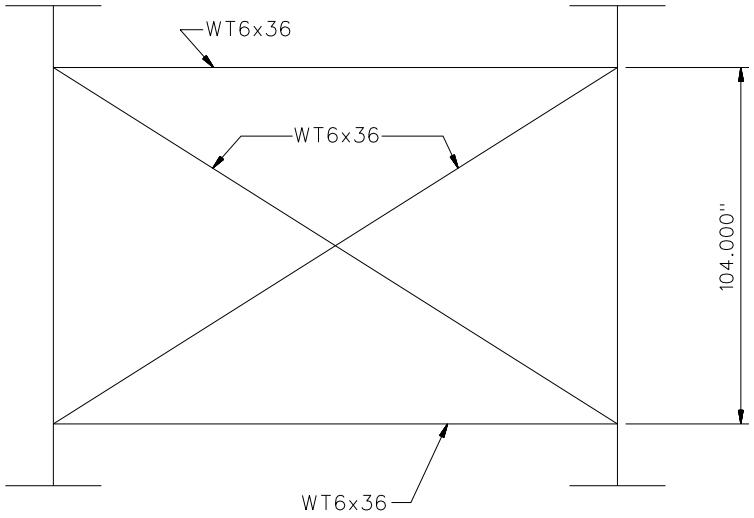

TYPICAL SUPPORT DIAPHRAGMS AND INTERMEDIATE DIAPHRAGMS

NOTES:

1. STEEL DEAD LOAD INCREASED BY 5% FOR MDX AND LARSA MODELS; 2% FOR 3D MODEL; AND 10% FOR APPROXIMATE ANALYSIS TO ACCOUNT FOR MISC. DETAILS.

2. FORMWORK LOAD OF 10PSF IS INCLUDED IN CONCRETE DEAD LOAD.

3. ADDITIONAL DESIGN PARAMETERS:
   A. 1.500' PARAPET WIDTH BOTH SIDES.
   B. 700 LB/FT UNIFORM LOAD ASSUMED FOR PARAPET WEIGHT.
   C. ROADWAY WIDTH = 26.500'.
   D. NUMBER OF DESIGN LANES = 2.
   E. HL93 LIVE LOAD.
   F. DESIGN SPEED = 35 MPH.

4. DIAPHRAGM MEMBER CALL-OUTS ARE IN UNITS OF INCHES.

NCHRP 12-79

BRIDGE NICCS13

MISC. DETAILS AND NOTES

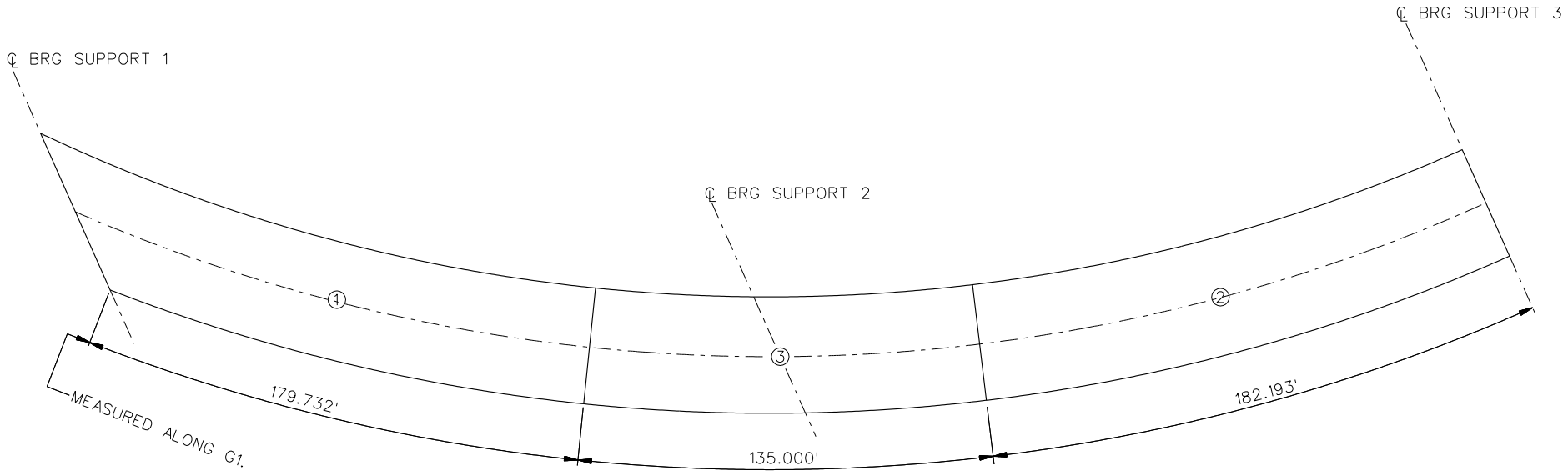

DECK POURING SEQUENCE

NCHRP 12-79

BRIDGE NICCS13

DECK POURING SEQUENCE

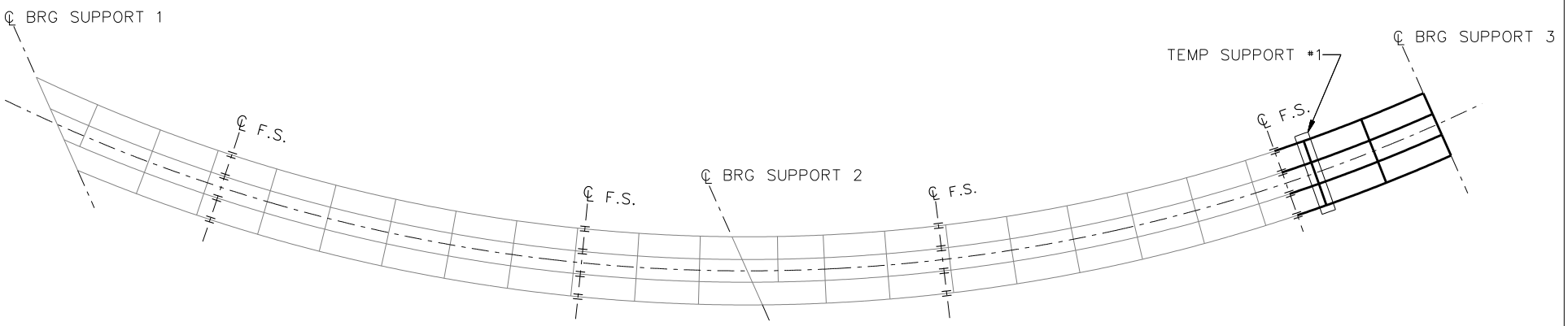

STAGE 4

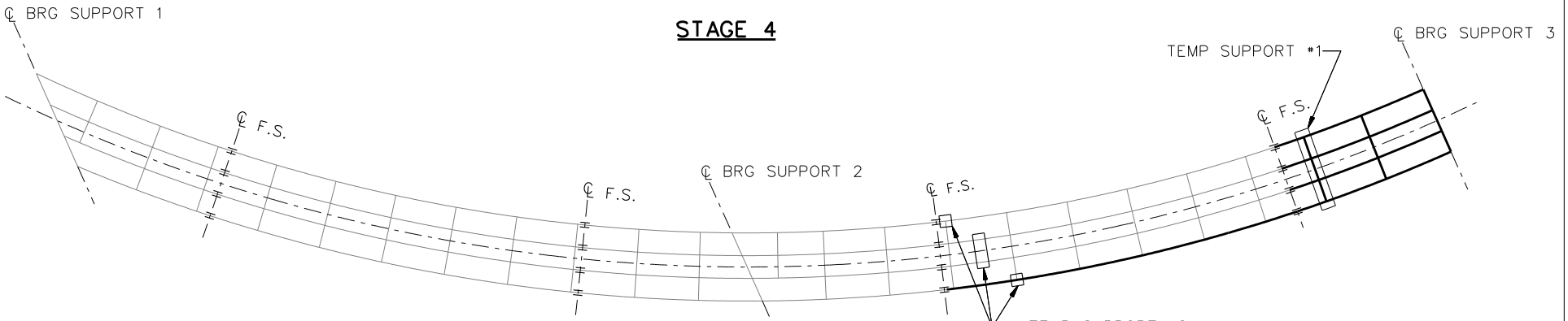

STAGE 5

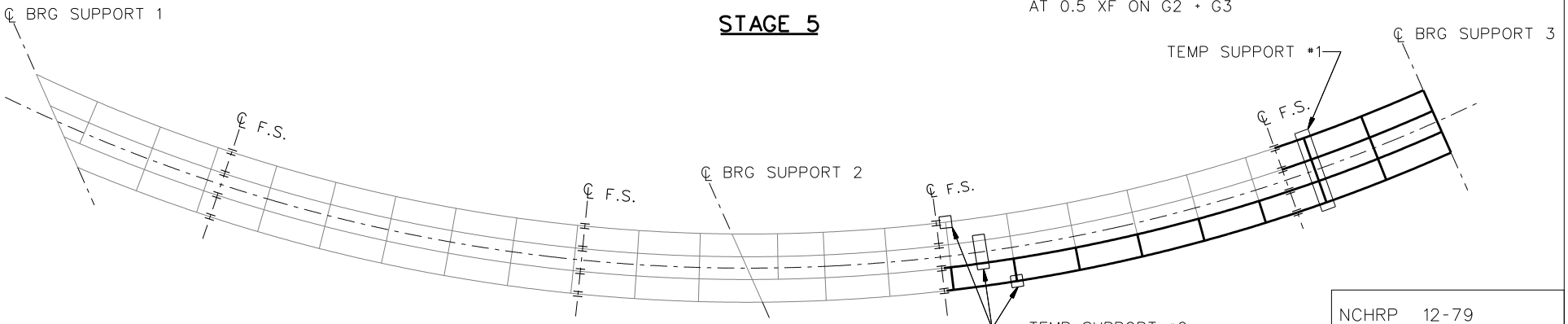

STAGE 6

LEGEND

▽ = HOLD OR LIFT CRANE

○ = TIE DOWN

□ = TEMPORARY SUPPORT STRUCTURE

NCHRP 12-79

BRIDGE NICCS13

GENERAL ERECTION PROCEDURE

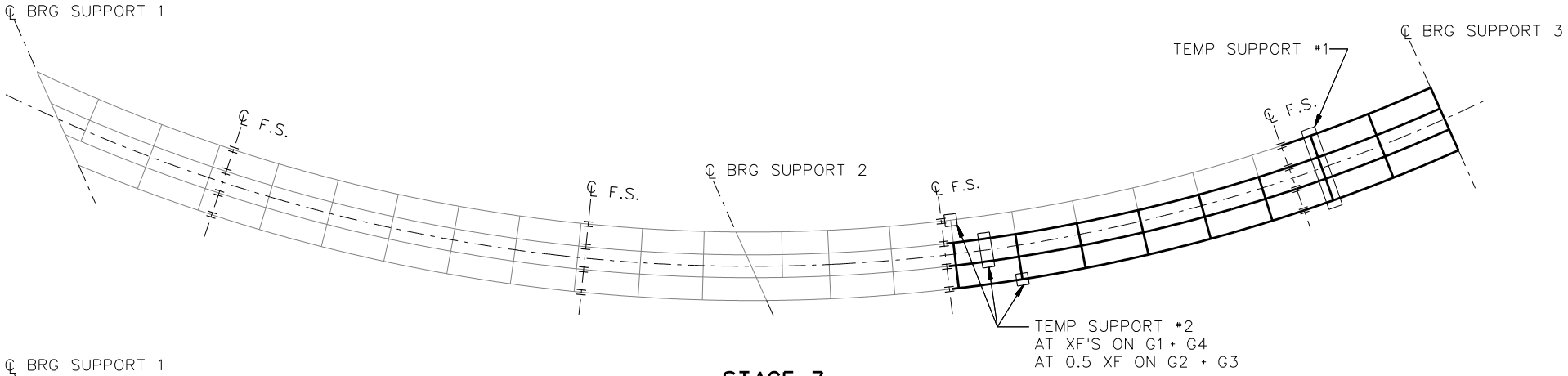

STAGE 7

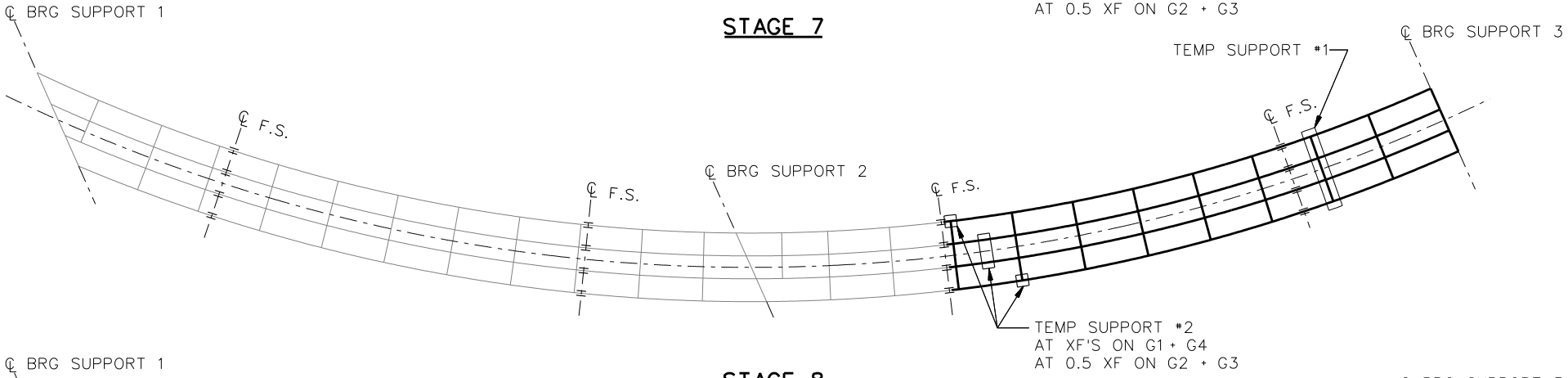

STAGE 8

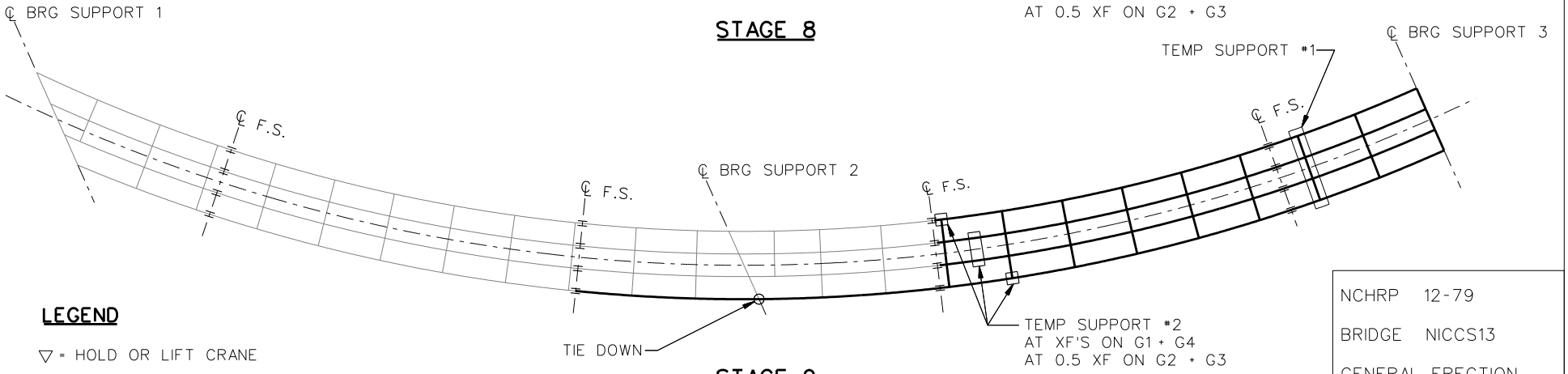

STAGE 9

LEGEND

▽ = HOLD OR LIFT CRANE

○ = TIE DOWN

□ = TEMPORARY SUPPORT STRUCTURE

NCHRP 12-79

BRIDGE NICCS13

GENERAL ERECTION PROCEDURE

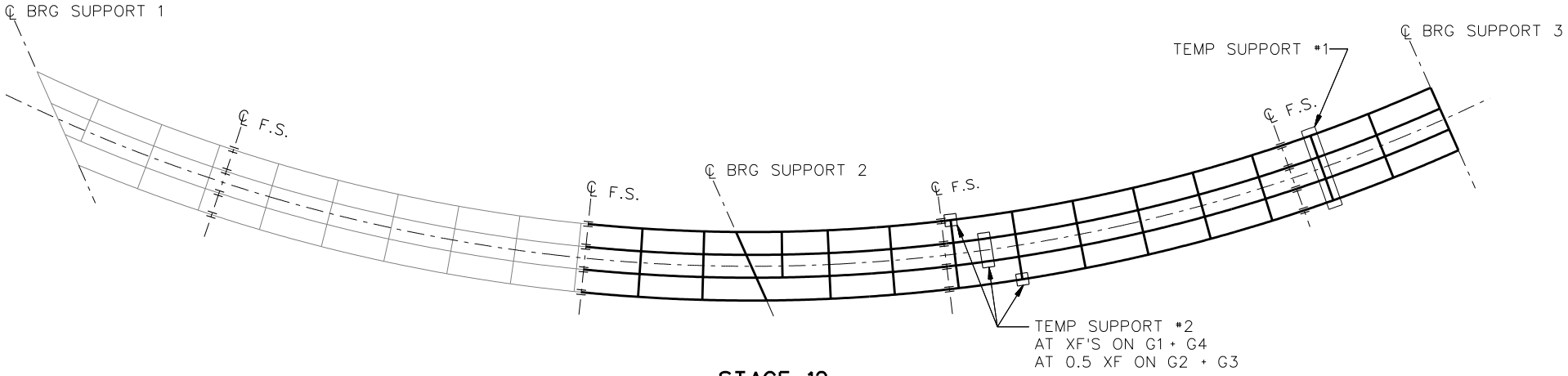

STAGE 12

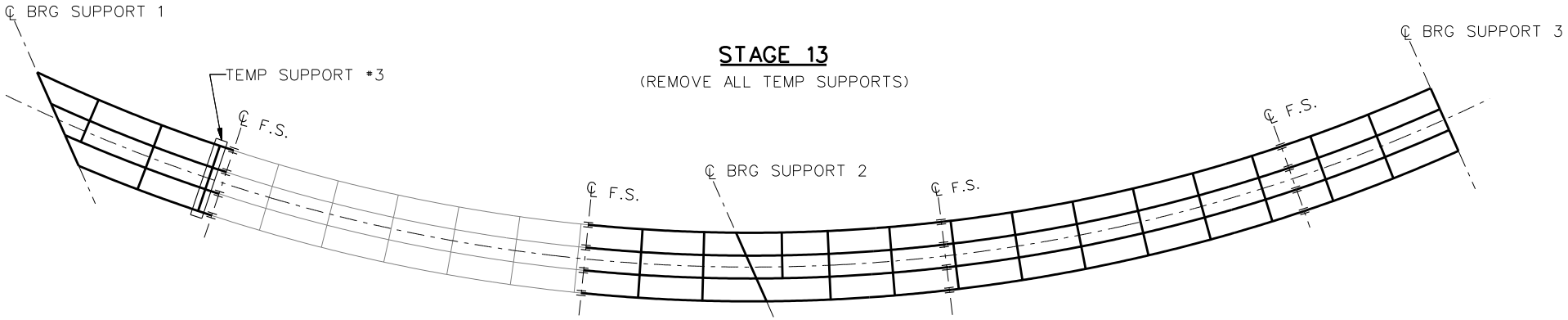

STAGE 13

(REMOVE ALL TEMP SUPPORTS)

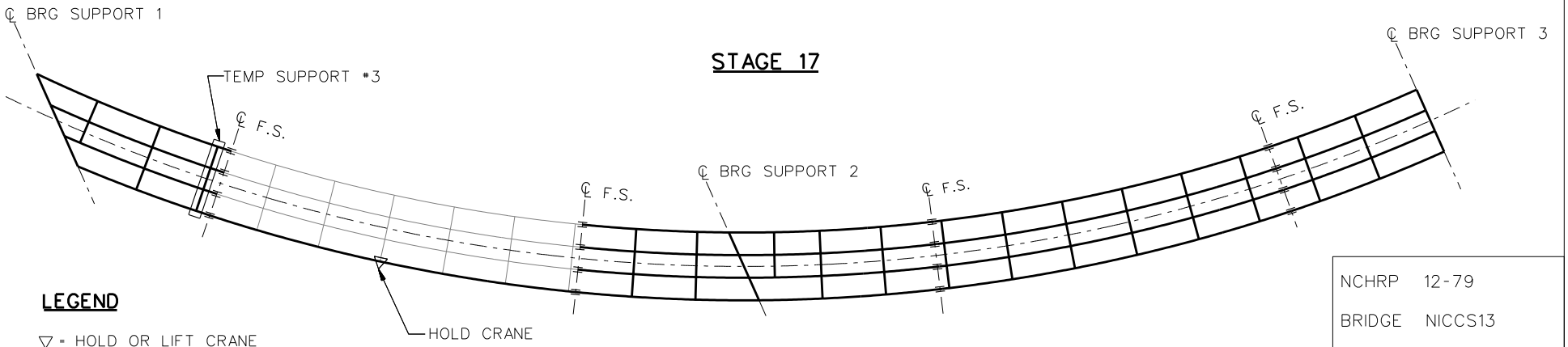

STAGE 17

STAGE 18

LEGEND

▽ = HOLD OR LIFT CRANE

○ = TIE DOWN

□ = TEMPORARY SUPPORT STRUCTURE

NCHRP 12-79

BRIDGE NICCS13

GENERAL ERECTION PROCEDURE

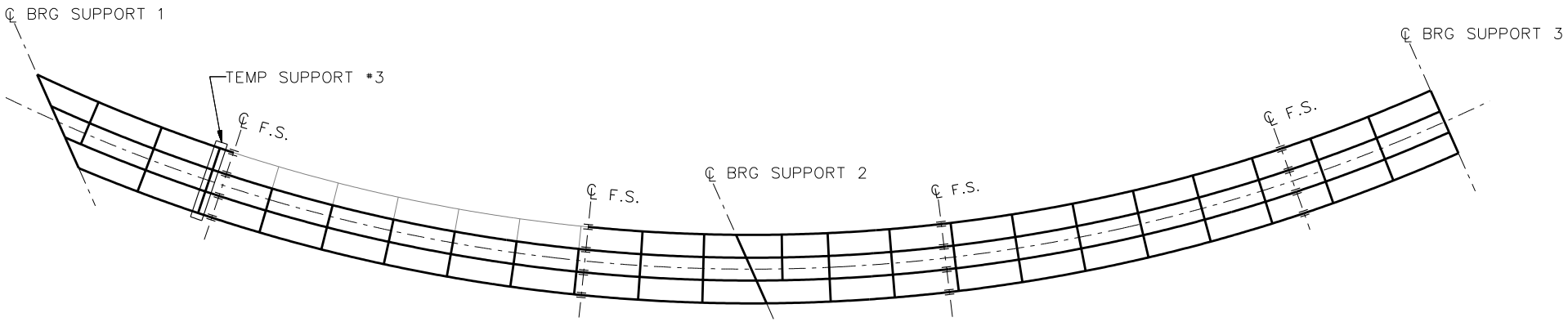

STAGE 20

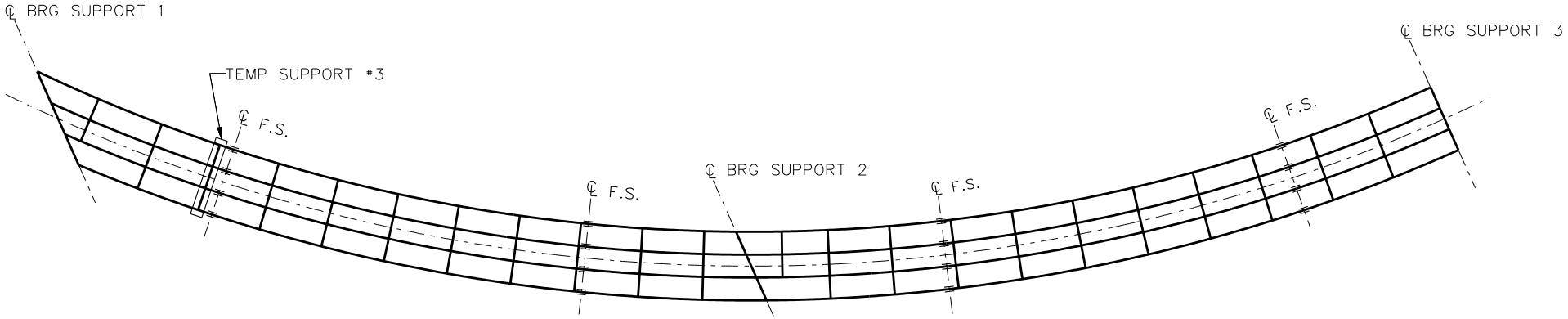

STAGE 21

STAGE 22
(REMOVE TEMP SUPPORT *3)

LEGEND

▽ = HOLD OR LIFT CRANE

○ = TIE DOWN

□ = TEMPORARY SUPPORT STRUCTURE

NCHRP 12-79

BRIDGE NICCS13

GENERAL ERECTION PROCEDURE

NCHRP 12-79

NICCS14

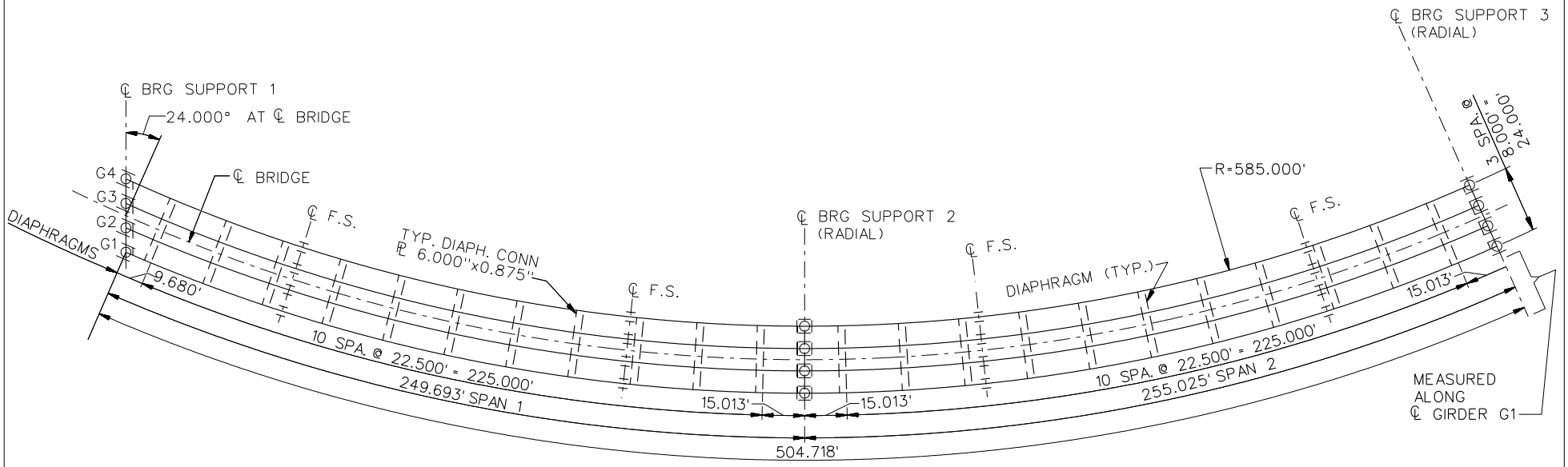

FRAMING PLAN

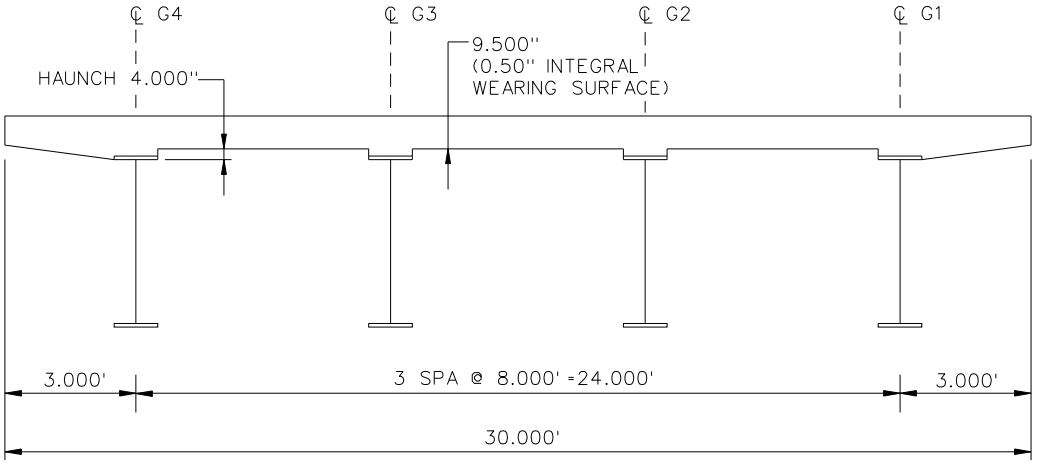

CROSS - SECTION

(DIAPHRAGMS NOT SHOWN)

BEARING LEGEND

- ○ NON-GUIDED
- ⊙ LONGITUDINALLY GUIDED
- |○| TRANSVERSELY GUIDED
- |⊙| FIXED

NCHRP 12-79

BRIDGE NICCS14

FRAMING PLAN AND CROSS-SECTION

SHEET 1 OF 9

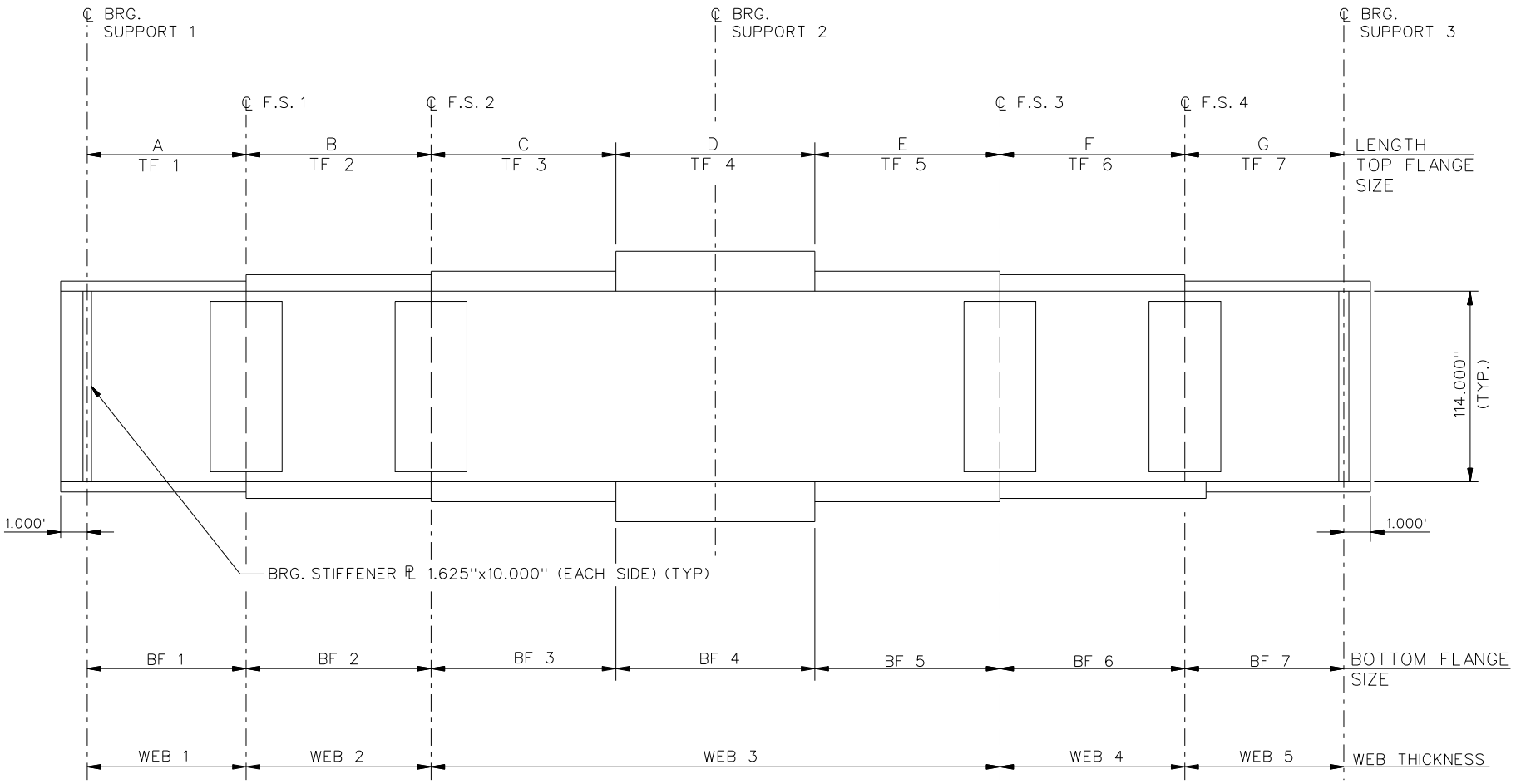

NOTE :

1. SEE TABLES ON SHEET 3 FOR GIRDER ELEVATION DIMENSIONS AND PLATE SIZES.

2. G1, G2 : WEB 1 = WEB 3 = WEB 5 = 1.000", WEB 2 = WEB 4 = 0.875"
   G3, G4: ALL WEBS = 0.875".

NCHRP 12-79

BRIDGE NICCS14

GIRDER ELEVATION

SHEET 2 OF 9

	GIRDER PLATE LENGTHS ✳			
LENGTH	G1	G2	G3	G4
A	56.693	62.391	65.099	67.816
B	125.000	123.358	121.716	120.074
C	40.000	39.475	38.949	38.424
D	50.000	49.343	48.686	48.029
E	40.000	39.475	38.949	38.424
F	125.000	123.358	121.716	120.074
G	65.025	64.171	63.317	62.463

✳ ALL DIMENSIONS ARE IN FEET.

	GIRDER FLANGE DIMENSIONS ✳✳							
TOP	G1		G2		G3		G4	
FLANGE	BF	TF	BF	TF	BF	TF	BF	TF
TF1	30.000	1.625	30.000	1.625	24.000	1.000	24.000	1.000
TF2	30.000	1.625	30.000	1.625	24.000	1.000	24.000	1.000
TF3	36.000	2.250	36.000	2.250	32.000	1.500	32.000	1.500
TF4	36.000	2.750	36.000	2.750	32.000	2.500	32.000	2.500
TF5	36.000	2.250	36.000	2.250	32.000	1.500	32.000	1.500
TF6	30.000	1.625	30.000	1.625	24.000	1.000	24.000	1.000
TF7	30.000	1.625	30.000	1.625	24.000	1.000	24.000	1.000

✳✳ ALL DIMENSIONS ARE IN INCHES.

	GIRDER FLANGE DIMENSIONS ✳✳							
BOTTOM	G1		G2		G3		G4	
FLANGE	BF	TF	BF	TF	BF	TF	BF	TF
BF1	30.000	2.250	30.000	2.250	24.000	1.000	24.000	1.000
BF2	30.000	2.250	30.000	2.250	24.000	1.000	24.000	1.000
BF3	36.000	2.250	36.000	2.250	32.000	2.000	32.000	2.000
BF4	36.000	3.000	36.000	3.000	32.000	2.500	32.000	2.500
BF5	36.000	2.250	36.000	2.250	32.000	2.000	32.000	2.000
BF6	30.000	2.250	30.000	2.250	24.000	1.000	24.000	1.000
BF7	30.000	2.250	30.000	2.250	24.000	1.000	24.000	1.000

✳✳ ALL DIMENSIONS ARE IN INCHES.

NCHRP 12-79

BRIDGE NICCS14

GIRDER ELEVATION TABLES

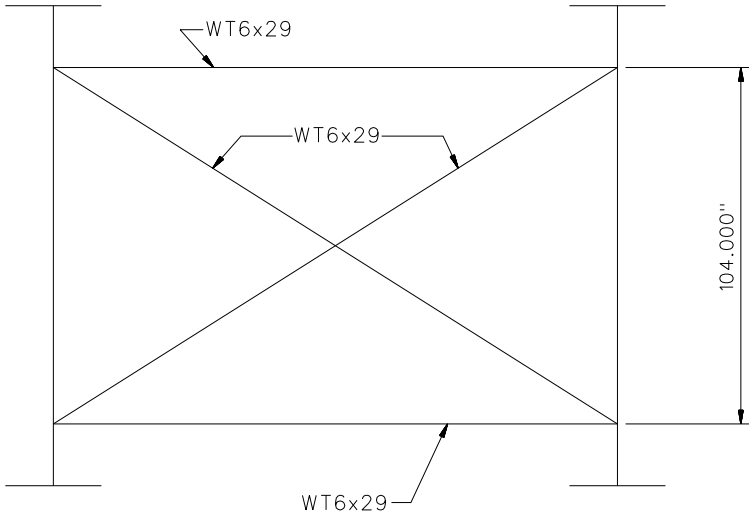

TYPICAL SUPPORT DIAPHRAGMS AND INTERMEDIATE DIAPHRAGMS

NOTES:

1. STEEL DEAD LOAD INCREASED BY 5% FOR MDX AND LARSA MODELS; 2% FOR 3D MODEL; AND 10% FOR APPROXIMATE ANALYSIS TO ACCOUNT FOR MISC. DETAILS.

2. FORMWORK LOAD OF 10PSF IS INCLUDED IN CONCRETE DEAD LOAD.

3. ADDITIONAL DESIGN PARAMETERS:
   A. 1.500' PARAPET WIDTH BOTH SIDES.
   B. 700 LB/FT UNIFORM LOAD ASSUMED FOR PARAPET WEIGHT.
   C. ROADWAY WIDTH = 26.500'.
   D. NUMBER OF DESIGN LANES = 2.
   E. HL93 LIVE LOAD.
   F. DESIGN SPEED = 35 MPH.

NCHRP 12-79

BRIDGE NICCS14

MISC. DETAILS AND NOTES

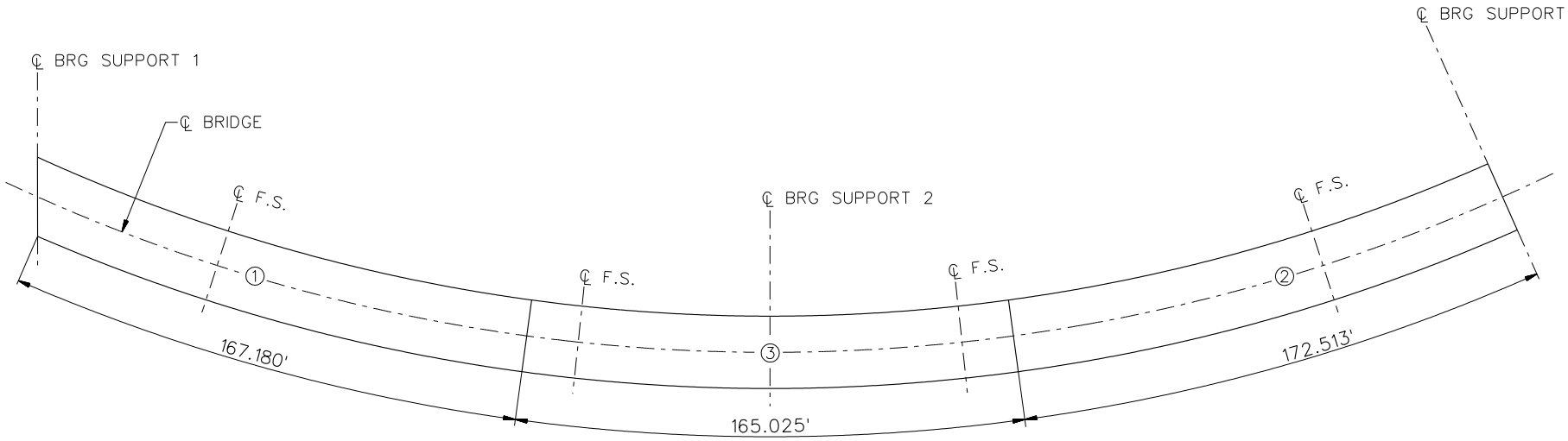

DECK POURING SEQUENCE

NOTE:

DECK POUR LENGTH ARE MEASURED ALONG ℄ G1.

NCHRP 12-79

BRIDGE NICCS14

DECK POURING SEQUENCE

SHEET 5 OF 9

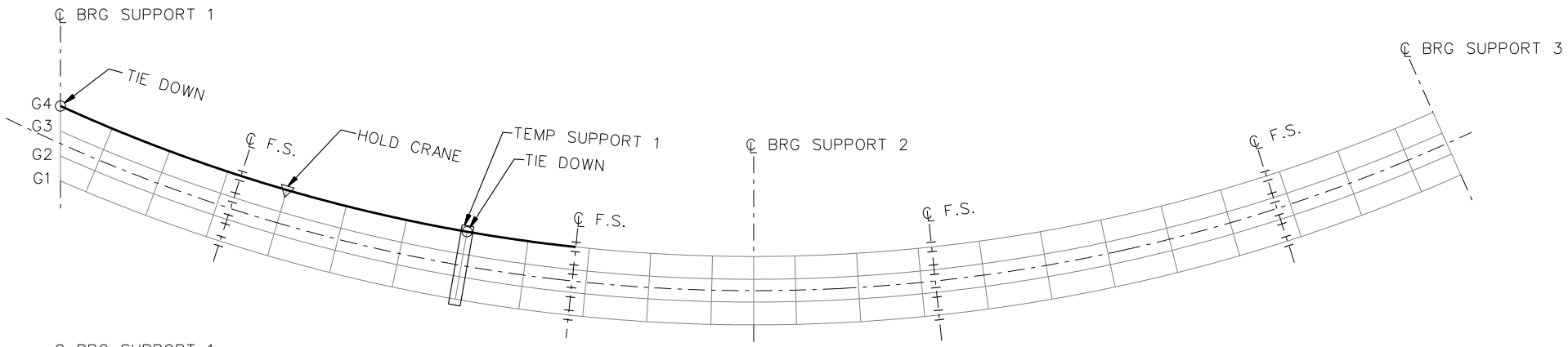

STAGE 1

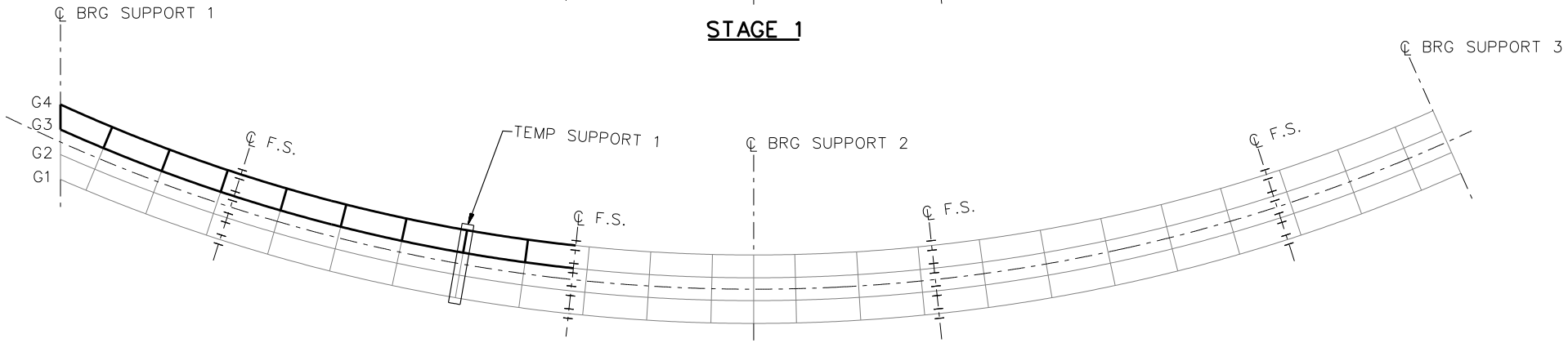

STAGE 2

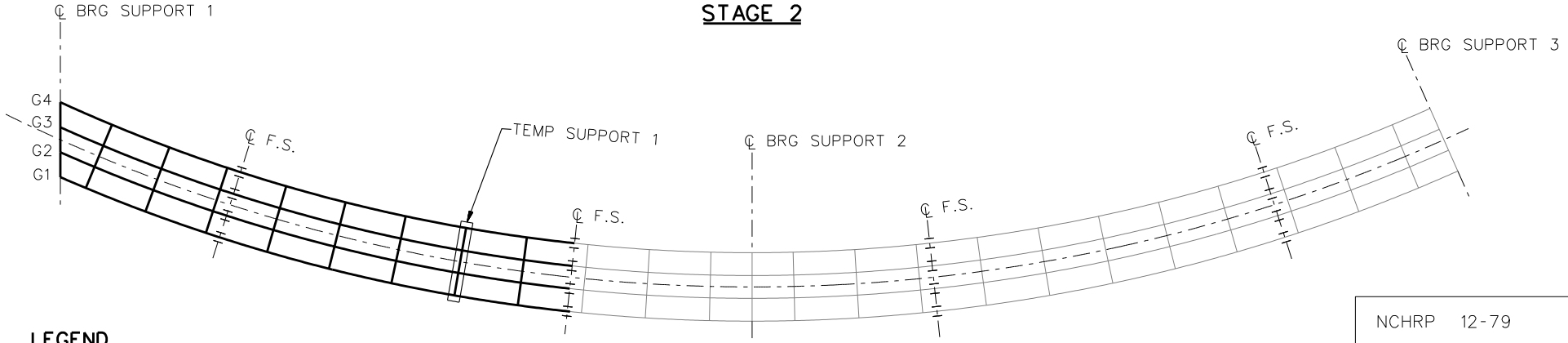

STAGES 3 AND 4

LEGEND

▽ = HOLD OR LIFT CRANE

○ = TIE DOWN

□ = TEMPORARY SUPPORT STRUCTURE

NCHRP 12-79

BRIDGE NICCS14

GENERAL ERECTION PROCEDURE

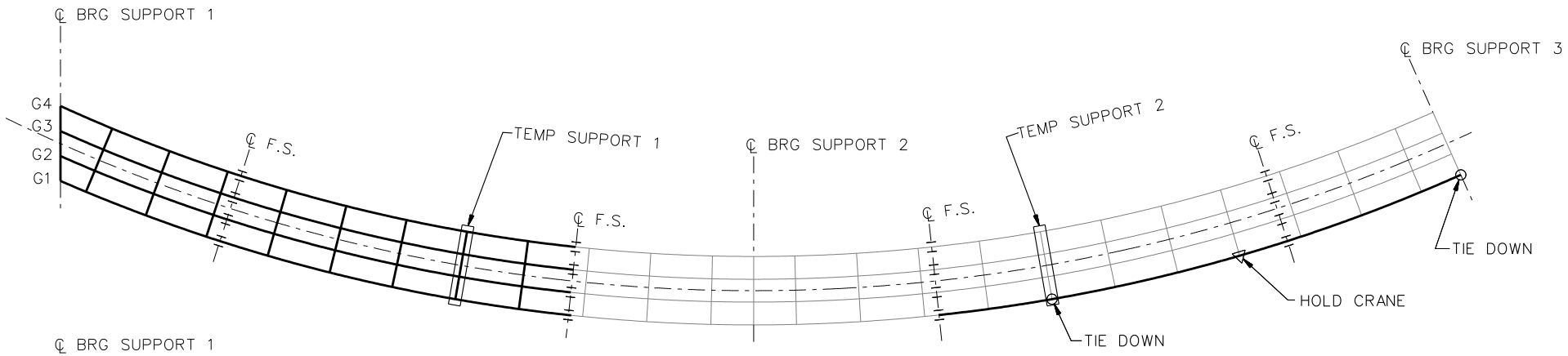

STAGE 5

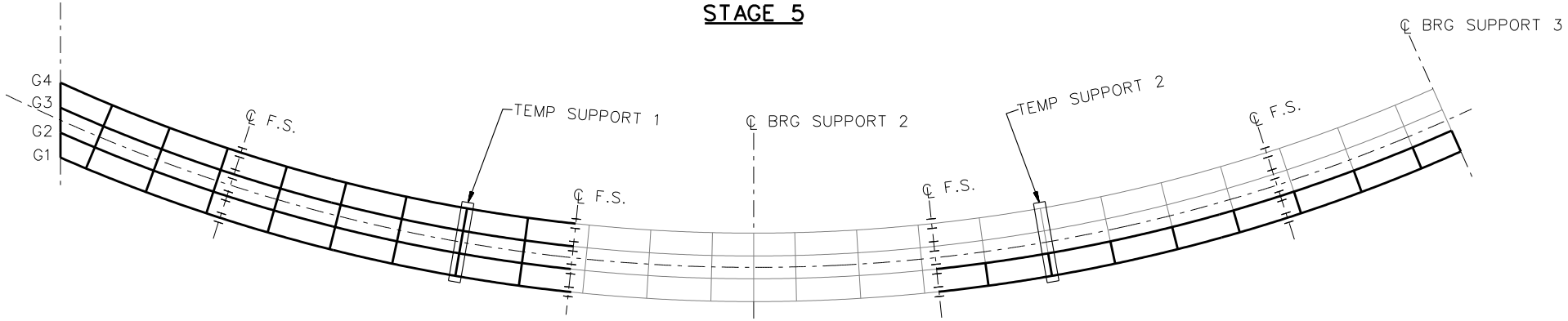

STAGE 6

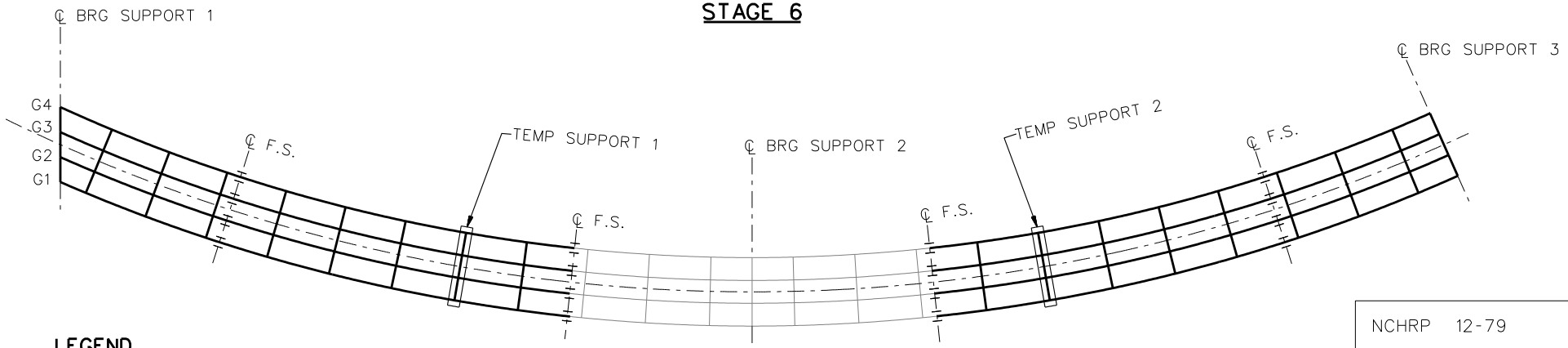

STAGES 7 AND 8

LEGEND

▽ = HOLD OR LIFT CRANE

○ = TIE DOWN

□ = TEMPORARY SUPPORT STRUCTURE

NCHRP 12-79

BRIDGE NICCS14

GENERAL ERECTION PROCEDURE

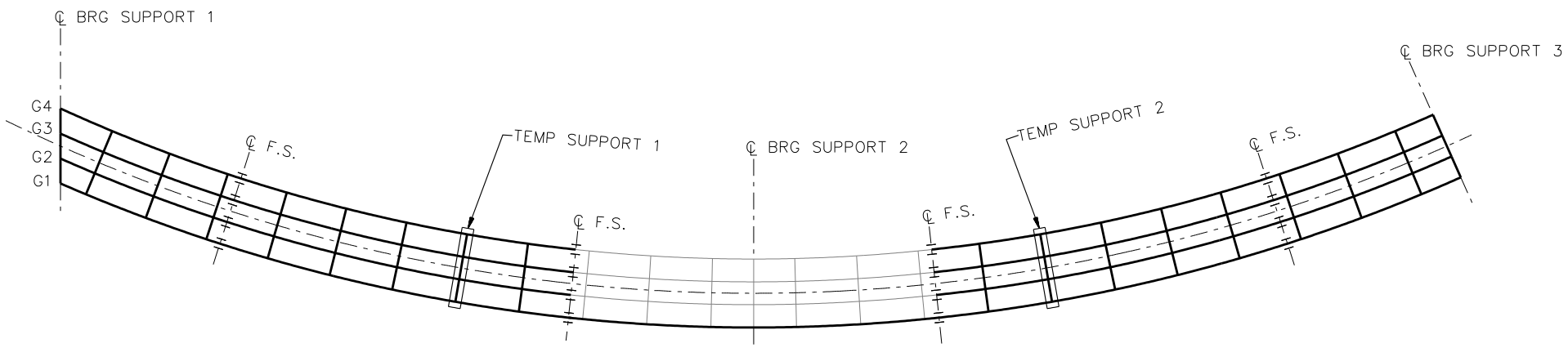

STAGE 9

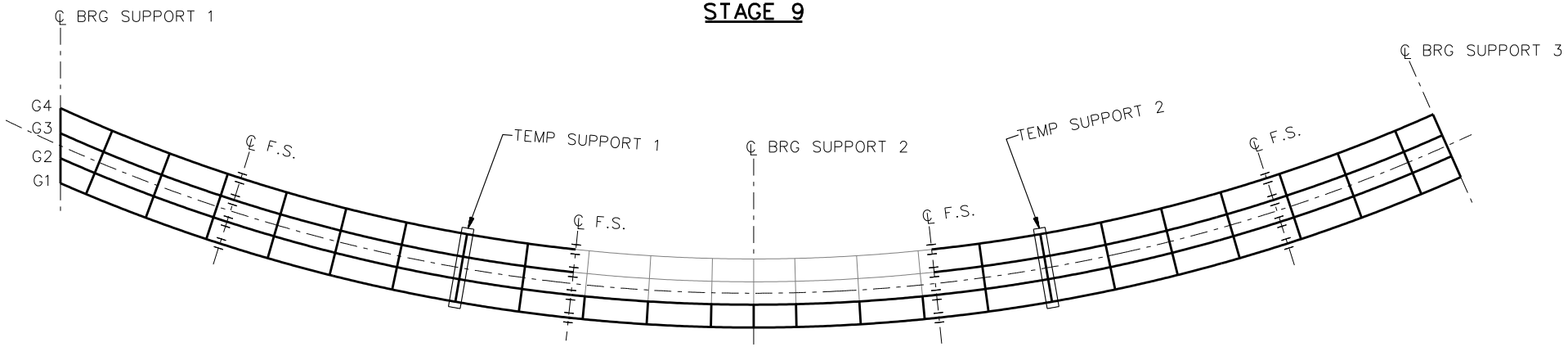

STAGE 10

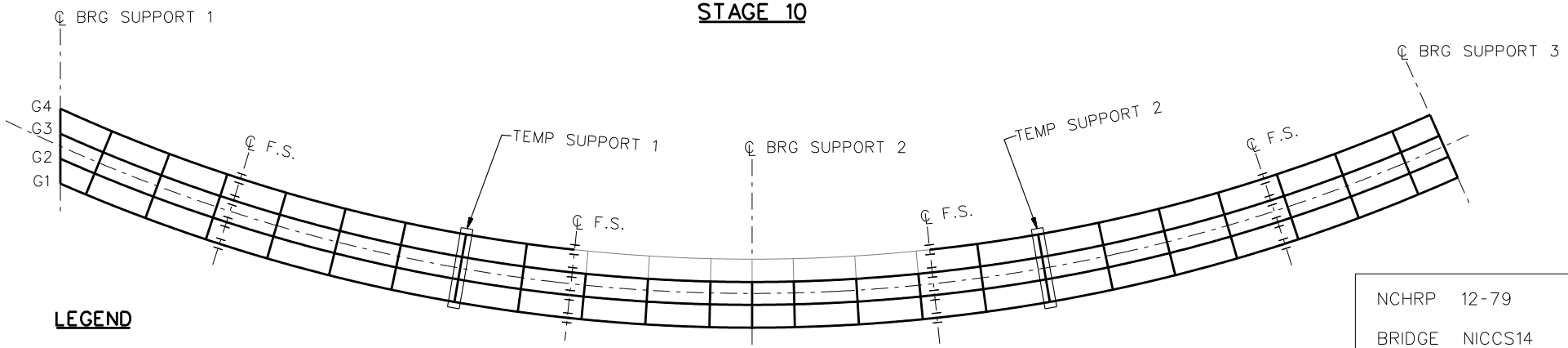

STAGE 11

LEGEND

▽ = HOLD OR LIFT CRANE

○ = TIE DOWN

□ = TEMPORARY SUPPORT STRUCTURE

NCHRP 12-79

BRIDGE NICCS14

GENERAL ERECTION PROCEDURE

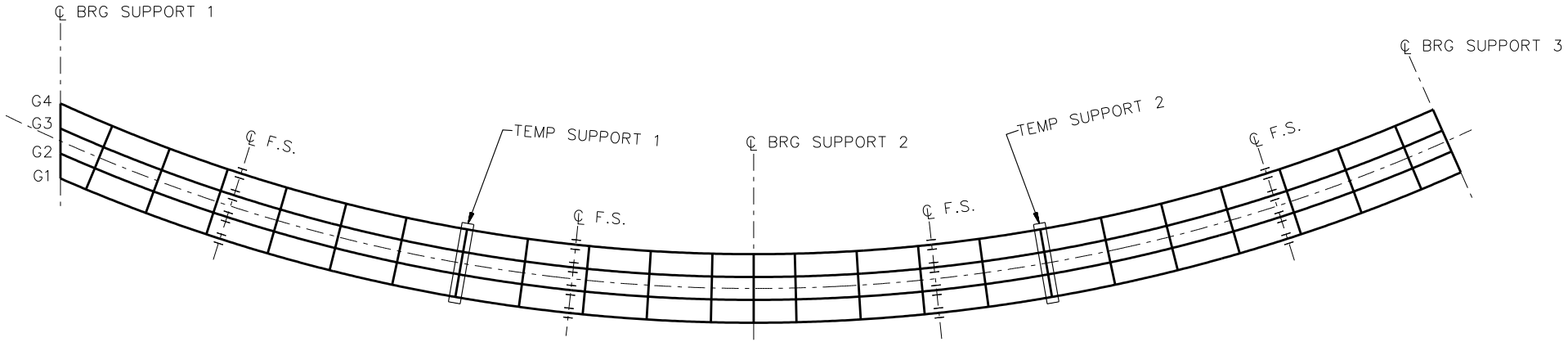

STAGE 12

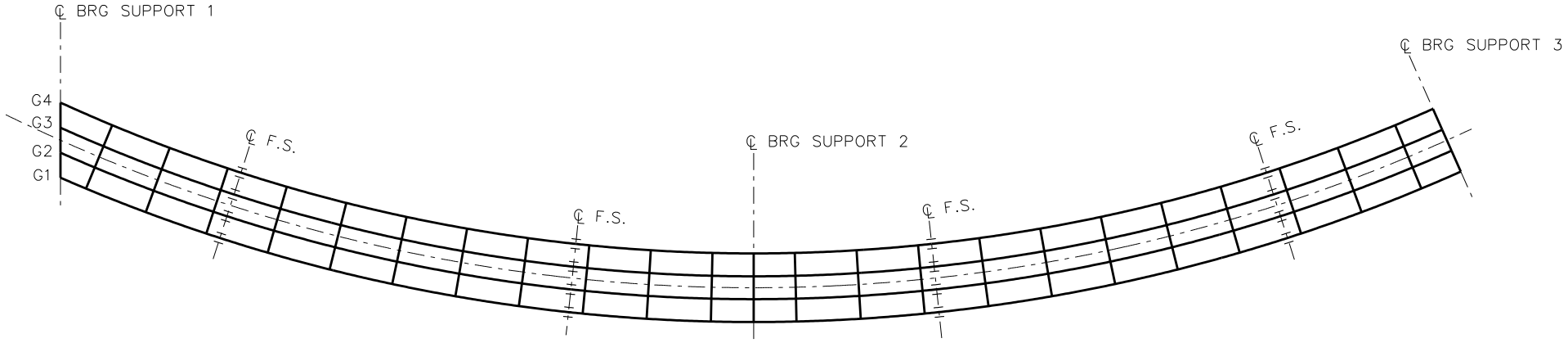

STAGE 13

LEGEND

▽ = HOLD OR LIFT CRANE

○ = TIE DOWN

□ = TEMPORARY SUPPORT STRUCTURE

NCHRP 12-79

BRIDGE NICCS14

GENERAL ERECTION PROCEDURE

NCHRP 12-79

NICCS24

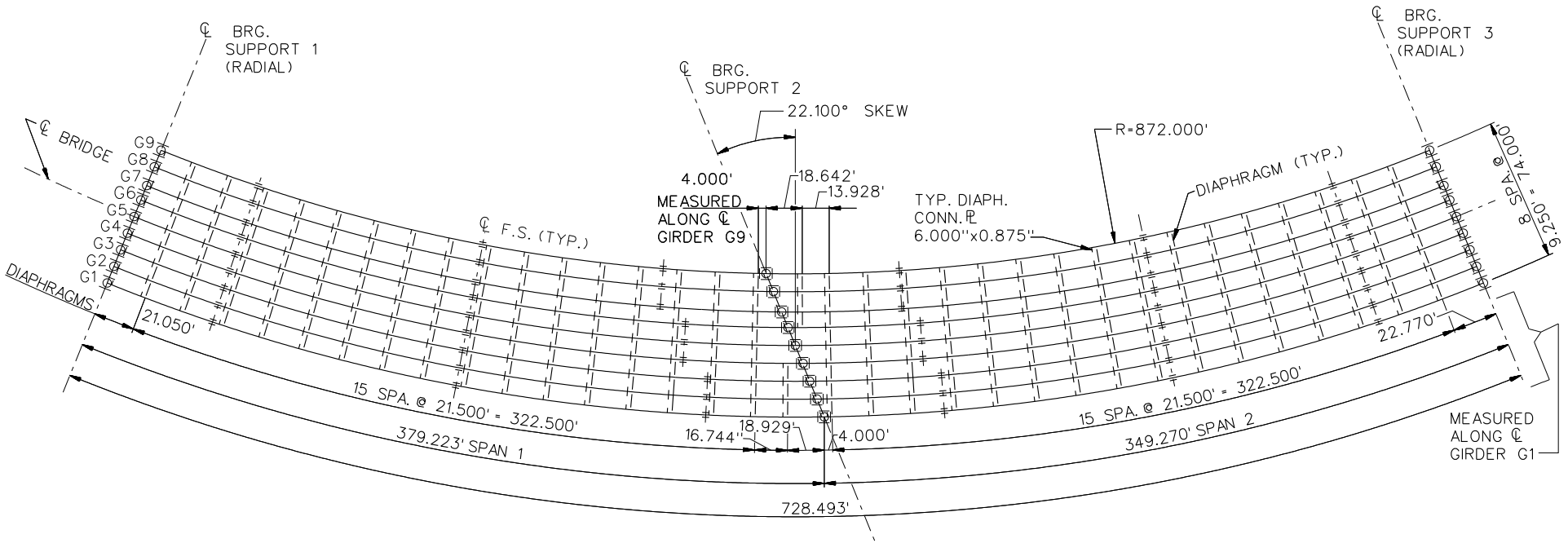

NOTE :

NO INTERMEDIATE TRANSV. STIFFS.
ALL BRG. STIFFENERS = 12.000"x2.000"

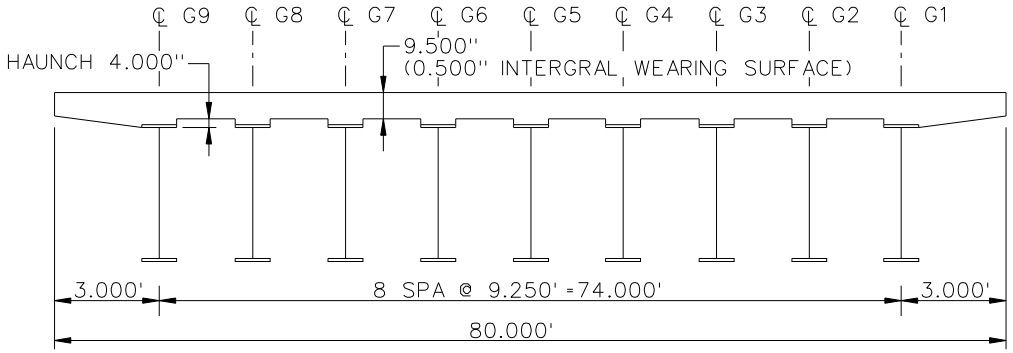

CROSS - SECTION

(DIAPHRAGMS NOT SHOWN)

BEARING LEGEND

- ○ NON-GUIDED
- ⊙ LONGITUDINALLY GUIDED
- |○| TRANSVERSELY GUIDED
- |⊙| FIXED

NCHRP 12-79

BRIDGE NICCS24

FRAMING PLAN AND CROSS-SECTION

SHEET 1 OF 11

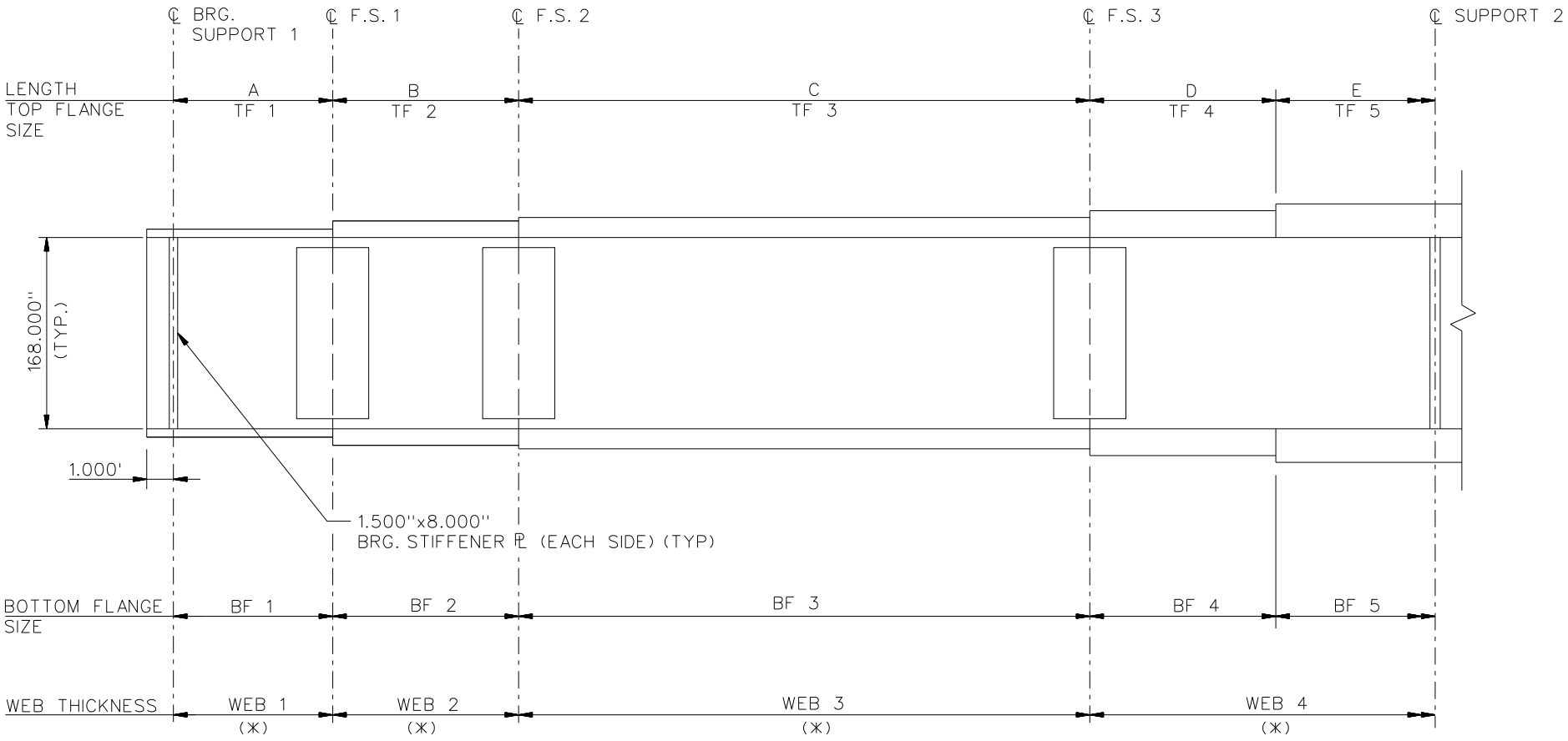

"E", "TF 5", "BF 5", WEB 4 INCLUDES LEFT AND RIGHT OF SUPPORT 2

NOTES:

SEE TABLES ON SHEETS 4 AND 5 FOR GIRDER ELEVATION DIMENSIONS AND PLATE SIZES.

(*) G1, G2, G3, WEB 1 = WEB 2 = WEB 3 = 1.125", WEB 4 = 1.375"
G4, G5, G6, WEB 1 = WEB 2 = WEB 3 = 1.125", WEB 4 = 1.250"
G7, G8, G9, WEB 1 = WEB 2 = WEB 3 = WEB 4 = 1.125"

NCHRP 12-79

BRIDGE NICCS24

GIRDER ELEVATION SPAN 1

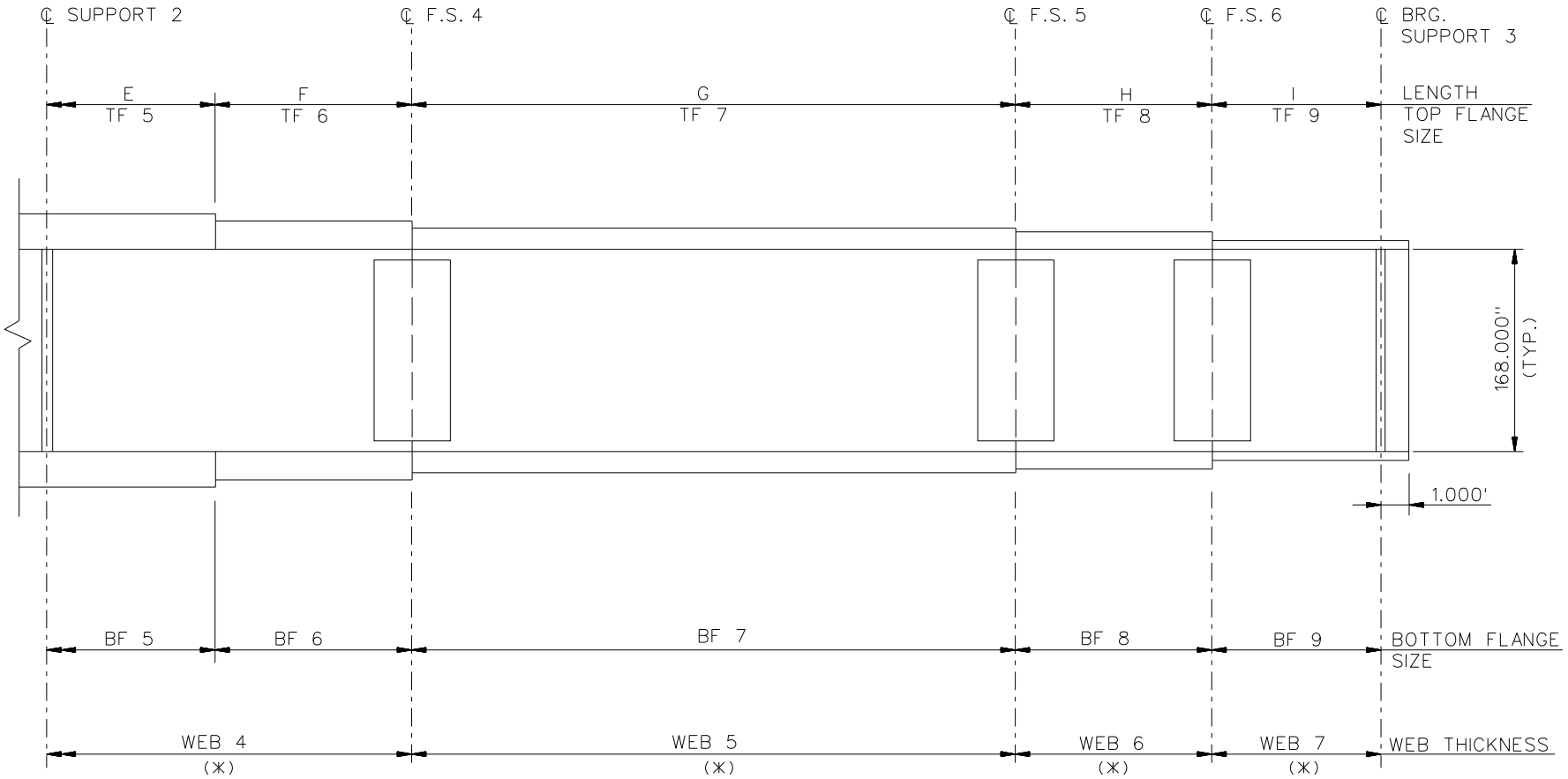

"E", "TF 5", "BF 5", WEB 4 INCLUDES
LEFT AND RIGHT OF SUPPORT 2

NOTES:

SEE TABLES ON SHEETS 4 AND 5 FOR GIRDER ELEVATION DIMENSIONS AND PLATE SIZES.

(*) G1, G2, G3, WEB 4 = 1.375", WEB 5 = WEB 6 = WEB 7 = 1.125"
G4, G5, G6, WEB 4 = 1.250", WEB 5 = WEB 6 = WEB 7 = 1.125"
G7, G8, G9, WEB 4 = WEB 5 = WEB 6 = WEB 7 = 1.125"

NCHRP 12-79

BRIDGE NICCS24

GIRDER ELEVATION
SPAN 2

	GIRDER PLATE LENGTHS ✳								
LENGTH	G1	G2	G3	G4	G5	G6	G7	G8	G9
A	57.980	57.413	56.846	56.279	55.712	55.145	54.578	54.011	53.444
B	130.000	128.729	127.458	126.187	124.915	123.644	122.373	121.102	119.831
C	130.000	128.729	127.458	113.130	111.990	110.850	96.155	95.156	94.157
D	34.281	33.946	33.611	34.502	34.154	33.806	34.747	34.386	34.026
E	48.597	48.121	47.646	48.843	48.352	47.860	49.118	48.608	48.097

✳ ALL DIMENSIONS ARE IN FEET.

	GIRDER FLANGE DIMENSIONS ✳✳					
TOP	G1, G2, G3		G4, G5, G6		G7, G8, G9	
FLANGE	BF	TF	BF	TF	BF	TF
TF1	36.000	2.000	30.000	1.500	28.000	1.250
TF2	36.000	2.000	30.000	1.500	28.000	1.250
TF3	36.000	2.000	30.000	1.500	28.000	1.250
TF4	42.000	2.250	36.000	2.000	34.000	1.750
TF5	42.000	3.000	36.000	2.750	34.000	2.500

✳✳ ALL DIMENSIONS ARE IN INCHES.

	GIRDER FLANGE DIMENSIONS ✳✳					
BOTTOM	G1, G2, G3		G4, G5, G6		G7, G8, G9	
FLANGE	BF	TF	BF	TF	BF	TF
BF1	36.000	2.250	30.000	1.500	28.000	1.250
BF2	36.000	2.250	30.000	1.500	28.000	1.250
BF3	36.000	2.250	30.000	1.500	28.000	1.250
BF4	42.000	2.250	36.000	2.000	34.000	1.750
BF5	42.000	3.000	36.000	2.750	34.000	2.500

✳✳ ALL DIMENSIONS ARE IN INCHES.

NCHRP 12-79

BRIDGE NICCS24

GIRDER ELEVATION TABLES SPAN 1

	GIRDER PLATE LENGTHS ✳								
LENGTH	G1	G2	G3	G4	G5	G6	G7	G8	G9
E	48.597	48.121	47.646	48.843	48.352	47.860	49.118	48.608	48.097
F	40.446	40.051	39.655	40.602	40.193	39.784	40.775	40.351	39.928
G	119.334	118.167	117.000	124.650	123.394	122.138	130.000	128.650	127.299
H	110.000	108.924	107.849	106.773	105.698	104.622	103.547	102.471	101.395
I	57.855	57.289	56.724	56.158	55.592	55.027	54.461	53.895	53.329

✳ ALL DIMENSIONS ARE IN FEET.

	GIRDER FLANGE DIMENSIONS ✳✳					
TOP	G1, G2, G3		G4, G5, G6		G7, G8, G9	
FLANGE	BF	TF	BF	TF	BF	TF
TF5	42.000	3.000	36.00	2.750	34.000	2.500
TF6	42.000	2.250	36.000	2.000	34.000	1.750
TF7	36.000	2.000	30.000	1.500	28.000	1.250
TF8	36.000	2.000	30.000	1.500	28.000	1.250
TF9	36.000	2.000	30.000	1.500	28.000	1.250

✳✳ ALL DIMENSIONS ARE IN INCHES.

	GIRDER FLANGE DIMENSIONS ✳✳					
BOTTOM	G1, G2, G3		G4, G5, G6		G7, G8, G9	
FLANGE	BF	TF	BF	TF	BF	TF
BF5	42.000	3.000	36.000	2.750	34.000	2.500
BF6	42.000	2.250	36.000	2.000	34.000	1.750
BF7	36.000	2.250	30.000	1.500	28.000	1.250
BF8	36.000	2.250	30.000	1.500	28.000	1.250
BF9	36.000	2.250	30.000	1.500	28.000	1.250

✳✳ ALL DIMENSIONS ARE IN INCHES.

NCHRP 12-79

BRIDGE NICCS24

GIRDER ELEVATION TABLES SPAN 2

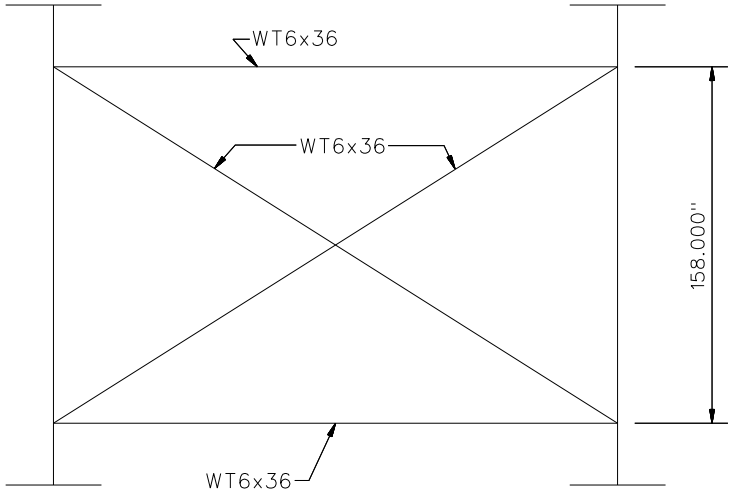

TYPICAL SUPPORT DIAPHRAGMS AND INTERMEDIATE DIAPHRAGMS

NOTES:

1. STEEL DEAD LOAD INCREASED BY 5% FOR MDX AND LARSA MODELS; 2% FOR 3D MODEL; AND 10% FOR APPROXIMATE ANALYSIS TO ACCOUNT FOR MISC. DETAILS.

2. FORMWORK LOAD OF 10PSF IS INCLUDED IN CONCRETE DEAD LOAD.

3. ADDITIONAL DESIGN PARAMETERS:
   A. 1.500' PARAPET WIDTH BOTH SIDES.
   B. 700 LB/FT UNIFORM LOAD ASSUMED FOR PARAPET WEIGHT.
   C. ROADWAY WIDTH = 76.500'.
   D. NUMBER OF DESIGN LANES = 6.
   E. HL93 LIVE LOAD.
   F. DESIGN SPEED = 35 MPH.

4. DIAPHRAGM MEMBER CALL-OUTS ARE IN ENGLISH UNITS.

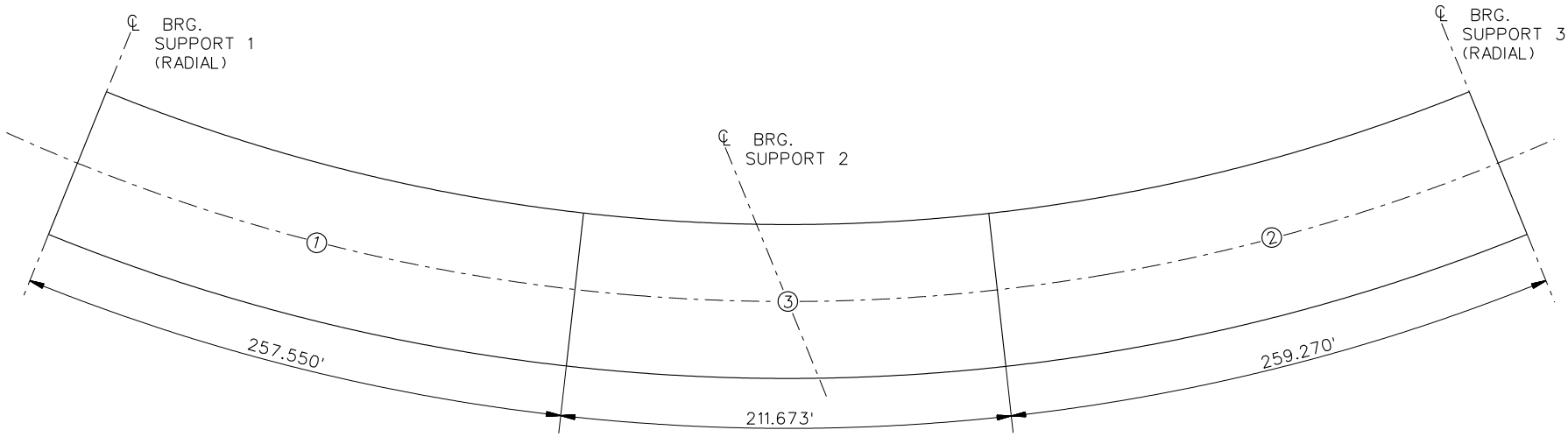

DECK POURING SEQUENCE

NCHRP 12-79

BRIDGE NICCS24

DECK POURING SEQUENCE

SHEET 7 OF 11

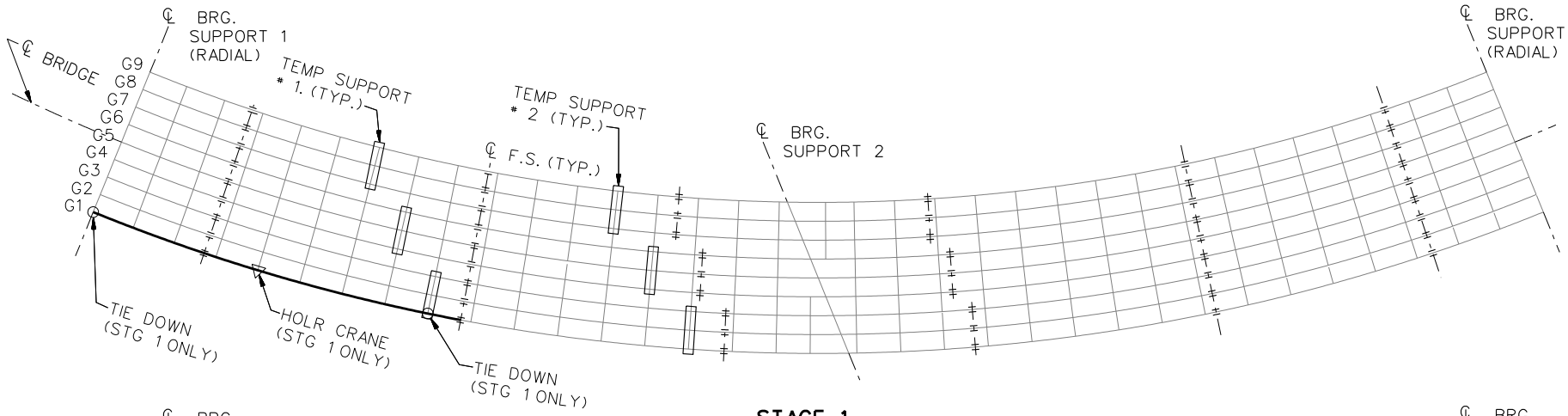

STAGE 1

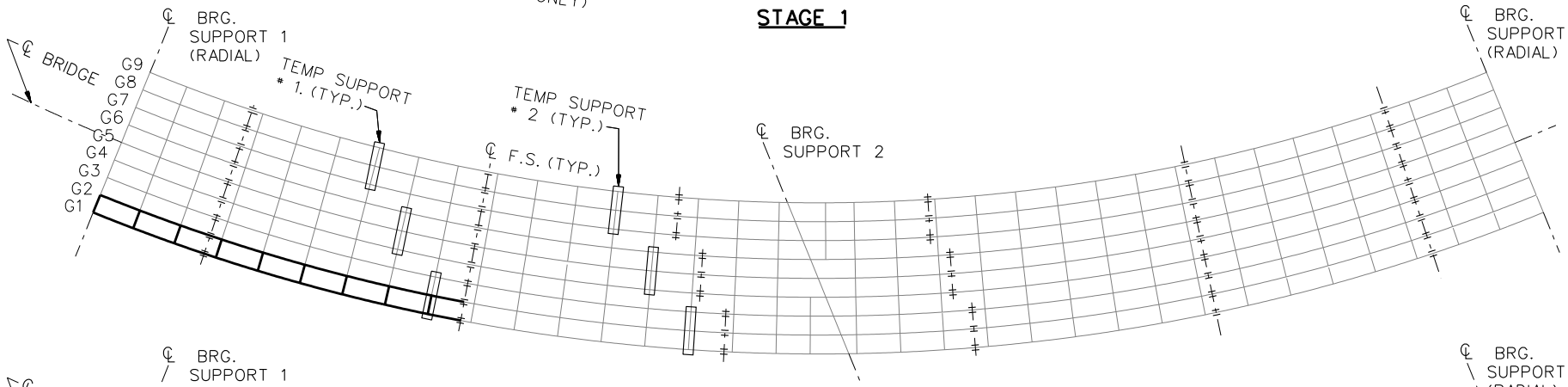

STAGE 2

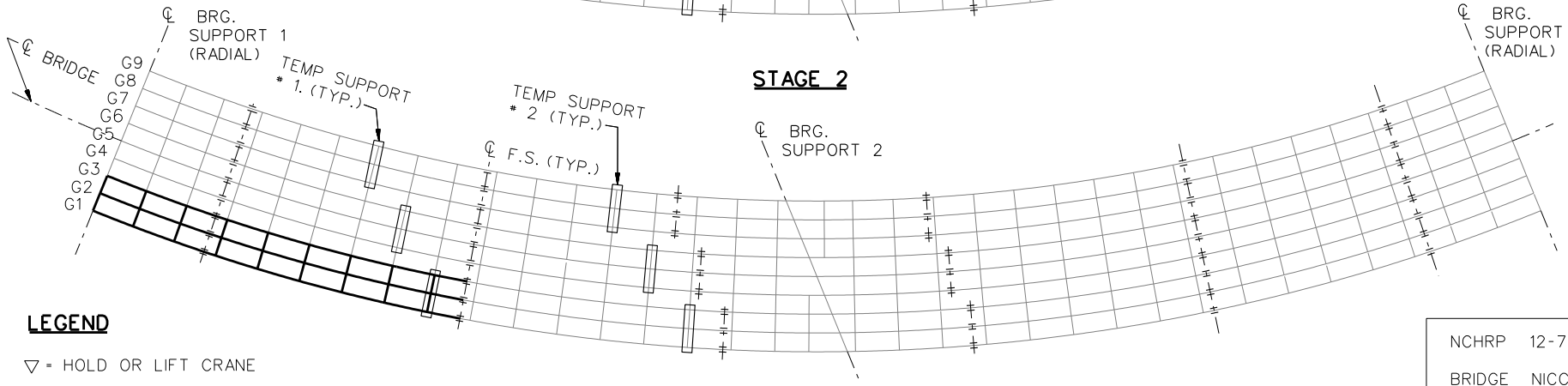

STAGE 3

LEGEND

▽ = HOLD OR LIFT CRANE

○ = TIE DOWN

□ = TEMPORARY SUPPORT STRUCTURE

NCHRP 12-79

BRIDGE NICCS24

GENERAL ERECTION PROCEDURE

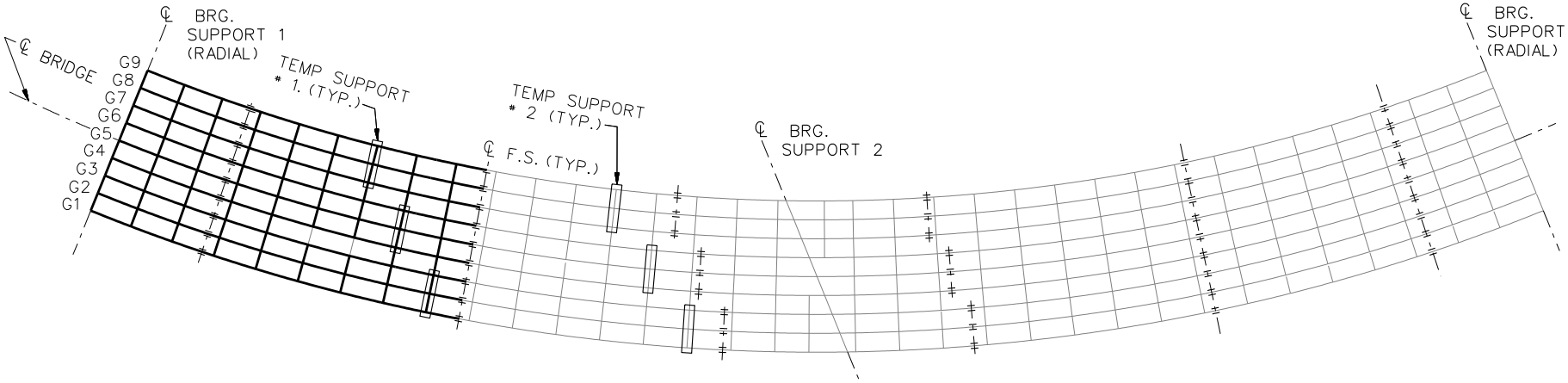

STAGES 4 THRU 9

(G4 THRU G9)

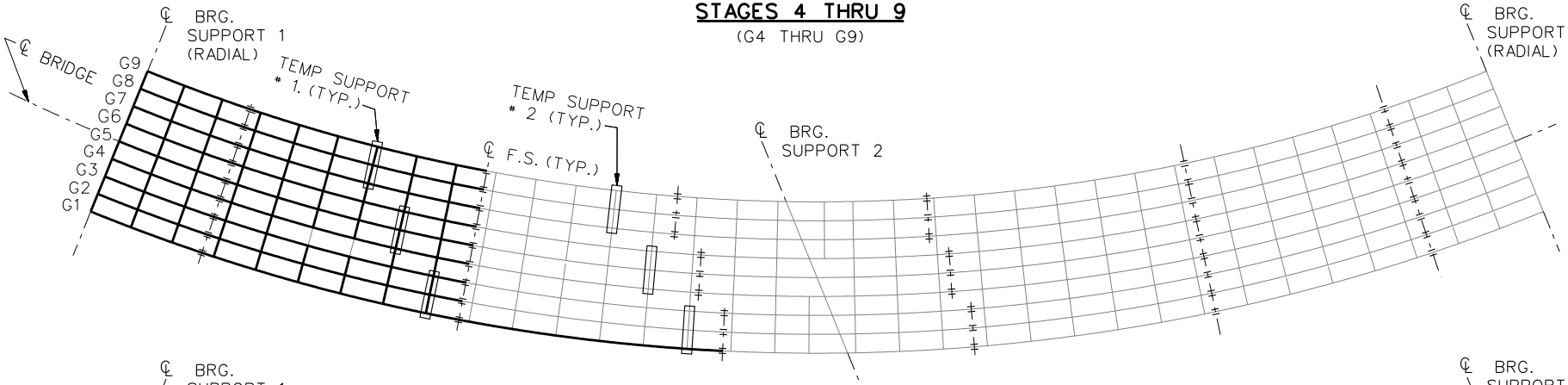

STAGE 10

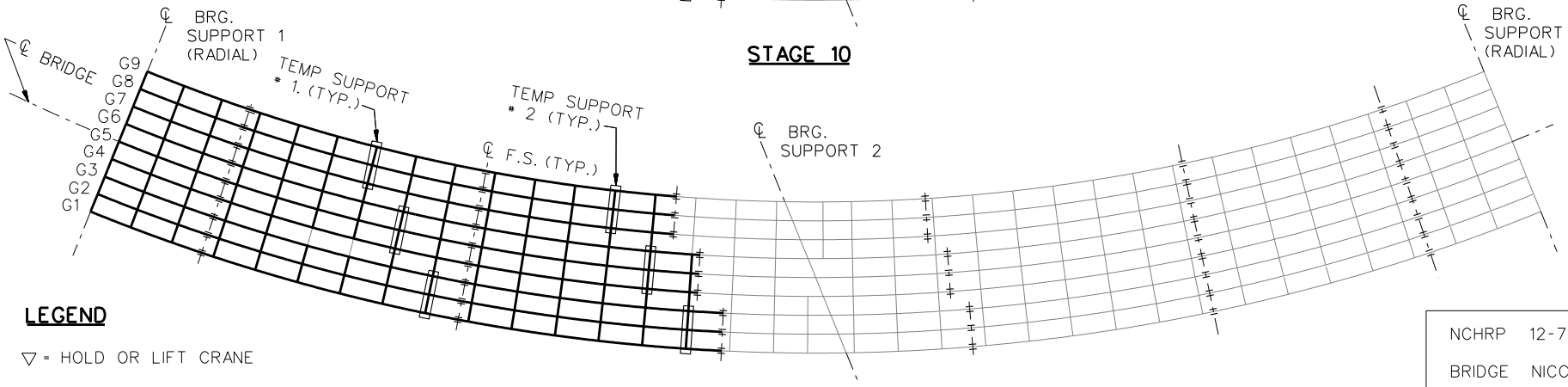

STAGES 11 - 18

LEGEND

▽ = HOLD OR LIFT CRANE

○ = TIE DOWN

□ = TEMPORARY SUPPORT STRUCTURE

NCHRP 12-79

BRIDGE NICCS24

GENERAL ERECTION PROCEDURE

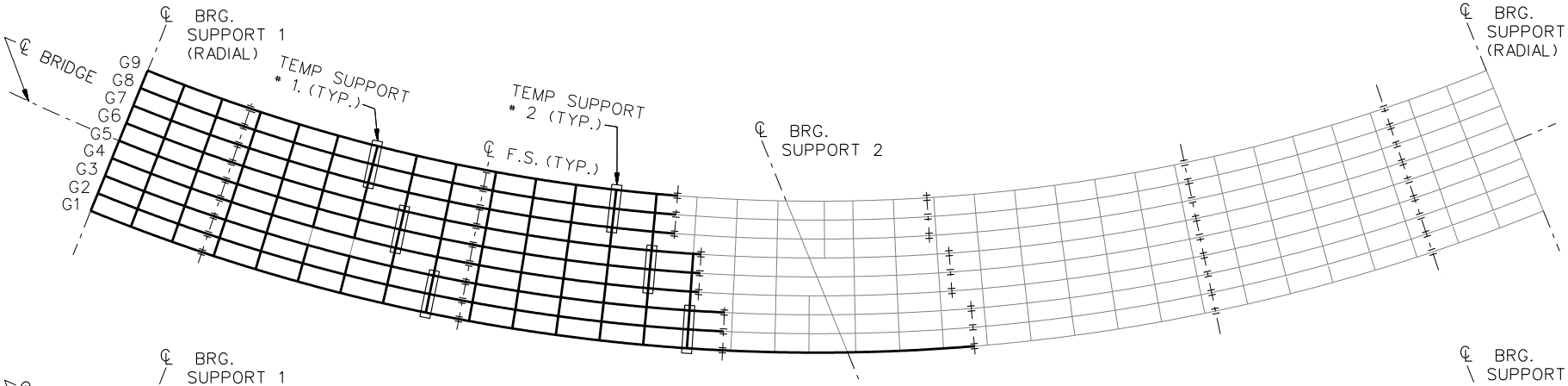

STAGE 19

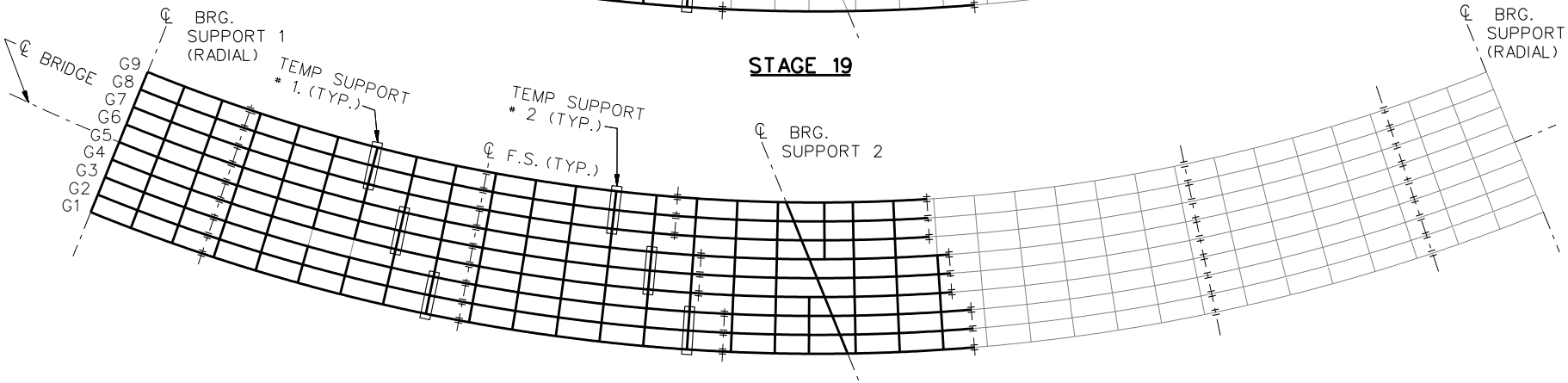

STAGES 20 THRU 27
(G2 THRU G9)

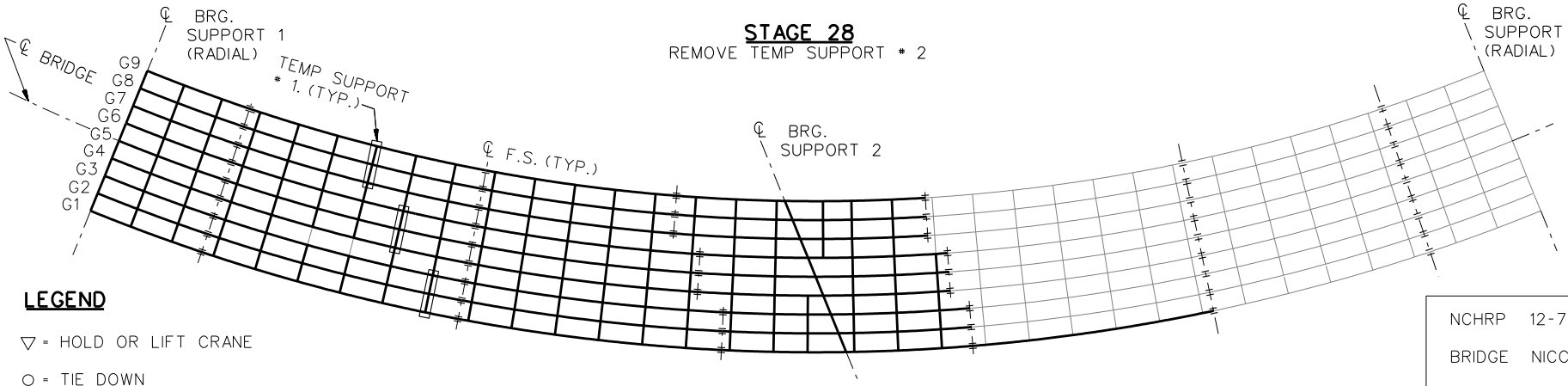

STAGE 28
REMOVE TEMP SUPPORT * 2

STAGE 29

LEGEND

▽ = HOLD OR LIFT CRANE

○ = TIE DOWN

□ = TEMPORARY SUPPORT STRUCTURE

NCHRP 12-79

BRIDGE NICCS24

GENERAL ERECTION PROCEDURE

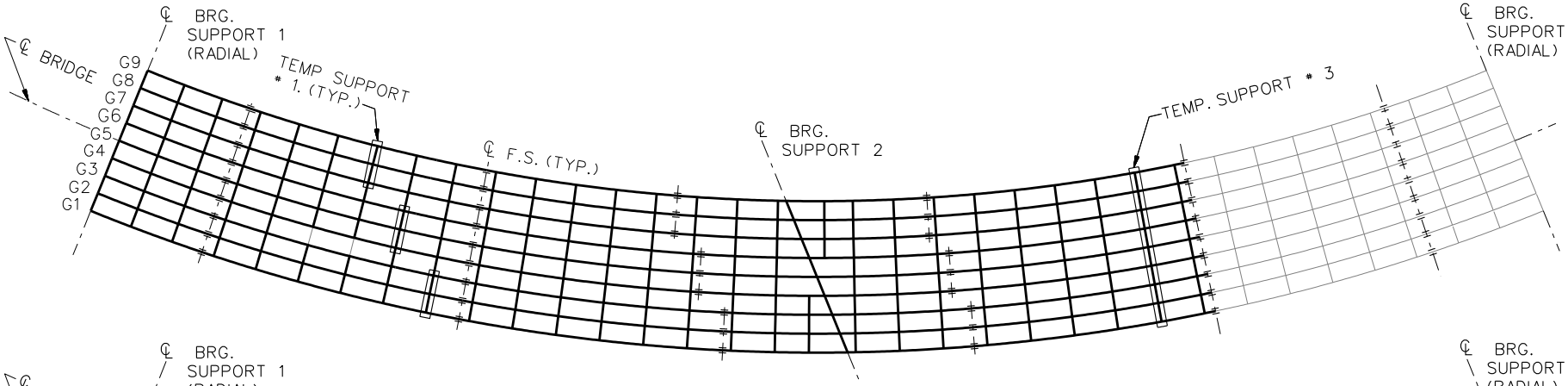

STAGES 30 THRU 37

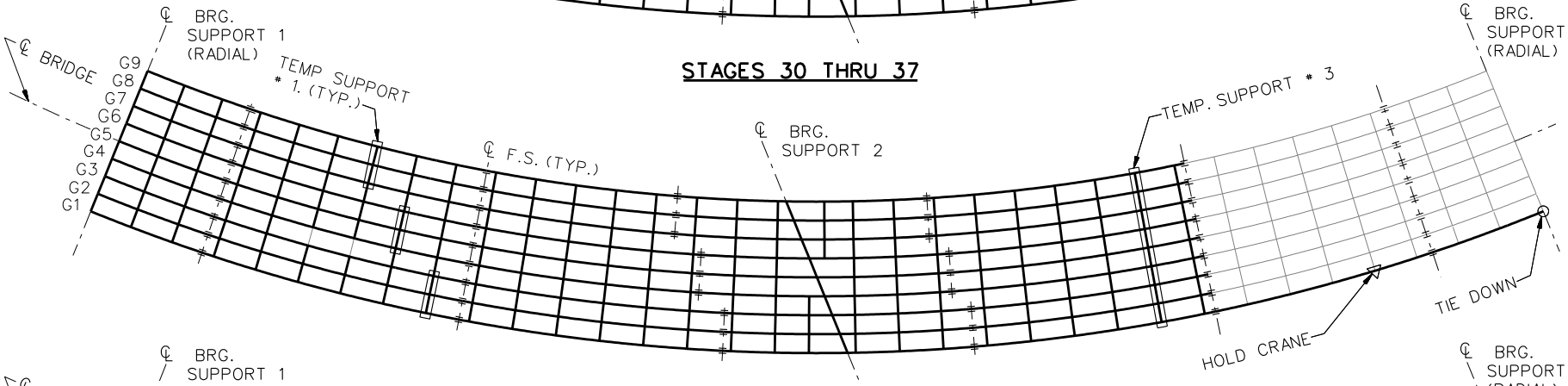

STAGE 38

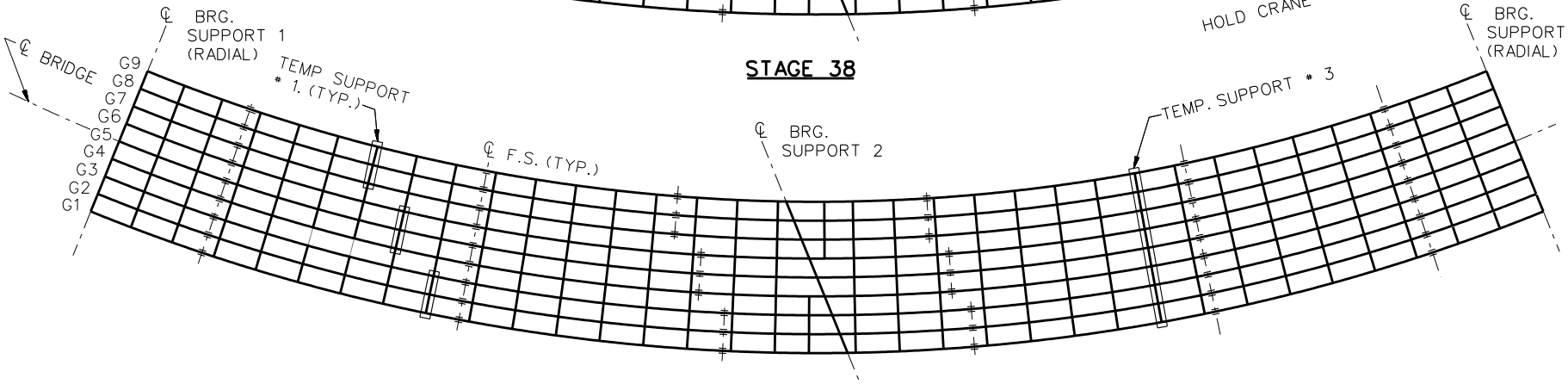

STAGES 39 THRU 46
(G2 THRU G9)

LEGEND

▽ = HOLD OR LIFT CRANE

○ = TIE DOWN

□ = TEMPORARY SUPPORT STRUCTURE

STAGE 47
REMOVE TEMP SUPPORT * 3

STAGE 48
REMOVE TEMP SUPPORT * 1

NCHRP 12-79

BRIDGE NICCS24

GENERAL ERECTION PROCEDURE

NCHRP 12-79

NICSS1

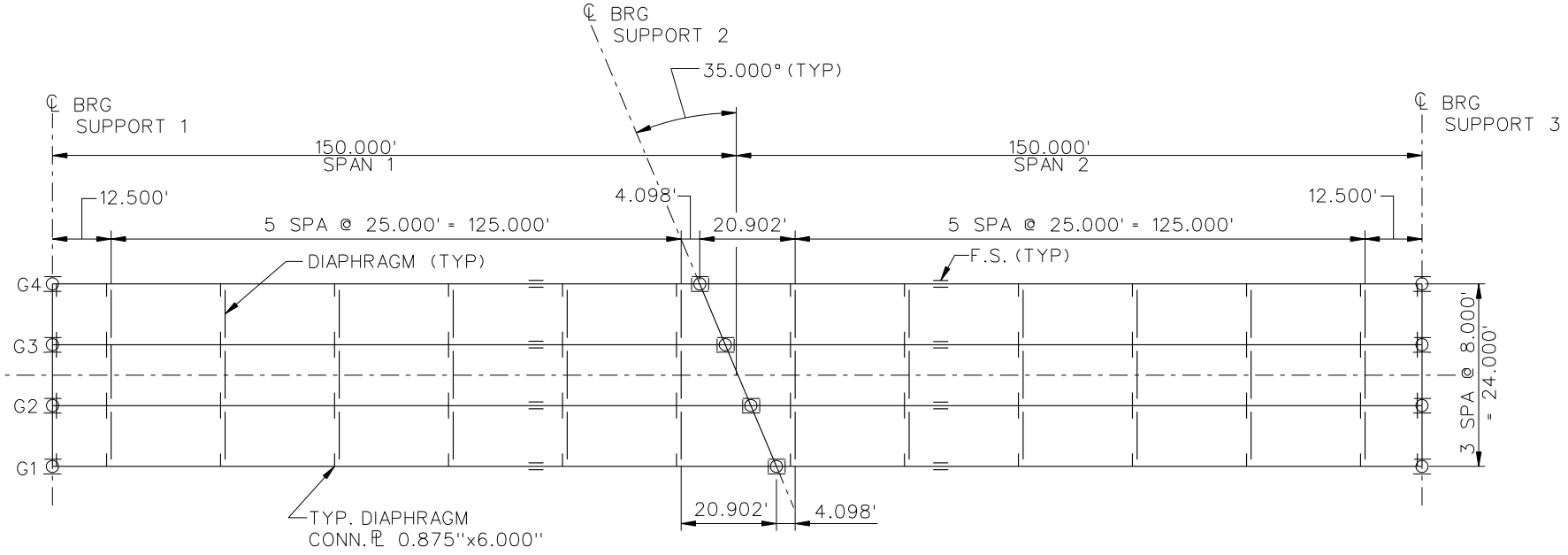

FRAMING PLAN

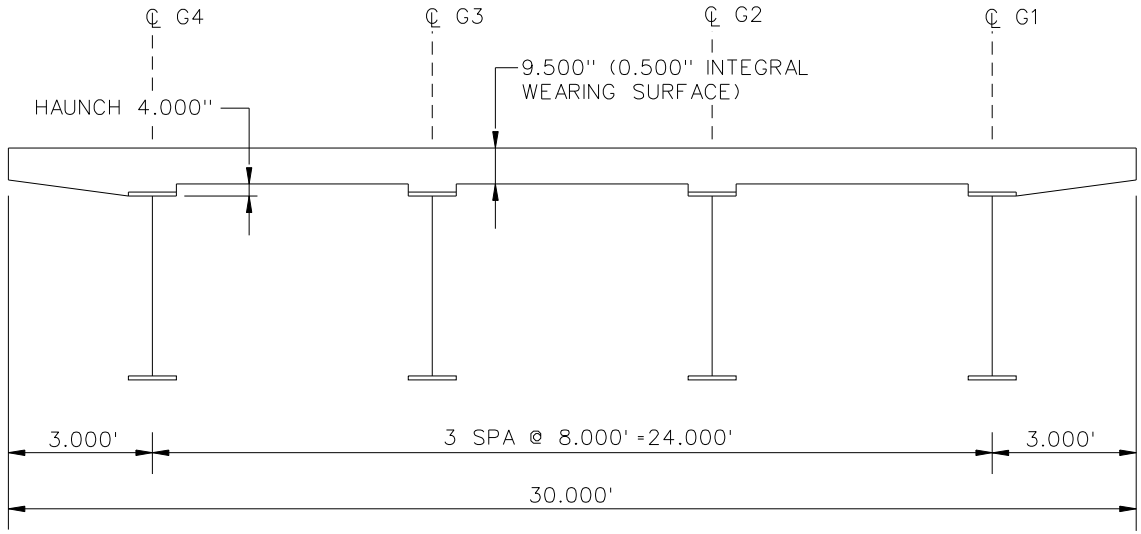

CROSS - SECTION

(DIAPHRAGMS NOT SHOWN)

BEARING LEGEND

- ○ NON-GUIDED
- ⊙ LONGITUDINALLY GUIDED
- |⊙| TRANSVERSELY GUIDED
- ⊡ FIXED

NCHRP 12-79

BRIDGE NICSS1

FRAMING PLAN AND CROSS SECTION

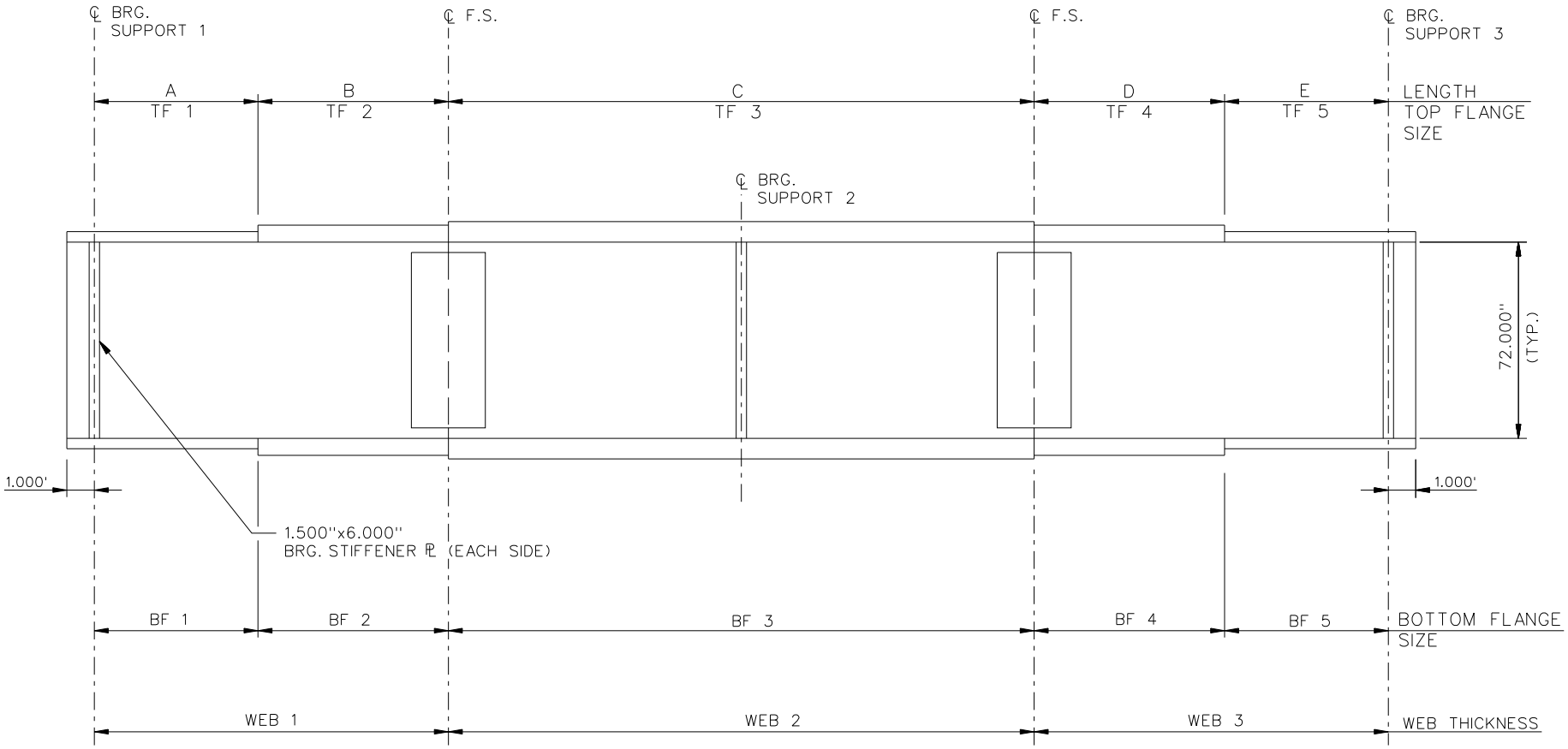

NOTES :

1. SEE TABLES ON SHEET 3 FOR GIRDER ELEVATION DIMENSIONS AND PLATE SIZES.

2. ALL GIRDERS, WEB 1 = WEB 3 = 0.5625"
   WEB 2 = 0.750".

NCHRP 12-79

BRIDGE NICSS1

GIRDER ELEVATION

SHEET 2 OF 9

	GIRDER PLATE LENGTHS ✳			
LENGTH	G1	G2	G3	G4
A	80.000	80.000	80.000	80.000
B	30.000	30.000	30.000	30.000
C	80.000	80.000	80.000	80.000
D	30.000	30.000	30.000	30.000
E	80.000	80.000	80.000	80.000

✳ ALL DIMENSIONS ARE IN FEET.

	GIRDER FLANGE DIMENSIONS ✳✳							
TOP	G1		G2		G3		G4	
FLANGE	BF	TF	BF	TF	BF	TF	BF	TF
TF1	16.000	1.000	16.000	1.000	16.000	1.000	16.000	1.000
TF2	16.000	0.875	16.000	0.875	16.000	0.875	16.000	0.875
TF3	16.000	1.875	16.000	1.875	16.000	1.875	16.000	1.875
TF4	16.000	0.875	16.000	0.875	16.000	0.875	16.000	0.875
TF5	16.000	1.000	16.000	1.000	16.000	1.000	16.000	1.000

✳✳ ALL DIMENSIONS ARE IN INCHES.

	GIRDER FLANGE DIMENSIONS ✳✳							
BOTTOM	G1		G2		G3		G4	
FLANGE	BF	TF	BF	TF	BF	TF	BF	TF
BF1	18.000	1.000	18.000	1.000	18.000	1.000	18.000	1.000
BF2	18.000	0.875	18.000	0.875	18.000	0.875	18.000	0.875
BF3	18.000	1.875	18.000	1.875	18.000	1.875	18.000	1.875
BF4	18.000	0.875	18.000	0.875	18.000	0.875	18.000	0.875
BF5	18.000	1.000	18.000	1.000	18.000	1.000	18.000	1.000

✳✳ ALL DIMENSIONS ARE IN INCHES.

NCHRP 12-79

BRIDGE NICSS1

GIRDER ELEVATION TABLES

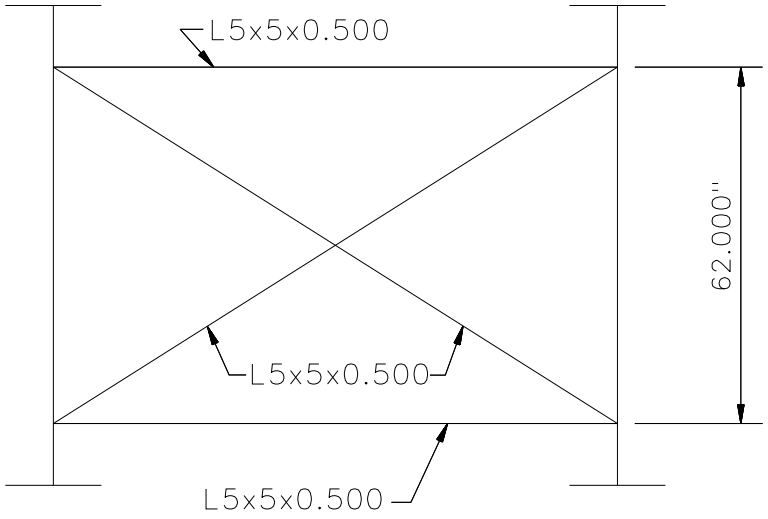

TYPICAL INTERMEDIATE DIAPHRAGM

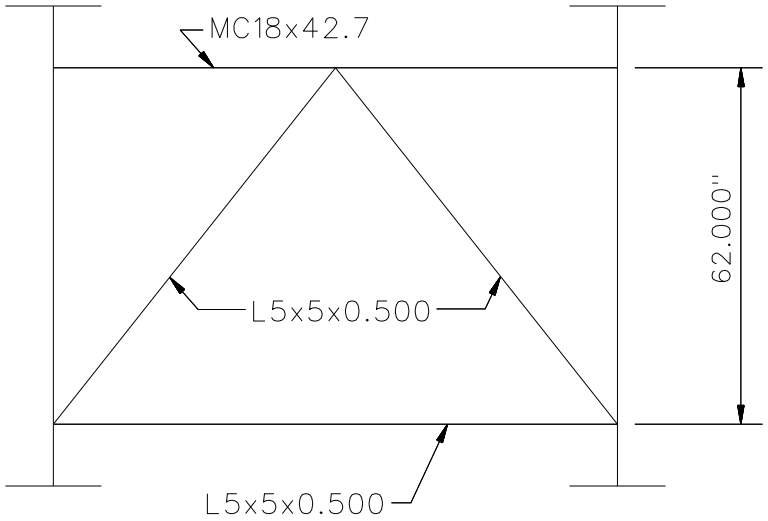

TYPICAL END DIAPHRAGM

NOTES:

1. STEEL DEAD LOAD INCREASED BY 5% FOR MDX AND LARSA MODELS; 2% FOR 3D MODEL; AND 10% FOR APPROXIMATE ANALYSIS TO ACCOUNT FOR MISC. DETAILS.

2. FORMWORK LOAD OF 10PSF IS INCLUDED IN CONCRETE DEAD LOAD.

3. ADDITIONAL DESIGN PARAMETERS:
   A. 1.500' PARAPET WIDTH BOTH SIDES.
   B. 700 LB/FT UNIFORM LOAD ASSUMED FOR PARAPET WEIGHT.
   C. ROADWAY WIDTH = 26.500'.
   D. NUMBER OF DESIGN LANES = 2.
   E. HL93 LIVE LOAD.

4. DIAPHRAGM MEMBER CALL-OUTS ARE IN UNITS OF INCHES.

NCHRP 12-79

BRIDGE NICSS1

MISC. DETAILS AND NOTES

SHEET 4 OF 9

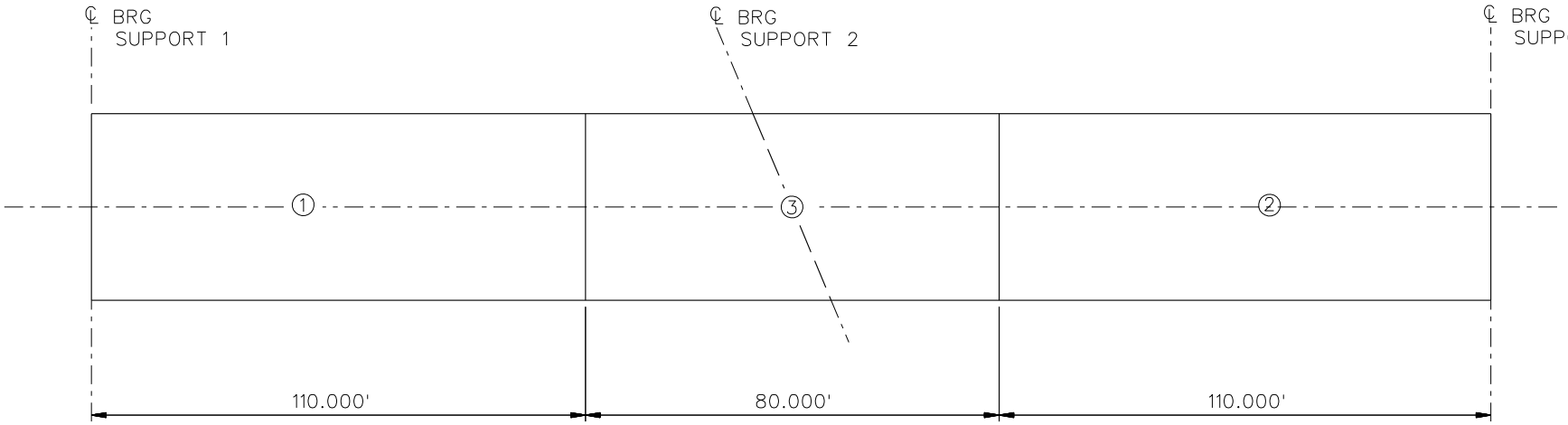

DECK POURING SEQUENCE

NCHRP 12-79

BRIDGE NICSS1

DECK POURING SEQUENCE

SHEET 5 OF 9

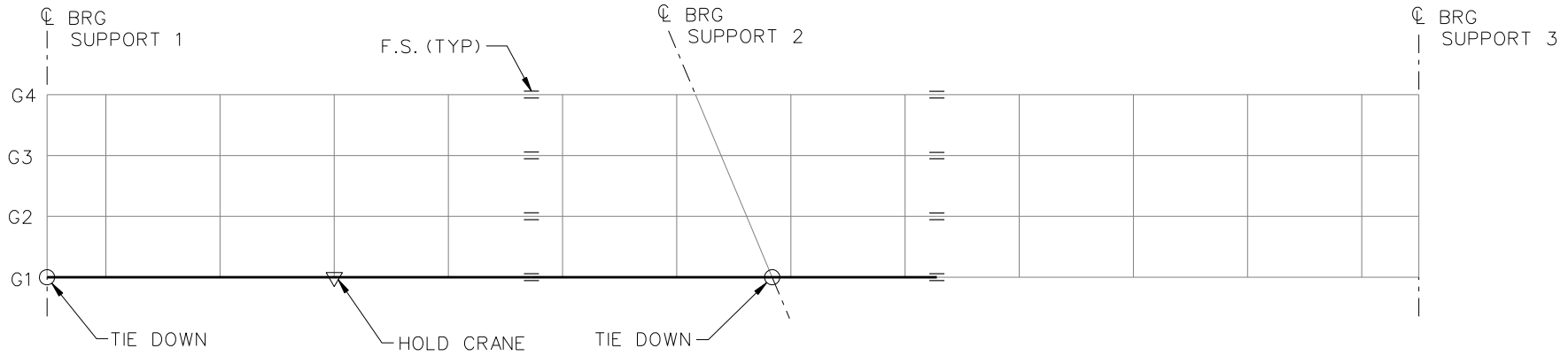

STAGE 1

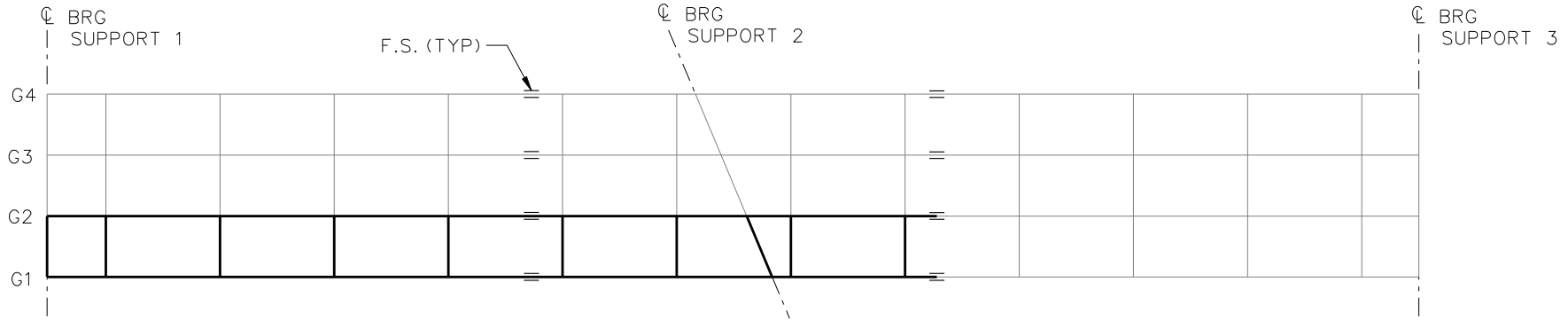

STAGE 2

LEGEND

▽ = HOLD OR LIFT CRANE

○ = TIE DOWN

□ = TEMPORARY SUPPORT STRUCTURE

NCHRP 12-79

BRIDGE NICSS1

GENERAL ERECTION PROCEDURE

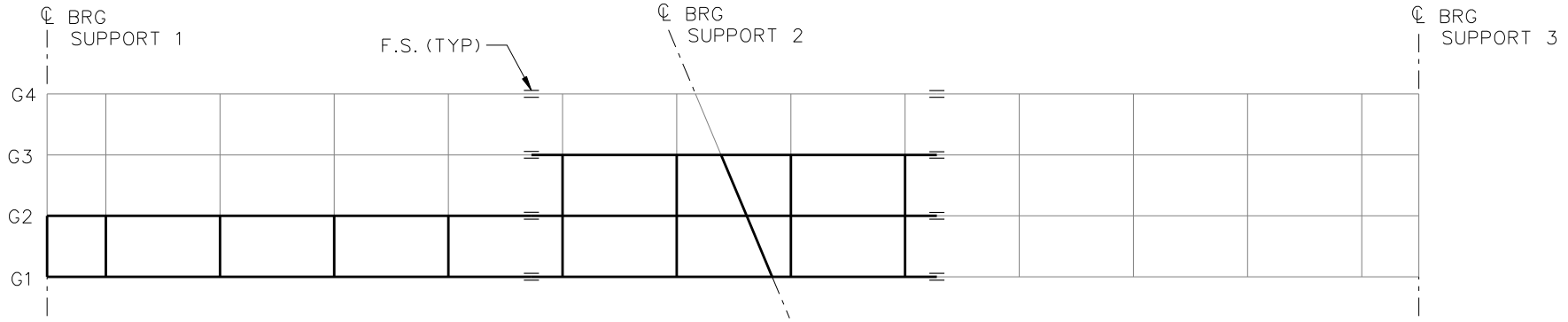

STAGE 3

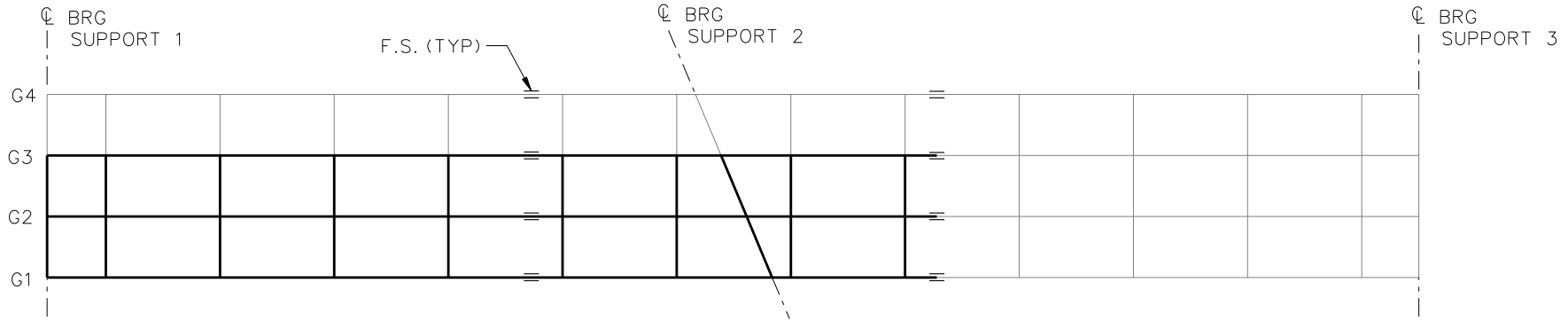

STAGE 4

LEGEND

▽ = HOLD OR LIFT CRANE

○ = TIE DOWN

□ = TEMPORARY SUPPORT STRUCTURE

NCHRP 12-79

BRIDGE NICSS1

GENERAL ERECTION PROCEDURE

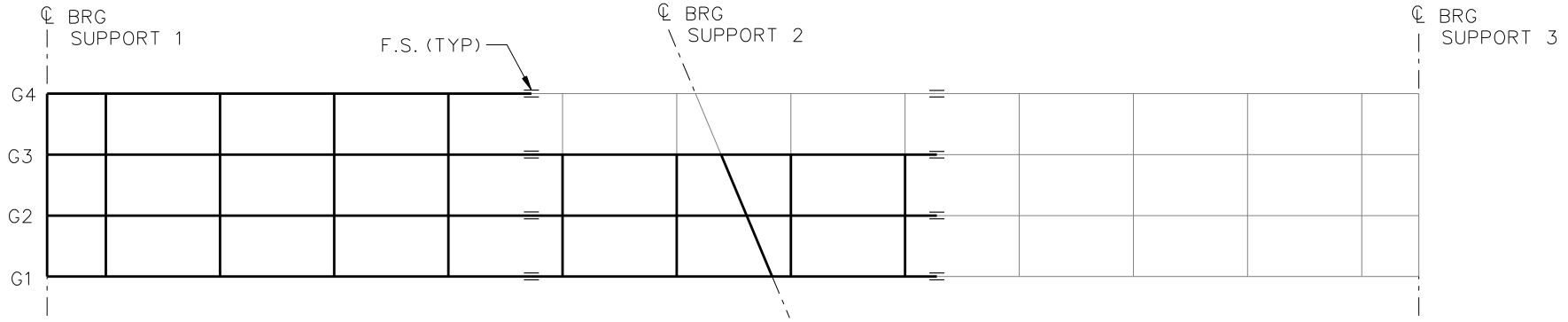

STAGE 5

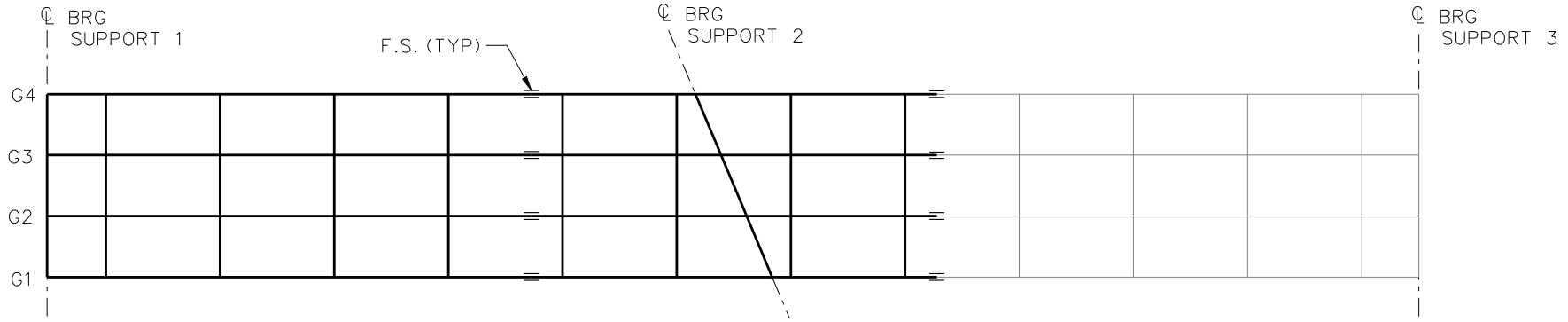

STAGE 6

LEGEND

▽ = HOLD OR LIFT CRANE

○ = TIE DOWN

□ = TEMPORARY SUPPORT STRUCTURE

NCHRP 12-79

BRIDGE NICSS1

GENERAL ERECTION PROCEDURE

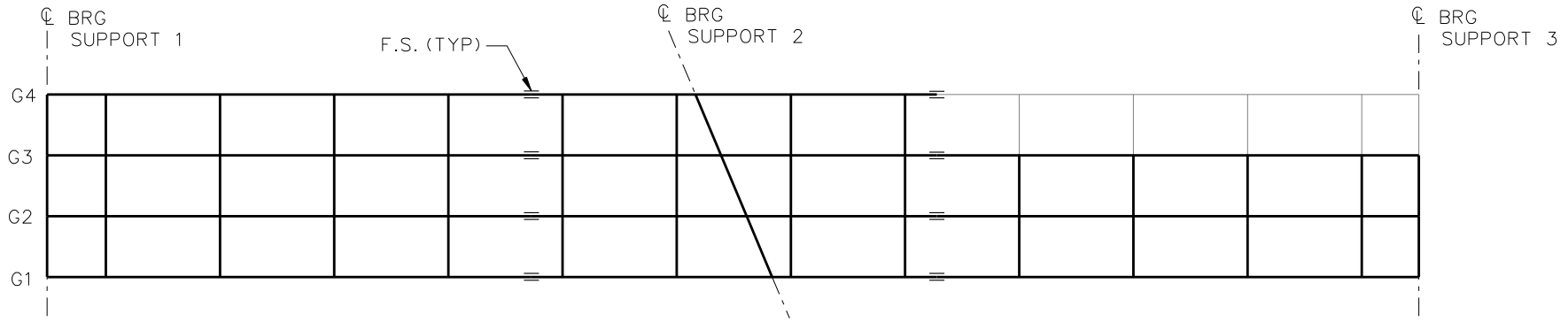

STAGE 9

NOTE:

STAGE 7 - ERECT G1, SPAN 2
STAGE 8 - ERECT G2 AND CROSS FRAMES, SPAN 2

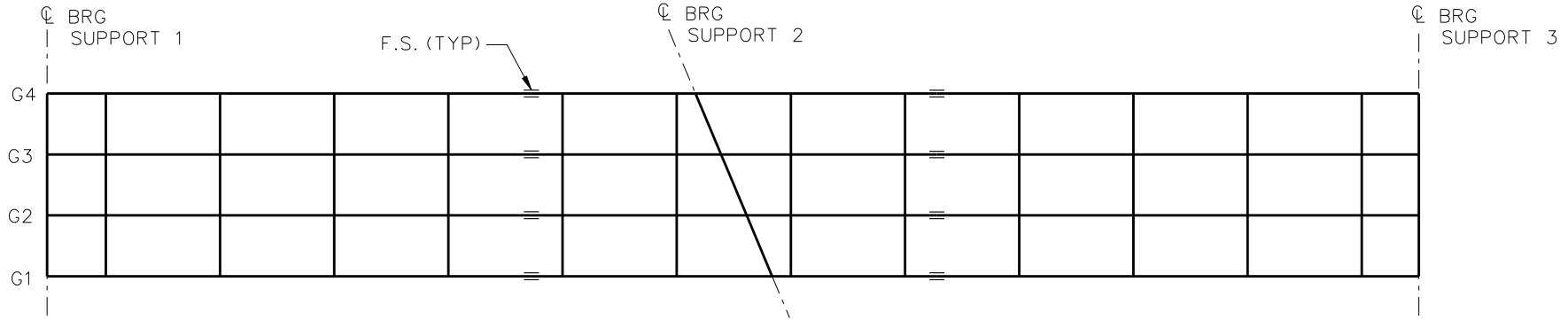

STAGE 10

LEGEND

▽ = HOLD OR LIFT CRANE

○ = TIE DOWN

□ = TEMPORARY SUPPORT STRUCTURE

NCHRP 12-79

BRIDGE NICSS1

GENERAL ERECTION PROCEDURE

NCHRP 12-79

NICSS3

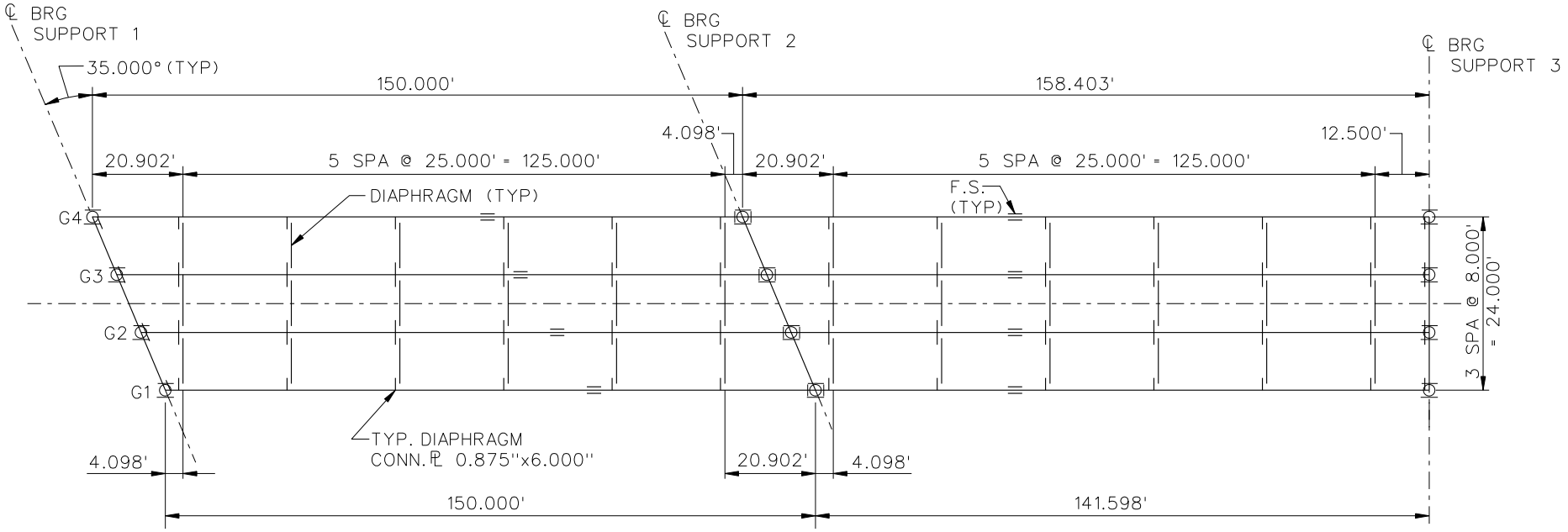

FRAMING PLAN

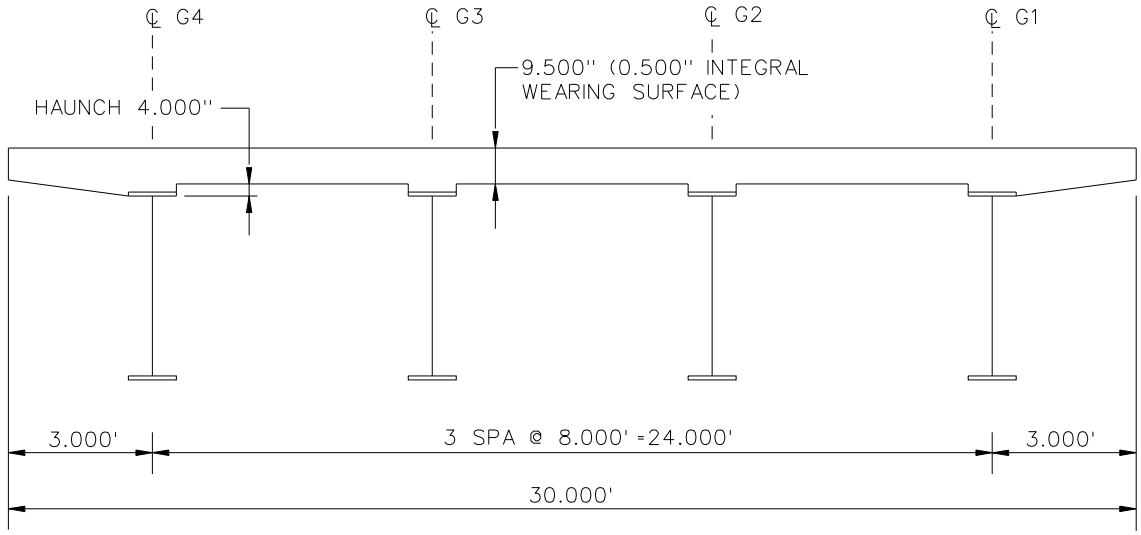

CROSS - SECTION

(DIAPHRAGMS NOT SHOWN)

BEARING LEGEND

- ○ NON-GUIDED
- ⊙ LONGITUDINALLY GUIDED
- |⊙| TRANSVERSELY GUIDED
- ⊡ FIXED

NCHRP 12-79

BRIDGE NICSS3

FRAMING PLAN AND CROSS SECTION

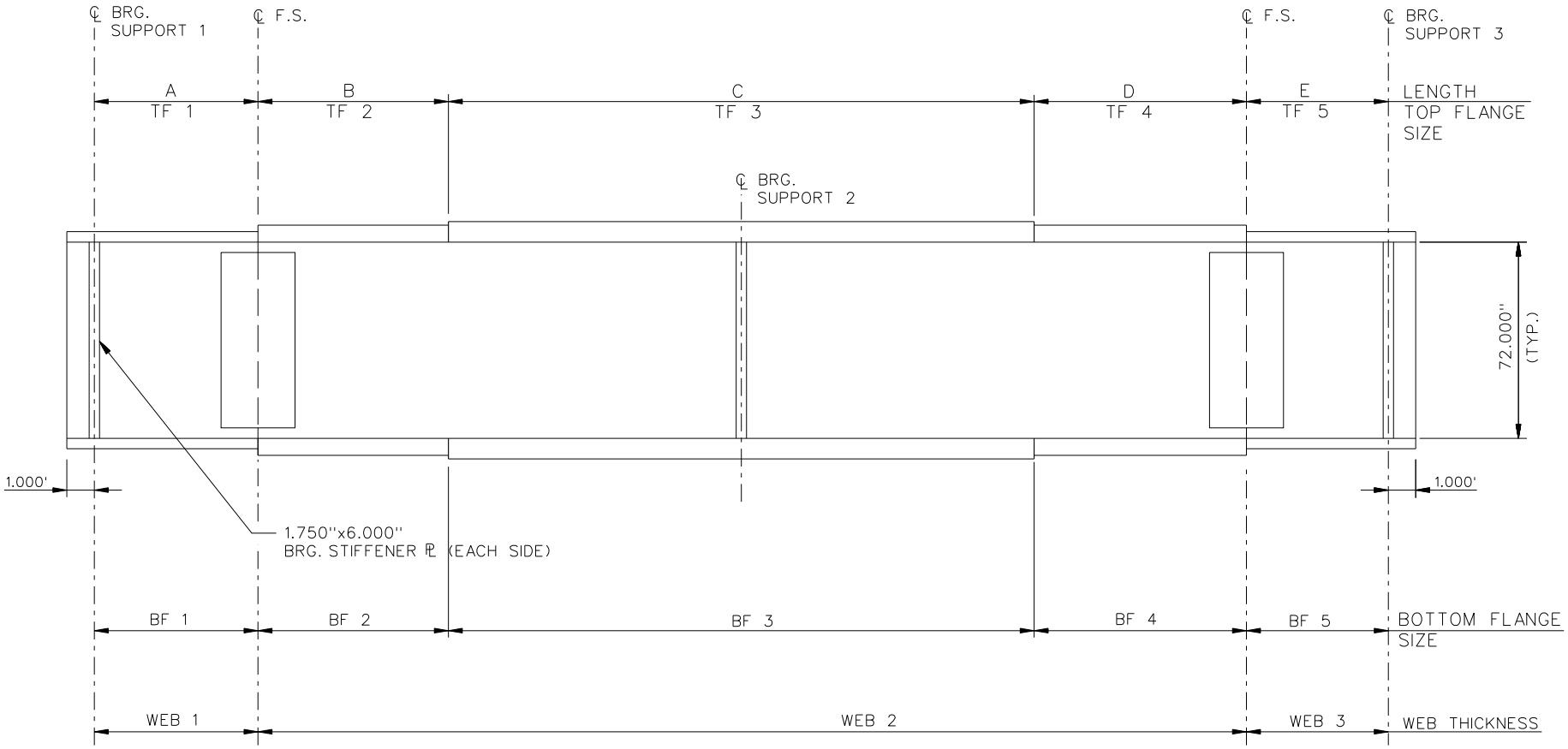

NOTE :

1. SEE TABLES ON SHEET 3 FOR GIRDER ELEVATION DIMENSIONS AND PLATE SIZES.

2. ALL GIRDERS, WEB 1 = WEB 3 = 0.5625"
   WEB 2 = 0.750".

NCHRP 12-79

BRIDGE NICSS3

GIRDER ELEVATION

SHEET 2 OF 8

	GIRDER PLATE LENGTHS ✳			
LENGTH	G1	G2	G3	G4
A	90.000	90.000	90.000	90.000
B	28.299	31.100	33.900	36.701
C	55.000	55.000	55.000	55.000
D	28.299	31.100	33.900	36.701
E	90.000	90.000	90.000	90.000

✳ ALL DIMENSIONS ARE IN FEET.

	GIRDER FLANGE DIMENSIONS ✳✳							
TOP	G1		G2		G3		G4	
FLANGE	BF	TF	BF	TF	BF	TF	BF	TF
TF1	16.000	1.000	16.000	1.000	18.000	1.000	18.000	1.000
TF2	16.000	0.875	16.000	0.875	18.000	0.875	18.000	0.875
TF3	16.000	1.750	16.000	1.750	18.000	1.750	18.000	1.750
TF4	16.000	0.875	16.000	0.875	18.000	0.875	18.000	0.875
TF5	16.000	1.000	16.000	1.000	18.000	1.000	18.000	1.000

✳✳ ALL DIMENSIONS ARE IN INCHES.

	GIRDER FLANGE DIMENSIONS ✳✳							
BOTTOM	G1		G2		G3		G4	
FLANGE	BF	TF	BF	TF	BF	TF	BF	TF
BF1	18.000	1.000	18.000	1.000	18.000	1.000	18.000	1.000
BF2	18.000	0.875	18.000	0.875	18.000	0.875	18.000	0.875
BF3	18.000	1.750	18.000	1.750	18.000	1.750	18.000	1.750
BF4	18.000	0.875	18.000	0.875	18.000	0.875	18.000	0.875
BF5	18.000	1.000	18.000	1.000	18.000	1.000	18.000	1.000

✳✳ ALL DIMENSIONS ARE IN INCHES.

NCHRP 12-79

BRIDGE NICSS3

GIRDER ELEVATION TABLES

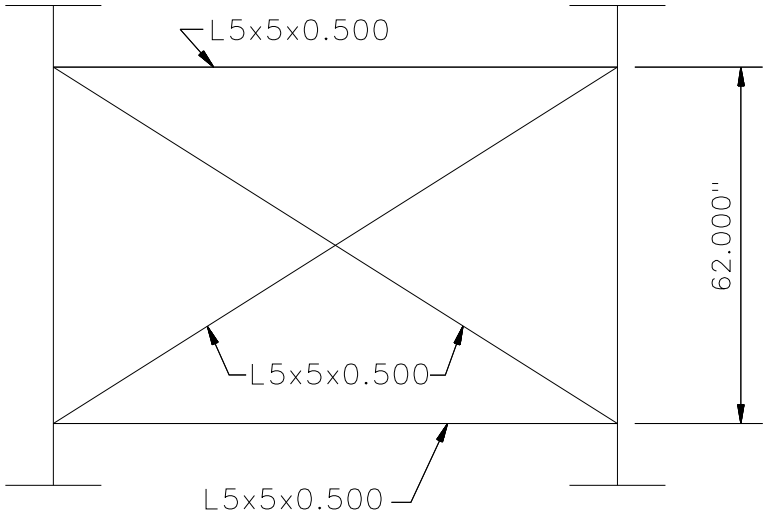

TYPICAL INTERMEDIATE DIAPHRAGM

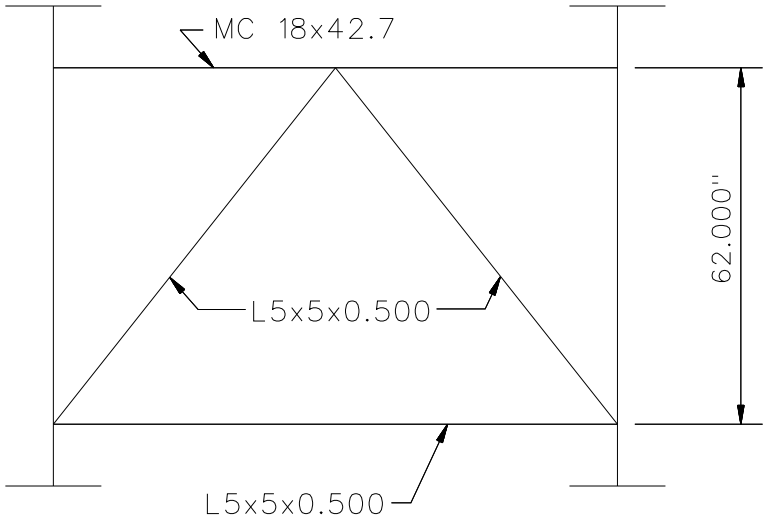

TYPICAL END DIAPHRAGM

NOTES:

1. STEEL DEAD LOAD INCREASED BY 5% FOR MDX AND LARSA MODELS; 2% FOR 3D MODEL; AND 10% FOR APPROXIMATE ANALYSIS TO ACCOUNT FOR MISC. DETAILS.

2. FORMWORK LOAD OF 10PSF IS INCLUDED IN CONCRETE DEAD LOAD.

3. ADDITIONAL DESIGN PARAMETERS:
   A. 1.500' PARAPET WIDTH BOTH SIDES.
   B. 700 LB/FT UNIFORM LOAD ASSUMED FOR PARAPET WEIGHT.
   C. ROADWAY WIDTH = 26.500'.
   D. NUMBER OF DESIGN LANES = 2.
   E. HL93 LIVE LOAD.

4. DIAPHRAGM MEMBER CALL-OUTS ARE IN UNITS OF INCHES.

NCHRP 12-79

BRIDGE NICSS3

MISC. DETAILS AND NOTES

SHEET 4 OF 8

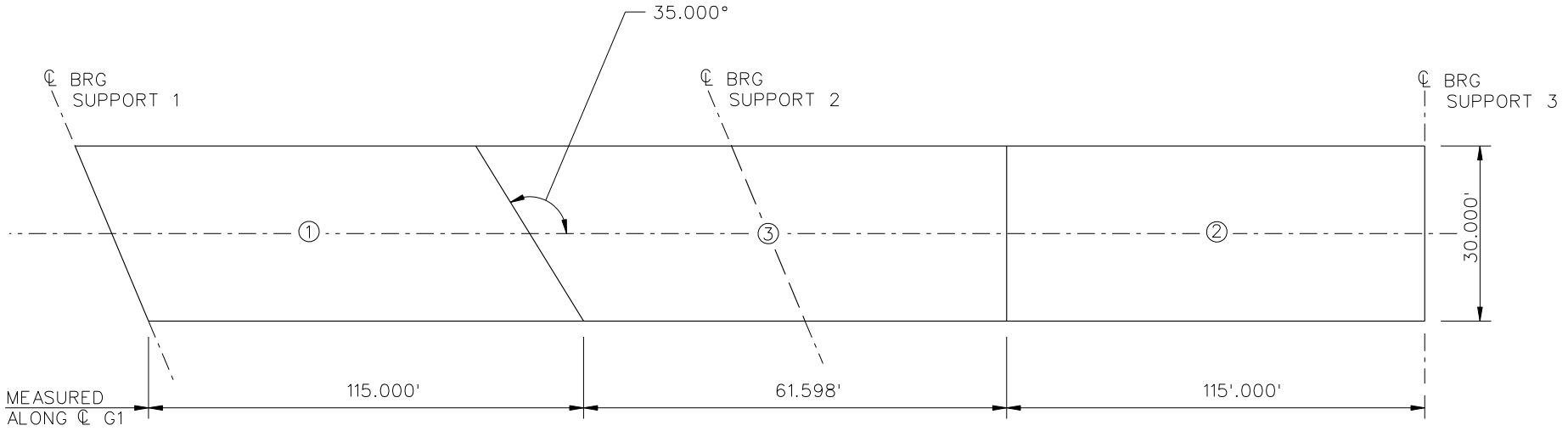

DECK POURING SEQUENCE

NCHRP 12-79

BRIDGE NICSS3

DECK POURING SEQUENCE

SHEET 5 OF 8

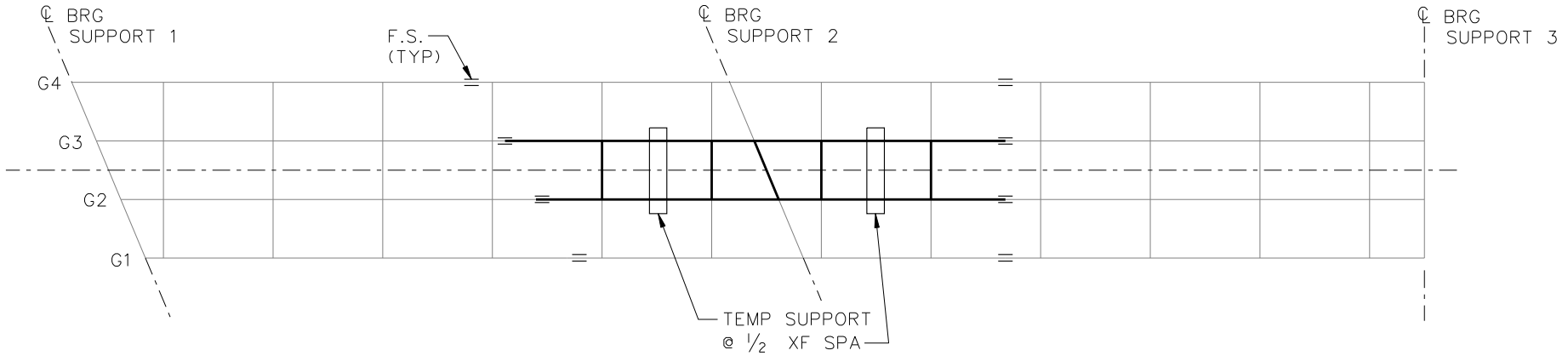

STAGE 1

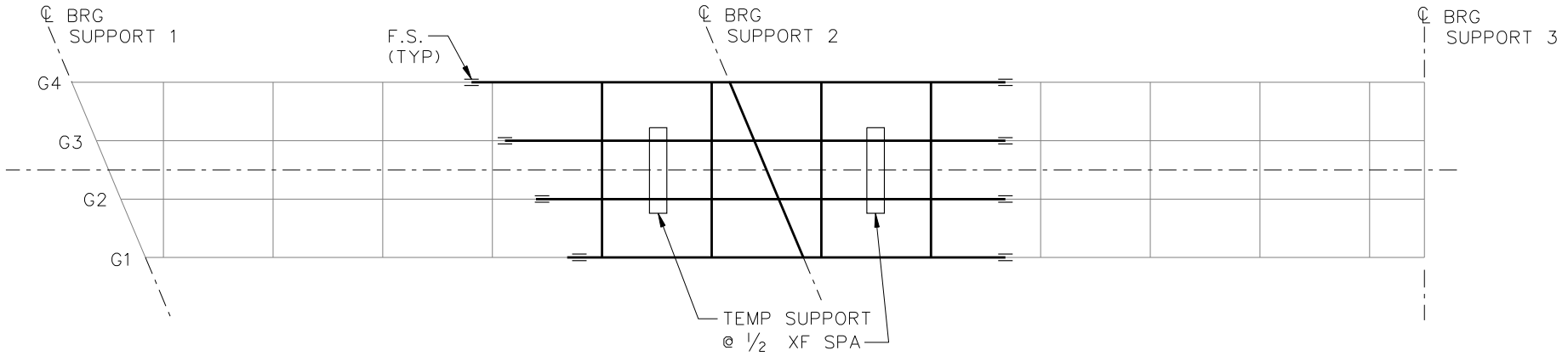

STAGE 3

LEGEND

▽ = HOLD OR LIFT CRANE

○ = TIE DOWN

□ = TEMPORARY SUPPORT STRUCTURE

STAGE 2 - ERECT G1 AND CROSS FRAMES
STAGE 3 - ERECT G4 AND CROSS FRAMES

NCHRP 12-79

BRIDGE NICSS3

GENERAL ERECTION PROCEDURE

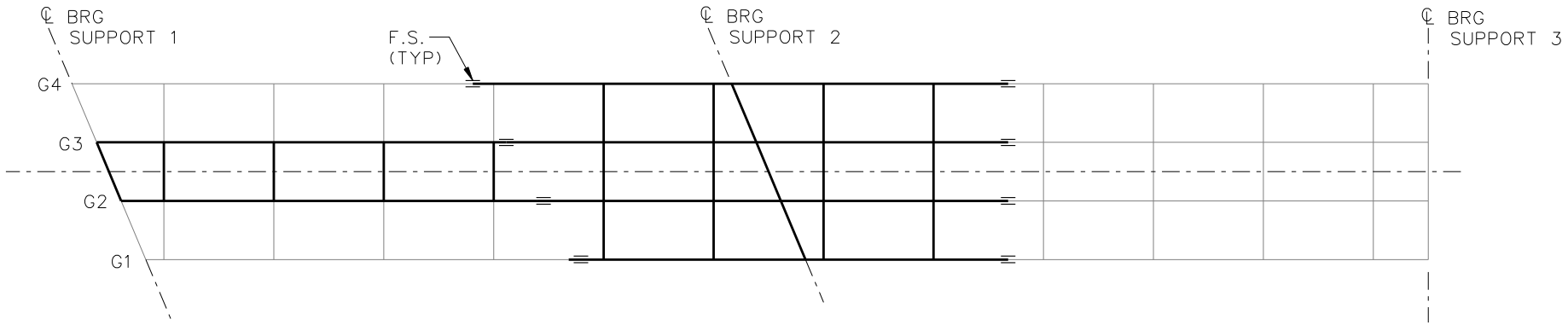

NOTES:

1. STAGE 4 - ERECT G2, TIE DOWN AT SUPPORT 1
2. STAGE 5 - ERECT G3 AND CROSS FRAMES
3. STAGE 6 - REMOVE ALL TEMP. SUPPORTS

STAGE 6

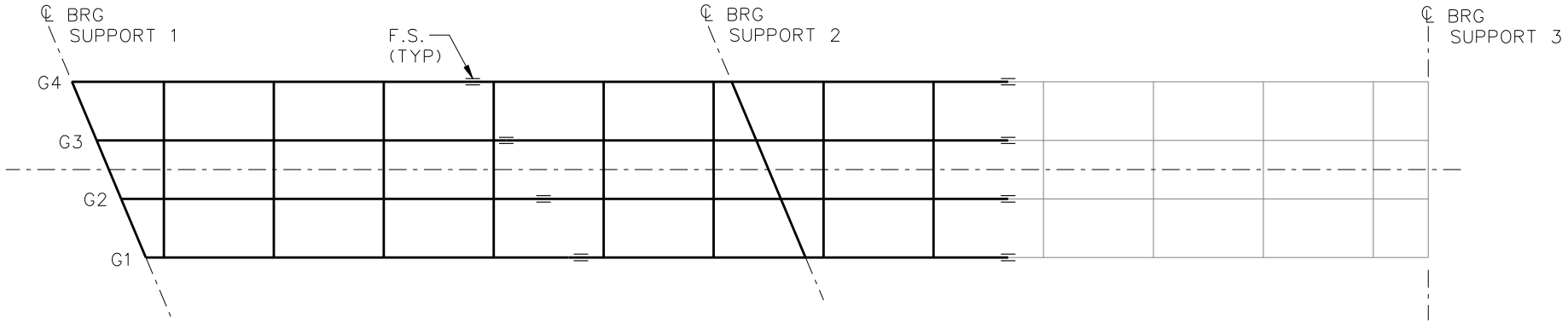

STAGE 8

LEGEND

▽ = HOLD OR LIFT CRANE

○ = TIE DOWN

□ = TEMPORARY SUPPORT STRUCTURE

NOTES:

1. STAGE 7 - ERECT G1 AND CROSS FRAMES
2. STAGE 8 - ERECT G4 AND CROSS FRAMES

NCHRP 12-79

BRIDGE NICSS3

GENERAL ERECTION PROCEDURE

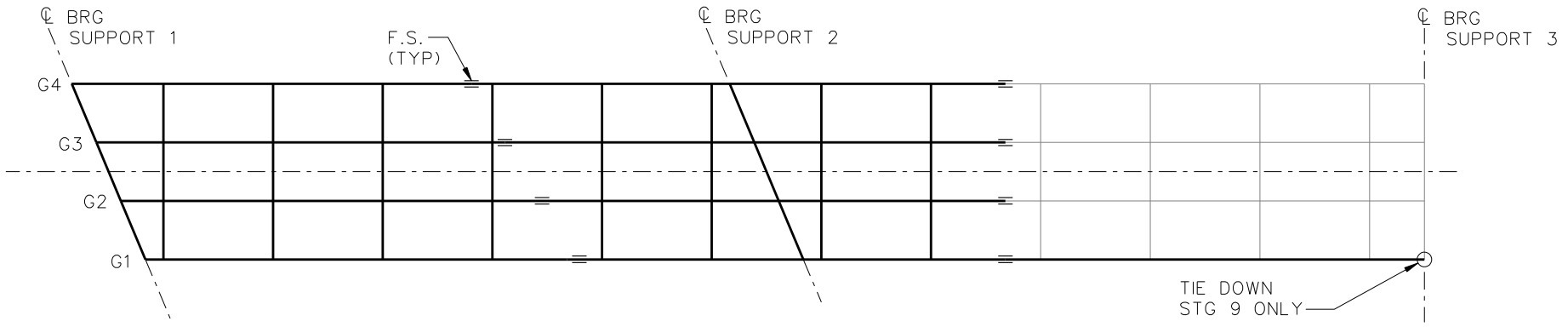

STAGE 9

NOTES:

1. STAGE 10 - ERECT G2 AND CROSS FRAMES
2. STAGE 11 - ERECT G3 AND CROSS FRAMES

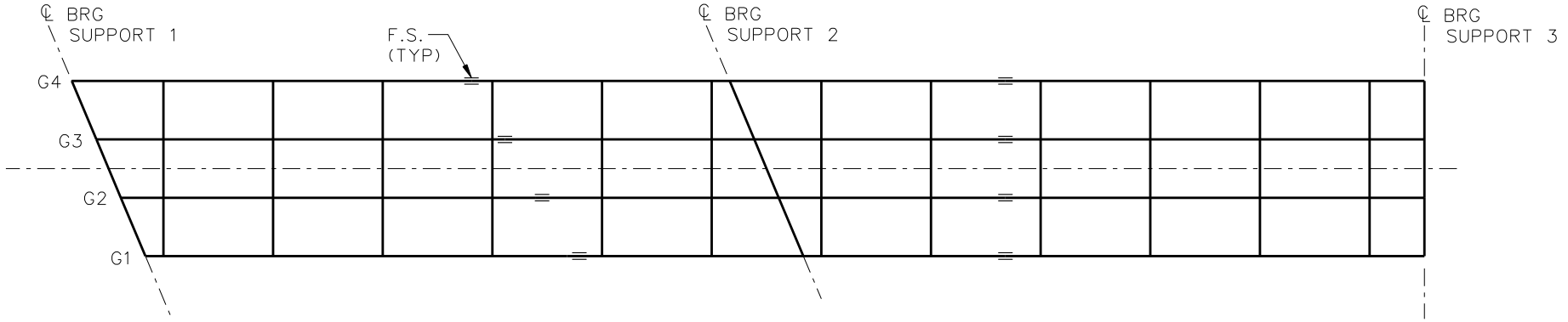

STAGE 12

LEGEND

▽ = HOLD OR LIFT CRANE

○ = TIE DOWN

□ = TEMPORARY SUPPORT STRUCTURE

NCHRP 12-79

BRIDGE NICSS3

GENERAL ERECTION PROCEDURE

NCHRP 12-79

NICSS16

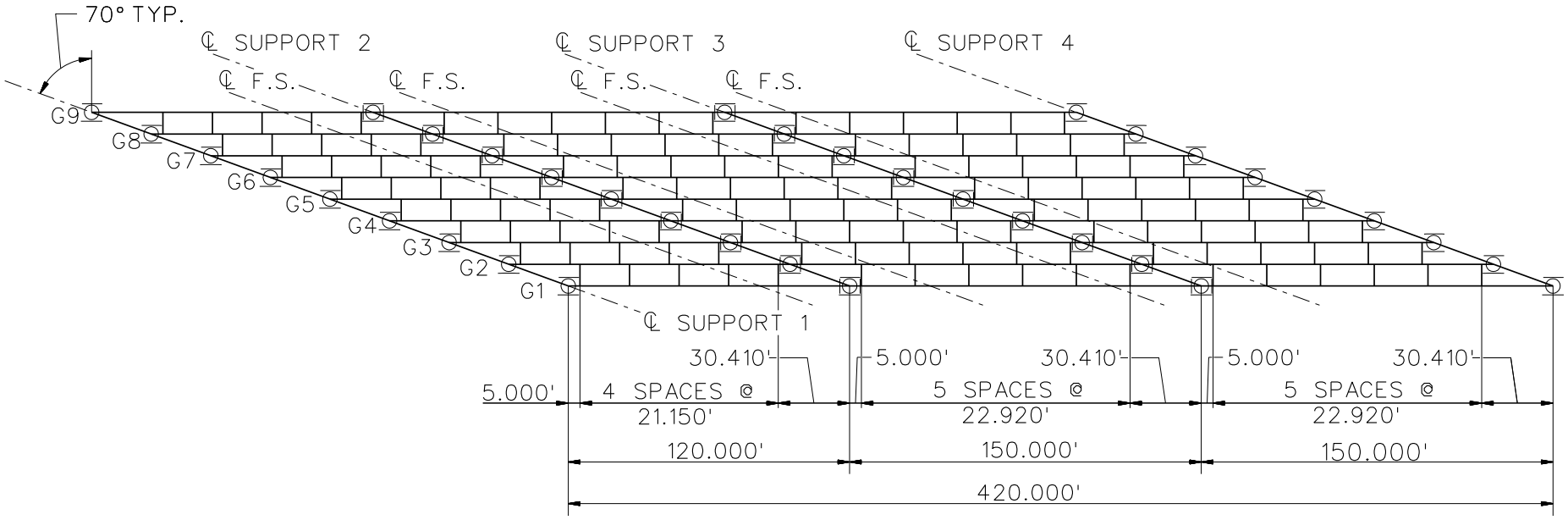

FRAMING PLAN

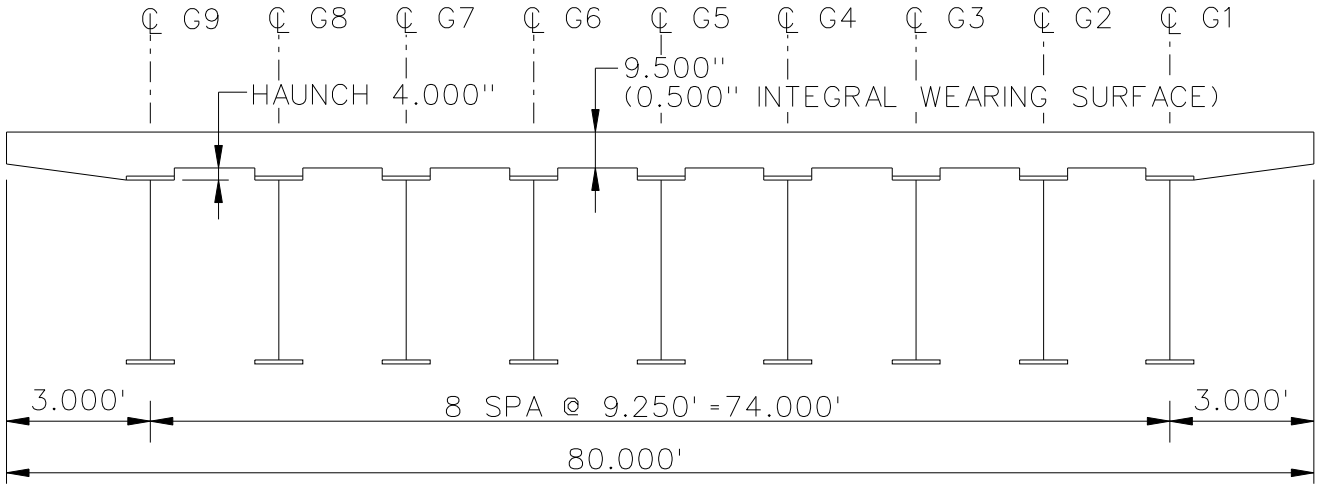

CROSS - SECTION
(DIAPHRAGMS NOT SHOWN)

BEARING LEGEND
- ○ NON-GUIDED
- ⊘ LONGITUDINALLY GUIDED
- ⊘ TRANSVERSELY GUIDED
- ⊘ FIXED

NCHRP 12-79

BRIDGE NICSS16

FRAMING PLAN AND CROSS SECTION

SHEET 1 OF 9

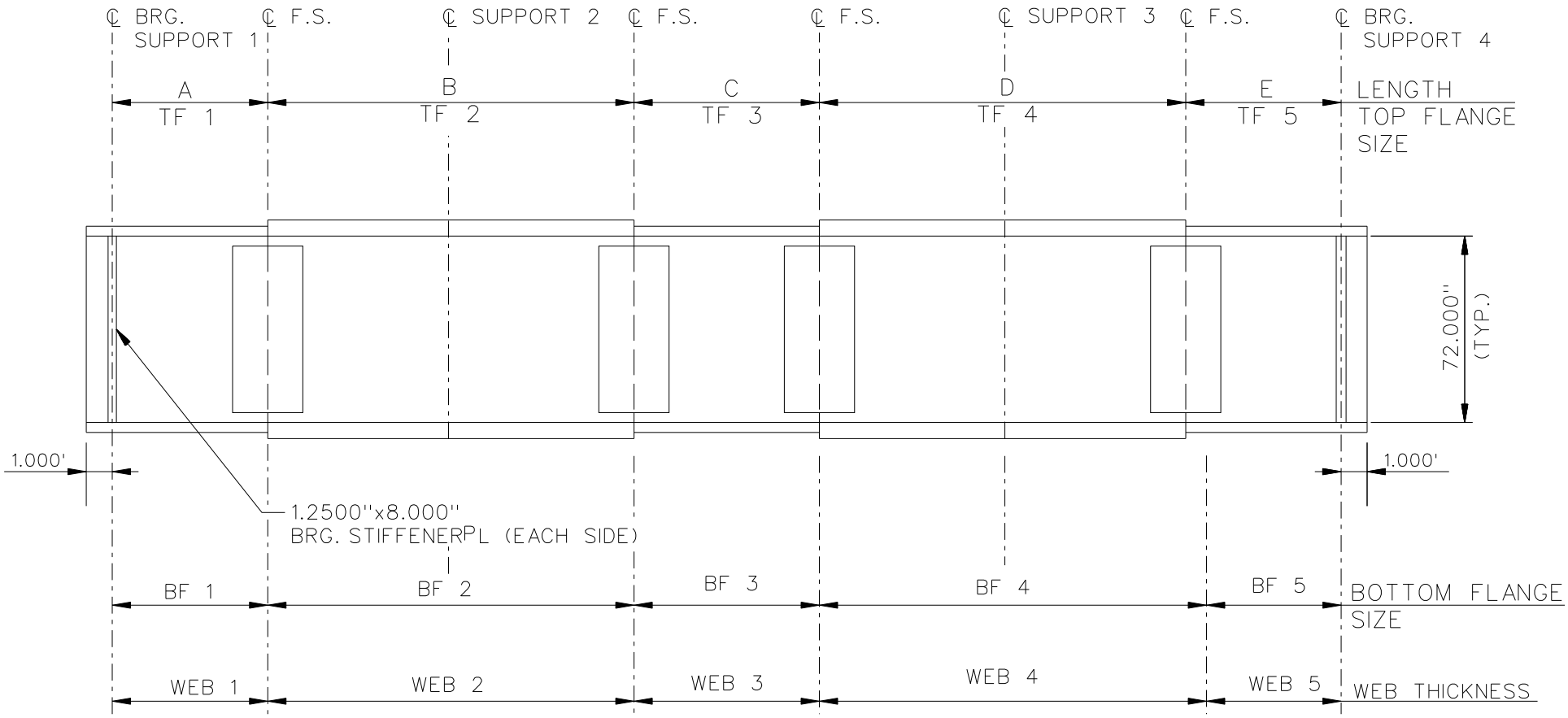

NOTE :

1. SEE TABLES ON SHEET 3 FOR GIRDER ELEVATION DIMENSIONS AND PLATE SIZES.
2. ALL GIRDERS, WEB = 0.6875" THICKNESS

NCHRP 12-79

BRIDGE NICSS16

GIRDER ELEVATION

SHEET 2 OF 9

	GIRDER PLATE LENGTHS ✳								
LENGTH	G1	G2	G3	G4	G5	G6	G7	G8	G9
A	90	90	90	90	90	90	90	90	90
B	65	65	65	65	65	65	65	65	65
C	70	70	70	70	70	70	70	70	70
D	75	75	75	75	75	75	75	75	75
E	120	120	120	120	120	120	120	120	120

✳ ALL DIMENSIONS ARE IN FEET.

	GIRDER FLANGE DIMENSIONS ✳✳	
TOP FLANGE	G1 THRU G9	
	BF	TF
TF1	18	0.75
TF2	18	1.75
TF3	18	0.75
TF4	18	1.75
TF5	18	0.75

✳✳ ALL DIMENSIONS ARE IN INCHES.

	GIRDER FLANGE DIMENSIONS ✳✳	
BOTTOM FLANGE	G1 THRU G9	
	BF	TF
BF1	18	0.75
BF2	18	1.75
BF3	18	0.75
BF4	18	1.75
BF5	18	0.75

✳✳ ALL DIMENSIONS ARE IN INCHES.

NCHRP 12-79

BRIDGE NICSS16

GIRDER ELEVATION TABLES

SHEET 3 OF 9

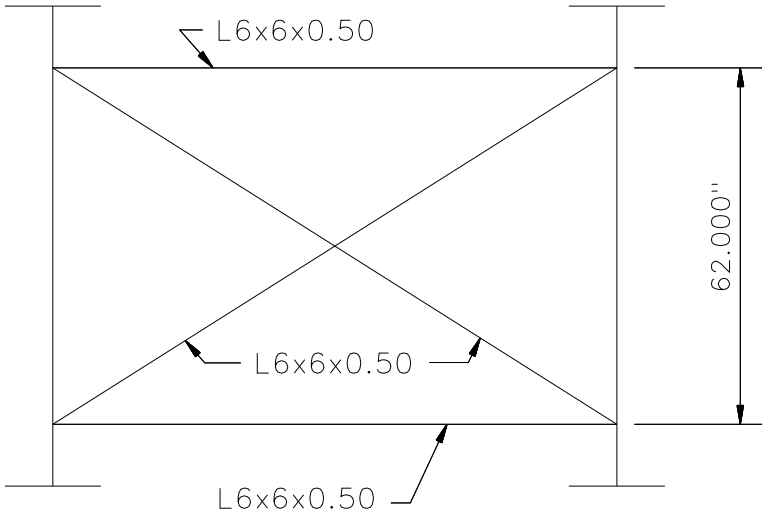

TYPICAL END DIAPHRAGM

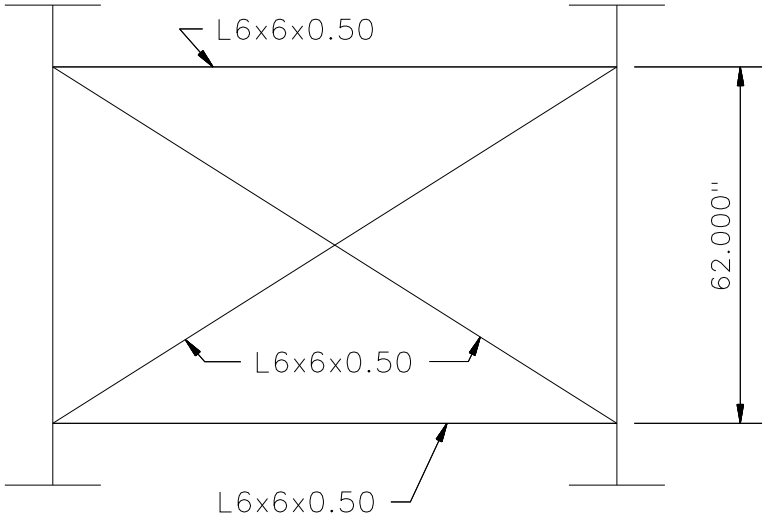

TYPICAL INTERMEDIATE DIAPHRAGM

NOTES:

1. STEEL DEAD LOAD INCREASED BY 5% FOR MDX AND LARSA MODELS; 2% FOR 3D MODEL; AND 10% FOR APPROXIMATE ANALYSIS TO ACCOUNT FOR MISC. DETAILS.

2. FORMWORK LOAD OF 10PSF IS INCLUDED IN CONCRETE DEAD LOAD.

3. DIAPHRAGM MEMBER CALL-OUTS ARE IN UNITS OF INCHES.

NCHRP 12-79

BRIDGE NICSS16

MISC. DETAILS AND NOTES

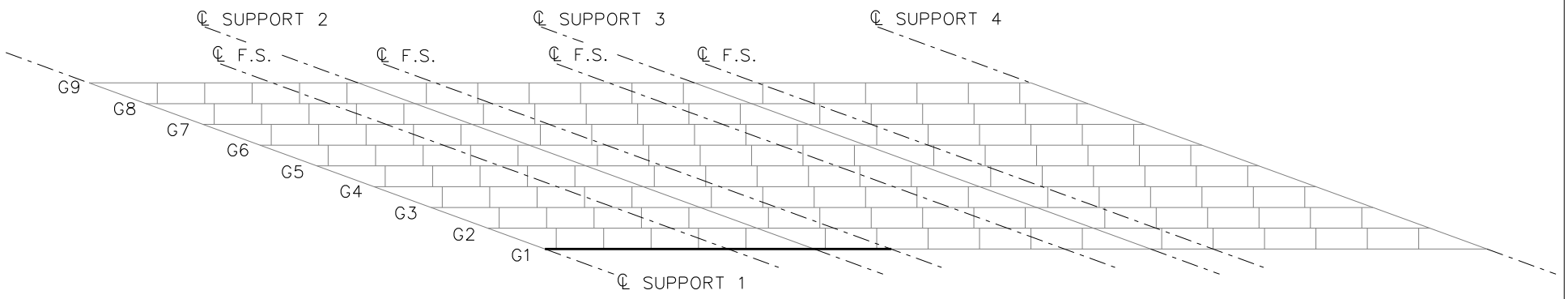

STAGE 1

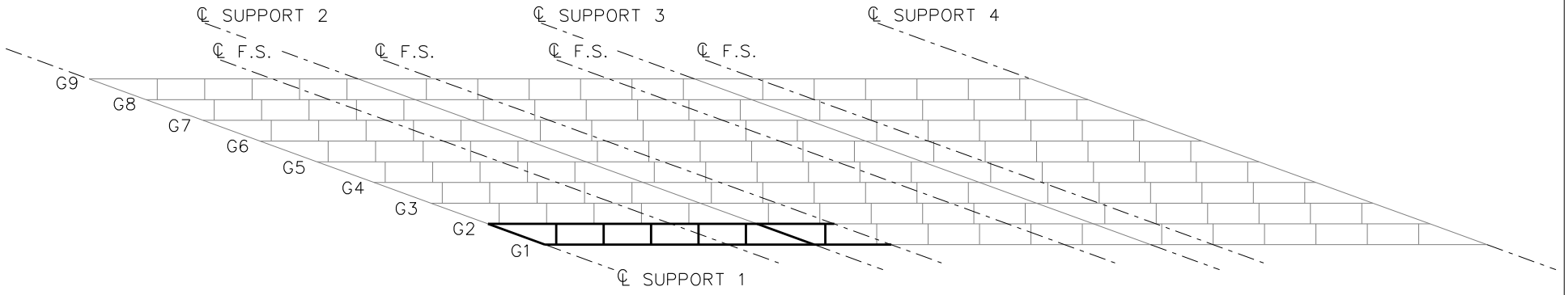

STAGE 2
(RESULTS REQ'D)

LEGEND

▽ = HOLD OR LIFT CRANE

○ = TIE DOWN

□ = TEMPORARY SUPPORT STRUCTURE

NCHRP 12-79

BRIDGE NICSS16

GIRDER ERECTION PROCEDURE

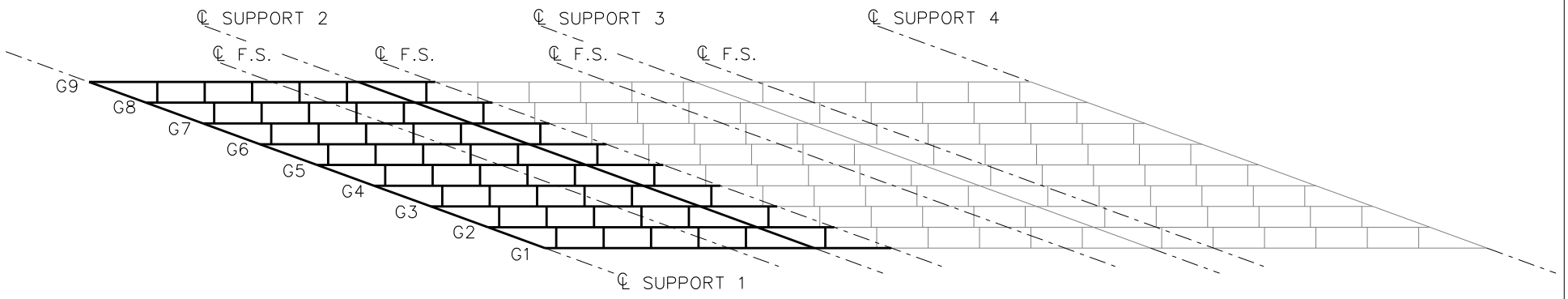

STAGES 3 THRU 9

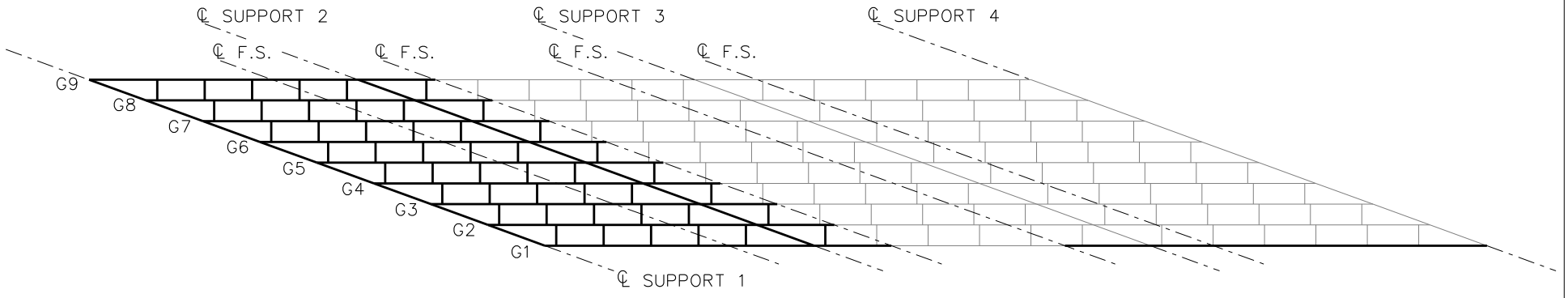

STAGE 10

LEGEND

▽ = HOLD OR LIFT CRANE

○ = TIE DOWN

□ = TEMPORARY SUPPORT STRUCTURE

NCHRP 12-79

BRIDGE NICSS16

GIRDER ERECTION PROCEDURE

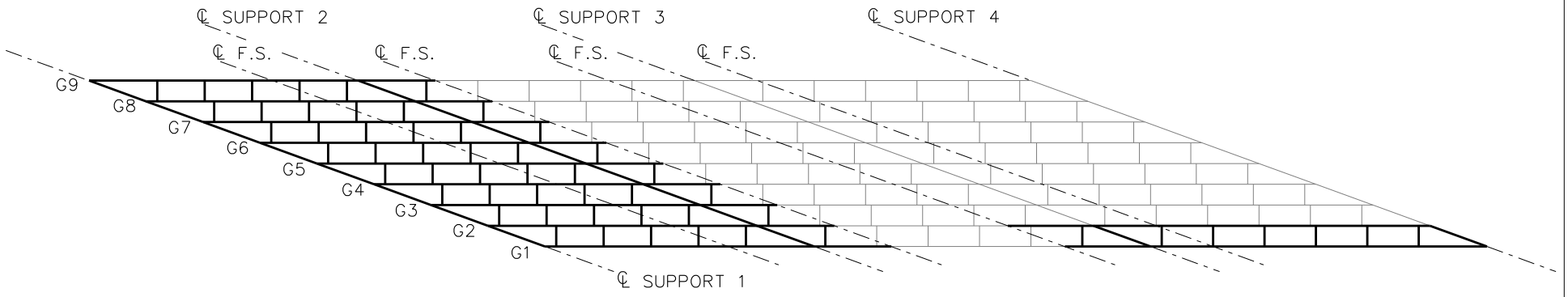

STAGE 11
(RESULTS REQ'D)

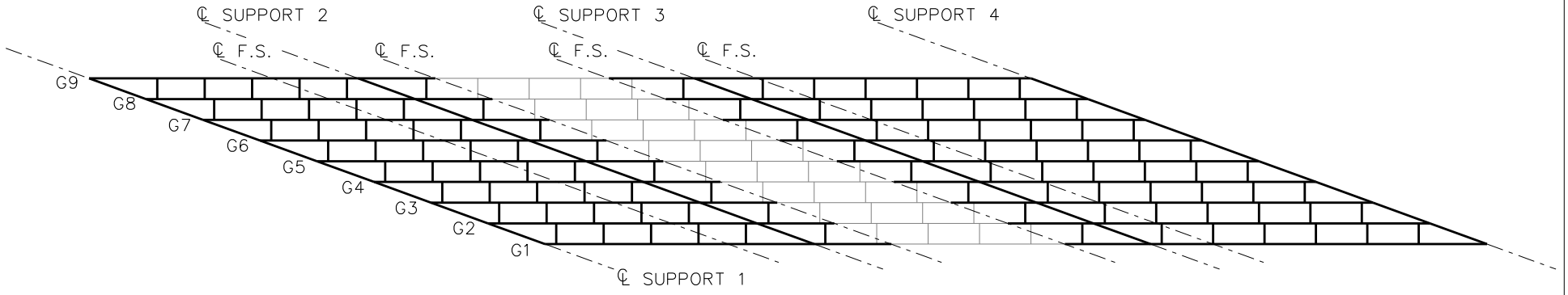

STAGES 12 THRU 18
(RESULTS REQ'D STG 18 ONLY)

LEGEND

▽ = HOLD OR LIFT CRANE

○ = TIE DOWN

□ = TEMPORARY SUPPORT STRUCTURE

NCHRP 12-79

BRIDGE NICSS16

GIRDER ERECTION PROCEDURE

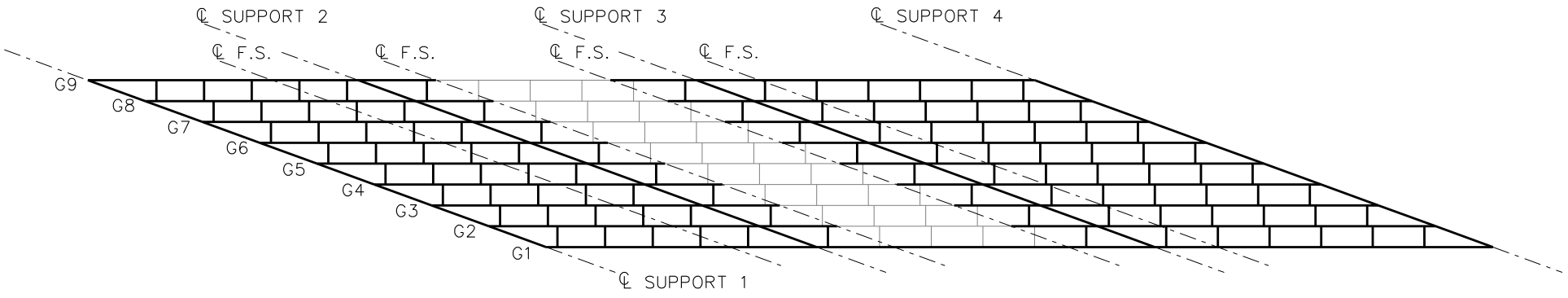

STAGE 19

(RESULTS REQ'D)

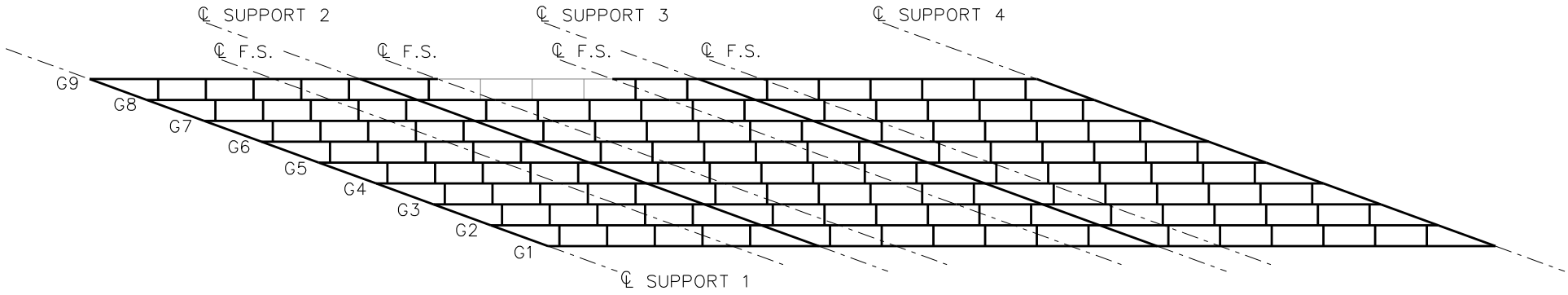

STAGES 20 THRU 26

(RESULTS REQ'D STG 26 ONLY)

LEGEND

▽ = HOLD OR LIFT CRANE

○ = TIE DOWN

□ = TEMPORARY SUPPORT STRUCTURE

NCHRP 12-79

BRIDGE NICSS16

GIRDER ERECTION PROCEDURE

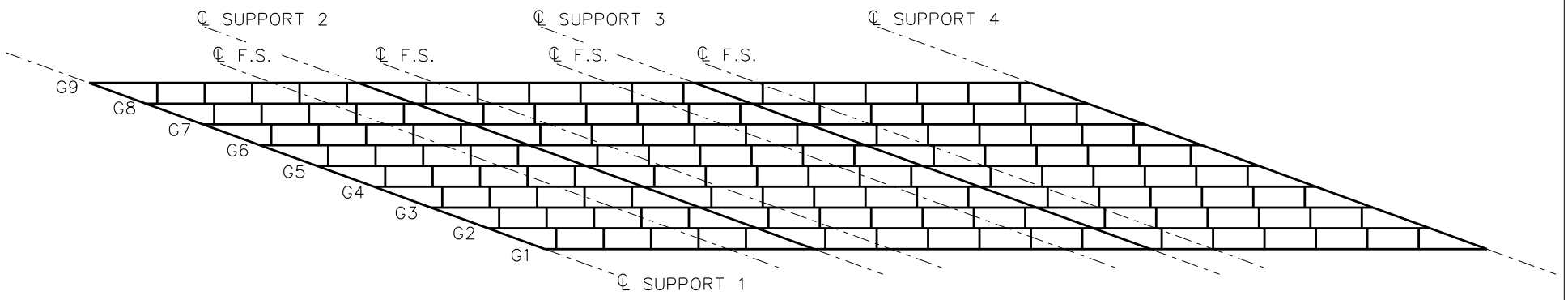

STAGE 27

STEEL DL RESULTS
TOTAL NONCOMP DL RESULTS

LEGEND

▽ = HOLD OR LIFT CRANE

○ = TIE DOWN

□ = TEMPORARY SUPPORT STRUCTURE

NCHRP 12-79

BRIDGE NICSS16

GIRDER ERECTION PROCEDURE

NCHRP 12-79

NICSS25

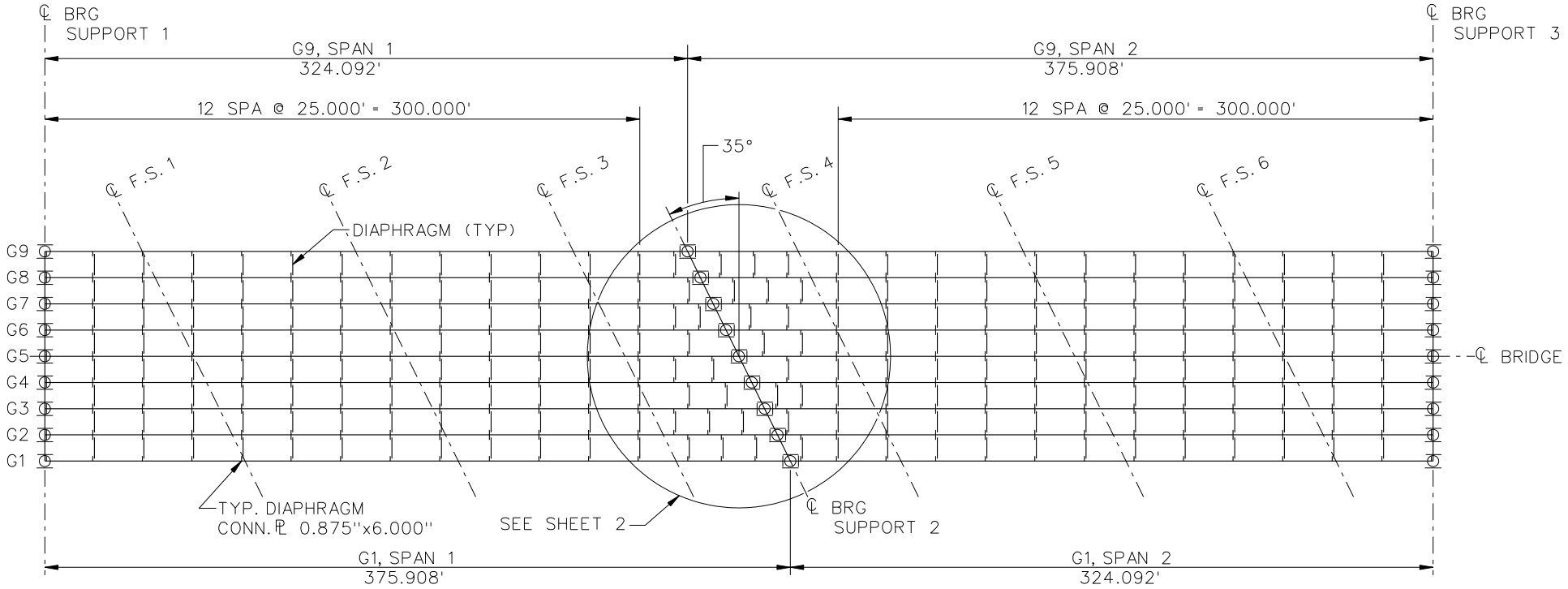

FRAMING PLAN

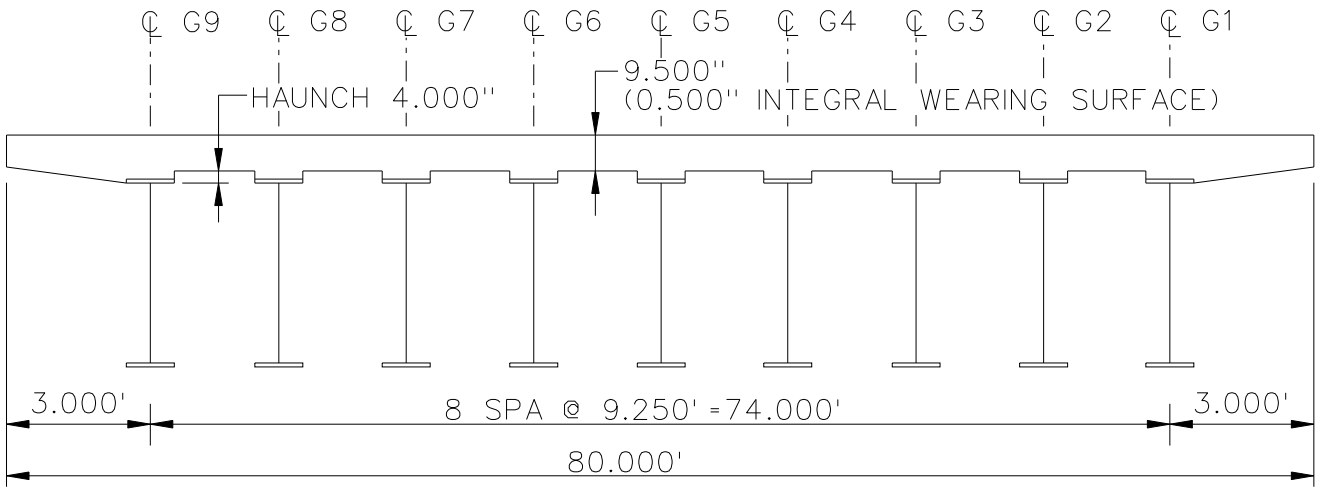

CROSS - SECTION

(DIAPHRAGMS NOT SHOWN)

BEARING LEGEND

- ○ NON-GUIDED
- ⊙ LONGITUDINALLY GUIDED
- |○| TRANSVERSELY GUIDED
- ▣ FIXED

NCHRP 12-79

BRIDGE NICSS25

FRAMING PLAN AND CROSS SECTION

SHEET 1 OF 9

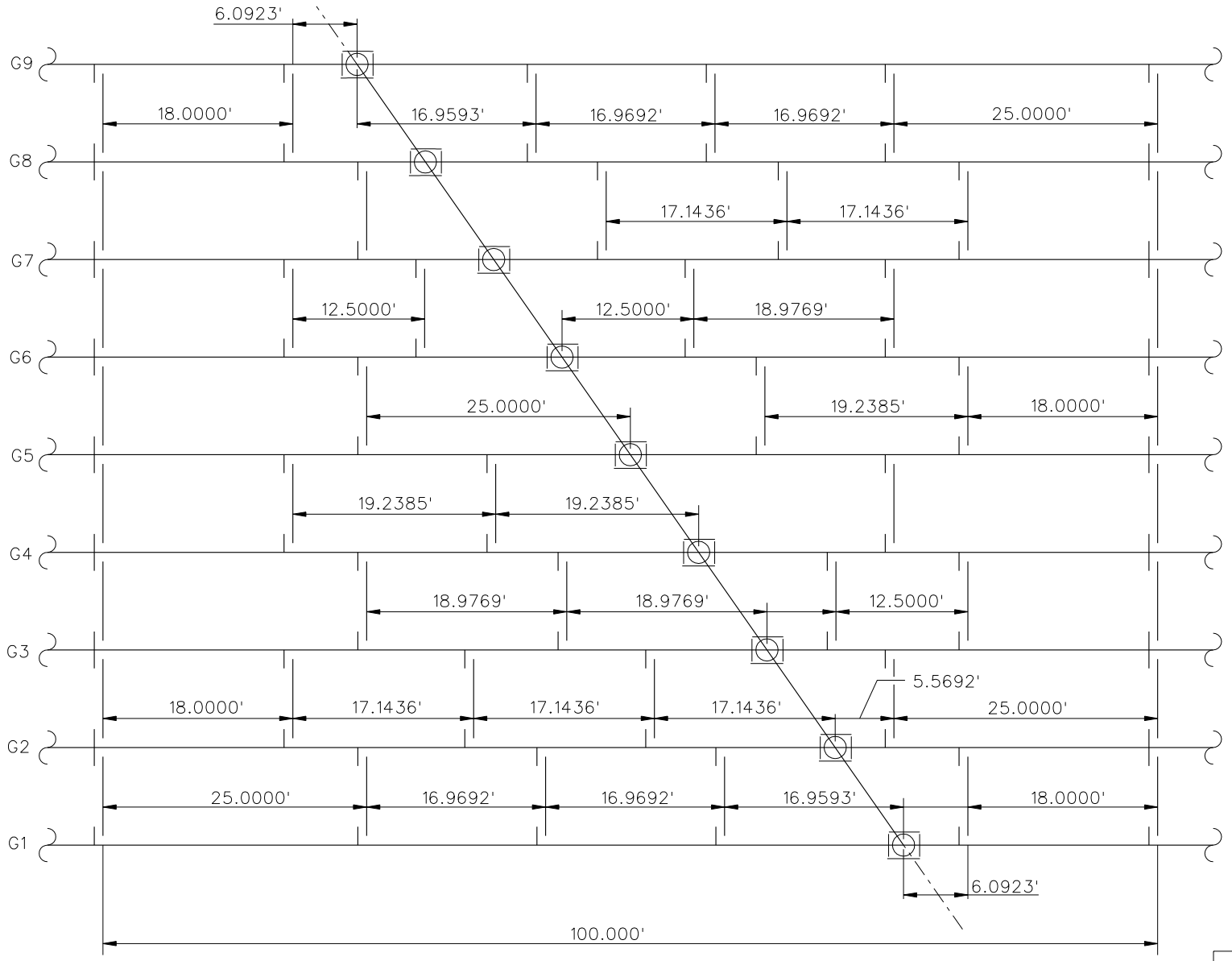

FRAMING PLAN
AT BRG SUPPORT 2

NCHRP 12-79
BRIDGE NICSS25
FRAMING PLAN
SHEET 2 OF 9

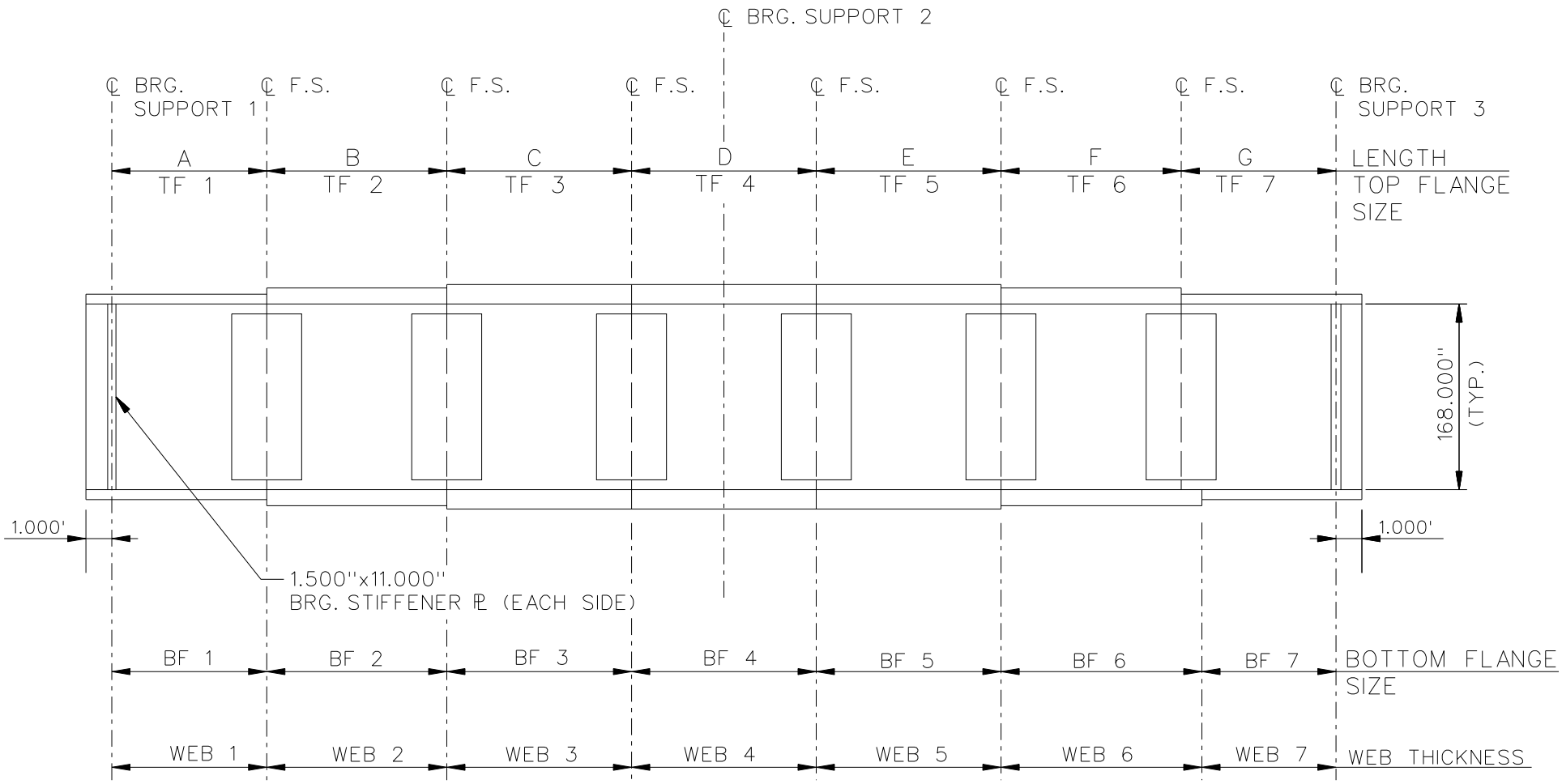

NOTE :

1. SEE TABLES ON SHEET 4 FOR GIRDER ELEVATION DIMENSIONS AND PLATE SIZES.

2. ALL GIRDERS, WEB 1 = WEB 3 = WEB 5 = WEB 7 = 1.125"
   WEB 2 = WEB 4 = WEB 6 = 1.250".

NCHRP 12-79

BRIDGE NICSS25

GIRDER ELEVATION

SHEET 3 OF 9

	GIRDER PLATE LENGTHS ✳								
LENGTH	G1	G2	G3	G4	G5	G6	G7	G8	G9
A	100.908	94.431	87.954	81.477	75.000	68.523	62.046	55.569	49.092
B	110.000	110.000	110.000	110.000	110.000	110.000	110.000	110.000	110.000
C	110.000	110.000	110.000	110.000	110.000	110.000	110.000	110.000	110.000
D	110.000	110.000	110.000	110.000	110.000	110.000	110.000	110.000	110.000
E	110.000	110.000	110.000	110.000	110.000	110.000	110.000	110.000	110.000
F	110.000	110.000	110.000	110.000	110.000	110.000	110.000	110.000	110.000
G	49.092	55.569	62.046	68.523	75.000	81.477	87.954	94.431	100.908

✳ ALL DIMENSIONS ARE IN FEET.

	GIRDER FLANGE DIMENSIONS ✳✳					
TOP FLANGE	G1, G2, G3		G4, G5, G6		G7, G8, G9	
	BF	TF	BF	TF	BF	TF
TF1	28.000	1.250	28.000	1.250	28.000	1.250
TF2	28.000	1.500	28.000	1.500	28.000	1.500
TF3	28.000	1.250	28.000	1.250	28.000	1.250
TF4	32.000	2.250	32.000	2.250	32.000	2.250
TF5	28.000	1.250	28.000	1.250	28.000	1.250
TF6	28.000	1.500	28.000	1.500	28.000	1.500
TF7	28.000	1.250	28.000	1.250	28.000	1.250

✳✳ ALL DIMENSIONS ARE IN INCHES.

	GIRDER FLANGE DIMENSIONS ✳✳					
BOTTOM FLANGE	G1, G2, G3		G4, G5, G6		G7, G8, G9	
	BF	TF	BF	TF	BF	TF
TF1	30.000	1.250	30.000	1.250	30.000	1.250
TF2	30.000	1.500	30.000	1.500	30.000	1.500
TF3	30.000	1.250	30.000	1.250	30.000	1.250
TF4	34.000	2.250	34.000	2.250	34.000	2.250
TF5	30.000	1.250	30.000	1.250	30.000	1.250
TF6	30.000	1.500	30.000	1.500	30.000	1.500
TF7	30.000	1.250	30.000	1.250	30.000	1.250

✳✳ ALL DIMENSIONS ARE IN INCHES.

NCHRP 12-79

BRIDGE NICSS25

GIRDER ELEVATION TABLES

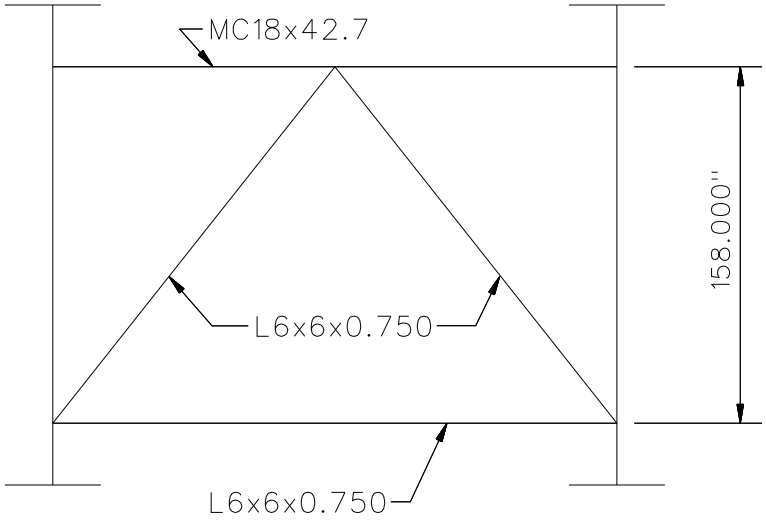

TYPICAL END DIAPHRAGM

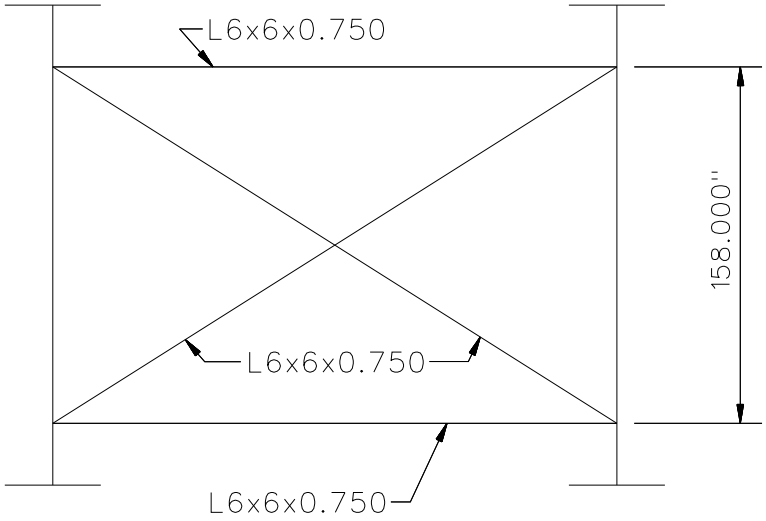

TYPICAL INTERMEDIATE DIAPHRAGM

NOTES:

1. STEEL DEAD LOAD INCREASED BY 5% FOR MDX AND LARSA MODELS; 2% FOR 3D MODEL; AND 10% FOR APPROXIMATE ANALYSIS TO ACCOUNT FOR MISC. DETAILS.

2. FORMWORK LOAD OF 10PSF IS INCLUDED IN CONCRETE DEAD LOAD.

3. ADDITIONAL DESIGN PARAMETERS :
   A. 1.5' PARAPET WIDTH BOTH SIDES.
   B. 700 $^{LB}/_{FT}$ UNIFORM LOAD ASSUMED FOR PARAPET WEIGHT.
   C. ROADWAY WIDTH = 77.000".
   D. NUMBER OF DESIGN LANES = 6.
   E. HL93 LIVE LOAD.

4. DIAPHRAGM MEMBER CALL-OUTS ARE IN UNITS OF INCHES.

NCHRP 12-79

BRIDGE NICSS25

MISC. DETAILS AND NOTES

SHEET 5 OF 9

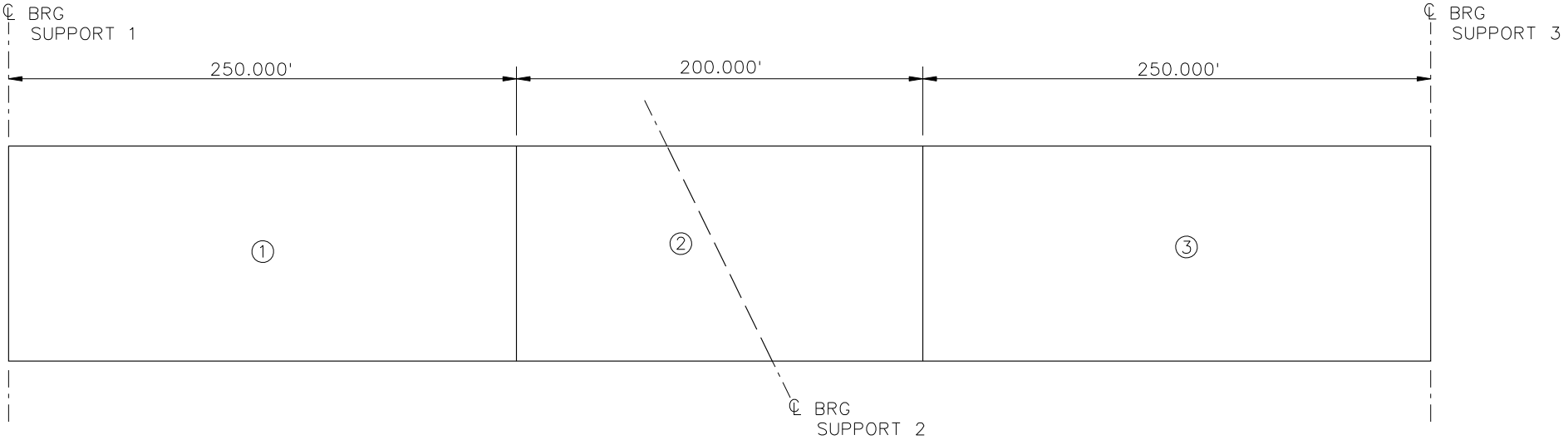

DECK POURING SEQUENCE

NCHRP 12-79

BRIDGE NICSS25

DECK POURING SEQUENCE

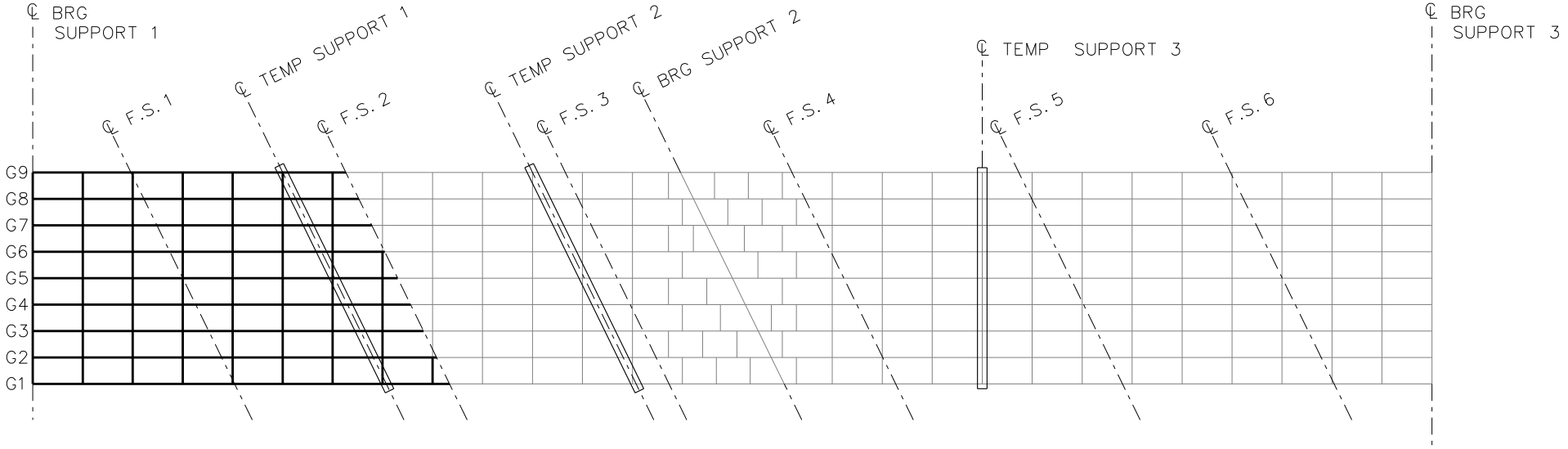

STAGES 1 THRU 9

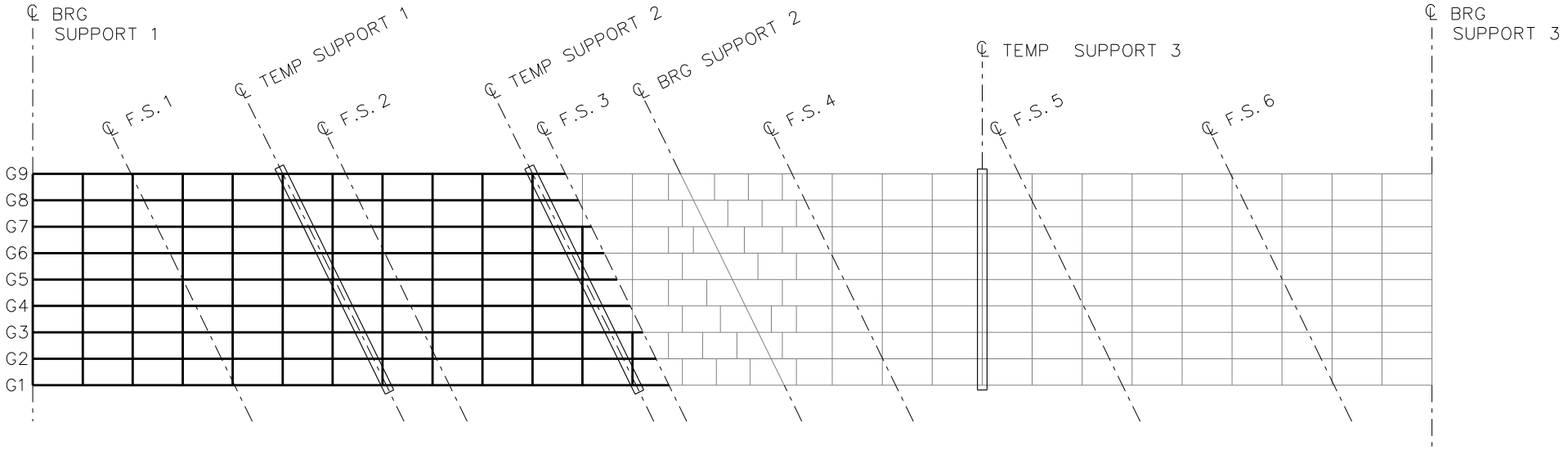

STAGES 10 THRU 18

NCHRP 12-79

BRIDGE NICSS25

GIRDER ERECTION PROCEDURE

SHEET 7 OF 9

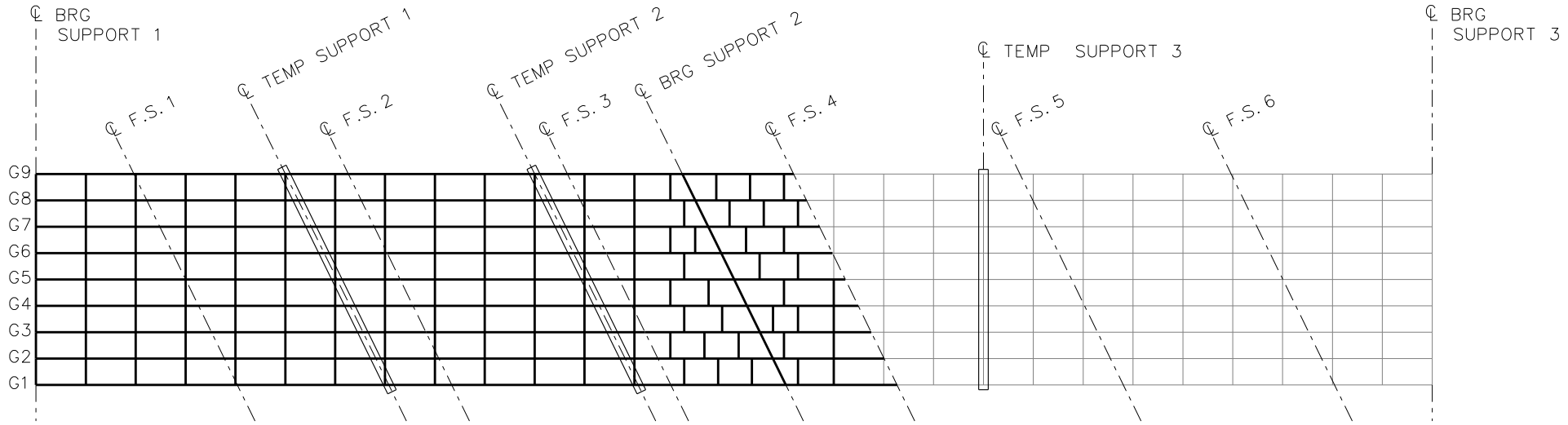

STAGES 19 THRU 27

STAGE 28

(REMOVE TEMP SUPPORT 2)

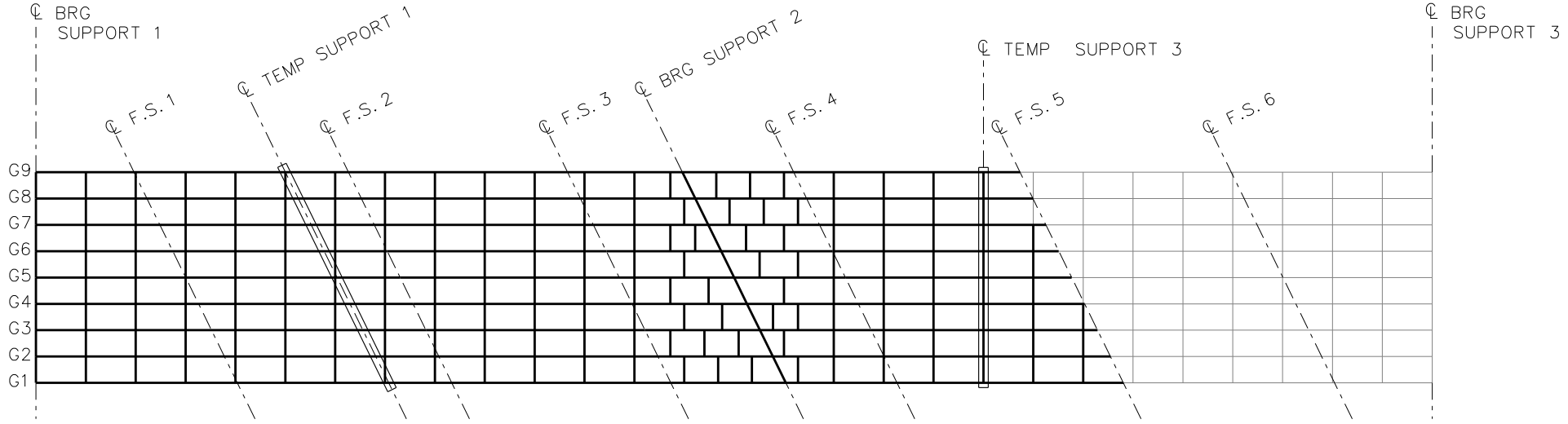

STAGES 29 THRU 37

NCHRP 12-79

BRIDGE NICSS25

GIRDER ERECTION PROCEDURE

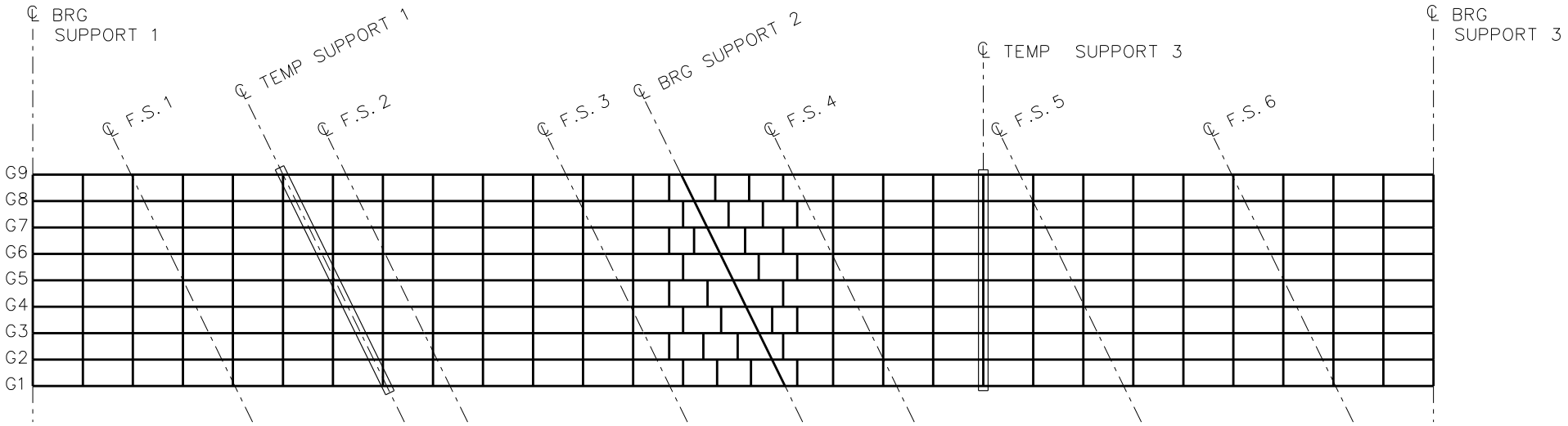

STAGES 38 THRU 46

STAGE 47

(REMOVE TEMP SUPPORTS 1AND 3)

NOTES:

1. LOCATION OF TEMP SUPPORT 1, 2
   G1, G5, G9 AT XF'S
   G2, G4, G6, G8 AT 0.25/0.75 XF SPACE
   G3, G7 AT 0.5 XF SPACE

NCHRP 12-79

BRIDGE NICSS25

GIRDER ERECTION PROCEDURE

NCHRP 12-79

NICSS27

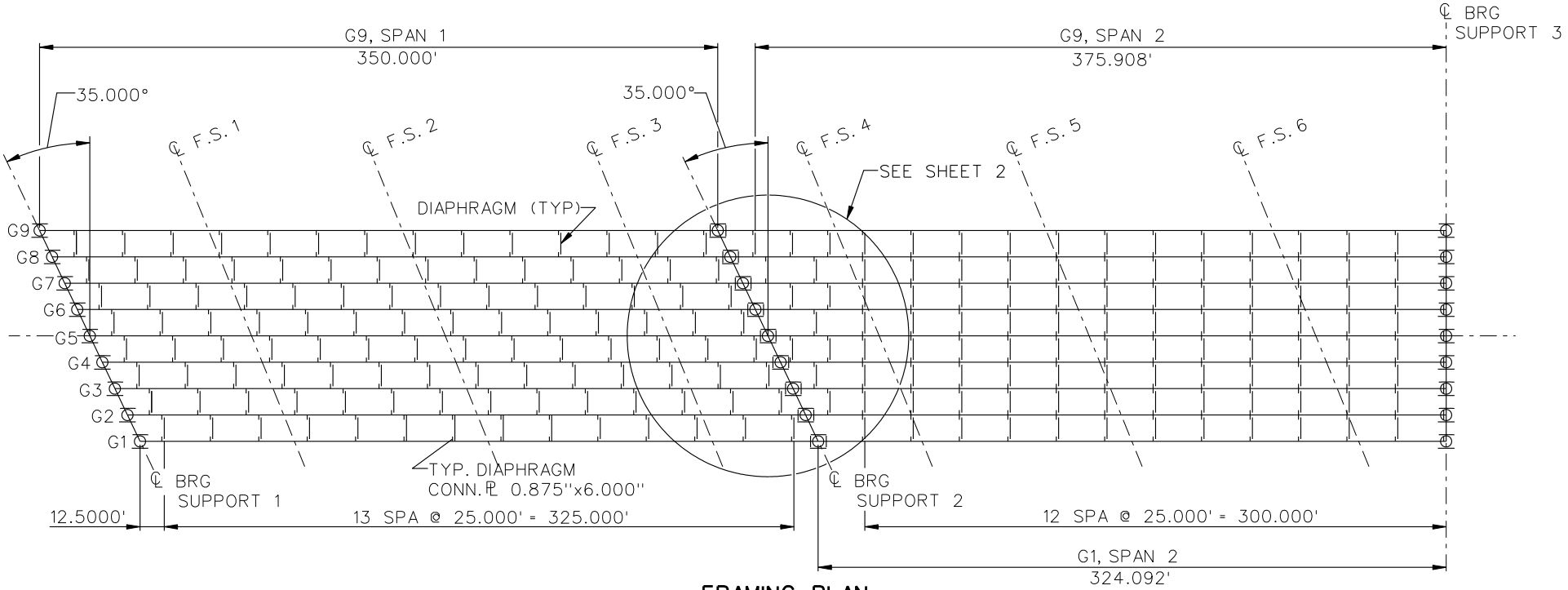

FRAMING PLAN

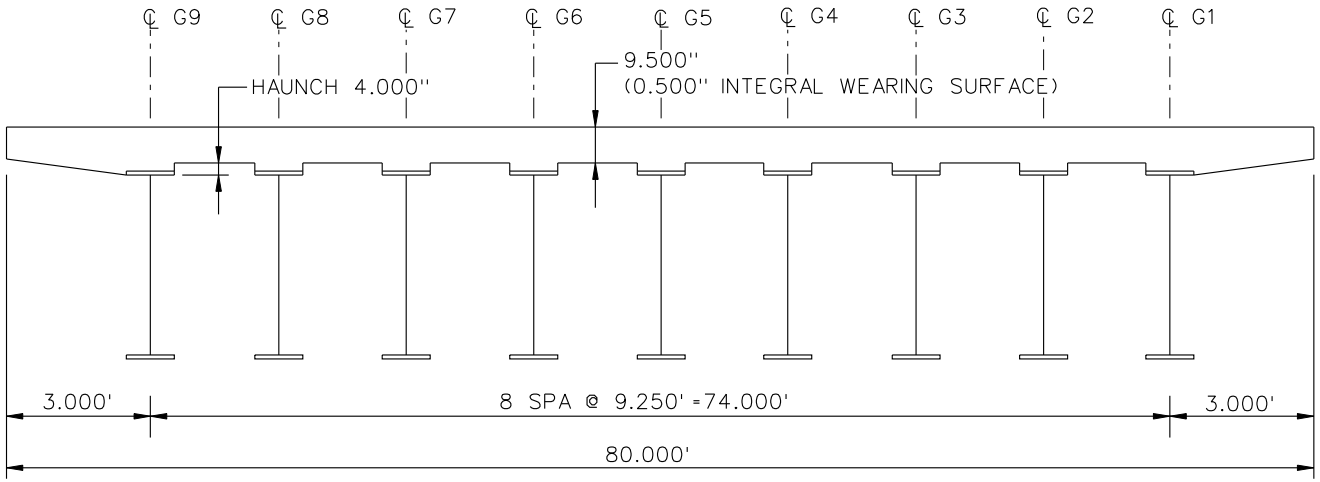

CROSS - SECTION

(DIAPHRAGMS NOT SHOWN)

BEARING LEGEND

- ○ NON-GUIDED
- ⊙ LONGITUDINALLY GUIDED
- ⊙ TRANSVERSELY GUIDED
- ⊙ FIXED

NCHRP 12-79

BRIDGE NICSS27

FRAMING PLAN AND CROSS SECTION

SHEET 1 OF 10

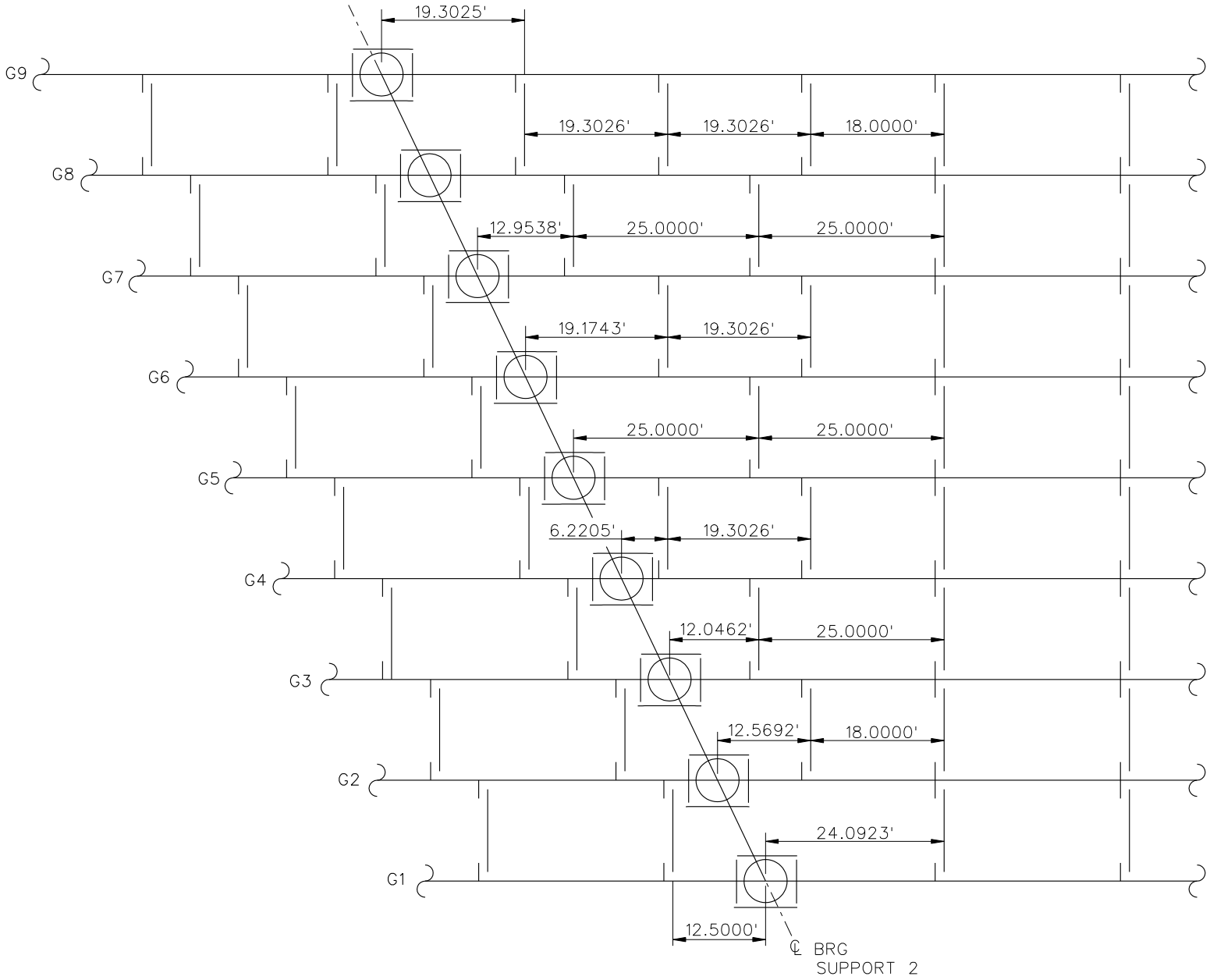

FRAMING PLAN
AT BRG SUPPORT 2

NCHRP 12-79
BRIDGE NICSS27
FRAMING PLAN
SHEET 2 OF 10

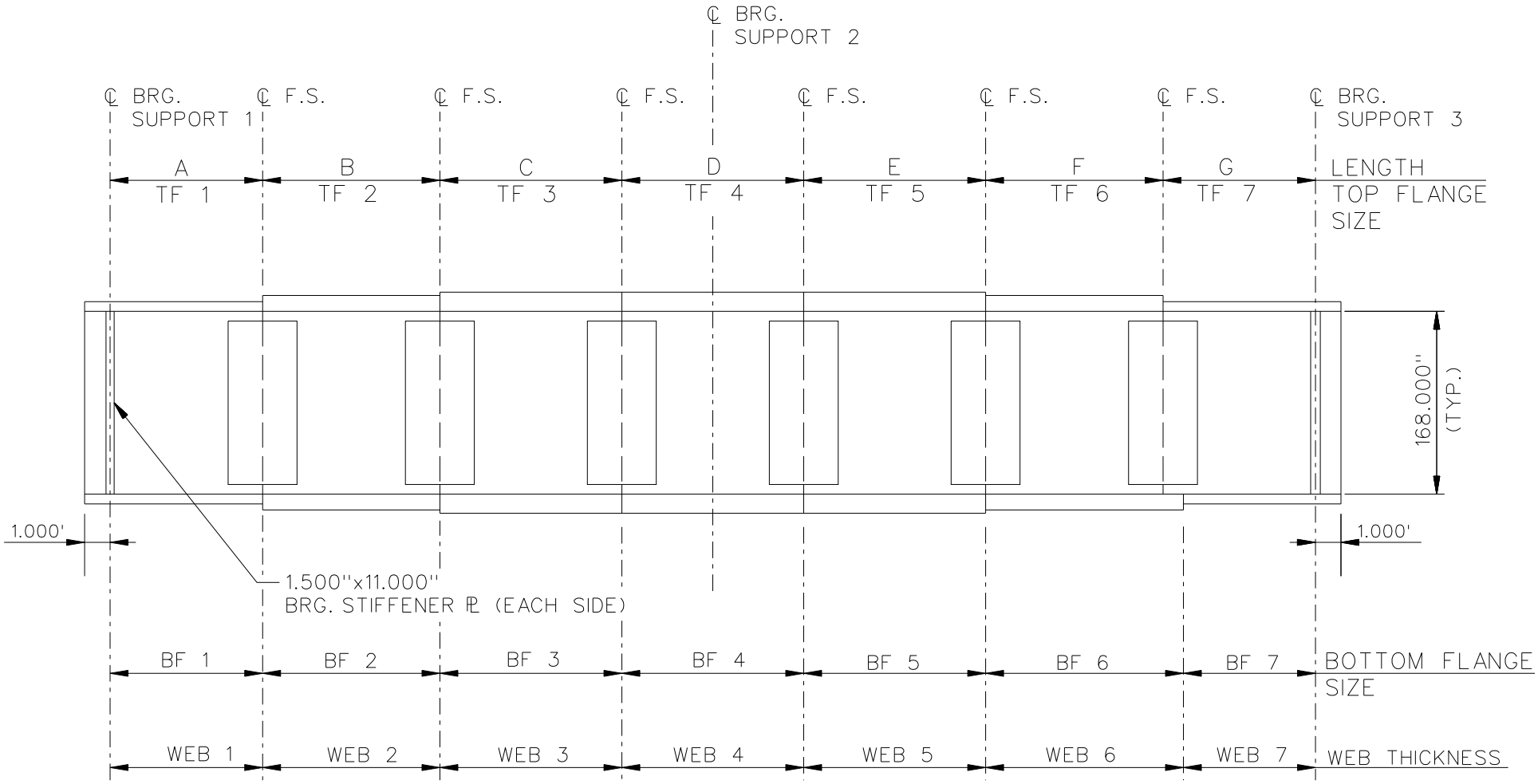

NOTE :

1. SEE TABLES ON SHEET 4 FOR GIRDER ELEVATION DIMENSIONS AND PLATE SIZES.

2. ALL GIRDERS, WEB 1 = WEB 3 = WEB 5 = WEB 7 = 1.125"
   WEB 2 = WEB 4 = WEB 6 = 1.250".

NCHRP 12-79

BRIDGE NICSS27

GIRDER ELEVATION

SHEET 3 OF 10

	GIRDER PLATE LENGTHS ✳								
LENGTH	G1	G2	G3	G4	G5	G6	G7	G8	G9
A	70.000	70.000	70.000	70.000	70.000	70.000	70.000	70.000	70.000
B	110.000	110.000	110.000	110.000	110.000	110.000	110.000	110.000	110.000
C	110.000	110.000	110.000	110.000	110.000	110.000	110.000	110.000	110.000
D	120.000	120.000	120.000	120.000	120.000	120.000	120.000	120.000	120.000
E	110.000	110.000	110.000	110.000	110.000	110.000	110.000	110.000	110.000
F	110.000	110.000	110.000	110.000	110.000	110.000	110.000	110.000	110.000
G	44.092	50.569	57.046	63.523	70.000	76.477	82.954	89.431	95.908

✳ ALL DIMENSIONS ARE IN FEET.

	GIRDER FLANGE DIMENSIONS ✳✳					
TOP	G1, G2, G3		G4, G5, G6		G7, G8, G9	
FLANGE	BF	TF	BF	TF	BF	TF
TF1	28.000	1.250	28.000	1.250	28.000	1.250
TF2	28.000	1.500	28.000	1.500	28.000	1.500
TF3	28.000	1.250	28.000	1.250	28.000	1.250
TF4	32.000	2.000	32.000	2.000	34.000	2.250
TF5	28.000	1.250	28.000	1.250	28.000	1.250
TF6	28.000	1.500	28.000	1.500	28.000	1.500
TF7	28.000	1.250	28.000	1.250	28.000	1.250

✳✳ ALL DIMENSIONS ARE IN INCHES.

	GIRDER FLANGE DIMENSIONS ✳✳					
BOTTOM	G1, G2, G3		G4, G5, G6		G7, G8, G9	
FLANGE	BF	TF	BF	TF	BF	TF
TF1	30.000	1.250	30.000	1.250	30.000	1.250
TF2	30.000	1.500	30.000	1.500	30.000	1.500
TF3	30.000	1.250	30.000	1.250	30.000	1.250
TF4	34.000	2.000	34.000	2.000	36.000	2.500
TF5	30.000	1.250	30.000	1.250	30.000	1.250
TF6	30.000	1.500	30.000	1.500	30.000	1.500
TF7	30.000	1.250	30.000	1.250	30.000	1.250

✳✳ ALL DIMENSIONS ARE IN INCHES.

NCHRP 12-79

BRIDGE NICSS27

GIRDER ELEVATION TABLES

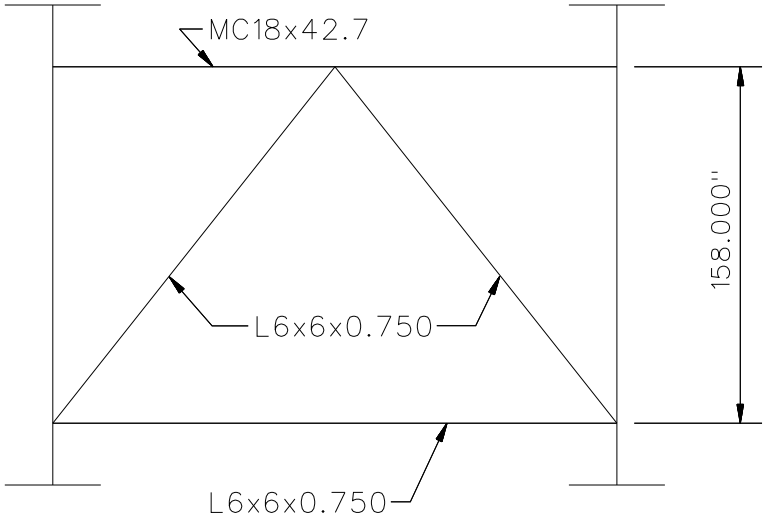

TYPICAL END DIAPHRAGM

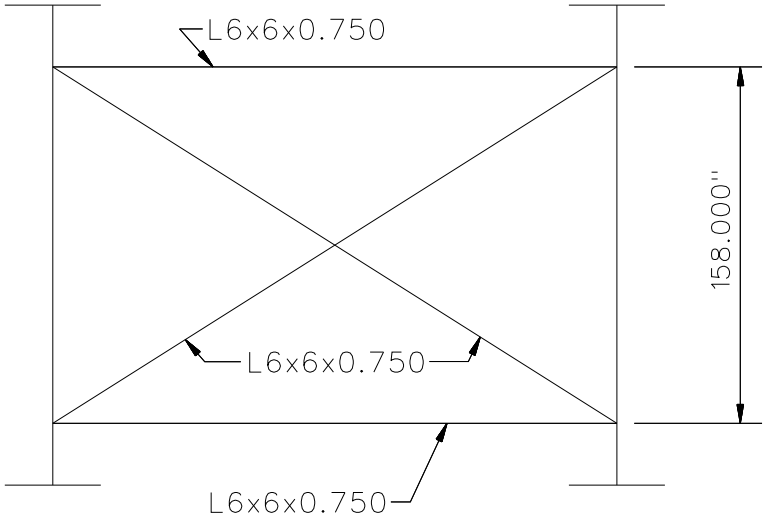

TYPICAL INTERMEDIATE DIAPHRAGM

NOTES:

1. STEEL DEAD LOAD INCREASED BY 5% FOR MDX AND LARSA MODELS; 2% FOR 3D MODEL; AND 10% FOR APPROXIMATE ANALYSIS TO ACCOUNT FOR MISC. DETAILS.

2. FORMWORK LOAD OF 10PSF IS INCLUDED IN CONCRETE DEAD LOAD.

3. ADDITIONAL DESIGN PARAMETERS :
   A. 1.500' PARAPET WIDTH BOTH SIDES.
   B. 700 $^{LB}/_{FT}$ UNIFORM LOAD ASSUMED FOR PARAPET WEIGHT.
   C. ROADWAY WIDTH = 77.000".
   D. NUMBER OF DESIGN LANES = 6.
   E. HL93 LIVE LOAD.

4. DIAPHRAGM MEMBER CALL-OUTS ARE IN UNITS OF INCHES.

NCHRP 12-79

BRIDGE NICSS27

MISC. DETAILS AND NOTES

SHEET 5 OF 10

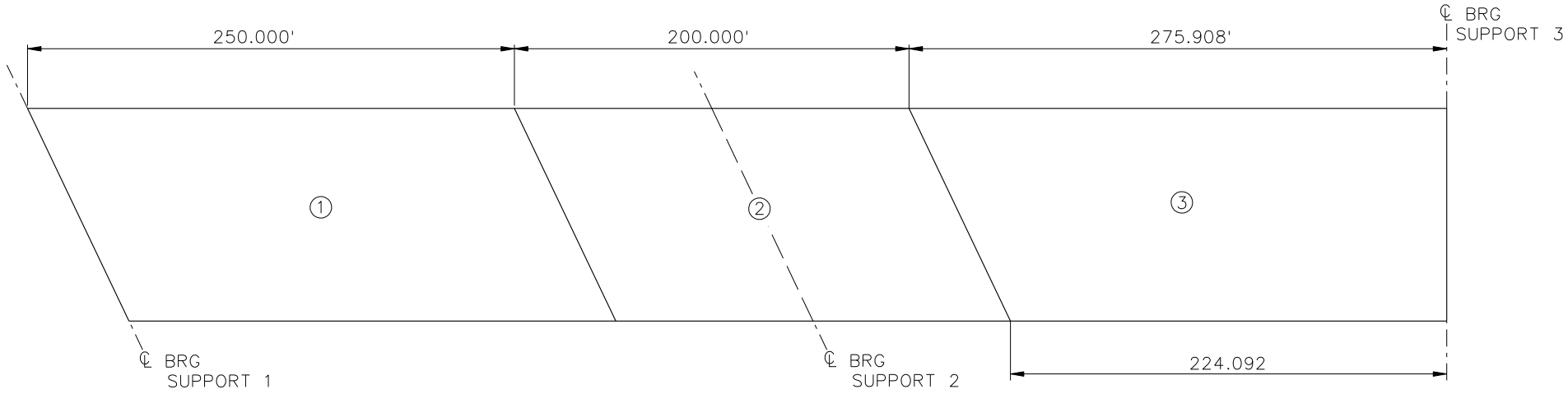

DECK POURING SEQUENCE

NCHRP 12-79

BRIDGE NICSS27

DECK POURING SEQUENCE

SHEET 6 OF 10

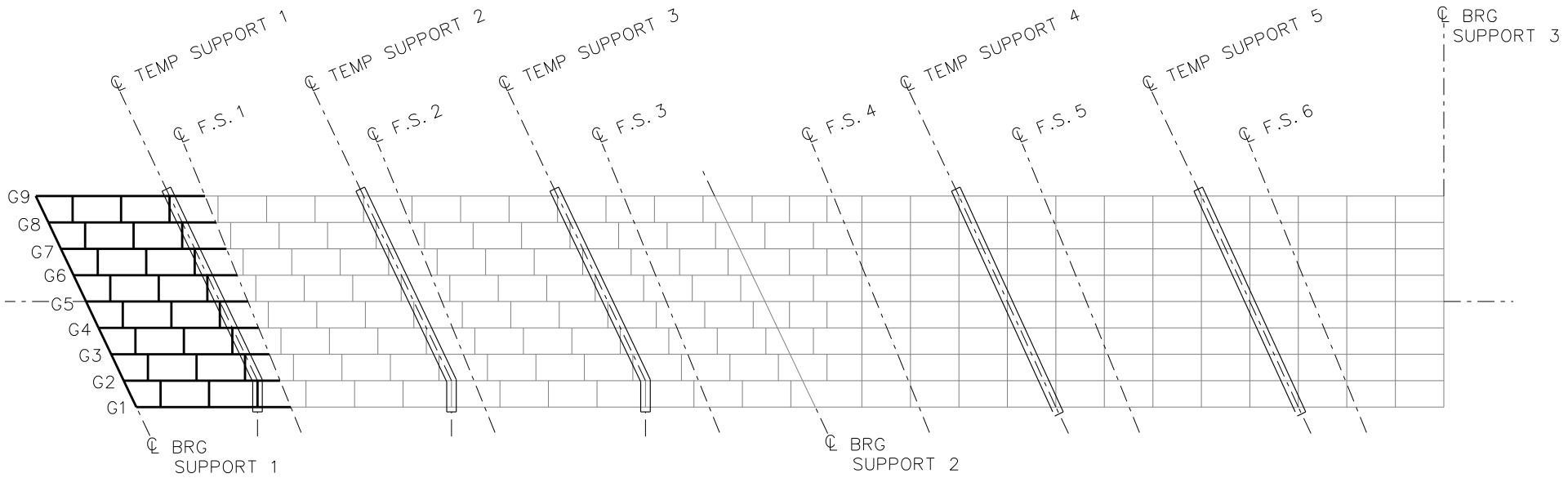

STAGES 1 THRU 9

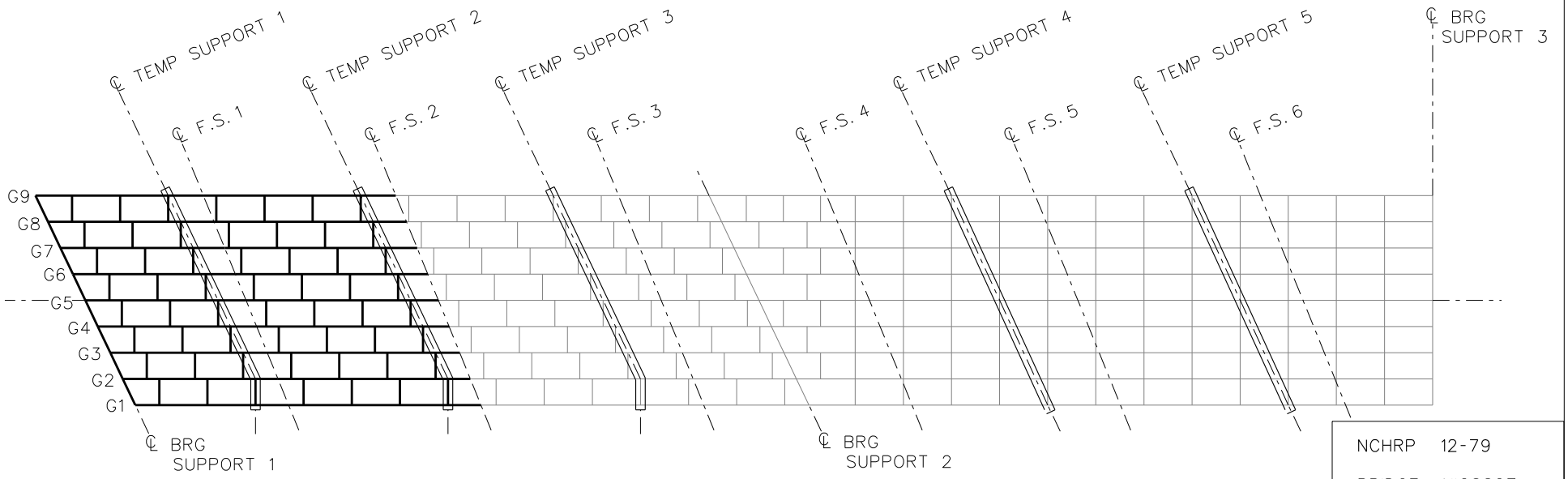

STAGES 10 THRU 18

NCHRP 12-79

BRIDGE NICSS27

GIRDER ERECTION PROCEDURE

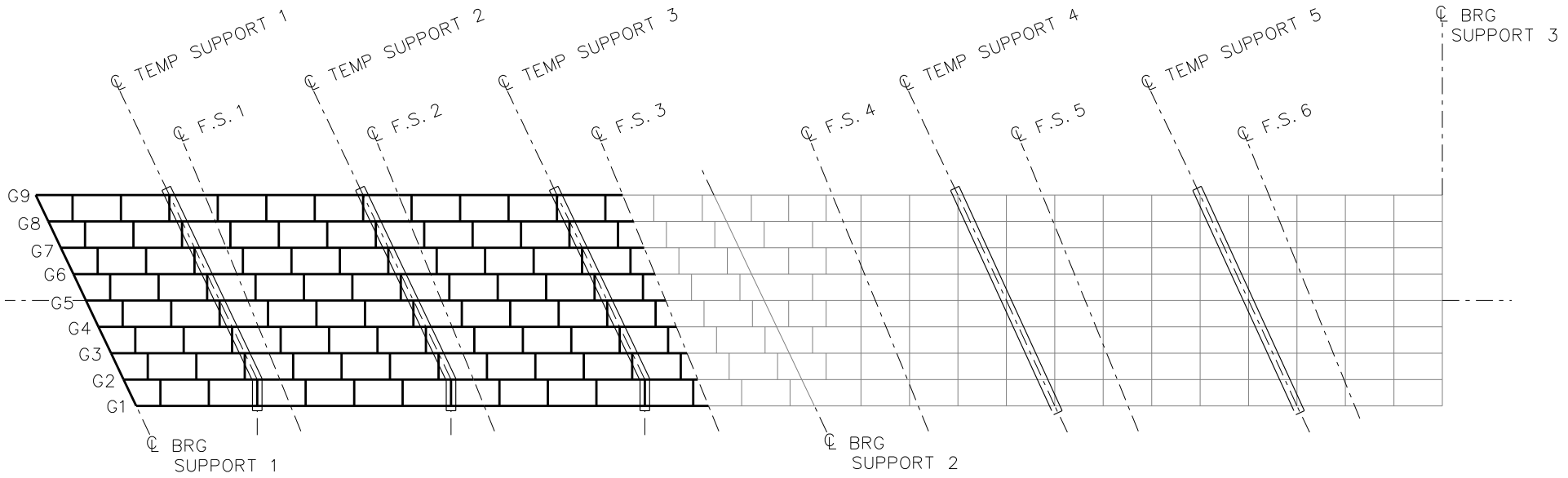

STAGES 19 THRU 27

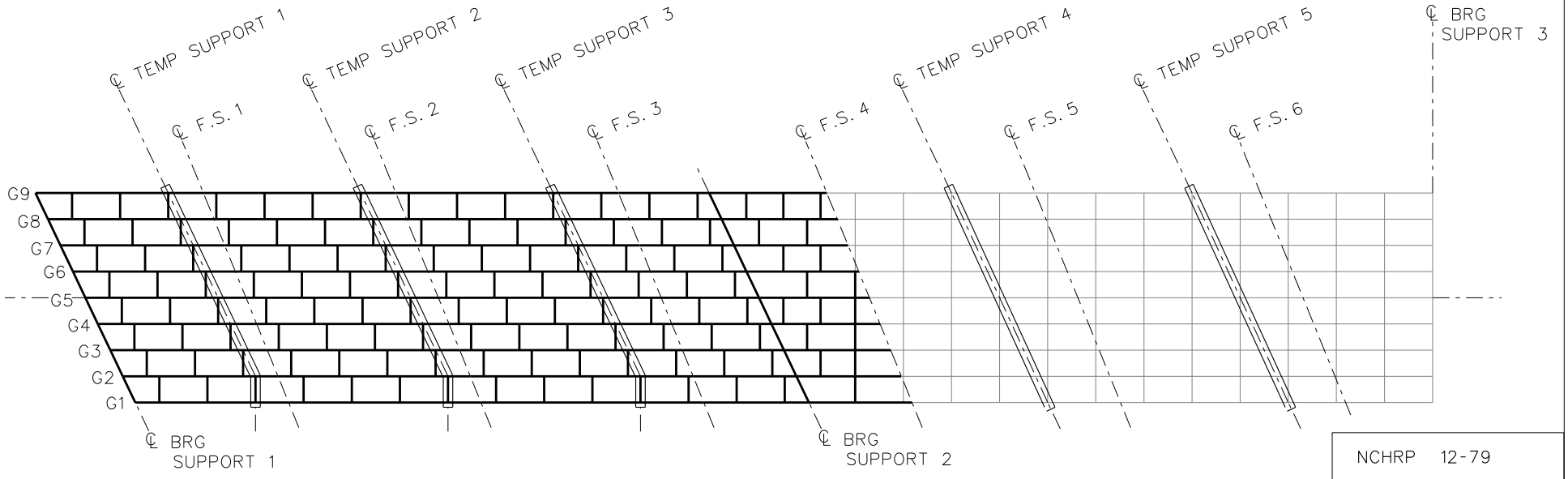

STAGES 28 THRU 36

STAGE 37

(REMOVE TEMP SUPPORTS 1 AND 3)

NCHRP 12-79

BRIDGE NICSS27

GIRDER ERECTION PROCEDURE

SHEET 8 OF 10

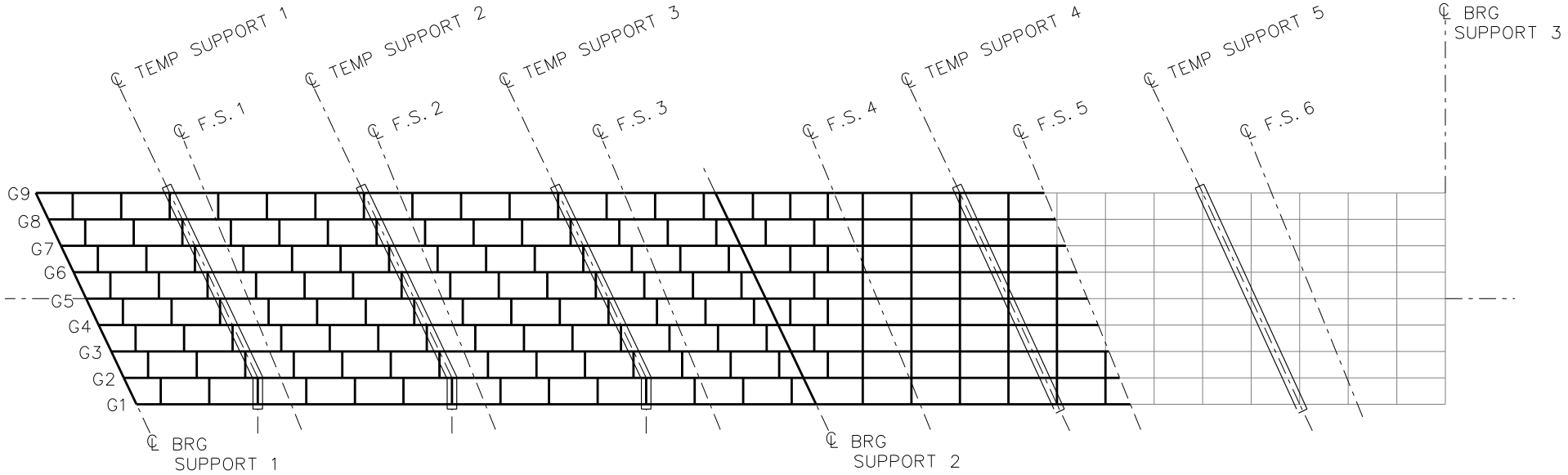

STAGES 38 THRU 46

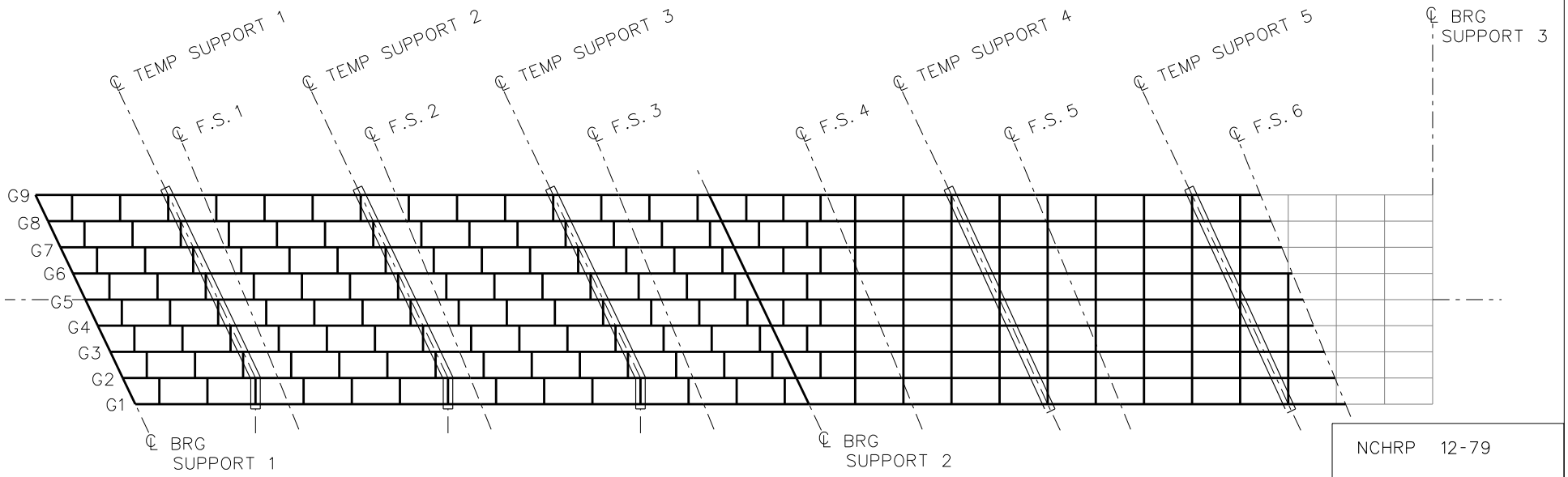

STAGES 47 THRU 55

NCHRP 12-79

BRIDGE NICSS27

GIRDER ERECTION PROCEDURE

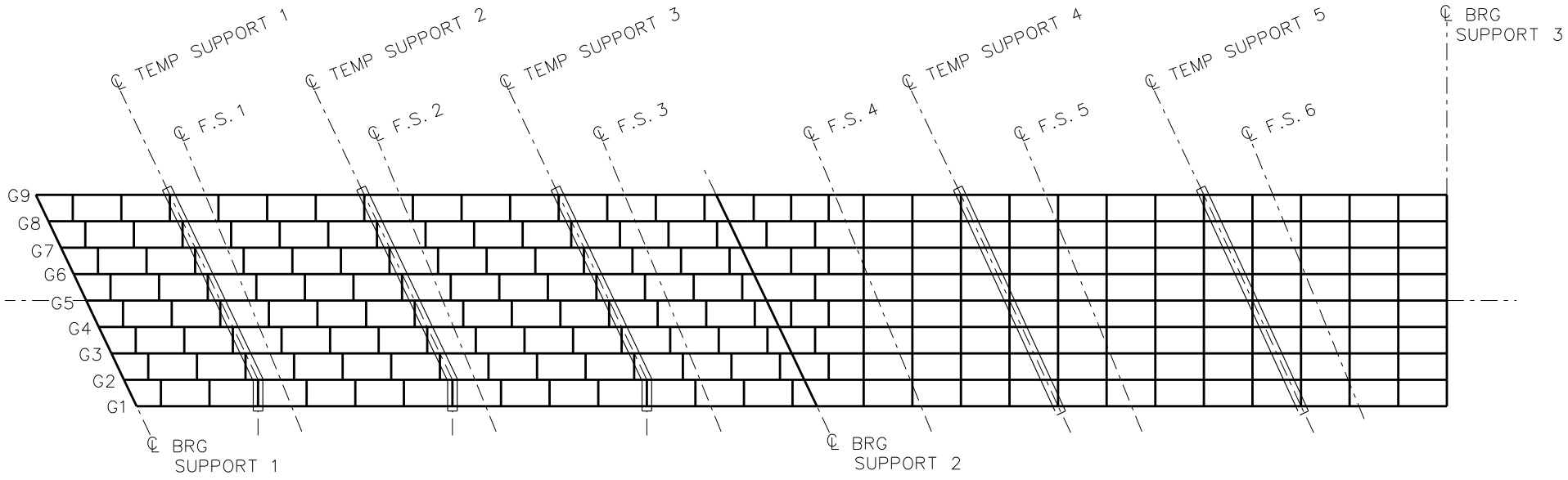

STAGES 56 THRU 64

STAGE 65

(REMOVE TEMP SUPPORTS 2, 4, AND 5)

NOTE:

1. LOCATION OF TEMP SUPPORT 4, 5
   G1, G5, G9 AT XF'S
   G2, G4, G6, G8 AT 0.25/0.75 XF SPACE
   G3, G7 AT 0.5 XF SPACE

NCHRP 12-79

BRIDGE NICSS27

GIRDER ERECTION PROCEDURE

NCHRP 12-79

NISCR1

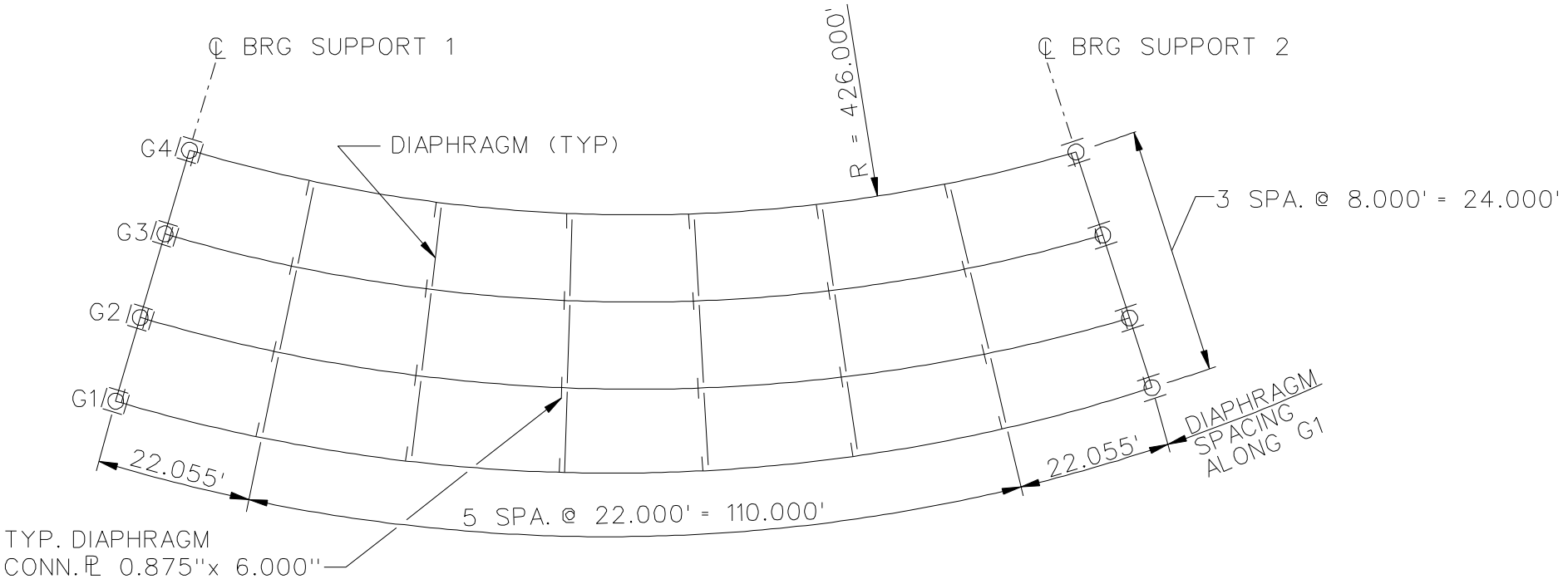

FRAMING PLAN

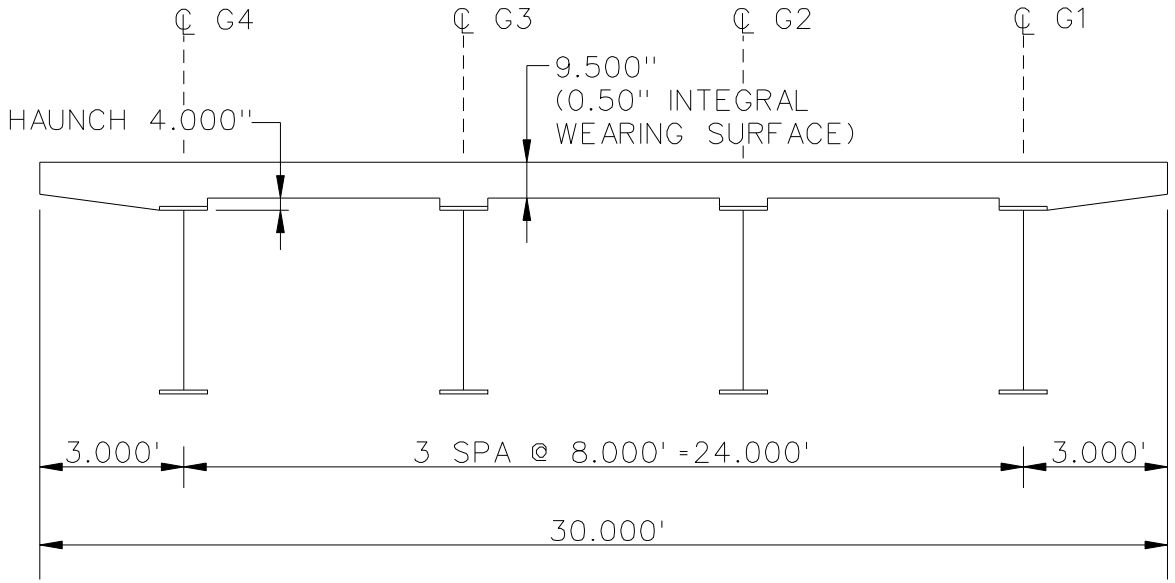

CROSS - SECTION

(DIAPHRAGMS NOT SHOWN)

BEARING LEGEND

- ○ NON-GUIDED
- ⊜ LONGITUDINALLY GUIDED
- |○| TRANSVERSELY GUIDED
- |⊜| FIXED

NCHRP 12-79

BRIDGE NISCR2

FRAMING PLAN AND CROSS-SECTION

SHEET 1 OF 6

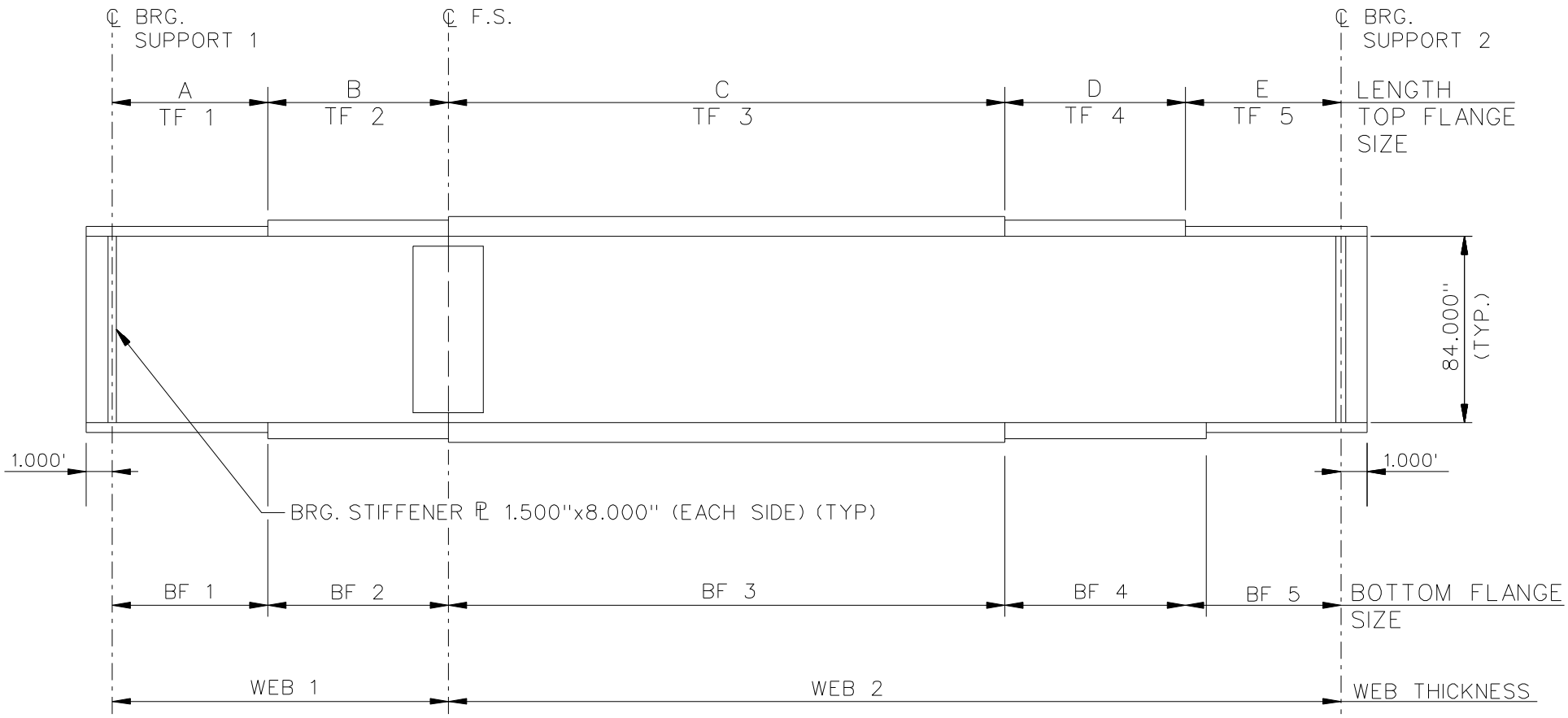

NOTE :

1. SEE TABLES ON SHEET 3 FOR GIRDER ELEVATION DIMENSIONS AND PLATE SIZES.
2. FOR G1 AND G2, WEB 1 = WEB 2 = 0.750"
3. FOR G3 AND G4, WEB 1 = WEB 2 = 0.625"

NCHRP 12-79

BRIDGE NISCR2

GIRDER ELEVATION

	GIRDER PLATE LENGTHS ✳			
LENGTH	G1	G2	G3	G4
A	20.000	19.644	19.289	18.933
B	20.000	19.644	19.289	18.933
C	74.110	72.793	71.475	70.158
D	20.000	19.644	19.289	18.933
E	20.000	19.644	19.289	18.933

✳ ALL DIMENSIONS ARE IN FEET.

	GIRDER FLANGE DIMENSIONS ✳✳							
TOP	G1		G2		G3		G4	
FLANGE	BF	TF	BF	TF	BF	TF	BF	TF
TF1	22.000	1.000	22.000	1.000	20.000	1.000	20.000	1.000
TF2	22.000	1.250	22.000	1.250	20.000	1.000	20.000	1.000
TF3	22.000	2.000	22.000	2.000	20.000	1.500	20.000	1.500
TF4	22.000	1.250	22.000	1.250	20.000	1.000	20.000	1.000
TF5	22.000	1.000	22.000	1.000	20.000	1.000	20.000	1.000

✳✳ ALL DIMENSIONS ARE IN INCHES.

	GIRDER FLANGE DIMENSIONS ✳✳							
BOTTOM	G1		G2		G3		G4	
FLANGE	BF	TF	BF	TF	BF	TF	BF	TF
BF1	26.000	1.250	26.000	1.250	24.000	1.000	24.000	1.000
BF2	26.000	2.000	26.000	2.000	24.000	1.250	24.000	1.250
BF3	26.000	2.750	26.000	2.750	24.000	2.000	24.000	2.000
BF4	26.000	2.000	26.000	2.000	24.000	1.250	24.000	1.250
BF5	26.000	1.250	26.000	1.250	24.000	1.000	24.000	1.000

✳✳ ALL DIMENSIONS ARE IN INCHES.

NCHRP 12-79

BRIDGE NISCR2

GIRDER ELEVATION TABLES

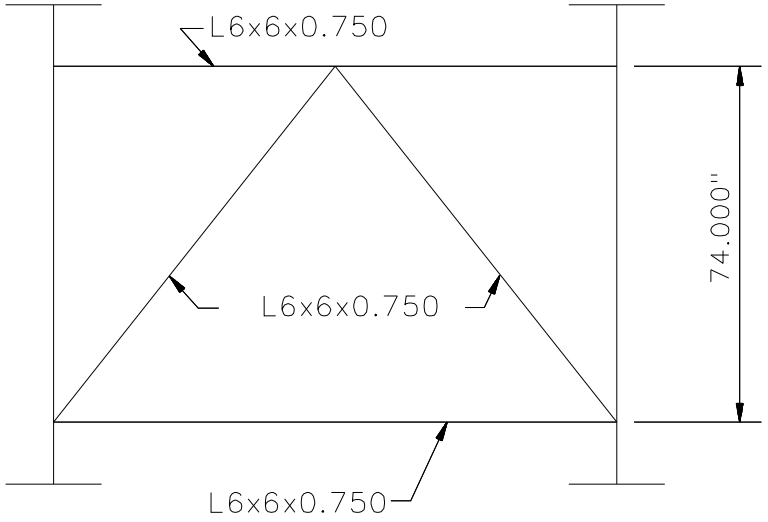

TYPICAL END DIAPHRAGM

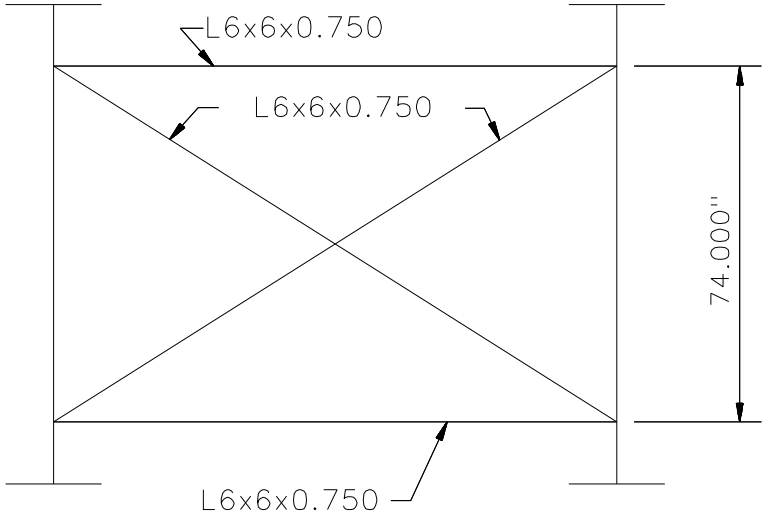

TYPICAL INTERMEDIATE DIAPHRAGM

NOTES:

1. STEEL DEAD LOAD INCREASED BY 5% FOR MDX AND LARSA MODELS; 2% FOR 3D MODEL; AND 10% FOR APPROXIMATE ANALYSIS TO ACCOUNT FOR MISC. DETAILS.

2. FORMWORK LOAD OF 10PSF IS INCLUDED IN CONCRETE DEAD LOAD.

3. ADDITIONAL DESIGN PARAMETERS:
   A. 1.500' PARAPET WIDTH BOTH SIDES.
   B. 700 LB/FT UNIFORM LOAD ASSUMED FOR PARAPET WEIGHT.
   C. ROADWAY WIDTH = 27.000'.
   D. NUMBER OF DESIGN LANES = 3.
   E. HL93 LIVE LOAD.

4. DIAPHRAGM MEMBER CALL-OUTS ARE IN UNITS OF INCHES.

NCHRP 12-79

BRIDGE NISCR2

MISC. DETAILS AND NOTES

SHEET 4 OF 6

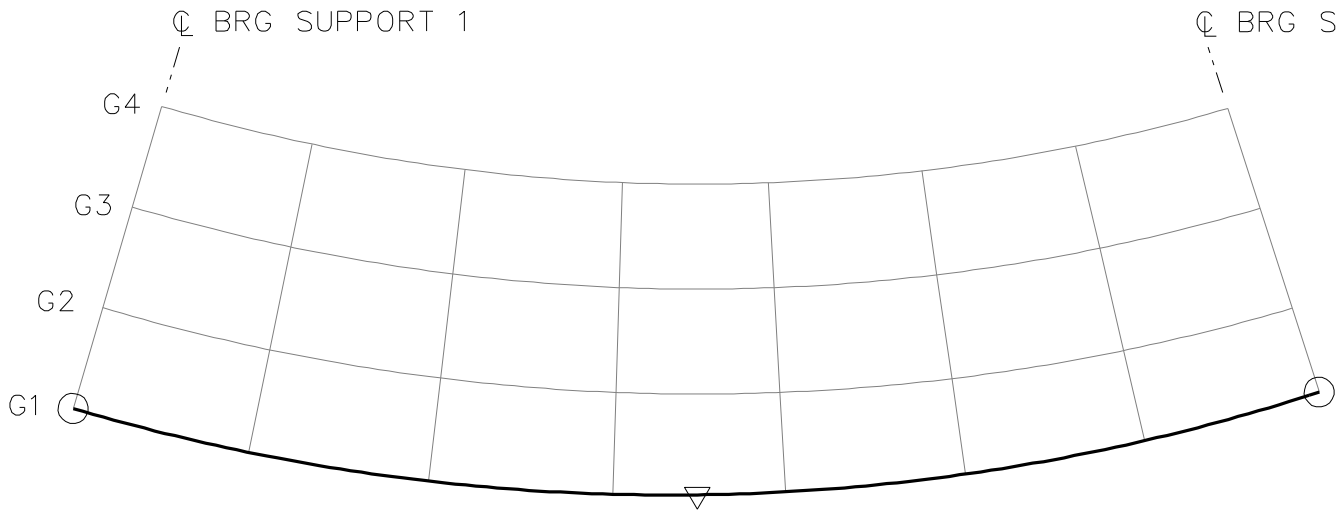

STAGE 1

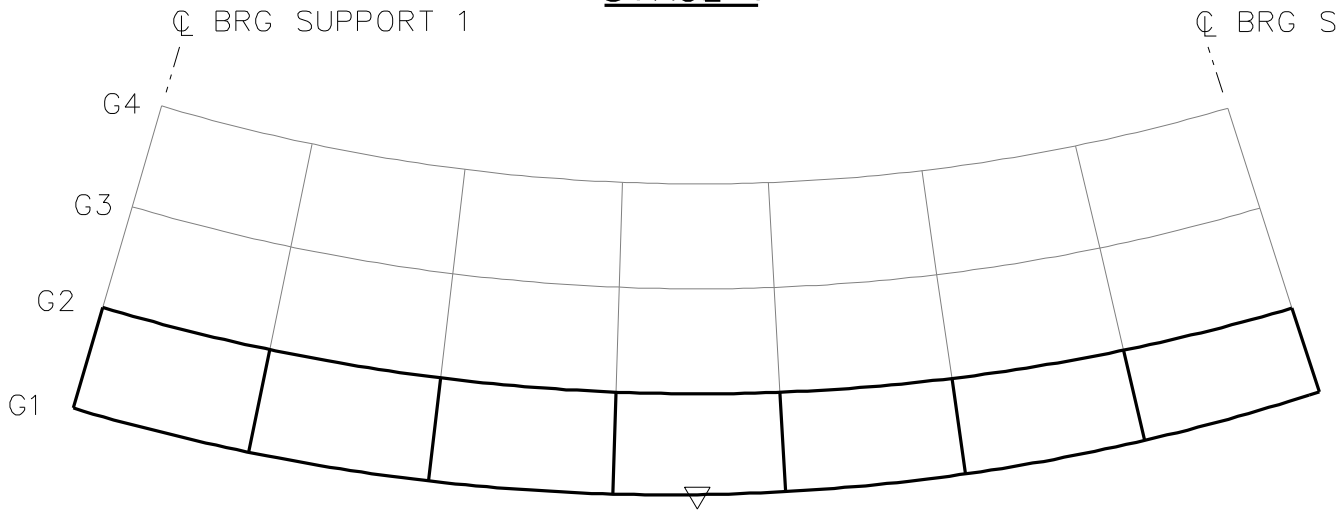

STAGE 2

LEGEND

▽ = HOLD OR LIFT CRANE

○ = TIE DOWN

□ = TEMPORARY SUPPORT STRUCTURE

NCHRP 12-79

BRIDGE NISCR2

GENERAL ERECTION PROCEDURE

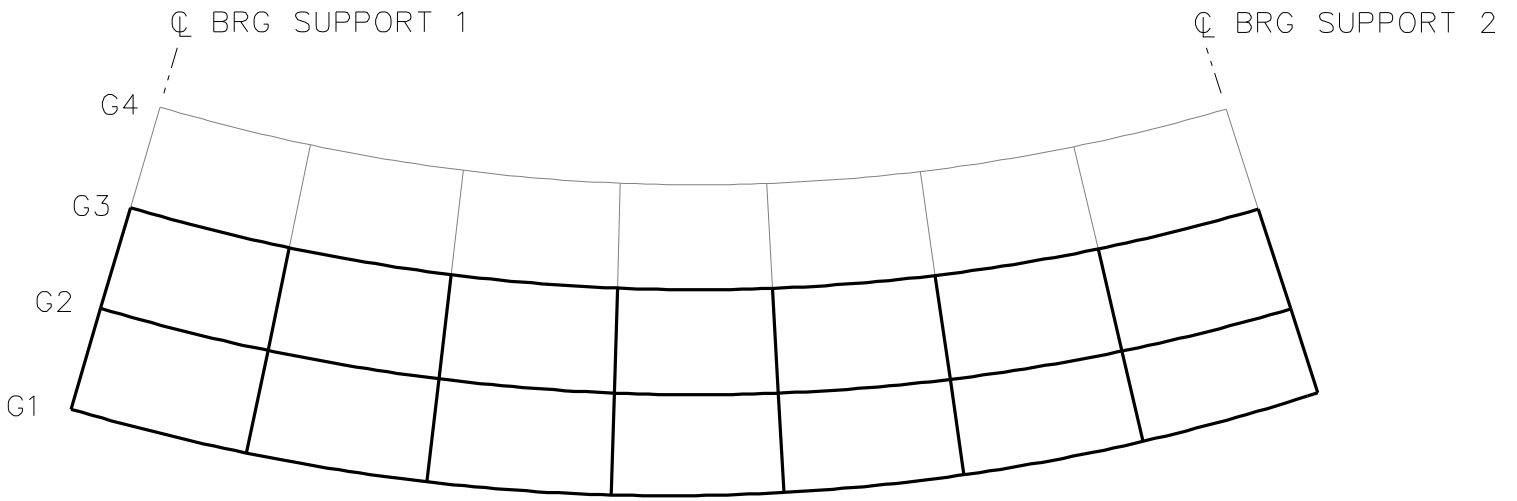

STAGE 3

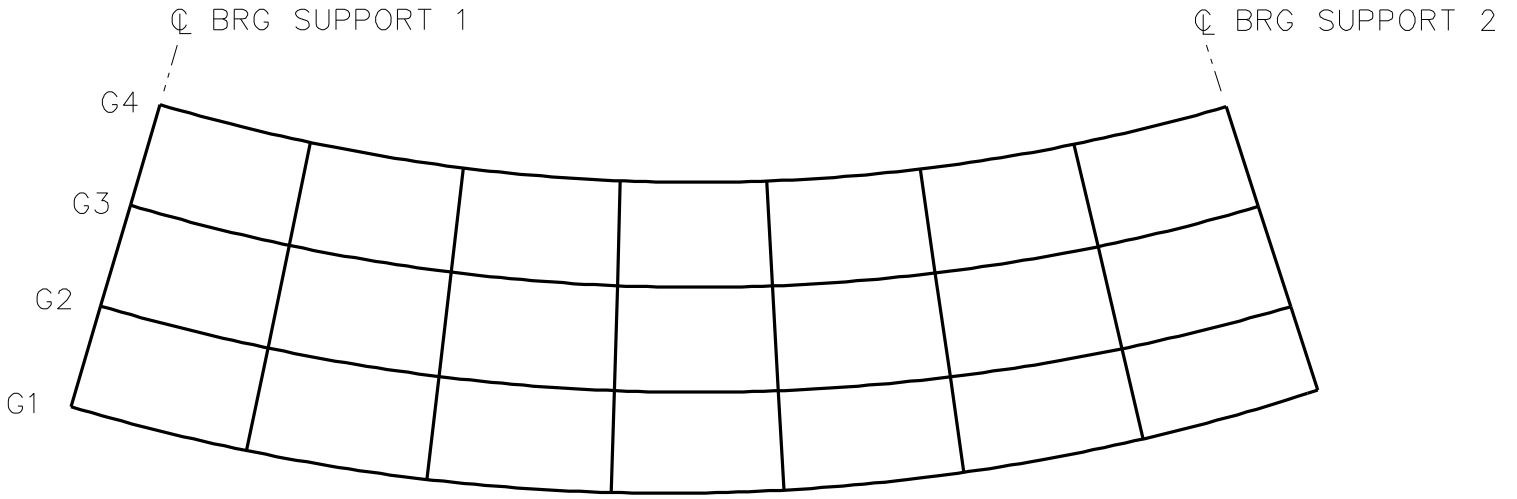

STAGE 4

LEGEND

▽ = HOLD OR LIFT CRANE

○ = TIE DOWN

□ = TEMPORARY SUPPORT STRUCTURE

NCHRP 12-79

BRIDGE NISCR2

GENERAL ERECTION PROCEDURE

NCHRP 12-79

NISCR5

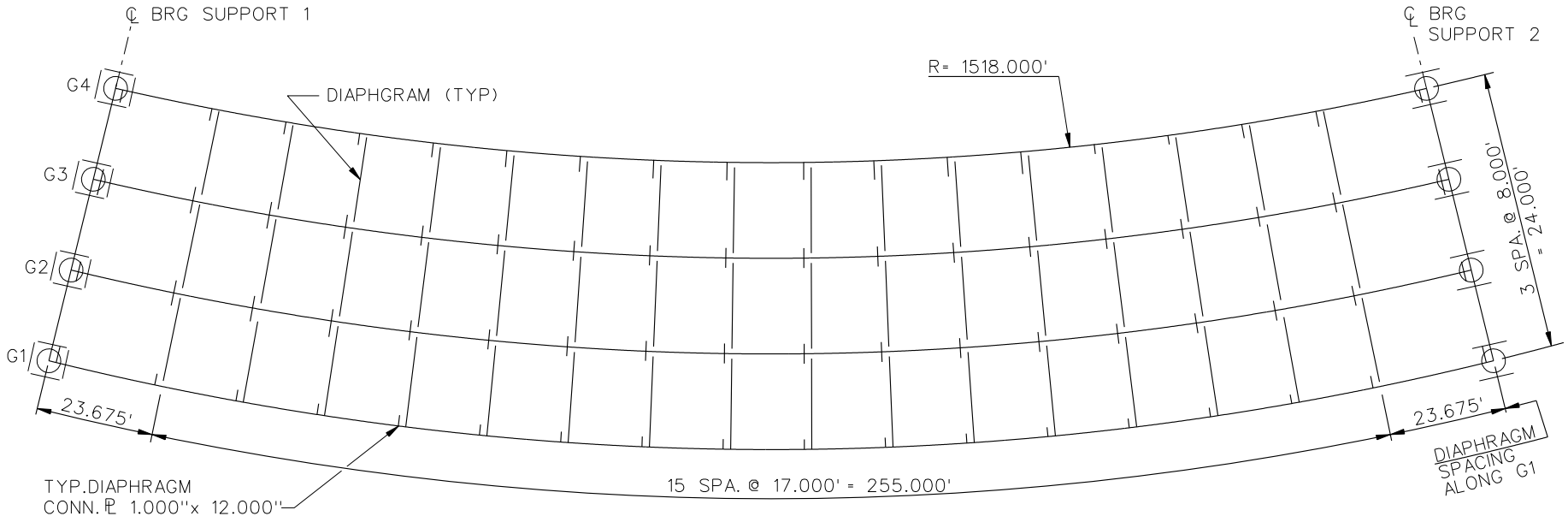

FRAMING PLAN

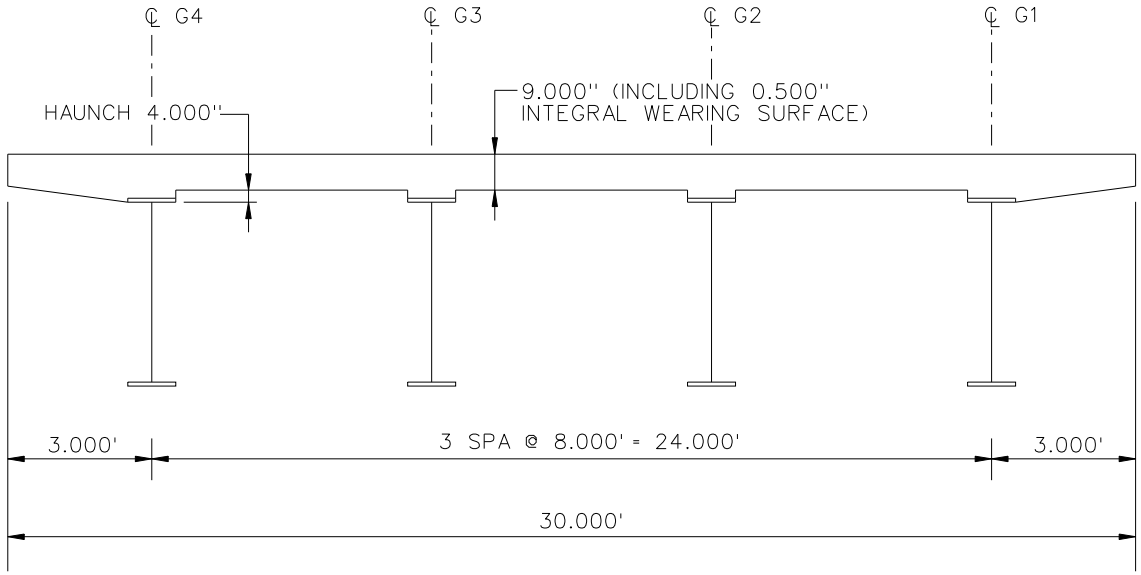

CROSS - SECTION

(DIAPHRAGMS NOT SHOWN)

BEARING LEGEND

- ○ NON-GUIDED
- ⊙ LONGITUDINALLY GUIDED
- |○| TRANSVERSELY GUIDED
- |⊙| FIXED

NCHRP 12-79

BRIDGE NISCR5

FRAMING PLAN AND CROSS-SECTION

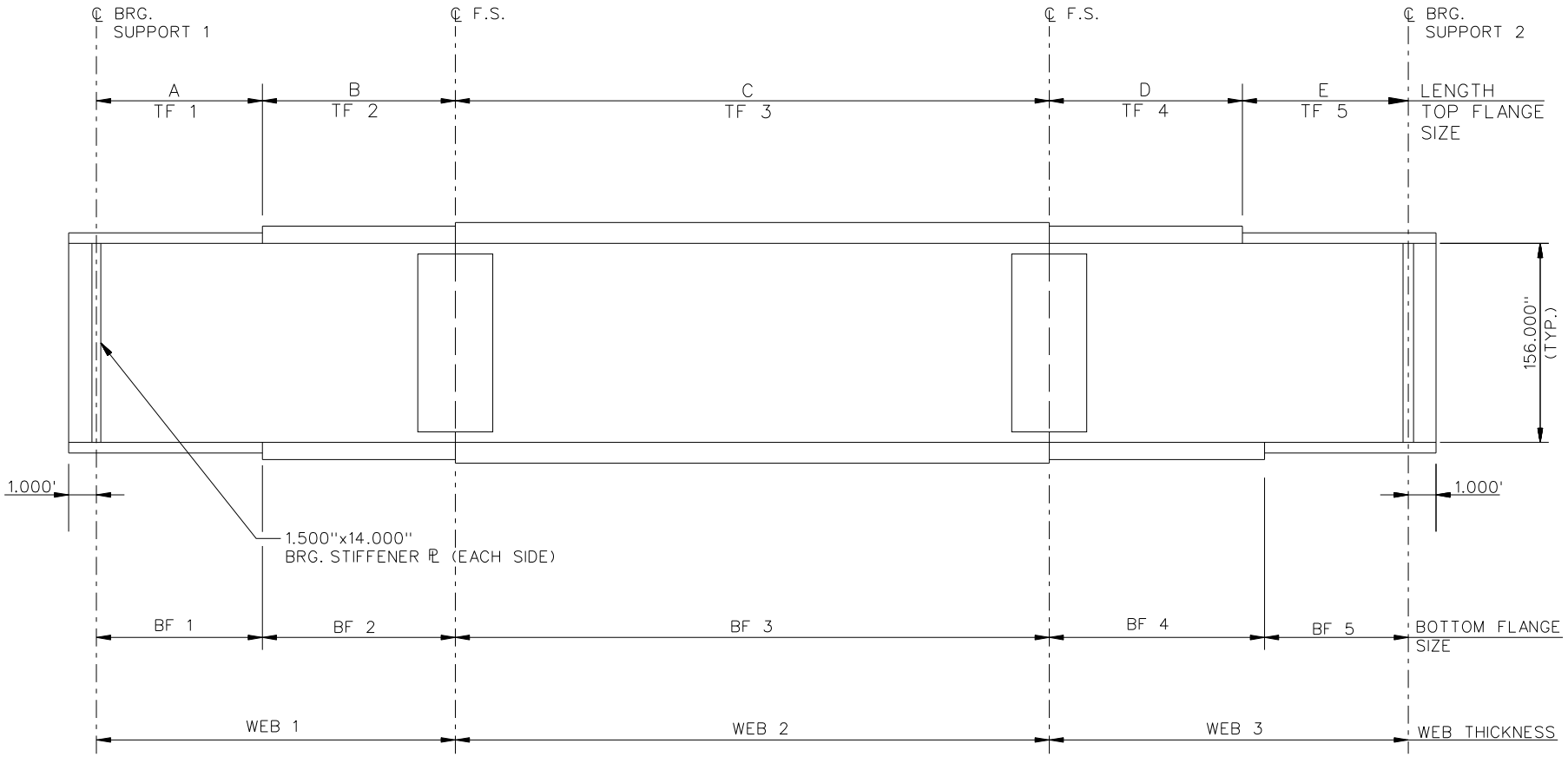

NOTE :

1. SEE TABLES ON SHEET 3 FOR GIRDER ELEVATION DIMENSIONS AND PLATE SIZES.

2. ALL GIRDERS, WEB 1 = WEB 2 = WEB 3 = 1.125".

NCHRP 12-79

BRIDGE NISCR5

GIRDER ELEVATION

SHEET 2 OF 8

	GIRDER PLATE LENGTHS ✳			
LENGTH	G1	G2	G3	G4
A	32.175	31.728	31.281	30.834
B	54.000	54.000	54.000	54.000
C	130.000	129.326	128.651	127.977
D	54.000	54.000	54.000	54.000
E	32.175	31.728	31.281	30.834

✳ ALL DIMENSIONS ARE IN FEET.

	GIRDER FLANGE DIMENSIONS ✳✳							
TOP	G1		G2		G3		G4	
FLANGE	BF	TF	BF	TF	BF	TF	BF	TF
TF1	38.000	1.500	38.000	1.500	32.000	1.375	32.000	1.375
TF2	38.000	2.750	38.000	2.750	32.000	1.375	32.000	1.375
TF3	38.000	3.250	38.000	3.250	32.000	2.000	32.000	2.000
TF4	38.000	2.750	38.000	2.750	32.000	1.375	32.000	1.375
TF5	38.000	1.500	38.000	1.500	32.000	1.375	32.000	1.375

✳✳ ALL DIMENSIONS ARE IN INCHES.

	GIRDER FLANGE DIMENSIONS ✳✳							
BOTTOM	G1		G2		G3		G4	
FLANGE	BF	TF	BF	TF	BF	TF	BF	TF
BF1	44.000	1.875	44.000	1.875	36.000	1.500	36.000	1.500
BF2	44.000	2.750	44.000	2.750	36.000	1.500	36.000	1.500
BF3	44.000	3.250	44.000	3.250	36.000	2.500	36.000	2.500
BF4	44.000	2.750	44.000	2.750	36.000	1.500	36.000	1.500
BF5	44.000	1.875	44.000	1.875	36.000	1.500	36.000	1.500

✳✳ ALL DIMENSIONS ARE IN INCHES.

NCHRP 12-79

BRIDGE NISCR5

GIRDER ELEVATION TABLES

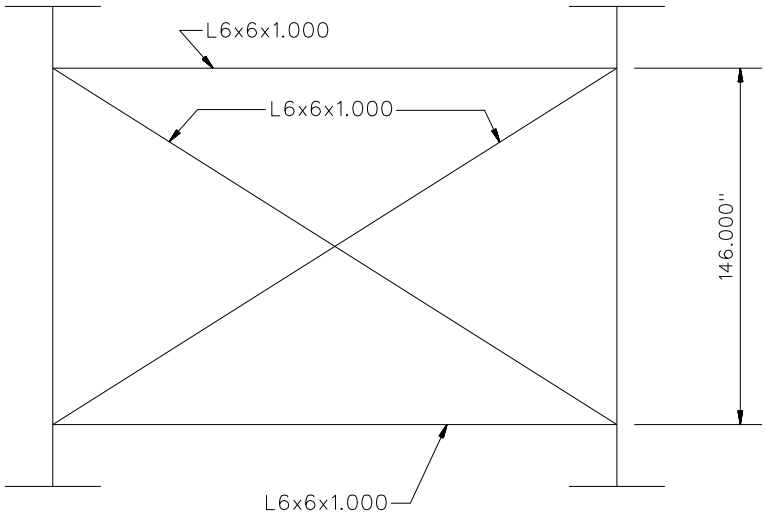

TYPICAL END AND INTERMEDIATE DIAPHRAGM

NOTES:

1. STEEL DEAD LOAD INCREASED BY 5% FOR MDX AND LARSA MODELS; 2% FOR 3D MODEL; AND 10% FOR APPROXIMATE ANALYSIS TO ACCOUNT FOR MISC. DETAILS.

2. FORMWORK LOAD OF 10PSF IS INCLUDED IN CONCRETE DEAD LOAD.

3. ADDITIONAL DESIGN PARAMETERS:
   A. 1.500' PARAPET WIDTH BOTH SIDES.
   B. 700 LB/FT UNIFORM LOAD ASSUMED FOR PARAPET WEIGHT.
   C. ROADWAY WIDTH = 26.500'.
   D. NUMBER OF DESIGN LANES = 2.
   E. HL93 LIVE LOAD.

4. DIAPHRAGM MEMBER CALL-OUTS ARE IN ENGLISH UNITS.

NCHRP 12-79

BRIDGE NISCR5

MISC. DETAILS AND NOTES

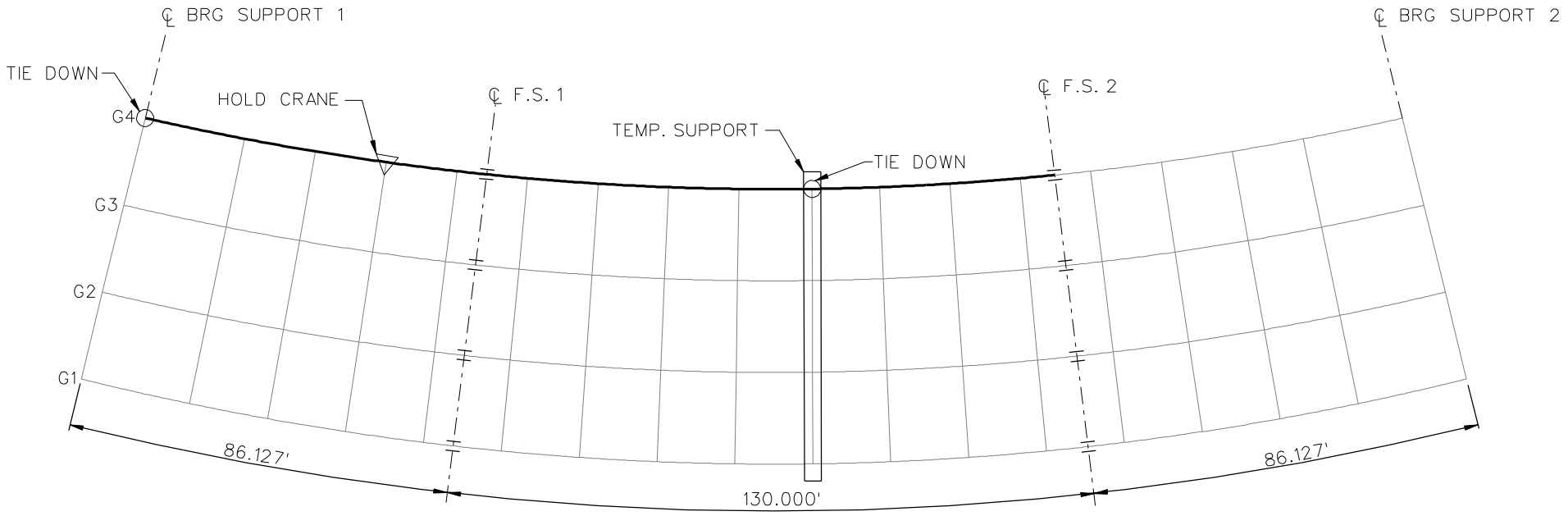

STAGE 1

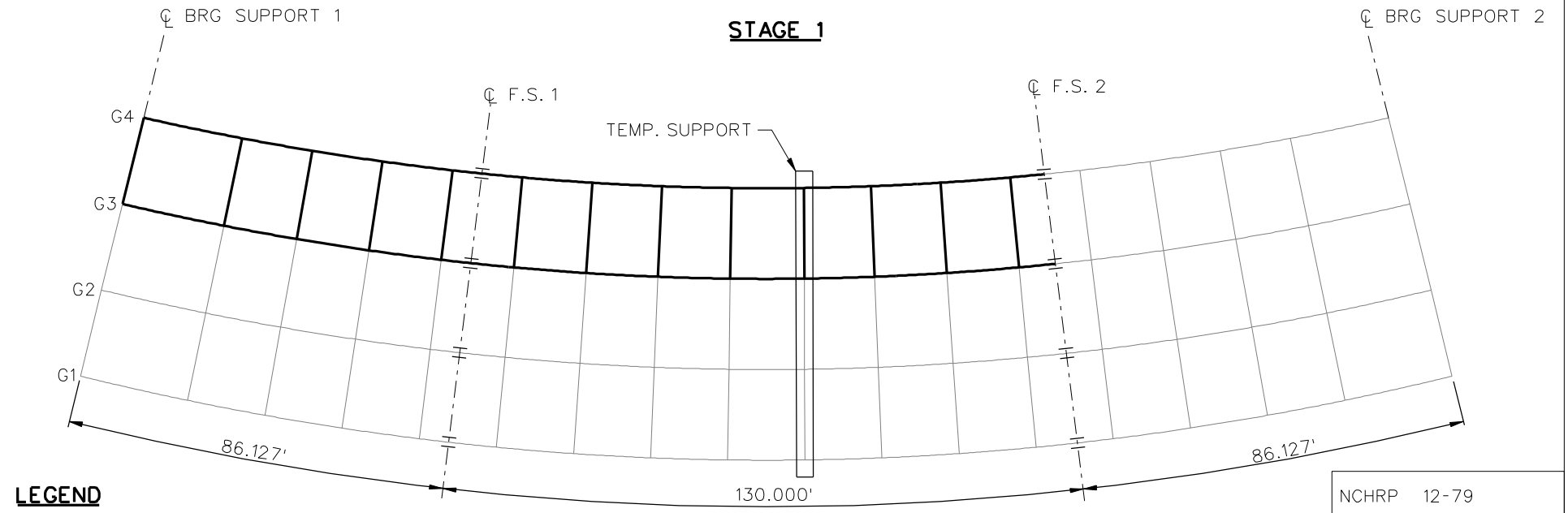

STAGE 2

LEGEND

▽ = HOLD OR LIFT CRANE

○ = TIE DOWN

□ = TEMPORARY SUPPORT STRUCTURE

NCHRP 12-79

BRIDGE NISCR5

GENERAL ERECTION PROCEDURE

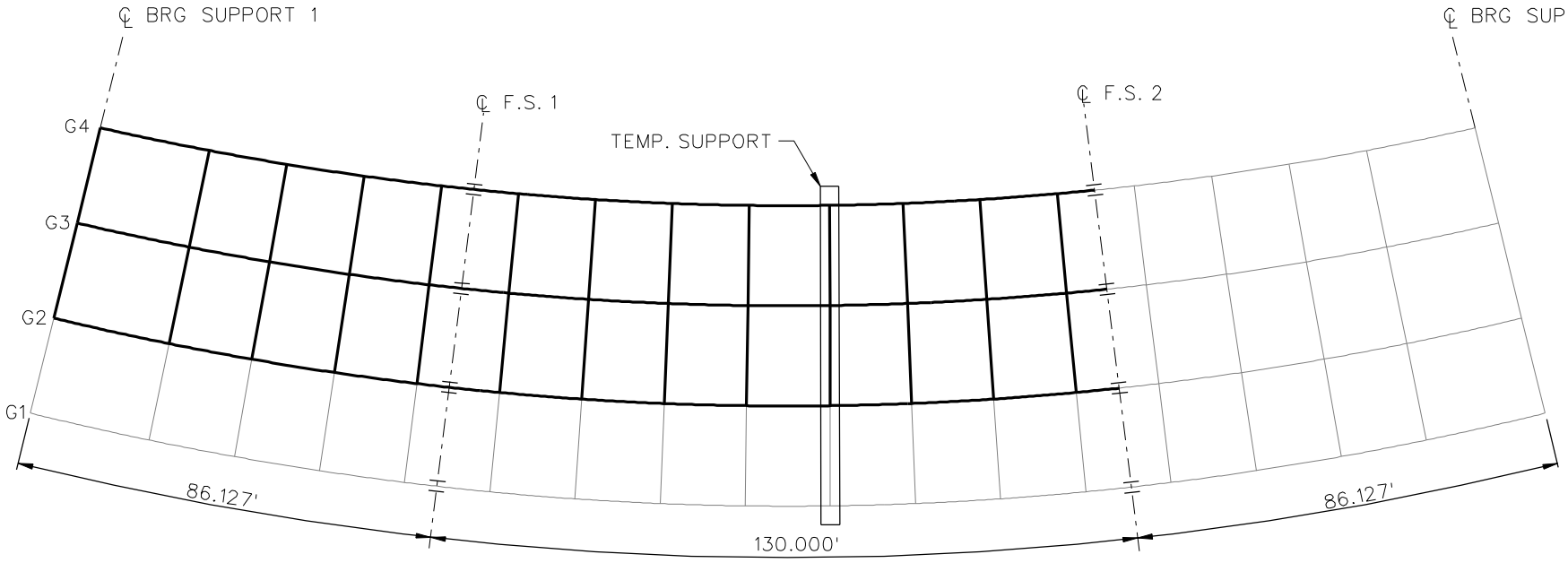

STAGE 3

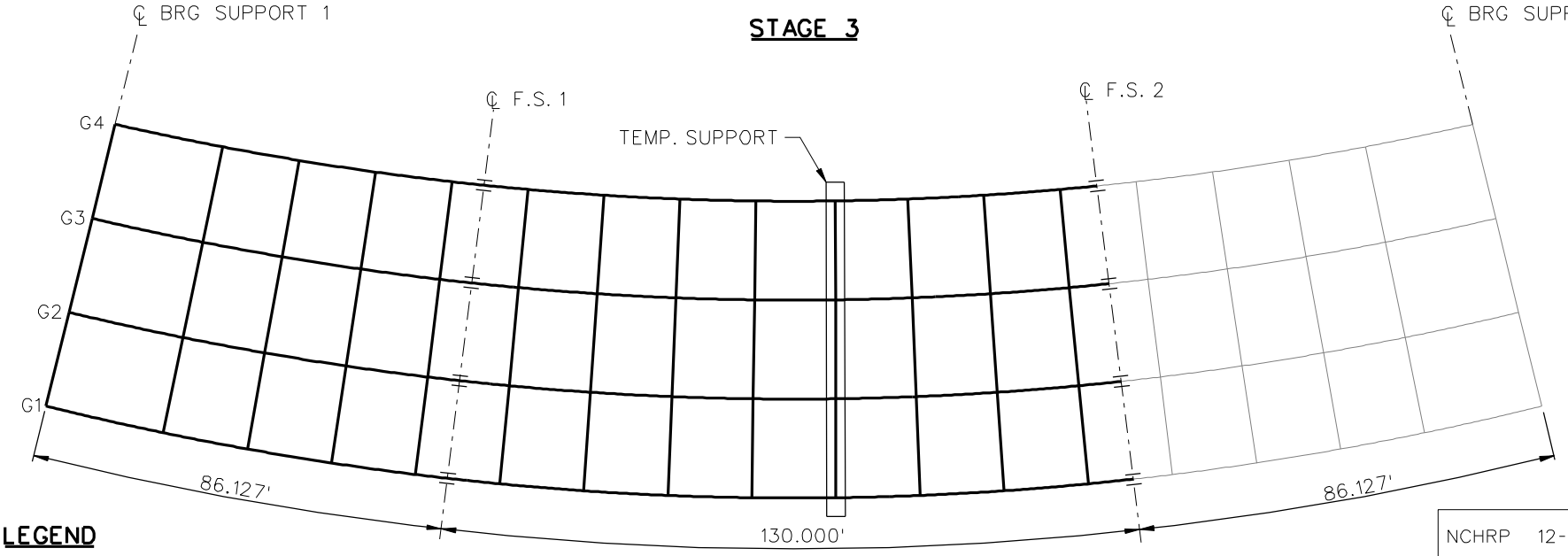

STAGE 4

LEGEND

▽ = HOLD OR LIFT CRANE

○ = TIE DOWN

□ = TEMPORARY SUPPORT STRUCTURE

NCHRP 12-79

BRIDGE NISCR5

GENERAL ERECTION PROCEDURE

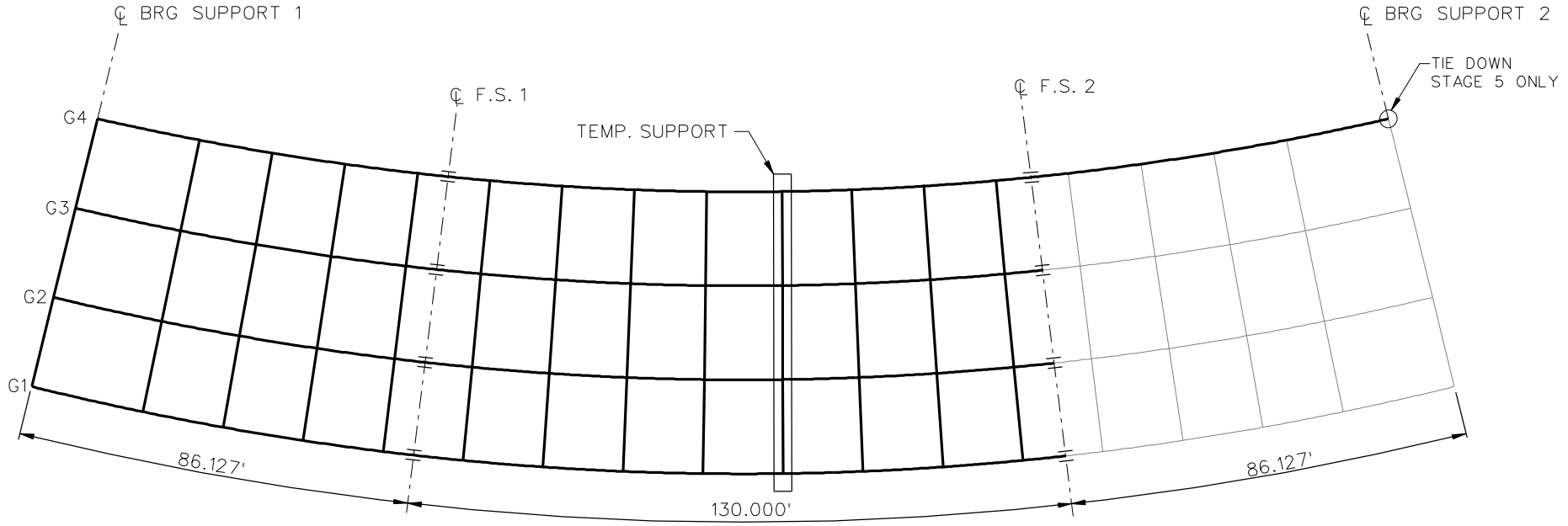

STAGE 5

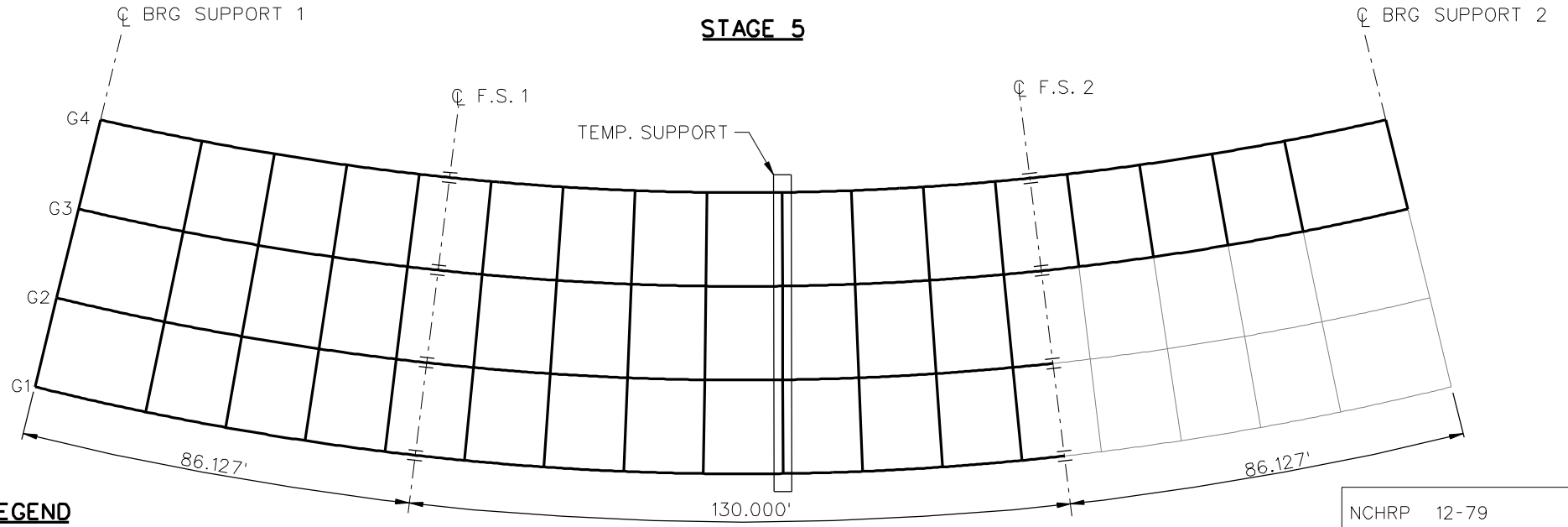

STAGE 6

LEGEND

▽ = HOLD OR LIFT CRANE

○ = TIE DOWN

□ = TEMPORARY SUPPORT STRUCTURE

NCHRP 12-79

BRIDGE NISCR5

GENERAL ERECTION PROCEDURE

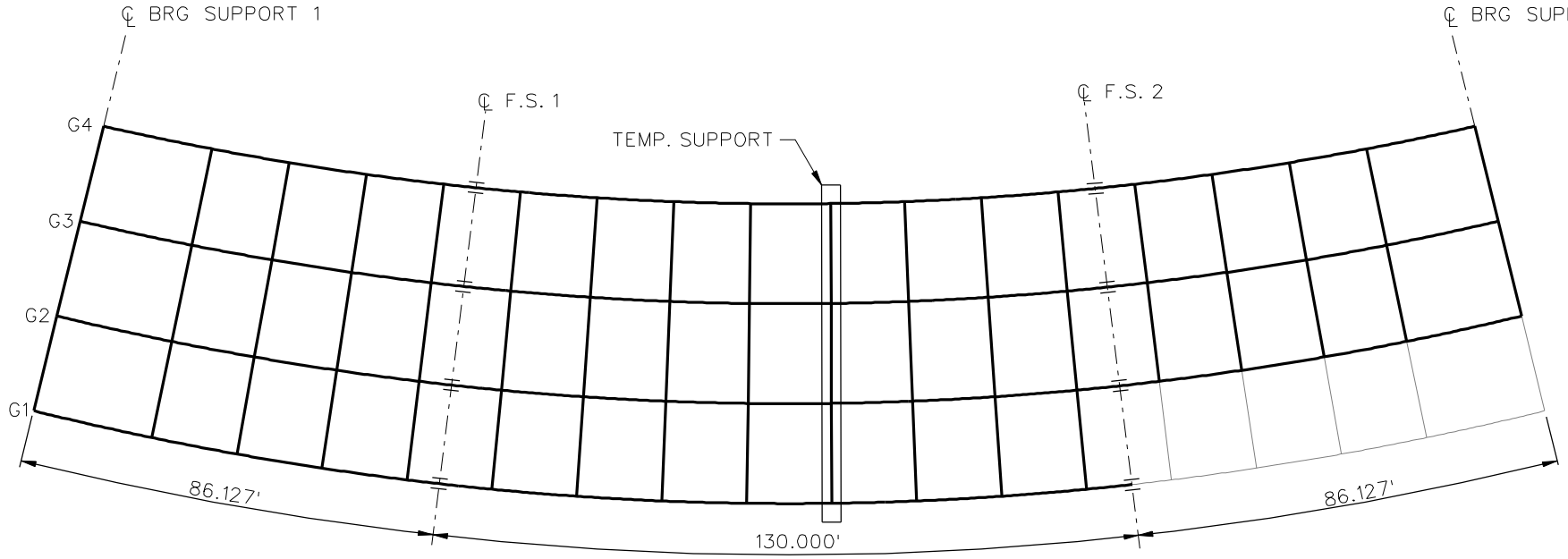

STAGE 7

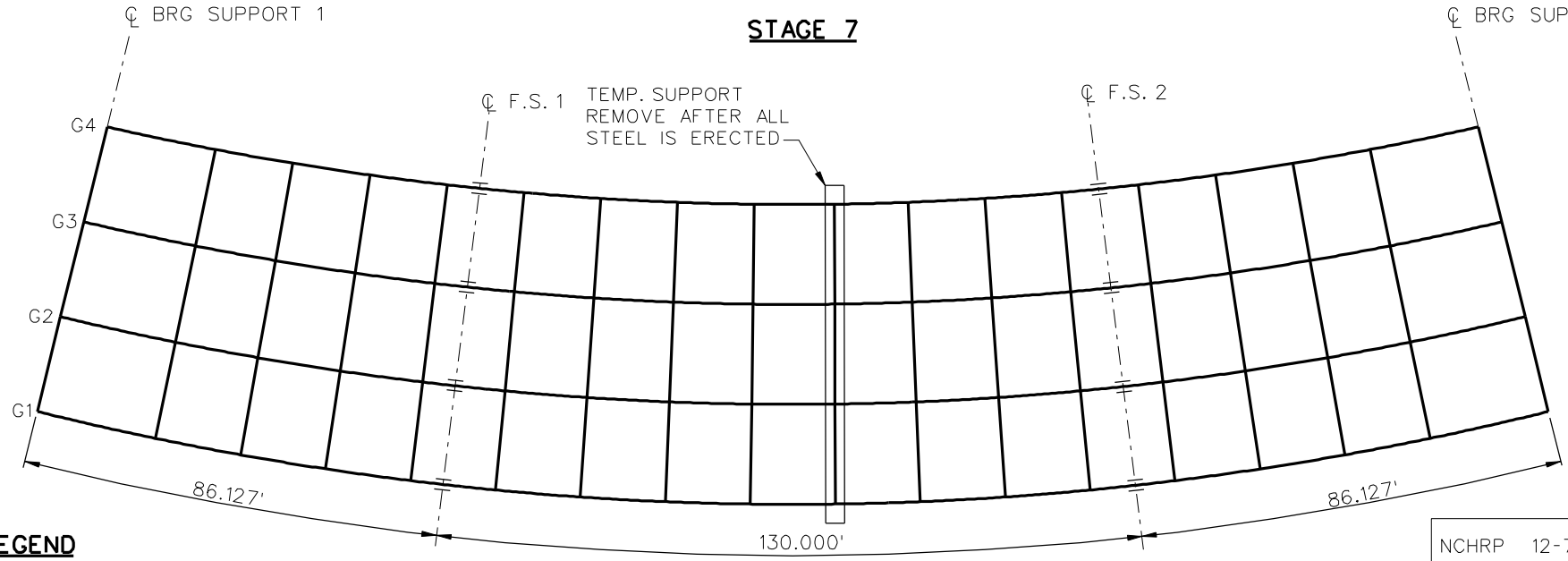

STAGE 8

LEGEND

▽ = HOLD OR LIFT CRANE

○ = TIE DOWN

□ = TEMPORARY SUPPORT STRUCTURE

NCHRP 12-79

BRIDGE NISCR5

GENERAL ERECTION PROCEDURE

SHEET 8 OF 8

NCHRP 12-79

NISCR7

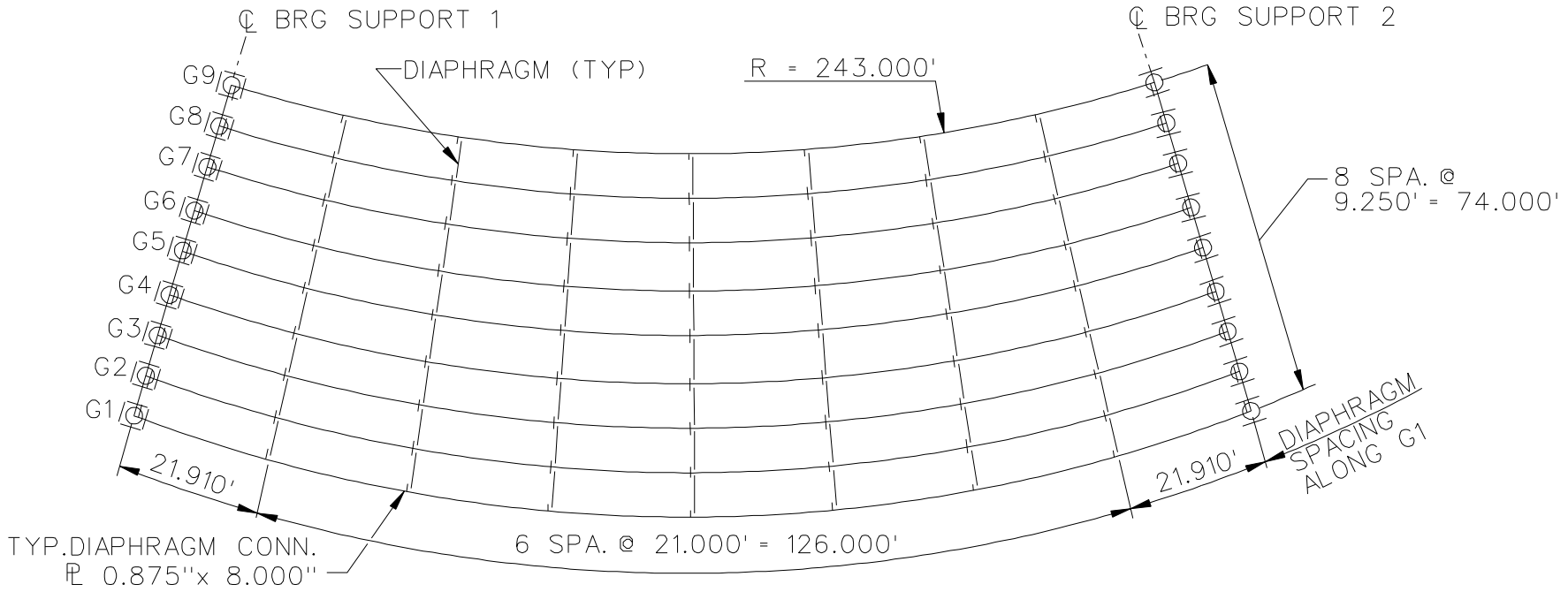

FRAMING PLAN

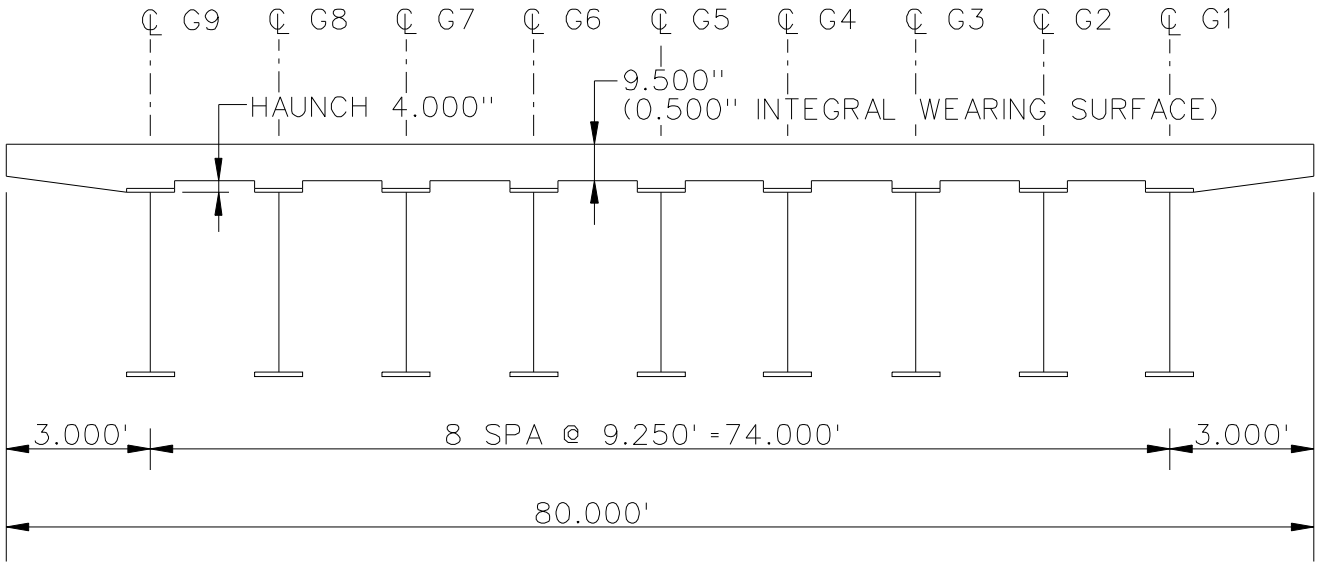

CROSS - SECTION

(DIAPHRAGMS NOT SHOWN)

BEARING LEGEND

- ○ NON-GUIDED
- ⊖ LONGITUDINALLY GUIDED
- |○| TRANSVERSELY GUIDED
- |⊖| FIXED

NCHRP 12-79

BRIDGE NISCR7

FRAMING PLAN AND CROSS-SECTION

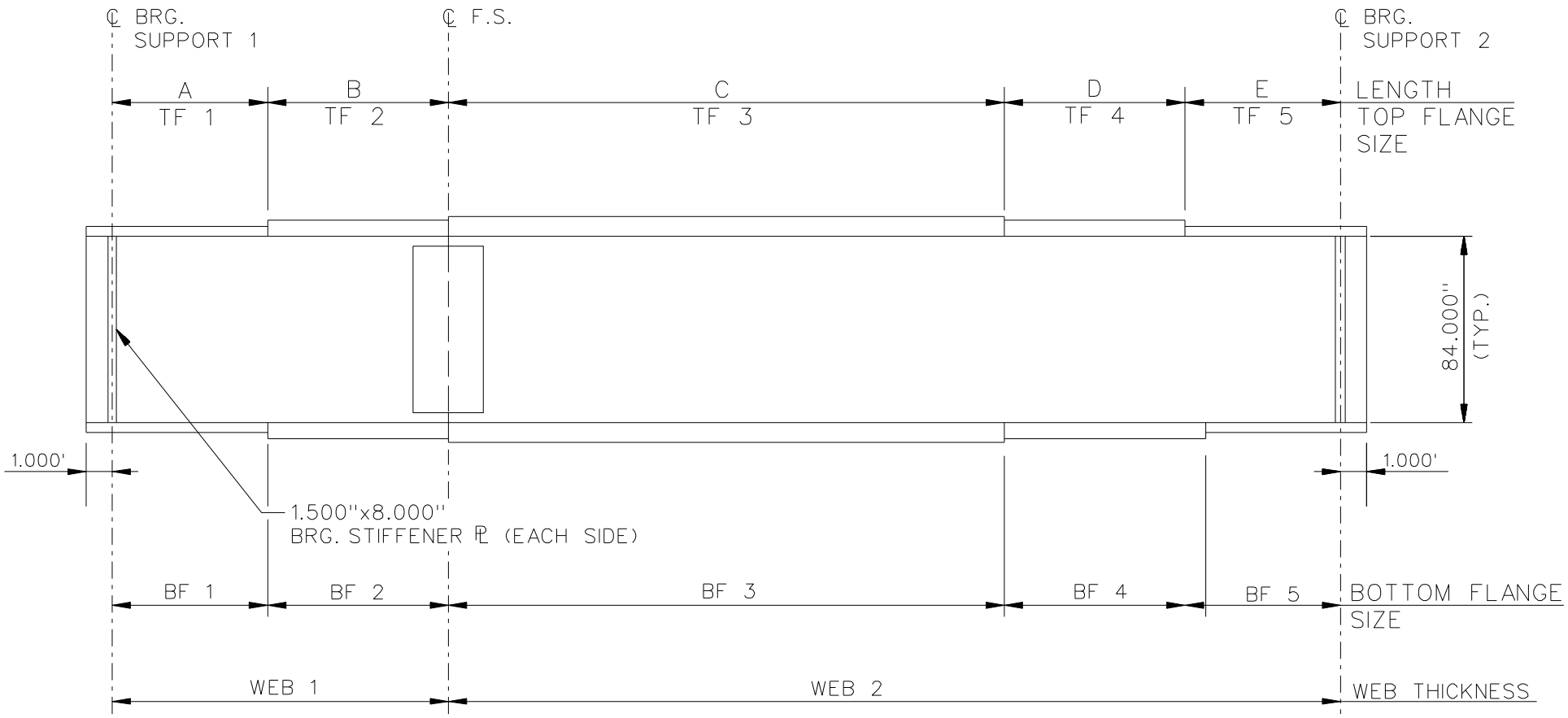

NOTE :

1. SEE TABLES ON SHEET 3 FOR GIRDER ELEVATION DIMENSIONS AND PLATE SIZES.
2. GIRDERS G1, G2, G3, WEB 1 = WEB 2 = 0.750".
3. GIRDERS G4 - G9, WEB 1 = WEB 2 = 0.625".

NCHRP 12-79

BRIDGE NISCR7

GIRDER ELEVATION

SHEET 2 OF 6

	GIRDER PLATE LENGTHS ✳								
LENGTH	G1	G2	G3	G4	G5	G6	G7	G8	G9
A	25.000	24.271	23.541	22.812	22.082	21.353	20.623	19.894	19.164
B	25.000	24.271	23.541	22.812	22.082	21.353	20.623	19.894	19.164
C	69.821	67.784	65.747	63.709	61.672	59.635	57.597	55.560	53.522
D	25.000	24.271	23.541	22.812	22.082	21.353	20.623	19.894	19.164
E	25.000	24.271	23.541	22.812	22.082	21.353	20.623	19.894	19.164

✳ ALL DIMENSIONS ARE IN FEET.

	GIRDER FLANGE DIMENSIONS ✳✳					
TOP	G1, G2, G3		G4, G5, G6		G7, G8, G9	
FLANGE	BF	TF	BF	TF	BF	TF
TF1	24.000	1.000	20.000	1.000	18.000	1.000
TF2	24.000	1.500	20.000	1.000	18.000	1.000
TF3	24.000	2.250	20.000	1.500	18.000	1.000
TF4	24.000	1.500	20.000	1.000	18.000	1.000
TF5	24.000	1.000	20.000	1.000	18.000	1.000

✳✳ ALL DIMENSIONS ARE IN INCHES.

	GIRDER FLANGE DIMENSIONS ✳✳					
BOTTOM	G1, G2, G3		G4, G5, G6		G7, G8, G9	
FLANGE	BF	TF	BF	TF	BF	TF
BF1	30.000	1.250	22.000	1.000	18.000	1.000
BF2	30.000	2.250	22.000	1.000	18.000	1.000
BF3	30.000	3.000	22.000	1.500	18.000	1.500
BF4	30.000	2.250	22.000	1.000	18.000	1.000
BF5	30.000	1.250	22.000	1.000	18.000	1.000

✳✳ ALL DIMENSIONS ARE IN INCHES.

NCHRP 12-79

BRIDGE NISCR7

GIRDER ELEVATION TABLES

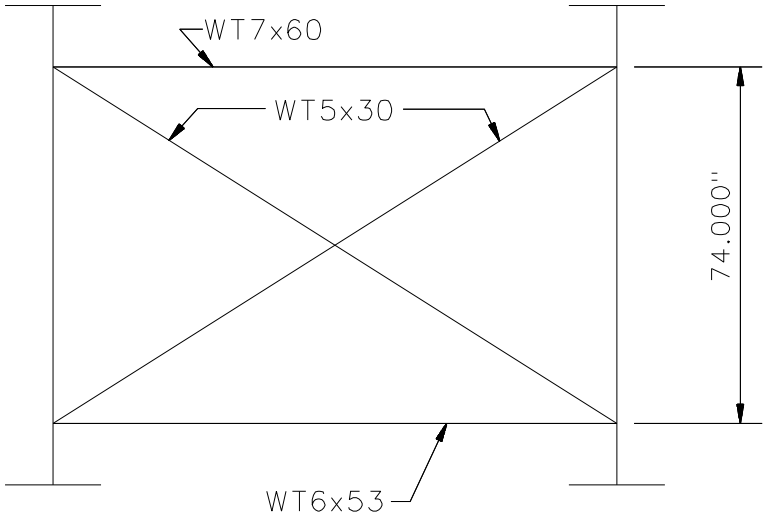

TYPICAL END AND INTERMEDIATE DIAPHRAGM

NOTES:

1. STEEL DEAD LOAD INCREASED BY 5% FOR MDX AND LARSA MODELS; 2% FOR 3D MODEL; AND 10% FOR APPROXIMATE ANALYSIS TO ACCOUNT FOR MISC. DETAILS.

2. FORMWORK LOAD OF 10PSF IS INCLUDED IN CONCRETE DEAD LOAD.

3. ADDITIONAL DESIGN PARAMETERS:
   A. 1.500' PARAPET WIDTH BOTH SIDES.
   B. 700 LB/FT UNIFORM LOAD ASSUMED FOR PARAPET WEIGHT.
   C. ROADWAY WIDTH = 77.000'.
   D. NUMBER OF DESIGN LANES = 6.
   E. HL93 LIVE LOAD.

4. DIAPHRAGM MEMBER CALL-OUTS ARE IN UNITS OF INCHES.

NCHRP 12-79

BRIDGE NISCR7

MISC. DETAILS AND NOTES

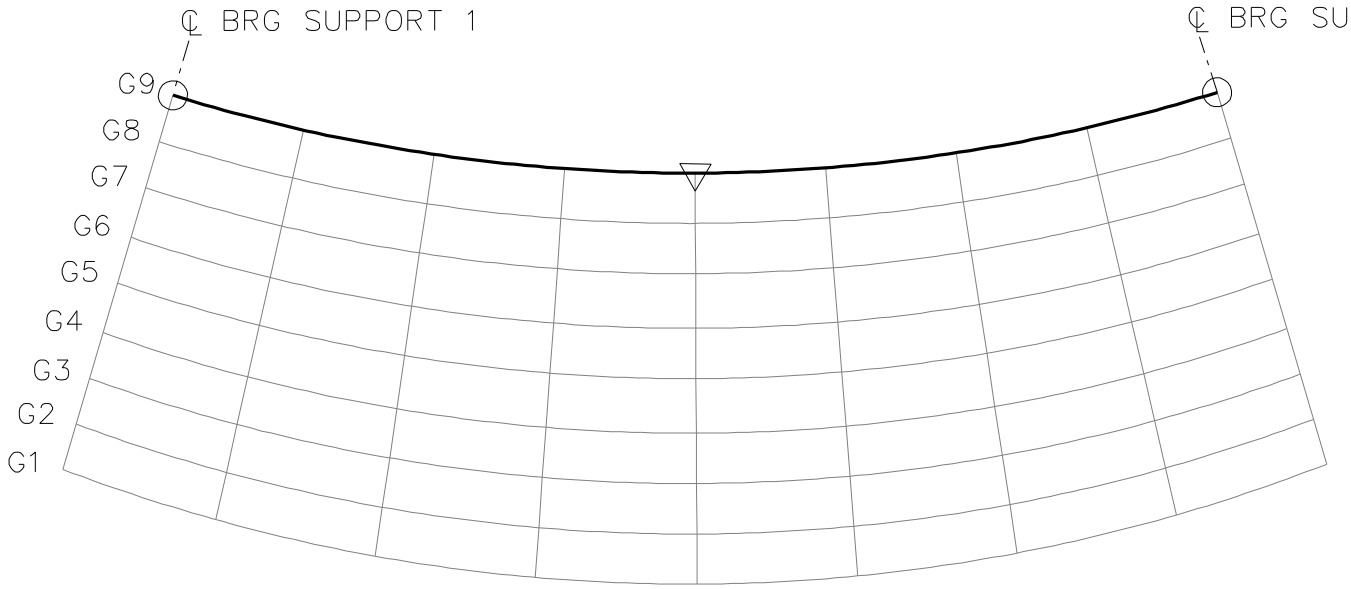

STAGE 1

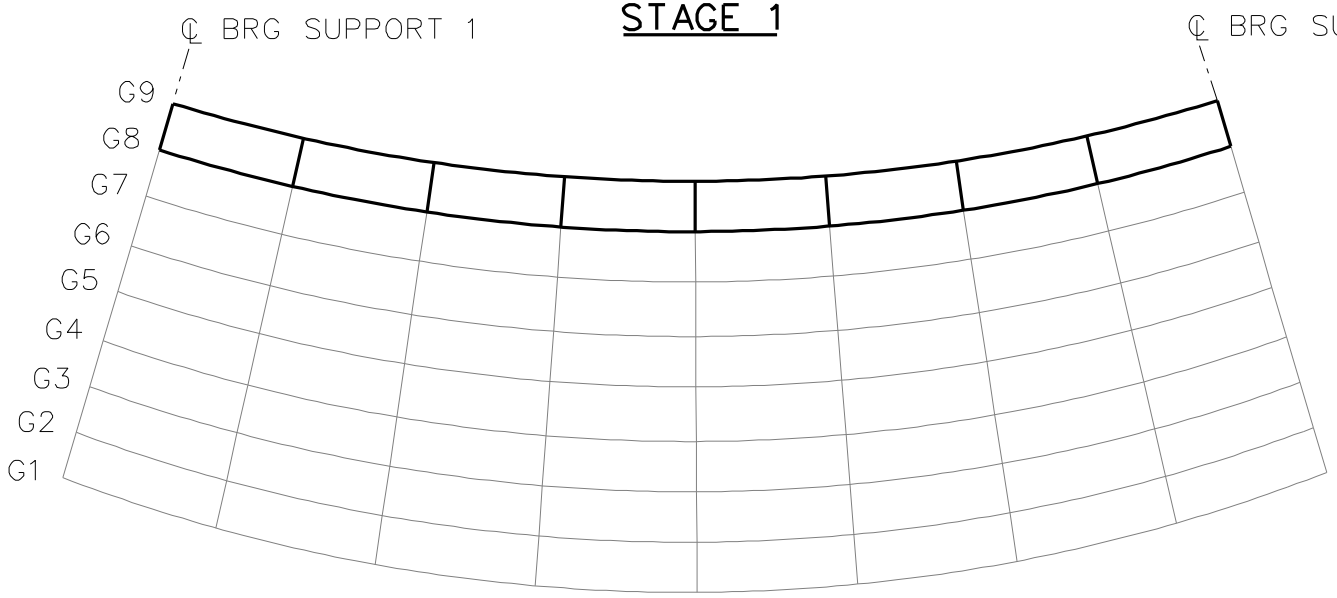

STAGE 2

LEGEND

▽ = HOLD OR LIFT CRANE

○ = TIE DOWN

□ = TEMPORARY SUPPORT STRUCTURE

NCHRP 12-79

BRIDGE NISCR7

GIRDER ERECTION PROCEDURE

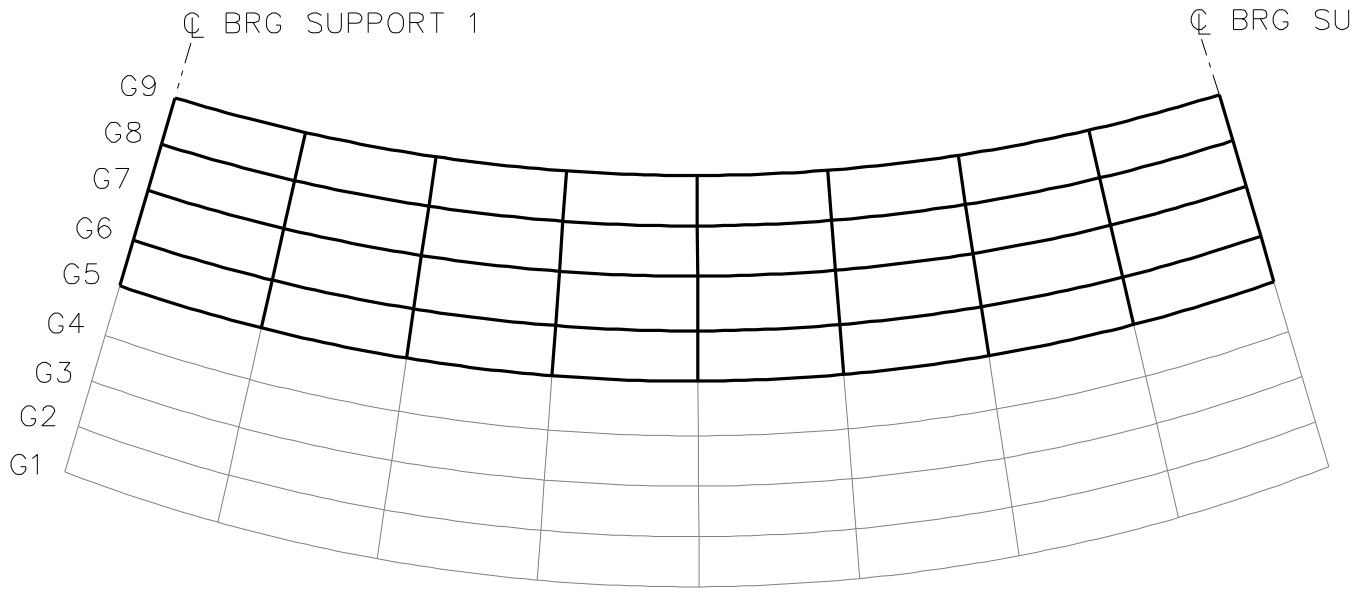

STAGE 5

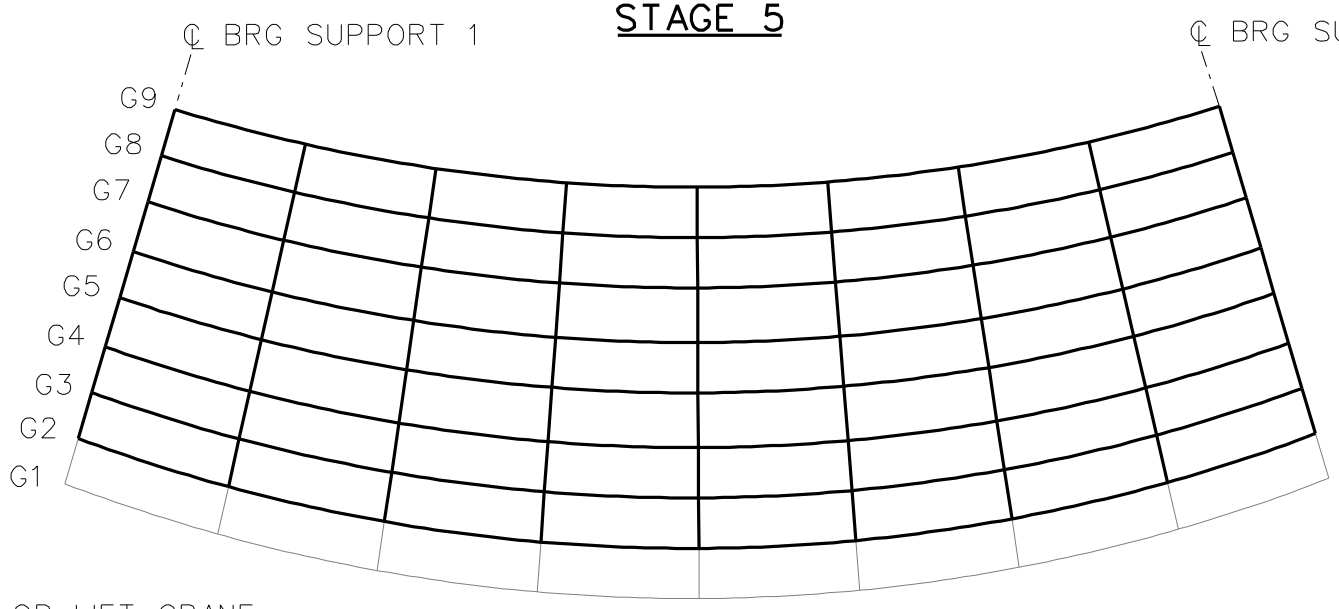

STAGE 8

LEGEND

▽ = HOLD OR LIFT CRANE

○ = TIE DOWN

□ = TEMPORARY SUPPORT STRUCTURE

NCHRP 12-79

BRIDGE NISCR7

GENERAL ERECTION PROCEDURE

NCHRP 12-79

NISCR8

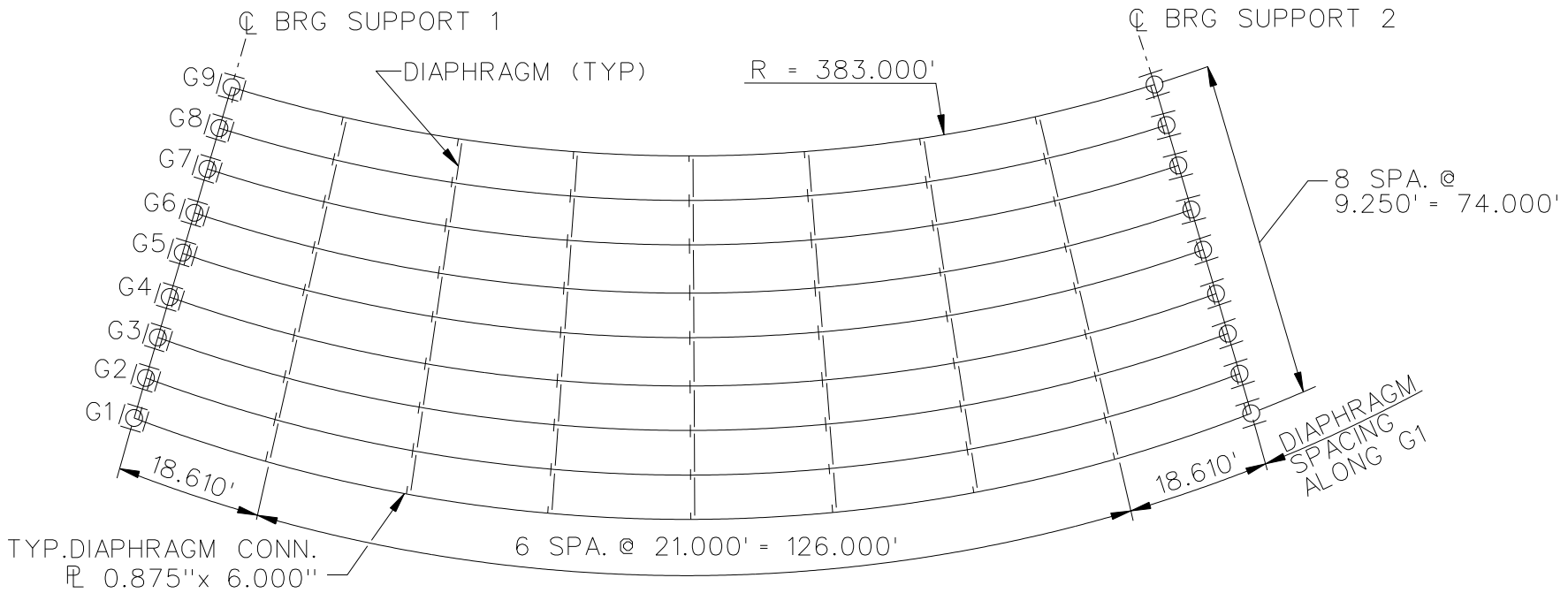

FRAMING PLAN

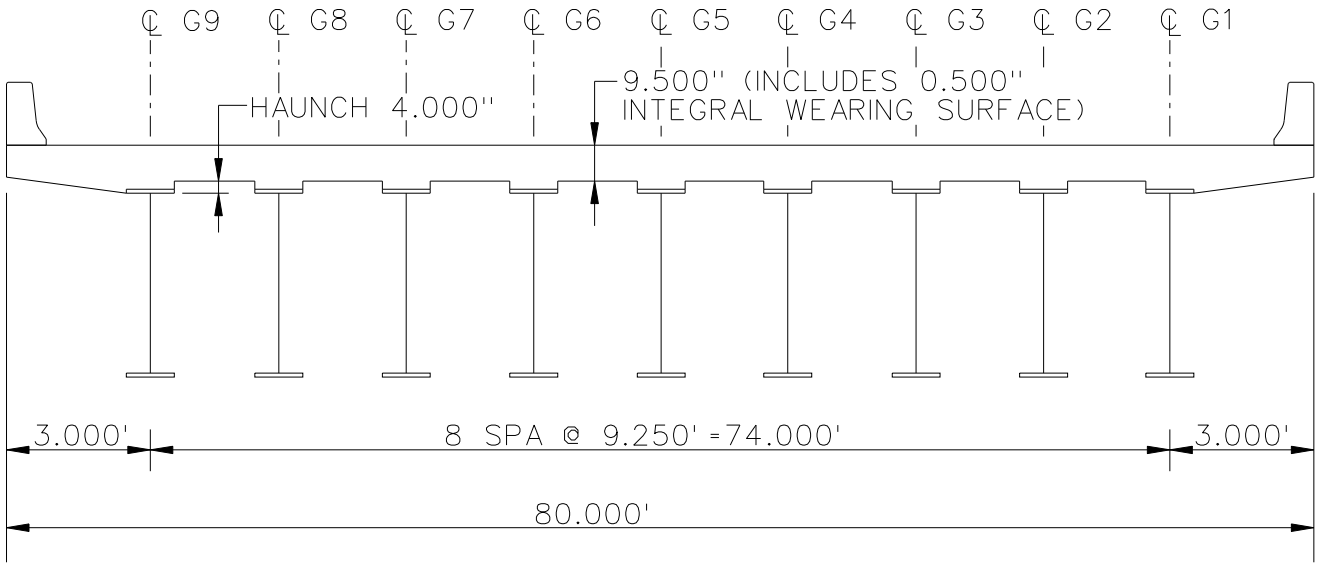

CROSS - SECTION

(DIAPHRAGMS NOT SHOWN)

BEARING LEGEND

- ○ NON-GUIDED
- ⊖ LONGITUDINALLY GUIDED
- |○| TRANSVERSELY GUIDED
- |⊖| FIXED

NCHRP 12-79

BRIDGE NISCR8

FRAMING PLAN AND CROSS-SECTION

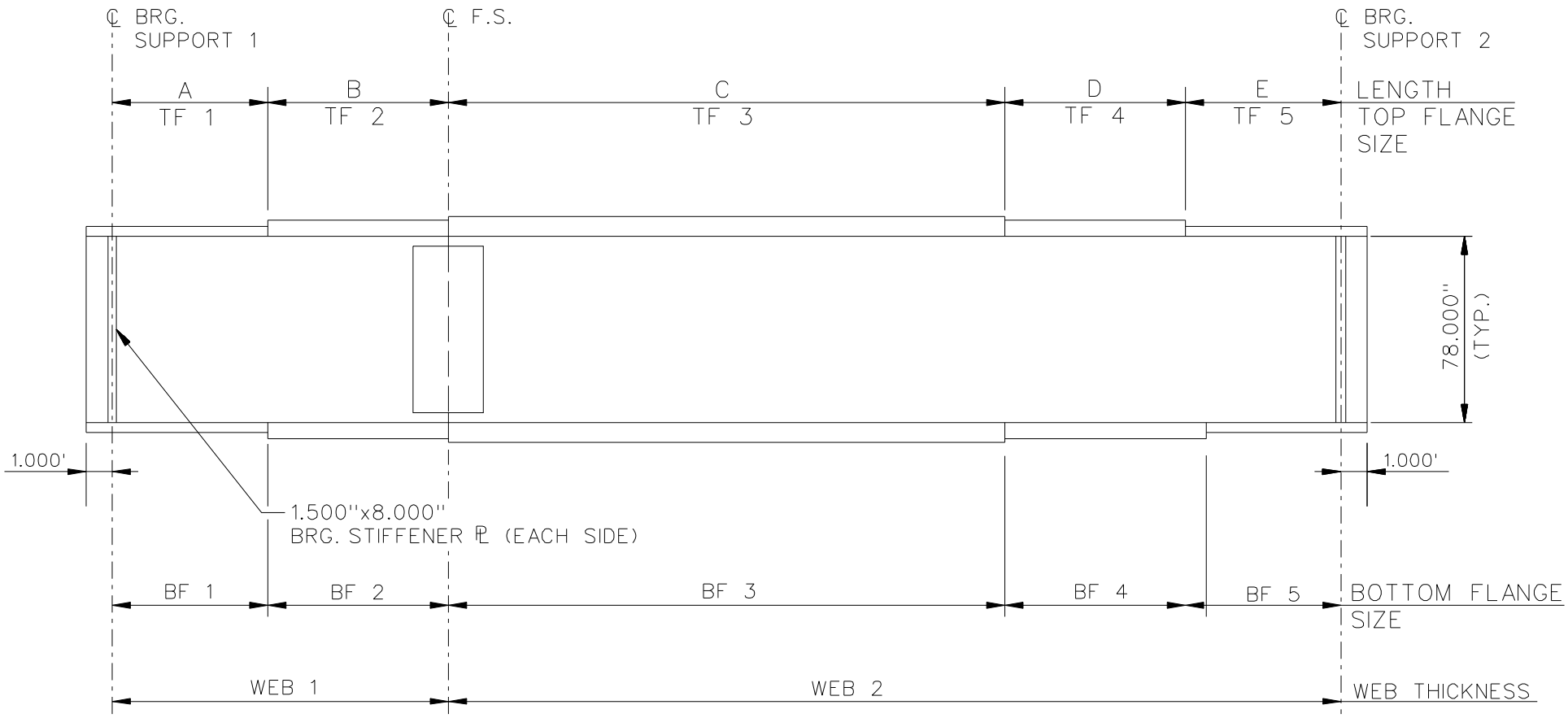

NOTE :

1. SEE TABLES ON SHEET 3 FOR GIRDER ELEVATION DIMENSIONS AND PLATE SIZES.
2. GIRDERS G1 - G4, WEB 1 = WEB 2 = 0.688".
3. GIRDERS G5 - G9, WEB 1 = WEB 2 = 0.625".

NCHRP 12-79

BRIDGE NISCR8

GIRDER ELEVATION

SHEET 2 OF 7

	GIRDER PLATE LENGTHS ✳								
LENGTH	G1	G2	G3	G4	G5	G6	G7	G8	G9
A	25.000	24.490	23.990	23.480	22.980	22.470	21.960	21.460	20.950
B	25.000	24.490	23.990	23.480	22.980	22.470	21.960	21.460	20.950
C	63.210	61.490	60.660	59.380	58.100	56.820	55.540	52.260	52.980
D	25.000	24.490	23.990	23.480	22.980	22.470	21.960	21.460	20.950
E	25.000	24.490	23.990	23.480	22.980	22.470	21.960	21.460	20.950

✳ ALL DIMENSIONS ARE IN FEET.

	GIRDER FLANGE DIMENSIONS ✳✳					
TOP	G1, G2, G3		G4, G5, G6		G7, G8, G9	
FLANGE	BF	TF	BF	TF	BF	TF
TF1	20.000	1.000	20.000	1.000	18.000	1.000
TF2	20.000	1.250	20.000	1.000	18.000	1.000
TF3	20.000	2.250	20.000	1.500	18.000	1.000
TF4	20.000	1.250	20.000	1.000	18.000	1.000
TF5	20.000	1.000	20.000	1.000	18.000	1.000

✳✳ ALL DIMENSIONS ARE IN INCHES.

	GIRDER FLANGE DIMENSIONS ✳✳					
BOTTOM	G1, G2, G3		G4, G5, G6		G7, G8, G9	
FLANGE	BF	TF	BF	TF	BF	TF
BF1	24.000	1.250	20.000	1.000	18.000	1.000
BF2	24.000	2.250	20.000	1.000	18.000	1.000
BF3	24.000	2.750	20.000	1.500	18.000	1.500
BF4	24.000	2.250	20.000	1.000	18.000	1.000
BF5	24.000	1.250	20.000	1.000	18.000	1.000

✳✳ ALL DIMENSIONS ARE IN INCHES.

NCHRP 12-79

BRIDGE NISCR8

GIRDER ELEVATION TABLES

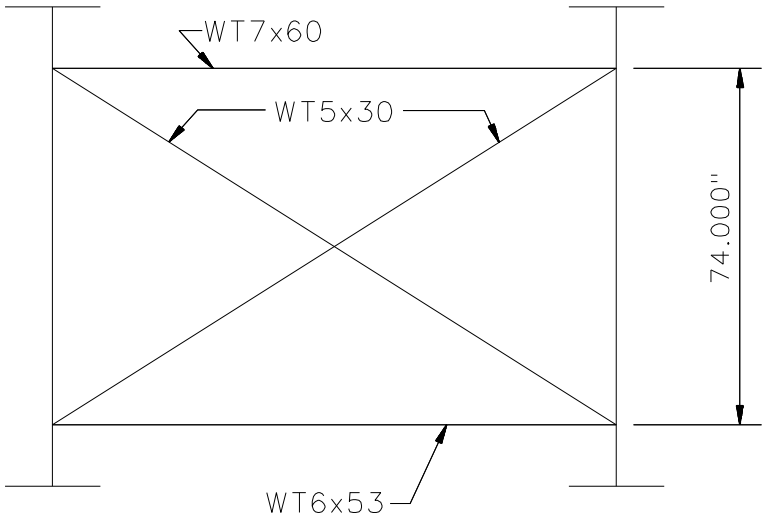

TYPICAL END AND INTERMEDIATE DIAPHRAGM

NOTES:

1. STEEL DEAD LOAD INCREASED BY 5% FOR MDX AND LARSA MODELS; 2% FOR 3D MODEL; AND 10% FOR APPROXIMATE ANALYSIS TO ACCOUNT FOR MISC. DETAILS.

2. FORMWORK LOAD OF 10PSF IS INCLUDED IN CONCRETE DEAD LOAD.

3. LIVE LOAD = HL93
   NO. OF DESIGN LANES = 6.

4. BARRIER WEIGHT = 700 LBS/LF (UNIFORM LOAD).

NCHRP 12-79

BRIDGE NISCR8

MISC. DETAILS AND NOTES

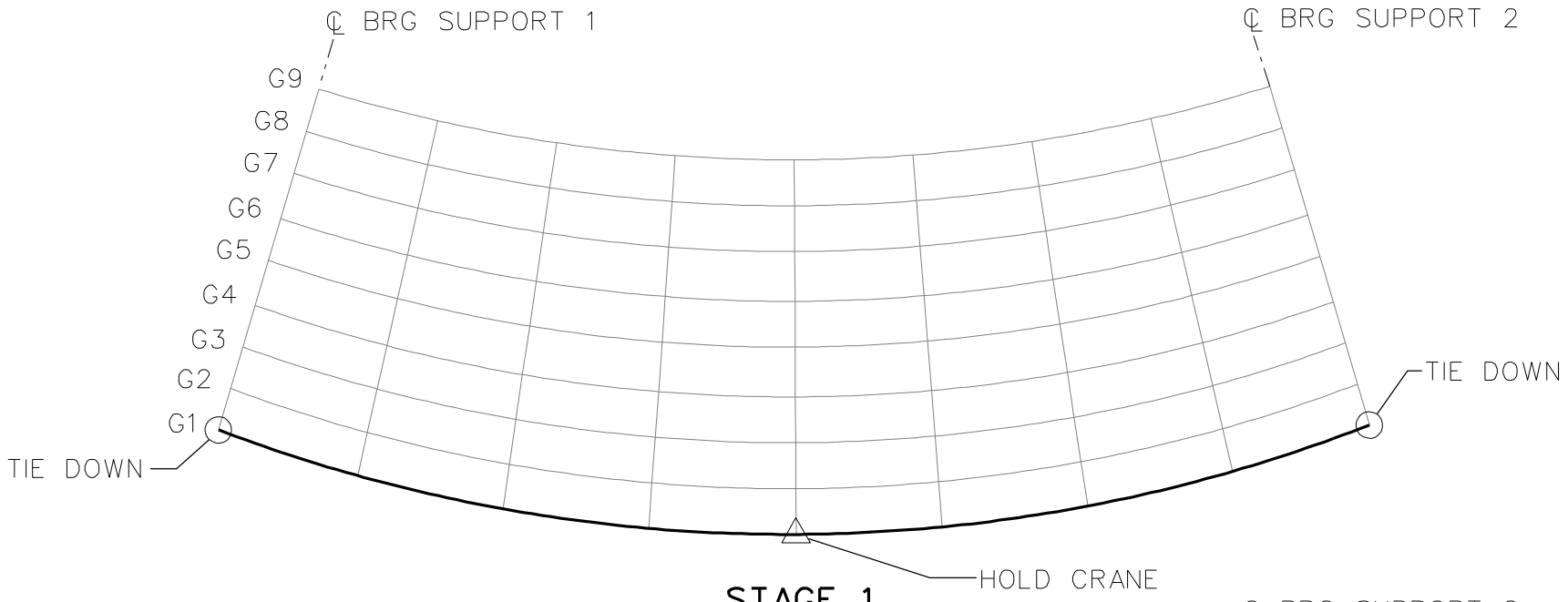

STAGE 1

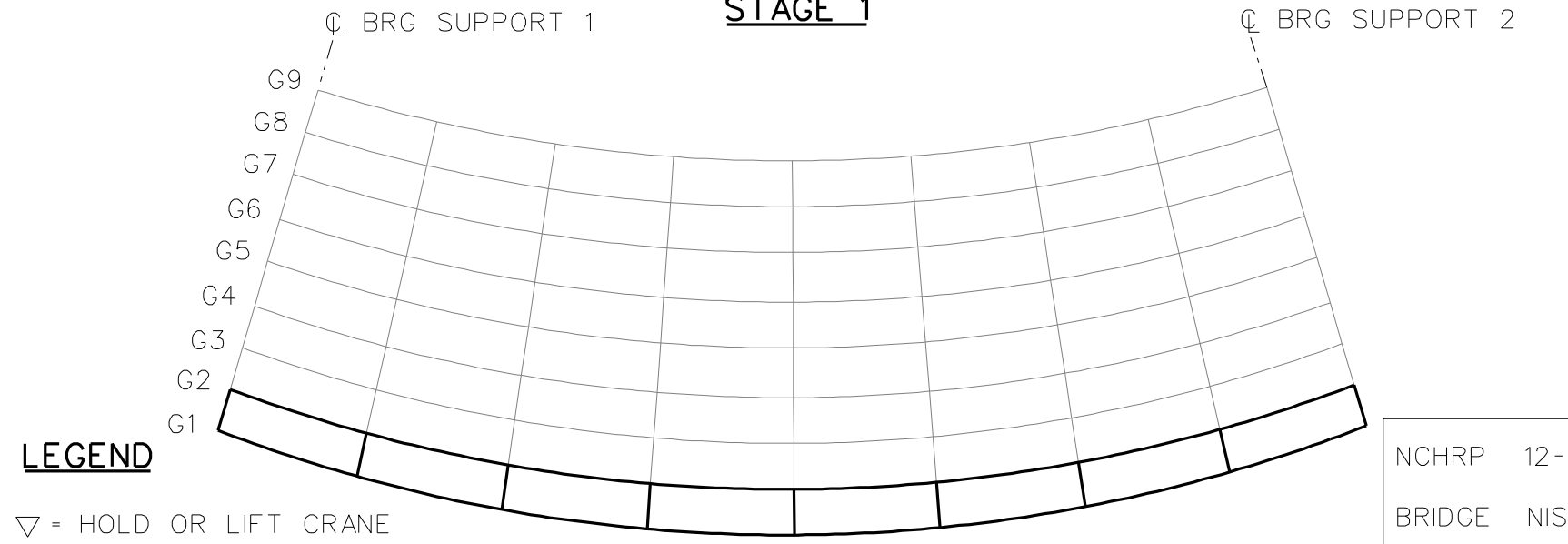

STAGE 2

LEGEND

▽ = HOLD OR LIFT CRANE

○ = TIE DOWN

□ = TEMPORARY SUPPORT STRUCTURE

NCHRP 12-79

BRIDGE NISCR8

GIRDER ELEVATION TABLES

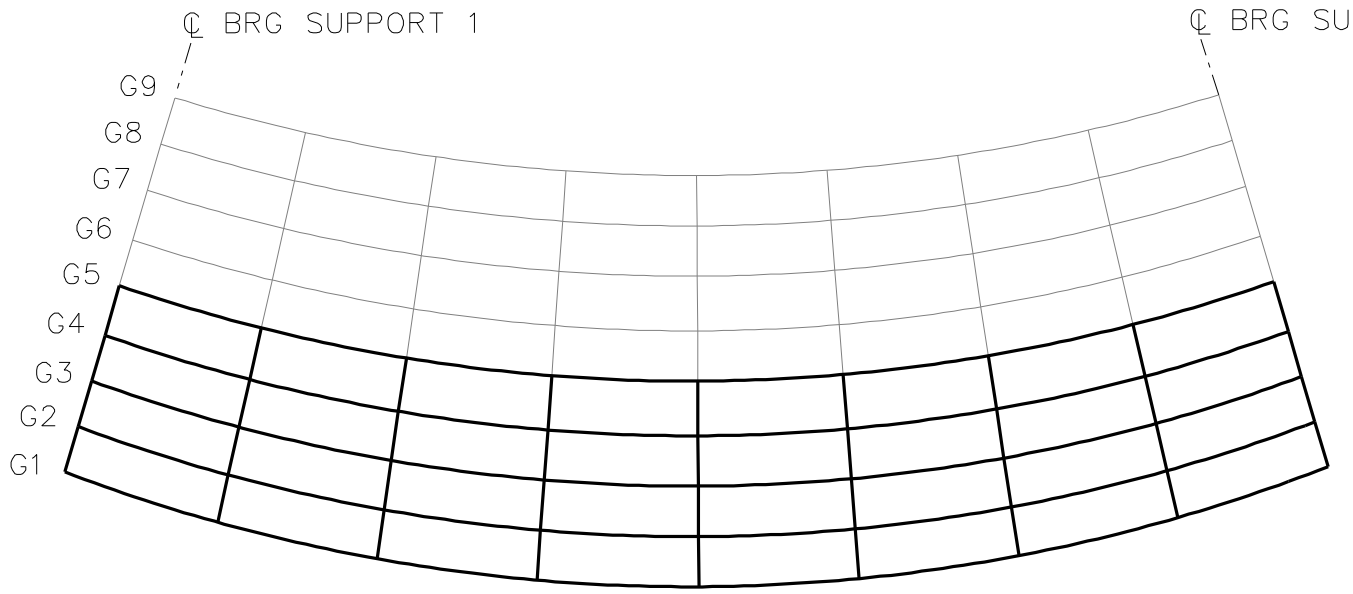

STAGE 5

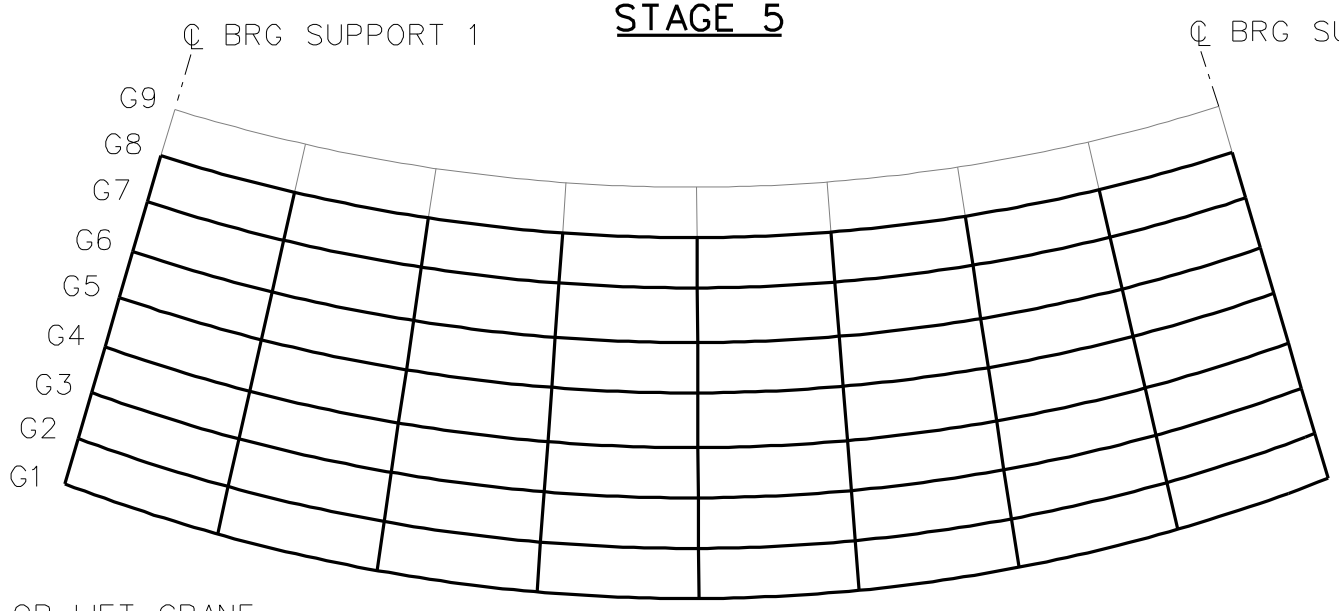

STAGE 8

LEGEND

▽ = HOLD OR LIFT CRANE

○ = TIE DOWN

□ = TEMPORARY SUPPORT STRUCTURE

NCHRP 12-79

BRIDGE NISCR8

GENERAL ERECTION PROCEDURE

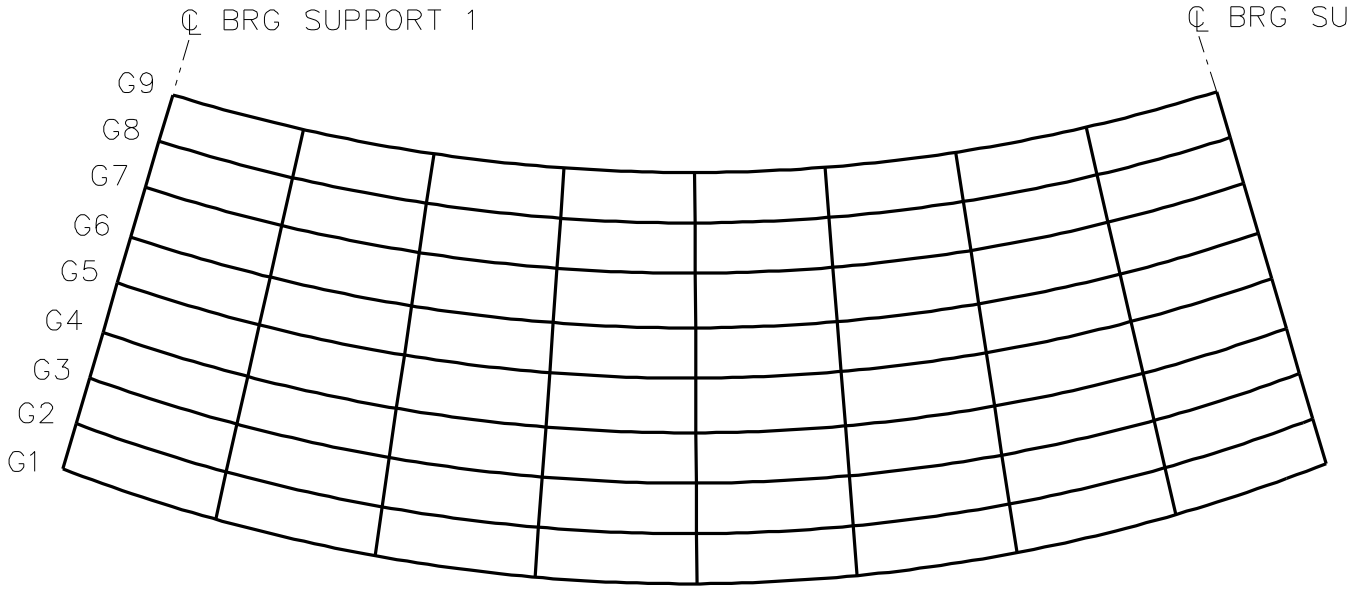

STAGE 9

LEGEND

▽ = HOLD OR LIFT CRANE

○ = TIE DOWN

□ = TEMPORARY SUPPORT STRUCTURE

NCHRP 12-79

BRIDGE NISCR8

GENERAL ERECTION PROCEDURE

NCHRP 12-79

NISCR10

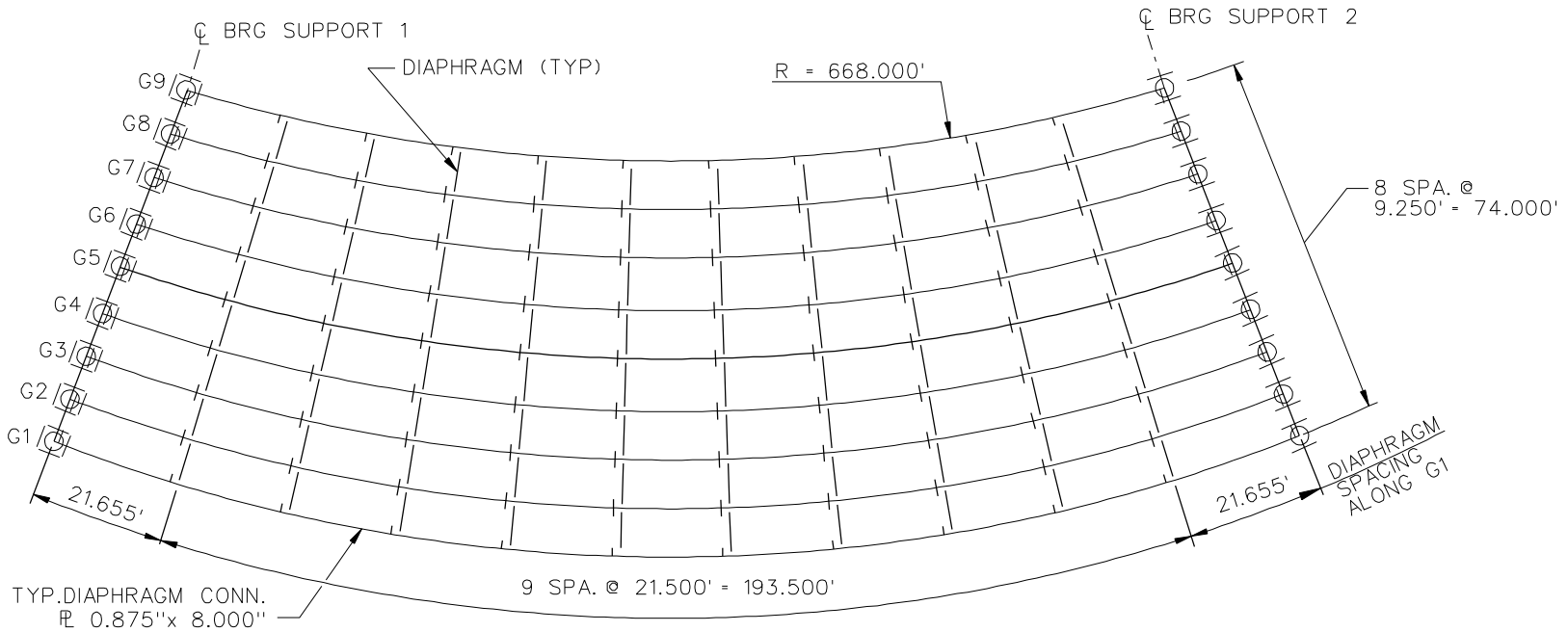

FRAMING PLAN

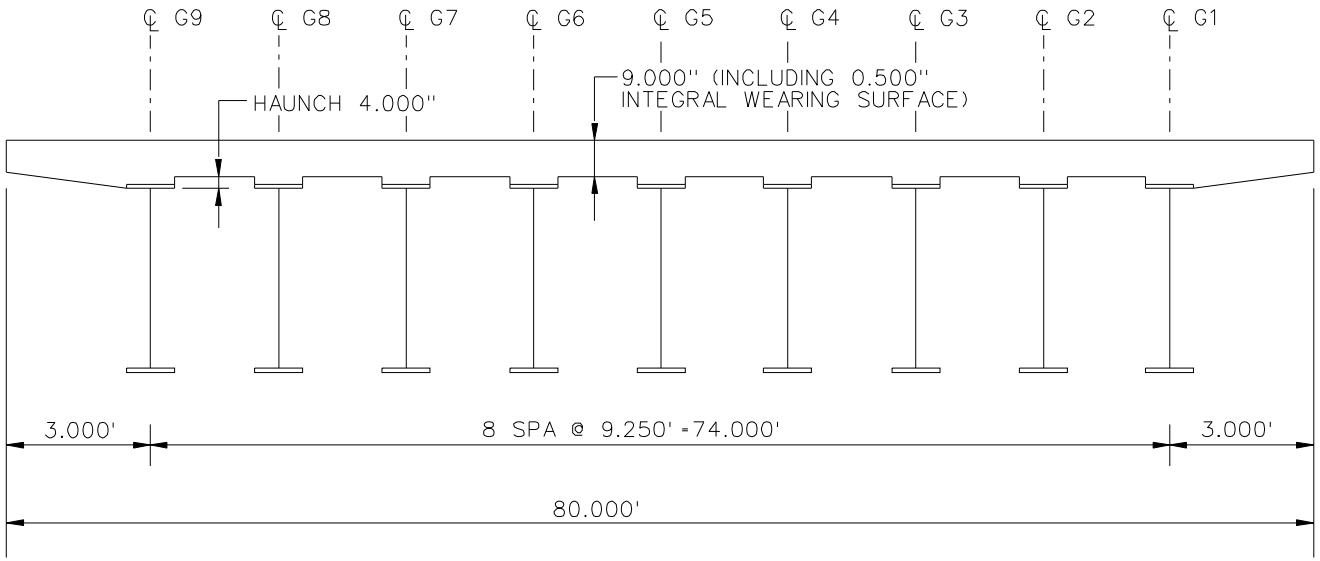

CROSS - SECTION

(DIAPHRAGMS NOT SHOWN)

BEARING LEGEND

- ○ NON-GUIDED
- ⊙ LONGITUDINALLY GUIDED
- |○| TRANSVERSELY GUIDED
- |⊙| FIXED

NCHRP 12-79

BRIDGE NISCR10

FRAMING PLAN AND CROSS-SECTION

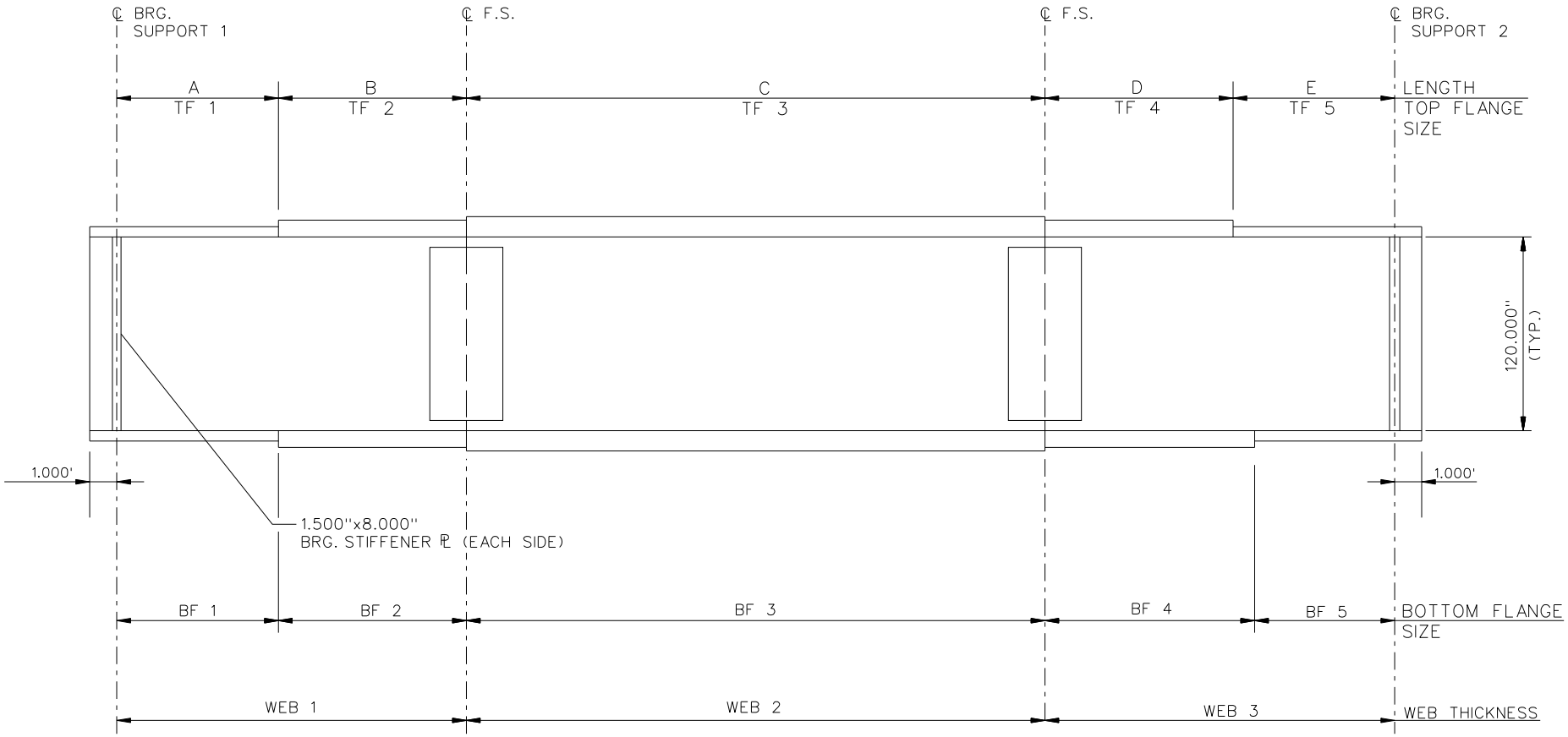

NOTE :

1. SEE TABLES ON SHEET 3 FOR GIRDER ELEVATION DIMENSIONS AND PLATE SIZES.

2. ALL GIRDERS, WEB 1 = WEB 2 = WEB 3 = 0.875".

NCHRP 12-79

BRIDGE NISCR10

GIRDER ELEVATION

SHEET 2 OF 8

	GIRDER PLATE LENGTHS ✳								
LENGTH	G1	G2	G3	G4	G5	G6	G7	G8	G9
A	28.405	27.739	27.073	26.408	25.742	25.076	24.410	23.745	23.079
B	25.000	25.000	25.000	25.000	25.000	25.000	25.000	25.000	25.000
C	130.000	128.379	126.759	125.138	123.518	121.897	120.276	118.656	117.035
D	25.000	25.000	25.000	25.000	25.000	25.000	25.000	25.000	25.000
E	28.405	27.739	27.073	26.408	25.742	25.076	24.410	23.745	23.079

✳ ALL DIMENSIONS ARE IN FEET.

	GIRDER FLANGE DIMENSIONS ✳✳					
TOP FLANGE	G1, G2, G3		G4, G5, G6		G7, G8, G9	
	BF	TF	BF	TF	BF	TF
TF1	24.000	1.000	20.000	1.000	20.000	1.000
TF2	24.000	1.750	20.000	1.000	20.000	1.000
TF3	24.000	3.000	20.000	1.000	20.000	1.000
TF4	24.000	1.750	20.000	1.000	20.000	1.000
TF5	24.000	1.000	20.000	1.000	20.000	1.000

✳✳ ALL DIMENSIONS ARE IN INCHES.

	GIRDER FLANGE DIMENSIONS ✳✳					
BOTTOM FLANGE	G1, G2, G3		G4, G5, G6		G7, G8, G9	
	BF	TF	BF	TF	BF	TF
BF1	30.000	1.250	20.000	1.000	20.000	1.000
BF2	30.000	2.250	20.000	1.000	20.000	1.000
BF3	30.000	3.250	20.000	1.500	20.000	1.500
BF4	30.000	2.250	20.000	1.000	20.000	1.000
BF5	30.000	1.250	20.000	1.000	20.000	1.000

✳✳ ALL DIMENSIONS ARE IN INCHES.

NCHRP 12-79

BRIDGE NISCR10

GIRDER ELEVATION TABLES

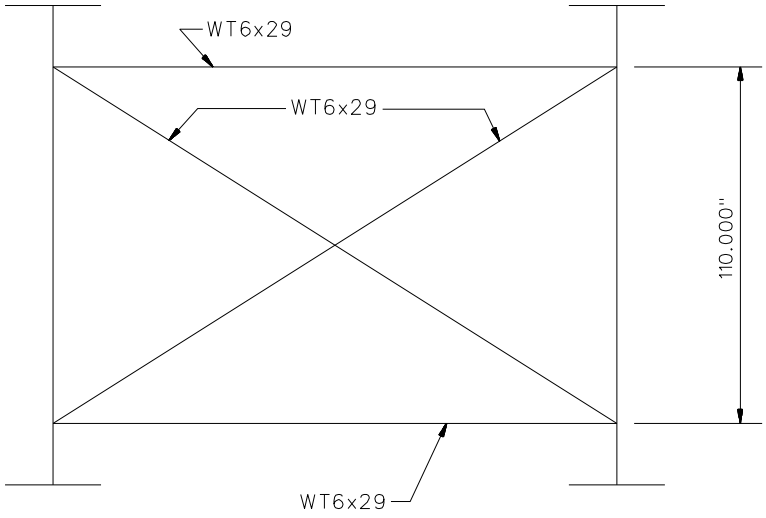

TYPICAL END AND INTERMEDIATE DIAPHRAGM

NOTES:

1. STEEL DEAD LOAD INCREASED BY 5% FOR MDX AND LARSA MODELS; 2% FOR 3D MODEL; AND 10% FOR APPROXIMATE ANALYSIS TO ACCOUNT FOR MISC. DETAILS.

2. FORMWORK LOAD OF 10PSF IS INCLUDED IN CONCRETE DEAD LOAD.

3. ADDITIONAL DESIGN PARAMETERS:
   A. 1.500' PARAPET WIDTH BOTH SIDES.
   B. 700 LB/FT UNIFORM LOAD ASSUMED FOR PARAPET WEIGHT.
   C. ROADWAY WIDTH = 77.000'.
   D. NUMBER OF DESIGN LANES = 6.
   E. HL93 LIVE LOAD.
   F. DESIGN SPEED = 45 MPH.

4. DIAPHRAGM MEMBER CALL-OUTS ARE IN ENGLISH UNITS.

NCHRP 12-79

BRIDGE NISCR10

MISC. DETAILS AND NOTES

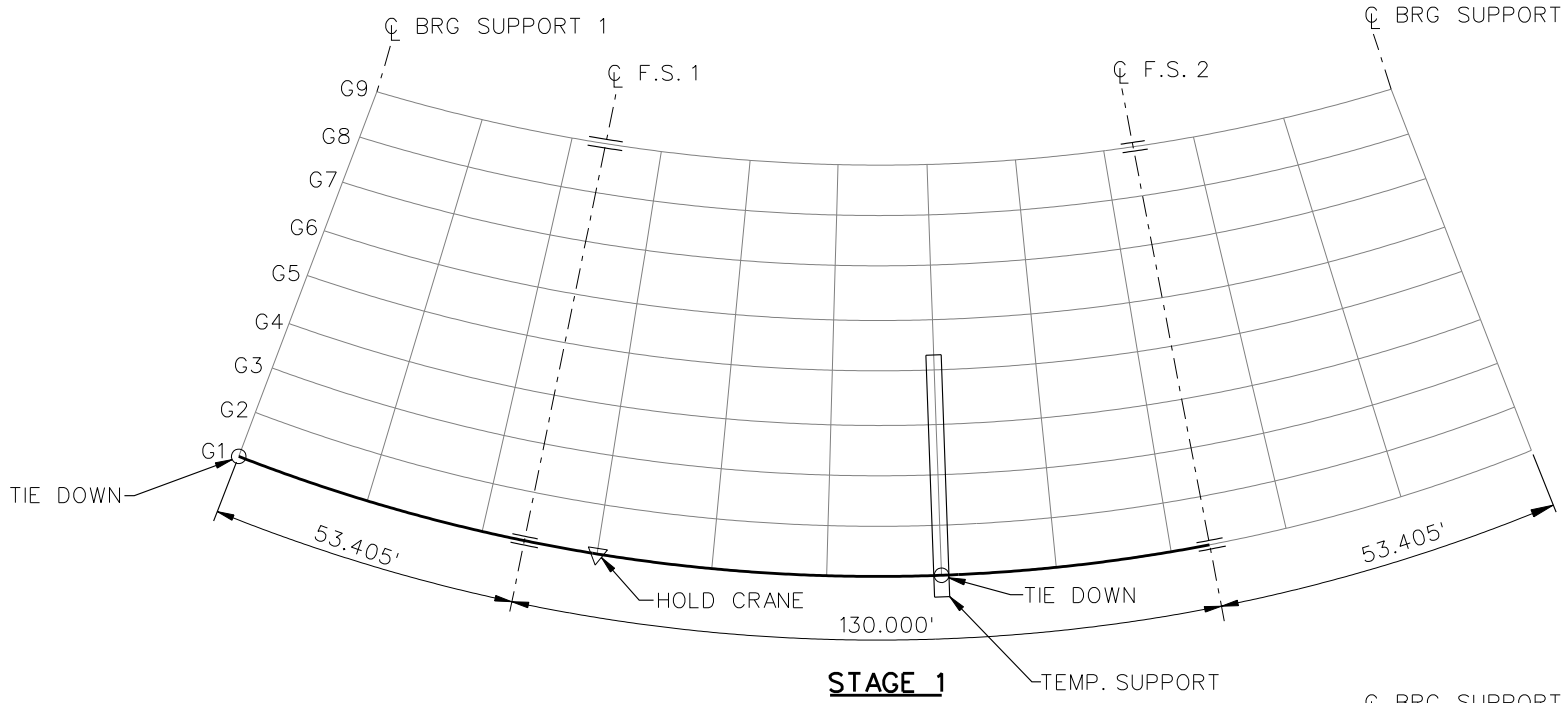

STAGE 1

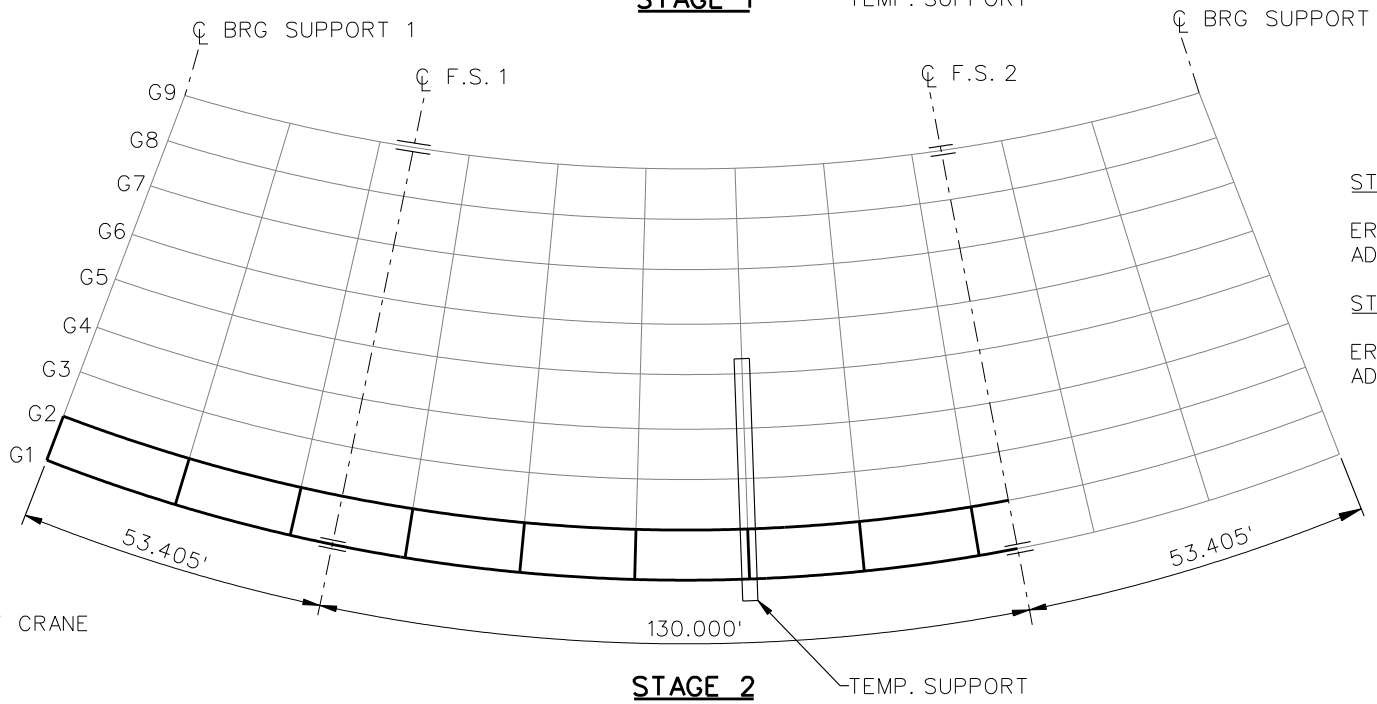

STAGE 2

STAGE 3

ERECT G3-1 AND G3-2 AND ADJACENT CROSS FRAMES

STAGE 4

ERECT G4-1 AND G4-2 AND ADJACENT CROSS FRAMES

LEGEND

▽ = HOLD OR LIFT CRANE

○ = TIE DOWN

□ = TEMPORARY SUPPORT STRUCTURE

NCHRP 12-79

BRIDGE NISCR10

GIRDER ELEVATION TABLES

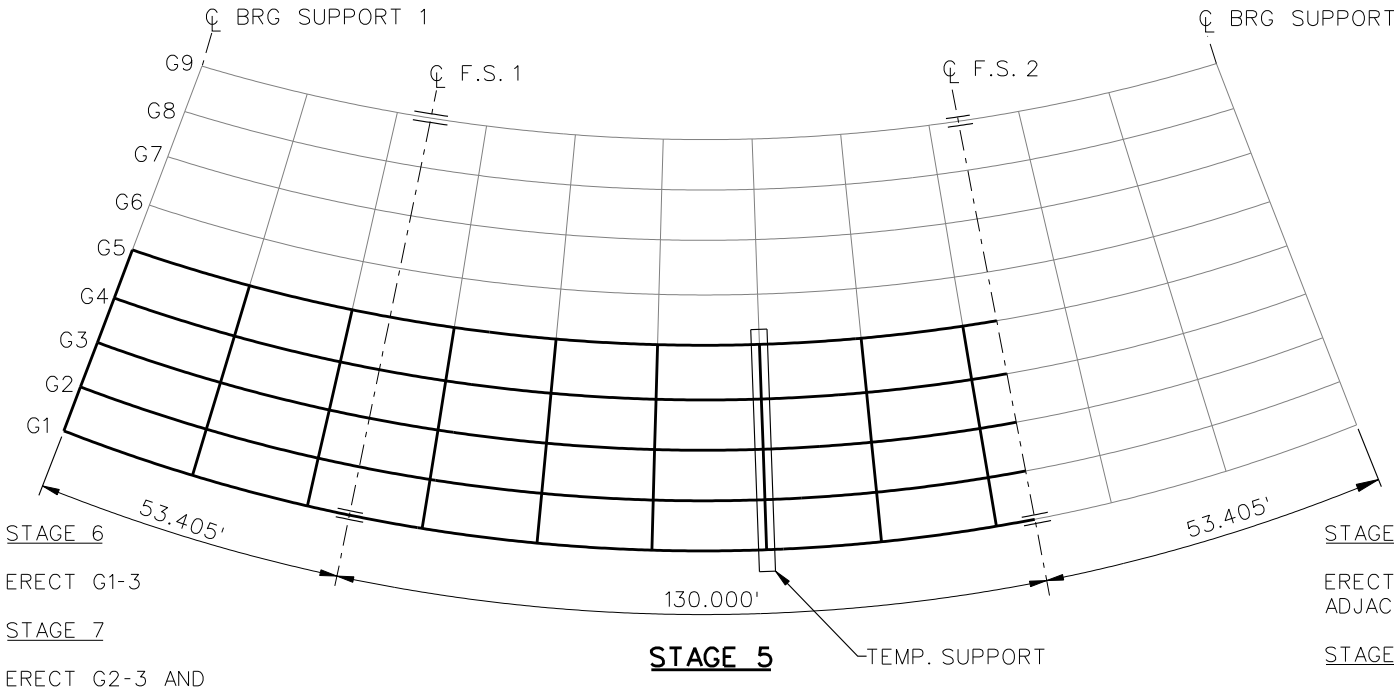

STAGE 5

STAGE 6

ERECT G1-3

STAGE 7

ERECT G2-3 AND
ADJACENT CROSS FRAMES

STAGE 8

ERECT G3-3 AND
ADJACENT CROSS FRAMES

STAGE 9

ERECT G4-3 AND
ADJACENT CROSS FRAMES

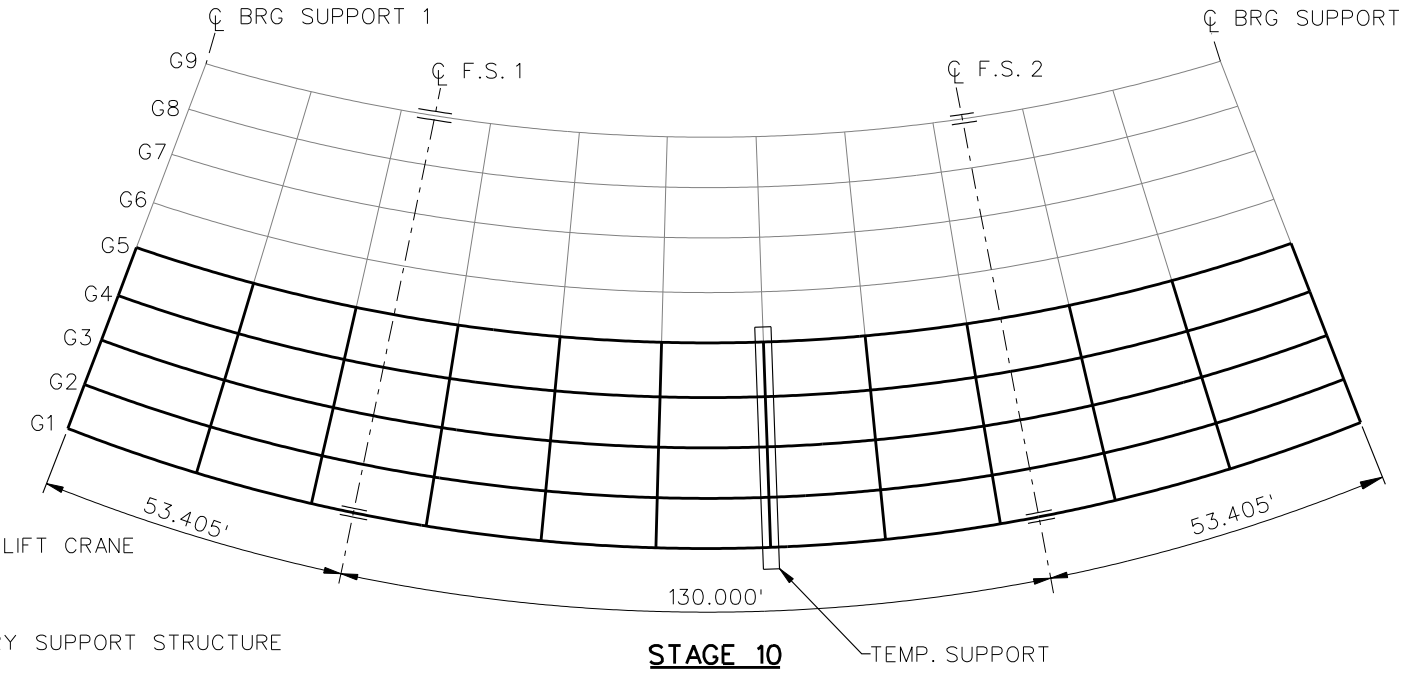

STAGE 10

LEGEND

▽ = HOLD OR LIFT CRANE

○ = TIE DOWN

□ = TEMPORARY SUPPORT STRUCTURE

NCHRP 12-79

BRIDGE NISCR10

GIRDER ELEVATION TABLES

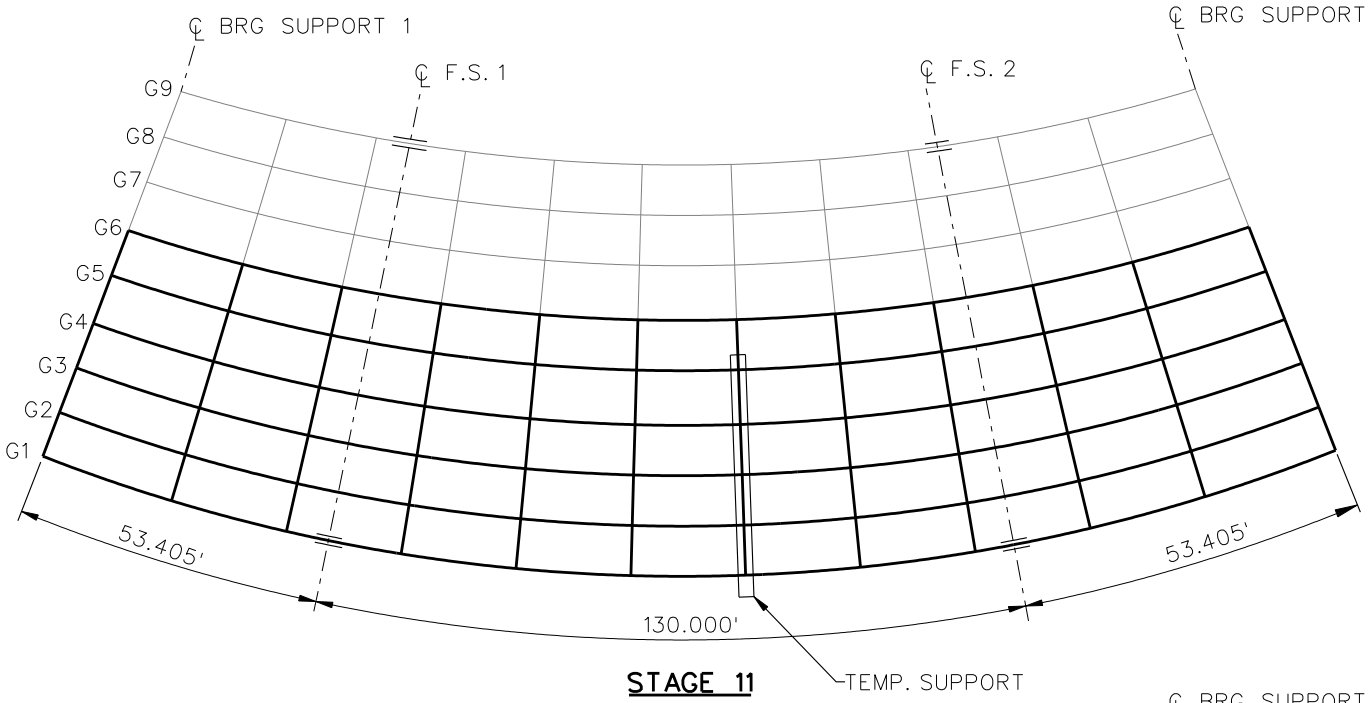

STAGE 11

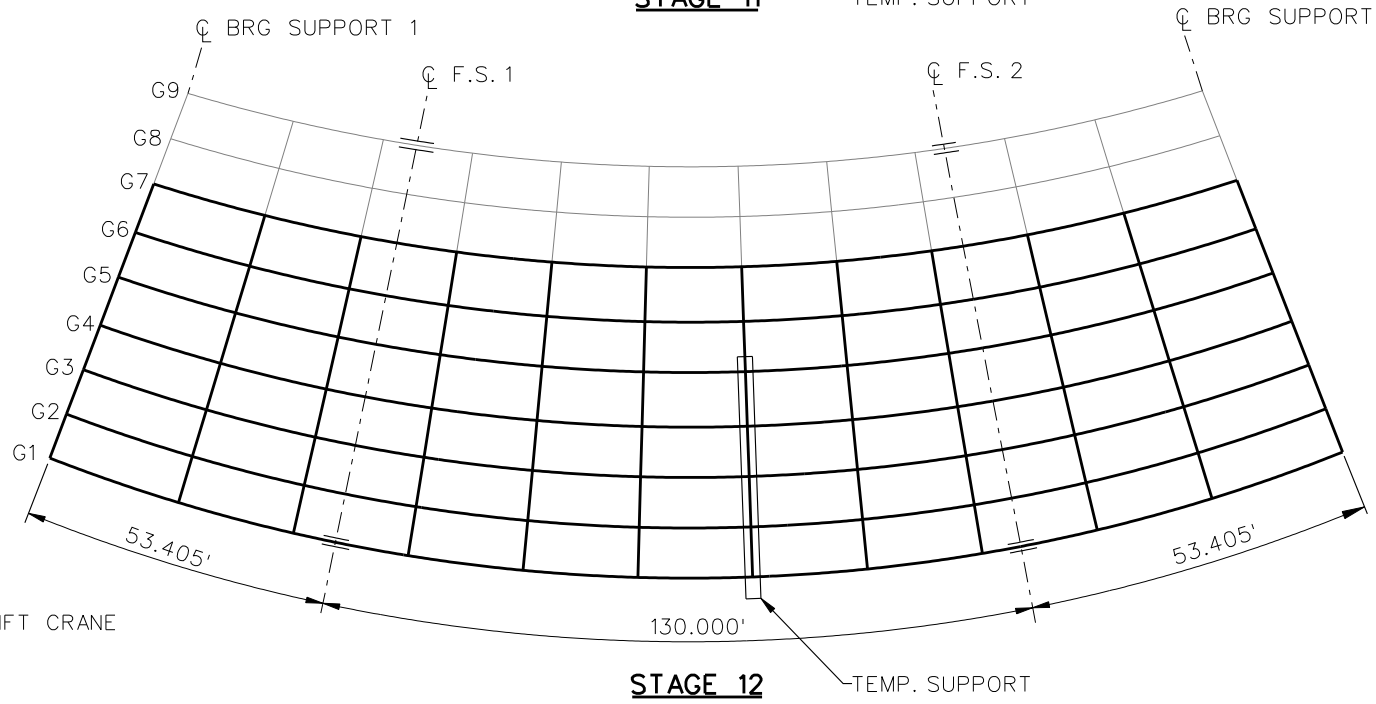

STAGE 12

LEGEND

▽ = HOLD OR LIFT CRANE

○ = TIE DOWN

□ = TEMPORARY SUPPORT STRUCTURE

NCHRP 12-79

BRIDGE NISCR10

GIRDER ELEVATION TABLES

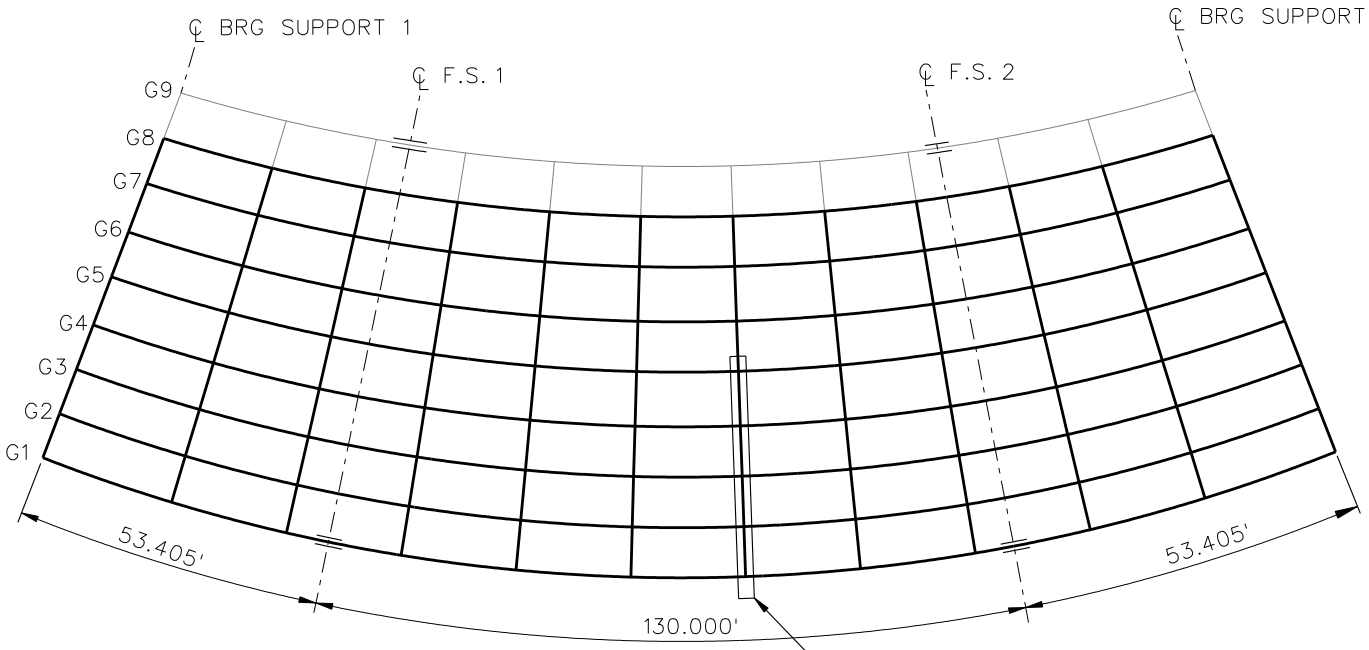

STAGE 13

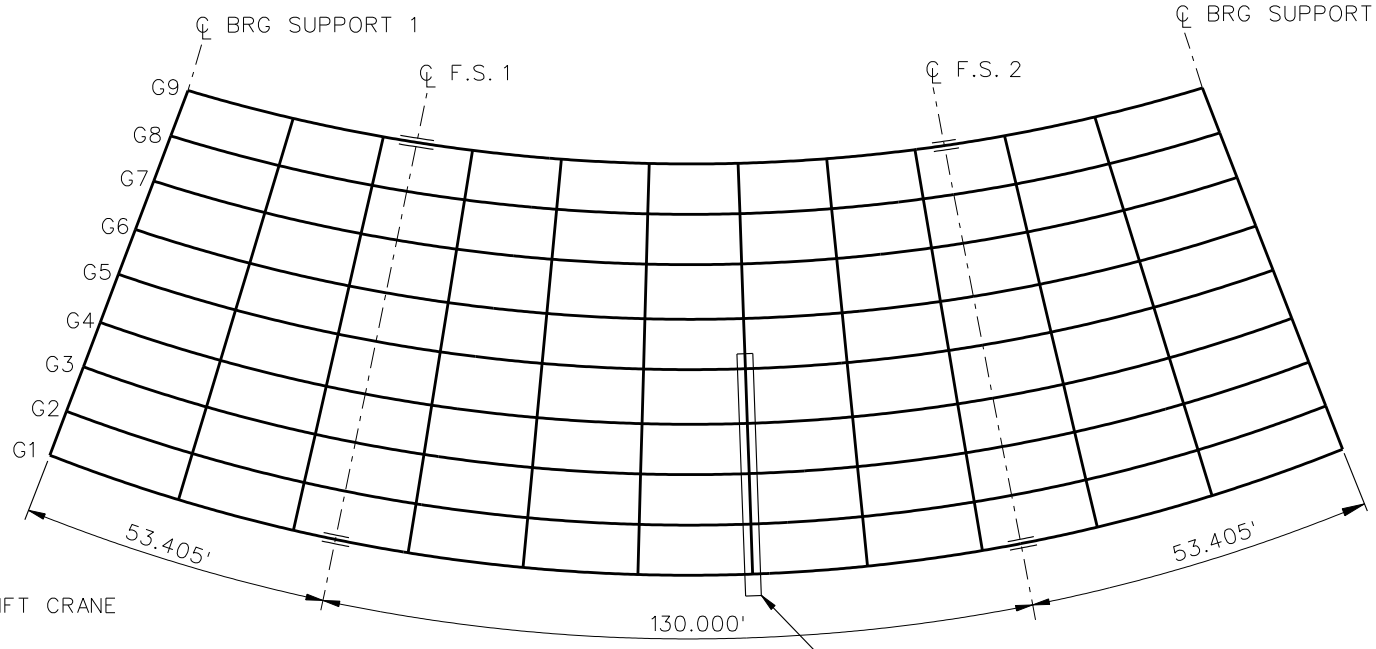

STAGE 14

LEGEND

▽ = HOLD OR LIFT CRANE

○ = TIE DOWN

□ = TEMPORARY SUPPORT STRUCTURE

NCHRP 12-79

BRIDGE NISCR10

GIRDER ELEVATION TABLES

NCHRP 12-79

NISCR11

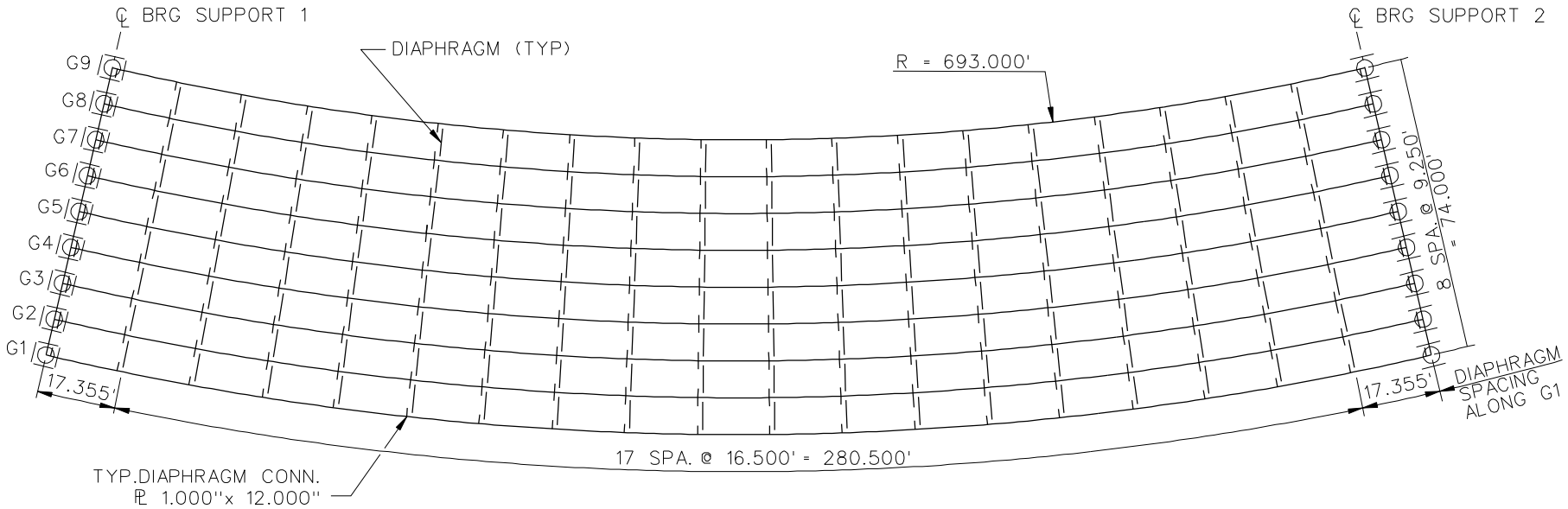

FRAMING PLAN

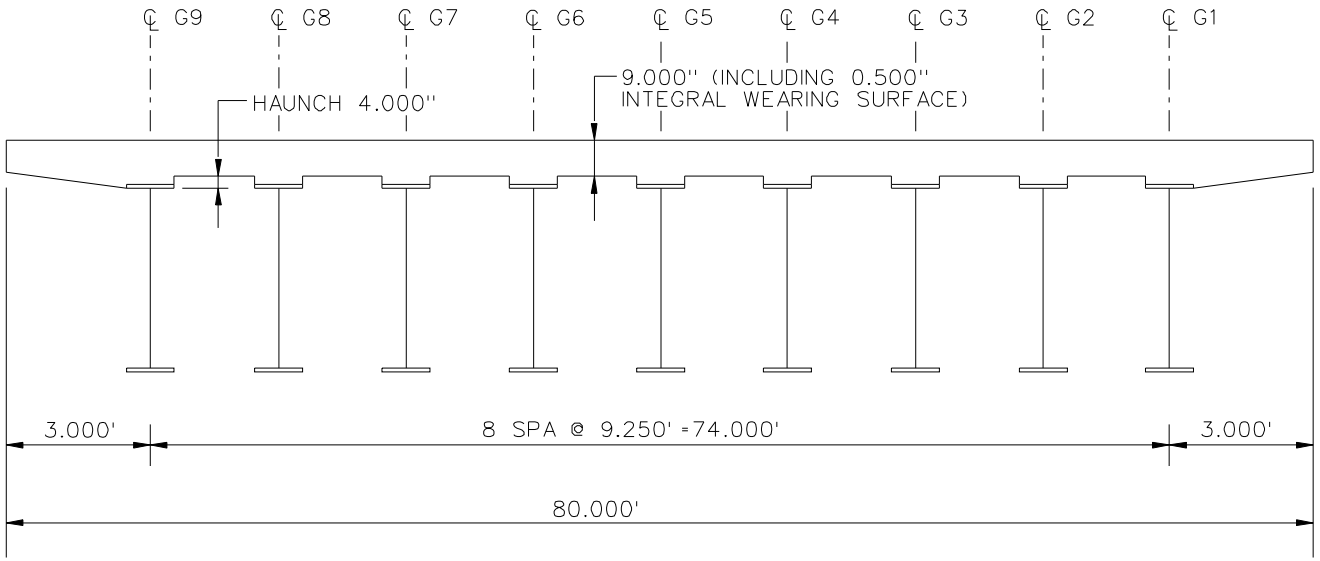

CROSS - SECTION

(DIAPHRAGMS NOT SHOWN)

BEARING LEGEND

O NON-GUIDED

O LONGITUDINALLY GUIDED

O TRANSVERSELY GUIDED

O FIXED

NCHRP 12-79

BRIDGE NISCR11

FRAMING PLAN AND CROSS-SECTION

SHEET 1 OF 8

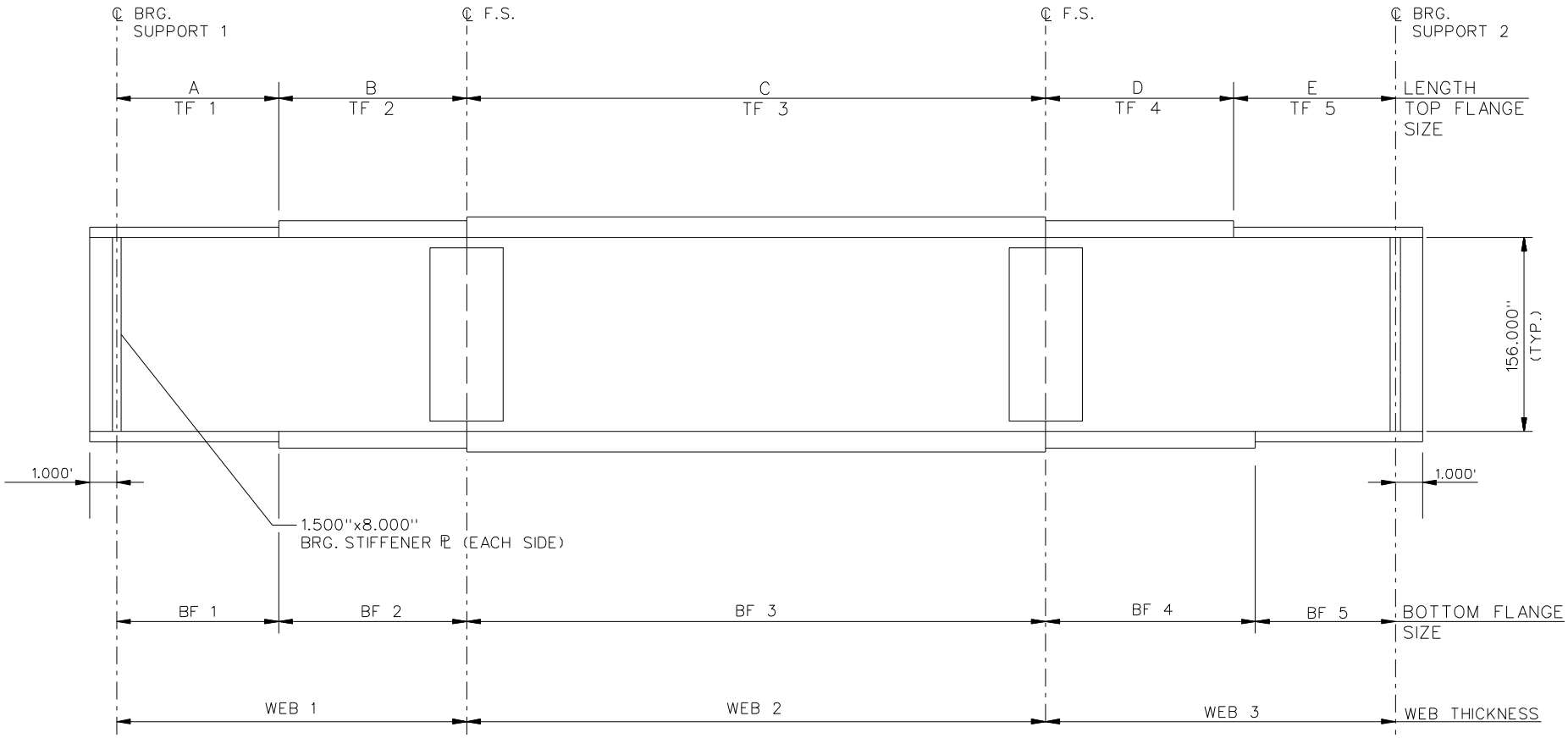

NOTE :

1. SEE TABLES ON SHEET 3 FOR GIRDER ELEVATION DIMENSIONS AND PLATE SIZES.

2. ALL GIRDERS, WEB 1 = WEB 2 = WEB 3 = 1.125".

3. BRG. STIFFENER WIDTH = 1.750"x18" FOR G1, G2, G3
   BRG. STIFFENER WIDTH = 1.500"x16" FOR G4, G5, G6
   BRG. STIFFENER WIDTH = 1.500"x12" FOR G7, G8, G9

NCHRP 12-79

BRIDGE NISCR11

GIRDER ELEVATION

	GIRDER PLATE LENGTHS ✳								
LENGTH	G1	G2	G3	G4	G5	G6	G7	G8	G9
A	46.105	44.898	43.690	42.483	41.276	40.069	38.861	37.654	36.447
B	54.000	54.000	54.000	54.000	54.000	54.000	54.000	54.000	54.000
C	115.000	113.613	112.226	110.839	109.452	108.066	106.679	105.292	103.905
D	54.000	54.000	54.000	54.000	54.000	54.000	54.000	54.000	54.000
E	46.105	44.898	43.690	42.483	41.276	40.069	38.861	37.654	36.447

✳ ALL DIMENSIONS ARE IN FEET.

	GIRDER FLANGE DIMENSIONS ✳✳					
TOP	G1, G2, G3		G4, G5, G6		G7, G8, G9	
FLANGE	BF	TF	BF	TF	BF	TF
TF1	40.000	1.750	32.000	1.500	28.000	1.250
TF2	40.000	2.750	32.000	2.000	28.000	1.250
TF3	40.000	3.250	32.000	2.500	28.000	1.250
TF4	40.000	2.750	32.000	2.000	28.000	1.250
TF5	40.000	1.750	32.000	1.500	28.000	1.250

✳✳ ALL DIMENSIONS ARE IN INCHES.

	GIRDER FLANGE DIMENSIONS ✳✳					
BOTTOM	G1, G2, G3		G4, G5, G6		G7, G8, G9	
FLANGE	BF	TF	BF	TF	BF	TF
BF1	46.000	2.000	38.000	1.750	28.000	1.250
BF2	46.000	2.750	38.000	2.250	28.000	1.250
BF3	46.000	3.250	38.000	3.000	28.000	1.250
BF4	46.000	2.750	38.000	2.250	28.000	1.250
BF5	46.000	2.000	38.000	1.750	28.000	1.250

✳✳ ALL DIMENSIONS ARE IN INCHES.

NCHRP 12-79

BRIDGE NISCR11

GIRDER ELEVATION TABLES

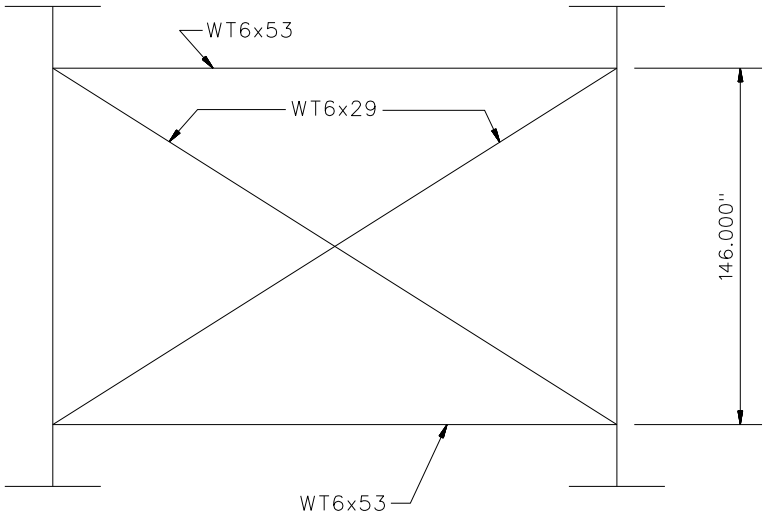

TYPICAL END AND INTERMEDIATE DIAPHRAGM

NOTES:

1. STEEL DEAD LOAD INCREASED BY 5% FOR MDX AND LARSA MODELS; 2% FOR 3D MODEL; AND 10% FOR APPROXIMATE ANALYSIS TO ACCOUNT FOR MISC. DETAILS.

2. FORMWORK LOAD OF 10PSF IS INCLUDED IN CONCRETE DEAD LOAD.

3. ADDITIONAL DESIGN PARAMETERS:
   A. 1.500' PARAPET WIDTH BOTH SIDES.
   B. 700 LB/FT UNIFORM LOAD ASSUMED FOR PARAPET WEIGHT.
   C. ROADWAY WIDTH = 77.000'.
   D. NUMBER OF DESIGN LANES = 6.
   E. HL93 LIVE LOAD.

4. DIAPHRAGM MEMBER CALL-OUTS ARE IN ENGLISH UNITS.

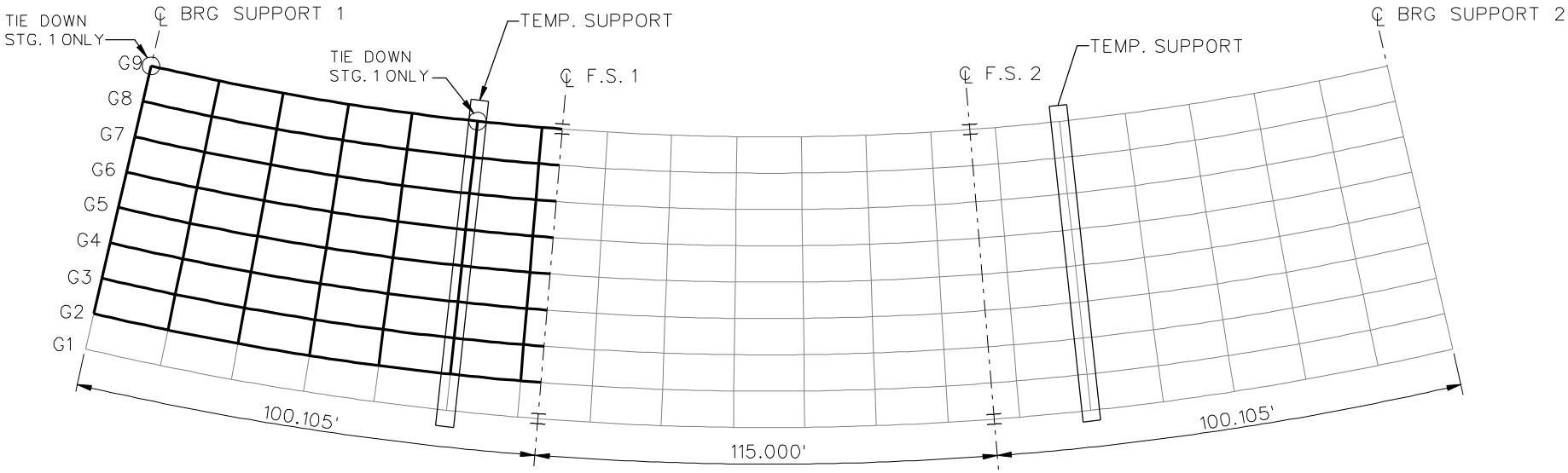

STAGE 8

STAGE 1 = ERECT G9 - 1

STAGE 2 = ERECT G8 - 1
AND XF'S BETWEEN G8 @ G9

STAGE 3 = ERECT G7 - 1 AND XF'S

STAGE 4 = ERECT G6 - 1 AND XF'S

STAGE 5 = ERECT G5 - 1 AND XF'S

STAGE 6 = ERECT G4 - 1 AND XF'S

STAGE 7 = ERECT G3 - 1 AND XF'S

STAGE 8 = ERECT G2 - 1 AND XF'S

LEGEND

▽ = HOLD OR LIFT CRANE

○ = TIE DOWN

□ = TEMPORARY SUPPORT STRUCTURE

NCHRP 12-79

BRIDGE NISCR11

GIRDER ELEVATION TABLES

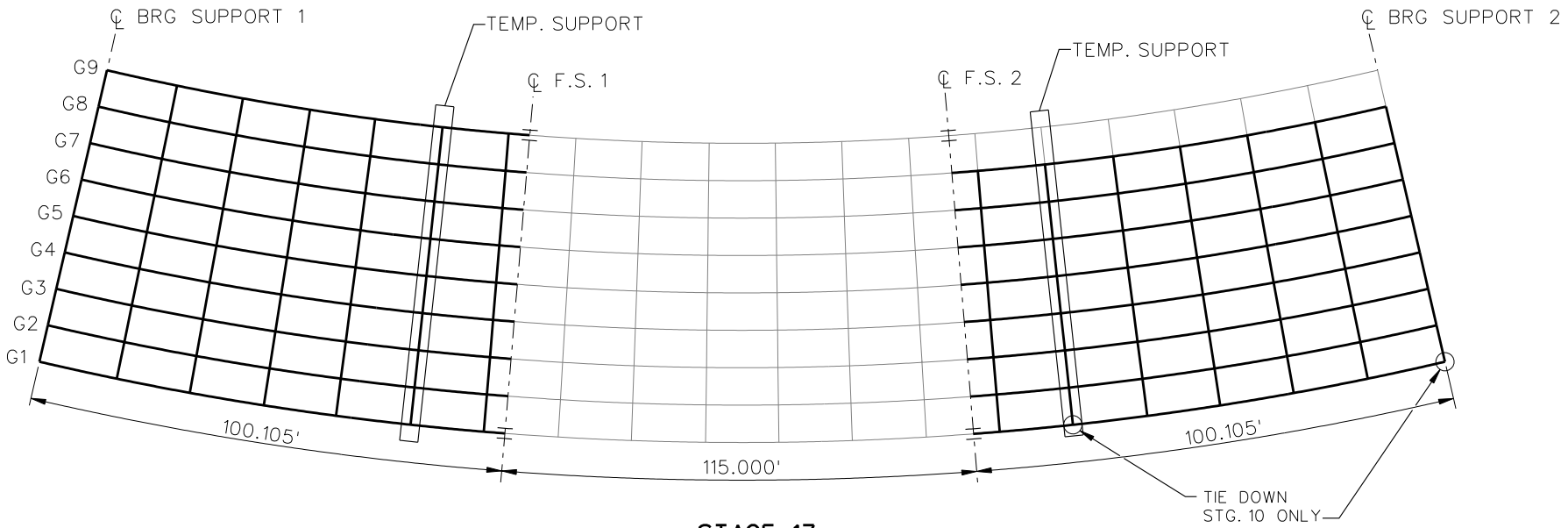

STAGE 17

STAGE 9 = ERECT G1 - 1 AND XF'S

STAGE 10 = ERECT G1 - 3 W/TIE DOWNS

STAGE 11 = ERECT G2 - 3 AND XF'S
BETWEEN G1 AND G2

STAGE 12 = ERECT G3 - 3 AND XF'S

STAGE 13 = ERECT G4 - 3 AND XF'S

STAGE 14 = ERECT G5 - 3 AND XF'S

STAGE 15 = ERECT G6 - 3 AND XF'S

STAGE 16 = ERECT G7 - 3 AND XF'S

STAGE 17 = ERECT G8 - 3 AND XF'S

LEGEND

▽ = HOLD OR LIFT CRANE

○ = TIE DOWN

□ = TEMPORARY SUPPORT STRUCTURE

NCHRP 12-79

BRIDGE NISCR11

GIRDER ELEVATION TABLES

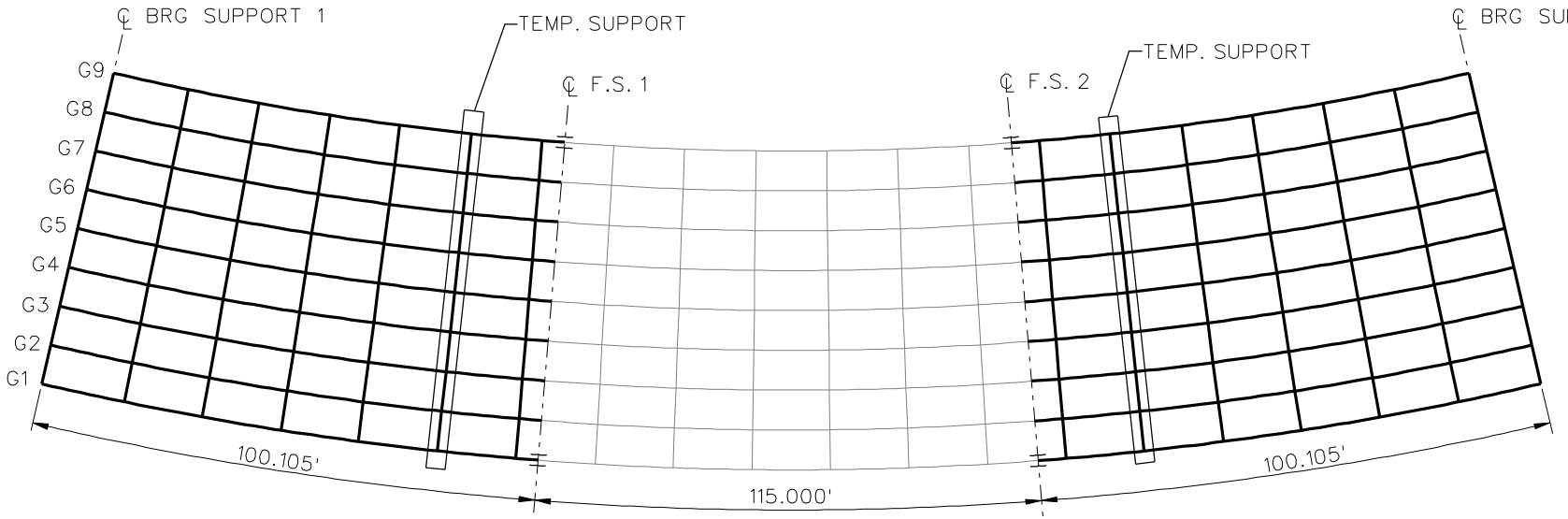

STAGE 18

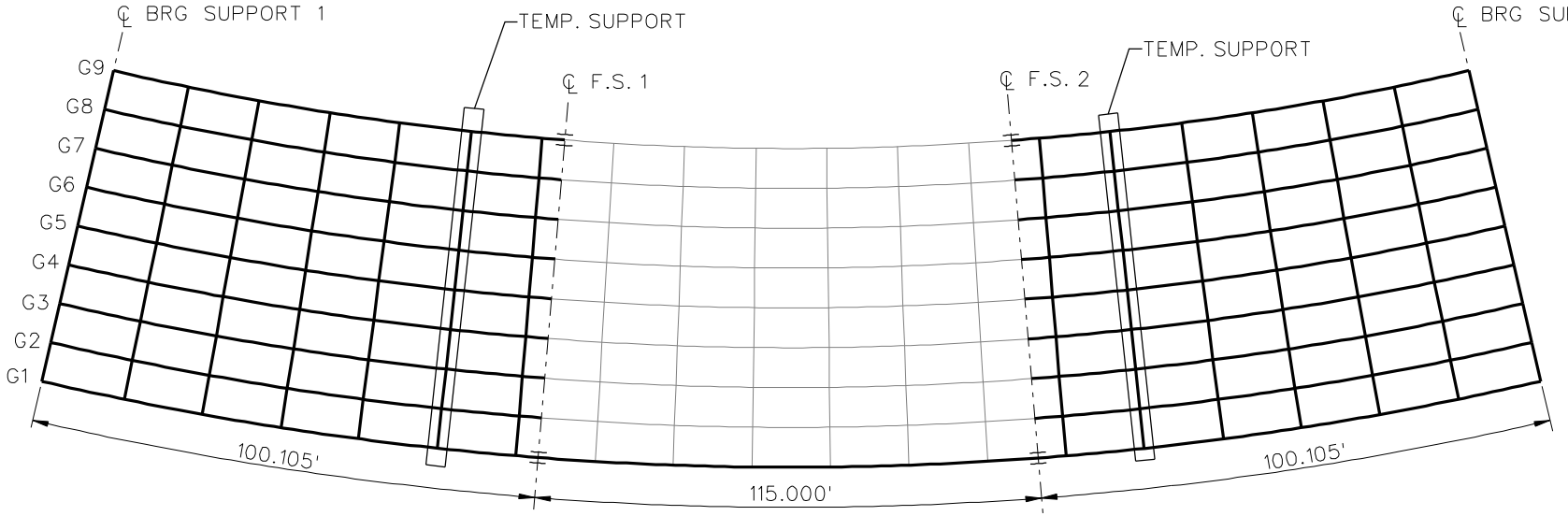

STAGE 19

LEGEND

▽ = HOLD OR LIFT CRANE

○ = TIE DOWN

□ = TEMPORARY SUPPORT STRUCTURE

NCHRP 12-79

BRIDGE NISCR11

GIRDER ELEVATION TABLES

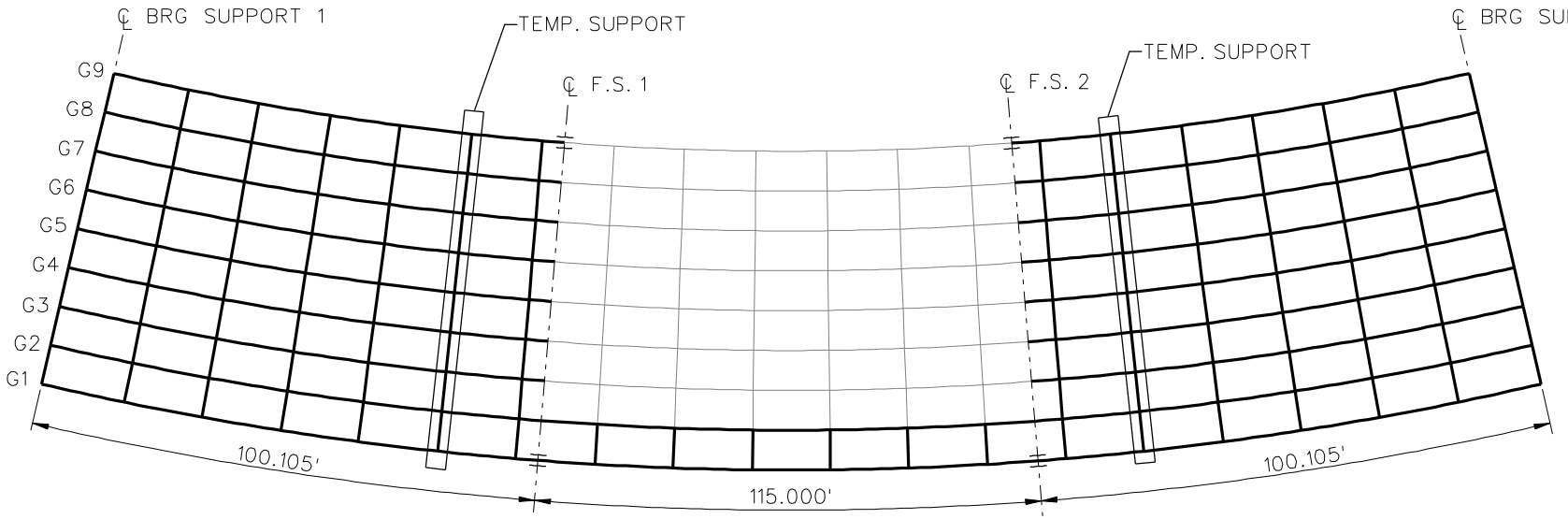

STAGE 20

STAGE 21 = ERECT G3 - 2 AND XF'S

STAGE 22 = ERECT G4 - 2 AND XF'S

STAGE 23 = ERECT G5 - 2 AND XF'S

STAGE 24 = ERECT G6 - 2 AND XF'S

STAGE 25 = ERECT G7 - 2 AND XF'S

STAGE 26 = ERECT G8 - 2 AND XF'S

STAGE 27 = ERECT G9 - 2 AND XF'S

STAGE 28 - REMOVE TEMP. SUPPORTS

LEGEND

▽ = HOLD OR LIFT CRANE

○ = TIE DOWN

□ = TEMPORARY SUPPORT STRUCTURE

NCHRP 12-79

BRIDGE NISCR11

GIRDER ELEVATION TABLES

NCHRP 12-79

NISCS3

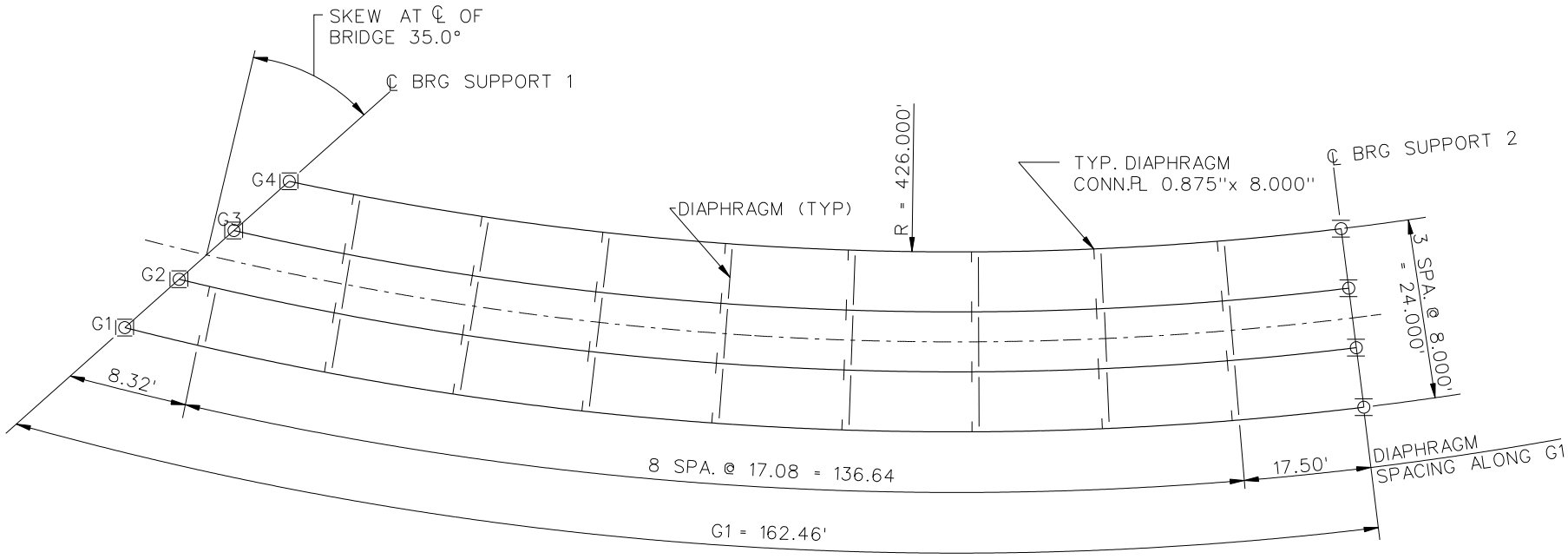

FRAMING PLAN

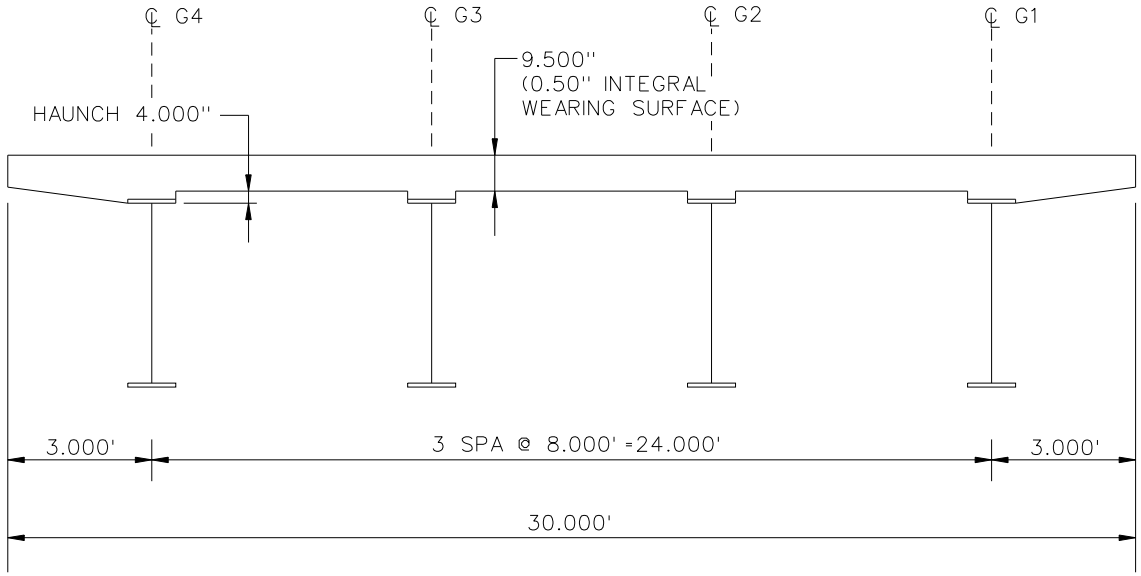

CROSS - SECTION
(DIAPHRAGMS NOT SHOWN)

BEARING LEGEND

- ○ NON-GUIDED
- ⊙ LONGITUDINALLY GUIDED
- |○| TRANSVERSELY GUIDED
- |⊙| FIXED

NCHRP 12-79

BRIDGE NISCS3

FRAMING PLAN AND CROSS-SECTION

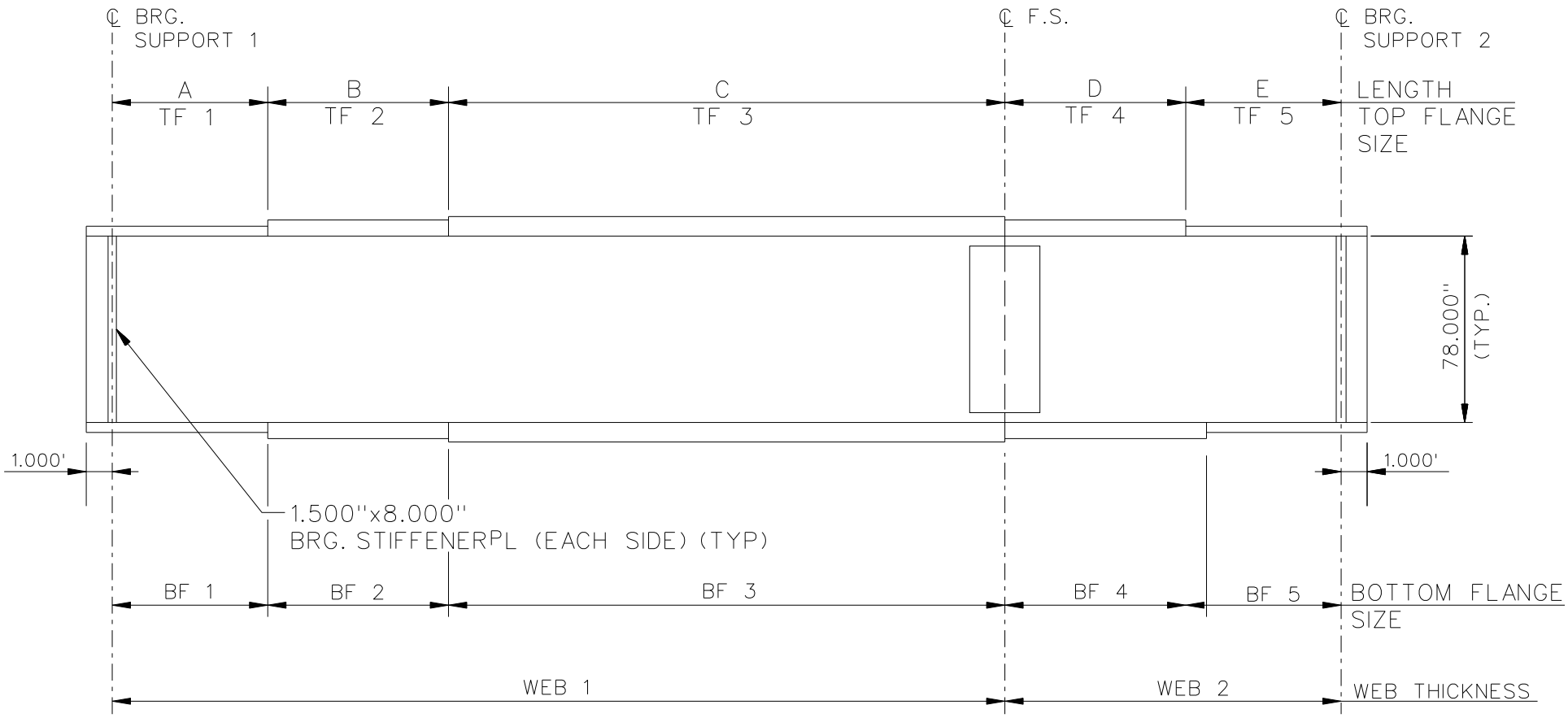

NOTE :

1. SEE TABLES ON SHEET 3 FOR GIRDER ELEVATION DIMENSIONS AND PLATE SIZES.

2. GIRDERS G1 AND G2, WEB 1 = WEB 2 = 0.750"
   GIRDERS G3 AND G4, WEB 1 = WEB 2 = 0.625"

NCHRP 12-79

BRIDGE NISCS3

GIRDER ELEVATION

SHEET 2 OF 6

	GIRDER PLATE LENGTHS ✳			
LENGTH	G1	G2	G3	G4
A	25.000	24.560	24.110	23.670
B	20.000	19.640	19.290	18.930
C	72.460	65.760	59.020	52.230
D	20.000	19.640	19.290	18.930
E	25.000	24.560	24.110	23.670

✳ ALL DIMENSIONS ARE IN FEET.

	GIRDER FLANGE DIMENSIONS ✳✳							
TOP	G1		G2		G3		G4	
FLANGE	BF	TF	BF	TF	BF	TF	BF	TF
TF1	24.000	1.000	18.000	1.000	18.000	1.000	18.000	1.000
TF2	24.000	1.750	18.000	1.000	18.000	1.000	18.000	1.000
TF3	24.000	2.750	18.000	1.000	18.000	1.000	18.000	1.000
TF4	24.000	1.750	18.000	1.000	18.000	1.000	18.000	1.000
TF5	24.000	1.250	18.000	1.000	18.000	1.000	18.000	1.000

✳✳ ALL DIMENSIONS ARE IN INCHES.

	GIRDER FLANGE DIMENSIONS ✳✳							
BOTTOM	G1		G2		G3		G4	
FLANGE	BF	TF	BF	TF	BF	TF	BF	TF
BF1	28.000	1.250	18.000	1.000	18.000	1.000	18.000	1.000
BF2	28.000	2.500	18.000	1.000	18.000	1.000	18.000	1.000
BF3	28.000	3.125	18.000	1.500	18.000	1.000	18.000	1.000
BF4	28.000	2.500	18.000	1.000	18.000	1.000	18.000	1.000
BF5	28.000	1.500	18.000	1.000	18.000	1.000	18.000	1.000

✳✳ ALL DIMENSIONS ARE IN INCHES.

NCHRP 12-79

BRIDGE NISCS3

GIRDER ELEVATION TABLES

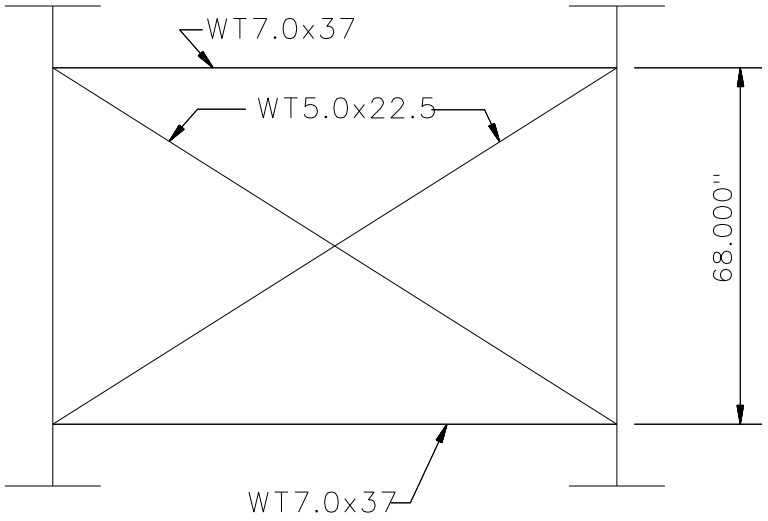

TYPICAL INTERMEDIATE AND END DIAPHRAGM

NOTES:

1. STEEL DEAD LOAD INCREASED BY 5% FOR MDX AND LARSA MODELS; 2% FOR 3D MODEL; AND 10% FOR APPROXIMATE ANALYSIS TO ACCOUNT FOR MISC. DETAILS.

2. FORMWORK LOAD OF 10PSF IS INCLUDED IN CONCRETE DEAD LOAD.

3. ADDITIONAL DESIGN PARAMETERS:
   A. 1.500' PARAPET WIDTH BOTH SIDES.
   B. 700 LB/FT UNIFORM LOAD ASSUMED FOR PARAPET WEIGHT.
   C. ROADWAY WIDTH = 27.000'.
   D. NUMBER OF DESIGN LANES = 2.
   E. HL93 LIVE LOAD.
   F. DESIGN SPEED = 45 MPH.

4. DIAPHRAGM MEMBER CALL-OUTS ARE IN ENGLISH UNITS.

NCHRP 12-79

BRIDGE NISCS3

MISC. DETAILS AND NOTES

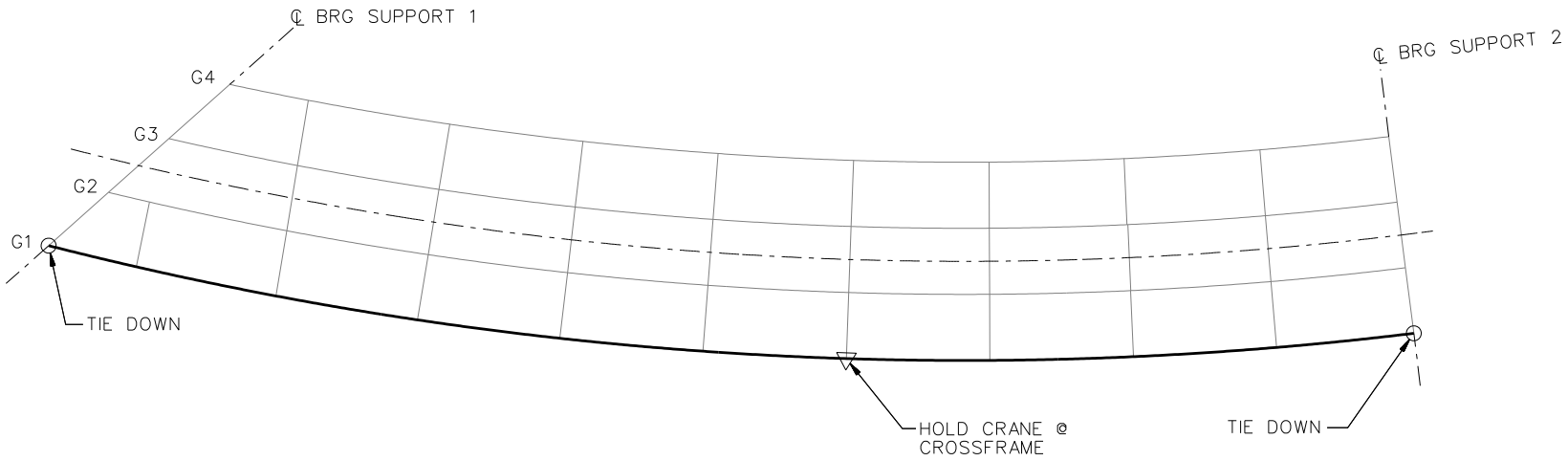

STAGE 1

(RESULTS NOT REQ'D)

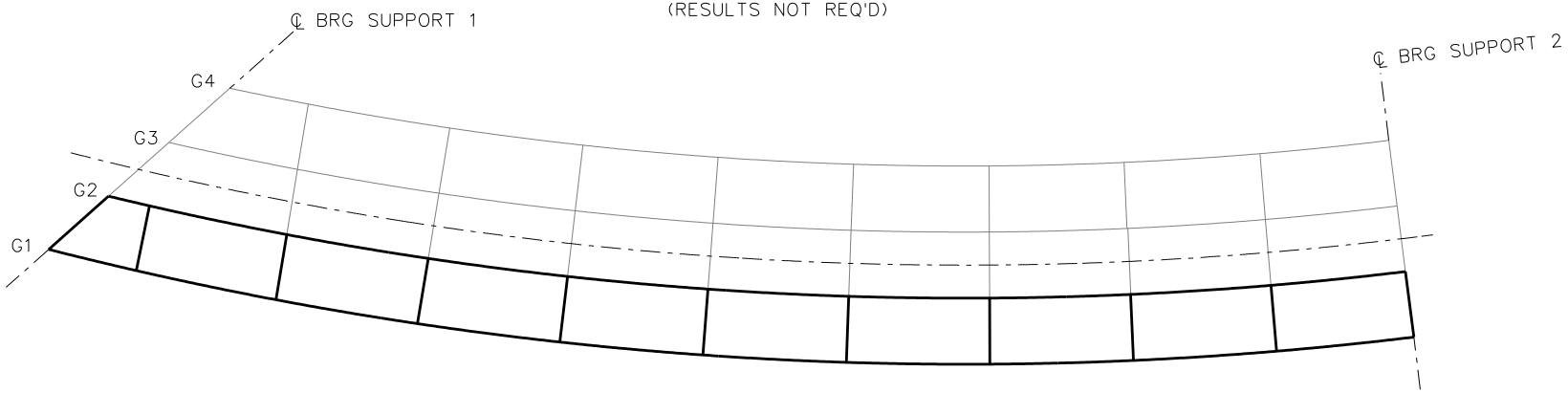

STAGE 2

(RESULTS REQ'D)

LEGEND

▽ = HOLD OR LIFT CRANE

○ = TIE DOWN

□ = TEMPORARY SUPPORT STRUCTURE

NCHRP 12-79

BRIDGE NISCS3

GIRDER ERECTION PROCEDURE

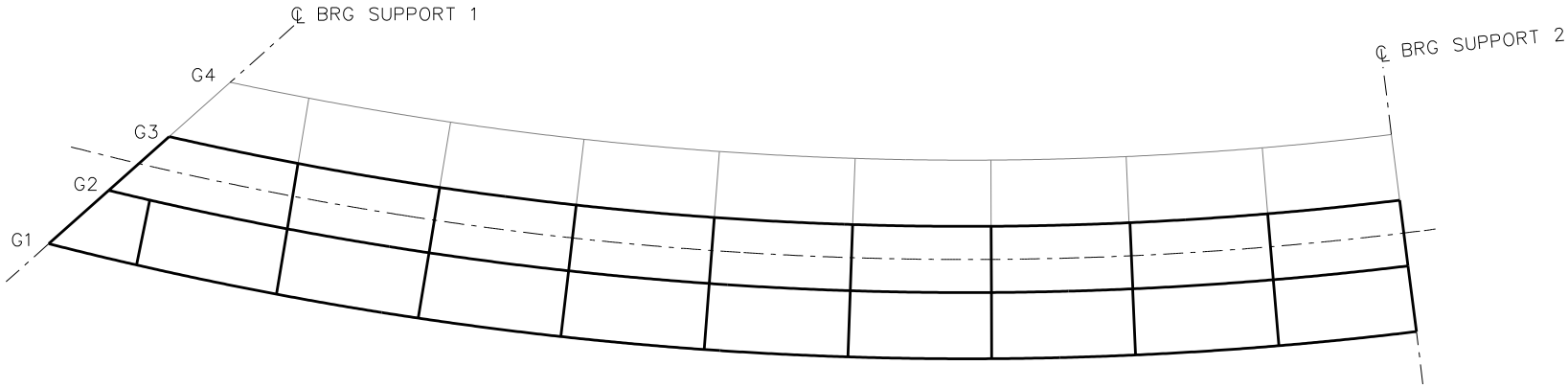

STAGE 3

(RESULTS REQ'D)

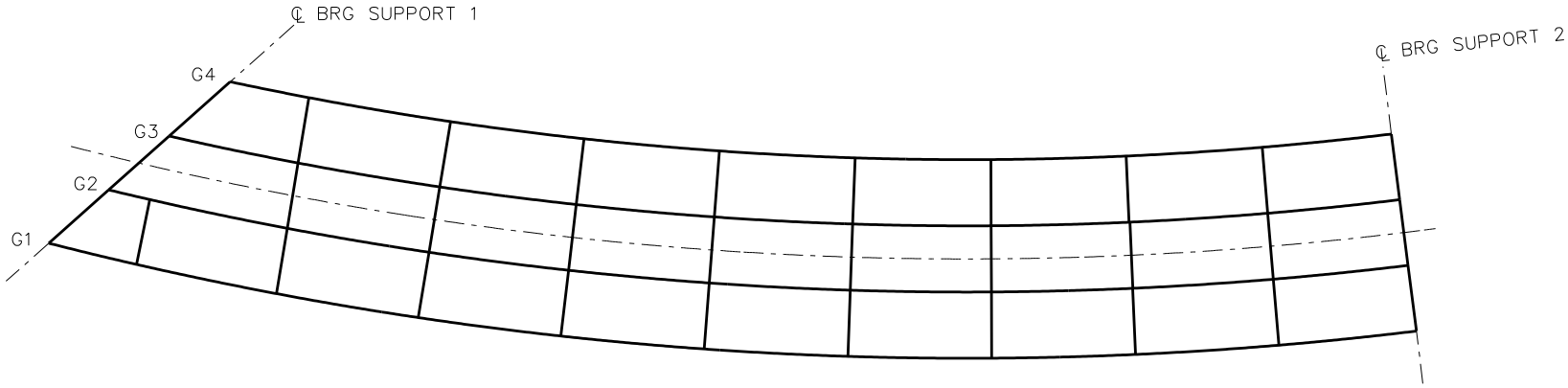

STAGE 4

STEEL DL + TOTAL NONCOMP DL RESULTS

LEGEND

▽ = HOLD OR LIFT CRANE

○ = TIE DOWN

□ = TEMPORARY SUPPORT STRUCTURE

NCHRP 12-79

BRIDGE NISCS3

GIRDER ERECTION PROCEDURE

NCHRP 12-79

NISCS9

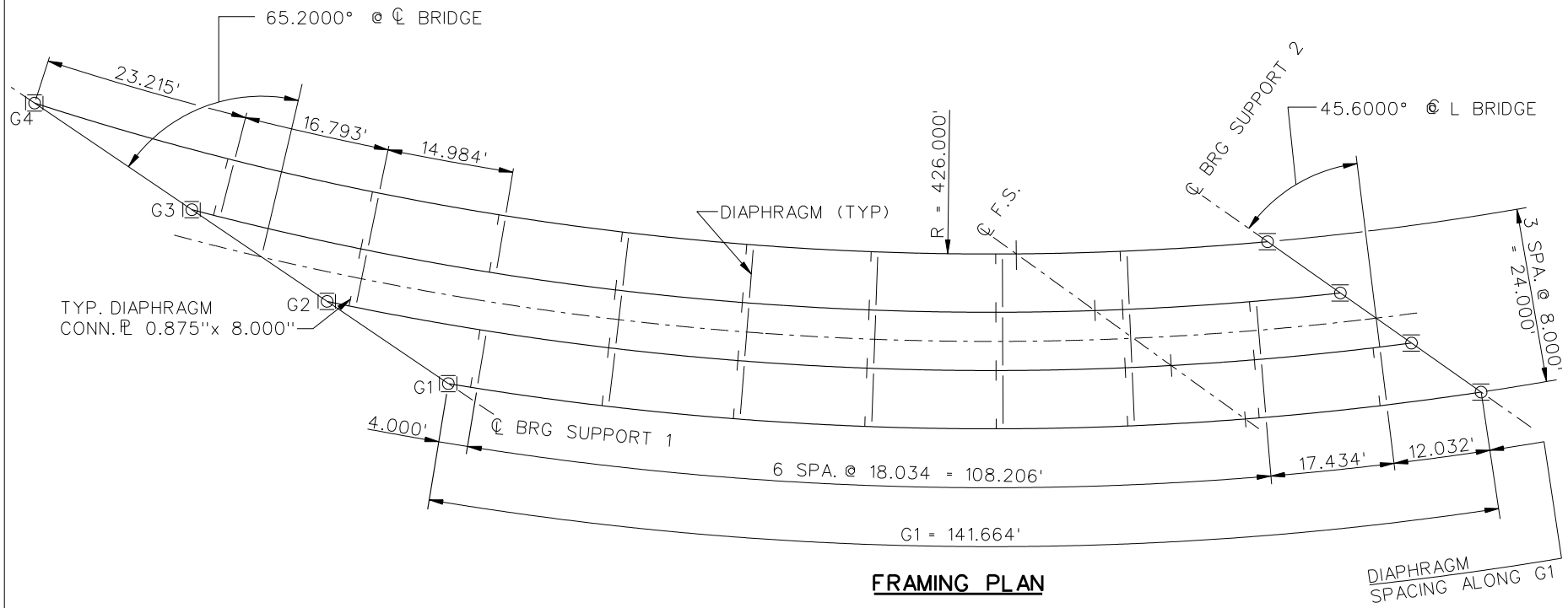

FRAMING PLAN

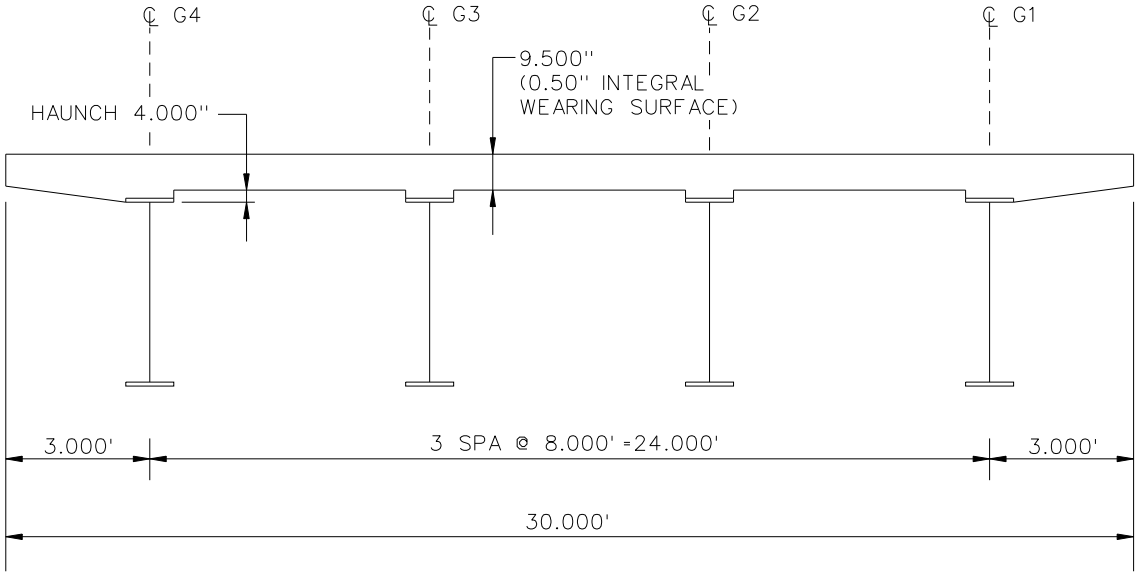

CROSS - SECTION
(DIAPHRAGMS NOT SHOWN)

BEARING LEGEND

- ○ NON-GUIDED
- ⊙ LONGITUDINALLY GUIDED
- |○| TRANSVERSELY GUIDED
- |⊙| FIXED

NCHRP 12-79

BRIDGE NISCS9

FRAMING PLAN AND CROSS-SECTION

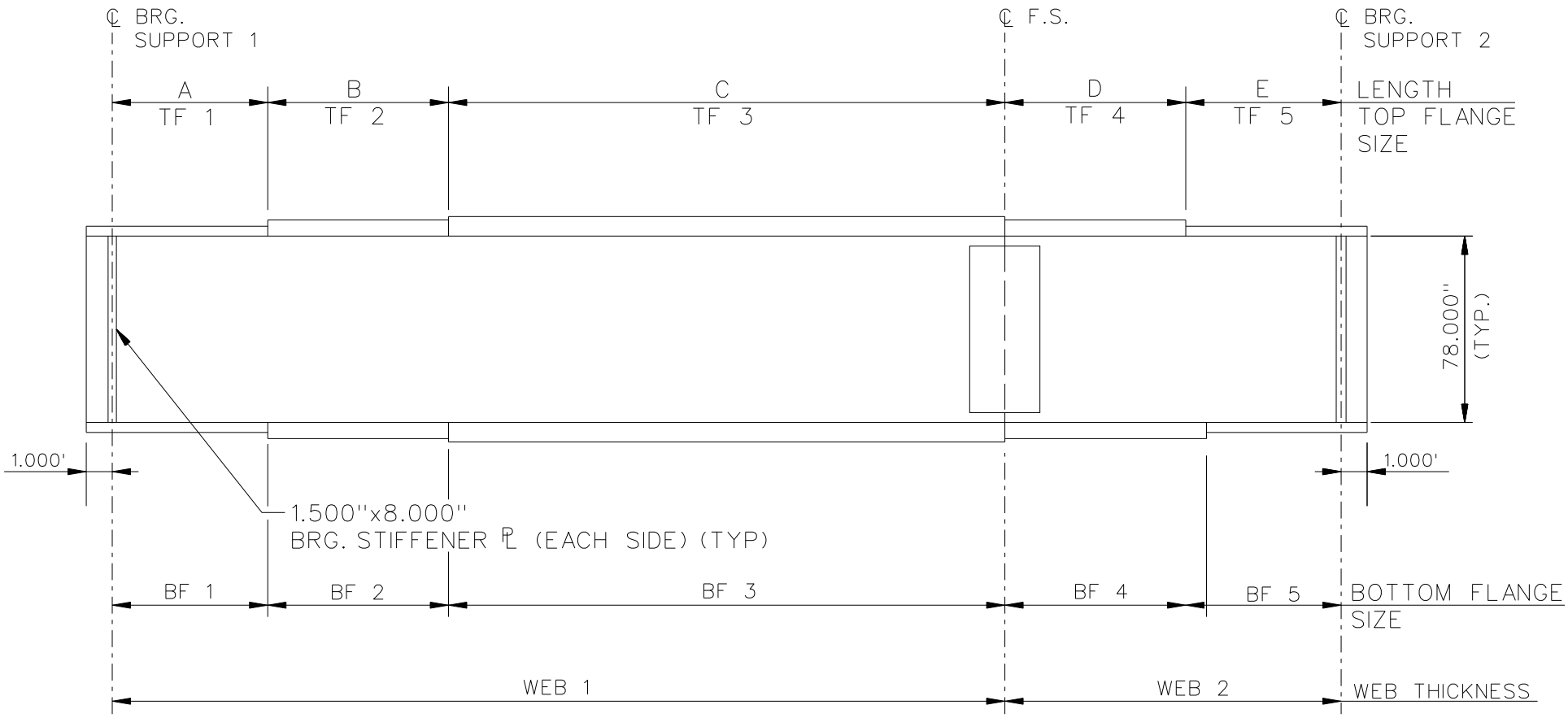

NOTES :

1. SEE TABLES ON SHEET 3 FOR GIRDER ELEVATION DIMENSIONS AND PLATE SIZES.

2. ALL GIRDERS, WEB 1 = WEB 2 = 0.750"

NCHRP 12-79

BRIDGE NISCS9

GIRDER ELEVATION

SHEET 2 OF 8

	GIRDER PLATE LENGTHS ✳			
LENGTH	G1	G2	G3	G4
A	18.000	21.000	21.000	22.000
B	18.000	21.000	21.000	22.000
C	71.663	70.954	77.378	84.427
D	17.000	17.000	17.000	16.500
E	17.000	17.000	17.000	16.500

✳ ALL DIMENSIONS ARE IN FEET.

	GIRDER FLANGE DIMENSIONS ✳✳							
TOP	G1		G2		G3		G4	
FLANGE	BF	TF	BF	TF	BF	TF	BF	TF
TF1	24.000	1.000	24.000	1.000	20.000	1.000	20.000	1.000
TF2	24.000	1.000	24.000	1.000	20.000	1.000	20.000	1.000
TF3	24.000	2.000	24.000	2.000	20.000	2.000	20.000	2.000
TF4	24.000	1.000	24.000	1.000	20.000	1.000	20.000	1.000
TF5	24.000	1.000	24.000	1.000	20.000	1.000	20.000	1.000

✳✳ ALL DIMENSIONS ARE IN INCHES.

	GIRDER FLANGE DIMENSIONS ✳✳							
BOTTOM	G1		G2		G3		G4	
FLANGE	BF	TF	BF	TF	BF	TF	BF	TF
BF1	28.000	1.500	28.000	1.500	24.000	1.000	24.000	1.000
BF2	28.000	1.500	28.000	1.500	24.000	1.000	24.000	1.000
BF3	28.000	2.250	28.000	2.250	24.000	2.000	24.000	2.000
BF4	28.000	1.500	28.000	1.500	24.000	1.000	24.000	1.000
BF5	28.000	1.500	28.000	1.500	24.000	1.000	24.000	1.000

✳✳ ALL DIMENSIONS ARE IN INCHES.

NCHRP 12-79

BRIDGE NISCS9

GIRDER ELEVATION TABLES

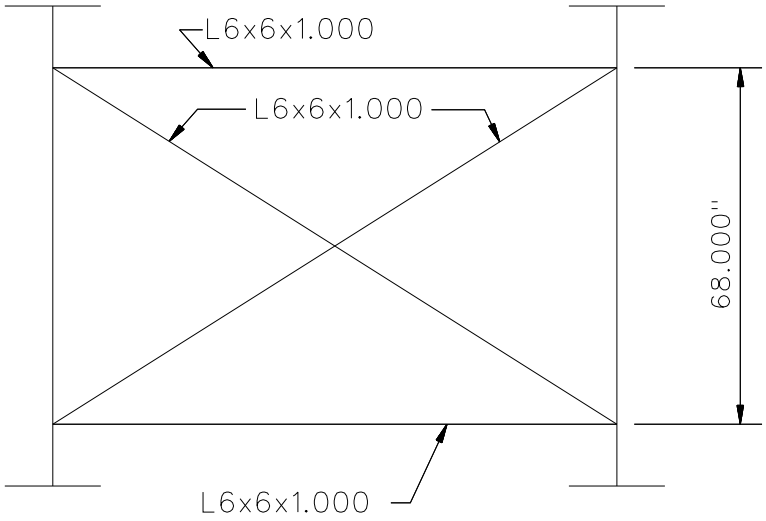

TYPICAL INTERMEDIATE AND END DIAPHRAGM

NOTES:

1. STEEL DEAD LOAD INCREASED BY 5% FOR MDX AND LARSA MODELS; 2% FOR 3D MODEL; AND 10% FOR APPROXIMATE ANALYSIS TO ACCOUNT FOR MISC. DETAILS.

2. FORMWORK LOAD OF 10PSF IS INCLUDED IN CONCRETE DEAD LOAD.

3. ADDITIONAL DESIGN PARAMETERS:
   A. 1.500' PARAPET WIDTH BOTH SIDES.
   B. 700 LB/FT UNIFORM LOAD ASSUMED FOR PARAPET WEIGHT.
   C. ROADWAY WIDTH = 77.000'.
   D. NUMBER OF DESIGN LANES = 6.
   E. HL93 LIVE LOAD.
   F. DESIGN SPEED = 35 MPH.

4. DIAPHRAGM MEMBER CALL-OUTS ARE IN ENGLISH UNITS.

NCHRP 12-79

BRIDGE NISCS9

MISC. DETAILS AND NOTES

SHEET 4 OF 8

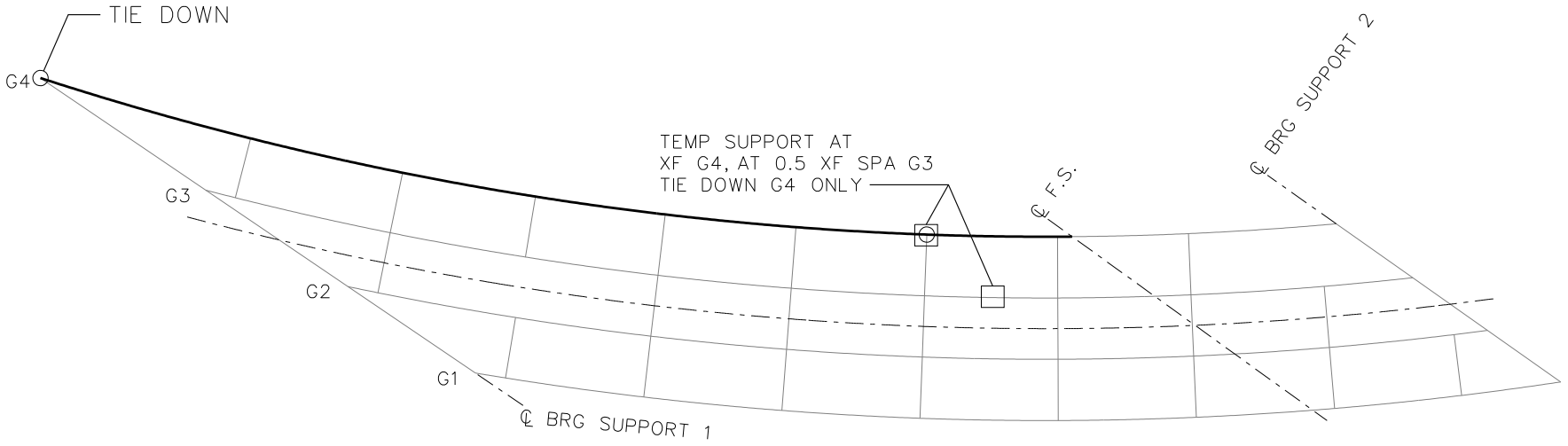

STAGE 1

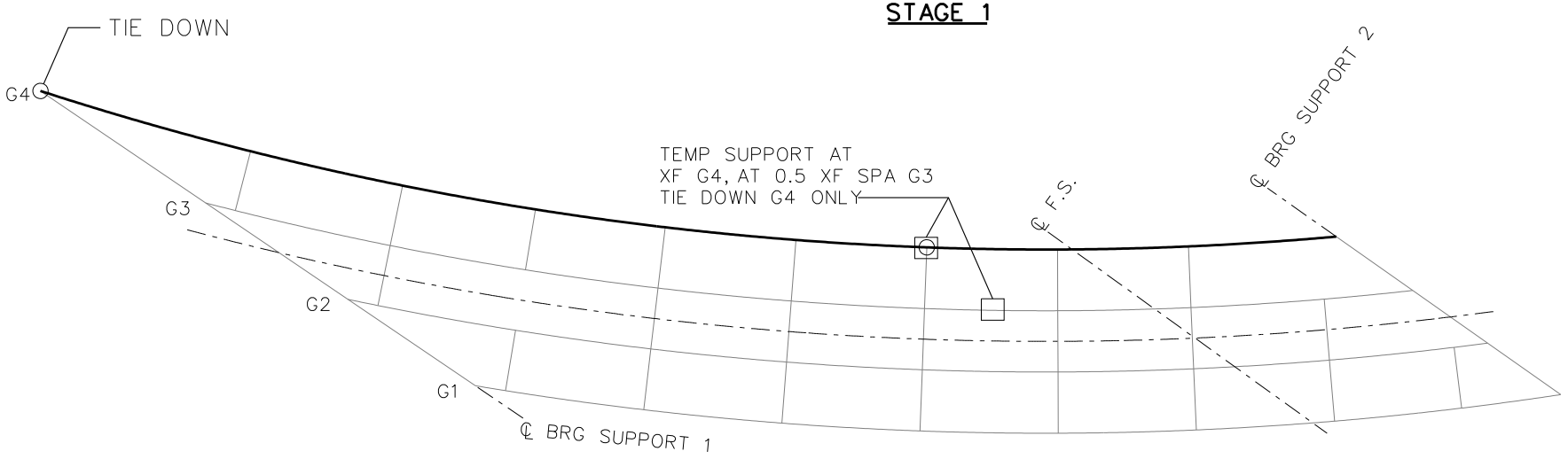

STAGE 2

LEGEND

▽ = HOLD OR LIFT CRANE

○ = TIE DOWN

□ = TEMPORARY SUPPORT STRUCTURE

NCHRP 12-79

BRIDGE NISCS9

GENERAL ERECTION PROCEDURE

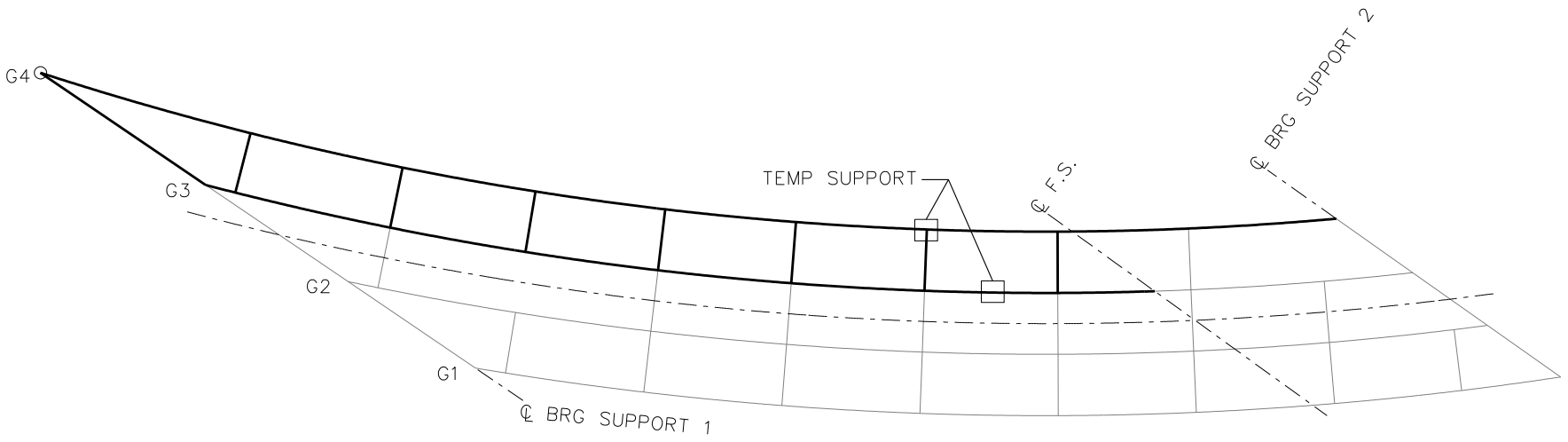

STAGE 3

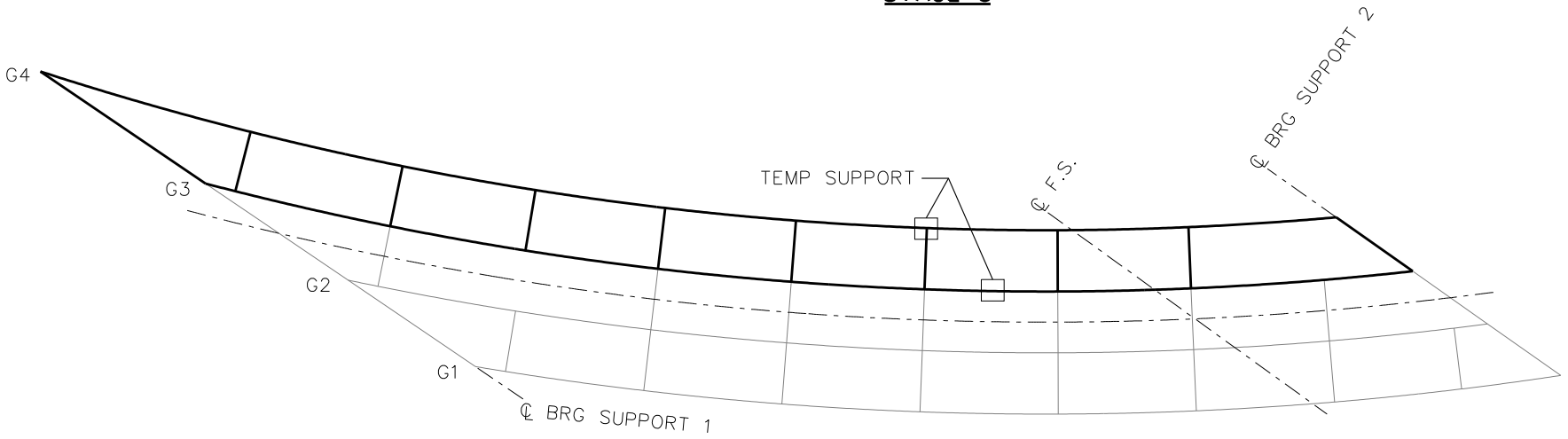

STAGE 4

LEGEND

▽ = HOLD OR LIFT CRANE

○ = TIE DOWN

□ = TEMPORARY SUPPORT STRUCTURE

NCHRP 12-79

BRIDGE NISCS9

GENERAL ERECTION PROCEDURE

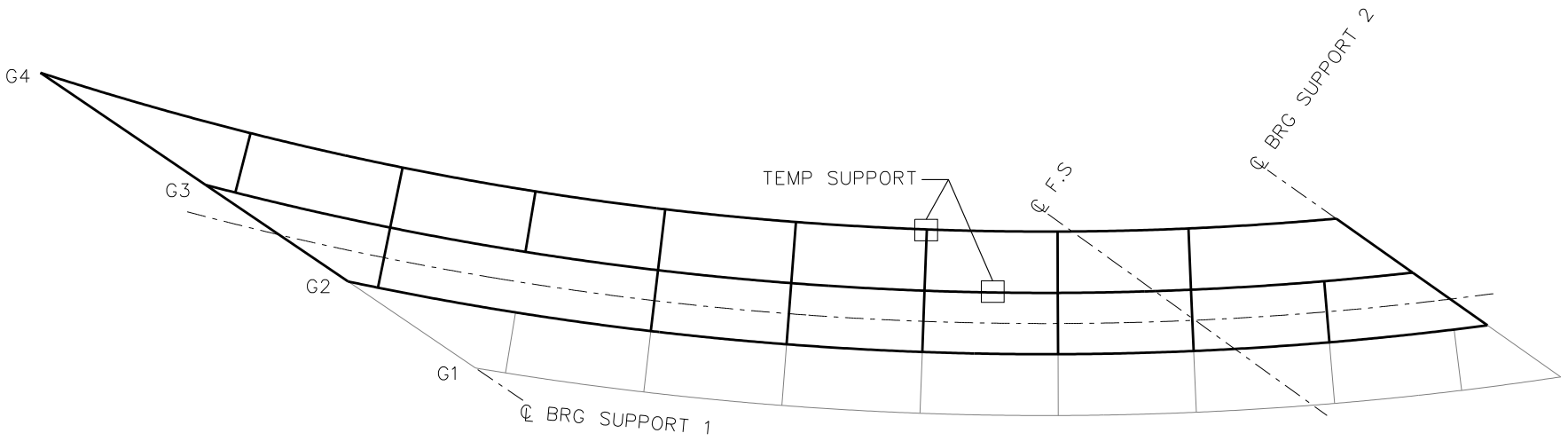

STAGE 5

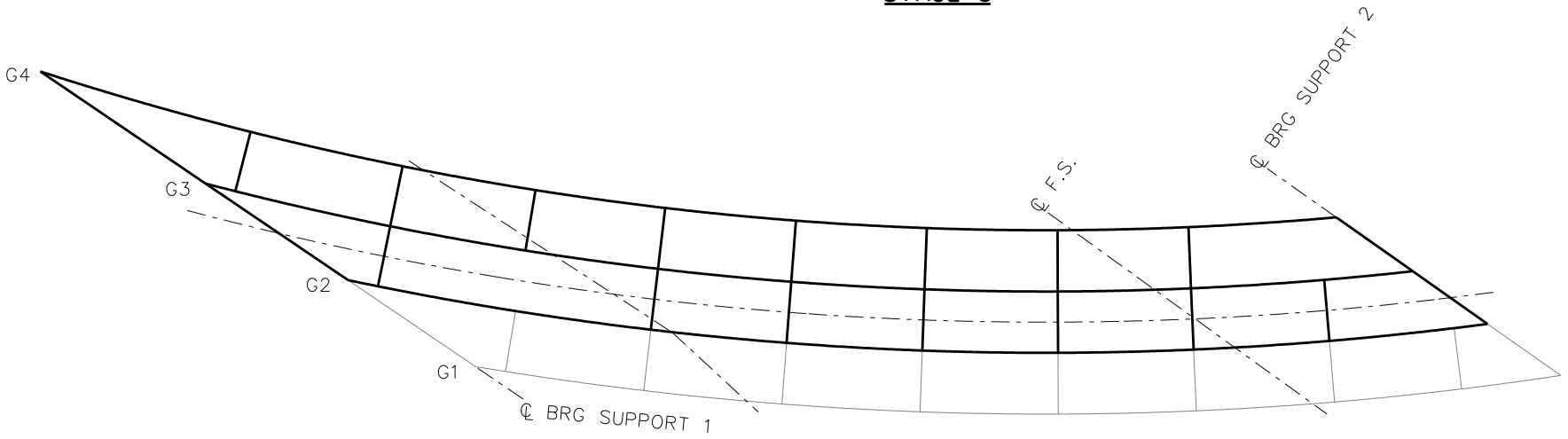

STAGE 6

ALL TEMP SUPPORTS REMOVED

LEGEND

▽ = HOLD OR LIFT CRANE

○ = TIE DOWN

□ = TEMPORARY SUPPORT STRUCTURE

NCHRP 12-79

BRIDGE NISCS9

GENERAL ERECTION PROCEDURE

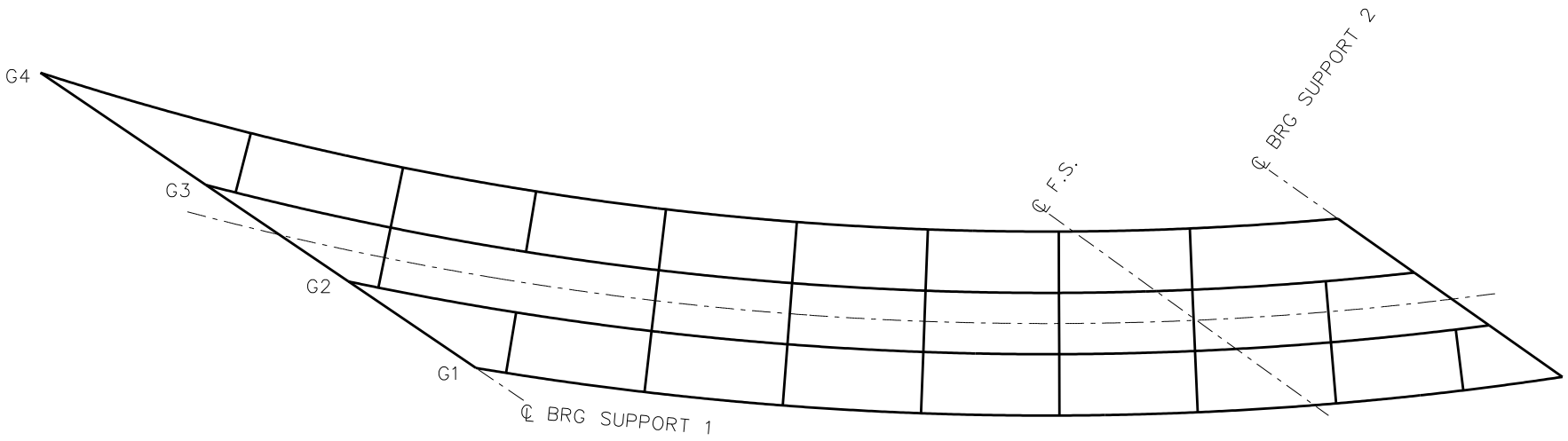

STAGE 7

LEGEND

▽ = HOLD OR LIFT CRANE

○ = TIE DOWN

□ = TEMPORARY SUPPORT STRUCTURE

NCHRP 12-79

BRIDGE NISCS9

GENERAL ERECTION PROCEDURE

NCHRP 12-79

NISCS14

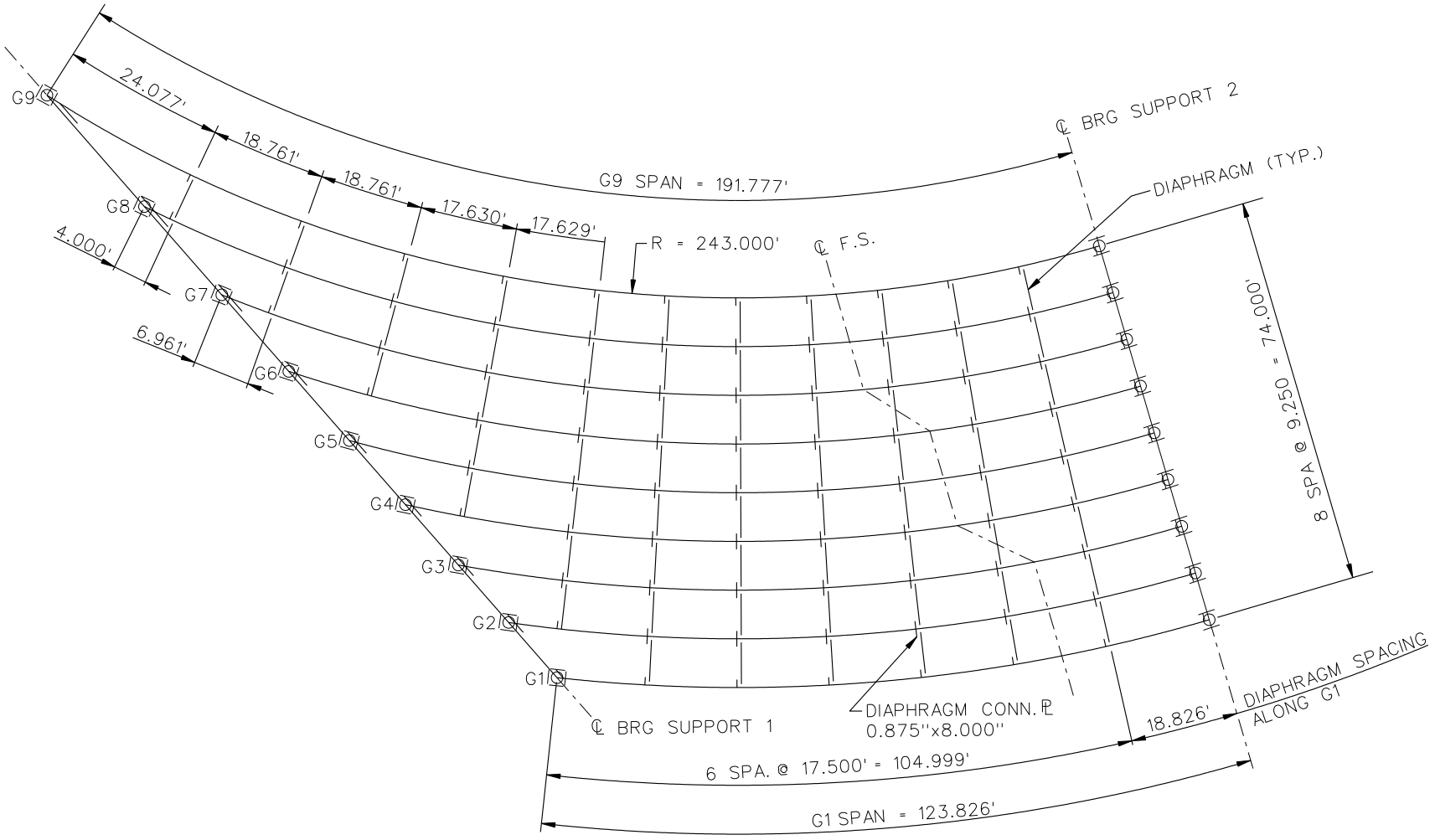

FRAMING PLAN

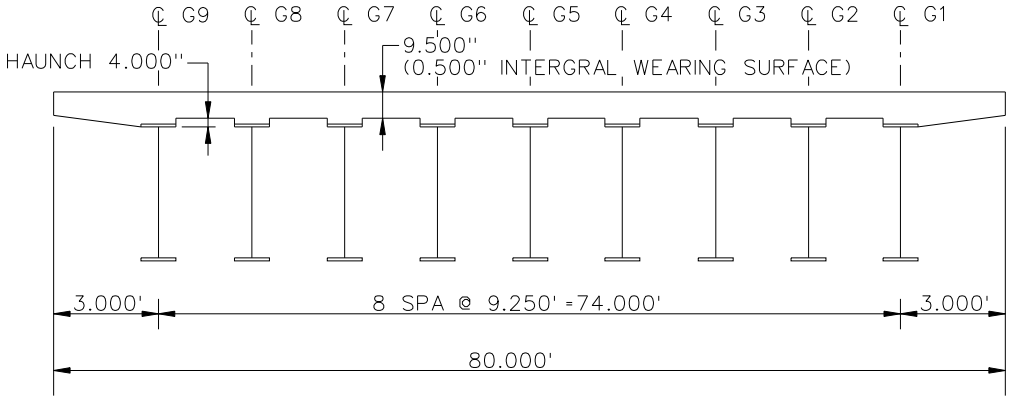

CROSS - SECTION

(DIAPHRAGMS NOT SHOWN)

BEARING LEGEND

- O NON-GUIDED
- O LONGITUDINALLY GUIDED
- O TRANSVERSELY GUIDED
- O FIXED

NCHRP 12-79

BRIDGE NISCS14

FRAMING PLAN AND CROSS-SECTION

SHEET 1 OF 9

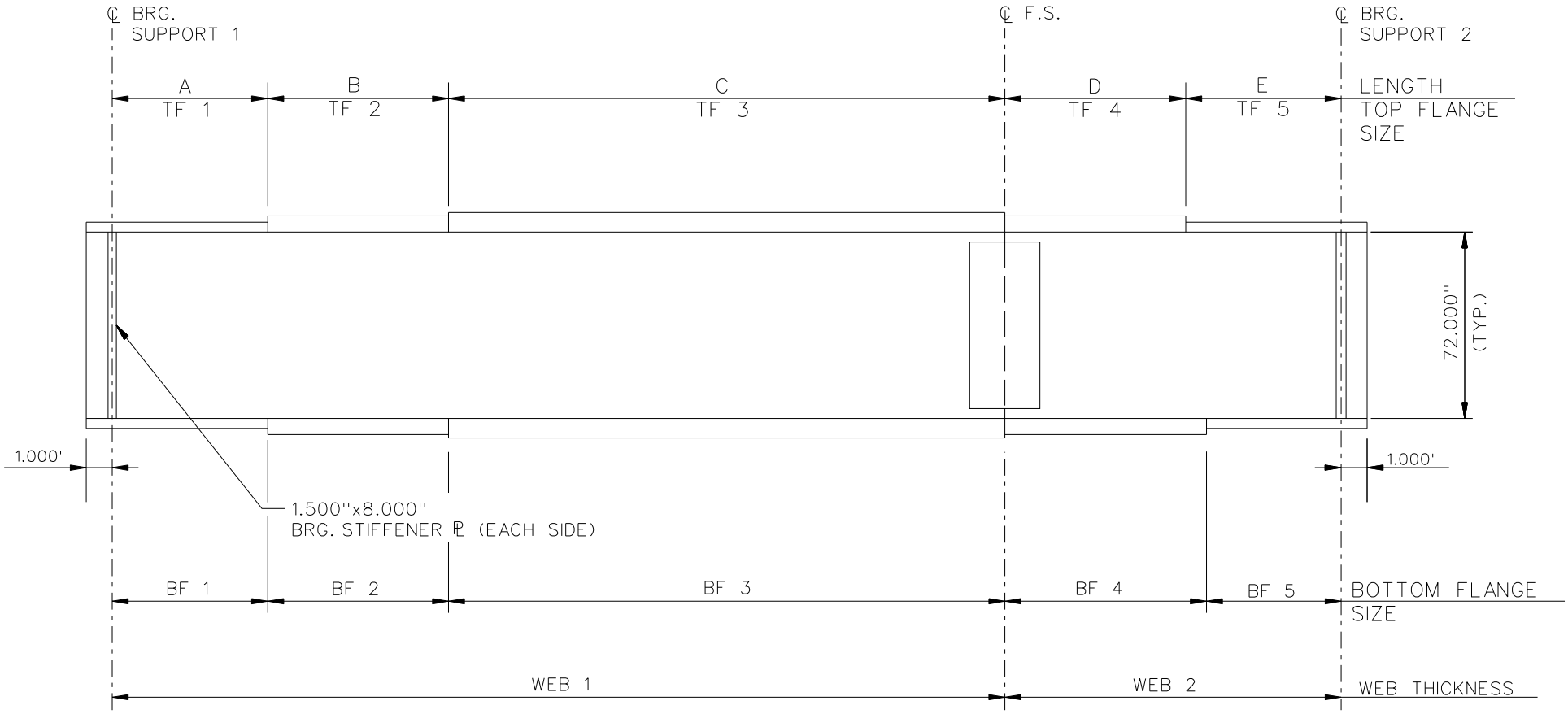

NOTES:

1. SEE TABLES ON SHEET 3 FOR GIRDER ELEVATION DIMENSIONS AND PLATE SIZES.

2. ALL GIRDERS, WEB 1 = WEB 2 = 0.750"

NCHRP 12-79

BRIDGE NISCS14

GIRDER ELEVATION

SHEET 2 OF 9

	GIRDER PLATE LENGTHS ✳								
LENGTH	G1	G2	G3	G4	G5	G6	G7	G8	G9
A	15.000	16.000	15.000	17.500	17.500	20.000	20.000	27.500	35.000
B	15.000	16.000	15.000	17.500	17.500	20.000	20.000	27.500	35.000
C	65.826	69.740	78.003	67.712	75.000	78.068	77.240	73.084	71.777
D	14.000	14.000	14.000	20.000	20.000	20.000	25.000	25.000	25.000
E	14.000	14.000	14.000	20.000	20.000	20.000	25.000	25.000	25.000

✳ ALL DIMENSIONS ARE IN FEET.

	GIRDER FLANGE DIMENSIONS ✳✳					
TOP	G1, G2, G3		G4, G5, G6		G7, G8, G9	
FLANGE	BF	TF	BF	TF	BF	TF
TF1	20.000	1.000	24.000	1.000	28.000	1.500
TF2	20.000	1.000	24.000	1.000	28.000	1.500
TF3	20.000	2.000	24.000	1.000	28.000	1.500
TF4	20.000	1.000	24.000	1.000	28.000	1.500
TF5	20.000	1.000	24.000	1.000	28.000	1.500

✳✳ ALL DIMENSIONS ARE IN INCHES.

	GIRDER FLANGE DIMENSIONS ✳✳					
BOTTOM	G1, G2, G3		G4, G5, G6		G7, G8, G9	
FLANGE	BF	TF	BF	TF	BF	TF
BF1	28.000	1.500	28.000	1.500	30.000	1.750
BF2	28.000	1.500	28.000	1.500	30.000	1.750
BF3	28.000	2.250	28.000	2.250	30.000	1.750
BF4	28.000	1.500	28.000	1.500	30.000	1.750
BF5	28.000	1.500	28.000	1.500	30.000	1.750

✳✳ ALL DIMENSIONS ARE IN INCHES.

NCHRP 12-79

BRIDGE NISCS14

GIRDER ELEVATION TABLES

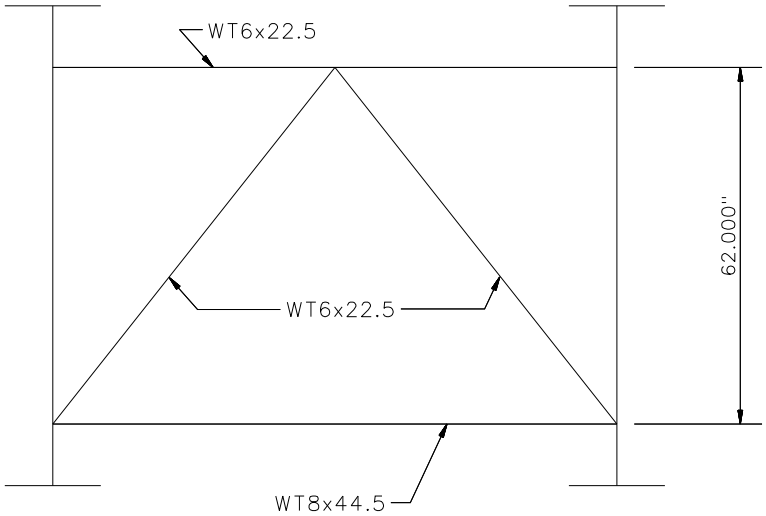

TYPICAL END DIAPHRAGM

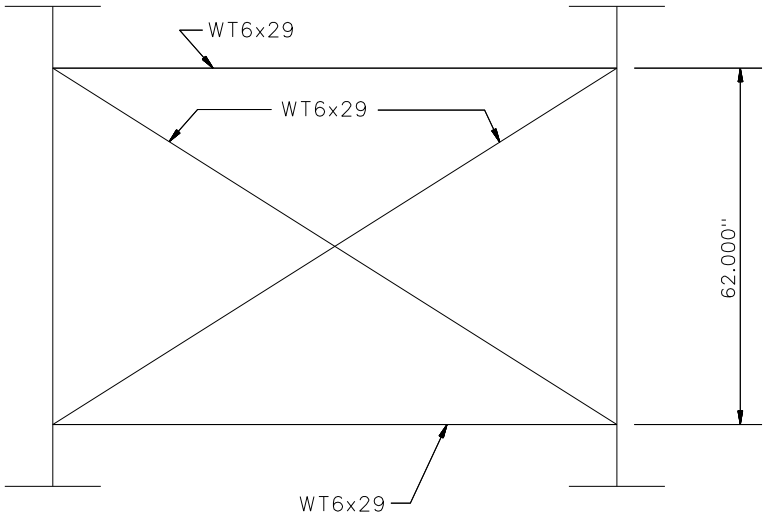

TYPICAL INTERMEDIATE DIAPHRAGM

NOTES:

1. STEEL DEAD LOAD INCREASED BY 5% FOR MDX AND LARSA MODELS; 2% FOR 3D MODEL; AND 10% FOR APPROXIMATE ANALYSIS TO ACCOUNT FOR MISC. DETAILS.

2. FORMWORK LOAD OF 10PSF IS INCLUDED IN CONCRETE DEAD LOAD.

3. ADDITIONAL DESIGN PARAMETERS:
   A. 1.500' PARAPET WIDTH BOTH SIDES.
   B. 700 LB/FT UNIFORM LOAD ASSUMED FOR PARAPET WEIGHT.
   C. ROADWAY WIDTH = 77.000'.
   D. NUMBER OF DESIGN LANES = 6.
   E. HL93 LIVE LOAD.
   F. DESIGN SPEED = 35 MPH.

4. DIAPHRAGM MEMBER CALL-OUTS ARE IN ENGLISH UNITS.

NCHRP 12-79

BRIDGE NISCS14

MISC. DETAILS AND NOTES

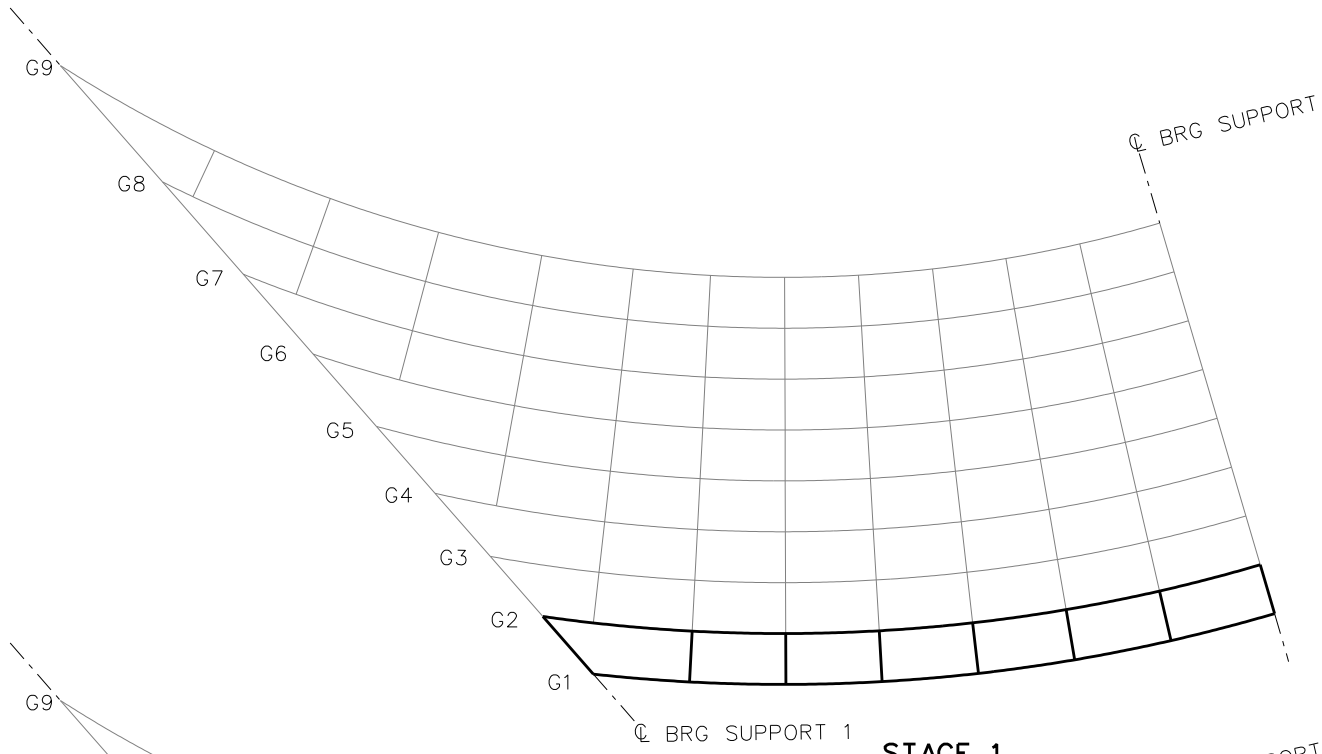

STAGE 1

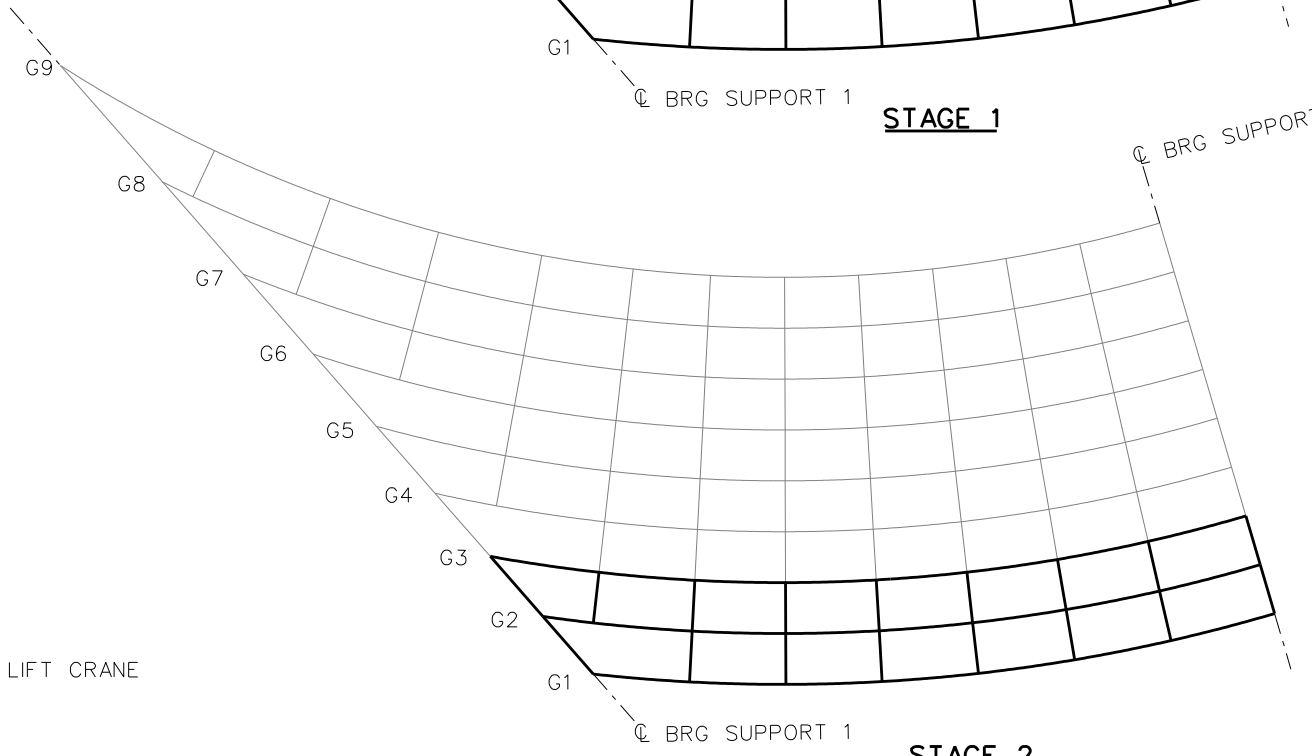

STAGE 2

LEGEND

▽ = HOLD OR LIFT CRANE

○ = TIE DOWN

□ = TEMPORARY SUPPORT STRUCTURE

NCHRP 12-79

BRIDGE NISCS14

GENERAL ERECTION PROCEDURE

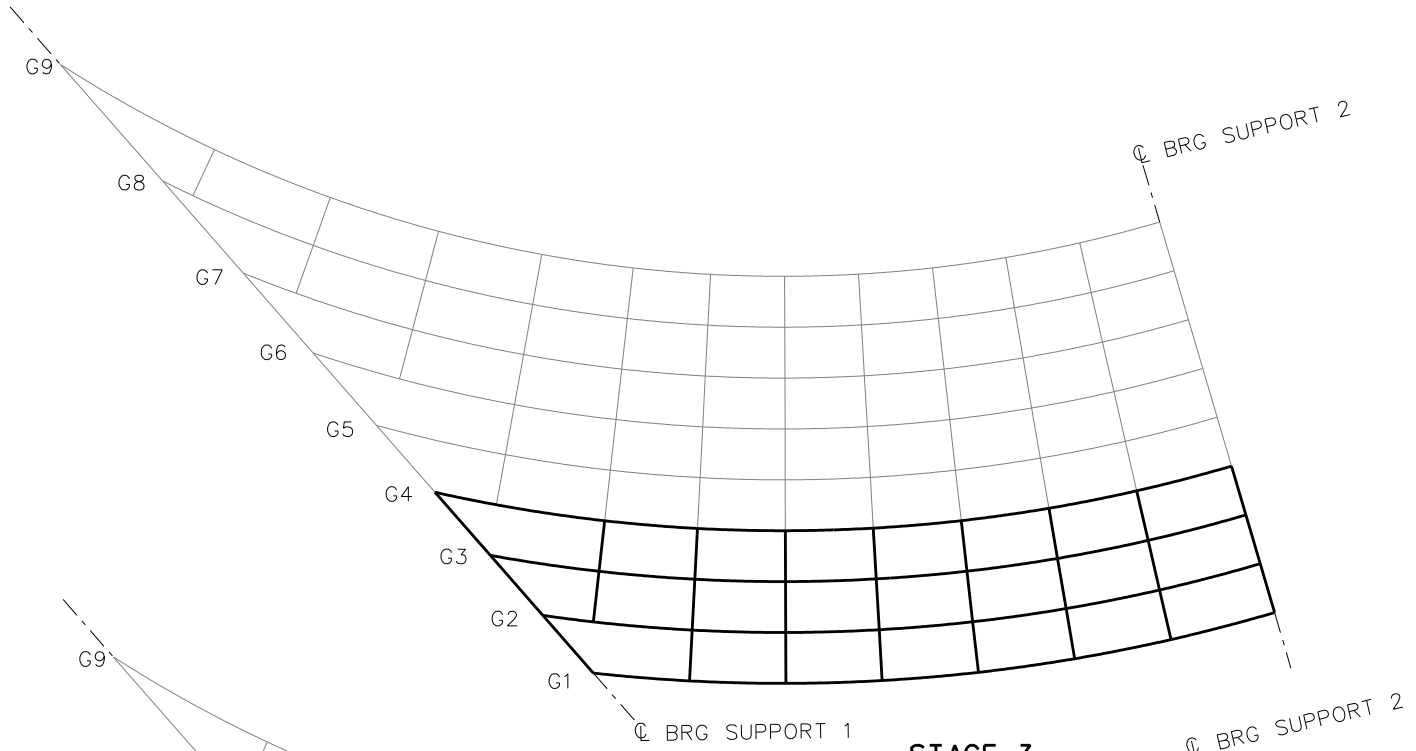

STAGE 3

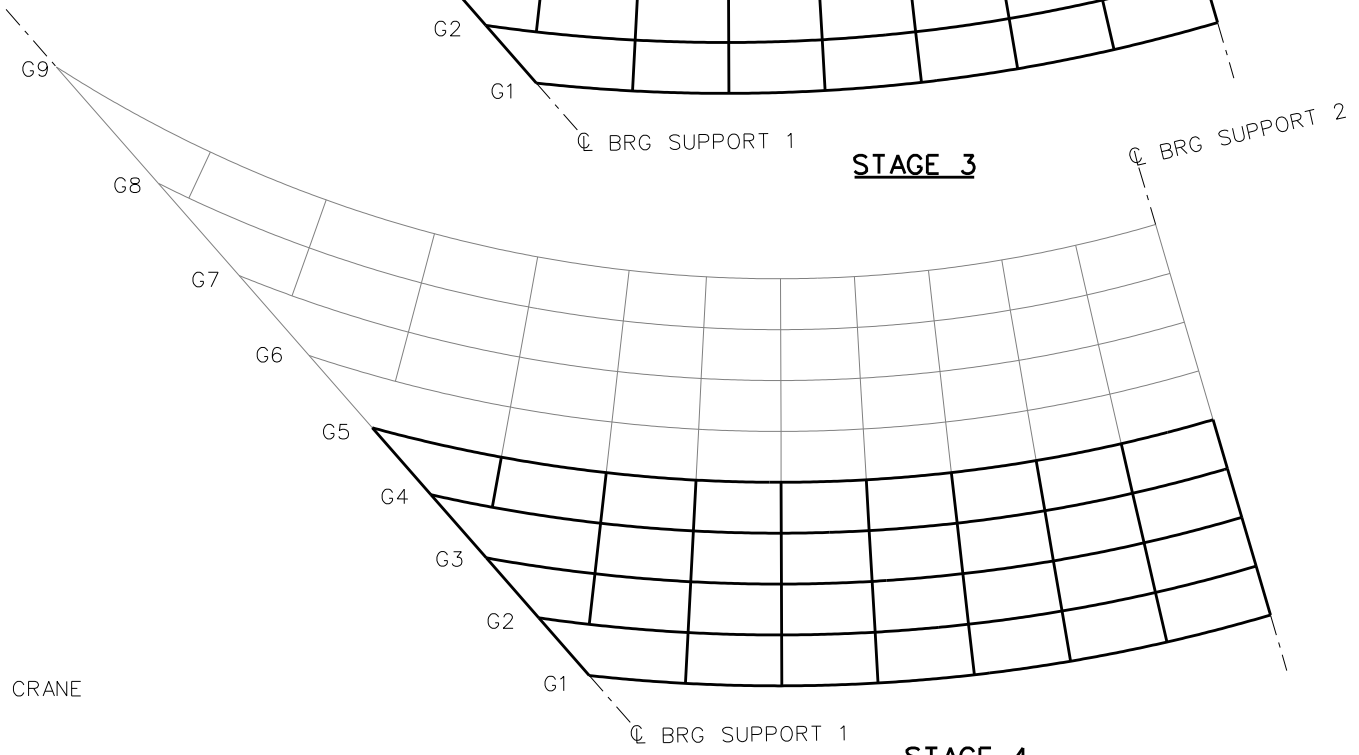

STAGE 4

LEGEND

▽ = HOLD OR LIFT CRANE

○ = TIE DOWN

□ = TEMPORARY SUPPORT STRUCTURE

NCHRP 12-79

BRIDGE NISCS14

GENERAL ERECTION PROCEDURE

SHEET 6 OF 9

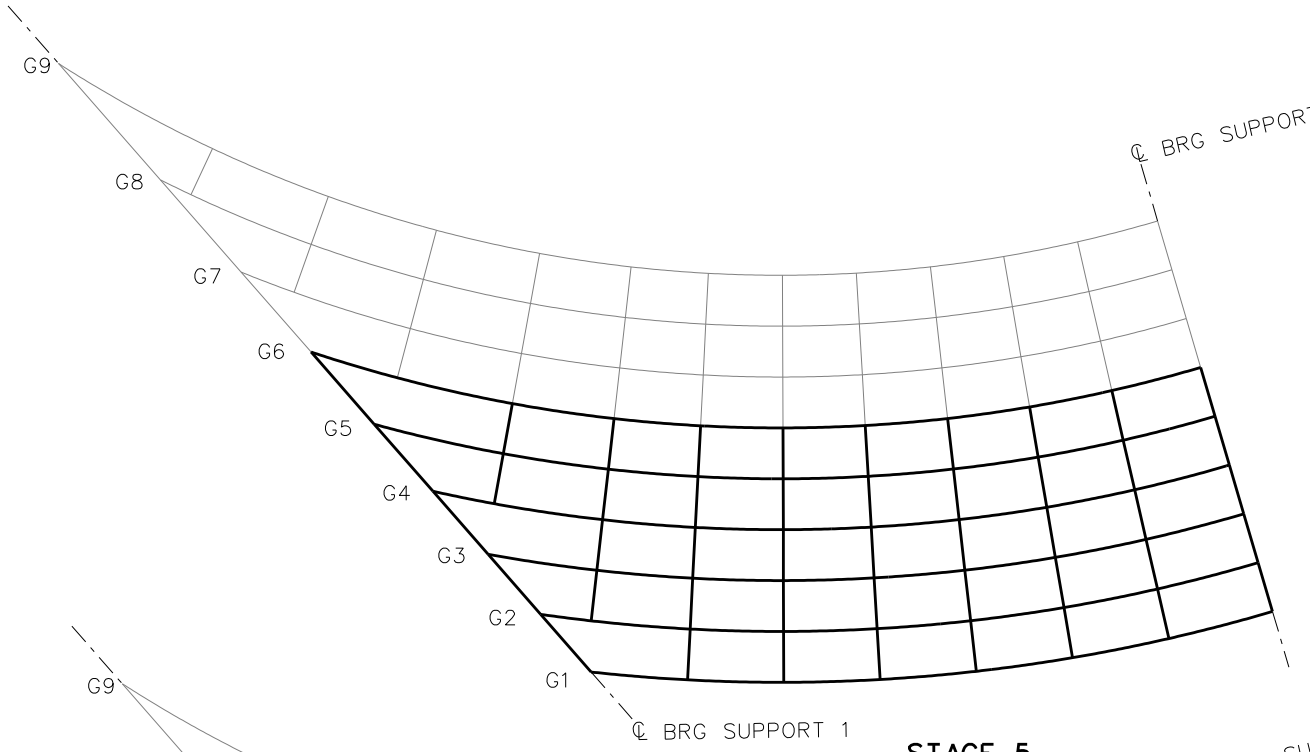

STAGE 5

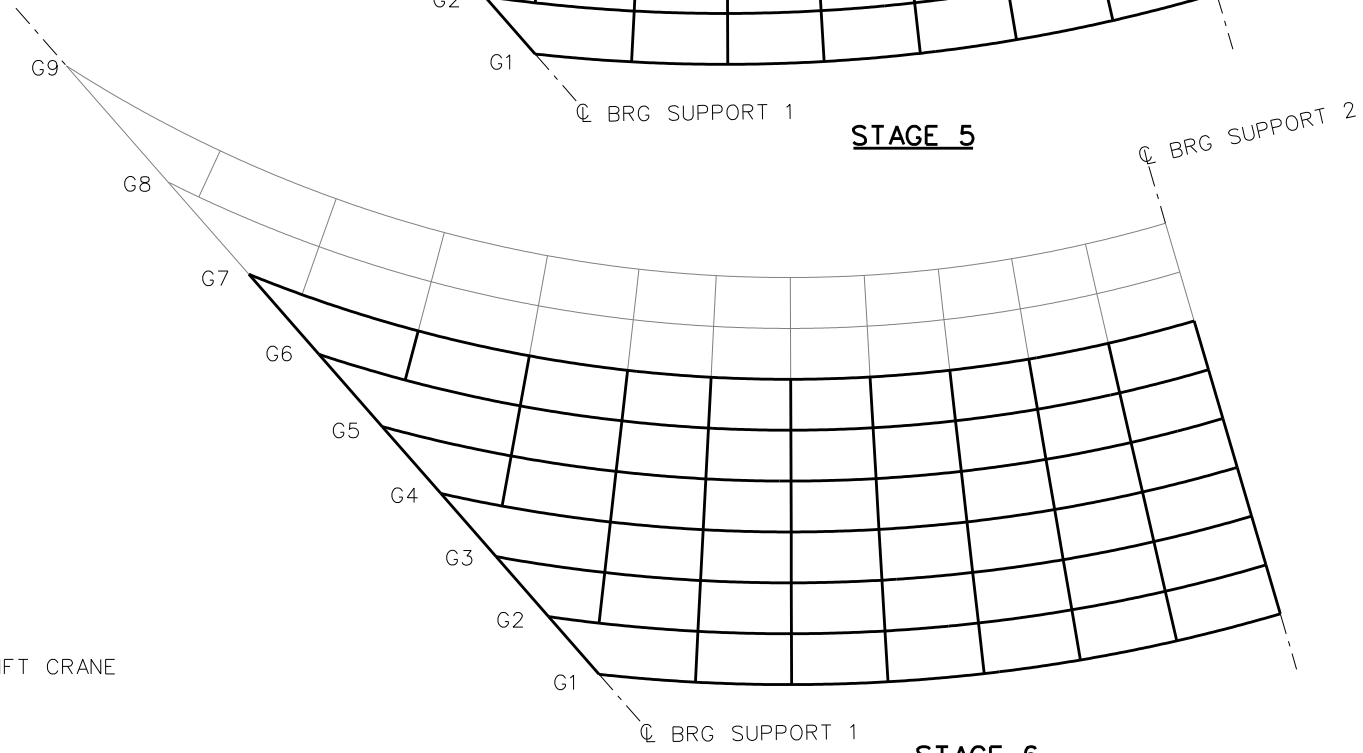

STAGE 6

LEGEND

▽ = HOLD OR LIFT CRANE

○ = TIE DOWN

□ = TEMPORARY SUPPORT STRUCTURE

NCHRP 12-79

BRIDGE NISCS14

GENERAL ERECTION PROCEDURE

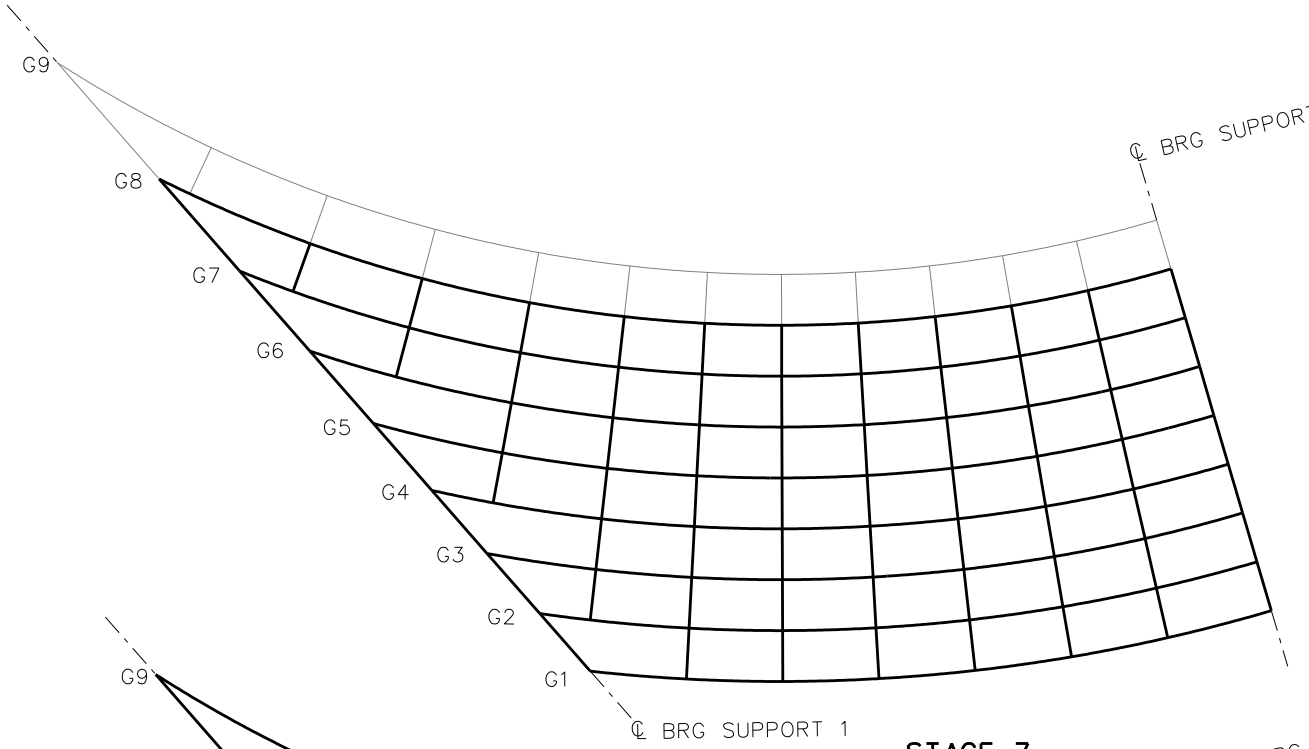

STAGE 7

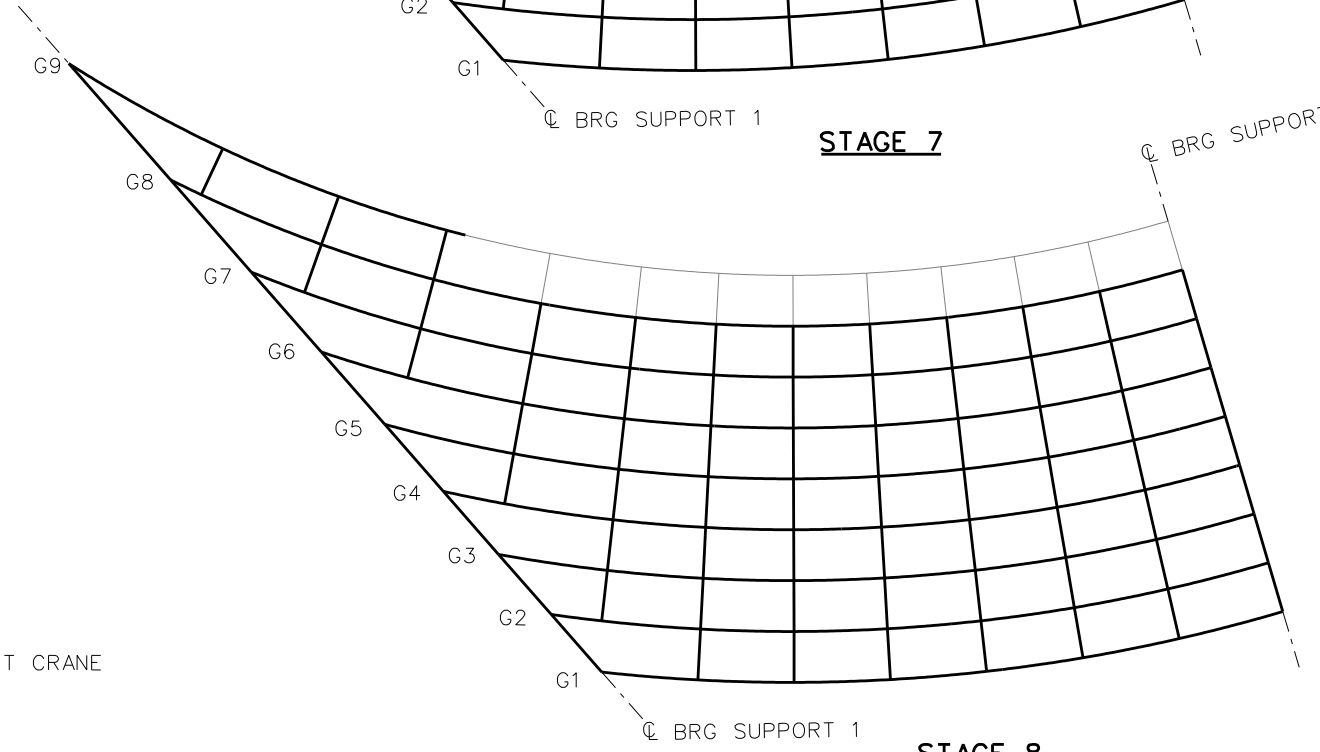

STAGE 8

LEGEND

▽ = HOLD OR LIFT CRANE

○ = TIE DOWN

□ = TEMPORARY SUPPORT STRUCTURE

NCHRP 12-79

BRIDGE NISCS14

GENERAL ERECTION PROCEDURE

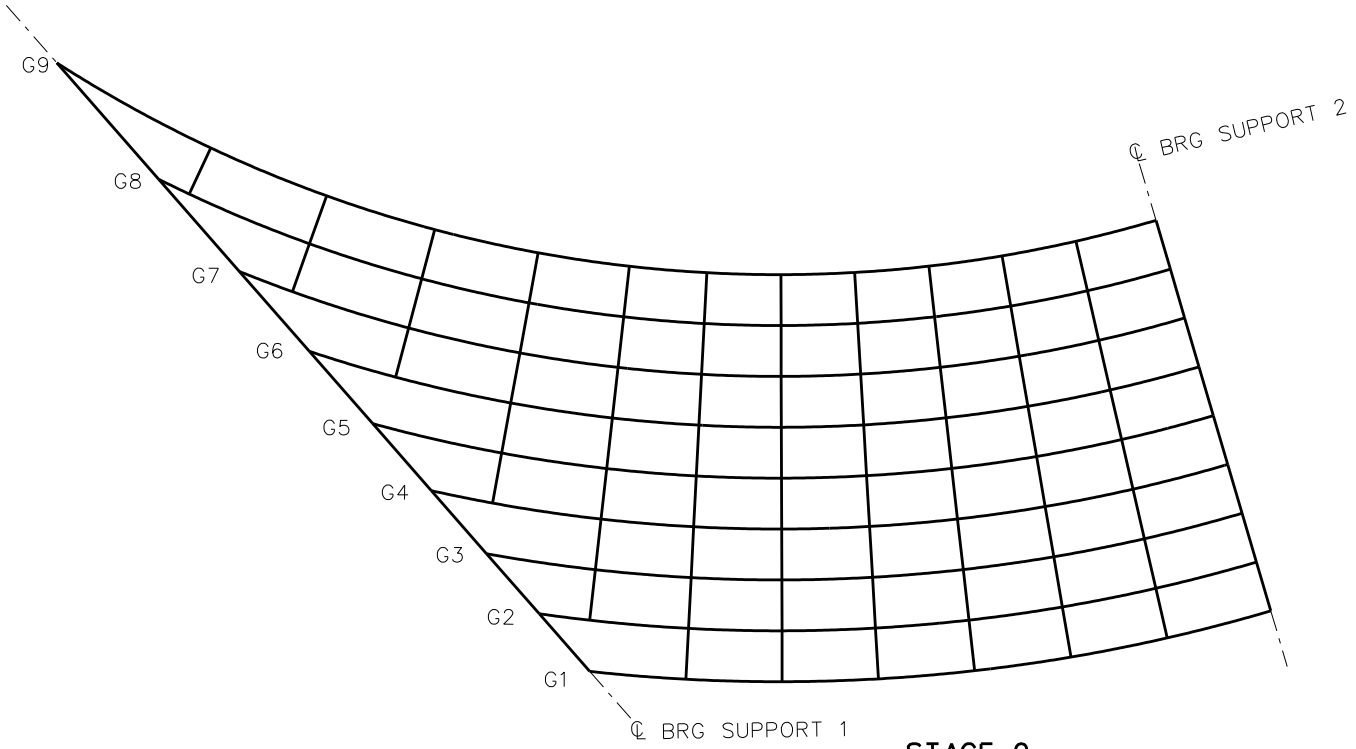

STAGE 9

LEGEND

▽ = HOLD OR LIFT CRANE

○ = TIE DOWN

□ = TEMPORARY SUPPORT STRUCTURE

NCHRP 12-79

BRIDGE NISCS14

GENERAL ERECTION PROCEDURE

SHEET 9 OF 9

NCHRP 12-79

NISCS15

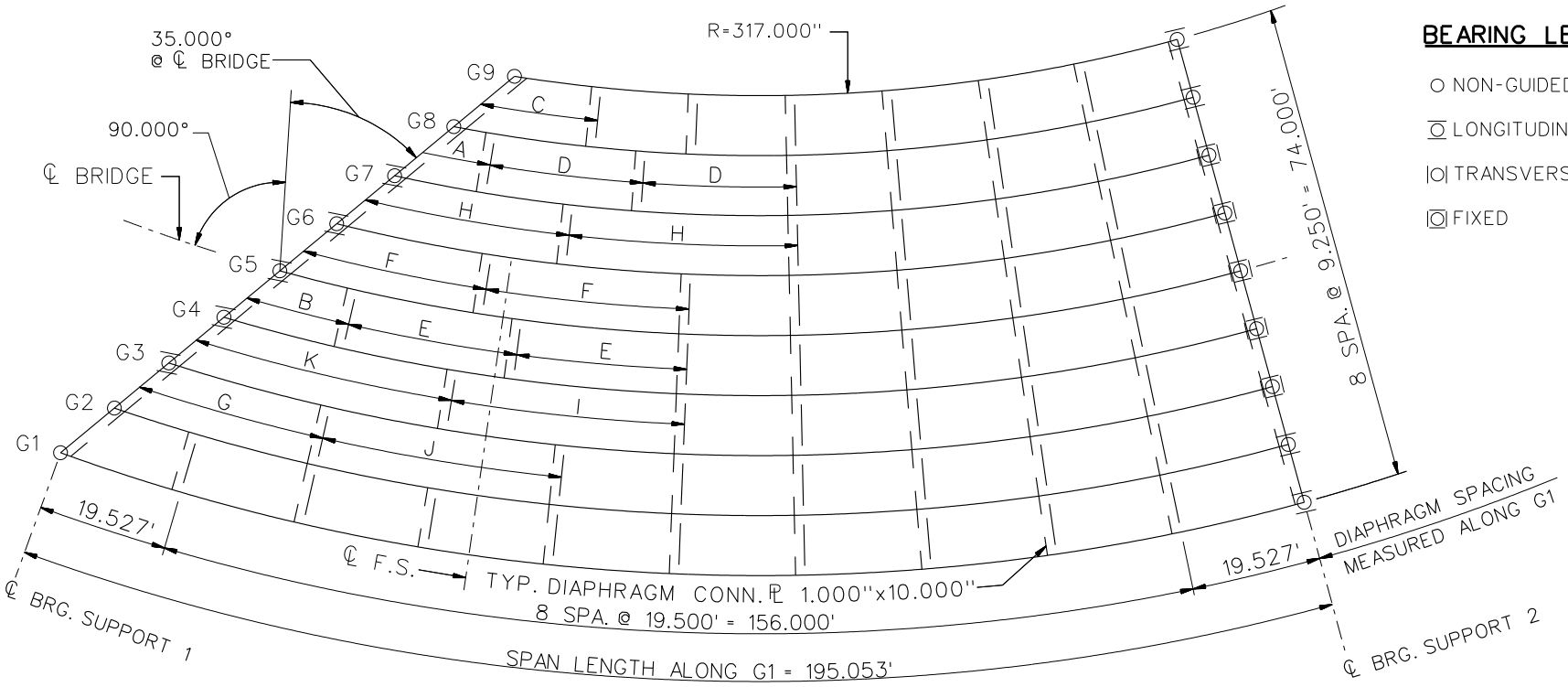

FRAMING PLAN

BEARING LEGEND

- ○ NON-GUIDED
- ⊙ LONGITUDINALLY GUIDED
- |⊙| TRANSVERSELY GUIDED
- |⊙| FIXED

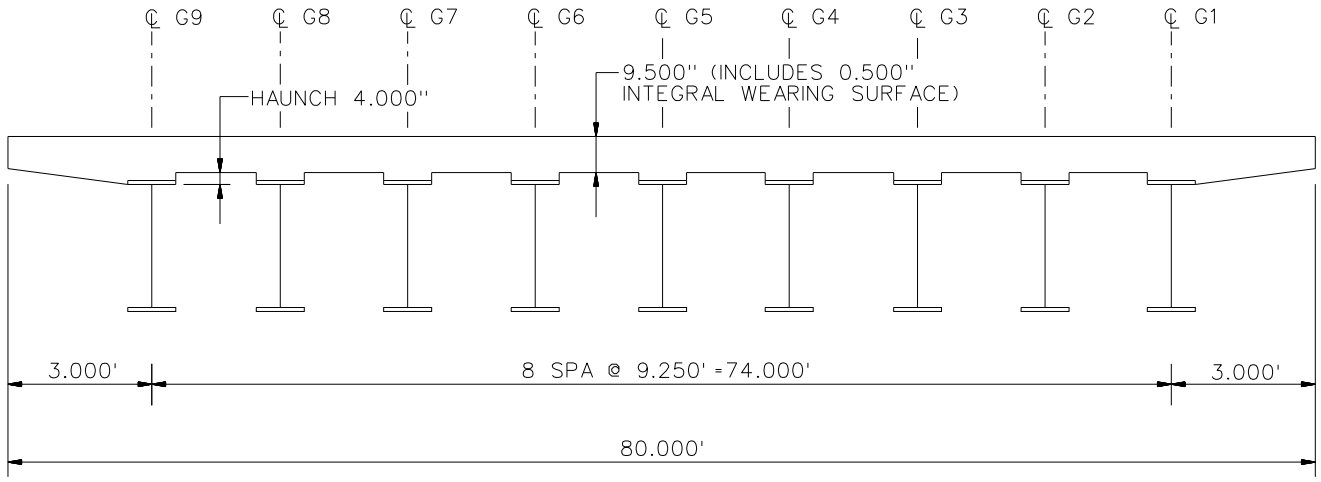

CROSS - SECTION

(DIAPHRAGMS NOT SHOWN)

CROSSFRAME SPACING			
A	14.273'	G	32.423'
B	19.015'	H	35.935'
C	22.004'	I	36.724'
D	24.129'	J	37.862'
E	26.689'	K	44.118'
F	31.928'		

NCHRP 12-79

BRIDGE NISCS15

FRAMING PLAN AND CROSS-SECTION

SHEET 1 OF 10

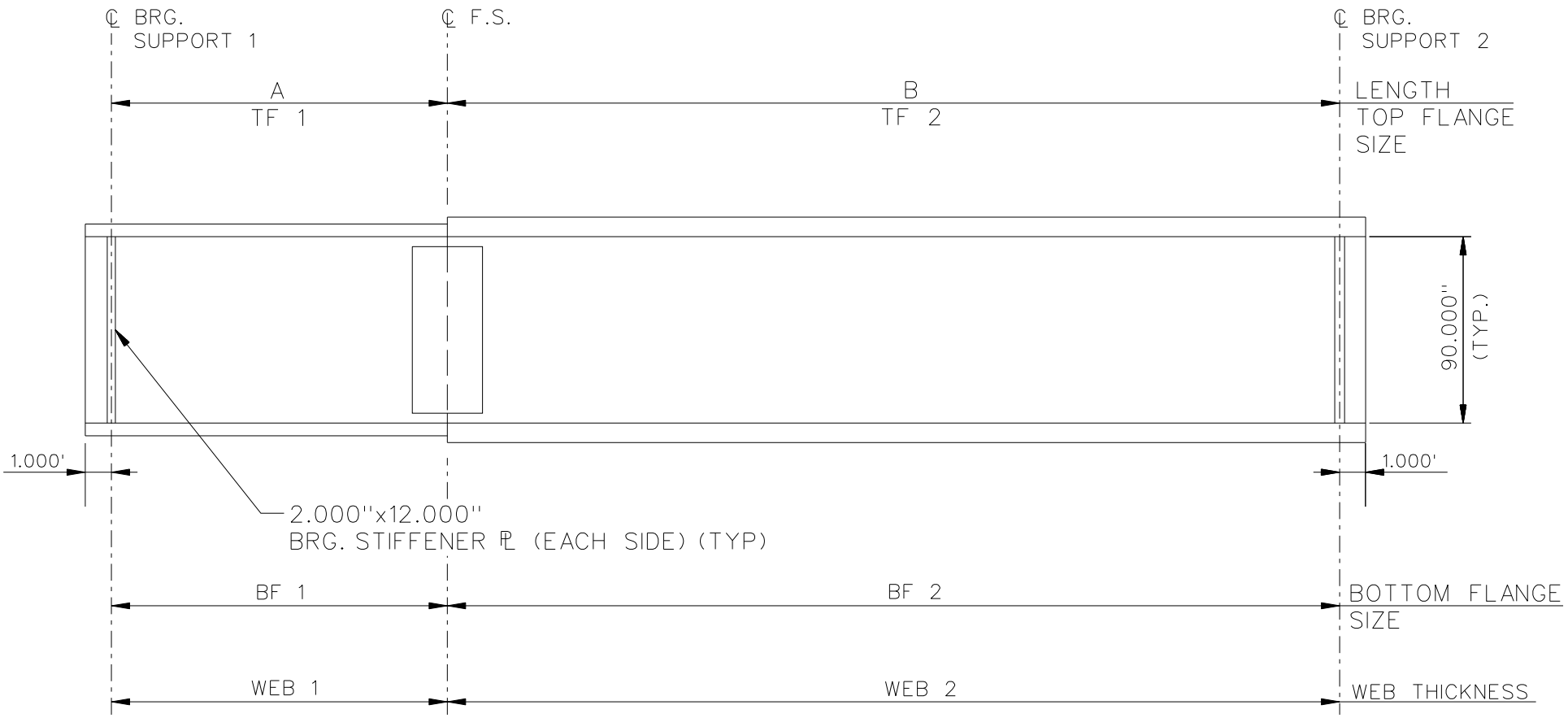

NOTE :

1. SEE TABLES ON SHEET 3 FOR GIRDER ELEVATION DIMENSIONS AND PLATE SIZES.

2. GIRDERS G1, G2, G3, WEB 1 = WEB 2 = 0.875"
   GIRDERS G4, G5, G6, WEB 1 = WEB 2 = 0.6875"
   GIRDERS G7, G8, G9, WEB 1 = WEB 2 = 0.625".

NCHRP 12-79

BRIDGE NISCS15

GIRDER ELEVATION

SHEET 2 OF 10

	GIRDER PLATE LENGTHS ✳								
LENGTH	G1	G2	G3	G4	G5	G6	G7	G8	G9
A	65.053	57.691	50.264	42.763	35.174	27.479	126.897	115.124	103.165
B	130.000	126.206	122.413	118.620	114.826	111.033	000.000	000.000	000.000

ALL DIMENSIONS ARE IN FEET.

	GIRDER FLANGE DIMENSIONS ✳✳					
TOP FLANGE	G1, G2, G3		G4, G5, G6		G7, G8, G9	
	BF	TF	BF	TF	BF	TF
TF1	30.000	2.750	26.000	2.750	24.000	1.500
TF2	30.000	2.750	26.000	2.750		

✳✳ ALL DIMENSIONS ARE IN INCHES.

	GIRDER FLANGE DIMENSIONS ✳✳							
TOP FLANGE	G1		G2, G3		G4, G5, G6		G7, G8, G9	
	BF	TF	BF	TF	BF	TF	BF	TF
BF1	32.000	3.250	32.000	3.000	28.000	2.000	24.000	1.500
BF2	32.000	3.250	32.000	3.000	28.000	2.000		

✳✳ ALL DIMENSIONS ARE IN INCHES.

NCHRP 12-79

BRIDGE NISCS15

GIRDER ELEVATION TABLES

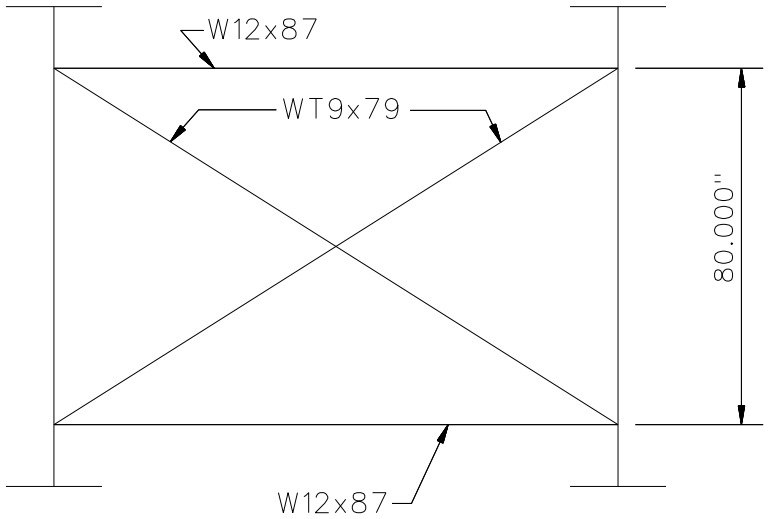

TYPICAL INTERMEDIATE AND END DIAPHRAGM

NOTES:

1. STEEL DEAD LOAD INCREASED BY 5% FOR MDX AND LARSA MODELS; 2% FOR 3D MODEL; AND 10% FOR APPROXIMATE ANALYSIS TO ACCOUNT FOR MISC. DETAILS.

2. FORMWORK LOAD OF 10PSF IS INCLUDED IN CONCRETE DEAD LOAD.

3. ADDITIONAL DESIGN PARAMETERS:
   A. 1.500' PARAPET WIDTH BOTH SIDES.
   B. 700 LB/FT UNIFORM LOAD ASSUMED FOR PARAPET WEIGHT.
   C. ROADWAY WIDTH = 76.500'.
   D. NUMBER OF DESIGN LANES = 6.
   E. HL93 LIVE LOAD.
   F. DESIGN SPEED = 35 MPH.

4. DIAPHRAGM MEMBER CALL-OUTS ARE IN ENGLISH UNITS.

NCHRP 12-79

BRIDGE NISCS15

MISC. DETAILS AND NOTES

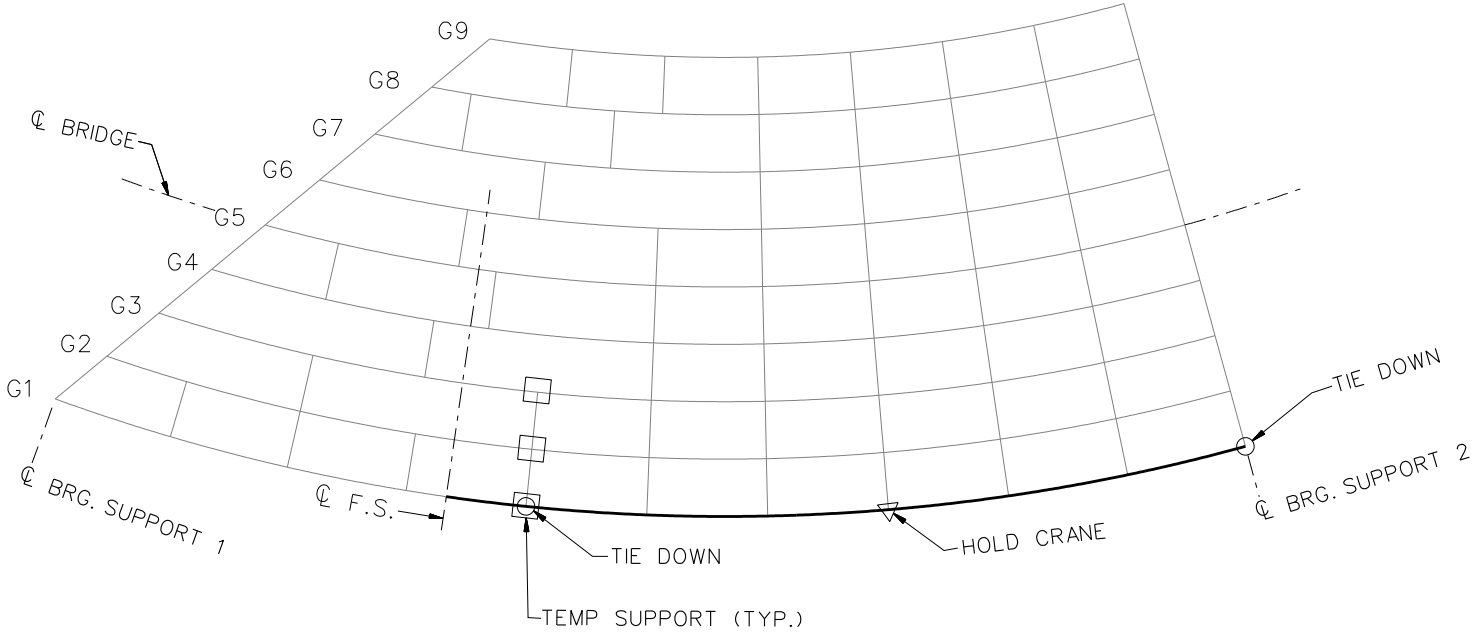

STAGE 1

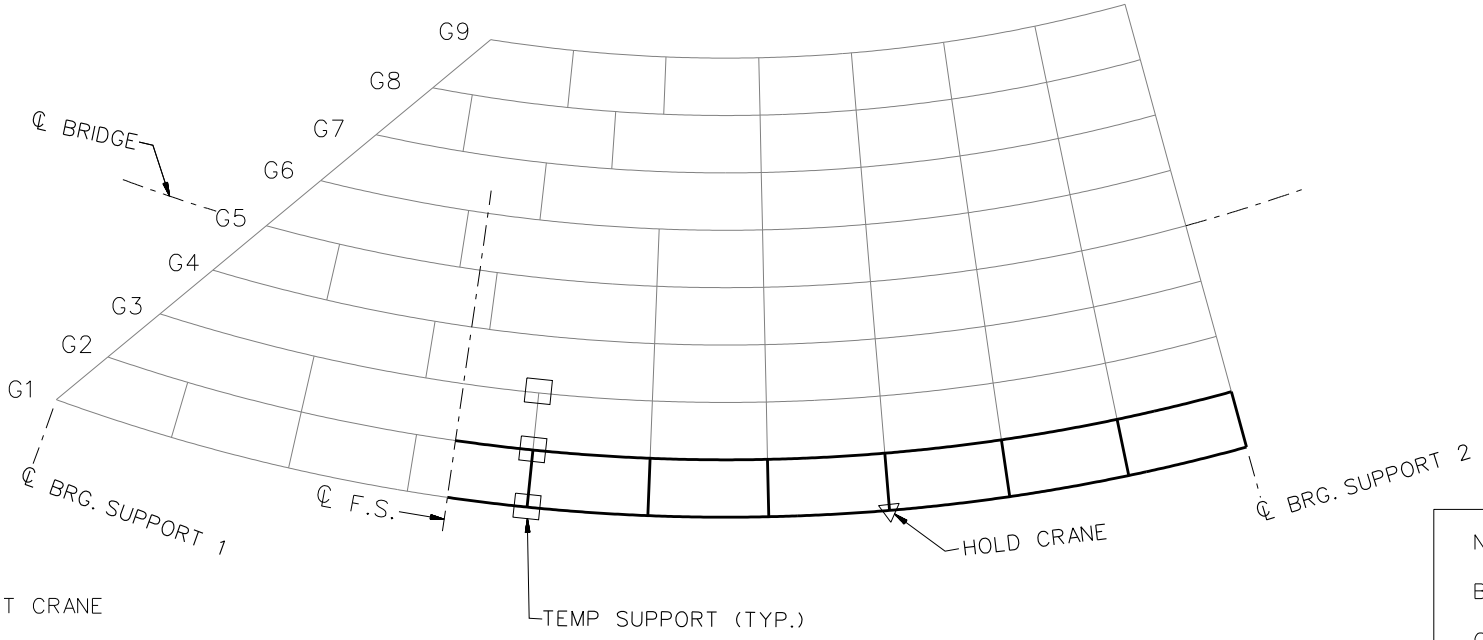

STAGE 2

LEGEND

▽ = HOLD OR LIFT CRANE

○ = TIE DOWN

□ = TEMPORARY SUPPORT STRUCTURE

NCHRP 12-79

BRIDGE NISCS15

GIRDER ERECTION PROCEDURE

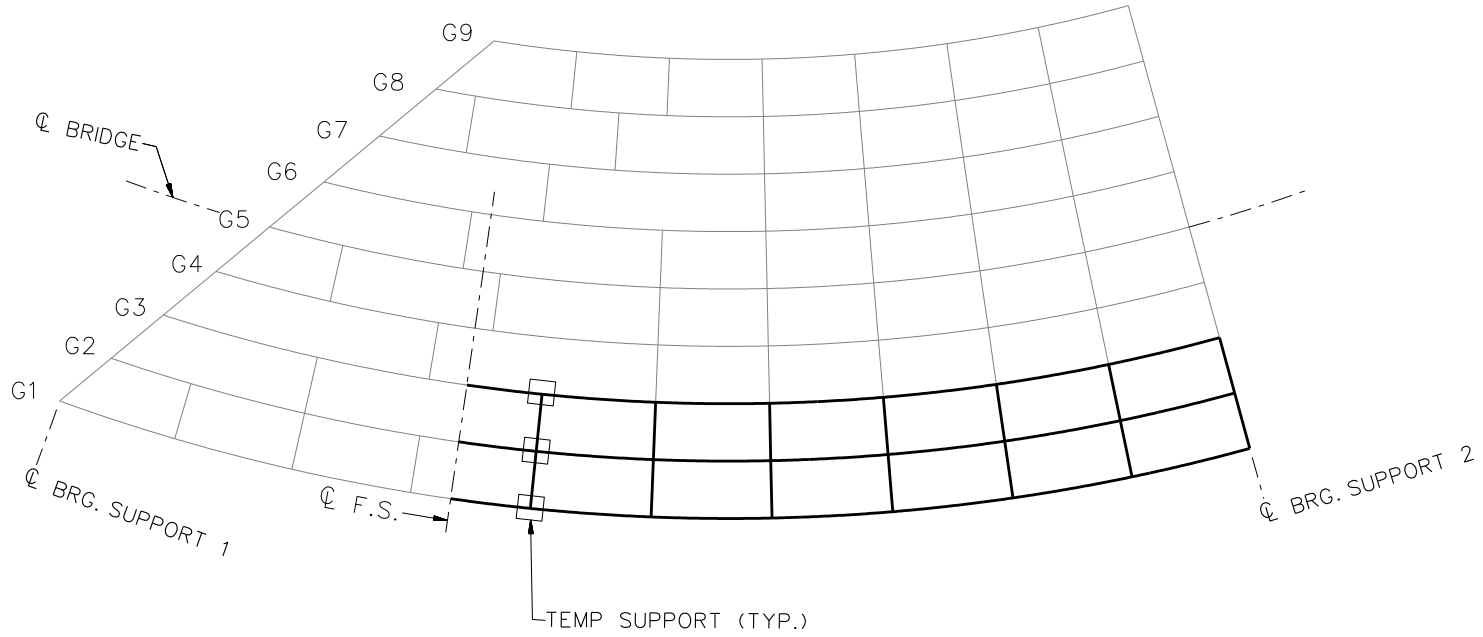

STAGE 3

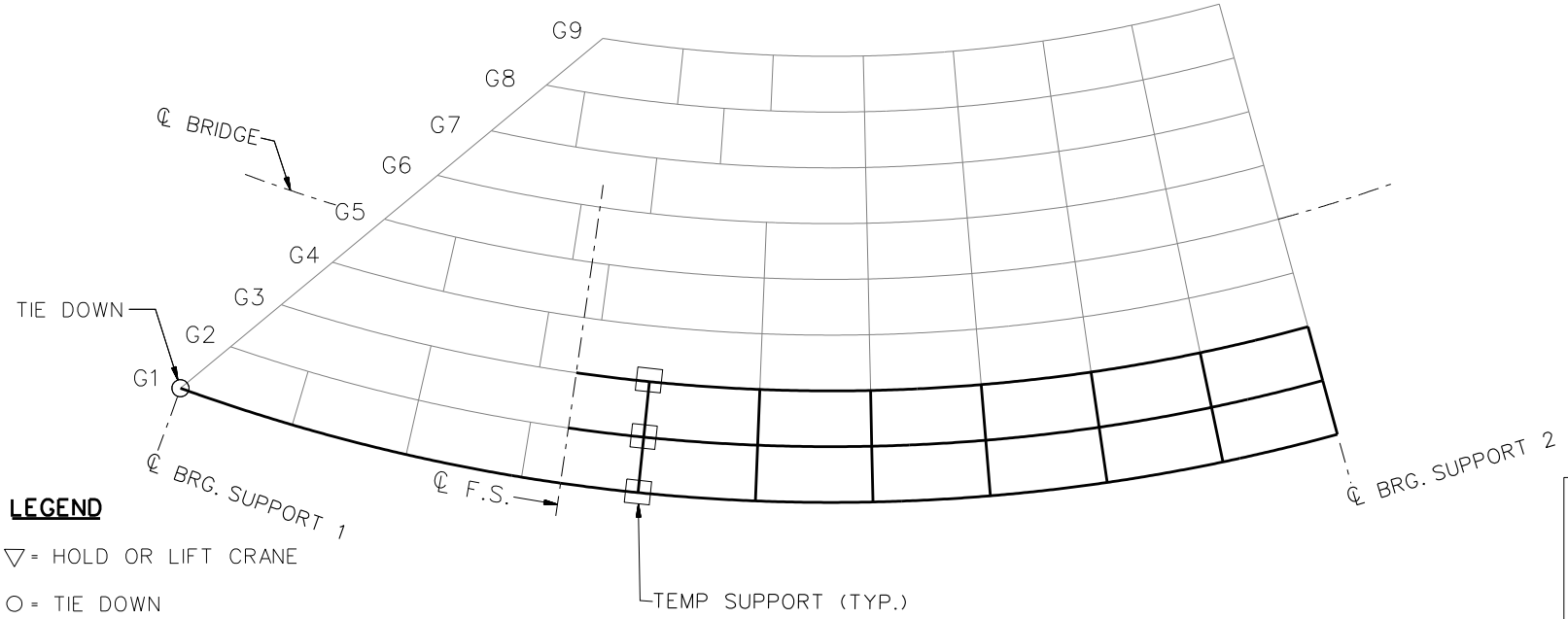

STAGE 4

LEGEND

▽ = HOLD OR LIFT CRANE

○ = TIE DOWN

□ = TEMPORARY SUPPORT STRUCTURE

NCHRP 12-79

BRIDGE NISCS15

GIRDER ERECTION PROCEDURE

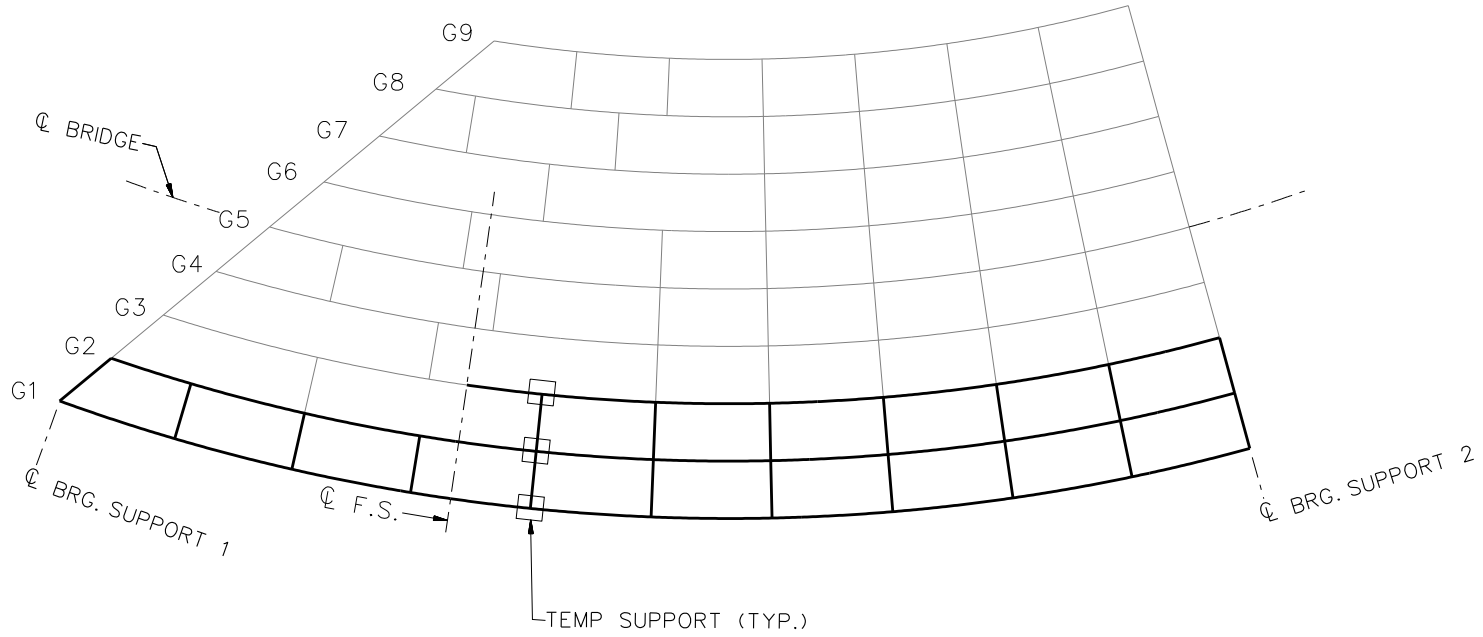

STAGE 5

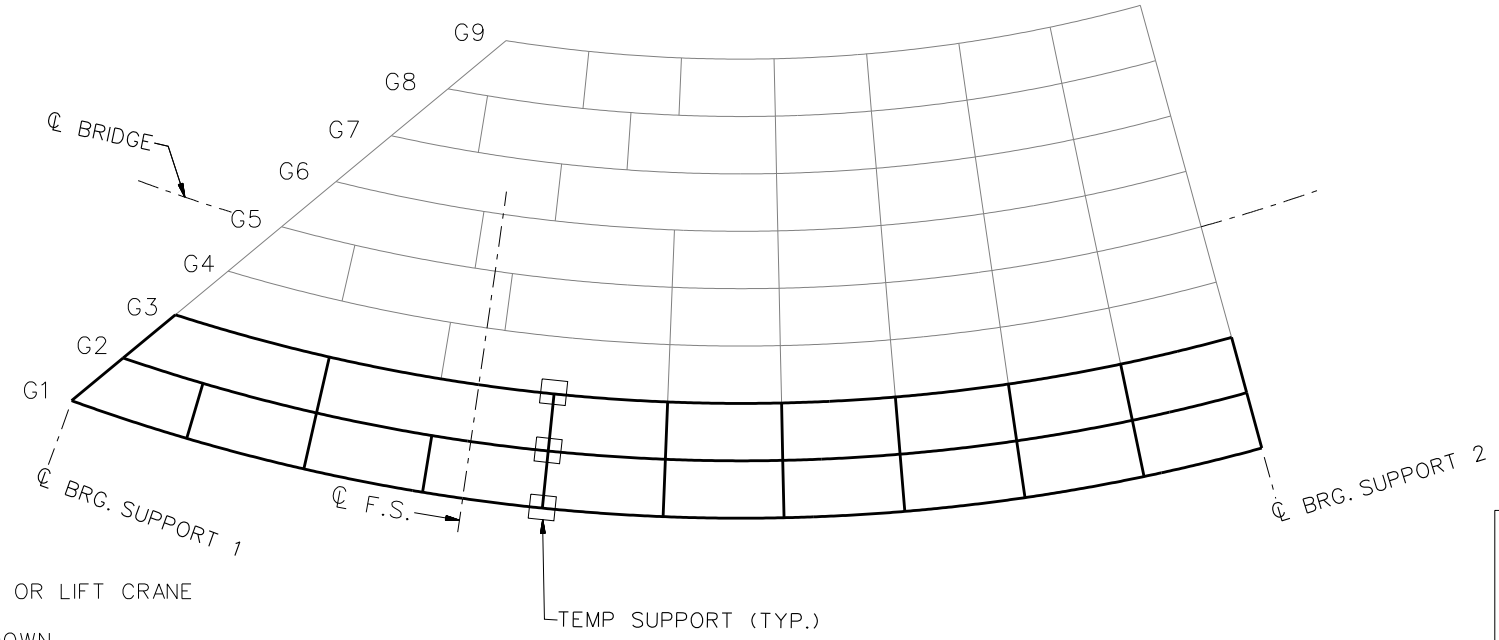

STAGE 6

LEGEND

▽ = HOLD OR LIFT CRANE

○ = TIE DOWN

□ = TEMPORARY SUPPORT STRUCTURE

NCHRP 12-79

BRIDGE NISCS15

GIRDER ERECTION PROCEDURE

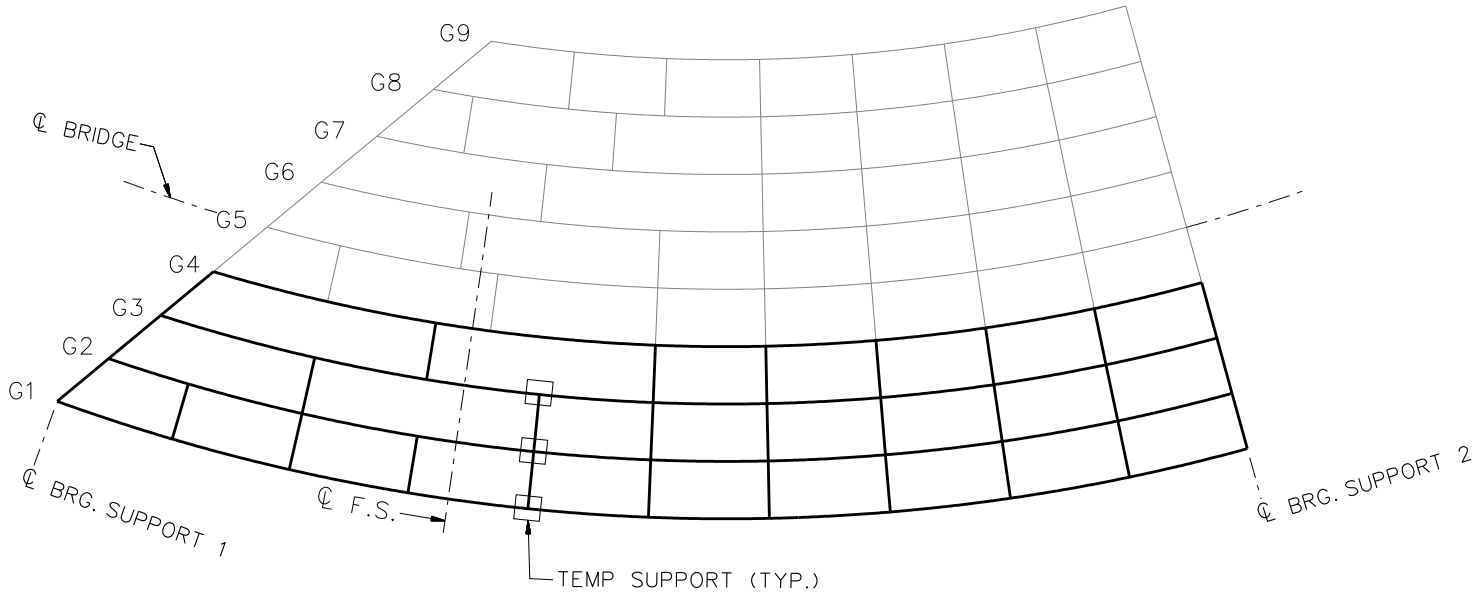

STAGE 7

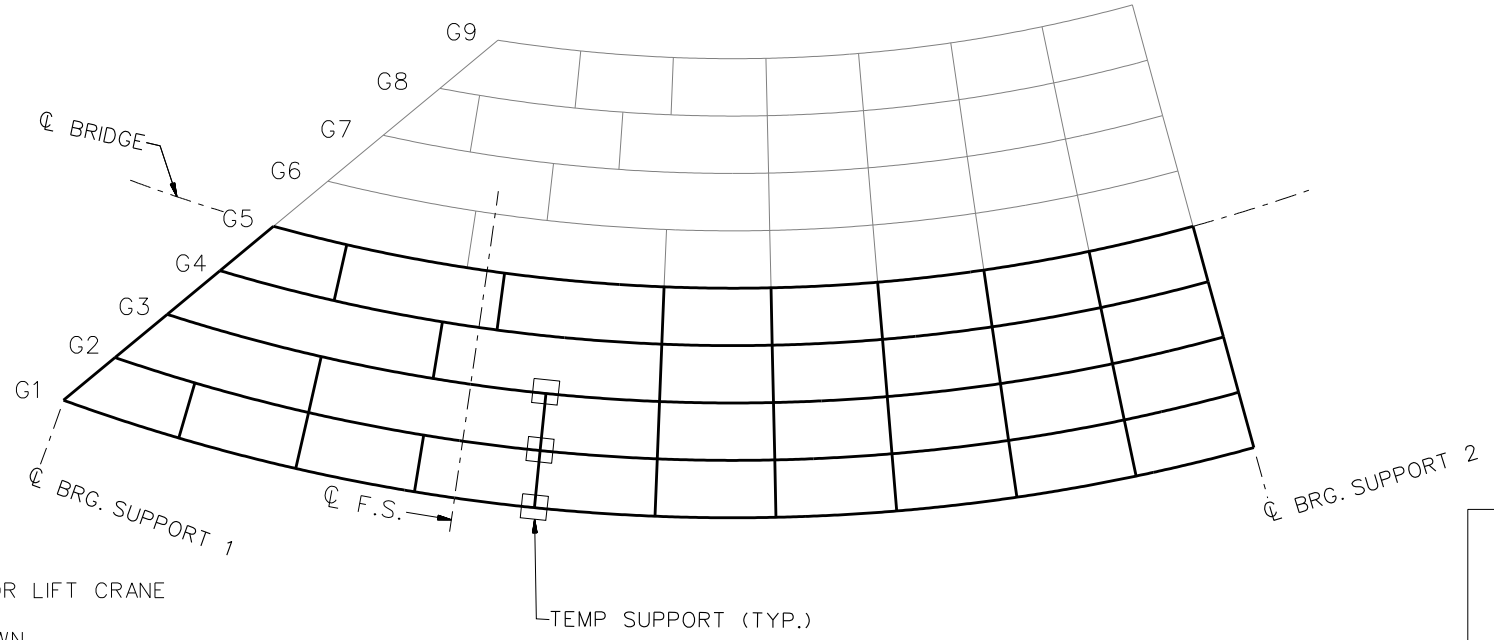

STAGE 8

LEGEND

▽ = HOLD OR LIFT CRANE

○ = TIE DOWN

□ = TEMPORARY SUPPORT STRUCTURE

NCHRP 12-79

BRIDGE NISCS15

GIRDER ERECTION PROCEDURE

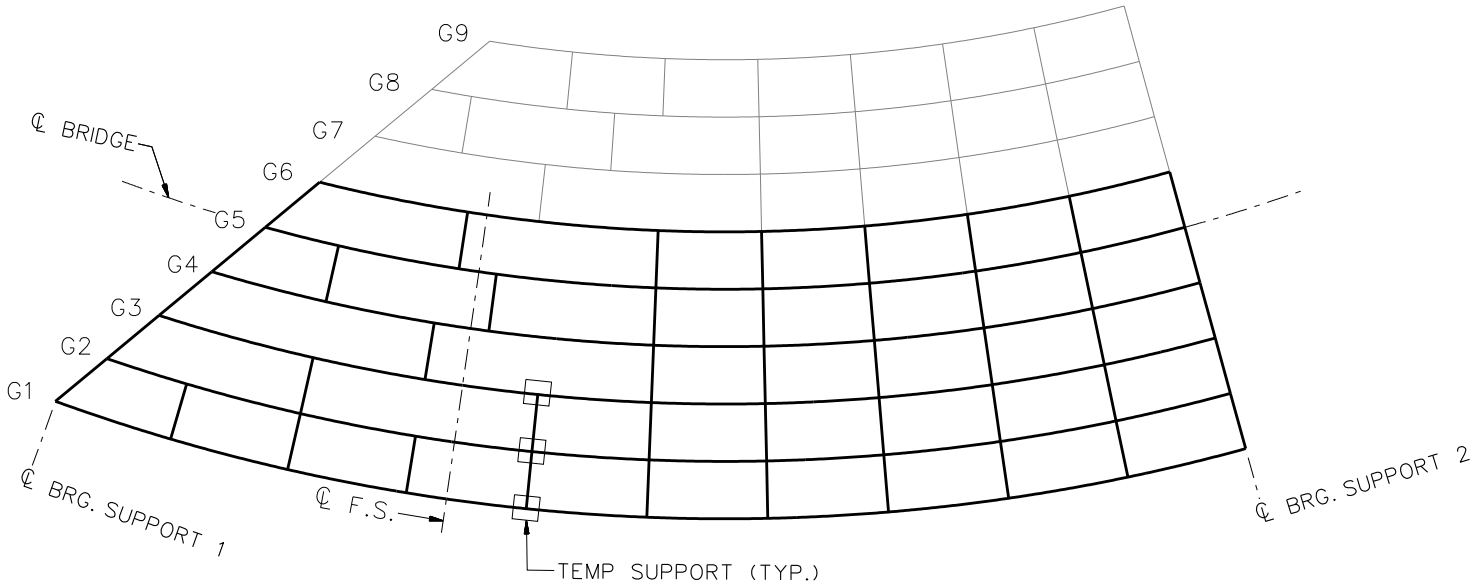

STAGE 9

STAGE 10

REMOVE TEMPORARY SUPPORTS

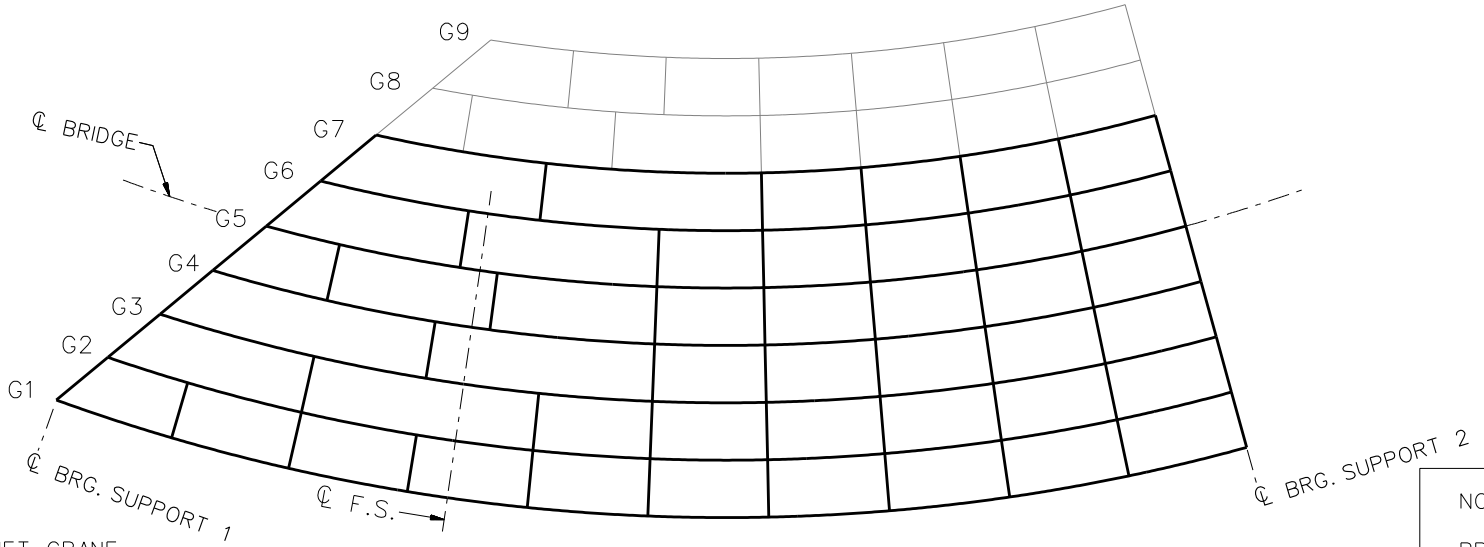

STAGE 11

LEGEND

▽ = HOLD OR LIFT CRANE

○ = TIE DOWN

□ = TEMPORARY SUPPORT STRUCTURE

NCHRP 12-79

BRIDGE NISCS15

GIRDER ERECTION PROCEDURE

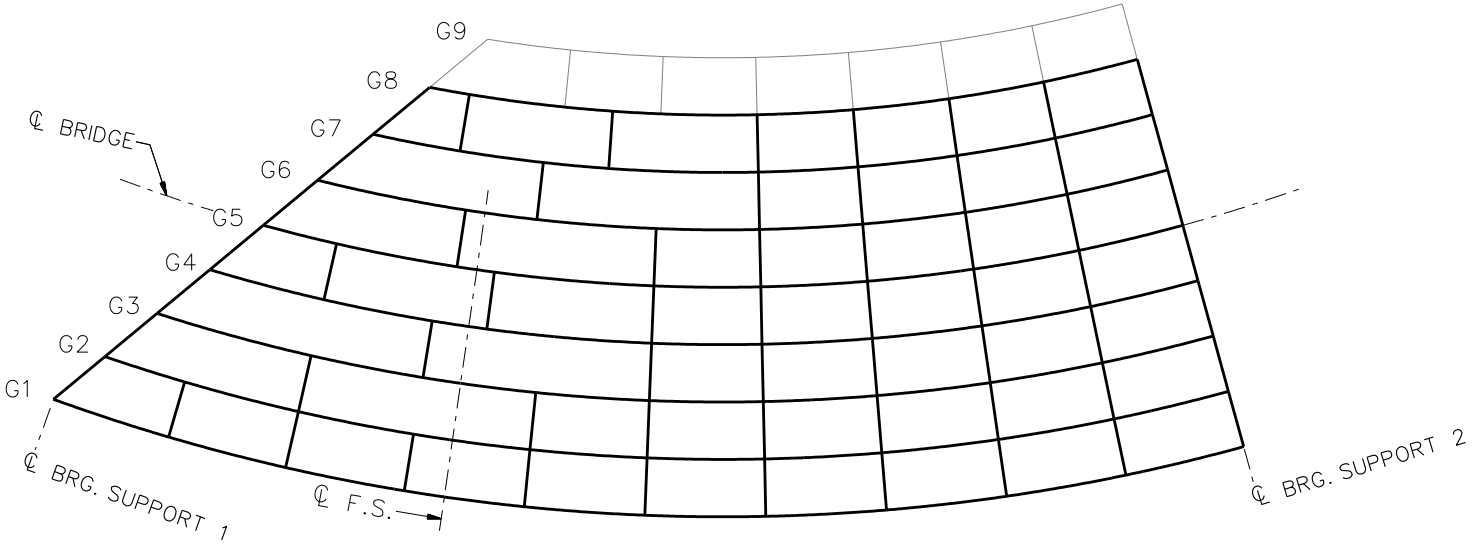

STAGE 12

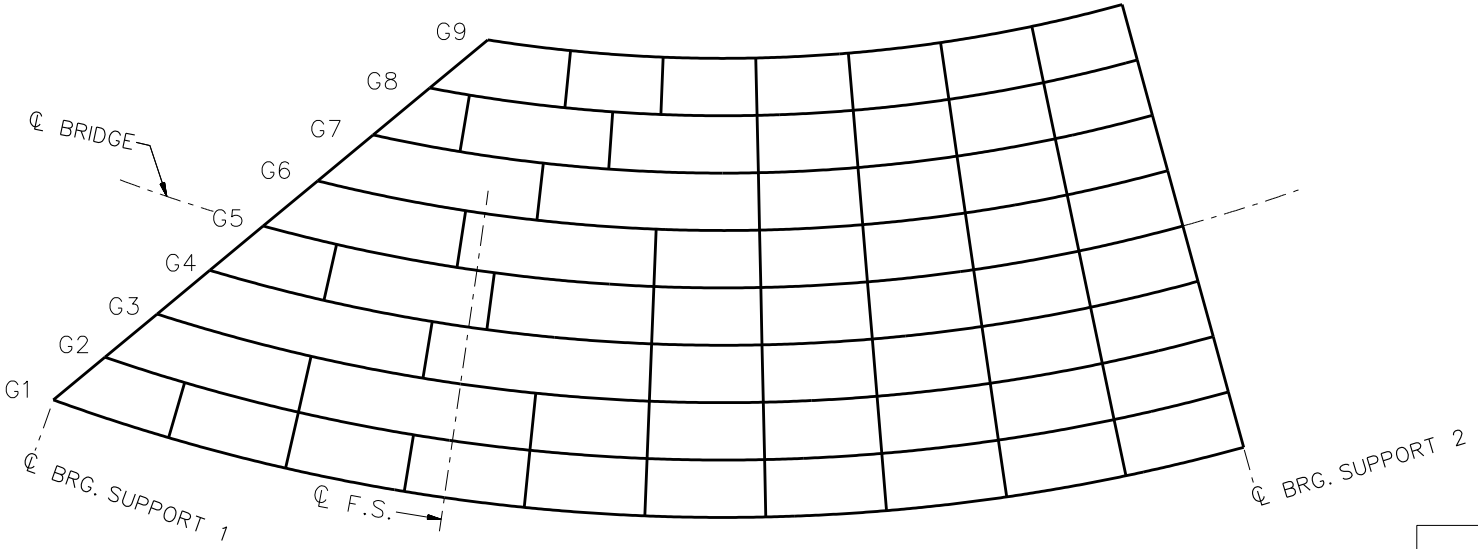

STAGE 13

LEGEND

▽ = HOLD OR LIFT CRANE

○ = TIE DOWN

□ = TEMPORARY SUPPORT STRUCTURE

NCHRP 12-79

BRIDGE NISCS15

GIRDER ERECTION PROCEDURE

NCHRP 12-79

NISCS37

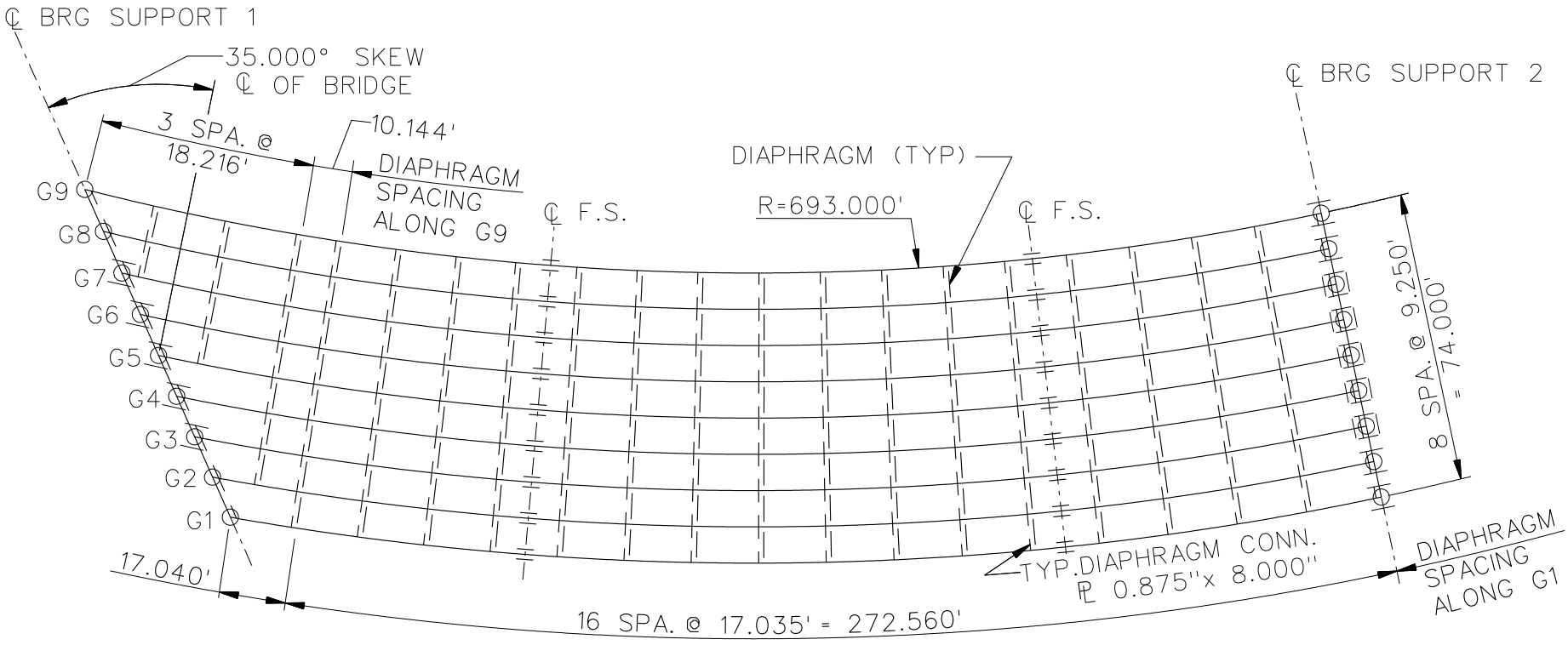

FRAMING PLAN

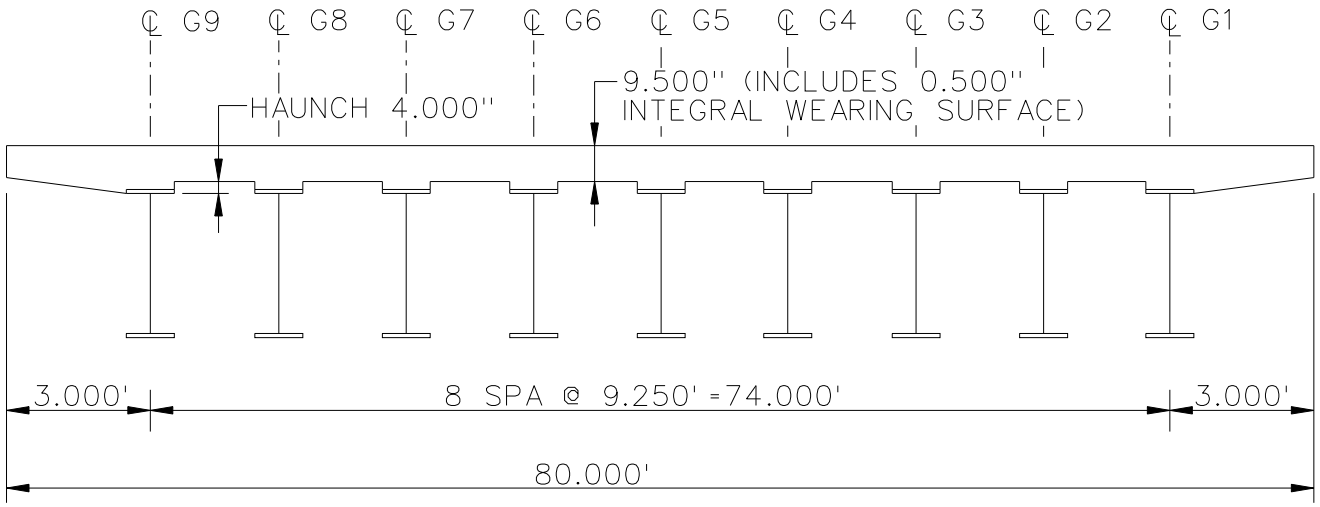

CROSS - SECTION

(DIAPHRAGMS NOT SHOWN)

BEARING LEGEND

- ○ NON-GUIDED
- ⎯○⎯ LONGITUDINALLY GUIDED
- |○| TRANSVERSELY GUIDED
- |⎯○⎯| FIXED

NCHRP 12-79

BRIDGE NISCS37

FRAMING PLAN AND CROSS-SECTION

SHEET 1 OF 6

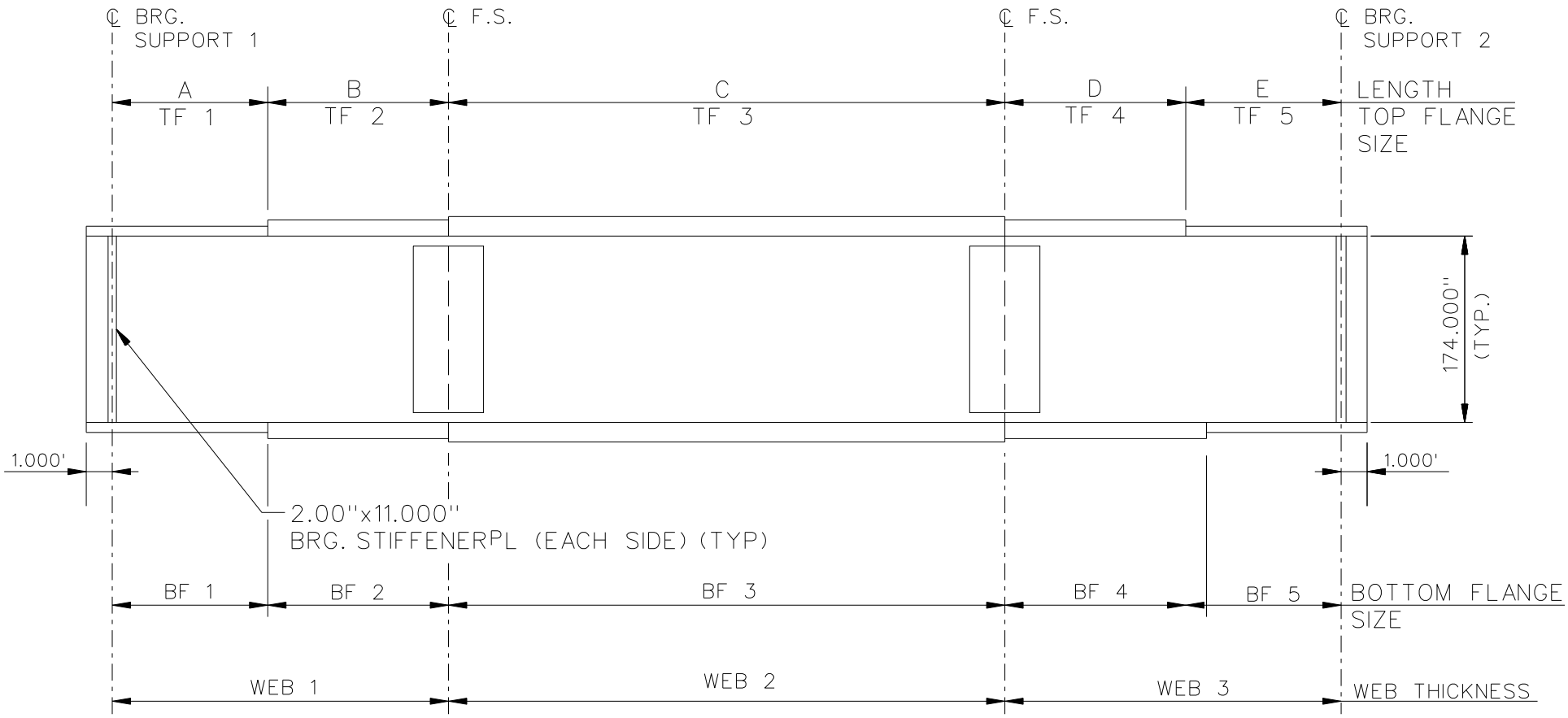

NOTE :

1. SEE TABLES ON SHEET 3 FOR GIRDER ELEVATION DIMENSIONS AND PLATE SIZES.

2. GIRDER G1: WEB 1 = WEB 2 = WEB 3 = 1.375"
   GIRDERS G2 & G3: WEB 1 = WEB 2 = WEB 3 = 1.125"
   GIRDERS G4 - G9: WEB 1 = WEB 2 = WEB 3 = 1.00"

NCHRP 12-79

BRIDGE NISCS37

GIRDER ELEVATION

SHEET 2 OF 6

	GIRDER PLATE LENGTHS ✳								
LENGTH	G1	G2	G3	G4	G5	G6	G7	G8	G9
A	35.000	35.000	35.000	35.000	35.000	35.000	35.000	35.000	35.000
B	44.8000	46.070	47.600	48.670	50.000	51.350	52.720	54.110	55.520
C	130.00	130.000	130.000	130.000	130.000	130.000	130.000	130.000	130.000
D	44.800	46.070	47.600	48.670	50.000	51.350	52.720	54.110	55.520
E	35.000	35.000	35.000	35.000	35.000	35.000	35.000	35.000	35.000

✳ ALL DIMENSIONS ARE IN FEET.

	GIRDER FLANGE DIMENSIONS ✳✳									
TOP	G1		G2		G3		G4-G6		G7-G9	
FLANGE	BF	TF	BF	TF	BF	TF	BF	TF	BF	TF
TF1	48.000	1.750	48.000	1.875	36.000	1.875	28.000	1.500	28.000	1.375
TF2	48.000	2.6250	48.000	2.000	36.000	2.000	28.000	1.500	28.000	1.375
TF3	48.000	3.375	48.000	2.500	36.000	2.000	28.000	1.500	28.000	1.375
TF4	48.000	2.500	48.000	2.000	36.000	2.000	28.000	1.500	28.000	1.375
TF5	48.000	1.750	48.000	1.875	36.000	1.875	28.000	1.500	28.000	1.375

✳✳ ALL DIMENSIONS ARE IN INCHES.

	GIRDER FLANGE DIMENSIONS ✳✳									
BOTTOM	G1		G2		G3		G4-G6		G7-G9	
FLANGE	BF	TF	BF	TF	BF	TF	BF	TF	BF	TF
BF1	48.000	1.750	48.000	1.875	36.000	1.875	28.000	1.500	28.000	1.375
BF2	48.000	2.6250	48.000	2.000	36.000	2.000	28.000	1.500	28.000	1.375
BF3	48.000	3.375	48.000	2.500	36.000	2.000	28.000	1.500	28.000	1.375
BF4	48.000	2.500	48.000	2.000	36.000	2.000	28.000	1.500	28.000	1.375
BF5	48.000	1.750	48.000	1.875	36.000	1.875	28.000	1.500	28.000	1.375

✳✳ ALL DIMENSIONS ARE IN INCHES.

NCHRP 12-79

BRIDGE NISCS37

GIRDER ELEVATION TABLES

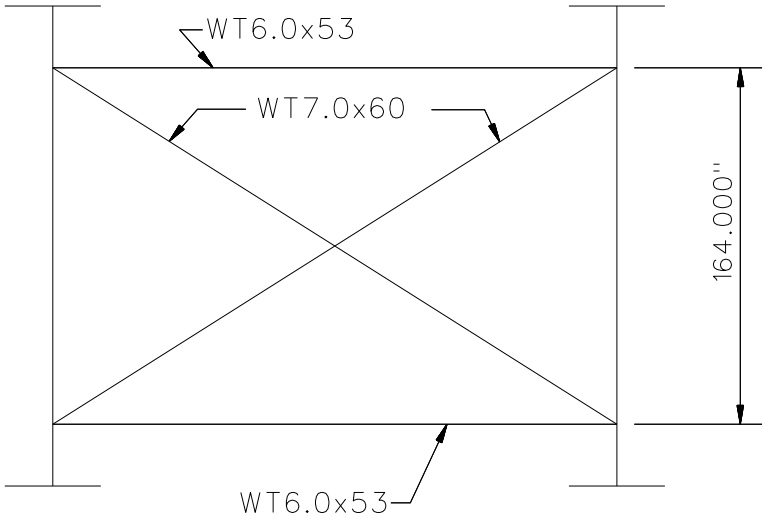

TYPICAL INTERMEDIATE AND END DIAPHRAGM

NOTES:

1. STEEL DEAD LOAD INCREASED BY 5% FOR MDX AND LARSA MODELS; 2% FOR 3D MODEL; AND 10% FOR APPROXIMATE ANALYSIS TO ACCOUNT FOR MISC. DETAILS.

2. FORMWORK LOAD OF 10PSF IS INCLUDED IN CONCRETE DEAD LOAD.

3. ADDITIONAL DESIGN PARAMETERS:
   A. 1.500' PARAPET WIDTH BOTH SIDES.
   B. 700 LB/FT UNIFORM LOAD ASSUMED FOR PARAPET WEIGHT.
   C. ROADWAY WIDTH = 76.500'.
   D. NUMBER OF DESIGN LANES = 6.
   E. HL93 LIVE LOAD.
   F. DESIGN SPEED = 45 MPH.

4. DIAPHRAGM MEMBER CALL-OUTS ARE IN ENGLISH UNITS.

NCHRP 12-79

BRIDGE NISCS37

MISC. DETAILS AND NOTES

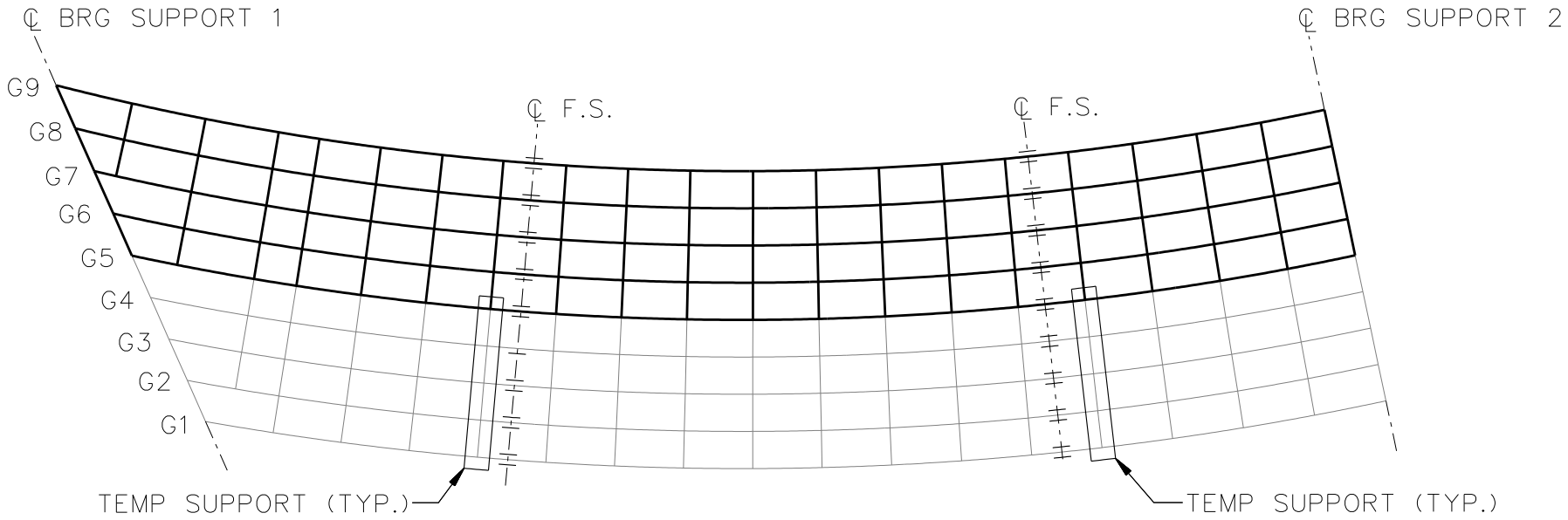

STAGES 1 THRU 15

(NO RESULTS REQ'D)

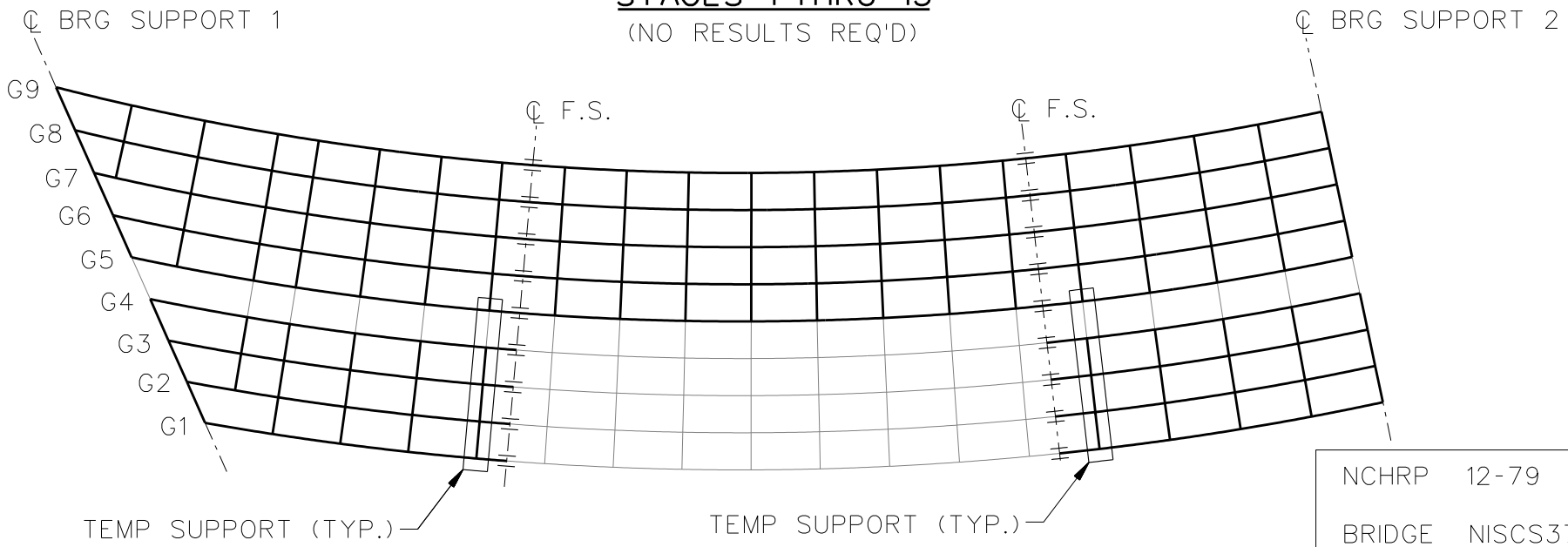

STAGES 16 THRU 23

(RESULTS REQ'D)

NCHRP 12-79

BRIDGE NISCS37

GIRDER ERECTION PROCEDURE

SHEET 5 OF 6

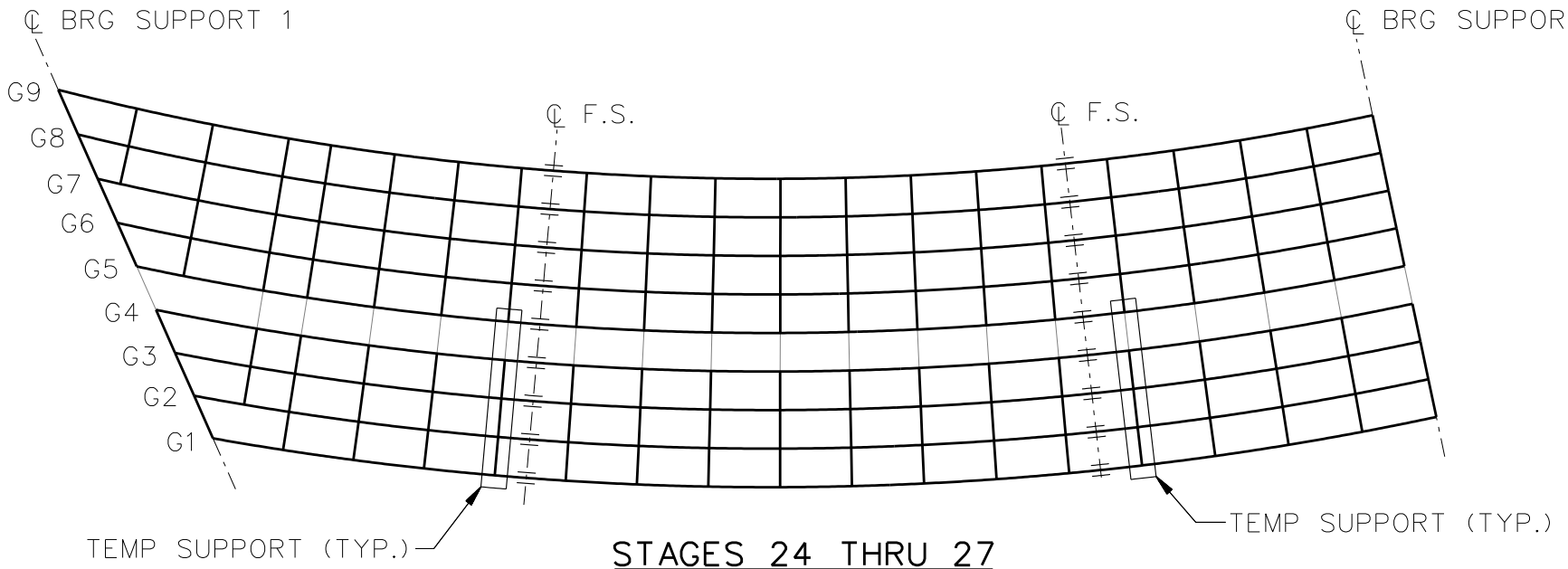

STAGES 24 THRU 27

(RESULTS REQ'D)

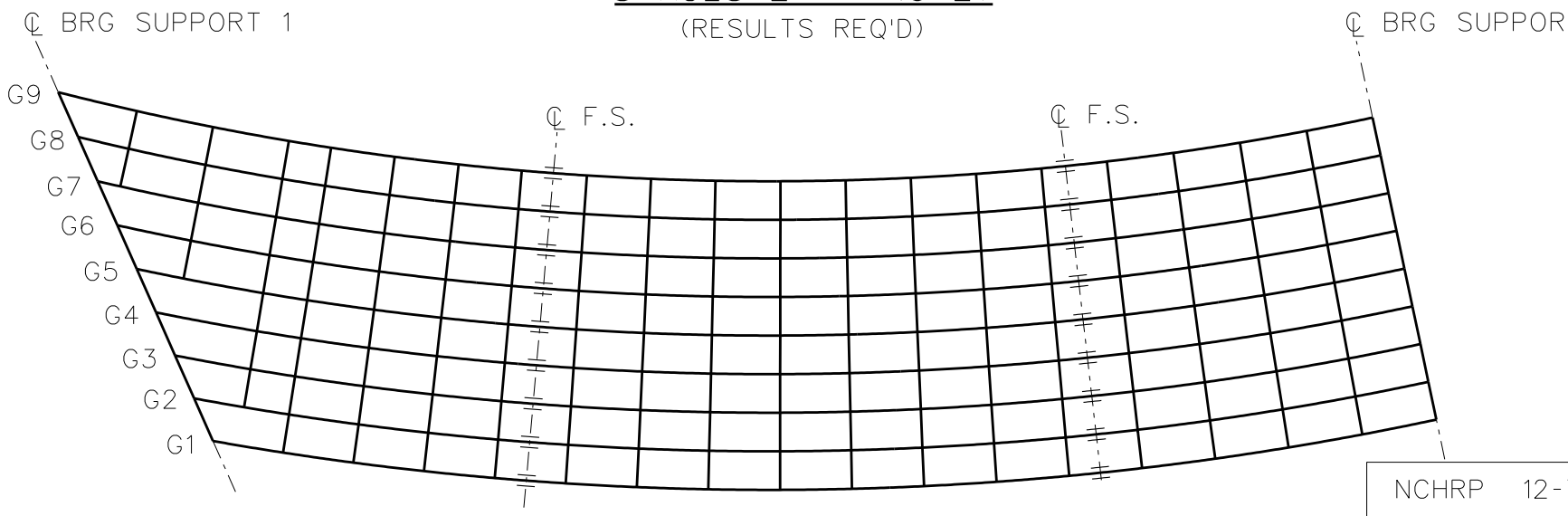

STAGE 28

REMOVE TEMP. SUPPORTS

STAGE 29

STEEL DL

CONCRETE DL

NCHRP 12-79

BRIDGE NISCS37

GIRDER ERECTION PROCEDURE

SHEET 6 OF 6

NCHRP 12-79

NISCS38

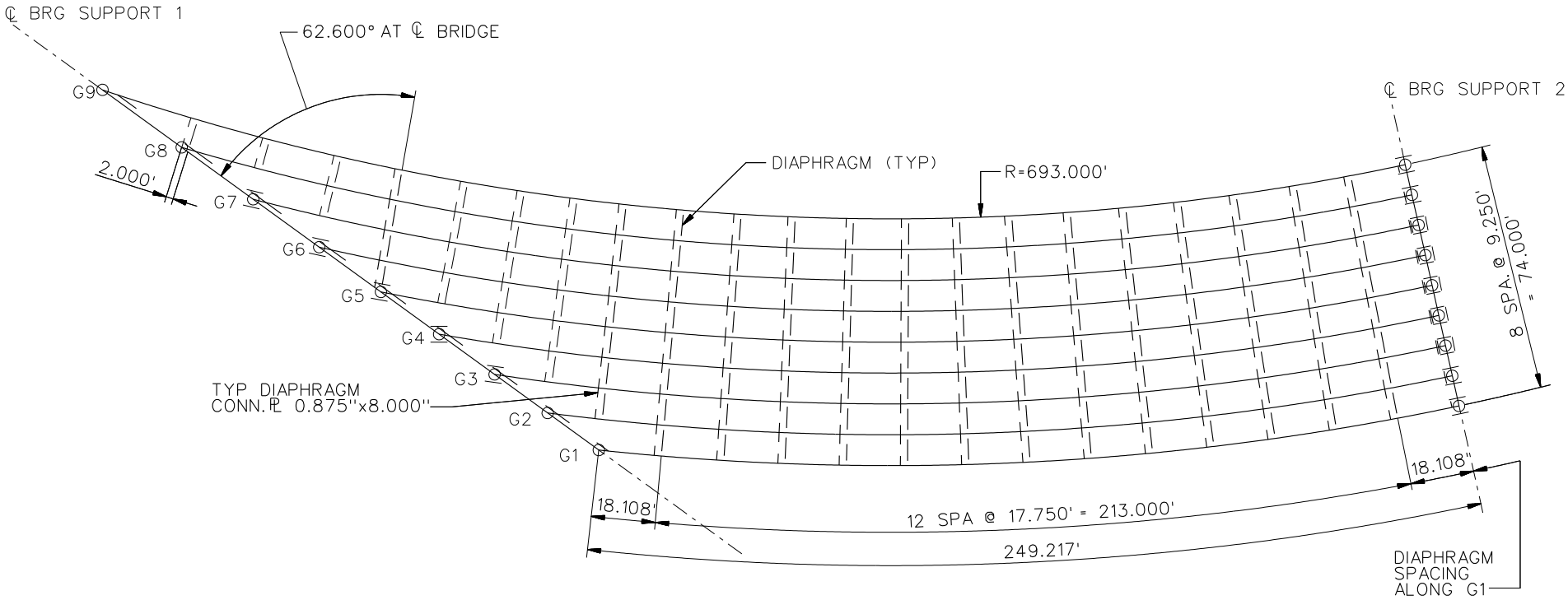

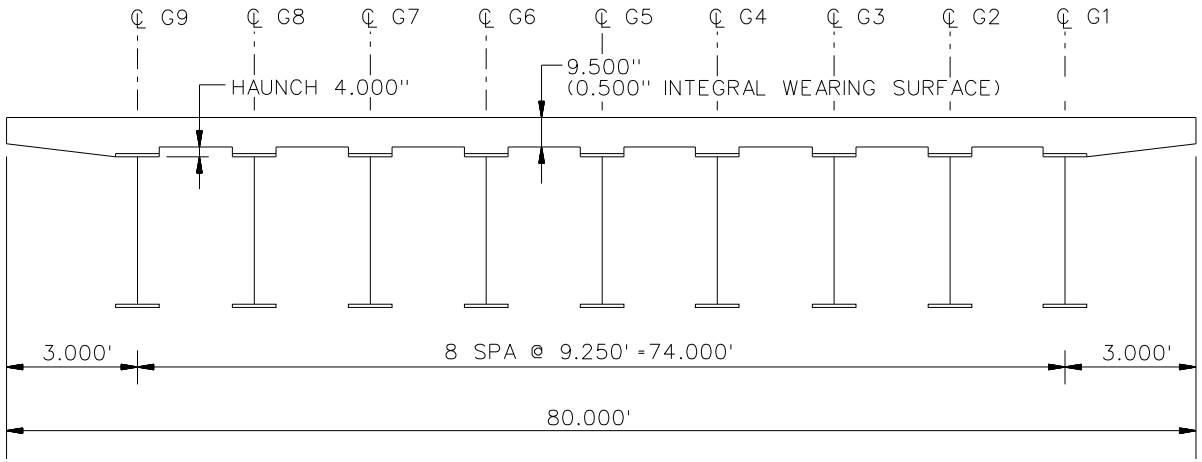

CROSS - SECTION

(DIAPHRAGMS NOT SHOWN)

BEARING LEGEND

○ NON-GUIDED

⊙ LONGITUDINALLY GUIDED

|⊙| TRANSVERSELY GUIDED

|⊙| FIXED

NCHRP 12-79

BRIDGE NISCS38

FRAMING PLAN AND CROSS-SECTION

SHEET 1 OF 8

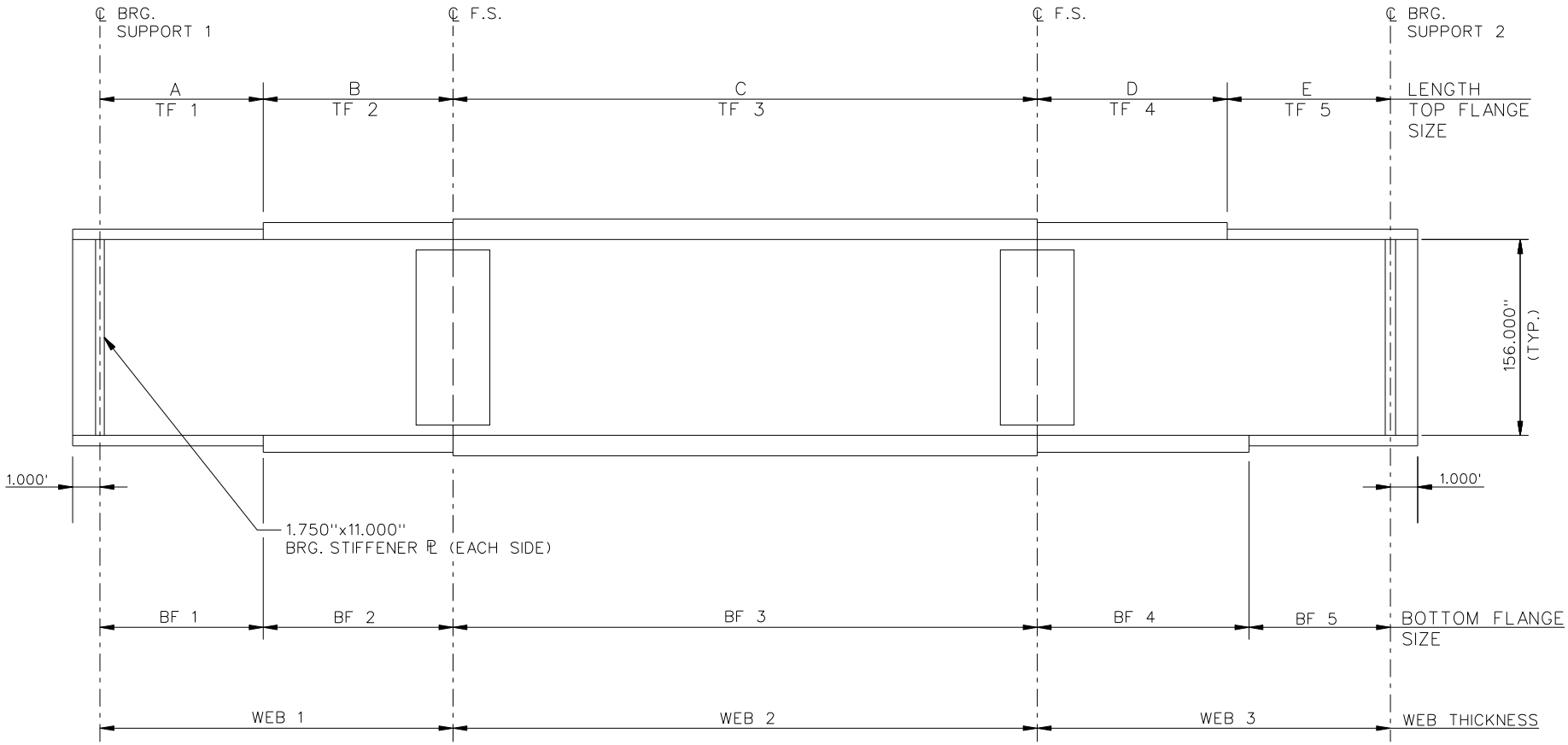

NOTES:

1. SEE TABLES ON SHEET 3 FOR GIRDER ELEVATION DIMENSIONS AND PLATE SIZES.

2. GIRDERS , WEB 1 = WEB 2 = WEB 3 = 1.125".

NCHRP 12-79

BRIDGE NISCS38

GIRDER ELEVATION

SHEET 2 OF 8

	GIRDER PLATE LENGTHS ✳								
LENGTH	G1	G2	G3	G4	G5	G6	G7	G8	G9
A	60.000	75.000	75.000	75.000	85.000	92.246	104.000	110.000	118.000
B	0	0	0	0	0	0	0	0	0
C	129.216	126.057	123.408	130.000	125.000	130.000	122.025	126.857	129.387
D	0	0	0	0	0	0	0	0	0
E	60.000	60.000	75.000	81.352	90.000	92.246	104.000	110.000	118.000

✳ ALL DIMENSIONS ARE IN FEET.

	GIRDER FLANGE DIMENSIONS ✳✳					
TOP	G1, G2, G3		G4, G5, G6		G7, G8, G9	
FLANGE	BF	TF	BF	TF	BF	TF
TF1	36.000	1.750	30.000	1.250	36.000	1.500
TF2	N/A	N/A	N/A	N/A	N/A	N/A
TF3	36.000	2.250	30.000	2.000	36.000	1.500
TF4	N/A	N/A	N/A	N/A	N/A	N/A
TF5	36.000	1.750	30.000	1.250	36.000	1.500

✳✳ ALL DIMENSIONS ARE IN INCHES.

	GIRDER FLANGE DIMENSIONS ✳✳					
BOTTOM	G1, G2, G3		G4, G5, G6		G7, G8, G9	
FLANGE	BF	TF	BF	TF	BF	TF
BF1	36.000	2.000	30.000	1.250	36.000	1.500
BF2	N/A	N/A	N/A	N/A	N/A	N/A
BF3	36.000	2.500	30.000	2.000	36.000	1.500
BF4	N/A	N/A	N/A	N/A	N/A	N/A
BF5	36.000	2.000	30.000	1.250	36.000	1.500

✳✳ ALL DIMENSIONS ARE IN INCHES.

NCHRP 12-79

BRIDGE NISCS38

GIRDER ELEVATION TABLES

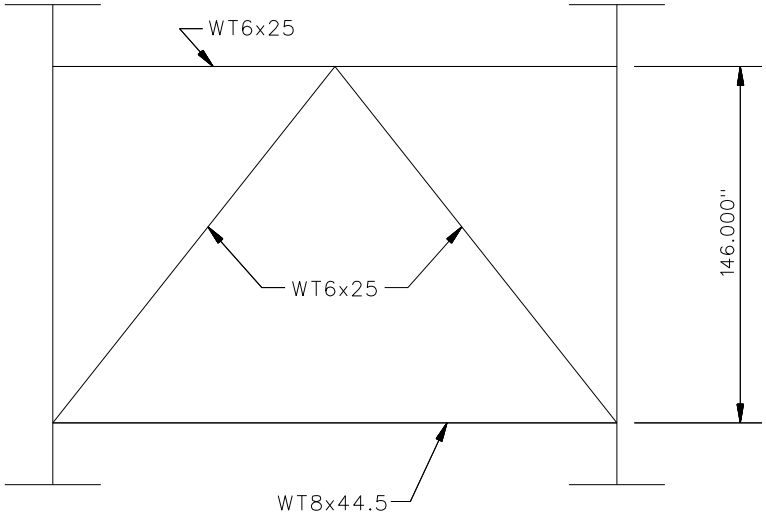

TYPICAL END DIAPHRAGM AT SUPPORT 1

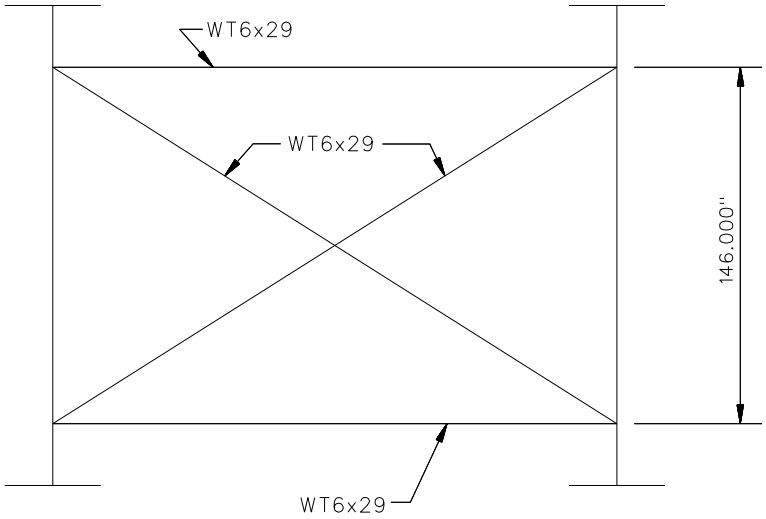

TYPICAL END AND INTERMEDIATE DIAPHRAGM AT SUPPORT 2

NOTES:

1. STEEL DEAD LOAD INCREASED BY 5% FOR MDX AND LARSA MODELS; 2% FOR 3D MODEL; AND 10% FOR APPROXIMATE ANALYSIS TO ACCOUNT FOR MISC. DETAILS.

2. FORMWORK LOAD OF 10PSF IS INCLUDED IN CONCRETE DEAD LOAD.

3. ADDITIONAL DESIGN PARAMETERS:
   A. 1.500' PARAPET WIDTH BOTH SIDES.
   B. 700 LB/FT UNIFORM LOAD ASSUMED FOR PARAPET WEIGHT.
   C. ROADWAY WIDTH = 77.000'.
   D. NUMBER OF DESIGN LANES = 6.
   E. HL93 LIVE LOAD.

4. DIAPHRAGM MEMBER CALL-OUTS ARE IN UNITS OF INCHES.

NCHRP 12-79

BRIDGE NISCS38

MISC. DETAILS AND NOTES

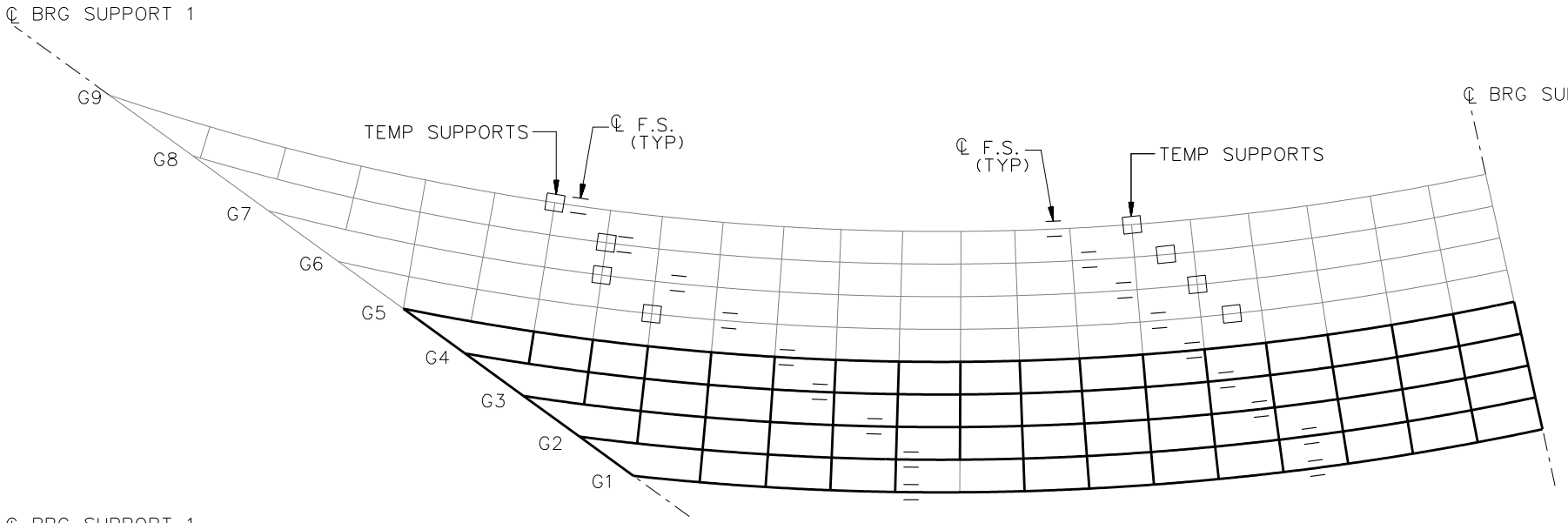

STAGE 15

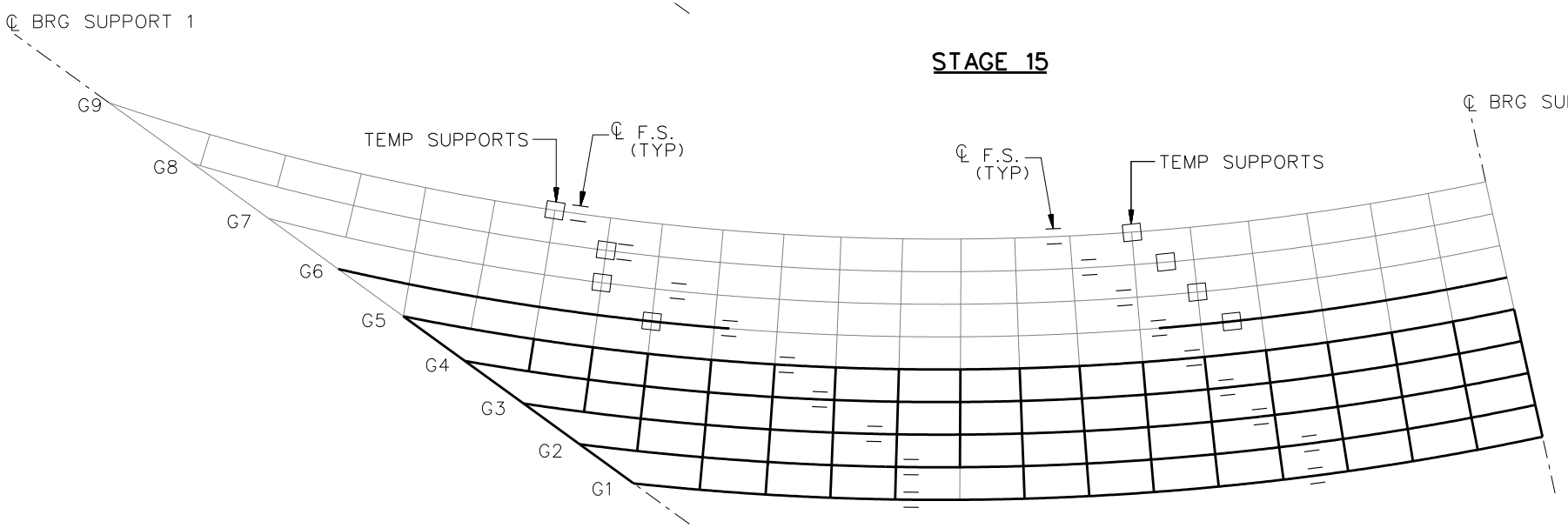

STAGE 16

LEGEND

▽ = HOLD OR LIFT CRANE

○ = TIE DOWN

□ = TEMPORARY SUPPORT STRUCTURE

NCHRP 12-79

BRIDGE NISCS38

GIRDER ERECTION PROCEDURE

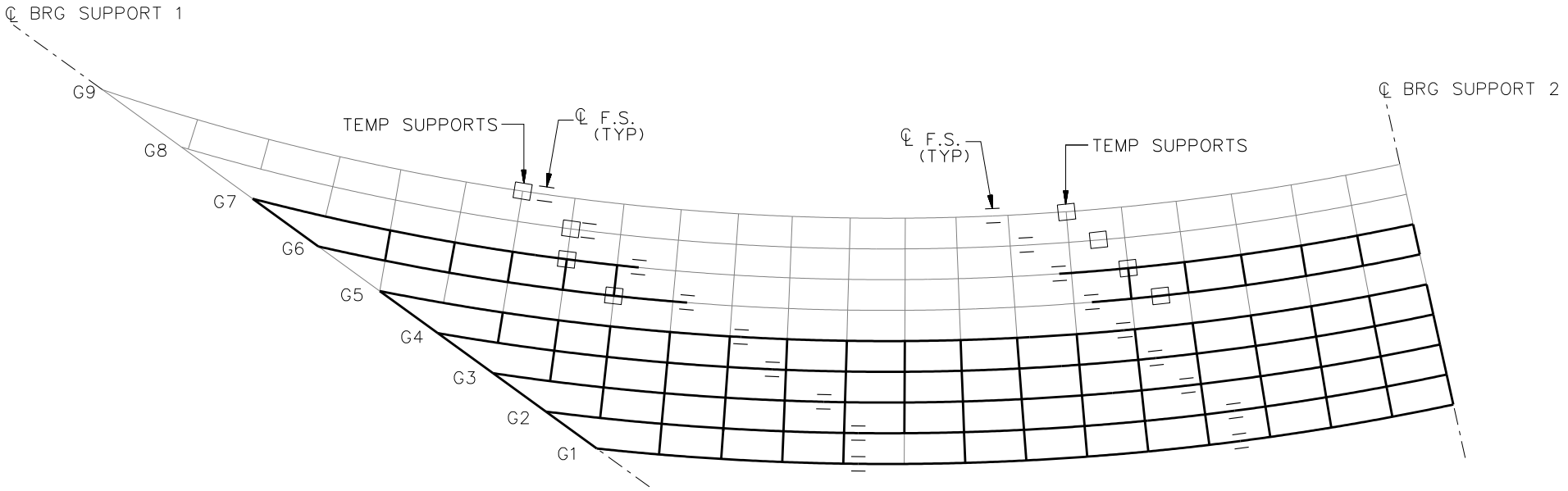

STAGE 17

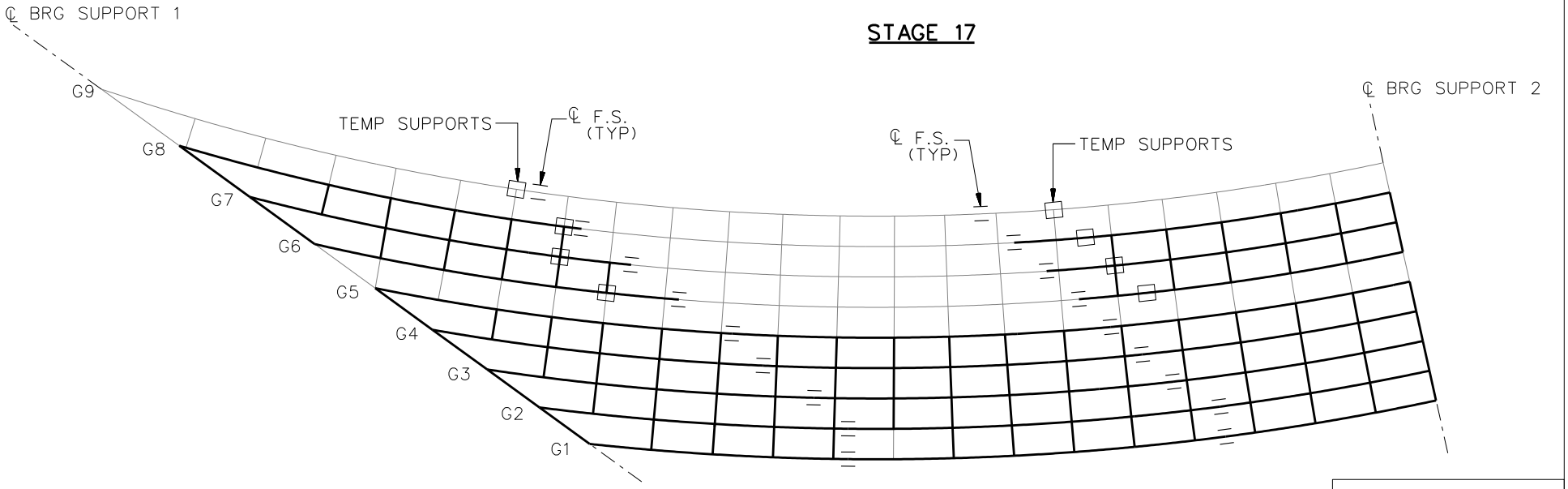

STAGE 18

LEGEND

▽ = HOLD OR LIFT CRANE

○ = TIE DOWN

□ = TEMPORARY SUPPORT STRUCTURE

NCHRP 12-79

BRIDGE NISCS38

GIRDER ERECTION PROCEDURE

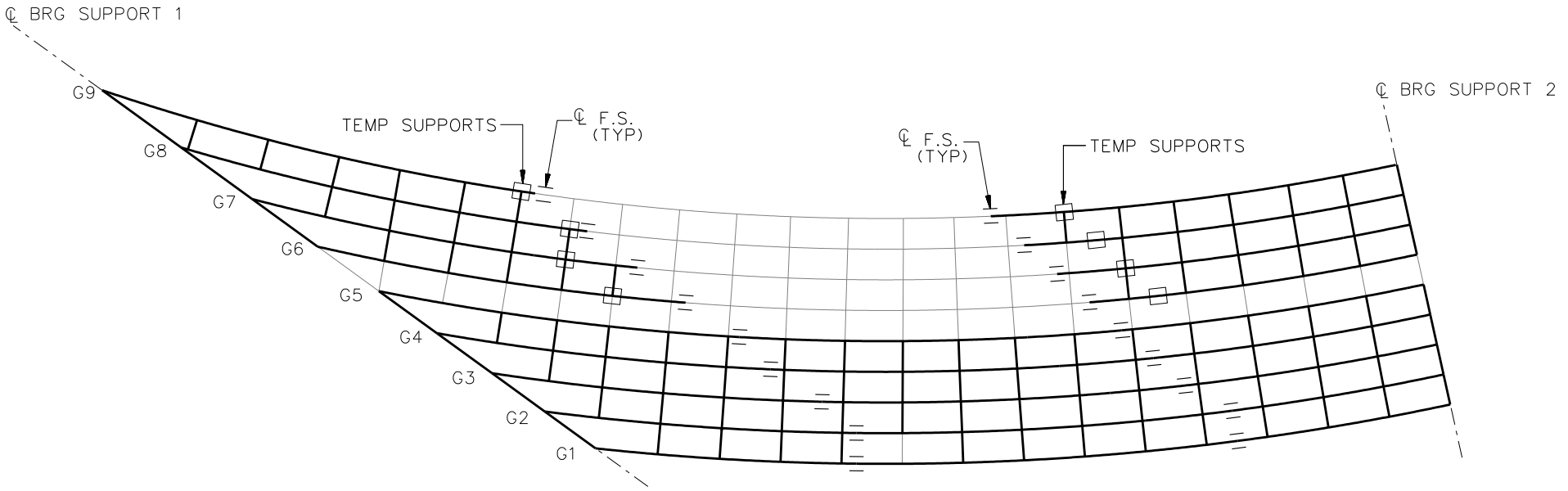

STAGE 19

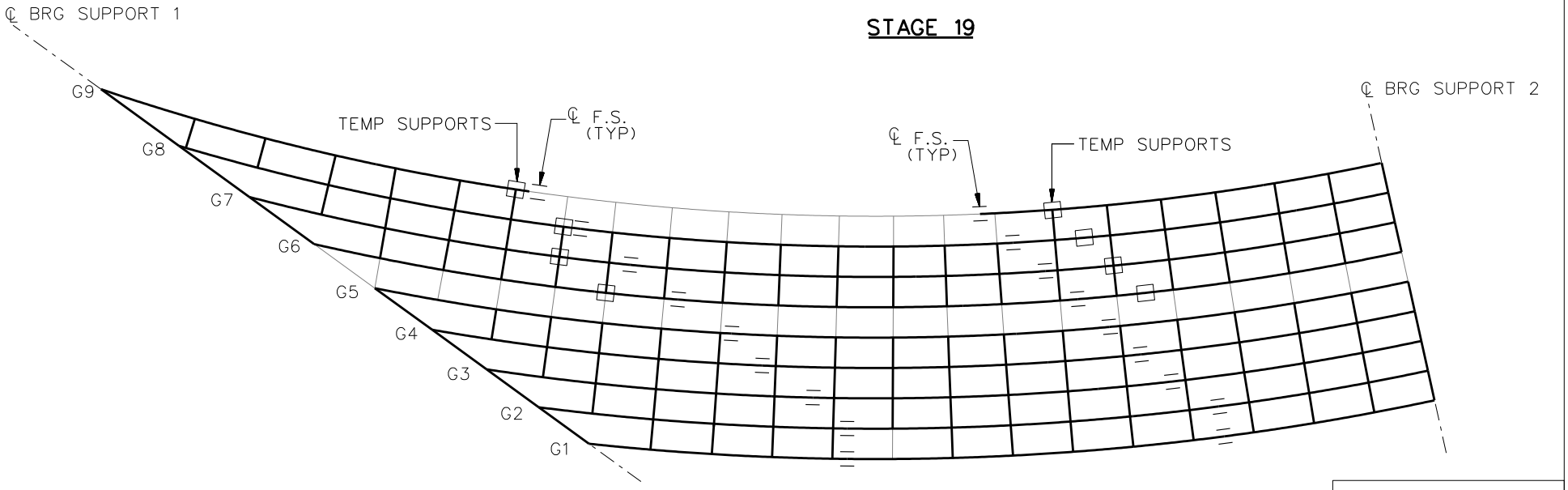

STAGE 22

LEGEND

▽ = HOLD OR LIFT CRANE

○ = TIE DOWN

□ = TEMPORARY SUPPORT STRUCTURE

NCHRP 12-79

BRIDGE NISCS38

GIRDER ERECTION PROCEDURE

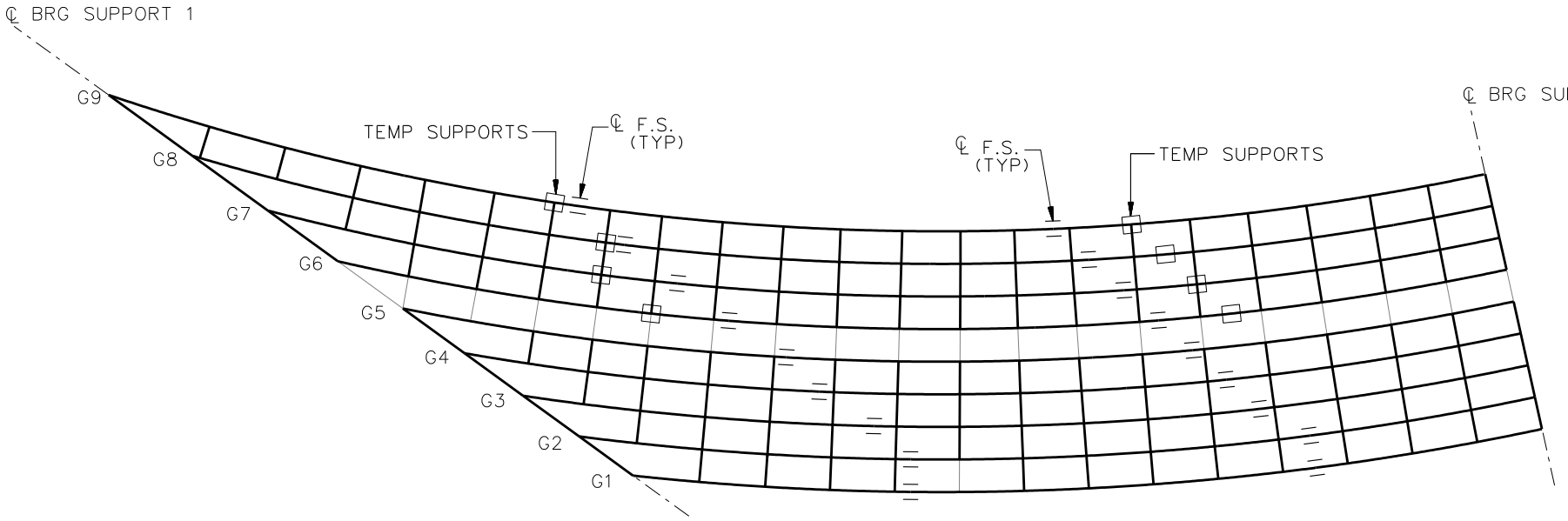

STAGE 23

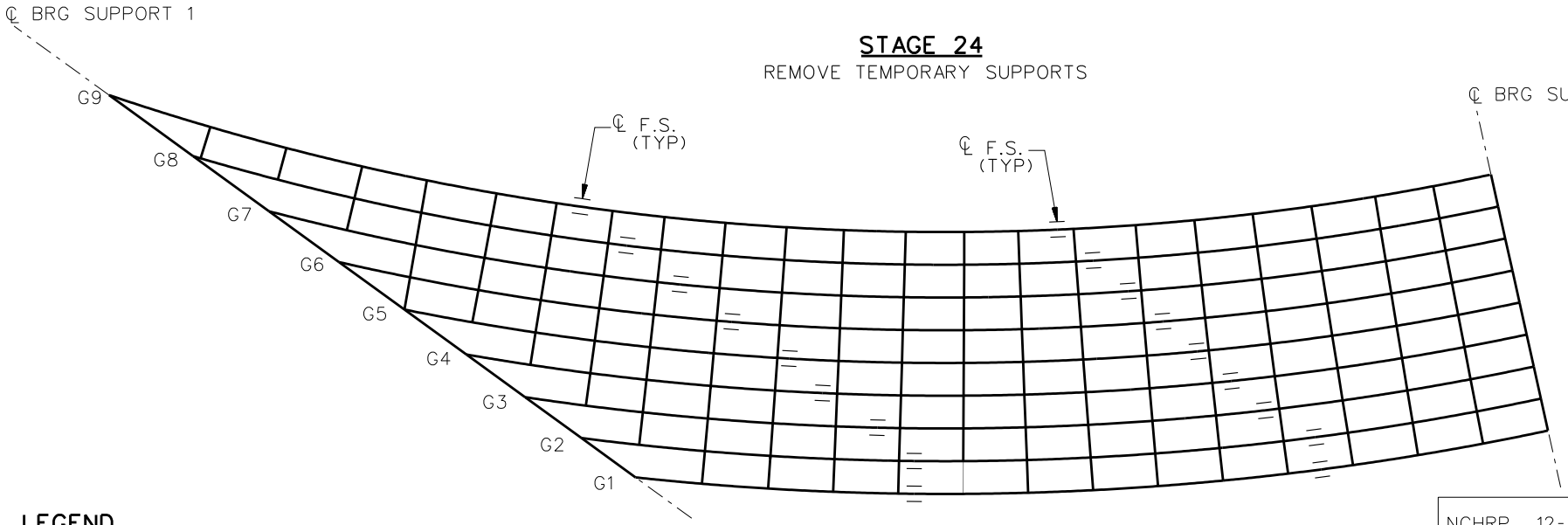

STAGE 24

REMOVE TEMPORARY SUPPORTS

STAGE 25

(RESULTS REQ'D)

LEGEND

▽ = HOLD OR LIFT CRANE

○ = TIE DOWN

□ = TEMPORARY SUPPORT STRUCTURE

NCHRP 12-79

BRIDGE NISCS38

GIRDER ERECTION PROCEDURE

NCHRP 12-79

NISCS39

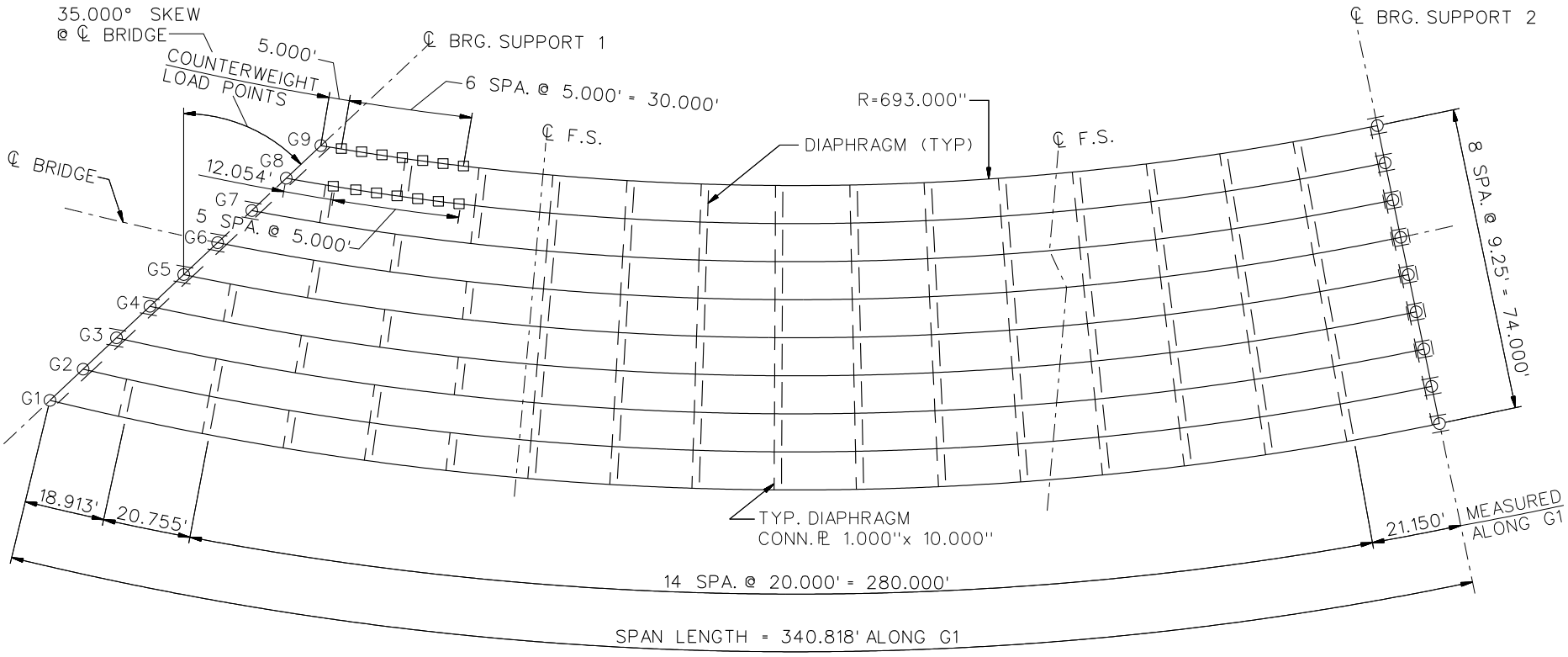

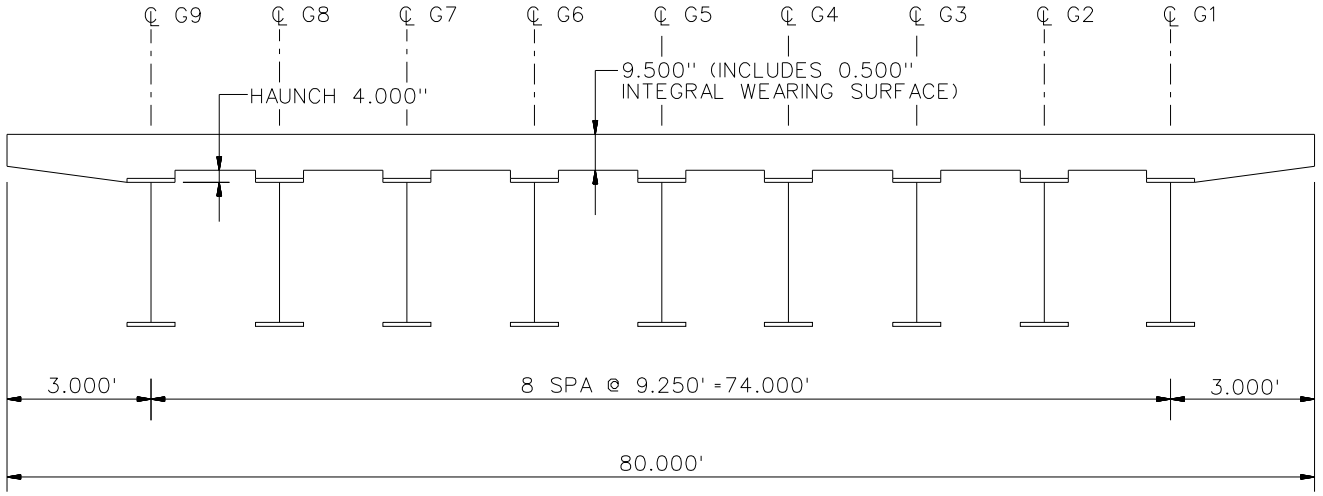

CROSS - SECTION

(DIAPHRAGMS NOT SHOWN)

BEARING LEGEND

○ NON-GUIDED

⊙ LONGITUDINALLY GUIDED

|○| TRANSVERSELY GUIDED

|⊙| FIXED

NCHRP 12-79

BRIDGE NISCS39

FRAMING PLAN AND CROSS-SECTION

SHEET 1 OF 8

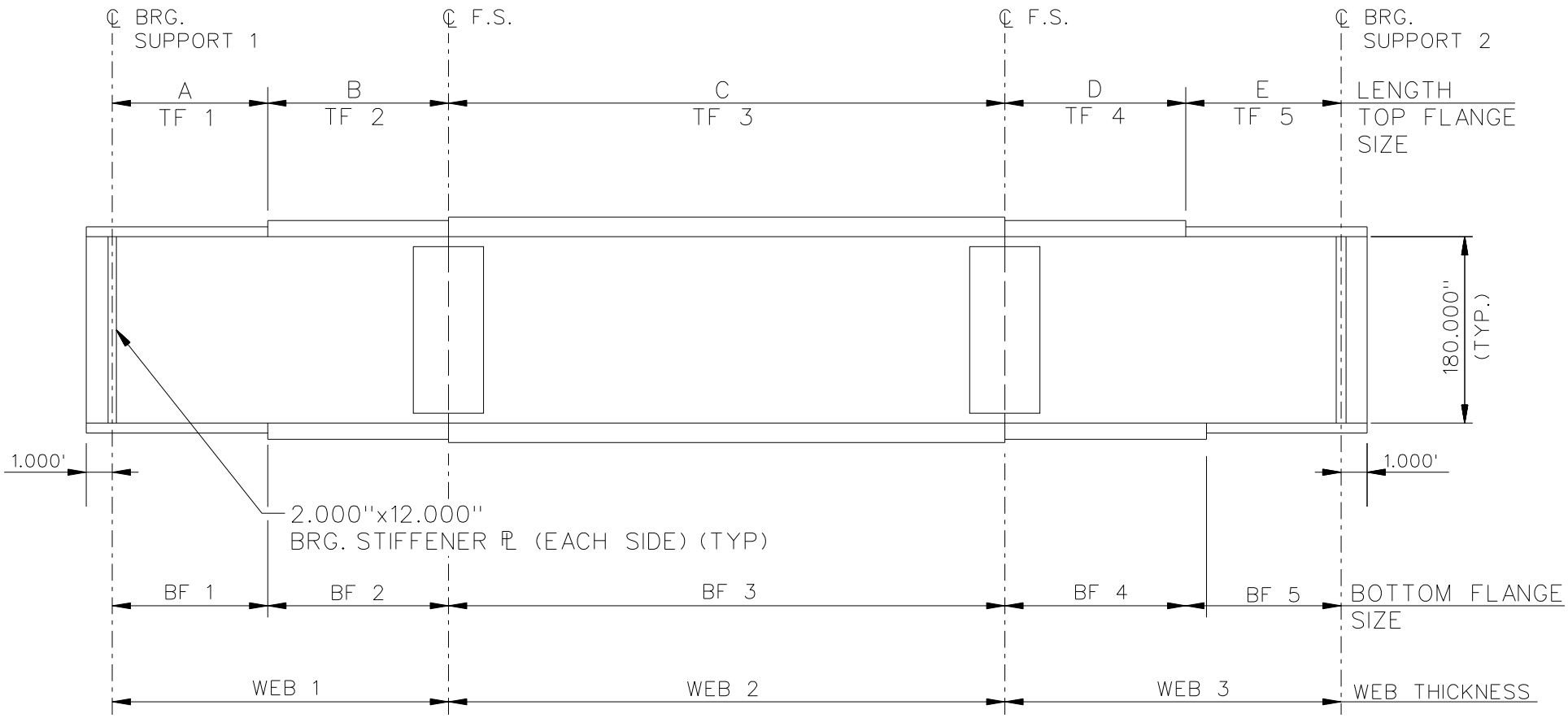

NOTE :

1. SEE TABLES ON SHEET 3 FOR GIRDER ELEVATION DIMENSIONS AND PLATE SIZES.

2. GIRDERS, WEB 1 = WEB 2 = WEB 3 = 1.250".

3. TOP FLANGE STEEL : G1, G2, G3 = HPS 70W
   G4 THRU G5 = GR 50W.

4. BOTTOM FLANGE : G1, G2, G3 = HPS 70W
   G4 THRU G5 = GR 50W.

5. WEB STEEL : ALL GIRDERS = GR 50W

NCHRP 12-79

BRIDGE NISCS39

GIRDER ELEVATION

SHEET 2 OF 8

	GIRDER PLATE LENGTHS ✳								
LENGTH	G1	G2	G3	G4	G5	G6	G7	G8	G9
A	115.000	107.570	100.108	92.610	85.075	77.499	69.881	62.216	54.501
B	35.001	35.362	35.724	36.086	36.448	36.810	34.671	35.033	35.395
C	59.999	59.276	58.552	57.828	57.105	56.381	55.658	54.934	54.210
D	35.001	35.362	35.724	36.086	36.448	36.810	34.671	35.033	35.395
E	95.818	93.095	90.371	87.648	84.925	82.202	84.478	81.755	79.032

✳ ALL DIMENSIONS ARE IN FEET.

	GIRDER FLANGE DIMENSIONS ✳✳					
TOP	G1, G2, G3		G4, G5, G6		G7, G8, G9	
FLANGE	BF	TF	BF	TF	BF	TF
TF1	44.000	2.500	36.000	1.750	30.000	1.500
TF2	44.000	3.000	36.000	1.750	30.000	1.500
TF3	44.000	3.000	36.000	2.000	30.000	1.500
TF4	44.000	3.000	36.000	1.750	30.000	1.500
TF5	44.000	2.500	36.000	1.750	30.000	1.500

✳✳ ALL DIMENSIONS ARE IN INCHES.

	GIRDER FLANGE DIMENSIONS ✳✳					
BOTTOM	G1		G2		G3	
FLANGE	BF	TF	BF	TF	BF	TF
BF1	46.000	2.500	38.000	1.750	32.000	1.500
BF2	46.000	3.500	38.000	2.500	32.000	1.500
BF3	46.000	3.500	38.000	2.500	32.000	1.500
BF4	46.000	3.500	38.000	2.500	32.000	1.500
BF5	46.000	2.500	38.000	1.750	32.000	1.500

✳✳ ALL DIMENSIONS ARE IN INCHES.

NCHRP 12-79

BRIDGE NISCS39

GIRDER ELEVATION TABLES

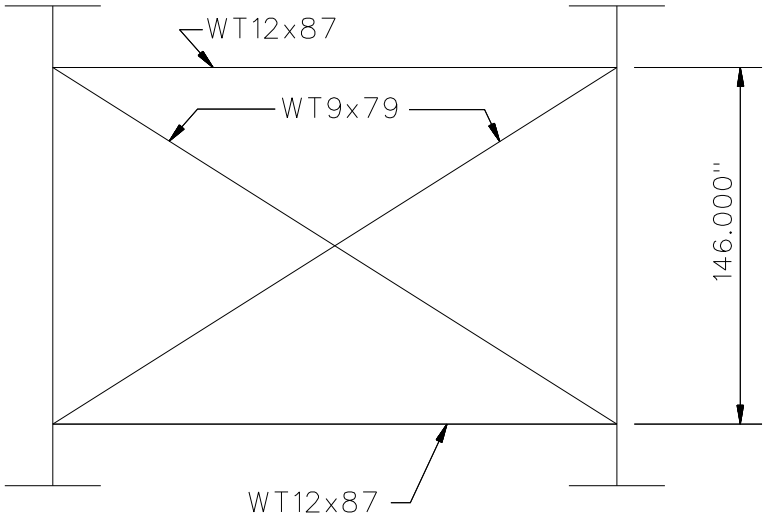

TYPICAL INTERMEDIATE AND END DIAPHRAGM

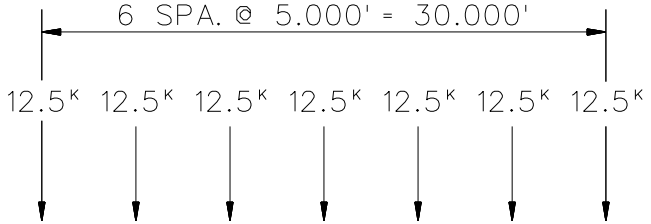

LOADING ON G8 AND G9

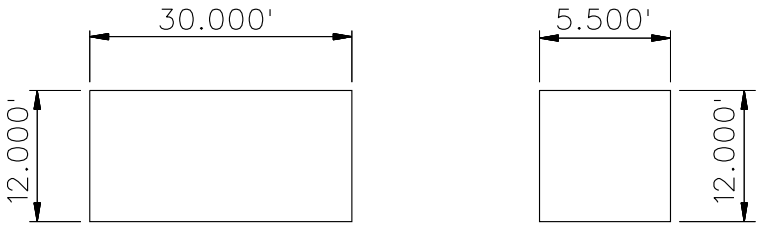

CONCRETE COUNTERWEIGHT INFORMATION

NOTES:

1. STEEL DEAD LOAD INCREASED BY 5% FOR MDX AND LARSA MODELS; 2% FOR 3D MODEL; AND 10% FOR APPROXIMATE ANALYSIS TO ACCOUNT FOR MISC. DETAILS.

2. FORMWORK LOAD OF 10PSF IS INCLUDED IN CONCRETE DEAD LOAD.

3. ADDITIONAL DESIGN PARAMETERS:
   A. 1.500' PARAPET WIDTH BOTH SIDES.
   B. 700 LB/FT UNIFORM LOAD ASSUMED FOR PARAPET WEIGHT.
   C. ROADWAY WIDTH = 77.000'.
   D. NUMBER OF DESIGN LANES = 6.
   E. HL93 LIVE LOAD.
   F. DESIGN SPEED = 35 MPH.

4. DIAPHRAGM MEMBER CALL-OUTS ARE IN ENGLISH UNITS.

NCHRP 12-79

BRIDGE NISCS39

MISC. DETAILS AND NOTES

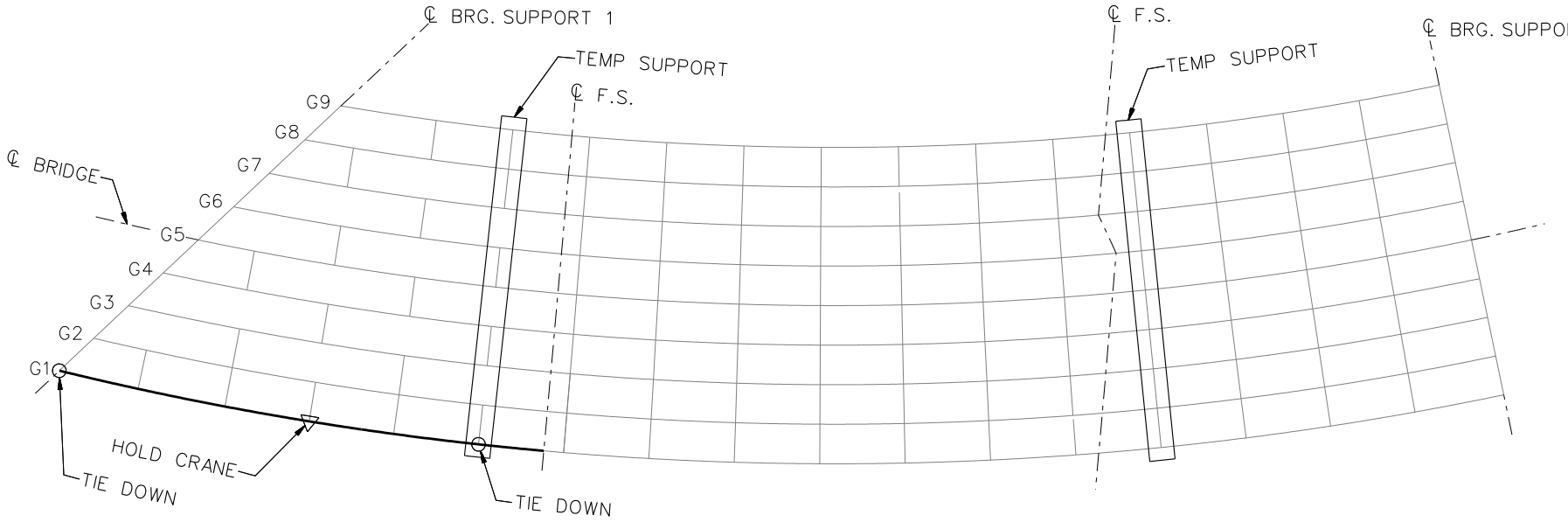

STAGE 1

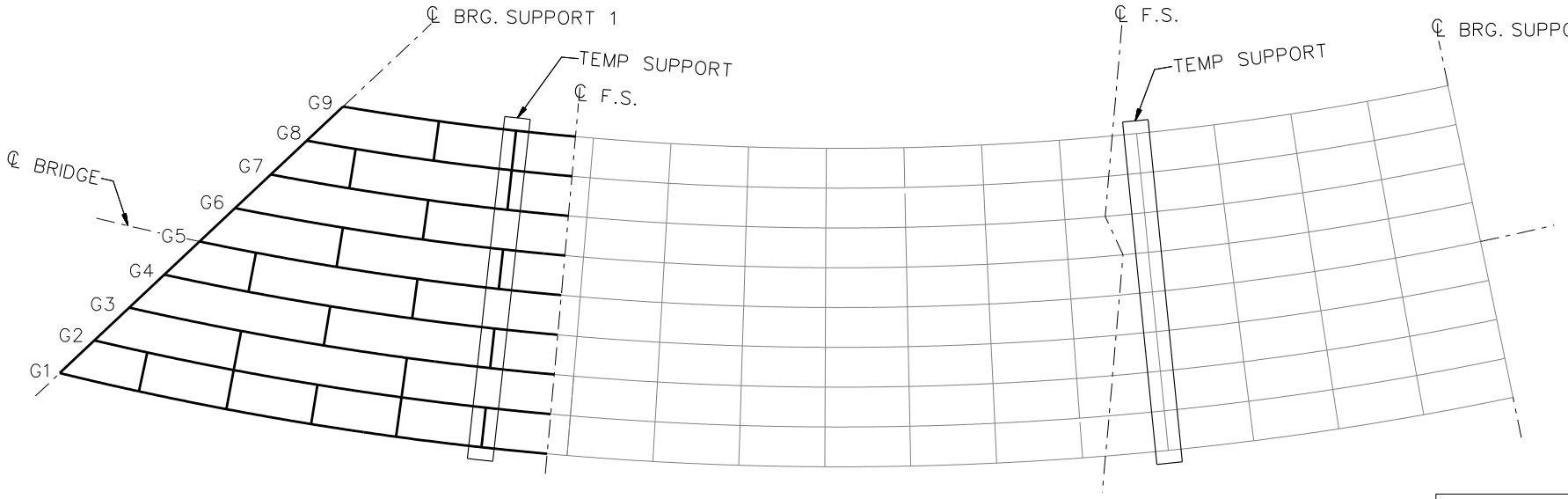

STAGES 2 THRU 9

LEGEND

▽ = HOLD OR LIFT CRANE

○ = TIE DOWN

□ = TEMPORARY SUPPORT STRUCTURE

NCHRP 12-79

BRIDGE NISCS39

GIRDER ERECTION PROCEDURE

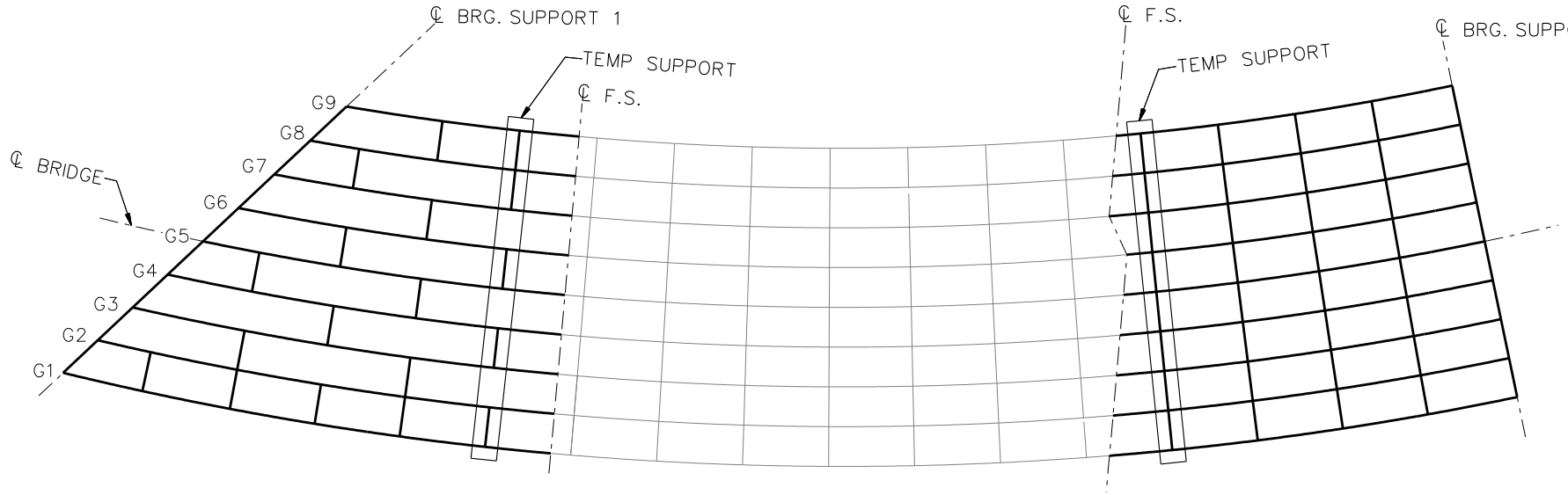

STAGES 10 THRU 18
(GIRDERS G1 THRU G9)

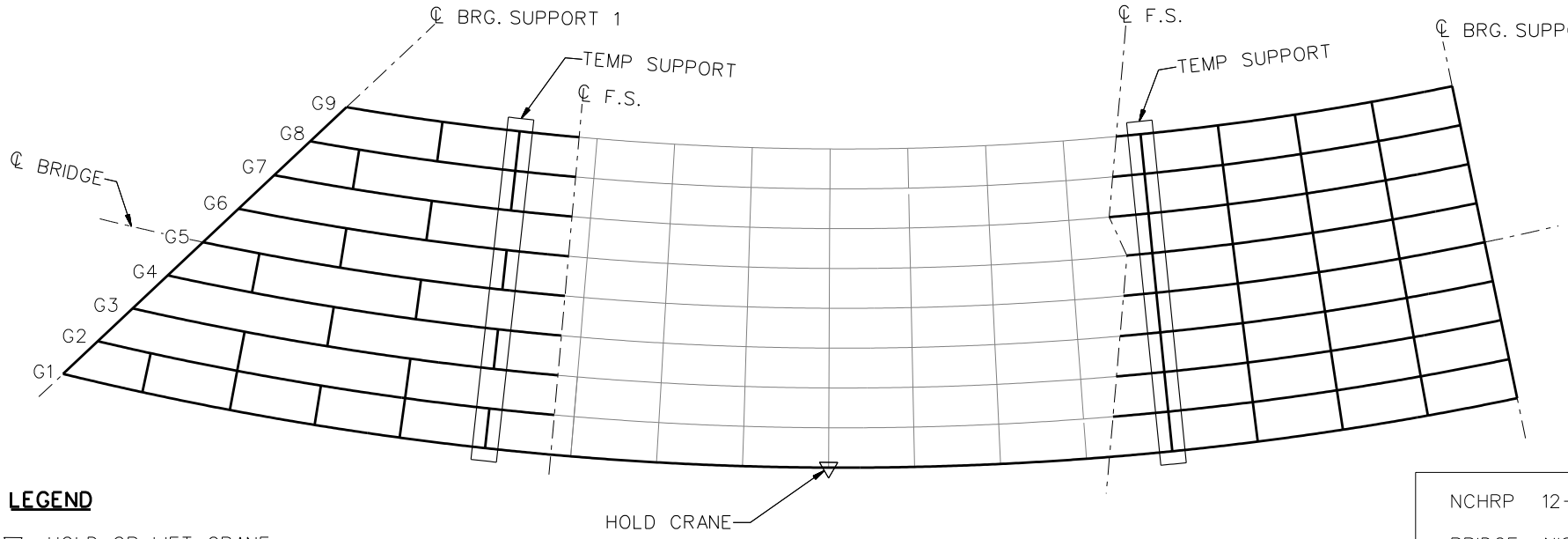

STAGE 19

LEGEND

▽ = HOLD OR LIFT CRANE

○ = TIE DOWN

□ = TEMPORARY SUPPORT STRUCTURE

NCHRP 12-79

BRIDGE NISCS39

GIRDER ERECTION PROCEDURE

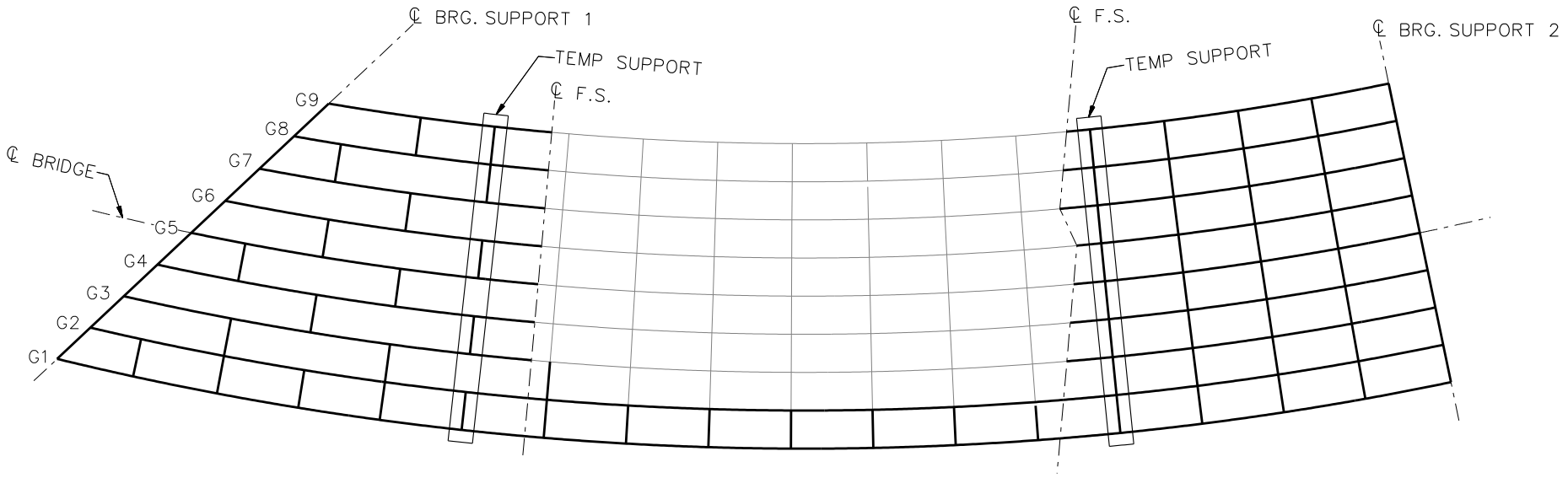

STAGE 20

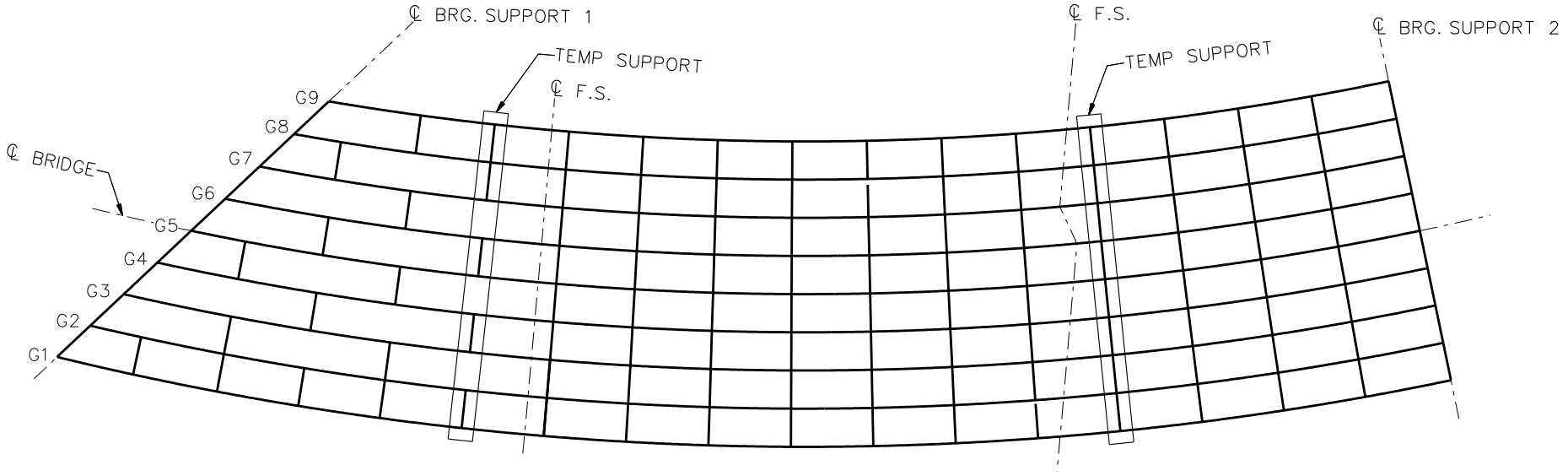

STAGES 21 THRU 27

LEGEND

▽ = HOLD OR LIFT CRANE

○ = TIE DOWN

□ = TEMPORARY SUPPORT STRUCTURE

NCHRP 12-79

BRIDGE NISCS39

GIRDER ERECTION PROCEDURE

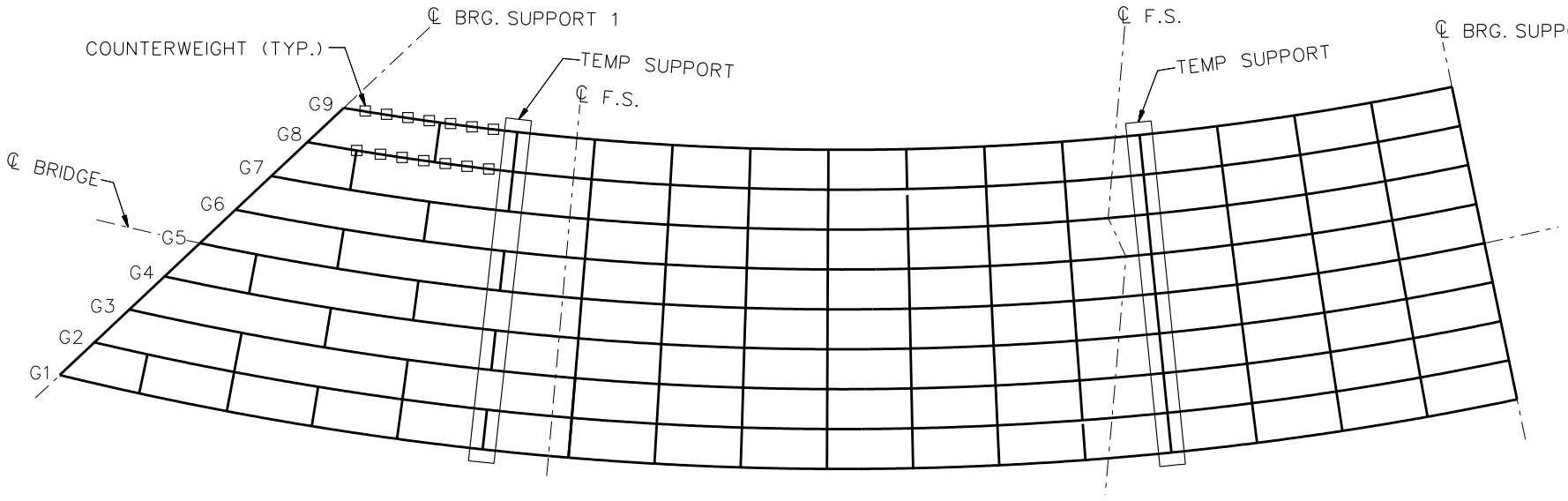

STAGE 28

PLACE COUNTERWEIGHT ON G8 + G9

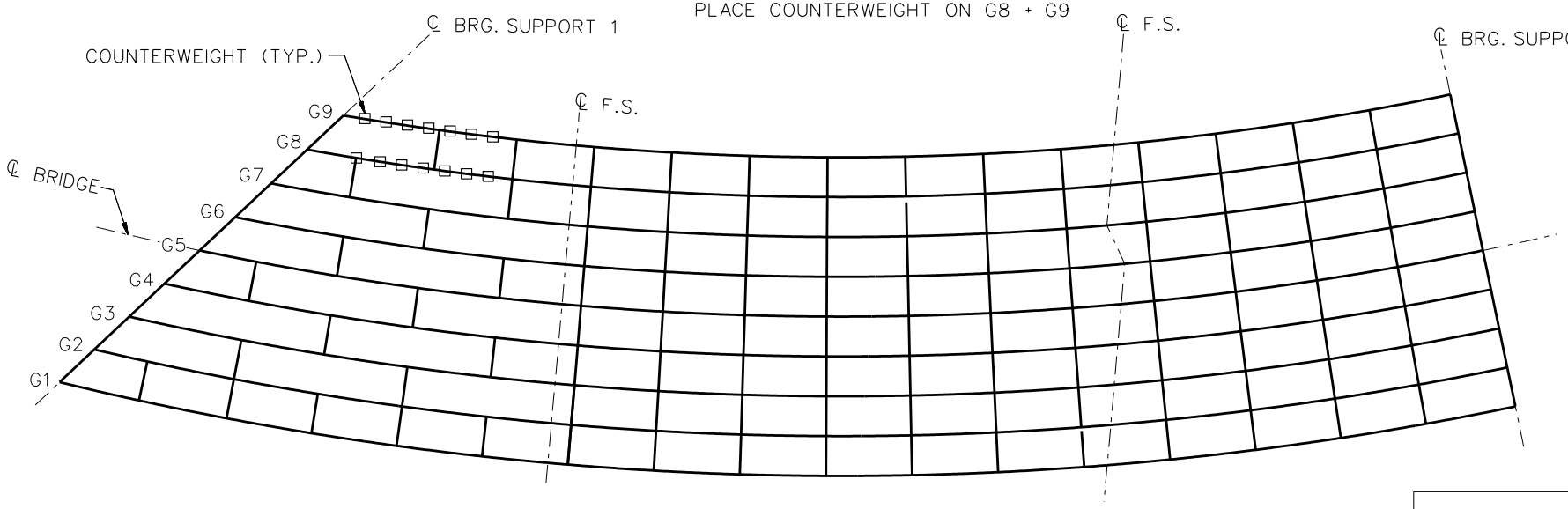

STAGE 29

REMOVE ALL TEMPORARY SUPPORTS

LEGEND

▽ = HOLD OR LIFT CRANE

○ = TIE DOWN

□ = TEMPORARY SUPPORT STRUCTURE

NCHRP 12-79

BRIDGE NISCS39

GIRDER ERECTION PROCEDURE

NCHRP 12-79

NISSS2

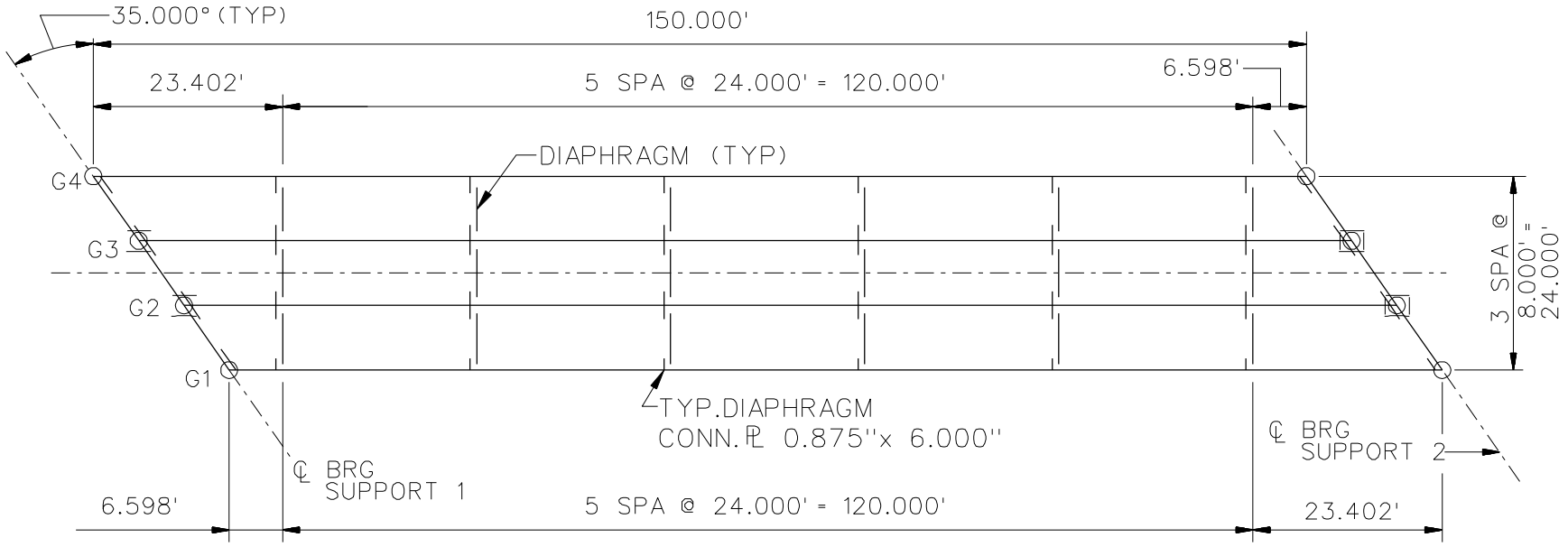

FRAMING PLAN

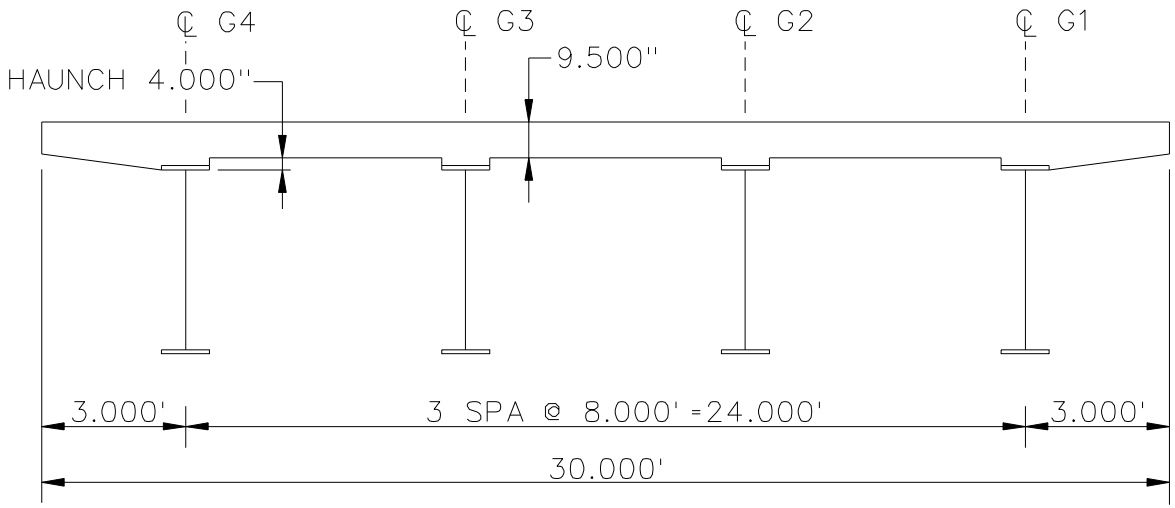

CROSS - SECTION

(DIAPHRAGMS NOT SHOWN)

BEARING LEGEND

- ○ NON-GUIDED
- ⊖ LONGITUDINALLY GUIDED
- ⊟ TRANSVERSELY GUIDED
- ⊡ FIXED

NCHRP 12-79

BRIDGE NISSS2

FRAMING PLAN AND CROSS SECTION

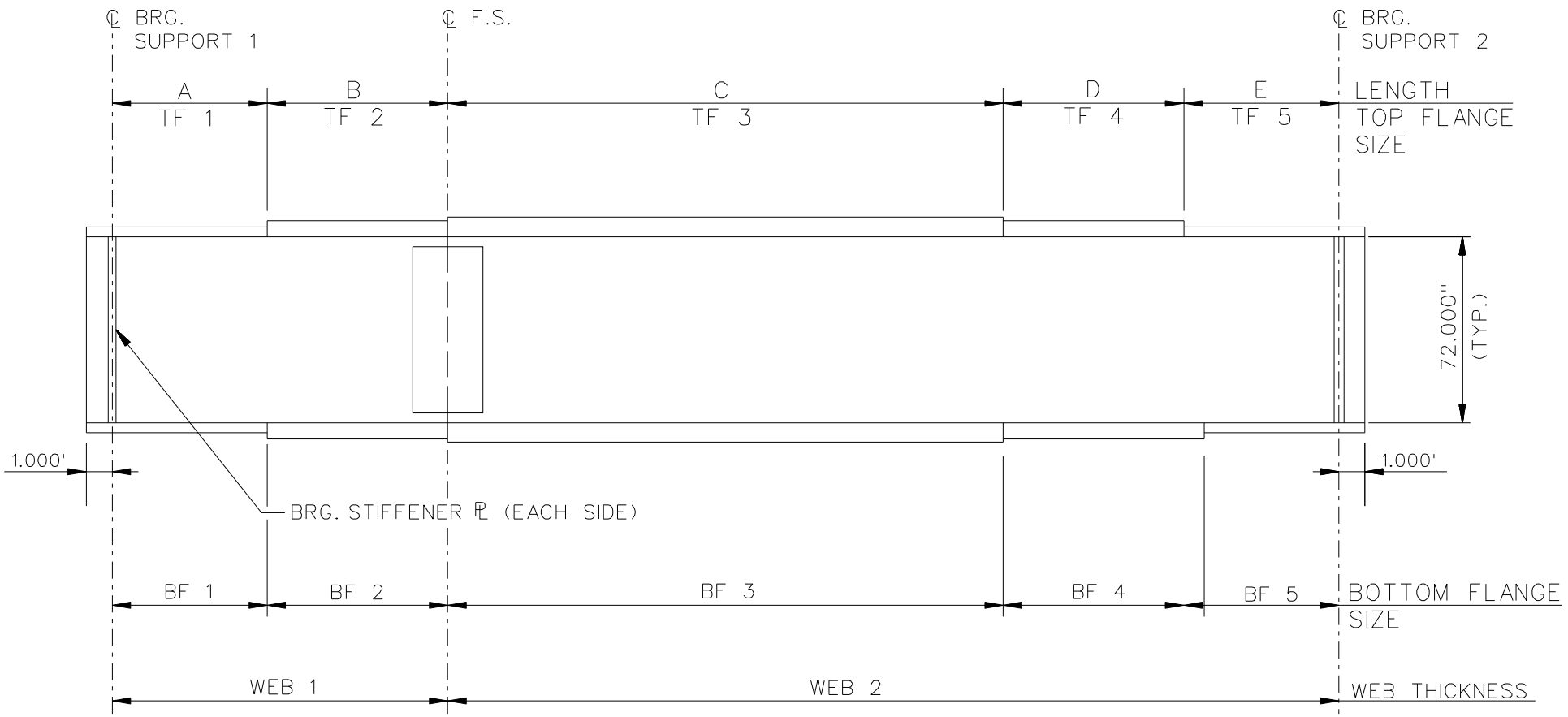

NOTE :

1. SEE TABLES ON SHEET 3 FOR GIRDER ELEVATION DIMENSIONS AND PLATE SIZES.

2. ALL GIRDERS, WEB 1 = WEB 2 = 0.6250".

NCHRP 12-79

BRIDGE NISSS2

GIRDER ELEVATION

SHEET 2 OF 6

	GIRDER PLATE LENGTHS ✳			
LENGTH	G1	G2	G3	G4
A	20.000	20.000	20.000	20.000
B	20.000	20.000	20.000	20.000
C	70.000	70.000	70.000	70.000
D	20.000	20.000	20.000	20.000
E	20.000	20.000	20.000	20.000

✳ ALL DIMENSIONS ARE IN FEET.

	GIRDER FLANGE DIMENSIONS ✳✳							
TOP	G1		G2		G3		G4	
FLANGE	BF	TF	BF	TF	BF	TF	BF	TF
TF1	16.000	0.875	16.000	0.875	16.000	0.875	16.000	0.875
TF2	16.000	0.875	16.000	0.875	16.000	0.875	16.000	0.875
TF3	16.000	1.250	16.000	1.250	16.000	1.250	16.000	1.250
TF4	16.000	1.000	16.000	1.000	16.000	1.000	16.000	1.000
TF5	16.000	1.000	16.000	1.000	16.000	1.000	16.000	1.000

✳✳ ALL DIMENSIONS ARE IN INCHES.

	GIRDER FLANGE DIMENSIONS ✳✳							
BOTTOM	G1		G2		G3		G4	
FLANGE	BF	TF	BF	TF	BF	TF	BF	TF
BF1	18.000	1.000	18.000	1.000	18.000	1.000	18.000	1.000
BF2	18.000	1.500	18.000	1.500	18.000	1.500	18.000	1.500
BF3	18.000	2.000	18.000	2.000	18.000	2.000	18.000	2.000
BF4	18.000	1.500	18.000	1.500	18.000	1.500	18.000	1.500
BF5	18.000	1.000	18.000	1.000	18.000	1.000	18.000	1.000

✳✳ ALL DIMENSIONS ARE IN INCHES.

NCHRP 12-79

BRIDGE NISSS2

GIRDER ELEVATION TABLES

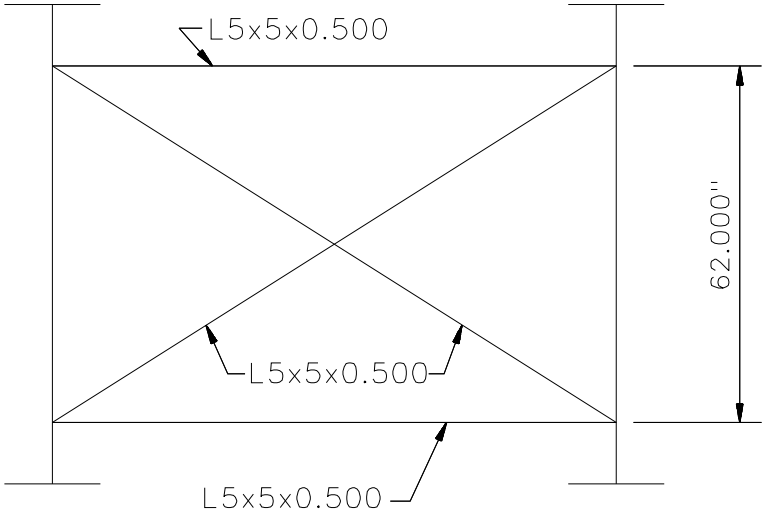

TYPICAL END AND INTERMEDIATE DIAPHRAGM

NOTES:

1. STEEL DEAD LOAD INCREASED BY 5% FOR MDX AND LARSA MODELS; 2% FOR 3D MODEL; AND 10% FOR APPROXIMATE ANALYSIS TO ACCOUNT FOR MISC. DETAILS.

2. FORMWORK LOAD OF 10PSF IS INCLUDED IN CONCRETE DEAD LOAD.

3. ADDITIONAL DESIGN PARAMETERS:
   A. 1.500' PARAPET WIDTH BOTH SIDES.
   B. 700 LB/FT UNIFORM LOAD ASSUMED FOR PARAPET WEIGHT.
   C. ROADWAY WIDTH = 26.500'.
   D. NUMBER OF DESIGN LANES = 2.
   E. HL93 LIVE LOAD.

4. DIAPHRAGM MEMBER CALL-OUTS ARE IN UNITS OF INCHES.

NCHRP 12-79

BRIDGE NISSS2

MISC. DETAILS AND NOTES

SHEET 4 OF 6

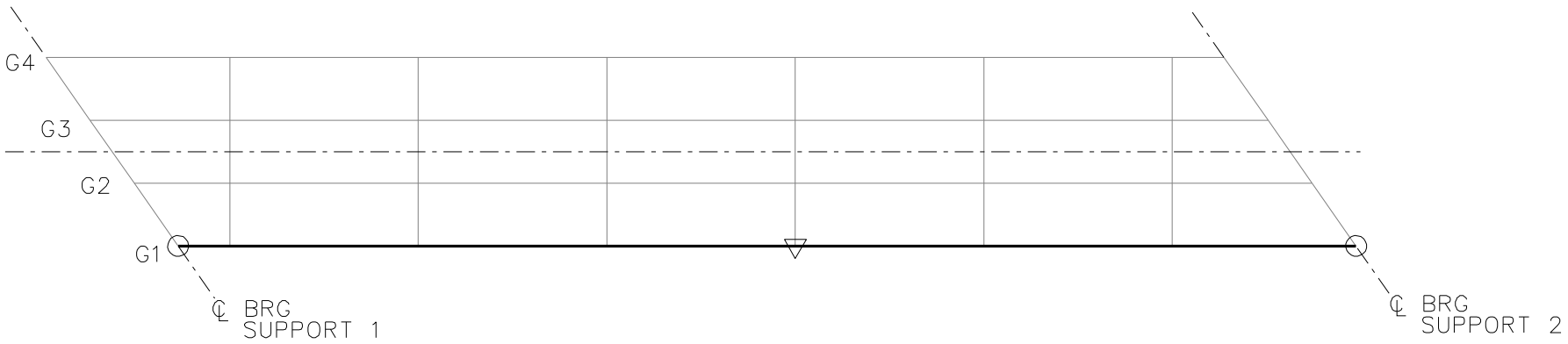

STAGE 1

STAGE 2

LEGEND

▽ = HOLD OR LIFT CRANE

○ = TIE DOWN

□ = TEMPORARY SUPPORT STRUCTURE

NCHRP 12-79

BRIDGE NISSS2

GENERAL ERECTION PROCEDURE

STAGE 3

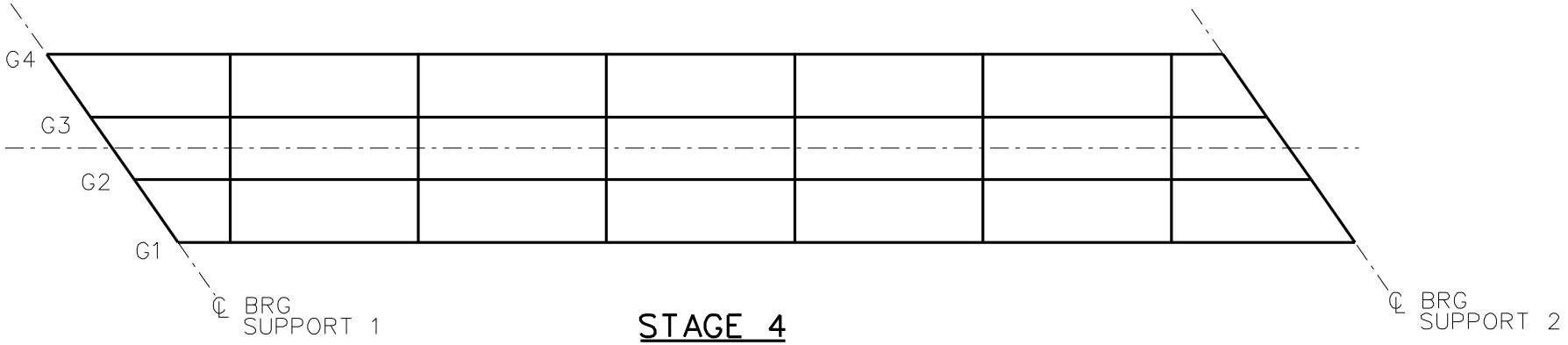

STAGE 4

LEGEND

▽ = HOLD OR LIFT CRANE

○ = TIE DOWN

□ = TEMPORARY SUPPORT STRUCTURE

NCHRP 12-79

BRIDGE NISSS2

GENERAL ERECTION PROCEDURE

NCHRP 12-79

NISSS4

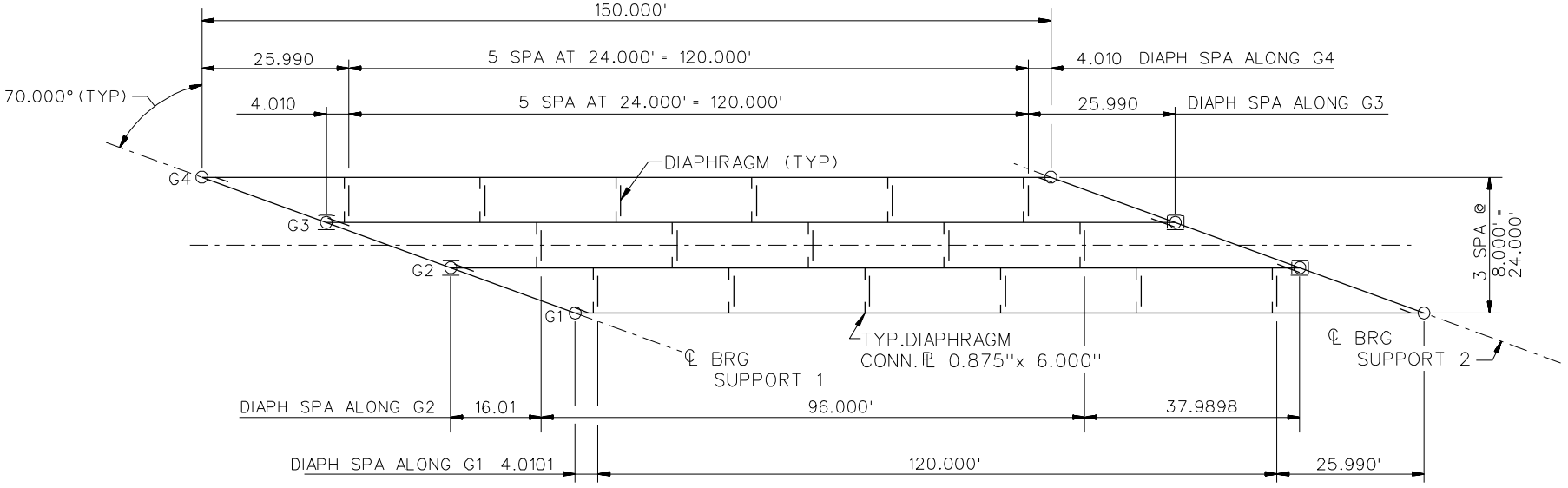

FRAMING PLAN

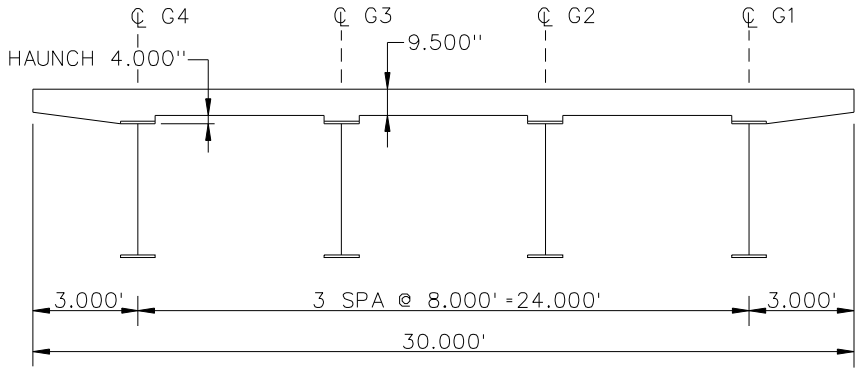

CROSS - SECTION

(DIAPHRAGMS NOT SHOWN)

BEARING LEGEND

- ○ NON-GUIDED
- ⊖ LONGITUDINALLY GUIDED
- |○| TRANSVERSELY GUIDED
- ⊡ FIXED

NCHRP 12-79

BRIDGE NISSS4

FRAMING PLAN AND CROSS SECTION

SHEET 1 OF 6

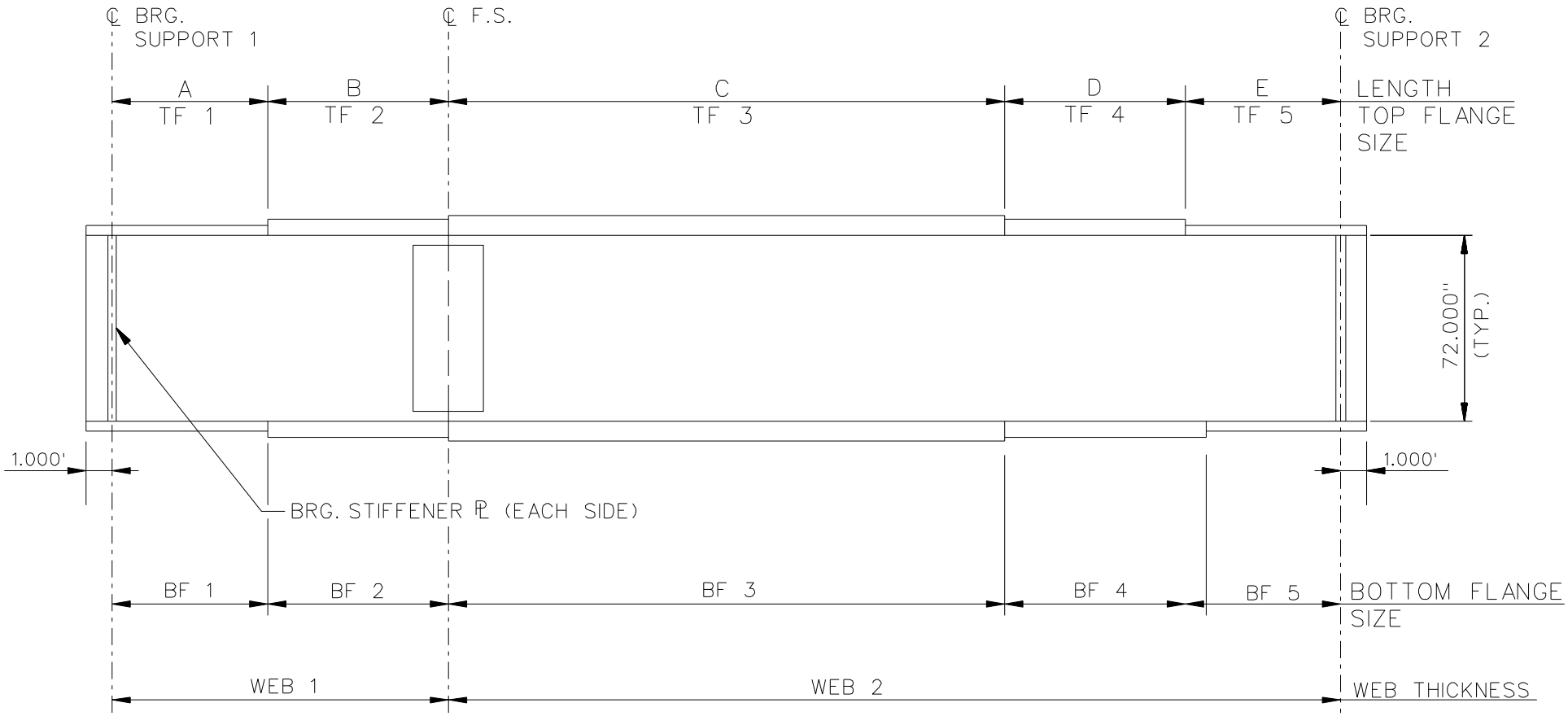

NOTE :

1. SEE TABLES ON SHEET 3 FOR GIRDER ELEVATION DIMENSIONS AND PLATE SIZES.
2. ALL GIRDERS, WEB 1 = WEB 2 = 0.6250".

NCHRP 12-79

BRIDGE NISSS4

GIRDER ELEVATION

SHEET 2 OF 6

	GIRDER PLATE LENGTHS ✳			
LENGTH	G1	G2	G3	G4
A	20.000	20.000	20.000	20.000
B	20.000	20.000	20.000	20.000
C	70.000	70.000	70.000	70.000
D	20.000	20.000	20.000	20.000
E	20.000	20.000	20.000	20.000

✳ ALL DIMENSIONS ARE IN FEET.

	GIRDER FLANGE DIMENSIONS ✳✳							
TOP	G1		G2		G3		G4	
FLANGE	BF	TF	BF	TF	BF	TF	BF	TF
TF1	16.000	0.875	16.000	0.875	16.000	0.875	16.000	0.875
TF2	16.000	0.875	16.000	0.875	16.000	0.875	16.000	0.875
TF3	16.000	1.125	16.000	1.125	16.000	1.125	16.000	1.125
TF4	16.000	1.000	16.000	1.000	16.000	1.000	16.000	1.000
TF5	16.000	1.000	16.000	1.000	16.000	1.000	16.000	1.000

✳✳ ALL DIMENSIONS ARE IN INCHES.

	GIRDER FLANGE DIMENSIONS ✳✳							
BOTTOM	G1		G2		G3		G4	
FLANGE	BF	TF	BF	TF	BF	TF	BF	TF
BF1	18.000	1.000	18.000	1.000	18.000	1.000	18.000	1.000
BF2	18.000	1.500	18.000	1.500	18.000	1.500	18.000	1.500
BF3	18.000	2.000	18.000	2.000	18.000	2.000	18.000	2.000
BF4	18.000	1.500	18.000	1.500	18.000	1.500	18.000	1.500
BF5	18.000	1.000	18.000	1.000	18.000	1.000	18.000	1.000

✳✳ ALL DIMENSIONS ARE IN INCHES.

NCHRP 12-79

BRIDGE NISSS4

GIRDER ELEVATION TABLES

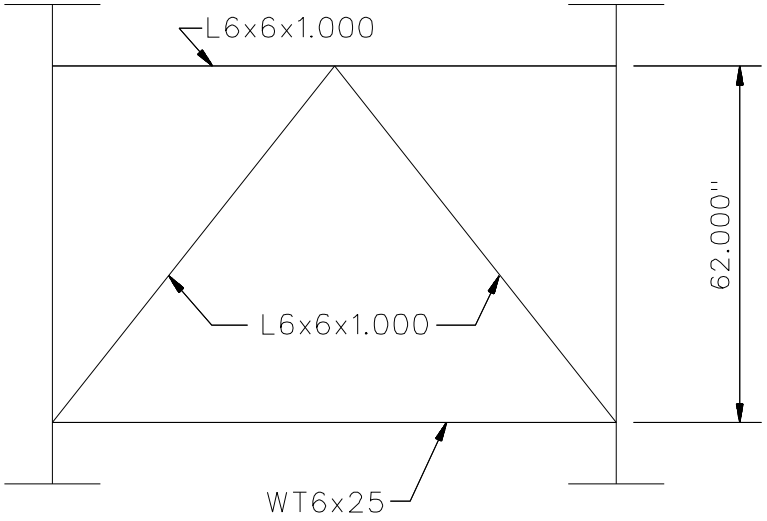

TYPICAL END AND INTERMEDIATE DIAPHRAGM

NOTES:

1. STEEL DEAD LOAD INCREASED BY 5% FOR MDX AND LARSA MODELS; 2% FOR 3D MODEL; AND 10% FOR APPROXIMATE ANALYSIS TO ACCOUNT FOR MISC. DETAILS.

2. FORMWORK LOAD OF 10PSF IS INCLUDED IN CONCRETE DEAD LOAD.

3. ADDITIONAL DESIGN PARAMETERS:
   A. 1.500' PARAPET WIDTH BOTH SIDES.
   B. 700 LB/FT UNIFORM LOAD ASSUMED FOR PARAPET WEIGHT.
   C. ROADWAY WIDTH = 26.500'.
   D. NUMBER OF DESIGN LANES = 2.
   E. HL93 LIVE LOAD.

4. DIAPHRAGM MEMBER CALL-OUTS ARE IN UNITS OF INCHES.

NCHRP 12-79

BRIDGE NISSS4

MISC. DETAILS AND NOTES

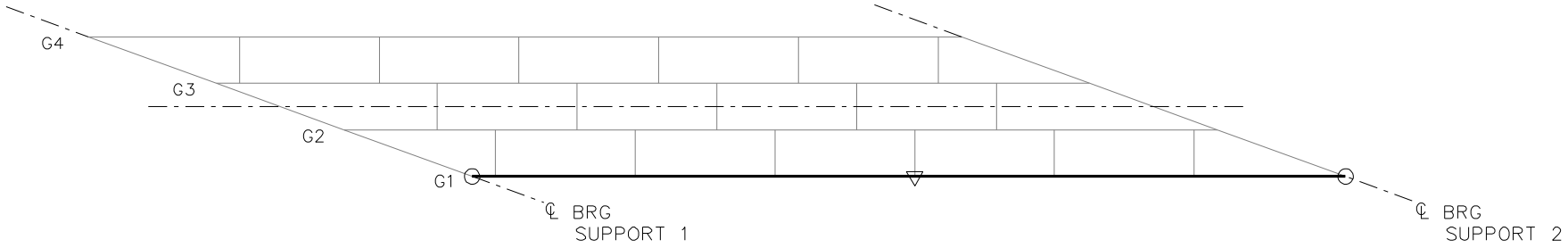

STAGE 1

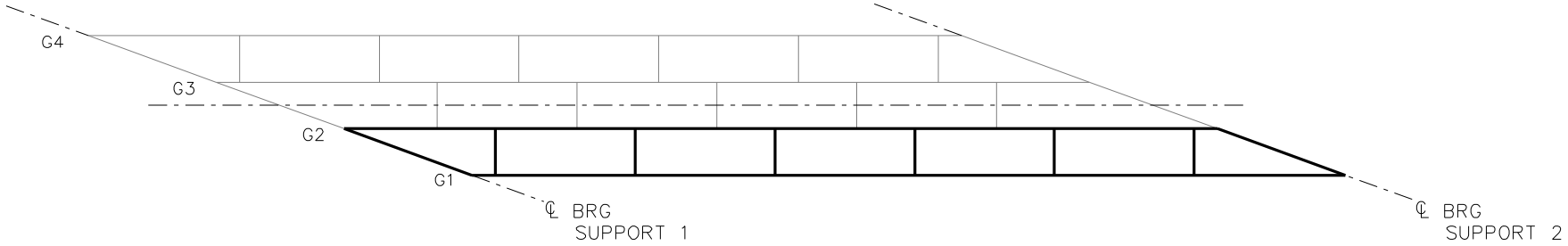

STAGE 2

LEGEND

▽ = HOLD OR LIFT CRANE

○ = TIE DOWN

□ = TEMPORARY SUPPORT STRUCTURE

NCHRP 12-79

BRIDGE NISSS4

GENERAL ERECTION PROCEDURE

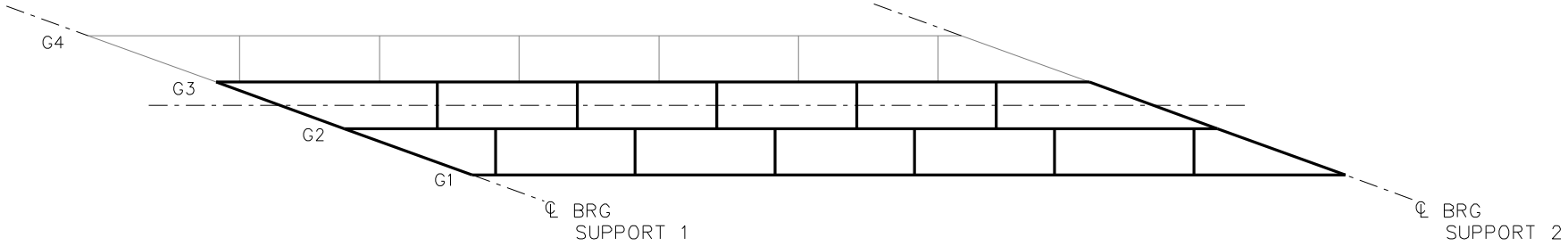

STAGE 3

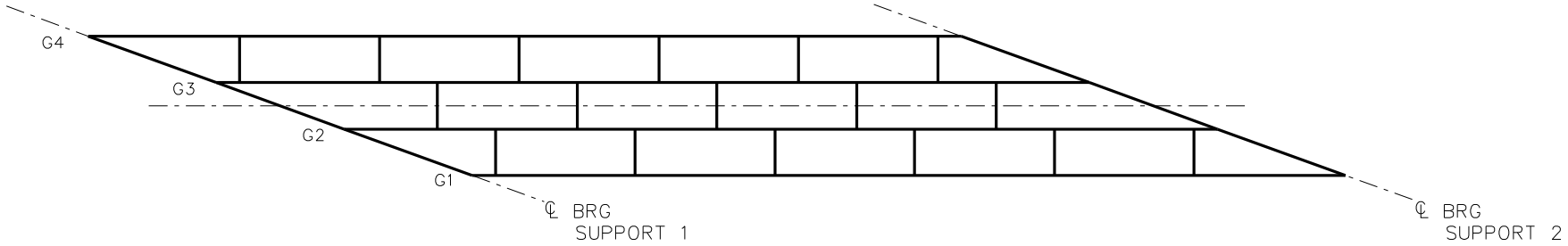

STAGE 4

LEGEND

▽ = HOLD OR LIFT CRANE

○ = TIE DOWN

□ = TEMPORARY SUPPORT STRUCTURE

NCHRP 12-79

BRIDGE NISSS4

GENERAL ERECTION PROCEDURE

NCHRP 12-79

NISSS6

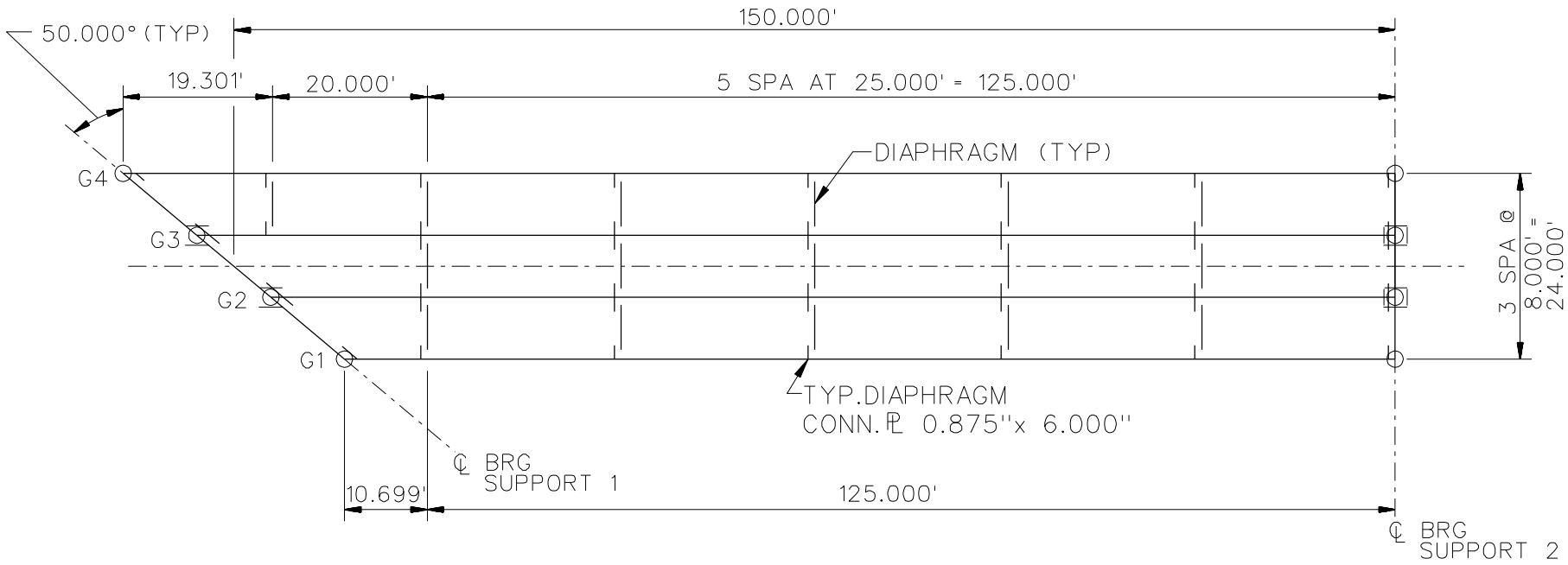

FRAMING PLAN

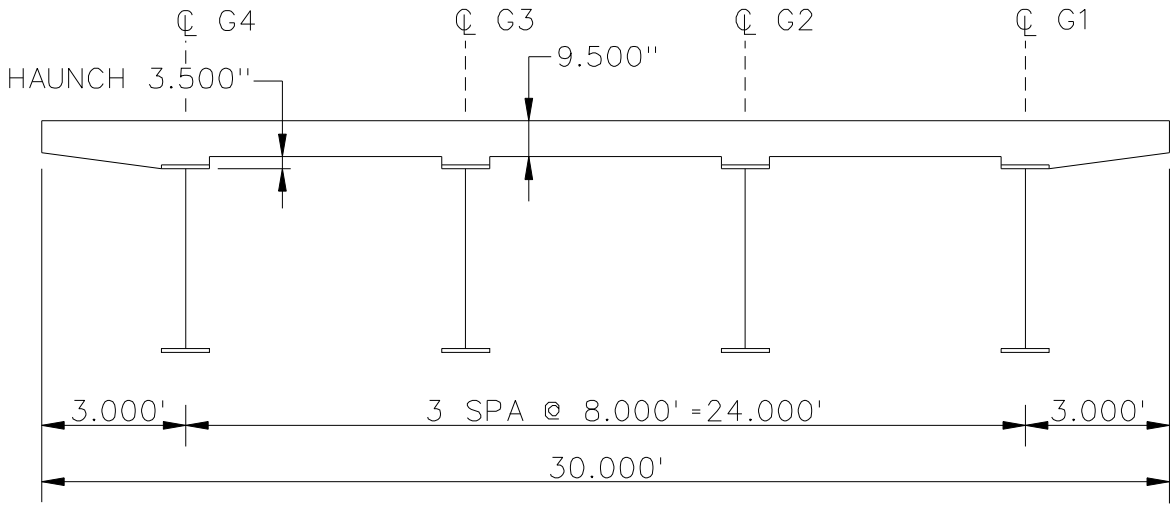

CROSS - SECTION

(DIAPHRAGMS NOT SHOWN)

BEARING LEGEND

- ○ NON-GUIDED
- ⊖ LONGITUDINALLY GUIDED
- |○| TRANSVERSELY GUIDED
- ⊡ FIXED

NCHRP 12-79

BRIDGE NISSS6

FRAMING PLAN AND CROSS SECTION

SHEET 1 OF 6

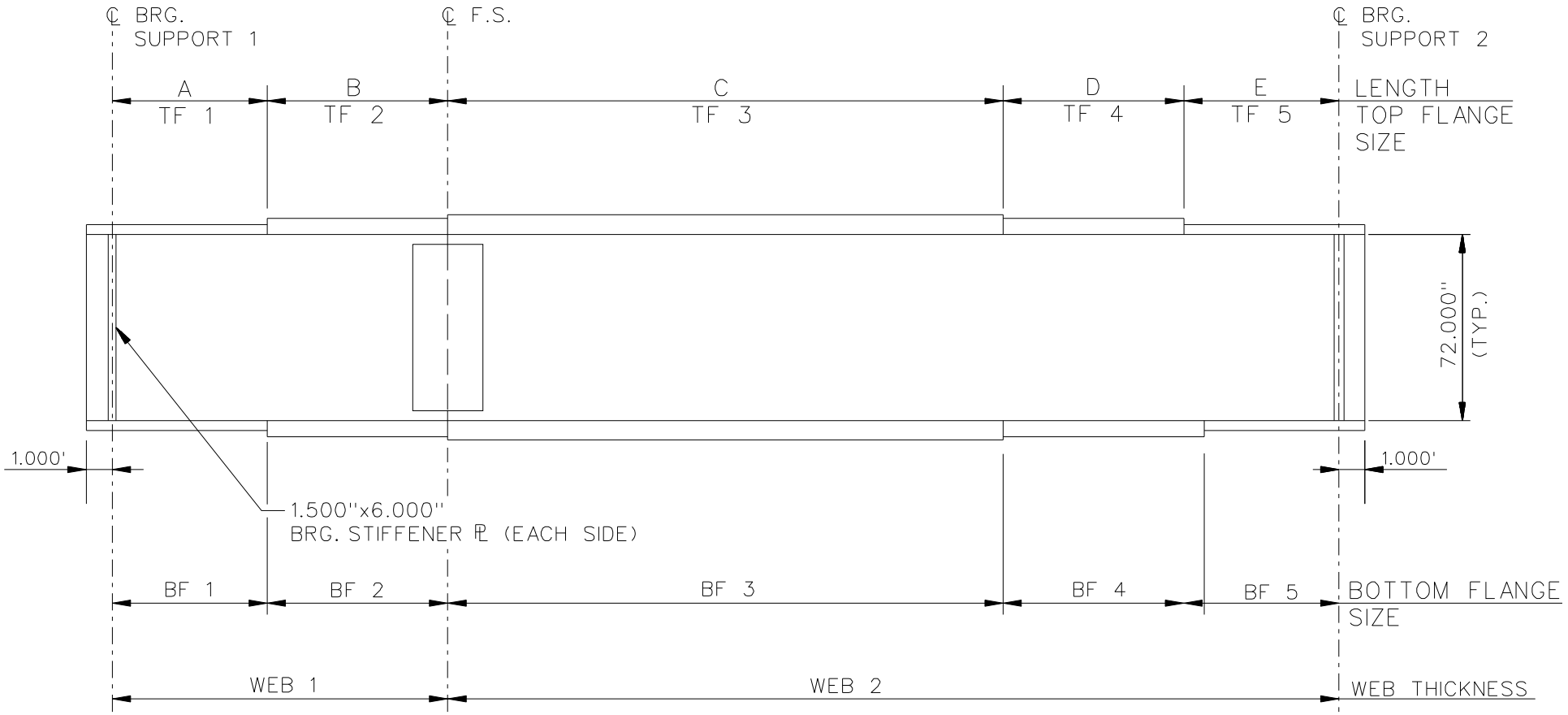

NOTE :

1. SEE TABLES ON SHEET 3 FOR GIRDER ELEVATION DIMENSIONS AND PLATE SIZES.

2. ALL GIRDERS, WEB 1 = WEB 2 = 0.6250".

NCHRP 12-79

BRIDGE NISSS6

GIRDER ELEVATION

SHEET 2 OF 6

	GIRDER PLATE LENGTHS ✳			
LENGTH	G1	G2	G3	G4
A	20.000	20.000	20.000	20.000
B	20.000	20.000	20.000	20.000
C	70.000	70.000	70.000	70.000
D	20.000	20.000	20.000	20.000
E	5.699	15.233	24.767	34.301

✳ ALL DIMENSIONS ARE IN FEET.

	GIRDER FLANGE DIMENSIONS ✳✳							
TOP	G1		G2		G3		G4	
FLANGE	BF	TF	BF	TF	BF	TF	BF	TF
TF1	18.000	0.875	18.000	0.875	18.000	0.875	18.000	0.875
TF2	18.000	0.875	18.000	0.875	18.000	0.875	18.000	0.875
TF3	18.000	1.250	18.000	1.250	18.000	1.250	18.000	1.250
TF4	18.000	1.000	18.000	1.000	18.000	1.000	18.000	1.000
TF5	18.000	1.000	18.000	1.000	18.000	1.000	18.000	1.000

✳✳ ALL DIMENSIONS ARE IN INCHES.

	GIRDER FLANGE DIMENSIONS ✳✳							
BOTTOM	G1		G2		G3		G4	
FLANGE	BF	TF	BF	TF	BF	TF	BF	TF
BF1	20.000	1.000	20.000	1.000	20.000	1.000	20.000	1.000
BF2	20.000	1.000	20.000	1.000	20.000	1.000	20.000	1.000
BF3	20.000	1.500	20.000	1.500	20.000	2.000	20.000	2.000
BF4	20.000	1.250	20.000	1.250	20.000	1.750	20.000	1.750
BF5	20.000	1.250	20.000	1.250	20.000	1.250	20.000	1.250

✳✳ ALL DIMENSIONS ARE IN INCHES.

NCHRP 12-79

BRIDGE NISSS6

GIRDER ELEVATION TABLES

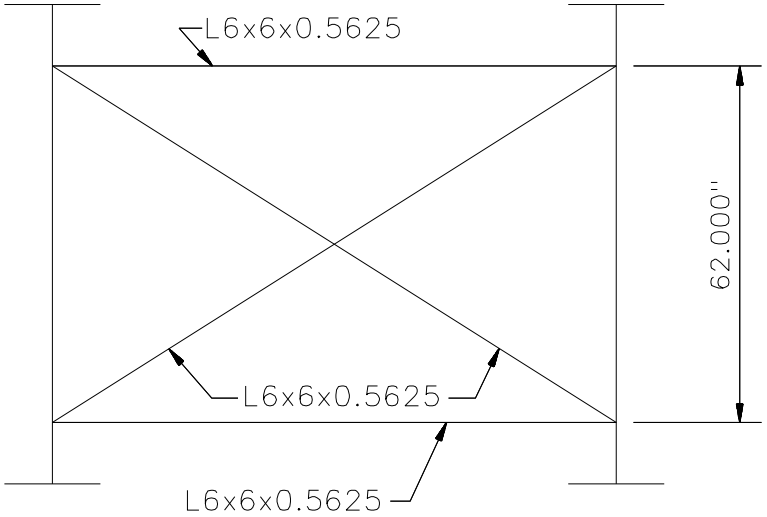

TYPICAL END AND INTERMEDIATE DIAPHRAGM

NOTES:

1. STEEL DEAD LOAD INCREASED BY 5% FOR MDX AND LARSA MODELS; 2% FOR 3D MODEL; AND 10% FOR APPROXIMATE ANALYSIS TO ACCOUNT FOR MISC. DETAILS.

2. FORMWORK LOAD OF 10PSF IS INCLUDED IN CONCRETE DEAD LOAD.

3. ADDITIONAL DESIGN PARAMETERS:
   A. 1.500' PARAPET WIDTH BOTH SIDES.
   B. 700 LB/FT UNIFORM LOAD ASSUMED FOR PARAPET WEIGHT.
   C. ROADWAY WIDTH = 26.500'.
   D. NUMBER OF DESIGN LANES = 2.
   E. HL93 LIVE LOAD.

4. DIAPHRAGM MEMBER CALL-OUTS ARE IN UNITS OF INCHES.

NCHRP 12-79

BRIDGE NISSS6

MISC. DETAILS AND NOTES

SHEET 4 OF 6

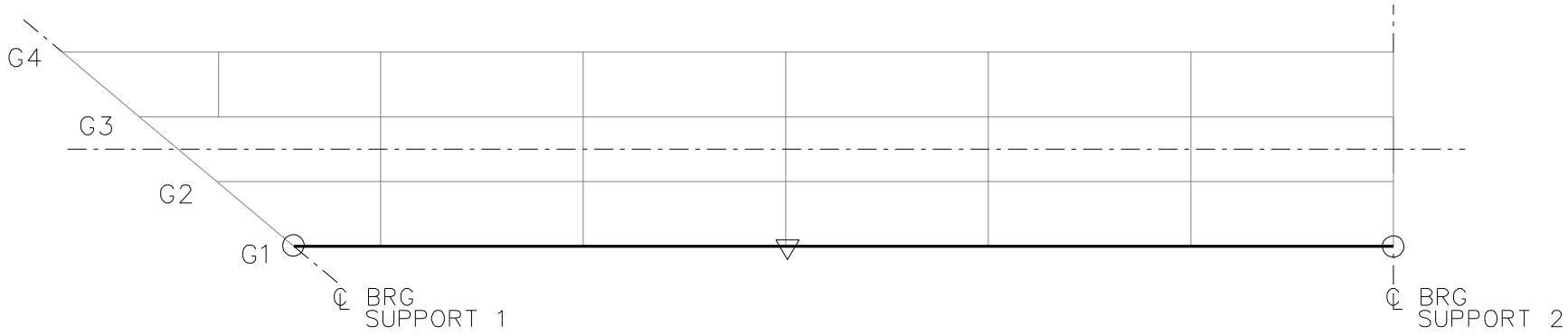

STAGE 1

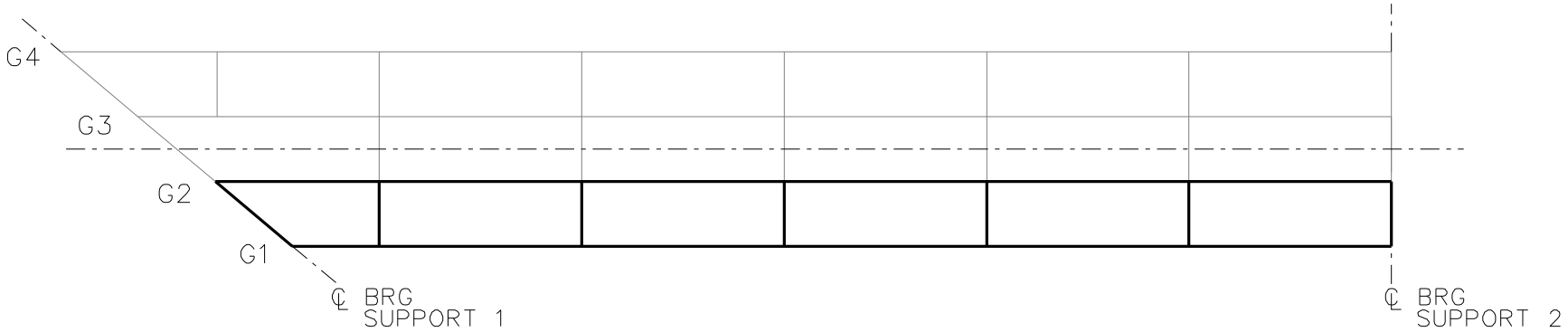

STAGE 2

LEGEND

▽ = HOLD OR LIFT CRANE

○ = TIE DOWN

□ = TEMPORARY SUPPORT STRUCTURE

NCHRP 12-79

BRIDGE NISSS6

GENERAL ERECTION PROCEDURE

STAGE 3

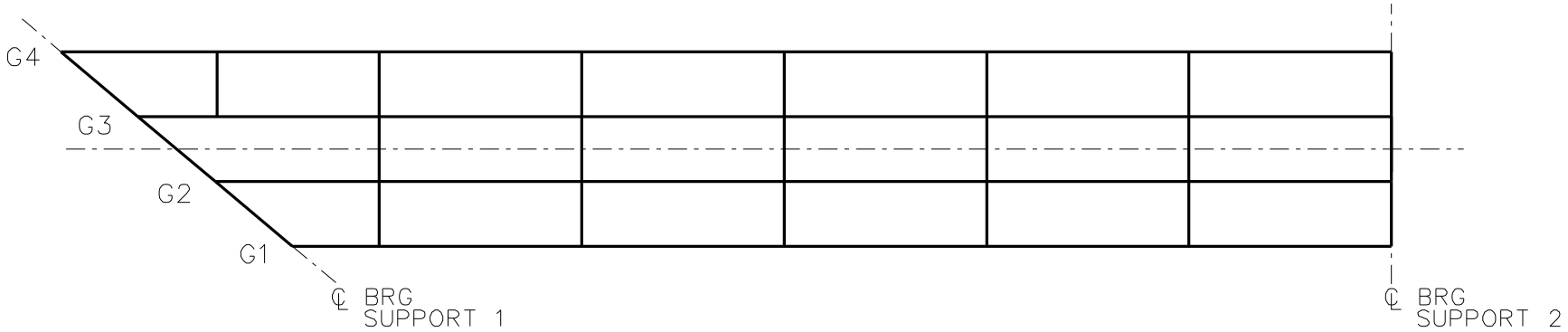

STAGE 4

LEGEND

▽ = HOLD OR LIFT CRANE

○ = TIE DOWN

□ = TEMPORARY SUPPORT STRUCTURE

NCHRP 12-79

BRIDGE NISSS6

GENERAL ERECTION PROCEDURE

NCHRP 12-79

NISSS11

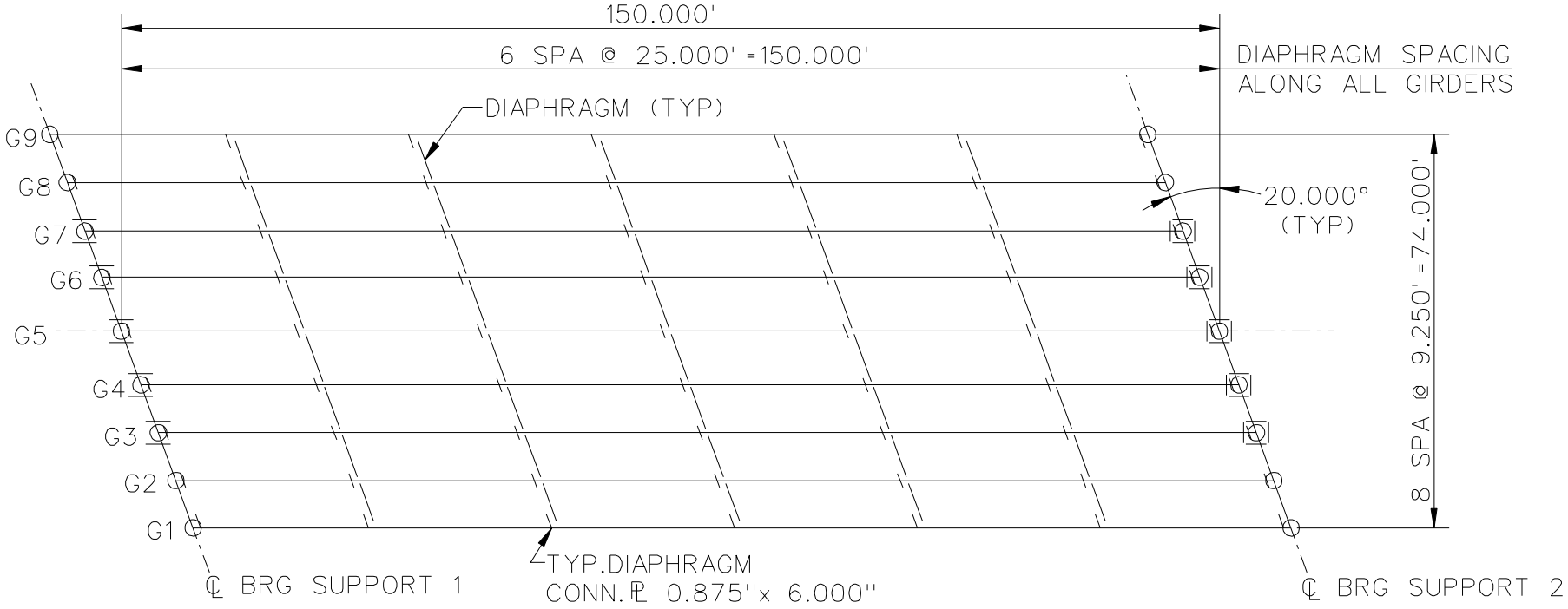

FRAMING PLAN

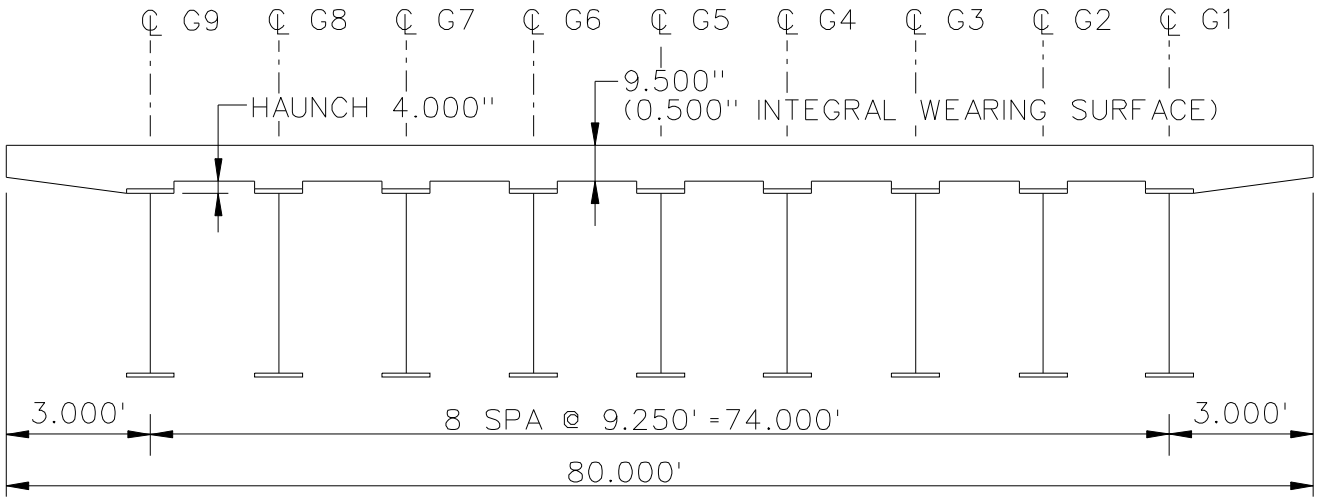

CROSS - SECTION

(DIAPHRAGMS NOT SHOWN)

BEARING LEGEND

- ○ NON-GUIDED
- ⊟○ LONGITUDINALLY GUIDED
- |○| TRANSVERSELY GUIDED
- ⊟○⊟ FIXED

NCHRP 12-79

BRIDGE NISSS11

FRAMING PLAN AND CROSS-SECTION

SHEET 1 OF 6

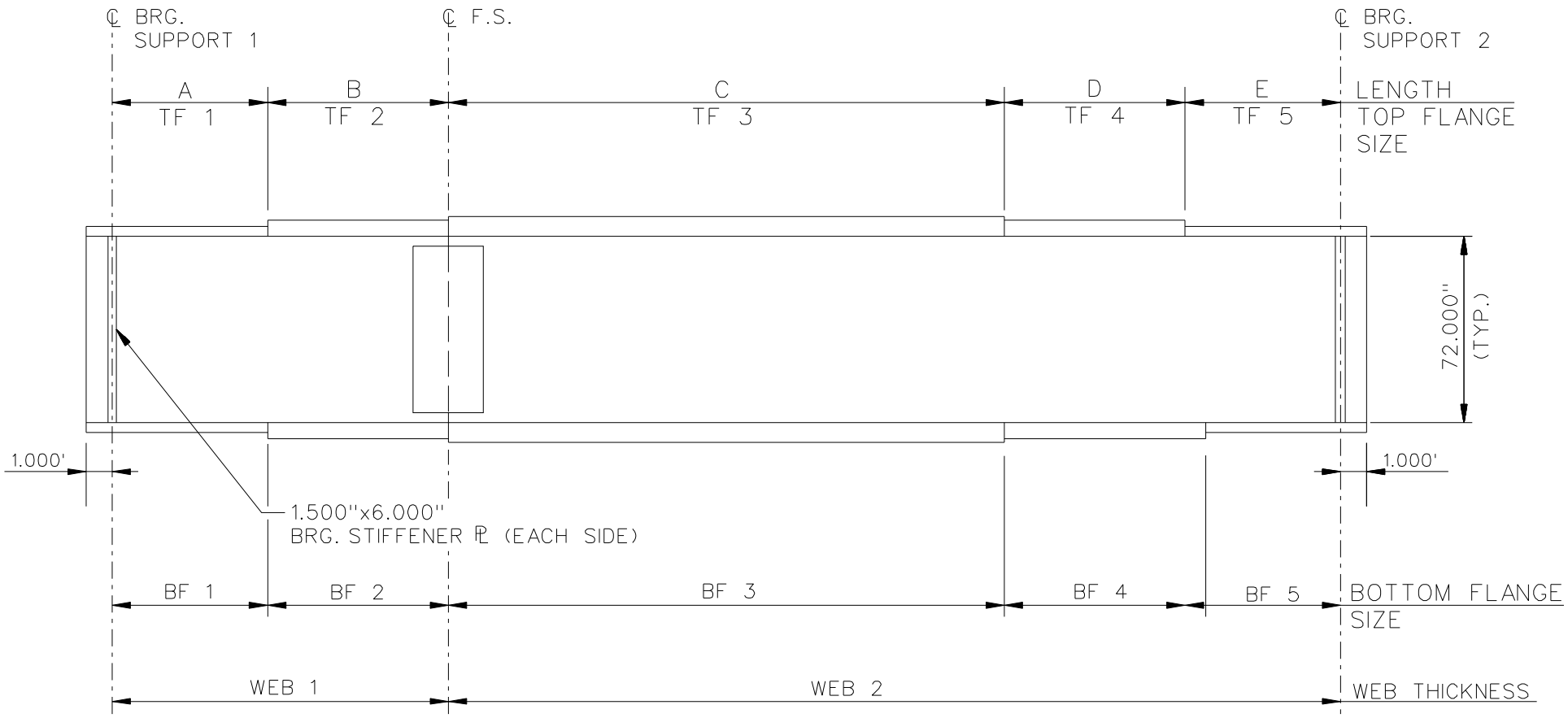

NOTE :

1. SEE TABLES ON SHEET 3 FOR GIRDER ELEVATION DIMENSIONS AND PLATE SIZES.
2. ALL GIRDERS, WEB 1 = WEB 2 = 0.6250".

NCHRP 12-79

BRIDGE NISSS11

GIRDER ELEVATION

SHEET 2 OF 6

	GIRDER PLATE LENGTHS ✳		
LENGTH	G1, G2, G3	G4, G5, G6	G7, G8, G9
A	20.000	20.000	20.000
B	20.000	20.000	20.000
C	70.000	70.000	70.000
D	20.000	20.000	20.000
E	20.000	20.000	20.000

✳ ALL DIMENSIONS ARE IN FEET.

	GIRDER FLANGE DIMENSIONS ✳✳					
TOP	G1, G2, G3		G4, G5, G6		G7, G8, G9	
FLANGE	BF	TF	BF	TF	BF	TF
TF1	16.000	0.750	16.000	0.750	16.000	0.750
TF2	16.000	0.750	16.000	0.750	16.000	0.750
TF3	16.000	1.000	16.000	1.000	16.000	1.000
TF4	16.000	0.750	16.000	0.750	16.000	0.750
TF5	16.000	0.750	16.000	0.750	16.000	0.750

✳✳ ALL DIMENSIONS ARE IN INCHES.

	GIRDER FLANGE DIMENSIONS ✳✳					
BOTTOM	G1, G2, G3		G4, G5, G6		G7, G8, G9	
FLANGE	BF	TF	BF	TF	BF	TF
BF1	18.000	1.000	18.000	1.000	18.000	1.000
BF2	18.000	1.500	18.000	1.500	18.000	1.500
BF3	18.000	2.000	18.000	2.000	18.000	2.000
BF4	18.000	1.500	18.000	1.500	18.000	1.500
BF5	18.000	1.000	18.000	1.000	18.000	1.000

✳✳ ALL DIMENSIONS ARE IN INCHES.

NCHRP 12-79

BRIDGE NISSS11

GIRDER ELEVATION TABLES

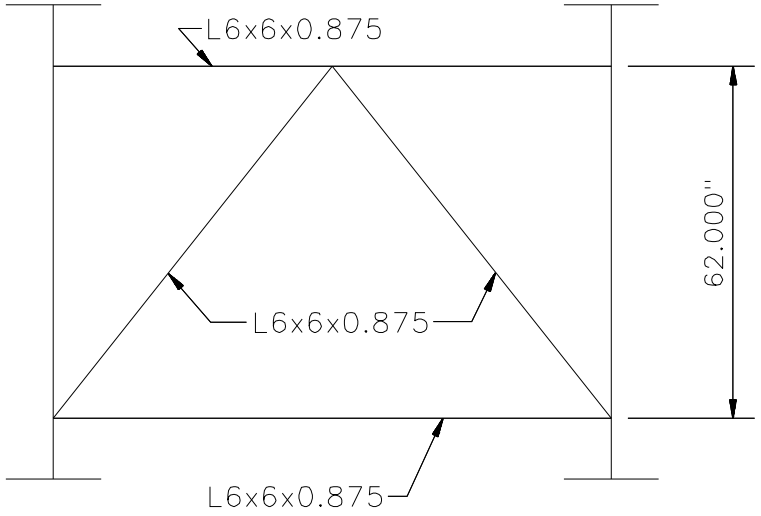

TYPICAL END AND INTERMEDIATE DIAPHRAGM

NOTES:

1. STEEL DEAD LOAD INCREASED BY 5% FOR MDX AND LARSA MODELS; 2% FOR 3D MODEL; AND 10% FOR APPROXIMATE ANALYSIS TO ACCOUNT FOR MISC. DETAILS.

2. FORMWORK LOAD OF 10PSF IS INCLUDED IN CONCRETE DEAD LOAD.

3. ADDITIONAL DESIGN PARAMETERS:
   A. 1.500' PARAPET WIDTH BOTH SIDES.
   B. 700 LB/FT UNIFORM LOAD ASSUMED FOR PARAPET WEIGHT.
   C. ROADWAY WIDTH = 77.000'.
   D. NUMBER OF DESIGN LANES = 6.
   E. HL93 LIVE LOAD.

4. DIAPHRAGM MEMBER CALL-OUTS ARE IN UNITS OF INCHES.

NCHRP 12-79

BRIDGE NISSS11

MISC. DETAILS AND NOTES

SHEET 4 OF 6

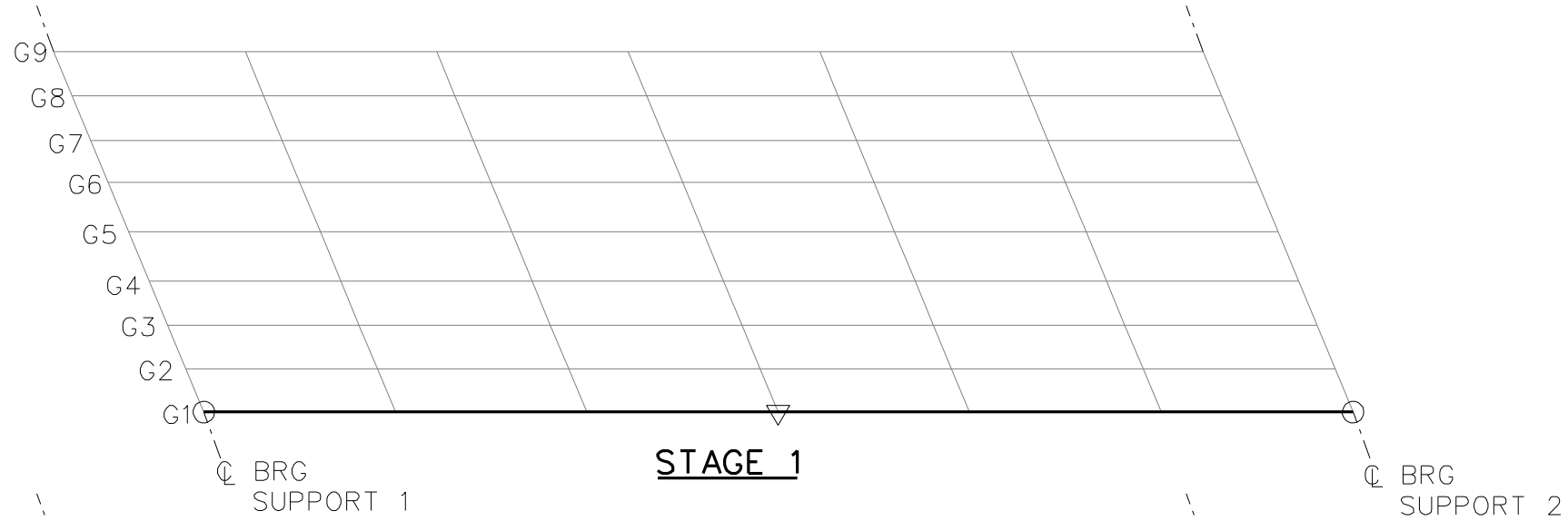

STAGE 1

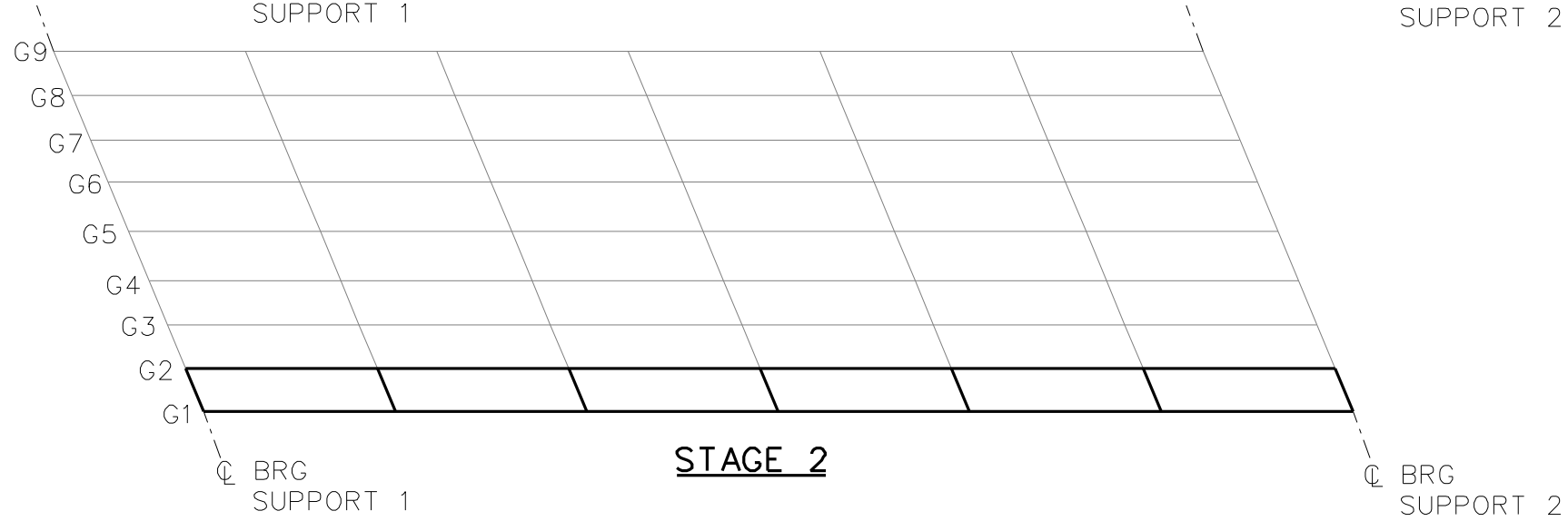

STAGE 2

LEGEND

▽ = HOLD OR LIFT CRANE

○ = TIE DOWN

□ = TEMPORARY SUPPORT STRUCTURE

STAGE 3 - ERECT G3 AND ADJACENT CROSS FRAMES
STAGE 4 - ERECT G4 AND ADJACENT CROSS FRAMES
STAGE 5 - ERECT G5 AND ADJACENT CROSS FRAMES
STAGE 6 - ERECT G6 AND ADJACENT CROSS FRAMES
STAGE 7 - ERECT G7 AND ADJACENT CROSS FRAMES

NCHRP 12-79

BRIDGE NISSS11

GENERAL ERECTION PROCEDURE

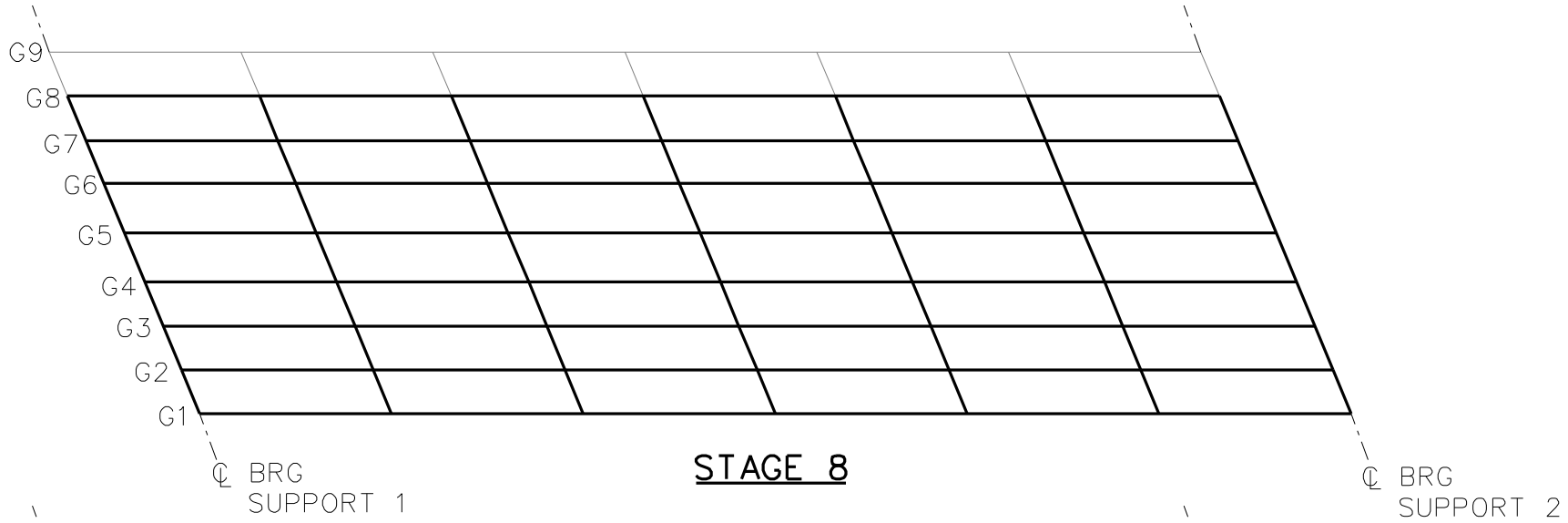

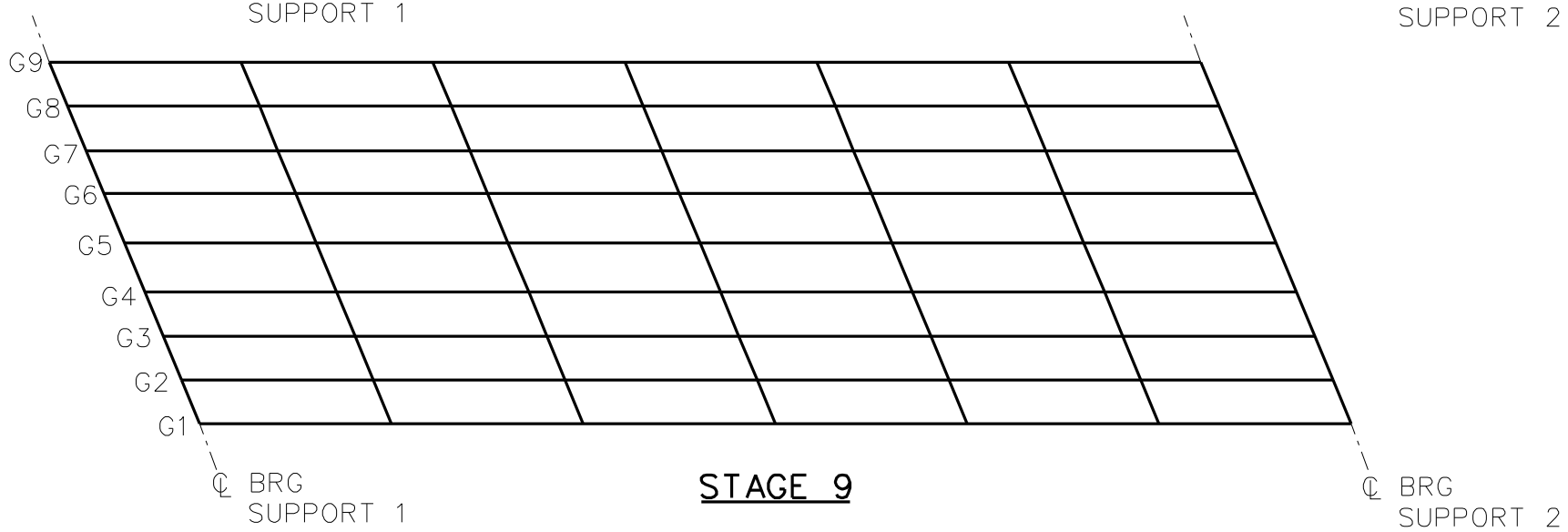

LEGEND

▽ = HOLD OR LIFT CRANE

○ = TIE DOWN

□ = TEMPORARY SUPPORT STRUCTURE

NCHRP 12-79

BRIDGE NISSS11

GENERAL ERECTION PROCEDURE

SHEET 6 OF 6

NCHRP 12-79

NISSS13

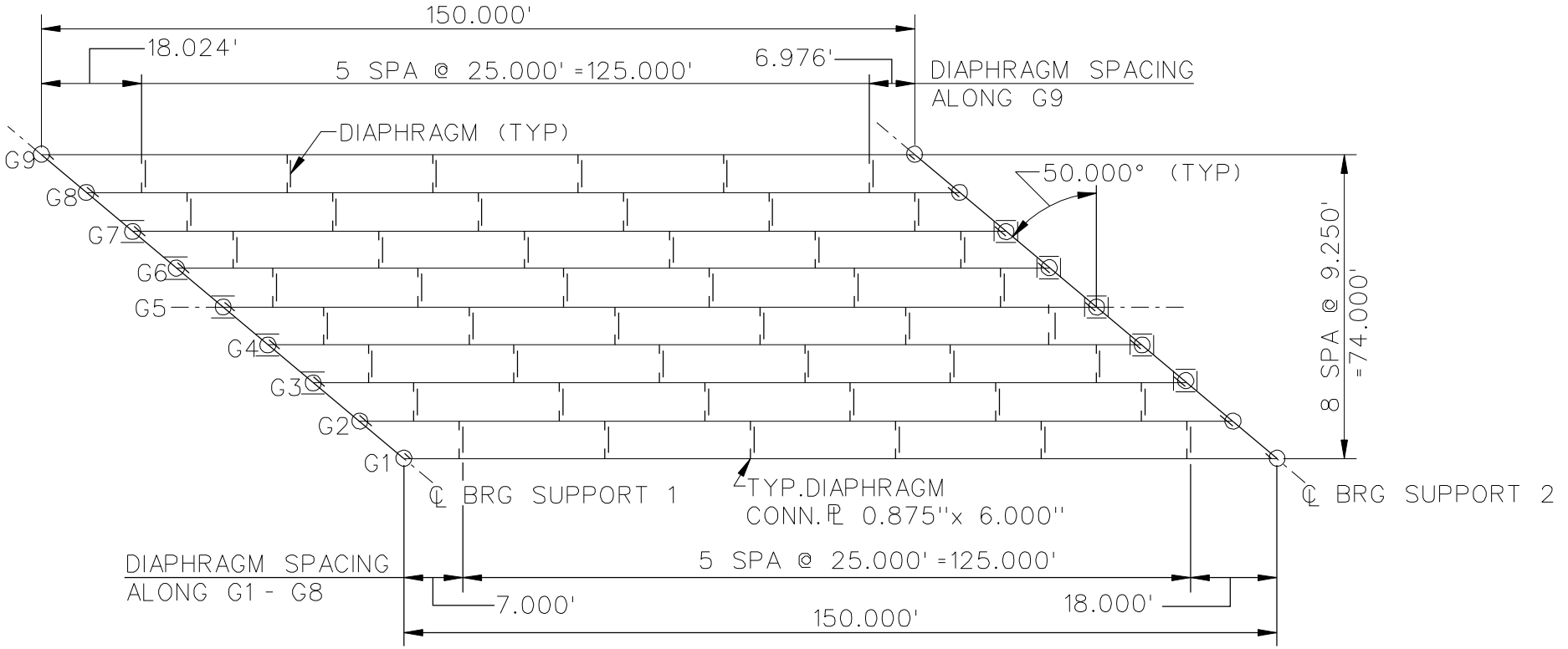

FRAMING PLAN

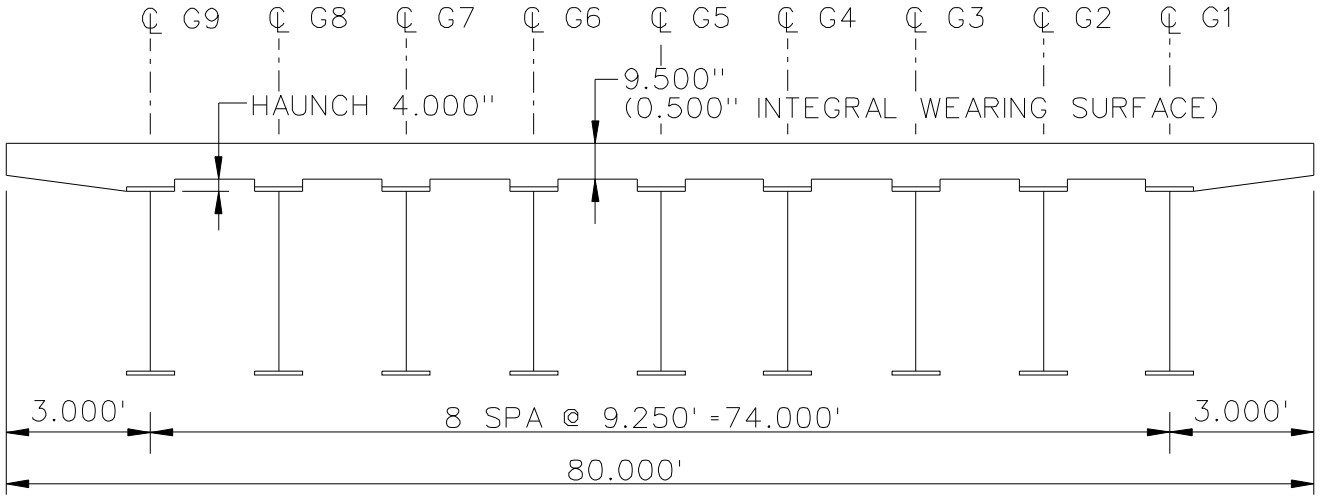

CROSS - SECTION

(DIAPHRAGMS NOT SHOWN)

BEARING LEGEND

- ○ NON-GUIDED
- ⊖ LONGITUDINALLY GUIDED
- |○| TRANSVERSELY GUIDED
- |⊖| FIXED

NCHRP 12-79

BRIDGE NISSS13

FRAMING PLAN AND CROSS-SECTION

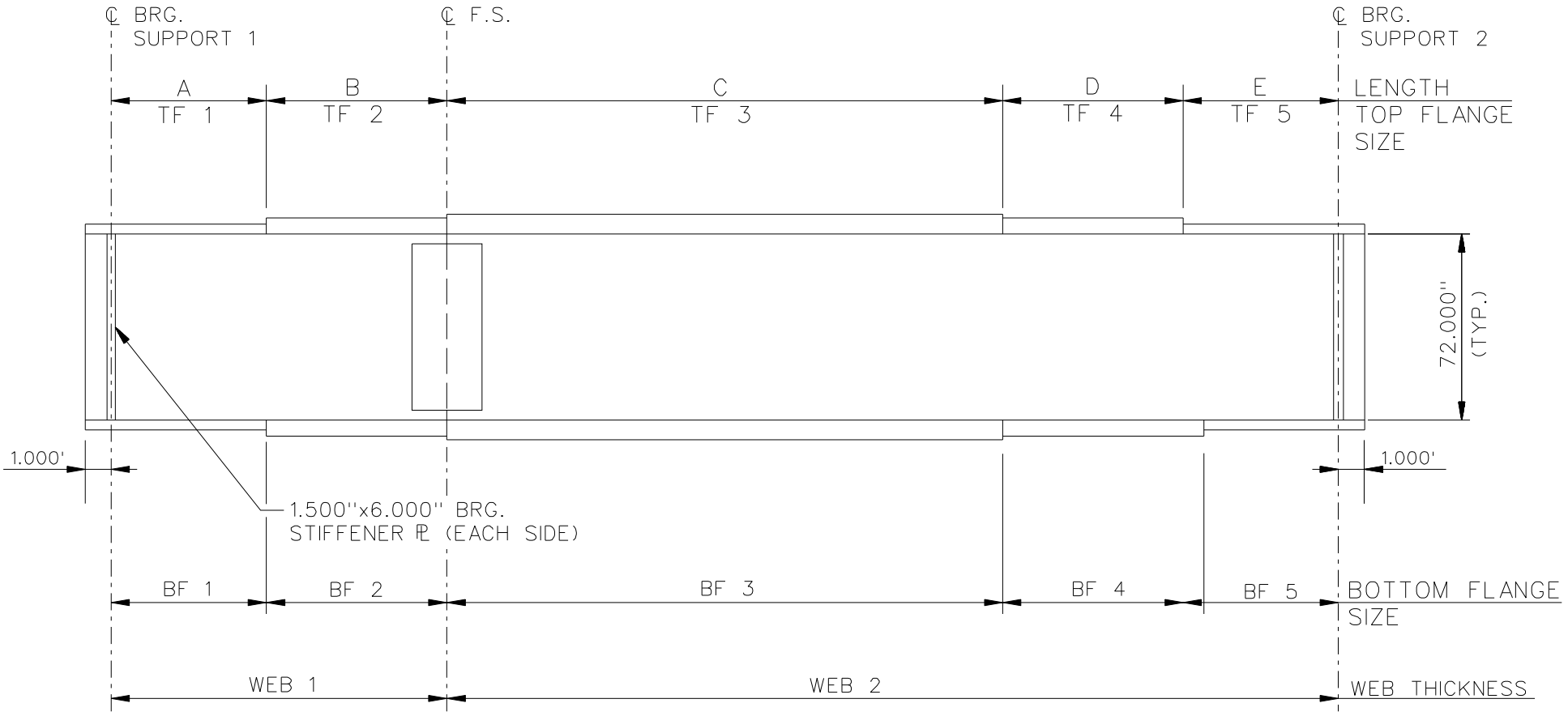

NOTE :

1. SEE TABLES ON SHEET 3 FOR GIRDER ELEVATION DIMENSIONS AND PLATE SIZES.
2. ALL GIRDERS, WEB 1 = WEB 2 = 0.6250".

NCHRP 12-79

BRIDGE NISSS13

GIRDER ELEVATION

SHEET 2 OF 7

	GIRDER PLATE LENGTHS ✳								
LENGTH	G1	G2	G3	G4	G5	G6	G7	G8	G9
A	20.000	20.000	20.000	20.000	20.000	20.000	20.000	20.000	20.000
B	20.000	20.000	20.000	20.000	20.000	20.000	20.000	20.000	20.000
C	70.000	70.000	70.000	70.000	70.000	70.000	70.000	70.000	70.000
D	20.000	20.000	20.000	20.000	20.000	20.000	20.000	20.000	20.000
E	20.000	20.000	20.000	20.000	20.000	20.000	20.000	20.000	20.000

✳ ALL DIMENSIONS ARE IN FEET.

	GIRDER FLANGE DIMENSIONS ✳✳					
TOP	G1, G2, G3		G4, G5, G6		G7, G8, G9	
FLANGE	BF	TF	BF	TF	BF	TF
TF1	16.000	0.750	16.000	0.750	16.000	0.750
TF2	16.000	0.750	16.000	0.750	16.000	0.750
TF3	16.000	1.250	16.000	1.250	16.000	1.250
TF4	16.000	0.750	16.000	0.750	16.000	0.750
TF5	16.000	0.750	16.000	0.750	16.000	0.750

✳✳ ALL DIMENSIONS ARE IN INCHES.

	GIRDER FLANGE DIMENSIONS ✳✳					
BOTTOM	G1, G2, G3		G4, G5, G6		G7, G8, G9	
FLANGE	BF	TF	BF	TF	BF	TF
BF1	18.000	1.000	18.000	1.000	18.000	1.000
BF2	18.000	1.500	18.000	1.500	18.000	1.500
BF3	18.000	2.000	18.000	2.000	18.000	2.000
BF4	18.000	1.500	18.000	1.500	18.000	1.500
BF5	18.000	1.000	18.000	1.000	18.000	1.000

✳✳ ALL DIMENSIONS ARE IN INCHES.

NCHRP 12-79

BRIDGE NISSS13

GIRDER ELEVATION TABLES

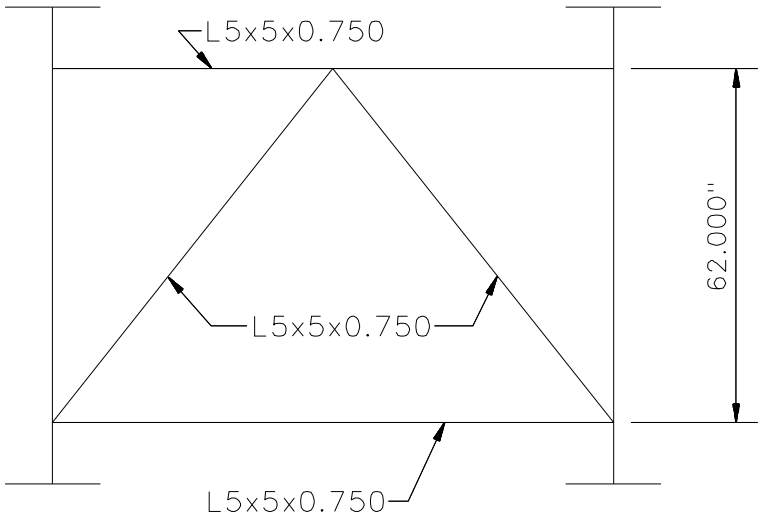

TYPICAL END AND INTERMEDIATE DIAPHRAGM

NOTES:

1. STEEL DEAD LOAD INCREASED BY 5% FOR MDX AND LARSA MODELS; 2% FOR 3D MODEL; AND 10% FOR APPROXIMATE ANALYSIS TO ACCOUNT FOR MISC. DETAILS.

2. FORMWORK LOAD OF 10PSF IS INCLUDED IN CONCRETE DEAD LOAD.

3. ADDITIONAL DESIGN PARAMETERS:
   A. 1.500' PARAPET WIDTH BOTH SIDES.
   B. 700 LB/FT UNIFORM LOAD ASSUMED FOR PARAPET WEIGHT.
   C. ROADWAY WIDTH = 77.000'.
   D. NUMBER OF DESIGN LANES = 6.
   E. HL93 LIVE LOAD.

4. DIAPHRAGM MEMBER CALL-OUTS ARE IN UNITS OF INCHES.

NCHRP 12-79

BRIDGE NISSS13

MISC. DETAILS AND NOTES

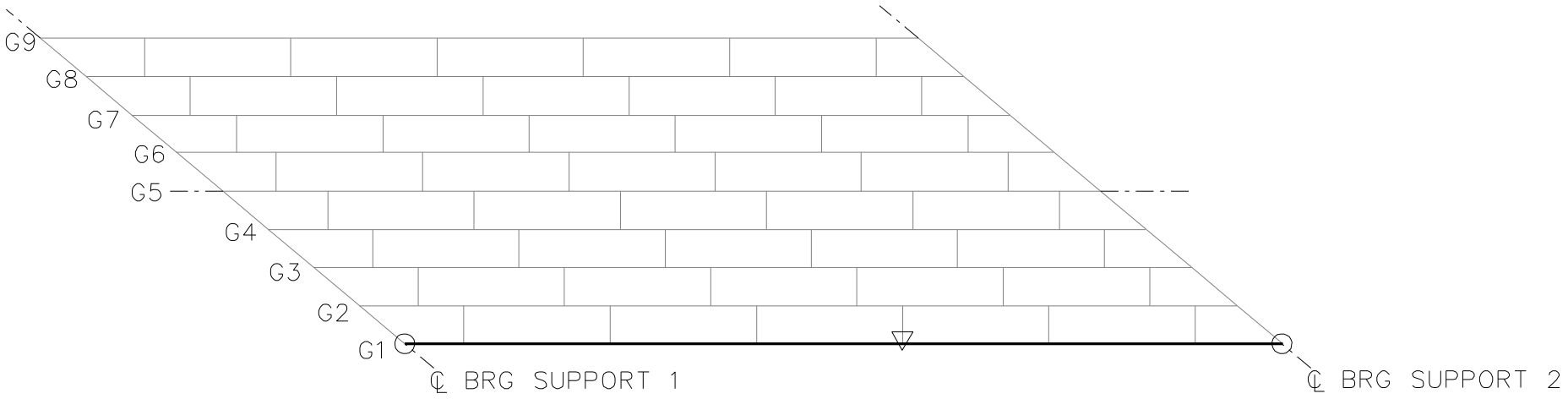

STAGE 1

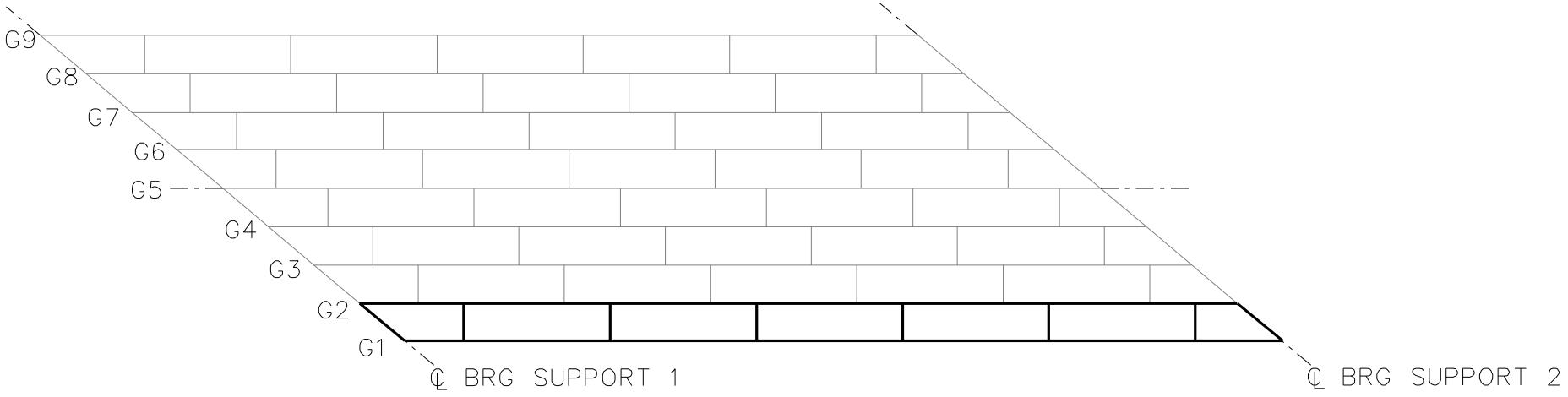

STAGE 2

LEGEND

▽ = HOLD OR LIFT CRANE

○ = TIE DOWN

□ = TEMPORARY SUPPORT STRUCTURE

NCHRP 12-79

BRIDGE NISSS13

GENERAL ERECTION PROCEDURE

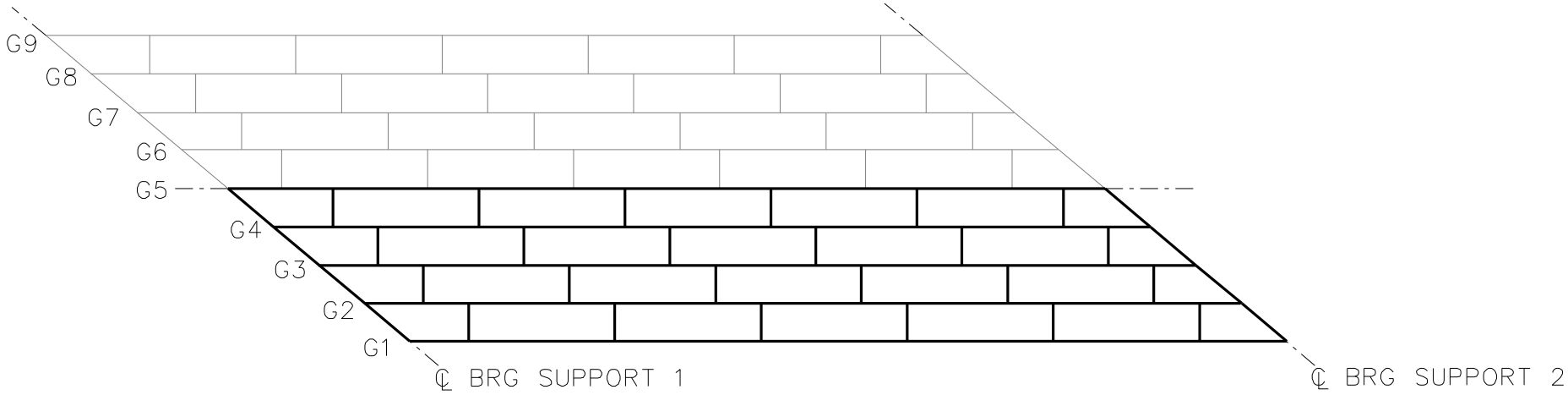

STAGE 5

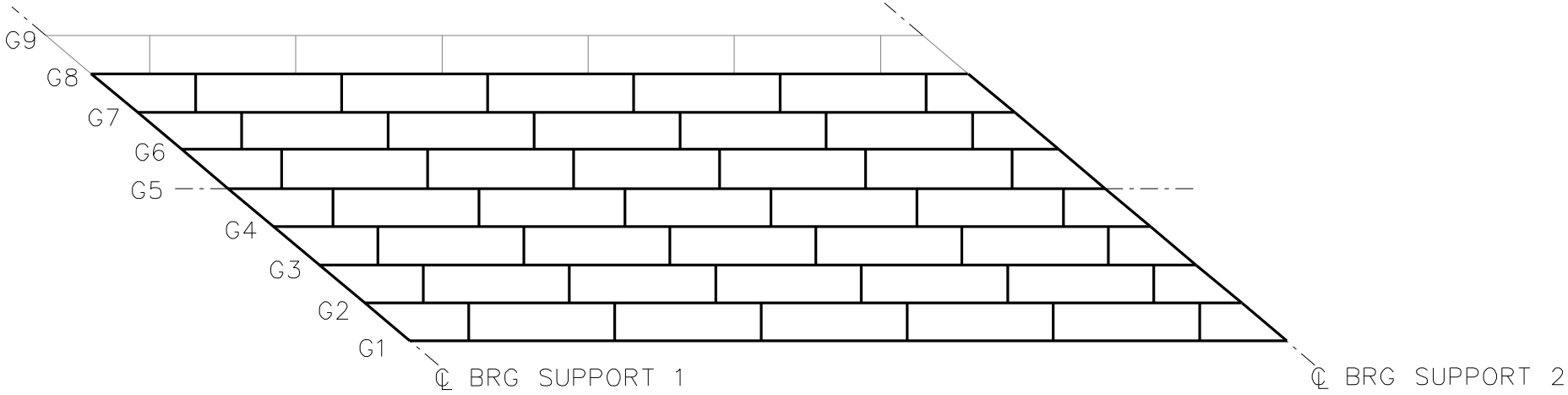

STAGE 8

LEGEND

▽ = HOLD OR LIFT CRANE

○ = TIE DOWN

□ = TEMPORARY SUPPORT STRUCTURE

NCHRP 12-79

BRIDGE NISSS13

GENERAL ERECTION PROCEDURE

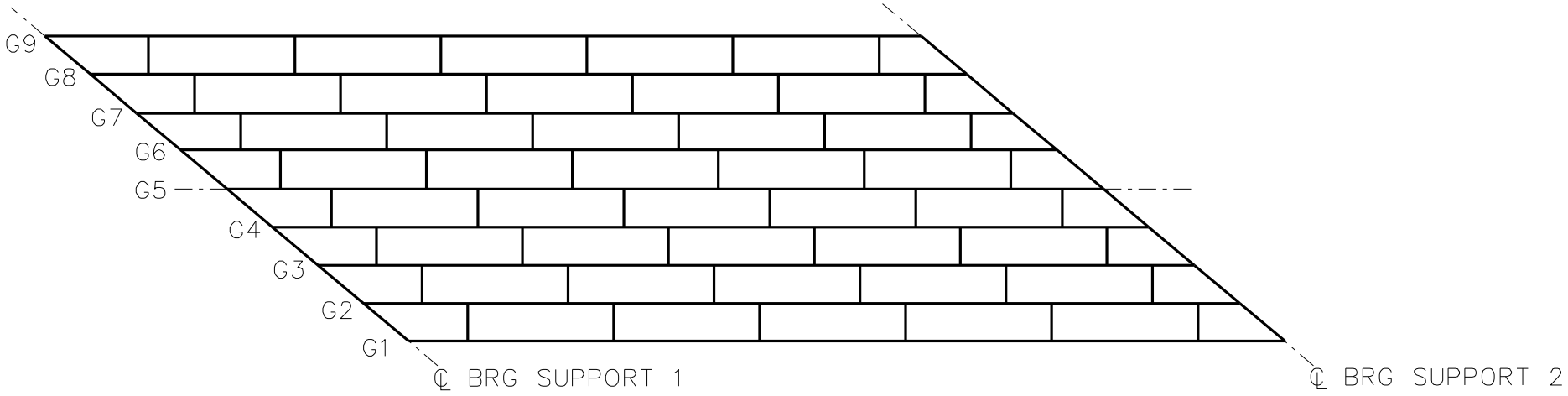

STAGE 9

LEGEND

▽ = HOLD OR LIFT CRANE

○ = TIE DOWN

□ = TEMPORARY SUPPORT STRUCTURE

NCHRP 12-79

BRIDGE NISSS13

GENERAL ERECTION PROCEDURE

NCHRP 12-79

NISSS14

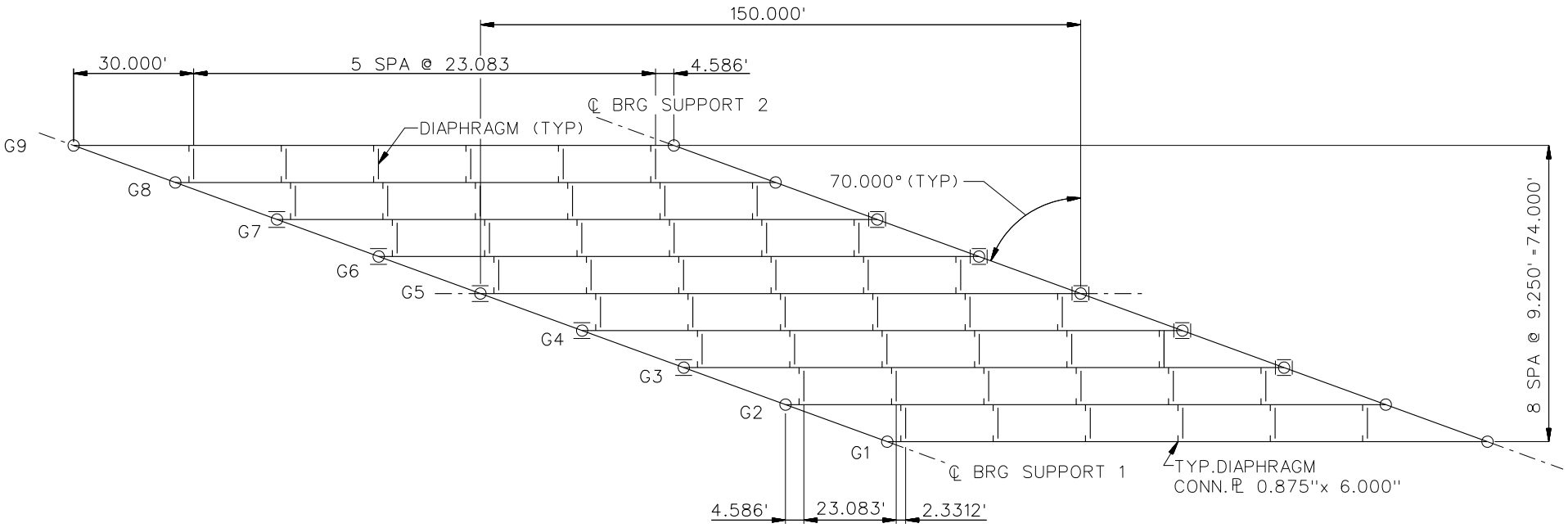

FRAMING PLAN

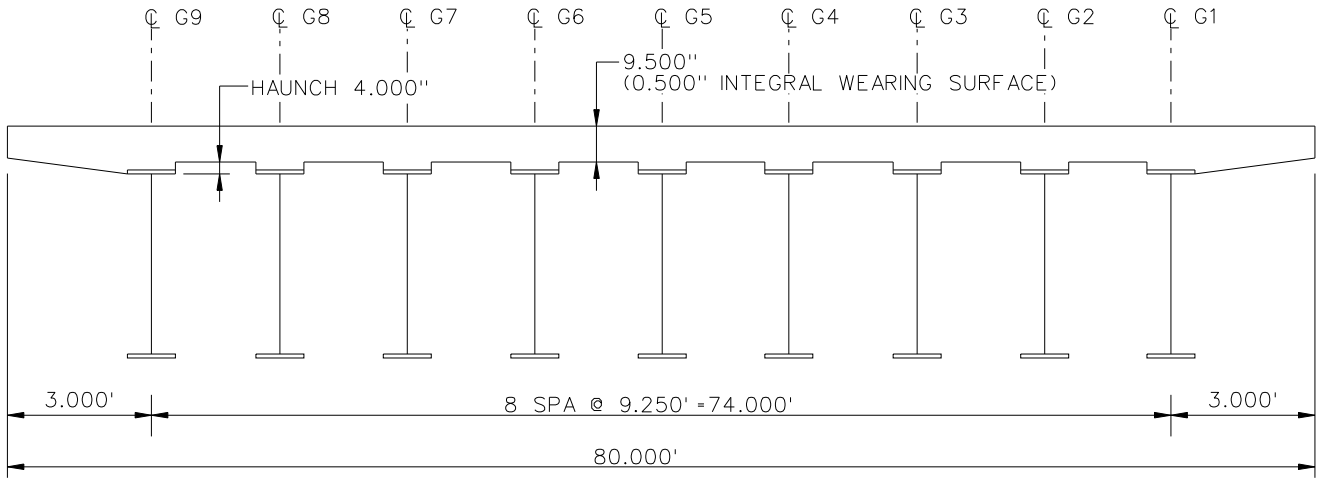

CROSS - SECTION

(DIAPHRAGMS NOT SHOWN)

BEARING LEGEND

- ○ NON-GUIDED
- ⊙ LONGITUDINALLY GUIDED
- |○| TRANSVERSELY GUIDED
- |⊙| FIXED

NCHRP 12-79

BRIDGE NISSS14

FRAMING PLAN AND CROSS-SECTION

SHEET 1 OF 6

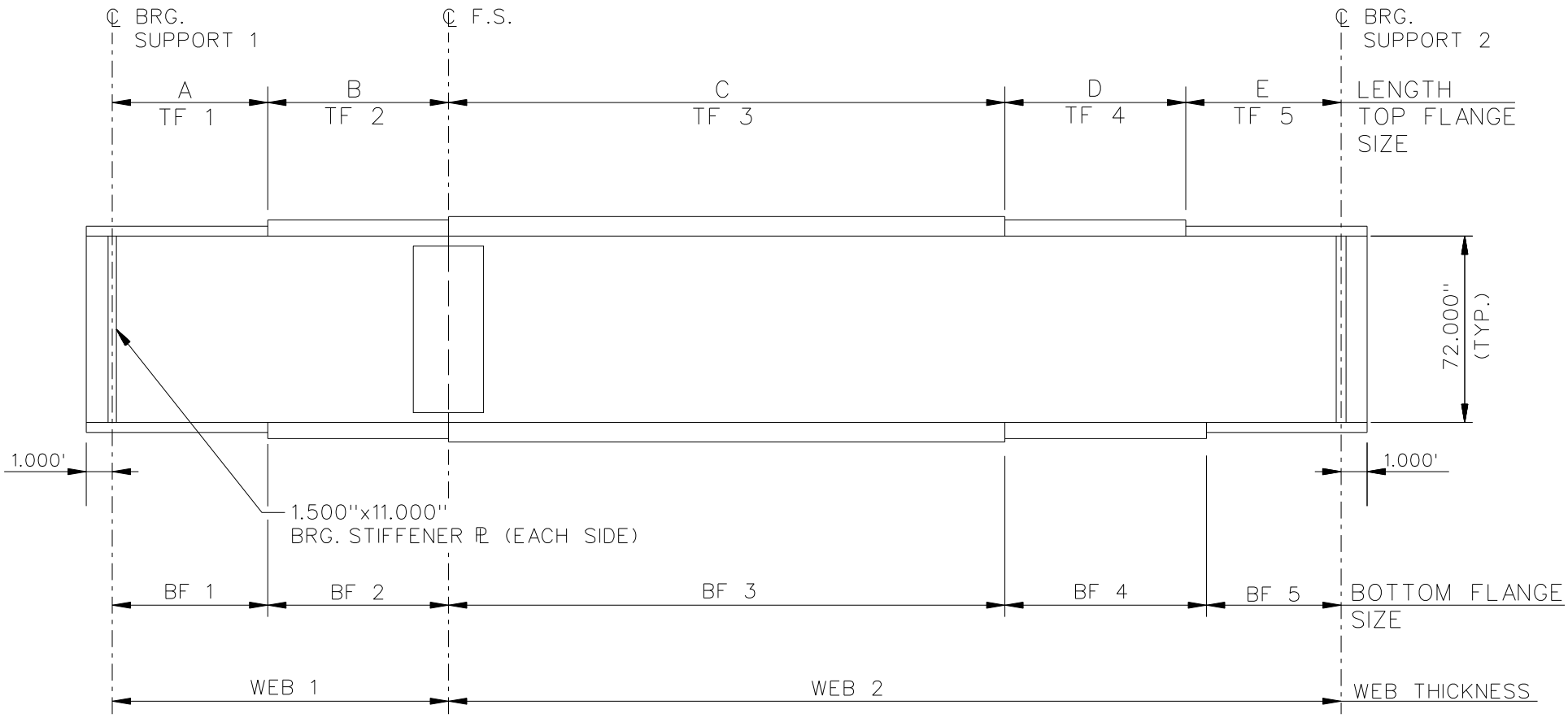

NOTE :

1. SEE TABLES ON SHEET 3 FOR GIRDER ELEVATION DIMENSIONS AND PLATE SIZES.
2. ALL GIRDERS, WEB 1 = WEB 2 = 0.6250".

NCHRP 12-79

BRIDGE NISSS14

GIRDER ELEVATION

SHEET 2 OF 6

	GIRDER PLATE LENGTHS ✳		
LENGTH	G1, G2, G3	G4, G5, G6	G7, G8, G9
A	20.000	20.000	20.000
B	20.000	20.000	20.000
C	70.000	70.000	70.000
D	20.000	20.000	20.000
E	20.000	20.000	20.000

✳ ALL DIMENSIONS ARE IN FEET.

	GIRDER FLANGE DIMENSIONS ✳✳					
TOP FLANGE	G1, G2, G3		G4, G5, G6		G7, G8, G9	
	BF	TF	BF	TF	BF	TF
TF1	16.000	0.750	16.000	0.750	16.000	0.750
TF2	16.000	0.750	16.000	0.750	16.000	0.750
TF3	16.000	1.000	16.000	1.000	16.000	1.000
TF4	16.000	0.750	16.000	0.750	16.000	0.750
TF5	16.000	0.750	16.000	0.750	16.000	0.750

✳✳ ALL DIMENSIONS ARE IN INCHES.

	GIRDER FLANGE DIMENSIONS ✳✳					
BOTTOM FLANGE	G1, G2, G3		G4, G5, G6		G7, G8, G9	
	BF	TF	BF	TF	BF	TF
BF1	18.000	1.000	18.000	1.000	18.000	1.000
BF2	18.000	1.500	18.000	1.500	18.000	1.500
BF3	18.000	2.000	18.000	2.000	18.000	2.000
BF4	18.000	1.500	18.000	1.500	18.000	1.500
BF5	18.000	1.000	18.000	1.000	18.000	1.000

✳✳ ALL DIMENSIONS ARE IN INCHES.

NCHRP 12-79

BRIDGE NISSS14

GIRDER ELEVATION TABLES

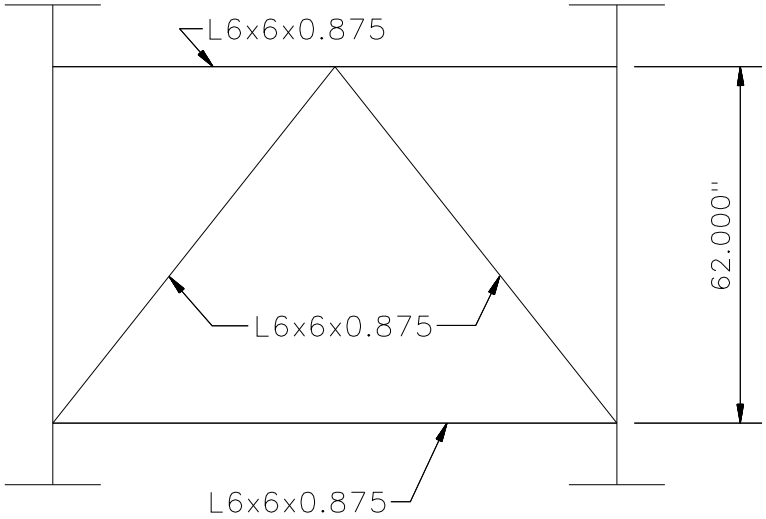

TYPICAL END AND INTERMEDIATE DIAPHRAGM

NOTES:

1. STEEL DEAD LOAD INCREASED BY 5% FOR MDX AND LARSA MODELS; 2% FOR 3D MODEL; AND 10% FOR APPROXIMATE ANALYSIS TO ACCOUNT FOR MISC. DETAILS.

2. FORMWORK LOAD OF 10PSF IS INCLUDED IN CONCRETE DEAD LOAD.

3. ADDITIONAL DESIGN PARAMETERS:
   A. 1.500' PARAPET WIDTH BOTH SIDES.
   B. 700 LB/FT UNIFORM LOAD ASSUMED FOR PARAPET WEIGHT.
   C. ROADWAY WIDTH = 77.000'.
   D. NUMBER OF DESIGN LANES = 6.
   E. HL93 LIVE LOAD.

4. DIAPHRAGM MEMBER CALL-OUTS ARE IN ENGLISH UNITS.

NCHRP 12-79

BRIDGE NISSS14

MISC. DETAILS AND NOTES

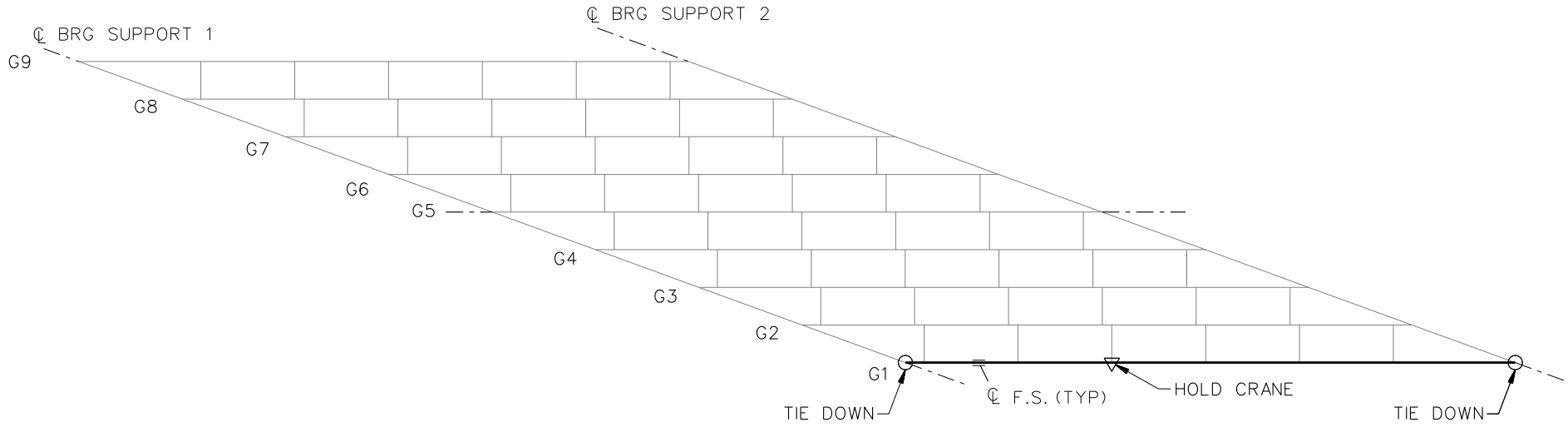

STAGE 1

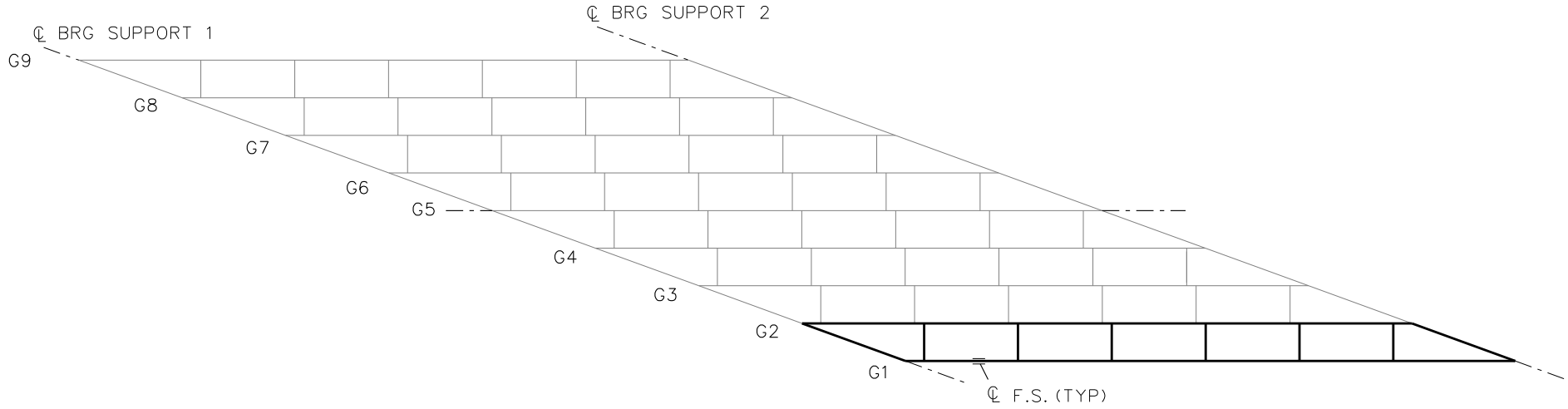

STAGE 2

LEGEND

▽ = HOLD OR LIFT CRANE

○ = TIE DOWN

□ = TEMPORARY SUPPORT STRUCTURE

STAGE 3 - ERECT G3 AND ADJACENT CROSS FRAMES
STAGE 4 - ERECT G4 AND ADJACENT CROSS FRAMES

NCHRP 12-79

BRIDGE NISSS14

GENERAL ERECTION PROCEDURE

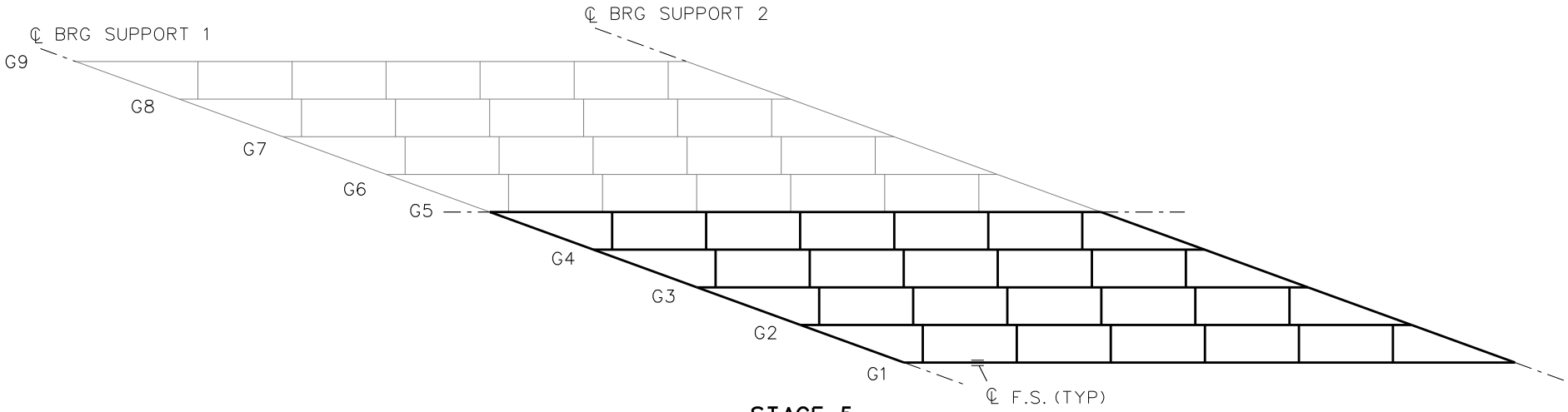

STAGE 5

STAGE 6 - ERECT G6 AND ADJACENT CROSS FRAMES
STAGE 7 - ERECT G7 AND ADJACENT CROSS FRAMES

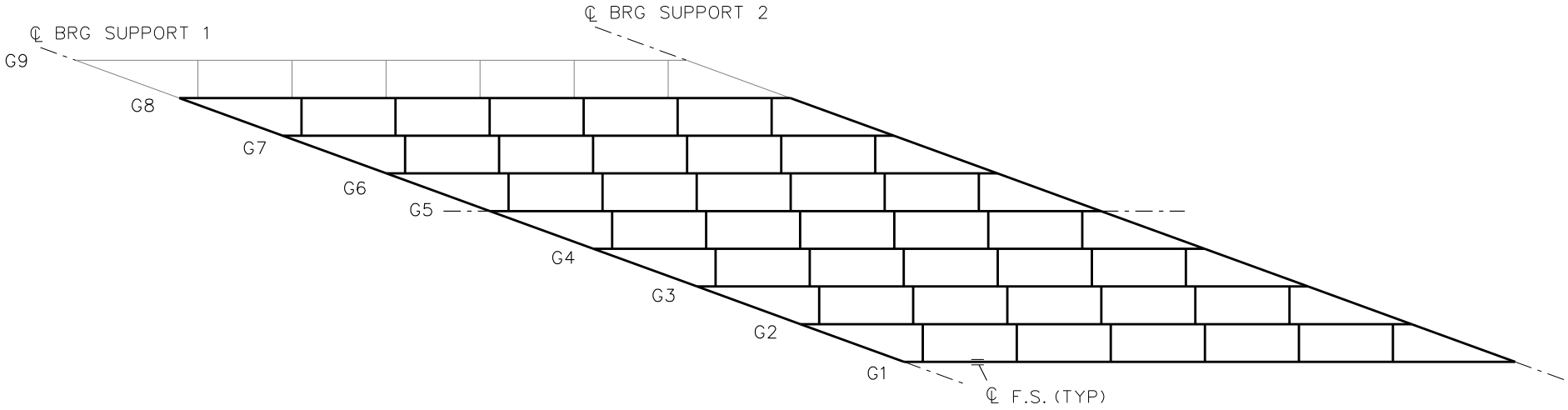

STAGE 8

LEGEND

▽ = HOLD OR LIFT CRANE

○ = TIE DOWN

□ = TEMPORARY SUPPORT STRUCTURE

STAGE 9 - ERECT G9 AND ADJACENT CROSS FRAMES

NCHRP 12-79

BRIDGE NISSS14

GENERAL ERECTION PROCEDURE

NCHRP 12-79

NISSS16

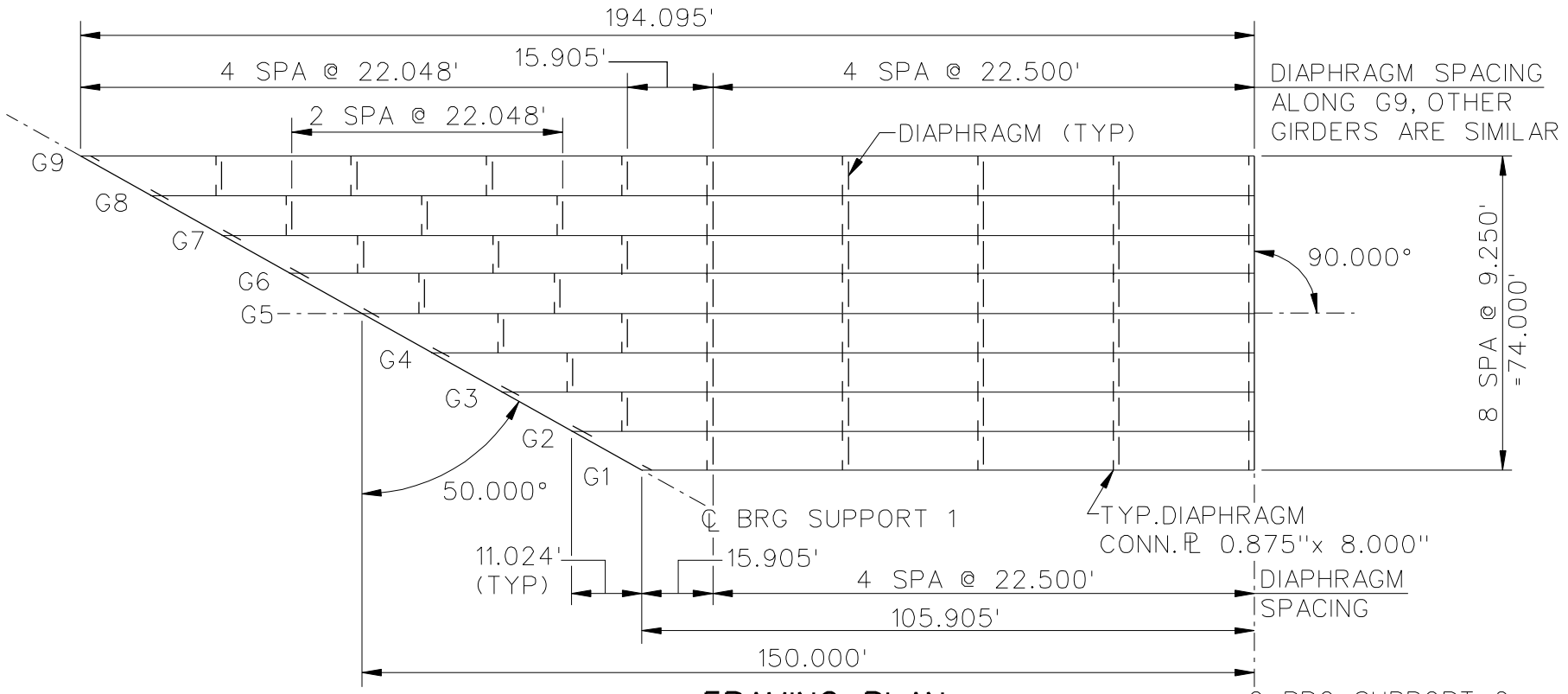

FRAMING PLAN

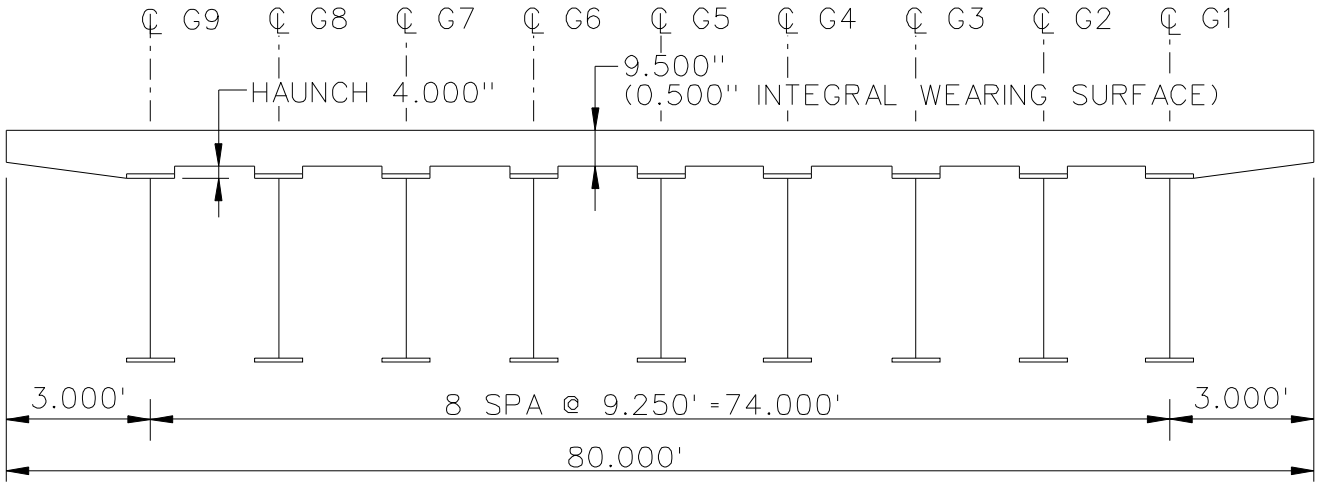

CROSS - SECTION

(DIAPHRAGMS NOT SHOWN)

BEARING LEGEND

○ NON-GUIDED

⊖ LONGITUDINALLY GUIDED

|○| TRANSVERSELY GUIDED

|⊖| FIXED

NCHRP 12-79

BRIDGE NISSS16

FRAMING PLAN AND CROSS-SECTION

SHEET 1 OF 6

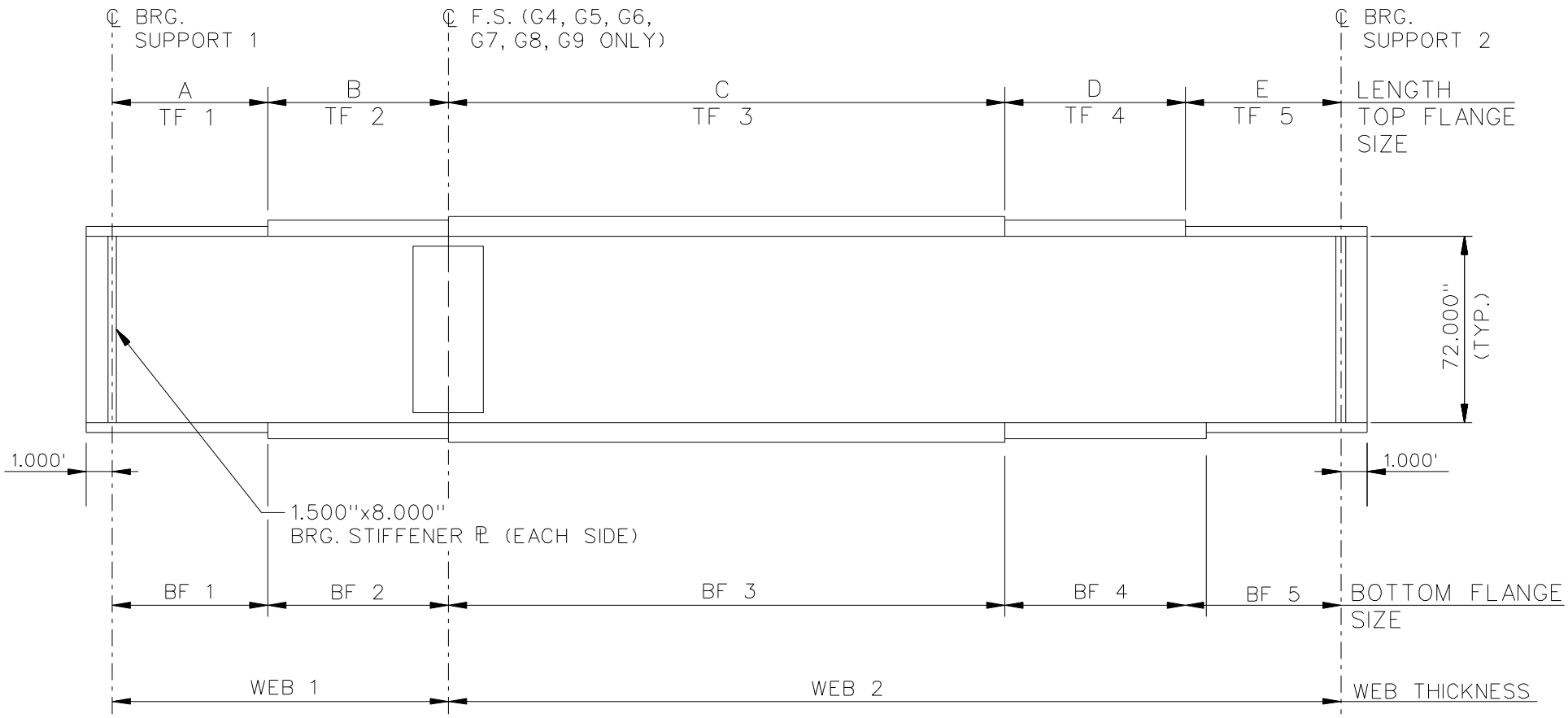

NOTE :

1. SEE TABLES ON SHEET 3 FOR GIRDER ELEVATION DIMENSIONS AND PLATE SIZES.
2. ALL GIRDERS, WEB 1 = WEB 2 = 0.6250".

NCHRP 12-79

BRIDGE NISSS16

GIRDER ELEVATION

SHEET 2 OF 6

	GIRDER PLATE LENGTHS ✳								
LENGTH	G1	G2	G3	G4	G5	G6	G7	G8	G9
A	25.453	30.964	36.476	19.488	20.000	25.512	25.000	25.000	25.000
B	0	0	0	20.000	25.000	25.000	30.000	35.000	40.000
C	55.000	55.000	55.000	60.000	60.000	60.000	62.047	63.071	64.095
D	0	0	0	20.000	25.000	25.000	30.000	35.000	40.000
E	25.453	30.964	36.476	19.488	20.000	25.512	25.000	25.000	25.000

✳ ALL DIMENSIONS ARE IN FEET.

	GIRDER FLANGE DIMENSIONS ✳✳					
TOP	G1, G2, G3		G4, G5, G6		G7, G8, G9	
FLANGE	BF	TF	BF	TF	BF	TF
TF1	18.000	0.750	18.000	1.000	20.000	1.000
TF2	N/A	N/A	18.000	1.000	20.000	1.250
TF3	18.000	1.000	18.000	1.250	20.000	1.500
TF4	N/A	N/A	18.000	1.000	20.000	1.250
TF5	18.000	0.750	18.000	1.000	20.000	1.500

✳✳ ALL DIMENSIONS ARE IN INCHES.

	GIRDER FLANGE DIMENSIONS ✳✳					
BOTTOM	G1, G2, G3		G4, G5, G6		G7, G8, G9	
FLANGE	BF	TF	BF	TF	BF	TF
BF1	18.000	1.000	20.000	1.000	22.000	1.000
BF2	N/A	N/A	20.000	1.500	22.000	1.750
BF3	18.000	1.250	20.000	2.000	22.000	2.250
BF4	N/A	N/A	20.000	1.500	22.000	1.750
BF5	18.000	1.000	20.000	1.000	22.000	1.000

✳✳ ALL DIMENSIONS ARE IN INCHES.

NCHRP 12-79

BRIDGE NISSS16

GIRDER ELEVATION TABLES

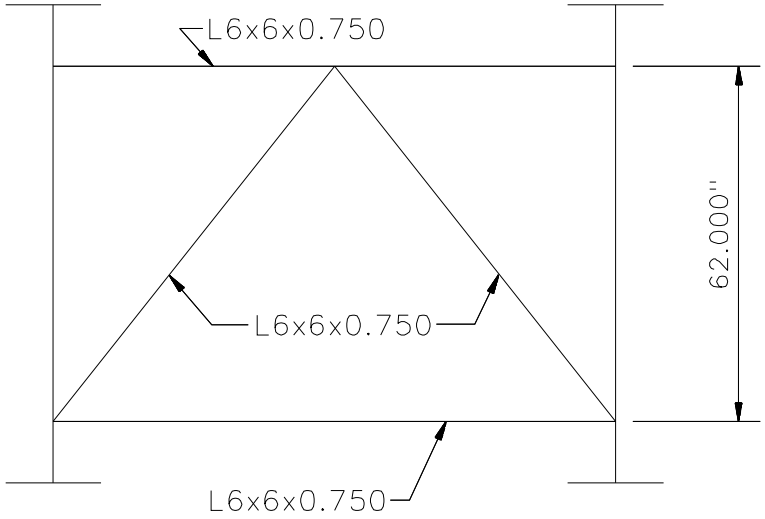

TYPICAL END AND INTERMEDIATE DIAPHRAGM

NOTES:

1. STEEL DEAD LOAD INCREASED BY 5% FOR MDX AND LARSA MODELS; 2% FOR 3D MODEL; AND 10% FOR APPROXIMATE ANALYSIS TO ACCOUNT FOR MISC. DETAILS.

2. FORMWORK LOAD OF 10PSF IS INCLUDED IN CONCRETE DEAD LOAD.

3. ADDITIONAL DESIGN PARAMETERS:
   A. 1.500' PARAPET WIDTH BOTH SIDES.
   B. 700 LB/FT UNIFORM LOAD ASSUMED FOR PARAPET WEIGHT.
   C. ROADWAY WIDTH = 77.000'.
   D. NUMBER OF DESIGN LANES = 6.
   E. HL93 LIVE LOAD.

4. DIAPHRAGM MEMBER CALL-OUTS ARE IN UNITS OF INCHES.

NCHRP 12-79

BRIDGE NISSS16

MISC. DETAILS AND NOTES

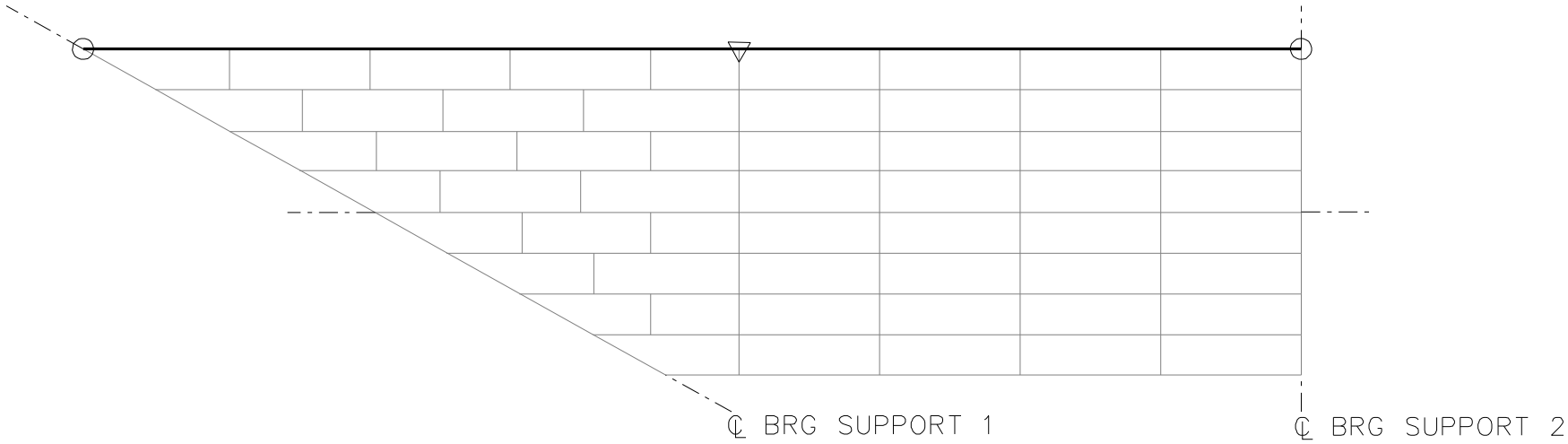

STAGE 1

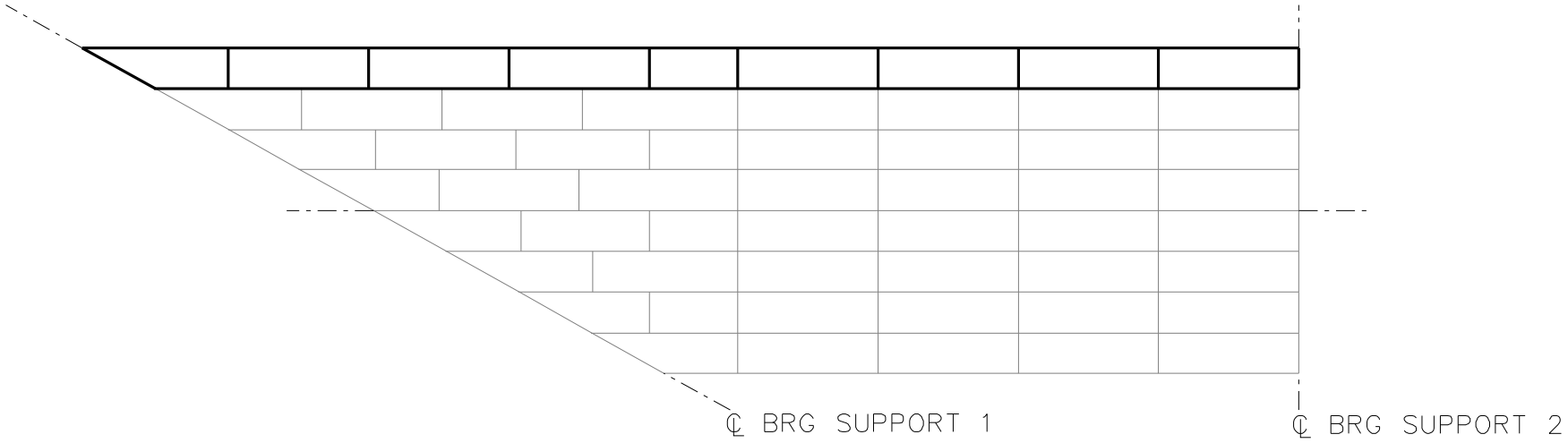

STAGE 2

LEGEND

▽ = HOLD OR LIFT CRANE

○ = TIE DOWN

□ = TEMPORARY SUPPORT STRUCTURE

NCHRP 12-79

BRIDGE NISSS16

GENERAL ERECTION PROCEDURE

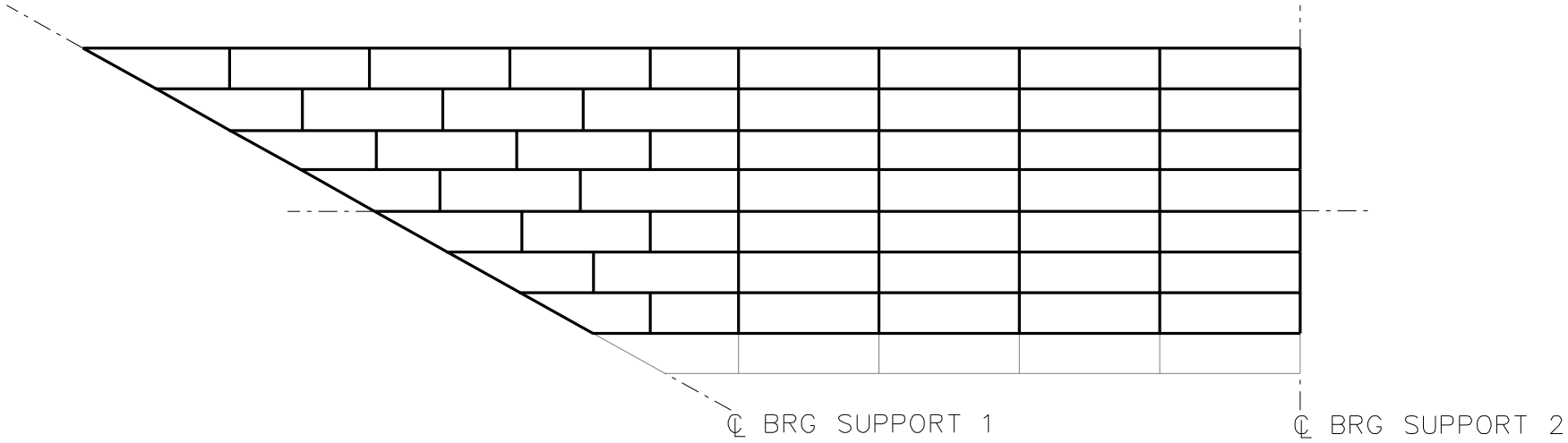

STAGE 8

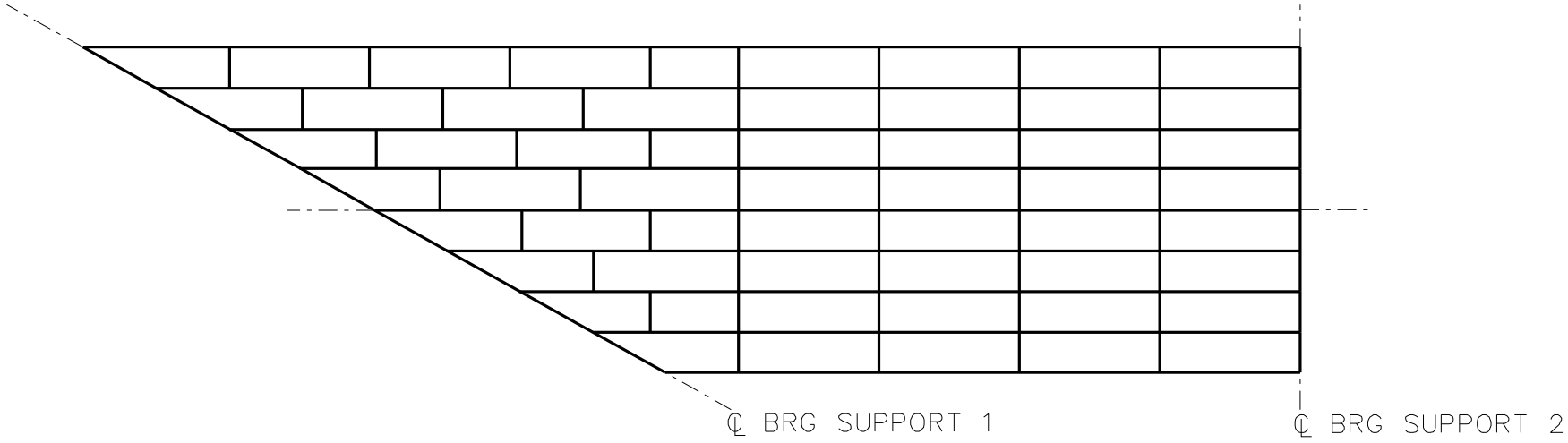

STAGE 9

LEGEND

▽ = HOLD OR LIFT CRANE

○ = TIE DOWN

□ = TEMPORARY SUPPORT STRUCTURE

NCHRP 12-79

BRIDGE NISSS16

GENERAL ERECTION PROCEDURE

NCHRP 12-79

NISSS36

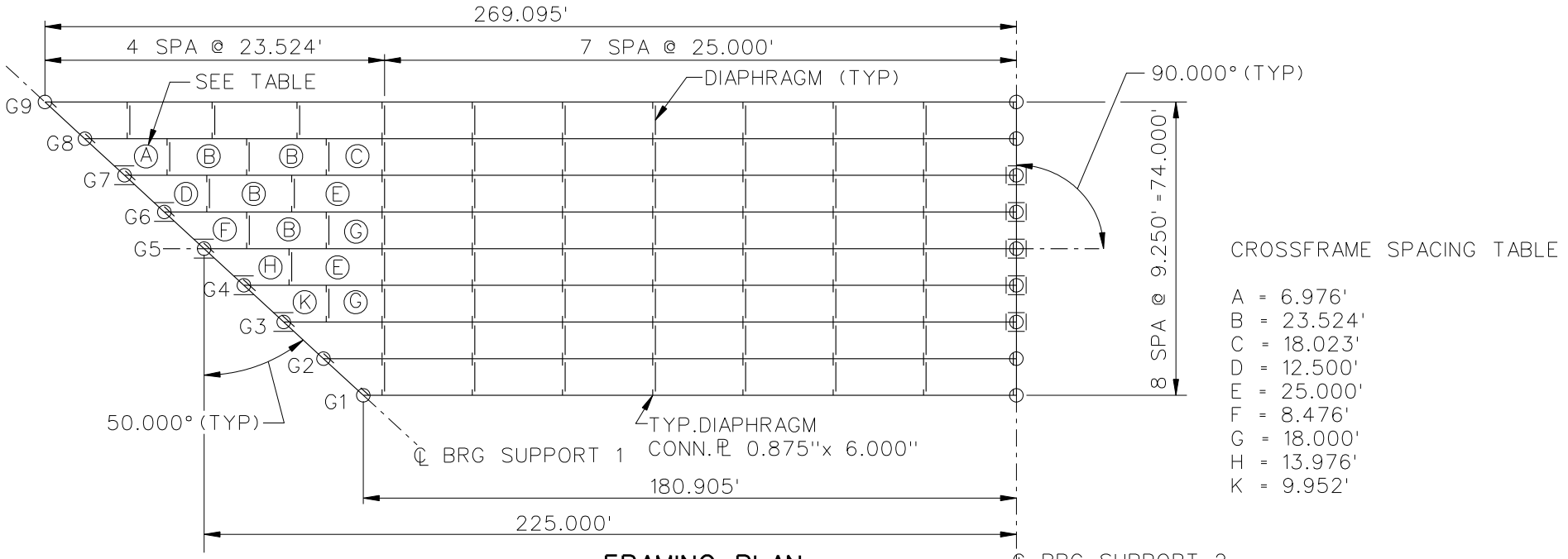

FRAMING PLAN

CROSSFRAME SPACING TABLE

A	6.976'
B	23.524'
C	18.023'
D	12.500'
E	25.000'
F	8.476'
G	18.000'
H	13.976'
K	9.952'

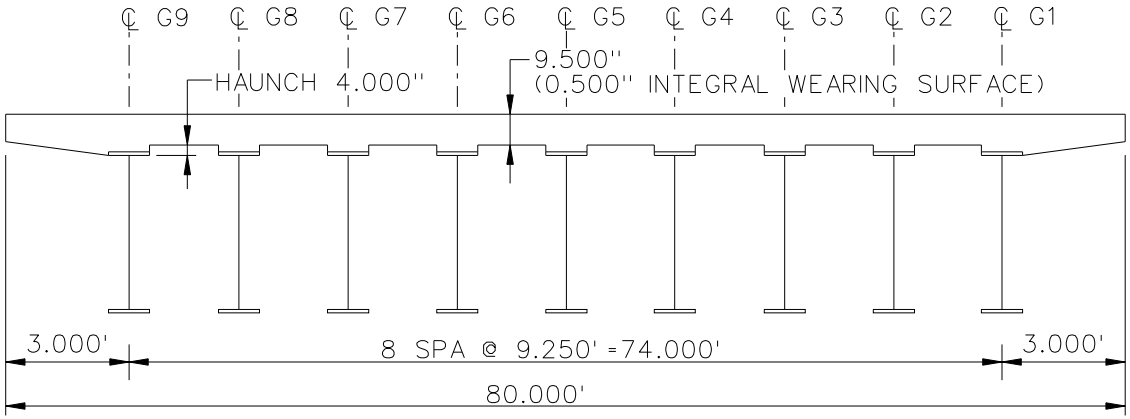

CROSS - SECTION

(DIAPHRAGMS NOT SHOWN)

BEARING LEGEND

○ NON-GUIDED

○ LONGITUDINALLY GUIDED

○ TRANSVERSELY GUIDED

○ FIXED

NCHRP 12-79

BRIDGE NISSS36

FRAMING PLAN AND CROSS-SECTION

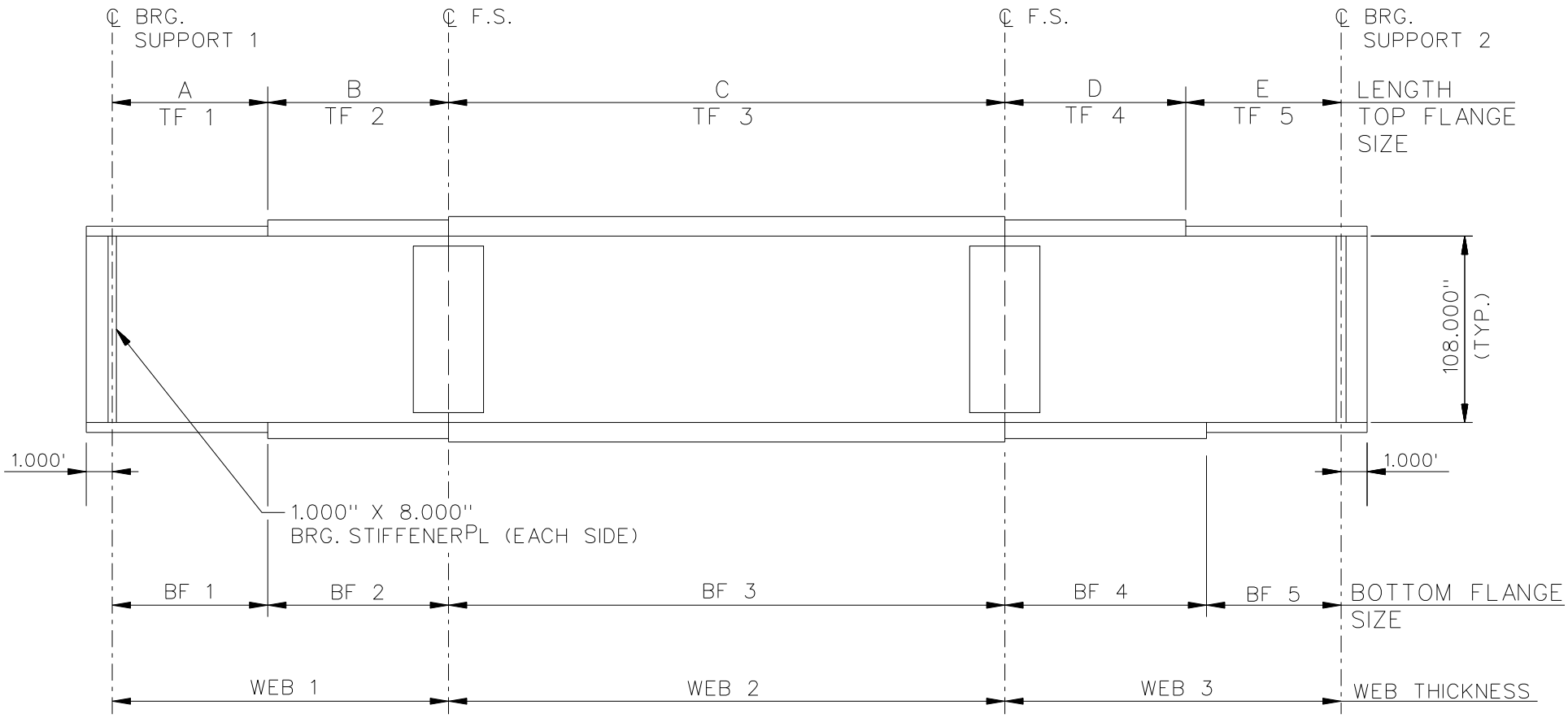

NOTES :

1. SEE TABLES ON SHEET 3 FOR GIRDER ELEVATION DIMENSIONS AND PLATE SIZES.
2. ALL GIRDERS, WEB 1 & WEB 3 = 0.875", WEB 2 = 1.000".

NCHRP 12-79

BRIDGE NISSS36

GIRDER ELEVATION

	GIRDER PLATE LENGTHS ✳								
LENGTH	G1	G2	G3	G4	G5	G6	G7	G8	G9
A	25.453	30.964	31.476	34.488	35.000	40.512	36.024	39.036	39.547
B	30.000	30.000	35.000	35.000	40.000	40.000	45.000	45.000	50.000
C	70.000	70.000	70.000	75.000	75.000	75.000	85.000	90.000	90.000
D	30.000	30.000	35.000	35.000	40.000	40.000	45.000	45.000	50.000
E	25.453	30.964	31.476	34.488	35.000	40.512	36.024	39.036	39.547

✳ ALL DIMENSIONS ARE IN FEET.

	GIRDER FLANGE DIMENSIONS ✳✳							
TOP	G1, G2		G3, G4, G5		G6, G7		G8, G9	
FLANGE	BF	TF	BF	TF	BF	TF	BF	TF
TF1	20.000	1.000	22.000	1.000	24.000	1.000	26.000	1.250
TF2	20.000	1.000	22.000	1.250	24.000	1.500	26.000	1.750
TF3	20.000	1.250	22.000	1.500	24.000	1.750	26.000	2.000
TF4	20.000	1.000	22.000	1.250	24.000	1.500	26.000	1.750
TF5	20.000	1.000	22.000	1.000	24.000	1.000	26.000	1.250

✳✳ ALL DIMENSIONS ARE IN INCHES.

	GIRDER FLANGE DIMENSIONS ✳✳							
BOTTOM	G1, G2		G3, G4, G5		G6, G7		G8, G9	
FLANGE	BF	TF	BF	TF	BF	TF	BF	TF
BF1	24.000	1.250	24.000	1.250	28.000	1.500	28.000	1.750
BF2	24.000	1.625	24.000	1.750	28.000	2.000	28.000	2.250
BF3	24.000	2.000	24.000	2.250	28.000	2.500	28.000	2.750
BF4	24.000	1.625	24.000	1.750	28.000	2.000	28.000	2.500
BF5	24.000	1.250	24.000	1.250	28.000	1.500	28.000	1.750

✳✳ ALL DIMENSIONS ARE IN INCHES.

NCHRP 12-79

BRIDGE NISSS36

GIRDER ELEVATION TABLES

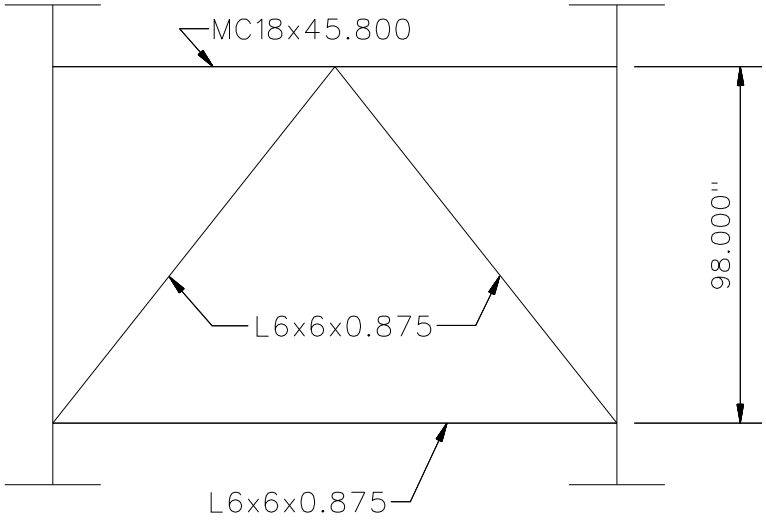

TYPICAL END DIAPHRAGM

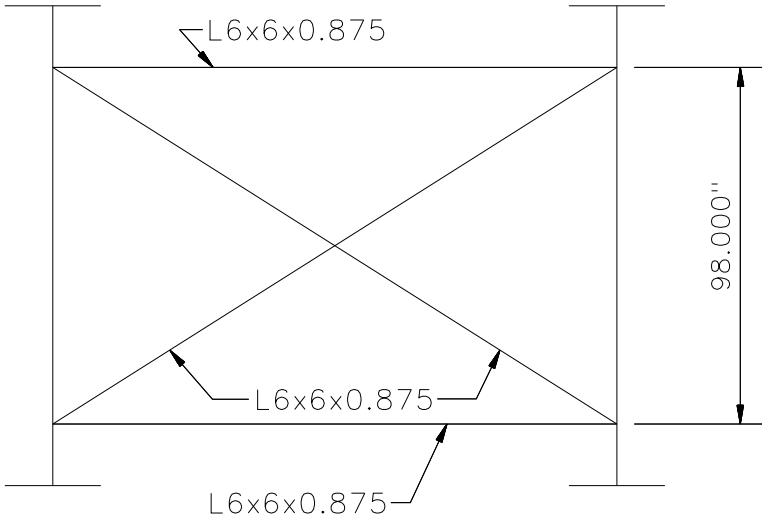

TYPICAL INTERMEDIATE DIAPHRAGM

NOTES:

1. STEEL DEAD LOAD INCREASED BY 5% FOR MDX AND LARSA MODELS; 2% FOR 3D MODEL; AND 10% FOR APPROXIMATE ANALYSIS TO ACCOUNT FOR MISC. DETAILS.

2. FORMWORK LOAD OF 10PSF IS INCLUDED IN CONCRETE DEAD LOAD.

3. ADDITIONAL DESIGN PARAMETERS:
   A. 1.500' PARAPET WIDTH BOTH SIDES.
   B. 700 LB/FT UNIFORM LOAD ASSUMED FOR PARAPET WEIGHT.
   C. ROADWAY WIDTH = 77.000'.
   D. NUMBER OF DESIGN LANES = 6.
   E. HL93 LIVE LOAD.
   F. DESIGN SPEED = 55 MPH.

4. DIAPHRAGM MEMBER CALL-OUTS ARE IN UNITS OF INCHES.

NCHRP 12-79

BRIDGE NISSS36

MISC. DETAILS AND NOTES

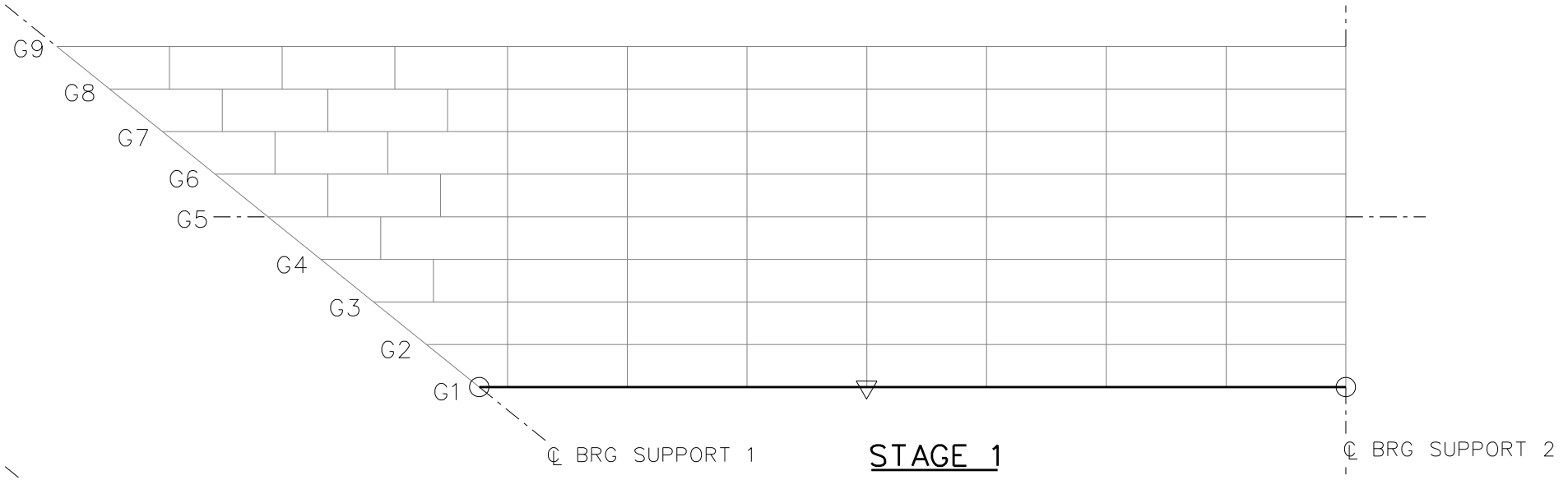

STAGE 1

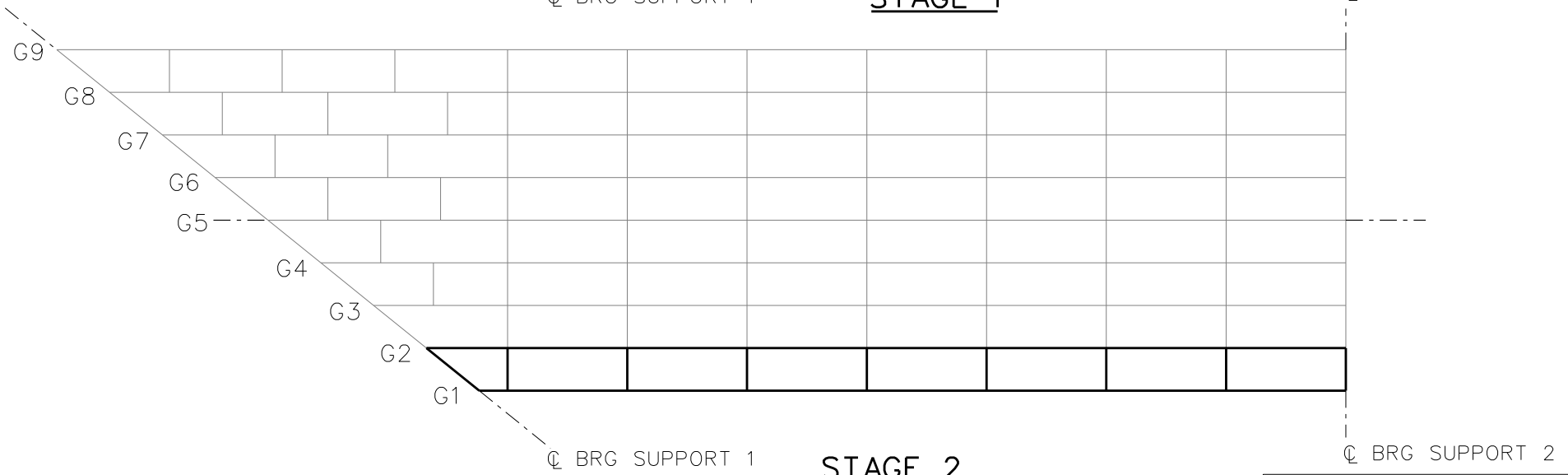

STAGE 2

LEGEND

▽ = HOLD OR LIFT CRANE

○ = TIE DOWN

□ = TEMPORARY SUPPORT STRUCTURE

STAGE 3 - ERECT G3 AND ADJACENT CROSS FRAMES
STAGE 4 - ERECT G4 AND ADJACENT CROSS FRAMES
STAGE 5 - ERECT G5 AND ADJACENT CROSS FRAMES
STAGE 6 - ERECT G6 AND ADJACENT CROSS FRAMES
STAGE 7 - ERECT G7 AND ADJACENT CROSS FRAMES

NCHRP 12-79

BRIDGE NISSS36

GENERAL ERECTION PROCEDURE

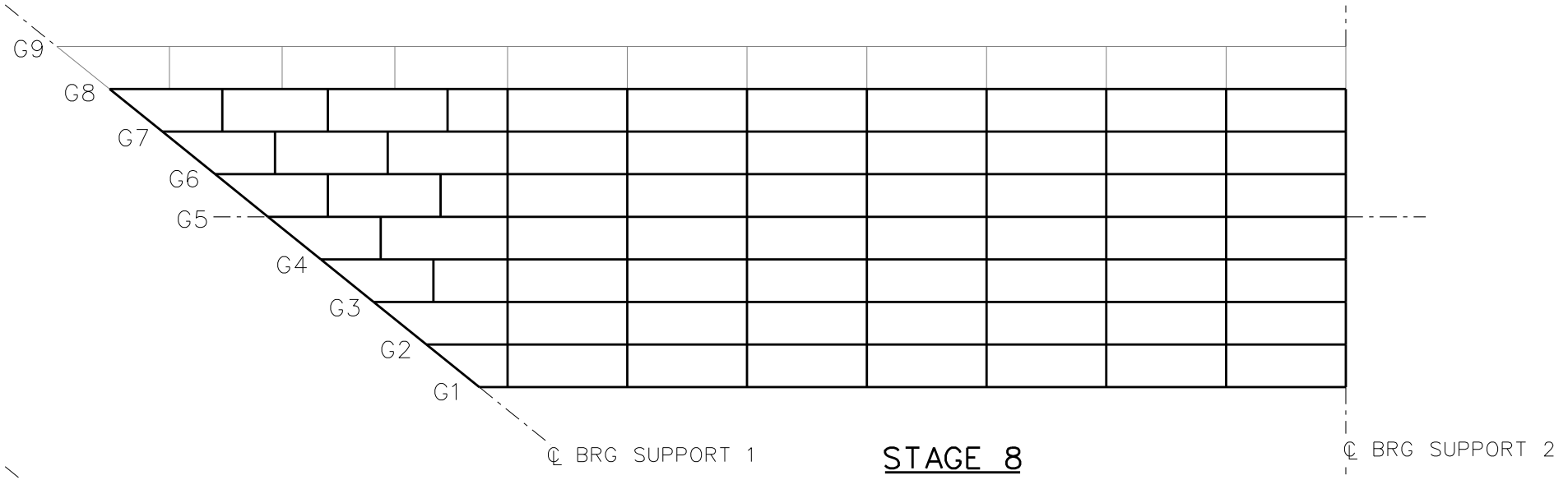

STAGE 8

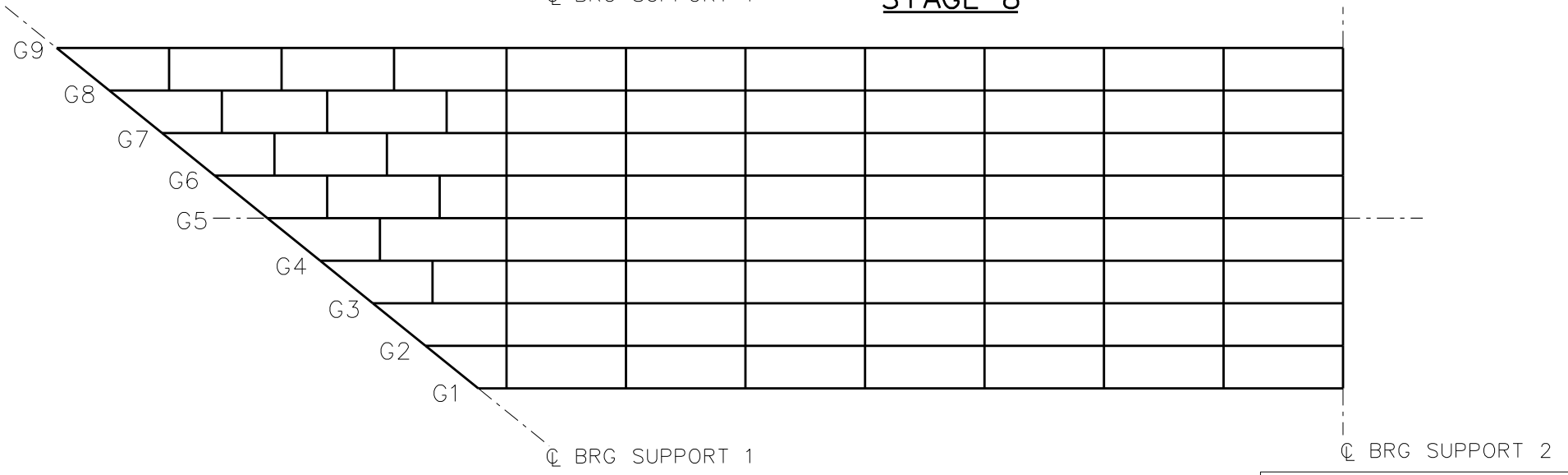

STAGE 9

LEGEND

▽ = HOLD OR LIFT CRANE

○ = TIE DOWN

□ = TEMPORARY SUPPORT STRUCTURE

NCHRP 12-79

BRIDGE NISSS36

GENERAL ERECTION PROCEDURE

NCHRP 12-79

NISSS37

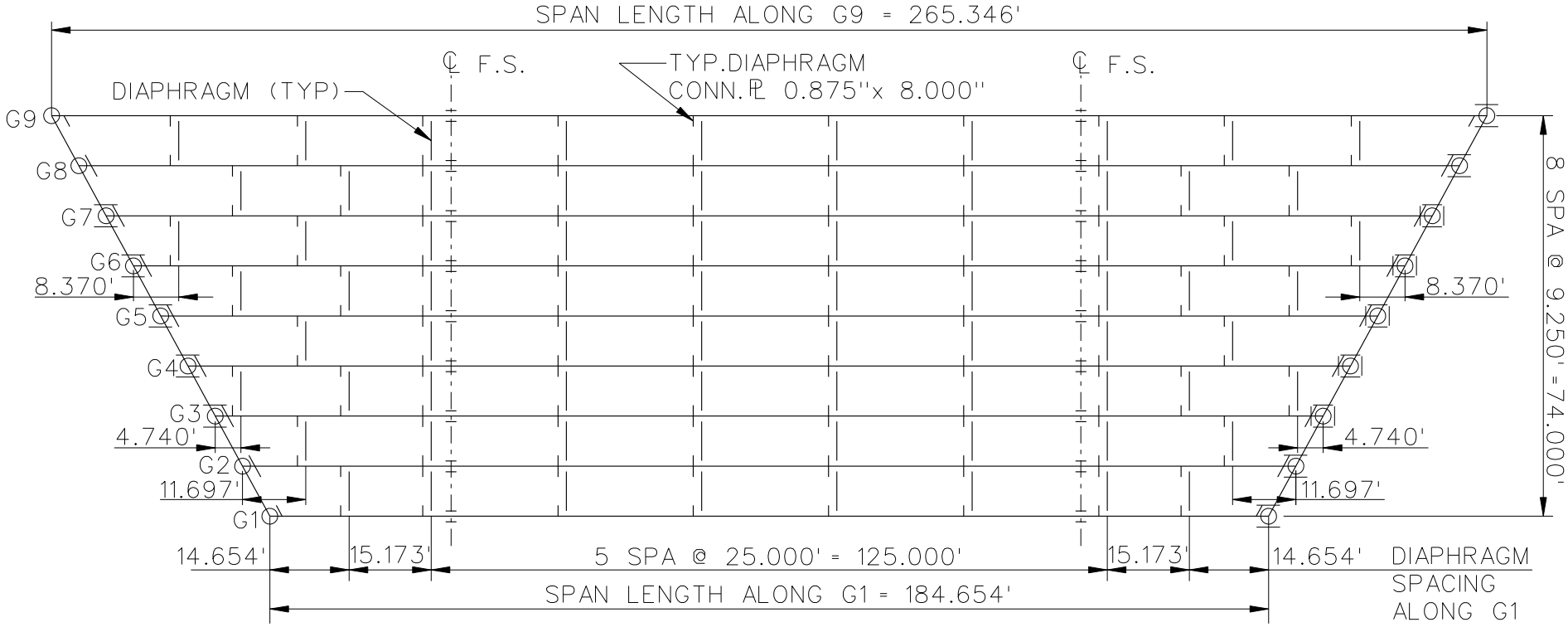

FRAMING PLAN

BEARING LEGEND

- ○ NON-GUIDED
- ⊜ LONGITUDINALLY GUIDED
- |○| TRANSVERSELY GUIDED
- |⊜| FIXED

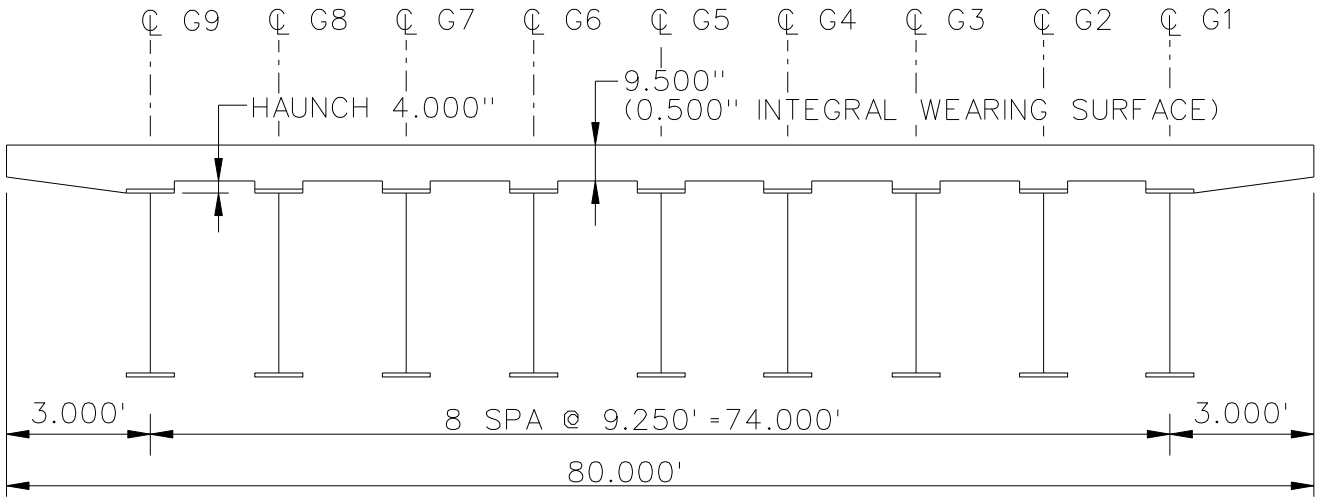

CROSS - SECTION

(DIAPHRAGMS NOT SHOWN)

NCHRP 12-79

BRIDGE NISSS37

FRAMING PLAN AND CROSS-SECTION

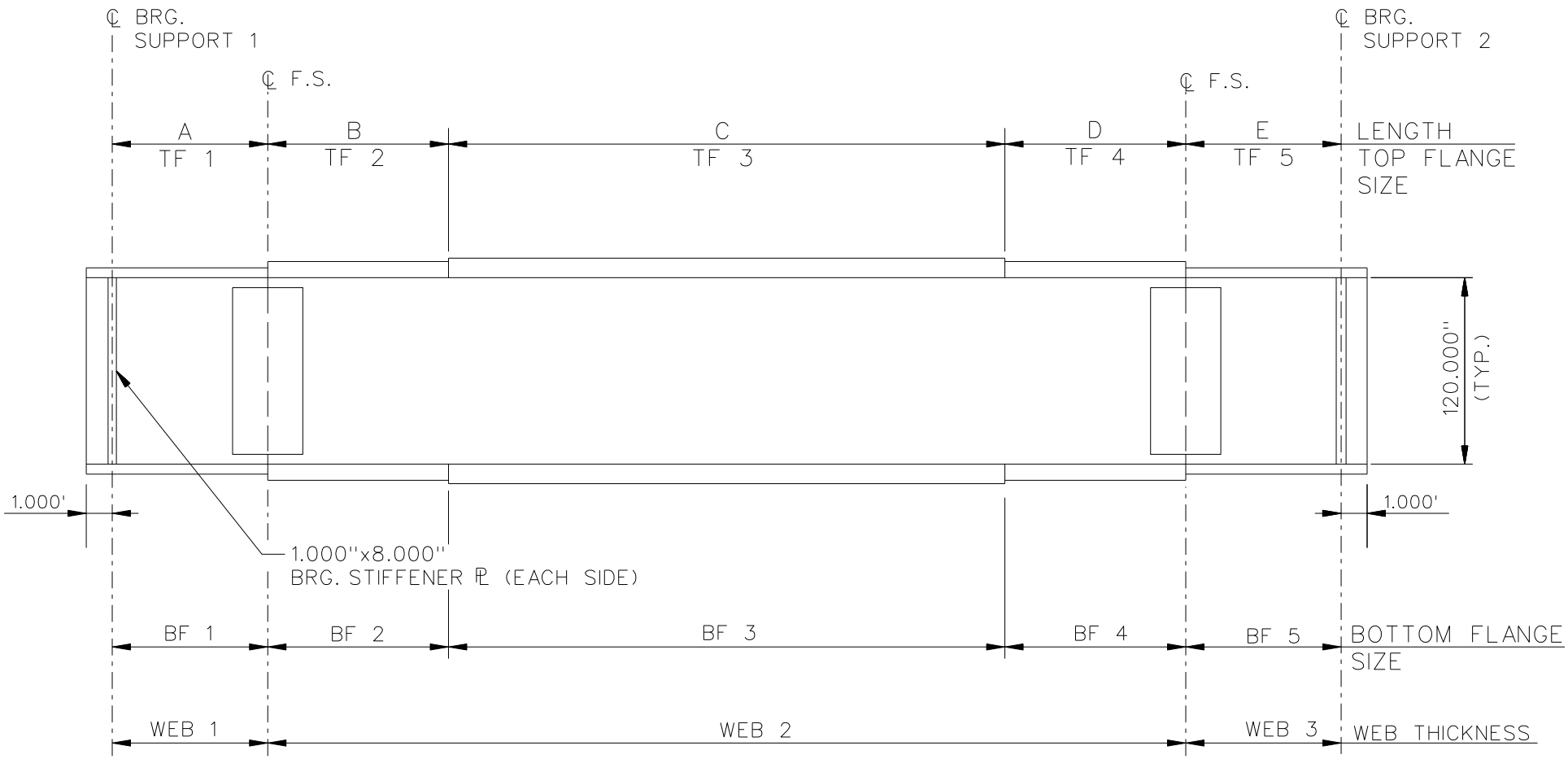

NOTE :

1. SEE TABLES ON SHEET 3 FOR GIRDER ELEVATION DIMENSIONS AND PLATE SIZES.

2. ALL GIRDERS, WEB 1 = WEB 2 = WEB 3 = 0.875".

NCHRP 12-79

BRIDGE NISSS37

GIRDER ELEVATION

SHEET 2 OF 6

	GIRDER PLATE LENGTHS ✳								
LENGTH	G1	G2	G3	G4	G5	G6	G7	G8	G9
A	33.827	38.870	43.941	48.957	54.000	59.043	64.087	69.130	74.173
B	25.000	25.000	25.000	25.000	25.000	25.000	25.000	25.000	25.000
C	67.000	67.000	67.000	67.000	67.000	67.000	67.000	67.000	67.000
D	25.000	25.000	25.000	25.000	25.000	25.000	25.000	25.000	25.000
E	33.827	38.870	43.941	48.957	54.000	59.043	64.087	69.130	74.173

✳ ALL DIMENSIONS ARE IN FEET.

	GIRDER FLANGE DIMENSIONS ✳✳					
TOP	G1, G2, G3		G4, G5, G6		G7, G8, G9	
FLANGE	BF	TF	BF	TF	BF	TF
TF1	20.000	1.000	24.000	1.000	28.000	1.250
TF2	20.000	1.000	24.000	1.500	28.000	1.750
TF3	20.000	1.000	24.000	2.000	28.000	2.250
TF4	20.000	1.000	24.000	1.500	28.000	1.750
TF5	20.000	1.000	24.000	1.000	28.000	1.250

✳✳ ALL DIMENSIONS ARE IN INCHES.

	GIRDER FLANGE DIMENSIONS ✳✳					
BOTTOM	G1, G2, G3		G4, G5, G6		G7, G8, G9	
FLANGE	BF	TF	BF	TF	BF	TF
BF1	24.000	1.000	28.000	1.500	32.000	1.500
BF2	24.000	1.000	28.000	1.750	32.000	1.750
BF3	24.000	1.000	28.000	2.250	32.000	2.250
BF4	24.000	1.000	28.000	1.750	32.000	1.750
BF5	24.000	1.000	28.000	1.500	32.000	1.500

✳✳ ALL DIMENSIONS ARE IN INCHES.

NCHRP 12-79

BRIDGE NISSS37

GIRDER ELEVATION TABLES

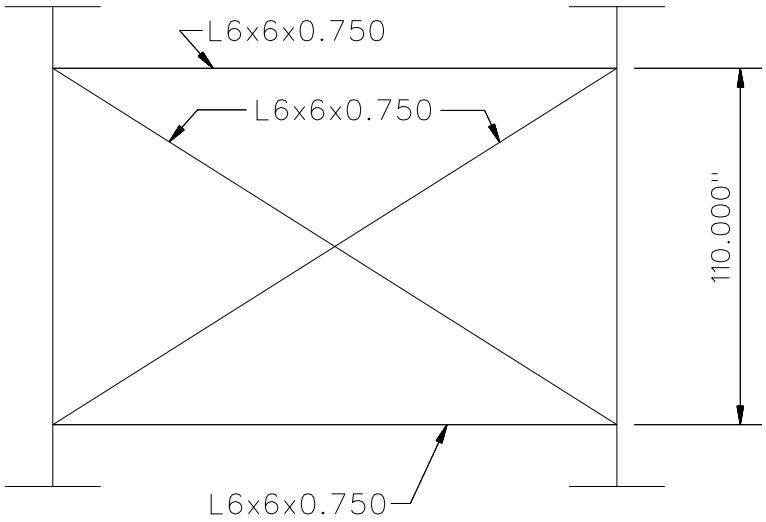

TYPICAL END AND INTERMEDIATE DIAPHRAGM

NOTES:

1. STEEL DEAD LOAD INCREASED BY 5% FOR MDX AND LARSA MODELS; 2% FOR 3D MODEL; AND 10% FOR APPROXIMATE ANALYSIS TO ACCOUNT FOR MISC. DETAILS.

2. FORMWORK LOAD OF 10PSF IS INCLUDED IN CONCRETE DEAD LOAD.

3. ADDITIONAL DESIGN PARAMETERS:
   A. 1.500' PARAPET WIDTH BOTH SIDES.
   B. 700 LB/FT UNIFORM LOAD ASSUMED FOR PARAPET WEIGHT.
   C. ROADWAY WIDTH = 77.000'.
   D. NUMBER OF DESIGN LANES = 6.
   E. HL93 LIVE LOAD.

4. DIAPHRAGM MEMBER CALL-OUTS ARE IN ENGLISH UNITS.

NCHRP 12-79

BRIDGE NISSS37

MISC. DETAILS AND NOTES

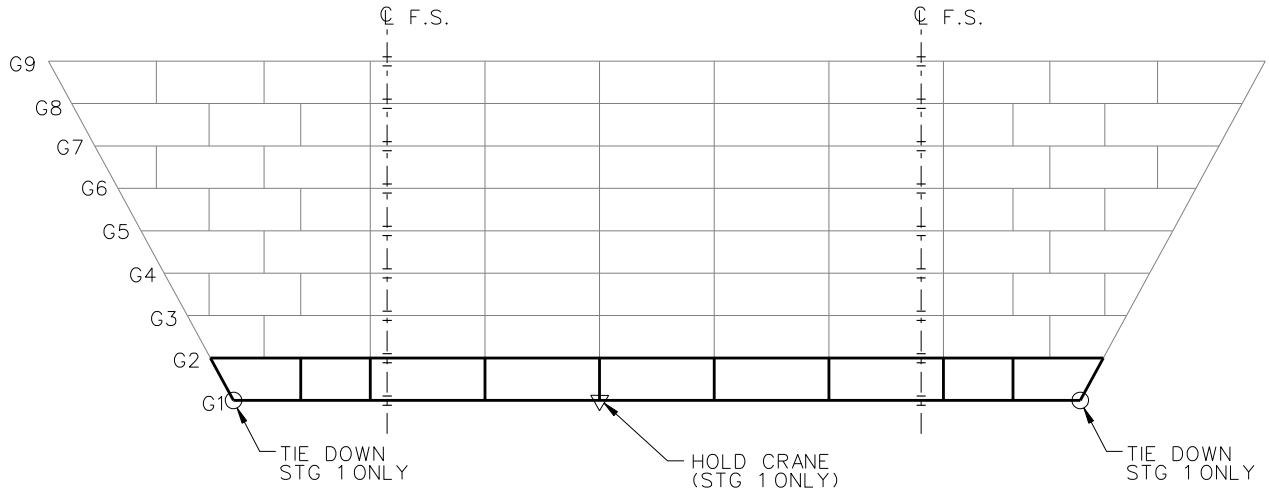

STAGE 2

NOTE:
STAGE 1 = G1 ERECTED.

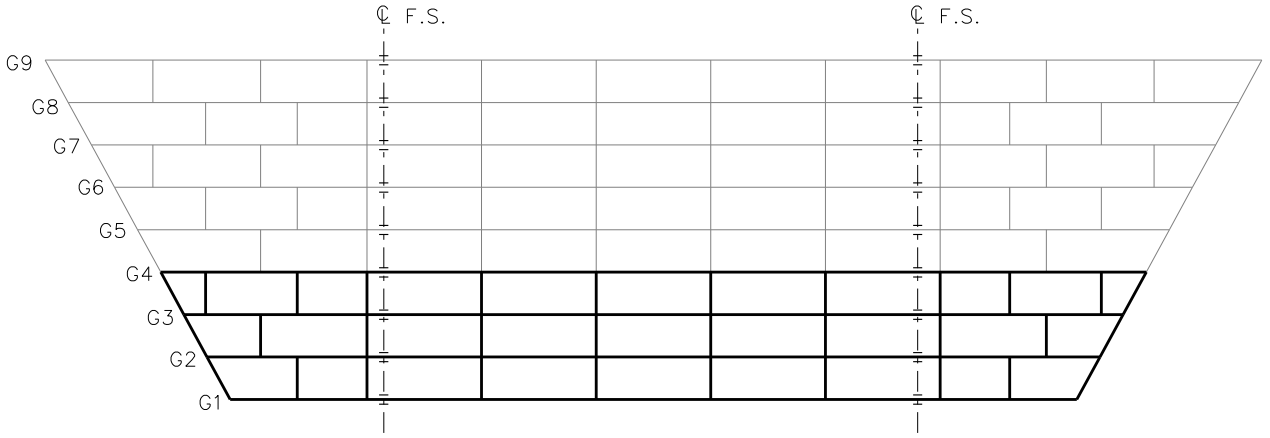

STAGE 4

NOTE:
STAGE 3 = G3 AND XF'S ERECTED.

LEGEND

▽ = HOLD OR LIFT CRANE

○ = TIE DOWN

□ = TEMPORARY SUPPORT STRUCTURE

NCHRP 12-79

BRIDGE NISSS37

GENERAL ERECTION PROCEDURE

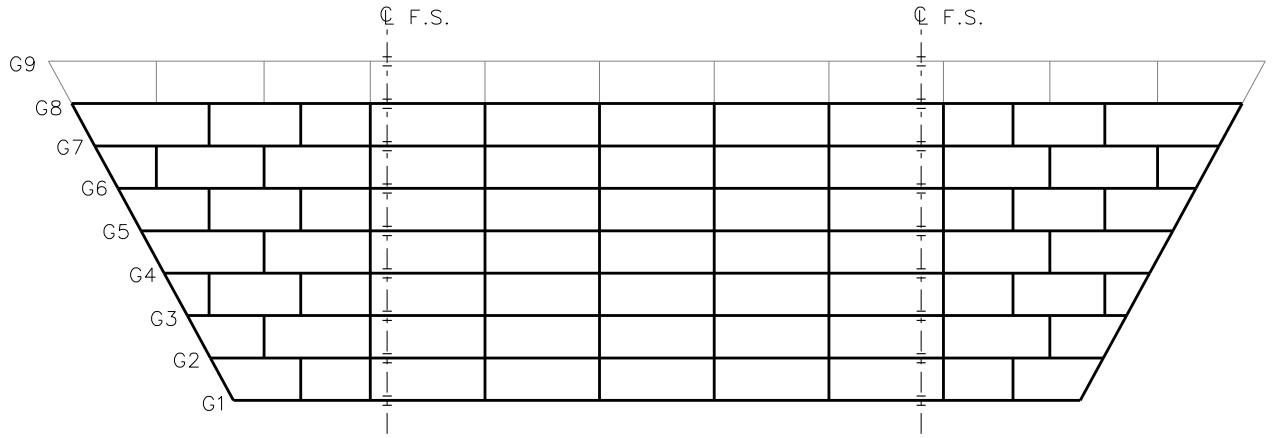

STAGE 8

NOTE:
STAGE 5 = G5 AND XF'S ERECTED
STAGE 6 = G6 AND XF'S ERECTED
STAGE 7 = G7 AND XF'S ERECTED.

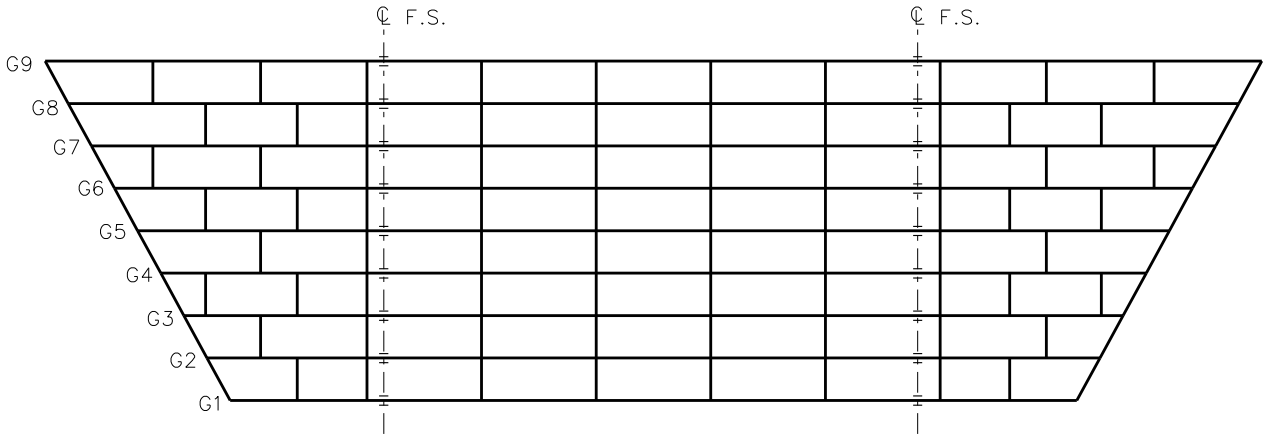

STAGE 9

LEGEND

▽ = HOLD OR LIFT CRANE

○ = TIE DOWN

□ = TEMPORARY SUPPORT STRUCTURE

NCHRP 12-79

BRIDGE NISSS37

GENERAL ERECTION PROCEDURE

SHEET 6 OF 6

NCHRP 12-79

NISSS53

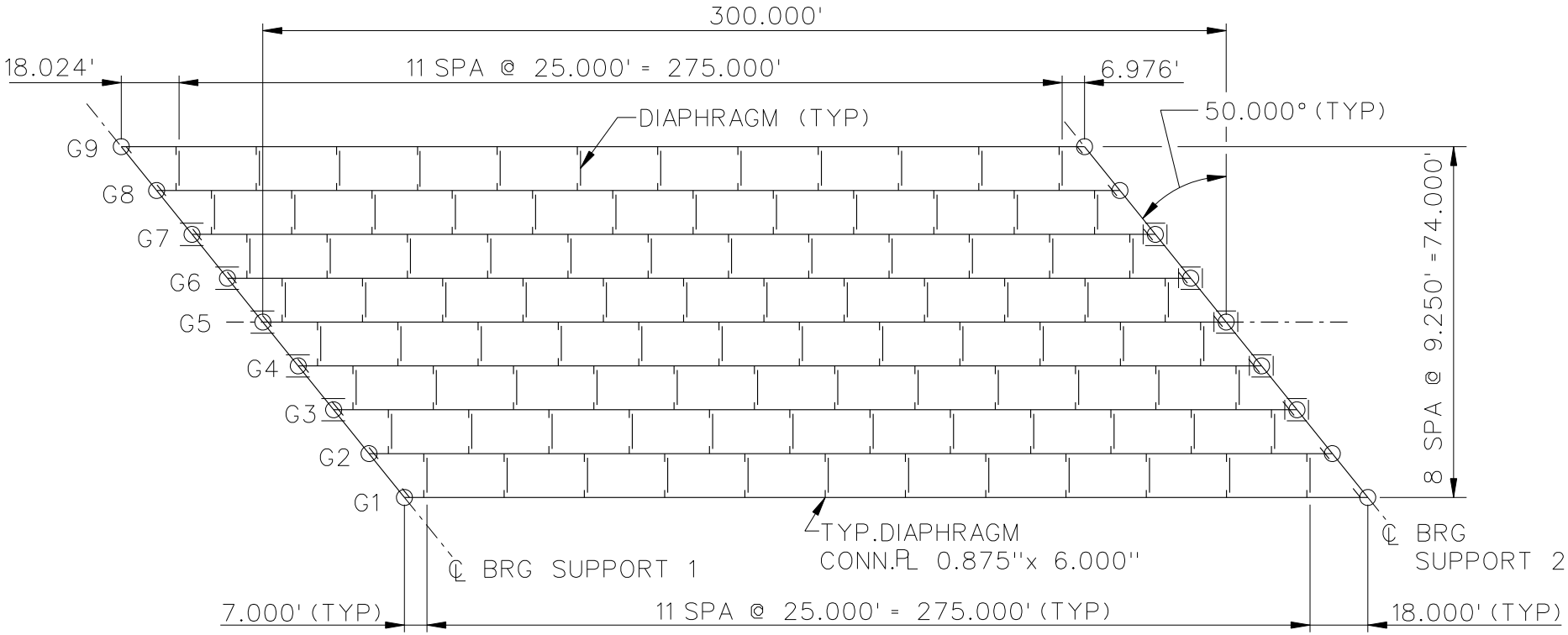

FRAMING PLAN

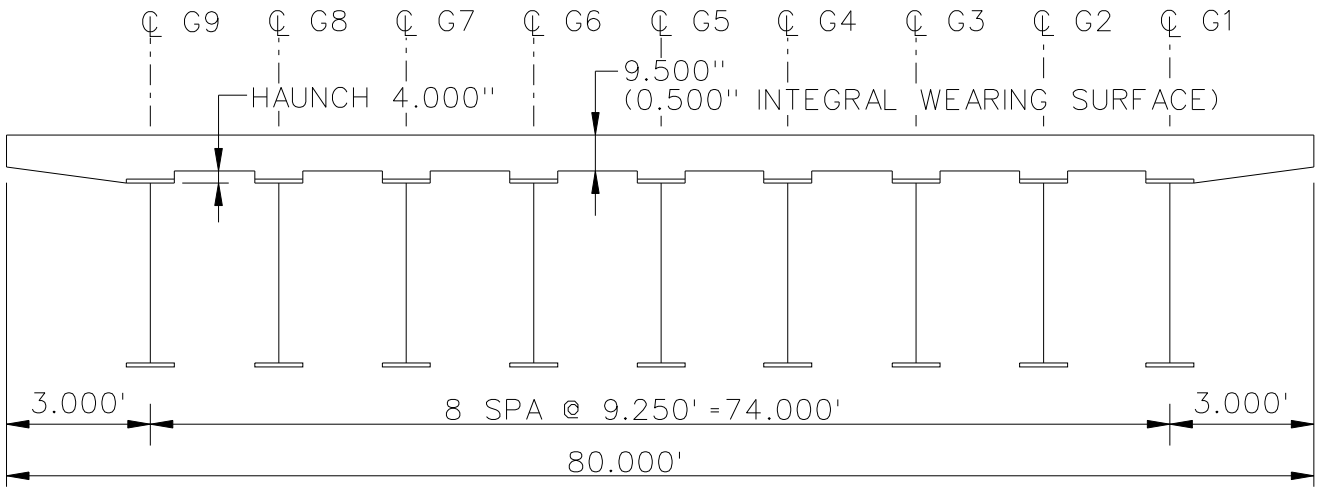

CROSS - SECTION

(DIAPHRAGMS NOT SHOWN)

BEARING LEGEND

- ○ NON-GUIDED
- ⎕○ LONGITUDINALLY GUIDED
- |○| TRANSVERSELY GUIDED
- |⎕○| FIXED

NCHRP 12-79

BRIDGE NISSS53

FRAMING PLAN AND CROSS-SECTION

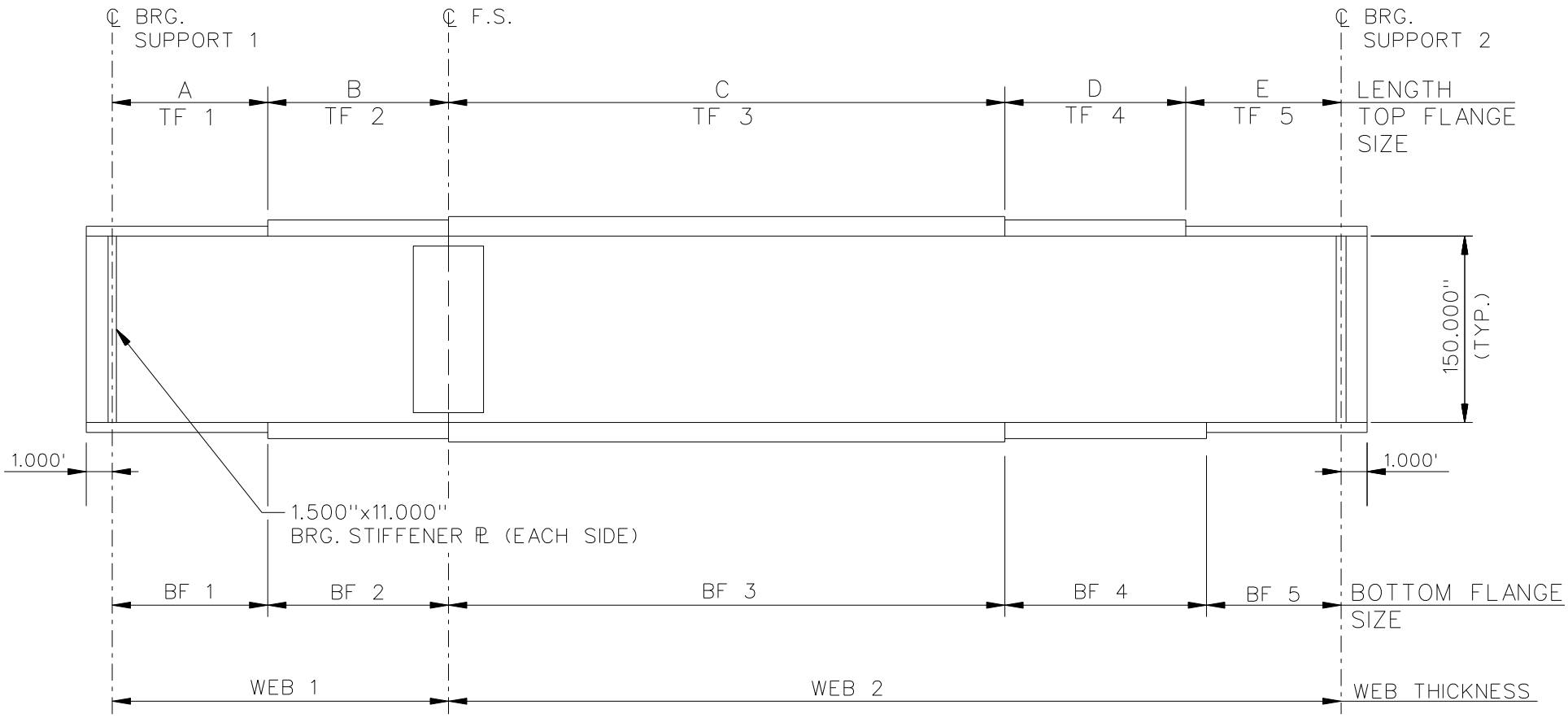

NOTE :

1. SEE TABLES ON SHEET 3 FOR GIRDER ELEVATION DIMENSIONS AND PLATE SIZES.
2. ALL GIRDERS, WEB 1 = WEB 2 = 1.000".

NCHRP 12-79

BRIDGE NISSS53

GIRDER ELEVATION

SHEET 2 OF 6

	GIRDER PLATE LENGTHS ✳		
LENGTH	G1, G2, G3	G4, G5, G6	G7, G8, G9
A	45.000	45.000	45.000
B	50.000	50.000	50.000
C	110.000	110.000	110.000
D	50.000	50.000	50.000
E	45.000	45.000	45.000

✳ ALL DIMENSIONS ARE IN FEET.

	GIRDER FLANGE DIMENSIONS ✳✳					
TOP	G1, G2, G3		G4, G5, G6		G7, G8, G9	
FLANGE	BF	TF	BF	TF	BF	TF
TF1	26.000	1.125	26.000	1.125	26.000	1.125
TF2	26.000	1.500	26.000	1.500	26.000	1.500
TF3	26.000	2.000	26.000	2.000	26.000	2.000
TF4	26.000	1.500	26.000	1.500	26.000	1.500
TF5	26.000	1.125	26.000	1.125	26.000	1.125

✳✳ ALL DIMENSIONS ARE IN INCHES.

	GIRDER FLANGE DIMENSIONS ✳✳					
BOTTOM	G1, G2, G3		G4, G5, G6		G7, G8, G9	
FLANGE	BF	TF	BF	TF	BF	TF
BF1	30.000	1.250	30.000	1.250	30.000	1.250
BF2	30.000	1.750	30.000	1.750	30.000	1.750
BF3	30.000	2.250	30.000	2.250	30.000	2.250
BF4	30.000	1.750	30.000	1.750	30.000	1.750
BF5	30.000	1.250	30.000	1.250	30.000	1.250

✳✳ ALL DIMENSIONS ARE IN INCHES.

NCHRP 12-79

BRIDGE NISSS53

GIRDER ELEVATION TABLES

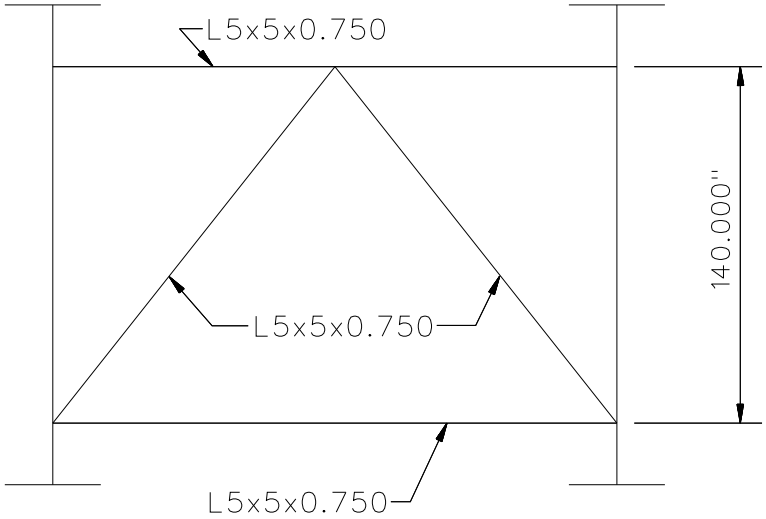

TYPICAL END AND INTERMEDIATE DIAPHRAGM

NOTES:

1. STEEL DEAD LOAD INCREASED BY 5% FOR MDX AND LARSA MODELS; 2% FOR 3D MODEL; AND 10% FOR APPROXIMATE ANALYSIS TO ACCOUNT FOR MISC. DETAILS.

2. FORMWORK LOAD OF 10PSF IS INCLUDED IN CONCRETE DEAD LOAD.

3. ADDITIONAL DESIGN PARAMETERS:
   A. 1.500' PARAPET WIDTH BOTH SIDES.
   B. 700 LB/FT UNIFORM LOAD ASSUMED FOR PARAPET WEIGHT.
   C. ROADWAY WIDTH = 77.000'.
   D. NUMBER OF DESIGN LANES = 6.
   E. HLP3 LIVE LOAD.

4. DIAPHRAGM MEMBER CALL-OUTS ARE IN UNITS OF INCHES.

NCHRP 12-79

BRIDGE NISSS53

MISC. DETAILS AND NOTES

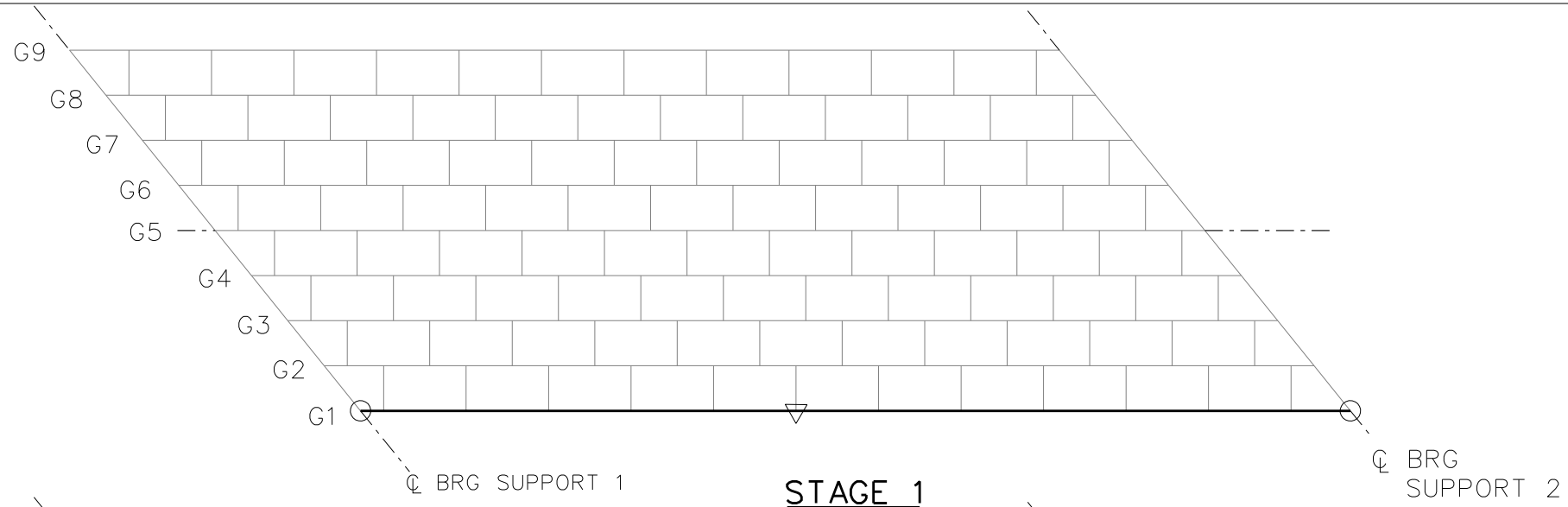

STAGE 1

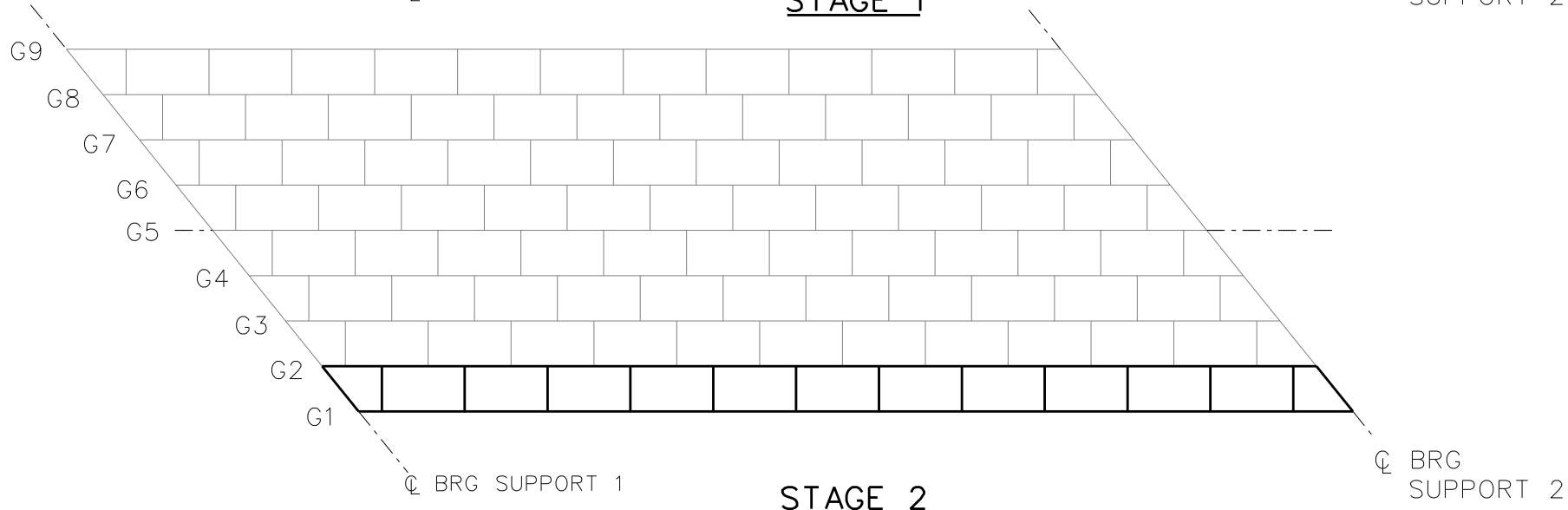

STAGE 2

LEGEND

▽ = HOLD OR LIFT CRANE

○ = TIE DOWN

□ = TEMPORARY SUPPORT STRUCTURE

STAGE 3 - ERECT G3 AND ADJACENT CROSS FRAMES
STAGE 4 - ERECT G4 AND ADJACENT CROSS FRAMES
STAGE 5 - ERECT G5 AND ADJACENT CROSS FRAMES
STAGE 6 - ERECT G6 AND ADJACENT CROSS FRAMES
STAGE 7 - ERECT G7 AND ADJACENT CROSS FRAMES

NCHRP 12-79

BRIDGE NISSS53

GENERAL ERECTION PROCEDURE

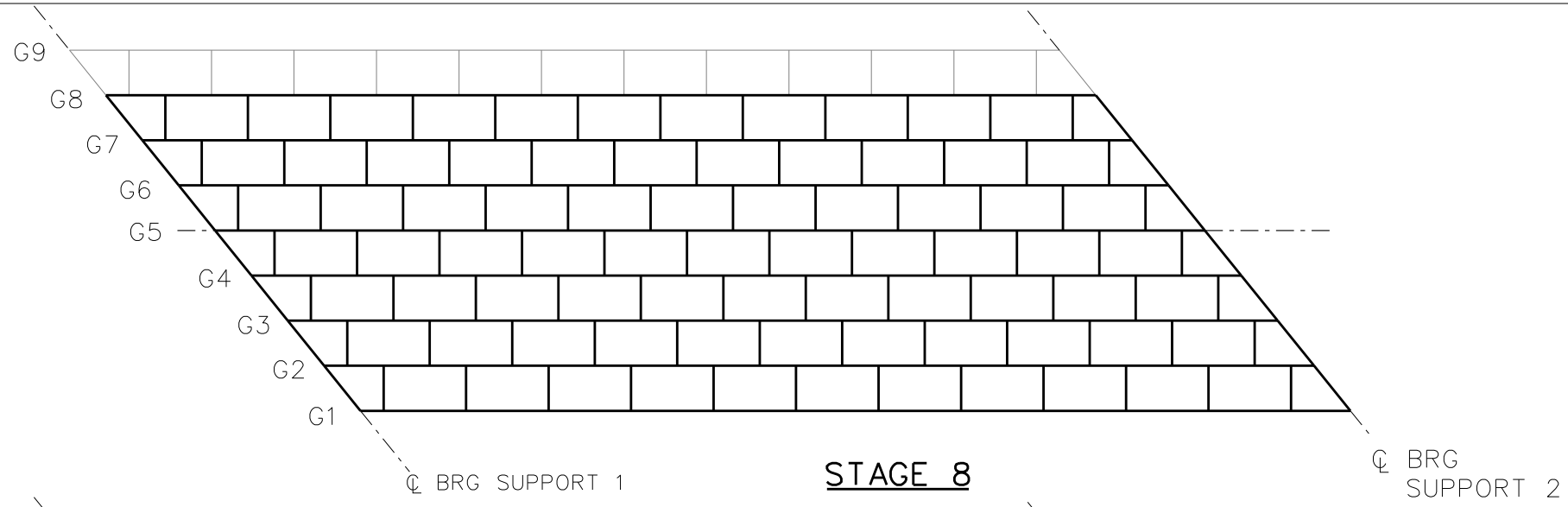

STAGE 8

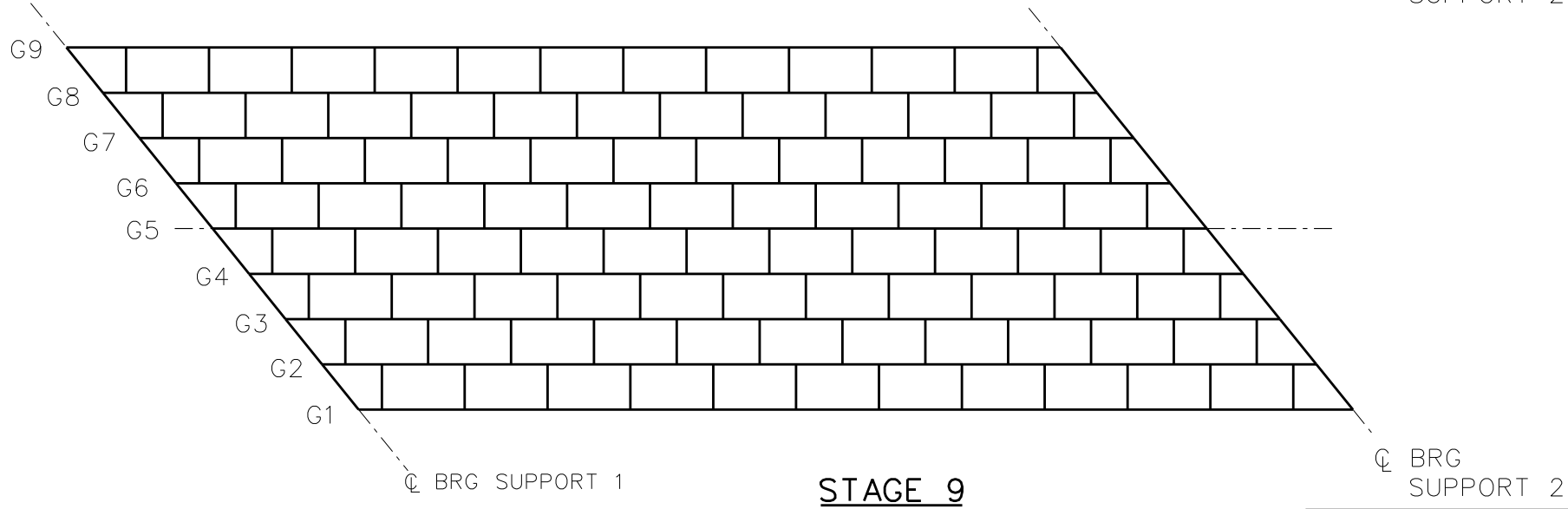

STAGE 9

LEGEND

▽ = HOLD OR LIFT CRANE

○ = TIE DOWN

□ = TEMPORARY SUPPORT STRUCTURE

NCHRP 12-79

BRIDGE NISSS53

GENERAL ERECTION PROCEDURE

SHEET 6 OF 6

NCHRP 12-79

NISSS54

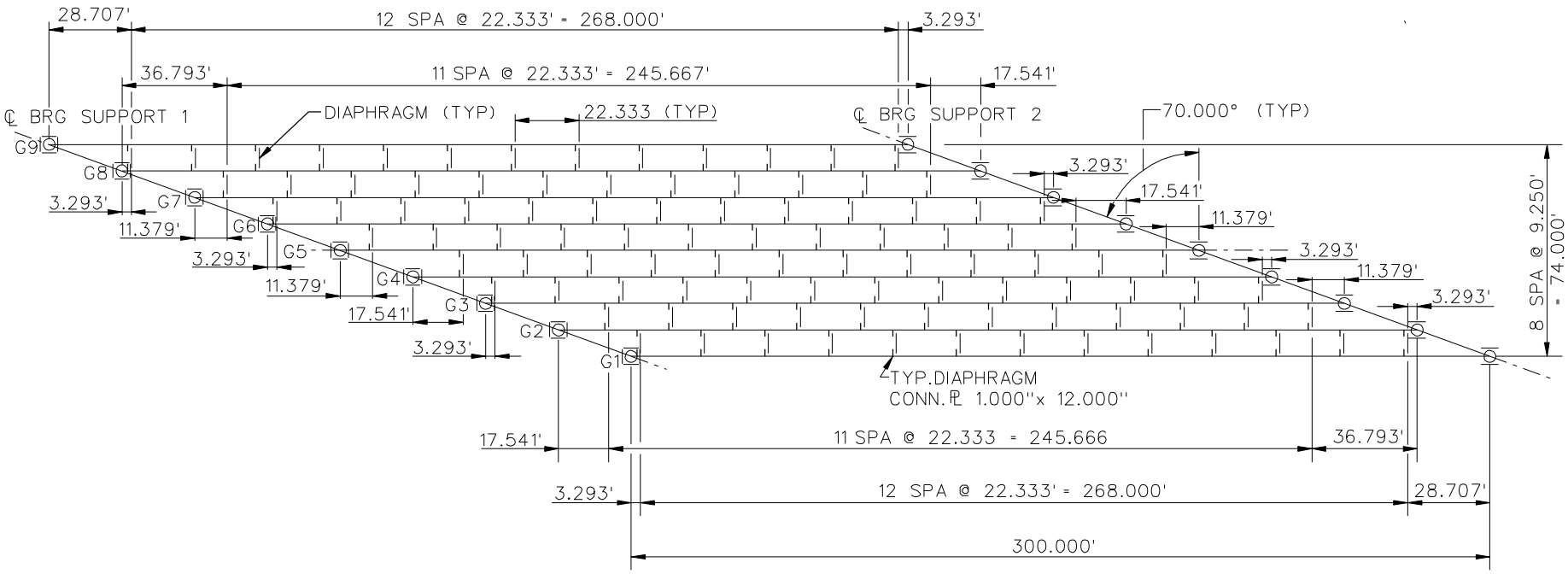

FRAMING PLAN

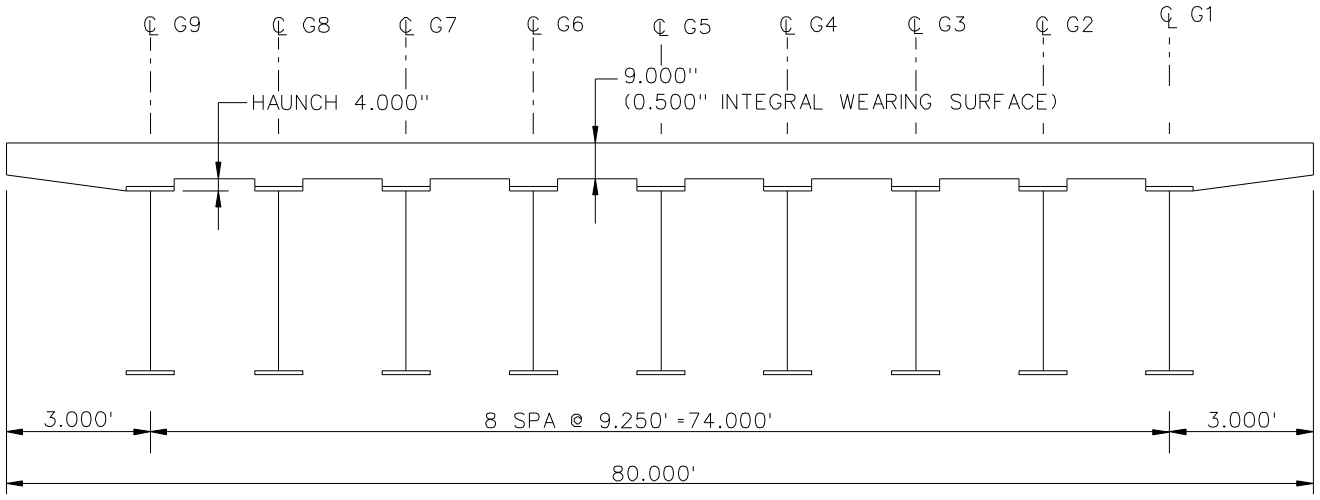

CROSS - SECTION

(DIAPHRAGMS NOT SHOWN)

BEARING LEGEND

- ○ NON-GUIDED
- ⊖ LONGITUDINALLY GUIDED
- |○| TRANSVERSELY GUIDED
- |⊖| FIXED

NCHRP 12-79

BRIDGE NISSS54

FRAMING PLAN AND CROSS-SECTION

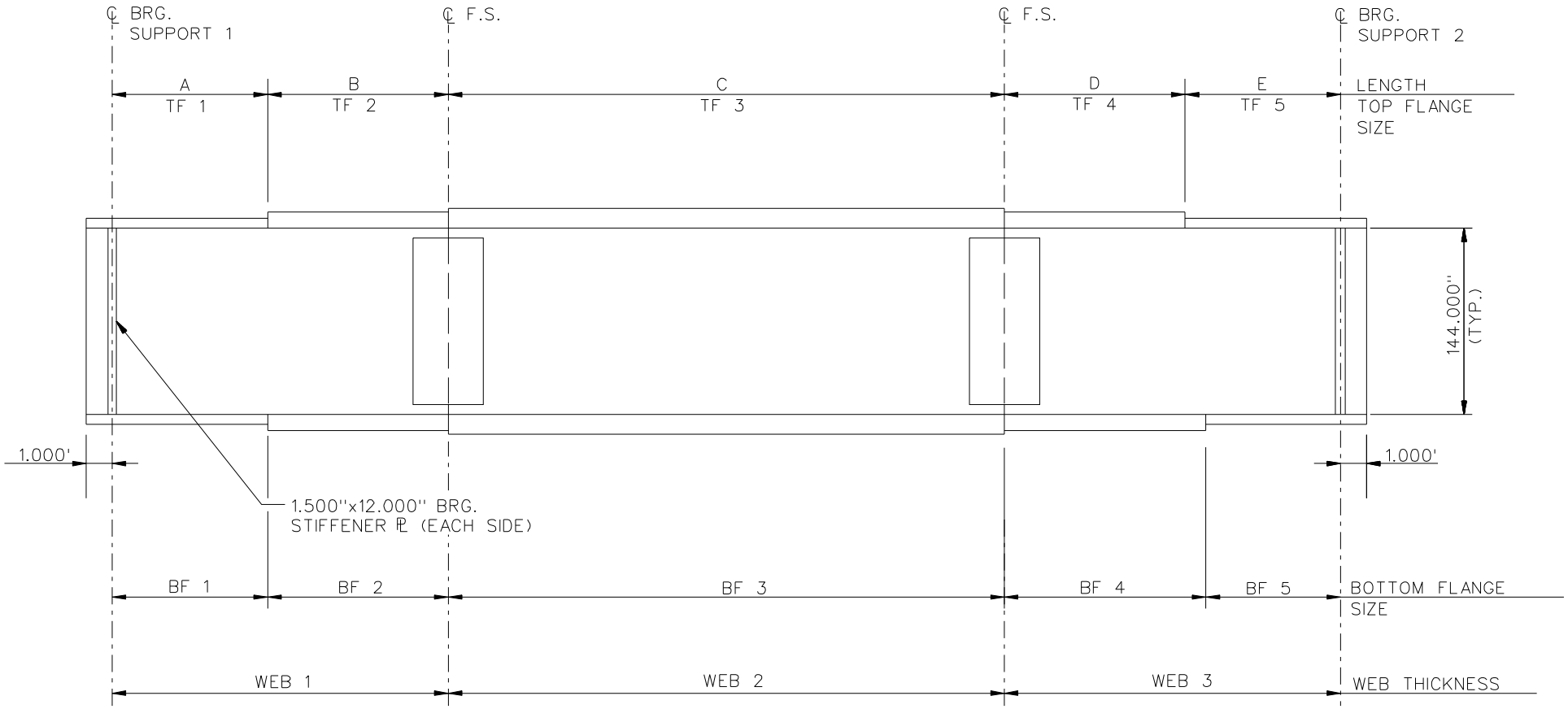

NOTE :

1. SEE TABLES ON SHEET 3 FOR GIRDER ELEVATION DIMENSIONS AND PLATE SIZES.

2. ALL GIRDERS, WEB 1 = WEB 2 = WEB 3 = 1.000".

NCHRP 12-79

BRIDGE NISSS54

GIRDER ELEVATION

SHEET 2 OF 10

	GIRDER PLATE LENGTHS ✳								
LENGTH	G1	G2	G3	G4	G5	G6	G7	G8	G9
A	45.000	45.000	45.000	45.000	45.000	45.000	45.000	45.000	45.000
B	45.000	45.000	45.000	45.000	45.000	45.000	45.000	45.000	45.000
C	120.000	120.000	120.000	120.000	120.000	120.000	120.000	120.000	120.000
D	45.000	45.000	45.000	45.000	45.000	45.000	45.000	45.000	45.000
E	45.000	45.000	45.000	45.000	45.000	45.000	45.000	45.000	45.000

✳ ALL DIMENSIONS ARE IN FEET.

	GIRDER FLANGE DIMENSIONS ✳✳					
TOP	G1, G2, G3		G4, G5, G6		G7, G8, G9	
FLANGE	BF	TF	BF	TF	BF	TF
TF1	28.000	1.250	28.000	1.250	28.000	1.250
TF2	28.000	2.000	28.000	2.000	28.000	2.000
TF3	28.000	2.000	28.000	2.000	28.000	2.000
TF4	28.000	2.000	28.000	2.000	28.000	2.000
TF5	28.000	1.250	28.000	1.250	28.000	1.250

✳✳ ALL DIMENSIONS ARE IN INCHES.

	GIRDER FLANGE DIMENSIONS ✳✳					
BOTTOM	G1		G2		G3	
FLANGE	BF	TF	BF	TF	BF	TF
BF1	30.000	1.250	30.000	1.250	30.000	1.250
BF2	30.000	2.250	30.000	2.250	30.000	2.250
BF3	30.000	2.750	30.000	2.750	30.000	2.750
BF4	30.000	2.250	30.000	2.250	30.000	2.250
BF5	30.000	1.250	30.000	1.250	30.000	1.250

ALL DIMENSIONS ARE IN INCHES.

NCHRP 12-79

BRIDGE NISSS54

GIRDER ELEVATION TABLES

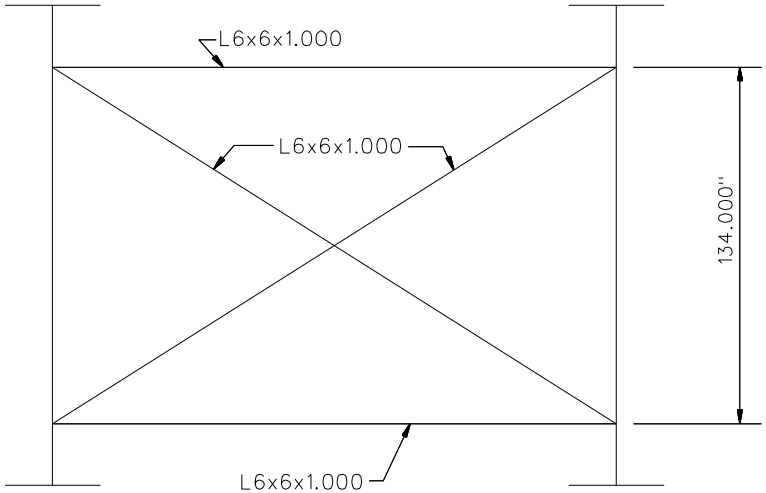

TYPICAL INTERMEDIATE DIAPHRAGM

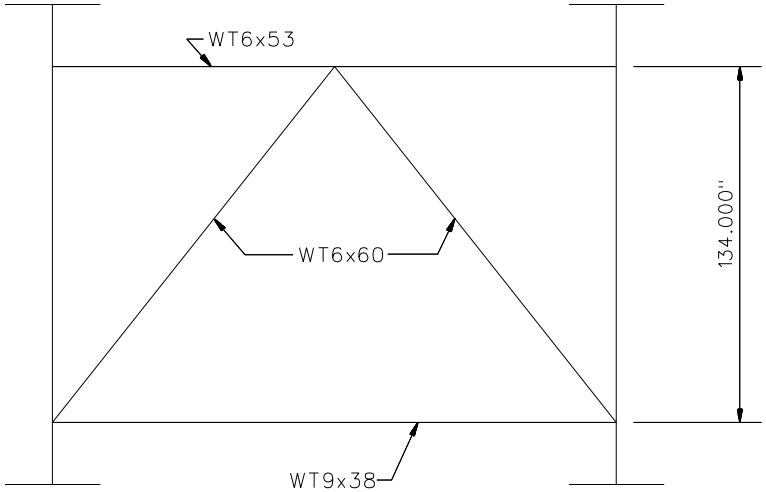

TYPICAL END DIAPHRAGM

NOTES:

1. STEEL DEAD LOAD INCREASED BY 5% FOR MDX AND LARSA MODELS; 2% FOR 3D MODEL; AND 10% FOR APPROXIMATE ANALYSIS TO ACCOUNT FOR MISC. DETAILS.

2. FORMWORK LOAD OF 10PSF IS INCLUDED IN CONCRETE DEAD LOAD.

3. ADDITIONAL DESIGN PARAMETERS:
   A. 1.500' PARAPET WIDTH BOTH SIDES.
   B. 700 LB/FT UNIFORM LOAD ASSUMED FOR PARAPET WEIGHT.
   C. ROADWAY WIDTH = 77.000'
   D. NUMBER OF DESIGN LANES = 6.
   E. HL93 LIVE LOAD

4. DIAPHRAGM MEMBER CALL-OUTS ARE IN UNITS OF INCHES.

NCHRP 12-79

BRIDGE NISSS54

MISC. DETAILS AND NOTES

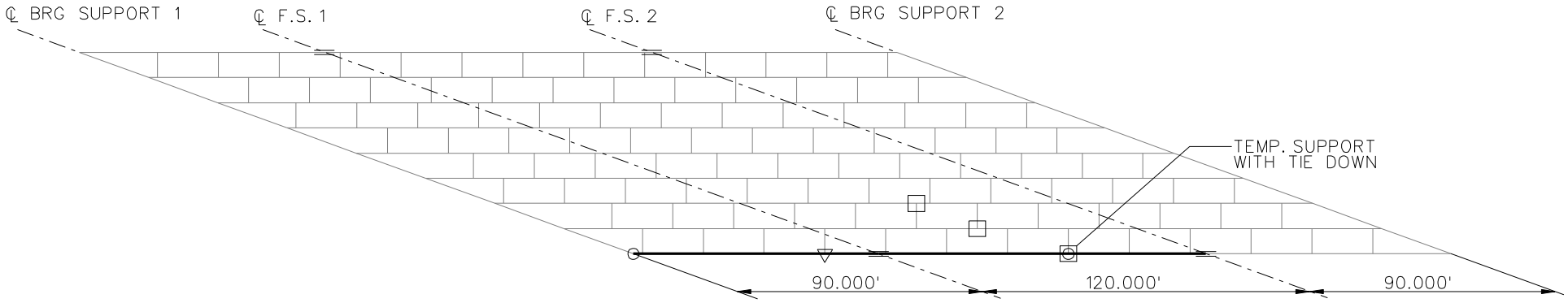

STAGE 1

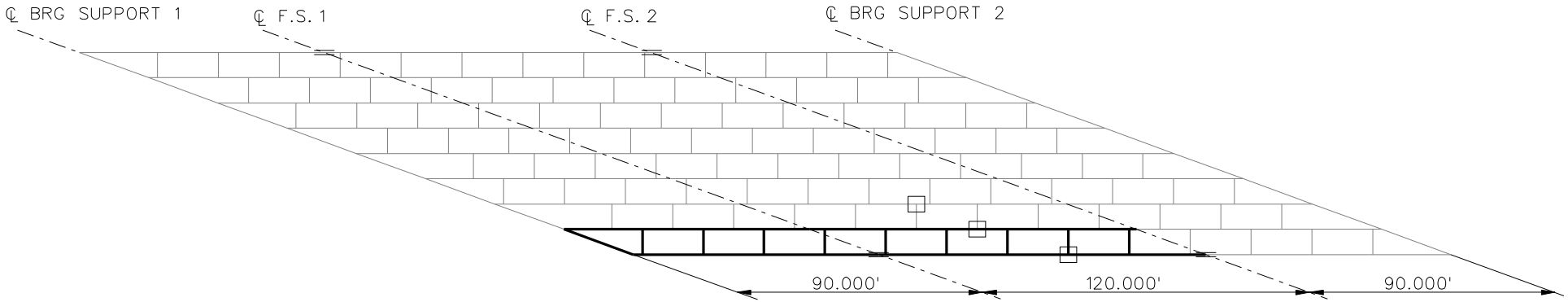

STAGE 2

LEGEND

▽ = HOLD OR LIFT CRANE

○ = TIE DOWN

□ = TEMPORARY SUPPORT STRUCTURE

NCHRP 12-79

BRIDGE NISSS54

GENERAL ERECTION PROCEDURE

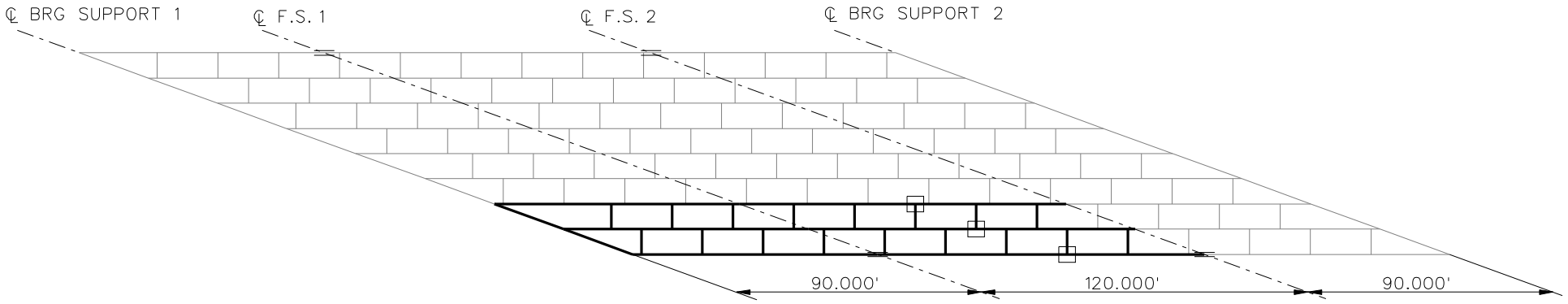

STAGE 3

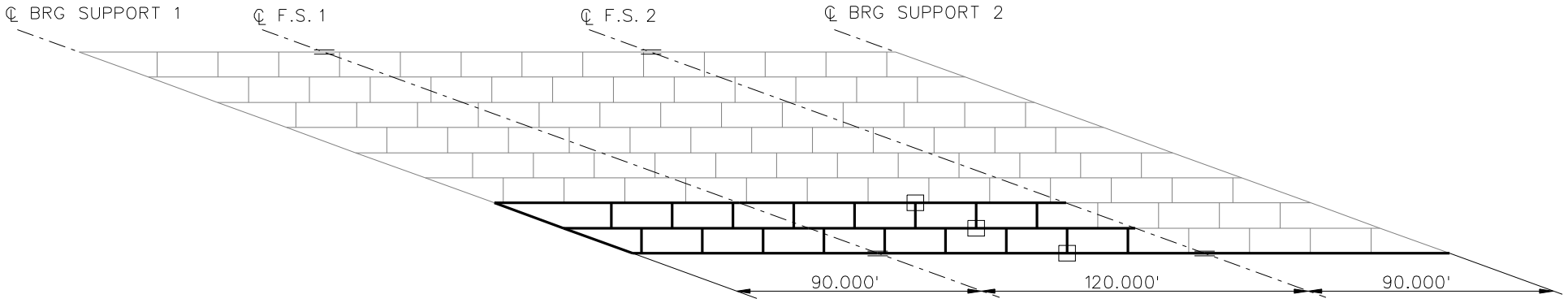

STAGE 4

LEGEND

▽ = HOLD OR LIFT CRANE

○ = TIE DOWN

□ = TEMPORARY SUPPORT STRUCTURE

STAGE 5 = G2-3 AND XF'S
STAGE 6 = G3-3 AND XF'S
REMOVE TEMP. SUPPORTS
AFTER STAGE 6.

NCHRP 12-79

BRIDGE NISSS54

GENERAL ERECTION PROCEDURE

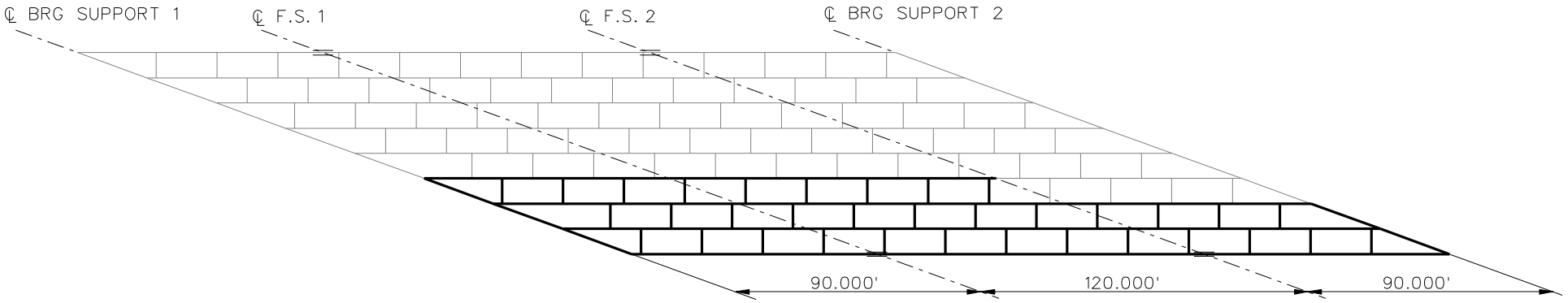

STAGE 7

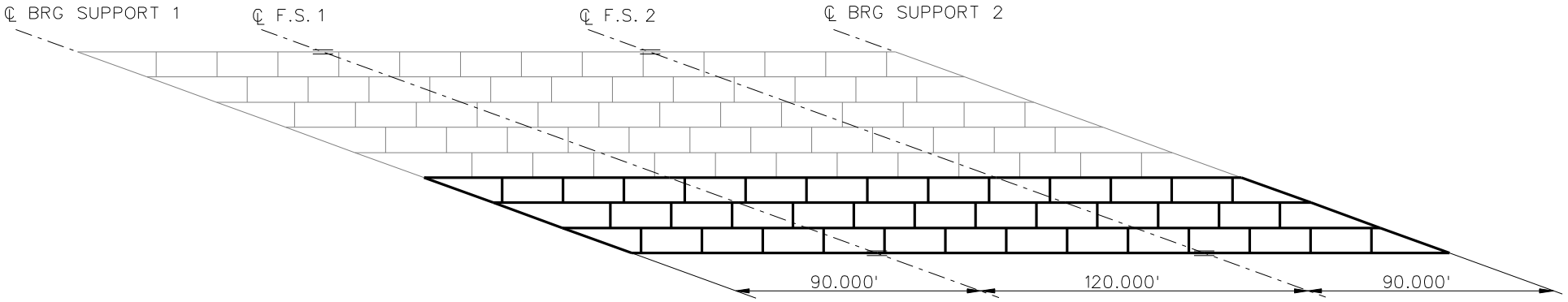

STAGE 8

LEGEND

▽ = HOLD OR LIFT CRANE

○ = TIE DOWN

□ = TEMPORARY SUPPORT STRUCTURE

NCHRP 12-79

BRIDGE NISSS54

GENERAL ERECTION PROCEDURE

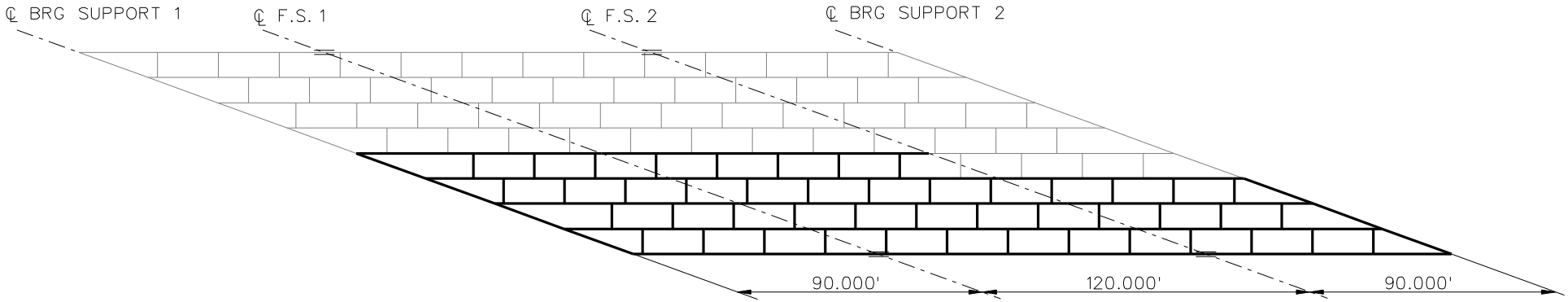

STAGE 9

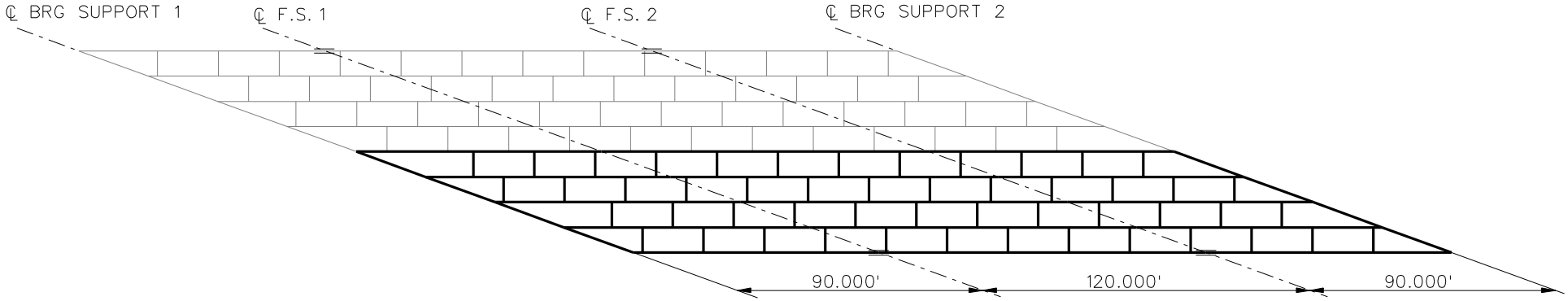

STAGE 10

LEGEND

▽ = HOLD OR LIFT CRANE

○ = TIE DOWN

□ = TEMPORARY SUPPORT STRUCTURE

NCHRP 12-79

BRIDGE NISSS54

GENERAL ERECTION PROCEDURE

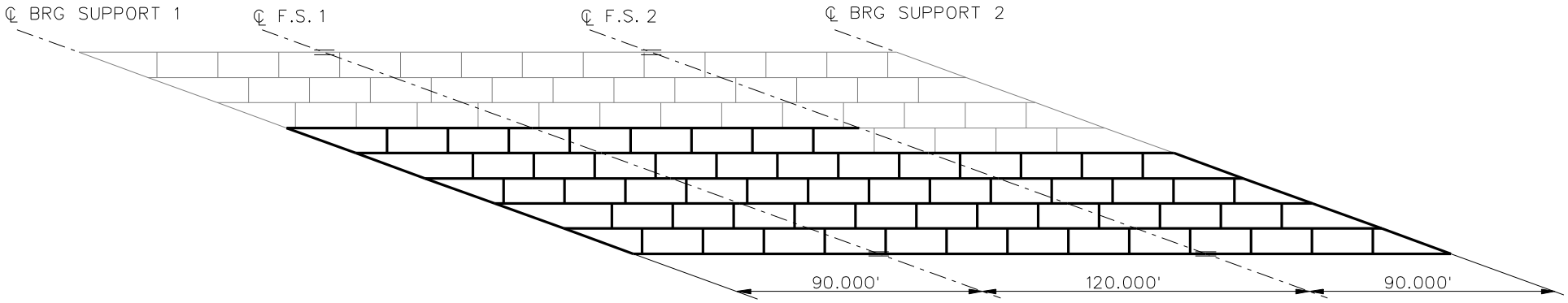

STAGE 11

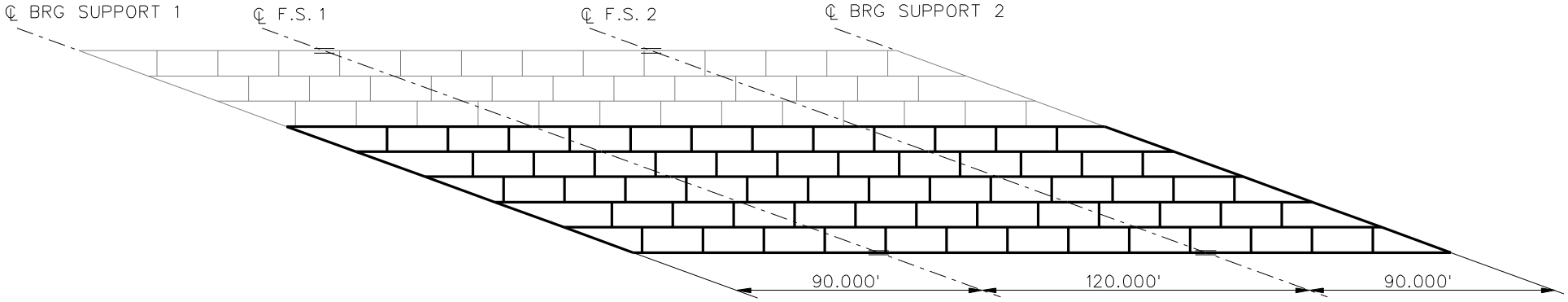

STAGE 12

STAGE 13 = G7-1, G7-2 AND XF'S
STAGE 14 = G7-3 AND XF'S
STAGE 15 = G8-1, G8-2 AND XF'S
STAGE 16 = G8-3 AND XF'S
STAGE 17 = G9-1, G9-2 AND XF'S

LEGEND

▽ = HOLD OR LIFT CRANE

○ = TIE DOWN

□ = TEMPORARY SUPPORT STRUCTURE

NCHRP 12-79

BRIDGE NISSS54

GENERAL ERECTION PROCEDURE

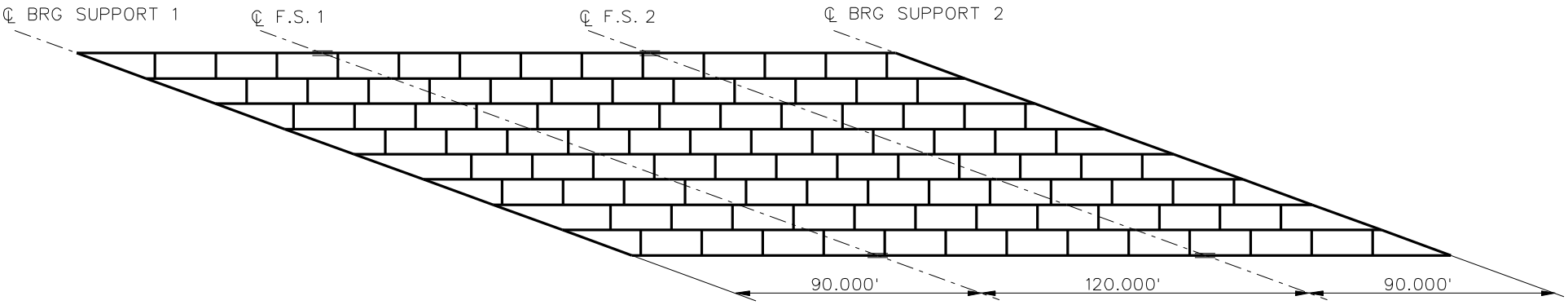

STAGE 18

LEGEND

▽ = HOLD OR LIFT CRANE

○ = TIE DOWN

□ = TEMPORARY SUPPORT STRUCTURE

NCHRP 12-79

BRIDGE NISSS54

GENERAL ERECTION PROCEDURE

NCHRP 12-79

NISSS56

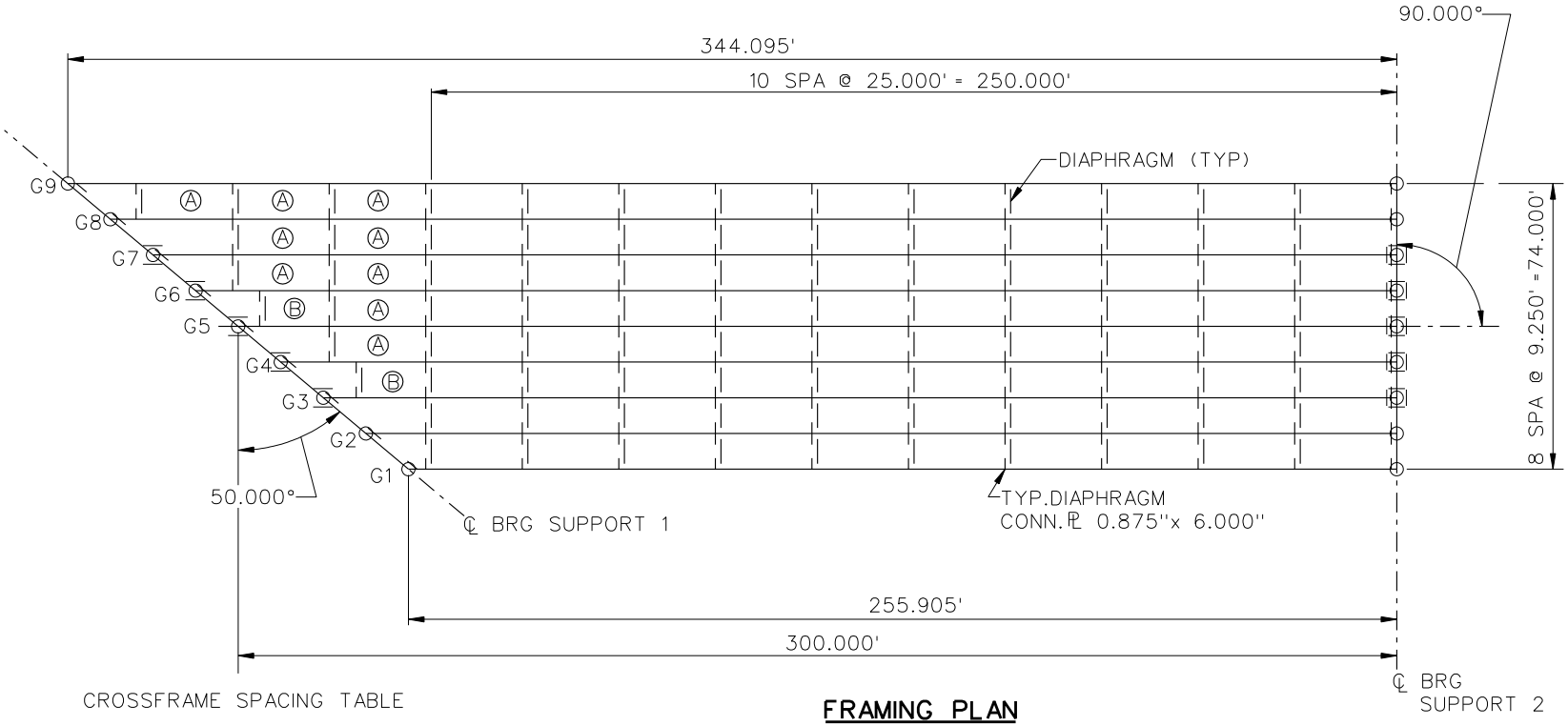

CROSSFRAME SPACING TABLE

A = 25.000'
B = 18.000'

FRAMING PLAN

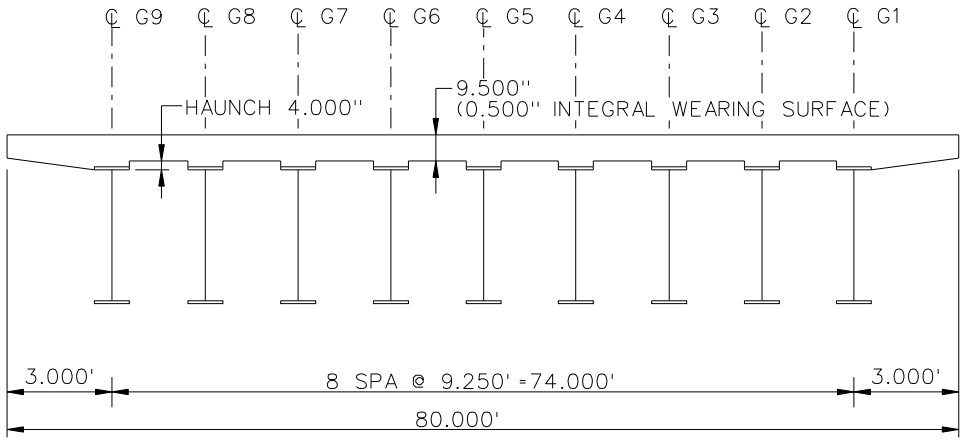

CROSS - SECTION

(DIAPHRAGMS NOT SHOWN)

BEARING LEGEND

- ○ NON-GUIDED
- ⊙ LONGITUDINALLY GUIDED
- |○| TRANSVERSELY GUIDED
- |⊙| FIXED

NCHRP 12-79

BRIDGE NISSS56

FRAMING PLAN AND CROSS-SECTION

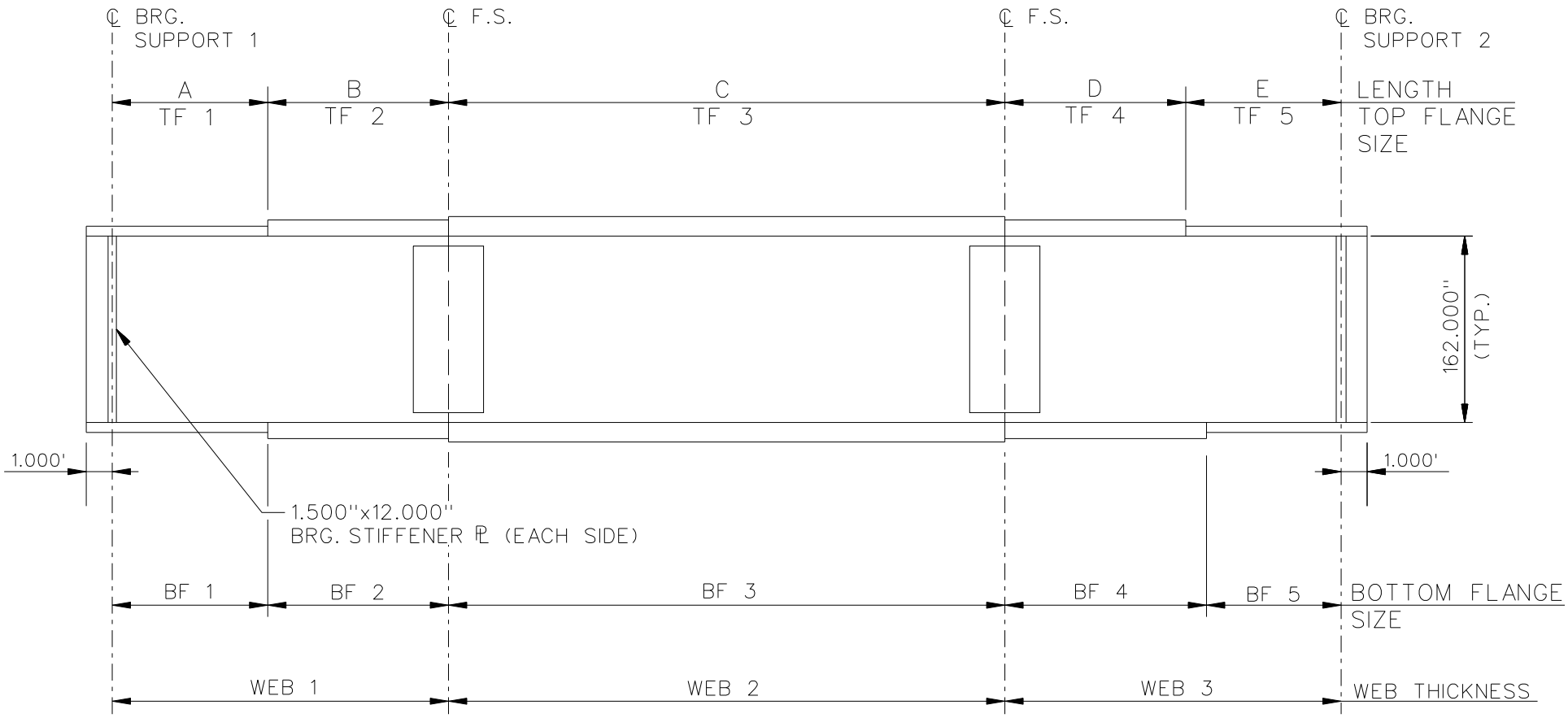

NOTES :

1. SEE TABLES ON SHEET 3 FOR GIRDER ELEVATION DIMENSIONS AND PLATE SIZES.
2. ALL GIRDERS, WEB 1 = WEB 2 = WEB 3 = 1.125".

NCHRP 12-79

BRIDGE NISSS56

GIRDER ELEVATION

SHEET 2 OF 7

	GIRDER PLATE LENGTHS ✳								
LENGTH	G1	G2	G3	G4	G5	G6	G7	G8	G9
A	17.953	23.465	28.977	34.488	40.000	45.512	51.024	56.536	62.048
B	17.953	23.465	28.977	34.488	40.000	45.512	51.024	56.536	62.048
C	110.000	110.000	110.000	110.000	110.000	110.000	110.000	110.000	110.000
D	55.000	55.000	55.000	55.000	55.000	55.000	55.000	55.000	55.000
E	55.000	55.000	55.000	55.000	55.000	55.000	55.000	55.000	55.000

✳ ALL DIMENSIONS ARE IN FEET.

	GIRDER FLANGE DIMENSIONS ✳✳											
TOP	G1, G2		G3, G4		G5		G6, G7		G8		G9	
FLANGE	BF	TF	BF	TF	BF	TF	BF	TF	BF	TF	BF	TF
TF1	28.000	1.250	28.000	1.250	28.000	1.250	28.000	1.250	28.000	1.250	30.000	1.500
TF2	28.000	1.250	28.000	1.250	28.000	1.250	28.000	1.250	28.000	1.500	30.000	2.250
TF3	28.000	1.250	28.000	1.500	28.000	1.750	28.000	1.750	28.000	2.000	30.000	2.500
TF4	28.000	1.250	28.000	1.250	28.000	1.250	28.000	1.250	28.000	1.500	30.000	2.250
TF5	28.000	1.250	28.000	1.250	28.000	1.250	28.000	1.250	28.000	1.250	30.000	1.500

✳✳ ALL DIMENSIONS ARE IN INCHES.

	GIRDER FLANGE DIMENSIONS ✳✳											
BOTTOM	G1, G2		G3, G4		G5		G6, G7		G8		G9	
FLANGE	BF	TF	BF	TF	BF	TF	BF	TF	BF	TF	BF	TF
TF1	30.000	1.250	30.000	1.250	30.000	1.250	28.000	1.250	30.000	1.250	32.000	1.500
TF2	30.000	1.250	30.000	1.250	30.000	1.250	28.000	1.500	30.000	1.750	32.000	2.250
TF3	30.000	1.250	30.000	1.500	30.000	1.750	28.000	1.750	30.000	2.000	32.000	2.500
TF4	30.000	1.250	30.000	1.250	30.000	1.250	28.000	1.500	30.000	1.750	32.000	2.250
TF5	30.000	1.250	30.000	1.250	30.000	1.250	28.000	1.250	30.000	1.250	32.000	1.500

✳✳ ALL DIMENSIONS ARE IN INCHES.

NCHRP 12-79

BRIDGE NISSS56

GIRDER ELEVATION TABLES

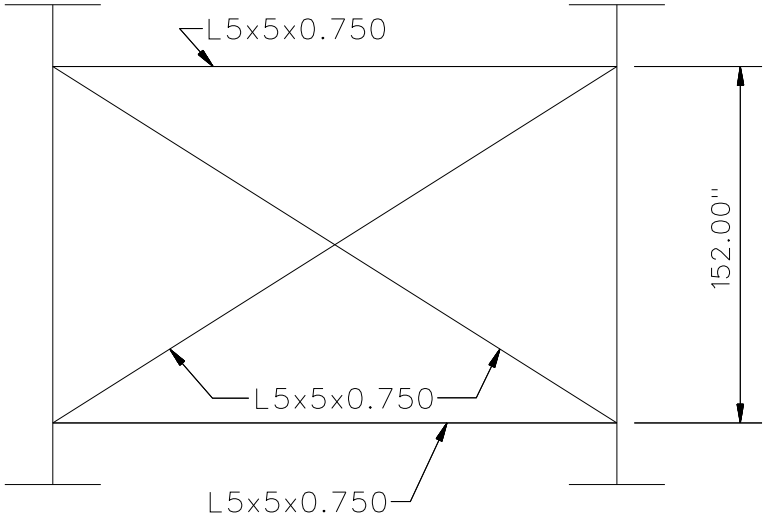

TYPICAL END AND INTERMEDIATE DIAPHRAGM

NOTES:

1. STEEL DEAD LOAD INCREASED BY 5% FOR MDX AND LARSA MODELS; 2% FOR 3D MODEL; AND 10% FOR APPROXIMATE ANALYSIS TO ACCOUNT FOR MISC. DETAILS.

2. FORMWORK LOAD OF 10PSF IS INCLUDED IN CONCRETE DEAD LOAD.

3. ADDITIONAL DESIGN PARAMETERS:
   A. 1.500' PARAPET WIDTH BOTH SIDES.
   B. 700 LB/FT UNIFORM LOAD ASSUMED FOR PARAPET WEIGHT.
   C. ROADWAY WIDTH = 77.000'.
   D. NUMBER OF DESIGN LANES = 6.
   E. HL93 LIVE LOAD.

4. DIAPHRAGM MEMBER CALL-OUTS ARE IN UNITS OF INCHES.

NCHRP 12-79

BRIDGE NISSS56

MISC. DETAILS AND NOTES

SHEET 4 OF 7

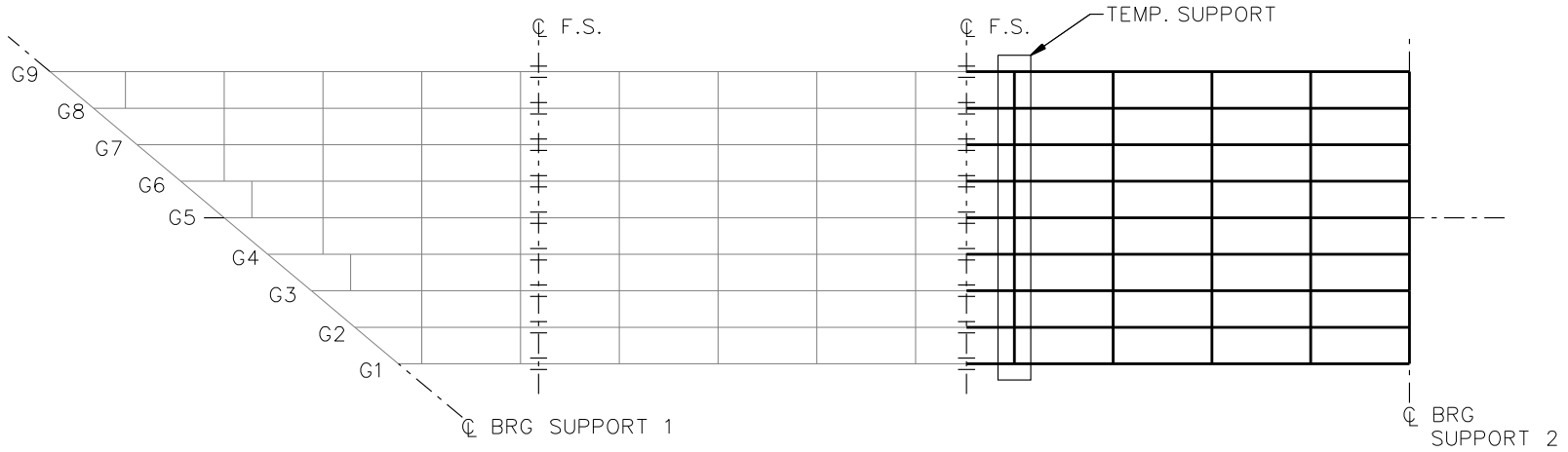

STAGE 9

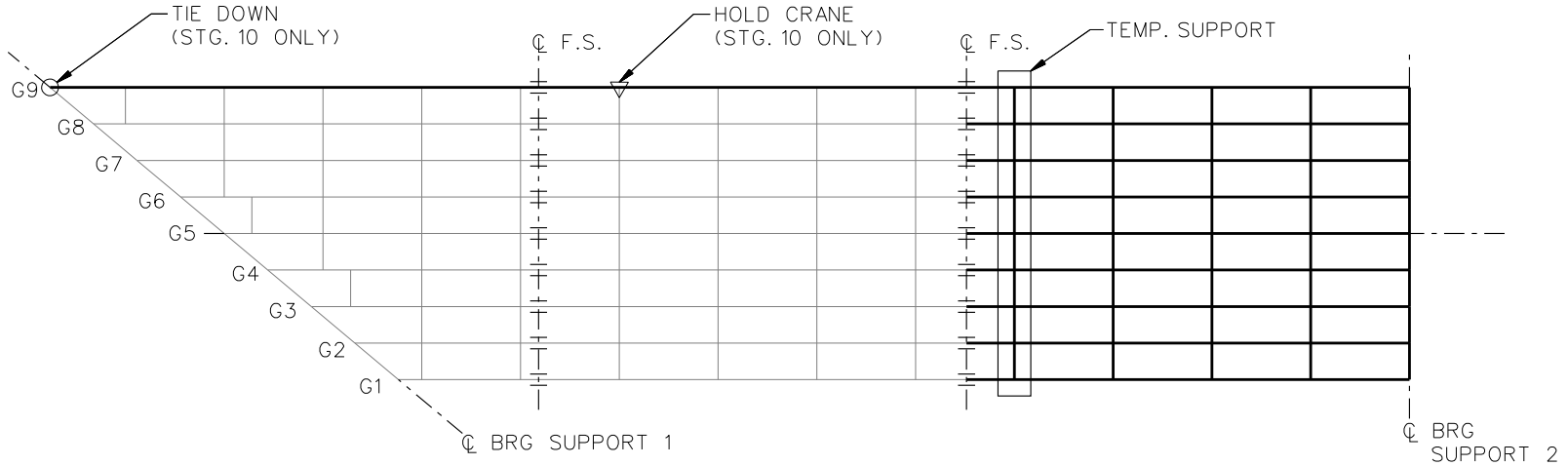

STAGE 10

LEGEND

▽ = HOLD OR LIFT CRANE

○ = TIE DOWN

□ = TEMPORARY SUPPORT STRUCTURE

NCHRP 12-79

BRIDGE NISSS56

GENERAL ERECTION PROCEDURE

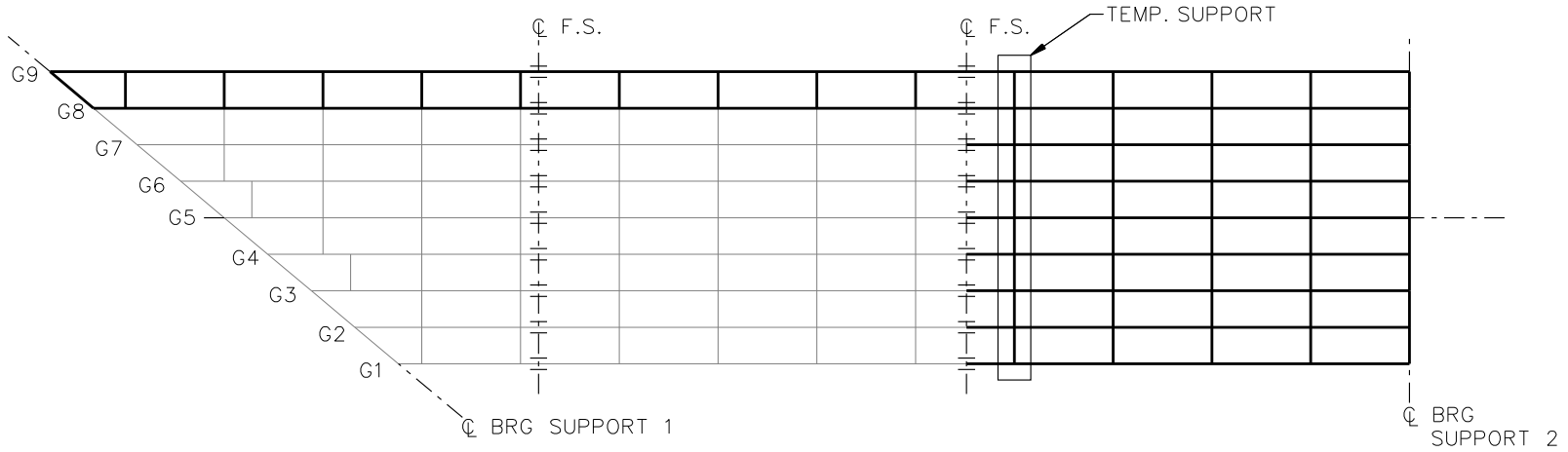

STAGE 11

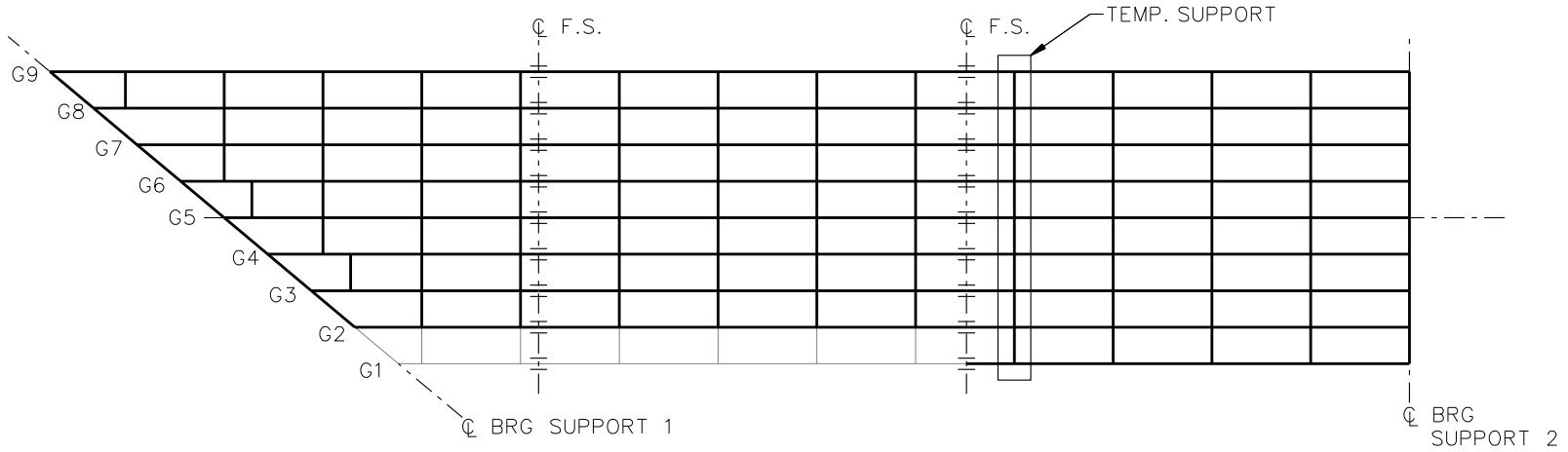

STAGE 17

LEGEND

▽ = HOLD OR LIFT CRANE

○ = TIE DOWN

□ = TEMPORARY SUPPORT STRUCTURE

NCHRP 12-79

BRIDGE NISSS56

GENERAL ERECTION PROCEDURE

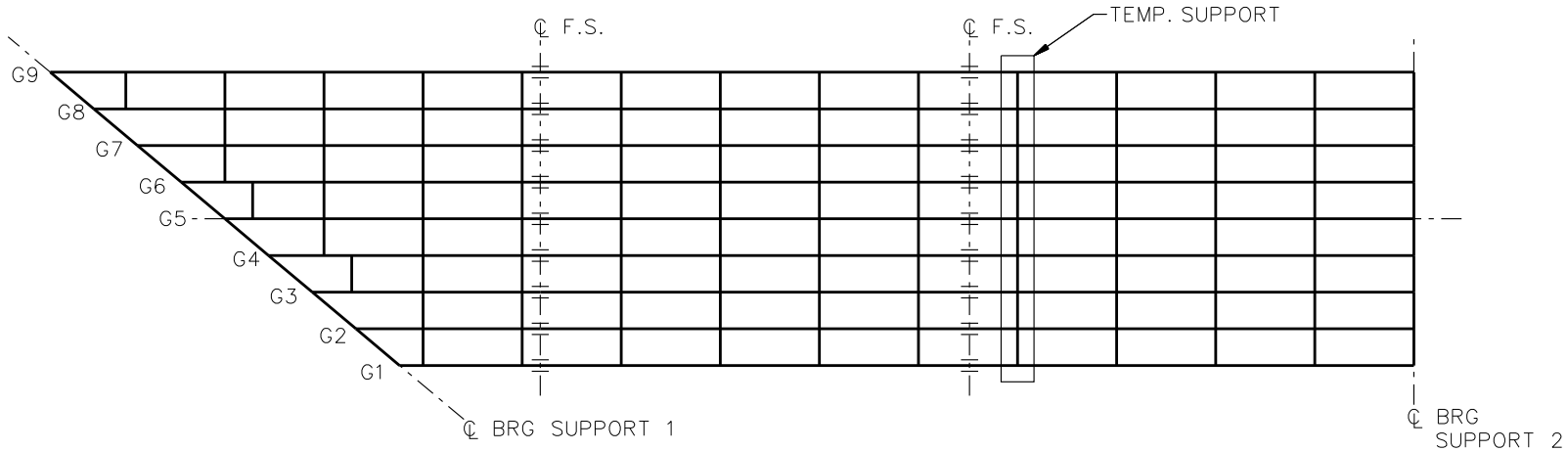

STAGE 18

LEGEND

▽ = HOLD OR LIFT CRANE

○ = TIE DOWN

□ = TEMPORARY SUPPORT STRUCTURE

NCHRP 12-79

BRIDGE NISSS56

GENERAL ERECTION PROCEDURE

NCHRP 12-79

NTCCR1

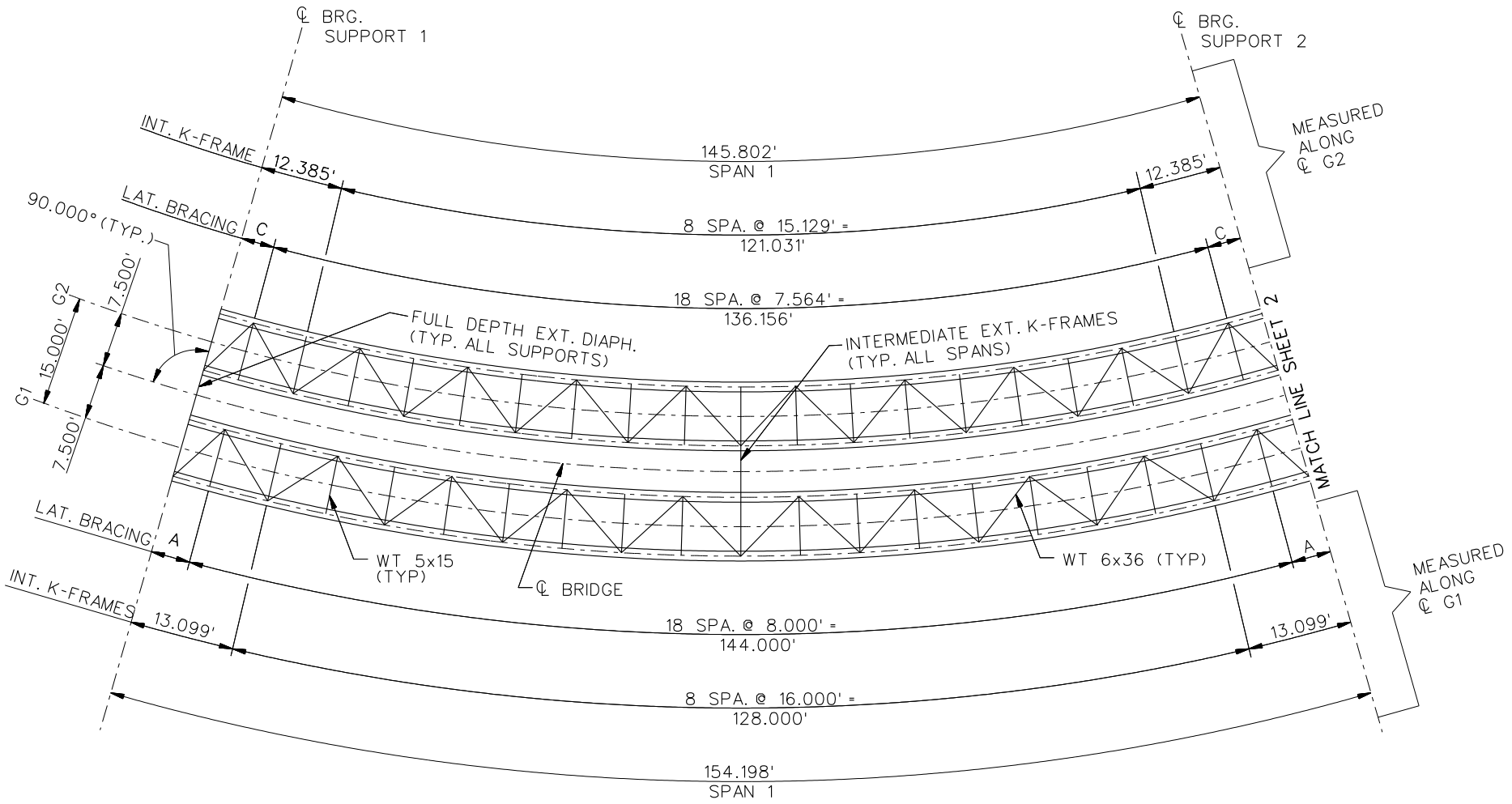

FRAMING PLAN

NOTES:

1. TYP. INTERNAL K-FRAME CONNECTION L = 0.875"x6.000'.
2. ALL BRG. STIFFENERS = 1.5000"x12.000".
3. DIMENSIONS: A = 5.099', B = 5.677', C = 4.823', D = 5.370.

NCHRP 12-79

BRIDGE NTCCR1

FRAMING PLAN AND CROSS-SECTION

SHEET 1 OF 13

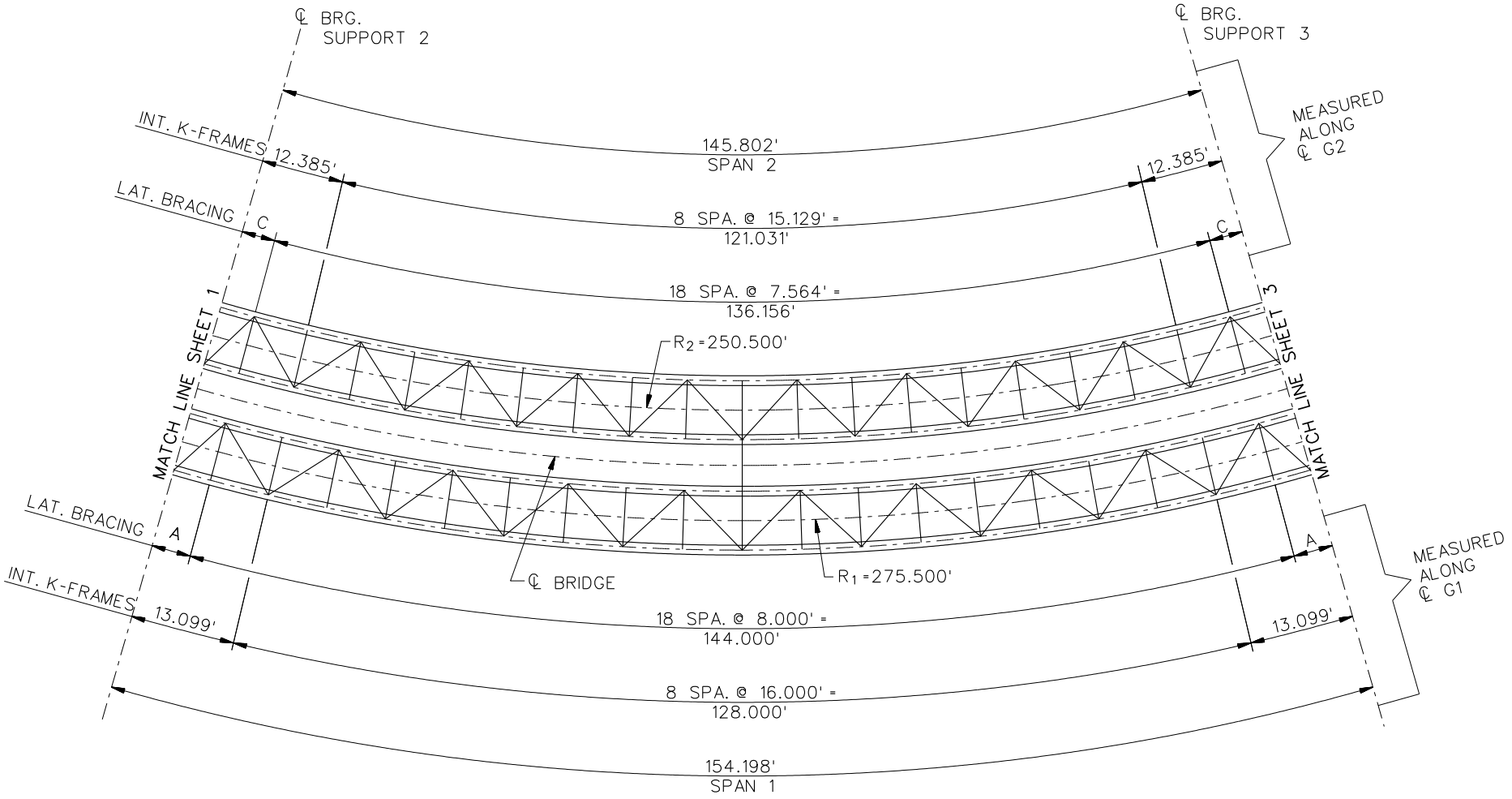

FRAMING PLAN

NOTES:
1. TYP. INTERNAL K-FRAME CONNECTION L = 0.875"x6.000'.
2. ALL BRG. STIFFENERS = 1.5000"x12.000".
3. DIMENSIONS: A = 5.099', B = 5.677', C = 4.823, D = 5.370.

NCHRP 12-79

BRIDGE NTCCR1

FRAMING PLAN AND CROSS-SECTION

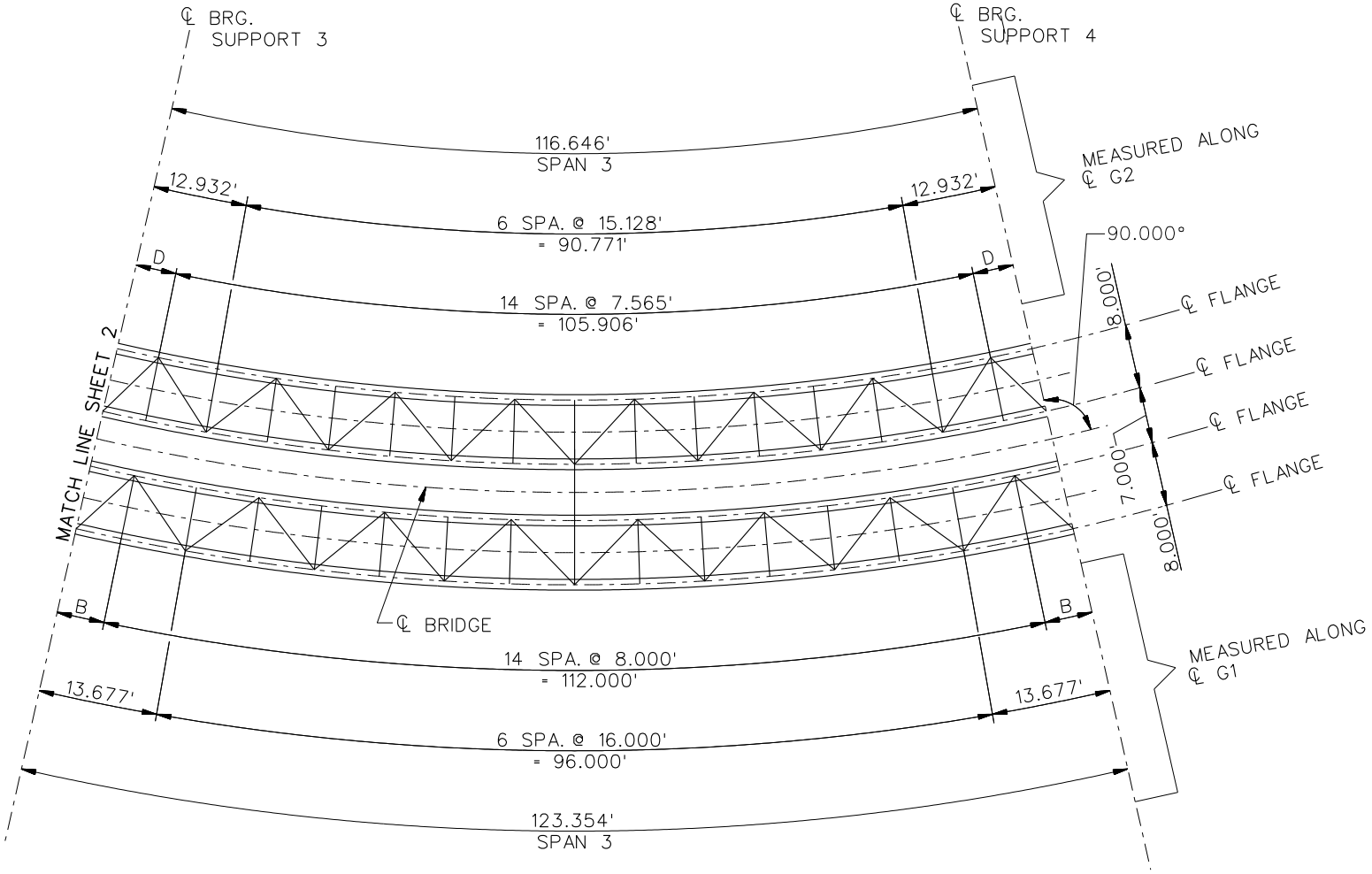

FRAMING PLAN

NOTES:
1. TYP. INTERNAL K-FRAME CONNECTION L = 0.875"x6.000'.
2. ALL BRG. STIFFENERS = 1.5000"x12.000".
3. DIMENSIONS: A = 5.099', B = 5.677', C = 4.823,
   D = 5.370.

NCHRP 12-79

BRIDGE NTCCR1

FRAMING PLAN AND CROSS-SECTION

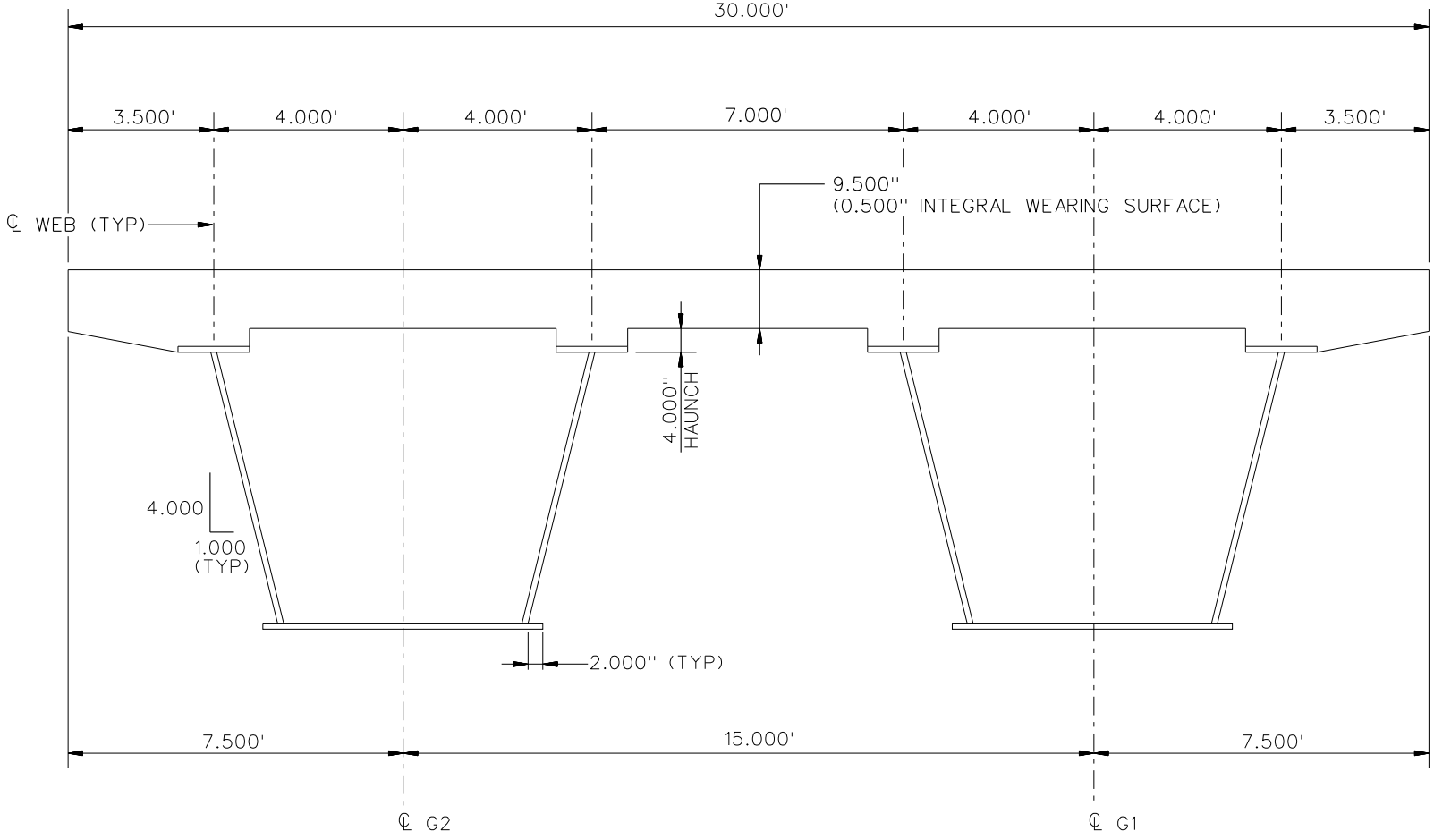

CROSS - SECTION

NCHRP 12-79

BRIDGE NTCCR1

TYPICAL SECTION

SHEET 4 OF 13

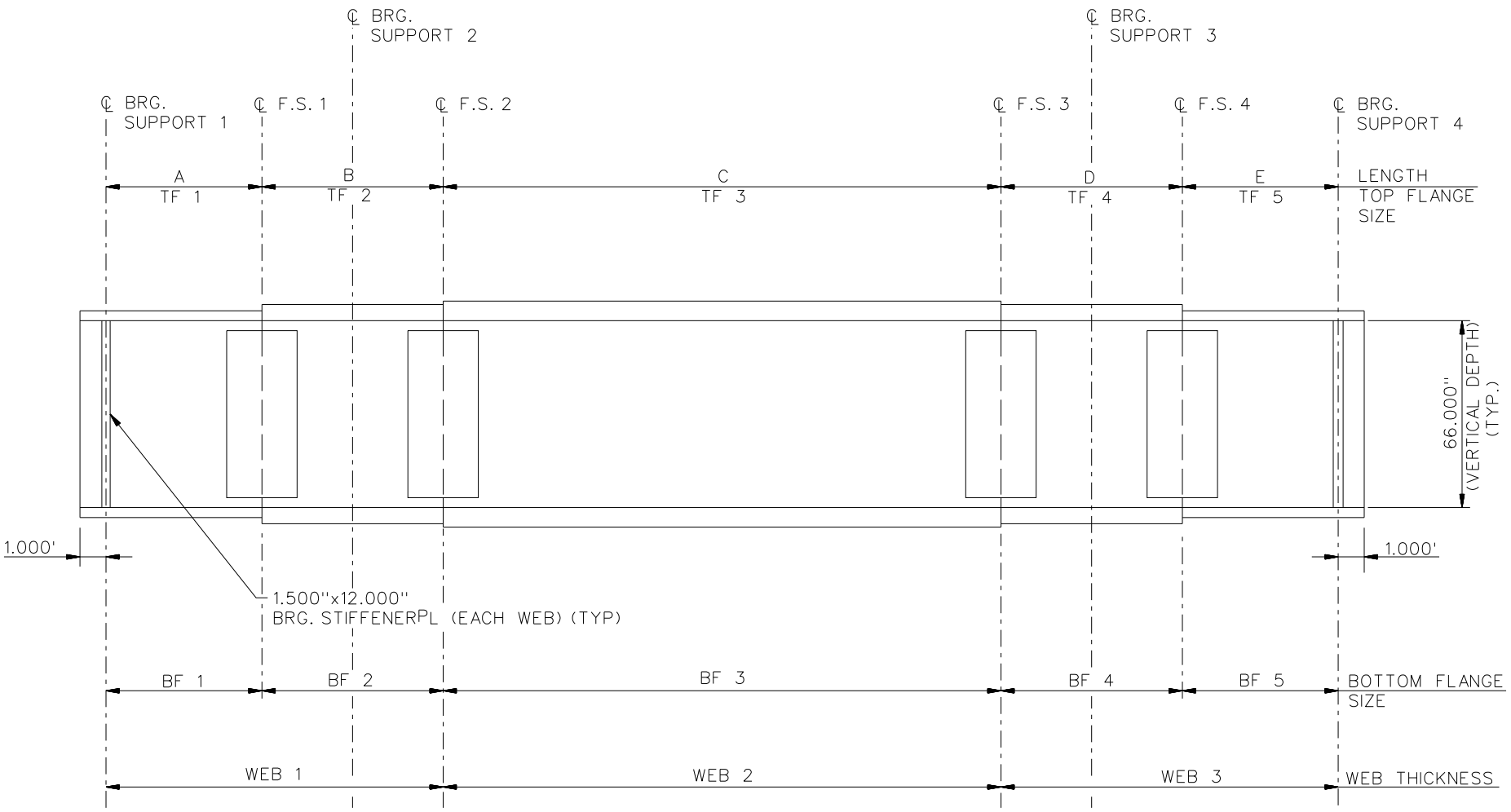

NOTES:

1. SEE TABLES ON SHEET 6 FOR GIRDER ELEVATION DIMENSIONS AND PLATE SIZES.
2. WEB 1 = WEB 2 = WEB 3 = 66.000"x0.6875" FOR G1
3. WEB 1 = WEB 2 = WEB 3 = 66.000"x0.6250" FOR G2

NCHRP 12-79

BRIDGE NTCCR1

GIRDER ELEVATION

	GIRDER PLATE LENGTHS ✳	
LENGTH	G1	G2
A	112.000	108.000
B	90.000	83.000
C	71.000	69.000
D	67.000	64.000
E	91.750	84.250

✳ ALL DIMENSIONS ARE IN FEET.

	GIRDER FLANGE DIMENSIONS ✳✳			
TOP	G1		G2	
FLANGE	BF	TF	BF	TF
TF1	16.000	0.875	16.000	0.875
TF2	16.000	2.125	16.000	1.625
TF3	16.000	0.875	16.000	0.875
TF4	16.000	1.375	16.000	1.250
TF5	16.000	0.875	16.000	0.875

✳✳ ALL DIMENSIONS ARE IN INCHES.

	GIRDER FLANGE DIMENSIONS ✳✳			
BOTTOM	G1		G2	
FLANGE	BF	TF	BF	TF
BF1	67.000	0.875	67.000	0.875
BF2	67.000	1.750	67.000	1.375
BF3	67.000	0.875	67.000	0.875
BF4	67.000	1.250	67.000	1.125
BF5	67.000	0.875	67.000	0.875

✳✳ ALL DIMENSIONS ARE IN INCHES.

NCHRP 12-79

BRIDGE NTCCR1

GIRDER ELEVATION TABLES

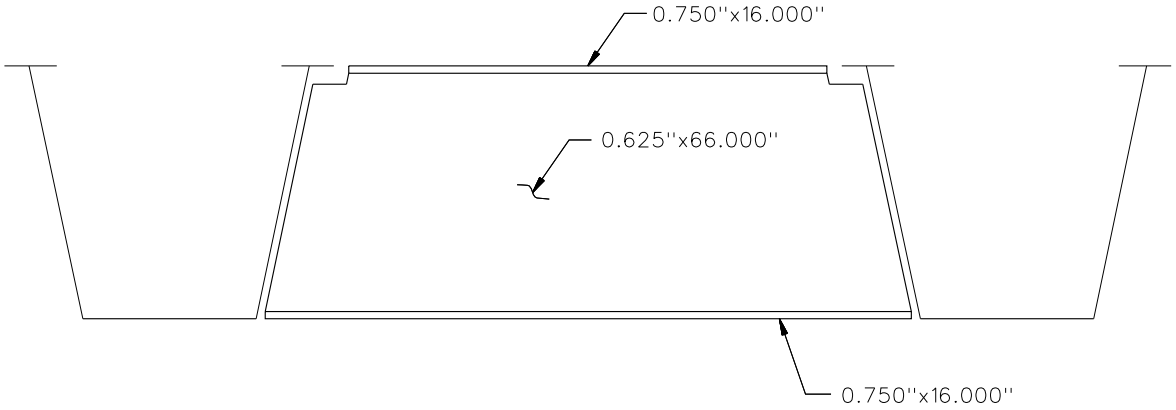

TYPICAL END DIAPHRAGM

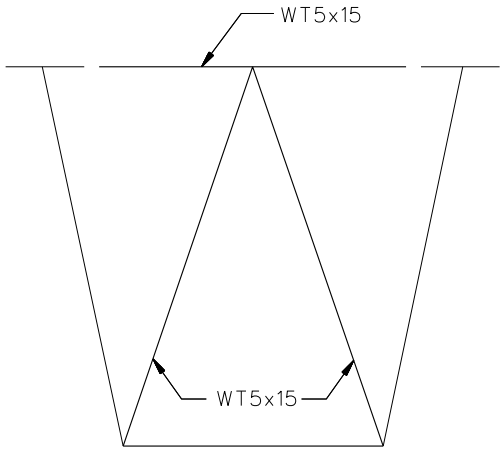

TYPICAL INTERNAL CROSS FRAME

NOTES:

1. STEEL DEAD LOAD INCREASED BY 15% FOR MDX AND LARSA MODELS; 2% FOR 3D MODEL; AND 20% FOR APPROXIMATE ANALYSIS TO ACCOUNT FOR MISC. DETAILS.

2. FORMWORK LOAD OF 10PSF IS INCLUDED IN CONCRETE DEAD LOAD.

3. ADDITIONAL DESIGN PARAMETERS:
   A. 1.500' PARAPET WIDTH BOTH SIDES.
   B. 700 LB/FT UNIFORM LOAD ASSUMED FOR PARAPET WEIGHT.
   C. ROADWAY WIDTH = 26.500'.
   D. NUMBER OF DESIGN LANES = 2.
   E. HL93 LIVE LOAD.
   F. DESIGN SPEED = 35 MPH.

4. DIAPHRAGM MEMBER CALL-OUTS ARE IN ENGLISH UNITS.

NCHRP 12-79

BRIDGE NTCCR1

MISC. DETAILS AND NOTES

SHEET 7 OF 13

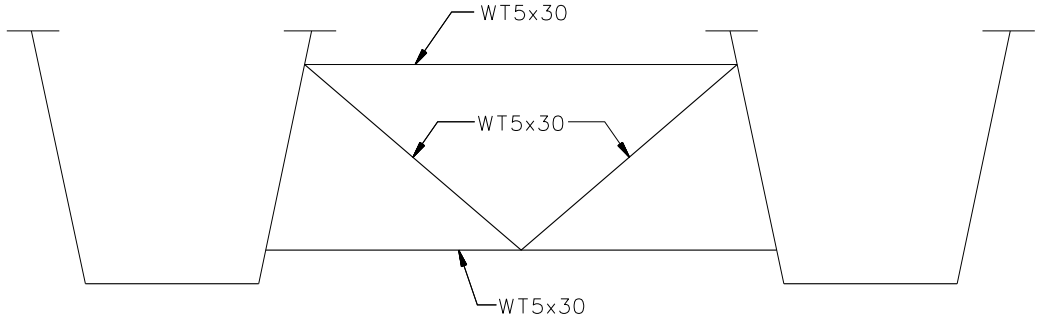

TYPICAL INTERMEDIATE EXTERNAL DIAPHRAGM

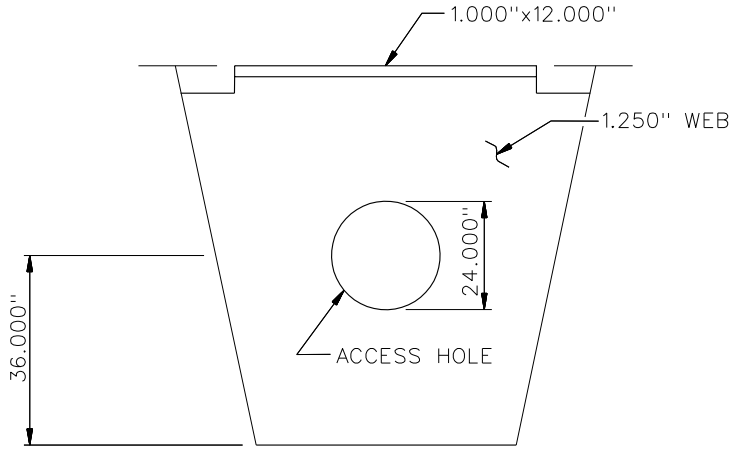

TYPICAL INTERNAL DIAPHRAGMS AT SUPPORTS

NCHRP 12-79

BRIDGE NTCCR1

MISC. DETAILS AND NOTES

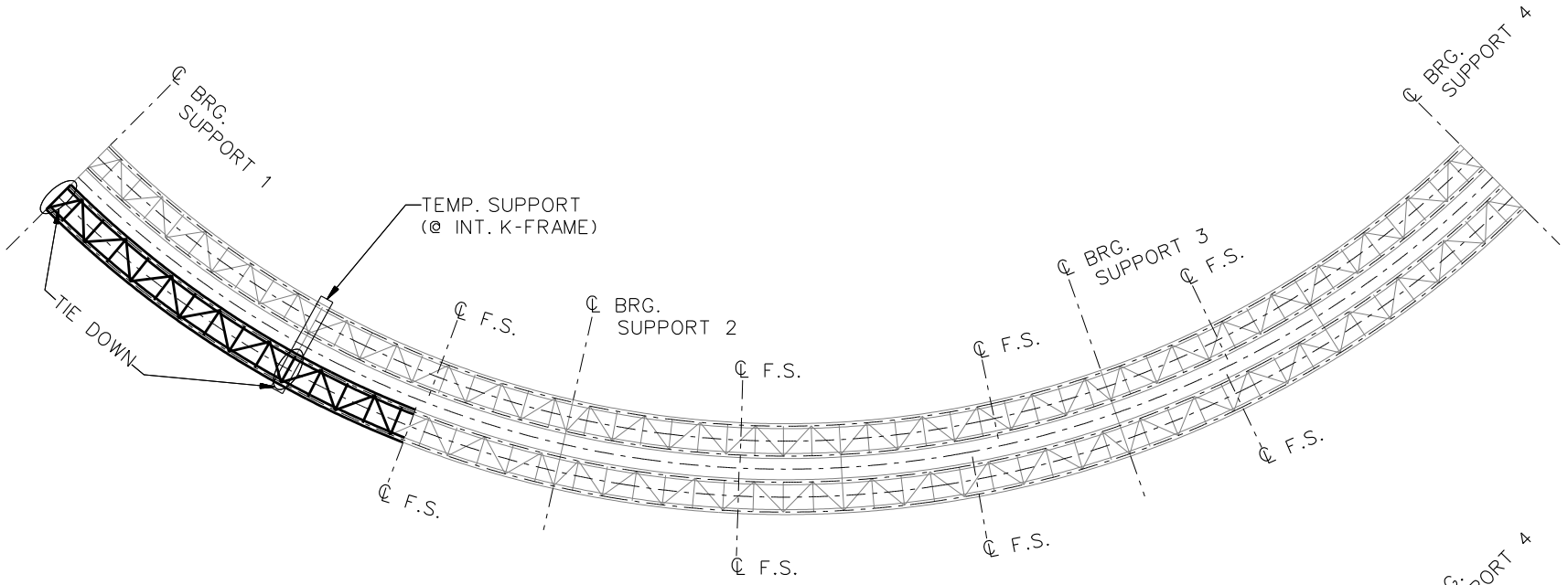

STAGE 1

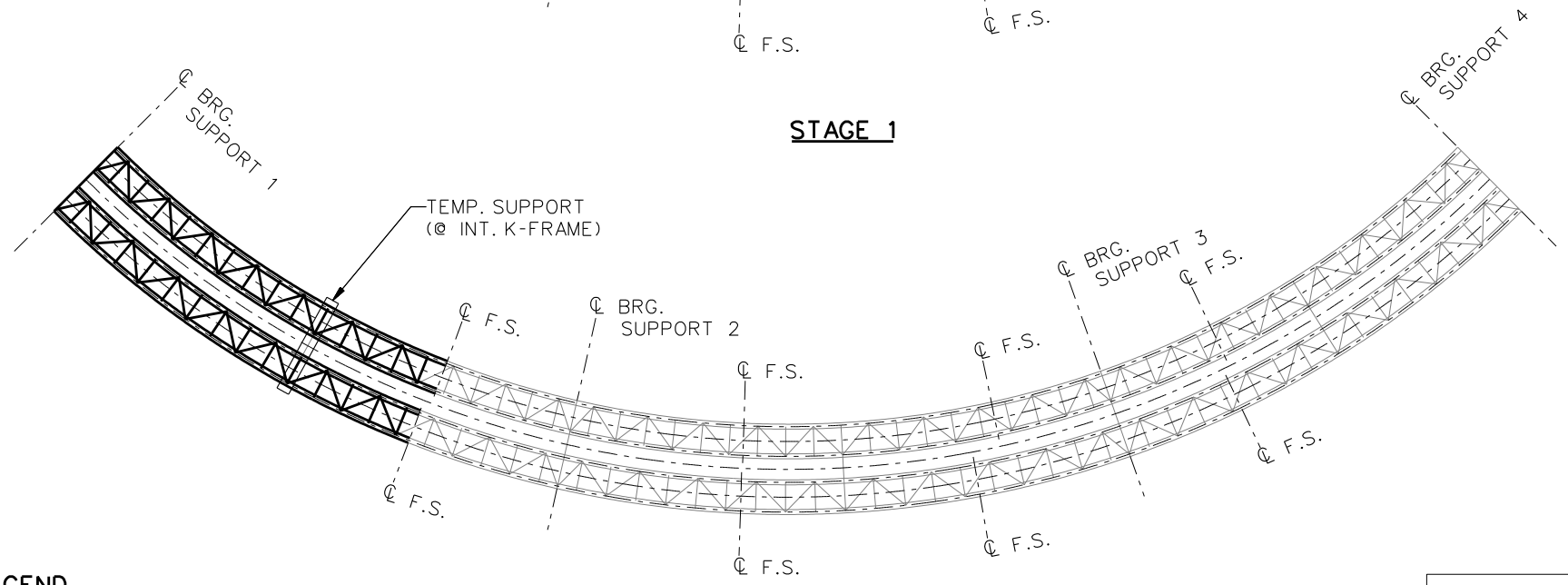

STAGE 2

LEGEND

▽ = HOLD OR LIFT CRANE

○ = TIE DOWN

□ = TEMPORARY SUPPORT STRUCTURE

NCHRP 12-79

BRIDGE NTCCR1

GENERAL ERECTION PROCEDURE

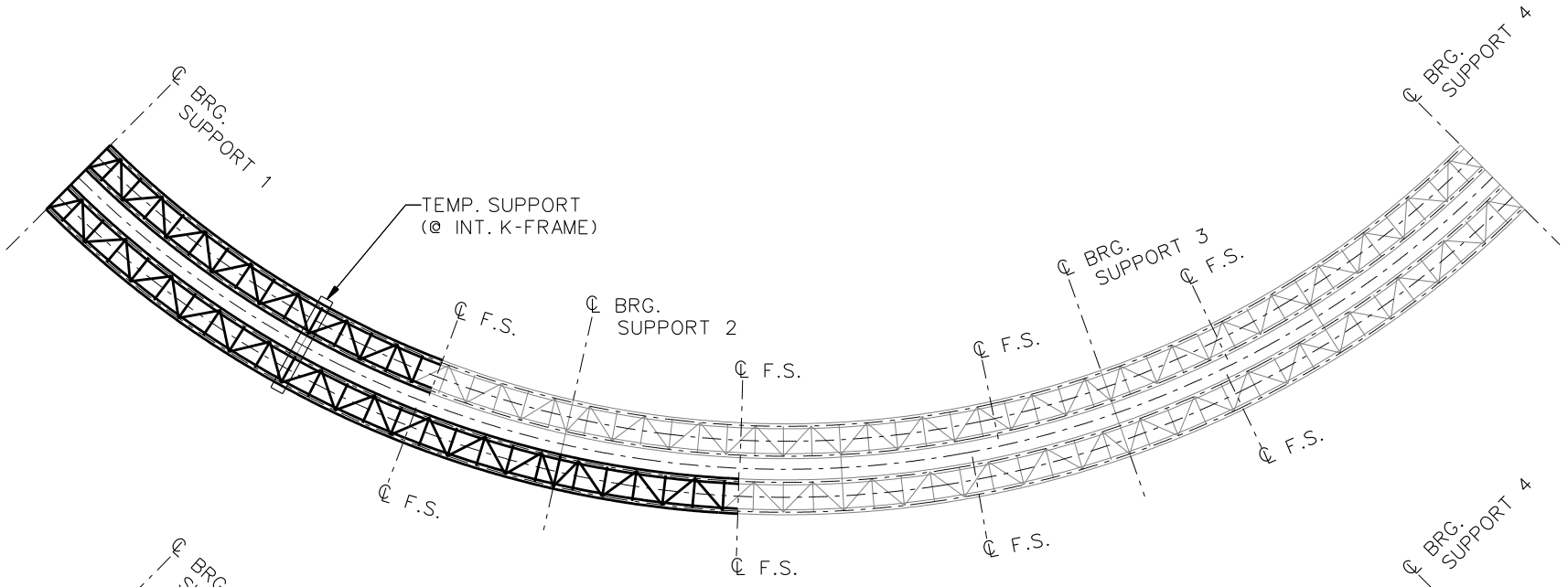

STAGE 3

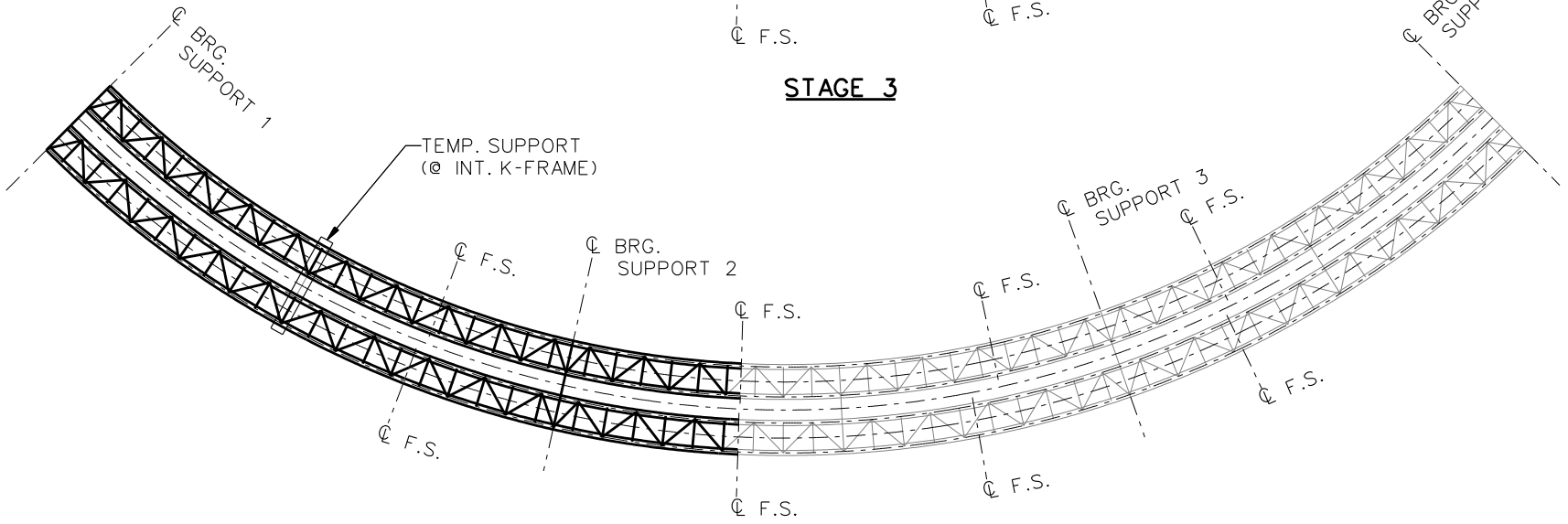

STAGE 4

LEGEND

▽ = HOLD OR LIFT CRANE

○ = TIE DOWN

□ = TEMPORARY SUPPORT STRUCTURE

STAGE 5

REMOVE TEMP. SUPPORT IN SPAN #1

NCHRP 12-79

BRIDGE NTCCR1

GENERAL ERECTION PROCEDURE

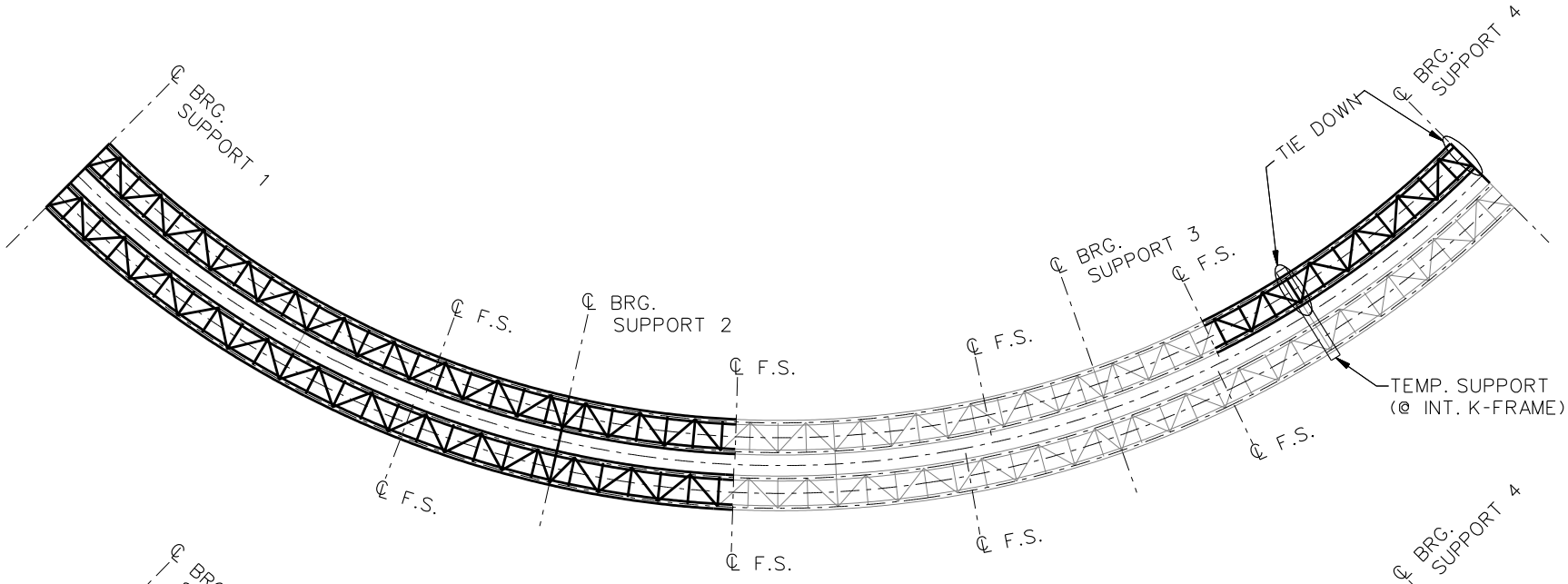

STAGE 6
(RESULTS REQ'D)

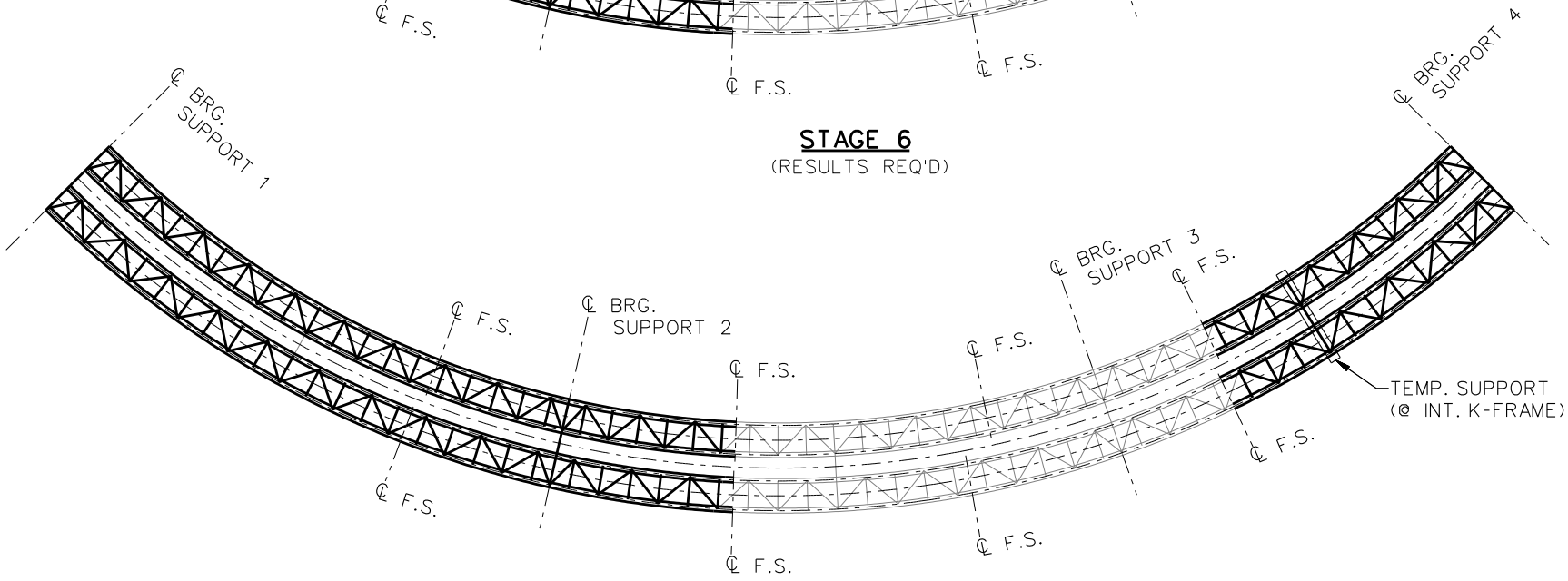

STAGE 7

LEGEND

▽ = HOLD OR LIFT CRANE

○ = TIE DOWN

□ = TEMPORARY SUPPORT STRUCTURE

NCHRP 12-79

BRIDGE NTCCR1

GENERAL ERECTION PROCEDURE

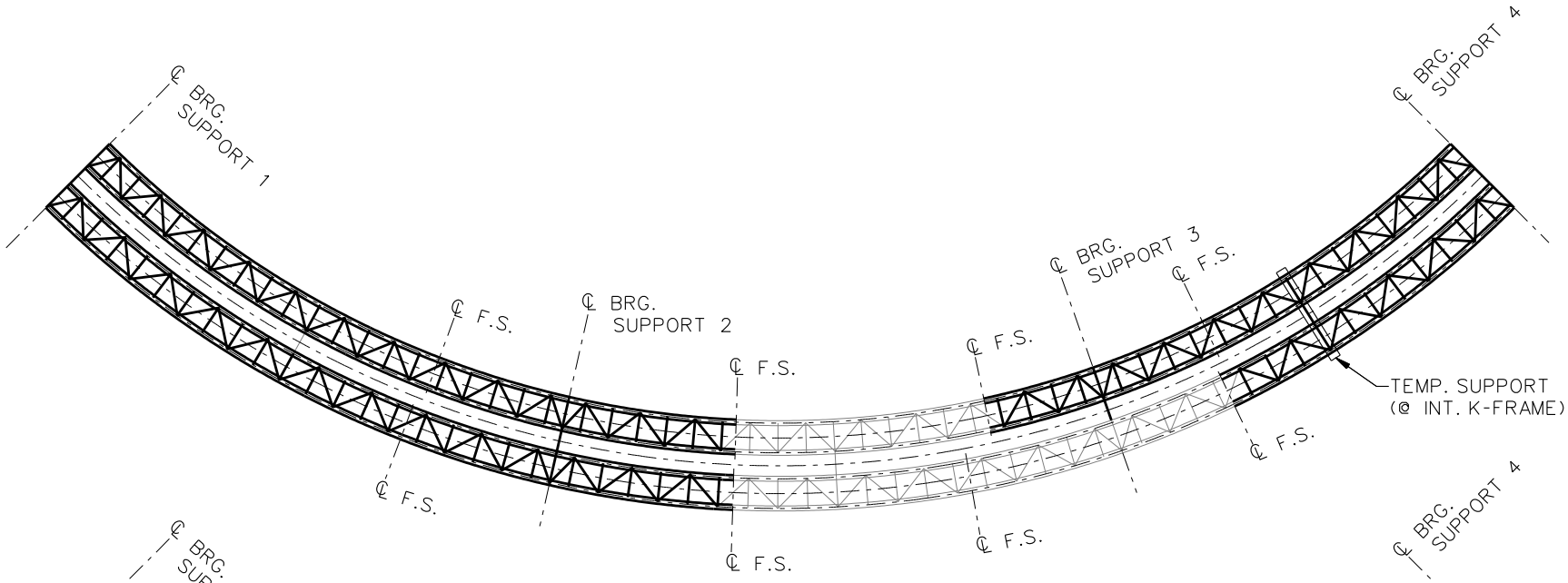

STAGE 8

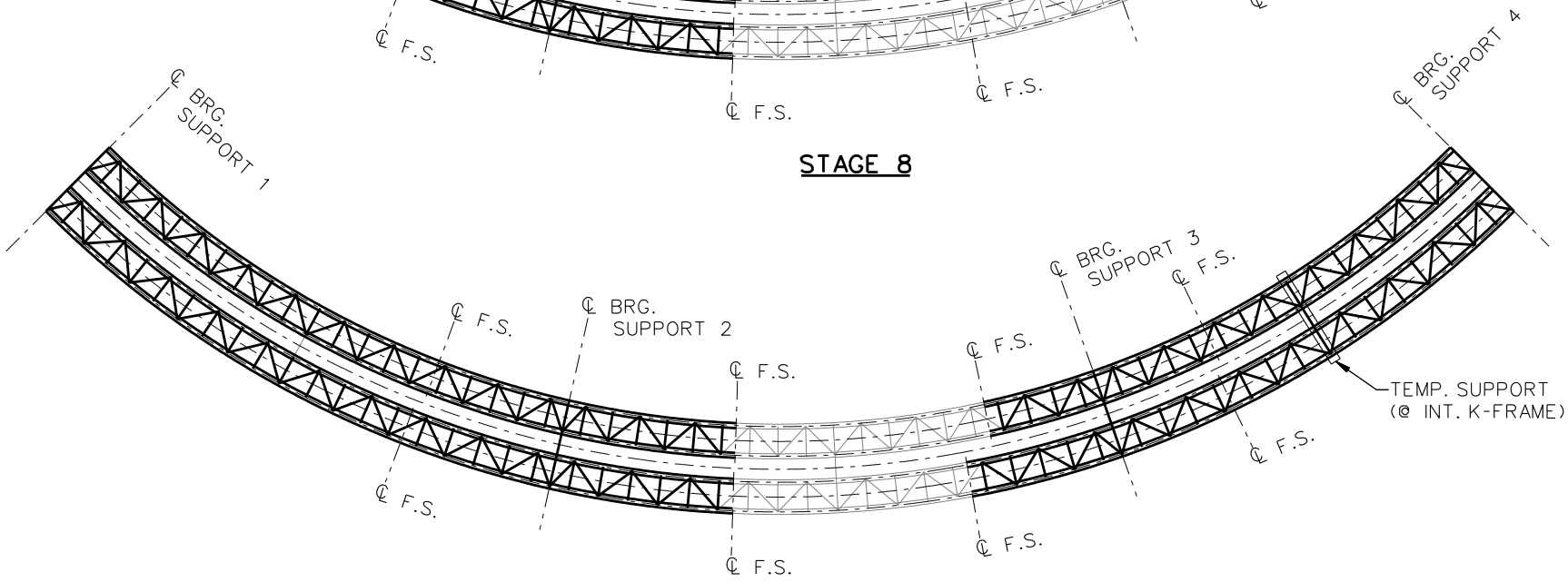

STAGE 9

LEGEND

▽ = HOLD OR LIFT CRANE

○ = TIE DOWN

□ = TEMPORARY SUPPORT STRUCTURE

STAGE 10

REMOVE TEMP. SUPPORT IN SPAN #3

NCHRP 12-79

BRIDGE NTCCR1

GENERAL ERECTION PROCEDURE

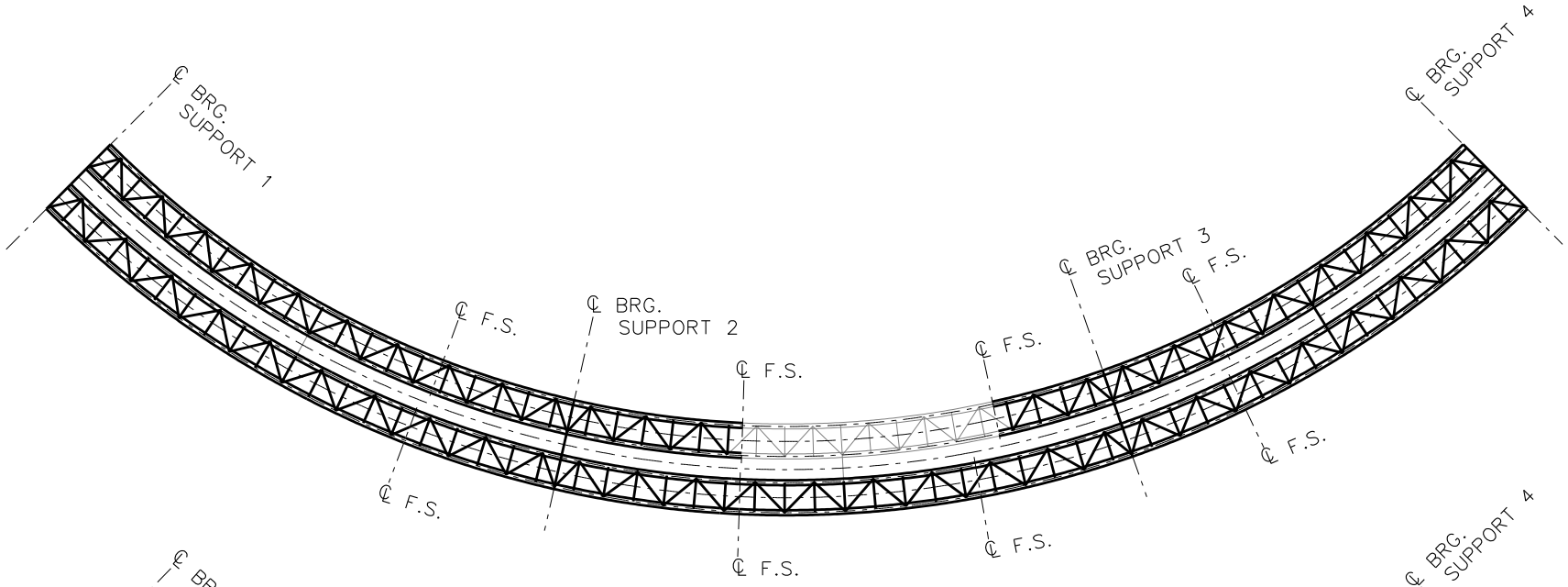

STAGE 11

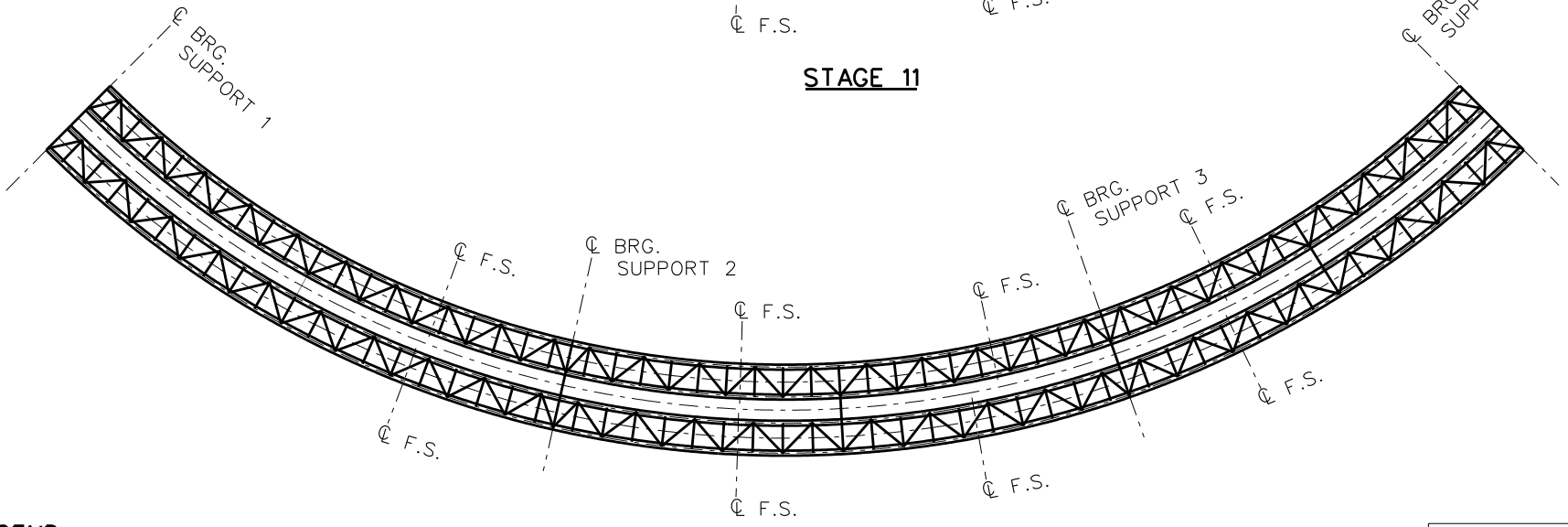

STAGE 12

LEGEND

▽ = HOLD OR LIFT CRANE

○ = TIE DOWN

□ = TEMPORARY SUPPORT STRUCTURE

NCHRP 12-79

BRIDGE NTCCR1

GENERAL ERECTION PROCEDURE

SHEET 13 OF 13

NCHRP 12-79

NTCCR5

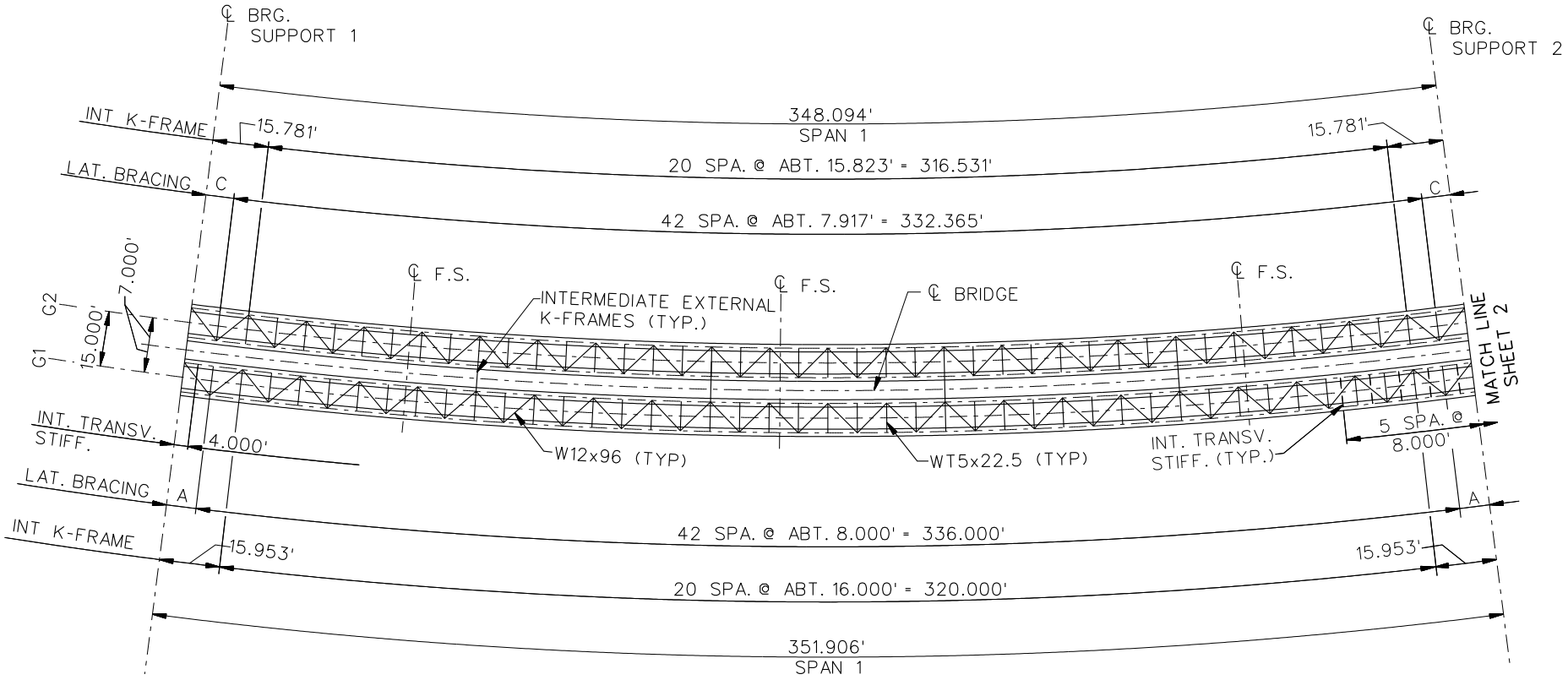

FRAMING PLAN

NOTE:

1. INT. TRANSV. STIFFS. AND INTERNAL K-FRAME CONNECTION PLATES = 0.875"x6.000"

2. DIMENSIONS
   A = 7.953'
   B = 4.760'
   C = 7.865'
   D = 4.708'

NCHRP 12-79

BRIDGE NTCCR5

FRAMING PLAN AND CROSS-SECTION

SHEET 1 OF 20

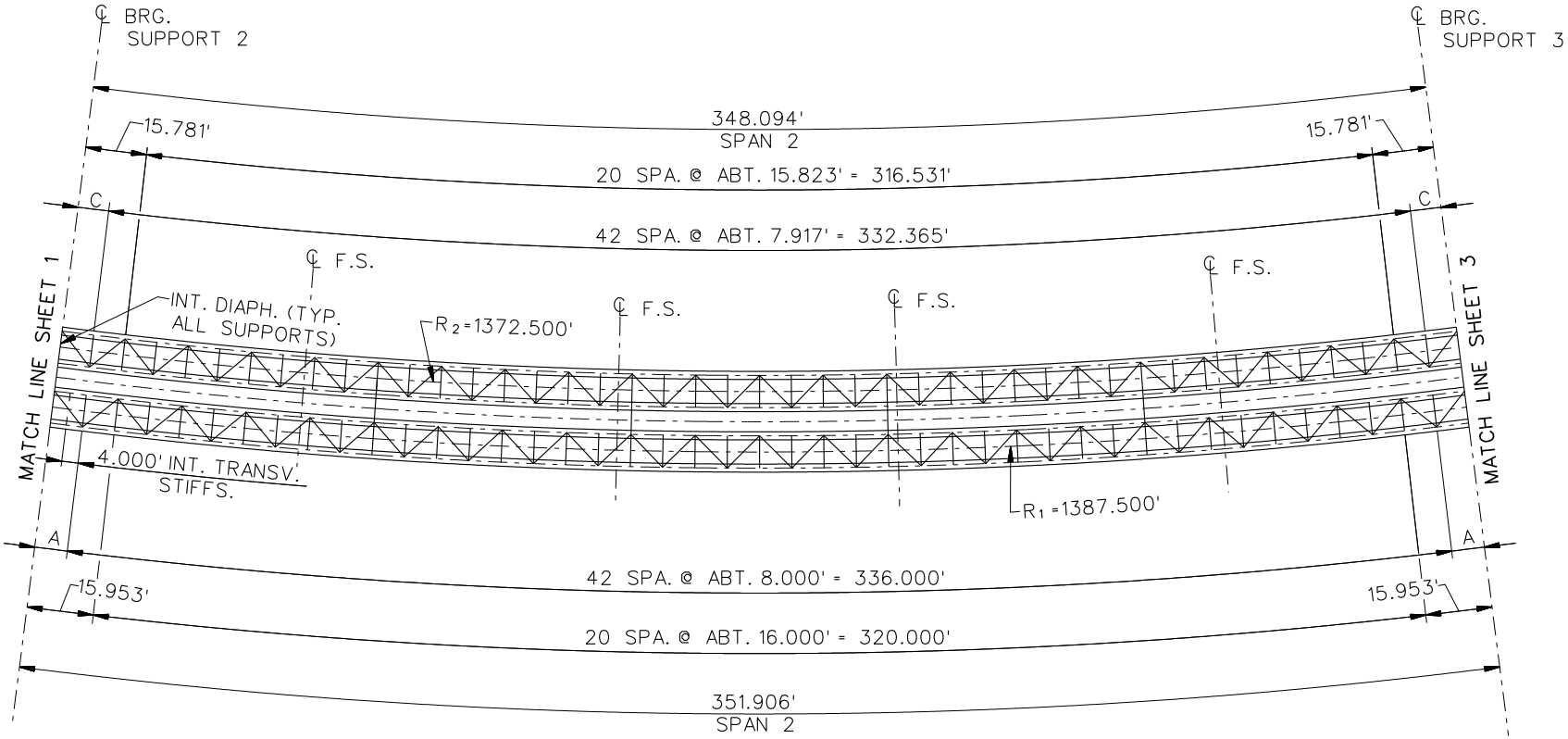

FRAMING PLAN

NCHRP 12-79

BRIDGE NTCCR5

FRAMING PLAN AND CROSS-SECTION

SHEET 2 OF 20

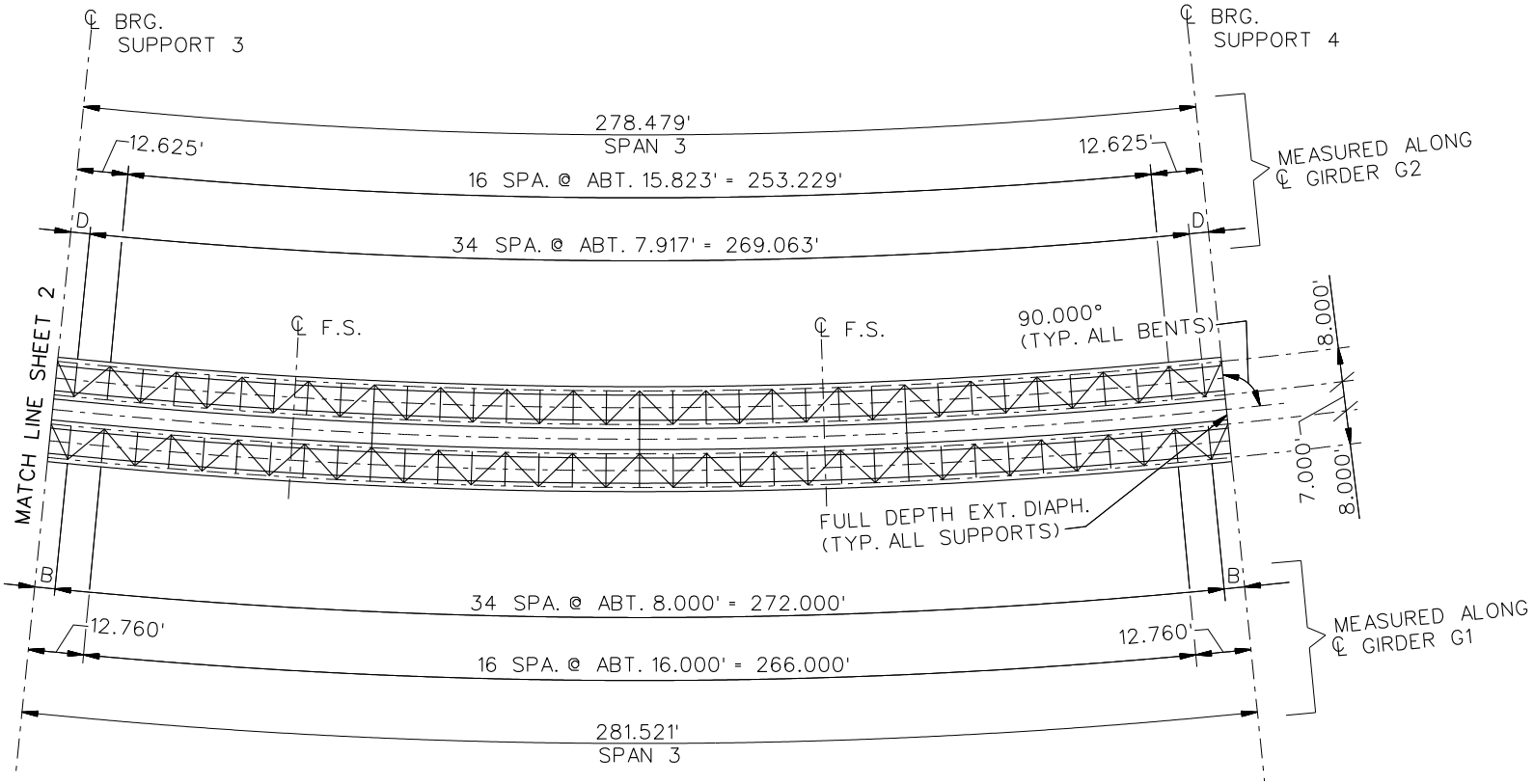

FRAMING PLAN

NCHRP 12-79

BRIDGE NTCCR5

FRAMING PLAN AND CROSS-SECTION

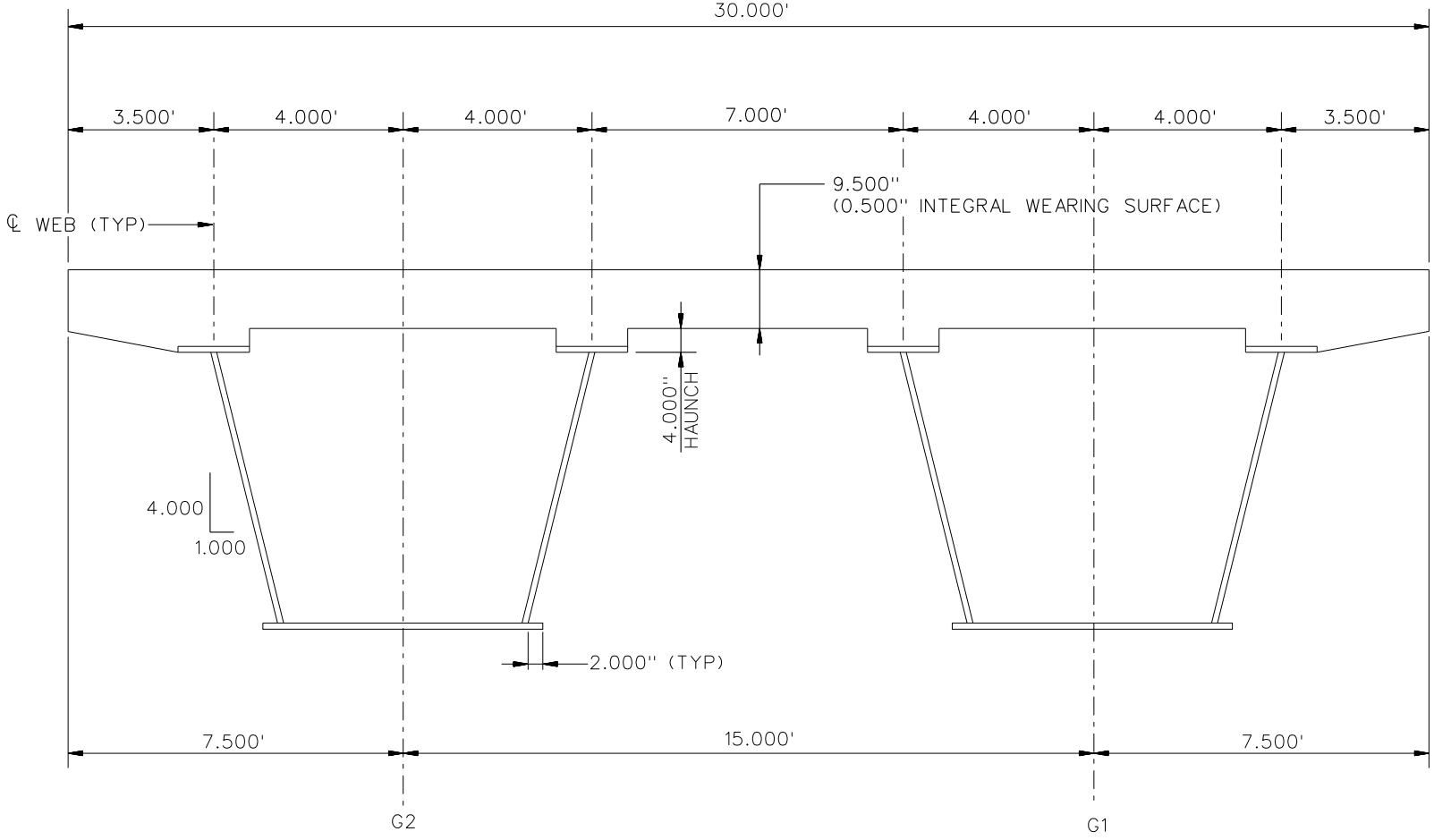

CROSS - SECTION

NCHRP 12-79

BRIDGE NTCCR5

TYPICAL SECTION

SHEET 4 OF 20

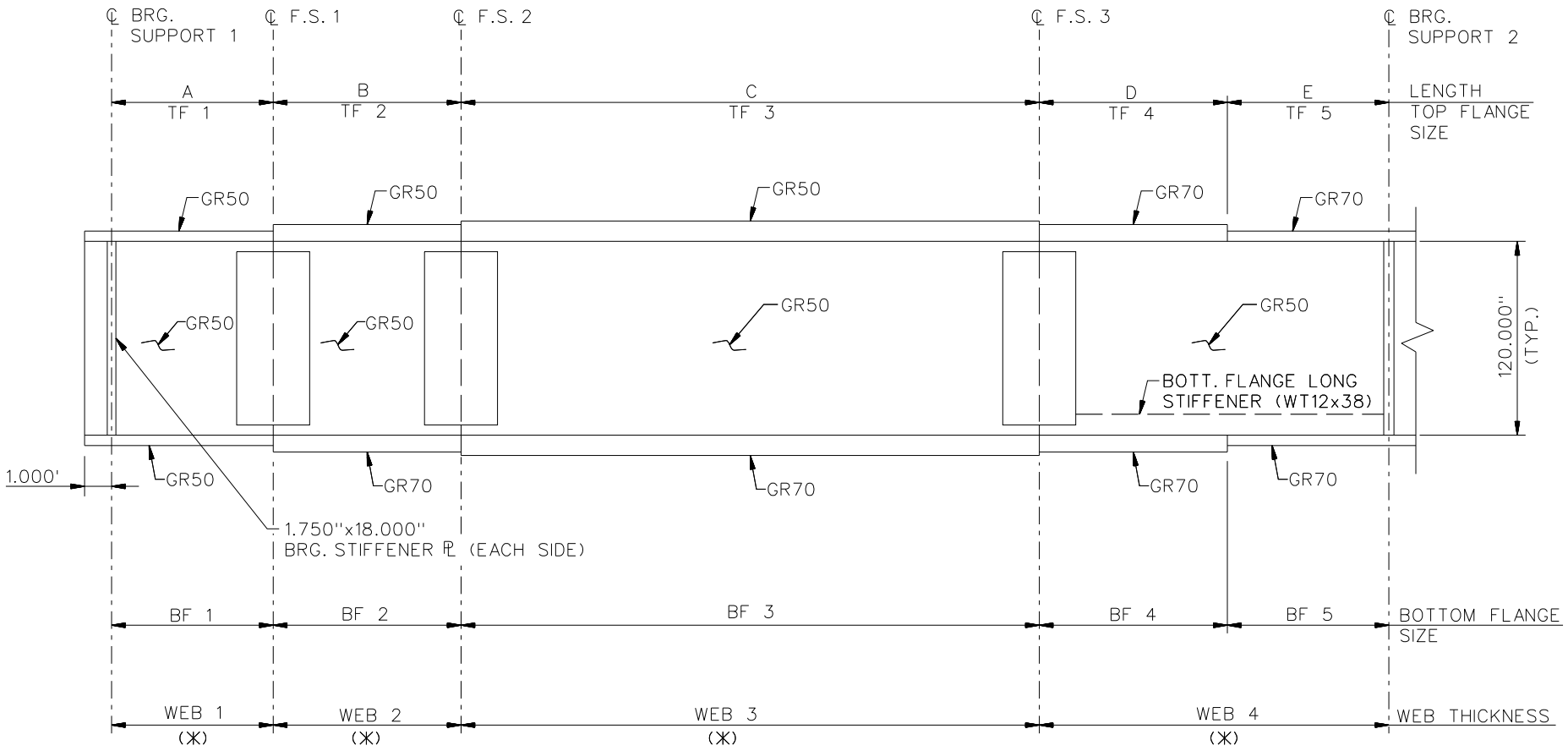

(*)	G1	G2
WEB 1	1.063"	1.063"
WEB 2	0.938"	0.938"
WEB 3	1.063"	1.063"
WEB 4	1.063"	1.063"

NOTES:

1. SEE TABLES ON SHEETS 8, 9 AND 10 FOR GIRDER ELEVATION DIMENSIONS AND PLATE SIZES.

NCHRP 12-79

BRIDGE NTCCR5

GIRDER ELEVATION (SPAN 1)

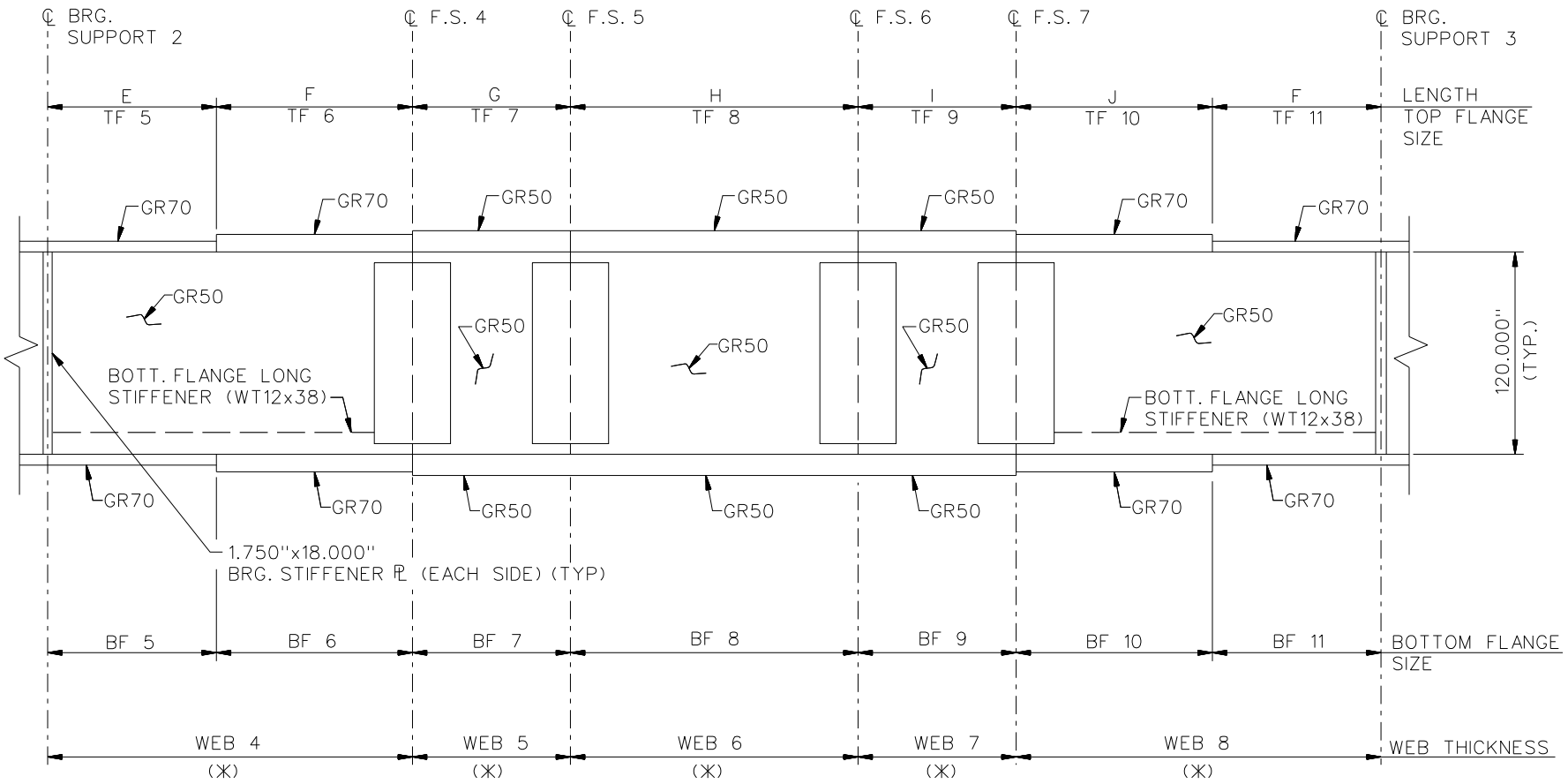

(*)	G1	G2
WEB 4	1.063"	1.063"
WEB 5	0.938"	0.938"
WEB 6	0.938"	0.938"
WEB 7	0.938"	0.938"
WEB 8	1.000"	1.000"

NOTES:

1. SEE TABLES ON SHEETS 8, 9 AND 10 FOR GIRDER ELEVATION DIMENSIONS AND PLATE SIZES.

NCHRP 12-79

BRIDGE NTCCR5

GIRDER ELEVATION (SPAN 2)

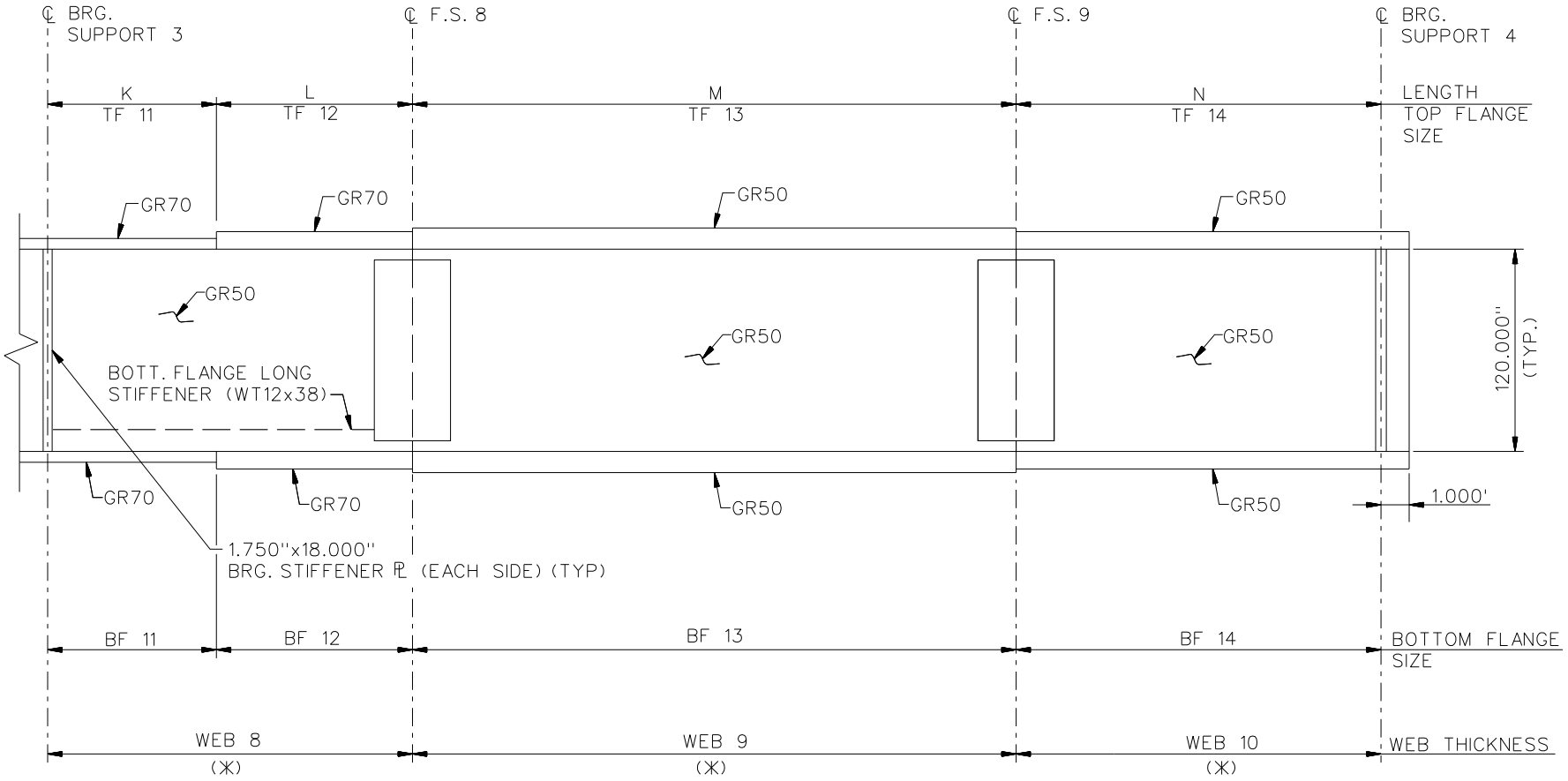

(*)	G1	G2
WEB 8	1.000"	1.000"
WEB 9	0.938"	0.938"
WEB 10	0.938"	0.938"

NOTES:

1. SEE TABLES ON SHEETS 8, 9 AND 10 FOR GIRDER ELEVATION DIMENSIONS AND PLATE SIZES.

NCHRP 12-79

BRIDGE NTCCR5

GIRDER ELEVATION (SPAN 3)

	GIRDER PLATE LENGTHS ✳	
LENGTH	G1	G2
A	66.900	60.100
B	96.000	101.000
C	128.000	126.000
D	32.000	32.000
E	58.000	58.000

✳ ALL DIMENSIONS ARE IN FEET.

	GIRDER FLANGE DIMENSIONS ✳✳			
TOP	G1		G2	
FLANGE	BF	TF	BF	TF
TF1	24.000	1.250	24.000	1.250
TF2	24.000	1.750	24.000	1.750
TF3	24.000	1.750	24.000	1.750
TF4	24.000	1.750	24.000	1.750
TF5	24.000	2.500	24.000	2.250

✳✳ ALL DIMENSIONS ARE IN INCHES.

	GIRDER FLANGE DIMENSIONS ✳✳			
BOTTOM	G1		G2	
FLANGE	BF	TF	BF	TF
BF1	40.000	2.000	40.000	1.750
BF2	40.000	2.500	40.000	2.500
BF3	40.000	2.500	40.000	2.500
BF4	40.000	1.750	40.000	1.750
BF5	40.000	3.000	40.000	2.750

✳✳ ALL DIMENSIONS ARE IN INCHES.

NCHRP 12-79

BRIDGE NTCCR5

GIRDER ELEVATION TABLES (SPAN 1)

	GIRDER PLATE LENGTHS ✳	
LENGTH	G1	G2
F	32.000	32.000
G	80.000	78.000
H	69.900	69.100
I	80.000	80.000
J	31.000	30.000

✳ ALL DIMENSIONS ARE IN FEET.

	GIRDER FLANGE DIMENSIONS ✳✳			
TOP	G1		G2	
FLANGE	BF	TF	BF	TF
TF6	24.000	1.750	24.000	1.750
TF7	24.000	1.250	24.000	1.250
TF8	24.000	1.250	24.000	1.250
TF9	24.000	1.250	24.000	1.250
TF10	24.000	1.500	24.000	1.500

✳✳ ALL DIMENSIONS ARE IN INCHES.

	GIRDER FLANGE DIMENSIONS ✳✳			
BOTTOM	G1		G2	
FLANGE	BF	TF	BF	TF
BF6	40.000	1.750	40.000	1.750
BF7	40.000	1.250	40.000	1.250
BF8	40.000	1.250	40.000	1.250
BF9	40.000	1.250	40.000	1.250
BF10	40.000	1.750	40.000	1.500

✳✳ ALL DIMENSIONS ARE IN INCHES.

NCHRP 12-79

BRIDGE NTCCR5

GIRDER ELEVATION TABLES (SPAN 2)

	GIRDER PLATE LENGTHS ✳	
LENGTH	G1	G2
K	58.000	58.000
L	30.000	29.000
M	128.000	126.000
N	95.500	95.500

✳ ALL DIMENSIONS ARE IN FEET.

	GIRDER FLANGE DIMENSIONS ✳✳			
TOP	G1		G2	
FLANGE	BF	TF	BF	TF
TF11	24.000	2.250	24.000	2.000
TF12	24.000	1.500	24.000	1.500
TF13	24.000	1.250	24.000	1.250
TF14	24.000	1.250	24.000	1.250

✳✳ ALL DIMENSIONS ARE IN INCHES.

	GIRDER FLANGE DIMENSIONS ✳✳			
BOTTOM	G1		G2	
FLANGE	BF	TF	BF	TF
BF11	40.000	2.500	40.000	2.250
BF12	40.000	1.750	40.000	1.500
BF13	40.000	1.750	40.000	1.250
BF14	40.000	1.750	40.000	1.250

✳✳ ALL DIMENSIONS ARE IN INCHES.

NCHRP 12-79

BRIDGE NTCCR5

GIRDER ELEVATION TABLES (SPAN 3)

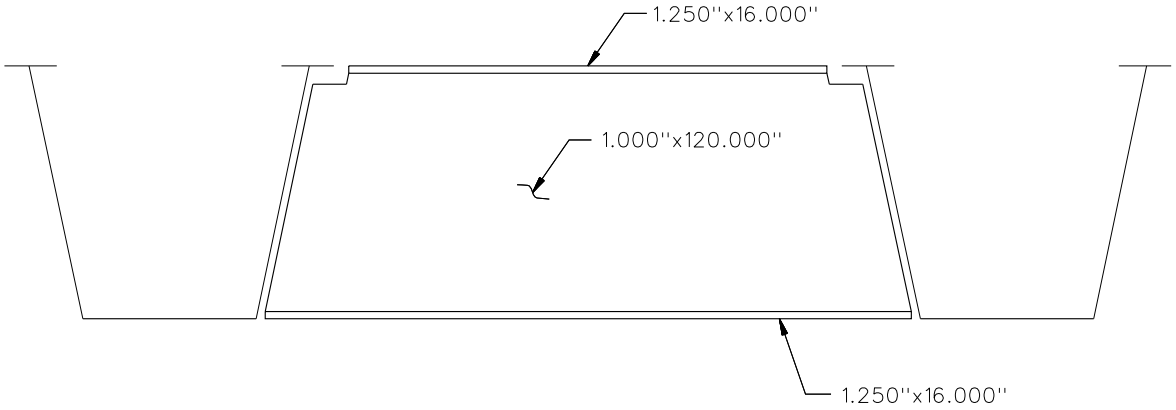

TYPICAL END DIAPHRAGM

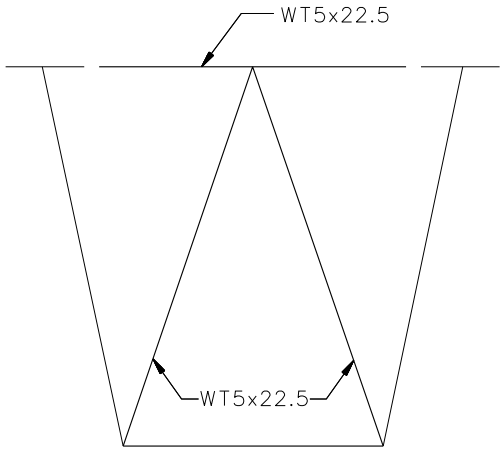

TYPICAL INTERNAL CROSS FRAME

NOTES:

1. STEEL DEAD LOAD INCREASED BY 15% FOR MDX AND LARSA MODELS; 2% FOR 3D MODEL; AND 20% FOR APPROXIMATE ANALYSIS TO ACCOUNT FOR MISC. DETAILS.

2. FORMWORK LOAD OF 10PSF IS INCLUDED IN CONCRETE DEAD LOAD.

3. ADDITIONAL DESIGN PARAMETERS:
   A. 1.500' PARAPET WIDTH BOTH SIDES.
   B. 700 LB/FT UNIFORM LOAD ASSUMED FOR PARAPET WEIGHT.
   C. ROADWAY WIDTH = 26.500'.
   D. NUMBER OF DESIGN LANES = 2.
   E. HL93 LIVE LOAD.
   F. DESIGN SPEED = 35 MPH.

4. DIAPHRAGM MEMBER CALL-OUTS ARE IN ENGLISH UNITS.

NCHRP 12-79

BRIDGE NTCCR5

MISC. DETAILS AND NOTES

SHEET 11 OF 20

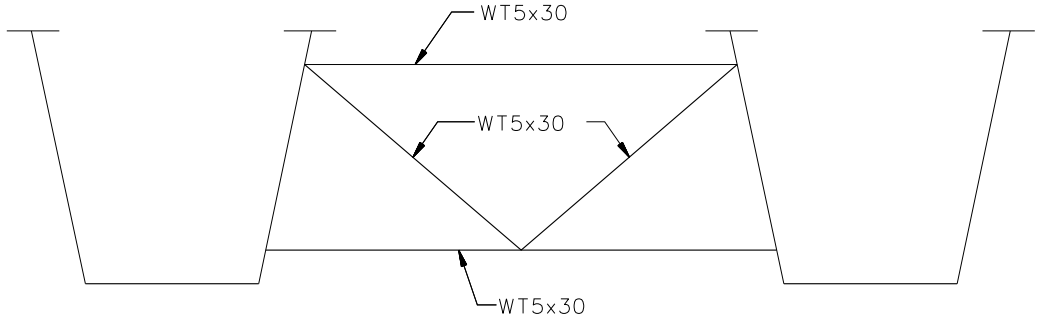

INTERMEDIATE EXTERNAL DIAPHRAGM

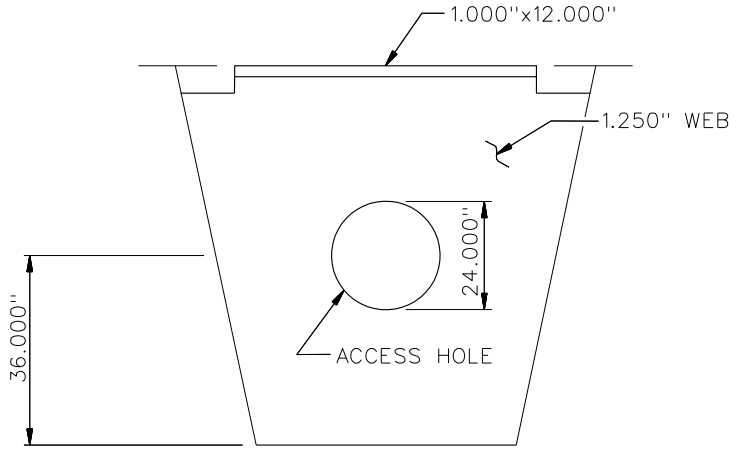

TYPICAL INTERNAL DIAPHRAGMS AT SUPPORTS

NCHRP 12-79

BRIDGE NTCCR5

MISC. DETAILS AND NOTES

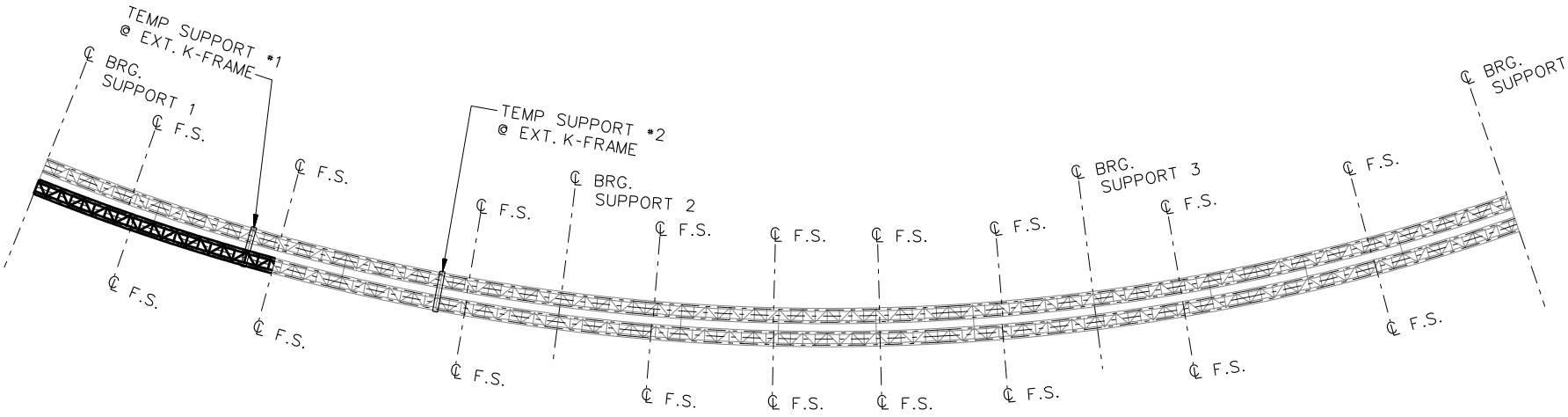

STAGE 1

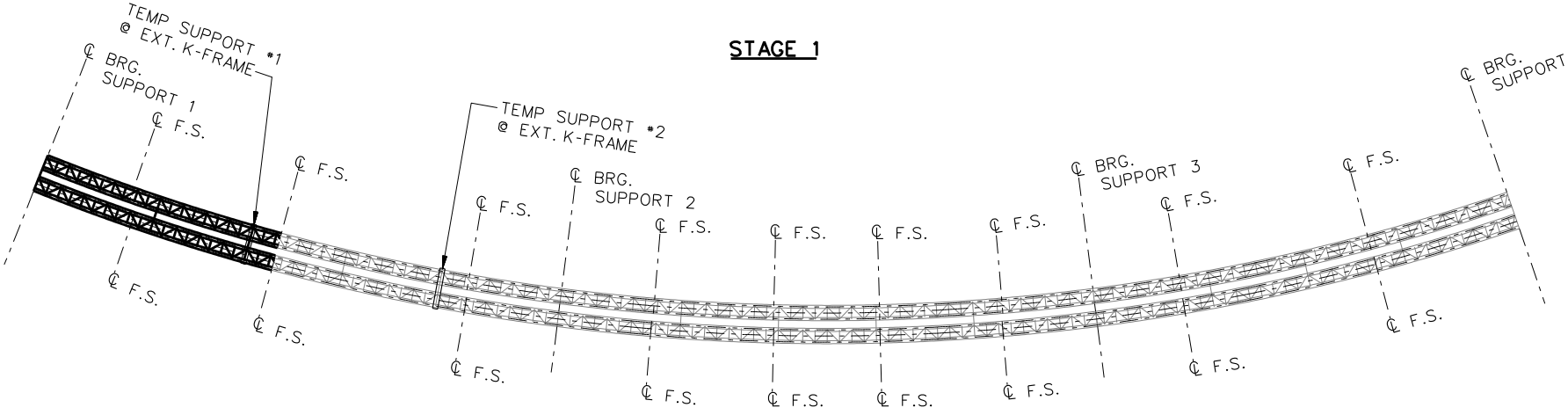

STAGE 2

LEGEND

▽ = HOLD OR LIFT CRANE

○ = TIE DOWN

□ = TEMPORARY SUPPORT STRUCTURE

NCHRP 12-79

BRIDGE NTCCR5

GENERAL ERECTION PROCEDURE

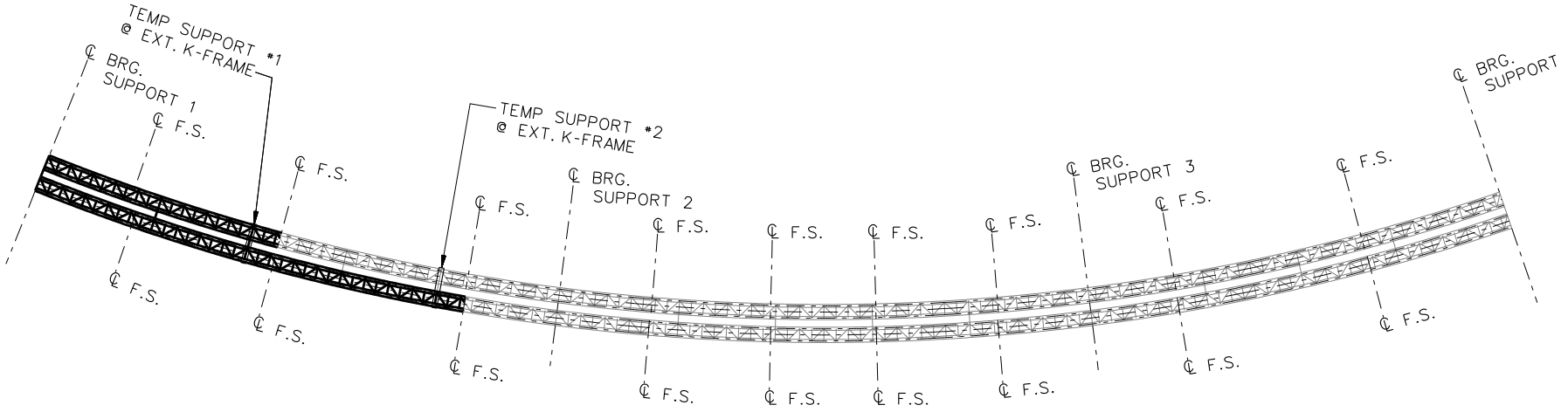

STAGE 3

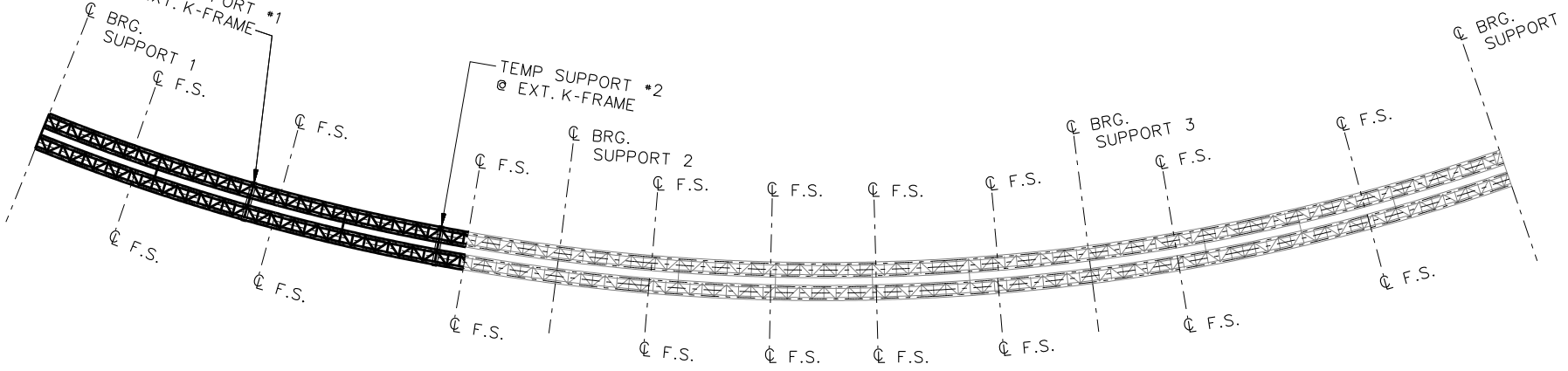

STAGE 4

LEGEND

▽ = HOLD OR LIFT CRANE

○ = TIE DOWN

□ = TEMPORARY SUPPORT STRUCTURE

NCHRP 12-79

BRIDGE NTCCR5

GENERAL ERECTION PROCEDURE

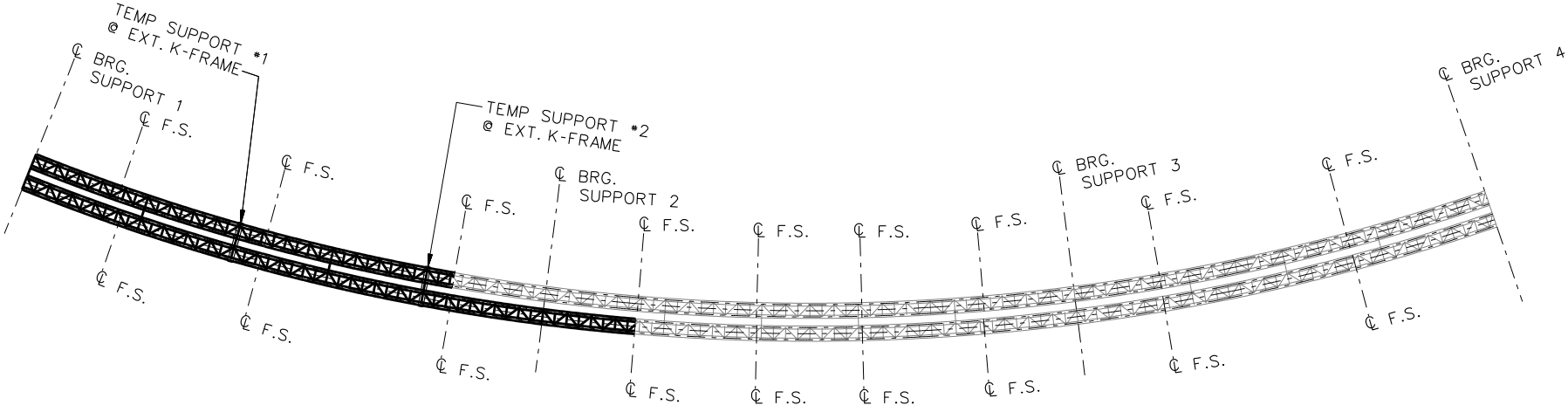

STAGE 5

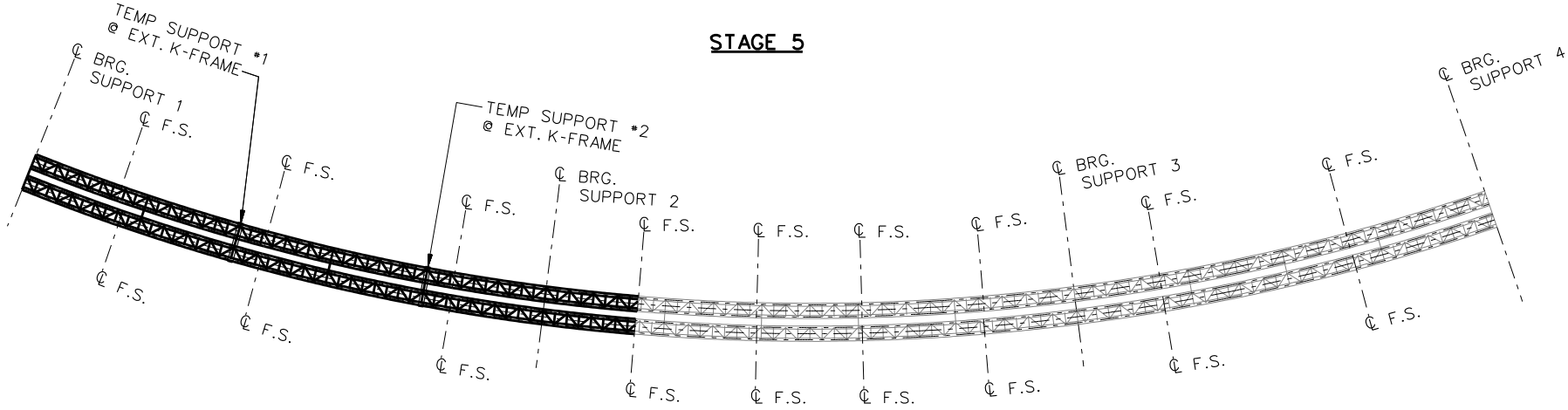

STAGE 6

LEGEND

▽ = HOLD OR LIFT CRANE

○ = TIE DOWN

□ = TEMPORARY SUPPORT STRUCTURE

STAGE 7

REMOVE TEMP SUPPORT *2

NCHRP 12-79

BRIDGE NTCCR5

GENERAL ERECTION PROCEDURE

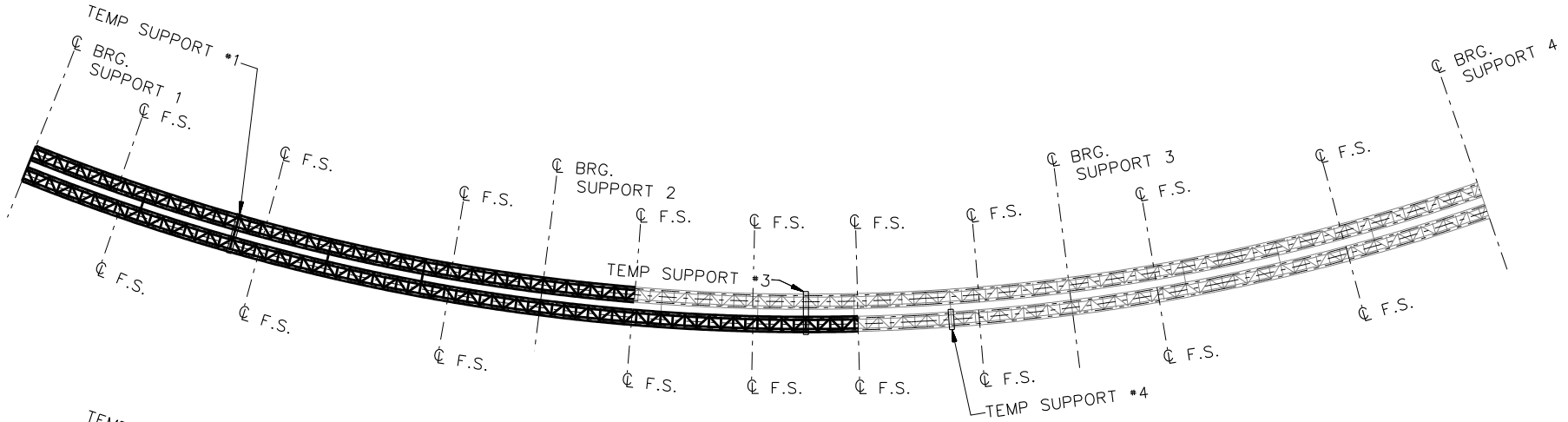

STAGE 8

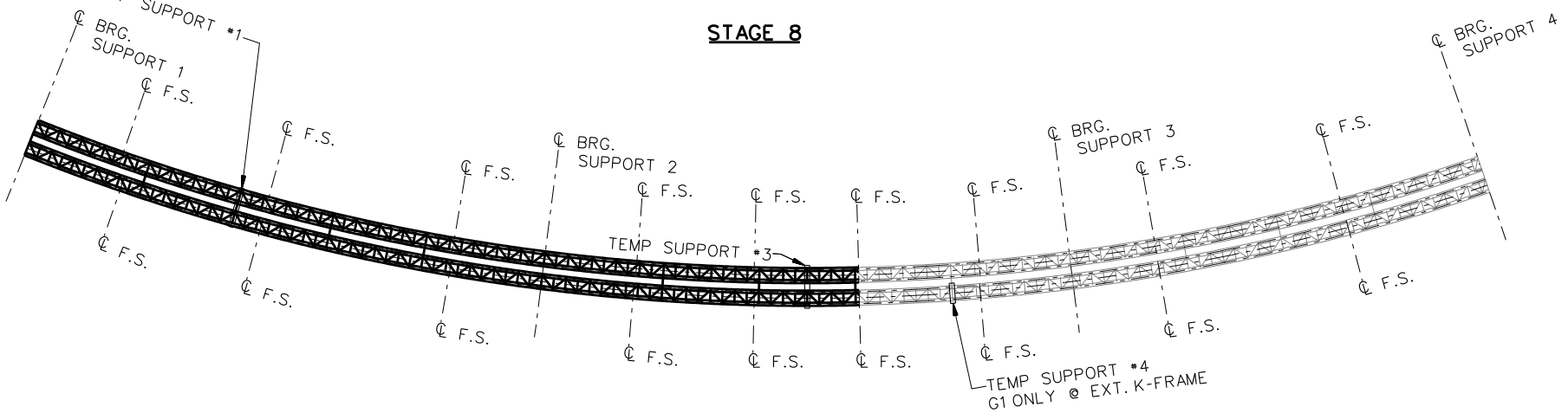

STAGE 9

LEGEND

▽ = HOLD OR LIFT CRANE

○ = TIE DOWN

□ = TEMPORARY SUPPORT STRUCTURE

NCHRP 12-79

BRIDGE NTCCR5

GENERAL ERECTION PROCEDURE

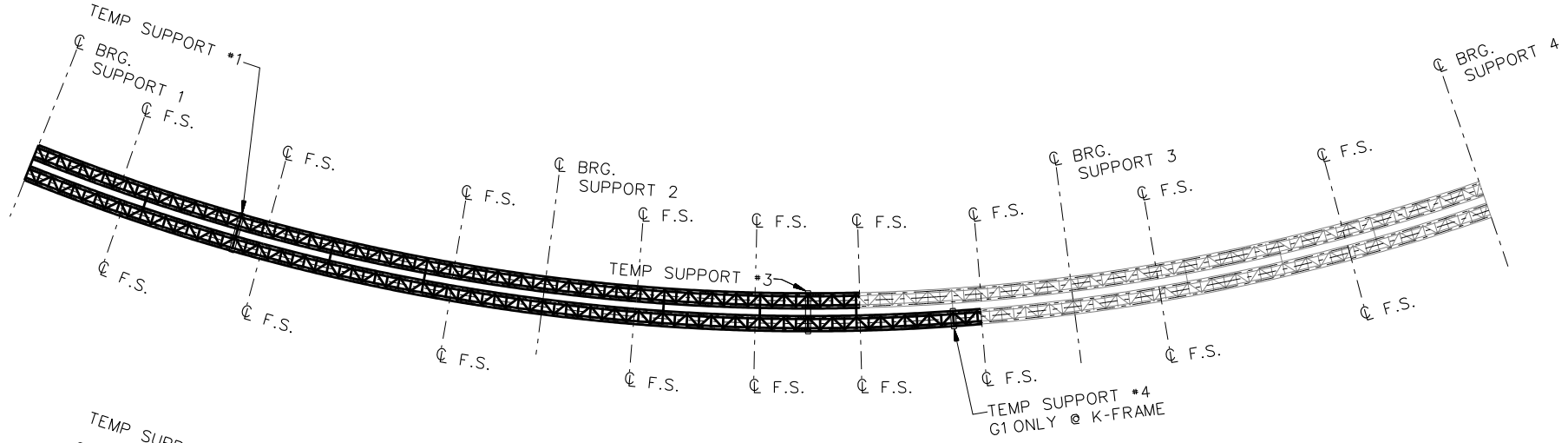

STAGE 10

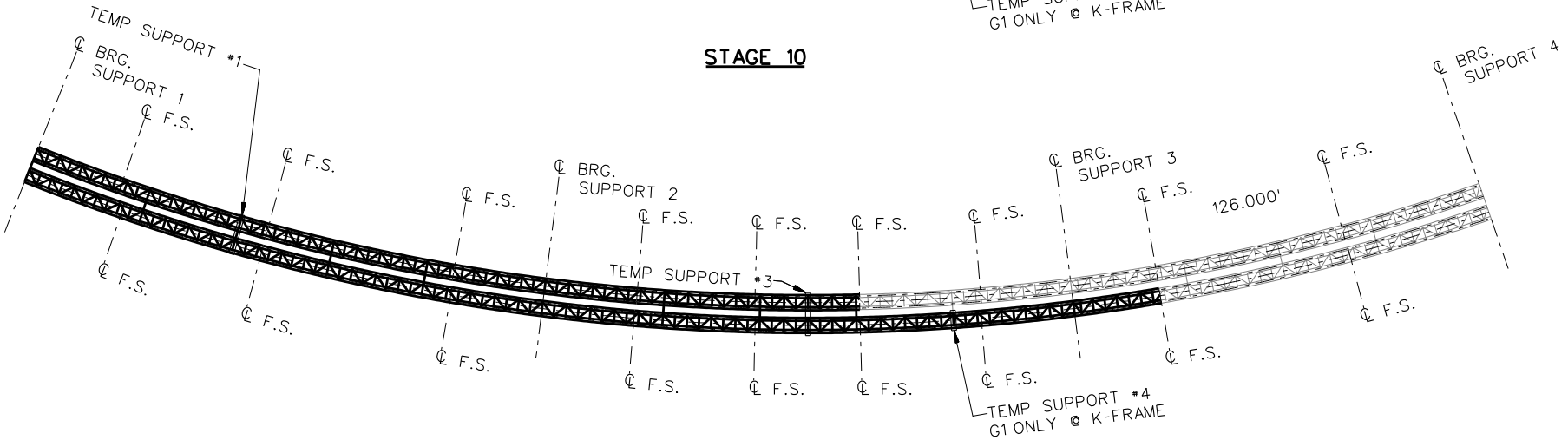

STAGE 11

STAGE 12

REMOVE TEMP SUPPORT *4

LEGEND

▽ = HOLD OR LIFT CRANE

○ = TIE DOWN

□ = TEMPORARY SUPPORT STRUCTURE

NCHRP 12-79

BRIDGE NTCCR5

GENERAL ERECTION PROCEDURE

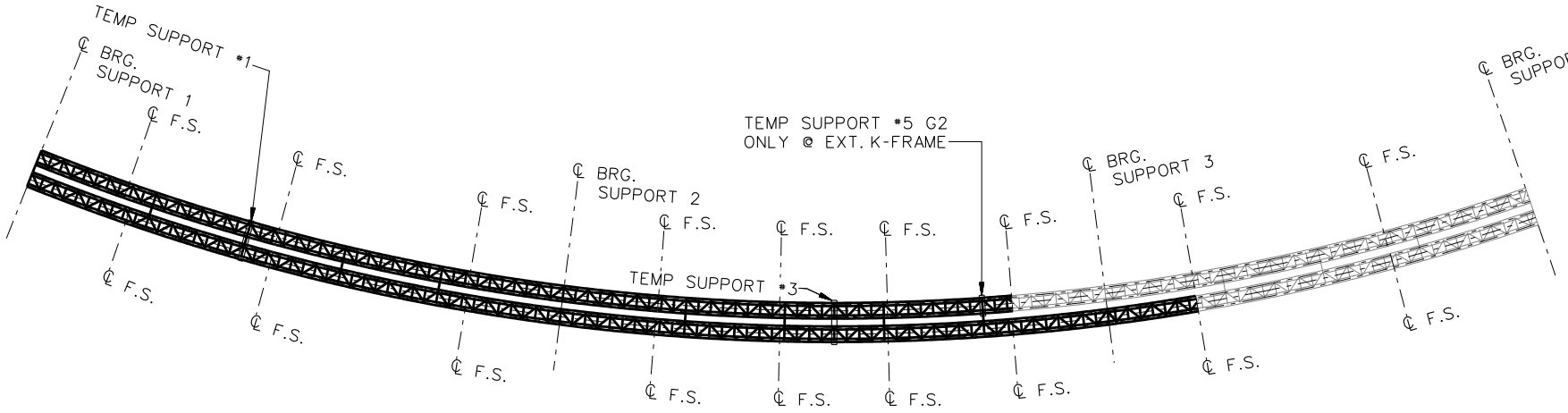

STAGE 13

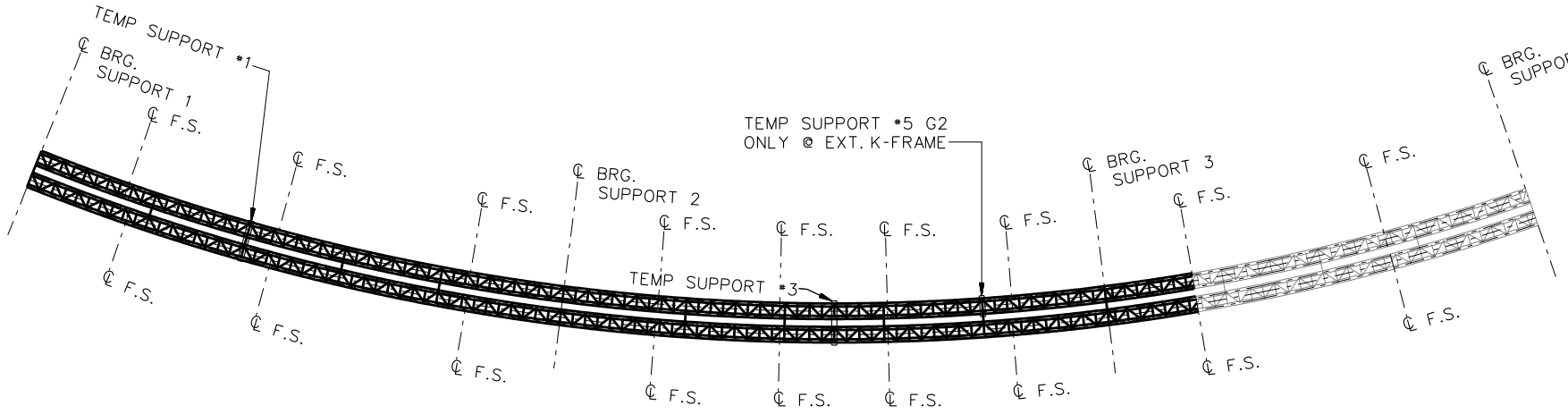

STAGE 14

LEGEND

▽ = HOLD OR LIFT CRANE

○ = TIE DOWN

□ = TEMPORARY SUPPORT STRUCTURE

STAGE 15

REMOVE TEMP SUPPORTS *1 AND *5

NCHRP 12-79

BRIDGE NTCCR5

GENERAL ERECTION PROCEDURE

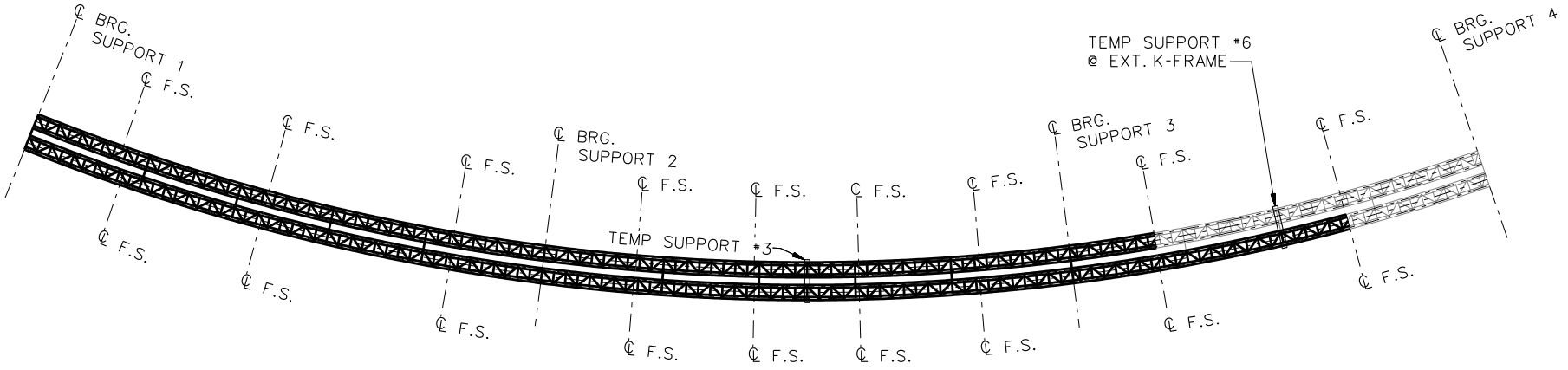

STAGE 16

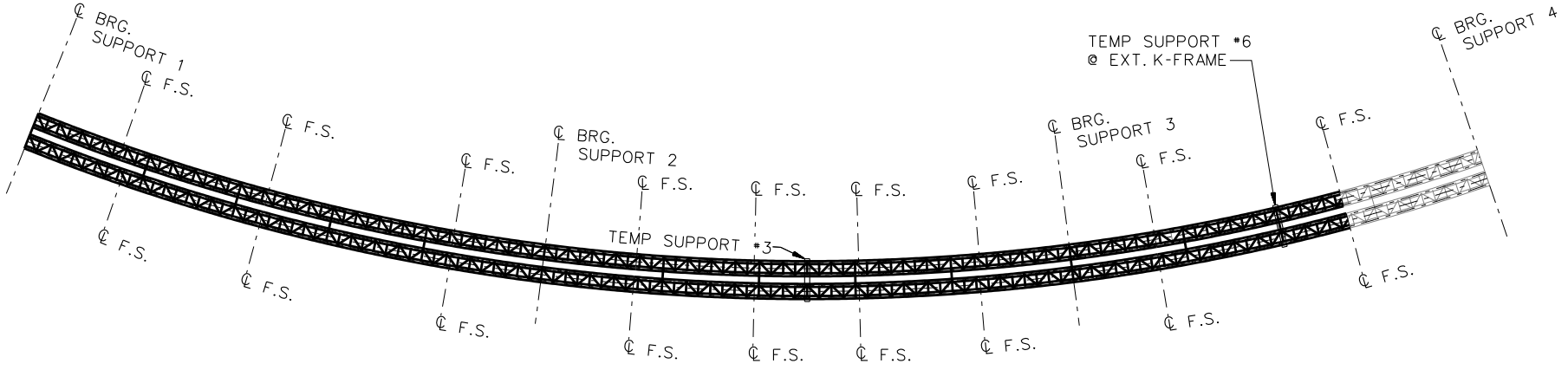

STAGE 17

LEGEND

▽ = HOLD OR LIFT CRANE

○ = TIE DOWN

□ = TEMPORARY SUPPORT STRUCTURE

NCHRP 12-79

BRIDGE NTCCR5

GENERAL ERECTION PROCEDURE

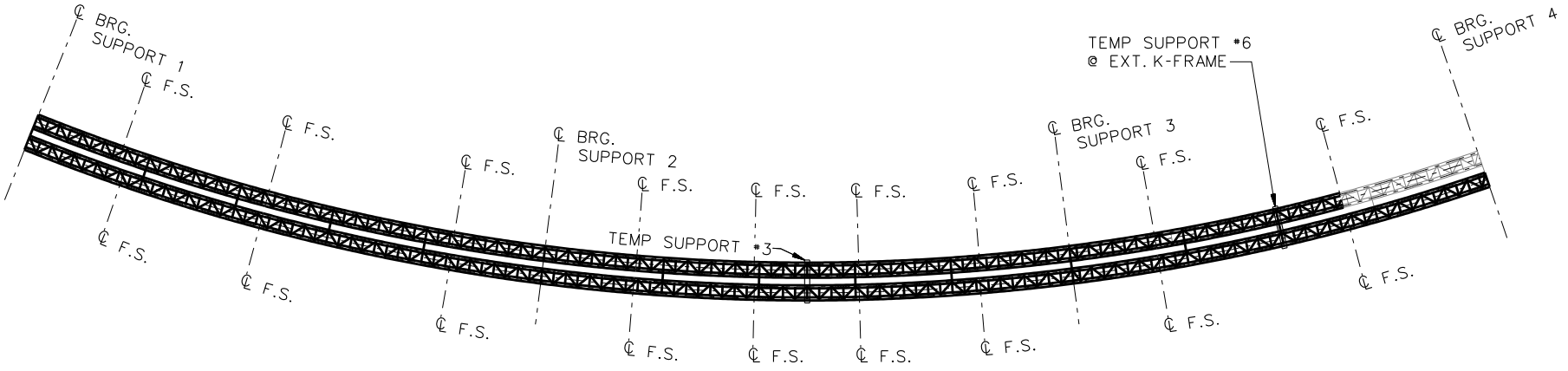

STAGE 18

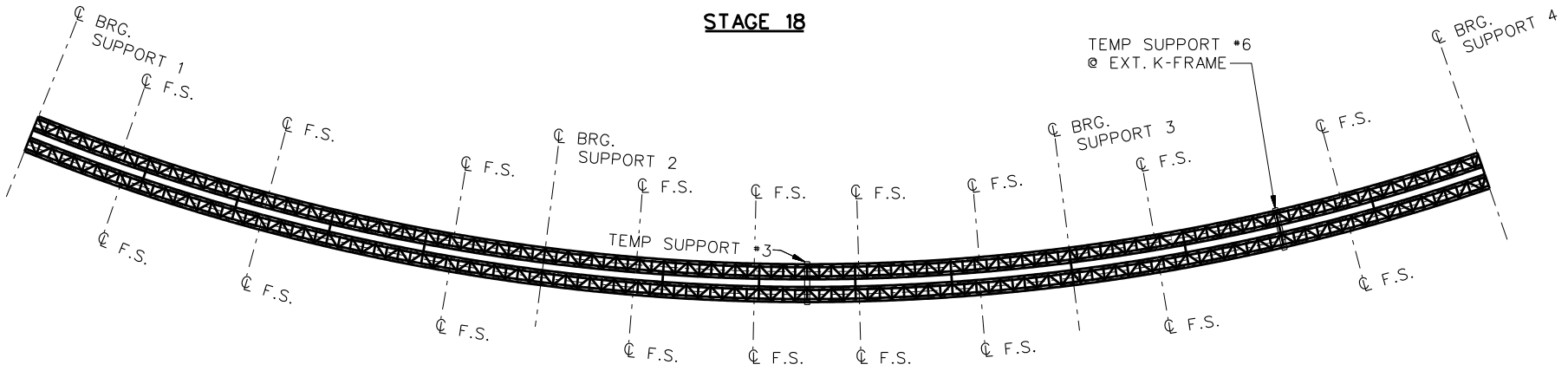

STAGE 19

STAGE 20

REMOVE TEMP SUPPORTS #3 AND #6

LEGEND

▽ = HOLD OR LIFT CRANE

○ = TIE DOWN

□ = TEMPORARY SUPPORT STRUCTURE

NCHRP 12-79

BRIDGE NTCCR5

GENERAL ERECTION PROCEDURE

NCHRP 12-79

NTCCS22

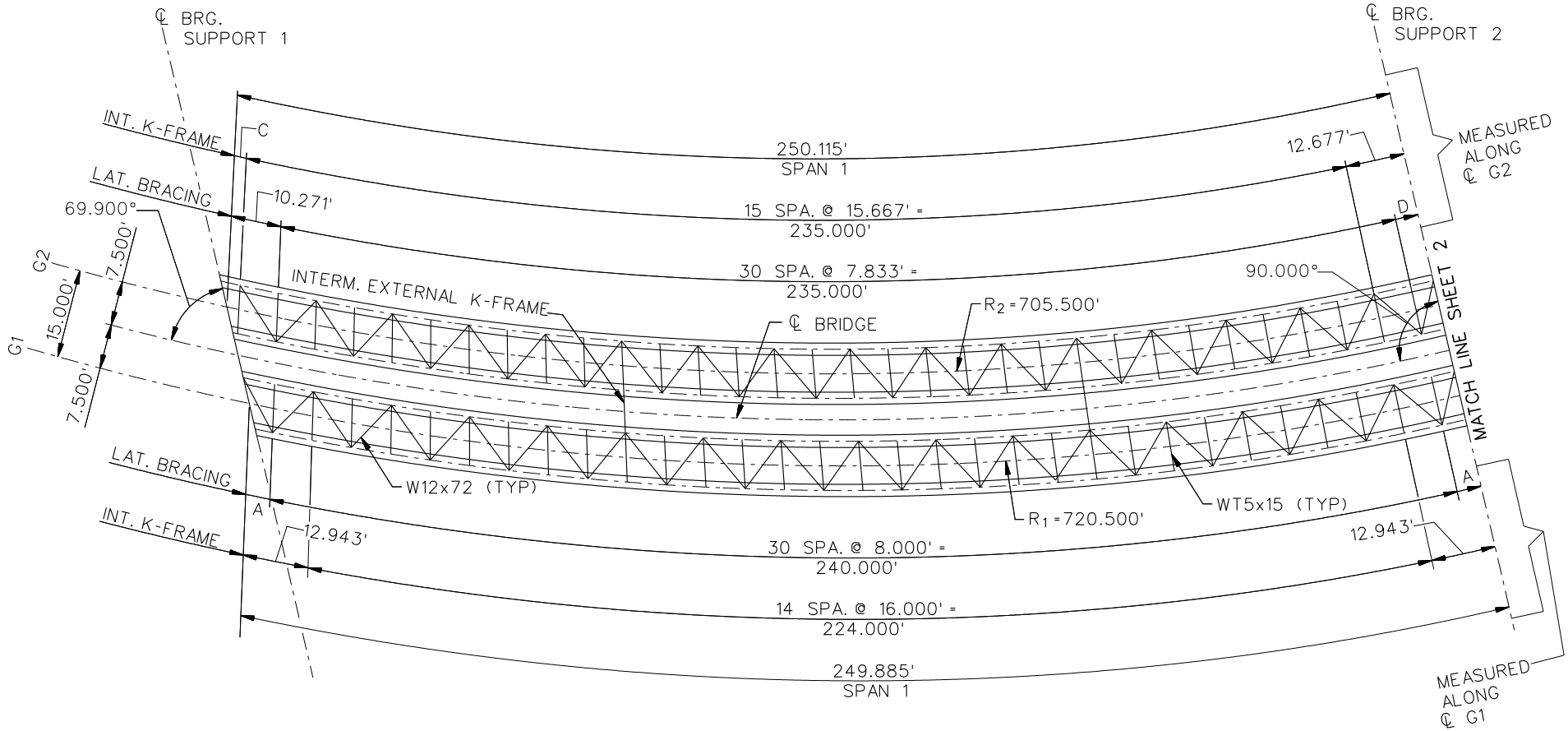

FRAMING PLAN

NOTES:

1. TYP. INTERNAL K-FRAME CONNECTION PLATE = 0.875"x6.000".
2. ALL BRG. STIFFENERS = 1.750"x20.000"
3. DIMENSIONS: A = 4.943', B = 6.313', C = 2.438', D = 4.844', E = 6.188'

NCHRP 12-79

BRIDGE NTCCS22

FRAMING PLAN AND CROSS-SECTION

SHEET 1 OF 11

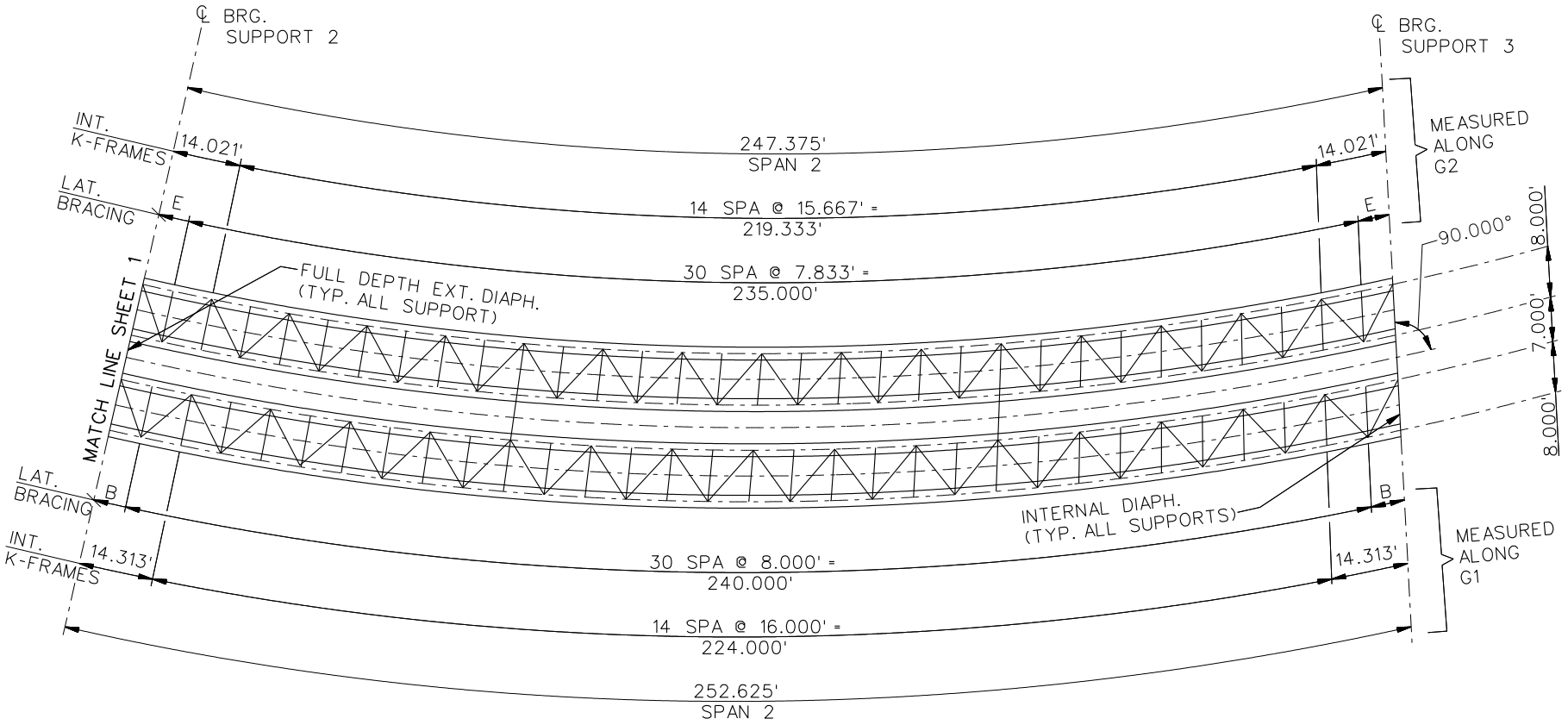

FRAMING PLAN

NOTES:

1. TYP. INTERNAL K-FRAME CONNECTION PLATE = 0.875"x6.000".
2. ALL BRG. STIFFENERS = 1.750"x20.000"
3. DIMENSIONS: A = 4.943', B = 6.313', C = 2.438',
   D = 4.844', E = 6.188'

NCHRP 12-79

BRIDGE NTCCS22

FRAMING PLAN AND
CROSS-SECTION

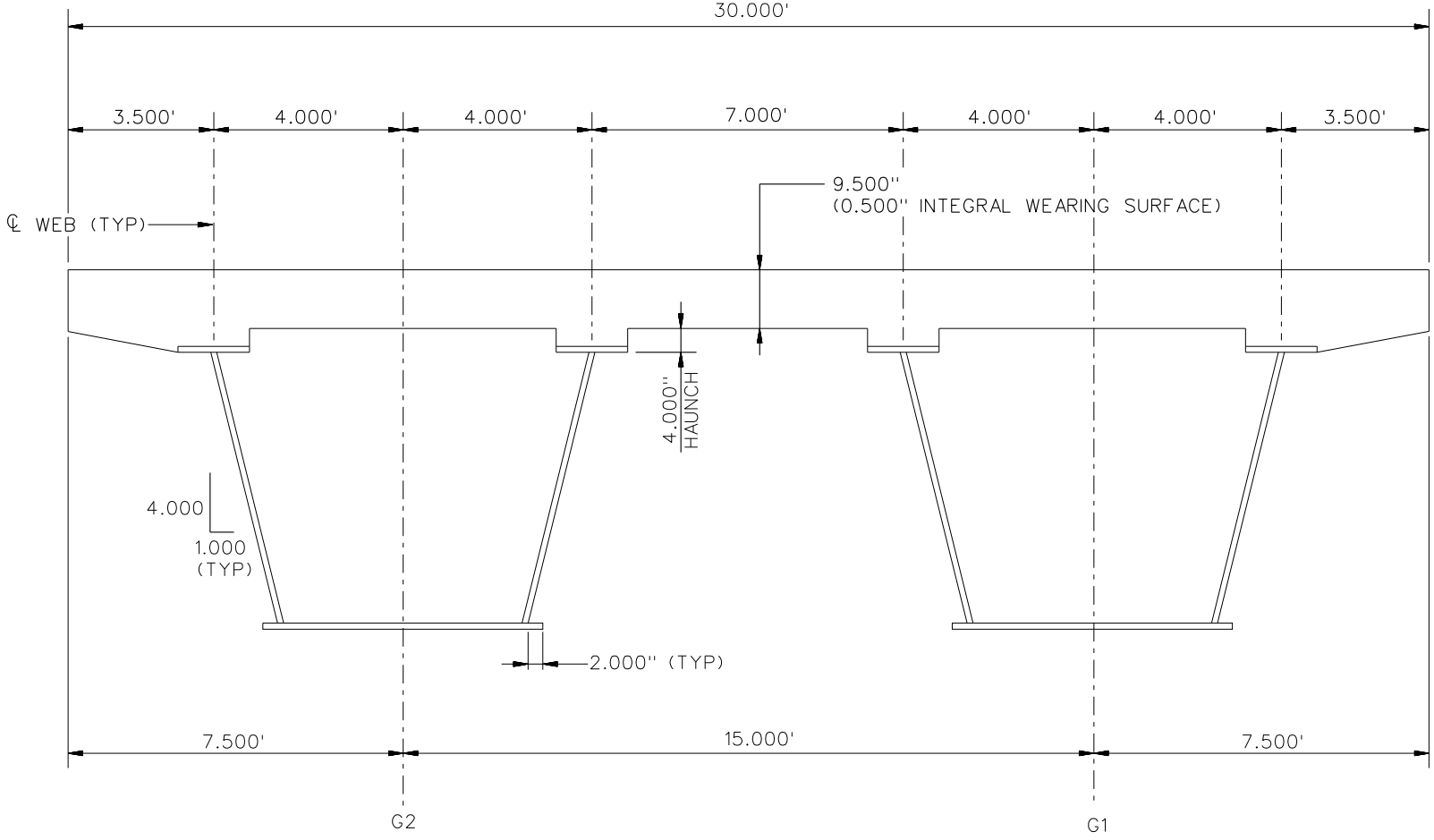

CROSS - SECTION

NCHRP 12-79

BRIDGE NTCCS22

TYPICAL SECTION

SHEET 3 OF 11

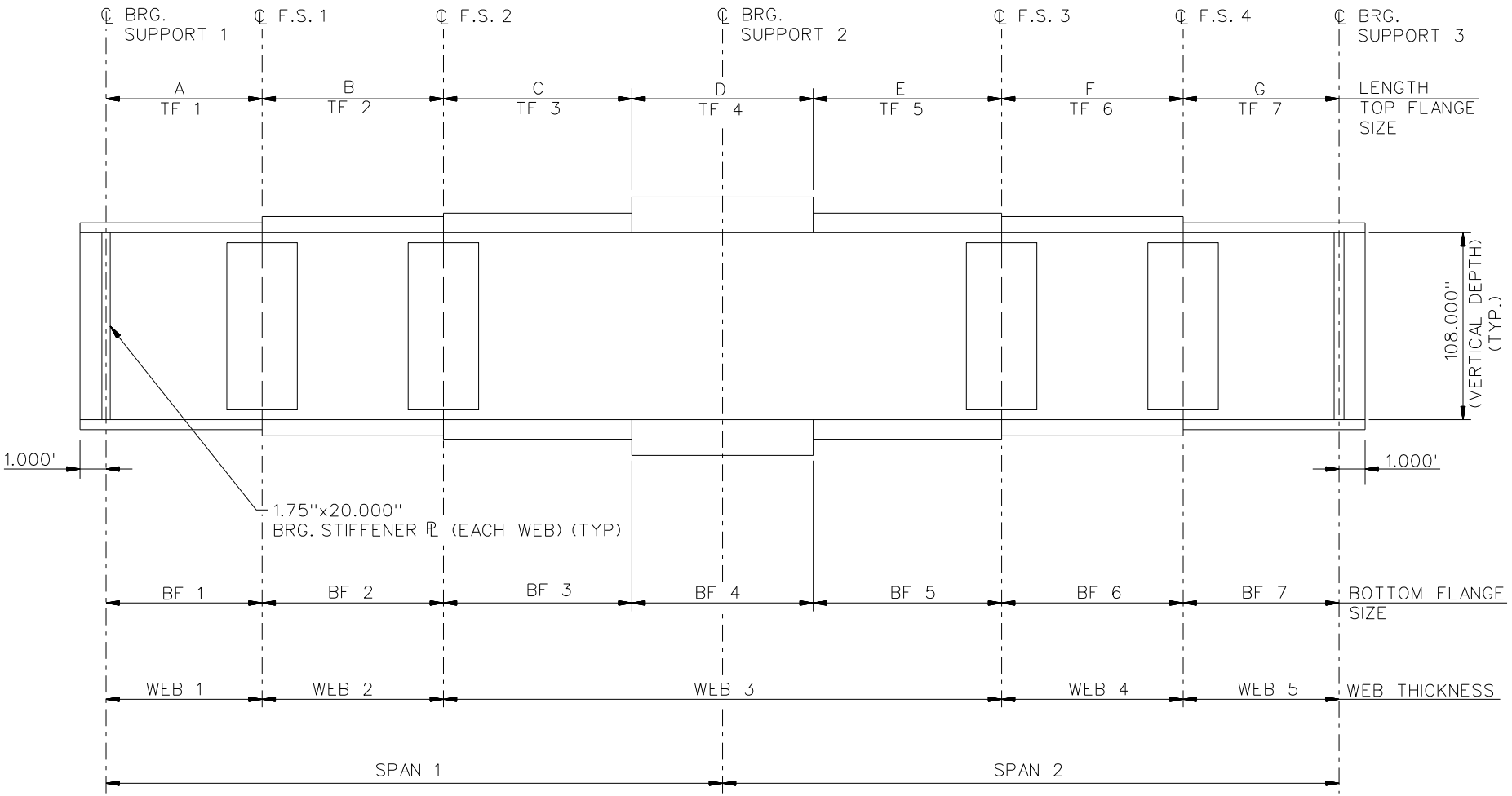

NOTES:

1. SEE TABLES ON SHEET 4 FOR GIRDER ELEVATION DIMENSIONS AND PLATE SIZES.
2. G1 WEB 1 THRU WEB 5 = 0.9375"
3. G2 WEB 1 THRU WEB 5 = 0.875".

NCHRP 12-79

BRIDGE NTCCS22
GIRDER ELEVATION

SHEET 4 OF 11

	GIRDER PLATE LENGTHS ✳	
LENGTH	G1	G2
A	54.750	55.083
B	130.000	130.000
C	35.000	35.000
D	60.000	60.000
E	35.000	35.000
F	130.000	127.000
G	57.500	55.333

✳ ALL DIMENSIONS ARE IN FEET.

	GIRDER FLANGE DIMENSIONS ✳✳			
TOP	G1		G2	
FLANGE	BF	TF	BF	TF
TF1	20.000	1.250	20.000	1.250
TF2	20.000	1.250	20.000	1.250
TF3	20.000	1.500	20.000	1.500
TF4	20.000	2.500	20.000	2.500
TF5	20.000	1.500	20.000	1.500
TF6	20.000	1.250	20.000	1.250
TF7	20.000	1.250	20.000	1.250

✳✳ ALL DIMENSIONS ARE IN INCHES.

	GIRDER FLANGE DIMENSIONS ✳✳			
BOTTOM	G1		G2	
FLANGE	BF	TF	BF	TF
BF1	46.000	1.250	46.000	1.250
BF2	46.000	1.250	46.000	1.250
BF3	46.000	1.500	46.000	1.500
BF4	46.000	2.750	46.000	2.500
BF5	46.000	1.500	46.000	1.500
BF6	46.000	1.250	46.000	1.250
BF7	46.000	1.250	46.000	1.250

✳✳ ALL DIMENSIONS ARE IN INCHES.

NCHRP 12-79

BRIDGE NTCCS22

GIRDER ELEVATION TABLES

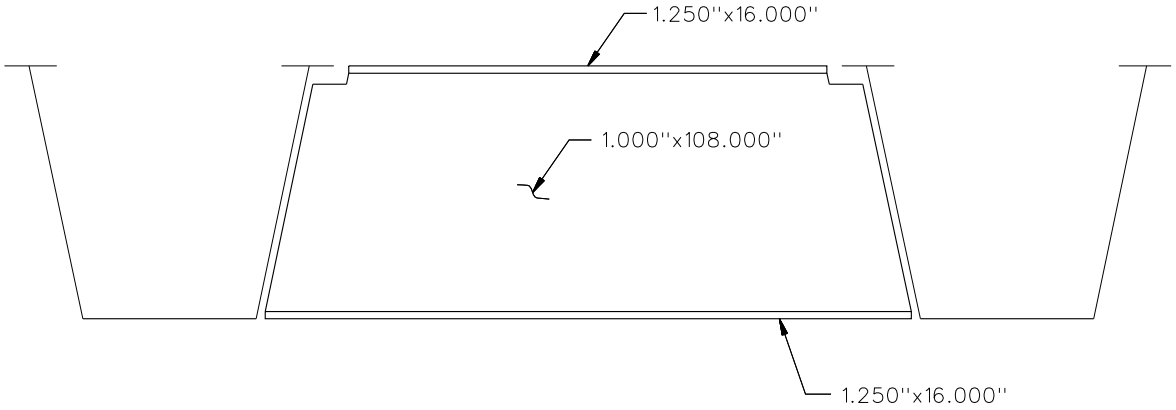

TYPICAL END DIAPHRAGM

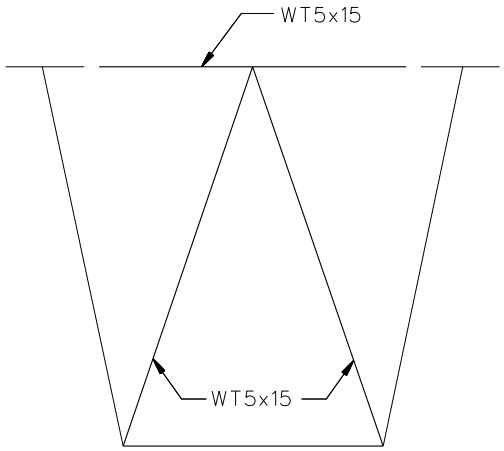

TYPICAL INTERNAL CROSS FRAME

NOTES:

1. STEEL DEAD LOAD INCREASED BY 15% FOR MDX AND LARSA MODELS; 2% FOR 3D MODEL; AND 20% FOR APPROXIMATE ANALYSIS TO ACCOUNT FOR MISC. DETAILS.

2. FORMWORK LOAD OF 10PSF IS INCLUDED IN CONCRETE DEAD LOAD.

3. ADDITIONAL DESIGN PARAMETERS:
   A. 1.500' PARAPET WIDTH BOTH SIDES.
   B. 700 LB/FT UNIFORM LOAD ASSUMED FOR PARAPET WEIGHT.
   C. ROADWAY WIDTH = 26.500'.
   D. NUMBER OF DESIGN LANES = 2.
   E. HL93 LIVE LOAD.
   F. DESIGN SPEED = 35 MPH.

4. DIAPHRAGM MEMBER CALL-OUTS ARE IN ENGLISH UNITS.

NCHRP 12-79

BRIDGE NTCCS22

MISC. DETAILS AND NOTES

SHEET 6 OF 11

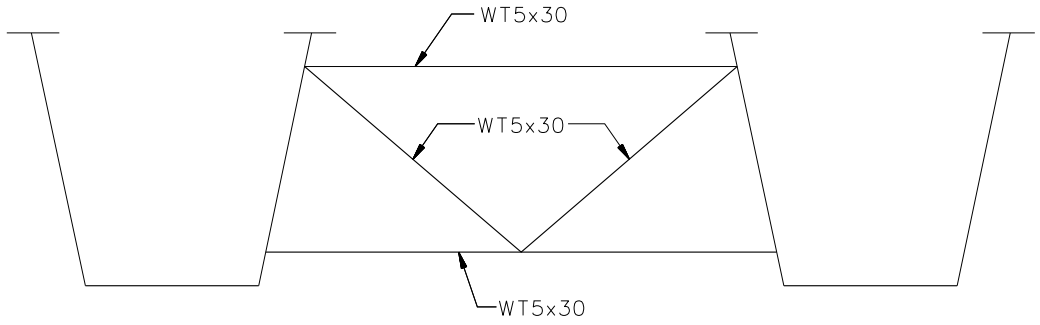

TYPICAL INTERMEDIATE EXTERNAL DIAPHRAGM

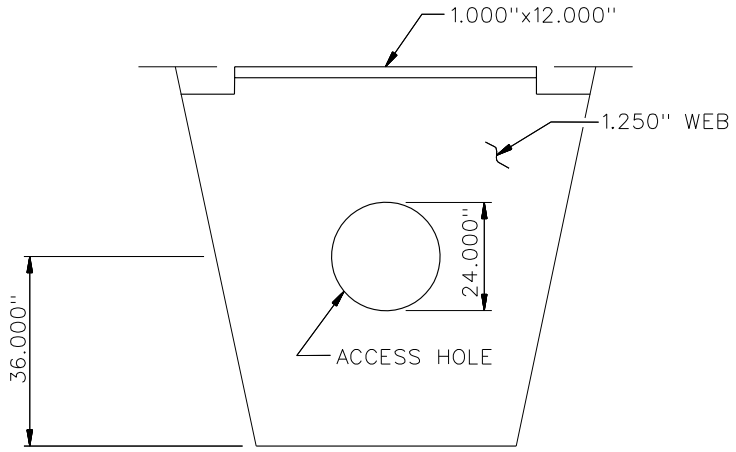

TYPICAL INTERNAL DIAPHRAGMS AT SUPPORTS

NCHRP 12-79

BRIDGE NTCCS22

MISC. DETAILS AND NOTES

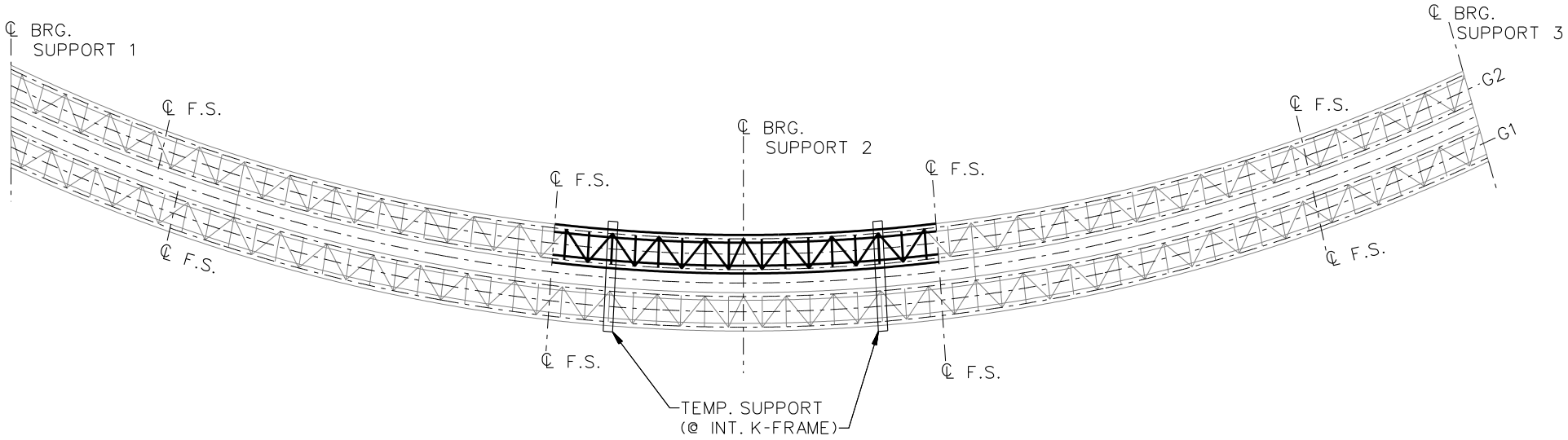

STAGE 1

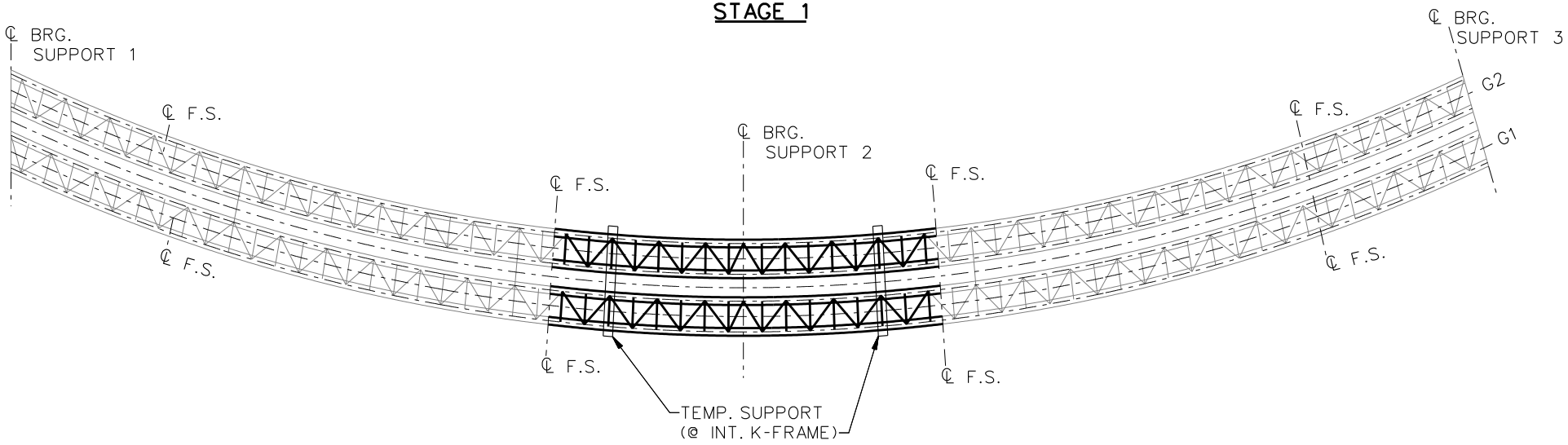

STAGE 2

LEGEND

▽ = HOLD OR LIFT CRANE

○ = TIE DOWN

□ = TEMPORARY SUPPORT STRUCTURE

NCHRP 12-79

BRIDGE NTCCS22

GENERAL ERECTION PROCEDURE

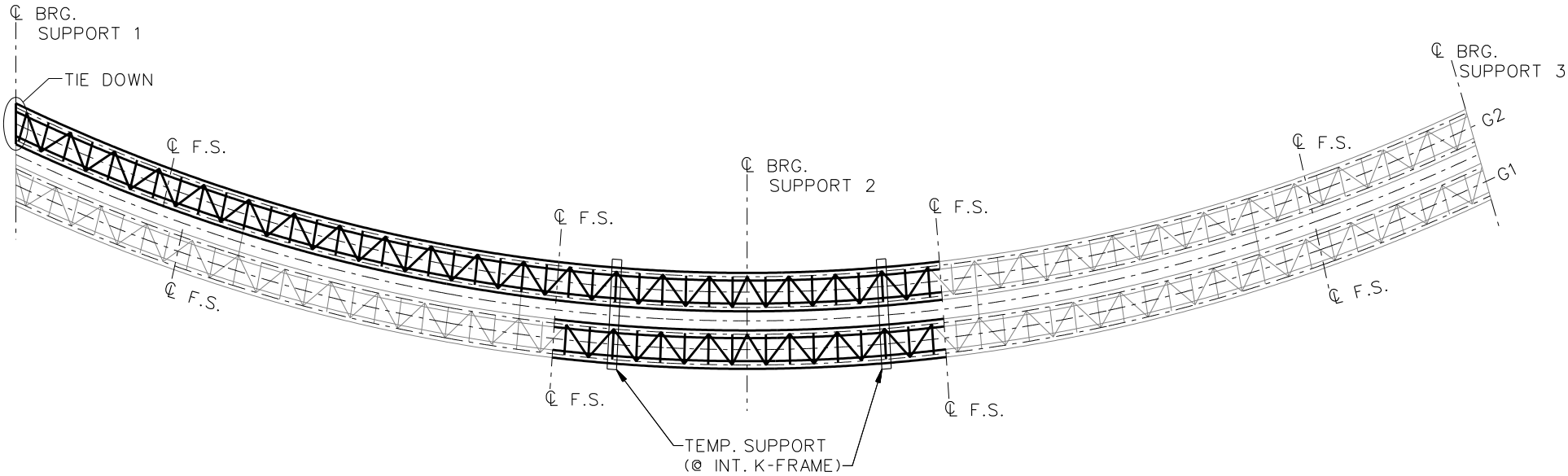

STAGE 3

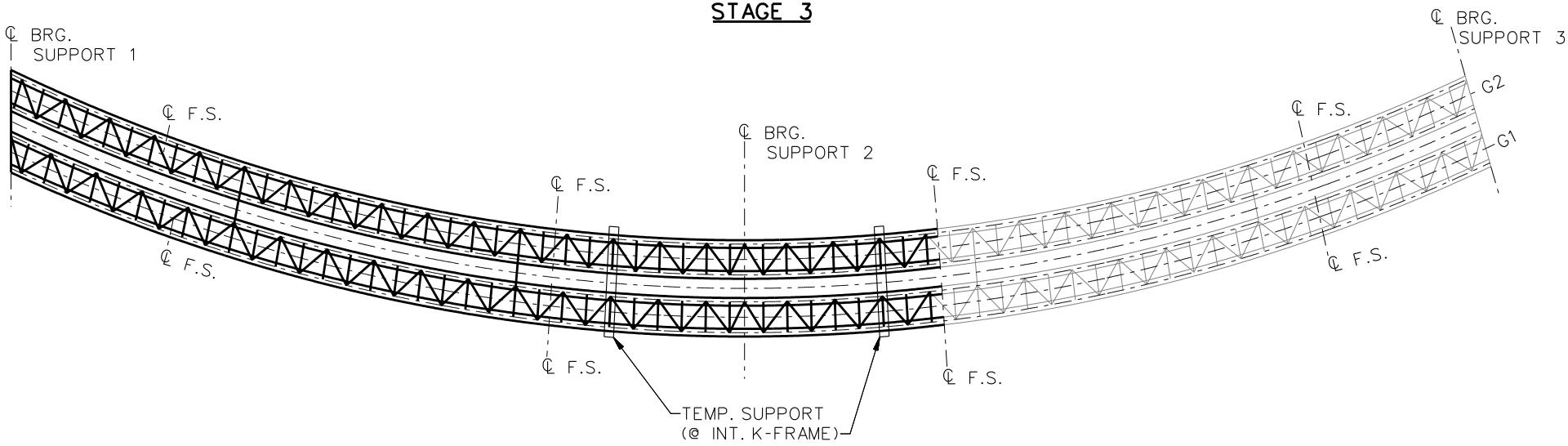

STAGE 4

LEGEND

▽ = HOLD OR LIFT CRANE

○ = TIE DOWN

□ = TEMPORARY SUPPORT STRUCTURE

STAGE 5

REMOVE ALL TEMP. SUPPORTS

NCHRP 12-79

BRIDGE NTCCS22

GENERAL ERECTION PROCEDURE

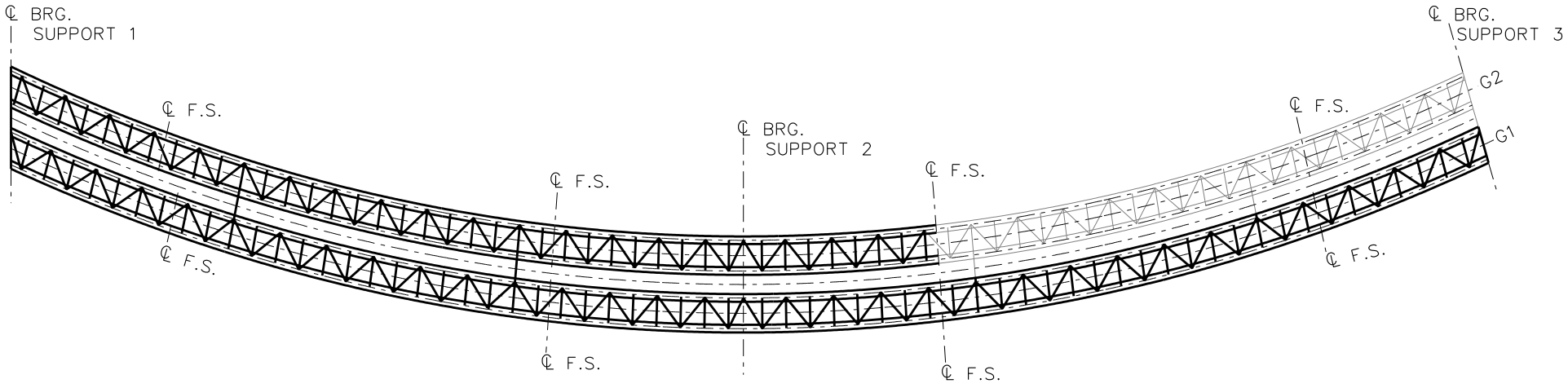

STAGE 6

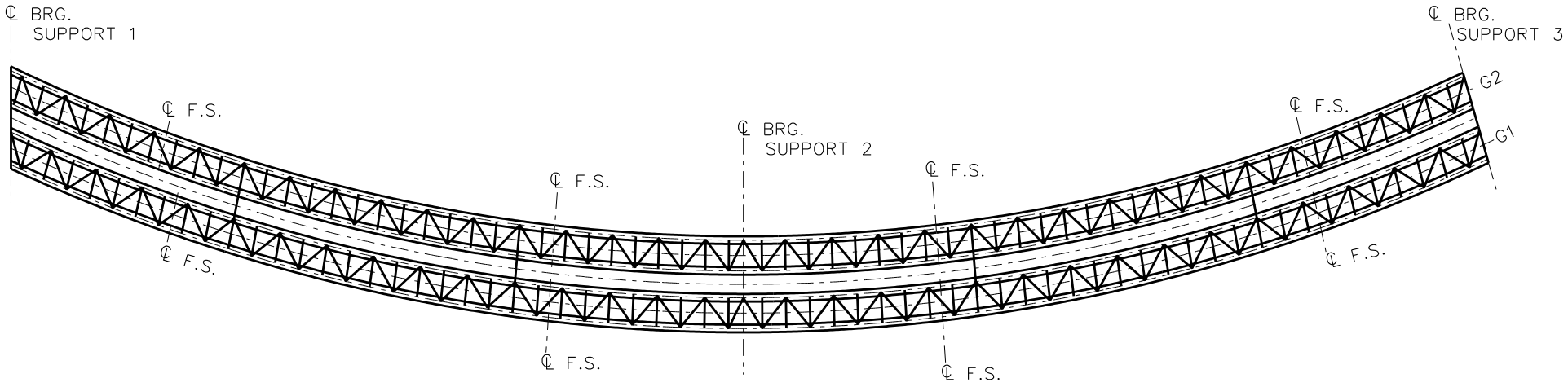

STAGE 7

LEGEND

▽ = HOLD OR LIFT CRANE

○ = TIE DOWN

□ = TEMPORARY SUPPORT STRUCTURE

NCHRP 12-79

BRIDGE NTCCS22

GENERAL ERECTION PROCEDURE

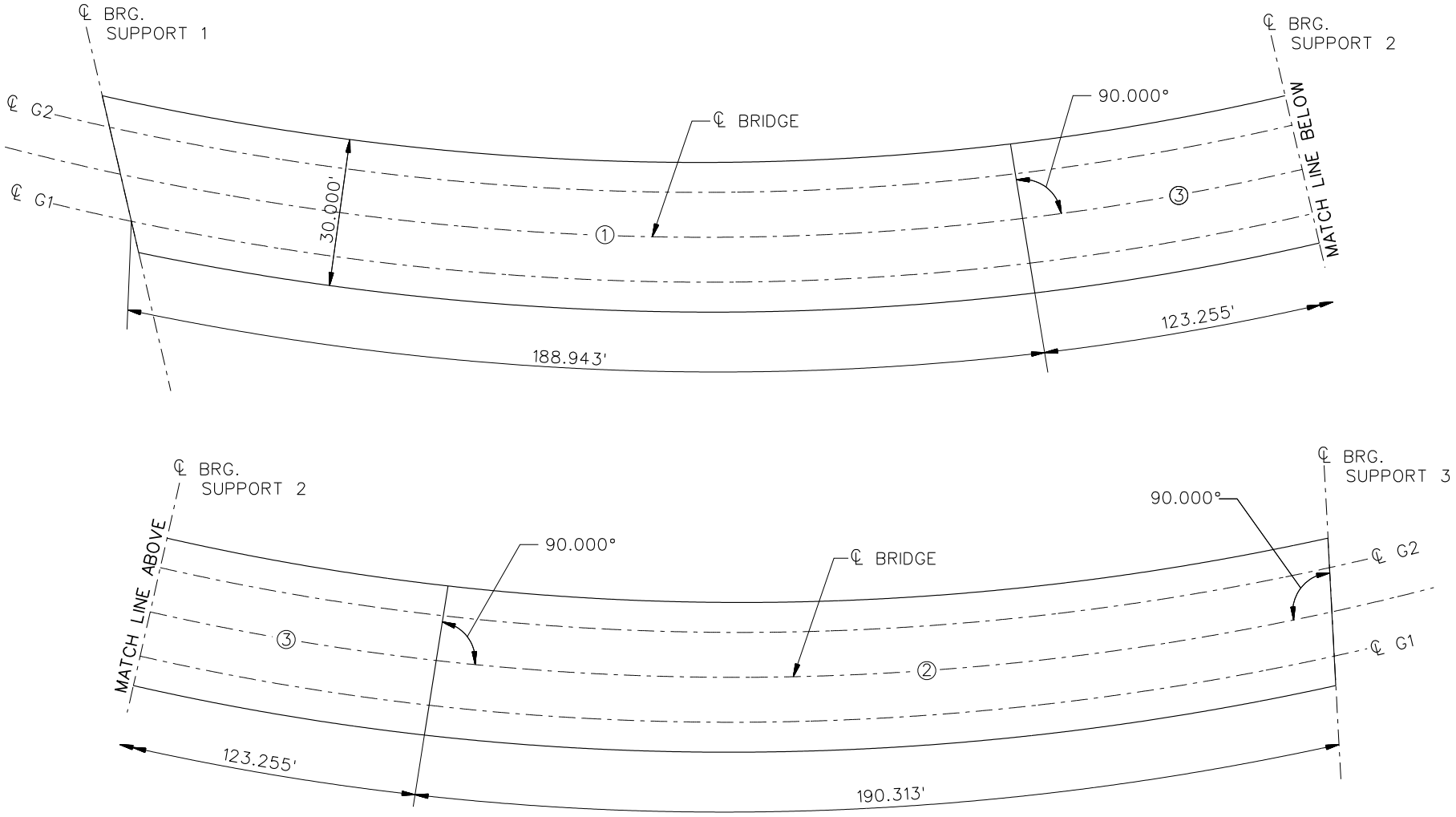

DECK POURING SEQUENCE

NCHRP 12-79
BRIDGE NTCCS22
DECK POURING SEQUENCE
SHEET 11 OF 11

NCHRP 12-79

NTSCR1

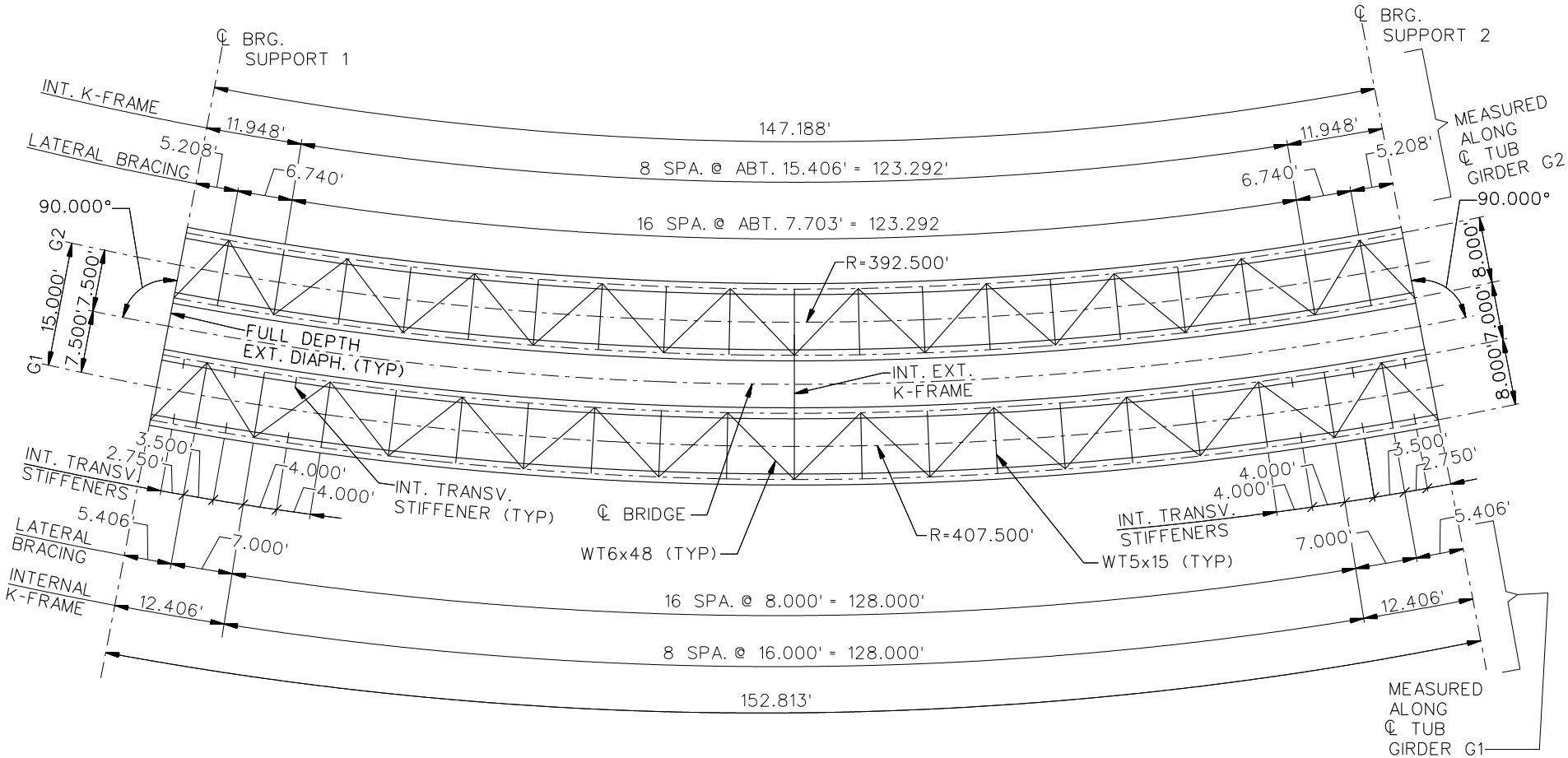

FRAMING PLAN

NOTE:
INT. TRANSV. STIFFENER + CONN PL = 6.000"x0.875"
BRG. STIFFENER = 8.000"x1.500"
ONE (1) INT. EXT. K-FRAME @ MIDSPAN

NCHRP 12-79

BRIDGE NTSCR1

FRAMING PLAN

SHEET 1 OF 7

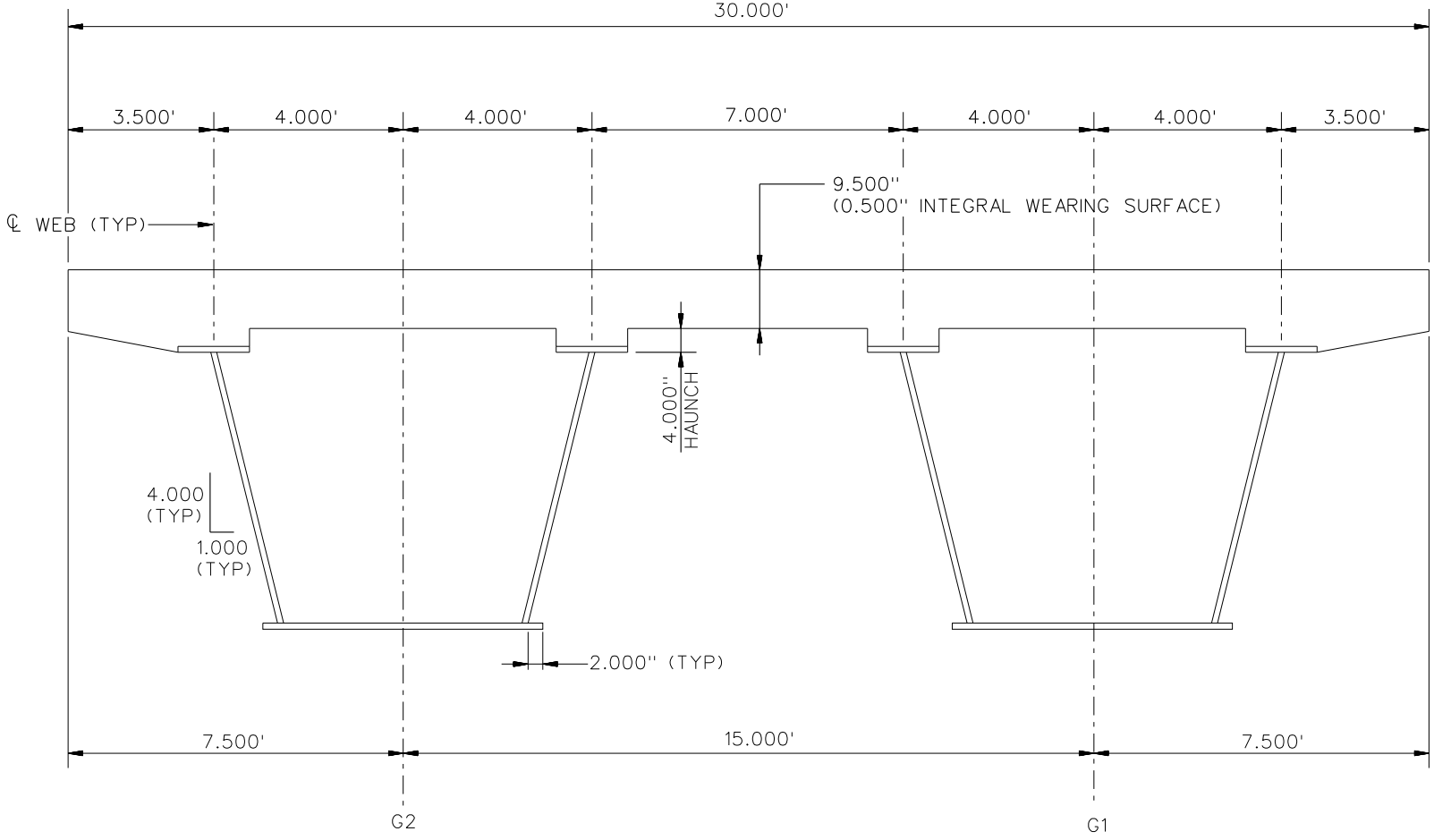

CROSS - SECTION

NCHRP 12-79

BRIDGE NTSCR1

TYPICAL SECTION

SHEET 2 OF 7

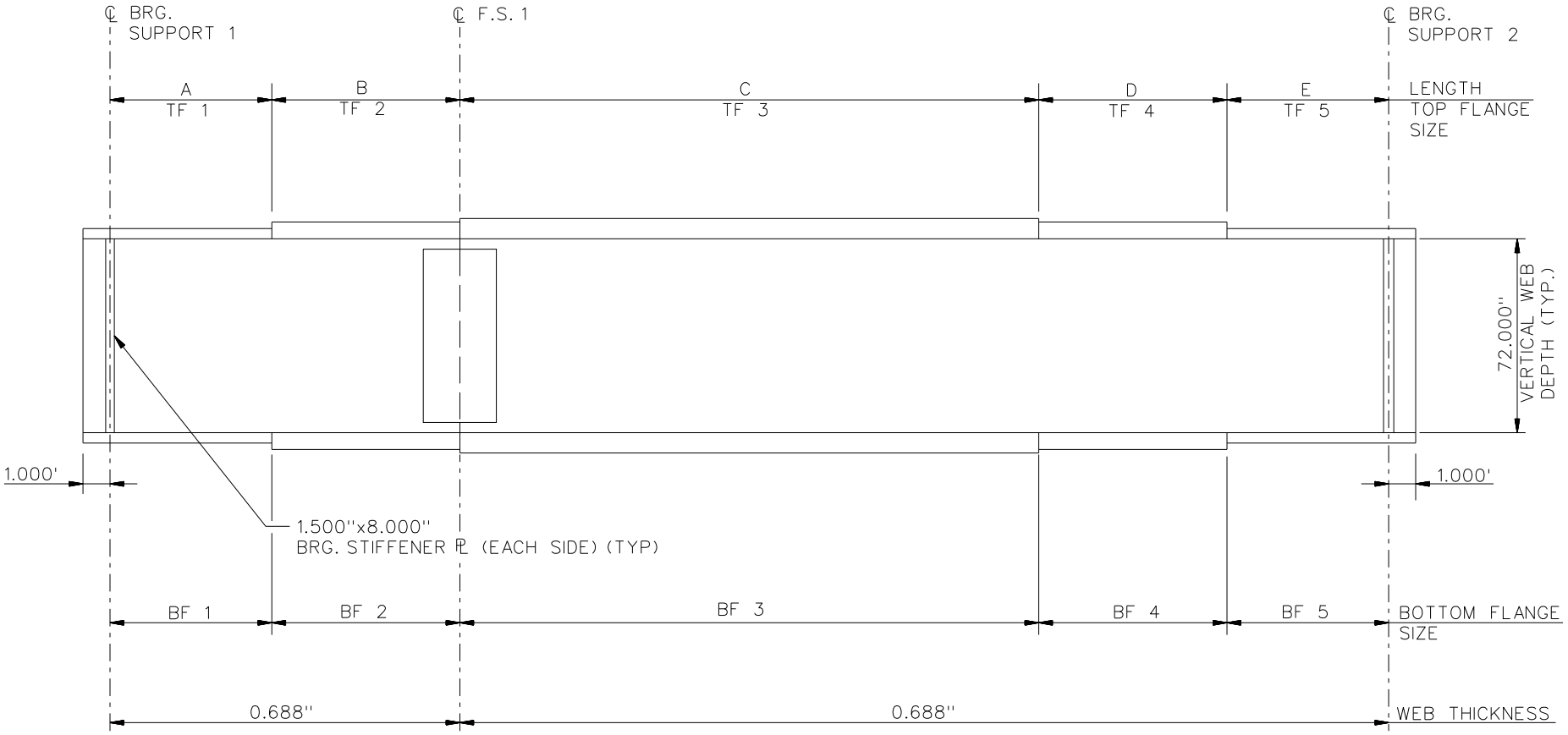

NOTES:

1. SEE TABLES ON SHEET 4 FOR GIRDER ELEVATION DIMENSIONS AND PLATE SIZES.

NCHRP 12-79

BRIDGE NTSCR1

GIRDER ELEVATION

SHEET 3 OF 7

	GIRDER PLATE LENGTHS ✳	
LENGTH	G1	G2
A	21.406	18.594
B	20.000	20.000
C	70.000	70.000
D	20.000	20.000
E	21.406	18.594

✳ ALL DIMENSIONS ARE IN FEET.

	GIRDER FLANGE DIMENSIONS ✳✳			
TOP	G1		G2	
FLANGE	BF	TF	BF	TF
TF1	16.000	0.875	16.000	0.875
TF2	16.000	0.875	16.000	0.875
TF3	16.000	0.875	16.000	0.875
TF4	16.000	0.875	16.000	0.875
TF5	16.000	0.875	16.000	0.875

✳✳ ALL DIMENSIONS ARE IN INCHES.

	GIRDER FLANGE DIMENSIONS ✳✳			
BOTTOM	G1		G2	
FLANGE	BF	TF	BF	TF
BF1	64.000	0.875	64.000	0.875
BF2	64.000	0.875	64.000	0.875
BF3	64.000	1.250	64.000	1.000
BF4	64.000	0.875	64.000	0.875
BF5	64.000	0.875	64.000	0.875

✳✳ ALL DIMENSIONS ARE IN INCHES.

NCHRP 12-79

BRIDGE NTSCR1

GIRDER ELEVATION TABLES

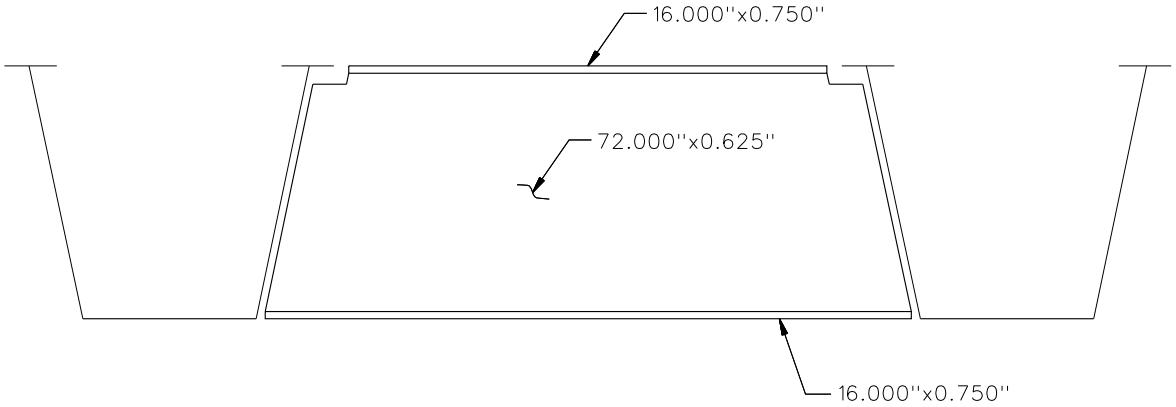

TYPICAL END DIAPHRAGM

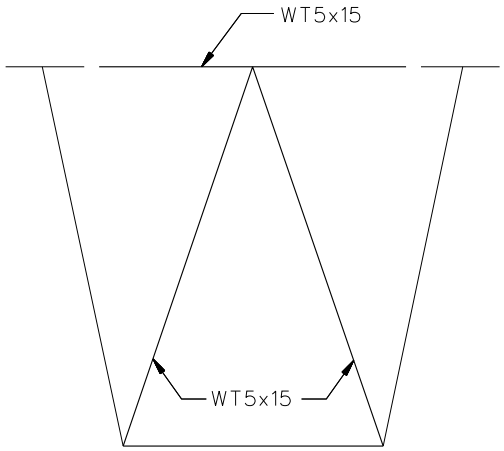

TYPICAL INTERNAL CROSS FRAME

NOTES:

1. STEEL DEAD LOAD INCREASED BY 5% FOR MDX AND LARSA MODELS; 2% FOR 3D MODEL; AND 10% FOR APPROXIMATE ANALYSIS TO ACCOUNT FOR MISC. DETAILS.

2. FORMWORK LOAD OF 10PSF IS INCLUDED IN CONCRETE DEAD LOAD.

3. ADDITIONAL DESIGN PARAMETERS:
   A. 1.500' PARAPET WIDTH BOTH SIDES.
   B. 700 LB/FT UNIFORM LOAD ASSUMED FOR PARAPET WEIGHT.
   C. ROADWAY WIDTH = 26.500'.
   D. NUMBER OF DESIGN LANES = 2.
   E. HL93 LIVE LOAD.
   F. DESIGN SPEED = 35 MPH.

4. DIAPHRAGM MEMBER CALL-OUTS ARE IN ENGLISH UNITS.

NCHRP 12-79

BRIDGE NTSCR1

MISC. DETAILS AND NOTES

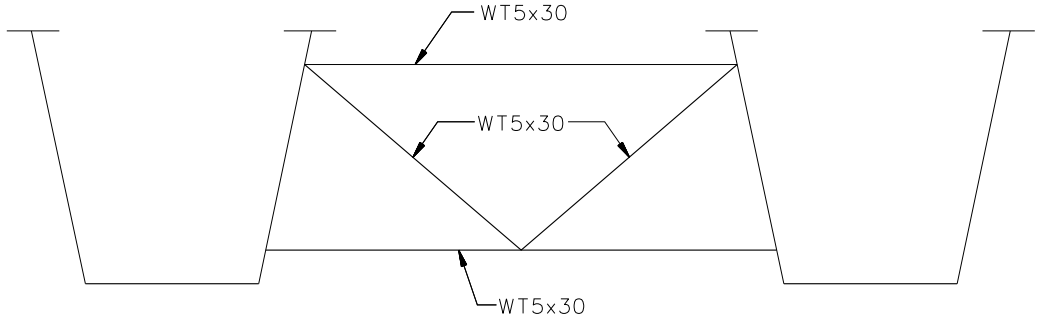

INTERMEDIATE EXTERNAL DIAPHRAGM

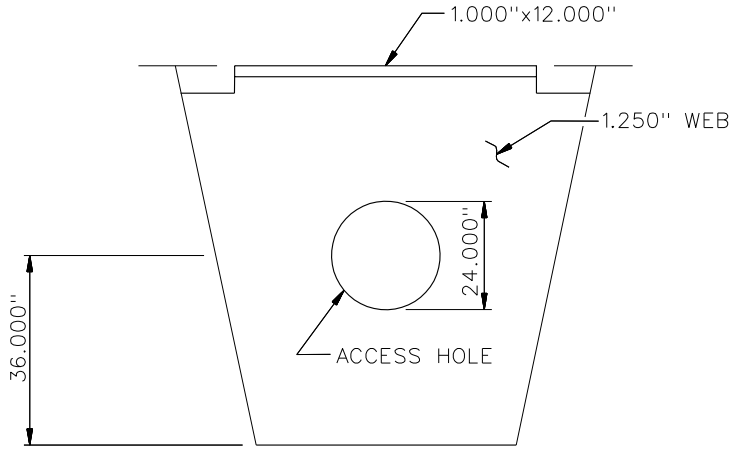

TYPICAL INTERNAL DIAPHRAGMS AT SUPPORTS

NCHRP 12-79

BRIDGE NTSCR1

MISC. DETAILS AND NOTES

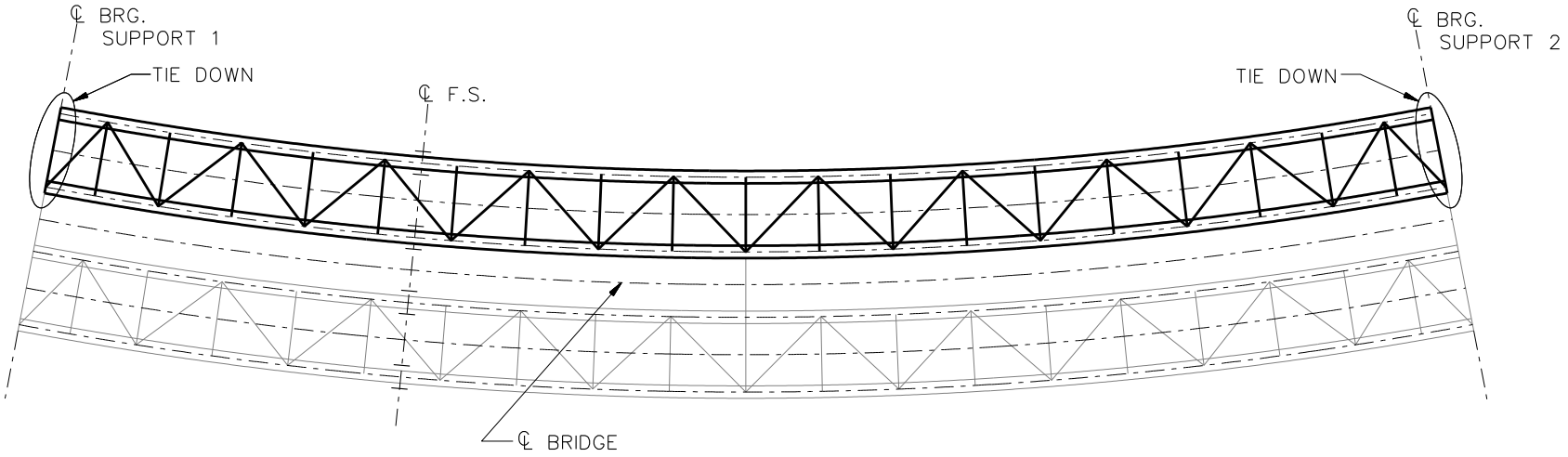

STAGE 1

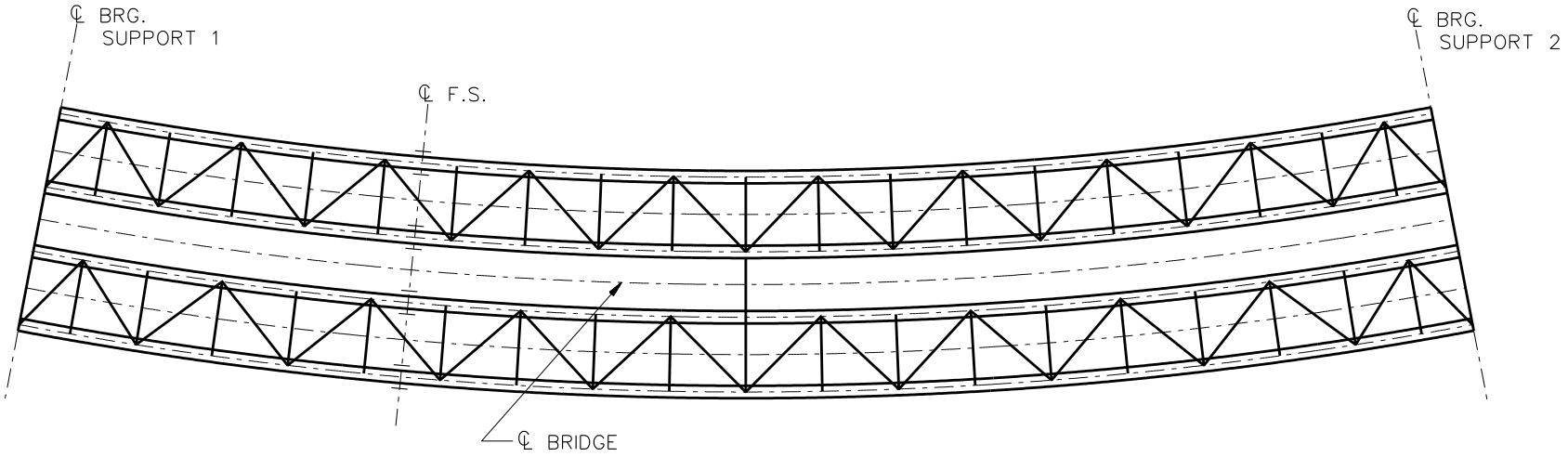

STAGE 2

LEGEND

▽ = HOLD OR LIFT CRANE

○ = TIE DOWN

□ = TEMPORARY SUPPORT STRUCTURE

NCHRP 12-79

BRIDGE NTSCR1

ERECTION PROCEDURE

NCHRP 12-79

NTSCR2

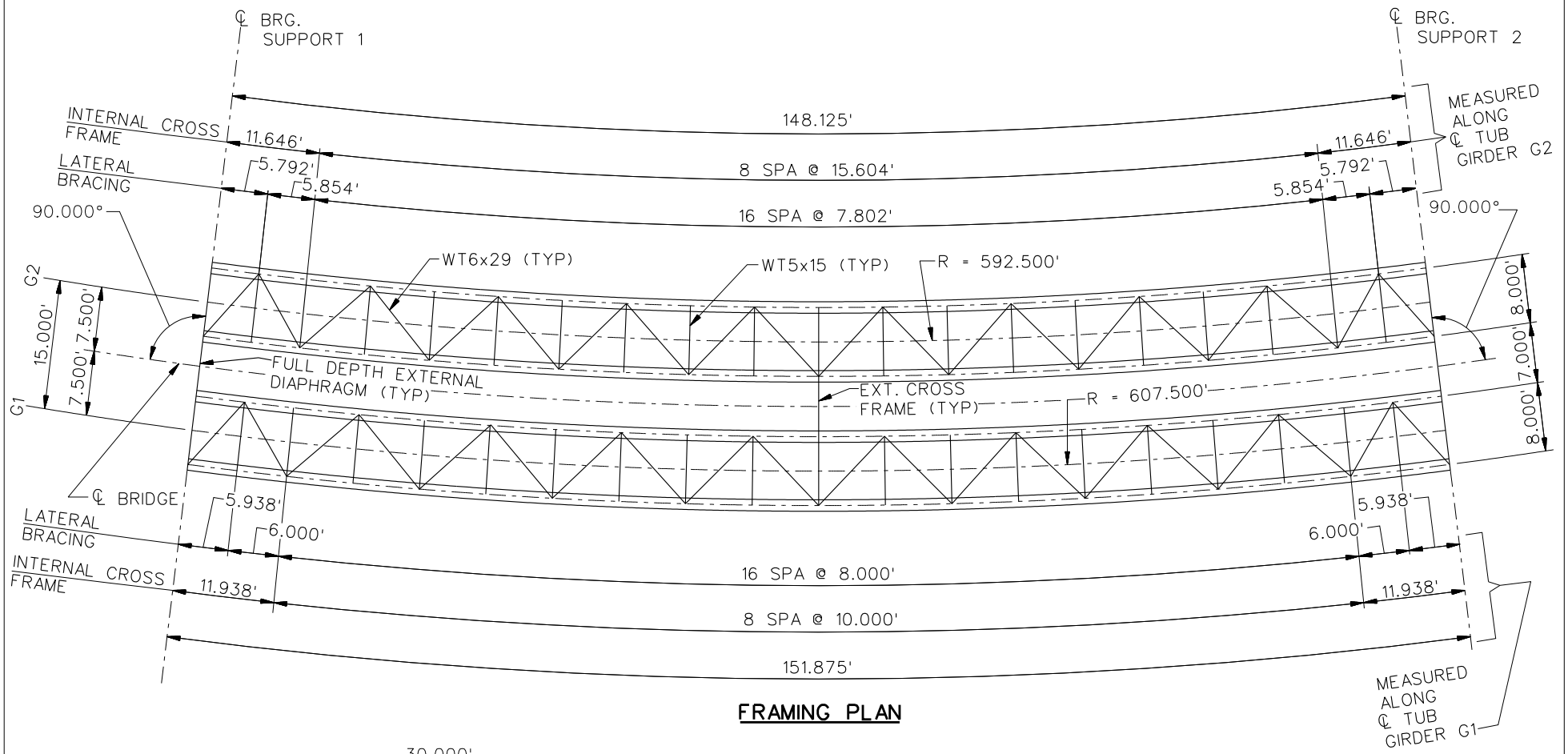

FRAMING PLAN

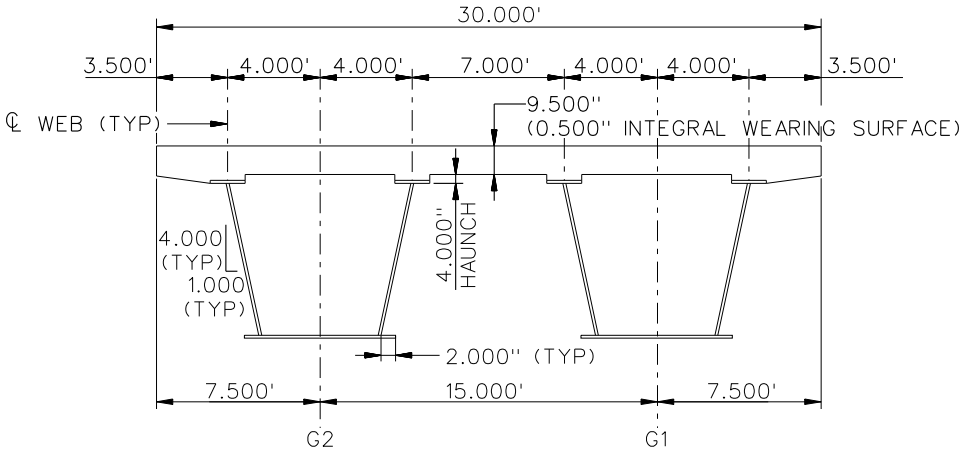

CROSS - SECTION

NOTE:
NO INT. TRANSV. STIFFENERS
CONN PL = 6.000"x0.875"
BRG. STIFFENER = 8.000"x1.500"
ONE INT. EXT. CROSS FRAME @ MIDSPAN (RADIAL)

NCHRP 12-79

BRIDGE NTSCR2

FRAMING PLAN AND CROSS-SECTION

SHEET 1 OF 7

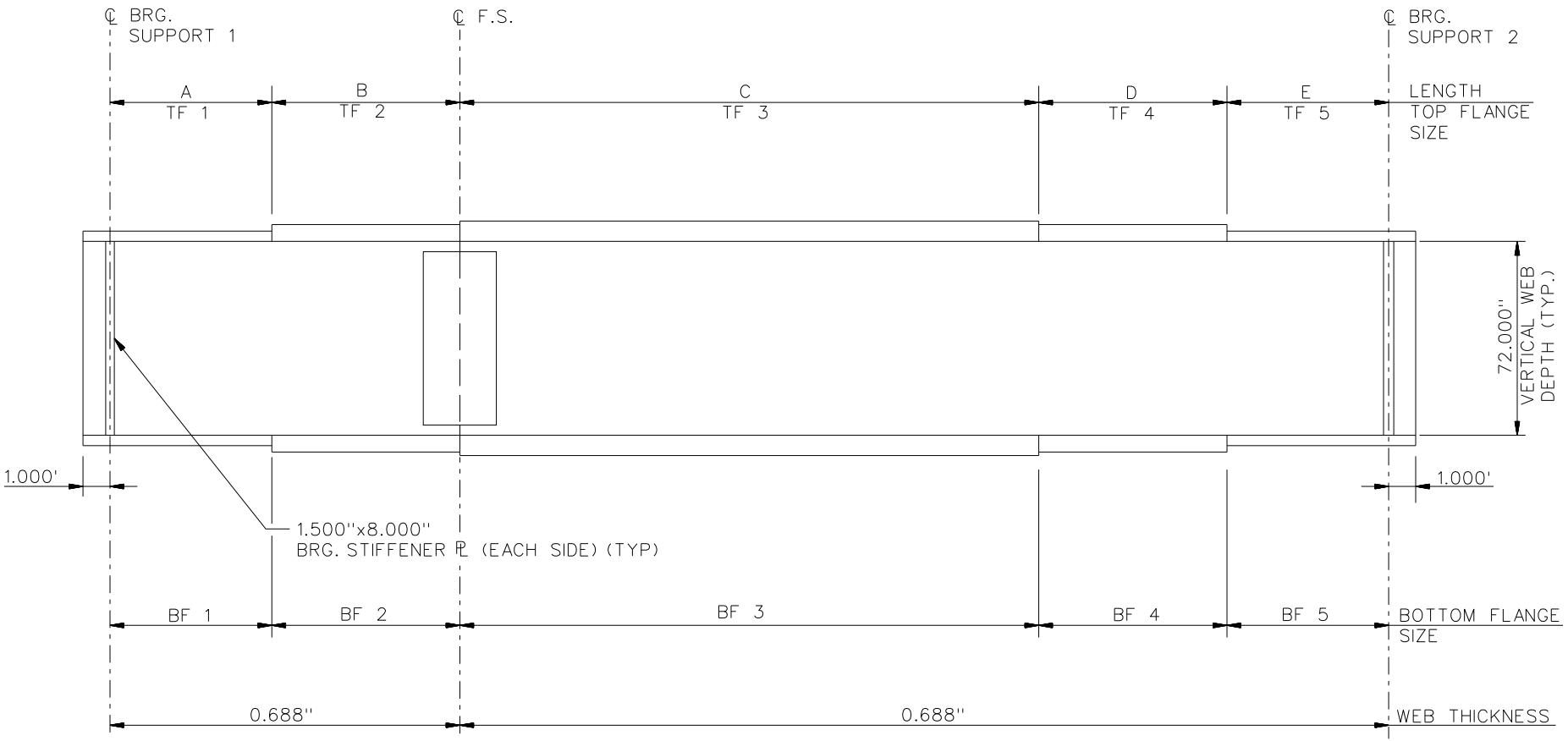

NOTES:

1. SEE TABLES ON SHEET 3 FOR GIRDER ELEVATION DIMENSIONS AND PLATE SIZES.

NCHRP 12-79

BRIDGE NTSCR2

GIRDER ELEVATION

SHEET 2 OF 7

	GIRDER PLATE LENGTHS ✳	
LENGTH	G1	G2
A	20.938	19.063
B	20.000	20.000
C	70.000	70.000
D	20.000	20.000
E	20.938	19.063

✳ ALL DIMENSIONS ARE IN FEET.

	GIRDER FLANGE DIMENSIONS ✳✳			
TOP FLANGE	G1		G2	
	BF	TF	BF	TF
TF1	16.000	0.875	16.000	0.875
TF2	16.000	0.875	16.000	0.875
TF3	16.000	0.875	16.000	0.875
TF4	16.000	0.875	16.000	0.875
TF5	16.000	0.875	16.000	0.875

✳✳ ALL DIMENSIONS ARE IN INCHES.

	GIRDER FLANGE DIMENSIONS ✳✳			
BOTTOM FLANGE	G1		G2	
	BF	TF	BF	TF
BF1	64.000	0.875	64.000	0.875
BF2	64.000	0.875	64.000	0.875
BF3	64.000	1.250	64.000	1.000
BF4	64.000	0.875	64.000	0.875
BF5	64.000	0.875	64.000	0.875

✳✳ ALL DIMENSIONS ARE IN INCHES.

NCHRP 12-79

BRIDGE NTSCR2

GIRDER ELEVATION TABLES

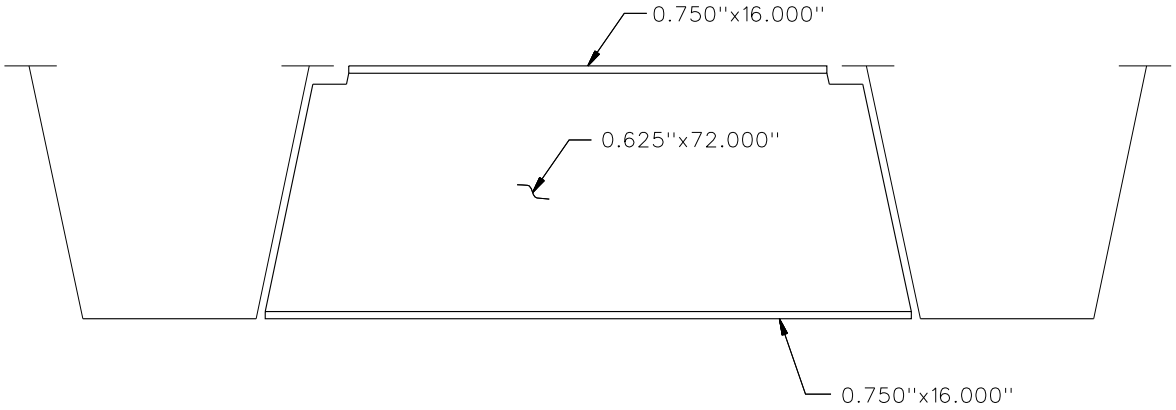

TYPICAL END DIAPHRAGM

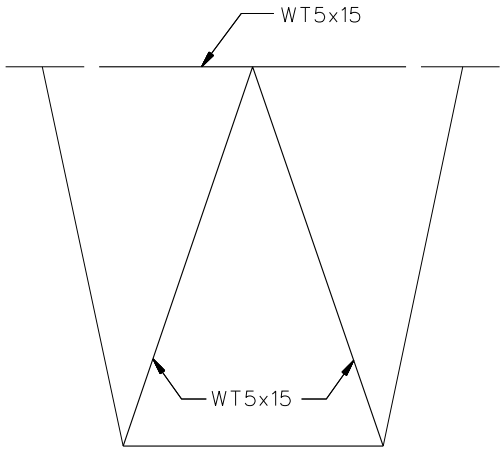

TYPICAL INTERNAL CROSS FRAME

NOTES:

1. STEEL DEAD LOAD INCREASED BY 5% FOR MDX AND LARSA MODELS; 2% FOR 3D MODEL; AND 10% FOR APPROXIMATE ANALYSIS TO ACCOUNT FOR MISC. DETAILS.

2. FORMWORK LOAD OF 10PSF IS INCLUDED IN CONCRETE DEAD LOAD.

3. ADDITIONAL DESIGN PARAMETERS:
   A. 1.500' PARAPET WIDTH BOTH SIDES.
   B. 700 LB/FT UNIFORM LOAD ASSUMED FOR PARAPET WEIGHT.
   C. ROADWAY WIDTH = 26.500'.
   D. NUMBER OF DESIGN LANES = 2.
   E. HL93 LIVE LOAD.
   F. DESIGN SPEED = 35 MPH.

4. DIAPHRAGM MEMBER CALL-OUTS ARE IN ENGLISH UNITS.

NCHRP 12-79

BRIDGE NTSCR2

MISC. DETAILS AND NOTES

SHEET 4 OF 7

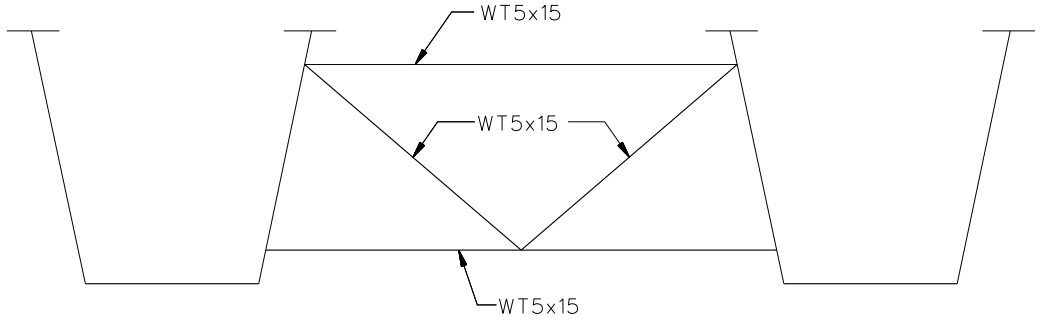

INTERMEDIATE EXTERNAL DIAPHRAGM

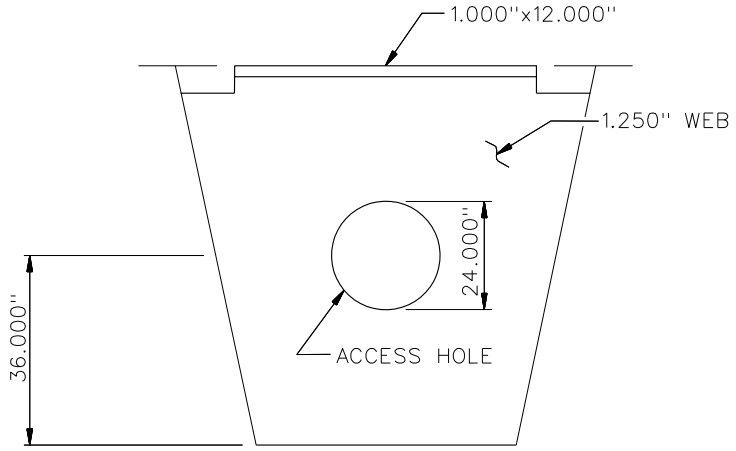

TYPICAL INTERNAL DIAPHRAGMS AT SUPPORTS

NCHRP 12-79

BRIDGE NTSCR2

MISC. DETAILS AND NOTES

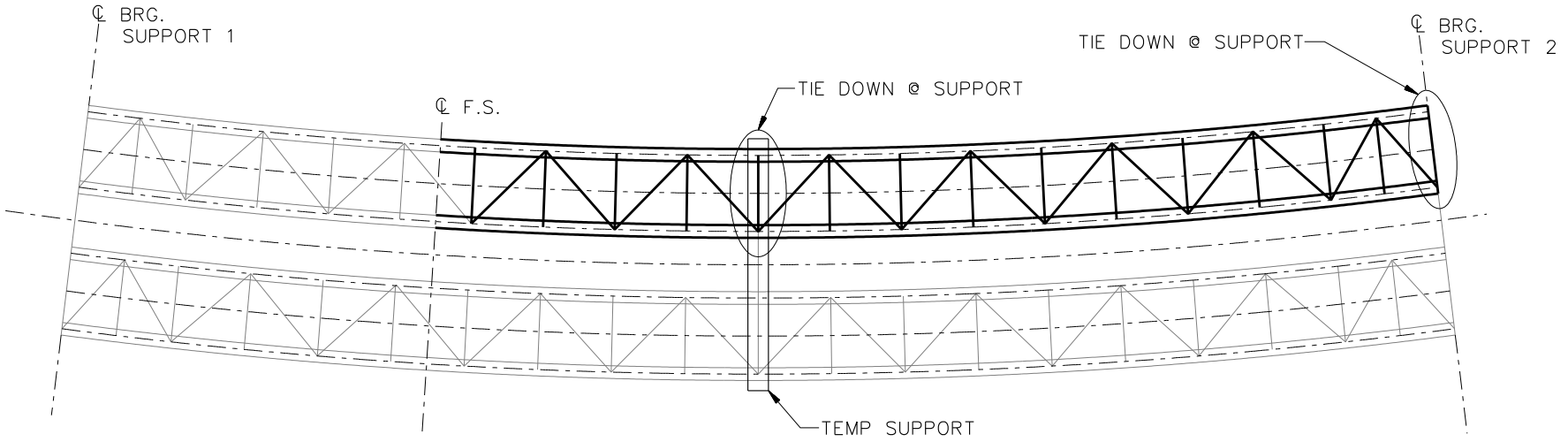

STAGE 1

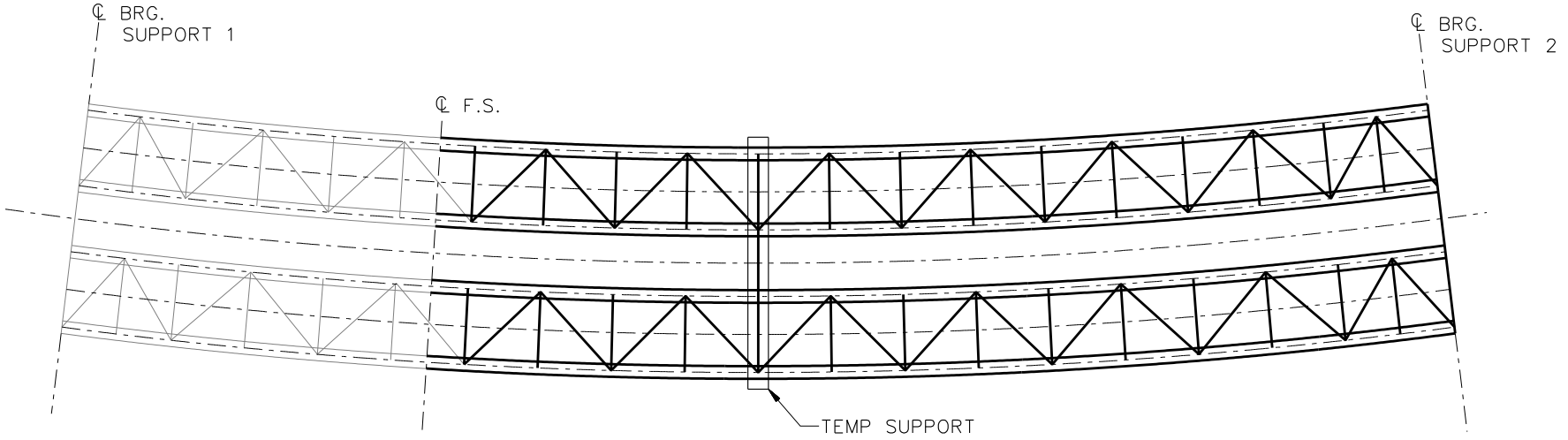

STAGE 2

LEGEND

▽ = HOLD OR LIFT CRANE

○ = TIE DOWN

□ = TEMPORARY SUPPORT STRUCTURE

NCHRP 12-79

BRIDGE NTSCR2

GENERAL ERECTION PROCEDURE

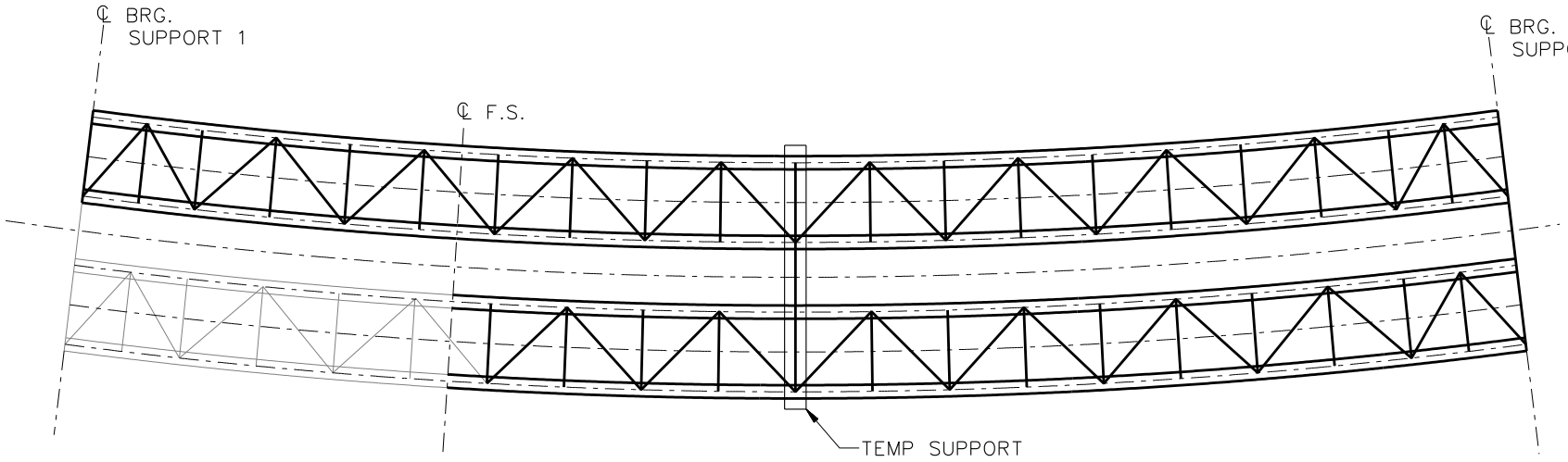

STAGE 3

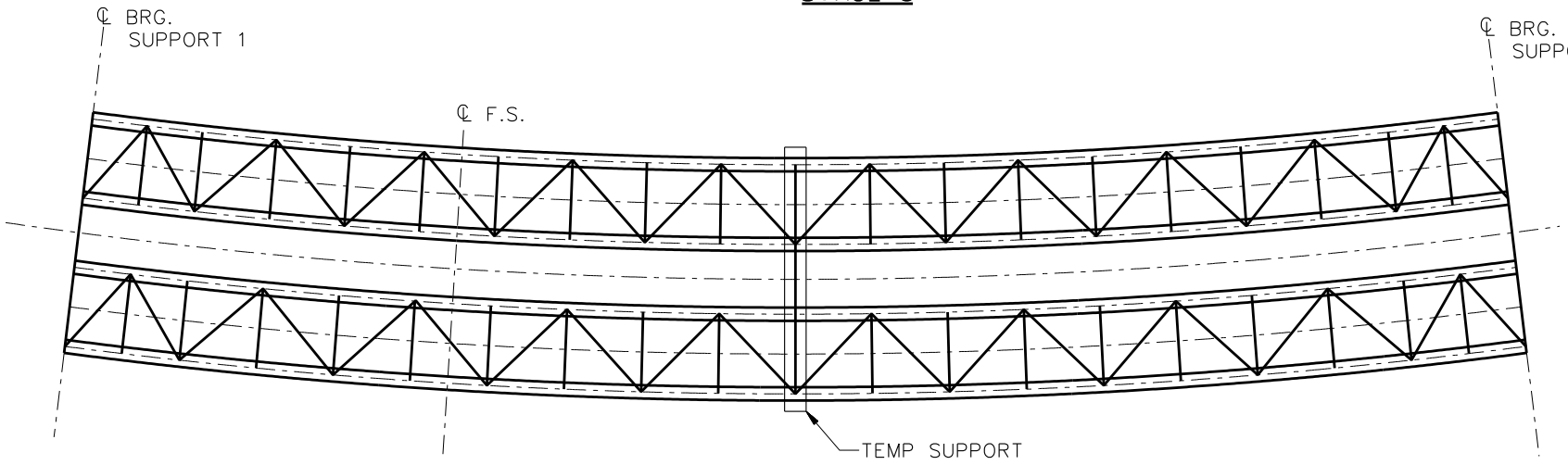

STAGE 4

LEGEND

▽ = HOLD OR LIFT CRANE

○ = TIE DOWN

□ = TEMPORARY SUPPORT STRUCTURE

STAGE 5

REMOVE TEMP SUPPORT

NCHRP 12-79

BRIDGE NTSCR2

GENERAL ERECTION PROCEDURE

NCHRP 12-79

NTSCR5

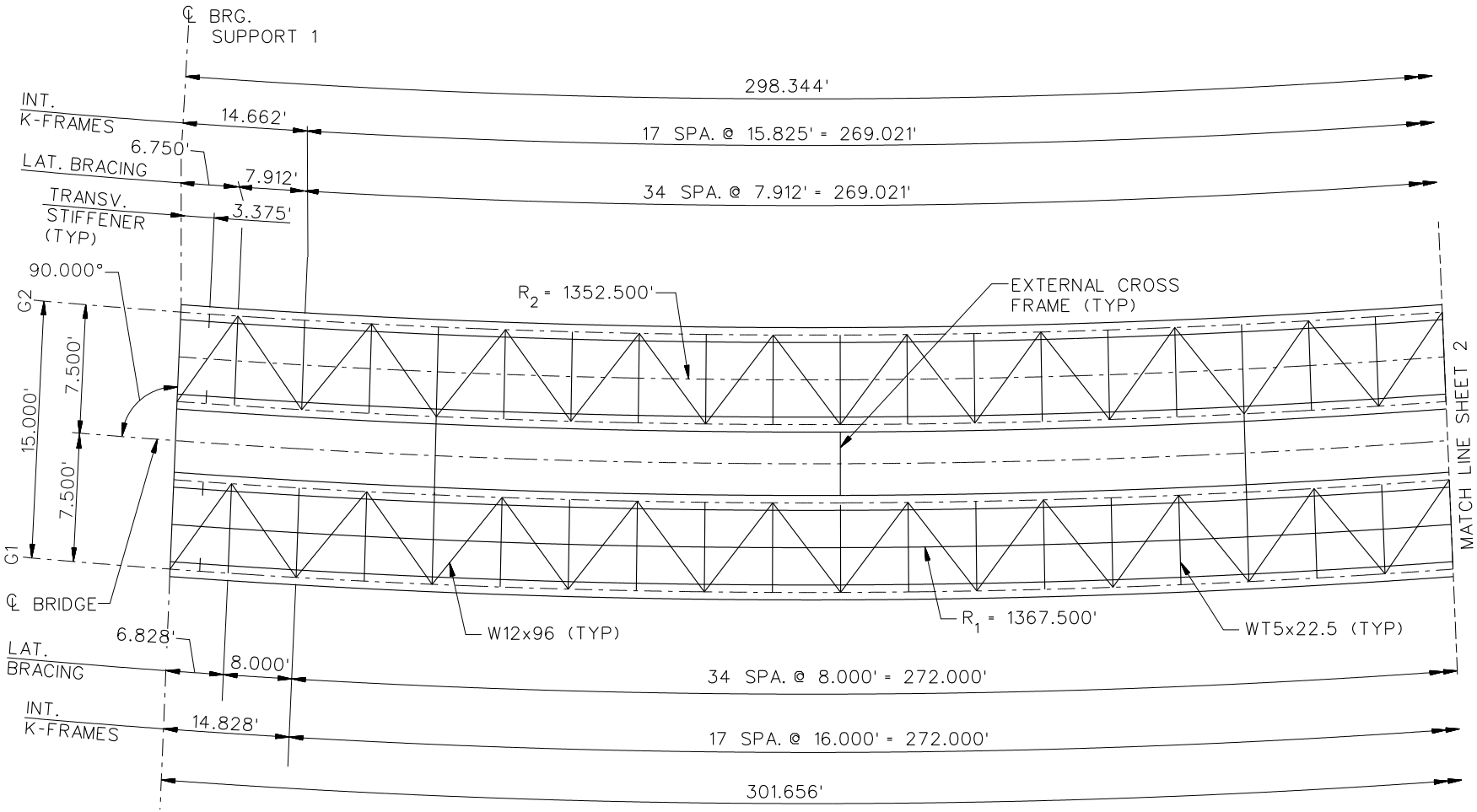

FRAMING PLAN

NOTES:
1. TYP. INTERNAL K-FRAMES CONNECTION PLATE = 0.875"x6.000".
2. ALL BRG. STIFFENERS = 1.500"x8.000".

NCHRP 12-79

BRIDGE NTSCR5

FRAMING PLAN AND CROSS-SECTION

SHEET 1 OF 9

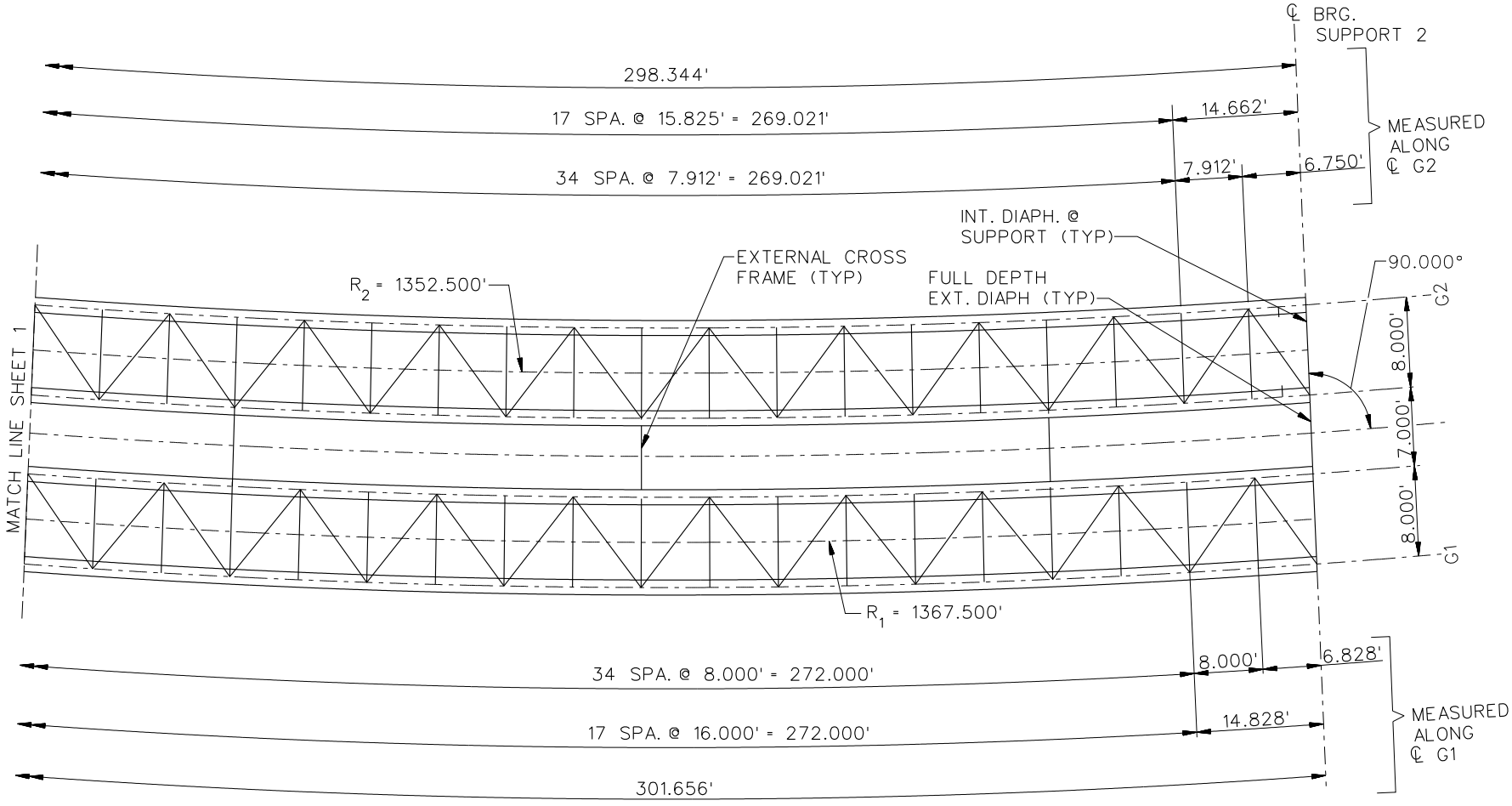

FRAMING PLAN

NOTE:
1. TYP. INTERNAL K-FRAMES CONNECTION PLATE = 0.875''x6.000''.
2. ALL BRG. STIFFENERS = 1.500''x8.000''

NCHRP 12-79

BRIDGE NTSCR5

FRAMING PLAN AND CROSS-SECTION

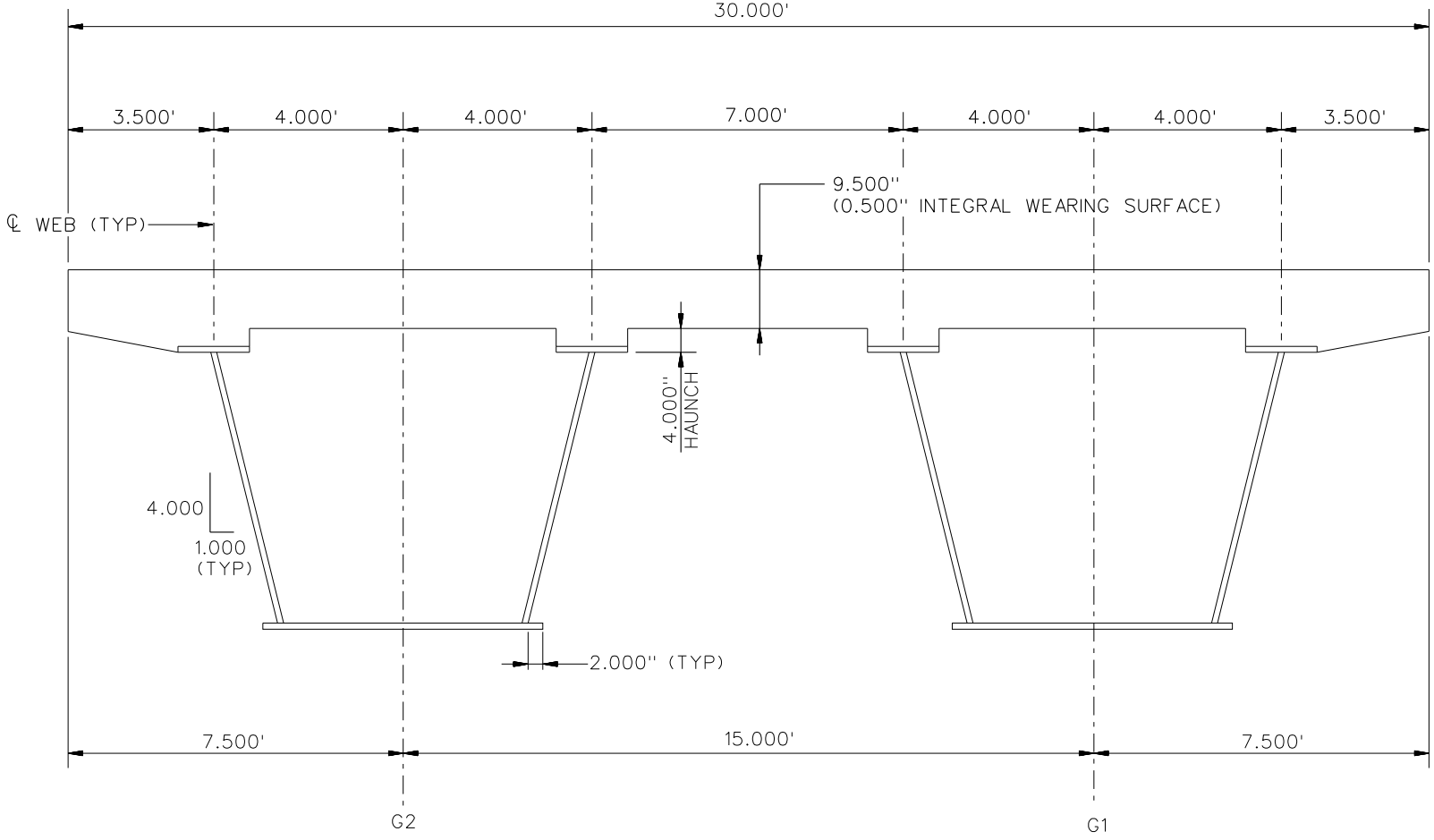

CROSS - SECTION

NCHRP	12-79
BRIDGE	NTSCR5
TYPICAL SECTION	
SHEET 3 OF 9	

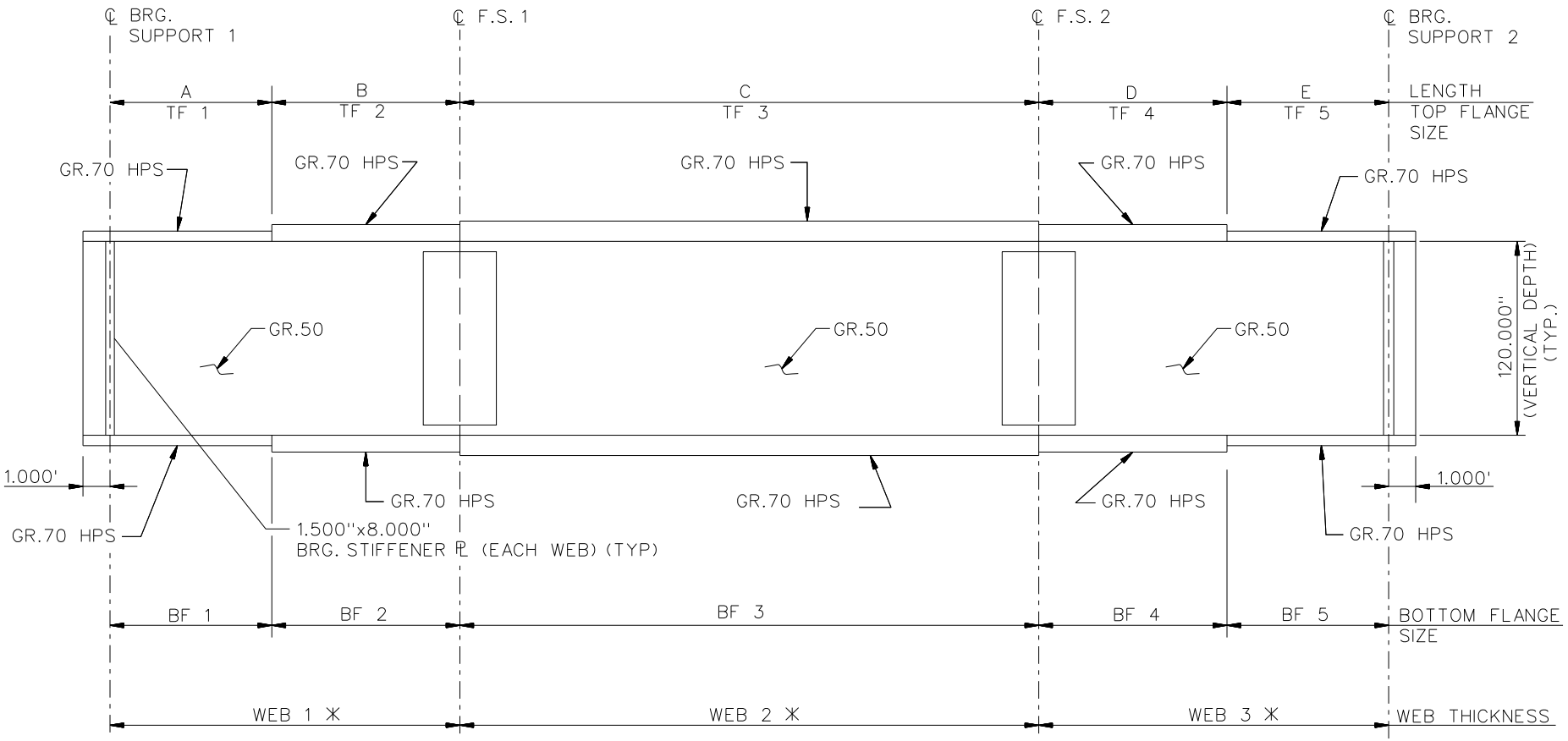

NOTES:

1. SEE TABLES ON SHEET 3 FOR GIRDER ELEVATION DIMENSIONS AND PLATE SIZES.

✳		G1	G2
	WEB 1	1.0625"	1.000"
	WEB 2	0.875"	0.875"
	WEB 3	1.0625"	1.000"

NCHRP 12-79

BRIDGE NTSCR5

GIRDER ELEVATION

SHEET 4 OF 9

	GIRDER PLATE LENGTHS ✳	
LENGTH	G1	G2
A	45.000	45.000
B	45.000	45.000
C	121.654	118.346
D	45.000	45.000
E	45.000	45.000

✳ ALL DIMENSIONS ARE IN FEET.

	GIRDER FLANGE DIMENSIONS ✳✳			
TOP	G1		G2	
FLANGE	BF	TF	BF	TF
TF1	24.000	1.500	24.000	1.250
TF2	24.000	1.500	24.000	1.250
TF3	24.000	2.250	24.000	1.750
TF4	24.000	1.500	24.000	1.250
TF5	24.000	1.500	24.000	1.250

✳✳ ALL DIMENSIONS ARE IN INCHES.

	GIRDER FLANGE DIMENSIONS ✳✳			
BOTTOM	G1		G2	
FLANGE	BF	TF	BF	TF
BF1	40.000	1.500	40.000	1.250
BF2	40.000	2.000	40.000	1.500
BF3	40.000	2.750	40.000	2.250
BF4	40.000	2.000	40.000	1.500
BF5	40.000	1.500	40.000	1.250

✳✳ ALL DIMENSIONS ARE IN INCHES.

NCHRP 12-79

BRIDGE NTSCR5

GIRDER ELEVATION TABLES

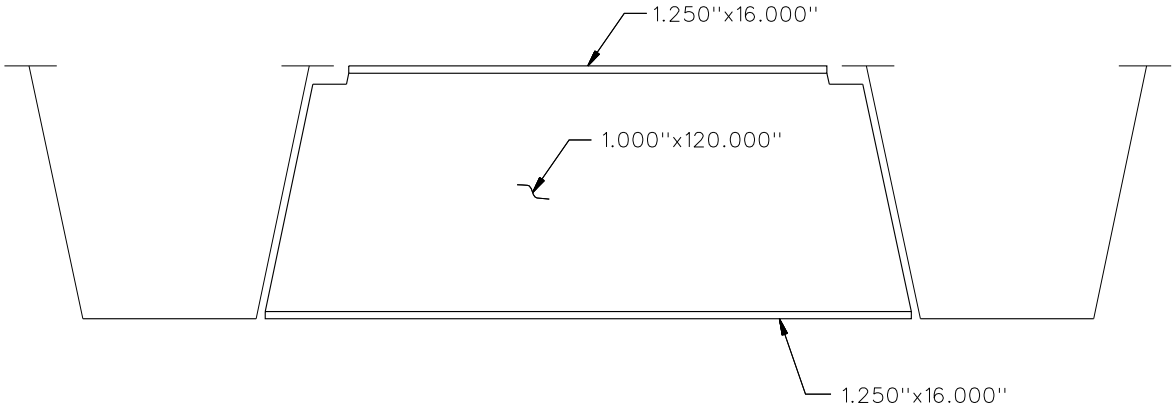

TYPICAL END DIAPHRAGM

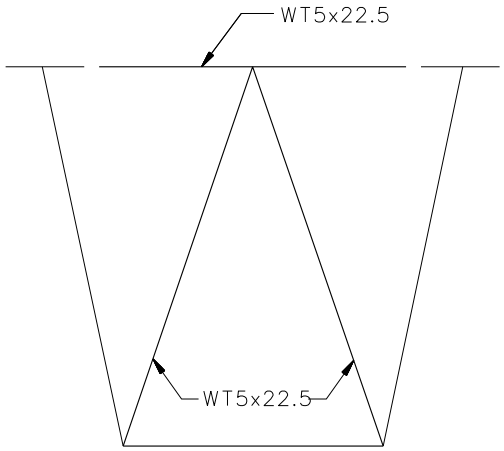

TYPICAL INTERNAL CROSS FRAME

NOTES:

1. STEEL DEAD LOAD INCREASED BY 15% FOR MDX AND LARSA MODELS; 2% FOR 3D MODEL; AND 20% FOR APPROXIMATE ANALYSIS TO ACCOUNT FOR MISC. DETAILS.

2. FORMWORK LOAD OF 10PSF IS INCLUDED IN CONCRETE DEAD LOAD.

3. ADDITIONAL DESIGN PARAMETERS:
   A. 1.500' PARAPET WIDTH BOTH SIDES.
   B. 700 LB/FT UNIFORM LOAD ASSUMED FOR PARAPET WEIGHT.
   C. ROADWAY WIDTH = 26.500'.
   D. NUMBER OF DESIGN LANES = 2.
   E. HL93 LIVE LOAD.
   F. DESIGN SPEED = 35 MPH.

4. DIAPHRAGM MEMBER CALL-OUTS ARE IN ENGLISH UNITS.

NCHRP 12-79

BRIDGE NTSCR5

MISC. DETAILS AND NOTES

SHEET 6 OF 9

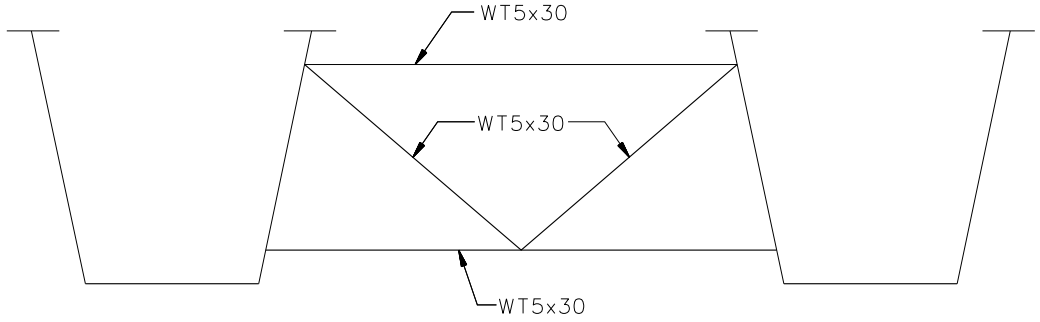

TYPICAL INTERMEDIATE EXTERNAL DIAPHRAGM

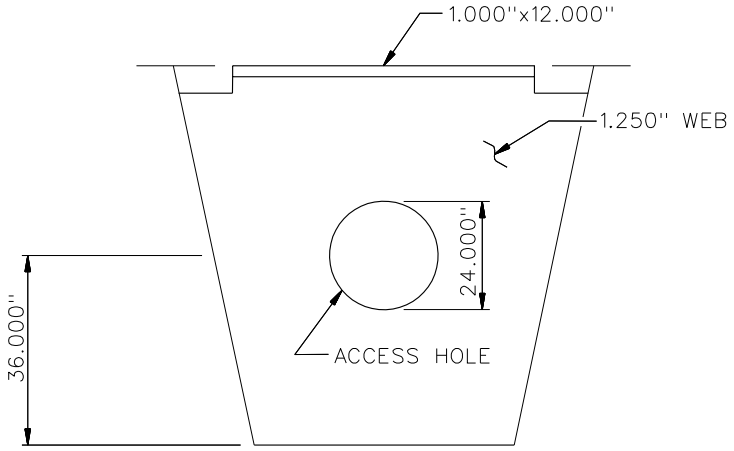

TYPICAL INTERNAL DIAPHRAGMS AT SUPPORTS

NCHRP 12-79

BRIDGE NTSCR5

MISC. DETAILS AND NOTES

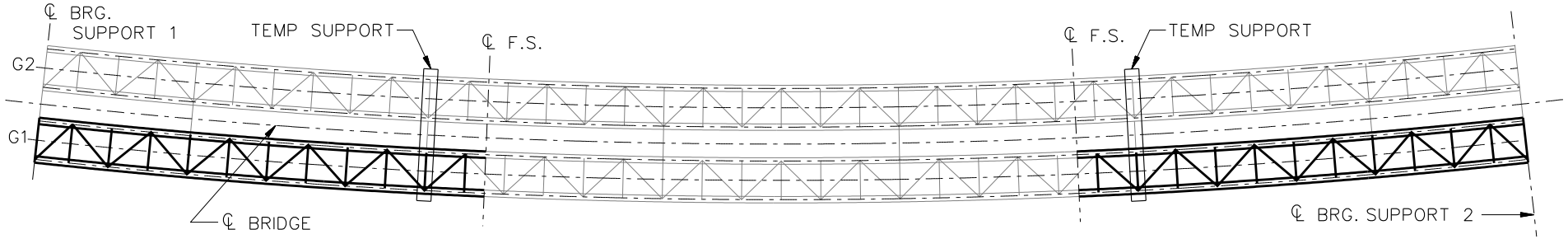

STAGE 1

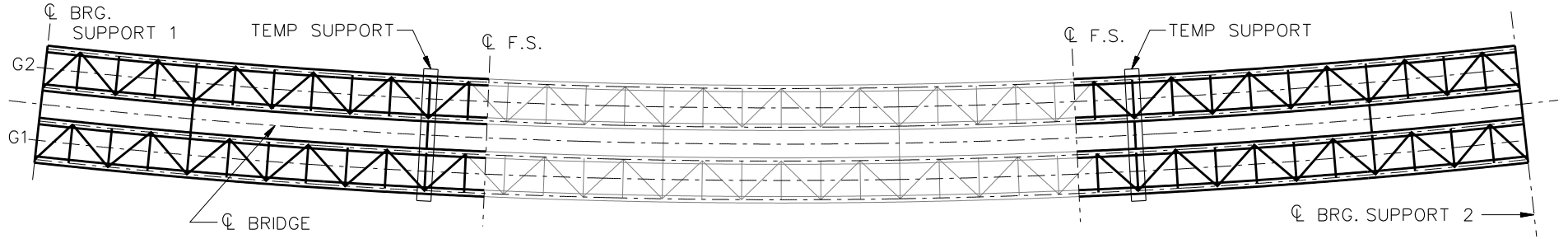

STAGE 2

LEGEND

▽ = HOLD OR LIFT CRANE

○ = TIE DOWN

□ = TEMPORARY SUPPORT STRUCTURE

NCHRP 12-79

BRIDGE NTSCR5

GENERAL ERECTION PROCEDURE

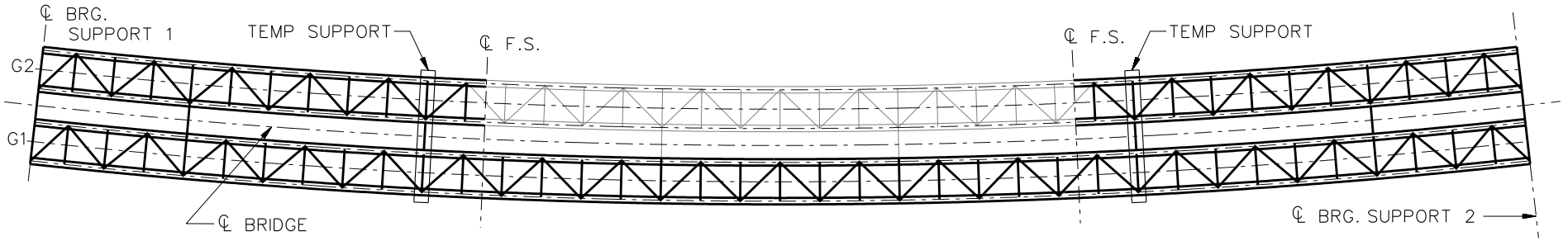

STAGE 3

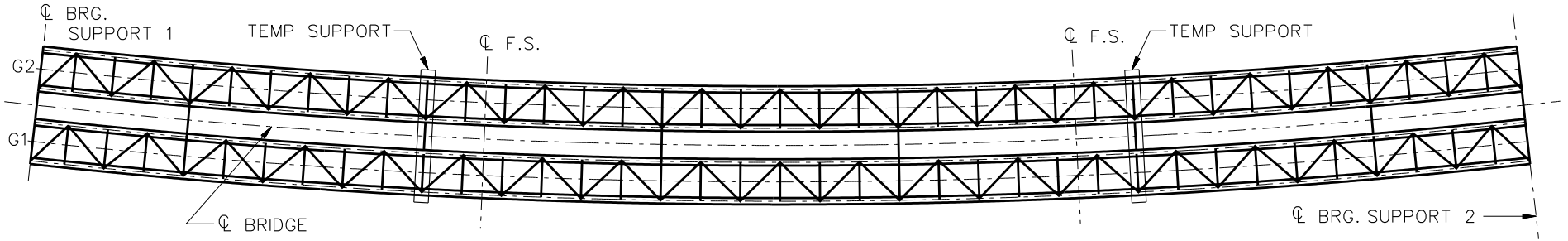

STAGE 4

LEGEND

▽ = HOLD OR LIFT CRANE

○ = TIE DOWN

□ = TEMPORARY SUPPORT STRUCTURE

STAGE 5

REMOVE ALL TEMP SUPPORTS

NCHRP 12-79

BRIDGE NTSCR5

GENERAL ERECTION PROCEDURE

NCHRP 12-79

NTSCS5

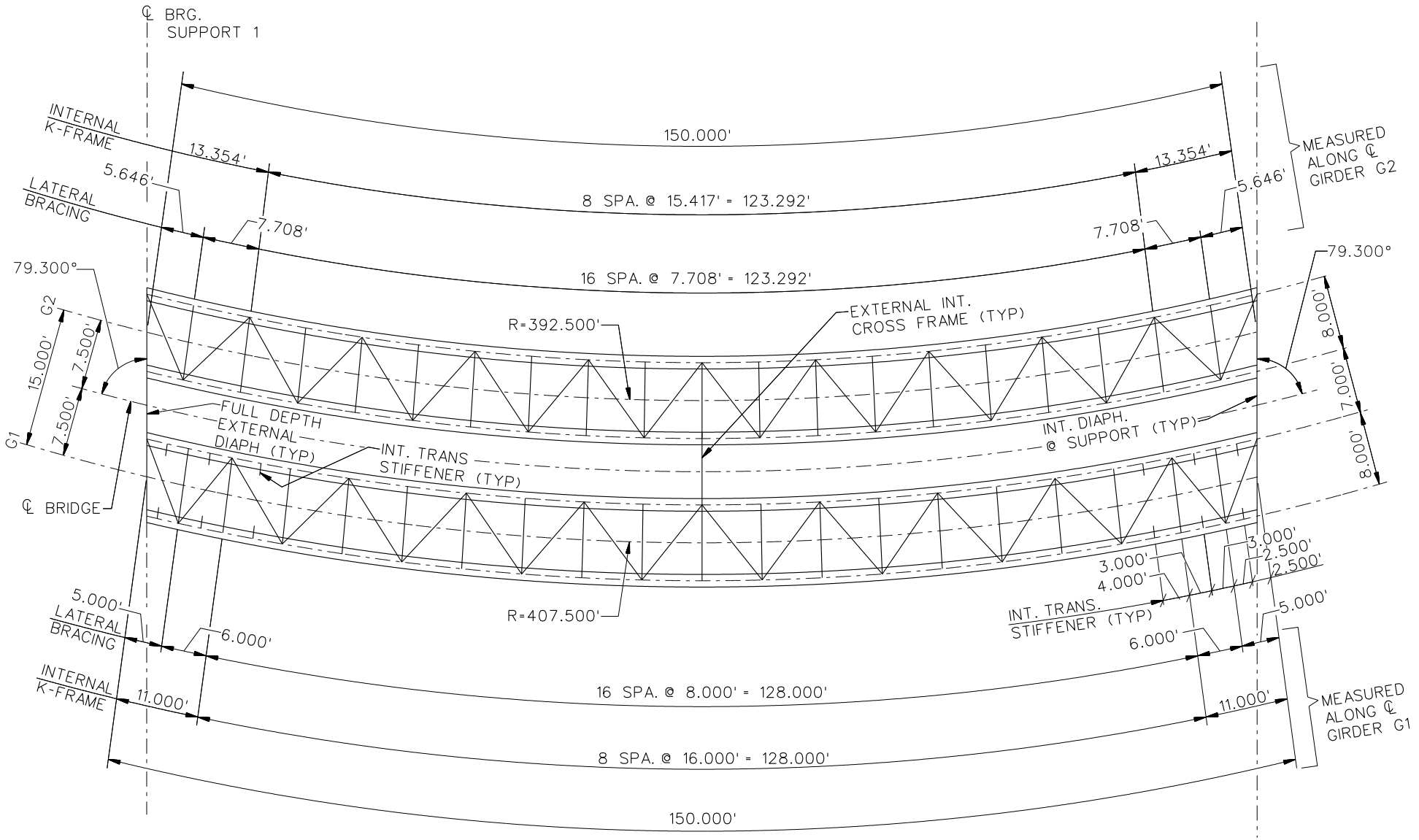

FRAMING PLAN

NOTES:

1. INT. TRANSV. STIFFENERS = 0.875"x6.000"
2. BRG. STIFFENER = 1.500"x12.000"

NCHRP 12-79

BRIDGE NTSCS5

FRAMING PLAN AND CROSS-SECTION

SHEET 1 OF 7

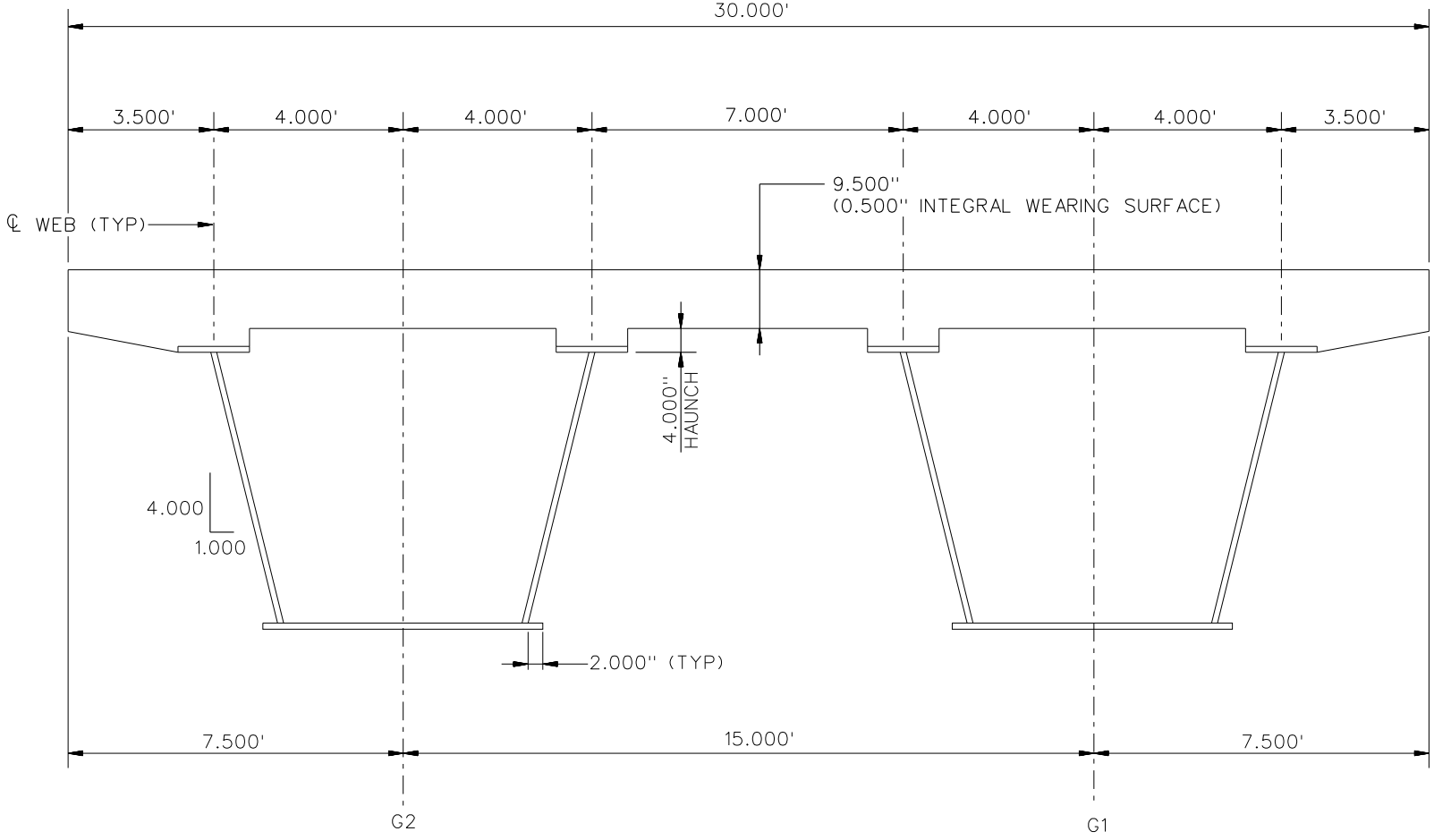

CROSS - SECTION

NCHRP 12-79

BRIDGE NTSCS5

TYPICAL SECTION

SHEET 2 OF 7

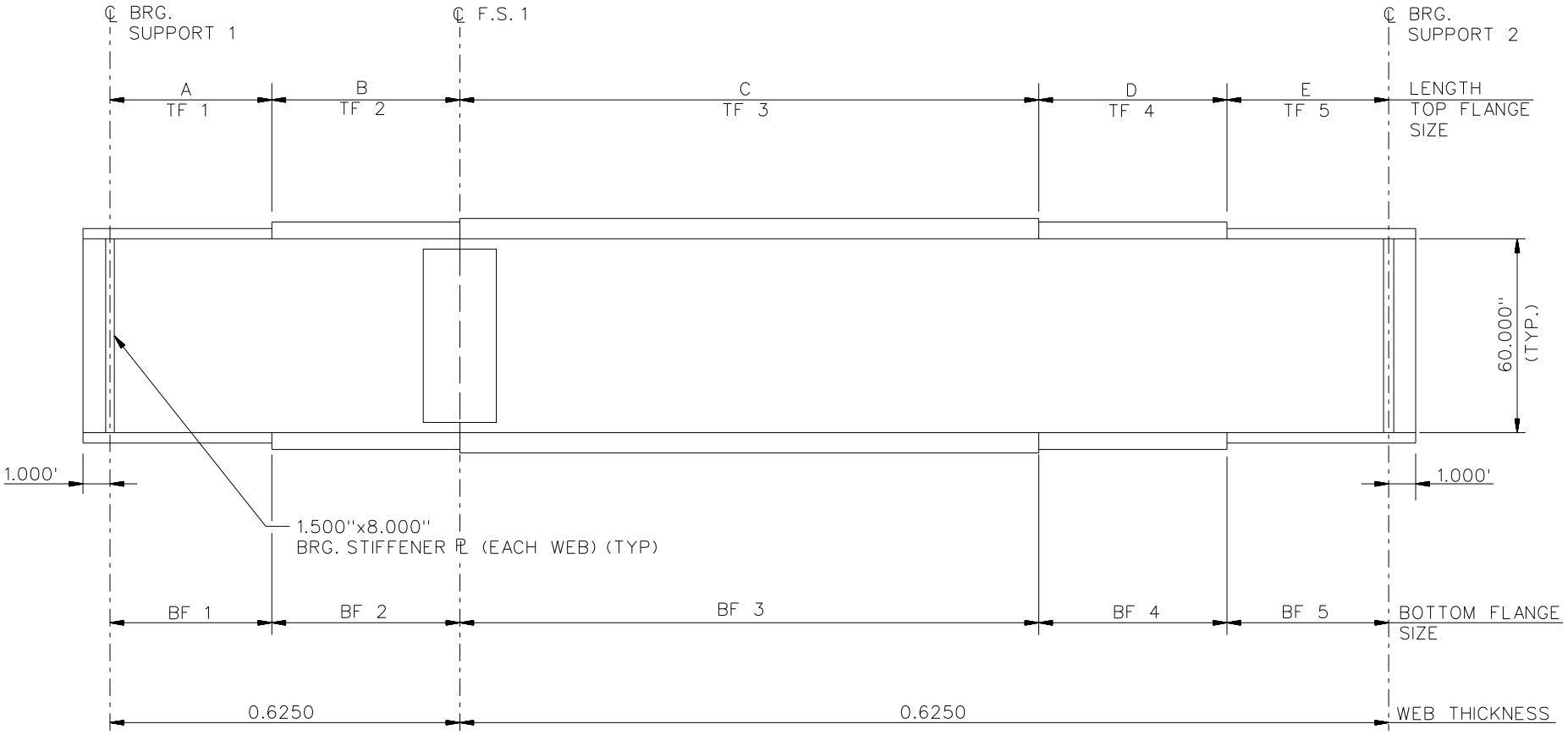

NOTES:

1. SEE TABLES ON SHEET 4 FOR GIRDER ELEVATION DIMENSIONS AND PLATE SIZES.

NCHRP 12-79

BRIDGE NTSCS5

GIRDER ELEVATION

SHEET 3 OF 7

	GIRDER PLATE LENGTHS ✳	
LENGTH	G1	G2
A	20.000	20.000
B	20.000	20.000
C	70.000	70.000
D	20.000	20.000
E	20.000	20.000

✳ ALL DIMENSIONS ARE IN FEET.

	GIRDER FLANGE DIMENSIONS ✳✳			
TOP	G1		G2	
FLANGE	BF	TF	BF	TF
TF1	16.000	0.875	16.000	0.875
TF2	16.000	0.875	16.000	0.875
TF3	16.000	1.250	16.000	0.875
TF4	16.000	0.875	16.000	0.875
TF5	16.000	0.875	16.000	0.875

✳✳ ALL DIMENSIONS ARE IN INCHES.

	GIRDER FLANGE DIMENSIONS ✳✳			
BOTTOM	G1		G2	
FLANGE	BF	TF	BF	TF
BF1	70.000	1.000	70.000	0.875
BF2	70.000	1.000	70.000	0.875
BF3	70.000	1.375	70.000	1.125
BF4	70.000	1.000	70.000	0.875
BF5	70.000	1.000	70.000	0.875

✳✳ ALL DIMENSIONS ARE IN INCHES.

NCHRP 12-79

BRIDGE NTSCS5

GIRDER ELEVATION TABLES

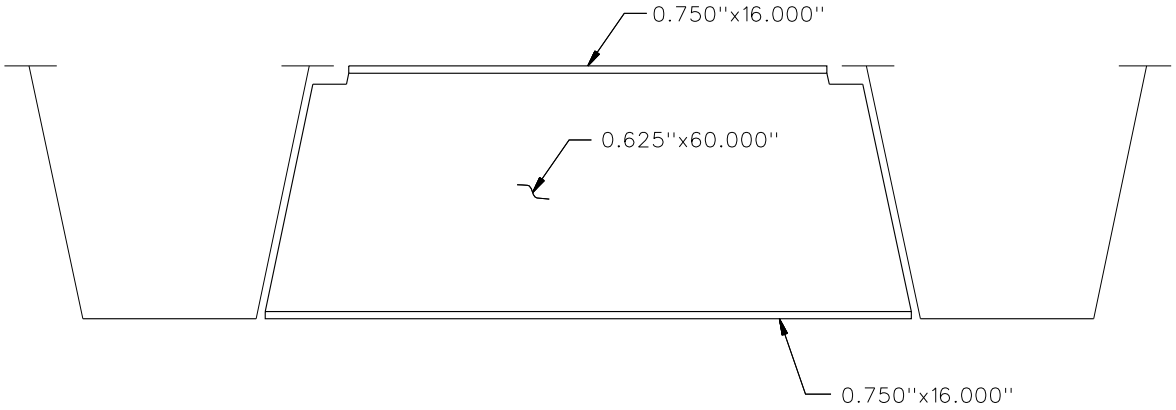

TYPICAL END DIAPHRAGM

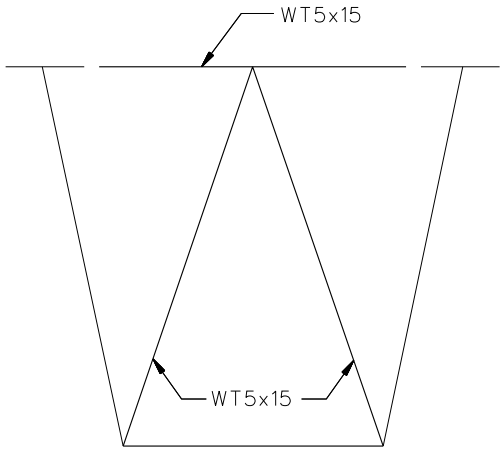

TYPICAL INTERNAL CROSS FRAME

NOTES:

1. STEEL DEAD LOAD INCREASED BY 15% FOR MDX AND LARSA MODELS; 2% FOR 3D MODEL; AND 20% FOR APPROXIMATE ANALYSIS TO ACCOUNT FOR MISC. DETAILS.

2. FORMWORK LOAD OF 10PSF IS INCLUDED IN CONCRETE DEAD LOAD.

3. ADDITIONAL DESIGN PARAMETERS:
   A. 1.500' PARAPET WIDTH BOTH SIDES.
   B. 700 LB/FT UNIFORM LOAD ASSUMED FOR PARAPET WEIGHT.
   C. ROADWAY WIDTH = 26.500'.
   D. NUMBER OF DESIGN LANES = 2.
   E. HL93 LIVE LOAD.
   F. DESIGN SPEED = 35 MPH.

4. DIAPHRAGM MEMBER CALL-OUTS ARE IN ENGLISH UNITS.

NCHRP 12-79

BRIDGE NTSCS5

MISC. DETAILS AND NOTES

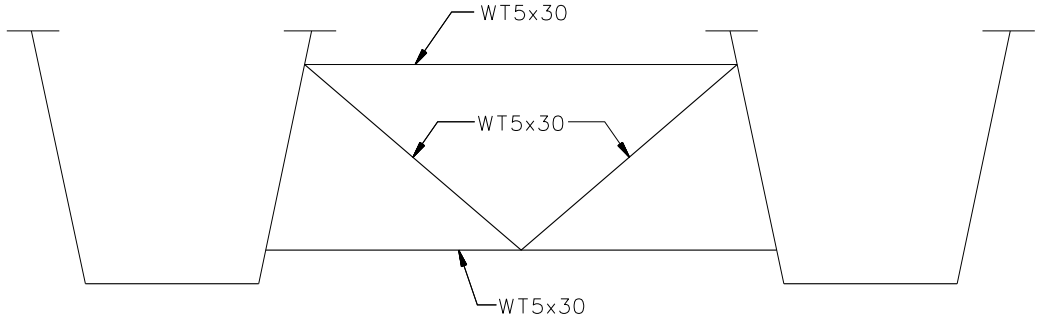

INTERMEDIATE EXTERNAL DIAPHRAGM

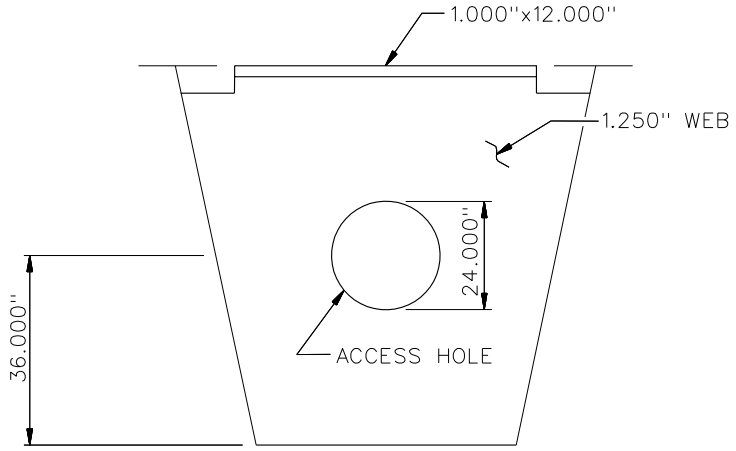

TYPICAL INTERNAL DIAPHRAGMS AT SUPPORTS

NCHRP 12-79

BRIDGE NTSCS5

MISC. DETAILS AND NOTES

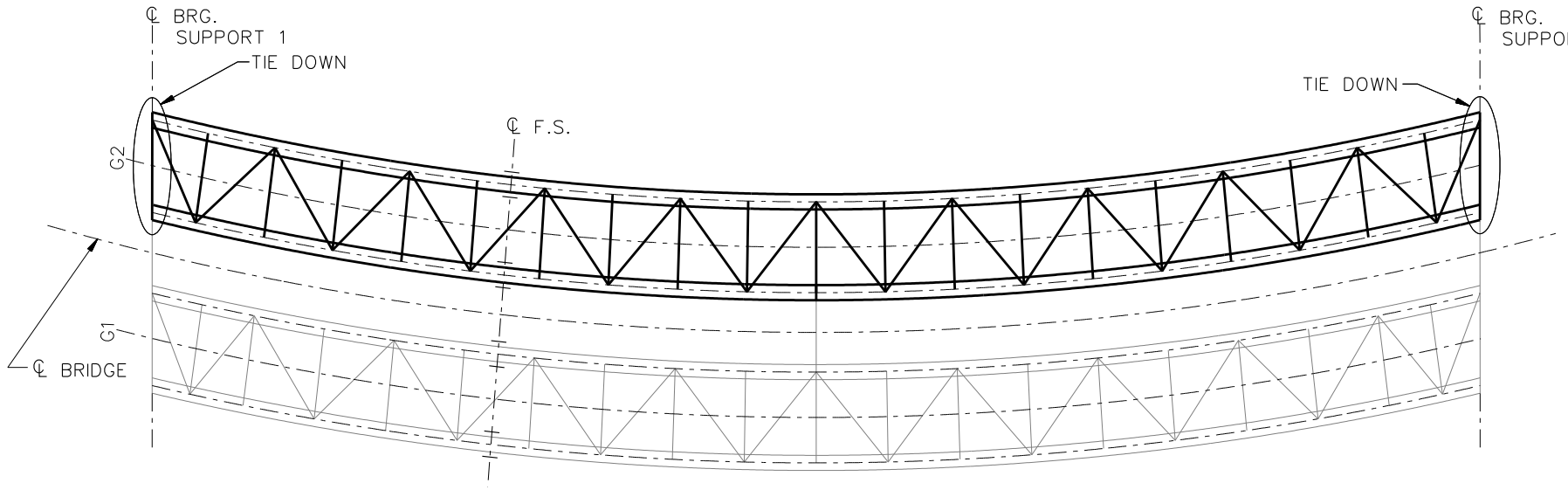

STAGE 1

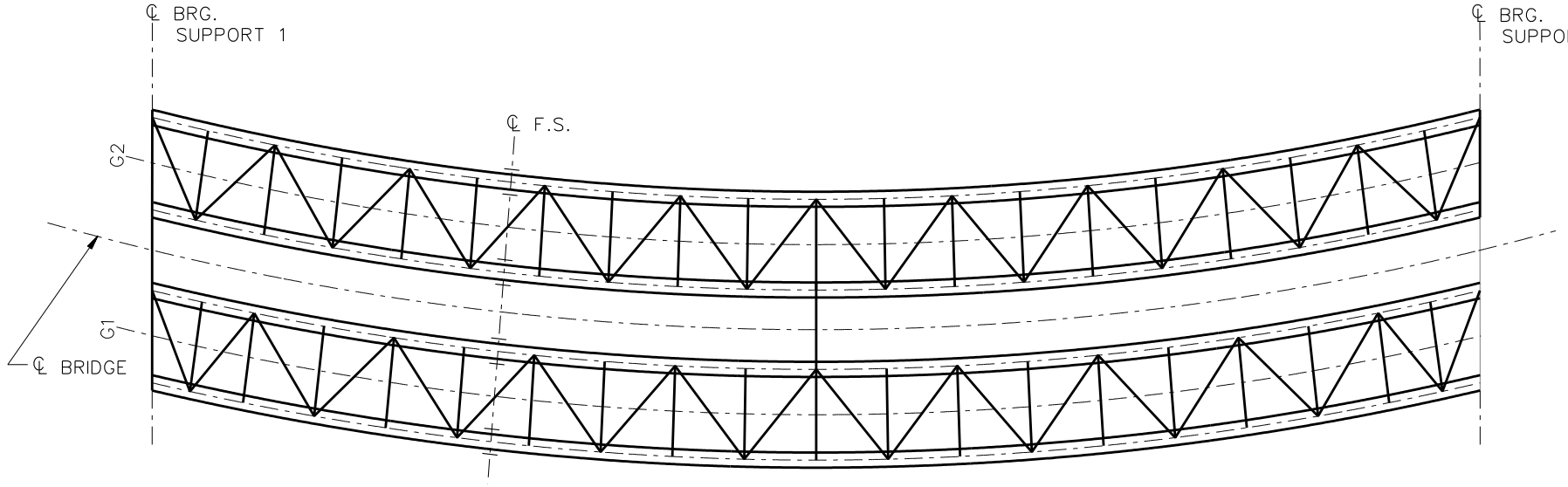

STAGE 2

LEGEND

▽ = HOLD OR LIFT CRANE

○ = TIE DOWN

□ = TEMPORARY SUPPORT STRUCTURE

NCHRP 12-79

BRIDGE NTSCS5

GENERAL ERECTION PROCEDURE

NCHRP 12-79

NTSCS29

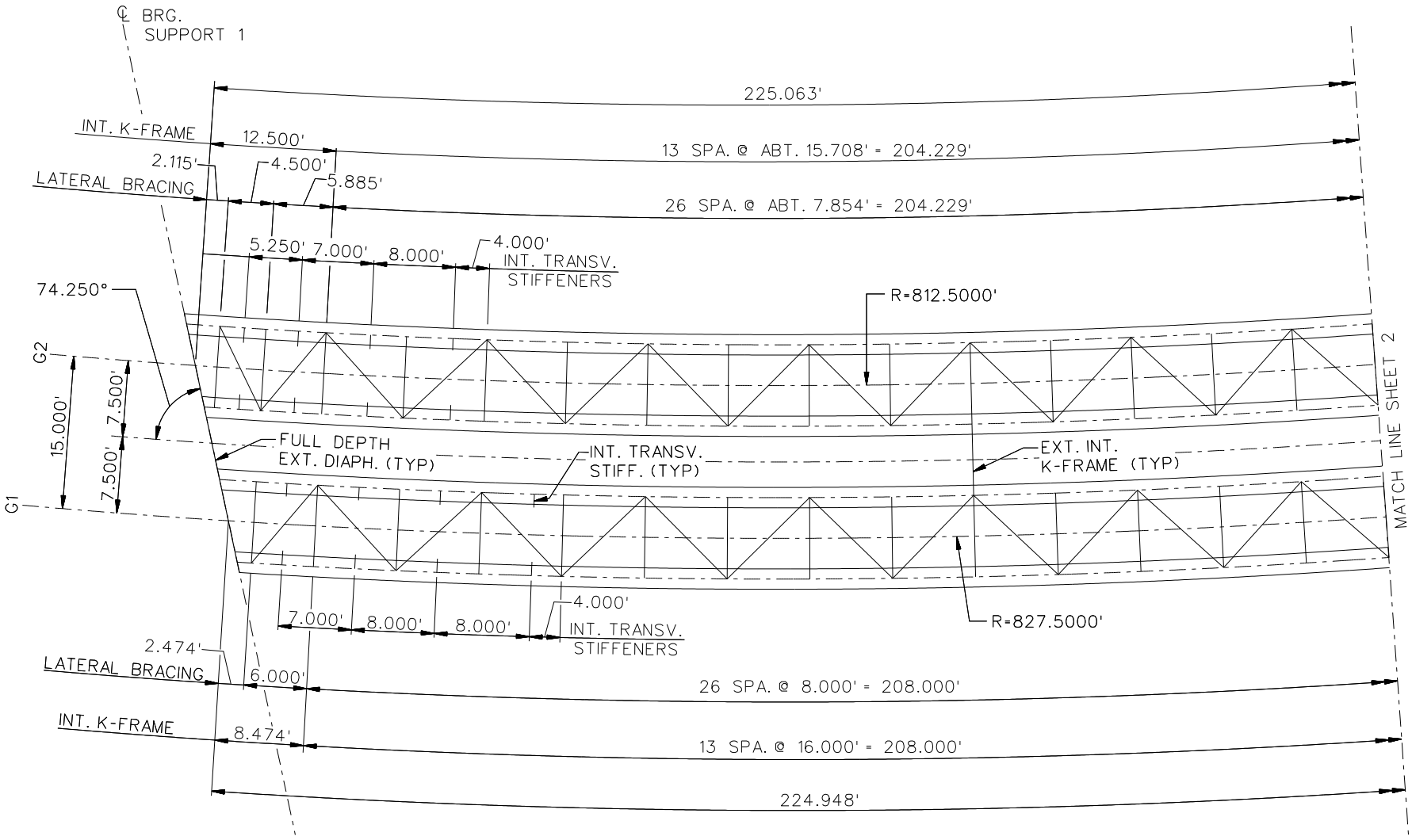

FRAMING PLAN

NOTE:
1. INT. TRANSV. STIFFENERS AND INT. K-FRAMES CONNECTION PLATES = 0.875"x6.000"

2. ALL BEARING STIFFENER = 1.500"x12.000"

NCHRP 12-79

BRIDGE NTSCS29

FRAMING PLAN AND CROSS-SECTION

SHEET 1 OF 9

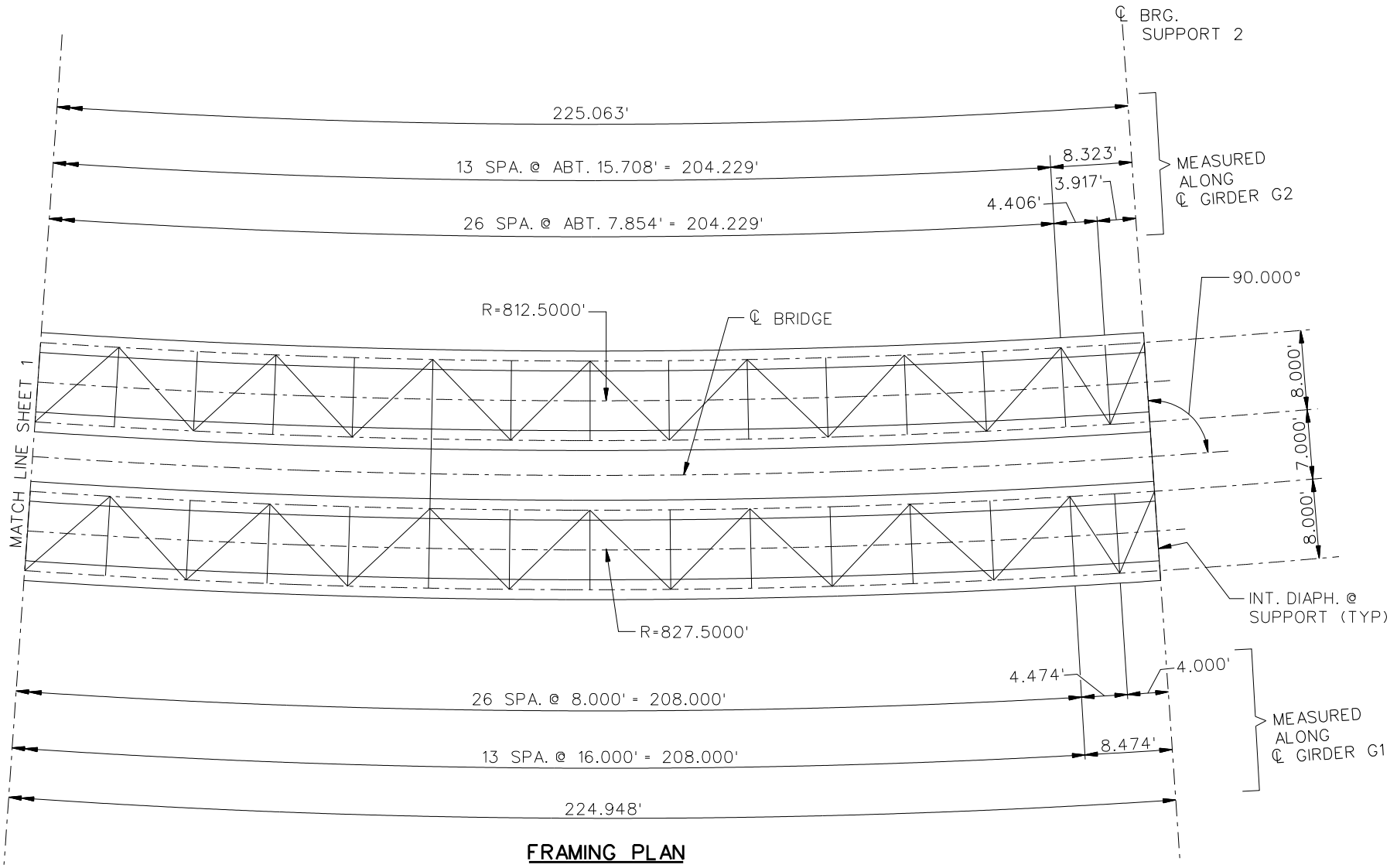

FRAMING PLAN

NCHRP 12-79

BRIDGE NTSCS29

FRAMING PLAN AND
CROSS-SECTION

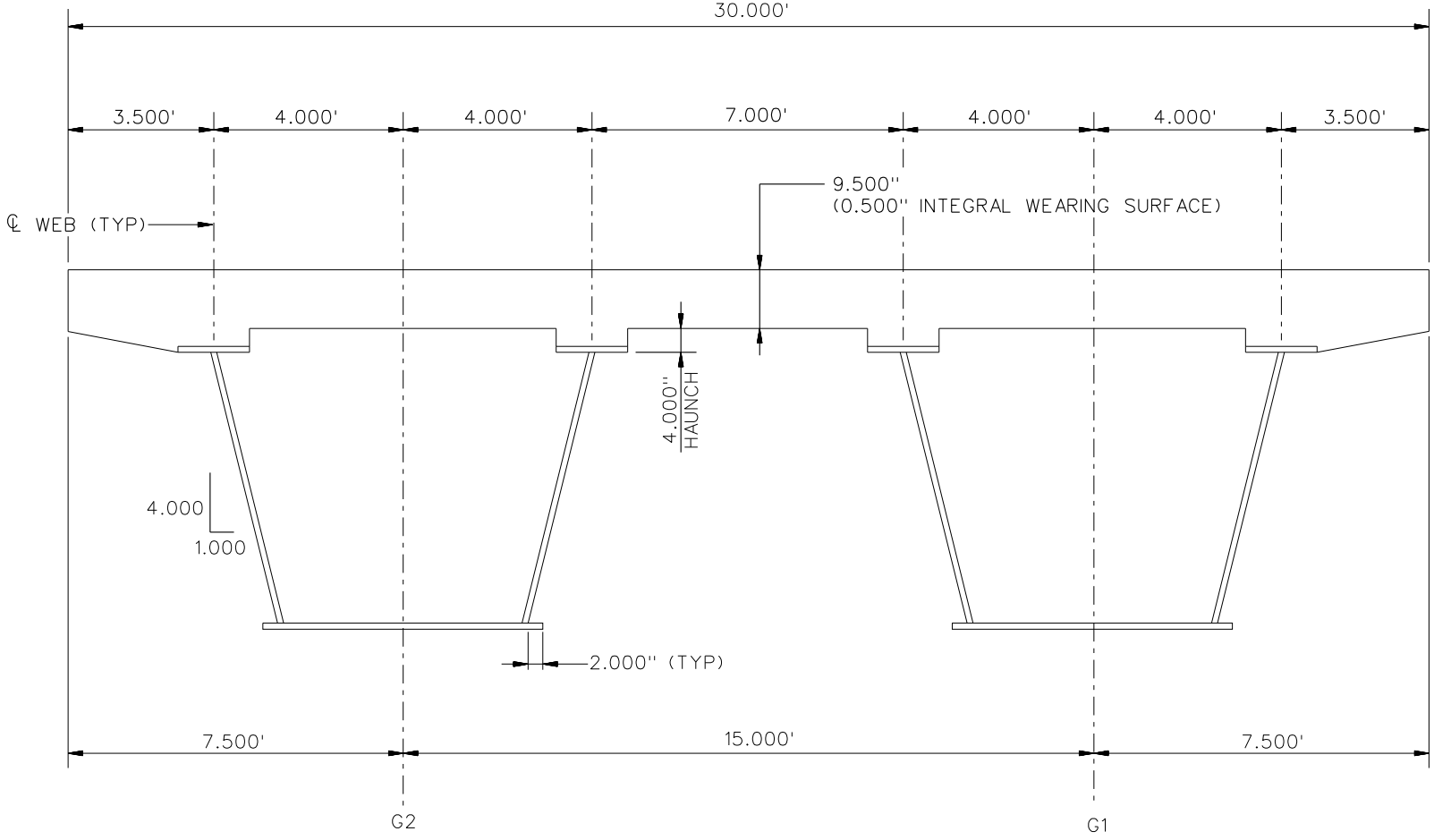

CROSS - SECTION

NCHRP	12-79
BRIDGE	NTSCS29
TYPICAL SECTION	
SHEET 3 OF 9	

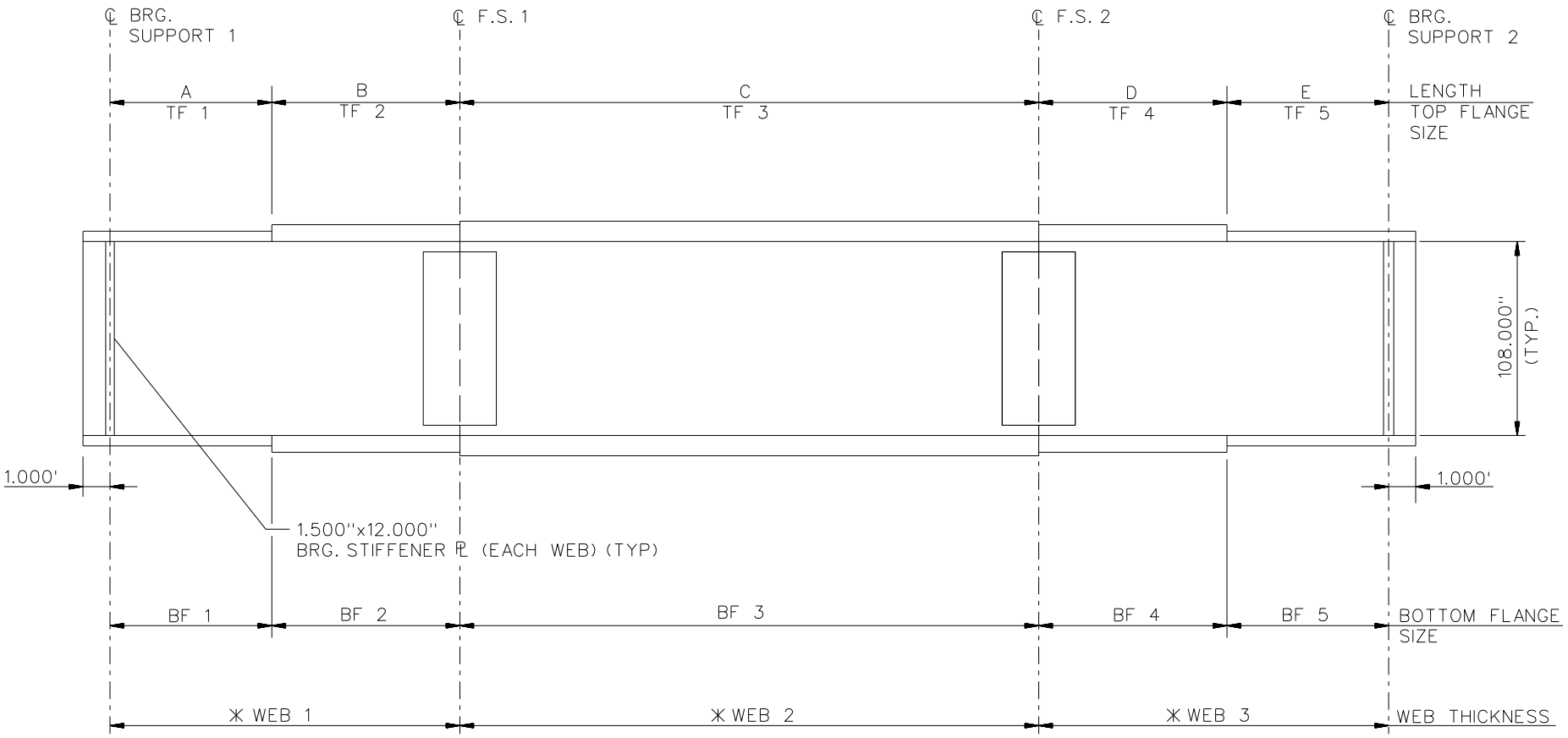

NOTES:

1. SEE TABLES ON SHEET 4 FOR GIRDER ELEVATION DIMENSIONS AND PLATE SIZES.

✳ G1 = 0.938" FOR WEB 1, WEB 2, WEB 3
G2 = 0.875" FOR WEB 1, WEB 2, WEB 3

NCHRP 12-79

BRIDGE NTSCS29

GIRDER ELEVATION

SHEET 4 OF 9

	GIRDER PLATE LENGTHS ✳	
LENGTH	G1	G2
A	29.000	29.000
B	29.000	29.000
C	108.950	109.050
D	29.000	29.000
E	29.000	29.000

✳ ALL DIMENSIONS ARE IN FEET.

	GIRDER FLANGE DIMENSIONS ✳✳			
TOP	G1		G2	
FLANGE	BF	TF	BF	TF
TF1	20.000	1.250	20.000	1.250
TF2	20.000	1.250	20.000	1.250
TF3	20.000	1.250	20.000	1.250
TF4	20.000	1.250	20.000	1.250
TF5	20.000	1.250	20.000	1.250

✳✳ ALL DIMENSIONS ARE IN INCHES.

	GIRDER FLANGE DIMENSIONS ✳✳			
BOTTOM	G1		G2	
FLANGE	BF	TF	BF	TF
BF1	46.000	1.250	46.000	1.250
BF2	46.000	1.500	46.000	1.250
BF3	46.000	2.000	46.000	1.750
BF4	46.000	1.500	46.000	1.250
BF5	46.000	1.250	46.000	1.250

✳✳ ALL DIMENSIONS ARE IN INCHES.

NCHRP 12-79

BRIDGE NTSCS29

GIRDER ELEVATION TABLES

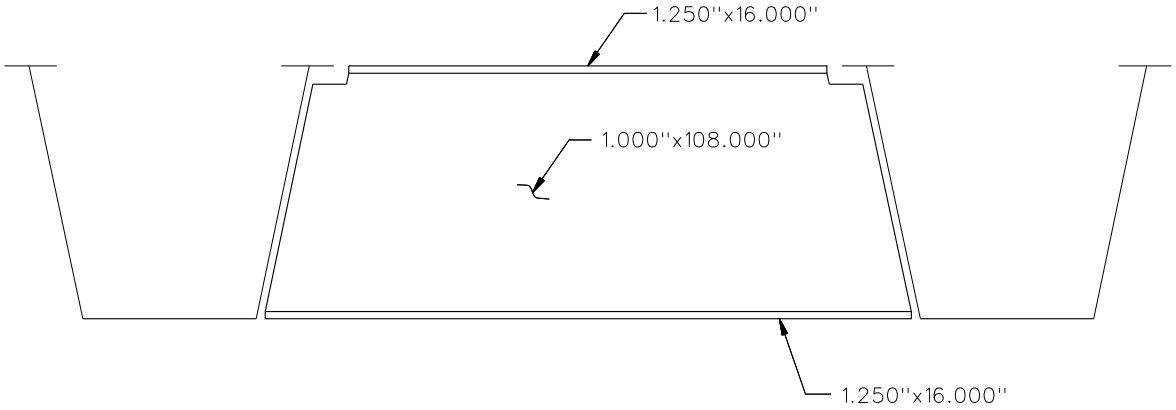

TYPICAL END DIAPHRAGM

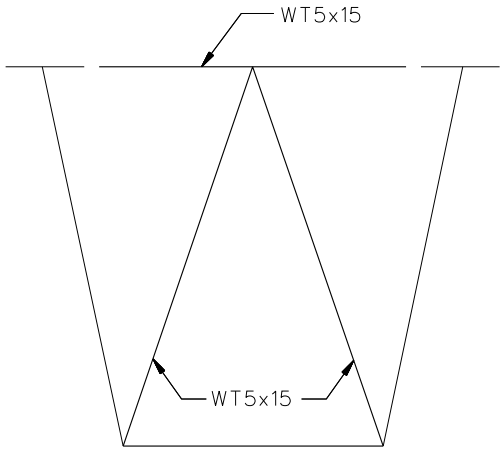

TYPICAL INTERNAL CROSS FRAME

NOTES:

1. STEEL DEAD LOAD INCREASED BY 15% FOR MDX AND LARSA MODELS; 2% FOR 3D MODEL; AND 20% FOR APPROXIMATE ANALYSIS TO ACCOUNT FOR MISC. DETAILS.

2. FORMWORK LOAD OF 10PSF IS INCLUDED IN CONCRETE DEAD LOAD.

3. ADDITIONAL DESIGN PARAMETERS:
   A. 1.500' PARAPET WIDTH BOTH SIDES.
   B. 700 LB/FT UNIFORM LOAD ASSUMED FOR PARAPET WEIGHT.
   C. ROADWAY WIDTH = 26.500'.
   D. NUMBER OF DESIGN LANES = 2.
   E. HL93 LIVE LOAD.
   F. DESIGN SPEED = 35 MPH.

4. DIAPHRAGM MEMBER CALL-OUTS ARE IN ENGLISH UNITS.

NCHRP 12-79

BRIDGE NTSCS29

MISC. DETAILS AND NOTES

SHEET 6 OF 9

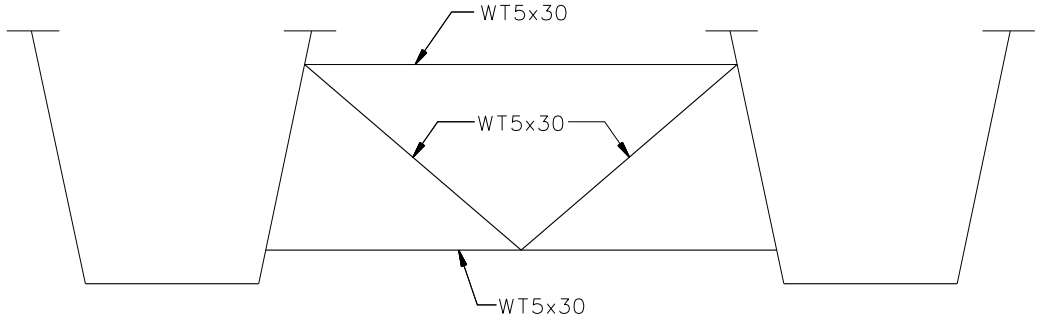

INTERMEDIATE EXTERNAL DIAPHRAGM

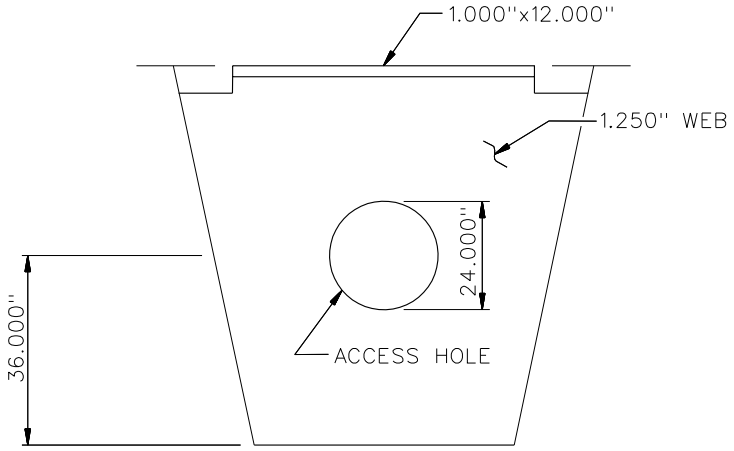

TYPICAL INTERNAL DIAPHRAGMS AT SUPPORTS

NCHRP 12-79

BRIDGE NTSCS29

MISC. DETAILS AND NOTES

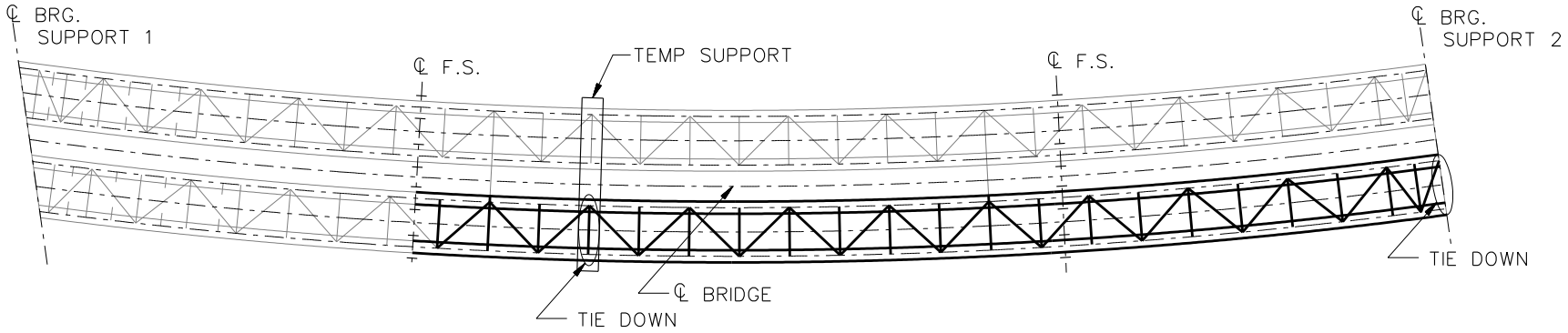

STAGE 1

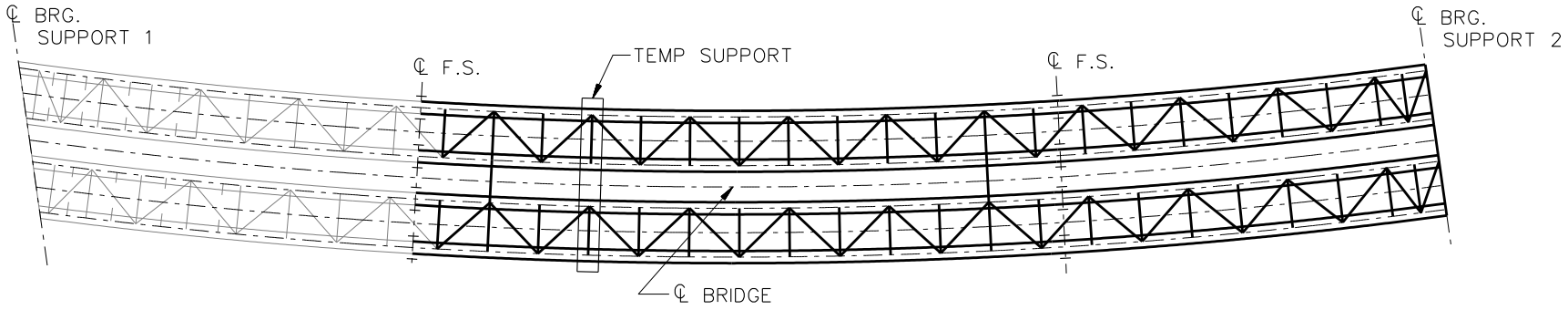

STAGE 2

LEGEND

▽ = HOLD OR LIFT CRANE

○ = TIE DOWN

□ = TEMPORARY SUPPORT STRUCTURE

NCHRP 12-79

BRIDGE NTSCS29

GENERAL ERECTION PROCEDURE

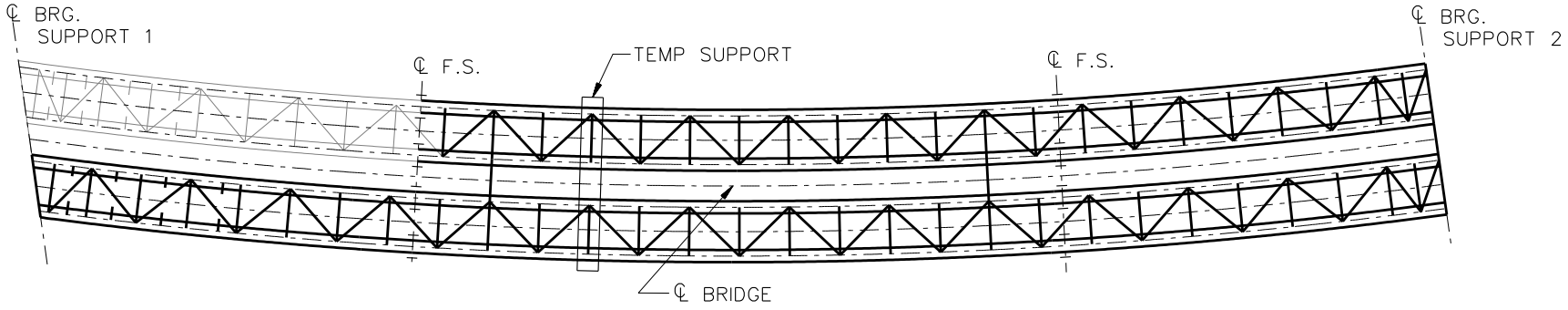

STAGE 3

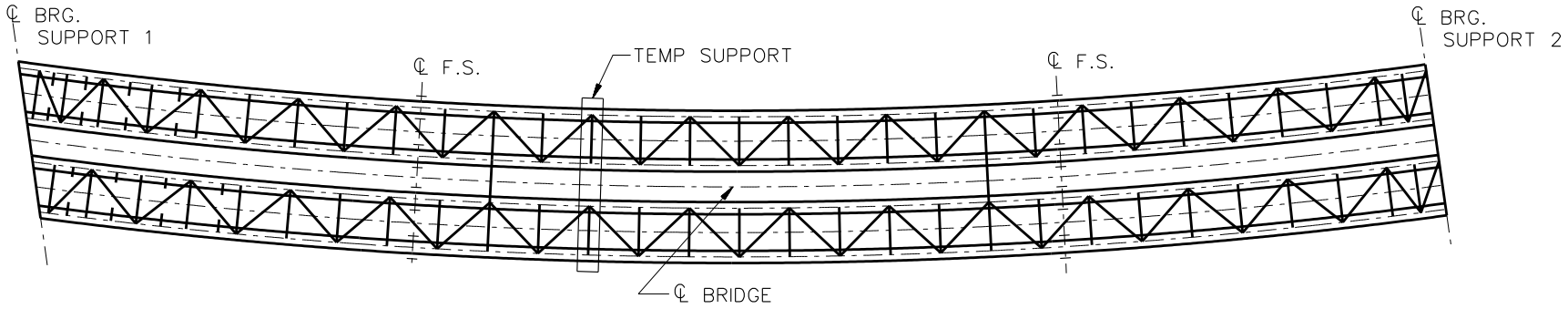

STAGE 4

LEGEND

▽ = HOLD OR LIFT CRANE

○ = TIE DOWN

□ = TEMPORARY SUPPORT STRUCTURE

STAGE 5

REMOVE TEMP SUPPORTS

NCHRP 12-79

BRIDGE NTSCS29

GENERAL ERECTION PROCEDURE

NCHRP 12-79

NTSSS1

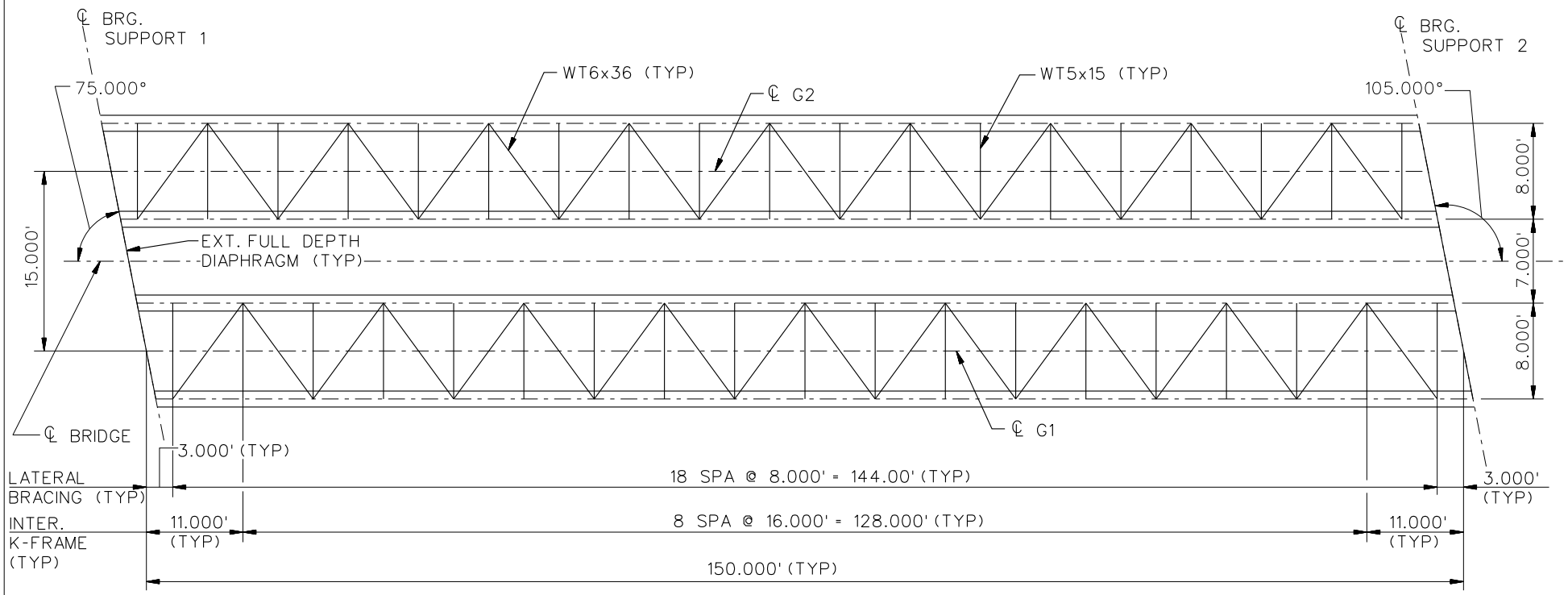

FRAMING PLAN

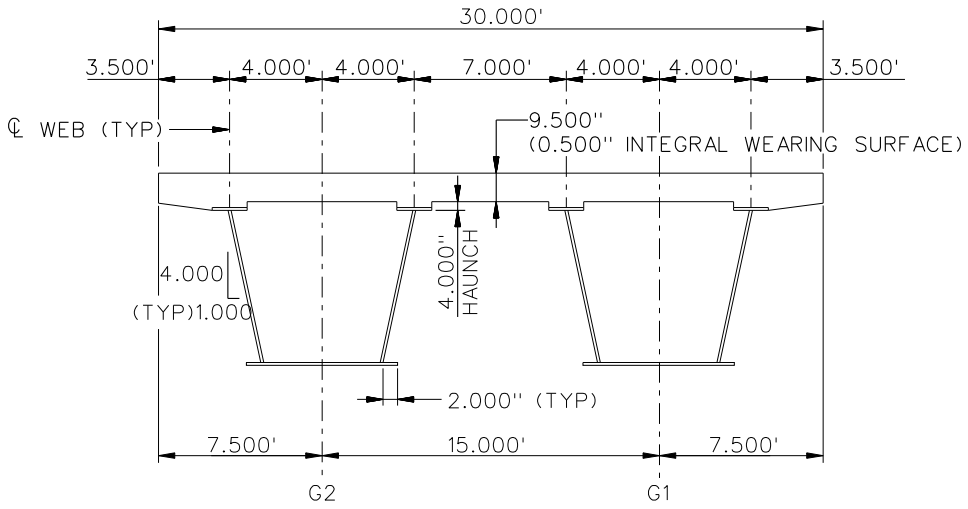

CROSS - SECTION

NOTES:
1. INTERNAL K-FRAME CONNECTION
   ℄ = 0.875" x 6.000'.

NCHRP 12-79

BRIDGE NTSSS1

FRAMING PLAN AND
CROSS-SECTION

SHEET 1 OF 6

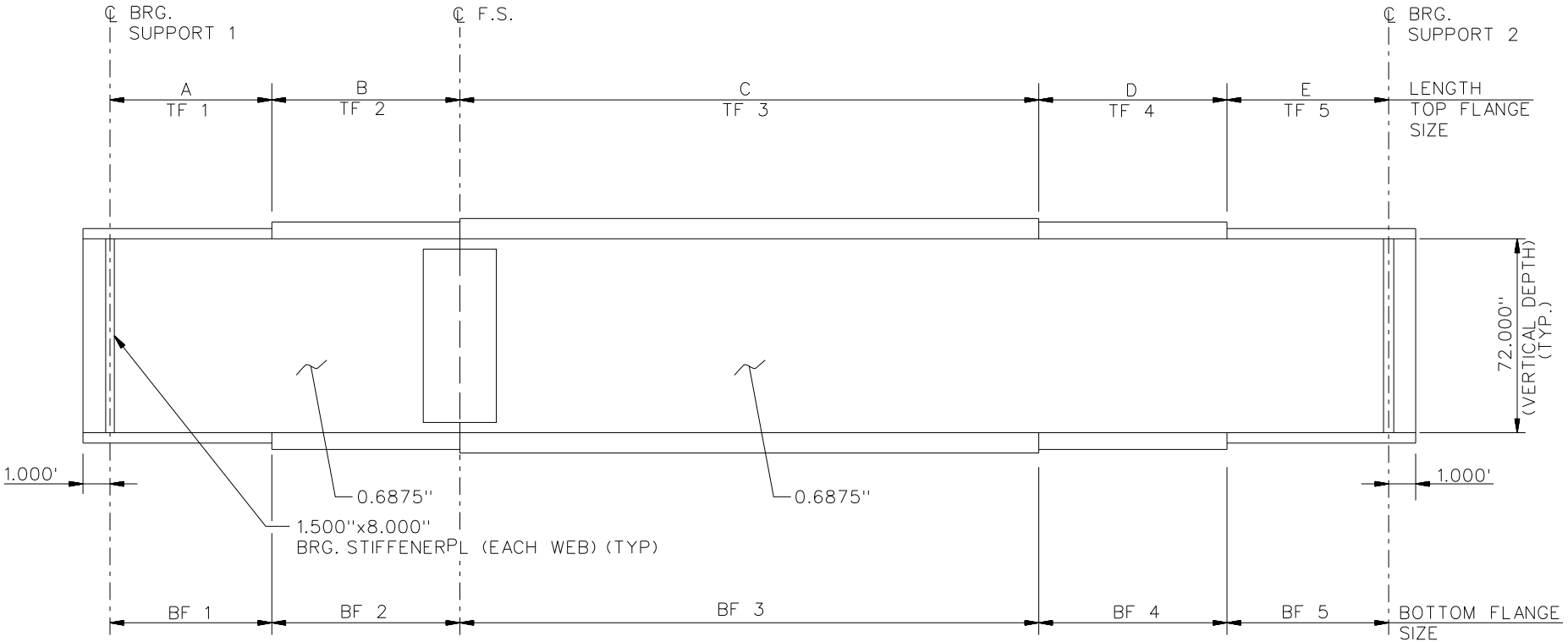

NOTES:

1. SEE TABLES ON SHEET 3 FOR GIRDER ELEVATION DIMENSIONS AND PLATE SIZES.

NCHRP 12-79

BRIDGE NTSSS1

GIRDER ELEVATION

SHEET 2 OF 6

	GIRDER PLATE LENGTHS ✳	
LENGTH	G1	G2
A	20.000	20.000
B	20.000	20.000
C	70.000	70.000
D	20.000	20.000
E	20.000	20.000

✳ ALL DIMENSIONS ARE IN FEET.

	GIRDER FLANGE DIMENSIONS ✳✳			
TOP	G1		G2	
FLANGE	BF	TF	BF	TF
TF1	16.000	0.875	16.000	0.875
TF2	16.000	0.875	16.000	0.875
TF3	16.000	0.875	16.000	0.875
TF4	16.000	0.875	16.000	0.875
TF5	16.000	0.875	16.000	0.875

✳✳ ALL DIMENSIONS ARE IN INCHES.

	GIRDER FLANGE DIMENSIONS ✳✳			
BOTTOM	G1		G2	
FLANGE	BF	TF	BF	TF
BF1	64.000	0.875	64.000	0.875
BF2	64.000	0.875	64.000	0.875
BF3	64.000	1.000	64.000	1.000
BF4	64.000	0.875	64.000	0.875
BF5	64.000	0.875	64.000	0.875

✳✳ ALL DIMENSIONS ARE IN INCHES.

NCHRP 12-79

BRIDGE NTSSS1

GIRDER ELEVATION TABLES

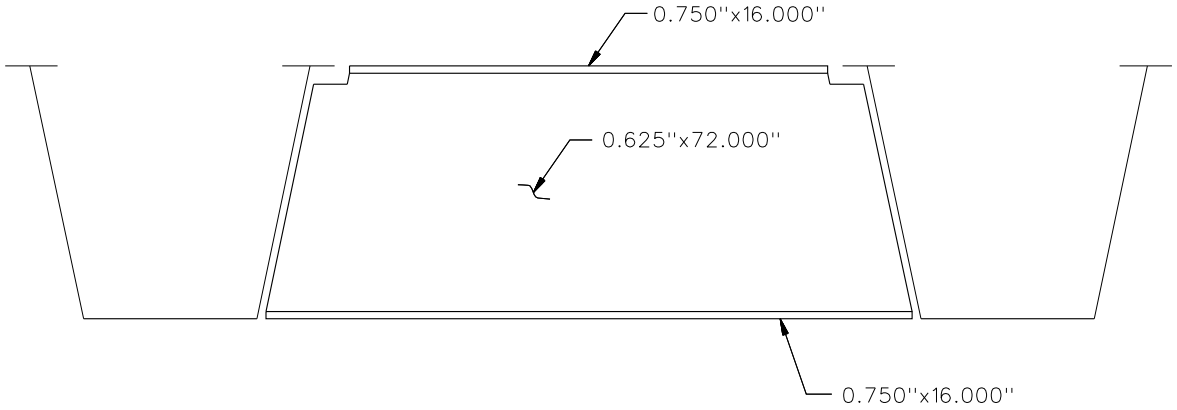

TYPICAL EXTERNAL END DIAPHRAGM

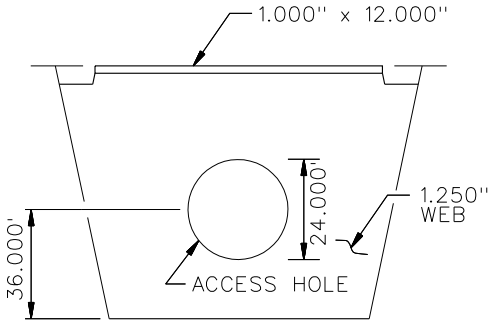

TYPICAL INTERNAL END DIAPHRAGM

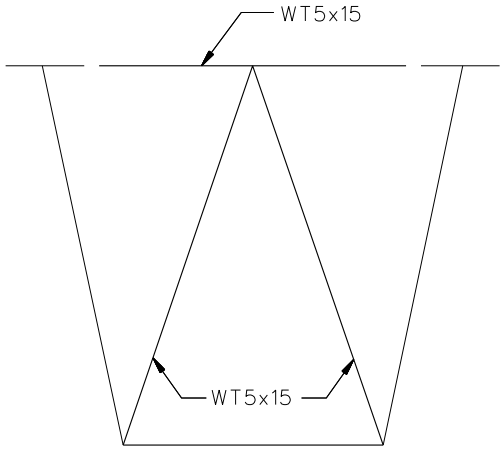

TYPICAL INTERNAL CROSS FRAME

NOTES:

1. STEEL DEAD LOAD INCREASED BY 15% FOR MDX AND LARSA MODELS; 2% FOR 3D MODEL; AND 20% FOR APPROXIMATE ANALYSIS TO ACCOUNT FOR MISC. DETAILS.

2. FORMWORK LOAD OF 10PSF IS INCLUDED IN CONCRETE DEAD LOAD.

3. ADDITIONAL DESIGN PARAMETERS:
   A. 1.500' PARAPET WIDTH BOTH SIDES.
   B. 700 LB/FT UNIFORM LOAD ASSUMED FOR PARAPET WEIGHT.
   C. ROADWAY WIDTH = 26.500'.
   D. NUMBER OF DESIGN LANES = 2.
   E. HL93 LIVE LOAD.
   F. DESIGN SPEED = 35 MPH.

4. DIAPHRAGM MEMBER CALL-OUTS ARE IN ENGLISH UNITS.

NCHRP 12-79

BRIDGE NTSSS1

MISC. DETAILS AND NOTES

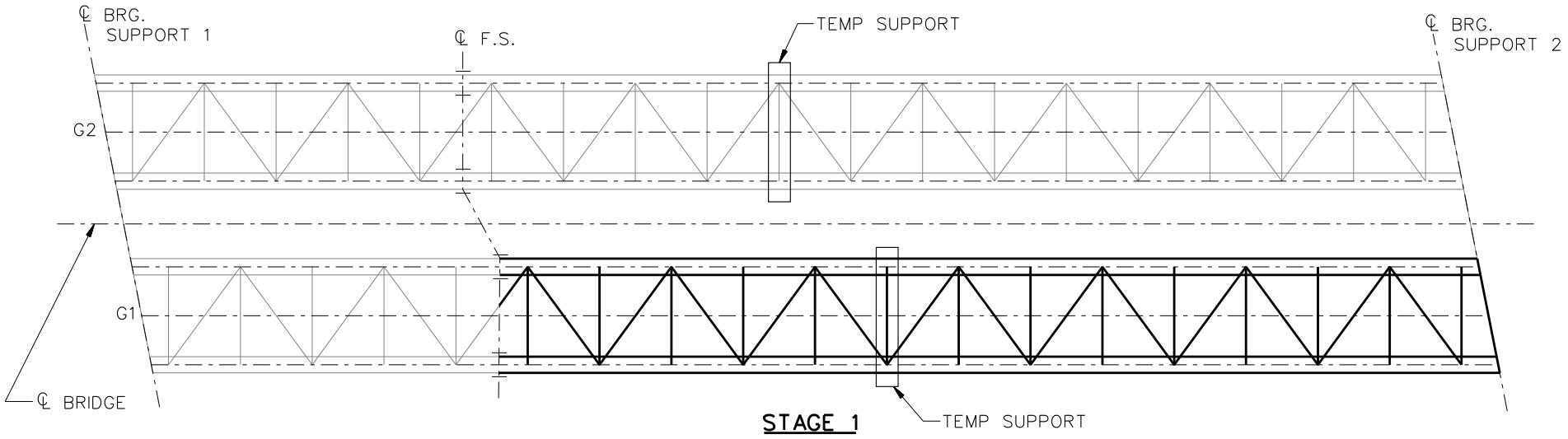

STAGE 1

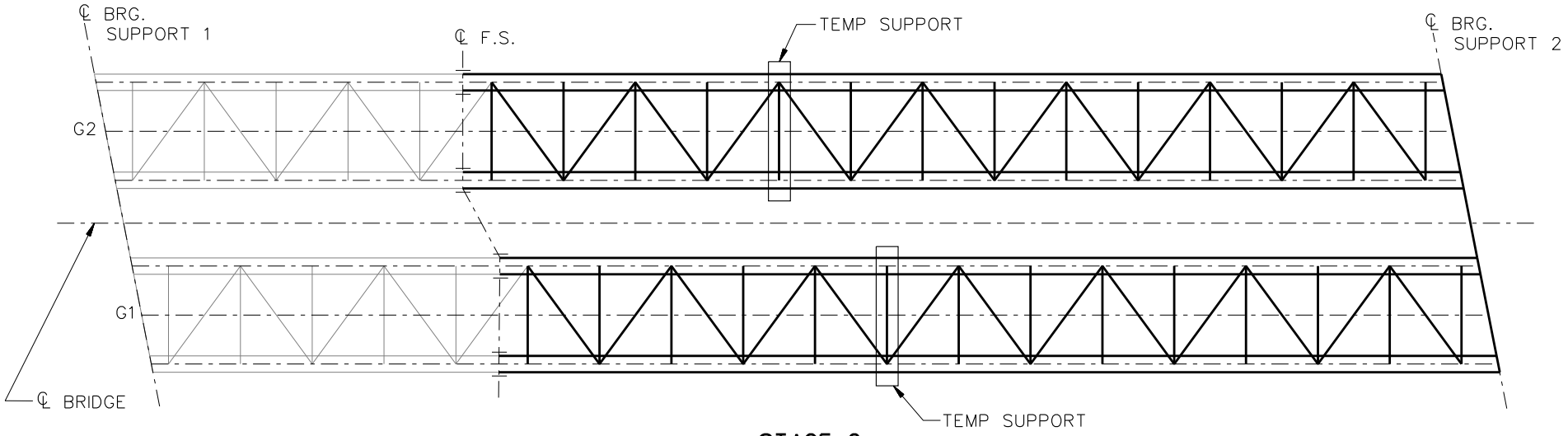

STAGE 2

LEGEND

▽ = HOLD OR LIFT CRANE

○ = TIE DOWN

□ = TEMPORARY SUPPORT STRUCTURE

NCHRP 12-79

BRIDGE NTSSS1

GENERAL ERECTION PROCEDURE

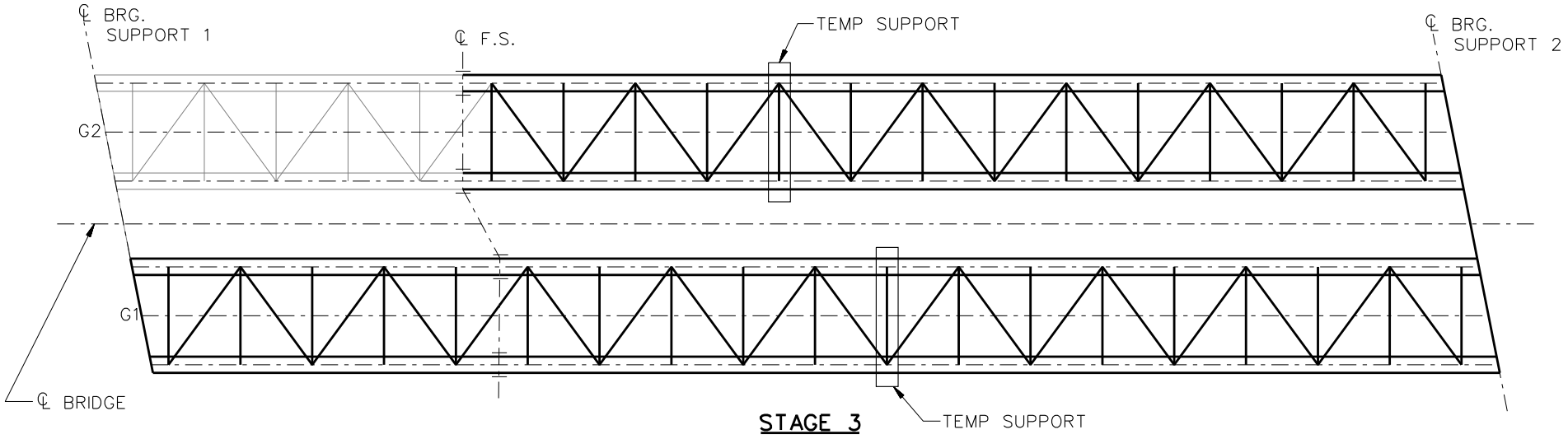

STAGE 3

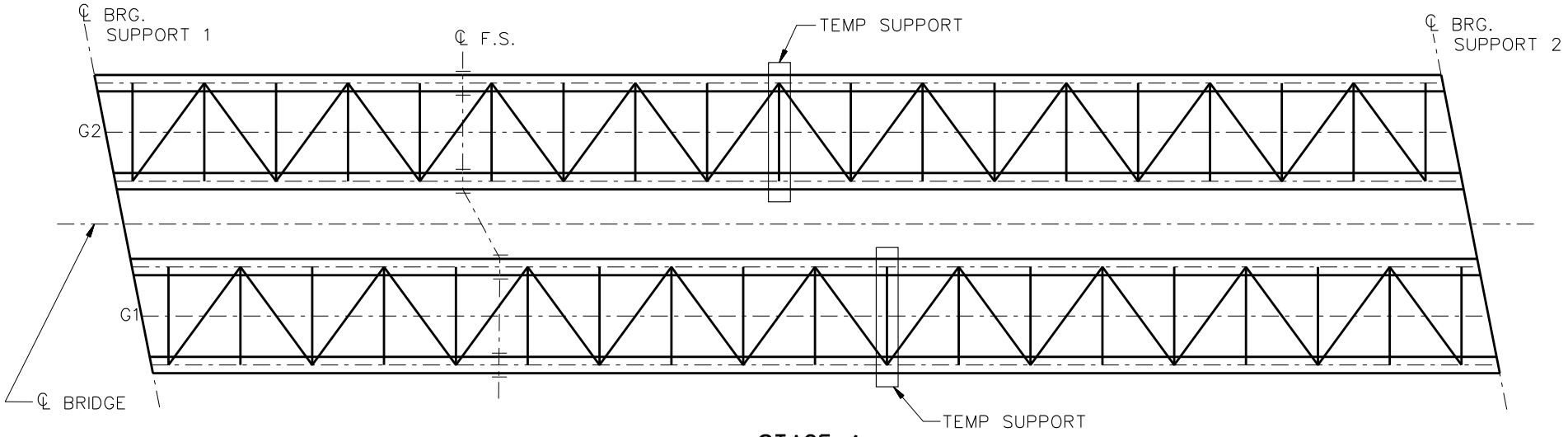

STAGE 4

LEGEND

▽ = HOLD OR LIFT CRANE

○ = TIE DOWN

□ = TEMPORARY SUPPORT STRUCTURE

STAGE 5

REMOVE ALL TEMP SUPPORTS

NCHRP 12-79

BRIDGE NTSSS1

GENERAL ERECTION PROCEDURE

NCHRP 12-79

NTSSS2

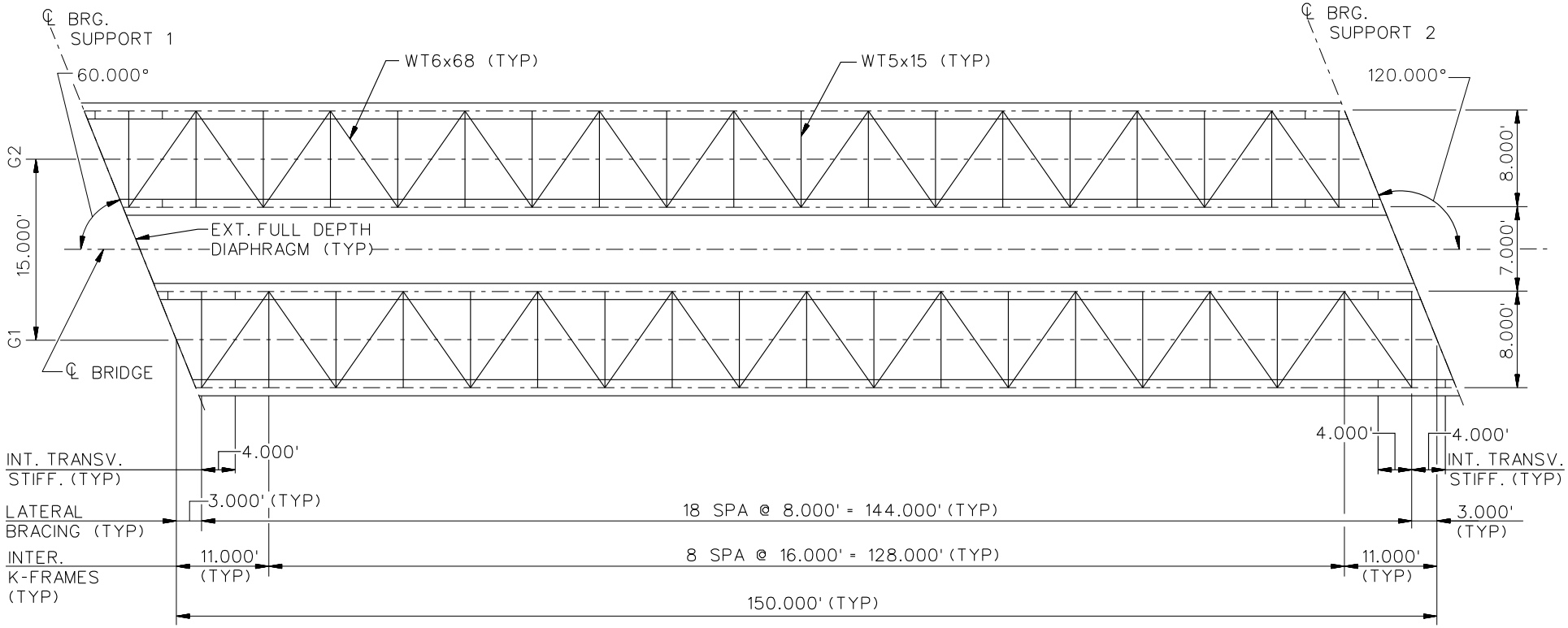

FRAMING PLAN

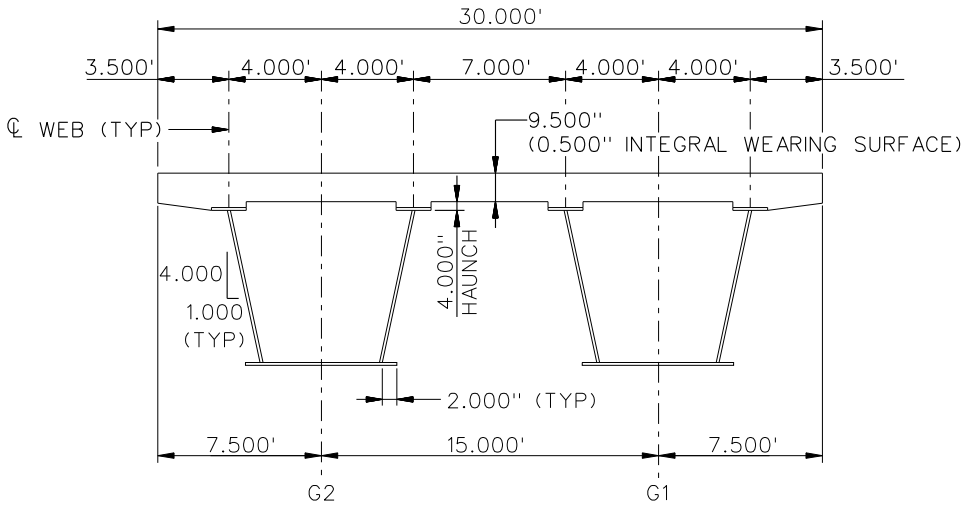

CROSS - SECTION

NOTES:

1. INTERMEDIATE TRANSVERSE STIFFENERS = 0.875"x6.000".
2. INTERNAL K-FRAMES CONNECTION PL = 0.875"x6.00".

NCHRP 12-79

BRIDGE NTSSS2

FRAMING PLAN AND CROSS-SECTION

SHEET 1 OF 6

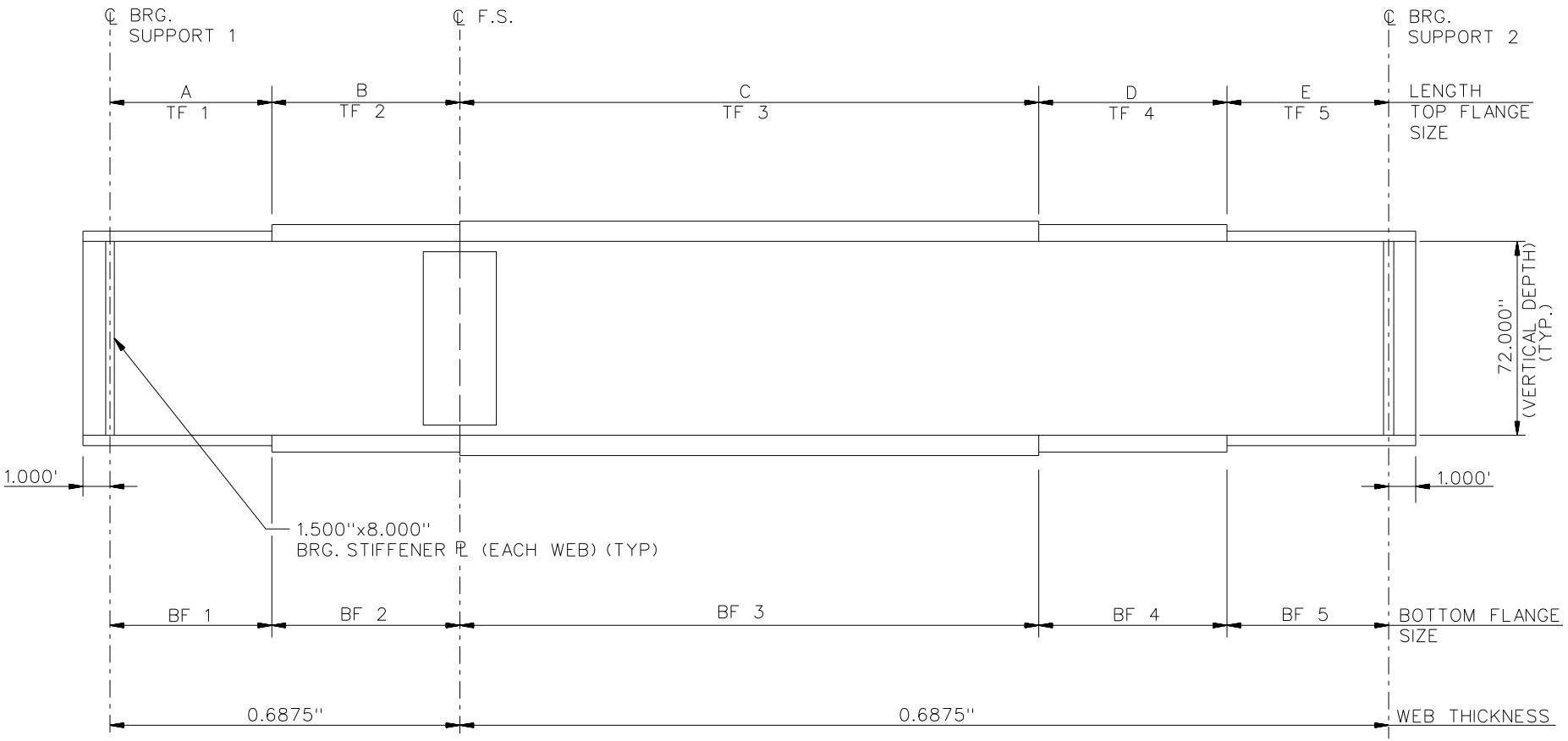

NOTES:

1. SEE TABLES ON SHEET 3 FOR GIRDER ELEVATION DIMENSIONS AND PLATE SIZES.

NCHRP 12-79

BRIDGE NTSSS2

GIRDER ELEVATION

SHEET 2 OF 6

	GIRDER PLATE LENGTHS ✳	
LENGTH	G1	G2
A	20.000	20.000
B	20.000	20.000
C	70.000	70.000
D	20.000	20.000
E	20.000	20.000

✳ ALL DIMENSIONS ARE IN FEET.

	GIRDER FLANGE DIMENSIONS ✳✳			
TOP FLANGE	G1		G2	
	BF	TF	BF	TF
TF1	16.000	0.875	16.000	0.875
TF2	16.000	0.875	16.000	0.875
TF3	16.000	0.875	16.000	0.875
TF4	16.000	0.875	16.000	0.875
TF5	16.000	0.875	16.000	0.875

✳✳ ALL DIMENSIONS ARE IN INCHES.

	GIRDER FLANGE DIMENSIONS ✳✳			
BOTTOM FLANGE	G1		G2	
	BF	TF	BF	TF
BF1	64.000	1.000	64.000	1.000
BF2	64.000	1.000	64.000	1.000
BF3	64.000	1.250	64.000	1.250
BF4	64.000	1.000	64.000	1.000
BF5	64.000	1.000	64.000	1.000

✳✳ ALL DIMENSIONS ARE IN INCHES.

NCHRP 12-79

BRIDGE NTSSS2

GIRDER ELEVATION TABLES

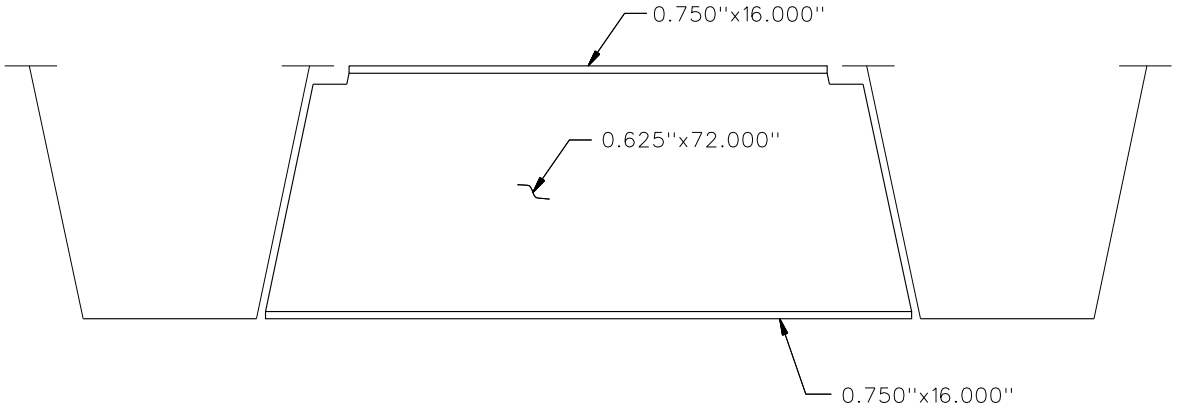

TYPICAL END DIAPHRAGM

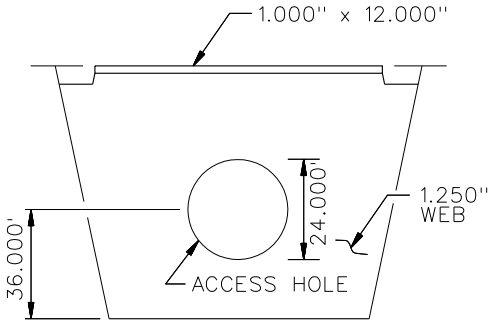

TYPICAL INTERNAL END DIAPHRAGM

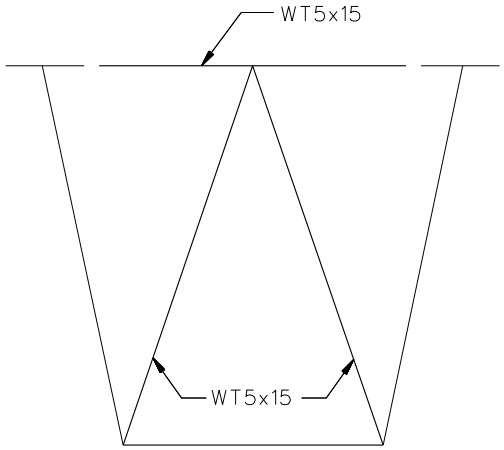

TYPICAL INTERNAL CROSS FRAME

NOTES:

1. STEEL DEAD LOAD INCREASED BY 15% FOR MDX AND LARSA MODELS; 2% FOR 3D MODEL; AND 20% FOR APPROXIMATE ANALYSIS TO ACCOUNT FOR MISC. DETAILS.

2. FORMWORK LOAD OF 10PSF IS INCLUDED IN CONCRETE DEAD LOAD.

3. ADDITIONAL DESIGN PARAMETERS:
   A. 1.500' PARAPET WIDTH BOTH SIDES.
   B. 700 LB/FT UNIFORM LOAD ASSUMED FOR PARAPET WEIGHT.
   C. ROADWAY WIDTH = 26.500'.
   D. NUMBER OF DESIGN LANES = 2.
   E. HL93 LIVE LOAD.
   F. DESIGN SPEED = 35 MPH.

4. DIAPHRAGM MEMBER CALL-OUTS ARE IN ENGLISH UNITS.

NCHRP 12-79

BRIDGE NTSSS2

MISC. DETAILS AND NOTES

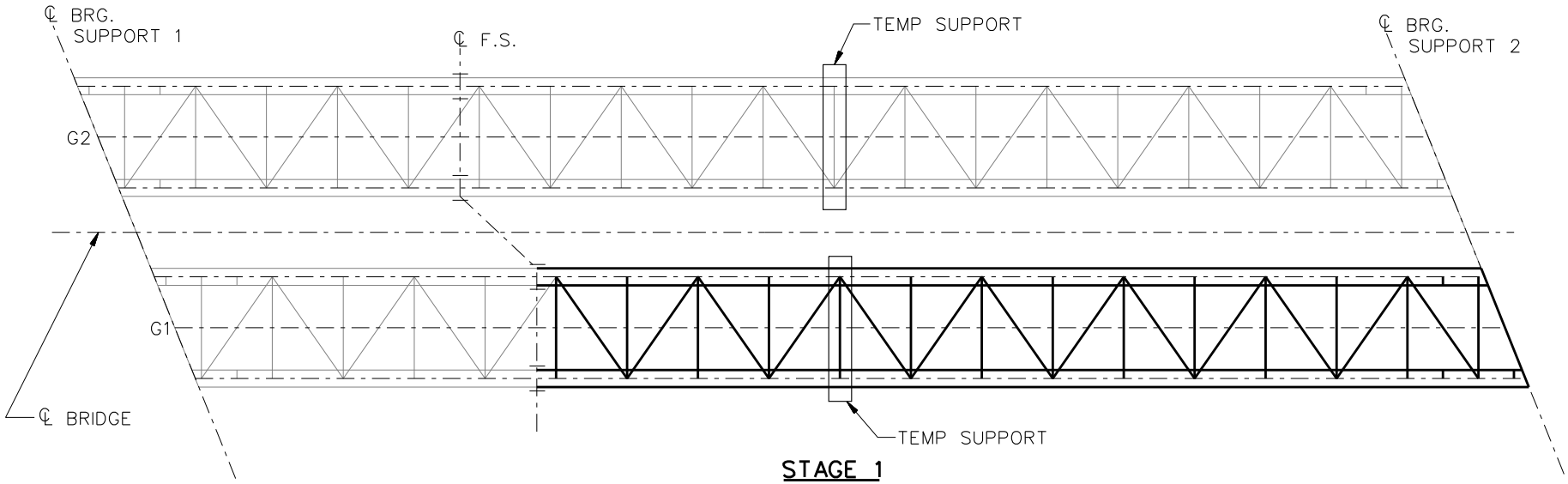

STAGE 1

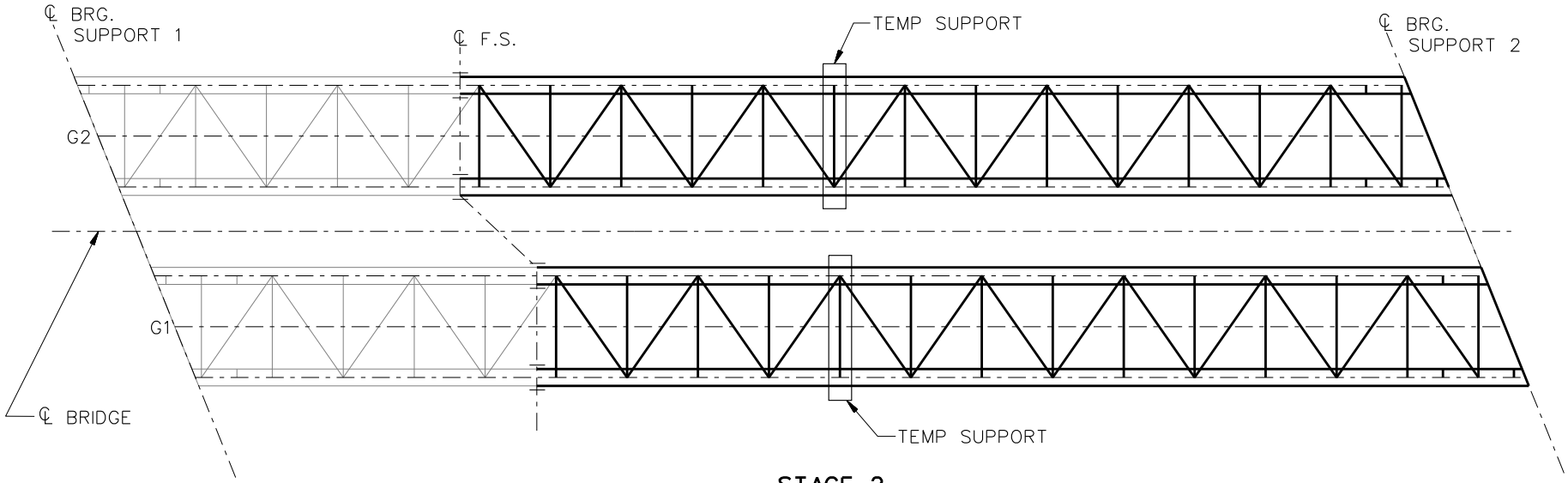

STAGE 2

LEGEND

▽ = HOLD OR LIFT CRANE

○ = TIE DOWN

□ = TEMPORARY SUPPORT STRUCTURE

NCHRP 12-79

BRIDGE NTSSS2

GENERAL ERECTION PROCEDURE

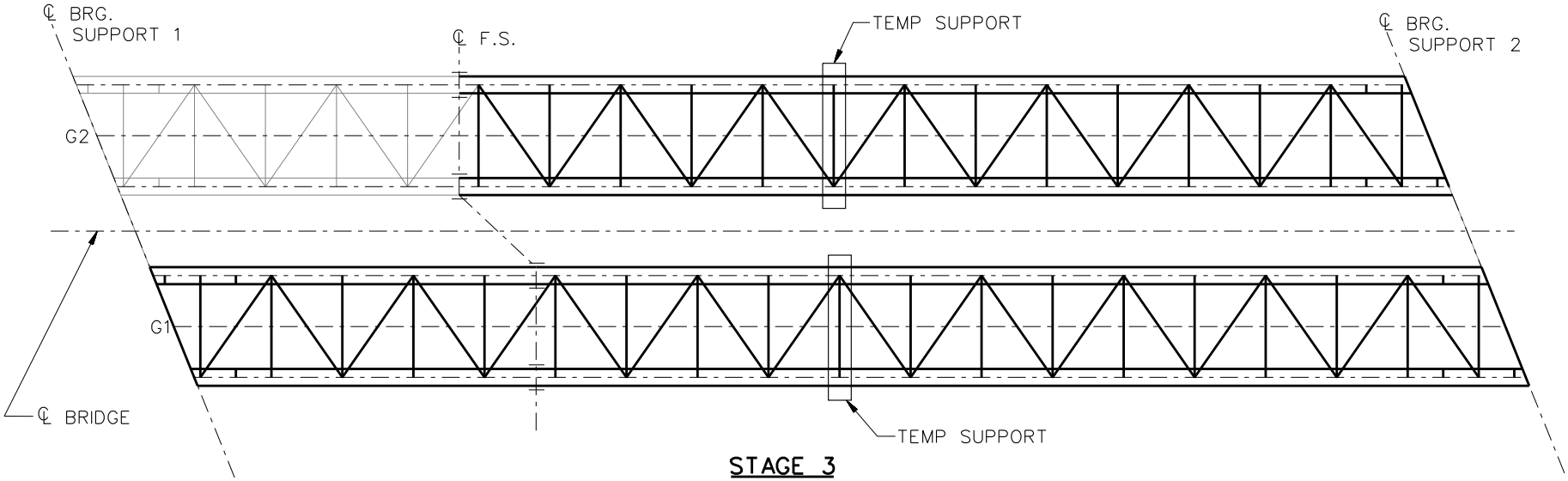

STAGE 3

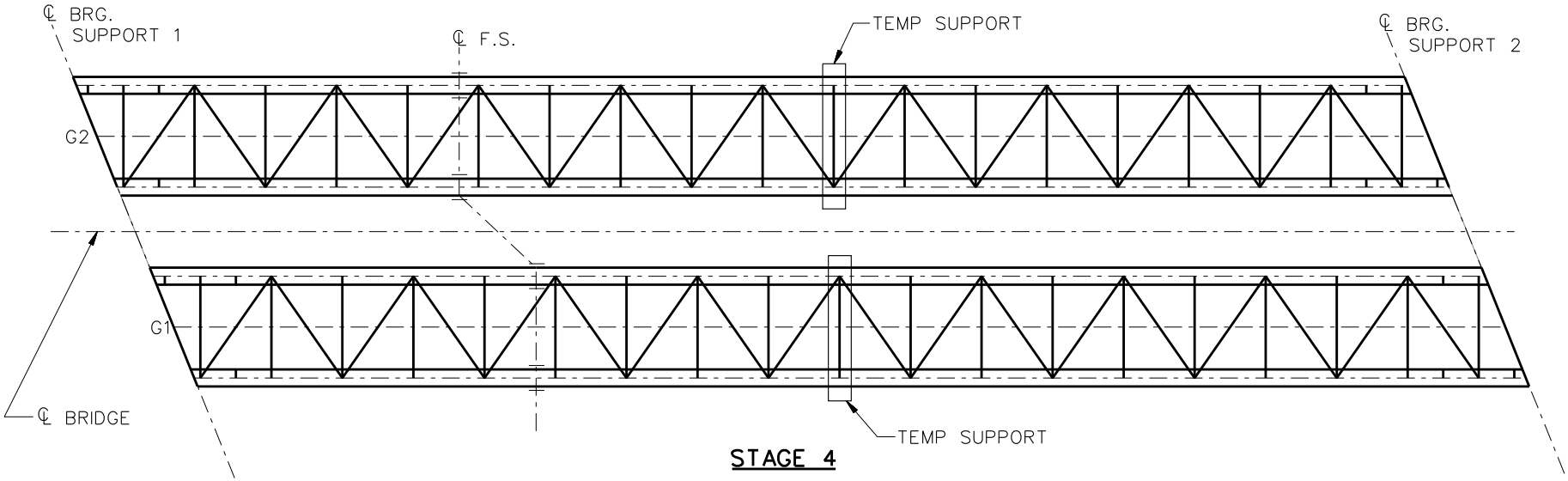

STAGE 4

LEGEND

▽ = HOLD OR LIFT CRANE

○ = TIE DOWN

□ = TEMPORARY SUPPORT STRUCTURE

STAGE 5

REMOVE TEMP ALL SUPPORTS

NCHRP 12-79

BRIDGE NTSSS2

GENERAL ERECTION PROCEDURE

NCHRP 12-79

NTSSS4

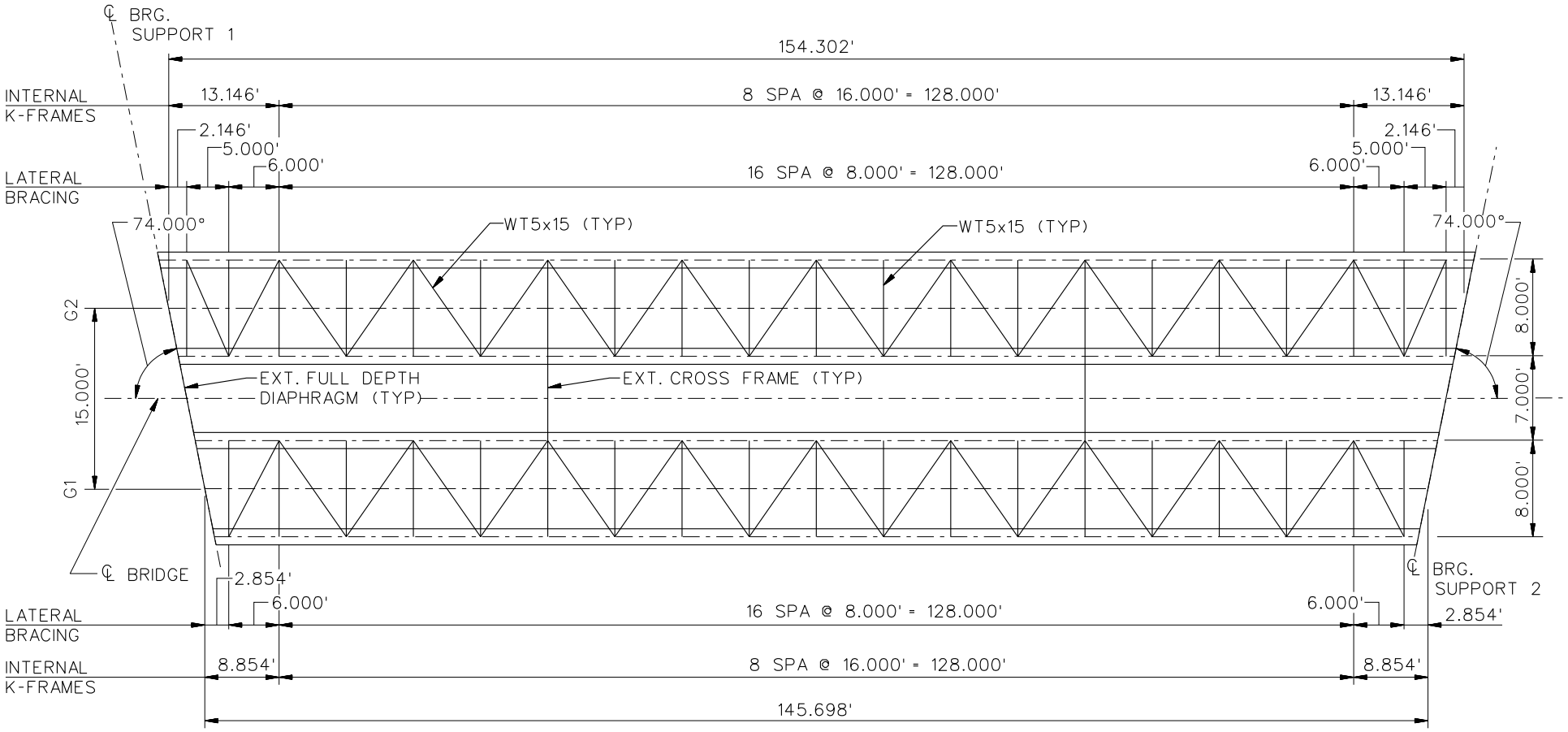

FRAMING PLAN

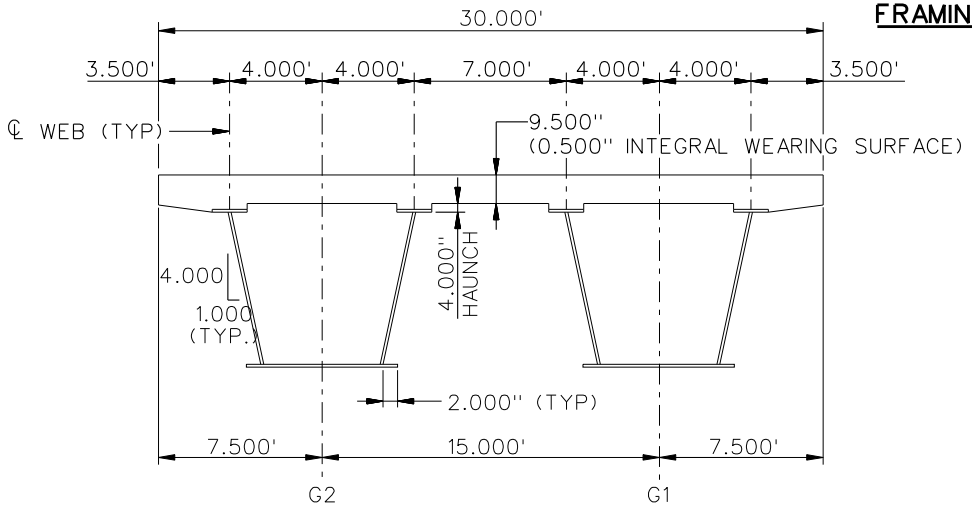

CROSS - SECTION

NOTES:

1. INTERNAL K-FRAME CONNECTION PL = 0.875"x6.000".

NCHRP 12-79

BRIDGE NTSSS4

FRAMING PLAN AND CROSS-SECTION

SHEET 1 OF 7

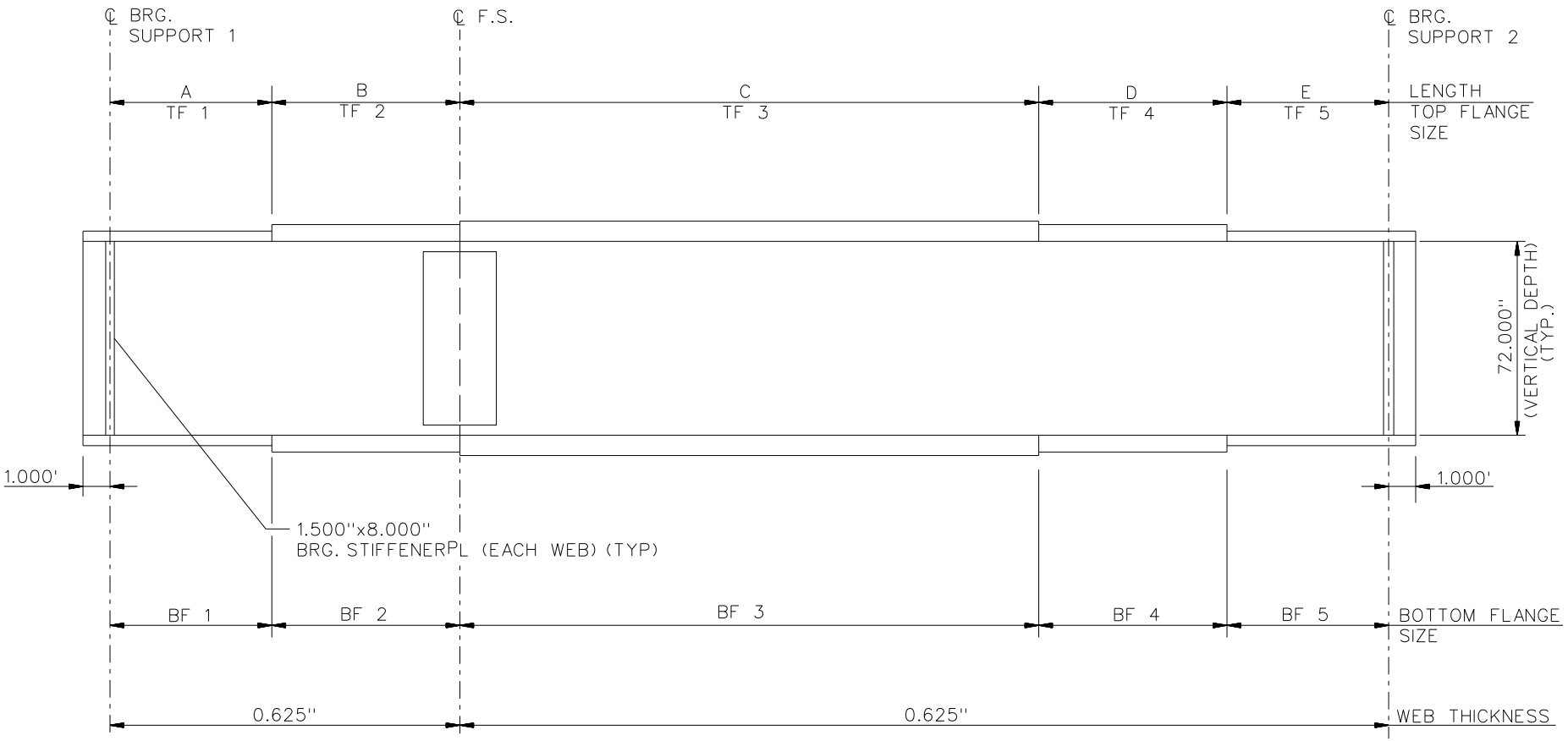

NOTES:

1. SEE TABLES ON SHEET 3 FOR GIRDER ELEVATION DIMENSIONS AND PLATE SIZES.

NCHRP 12-79

BRIDGE NTSSS4

GIRDER ELEVATION

SHEET 2 OF 7

	GIRDER PLATE LENGTHS ✳	
LENGTH	G1	G2
A	17.854	22.146
B	20.000	20.000
C	70.000	70.000
D	20.000	20.000
E	17.854	22.146

✳ ALL DIMENSIONS ARE IN FEET.

	GIRDER FLANGE DIMENSIONS ✳✳			
TOP	G1		G2	
FLANGE	BF	TF	BF	TF
TF1	16.000	0.875	16.000	0.875
TF2	16.000	0.875	16.000	0.875
TF3	16.000	0.875	16.000	0.875
TF4	16.000	0.875	16.000	0.875
TF5	16.000	0.875	16.000	0.875

✳✳ ALL DIMENSIONS ARE IN INCHES.

	GIRDER FLANGE DIMENSIONS ✳✳			
BOTTOM	G1		G2	
FLANGE	BF	TF	BF	TF
BF1	64.000	0.875	64.000	0.875
BF2	64.000	0.875	64.000	0.875
BF3	64.000	1.000	64.000	1.000
BF4	64.000	0.875	64.000	0.875
BF5	64.000	0.875	64.000	0.875

✳✳ ALL DIMENSIONS ARE IN INCHES.

NCHRP 12-79

BRIDGE NTSSS4

GIRDER ELEVATION TABLES

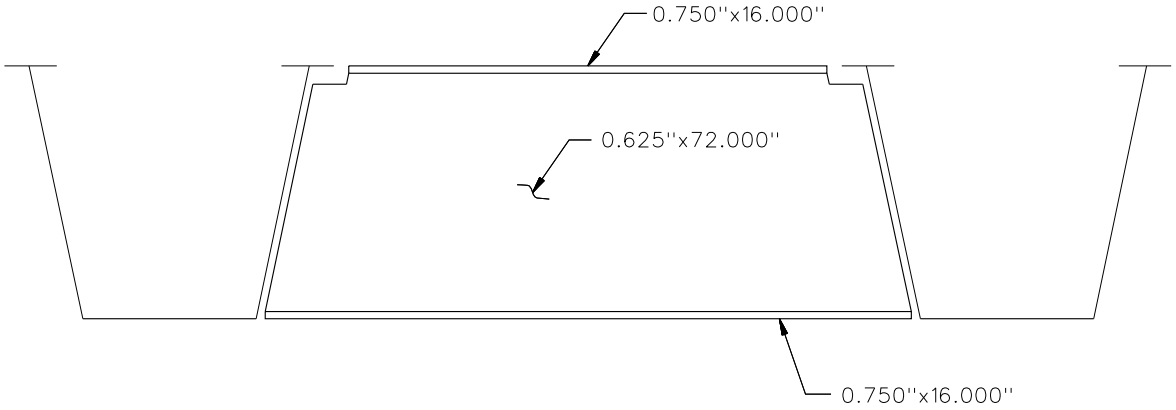

TYPICAL END DIAPHRAGM

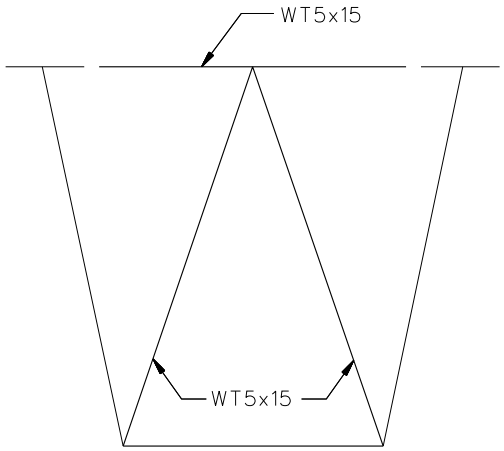

TYPICAL INTERNAL CROSS FRAME

NOTES:

1. STEEL DEAD LOAD INCREASED BY 15% FOR MDX AND LARSA MODELS; 2% FOR 3D MODEL; AND 20% FOR APPROXIMATE ANALYSIS TO ACCOUNT FOR MISC. DETAILS.

2. FORMWORK LOAD OF 10PSF IS INCLUDED IN CONCRETE DEAD LOAD.

3. ADDITIONAL DESIGN PARAMETERS:
   A. 1.500' PARAPET WIDTH BOTH SIDES.
   B. 700 LB/FT UNIFORM LOAD ASSUMED FOR PARAPET WEIGHT.
   C. ROADWAY WIDTH = 26.500'.
   D. NUMBER OF DESIGN LANES = 2.
   E. HL93 LIVE LOAD.
   F. DESIGN SPEED = 35 MPH.

4. DIAPHRAGM MEMBER CALL-OUTS ARE IN ENGLISH UNITS.

NCHRP 12-79

BRIDGE NTSSS4

MISC. DETAILS AND NOTES

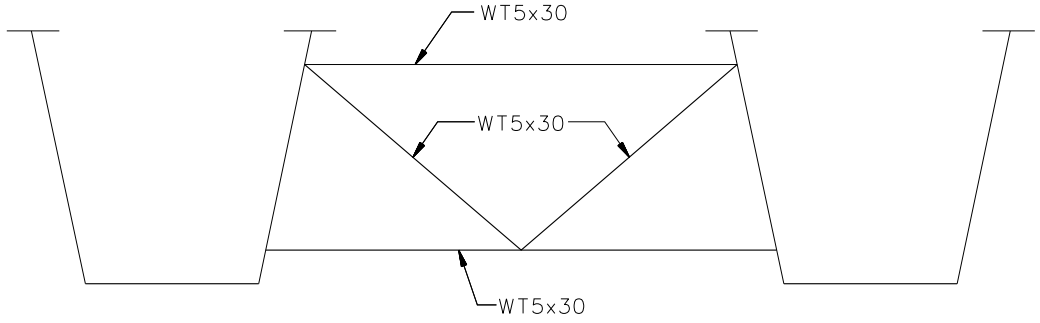

TYPICAL INTERMEDIATE EXTERNAL DIAPHRAGM

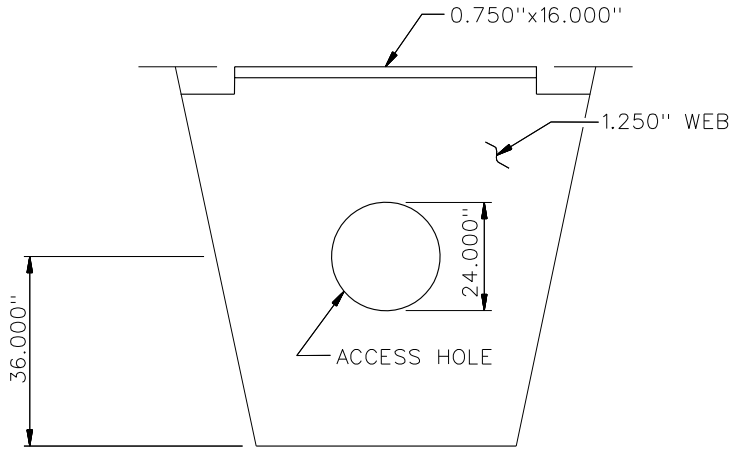

TYPICAL INTERNAL DIAPHRAGMS AT SUPPORTS

NCHRP 12-79

BRIDGE NTSSS4

MISC. DETAILS AND NOTES

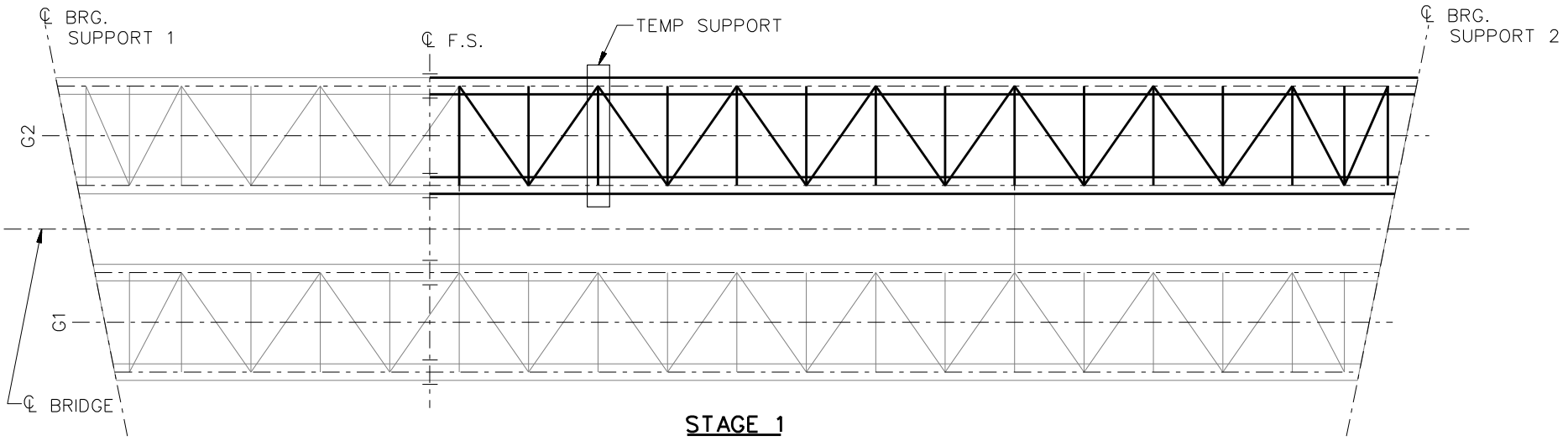

STAGE 1

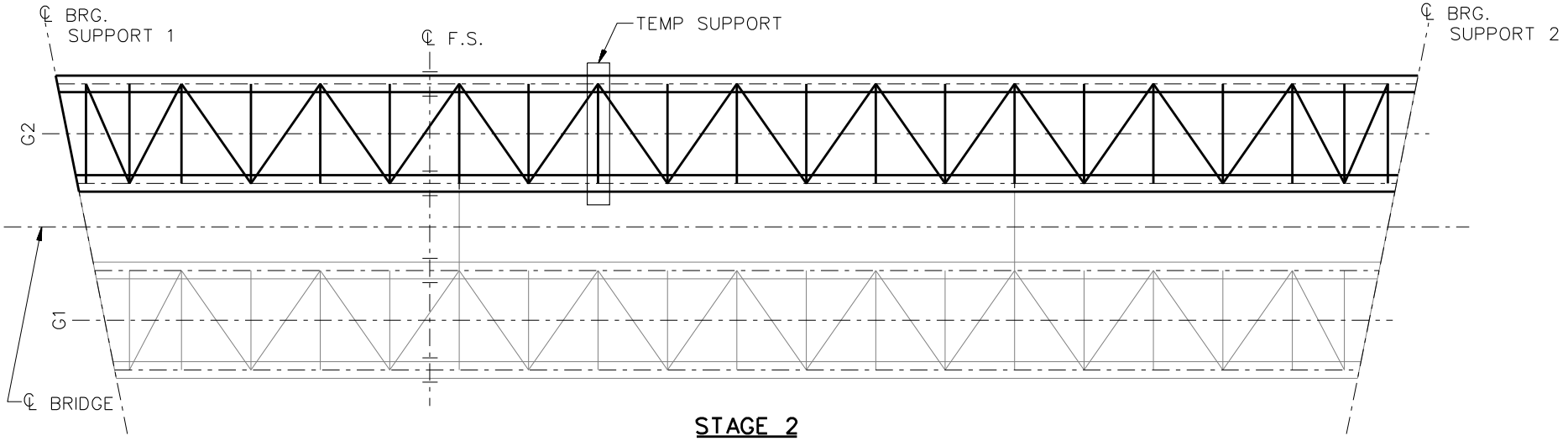

STAGE 2

LEGEND

▽ = HOLD OR LIFT CRANE

○ = TIE DOWN

□ = TEMPORARY SUPPORT STRUCTURE

STAGE 3

REMOVE TEMP. SUPPORT

NCHRP 12-79

BRIDGE NTSSS4

GENERAL ERECTION PROCEDURE

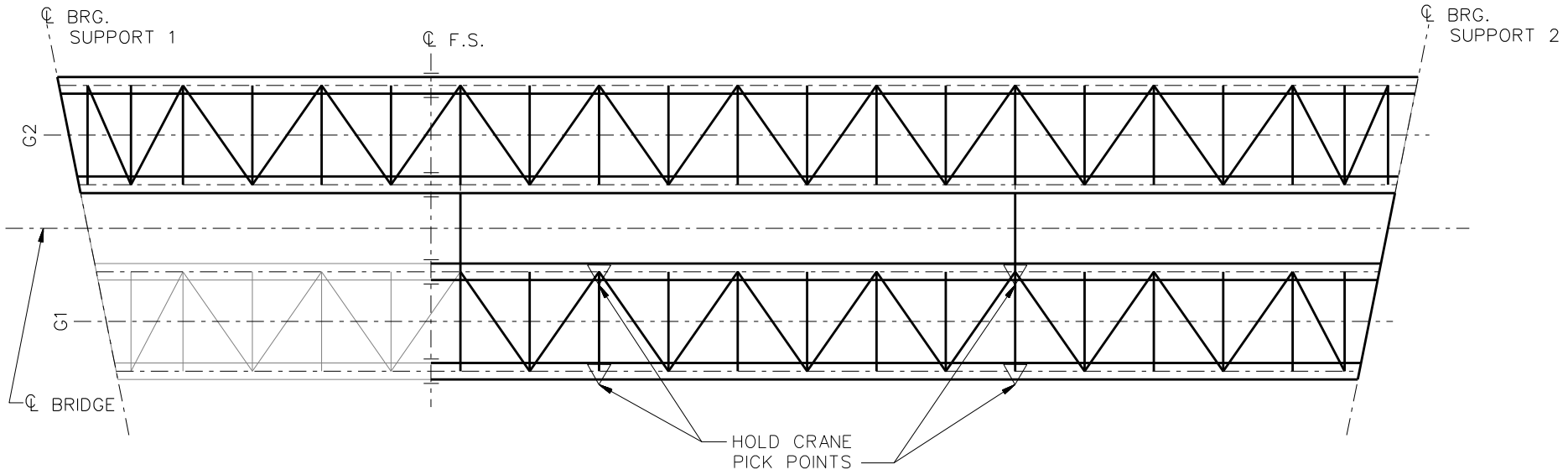

STAGE 4

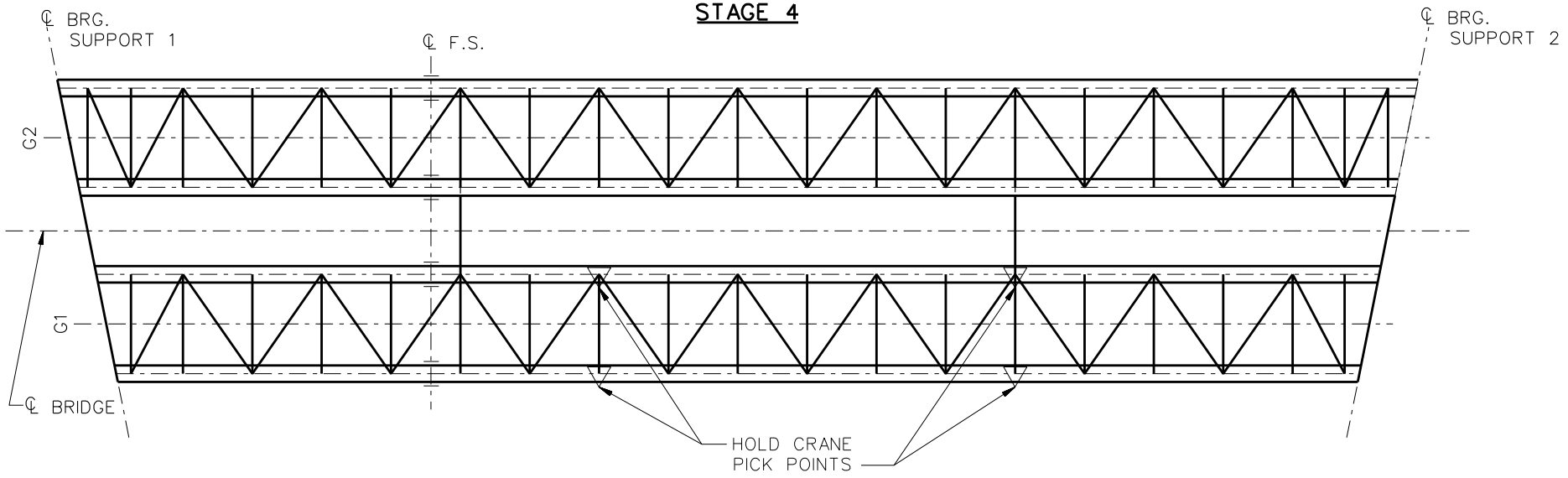

STAGE 5

LEGEND

▽ = HOLD OR LIFT CRANE

○ = TIE DOWN

□ = TEMPORARY SUPPORT STRUCTURE

STAGE 6

REMOVE HOLD CRANES

NCHRP 12-79

BRIDGE NTSSS4

GENERAL ERECTION PROCEDURE

NCHRP 12-79

XICCS7

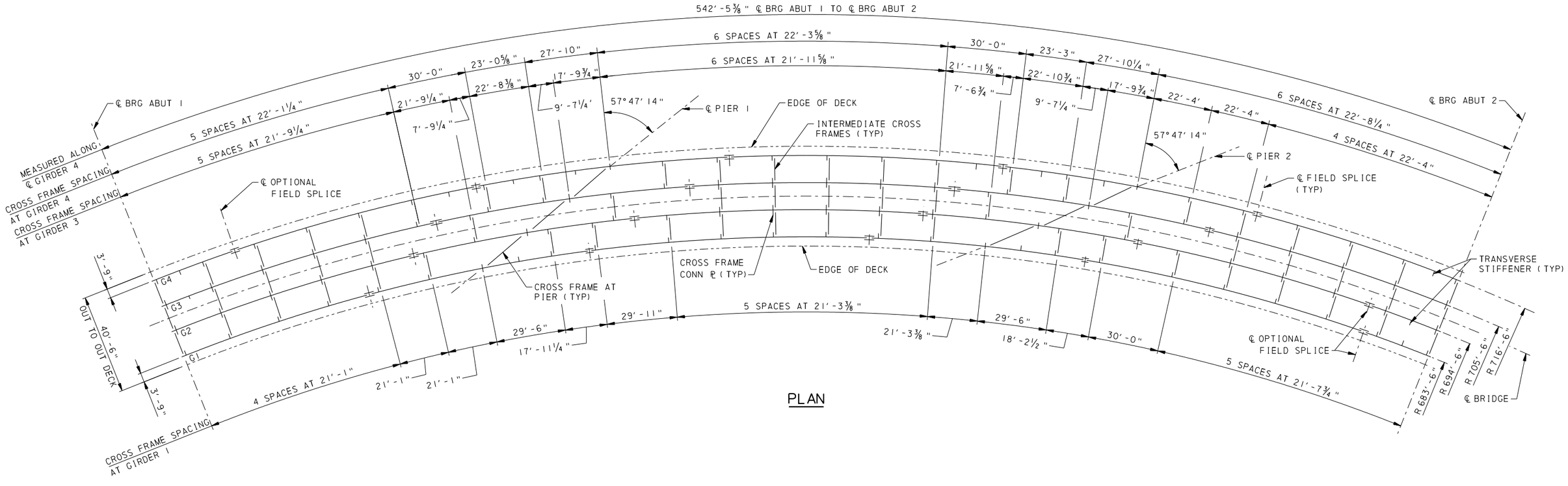

PLAN

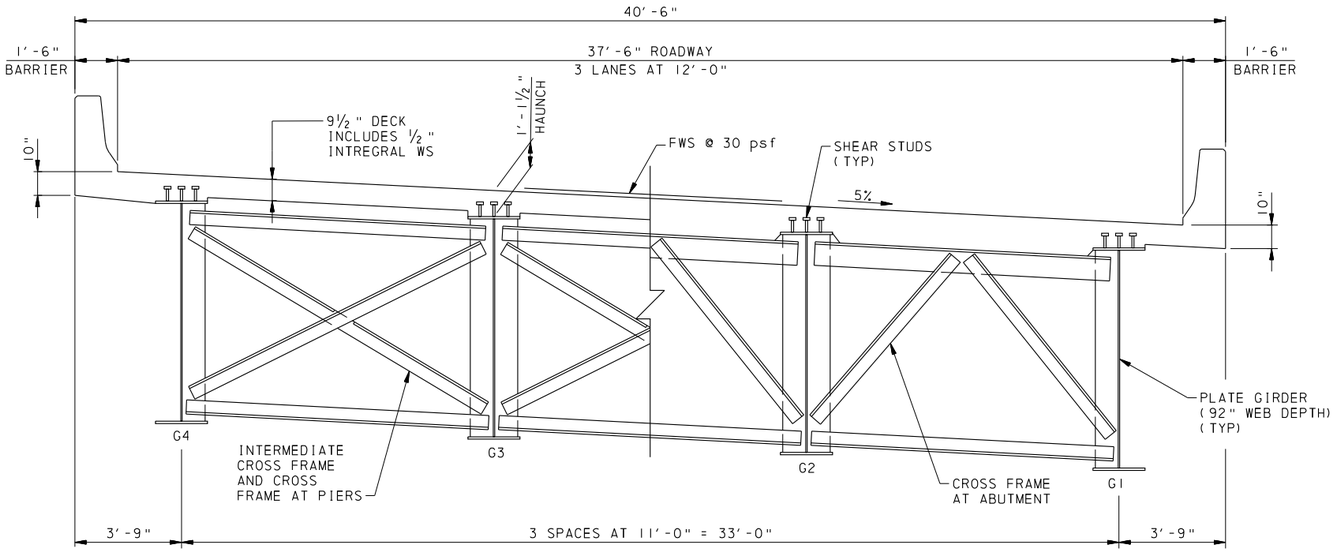

HALF SECTION AT PIERS AND INTERIOR GIRDERS

HALF SECTION AT ABUTMENTS

TYPICAL CROSS SECTION

NHI COURSE NO. 130095
LRFD AND ANALYSIS OF SKEWED AND CURVED STEEL BRIDGES
I-GIRDER DESIGN EXAMPLE

RECOMMENDED July 14, 2009

CHECK PRINT	No.: 1	7/14/2009	CORRECTIONS CHECKED BY:
DRAWING ORIGINATOR:			CHANGES MADE BY:
CHECKED BY:			CHANGES VERIFIED BY:

USER: ksiffey
PATH: 000001\0000000010906\13.00_CAD\13.01_Bridge\13.01.08_Miscellaneous
FILE: Yoda-FRMPLN01.DGN
PLOT DATE: 7/14/2009 7:32:25 AM
MODEL: Default

DES:	DWG:	CKD:

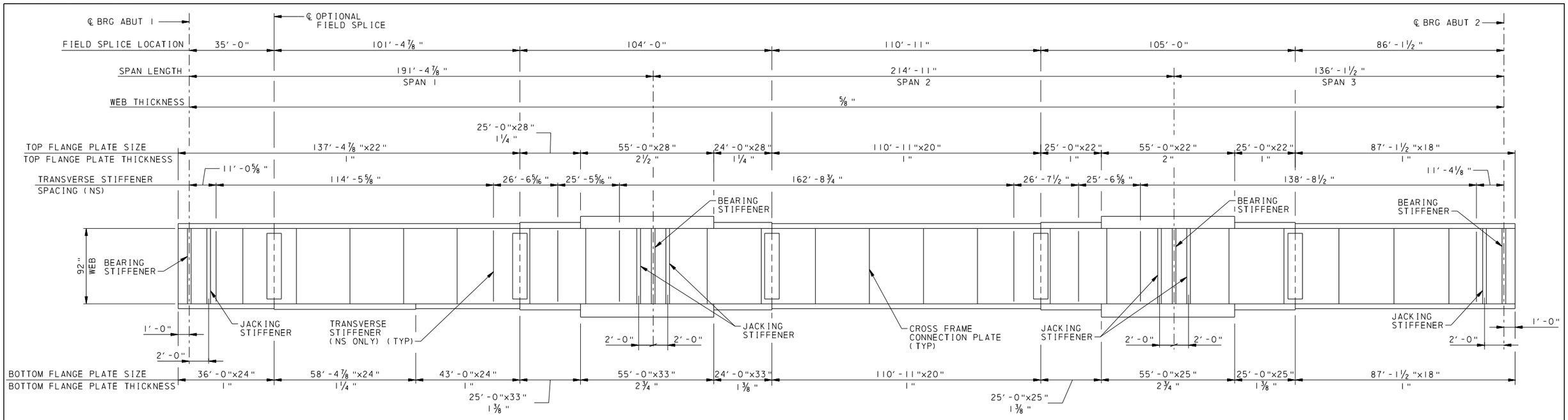

GIRDER ELEVATION - G4

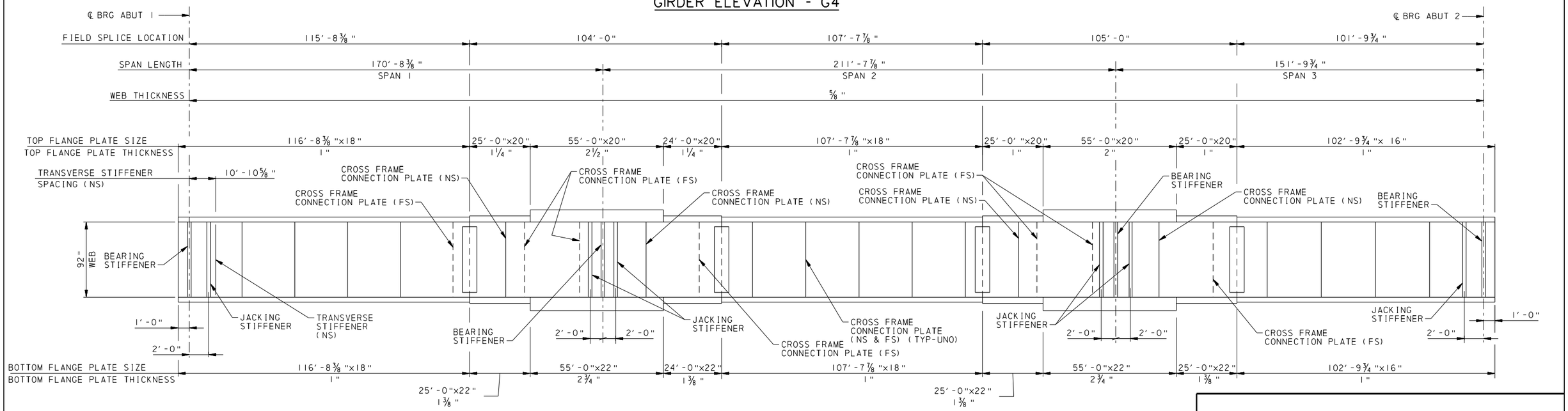

GIRDER ELEVATION - G3

NHI COURSE NO. 130095
LRFD AND ANALYSIS OF SKEWED AND CURVED STEEL BRIDGES
I-GIRDER DESIGN EXAMPLE

RECOMMENDED July 14, 2009

SHEET 2 OF 3

S -

DES: | DWG: | CKD:

FHWA CHECK PRINT
DRAWING ORIGINATOR:
CHECKED BY:

No.: 1 | 7/14/2009 | CORRECTIONS CHECKED BY:
CHANGES MADE BY:
CHANGES VERIFIED BY:

USER:ksliffey
PATH: 00000\\0000000010906\13.00_CAD\13.01_Bridge\13.01.08_Miscellaneous
FILE: Yods-GirderElev01.DGN
PLOT DATE: 7/14/2009 7:32:27 AM
MODEL: Default

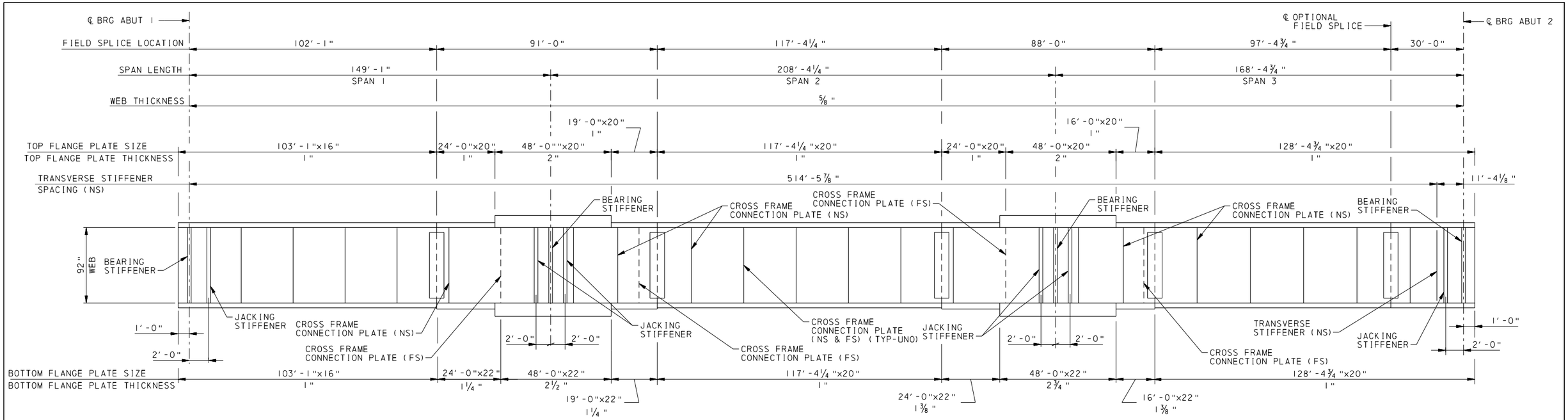

GIRDER ELEVATION - G2

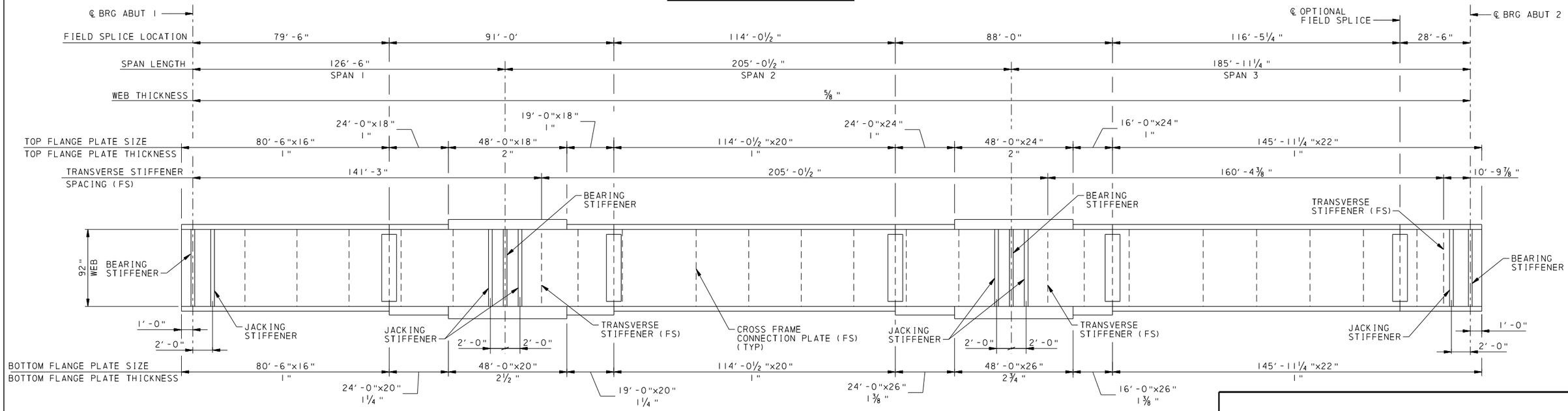

GIRDER ELEVATION - G1

NHI COURSE NO. 130095
LRFD AND ANALYSIS OF SKEWED AND CURVED STEEL BRIDGES
I-GIRDER DESIGN EXAMPLE

RECOMMENDED July 14, 2009

SHEET 3 OF 3

S -

DES: | DWG: | CKD:

CHECK PRINT
DRAWING ORIGINATOR:
CHECKED BY:

No.: 1 | 7/14/2009 | CORRECTIONS CHECKED BY: | CHANGES MADE BY: | CHANGES VERIFIED BY:

USER:ksritfey
PATH:000001\000000001\0906I\13.00_CAD\13.01_Bridge\13.01.08_Miscellaneous
FILE:Yods-GirderElev02.DGN
PLOT DATE: 7/14/2009 7:32:30 AM
MODEL:Default

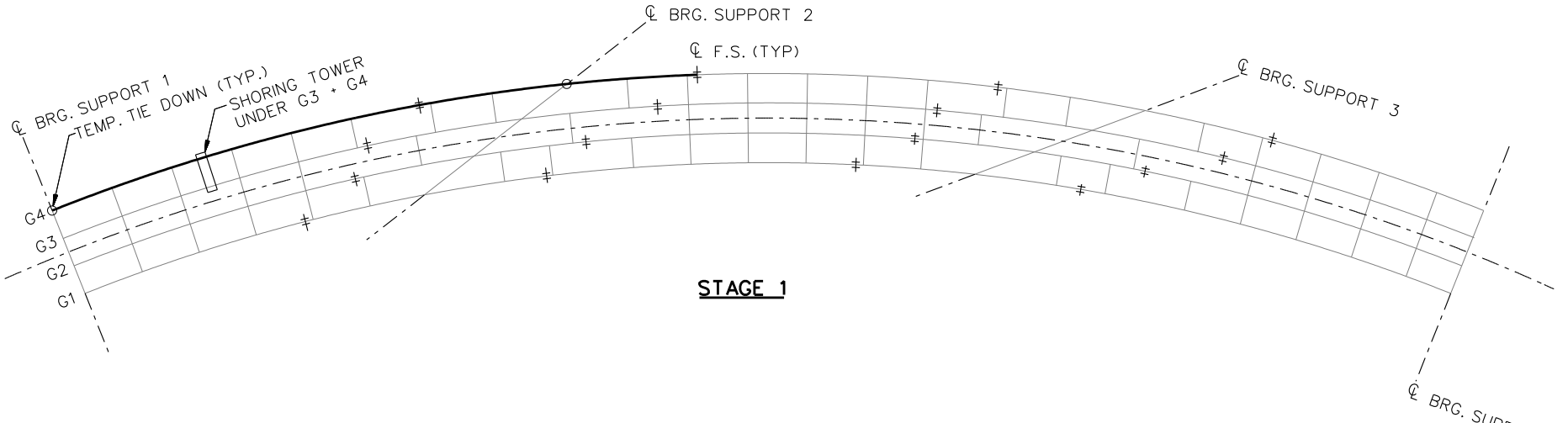

STAGE 1

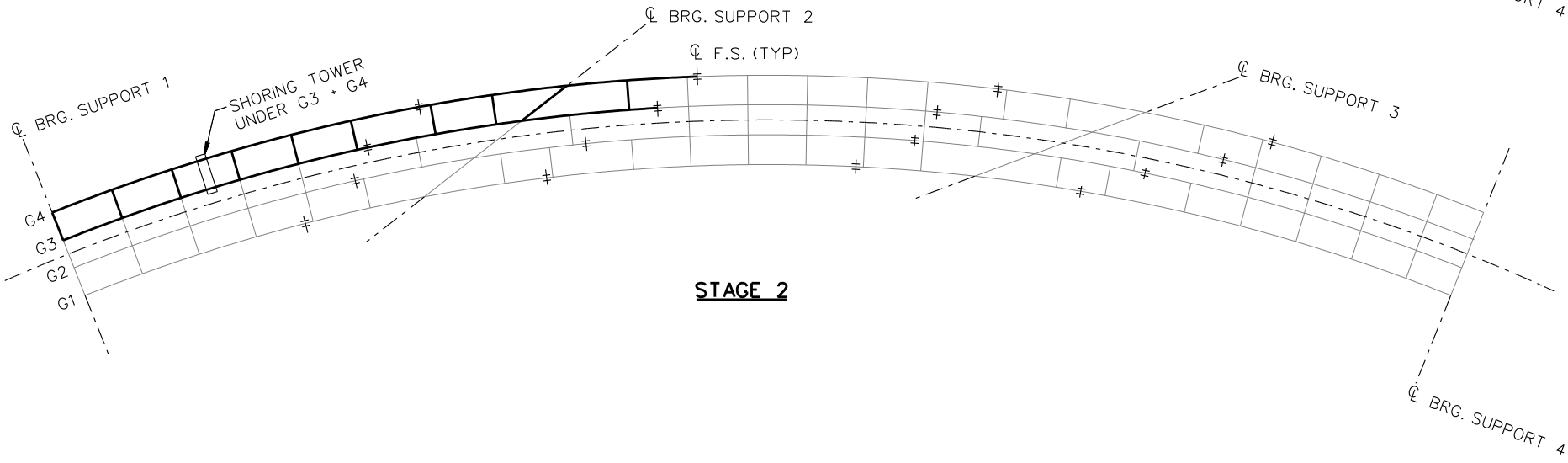

STAGE 2

LEGEND

▽ = HOLD OR LIFT CRANE

○ = TIE DOWN

□ = TEMPORARY SUPPORT STRUCTURE

NCHRP 12-79

BRIDGE XICCS7

GIRDER ERECTION PROCEDURE

SHEET 1 OF 3

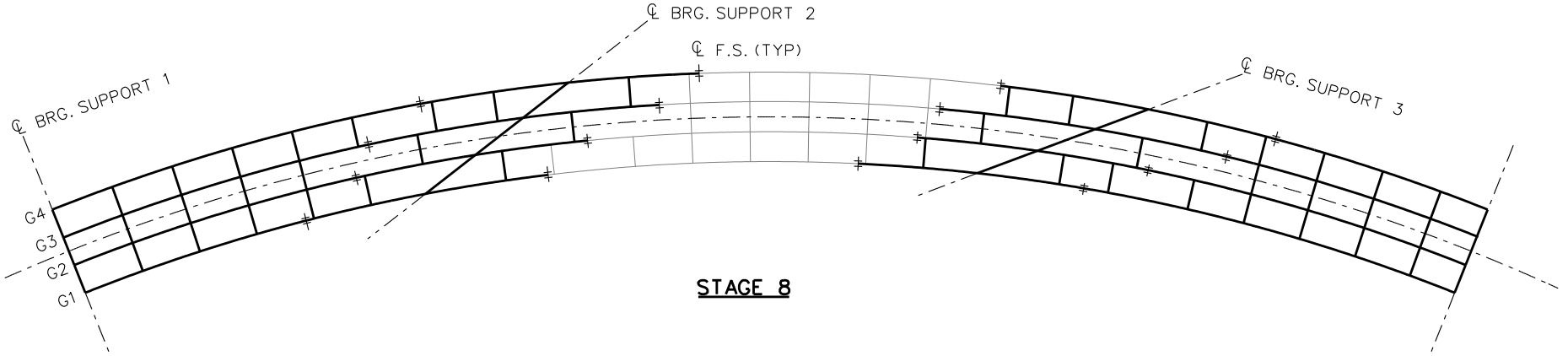

STAGE 8

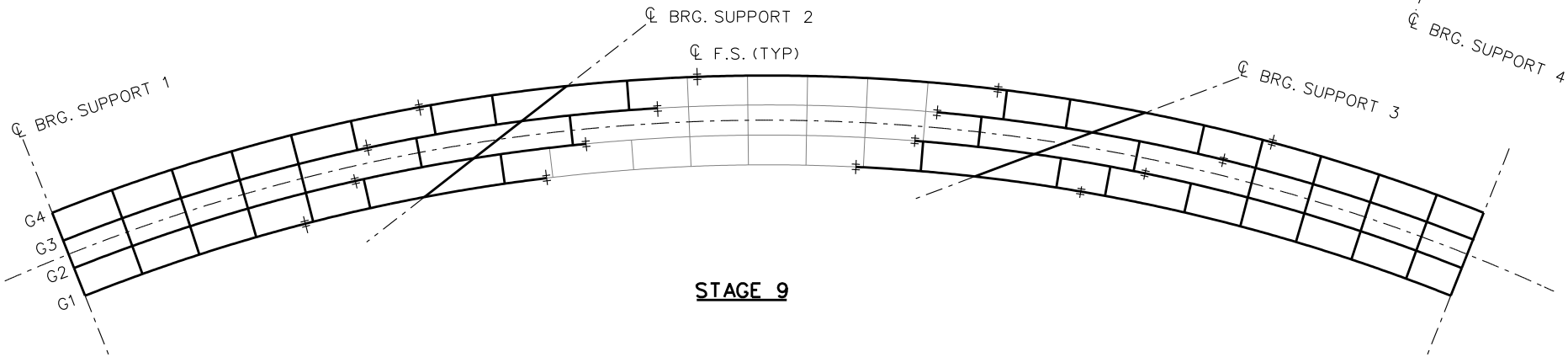

STAGE 9

LEGEND

▽ = HOLD OR LIFT CRANE

○ = TIE DOWN

□ = TEMPORARY SUPPORT STRUCTURE

NCHRP 12-79

BRIDGE XICCS7

GIRDER ERECTION PROCEDURE

SHEET 2 OF 3

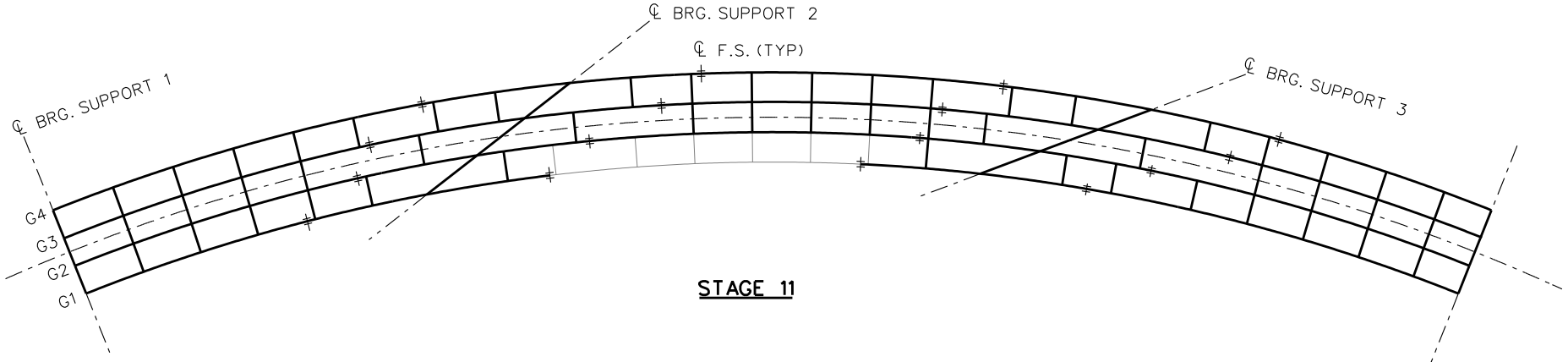

STAGE 11

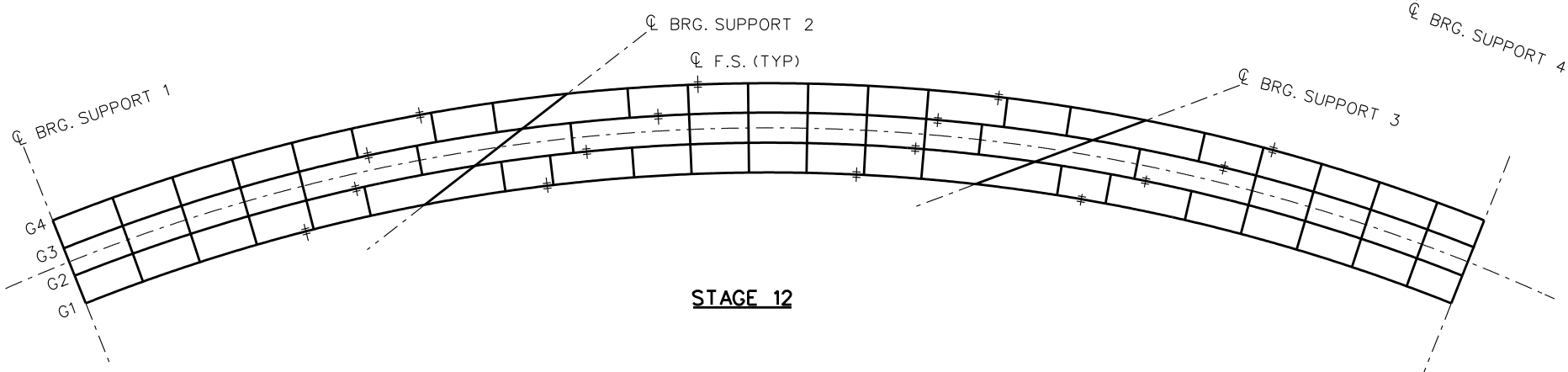

STAGE 12

LEGEND

▽ = HOLD OR LIFT CRANE

○ = TIE DOWN

□ = TEMPORARY SUPPORT STRUCTURE

NCHRP 12-79

BRIDGE XICCS7

GIRDER ERECTION PROCEDURE

SHEET 3 OF X 3

NCHRP 12-79

XICSN1

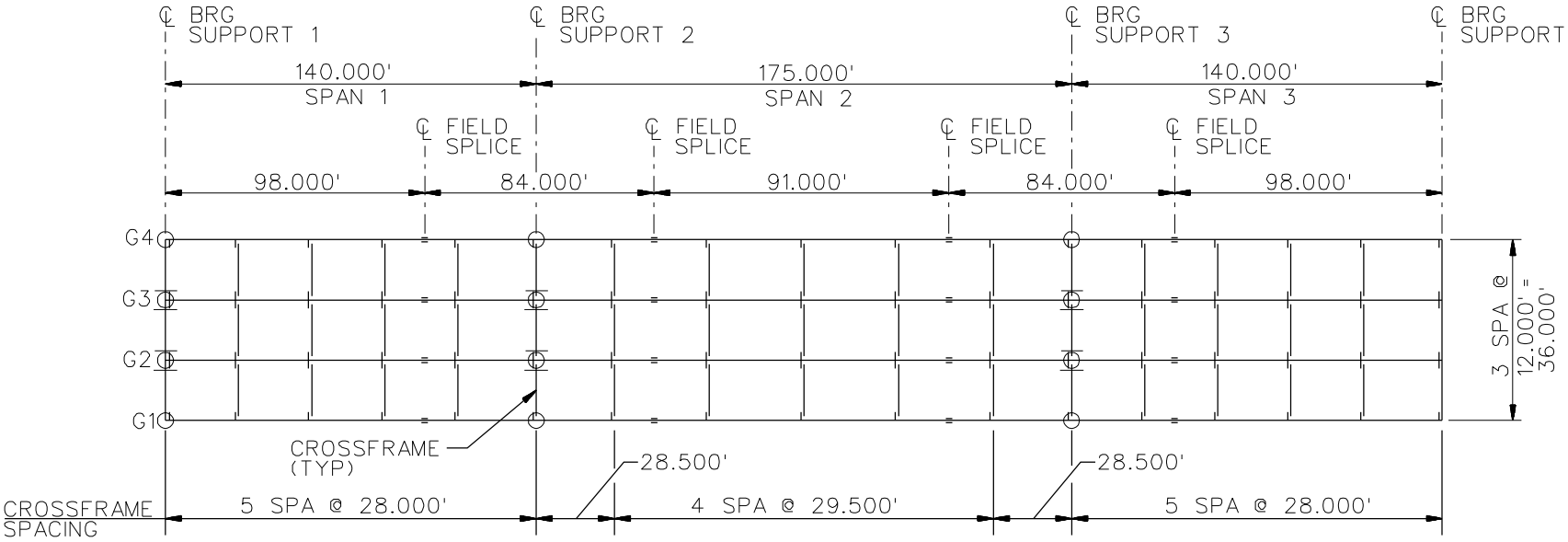

FRAMING PLAN

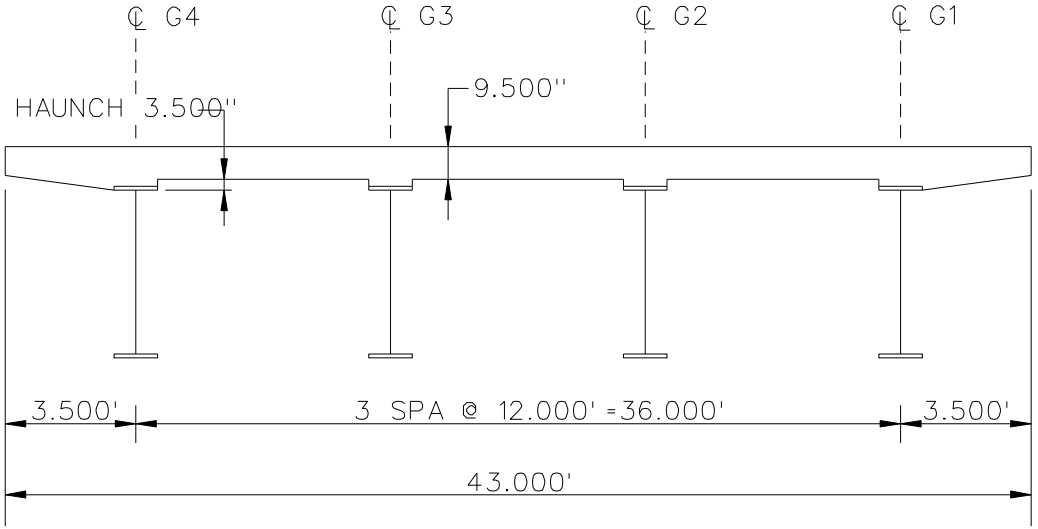

CROSS - SECTION

(DIAPHRAGMS NOT SHOWN)

BEARING LEGEND

- ○ NON-GUIDED
- ⊖ LONGITUDINALLY GUIDED
- |○| TRANSVERSELY GUIDED
- ⊡ FIXED

NCHRP 12-79

BRIDGE XICSN1

FRAMING PLAN AND CROSS SECTION

SHEET 1 OF 11

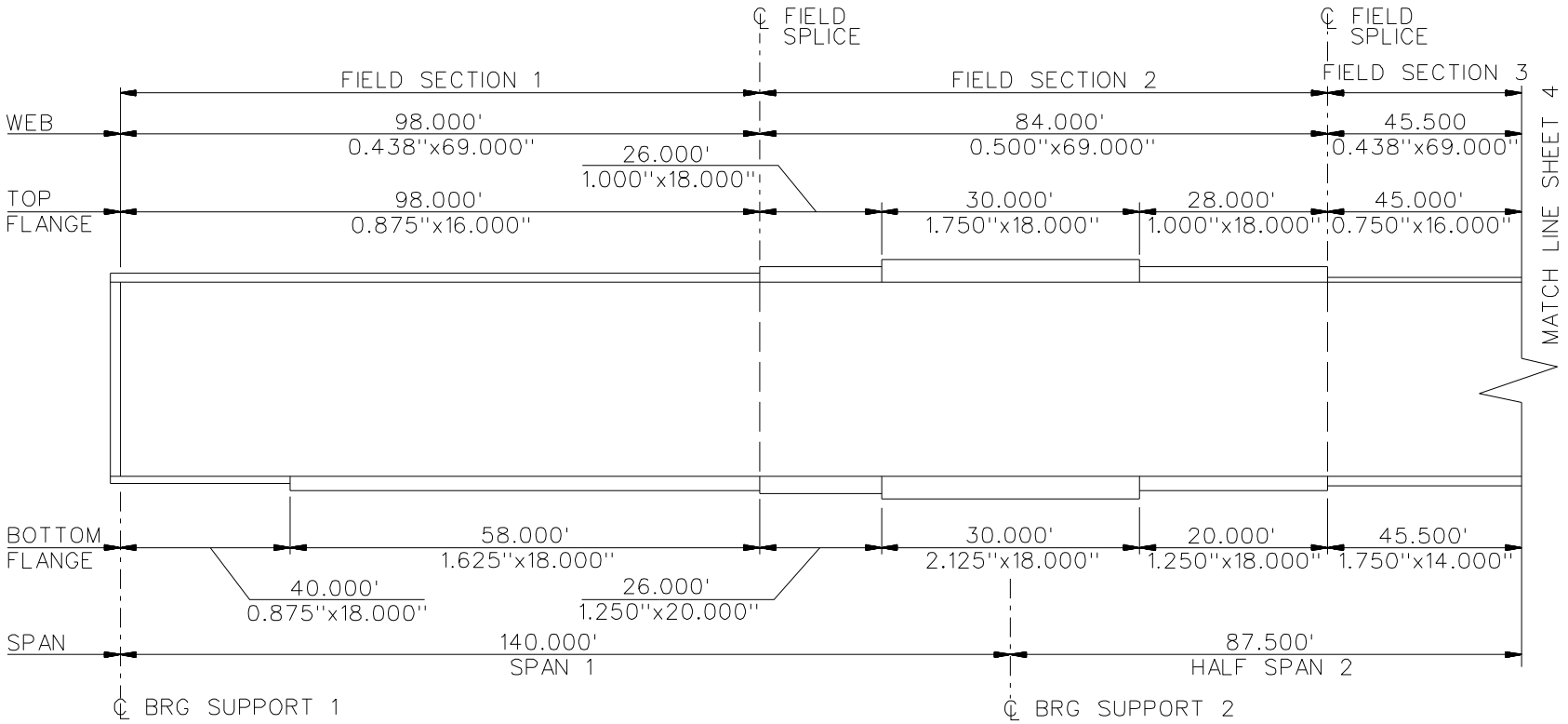

GIRDER ELEVATION

(ALL GIRDERS)
(NOT TO SCALE)

NCHRP 12-79

BRIDGE XICSN1

GIRDER ELEVATION

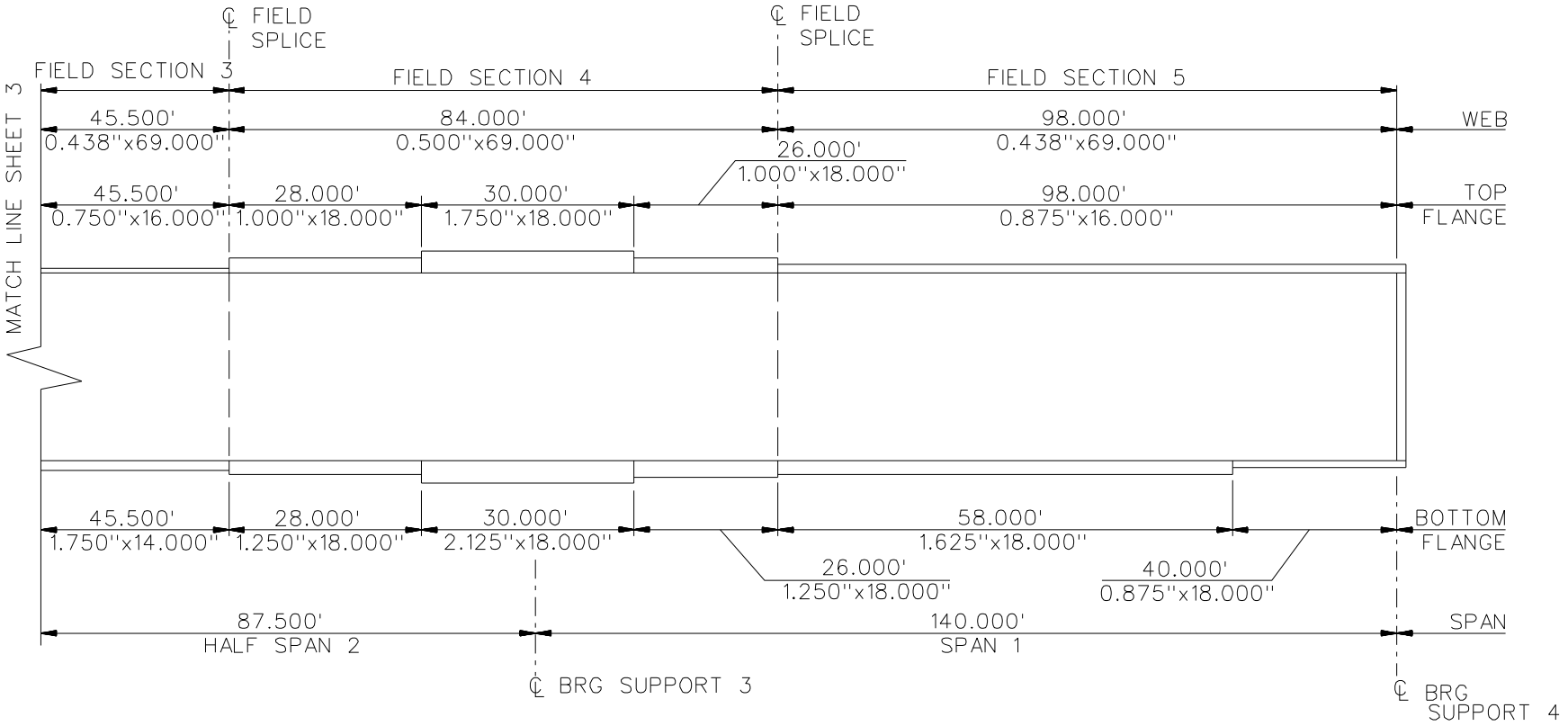

GIRDER ELEVATION

(ALL GIRDERS)
(NOT TO SCALE)

NCHRP 12-79

BRIDGE XICSN1

GIRDER ELEVATION

SHEET 3 OF 11

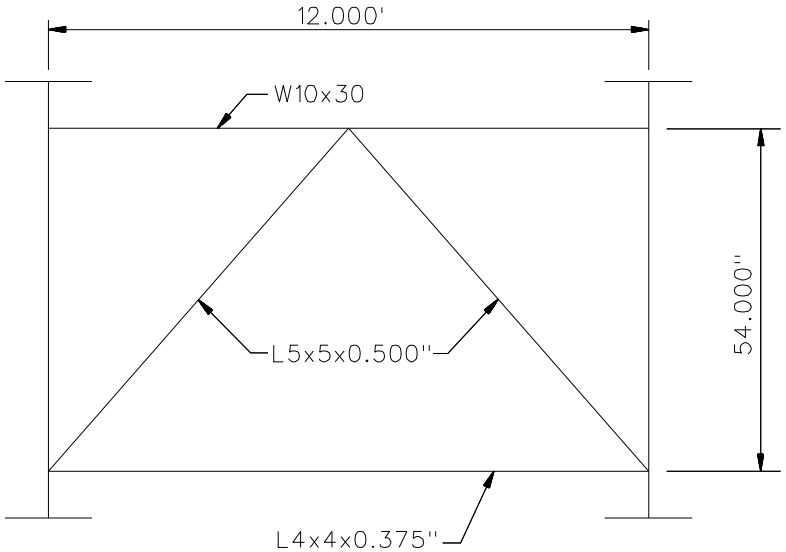

END CROSS FRAME

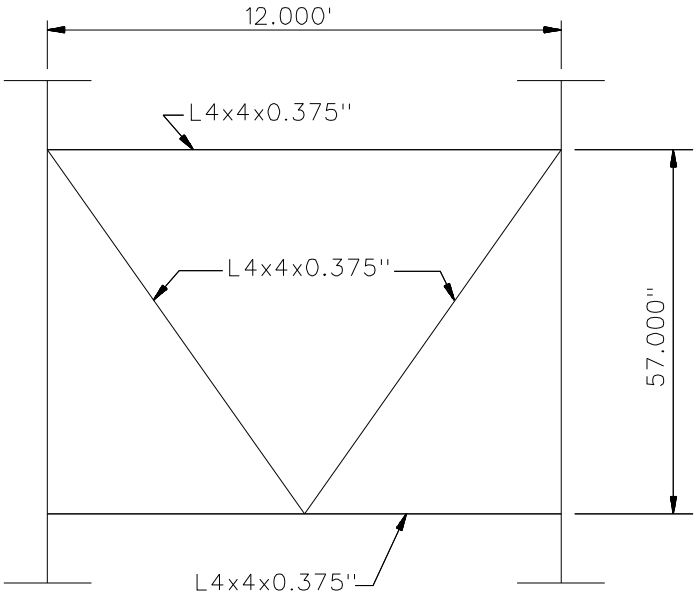

INTERMEDIATE CROSS FRAME

NOTES:

1. STEEL DEAD LOAD INCREASED BY 5% (MDX AND LARSA), 10% (APPROX), AND 2% (3D) TO ACCOUNT FOR MISC. DETAILS.

2. FORMWORK LOAD OF 10 PSF IS INCLUDED IN CONCRETE DEAD LOAD.

NCHRP 12-79

BRIDGE XICSN1

MISC. DETAILS AND NOTES

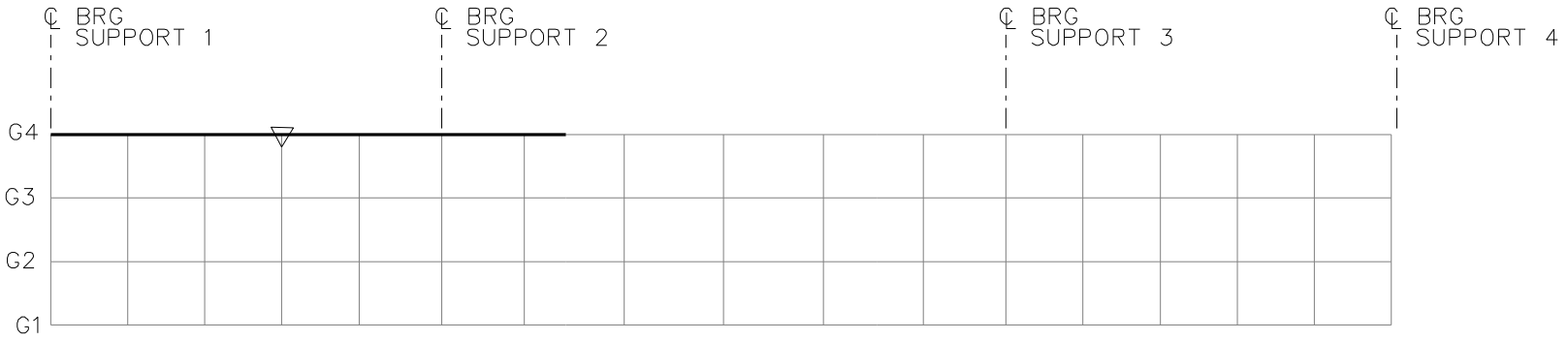

STAGE 1

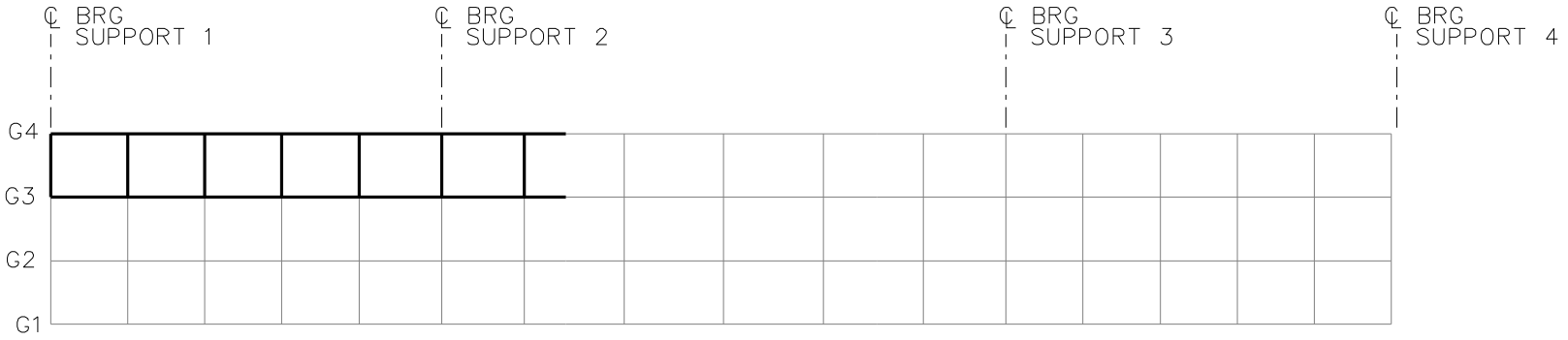

STAGE 2

LEGEND

▽ = HOLD OR LIFT CRANE

○ = TIE DOWN

□ = TEMPORARY SUPPORT STRUCTURE

NCHRP 12-79

BRIDGE XICSN1

GENERAL ERECTION PROCEDURE

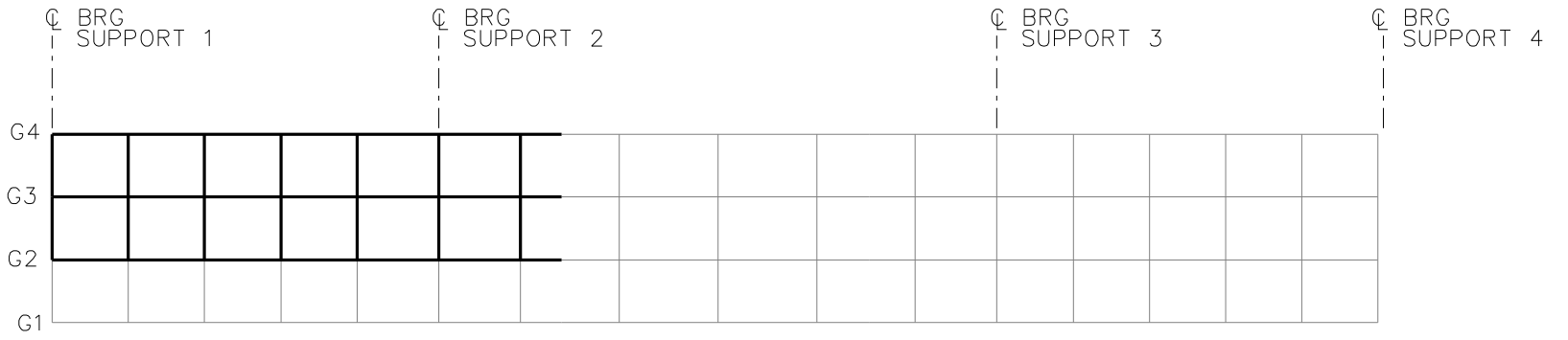

STAGE 3

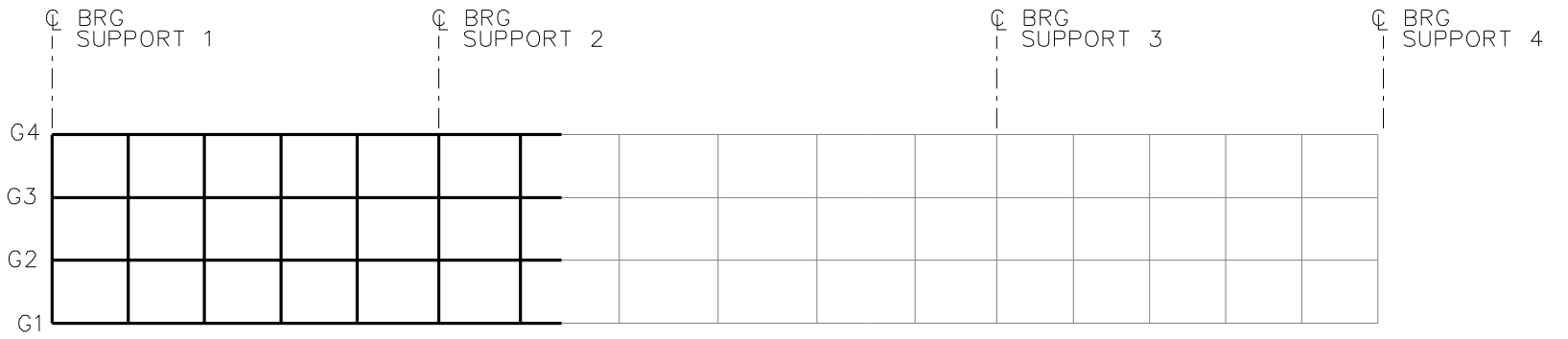

STAGE 4

LEGEND

▽ = HOLD OR LIFT CRANE

○ = TIE DOWN

□ = TEMPORARY SUPPORT STRUCTURE

NCHRP 12-79

BRIDGE XICSN1

GENERAL ERECTION PROCEDURE

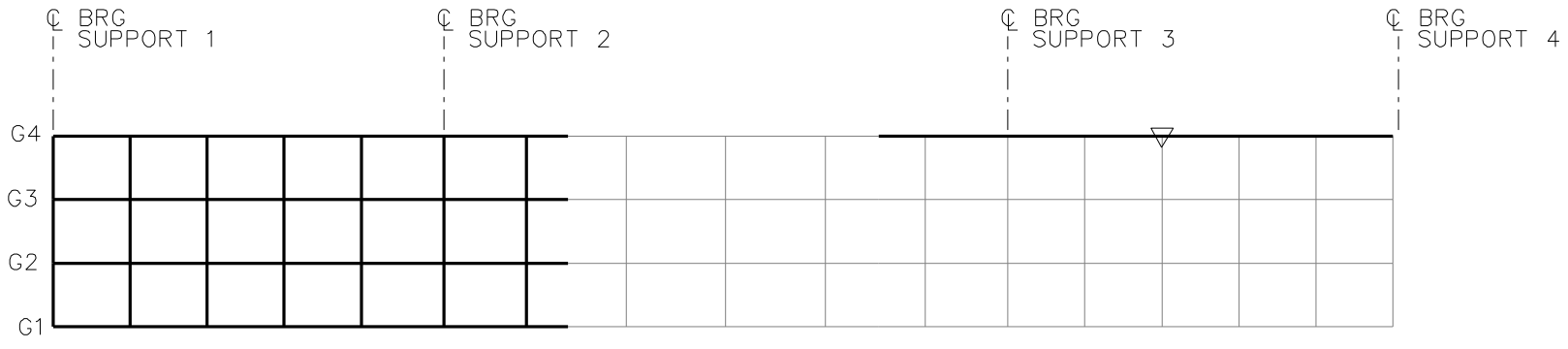

STAGE 5

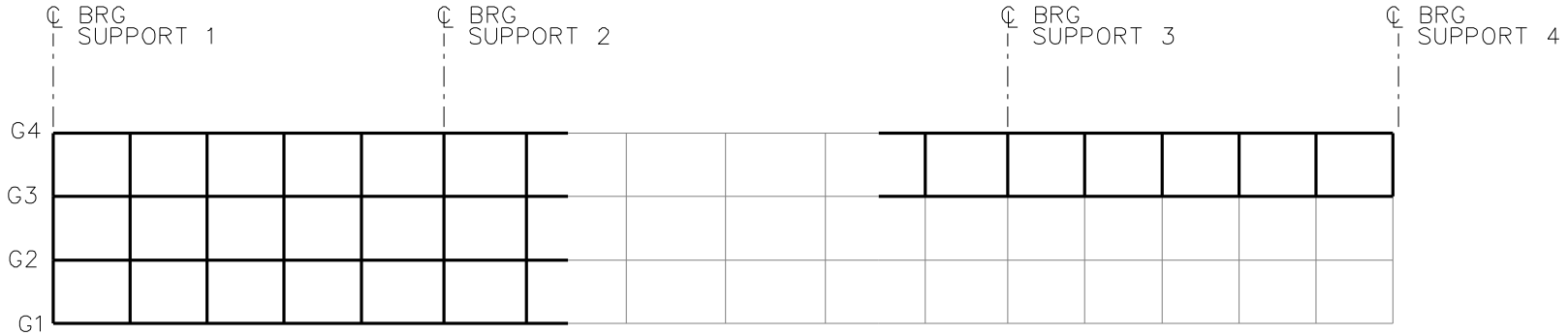

STAGE 6

LEGEND

▽ = HOLD OR LIFT CRANE

○ = TIE DOWN

□ = TEMPORARY SUPPORT STRUCTURE

NCHRP 12-79

BRIDGE XICSN1

GENERAL ERECTION PROCEDURE

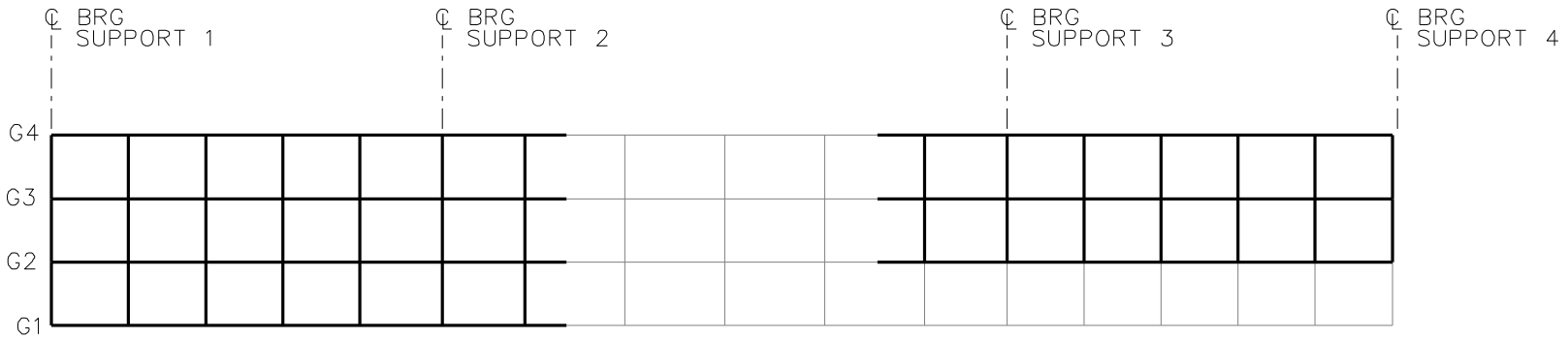

STAGE 7

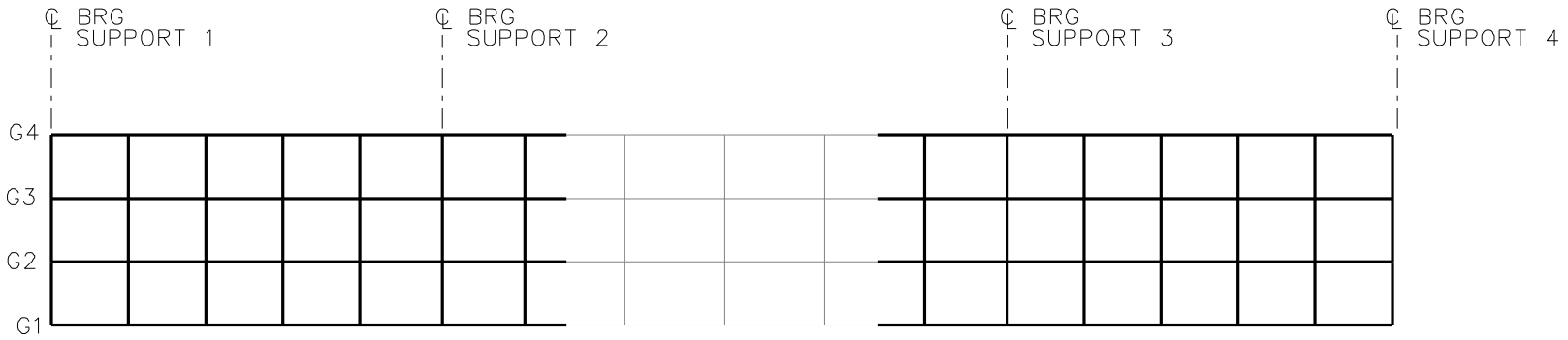

STAGE 8

LEGEND

▽ = HOLD OR LIFT CRANE

○ = TIE DOWN

□ = TEMPORARY SUPPORT STRUCTURE

NCHRP 12-79

BRIDGE XICSN1

GENERAL ERECTION PROCEDURE

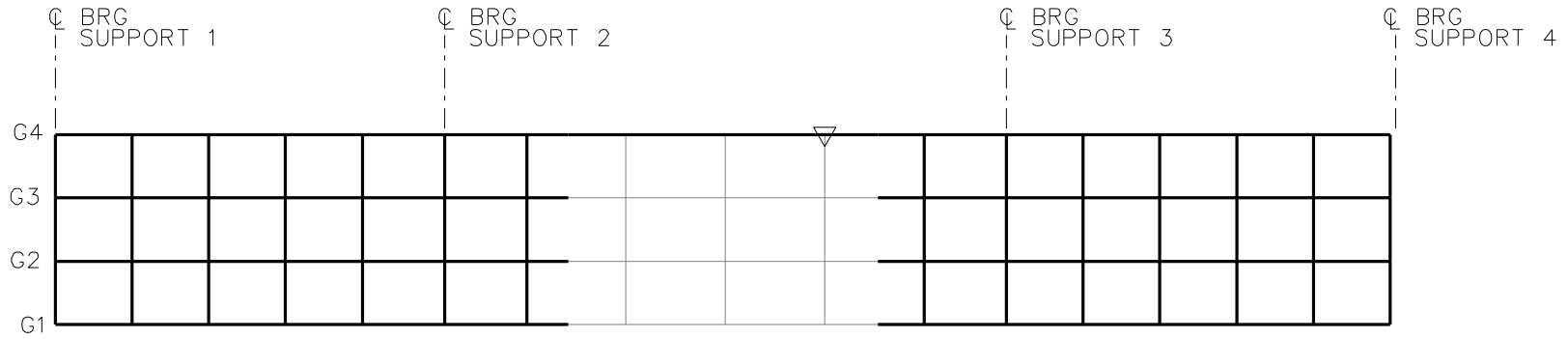

STAGE 9

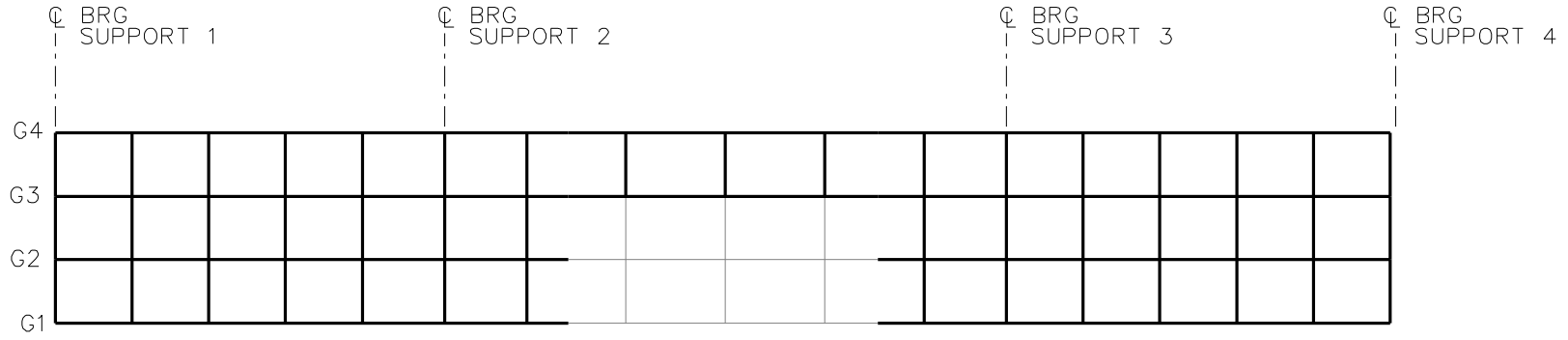

STAGE 10

LEGEND

▽ = HOLD OR LIFT CRANE

○ = TIE DOWN

□ = TEMPORARY SUPPORT STRUCTURE

NCHRP 12-79

BRIDGE XICSN1

GENERAL ERECTION PROCEDURE

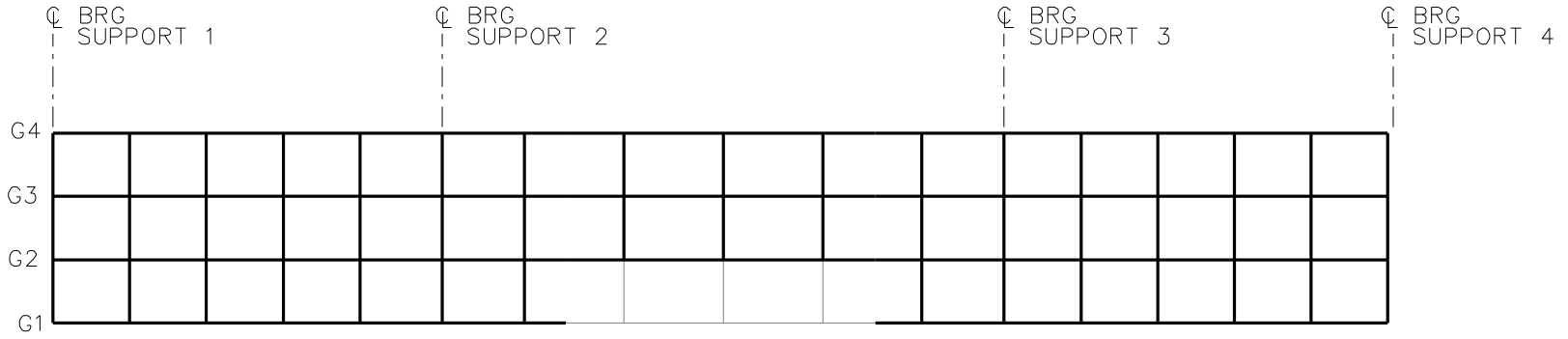

STAGE 11

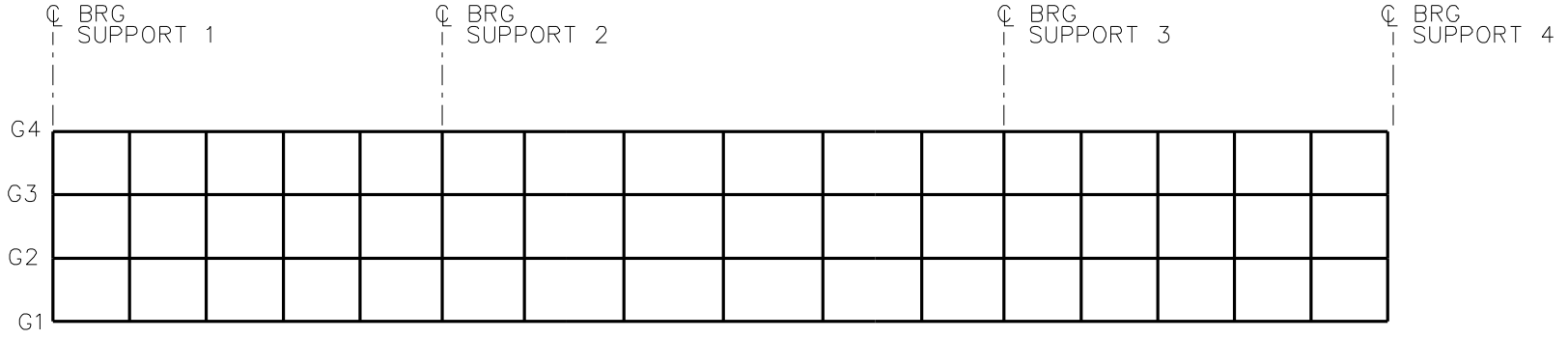

STAGE 12

LEGEND

▽ = HOLD OR LIFT CRANE

○ = TIE DOWN

□ = TEMPORARY SUPPORT STRUCTURE

NCHRP 12-79

BRIDGE XICSN1

GENERAL ERECTION PROCEDURE

NCHRP 12-79

XICSS5

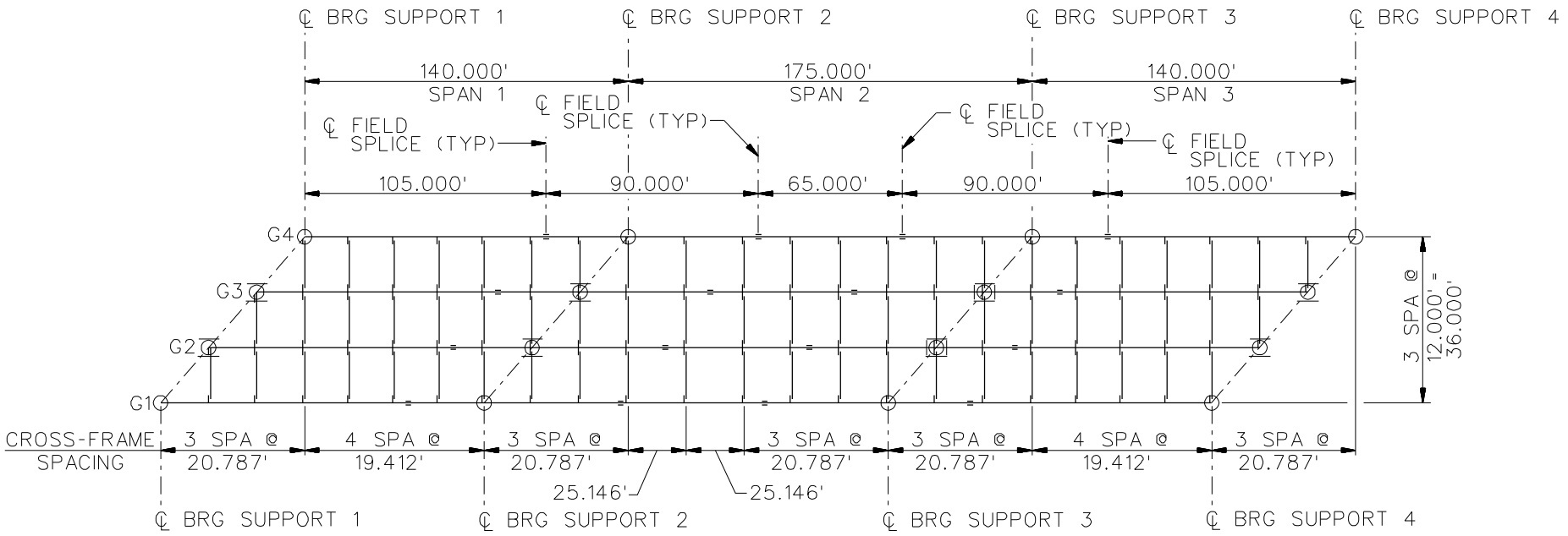

FRAMING PLAN

BEARING LEGEND

- ○ NON-GUIDED
- ⊖ LONGITUDINALLY GUIDED
- |○| TRANSVERSELY GUIDED
- ⊡ FIXED

NCHRP 12-79

BRIDGE XICSS5

FRAMING PLAN

SHEET 1 OF 11

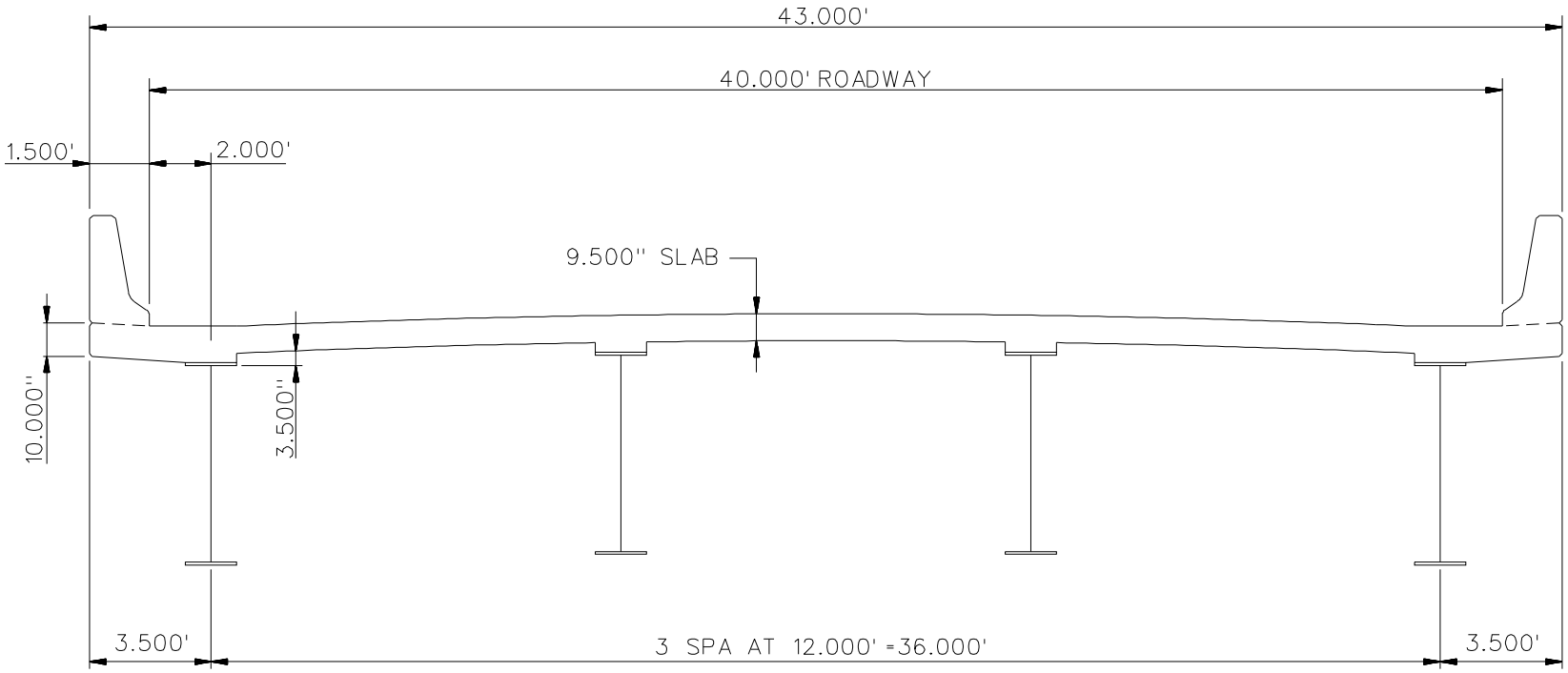

TYPICAL SECTION

NCHRP 12-79

BRIDGE XICSS5

TYPICAL SECTION

SHEET 2 OF 11

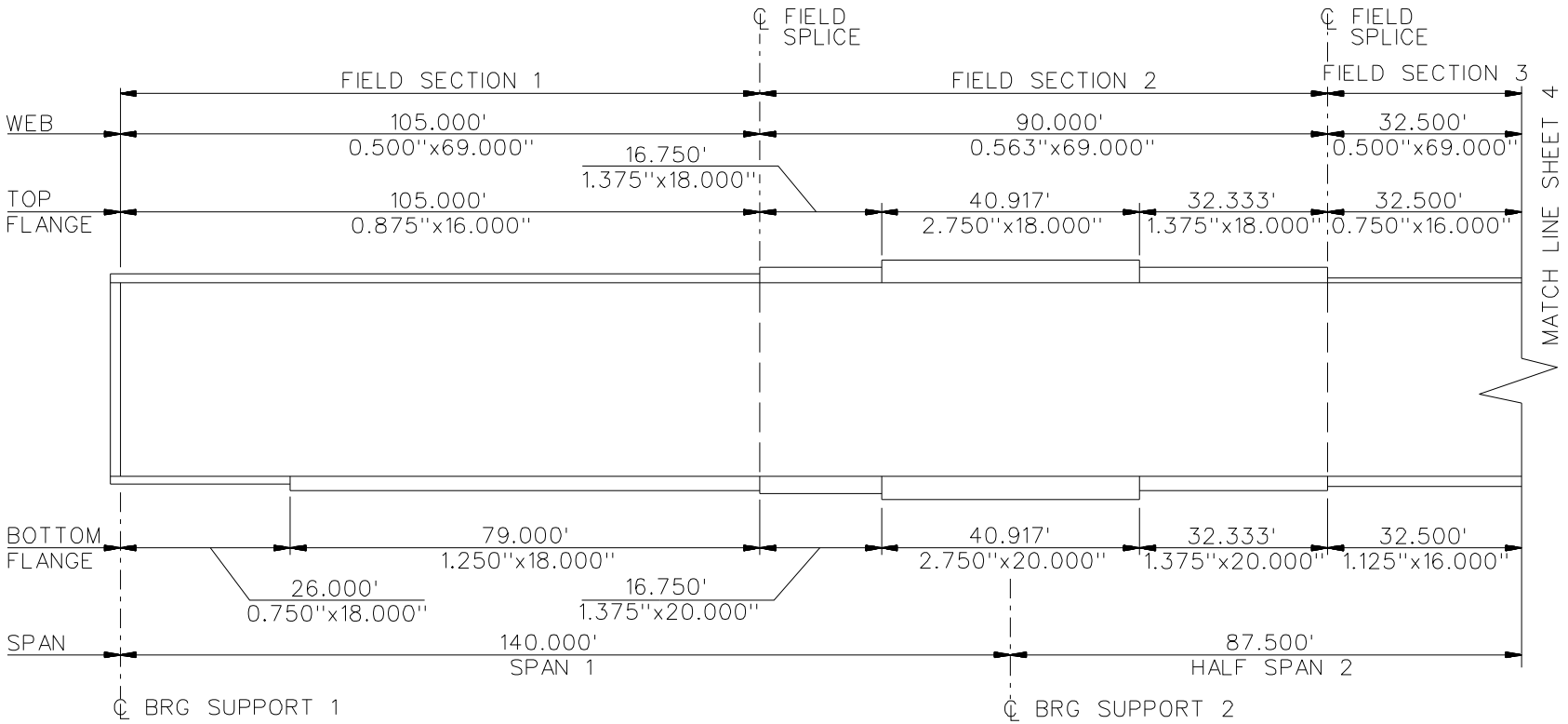

GIRDER ELEVATION

(ALL GIRDERS)

NCHRP 12-79

BRIDGE XICSS5

GIRDER ELEVATION

SHEET 3 OF 11

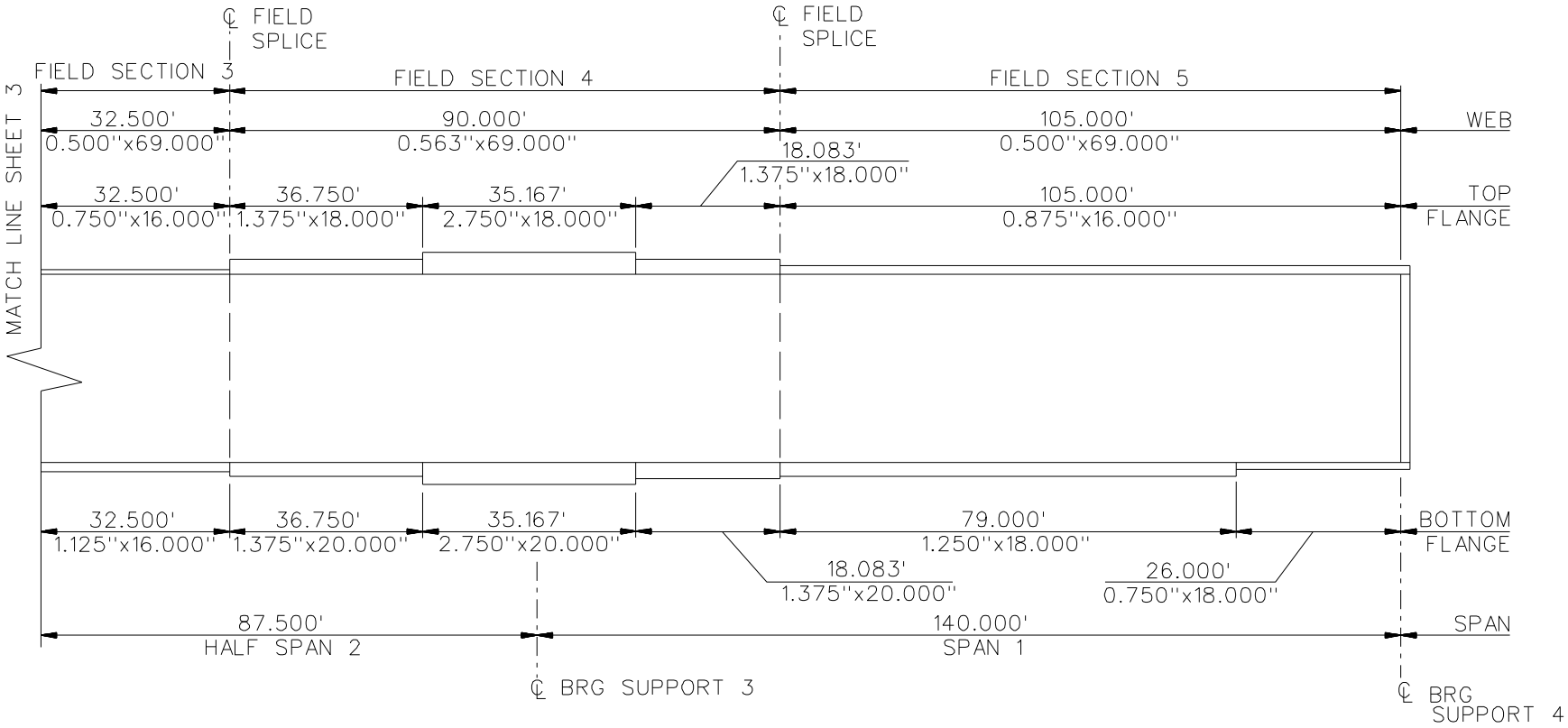

GIRDER ELEVATION

(ALL GIRDERS)

NCHRP 12-79

BRIDGE XICSS5

GIRDER ELEVATION

SHEET 4 OF 11

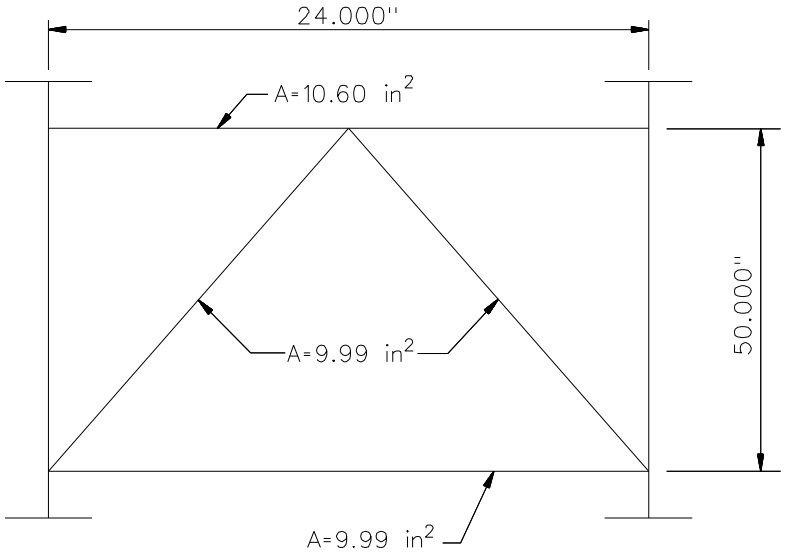

END CROSS FRAME

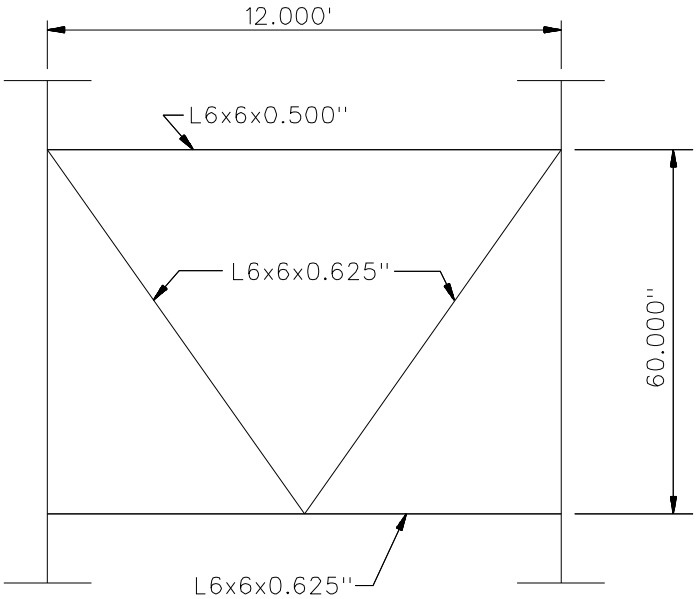

INTERMEDIATE CROSS FRAME

NOTES:

1. STEEL DEAD LOAD INCREASED BY 5% (MDX AND LARSA), 10% (APPROX), AND 2% (3D) TO ACCOUNT FOR MISC. DETAILS.

2. FORMWORK LOAD OF 10 PSF IS INCLUDED IN CONCRETE DEAD LOAD.

NCHRP 12-79

BRIDGE XICSS5

MISC. DETAILS AND NOTES

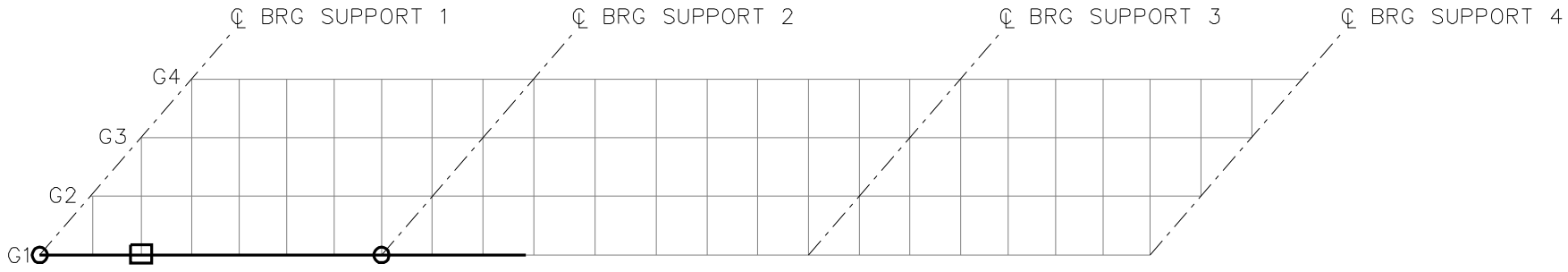

STAGE 1

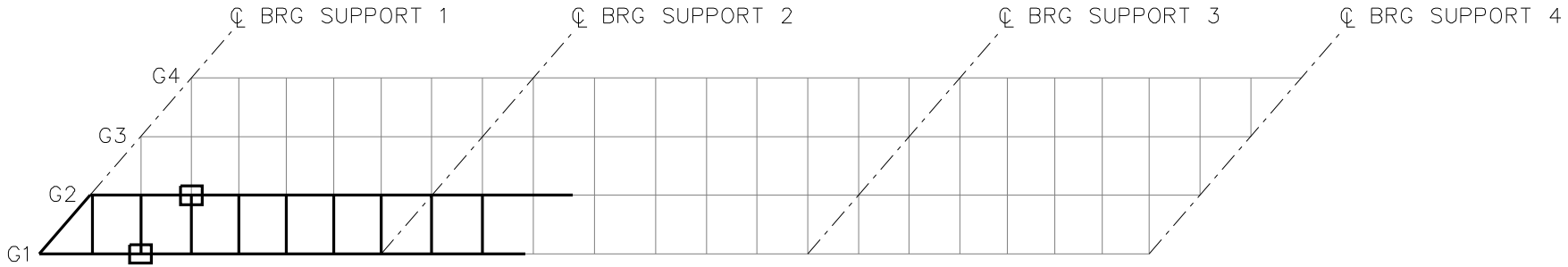

STAGE 2

LEGEND

▽ = HOLD OR LIFT CRANE

○ = TIE DOWN

□ = TEMPORARY SUPPORT STRUCTURE

NCHRP 12-79

BRIDGE XICSS5

GENERAL ERECTION PROCEDURE

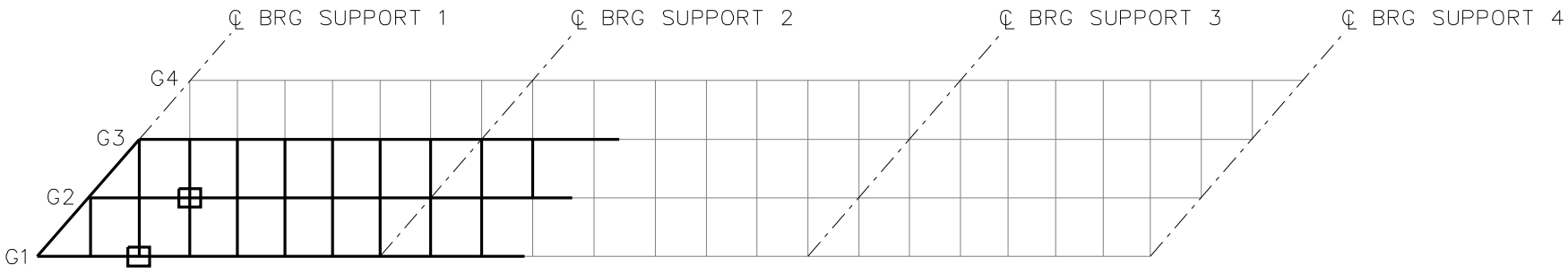

STAGE 3

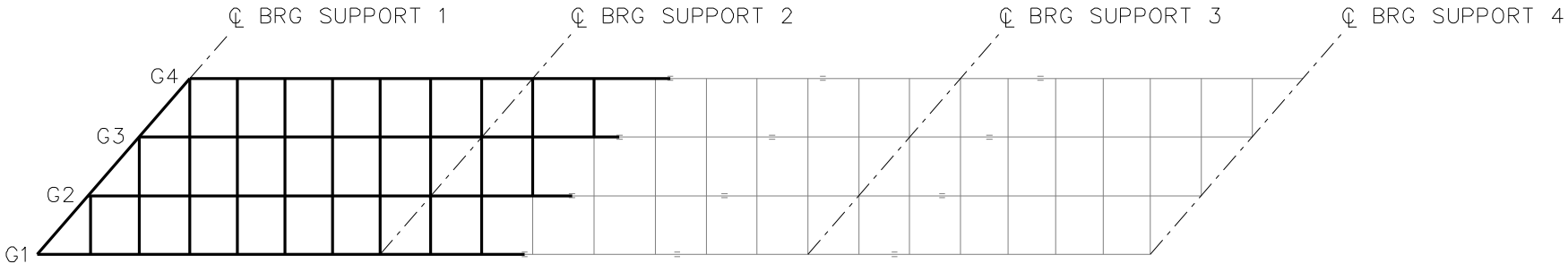

STAGE 4

LEGEND

▽ = HOLD OR LIFT CRANE

○ = TIE DOWN

□ = TEMPORARY SUPPORT STRUCTURE

NCHRP 12-79

BRIDGE XICSS5

GENERAL ERECTION PROCEDURE

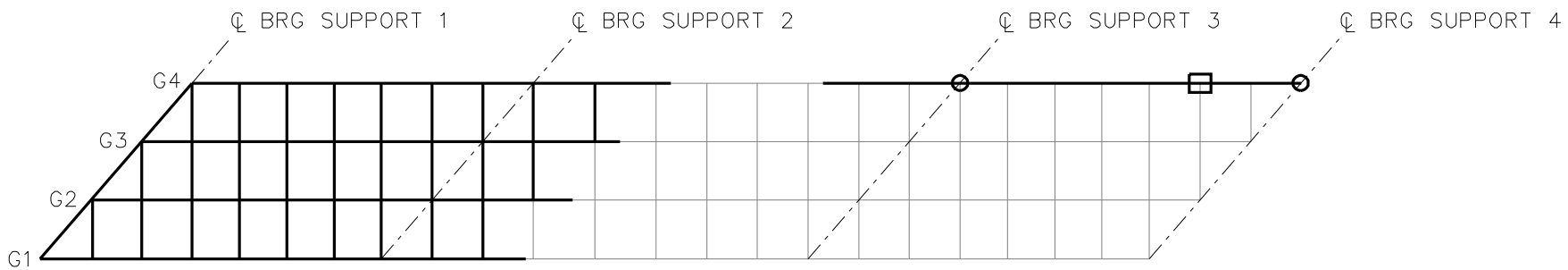

STAGE 5

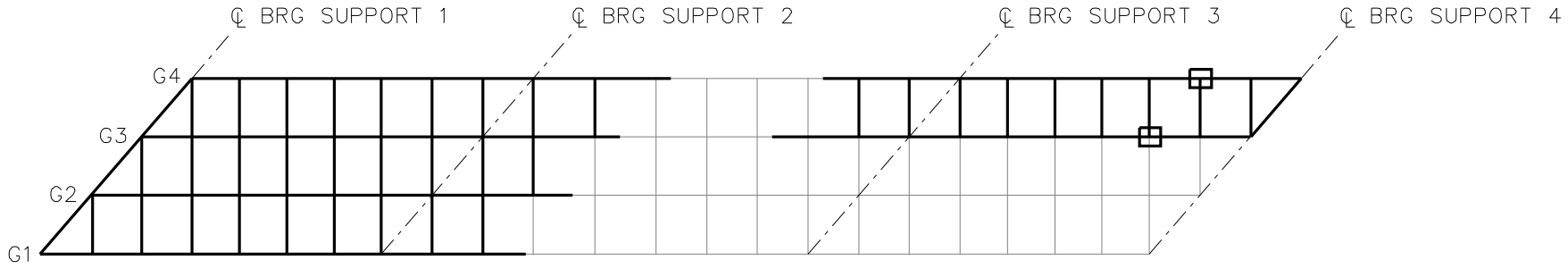

STAGE 6

LEGEND

▽ = HOLD OR LIFT CRANE

○ = TIE DOWN

□ = TEMPORARY SUPPORT STRUCTURE

NCHRP 12-79

BRIDGE XICSS5

GENERAL ERECTION PROCEDURE

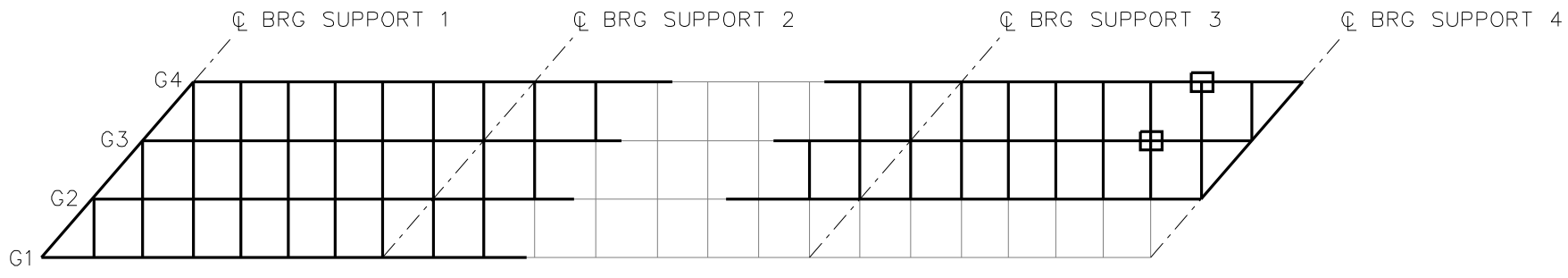

STAGE 7

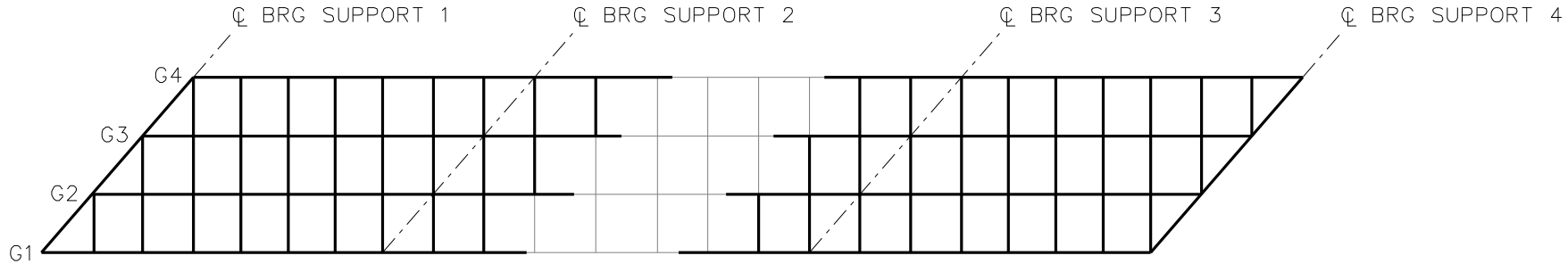

STAGE 8

LEGEND

▽ = HOLD OR LIFT CRANE

○ = TIE DOWN

□ = TEMPORARY SUPPORT STRUCTURE

NCHRP 12-79

BRIDGE XICSS5

GENERAL ERECTION PROCEDURE

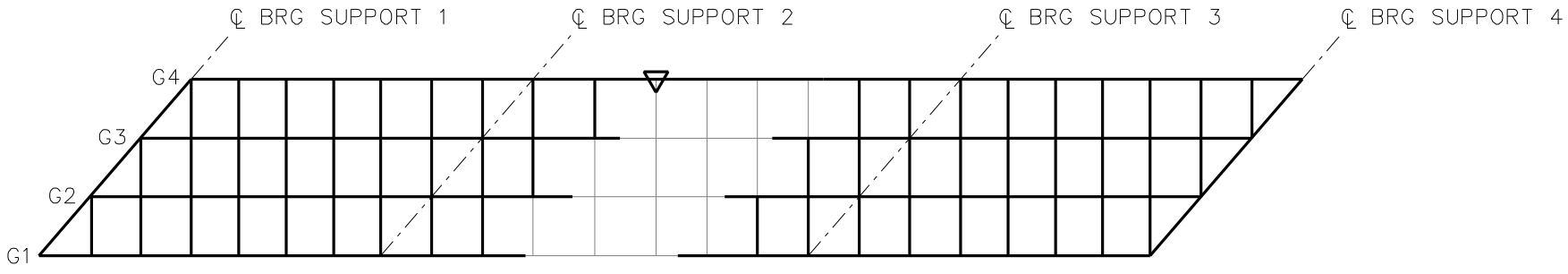

STAGE 9

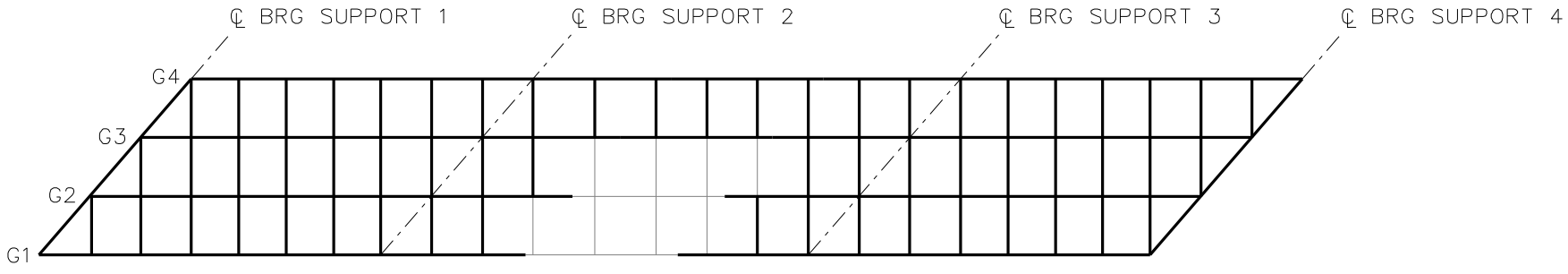

STAGE 10

LEGEND

▽ = HOLD OR LIFT CRANE

○ = TIE DOWN

□ = TEMPORARY SUPPORT STRUCTURE

NCHRP 12-79

BRIDGE XICSS5

GENERAL ERECTION PROCEDURE

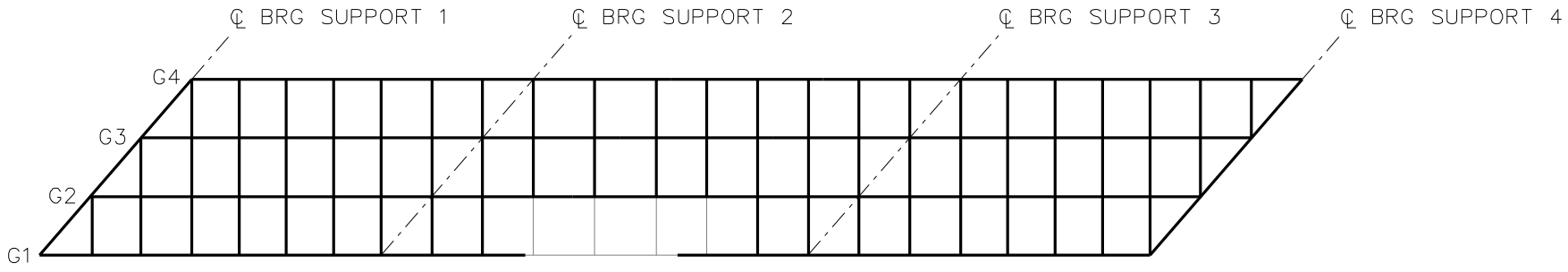

STAGE 11

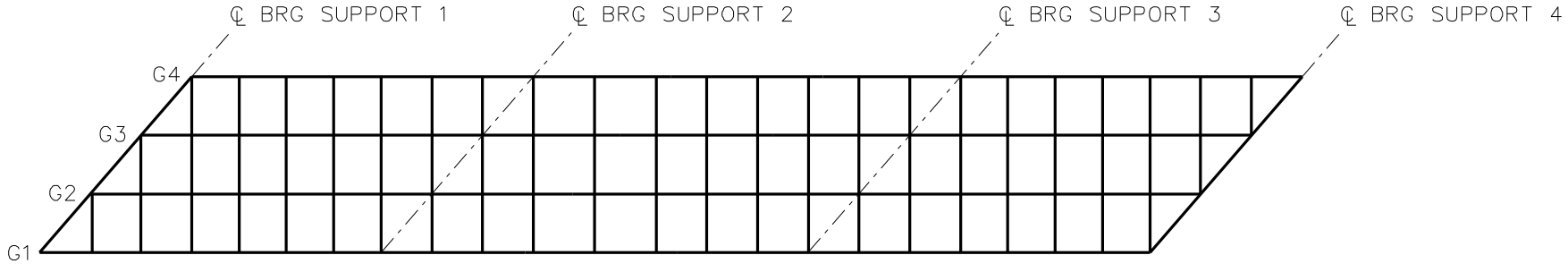

STAGE 12

LEGEND

▽ = HOLD OR LIFT CRANE

○ = TIE DOWN

□ = TEMPORARY SUPPORT STRUCTURE

NCHRP 12-79

BRIDGE XICSS5

GENERAL ERECTION PROCEDURE

NCHRP 12-79

XTCCR8

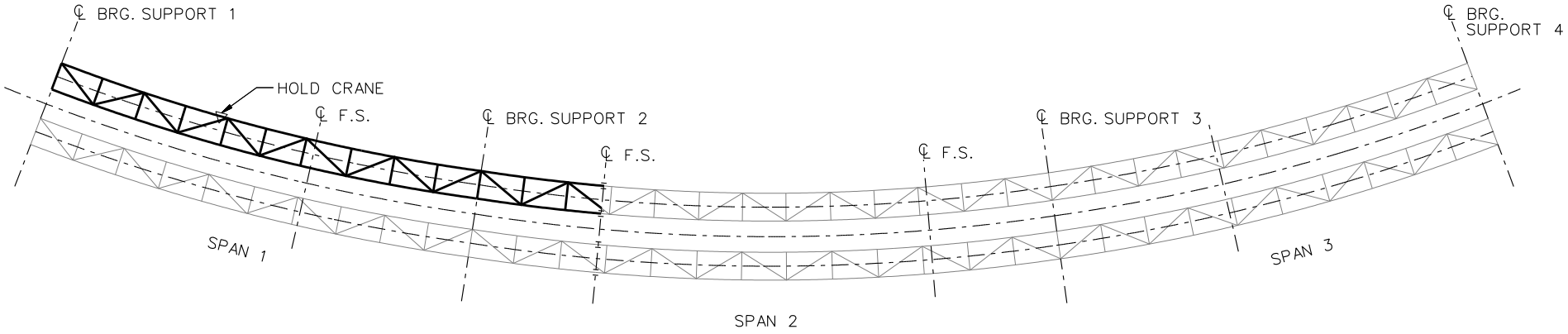

STAGE 1

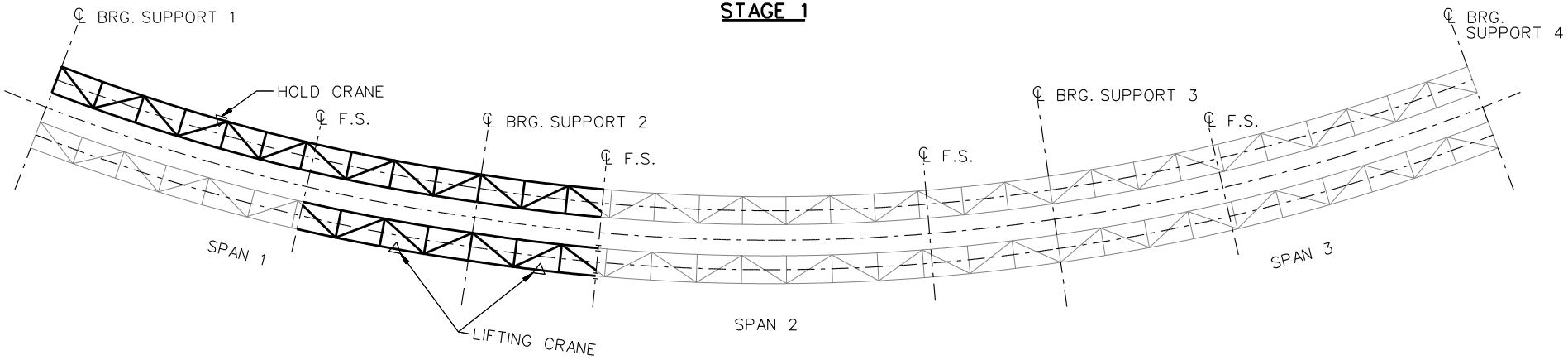

STAGE 2

LEGEND

▽ = HOLD OR LIFT CRANE

○ = TIE DOWN

□ = TEMPORARY SUPPORT STRUCTURE

NCHRP 12-79

BRIDGE XTCCR8

GIRDER ERECTION PROCEDURE

SHEET 1 OF 4

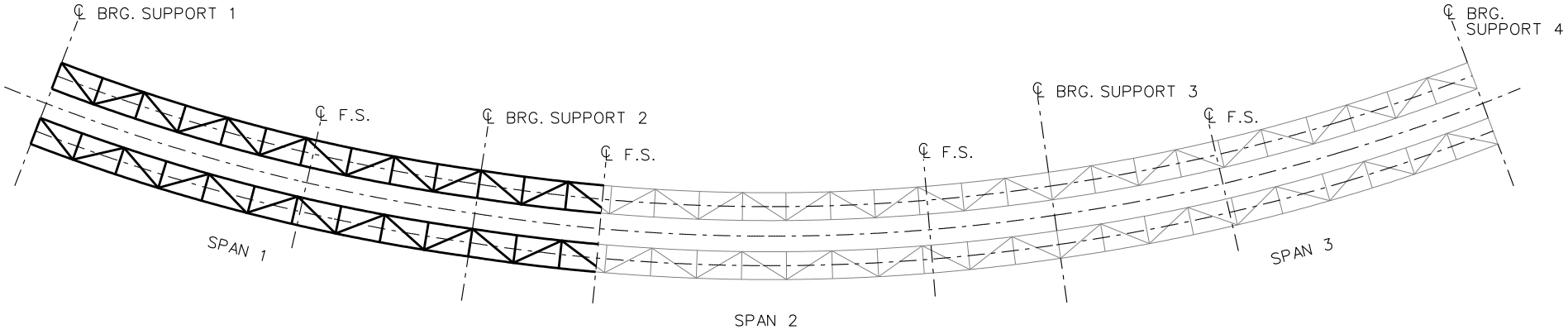

STAGE 3

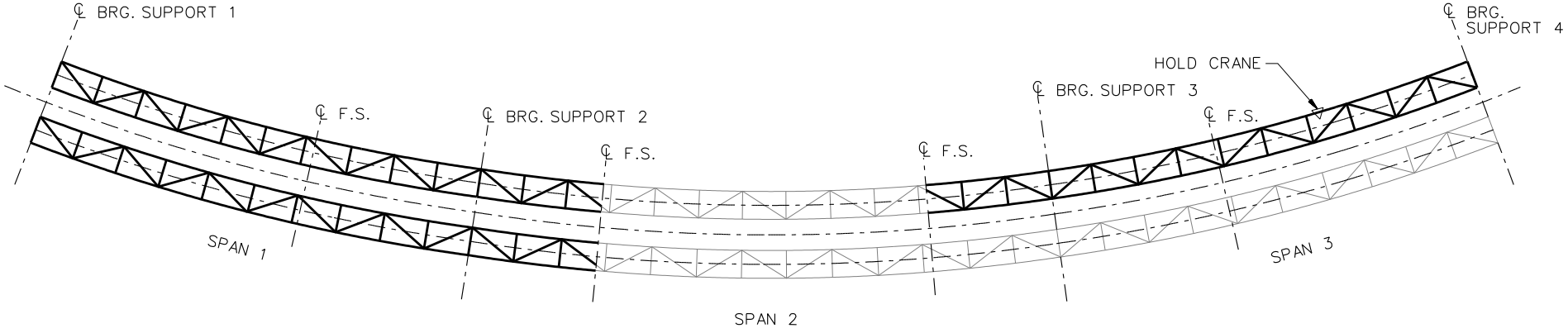

STAGE 4

LEGEND

▽ = HOLD OR LIFT CRANE

○ = TIE DOWN

□ = TEMPORARY SUPPORT STRUCTURE

NCHRP 12-79

BRIDGE XTCCR8

GIRDER ERECTION PROCEDURE

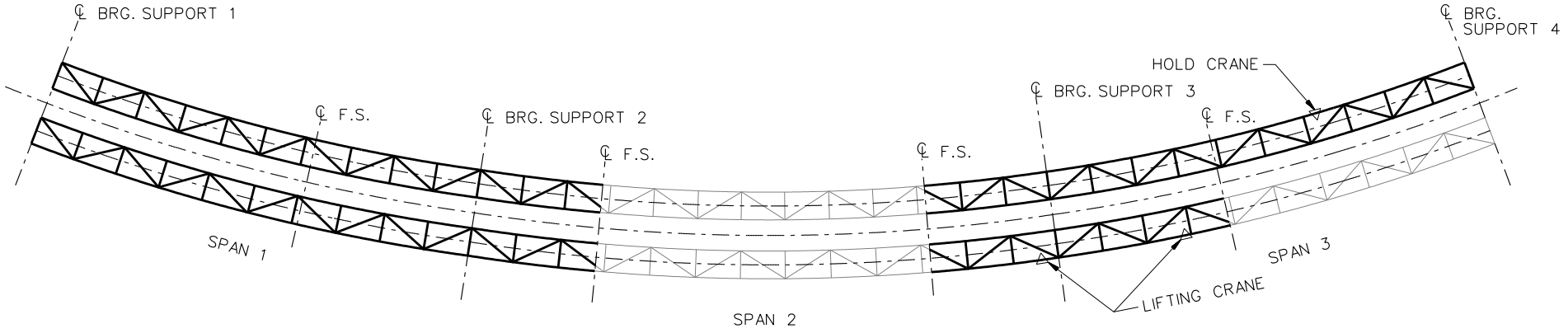

STAGE 5

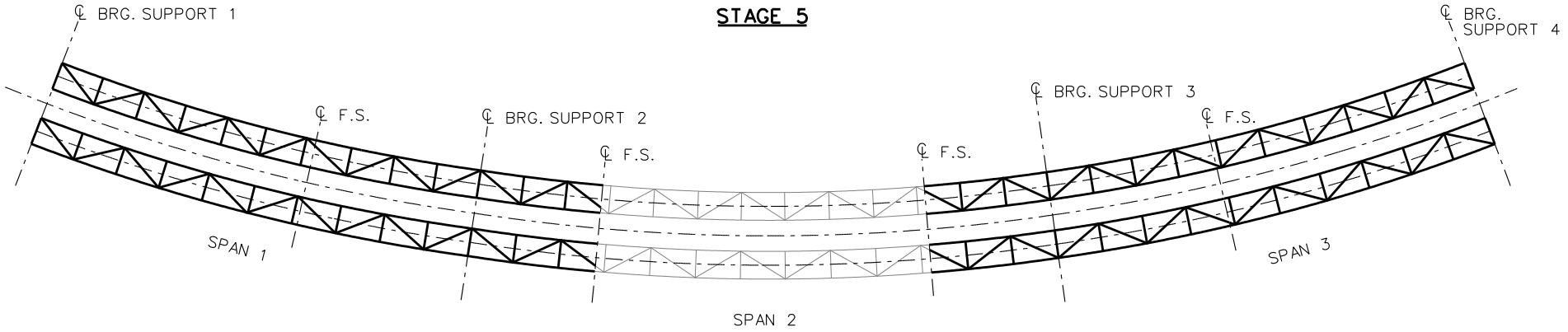

STAGE 6

LEGEND

▽ = HOLD OR LIFT CRANE

○ = TIE DOWN

□ = TEMPORARY SUPPORT STRUCTURE

NCHRP 12-79

BRIDGE XTCCR8

GIRDER ERECTION PROCEDURE

SHEET 3 OF 4

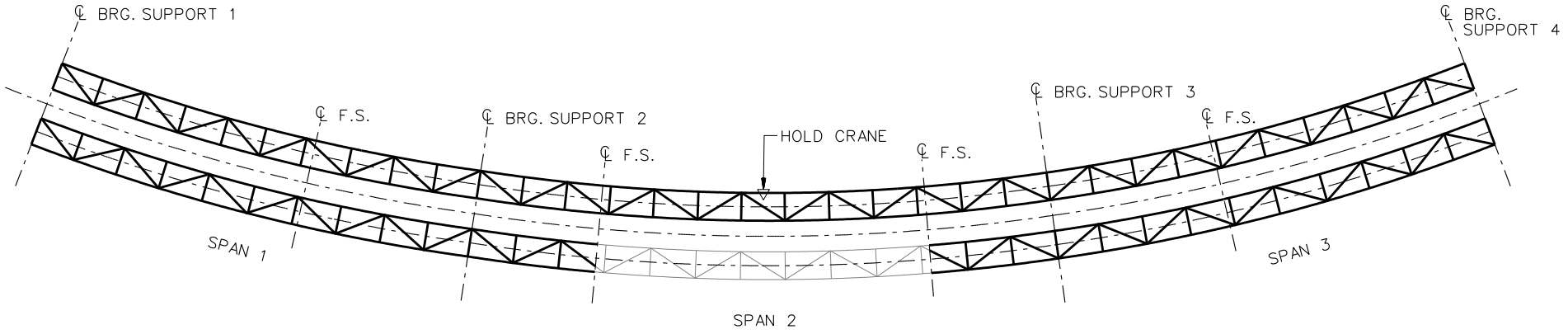

STAGE 7

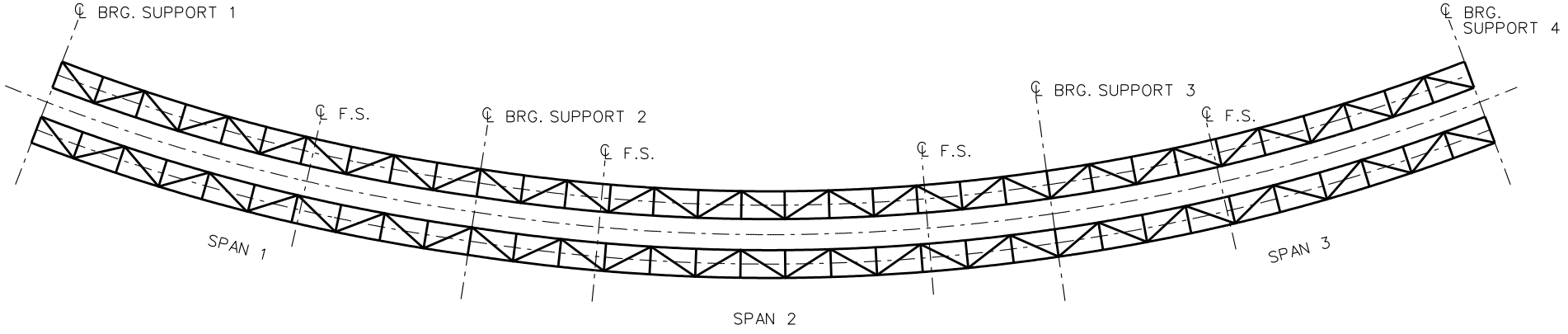

STAGE 8

LEGEND

▽ = HOLD OR LIFT CRANE

○ = TIE DOWN

□ = TEMPORARY SUPPORT STRUCTURE

NCHRP 12-79

BRIDGE XTCCR8

GIRDER ERECTION PROCEDURE

SHEET 4 OF 4

NCHRP 12-79

XTCSN3

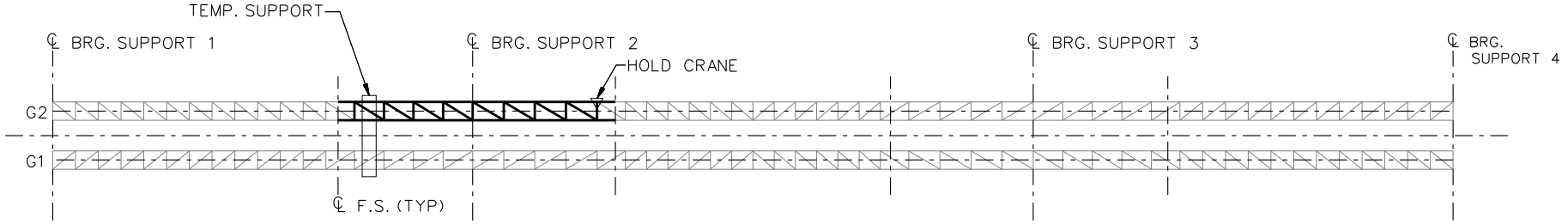

STAGE 1

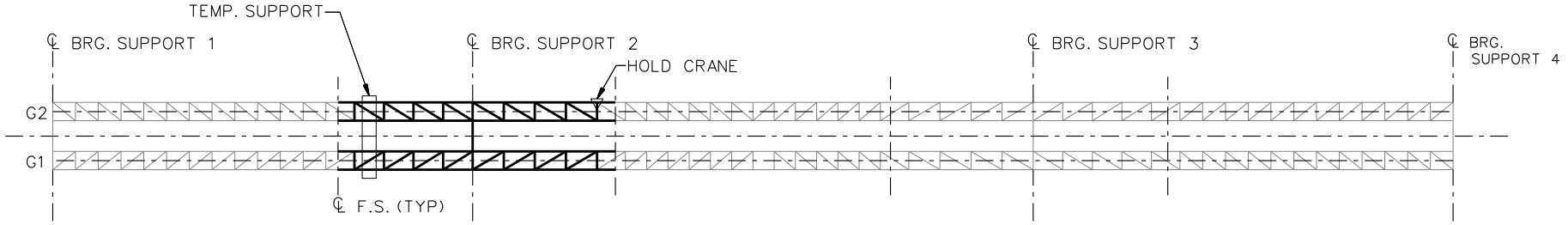

STAGE 2

LEGEND

▽ = HOLD OR LIFT CRANE

○ = TIE DOWN

□ = TEMPORARY SUPPORT STRUCTURE

NCHRP 12-79

BRIDGE XTCSN3

GIRDER ERECTION PROCEDURE

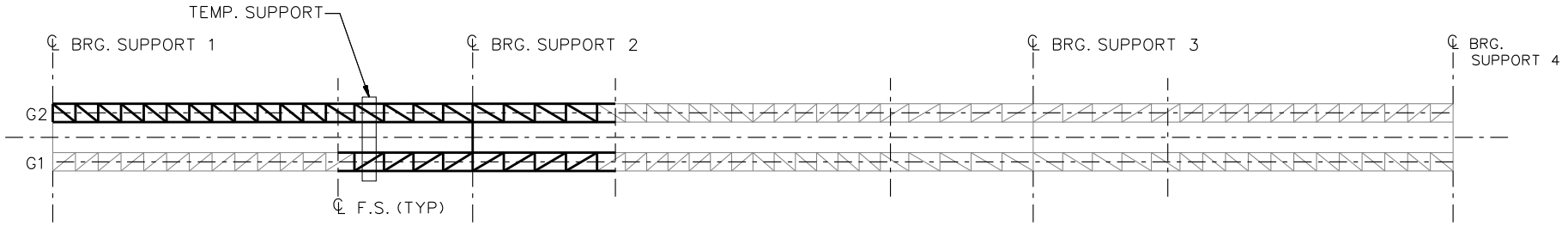

STAGE 3

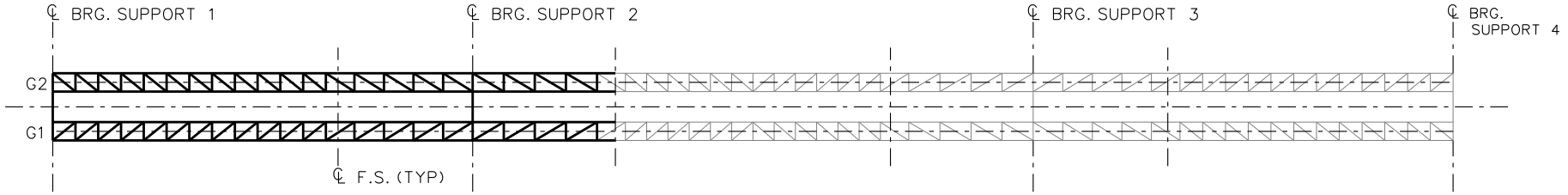

STAGE 4

LEGEND

▽ = HOLD OR LIFT CRANE

○ = TIE DOWN

□ = TEMPORARY SUPPORT STRUCTURE

NCHRP 12-79

BRIDGE XTCSN3

GIRDER ERECTION PROCEDURE

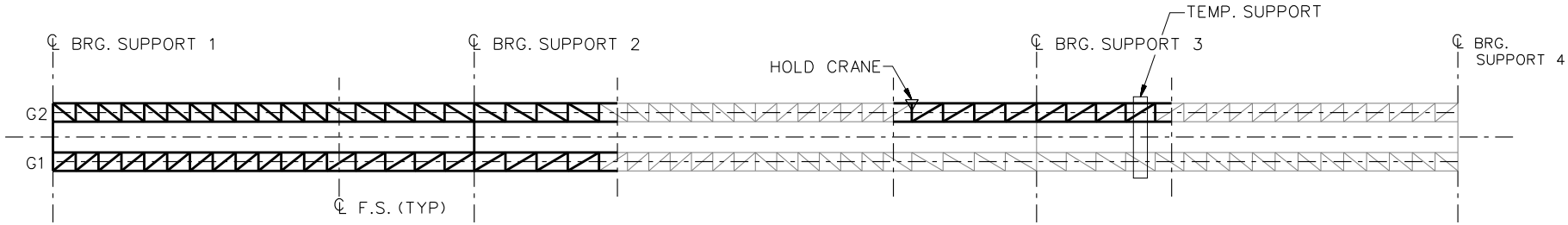

STAGE 5

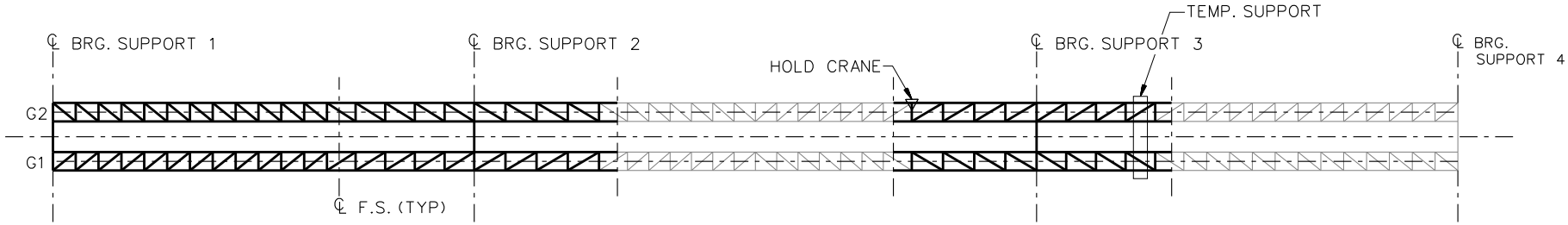

STAGE 6

LEGEND

▽ = HOLD OR LIFT CRANE

○ = TIE DOWN

□ = TEMPORARY SUPPORT STRUCTURE

NCHRP 12-79

BRIDGE XTCSN3

GIRDER ERECTION PROCEDURE

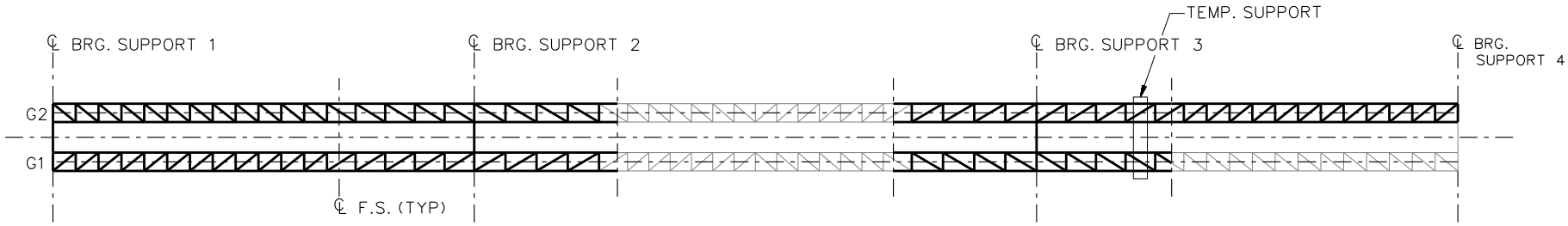

STAGE 7

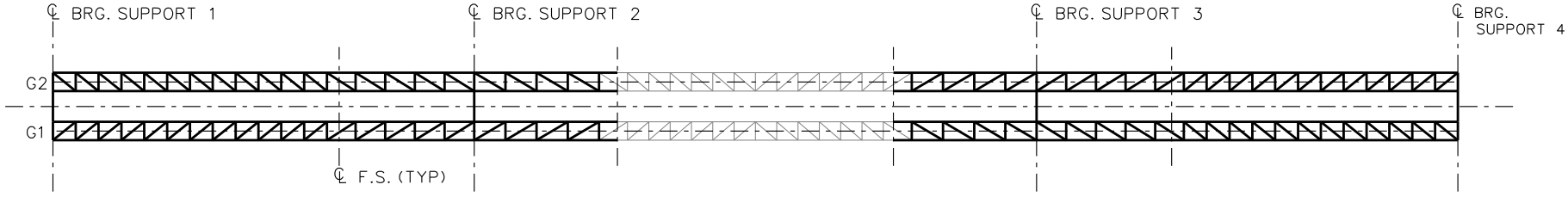

STAGE 8

LEGEND

▽ = HOLD OR LIFT CRANE

○ = TIE DOWN

□ = TEMPORARY SUPPORT STRUCTURE

NCHRP 12-79

BRIDGE XTCSN3

GIRDER ERECTION PROCEDURE

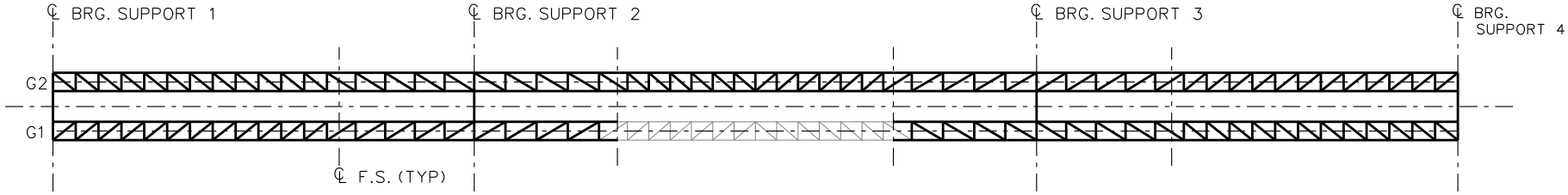

STAGE 9

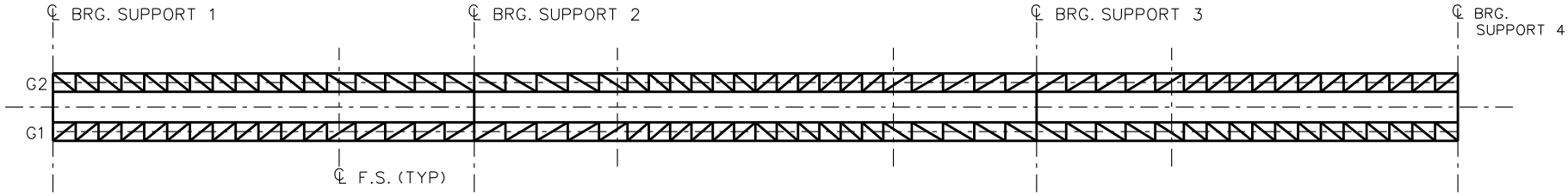

STAGE 10

LEGEND

▽ = HOLD OR LIFT CRANE

○ = TIE DOWN

□ = TEMPORARY SUPPORT STRUCTURE

NCHRP 12-79

BRIDGE XTCSN3

GIRDER ERECTION PROCEDURE

Appendix K. Organization of Electronic Data

This Appendix describes the information provided in electronic format. The electronic data is organized by folders that contain the information of each of the 58 I-girder bridges and the 18 tub-girder bridges studied in the NCHRP 12-79 Project. The electronic data is comprised of 76 main folders (one for each bridge) that are organized as follows:

Sub-Folder 1, Bridge Information:

Design Drawings: The design drawings include the plan view, the dimensions of all the bridge structural components, bearing types, and the dimensions of the concrete slab. In general, the design drawings describe the bridge geometry and contain all the information required to model and analyze the structure.

Erection and Deck Placement Drawings: These drawings describe the erection plan considered for the construction of the steel structure. In addition, the drawings include the deck placement sequence for the bridges where the deck was placed in more than one step.

Bridge Worksheet: This is a spreadsheet that contains information extracted from the design drawings and was used to generate the 3D FE models. This spreadsheet can be used to reproduce the 3D FE models of the bridges studied in the NCHRP 12-79 Project.

Sub-Folder 2, Analysis Results:

This folder contains the spreadsheets with the results obtained from the approximate analysis methods and the 3D FEA. Depending on the bridge type and geometry, the 1D analysis results correspond to the line-girder analysis obtained from one of the two following programs. For straight I-girder bridges, analyses were performed using the STLBRIDGE package (Bridgesoft, Inc., 2010). For curved I-girder bridges, the analyses were conducted based on the V-load method using the program VANCK (1996). All of the 1D analysis conducted in tub-girder bridges, for both straight and curved, were performed using the STLBRIDGE package. In the case of the 2D-grid

analyses, they were implemented using MDX (MDX Software, 2010) and LARSA 4D (LARSA, 2010) software packages for all the studies conducted in both I-girder and tub-girder bridges. The reader is referred to Chapters 2 and 5 for more information regarding the analysis methods and the software packages used in the NCHRP 12-79 Project.

The results of the 1D line-girder analyses are provided for two construction stages. The first is the stage where all the components of the steel structure are erected, typically known as steel dead load (SDL) condition. The second stage corresponds to the total dead load (TDL) condition, where the full noncomposite load is acting on the structure, and the concrete deck is applied in a single step.

The results of the 2D-grid models conducted with the MDX package are provided at the SDL condition and also, for the different stages considered in the sequential deck placement. The results obtained from the 2D-grid LARSA models are provided for selected steel erection stages, as well as, for the SDL and TDL condition.

The 3D model results are provided for the same steel erection stages analyzed with the LARSA software. In addition, except for bridges XICSS5 and EICSS1, all the 3D FEA results are shown at the TDL condition. For these two bridges, sequential deck placement analyses were performed.

Sub-Folder 3, Comparison of Results:

This folder contains spreadsheets that combine the information of Sub-Folder 2. In these spreadsheets the results of the approximate 1D and 2D analysis methods are plotted and compared to the 3D FEA solutions. The spreadsheets contain the calculations of the error index used to determine the accuracy of the approximate methods, as discussed in Chapter 5.